Can. J. Chem. Downloaded from www.nrcresearchpress.com by 210.87.254.105 on 09/05/12
For personal use only.

Canadian Journal of Chemistry

Published by THE NATIONAL RESEARCH COUNCIL OF CANADA

VOLUME 50 JANUARY 1, 1972 NUMBER 1

Collisional Deactivation Rates of Electronically Excited Molecular Ions. II

G. I. MACKAY AND R. E. MARCH

Department of Chemistry, Trent University, Peterborough, Ontario

Received July 5, 1971

Total deactivation rate constants have been determined for $N_2^+(B^2\Sigma_u^+)$ and the $(A^2\Pi_u)$ and $(B^2\Sigma_u^+)$ states of CO_2^+ with a number of quenchers. The energy specific total deactivation rate constant is compared to the total radiative lifetime of the excited species. A particular novelty of the technique is that it does not require a complete knowledge of the formation modes for the excited species. The results are compared with theoretical values obtained from the ion-induced dipole model. Individual deactivation rate constants are presented for $N_2^+(B^2\Sigma_u^+)$ ions in the $v = 0$, 1, and 2 vibrational levels quenched by N_2, O_2, H_2, and CO_2; and for the $(A^2\Pi_u)$ and $(B^2\Sigma_u^+)$ states of CO_2^+ quenched by CO_2, N_2, O_2, NO, and H_2. Charge transfer is the most probable mode of deactivation except in the CO_2^+–H_2 reactions where H-atom abstraction is more probable.

Les constantes de vitesse de désactivation totale ont été déterminées pour $N_2^+(B^2\Sigma_u^+)$ et pour les états $(A^2\Pi_u)$ et $(B^2\Sigma_u^+)$ de CO_2^+ avec un certain nombre d'accepteurs. L'énergie spécifique correspondant à la constante de vitesse de désactivation totale est comparée à la durée de vie radiative totale des espèces excitées. Une nouveauté particulière de la technique est qu'elle ne nécessite pas une connaissance complète des modes de formation des espèces excitées. Les résultats sont comparés avec les valeurs théoriques issues du modèle ion-dipôle induit. Les constantes de vitesse de désactivation sont données individuellement pour les ions $N_2^+(B^2\Sigma_u^+)$ dans les niveaux vibrationnels $v = 0$, 1 et 2, piégés par N_2, O_2, H_2 et CO_2; et pour CO_2^+ dans les niveaux $(A^2\Pi_u)$ et $(B^2\Sigma_u^+)$, piégés par CO_2, N_2, O_2, NO et H_2. Le transfert de charge est le mode de désactivation le plus probable sauf pour le système CO_2^+–H_2 où l'arrachement de l'hydrogène est plus probable.

Canadian Journal of Chemistry **50**, 1 (1972)

Thermal energy positive ion–neutral deactivation rate constants have been determined for electronically excited molecular ions, produced in a high energy electron beam. Deactivation rate constants are presented for the ground vibrational level ($v = 0$) of the $N_2^+(B^2\Sigma_u^+)$ ion and for the $v = 1$ and $v = 2$ levels, and for electronically excited molecular ions of carbon dioxide deactivated by carbon dioxide, oxygen, nitrogen, nitric oxide, and hydrogen.

The acquisition of ultraviolet spectra of Mars from the flyby flights of Mariners 6 and 7 has led to a renewed interest in the photochemistry of carbon dioxide. The Martian dayglow spectrum consists of a variety of emission features associated with CO_2^+, CO, O, C, and H. This paper is concerned partially with loss processes of excited CO_2^+ ions which may be either of atmospheric interest or of relevance to the CO_2 atmospheric laser.

Experimental

A differentially pumped beam of electrons, accelerated to 20 keV through an orifice 0.022 in. in diameter, was directed into a cylindrical observation chamber located in a flow system. The beam which was perpendicular to the direction of flow was maintained by adjustment of the filament voltage at a constant current of approximately 1 mA. The current was measured by a Faraday cup grounded through a Keithley 601 electrometer. The flow rate of each component was determined initially from the decrease in pressure of a known volume of gas; a calibrated McLeod gauge was used for the total pressure. An image of the slit of the spectrometer at a magnification of unity was formed along the axis of the beam using a combination of lens and front-surfaced mirror. Direct observation of the first negative system (1N) of nitrogen and the $(\tilde{B} \rightarrow \tilde{X})$ and $(\tilde{A} \rightarrow \tilde{X})$ systems of carbon dioxide was made with a SPEX 1700-II Czerny-Turner spectrometer equipped with a 100 mm × 100 mm grating (1200 lines/mm)

Can. J. Chem. Downloaded from www.nrcresearchpress.com by 210.87.254.105 on 09/05/12
For personal use only.

blazed at 3000 Å. The spectra were scanned in the first order. The beam diameter was 0.15 cm. The signal was detected with an EMI 6256S photomultiplier, amplified with an Ortec 486 Amplifier–Pulse Height Analyzer coupled with an Ortec 441 Linear Ratemeter and recorded with a Speedomax W Azar Recorder. The signal intensity was taken as the integrated area of an entire vibrational band.

Results and Discussion

Electronically excited molecular ions are produced by electron impact, as the beam traverses the gas filled observation chamber. Those states from which radiative transitions are allowed were monitored spectroscopically. The effects of secondary electron excitation are small at the pressures used here (0.1–1 Torr). With nitrogen the following bands of the N_2 IN system were monitored; the (0,0) band at 3914 Å, the (1,2) band at 4236 Å, and the (2,4) band at 4597 Å. The essential features of the carbon dioxide electron impact induced fluorescence spectrum arise from the ($A^2\Pi_u$) and ($B^2\Sigma_u^+$) states of the carbon dioxide ion, CO_2^+.

$CO_2^+(\tilde{B}^2\Sigma^+ \rightarrow \tilde{X}^2\Pi_g)$

Emission of a very strong double-peaked band (1) at 2875–2905 Å is due to the $CO_2^+(B^2\Sigma_u^+ \rightarrow \tilde{X}^2\Pi_g)$ transition. The excitation potential of this band is around 18.0 eV. The high intensity of this band (as compared with other possible bands in the same system) suggests that there is very little vibration in the upper state. This may be due to the operation of the Franck–Condon principle in the excitation process, since the values of the rotational constant B of the CO_2 ground state, the $CO_2^+(B^2\Sigma_u^+)$ state and the $CO_2^+(X^2\Pi_g)$ state are almost equal ($B = 0.381$, 0.379, and 0.350 cm^{-1}, respectively (2)) and the molecule is linear in all three states.

$CO_2^+(\tilde{A}^2\Pi_u \rightarrow \tilde{X}^2\Pi_g)$

The band spectrum appearing in emission in the region 2900–4300 Å (and often referred to as the Fox, Duffendack and Barker (3) system) has been identified (4) as a $^2\Pi$–$^2\Pi$ transition of CO_2^+. The system is composed of two sub-bands corresponding to the ($^2\Pi_{3/2} \rightarrow {}^2\Pi_{3/2}$) and ($^2\Pi_{1/2} \rightarrow {}^2\Pi_{1/2}$) transitions. The band sequence at 3247–3275 Å, which was found to be free of overlapping nitrogen bands, is due to (v_1', v_1'') transitions with $v_2' = v_2'' = v_3' = v_3'' = 0$ and it was possible to resolve the (2,0) and (3,1) transitions in each of the sub-bands. The (2,0) band of the ($^2\Pi_{3/2u} \rightarrow {}^2\Pi_{3/2g}$) transition is situated on the short wavelength side of the sequence and since all bands are degraded towards the red, a band-width of 6 Å was isolated free from overlappings. The remaining bands of the sequence overlap other bands lying at longer wavelengths, *i.e.* the (2,0) band of the ($^2\Pi_{1/2u} \rightarrow {}^2\Pi_{1/2g}$) transition is overlapped by the (2,0) band of the ($^2\Pi_{3/2u} \rightarrow {}^2\Pi_{3/2g}$) transition and, in turn, overlaps the (3,1) band of the ($^2\Pi_{1/2u} \rightarrow {}^2\Pi_{1/2g}$) transition which overlaps the (3,1) band of the ($^2\Pi_{3/2u} \rightarrow {}^2\Pi_{3/2g}$) transition. The extent of overlap of the last three bands described above was estimated to be less than 10%. When a correction for this overlap was applied to the data, it had little effect due to the similarity of the self-deactivation rate constants.

For a single gas, A, the steady state equation for the intensity of a given band, I is of the form

$$[1] \qquad \frac{1}{I} = \frac{1}{k_1 c[\mathrm{A}]} + \frac{k_3}{k_1 k_2 c}$$

where c is the electron beam current, k_1 is related to the cross-section for formation of an excited ion, k_2 is the reciprocal of the lifetime τ of the radiative transition, and k_3 is the deactivation rate constant for parent molecules. A plot of I^{-1} *vs.* $[\mathrm{A}]^{-1}$ yields $k_3 = (\text{intercept}/\tau\ \text{slope})$.

In the presence of added quencher and at constant total pressure, P, the intensity of a given band I_q is of the form

$$[2] \qquad \frac{1}{I_q} = \frac{(k_2 + k_4)P}{k_1 k_2 c[\mathrm{A}]} + \frac{(k_3 - k_4)}{k_1 k_2 c}$$

where k_4 is the quencher deactivation rate constant. Thus from a plot of I_q^{-1} *vs.* $[\mathrm{A}]^{-1}k_4$ may be evaluated provided that the lifetime of the radiative state is known. The experimental uncertainty in the reported value for k_2 is reflected directly in this evaluation of k_4. A summary is given in Table 1 of the lifetimes of the $N_2^+(B)$ and $CO_2^+(A)$ and (B) states reported in the past seven years.

The method outlined above is particularly convenient for flow systems with calibrated flow rates in that it offers the advantage over the treatment of, for example, Brown and Miller (5) in that it obviates the evaluation of k_1. Population of the observed radiative states by collision induced cascade processes from higher vibrational levels may well occur in these systems. It has been assumed here that k_1 is a total rate con-

Can. J. Chem. Downloaded from www.nrcresearchpress.com by 210.87.254.105 on 09/05/12
For personal use only.

TABLE 1. Lifetimes of excited states

State	Lifetime (ns)	Reference
$N_2^+(B^2\Sigma_u^+)$	65.8 ± 3.5	21
	60	22
	65 ± 2	23
	40 ±20	24
	82 ± 8	25
	71.5 ± 4	26
	66.6 ± 1.3	27
	59.2 ± 6	28
	65.9 ± 1.0	29
	58.6 ± 5	30
	$(62.5 \pm 5)_{v'=1}$	30
$CO_2^+(\tilde{A}^2\Pi_g)$	139	31
	100 ±40	32
	113 ±12	28
$CO_2^+(\tilde{B}^2\Sigma_u^+)$	118 ±12	28

stant for all pressure dependent production processes for the radiative state. The linearity of the subsequent plots of I^{-1} *vs.* $[A]^{-1}$ demonstrates the constancy of k_1 over the pressure range and justifies the assumption of negligible cascade population. The population of the excited states by electronic transitions from higher energy levels does not appear likely. Such transitions populating the states under observation would be accompanied by emissions comparable in intensity to those observed. No such emissions have been reported in the literature. Other electronic states of N_2^+ other than $N_2^+(B)$ have been identified, but these states combine only with ground state $N_2^+(X)$. Both the $CO_2^+(A^2)$ and (B^2) states combine only with ground state $CO_2^+(X^2)$.

The polarization theory of ion–molecule collisions (6, 7) predicts a collision rate constant (collisions referring to orbiting collisions) which is given by $k_c = 2\pi e(\alpha/\mu)^{1/2}$ where e is the electronic charge, α is the polarizability of the molecule, and μ is the reactant pair reduced mass. It is convenient to compare the total deactivation rate constant with k_c as the ratio affords a measure of the reaction efficiency *i.e.* the probability of a reactive encounter per orbiting collision. While it is recognized that the induced dipole model was not intended to describe reactions of electronically excited ions and their quenching the model does provide a form of reference for these results. The rotational temperature as determined from the R branch of the N_2^+IN (0,0) band varied only between 308–320 °K over the pressure range 1–0.05 Torr, thus as translational–rotational equilibrium is attained rapidly, the kinetic energy of the ions will be thermalized.

In brief the present technique is restricted to those molecules which may be ionized on electron impact to an excited ion energy level from which radiative transfer can be observed. Charge transfer may then occur with a quencher molecule which has an ion energy level (or levels, wherein multiple pathways will be available) which is at a lower energy than the level initially excited (including vibrational energy). In Fig. 1 are shown the ion energy levels of the species studied in this work. It is readily seen that charge transfer is exothermic for H_2, O_2, NO, and CO_2, with $N_2^+(B)$, and for H_2, O_2, N_2, NO, and CO_2 with $CO_2^+(A^2)$ and (B^2), provided that the final ion states produced are those shown in this figure. The only exception is in the CO_2^+–H_2 reactions where it appears (8) that hydrogen-

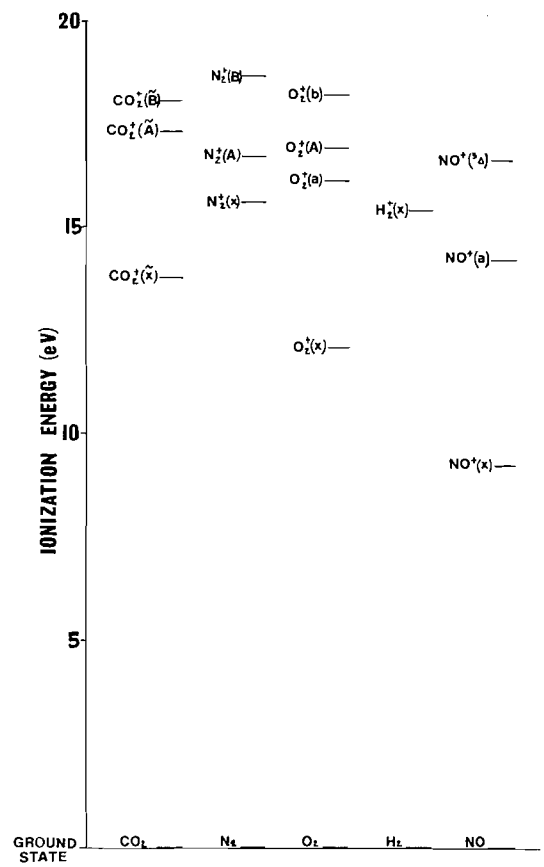

FIG. 1. Schematic representation of the ion electronic energy levels of molecules used in this study.

Can. J. Chem. Downloaded from www.nrcresearchpress.com by 210.87.254.105 on 09/05/12
For personal use only.

atom abstraction to produce CO_2H^+ ions is more probable. It is also apparent that while charge transfer of vibrationally "cool" $O_2^+(X)$ with N_2 is highly endothermic, charge transfer of $O_2^+(B)$ with N_2 (to produce $N_2^+(X)$) is highly exothermic and that measurement of its rate is possible from observation of the oxygen (IN) system. This work will be reported later.

Nitrogen

A summary of the self-quenching rate data for nitrogen is given in Table 2 and the results are shown graphically in Fig. 2. The radiative lifetimes of the $v' = 0$ and $v' = 1$ levels were taken as 58.6 ± 5 and 62.5 ± 5 ns, respectively (11), while that of the $v' = 2$ level was taken as 70 ± 5 ns (12). On the addition of quencher (CO_2, O_2 or NO), it was possible to measure the deactivation rates for the $N_2^+(B)$ $v' = 0$ and 1 levels only due to overlap of a quencher band with the $N_2^+(2,4)$ band. With hydrogen as quencher individual rate constants were obtained for $v' = 0$, 1, and 2 of $N_2^+(B)$. The results are presented in Table 3. The values presented in Tables 2 and 3 are mean values from several determinations; the variation in the mean indicates the spread presented by individual runs in which the experimental error was not greater than 5%.

The rate constants for the deactivation of $N_2^+(B)$ in $v' = 0$ and 1 by nitrogen are in good agreement with our earlier published values (16), and the variation in each value is somewhat diminished. The relative ratio for the $v' = 0$, 1, and 2 levels is presented with more certainty than the given variations would tend to indicate. The values for $k_{3,v'=0}$ and $k_{3,v'=2}$ are virtually the same, but $k_{3,v'=1}$ is appreciably lower. k_3 may be regarded as the sum of electronic and vibrational quenching constants for the $v' = 1$ and 2 levels, but can represent only the electronic quenching constant for the $v' = 0$ level, *i.e.* $k_{3,0}$.

TABLE 2. Self-quenching constants for $N_2^+(B^2\Sigma_u^+)$

		k(l mol^{-1} s^{-1} × 10^{-10})		
$k_{3,v'}$	Quencher	This work	Other workers	k_c*
$v' = 0$	N_2	35 ± 5	24 ± 9†; 27 ± 3‡	49
$v' = 1$	N_2	21 ± 3		49
$v' = 2$	N_2	$35(+20, -10)$		49

*Collision rate constant $k_c = 2\pi e(\alpha/\mu)^{1/2}$.
†Reference 9.
‡Reference 10.

As the energy difference between the $v' = 1$ and $v' = 0$ levels of the $B^2\Sigma_u^+$ state of nitrogen is 0.2934 eV, which is greater than the corresponding energy difference for many other states of nitrogen (*e.g.* $N_2(X'_g{}^+)$ 0.2889 eV; $N_2(C^3\Pi_u)$

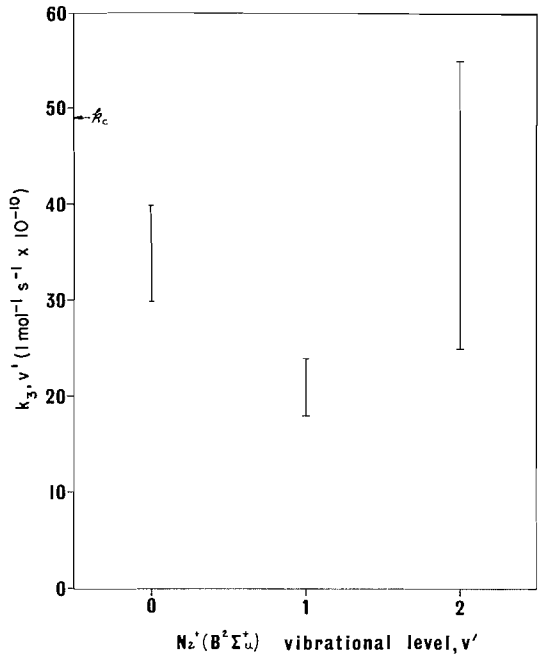

FIG. 2. Deactivation rate constant $k_{3,v'}$ as a function of vibrational level of $N_2^+(B^2\Sigma_u^+)$ for the reaction $N_2^+(B) + N_2 \rightarrow N_2 + N_2^+(X)$. The calculated value of the collision rate constant k_c is shown.

TABLE 3. Quenching constants for $N_2^+(B^2\Sigma_u^+)$

		k(l mol^{-1} s^{-1} × 10^{-10})		
$k_{5,v'}$	Quencher	This work	Other workers	k_c*
$v' = 0$	CO_2	60 ± 6	(54)†	61
$v' = 1$	CO_2	60 ± 6		61
$v' = 0$	H_2	70	(100)‡	90
$v' = 1$	H_2	50 ± 10		90
$v' = 2$	H_2	85		90
$v' = 0$	O_2	44 ± 8	(2.6–12)§	46
$v' = 1$	O_2	24 ± 4		46
$v' = 0$	NO		46 ± 9‖ (20 ± 7)¶	48
$v' = 1$	NO		14(6, −3)‖	48

*Collision rate constant $k_c = 2\pi e(\alpha/\mu)^{1/2}$.
†Reference 13 (ground state ion, $N_2^+(X)$).
‡Reference 14 (ground state ion, $N_2^+(X)$).
§Reference 15 (ground state ion, $N_2^+(X)$).
‖Reference 16.
¶Reference 17 (ground state ion, $N_2^+(X)$).

Can. J. Chem. Downloaded from www.nrcresearchpress.com by 210.87.254.105 on 09/05/12
For personal use only.

0.2471 eV; $N_2^+(X^2{}_g^+)$ 0.2697 eV), we may assume that vibrational quenching is relatively slow and that the observed value of $k_{3,1}$ represents mainly electronic quenching. Calo and Axtmann (18) have shown that in the deactivation of the $C^3\Pi_u$ state of nitrogen by ground state nitrogen molecules the ratio of electronic quenching cross-sections for the $v' = 0$ and $v' = 1$ levels ≈ 1.5 which is in agreement, albeit fortuitously, with the ratio for $k_{3,0}/k_{3,1}$ obtained here for $N_2^+(B)$. The diminution of the deactivation rate constant for $N_2^+(B)_{v'=1}$ as shown in Fig. 2 is not limited to deactivation by nitrogen molecules. We reported earlier (16) that the rate constant for deactivation of $N_2^+(B)$ by nitric oxide is decreased by a factor of 3 on the acquisition by the ion of a single vibrational quantum. However, in the quenching by nitric oxide it was not possible, due to overlapping of bands, to determine the rate constant for deactivation of the $N_2^+(B)$ $v' = 2$ level. It would be of interest to know in this system whether or not the rate constant for $v' = 2$ is comparable to that for $v' = 0$. Deactivation of $N_2^+(B)$ by molecular hydrogen exhibits the same minimum in the deactivation rate constant at $v' = 1$, and deactivation with molecular oxygen also shows diminution of the rate for $v' = 1$ relative to $v' = 0$. Of particular interest in aeronomy is the appreciable enhancement of the deactivation rate of the excited nitrogen ion by molecular oxygen compared to that of the ground state ion (15).

Hydrogen-atom abstraction from H_2 by positive ions has been shown previously to be a rapid reaction when exothermic. In this work we made no attempt to determine the nature of the products of the reaction of $N_2^+(B)$ with hydrogen, but assumed that the excitation of the ion would not cause any departure from the pathway proposed by Moran and Friedman (19), in which the hydride ion is formed.

[3] $$N_2^+ + H_2 \rightarrow N_2H^+ + H$$

Chupka and Russell (20) have shown that NH_3^+ in higher vibrational states reacts less efficiently with NH_3 to produce NH_4^+ while vibrational excitation has virtually no effect on the NH_3^+–H_2O reaction. Both reactions are exothermic.

In contrast, the rate constant for deactivation of $N_2^+(B)$ by carbon dioxide is greater than the corresponding constant with nitrogen or nitric oxide and fails to exhibit any difference in activity between the $v' = 0$ and $v' = 1$ levels for $N_2^+(B)$. The values obtained here, and shown in Table 3, agree well with the value reported by Ferguson and co-workers (13) for deactivation of the ground state ion $N_2^+(X)$ by carbon dioxide. In each case the deactivation rate constant approaches the collision rate constant, k_c. The conclusions which may be drawn at this stage are as follows:

(*i*) That when the charge transfer rate of ground state N_2^+ with diatomic molecules is slow (relative to the maximum value which is taken here as k_c), electronic excitation of the ion will lead to enhancement of the charge transfer rate (though mindful of the distinction between deactivation and charge transfer and in particular that the rate of the latter process must be equal to or less than that of the former process).

(*ii*) That electronic excitation of N_2^+ does not lead to any diminution of the overall deactivation rate in comparison to that of the ground state ion when charge transfer of the ground state ion is rapid as was observed with H_2 and CO_2.

(*iii*) Deactivation by diatomic molecules of $N_2^+(B)$ ions possessing a single vibrational quantum appears to proceed generally at a rate which is slower by a factor of 2–3 in comparison to the respective rate for ions in the zeroth vibrational level. This effect on $N_2^+(B)_{v'=1}$ was observed with nitrogen, hydrogen, oxygen, and nitric oxide. No such effect was observed with carbon dioxide. One is thus led to speculate that the first quantum of vibrational energy in the $N_2^+(B)$ ion which is large in comparison to other vibrational quanta in nitrogen decreases the probability of a reactive encounter with a diatomic molecule. This effect was non-existent with a polyatomic molecule possessing several modes of vibration. Exhibition of this effect in the $N_2^+(B)$–H_2 reaction was somewhat surprising in view of Moran and Friedman's proposal concerning hydride formation in which the total number of vibrational modes would be increased.

(*iv*) Deactivation by diatomic molecules (N_2 and H_2) of $N_2^+(B)$ ions with two vibrational quanta appears to proceed at a rate which is comparable to that for ions in the zeroth vibrational level and to the collision rate.

Can. J. Chem. Downloaded from www.nrcresearchpress.com by 210.87.254.105 on 09/05/12
For personal use only.

Carbon Dioxide

The self-quenching rate constants shown in Table 4 are the least accurate due to the requirement of the evaluation of the intercept from the plot of I^{-1} *vs.* $[CO_2]^{-1}$. A relatively small change in slope can produce a large change in the intercept and hence there is a relatively large uncertainty in the value for k_5. However, two points may be made here. (*i*) That within the stated uncertainty limits the data can be interpreted as following the trend previously observed that ions in high electronic states are deactivated more rapidly than those in lower electronic states. (*ii*) That the deactivation rate constants appear to exceed the collision rate constant. Thus the self-quenching reaction for carbon dioxide may be yet another example for which the ion-induced dipole model is inadequate for the explanation of reactions of excited ions.

CO_2^+–O_2

The quenching constants for this reaction are shown in Table 5. The value for the $CO_2^+(B)$ state is more accurate than that for the $CO_2^+(A)$ state. Thus we are able to report with some certainty that deactivation of the $CO_2^+(B)$ state by O_2 proceeds at a rate in excess of that predicted by the ion-induced dipole model. A similar observation has been reported by Giomousis and Stevenson (7) for the reaction of O_2 with H_2^+ and D_2^+ ions, and although their values lack some precision as the ion residence times were not measured, the O_2 reactions were unique in that the experimental rate constants exceeded the theoretical value (k_c) by a factor ~ 2. Thus it appears that the ion-induced dipole model is not applicable generally to O_2 reactions possibly due to the polarizability tensor of oxygen which is not isotropic.

It is of interest to note in this series of reactions of carbon dioxide ions with molecular oxygen that a linear relationship appears to exist between the logarithm of the deactivation rate constant and the energy of the ion.

CO_2^+–N_2

In Table 5 we report the deactivation rate constants for the $CO_2^+(\tilde{A})$ and $CO_2^+(\tilde{B})$ ions with N_2. The energetic ion is deactivated at an enhanced rate in comparison to the less energetic ion.

TABLE 4. Self-quenching constants for CO_2^+

Quencher	State	$1/k_2$ (ns)	k_3*	k_c*†
CO_2	$CO_2^+(\tilde{X})$	—	—	49
CO_2	$CO_2^+(\tilde{A})$	113 ± 12	120 ± 60	49
CO_2	$CO_2^+(\tilde{B})$	118 ± 12	66 ± 24	49

*In l mol^{-1} s^{-1}.
†Collision rate constant $k_c = 2\pi e(\alpha/\mu)^{1/2}$.

TABLE 5. Quenching constants for CO_2^+

Quencher	State	k_5*	k_c*
O_2	$CO_2^+(\tilde{X})$	(3 ± 1)†	62
O_2	$CO_2^+(\tilde{A})$	84 ± 18	62
O_2	$CO_2^+(\tilde{B})$	132 ± 24	62
N_2	$CO_2^+(\tilde{X})$	Endoergic	
N_2	$CO_2^+(\tilde{A})$	15 ± 9	43
N_2	$CO_2^+(\tilde{B})$	33 ± 6	43
NO	$CO_2^+(\tilde{X})$	(7.2 ± 2)†	43
NO	$CO_2^+(\tilde{A})$	(26 ± 5)‡	43
NO	$CO_2^+(\tilde{B})$	33 ± 6	43
H_2	$CO_2^+(\tilde{B})$	60 ± 12	90

*In l mol^{-1} s^{-1}.
†Reference 17.
‡An interpolation, see Discussion.

An attempt was made to determine the effect of vibrational excitation in the $CO_2^+(\tilde{A})$ ion on the deactivation rate with nitrogen. The bands selected were the (2,0) and (3,1) of the $\Pi_{1/2}$ system and the (2,0) and (3,1) of the $\Pi_{3/2}$ system which overlap each other as discussed above. A common lifetime was assumed. It was found that within each of these systems the $v_1 = 2$ state was deactivated at a slightly enhanced rate ($\sim$30–40%) in comparison to the $v_1 = 3$ state. The $\Pi_{3/2}$ system exhibited a similar enhancement ($\sim$50–60%) in comparison to the $\Pi_{1/2}$ system. The effect is small and may not be real.

CO_2^+–NO

The $CO_2^+(\tilde{A} \rightarrow \tilde{X})$ system is overlapped by emission from nitric oxide molecules excited by the electron beam. The deactivation rate constant for the $CO_2^+(\tilde{B})$ state ion is given in Table 5 along with the value obtained by Ferguson and co-workers (17) for charge transfer from the ground state ion. Again in this series the excited ion ($\tilde{B}$) is deactivated at an enhanced rate compared to the ground state ion but somewhat less than the collision rate. On the assumption that a similar relationship exists in the CO_2^+–NO system as in the CO_2^+–O_2 system one may

estimate that the deactivation rate constant for $CO_2^+(\tilde{A})$ by NO is $26 \pm 5 \times 10^{10}$ l s^{-1}.

It should be emphasized that the data obtained for the $CO_2^+(\tilde{B})$ ion are more accurate than for the $CO_2^+(\tilde{A})$ ion due to the high intensity of the double peaked emission from the $CO_2^+(\tilde{B})$ ion in a spectral region free from background interference and overlap.

The experimental uncertainties for the rate constants quoted in Table 5 include an uncertainty of $\pm 10\%$ from the value of the lifetime, thus the relative value of a given rate constant to another is somewhat more accurate than the quoted uncertainties would indicate.

The authors gratefully acknowledge the financial support of the National Research Council of Canada and Imperial Oil Limited (Canada).

1. F. BUESO-SANLLEHI. Phys. Rev. **60**, 556 (1941).
2. S. MROZOWSKI. Rev. Mod. Phys. **14**, 216 (1942).
3. G. W. FOX, O. S. DUFFENDACK, and E. F. BARKER. Proc. Nat. Acad. **13**, 320 (1927).
4. S. MROZOWSKI. Phys. Rev. **72**, 682, 691 (1947).
5. L. O. BROWN and N. MILLER. Trans. Faraday Soc. **53**, 748 (1957).
6. H. EYRING, J. O. HIRSCHFELDER, and H. S. TAYLOR. J. Chem. Phys. **4**, 479 (1966).
7. G. GIOMOUSIS and D. P. STEVENSON. J. Chem. Phys. **29**, 294 (1958).
8. F. C. FEHSENFELD, A. L. SCHMELTEKOPF, and E. E. FERGUSON. J. Chem. Phys. **46**, 2802 (1967); T. F. MORAN and L. FRIEDMAN. J. Chem. Phys. **42**, 2391 (1965).
9. B. BROCKLEHURST and F. A. DOWNING. J. Chem. Phys. **46**, 2976 (1967).
10. K. B. MITCHELL. J. Chem. Phys. **53**, 1795 (1970).
11. C. E. HEAD. Phys. Lett. **34A**, 92 (1971).
12. M. JEUNEHOMME. J. Chem. Phys. **44**, 2672 (1966).
13. F. C. FEHSENFELD, A. L. SCHMELTEKOPF, and E. E. FERGUSON. J. Chem. Phys. **44**, 4537 (1966).
14. F. C. FEHSENFELD, A. L. SCHMELTEKOPF, and E. E. FERGUSON. J. Chem. Phys. **46**, 2802 (1967).
15. F. C. FEHSENFELD, A. L. SCHMELTEKOPF, and E. E. FERGUSON. Planet. Space Sci. **13**, 219 (1965); **13**, 919 (1965); P. D. GOLDAN, A. L. SCHMELTEKOPF, F. C. FEHSENFELD, H. I. SCHIFF, and E. E. FERGUSON. J. Chem. Phys. **44**, 4095 (1966); D. B. DUNKIN, F. C. FEHSENFELD, A. L. SCHMELTEKOPF, and E. E. FERGUSON. J. Chem. Phys. **49**, 1365 (1968).
16. G. I. MACKAY and R. E. MARCH. Can. J. Chem. **49**, 1268 (1971).
17. F. C. FEHSENFELD, D. B. DUNKIN, and E. E. FERGUSON. Planet. Space Sci. **18**, 1267 (1970).
18. J. M. CALO and R. C. AXTMANN. J. Chem. Phys. **54**, 1332 (1971).
19. T. F. MORAN and L. FRIEDMAN. J. Chem. Phys. **42**, 2391 (1965).
20. W. A. CHUPKA and M. E. RUSSELL. J. Chem. Phys. **48**, 1527 (1968).
21. R. G. BENNETT and F. W. DALBY. J. Chem. Phys. **31**, 434 (1964).
22. E. FINK and K. H. WELGE. Z. Naturforsch. **19a**, 1193 (1964).
23. D. I. SEBACHER. J. Chem. Phys. **42**, 1368 (1965).
24. H. ANTON. Ann. Phys. **18**, 178 (1966).
25. R. G. FOWLER and T. M. HOLZBERLEIN. J. Chem. Phys. **45**, 1123 (1966).
26. M. JEUNEHOMME. J. Chem. Phys. **44**, 2672 (1966).
27. J. DESESQUELLES, M. DUFAY, and M. C. POULIZAC. Phys. Lett. **27A**, 96 (1968).
28. J. E. HESSER. J. Chem. Phys. **48**, 2518 (1968).
29. L. L. NICHOLS and W. E. WILSON. Appl. Opt. **7**, 167 (1968).
30. C. E. HEAD. Phys. Lett. **34A**, 92 (1971).
31. R. P. SCHWENKER. J. Chem. Phys. **42**, 2618 (1965).
32. H. ANTON. Ann. Physik. **18**, 178 (1966).

Can. J. Chem. Downloaded from www.nrcresearchpress.com by 210.87.254.105 on 09/05/12
For personal use only.

Studies of β-Diketone Complexes of Rhenium. I. Trispentane-2,4-dionatorhenium(III) and Tris(1,1,1,5,5,5-hexafluoropentane-2,4-dionato)rhenium(III)

W. D. COURRIER, W. FORSTER, C. J. L. LOCK,[1] AND G. TURNER
Institute for Materials Research, McMaster University, Hamilton, Ontario

Received July 7, 1971

Pure samples[2] of $Re(hfac)_3$ and $Re(acac)_3$ have been prepared and their physical properties studied by ultraviolet–visible and infrared spectroscopy, mass spectrometry, magnetic susceptibility measurements, and X-ray diffraction. The compounds are monomeric and the physical properties may be explained if the rhenium atom sits in an essentially octahedral ligand field. $Re(hfac)_3$ has a hexagonal unit cell and the acetylacetone complex adopts the monoclinic cell of the α-form of the three typical crystal structure types which Astbury (1) observed for trispentane-2,4-dionatometal(III) compounds. The properties observed for trispentane-2,4-dionatorhenium(III) differ from those reported previously (2, 3). The difficulties experienced in obtaining pure $Re(C_5H_7O_2)_3$ were caused by the ease with which the material is oxidized.

On a préparé des échantillons purs[2] de $Re(hfac)_3$ et $Re(acac)_3$ et étudié leurs propriétés physiques par la spectroscopie ultraviolette–visible et infrarouge, la spectrométrie de masse, des mesures de susceptibilité magnétique et la diffraction de rayons-X. Les composés sont monomériques et on peut expliquer les propriétés physiques si l'atome de rhénium se trouve dans un champ de ligand essentiellement octaédrique. $Re(hfac)_3$ possède une maille hexagonale et le complexe acétylacétone adopte la maille monoclinique de forme α des trois genres de structure cristalline typiques que Astbury (1) a observé pour les composés trispentane-2,4-dionatométalliques. Les propriétés observées pour le trispentane-2,4-dionatorhénium(III) diffèrent de celles rapportées précédemment (2, 3). Les difficultés rencontrées pour obtenir le $Re(C_5H_7O_2)_3$ pur furent causées par la facilité avec laquelle le matériel est oxydé.

Canadian Journal of Chemistry, **50**, 8 (1972)

Introduction

Tris(pentane-2,4-dionato)rhenium(III) was first described in 1960 (2, 3). We attempted to prepare some crystals of the material for X-ray diffraction studies, but had great difficulty isolating any solid. The products usually obtained by us were tars. In 1969 (4) a different method was described for the preparation of tris(1,1,1,5,5,5-hexafluoropentane-2,4-dionato)-rhenium(III) in which the sodium salt of the β-diketone and rhenium trichloride were destructively distilled. This suggested an alternative preparation for $Re(C_5H_7O_2)_3$ which is described herein. As the properties of the material we obtained were so different from those of the material described previously we have made extensive physical measurements on our compound with the dual purpose of contrasting it with previous work and showing that our material was really $Re(C_5H_7O_2)_3$. No physical measurements of $Re(C_5F_6HO_2)_3$ have been described previously so we have made a set of measurements on this compound, similar to those for $Re(C_5H_7O_2)_3$.

Experiments

Carbon and hydrogen analyses were performed by Alfred Bernhardt Microanalytisches Laboratorium, West Germany. Infrared spectra were recorded for solid samples ground into a mull with Nujol. The Nujol had been dried by refluxing with phosphorus pentoxide followed by vacuum distillation. The mull samples were mounted between potassium bromide or polyethylene plates and spectra were recorded on Perkin–Elmer 337 and 301 spectrometers. X-Ray diffraction photographs of powdered samples were recorded on a Debye–Scherrer camera. Samples were sealed inside quartz tubes and nickel-filtered copper radiation was used for recording the photographs. Line intensities were measured from the powder photographs using a Joyce–Loebl microdensitometer.

The densities of the compounds were measured using a float – no float technique in aqueous $ZnBr_2$ solutions which had been vacuum degassed. For $Re(acac)_3$ we had up to 10 min to do the measurements before significant decomposition occurred. The extent of decomposition was checked by dissolving the crystals in diethyl ether after the measurement since the oxidation products are insoluble in ether.

Electronic spectra were recorded for methylene chloride solutions in matched 1 cm silica cells on a Cary 14 spectrometer. Mass spectra were recorded on a Consolidated Electrodynamics Corp. Mass Spectrometer Model 21-110B.[3]

[1]To whom correspondence should be addressed.

[2]hfac is the anion of the β-ketoenol form of 1,1,1,5,5,5-hexafluoropentane-2,4-dione, $(C_5F_7HO_2)^-$, and acac is the corresponding anion of acetylacetone, $(C_5H_7O_2)^-$.

[3]Mass spectra were recorded through the courtesy of Professor D. B. McLean.

Can. J. Chem. Downloaded from www.nrcresearchpress.com by 210.87.254.5 on 09/05/12
For personal use only.

Can. J. Chem. Downloaded from www.nrcresearchpress.com by 210.87.254.5 on 09/05/12
For personal use only.

Measurements of magnetic susceptibility were made by the Gouy method. The apparatus used is described in detail elsewhere (5).

Tris(1,1,1,5,5,5-hexafluoropentane-2,4-dionato)rhenium(III)

A finely ground mixture of sodium hexafluoroacetylacetonate and dichloro(1,1,1,5,5,5-hexafluoropentane-2,4-dionato)bis(triphenylphosphine)rhenium(III) (6) (2:1 by weight) was heated *in vacuo* for 12 h at 110 °C. The product, which sublimed from the mixture, was collected in a cold trap (solid carbon dioxide – acetone or liquid nitrogen). In a typical experiment 3.0 g of the mixture gave 0.45 g of dark purple crystals (yield 40%).

Anal. Calcd. for $C_{15}H_3F_{18}O_6Re$: C, 22.3; H, 0.40. Found: C, 22.7; H, 0.61.

Tris(pentane-2,4-dionato)rhenium(III)

(*a*) A finely ground mixture of sodium acetylacetonate and dichlorobis(pentane-2,4-dionato)rhenium(IV) (6, 7) (2:1 by weight) was heated *in vacuo* (10^{-4} mm Hg) for 24 h at 175 °C. The product collected just outside the hot zone as dark red crystals. In a typical experiment 3 g of mixture gave 0.4 g of crystals (yield 38%).

Anal. Calcd. for $C_{15}H_{21}O_6Re$: C, 37.4; H, 4.39. Found: C, 37.1; H, 4.48.

Best yields were obtained when an excess of sodium acetylacetonate was used and when the sodium acetylacetonate had been recrystallized from methanol/benzene and the dichlorobis(pentane-2,4-dionato)rhenium(IV) from dichloromethane before use.

(*b*) $Re(acac)_3$ may be prepared in a similar manner to the above using dichloropentane-2,4-dionatobis(triphenylphosphine)rhenium(III) (6) as the starting material. The sublimed product was contaminated with triphenylphosphine and was purified by recrystallization from a very carefully deoxygenated anhydrous ether/hexane mixture.

Results and Discussion

The existence of $Re(acac)_3$ and $Re(hfac)_3$ was clearly demonstrated from the analyses and the mass spectral results for the two compounds. In both cases the parent ions were observed in relatively high intensities. The mass spectral results are presented in Tables 1 and 2. It is apparent that the mass spectra of the two compounds are quite different, the main difference being the transfer of fluorine atoms to the metal for $Re(hfac)_3$. This difference is hardly surprising since the Re—F bond is likely to be fairly strong, whereas Re—H (the analogous bond for the acetylacetone case) is not likely to be formed very readily.

The $Re(hfac)_3$ breakdown pattern is of interest since it is quite unlike that of $Cr(hfac)_3$ (see Table 1). This difference might indicate that the mechanism of breakdown is quite different for the two compounds. The presence of the L_2ReO^+ ion may be caused by C—O bond fission and elimination of a C_5HF_6O fragment. This type of mechanism has been suggested by Bancroft *et al.* (11) for $Ti(acac)_3$ and $V(acac)_3$ and related to the tendency of titanium and vanadium to form the MO^{2+} grouping. Many compounds of rhenium(V) containing the ReO grouping are known and a similar mechanism may apply to $Re(hfac)_3$.

It is possible, however, that despite the differences in breakdown pattern, the mechanism of breakdown may be the same. We have suggested possible breakdown schemes in Fig. 1. They are based on the suggestion by Bancroft *et al.* (9) that the initial process involves "fission of one M—O bond followed by a rotation of part of the ligand about the 2,3 C—C bond, which brings the halogens close to the metal atom. In a presumed concerted process the metal–fluorine bond is formed and a neutral species, such as CF_2, is eliminated". The differences in the

TABLE 1. Mass spectra of $M(hfac)_3$ species

Ion	*m/e*	Intensity Re	Intensity Cr
L_3M^+	*p* (parent)	100	20
$(L_3M - F)^+$	*p* − 19	36	4
$(L_3M - CF_3)^+$	*p* − 69	—	6
$L_2MF_2^+$	*p* − 169	<2	—
L_2MF^+	*p* − 188	54	—
L_2MO^+	*p* − 191	22	—
L_2M^+	*p* − 207	4	100
$(L_2M - CF_2)^+$	*p* − 257	—	21
$(L_2M - CF_3)^+$	*p* − 276	—	3
$LMOF_2^+$	*p* − 360	40	—
LMF_2^+	*p* − 376	38	—
$LMOF^+$	*p* − 379	34	—
LMF^+	*p* − 395	78	—
LM^+	*p* − 414	5	64
$(LMOF - CF_2)^+$	*p* − 429	10	—
$(LM - F)^+$	*p* − 433	—	23
$(LMF - CF_2)^+$	*p* − 445	10	—
$(LMO - CF_2)^+$	*p* − 448	9	—
$(LM - CF_2)^+$	*p* − 464	5	35
$(LM - CF_3)^+$	*p* − 483	—	38
$MO_2F_2^+$	*p* − 551	36	—
MOF_2^+	*p* − 567	11	—
MO_2F^+	*p* − 570	<2	—

Other fragments from $Re(hfac)_3$

Ion	*m/e*	Intensity	Ion	*m/e*	Intensity
$C_5HF_6^+$	175	8	$C_3O_2F_3^+$	125	50
$C_5HOF_5^+$	172	9	$C_4OF_3^+$	119	22
$C_5HO_2F_4^+$	169	18	$C_4F_3^+$	103	28
$C_5HF_5^+$	156	4	$C_3F_3^+$	91	21
$C_5HOF_4^+$	153	22	CF_3^+	69	13
$C_4O_2F_3^+$	137	6	$Re(hfac)_3^{2+}$	403, 404	<2

Can. J. Chem. Downloaded from www.nrcresearchpress.com by 210.87.254.5 on 09/05/12
For personal use only.

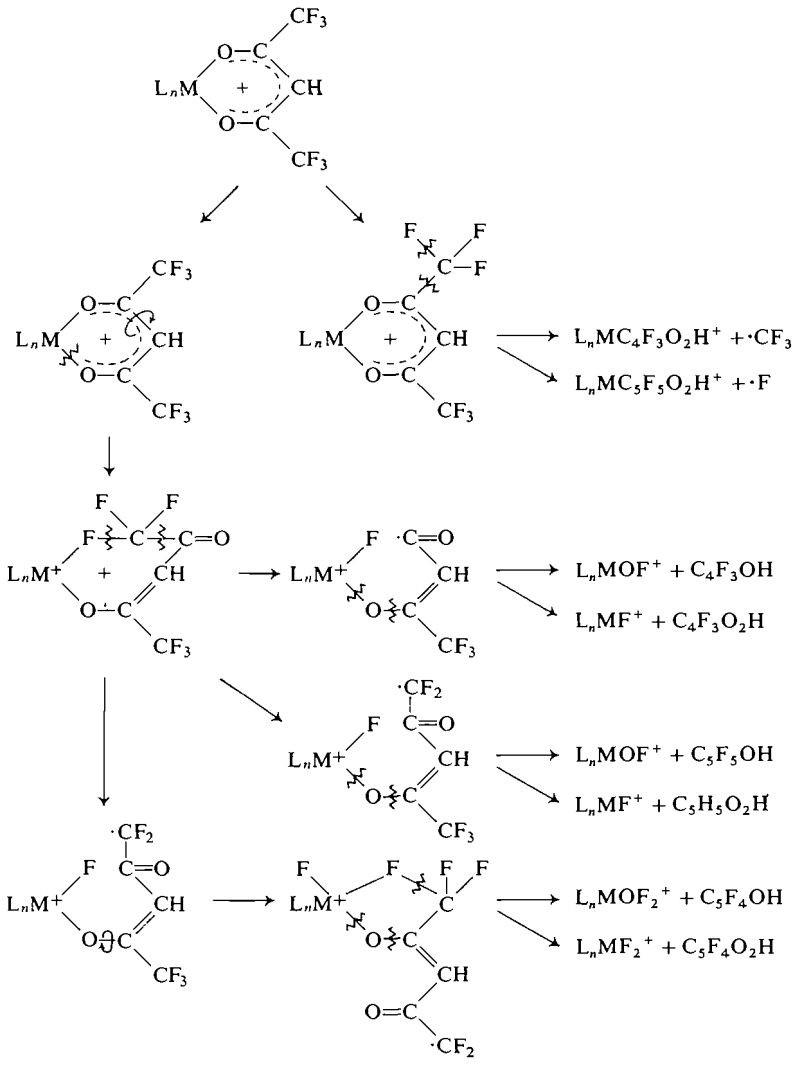

FIG. 1. Possible break-up mechanism for $Re(hfac)_3$ in the mass spectrometer: ↻, indicates rotation about bond; ≷ possible bond breaking points.

spectra of $Re(hfac)_3$ and $Cr(hfac)_3$ are assumed to arise because of subsequent steps. McDonald and Shannon (10) have related the stable valences of the metal to the observed mass spectra of several acetylacetonates, and Bancroft *et al.* (11) explained the spectra of $Ti(acac)_3$ and $V(acac)_3$ in terms of oxidation to Ti(IV) and V(IV), respectively. In addition they showed that in $Cr(acac)_3$ the Cr(III) state was particularly stable. Thus the absence of stable peaks of the type L_nMF^+, $L_nMF_2{}^+$, LMF_2O^+ for chromium is not unusual since their presence would imply oxidation of the Cr(III). The metastable ions $L_nMF(C_4F_3O_2H)^+$ decompose directly to L_nM^+. For rhenium, however, Re(IV), Re(V), and Re(VII) states are more stable than monomeric Re(III) species, particularly in the presence of fluoro- or oxo-groups so that decomposition of the initial ion to give ions of the type shown above is to be expected.

The mass spectrum of $Re(acac)_3$ has been compared with those of $M(acac)_3$ (M = Ti, V, Cr, Mn) in Table 2. The results for rhenium show considerable similarity to those for vanadium,

TABLE 2. Relative intensities of major fragments in the breakdown of some $M(acac)_3$ compounds

Ion	Mass	Intensity				
		Ti	V	Re	Cr	Mn
$M(acac)_3^+$	p(parent)	100	32	100	23	16
$MOH(acac)_2^+$	$p-82$	37	3	—	—	—
$MO(acac)_2^+$	$p-83$	—	4	22	—	—
$M(acac)_2^+$	$p-99$	55	100	35	100	100
$MOH(acac)C_5H_5O^+$	$p-100$	80	—	—	—	—
$M(acac)(C_4H_4O_2)^+$	$p-114$	—	—	—	5	32
$MOH(C_5H_5O)_2^+$	$p-118$	12	—	—	—	—
$MOH(acac)(C_3H_5O)^+$	$p-124$	7	—	—	—	—
$M(acac)(C_3H_5O)^+$	$p-141$	—	—	—	—	6
$MO_2H_2(acac)^+$	$p-164$	7	—	—	—	—
$MO_2H(acac)^+$	$p-165$	—	7	14	—	—
$MOH_2(acac)^+$	$p-180$	16	—	—	—	—
$MOH(acac)^+$	$p-181$	36	10	10	12	—
$MO(acac)^+$	$p-182$	64	26	18	—	—
$MO(C_4H_5O_2)^+$	$p-193$	—	3	—	—	—
$M(acac)^+$	$p-198$	—	5	<2	45	70
$MO(C_5H_5O)^+$	$p-200$	18	3	—	—	—
$M(C_4H_4O_2)^+$	$p-213$	—	—	—	4	3
$M(C_5H_5O)^+$	$p-216$	—	—	—	3	3
Not assigned	$p-218$	17	—	—	—	—
MO^+	$p-281$	—	34	—	—	—

the only significant difference being a somewhat greater tendency to form MO groups rather than MOH groups. As with $Re(hfac)_3$ oxidation to Re(IV) is to be expected, since it has been shown (8) that Re(III) compounds such as $Re(acac)Cl_2[P(C_6H_5)_3]_2$ are readily oxidized to very stable Re(IV) compounds like $Re(acac)_2Cl_2$. In addition $Re(acac)_3$ is very easily oxidized (*vide infra*).

The data from the electronic spectra of both rhenium compounds are given in Table 3. Attempts to assign the observed bands to specific electronic transitions for the d^4-system developed by Kamimura *et al.* (12) have been unsuccessful. The magnitudes of the extinction coefficients of the bands are more characteristic of absorptions arising from charge transfer processes than from d–d transitions.

Both rhenium compounds show essentially temperature independent paramagnetism over the temperature range 80–290 °K. This behavior is like that observed previously for Re(III) in a close to octahedral environment (13) and the magnitude of the magnetic susceptibility lies in the range $1200–1900 \times 10^{-6}$ c.g.s. units observed previously. Like previous workers we find that the value of the spin-orbit coupling constant ζ_{5d} calculated using conventional magnetic relationships (13) is approximately 4500 cm^{-1}, nearly twice the free ion value of 2500 cm^{-1}.

The infrared spectra of $Re(acac)_3$ and $Re(hfac)_3$ are reported in Table 5. Raman spectra were not obtained as solid samples absorbed the laser light, melted, and volatilized. No signal could be obtained from solutions because of absorption.

TABLE 3. Electronic spectra of $Re(acac)_3$ and $Re(hfac)_3$

$Re(acac)_3$		$Re(hfac)_3$	
Wavenumber (cm^{-1})	$\varepsilon_{max} \times 10^{-3}$	Wavenumber (cm^{-1})	$\varepsilon_{max} \times 10^{-3}$
38 900	5.3	37 300	6.6
37 500	5.7	35 700	6.5
29 300	3.1	28 100	4.7
24 850	3.2	26 300	4.5
21 500	1.6	20 000	4.5
18 400	2.1		
17 450	2.2	14 800	5.4
5 400	0.15	6 100	0.43

Can. J. Chem. Downloaded from www.nrcresearchpress.com by 210.87.254.5 on 09/05/12
For personal use only.

The assignments of the vibrational transitions for $Re(acac)_3$ and $Re(hfac)_3$ were made by comparison with previous work.

The vibrational spectra of metal acetylacetonates have been extensively studied (14–23) and bands at 1365, 1274, 1190, 1022, 780, 652, 620 cm^{-1} for $Re(acac)_3$ correspond to bands reported previously for similar compounds and for

TABLE 4. Magnetic properties of $Re(acac)_3$ and $Re(hfac)_3$

$Re(acac)_3$			$Re(hfac)_3$		
T(°K)	$10^6\chi_m'$ (c.g.s.)	μ (B.M.)	T(°K)	$10^6\chi_m'$ (c.g.s.)	μ (B.M.)
83	1437	0.98	79	1337	0.92
93	1430	1.04	95	1227	0.97
104	1437	1.10	104	1210	1.01
113	1437	1.14	113	1213	1.05
124	1432	1.20	124	1227	1.11
136	1432	1.25	137	1241	1.17
151	1430	1.32	152	1256	1.24
163	1437	1.37	164	1266	1.29
177	1437	1.43	177	1273	1.35
193	1430	1.49	193	1284	1.41
209	1425	1.55	208	1284	1.41
225	1421	1.61	225	1291	1.53
241	1412	1.66	258	1291	1.64
258	1405	1.71	271	1291	1.68
273	1405	1.76	290	1287	1.74
289	1402	1.81			

TABLE 5. Infrared spectra of $Re(acac)_3$ and $Re(hfac)_3$*

$Re(acac)_3$			$Re(hfac)_3$		
Band position (cm^{-1})	Intensity	Assignment	Band position (cm^{-1})	Intensity	Assignment
1545	sh	CO str	1560	s	CO str
1530	sh	CH out-of-plane bend combination	1535	m	CC str
1515	vs	CC str			
1420	m	CH_3 deg def	1415	vs	?
1380	vs	CO str + CH bend	1325	vs	CC str + CF_3 str
1365	vs	CH_3 sym def			
1274	s	CC str + CCH_3 str	1267	vs	CF_3 str
			1225	m	?
			1205	m	?
			1175	sh	
1190	m	CH in-plane bend	1164	m	CH in-plane bend
			1148	m	
1022	m	CH_3 rock	1105	m	?
935	m	C—CH_3 str + CO str	946	m	?
910	vw	Oxidation product?	830	m	C—CF_3 str + CH out-of-plane bend
780	m	CH out-of-plane bend	750	m	C—CF_3 str
652	m	Ring def + ReO str	686	s	Ring def + ReO str
620	s	C—CH_3 bend + ReO str	608	m	CCF_3 bend + ReO str
614	sh	C—C(C)O out-of-plane bend	590	vw	?
545	vw	Ring mode?†			
444	m	ReO str			
421	sh	Ring out-of-plane mode‡			
418	m	Ring mode?‡	417	m	Ring mode
401	s	ReO str	394	s	ReO str
321	m	ReO str	314	m	ReO str or ring def
296	vw	C—CH_3 bend§			

*sh, shoulder; v, very; s, strong; m, medium; w, weak; str, stretch; deg, degenerate; def, deformation; sym, symmetric.
†References 15, 16, 20.
‡References 13, 15, 16.
§References 13, 15, 22.

Can. J. Chem. Downloaded from www.nrcresearchpress.com by 210.87.254.5 on 09/05/12
For personal use only.

Can. J. Chem. Downloaded from www.nrcresearchpress.com by 210.87.254.5 on 09/05/12
For personal use only.

which there is unanimity of assignment. Bands at 1545, 1530, 1515, 1420, 1380 cm^{-1} correspond to bands reported previously, but over which there has been some controversy. The assignment we have used is based on the more recent analyses of spectra (21–23). The three highest bands are at somewhat lower energies than usual (27). The band at 1530 cm^{-1} may arise from splitting of one of the neighboring bands or more probably from a C—H out of plane vibration coupled either with the infrared inactive CH out-of-plane vibration (23) or CO stretch (14), since it has been shown that the band (when observed) disappears on deuteration (23). No assignment has been made previously of the band at 910 cm^{-1}, although calculations show a C—CH_3 stretch may occur near this value (14). It is also possible that this band may arise from a small amount of oxidation product, since strong absorptions for Re=O stretches occur in this region (28). The band at 614 cm^{-1} is probably a C—C(C)—O out-of-plane bend (14, 15, 17). The assignment of the remaining bands is a matter of some controversy. Gillard *et al.* (17) have shown that there should be three M—O stretches in this region of which two should be strong and three bands have been reported for $Fe(acac)_3$ at 433, 415, and 298 cm^{-1}.

Unfortunately, the stretches are necessarily very metal sensitive and may shift considerably from the above frequencies. Typical ranges for these bands are 420–480, 390–450, and 290–390 cm^{-1}(14–21, 23) and on this basis we have assigned the bands at 321, 401, and 444 cm^{-1} to M—O stretches. The first two bands are also observed for $Re(hfac)_3$, but no band is observed near 444 cm^{-1}. Another band of comparable strength occurs at 418(1) cm^{-1} for both compounds, but is unlikely to be an Re—O stretch, since a medium-strong metal-insensitive band at 420 ± 10 is observed in nearly all acetylacetone complexes (37) and Nakamoto *et al.* (24) have shown that for the series $M(C_5H_7O_2)_2$, $M(C_5H_4F_3O_2)_2$, and $M(C_5F_6HO_2)_2$(M = Ni, Cu) the intensity of the M—O stretch in these compounds drops markedly as hydrogen is substituted for fluorine, almost disappearing for the hexafluoroacetylacetone complexes. The source of the assignment of the remaining bands is indicated in the table.

The vibrational spectra of metal hexafluoroacetylacetonates have been studied less extensively. The assignments for $Re(hfac)_3$ are based on comparisons with the work of Nakamoto *et al.* (24) and Morris *et al.* (25) and are incomplete. Nevertheless, one feature of the spectrum is particularly interesting and this is that the highest frequency bands of $Re(hfac)_3$ are nearly identical in energy to those of $Re(acac)_3$. This is in complete contrast to the results of Nakamoto *et al.* (24) which show a strong shift to higher energies of the C=O and C=C stretches when CH_3 is substituted by CF_3 in metal β-ketoenolates. Nakamoto *et al.* postulated that the effect is caused by the inductive effect of the fluorine atoms which causes strengthening of the C=O and C=C bonds and a decrease in the MO bond strength.

Morris *et al.* (25) noticed in their studies on $M(hfac)_3$ and $M(hfac)_2.1$ or $2H_2O$ compounds that there were two groups of CO stretching frequencies and related these to the charge/radius ratio of the central metal, assuming an ionic model (q/r 2.2–2.6, ν(CO) = 1650 cm^{-1}; q/r 4–6, ν(CO) = 1610 cm^{-1}). $Re(hfac)_3$, with q/r for Re(III) roughly 5.4, does not fit this simple relationship. Nevertheless, we feel the picture is capable of extension. The covalent bond strength will be related to q/r, and we feel that it is the strength of the MO bond, in particular the π bond, (pπO—dπM) which is related to the position of ν(CO). Following the argument of Nakamoto *et al.* (24), we have a competitive process for the electrons associated with the MO bond. The shift of electron density will depend on the ability of the metal to attract the electrons relative to the fluorine atoms. The greater this ability (reflected in greater MO π bond strength), the less will be the upward shift of ν(CO). The importance of this π bonding (pπO→dπM donation) has already been commented on by Cotton and Holm (29) in explaining the electronic spectra and Hester and Plane (20) the Raman spectra of metal acetylacetonates. If the explanation is correct, one would expect a parallel effect to be observed for corresponding acetylacetonates as is the case. Indeed, Holtzclaw and Collmann (30) and West and Riley (31) have already related the position of ν(CO) to the stability constants of metal acetylacetonates; the lower the energy, the greater is the stability constant. Nakamoto (27) has criticized this relationship; nevertheless, as is shown in Fig. 2, there is a broad correlation between ν(CO)

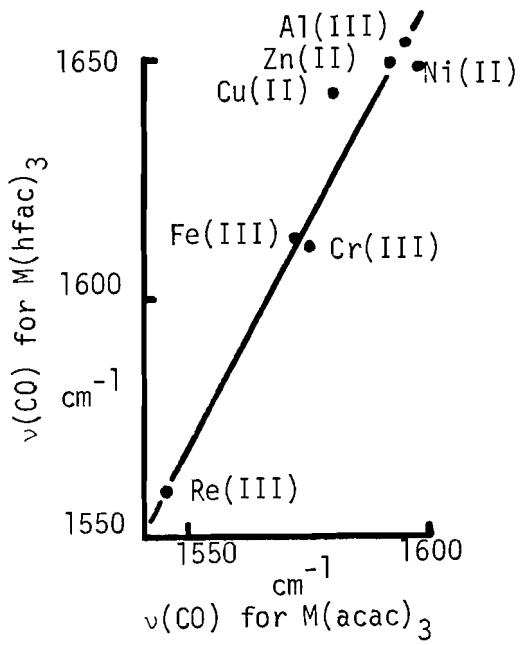

FIG. 2. The relationship between ν(CO) in $M(acac)_3$ and $M(hfac)_3$.

stretching frequencies for corresponding metal acetylacetonates and hexafluoroacetylacetonates, as would be expected from the above model.

Whether a direct relationship can be drawn between π-bond strength and ν(CO) remains a matter of conjecture. Nakamoto has pointed out (27) a measure of the MO bond strength is the MO force constant. The bands we have assigned to ν(ReO) do not shift much from $Re(acac)_3$ to $Re(hfac)_3$, as expected, but our assignment is not unambiguous. Detailed force constant calculations of a number of compounds will be necessary to test the relationship suggested.

The X-ray powder diffraction patterns of both rhenium compounds were recorded primarily for identification purposes and to see whether the compounds were isomorphous with known $M(acac)_3$ and $M(hfac)_3$ compounds. The data are presented in Table 6.

The data for $Re(acac)_3$ can be indexed in terms of a monoclinic cell, $a = 14.10(1)$ Å, $b = 7.52(1)$ Å, $c = 16.56(1)$ Å, and $\beta = 99.15(5)°$, space group $P2_1/c$, $Z = 4$, $D_{calcd} = 1.85$ g cm^{-3}, $D = 1.92$ g cm^{-3}. Thus the compound has the α-form of the three common unit cells for $M(acac)_3$ compounds first noted by Astbury (1). A comparison of the powder pattern of $Re(acac)_3$ with that for $Ir(acac)_3$ (32) shows a fair similarity between the intensities of the corresponding lines, and good agreement is shown with the calculated intensities which were obtained by placing rhenium atoms at coordinates found for

TABLE 6. X-Ray data for powdered samples of $Re(hfac)_3$ and $Re(acac)_3$

(*a*) $Re(hfac)_3$

d_{obs} (Å)	d_{calcd} (Å)	*hkl*	Intensity	d_{obs} (Å)	d_{calcd} (Å)	*hkl*	Intensity	d_{obs} (Å)	d_{calcd} (Å)	*hkl*	Intensity
9.359	9.256	110	100	2.560	2.567	520	15	1.897	1.902	614	<3
5.717	5.666	102	48	2.442	2.445	610	11		1.903	802	
5.372	5.343	300	9	2.411	2.417	432	10	1.838	1.839	640	8
5.096	5.068	112	14	2.341	2.338	324	11	1.802	1.804	730	4
4.861	4.832	200	44	2.292	2.290	530	26	1.771	1.769	326	5
4.623	4.628	220	48			700		1.751	1.749	820	≪3
4.270	4.283	212	78	2.262	2.267	612	13	1.737	1.739	714	5
4.004	4.008	400	58	2.159	2.162	442	13	1.722	1.729	732	6
3.678	3.678	320	<3		2.161	334		1.708	1.709	902	<3
3.583	3.584	312	25	2.137	2.142	532	18		1.706	506	
3.493	3.498	410	30			702		1.675	1.680	822	5
3.339	3.342	402	24		2.142	424			1.671	804	
3.143	3.144	322	5	2.113	2.123	710	11	1.654	1.653	516	4
3.079	3.085	330	24	2.085	2.087	622	15	1.612	1.611	606	6
2.885	2.879	510	18		2.087	514		1.558	1.556	616	6
2.827	2.833	204	22	2.047	2.053	540	15	1.533	*	*	4
	2.834	502		1.981	1.988	434	8	1.511	*	*	8
2.706	2.710	422	6		1.972	116		1.492	*	*	<3
	2.709	214		1.955	1.958	720	13	1.475	*	*	<3
2.640	2.635	430	6	1.937	1.944	542	8	1.402	*	*	4
2.596	2.600	512	20	1.918	1.916	632	<3				
					1.916	216					

*Several possibilities. Hexagonal cell, $a = 18.44(1)$ Å, $c = 12.13(1)$ Å, $Z = 6$, $D_{calcd} = 2.25$ g cm^{-3}, $D_m = 2.26$ g cm^{-3}.

Can. J. Chem. Downloaded from www.nrcresearchpress.com by 210.87.254.5 on 09/05/12
For personal use only.

TABLE 6. (*Concluded*)
(*b*) $Re(acac)_3$

d_{obs} (Å)	d_{calcd} (Å)	*hkl*	I_{calcd}*	I_{obs}	d_{obs} (Å)	d_{calcd} (Å)	*hkl*	I_{calcd}*	I_{obs}	d_{obs} (Å)	d_{calcd} (Å)	*hkl*	I_{calcd}*	I_{obs}
8.343	8.175	002	75	75	2.966	2.965	123	10	12	1.886	1.886	51$\bar{7}$	24	15
7.625	7.596	10$\bar{2}$	10	14	2.789	2.784	500	2	5	1.861	1.863	622	22	17
6.970	6.960	200	86	85	2.693	2.694	41$\bar{4}$	4	8	1.832	1.833	23$\bar{6}$	28	20
6.606	6.616	110	84	100	2.611	2.611	510	50	26	1.812	1.812	24$\bar{1}$	8	8
	6.605	102	16		2.525	2.529	21$\bar{6}$	44	36	1.758	1.759	516	—	<5
5.788	5.772	20$\bar{2}$	40	49	2.475	2.479	421	1.9	<5		1.758	720	—	
5.343	5.344	11$\bar{2}$	33	30		2.473	323	0.3		1.737	1.738	236	—	<5
5.139	5.108	210	1	5	2.433	2.429	131	0.5	<5	1.711	1.713	62$\bar{6}$	—	<5
4.954	4.963	112	65	45	2.386	2.386	512	34	25	1.689	1.689	34$\bar{3}$	—	<5
4.636	4.640	300	19	8	2.356	2.360	422	35	23	1.651	1.652	219	—	
4.373	4.372	11$\bar{3}$	0.3	5	2.278	2.277	033	5	5		1.651	20$\bar{1}$0	—	<5
4.122	4.121	212	25	35	2.224	2.224	133	25	18		1.651	408	—	
3.972	3.965	21$\bar{3}$	22	32	2.166	2.169	52$\bar{3}$	16	15	1.625	1.625	30$\bar{1}$0	—	<5
3.785	3.785	302	67	65	2.122	2.124	50$\bar{6}$	30	12	1.596	1.597	625	—	<5
3.591	3.591	014	20	20	2.096	2.092	23$\bar{4}$	3	7		1.596	13$\bar{8}$	—	
3.480	3.480	400	45	46	2.065	2.065	514	12	5	1.541	1.540	24$\bar{6}$	—	<5
3.389	3.390	21$\bar{4}$	27	58	2.051	2.051	20$\bar{8}$	0.5	<5	1.506	1.507	2110	—	<5
	3.384	312	49		1.999	1.997	13$\bar{5}$	4	15		1.506	542	—	
3.309	3.308	220	60	41	1.975	1.975	620	—	<5	1.466	1.467	152	—	<5
3.165	3.158	410	3	7	1.932	1.932	432	—	<5	1.416	1.416	627	—	<5
3.100	3.100	41$\bar{2}$	3	7	1.894	1.896	33$\bar{5}$	—	<5					
3.058	3.054	31$\bar{4}$	42	26		1.893	43$\bar{4}$	—						

*Calculated using rhenium atoms only at coordinates given for Mn in $Mn(acac)_3$ (33). Monoclinic cell, $a = 14.10(1)$ Å; $b = 7.52(1)$ Å; $c = 16.56(1)$ Å; $\beta = 99.15(5)°$, $P2_1/C$, $Z = 4$, $D_{calcd} = 1.85$ g cm^{-3}, $D_m = 1.92$ g cm^{-3}.

manganese in $Mn(acac)_3$ (33), and applying appropriate Lorenz-Polarization and multiplicity corrections (see Table 6). A calculation of the residual $R = \Sigma\|F_o| - |F_c\|/\Sigma F_o$ using this data without refinement gave $R = 0.21$, suggesting that $Re(acac)_3$ and $Mn(acac)_3$ are structurally similar as well as isomorphous. It should be noticed that our indexing differs significantly from that proposed for $Ir(acac)_3$, for which some indices are used which are forbidden by the systematic absence requirements of the space group.

The powder data for $Re(hfac)_3$ can be indexed in terms of a hexagonal unit cell with $a = 18.44(1)$ Å, $c = 12.13(1)$ Å, $Z = 6$, $D_{calcd} = 2.25$ g cm^{-3}, $D_m = 2.26$ g cm^{-3}. These data show a very close relationship to those reported for $Ir(hfac)_3$ and $Rh(hfac)_3$ (34), where for iridium $a = 18.2$ Å, $c = 6.16$ Å and for rhodium $a = 18.27$ Å, $c = 6.175$ Å. The iridium and rhodium compound parameters were derived from powder data. Our powder data also would indicate a *c* axis length one half of what we have reported. However, single crystal measurements (35) show very weak superstructure spots indicating the powder *c*-axis length should be doubled. It is probable that all three compounds are isomorphous. At present the single crystal data are inadequate to give full structural details. From the small amount of data for the *hk*0 zone it is possible to say that the $Re(hfac)_3$ units are monomeric and have a threefold axis. Patterson synthesis showed rhenium atoms at (0,0,0), 1/3,2/3,*Z*, and 2/3,1/3,*Z* and subsequent Fourier synthesis located the oxygen atoms, which are in a six-fold array around the rhenium atom in projection. There is no evidence of polymerization. However, there are considerable problems in refinement of data containing information along the *c*-axis. This may be caused by disorder of left-handed and right-handed molecules or a form of "microtwinning" similar to that reported by Beurskens and Cras (36).

Now that we have prepared $Re(acac)_3$ and examined its properties it is easy to understand why it was so difficult to prepare. Unlike $Re(hfac)_3$, $Re(acac)_3$ is extremely susceptible to oxidation. If a sample of $Re(acac)_3$, prepared in a dry box and handled with precautions to exclude air, is used for infrared spectroscopy the spectrum

Can. J. Chem. Downloaded from www.nrcresearchpress.com by 210.87.254.5 on 09/05/12
For personal use only.

TABLE 7. Comparison of the properties of two samples of $Re(acac)_3$

Property	This work		Reference 3
Analysis C	37.1%*	37.3%†	37.7%*
H	4.5%*	4.4%†	3.7%*
O	—	19.7%†	20.1%*
Re	—	38.3%†	38.9%*
Molecular weight	483/485 Mass spec.	483/485	471 (ebullioscopic)
Melting point	Does not melt, sublimes 160–180 °C		Not given
Color	Purple		Brown
Solubility in ether	Soluble		Insoluble
Magnetism	χ_m = constant $\mu \propto T^{1/2}$ μ_{298} = 1.81 B.M.		$\chi_m \propto 1/(T+\theta)$ $\mu \propto (T+\text{constant})$ μ_{298} = 2.33 B.M.

*Observed value.
†Calculated value.

described in Table 5 is obtained. If the containing plates are opened in air for a few seconds, and then closed and the spectra recorded, extra bands in the 800–1000 cm^{-1} region are observed, which we postulate are caused by Re=O or Re—O—Re groups. The nature of the oxidation is complex since the frequency and number of bands in the 800–1000 cm^{-1} region depend on the time of exposure to air. A complex pattern is also observed if a solution of $Re(acac)_3$ is allowed to stand in air. The purple solution soon turns red and eventually brown after a few hours. These reactions can be speeded-up considerably by bubbling oxygen through the solution. Solid $Re(acac)_3$ becomes brown on standing and ether-insoluble. $Re(hfac)_3$ is much more stable to oxidation and can be handled in air at room temperature for hours with little sign of decomposition. However, both the solid and solutions can be oxidized if they are heated for any length of time in air. Again, reaction is much more rapid in an atmosphere of oxygen.

Comparison of the chemical and physical properties of $Re(acac)_3$ and those of the compound described previously (3), suggest that the two compounds are different. Some properties are compared in Table 7. Since our compound has been shown to be $Re(acac)_3$, we suggest that the previous description of $Re(acac)_3$ was incorrect. In light of our results we suspect that the sample described previously was at least partly oxidized.

We thank the National Research Council of Canada for financial support of this work and the award of Graduate Scholarships to three of us (W.D.C., W.F., and G.T.).

1. W. T. ASTBURY. Proc. Roy. Soc. **112A**, 448 (1926).
2. R. COLTON, R. LEVITUS, and G. WILKINSON. Nature, **186**, 233 (1960).
3. R. COLTON, R. LEVITUS, and G. WILKINSON. J. Chem. Soc. 4121 (1960).
4. H. J. ANDERSON and A. BRENNER. J. Electrochem. Soc. **116**, 513 (1969).
5. P. W. FRAIS, A. GUEST, and C. J. L. LOCK. Can. J. Chem. **47**, 1069 (1969).
6. D. E. GROVE, N. P. JOHNSON, C. J. L. LOCK, and G. WILKINSON. J. Chem. Soc. 490 (1965).
7. C. J. L. LOCK and C. WAN. Chem. Commun. 1109 (1967).
8. W. D. COURRIER. Ph.D. Thesis. McMaster University, Hamilton, Ontario. 1971.
9. G. M. BANCROFT, C. REICHERT, and J. B. WESTMORE. Inorg. Chem. **7**, 870 (1968).
10. C. G. MCDONALD and J. S. SHANNON. Aust. J. Chem. **19**, 1545 (1966).
11. G. M. BANCROFT, C. REICHERT, J. B. WESTMORE, and H. D. GESSER. Inorg. Chem. **8**, 474 (1969).
12. K. KAMIMURA, S. KOIDE, H. SEKIYAMA, and S. SUGANO. J. Phys. Soc. Jap. **15**, 1264 (1960).
13. A. EARNSHAW, B. N. FIGGIS, J. LEWIS, and R. D. PEACOCK. J. Chem. Soc. 3132 (1961).
14. K. NAKAMOTO and A. E. MARTELL. J. Chem. Phys. **32**, 588 (1960).
15. K. NAKAMOTO, P. J. MCCARTHY, A. RUBY, and A. E. MARTELL. J. Am. Chem. Soc. **83**, 1066, 1272 (1961).
16. R. C. FAY and T. J. PINNAVAIA. Inorg. Chem. **7**, 508 (1968).
17. R. D. GILLARD, H. G. SILVER, and J. L. WOOD. Spectrochim. Acta, **20**, 63 (1964).
18. B. F. JOHNSON, J. LEWIS, and M. S. SUBRAMANIAN. J. Chem. Soc. A, 1993 (1968).
19. J. LEWIS, R. F. LONG, and C. OLDHAM. J. Chem. Soc. 6470 (1965).
20. R. E. HESTER and R. A. PLANE. Inorg. Chem. **3**, 513 (1964).
21. Y. KAWASAKI, T. TANAKA, and R. OKAWARA. Spectrochim. Acta, **22**, 1571 (1966).
22. G. T. BEHNKE and K. NAKAMOTO. Inorg. Chem. **6**, 433 (1967).

Can. J. Chem. Downloaded from www.nrcresearchpress.com by 210.87.254.5 on 09/05/12
For personal use only.

23. M. M. MIKAMI, I. NAKAWAGA, and T. SHINAMOUCHI. Spectrochim. Acta, **23A**, 1037 (1967).
24. K. NAKAMOTO, Y. MORIMOTO, and A. E. MARTELL. J. Phys. Chem. **66**, 346 (1962).
25. M. L. MORRIS, R. W. MOSHIER, and R. E. SIEVERS. Inorg. Chem. **2**, 411 (1963).
26. J. P. DISMUKES, L. H. JONES, and J. C. BAILAR, JR. J. Phys. Chem. **65**, 729 (1961).
27. K. NAKAMOTO. Infrared spectra of inorganic and coordination compounds. Wiley, New York, 1963. p. 217.
28. N. P. JOHNSON, C. J. L. LOCK, and G. WILKINSON. J. Chem. Soc. 1054 (1964).
29. F. A. COTTON and R. H. HOLM. J. Am. Chem. Soc. **82**, 2979 (1960).
30. H. F. HOLTZCLAW and J. P. COLLMAN. J. Am. Chem. Soc. **79**, 3318 (1957).
31. R. WEST and R. RILEY. J. Inorg. Nucl. Chem. **5**, 295 (1958).
32. L. DAVIGNON, A. DEREIGNE, J. M. MANOLI, and P. DAVOUS. J. Less-Common Metals, **21**, 345 (1970).
33. B. MOROSIN and J. R. BRATHOVDE. Acta Cryst. **17**, 705 (1964).
34. L. DAVIGNON, J. M. MANOLI, and A. DEREIGNE. J. Less-Common Metals, **21**, 341 (1970).
35. W. FORSTER and C. J. L. LOCK. Unpublished work. 1970.
36. P. T. BEURSKENS and J. A. CRAS. J. Crystal Mol. Struct. **1**, 63 (1971).

Can. J. Chem. Downloaded from www.nrcresearchpress.com by 210.87.254.5 on 09/05/12
For personal use only.

Formation des dérivés *N*- et *C*-substitués au cours de l'alkylation de l'indol-2(3*H*)-one

ILONA GRUDA

Département de chimie–biologie, Université du Québec à Trois-Rivières, Trois-Rivières, Québec

Reçu le 27 juillet 1971

The alkylation of indol-2(3*H*)-one (oxindole) and of some of its mono and dialkyl derivatives has been investigated.

Chromatographic methods for preparative separation and quantitative determination of the five compounds formed in the reaction between oxindole and benzyl chloride in the presence of a base are reported.

A kinetic approach to these reactions shows that in unsubstituted indol-2(3*H*)-one the 3-position is twice as reactive as the 1-position. In the already 3-monosubstituted compound the reactivity of the 3-position is about 30 times greater than that of the 1-position.

On a étudié l'alkylation de l'indol-2 (3*H*)-one et de quelques uns de ses dérivés mono et dialkylés.

On rapporte des méthodes chromatographiques pour la séparation préparative et la détermination quantitative des cinq composés formés au cours de la réaction entre l'oxindole et le chlorure de benzyle en présence d'une base.

Une approche cinétique dans le cas de ces réactions nous montre que pour l'indol-2 (3*H*)-one, la position 3 est deux fois plus réactive que la position 1. Pour le composé qui est déjà mono-substitué en position 3, la réactivité de la position 3 est environ trente fois plus grande que celle de la position 1.

Canadian Journal of Chemistry, **50**, 18 (1972)

La réaction de l'alkylation directe de l'indol-2(3*H*)-one (oxindole) et de ses dérivés a fait l'object d'un certain nombre de publications (1–9).

Les résultats obtenus sont assez contradictoires. Ainsi certains auteurs (4, 5) affirment que l'introduction d'un substituant sur le carbone 3 de l'oxindole n'est possible que dans le cas d'un composé déjà 3-monosubstitué. D'autres, (1, 3, 6, 7) par contre, ont démontré que l'alkylation directe de l'oxindole et des *N*-alkyloxindoles était facile et que les produits obtenus étaient principalement des dérivés 3,3-disubstitués. Certains auteurs ont réussi également à isoler des dérivés 1,3,3-trisubstitués (3, 7).

D'après les résultats de la plupart des auteurs il semblerait que, en général, la réaction de l'oxindole avec des halogénures actifs tels que les halogénures d'allyle, de benzyle ou de carbalkoxyméthyle dans un milieu homogène mène uniquement à des produits polysubstitués tandis que la monosubstitution n'a lieu qu'avec des halogénures peu actifs ou dans un milieu hétérogène.

Dans une étude approfondie Daisley et Walker (9) ont démontré récemment que dans un milieu hétérogène le *N*-méthyloxindole réagit avec de différents halogénures en donnant des mélanges de produits mono- et disubstitués. La réactivité de l'azote n'a pas été étudiée par ces auteurs.

En ce qui concerne les voies réactionnelles de l'alkylation directe de l'oxindole et de ses dérivés alkylés les résultats décrits jusqu'à présent sont assez fragmentaires.

Le schéma 1 montre les voies possibles menant au produit 1,3,3-trisubstitué.

D'après les produits principalement obtenus (CC et NCC) par la plupart des auteurs, on aurait pu conclure que la voie oxindole $\xrightarrow{k_1}$ C $\xrightarrow{k_2}$ CC $\xrightarrow{k_3}$ NCC est la voie dominante avec $k_1 \ll k_2$, $k_3 < k_2$, et k_4 et $k_7 \simeq 0$. Ceci laisserait supposer une réactivité beaucoup plus grande du carbone 3 que de l'azote dans une attaque nucléophile. Par contre, Wenkert et Blossey (2) obtiennent dans la réaction entre l'oxindole et l'iodure d'éthyle 3 fois plus de produit *N*-substitué que de produit substitué sur le carbone et ne constatent pas la présence de dérivés polysubstitués.

Donc d'après ces auteurs $k_4 > k_1$ et $k_1 \gg k_2$, $k_4 \gg k_5$. Le but de ce travail a été d'examiner les étapes de l'alkylation de l'oxindole et de comparer la réactivité nucléophile de l'azote et du carbone 3.

Can. J. Chem. Downloaded from www.nrcresearchpress.com by 210.87.254.40 on 09/05/12
For personal use only.

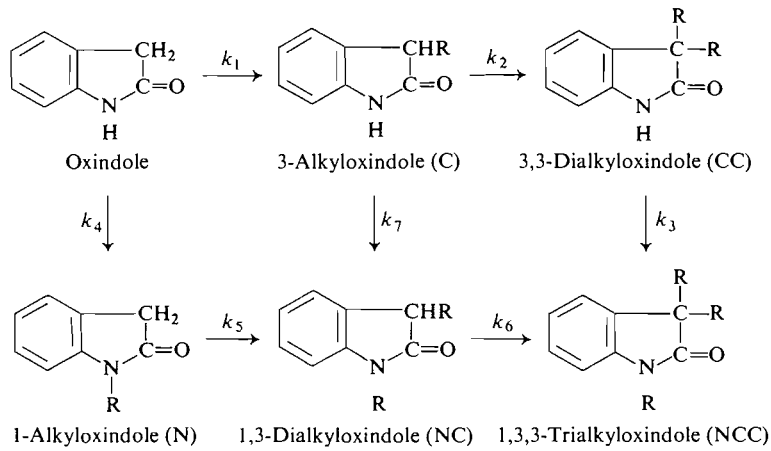

SCHÉMA 1

Résultats et discussion

Le système réactionnel représenté dans le schéma 1 semble trop complexe pour qu'on puisse déterminer les constantes de vitesse. Il faut indiquer en outre que chaque réaction du schéma est en réalité composée de deux réactions (eq. 1).

Il fallait donc envisager l'étude du problème d'une façon approchée.

Le système choisi dans ce travail était: l'oxindole, le chlorure de benzyle et une base (NaOH ou $NaOC_2H_5$) dans le rapport 1:1:1, dans l'éthanol. En séparant le mélange après la réaction par chromatographie sur colonne on a isolé six composés: l'oxindole et ses produits de substitution N, C, NC, CC, NCC, donc tous les produits du schéma 1. Leur structure a été établie par l'analyse élémentaire et les spectres i.r. et confirmée par comparaison avec les mêmes composés synthétisés par d'autres méthodes.

Afin d'étudier le cours de la réaction on a utilisé la c.p.v. quantitative.

Les résultats sont représentés par les figs. 1 et 2.

Il en résulte que l'agent électrophile attaque simultanément l'azote et le carbone 3 de l'oxindole, le rapport des produits formés étant N/C = 1/2 au début de la réaction. Ce rapport change par la suite à cause de la formation des dérivés polysubstitués.

La forme des courbes dans les fig. 1 et 2 suggère que l'accumulation rapide du produit CC est dûe à une grande réactivité de C et éventuellement à une diminution de la réactivité de l'azote causée par les substituants sur le carbone 3.

Pour vérifier cette hypothèse on a étudié le cours de réactions suivantes:

[*a*] N + chlorure de benzyle

[*b*] C + chlorure de benzyle

[1]

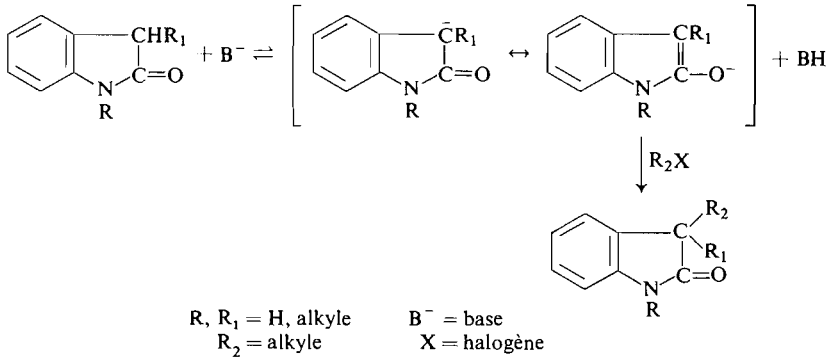

Can. J. Chem. Downloaded from www.nrcresearchpress.com by 210.87.254.40 on 09/05/12
For personal use only.

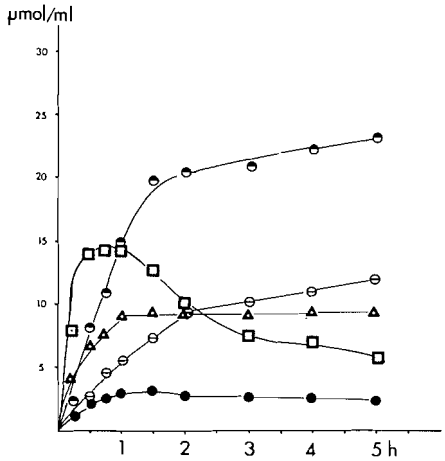

FIG. 1. Oxindole + chlorure de benzyle + $NaOC_2H_5$ (1:1:1); concentrations, 230 μmol/ml; température, 40° -●-. 3,3-Dibenzyloxindole; -□-, 3-benzyloxindole; -△- l-benzyloxindole; -⊖-, 1,3,3-tribenzyloxindole; -●-, 1,3-dibenzyloxindole.

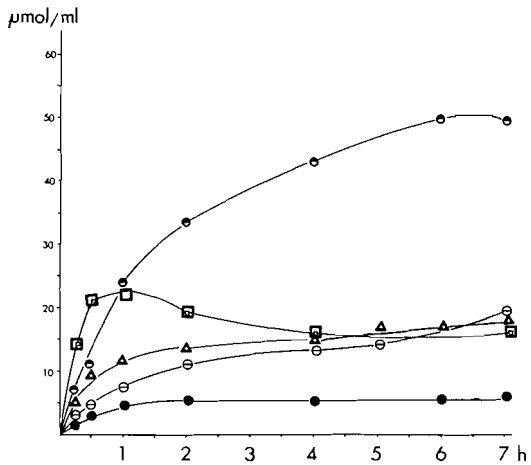

FIG. 2. Oxindole + chlorure de benzyle + NaOH (1:1:1); concentrations, 230 μmol/ml; température, 40°. -●-, 3,3-Dibenzyloxindole; -□-, 3-benzyloxindole; -△-, l-benzyloxindole; -⊖-, 1,3,3-tribenzyloxindole; -●- 1,3-dibenzyloxindole.

[c] NC + chlorure de benzyle

[d] CC + chlorure de benzyle

En effectuant les réactions *a*, *b*, et *c* dans l'atmosphère ambiante on constate sur le chromatogramme l'apparition de produits qui ne furent pas détectés auparavant dans la réaction à partir de l'oxindole. Un de ces composés a été

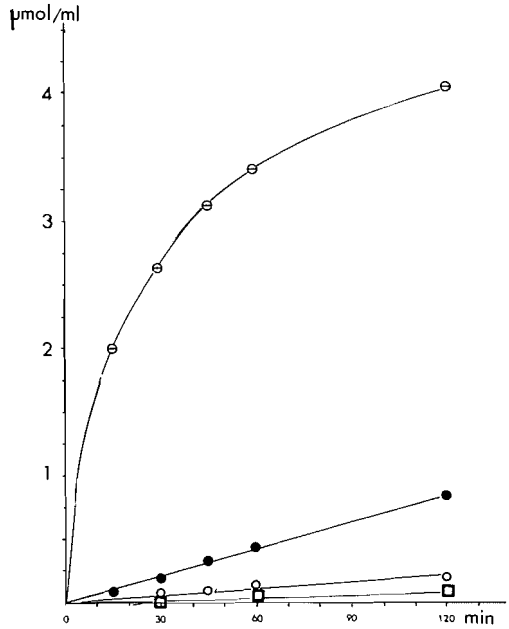

FIG. 3. Formation du 1,3,3-tribenzyloxindole, -⊖-, À partir du 1,3-dibenzyloxindole (10 μmol/ml); -●- à partir du l-benzyloxindole (10.7 μmol/ml); -○-, à partir du 3,3-dibenzyloxindole (10 μmol/ml); -□-, à partir du 3-benzyloxindole (10.7 μmol/ml).

isolé et identifié comme étant un dérivé du dioxindole ce qui est en accord avec les observations de Ghosal et Dutta (10) qui obtinrent différents 3-phényldioxindoles en introduisant l'oxygène dans une solution alcaline des oxindoles correspondants. Les essais suivants pour ces réactions furent donc menés dans l'atmosphère de l'azote.

Les résultats sont représentés dans la fig. 3 et les tableaux 1, 2, 3,[1] et 4.

Il en résulte que les composés NC et NCC ne se forment pratiquement qu'à partir de N.

On peut donc déduire que:

$$(1) \qquad C \xrightarrow{k_2} CC \xrightarrow{k_3} NCC \qquad k_2 \gg k_3$$

$$(2) \qquad N \xrightarrow{k_5} NC \xrightarrow{k_6} NCC \qquad k_6 \gg k_3$$

$$(3) \qquad C \xrightarrow{k_7} NC \qquad k_7 \cong 0$$

[1]On peut remarquer dans le tableau 3 une baisse considérable de la quantité du substrat dans les premières minutes de la réaction. Cette baisse est accompagnée de l'apparition d'un produit inconnu dont la quantité diminue par la suite proportionnellement à la quantité de NCC formé. L'étude de ce produit est en cours.

Can. J. Chem. Downloaded from www.nrcresearchpress.com by 210.87.254.40 on 09/05/12
For personal use only.

Can. J. Chem. Downloaded from www.nrcresearchpress.com by 210.87.254.40 on 09/05/12
For personal use only.

TABLEAU 1. 1-Benzyloxindole + chlorure de benzyle + C_2H_5ONa; température, 40°

Temps (min)	1-Benzyloxindole		Chlorure de benzyle		1,3-Dibenzyloxindole		1,3,3-Tribenzyloxindole	
	μmol/ml	%	μmol/ml	%	μmol/ml	%	μmol/ml	%
0	10.00	100	180.0	100	0	0	0	0
5	8.23	82.3	—	—	0.21	2.1	traces	
10	7.68	76.8	—	—	0.37	3.7	0.03	0.3
15	7.88	78.8	—	—	0.53	5.3	0.07	0.7
30	7.07	70.7	—	—	0.82	8.2	0.21	2.1
45	6.46	64.6	—	—	1.13	11.3	0.33	3.3
60	6.01	60.1	—	—	1.23	12.3	0.46	4.6
120	5.30	53.0	—	—	1.44	14.4	0.85	8.5

TABLEAU 2. 3-Benzyloxindole + chlorure de benzyle + C_2H_5ONa; température, 40°

Temps (min)	3-Benzyloxindole		Chlorure de benzyle		1,3-Dibenzyloxindole		3,3-Dibenzyloxindole		1,3,3-Tribenzyloxindole	
	μmol/ml	%	μmol/ml	%	μmol/ml	%	μmol/ml	%	μmol/ml	%
0	10.00	100	180.0	100	0	0	0	0	0	0
5	7.62	76.2	—	—	0	0	0.44	4.4	0	0
10	7.00	70.0	—	—	0	0	0.71	7.1	0	0
15	6.49	64.9	—	—	0	0	0.78	7.8	0	0
30	5.70	57.0	—	—	0	0	1.20	12.0	0	0
45	4.90	49.0	—	—	traces	—	1.86	18.6	traces	—
60	4.87	48.7	—	—	"	—	2.02	20.2	0.03	0.3
120	4.87	48.7	—	—	"	—	2.71	27.1	0.07	0.7

TABLEAU 3. 1,3-Dibenzyloxindole + chlorure de benzyle + C_2H_5ONa; température, 40°

Temps (min)	1,3-Dibenzyloxindole		Chlorure de benzyle		1,3,3-Tribenzyloxindole	
	μmol/ml	%	μmol/ml	%	μmol/ml	%
0	10.70	100	180.0	100	0	0
5	3.72	34.8	—	—	1.09	10.2
10	3.95	36.9	—	—	1.55	14.5
15	3.81	35.6	—	—	1.97	18.4
30	3.51	32.8	—	—	2.64	24.7
45	3.81	35.6	—	—	3.14	29.3
60	3.68	34.4	—	—	3.40	31.8
120	3.58	33.4	—	—	4.05	37.8

TABLEAU 4. 3,3-Dibenzyloxindole + chlorure de benzyle + C_2H_5ONa; température, 40°

Temps (min)	3,3-Dibenzyloxindole		Chlorure de benzyle		1,3,3-Tribenzyloxindole	
	μmol/ml	%	μmol/ml	%	μmol/ml	%
0	10.70	100	184.0	100	0	0
5	7.90	73.8	—	—	traces	—
10	7.80	72.9	—	—	"	—
15	7.30	68.2	—	—	0.05	0.47
30	7.30	68.2	—	—	0.08	0.75
45	7.21	67.4	—	—	0.11	1.03
60	7.08	66.2	—	—	0.15	1.40
120	7.05	65.9	—	—	0.21	1.96

Can. J. Chem. Downloaded from www.nrcresearchpress.com by 210.87.254.40 on 09/05/12
For personal use only.

On en vient donc à conclure que l'expression $r = (N + NC + NCC)/(C + CC)$ peut être considérée avec une certaine approximation comme mesure de la réactivité relative de l'azote et du carbone 3, surtout au début de la réaction quand les différences en concentration de NC et CC ne sont pas encore trop grandes.

Les valeurs de r calculées à partir des résultats des figs. 1 et 2 sont représentées dans le tableau 5.

Comme on voit le carbone 3 de l'oxindole est environ deux fois plus réactif que l'azote. Cette différence en réactivité est beaucoup plus prononcée dans le cas des dérivés de l'oxindole substitués en 3. Le tableau 6 montre que la vitesse de la transformation $CC \rightarrow NCC$ (V_n) est environ 30 fois plus faible que la vitesse de la transformation $NC \rightarrow NCC$ (V_c). Autrement dit $r' = V_n/V_c \cong 1/30$.

Cette différence considérable entre r et r' n'est expliquable que partiellement par la croissance de la réactivité du carbone 3 dans les dérivés 3-substitués. Si on compare la vitesse des transformations $N \rightarrow NC$ et $NC \rightarrow NCC$ (tableaux 1 et 3) on aperçoit que la différence en réactivité entre les composés N et NC n'est que de l'ordre de 3–5. Il faut donc admettre qu'il existe un autre facteur responsable de la valeur basse de r', notamment une diminution de la réactivité nucléophile de l'azote par les substituants en carbone-3. Cela est dû probablement à une plus importante délocalisation du doublet libre de l'azote (structure **2**) dans les composés 3,3-disubstitués en comparaison avec les dérivés non ou monosubstitués formant les ions énolates dans lesquels est favorisée la structure **4** (éq. **3**).

TABLEAU 5.

$$r = \frac{N + NC + NCC}{C + CC}$$

Temps (min)	r	
	Base NaOH	Base $NaOC_2H_5$
15	0.48	0.58
30	0.48	0.55
60	0.51	0.64
120	0.55	0.67
180	0.57	0.73
240	0.57	0.73

TABLEAU 6.

$$r' = \frac{V_n}{V_c}$$

Vitesse (μmol $min^{-1}ml^{-1}$		Temps (min)	r'
V_n	V_c		
0.0033	0.13	15	0.025
0.0027	0.088	30	0.030
0.0024	0.070	45	0.034
0.0025	0.057	60	0.043
0.0017	0.034	120	0.050

[2] 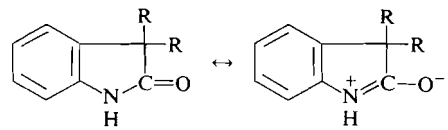

1 2

[3] 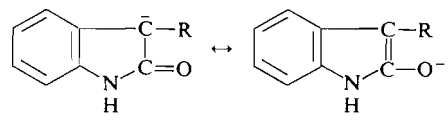

3 4

Partie expérimentale

Les points de fusion, non corrigés, ont été pris sur un appareil Mettler FPI.

Les c.p.v. analytiques ont été effectuées sur un Varian Aerograph 1700. Les spectres i.r. ont été déterminés au moyen d'un appareil Unicam SP 200 G.

L'oxindole provient de chez Baker, Baker Grade; le chlorure de benzyle, Fisher Scientific, Reagent Grade.

(A) Partie préparative

Benzylation de l'oxindole

A 2.0 g (0.015 mol) d'oxindole dissous dans 20 ml d'éthanol on ajoute une solution de 0.6 g (0.015 mol) de NaOH dans 80 ml d'éthanol et 1.9 g (0.015 mol) de chlorure de benzyle dissous dans 7 ml d'éthanol. On chauffe ce mélange à reflux pendant 4 h. Après avoir refroidi la solution on l'acidifie (HCl), évapore sous vide, ajoute 25 ml de benzène, essore le NaCl et évapore la solution à sec sous vide.

On obtient ainsi 3.4 g d'une huile jaune foncé qu'on dissout par la suite dans une quantité minimale de benzène et sépare sur une colonne de 100 g de gel de silice. L'élution avec un mélange benzène–hexane (2:1) donne 0.49 g de 1,3,3-tribenzyloxindole, rendement, 8.1%; p.f., 116.4° (éthanol). Spectres i.r. (CCl_4): 1708 cm^{-1} ($\nu_{(C=O)}$).

L'élution avec le benzène donne 0.169 g de 1,3-dibenzyloxindole, rendement 3.6%; p.f., 100.0° (éthanol).

Anal. calc. pour $C_{22}H_{19}NO$: C, 84.34; H, 6.04; N, 4.47. Trouvé: C, 83.95; H, 6.31; N, 4.46.

Spectres i.r. (CCl_4): 1708, 1712 cm^{-1} ($\nu_{(C=O)}$).

Dans les fractions benzéniques suivantes on trouve 0.217 g de 1-benzyloxindole, rendement, 6.5%; p.f., 75.5° (éthanol).

Anal. calc. pour $C_{15}H_{13}NO$: C, 80.72; H, 5.83; N, 6.28. Trouvé: C, 80.93; H, 6.06; N, 6.35.

Spectres i.r. (CCl_4): 1705, 1715 cm^{-1} ($\nu_{(C=O)}$). Ce produit est identique avec le 1-benzyloxindole obtenu à partir de la 1-benzylisatine (8).

L'élution avec le mélange benzène–chloroforme (2:1) donne 0.95 g de 3,3-dibenzyloxindole, rendement, 20.2%; p.f., 204.2° (éthanol).

Spectres i.r. (CCl_4): 1704, 1728 ($\nu_{(C=O)}$); 3445, 3190 cm^{-1} ($\nu_{(N-H)}$).

L'élution avec le chloroforme donne 0.435 g de 3-benzyloxindole, rendement, 13%; p.f., 132° (éthanol).

Anal. calc. pour $C_{15}H_{13}NO$: C, 80.72; H, 5.83; N, 6.28. Trouvé; C, 80.94; H, 5.91; N, 6.49.

Spectres i.r. (CCl_4): 1702, 1724, 1730 ($\nu_{(C=O)}$) 3448, 3200 cm^{-1} ($\nu_{(N-H)}$).

Il est identique avec le 3-benzyloxindole synthétisé par la réduction du 3-benzylidènoxindole avec le $NaBH_4$ (11).

En continuant l'élution avec le chloroforme on obtient 0.778 g (39%) d'oxindole.

Synthèse du 1,3-dibenzyloxindole à partir du 3-benzylidènoxindole

A une solution de $NaOC_2H_5$ (à partir de 0.8 g de Na) dans 50 ml d'éthanol ou ajoute 7.1 g (0.032 mol) de 3-benzylidènoxindole; on ajoute alors par portions 15.2 g (0.12 mol) de chlorure de benzyle et porte le mélange à reflux pendant 15 h. On évapore à sec sous vide, reprend le résidu par du benzène, lave avec de l'eau, sèche la solution benzénique sur le $MgSO_4$ anhydre. Après avoir chassé le solvant on dissout le résidu dans 150 ml d'éthanol à 50% et réduit par le $NaBH_4$. Une fois la réduction terminée on concentre sous vide et reprend par du benzène.

On sépare la solution dans le benzène sur une colonne de gel de silice.

L'élution par le benzène donne 4 g (40%) de 1,3-dibenzyloxindole, p.f., 92°, après une cristallisation dans l'éthanol, p.f., 99.8°.

L'élution par le chloroforme donne 3.2 g de 3-benzyloxindole.

1,3-Dibenzyldioxindole

A une solution de 0.276 g (0.00088 mol) de 1,3-dibenzyloxindole on ajoute 1.2 g (0.009 mol) de chlorure de benzyle et 17 ml d'une solution 0.05 *M* de NaOH dans l'éthanol. On chauffe à 40° pendant 5 h, acidifie avec du HCl, évapore à sec, ajoute du benzène, essore le NaCl et sépare la solution benzénique sur une colonne de 12 g de gel de silice.

Eluant avec du benzène on obtient le 1,3,3-tribenzyloxindole. Le chloroforme élue 0.12 g de 1,3-dibenzyldioxindole, p.f., 170°, après une cristallisation dans l'éthanol, p.f., 178.5°, lit. (12) p.f., 176–177°.

Anal. calc. pour $C_{22}H_{19}NO_2$: C, 80.24; H, 5.77; N, 4.26. Trouvé: C, 79.89; H, 6.08; N, 4.48.

Spectres i.r. (CCl_4): 1710 ($\nu_{(C=O)}$), 3560 cm^{-1} ($\nu_{(O-H)}$)

(B) Partie analytique

On chauffe une solution de l'oxindole ou d'un de ces dérivés mono- ou disubstitués, du chlorure de benzyle et de la base (le NaOH ou le $NaOC_2H_5$) en agitant sur un bain thermostaté. Les concentrations de chaque produit sont données dans les graphiques et les tableaux.

On prélève les échantillons aux temps indiqués, les acidifie, chasse le solvant, ajoute du benzène, essore le NaCl et ajuste le volume de la solution avec du benzène. On injecte ensuite des échantillons de 5–20 μl sur une colonne de c.p.v.

On utilise les colonnes de 10% Versamide 900 (3 ft × 1/8 in.) avec un programme 200→300° 15°/min, *T*(det.), 320°; *T* (inj.), 310°, N_2 30 cm^3/min, ou bien les colonnes de 10% SE 30 (5 ft × 1/8 in.) avec un programme 170→320° 10°/min, autres conditions identiques. Les temps de retension avec le Versamide: oxindole, 3.5; 1-benzyloxindole, 5.8; 3-benzyloxindole, 8; 1,3-dibenzyloxindole, 10.7; 3,3-dibenzyloxindole, 12.7; 1,3,3-dibenzyloxindole, 16.3 min; avec le SE-30: oxindole, 2.2 min; 1-benzyloxindole, 8; 3-benzyloxindole, 9; 1,3-dibenzyloxindole, 13.6; 3,3-dibenzyloxindole, 14.1; 1,3,3-tribenzyloxindole, 18 min.

On calcule la quantité de chaque dérivé à partir des hauteurs des pics, après avoir calibré l'appareil avec un mélange des composés purs. On répète la calibration quelques fois durant la journée. L'erreur estimée de la méthode: 10%.

Dans les réactions menées dans l'atmosphère de l'azote on introduit ce gaz après l'avoir saturé en éthanol à la température de l'eau du robinet.

Ce travail a été partiellement financé par une subvention du Conseil National de Recherches du Canada.

L'auteur remercie bien vivement MM. D. Fletcher et M. Bergeron pour leur assistance technique efficace.

1. E. WENKERT, N. BHATTACHARYYA, T. L. REID, et T. E. STEVENS. J. Am. Chem. Soc. **78**, 797 (1956).
2. E. WENKERT et E. BLOSSEY. J. Org. Chem. **27**, 4656 (1962).
3. B. WITKOP et A. EK. J. Am. Chem. Soc. **73**, 5664 (1951).
4. P. JULIAN, E. MEIER, et M. Printy. *Dans* Heterocyclic compounds. Vol. 3. Elderfield. 1952. p. 159.
5. W. SUMPTER et E. MILLER. Heterocyclic compounds with indole and carbazole systems. New York, N.Y. 1954. p. 146.
6. B. BOBRANSKI et Z. ZBORUCKI. Roczniki Chem. **42**, 487 (1968).
7. I. GRUDA. Roczniki Chem. **40**, 1323 (1966).
8. G. PALAZZO et V. ROSNATI. Gazz. Chim. Ital. **83**, 211 (1953).
9. R. W. DAISLEY et J. WALKER. J. Chem. Soc. C 1375, (1971).
10. S. GHOSAL et S. K. DUTTA. Indian J. Chem. **8**, 687 (1970).
11. I. W. ELLIOTT et P. RIVERS. J. Org. Chem. **29**, 2438 (1964).
12. G. HALLMANN. Chem. Ber. **95**, 1138 (1962).

Can. J. Chem. Downloaded from www.nrcresearchpress.com by 210.87.254.40 on 09/05/12
For personal use only.

Kinetics of Proton Transfer Reactions of Carbon Acids. II.[1] Reaction of Di-(4-nitrophenyl)methane with Alkoxide Bases

A. JARCZEWSKI[2] AND K.T. LEFFEK
Chemistry Department, Dalhousie University, Halifax, Nova Scotia

Received July 12, 1971

The second-order rate constants have been measured over a range of temperatures for the proton-transfer reactions from di-(4-nitrophenyl)methane to ethoxide, isopropoxide, and *t*-butoxide ions in solvents consisting of the corresponding alcohols containing 10% toluene by volume. The activation parameters $\Delta H^{\ddagger}$ and $\Delta S^{\ddagger}$ have been calculated and an interpretation of them is given in terms of solvation effects during the activation process. A comparison between the activation parameters for proton transfers and E2 olefin-forming β-elimination reactions is made and discussed with respect to transition state character of the latter reactions.

On a mesuré les constantes de vitesse de second ordre à plusieurs températures pour les réactions de transfert de proton du di-(4-nitrophényl)méthane aux ions éthoxyde, isopropoxyde et butoxyde tertiaire dans des solvants consistant en les alcools correspondants contenant 10% de toluène par volume. On a calculé les paramètres d'activation $\Delta H^{\ddagger}$ et $\Delta S^{\ddagger}$ et on les interprète en termes d'effets de solvation durant le procédé d'activation. On fait une comparaison entre les paramètres d'activation pour les transferts de proton et les réactions E2 de formation d'oléfine par élimination-β et on discute par rapport au caractère d'état de transition de ces dernières réactions.

Canadian Journal of Chemistry, **50**, 24 (1972)

Introduction

The kinetics of proton-transfer reactions between substituted methanes and bases in organic solvents have been studied by Caldin and co-workers (1–4). This paper presents part of a systematic study of the activation parameters of this type of reaction.

The addition of sodium alkoxide to di-(4-nitrophenyl)methane in alcohol yields a violet colored solution. The reaction is presumed to be a reversible proton-transfer by analogy with the reaction with tri-(4-nitrophenyl)methane, which has been investigated in detail (2) and also from the fact that neutralization of the basic solution with deuterated hydrochloric acid yields a colorless solution from which the original di-(4-nitrophenyl)methane can be recovered, deuterated on the aliphatic carbon atom. Some work has been carried out by Shapiro *et al.* (5) on the formation of anion radicals from di-(4-nitrophenyl)methane and hydroxyl ions in non-hydroxylic solvents. In some cases the colored solution yielded an e.p.r. signal and in others it did not, but in all cases the appearance of the color preceded the appearance of the e.p.r. signal. It is, therefore, concluded that the second-order rate constant corresponding to the appearance of the color is the k_2 of eq. 1.

$$[1] \quad (NO_2C_6H_4)_2CH_2 + \bar{O}Alk \overset{k_2}{\rightleftarrows} [(NO_2C_6H_4)_2CH]^- + HOAlk$$

The anion has a maximum absorption at about 530 nm, hence the velocity of the reaction may be conveniently followed spectrophotometrically.

Results and Discussion

Optical density measurements were made on equilibrium mixtures for solutions containing a constant concentration of the substrate and various concentrations of sodium ethoxide. These are given in Table 1. From eq. 1 the expression for the equilibrium constant may be written as eq. 2, since the concentration of

$$[2] \quad \frac{K}{[C_2H_5OH]} = K' = \frac{[A^-]}{[C_2H_5O^-]([AH]-[A^-])}$$

ethoxide is in large excess over that of the anion. AH is the substituted methane and A^- its anion. Substitution of the anion concentration by the optical density (o.d.) and molar

[1]Part I is considered to be ref. 1.

[2]Post-doctoral Fellow 1969-1970. Permanent address: Zaklad Chemii ogólnej UAM, Poznan, Grunwaldzka 6, Poland.

Can. J. Chem. Downloaded from www.nrcresearchpress.com by 210.87.254.6 on 09/05/12
For personal use only.

Can. J. Chem. Downloaded from www.nrcresearchpress.com by 210.87.254.6 on 09/05/12
For personal use only.

TABLE 1. Optical density measurements for mixtures of di-(4-nitrophenyl)-methane and sodium ethoxide in ethanol–toluene* solvent at equilibrium; $[(NO_2C_6H_4)_2CH_2] = 2 \times 10^{-3}$ *M*; temperature = 25.0 °C

C_2H_5ONa (*M*)	Optical density
0.0392	0.222
0.0784	0.395
0.0979	0.485
0.1175	0.580
0.1371	0.675
0.176	0.861
0.196	0.960

*10% v/v toluene in ethanol.

absorptivity (ε) according to de Beer's Law leads (4) to eq. 3.

[3] $$[AH]/(o.d.) = 1/K'\varepsilon[\bar{O}C_2H_5] + 1/\varepsilon$$

The results of Table 1 plotted in the form of [AH]/(o.d.) *vs.* $1/[\bar{O}C_2H_5]$ give a good straight line, which demonstrates the validity of de Beer's Law for the anion and also the form in which eq. 1 is written. Although these results may be used to evaluate ε for the anion and K' for the system, it is not possible to do so to a good precision because the intercept of the graph, equal to $1/\varepsilon$, contains a large percentage uncertainty which also appears in K' which is calculated from the slope of the graph (slope = $1/K\varepsilon$). However, the values obtained are $\varepsilon \sim$ 11 000 l mol^{-1} cm^{-1} and $K' \sim$250 l mol^{-1}.

The kinetic measurements were made using a large excess of base and first-order rate constants were calculated using eq. 4 (see Experimental) derived from the equilibrium shown in eq. 1. These are shown in Table 2 for the reaction with ethoxide, isopropoxide, and *t*-butoxide in solvents consisting of the corresponding alcohol containing 10% toluene by volume. These rate constants were measured at a number of temperatures between 0 and 50 °C. The slope of the graph of the first order rate constant against the base concentration is the second order rate constant k_2 of eq. 1. The values of k_2, which were actually obtained by a least squares computation, are given in Table 3 together with their standard deviations. These second order rate constants were fitted to the transition state theory equation ($\log_{10} k_2$ *vs.* $1/T$) by a second least squares computation and the resulting activation parameters are shown in Table 4, with their standard deviations. Within the limits of the experimental precision the activation parameters for the ethoxide and isopropoxide reactions are the same but those for the tertiary butoxide attack show a lower enthalpy of activation which is compensated by a much more negative entropy of activation.

Caldin (6) has discussed the interpretation of energies of activation of some aromatic nitrocompounds, including the proton-abstraction from 2,4,6-trinitrotoluene by ethoxide ion in ethanol containing 1% toluene. This particular reaction gave a $\Delta H^{\ddagger}$ of 13.0 kcal mol^{-1} and a $\Delta S^{\ddagger}$ of -5.6 cal mol^{-1} deg^{-1}. Other measurements of the activation parameters for proton-abstraction by ethoxide in ethanolic solvents gave results of the same order of magnitude, *i.e.* for 4-nitrobenzyl cyanide (4), $\Delta H^{\ddagger} = 8.57$ kcal mol^{-1}, $\Delta S^{\ddagger} = -0.6$ cal mol^{-1} deg^{-1} and for tri(4-nitrophenyl)methane (2), $\Delta H^{\ddagger} = 11.6$ kcal mol^{-1}, $\Delta S^{\ddagger} = -11.1$ cal mol^{-1} deg^{-1}. Thus the result of approximately 10 kcal mol^{-1} for the enthalpy of activation for the ethoxide and isopropoxide reactions is within the range of typical proton abstraction reactions.

Enthalpies of Activation

Caldin's discussion (6) was made in terms of the four factors which contribute to the activation energies of bimolecular reactions in solution which had been recognized much earlier by Polanyi and co-workers (7, 8), *i.e.* bond breaking and making, non-bonded repulsions, electrostatic interactions, and solvation changes. It was concluded that the reorganization of solvent molecules could account for the major part of the activation energy. The point of interest of the results in Table 4 is, therefore, whether the enthalpies and entropies of activation confirm or cast doubt upon Caldin's conclusions.

When the reagent is changed from ethoxide ion to *t*-butoxide ion with each reaction run in its conjugate acid solvent, the reagent ($\bar{O}Bu$) becomes larger and more strongly basic and the solvent becomes less well able to facilitate ionization and solvate ions. Thus, the ethoxide ion is strongly solvated in ethanol, whereas the larger, more basic *t*-butoxide ion is less strongly solvated in *t*-butanol. Cram has suggested (9) that potassium *t*-butoxide at concentrations above 0.01 *M* in *t*-butanol exists as ion-pairs.

TABLE 2. First-order rate constants for the reaction of di-(4-nitrophenyl)methane with alkoxide ions

(a) Ethoxide in 10% v/v toluene in ethanol; initial concentration $(NO_2C_6H_4)_2CH_2 = 2 \times 10^{-3}$ *M*

	Ethoxide (*M*)				
	0.0392	0.0784	0.0979	0.1175	0.1620
Temperature (°C)	$k_1(s^{-1})$				
0.0	0.39_5	0.44	0.48	0.51	0.56
5.0	0.55	0.64	0.66	0.70	0.75
10.0	0.72	0.88	0.93	0.97_5	1.06
20.0	1.48	1.70	1.81	1.97	2.01
25.0	2.28	2.49	2.55	2.62	3.01
30.0	3.15	3.24	3.50	3.70	4.20
40.0	—	5.95	6.09	6.65	7.30
50.0	9.11	10.42	10.78	11.30	12.52

(b) Isopropoxide in 10% v/v toluene in isopropanol; initial concentration $(NO_2C_6H_4)_2CH_2 = 2 \times 10^{-4}$ *M*

	Isopropoxide (*M*)			
	0.0124	0.0558	0.116	0.1278
Temperature (°C)	$k_1(s^{-1})$			
0.0	0.087	0.093	0.114	0.117
5.0	0.109	0.106	0.126	0.139
10.0	0.131	0.144	0.160	0.168
20.0	0.206	0.201	0.245	0.240
25.0	0.245	0.262	0.319	0.368
30.0	0.301	0.341	0.413	0.456
40.0	0.446	0.524	0.711	0.744
50.0	0.634	0.746	1.130	1.220

(c) t-Butoxide in 10% v/v toluene in t-butanol; initial concentration $(NO_2C_6H_4)_2CH_2 = 5 \times 10^{-5}$ *M*

	t-Butoxide (*M*)			
	0.0023	0.00465	0.00931	0.0186
Temperature (°C)	$10^2\ k_1(s^{-1})$			
20.0	0.55	1.04	1.74	2.50
25.0	0.61_5	1.15	1.86	2.80
30.0	0.71_5	1.27_5	2.08	3.86
35.0	0.85	1.50_5	2.53	4.55
40.0	1.02	1.73_5	2.98	5.28

Therefore, it is probable that there is a qualitative difference in the initial state of the reagent between ethoxide and *t*-butoxide which should appear as a quantitative difference in the activation parameters even though both reactions exhibit the same type of second-order kinetics. If a major part of the activation energy is the breaking down of a strong solvation shell around the ethoxide ion in ethanol, then the enthalpy of activation for *t*-butoxide attack should be smaller since its solvation shell is weaker, and the more so if it does indeed exist predominantly in an ion-paired state.

Entropies of Activation

The activation entropies shown in Table 4 are all negative but of larger magnitude than those for the other proton-transfers quoted above. Such entropies of activation indicate a marked increase in the order of the system during the

Can. J. Chem. Downloaded from www.nrcresearchpress.com by 210.87.254.6 on 09/05/12
For personal use only.

Can. J. Chem. Downloaded from www.nrcresearchpress.com by 210.87.254.6 on 09/05/12
For personal use only.

TABLE 3. Second-order rate constants for the reaction of di-(4-nitrophenyl)methane with alkoxide ions

Temperature (°C)	0.0	5.0	10.0	20.0	25.0	30.0	35.0	40.0	50.0
Ethoxide k_2*	1.37 ±0.12	1.65 ±0.15	2.58 ±0.41	4.94 ±0.73	5.85±0.65	9.37±1.2	—	16.6±1.0	27.2±1.2
Isopropoxide k_2*	0.281±0.02	0.260±0.09	0.313±0.03	0.802±0.02	1.01±0.23	1.27±0.21	—	2.76±0.21	5.32±0.68
t-Butoxide k_2*	—	—	—	1.19 ±0.09	1.30±0.09	1.90±0.03	2.24±0.03	2.61±0.05	—

*l mol^{-1} s^{-1}.

TABLE 4. Activation parameters of proton-transfer reactions from di-(4-nitrophenyl)methane to alkoxide bases

Base	$\Delta H^{\ddagger}$(kcal mol^{-1})	$\Delta S^{\ddagger}$(cal mol^{-1} deg^{-1})
Ethoxide	10.2 ± 0.3	-20.6 ± 1.0
Isopropoxide	10.4 ± 0.8	-23.5 ± 2.6
t-Butoxide	7.1 ± 0.9	-34.0 ± 2.9

activation process. This will result automatically for any bimolecular reaction, but if the activation parameters are to be interpreted on the basis of a major contribution from solvation effects, then it must be assumed that the transition states for these reactions have more solvent molecules tied down than do the corresponding initial states. For the ethoxide reaction a strongly solvated initial state contains ethanol molecules hydrogen-bonded to the negatively charged oxygen atom. In the transition state the negative charge is dispersed partly onto the carbon atom of the incipient carbanion with the whole entity solvated by an ethanol sheath which must contain a lot of solvent–hydrogen-bonded interaction and a much reduced ethanol-ethoxide interaction. Thus, it is possible to have more solvent molecules constrained in the transition state than in the initial state, with a concomitant decrease in entropy.

The much larger entropy of activation encountered with the *t*-butoxide reaction may result from the ion-pair state of sodium *t*-butoxide in *t*-butanol. The weak solvation of the initial state becomes stronger on activation by a mechanism analogous to that postulated for the ethoxide reaction. In addition, a strong solvation shell must form around the sodium ion since it will become a more independent entity as the negative charge is dispersed between the oxygen and carbon atoms. Such an explanation would predict that the entropy of activation for the *t*-butoxide attack in *t*-butanol should be largely independent of the structure of the substrate molecule. Caldin and Hyde[3] have found $\Delta S^{\ddagger} = -35$ cal mol^{-1} deg^{-1} for tri-(4-nitrophenyl)methane under almost the same conditions as the present work, which is essentially the same as our value in Table 4. On the other hand for the ethoxide attack in ethanol the entropies of activation are quite different; -11 cal mol^{-1} deg^{-1} for tri-(4-nitrophenyl)methane and -21 cal mol^{-1} deg^{-1} for di-(4-nitrophenyl)methane.

It is concluded that the major part of the observed activation parameters may be satisfactorily interpreted in terms of solvation effects in a manner consistent with the earlier treatment of Caldin (6) by using arguments similar to those used by others in discussions of solvation effects, particularly those of Robertson in his review of the characteristics of solvolysis reactions of alkyl halides and sulfonates in water (10).

Comparison with β-Elimination Reactions

It is of interest to compare the above proton abstraction reactions with olefin-forming β-eliminations which involve the removal of a halide with its bonding electrons from an α-carbon atom and also the removal of a proton from the β-carbon atom of an alkyl halide to yield an olefin. Of the three main mechanisms possible, E1, E2, and E1cB, the E2 is by far the most common. The unimolecular elimination from the conjugate base of the alkyl halide (E1cB) would involve the initial formation of a carbanion followed by rapid loss of halide. This mechanism seems to be quite rare for reactions which produce simple olefins (11, 12). Since the first step is a proton transfer, the activation parameters of an E1cB reaction might be expected to be similar to those in Table 4 under certain mechanistic conditions. The conditions are that the carbanion intermediates should decompose to olefins at roughly the same rate as they re-protonate to form the original molecule, so that the first proton-abstraction step would play a major role in controlling the rate of the overall reaction. This type of E1cB mechanism merges smoothly into an E2 process as the rate at which the carbanion decomposes to olefin is increased in relation to the re-protonation step (13). Thus, the E2 reaction may have a symmetrical transition state with equal amounts of β-carbon–hydrogen and α-carbon–halogen bond breaking, or the transition state may be unsymmetrical, either E1-like with more carbon–halogen bond breaking or E1cB-like with more carbon–hydrogen bond breaking. Such different transition states have been postulated several times (12–15) and correlated with kinetic isotope effects (15–17).

Despite the fact that Cristol *et al.* (18) estimated that the energy required to form a sym-

[3]Personal communication.

Can. J. Chem. Downloaded from www.nrcresearchpress.com by 210.87.254.6 on 09/05/12
For personal use only.

Can. J. Chem. Downloaded from www.nrcresearchpress.com by 210.87.254.6 on 09/05/12
For personal use only.

metrical E2 transition state was lower than that required for a carbanion transition state by 7 to 14 kcal mol^{-1} for a molecule with no resonance stabilization of the carbanion, it seems reasonable to postulate, in the light of the results in Table 4, that an increase in carbanion character in the transition state of an E2 reaction would be accompanied by a decrease in ethalpy of activation, for molecules in which some amount of stabilization of the carbanion is to be expected. The reduction in the enthalpy of activation is achieved by a reduction in the energy contribution from the stretching of the carbon–halogen bond. This postulate may be used to interpret some activation parameter changes which have been observed, *e.g.* with β-phenylethyl tosylate and bromide undergoing E2 reactions with ethoxide in ethanol and *t*-butoxide in *t*-butanol. For the bromide $\Delta H^{\ddagger}$ falls from 20.4 to 13.0 kcal mol^{-1} while $\Delta S^{\ddagger}$ changes from −6.8 to −25.0 cal mol^{-1} deg^{-1} on changing from ethoxide to *t*-butoxide (19, 20). A very similar change is also found for the tosylate (19). These parameters might reasonably be interpreted as an indication that the elimination reaction with *t*-butoxide is going through a transition state with more carbanion character than that of the ethoxide reaction. The bromide shows a primary β-deuterium isotope effect (k_H/k_D) of between 7 and 8 (20) for both the ethoxide and tertiary butoxide, and also the same Hammett ρ-value (19), indicating that the reacting proton is symmetrically placed between the carbon atom and the base in this transition state (21). Thus, any difference in the transition states of the two reactions must lie in the amount of stretching of the carbon-bromine bond. It may be possible, therefore, to deduce the character of an E2 transition state, for particular types of substrate molecules, from the magnitude of the activation parameters.

Examples of the E1cB mechanism may be found in the future by first studying the proton-transfer reaction and then adjusting the structure of the formed carbanion so that it has the correct stability and also the ability to eliminate a halogen or some other group at an appropriate rate. An example, using essentially this approach, has been reported recently (22).

Experimental

Materials

Di-(4-nitrophenyl)methane was prepared by adding diphenylmethane (75 g) slowly to a vigorously stirred solution of concentrated nitric acid (390 g) and concentrated sulfuric acid (470 g) maintained at −10 to −15 °C. Stirring was continued for 45 min keeping the temperature below −10°, after which the solution was poured into an excess of ice-water. The yellow precipitate which formed was filtered off and washed successively with water, methanol, and diethyl ether. The nitro compound was recrystallized from benzene several times yielding yellow needles m.p. 183–185° (lit. 183° (23)).

Ethanol was purified by refluxing with potassium hydroxide and silver nitrate to remove the aldehydes (24), then dried by the method of Lund and Bjerrum (24). Traces of bases were finally removed by redistilling with a little 2,4,6-trinitrobenzoic acid (24).

2-Propanol was dried for several days over Drierite, then with calcium hydride. After heating under reflux with stannous chloride, the 2-propanol was fractionally distilled.

t-Butanol was dried over calcium hydride and then fractionally distilled from dibutylphthalate.

Toluene was dried with sodium metal and fractionally distilled.

Equilibrium Measurements

The o.d. measurements were made on a Unicam SP800 Spectrophotometer, fitted with a constant-temperature bath to control the temperature of the cell block.

Kinetic Measurements

Alkoxide stock solutions were prepared in the alcohols containing 10% toluene by volume, by dissolving clean sodium metal in the solvents in flasks protected from absorption of moisture and carbon dioxide from the atmosphere. The solutions were stored under nitrogen. The concentrations of the alkoxide solutions were determined by titration against standard HCl solutions, using methyl orange as the indicator.

For the ethoxide and isopropoxide reactions the velocities were observed using a Durrum-Gibson stopped-flow spectrophotometer with a Kel-F flow system and an optical cell of 2 mm light-pathlength. The instrument was fitted with a constant-temperature system which maintained the reservoir, in which the drive syringes of the apparatus are immersed, at the temperatures quoted in Table 2 to ±0.03 °C.

The concentrations in the ethoxide reaction were chosen so that the traces showing transmittance *vs.* time, which were displayed on a Tektronix 564 storage oscilloscope screen, covered the range of 80–100% transmittance. Several runs under identical reaction conditions were displayed on the screen consecutively then this was photographed with a Polaroid camera. The photographs were enlarged and the first-order rate constants were calculated by the Guggenheim method (25) assuming that the transmittance was proportional to the substrate concentration.

For the isopropoxide reaction, it was not convenient to work in the 80–100% transmittance range, so in this case the color change was monitored over a wider transmittance range and converted to absorbance before calculation of the rate constants.

The *t*-butoxide reaction was followed on the Unicam SP 800 spectrophotometer by scanning at a fixed wavelength of 530 nm against time. The absorbance values were read directly from the chart paper and the first-order rate constants were again calculated by the Guggenheim method.

Can. J. Chem. Downloaded from www.nrcresearchpress.com by 210.87.254.6 on 09/05/12
For personal use only.

TABLE 5*a*. Run 343; temperature 25.0 °C; initial concentration $(NO_2C_6H_4)_2CH_2 = 2 \times 10^{-3}$ *M*; initial concentration $C_2H_5\bar{O}\dot{N}a = 0.784$ *M*

Time (ms)	x_1*	x_2*
0	228.5	52.5
20	215.5	49.5
40	203.0	47.0
60	192.5	44.0
80	181.5	41.5
100	172.5	39.5
120	162.5	38.0
140	154.5	35.5
160	146.5	33.5
180	138.5	31.5
200	132.0	29.0
220	125.5	27.5
240	119.0	26.0
260	112.5	24.5
280	107.0	23.0

Guggenheim analysis yields $k_1 = 2.59$ s^{-1}

*x_1 and x_2 are readings in mm from the enlarged reaction trace corresponding to transmittance decreasing with time.

TABLE 5*b*. Run 460; temperature 20.0 °C; initial concentration $(NO_2C_6H_4)_2CH_2 = 5 \times 10^{-5}$ *M*; initial concentration t-$C_4H_9\bar{O}\dot{N}a = 0.00931$ *M*

Time (1 unit = 5.657 s)	x_1(absorbance)	x_2(absorbance)
0	0.208	0.554
1	0.258	0.566
2	0.302	0.578
3	0.338	0.588
4	0.366	0.598
5	0.398	0.604
6	0.424	0.612
7	0.448	0.620
8	0.472	0.624
9	0.492	0.630
10	0.508	0.636
11	0.525	0.640
12	0.540	0.644

Guggenheim analysis yields $k_1 = 1.76 \times 10^{-2}$ s^{-1}

The values reported in Table 2 are the means of three or four runs. Two example runs are shown in Table 5.

The first order rate constants were calculated using eq. 4

$$[4] \qquad (x_e - x)/x_e = \exp\,[-(k_2 b + k_{-2})t]$$

where x_e is the equilibrium concentration of carbanion, x is its concentration at time t and the term $(k_2 b + k_{-2})$ is the observed first-order rate constant in which b is the alkoxide concentration, k_2 is the second-order rate constant for the forward reaction and k_{-2} that for the reverse reaction multiplied by the concentration of solvent alcohol (2).

The authors are grateful for financial support by the National Research Council of Canada and to Professor E. F. Caldin for helpful comments.

1. E. F. CALDIN, A. JARCZEWSKI, and K. T. LEFFEK. Trans. Faraday Soc. **67**, 110 (1971).
2. E. F. CALDIN and J. C. TRICKETT. Trans. Faraday Soc. 772 (1954).
3. E. F. CALDIN and G. LONG. Proc. Roy. Soc. A**228**, 263 (1955).
4. E. F. CALDIN, M. KASPARIAN, and G. TOMALIN. Trans. Faraday Soc. **64**, 2802 (1968).
5. B. I. SHAPIRO, V. M. KAZAKOVA, and YA. K. SYRKIN. Dok. Akad. Nauk SSSR **165**, 619 (1965); Dok. Phys. Chem. **165**, 828 (1965) (Engl.).
6. E. F. CALDIN. J. Chem. Soc. 3345 (1959).
7. R. A. OGG, JR. and M. POLANYI. Trans. Faraday Soc. **31**, 604 (1935).
8. M. G. EVANS and M. POLANYI. Trans. Faraday Soc. **34**, 11 (1938).
9. D. J. CRAM. Fundamentals of carbanion chemistry. Academic Press, New York, N.Y. 1965. p. 34.
10. R. E. ROBERTSON. Prog. Phys. Org. Chem. **4**, 213 (1967).
11. C. K. INGOLD. Structure and mechanism in organic chemistry. Cornell University Press, Ithaca, N.Y. 1969. Chapt. IX.
12. D. J. MCLENNAN. Quart. Rev. **21**, 490 (1967).
13. D. V. BANTHORPE. Elimination reactions. Elsevier Publishing Co., Amsterdam. 1963. Chapt. 4.
14. J. F. BUNNETT. Angew. Chem. Int. Ed. Engl. **1**, 225 (1962).
15. G. AYREY, A. N. BOURNS, and V. A. VYAS. Can. J. Chem. **41**, 1759 (1963).
16. W. H. SAUNDERS, JR. and S. ASPERGER. J. Am. Chem. Soc. **79**, 1612 (1957).
17. G. AYREY, E. BUNCEL, and A. N. BOURNS. Proc. Chem. Soc. 458 (1961).
18. S. L. CRISTOL, N. L. HAUSE, and J. S. MEEK. J. Am. Chem. Soc. **73**, 674 (1951).
19. C. H. DEPUY and C. A. BISHOP. J. Am. Chem. Soc. **82**, 2532 (1960).
20. W. H. SAUNDERS, JR. and D. H. EDISON. J. Am. Chem. Soc. **82**, 138 (1960).
21. F. H. WESTHEIMER. Chem. Revs. **55**, 265 (1961).
22. A. BERNDT. Angew. Chem. Int. Ed. Engl. **8**, 613 (1969).
23. Directory of organic compounds. Eyre and Spottiswoode Ltd., London. **4**, 2473 (1965).
24. D. D. PERRIN, W. L. F. ARMAREGO, and D. R. PERRIN. Purification of laboratory chemicals. Pergamon Press, Oxford. 1966. p. 157.
25. E. A. GUGGENHEIM. Phil. Mag. **2**, 538 (1926).

Diffusion of some Hydrocarbons in Air: a Regularity in the Diffusion Coefficients of a Homologous Series[1]

ROBERT W. ELLIOTT[2] AND HARRY WATTS

Research Department, Dow Chemical of Canada, Limited, Sarnia, Ontario

Received March 17, 1971

Diffusion coefficients in air at 298.2 °K and 1 atm pressure are reported for ethane, ethene, ethyne, cyclopropane, propene, propadiene, propyne, butane, 1-butene, 2-methylpropene, *cis*-2-butene, *trans*-2-butene, 1,3-butadiene, 1-butyne, 2-methylbutane, 2,2-dimethylpropane, cyclopentane, and 1-pentene.

A linear relationship, valid for alkanes and alkenes, has been found between the diffusion coefficient and the reduced molecular weight of the members of a homologous series and air.

Diffusion coefficients calculated by ten prediction equations were generally lower than those observed.

Les coefficients de diffusion dans l'air à 298.2 °K et sous une pression de une atmosphère sont rapportés pour l'éthane, l'éthène, l'éthyne, le cyclopropane, le propène, le propadiène, le propyne, le butane, le butène-1, le méthyl-2 propène, le butène-2 *cis*, le butène-2 *trans*, le butadiène-1,3, le butyne-1, le méthyl-2 butane, le diméthyl-2,2 propane, le cyclopentane et le pentène-1.

Une relation linéaire, valable pour les alcanes et les alcènes, existe entre le coefficient de diffusion et la masse moléculaire réduite des membres d'une série homologue et l'air.

Les coefficients de diffusion, calculés à partir de dix équations de prédiction, sont généralement plus bas que ceux observés.

Canadian Journal of Chemistry, **50**, 31 (1972)

Introduction

Measurements of gaseous diffusion coefficients are of great value for both theoretical and practical reasons. The detailed kinetic theory of gases relates the diffusion coefficient in a binary mixture to the intermolecular forces acting between the diffusing species (1). In principle, it is possible to calculate a diffusion coefficient from intermolecular forces. However, knowledge of intermolecular forces is far from complete; hence data necessary for this calculation must be obtained from measurements of some other property, such as viscosity, which can also be related to intermolecular forces. Alternately, data on diffusion coefficients may be used to give information on intermolecular forces (2). The practical need in engineering design for reasonable values of diffusion coefficients has produced a rash of semi-empirical prediction equations. Most of these are soundly based on theory, but have been forced to empiricism because of our incomplete knowledge of intermolecular forces.

Dichotomy of interest has divided diffusion coefficient measurements into two groups, those aimed at gaining greater understanding of intermolecular forces, and those aimed at obtaining data on systems of practical importance. Most studies of gaseous diffusion have been fragmentary and few systematic investigations of related systems have been made. Recent notable exceptions have been the investigations of noble gas mixtures by Van Heijningen, Harpe, and Beenakker (2) and the diffusion of 147 compounds in air by Lugg (3).

In this paper we report the results of a systematic investigation of the diffusion of some hydrocarbons in air. These results have revealed a regularity in the diffusion coefficients of a homologous series that has apparently not been previously observed.

Experimental

The apparatus and experimental techniques have been described previously (4, 5). All data were corrected to 1 atm pressure and 25 °C as before. In an attempt to refine techniques two possible sources of experimental error were investigated. Previously it had been considered that the effect of small atmospheric pressure fluctuations would be negligible from the point of view of their effect upon the magnitude of the diffusion coefficient. However, if the atmospheric pressure fell steadily during an experiment the rate of loss of diffusing gas from the cell would be enhanced, due to expansion of the cell contents, and if it rose steadily during an experiment the rate of loss would be lowered, due to contraction of the cell contents. If this effect were significant, then experiments performed with a steady pressure

[1]Contribution No. 190.

[2]Present address: The International Nickel Company of Canada Limited, J. Roy Gordon Research Laboratory, Sheridan Park, Clarkson, Ontario.

Can. J. Chem. Downloaded from www.nrcresearchpress.com by 210.87.254.5 on 09/05/12
For personal use only.

TABLE 1. Diffusion coefficients at 298.2 °K

Compound	Infrared frequency (cm^{-1})	No. of data	Diffusion coefficients in $cm^2\ s^{-1}$	
			Experimental	Calculated
Ethane	2950	6	0.1531±0.0038	0.1453
Ethene	3123	6	0.1655±0.0021	0.1543
Ethyne	3307	5	0.1457±0.0015	0.1597
Cyclopropane	1028	6	0.1277±0.0012	0.1219
Propene	2953	6	0.1318±0.0017	0.1204
Propadiene	1969	6	0.1392±0.0018	0.1160
Propyne	3346	6	0.1316±0.0011	0.1236
Butane	2965	8	0.1021±0.0013	0.0981
1-Butene	2969	6	0.1092±0.0016	0.1019
2-Methylpropene	2963	6	0.1072±0.0032	0.1000
cis-2-Butene	3036	6	0.1087±0.0013	0.1011
trans-2-Butene	961	6	0.1131±0.0012	0.1091
1,3-Butadiene	3110	6	0.1158±0.0018	0.1039
1-Butyne	3340	6	0.1163±0.0020	0.0945
2-Methylbutane	2967	6	0.0935±0.0020	0.0876
2,2-Dimethylpropane	2957	6	0.0877±0.0021	0.0883
Cyclopentane	2967	6	0.0919±0.0025	0.0920
1-Pentene	2967	6	0.0958±0.0011	0.0926

drop would give diffusion coefficients showing positive deviations from the mean of a set and those performed with a steady pressure increase would show negative deviations. Statistical analysis of experiments in which these conditions obtained showed no such systematic trend in the diffusion coefficients. We therefore conclude that any effect of small systematic atmospheric pressure changes during an experiment is negligible.

The frequencies of the i.r. absorption bands used to follow concentration changes in the diffusion cell lay near the OH stretching vibration frequency of water, consequently changes in atmospheric humidity during an experiment might effect the results due to changes in atmospheric absorbance in the reference beam of the i.r. spectrophotometer used to follow concentration changes in the cell. Consequently the relative humidity of the room was measured during experiments. Analysis of results showed no trend in diffusion coefficient with humidity.

Materials

The compounds studied were pure grade (99 mol% or better) and were obtained from the following sources: ethane, propene, *n*-butane, 2-methylpropene, 1-butene, *cis*-2-butene, *trans*-2-butene, 1,3-butadiene, 2-methylbutane, 1-pentene, and cyclopentane (95 mol%), Phillips Petroleum Company; ethyne, cyclopropane, propadiene, propyne, 1-butyne, and 2,2-dimethylpropane, Matheson of Canada, Ltd.; ethylene, Imperial Oil, Limited.

Results and Discussion

Table 1 gives the mean observed diffusion coefficients in air of the compounds studied together with their root-mean-square deviations, the number of data obtained, and the i.r. frequency used to follow concentration changes of the diffusing gas. Inspection of the data reveals some systematic trends. The diffusion coefficients of the alkenes, ethene, propene, 1-butene, and 1-pentene, are all higher than those for the corresponding alkanes. Propane and *n*-pentane were determined previously (5) and have the values 0.1144 ± 0.0015 and 0.0856 ± 0.0035 $cm^2\ s^{-1}$, respectively. Propadiene and 1,3-butadiene have higher diffusion coefficients than the corresponding alkenes. The values for cyclopropane and cyclopentane are both higher than the respective straight chain alkanes quoted above. Lugg (3) reported that the diffusion coefficients of chain isomers of many substituted alkanes was in the order *iso* > *n*. This order is observed with pentane but not with butane. Beatty (6) observed that the binary diffusion coefficient for the system 2,2-dimethylpropane–pentane was higher than the self diffusion coefficient of pentane; consistent with this we find the diffusion coefficients in air to be ordered 2,2-dimethylpropane > pentane. We also note a significant difference between the *cis* and *trans* isomers of 2-butene.

Diffusion coefficients were calculated from the detailed kinetic theory equation (1) as in previous work (4, 7) and from nine other prediction equations using modified versions of the computer programmes of Jarvis and Lugg (8). The equations used are named in order of decreasing accuracy of their predictions, together with the root-mean-square deviations in $cm^2\ s^{-1}$ of the predicted from our experimental results: Wilke–Lee (9), ±0.0087; Slattery-Bird (10),

Can. J. Chem. Downloaded from www.nrcresearchpress.com by 210.87.254.5 on 09/05/12
For personal use only.

Can. J. Chem. Downloaded from www.nrcresearchpress.com by 210.87.254.5 on 09/05/12
For personal use only.

±0.0092; the kinetic theory equation (1), ±0.0105; Chen–Othmer (11), ±0.0106; Fuller, Schettler, and Giddings (12), ±0.0122; Hirschfelder, Bird, and Spotz (13), ±0.0141; Othmer–Chen (14), ±0.0147; Andrussow (15), ±0.0202; Gilliland (16), ±0.0220; and Arnold (17), ±0.0414. In general, all of these equations predicted diffusion coefficients lower than the experimental values, and none was completely successful in arranging the diffusion coefficients of isomers in the correct order. Indeed the equations of Gilliland (16), Andrussow (15), and Fuller, Schettler, and Giddings (12) are unable to distinguish between isomers at all!

If good data for its use were available, the kinetic theory equation should be superior to the other equations because of its sound theoretical basis. In our calculations we used tabulated values of the Lennard–Jones potential parameters for the hydrocarbons obtained from viscosity measurements (1), where available; where these data were not available they were estimated from critical properties listed by Kudchadkar, Alani, and Zwolinski (18) by the method of Stiel and Thodos (19). Where critical properties were not available they were estimated by standard methods (19). Potential parameters for the mixture were calculated from those for the pure components as before (7) using the Hudson–McCoubrey combining rules (20) and ionization potentials as follows: ethane, ethene, ethyne, propene, propadiene, propyne, 1-butene, 1,3-butadiene, and 1-butyne from Herzberg (21), butane, 2-methylpropene, *cis*-2-butene, *trans*-2-butene from Bernecker and Long (22), 2-methylbutane, 2,2-dimethylpropane, and cyclopentane from Lorquet (23), cyclopropane from Cermak (24), and 1-pentene from Honig (25). It is probably this estimation of data that causes the kinetic theory equal ion to be slightly inferior to the Wilke–Lee and Slattery–Bird equations for the present systems.

In Fig. 1 are plotted the observed diffusion coefficients against the reduced molecular weight of each system, defined by

$$[1] \qquad \mu = \frac{M_A M_H}{M_A + M_H}$$

where M_A is the mean molecular weight of air and M_H is the molecular weight of the hydrocarbon. Data for the *n*-alkanes and *n*-alkenes

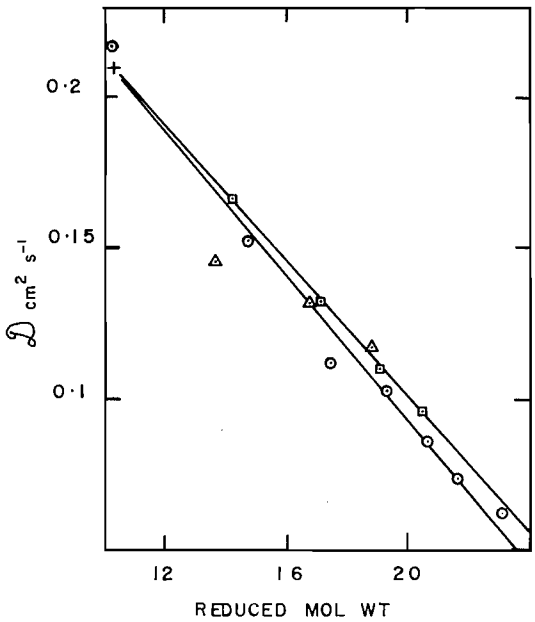

FIG. 1. Linear plots of diffusion coefficient in air at 25 °C against reduced molecular weight for the diffusion of *n*-alkanes, ⊙; *n*-alkenes, ⊡; and *n*-alkynes, △. The intersection of lines for alkanes and alkenes is marked +.

gave good straight lines. A least square fit to the equation:

$$[2] \qquad \mathcal{D} = m\mu + c$$

gave values for the slope m, intercept c, intercept on the μ axis, correlation coefficients, and standard deviations of experimental value of $\mathcal{D}$ from the fitted line listed in Table 2. The probability of obtaining these values of the correlation coefficients by chance alone is less than 0.01, indicating that the data are well represented by a linear relationship (26). To increase the number of data used in this calculation we included our previous values for methane (4) and propane (5) and Lugg's values for hexane and octane (3).

The intercepts of these lines on the reduced molecular weight axis are very close to the mean molecular weight of air, 28.967. This is consistent with the limit of $\mu \to M_A$ as $M_H \to \infty$, and the expectation that $\mathcal{D} \to 0$ as $M_H \to \infty$.

Figure 1 shows that the lines for the *n*-alkanes and *n*-alkenes intersect close to the point for methane. This would imply that, as far as diffusion is concerned, methane can be regarded as the first member of the alkene series. No

TABLE 2. Values for least squares fit to eq. 3

Hydrocarbon	m	c	μ axis intercept	Standard deviation	Correlation coefficients
n-alkanes	0.3344	−0.01206	27.73	0.0062	−0.9945
n-alkenes	0.3261	−0.01130	28.85	0.001	−0.9996

linear correlation was observed with the alkynes but our data are insufficient to draw any conclusion about the trend of diffusion coefficient with reduced molecular weight in this series.

The kinetic theory equation can be written in the form

$$[3] \qquad \mathscr{D}_{12} = \frac{bT^{3/2}}{\mu^{1/2}\sigma_{12}^{2}\Omega(T^*)}$$

where T is the absolute temperature and $\Omega(T^*)$ is a collision integral at a reduced temperature of $T^* = kT/\varepsilon_{12}$ and ε_{12} and σ_{12} are molecular interaction parameters characteristic of a 1–2 interaction; b is a constant, and k is the Boltzmann constant. The implications of eqs. 2 and 3 are that $\sigma_{12}^{2}\Omega(T^*)$ varies in a systematic, but not simple, way with reduced molecular weight for a homologous series. The discovery of this regularity in diffusion coefficients points to the need for further experimental work on other homologous series and to the need for further theoretical work. Analysis of literature data, now in progress, indicates that the linear variation of diffusion coefficient with reduced molecular weight is a general phenomenon for other classes of compounds (27).

We suggest that our linear relationship may be used for the empirical prediction of diffusion coefficients and predict the following for $\mathscr{D}$ in $cm^2\ s^{-1}$: heptane, 0.0635; nonane, 0.0495; decane, 0.0442. We might expect that the value for heptane in air would be reliable because it is an interpolated value and it will be interesting to see if future measurement bears out these predictions.

1. J. O. HIRSCHFELDER, C. F. CURTISS, and R. B. BIRD. Molecular theory of gases and liquids. John Wiley and Sons, Inc., New York. 1954.
2. R. J. J. VAN HEIJNINGEN, J. P. HARPE, and J. J. M. BEENAKKER. Physica, **38**, 1 (1968).
3. G. A. LUGG. Anal. Chem. **40**, 1072 (1968).
4. M. COWIE and H. WATTS. Can. J. Chem. **49**, 74 (1971).
5. R. F. BARR and H. WATTS. J. Chem. Eng. Data. In press.
6. J. W. BEATTY. J. Chem. Phys. **51**, 4673 (1969).
7. H. WATTS. Can. J. Chem. **49**, 67 (1971).
8. M. W. JARVIS and G. A. LUGG. Report 318, Department of Supply, Australian Defence Scientific Service, Defence Standards Laboratories, Maribyrnong, Victoria, Australia.
9. C. R. WILKE and C. Y. LEE. Ind. Eng. Chem. **47**, 1253 (1955).
10. J. C. SLATTERY and R. B. BIRD. A.I.Ch.E. J. **4**, 137 (1958).
11. N. H. CHEN and D. F. OTHMER. J. Chem. Eng. **7**, 37 (1962).
12. E. N. FULLER, P. D. SCHETTLER, and J. C. GIDDINGS. Ind. Eng. Chem. **58**, 19 (1966).
13. J. O. HIRSCHFELDER, R. B. BIRD, and E. L. SPOTZ. Trans. Am. Soc. Mech. Eng. **71**, 921 (1949).
14. D. F. OTHMER and H. T. CHEN. Ind. Chem. Eng., Prod. Res. Dev. **1**, 249 (1962).
15. L. ANDRUSSOW. Z. Elecktrochem. **54**, 566 (1950).
16. E. R. GILLILAND. Ind. Eng. Chem. **26**, 681 (1934).
17. J. H. ARNOLD. Ind. Eng. Chem. **22**, 1091 (1930).
18. A. P. KUDCHADKER, G. H. ALANI, and B. J. ZWOLINSKI. Chem. Rev. **68**, 659 (1968).
19. R. C. REID and T. K. SHERWOOD. The properties of gases and liquids. 2nd ed. McGraw-Hill, New York. 1966.
20. G. H. HUDSON and J. D. MCCOUBREY. Trans. Faraday Soc. **56**, 761 (1960).
21. G. HERZBERG. Molecular spectra and molecular structure, Vol. III. Electronic spectra and electronic structure of polyatomic molecules. Van Nostrand, Princeton, New Jersey. 1966.
22. R. R. BERNECKER and F. A. LONG. J. Phys. Chem. **65**, 1566 (1961).
23. J. C. LORQUET. Adv. Mass Spectrosc. **3**, 443 (1966).
24. V. CERMAK. Coll. Czeck. Chem. Comm. **33**, 2739 (1968).
25. R. E. HONIG. J. Chem. Phys. **16**, 105 (1948).
26. W. VOLK. Applied statistics for engineers. McGraw-Hill, New York, New York. 1958.
27. R. W. ELLIOTT and H. WATTS. Nature. In press.

Can. J. Chem. Downloaded from www.nrcresearchpress.com by 210.87.254.5 on 09/05/12
For personal use only.

Can. J. Chem. Downloaded from www.nrcresearchpress.com by 210.87.254.6 on 09/05/12
For personal use only.

Vibrational Spectra of SiH_4 and SiD_4–SiH_4 Mixtures in the Condensed States

R. P. FOURNIER AND R. SAVOIE
Centre de recherches sur les atomes et les molécules et Département de chimie, Université Laval, Québec

AND

NGUYEN DINH THE, R. BELZILE, AND A. CABANA
Département de chimie, Université de Sherbrooke, Sherbrooke, Québec

Received August 13, 1970

FOR ERRATA SEE V.50 #7 1972 P. 1442

The i.r. and Raman spectra of liquid and crystalline SiH_4 and SiD_4–SiH_4 mixtures have been recorded. The spectra show striking changes when the crystal undergoes the solid–solid phase transition. Phase I is disordered. Possible site, and factor groups for the low temperature crystalline phase are proposed.

Les spectres i.r. et Raman de SiH_4 et de mélanges SiD_4–SiH_4 dans la phase liquide et les deux phases cristallines furent enregistrées. Les spectres sont profondément modifiés au point de transition solide–solide. La phase I est désordonnée. On propose certains groupes de site et certains groupes facteurs possibles pour la phase cristalline de basse température.

Canadian Journal of Chemistry, **50**, 35 (1972)

Introduction

It is well known that the analysis of vibrational spectra may lead to the determination of the site and factor groups, of crystals, although such an analysis is seldom sufficient to allow a unique choice of space group (1–4). This method is particularly useful with solids which are not well suited for diffraction studies, as is the case with molecules containing light atoms or when single crystals cannot be obtained. Solid methane, which provides a typical example of this, has received considerable attention, although some doubt still remains about the structure of its low-temperature phases (5–8). Monosilane (SiH_4) appeared to be another compound appropriate to this kind of study. The solid (m.p. 88 °K) is known to exhibit a λ-type phase transition at 63.75 °K (9), but no crystallographic data are as yet available on either solid phase. Clusius (10) has observed that the high-temperature phase (phase I) is weakly optically anisotropic, whereas phase II is strongly birefringent. This suggests that solid SiH_4, at least in its low-temperature modification, has a non-cubic crystal structure.

Vibrational spectra of silane in both the gas (11) and condensed phases (12–15) have been previously reported. However, previous works on the solid were not performed in the best of experimental conditions. The i.r. spectrum of McKean and Chalmers (13), believed to be that of the solid in its phase II, was recorded at a temperature very close to the transition point, and our results indicate that phase II was not always attained in that previous work. In the two other reported studies (12–14), the solid samples were prepared by direct deposition of the gas on a cold window. Preliminary experiments from our part indicated that spectra thus obtained were usually not reproducible, and were often very different from one another, even when attempts were made to anneal the solid deposits. We have therefore carefully rerun the i.r. spectra and recorded the Raman spectra of liquid and solid SiH_4, the solid samples being grown from the melt. In addition, studies were performed on solutions of SiD_4 in SiH_4 in order to gather information on the site symmetry (16) in the solid phases of silane.

Experimental

The SiH_4 (semi-conductor grade) used in our experiments was obtained from the Matheson Co. and used without purification. The SiD_4, from Merck, Sharp, and Dohme of Canada, Ltd., was analyzed by mass spectrography and found to contain ~4 at.% H. This material, although suitable for obtaining the spectra of SiD_4 diluted in SiH_4, could not be used for obtaining the spectra of pure solid SiD_4.

The mid-infrared spectra (400–4000 cm^{-1}) were recorded on a Perkin–Elmer Model 125 prism-grating spectrometer calibrated with references at the I.U.P.A.C. tables (17). Far-infrared spectra (10–400 cm^{-1}) were obtained with a Michelson interferometer (Research and Industrial Instruments Co., model FS–720) coupled to a Fourier transform computer (model FTC–100). The frequency accuracy for both instruments is probably close to 0.5 cm^{-1} in the regions of interest. A conventional variable temperature liquid helium cryostat supplied by Andonian Associates was used

Can. J. Chem. Downloaded from www.nrcresearchpress.com by 210.87.254.6 on 09/05/12
For personal use only.

for the i.r. experiments. The gaseous mixtures were prepared in a Pyrex system previously evacuated to a pressure lower than 1×10^{-6} mm Hg. The samples were prepared by condensing the pure gas, or the appropriate isotopic mixtures, to the liquid between two circular windows sealed off into a closed compartment by means of indium gaskets. The window material was either sapphire ($\nu > 2000$ cm^{-1}), germanium (400–2000 cm^{-1}), or crystalline quartz ($\nu < 200$ cm^{-1}). Germanium windows are known to distort i.r. band shapes because of its high refractive index; however, this effect was found to be unimportant in our study. The crystals, slowly grown from the liquid, always yielded reproducible spectra. The rate of cooling at the freezing and solid transition temperatures was of the order of one half of a degree per hour. Reproducible spectra were always obtained when the samples were repeatedly cycled through the transition temperatures. The sample thickness was ~1 micron for pure SiH_4 and ~50 microns for the isotopic mixtures in the mid-infrared, whereas very thick films (~2 mm) were needed in the far-infrared.

The Raman spectra, obtained with two different sets of spectrometers and cryostats, were identical except that better resolution was achieved with the more powerful laser source. One of the two spectrometers consisted of a Spex Model 1400 double monochromator with a Spectra Physics Model 125 He–Ne laser operated at ~70 mW, an ITT (FW-130) phototube, and direct current amplification. The other instrument contained a Jarrell–Ash Model 25–100 double monochromator with a Coherent Radiation Laboratory Model 52–A argon ion laser operated at 100–800 mW, an ITT (FW-130) phototube, and photon counting detection system. Both instruments were calibrated using Ne and Kr discharge lamps and the frequency accuracy is estimated at ± 0.5 cm^{-1} for sharp peaks. The Pyrex cells for Raman studies, 8 mm in diameter, were either fixed at the base of a commercial Andonian cryostat and cooled by a flow of helium gas, or directly dipped into liquid helium in an all-glass cryostat. In this latter technique, appreciable scattering of the laser beam occurred from frozen particles of N_2, O_2, and CO_2 which gathered around the sample cell at the bottom part of the cryostat. Since very little change was observed in the spectra when the temperature was lowered from the solid I–solid II transition point to 4.2 °K, most experiments were performed with the Andonian cryostat, at a temperature of ~40 °K. The samples studied were usually quite transparent in the high-temperature phase but shattered upon cooling to phase II.

Results and Discussion

The SiH_4 molecule (of T_d symmetry) has four normal modes of vibration, of which all are Raman active but only the two F_2 vibrations are infrared active. Although it was relatively easy to obtain the $\nu_1(A_1)$, $\nu_2(E)$, and $\nu_3(F_2)$ bands in the Raman spectra of the liquid and solid, no band could be detected in the $\nu_4(F_2)$ region, even when very wide slits were used. This implies that the ν_4 band in the Raman spectrum of silane is at least 500 times weaker than the ν_1 band. Similarly, the ν_2 band was not found in the i.r. spectrum, even with samples 50 times thicker than those used for the study of the gas-phase allowed fundamentals. As for ν_1, it was impossible to check for its i.r. activity in the liquid and solid I, since its frequency is almost identical to that of ν_3 which gives a very strong absorption band. This makes the assignment of the observed bands in the ν_1–ν_3 region particularly difficult in SiH_4 in phase II.

A. Infrared and Raman Spectra of Liquid and Solid I Silane

The i.r. and Raman spectra of liquid and solid I SiH_4 are reproduced in Fig. 1 and measured frequencies and bandwidths are listed in Table 1. Polarization studies of the ν_3–ν_1 bands in the liquid show that the observed band cannot be entirely extinguished, the ~10% residual intensity indicating frequency overlapping and possible partial mixing of the two modes.

The vibrational spectra of solid SiH_4 in phase I are quite similar to those of the liquid, except for a slight narrowing of the bands in the solid. The frequency shifts from the liquid to phase I are also very small (less than 2 cm^{-1}), as can be seen in Table 1. The large bandwidths indicate that the molecules are being subjected to a great variety of fields in these two phases. It is likely that molecular rotation is only partially hindered, even in phase I, and that orientational disorder therefore prevails in the solid. A similar situation was encountered in CH_4, CD_4, and CF_4 in their high-temperature solid phase (5, 7, 18). An identical conclusion can be deduced from the vibrational spectra of SiD_4 in a solution of 1.8% SiD_4 in SiH_4 (see Fig. 2 and Table 2). The ν_4 region of that spectrum was not investigated although it is obvious that it should show some spectral activity. However, it would not yield additional information. The far-infrared spectrum of liquid SiH_4 and that of the solid in phase I (Fig. 3) also point to the plasticity of the high-temperature solid phase of this compound.

B. Spectra of SiD_4–SiH_4 Isotopic Solutions in Phase II

The vibrational frequencies of SiD_4 being sufficiently different from those of SiH_4, the vibrational modes of this molecule should be largely uncoupled from those of the SiH_4 host molecules in an isotopic solution. The i.r. spectrum of a 1% solution, and the Raman spectrum

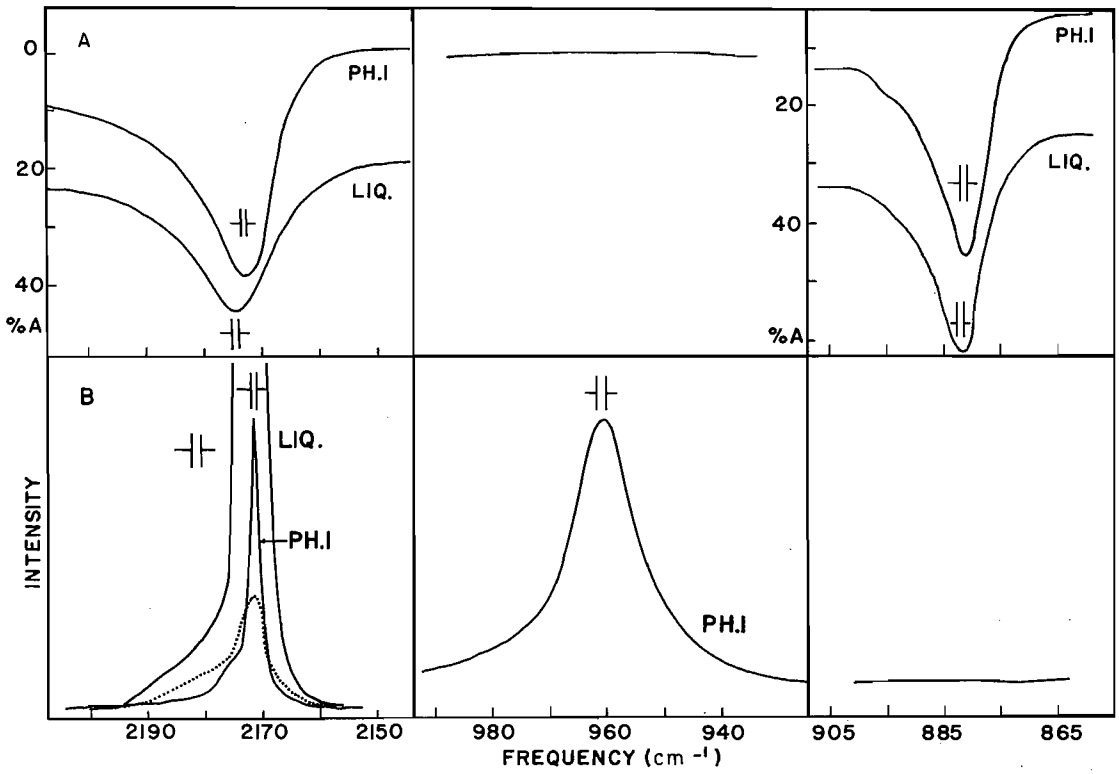

FIG. 1. (*A*) Infrared spectra of a ~1 micron thick sample of (*a*) liquid (98 °K) and (*b*) solid in phase I (77 °K) SiH_4. (*B*) Corresponding Raman spectra, with laser beam polarized perpendicular (—) and parallel (...) to spectrometer axis.

TABLE 1. Vibrational frequencies of SiH_4 (in cm^{-1})

Gas (i.r.) (ref. 11)	Liquid (98 °K)*		Crystal I (77 °K)*		Crystal II†		Assignment
	i.r.	Raman	i.r.	Raman	i.r. (10 °K)	Raman (40 °K)	
2191	2174(18)	2171(3.8)	2172.5(15)	2170.4(3.5)	2189.6m 2183.3ms 2181.2w — 2175.9s 2174.2s 2171.1s 2168.6s 2167sh 2162sh	— — 2181.8m 2179.9w 2175.6w 2174.1s 2171.0w 2168.7s — 2163.4s	ν_3, ν_1
975	—	961.7(17)	—	960.4(13)	—	961.7sh 960.6 959.9 957.5w	ν_2
914	881.7(25)	—	880.7(21)	—	890.4 889.1 883.9 879.6 874.6	—	ν_4

*Numbers in parentheses following frequencies refer to bandwidths at half-height.
†s = strong, m = medium, w = weak, sh = shoulder.

Can. J. Chem. Downloaded from www.nrcresearchpress.com by 210.87.254.6 on 09/05/12
For personal use only.

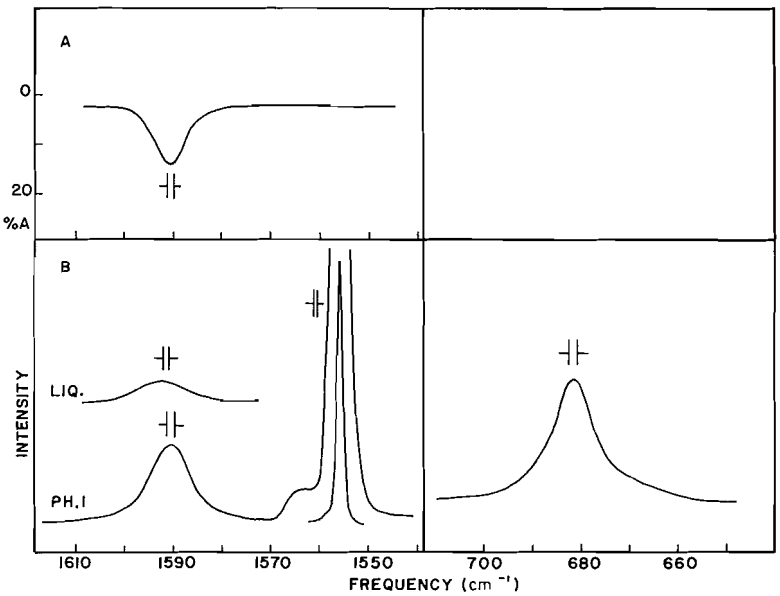

FIG. 2. (*A*) The ν_3 infrared band of SiD_4 in a 1% solution of SiD_4 in SiH_4 in phase I at 77 °K (sample thickness: 50 microns). (*B*) Corresponding Raman spectra of a 1.8% solution in the liquid state (*a*) at 98 °K and in the solid phase I, (*b*) at 77 °K.

of a 1.8% solution of SiD_4 in SiH_4 in phase II are reproduced in Fig. 4. Vibrational frequencies and bandwidths are given in Table 2. Only the two gas-phase F_2 modes were detected in each case. McKean and Chalmers (13) have reported an intense ν_1 absorption band for GeH_4 and SnH_4 isolated in a SiH_4 matrix in phase II, whereas in the present study the ν_1 band of SiD_4 was not observed. The different sizes of guest and host molecules used in the previous investigation, and possibly crystal imperfections resulting from rapid deposition of the gaseous mixtures, are probably responsible for this discrepancy. The splitting into three components of the ν_4 band of SiD_4 in solution in SiH_4 in phase II has already been reported by Shrinivasan and Wilde (14).

The Raman spectrum is particularly informative in this case since all the fundamentals are active, yielding one, two, and three components for the gas phase A_1, E, and F_2 vibrations, respectively (the weak Raman bands between ν_1 and ν_3 (Fig. 4) of SiD_4 arise from impurities of partially deuterated silane). The site splitting of the degenerate vibrations of SiD_4 in solution in SiH_4

TABLE 2. Vibrational frequencies (cm^{-1}) of SiD_4 isolated in SiH_4*

Liquid (98 °K) Raman	Crystal I (77 °K)†		Crystal II†		Assignment
	i.r.	Raman	i.r. (10 °K)	Raman (40 °K)	
1591.0(11)	1591(7)	1590.5(8.5)	1592.7(1.6) 1589.2(2.7) 1584.7(2.0)	1593.5(2.8) 1590.0(2.8) 1585.7(3.0)	ν_3
1555.5(2)	—	1554.8(2)	—	1553.8(2)	ν_1
680(12)	—	681.7(10.5)	—	681.8 680.5 (2.6)	ν_2
—	—	—	664.5(1.0) 663.1(0.7) 661.5(1.0)	—	ν_4

*Concentration of SiD_4: 1% for the infrared and 1.8% for the Raman.
†Numbers in parentheses following frequencies refer to bandwidths at half-height. Bandwidths of sharp Raman bands are largely influenced by instrumental slit widths.

Can. J. Chem. Downloaded from www.nrcresearchpress.com by 210.87.254.6 on 09/05/12
For personal use only.

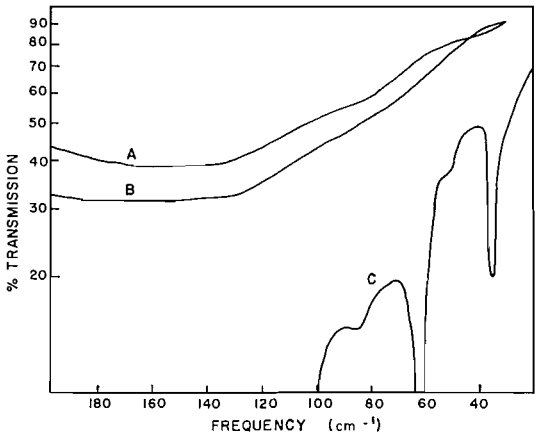

FIG. 3. Far-infrared spectra of a 2 mm thick sample of SiH_4;(*A*) liquid at 98 °K, (*B*) solid in phase I at 77 °K, and (*C*) solid in phase II at ~15 °K.

in phase II proves the absence of threefold or higher symmetry axis at the site in this solid. Acceptable site symmetries are then limited to the following: D_2, C_{2v}, C_2, C_s and C_1. In addition, the observation of a singlet for the A_1 mode proves that only one set of equivalent sites is occupied in the crystal.

The apparent i.r. inactivity of the ν_1 vibration of SiD_4 in SiH_4 in phase II suggests a D_2 site symmetry since, among the groups cited above, this is the only one in which a totally symmetric vibration would be infrared inactive. However, as will be shown below, a site of D_2 symmetry fails to account for the multiplicity of bands in the spectra of the pure solid and has to be rejected. We therefore surmise that the ν_1 vibration of SiD_4 in SiH_4 in phase II should be weakly i.r. active, and has not been observed because of its very low intensity.

C. Spectra of Pure SiH_4 in its Solid Phase II

The i.r. spectrum of pure SiH_4 in its low-temperature modification is reproduced in Fig. 5 and measured frequencies are listed in Table 1.

The ν_3 and ν_4 bands reproduced here were

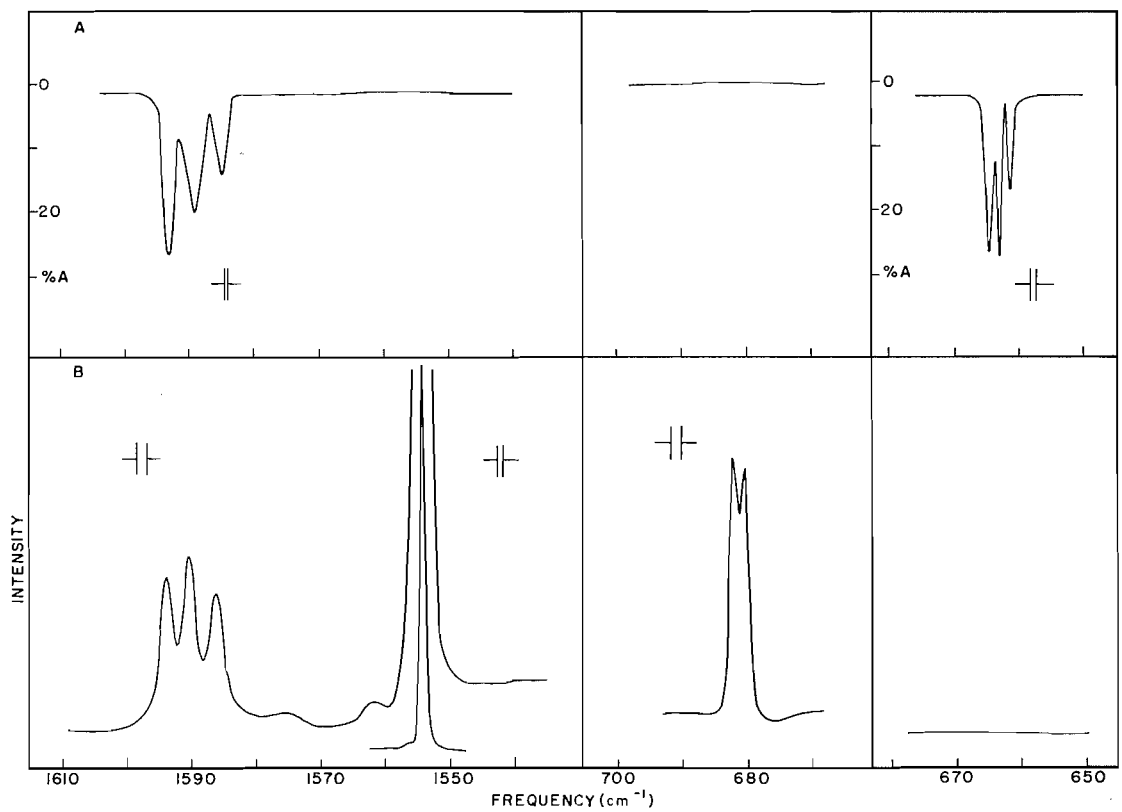

FIG. 4. (*A*) Infrared spectrum of SiD_4 in a 1% solution of SiD_4 in SiH_4 in phase II at ~10 °K (sample thickness: 50 microns). (*B*) Corresponding Raman spectrum of a 1.8% solution at ~40 °K.

Can. J. Chem. Downloaded from www.nrcresearchpress.com by 210.87.254.6 on 09/05/12
For personal use only.

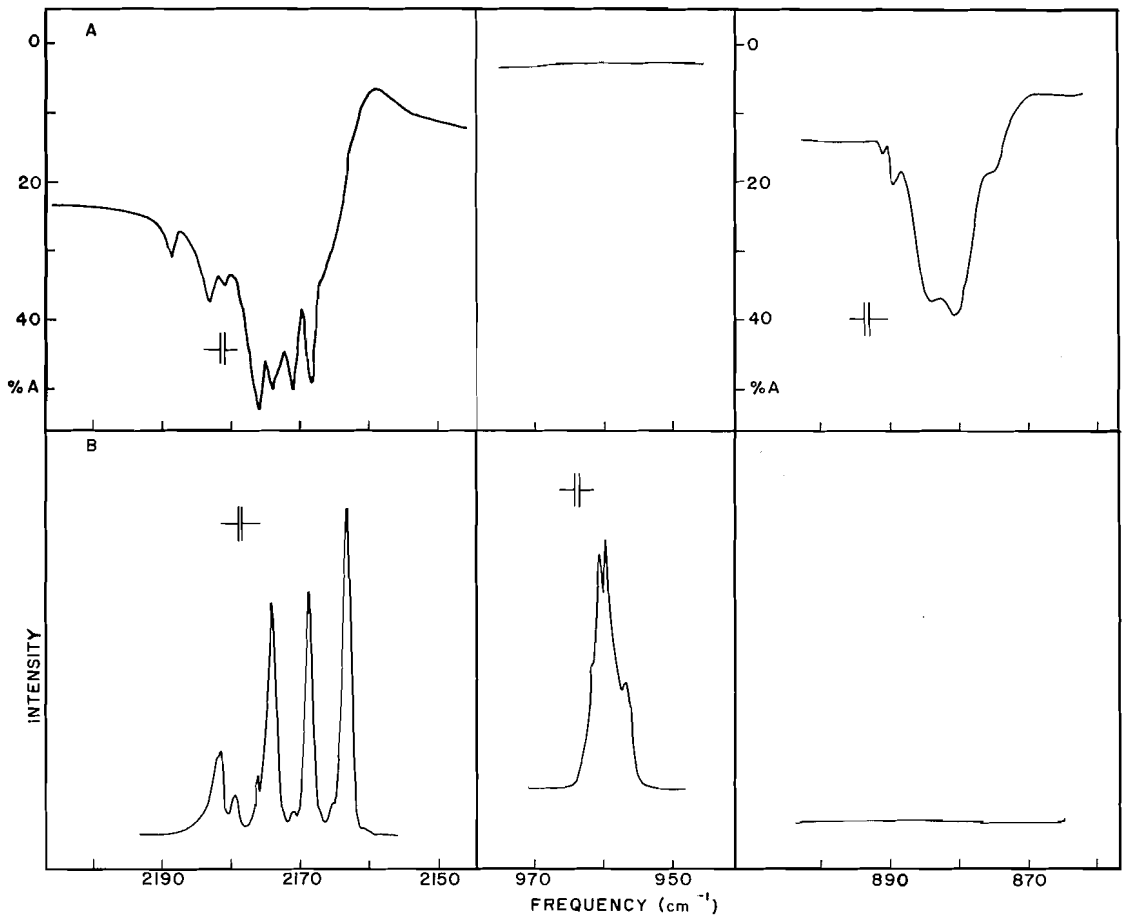

FIG. 5. (*A*) Infrared spectrum of a 1 micron thick sample of pure SiH_4 in phase II at ~10 °K. (*B*) Raman spectrum at ~40 °K.

obtained with different samples, such that their relative intensity is not meaningful. When the same sample thickness was used in both regions, these two bands had almost equal intensities. Seven resolved components and two shoulders on the low frequency side of the main features are seen in the ν_3 region, whereas a complicated structure is also observed in the ν_4 region. As in the liquid or in the solid in phase I, ν_2 could not be detected, even with very thick films.

The far-infrared spectrum of solid SiH_4 in its phase II at ~15 °K is reproduced in Fig. 3. Two sharp peaks are observed at 35 and 61 cm^{-1}, together with two much weaker bands at 53 and 85 cm^{-1}. The strong absorption at higher frequencies is believed to be caused by reflection of the incident beam by crystal defects in the very thick samples used. The far-infrared spectrum of solid SiH_4 is of little help in elucidating the crystal structure of the low-temperature modification of this compound. The narrowness of the observed peaks, together with their location close to the Debye frequency, 69 cm^{-1} (10, 19), suggest that they arise from translational modes. The librational modes are probably located at higher frequencies and were not observed in this study. A similar situation was encountered in CH_4 in its solid phase II (7).

The Raman spectrum of SiH_4 in phase II at ~40 °K is shown in Fig. 5 and measured frequencies are collected in Table 1. At least seven bands are resolved in the ν_3–ν_1 region and four components are present in the ν_2 region. Although it is impossible to assign all the lines

Can. J. Chem. Downloaded from www.nrcresearchpress.com by 210.87.254.6 on 09/05/12
For personal use only.

Can. J. Chem. Downloaded from www.nrcresearchpress.com by 210.87.254.6 on 09/05/12
For personal use only.

individually in both type of spectra, the multiplicity of components for the observed fundamentals indicates that there are at least two molecules per primitive cell in this solid.

D. Silicon Isotope Effects

Natural silicon contains 92.28% of ^{28}Si, 4.67% of ^{29}Si, and 3.05% of ^{30}Si. The ν_3 gas vibrational frequencies of the three corresponding silane molecules are 2189.16, 2187.63, and 2186.19 cm^{-1}, respectively (11). Isotopic shifts are expected to be smaller for ν_4 and almost negligible for ν_1 and ν_2 in the condensed states. Observed bands of SiD_4 in SiH_4 cannot be explained by an isotopic effect since their relative intensities are not appropriate and their spacings are not as expected. Thus, it is believed that the main bands are due to the most abundant isotopic variety, the other species mainly contributing to bandwidths. However, some weak features or shoulders, particularly in the ν_3–ν_1 region of the spectra of the pure solid, could result from the presence of the less abundant varieties.

E. Crystal Structure of SiH_4 on Phase II

Possible site symmetries for SiH_4 in phase II (D_2, C_{2v}, C_2, C_s, and C_1) have been deduced above from the i.r. and Raman spectra of mixed isotopic crystals. The multiplicity of bands in the i.r. and Raman spectra of the pure crystal may now be used to search for acceptable factor groups. This can be accomplished by selecting, amongst the super-groups of these site groups, those compatible with the number of components observed in the spectra of the pure crystal. This somewhat tedious process is straightforwardly carried out using standard group theoretical procedures (2, 3). Basic assumptions are that only one set of equivalent sites is occupied (the opposite would be exceptional in a molecular crystal), and that all the observed components are due to the site and coupling effects only.

Among the groups cited above, the D_2 site group can readily be discarded since, for any appropriate factor group, ν_1 should be infrared inactive and ν_3 is predicted to give three components whereas seven resolved peaks (and two shoulders) are observed in the ν_3–ν_1 region of the infrared spectrum (Fig. 5). The C_{2v} site group can also be rejected since it predicts a maximum of four infrared-active components in the ν_3–ν_1 region, and a maximum of three in the ν_4 region (five are observed). As for the C_2 and C_s sites, for which a maximum of 6 and 7 infrared-active components are respectively predicted in the ν_3–ν_1 region, they can be tentatively eliminated, in as much as the weak band at 2181.2 cm^{-1} and the shoulders at 2167 and 2162 cm^{-1} in the i.r. spectrum are assumed to be genuine components of the ν_1 and ν_3 fundamentals. Finally, if the site symmetry is C_1, a maximum of 3 and 9 infrared components is predicted for ν_1 and ν_3, respectively, which could certainly account for the multiplicity of bands in the ν_3–ν_1 region of the infrared spectrum. It is therefore likely that the molecules occupy general positions of the unit cell in SiH_4 in phase II. Speculating further, it is possible that the three intense peaks in the ν_3–ν_1 region of the Raman spectrum are all due to ν_1, since this mode is expected to be appreciably more intense than ν_3. If this is the case, acceptable crystals systems are then limited to tetragonal (factor groups: S_4, C_4, C_{4h}), trigonal (factor groups: C_{3v}, D_3, D_{3d}) or hexagonal (factor groups: C_{3h}, C_6, C_{6h}). Further elimination would be possible by determining whether or not the crystal is piezoelectric.

The frequency coincidence of many of the i.r. and Raman bands in the ν_3–ν_1 region suggests a non-centrosymmetric crystal structure. However, in such a case a longitudinal component, or a shoulder extending to the longitudinal frequency, should have been observed on the high-frequency side of ν_3 in the Raman spectrum. Using the relation of Haas and Hornig (20), the known value of $\partial\mu/\partial Q$ for ν_3 in gaseous SiH_4 (21), the crystal density (22), and an assumed index of refraction of 1.3, it is found that the longitudinal frequency associated to ν_3 should be about 17 cm^{-1} above that of the transverse mode. No feature unambiguously attributable to a longitudinal mode is found in our Raman spectrum, but this cannot be taken as a proof that the crystal is centrosymmetric.

The authors wish to thank the National Research Council of Canada for grants in support of research and for the award of a post-graduate scholarship to one of us (R.P.F.). Financial assistance to one of us (A.C.) from the Ministère de l'Education de la Province de Québec is gratefully acknowledged.

1. S. BHAGAVANTAM and T. VENKATARAYUDU. Proc. Indian. Acad. Sci. **9A**, 224 (1939).
2. R. S. HALFORD. J. Chem. Phys. **14**, 8 (1946). H. WINSTON and R. S. HALFORD. J. Chem. Phys. **17**, 607 (1949).
3. D. F. HORNIG. J. Chem. Phys. **16**, 1063 (1948).
4. W. VEDDER and D. F. HORNIG. Adv. Spectr. **2**, 189 (1961).
5. G. B. SAVITSKY and D. F. HORNIG. J. Chem. Phys. **36**, 2634 (1962).
6. A. ANDERSON and R. SAVOIE. J. Chem. Phys. **43**, 3468 (1965).
7. R. SAVOIE and R. P. FOURNIER. Chem. Phys. Lett. **7**, 1 (1970).
8. C. CHAPADOS and A. CABANA. Chem. Phys. Lett. **7**, 191 (1970).
9. M. L. KLEIN, J. A. MORRISON, and R. D. WEIR, Discuss. Faraday Soc. **48**, 93 (1969).
10. K. CLUSIUS. Z. Phys. Chem. **B23**, 213 (1933).
11. C. H. TINDAL, J. W. STRALEY, and H. H. NEILSON. Phys. Rev. **62**, 151 (1942); **58**, 1002 (1940). G. R. WILKINSON and M. K. WILSON. J. Chem. Phys. **44**, 3867 (1966).
12. R. M. HEXTER and D. E. MILLIGAN. Proceedings of the Fourth International Symposium on Free Radical Stabilization. 1959.
13. D. C. MCKEAN and A. A. CHALMERS. Spectrochim. Acta, **23A**, 777 (1967).
14. R. E. WILDE and T. K. K. SHRINIVASAN. 24th Symposium on Molecular Structure and Spectroscopy, Ohio State University, Ohio. 1969.
15. F. B. STITT and D. M. YOST. J. Chem. Phys. **4**, 82 (1936).
16. G. L. HIEBERT and D. F. HORNIG. J. Chem. Phys. **20**, 918 (1952).
17. Tables of Wavemembers for the Calibration of Infra-Red Spectrometers, Butterworths Inc., Washington, D.C. (1961).
18. R. P. FOURNIER, R. SAVOIE, F. BESSETTE, and A. CABANA, J. Chem. Phys. **49**, 1159 (1968).
19. A. ANDERSON and H. A. GEBBIE. Spectrochim. Acta, **21**, 883 (1965).
20. C. HAAS and D. F. HORNIG. J. Chem. Phys. **26**, 707 (1957).
21. D. F. BALL and D. C. MCKEAN. Spectrochim. Acta, **18**, 1019 (1962).
22. J. W. STEWART. J. Chem. Phys. **36**, 400 (1962).

Can. J. Chem. Downloaded from www.nrcresearchpress.com by 210.87.254.6 on 09/05/12
For personal use only.

Electron Spin Resonance of γ-Irradiated Taurine

G. LIND AND R. KEWLEY[1]

Department of Chemistry, Queen's University, Kingston, Ontario

Received July 19, 1971

The 9.5 GHz electron spin resonance (e.s.r.) spectra of single crystal and powder samples of γ-irradiated taurine, $H_3\overset{+}{N}CH_2CH_2SO_3^-$, have been recorded. Overlapping spectra from three distinct radicals are present. The first of these is the species SO_3^- with an isotropic *g*-value of 2.0035 and a ^{33}S hyperfine coupling tensor with principal values 135.2, 99.2, and 97.9 G. The second radical is a π-electron species with the unpaired electron mainly on carbon and exhibiting hyperfine interaction from at least four protons, probably $H_3\overset{+}{N}CH_2CH_2$ or $H_3\overset{+}{N}CH_2CHSO_3^-$, and with principal *g*-values 2.0021, 2.0027, and 2.0034. The third radical has principal *g*-values 2.0024, 2.0056, and 2.0097 and principal values of the ^{33}S hyperfine tensor of 49.6, 9.1, and 1.2 G. The proposed structure for this radical is $H_3\overset{+}{N}CH_2CH_2SO_2$.

Les spectres de résonance paramagnétique électronique (r.p.e.) à 9.5 GHz de l'état cristallin et de poudre de la taurine $H_3\overset{+}{N}CH_2CH_2SO_3^-$ irradiée aux rayons-γ sont rapportés. On observe un recouvrement de spectres de trois radicaux distincts. Le premier est l'espèce SO_3^- avec une valeur de *g* isotropique de 2.0035 et des tenseurs hyperfins du ^{33}S de 135.2, 99.2 et 97.9 G. Le second radical est une espèce à électron π ayant l'électron non pairé principalement sur le carbone et les interactions hyperfines pour au moins quatre protons, probablement $H_3\overset{+}{N}CH_2CH_2$ ou $H_3\overset{+}{N}CH_2CHSO_3^-$, ont des valeurs de *g* de 2.0021, 2.0027 et 2.0034. Le troisième radical a des valeurs de *g* de 2.0024, 2.0056 et 2.0097 et les tenseurs hyperfins du ^{33}S sont de 49.6, 9.1 et 1.2 G. La structure proposée pour ce radical est $H_3\overset{+}{N}CH_2CH_2SO_2$.

Canadian Journal of Chemistry, **50**, 43 (1972)

Introduction

In the past detailed electron spin resonance (e.s.r.) studies have been made of a number of radicals produced by irradiation of amino-acids and amino-acid derivatives (1–4). As is well known the most common product is the type of radical formed by loss of a hydrogen atom from a carbon atom adjacent to a carboxyl group. In a few cases detachment of an NH_2 group may occur and in sulfur-containing amino-acids a C—S or S—S bond may break; for example, when the radical $HOOCCH(NH_3^+Cl^-)CH_2S$ is formed during the γ-irradiation of L-cystine hydrochloride (5). Except for a qualitative study in which the e.s.r. spectrum of a single crystal was reported but no *g*-values given (6), no work appears to have been done on the naturally occurring amino-acid taurine, $H_2NCH_2CH_2SO_3H$. It was therefore considered worthwhile to carry out a careful study of the e.s.r. spectrum of this substance with a view to discovering how this amino-acid is broken down by γ-irradiation.

[1]On sabbatical leave until August 31, 1972 at Department of Chemistry, Rice University, Houston, Texas 77001.

Experimental

Commercial taurine from the Nutritional Biochemicals Corporation was used without further purification. Single crystals were grown easily by slow evaporation from aqueous solution. Such crystals were reported to be monoclinic with space group $P2_1/c$ and having the greatest length along the *a*-axis (7). For the $P2_1/c$ space group there should be two magnetically distinct sites for each molecule in the crystal. This is seen to be the case when the e.s.r. spectra are well resolved. From the angular dependence of the spectra on magnetic field direction and by examining the shape of the crystal there was no difficulty in identifying the axes of the crystal used.

The crystal had a tabular appearance with the *a*-axis lying along the largest dimension as expected. The *b*-axis is perpendicular to the largest face and to the *a*-direction. The *c'*-axis was chosen to be in the largest face at 4° 12′ to the crystal *c*-axis and perpendicular to *a* and *b* in a right-handed cartesian system, see Fig. 1. The magnetic field was rotated around the *a*, *b*, and *c'* axes as well as around the two axes in the *ac'* plane at 45 and 135° from *c'* towards *a*, $\beta = 45$ and 135° in Fig. 1.

The single crystal and also a powder sample were irradiated for periods from 5 min to 3 h at a γ-ray dosage of 5.7×10^{17} eV/g min in a ^{60}Co Gammacell (A.E.C.L.) at room temperature. No change in the character of the e.s.r. spectrum, other than an increase in intensity, was noticed in this time range. Neither the unirradiated powder nor the unirradiated single crystal gave an e.s.r. signal. Further details of the experimental procedure have been given earlier (8).

Can. J. Chem. Downloaded from www.nrcresearchpress.com by 210.87.254.5 on 09/05/12
For personal use only.

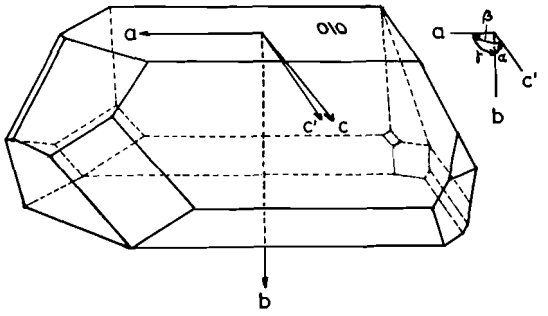

FIG. 1. The form of the taurine single crystal and the choice of reference axes. The c'-axis is at 90° to the a-axis and at 4° 17′ from the c-axis.

Results and Discussion

(1) Single Crystal

The e.s.r. spectrum of a single crystal of γ-irradiated taurine shows the presence of four different radical species, see Fig. 2.

(*A*) The e.s.r. spectrum of the first radical (radical A) is a single line of width 2 G. This line is masked over a wide range of orientations by the more intense spectrum of radical C. described below, but seems to have an almost isotropic **g**-tensor with $g = 2.0035$. There is an unidentified bump on the high field side of the line at a distance of about 5 G and with intensity about 1/7 of the line itself. There is no way of finding out if there is a corresponding bump on the low field side as there is no orientation where such a line would be far enough separated from the radical C spectrum.

The single line is thought to be the e.s.r. spectrum of the species SO_3^-. This radical could be produced with the scission of only one covalent bond provided that taurine consists of the "zwitterion" form, $H_3\overset{+}{N}CH_2CH_2SO_3^-$. Two bonds would have to break for SO_3^- to be formed from the molecular form of taurine, $H_2NCH_2CH_2SO_3H$. Thus it is considered that the "zwitterion" structure is the more accurate representation for the solid. This question was left undecided by the X-ray work (7). There are several earlier reports describing e.s.r. spectra following irradiation of molecules containing one or more $-SO_3^-$ groups and in which the radical SO_3^- was identified, with an isotropic **g**-tensor having $g = 2.004$ (9–11). In the present study at high gain and modulation amplitude the four weak isotopic lines due to $^{33}SO_3^-$ in 0.76% natural abundance were observed. The same downfield shift of the ^{33}S hyperfine pattern relative to the single line of the ^{32}S spectrum was found as that reported by Chantry *et al.* (10). This effect is expected if second order terms are retained in the derivation of the line positions from the spin Hamiltonian (12). For a typical spectrum, for example at the orientation $H_0 \| a (\gamma = 0°)$, the downfield shift was 2.6 G for the outer ^{33}S lines ($M_I = \pm 3/2$) and 6.1 G for the inner lines ($M_I = \pm 1/2$). The unidentified bump seen close to the single ^{32}S line seems to manifest itself in the ^{33}S pattern as a peak on the high field side of the high field line ($M_I = -3/2$) at most orientations. There is also a similar peak on the low field side of the low field line ($M_I = +3/2$) but no such peaks associated with the inner lines ($M_I = \pm 1/2$). At present the significance of these bumps is not understood.

The principal values of the $^{33}SO_3^-$ **A**-tensor are given in Table 1 and agree very well with those reported by Chantry *et al.* (10). The tensor shows cylindrical symmetry and all three elements must have the same sign, otherwise the atomic ^{33}S anisotopic coupling ($2B$) of 56 G would be exceeded. The spin densities at sulfur calculated from the principal **A**-tensor elements are $\rho_S^s = 0.11$ and $\rho_S^p = 0.43$.

Chantry *et al.* (10) calculated the angle between the direction corresponding to the largest **A**-tensor element of SO_3^- and the two distinguishable C—S bonds in the host crystal of $K_2CH_2(SO_3)_2$ and obtained the values 7 and 53°. They considered it unlikely that the SO_3^- fragment would be grossly displaced from its position prior to irradiation and therefore selected the angle 7° as the one through which the SO_3^- axis moves on irradiation. However, in the present case the angle between the direction for the largest **A**-tensor element (135.2 G) and the C—S bond in unirradiated taurine is 56 and 85° for the two different magnetic sites. This indicates a surprisingly large change in orientation for the SO_3^- species, which may be due to hydrogen bonding forces in taurine which would not be important in $K_2CH_2(SO_3)_2$.

(*B*) The second radical (radical B) has a spectrum of many lines which is typical of a π-electron species with the unpaired electron located primarily at a carbon atom but able to undergo hyperfine interactions with nearby protons. This spectrum is about 1/10 of the intensity of that of radical A. In this radical there

Can. J. Chem. Downloaded from www.nrcresearchpress.com by 210.87.254.5 on 09/05/12
For personal use only.

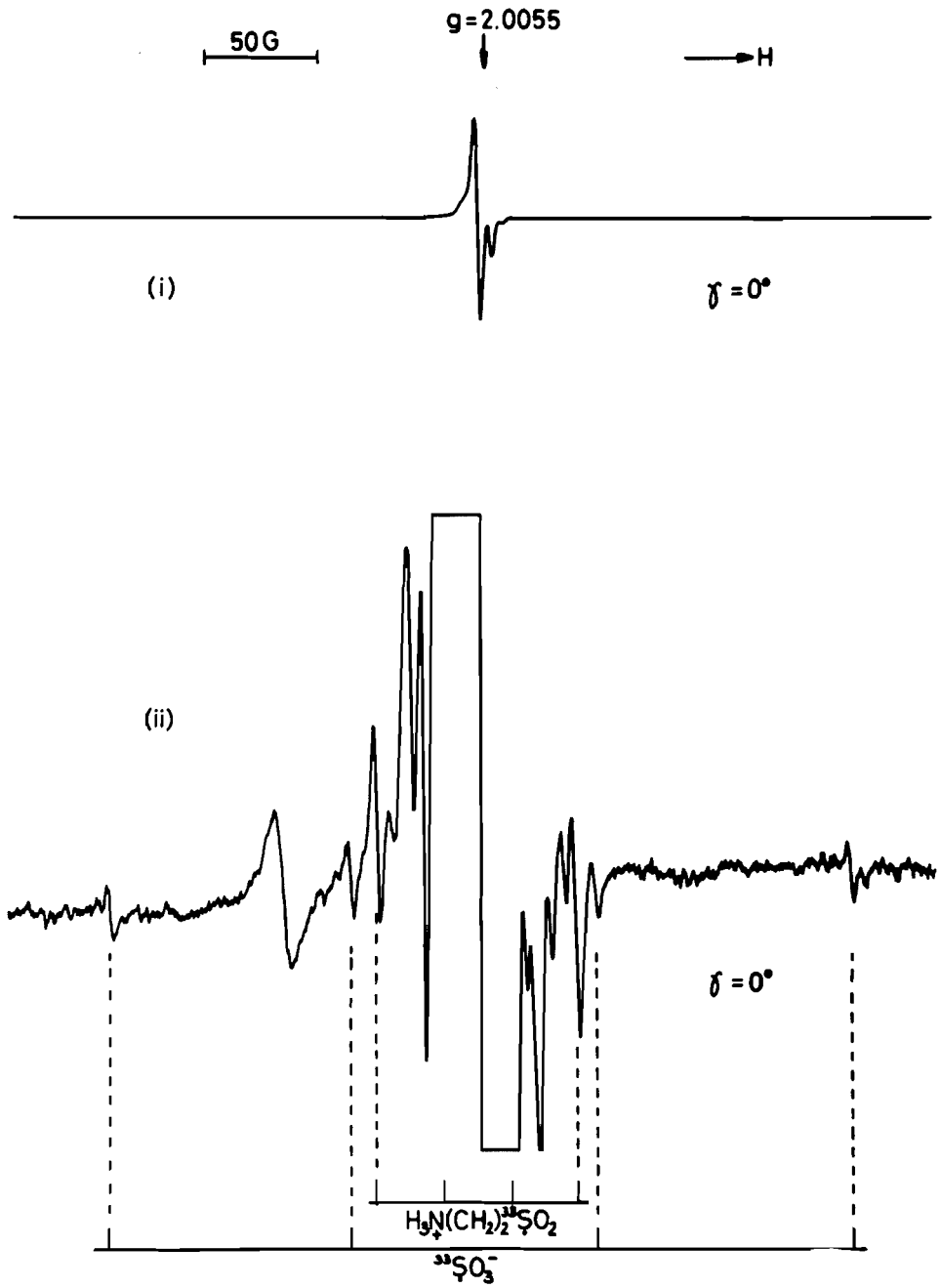

FIG. 2. Electron spin resonance spectrum of the taurine single crystal for the orientation $H_0 \| a(\gamma = 0°)$. (*i*) Low gain and modulation amplitude; (*ii*) Gain increased by 1000 times at same modulation amplitude. The broad line of width 8 G situated between the two low field peaks due to ^{33}S hyperfine splitting is that due to the unidentified species (D). The klystron frequency was 9.5 GHz.

Can. J. Chem. Downloaded from www.nrcresearchpress.com by 210.87.254.5 on 09/05/12
For personal use only.

TABLE 1. Principal values and directions of hyperfine coupling and **g**-tensors in the γ-irradiated taurine single crystal

Radical	Principal values	Direction cosines in *abc'* system
A. $^{32}SO_3^-$	$g = 2.0035\ (0.0004)$	Isotropic
$^{33}SO_3^-$	$A_1 = 135.2\ (4.0)$ G	$(0.516 \mp 0.540 \quad 0.665)$
	$A_2 = 99.2\ (4.0)$ G	$(0.714 \pm 0.700 \quad 0.014)$
	$A_3 = 97.9\ (4.0)$ G	$(0.473 \mp 0.468 \quad -0.747)$
B. $H_3\overset{+}{N}CH_2CH_2$	$g_1 = 2.0021\ (0.0004)$	$(0.590 \quad 0.060 \quad -0.805)$
or	$g_2 = 2.0027\ (0.0004)$	$(0.807 \quad -0.065 \quad 0.587)$
$H_3\overset{+}{N}CH_2CHSO_3^-$	$g_3 = 2.0034\ (0.0004)$	$(0.017 \quad 0.996 \quad 0.087)$
C. $H_3\overset{+}{N}CH_2CH_2{}^{32}SO_2$	$g_1 = 2.0024\ (0.0004)$	$(0.527 \mp 0.504 \quad 0.684)$
	$g_2 = 2.0056\ (0.0004)$	$(0.586 \pm 0.798 \quad 0.137)$
	$g_3 = 2.0097\ (0.0004)$	$(0.615 \mp 0.329 \quad 0.716)$
$H_3\overset{+}{N}CH_2CH_2{}^{33}SO_2$	$A_1 = 49.6\ (1.5)$ G	$(0.593 \mp 0.454 \quad 0.666)$
	$A_2 = 9.1\ (1.5)$ G	$(0.577 \pm 0.815 \quad 0.042)$
	$A_3 = 1.2\ (1.5)$ G	$(0.562 \mp 0.360 \quad -0.745)$

are at least four protons interacting with the unpaired electron. These protons may be attached to both nitrogen and carbon, although no ^{14}N hyperfine splitting was noticed. An unambiguous identification of this radical has not been possible but it is thought to be either the $H_3\overset{+}{N}CH_2CH_2$ residue, from the loss of SO_3^-, or $H_3\overset{+}{N}CH_2CHSO_3^-$. At all orientations the middle part of this spectrum was completely overlapped by the spectra of radicals A and C so only the wings of spectrum B could be studied. Attempts to remove the spectra of radicals A and C by heating were not successful. Although the elements of the several proton **A**-tensors could not be determined the principal *g*-values (Table 1) are those of a typical carbon-centered π-radical. It should be noted that the proximity of the sulfur in an $-SO_3^-$ group, attached to the carbon in question would not be expected to be reflected in the **g**-tensor values since in the radical $CH(SO_3^-)_2$ the principal values are 2.0033, 2.0025, and 2.0019 (9).

The angle between the direction corresponding to the **g**-tensor element 2.0021 (Table 1, radical B), which should be that for the axis of the carbon 2p orbital, and the direction of the C—C bonds in the undamaged taurine crystal is calculated to be 79°, which confirms the π-electron nature of radical B. There appears to be only one magnetically distinct site as regards the **g**-tensor of this radical, within the limits of experimental error.

(*C*) The spectrum of radical C is a single line of width 3.5 G when the magnetic field is in the *ab* or *ac'* plane. There is also on each side of this line a bump at a distance of about 6 G and of about 1/20 of the intensity. These bumps appear to follow the movement of the main line with change of orientation of the crystal. These extra peaks have not yet been explained. The **g**-tensor of radical C is noticeably anisotropic (Table 1), which results in the appearance of two lines, from the two magnetically inequivalent sites, at most orientations in the *bc'* plane. The principal **g**-tensor elements indicate that the radical is one in which the unpaired electron is at least partially on a sulfur atom.

At high gain and modulation amplitude further lines were seen which can be assigned to the ^{33}S isotopic form of the radical. Only the two outer lines of the hyperfine pattern could be observed for each magnetic site. The **A**-tensor is anisotropic (Table 1) and the direction of the largest principal value (49.6 G) coincides well with the direction of the smallest principal value 2.0024 of the **g**-tensor which would be the direction of the p-orbital containing the odd electron for a radical of the π-electron type.

For several reasons it was thought initially that radical C might be the species SO_2^-. The observed principal *g*-values (Table 1) are close to 2.0018, 2.0103, and 2.0055 observed by Atkins *et al.* for SO_2^- in irradiated potassium metabisulfite, $K_2S_2O_5$, (13). The a_{iso} for the radical C of 20.0 G, assuming all three ^{33}S **A**-tensor elements to be of like sign, and the a_{iso} for SO_2^- of 14.2 G (13) are also quite similar. Also no

Can. J. Chem. Downloaded from www.nrcresearchpress.com by 210.87.254.5 on 09/05/12
For personal use only.

Can. J. Chem. Downloaded from www.nrcresearchpress.com by 210.87.254.5 on 09/05/12
For personal use only.

resolved proton hyperfine splitting was found at any orientation in the spectrum of radical C. On the other hand the similarity in the g-values is by no means conclusive evidence since the $S_2O_2^-$ observed in X-irradiated $Na_2S_2O_3 \cdot 5H_2O$ by Morton (14) also has g-values similar to those of SO_2^-, 2.0083, 2.0050, and 2.0030. Furthermore in e.s.r. studies of irradiated solids it is unusual to find a radical formed by breakage of two covalent bonds, which would be required if the C—S and S---O bonds break as SO_2^- is formed from $H_3\overset{+}{N}CH_2CH_2SO_3^-$. There are, however, a number of instances in which an oxy-radical is produced by loss of an O^- from an oxy-ion. The formation of $S_2O_2^-$ from $S_2O_3^{2-}$ cited above is one example. Others occur in the formation of SeO_3^- from SeO_4^{2-} (15) and the formation of AsO_3^{2-} from AsO_4^{3-} (16). So although SO_2^- cannot be ruled out we consider an alternative possibility to be more likely. This is the radical $H_3\overset{+}{N}CH_2CH_2SO_2$.

Radicals of the type RSO_2 have been observed previously in γ-irradiated sulfones and polysulfones and in γ-irradiated hydrocarbon polymers on exposure to SO_2 gas (17–19). The typical RSO_2 e.s.r. spectrum for a powder was reported to be a peak of width 3–5 G showing no resolved proton hyperfine structure (19), indicating that the odd electron is located mainly on sulfur. This spectrum is similar in appearance to that of radical C in both taurine single crystal and powder. The g-values for RSO_2 type radicals were estimated as $g_\perp = 2.002$ and $g_\parallel = 2.005$ from the spectra in amorphous matrices (19), which are somewhat lower than the principal g-values of radical C. For both $H_3\overset{+}{N}CH_2CH_2SO_2$ and RSO_2 type radicals the electronic environment at sulfur should not be markedly different from that in the SO_2^- radical, the lone pair of electrons on sulfur in SO_2^- being replaced by the C—S bonding pair in $H_3\overset{+}{N}CH_2CH_2SO_2$ and RSO_2.

The calculated spin densities at sulfur in $H_3\overset{+}{N}CH_2CH_2SO_2$, assuming all three principal **A**-tensor elements to be of the same sign, are $\rho_S^s \simeq 0.02$ and $\rho_S^p \simeq 0.54$, showing that the radical is of the π-electron type with the unpaired electron concentrated mainly in a sulfur 3p-orbital. This is supported by the calculation of the angle between the principal **g**-value 2.0024, $A_1 = 49.6$ G, direction and that of the C—S bond in the undamaged structure. The result obtained is 86.5°, using the atom parameters of Sutherland and Young (7).

The lack of any proton hyperfine splitting in the spectrum of $H_3\overset{+}{N}CH_2CH_2SO_2$ requires some explanation. The accepted formula for the isotropic splitting of β-protons when an unpaired electron is located at an α-carbon atom is (20)

$$a_H = B_0 + B_2 \cos^2 \theta$$

where θ is the angle between the plane defined by $C_\alpha C_\beta H_\beta$ and the symmetry axis of the C_α 2p-orbital and $B_2 \gg B_0$ with $0 < B_0 < 3.5$ G (21). The calculated angles θ between the $g = 2.0024$ principal direction and the S—C—H_1 and S—C—H_2 planes, where the designations H_1 and H_2 are taken from the X-ray study (7), are respectively 19.5 and 39.5°. Using the simplified formula

$$a_H = A_0 \cos^2 \theta$$

with $A_0 \simeq 9$ G as given by Kurita and Gordy (5) for the isotropic β-proton splitting when the unpaired electron is located at an α-sulfur atom, we arrive at the values $a_{H_1} = 8.0$ G and $a_{H_2} = 5.3$ G. However the observed spin density at sulfur in $H_3\overset{+}{N}CH_2CH_2SO_2$ is only about 50% so it may well be that the β-proton splittings are of the same magnitude as the line width and were therefore not detached.

(*D*) In addition to the spectra of the radicals discussed in *A*, *B*, and *C* above there is an unexplained feature (*D*) consisting of an orientation dependent, broad line of width 8 G, see Fig. 2.

(2) Powder

The e.s.r. spectrum of γ-irradiated taurine powder fully confirms the results of the single crystal study, see Fig. 3. The observed pattern is an overlapping of the single g-value powder spectrum of SO_3^- with the three g-value powder spectrum of $H_3\overset{+}{N}CH_2CH_2SO_2$. These g-values are shown in Table 2 and agree very closely with the corresponding ones in Table 1. The spectrum of the π-electron species radical B, $H_3\overset{+}{N}CH_2CH_2$ or $H_3\overset{+}{N}CH_2CHSO_3^-$, is much less intense and lies beneath the other two overlapping patterns. At higher gain and modulation amplitude the

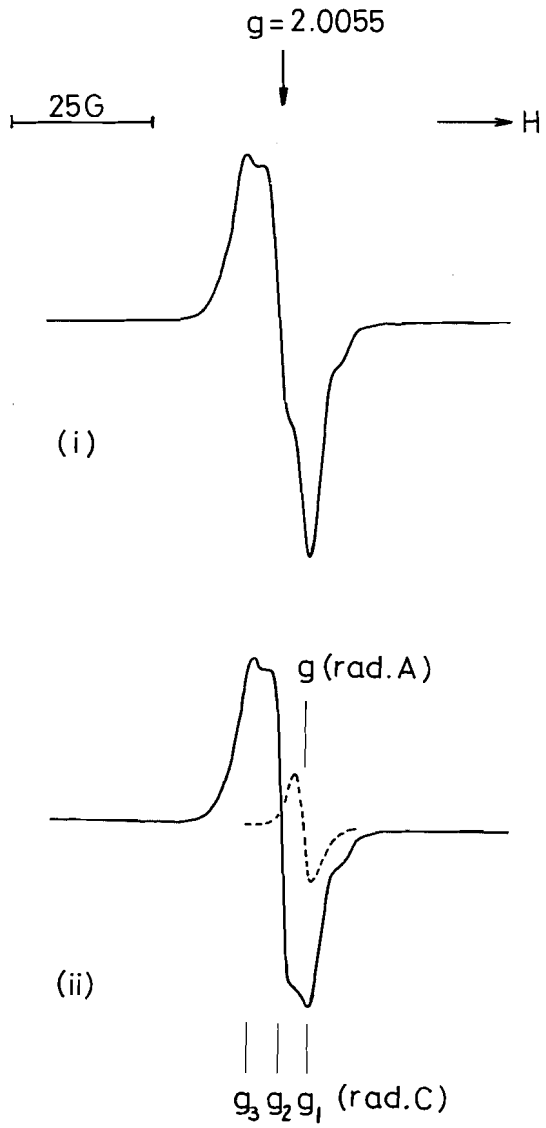

FIG. 3. (*i*) Electron spin resonance spectrum of taurine powder at low gain and modulation amplitude and at a klystron frequency of 9.5 GHz. (*ii*) Approximate reconstruction of the spectrum using the *g*-values of $H_3\overset{+}{N}CH_2CH_2SO_2$ and SO_3^- observed in the single crystal.

^{33}S lines in natural abundance for both SO_3^- and $H_3\overset{+}{N}CH_2CH_2SO_2$ were observed, see Fig. 4, yielding the additional confirmatory data of Table 2.

TABLE 2. Principal values of hyperfine and **g**-tensors derived from the spectrum of γ-irradiated taurine powder

Radical	Principal values
A. $^{32}SO_3^-$ $^{33}SO_3^-$	$g = 2.0034\ (0.0004)$ $A_1 = 135.0\ (4.0)$ G $A_2 = 100.0\ (4.0)$ G A_3 = not observed
C. $H_3\overset{+}{N}CH_2CH_2{}^{32}SO_2$	$g_1 = 2.0025\ (0.0004)$ $g_2 = 2.0058\ (0.0004)$ $g_3 = 2.0093\ (0.0004)$
$H_3\overset{+}{N}CH_2CH_2{}^{33}SO_2$	$A_1 = 48.6\ (1.5)$ G A_2, A_3 not observed

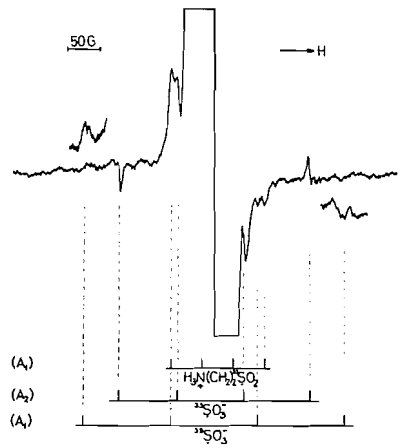

FIG. 4. Electron spin resonance spectrum of taurine powder showing the lines due to ^{33}S hyperfine splitting. The gain is 8 times and the modulation amplitude 20 times greater than those at which the spectrum in Fig. 3(*i*) was taken. The klystron power was lowered by 5 db to counteract saturation of the ^{33}S lines.

We are pleased to acknowledge that this project was made possible by the support of the National Research Council of Canada, through operating grants.

1. P. B. AYSCOUGH. Electron spin resonance in chemistry. Methuen 1967. p. 228, Table 7.9.
2. M. KATAYAMA. J. Mol. Spectrosc. **9**, 429 (1962).
3. I. MIYAGAWA, Y. KURITA, and W. GORDY. J. Chem. Phys. **33**, 1599 (1960).
4. M. KATAYAMA. J. Chem. Phys. **37**, 2143 (1962).
5. Y. KURITA and W. GORDY. J. Chem. Phys. **34**, 282 (1961).
6. G. LOMAGLIO. C. R. Acad. Sc. Paris, Ser. B. **265**, 219 (1967).
7. H. H. SUTHERLAND and D. W. YOUNG. Acta Cryst. **16**, 897 (1963).
8. G. LIND and R. KEWLEY. Can. J. Chem. **49**, 2514 (1971).

Can. J. Chem. Downloaded from www.nrcresearchpress.com by 210.87.254.5 on 09/05/12
For personal use only.

9. A. HORSFIELD, J. R. MORTON, J. R. ROWLANDS, and D. H. WHIFFEN. Mol. Phys. **5**, 241 (1962).
10. G. W. CHANTRY, A. HORSFIELD, J. R. MORTON, J. R. ROWLANDS, and D. H. WHIFFEN. Mol. Phys. **5**, 233 (1962).
11. J. R. ROWLANDS and D. H. WIFFEN. Nature, **193**, 62 (1962).
12. A. HORSFIELD, J. R. MORTON, and D. H. WHIFFEN. Mol. Phys. **4**, 475 (1961).
13. P. W. ATKINS, A. HORSFIELD, and M. C. R. SYMONS. J. Chem. Soc. 5220 (1964).
14. J. R. MORTON. Can. J. Chem. **43**, 1948 (1965).
15. P. W. ATKINS, M. C. R. SYMONS, and H. W. WARDALE. J. Chem. Soc. 5215 (1964).
16. W. C. LIN and C. A. MCDOWELL. Mol. Phys. **7**, 223 (1964).
17. Z. KURI, H. UEDA, and S. SHIDA. J. Chem. Phys. **32**, 371 (1960).
18. P. B. AYSCOUGH, K. J. IVIN, and J. H. O'DONNELL. Proc. Chem. Soc. 71 (1961).
19. P. B. AYSCOUGH, J. H. O'DONNELL, and K. J. IVIN. Trans. Faraday Soc. **61**, 1110 (1965).
20. A. CARRINGTON and A. D. MCLACHLAN. Introduction to magnetic resonance. Harper and Row. 1967. p. 109.
21. J. R. MORTON. Chem. Rev. 453 (1964).

Can. J. Chem. Downloaded from www.nrcresearchpress.com by 210.87.254.5 on 09/05/12
For personal use only.

The Pyrolysis of Tetramethyltin

R. P. JOHNSON AND S. J. W. PRICE
Chemistry Department, University of Windsor, Windsor 11, Ontario
Received July 29, 1971

The pyrolysis of tetramethyltin has been studied in a toluene carrier flow system from 803–941 °K using total pressures of 10.6 to 52.4 mm. Contact times varied from 0.49 to 13.8 s and the amount of decomposition from 1.35–98.7%. The progress of the reaction was followed by measuring the amount of methane, ethane, ethylene, and ethylbenzene formed. No appreciable heterogeneous reaction was detected and the first order rates constants appear to have been determined at the high pressure limit. The quantity of undecomposed alkyl was also measured and was found to be in agreement with the product analysis if four methyl radicals are released for each molecule undergoing reaction.

Least squares analysis gives

$$\log_{10} k/\mathrm{s} = 15.7 - (64\,500/2.3\,RT)$$

with an estimated uncertainty in E of ± 1 kcal mol^{-1}. The activation energy should be a good approximation to $D[(CH_3)_3Sn—CH_3]$.

La pyrolyse du tétraméthyl étain a été étudiée dans un système à courant porteur de toluène entre 803 et 941 °K et en utilisant des pressions totales de 10.6 à 52.4 mm. Les temps de contact varient entre 0.49 et 13.8 s et le degré de décomposition de 1.35 à 98.7%. L'avancement de la réaction est suivie en mesurant la quantité formée de méthane, d'éthane d'éthylène et d'éthylbenzène. Aucune réaction hétérogène appréciable n'a été détectée et les constantes de vitesse du premier ordre semblent avoir été déterminées à la limite des hautes pressions. La quantité d'alkyle non décomposée est également mesurée et est en accord avec l'analyse du produit si quatre radicaux méthyles sont libérés pour chaque molécule subissant la réaction.

L'analyse par la méthode des moindres carrés donne:

$$\log_{10} k/\mathrm{s} = 15.7 - (64\,500/2.3\,RT)$$

l'incertitude estimée sur E étant de ± 1 kcal mol^{-1}. L'énergie d'activation devrait être une bonne approximation à $D[(CH_3)_3Sn—CH_3]$.

Canadian Journal of Chemistry, **50**, 50 (1972)

Introduction

Two previous investigations of the pyrolysis of tetramethyltin have been reported. The first investigation (1) showed approximately first order kinetics and gave $k = 8.3 \times 10^{21}$ exp $(-82\,400/RT)$ s^{-1}. A later investigation reported the overall decomposition was 3/2 order and gave an activation energy of 75.9 kcal mol^{-1} (2). The suggested mechanism explained the observed order but leads to the conclusion

[1] $$Sn(CH_3)_4 \rightarrow Sn(CH_3)_3 + CH_3$$

that $E_1 = 121$ kcal mol^{-1}. Neither investigation is satisfactory.

A related alkyl, dimethyltindichloride, has been studied in a toluene carrier system similar to that used in the present investigation (3). The decomposition was first order and homogeneous. For reaction 1*a* the Arrhenius equation obtained

[1*a*] $$(CH_3)_2SnCl_2 \rightarrow CH_3SnCl_2 + CH_3$$

was $k = 3.3 \times 10^{13} \exp(-56\,100/RT)$ s^{-1}. However, no allowance was made for the methyl radicals which combine with benzyl to form ethylbenzene. Based on our experience with other alkyls we would estimate that full analysis would have led to approximately $k = 2 \times 10^{14}$ exp $(-58\,000/RT)$ s^{-1}. This activation energy should be approximately equal to $D[CH_3Cl_2Sn—CH_3]$. Thermochemical results (4, 5) then lead to $D[Cl_2Sn—CH_3] = 32$ kcal mol^{-1}. The mean bond dissociation energy in tetramethyltin is 55 kcal mol^{-1} (4, 5) some 10 kcal stronger than the mean of the two Sn—C bonds in dimethyltindichloride. $D[(CH_3)_3Sn—CH_3]$ might be expected to be somewhat greater than $D[CH_3Cl_2Sn-CH_3]$ but not to the extent suggested by the two previous studies of this tetramethyl compound.

Experimental

Materials

(*a*) Toluene from sulfonic acid (Eastman Organic X325) was prepared for use by refluxing over sodium under vacuum and then degassing by bulb-to-bulb distillation.

TABLE 1. Selected results for the pyrolysis of tetramethyltin

T^* (°K)	P (mm)	Time† (min)	Toluene / Alkyl (molar ratio)	Alkyl used (moles × 10^4)	Products (moles × 10^4) CH_4	C_2H_6	C_2H_4	$C_6H_5C_2H_5$	t_c (s)	k_1 (s^{-1})
941 P	23.0	5,35,5	842	1.12	3.78	0.003	0.038	0.50	1.02	4.01
941 P	21.4	5,35,5	374	2.25	7.04	0.082	0.082	1.51	1.06	4.08
908 —	17.8	5,30,5	179	3.69	8.28	0.200	0.130	2.40	0.98	1.33
908 —	16.7	5,30,5	562	2.70	5.22	0.058	0.032	0.90	0.60	1.44
879 P	18.6	5,20,5	112	4.07	4.67	0.102	0.070	1.15	1.04	0.46
877 —	13.1	5,36,4	453	3.28	2.69	0.022	0.016	0.40	0.68	0.41
867 —	20.1	5,20,5	129	3.20	3.49	0.048	0.048	0.85	1.85	0.24
866 —	23.9	5,20,5	13	6.61	16.36	1.45	1.32	1.74	10.19	0.22
856 —	15.4	5,20,5	78	4.03	3.17	0.085	0.051	0.68	1.87	0.16
850 P	17.7	5,20,5	89	4.02	1.93	0.047	0.017	0.38	1.31	0.13
845 —	22.5	5,35,5	154	5.56	2.97	0.033	0.018	0.33	1.79	0.093
836 P	22.7	5,21,4	319	5.46	0.59	0.008	0.006	0.21	0.49	0.079
836 P	16.7	5,20,5	26	26.89	3.54	0.171	0.058	1.22	0.59	0.078
822 P	16.9	5,25,5	157	5.72	0.39	0.003	0.003	0.13	0.57	0.042
822 —	23.2	5,50,5	67	19.70	3.70	0.038	0.031	0.51	1.75	0.032
803 P	22.7	5,35,5	67	3.93	0.92	0.016	0.012	0.35	6.21	0.014

*P runs in packed reaction vessel.
†Prerun, duration of alkyl flow, postrun.

(*b*) Tetramethyltin was purchased from Alfa Inorganics [No. SN-145]. The vapor pressure curve was checked against that of Bullard and Haussman (6) and found to correspond. Refractive index and specific gravity measurements also agreed with literature values (1).

Apparatus

The experiments were carried out using the same system previously used in studying the decomposition of dimethylmercury in a benzene carrier (7). The gaseous products were analyzed using a Perkin–Elmer 154 gas chromatograph equipped with a 1/4 in. × 6 ft silica gel column. The column was maintained at 80 °C and a helium flow rate of 20 cc/min was used. The liquid products condensed along with the toluene in an acetone – Dry Ice trap were analyzed using a Perkin–Elmer model 800 gas chromatograph equipped with a 150 ft × 0.02 in. inside diameter Golay Column coated with poly(propylene glycol) (isothermal operation at 60 °C, flow rate N_2 carrier 10 cc/min).

The contact times used in the toluene carrier flow system were selected to minimize both thermal equilibrium and diffusion errors (8, 9). The unpacked reaction vessel had a volume of 171 cc. The packed reaction vessel had a volume of 117 cc and a surface-to-volume ratio 17 times that of the unpacked vessel. Before use both vessels were treated with boiling concentrated nitric acid and vacuum baked without rinsing.

Results and Discussion

Selected[1] experimental results are given in Table 1. They may be discussed in terms of the following mechanism.

[1] $Sn(CH_3)_4 \rightarrow Sn(CH_3)_3 + CH_3$

[2] $Sn(CH_3)_3 \rightarrow Sn(CH_3)_2 + CH_3$

[3] $Sn(CH_3)_2 \rightarrow Sn(CH_3) + CH_3$

[4] $Sn(CH_3) \rightarrow Sn + CH_3$

[5] $CH_3 + C_6H_5CH_3 \rightarrow C_6H_5CH_2 + CH_4$

[6] $2CH_3 \rightarrow C_2H_6$

[7] $CH_3 + C_6H_5CH_2 \rightarrow C_6H_5C_2H_5$

[8] $2C_6H_5CH_2 \rightarrow (C_6H_5CH_2)_2$

[9] $CH_3 + C_2H_6 \rightarrow CH_4 + C_2H_5$

[10] $C_2H_5 \rightarrow C_2H_4 + H$

[11] $H + C_6H_5CH_3 \rightarrow C_6H_5CH_2 + H_2$

[12] $H + C_6H_5CH_3 \rightarrow C_6H_6 + CH_3$

It is apparent from the results that the bulk of the methyl radicals are removed by reactions 5 and 7. The small yields of ethylene seem somewhat higher than might be expected from reactions 9 and 10. This may be due to reaction 13.

[13] $C_6H_5C_2H_5 \rightarrow C_6H_6 + C_2H_4$

In a conditioned reaction vessel this reaction should be completely negligible under the conditions of temperature, pressure, and residence time used in the present work (10). However, as shown in reference 10 reaction 13 is extremely sensitive to the nature of the surface and may be catalyzed by the tin released in the present reaction.

[1]Complete set of tables is available from the Depository of Unpublished Data, National Science Library, National Research Council of Canada, Ottawa, Canada K1A 0S2.

TABLE 2. Effect of alkyl concentration on k_1 at 856 °K

% decomposition			
Product analysis	Residual alkyl analysis*	$Sn(CH_3)_4$ conc. (mol/cc × 10^9)	k_1 (s^{-1})
26.8	26.3	5.45	0.160
25.5	24.9	3.70	0.159
25.7	23.4	2.70	0.158
38.4	39.4	1.64	0.159
25.9	25.9	0.30	0.157

*% decomposition based on alkyl used – alkyl recovered.

TABLE 3. Effect of pressure on k_1

T (°K)	P (mm)	% decomposition		k_1 (s^{-1})
		Product analysis	Residual alkyl analysis	
866	52.4	79.6	76.1	0.214
866	40.6	93.7	94.8	0.201
866	23.9	89.5	—	0.221
867	14.9	34.6	38.0	0.211
867	10.6	25.3	25.3	0.210

In Tables 2, 3, and 4 a comparison is shown between the percent decomposition based on products analysis (assuming four CH_3 are released for each molecule undergoing reaction 1) and the percent decomposition calculated from the undecomposed alkyl. The basic agreement over a wide range of decomposition (approximately 13%–90%) indicates that each time reaction 1 occurs it is followed in rapid sequence by reactions 2, 3, and 4 or some equivalent processes. Rate constants have therefore been calculated from the usual first order equation

$$k = \frac{2.303}{t_c} \log \frac{1}{1-x}$$

where t_c is the average residence time in the reaction zone and the fraction decomposed, x, is given by

$$x = \frac{\text{moles } CH_4 + \text{moles ethylbenzene} + 2\,(\text{moles } C_2H_6 + C_2H_4)}{4\,(\text{moles } Sn(CH_3)_4 \text{ used})}$$

To the extent that reaction 12 occurs the value of x calculated in this way will be too high. However, even if reaction 13 is completely negligible the maximum contribution of reaction 12 is 0.3 × moles C_2H_4 (11). Any correction for reaction 12 is therefore negligible.

The results in Table 2 show the reaction follows first order kinetics. For a molecule as complex as $Sn(CH_3)_4$ no unimolecular pressure effects were expected at the temperatures and pressures used. The limited tests shown in Table 3 are in agreement with this expectation. Although most of the contact times used conform to the recommendations of Mulcahy and Pethard (9) a significant number of runs were done with $t_c/P < 0.5$. However, the results in Table 4 indicate that even at $t_c/P = 0.28$ no significant change in k_1 has occurred.

The Arrhenius plot for k_1 is shown in Fig. 1. It is clear that within the limits of the experimental method the extent of heterogeneous decomposition of the alkyl is undetectably small except for a very small contribution at the lowest temperatures used. The Arrhenius equation obtained by least squares analysis of the runs in the unpacked vessel is $k = 4.7 \times 10^{15} \exp(-64\,500 \pm 1\,000/RT)\ s^{-1}$. The activation energy should be a good approximation to

TABLE 4. Effect of contact times on k_1

T (°K)	t_c (s)	P (mm)	% decomposition		k_1 (s^{-1})
			Product analysis	Residual alkyl analysis	
866	10.2	24	89.5	—	0.22
867	2.60	20	48.0	50.6	0.25
867	1.85	20	35.4	34.2	0.24
867	1.83	23	37.5	—	0.26
867	1.73	23	37.9	40.4	0.28
867	0.94	20	19.5	22.7	0.23
867	0.57	20	13.4	14.3	0.25

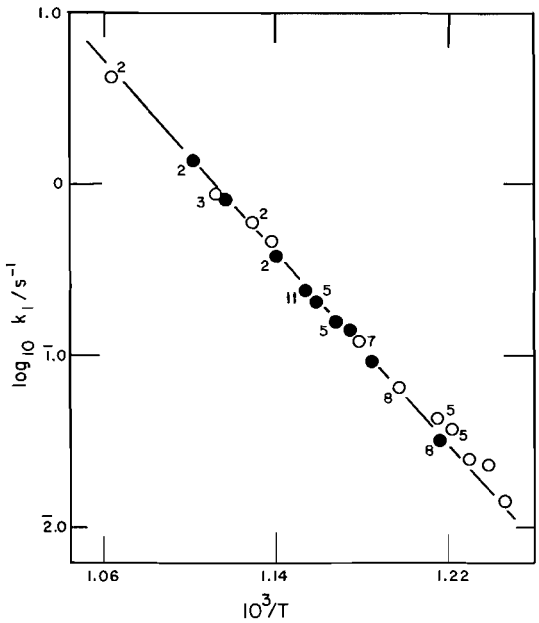

FIG. 1. Arrhenius plot of k_1. Full circles, unpacked vessel; open circles, packed vessel. Numbers indicate number of runs average to obtain the given point.

$D[(CH_3)_3Sn—CH_3]$. Thus $D_1 = 64.5 \pm 1$ kcal mol^{-1}. This value is in fair agreement with a value derived from a combination of mass spectral and thermochemical data (12) 66.5 kcal mol^{-1} (actually 67.5 as calculated by Lappert *et al.* (12) but this is based on $\Delta H_f^0(CH_3) =$ 34.8 kcal mol^{-1}). The kinetic energy of the fragments ion is expected to be no more than 0.05 eV but even this would lower D_1 to about 65.3 kcal mol^{-1}. It is difficult to estimate the probable error limits on this value but ± 2 kcal is probably a fair guess. The extent of agreement with the present results for D_1 is therefore well within the combined experimental error.

Although no further quantitative conclusions can be reached it is interesting to speculate on the relative magnitudes of D_1, D_2, D_3, and D_4 and how they relate to the proposed mechanism. From previous studies in our laboratory (3, 13–16) it seems reasonable to assign the following approximate values

$$A_2 = 10^{15}\ s^{-1}$$

$$A_3 = 10^{14}\ s^{-1}$$

Then in order to establish reaction 1 as rate controlling we arbitrarily set $5k_1 = k_2 = k_3 = k_4$. At approximately the middle of our temperature range, 850 °K, $k_1 = 0.126$. Therefore $k_2 = k_3 = k_4 = 0.630$ and $E_2 = 59$ kcal mol^{-1}. This should be close to D_2 at the temperature and pressures used. Similarly, $E_3 = 55$ kcal mol^{-1} but due to unimolecular pressure effects, D_3 is probably about 4 kcal greater than E_3. Thus D_3 is approximately 59 kcal mol^{-1}. Since $(D_1 + D_2 + D_3 + D_4) = 220$ kcal, $D_4 = 37.5$ or again estimating the effect of pressure on E_4, E_4 should be approximately 34 kcal mol^{-1}. This leads to $A_4 = 8.5$ s^{-1}. Because of the way the calculation has been done these values of E_4 and A_4 are probably a reasonable estimate of minimum values. Based on experience with methylindium A_4 might be as large as 10^{11} s^{-1} (15). This would set an approximate maximum value of $E_4 = 43.5$ kcal mol^{-1}. If E_3 is not changed then E_2 could now be as low as 49 kcal mol^{-1}. In relation to E_1 this would be more in line with the relative E_1 and E_2 values for dimethyltindichloride. Therefore values of $D_1:D_2:D_3:D_4 = 65:49:59:47$ kcal mol^{-1} would be consistent with the proposed mechanism and the experimental evidence that is available. However, the whole process used to reach this conclusion is extremely speculative and the results obtained are at best an indication that decomposition by simple consecutive release of methyl radicals is plausible.

We are indebted to Professor Lappert who supplied a prepublication copy of his paper "Bonding Studies of Compounds of Boron and the Group IV Elements, Part VI".

This work was supported by a grant from the National Research Council of Canada.

1. C. E. WARING and W. S. HORTON. J. Am. Chem. Soc. **67**, 540 (1945).
2. T. V. SATHYAMURTHY, S. SWAMINATHAN, and L. M. YEDDANAPALLI. J. Indian Chem. Soc. **27**, 509 (1950).
3. S. J. W. PRICE and A. F. TROTMAN-DICKENSON. Trans. Faraday Soc. **54**, 1630 (1958).
4. Selected values of chemical thermodynamic properties. Natl. Bur. Std. U.S. Tech. Notes, No. 270–3, 1968.
5. G. A. NASH, H. A. SKINNER, and W. F. STACK. Trans. Faraday Soc. **61**, 640 (1965).
6. H. BULLARD and M. HAUSSMANN. J. Phys. Chem. **34**, 743 (1930).
7. M. KRECH and S. J. PRICE. Can. J. Chem. **41**, 224 (1963).
8. J. J. BATTEN. Aust. J. Appl. Sci. **12**, 11 (1961).
9. M. F. R. MULCAHY and M. R. PETHARD. Aust. J. Chem. **16**, 527 (1963).
10. W. D. CLARK and S. J. PRICE. Can. J. Chem. **48**, 1059 (1970).

11. S. J. PRICE. Can. J. Chem. **40**, 1310 (1962).
12. M. F. LAPPERT, J. B. PEDLEY, J. SIMPSON, and T. R. SPALDING. J. Organomet. Chem. **29**, 195 (1971).
13. R. J. KOMINAR and S. J. PRICE. Can. J. Chem. **47**, 1560 (1963).
14. M. G. JACKO and S. J. W. PRICE. Can. J. Chem. **41**, 1560 (1963).
15. M. G. JACKO and S. J. W. PRICE. Can. J. Chem. **42**, 1198 (1964).
16. S. J. W. PRICE and J. P. RICHARD. Can. J. Chem. **48**, 3209 (1970).

The Photodecomposition of an Analogue of DDT

H. J. Liu, P. J. Silk, and I. Unger

Department of Chemistry, University of New Brunswick, Fredericton, New Brunswick

Received July 22, 1971

The photodecomposition of 1,1,1-trichloro-2,2-bis(5′-chloro-2′-methoxyphenyl)ethane (MPA) has been carried out both in solution and solid phase with exciting light > 300 nm. The major products of the solid phase photolyses are HCl and 1,1-dichloro-2,2-bis(5′-chloro-2′-methoxyphenyl)ethylene (MPE), 5,5′-chloro-2,2′-methoxybenzophenone (MPO), 1,1-dichloro-2,2-bis(5′-chloro-2′-methoxyphenyl)ethane (MPD), and 1-chloro-2,2-bis(5′-chloro-2′-methoxyphenyl)ethane (MPC). In liquid phase and in the presence of O_2 the photodecomposition yields many products, the major ones, in addition to HCl, being MPE, MPD, MPC, and MPO. In the absence of O_2 in liquid phase only HCl, MPD, MPC, and MPE were observed. In the O_2 free photolysis MPD and MPC are produced in larger quantity than MPE. A preliminary investigation has shown that MPE irradiated at $\lambda > 300$ nm also photodecomposes. A check carried out by the Canada Department of Agriculture indicates that MPA is a pesticide although it may not be as effective as DDT.

La photodécomposition du trichloro-1,1,1 bis(chloro-5′ méthoxy-2′ phényl)-2,2 éthane (MPA) a été menée à bien à la fois en solution et en phase solide, avec une lumière excitatrice >300 nm. Les produits principaux de la photolyse en phase solide sont HCl et le dichloro-1,1 bis(chloro-5′ méthoxy-2′ phényl)-2,2 éthylène (MPE), le chloro-5,5′ méthoxy-2,2′ benzophénone (MPO), le dichloro-1,1 bis(chloro-5′ méthoxy-2′ phényl)-2,2′ éthane (MPD), et le chloro-1 bis(chloro-5′ mèthoxy-2′ phényl)-2,2 éthane (MPC). En phase liquide et en présence d'O_2 la photodécomposition donne de nombreux produits; en plus de HCl, les produits majoritaires sont le MPE, MPD, MPC, et MPO. En l'absence d'O_2 et en phase liquide on observe uniquement la présence d'HCl, MPD, MPC, et MPE. Dans la photolyse en l'absence d'O_2, le MPD et le MPC sont formés en plus grande quantité que le MPE. Des recherches préliminaires ont montré que le MPE. Des recherches préliminaires ont montré que le MPE irradié à $\lambda > 300$ nm subit également une photodécomposition. Des recherches entreprises par le Département d'Agriculture du Canada montrent que le MPA est un pesticide bien qu'il ne soit pas aussi efficace que le DDT.

Canadian Journal of Chemistry, **50**, 55 (1972)

Introduction

The persistence of DDT, and related chlorinated pesticides, in the environment is due to two reasons: (*a*) they do not absorb appreciably in the solar spectrum, and (*b*) they resist degradation by microorganisms. A technique to overcome the former difficulty has been suggested by Miller and Narang (1), who showed that absorption by a variety of aromatic amines in the presence of DDT resulted in the decomposition of DDT, and postulated that the reaction occurred via a charge transfer from the amine to DDT. Since intramolecular energy transfer has been shown to occur in a variety of systems such as naphthalene–anthracene (2), naphthalene–benzophenone (3), and benzene–olefin (4–6) and since DDT may be thought of as consisting of three distinct moieties (the two chlorophenyl groups and the chlorinated ethane moiety), then an alternative procedure to that described by Miller and Narang would be to produce a bathochromic shift in DDT by a suitable modification in the chlorophenyl part of the molecule with the expectation that the resulting molecule may exhibit intramolecular sensitized decomposition. We report here the results of such a study.

Experimental

(1) Equipment and Materials

Infrared spectra were determined using a Perkin–Elmer grating Infra-Red Spectrophotometer, Model 457. Ultraviolet spectra were determined either on a Perkin–Elmer 402 UV-Visible Spectrophotometer, or an Hitachi EPS-3T Spectrophotometer. The n.m.r. spectra were recorded on a Varian T-60 NMR spectrometer; tetramethylsilane was used as an internal standard. Mass spectra were recorded using an Hitachi Perkin–Elmer RMU-6D Mass Spectrometer. Melting points were determined on a Kofler hot-stage apparatus and are uncorrected.

The photolyses were performed using a 1 KW Hanovia high-pressure xenon–mercury lamp contained in a Schoeffel housing, air-cooled to a temperature of 110 °C. Radiation from the lamp was filtered using two Corning 0-54(0160) filters, each being 2.1 mm thick and with an exact wavelength cut-off at 300 nm. Solution and solid phase photolyses were performed in cylindrical quartz cells (5 × 1 cm). The cells were always placed 20 cm from the focusing device of the lamp housing.

The v.p.c. was performed either on a Hewlett–Packard 7620A Chromatograph equipped with a flame ionization and a thermal conductivity detector, or a Varian Aerograph, Model 705 equipped with a flame ionization detector. Helium was used as a carrier gas throughout Columns for

Can. J. Chem. Downloaded from www.nrcresearchpress.com by 210.87.254.5 on 09/05/12
For personal use only.

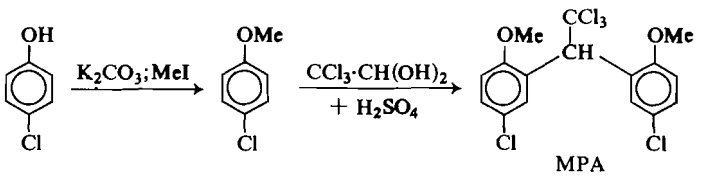

SCHEME 1

the HP were either 4 or 6 ft long constructed from 1/8 in. stainless-steel. Liquid phases used were DC-200 (12500-cnstk), OV-17, or QF-1, on Chromosorb Q (100/120 mesh) at 10% w/w loading. Column temperature was 210° with a helium flow-rate of ~60 ml/min. The column used for the Varian Aerograph was 10 ft × 1/4 in. stainless-steel packed with 5% w/w QF-1 on Chromosorb W (60/80 mesh). The injectors and detectors on both instruments were maintained at 230 and 260 °C, respectively. Sample introduction was by Hamilton Precision syringes, solid samples being injected as benzene solutions through self-sealing rubber septa. "On-column" injection was used throughout.

Cyclohexane used for solution photolyses and u.v. spectra was fluorometric grade obtained from Harleco and was used without further purification. A standard cyclohexane solution of MPA (4g/l) was used for all photolyses.

(2) Preparation of MPA

MPA was prepared by the overall reaction sequence shown in Scheme 1.

p-Chloroanisole was prepared in 98% yield by reacting *p*-chlorophenol with methyl iodide in the presence of potassium carbonate under an atmosphere of nitrogen. This was done at room temperature and the reaction mixture was stirred overnight. The mixture was then poured into water and the product was extracted with chloroform. The extract was dried with magnesium sulfate, filtered, and concentrated to yield *p*-chloroanisole.

The general method of preparing 1,1,1-trichloro-2,2-bis(*p*-chlorophenyl)ethane (DDT) was adapted (7) for the synthesis of MPA. Chloral hydrate crystals (23 g) and *p*-chloroanisole in a round-bottomed flask (1 l) were warmed in a water bath until all crystals were dissolved. The solution was cooled and concentrated sulfuric acid (270 ml) was slowly added. After stirring at room temperature for 3 h, the mixture was poured into cold water (1 l), filtered through a sintered-glass funnel and washed with water (3 × 500 ml). The solid was then stirred with 100 ml of 2% sodium carbonate solution and washed with distilled water followed by absolute ethanol (3 × 25 ml). The residue was dried in an oven at 70 °C. The MPA produced in this way was in 69% yield; crude m.p. 142–143 °C; ethanol recrystallized product m.p. 146–147 °C; i.r. ($CHCl_3$) 1600 cm^{-1} (benzene); n.m.r. ($CDCl_3$) τ 2.23 (d, 2 Hz, 2H, $=C-CH=C-$, Cl), 2.80 (d of d, 2 and 8 Hz, 2H, $-CH=CH-CCl=$), 3.24 (d, 8 Hz, 2H, $-CH=C(OCH_3-)$), 3.67 (s, 1H, $>CH-CCl_3$), and 6.17 (s, 6H, $-OCH_3$); mass spectrum: M^+ 412 (with peaks at 414, 416, 418, 420 in the ratio corresponding to five Cl atoms in the molecule (8)); u.v.: (C_6H_{12}) λ_{max} 289 nm. No impurities were detected, by v.p.c., in the recrystallized MPA.

(3) The Preparation of Photolysis Products for Comparison Purposes

(a) Synthesis of MPE

MPE was synthesized in 98% yield by the alkaline dehydrochlorination of MPA the method being adapted from a similar procedure (9). To a solution of MPA (4 g) in 95% ethanol (50 ml) was added 50 ml of a 5% sodium hydroxide solution. The mixture was then refluxed and stirred for 3 h. The mixture was then cooled and then alcohol mostly removed by placing the mixture under vacuum in a rotary evaporator. The product was then extracted with ether, washed with water (3 × 50 ml), and the ethereal solution dried over magnesium sulfate overnight. The solution was filtered and the ether removed from the extract on the rotary evaporator. The crude product was then recrystallized from hot absolute ethanol and dried in an air-oven at 70 °C; v.p.c., (6 ft DC-200, HP, at 200 °C, benzene) showed the material to have a purity of 98%. The spectral data for MPE and MPD are given in the Results section of this paper.

(b) Synthesis of MPD

Two general methods were adopted:

(*i*) MPD was produced in >90% yield by the photolysis of pure MPA in cyclohexane in the absence of $O_2(N_2)$ at λ > 300 nm (see Table 1). The cyclohexane was then evaporated from the solution and the product recrystallized in absolute ethanol.

(*ii*) MPD was also produced in ~10% yield from a Clemmensen reduction (7) of MPA along with three other products, MPC, $R_2-CH-CH_3$ (n.m.r.), and a rearranged product (9). The n.m.r. ($CDCl_3$) on the mixture indicates τ 3.85 (d, 7 Hz, 2H, $>CH-CH_2Cl$)(10), α-proton triplet obscured by other compounds present including $>CH-CH_3$ (n.m.r. ($CDCl_3$) τ 8.53 (d, 4 Hz, 3H, $>CH-CH_3$), 5.25 (q, 4 Hz, $>CH-CH_3$)) and MPD.

(c) Synthesis of MPO

Several methods of producing MPO from MPE were attempted. These included oxidation with IO_4^-/MnO_4^- in K_2CO_3 and IO_4^-/OsO_4. Both were unsuccessful in that they produced MPO in very low yield, 99% of MPE being recovered from the starting material. MPO was finally produced in ~10% yield by the oxidation of MPE in acetone by Jones' reagent (7, 9) ($CrO_3 + H_2SO_4$) the product being extracted into ether and dried with magnesium sulfate. MPO was not separated from MPE and was used as such in benzene solution for v.p.c. analysis using peak-matching techniques (in two different columns) for comparison with photolysis samples; i.r. (Nujol mull) 1715 cm^{-1} (ν C=O); n.m.r. ($CDCl_3$) similar to MPE, no other proton containing impurities present.

Can. J. Chem. Downloaded from www.nrcresearchpress.com by 210.87.254.5 on 09/05/12
For personal use only.

Can. J. Chem. Downloaded from www.nrcresearchpress.com by 210.87.254.5 on 09/05/12
For personal use only.

TABLE 1. MPA photolysis products

Phase	O_2 or N_2	Photolysis time	Irradiation source	% MPA remaining	% MPE formed	% MPD formed	% MPC formed	% MPO formed	Others
Solution	N_2	2 h	Hg lamp	97.3	0.97	0	1.7	—	Volatiles
"	N_2	4 "	"	95.9	0.12	3.8	0.09	—	"
"	N_2	8 "	"	47.8	0.22	48.9	3.1	—	"
"	N_2	23 "	"	3.8	0.27	95.8	0.18	—	"
"	O_2	2 "	"	96.5	1.76	0.16	1.35	Trace	0.2% volatiles + traces of two higher molecular weight compounds
"	O_2	4 "	"	72.9	2.4	11.4	11.1	0.05	0.2% volatiles + 2% of two higher molecular weight compounds
"	O_2	23 "	"	3.2	1.7	78.6	11.9	0.24	0.5% volatiles + 4% of two higher molecular weight compounds
Solid	Air	18 "	"	98.8	0.27	0.39	0.11	Trace	0.4% volatiles + traces of two higher molecular weight compounds
"	"	24 "	"	97.9	0.14	0.13	0.06	Trace	0.3% volatiles + traces of two higher molecular weight compounds
"	"	48 "	"	97.1	0.94	1.14	0.34	Trace	Traces of volatiles + traces of higher molecular weight compounds
"	"	14 days	Sunlight	99.0*	0.48	0.43	0.07	Trace	Traces of higher molecular weight compounds
"	"	20 "	"	97.8*	1.5	0.55	0.19	Trace	Traces of higher molecular weight compounds
"	"	28 "	"	95.0*	2.32	1.39	0.79	Trace	Traces of higher molecular weight compounds

*Based on material present after irradiation, no attempt was made to collect any volatile products.

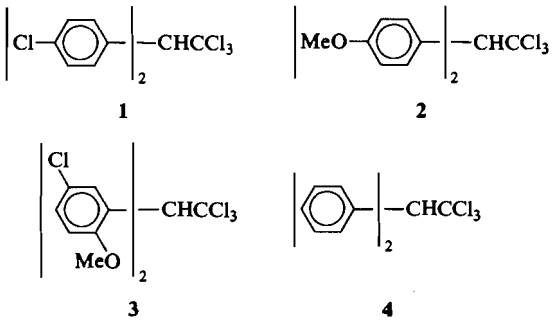

Results and Discussion

The absorption spectra of *p,p'*-DDT, **1**, methoxychlor, **2**, and MPA, **3**, are given in Fig. 1. It is interesting to compare the spectra of the above molecules with the published spectrum of 1,1-diphenyl-2,2,2-trichloroethane (**4**) (11). The π,π^* absorption (12) of **4** begins at about 275 nm and exhibits six clearly discernible vibrational bands. On substituting a chlorine atom for an H atom in the para position, thus forming *p,p'*-DDT **1**, the absorption is red shifted by about 6 nm and some of the structure begins to disappear. Similarly substituting an MeO group in the para position of **4**, to yield methoxychlor **2**, produces a red shift of approximately 10 nm and eliminates most of the vibrational bands. The addition of both Cl and MeO to **4**, to give MPA **3** results in a bathochromic shift of about 30 nm, and the almost total disappearance of vibrational structure.

The photolysis of MPA was carried out in solution (cyclohexane solvent) in the presence and absence of O_2, by bubbling either O_2 or N_2 through the solution prior to and during photolysis. Photolysis was performed on MPA, with filtered light $\lambda > 300$ nm and in direct sun-

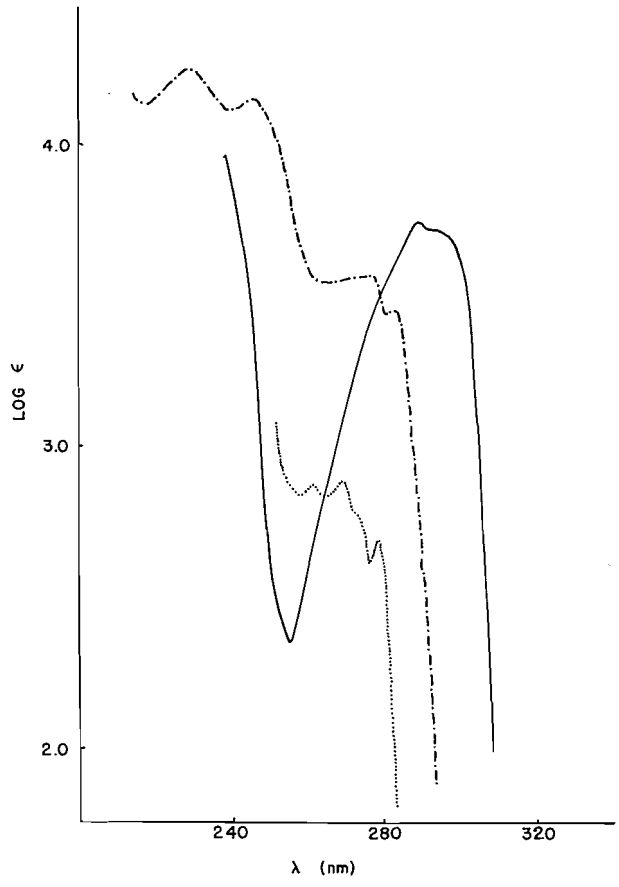

FIG. 1. The absorption spectra of DDT (·····), MPA (——), methoxychlor (–·–·–·–).

Can. J. Chem. Downloaded from www.nrcresearchpress.com by 210.87.254.5 on 09/05/12
For personal use only.

Can. J. Chem. Downloaded from www.nrcresearchpress.com by 210.87.254.5 on 09/05/12
For personal use only.

light. The results of these experiments are summarized in Table 1. The major products of photolysis are MPE **5**, MPD, **6**, MPC, **7**, MPO, **8**, and HCl. These molecules were identified by the following means.

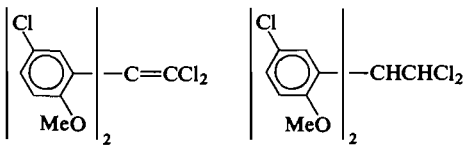

5 **6**

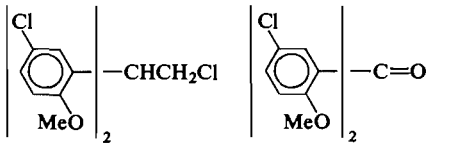

7 **8**

In solution photolysis in cyclohexane (both in O_2 and N_2) a small quantity of a white solid was precipitated. This solid, collected from several photolysis experiments was found to be identical, spectrally, with MPE, prepared by the alkaline dehydrochlorination of MPA. White solid; m.p. 164–165 °C; i.r. ($CHCl_3$) 1600 cm^{-1}; n.m.r. ($CDCl_3$) τ 6.16 (s, 6H, —OCH_3); ratio of 2 × (—OCH_3): aromatic protons, 1:1; mass spectrum: M^+ 376 (with peaks at 378, 380, 382, 384 in ratio corresponding to four Cl atoms in the molecule (8)); u.v. (C_6H_{12}) λ_{max} 295.5 and 214 nm; MPD was isolated in a similar way from the photolyses of MPA (C_6H_{12}) under N_2. Again the spectral properties of the product isolated from the photolysis was identical to synthesized MPD; mass spectrum: M^+ 378 (peaks at 380, 382, 384 ratio corresponding to four Cl atoms in the molecule); n.m.r. ($CDCl_3$) τ 6.16 (s, 6H,—OCH_3), 4.80 (d, 6 Hz, 1H, $\rangle$CH—$CHCl_2$), 3.79 (d, 6 Hz, 1H, $\rangle$$CH$—$CHCl_2$); AB system of α,β-ethane protons (10), aromatic protons, see synthesis of MPA; ratio 2 × (—OCH_3) + α,β ethane protons : aromatic protons 4:3; some impurities evident from n.m.r. spectrum. In the case of MPC and MPO, together with other photolysis products, v.p.c. peak matching (retention times) was employed as a method of identification. Two different columns (DC-200, QF-1) were used in retention time matching to ensure proper identification of the products. A standard solution (benzene) of MPA, MPD, MPC, MPE, and MPO was prepared in order to provide a peak matching reference before and after each analysis of photolyzed material. HCl gas, evolved from *all* photolyses both in solution and from the solid, was identified by collecting the gas (~2 cm pressure) *in vacuo* in a 10 cm i.r. gas cell from various photolysis experiments. The typical i.r. spectrum of gaseous HCl was obtained.

Inspection of the data in Table 1 shows that MPE, MPD, and MPC are formed in both liquid and solid phase, in the absence as well as in the presence of O_2. Trace quantities of MPO and higher molecular weight compounds are produced only in the presence of O_2. MPE and MPC are formed in small amounts and their production does not appear to be dependent on photolysis time. MPD is produced in large quantities, its concentration is dependent on irradiation time and it may have an induction period. Our experimental results show that π,π^* absorption in MPA leads to photodecomposition in the chloroethane part of the molecule. In view of the fact that intramolecular energy transfer is known to occur much more efficiently than intermolecular energy transfer (2, 3, 13) it is possible that MPA photodissociation occurs via intramolecular sensitization. While our data do not permit any conclusions about the mechanism of the reaction, the knowledge that photodecomposition of DDT (14–16), carried out at exciting wavelengths ranging from 280–250 nm, proceeds via a free radical mechanism, (C—Cl bond cleavage occurs from both the ethane and the aromatic parts of the molecule with the latter being favored at shorter wavelengths) suggests that MPA photolysis occurs via a mechanism similar to the photolysis of DDT at high wavelengths. This contention is supported by the fact that the major products in the DDT photolysis (16), are analogous to the products of MPA photolysis. At the same time since molecular elimination of HCl is known to occur in the photolysis of chlorinated hydrocarbons (17, 18), it is possible that MPE results from such a reaction. Since MPE has a large extinction coefficient in the 300 nm region ($\simeq 7.5 \times 10^3$) it is possible that it undergoes secondary photolysis, one or more of the observed products could conceivably be due to

this reaction. Further work, which should elucidate the mechanism of photodecomposition of MPA, is underway in our laboratory.

Two other points are also worth noting; a preliminary investigation shows that MPE dissociates when excited by light of $\lambda > 300$ nm, MPA has been shown by the Canada Department of Agriculture (Fredericton, New Brunswick Experimental Station) to have pesticidal properties.

We wish to thank professors G. P. Semeluk and Z. Valenta for many valuable discussions. We are indebted to Mr. D. Pond of the Canada Department of Agriculture, Fredericton for carrying out the toxocological tests on MPA. We thank Mr. J. Addison and Mr. M. Chalmers for technical assistance. We are grateful for financial aid for this project from the University of New Brunswick Research Fund.

1. L. I. MILLER and R. S. NARANG. Sci. **169**, 368 (1970).
2. O. SCHNEPP and M. LEVY. J. Am. Chem. Soc. **84**, 172 (1962).
3. A. A. LAMOLA, P. A. LEERMAKERS, G. W. BYERS, and G. S. HAMMOND. J. Am. Chem. Soc. **87**, 2322 (1965).
4. H. MORRISON and R. PEIFFER. J. Am. Chem. Soc. **90**, 3428 (1968).
5. M. COMTET. J. Am. Chem. Soc. **91**, 7761 (1969).
6. K. SALISBURY. J. Chem. Soc. 931 (1971).
7. A. I. VOGEL. A textbook of practical organic chemistry including qualitative organic analyses. 3rd Ed. Longmans, London. 1956.
8. J. M. BEYNON. The mass spectra of organic molecules. Elsevier, London. 1966.
9. G. S. HARTLEY and T. F. WEST. Chemicals for pest control. Pergamon, London. 1966.
10. N. E. SHARPLESS and R. B. BRADLEY. Appl. Spectrosc. **19** (5), 150–154 (1965).
11. H. KELLER, M. HOCHWEBER, and H. V. HALBAN. Helv. Chim. Acta, **29**, 761 (1946).
12. F. SMITH and L. M. TURTON. J. Chem. Soc. 1350 (1955).
13. T. FOERSTER. Discuss. Faraday Soc. **27**, 7 (1959).
14. E. E. FLECK. J. Am. Chem. Soc. **71**, 1034 (1949).
15. A. R. MOSIER, W. D. GUENZI, and L. L. MILLER. Sci. **164**, 1083 (1969).
16. J. R. PLIMMER, U. I. KLINGEBIEL, and B. E. HUMMER. Sci. **167**, 67 (1970).
17. M. H. J. WIJNEN. J. Am. Chem. Soc. **83**, 4109 (1961).
18. J. R. MAJER and J. P. SIMMONS. Adv. in Photochem. **2**, 137 (1964).

Can. J. Chem. Downloaded from www.nrcresearchpress.com by 210.87.254.5 on 09/05/12
For personal use only.

Vapor Phase Catalytic Transformations of Terpene Hydrocarbons in the $C_{10}H_{16}$ Series. I. Isomerization of α-Pinene over Alumina[1]

A. STANISLAUS[2] AND L. M. YEDDANAPALLI
Department of Chemistry, Loyola College, Madras, India

Received April 1, 1971

The isomerization of α-pinene in the vapor phase over alumina catalysts of varying acid strength has been studied. The isomerization proceeds via two parallel paths, one giving bi- and tricyclic products such as camphene, β-pinene, tricyclene, and bornylene and the other giving rise to monocyclic compounds such as dipentene, terpinolene, α-terpinene, γ-terpinene, *p*-cymene, and *p*-menthene. Dependence of the distribution of reaction products on space time reveals that camphene, β-pinene, tricyclene, dipentene, and terpinolene are the primary products. The acid strength of alumina catalysts has a remarkable influence on the selectivity ratio of bi- and tricyclic to monocyclic products, the strong acid sites favoring the formation of monocyclic products. From the study of the reactions of camphene and tricyclene over the same catalysts under similar conditions it has been concluded that the decrease in the selectivity ratio with increasing acid strength of the catalysts is mainly due to the further isomerization of the bi- and tricyclic compounds to monocyclic products which takes place only on the strong acid sites.

L'isomérisation de α-pinène en phase vapeur sur catalyseurs d'alumine d'acidité variable a été étudiée. L'isomérisation procède par deux voies parallèles, l'une donnant des produits bi et tricycliques tels que le camphène, le β-pinène, le tricyclène et le bornylène et l'autre permettant d'obtenir des composés monocycliques tels que le dipentène, le terpinolène, l'α-terpinène, le γ-terpinène, le *p*-cymène et le *p*-menthène. La relation entre la distribution des produits de réaction et du temps de contact révèle que le camphène, le β-pinène, le tricyclène, le dipentène et le terpinolène sont des produits primaires. L'acidité des catalyseurs d'alumine a une influence notable sur le rapport de sélectivité: produits bi et tricycliques sur produits monocycliques; les sites fortement acides favorisent la formation de produits monocycliques.

Canadian Journal of Chemistry, **50**, 61 (1972).

Introduction

Alumina has been used as a catalyst and catalyst support in this laboratory for the vapor phase catalytic transformations of terpene compounds (1–5). Studies (6, 7*a*) on the nature of the active sites of alumina have revealed that aluminas can vary widely in their activity for skeletal and double bond isomerization reactions depending upon the strength of acid sites on their surface. A survey of literature reveals that a systematic investigation of the isomerization of α-pinene over alumina catalysts of varying acid strength in vapor phase has not been carried out. The influence of the acid strength of alumina on the rate and the distribution of products of the isomerization of α-pinene was, therefore, studied and the results of such studies are presented in this paper.

[1]This investigation is dedicated to the memory of Professor L. M. Yeddanapalli who died on June 6, 1970.

[2]Present address: Department of Chemistry & Chemical Engineering, Royal Military College of Canada, Kingston, Ontario.

Experimental

(1) Materials

α-Pinene was obtained from the first quality Indian turpentine oil supplied by the Government Turpentine and Rosin Company Ltd., Bareilly, India, by fractionation using a 5 ft column packed with stainless steel helices (containing 20 theoretical plates) at reduced pressure (10 mm Hg). The purity was found to be better than 99% by gas chromatographic analysis.

Camphene: Pure camphene (BDH) was further fractionated and the liquid distilling at 158–159 °C/760 mm was collected and stored in brown bottles. By gas chromatographic analysis the purity was established to be better than 99%.

Tricyclene: Tricyclene (99% pure) generously gifted by Hercules Powder Company, U.S.A., was used without further purification.

Alumina A was prepared by hydrolyzing aluminum isopropoxide with water. The precipitated aluminum hydroxide was filtered with a Buckner funnel, washed thoroughly with distilled water, cut into cakes, and dried at 120 °C for 24 h. The material was then activated at 500 °C in a stream of dry air for 24 h. The activated material was crushed into a powder and then pelletized to give 4 × 4 mm cylindrical pellets.

Aluminas B, C, and D were prepared by doping alumina A with appropriate amounts of sodium carbonate solution to give 0.6, 1.0, and 1.5% by weight of sodium in the catalysts, respectively.

Can. J. Chem. Downloaded from www.nrcresearchpress.com by 210.87.254.6 on 09/05/12
For personal use only.

TABLE 1. Acid strength distribution of alumina catalysts

Catalyst	*n*-Butylamine mequiv/g		
	pK_a < -5.7	pK_a -3.0 to -5.7	pK_a* 3.3 to -3.0
Alumina C	0.0	0.24	0.0
Alumina A	0.19	0.05	0.01
Alumina E	0.21	0.20	0.00

*Compared to sulfuric acid water system acid sites having pK_a values in the three ranges 3.3 to -3.0, -3.0 to -5.7, and -5.7 and less are 3×10^{-4} to 48% H_2SO_4, 48 to 72% H_2SO_4, and stronger than 72% H_2SO_4, respectively.

Alumina E was prepared by impregnating alumina A with appropriate amounts of HF acid (40% E. Merck) to give 5% by weight of HF in the catalyst. The activation of these catalysts were carried out in a manner similar to that employed in the preparation of alumina A.

The distribution of acid strengths in aluminas A, C, and E was determined by the *n*-butylamine titration method (*7b*). The results are summarized in Table 1. Pure alumina appears to have a continuous distribution of acid strength although most of the acidity is strong ($pK_a < -5.7$). The treatment with HF increases acid sites having pK_a values -3.0 to -5.7 considerably. On the other hand addition of 1% sodium to pure alumina results in the removal of all strong acid sites.

(2) Apparatus and Procedure

The reactions were carried out in a fixed bed flow type reactor. Five grams of alumina (4 × 4 mm cylindrical pellets) was placed in a Pyrex reaction tube of 25 cm long and 3 cm internal diameter. Above the catalyst bed Pyrex glass beads (4 mm diameter) were placed to a height of 5 cm. The tube was inserted into the furnace (a cylindrical steel tube of internal diameter 4 cm coated with thin layer of asbestos and wound uniformly with the nichrome wire) and heated electrically to the requisite temperature. α-Pinene was passed over the catalyst using a constant feed-rate syringe pump that could be operated at different feed rates.

The products of the isomerization were analyzed by gas chromatography using a Perkin–Elmer Vapor Fractometer Model 154-D with a thermal conductivity cell detector. Hydrogen was used as the carrier gas. Perkin–Elmer Column K consisting of 2 m column of Carbowax on Chromosorb was used. The column temperature for the best resolution within a reasonable time was found to be 115 °C with the hydrogen inlet pressure of 15 psig and flow rate of 112 cc/min. For the identification of different peaks in a chromatogram, retention times for the different compounds were found by introducing pure substances gifted generously by Hercules Powder Company, U.S.A.

For quantitative analysis exactly reproducible quantities of synthetic mixtures containing the different compounds in varying proportion were introduced and calibration curves relating the concentration with the peak heights were drawn. Since the peaks obtained were sharp and symmetrical, peak heights were used as a measure of concentration without any serious error. Initial experiments in which both peak heights and the total areas were compared using mixtures of known concentrations, gave identical results. Therefore, in subsequent work all analyses were based on comparison of peak heights.

Results and Discussion

Isomerization of α-Pinene

Effect of Sodium

Figure 1 shows the influence of sodium content of the catalyst on the distribution of products resulting from the isomerization of α-pinene. As can be seen from Fig. 1, a change in the sodium content of the catalyst markedly changes the distribution of products. With increasing amount of sodium in the catalyst the concentrations of camphene and dipentene in the product are increased at the expense of α- and γ-terpinenes. With a catalyst containing 1.5% sodium the isomerization product contained only camphene, tricyclene, dipentene, β-pinene, and terpinolene, the concentrations of the other products being reduced to zero.

Addition of sodium ions to pure alumina reduces the strength of its surface acidity (Table 1). A catalyst impregnated with 1% sodium has lost all the strong acid sites having pK_a values less than -5.7 originally present in pure alumina. It has been shown by a number of workers (*7a*, 8) that aluminas containing only weak acid sites do not promote secondary reactions. Based on this fact it may be concluded that camphene, tricyclene, β-pinene, dipentene, and terpinolene (the only products obtained from α-pinene over a catalyst containing 1.5% sodium) are the primary products of the isomerization of α-pinene.

Effect of Space–Time[3]

Figures 2, 3, and 4 illustrate the effect of space–time on the distribution of the reaction products over aluminas A, C, and E, respectively. As can be seen from Fig. 2, the concentrations of camphene, dipentene, terpinolene,

[3]Space–time = 1/WHSV; WHSV = the number of grams of α-pinene passed per gram of the catalyst per hour.

Can. J. Chem. Downloaded from www.nrcresearchpress.com by 210.87.254.6 on 09/05/12
For personal use only.

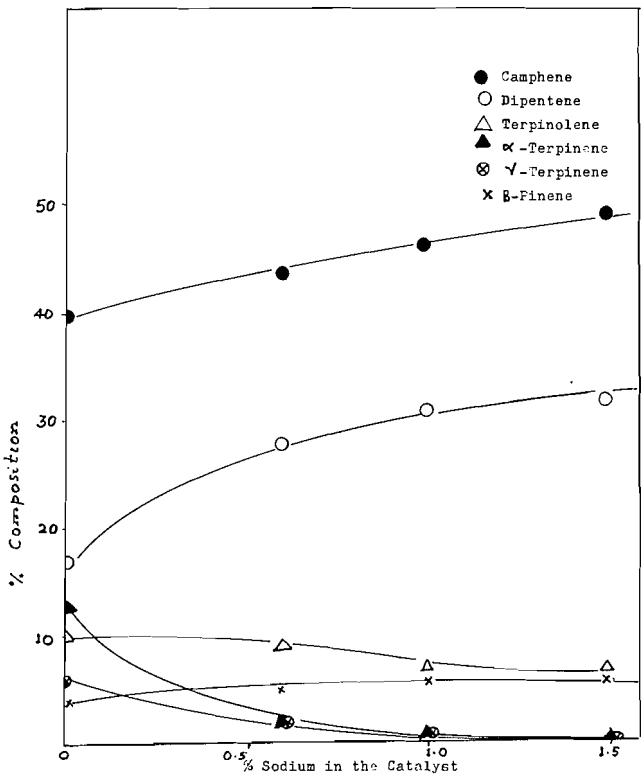

FIG. 1. Effect of sodium on the distribution of products of isomerization of α-pinene; temperature, 210 °C; WHSV, 1.

β-pinene, and tricyclene reach a maximum at a relatively low space–time and then fall rapidly with further increase in space–time. Also the rate of formation of camphene is appreciably faster. The concentrations of α- and γ-terpinenes increase with increasing space–time, the amount of α-terpinene being much higher than that of γ-terpinene. At high space–times, *p*-cymene and *p*-menthenes are formed and their concentrations continue to increase with space–time. Essentially the same reaction pattern is presented in Figs. 3 and 4. These results indicate that camphene, β-pinene, dipentene, tricyclene, and terpinolene are the primary isomerization products of α-pinene. α- and γ-terpinenes, and *p*-cymene and *p*-menthenes are secondary and tertiary products, respectively.

Carber *et al.* (9) from the results of their study of the kinetics of isomerization of α-pinene in the liquid phase in presence of cobalt molybdenite catalysts have shown that camphene and dipentene are the primary products. The results of the present investigation show that in addition to these two products, β-pinene, terpinolene, and tricyclene are also formed in the primary step.

Dipentene and terpinolene which are formed in the first step undergo subsequently a double bond isomerization to α- and γ-terpinenes. The terpinenes are then converted to *p*-cymene and *p*-menthene by disproportionation or by direct dehydrogenation. This is in accordance with the results of Hunter and Brogden (10) who from their studies of the kinetics of isomerization of dipentene in the presence of silica gel in the liquid phase showed that dipentene undergoes isomerization to α- and γ-terpinenes which are then converted to *p*-cymene and *p*-menthenes at high contact times.

β-Pinene can isomerize similarly over acid catalyst giving α-pinene, camphene, tricyclene, dipentene, and terpinolene (11). Camphene has been reported to yield tricyclene and bornylene in an equilibrium composition of 73% camphene, 24% tricyclene, and 3% bornylene in the presence of alumina catalysts (12). The decrease

Can. J. Chem. Downloaded from www.nrcresearchpress.com by 210.87.254.6 on 09/05/12
For personal use only.

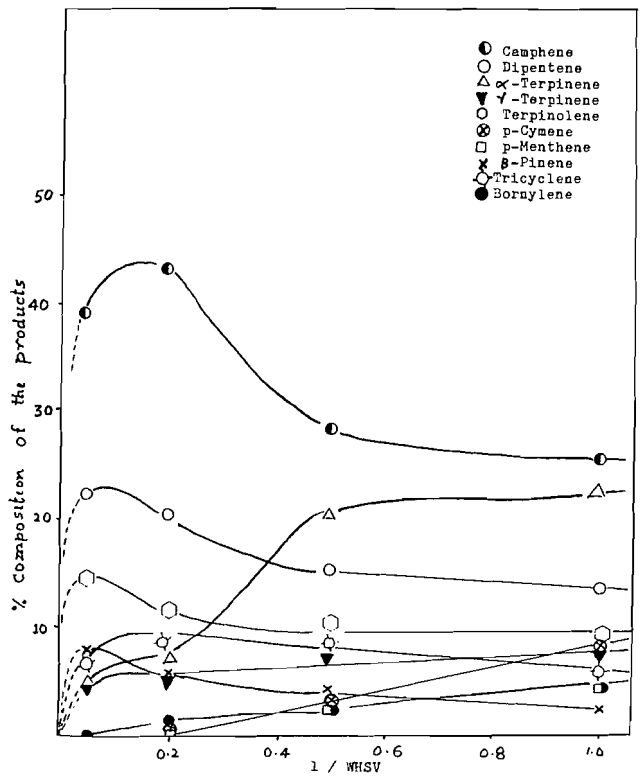

FIG. 2. Isomerization of α-pinene over alumina A. Influence of space–time; temperature, 235 °C.

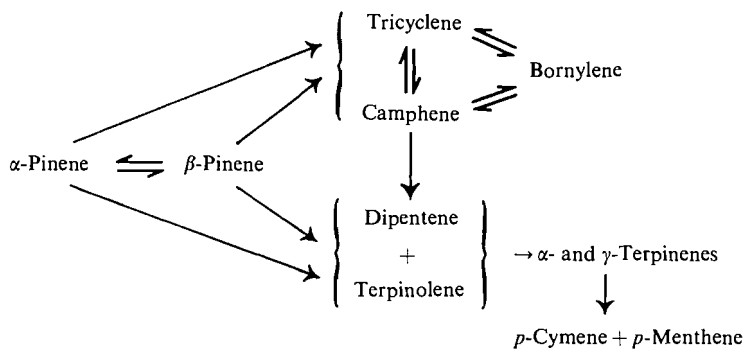

SCHEME 1

in concentration of camphene at high space–times after a maximum at a relatively low space–time over strongly acidic aluminas shows that camphene undergoes further reaction over these catalysts.

The sequence shown in Scheme 1 may, therefore, be proposed for the isomerization of α-pinene.

Isomerization of Camphene and Tricyclene

The reactions of camphene and tricyclene were studied separately under similar conditions of the isomerization of α-pinene in order to obtain further support to the kinetic sequence proposed for the isomerization of α-pinene.

Table 2 gives the results obtained from the reactions of camphene over different alumina

Can. J. Chem. Downloaded from www.nrcresearchpress.com by 210.87.254.6 on 09/05/12
For personal use only.

Can. J. Chem. Downloaded from www.nrcresearchpress.com by 210.87.254.6 on 09/05/12
For personal use only.

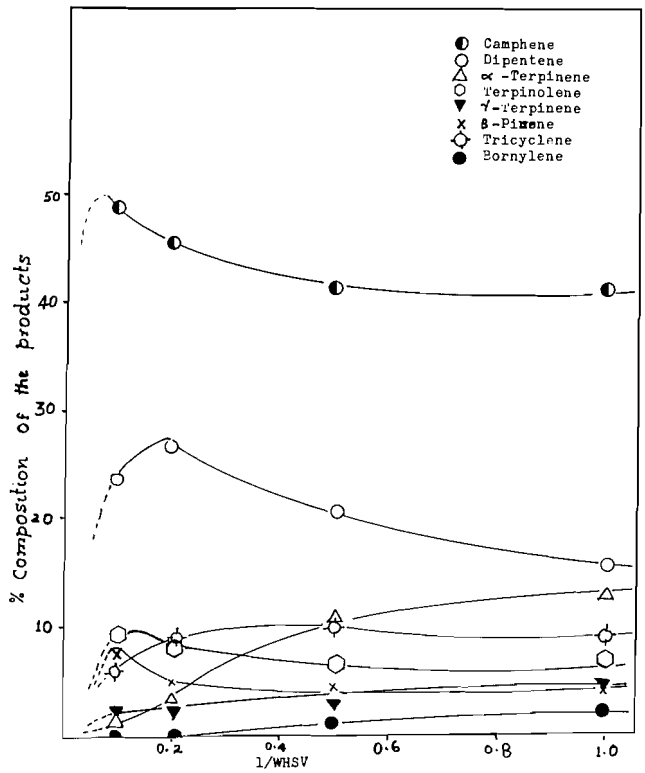

FIG. 3. Isomerization of α-pinene over alumina C. Influence of space–time; temperature, 235 °C.

TABLE 2. Isomerization of camphene. Catalyst type and reactivity; temperature, 250 °C; WHSV, 1

Catalyst	% camphene reacted	% composition of the products		
		Tricyclene	Monocyclics	Bornylene
Alumina C	24	90	0	10
Alumina A	32	70	17	13
Alumina E	49	46	40	14

catalysts. As can be seen from Table 2 the extent of camphene undergoing isomerization increases from 24 to 49% in going from the weakly acidic sodium doped alumina to the strongly acidic HF treated alumina. It appears also from Table 2 that over weakly acidic sodium doped catalyst (alumina C) camphene does not undergo conversion to monocyclic products but undergoes isomerization to only tricyclene and bornylene. Over strongly acidic HF treated alumina (alumina E) it undergoes ring opening giving monocyclic products which include dipentene, terpinolene, α- and γ-terpinenes, *p*- and *m*-cymenes and menthenes.

Another notable feature of the results presented in Table 2 is that the concentration of tricyclene in the product decreases and that of monocyclic products increases with increasing acid strength. Thus the concentration of tricyclene decreases from 90 to 46% and that of monocyclics increases from 0 to 40% in going from the weakly acidic sodium doped alumina (alumina C) to the strongly acidic HF treated alumina (alumina E).

Table 3 presents the results obtained by subjecting tricyclene to isomerization over various alumina catalysts. The amount of tricyclene undergoing reaction increases from 77 to 87%

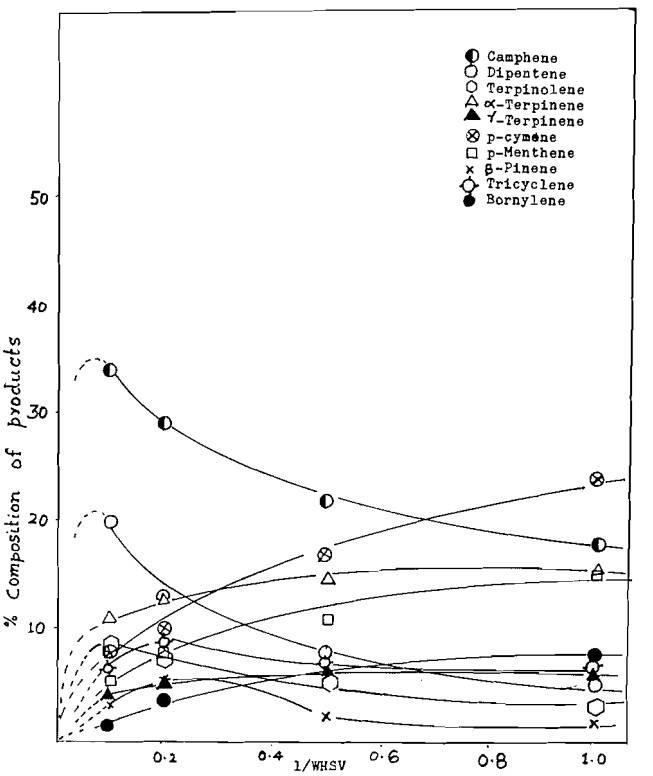

FIG. 4. Isomerization of α-pinene over alumina E. Influence of space–time; temperature, 235 °C.

TABLE 3. Isomerization of tricyclene. Catalyst type and reactivity; temperature, 250 °C; WHSV, 1

Catalyst	% tricyclene reacted	% composition of the products		
		Camphene	Monocyclics	Bornylene
Alumina C	77	96	0	4
Alumina A	80	85	7	8
Alumina E	87	40	45	15

in going from the weakly acidic sodium containing alumina to the HF treated alumina having strong acid sites. Also over the sodium doped alumina tricyclene does not undergo conversion to monocyclic products, but isomerizes to give only camphene and bornylene. In going from sodium doped alumina to HF treated alumina catalyst the amount of camphene in the product decreases from 96 to 40% while that of monocyclic products increases from 0 to 45%.

A comparison of the results in Tables 2 and 3 shows that for a given catalyst at constant temperature and space velocity, tricyclene is more reactive than camphene. Thus, while 80% of tricyclene undergoes reaction over alumina A at 250 °C, only 32% of camphene reacts under similar conditions. This is not surprising in view of the greater strain in the molecule of tricyclene.

The following conclusions can be drawn from these results: (*1*) Over weakly acidic sodium doped catalyst both camphene and tricyclene undergo interconversion but do not isomerize to monocyclic products. (*2*) The extent of interconversion decreases with increasing acid strength. (*3*) Strong acid sites are necessary for

Can. J. Chem. Downloaded from www.nrcresearchpress.com by 210.87.254.6 on 09/05/12
For personal use only.

TABLE 4. Effect of pyridine poisoning on the isomerization of camphene; temperature, 250 °C; WHSV, 1

Feed	Catalyst: alumina A				Catalyst: alumina E			
	% camphene reacted	% composition of the products			% camphene reacted	% composition of the products		
		Tricyclene	Bornylene	Monocyclics		Tricyclene	Bornylene	Monocyclics
Camphene	32	70	13	17	49	40	13	47
Camphene + Pyridine (5% wt)	26	92	8	0	30	75	10	15

TABLE 5. Effect of pyridine poisoning on the isomerization of tricyclene; temperature, 250 °C; WHSV, 1

Feed	Catalyst: alumina A				Catalyst: alumina E			
	% tricyclene reacted	% composition of the products			% tricyclene reacted	% composition of the products		
		Camphene	Bornylene	Monocyclics		Camphene	Bornylene	Monocyclics
Tricyclene	80	85	8	7	87	40	15	45
Tricyclene + Pyridine (5% wt)	51	95	5	0	65	77	7	16

the conversion of camphene and tricyclene to monocyclic products. (*4*) Tricyclene is more reactive than camphene.

The effect of pyridine on the reaction was studied with a view to ascertaining whether only the strong acid sites of the catalysts are involved in the conversion of camphene and tricyclene to monocyclic products. The reactions were carried out over HF treated alumina and pure alumina catalysts. The results obtained for camphene are presented in Table 4. The corresponding results for tricyclene are given in Table 5.

It is seen that pyridine, apart from reducing the activity of the catalyst for total isomerization, brings out marked decrease in the proportion of monocyclic products formed from both camphene and tricyclene. In the case of pure alumina the added pyridine (5% by weight) is sufficient to neutralize all strong acid sites and completely suppress the formation of monocyclic products. In the case of HF treated alumina the concentration of monocyclic products decreases from 47 to 15% by the addition of the same amount of pyridine. In this case the amount of pyridine added is probably not sufficient to neutralize all the strong acid sites. These results support the conclusion that strong acid sites are involved in the conversion of camphene and tricyclene to monocyclic products.

The effect of space–time on the isomerization of camphene and tricyclene over pure alumina and HF doped alumina has been studied in an attempt to arrive at the sequence of the reaction steps. The compositions of the products formed from camphene and tricyclene over HF treated alumina (alumina E) are plotted in Figs. 5 and 6 respectively, as a function of space–time.

As can be seen from Fig. 5 the amount of tricyclene formed from camphene reaches a maximum and falls rapidly with increasing space–time. Thus tricyclene is formed in the rapid initial stage and undergoes further isomerization to monocyclic products whose concentrations in the product increase with increasing space–time.

Starting with tricyclene (Fig. 6) the amount of camphene produced falls steadily with space–time after a maximum at low space–time region.

These results indicate that camphene and tricyclene undergo isomerization to monocyclic

Can. J. Chem. Downloaded from www.nrcresearchpress.com by 210.87.254.6 on 09/05/12
For personal use only.

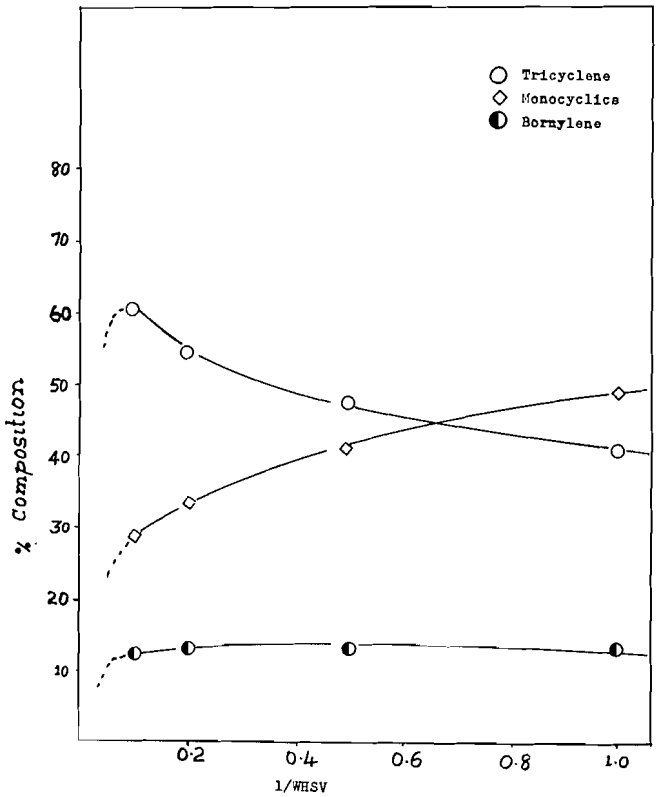

FIG. 5. Isomerization of camphene over alumina E. Influence of space–time; temperature, 250 °C.

products and interconversion simultaneously over acid catalysts (see Scheme 2).

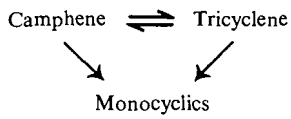

SCHEME 2

The change in the composition of monocyclic products with space–time is shown in Fig. 7. It is evident from Fig. 7 that the concentrations of dipentene and terpinolene in the product decrease while those of α- and γ-terpinenes increase with space–time. This indicates that dipentene and terpinolene are the first to be formed which then undergo double bond isomerization to α- and γ-terpinenes. At higher contact times *p*-cymene and menthene are formed. In general, the change in the composition of monocyclic products is similar to that observed in the case of the isomerization of α-pinene. The complete sequence of the reactions of camphene and tricyclene over alumina E may, therefore, be written as Scheme 3.

These results confirm the kinetic sequence suggested for the isomerization of α-pinene over strongly acidic alumina catalysts.

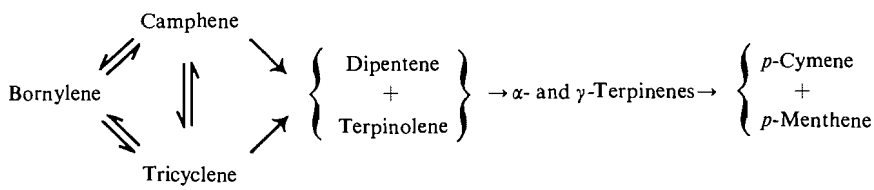

SCHEME 3

Can. J. Chem. Downloaded from www.nrcresearchpress.com by 210.87.254.6 on 09/05/12
For personal use only.

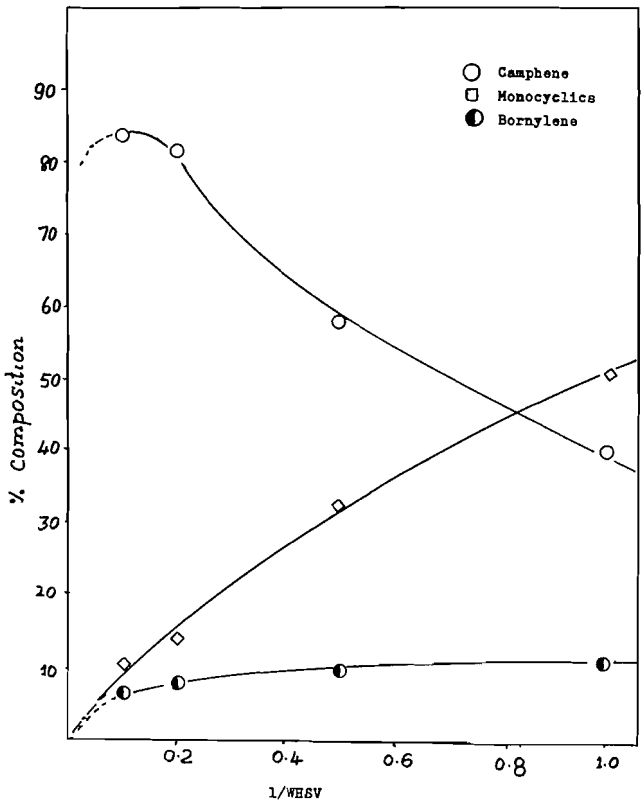

FIG. 6. Isomerization of tricyclene over alumina E. Influence of space–time; temperature, 250 °C.

Mechanism of Isomerization of α-Pinene over Alumina

It has been well established that alumina surface contains both Bronsted and Lewis acid sites. Several mechanisms have been proposed for the isomerization of olefins over solid acid catalysts. These include the carbonium ion theory of Whitmore (13) and hydrogen switch mechanism of Turkevich and Smith (14). In recent years Pines and Haag (15) have proposed that the isomerization proceeds through an intermediate π-complex of the olefin and a proton from the catalyst. All these mechanisms assume proton addition to the olefin double bond accompanied by a subsequent or simultaneous proton elimination from another part of the carbonium ion thus formed.

Carbonium ions on the surface of solid acid catalysts have been identified by Leftin and Hermana (16).

Osaki and Kimura (17) have suggested a proton donor–acceptor mechanism for butene isomerization over solid acid catalysts, either the Bronsted acid sites on the surface of the catalysts or the carbonium ions formed by the adsorption of olefins on Lewis acid sites serving as proton donors.

The isomerization of α-pinene over alumina catalysts will be interpreted in terms of carbonium ions adsorbed on the surface of the catalyst.

The isomerization of α-pinene proceeds via two parallel directions one giving bi- and tricyclic products (camphene, β-pinene, and tricyclene) and the other giving rise to monocyclic products (dipentene, terpinolene, α-terpinene, and γ-terpinene).

The direction of the reaction is determined by the nature of orientation of α-pinene molecule to the surface of the catalyst. α-Pinene can be adsorbed on the catalyst surface in three ways, as shown by structures **1**, **2**, and **3**.

In type **1** adsorption the acid site acts on the double bond on the side away from the *gem-*

Can. J. Chem. Downloaded from www.nrcresearchpress.com by 210.87.254.6 on 09/05/12
For personal use only.

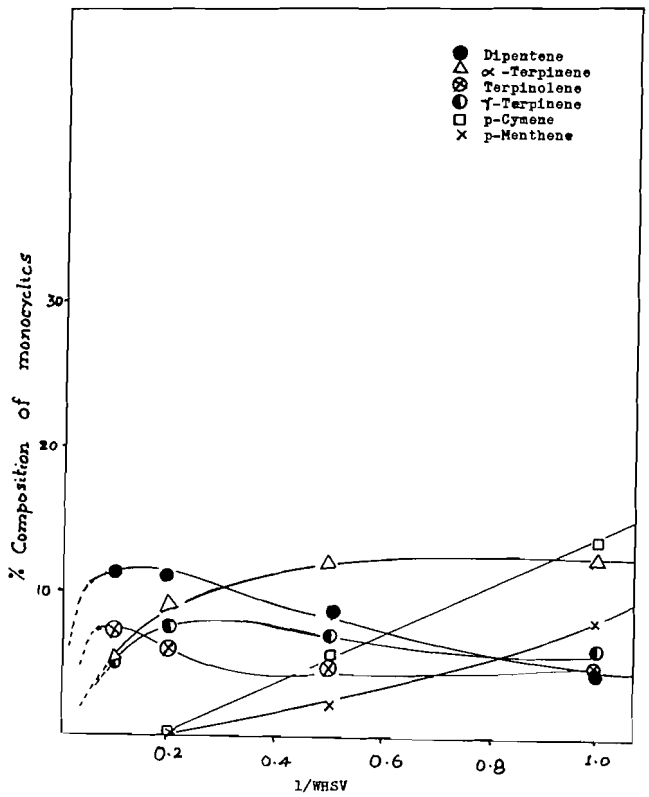

FIG. 7. Isomerization of camphene over alumina E. Influence of space–time on the distribution of monocyclic products; temperature, 250 °C.

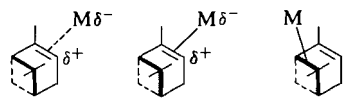

(M is an acid site in the catalyst surface)

dimethyl group because of its bulkiness. This mode of adsorption is sterically favored.

In type **2** the acid site acts on the double bond from the side of the *gem*-dimethyl group. This mode of adsorption is sterically unfavorable.

In type **3** the cyclobutane ring of α-pinene is attached to the acid site. This mode of adsorption will be favored within the pores of the catalyst.

According to Rudakov (18) if the double bond of α-pinene molecule is directed towards the surface of the catalyst bi- and tricyclic compounds are formed, while if the four-membered ring is directed towards the catalyst surface monocyclic products are formed.

Thus type **1** and **2** mode of adsorption must lead to the formation of bi- and tricyclic products. But due to steric reasons only the mode of adsorption corresponding to **1** can give rise to these products.

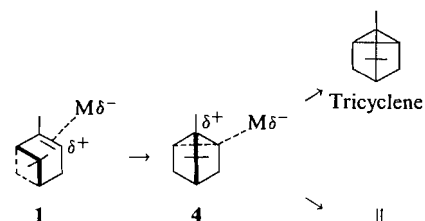

SCHEME 4

The formation of camphene and tricyclene from **1** can be represented by Scheme 4. The surface complex **1** is converted into camphene through the nonclassical ion **4**. This intermediate nonclassical ion is similar to that occurring in the well known isobornylchloride –

Can. J. Chem. Downloaded from www.nrcresearchpress.com by 210.87.254.6 on 09/05/12
For personal use only.

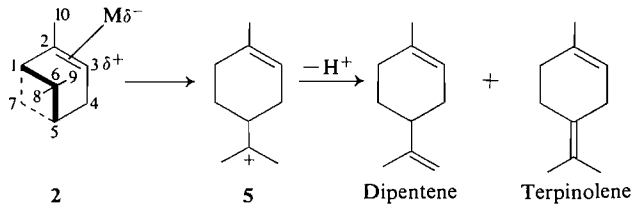

SCHEME 5

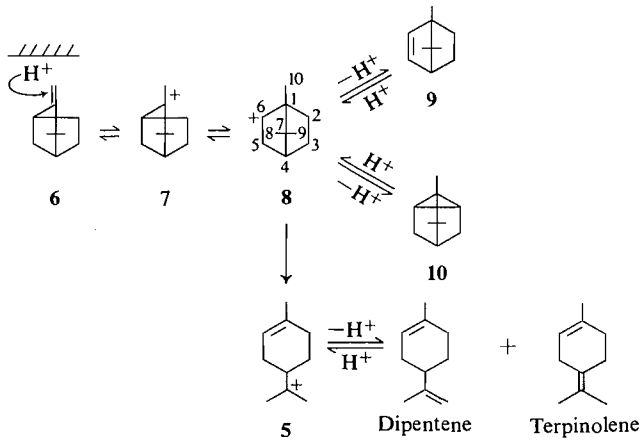

SCHEME 6

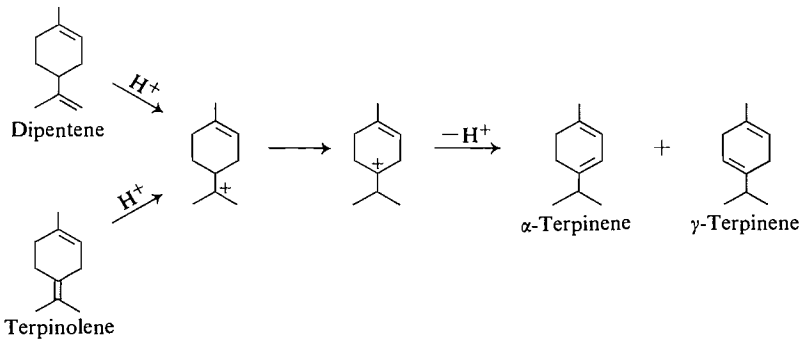

SCHEME 7

camphene interconversion. Analogous conversion from **2** is sterically hindered.

The formation of dipentene and terpinolene from α-pinene involves the bond rearrangements shown in Scheme 5. The bond between C-6 and -1 is ruptured resulting in the formation of the classical carbonium ion **5** which on subsequent proton elimination gives dipentene and terpinolene. The rupture of the C_6—C_1 bond of α-pinene molecule is favored by type **2** and **3** adsorptions.

The formation of dipentene and terpinolene from camphene and tricyclene may be represented by Scheme 6. The catalyst surface interacts with the double bond of camphene molecule (**6**) resulting in the formation of the carbonium ion (**7**). This carbonium ion rearranges to another carbonium ion (**8**) which with the elimination of a proton from C-5 forms bornylene (**9**). Elimination of a proton from C-2 results in the formation of tricyclene (**10**). Over strong acid sites the carbonium ion (**8**) re-

Can. J. Chem. Downloaded from www.nrcresearchpress.com by 210.87.254.6 on 09/05/12
For personal use only.

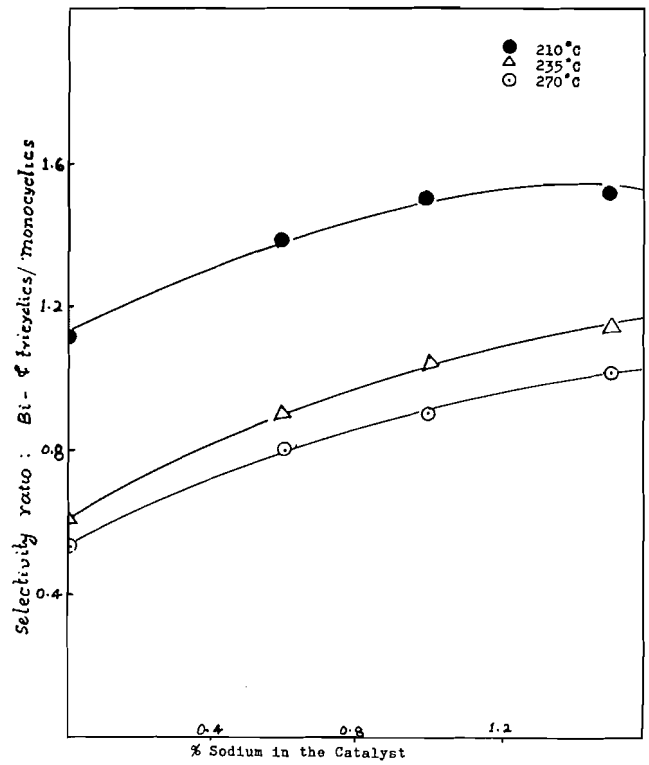

FIG. 8. Isomerization of α-pinene. Influence of sodium on the selectivity ratio.

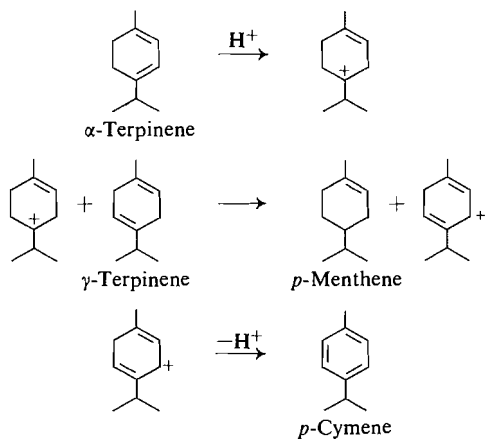

SCHEME 8

arranges to the monocyclic carbonium ion (**5**) by breaking of C_1—C_7 bond. Removal of a proton from **5** leads to the formation of dipentene and terpinolene.

α- and γ-terpinenes are formed from dipentene and terpinolene by further double bond isomerization as shown in Scheme 7.

p-Cymene and menthene are probably formed from α- and γ-terpinenes by disproportionation or hydrogen exchange (Scheme 8).

It has been shown by Tung and McInninch (19) that Lewis acid sites of alumina can catalyze dehydrogenation and hydrogenation reactions. *p*-Cymene may also be formed by direct dehydrogenation of α-terpinene by the Lewis acid sites of alumina (Scheme 9).

The Lewis acid site abstracts a hydride ion from α-terpinene molecule generating a carbonium ion. This then loses a proton to an adjacent oxide ion forming the dehydrogenated compound (*p*-cymene). The hydrogen liberated in this process may hydrogenate α- and γ-terpinenes to *p*-menthene.

Influence of Acid Strength of the Catalyst on the Selectivity Ratio

The influence of sodium on the selectivity ratio of bicyclic to monocyclic products is shown in Fig. 8. It is evident that the selectivity ratio increases with increasing sodium content

Can. J. Chem. Downloaded from www.nrcresearchpress.com by 210.87.254.6 on 09/05/12
For personal use only.

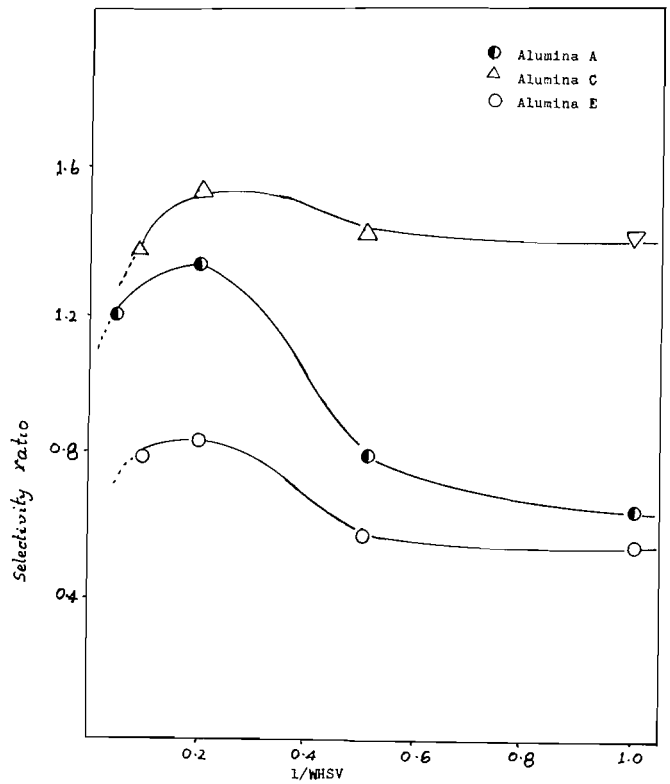

FIG. 9. Isomerization of α-pinene. Influence of space–time on the selectivity ratio; temperature, 235 °C; WHSV, 1.

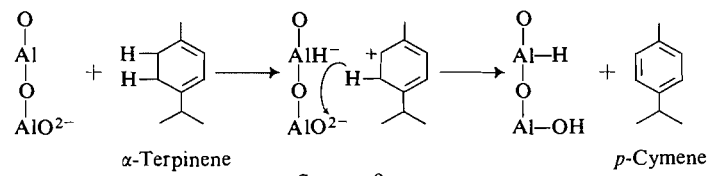

SCHEME 9

of the catalyst. This means that the rates of the two paths of the reaction one giving bi- and tricyclics (camphene, β-pinene, and tricyclene) and the other giving monocyclics (dipentene and terpinolene) depend on the sodium content or in other words the acidic strength of the catalyst. This may be due to three factors which may act separately or jointly depending on the conditions:

(*1*) The strong acid sites of the catalyst may cause an increase in the type **2** adsorption despite the steric hinderance and thus lead to the formation of more monocyclics.

(*2*) The strong acid sites of the catalyst may cause further isomerization of bicyclic products to monocyclics and thus bring about an increase in the amount of monocyclics.

(*3*) The substance (sodium or HF) added to the catalysts, in order to decrease or increase their acid strength may modify the structure and texture of the catalyst. The changes in the texture of the catalyst may affect the nature of orientation of the molecules to the surface. The narrow pores of alumina and modified alumina catalysts can act as a pseudo-solvent (20). Within the narrow pores an attack on the cyclobutane ring may take place leading to the formation of monocyclics.

Rudakov and Ivanova (21) have recently shown that the course of the reaction (in the

Can. J. Chem. Downloaded from www.nrcresearchpress.com by 210.87.254.6 on 09/05/12
For personal use only.

liquid phase) does not depend on the pore structure of the catalyst.

The acid strength of the catalyst is, therefore, the major factor in deciding the course of the reaction. The next question to answer is whether the strong acid sites of alumina cause the observed change in the selectivity ratio by mechanism *1* or *2*.

The results of the influence of contact time on the selectivity ratio (Fig. 9) suggest that mechanism *2* is mainly operative.

Over strongly acidic alumina catalysts the selectivity ratio of bicyclic to monocyclic products increases, reaches a maximum and then decreases rapidly with increasing contact time. On the other hand over weakly acidic sodium doped alumina there is not much fall in the selectivity ratio after reaching the maximum even at high contact times. This means that over catalysts having strong acid sites further conversion of the bi- and tricyclic products (camphene and tricyclene) to monocyclic products occurs. This is further supported by the results of the study of the reaction of camphene and tricyclene over various alumina catalysts under similar conditions. Mechanism *1* may also contribute partly to the formation of monocyclic products by favoring type **2** adsorption on the strong acid sites.

We wish to thank the Council of Scientific and Industrial Research for financial help.

1. P. DESIKAN and L. M. YEDDANAPALLI. J. Sc. Ind. Res. **21B**, 116 (1962).
2. L. M. XAVIER, J. VERGHESE, and L. M. YEDDANAPALLI. Symposium on Contact Catalysis, Calcutta, India. 1956.
3. J. VERGHESE and L. M. YEDDANAPALLI. J. Sc. Ind. Res. **16B**, 224 (1957).
4. A. STANISLAUS. Ph.D. Thesis. Madras University, Madras, India. 1967.
5. V. KRISHNASAMY. Ph.D. Thesis. Madras University, Madras, India. 1968.
6. H. PINES and W. O. HAAG. J. Am. Chem. Soc. **82**, 2471 (1960).
7. (*a*) H. PINES and W. O. HAAG. J. Am. Chem. Soc. **83**, 2487 (1961). (*b*) H. A. BENESI. J. Phys. Chem. **61**, 970 (1957).
8. H. PINES and C. N. PILLAI. J. Am. Chem. Soc. **83**, 3270 (1961).
9. V. P. WYSTRACH, L. H. BARNUM, and H. GARBER. J. Am. Chem. Soc. **79**, 5786 (1957).
10. G. L. K. HUNTER and W. B. BROGDEN. J. Org. Chem. **28**, 1679 (1963).
11. P. RATANASAMY and L. M. YEDDANAPALLI. Unpublished results.
12. H. PINES, C. N. PILLAI, and K. WATANABE. J. Am. Chem. Soc. **84**, 3934 (1962).
13. F. C. WHITMORE. Chem. Eng. News, **26**, 668 (1948).
14. J. TURKEVICH and R. K. SMITH. J. Chem. Phys. **16**, 466 (1948).
15. H. PINES and W. O. HAAG. J. Am. Chem. Soc. **82**, 2488 (1960).
16. H. P. LEFTIN and T. E. HERMANA. Proceedings of the Third International Congress on Catalysis, Amsterdam. **I**, 31 (1964).
17. A. OSAKI and K. KIMURA. J. Catal. **3**, 395 (1964).
18. G. A. RUDAKOV. Chemistry and technology of camphor. Moscow-Leningrad, 1961.
19. S. E. TUNG and MCINNINCH. Proceedings of the Third International Congress on Catalysis, Amsterdam. I, 42 (1964).
20. H. PINES and J. MANASSEN. Adv. Catal. **16**, 49 (1966).
21. G. A. RUDAKOV and L. S. IVANOVA. Dok. Akad. Nauk. SSSR. **163**, 113 (1965).

Can. J. Chem. Downloaded from www.nrcresearchpress.com by 210.87.254.6 on 09/05/12
For personal use only.

Chlorocuprate(II) and Chlorocobaltate(II) Salts of the Aminodiphenylphosphonitrileaminodiphenylphosphonium Ion

R. M. CLIPSHAM[1] AND M. A. WHITEHEAD[2]

Department of Chemistry, McGill University, The Royal Institution for the Advancement of Learning, P.O. Box 6070, Montréal 110, Québec

Received April 22, 1971

Two new compounds $[NH_2(C_6H_5)_2PNP(C_6H_5)_2NH_2]_2[CoCl_4]$ and $[NH_2(C_6H_5)_2PNP(C_6H_5)_2NH_2][CoCl_4]CH_2Cl_2$ have been isolated, and characterized by spectrometry, as examples of the general series of quaternary amine transition metal chloride salts. Three other compounds containing the same cations, with empirical formulae, $CuP_2N_3C_{25}H_{32}OCl_3$ (**1**), $CuP_2N_3C_{24}H_{28}Cl_3$ (**2**), and $Cu_3P_4N_6C_{50}H_{64}O_2Cl_8$ (**3**) have been isolated and studied by spectrometry. The formulae $[NH_2(C_6H_5)_2PNP(C_6H_5)_2NH_2]_2[Cu_2Cl_6]$ and $[NH_2(C_6H_5)_2PNP(C_6H_5)_2NH_2]_2[Cu_2Cl_6]$. $2CH_3OH$ are proposed for (**2**) and (**1**) by comparison with the cobalt compounds, and interpretation of the electronic structure. These compounds were produced during attempts to synthesize mixed ring compounds of (PN) and (SN) units.

Deux nouveaux composés $[NH_2(C_6H_5)_2PNP(C_6H_5)_2NH_2]_2[CoCl_4]$ et $[NH_2(C_6H_5)_2PNP(C_6H_5)_2NH_2][CoCl_4]CH_2Cl_2$ ont été isolés et caractérisés par spectrométrie; ils appartiennent à la série générale des sels des chlorures des métaux de transition et des amines quaternaires. Trois autres composés contenant les mêmes cations, et ayant pour formule empirique, $CuP_2N_3C_{25}H_{32}Cl_3$ (**1**), $CuP_2N_3C_{24}H_{28}Cl_3$ (**2**) et $Cu_3P_4N_6C_{50}H_{64}O_2Cl_8$ (**3**) ont été isolés et étudiés par spectrométrie. Les formules $[NH_2(C_6H_5)_2PNP(C_6H_5)_2NH_2]_2[Cu_2Cl_6]$ et $[NH_2(C_6H_5)_2PNP(C_6H_5)_2NH_2]_2[Cu_2Cl_6]$. $2CH_3OH$ ont été proposées pour les composés (**2**) et (**1**), par comparaison avec les composés du cobalt et par l'interprétation de la structure électronique. Ces composés ont été fabriqués pendant l'essai de synthèse de composés à cycle mixte des unités (PN) et (SN).

Canadian Journal of Chemistry, **50**, 75 (1972)

Introduction

In the course of research into the possibility of producing mixed rings containing PN and SN units (1), the cation $[NH_2(C_6H_5)_2PNP(C_6H_5)_2NH_2]^+$ was studied. Models of the cation, showed that the amino groups could be oriented "*cis*" or "*trans*" with no "visible" preference. For a "*trans*" orientation, formation of a linear chain would be more likely than the formation of a ring. (Preliminary X-ray analysis of the molecular structure published subsequent to these studies confirms a "*trans*" orientation (2).) Coordination of both amino groups of a single molecule to an appropriate transition metal atom would lock the NPNPN skeleton into a ring structure, and this chelate could then react with a suitable sulfur compound to substitute a sulfur atom for the metal and form a mixed ring. The positive charge of the phosphonitrile could hinder coordination to another positively charged species. To minimize this possibility, initial chelate formation attempts were made with copper(II) salts. When crystalline solids were isolated, reactions with other transition metal salts were also investigated. Only copper(II) and cobalt(II) chloride compounds were obtained. Subsequent characterization of these indicated they were not the chelates desired, but salts containing the phosphonitrile cations and cobalt(II) or copper(II) chloride anions.

$$[H_2N(C_6H_5)_2PNP(C_6H_5)_2NH_2]Cl + \underset{CuCl_2}{CoCl_2} \text{ or } \rightarrow \begin{matrix} \text{A, } L_2Cu_2Cl_6 \cdot 2CH_3OH \\ \text{B, } L_2Cu_2Cl_6 \\ \text{C, } L_2Cu_3Cl_8 \cdot 2CH_3OH \\ \text{D, } L_2CoCl_4 \\ \text{E, } L_2CoCl_4 \cdot CH_2Cl_2 \end{matrix}$$

[1]Present address: Dawson College, Montréal, Québec.

[2]Present address: University Chemical Laboratories, Lensfield Road, Cambridge CB2-1EW, England.

Can. J. Chem. Downloaded from www.nrcresearchpress.com by 210.87.254.5 on 09/05/12
For personal use only.

TABLE 1. Comparison of analytical results found and calculated for copper(II) and cobalt(II) chlorides of $[NH_2(C_6H_5)_2PNP(C_6H_5)_2NH_2]^+$*

Compound	Analysis, %						
	Cu or Co	P	N	Cl	C	H	O
A	10.36	9.87	7.28	17.4	48.7	4.48	2.61
B	10.87			18.2			
C	13.94	8.81	6.20	20.5	43.7	4.01	2.68
$CuLCl_3$	10.84	10.57	7.17	18.14	49.18	4.10	0
$CuLCl_3 \cdot 2H_2O$	10.21	9.96	6.75	17.09	46.33	4.51	5.14
$CuLCl_3 \cdot CH_3OH$	10.28	10.02	6.80	17.20	48.58	4.54	2.59
$Cu_3L_2Cl_8$	14.59	9.48	6.43	21.70	44.12	3.68	0
$Cu_3L_3Cl_8 4H_2O$	13.83	8.98	6.08	20.57	41.81	4.07	4.64
$Cu_3L_2Cl_8 \cdot 2CH_3OH$	13.91	9.04	6.13	20.69	43.83	4.09	2.34
D	5.61	11.6	8.26	14.2	54.6	4.88	<0.5
E	5.23	11.0	7.65	18.2	52.4	4.95	<0.5
CoL_2Cl_4	5.70	11.99	8.13	13.72	55.80	4.65	0
$CoL_2Cl_4 \cdot H_2O$	5.61	11.78	7.99	13.49	54.85	4.76	1.52
$CoL_2Cl_4 \cdot CH_3OH$	5.53	11.63	7.89	13.31	55.25	4.89	1.50
$CoL_2Cl_4 \cdot CH_2Cl_2$	5.27	11.08	7.51	19.02	52.64	4.48	0
$CoLCl_3$	10.05	10.65	7.23	18.28	49.57	4.13	0

*$L^+ = [NH_2(C_6H_5)_2PNP(C_6H_5)_2NH_2]^+$.

Experimental

All starting materials were reagent grade. The Cu(II) and Co(II) chlorides were dried Fisher reagent grade salts, $CuCl_2 \cdot 2H_2O$ and $CoCl_2 \cdot XH_2O$, and were kept at 120 °C for several hours and stored over silica gel.

Aminodiphenylphosphonitrileaminodiphenylphosphonium Chloride

$[NH_2(C_6H_5)_2PNP(C_6H_5)_2NH_2]Cl$ was prepared from the controlled ammonolysis of diphenyltrichlorophosphorane in chloroform solution (3). Diphenyltrichlorophosphorane was prepared by chlorination of diphenylchlorophosphine in controlled ratio in carbontetrachloride.

Reactions of Aminodiphenylphosphonitrileaminodiphenylphosphonium Chloride with Transition Metal Halides

Initial attempts to use other salts of copper(II), the nitrate, sulfate, and bromide, in a similar preparation to that for compounds of the phosphonitrile and copper(II) chloride, were unsuccessful; only copper(II) chloride in either dried or hydrated form resulted in "complex" formation. This was also found for cobalt(II) salts. Similar preparative attempts were unsuccessful for hydrated chlorides of iron(III), iron(II), chromium(III), nickel(II), and anhydrous zinc(II) chloride. No other preparative method was tried.

Copper(II) Compounds[3]

A, ($CuLCl_3 \cdot CH_3OH$): crystallized from methanol solution; 2.0 g (0.0044 mol) LCl and 0.57 g (0.0042 mol) dried $CuCl_2$ were added to enough methanol to just dissolve the combined substances, and the green solution warmed to 60 °C. Then anhydrous diethylether was added slowly, until the point of cloudiness. The solution was allowed to stand until red-green plates formed, which were filtered, washed with a mixture of methanol and ether, and stored in methanol atmosphere. A slight excess of LCL must be present for reprecipitation from methanol.

B, ($CuLCl_3$): prepared by heating powdered samples of A at 100 °C until constant weight, or by precipitation from acetonitrile or methylene chloride as for A. Yellow-gold needles or plates precipitated from orange solution and were filtered, washed in a mixture of solvent and ether, then in ether to dry, and stored over silica gel. A slight excess of LCL must be present for reprecipitation from methylene chloride or acetonitrile.

C, ($Cu_3L_2Cl_8 \cdot 2CH_3OH$): precipitated from methanol as for A, using a 1:2 molar ratio of LCL:dried $CuCl_2$. Red needle clusters obtained were filtered, washed in a methanol–ether mixture, and stored in methanol atmosphere. The substance lost methanol when heated to 100 °C, but the product did not melt sharply. From i.r. analysis, it was a mixture of B and another substance which was not anhydrous copper(II) chloride.

Cobalt(II) Compounds

D, (CoL_2Cl_4): precipitated from methanol solution of LCl and dried $CoCl_2$ as for A (1:1 molar ratio). Royal blue diamonds formed which were filtered, washed with a mixture of methanol and ether, then ether to dry, and stored over silica gel.

E, ($CoL_2Cl_4 \cdot CH_2Cl_2$): precipitated from methylene chloride solution as for A (1:1 molar ratio). Turquoise needles or plates were obtained and stored over silica gel at room temperature without decomposition from loss of methylene chloride. When heated above 90 °C, E lost methylene chloride to become D.

The analytical results for these molecules are given in Table 1.

Copper(II) and Cobalt(II) Chlorides of Aminodiphenylphosphonitrileaminodiphenylphosphonium Ion

The phosphonitrile cation, $[NH_2(C_6H_5)_2PNP(C_6H_5)_2NH_2]^+$, is designated L^+, and the phosphonitrile chloride as LCl. The copper compounds are referred to as A, B, and C;

[3]Empirical formulae: $L = P_2N_3C_{24}H_{24}$. The phosphonitrile cation is referred to as L^+ and the chloride as $LCl \equiv [NH_2(C_6H_5)_2PNP(C_6H_5)_2NH_2]Cl$.

Can. J. Chem. Downloaded from www.nrcresearchpress.com by 210.87.254.5 on 09/05/12
For personal use only.

Can. J. Chem. Downloaded from www.nrcresearchpress.com by 210.87.254.5 on 09/05/12
For personal use only.

and the cobalt compounds as D and E, following the outline and formulae in the experimental section.

There has been one report of complex chelate formation (52), $[N_6P_6(NMe_2)_{12}Cu^{II}Cl]^+$ Cu^ICl_2, but none from phosphonitrile chlorides; however, a blue compound, $Cu(NH(C_6H_5)_2PNP(C_6H_5)_2NH)_2$ (m.p. 178–180 °C with decomposition), prepared from methanol solution of the ionic phosphonitrile and $CuCl_2 \cdot 2H_2O$, has been reported (4). After treatment with sodium methoxide, a green precipitate was obtained which became the copper compound on hydrolysis. It was insoluble in water and could be crystallized from polar organic solvents or benzene.

When compounds are formed by an amino group nitrogen atom coordinating to copper(II) or cobalt(II) halides, they usually contain polymeric distorted octahedral copper(II), and octahedral or tetrahedral cobalt(II) in a non-ionic structure (5–8). Cobalt(II) halides form complex ionic compounds for some ligands, particularly at low metal : ligand ratios, where the cations are ligand-coordinated cobalt(II) ions and the anions are tetrahedral tetrachlorocobaltate(II) (9). Similar behavior occurs for copper(II) halides (10, 11).

The donor properties of positively charged ligand quaternary amines and phosphines have been studied (11–14), and it has been suggested that a positive charge on a ligand does not necessarily prevent its coordination to a positively charged metal ion, but may stabilize unusual stoichiometries and structures. Tetracoordinate cobalt(II) and nickel(II) complexes containing monoquaternized ditertiary phosphines have been reported with stoichiometry $MX_2 \cdot \P X$, where ¶ is the monocharged phosphonium ion. Although these compounds are supposed to contain non-ionic monomeric transition metal species, they have high thermal stabilities and low solubilities in non-polar solvents, which has been attributed to high lattice energies from interaction of polar $\P^{\delta+}$–$MX_3^{\delta-}$ sites of neighboring units.

On the other hand, there are many examples of ionic compounds containing bulky quaternary amine (15, 16) or other cations (17) and transition metal halide anions, including tetracoordinate copper(II) and cobalt(II) chlorides (16, 18–21).

From the solubility, conductivity, and melting point characteristics, and the similarity of their electronic spectra to those of anionic copper(II) and cobalt(II) chlorides, it was concluded that the compounds prepared could be ionic compounds with $\P^{\delta+}MX_3^{\delta-}$ structure. However, the pseudo-tetrahedral "polarized" phosphonium $MX_2\P X$ structure might occur.

Physical and Chemical Properties

The compounds were soluble in polar, and insoluble in non-polar organic solvents. In aqueous solution, or in wet organic solvents, decomposition occurred with formation of the phosphonitrile chloride and octahedral aquo copper(II) or cobalt(II) ions. Decomposition also occurred in pyridine, with formation of the phosphonitrile chloride and copper(II) or cobalt(II) pyridine complexes.

The solid state copper(II) compounds exhibited color changes on variation of temperature. For example, B changed from brown, through gold, to yellow as the temperature was lowered from the melting point, 430 °K, to 77 °K. The change was gradual, with no evidence of a sharp transition. Single crystals of all the copper(II) compounds were pleochroic: viewed in one direction, plates of A appear green-brown, while in perpendicular view, they are deep red.

TABLE 2. *g*-Values from electron paramagnetic resonance measurements for some copper(II) chloride compounds

	Compound*	*g*-Value† 294 °K	*g*-Value† 124 °K
A	$CuLCl_3 \cdot CH_3OH$	2.098	2.092
B	$CuLCl_3$	2.107	2.113
C	$Cu_3L_2Cl_8 \cdot 2CH_3OH$	2.096	2.094
	Dried $CuCl_2$	2.096	2.089

*Empirical formulae, $[NH_2(C_6H_5)_2PNP(C_6H_5)_2NH_2]^+ = L^+$; polycrystalline.

†A varian spectrometer, V4500-10A was used for these measurements on both the solid state and solution. Samples were contained in dried, sealed quartz tubes 4 mm diameter. The limit of error in the *g*-value is ±0.005 from 3 measurements per sample for duplicate samples. No signal was detected for A, B, or C in any solvent.

Conductance measurements indicated B was more ionic than the phosphonitrile chloride (22) in nitrobenzene. However, solvation occurred to a varying extent for all compounds. For each metal ion, the same solution spectrum was obtained for all compounds, and because of their insolubility in solvents with low coordination (23), no further conductance studies were attempted.

Spectrometric Results

(1) ^{35}Cl Nuclear Quadrupole Resonance (1): Solid samples of all molecules were scanned through 9–54 MHz. No interactions were detected.

(2) Electron Paramagnetic Resonance: See Table 2.

(3) Infrared Spectra: Few changes in solid state or solution spectra occur on compound formation. Those which are observed are minor shifts or "splitting" of bands assigned to phosphonitrile amino or P—NH_2 group vibrations, which could be attributable to a solvent shift or crystal packing effect (24).

(4) Ultraviolet, Visible, and Near-infrared Spectra: Dried $CuCl_2$ and $CoCl_2$ were insoluble in methylene chloride or nitromethane. All cobalt(II) and copper(II) compounds were soluble in both solvents, and in the absence of moisture no changes in their solution spectra occurred during periods of 2 h. Tables 3, 4, and 5.[4]

Discussion

1. *Empirical Formulae*

From solution i.r. spectra of A and C, the molecules are probably methanolates.

[4]Footnote to Tables 3, 4 and 5: Solution spectra were obtained using matched silica cells of 10 mm path length on a Beckman D.U. manual spectrometer, or a Unicam SP 800 recording spectrometer (13 500 – 47 500 cm^{-1}), and on the former, or a Perkin–Elmer 350 spectrophotometer (4 000–16 800 cm^{-1}), solvent permitting. Solid state spectra were obtained using Nujol mulls on Whatman no. 1 filter paper strips held in place by matched silica cells (26); a strip painted with Nujol was used as a reference. The spectra are qualitative since values of molar extinction coefficient cannot be calculated. However, this technique is as reproducible as reflectance measurements on powdered samples, and as useful for solid state spectra where samples can be ground sufficiently fine to make a good mull suspension.

TABLE 3. Electronic spectra of some cobalt(II) chlorides*

LCl (solution, CH_2Cl_2)	D, L_2CoCl_4 (solution, CH_2Cl_2)†	D, L_2CoCl_4 Solid	$(NH_4)_2CoCl_4$ (25) (solid)	$((C_4H_9)_4N)_2CoCl_4$ (15) (solid)
	6300–4500 (55_{av})	4545–6250	4250–6600	4780–5920
	14 500 (565)	14 550	14 450	14 300
	15 100 (535)	15 000	15 040	14 900
	15 750 sh	15 700 sh	15 500	15 750
	15 850 (385)	15 800	15 870	
	16 500 sh	16 250 sh	16 210 sh	16 230 sh
				17 300 sh
			18 182 sh	18 100 sh
	19 000 (5–10)	19 000 w	18 760	18 900
	23 000 (< 5)	23 000	22 220	22 000
			24 390	
36 340 (2240)‡	36 400 (2240)‡	36 230‡	31 250 sh	
37 200 (2890)	37 250 (2880)	37 200		
38 000 (2430)	38 100 (2380)	38 000		
38 950 sh	39 050 sh	sh		
		42 200	45 450	

*Positions of maximum absorption in cm^{-1} ($\pm 200\ cm^{-1}$); $L^+ \equiv [NH_2(C_6H_5)_2PNP(C_6H_5)_2NH_2]^+$; sh = shoulder, w = weak.
†Molar extinction coefficient in brackets based on formula L_2CoCl_4 (± 5 l/mol cm), values low compared with $CoCl_4^{2-}$ (15) because excess Cl^- not present.
‡Phenyl bands, 36 200–39 000 cm^{-1}.

TABLE 4. Electronic spectra of copper(II) chlorides; solid state, $L^+ \equiv [NH_2(C_6H_5)_2PNP(C_6H_5)_2NH_2]^+$*

A $LCuCl_3 \cdot CH_3OH$†	B $LCuCl_3$	C $L_2Cu_3Cl_8 \cdot 2CH_3OH$
10 500‡	10 000 sh§	9 800 sh‖
12 000 sh	12 500	12 100
18 600		18 800
23 800	22 700	23 600
¶	25 700 (w,sh)	25 600 (w,sh)
	27 000 (vw,sh)	¶
	32 000	
	36 400	
	37 500	
	¶	

*Position of maximum absorption in cm^{-1}; sh = shoulder, w = weak, vw = very weak.
†Empirical formulae.
‡Broad, slightly asymmetric to higher cm^{-1}.
§Very broad, at least two components, asymmetric to lower cm^{-1}, 9 000–14 000 cm^{-1} spread.
‖Intermediately broad, slightly asymmetric to lower cm^{-1}.
¶Higher energy components not distinguishable.

TABLE 5. Solution electronic spectrum of copper(II) compounds of $[NH_2(C_6H_5)_2PNP(C_6H_5)_2NH_2]^+$, L^+*

Maximum absorption, cm^{-1} A, B, or C	
11 300	slightly asymmetric to lower cm^{-1} broad band
17 500	
24 200	
31 600	
35 400	
37 200 }	phenyl bands
37 600 }	
39 100 sh	

*Methylene chloride solution; A, B, and C as in Table 4; sh = shoulder.

Melting point characteristics of A, C, and E also indicate these compounds are solvates. From a comparison of the analytical results (Table 1) the empirical formulae for A, B, and C are $CuLCl_3 \cdot CH_3OH$, $CuLCl_3$, and $Cu_3L_2Cl_8 \cdot 2CH_3OH$, respectively; and A and C are methanolates rather than hydrates. Empirical formulae concluded for D and E are less certain. Infrared spectra indicate neither is a methanolate. Low percent oxygen values for both compounds are also evidence that neither is a methonalate nor a hydrate. From its

Can. J. Chem. Downloaded from www.nrcresearchpress.com by 210.87.254.5 on 09/05/12
For personal use only.

Can. J. Chem. Downloaded from www.nrcresearchpress.com by 210.87.254.5 on 09/05/12
For personal use only.

analysis, E is most likely a solvate of methylene chloride, with the empirical formula $CoL_2Cl_4 \cdot CH_2Cl_2$; comparing spectral characteristics and other behavior with E, the empirical formula of D is CoL_2Cl_4.

2. Cobalt(II) Compounds; Ionic Type $[L]_2[CoCl_4]$

Solid state and solution electronic spectra for D and E indicate that the cobalt(II) species in both is tetracoordinate (Table 3). Comparison of the solid state spectra of D and E suggests that the latter contains a more distorted ligand arrangement. That is, the minor shifts in band shape observed are similar to those expected for a more "solvolyzed" structure (27). Given the empirical formula, CoL_2Cl_4, for D, the possibilities which must be considered for the solid state structure are: (*a*), $[CoL_2^{4+}][Cl^-]_4$; (*b*), a eutectic mixture of $CoLCl_3$ and LCl; and (*c*), $[L^+]_2[CoCl_4^{2-}]$; in a crystal lattice which is ionic ((*a*) or (*c*)) or pseudoionic (*b*). Possibility (*a*) is least likely because of the high formal charge of the cobalt cation, and can be ruled out because the major spectral changes which would be expected on solution do not occur. The electronic spectrum of pseudotetrahedral $CoCl_3$¶ where ¶ is a monoquaternized phosphine cation, has been described as very similar to that of tetrahedral $CoCl_4^{2-}$ (12). Thus, the electronic spectral evidence is consistent with either (*b*) or (*c*). Possibility (*b*) is less likely on the basis of i.r. spectra, since the solid state spectrum would then be a superposition of unchanged phosphonitrile chloride and the pseudotetrahedral complex spectra. This is not observed. Therefore the most likely structure for D is a lattice of phosphonitrile cations, and somewhat distorted tetrahedral $CoCl_4^{2-}$ anions. E can then be considered as a solvate containing methylene chloride "of crystallization", which further distorts the solid state $CoCl_4^{2-}$ anions from a strictly tetrahedral arrangement. A pentacoordinate cobalt(II) arrangement for E is not likely by comparison of its electronic spectrum with that reported for pentacoordinate arrangements (11). The relatively strong band expected at $\simeq 10\,500$ cm^{-1} is not observed.

3. Copper(II) Compounds; Ionic Type $[L]_2[Cu_2Cl_6]$

From the similarity to the cobalt compounds in their i.r. spectra and solubility, and the qualitative conductivity of B, the copper compounds are also ionic and possibly contain analogous copper(II) chloride anions. The same preparative system was used for monoalkylammoniumtetrachlorocuprates(II) (28) and acetamidinium tetrachlorocuprate(II) (29), which is chemical evidence for the ionic formulation as well as for the possible presence of tetracoordinate copper(II) anions.

Several tetracoordinate copper(II) chloride anions are known, and there is X-ray structural evidence for the existence of the types: discrete distorted tetrahedral, $CuCl_4^{2-}$ (20, 31–32); trigonal bipyramidal, $CuCl_5^{3-}$ (33), square planar ("long"-bonded, tetragonally distorted octahedral), $CuCl_4^{2-}$; and dimeric square planar, $Cu_2Cl_6^{2-}$ (34, 35). Electronic d–d bands and some charge-transfer bands observed for compounds containing these anions have been used to differentiate between possible arrangements. From comparison of the spectrum of B (or A, Table 4) with the spectra for these types (Table 6), it is apparent that neither is tetrahedral nor trigonal bipyramidal as the d–d bands occur at too high energies. The solid state electronic spectrum of A indicates the copper absorbing species is very similar to that which exists in methylene chloride in the absence of excess chloride ion, so that the copper species in compound A is probably a "solvated" form of that in B. Both solids probably contain square planar, or distorted square planar anions.

Thermochromic and pleochroic behavior similar to that observed for A, B, and C has been noted for solid state compounds containing tetragonal copper(II) chloride anions, either approximately square planar (29, 39–41), or distorted square planar, $Cu_2Cl_6^{2-}$ (38), and cited as evidence for the existence of this arrangement (29). However, dichroism has also been noted for compounds containing discrete flattened tetrahedral anions (19, 42). Thus, it is likely that the use of such behavior as a diagnostic tool is invalid.

The empirical formulae of A and B or C indicate that a discrete tetracoordinate anion arrangement, analogous to that proposed for D and E, does not occur, and that A and B, at least, are probably similar to the dimeric square planar compounds (Table 6).

The presence of a band at 18 500 – 18 800 cm^{-1} has been used to distinguish between dimeric

TABLE 6. Electronic spectra for some copper(II) chloride anions*

$CuCl_4^{2-}$ discrete tetrahedral (36)	$CuCl_5^{3-}$ bipyramidal (37)	$Cu_2Cl_6^{2-}$ dimeric square planar (38)	$CuCl_4^{2-}$ square planar (38)	B†
4 800				
5 550				
7 900	8 330–8 500‡	10 800–11 500 sh	10 500 sh	10 000 sh
9 050	9 900–10 200	12 900–12 500 †	12 800 †	12 500
23 000 sh		18 800–18 500		
24 800	23 800–24 400 sh	22 700–25 000	24 000	22 700
29 000	27 030–27 470	34 000 †	33 000 †	25 700
34 000				27 000
	39 060–37 000		38 500	
34 500		44 500		32 000
42 400		49 000	49 000	
R_2CuCl_4§ $R = Cs^+, R_4N^+$	$M(NH_3)_6CuCl_5$§ M(III) = Cr, Co	$RCuCl_3$§ $R = R_2NH_2^+ K^+, Cs^+$	R_2CuCl_4§ $R = RNH_3^+, NH_4^+$	

*Solid state; position of maximum absorption in cm^{-1}.
†See Table 4 for spectra of A, B, and C.
‡More intense.
§Compound type, empirical formulae.

($Cu_2Cl_6^{2-}$) and discrete ($CuCl_4^{2-}$) square planar arrangements being indicative of the former (38). On the "dimer" band basis, however, A (and C) should be considered to contain $Cu_2Cl_6^{2-}$ ions, and B should not. This is unlikely, considering the ease with which B and A can be interconverted in the solid state. It is more probable that a dimeric arrangement exists for both A and B, and the "dimer" band does not indicate the $Cu_2Cl_6^{2-}$ arrangement, but the distortion from square planar symmetry.

The possibility remains that instead of a lattice of discrete anions, a pseudotetrahedral system occurs, MX_2¶X as for the quaternary phosphines (11–14). Since the electronic spectra of the phosphines (11–14) resemble those of tetrahedral cobalt(II) and nickel(II) species, a pseudotetrahedrally coordinated metal ion structure has been proposed (11–14). A similar quaternary phosphine of copper(II) would be even more distorted from this arrangement, and might possess the d–d band spectra observed for A and B. However, the cobalt(II) and nickel(II) halides required rigorously anhydrous preparative conditions, as well as excess halide ion, quite different conditions from those used to prepare the copper(II) and cobalt(II) phosphonitrile compounds. Consequently, it is preferable to formulate B and A as the ionic compounds $[L^+]_2[Cu_2Cl_6^{2-}]$ and $[L^+]_2[Cu_2Cl_6^{2-}]\cdot 2CH_3OH$.

The Copper(II) Compound, $Cu_3L_2Cl_8\cdot 2CH_3OH$

The solid state electronic spectrum of C suggests that two forms of copper(II) could be present: both tetragonally distorted from square planar, one more so than the other. It is possible that C is a methanolate containing trimeric anionic groups $Cu_3Cl_8^{2-}$, analogous to the dimeric structures proposed for A and B. Such a compound would have a similar solid state electronic spectrum to A, with smaller components from copper(II), in a completely bridged environment. The latter would also be derived from square planar symmetry and this is consistent with the electronic spectrum of C. Considering the changes in the infrared spectra of the phosphonitrile cation, on replacement of the Cl^- counterion by $Cu_2Cl_6^{2-}$, similar changes to those observed would be expected on replacement of the Cl^- by $Cu_3Cl_8^{2-}$. The crystal structure of a compound containing molecules with a related trimeric structure, $Cu_3Cl_6(CH_3CN)_2$, has been reported (43). Melting point behavior of C indicates that, on drying, decomposition occurs, so that the remaining substance is not a single compound. Thus, instead of discrete $Cu_3Cl_8^{2-}$ ions, C may contain a more complex ionic structure, involving three-dimensional bridging to form infinite chains, which decomposes on loss of methanol to a mixture containing units of B.

Further Evidence

Electron Paramagnetic Resonance: *g*-Values from e.p.r. measurements on polycrystalline samples of A, B, and C and dried copper(II) chloride are almost the same, and within the accuracy of measurement the paramagnetism is

Can. J. Chem. Downloaded from www.nrcresearchpress.com by 210.87.254.5 on 09/05/12
For personal use only.

TABLE 7. Some copper(II) and cobalt(II) chloride stretching frequency assignments for solid state infrared spectra

Anion	Compound	M—Cl stretch (cm^{-1})*	Reference
Bipyramidal $CuCl_5^{3-}$	$Co(NH_3)_6CuCl_5$	273	37
Tetrahedral $CuCl_4^{2-}$	Cs_2CuCl_4	298 sh, 268 s, 247 m	27
Tetragonal square planar $Cu_2Cl_6^{2-}$		terminal bridging	46
	$CsCuCl_3$	293 s, 287 s, 263 s	
	NH_4CuCl_3	311 s, 280 s, 230 m	
	$KCuCl_3$	301 s, 278 s, 236 m	
	$LiCuCl_3 \cdot 2H_2O$	295 s, 272 s, 222 m	
Square planar $CuCl_4^{2-}$	$CuCl_2$	328 m, 275 s	46
Tetrahedral $CoCl_4^{2-}$	R_2CoCl_4	300 s, 281 sh	27
		297 s,	48
B	$LCuCl_3$	315 w, 303 mw	
D	L_2CoCl_4	304 w, 290 w	
E	$L_2CoCl_4 \cdot CH_2Cl_2$	303 vw, 292 w	

*sh = shoulder, s = strong, m = medium, w = weak, vw = very weak.

temperature independent (Table 2). The average g-value is 2.10 ± 0.01, within the range for an "unpaired" copper(II) electron in a complex molecule. However, this does not rule out the dimeric anion arrangement. No anomalies in the magnetic susceptibility of $CsCuCl_3$ due to exchange interactions have been observed down to 80 °K (44), and g-values from e.p.r. measurements at room temperature on other compounds containing $Cu_2Cl_6^{2-}$ dimers are similar to those for square planar (40) or trigonal bipyramidal (45) chloride anion arrangements, and lie within the "normal" range.

Metal-Chlorine Vibrational Stretching Modes: Some assignments for copper(II) and tetrahedral cobalt(II) chloride anions for solid state measurements are shown in Table 7 in comparison with tentative assignments for the ionic phosphonitrile prepared. Assignments of bands at 304 and 290 cm^{-1} to cobalt(II) chloride stretching modes agrees with those reported for tetrahedral tetrachlorocobaltate(II) compounds (47). Considering that the anion arrangement for D is flattened tetrahedral in the solid state, it is likely that two bands in the expected region are observed. Thus, the ionic structures suggested for D and E are substantiated. If B contains dimeric $Cu_2Cl_6^{2-}$ anions, a third band (attributable to a bridging chloride mode) should occur at lower energy, though the limits of measurement may have precluded its observation. The positions of the bands which are observed, 315 and 300 cm^{-1}, suggest that the arrangement for B could be tetragonally distorted square planar. At most, it can be concluded that these assignments are consistent with other evidence in support of the ionic structures proposed.

Chelate Formation for Aminodiphenylphosphonitrileaminodiphenylphosphonium Ion Reassessed

Initially, it was considered that the positive charge repulsion hindrance to chelation or coordination via the amino groups might not prevent formation of covalent bonds with a positive transition metal ion. Based on the observation of a single ^{31}P n.m.r. interaction and only a single broad interaction attributable to the nitrogen hydrogen atoms, the phosphorus atoms are equivalent, and the positive charge can be considered as delocalized over the PNP portion of the skeleton (49).

The recent preliminary crystal structure report (50) indicates a possible reason for the non-occurrence of chelation or coordination. The phosphorus–nitrogen interatomic distances for the PNP portion are equal and short (1.57 Å), comparable with those of cyclic phosphonitriles, as expected for a delocalized multiple bonding system. However, the phosphorus–nitrogen distance for the P—NH_2 bonds are also short (1.65 Å) compared with that usually considered as the single bond value (1.78 Å). They are of the order calculated for a phosphorus–nitrogen "pure" double bond (1.64 Å) (51). This is evidence for a π_s-type bond system involving the whole phosphorus–nitrogen skeleton (51). Thus, the amino group lone-pairs must be even

Can. J. Chem. Downloaded from www.nrcresearchpress.com by 210.87.254.5 on 09/05/12
For personal use only.

less "available" for donation to any external acceptor site. This substantiates the proposal of ionic structures for the copper(II) and cobalt(II) compounds prepared. It also indicates that formation of a covalent bond to a sulfur atom, for example, through an addition mechanism, would require substantial rearrangement of the charge distribution for the phosphonitrile, possibly resulting in a destabilized skeleton. This might favor chain polymerization, thus contributing to the problem of obtaining an experimental compromise between conditions necessary for reaction and also favorable to intramolecular cyclization.

This research was supported by the Defence Research Board of Canada, Grant No. DRB-9530-55. R.M.C. thanks the National Research Council of Canada for Scholarships 1966-1968 and McGill University for Scholarships 1968-1970. The referees are sincerely thanked for their thorough and painstaking review of the paper which contributed to its final form.

1. R. M. Clipsham, R. M. Hart, and M. A. Whitehead. Inorg. Chem. **8**, 2431 (1969).
2. J. W. Cox and E. R. Corey. Chem. Commun. 205 (1969).
3. I. I. Bezman and J. H. Smalley. Chem. Ind. 839 (1960).
4. A. Schmidpeter, R. Bohn, and H. Groeger. Angew. Chem. Int. Ed. Engl. **3**, 704 (1964)
5. B. J. Hathaway, D. E. Billing, P. Nicholls, and I. M. Procter. J. Chem. Soc. 312, 319 (1969).
6. I. M. Procter, B. J. Hathaway, and P. Nicholls. J. Chem. Soc. 1678 (1968).
7. R. Nasanen, I. Virtamo, and H. Erikkila. Suom. Kemistil. B**38**, 278 (1965); B**40**, 23 (1967); B**20**, 108 (1967); B**42**, 11 (1969).
8. E. J. Duff. J. Chem. Soc. 434 (1968).
9. G. C. Kulasingham and W. R. McWhinnie. J. Chem. Soc. 1253 (1967).
10. M. Mori. Bull. Chem. Soc. Jap. **33**, 985 (1960).
11. V. L. Goedken, J. V. Quagliano, and L. M. Vallarino. Inorg. Chem. **8**, 2331 (1969).
12. C. Ercolani, J. V. Quagliano, and L. M. Vallarino. Inorg. Chim. Acta, **3**, 421 (1969).
13. J. V. Quagliano, J. T. Summers, S. Kida, and L. M. Vallarino. Inorg. Chem. **3**, 1557 (1964).
14. D. Berglund and D. W. Meek. Inorg. Chem. **8**, 2602 (1969).
15. F. A. Cotton, D. M. L. Goodgame, and M. Goodgame. J. Am. Chem. Soc. **83**, 4690 (1961).
16. N. S. Gill and R. S. Nyholm. J. Chem. Soc. 3997 (1959).
17. G. A. Heath, R. L. Martin, and I. M. Stewart. Chem. Commun. 54 (1969).
18. C. Furlani and G. Morpurgo. Theor. chim. Acta, **1**, 102 (1963).
19. M. Bonamico, G. Dessy, and A. Vaciago. Theor. chim. Acta, **7**, 367 (1967).
20. C. Furlani, E. Cervone, F. Calzona, and B. Baldanza. Theor. chim. Acta, **7**, 375 (1967).
21. M. L. Good, C-C Chang, D. W. Wertz, and J. R. Durig. Spectr. chim. Acta, **25A**, 1303 (1969).
22. I. Y. Ahmed and C. D. Schmulbach. J. Phys. Chem., **71**, 2358 (1967).
23. R. S. Drago and K. F. Purcell. Non-aqueous solvent systems, Chapt 5, Academic Press, New York, N.Y. (1965).
24. L. J. Bellamy. The Infra-red spectra of complex molecules, John Wiley and Sons, New York, N.Y. (1965).
25. N. Fogel, C. C. Lin, C. Ford, and W. Grindstaff. Inorg. Chem. **3**, 720 (1964).
26. R. H. Lee, E. Griswold, and J. Kleinberg. Inorg. Chem. **3**, 1278 (1964).
27. R. J. H. Clark and T. M. Dunn. J. Chem. Soc. 1198 (1963).
28. H. Remy and G. Laves. Ber. **66**, 401 (1933).
29. L. A. Bares, K. Emerson, and J. E. Drumheller. Inorg. Chem. **8**, 131 (1969).
30. L. Helmholtz and R. F. Kruh. J. Am. Chem. Soc. **74**, 1176 (1952).
31. B. Morosin and E. C. Lingafelter. J. Phys. Chem. **65**, 50 (1961).
32. M. Bonomico and G. Dessy. Acta Crystallogr. A**21**, 136 (1966).
33. M. Mori, Y. Saito, and T. Watanabe. Bull. Chem. Soc. Jap. **34**, 245 (1961).
34. P. H. Vossos, D. R. Fitzwater, and R. E. Rundle. Acta Crystallogr. **16**, 1037, (1963).
35. R. D. Willett, C. Dwiggins, R. F. Kruh, and R. E. Rundle. J. Chem. Phys. **38**, 2429 (1962).
36. J. Ferguson. J. Chem. Phys. **40**, 3406 (1964).
37. G. C. Allen and N. S. Hush. Inorg. Chem. **6**, 4 (1967).
38. R. D. Willett and O. L. Liles. Inorg. Chem. **6**, 1666 (1967).
39. R. D. Willett. J. Chem. Phys. **41**, 2243 (1964).
40. R. D. Willett, O. L. Liles, and C. Michelson. Inorg. Chem. **6**, 1886 (1967).
41. J. E. Drumheller, P. H. Amundson, and K. Emerson. J. Chem. Phys. **51**, 5729 (1969).
42. J. H. Russell and S. C. Wallwork. Acta. Crystallogr. B**25**, 1691, (1969).
43. R. D. Willett and R. E. Rundle. J. Chem. Phys. **40**, 838 (1964).
44. G. F. Kokoszka, H. C. Allen, and G. Gordon. J. Chem. Phys. **46**, 3013 (1967).
45. W. E. Hatfield and T. S. Piper. Inorg. Chem. **3**, 841 (1964).
46. R. J. Clark. Spectrochim. Acta, **21**, 955 (1965).
47. A. Sabatini and L. Sacconi. J. Am. Chem. Soc., **86**, 17 (1964).
48. H. H. Sisler, H. S. Ahuja, and N. L. Smith. Inorg. Chem. **1**, 84 (1962).
49. J. W. Cox and E. R. Corey. Chem. Commun. 205 (1969).
50. L. G. Hoard and R. A. Jacobson. J. Chem. Soc. 1203 (1966).
51. R. M. Clipsham and M. A. Whitehead, to be published.
52. W. C. Marsh and J. Trotter. J. Chem. Soc. 1482 (1971).

Can. J. Chem. Downloaded from www.nrcresearchpress.com by 210.87.254.5 on 09/05/12
For personal use only.

Isotope Effects and Hydrogen Yields in the Radiolysis of H_2O–D_2O Mixtures at Very High Dose Rates[1]

A. W. BOYD, C. WILLIS,[2] AND G. C. LALOR[3]

Physical Chemistry Branch, Chalk River Nuclear Laboratories, Atomic Energy of Canada Limited, Chalk River, Ontario

Received April 15, 1971

Total hydrogen yields and their isotopic ratios have been measured in the single pulse, high dose rate radiolysis of H_2O–D_2O mixtures and acidic, basic, and nitrous oxide solutions. The yield from D_2O is $\sim 11\%$ lower than in H_2O at 7×10^{27} eV g^{-1} s^{-1}. In acid solutions the yields from H_2O and D_2O are the same within 5%. This yield, $G(H_2) = 1.15 \pm 0.05$ has been used to derive a value of $k_{H+OH} = 2.5 \pm 0.3 \times 10^{10}$ M^{-1} s^{-1}.

Using the literature values for primary yield data and for the reaction rate constants, values of α have been determined for the various hydrogen forming processes by computer calculation. We obtain values for hydrogen formation of $\alpha_{spur} = 2.1 \pm 0.1$, $\alpha_{e+e} = 6.0 \pm 0.1$, α_{H+H} (effective) $= 3.2 \pm 0.1$, and α_{e+H} (effective) $= 1.3 \pm 0.2$. Detailed consideration of the mechanisms involved suggest that there are little or no isotopic preferences in H + H and e + H reactions.

Les rendements totaux en hydrogène et leurs rapports isotopiques ont été mesurés par radiolyse à un seul faisceau et à vitesse à haute dose de mélanges H_2O–D_2O et de solutions acides, basiques et de solutions d'oxyde nitreux. Le rendement à partir de D_2O est de environ 11% plus faible que dans H_2O à 7×10^{27} eV g^{-1} s^{-1}. En solutions acides, les rendements à partir de H_2O et D_2O sont les mêmes à 5% près. Ce rendement, $G(H_2) = 1.15 \pm 0.05$ a été utilisé pour obtenir une valeur de $k_{H+OH} = 2.5 \pm 0.3 \times 10^{10}$ M^{-1} s^{-1}.

En utilisant les valeurs de la littérature pour les données des rendements primaires et pour les constantes de vitesse de réaction, des valeurs de α ont été déterminées pour les nombreux procédés de formation de l'hydrogène par calculateur électronique. Nous obtenons des valeurs pour la formation de l'hydrogène $\alpha_{spur} = 2.1 \pm 0.1$, $\alpha_{e+e} = 6.0 \pm 0.1$, α_{H+H} (effectif) $= 3.2 \pm 0.1$ et α_{e+H} (effectif) $= 1.3 \pm 0.2$. Une analyse détaillée des mécanismes impliqués permet d'avancer qu'il y a peu de préférences ou des préférences non isotopiques dans les réactions H + H et e + H.

Canadian Journal of Chemistry, **50**, 83 (1972)

Introduction

Isotope effects in hydrogen formation in the radiolysis of H_2O–D_2O mixtures can be divided into three classes: (*a*) isotope effects in the spur processes leading to molecular and atomic hydrogen, (*b*) isotope effects in the bimolecular reactions of e_{aq}^- and H atoms which form hydrogen, (*c*) isotope effects in other reactions involving e_{aq}^- and H atoms which do not directly form hydrogen. The reactions of importance in these three classes are

(*a*)

[1] $H_2O \rightsquigarrow H_2$ } spur processes

[2] $H_2O \rightsquigarrow H$ }

(*b*)

[3] $e^- + e^- \rightarrow H_2 + 2OH^-$

[4] $e^- + H \rightarrow H_2 + OH^-$

[5] $H + H \rightarrow H_2$

(*c*)

[6] $e^- + H_3O^+ \rightarrow H + H_2O$

[7] $OH + H_2 \rightarrow H + H_2O$

[8] $H + OH \rightarrow H_2O$

[9] $H + H_2O_2 \rightarrow OH + H_2O$

[10] $H + O_2 \rightarrow HO_2$

[11] $H + HO_2 \rightarrow H_2O_2$

[12] $H + OH^- \rightarrow e^-$

Reactions of e^- and OH, other than those producing H atoms, are not included in (*a*) and (*c*), as these species rapidly equilibrate with the bulk solvent whereas H atoms do not. A comprehensive review of isotope effects has been given by Anbar and Meyerstein (1).

The isotope effect in reaction 1, α_1, has been shown to be 2.2 ± 0.2 (1) for a variety of conditions in low linear energy transfer (l.e.t.) radiolysis.[4] Values of $\alpha_2 = 2.6 \pm 0.2$ (1) have been determined from the radiolysis of solutions of radical scavengers where conversion of e^- to

[1]A.E.C.L. No. 4047.

[2]Present address: Chemistry Department, University of the West Indies, Jamaica.

[3]Canadian International Development Agency Fellow from the University of the West Indies, Jamaica.

[4]We shall define α = (H/D) product measured/(H/D) reactants.

Can. J. Chem. Downloaded from www.nrcresearchpress.com by 210.87.254.40 on 09/05/12
For personal use only.

Can. J. Chem. Downloaded from www.nrcresearchpress.com by 210.87.254.40 on 09/05/12
For personal use only.

H atoms (reaction 6) is suppressed. By addition of a deuterated compound from which H atoms can abstract, reaction 13, the isotope effect in

[13] $\quad H(\text{or } D) + RD \rightarrow HD(\text{or } D_2) + R\cdot$

reaction 2 can be derived from the ratio of HD to D_2 in the hydrogen produced. Since H atoms are not in equilibrium with the bulk solvent and since they all must undergo reaction 13, any isotope effect in reaction 13 itself will not be reflected in the ratio of HD to D_2.

The most important reaction in class *c* is [6]. The isotope effect in this reaction, $\alpha_6 = 3.5 \pm 0.3$, has been determined in the same way as α_2 by irradiating acidic solutions of RD in H_2O–D_2O mixtures (1). Results from both radiolysis and photodetachment are in good agreement (2, 3).

Since all other contributions to the hydrogen yield are completely suppressed by the addition of radical scavengers the measurement of α_1 is unambiguous. The derivation of α_2 and α_6 depend upon both the contribution of these and that of reaction 1 to the hydrogen yield but these contributions can be determined with good precision. Values of α_1, α_2, and α_6 should then be meaningful. The determination of α_3, α_4, and α_5 is more complex. Not only are the contributions of these reactions often uncertain but also they reflect isotope effects in other reactions.

Anbar and Meyerstein have reported determinations of α_3 by studying the reactions of electrons produced by photodetachment (4) and by radiolysis (5). In the former paper (4) they obtained values of α_3 of 3.9 ± 0.2, 4.7 ± 0.2, and 5.5 ± 0.2 for 25, 50, and 75% D_2O in H_2O, but state their values to be lower limits. The uncertainty is due to reactions of OH radicals with the hydrogen formed (reaction 7). In the latter paper (5) they irradiated solutions of 0.1 *M* CD_3OH in H_2O–D_2O mixtures at pH = 14 and a dose rate of $\sim 4 \times 10^{23}$ eV g^{-1} s^{-1}. Under these conditions all the OH radicals react with the CD_3OH and the H atoms are converted to e^- (reaction 12). Their measured α value, 3.4 to 3.7, was corrected for the contribution of α_1 ($G_{H_2} = 0.45$) by assuming the yield from reaction 3 was $\frac{1}{2}(G_e + G_H - G_{H_2O_2}) = 1.2$, giving $\alpha_3 = 4.6 \pm 0.2$. This neglects the reactions of e^- with O_2, CO_2, and other electron scavenging impurities which may be significant at their dose rates. Thus their radiolytic values of α_3 should also be considered as lower limits.

Using the same system they also derived values of α_4 and α_5 (5). They report α_4(effective) $= 1.5 \pm 0.3$ using rough estimates of the contributions of reactions 1, 3, 4, and 5 to the total hydrogen yield. This should be considered an effective value because isotope effects in the formation of H atoms are not taken into account.

Under their conditions, at p$H = 1.1$, all e^- form H atoms by reaction 6. A value of α_5(effective) $= 3.5 \pm 0.2$ was obtained by assuming the contribution of reaction 5 to the total hydrogen yield to be $\frac{1}{2}(G_e + G_H) = 1.6$. This means that all the H atoms formed disappear by reaction 5. Therefore any isotope effect in reaction 5 cannot be reflected in the results. What is then being measured is a weighted mean of α_2 and α_6.

From the above discussion it is obvious that further work on the determination of α_3, α_4, and α_5 is desirable.

We have previously shown (6) that single pulse irradiations of pure H_2O at dose rates of 10^{26} to 10^{28} eV g^{-1} s^{-1} give hydrogen yields with $G(H_2) \approx 1$. These are made up of the molecular hydrogen yield and the reactions outside the spurs of e^- and H. They are in agreement with computer calculations (7) of the yields from rate constant and primary yield data. These computer calculations also give the contributions of the various reactions. In this paper we describe the determination of hydrogen yields and H/D separation factors in the irradiation of H_2O–D_2O solutions under the above conditions. By combining the measured values of the isotopic composition with the calculated contributions we can estimate α_1, α_3, α_4, and α_5.

Experimental

Irradiations

As in ref. 6, the irradiations were done with a Febetron 705.[5] Pure H_2O, D_2O, and H_2O–D_2O mixtures and solutions containing N_2O were irradiated in the stainless steel cells described in ref. 6. The acidic and basic solutions were irradiated by putting 2 to 3 ml of solution in the 75 ml quartz cells used for irradiation of gases (8). Quartz cells filled with liquid shatter when irradiated with high intensity electron pulses (6). With this partial filling technique only one cell was shattered in 25 irradiations.

Dosimetry

Previously, good agreement was obtained between experimental yields (based on calorimetric dosimetry (9)) and

[5]Manufactured by Field Emission Corporation, McMinnville, Oregon, U.S.A.

Can. J. Chem. Downloaded from www.nrcresearchpress.com by 210.87.254.40 on 09/05/12
For personal use only.

calculated yields for hydrogen from water for single pulses from 0.1 to 8.0 Mrad per pulse giving dose rates of 10^{26}–10^{28} eV $g^{-1}s^{-1}$ (6). In the present work the hydrogen from H_2O was used to determine the absorbed dose in H_2O–D_2O mixtures. The energy absorbed per unit volume of D_2O was taken to be the same as that for light water. The increase in density in going from H_2O to D_2O compensates almost exactly for the decrease in stopping power per gram.

Analyses

The volume of radiolytic gas, non-condensible at 77 °K, was measured by conventional vacuum line techniques using a McLeod gauge. The H_2, HD, and D_2 ratios and total hydrogen content of this gas were determined by mass spectrometry.

The mass spectrometers were calibrated with known mixtures of H_2, HD, and D_2. Mixtures for the range 20–95% H were prepared by equilibrating appropriate mixtures of H_2 and D_2 on a platinum filament at 900–930 °C.

Most of the work reported here was obtained using a CEC-21-130[6] mass spectrometer. To obtain an accurate value of the isotopic composition of the hydrogen samples, we used essentially three different mass spectrometers, the CEC-21-130 and a CEC-21-614[6] with either a type 614-1 or a 614-2 cycloid tube. The radiolytic hydrogen from a mixture of equal volumes of H_2O and D_2O was compared using these instruments to a standard mixture of approximately the same composition (H_2:HD:D_2::1.0:0.8:0.2) at the same inlet pressure. In these determinations, standard mixtures and radiolytic samples were analyzed alternately.

The radiolytic samples containing very low deuterium concentrations were compared with a standard hydrogen mixture containing 120.9 p.p.m. D. This was used to attempt to correct for both memory effects of the mass spectrometer and also for the contribution of H_3^+ to the $m/e = 3$ peak. Again pressures of the standard were matched to those of the samples and standard and sample were analyzed alternately. For radiolytic samples containing very high deuterium concentrations, comparison was made with a standard deuterium sample of 99.682% isotopic purity. Both H_2 and D_2 standards were originally analyzed by conversion to water and determining the isotopic content of the water by infrared analysis. Although the errors at both low and high deuterium concentrations were significantly reduced by these standardizations, the remaining errors are much larger than those for intermediate concentrations. Further reductions in these errors could only be made by using a large range of low and high deuterium standards. This was not done because of the difficulty of obtaining these standards.

The precision of the measured total hydrogen yields depends only on the reproducibility of the experimental techniques as basically a comparative measurement was involved. Exchange in the mass-spectrometer does not significantly affect the hydrogen to nitrogen, oxygen sensitivities. Overall errors should be less than ±2%. The errors involved in the α value determinations are much more difficult to assess but should be less than ±5% over most of the range of composition.

Materials

Both the H_2O (isotopic D content 150 p.p.m.) and D_2O (isotopic purity 99.58 and 99.949%) were pre-irradiated and triply distilled. Gases non-condensible at 77 °K were removed by several freeze–pump–thaw cycles. The N_2O was McDuff medical grade and was also freed of gases non-condensible at 77 °K. The acidic and basic solutions were prepared by diluting "acculute" standard solutions (Anachemia Chemicals) of 2 *N* H_2SO_4 and 2 *N* NaOH with appropriate H_2O–D_2O mixtures, making corrections for the isotopic dilution introduced by the solutes.

[6]Manufactured by Dupont Instrumental Products Division, Monrovia, California, U.S.A.

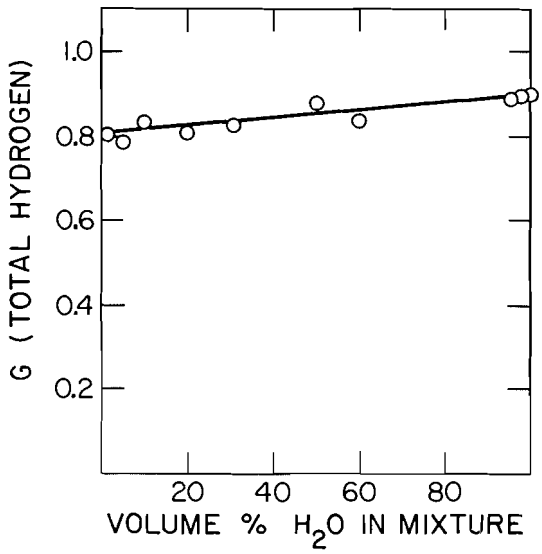

FIG. 1. Total hydrogen yield from H_2O–D_2O mixtures at 7×10^{27} eV g^{-1} s^{-1}.

Results

Pure H_2O–D_2O Mixtures

The total yield of hydrogen (H_2, HD, and D_2) from single pulse irradiations of 3.5×10^{20} eV g^{-1} (7×10^{27} eV g^{-1} s^{-1}) as a function of H_2O concentration is shown in Fig. 1. The yield from pure H_2O at this dose rate and dose per pulse is $G(H_2) = 0.90$ (6). This decreases to $G(D_2) = 0.81$ for pure D_2O.

The values of $\alpha = (H/D)_{\text{radiolytic hydrogen}}/(H/D)_{H_2O-D_2O\text{ solution}}$ and $K = (HD)^2/(H_2)(D_2)$ (radiolytic hydrogen) as a function of H_2O concentration at dose rates of 7×10^{27} and 5×10^{26} eV g^{-1} s^{-1} are shown in Figs. 2 and 3, respectively. The uncertainties in the α values at both high and low H_2O concentrations are due to the mass spectrometric exchange discussed above. Values for *K* are given only for intermediate concentrations where exchange does not contribute significantly. The values of *K* obtained, 3.7–3.8, are higher than the calculated equilibrium value at room temperature, 3.25 (1), but

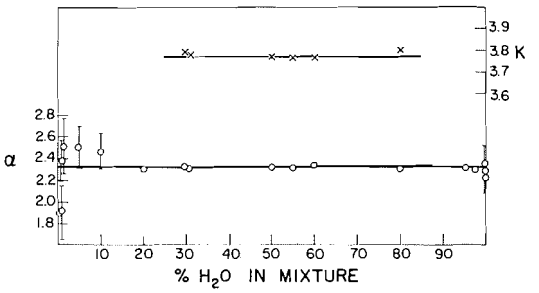

FIG. 2. α and K values in the radiolysis of H_2O–D_2O mixtures at 7×10^{27} eV g^{-1} s^{-1}. The uncertainties are represented by the circles or by the error bars.

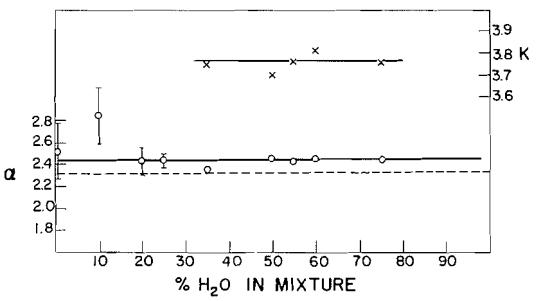

FIG. 3. α and K values in the radiolysis of H_2O–D_2O mixtures at 5×10^{26} eV g^{-1} s^{-1}. --- line from 7×10^{27} eV g^{-1} s^{-1}.

are close to a value of 4.0 expected on a statistical basis. As can be seen in Fig. 3, the α value at 5×10^{26} eV g^{-1} s^{-1} is significantly higher than that at 7×10^{27} eV g^{-1} s^{-1}.

The α value obtained using three different mass spectrometers and a 50 mol% H_2O–D_2O mixture are given in Table 1. The agreement between the α values obtained using the three different mass spectrometers is most satisfactory and gives confidence in the accuracy of the measurements, at least for 50:50 mixtures.

H_2O–D_2O–N_2O Mixtures

At 7×10^{27} eV g^{-1} s^{-1} the addition of N_2O up to 0.05 M has little effect on the hydrogen yield (6) from H_2O. The effect of N_2O on the hydrogen yield from mixtures of H_2O and D_2O is shown in Fig. 4 and the effect of N_2O on α and K for the same mixtures is shown in Fig. 5 both for a dose rate of 5×10^{26}.

H_2O–D_2O with H_2SO_4 or NaOH

The effect of pH on α in the irradiation of mixtures of equal volumes of H_2O and D_2O is shown in Fig. 6. The dose and dose rate in these

TABLE 1. Values of α for a mixture of equal volumes of H_2O and D_2O for a dose of 3.5×10^{19} eV g^{-1} at 7×10^{27} eV g^{-1} s^{-1}

Mass spectrometer	α
CEC-21-130	2.35 ± 0.06
CEC-21-614-1	2.30 ± 0.04
CEC-21-614-2	2.32 ± 0.02

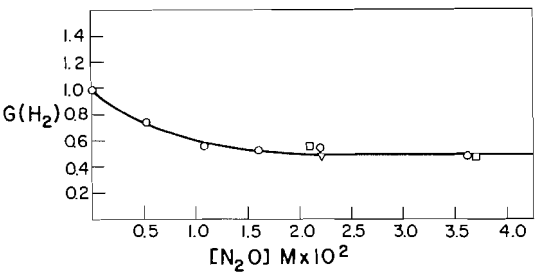

FIG. 4. Total hydrogen yield from H_2O–D_2O mixtures with N_2O at 5×10^{26} eV g^{-1} s^{-1}. ○, 50:50 H_2O:D_2O; □, 75:25 H_2O:D_2O; ▽, 25:75 H_2O:D_2O.

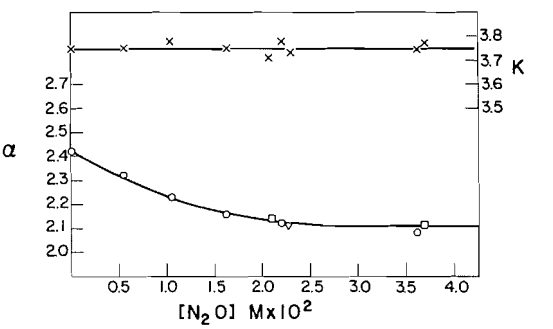

FIG. 5. α and K values in the radiolysis of N_2O solutions at 5×10^{26} eV g^{-1} s^{-1}. ○, 50:50 H_2O:D_2O; □, 75:25 H_2O:D_2O; ▽, 25:75 H_2O: D_2O.

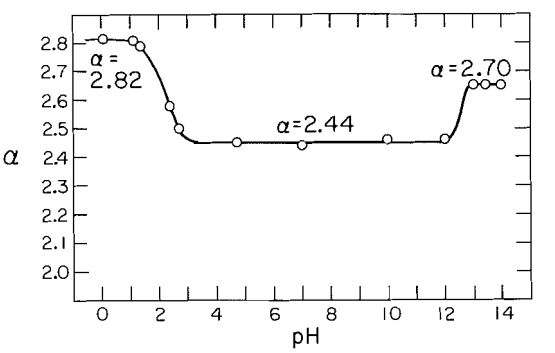

FIG. 6. α values as a function of pH from the radiolysis of 50:50 H_2O:D_2O mixtures at $\sim 1 \times 10^{27}$ eV g^{-1} s^{-1}.

Can. J. Chem. Downloaded from www.nrcresearchpress.com by 210.87.254.40 on 09/05/12
For personal use only.

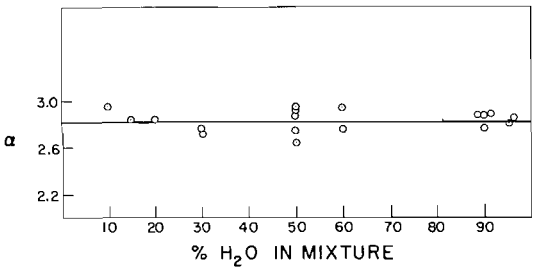

FIG. 7. α values from the radiolysis of 0.2 *N* H_2SO_4 solutions at $\sim 1 \times 10^{27}$ eV g^{-1} s^{-1}.

irradiations are estimated to be 7×10^{19} eV g^{-1} and 1×10^{27} eV g^{-1} s^{-1}, respectively.

Figure 7 shows the dependence of measured α values on concentration of H_2O for 0.2 *N* H_2SO_4 solutions. The total measured yield of hydrogen from these samples gave $G(H_2)_{total} = 1.15 \pm 0.05$ over the whole range of H_2O–D_2O concentrations.

Discussion

Hydrogen Yields from H_2O and D_2O

In our previous paper on the high dose rate radiolysis of liquid water (6) we obtained good agreement between measured values and those calculated from primary yield and reaction rate constant data. From the present work, as shown in Fig. 1, in going from pure H_2O to pure D_2O there is a decrease in the total hydrogen yield of $\sim 11\%$ at the highest dose rate of 7×10^{27} eV g^{-1} s^{-1}.

The yields of the primary radiolytic species in H_2O and D_2O and the rate constants for the reactions of these species that are important at Febetron dose rates are listed in Tables 2 and 3. The yield of hydrogen calculated with the values in these tables and the computer program, WR 16 of Schmidt (7), for the single pulse irradiations at 7×10^{27} eV g^{-1} s^{-1} is $G(H_2) = 0.90$ for both H_2O and D_2O.

The accuracy of the results obtained with the computer program is dependent on the values of the rate constants and primary yields used. It is also dependent on the applicability of calculations based on a homogeneous distribution of reactants to the high dose rate situation when reactions take place while the spurs expand, an essentially non-homogeneous situation. We have already discussed this (6) and concluded that, for pure systems, the calculated final yields should not be seriously in error. As stated the precision of the measured yields is estimated to be within $\pm 2\%$. The difference between the measured value of $G(D_2) = 0.81$ and the calculated value of $G(D_2) = 0.90$ is most probably due to errors in the values used for the primary yields and rate constants. The errors in the experimental primary yield data seem to be much less than for the rate constant data. To determine the effect of uncertainties in the latter we have calculated hydrogen yields for various values of the rate constants of the most important reactions. The results of these are shown in Table 4. Changes of 20% in a few of these rate constants will reduce the calculated value of $G(D_2)$ to the observed value and, within the precision of the rate constant data, it is easy to obtain calculated yields which agree with our experimental data. Any choice of values for these rate constants to give $G(D_2) = 0.8$ is somewhat arbitrary. We used the following values for H_2O and D_2O for the important reactions which are listed in Table 4: $k_{3H} = k_{3D} = 4.5 \times 10^9$; $k_{4H} = 2.5 \times 10^{10}$, $k_{4D} = 2.0 \times 10^{10}$; $k_{5H} = 1.0 \times 10^{10}$, $k_{5D} = 8.0 \times 10^9$; $k_{6H} = 2.2 \times 10^{10}$; $k_{6D} = 1.7 \times 10^{10}$; $k_{8H} = 2.5 \times 10^{10}$, $k_{8D} = 2.4 \times 10^{10}$; $k_{14H} = 3.0 \times 10^{10}$, $k_{14D} = 2.8 \times 10^{10}$; $k_{15H} = k_{15D} = 1.2 \times 10^{10}$; $k_{16H} = 1.43 \times 10^{11}$, $k_{16D} = 1.23 \times 10^{11}$; $k_{17H} = 5.0 \times 10^9$, $k_{17D} = 4.0 \times 10^9$. All have units l mol^{-1} s^{-1}; suffix H signifies H_2O, D signifies D_2O. The only values which are different by more than the present uncertainty in the value for H_2O are k_{6D} and k_{16D} but these are in line with experimentally observed differences, see Table 3.

In 0.2 *N* acid solutions we find $G(H_2)_{total} = 1.15 \pm 0.05$ in both H_2O and D_2O. This value

TABLE 2. Primary yields in the radiolysis of H_2O and D_2O*

	G	
Species	H_2O	D_2O
e^-	2.7	2.9
H	0.56	0.44
H_2	0.45	0.40
H^+	2.9	3.2
OH^-	0.2	0.3
OH	2.75	2.9
HO_2	0.02	0.02
H_2O_2	0.7	0.62

*Initial O_2 concentration assumed to be 10^{-6} *M*. The yield data are taken from refs. 16–18.

Can. J. Chem. Downloaded from www.nrcresearchpress.com by 210.87.254.40 on 09/05/12
For personal use only.

Can. J. Chem. Downloaded from www.nrcresearchpress.com by 210.87.254.40 on 09/05/12
For personal use only.

TABLE 3. Rate constants for reactions occurring in irradiated water at very high dose rates

	Reaction	Rate constant (l mol^{-1} s^{-1}) H_2O*	D_2O†
[3]	$e^- + e^- \rightarrow H_2 + 2\,OH^-$	4.5×10^9	4.5×10^9‡
[4]	$e^- + H \rightarrow H_2 + OH^-$	2.5×10^{10}	2.8×10^{10}
[5]	$H + H \rightarrow H_2$	1.0×10^{10}	8×10^9
[6]	$e^- + H^+ \rightarrow H$	2.2×10^{10}	1.7×10^{10}
[7]	$OH + H_2 \rightarrow H_2O + H$	4.5×10^7	1.6×10^7
[8]	$H + OH \rightarrow H_2O$	2.5×10^{10}	2×10^{10}
[9]	$H + H_2O_2 \rightarrow H_2O + OH$	9×10^7†	§
[10]	$H + O_2 \rightarrow HO_2$	2×10^{10}	§
[11]	$H + HO_2 \rightarrow H_2O_2$	2×10^{10}	§
[12]	$H + OH^- \rightarrow e^- + H_2O$	2.0×10^7	2×10^7
[14]	$e^- + OH \rightarrow OH^-$	3.0×10^{10}	2.8×10^{10}
[15]	$e^- + H_2O_2 \rightarrow OH + OH^-$	1.2×10^{10}	1.2×10^{10}
[16]	$H^+ + OH^- \rightarrow H_2O$	1.43×10^{11}	1.2×10^{11}
[17]	$OH + OH \rightarrow H_2O_2$	5×10^9	4×10^9
[18]	$OH + H_2O_2 \rightarrow H_2O + HO_2$	4.5×10^7	4.5×10^7
[19]	$e^- + O_2 \rightarrow O_2^-$	2×10^{10}	1.5×10^{10}
[20]	$HO_2 \rightarrow H^+ + O_2^-$	2.5×10^6	§
[21]	$H^+ + O_2^- \rightarrow HO_2$	5×10^{10}	§
[22]	$OH + HO_2 \rightarrow H_2O + O_2$	1.2×10^{10}	§
[23]	$OH + O_2^- \rightarrow OH^- + O_2$	1.5×10^{10}	§
[24]	$e^- + HO_2 \rightarrow H_2O_2 + H^+$	2.0×10^{10}	§

*Values from ref. 2 except as noted.
†Values from ref. 16.
‡Values from ref. 17.
§Value assumed to be the same as for H_2O.

is in very good agreement with previously obtained yields of $G(H_2) = 1.17 \pm 0.05$ (10) and $G(H_2) = 1.16$ (11) in acidic H_2O solutions at high dose rates. The calculated values are dependent only on the primary yields and the rate constants for reactions 5, 8 and 17

[5] $H + H \rightarrow H_2$

[8] $H + OH \rightarrow H_2O$

[17] $OH + OH \rightarrow H_2O_2$

Taking as best values $k_5 = 1 \pm 0.1 \times 10^{10}\ M^{-1}\ s^{-1}$, $k_7 = 5 \pm 1 \times 10^9\ M^{-1}\ s^{-1}$ (12), and the primary yields in Table 2 and the value of $G(H_2) = 1.15 \pm 0.03$ the computer calculations show that $k_8 = 2.5 \pm 0.3 \times 10^{10}\ M^{-1}\ s^{-1}$. This is slightly lower than the value of $k_8 = 3.2 \times 10^{10}\ M^{-1}\ s^{-1}$ of Fricke and Thomas (11) derived by similar methods but higher than the value used by Pagsberg *et al.* (12) of $k_8 = 1.0 \times 10^{10}\ M^{-1}\ s^{-1}$ (13).

TABLE 4. Rate constants controlling the yield of hydrogen in the pulse radiolysis of water at 7×10^{27} eV g^{-1} s^{-1} for a dose of 3.5×10^{20} eV g^{-1}

	Reaction	Rate constant	Percent uncertainty	Reference	% Change in $G(H_2)$ for 10% increase in rate constant
[3]	$e^- + e^- \rightarrow H_2 + 2\,OH^-$	4.5×10^9	33	19, 20	+0.45
[4]	$e^- + H \rightarrow H_2 + OH^-$	2.5×10^{10}	24	19, 20, 23	+1.0
[5]	$H + H \rightarrow H_2$	1.0×10^{10}	30	27, 28, 12	+0.25
[6]	$e^- + H^+ \rightarrow H$	2.2×10^{10}	10	20, 21, 22	+0.40
[8]	$H + OH \rightarrow H_2O$	2.5×10^{10}	33	11, 29, 16*	−1.0
[14]	$e^- + OH \rightarrow OH^-$	3×10^{10}	23	19, 20, 23	−0.81
[15]	$e^- + H_2O_2 \rightarrow OH^- + OH$	1.2×10^{10}	12	20, 21	−0.68
[16]	$H^+ + OH^- \rightarrow H_2O$	1.43×10^{11}	10	12, 24–26	−0.13
[17]	$OH + OH \rightarrow H_2O_2$	5×10^9	40	11, 12, 29, 16*	+0.6

*Reference 16, p. 76.

TABLE 5. α values for the radiolysis of H_2O–D_2O mixtures at high dose rates

	Dose rate ($eV\ g^{-1}\ s^{-1}$)	α
Limiting low p*H*	$\sim 1 \times 10^{27}$	2.82
Neutral	7×10^{27}	2.32
	5×10^{26}	2.44
Limiting N_2O solution	5×10^{26}	2.11
Limiting high p*H*	$\sim 1 \times 10^{27}$	2.70

α *Values for* H_2O–D_2O *Mixtures*

General

Our experimental observations of the isotope effects in hydrogen formation consist of α values for five different systems. These are listed in Table 5. As shown in Figs. 2, 3, and 7 these values appear to be independent of H_2O concentration from <10 to >90% H_2O in D_2O.

The hydrogen from water irradiated under our conditions results from four processes

[1] $H_2O \rightsquigarrow H_2$

[3] $e^- + e^- \rightarrow H_2$

[4] $e^- + H \rightarrow H_2$

[5] $H + H \rightarrow H_2$

In H_2O or D_2O solutions the contributions of each of these to the hydrogen yield can be calculated with the computer program within the accuracy of the data in Tables 2 and 3.

As we have discussed in (6) the non-homogeneous part of the reaction sequence leads to errors in the calculations for other than pure water but for limiting conditions these errors are small. In the following discussion we shall consider in turn the N_2O, the acidic, and the basic solutions. The α values for the individual reactions thus obtained will be applied to the mixtures of "pure" D_2O–H_2O. To calculate the effective contributions from mixtures we shall use the calculations for D_2O and H_2O and take the mean.

N_2O Solutions

For conditions identical to those of the present experiments the effective rate constant for reaction 25 was shown to be $2 \times 10^9\ M^{-1}\ s^{-1}$ (6).

[25] $N_2O + e^- \rightarrow N_2 + OH + OH^-$

Using this value the calculated effect of 0.05 *M* N_2O in both H_2O and D_2O is to reduce the total contribution of reactions 3, 4, and 5 to the hydrogen yield to less than 10%. The reduction in [5] is due to the increased concentration of OH radicals in the system and the consequent increase in the reaction H + OH. The calculation is supported by the measured reduction of the total hydrogen yield in N_2O solutions to $G(H_2) \approx 0.45$, which is paralleled by the reduction in the measured α values. Since

$$\alpha_{\text{measured}} = \alpha_1 f_1 + \alpha_3 f_3 + \alpha_4 f_4 + \alpha_5 f_5$$

where $f\alpha$ is the fractional contribution to the hydrogen yield of reaction [*a*],

[26] $$\alpha_1 = \frac{2.11 - 0.1\,(\text{mean effective } \alpha \text{ for [3], [4], and [5]})}{0.9}$$

Assuming that the mean α for [3], [4], and [5] is 2 ± 1 we have $\alpha(\text{spur}) = 2.1 \pm 0.1$. This is in good agreement with previous work (1).

Acidic Solutions

In acid solutions the electron reacts with H_3O^+ giving H atoms and under limiting conditions hydrogen is formed only by reactions 1 and 5. Using the calculated contributions of these two reactions to the hydrogen yield an effective value for α_5 can be obtained

[27] $$\alpha_5(\text{effective}) = \frac{2.82 - 0.37(2.1)}{0.63} = 3.24 \pm 0.06$$

Relating this effective α value to the isotope effects in reaction 5 is complex. The H atoms reacting in reaction 5 are produced both by reactions 2 and 6, each of which has a large isotope effect, $\alpha_2 = 2.6$ and $\alpha_6 = 3.5$. Since H atoms are not in equilibrium with the bulk solvent, their initial concentration will differ from the H_2O/D_2O ratio by the weighted mean of α_2 and α_6, which for acid solutions is $\overline{\alpha_{2,6}} = 3.3$. The observed effective α value is a function of this initial ratio and of the true isotope effects in reactions 5 and also in reaction 8.

Reaction 5 can be written

[5*a*] $H + H \rightarrow H_2$

[5*b*] $H + D \rightarrow HD$

[5*c*] $D + D \rightarrow D_2$

Can. J. Chem. Downloaded from www.nrcresearchpress.com by 210.87.254.40 on 09/05/12
For personal use only.

TABLE 6. Calculated fractional contributions to the hydrogen yield for alkaline conditions ($\sim 1 \times 10^{27}$ eV g^{-1} s^{-1}) and at 7×10^{27} eV g^{-1} s^{-1} (HDR), and 5×10^{26} eV g^{-1} s^{-1} (LDR) for H_2O and D_2O

		H_2O			D_2O		
		p*H* 14	HDR	LDR	p*H* 14	HDR	LDR
(1)	Spur	0.550	0.492	0.453	0.597	0.497	0.456
(3)	$e^- + e^-$	0.193	0.093	0.112	0.200	0.122	0.146
(4)	$e^- + H$	0.236	0.325	0.331	0.188	0.314	0.316
(5)	H+H	0.021	0.089	0.104	0.014	0.067	0.081

so that,

[28] $$\alpha_5(\text{true}) = \frac{2k_{5a}[H]^2 + k_{5b}[H][D]}{2k_{5c}[D]^2 + k_{5b}[H][D]} [H]/[D] = \frac{2k_{5a}[H]/[D] + k_{5b}}{2k_{5c} + k_{5b}[H]/[D]}$$

Since under our pulsed conditions we do not have stationary state kinetics the above equation cannot be directly applied. What we have done is to compare our experimental values of α in acid solutions with the computer calculated values based on assumed rate constants. We have assumed H and D atoms are produced from H_2O–D_2O 0.2 *N* acid mixtures with an isotope effect of $\overline{\alpha_{2,6}} = 3.3$ and that $k_{5a} = 1.0 \times 10^{10}$ M^{-1} s^{-1}, $k_{5b} = 1.8 \times 10^{10}$ M^{-1} s^{-1}, $k_{5c} = 0.8 \times 10^{10}$ M^{-1} s^{-1}, $k_{8H} = 2.5 \times 10^{10}$ M^{-1} s^{-1}, $k_{8D} = 2.0 \times 10^{10}$ M^{-1} s^{-1}, and $k_{17} = 0.5 \times 10^{10}$ M^{-1} s^{-1}. The value of k_{5b} is taken as twice the average of k_{5a} and k_{5c}. The value of α in acid solutions calculated from these data is 2.74 ± 0.02 over the concentration range in Fig. 7. (The calculated α_5 value will be dependent on the ratio of H_2O to D_2O unless $k_{5a} \approx k_{5c} \approx 0.5k_{5b}$.) Exact agreement with the experimental value of $\alpha = 2.82$ can be obtained by increasing $\overline{\alpha_{2,6}}$ to 3.5. These results imply that there is little isotopic preference in reaction 5.

Alkaline Solutions

The limiting condition in which all the hydrogen atoms are converted to electrons cannot be obtained at our dose rates. The computer calculations indicate however that at p$H = 12$, reaction 6 is completely suppressed and even at p$H = 14$ less than 10% of H atoms react via [12]. Since inhomogeneities will reduce the effective concentration of OH^-, the limiting condition can be considered to be where e and H are not interconverted and react in proportion to their primary yields. Assuming this to be the limiting condition the computer calculated contributions of reactions 1, 3, 4, and 5 are given in Table 6. We have not taken into account the uncertainty which exists at high p*H* due to the ionization of the OH radical.

From these values using values for α_1 and α_5 we can derive relationships between α_3 and α_4 for H_2O and D_2O, respectively. For H_2O

[29] $$\alpha_{\text{measured}} = 0.55\alpha_1 + 0.193\alpha_3 + 0.236\alpha_4 + 0.021\alpha_5$$

Taking α_5(effective) (p*H* 14) $= \overline{\alpha_{2,6}}$(p*H* 14) $= \alpha_2 = 2.6$, $\alpha_{\text{measured}} = 2.70$, and $\alpha_1 = 2.1$

[30] $$\alpha_3 = 7.72 - 1.22\alpha_4$$

Similarly for D_2O

[31] $$\alpha_3 = 7.05 - 0.94\alpha_4$$

"Pure" H_2O–D_2O Mixtures

For pure H_2O and D_2O the calculated contributions to the hydrogen yields at low (LDR) and high dose rates (HDR) are given in Table 6. The relationships between α_3 and α_4 for the four sets of conditions are:

H_2O

[32] HDR $\alpha_3 = 10.87 - 3.49\alpha_4$

[33] LDR $\alpha_3 = 10.41 - 2.96\alpha_4$

D_2O

[34] HDR $\alpha_3 = 8.76 - 2.57\alpha_4$

[35] LDR $\alpha_3 = 8.43 - 2.16\alpha_4$

In all four expressions α_5 has been taken to be $\overline{\alpha_{2,6}}$ (p*H* 7) = 3.1.

Calculation of α_3 and α_4

Assuming effective values of α_3 and α_4 do not vary between p*H* 7 and p*H* 14 eq. 30 can be com-

Can. J. Chem. Downloaded from www.nrcresearchpress.com by 210.87.254.40 on 09/05/12
For personal use only.

Can. J. Chem. Downloaded from www.nrcresearchpress.com by 210.87.254.40 on 09/05/12
For personal use only.

bined with eq. 32 or eq. 33 and eq. 31 with eq. 34 or eq. 35 to obtain four sets of values. The averages of these four sets are

$$\alpha_3(\text{effective}) = 5.98 \pm 0.07$$
$$\alpha_4(\text{effective}) = 1.28 \pm 0.19$$

This value of $\alpha_3 = 6.0$ should be a "true" value. Electrons are solvated in less than 20 ps (14) and equilibration of the solvent shell with the bulk solvent should be very rapid. The relatively high value of α_3, particularly since $k_{3H} \simeq k_{3D}$, is generally considered (4) to be due to preferential decomposition of the solvated dimer $(e_{aq}^-)_2$ transition state to form light hydrogen. A similar argument is used to explain $\alpha_6 = 3.5$ but it is by no means certain that a solvated complex is formed in reaction 4.

It has been proposed (15) that reaction 4 takes place via a hydride mechanism involving formation of H^- and reaction of this with the solvent to give hydrogen as in reaction 36.

[36] $$H^- + H_2O \rightarrow H_2 + OH^-$$

Also it has been demonstrated that reaction 36 has no isotope effect.

Accepting this mechanism reaction 4 can be written

[4*a*] $$e + (H)_{solvent} + H \rightarrow H_2$$
[4*b*] $$e + (H)_{solvent} + D \rightarrow HD$$
[4*c*] $$e + (D)_{solvent} + H \rightarrow HD$$
[4*d*] $$e + (D)_{solvent} + D \rightarrow D_2$$

Assuming there is no true isotope effect in reaction 4, *i.e.* $k_{4a} = k_{4b} = k_{4c} = k_{4d}$ and that $[H]/[D] = \overline{\alpha_{2,6}}\ (H/D)_{solvent}$ and $(H)_{solvent}/(D)_{solvent} = (H/D)_{solvent}$ for stationary state conditions,

[37] $$\alpha_4(\text{effective}) = \frac{2\overline{\alpha_{2,6}}(H/D)_{solvent} + \overline{\alpha_{2,6}} + 1}{2 + (1 + \overline{\alpha_{2,6}})(H/D)_{solvent}}$$

The terms $(H)_{solvent}$, $(D)_{solvent}$ in reactions 4*a* to 4*d* refer to the solvent with which the H^- ion will react on its formation. If

$$\overline{\alpha_{2,6}} = 1$$

then

$$\alpha_4(\text{effective}) = 1 \text{ at any ratio of } H_2O/D_2O$$

but taking

$$\alpha_{2,6} = 3.0$$

as the approximation mean of the values at p*H* 7 and p*H* 14, eq. 37 becomes

[38] $$\alpha_4(\text{effective}) = \frac{2 + 3(H/D)_{solvent}}{1 + 2(H/D)_{solvent}}$$

This equation indicates that α_4 will vary between 2 and 1.5 over the total range of H_2O concentration for this ideal steady state condition. Under our conditions the variation would presumably be reduced and be within our experimental uncertainty.

Our experimentally derived value of $\alpha_4 = 1.3 \pm 0.2$ is close to the value given by eq. 38 and implies that in reaction 4 as well as reaction 5 the true isotope effect is very small and the observed effective α values are due to isotope effects in precursor reactions.

We can compare our values of α_3 and α_4 to those obtained in previous work. Our value of $\alpha_3 = 6.0$ is higher than the value of Anbar and Meyerstein (4, 5) of about 4.6 but as we discussed in the introduction, their value should properly be considered a lower limit. Also our value of $\alpha_4(\text{effective}) \simeq 1.3 \pm 0.2$ for p*H* 7 and 14 is not too different from the value found by these workers (5) ($\alpha = 1.5 \pm 0.3$).

Conclusions

Our value of $\alpha_1 = 2.1 \pm 0.1$ is in good agreement with the values obtained at low dose rates. Since the previous values of α_3 were lower limits the fact that our value $\alpha_3 = 6.0 \pm 0.1$ is higher is not unexpected. Our observed effective α values for reactions 4 and 5 are in good agreement with previous work. From our treatment of the kinetics of these reactions it is suggested that there is little or no isotopic preference in these reactions. The fairly high effective α values in these reactions are attributed to isotope effects in the formation of H atoms.

We thank Mr. W. M. Thurston, General Chemistry Branch, CRNL for providing the standardized hydrogen, deuterium, and D_2O samples and Mr. W. J. Olmstead, also of the General Chemistry Branch, for his extensive help in preparing reliable H_2:HD:D_2 standards and his help and advice in our mass spectrometric calibrations.

We are also very grateful to Dr. J. W. Fletcher, Physical Chemistry Branch, CRNL, for many helpful discussions which greatly enhanced our understanding of the subject in preparing the manuscript.

1. M. ANBAR and D. MEYERSTEIN. Radiation Chemistry of Aqueous Solutions. Proc. of 19th L. Farkas Memorial Symposium. Jerusalem. December 1967. *Edited by* G. Stein. pp. 109–155.
2. M. ANBAR and D. MEYERSTEIN. J. Phys. Chem. **69**, 698 (1965).
3. S. OHNO. Bull. Chem. Soc. Jap. **41**, 1302 (1968).
4. M. ANBAR and D. MEYERSTEIN. Chem. Commun. 57 (1966).
5. M. ANBAR and D. MEYERSTEIN. Trans. Faraday Soc. **62**, 2121 (1966).
6. C. WILLIS, A. W. BOYD, A. E. ROTHWELL, and O. A. MILLER. Int. J. Radiat. Phys. Chem. **1**, 373 (1969).
7. K. H. SCHMIDT. A.E.C. Research and Development Report ANL-7199 (1966).
8. C. WILLIS, A. W. BOYD, and O. A. MILLER. Can. J. Chem. **47**, 3007 (1969).
9. C. WILLIS, A. E. ROTHWELL, O. A. MILLER, and A. W. BOYD. Radiat. Res. **35**, 428 (1968).
10. J. K. THOMAS and E. J. HART. Radiat. Res. **17**, 408 (1962).
11. H. FRICKE and J. K. THOMAS. Radiat. Res. Suppl. **4**, 35 (1964).
12. P. PAGSBERG, H. CHRISTENSEN, J. RABANI, G. NILSSON, J. FENGER, and S. O. NIELSEN. J. Phys. Chem. **73**, 1029 (1969).
13. J. K. THOMAS. J. Phys. Chem. **67**, 2593 (1963).
14. M. J. BRONSKILL, R. K. WOLFF, and J. W. HUNT. J. Chem. Phys. **53**, 4201 (1970); **53**, 4211 (1970).
15. M. ANBAR. Solvated electron. *Edited by* E. J. Hart. A.C.S. Publ. **50**, 55 (1965).
16. E. J. HART and M. ANBAR. The hydrated electron. Wiley Interscience. New York. 1970.
17. M. S. MATHESON and L. M. DORFMAN. Pulse radiolysis. MIT Press, Cambridge, Mass. 1969.
18. K. H. SCHMIDT and S. M. ANDER. J. Phys. Chem. **73**, 2846 (1969).
19. M. S. MATHESON and J. RABANI. J. Phys. Chem. **69**, 1324 (1965).
20. S. GORDON, E. J. HART, M. S. MATHESON, J. RABANI, and J. K. THOMAS. Discuss. Faraday Soc. **36**, 193 (1963).
21. J. P. KEENE. Radiat. Res. **22**, 1 (1964).
22. L. M. DORFMAN and I. A. TAUB. J. Am. Chem. Soc. **85**, 2370 (1963).
23. E. J. HART, J. K. THOMAS, and S. GORDON. Radiat. Res. Suppl. **4**, 74 (1964).
24. M. EIGEN and L. DEMAEYER. Z. Elektrochem. **59**, 986 (1955).
25. G. ERTL and H. GERISCHER. Z. Elektrochem. **65**, 629 (1961).
26. G. C. BARKER and D. C. SAMMON. Nature, **213**, 65 (1967).
27. J. P. SWEET and J. K. THOMAS. J. Phys. Chem. **68**, 1363 (1964).
28. H. A. SCHWARZ. J. Phys. Chem. **67**, 2827 (1962).
29. H. A. SCHWARZ. Radiat. Res. Suppl. **4**, 89 (1964).

Can. J. Chem. Downloaded from www.nrcresearchpress.com by 210.87.254.40 on 09/05/12
For personal use only.

The Crystal and Molecular Structure of 3-Chloro-3-deoxy-1,2;5,6-di-*O*-isopropylidene-β-D-idose

F. W. B. EINSTEIN AND K. N. SLESSOR

Department of Chemistry, Simon Fraser University, Burnaby 2, British Columbia

Received August 4, 1971

The crystal and molecular structure of 3-chloro-3-deoxy-1,2;5,6-di-*O*-isopropylidene-β-D-idose has been determined from three dimensional X-ray data collected by counter methods. The structure was refined by full-matrix least-squares techniques to a conventional *R* factor of 5.7% for the 817 observed reflections. The compound crystallizes in the orthorhombic space group $P2_12_12_1$ with four molecules in a cell of dimensions $a = 9.744(6)$, $b = 26.76(2)$, $c = 5.403(3)$ Å.

The structure analysis has served to confirm the site of halogenation and that it occurs stereospecifically. The conformation of the furan ring is an envelope arrangement with C(4) displaced from the mean plane.

La structure cristalline et moléculaire du 3-chloro-3-déoxy-1,2;5,6-di-*O*-isopropylidène-β-D-idose a été déterminée à partir des données tridimensionnelles de rayons-X obtenues par des méthodes de comptage. La structure a été affinée par moindres carrés (matrice complète) jusqu'à un facteur d'accord $R = 5.7\%$ pour 817 réflexions observées. Le composé cristallise dans le système orthorhombique groupe d'espace $P2_12_12_1$, avec quatre molécules dans une maille de dimensions $a = 9.744(6)$, $b = 26.76(2)$, $c = 5.403(3)$ Å.

La détermination de la structure a servi à confirmer le site de l'halogénation ainsi que le fait de sa stéréospécificité. La conformation du noyau du furanne est un arrangement en enveloppe avec le C_4 déplacé par rapport au plan central.

Canadian Journal of Chemistry, **50**, 93 (1972)

Introduction

It has been found that some procedures (1, 2) for halogenation of sugars have resulted in the rearrangement of the acetal linkage. In order to both establish unequivocally the position of chlorination in the triphenylphosphine/carbon tetrachloride (TPP/CCl_4) reaction (3) with 1,2;5,6-di-*O*-isopropylidene-β-D-talose (**1**), and also to examine the detailed conformation of the molecule we have determined the crystal structure of the title compound (**2**).

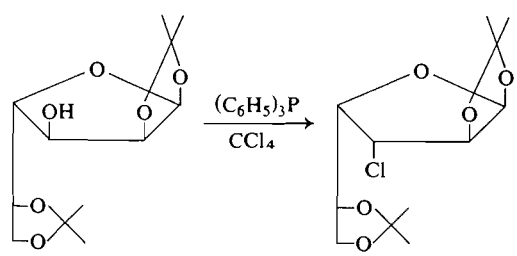

1 **2**

Experimental

Compound **2** was prepared by reacting 1,2;5,6-di-*O*-isopropylidene-β-D-talose with TPP/CCl_4 (3). Colorless needle-shaped single crystals suitable for diffraction studies were obtained by recrystallization from petroleum ether (b.p. 30–60°). Weissenberg photographs of the nets *hk*0–*hk*2 inclusive using CrKα radiation together with precession photographs of the zones *h*0*l*, and 0*kl* using MoKα radiation, showed systematic absences for *h*00: $h = 2n + 1$, 0*k*0: $k = 2n + 1$, 00*l*: $l = 2n + 1$. This combined with the Laue group *mmm*, indicated unambiguously the space group $P2_12_12_1$.

Crystal Data

$C_{12}H_{19}ClO_5$ f.w. = 278.7

Orthorhombic, $a = 9.744(6)$, $b = 26.76(2)$, $c = 5.403(3)$ Å, $V = 1408.8$ Å^3, ρo 1.27 g cm^{-3}, $Z = 4$, ρc 1.31 g cm^{-3}, 22 °C, μ(MoKα) = 2.9 cm^{-1}, λMoKα = 0.7107 Å.

Two crystals were used to provide the diffraction data; the crystal used for intensity measurements had dimensions 0.14 × 0.11 × 0.51 mm. The direction of greater elongation (*c* axis) was parallel to Φ. Cell constants were determined using MoKβ radiation $\lambda = 0.63225$ Å by applying a least-squares fit to 12 high angle reflections (the numbers in parentheses are the estimated standard errors).

Reflection intensities for the unique set of intensity data were manually measured using a Picker 4 circle goniostat equipped with our own semiautomation. Niobium filtered MoKα radiation was used in conjunction with a scintillation detector and pulse-height analysis. Measurements were made using a 1.5° take-off angle with a symmetrical θ–2θ scan of 1.6° width (carried out at a rate of 2°/min). Background counts of 24 s were measured at both scan limits. Of the 1119 intensities recorded in the range $0° < 2\theta < 45°$, 817 were above 1.8σ and were considered as observed reflections ($\sigma = \sqrt{N}$ where *N* is the scan count plus the total of both background counts). Three standard reflections were measured at least every 90 min and their intensities decreased steadily during the data collection. A decrease in crystal size, and a decrease in overall scale of approximately 20% during data collection can both be attributed to sublimation.

Can. J. Chem. Downloaded from www.nrcresearchpress.com by 210.87.254.42 on 09/05/12
For personal use only.

Can. J. Chem. Downloaded from www.nrcresearchpress.com by 210.87.254.42 on 09/05/12
For personal use only.

TABLE 1. Phases used to indicate the tangent refinement procedure

h	k	l	E	Phase
0	1	1	2.05	$-\pi/2$
7	15	0	2.03	$\pi/2$*
0	9	4	1.97	$-\pi/2$
10	1	0	1.82	0†
2	10	0	2.49	0‡

*Origin defining.
†Enantiomorph defining.
‡Variable.

Coincidence losses were shown to be negligible by measurement of all outstanding and some intermediate intensity reflections at low incident beam strength. No absorption corrections were made; the maximum error in F^2 which can result would be less than 1%. Lorentz and polarization factors were applied to give structure factors in the usual way.

Structure Determination

It was intended to solve the structure using three dimensional Patterson superposition techniques, however, after an examination of the sharpened Patterson function it became clear that there was considerable overlap and the chlorine–chlorine vectors were in doubt. Examination of the final coordinates shows vectors falling on or near lines of *mm* symmetry.

The structure was solved using the tangent refinement procedure (4, 5). One enantiomorph defining and three origin determining reflections were chosen together with an additional reflection of variable sign. These are shown in Table 1. *R*-Karle (4) was 0.18 for the correct sign (0) and 0.25 for the incorrectly signed (π) reflection.

Two electron density Fourier maps were computed (one for each sign of the variable), each map was phased on the signed structure factors of the 128 largest phased *E*'s. Seventeen of the 18 non-hydrogen atoms of the molecule were located in the correctly signed map.

Full-matrix least-squares refinement of all the non-hydrogen atoms commenced with $R = 0.34$ and proceeded with isotropic temperature factors to $R = 0.15$. Electron-density difference maps indicated anisotropic motion and, at a later stage, the position of the hydrogen atoms. The final refinement was computed allowing all non-hydrogen atom parameters to vary. Hydrogen atoms were given thermal motion parameters one unit larger than the atom to which they were bonded. The final value of $R = 0.057$.

All the variables introduced were justified by improved agreement meeting Hamilton's criterion (6). A constant weighting scheme was used with $\sigma F = 1.3$ until the final three cycles of refinement. At this point down-weighting of the weak reflections was indicated by an analysis of $\omega\Delta^2$ as a function of $\sin\theta/\lambda$, $|F_0|$, and h, k, and l. The final weighting scheme was such that $\sigma F = 1.14$ for $F_0 \geq 12.0$ and $\sigma F = 3.95/(F_0)^{1/2}$ for $F_{obs} < 12.0$. The error of fit $[\Sigma\omega(|F_0| - |F_c|)^2/(N_o - N_v)]^{1/2}$ where $N_o - N_v$ = number of observations − number of variables, was 0.92 (indicating the assigned standard errors were slightly too large). No trends in $\omega\Delta^2$ were present in an analysis of structure factor agreement after refinement was completed. The final value of $\omega R(\Sigma\omega(|F_0| - |F_c|)^2/\Sigma|F_0|^2)^{1/2}$ was 0.049.

TABLE 2. Coordinate parameters $\times 10^4$ where four significant figures are given and $\times 10^3$ where three are given

Atom	x	y	z	B(Å^2)
Cl(1)	−0256(2)	1040(1)	4185(7)	*
O(1)	2581(5)	2445(2)	4784(10)	*
O(2)	1119(5)	2314(2)	1616(9)	3.5(1)
O(4)	2462(5)	1606(2)	5809(9)	*
O(5)	4311(6)	0812(2)	4232(13)	*
O(6)	3869(6)	0188(2)	1523(13)	*
C(1)	1714(7)	2057(3)	559(1)	3.6(2)
C(2)	0683(7)	1985(2)	349(1)	3.3(1)
C(3)	0943(8)	1442(3)	265(1)	4.1(2)
C(4)	2398(8)	1355(2)	349(1)	3.4(1)
C(5)	2882(8)	0820(3)	379(2)	4.6(2)
C(6)	2699(9)	0509(3)	149(2)	5.7(2)
C(7)	0989(9)	3103(3)	380(2)	5.9(2)
C(8)	1905(7)	2693(3)	280(1)	3.1(1)
C(9)	2958(8)	2875(3)	097(2)	5.3(2)
C(10)	5664(12)	0775(4)	056(3)	9.9(3)
C(11)	4932(10)	0477(3)	256(2)	*
C(12)	5882(11)	0121(4)	395(2)	7.3(3)
H(1)	137	208	723	5.
H(2)	−024	200	379	4.
H(3)	089	143	114	5.
H(4)	300	152	237	5.
H(5)	233	067	506	6.
H(61)	184	034	167	7.
H(62)	290	068	008	7.
H(71)	158	335	451	7.
H(72)	034	292	496	7.
H(73)	039	317	241	7.
H(91)	346	259	076	6.
H(92)	332	312	191	6.
H(93)	245	302	−038	6.
H(101)	490	100	011	11.
H(102)	626	082	120	11.
H(103)	610	050	−010	11.
H(121)	537	003	529	8.
H(122)	597	−006	252	8.
H(123)	651	034	434	8.

Atom	U_{11}†	U_{22}	U_{33}	U_{12}	U_{13}	U_{23}
Cl(1)	63(2)	61(1)	144(3)	−20(1)	13(2)	7(2)
O(1)	52(3)	48(3)	39(3)	−8(3)	−14(3)	3(3)
O(4)	65(4)	52(3)	36(3)	12(3)	−12(3)	−5(3)
O(5)	72(4)	76(4)	84(5)	30(3)	−35(4)	−33(4)
O(6)	73(4)	49(3)	95(5)	8(3)	−19(4)	−30(4)
C(11)	83(7)	44(4)	58(5)	0(5)	1(6)	0(5)

*Anisotropic thermal parameter (Å^2 × 10^3).
†These values were obtained from $\beta_{ij} = 2\pi^2 b_i b_j U_{ij}$ where β_{ij} appear as the temperature effect through $\exp[-(\beta_{11}h^2 \ldots + 2\beta_{12}hk \ldots)]$ in the structure factor expression and b_i are the reciprocal lattice vectors.

An electron density difference map computed after the refinement was complete showed large peaks and troughs of +0.22 (near C(6)) and −0.24 eÅ^{-3} (near C(7)) respectively, the standard error in the electron density is 0.12 eÅ^{-3}.

Scattering factors used throughout were taken from "International Tables for X-ray Crystallography" (7) and included both components of the anomalous scattering in the case of the chlorine atom.

Table 2 gives the final atomic parameters. Table 3 lists the relevant interatomic distances and angles. Estimated standard errors appear in parentheses and, where appropriate, include contribution from the cell dimensions and those

TABLE 3. Interatomic distances and angles (Å and degrees)

(*a*) Distances

Bonded contacts			
Cl(1)—C(3)	1.793(8)	C(1)—C(2)	1.525(10)
O(1)—C(1)	1.406(8)	C(2)—C(3)	1.545(10)
O(1)—C(8)	1.423(8)	C(3)—C(4)	1.507(10)
O(2)—C(2)	1.409(8)	C(4)—C(5)	1.516(10)
O(2)—C(8)	1.423(8)	C(5)—C(6)	1.510(12)
O(4)—C(1)	1.415(8)	C(7)—C(8)	1.514(10)
O(4)—C(4)	1.424(8)	C(8)—C(9)	1.507(10)
O(5)—C(5)	1.413(9)	C(10)—C(11)	1.521(14)
O(5)—C(11)	1.407(10)	C(11)—C(12)	1.524(12)
O(6)—C(6)	1.428(10)		
O(6)—C(11)	1.410(10)		
Intermolecular contacts <3.5 Å (not involving hydrogen atoms)			
O(2) .... C(1)	3.35	$x, y, z-1$*	
O(2) .... C(9)	3.43	$-\frac{1}{2}+x, \frac{1}{2}-y, -z$*	

*Symmetry operation involved to generate the second atom of the contact.

(*b*) Angles

C(8)—O(1)—C(1)	107.4(5)	O(5)—C(5)—C(4)	109.9(6)
C(8)—O(2)—C(2)	106.5(5)	O(5)—C(5)—C(6)	104.2(7)
C(1)—O(4)—C(4)	107.8(6)	C(4)—C(5)—C(6)	113.2(7)
C(5)—O(5)—C(11)	109.1(7)	O(6)—C(6)—C(5)	103.1(7)
C(6)—O(6)—C(11)	105.2(6)	O(1)—C(8)—O(2)	104.7(6)
O(1)—C(1)—O(4)	110.2(6)	O(1)—C(8)—C(7)	110.0(6)
O(1)—C(1)—C(2)	105.1(6)	O(1)—C(8)—C(9)	109.3(6)
O(4)—C(1)—C(2)	107.1(6)	O(2)—C(8)—C(7)	111.1(6)
O(2)—C(2)—C(1)	104.9(5)	O(2)—C(8)—C(9)	107.6(6)
O(2)—C(2)—C(3)	108.9(6)	C(7)—C(8)—C(9)	113.6(7)
C(1)—C(2)—C(3)	103.4(6)	O(5)—C(11)—O(6)	106.8(7)
Cl(1)—C(3)—C(2)	108.7(6)	O(5)—C(11)—C(10)	108.8(7)
Cl(1)—C(3)—C(4)	112.3(5)	O(5)—C(11)—C(12)	110.2(8)
C(2)—C(3)—C(4)	102.1(6)	O(6)—C(11)—C(10)	110.4(8)
O(4)—C(4)—C(3)	103.5(6)	O(6)—C(11)—C(12)	107.4(6)
O(4)—C(4)—C(5)	109.7(6)	C(10)—C(11)—C(12)	113.1(9)

from the variance–covariance matrix. No corrections to bond lengths for anisotropic thermal motion were made. A table listing $|F_o|, |F_c| = (A^2 + B^2)^{1/2}$, and α for each measured reflection can be obtained from the Depository of Unpublished Data, National Science Library, National Research Council of Canada, Ottawa K1A 0S2. (Accidentally unobserved reflections are indicated as $-\sigma/2$ in place of $|F_o|$.) Figure 1 shows the packing of the molecules within the unit cell, viewed down the *c* axis.

The major programs used are listed in ref. 8, in addition the NRCC Tangent Refinement Program was used in the structure solution. Calculations were carried out at the Simon Fraser University Computing Centre on an IBM 360/50.

Discussion

The crystal structure analysis has shown (Table 3) that there are no significant intermolecular interactions; while this is an advantage in eliminating any conformational changes which may result from hydrogen bonding, it has also permitted a larger amount of thermal motion (with a corresponding decrease in accuracy). The bond lengths and angles show chemically expected variations and are close to accepted values.

Two major structural features are important in this molecule and both are related to the method of preparation of this chloro sugar (3). Firstly, the site of halogenation is clearly at C(3), confirming that substitution of chlorine for hydroxyl took place without rearrangement of the acetal functions. Several closely related reagents (1, 2) have been shown to effect halogenation only after extensive rearrangement of the acetal blocking groups. Clearly such rearrangements are not involved in the chlorination of 1,2;5,6-di-*O*-isopropylidene-β-D-talofuranose. Secondly, the configuration about C(3) shows that replacement of the hydroxyl in the talofuranose derivative occurred stereospecifically and with inversion to give the idofuranose derivative. Nuclear magnetic spectroscopy (15)

Can. J. Chem. Downloaded from www.nrcresearchpress.com by 210.87.254.42 on 09/05/12
For personal use only.

Can. J. Chem. Downloaded from www.nrcresearchpress.com by 210.87.254.42 on 09/05/12
For personal use only.

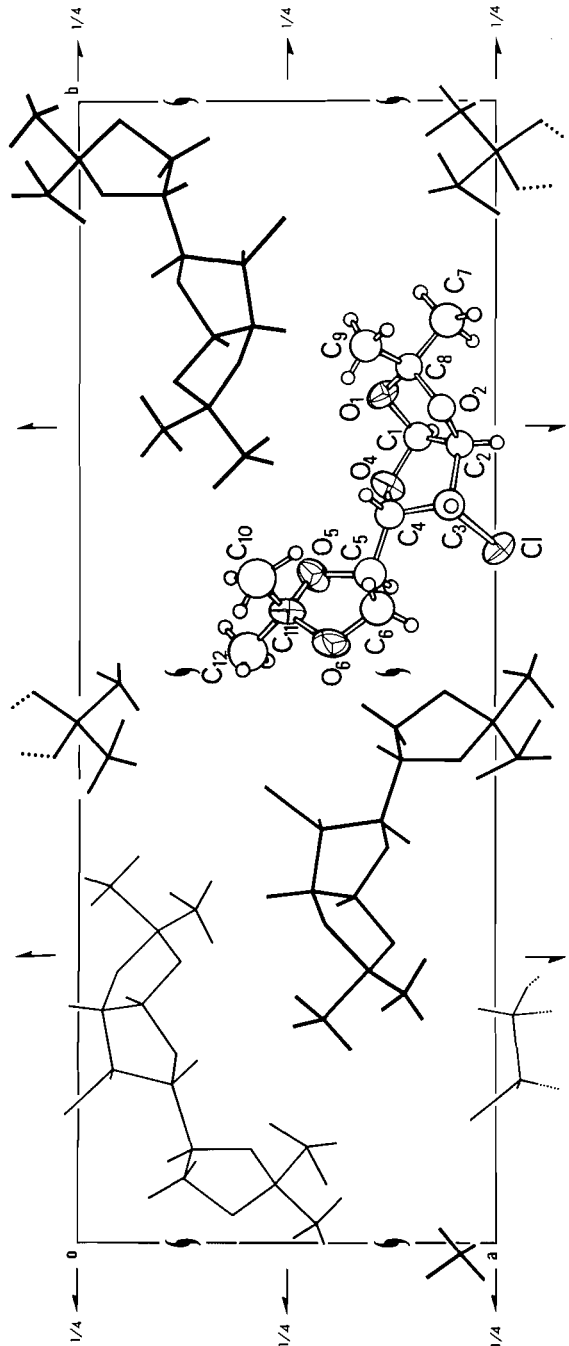

FIG. 1. The crystal structure of 3-chloro-3-deoxy-1,2;5,6-di-*O*-isopropylidene-β-D-idose viewed down the *c* axis.

TABLE 4. Equations of selected planes*

Plane	*A*	*B*	*C*	*D*	χ^2
O(1),C(1),C(2)	0.6068	−0.6723	−0.4240	−3.9678	—
C(1),C(2),O(2)	0.5737	−0.7224	−0.3860	−4.1844	—
O(5),C(5),C(6)	0.1086	0.8198	−0.5622	0.9518	—
C(5),C(6),O(6)	0.5184	0.6754	−0.5246	1.8626	—
O(4),C(1),C(2),C(3)	0.6704	0.3330	−0.6631	0.9567	1.7
O(1),C(1),C(2),O(2)	0.6133	−0.6939	−0.3774	−3.9646	35.4†

*The equation has the form $Ax + By + Cz - D = 0$ where x, y, and z are expressed in Å.
†These atoms are *not* coplanar within the limits of error.

had indicated this to be the case but this crystal structure determination settles the point unambiguously.

Conformations of five-membered rings, especially those containing oxygen atoms, are of considerable interest since the furan ring is a component of the biologically important nucleotides and nucleic acids. Extensive X-ray crystal structural studies have shown the furan ring in nucleotides adopts a conformation with either carbon atoms 2 and/or 3 out of the plane of the ring (9), in keeping with earlier suggestions that such a ring puckering would be the most stable (10, 11). The structure of 3-chloro-3-deoxy-1,2;5,6-di-*O*-isopropylidene-β-D-idofuranose (**2**) is clearly of interest in this respect since it contains three five-membered rings, one of which is a furan ring (C(1)—C(2)—C(3)—C(4)—O(4)). Inspection of the molecular structure and Table 4 shows the furan ring conformation as an envelope with carbon atom four displaced from the mean plane of C(1), C(2), C(3), and O(4), ^4V in Hall's designation (12), and quite out of keeping with previous suggestions (10, 11). A similar furanose conformation was found for the crystal structure of 6-azido-5,6-dideoxy-5-iodo-1,2-*O*-isopropylidene-β-L-idofuranose (**3**) (13). However, a recent communication (14) revealing the crystal structure of the methyl ester of 1,2,3,5-tetra-*O*-acetyl-β-D-galactofuranuronate (**4**) to be one in which C(1) is displaced in from the mean plane (^1V) suggests the *cis* fused 1,2-*O*-isopropylidene ring is not responsible for this apparently anomalous behavior. Recent n.m.r. studies (15) indicate that position of substitution is an important criterion in the conformational preference of furanose rings in solution.

The conformation of the two remaining five-membered dioxolane rings are most difficult to describe since they adopt twist conformations to different extents. Table 4 describes equations of planes formed by atoms in these rings. The 1,2-*O*-isopropylidene ring is the less twisted of two with the dihedral angle O(1)—C(1)—C(2)—O(2) being 4.1(7)° with C(8) being displaced in an *exo* fashion from the fused ring system. This is in keeping with recent n.m.r. spectroscopic work (15) and the two other crystal structures (**3** and **5**) reporting this structural feature (13, 16). The 5,6-*O*-isopropylidene ring is twisted to a great extent, the dihedral angle O(5)—C(5)—C(6)—O(6) being 25.2(9)°. Again, this agrees well with n.m.r. (15) and the only other structure (16) reporting this molecular arrangement, **5**.

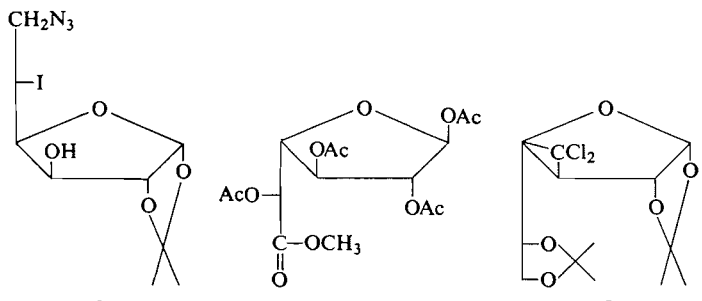

Can. J. Chem. Downloaded from www.nrcresearchpress.com by 210.87.254.42 on 09/05/12
For personal use only.

We are pleased to thank the National Research Council of Canada for financial support in the form of Operating Grants. We also wish to thank Drs. F. R. Ahmed, C. Huber, and B. R. Penfold for providing us with their computer programs.

1. S. HANESSIAN and N. R. PLESSAS. Chem. Commun. 1152 (1967); J. Org. Chem. **34**, 2162 (1969).
2. N. K. KOCHETKOV and A. I. USOV. Tetrahedron, **19**, 973 (1963).
3. C. R. HAYLOCK, L. D. MELTON, K. N. SLESSOR, and A. S. TRACEY. Carbohydr. Res. **16**, 375 (1971).
4. J. KARLE and I. L. KARLE. Acta Cryst. **21**, 849 (1966).
5. J. KARLE. Acta Cryst. B**24**, 182 (1968).
6. W. C. HAMILTON. Statistics in physical sciences. Ronald Press, New York, 1964. p. 217.
7. International tables for X-ray crystallography. Vol. III. Sect. 3.3 (1965).
8. L. Y. Y. CHAN and F. W. B. EINSTEIN. Can. J. Chem. **49**, 468 (1971).
9. B. CAPON. Chem. Rev. **69**, 412 (1969).
10. M. SPENCER. Acta Cryst. **12**, 59 (1959).
11. R. U. LEMIEUX and R. NAGARAJAN. Can. J. Chem. **42**, 1270 (1964).
12. L. D. HALL, P. R. STEINER, and C. PEDERSEN. Can. J. Chem. **48**, 1155 (1970).
13. J. S. BRIMACOMBE, J. G. H. BRYAN, and T. A. HAMOR. J. Chem. Soc. (B), 514 (1970).
14. J. P. BEALE, N. C. STEPHENSON, and J. D. STEVENS. Chem. Commun. 25 (1971).
15. K. N. SLESSOR and A. S. TRACEY. Unpublished results.
16. J. S. BRIMACOMBE, P. A. GENT, and T. A. HAMOR. J. Chem. Soc. (B), 1566 (1968).

Can. J. Chem. Downloaded from www.nrcresearchpress.com by 210.87.254.42 on 09/05/12
For personal use only.

Dielectric and Association Behavior of 1-Propanol, 2-Propen-1-ol, and 2-Propyn-1-ol in Non-polar Solvents

G. E. RAJALA AND J. CROSSLEY

Department of Chemistry, Lakehead University, Thunder Bay, Ontario

Received August 31, 1971

Dielectric constants and losses of 1-propanol, 2-propen-1-ol, and 2-propyn-1-ol in *p*-xylene, and 1-propanol and 2-propen-1-ol in cyclohexane have been measured at up to 10 frequencies in the range 1–145 GHz at 25 °C. The low frequency dielectric constants have also been measured at 2 MHz. An analysis in terms of two relaxation times has been obtained for each system. The short relaxation times are relatively independent of the alcohol, its concentration, and the solvent. Conversely, the longer relaxation times lengthen with increased alcohol concentration, lengthen in the order 2-propyn-1-ol, 2-propen-1-ol, 1-propyn-1-ol and are considerably shorter in *p*-xylene than in cyclohexane.

On a mesuré les pertes et les constantes diélectriques du 1-propanol, du 2-propène-1-ol, et du 2-propyne-1-ol dans le *p*-xylène et celles du 1-propanol et du 2-propène-1-ol dans le cyclohexane, jusqu'à dix fréquences dans la région de 1–145 GHz à 25 °C. On a aussi mesuré les constantes diélectriques à basse fréquence à 2 MHz. On a obtenu une analyse en termes de deux temps de relaxation pour chaque système. Les temps de relaxation courts sont relativement indépendants du type d'alcool utilisé, de sa concentration et du solvant. D'autre part, les temps de relaxation longs augmentent avec la concentration en alcool, cette augmentation se faisant dans l'ordre suivant: 2-propyne-1-ol, 2-propène-1-ol, 1-propyne-1-ol; ils sont considérablement plus courts dans le *p*-xylène que dans le cyclohexane.

Canadian Journal of Chemistry, **50**, 99 (1972)

Can. J. Chem. Downloaded from www.nrcresearchpress.com by 210.87.254.42 on 09/05/12
For personal use only.

Introduction

In dilute solution the microwave absorption of aliphatic alcohols may be characterized by two relaxation times (1–4). The high frequency process is undoubtedly due to the rotation of hydroxyl groups about their C—O bonds. Reorientation of monomers and low polymers, together with —OR groups in polymers, has received strong support as the most likely mechanism for the longer relaxation time. The magnitude of this relaxation time, its weight factor, and the apparent dipole moment are sensitive to the alcohol chain length, its concentration, the basicity of the solvent, and the steric environment of the hydroxyl group. At higher alcohol concentrations a third low frequency process, which is responsible for almost the entire absorption of pure liquid *n*-alkanols, emerges (5).

Recently the dielectric properties of pure liquid 2-propen-1-ol and 2-propyn-1-ol have been measured (6), at frequencies less than 500 MHz, and the results compared with those previously reported for 1-propanol (7). It was considered that the unsaturation in alkenols and alkynols may enhance molecular interactions not possible in alkanols. Very little difference was in fact observed for the equilibrium dielectric constants and their temperature dependence, and the dielectric dispersion of 2-propen-1-ol was typical of the monoalkanols. However, the Arrhenius activation parameters for 1-propanol and 2-propen-1-ol differed significantly. The high frequency relaxation processes were not examined, and liquid 2-propyn-1-ol could not be cooled sufficiently to bring its main dispersion into their frequency range.

One of us (4) has examined the disassociating effect of electron donor solvents on alkanols by dielectric relaxation measurements. We decided to investigate the effect of solute–solute interactions on the two high frequency relaxation processes of alcohols by measuring 1-propanol, 2-propen-1-ol and 2-propyn-1-ol in solution, in the microwave region at 25 °C.

Experimental

The apparatus and procedure for determining the dielectric constant and loss at the frequencies (up to 10 in the range 1–145 GHz) employed in this study have been described previously (8–10).

Materials

1-Propanol and 2-propen-1-ol were dried over calcium hydride and fractionally distilled under reduced pressure. 2-Propyn-1-ol, which polymerizes on standing, was dried over calcium hydride, distilled under reduced pressure, and finally purified by molecular distillation and stored under

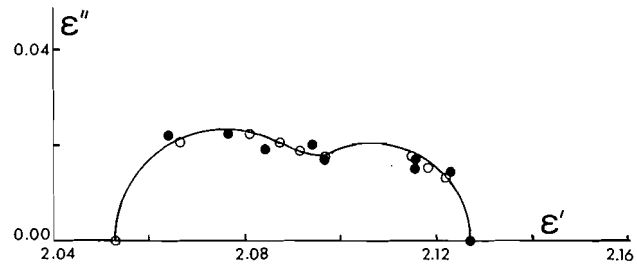

FIG. 1. Cole–Cole plot for 1-propanol at 0.0588 mol fraction in cyclohexane. Solid circles are experimental points and open circles are points calculated for the same frequencies using the relaxation parameters given in Table 1.

TABLE 1. Static dielectric constant, high frequency dielectric constant, relaxation time (ps), weight factor, and apparent dipole moment (in D units) data for 1-propanol, 2-propen-1-ol, and 2-propyn-1-ol at several mol fractions (f_2) in cyclohexane and *p*-xylene solution at 25 °C

f_2	Solvent	τ_2	τ_3	C_2	ε_∞	μ	ε_0
			1-Propanol				
0.0492	Cyclohexane	41	3.0	0.42	2.050	1.05	2.1071
0.0588		48	3.2	0.44	2.053	1.09	2.1263
0.0789		55	3.4	0.49	2.065	1.13	2.1737
0.1020		68	3.6	0.54	2.083	1.18	2.2402
0.1201		102	4.6	0.57	2.090	1.25	2.3016
0.1487		141	5.5	0.63	2.112	1.36	2.4315
0.1987		185	4.9	0.72	2.140	1.56	2.7328
0.0441	*p*-Xylene	19	2.6	0.50	2.290	1.51	2.3953
0.0668		27	2.9	0.48	2.295	1.53	2.4612
			2-Propen-1-ol				
0.0521	Cyclohexane	24	1.2	0.53	2.036	1.31	2.1304
0.0588		33	3.0	0.50	2.050	1.24	2.1461
0.0794		41	3.1	0.53	2.060	1.28	2.2034
0.0981		43	3.5	0.56	2.075	1.31	2.2634
0.1221		61	4.5	0.57	2.099	1.36	2.3566
0.1508		83	6.3	0.60	2.150	1.37	2.4924
0.0448	*p*-Xylene	15	2.8	0.54	2.300	1.49	2.405
0.0638		23	2.9	0.45	2.300	1.56	2.4683
			2-Propyn-1-ol				
0.0475	*p*-Xylene	14	2.4	0.51	2.290	1.54	2.4103
0.0651		12	2.1	0.66	2.310	1.54	2.4779

vacuum. This alcohol is insoluble in cyclohexane and tends to polymerize when allowed to stand in *p*-xylene solution. All the measurements on each 2-propyn-1-ol solution were made in a single day. There was no evidence of polymerization during that time and the static dielectric constants were the same before and after the microwave measurements.

Cyclohexane and *p*-xylene were dried over and distilled from sodium.

Results

Cole–Cole plots (11) for all the systems were unsymmetrical (Fig. 1) and it was possible to analyze each set of dielectric data for two relaxation times τ_2 and τ_3, their weight factors C_2 and C_3 respectively, and the high frequency dielectric constant ε_∞. The computer method used to obtain the analyses has been described previously (3). The errors involved in the measurements and analyses have been discussed elsewhere (12).

As before (3) apparent dipole moments μ were calculated using the Onsager equation.

The experimental dielectric constant and loss values have been placed in a depository.[1] Static dielectric constants ε_0, very high frequency dielectric constants ε_∞, relaxation times τ_2 and τ_3, weight factors C_2, and apparent dipole moments μ are presented in Table 1.

[1]Copies of material in the depository may be obtained from: Depository of Unpublished Data, National Science Library, National Research Council of Canada, Ottawa, Canada K1A 0S2.

Can. J. Chem. Downloaded from www.nrcresearchpress.com by 210.87.254.42 on 09/05/12
For personal use only.

Can. J. Chem. Downloaded from www.nrcresearchpress.com by 210.87.254.42 on 09/05/12
For personal use only.

Discussion

The dielectric dispersions for all the solutions examined can not be represented by either a single Debye relaxation or a Cole–Cole distribution. The complex plane plots are obviously unsymmetrical and analyses in terms of two relaxation times give a satisfactory representation of the experimental data. The relaxation times, shown in Table 1, are consistent and compare favorably with values obtained previously for monohydric alkanols in non-polar solvents (1–4).

The short relaxation times τ_3 are very similar to those reported for phenols (13, 14) and other alcohols, as the pure liquids (5) or in solution (1–4). They are relatively independent of the alcohol and the solvent, and are probably associated with the reorientation of —OH dipoles about their C—O bonds. This process is the predominant mechanism in very dilute solution (15). For 2-propen-1-ol and 2-propyn-1-ol an additional fast relaxation process, involving the rotation of $—C{=}CH_2$ and $—C{\equiv}CH$ groups about their C—C bonds, is possible (16). However, the dipole component perpendicular to the axis of rotation for these groups, and thus the contribution to the absorption, is very small compared to that for the —OH group. In addition, it is anticipated that the relaxation times for —OH, $—C{=}CH_2$, and $—C{\equiv}CH$ group rotations would be very similar.

The possible origins of the relaxation time τ_2 have been discussed in detail elsewhere (1, 17). Its magnitude and weight factor are dependent upon the alcohol size, its concentration, and the solvent. Figure 2 shows the concentration dependence of τ_2 for 1-propanol, 2-propen-1-ol, and 1-butanol (4) in cyclohexane (2-propyn-1-ol is insoluble in cyclohexane). It is apparent that τ_2 decreases in the order 1-butanol, 1-propanol, 2-propen-1-ol in all concentrations. The longer values for 1-butanol are consistent with Johari and Smyth's (18) hypothesis that, in dilute solution, monomer reorientation is the major mechanism responsible for τ_2. However, l-propanol and 2-propen-1-ol are essentially the same shape and size and the considerably shorter τ_2 values for the latter must, in some way, be due to the olefinic linkage. In *p*-xylene solution τ_2 decreases in the order 1-propanol, 2-propen-1-ol, 2-propyn-1-ol, *i.e.* with increased multiple bond character of the terminal carbon–carbon bond. Also, as noted previously (4), the τ_2 values in cyclohexane are longer than those in *p*-xylene solution at similar concentrations. The low frequency relaxation process τ_1, which is responsible for almost the entire absorption of pure liquid *n*-alkanols (5), has been detected above about 0.15 mol fraction and undoubtedly makes some contribution at lower concentrations (1). The absence of any dielectric loss data at frequencies below 1 GHz did not allow us to observe τ_1 or to analyze our data for three relaxation times. It is probable that our τ_2 values contain some contribution from τ_1 and the slopes (Fig. 2) do appear to increase sharply above about 0.08–0.1 mol fraction alcohol.

The dipole moments of 1-butanol and 1-propanol in cyclohexane are almost the same but, at concentrations less than 0.12 mol fraction, they are significantly smaller than those for 2-propen-1-ol. In *p*-xylene the dipole moments of 1-butanol (3), 1-decanol (4), 1-propanol, 2-propen-1-ol, and 2-propyn-1-ol are similar and relatively independent of concentration. The dipole moment of a monomeric alkanol in the gaseous phase is about 1.7 D. In dilute solution alcohol self association predominantly involves the formation of small weakly polar multimers, with increased concentration association into larger highly polar multimers becomes progressively more important and the dipole moments of *n*-alkanols increase markedly with increased concentration (2). Electron donor solvents, such as *p*-xylene have a disassociating effect on alcohol multimers (19). At those concentrations where weakly polar multimers are the most important associated species, the dipole moments increase with increased solvent basicity and are smallest in inert solvents, such as cyclohexane, in which alcohol self association is the most extensive. Conversely, when highly polar multimers are predominant the dipole moments decrease with increased solvent basicity, and are largest in inert solvents (4). The dipole moment of 1-propanol in cyclohexane increases with increased alcohol concentration, which indicates that large highly polar multimers become progressively more important. For 2-propen-1-ol the dipole moment in cyclohexane shows only small changes in this concentration range which suggests that association into large multimers is less extensive than for 1-propanol.

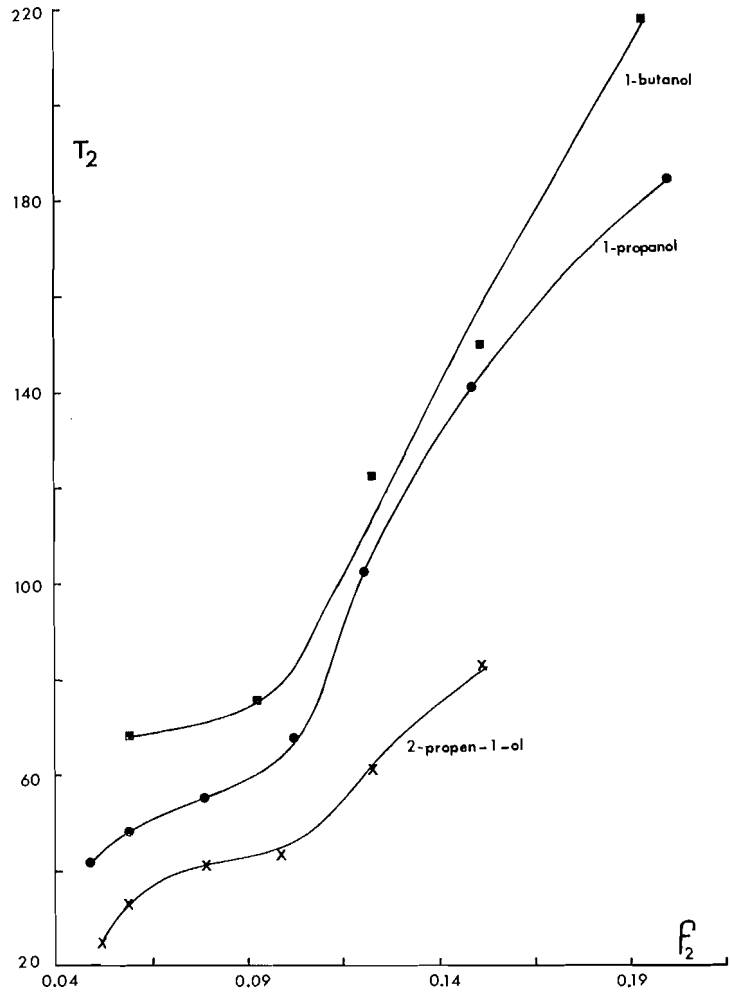

FIG. 2. Relaxation time τ_2 (ps) at 25 °C for 1-butanol, 1-propanol, and 2-propen-1-ol in cyclohexane.

The differences in the dielectric properties of 1-propanol, 2-propen-1-ol, and 2-propyn-1-ol are somewhat analogous to those observed for an alkanol in an inert and an electron donor solvent. In both situations an alternative to the O—H···O type of molecular interaction is probably responsible. For 2-propen-1-ol and 2-propyn-1-ol interactions involving the hydroxyl group and the unsaturated carbon–carbon bond and/or the terminal hydrogen atoms may provide additional molecular interactions which are not possible for 1-propanol. The shorter τ_2 values and larger dipole moments observed for the unsaturated alcohols suggest that such interactions are not negligible. This disassociating effect appears to be greatest for 2-propyn-1-ol which has the most acidic terminal hydrogen atom, and is most evident in the relatively inert cyclohexane. Interactions between the hydroxyl hydrogen atoms and the π-electrons of the solvent are possible for all three alcohols in *p*-xylene.

1. J. CROSSLEY, L. GLASSER, and C. P. SMYTH. J. Chem. Phys. **55**, 2197 (1971).
2. J. CROSSLEY, L. GLASSER, and C. P. SMYTH. J. Chem. Phys. **52**, 6203 (1970).
3. J. CROSSLEY. Can. J. Chem. **49**, 712 (1971).
4. J. CROSSLEY. J. Phys. Chem. **75**, 1790 (1971).
5. S. K. GARG and C. P. SMYTH. J. Phys. Chem. **69**, 1294 (1965).
6. W. DANNHAUSER, R. GUERIN, and A. F. FLUECKINGER. J. Chem. Phys. **52**, 6446 (1970).
7. D. W. DAVIDSON and R. H. COLE. J. Chem. Phys. **19**, 1484 (1951); **20**, 1389 (1952).

Can. J. Chem. Downloaded from www.nrcresearchpress.com by 210.87.254.42 on 09/05/12
For personal use only.

8. S. K. GARG, H. KILP, and C. P. SMYTH. J. Chem. Phys. **43**, 2341 (1965).
9. W. F. HASSELL, M. D. MAGEE, S. W. TUCKER, and S. WALKER. Tetrahedron, **20**, 2137 (1964).
10. S. E. KEEFE and E. H. GRANT. Rev. Sci. Instrum. **39**, 1800 (1968).
11. K. S. COLE and R. H. COLE. J. Chem. Phys. **9**, 341 (1941).
12. M. D. MAGEE and S. WALKER. Trans. Faraday Soc. **62**, 3093 (1966).
13. F. K. FONG and C. P. SMYTH. J. Am. Chem. Soc. **85**, 1565 (1963).
14. M. D. MAGEE and S. WALKER. Trans. Faraday Soc. **62**, 1748 (1966).
15. Y. LEROY. Thesis. Université de Lille, France, 1964.
16. G. E. RAJALA and J. CROSSLEY. Unpublished results of liquid 1-alkenes.
17. L. GLASSER, J. CROSSLEY, and C. P. SMYTH. J. Chem. Phys. To be published.
18. G. P. JOHARI and C. P. SMYTH. J. Am. Chem. Soc. **91**, 6215 (1969).
19. J. MALECKI. J. Chem. Phys. **43**, 1351 (1965).

Can. J. Chem. Downloaded from www.nrcresearchpress.com by 210.87.254.42 on 09/05/12
For personal use only.

Selectivity in NBS Bromination. I. The Reaction of Methyl Enol Ethers of Cyclohexane-1,3-diones. A Reexamination

D. V. C. AWANG,[1] A. VINCENT, W. L. WILSON, AND H. W. AVDOVICH
Department of National Health and Welfare, Tunney's Pasture, Ottawa, Canada K1A OL2

Received May 19, 1971

The n.m.r. spectral analysis utilising solvent- and $Eu(DPM)_3$-induced chemical shifts demonstrates that the reaction of *N*-bromosuccinimide with the methyl enol ethers of cyclohexane-1,3-dione and dimedone leads to bromine substitution at the carbon atom allylic to the olefinic bond, and not at the olefinic site or α to carbonyl, respectively, as previously claimed.

Par l'utilisation en r.m.n. des déplacements chimiques induits par les solvants et $Eu(DPM)_3$, il est prouvé que la réaction entre le *N*-bromosuccinimide et l'éther méthyl énolique de la cyclohexanedione-1,3 conduit à une substitution par le brome sur le carbone allylique à la double liaison, et non pas sur le site oléfinique ou en α du carbonyle, comme cela avait été respectivement annoncé.

Canadian Journal of Chemistry, **50**, 104 (1972)

Can. J. Chem. Downloaded from www.nrcresearchpress.com by 210.87.254.42 on 09/05/12
For personal use only.

The remarkable antibacterial activity of tetracyclines has been imputed to their characteristic A-ring (1), whose salient chemical features are represented by cyclohexane-1,3-diones bearing carbamoyl and dimethylamino substituents at the 2- and 4-positions, respectively. One of the general approaches to synthesis of model compounds for study of structure–activity relationships and stability factors involves derivatization of 1,3-diones; carbamoylation at the 2-position of 1,3-diones, unsubstituted at that site, can readily be achieved (1, 2), but functionalization of the 4-position is not so easily accomplished.

Bromination of cyclohexane-1,3-dione, dimedone, and monoenolates of 5-phenylcyclohexane-1,3-diones using *N*-bromosuccinimide (NBS) under radical-promoting conditions leads to substitution at the 2-position (3). It has been reported, however (4), that the methyl enol ether of dimedone, 3-methoxy-5,5-dimethylcyclohex-2-enone (**1**), undergoes substitution at the 6-position upon reaction with NBS under similar conditions. In the case of the enolates of symmetrical cyclohexane-1,3-diones, the question of whether substitution occurs at the 4- or 6-position, although a matter of some fundamental significance,[2] does not jeopardize the potential

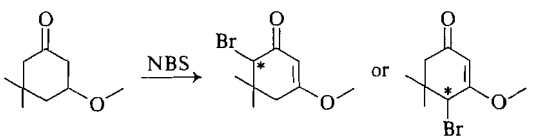

1 **2** **3**

of the synthetic plan, since hydrolysis of both 4- and 6-bromoenolates would lead to 4-bromo-1,3-dione; but the answer may be of crucial importance to the application of any synthetic scheme which involves this bromination step in the derivatization of *unsymmetrical* cyclohexane-1,3-diones. Arakawa (4) has based his conclusion that **2** rather than **3** is the product of NBS reaction with **1** on what appears to be rather tenuous *chemical* evidence: easy condensation of the bromination product with nitrogen bases and ready reaction with Brady's reagent were thought to be indicative of an α-haloketone, as was formation of an "osazone"[3] rather than a tris(2,4-dinitrophenylhydrazone) upon treatment of the initially formed bromohydrazone[3]

[1]To whom correspondence should be addressed.

[2]The bromine atom, which is the chain-carrying species in NBS allylic bromination is a strong acceptor radical (5). The passivity of cyclohexanone towards NBS in the presence of cyclohexene is imputed to polar factors affecting the stability of the transition state for hydrogen abstraction: the carbonyl dipole militates against the development of positive charge at the α carbon.

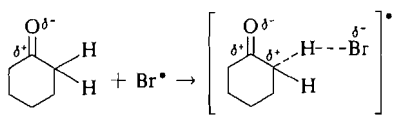

While the same rationale can be expected to apply to the case of simple α,β-unsaturated ketones, the effect of polar substituent groups on the selectivity of bromine substitution in such systems cannot be readily surmised.

[3]The detailed structures of the "osazone" and bromohydrazone were not elucidated.

Can. J. Chem. Downloaded from www.nrcresearchpress.com by 210.87.254.42 on 09/05/12
For personal use only.

with an excess of Brady's reagent. Arakawa's decision seemed unjustified, since the relative reactivity of α'- and γ-brominated α,β-unsaturated ketones was not considered, and since it has been established unequivocally by n.m.r. spectral analysis (6) that NBS bromination of cyclopent-2-enone leads to substitution at the 4-position.[4] Also, the claim by Arakawa and Irie (3) that monoenolates of cyclohexane-1,3-dione yield 2-bromo derivatives upon reaction with NBS appeared enigmatic, in face of the claimed dimedone enol ether result. Because of these apparent inconsistencies, and the possible theoretical and synthetic implications a re-examination of these reactions was undertaken.

The n.m.r. spectral analysis of the product of reaction of NBS with **1** establishes that bromine substitution takes place at carbon atom 4 rather than at carbon atom 6, yielding **3** instead of **2** as previously claimed (4); similar examination of the product of NBS reaction of isophorone confirms, as expected, the conclusion by earlier workers (8) that substitution occurs at the 4-position. The reaction of NBS with the methyl enol ether of cyclohexane-1,3-dione also leads to substitution at the 4-position, rather than at the 2-position as formerly reported (3).

The disposition of bromine in the products of the NBS reaction is clear from a consideration of the solvent-induced chemical shifts (Table 1) observed in the n.m.r. spectrum on passing from dilute solution in carbon tetrachloride to dilute solution in benzene ($\Delta = \delta(CCl_4) - \delta(C_6H_6)$ p.p.m.); the signs and magnitudes of the observed shifts are in accord with the generalization that the signals of protons lying behind a reference plane, perpendicular to the αC—CO—α'C plane through the carbonyl carbon atom, suffer positive shifts whereas those of protons in front of the plane undergo negative shifts and those of protons close to the plane exhibit very small and variable shifts (10). The downfield shifts induced by trifluoroacetic acid (TFA) ($\Delta = \delta(CDCl_3) - \delta(TFA)$ p.p.m.) also support these assignments, on the premise that protonation of carbonyl oxygen predominates.

The structures indicated by the solvent shift observations eminently satisfy the data (Table 2) available from reagent shift studies employing $Eu(DPM)_3$, if one assumes complexation of the shift reagent at the carbonyl oxygen (11).

It seems clear from this work that substitution of the methoxyl group for the C-3 hydrogen of cyclic 2-enone systems[6] does not promote a departure from the general rule that radical bromination by NBS effects substitution at the carbon atom allylic to the olefinic bond.

Experimental

The n.m.r. spectra were recorded on a Varian A-60A spectrometer operated at an ambient probe temperature of 40 ± 2 °C. The i.r. spectra were obtained using a Perkin–Elmer Model 621 spectrophotometer.

Materials

Dimedone, 1,3-cyclohexanedione, and isophorone were obtained commercially. The latter liquid was purified by vacuum distillation. The enol ethers were prepared by methylation of the diones using methanol – sulfuric acid according to the procedure of Arakawa and Irie (3).

General Bromination Procedure

NBS brominations were conducted in the standard manner (12) employing a 100 W, Photoflood No. 2 lamp to maintain reflux of carbon tetrachloride while providing a catalytic radiative source. Irradiation was halted as soon as it was estimated, visually, that the NBS had been consumed. The reaction product was quickly cooled, succinimide filtered off and the filtrate concentrated.

The n.m.r. analysis of the filtrates indicated that better than 95% conversion to product was achieved in all cases.

Bromination products were purified by preparative t.l.c. on silica gel GF_{254} using benzene–ether (9:1). Satisfactory microanalyses were obtained for all products.

4-Bromo-5,5-dimethyl-3-methoxycyclohex-2-enone (3)

Compound **3** had m.p. 87–88° (lit. (4) 90–91°); i.r. ($CHCl_3$) ν 1645 (C=O), 1600 (C=C), 1150 (C—O—C) cm^{-1}.

6-Bromo-5,5-dimethyl-3-methoxycyclohex-2-enone (2)

The product of hydrolysis of **3** (13) was treated with ethereal diazomethane to yield ethers **2** and **3** in a 3:2 ratio. Compound **2** was obtained by preparative t.l.c., as described above, in the form of an oil which resisted attempts at crystallization. Its i.r. spectrum showed characteristic absorption at ν 1650 (C=O), 1600 (C=C), 1150 (C—O—C) cm^{-1}.

4-Bromo-3-methoxycyclohex-2-enone

This compound was obtained as an oil and showed characteristic i.r. absorption at ν 1650 (C=O), 1600 (C=C), 1160 (C—O—C) cm^{-1}.

[4]There is also chemical evidence which supports the direction of substitution of cyclopenten-2-ones (6*a*, 7) as well as for isophorone (8) but Hafner and Goliasch (9) have assigned the wrong structure to the product of NBS bromination of cyclopenten-2-one on the basis of observed chemical transformation.[5]

[5]See commentary in ref. 6*a*.

[6]An examination of conformationally labile acyclic enone systems and of the theoretical implications of selective bromination of such systems is in progress.

Can. J. Chem. Downloaded from www.nrcresearchpress.com by 210.87.254.42 on 09/05/12
For personal use only.

TABLE 1. The n.m.r. solvent shift data (in p.p.m. downfield from internal TMS)*

Compound		2 H	4 H	6 H	3 OCH_3	3 CH_3	5 H	5 CH_3
5,5-Dimethyl-3-methoxy-cyclohex-2-enone (**1**)	CCl_4	5.25	2.21†	2.07†	3.68			1.04
	$\Delta^{CCl_4}_{C_6H_6}$	−0.07	+0.26	+0.01	+0.59			+0.26
6-Bromo-5,5-dimethyl-3-methoxycyclohex-2-enone (**2**)	CCl_4	5.19	2.58, 2.00 (J_{AB} = 18 Hz)	3.86	3.71			1.20
	$\Delta^{CCl_4}_{C_6H_6}$	−0.01	+0.16, +0.26	−0.10	+0.77			+0.34, +0.39
4-Bromo-5,5-dimethyl-3-methoxycyclohex-2-enone (**3**)	CCl_4	5.28	4.24 ($J_{4,6}$ = 1.5 Hz)	2.47, 2.02 (J_{AB} = 16 Hz)‡	3.76			1.23, 1.20
	$\Delta^{CCl_4}_{C_6H_6}$	+0.08	+0.19	−0.04, 0	+0.76			+0.32, +0.39
3-Methoxy-cyclohex-2-enone	CCl_4	5.23	2.36 (t) ($J_{4,5}$ = 6 Hz)	2.11 (t) ($J_{5,6}$ = 6.5 Hz)	3.68		2.0 (m)	
	$\Delta^{CCl_4}_{C_6H_6}$	−0.08	+0.33	−0.02	+0.53		+0.5	
4-Bromo-3-methoxy-cyclohex-2-enone	CCl_4	5.28	4.62 (t) ($J_{4,5}$ = 3.5 Hz)	2.4 (m)	3.76		2.4 (m)	
	$\Delta^{CCl_4}_{C_6H_6}$	+0.13	+0.48	+0.1	+0.88		+0.8	
6-Bromo-3-methoxy-cyclohex-2-enone	CCl_4	5.26	*ca.* 2.8 (t) ($J_{4,5}$ = 9 Hz)	4.29 (t) ($J_{5,6}$ = 4 Hz)	3.74		2.35 (m)	
	$\Delta^{CCl_4}_{C_6H_6}$	+0.10	+0.5	+0.14	+0.87		+0.7	
3,5,5-Trimethylcyclohex-2-enone	CCl_4	5.73 (m)	2.13	2.05		1.90 (t)		1.01
	$\Delta^{CCl_4}_{C_6H_6}$	−0.12	+0.47	+0.03		+0.41		+0.24
4-Bromo-3,5,5-trimethyl-cyclohex-2-enone	CCl_4	5.76 (m)	4.35 (d) ($J_{2,4}$ = 1.4 Hz)	2.50, 2.07 (J_{AB} = 17 Hz)		2.10 (d) ($J_{2,3}$ = 1.4 Hz)		1.26, 1.15
	$\Delta^{CCl_4}_{C_6H_6}$	+0.06	+0.52	+0.06, +0.09		+0.45		+0.30, +0.41

*d, Doublet; t, triplet; m, multiplet.

†The signal at lower field, due to the protons allylic to the olefinic bond, is of appreciably greater line-width than that of the protons α to carbonyl, presumably because of coupling of C-4 protons with the vinylic proton.

‡The doublet character of the two high-field components of the 6 H AB quartet and the corresponding splitting of the 4H proton signal suggests long-range W-coupling between two quasi-equatorial protons and therefore, a quasi-axial conformation for the bromine substituent. The spectra of the other bromination products are complicated by allylic coupling and do not lend themselves as readily to such detailed analysis.

Can. J. Chem. Downloaded from www.nrcresearchpress.com by 210.87.254.42 on 09/05/12
For personal use only.

TABLE 2. The n.m.r. reagent* shift data (in p.p.m. downfield from internal TMS)

Compound		2 H	4 H	6 H	3 OCH_3	3 CH_3	5 H	5 CH_3
5,5-Dimethyl-3-methoxy-cyclohex-2-enone (**1**)	0.18 *M* ($CDCl_3$)	5.37	2.27	2.21	3.70			1.06
	$\Delta^{CDCl_3}_{0.024\ M\ Eu(DPM)_3}$	0.87	0.32	0.97	0.13			0.27
6-Bromo-5,5-dimethyl-3-methoxycyclohex-2-enone (**2**)	0.14 *M* ($CDCl_3$)	5.35	2.63, 2.10 (J_{AB} = 18 Hz)	4.06	3.73			1.20
	$\Delta^{CDCl_3}_{0.023\ M\ Eu(DPM)_3}$	0.52	0.19, 0.27	0.75	0.03			0.18, 0.23
4-Bromo-5,5-dimethyl-3-methoxycyclohex-2-enone (**3**)	0.12 *M* ($CDCl_3$)	5.36	4.30	2.60, 2.13 (J_{AB} = 16 Hz)	3.77			1.25, 1.20
	$\Delta^{CDCl_3}_{0.023\ M\ Eu(DPM)_3}$	1.08	0.35	1.18, 1.32	0.16			0.25, 0.42
3-Methoxycyclohex-2-enone	0.21 *M* ($CDCl_3$)	5.38	2.40 (t) ($J_{4,5}$ = 6 Hz)	2.35 (t) ($J_{5,6}$ = 6.5 Hz)	3.70		*ca.* 2.0 (m)	
	$\Delta^{CDCl_3}_{0.038\ M\ Eu(DPM)_3}$	0.84	0.31	0.93	0.13		0.3	
4-Bromo-3-methoxy-cyclohex-2-enone	0.15 *M* ($CDCl_3$)	5.41	4.70 (t) ($J_{4,5}$ = 3.5 Hz)	2.8 (m)	3.76		*ca.* 2.4 (m)	
	$\Delta^{CDCl_3}_{0.025\ M\ Eu(DPM)_3}$	0.55	0.17	0.4	0.09		0.2	
6-Bromo-3-methoxy-cyclohex-2-enone	0.10 *M* ($CDCl_3$)	5.39	*ca.* 2.7 (t) ($J_{4,5}$ = 9 Hz)	4.42 (t) ($J_{5,6}$ = 4 Hz)	3.73		*ca.* 2.4 (m)	
	$\Delta^{CDCl_3}_{0.015\ M\ Eu(DPM)_3}$	0.61	0.2	0.65	0.10		0.3	
3,5,5-Trimethylcyclohex-2-enone	0.14 *M* ($CDCl_3$)	5.89	2.16	2.18		1.93		1.02
	$\Delta^{CDCl_3}_{0.023\ M\ Eu(DPM)_3}$	1.07	0.40	1.15		0.25		0.34
4-Bromo-3,5,5-trimethyl-cyclohex-2-enone	0.15 *M* ($CDCl_3$)	5.84	4.30 (d) ($J_{2,4}$ = 1.4 Hz)	2.61, 2.14 (J_{AB} = 17 Hz)		2.10 (d) ($J_{2,3}$ = 1.5 Hz)		1.26, 1.15
	$\Delta^{CDCl_3}_{0.027\ M\ Eu(DPM)_3}$	1.03	0.31	1.02, 1.14		0.24		0.25, 0.40

*Eu-Resolve, $Eu(DPM)_3$, (Alpha Inorganics) added to $CDCl_3$ solutions in the amounts indicated. d, Doublet; t, triplet; m, multiplet.

6-Bromo-3-methoxycyclohex-2-enone

A methylene chloride solution of 4-bromo-3-methoxycyclohex-2-enone stored for 3 days in the refrigerator underwent isomerization[7] to produce a 1:1 ratio of 4-bromo and 6-bromo isomers, also separated by preparative t.l.c. The latter isomer showed characteristic i.r. absorption at ν 1650 (C═O), 1590 (C═C), 1155 (C—O—C) cm^{-1}.

The authors are grateful to Mr. H. Séguin of NRCC for the elemental microanalyses and to Mr. J. C. Ethier for recording of the i.r. spectra.

1. T. Ukita and K. Arakawa. Chem. Pharm. Bull. Tokyo, **5**, 535 (1957).
2. K. Tomino. Chem. Pharm. Bull. Tokyo, **6**, 320 (1958). M. M. Shemyakin, Y. A. Arbuzov, M. N. Kolosov, G. A. Shatenshtein, V. V. Onoprienko, and Y. U. Kounova. Zh. Obshch. Kim. **30**, 542 (1960).
3. K. Arakawa and M. Irie. Chem. Pharm. Bull. Tokyo, **5**, 525 (1957).
4. K. Arakawa. Chem. Pharm. Bull. Tokyo, **5**, 531 (1957).

[7]The mechanism of this isomerization is under investigation.

5. R. S. Davidson. Quart. Rev. **21** (2), 249 (1967).
6. (*a*) C. H. Depuy, M. Isaks, K. L. Eilers, and G. F. Morris. J. Org. Chem. **29**, 3503 (1964); (*b*) C. H. Depuy, C. E. Lyons, and L. B. Rodewald. J. Chem. and Eng. Data, **11**, 102 (1966).
7. L. Crombie, M. Elliott, and S. H. Harper. J. Chem. Soc. 971 (1950).
8. A. J. B. Edgar, S. H. Harper, and M. A. Kazi. J. Chem. Soc. 1083 (1957).
9. K. Hafner and K. Goliasch. Ber. **94**, 2909 (1961).
10. D. V. C. Awang. Can. J. Chem. **49**, 2672 (1970). J. Ronayne and D. H. Williams. *In* Annual review of NMR spectroscopy. *Edited by* E. F. Mooney. Vol. 2. Academic Press, London, 1969. p. 118.
11. J. K. M. Sanders and D. H. Williams. Chem. Commun. 422 (1970). H. Hart and G. M. Love. Tetrahedron Lett. 625 (1971).
12. L. Horner and E. H. Winklemann. *In* Newer Methods of Preparative Organic Chemistry. *Edited by* W. Foerst. Vol. 3. Academic Press, London, 1964. p. 151.
13. K. Arakawa. Chem. Pharm. Bull. Tokyo, **5**, 528 (1957).

Can. J. Chem. Downloaded from www.nrcresearchpress.com by 210.87.254.42 on 09/05/12
For personal use only.

Can. J. Chem. Downloaded from www.nrcresearchpress.com by 210.87.254.105 on 09/05/12
For personal use only.

Structure of Grandiflorenic Acid

F. PIOZZI,[1] S. PASSANNANTI,[1] M. L. MARINO,[1] AND V. SPRIO[2]
Institute of Organic Chemistry, University of Palermo, Palermo, Italy
Received July 13, 1971

Grandiflorenic acid is determined to be structure **2**, (−)-kaura-9(11),16-dien-19-oic acid.

L'acide grandiflorénique a la structure **2**, l'acide (−)-kaura-9(11),16-diène-19-oique.
Canadian Journal of Chemistry, **50**, 109 (1972)

We wish to present definitive evidence concerning the structure of grandiflorenic acid, extracted from the acid fraction of the resin of *Espeletia grandiflora* Humb. et Bonpl. (Compositae). This fraction also contains grandiflorolic acid, whose structure elucidation we have already reported (1) and (−)-kaur-16-en-19-oic acid (2). The neutral fraction of the resin contains (−)-kaur-16-ene, (−)-kaur-16-en-19-ol, and (−)-kaur-16-en-19-al (2).

Grandiflorenic acid $C_{20}H_{28}O_2$ contains two double bonds (as proved by perbenzoic acid titration and by selective hydrogenation to dihydro-grandiflorenic acid $C_{20}H_{30}O_2$ and tetrahydro-grandiflorenic acid $C_{20}H_{32}O_2$) in the form of an exocyclic methylene group (confirmed also by formation of formaldehyde upon ozonolysis) and of a trisubstituted C=CH— system, as indicated by n.m.r. and i.r. data. The n.m.r. spectrum of grandiflorenic acid also reveals the occurrence of two tertiary methyls; the i.r. spectrum of methyl grandiflorenate has the typical band at 1147 cm^{-1} for an axial $COOCH_3$ group. Physical constants of tetrahydro-grandiflorenic acid agree with those reported (3) for 16β-(−)-kauran-19-oic acid (**3**); the identification is confirmed by direct comparison (mixed m.p., g.l.c., m.s.) with a sure specimen of **3** prepared from a sample of (−)-kaur-16-en-19-oic acid, and by lithium aluminum hydride reduction to the known (4) 16β-(−)-kauran-19-ol (**4**). This identification is confirmed also by comparison with a specimen of **4**.

On the basis of such evidence, we had tentatively suggested (5) the structure **1** for grandiflorenic acid, although the alternative structure **2** could not be ruled out.

Grandiflorenic acid was isolated concurrently by Kloss (6) from the related species *Espeletia schultzii* Wedd. After comparison of his experimental results with those we had communicated, Kloss suggested structure **1**: however, his considerations, based on mass spectra, seemed to us to be not probative.

Grandiflorenic acid is clearly identical with "S 1 acid", extracted by Brieskorn and Pöhlmann (7) from *Espeletia schultzii* Wedd. These workers preferred the structure **2** on the basis of results similar to ours and of two other considerations: (*a*) the acid does not decarboxylate easily, while a β,γ-unsaturated acid such as **1** should do so; (*b*) the sequence ozonization, lithium aluminum hydride reduction – selenium dehydrogenation of the dihydro-acid, gives 1,5-dimethylnaphthalene.

Our own more recent results demonstrate the correctness of formula **2**.

Comparative determinations[3] of pK_{MCS}* gave 8.49 for grandiflorenic acid, 8.53 for dihydro-grandiflorenic acid, and 8.66 for tetrahydro-grandiflorenic acid.[4] These results can be rationalized only by assuming that in the three products there are three 1,3-interactions with a 4α-COOH (calcd. 8.50 for three and 8.25 for two 1,3-interactions). The small increment in the pK_{MCS}* when passing from the dihydro-acid to the tetrahydro-acid seems to us not sufficient to postulate the formation of an additional

[1]Faculty of Sciences.
[2]Faculty of Pharmacy.
[3]By the courtesy of Professor W. Simon, E. T. H., Zürich.
[4]Brieskorn and Pöhlmann (7) reported pK_{MCS}* 8.70 for their tetrahydro-acid.

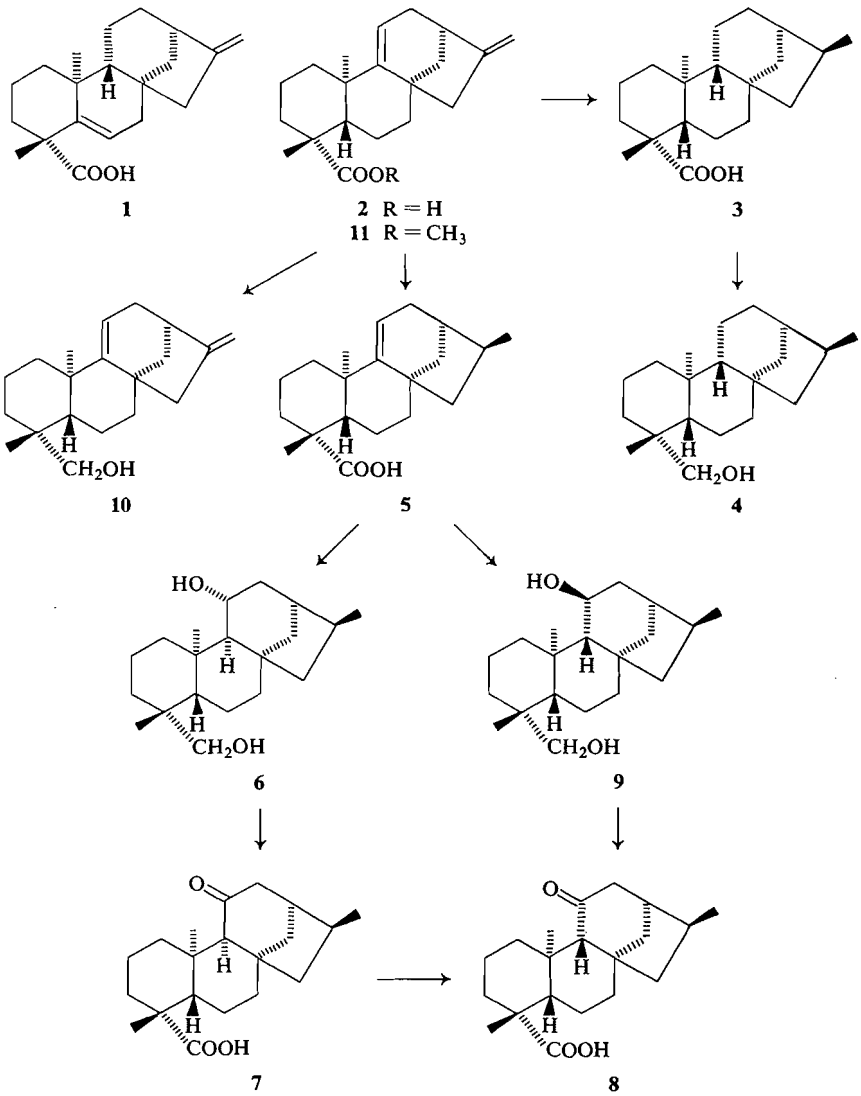

1,3-interaction. Hence the double bond cannot be at position 5,6.

The comparison of the n.m.r. chemical shift values for 4β-CH_3 and 10α-CH_3 indicates that 4β-CH_3 is not substantially shifted when passing from grandiflorenic to dihydro- and thence to tetrahydro-acid: 1.25, 1.24, and 1.22 δ respectively. On the contrary, the 10α-CH_3 is shifted moderately upfield: 1.03, 1.00, and 0.94 δ respectively. The same results are observed for methyl grandiflorenate and methyl tetrahydrograndiflorenate: 4β-CH_3 1.16 and 1.16 δ, 10α-CH_3 0.92 and 0.82 δ respectively. Such behavior agrees with the presence of a 9,11-double bond as in **2**, but is less likely in the case of a 5,6-double bond as in **1**.

Hence, the most probable structures are **2** for grandiflorenic acid and **5** for dihydro-grandiflorenic acid.

Hydroboration–oxidation of dihydro-grandiflorenic acid gives as main product a $C_{20}H_{34}O_2$ diol whose n.m.r. spectrum shows a complex multiplet at 4.07 δ for the —C*H*OH— proton. This signal is an apparent sextet with three coupling constants of 10.50, 9.75, and 6.75 Hz. Chromic oxidation of the diol affords a

Can. J. Chem. Downloaded from www.nrcresearchpress.com by 210.87.254.105 on 09/05/12
For personal use only.

Can. J. Chem. Downloaded from www.nrcresearchpress.com by 210.87.254.105 on 09/05/12
For personal use only.

$C_{20}H_{30}O_3$ ketoacid, having pK_{MCS}* 8.66: this result definitively excludes the occurrence of a keto group at C-6, because it is known (4) in the case of 6-keto-(−)-kaur-16-en-19-oic acid that hydrogen bonding of the carboxyl with the keto group at C-6 increases the pK_{MCS}* to 9.25. Therefore the carbonyl of the present ketoacid must be at C-11.

The three coupling constants reported for the diol can be interpreted as belonging to axial–axial, axial–axial, and axial–equatorial couplings. These relationships can be fulfilled only by structure **6** with a 9α-H configuration, deriving from *cis*-addition from the least hindered α side of the 9,11-double bond. A similar result has been reported (8) recently in the hydroboration of an abietane skeleton with a 9,11-double bond. Hence, our ketoacid has the structure **7** with 9α-H configuration. This product can be epimerized easily by base to the more stable 9β-H derivative **8**. The o.r.d. and c.d. have been obtained for **7** and **8**. The Cotton effect is positive for both products but is rather weak in **7** and more intense in **8**.

Hydroboration of **5** gives also as a minor product the isomeric diol **9**. In its n.m.r. spectrum 11α-H appears as a broad signal at 3.89 δ with $w_{1/2} = 6.5$ Hz, as can be foreseen for equatorial–equatorial, equatorial–equatorial, and equatorial–axial relationships. Jones oxidation of **9** affords as expected the ketoacid **8**.

Lithium aluminum hydride reduction of grandiflorenic acid affords the dienol $C_{20}H_{30}O$ described by Kloss (6). On the basis of previous evidence, this product must be assigned the structure **10**, (−)-kaura-9(11),16-dien-19-ol.

The above reported results allow us to assign grandiflorenic acid the structure **2**.

Experimental

Melting points (capillary tubes) are uncorrected. The i.r. spectra were measured on a Perkin–Elmer Infracord 137, Nujol mull; n.m.r. spectra, C-60 H Jeol, TMS internal standard with $\delta = 0$; m.s., Hitachi Perkin–Elmer RMU-6D, 70 eV (courtesy of Dr. A. Selva, Institute of Chemistry, Politechnic of Milano); g.l.c. analyses, 1440 Varian Aerograph with flame ionization detector, carrier gas N_2, columns 1% GE XE 60 at 180° or 3% SE 30 at 200°; $[\alpha]_D^{20°}$, Perkin–Elmer 141 polarimeter.

Extraction

The resin, collected from trees growing at Pàramo de Guadalupe, Bogotà, Colombia at 3400 meters above sea level, is dissolved in ether and extracted with 3% sodium hydroxyde solution; the latter is acidified and extracted with ether. The acidic fraction obtained is chromatographed on silica gel with benzene – ethyl acetate, eluting in the order: pure grandiflorenic acid, a mixture of grandiflorenic and (−)-kaur-16-en-19-oic acid, pure grandiflorolic acid. No trace of acetyl-grandiflorolic acid (= "S 2 acid" of Brieskorn and Pöhlmann (7)) is present.

Grandiflorenic Acid (2)

The pure acid has m.p. 158–160° (from ethyl acetate then from methanol); $[\alpha]_D^{20°}$ +38° (ethanol; *c*, 1.02).

Anal. Calcd. for $C_{20}H_{28}O_2$: C, 79.95; H, 9.39. Found: C, 79.65; H, 9.35.

The i.r.: 1695 (COOH), 1655 and 876 (C=CH_2), 810 cm^{-1} (C=CH); n.m.r. ($CDCl_3$): 1.03 and 1.25 (s, *t*-CH_3), 4.80 and 4.90 (C=CH_2), 5.26 (t of 3 Hz, C=C*H*—CH_2), ~10 δ (broad, COOH); m.s.: 300 *m/e* (M^+), 285 (M-15), 239 (M-15-46); TNM test: positive; determination of pK_{MCS}*: found 8.49.

Methyl grandiflorenate (**11**) is obtained by treatment of the acid with ethereal diazomethane and is purified by chromatography on neutral alumina eluting with cyclohexane: uncrystallizable viscous oil, one component by t.l.c. and g.l.c. The i.r. (liquid): 1725 ($COOCH_3$), 1655 and 877 (C=CH_2), 1147 (axial $COOCH_3$ on C-4), 810 cm^{-1} (C=CH); n.m.r. (CCl_4): 0.92 and 1.16 (s, *t*-CH_3), 3.62 (s, $COOCH_3$), 4.76 and 4.89 (C=CH_2), 5.21 δ (t of 3 Hz, C=C*H*—CH_2). Titrations with perbenzoic acid: 2.20 and 2.10 double bonds (two determinations).

Methyl grandiflorenate (**11**) (150 mg) is reduced with excess of lithium aluminum hydride in ether solution (6 h reflux); the isolated product is chromatographed on silica gel (eluent benzene – ethyl acetate 9:1) and crystallized from cyclohexane: (−)-kaura-9(11),16-dien-19-ol (**10**) has m.p. 114–115°, $[\alpha]_D^{20°}$ +43° (ethanol; *c*, 0.38); i.r.: 3330 (OH), 1655 and 877 (C=CH_2), 810 cm^{-1} (C=CH); n.m.r. ($CDCl_3$): 0.95 and 1.03 (s, *t*-CH_3), 3.62 and 3.83 (q, $J_{AB} = 11$ Hz, axial CH_2OH on C-4), 4.78 and 4.89 (C=CH_2), 5.16 δ (t of 3 Hz, C=C*H*—CH_2); m.s.: 286 *m/e* (M^+), 271 (M-15), 255 (M-31). Kloss (6) reported m.p. 114–115°, $[\alpha]_D^{20°}$ +45°, and identical m.s.

Dihydro-grandiflorenic Acid (5)

A sample of grandiflorenic acid (200 mg) in methanol solution is hydrogenated on PtO_2 (20 mg) at room temperature (H_2 absorbed corresponding to 1.02 double bonds after 1 h): m.p. 166–168° (from aqueous ethanol); $[\alpha]_D^{20°}$ +43° (ethanol; *c*, 0.30); i.r.: 1695 (COOH), 815 cm^{-1} (C=CH); n.m.r. ($CDCl_3$): 0.98 (d, $J = 6$ Hz, *s*-CH_3), 1.00 and 1.24 (s, *t*-CH_3), 5.17 δ (t of 3 Hz, C=C*H*—CH_2); m.s.: 302 *m/e* (M^+), 287 (M-15), 241 (M-15-46); TNM test: positive; determination of pK_{MCS}*: found 8.53.

Transformation of samples of the dihydro-acid into its methyl ester (not characterized) and g.l.c. determinations indicate that the crude acid is a 80:20 mixture of 16β-CH_3 and 16α-CH_3 epimers; the crystallized acid contains ~85% of the 16β-CH_3 epimer.

Tetrahydro-grandiflorenic Acid (3)

A sample of grandiflorenic acid (200 mg) in ethanol solution is hydrogenated on 10% Pd–C at room temperature (H_2 absorbed corresponding to 1.98 double bonds after 24 h): m.p. 209–210° (from methanol); $[\alpha]_D^{20°}$ −80° (ethanol; *c*, 0.44); i.r.: 1690 cm^{-1} (COOH); n.m.r. ($CDCl_3$): 0.94 and

Can. J. Chem. Downloaded from www.nrcresearchpress.com by 210.87.254.105 on 09/05/12
For personal use only.

1.22 (s, t-CH_3), 0.99 δ (d, $J = 6$ Hz, s-CH_3); m.s.: 304 m/e (M^+), 289 (M-15), 243 (M-15-46); TNM test: negative; determination of pK_{MCS}*: found 8.66.

Transformation of samples of the tetrahydro-acid into its methyl ester and g.l.c. determinations indicate that the crude acid is a 80:20 mixture of 16β-CH_3 and 16α-CH_3 epimers. The crystallized acid contains only the pure 16β-CH_3 epimer. This finding agrees with common assumption that catalytic hydrogenation of the exocyclic double bond of (−)-kaur-16-ene derivatives gives mainly 16β-CH_3 epimers.

The characteristics of the crystallized acid agree sufficiently with those reported (3) for 16β-(−)-kauran-19-oic acid, *i.e.* m.p. 210–214° and $[\alpha]_D^{20}$ −68°. Direct comparison with a sure sample, prepared by hydrogenation of (−)-kaur-16-en-19-oic acid extracted (2) from *Espeletia grandiflora* and having m.p. 209–211°, shows no depression at mixed m.p., identical m.s., identical retention volume as methyl ester at g.l.c. (crossed injection).

A sample of the crystallized acid is then methylated and reduced with lithium aluminum hydride: the product has m.p. 146–147° (from aqueous ethanol), in agreement with m.p. 148–150° reported (4) for 16β-(−)-kauran-19-ol (**4**). Direct comparison with a sure specimen, prepared from sure 16β-(−)-kauran-19-oic acid and having m.p. 147–148°, shows no depression at mixed m.p. and identical retention volume at g.l.c. (crossed injection).

Hydroboration of **5**: *Diol* **9** *and Diol* **6**

A solution of **5** (250 mg) in anhydrous tetrahydrofuran (100 ml) is added at 0° with sodium borohydride (3 g) and boron trifluoride etherate (6 ml). After 24 h, water (30 ml), 3 *N* sodium hydroxide (15 ml) and hydrogen peroxide (30% solution, 15 ml) are added dropwise. Repeated ether extractions afford a solid residue that is chromatographed on silica gel (50 g; eluent benzene – ethyl acetate 9:1, 10 ml fractions): fractions 80–90 yield 10 mg of diol **9**, fractions 100–145 give 150 mg of diol **6**.

The first product has m.p. 158–160° with pseudo m.p. 70° (from cyclohexane); m.s.: 306 m/e (M^+), 288 (M-18), 275 (M-31), 257 (M-18-31); n.m.r. ($CDCl_3$): 0.88 and 0.97 (s, t-CH_3), 1.11 (d, $J = 6.5$ Hz, s-CH_3), 3.44 and 3.69 (q, $J_{AB} = 11$ Hz, axial CH_2OH), 3.89 δ (broad, $w_{1/2}$ 6.5 Hz, 11α-H). These data are consistent with the structure **9** of 16β-(−)-kauran-11β,19-diol.

The second product has m.p. 57–58° (from cyclohexane), $[\alpha]_D^{20}$ −27° (ethanol; *c*, 0.35); m.s.: same peaks as **9** but with different intensities; n.m.r. ($CDCl_3$): 1.00 and 1.08 (s, t-CH_3), 1.01 (d, $J = 6.5$ Hz, s-CH_3), 3.57 and 3.93 (q, $J_{AB} = 11$ Hz, axial CH_2OH), 4.07 δ (six-line pattern, $J_{ax,ax} = 10.50$, $J_{ax,ax} = 9.75$, $J_{ax,eq} = 6.75$ Hz, 11β-H). In the n.m.r. spectrum ($CDCl_3$) of its diacetate (not characterized) the latter signals are shifted downfield: 3.88 and 4.18 (q_{AB}, CH_2OAc), 5.00 δ (six-line pattern, 11β-H). Such data support the structure **6** of 16β,9α-(−)-kauran-11α,19-diol.

Oxidation of Diol **6**: *Ketoacid* **7**

The diol (100 mg) is oxidized with Jones reagent at 0°; after usual work-up, the crude ketoacid is chromatographed on silica gel (eluent benzene – ethyl acetate 9:1), obtaining 40 mg of **7**, m.p. 210° (from benzene–cyclohexane); $[\alpha]_D^{20}$ −68° (ethanol; *c*, 0.19); m.s.: 318 m/e (M^+), 300 (M-18), 285 (M-18-15), 274 (M-44), 272 (M-18-28), 257 (M-18-28-15), 229 (257-28); determination of pK_{MCS}*: found 8.66; o.r.d. (ethanol; *c*, 0.19; 27°): $[\alpha]_{400}$ −140, $[\alpha]_{330}$ +40 (peak), $[\alpha]_{270}$ −1200° (sh); c.d.[5]: 330 (sh), 320 (sh), 309 ($\Delta\varepsilon$ +0.65), 303 ($\Delta\varepsilon$ +0.65), 292 nm (sh).

The product (examined as methyl ester, uncharacterized) is pure by g.l.c.

A sample of the ketoacid **7** (20 mg) is dissolved in 10% methanolic potassium hydroxide (5 ml) and refluxed 1 h: the epimeric ketoacid **8** has m.p. 187–188°. The product (examined as methyl ester, not characterized) is pure by g.l.c.: it differs from **7** but is identical with the product obtained by oxidation of **9** (see below); also mixed m.p. shows no depression, i.r. and m.s. are identical.

Oxidation of Diol **9**: *Ketoacid* **8**

Jones oxidation of the diol (20 mg) gives the ketoacid **8** (8 mg), m.p. 186–187° (from cyclohexane); $[\alpha]_D^{20}$ +32° (ethanol; *c*, 0.14); m.s.: almost identical peaks as in **7**, but with different intensities; o.r.d. (ethanol; *c*, 0.14; 27°): $[\alpha]_{400}$ +190, $[\alpha]_{326}$ +1460 (peak), $[\alpha]_{282}$ −1880 (trough), $[\alpha]_{255}$ −1560° (peak); c.d.: 330 (sh), 320 (sh), 309.5 ($\Delta\varepsilon$ +2.37), 304 (sh), 294 nm (sh). The product (examined as methyl ester, uncharacterized) is pure by g.l.c. and different from **7**.

This work has been supported by C.N.R. (National Research Council), Roma.

1. F. Piozzi, V. Sprio, S. Passannanti, and R. Mondelli. Gazz. Chim. Ital. **98**, 907 (1968).
2. F. Piozzi, S. Passannanti, M. P. Paternostro, and V. Sprio. Phytochem. **10**, 1164 (1971).
3. C. A. Henrick and P. R. Jefferies. Austral. J. Chem. **17**, 915 (1964).
4. B. E. Cross, R. H. B. Galt, and J. R. Hanson. J. Chem. Soc. 2944 (1963).
5. F. Piozzi *et al.* 5th IUPAC Symposium on the Chemistry of Natural Products. London, July, 1968. Abstracts Book. p. 313.
6. P. Kloss. Arch. Pharm. (Weinheim), **302**, 376 (1969); Chem. Abstr. **71**, 57535 (1969).
7. C. H. Brieskorn and E. Pöhlmann. Tetrahedron Lett. 5661 (1968); Chem. Ber. **102**, 2621 (1969).
8. W. Herz and J. J. Schmid. J. Org. Chem. **34**, 3464 (1969).

---

[5]Our thanks are due to Dr. P. Salvadori (Institute of Industrial Organic Chemistry, University of Pisa) who recorded o.r.d. and c.d. curves.

Vapor Phase Catalytic Transformations of Terpene Hydrocarbons in the $C_{10}H_{16}$ Series. II. Aromatization of α-Pinene over Chromia–Alumina[1]

A. STANISLAUS[2] and L. M. YEDDANAPALLI
Department of Chemistry, Loyola College, Madras, India

Received April 1, 1971

The aromatization of α-pinene in the vapor phase over chromia gel and chromia–alumina catalysts prepared from aluminas of different acidity has been studied. The acidity of alumina support has a remarkable influence on the composition of the aromatics resulting from the dehydrogenation of α-pinene. Over weakly acidic chromia–alumina doped with 1% sodium catalyst, α-pinene is aromatized to *p*-cymene, 1,2,4- and 1,2,3-trimethylbenzenes with traces of toluene and xylenes, whereas over the strongly acidic chromia – pure alumina and chromia–alumina containing 5% HF catalysts it gives considerable amount of *m*-cymene, toluene, and tetramethylbenzenes. A satisfactory mechanism to explain the formation of these compounds is offered.

L'aromatisation de l'α-pinène en phase vapeur sur catalyseurs gel de chrome et chrome–aluminium préparés à partir d'alumine d'acidité différente a été étudiée. L'acidité du support d'alumine a une influence notable sur la composition des produits aromatiques résultant de la déshydrogénation de l'α-pinène sur un catalyseur chrome–alumine faiblement acide dopé par 1% de sodium, l'α-pinène s'aromatise en *p*-cymène et en benzènes triméthylés en 1,2,4- et 1,2,3 avec des traces de toluène et de xylènes tandis que, sur des catalyseurs chrome–alumine pure faiblement acide et chrome–alumine contenant 5% HF, on obtient une quantité considérable de *m*-cymène, de toluène et de benzènes tétraméthylés. Un mécanisme satisfaisant pour expliquer la formation de ces composés est offert.

Canadian Journal of Chemistry, **50**, 113 (1972)

Introduction

Chromia–alumina has been used extensively as a catalyst for dehydrogenation and aromatization studies. It has been shown recently that the alumina influences the catalytic properties of chromia–alumina catalysts and that the products resulting from such aromatization reactions depend to a great extent upon the type of alumina (1–3). The present study was undertaken in order to determine the effect of different types of alumina in chromia–alumina catalysts upon the aromatization of α-pinene. Chromia gel, chromia–alumina doped with 1% sodium, chromia – pure alumina, and chromia–alumina containing 5% hydrogen fluoride were used as catalysts.

Experimental

Materials

α-Pinene: First quality Indian turpentine oil supplied by the Government Turpentine and Rosin Company Ltd., Bareilly, India, contains 50% carene, 40% α-pinene, and 10% β-pinene. α-Pinene was obtained from this oil by fractionation using a 5 ft column packed with stainless steel helices (containing 20 theoretical plates) at reduced pressure (10 mm Hg). The purity was found to be better than 99% by gas chromatographic analysis.

Catalysts

Chromia Gel

Hydrated chromium nitrate (Rideal) (100 g) and ammonium acetate (33 g) were dissolved in water (625 ml). The solution was heated to boiling for a brief interval and cooled to room temperature. A solution of ammonium hydroxide (*d.* 0.885; 90 ml) in water (250 ml) was then added with stirring and the whole slowly warmed on a water bath, where upon a strong, homogeneous jelly was obtained. This jelly was cut into cubes and partially dried at 50 to 60 °C for 12 h. The cubes were then washed by decantation with distilled water until the nitrate and ammonium ions were completely removed. The cubes were then activated at 50 to 60 °C to a hard black vitreous material which before use was raised slowly in temperature with further elimination of water and finally held over 12 h at 400 °C.

Chromia–Alumina A

It was prepared by impregnating alumina A (prepared by hydrolyzing aluminum isopropoxide with water) with requisite amount of chromic acid solution to give 6% chromium in the catalyst. It was dried at 120 °C for 24 h, made into pellets (4 × 4 mm), and calcined at 500 °C for 24 h.

Chromia–Alumina C

It was prepared by impregnating alumina C (prepared by doping alumina A with appropriate amount of sodium carbonate solution to give 1% sodium in the catalyst) with requisite amount of chromic acid solution to give 6% chromium in the catalyst. It was dried at 120 °C for 24 h, made into pellets (4 × 4 mm), and calcined at 500 °C for 24 h.

[1]This investigation is dedicated to the memory of Professor L. M. Yeddanapalli who died on June 6, 1970.

[2]Present address: Department of Chemistry & Chemical Engineering, Royal Military College of Canada, Kingston, Ontario.

Can. J. Chem. Downloaded from www.nrcresearchpress.com by 210.87.254.6 on 09/05/12
For personal use only.

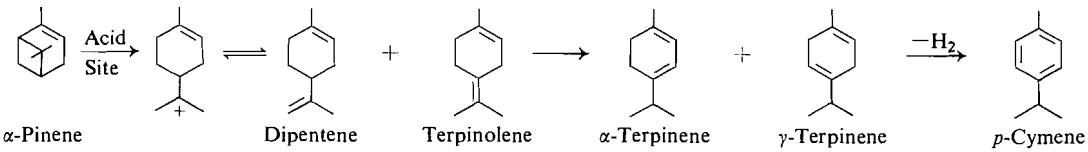

SCHEME 1

Chromia–Alumina E

It was prepared by impregnating alumina E (obtained by doping alumina A with appropriate amount of HF acid to give 5% by weight of HF in the catalyst) with requisite amount of chromic acid solution to give 6% chromium in the catalyst. The method of activation of the catalyst was similar to that employed in preparing chromia–alumina A.

Apparatus and Procedure

Apparatus, procedure and analytical techniques were essentially the same as described in paper I of these series (9).

Results and Discussion

Table 1 summarizes the data on the rate and distribution of products of aromatization of α-pinene over the different chromia–alumina catalysts at 390 °C. The results obtained at 425 and 460 °C are given in Tables 2 and 3, respectively. It appears from these tables that there is a marked change in the distribution of products as the acid strength of alumina support is increased. In the case of chromia–alumina prepared from weakly acidic sodium doped alumina, the aromatic fraction contains mainly *p*-cymene with small amounts of *m*-cymene, toluene, and xylenes and trimethylbenzenes. Over the strongly acidic HF treated chromia–alumina catalyst the concentration of *m*-cymene, toluene, and xylenes are increased. In addition to these tetramethylbenzenes are also formed.

The formation of *p*-cymene from α-pinene under aromatizing conditions is well known (4–6) (see Scheme 1). Breaking of the cyclobutane ring to give *p*-menthadienes followed by dehydrogenation is the mechanism proposed by these authors to explain the formation of *p*-cymene from α-pinene. Chromia–alumina and chromia catalysts are poly functional catalysts. They contain two types of sites, one catalyzing the isomerization and the other dehydrogenation reactions. The isomerization activity is associated with the acidity of the catalysts whereas the dehydrogenation activity is associated with Cr(II) and Cr(III) ions. In the formation of *p*-cymene first α-pinene is isomerized on the acid sites to dipentene and terpinolene. The dipentene and terpinolene undergo further isomerization to α- and γ-terpinenes which are then dehydrogenated to *p*-cymene.

The production of 1,2,3- and 1,2,4-trimethylbenzenes may be explained by assuming that the hydrogen liberated in the formation of *p*-cymene acts upon the unreacted portion of α-pinene to form 1,1,2,3- and 1,1,2,5-tetramethylcyclohexanes by breaking the bonds III and IV by hydrogenolysis followed by dehydrogenation and demethanation as shown in Scheme 2. Ipatieff and Pines (6) have proposed a similar mechanism to explain the formation of 1,2,3- and 1,2,4-trimethylbenzenes from pinane during dehydrogenation over Pt–alumina.

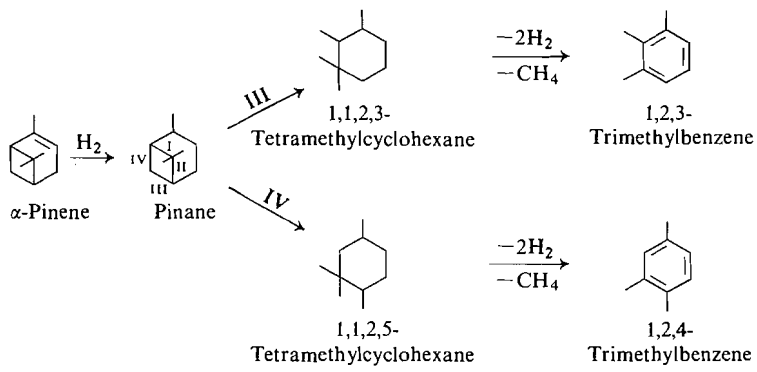

SCHEME 2

Can. J. Chem. Downloaded from www.nrcresearchpress.com by 210.87.254.6 on 09/05/12
For personal use only.

Can. J. Chem. Downloaded from www.nrcresearchpress.com by 210.87.254.6 on 09/05/12
For personal use only.

TABLE 1. Aromatization of α-pinene. Influence of alumina support; temperature, 390 °C; WHSV*, 1

Catalyst	% aromatics	% composition of aromatics						
		Toluene	Xylenes	1,2,4-Trimethylbenzene	1,2,3-Trimethylbenzene	*p*-Cymene†	*m*-Cymene†	Tetramethylbenzenes
Chromia gel	20	2.0	1.0	3.0	2.0	92	0	0
Chromia–alumina C	63	1.0	1.0	12	5.0	81	0	0
Chromia–alumina A	50	1.4	1.5	5.8	3.3	88	0	0
Chromia–alumina E	70	17	1.3	8.0	8.0	52	8	6.7

*WHSV, the number of grams of α-pinene passed per gram of the catalyst per hour.
†*p*- and *m*-Cymenes were estimated using Perkin–Elmer Infracord spectrophotometer Model 137. The characteristic peaks selected were 12.28 and 12.78 μ for *p*-cymene and *m*-cymene, respectively.

TABLE 2. Aromatization of α-pinene. Influence of alumina support; temperature, 425 °C; WHSV, 1

Catalyst	% aromatics	% composition of aromatics						
		Toluene	Xylenes	1,2,4-Trimethylbenzene	1,2,3-Trimethylbenzene	*p*-Cymene	*m*-Cymene	Tetramethylbenzenes
Chromia gel	28	2.5	1.5	4.0	2.0	87	3.0	0
Chromia–alumina C	68	1.0	1.0	14	6.0	78	0	0
Chromia–alumina A	56	2.0	1.5	6.5	4.7	81.3	4	1
Chromia–alumina E	72	29	2.5	5.5	5.0	35	14	9

TABLE 3. Aromatization of α-pinene. Influence of alumina support; temperature, 460 °C; WHSV, 1

Catalyst	% aromatics	% composition of aromatics						
		Toluene	Xylenes	1,2,4-Trimethylbenzene	1,2,3-Trimethylbenzene	*p*-Cymene	*m*-Cymene	Tetramethylbenzenes
Chromia gel	37	4.0	1.5	6.0	3.0	79.5	4.0	2.0
Chromia–alumina C	70	3.2	1.3	16.5	7.0	72	0	0
Chromia–alumina A	63	3.0	1.5	7.0	3.0	77	6.0	2.5
Chromia–alumina E	72	36	2.5	4.0	4.0	32	10	11.5

Can. J. Chem. Downloaded from www.nrcresearchpress.com by 210.87.254.6 on 09/05/12
For personal use only.

TABLE 4. Isomerization of *p*-cymene over alumina catalysts; temperature, 460 °C; WHSV, 1

Catalyst	% *m*-cymene
Alumina C	0
Alumina A	6
Alumina E	13

Tetramethylbenzenes, *m*-cymene, and toluene are formed only when the catalyst contains strong acid sites. The tetramethylbenzenes are probably formed by skeletal isomerization of 1,1,2,3- and 1,1,2,5-tetramethylcyclohexanes to 1,2,3,4-, 1,2,3,5-, and 1,2,4,5-tetramethylcyclohexanes followed by dehydrogenation.

Skeletal isomerization may be interpreted in terms of a carbonium ion mechanism involving the strong acid sites of alumina. The saturated hydrocarbons 1,1,2,3- and 1,1,2,5-tetramethylcyclohexanes could form the corresponding cyclohexyl carbonium ion either by partial dehydrogenation to the corresponding tetramethylcyclohexenes followed by proton exchange or by a direct hydride ion removal from the saturated compound. The carbonium ion thus formed would give through a methide migration, isomerized cyclohexyl carbonium ion which would then aromatize to the corresponding tetramethylbenzenes. Such skeletal isomerization preceding aromatization over chromia–alumina catalysts having strong intrinsic acidity have been reported by Pines and Chen (3).

m-Cymene is formed by the isomerization of *p*-menthadienes to *m*-menthadienes over strong acid sites and subsequent dehydrogenation or directly from *p*-cymene by isomerization. The latter view is supported by the fact that *p*-cymene itself undergoes isomerization to *m*-cymene over strongly acidic HF treated alumina as shown in Table 4. Similar isomerizations involving xylenes have already been reported by Pines and Covini (7) over strongly acidic molybdena–alumina catalysts. Cracking of the isopropyl group of both *p*- and *m*-cymenes on the strong acid sites results in the formation of toluene.

It also appears from Tables 1, 2 and 3 that both the weakly acidic sodium doped and strongly acidic HF treated chromia–alumina are more active than chromia – pure alumina for aromatization of α-pinene. The high activity of chromia–alumina catalyst prepared from sodium doped alumina may be explained on the basis of the fact that alkali metal ions doped on chromia–alumina promote the dehydrogenation activity of the catalyst by neutralizing the strong acid sites of alumina and thus preventing the undesirable side reactions leading to the formation of alkyl cyclopentenes which act as poisons for dehydrogenation sites (8). The high aromatization activity of chromia–alumina–HF catalyst can be explained as follows. Camphene and tricyclene are formed from α-pinene in the primary isomerization step to an extent of 30–40%. Strong acid sites are necessary for the conversion of camphene to monocyclics (9) and consequently its aromatization will be favored by only catalysts possessing strong acid sites. Since HF treated chromia–alumina contains a large number of such strong acid sites, it can cause the further isomerization of camphene to menthadienes which are then dehydrogenated to *p*-cymene.

Effect of Pyridine

From the results of the influence of acidic strength of alumina in chromia–alumina catalysts on the distribution of products of the aromatization of α-pinene it was concluded that strong acid sites are necessary for the formation of tetramethylbenzenes, *m*-cymene, and toluene. Selective poisoning of these sites by bases like pyridine was employed to verify the validity of this conclusion. At low partial pressures pyridine should get adsorbed preferentially on the stronger acid sites than on the weaker acid sites.

α-Pinene in presence of varying amounts of pyridine was subjected to aromatization over chromia–alumina E and the results are summarized in Table 5. It appears from Table 5 that the yield of aromatics is decreased by the addition of pyridine to the reactant. In the absence of pyridine 72% of aromatics are obtained whereas in the presence of 5% by weight of pyridine the yield of aromatics is only 48%. Among the aromatics the concentrations of *m*-cymene, tetramethylbenzenes, and toluene are decreased by pyridine supporting the conclusion that the formation of these compounds involves strong acid sites. The concentration of camphene in the products is increased by the addition of pyridine. This shows that in the presence of pyridine camphene formed from α-pinene in the primary isomerization step does not undergo

Can. J. Chem. Downloaded from www.nrcresearchpress.com by 210.87.254.6 on 09/05/12
For personal use only.

TABLE 5. Aromatization of α-pinene. Influence of pyridine; catalyst, chromia–alumina E; temperature, 460 °C; WHSV, 1

% pyridine in the reactant	% α-pinene reacted	% camphene	% menthadienes	% total aromatics	% composition of aromatics						
					Toluene	Xylene	1,2,4-Trimethyl-benzene	1,2,3-Trimethyl-benzene	*p*-Cymene	*m*-Cymene	Tetramethyl-benzenes
0	100	12	16	72	36	2.0	4.0	4.5	32	10	11.5
2	89	17	11	61	13.7	4.7	4.7	5.9	56	6	6.0
5	80	19	13	48	7.2	3.6	5.0	7.2	73	2	2.0

further conversion to monocyclics and then to aromatics. The fall in the concentration of aromatics is, therefore, not surprising.

A. Stanislaus wishes to thank the Council of Scientific and Industrial Research for the research fellowship award.

1. C. T. CHEN, W. O. HAAG, and H. PINES. Chem. Ind. (Lond.) 1379 (1959).
2. H. PINES and C. T. CHEN. Actes Deuxieme Congres Intern. Catalyse, Paris. **I**, 367 (1960).
3. H. PINES and C. T. CHEN. J. Am. Chem. Soc. **82**, 3562 (1960).
4. L. M. YEDDANAPALLI and J. VERGHESE. J. Sci. Ind. Res. **16B**, 224 (1957).
5. R. P. LINSTEAD. J. Am. Chem. Soc. 1139 (1940).
6. V. N. IPATIEFF and H. PINES. J. Am. Chem. Soc. **70**, 533 (1948).
7. H. PINES and ROMANO COVINI. J. Catal. **4**, 454 (1965).
8. J. M. BRIDGES, G. T. RYMER, and D. S. MCIVER. J. Phys. Chem. **66**, 871 (1962).
9. A. STANISLAUS and L. M. YEDDANAPALLI. Can. J. Chem. This issue.

Base-catalyzed Deuteration of Tricarbonylchromium Complexes[1]

M. ASHRAF[2]
Department of Chemistry, Queen's University, Belfast, N. Ireland

Received June 16, 1971

Hydrogen–deuterium exchange in tricarbonylchromium complexes of anisole, ethylbenzoate, and *N,N*-dimethylaniline has been studied for solutions in ethanol-*O*-d_1, containing sodium ethoxide. The extent of deuteration has been estimated mass spectroscopically and the position of deuteration by n.m.r. spectroscopy. In this kinetically controlled reaction ortho-substitution has been found to be predominantly preferred in case of anisole complex, whereas random substitution was observed (n.m.r.) for ethylbenzoate complex. The results are interpreted in terms of chelative, inductive, mesomeric, and steric effects of the substituents.

L'échange hydrogène–deutérium dans les complexes du chrome tri-carbonyle de l'anisole, de l'éthylbenzoate et de la *N,N*-diméthyl aniline a été étudié pour des solutions dans l'éthanol-*O*-d_1, contenant de l'éthylate de sodium. Le domaine de deutération a été estimé par spectroscopie de masse et la position de deutération par spectroscopie r.m.n. Dans cette réaction contrôlée cinétiquement la substitution en ortho a été trouvée prédominante dans le cas du complexe de l'anisole tandis qu'une substitution annexe a été observée par r.m.n. pour le complexe de l'éthylbenzoate. Les résultats sont interprétés en termes de chélation, d'induction, de mésomérie et d'effets stériques des substituants.

Canadian Journal of Chemistry, **50**, 118 (1972)

Introduction

The ability of a tricarbonylchromium group to stabilize a negative charge on or adjacent to a benzene ring has been shown by the ease of nucleophilic displacement of chloride and fluoride ions from tricarbonyl(chloro- and fluorobenzene)chromiums and in the increased acid strength of tricarbonyl(benzoic acid)chromium relative to that of benzoic acid (1). Russian workers (2) have shown that when a solution of tricarbonyl(benzene)chromium in ethanol-*O*-d_1 containing sodium ethoxide is heated for 20 h at 100° almost half of the hydrogen is replaced by deuterium. They also found that the tendency of hydrogen atoms to undergo protophilic hydrogen–deuterium exchange in the aromatic ring was very much greater in tricarbonyl(toluene)chromium than in toluene (3).

We have extended this work by studying the degree and nature of hydrogen-deuterium exchange reactions in tricarbonylchromium complexes of anisole, ethylbenzoate, and *N,N*-dimethylaniline.

Results and Discussion

Deuteration of Tricarbonyl(anisole)chromium

When a solution of tricarbonyl(anisole)-chromium was heated for 24 h at 100° appreciable decomposition occurred and *ca.* 14% of the anisole complex was recovered. The amount

[1]This work is a part of Ph.D. thesis of the author at Queen's University of Belfast.

[2]Present address: 40-Urdu Bazar Lahore, West Pakistan.

Can. J. Chem. Downloaded from www.nrcresearchpress.com by 210.87.254.6 on 09/05/12
For personal use only.

further conversion to monocyclics and then to aromatics. The fall in the concentration of aromatics is, therefore, not surprising.

A. Stanislaus wishes to thank the Council of Scientific and Industrial Research for the research fellowship award.

1. C. T. CHEN, W. O. HAAG, and H. PINES. Chem. Ind. (Lond.) 1379 (1959).
2. H. PINES and C. T. CHEN. Actes Deuxieme Congres Intern. Catalyse, Paris. **I**, 367 (1960).
3. H. PINES and C. T. CHEN. J. Am. Chem. Soc. **82**, 3562 (1960).
4. L. M. YEDDANAPALLI and J. VERGHESE. J. Sci. Ind. Res. **16B**, 224 (1957).
5. R. P. LINSTEAD. J. Am. Chem. Soc. 1139 (1940).
6. V. N. IPATIEFF and H. PINES. J. Am. Chem. Soc. **70**, 533 (1948).
7. H. PINES and ROMANO COVINI. J. Catal. **4**, 454 (1965).
8. J. M. BRIDGES, G. T. RYMER, and D. S. MCIVER. J. Phys. Chem. **66**, 871 (1962).
9. A. STANISLAUS and L. M. YEDDANAPALLI. Can. J. Chem. This issue.

Base-catalyzed Deuteration of Tricarbonylchromium Complexes[1]

M. ASHRAF[2]
Department of Chemistry, Queen's University, Belfast, N. Ireland

Received June 16, 1971

Hydrogen–deuterium exchange in tricarbonylchromium complexes of anisole, ethylbenzoate, and *N,N*-dimethylaniline has been studied for solutions in ethanol-*O*-d_1, containing sodium ethoxide. The extent of deuteration has been estimated mass spectroscopically and the position of deuteration by n.m.r. spectroscopy. In this kinetically controlled reaction ortho-substitution has been found to be predominantly preferred in case of anisole complex, whereas random substitution was observed (n.m.r.) for ethylbenzoate complex. The results are interpreted in terms of chelative, inductive, mesomeric, and steric effects of the substituents.

L'échange hydrogène–deutérium dans les complexes du chrome tri-carbonyle de l'anisole, de l'éthylbenzoate et de la *N,N*-diméthyl aniline a été étudié pour des solutions dans l'éthanol-*O*-d_1, contenant de l'éthylate de sodium. Le domaine de deutération a été estimé par spectroscopie de masse et la position de deutération par spectroscopie r.m.n. Dans cette réaction contrôlée cinétiquement la substitution en ortho a été trouvée prédominante dans le cas du complexe de l'anisole tandis qu'une substitution annexe a été observée par r.m.n. pour le complexe de l'éthylbenzoate. Les résultats sont interprétés en termes de chélation, d'induction, de mésomérie et d'effets stériques des substituants.

Canadian Journal of Chemistry, **50**, 118 (1972)

Introduction

The ability of a tricarbonylchromium group to stabilize a negative charge on or adjacent to a benzene ring has been shown by the ease of nucleophilic displacement of chloride and fluoride ions from tricarbonyl(chloro- and fluorobenzene)chromiums and in the increased acid strength of tricarbonyl(benzoic acid)chromium relative to that of benzoic acid (1). Russian workers (2) have shown that when a solution of tricarbonyl(benzene)chromium in ethanol-*O*-d_1 containing sodium ethoxide is heated for 20 h at 100° almost half of the hydrogen is replaced by deuterium. They also found that the tendency of hydrogen atoms to undergo protophilic hydrogen–deuterium exchange in the aromatic ring was very much greater in tricarbonyl(toluene)chromium than in toluene (3).

We have extended this work by studying the degree and nature of hydrogen-deuterium exchange reactions in tricarbonylchromium complexes of anisole, ethylbenzoate, and *N,N*-dimethylaniline.

Results and Discussion

Deuteration of Tricarbonyl(anisole)chromium

When a solution of tricarbonyl(anisole)-chromium was heated for 24 h at 100° appreciable decomposition occurred and *ca.* 14% of the anisole complex was recovered. The amount

[1]This work is a part of Ph.D. thesis of the author at Queen's University of Belfast.

[2]Present address: 40-Urdu Bazar Lahore, West Pakistan.

Can. J. Chem. Downloaded from www.nrcresearchpress.com by 210.87.254.42 on 09/05/12
For personal use only.

TABLE 1. Deuteration of tricarbonylchromium compounds

Compound	Relative intensities for peaks of *m/e*							Ionizing voltage (eV)
	107	108	109	110	111	112		
Tricarbonyl(anisole)chromium	1.2	28.9	3.9	0.3	0.0	0.0		70
" " "	1.3	100.0	8.5	0.6	0.0	0.0		12
Deuterated sample	0.65	15.0	25.9	17.5	7.5	1.6		70
" "	0.70	60.7	100.0	69.5	21.4	0.0		12
	149	150	151	152	153	154	155	
Tricarbonyl(ethylbenzoate)chromium	0.2	2.5	0.29	0.09	0.0	0.0	0.0	70
" " "	1.94	50.7	4.4	0.0	0.0	0.0	0.0	12
Deuterated sample	0.0	2.35	5.5	9.9	11.3	7.3	3.0	70
" "	0.0	2.7	9.2	18.9	21.4	14.3	6.0	12
	122	123	124	125	126	127		
Tricarbonyl(benzoic acid)chromium	25.0	2.2	1.7	0.0	0.0	0.0		70
" " " "	100.0	8.5	0.0	0.0	0.0	0.0		12
Deuterated sample	31.8	21.2	33.3	25.6	13.7	4.5		70
" "	88.0	56.4	93.2	100.0	54.6	15.8		12
% of deuterated molecules in	0D	1D	2D	3D	4D	5D		
Anisole complex	23.0	36.0	22.0	8.6				70
	26.0	41.0	26.0	6.7				12
Ethylbenzoate complex	6.8	15.0	27.0	29.0	17.0	6.0		70
	4.0	13.3	27.0	29.5	18.6	7.3		12
Benzoic acid complex	28.3	16.3	26.2	20.0	9.0	2.0		70
	24.0	12.3	24.0	25.0	12.5	3.0		12

of hydrogen–deuterium exchange was estimated by comparison of the mass spectrum of the deuterated sample with that of tricarbonyl(anisole)chromium. The parent molecular ion was not used for measuring the amount of deuterium incorporation because of the difficulties associated with chromium isotopes. Instead the peaks associated with the anisole ion, *m/e* 108 were used. The spectra were obtained with a beam energy of 70 and 12 eV and the results are shown in Table 1. The average of these results indicated that the deuterated sample contained 24.5% of molecules with no deuterium, 38.5% with 1D, 24% with 2D, and 7.6% with 3D.

The n.m.r. spectrum of tricarbonyl(anisole)-chromium ($CDCl_3$) at 100 MHz showed the aromatic protons as well resolved signals at τ 4.46 (triplet, meta), 4.90 (doublet, ortho), and 5.14 (triplet, para) with the methoxy protons at τ 6.34, in agreement with a published spectrum (4). The deuterated sample had a similar spectrum with two distinctions. The meta-triplet, $J = 6$ Hz was now a five-line multiplet consisting of the original triplet together with a doublet, $J = 6$ Hz, also centered at τ 4.46. The integral was now in the ratio 1.9 meta:1.25 ortho:0.9 para:3 methoxy protons, suggesting a deuterium exchange of 5% of the meta, 38% of the ortho and 10% of the para hydrogen atoms. These results are in agreement with an independent Russian study which was published during the course of this work (5).

Deuteration of Tricarbonyl(ethylbenzoate)-chromium

The deuteration of tricarbonyl(ethylbenzoate)chromium, as described in the Experimental recovered only *ca.* 7% of the ester complex from the ethereal extract of the reaction mixture. However, the aqueous layer on acidification afforded tricarbonyl(benzoic acid)chromium (*ca.* 46%). The amount of deuterium incorporation in both substances was measured using the peaks associated with ethylbenzoate and benzoic acid ions, *m/e* 150 and 122 respectively. No correction was used for oxygen isotopes. The relevant spectra for both of these complexes, obtained with an ionizing voltage

Can. J. Chem. Downloaded from www.nrcresearchpress.com by 210.87.254.42 on 09/05/12
For personal use only.

Can. J. Chem. Downloaded from www.nrcresearchpress.com by 210.87.254.42 on 09/05/12
For personal use only.

of 70 and 12 eV, are given in Table 1. The average of these results indicated *ca.* 5% of molecules with no deuterium, 14% with 1D, 27% with 2D, 29% with 3D, 18% with 4D, and 7% with 5D in the ethylbenzoate complex, while the corresponding percentages in the benzoic acid complex were 26, 14, 25, 23, 11, and 3% for the molecules containing 0D to 5D respectively. The rather large variation of deuterium incorporation in these compounds might be due to the hydrolysis of the ester complex partly during the course of the reaction (due to some moisture content) and partly during work-up of the hot reaction mixture.

The n.m.r. spectrum of tricarbonyl(ethylbenzoate)chromium in $CDCl_3$ at 100 MHz showed well resolved signals at τ 8.64 (triplet, methyl), 5.65 (quartet, methylene), 4.74 (triplet, meta), 4.47 (triplet, para, $J = 6.0$ Hz), and 3.90 (doublet, ortho, $J = 6.5$ Hz). In the case of the deuterated sample the spectrum was very different in the aromatic region. The meta-triplet now appeared as a five-line multiplet centered on τ 4.74, the para-proton as a partially resolved multiplet on 4.47, and the ortho-protons as a well resolved triplet on 3.9, suggesting that deuteration occurred on all available positions. The integral intensity was now in the ratio 1 meta:0.6 para:0.8 ortho:2 methylene:3 methyl protons indicating that 50% of the meta, 40% of the para, and 60% of the ortho protons had been exchanged by deuterium.

The n.m.r. spectrum of the tricarbonyl(benzoic acid)chromium in CD_3COCD_3 showed signals at τ 4.39 (triplet, meta), 4.11 (triplet, para), and 3.74 (doublet, ortho). The n.m.r. spectrum of the deuterated sample was almost identical to the deuterated sample of the ester complex as regarded the coupling pattern of the signals. The signals were, however, centered on the same positions as that of the undeuterated acid complex. The integrated intensities in the deuterated sample of the benzoic acid complex were in the ratio 1.0 meta:0.6 para:1.0 ortho suggesting an exchange of 50, 40, and 50% protons from the meta, para, and ortho positions respectively. This ratio is slightly different from that in the ester complex. This could again be explained by hydrolysis of some of the ester complex giving the complexed benzoate ion which would not be expected to exchange readily.

Attempted Deuteration of Tricarbonyl-(N,N-dimethylaniline)chromium

When the deuteration of tricarbonyl(*N*,*N*-dimethylaniline)chromium was now attempted under conditions similar to previous reactions, *ca.* 18% of the complex was recovered. The mass spectrum of this sample showed no enhancement of various peaks as compared with starting material. The n.m.r. spectrum of the recovered sample was also identical to the undeuterated sample with no difference in the integral intensities of various protons.

The results of the deuteration of the anisole complex indicate that the exchange reaction must be predominantly kinetically controlled and that the exchange of ortho-protons is kinetically preferred over that of the meta- or para-protons. The metallation of anisole with *n*-butyllithium has been reported to give exclusive (99.9%) ortho-substitution (6). The high selectivity in metallation reflects the relative thermodynamic stability of the isomeric lithiated anisoles, whereas the preference for ortho-substitution in this work reflects a lower transition state energy for proton abstraction from the ortho-position. However, in analogy with the metallation reaction it would appear that inductive and possibly chelative effects of the methoxy group can stabilize the transition state leading to ortho-deuteration.

The kinetically controlled deuterium exchange reaction of tricarbonyl(ethylbenzoate)-chromium gives an almost statistical exchange pattern of ortho:meta:para. The carboxyethyl group can withdraw electrons by both inductive and mesomeric effects, and thus help stabilize a negatively charged transition state in any position. Possibly slightly higher deuteration may be expected at the ortho- and para-positions of this compound but results give marginal support for this suggestion.

Tricarbonyl(*N*,*N*-dimethylaniline)chromium should be comparatively more susceptible to hydrogen–deuterium exchange reaction because of strongly electron-withdrawing power of $Cr(CO)_3$ group. Moreover, electronegative nitrogen could also activate the ortho-hydrogens inductively. But no deuteration takes place even in the chromium complex of *N*,*N*-dimethylaniline. This could be due to weak inductive effect of nitrogen as compared with oxygen in anisole. It is also possible that flanking methyl

groups of *N,N*-dimethylamino group inhibit sterically the exchange of ortho-protons.

In conclusion, the base-catalyzed hydrogen-deuterium exchange reactions in these tricarbonylchromium complexes can be rationalized by considering the well-known inductive, mesomeric, and steric effects of the substituents.

Experimental

Spectra

Mass spectra were determined with an AE1 MS9, using the heated inlet system and operating at 70 and 12 eV. The n.m.r. spectra were recorded for $CDCl_3$ and CD_3COCD_3 solutions (as specified) containing TMS as internal standard using a Varian HA 100 spectrometer.

Materials

Tricarbonylchromium complexes of anisole had m.p. 85–86° (lit. 86–87° (1)) and that of *N,N*-dimethylaniline, m.p. 143–144° (lit. 145.8–146.5° (1)). Tricarbonyl(ethyl-benzoate)chromium, m.p. 52–53° from ether–light petroleum, was prepared by the method of Nicholls and Whiting (1).

Anal. calcd. for $C_{12}H_{10}CrO_5$: C, 50.3; H, 3.5. Found: C, 50.1; H, 3.5.

Ethanol-*O*-d_1, was prepared by the method of Shiner and Smith (7).

Deuteration of Tricarbonyl(anisole)chromium

A solution of tricarbonyl(ethyl benzoate)chromium (0.4 g) in ethanol-*O*-d_1 (100 ml) was placed in a thick-walled glass tube and sodium ethoxide, prepared from sodium (2.0 g), added under a nitrogen atmosphere. The solution was flushed well with nitrogen, the tube sealed and heated at 100° for 24 h. The cooled reaction mixture was poured into ice water and the product (55 mg) isolated in benzene. One crystallization from light petroleum gave tricarbonyl-(anisole)chromium (34 mg), m.p. 86–87°.

Another reaction on an identical scale which was heated for 24 h recovered tricarbonyl(anisole)chromium (68 mg, 17%). The mass spectrum indicated that *ca.* 15% of mono-deuteration had taken place and n.m.r. spectrum showed that this had occurred mainly in the ortho-position (see Discussion).

Deuteration of Tricarbonyl(ethyl benzoate)chromium

A solution of tricarbonyl(ethyl benzoate)chromium (0.4 g) and sodium ethoxide in ethanol-*O*-d_1 (100 ml) was heated similar to the anisole complex. After 26 h the solvent was removed on the water-bath and the hot residue poured in water. The ethereal extract gave the yellow oil (0.112 g) which on crystallization from ether–light petroleum provided only small amount (30 mg) of the ester complex, m.p. 50–51°.

The aqueous layer on acidification and routine extraction gave crude tricarbonyl(benzoic acid)chromium (0.164 g). Crystallization from ether–light petroleum afforded the acid complex (0.135 g), m.p. 195–196° (dec.) (lit. 194° (1)).

Attempted Deuteration of Tricarbonyl(N,N-dimethylaniline)chromium

A solution of tricarbonyl(*N,N*-dimethylaniline)chromium (0.4 g) and sodium ethoxide, in ethanol-*O*-d_1 (80 ml) was heated as already described. Work-up after 24 h recovered the complex (73 mg, 18%), which on crystallization from ether–light petroleum afforded the complex (49 mg), m.p. 143–146° (dec.).

A repeat experiment on an identical scale gave the complex (53 mg).

The author wishes to thank Dr. W. R. Jackson and Dr. J. Grimshaw of this Department for their helpful discussion. Thanks are also due to Mr. T. G. Kee who performed a section of the experimental work. The award of a visiting studentship from this University is also acknowledged.

1. B. Nicholls and M. C. Whiting. J. Chem. Soc. 551 (1959).
2. V. N. Setkina, N. K. Baranetskaya, K. N. Anisimov, and D. N. Kursanov. Izvest. Akad. Nauk. S.S.S.R. Ser. Kim. 1873 (1964).
3. Reference 2. 1622 (1968).
4. W. McFarlane and S. O. Grim. J. Organomet. Chem. **5**, 147 (1966).
5. D. N. Kursanov, V. N. Setkina, N. K. Baranetskaya, E. I. Fedin, K. N. Anisimov, and V. M. Urinyuk. Doklady Akad. Nauk. S.S.S.R. **183**, 1340 (1968).
6. D. A. Shirley, J. R. Johnson, Jr., and J. P. Hendrix. J. Organomet. Chem. **11**, 209 (1968).
7. V. J. Shiner and M. L. Smith. J. Am. Chem. Soc. **83**, 593 (1961).

Can. J. Chem. Downloaded from www.nrcresearchpress.com by 210.87.254.42 on 09/05/12
For personal use only.

Stereochemistry of some Altersolanol B Derivatives and their Correlation with Bostrycin[1]

M. GORDON, A. STOESSL, AND J. B. STOTHERS

Department of Chemistry, University of Western Ontario and the Research Institute, Canada Department of Agriculture, London, Ontario

Received August 25, 1971

The results of a complete analysis of the proton spectra of altersolanol B acetonide indicate that this compound exists preferentially in the half-chair conformation corresponding to that favored by the parent pigment in the solid state, as shown by previous X-ray studies. In contrast, the triacetate derivative apparently adopts the alternative half-chair conformation.

Les résultats d'une analyse complète r.m.n. de l'altersolanol B acétonide indique que ce composé existe préférentiellement sous la forme demi-chaise correspondant à celle favorisée par le pigment de base dans l'état solide, comme l'ont montré de précédentes études rayons-X. En revanche, le dérivé triacétate adopte apparemment la conformation demi-chaise alternative.

Canadian Journal of Chemistry, **50**, 122 (1972)

Can. J. Chem. Downloaded from www.nrcresearchpress.com by 210.87.254.40 on 09/05/12
For personal use only.

In an earlier paper on some metabolites of *Alternaria solani* (1), structures were proposed for altersolanol B (**1**, R = R′ = H), its triacetate (**1**, R = R′ = Ac) and isopropylidene (**2**) derivatives. To confirm the assigned structures and to obtain information bearing on the probable conformations of these materials, a complete analysis of the proton spectrum of acetonide **2** was undertaken. In the interim Noda *et al.* (2) reported the results of their structural study of bostrycin (**3**), a closely related tetrahydroanthraquinone pigment. These authors found that treatment of hydrogenation products of **3** with *p*-bromobenzoyl chloride in pyridine yielded a crystalline ester which was subsequently hydrolyzed in these laboratories to give altersolanol B as judged by t.l.c. and u.v. spectra. X-Ray diffraction results for the *p*-bromobenzoate **1** (R = H, R′ = *p*-BrC_6H_4CO) were presented by Takenaka *et al.* (3). As a further check on the correspondence between the two pigments a sample of acetonide **2** was treated with *p*-bromobenzoic anhydride in tetrahydrofuran containing some γ-dimethylaminopyridine to yield an acetonide ester. Upon removal of the isopropylidene group, the resulting *p*-bromobenzoate was compared to an authentic sample of the degradation product obtained by Noda *et al.* (2) and found to be identical by m.p., mixture m.p., i.r. and u.v. spectra and specific rotation. Consequently, the structures originally proposed are undoubtedly correct but the question of preferred conformation remained.

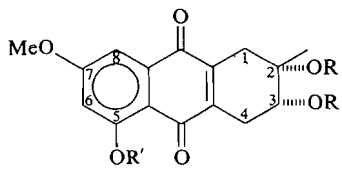

1

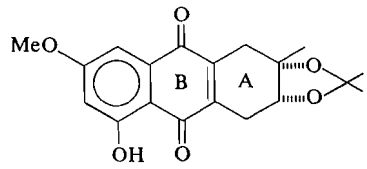

2

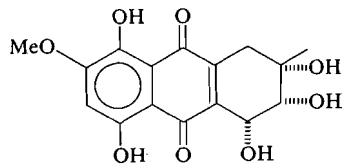

3

In addition to the methyl proton absorptions, the high field region of the proton spectrum of **2** consists of two overlapping AB patterns one of which is part of an ABX system; since the two AB patterns are long-range coupled a better description of the spin system may be ABMNX. To

[1]Contribution No. 496 from the Research Institute and Part XXIV in the series NMR Studies (for Part XXIII see ref. 7).

Can. J. Chem. Downloaded from www.nrcresearchpress.com by 210.87.254.40 on 09/05/12
For personal use only.

analyze this portion of the spectrum the LAOCOON III program was utilized with spectra obtained at 60 and 100 MHz. Since the amount of material was limited, time-averaging was employed to obtain spectra having suitable S/N ratios. The averaged results of these analyses are listed in Table 1. The acetonide methyl protons absorb at δ 1.22 and 1.37 while the quaternary methyl protons appear at δ 1.46; the *gem*-dimethyl absorptions are readily identified since each appears as a quartet ($J = 0.6$ Hz) due to mutual long-range coupling. The relatively small shift between the *gem*-dimethyl protons offers strong evidence that these groups do not lie close to the double bond of the B-ring, *i.e.*, this acetonide does not exist in a boat conformation analogous to that found for altersolanol A acetonide (4).

The lowest field pattern, readily assigned to the C-3 proton, has the typical appearance of the X-absorption for an ABX spin system; there is no evidence of coupling between the X proton (C-3 H) and the C-1 methylene protons. The sum of the vicinal coupling constants, $J_{AX} + J_{BX}$, is obtained directly from the X-pattern and the value of 6.5 Hz indicates the absence of a *trans*-diaxial interaction. This observation rules out the alternative boat conformation for the A-ring in which the acetonide grouping is in a pseudo-equatorial orientation. The intensity of the X pattern increases by 14% upon simultaneous irradiation of the δ 1.46 methyl protons; this nuclear Overhauser enhancement confirms the *cis* relation of X with respect to the quaternary methyl.

On the basis of the foregoing it follows that the A-ring exists in a half-chair conformation for which there are two possibilities, **4** and **5**. To illustrate the relative orientations of the ABX protons in each of these conformations, Newman projections along the C_3—C_4 bond are shown

TABLE 1. Proton parameters for the ABMNX pattern of acetonide **2***

	A	B	M	N	X
A	244.8	-17.8_5	2.1_9	1.3_5	4.2_8
B		335.4	0.2_7	0.9_4	2.4_2
M			229.2	-17.3_1	0.0
N				308.9	0.0
X					430.6

*The values on the diagonal are the chemical shifts in Hz from TMS (at 100 MHz) while the off-diagonal values are the coupling constants.

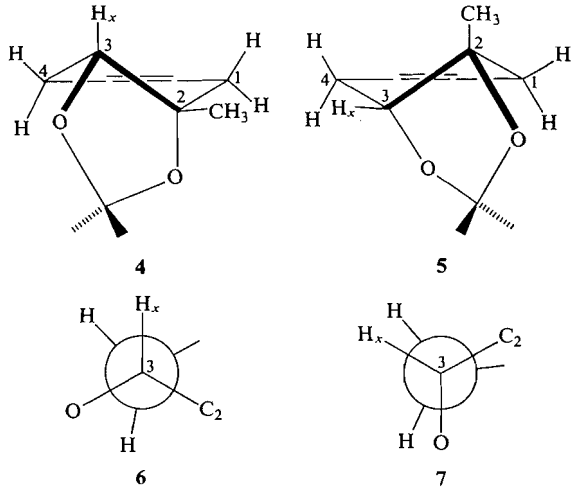

4 5

6 7

as **6** and **7**, respectively. Since **4** requires an essentially *trans*-diaxial disposition of the X proton with respect to one of the vicinal protons and the vicinal couplings are 4.3 and 2.4 Hz it appears that **5** is the preferred conformation. The dihedral angles between vicinal protons in this form are approximately 75 and 45°, which are consistent with the observed couplings. It is interesting that the geminal coupling constants for the C-1 and -4 methylene groups differ slightly, -17.3 and -17.9 Hz, respectively. This difference may be taken to indicate that the C-4 protons are more symmetrically disposed relative to the double bond than the C-1 methylene protons (5) which suggests a slight warping of half-chair **5**. There remains the assignment of the long-range, homoallylic couplings. Since it is generally found that protons lying near the plane of the π-system in the HC—C=C—C—H fragment exhibit small coupling constants while diaxial protons are the most strongly coupled nuclei in such systems (6), the following assignments may be made: $J_{1a',4a'}$ 2.2; $J_{1e',4a'}$ 1.3; $J_{1a',4e'}$ 0.2; and $J_{1e',4e'}$ 0.9 Hz. The chemical shifts of the methylene protons are consistent with these assignments in that the pseudo-axial protons are significantly shielded relative to their pseudo-equatorial counterparts.

On the basis of the X-ray diffraction results for the *p*-bromobenzoate of altersolanol B, it follows that the preferred conformation for the parent pigment, in the solid state, is also the half-chair form corresponding to **5**. Although we have been unable to complete the analysis of the

spectrum of altersolanol B triacetate (**1**, R = R′ = Ac), the absorption of the C-3 proton is distinctively the X-portion of an ABX system in which $(J_{AX} + J_{BX}) = 10.5$ Hz, significantly larger than that found for the acetonide. This finding strongly suggests that altersolanol B triacetate preferentially exists in the alternative half-chair conformation in which the C-3 proton is *trans*-diaxial with respect to one of the vicinal protons as in **6**.

The correlation with the *p*-bromobenzoyl derivative of bostrycin establishes **1** (R = R′ = H) as a representation of the absolute stereochemistry of altersolanol B. It is most probable that altersolanol A, a cometabolite of altersolanol B, will have the same configuration at C-2 and -3. Therefore, the absolute stereochemistry of altersolanol A is the mirror image of that depicted in an earlier communication (4).

Experimental

Nuclear Magnetic Resonance Spectra

The proton spectra were obtained with Varian HA-60 and HA-100 instruments using dilute solutions in $CDCl_3$. To increase the sensitivity, time-averaged spectra were collected using a Varian C-1024 device; in each case 100–200 scans over sweep widths of 100–500 Hz were employed. Spectral analysis was accomplished using the LAOCOON III program of Bothner-By and Castellano with the University of Western Ontario 7040 computer. Comparisons of the observed spectra with those calculated were aided by generating the latter using a plot program kindly supplied by Dr. Castellano in conjunction with the Cal-Comp plotter of the University of Western Ontario computer center. The precision of the chemical shifts and coupling constants is judged to be ±0.05 Hz; both 60 and 100 MHz spectra were fitted with an overall r.m.s. error of 0.05.

Altersolanol B 5-p-Bromobenzoate

Altersolanol B acetonide (35 mg; 0.104 mmol) in tetrahydrofuran (1.5 ml) was added to an ice-cold suspension of *p*-bromobenzoic anhydride (153 mg; 0.40 mmol) in a solution of 4-dimethylaminopyridine (48 mg; 0.40 mmol) in tetrahydrofuran (2.5 ml), which was then allowed to warm to room temperature. After gentle shaking during 2 h, the clear solution was poured on ice (10 ml), sodium hydrogen carbonate solution (5%, 2 ml) was added, and the solution extracted with ethyl acetate (3 × 10 ml). After washing with dilute sodium hydrogen carbonate, water, ice-cold *N*/10 hydrochloric acid, and repeatedly with water, the extracts were dried, filtered, and evaporated *in vacuo*. The bright yellow band obtained on preparative t.l.c. of the residue (silica gel (Camag DF-5), with ether–petroleum ether (b.p. 37–67°)–acetic acid (30:70:2) as irrigant) was eluted. A little more of the same material was obtained by irrigating a band, which had remained at the origin, with methanol–chloroform–acetic acid (10:90:2). The combined product was crystallized and recrystallized from ether, to give altersolanol B acetonide-5-*p*-bromobenzoate (12.6 mg); m.p. 209–212°; λ_{max} 375, 340, 284 (sh), 266 (sh), and 252 nm (log ε 3.24, 3.30, 4.23, 4.48, and 4.49).

To a solution of the acetonide 5-*p*-bromobenzoate (8.6 mg) in chloroform (1 ml)–methanol (1.8 ml) was added aqueous hydrochloric acid (0.2 ml 1 *N*). After 22 h at room temperature, the solution was evaporated *in vacuo* and the product recrystallized from ethanol. It was identical with an authentic specimen of the *p*-bromobenzoate derived from bostrycin by m.p., mixture m.p., i.r. spectrum (in $CHCl_3$), u.v. spectrum (λ_{max} 375, 340, 281 (sh), and 248 nm (log ε 3.19, 3.30, 4.18, and 4.47). Both specimens exhibited the same specific rotation ($[\alpha]_D^{23}$ +23°; *c*, 0.40 in $CHCl_3$).

We thank Dr. T. Noda for a generous gift of bostrycin and its *p*-bromobenzoate derivative; Mr. G. Rock and Miss P. M. Pellitt for valuable technical assistance; and Dr. S. Castellano, Carnegie-Mellon University, for kindly supplying the plotter program. The financial support of the National Research Council of Canada is gratefully acknowledged.

1. A. Stoessl. Can. J. Chem. **47**, 767 (1969).
2. T. Noda, T. Take, T. Watanabe, and J. Abe. Tetrahedron, **26**, 1339 (1970).
3. A. Takenaka, A. Furusaki, T. Watanabe, T. Noda, T. Take, T. Watanabe, and J. Abe. Tetrahedron Lett. 6091 (1968).
4. A. Stoessl. Can. J. Chem. **47**, 777 (1969).
5. J. A. Pople and A. A. Bothner-By. J. Chem. Phys. **42**, 1339 (1965).
6. A. W. Brinkman, M. Gordon, R. G. Harvey, P. W. Rabideau, J. B. Stothers, and A. L. Ternay. J. Am. Chem. Soc. **92**, 5912 (1970), and refs. therein.
7. H. Brouwer and J. B. Stothers. Can J. Chem. **49**, 2152 (1971).

Can. J. Chem. Downloaded from www.nrcresearchpress.com by 210.87.254.40 on 09/05/12
For personal use only.

The Adsorption of Alkylchlorosilanes on Quartz Crystal Surfaces

G. M. KHAN
Institute of Chemistry, University of Islamabad, Rawalpindi, Pakistan

Received June 29, 1971

The piezogravimetric method has been used to study the adsorption of dimethyl and trimethylchlorosilanes on quartz crystal surfaces by varying the mode of treatment. The nature of the resulting low-energy surfaces has been discussed in the light of the extent of adsorption of *n*-hexane and water, calculated at different relative pressures, from their isotherms. The results obtained permit the conclusion that after the adsorption of silanes at 240 °C, the modified surface may be described as close-packed methyl surface, impenetrable to *n*-alkane and water vapor.

La méthode piézogravimétrie a été utilisée pour étudier l'adsorption des diméthyl et triméthylchlorosilanes, sur des surfaces en cristaux de quartz, en modifiant les modes de traitement. La nature des surfaces à faible énergie ainsi obtenues a été discutée à la lumière du degré d'adsorption en *n*-hexane et eau, calculé à différentes pressions relatives, à partir de leurs isothermes. Les résultats obtenus permettent de conclure qu'après l'adsorption des silanes à 240 °C, la surface modifiée peut être décrite comme étant une surface méthylée très tassée, impénétrable aux *n*-alkanes et à la vapeur d'eau.

Canadian Journal of Chemistry, **50**, 125 (1972)

Can. J. Chem. Downloaded from www.nrcresearchpress.com by 210.87.254.40 on 09/05/12
For personal use only.

Introduction

The ability of alkylchlorosilanes to chemisorb onto many high energy surfaces, and convert them to low energy ones, is well-known. Most of the previous work has been concerned, for technological reasons, with glass substrates. Glass differs from quartz in the well-known sense that the very term 'glass' implies a measure of uncertainty; the type of glass, and its mode of preparation, needs to be specified. The term 'quartz' is more precise, particularly when a certain modification, and crystal cut are specified. Nevertheless, glass and quartz crystals possess some features in common. With particular respect to the chemisorption of alkylchlorosilanes, the critical feature concerns the number and distribution of residual hydroxyl groups on the surface, these being dependent both upon the basic nature of the substrate and upon the history of its pretreatment.

Surface hydroxyl groups, or residual adsorbed water molecules upon glass or quartz surfaces must obviously play a predominant role in the chemisorption of alkylchlorosilane vapors to which they are exposed. Presently available information in the literature is helpful, but not definitive (1–3). There are, for example, indications that not all of the hydroxyl groups are removed during the vapor phase adsorption of trichloroalkylsilanes on hydrated porous glass samples at room temperature (2, 3). The findings from the present studies fall into the same class; they are indicative, rather than definitive.

Experimental

The core feature of the piezogravimetric method is that a suitably chosen quartz crystal, capable of resonating at its characteristic frequency between two exciting electrodes, be coupled with an auxiliary device for measuring frequency shifts at various pressures of the adsorbate vapor, at equilibrium with the adsorbent phase, in an accurately temperature controlled cell. The vacuum system and circuits used in this work have been described, in detail, elsewhere (4). However, for convenience, Fig. 1 is given here which shows the details of the experimental cell and the quartz crystal mounting assembly.

Before use, the cell, stainless steel components, and the crystal assembly were treated with chromic acid – sulfuric acid mixture followed by repeated rinsing with triply-distilled water. Prior to each set of observations, the cell with crystal assembly was heated at 240 °C and the vacuum line was thoroughly baked at 80 °C for about 48 h. Special attention was paid to the purity of the adsorbate sample of *n*-hexane obtained from Matheson Coleman and Bell Co. (U.S.A.), listed as being of chromatoquality, which was further dried thoroughly by passing through molecular sieve and finally degassed by trap-to-trap distillation and repeated freezing and thawing in vacuum. The water used as adsorbate was, of course, triply-distilled, and the alkylchlorosilanes were kindly provided by Dr. A. C. Lowe (5). They had been purified by trap-to-trap distillation under grease-free conditions.

The crystal assembly mounted in the experimental cell and connected to the oscillator was placed in the air-stirred constant temperature thermostat and the whole system was evacuated for a period of about 24 h, till the system had attained a full stability shown by a constant value of the resonant frequency. As the temperature of the adsorbate

Can. J. Chem. Downloaded from www.nrcresearchpress.com by 210.87.254.40 on 09/05/12
For personal use only.

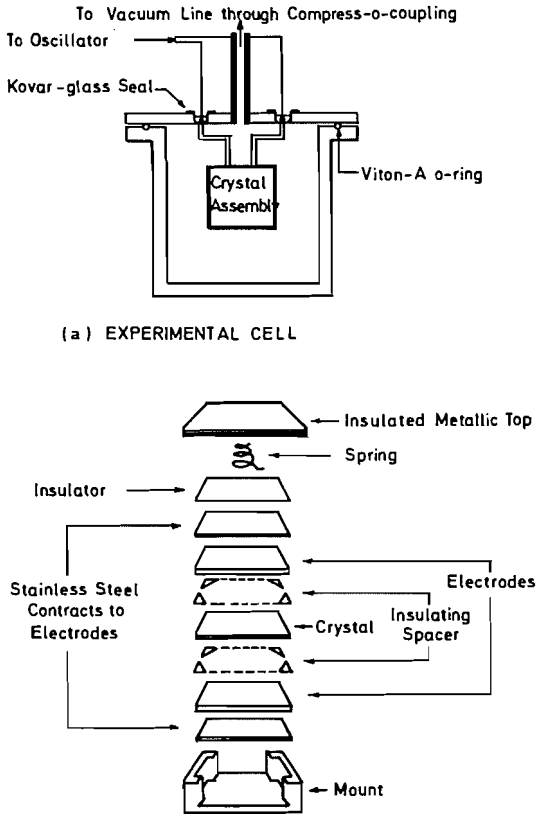

FIG. 1. The schematic diagram of (*a*) the experimental cell, (*b*) the quartz crystal mounting assembly.

vapor differed from that of the quartz surface, the former was preheated in a preliminary thermostating compartment before admitting it into the cell. At each run the vapor was introduced gradually by increasing the pressure in small steps. Following the introduction of vapor, the frequency was monitored as a function of time over a period of about 30 min for each run until equilibrium had been attained. After the determination of a particular isotherm, the system was outgassed till a stable value for the resonant frequency was obtained again.

Three AT-cut crystals, A, B, and C have been used during these studies. Their apparent (geometric) available areas for adsorption and their masses are shown in Table 1, which also summarizes the treatments to which the crystals were submitted and the designations given to each treated surface.

Crystal A cleaned and mounted in standard fashion, and stable to the extent shown in Table 2, was placed in the experimental cell and outgassed as mentioned before. It was named surface 'A' and the adsorption of *n*-hexane and water vapors was studied on this surface. The experimental system was outgassed hard, at 200 °C, and surface 'AS2' prepared by adsorbing $(CH_3)_2SiCl_2$ on the crystal at 26.7 °C. The process was monitored by measuring the change in crystal frequency. When the latter approached constancy, excess silane was removed by the pump. The stability of this coated crystal is also shown in Table 2, and appeared to be somewhat better than the uncoated crystal. The term 'S2' is simply a convenient notation for dichloromethylsilane. After adsorption studies on 'AS2' surfaces above, the experimental cell was outgassed and heated to 160 °C for about 5 h before being allowed to cool. The adsorption of *n*-hexane and water vapor was studied on the resulting surface termed 'AS2H'.

Crystal B, essentially similar to A, was coated with $(CH_3)_2SiCl_2$ by exposure to the vapor at 240 °C for approximately 8 h and the adsorption of *n*-hexane and water vapor was studied on the resulting surface termed 'BS2HA'. The surface 'CS3HA' was prepared in the same manner as 'BS2HA' except that crystal 'C' was coated with $(CH_3)_3SiCl$ by exposure to the vapor under the same conditions and the adsorption studies of *n*-hexane and water vapor were studied as mentioned before.

Results and Discussion

Figures 2 and 3 show the observed extent of adsorption measured by the change in frequency, $\Delta\nu$, for *n*-hexane and of water vapor in comparative form for these different surfaces as a function of pressure. As expected, the extent of adsorption was always highest upon the clean quartz surface 'A'. Of more interest, adsorption decreases in passing from the 'AS2' surface,

TABLE 1. Nomenclature of the surfaces (all crystals used were AT-cut)

Crystal	Apparent area used for adsorption (cm^2)	Mass (g)	Treatment	Designation of surface
A	3.765	0.0807	General cleaning 'A'	'A'
			coated with $(CH_3)_2SiCl_2$ at 26.7 °C	'AS2'
			'AS2' heated at 160 °C for about 5 h	'AS2H'
B	3.779	0.813	Coated with $(CH_3)_2SiCl_2$ at 240 °C for about 8 h	'BS2HA'
C	3.788	0.0817	Coated with $(CH_3)_3SiCl$ at 240 °C for about 8 h	'CS3HA'

TABLE 2. The stability of the resonance frequency of surfaces 'A' and 'AS2' at 240 °C, with time, under vacuum

	Frequency (c/s)	
Time (min)	Surface 'A'	Surface 'AS2'
0	10 013 309.1	10 013 274.8
30	09.4	74.6
60	09.2	74.3
90	09.9	74.1
120	09.7	74.2
150	09.6	74.3
180	09.8	74.5
210	10.3	74.7
240	10.0	74.6
270	10.2	74.3
300	10.2	74.3
	Ave. 10 013 309.7 ± 0.5	Ave. 10 013 274.4 ± 0.4

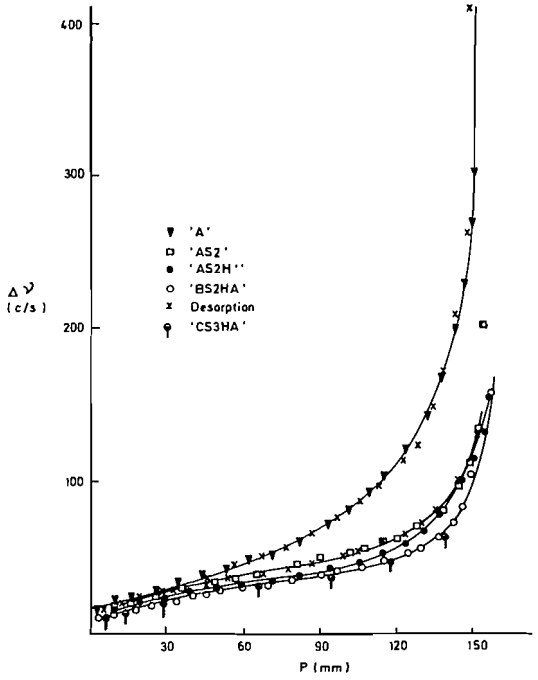

FIG. 2. Extent of *n*-hexane adsorption on 'A', 'AS2', 'AS2H', 'BS2HA', and 'CS3HA' at 26.7 °C.

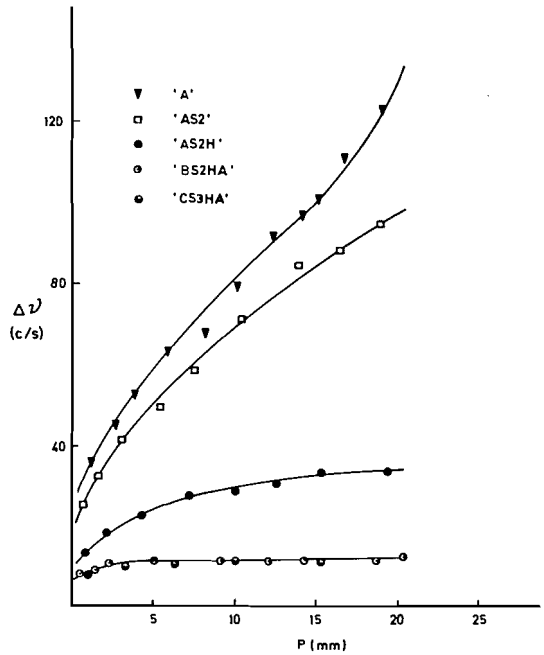

FIG. 3. Extent of water adsorption on 'A', 'AS2', 'AS2H', 'BS2HA', and 'CS3HA' at 26.7 °C.

through the 'AS2H', 'BS2HA', and 'CS3HA'. The differences between the 'AS2H' and 'BS2HA' surfaces are smaller than those found for the 'AS2' surface, but are sufficiently large as to indicate a marked difference between a heat-cured surface prepared by silane deposition at 26.7 °C, followed by heating at 160 °C, and the surface prepared by deposition at 240 °C.

From Fig. 2, the adsorption of *n*-hexane on the 'AS2' surface is not too dissimilar from the behavior found for the 'AS2H', 'BS2HA', and 'CS3HA' surfaces. This presumably reflects the size of the adsorbate molecule as compared with the possibility of its penetrating the surface layer. For the smaller water molecule (see Fig. 3), there is a much greater spread in the extent

Can. J. Chem. Downloaded from www.nrcresearchpress.com by 210.87.254.40 on 09/05/12
For personal use only.

of adsorption upon the three coated surfaces, adsorption on 'AS2' now tending towards the values found for the clean quartz surface. This must mean that water molecules can penetrate through gaps in the silane layer deposited at 26.7 °C. These gaps are reduced in number or diameter by subsequent curing at 160 °C, and still further by deposition at 240 °C.

From a practical point of view it is clear that when a silane layer is deposited upon a quartz surface under moderate conditions, the resulting surface is more hydrophilic than when the same surface is heated prior to exposure to water vapor, or when the initial silane deposition is conducted at elevated temperature. Whether heat is necessary to bond the silane layer fully to the surface, either during the initial act of deposition, or subsequently, and the mode of such treatments, are matters upon which the present studies can give no clear guide, although it should be noted that Armstead and Hockey have shown that reactions between methylchlorosilanes and silica surfaces are completed in 1 h at temperatures in excess of 280 °C. In the present studies, the use of curing temperature around 240 °C, for periods of approximately 8 h would suggest similar completion.

The author wishes to express his thanks to the National Research Council of Canada for support of this work, and to the Department of Chemistry, University of Victoria, Victoria, British Columbia for providing necessary research facilities, and Professor A. C. Riddiford for his guidance throughout this work.

1. R. L. Bass. Chem. Ind. 912 (1959).
2. T. D. Blake. Ph.D. Thesis. University of Bristol, Bristol, England, 1968.
3. C. G. Armstead and J. A. Hockey. Trans. Faraday Soc. **63**, 2549 (1967).
4. G. M. Khan. Ph.D. Thesis. University of Southampton, Southampton, England, 1970.
5. A. C. Lowe. Ph.D. Thesis. University of Southampton, Southampton, England, 1969.

Can. J. Chem. Downloaded from www.nrcresearchpress.com by 210.87.254.40 on 09/05/12
For personal use only.

Can. J. Chem. Downloaded from www.nrcresearchpress.com by 210.87.254.40 on 09/05/12
For personal use only.

An Aromatic Amine—1,3,5-Trinitrobenzene σ-Complex

E. BUNCEL AND J. G. K. WEBB

Department of Chemistry, Queen's University, Kingston, Ontario

Received September 7, 1971

Interaction between aniline and the 1,3,5-trinitrobenzene–methoxide ion adduct **1** in DMSO solution results in spectral changes which are characteristic of σ-complex formation, the first such case involving an aromatic amine.

L'intéraction entre l'aniline et le produit d'addition trinitro-1,3,5 benzène–ion méthylate **1**, en solution dans le DMSO, provoque des modifications spectrales caractéristiques de la formation d'un complexe σ. Ce cas est le premier qui implique une amine aromatique.

Canadian Journal of Chemistry, **50**, 129 (1972)

The interaction between aromatic polynitro compounds and a variety of anionic reagents is now well established to give rise to covalently bonded adducts, generally called Meisenheimer or σ-complexes (1). The relevance of such complexes in nucleophilic aromatic substitution has been discussed (1). The 1,3,5-trinitrobenzene–methoxide ion adduct **1**, for instance, has been characterized through n.m.r., visible, and i.r. spectroscopy. σ-Complex formation between polynitro aromatics and primary or secondary aliphatic amines is likewise established (2, 3). In contrast, the interaction between aromatic amines and polynitro aromatics which has been characterized hitherto (4, 5) is the weaker electron-donor–acceptor type of interaction (6, 7), leading to charge transfer complexes which can be represented by **2**. The presumed lack of formation of σ-adducts with aromatic amines could be rationalized on the ground of their very much weaker basicity in comparison with aliphatic amines.

We have now obtained evidence which is strongly indicative of the formation of a σ-complex between 1,3,5-trinitrobenzene and aniline. The complex appears to be formed in the interaction between aniline and adduct **1** in dimethylsulfoxide (DMSO) solution. The characterization involves n.m.r. and visible spectroscopy.

The substance **1**, prepared (8) as the potassium salt from 1,3,5-trinitrobenzene and potassium methoxide, showed in the n.m.r. spectrum in DMSO-d_6 signals (quoted downfield in p.p.m. from tetramethylsilane as internal standard) at 8.57 (doublet, J 1.2 Hz), 6.25 (unresolved triplet), and 3.30 (singlet), corresponding respectively to the H_α, H_β, and OCH_3 proton resonances. Addition of aniline in DMSO-d_6 (the initial solution concentrations being *ca.* aniline, 0.5 M; **1**, 0.4 M) resulted in spectral changes with time as follows. A spectrum taken 10 min after mixing exhibited the H_α, H_β, and OCH_3 absorptions due to **1**, a multiplet centered at 6.9 p.p.m. due to the ring protons of aniline and a broad signal at 4.9 p.p.m. due to the amino protons of aniline; in addition there were present a small peak upfield by 0.1 p.p.m. from H_α and assigned to H'_α of **3**, a doublet 0.4 p.p.m. upfield from H_β, interpreted as half the NH—H'_β AB quartet expected for **3**, and peaks due to methanol at 4.1 and 3.2 p.p.m. The spectrum obtained

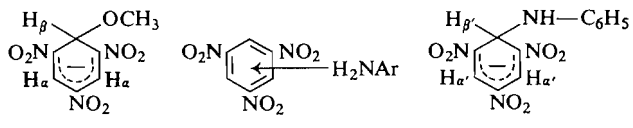

1 **2** **3**

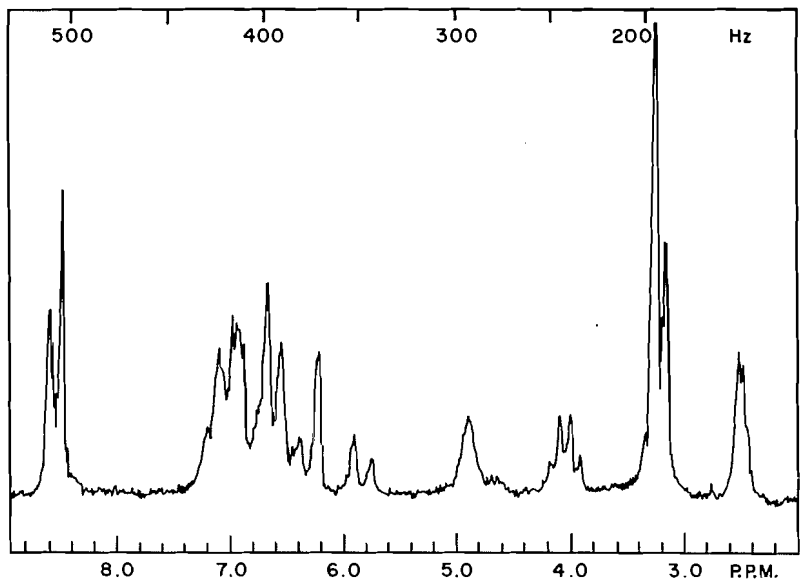

FIG. 1. The n.m.r. spectrum at 60 MHz for reaction of TNB–methoxide ion σ-complex with aniline in DMSO taken after 75 min.

after 75 min is shown in Fig. 1 and exhibits further development of the H_α' signal at the expense of H_α and a clearer emergence of the NH—H_β' quartet. The NH_2 signal has become correspondingly diminished and the methanol signals increased. The multiplet at 2.5 p.p.m. represents residual DMSO-d_5 in the solvent. A spectrum taken after 26 h shows these changes to be substantially complete. Addition of a small amount of D_2O to the solution results in a collapse of the NH—H_β' quartet into a single slightly broadened peak at 6.30 p.p.m. as a result of deuteration of NH, and at the same time a sharp OH signal at 4.00 p.p.m. is produced. Thus the n.m.r. assignments for the σ-adduct **3** are: H_α' 8.45, H_β' 6.30, NH 5.88 p.p.m., J(NH—H_α') 8.8 Hz. Isolation of the complex in the pure state has not yet been found feasible.

The reaction between aniline and **1** in DMSO was also followed by visible spectroscopy. Using the solution prepared for the n.m.r. measurements, 0.05 ml aliquots were withdrawn periodically, diluted to 5 ml with DMSO, and the spectra taken in a 0.1 mm cell. Reaction was thus seen to be accompanied by a decrease in the 427 and 509 nm absorptions characteristic of **1** and the growth of peaks at 443 and 520 nm due to product formation. Reasonably tight isobestic points were maintained for interconversion of the two absorbing species. These spectral characteristics of the reaction product, *i.e.* twin absorptions with the higher energy maximum being more intense, are typical of σ-complexes in the trinitrobenzene series (1, 9).

Thus the n.m.r. and visible spectral characteristics observed in the interaction of aniline with adduct **1** are fully in accord with formation of σ-complex **3**. In continuation, it should be of interest to determine whether substituents in the aryl amine moiety can lead to useful information concerning structural characteristics of these σ-complexes. Systematic studies, through kinetic and thermodynamic measurements, are underway to investigate this possibility. The detailed mechanism for formation of **3** should then also be clarified.

Support of this research by the National Research Council of Canada is gratefully acknowledged.

1. (*a*) R. FOSTER and C. A. FYFE. Rev. Pure Appl. Chem. **16**, 61 (1966). (*b*) E. BUNCEL, A. R. NORRIS, and K. E. RUSSELL. Quart. Rev. **22**, 123 (1968). (*c*) M. R. CRAMPTON. Advan. Phys. Org. Chem. **7**, 211 (1969). (*d*) M. J. STRAUSS. Chem. Rev. **70**, 667 (1970). (*e*) E. J. FENDLER, D. M. CAMAIONI, and J. H. FENDLER. J. Org. Chem. **36**, 1544 (1971).
2. R. FOSTER and C. A. FYFE. Tetrahedron, **22**, 1831 (1966).

Can. J. Chem. Downloaded from www.nrcresearchpress.com by 210.87.254.40 on 09/05/12
For personal use only.

3. M. R. CRAMPTON and V. GOLD. J. Chem. Soc. B, 23 (1967).
4. R. E. MILLER and W. F. K. WYNNE-JONES. J. Chem. Soc. 2375 (1959).
5. R. FOSTER and J. W. MORRIS. J. Chem. Soc. B, 703 (1970).
6. R. S. MULLIKEN. J. Am. Chem. Soc. **74**, 811 (1952).
7. G. BRIEGLEB. Electronen Donator-Akzeptor Komplexe. Springer Verlag. Berlin, 1961.
8. L. K. DYALL. J. Chem. Soc. 5160 (1960).
9. (*a*) E. BUNCEL, A. R. NORRIS, W. PROUDLOCK, and K. E. RUSSELL. Can J. Chem. **46**, 2759 (1968). (*b*) A. R. NORRIS. J. Org. Chem. **34**, 1486 (1969).

Can. J. Chem. Downloaded from www.nrcresearchpress.com by 210.87.254.40 on 09/05/12
For personal use only.

Can. J. Chem. Downloaded from www.nrcresearchpress.com by 210.87.254.5 on 09/05/12
For personal use only.

Canadian Journal of Chemistry

Published by THE NATIONAL RESEARCH COUNCIL OF CANADA

VOLUME 50 JANUARY 15, 1972 NUMBER 2

Aqueous Solutions of Nonpolar Compounds. Heat-Capacity Effects[1]

R. D. WAUCHOPE[2] AND R. HAQUE

Department of Agricultural Chemistry and Environmental Health Sciences Center, Oregon State University, Corvallis, Oregon 97331

Received July 19, 1971

The method of Clarke and Glew has been used to obtain estimates of the precision of measurement of the thermodynamic functions for the solution of hydrocarbons, the noble gases, and inert diatomic gases in water. In some cases, the precision of the data is such that a statistically significant value for the temperature coefficient of the heat-capacity change for the solution process is obtained. Comparison with the theory of Némethy and Scheraga shows that their calculations of heat-capacity changes at 25 °C are better than previously believed, but that their prediction of a positive temperature coefficient for this quantity is in contradiction with most data.

On a utilisé la méthode de Clarke et Glew pour obtenir des estimés de la précision des mesures des fonctions thermodynamiques dans le cas de solutions d'hydrocarbures, de gaz nobles et de gaz diatomiques inertes dans l'eau. Dans quelques cas, la précision des données est telle qu'on obtient une valeur statistiquement significative pour le coefficient de température du changement de capacité calorifique pour le procédé de solution. Une comparaison avec la théorie de Némethy et Scheraga montre que leurs calculs de changement de capacité calorifique à 25 °C sont plus valables qu'on le croyait antérieurement, mais que leur prédiction d'un coefficient de température positif pour cette quantité est en contradiction avec la plupart des données.

Canadian Journal of Chemistry, **50**, 133 (1972)

Introduction

The aqueous solubility of nonpolar compounds plays a major role in explaining the behavior of such chemicals in various phases of the environment. Theories of the effects of water-structure on solubility, some quite elegant (1–8), have been advanced which account for most of the unusual properties of aqueous solutions of nonpolar species, but the large partial molar heat capacities observed for these solutes are difficult to predict from theory (8). The analysis of this problem is pivotal in the understanding of these solutions, and in understanding the biochemical effects for which these solutions have served as models (4, 9, 10). We have reviewed the best solubility data from the literature to determine how much is known from experiment. In particular, since the heat-capacity change for the solution process is a second derivative quantity requiring precise solubility *vs.* temperature data for its determination, we wished to know the limits of error with which this quantity has been determined for various nonpolar solutes, and, if possible, its dependence on temperature.

The calculation of thermodynamic functions from equilibrium constant data involves "curve fitting" to a model temperature function. Much of the solubility data for nonpolar solutes has been correlated using the Valentiner equation (11, 12) where K_s

$$[1] \qquad \ln K_s = AT^{-1} + B \ln T + C$$

is the solubility at temperature T. For accurate

[1]Research supported by N.I.E.H. Grant No. ES-00210 from U.S. Public Health Service, and the manuscript issued as a Technical Paper No. 3188 from Oregon Agricultural Experiment Station.

[2]N.I.E.H. Post Doctoral Trainee. To whom correspondence should be addressed.

TABLE 1. Sources of solubility data

Solute[a]	Temperature range (°C)	References
Oxygen	7[b]–35	Murray and Riley (20), Carpenter (21), Klots and Benson (22)
Argon	5[b]–30	Douglas (23), Klots and Benson (22)
Nitrogen	8[b]–31	Murray *et al.* (24), Klots and Benson (22)
Hydrogen	12–72	Morrison and Billett (19)
Ethylene	14–73	Morrison and Billett (19)
Isopropylbenzene	25–80	Glew and Robertson (25)
Neon	9–74	Morrison and Johnstone (26)
Helium	4–73	Morrison and Johnstone (26)
Methane	12–75	Morrison and Billett (19)
Ethane	14–73	Morrison and Billett (19)
Propane	1–74	Morrison and Billett (19), Schneider (private communication)
n-Butane	1–76	Morrison and Billett (19), Schneider (private communication)
Krypton	7–75	Morrison and Johnstone (26)
Xenon	13–72	Morrison and Johnstone (26)
Benzene	5–63	Franks *et al.* (16), Arnold *et al.* (27)
Toluene	0–45	Bohon and Claussen (28)
Ethylbenzene	"	Bohon and Claussen (28)
p-, *m*-Xylene	"	Bohon and Claussen (28)
Naphthalene	0–73	Bohon and Claussen (28), Wauchope and Getzen (in preparation)
Biphenyl	0–65	Wauchope and Getzen (in preparation)
Acenaphthene	25–75	Wauchope and Getzen (in preparation)
Fluorene	"	Wauchope and Getzen (in preparation)
Phenanthrene	"	Wauchope and Getzen (in preparation)
Anthracene	"	Wauchope and Getzen (in preparation)
Pyrene	"	Wauchope and Getzen (in preparation)

[a]Solutes are arranged in order of decreasing precision, based on dev. from least-squares fit.
[b]Points for lower temperatures deleted (see text).

solubility data, however, covering a wide range of temperatures, eq. 1 fails and an equation which describes functional dependence of ΔC_p on T is needed. Himmelblau (13) used an expression of the form

$$[2] \quad A(\log K_s)^2 + BT^{-2} + CT^{-1} \log K_s + D \log K_s + ET^{-1} - 1 = 0$$

to fit gas solubilities up to near the critical point of water, but for solubilities in the region of room temperature a simple expansion of the heat capacity in powers of T has been sufficient for most data (14, 15), giving an expression of the form

$$[3] \quad \ln K_s = AT^{-1} + B \ln T + C + DT + ET^2 + \ldots$$

Glew (14) fitted the data for methane to the four-term form of eq. 3, obtaining a linear temperature coefficient of ΔC_p for the solution process. On the other hand, Franks *et al.* (16) found that a simple power series in T fitted the data for benzene better than eq. 3.

Clarke and Glew (17) have derived a general family of equations to describe the temperature dependence of equilibrium constants. These are equivalent in functional form to eq. 3 but allow the unbiased estimate of the standard errors of the derived thermodynamic functions. A stepwise least-squares regression fit to successively higher-order variables in T is performed, and standard statistical tests (17, 18) allow an objective decision to be made as to whether $d\Delta C_p/dT$ or higher-order derivatives of ΔC_p are significantly different from zero. In the present paper the method of Clarke and Glew has been applied to the available solubility data because of its generality and because it provides estimates of the precision with which the thermodynamic functions have been determined.

Sources and Treatment of the Data

Sources of data are listed in Table 1 in approximate order of decreasing internal precision, as estimated from the present curve-fitting procedure. In several cases, independent investigations of a solute have been made of near-equal

Can. J. Chem. Downloaded from www.nrcresearchpress.com by 210.87.254.5 on 09/05/12
For personal use only.

Can. J. Chem. Downloaded from www.nrcresearchpress.com by 210.87.254.5 on 09/05/12
For personal use only.

precision, and each is shown. For methane, a solute which has been studied many times, only the data of Morrison and Billett (19) are presented: Glew (14) previously analyzed these and other data with results in substantial agreement with ours.

Unsmoothed solubility data from the various sources were all converted (29) to Henry's law coefficients,

$$[4] \qquad K_T\,(\text{atm}) = f_s/X_s$$

where f_s is the fugacity of the solute over a saturated solution of mole fraction X_s. The standard free energy of solution at temperature T is then calculated from

$$[5] \qquad \Delta G_T^0\,(\text{cal/mol}) = RT \ln K_T$$

and the standard enthalpy, etc., of solution are obtained through standard thermodynamic relations from the temperature dependence of $\ln K_T$. All standard thermodynamic functions thus refer to the process

$$[6] \qquad \text{gas, 1 atm, } T \rightarrow \text{soln, } X_s = 1, T$$

in which the effects of solute condensed state are removed, allowing a comparison of "hydration" effects only (30). For liquids and solids, f_s was taken to be the saturation vapor pressure of the pure solute, neglecting the effects of water dissolution in the solute phase. Vapor pressures for the liquid hydrocarbons and naphthalene were taken from the compilation by Dreisbach (31); the data of Bradley and Cleasby (32) were used for the other solid hydrocarbons. No corrections were made for the small expansion of the aqueous phase with dissolution of the solute; according to Weiss (15), the effect for nitrogen and argon is approximately 0.14% but for most solutes this quantity, and its dependence on temperature, is not known.

Eley (34) suggested that comparisons of thermodynamic functions for the dissolution of nonpolar solutes in water should be made at 4 °C, where the entropy and enthalpy of cavity formation is at a minimum. However, most of the data in Table 1 span ranges near room temperature, and the usual comparison at 25 °C seemed more appropriate. Furthermore, very accurate studies (20–22, 24) of argon, nitrogen, and oxygen showed complicated temperature dependences of the solubility near 4 °C; thus, for purposes of comparison with the other solutes, data points in this low-temperature region were deleted, as shown in Table 1. A stepwise regression program based on the model of Clarke and Glew (17) was written for the Oregon State University CDC 3300 computer,[3] and tested with the data of Feates and Ives (33) with results identical to those obtained by Clarke and Glew.

Results and Discussion

Table 2 gives the calculated standard thermodynamic functions and errors obtained from the Clarke and Glew procedure. All data sets required at least a three-constant or Valentiner-type, equation representation, and some, as shown required four or five constants. In the four and five constant cases, a linear and quadratic dependence of ΔC_p^0 on temperature, respectively, is assumed. Rejection of fourth and fifth terms was arbitrarily made if standard statistical tests (17, 18) indicated a 20% or greater probability that the improvement in fit was due to chance.

The relationships between the standard free energies, enthalpies, and entropies of solution for the inert gases and hydrocarbons are shown in Fig. 1, plotted against molecular volumes. The results for the solid hydrocarbons will be presented elsewhere[4] but they are included in Table 2 since the present study has allowed an estimate of the precision of that data. Miller and Hildebrand (35) have discussed the trends for the entropies of the gases, and those authors' values for molecular volumes have been used to relate the volumes of methane and the smaller gases. Volumes for the hydrocarbons were taken from the data used by McAuliffe (36). Plots based on molecular surface area (35) or second virial coefficient (13) show similar trends. From Fig. 1 we find (*a*) a smaller volume for H_2 and a larger one for O_2 are required to bring them "in line" with the other small gases; (*b*) helium appears to belong to the left of neon; (*c*) based on McAuliffe's (36 and references therein) molar volume data, a comparison of benzene with the paraffin hydrocarbons indi-

[3]The authors are grateful to Mr. H. Pendell for much help with the programming.

[4]R. D. Wauchope and F. W. Getzen, in preparation.

TABLE 2. Standard thermodynamic functions for dissolution of nonpolar species in water at 25° C, with standard errors

Solute[a]	$\Delta G^0_{298.15}$ (cal/mol)	$\Delta H^0_{298.15}$ (cal/mol)	$(\Delta C^0_p)_{298.15}$ (cal/deg mol)	$(d\Delta C^0_p/dT)_{298.15}$ (cal/deg mol)	$(d^2\Delta C^0_p/dT^2)_{298.15}$ (cal/deg^3 mol)
Helium	7049.6± 0.8	−443± 24	48 ± 2	0.4±0.3	−0.07±0.03
Neon	6937.5± 1.6	−1007± 54	36 ± 5	−1.1±1.1	0.1 ±0.06
Hydrogen	6613.1± 0.5	−992± 16	24 ± 2	0.8±0.5	−0.05±0.03
Oxygen (21)	6348.4± 0.2	−3178± 20	53 ± 4	−6.3±1.3	−2.6 ±0.4
Oxygen (20)	6346.4± 0.2	−3202± 9	12 ± 2	−3.2±0.4	
Oxygen (22)	6328.8± 0.8	−2897± 41	48 ±11		
Argon (23)	6274.2± 0.1	−2854± 8	43 ± 4	−3.0±1.4	−0.4 ±0.2[c]
Argon (22)	6271.0± 0.6	−2778± 26	53 ± 3		
Nitrogen (24)	6731.4± 0.4	−2599± 12	42 ± 2		
Nitrogen (22)	6722.7± 1.1	−2497± 42	49 ± 5		
Krypton	5956 ± 1	−3499± 20	40 ± 1		
Methane	6298 ± 2	−3232± 32	65 ± 6	−0.6±0.3	
Xenon	5614 ± 1	−4374± 59	43 ± 4		
Ethylene	5549.5± 1.5	−3803± 43	65 ± 9	−3.3±1.5	0.17±0.08
Ethane	6158 ± 1	−4049± 24	69 ± 5	−0.6±0.3	
Propane (19)	6238 ± 2	−5109± 40	80 ± 6	−0.6±0.4	
Propane[b]	6224 ± 2	−5387± 45	86 ± 2	−1.1±0.5	
Butane (19)	6385.4± 0.9	−5739± 17	69 ± 3	0.2±0.2[c]	
Butane[b]	6336 ± 2	−6113± 61	107 ± 3	−1.1±0.7	
Benzene (16)	3407 ± 1	−7630± 51	84 ± 2	−1.5±0.6	
Benzene (27)	3405 ± 1	−7623± 20	72 ± 2		
Toluene	3389.9± 0.7	−8648± 21	84 ± 2		
m-Xylene	3439 ± 4	−9560± 81	98 ±10		
p-Xylene	3465 ± 2	−9553± 39	80 ± 8		
Et-benzene	3483 ± 2	−9584± 35	78 ± 4		
i-Pr-benzene	3690 ± 1	−9911± 16	80.6± 0.6		
Naphthalene (28)	1832 ± 4	−10210± 70	82 ± 8		
Naphthalene[d]	1885 ± 4	−11200±280	70 ±35	3 ±2	
Acenaphthene	912 ±34	−11860±470	93 ±18		
Fluorene	860 ±10	−12700±650	256 ±69	−8 ±3	
Phenanthrene	390 ±15	−13000±910	263 ±94	−9 ±4	
Pyrene	−812 ±18	−15200±230	130 ±10		
Anthracene	−2290 ±63	−14000±770	48 ±26		

[a]Reference numbers in parentheses.
[b]H. Schneider, private communication.
[c]75% probability.
[d]R. D. Wauchope and F. W. Getzen, in preparation.

cates that the enthalpy of solution for the aromatic species is more negative than for similar-sized paraffin molecules, and differences in the entropies of solution for the two types are less than previously stated.[4]

Examination of Table 2 shows that ΔC^0_p at 25 °C does increase with molecular size as has been stated (2, 4), but that the major increase occurs in the methane–butane region, with fairly constant values near 50 cal/deg mol below and 80–100 cal/deg mol above this region, respectively. Finer comparisons are made difficult by the variety of temperature intervals of the source data, and perhaps by other complications in the temperature dependence of ΔC^0_p. Regressions based on eq. 3 give non-comparable results when the data for different solutes are taken over different temperature ranges. Thus, there is little consistency in the last column of Table 2, and this may be due to wild oscillation of $d^2\Delta C^0_p/dT^2$, as suggested by the plot of ΔC^0_p *vs.* T given by Franks *et al.* (16) for benzene.

Nevertheless, some agreement between compounds is seen for the first derivative of ΔC^0_p at 25 °C; most of the entries in the fifth column of Table 2 are negative, and eight compounds, having data over similar temperature intervals, have values between −0.5 and −1.5 cal/deg^2 mol. A single value of −0.5 cal/deg^2 mol was assumed for these eight solutes (this "low"

Can. J. Chem. Downloaded from www.nrcresearchpress.com by 210.87.254.5 on 09/05/12
For personal use only.

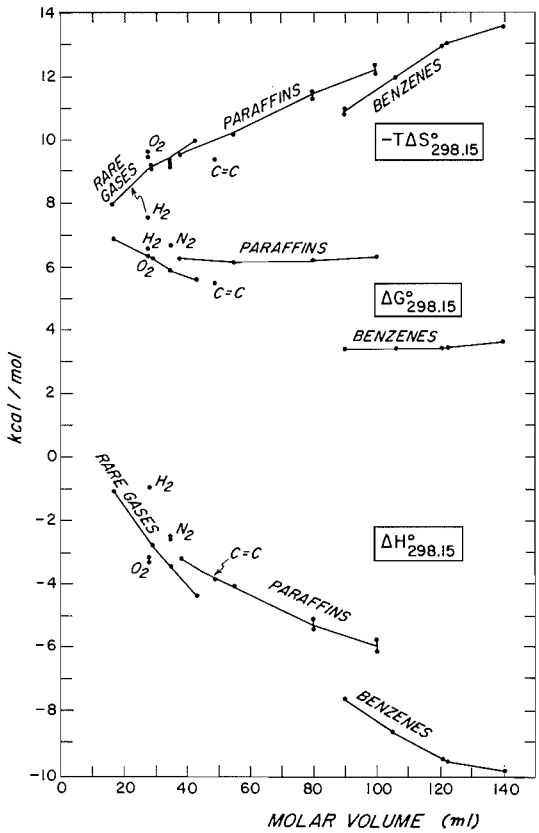

FIG. 1. Standard thermodynamic function changes for solution of gaseous compounds in water at 298.15 °K, as a function of molar volume.

average for $d\Delta C_p^0/dT$ takes into account the near-zero value which is indicated by the very accurate nitrogen and argon data, and is also closer to the values obtained by Glew (14) for methane). The values for ΔC_p^0 obtained from the three-constant step of the regression procedure, which are associated with the mid-point temperature of the data, were corrected to 25 °C using this value. The results are shown in Table 3. This assumption of a common *linear* dependence of ΔC_p^0 on temperature is doubtless an oversimplification, but it provides a first-approximation correction to ΔC_p^0 for differences in temperature range and the relation of the other solutes to the paraffins is seen. We believe these "corrected" values to be the best available for comparison with the predictions of theory. The theory of Némethy and Scheraga (4) is seen to calculate ΔC_p^0 values better than they themselves had thought, at 25 °C. However, their prediction of a positive temperature dependence of ΔC_p^0 does not agree with experiment.

NOTE ADDED IN REVISION

After submission of this study for publication, a paper by Alexander, Hill, and White (37) appeared, in which the Clarke and Glew method was used to analyze the benzene solubility data, and much of the gas solubility data, cited in the present work. In most cases their results confirm ours in detail. However, a

TABLE 3. Standard heat-capacity changes, corrected to 25 °C assuming a common value for $d\Delta C_p^0/dT$ of −0.5 cal/deg. mol

Solute[a]	Mid-point of data temperature range (°C)	$d(\Delta C_p^0)/dT$[b] (cal/deg² mol)	Average[c] ΔC_p^0 (cal/deg mol)	$(\Delta C_p^0)_{298}$ (cal/deg mol)	
				Corrected	Theory[d]
Helium	39	−0.5±0.1	40±1	47	
Neon	42	−0.5±0.3	39±2	48	
Methane	44	−0.6±0.3	54±1	64	64
Ethane	44	−0.6±0.3	60±1	70	79
Propane (19)	43	−0.6±0.4	71±2	80	90
Propane[e]	28	−1.1±0.5	85±3	87	90
Butane[e]	28	−1.1±0.7	105±3	107	99
Benzene (16)	40	−1.5±0.6	66±3	74	73

[a]Reference numbers in parentheses.
[b]Taken from four-constant fit: average over temperature range of data.
[c]Taken from three-constant fit: average over temperature range of data.
[d]Reference 4.
[e]H. Scheider, private communication.

Can. J. Chem. Downloaded from www.nrcresearchpress.com by 210.87.254.5 on 09/05/12
For personal use only.

consistent error appears to exist in their analyses of the nitrogen, argon, and oxygen data of Klots and Benson (22), as their reported values for the standard free energy of solution at 298.16 °K yields a Henry's constant which is 0.59 that reported by Klots and Benson in all three cases.

1. D. D. ELEY. Trans. Faraday Soc. **35**, 1281 (1939).
2. H. S. FRANK and M. W. EVANS. J. Chem. Phys. **13**, 507 (1945).
3. W. F. CLAUSSEN and M. F. POLGLASE. J. Am. Chem. Soc. **74**, 4817 (1952).
4. G. NÉMETHY and H. A. SCHERAGA. J. Chem. Phys. **36**, 3382 (1962); **36**, 3401 (1962).
5. A. YU. NAMIOT. Russ. J. Struct. Chem. **2**, 381 (1961) (Zhur. Strukt. Khim. **2**, 408).
6. D. N. GLEW. J. Phys. Chem. **66**, 605 (1962).
7. A. BEN-NAIM. J. Phys. Chem. **69**, 3240 (1964); **69**, 3245 (1964).
8. R. B. HERMANN. J. Phys. Chem. **75**, 363 (1971).
9. W. KAUZMANN. In Advances in protein chemistry, Vol 14. *Edited by* C. B. Anfinson, M. L. Anson, K. Bailey, and J. T. Edsall. Academic Press, New York, N.Y. 1959.
10. J. L. KAVANAU. Structure and function in biological membranes. Vols. I and II, Holden-Day, Inc., San Francisco. 1965.
11. S. VALENTINER. Z. Phys. **42**, 253 (1927).
12. T. J. MORRISON. J. Chem. Soc. 3814 (1952).
13. D. M. HIMMELBLAU. J. Phys. Chem. **63**, 1803 (1959).
14. D. N. GLEW. J. Phys. Chem. **66**, 605 (1962).
15. R. F. WEISS. Deep-Sea Res. **17**, 721 (1970).
16. F. FRANKS, M. GENT, and H. H. JOHNSON. J. Chem. Soc. 2716 (1963).
17. E. C. W. CLARKE and D. N. GLEW. Trans. Faraday Soc. **62**, 539 (1966).
18. P. D. BOLTON. J. Chem. Ed. **47**, 638 (1970).
19. T. J. MORRISON and F. BILLETT. J. Chem. Soc. 3819 (1952).
20. C. N. MURRAY and J. P. RILEY. Deep-Sea Res. **16**, 311 (1969).
21. J. H. CARPENTER. Limn. Oceanography, **11**, 264 (1966).
22. C. E. KLOTS and B. B. BENSON. J. Mar. Res. **21**, 48 (1963).
23. E. DOUGLAS. J. Phys. Chem. **68**, 169 (1964).
24. C. N. MURRAY, J. P. RILEY, and T. R. S. WILSON. Deep-Sea Res. **16**, 297 (1969).
25. D. N. GLEW and R. E. ROBERTSON. J. Phys. Chem. **60**, 332 (1956).
26. T. J. MORRISON and N. B. JOHNSTONE. J. Chem. Soc. 3441 (1954).
27. D. S. ARNOLD, C. A. PLANK, E. E. ERICKSON, and F. P. PIKE. J. Chem. Eng. Data **3**, 253 (1958).
28. R. L. BOHON and W. F. CLAUSSEN. J. Am. Chem. Soc. **73**, 1571 (1951).
29. A. E. MARKHAM and K. A. KOBE. Chem. Rev. **28**, 519 (1941).
30. J. A. V. BUTLER. Chemical thermodynamics. 5th ed., Macmillan, London. 1962.
31. R. R. DREISBACH. Physical properties of chemical compounds. Advances in Chemistry Series, Vol. 15, American Chemical Society, Washington, D.C. 1955.
32. R. S. BRADLEY and T. G. CLEASBY. J. Chem. Soc. 1960 (1953).
33. F. S. FEATES and D. J. G. IVES. J. Chem. Soc. 2798 (1956).
34. D. D. ELEY. Trans. Faraday Soc. **40**, 481 (1944).
35. K. W. MILLER and JOEL H. HILDEBRAND. J. Am. Chem. Soc. **90**, 3001 (1968).
36. C. MCAULIFFE. J. Phys. Chem. **70**, 1267 (1966).
37. D. M. ALEXANDER, D. J. T. HILL, and L. R. WHITE. Aust. J. Chem. **24**, 1143 (1971).

Can. J. Chem. Downloaded from www.nrcresearchpress.com by 210.87.254.5 on 09/05/12
For personal use only.

Theoretical Anisotropic Hyperfine Tensors in Neutral Radicals

H. R. FALLE[1] AND M. A. WHITEHEAD
Department of Chemistry, McGill University, Montréal, Québec

Received December 23, 1970[2]

Anisotropic hyperfine tensors were calculated for C—H, (C—CH_3), allyl, and perinaphthenyl. In the McConnell and Strathdee theory, the anisotropic proton tensor depends primarily on the STO exponent chosen for the $2p_\pi$ carbon atom orbital. By decreasing the exponent ζ_π from the normal Slater value to ~1.3, the effect of σ-spin density in the C—H bond could be taken into account. However, this reduction in ζ_π yields too small a value for $\langle r^{-3} \rangle$, which governs the anisotropic ^{13}C tensor. Contributions to the anisotropic proton and ^{13}C hyperfine tensors are discussed, and the results compared with recent *ab initio* calculations, as well as single-crystal and liquid crystal data.

Les tenseurs anisotropiques hyperfins ont été calculés pour les groupements C—H, C—CH_3, allyle et perinaphthényle. Dans la théorie de McConnell et Strathdee, le tenseur anisotropique du proton dépend en premier de l'exposant STO choisi pour l'orbitale de l'atome de carbone $2p_\pi$. En faisant décroître l'exposant ζ_π à partir de la valeur normale de Slater approximative de 1.3, l'effet de la densité σ-spin dans la liaison C—H a pû être prise en compte. Cependant, cette réduction du ζ_π amène à valeur trop petite pour $\langle r^{-3} \rangle$ qui gouverne le tenseur anisotropique du carbone 13. Les contributions aux tenseurs anisotropiques hyperfins du proton et du carbone 13 sont discutées et les résultats comparés avec les récents calculs *ab initio*, ainsi que les données des cristals unique et d'un cristal liquide.

Canadian Journal of Chemistry, **50**, 139 (1972)

Can. J. Chem. Downloaded from www.nrcresearchpress.com by 210.87.254.5 on 09/05/12
For personal use only.

Introduction

The use of nematic liquid crystals as solvents in e.p.r. studies of π-electron free radicals (1–4) has provided valuable qualitative information: for example, confirmation of negative spin densities in perinaphthenyl (2). However, certain quantitative descriptions have been more difficult because of inaccuracies in the theoretical anisotropic hyperfine tensors. This difficulty is evident from the calculations of anisotropic proton tensors in perinaphthenyl (4).

McConnell and Strathdee (5) have calculated the anisotropic hyperfine tensor components for a proton bonded to a sp^2 hybridized carbon atom. Comparison with experimental results for isolated C—H fragments shows that the dominant contribution to the anisotropic proton tensor comes from the dipolar interaction between the proton and the unpaired electron in the $2p_\pi$ carbon atom orbital (5, 6). Calculation of the anisotropic hyperfine tensor for a proton in a delocalized π-electron radical requires the summation of contributions which are proportional to the unpaired π-spin densities borne by the constituent atoms (1, 7, 8). In the case of perinaphthenyl, calculations were found to agree with experiment when only the adjacent and the two nearest-neighbor π-spin density contributions were included (2). However, it was also found that, although contributions from carbon atoms further removed were significant, the inclusion of all the π-contributions in the radical led to a large discrepancy between theory and experiment (4).

The observations above were based on calculations which employed a Slater $2p_\pi$ carbon atom orbital

$$[1] \qquad \varphi(2p_\pi) \sim r \exp(-\zeta_\pi r)$$

with exponent ζ_π equal to 1.59 or 1.63, and which also neglected the effect of unpaired spin density in the σ-orbitals. The σ-spin density in the C—H bond of course gives rise to the isotropic proton coupling and, in fact, is quite substantial; in $HC(CO_2H)_2$ for example, it is roughly 5% of the π-spin density (9). Modification of the carbon orbital functions should obviously have a considerable effect on the π- and σ-contributions to the anisotropic proton tensor calculated for the hypothetical molecular fragment $\rangle\dot{C}$—H. However, it is noteworthy that the outcome obtained with Hartree–Fock ^5S carbon valence-state functions (10) is not very different from *ab initio* calculations which used a minimal basis set of Slater orbitals (6). Clearly, the inclusion

[1]Postdoctoral Teaching Fellow, McGill University, 1967–1969. Present address: Cookridge High Energy Radiation Research Centre, Cookridge Hospital, LEEDS LS16 6QB, England.

[2]Revision received August 25, 1971.

Can. J. Chem. Downloaded from www.nrcresearchpress.com by 210.87.254.5 on 09/05/12
For personal use only.

of the σ-contributions only serves to increase the discrepancy between theory and experiment. On the other hand, allowance can be made for the effect of σ-spin density when the exponent ζ_π is reduced to 1.3 (10).

In order to enquire further into the disparity between the theoretical and experimental results, we have undertaken calculation of the anisotropic hyperfine tensors in perinaphthenyl with the following Slater-type (STO) atomic orbital functions:

(*A*) The STO exponents obtained from s.c.f. calculations of atomic screening constants were used; for the carbon atom $2p_\pi$ orbital, $\zeta_\pi = 1.5679$ (11).

(*B*) Using a valence-state model, the charge density dependence of the isotropic hyperfine coupling in C—H has been evaluated and STO exponents given as a function of the spin density, $\rho_{\pi\pi}$, in the $2p_\pi$ orbital; for unit $\rho_{\pi\pi}$, $\zeta_\pi = 1.5387$ (12). For the cases in which the π-spin density differs from unity, we have employed the equation

$$[2] \qquad \zeta_\pi = 1.2969 + 0.2418\rho_{\pi\pi}^2$$

This expression gives a close approximation to the results of Kay and Silverstone, except that ζ_π should be 1.2929 when $\rho_{\pi\pi}$ is zero.

(*C*) For the purpose of comparison, we have included the valence-state integral *n* minimal STO derived for alternant hydrocarbon ground-states (13). The closed-shell $2\rho_\pi$ exponent has the same value as a neutral radical with $\rho_{\pi\pi} = 0$, namely $\zeta_\pi = 1.2929$.

(*D*) Chang, Davidson, and Vincow (14, 15) have done extensive *ab initio* calculations concerning the isotropic hyperfine interactions in C—H and CH_3, employing in particular a minimal STO basis set with exponents optimized by minimization of the s.c.f. energy. The optimized $2p_\pi$ orbital exponent is $\zeta_\pi = 1.46$ (15).

While the calculated anisotropic proton tensor is most dependent on the $2p_\pi$ orbital exponent (6), the isotropic hyperfine coupling shows a significant dependence on the hydrogen 1s orbital exponent ζ_h (15). In the optimized basis set D, $\zeta_h = 1.19$ whereas a ζ_h of unity was employed in cases *A*, *B*, and *C*. Orthogonalized 2s orbitals were used in all the above cases.

In the next section, we shall review the theories of isotropic and anisotropic hyperfine interactions in the C—H fragment. The foregoing STO functions will then be applied to the calculation of the anisotropic proton tensor for C—H and for the allyl radical, in order to provide a background for the similar calculations on perinaphthenyl. The anisotropic β-proton hyperfine tensor for a freely rotating methyl group will also be included.

The C—H Fragment

The total hyperfine coupling for the proton in the trigonal fragment $\rangle$C—H is comprised of two parts; the anisotropic electron–nucleus dipolar interaction and the isotropic contact interaction (16, 17). Following the treatment by McConnell and Strathdee (5), the spin Hamiltonian for the anisotropic dipolar interaction can be written in the form

$$[3] \qquad \mathscr{H}_d = \boldsymbol{S}\cdot[-K\boldsymbol{\tau}]\cdot\boldsymbol{I}$$

where the constant K is $g\beta(\gamma/h)$ in the notation of atomic units, and takes the value 533.53 MHz a.u.[3] The tensor $\boldsymbol{\tau}$ is given by

$$[4] \qquad \boldsymbol{\tau} = \int\rho(\boldsymbol{r})\mathbf{T}\mathrm{d}v$$

in which $\rho(\boldsymbol{r})$ is the unpaired spin density distribution function, and

$$[5] \qquad \mathbf{T} = (r^{-3})[\mathbf{U} - 3\boldsymbol{rr}(r^{-2})]$$

U is the unit tensor and $\boldsymbol{r}$ is the vector position of the electron. When the complete molecular wave function is described in terms of a set of atomic orbitals $\{\phi_\lambda\}$, the spin density function has the form

$$[6] \qquad \rho(\boldsymbol{r}) = \sum_{\lambda\mu}\rho_{\lambda\mu}\phi_\lambda^*\phi_\mu$$

It follows from [4] and [6] that

$$[7] \qquad \boldsymbol{\tau} = \sum_{\lambda\mu}\rho_{\lambda\mu}\langle\phi_\lambda|\mathbf{T}|\phi_\mu\rangle$$

The spin density function can be separated into π- and σ-contributions

$$[8] \qquad \rho(\boldsymbol{r}) = \rho^\pi(\boldsymbol{r}) + \rho^\sigma(\boldsymbol{r})$$

and we can subsequently write

$$[9] \quad \boldsymbol{\tau} = \boldsymbol{\pi} + \boldsymbol{\sigma} = \sum_{\pi\pi'}\rho_{\pi\pi'}\langle\phi_{\pi'}|\mathbf{T}|\phi_\pi\rangle + \sum_{\sigma\sigma'}\rho_{\sigma\sigma'}\langle\phi_{\sigma'}|\mathbf{T}|\phi_\sigma\rangle$$

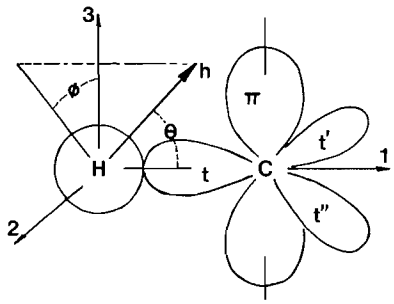

FIG. 1. The angles θ and ϕ define the direction of the external magnetic field h with respect to the principal axes $i = 1, 2, 3$ of the proton hyperfine tensor for C—H (5)

For the C—H fragment, the π-contribution to τ is simply

$$[10] \qquad \boldsymbol{\pi} = \rho_{\pi\pi}\langle\pi|\mathbf{T}|\pi\rangle$$

where $\rho_{\pi\pi}$ is the unpaired spin density in the $2p_\pi$ orbital π. When localized sp^2 hybrid orbitals, t, t', and t'' as in Fig. 1, are used to represent the σ-orbitals in C—H, the σ-spin density matrix is diagonal. By symmetry, the spin densities in the orbitals t' and t'' will be equal, though not necessarily the same as the spin density in t. The σ-contribution to τ can then be written

$$[11] \quad \boldsymbol{\sigma} = \rho_{\sigma\sigma}\langle t|\mathbf{T}|t\rangle + \rho_{\sigma'\sigma'}[\langle t'|\mathbf{T}|t'\rangle + \langle t''|\mathbf{T}|t''\rangle]$$

The established explanation for the isotropic hyperfine coupling in $\rangle$C—H is the finite unpaired spin density $\rho^\sigma(\boldsymbol{r}_H)$ at the proton, due essentially to configuration interaction (16, 17). To first-order (18),

$$[12] \quad \rho^\sigma(\boldsymbol{r}_H) = -2[\langle\sigma\pi|e^2/r|\pi\sigma^*\rangle/\Delta E]\sigma(\boldsymbol{r}_H)\sigma^*(\boldsymbol{r}_H)$$

Neglecting overlap and writing the bonding and antibonding orbitals as $\sigma = (t + h)/\sqrt{2}$ and $\sigma^* = (t - h)/\sqrt{2}$, respectively, [12] reduces to

$$[13] \quad \rho^\sigma(\boldsymbol{r}_H) = (K_{\pi t} - K_{\pi h})[|t(\boldsymbol{r}_H)|^2 - |h(\boldsymbol{r}_H)|^2]$$

in which the exchange interaction term is

$$[14] \quad (K_{\pi t} - K_{\pi h}) = (-1/2\Delta E)[\langle t\pi|\pi t\rangle - \langle h\pi|\pi h\rangle]$$

ΔE is the $\sigma \rightarrow \sigma^*$ one-electron excitation energy, t is the carbon sp^2 hybrid orbital and h the hydrogen 1s orbital. The orbital densities $|h(\boldsymbol{r}_H)|^2$ and $|t(\boldsymbol{r}_H)|^2$ are obtained by evaluating the square of h and t at the proton; in the axis system in Fig. 1,

$$[15] \qquad t = \sqrt{1/3}(2s) - \sqrt{2/3}(2p_\sigma)$$

The magnitude of the $\pi - \sigma$ exchange interaction $(K_{\pi t} - K_{\pi h})$, and hence the magnitude of the isotropic hyperfine coupling a, depends on the unpaired spin density in the orbital π. The McConnell relation

$$[16] \qquad a/\rho_{\pi\pi} = (8\pi/3)K\rho^\sigma(\boldsymbol{r}_H) = Q$$

assumes the same direct proportionality, between the isotropic proton coupling and the π-spin density, for all C—H type bonds in π-radicals. For neutral aromatic radicals, Q generally lies in the vicinity of -80 MHz (7, 17, 19) whereas -64 to -76 is quoted as the "experimental" range of Q for the fragment $\rangle$C—H (14). Now the unpaired σ-spin density in h is opposite in sign and, to first-order, equal in magnitude to that in the orbital t forming the C—H bond (16, 17). It follows that a reasonable estimate of the σ-spin density in t can be derived from the isotropic proton coupling on substitution into the equation

$$[17] \quad \rho_{\sigma\sigma} = a/\{(8\pi/3)K[|t(\boldsymbol{r}_H)|^2 - |h(\boldsymbol{r}_H)|^2]\}$$

If the three trigonal orbitals in the C—H fragment are assumed equivalent, that is to set $\rho_{\sigma'\sigma'} = \rho_{\sigma\sigma}$, then the principal components of the σ-contribution to τ can be reformulated from [11] as

$$[18] \qquad \sigma_{ii} = \rho_{\sigma\sigma}r^{-3}V(3\cos^2\theta - 1)$$

Similarly, the π-contribution to τ can be written

$$[19] \quad \pi_{ii} = \rho_{\pi\pi}r^{-3}[P(3\cos^2\theta - 1) + Q(1 - \cos 2\phi)]$$

The carbon–hydrogen internuclear distance is r a.u. (the atomic unit of distance is 52.9167 pm). The subscripts i refer to the axis system 1, 2, 3 and the angles θ and ϕ define the direction of the external magnetic field h, in Fig. 1. The terms V, P, and Q involve the parameter $a = \zeta r(5, 20)$ and are reproduced below for the standard STO functions $\varphi(2s) \sim r\exp(-\zeta r) \sim \varphi(2p)$.

Can. J. Chem. Downloaded from www.nrcresearchpress.com by 210.87.254.5 on 09/05/12
For personal use only.

TABLE 1. Anisotropic proton hyperfine tensor components (in MHz), calculated for the hypothetical >Ċ—H fragment, assuming $r_{C-H} = 2.05$ a.u.

STO function	Anisotropic principal component
A, s.c.f. screening constants (11)	$A'_{11} = 41.99\ \rho_{\pi\pi} + 145.2\ \rho_{\sigma\sigma} + 74.4\ \rho_{\sigma'\sigma'}$ $A'_{33} = -3.60\ \rho_{\pi\pi} - 72.6\ \rho_{\sigma\sigma} - 54.6\ \rho_{\sigma'\sigma'}$
B, Valence-state (unit $\rho_{\pi\pi}$) STO (12)	$A'_{11} = 40.30\ \rho_{\pi\pi} + 147.3\ \rho_{\sigma\sigma} + 74.8\ \rho_{\sigma'\sigma'}$ $A'_{33} = -2.58\ \rho_{\pi\pi} - 73.7\ \rho_{\sigma\sigma} - 54.6\ \rho_{\sigma'\sigma'}$
D, *ab initio* C—H optimized STO (14)	$A'_{11} = 35.72\ \rho_{\pi\pi} + 181.5\ \rho_{\sigma\sigma} + 91.4\ \rho_{\sigma'\sigma'}$ $A'_{33} = +0.15\ \rho_{\pi\pi} - 90.7\ \rho_{\sigma\sigma} - 61.4\ \rho_{\sigma'\sigma'}$
Hartree–Fock ^{5}S valence-state (10) ($r_{C-H} = 2.0$ a.u.)	$A'_{11} = 42.3\ \rho_{\pi\pi} + 144.3\ \rho_{\sigma\sigma} + 77.4\ \rho_{\sigma'\sigma'}$ $A'_{33} = -3.1\ \rho_{\pi\pi} - 72.2\ \rho_{\sigma\sigma} - 56.8\ \rho_{\sigma'\sigma'}$

$$[20]\quad V = 3 + \frac{9}{a^2} - e^{-2a}\left(\frac{16a^5}{9} + \frac{8a^4}{3} + \frac{19a^3}{3} + 12a^2 + 18a + 21 + \frac{18}{a} + \frac{9}{a^2}\right)$$

$$[21]\quad P = 1 - \frac{9}{a^2} + e^{-2a}\left(a^3 + 4a^2 + 10a + 17 + \frac{18}{a} + \frac{9}{a^2}\right)$$

$$[22]\quad Q = \frac{9}{2a^2} - e^{-2a}\left(a^3 + 3a^2 + 6a + 9 + \frac{9}{a} + \frac{9}{2a^2}\right)$$

(The correction made by Pitzer *et al.* (20) on the McConnell and Strathdee form of V essentially entails examination of the dipolar interaction in the region of the nucleus which requires introduction of the term $-(16a^5/9)\ e^{-2a}$. The terms P and Q are not affected since the proton lies in the nodal plane of the orbital π). Hence, the principal components of the anisotropic hyperfine tensor for the proton in >Ċ—H will be given by

$$[23]\quad A'_{ii} = K(\pi_{ii} + \sigma_{ii})$$

The total hyperfine tensor is of course $\mathbf{A} = a\mathbf{U} + \mathbf{A}'$, and $A'_{22} = -A'_{11} - A'_{33}$.

Numerical values of the principal components of the anisotropic proton tensor for the C—H fragment are listed in Table 1, in terms of the requisite spin densities. Provided that Q is known and that $\rho_{\sigma'\sigma'}$ can be related to $\rho_{\sigma\sigma}$, comparisons between experimental and theoretical values of the $A'^{(H)}_{ii}$ can be made. In order to obtain the results in Table 2, we have assumed a Q of -80 MHz and have taken $\rho_{\sigma'\sigma'} = \rho_{\sigma\sigma}$. An experimental estimate of the anisotropic proton tensor for C—H is now required with which to assess these rather wide-ranging results. To do this, we have selected the single-crystal data in Table 3, and have expressed the anisotropic principal components in terms of the corresponding isotropic coupling. The principal components of the total proton tensor in these radicals, and hence $a = (1/3)\sum A_{ii}$, are all negative in sign (16, 21). By taking the ratios A'_{ii}/a for each radical, as in Table 3, Q remains an unknown. The "experimental" principal components $A'^{(H)}_{ii}$ for the fragment >Ċ—H were subsequently derived from the averages $\langle A'_{ii}/a \rangle$ assuming two values of Q.

TABLE 2. Theoretical anisotropic proton tensor components for >Ċ—H derived assuming equivalent trigonal orbitals, and $Q = -80$ MHz

$(\rho_{\sigma'\sigma'} = \rho_{\sigma\sigma})$	A'_{11}	A'_{22}	A'_{33}	$\lvert\psi(r_H)\rvert^2$
A	55.5	−44.1	−11.4	0.0268
B	53.9	−43.5	−10.5	0.0266
C	40.1	−37.5	−2.7	0.0256
D	45.2	−40.1	−5.1	0.0213
*	51.5	−43.4	−8.1	—

*From Vincow *et al.* (6).

As indicated by the results in Table 1, the σ-spin density terms cannot be satisfactorily included under *A*, *B*, or the Hartree–Fock case. Comparison of Tables 2 and 3 shows that when the σ-contributions are included, assuming $\rho_{\sigma'\sigma'} = \rho_{\sigma\sigma}$, the closed-shell function *C* provides the closest agreement between theory and experiment. Although the anisotropic proton tensor components are over-estimated by *A* and *B*, this can be compensated for, as in *C*, by

Can. J. Chem. Downloaded from www.nrcresearchpress.com by 210.87.254.5 on 09/05/12
For personal use only.

TABLE 3. "Experimental" anisotropic proton tensor components for $\rangle\dot{C}$—H derived from high-field single-crystal data and zero-field data

Radical	a	A'_{11}/a	A'_{22}/a	A'_{33}/a	Reference
$H\dot{C}(CO_2H)_2$	−59.1	−0.511	0.534	−0.022	9
	−59.2	−0.520	0.561	−0.041	22
	−59.6	−0.520	0.556	−0.034	23
$H\dot{C}(CONH_2)_2$	−59.0	−0.517	0.514	+0.002	24
	−58.6	−0.623	0.575	+0.048	25
$HO_2C\dot{C}HCO_2^-K^+$	−56.8	−0.528	0.560	−0.032	22
	−55.9	−0.499	0.540	−0.041	26
$H\dot{C}(CO_2^-Na^+)_2$	−61.3	−0.351	0.436	−0.090	27
$H\dot{C}(CO_2^-K^+)_2$	−58.1	−0.556	0.587	−0.029	22
$H\dot{C}(SO_3^-K^+)_2$	−60	−0.533	0.583	−0.050	28
$H\dot{C}CONHCONHCO$	−55.3	−0.541	0.519	+0.020	23
	−57.6	−0.455	0.460	−0.007	29
$\dot{C}H_3$	−62.5	—	—	—	30
$\langle A'_{ii}/a \rangle$	=	−0.513	0.535	−0.023	
$(Q = -80)$	A'_{ii} =	41.0*	−42.8	+1.8	
$(Q = -66.5)$	A'_{ii} =	34.1*	−35.6	+1.5	

*Anisotropic proton tensor components for $\rangle\dot{C}$—H in the principal axis system $i = 1, 2, 3$ in Fig. 1.

a decrease in the effective nuclear charge on the carbon atom. The magnitudes of the *ab initio* optimized orbital exponents for carbon are smaller than the standard Slater exponents and hence, the former give correspondingly better agreement (6). It should be noted that as $\rho_{\pi\pi}$ tends to zero, the outcome for B approaches that obtained with C. An estimate of the effectiveness of the approximations embodied by [11] and [17] can be gained by comparing the results under D with the *ab initio* based $A'^{(H)}_{ii}$ calculated by Vincow *et al.* (6). Thus the σ-contributions obtained following the above approximations are roughly two-thirds the magnitudes of those derived by incorporating the complete σ-spin density matrix; the π-contributions should of course be the same.

Although the most important consideration in the foregoing calculations is certainly the form of the carbon STO functions, there are other factors which should be mentioned. One, which has a bearing on the magnitude of Q, is the sensitive dependence of the isotropic proton coupling on the hydrogen 1s orbital exponent (14). Chang *et al.* (16) have found that the use of $\zeta_h = 1.0$ along with the optimized STO exponents yielded a more reasonable proton coupling than $\zeta_h = 1.19$, whereas the latter led to a better total s.c.f. energy. However, when ζ_h under D is changed from 1.19 to unity, as in Table 4, the σ-spin density contributions to the $A'^{(H)}_{ii}$ become larger. That is, although an increase in ζ_h is reflected in a Q of increased magnitude (14), the accompanying increase in $|a|$ and $|h(\mathbf{r}_H)|^2$ would leave the $\rho_{\sigma\sigma}$ derived from [17] comparatively unchanged. Changes in carbon–hydrogen bond length have a significant effect but variations within the normal range of r_{C-H}, like changes in ζ_h and Q, would be difficult to assess. Other calculations have shown that small changes in bond-angle and hybridization do not markedly affect either the anisotropic σ-contributions (31) or the magnitude of Q (32).

Also from Table 4, a change in Q from the more or less arbitrary value of −80 to the −66.5 MHz calculated for the fragment $C'_2\dot{C}$—H (33) has a relatively small effect. In fact, setting $\rho_{\sigma'\sigma'}$ equal to zero has more effect on the theoretical $A'^{(H)}_{ii}$ than the change in Q. On the basis of theoretical results, the difference between $\rho_{\sigma'\sigma'}$ and $\rho_{\sigma\sigma}$ in the C—H fragment is small (33). However, contributions to the anisotropic proton tensor from the orbitals t' and t'' might be at least partially cancelled by unpaired spin density in the trigonal orbitals of contiguous carbon atoms. To gauge this possibility, we have included the two extra orbitals forming the C′—C bonds in $C'_2\dot{C}$—H; the spin density in these two extra orbitals was assumed equal to $-\rho_{\sigma\sigma}$. The effect is not large, but could conceivably be more significant in an odd-alternant radical such as allyl.

At this point, it will be useful to calculate the anisotropic proton tensors for the allyl radical,

Can. J. Chem. Downloaded from www.nrcresearchpress.com by 210.87.254.5 on 09/05/12
For personal use only.

TABLE 4. Anisotropic proton tensor principal components for C—H, calculated with *ab initio* optimized STO in case *D*, subject to the parameter changes indicated

Fragment	A'_{11}	A'_{22}	A'_{33}	Remarks
	45.2	−40.1	−5.1	*
	42.0	−39.0	−3.0	$\rho_{\sigma'\sigma'} = 0$
	44.9	−40.1	−4.8	$\rho'_{\sigma'\sigma'} = -\rho_{\sigma\sigma}$
	43.6	−39.4	−4.2	$Q = -66.5$
	52.2	−43.1	−9.0	$\zeta_h = 1.00$
	44.3	−38.2	−6.0	$r_{C-H} = 2.10$
	42.3	−39.0	−3.4	$Q = -62.5$
	49.1	−42.5	−6.6	From ref. 6

*The basic parameters were $Q = -80$ MHz, $\rho_{\pi\pi} = 1$, $\rho_{\sigma'\sigma'} = \rho_{\sigma\sigma}$, $\zeta_h = 1.19$ and $r_{C-H} = 2.05$ a.u.

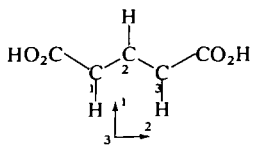

FIG. 2. Molecular axis system *1*, *2*, *3* for the allyl-type fragment observed in x-irradiated glutaconic acid (8).

since it is in many respects similar to perinaphthenyl. Heller and Cole (8) have shown that X-ray irradiation of a single crystal of glutaconic acid yields the allyl-type radical in Fig. 2, and have demonstrated conclusively the positive sign of the isotropic coupling for proton 2. The experimental anisotropic proton tensor principal components and isotropic couplings in MHz were found to be

$$\begin{aligned} A_{ii}'^{(H_1,H_3)} &= 27.7,\ -27.3,\ -0.3 \\ a^{(H_1,H_3)} &= -35.7 \\ A_{ii}'^{(H_2)} &= 0.0,\quad 5.0,\ -5.0 \\ a^{(H_2)} &= 12.0 \end{aligned} \qquad [24]$$

and it was noted that the principal axes for protons 1 and 3 were slightly different. Since the unpaired electron is delocalized, mainly within a three carbon π-orbital (8), significant contributions to the anisotropic tensor for a given proton arise from spin density associated with the neighboring carbon atoms in addition to contributions from the adjacent carbon atom. The complete π-spin density contribution for the proton in position k will be given by

$$\boldsymbol{\pi}^{(k)} = \sum_{ij} \rho_{ij}^{\pi} \langle \pi^{(i)} | \mathbf{T}^{(k)} | \pi^{(j)} \rangle \qquad [25]$$

McConnell (34) has calculated the atomic orbital π-spin density matrix for allyl using the self-consistent unrestricted wave function given by Berthier (35) and found, after elimination of the quartet spin component,

$$\rho_{ij}^{\pi} = \begin{bmatrix} 0.609 & -0.005 & -0.345 \\ -0.005 & -0.185 & -0.005 \\ -0.345 & -0.005 & 0.609 \end{bmatrix} \qquad [26]$$

If, for the moment, the off-diagonal elements of ρ_{ij}^{π} are neglected, then [25] becomes

$$\boldsymbol{\pi}^{(k)} = \sum_{i} \rho_{ii}^{\pi} \langle \pi^{(i)} | \mathbf{T}^{(k)} | \pi^{(i)} \rangle \qquad [27]$$

where the various contributions are by definition not in the same axis system. The transformation of a tensor in an axis system, *a*, *b*, *c* into another system α, β, γ is given by (16)

$$\boldsymbol{T}_{\alpha\beta} = \sum l_{\alpha a} T_{ab} l_{b\beta} \qquad [28]$$

where $l_{\alpha a}$ is the direction cosine between the axes α and *a*. In calculating the proton tensors, each of the carbon atoms of allyl was considered as an isolated sp^2 hybridized fragment. Equation 27 was used to calculate the π-contributions and, except as outlined below, σ-spin density

Can. J. Chem. Downloaded from www.nrcresearchpress.com by 210.87.254.5 on 09/05/12
For personal use only.

TABLE 5. Theoretical anisotropic proton tensors for the allyl radical, in the molecular axis system *1*, *2*, *3* in Fig. 2

Case	A'_{ij}	Case	A'_{ij}
$(\overset{B}{>}\dot{C}—H)$	$A'^{(H_1)} = \begin{bmatrix} 23.19 & -0.86 & 0 \\ -0.86 & -20.13 & 0 \\ 0 & 0 & -3.06 \end{bmatrix}$	$(\overset{B}{>}\dot{C}—H)$	$A'^{(H_2)} = \begin{bmatrix} -1.08 & 0 & 0 \\ 0 & 5.95 & 0 \\ 0 & 0 & -4.87 \end{bmatrix}$
$(\overset{B}{>}\dot{C}—H)$	$A'^{(H_2)} = \begin{bmatrix} -0.37 & 0 & 0 \\ 0 & 5.75 & 0 \\ 0 & 0 & -5.38 \end{bmatrix}$	$(\overset{C'}{\underset{C'}{>}}\overset{B}{\dot{C}}—H)$	$A'^{(H_2)} = \begin{bmatrix} -0.83 & 0 & 0 \\ 0 & 5.98 & 0 \\ 0 & 0 & -5.15 \end{bmatrix}$
$(\overset{D}{>}\dot{C}—H)$	$A'^{(H_1)} = \begin{bmatrix} 23.65 & -0.86 & 0 \\ -0.86 & -20.37 & 0 \\ 0 & 0 & -3.28 \end{bmatrix}$	$(\overset{D}{>}\dot{C}—H)$	$A'^{(H_2)} = \begin{bmatrix} -0.87 & 0 & 0 \\ 0 & 6.08 & 0 \\ 0 & 0 & -5.21 \end{bmatrix}$

TABLE 6. Individual contributions to the principal component $A'^{(H)}_{33}$ for the protons of allyl, including both diagonal and off-diagonal terms

Proton	ρ^{π}_{11}	ρ^{π}_{22}	ρ^{π}_{33}	$\rho_{\sigma\sigma}$	$2\rho_{\sigma'\sigma'}$	$2\rho'_{\sigma'\sigma'}$	$K\sum_{i,j\,(i\neq j)}\pi_{ij}$	Sum
B (1, 3)	1.58	0.85	−1.85	−2.11	−1.54	—	0.62	−2.45
(2)	−2.81	−0.48	−2.81	0.71	0.52	−0.28	0.48	−4.67
D (1, 3)	0.09	0.91	−1.92	−0.95	−0.45	—	0.62	−1.70
(2)	−2.99	−0.03	−2.99	0.47	0.32	−0.16	0.48	−4.90

contributions were confined to the $>\dot{C}—H$ portion containing the proton in question. Now the two sites of large positive π-spin density which flank the negative $\rho_{\pi\pi}$ site could affect the σ-contribution for proton 2 to the extent that the approximation $\rho_{\sigma'\sigma'} = \rho_{\sigma\sigma}$ loses validity. Two possibilities have been entertained in this regard: one is to set $\rho_{\sigma'\sigma'}$ equal to zero and consider only the σ-spin density in the C—H bond, whereas the other effectively considers the fragment $C'_2\dot{C}—H$. In the latter case, the σ-spin densities in the trigonal orbitals forming the C′—C bonds are derived from the isotropic couplings of the protons bonded to the respective carbon atoms. As can be seen from the results in Table 5, the differences between these choices for proton 2 are quite small.

The results for allyl under *B* were obtained using the expression [2] for the sites with $\rho_{\pi\pi} > 0$; for the negative $\rho_{\pi\pi}$ site, ζ_{π} was assigned the closed-shell value from *C*. The σ-spin density terms showed little overall change with $\rho_{\pi\pi}$ and so the case *C* STO functions were also used to derive the σ-terms in this instance. The carbon-hydrogen and carbon–carbon bond lengths used were 2.05 and 2.65 a.u., respectively, and all bond angles were 120°. The anisotropic tensor calculated for proton 2 is diagonal in the molecular axis system *1*, *2*, *3* in Fig. 2, whereas the angle between the axis corresponding to the positive principal component of $\mathbf{A}'^{(H_1)}$ and the axis *1* is $\cong 1°$. The agreement between the calculated principal components in Table 5 and the experimental values [24] is reasonable for proton 2 but less so for protons 1 and 3.

The anisotropic hyperfine tensor component which is perpendicular to the molecular plane is the one essential to the discussion of the liquid-crystal results for perinaphthenyl. Hence, it is worthwhile to consider the breakdown of the various contributions to the $A'^{(H)}_{33}$ in the allyl radical, and also to gauge the importance of terms arising from the off-diagonal elements of ρ^{π}_{ij}. The sum of the off-diagonal π-contributions to the $A'^{(H)}_{33}$ are given in Table 6, along with the various diagonal π- and σ-terms. The off-diagonal contributions were approximated (8) as being of the order of $\langle r^{-3}\rangle\rho^{\pi}_{ij}\langle i|j\rangle$, where $\langle i|j\rangle$ represents the overlap between $2p_{\pi}$ atomic orbitals on centers *i* and *j*; from benzene, $\langle 1|2\rangle = \langle 2|3\rangle = 0.260$ and $\langle 1|3\rangle = 0.039$ (36). In effect, we have thus considered point-dipoles of magnitude $\rho^{\pi}_{ij}\langle i|j\rangle$ located midway between carbon atoms *i* and *j* at the distances *r* from the proton concerned. The magnitude of the sum of the off-diagonal contributions for proton 1 is small compared with the in-plane anisotropic components, but significant when compared with the diagonal contributions to $A'^{(H_1)}_{33}$; for proton 2, the off-diagonal terms contribute

Can. J. Chem. Downloaded from www.nrcresearchpress.com by 210.87.254.5 on 09/05/12
For personal use only.

Can. J. Chem. Downloaded from www.nrcresearchpress.com by 210.87.254.5 on 09/05/12
For personal use only.

roughly 10% of the total $A_{33}^{\prime(H_2)}$ given in Table 6. However, off-diagonal σ-spin density elements are often avoided by neglect of overlap (17) and, in so doing, π-spin densities compatible with [16] and obeying the relation $\sum_i \rho_{\pi\pi}^{(i)} = 1$ can be obtained. For the allyl radical, Snyder and Amos find $\rho_{\pi\pi}^{(1)} = \rho_{\pi\pi}^{(3)} = 0.547$, $\rho_{\pi\pi}^{(2)} = -0.094$ as the unrestricted Hartree–Fock values (ρ_{aa}) after annihilation of the quartet spin component (37). With the off-diagonal contributions thus neglected, these $\rho_{\pi\pi}^{(i)}$, in conjunction with B, yield $A_{33}^{\prime(H_1,H_3)} = -3.46$ and $A_{33}^{\prime(H_2)} = -4.35$ MHz. It is nevertheless evident that the term arising from $\rho_{\sigma\sigma}$ is significant compared with the total perpendicular component A'_{33} and, to anticipate results to follow, perinaphthenyl is similar in this regard.

Perinaphthenyl

In general, the motion of a paramagnetic molecule dissolved in a nematic mesophase is constrained by the partial alignment of the solvent molecules in the presence of an external magnetic field (38). Hence, the anisotropic magnetic interactions within a π-radical are not completely lost through motional averaging and the hyperfine splittings and g-factor are found to differ from those values observed in isotropic solvent media. For a particular nucleus, the average hyperfine coupling $\bar{a}$ in the aligned nematic environment is related to the anisotropic hyperfine tensor A'_{ij} by the expression (4)

$$[29] \qquad \bar{a} = a + \tfrac{2}{3} \sum_{ij} \vartheta_{ij} A'_{ij}$$

The quantity a is normally identified with the isotropic hyperfine coupling observed above the transition from the nematic to the isotropic solvent phase.

The alignment of the solute molecule, which is governed primarily by its physical shape, is described in terms of the traceless ordering matrix $\mathbf{\vartheta}$. Because of the D_{3h} symmetry of the planar radical perinaphthenyl, no preferential ordering occurs with respect to the in-plane molecular axes *1* and *2* shown in Fig. 3. The ordering matrix therefore has axial symmetry with diagonal elements $\vartheta_{11} = \vartheta_{22} = -\vartheta_{33}/2$ (39), so that [29] reduces to

$$[30] \qquad \delta a = (\bar{a} - a) = \vartheta_{33} A'_{33}$$

That is, the degree of alignment ϑ_{33} can be derived from the experimental shift δa and the calculated anisotropic hyperfine tensor. Subsequent correlation of other shifts and anisotropic tensors using this ϑ_{33} should then reveal any inconsistencies in the theoretical results under consideration.

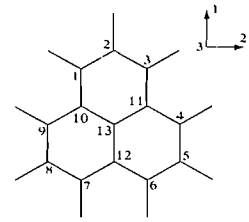

FIG. 3. Molecular axis system *1*, *2*, *3* for the π-electron free radical perinaphthenyl.

The proton hyperfine e.p.r. spectra of perinaphthenyl dissolved in 4,4′-dimethoxyazoxybenzene consist of a large septet splitting and a smaller quartet splitting (1–3). The quartet splitting arises from the symmetrically equivalent protons labelled 2, 5, and 8 in Fig. 3. The isotropic hyperfine couplings and shifts for the two sets of protons in MHz (2) are

$$[31] \qquad a^{(H_1)} = -17.6, \qquad \delta a^{(H_1)} = 0.0$$

and

$$a^{(H_2)} = 5.10, \qquad \delta a^{(H_2)} = 0.65$$

The magnitude of the larger proton coupling requires that the π-spin density $\rho_{\pi\pi}^{(1)}$ be positive. Now irrespective of whether the sign of $\rho_{\pi\pi}^{(2)}$ is positive or negative, the calculated tensor component A'_{33} for proton 2 is negative, ϑ_{33} is also negative, so that the predicted shift $\delta a^{(H_2)}$ is positive (2, 38). From experiment, $|\bar{a}| > |a|$ for proton 2, which means that $a^{(H_2)}$ must therefore be positive and $\rho_{\pi\pi}^{(2)}$ negative. This outcome is supported by the signs of the ^{13}C couplings obtained from the experimental shifts (2)

$$[32] \quad \delta a^{(C_1)} = -11.13 \text{ and } \delta a^{(C_2,C_{10})} = 3.22 \text{ MHz}$$

In using the foregoing STO functions to calculate the proton tensor components required by [30], we have employed the π-spin densities (ρ_{aa}) for perinaphthenyl given by Snyder and Amos; annihilation of the undesired spin multiplicities resulting from the self-consistent unrestricted treatment yielded (37)

$$[33] \qquad \rho_{\pi\pi}^{(1)} = 0.219, \qquad \rho_{\pi\pi}^{(2)} = -0.064,$$
$$\rho_{\pi\pi}^{(10)} = -0.054, \quad \rho_{\pi\pi}^{(13)} = 0.044.$$

TABLE 7. Theoretical anisotropic proton tensor components (in MHz) perpendicular to the molecular plane in perinaphthenyl

	Proton 1		Proton 2			
	$K\sum\pi_{33}$	A'_{33}	$K\sum\pi_{33}$	A'_{33}	ϑ^*_{33}	$\delta a^{(H_1)}$
A	−1.479	−3.200	−2.351	−1.853	−0.351	1.12
B	0.411	−1.388	−2.449	−1.928	−0.337	0.47
C	0.513	−1.286	−2.444	−1.923	−0.338	0.43
D	−0.662	−1.825	−2.426	−2.089	−0.311	0.57

*From $\delta a^{(H_2)} = 0.65$ MHz.

TABLE 8. Analysis of contributions to the $A'^{(H)}_{33}$ for perinaphthenyl

Proton	$\rho^{(1)}_{\pi\pi}$	$\rho^{(2)}_{\pi\pi}$	$\rho^{(3)}_{\pi\pi}$	$K\sum\pi_{33}$	$\rho_{\sigma\sigma}$	$2\rho_{\sigma'\sigma'}$	$2\rho'_{\sigma'\sigma'}$
B (1)	1.108	0.272	−0.353	0.411	−1.041	−0.758	—
(2)	−0.930	−0.324	−0.930	−2.444	0.302	0.219	−0.138
D (1)	0.033	0.314	−0.370	−0.662	−0.694	−0.469	—
(2)	−1.074	−0.010	−1.074	−2.426	0.201	0.136	−0.080

The bond lengths used were again $r_{C-H} = 2.05$ and $r_{C-C} = 2.65$ a.u., and all bond angles were 120°. The sum of the thirteen π-contributions we have denoted by $K\sum\pi_{33}$, and so for a given proton

$$[34] \qquad A'_{33} = K(\sum\pi_{33} + \sigma_{33})$$

Only the σ-spin densities in the C—H portion under consideration were included in the derivation of σ_{33} and, in obtaining the results in Table 7, we have assumed [18] to be valid; that is $\rho_{\sigma'\sigma'} = \rho_{\sigma\sigma}$. The isotropic proton couplings [31] were used to find the $\rho_{\sigma\sigma}$ from [17]. The shift $\delta a^{(H_2)} = 0.65$ MHz was then used in conjunction with the various $A'^{(H_2)}_{33}$ to determine the degree of alignment from [30]. Now the product of ϑ_{33} and $A'^{(H_1)}_{33}$ should yield a shift near zero for the protons at the positive $\rho_{\pi\pi}$ sites. As can be seen from Table 7, cases *B* and *C* provide comparable agreement with experiment, and thus represent a substantial improvement over *A*, as well as previous calculations which used $\zeta_\pi \sim 1.6$ (1–4). The perinaphthenyl results under *B* were derived using [2] for sites with $\rho_{\pi\pi} > 0$; contributions from positions of negative $\rho_{\pi\pi}$ and from the σ-spin densities were obtained with the closed-shell functions *C*. The similarity between the results of *B* and *C* is not unexpected, since the magnitude of $\rho^{(1)}_{\pi\pi}$ is relatively small.

Essentially the same trends are evident from Table 7 as those already noted for the C—H fragment, and it is clear that inclusion of the σ-contributions to the anisotropic proton tensor makes a considerable difference. For *A* better, though certainly not good, agreement between theory and experiment is obtained when the σ_{33} are omitted. Under *B* and *C*, however, the sign of $K\sum\pi_{33}$ for proton 1 is opposite to that for the total component $A'^{(H_1)}_{33}$. Clearly, the outcome in these cases would be further improved by applying the approximation $\rho_{\sigma'\sigma'} = 0$ in determining the σ_{33}. Thus we find for *B* that $A'^{(H_1)}_{33} = -0.603$ and $A'^{(H_2)}_{33} = -2.147$ MHz, whence $\vartheta_{33} = -0.302$ which predicts $\delta^{(H_1)}_a = 0.19$ MHz. Setting $\rho_{\sigma'\sigma'} = 0$ in case *D* also improves agreement with experiment. In Table 8, we show separately some of the more important diagonal contributions to the anisotropic proton tensors for perinaphthenyl. It should be noted that a significant contribution to $A'^{(H_1)}_{33}$ comes from the π-spin density on carbon atom 9; under *B*, the magnitude of this term is −0.635 MHz.

To extend the present discussion, an independent estimate of ϑ_{33} was obtained from the experimental ^{13}C shifts. Neglecting the effect of σ-spin density, the necessary anisotropic tensor component for carbon atom *i* is given by

$$[35] \quad A'^{i(C_1)}_{33} = \rho^{(i)}_{\pi\pi} K(\tfrac{4}{5})\langle r^{-3}\rangle - \sum_{j\neq i} \rho^{(j)}_{\pi\pi} K r_{ij}^{-3}(P - Q)$$

in which *K* takes the value 134.15 MHz a.u.[3] The π-spin density on carbon *i*, in the first term, yields the axially symmetric part (21), whereas the second term of [35] comprises the

Can. J. Chem. Downloaded from www.nrcresearchpress.com by 210.87.254.5 on 09/05/12
For personal use only.

TABLE 9. Calculated proton hyperfine shifts and anisotropic tensor components for perinaphthenyl, assuming $\rho_{\sigma'\sigma'} = 0$

Q	$A''^{(C_1)}_{33}$	$A''^{(C_2,C_{10})}_{33}$	ϑ^{*}_{33}	$A''^{(H_1)}_{33}$	$A''^{(H_2)}_{33}$	$\delta a^{(H_1)}$	$\delta a^{(H_2)}$
$B\,(\rho_{aa})$	39.40	−11.29	−0.284	−0.630	−2.147	0.18	0.61
B −80	39.58	−12.20	−0.272	−0.603	−2.143	0.16	0.58
B −66.5	47.67	−14.53	−0.228	−0.233	−2.405	0.05	0.55
$D\,(\rho_{aa})$	39.44	−9.77	−0.306	−1.356	−2.225	0.41	0.68

*Average degree of alignment using the $\delta a^{(C)}$ from [32].

TABLE 10. ^{13}C hyperfine tensor components from single-crystal data

Radical	a	A'_{11}	A'_{22}	A'_{33}	Reference
$\dot{C}H(CO_2H)_2$	92.6	−50.4	−69.8	120.1	9
$\dot{C}H(SO_3^-K^+)_2$	125.7	−63.7	−70.7	134.3	28
$\dot{C}H_3$	105.7	—	—	126.1	30

sum of the π-terms from neighboring carbon atoms; the first term represents the dominant contribution to the $A''^{(C_1)}_{33}$ for perinaphthenyl. However, the $2p_\pi$ STO under B, as $\rho_{\pi\pi}$ tends to zero, yields an average value of $\langle r^{-3}\rangle$ which becomes considerably smaller than the s.c.f. value of 1.692 a.u.$^{-3}$ (21). In fact, the anisotropic ^{13}C tensor components calculated entirely with B lead to invalid estimates of $|\vartheta_{33}| > 0.5$. Alternatively, if the s.c.f. $\langle r^{-3}\rangle$ is taken for the first term, along with the results from B for the remainder of [35], we obtain $A''^{(C_1)}_{33} = 39.4$, $A''^{(C_2)}_{33} = -12.13$ and $A''^{(C_{10})}_{33} = -10.46$ MHz. The average of the anisotropic tensors for carbon atoms 2 and 10 was taken, since the experimental isotropic couplings and shifts for these positions were not distinguishable (1–3). The ^{13}C shifts [32] thus yield ϑ_{33} values of −0.283 and −0.285, respectively, the average of which subsequently predicts the proton shifts 0.18 and 0.61 MHz in Table 9. Also from Table 9, the use of experimental π-spin densities (4) does not markedly alter the theoretical proton shifts. Similar overall agreement is obtained with the experimental data for perinaphthenyl in refs. 1 and 3. If the trigonal orbitals in the C—H fragment are assumed equivalent, then the spin densities in the 2s and the two $2p_\sigma$ orbitals are essentially the same and equal to $\rho_{\sigma\sigma}$ (5). The first term of [35] thus becomes

$$[36] \qquad (\rho^{(i)}_{\pi\pi} - \rho^{(i)}_{\sigma\sigma})K(\tfrac{4}{5})\langle r^{-3}\rangle$$

and when this modification is included, the $A''^{(C)}_{33}$ decrease in magnitude and consequently the $\delta a^{(H)}$ increase by about 6% over the values given in Table 9.

Discussion

Apart from differences between trapping sites in the host crystal (33), an obvious problem in the correlation of single-crystal data for species RCHR′ with theoretical results is the difficulty in gauging anisotropic contributions from neighboring groups of atoms such as $-CO_2H$. The difficulty in evaluating the effect of unpaired spin density in the C—H portion alone is emphasized by comparing the data for $\dot{C}H(CO_2H)_2$ and $\dot{C}H(SO_3^-)_2$, in Tables 3 and 10. These two radicals have similar proton tensor principal values and so the anisotropic hyperfine interactions and the $\rho_{\pi\pi}$ are essentially the same, insofar as the proton is concerned. But the ^{13}C hyperfine tensors are quite different. The deviation from axial symmetry in $\mathbf{A}''^{(C)}$, $A'_{33}/2 + A'_{11}$, for $\dot{C}H(CO_2H)_2$ is −9.7 MHz compared with only −3.5 MHz for $\dot{C}H(SO_3^-)_2$, whereas the isotropic coupling $a^{(C)}$ is substantially larger in the latter radical. The approximation $\rho_{\sigma'\sigma'} = 0$ can account for only part of the observed deviation from axial symmetry in these two ^{13}C tensors, and consequently any choice between $\rho_{\sigma'\sigma'}$ equal to $\rho_{\sigma\sigma}$ or to zero remains unresolved. The isotropic ^{13}C coupling generally reflects differences in Q^{C}_{CX} for different C—X bonds (33).

In the foregoing calculations, the σ-spin density contributions to the $A'^{(H)}_{ii}$ have been satisfactorily accommodated, but even so are not strictly necessary for experimental agreement, by reducing ζ_π from ~1.6 to 1.3. But in addition to the decrease in the absolute magnitudes of the

Can. J. Chem. Downloaded from www.nrcresearchpress.com by 210.87.254.5 on 09/05/12
For personal use only.

Can. J. Chem. Downloaded from www.nrcresearchpress.com by 210.87.254.5 on 09/05/12
For personal use only.

$A'^{(H)}_{ii}$, the magnitude of $\langle r^{-3}\rangle$, which governs $\mathbf{A}'^{(C)}$, also decreases. That is, decreasing ζ_π in order to incorporate the σ-terms results in too small a value for $\langle r^{-3}\rangle$. The ζ_π under C yields 0.720 a.u.$^{-3}$ for $\langle r^{-3}\rangle$, compared with 1.214 a.u.$^{-3}$ from B ($\rho_{\pi\pi} = 1$). The $A'^{(C)}_{33}$ for CH_3 in Table 10, when substituted into [35], leads to $\langle r^{-3}\rangle \cong 1.24$ a.u.$^{-3}$. The s.c.f. value of $\langle r^{-3}\rangle$ (21), which gives $A'^{(C)}_{33} = 181$ MHz for unit $\rho_{\pi\pi}$, thus seems too large. Using the optimized basis set D and including all contributions, Vincow *et al.* (6) have calculated $A'^{(C)}_{33}$ for CH_3 to be 106 MHz. If the axially symmetric parts of the $A'^{(C)}_{33}$ for perinaphthenyl are scaled in accord with the experimental value for CH_3 rather than s.c.f. value, an alignment factor of $\vartheta_{33} \cong 0.40$ is obtained. But with this larger ϑ_{33}, the calculated proton shifts would no longer be in reasonable agreement with the experimental shifts. From these observations, the difficulty in obtaining adequate results for both proton and carbon-13 anisotropic hyperfine tensors by means of the same ζ_π is of course clear.

Further improvement could perhaps be provided by a change in the form of the $2p_\pi$ orbital, since this orbital is certainly the most important consideration in these calculations. The π-terms, which are governed by ζ_π, represent the dominant contributions to the $A'^{(H)}_{ii}$, and so the σ-terms must be judged in relation to the π_{ii}. The important factor in determining the σ-contributions is the hydrogen orbital exponent. The term $|h(\mathbf{r}_H)|^2$ in [17] is equal to ζ_h^3/π, so that an increase in ζ_h leads to a decrease in the magnitudes of the σ_{ii}. However, Pople *et al.* (40) have compared minimal basis semi-empirical INDO-UHF calculations of unpaired σ-spin densities with experimental a^H for a large variety of π-electron radicals; the best value found for $|h(\mathbf{r}_H)|^2$, equal to 0.338 a.u.$^{-3}$, corresponds to $\zeta_h = 1.02$. This outcome supports the use of unit ζ_h in the foregoing approximations. Chang *et al.* (15) have found that the magnitudes of $a^{(H)}$ and $a^{(C)}$, calculated by s.c.f.-c.i. methods which included all appropriate singly and doubly excited configurations, were improved considerably when the expanded STO basis developed by Clementi (41) was employed for the carbon atom. But these double ζ STO functions unfortunately present some major complications and become rather cumbersome when applied to the calculation of anisotropic hyperfine tensors.

TABLE 11. Anisotropic tensor components (in MHz) for a methyl proton in $(CH_3)_2\dot{C}CO_2H$, subject to free rotation of the methyl group

	$\langle A'_{11}\rangle$	$\langle A'_{22}\rangle$	$\langle A'_{33}\rangle$
Experimental (44)	5.8	−2.2	−3.7
A	7.78	−2.79	−4.99
	(2.40)	(1.02)	(−3.48)
B	6.63	−3.05	−3.57
(CH_4 STO)*	(1.76)	(0.79)	(−2.55)
C	6.94	−2.65	−4.30
	(2.54)	(1.15)	(−3.69)
D	6.76	−3.09	−3.66
	(1.70)	(0.77)	(−2.47)

*σ-Contribution derived using the s.c.f. ($r_{C-H} = 2.05$ a.u.) STO exponents for methane (46).

The calculation of anisotropic β-proton hyperfine tensors, in the fragment $\rangle\dot{C}—CH_3$ for example, is in some respects analogous to the foregoing procedure for C—H (42, 43). Extension of the McConnell and Strathdee theory for a proton lying not necessarily in the nodal plane of the 2p orbital bearing the unpaired electron has been demonstrated by Derbyshire (42), and we have again incorporated the σ-term correction of Pitzer *et al.* (20). The isotropic hyperfine coupling for the protons of the freely rotating methyl group in $C—CH_3$ is related to the π-spin density by (30)

$$[37] \qquad a^{(Me)} = \rho_{\pi\pi}(Q' + Q'' \langle \cos^2 \beta\rangle)$$

where β is the angle between the proton and the plane defined by the C—C bond and the axis of the $2p_\pi$ orbital. From ENDOR studies of $(CH_3)_2\dot{C}CO_2H$ (44), $\rho_{\pi\pi}Q' = 3.2$ MHz and $\rho_{\pi\pi}Q'' = 123.2$ MHz, and the anisotropic tensor components for the methyl group undergoing free rotation at room temperature appear in Table 11. The principal axis *1* lies along the bond between the sp^2 and sp^3 hybridized carbon atoms and the axis *3*, which corresponds to the direction of minimum hyperfine coupling (44), lies parallel to the symmetry axis of the $2p_\pi$ orbital. The isotropic hyperfine coupling for the α-proton in $CH_3\dot{C}HCO_2H$ is −54.7 MHz (45) which yields $\rho_{\pi\pi} = 0.68$, and we have taken $\rho_{\pi\pi}$ in $(CH_3)_2\dot{C}CO_2H$ to be the same. The bond lengths used in obtaining the results in Table 11 were $r_{C-H} = 2.05$ and $r_{C-C} = 2.75$ a.u., along with the usual tetrahedral angle of 109.5°. The σ-spin density required in determining the anisotropic contribution from the C—H tetrahedral orbital was obtained using an equation analogous to

Can. J. Chem. Downloaded from www.nrcresearchpress.com by 210.87.254.5 on 09/05/12
For personal use only.

[17]. These tetrahedral orbital terms are included in parentheses in Table 11; all other σ-spin densities in the radical were neglected. The direction of the minimum hyperfine coupling is correctly predicted in all cases, and case *B*, in which the C—H tetrahedral orbital portion was obtained using the s.c.f. minimal STO exponents for methane (46), provides the closest agreement with experiment.

To summarize: the calculations on C—H show that the σ-contributions to the $A_{ii}^{\prime(H)}$ are quite substantial; the σ-terms based on the approximations herein are roughly two-thirds those derived with the complete σ-spin density matrix (6). In relation to the π-contributions, the inclusion of the σ-terms is not required for agreement with experiment when $\zeta_\pi \sim 1.6$ is employed. When the theory is extended to delocalized π-electron radicals, for example perinaphthenyl-3-carboxylic acid dissolved in 4-(*n*-pentyloxy)-benzoic acid (4), it becomes necessary to include π-contributions from neighboring atoms. However, when all the contributions arising from the $\rho_{\pi\pi}$ in perinaphthenyl are included using $\zeta_\pi \sim 1.6$, the results are clearly unsatisfactory: more so when it is noted that the σ-terms are comparable in magnitude to most of the π-contributions to the $A_{33}^{\prime(H)}$. These difficulties, insofar as the proton tensors are concerned, can be alleviated by reducing ζ_π to 1.3, when at least the $\rho_{\sigma\sigma}$ portion can be accommodated along with the terms from the $\rho_{\pi\pi}$. Although optimization of the STO exponents for C—H led to a decrease from the Slater values for carbon (6), the reduction in ζ_π to 1.3, or perhaps further to 1.25, is difficult to support. Such a decrease in ζ_π does lead to more reasonable anisotropic components for the proton tensor, but at the same time $\langle r^{-3} \rangle$ becomes smaller. Presumably the divergent dependence of $\mathbf{A}^{\prime(H)}$ and $\mathbf{A}^{\prime(C)}$ on ζ_π is a limitation of STO functions which extends to other π-electron fragments, particularly N—H.

Calculation of the anisotropic hyperfine tensors in C—F and C—Cl fragments (47) is a more complex problem than in C—H because of the non-vanishing anisotropic interaction due to spin density in the p-orbitals of the halogen atom. Spin polarization in the C—F bond of $FC(CONH_2)_2$ plays a significant part in the deviation of $\mathbf{A}^{\prime(F)}$ from axial symmetry (48). The question remains as to whether a similar reduction in ζ_π for nitrogen and oxygen is necessary in π-radicals such as carbazole-*N*-oxyl (4). Analyses of other liquid crystal data are complicated by the fact that the majority of radicals studied thus far have two-fold, or lower, symmetry. Würster's blue cation, for example, requires two parameters with which to describe its alignment in the nematic mesophase (4). Uncertain π-spin density distributions, and flexible radical geometry as in triphenylmethyl, are additional complicating features.

This research was supported by the National Research Council of Canada, and by the Defence Research Board of Canada, Grant number 9530-55. We are very grateful to Dr. G. R. Luckhurst for the benefit of numerous discussions, and to Dr. G. Vincow for placing a preprint of (6) at our disposal along with valuable comments concerning the present work.

1. S. H. GLARUM and J. H. MARSHALL. J. Chem. Phys. **44**, 2884 (1966).
2. H. R. FALLE and G. R. LUCKHURST. Mol. Phys. **11**, 299 (1966).
3. K. MÖBIUS, H. HAUSTEIN, and M. PLATO. Z. Naturforsch. A **23**, 1626 (1968).
4. H. R. FALLE and G. R. LUCKHURST. J. Magn. Resonance **3**, 161 (1970).
5. H. M. MCCONNELL and J. STRATHDEE. Mol. Phys. **2**, 129 (1959).
6. G. VINCOW, S. Y. CHANG, and E. R. DAVIDSON. J. Chem. Phys. **54**, 4121 (1971).
7. H. J. SILVERSTONE, D. E. WOOD, and H. M. MCCONNELL. J. Chem Phys. **41**, 2311 (1964).
8. C. HELLER and T. COLE. J. Chem. Phys. **37**, 243 (1962).
9. T. COLE and C. HELLER. J. Chem. Phys. **34**, 1085 (1961).
10. G. M. ZHIDOMIROV and P. V. SCHASTNEV. Zh. Strukt. Khim. **7**, 66 (1966).
11. E. CLEMENTI and D. L. RAIMONDI. J. Chem. Phys. **38**, 2686 (1963).
12. K. G. KAY and H. J. SILVERSTONE. J. Chem. Phys. **46**, 2854 (1967).
13. H. J. SILVERSTONE and H. W. JOY. J. Chem. Phys. **47**, 1384 (1967).
14. S. Y. CHANG, E. R. DAVIDSON, and G. VINCOW. J. Chem. Phys. **49**, 529 (1968).
15. S. Y. CHANG, E. R. DAVIDSON, and G. VINCOW. J. Chem. Phys. **50**, 1740 (1970).
16. A. CARRINGTON and A. D. MCLACHLAN. Introduction to magnetic resonance. Harper and Row, New York. 1967.
17. K. D. SALES. Adv. Free Radical Chem. **3**, 139 (1969). G. M. Zhidomirov and P. V. Schastnev. Zh. Strukt. Khim. **8**, 974 (1967).
18. J. -P. MALRIEU. J. Chem. Phys. **46**, 1654 (1967).
19. J. W. VANDER Hart. Mol. Phys. **19**, 75 (1970).
20. R. M. PITZER, C. W. KERN, and W. N. LIPSCOMB. J. Chem. Phys. **37**, 267 (1962).
21. J. R. MORTON. Chem. Rev. **64**, 453 (1964).

22. T. COLE, T. KUSHIDA, and H. C. HELLER. J. Chem. Phys. **38**, 2915 (1963).
23. M. BIRKLE and G. SCHOFFA. J. Chem. Phys. **49**, 3191 (1968).
24. H. N. REXROAD, Y. H. HAHN, and W. J. TEMPLE. J. Chem. Phys. **42**, 324 (1965).
25. N. CYR and W. C. LIN. J. Chem. Phys. **50**, 3701 (1969).
26. W. C. LIN and C. A. MCDOWELL. Mol. Phys. **4**, 343 (1961).
27. B. L. BALES, R. N. SCHWARTZ, and M. W. HANNA. J. Chem. Phys. **51**, 5178 (1969).
28. A. HORSFIELD, J. R. MORTON, J. R. ROWLANDS, and D. H. WHIFFEN. Mol. Phys. **5**, 241 (1962).
29. W. BERNHARD and W. SNIPES. J. Chem. Phys. **44**, 2817 (1966).
30. M. T. ROGERS and L. D. KISPERT. J. Chem. Phys. **46**, 221 (1967).
31. J. HIGUCHI. J. Chem. Phys. **41**, 2084 (1964).
32. J. HIGUCHI. J. Chem. Phys. **39**, 3455 (1963).
33. M. KARPLUS and G. K. FRAENKEL. J. Chem. Phys. **35**, 1312 (1961).
34. H. M. MCCONNELL. J. Chem. Phys. **29**, 244 (1958).
35. G. BERTHIER. J. Chim. Phys. **52**, 141 (1954).
36. R. G. PARR, D. P. CRAIG, and I. G. ROSS. J. Chem. Phys. **18**, 1561 (1950).
37. L. C. SNYDER and T. AMOS. J. Chem. Phys. **42**, 3670 (1965).
38. G. R. LUCKHURST. Royal Inst. Chem. Rev. **3**, 61 (1970).
39. G. R. LUCKHURST. Mol. Cryst. Liquid Cryst. **2**, 363 (1967).
40. J. A. POPLE, D. L. BEVERIDGE, and P. A. DOBOSH. J. Am. Chem. Soc. **90**, 4201 (1968).
41. E. CLEMENTI. J. Chem. Phys. **40**, 1944 (1964); IBM Tech. Rept. RJ-256 (1963).
42. W. DERBYSHIRE. Mol. Phys. **5**, 225 (1962).
43. R. REITBÖCK. Z. Naturforsch. A **24**, 279 (1969).
44. J. W. WELLS and H. C. BOX. J. Chem. Phys. **46**, 2935 (1967).
45. J. R. MORTON and A. HORSFIELD. J. Chem. Phys. **35**, 1142 (1961).
46. R. M. PITZER. J. Chem. Phys. **46**, 4871 (1967).
47. R. P. KOHIN. J. Chem. Phys. **50**, 5356 (1969).
48. M. IWASAKI, S. NODA, and K. TORIYAMA. Mol. Phys. **18**, 201 (1970).

Can. J. Chem. Downloaded from www.nrcresearchpress.com by 210.87.254.5 on 09/05/12
For personal use only.

Infrared Studies on Rotational Isomerism. VI. Normal-Coordinate Analysis of 2-Chloro-, 2-Bromo-, and 2-Cyanoethanol

PAUL A. GIGUÈRE AND MICHEL SCHNEIDER[1]

Département de chimie, Université Laval, Québec, Québec

Received August 9, 1971

A normal-coordinate analysis of three substituted ethanol molecules X—CH_2—CH_2—OH (where X = Cl, Br, or CN) was carried out using the simple valence force field model, and a computer program of Schachtschneider translated into Fortran language by Brooks. The effect of internal hydrogen bonding was studied by adding one extra symmetry coordinate, H . . . X (two, H . . . C and H . . . N, in the case of 2-cyanoethanol). The corresponding force constants show a good correlation with the hydrogen bond strengths. Most of the other force constants maintain the same value in the *gauche* and the *trans* rotamers. In general the calculated fundamental frequencies agree closely with the observed ones. The potential energy distribution confirms the extensive coupling between certain vibrations; particularly the skeleton stretching and the CH_2 twisting and rocking. Only the C—X stretching and the skeleton bending vibrations are strongly affected by rotational isomerism.

Dans l'hypothèse du champ de force de valence et à l'aide d'un programme de Schachtschneider transcrit en langage Fortran IV par Brooks nous avons analysé en coordonnées normales trois molécules d'éthanol substitué: X—CH_2—CH_2—OH, où X = Cl, Br ou CN. Pour mieux étudier l'effet de la liaison hydrogène intramoléculaire nous avons ajouté une coordonnée de symétrie supplémentaire H . . . X (et deux, H . . . C et H . . . N, pour le cyano-2 éthanol). Les constantes de force correspondantes montrent nettement une corrélation avec l'énergie des liaisons hydrogène. La transférabilité des constantes de force entre rotamères *gauche* et *trans* est excellente dans la plupart des cas. Les fréquences de vibration ainsi calculées s'accordent très bien avec les valeurs expérimentales en général. Les calculs de distribution de l'énergie potentielle confirment que certaines vibrations sont fortement couplées: en particulier les modes de valence du squelette et celles de torsion et de rotation des groupes CH_2. Seules les vibrations de valence C—X et de déformation du squelette sont fortement affectées par l'angle azimutal.

Canadian Journal of Chemistry, **50**, 152 (1972)

Introduction

Normal-coordinate analysis of the fundamental vibrations of small molecules of known structure is usually carried out to test the assignment of the various bands in their spectra. Since the force constants thus calculated depend to some extent on the model chosen they do not always lead to definite answer in dubious cases. Nevertheless, they provide much useful information. For instance, the extent of coupling or mixing of neighboring vibrations may be derived from the potential energy distribution. Furthermore, in molecules showing rotational isomerism the force constants may be expected to remain roughly the same in the different rotamers. Therefore, it becomes possible to evaluate the dependance of certain vibrational frequencies on the azimuthal angle.

As a complement to this series of spectroscopic studies on 2-substituted ethanols (1) we have applied this theoretical method in order to learn more about the nature of the intramolecular hydrogen bond in the *gauche* conformers. The structural (2) and spectroscopic data (3, 4) available on the three alcohols 2-chloro-, 2-bromo-, and 2-cyanoethanol are adequate to determine their potential energy functions.

Method of Calculation

The **F** and **G** matrix method of Wilson (5) was followed, using a program developed by Schachtschneider (6) and transcribed in FORTRAN IV language by Brooks and Haas (7). The initial force constants were taken from the study by the latter authors of carboxylic and percarboxylic acids as well as from other similar studies on methanol (8), acetone (9), and 2,3-dibromobutane (10). Thus, 18 of the 32 force constants were left independent in the case of 2-chloroethanol. Taking into account the data for the OD deuterated molecule (3) increased that number to 26. The Cartesian coordinates for setting up the **G** matrix were taken from the microwave data for the *gauche* rotamers of 2-chloro-, and 2-bromoethanol (2). The remain-

[1]Present address: Institut Battelle, Carouge/Genève, Suisse.

Can. J. Chem. Downloaded from www.nrcresearchpress.com by 210.87.254.42 on 09/05/12
For personal use only.

Can. J. Chem. Downloaded from www.nrcresearchpress.com by 210.87.254.42 on 09/05/12
For personal use only.

TABLE 1. Symmetry coordinates for X—CH_2—CH_2—OH (X = Cl or Br)

Class A'	
$S_1 = \Delta r_1$	C—X stretching
$S_2 = (\Delta r_2 + \Delta r_3 + \Delta r'_2 + \Delta r'_3)/2$	C—H "
$S_3 = (\Delta r_2 + \Delta r_3 - \Delta r'_2 - \Delta r'_3)/2$	C—H "
$S_4 = \Delta R$	C—C "
$S_5 = \Delta r'_1$	C—O "
$S_6 = \Delta r_4$	O—H "
$S_7 = (4\Delta\alpha_{23} - \Delta\beta_2 - \Delta\beta_3 - \Delta\alpha_{13} - \Delta\alpha_{12} + 4\Delta\alpha'_{23} - \Delta\beta'_2 - \Delta\beta'_3 - \Delta\alpha'_{13} - \Delta\alpha'_{12})/\sqrt{40}$	CH_2 scissoring*
$S_8 = (4\Delta\alpha_{23} - \Delta\beta_2 - \Delta\beta_3 - \Delta\alpha_{13} - \Delta\alpha_{12} - 4\Delta\alpha'_{23} + \Delta\beta'_2 + \Delta\beta'_3 + \Delta\alpha'_{13} + \Delta\alpha'_{12})/\sqrt{40}$	CH_2 " †
$S_9 = (\Delta\beta_2 + \Delta\beta_3 - \Delta\alpha_{13} - \Delta\alpha_{12} + \Delta\beta'_2 + \Delta\beta'_3 - \Delta\alpha'_{13} - \Delta\alpha'_{12})/\sqrt{8}$	CH_2 wagging*
$S_{10} = (\Delta\beta_2 + \Delta\beta_3 - \Delta\alpha_{13} - \Delta\alpha_{12} - \Delta\beta'_2 - \Delta\beta'_3 + \Delta\alpha'_{13} + \Delta\alpha'_{12})/\sqrt{8}$	CH_2 " †
$S_{11} = (5\Delta\beta_1 - \Delta\beta_2 - \Delta\beta_3 - \Delta\alpha_{12} - \Delta\alpha_{13} - \Delta\alpha_{23})/\sqrt{30}$	CCX bending
$S_{12} = (5\Delta\beta'_1 - \Delta\beta'_2 - \Delta\beta'_3 - \Delta\alpha'_{12} - \Delta\alpha'_{13} - \Delta\alpha'_{23})/\sqrt{30}$	CCO "
$S_{13} = \Delta\phi$	COH "
$S_{14} = \Delta r_5$	H . . . X stretching
Class A"	
$S_{15} = (\Delta r_2 - \Delta r_3 + \Delta r'_2 - \Delta r'_3)/2$	C—H stretching
$S_{16} = (\Delta r_2 - \Delta r_3 - \Delta r'_2 + \Delta r'_3)/2$	C—H "
$S_{17} = (\Delta\beta_2 - \Delta\beta_3 - \Delta\alpha_{12} + \Delta\alpha_{13} + \Delta\beta'_2 - \Delta\beta'_3 - \Delta\alpha'_{12} + \Delta'_{13})/\sqrt{8}$	CH_2 twisting*
$S_{18} = (\Delta\beta_2 - \Delta\beta_3 - \Delta\alpha_{12} + \Delta\alpha_{13} - \Delta\beta'_2 + \Delta\beta'_3 + \Delta\alpha'_{12} - \Delta\alpha'_{13})/\sqrt{8}$	CH_2 " †
$S_{19} = (\Delta\beta_2 - \Delta\beta_3 + \Delta\alpha_{12} - \Delta\alpha_{13} + \Delta\beta'_2 - \Delta\beta'_3 + \Delta\alpha'_{12} - \Delta\alpha'_{13})/\sqrt{8}$	CH_2 rocking*
$S_{20} = (\Delta\beta_2 - \Delta\beta_3 + \Delta\alpha_{12} - \Delta\alpha_{13} - \Delta\beta'_2 + \Delta\beta'_3 - \Delta\alpha'_{12} + \Delta\alpha'_{13})/\sqrt{8}$	CH_2 " †
$S_{21} = \Delta t$	C—C torsion
$S_{22} = \Delta t_{OH}$	C—O "

*In-phase
†Out-of-phase.

ing undetermined parameters were given the following probable values: $r_{C-H} = 1.09$ Å, $\angle_{CCH} = 111.4°$, and $\angle_{HCH} = 108.7°$. The same parameters were used for the *trans* rotamers except, of course, for the azimuthal angle, and the O—H bond length, 0.95 Å and bond angle, 108.5°. In the case of 2-cyanoethanol the probable values (11) of 1.17 Å and 1.48 Å were chosen, respectively, for the C—CN and C ≡ N bonds.

A valence force field model was adopted in preference to a Urey–Bradley force field in view of a better transferability of force constants between related molecules. In the former model the force field is described in terms of bond stretching and deformation, plus bond–bond, bond–angle, and angle–angle interactions.

There are 23 internal coordinates in the 2-halogen substituted ethanol molecules but only 21 vibrations (26 and 24, respectively, in 2-cyanoethanol.) The two redundant coordinates were eliminated by means of the symmetry coordinates S listed in Tables 1 and 2. On the other hand an extra coordinate corresponding to the X . . . H stretching vibration was added to study the effect of the intramolecular hydrogen bond in the *gauche* isomers (Fig. 1). For 2-cyanoethanol two extra coordinates, C . . . H and N . . . H, were introduced to give still better insight into this phenomenon.

On the assumption of a C_s symmetry the *trans* molecules have 14 vibrations of class A' and 8 of class A'', (17 and 9, respectively, in cyano-

TABLE 2. Symmetry coordinates for $CN—CH_2—CH_2—OH$

Class A'	
$S_1 = \Delta r_7$	C≡N stretching
$S_2 = \Delta r_1$	C—CN "
$S_3 = (\Delta r_2 + \Delta r_3 + \Delta r'_2 + \Delta r'_3)/2$	C—H "
$S_4 = (\Delta r_2 + \Delta r_3 - \Delta r'_2 - \Delta r'_3)/2$	C—H "
$S_5 = \Delta R$	C—C "
$S_6 = \Delta r'_1$	C—O "
$S_7 = \Delta r_4$	O—H "
$S_8 = (4\Delta\alpha_{23} - \Delta\beta_2 - \Delta\beta_3 - \Delta\alpha_{13} - \Delta\alpha_{12} + 4\Delta\alpha'_{23} - \Delta\beta'_2 - \Delta\beta'_3 - \Delta\alpha'_{13} - \Delta\alpha'_{12})/\sqrt{40}$	CH_2 scissoring*
$S_9 = (4\Delta\alpha_{23} - \Delta\beta_2 - \Delta\beta_3 - \Delta\alpha_{13} - \Delta\alpha_{12} - 4\Delta\alpha'_{23} + \Delta\beta'_2 + \Delta\beta'_3 + \Delta\alpha'_{13} + \Delta\alpha'_{12})/\sqrt{40}$	CH_2 " †
$S_{10} = (\Delta\beta_2 + \Delta\beta_3 - \Delta\alpha_{13} - \Delta\alpha_{12} + \Delta\beta'_2 + \Delta\beta'_3 - \Delta\alpha'_{13} - \Delta\alpha'_{12})/\sqrt{8}$	CH_2 wagging*
$S_{11} = (\Delta\beta_2 + \Delta\beta_3 - \Delta\alpha_{13} - \Delta\alpha_{12} - \Delta\beta'_2 - \Delta\beta'_3 + \Delta\alpha'_{13} + \Delta\alpha'_{12})/\sqrt{8}$	CH_2 " †
$S_{12} = (5\Delta\beta_1 - \Delta\beta_2 - \Delta\beta_3 - \Delta\alpha_{12} - \Delta\alpha_{13} - \Delta\alpha_{23})/\sqrt{30}$	CCC bending
$S_{13} = (5\Delta\beta'_1 - \Delta\beta'_2 - \Delta\beta'_3 - \Delta\alpha'_{12} - \Delta\alpha'_{13} - \Delta\alpha'_{23})/\sqrt{30}$	CCO "
$S_{14} = \Delta\partial_1$	CCN "
$S_{15} = \Delta\phi$	COH "
$S_{16} = \Delta r_5$	H . . . C stretching
$S_{17} = \Delta r_6$	H . . . N
$S_{18} = (\Delta r_2 - \Delta r_3 + \Delta r'_2 - \Delta r'_3)/2$	C—H stretching
$S_{19} = (\Delta r_2 - \Delta r_3 - \Delta r'_2 + \Delta r'_3)/2$	C—H "
$S_{20} = (\Delta\beta_2 - \Delta\beta_3 - \Delta\alpha_{12} + \Delta\alpha_{13} + \Delta\beta'_2 - \Delta\beta'_3 - \Delta\alpha'_{12} + \Delta\alpha'_{13})/\sqrt{8}$	CH_2 twisting*
$S_{21} = (\Delta\beta_2 - \Delta\beta_3 - \Delta\alpha_{12} + \Delta\alpha_{13} - \Delta\beta'_2 + \Delta\beta'_3 + \Delta\alpha'_{12} - \Delta\alpha'_{13})/\sqrt{8}$	CH_2 "
$S_{22} = (\Delta\beta_2 - \Delta\beta_3 + \Delta\alpha_{12} - \Delta\alpha_{13} + \Delta\beta'_2 - \Delta\beta'_3 + \Delta\alpha'_{12} - \Delta\alpha'_{13})/\sqrt{8}$	CH_2 rocking*
$S_{23} = (\Delta\beta_2 - \Delta\beta_3 + \Delta\alpha_{12} - \Delta\alpha_{13} - \Delta\beta'_2 + \Delta\beta'_3 - \Delta\alpha'_{12} + \Delta\alpha'_{13})/\sqrt{8}$	CH_2 " †
$S_{24} = \Delta\partial_2$	CCN bending‡
$S_{25} = \Delta t$	C—C torsion
$S_{26} = \Delta t_{OH}$	C—O "

*In-phase.
†Out-of-phase.
‡Out-of-plane.

ethanol). The *gauche* molecules having no symmetry, all their vibrations are of class *A*.

Discussion

2-Chloro- and 2-Bromoethanol

The force constants given in Table 3 were obtained independently for the *trans* and *gauche* rotamers. The transferability between the two sets for a given compound, as well as between the chloro and bromo compounds is seen to be good in most cases. For vibrations which show little or no coupling the equations could be determined with high accuracy. However, for constants which always occur simultaneously, the dispersion was of the order of 10%.

Examination of the calculated frequencies and the p.e.d. listed in Tables 4 and 5 reveals some interesting features. (*1*) Vibrations in the middle range of the spectra are quite complex in nature. For instance, that at 1394 cm^{-1}

Can. J. Chem. Downloaded from www.nrcresearchpress.com by 210.87.254.42 on 09/05/12
For personal use only.

TABLE 3. Force constants for 2-chloro- and 2-bromoethanol*

Modes		2-Chloroethanol		2-Bromoethanol	
		Trans	*Gauche*	*Trans*	*Gauche*
Stretching C—X	F_{CX}	3.310	3.322	2.620	2.614
" C—C	F_{CC}	4.470	4.421	4.444	4.412
" C—H	F_{CH}	4.731	4.722	4.734	4.731
" C—O	F_{CO}	5.244	5.206	5.257	5.215
" O—H	F_{OH}	7.518	7.377	7.526	7.298
" H...X	$F_{H...X}$	0 f	0.135	0 f	0.146
Bending CCX	H_{CCX}	1.053	1.056	1.065	1.056
" CCO	H_{CCO}	1.016	1.000	1.027	1.000
" HCX	H_{HCX}	0.662	0.709	0.665	0.731
" HCO	H_{HCO}	0.671	0.690	0.682	0.731
" HCH	H_{HCH}	0.53 f	0.53 f	0.53 f	0.53 f
" CCH	H_{CCH}	0.577	0.612	0.563	0.615
" COH	H_{COH}	0.683	0.873	0.663	0.880
Bond–bond interaction					
C—X/C—C	$F_{CX/CC}$	0.325	0.316	0.327	0.329
C—C/C—O	$F_{CC/CO}$	0.405	0.425	0.384	0.419
C—O/O—H	$F_{CO/OH}$	0.097	0.097	0.100	0.099
Bond–angle interaction					
C—X/CCX	$F'_{CX/CCX}$	0.448	0.416	0.402	0.403
C—X/HCX	$F'_{CX/HCX}$	0.122	0.215	0.170	0.238
C—C/CCX	$F'_{CC/CCX}$	0.043	0.097	0.091	0.114
C—C/CCH	$F'_{CC/CCH}$	0.207	0.243	0.200	0.367
C—C/CCO	$F'_{CC/CCO}$	0.061	0.118	0.087	0.123
C—O/CCO	$F'_{CO/CCO}$	0.391	0.411	0.385	0.399
C—O/HCO	$F'_{CO/HCO}$	0.174	0.169	0.159	0.237
C—O/COH	$F'_{CO/COH}$	0.255	0.149	0.231	0.110
O—H/COH	$F'_{OH/COH}$	0.043	0.041	0.051	0.050
Angle–angle interaction					
XCC/CCO	$H_{XCC/CCO}$	0.187	0.125	0.214	0.182
CCO/COH	$H_{CCO/COH}$	−0.142	−0.058	−0.158	−0.100
HCC/CCH	$H_{HCC/CCH}$	−0.021	−0.010	−0.031	−0.061
CCO/HCO	$H_{CCO/HCO}$	−0.128	−0.059	−0.146	−0.045
CCX/HCX	$H_{CCX/HCX}$	−0.046	−0.051	−0.049	−0.029
Torsion					
C—O	t_{OH}	0.030	0.034	0.030	0.030
C—C	t_{CC}	0.080	0.160	0.080	0.160

*Units for bond stretching, mdyn/Å; bond bending, mdyn Å/(radian)^2; bond–bond interaction, mdyn/Å; bond–angle interaction, mdyn/radian; angle–angle interaction, mdyn Å/(radian)^2. f = fixed force constants.

in *gauche* 2-chloroethanol is made up of five components, none of which contributes more than one-third of the whole. (Minor contributions of only a few % were left out.) (*2*) The CH_2 wagging and twisting modes have been described so far as in-phase and out-of-phase. Now the p.e.d. shows this to be inexact, particularly in the *trans* rotamers. Indeed, the high-frequency components of these two modes belong mostly to the CH_2 group adjacent to the OH group, whereas those of low frequency are due to the other CH_2 group. This explains why these modes are not appreciably affected by rotational isomerism. In contrast, the rocking modes involve both CH_2 groups; accordingly their frequencies are widely separated in the two conformers. (*3*) The OH bending mode is more strongly coupled to the CH_2 wagging in the *gauche* than in the *trans* isomers as could be expected on mechanical grounds. (*4*) The tightly coupled C—C and C—O stretching vibrations are quite insensitive to the azimuthal angle.

Can. J. Chem. Downloaded from www.nrcresearchpress.com by 210.87.254.42 on 09/05/12
For personal use only.

TABLE 4. Potential energy distribution in 2-chloroethanol

Frequencies (cm^{-1})		
Obsd.*	Calcd.	Contribution of principal force constants (%)
Trans		
Class A'		
3674	3669	$F_{OH}(100)$
2927	2915	$F_{CH}(99)$
2884	2906	$F_{CH}(100)$
1436	1446	$H_{HCH}(77) + H_{CCH}(17)$
	1417	$H_{HCH}(80) + H_{CCH}(10) + H_{HCO}(4) + H_{HCX}(5)$
1394	1365	$H_{CCH}(25) + H_{HCO}(45) + H_{COH}(12)$
1293	1279	$H_{CCH}(41) + H_{HCX}(51)$
1170	1172	$H_{COH}(83) + H_{CCH}(12) + H_{HCO}(5)$
1060	1053	$F_{CO}(61) + F_{CC}(6) + H_{CCH}(15) + H_{HCO}(4)$
1045	1031	$F_{CC}(48) + F_{CO}(12) + H_{CCH}(16) + H_{HCO}(16)$
767	770	$F_{CX}(79) + H_{CCX}(7) + H_{CCO}(9)$
395†	387	$H_{CCO}(38) + F_{CX}(19) + F_{CC}(13) + H_{CCX}(7)$
258	254	$H_{CCX}(71) + H_{CCO}(30)$
Class A''		
3010	2985	$F_{CH}(99)$
2957	2979	$F_{CH}(100)$
1200	1209	$H_{CCH}(43) + H_{HCO}(54)$
	1181	$H_{CCH}(49) + H_{HCX}(48)$
850	905	$H_{CCH}(39) + H_{HCO}(28) + H_{HCX}(30)$
—	724	$H_{CCH}(58) + H_{HCO}(17) + H_{HCX}(21)$
(270)	263	$t_{OH}(99)$
115†	110	$t_{CC}(99)$
Gauche		
Class A		
3628	3630	$F_{OH}(100)$
3010	2981	$F_{CH}(99)$
2957	2977	$F_{CH}(100)$
2927	2909	$F_{CH}(99)$
2884	2904	$F_{CH}(100)$
1436	1448	$H_{HCH}(65) + H_{CCH}(27)$
	1429	$H_{HCH}(75) + H_{CCH}(11) + H_{HCO}(5) + H_{HCX}(7)$
1394	1393	$H_{CCH}(11) + H_{HCO}(32) + H_{HCX}(4) + H_{COH}(31) + H_{HCH}(14)$
1352	1349	$H_{COH}(47) + H_{CCH}(22) + H_{HCO}(10) + H_{HCX}(18)$
1293	1281	$H_{CCH}(47) + H_{HCO}(17) + H_{HCX}(28) + H_{COH}(7)$
1200	1230	$H_{CCH}(41) + H_{HCO}(44) + H_{HCX}(8) + H_{COH}(4)$
	1220	$H_{CCH}(43) + H_{HCO}(5) + H_{HCX}(46)$
1060	1058	$F_{CO}(45) + F_{CC}(27) + H_{CCH}(8) + H_{HCO}(9) + H_{HCX}(2)$
1045	1018	$F_{CC}(30) + F_{CO}(28) + H_{HCX}(16) + H_{CCH}(7) + H_{HCO}(2)$
930	904	$H_{CCH}(33) + H_{HCO}(27) + H_{HCX}(10) + F_{CC}(8) + F_{CX}(10)$
850	816	$H_{CCH}(42) + H_{HCO}(7) + H_{HCX}(24)$
672	687	$F_{CX}(81) + H_{CCH}(14) + H_{HCO}(5)$
472	464	$H_{CCO}(57) + H_{CCX}(20) + H_{CCH}(14)$
340	339	$t_{OH}(53) + F_{H\ldots X}(37)$
288	297	$H_{CCX}(50) + H_{CCO}(9) + F_{H\ldots X}(8) + t_{CC}(5)$
153	157	$t_{CC}(66) + t_{OH}(22)$

*Values in parentheses denote probable frequency.
†Observed only in condensed phases.

(5) The C—X stretching and the CCO and CCX bending vibrations are the only ones strongly affected by rotational isomerism. This is mainly a structural effect since their force constants are the same in both isomers.

2-Cyanoethanol

Here again (Table 6) the force constants are essentially the same for both isomers. They also show good agreement with the corresponding ones in the two haloethanols. To avoid con-

Can. J. Chem. Downloaded from www.nrcresearchpress.com by 210.87.254.42 on 09/05/12
For personal use only.

TABLE 5. Potential energy distribution in 2-bromoethanol

Frequencies (cm^{-1})		
Obsd.*	Calcd.	Contribution of principal force constants (%)
Trans		
Class A'		
3670	3671	$F_{OH}(100)$
2930	2917	$F_{CH}(99)$
2865	2908	$F_{CH}(100)$
1430	1440	$H_{HCH}(77) + H_{CCH}(18)$
	1409	$H_{HCH}(80) + H_{CCH}(12)$
1385	1365	$H_{CCH}(24) + H_{HCO}(46) + F_{CC}(15)$
1263	1253	$H_{CCH}(40) + H_{HCX}(55)$
1160	1162	$H_{COH}(86) + H_{CCH}(9) + H_{HCO}(3) + H_{HCX}(2)$
1049	1051	$F_{CO}(64) + F_{CC}(2) + H_{HCO}(8) + H_{CCO}(5)$
1035	1020	$F_{CC}(53) + F_{CO}(3) + H_{CCH}(16) + H_{HCO}(5)$
685	688	$F_{CX}(65) + H_{CCO}(16) + H_{CCX}(11)$
340†	337	$H_{CCO}(39) + F_{CX}(38)$
	225	$H_{CCX}(74) + H_{CCO}(26)$
Class A"		
3010	2985	$F_{CH}(99)$
2955	2978	$F_{CH}(100)$
1182	1204	$H_{CCH}(41) + H_{HCO}(57)$
	1176	$H_{CCH}(48) + H_{HCX}(48)$
840	895	$H_{CCH}(41) + H_{HCO}(27) + H_{HCX}(29)$
	714	$H_{CCH}(58) + H_{HCO}(16) + H_{HCX}(22)$
(270)	263	$t_{OH}(100)$
	105	$t_{CC}(99)$
Gauche		
Class A		
3620	3620	$F_{OH}(100)$
3010	2985	$F_{CH}(99)$
2955	2980	$F_{CH}(100)$
2930	2913	$F_{CH}(99)$
2865	2908	$F_{CH}(100)$
1430	1433	$H_{HCH}(67) + H_{CCH}(23)$
	1423	$H_{HCH}(72) + H_{CCH}(9) + H_{HCX}(9) + H_{HCO}(8)$
1385	1381	$H_{CCH}(12) + H_{HCO}(29) + H_{HCX}(11) + H_{COH}(31) + H_{HCH}(11)$
1353	1361	$H_{COH}(51) + H_{CCH}(23) + H_{HCX}(17) + H_{HCO}(9)$
1263	1266	$H_{CCH}(53) + H_{HCO}(26) + H_{HCX}(18)$
1182	1259	$H_{CCH}(37) + H_{HCO}(24) + H_{HCX}(34)$
	1160	$H_{CCH}(55) + H_{HCO}(26) + H_{HCX}(28)$
1076	1075	$F_{CO}(49) + F_{CC}(40)$
1035	1023	$F_{CC}(35) + F_{CO}(27) + H_{HCX}(15) + H_{CCO}(10)$
917	914	$H_{CCH}(37) + H_{HCO}(26) + H_{HCX}(10) + F_{CC}(13)$
840	830	$H_{CCH}(47) + H_{HCO}(11) + H_{HCX}(22)$
580	573	$F_{CX}(89) + H_{CCX}(14)$
451	440	$H_{CCO}(63) + H_{CCX}(10) + H_{CCH}(13)$
338	337	$t_{OH}(46) + F_{H\ldots X}(41)$
	262	$H_{CCX}(54)$
	163	$t_{CC}(60) + t_{OH}(26)$

*Values in parentheses denote probable frequency.
†Observed only in condensed phases.

fusion we have represented by H_{HCX} the HCC deformation in which the last carbon is that of the cyano group. Likewise, the C—CN stretching constant was denoted by F_{CCN}. As far as the coupling of vibrations is concerned (Table 7), the situation resembles that in 2-chloro or 2-bromoethanol; except for the OH bending which is less strongly coupled to the CH_2 wagging. The C—CN stretching mode exhibits little coupling in the *trans* isomer, but rather strong coupling

Can. J. Chem. Downloaded from www.nrcresearchpress.com by 210.87.254.42 on 09/05/12
For personal use only.

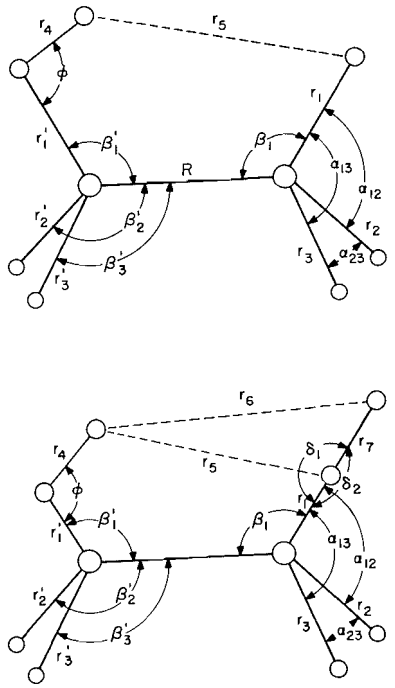

FIG. 1. Structural coordinates for the *gauche* rotamer of the 2-haloethanols (top) and 2-cyanoethanol (bottom). For clarity some of the angular coordinates are not shown.

with a CH_2 bending and the C—C stretching in the *gauche*.

It is noteworthy that the torsion modes are appreciably coupled to other modes. According to some authors (5, 8), these motions do not affect noticeably the other vibrations of the molecule. Nevertheless, we think they should be taken into account since at least the order of magnitude of the results is significant. For instance, in the case of dichloroethane (12) the CCCl bending frequency could only be adjusted after the C—C torsion had been included. To be sure the harmonic-oscillator approximation does not fit these modes too well; especially when the potential barriers are low, and the amplitudes of motion wide. However, the anharmonicity of their potential function apparently introduces no complication (13).

At the beginning we have alluded to the hazard of using force constants to decide between different assignments of bands. Nonetheless the present study provides examples where such data were useful in that connection. (*1*) The H_{CCO} constant has a remarkably constant value in a great variety of molecules. From that we could decide that the 392 and 305 cm^{-1} bands correspond to the *gauche* and *trans* bending

TABLE 6. Force constants for 2-cyanoethanol

Modes		*Trans*	Gauche
Stretching			
C≡N	F_{CN}	17.698	17.704
C—CN	F_{CCN}	5.227	5.215
C—C	F_{CC}	4.423	4.421
C—H	F_{CH}	4.706	4.712
C—O	F_{CO}	5.261	5.203
O—H	F_{OH}	7.553	7.378
H...C	$F_{H...C}$	0 f†	0.045
H...N	$F_{H...N}$	0 f‡	0.030
Bending			
CCN*	H_{CCN}	0.201	0.208
CCN†	H'_{CCN}	0.177	0.385
CCC	H_{CCC}	2.143	2.138
CCO	H_{CCO}	1.000	1.023
HCC	H_{HCX}	0.510	0.556
HCO	H_{HCO}	0.591	0.765
HCH	H_{HCH}	0.53f	0.53f
CCH	H_{CCH}	0.656	0.656
COH	H_{COH}	0.663	0.835
Torsion			
C—O	t_{OH}	0.030	0.030
C—C	t_{CC}	0.080	0.110
Bond–bond interaction			
C—CN/C≡N		0.150	0.134
C—C/C—CN		0.354	0.373
C—C/C—O		0.380	0.442
C—O/O—H		0.101	0.101
Bond–angle interaction			
C—N/CCN*		0.014	0.028
C—N/CCN†		0.0	0.053
C—C/CCN*		0.056	0.146
C—C/CCN†		0.0	0.214
C—CN/CCC		0.508	0.461
C—C/CCC		0.253	0.184
C—CN/HCX		0.047	0.225
C—C/CCH		0.236	0.287
C—O/CCO		0.429	0.408
C—O/HCO		0.116	0.203
C—O/COH		0.286	0.276
O—H/COH		0.053	0.053
C—O/CCO		0.202	0.116
Angle–angle interaction			
CCN*/CCC		0.341	0.251
CCN†/CCC		0.0	0.096
CCC/CCO		0.377	0.175
CCO/HCO		−0.012	−0.108
CCO/COH		−0.124	−0.120
HCC/CCH		−0.021	−0.021
CCC/HCX		−0.106	−0.067

*In-plane.
†Out-of-plane.
‡f = fixed constants.

Can. J. Chem. Downloaded from www.nrcresearchpress.com by 210.87.254.42 on 09/05/12
For personal use only.

Can. J. Chem. Downloaded from www.nrcresearchpress.com by 210.87.254.42 on 09/05/12
For personal use only.

TABLE 7. Potential energy distribution in 2-cyanoethanol

Frequencies (cm^{-1})		
Obsd.	Calcd.	Contribution of principal force constants (%)
Trans		
Class A'		
3678	3677	$F_{OH}(100)$
	2910	$F_{CH}(99)$
2901	2900	$F_{CH}(99)$
2262	2256	$F_{CN}(89) + F_{CCN}(11)$
	1455	$H_{HCH}(69) + H_{CCH}(30)$
1420	1433	$H_{HCH}(71) + H_{CCH}(27)$
1386	1374	$H_{CCH}(23) + H_{HCO}(35) + F_{CO}(25) + F_{CC}(10)$
1312	1311	$H_{CCH}(24) + H_{HCX}(40) + F_{CCN}(13) + F_{CC}(6)$
	1180	$H_{COH}(80) + F_{CO}(7) + F_{CC}(6)$
1076	1074	$F_{CO}(57) + F_{CC}(32)$
1030	1027	$F_{CC}(38) + F_{CO}(27) + H_{HCO}(16)$
939	927	$F_{CCN}(51) + F_{CC}(15) + F_{CO}(5) + H_{HCX}(10)$
524*	490	$H_{CCC}(36) + F_{CC}(17) + F_{CCN}(13) + H_{CCO}(7) + H_{CCN}(5)$
305	311	$H_{CCO}(78) + H_{CCN}(15)$
180*	179	$H_{CCN}(100)$
Class A"		
2976	2977	$F_{CH}(99)$
2952	2970	$F_{CH}(100)$
1210	1212	$H_{CCH}(69) + H_{HCO}(28)$
1175	1160	$H_{CCH}(59) + H_{HCO}(12) + H_{HCX}(27)$
—	880	$H_{CCH}(20) + H_{HCO}(36) + H_{HCX}(41)$
720	728	$H_{CCH}(45) + H_{HCO}(24) + H_{HCX}(28)$
280*	278	$H'_{CCN}(84) + t_{OH}(3) + t_{CC}(9)$
(270)†	262	$t_{OH}(96) + H'_{CCN}(4)$
125*	100	$t_{CC}(90) + H'_{CCN}(10)$
Gauche		
Class A		
3640	3637	$F_{OH}(100)$
2976	2980	$F_{CH}(99)$
2952	2975	$F_{CH}(99)$
—	2908	$F_{CH}(99)$
2901	2904	$F_{CH}(99)$
2262	2255	$F_{CN}(89) + F_{CCN}(11)$
—	1450	$H_{HCH}(63) + H_{CCH}(34)$
1420	1438	$H_{HCH}(75) + H_{CCH}(16)$
1386	1396	$H_{CCH}(30) + H_{HCO}(51) + H_{HCH}(12) + H_{COH}(5)$
1332	1325	$H_{COH}(74) + H_{CCH}(5) + H_{HCX}(3) + H_{HCO}(7)$
1312	1300	$H_{CCH}(50) + H_{HCO}(34) + H_{HCX}(11)$
1221	1227	$H_{CCH}(32) + H_{HCX}(37) + H_{HCO}(14)$
1190	1190	$H_{CCH}(59) + H_{HCX}(27) + H_{HCO}(4)$
1070	1086	$F_{CO}(37) + F_{CC}(28) + H_{CCH}(8) + H_{HCO}(10)$
1015	1012	$F_{CC}(34) + F_{CO}(30) + H_{HCX}(21) + H_{CCH}(5) + H_{HCO}(9)$
990	990	$F_{CCN}(34) + F_{CC}(20) + H_{CCH}(5) + H_{HCO}(8) + H_{HCX}(7)$
859	859	$H_{CCH}(26) + H_{HCX}(33) + H_{HCO}(3) + F_{CCN}(10)$
834	805	$H_{CCH}(38) + H_{HCX}(8) + H_{HCO}(16) + F_{CCN}(22)$
566	555	$H_{CCC}(58) + H_{CCO}(19) + H_{CCH}(15) + H'_{CCN}(7)$
392	389	$H_{CCO}(55) + H'_{CCN}(25)$
380	381	$H'_{CCN}(34) + H_{CCO}(24) + H_{CCC}(14)$
296	299	$t_{OH}(61) + F_{C\ldots H}(20) + F_{N\ldots H}(8)$
215*	219	$H_{CCN}(87) + F_{N\ldots H}(7)$
140*	128	$t_{CC}(65) + t_{OH}(14)$

*Observed only in condensed phases.
†Values in parentheses denote probable frequency.

Can. J. Chem. Downloaded from www.nrcresearchpress.com by 210.87.254.42 on 09/05/12
For personal use only.

modes, respectively. (2) The C—CN stretching constant is quite different from the stretching constant of the central C—C bond (14). The value of 5.2 mdyn/Å for the former leads to frequencies of 990 and 930 cm^{-1} in the *gauche* and *trans* rotamers. (3) From the close transferability of the force constants between the two rotamers a value of 490 cm^{-1} may be predicted for the CCC deformation in the *trans* 2-cyanoethanol molecule. That vibration could not be observed in the spectrum of the vapor. (4) *A priori* one might expect nearly equal force constants for the in-plane and the out-of-plane CCN deformations. This was confirmed in the *trans* conformer. The fact that the H'_{CCN} constant of the *gauche* molecule is much larger than the other three must be due to the intramolecular hydrogen bond and/or some other sort of coupling. At any rate the calculations show that for the pair of bands at 215/380 cm^{-1} in the *gauche* and at 180/280 cm^{-1} in the *trans* isomer, the low-frequency components belong to the in-plane deformations.

The Intramolecular Hydrogen Bonds

The force constants for the various displacements of the hydroxyl proton characterize the intramolecular hydrogen bond in the *gauche* conformers. Three different methods were used to derive these constants. In the first, $F_{H...X}$ was made equal to zero. Adjustment of the other constants led to excellent agreement of the calculated frequencies. The following values of the constants were obtained:

	F_{OH}	H_{COH}	t_{OH}
Chloro-	7.359	0.947	0.0488
Bromo-	7.307	0.930	0.055
Cyano-	7.378	0.835	0.03

In a second method the three constants were given their value in the *trans* isomer and the extra constants $F_{H...X}$ were adjusted. They turned out to be of the order of 0.25 mdyn/Å but the convergence was poor. For instance the OH bending frequency was too low by some 20 cm^{-1} and the OH stretching and torsion frequencies were too high by 30 and 10 cm^{-1}, respectively. Similar results have been reported for the percarboxylic acids (7). Lastly, by allowing all the constants to "float" the values considered most reliable (in Tables 3 and 6) were arrived at. As may be seen, the $F_{H...X}$ constants for the three alcohols are not only in the same order as, but also proportional to the strength of the intramolecular hydrogen bonds. (For 2-cyanoethanol it is logical to take the sum of the two constants $F_{H...C}$ and $F_{H...N}$.) This relationship even holds for the case of the percarboxylic acids (7, 15). In fact the correlation is a fairly close one; but this must be fortuitous as the other OH force constants also are involved here.

The trend in the latter is equally instructive. For instance, the decrease of F_{OH} in the *gauche* isomers follows from the weakening of that bond as revealed by microwave spectrometry (2). Such decrease, however, remains quite small compared to the corresponding increase in H_{COH} (of the order of 20 to 30%). On structural grounds this is understandable since the force acting on the proton is presumably oriented towards a lone pair orbital on the acceptor atom. The larger upward shifts of the OH bending frequencies in the *gauche* rotamers are, therefore, seen not to arise from mixing with other vibrations. Contrary to linear hydrogen bonds, the geometry plays a considerable rôle in intramolecular hydrogen bonds. As we explained before (1) the various semi-empirical correlations based on ν_{O-H} cannot be expected to hold in strongly bent hydrogen bonds. For instance, in the series of the haloethanols (16), the shifts of that frequency in the *gauche* isomers increase in the inverse order of the electronegativity of the halogen.

In the case of 2-cyanoethanol the two extra force constants $F_{H...C}$ and $F_{H...N}$ are found to be of the same magnitude. This agrees with the conclusion, based on structural considerations, that the π electrons of the C≡N bond act as proton acceptor. The relative weakness of that hydrogen bond is due largely to the non-directional character of that electron cloud. Finally it is interesting to note that the t_{CC} force constants show considerable increase from the *trans* to the *gauche*, as expected.

The authors are very grateful to Dr. W. V. F. Brooks, from the University of New Brunswick, for the gift of the FORTRAN IV program with the complete set of punched cards, as well as for much valuable advice on its use. The computations were carried out at the *Centre de Traitement de l'Information de l'Université Laval* (on an IBM 360/50 Model OS computer with a fast memory of 500 000 digits). The cooperation of the Director and the staff is gratefully acknowledged. This research was made possible thanks to an

operating grant of the National Research Council of Canada.

1. P. BUCKLEY and P. A. GIGUÈRE. Can. J. Chem. **45**, 397 (1967).
2. R. G. AZRAK and E. BRIGHT WILSON. J. Chem. Phys. **52**, 5299 (1970).
3. P. BUCKLEY, P. A. GIGUÈRE, and M. SCHNEIDER. Can. J. Chem. **47**, 901 (1969).
4. M. SCHNEIDER and P. A. GIGUÈRE. Can. J. Chem. **47**, 4685 (1969).
5. E. B. WILSON, JR., J. C. DECIUS, and P. C. CROSS. Molecular vibrations. McGraw-Hill Book Co. New York. 1955. p. 54.
6. J. H. SCHACHTSCHNEIDER. Technical Report No. 263-62, Shell Development Co.
7. W. V. F. BROOKS and C. M. HAAS. J. Phys. Chem. **71**, 650 (1967).
8. M. MARGOTTIN-MACLOU. J. Phys. Radium, **21**, 634 (1960).
9. P. COSSEE and J. H. SCHACHTSCHNEIDER. J. Chem. Phys. **44**, 97 (1966).
10. R. G. SNYDER. J. Mol. Spectrosc. **28**, 273 (1968).
11. L. E. SUTTON (*Editor.*) Chem. Soc. (London), Special Public. **11**, (1958).
12. T. MIYAZAWA and K. FUKUSHIMA. J. Mol. Spectrosc. **15**, 308 (1965).
13. T. MIYAZAWA and K. S. PITZER. J. Chem. Phys. **30**, 1076 (1959).
14. G. HERZBERG. Spectra of diatomic molecules. D. Van Nostrand Co. New York. 1955. p. 74.
15. P. A. GIGUÈRE and A. WEINGARTSHOFER-OLMOS. Can. J. Chem. **30**, 821 (1952).
16. M. KUHN, W. LÜTTKE, and R. MECKE. Z. Anal. Chem. **170**, 106 (1959).

Can. J. Chem. Downloaded from www.nrcresearchpress.com by 210.87.254.42 on 09/05/12
For personal use only.

An Electron Spin Resonance Study of High Energy Radiation Damage in Tetrapotassium Hexacyanoruthenate Trihydrate, $K_4Ru(II)(CN)_6.3H_2O$

R. S. EACHUS[1] AND F. G. HERRING

Chemistry Department, University of British Columbia, Vancouver 8, British Columbia

Received March 8, 1971[2]

Gamma-ray irradiation at 77 °K and X-ray irradiation at room temperature of single crystals of the diamagnetic tetrapotassium hexacyanoruthenate trihydrate have been shown to produce a number of interesting paramagnetic species. At room temperature the e.s.r. spectra can be interpreted in terms of the species $[Ru(CN)_5(NC)]^{5-}$. At liquid nitrogen temperature the species $[Ru(CN)_4(NC)_2]^{5-}$ is observed and the HCN^- radical is produced in an environment which does not permit it to rapidly reorientate at 77 °K. The HCN^- radical is believed to be in close association with a ruthenium(II) ion.

On a montré que l'irradiation par rayons-gamma à 77 °K et par rayons-X à la température de la pièce, de cristaux uniques de la molécule diamagnétique d'hexacyanoruthénate de tétrapotassium trihydraté produit un certain nombre d'espèces paramagnétiques intéressantes. A la température de la pièce, le spectre rpe peut être interprété en termes des espèces $[Ru(CN)_5(NC)]^{5-}$. A la température de l'azote liquide, on observe les espèces $[Ru(CN)_4(NC)_2]^{4-}$ et le radical HCN^- est produit dans un environnement qui ne lui permet pas de se réorienter rapidement à 77 °K. On croit que le radical HCN^- est associé de près avec un ion ruthénium(II).

Canadian Journal of Chemistry, **50**, 162 (1972)

Recently there has been considerable interest in the effects of high energy radiation on transition metal cyanides (1–4). There are two reports of radiation damage in $K_3Co(CN)_6$; the first (1) reports that the effect of 2 MeV electrons at liquid nitrogen temperature is to produce the stabilized complex $[Co(II)(CN)_4(NC)_2]^{4-}$. These conclusions being supported by the observation of superhyperfine interactions due to two nitrogen nuclei for the center at 77 °K and no such superhyperfine interaction for the second species. The second report (2) refers to the X-irradiation of $K_3Co(CN)_6$ at room temperature, the spin Hamiltonian parameters of the paramagnetic center produced being identical to those characterising the second radical reported by Danon *et al.* (1). Lin *et al.* (2) interpret the spin Hamiltonian parameters of this second center in terms of a d^7 octahedral system with a weak tetragonal elongation. In such situations the odd electron will occupy the d_{z^2} orbital of the Co(II) atom.

Subsequently Root and Symons (3) reported radiation damage studies on $K_4Fe(CN)_6$ doped in Group IA halides, the paramagnetic center produced in this case being the mon-isocyanide $[Fe(CN)_5NC]^{5-}$. Danon and co-workers (4) have suggested that the formation of Fe(I) and Co(II) isocyanides on irradiation of alkali metal halides doped with the corresponding transition metal cyanides is due to the influence of cation vacancies produced in the lattice by the substitution of the cyanide complex. In all of the cases referred to above the spin Hamiltonian parameters correspond to a ground state in which the odd electron is accommodated in the d_{z^2} orbital. The stabilization of the d_{z^2} orbital relative to the $d_{x^2-y^2}$ orbital is brought about by the fact that the nitrogen end of the CN^- ligand leads to a lower ligand-field strength (5) than the carbon end. The possibility of a CN^- flip had already been suggested by Shriver *et al.* (5).

We wish to report an e.s.r. study of X- and γ-ray irradiated $K_4Ru(II)(CN)_6 3H_2O$ both at liquid nitrogen temperature and room temperature.

Experimental

Single crystals of $K_4Ru(CN)_6.3H_2O$ were grown by slow evaporation of aqueous solutions containing approximately 4% KOH as described by Tsang and O'Reilly (6). Suitable crystals were irradiated with either 65 kV X-rays at 300 °K or ^{60}Co γ-rays at 77 °K. The e.s.r. spectra were observed both at room temperature and at liquid nitrogen temperature.

The room temperature crystal structure of $K_4Ru(CN)_6$-$3H_2O$ is monoclinic with a pseudotetragonal unit cell containing four molecules (7). The crystals grew as flat platelets with the $\langle 010 \rangle (b-)$ axis perpendicular to the plate. Rotations were performed about the crystallographic *a*, *b*-, and *c*-axes for our e.s.r. studies.

[1]Present address: Research Laboratories, Eastman Kodak Company, Rochester, New York 14650.

[2]Revision received September 22, 1971.

Can. J. Chem. Downloaded from www.nrcresearchpress.com by 210.87.254.5 on 09/05/12
For personal use only.

TABLE 1. The spin Hamiltonian parameters of the centers produced in $K_4Ru(CN)_6.3H_2O$ by γ-irradiation at 77 °K and X-irradiation at room temperature

Assigned species	Temperature		Hyperfine tensors w.r.t. a	b	c*	g-Tensor w.r.t. a	b	c
$[Ru(CN)_5(HCN)]^{4-}$	77 °K	^{14}N	5.3±1.0	22.0±2.0	17.0±2.0	2.0132	1.991	2.0128±0.0005
		^{1}H	$a_{iso} = 117 \pm 3$					
$[Ru(CN)_4(NC)_2]^{5-}$	77 °K	^{14}N	$a_{iso} = 3.0$			2.0855	1.9982	2.0855±0.0005
$[Ru(CN)_5(NC)]^{5-}$	298 °K	^{99}Ru	5.0	38.4	5.0	2.0884	1.9984	2.0884±0.0005
		^{101}Ru	5.0	35.1	5.0			
		^{14}N	$a_{iso} = 4.5$					

*The units are gauss and *a*, *b*, *c* refer to the crystal axes.

Results

At room temperature the e.s.r. spectrum consisted of a single intense line which was accompanied by six weaker symmetrically disposed features; a typical spectrum is shown in Fig. 1. These satellite lines can be attributed to the naturally occurring isotopes of ruthenium (^{100}Ru, I = 0, 70.21%; ^{99}Ru, I = 5/2, 12.81%, $\mu_N = -0.63$ N.M.; ^{101}Ru, I = 5/2, 16.98%, $\mu_N = -0.69$ N.M.). The line width of the resonances precluded the resolution of the individual ^{99}Ru and ^{101}Ru isotope lines and two of the six lines are obscured by the resonance due to ^{100}Ru. The line to the left, in Fig. 1, is due to an unknown species. The experimental data was interpreted using the spin Hamiltonian

$$\mathcal{H} = \boldsymbol{H}\cdot\mathbf{g}\cdot\boldsymbol{S} + \boldsymbol{S}\cdot\mathbf{A}\cdot\boldsymbol{I}$$

Both the hyperfine and **g**-tensors of this centre were found to be axial within experimental error and the unique components of these tensors proved to be parallel to the *b*-axis of the crystal. The results are given in Table. 1.

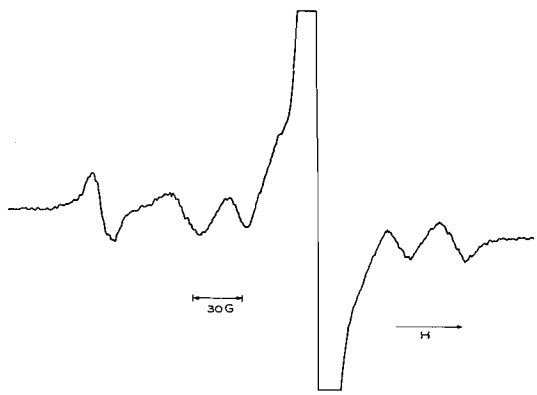

FIG. 1. The electron spin resonance spectrum at room temperature of X-irradiated $K_4Ru(CN)_6.3H_2O$. The magnetic field is parallel to the *b*-axis.

On cooling a sample of the $K_3Ru(CN)_6.3H_2O$, which had been X-irradiated at room temperature, and observing the e.s.r. spectrum it was found that the intense line due to the ^{100}Ru isotope exhibited nitrogen superhyperfine structure corresponding to one nitrogen atom. The splitting was found to be a maximum (5.1 ± 0.25 G) along the *a*-axis of the crystal and less than 4.0 G along the *b*- and *c*-directions (this last value being estimated from the line width).

The results described above suggest that the center produced at room temperature is either of the electron excess centers $[Ru(CN)_5NC]^{5-}$ or $[Ru(CN)_4NC]^{4-}$. The assignment of the presence of an isocyanide linkage at room temperature assumes that no intramolecular rearrangement occurred on cooling the crystal to liquid nitrogen temperature.

The results of γ-irradiation at liquid nitrogen temperatures are substantially more complex than those at room temperature. Three radicals are formed, two of which have been identified. The radical which was not identified had a completely isotropic spectrum consisting of three lines of approximate heights 1:4:1 with approximate line widths 2:1:2. The splitting between the lines is 21.2 ± 0.1 G and the *g*-value of the radical is 2.002 ± 0.001. This radical could be tentatively assigned as the H_2O^- radical rapidly reorientating in the crystal lattice. The extra electron would be accommodated in the antibonding b_1 orbital of H_2O; this orbital contains a contribution from the hydrogen 1s orbitals and a splitting of 20 G is not unreasonable. The H_2O^- radical could be formed in a number of ways, for example, H atoms, produced by the radiation damage of water could

Can. J. Chem. Downloaded from www.nrcresearchpress.com by 210.87.254.5 on 09/05/12
For personal use only.

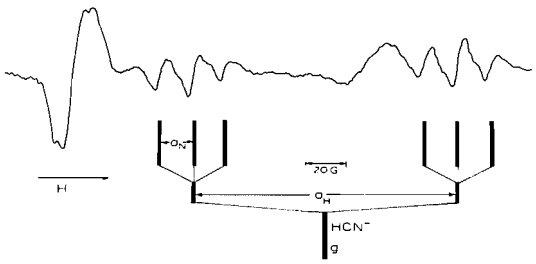

FIG. 2. The electron spin resonance spectrum at 77 °K of γ-irradiated $K_4Ru(CN)_6.3H_2O$. The magnetic field is parallel to the *c*-axis.

react with OH^- impurities in the lattice. Fortunately this radical could be annealed out on warming very slightly without significant reduction in the intensity of the other two centers produced, Fig. 2 shows a spectrum of a crystal treated in such a way.

The stronger resonance at low field, see Fig. 2, proved to be $[Ru(I)(CN)_4(NC)_2]^{5-}$. This identification is based upon the observed *g*-values of $g_{||} = 1.9982 \pm 0.0005$ and $g_{\perp} = 2.0855 \pm 0.0005$, where $g_{||}$ is parallel to the *b*-axis of the crystal and hyperfine splitting due to two nitrogen atoms. The *g*-values of this center are identical to those of the major species observed at room temperature; unfortunately the ^{99}Ru and ^{101}Ru splitting could not be observed.

The second feature shown in Fig. 2 is a doublet of triplets, the hyperfine parameters are given in Table 1. We attribute this center as being due to a HCN^- radical associated with a $Ru(II)(CN)_5^{3-}$ complex in which most of the spin density is on the HCN^-. The hyperfine coupling parameters for this species are also given in Table 1. There are two previous reports of the HCN^- radical, the first is by Root *et al.* (8) who observed it in alkali halide matrices at 77 °K. Under their experimental conditions the radical is rapidly rotating. On cooling to 4.2 °K, however, Adrian *et al.* (9) succeeded in obtaining the oriented HCN^- radical and measured the anisotropy of the spin Hamiltonian parameters. The differences between the parameters measured in this work and the work of Adrian *et al.* together with the fact that the HCN^- radical is not rotating at 77 °K in $K_4Ru(CN)_6.3H_2O$ may be satisfactorily interpreted by postulating that the HCN^- is associated with the Ru atom; this is discussed later. In addition to these three major centers very weak signals were observed for two species with **g**-tensors identical to that of $[Ru(I)(CN)_4(NC)_2]^{5-}$ except that in one case *g* is along a direction 65° from the *a*-axis and in the other along a direction 65° from the *c*-axis. The two signals are therefore expected to be due to a small concentration of $[Ru(I)(CN)_4(NC)_2]^{5-}$ formed in the *ac* plane. The direction of the unique axes for these species corresponded very closely to the RuCN directions in the *ac* plane.

When a crystal which has been γ-irradiated at 77 °K is annealed to room temperature only a ruthenium(I) species is left. The e.s.r. data show that this center is the same as that produced by X-irradiation at room temperature.

Discussion

At liquid nitrogen temperatures the irradiation of iron group transition metal cyanides produces an electron excess center at the transition metal ion. If the original complex is octahedral then the additional electron must be accommodated in the degenerate e_g level and consequently the e.s.r. spectrum of such a system would be difficult to observe. The results of Danon and co-workers (1, 4) and Root and Symons (3) show that a distortion occurs which causes the e_g level to split; this distortion takes the form of a rearrangement to form isocyanide linkages as is evidenced by the observation of nitrogen superhyperfine structure. In the pure cobalt(III) cyanide this center is unstable to warming and decays to a pentacoordinate species (1 4); however, when the cyanide is doped in the alkali halide the isocyanide center is stable indefinitely. The stability being ascribed to the interaction of the complex with cation vacancies. The results of the present study show that at liquid nitrogen temperatures the $[Ru(CN)_4(NC)_2]^{5-}$ center is the species formed. The hyperfine splitting for two equivalent nitrogens is about 3.0 G, with a small anisotropy, indicating that the majority of the spin density resides on the Ru atom. On warming to room temperature this radical decays to the $[Ru(CN)_5(NC)]^{5-}$ or $[Ru(CN)_4(NC)]^{4-}$, observed at room temperature after X-irradiation. On the basis of our results it is not possible to decide unequivocally between 5 or 6 ligands but the reversal of one isocyanide linkage may be rationalized on the basis of the crystal structure of $K_4Ru(CN)_6.3H_2O$.

The results of the structure determination by Kiriyama *et al.* (7) show that there are double

Can. J. Chem. Downloaded from www.nrcresearchpress.com by 210.87.254.5 on 09/05/12
For personal use only.

Can. J. Chem. Downloaded from www.nrcresearchpress.com by 210.87.254.5 on 09/05/12
For personal use only.

layers of cyanide octahedra with water molecules in between. The work of Tsang and O'Reilly (6) suggests that only one cyanide ligand from each octahedron in the double layer can hydrogen bond with this water molecule along the *b*-axis of the crystal. We would like to propose that when the $Ru(CN)_6^{4-}$ traps a thermalized electron the resultant $Ru(CN)_6^{5-}$ stabilizes itself by destroying the hydrogen bonding and forms two isocyanide linkages along the *b*-axis; this is supported by the fact that the unique axis of the **g**-tensor is along the *b*-axis. On warming we believe the isocyanide ligand which arose from that cyanide which participated in hydrogen bonding in the undamaged crystal returns to a normal form of linkage and is stabilized by the hydrogen bonding. The remaining isocyanide ligand remains to cause sufficient distortion to the octrahedron to afford a splitting of the e_g level. The existence of only one isocyanide ligand is confirmed by our e.s.r. results. The observation that the **g**-tensors of $[Ru(I)(CN)_4(NC)_2]^{5-}$ seen at 77 °K and the species observed at room temperature, which exhibits superhyperfine features due to one nitrogen only, are the same, leads us to believe that the room temperature center is the six coordinate moiety $[Ru(I)(CN)_5(NC)]^{5-}$. There is however a slight inconsistency in this analysis in as much as the maximum nitrogen hyperfine splitting for the postulated species $[Ru(I)(CN)_5(NC)]^{5-}$ is along the *a*-axis and not along the *b*-axis as may be expected if the nitrogen $2p_\sigma$ orbital (along the *b*-axis) contains the bulk of the density located on the nitrogen. This discrepancy is not readily explained but may indicate that the "flipped" CN^- ligand does not rotate fully through 180°.

The HCN^- radical, as mentioned before, has been observed in KCl at 4.2 °K (9). The anisotropy of the nitrogen hyperfine splitting constant arises from spin density in the nitrogen 2p orbital in the HCN plane and perpendicular to the CN bond. The total tensor has the form (A,0,0) (9) so that the Fermi-contact term is positive and just cancels the anisotropy perpendicular to the axis of the 2p orbital. In the present case, however, we have suggested that the HCN^- radical is associated with a Ru(II) ion in the form of a $[Ru(II)(CN)_5(HCN)]^{4-}$ complex, consequently, we may expect the nitrogen hyperfine tensor to be quite different.

The form of the nitrogen hyperfine tensor can shed some light on both the structure and the orientation of this radical. Within experimental error the diagonal nitrogen hyperfine coupling tensor elements are $|a_{bb}| = 22$, $|a_{aa}| = 5.0$, and $|a_{cc}| = 17.0$ G, where the subscripts refer to the crystal axes. The HCN^- ligand will most likely be bent so that the $[Ru(CN)_5(HCN)]^{4-}$ species will have very little symmetry and the odd electron orbital could in practice contain all the atomic orbitals on nitrogen. However, it is very likely that a reflexion plane could be preserved so that the 2p orbital perpendicular to the plane of the HCN^- radical can be ignored. Unlike the HCN^- radical observed in KCl (and HCO as discussed by Adrian *et al.* (10)) the fact that the largest hyperfine component is along the *b*-axis suggests that the 2p orbital in this direction dominates the odd electron orbital and the in-plane 2p orbital perpendicular to the CN bond contributes to a smaller degree. Les us denote the molecular orbital coefficient of these atomic orbitals by C_σ and C_δ, respectively, then we may write

$$a_1 = a_{iso} + (2C_\sigma^2 - C_\delta^2)B$$

$$a_2 = a_{iso} + (-C_\sigma^2 + 2C_\delta^2)B$$

$$a_3 = a_{iso} + (-C_\sigma^2 - C_\delta^2)B$$

where $B = g_e g_N \beta_e \beta_N \langle r^{-3} \rangle_{2p}$ and a_{iso} is the isotropic part of the coupling tensor and if the odd electron is in a σ orbital, as we believe, then it will likely be positive. Thus if $C_\sigma > C\delta$ then $a_1 > 0$, $a_1 > a_2$, and a_3 will be small and possibly negative. Since two of the hyperfine components are almost equal (a_{bb} and a_{cc}) we assign these to be a_1 and a_2, *i.e.* the plane of the HCN^- radical is in the *bc* plane. The third component $a_{aa} = a_3$ will almost certainly be negative. This assignment ($a_{bb} = +22$, $a_{cc} = +17$, and $a_{aa} = -5$ G) leads to a Fermi contact term of +11 G. These values of the anisotropy indicate that the odd electron spends about 50% of its time in the nitrogen 2p orbitals. The large isotropic coupling observed for the hydrogen nucleus is in accord with the above description of the HCN^- center and corresponds to about a 20% occupancy of the hydrogen 1s orbital. The slightly reduced **g**-tensor no doubt reflects the spin–orbit interaction from the ruthenium atom which has a large spin–orbit coupling constant.

It is of some interest to compare the bonding parameters in $[Ru(CN)_5(NC)]^{5-}$ and those in $[Fe(CN)_5(NC)]^-$ which may be inferred from the data given by Danon *et al.* (4).

Can. J. Chem. Downloaded from www.nrcresearchpress.com by 210.87.254.5 on 09/05/12
For personal use only.

The formation of the isocyanide linkage brings the nitrogen end of CN^- toward the metal atom; this, because the nitrogen end has a weaker ligand field splitting than the carbon end, causes the d_{z^2} orbital to be stabilized relative to the $d_{x^2-y^2}$ orbital. The ground state for this C_{4v} symmetry can be represented by $|E^4B_2^2A_1|$ and the corresponding g-values are (2) $g_{||} = 2.00$; $g_\perp = 2.0 - 6\lambda K_\perp/\Delta E$; where ΔE is the energy difference between the $|E^3B_2^2A_1^2|$ excited state and the ground state, λ is the spin orbit coupling parameter which has a value of approximately $-1000\ cm^{-1}$ (11) and $k_\perp$ is an orbital reduction parameter. The observed g-values are in accord with this assignment of the ground state. The form of the hyperfine tensor will be determined, to a large extent, by the spin density in the d_{z^2} which constitutes part of the A_1 orbital. If the coefficient of the d_{z^2} orbital is α then we have

$$a_{||} = -k + \tfrac{4}{7}\alpha^2 P - \tfrac{1}{7}\Delta g_\perp P$$

$$a_\perp = -k - \tfrac{2}{7}\alpha^2 P + \tfrac{15}{14}\Delta g_\perp P$$

where $P = g_e g_N \beta_e \beta_N \langle r^{-3} \rangle_{4d}$ and has a value of about $-42 \times 10^{-4}\ cm^{-1}$. This value was obtained by extrapolation of the values for Ru^{2+} and Ru^{3+} given by Abragam and Bleaney (11). Since P is negative it is almost certain that $a_{||} < 0$ and $a_\perp < 0$.

The expression for the hyperfine tensor can be used to deduce k and α^2 for a given choice of sign for $a_{||}$ and $a_\perp$. If the relative sign $a_{||} < 0$ and $a_\perp > 0$ are chosen a value of $\alpha^2 > 1$ is obtained which is not consistent with the usual chemical ideas of a high degree of covalency in a cyanide complex. The combination $a_{||} = -38.4$ and $a_\perp = 5.0$ for ^{101}Ru gives $k = +0.00126\ cm^{-1}$ and $\alpha^2 = 0.91$. The value of α^2 is somewhat higher than the values computed by Danon *et al.* (4), reflecting a slightly more ionic σ-bonding for Ru(I) relative to Co(II). Similarly the reduced nitrogen superhyperfine in $[Ru(CN)_5(NC)]^{5-}$ relative to that for $[Fe(CN)_5(NC)]^{5-}$ reinforces the above notion. Second row transition metals are generally thought to exist in more ionic bonding situations in their complexes relative to first row transition elements.

The value of k can now be used to compute the quantity χ (12), i.e. the spin density, defined by

$$\chi = \frac{4\pi}{S}\left\langle \psi \left| \sum_i \delta(r_i) S_{zi} \right| \psi \right\rangle = \frac{-3}{2} \frac{hca_0^3}{g_e g_N \beta_e \beta_N} k\,(\text{a.u.})$$

the value is $+2.15$. The nuclear magnetic moment of the ruthenium isotopes is negative so that if k is positive $\chi > 0$, and a positive value of χ indicates a direct s orbital contribution to the Ru molecular orbital in which the odd electron resides, which is in accord with the assignment of a $^2A_1$ ground state. Core polarization of the inner s orbitals will create negative spin density which will tend to reduce the overall value of χ.

The magnitude of $\Delta g_\perp$ suggests that there is a fairly substantial orbital reduction in the xz and yz orbitals of ruthenium; a reasonable estimate for ΔE ($20\,000\ cm^{-1}$) gave $k_\perp \simeq 0.4$. This low value is presumably due to substantial ligand–metal π back bonding which is needed to stabilize the low oxidation state.

The authors wish to thank Professor C. A. McDowell for his interest in this work and the National Research Council of Canada for financial support.

1. J. Danon, R. P. A. Muniz, A. D. Caride, and I. Wolfsen. J. Mol. Struct. **1**, 127 (1968).
2. W. C. Lin, C. A. McDowell, and D. J. Ward. J. Chem. Phys. **49**, 2883 (1968).
3. K. D. J. Root and M. C. R. Symons. J. Chem. Soc. (A) 2366 (1968).
4. A. O. Caride, S. I. Zanette, and J. Danon. J. Chem. Phys. **52**, 4911 (1970).
5. D. F. Shriver, S. A. Shriver, and S. E. Anderson. Inorg. Chem. **4**, 725 (1965).
6. T. Tsang and D. E. O'Reilly. J. Chem. Phys. **43**, 4234 (1965).
7. R. Kiriyama, H. Kiriyama, T. Wada, N. Niizeki, and H. Hirabayarhi. J. Phys. Soc. Jap. **19**, 540 (1964).
8. K. D. J. Root, M. C. R. Symons, and B. C. Weatherley. Mol. Phys. **11**, 161 (1966).
9. F. J. Adrian, E. L. Cochran, V. A. Bowers, and B. C. Weatherley. Phys. Rev. **177**, 129 (1969).
10. F. J. Adrian, E. L. Cochran, and V. A. Bowers. J. Chem. Phys. **44**, 4626 (1966).
11. A. Abragam and B. Bleaney. Electron paramagnetic resonance of transition ions. Clarendon Press. 1970. p. 474.
12. B. R. McGarvey. J. Phys. Chem. **71**, 51 (1967).

An Examination of the Heat Capacity of Activation for the Hydrolysis of *t*-Butyl Chloride in Water

J. M. W. SCOTT[1] AND R. E. ROBERTSON

Department of Chemistry, The University of Calgary, Calgary 44, Alberta

Received June 22, 1970[2]

The influence of ion-pair intermediates on solvolytic displacement reactions is considered for cases where the observed rate constant is complex.

Such complex and composite rate constants under certain conditions may show deviations from the Arrhenius temperature dependence law. The deviations will manifest themselves as "spurious" positive and/or negative heat capacities of activation, superimposed on the real heat capacity terms.

The hypothesis of Albery and Robinson (1) which proposes that the heat capacity of activation for *t*-butyl chloride is entirely "spurious" in the sense outlined above, is critically evaluated and rejected. An alternative hypothesis that considers the heat capacity to be a manifestation of solvation effects is retained.

The mechanism of the hydrolysis of both the methyl and *t*-butyl halides in water is discussed and the kinetic laws appropriate to each are shown to be consistent with real heat capacities of activation. The mechanism proposed differs from the classical S_N1–S_N2 description. Both series of substrates are considered to give rise to intimate-ion-pairs but in the case of the methyl halides these react further by a path which involves the nucleophilicity of the solvent in a kinetically significant way. In the cases of the tertiary compounds, solvent separation of ion-pairs becomes kinetically significant. The nucleophilic component which characterizes the destruction of the solvent-separated ion-pairs for the tertiary compounds is kinetically insignificant.

On étudie l'influence des paires d'ions intermédiaires sur les réactions de déplacement solvolytique dans le cas où la constante de vitesse observée est complexe.

Des constantes de vitesses complexes ou composées peuvent, sous certaines conditions, montrer des déviations à la loi d'Arrhénius sur la dépendance de la température. Les déviations se manifestent comme des "pseudo" capacités de chaleur d'activation, positives et/ou négatives qui se superposent aux termes réels de capacité calorifique.

L'hypothèse de Albery et Robinson (1) qui propose que la capacité calorifique d'activation pour le chlorure de tertio-butyl est entièrement "pseudo", dans le sens exprimé plus haut, est examinée et rejetée. Une hypothèse différente, qui considère la capacité de chaleur comme étant une manifestation des effets de solvatation est plutôt émise.

On discute du mécanisme d'hydrolyse des halogénures de méthyle et de tertio-butyle dans l'eau et on montre que les lois de cinétique appropriées à chacun sont consistantes avec les capacités calorifiques d'activation réelles. Le mécanisme proposé diffère de la description classique S_N1–S_N2. On considère que les deux séries de substrats donnent lieu à des paires d'ions liés, mais dans le cas des halogénures de méthyle, ceux-ci réagissent plus loin par un mécanisme impliquant la nucléophilicité du solvant et ceci de façon cinétiquement importante. Le composé nucléophile caractérisant la destruction des paires d'ions séparées du solvant pour les composés tertiaires est cinétiquement négligeable.

Canadian Journal of Chemistry, **50**, 167 (1972)

Recently Albery and Robinson (1) have chosen to interpret the large negative temperature dependence of the enthalpy of activation ($\Delta H^{\ddagger}$) characteristic of the hydrolysis of *t*-butyl chloride in water in a manner which casts serious doubts on that hypothesis based on solvent-structure reorganization which has been found useful (2). Instead of using the classical kinetic formulation for the S_N1 reaction proposed by Hughes and Ingold (3)

$$[1] \qquad RX \underset{k_2}{\overset{k_1}{\rightleftharpoons}} R^+ + X^- \xrightarrow{k_3} \text{Products}$$

which involves the substrate RX and the kinetically free ions R^+ and X^- together with k_1 rate determining, Robinson and Albery examine the temperature dependence of an S_N1-like reaction where the intermediate is possibly an ion-pair

[1]Honorary Visiting Professor on leave from the Chemistry Department, Memorial University of Newfoundland, St. John's, Newfoundland. Author to whom correspondence should be addressed (at Memorial University of Newfoundland).

[2]Revision received August 18, 1971.

Can. J. Chem. Downloaded from www.nrcresearchpress.com by 210.87.254.105 on 09/05/12
For personal use only.

rather than the kinetically free ions

$$[2] \qquad RX \underset{k_{-1}}{\overset{k_1}{\rightleftharpoons}} R^+ + X^- \xrightarrow{k_2} \text{Product or further intermediates}^3$$

with the condition that $k_{-1} \simeq k_2$.

Reaction 2 is similar to Sneen's truncated version of the detailed mechanism proposed by Winstein and co-workers (4) where the truncated

$$[3] \qquad \begin{array}{ccccccc} RX & \underset{k_2}{\overset{k_1}{\rightleftharpoons}} & R^+X^- & \underset{k_4}{\overset{k_3}{\rightleftharpoons}} & R^+\|X^- & \underset{k_6}{\overset{k_5}{\rightleftharpoons}} & R^+ + X^- \\ \downarrow k_{1n} & & \downarrow k_{2n} & & \downarrow k_{3n} & & \downarrow k_{4n} \\ P & & P & & P & & P \end{array}$$

version confines attention to k_1, k_2, and k_{2n} and the remaining rate constants in reaction 3 contribute nothing to the observed rate. The species R^+X^- and $R^+\|X^-$ are respectively intimate and solvent-separated ion-pairs. The solvent separated ion pair is required to accommodate, among other things, some of the stereochemical consequences of substitution. For instance, according to Sneen (5) the intimate-ion-pair leads exclusively to inversion in nucleophilic (aqueous) media, even for reactive (S_N1 tending) substrates.

Although the kinetic complexity of these reactions has been recognized, k_1 in reactions 1, 2, and 3 has invariably been assumed to be rate determining (however, see ref. 6). The ubiquity of this assumption does not guarantee its validity and the gist of the proposals put forward by Albery and Robinson (1) is to question this sort of assumption particularly with respect to their own scheme.[4] If their proposals are accepted and applied to reaction 3*a* (footnote 4) the observed rate (k^0) for a process proceeding by this reaction will be given by

$$[4] \qquad k^0 = k_1k_{2n}/(k_2 + k_{2n}) = k_1/(1 + \alpha)$$

where

$$k_2/k_{2n} = \alpha$$

The relative values of α will clearly have a strong effect on k^0. If α is small then $k^0 = k_1$ and subsequent steps are not kinetically significant. If the rate of return (k_2) is much greater than the k_{2n} step, then $k^0 = k_1k_{2n}/k_2 = K_{el}k_{2n}$, *i.e.*, that rate becomes dependent on an equilibrium constant K_{el} and the rate constant k_{2n} which leads to product formation. There is also the situation where k_2 and k_{2n} are comparable. In their scheme (reaction 2) Albery and Robinson place the hydrolysis of *t*-butyl chloride in a similar category; more specifically they consider k_{-1} and k_2 to be comparable. Granted certain premises, which seem unlikely (see below), they then go on to show that if k_{-1} and k_2 are comparable in their scheme, the temperature dependence of $\Delta H^{\ddagger}$ will logically result from an apparent or "spurious" heat capacity of activation which is unrelated to solvent reorganization.

The recognition of the importance of ion-pair intermediates in solvolytic displacements is not new (see refs. 4–6). Neither is the rationalization of non-Arrhenius behavior of rate constants in terms of a non-unitary process (7). The studies of Winstein and co-workers (4, 6), Goering and co-workers (8–10), and the more recent studies of Shiner (11) and of Sneen (5, 12, 13) provide ample evidence for the existence of ion-pair intermediates. However, whether the observed heat capacity for the hydrolysis of *t*-butyl chloride is a manifestation of the existence of ion-pair intermediates and thereby spurious or real as a consequence of solvent reorganization, or alternatively a combination of both these possibilities, is not easily established. The existence of a spurious heat capacity depends on the ratio k_2/k_{2n} (or on k_{-1}/k_2 for reaction 2 and k_2/k_3 for reaction 1). A feature common to all these mechanisms is the difficulty of establishing the magnitude of the appropriate ratios. Ritchie (6) in a detailed discussion of the Winstein mechanism (reaction 3) concludes that k_2 is the fastest rate of the ten rate constants which define the mechanism. This conclusion can reasonably be extrapolated to the Sneen truncated version

[3] Albery and Robinson do not specify the nature of the k_2 reaction in their scheme which is algebraically equivalent to reaction 1 and Sneen's truncated version of reaction 3 (see below).

[4] We draw attention to the fact that reactions 1, 2 and Sneen's truncated version of reaction 3 are all algebraically equivalent. The last, which is

$$[3a] \qquad RX \underset{k_2}{\overset{k_1}{\rightleftharpoons}} R^+X^- \xrightarrow{k_{2n}} \text{Product}$$

will be used subsequently to establish the consequences of this kind of rate law on the thermodynamic parameters which characterize such a process.

Can. J. Chem. Downloaded from www.nrcresearchpress.com by 210.87.254.105 on 09/05/12
For personal use only.

Can. J. Chem. Downloaded from www.nrcresearchpress.com by 210.87.254.105 on 09/05/12
For personal use only.

of reaction 3. However, the question of how k_2 might alter with the structure of RX remains open.

In their discussion Albery and Robinson maintain k_{-1}/k_2 is unity for *t*-butyl chloride reacting in water at $T = 33.4$ °C. To arrive at this value from their experimental data they assume that there are no real heat capacity terms associated with the activation of *t*-butyl chloride in water. Sneen and Larsen find values of α (see eq. 4) which are close to unity but their interpretation of their own data is open to criticism (14).

Alternative interpretations of non-Arrhenius behavior which assume the apparent heat capacities to be real and to be a manifestation of solvation phenomena have been reviewed by Kohnstam (15) and by Robertson (2). A more general review of non-Arrhenius behavior has been presented by Hullett (16).

While we are inclined to accept the hypothesis that all substitutions at the saturated carbon atom involve ion-pair intermediates (and this includes those examples which have been described traditionally as reacting by an S_N2 mechanism),[5] we are less inclined to accept the kinetic analysis provided by Sneen and Larsen (13), or alternatively the temperature dependence of *t*-butyl chloride hydrolysis presented by Albery and Robinson (1). Neither of the interpretations offered by the above authors is unique.

Granted their assumptions, the treatment of the temperature dependence of the hydrolysis of *t*-butyl chloride in water proposed by Albery and Robinson is correct in principle. However, there is good reason to believe that $\Delta C^{\ddagger}_{p0}$ (*i.e.* non-Arrhenius behavior) is a manifestation of solvent reorganization with little or no contribution from kinetic complexity.

Aside from this study by Albery and Robinson, the consequences of the Winstein or Winstein-like mechanisms with respect to temperature dependence for solvolytic displacements has been neglected. In view of the current interest, an analysis of temperature effects on this mechanism is highly desirable.

[5]Such a hypothesis provides a natural explanation for the similarity of the kinetic solvent isotope effect for the hydrolysis of primary and tertiary halides. The absence of any significant primary isotope effect associated with the solvolysis of the primary halides is regarded as particularly significant in this connection (17).

Some Thermodynamic Consequences of the Winstein Mechanism

In deriving pseudo-thermodynamic parameters it is normally assumed that the reaction involves a single energy barrier and that the temperature dependence of the rate provides a means for investigating the energetics of the reaction. However, if the Winstein mechanism is accepted for solvolytic displacement reactions, the identification of the observed rate constant with a single energy barrier is likely to be an oversimplification. While the steady state treatment of the complete Winstein mechanism is possible the resulting expression will be unwieldy, and provide little insight to the problem. Fortunately, the kinetic behavior of certain systems of interest permits a simplified treatment.

(a) S_N1-like Processes

These are cases where $k_{1n} \rightarrow k_{4n} \gg k_1, k_3, k_5$ giving rise to the following rate laws

$$[5] \qquad k^0 = k_1$$

where k_1 is rate determining

$$[6] \qquad k^0 = k_1k_3/k_2 = K_{e1}k_3$$

where k_3 is rate determining and finally where k_5 is rate determining[6]

$$[7] \qquad k^0 = k_1k_3k_5/k_2k_4 = K_{e1}K_{e2}k_5$$

Each of these rate laws is consistent with the S_N1 mechanism within the framework of the Hughes–Ingold scheme. In each of the reactions represented by the kinetic eqs. 5→7, one molecule is altering its bonding via heterolytic fission to give a more ionic species. The difference between these mechanisms and the classical S_N1 scheme is the recognition that complete heterolysis, *i.e.* the formation of kinetically free ions, does not necessarily occur in a single step.

(b) S_N2-like Processes

For these examples, $k_{2n} \rightarrow k_{4n}$ are kinetically significant. In cases where the rate of nucleophilic attack becomes either rate determining or

[6]There will also be transitional situations where k_2 is comparable to k_3 and where k_4 is comparable to k_5. The form of the rate laws in these regions can be established by an appropriate steady state treatment which we ignore here for the sake of economy. The behavior of the thermodynamic parameters in these regions can be inferred from considerations elaborated below.

Can. J. Chem. Downloaded from www.nrcresearchpress.com by 210.87.254.105 on 09/05/12
For personal use only.

comparable with the return rates (k_2, k_4, k_6) or further heterolytic rates (k_3, k_5), the observed rates will contain both nucleophilic and heterolytic components and correspond to what has usually been described as "borderline" kinetic situations (18). The designation S_N2-like is justified in the sense that nucleophilic components form part of the observed rate constant. But if, following Sneen (13), k_{1n} is deemed kinetically insignificant (see also ref. 14) then the resemblance of the remaining kinetic possibilities to the classical S_N2 description is superficial. A more complete kinetic analysis will require due consideration be given to the nine remaining rate constants in reaction 3.

When both the nucleophilic components (k_n) and the heterolytic components contribute to the observed rate a much wider selection of rate laws is possible and some examples of these, particularly with respect to the temperature dependence problem, can be examined via the truncated scheme

[8] $$RX \underset{k_2}{\overset{k_1}{\rightleftharpoons}} R^+X^- \underset{k_4}{\overset{k_3}{\rightleftharpoons}} R^+\|X^-$$
$$\downarrow k_{2n} \qquad \downarrow k_{3n}$$
$$P \qquad P$$

We retain the assumption originally made by Sneen and Larsen (13) that k_{1n} is kinetically insignificant in all cases, *i.e.* direct attack on the unactivated initial state of RX is unlikely.

The Sneen mechanism is evidently a truncated version of reaction 8 which confines attention to k_1, k_2, and k_{2n}. For this particular simplification we may define three kinetic regions:[7] Region I ($\alpha < 0.01$), Region II ($0.01 < \alpha < 100$), and Region III ($\alpha > 100$), with rate laws $k^0 = k_1$ (Region I), $k^0 = k_1k_{2n}/(k_2 + k_{2n})$ (Region II), and $k^0 = k_1k_{2n}/k_2 = K_{1e}k_{2n}$ (Region III). The corresponding pseudo-thermodynamic parameters for Regions I and III are:

	Region I	*Region III*
[9]	$\Delta G^{\ddagger}_0 = \Delta G^{\ddagger}_1 = \Delta G^{\ddagger}_1 - \Delta G^{\ddagger}_2 + \Delta G^{\ddagger}_{2n} =$	$\Delta G^{\ddagger}_{1e} + \Delta G^{\ddagger}_{2n}$
[10]	$\Delta S^{\ddagger}_0 = \Delta S^{\ddagger}_1 = \Delta S^{\ddagger}_1 - \Delta S^{\ddagger}_2 + \Delta S^{\ddagger}_{2n} =$	$\Delta S^{\ddagger}_{1e} + \Delta S^{\ddagger}_{2n}$
[11]	$\Delta H^{\ddagger}_0 = \Delta H^{\ddagger}_1 = \Delta H^{\ddagger}_1 - \Delta H^{\ddagger}_2 + \Delta H^{\ddagger}_{2n} =$	$\Delta H^{\ddagger}_{1e} + \Delta H^{\ddagger}_{2n}$
[12]	$\Delta C^{\ddagger}_{p0} = \Delta C^{\ddagger}_{p1} = \Delta C^{\ddagger}_{p1} - \Delta C^{\ddagger}_{p2} + \Delta C^{\ddagger}_{p2n} =$	$\Delta C^{\ddagger}_{p1e} + \Delta C^{\ddagger}_{p2n}$

In Region II the expressions are more complex:

[13] $$\Delta G^{\ddagger}_0 = \Delta G^{\ddagger}_1 + RT \ln (1 + \alpha)$$

[14] $$\Delta S^{\ddagger}_0 = \Delta S^{\ddagger}_1 + \frac{\alpha}{1+\alpha}\frac{(\Delta H^{\ddagger}_{2n} - \Delta H^{\ddagger}_2)}{T} - R \ln (1 + \alpha)$$

or $$= \Delta S^{\ddagger}_1 + \frac{\alpha}{1+\alpha}(\Delta S^{\ddagger}_{2n} - \Delta S^{\ddagger}_2) + \frac{\alpha}{1+\alpha} R \ln \alpha - R \ln (1 + \alpha)$$

[15] $$\Delta H^{\ddagger}_0 = \Delta H^{\ddagger}_1 + \frac{\alpha}{1+\alpha}(\Delta H^{\ddagger}_{2n} - \Delta H^{\ddagger}_2)$$

[16] $$\Delta C^{\ddagger}_{p0} = \Delta C^{\ddagger}_{p1} + \frac{\alpha}{1+\alpha}(\Delta C^{\ddagger}_{p2n} - \Delta C^{\ddagger}_{p2}) - \frac{\alpha}{(1+\alpha)^2}\frac{(\Delta H^{\ddagger}_{2n} - \Delta H^{\ddagger}_2)^2}{RT^2}$$

Equations 9–16 show that solvolytic displacements proceeding via the Sneen or Albery mechanism will give rise to values of $\Delta H^{\ddagger}_0$, $\Delta S^{\ddagger}_0$, and $\Delta C^{\ddagger}_{p0}$ which are complex functions of the thermodynamic quantities which characterize the individual steps k_1, k_2, and k_{2n}, (or k_1, k_{-1}, and k_2 for reaction 2). Particular attention is directed to eq. 16 which contains three real heat capacity terms $\Delta C^{\ddagger}_{p1}$, $\Delta C^{\ddagger}_{p2}$, and $\Delta C^{\ddagger}_{p2n}$ and a third "spurious" term which must always be negative irrespective of the sign of $\Delta H^{\ddagger}_{2n} - \Delta H^{\ddagger}_2$ since the "spurious" term depends on the square of this quantity. The other

[7] Operationally Sneen and Larsen define these regions more narrowly: Region I, $\alpha < 0.10$; Region II, $0.10 < \alpha < 10$; and Region III, $\alpha > 10$.

Can. J. Chem. Downloaded from www.nrcresearchpress.com by 210.87.254.105 on 09/05/12
For personal use only.

quantities in the "spurious" term R, T, and α are all necessarily positive.

The pith of the Albery-Robinson treatment is to assume that in similar equations related to reaction 2, real heat capacity terms are zero. Alternatively, and more specifically, they assume, without any real justification, that quantities such as $\Delta H^{\ddagger}_1$, $\Delta H^{\ddagger}_2$, and $\Delta H^{\ddagger}_{2n}$, or those related to their own scheme, are all true constants and that the experimentally observed heat capacity derives entirely from the existence of the ion-pair, *i.e.*, the "spurious" heat capacity is the only sizeable term in eq. 16. We shall evaluate this assumption more critically below. In the meantime a further examination of the mechanism (eq. 8) with respect to the temperature dependence of solvolytic displacements is of interest.

Consider a system reacting according to eq. 8 where the ratio k_4/k_{3n} is small and k_2/k_{2n} large. The appropriate steady state expression with these constants is

$$[17]\quad k^0 = K_e\{k_{2n} + k_3\} = K_e k_3\{1 + k_{2n}/k_3\} = K_e k_3\{1 + \beta\}$$

where $\beta = k_{2n}/k_3$

This constitutes a "mixed kinetics" situation with a nucleophilic component k_{2n} and a further heterolytic component k_3: both contributing to the observed rate. Such a kinetic scheme will also have a profound effect on the temperature dependence which differs from the situation represented by reaction 2. A brief analysis of an analogous situation has been presented by Kohnstam (15) within the framework of a mixed classical S_N1/S_N2 case, *i.e.*, he considers $k^0 = k_1 + k_{1n}$ using the Arrhenius rather than the absolute rate theory formalism.[8]

Equation 17 also gives rise to three kinetic regions which depend on the magnitude of β. These regions are Region I*a* ($\beta < 0.01$), Region II*a* ($0.01 < \beta < 100$) and Region III*a* ($\beta > 100$).

Region III*a* corresponds to Region III in the treatment given above and Region I*a* corresponds to an S_N1 type reaction given in eq. 6. The expressions for the thermodynamic parameters have already been given for Region III and those for Region I*a* are straightforward and require no elaborate discussion. It will suffice to note that in both these regions, the heat capacity of activation will contain no "spurious" terms. On the other hand, in Region II*a* the thermodynamic parameters are given by

$$[18]\quad \Delta G^{\ddagger}_0 = \Delta G^{\ddagger}_e + \Delta G^{\ddagger}_3 - RT\ln(1+\beta)$$

$$[19]\quad \Delta S^{\ddagger}_0 = \Delta S^{\ddagger}_e + \Delta S^{\ddagger}_3 + \frac{\beta}{1+\beta}\frac{(\Delta H^{\ddagger}_3 - \Delta H^{\ddagger}_{2n})}{T} + R\ln(1+\beta)$$

$$[20]\quad \Delta H^{\ddagger}_0 = \Delta H^{\ddagger}_e + \frac{1}{1+\beta}\Delta H^{\ddagger}_3 + \frac{\beta}{1+\beta}\Delta H^{\ddagger}_{2n}$$

$$[21]\quad \Delta C^{\ddagger}_{p0} = \Delta C^{\ddagger}_{pe} + \frac{1}{1+\beta}\Delta C^{\ddagger}_{p3} + \frac{\beta}{1+\beta}\Delta C^{\ddagger}_{p2n} + \frac{\beta}{(1+\beta)^2}\frac{(\Delta H^{\ddagger}_{2n} - \Delta H^{\ddagger}_3)^2}{RT^2}$$

We specifically draw attention to the "spurious" heat capacity term in eq. 21 (the final expression on the r.h.s.) which, contrasting with eq. 16, must always be positive. The kinetic schemes represented by eq. 17 and eq. 14 are the simplest forms of the "bifurcated" and "intermediate" mechanisms. It follows that a complete steady state treatment of the Winstein mechanism would by inference and analogy contain both positive and negative "spurious" heat capacity terms as well as the real terms associated with the individual steps. In such a case the apparent heat capacity of activation becomes a dull tool for mechanistic diagnosis. In practice it is sharpened by noting that for every solvolytic displacement reaction in water and mixed aqueous solvents examined with sufficient care (2, 15), the apparent $\Delta C^{\ddagger}_{p0}$'s have negative values. This would suggest that the negative components (real or "spurious") dominate the situation in every case.

In a recent paper, one of us firmly placed the mechanism for substitution at the primary carbon atom in water in Region III. This

[8] k_1 here refers to reaction 1, not reaction 2.

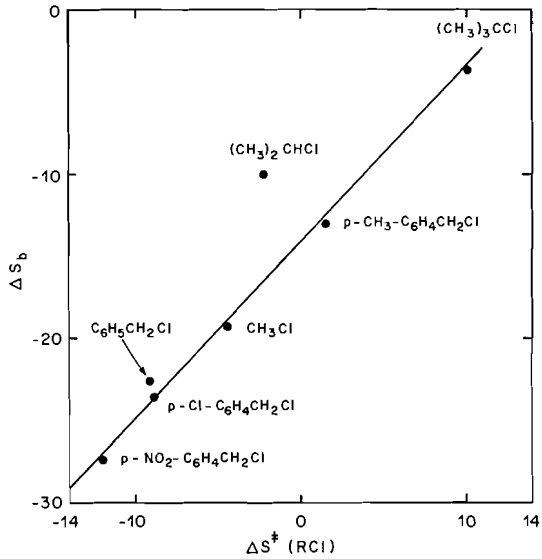

FIG. 1. A correlation between the entropy of activation for a series of alkyl and arylmethyl chlorides and the entropy of ionization of a series of structurally related amines.

hypothesis requires that the observed heat capacities of activation for the hydrolysis of the methyl halides in water are real. We therefore see no reason for abandoning the previous interpretation of $\Delta C^{\ddagger}_{p0}$ for the methyl halides (2) except to recognize that these quantities now derive from an equilibrium constant together with a term from a rate-determining nucleophilic component (eq. 12, Region III). The division of the overall heat capacity ($\Delta C^{\ddagger}_{p0}$) for the methyl halides into $\Delta C^{\ddagger}_{p1e}$ and $\Delta C^{\ddagger}_{p2n}$ is an important problem to which we can offer no solution at the present time. However, the problem represented by $\Delta C^{\ddagger}_{p0}$ for the hydrolysis of *t*-butyl chloride merits examination in terms of eqs. 9 and 21.

The Heat Capacity of Activation for the Hydrolysis of *t*-Butyl Chloride and the Mechanism for the Hydrolysis of Tertiary Halides in Water

Irrespective of the mechanistic region postulated for the hydrolysis of *t*-butyl chloride and similar substrates, we feel safe in assuming that these substances are required to pass from a weakly polar initial state, characterized by a solvation shell in which water–water interactions dominate, to a transition state in which these interactions are broken down. The likely consequences of such a change with respect to the heat capacity of activation are most clearly seen if it is recalled that the heat capacities for the ionogenic processes

[22] $R_1R_2R_3N + H_2O \rightarrow R_1R_2R_3NH^+ + OH^-$

where $R_1 = R_2 = H$, $R_3 = Me$; $R_1 = R_2 = Me$, $R_3 = H$; and $R_1 = R_2 = R_3 = Me$ are, respectively, -60, -68, and -90 cal deg^{-1} mol^{-1} (19, 20). The heat capacity terms for these equilibria are necessarily real and free of kinetic ambiguity and provide a useful model for solvolytic displacements. As models, they are also in keeping with that approach of analyzing the thermodynamics of ionic transition states using thermodynamically stable ions as analogues. The linear correlation between the Grunwald–Winstein *Y* parameter for methanol–water mixtures and the free-energy of solvation of potassium and chloride ions in the same solvent mixtures represents an early instance of this tactic (21). More recently, Arnett and coworkers (22, 23) have used the parallelism between changes in the heat content of the transition state for *t*-butyl chloride in ethanol–water mixtures with changes in the heat content of potassium and chloride ions in the same solvent mixtures as evidence for the ionic character of the transition state. The appropriate differentiation with respect to temperature of these relationships implies a corresponding relationship between the heat capacities of activation and the thermodynamic heat capacities.

The relationship between the entropy of activation and the entropy of ionization for structurally related amines, first noted by Evans and Hamman (24), also demands a corresponding relationship between the heat capacity of ionization of the amines and the corresponding solvolytic quantities. A good correlation for a series of chlorides is given in Fig. 1 (see also Table 1), although it may be of limited significance because of the variable nature of the rate determining step along the reaction series (see below). However, in spite of possible variations in the nature of the rate determining step, entropy changes ($\delta_R \Delta S^{\ddagger}$) will still be influenced by solvation changes between the initial and the transition states because all displacement processes have considerable ionogenic character[9] irrespec-

[9]Intimate-ion-pairs are considered to be common to all the displacements included in the entropy correlation.

Can. J. Chem. Downloaded from www.nrcresearchpress.com by 210.87.254.105 on 09/05/12
For personal use only.

TABLE 1. Entropy data for the ionization of aliphatic and aromatic amines and entropy data appropriate to the hydrolysis of structurally related alkyl and arylmethyl chlorides; $T = 25$ °C

Amine	$-\Delta S_b$	Reference	RX	$\Delta S^{\ddagger}$	Reference
$(CH_3)_3N$	3.63	19	*t*-BuCl	10.14	2
NH_3	19.06	20	CH_3Cl	−4.31	2
$PhNH_2$	22.60	20	$PhCH_2Cl$	−9.09	2
$(CH_3)_2NH$	10.00	20	$(CH_3)_2CHCl$	−2.10	2
p-CH_3—$C_6H_4NH_2$	13.02	25	*p*-CH_3—$C_6H_4CH_2Cl$	1.50	27
p-Cl—$C_6H_4NH_2$	23.51	26	*p*-Cl—$C_6H_4CH_2Cl$	−8.91	27
p-NO_2—$C_6H_4NH_2$	27.29	26	*p*-NO_2—$C_6H_4CH_2Cl$	−12.00	27

tive of whether the nucleophilic component is kinetically significant. Hence the correlation between the thermodynamic amine entropies and the pseudo-thermodynamic entropies ($\Delta S^{\ddagger}$) demands a similar relationship between the heat capacities for the ionization and the corresponding kinetic quantities. The various correlations mentioned above provide scant justification for the cavalier dismissal of the real heat capacity terms in eq. 16.

The above qualitative considerations with respect to the entropy, free energy, and enthalpy correlations and their implications with respect to the reality of $\Delta C^{\ddagger}_{p0}$ are supported by a closer scrutiny of the quantitative methods employed by Albery and Robinson to extract the temperature dependence of $\Delta C^{\ddagger}_{p0}$ demanded by their model (see also ref. 28).

To establish the ion-pair mechanism quantitatively these authors add a further linear term in T to the empirical equation used extensively to represent the temperature dependence of solvolytic rates (2), *i.e.*

$$[23] \qquad \log k = \frac{A}{T} + B \log T + C$$

becomes

$$[24] \qquad \log k = \frac{A}{T} + B \log T + C + DT$$

The latter equation leads to a heat capacity of activation which is a linear function of temperature or alternatively to a quadratic temperature dependence of $\Delta H^{\ddagger}$. If the heat capacity of activation is calculated by the equation

$$[25] \quad \Delta C^{\ddagger}_{p0} = \frac{\alpha}{(1+\alpha)^2} \frac{(\Delta H^{\ddagger}_{2n} - \Delta H^{\ddagger}_{2})^2}{RT^2}$$

with $\alpha = 1$ ($T = 33.4$ °C) and $\Delta H^{\ddagger}_{2n} - \Delta H^{\ddagger}_{2} = \pm 8943$ cal (see ref. 1), the resulting temperature dependence of $\Delta C^{\ddagger}_{p0}$ is a bell-shaped curve (Fig. 2) and is only *very* approximately linear over the temperature interval (0→35 °C) used to establish the temperature dependence of $\Delta H^{\ddagger}$ by an innovative differential method. Thus, whilst the temperature dependence of $\Delta C^{\ddagger}_{p0}$ established by Albery and Robinson is not inconsistent with their mechanism, it does not establish definitely the spurious spike in $\Delta C^{\ddagger}_{p0}$ required by eq. 25 (see Fig. 2) since the range of temperature investigated was *much too small.*

In searching for an alternative to the mechanistic description proposed by Albery and Robinson for the hydrolysis of *t*-butyl chloride in water, we recognize that the order of reactivity (k^0) for the hydrolysis of the *t*-butyl halides is F < Cl < Br < I (see Table 2) while the order

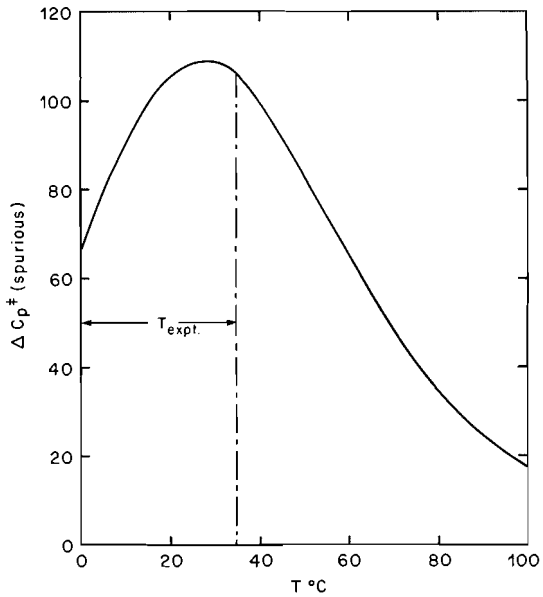

FIG. 2. The variation of the "spurious" heat capacity term (eq. 25) with temperature.

Can. J. Chem. Downloaded from www.nrcresearchpress.com by 210.87.254.105 on 09/05/12
For personal use only.

TABLE 2. Rate constants and related data for the hydrolysis of t-BuX, $T = 25$ °C

X	$-\log k^0$ (t-BuX)*	$\Delta G^{\ddagger}$	Reference	ΔG_{e1} (MeX)§
F	6.25†	8.53	29	18.97
Cl	1.536; 1.527	2.09	2, 30	12.02
Br	0.119; 0.126‡	0.17	30, 31	9.81
I	−0.186	−0.25	30	9.11

*Mean values used for calculating $\Delta G^{\ddagger}$; the latter quantities are reported without the constant $RT \ln (kT/h)$ term.
†Calculated from $\Delta H^{\ddagger} = 22.61$ kcal/mol and $\Delta S^{\ddagger} = -11.26$ e.u. (29).
‡Calculated via the Grunwald–Winstein relationship.
§Reference 14.

for the methyl, allyl, and isopropyl halides is F < Cl < I < Br. In a previous paper (14) one of us postulated that the anomalous order found in the latter series was dependent on the nucleophilic component of the activation process, *i.e.* a consequence of the fact that log K_{e1} and log k_{2n} show differing dependencies on the nature of the leaving group and add so that the bromide reaction rate (k^0) is the fastest. The observation that $\Delta G^{\ddagger}_0$ for the hydrolysis of t-butyl X (X = F, Cl, Br, I) gives an excellent correlation with ΔG_e(MeX) (see Fig. 3 and Table 2) supports the long standing assumption that the mechanism for the hydrolysis of tertiary halides differs from that for primary halides. We retain Ritchie's proposal that k_2 is the fastest step in reaction 3, hence the intimate-ion-pair remains an important intermediate in both mechanisms. Whereas the rate controlling step for the primaries and secondaries involves k_{2n}, the corresponding step for the tertiaries involves displacement of the X^- to give a solvent separated ion-pair which shows no important tendency to return to the intimate-ion-pair stage. Further, the destruction of the solvent-separated-ion-pair, whether by front-side or back-side attack, is kinetically insignificant.

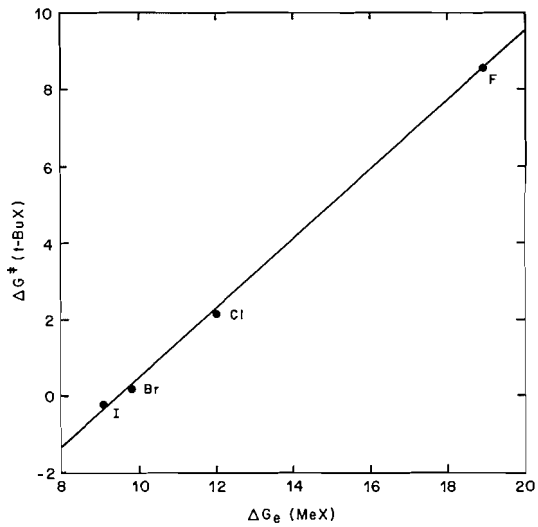

FIG. 3. A correlation between $\Delta G^{\ddagger}$ for the hydrolysis of the t-butyl halides and the free energies calculated from the ion-pair equilibrium constants for the methyl halides.

We believe that the correlation (Fig. 3) establishes three other points. Firstly, the heat capacity of activation characteristic of the hydrolysis of t-butyl chloride in water must be real if the observed rate is given by $k^0 = K_{e1}k_3$ since the latter expression cannot give rise to "spurious" terms. Hence we retain the hypothesis based on solvent reorganization for the hydrolysis of t-butyl chloride in water, and we reject the alternative interpretation proposed by Albery and Robinson. Secondly, the log K_{e1} (MeX) values appropriate to the correlation shown in Fig. 3 were calculated on the assumption of the generality of the selectivities of OH^- and H_2O acting as nucleophiles on free carbonium ions. The consistency which emerges from acceptance of this hypothesis in our view vindicates our earlier description of the mechanism for the hydrolysis of the methyl halides. Thirdly, and finally, it would seem that the anomalous order of the rate of hydrolysis of the bromide with respect to the iodide (32, 33) for displacement reactions in water is typical of processes where the nucleophilic component of the displacement rate is partly or wholly rate determining. This places the isopropyl and allyl halides securely in such a category. Thus, in water, the bromide/iodide ratios become useful tools for mechanistic diagnosis.

Can. J. Chem. Downloaded from www.nrcresearchpress.com by 210.87.254.105 on 09/05/12
For personal use only.

The authors wish to express their gratitude for financial support from the National Research Council of Canada. One of us (J.M.W.S.) thanks the University of Calgary for its hospitality during the academic year 1969–1970. The latter author also wishes to thank Memorial University for its generosity in granting a sabbatical leave of absence during the same period.

1. W. J. ALBERY and B. H. ROBINSON. Trans. Faraday Soc. **65**, 980 (1969).
2. R. E. ROBERTSON. Advances in physical organic chemistry. Vol. 4. *Edited by* A. J. Streitwieser, Jr. and R. W. Taft. Interscience John Wiley, London and N.Y. 1967. p. 213 and references therein.
3. C. K. INGOLD. Structure and mechanism in organic chemistry. Cornell University Press, Ithaca, N.Y. 1953. Chap. 7.
4. S. WINSTEIN, P. P. KLINEDIST, Jr., and C. G. ROBINSON. J. Am. Chem. Soc. **83**, 885 (1961) and references therein.
5. R. A. SNEEN and H. WEINER. J. Am. Chem. Soc. **87**, 287 (1965).
6. C. D. RITCHIE. Solute–solvent interactions. *Edited by* C. D. Ritchie and J. F. Coetzee. Marcel Dekker, N.Y. and London. 1969. Section 4. p. 272 and references therein.
7. C. HINSHELLWOOD. Kinetics of homogeneous gas reactions. Oxford University Press. 1929. p. 42.
8. H. L. GOERING and J. F. LEVY. J. Am. Chem. Soc. **84**, 3853 (1962).
9. H. L. GOERING and R. W. THEIS. J. Am. Chem. Soc. **90**, 2967 (1962).
10. H. L. GOERING, J. T. DOI, and K. D. MCMICHAEL. J. Am. Chem. Soc. **86**, 1951 (1964).
11. V. J. SHINER, JR. and W. DOWD. J. Am. Chem. Soc. **91**, 6528 (1969).
12. R. A. SNEEN and J. W. LARSEN. J. Am. Chem. Soc. **91**, 362 (1969).
13. R. A. SNEEN and J. W. LARSEN. J. Am. Chem. Soc. **91**, 6031 (1969).
14. J. M. W. SCOTT. Can. J. Chem. **48**, 3807 (1970).
15. G. KOHNSTAM. Advances in physical organic chemistry. Vol. 5. *Edited by* V. Gold. Academic Press, London and N.Y. 1967. p. 121.
16. J. R. HULETT. Quart. Rev. Chem. Soc. London, **18**, 227 (1964).
17. R. E. ROBERTSON and P. M. LAUGHTON. *In* Solute–solvent interactions. *Edited by* C. D. Ritchie and J. Coetzee. Marcel Dekker, N.Y. and London. 1969. Section 7, p. 424.
18. S. WINSTEIN, E. GRUNWALD, and H. W. JONES. J. Am. Chem. Soc. **73**, 2700 (1951).
19. D. NORTHCUTT and R. E. ROBERTSON. J. Phys. Chem. **73**, 1559 (1969).
20. J. W. LARSON and L. G. HEPLER. *In* Solute–solvent interactions. *Edited by* C. D. Ritchie and J. Coetzee. Marcel Dekker, N.Y. and London, 1969, Section 1, p. 1.
21. R. F. HUDSON and B. SAVILLE. J. Chem. Soc. 4114 (1956).
22. F. FRANKS, E. M. ARNETT, W. G. BENTRUDE, J. J. BURKE, and P. MCC. DUGGLEBY. J. Am. Chem. Soc. **85**, 1350 (1965).
23. E. M. ARNETT, W. G. BENTRUDE, J. J. BURKE, and P. MCC. DUGGLEBY. J. Am. Chem. Soc. **87**, 1541 (1965).
24. A. G. EVANS and S. D. HAMMAN. Trans. Faraday Soc. **47**, 25 (1951).
25. K. LAIDLER, T. W. ZADWIDSKI, H. M. PAPÉE and W. J. CANADY. Trans. Faraday Soc. **55**, 1734 (1959).
26. P. D. BOLTON and F. M. HALL. J. Chem. Soc. (B) 259 (1969).
27. R. E. ROBERTSON and W. STRACHAN. Unpublished data.
28. G. KOHNSTAM and co-workers. Private communication.
29. R. E. ROBERTSON, R. L. HEPPOLETTE, and J. M. W. SCOTT. Can. J. Chem. **37**, 803 (1959).
30. E. A. MOELWYN-HUGHES. J. Chem. Soc. 4301 (1962).
31. E. GRUNWALD and S. WINSTEIN. J. Am. Chem. Soc. **70**, 846 (1948).
32. R. E. ROBERTSON and J. M. W. SCOTT. J. Chem. Soc. 1596 (1961).
33. R. E. ROBERTSON and R. L. HEPPOLETTE. Proc. Roy. Soc. London, **A252**, 273 (1959).

Can. J. Chem. Downloaded from www.nrcresearchpress.com by 210.87.254.105 on 09/05/12
For personal use only.

Spin–Orbit Relaxation of $Hg(6^3P_1)$ by Various Gases

A. C. VIKIS, G. TORRIE, AND D. J. LE ROY

Lash Miller Chemical Laboratories, University of Toronto, Toronto 181, Ontario

Received August 16, 1971

The spin–orbit relaxation of $Hg(6^3P_1)$ to yield $Hg(6^3P_0)$ was investigated in the presence of various gases. The quantum yields of $Hg(6^3P_0)$ formation (defined as relaxation to $Hg(6^3P_0)$/total relaxation) in the presence of CO, CO_2, NH_3, ND_3, H_2O, D_2O, C_2H_6, *c*-C_3H_6, $C(CH_3)_4$, C_3H_8, 2,2-$C_3H_6D_2$, C_3D_8, *n*-C_4H_{10} and *i*-C_4H_{10} were: 0.88 ± 0.07, <0.01, 1.05 ± 0.05, 1.00 ± 0.08, 0.76 ± 0.18, 1.06 ± 0.26, 0.64 ± 0.16, 0.56 ± 0.10, 0.58 ± 0.02, 0.14 ± 0.01, 0.51 ± 0.07, 0.47 ± 0.10, 0.11 ± 0.01, and 0.05 ± 0.01, respectively. The extent of the spin–orbit relaxation process appears to be related in an inverse manner to the availability and accessibility of channels leading to the formation of $Hg(6^1S_0)$, rather than to the fulfillment of electronic–vibrational resonance conditions. This in turn suggests the existence of $Hg(6^3P_1)$—quencher intermediates having lifetimes long enough to permit several vibrations.

La relaxation spin–orbitale de $Hg(6^3P_1)$ pour donner $Hg(6^3P_0)$ a été étudiée en présence de nombreux gaz. Les rendements quantiques de la formation de $Hg(6^3P_0)$ (définis par relaxation de $Hg(6^3P_0)$ sur relaxation totale) en présence de CO, CO_2, NH_3, ND_3, H_2O, D_2O, C_2H_6, *c*-C_3H_6, $C(CH_3)_4$, C_3H_8, 2,2-$C_3H_6D_2$, C_3D_8, *n*-C_4H_{10} et *i*-C_4H_{10} sont: 0.88 ± 0.07, <0.01, 1.05 ± 0.05, 1.00 ± 0.08, 0.76 ± 0.18, 1.06 ± 0.26, 0.64 ± 0.16, 0.56 ± 0.10, 0.58 ± 0.02, 0.14 ± 0.01, 0.51 ± 0.07, 0.47 ± 0.10, 0.11 ± 0.01 et 0.05 ± 0.01. Le domaine du procédé de relaxation spin orbitale apparaît comme étant en sens inverse de la disponibilité et de l'accessibilité des canaux menant à la formation de $Hg(6^1S_0)$ plutôt que du remplissage des conditions de résonance électronique-vibrationnelle. Ceci suggère l'existence d'intermédiaires de piégeage $Hg(6^3P_1)$ qui ont des temps de vie assez longs pour permettre plusieurs vibrations.

Canadian Journal of Chemistry, **50**, 176 (1972)

Can. J. Chem. Downloaded from www.nrcresearchpress.com by 210.87.254.42 on 09/05/12
For personal use only.

In a recent communication from this laboratory (1) we have presented preliminary data on the spin–orbit relaxation of $Hg(6^3P_1)$ atoms to yield $Hg(6^3P_0)$ in the presence of various gases. Because of the importance of these measurements in the elucidation of the energy transfer process in mercury photosensitization (2–9) and the controversial nature of the problem (10–14), we have investigated the spin–orbit relaxation process in greater detail and extended our measurements to more molecules.

Particular attention was focused on molecules such as CO, CO_2, H_2O, D_2O, NH_3 and ND_3, that have been previously considered (2–4, 10, 15) from the point of view of the resonance theory of spin–orbit relaxation,

[1] $Hg(6^3P_1) + Q(v = 0) \rightarrow Hg(6^3P_0) + Q(v = 1) + \Delta E$

The relative increase of the total $Hg(6^3P_1)$ quenching cross section with the relative decrease of the energy discrepancy, ΔE, of the electronic and the vibrational transition, were cited as basis for the resonance theory. However, there were only few direct measurements such as rate constants for the occurrence of reaction 1. The result of Scheer and Fine (10) for CO has recently been questioned (14, 12*b*).

Also, of particular interest were the alkanes which have been thoroughly studied in the past and were shown to exhibit a number of interesting trends (8, 9), as far as their reactions with $Hg(6^3P_1)$ are concerned. Qualitative studies of $Hg(6^3P_0)$ formation in these systems were reported by Penzes *et al.* (16) using 4047 Å light absorption to monitor $Hg(6^3P_0)$ steady state populations. They had concluded that deuteration of the alkanes enhanced the rate of $Hg(6^3P_0)$ formation and that the discrepancies between $Hg(6^3P_1)$ physical and chemical quenching cross sections were due to $Hg(6^3P_0)$ formation. Yang (6*b*) arrived at a similar conclusion based on conservation of total electronic angular momentum, symmetry considerations and the phase space theory of chemical reactions. The effect of $Hg(6^3P_0)$ quenching by the molecules that form it was not taken into consideration, however. The result of this effect would be to show a greater rate of $Hg(6^3P_0)$ formation in the deuterated alkanes in comparison with the undeuterated alkanes. Also, it would tend to

Can. J. Chem. Downloaded from www.nrcresearchpress.com by 210.87.254.42 on 09/05/12
For personal use only.

make physical and chemical quenching cross sections similar.

Experimental

The method of studying $Hg(6^3P_0)$ formation and decay in the presence of various molecules has been outlined in previous publications (1, 14, 17). It is based on the enhancement of the mercury photosensitized decomposition of C_2H_4 under incomplete quenching of $Hg(6^3P_1)$. The enhancement effect is due to the formation of $Hg(6^3P_0)$ atoms and their long lifetime.

A diagram of the apparatus used is shown in Fig. 1. The experiments were carried out in a flow system employing argon as the carrier gas at a flow rate of 27 cc/min and a total pressure of 20 Torr. Small partial pressures (10^{-3} to 2 Torr) of the reagent gases were introduced to the main flow through calibrated capillaries, except for H_2O and D_2O for which the carrier gas was saturated at various pressures by passage through a saturator containing H_2O and D_2O and maintained at the desired temperature with a cooled ethyl alcohol bath. The carrier gas was saturated with mercury at the desired temperature (−5 to +0.5 °C) by passage through a presaturator containing a pool of mercury maintained at 25 °C, followed by a multistage desaturator maintained at the desired saturation temperature to within ±0.2 °C. The $Hg(6^3P_1)$ lifetimes with respect to emission, τ^*, for the reaction cell used, were 1.54×10^{-7} s and 2.06×10^{-7} s, for the mercury saturation temperatures of -5.0 ± 0.2 °C and $+0.5 \pm 0.2$ °C, respectively. These were determined according to eq. 2 by observing the 2537 Å fluorescence intensity, with a Westinghouse type WL-775 photodiode, as a function of the partial pressure of C_2H_4,

$$[2] \qquad I_0/I = 1 + \tau^* k_E^1 [C_2H_4]$$

where I_0 is the fluorescence intensity in the absence of C_2H_4 and k_E^1 is the total quenching rate constant of $Hg(6^3P_1)$ by C_2H_4 which was taken to be $36 \times 10^{10}\ M^{-1}\ s^{-1}$ (8).

The reaction cell was a cylindrical quartz tube 20 cm long and 3.1 cm i.d., surrounded by an outer quartz tube, 28 cm long and 5.5 cm i.d. A nickel sulfate filter solution thermostated at 25 °C was circulated in the outer tube to attenuate radiation in the 4000 Å region which depopulates $Hg(6^3P_1)$ and $Hg(6^3P_0)$ atoms to higher states. The middle region of the reaction cell, 18 cm long, was irradiated at low light intensities with two U-shaped, cold cathode low pressure mercury lamps, which were placed parallel to and on opposite sides of the reaction cell. The lamps were operated from a Kepco regulated d.c. power supply.

The progress of the reaction was monitored by the rate of hydrogen production, from the photosensitized decomposition of C_2H_4. The H_2 detection system was similar to the one described in ref. 14 with the sensitivity improved by a factor of approximately ten. For C_3H_8, n-C_4H_{10}, and i-C_4H_{10} the rate of C_2H_2 formation was used, because of significant extraneous hydrogen formation resulting from hydrogen atom abstraction reactions. The acetylene was sampled from the flow system by condensing in a cold trap maintained at 65–67 °K with pumped liquid nitrogen. Acetylene separation and detection was accomplished with

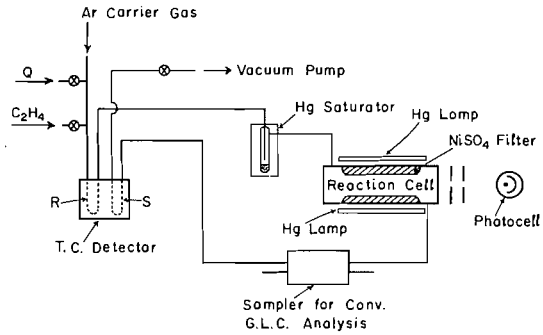

FIG. 1. Reaction and analysis system.

conventional gas chromatographic methods using helium as the carrier gas and a thermal conductivity detector.

The reagents and the manufacturer's stated minimum purity were as follows: Matheson; Ar (99.999), CO (99.9), CO_2 (99.995), NH_3 (anhydrous, 99.99), c-C_3H_6 (99.0). Phillips; C_2H_4 (99.98), C_2H_6 (99.99), $C(CH_3)_4$ (99.88), C_3H_8 (99.99), n-C_4H_{10} (99.8), i-C_4H_{10} (99.9). Merck, Sharp & Dohme; ND_3 (99% atom D), D_2O (99.7% atom D), 2,2-$C_3H_6D_2$ (98% atom D), C_3D_8 (99% atom D). Distilled water (degassed). Gases which are condensible at Dry Ice–acetone or liquid nitrogen temperatures were additionally degassed by freezing and pumping. With the exception of H_2O and D_2O all gases were passed through a spiral trap cooled at Dry Ice–acetone temperatures before entering the reaction cell.

Results

Typical enhancement curves of the decomposition of ethylene as a function of the partial pressure of quencher, Q, are shown in Fig. 2. These enhancement effects cannot be realized in terms of simple competitive quenching between C_2H_4 and Q since this would cause the S/S_0 curves to lie below the dotted line as in the case of CO_2. The effect is attributed to $Hg(6^3P_0)$ formation and we propose the following mechanism (1, 14):

$$[3] \qquad Hg + h\nu^* \longrightarrow Hg^*$$

$$[4] \qquad Hg^* \xrightarrow{1/\tau^*} Hg + h\nu^*$$

$$[5] \qquad Hg^* + Q \xrightarrow{k_Q^{*g}} Hg + Q'$$

$$[6] \qquad Hg^* + Q \xrightarrow{k_Q^{*0}} Hg^0 + Q''$$

$$[7] \qquad Hg^* + C_2H_4 \xrightarrow{k_E^{*g}} Hg + C_2H_2 + H_2$$

$$[8] \qquad Hg^0 + C_2H_4 \xrightarrow{k_E^{0g}} Hg + C_2H_2 + H_2$$

$$[9] \qquad Hg^0 + Q \xrightarrow{k_Q^{0g}} Hg + Q'''$$

$$[10] \qquad Hg^0 \xrightarrow{1/\tau^0} Hg$$

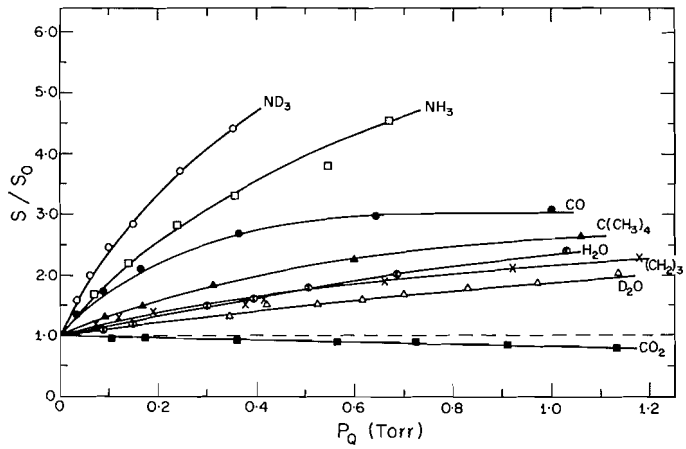

FIG. 2. Enhancement of the photosensitized decomposition of C_2H_4 by various molecules. (S/S_0 is the ratio of the rates of H_2 formation in the presence to the absence of quencher, Q. The C_2H_4 pressure in Torr $\times 10^3$ for NH_3, $(CH_2)_3$, ND_3, H_2O, D_2O, $C(CH_3)_4$, CO, and CO_2 were 11.7 ± 0.9, 10.5 ± 0.7, 10.6 ± 0.7, 11.6, 16.3, 4.3 ± 0.6, 18.4 ± 1.0, and 6.3 ± 0.7, respectively.

in which Hg*, Hg^0, and Hg represent $Hg(6^3P_1)$, $Hg(6^3P_0)$, and $Hg(6^1S_0)$, respectively. Reactions 4 and 10 include all processes, besides radiative decay, which are first or pseudo-first order under our experimental conditions (constant mercury pressure and constant total pressure). Quenching to $Hg(6^3P_0)$ by ethylene or argon is negligible and the relevant reactions are omitted from the mechanism (*cf.* Appendix 1). The reverse of reaction 6 can also be shown unimportant under our experimental conditions (12*b*, 17).

On the basis of the above mechanism the ratio of the rates of H_2 or C_2H_2 formation in the presence to that in the absence of Q is

$$[11] \qquad \frac{S}{S_0} = \frac{1 + \{\phi_E^{0g} k_E^{0g} k_Q^{*0}[Q]\}/[\phi_E^{*g} k_E^{*g}\{k_E^{0g}[C_2H_4] + k_Q^{0g}[Q] + (1/\tau^0)\}]}{1 + \{k_Q^{l}[Q]\}/\{(1/\tau^*) + k_E^{*g}[C_2H_4]\}}$$

where, k_Q^l is $k_Q^{*g} + k_Q^{*0}$ and ϕ_E^{*g}, ϕ_E^{0g} are the efficiencies of H_2 formation from reactions 7 and 8, respectively. The denominator of eq. 11 can either be calculated using the published rate constants k_Q^l and k_E^{*g} or be obtained experimentally by simultaneous observation of the ratio of $Hg(6^3P_1)$ fluorescence in the absence to that in the presence of Q, I_0/I,

$$[12] \qquad I_0/I = 1 + k_Q^l[Q]/\{(1/\tau^*) + k_E^{*g}[C_2H_4]\}$$

Experimentally determined I_0/I values were used in all cases except for $C(CH_3)_4$. The observation of the fluorescence intensity as a function of Q, either in the presence of ethylene or in its absence, was also used to obtain total quenching rate constants for the various gases used in the present experiments. This was done using eq. 12 or the analogous expression in the absence of C_2H_4. Substitution of eq. 12 in eq. 11 and rearrangement yields eq. 13,

$$[13] \qquad \left[\frac{S}{S_0}\frac{I_0}{I} - 1\right]^{-1} = \frac{\phi_E^{*g} k_E^{*g} k_Q^{0g}}{\phi_E^{0g} k_E^{0g} k_Q^{*0}} + \{(1/\tau^0) + k_E^{0g}[C_2H_4]\}\frac{\phi_E^{*g} k_E^{*g}}{\phi_E^{0g} k_E^{0g} k_Q^{*0}}\frac{1}{[Q]}$$

The values of $[C_2H_4]$ were in the range of 5×10^{-3} to 25×10^{-3} Torr and those of [Q] in the range of 10^{-2} to 2 Torr. The total pressure was kept constant at 20 Torr using argon; the latter had a threefold purpose: (*a*) it eliminated any pressure broadening of the $Hg(6^1S_0) \rightarrow Hg(6^3P_1)$ absorption, (*b*) it kept the rate constant of reaction 10 and possibly reaction 4

Can. J. Chem. Downloaded from www.nrcresearchpress.com by 210.87.254.42 on 09/05/12
For personal use only.

TABLE 1. Spin–orbit relaxation of $Hg(6^3P_1)$ by various gases[a]

Gas	$k^1(M^{-1}\,s^{-1}\times10^{-9})$	$k^{*0}(M^{-1}\,s^{-1}\times10^{-9})$	ϕ^{*0}
CO	55.6±1.3 (55.9)	48.7 ±3.9	0.88±0.07 (0.85)
CO_2	27.1 (28.0)	<0.3	<0.01 (~0.02)
NH_3	51.7±1.8 (50.4)	54.3 ±1.8	1.05±0.05 (0.62)
ND_3	53.0±1.8 (17.4)	52.8 ±3.5	1.00±0.08
H_2O	12.6±2.0 (16.7)	9.6 ±1.4	0.76±0.18 (0.38)
D_2O	5.4±1.1 (7.4)	5.6 ±1.0	1.06±0.26
C_2H_6	1.3±0.3 (1.5)	0.85±0.08	0.64±0.16 (0.80)
c-C_3H_6	12.5±0.4 (13)	7.0 ±1.2	0.56±0.10
$C(CH_3)_4$	(14)	8.0 ±0.3	0.58±0.02
C_3H_8	15.3±0.7 (18)	2.2 ±0.1	0.14±0.01 (0.38)
2,2-$C_3H_6D_2$	5.8±0.5 (4.3)†	2.9 ±0.3	0.51±0.07
C_3D_8	4.8±0.2 (3.3)†	2.2 ±0.2	0.47±0.10
n-C_4H_{10}	45.0±2.0 (40)	4.9 ±0.1	0.11±0.01
i-C_4H_{10}	48.7±2.0 (50)	2.4 ±0.3	0.05±0.01

[a]Quantum yields of $Hg(6^3P_0)$ formation, ϕ^{*0}, are defined as k^{*0}/k^1. Values in parentheses for k^1 and ϕ^{*0} are from refs. 8 and 12*b*, respectively, except those marked by † which are from ref. 16*a*. Plus and minus values are standard deviations of the mean.

constant from any third order effects, and (*c*) it kept ϕ_E^{*g} and ϕ_E^{0g} constant and the ratio $(\phi_E^{*g}/\phi_E^{0g})$ close to unity (17).

The rate constant ratios k_E^{*g}/k_Q^{*0} were determined from plots of the left hand side of eq. 13 *vs.* $[Q]^{-1}$ at fixed $[C_2H_4]$; the slopes of these plots were then plotted again *vs.* $[C_2H_4]$ to obtain $\phi_E^{*g}k_E^{*g}/\phi_E^{0g}k_Q^{*0}$. The absolute values of k_Q^{*0} were calculated using the value of $36\times10^{10}\ M^{-1}\ s^{-1}$ for k_E^{*g} (8) and assuming $(\phi_E^{*g}/\phi_E^{0g})\sim1$ (17). Values of k_Q^{0g}/k_E^{0g} can also be determined by this method; however, the present experiments were done under conditions where quenching of $Hg(6^3P_0)$ by Q was minimal in relation to that by ethylene and the determined values are not as meaningful.

The results are shown in Table 1. Literature values are cited for comparison wherever they are available. The agreement of the present total rate constants with the literature ones is very good in all cases with the exception of ND_3. Unless rapid exchange of ND_3 to form NH_3 occurred in the Pyrex surfaces leading from the gas cylinder to the reaction vessel, this discrepancy could be accounted for by the $Hg(6^3P_1)$–ND_3 and $Hg(6^3P_0)$–ND_3 excimer emission (18). We found that even though the WL-775 photodiode we used had a wavelength cut-off of 3000 Å, the excimer emission was significant enough in this region to reduce the quenching rate constant by a factor of two in the range of 0.5 to 2.0 Torr. The present value was obtained at ND_3 pressures less than 0.5 Torr and in the presence of small amounts of C_2H_4 which suppresses the excimer emission but leaves the $Hg(6^3P_1)$ emission unaffected. The literature value (15) was obtained under conditions where excimer emission would be significant. The new quantum yields of $Hg(6^3P_0)$ formation obtained by Callear and McGurk (12*b*) are in close agreement with the present results wherever data overlap. The results on C_2H_6 were obtained by the method described in Appendix 1.

Conclusions

These results allow us to come to the following conclusions:

(*1*) Spin–orbit relaxation is important to a predominant route for all cases studied with the exception of CO_2, C_2H_4, and i-C_4H_{10}.[1] Thus, in a large number of cases studied in the past it was not $Hg(6^3P_1)$ but $Hg(6^3P_1)$ and $Hg(6^3P_0)$ reactions that were being studied, with the relative importance of each depending on the $Hg(6^3P_0)$ quantum yield and the partial pressure of the quencher Q. For this reason chemical cross sections which are reported in the literature are in many cases of questionable validity and a correct analysis of those data should be applied (21). Such an analysis is discussed in Appendix 2.

[1]A possible explanation for the CO_2 behavior may be fast electronic–electronic energy transfer from $^3P_1$ to an adjacent CO_2 triplet state. A $CO_2(^3\Pi)$ state of 4.86 eV (19) was previously proposed (20) to account for the $Hg(6^3P_1)$ reactions of CO_2.

Can. J. Chem. Downloaded from www.nrcresearchpress.com by 210.87.254.42 on 09/05/12
For personal use only.

(*2*) Does the resonance hypothesis have anything to do with the spin–orbit relaxation? The present result with CO in combination with the result on N_2 (22) seem to be in line with such a proposition. However, such statement would have to be qualified, because we are dealing with two different electronic structures. The rest of the molecules studied do not seem to be in line with resonance, because neither their spin–orbit relaxation rate constants nor their quantum yields indicate such a simple trend. Most of all, molecules such as NH_3 and H_2O have been shown (18, 23) to give significant excimer emission in quenching $Hg(6^3P_0)$. It is most likely that complex formation occurs with $Hg(6^3P_1)$ as well, whence the presence of resonance or not will not be as important in determining the magnitude of the spin–orbit relaxation process, because the system could pass several times over the configuration leading to $Hg(6^3P_0)$.

(*3*) Deuteration of the C—H bonds in the alkanes does not enhance the spin–orbit relaxation since undeuterated alkanes show comparable spin–orbit relaxation. We attribute the previous conclusions (*6b*, *16a*) which were based on chemical *vs.* physical quenching cross section discrepancies or on spectroscopic investigations of the $Hg(6^3P_0)$ steady state populations,

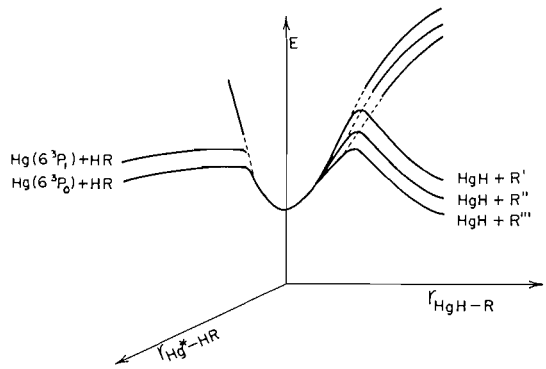

FIG. 3. Hypothetical potential energy surfaces for the quenching of excited mercury atoms by the alkanes (7).

to failure to take into account removal of $Hg(6^3P_0)$ by the molecules that form it. In comparison to the undeuterated molecules, deuterated molecules are known to be weaker quenchers of $Hg(6^3P_1)$; and particularly weaker quenchers of $Hg(6^3P_0)$ (17).

(*4*) A better approach towards an explanation of these results seems to be formation of a complex between $Hg(6^3P_1)$ and the quencher, Q. Such a process is illustrated in Fig. 3 for the alkanes (7), but it could also have wider applicability. A $Hg(6^3P_1)$ atom and an alkane, RH, form a complex, which could decompose

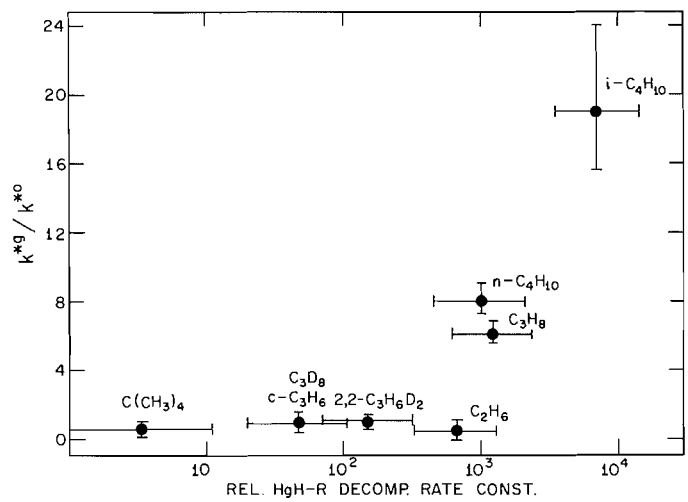

FIG. 4. (Quenching to the ground state/quenching to the $Hg(6^3P_0)$ state) *vs.* calculated relative HgH—R decomposition rate constants. (The calculated relative HgH—R decomposition rate constants are from ref. 7. The quenching rate constant ratios are from this work. They are related to each other by $k^{*g}/k^{*0} = f(k_d/k^0_{-1})$, where k_d is the HgH—R decomposition rate constant and k^0_{-1} is the rate constant for decomposition to $Hg(6^3P_0) + RH$. Vertical bars are error limits for the experimental results. Horizontal bars are relative variations of the calculated rate constants assuming relative changes of ± 1 kcal/mol in the R—HHg decomposition barrier (7)).

Can. J. Chem. Downloaded from www.nrcresearchpress.com by 210.87.254.42 on 09/05/12
For personal use only.

by several channels. For the alkanes these channels are: (*a*) decomposition to the original reactants; (*b*) decomposition to $Hg(6^3P_0)$ and RH; (*c*) R—HHg bond decomposition; (*d*) excimer emission.

A model of this form was previously proposed by Yang (6*a*) to account for the C—H *vs.* C—D isotope effects in $Hg(6^3P_1)$ photosensitization. Vikis and Moser (7) investigated this model and found that the relative trends and isotope effects shown by the alkanes towards $Hg(6^1P_1)$, $Hg(6^3P_1)$, and $Hg(6^3P_0)$ are sufficiently explained, by assuming that the major variations among the alkanes are due to fractional differences in the C—HHg bond decomposition rate constants. The present results are in accord with this model because molecules with stronger bonds exhibit higher $Hg(6^3P_0)$ quantum yields. The correlation is shown in Fig. 4, which was constructed from the relative decomposition rate constants calculated in ref. 7 and the present results. The correlation separates the alkanes into three rough categories according to their bond strength (primary, secondary, tertiary).

One can infer from the above that in the absence of an accessible channel for bond rupture the excimer is bound to decompose via the $Hg(6^3P_0)$ channel even though resonance is not well obeyed. It could also be deactivated by emission but this is apparently a less important process for $Hg(6^3P_1)$ quenching.

Appendix 1

In the present work ethylene was used as the standard to detect $Hg(6^3P_1)$ and $Hg(6^3P_0)$ atoms by reacting to give C_2H_2 and H_2. Also, argon was used as the carrier gas at a pressure of 20 Torr. Both gases would influence the present results if they quench $Hg(6^3P_1)$ to $Hg(6^3P_0)$, or if Ar quenches $Hg(6^3P_0)$, significantly. These effects, when included, modify eq. 13 to eq. 14,

$$[14]\quad \frac{S}{S_0}\cdot\frac{I_0}{I}=\left[1+\frac{\phi_E^{0g}k_E^{0g}}{\phi_E^{*g}k_E^{*g}}\frac{(k_{Ar}^{*0}[Ar]+k_E^{*0}[C_2H_4]+k_Q^{*0}[Q])}{((1/\tau^0)+k_{Ar}^{0g}[Ar]+k_E^{0g}[C_2H_4]+k_Q^{0g}[Q])}\right]\times\left[1+\frac{\phi_E^{0g}k_E^{0g}}{\phi_E^{*g}k_E^{*g}}\frac{(k_{Ar}^{*0}[Ar]+k_E^{*0}[C_2H_4])}{((1/\tau^0)+k_{Ar}^{0g}[Ar]+k_E^{0g}[C_2H_4])}\right]^{-1}$$

where the symbolism is the one adopted in this paper. This effect was investigated by the study of the rate of H_2 production in the absence of Q, according to eq. 15,

$$[15]\quad S_0\left(1-\frac{I_0}{I_{00}}\right)=I_a\phi_E^{*g}\frac{k_E^{*g}}{k_E^{t}}\left[1+\frac{\phi_E^{0g}k_E^{0g}}{\phi_E^{*g}k_E^{*g}}\frac{k_{Ar}^{*0}[Ar]+k_E^{*0}[C_2H_4]}{\{(1/\tau^0)+k_{Ar}^{0g}[Ar]+k_E^{0g}[C_2H_4]\}}\right]$$

where, I_{00} is the fluorescence intensity in the absence of ethylene and I_a is the rate of reaction 3. The left hand side of eq. 15 was found to be independent of ethylene in the range of 4.6×10^{-3} to 0.26 Torr of ethylene. This means that either $k_{Ar}^{*0}[Ar]\gg k_E^{*0}[C_2H_4]$ and $(1/\tau^0)+k_{Ar}^{0g}[Ar]\gg k_E^{0g}[C_2H_4]$, or $k_E^{*0}[C_2H_4]\gg k_{Ar}^{*0}[Ar]$ and $k_E^{0g}[C_2H_4]\gg(1/\tau^0)+k_{Ar}^{0g}[Ar]$. The former possibility is excluded on the basis of the dependence of the function $(S/S_0)(I_0/I)$ on $[C_2H_4]$, *e.g.*, for 0.9 Torr of CO $(S/S_0)(I_0/I)$ increases from 3.5 at 34×10^{-3} Torr of C_2H_4 to 6.0 at 6.8×10^{-3} Torr of C_2H_4. Also, according to ref. 12*b* $(k_E^{*0}/k_E^{t})<0.1$. Thus, eq. 14 can be reduced to eq. 13, with a good approximation.

Ethane, because of its low quenching rate constant, could not be studied under the same conditions that the other gases were studied, without the addition of large partial pressures of it to the carrier gas. Therefore, we modified the method using ethane itself as the carrier gas. Equation 16 which is analogous to eq. 15 can be derived for the modified method.

$$[16]\quad S\left(1-\frac{I}{I_0}\right)=I_a\phi_E^{*g}\left[1+\frac{\phi_E^{0g}k_E^{0g}}{\phi_E^{*g}k_E^{*g}}\frac{k_{Et}^{*0}[C_2H_6]}{\{(1/\tau^0)+k_{Et}^{0g}[C_2H_6]+k_E^{0g}[C_2H_4]\}}\right]$$

By observing S and I/I_0 *vs.* $[C_2H_4]$ at fixed $[C_2H_6]$ we obtained an average value for k_{Et}^{*0} of $(0.85\pm0.08)\times10^9\ M^{-1}\ s^{-1}$. Three total pressures of C_2H_6 were investigated 2.5, 3.3, and 4.5 Torr. At these pressures quenching of $Hg(6^3P_0)$ by C_2H_6 is negligible by comparison to that by C_2H_4 (17).

Can. J. Chem. Downloaded from www.nrcresearchpress.com by 210.87.254.42 on 09/05/12
For personal use only.

Can. J. Chem. Downloaded from www.nrcresearchpress.com by 210.87.254.42 on 09/05/12
For personal use only.

Appendix 2

The discrepancy between quenching cross sections determined by the physical method and those determined by the chemical method has been considered in the past (6*b*, 8, 16*a*, 21) as an indication of $Hg(6^3P_0)$ formation by the quencher. In this Appendix the N_2O chemical method is examined in terms of a mechanism that takes into consideration $Hg(6^3P_0)$ atom formation. The results of this approach are compared to those of the present work.

The mechanism postulated for conditions of complete quenching is as follows,

[17] $Hg + h\nu \longrightarrow Hg^*$

[18] $Hg^* + N_2O \xrightarrow{k_N^{*g}} Hg + N_2 + O$

[19] $Hg^* + N_2O \xrightarrow{k_N^{*0}} Hg^0 + N_2O$

[20] $Hg^* + Q \xrightarrow{k_Q^{*g}} Hg + Q'$

[21] $Hg^* + Q \xrightarrow{k_Q^{*0}} Hg^0 + Q''$

[22] $Hg^0 + N_2O \xrightarrow{k_N^{0g}} Hg + N_2 + O$

[23] $Hg^0 + Q \xrightarrow{k_Q^{0g}} Hg + Q'''$

The symbolism is the one adopted throughout this paper.

This mechanism yields eq. 24 for the quantum yield of N_2 formation, ϕ_N,

[24] $$\phi_N^{-1} = \frac{(k_N^t/k_N^{*g}) + \{k_Q^t[Q]/k_N^{*g}[N_2O]\}}{1 + \dfrac{(k_N^{*0}/k_N^{*g}) + \{k_Q^{*0}[Q]/k_N^{*g}[N_2O]\}}{1 + k_Q^{0g}[Q]/k_N^{0g}[N_2O]}}$$

Under conditions where $k_Q^{0g}[Q] \ll k_{N_2O}^{0g}[N_2O]$, which are easily obtainable for some alkanes, RH, (17, 12*b*), eq. 24 reduces to eq. 25,

[25] $$\phi_N^{-1} = 1 + \{k_{RH}^{*g}[RH]/[N_2O]\}/\{k_N^t + k_{RH}^{*0}[RH]/[N_2O]\}$$

The slope of eq. 25 at low $[RH]/[N_2O]$ ratios, where ϕ_N^{-1} is linear with $[RH]/[N_2O]$, is k_{RH}^{*g}/k_N^t. Thus, data obtained in this manner (24) give low quenching rate constants k_{RH}^{*g} by comparison to the ones determined by the physical method which determines $k_{RH}^{*g} + k_{RH}^{*0}$. At higher $[RH]/[N_2O]$ ratios a deviation from linearity should be observed for those molecules that quench significantly to the $Hg(6^3P_0)$ state. This situation is illustrated by the results of Yang (6*b*). Employing eq. 25 for the $Hg(6^3P_1)$–$C(CH_3)_4$ and $Hg(6^3P_1)$–C_3H_8 systems studied by Yang (6*b*), we determine, using his data, k_{RH}^{*g} and k_{RH}^{*0}/k_{RH}^{*g} for $C(CH_3)_4$ and C_3H_8. These values are $1.36 \times 10^{10}\ M^{-1}\ s^{-1}$ and 0.16 for C_3H_8; $0.47 \times 10^{10}\ M^{-1}\ s^{-1}$ and 1.4 for $C(CH_3)_4$. They correspond to 14% and 58% quenching to the $Hg(6^3P_0)$ state by C_3H_8 and $C(CH_3)_4$, respectively, and are comparable to the values of 14% and 58% determined in this work. Cvetanovic (21) has examined Yang's (6*b*) data from the same point of view and arrived at similar conclusions. Also, additional data obtained in his laboratory (25) using the N_2O chemical method are in line with the results of the present work.

The authors gratefully acknowledge the financial support received from the National Research Council of Canada.

1. A. C. Vikis, G. Torrie, and D. J. Le Roy. Can. J. Chem. **48**, 3771 (1970).
2. A. C. G. Mitchell and M. W. Zemansky. Resonance radiation and excited atoms. Cambridge University Press, New York. 1961.
3. V. K. Bykhovskii and E. E. Nikitin. Opt. Spectrosc. **16**, 111 (1964).
4. P. G. Dickens, J. W. Linnett, and O. Sovers. Discuss. Faraday Soc. **33**, 52 (1962).
5. G. Karl, P. Kruus, and J. C. Polanyi. J. Chem. Phys. **46**, 224 (1967).
6. (*a*) K. Yang. J. Am. Chem. Soc. **87**, 5294 (1965). (*b*) K. Yang. J. Am. Chem. Soc. **89**, 5344 (1967).
7. A. C. Vikis and H. C. Moser. J. Chem. Phys. **53**, 2333 (1970).
8. R. J. Cvetanovic. Prog. React. Kinet. **2**, 41 (1964).
9. J. G. Calvert and J. N. Pitts. Photochemistry. John Wiley and Sons, Inc., New York. 1966.
10. M. D. Scheer and J. Fine. J. Chem. Phys. **36**, 1264 (1962).
11. B. De B. Darwent and F. G. Hurtubise. J. Chem. Phys. **20**, 1684 (1952).
12. (*a*) A. B. Callear and R. E. M. Hedges. Trans. Faraday Soc. **66**, 605 (1970). (*b*) A. B. Callear and J. McGurk. Chem. Phys. Lett. **7**, 491 (1970).
13. J. B. Homer and F. P. Lossing. Can. J. Chem. **44**, 143 (1966).
14. G. London, A. C. Vikis, and D. J. Le Roy. Can. J. Chem. **48**, 1420 (1970).

15. M. G. EVANS. J. Chem. Phys. **2**, 445 (1934).
16. (*a*) S. PENZES, A. J. YARWOOD, O. P. STRAUSZ, and H. E. GUNNING. J. Chem. Phys. **43**, 4524 (1965). (*b*) S. PENZES, O. P. STRAUSZ, and H. E. GUNNING. J. Chem. Phys. **45**, 2322 (1966).
17. A. C. VIKIS and H. C. MOSER. J. Chem. Phys. **53**, 1491 (1970).
18. R. H. NEWMAN, C. G. FREEMAN, M. J. MCEWAN, R. F. C. CLARIDGE, and L. F. PHILLIPS. Trans. Faraday Soc. **66**, 2827 (1970).
19. R. G. W. NORRISH. Energy transfer in gases. *Edited by* R. Stoops, Interscience Publishers, New York. 1962.
20. O. P. STRAUSZ and H. E. GUNNING. Can. J. Chem. **39**, 2244 (1961).
21. R. J. CVETANOVIC. Fifth International Photochemistry Conference, Sept. 2–5, 1969. IBM Research Center, York Town, New Jersey.
22. C. G. MATLAND. Phys. Rev. **92**, 637 (1953).
23. C. G. FREEMAN, M. J. MCEWAN, R. F. C. CLARIDGE, and L. F. PHILLIPS. Trans. Faraday Soc. **66**, 2974 (1970).
24. Y. ROUSSEAU and H. E. GUNNING. Can. J. Chem. **41**, 465 (1963).
25. R. J. CVETANOVIC. Private communication.

Can. J. Chem. Downloaded from www.nrcresearchpress.com by 210.87.254.42 on 09/05/12
For personal use only.

Etude des oxynitrates de plomb (II). Synthèse des oxynitrates de plomb hydratés et de l'oxyde de plomb anhydre ou hydraté

H. BRUSSET, J. J. P. MARTIN, C. MARTIN-LEFEVRE, Y. REPELIN, E. HUSSON ET B. DESPAGNE

Laboratoire de Recherche de Chimie Systématique, Ecole Normale Supérieure, 24, rue Lhomond et Université Paris VI, Bât, F. 8, rue Cuvier, Paris 5ème

Reçu le 5 fevrier 1971[1]

Les dosages potentiométriques et conductimétriques effectués à 27 ± 0.2 °C à partir de solutions de soude et de nitrate de plomb ont prouvé l'existence des monoxynitrate, dioxynitrate, heptoxytrinitrate et pentoxynitrate de plomb hydratés. Il a été montré que la présence de traces de silice inhibe la formation de l'oxyde de plomb anhydre et favorise celle de l'oxyde de plomb hydraté. La synthèse des oxynitrates de plomb et de l'oxyde de plomb hydraté a été effectué dans un large domaine de température avec diverses concentrations des réactifs.

Potentiometric and conductimetric measurements of solutions of sodium hydroxide and lead nitrate at 27 ± 0.2 °C have established the existence of hydrated lead monoxynitrate, dioxynitrate, heptoxytrinitrate and pentoxynitrate. It was shown that the presence of silica inhibits the formation of anhydrous lead oxide but favors that of hydrated lead oxide. The preparation of lead oxynitrates and hydrated lead oxide was carried out over a wide range of temperatures at various concentrations of reactants.

Canadian Journal of Chemistry, **50**, 184 (1972)

Introduction

Les oxynitrates de plomb hydratés présentent un intérêt particulier en tant que catalyseurs d'oxydation des aldehydes α-halogénés (1). La connaissance de l'effet catalytique d'un ou plusieurs de ces oxynitrates dans de telles réactions d'oxydation nécessite la maitrise de leur synthèse avec un bon degré de pureté.

Il s'est avéré que les résultats obtenus au cours d'un travail préliminaire (2) devaient être précisés. Nous avons donc entrepris l'étude systématique de l'évolution de la réaction de solutions aqueuses de soude sur des solutions aqueuses de nitrate de plomb, à la température de 27 ± 0.2 °C, soit par dosages conductimétriques, soit par dosages potentiométriques. Ceci nous a amené à préciser les conditions d'obtention des différents composés mis en évidence, lorsqu'on opère à 3 ± 0.5 °C, 20 ± 0.3 °C, 27 ± 0.3 °C, 50 ± 0.3 °C.

Techniques expérimentales

La conductivité du milieu réactionnel a été mesurée avec un conductimètre "Philips GM 4249". Pour tenir compte des volumes de réactifs ajoutés, on a effectué les corrections de dilution. La précision des mesures est de 2%.

Les mesures de p*H* des solutions ont été réalisées avec un p*H*-mètre "Heito PS 18". L'électrode employée est une électrode de verre combinée avec une électrode de référence au calomel. L'incertitude sur la mesure est de 0.02 unité de p*H*.

La caractérisation structurale des composés est basée sur la diffractométrie aux rayons X d'échantillons de poudres, suivant la méthode de Debye et Scherrer. Nous avons utilisé un diffractomètre à compteur de la "Compagnie Générale de Radiologie, Theta 60". Le rayonnement X est le rayonnement K_α du cuivre. Le diffractomètre est utilisé avec un montage par transmission et le domaine exploré est celui des petits angles de Bragg entre 4 et 35°.

Les solutions aqueuses de nitrate de plomb sont préparées à partir de sel cristallisé pur ("Carlo Erba" Italie).

Les solutions aqueuses de soude sont préparées à partir de pastilles de soude ("Prolabo", France).

Les oxynitrates de plomb ont été dosés selon une méthode connue (2). Elle permet de connaitre le nombre N_1 d'atomes-g de plomb engagés sous forme PbO et le nombre N_2 d'atomes-g de plomb engagés sous forme $Pb(NO_3)_2$. La formule d'un oxynitrate de plomb s'écrira alors sous la forme dualistique: $Pb(NO_3)_2.N_1/N_2PbO.xH_2O$.

L'incertitude sur la valeur du rapport N_1/N_2 est égale à 0.2.

Les expériences ont toutes été effectuées avec des solutions décarbonatées conservées une quinzaine de jours en récipients de verre "Pyrex". Pour éviter tout risque de carbonatation, elles ont été réalisées en boite à gants, sous courant d'azote.

Les dosages conductimétriques ont été effectués en versant cm^3 par cm^3 la solution de soude dans 50 cm^3 de solution de nitrate de plomb. Le mélange obtenu est agité dix minutes, à l'aide d'un agitateur magnétique, après chaque addition de soude. Avant chaque mesure de conductivité de la solution, on attend la décantation totale du solide formé.

Le p*H* du milieu réactionnel a été mesuré lorsque celui-ci devenait invariant. Ceci nécessite une attente de un à vingt jours. Nous avons donc opéré de la façon suivante: dans des flacons contenant 75 cm^3 de solution de nitrate de

[1]Revision reçu le 21 septembre 1971.

Can. J. Chem. Downloaded from www.nrcresearchpress.com by 210.87.254.105 on 09/05/12
For personal use only.

Can. J. Chem. Downloaded from www.nrcresearchpress.com by 210.87.254.105 on 09/05/12
For personal use only.

plomb, on introduit des volumes déterminés de solution de soude. Les flacons sont bouchés hermétiquement entre chaque mesure de pH.

La synthèse des oxynitrates de plomb hydratés a été effectuée en agitant pendant dix minutes, à une température fixe, dans un bain thermostaté, le mélange de 50 cm^3 de solution de nitrate de plomb et de V cm^3 de solution de soude préalablement portées à la température choisie. Les précautions élémentaires sont prises pour éviter toute évaporation pendant la préparation. Les solides obtenus sont séparés par décantation et identifiés par diffractométrie X.

Résultats expérimentaux et discussions

Dosages réalisés avec une solution de soude 0.4 mol l^{-1} et une solution de nitrate de plomb 0.4 mol l^{-1}

En appelant: M_s, la molarité de la solution de soude; M_n, la molarité de la solution de nitrate de plomb; a, le volume utilisé de la solution de soude; b, le volume utilisé de la solution de nitrate de plomb; on a les relations:

$$[1] \qquad (s) = M_s.a/(a+b)$$

$$[2] \qquad (n) = M_n.b/(a+b)$$

et on définit un rapport R par

$$[3] \qquad R = (s)/(n) = M_s.a/M_n.b$$

D'autre part, l'équation de réaction correspondant à la formation stoechiométrique des oxynitrates de plomb peut s'écrire d'une façon générale:

$$[4] \quad (m+1)\,Pb(NO_3)_2 + 2m\,NaOH \rightarrow Pb(NO_3)_2.m\,PbO.\text{hydraté} + 2m\,NaNO_3 + m\,H_2O$$

Par conséquent, le rapport R est défini par la relation

$$[5] \qquad R = M_s.a/M_n.b = 2m/(m+1)$$

On observe, sur la courbe conductimétrique (Fig. 1), des ruptures de pente pour les valeurs: $R = 0.16$, $R = 0.63$, $R = 1.00$, $R = 1.40$ et $R = 1.66$. Les valeurs $R = 1.00$, $R = 1.40$ et $R = 1.66$ correspondent respectivement à la précipitation stoechiométrique du monoxynitrate, de l'heptoxytrinitrate et du pentoxynitrate de plomb hydratés suivant les équations

$$[6] \quad 2Pb(NO_3)_2 + 2NaOH \rightarrow Pb(NO_3)_2.PbO.\text{hydraté} + 2NaNO_3 + H_2O \quad (R = 2/2 = 1)$$

$$[7] \quad 10Pb(NO_3)_2 + 14NaOH \rightarrow 3Pb(NO_3)_2.7PbO.\text{hydraté} + 14NaNO_3 + 7H_2O \quad (R = 14/10 = 1.40)$$

$$[8] \quad 6Pb(NO_3)_2 + 10NaOH \rightarrow Pb(NO_3)_2.5PbO.\text{hydraté} + 10NaNO_3 + 5H_2O \quad (R = 10/6 = 1.66)$$

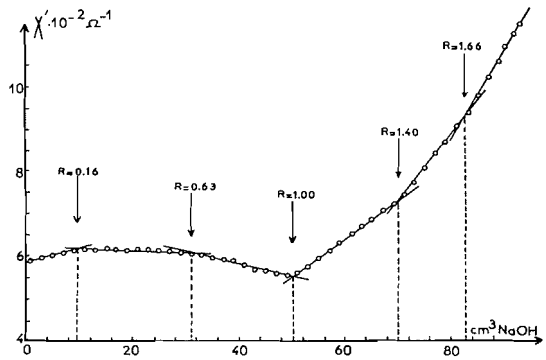

FIG. 1. Dosage conductimétrique de 50 cm^3 d'une solution de nitrate de plomb 0.4 mol l^{-1} par une solution de soude 0.4 mol l^{-1}. χ' = conductivité de la solution rapportée au volume initial, $\chi' = (1/r)(V_0 + V)/V_0$; où V_0 = volume initial de la solution, V = volume du réactif ajouté, r = résistance de la solution.

Par contre, les deux ruptures de pente observées pour $R = 0.16$ et $R = 0.63$ ne correspondent pas à la formation d'autres oxynitrates. En effet, l'analyse aux rayons X des solides obtenus pour $R < 1$ révèle la seule présence du monoxynitrate hydraté. Ces ruptures de pente mettent en évidence des propriétés particulières à la solution mais non des phénomènes de transition entre phases solides.

La courbe potentiométrique (Fig. 2, *a*) laisse tout d'abord apparaitre une brusque élévation du pH de la solution de p$H = 3.9$ (solution de $Pb(NO_3)_2$ pur) à p$H = 4.5$ après addition de 0.5 cm^3 de soude.

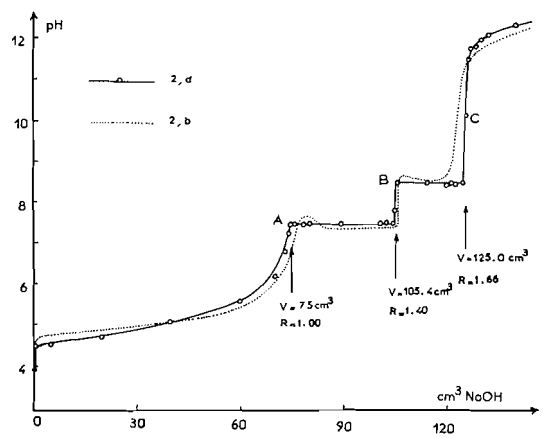

FIG. 2. Dosages potentiométriques de 75 cm^3 d'une solution de nitrate de plomb 0.4 mol l^{-1} par une solution de soude 0.4 mol l^{-1} (commentaires dans le texte).

Can. J. Chem. Downloaded from www.nrcresearchpress.com by 210.87.254.105 on 09/05/12
For personal use only.

On observe alors le début de précipitation du monoxynitrate de plomb $Pb(NO_3)_2.PbO$.hydraté. Le pH de la solution croit ensuite jusqu'à la valeur 7.5 après addition de 75 cm^3 de soude. Le point (A) correspond au rapport $R = 1.00$, en excellent accord avec le rapport R théorique de fin de précipitation du monoxynitrate de plomb. On constate ensuite que le pH reste constant (p$H = 7.5$) lorsque le volume de soude ajouté à la solution de nitrate de plomb est compris entre 75 et 104 cm^3. Le pH de la solution croit alors brusquement puis se fixe à la valeur p$H = 8.5$ après addition de 105.4 cm^3 de soude. Le point (B) correspond au rapport $R = 1.40$, en excellent accord avec le rapport R théorique de fin de formation de l'heptoxytrinitrate de plomb $3Pb(NO_3)_2.7PbO$.hydraté. Le pH de la solution reste alors constant (p$H =$ 8.50) lorsque le volume de soude ajouté est compris entre 105.4 et 124.5 cm^3. Le pH de la solution s'accroit alors brusquement. Le point C (p$H = 10.1$) correspond au rapport $R = 1.66$ en excellent accord avec le rapport R théorique de fin de formation du pentoxynitrate $Pb(NO_3)_2.$-$5PbO$.hydraté.

La solubilité du monoxynitrate étant faible (environ 14 g par l), la concentration des ions provenant de cette solubilisation reste constante et le pH du milieu réactionnel ne peut évoluer tant que la transformation en heptoxytrinitrate n'est pas achevée.

De même, l'heptoxytrinitrate étant peu soluble (environ 7 g par l), la concentration en ions provenant de sa solubilisation reste constante et impose le pH du milieu réactionnel tant que la transformation en pentoxynitrate n'est pas achevée.

Action des solutions de soude sur le pentoxynitrate de plomb hydraté

Si on poursuit les dosages précédents en continuant l'addition de soude, on constate la disparition progressive du solide précipité et la solution devient limpide.

Cependant, l'analyse aux rayons X des solides formés, montre que le pentoxynitrate n'est pas pur après addition d'un volume de soude supérieur à 250 cm^3. Elle révèle l'existence d'un autre composé qui a pu être isolé pur en laissant pendant trois jours le solide formé au contact de la solution, quelles que soient les concentration des solutions de soude ou de nitrate de plomb. C'est ainsi que nous avons préparé ce solide à partir de solutions de soude et de nitrate de plomb 0.1 mol l^{-1} lorsque le rapport R est supérieur ou égal à 7 ou lorsque le rapport R est supérieur à 5 en utilisant des solutions de soude 0.4 mol l^{-1} ou 1 mol l^{-1} réagissant sur des solutions de nitrate de plomb 0.4; 0.6; 0.8 ou 1 mol l^{-1}.

L'analyse chimique et l'analyse thermogravimétrique ont permis d'identifier ce solide à l'oxyde de plomb hydraté $PbO.\frac{1}{3}H_2O$. Cet oxyde, de couleur blanche, chauffé dans l'air à la vitesse de 150 °C par heure perd son eau d'hydratation entre 145 et 175 °C et conduit à la formation de l'oxyde de plomb jaune $PbO\beta$. L'analyse chimique a montré l'absence d'ions nitrate et sodium dans le solide. La teneur en plomb a été trouvée égale à $90.2 \pm 0.5\%$ (pourcentage en masse) alors que la teneur théorique est de 90.4%. La teneur en eau, calculée d'après les thermogrammes, est de $2.5 \pm 0.2\%$ (pourcentage en masse), en bon accord avec la teneur théorique égale à 2.62%. De plus, le diagramme de diffraction des rayons X présente toutes les raies caractéristiques de $PbO.\frac{1}{3}H_2O$ dont on connait la préparation par action d'une solution d'ammoniaque sur une solution d'acétate de plomb (3). Pour notre part, nous avons tenté la synthèse de cet oxyde de plomb hydraté en faisant réagir à la température ambiante ($21 \pm$ 2 °C), des solutions d'ammoniaque diluées ou concentrées sur une solution de nitrate de plomb de concentration 0.4 mol l^{-1}. Nous avons pu préparer ainsi tous les oxynitrates de plomb obtenus, par ailleurs, en faisant réagir des solutions de soude et de nitrate de plomb mais nous n'avons jamais observé la formation de l'oxyde de plomb hydraté.

La formation de l'oxyde de plomb hydraté a pu être observée par dosages conductimétriques ou potentiométriques. Nous avons utilisé une solution de nitrate de plomb de concentration 0.4 mol l^{-1} et des solutions de soude de concentration 1 mol l^{-1} ou 4 mol l^{-1}. Nous avons préparé une série de flacons contenant 50 cm^3 de solution de nitrate de plomb 0.4 mol l^{-1} auxquels nous avons ajouté des volumes de soude 1 mol l^{-1} compris entre 35 et 57.5 cm^3 ou des volumes de soude 4 mol l^{-1} compris entre 8.5 et 15 cm^3. La conductivité et le pH des solutions sont mesurés à intervalles réguliers entre 3 et 21 jours. Au bout de 5 à 7 jours, les

Can. J. Chem. Downloaded from www.nrcresearchpress.com by 210.87.254.105 on 09/05/12
For personal use only.

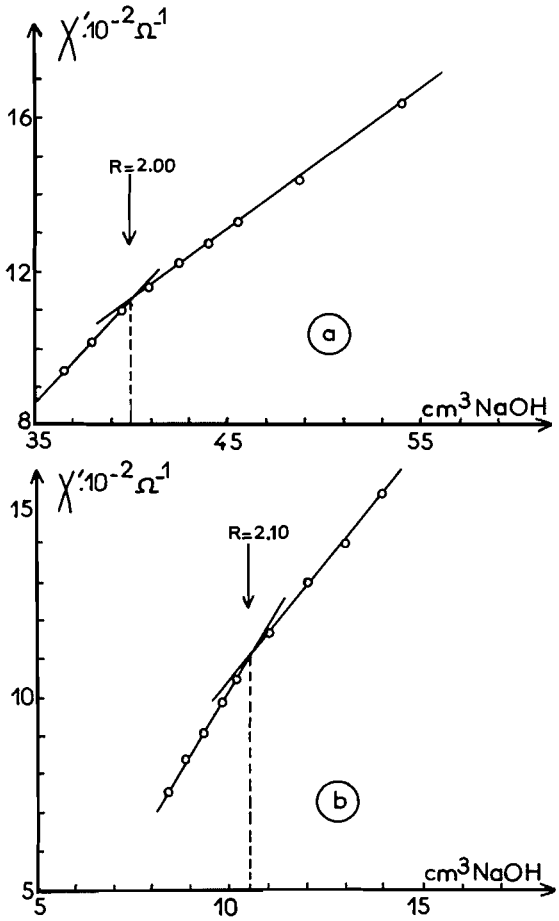

FIG. 3. Dosages conductimétriques de 50 cm³ d'une solution de nitrate de plomb 0.4 mol l^{-1} par (*a*) une solution de soude 1 mol l^{-1}, (*b*) une solution de soude 4 mol l^{-1} (commentaires dans le texte).

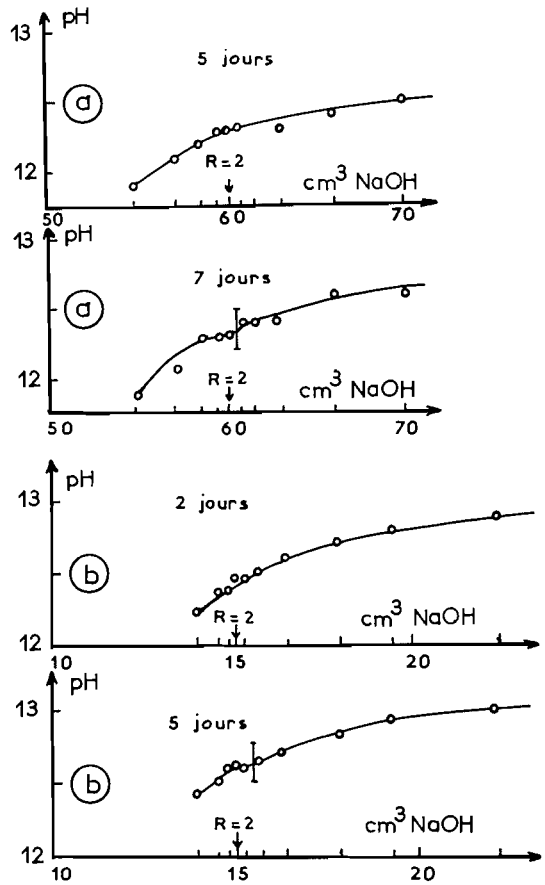

FIG. 4. Dosages potentiométriques de 75 cm³ d'une solution de nitrate de plomb 0.4 mol l^{-1} par (*a*) une solution de soude 1 mol l^{-1}, (*b*) une solution de soude 4 mol l^{-1} (commentaires dans le texte).

courbes conductimétriques (Fig. 3) font apparaitre une rupture de pente pour une valeur de R compris entre 2.0 et 2.1 et les courbes potentiométriques (Fig. 4) présentent un point d'inflexion pour cette même valeur du rapport R, le pH de la solution étant égal à 12.6. Cette valeur du rapport $R = 2$ correspond à la formation de l'oxyde de plomb hydraté selon l'équation:

[9] $Pb(NO_3)_2 + 2NaOH \rightarrow PbO.\text{hydraté} + 2NaNO_3 + H_2O \quad (R = 2/1 = 2)$

L'analyse aux rayons X des solides formés montre que pour $R < 2$, on a affaire au pentoxynitrate pur. L'oxyde de plomb hydraté peut être détecté pour $R > 3$ lorsque les dosages sont effectués à partir d'une solution de soude de concentration 1 mol l^{-1} et pour $R > 2$ si la concentration de la soude est 4 mol l^{-1}.

Dosages réalisés avec des solutions de soude 1 mol l^{-1} ou 4 mol l^{-1} et une solution de nitrate de plomb 0.4 mol l^{-1}

Les oxynitrates mis en évidence au cours des dosages conductimétriques sont ceux déjà cités mais les courbes conductimétriques ne présentent plus de rupture de pente pour des valeurs de $R < 1$. Cependant, en modifiant les conditions opératoires, nous avons pu montrer l'existence d'un autre oxynitrate de plomb. C'est ainsi que nous avons effectué le dosage de 50 cm³ d'une solution de nitrate de plomb

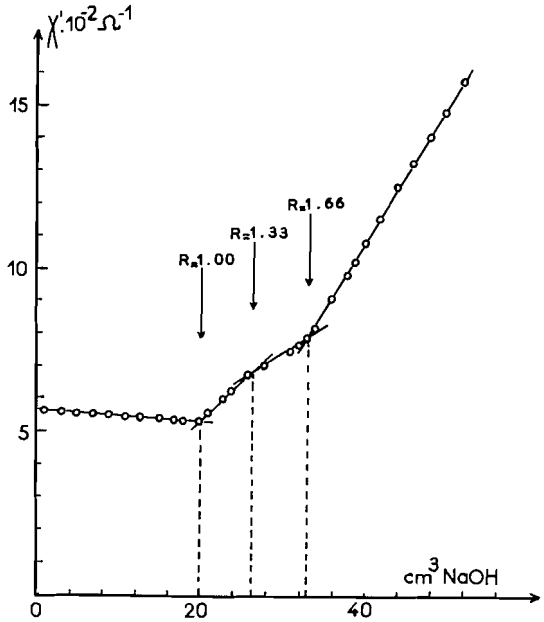

FIG. 5. Dosage conductimétrique de 50 cm^3 d'une solution de nitrate de plomb 0.4 mol l^{-1} par une solution de soude 1 mol l^{-1}.

0.4 mol l^{-1} avec de la soude de concentration 1 mol l^{-1} en versant, tout d'abord, en une seule fois, le volume de soude nécessaire à la précipitation totale du monoxynitrate (20 cm^3) avant de poursuivre l'addition de la base cm^3 par cm^3. La courbe conductimétrique (Fig. 5), tracée à partir des mesures de conductivité effectuées après agitation pendant cinq minutes et décantation des solides formés, met en évidence trois ruptures de pente pour les valeurs: $R = 1.00$, $R = 1.33$ et $R = 1.66$.

Les valeurs $R = 1.00$ et $R = 1.66$ correspondent respectivement à la précipitation stoechiométrique du monoxynitrate et du pentoxynitrate de plomb hydratés. La valeur $R = 1.33$ correspond à la formation du dioxynitrate de plomb hydraté selon l'équation:

[10] $3Pb(NO_3)_2 + 4NaOH \rightarrow Pb(NO_3)_2.2PbO.\text{hydraté} + 4NaNO_3 + 2H_2O \quad (R = 4/3 = 1.33)$

Par contre, si on effectue le dosage comme précédemment jusqu'à la précipitation totale du monoxynitrate et qu'on attende au moins une heure avant de poursuivre l'addition de la soude, on n'observe plus, sur la courbe conductimétrique, une rupture de pente pour la valeur $R = 1.33$ mais pour $R = 1.40$. Il y a donc, dans ces conditions, formation de l'heptoxytrinitrate et non du dioxynitrate de plomb hydraté.

Par conséquent, suivant le mode opératoire, la soude peut réagir sur le monoxynitrate de plomb selon deux processus différents. Il peut se former soit l'heptoxytrinitrate soit le dioxynitrate de plomb hydraté.

Les courbes potentiométriques sont analogues à celle obtenue en effectuant le dosage de la solution de nitrate de plomb 0.4 mol l^{-1} avec une solution de soude 0.4 mol l^{-1}. Les seuls oxynitrates formés sont le monoxynitrate, l'heptoxytrinitrate et le pentoxynitrate de plomb. On observe une invariance de pH de la solution au cours de la transformation du monoxynitrate en heptoxytrinitrate (pH compris entre 7.50 et 7.60) et au cours de la transformation de l'heptoxytrinitrate en pentoxynitrate (pH compris entre 8.60 et 8.80). Le pH des solutions ne se stabilise que très lentement. Il est souvent nécessaire d'attendre une vingtaine de jours avant d'observer que le pH n'évolue plus au voisinage des points correspondant à la formation des oxynitrates purs. Par exemple, la courbe potentiométrique (Fig. 2, *b*) traduit les résultats obtenus lorsque la variation de pH ne dépasse pas 0.02 unité pendant 5 min. Par conséquent, les mesures de pH effectuées au cours de dosages rapides n'ont aucune signification. Les dosages potentiométriques ne permettent donc pas de mettre en évidence la formation de dioxynitrate de plomb hydraté.

Dosages inverses réalisés avec une solution de nitrate de plomb 0.4 mol l^{-1} et une solution de soude 0.4 mol l^{-1}

Le mode opératoire est le même que lors des dosages précédents, mais ceux-ci sont effectués en versant la solution de nitrate de plomb dans un volume de soude égal à 50 cm^3 pour les dosages conductimétriques et 75 cm^3 pour les dosages potentiométriques.

La courbe conductimétrique (Fig. 6) présente quatre ruptures de pente pour les valeurs $R = 8.9$, $R = 1.80$, $R = 1.39$ et $R = 1.06$.

La première rupture de pente ($R = 8.9$) correspond à l'apparition du précipité de pentoxynitrate de plomb. Les autres ruptures de pente correspondent respectivement à la fin de formation du pentoxynitrate, de l'heptoxytrinitrate et du monoxynitrate de plomb. Cependant, les

Can. J. Chem. Downloaded from www.nrcresearchpress.com by 210.87.254.105 on 09/05/12
For personal use only.

Can. J. Chem. Downloaded from www.nrcresearchpress.com by 210.87.254.105 on 09/05/12
For personal use only.

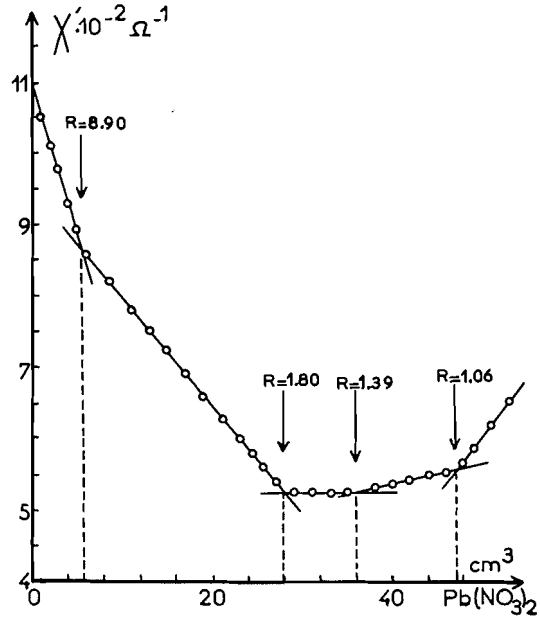

FIG. 6. Dosage conductimétrique de 50 cm^3 d'une solution de soude 0.4 mol l^{-1} par une solution de nitrate de plomb 0.4 mol l^{-1}.

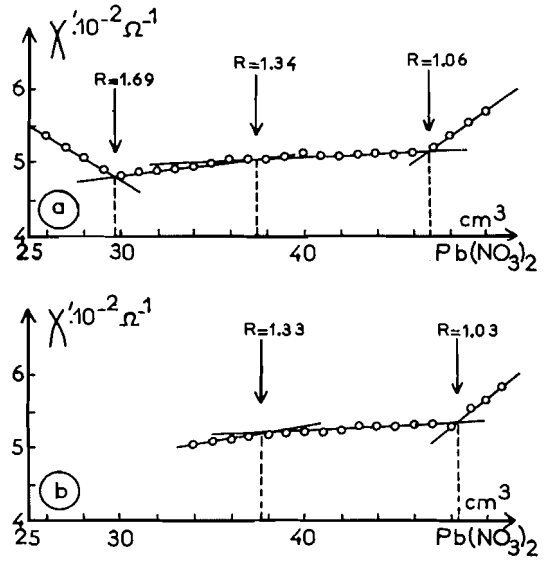

FIG. 7. Dosages conductimétriques de 50 cm^3 d'une solution de soude 0.4 mol l^{-1} par une solution de nitrate de plomb 0.4 mol l^{-1} (commentaires dans le texte).

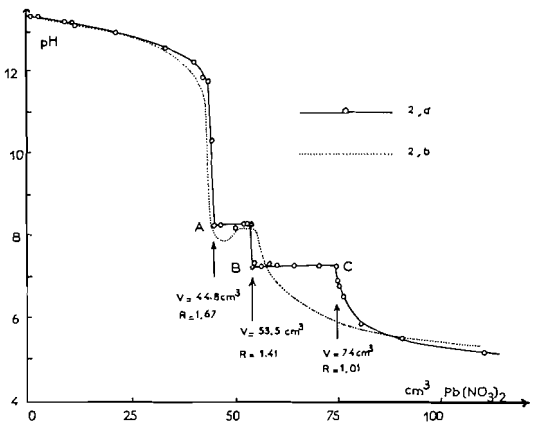

FIG. 8. Dosages potentiométriques de 75 cm^3 d'une solution de soude 0.4 mol l^{-1} par une solution de nitrate de plomb 0.4 mol l^{-1} (commentaires dans le texte).

valeurs expérimentales de R sont légèrement supérieures aux valeurs théoriques de R correspondant à la fin de formation du pentoxynitrate ($R = 1.66$) et du monoxynitrate ($R = 1.00$). Si on verse tout d'abord en une seule fois 25 cm^3 de la solution de nitrate de plomb 0.4 mol l^{-1} avant de poursuivre le dosage, la courbe conductimétrique (Fig. 7, *a*) présente trois ruptures de pente pour les valeurs $R = 1.69$, $R = 1.34$ et $R = 1.06$. La valeur $R = 1.69$ est en bon accord avec la valeur théorique du rapport R correspondant à la précipitation totale du pentoxynitrate de plomb. La rupture de pente observée pour $R = 1.34$ atteste la formation du dioxynitrate de plomb. De même, si on verse tout d'abord en une seule fois 35 cm^3 de la solution de nitrate de plomb avant de poursuivre le dosage, la courbe conductimétrique (Fig. 7, *b*) présente deux ruptures de pente pour $R = 1.33$ et $R = 1.03$. Le rapport $R = 1.33$ correspond exactement à la valeur R théorique de formation du dioxynitrate de plomb.

Ainsi en versant la solution de nitrate de plomb dans la soude, on obtient les mêmes oxynitrates de plomb hydratés que ceux déjà mentionnés lors de l'étude des dosages effectués en versant la soude dans la solution de nitrate de plomb.

La courbe potentiométrique (Fig. 8, *a*) montre que le pH de la solution décroit jusqu'à la valeur 8.30 après addition de 44.8 cm^3 de solution de nitrate de plomb. Le point (A) correspond au rapport $R = 1.67$ en accord avec le rapport R théorique de fin de précipitation du pentoxynitrate de plomb. On constate ensuite que le pH reste constant (p$H = 8.30$) jusqu'à ce

Can. J. Chem. Downloaded from www.nrcresearchpress.com by 210.87.254.105 on 09/05/12
For personal use only.

que le volume de nitrate de plomb ajouté soit égal à 53.5 cm^3. Le pH de la solution décroit alors brusquement et se fixe à la valeur p$H = 7.30$ après addition de 53.6 cm^3 de solution de nitrate de plomb. Le point (B) correspond au rapport $R = 1.41$, en accord avec le rapport R théorique de fin de formation de l'heptoxytrinitrate de plomb. Le pH de la solution reste alors constant (p$H = 7.30$) lorsque le volume de solution de nitrate de plomb est compris entre 53.5 et 74 cm^3. Le pH de la solution décroit ensuite brusquement et le point (C) correspond au rapport $R = 1.01$ en accord avec le rapport R théorique de fin de formation du monoxynitrate de plomb hydraté.

Le pH des solutions ne se stabilise que très lentement. Ainsi, la courbe potentiométrique (Fig. 8, *b*) est obtenue lorsque la variation de pH ne dépasse pas 0.02 unité pendant cinq minutes. Il apparait, en ce cas, que les points correspondant à la formation des oxynitrates de plomb purs ne sont pas définis d'une façon précise. En particulier, on remarque qu'aucun accident ne se manifeste sur la courbe potentiométrique pour la valeur $R = 1.00$ devant indiquer la fin de formation du monoxynitrate. La nécessité d'attendre une vingtaine de jours l'invariance du pH des solutions ne permet pas de mettre en évidence la formation du dioxynitrate de plomb pour les mêmes raisons que celles évoquées à propos des dosages effectués en versant la solution de soude dans celle de nitrate de plomb.

Synthèse des oxynitrates de plomb

Les dosages que nous avons effectués ont révélé que la soude réagit sur une solution de nitrate de plomb pour former les monoxynitrate, dioxynitrate, heptoxytrinitrate et pentoxynitrate de plomb hydratés.

Nous avons également montré qu'il est possible de préparer l'oxyde de plomb hydraté. Nous avons donc étudié les conditions de synthèse des oxynitrates de plomb hydratés et de l'oxyde de plomb hydraté dans un large domaine de température en utilisant plusieurs concentrations de solution aqueuses de soude et de nitrate de plomb. Afin de simplifier leur écriture, nous avons affecté aux différents composés les symboles suivants: $Pb(NO_3)_2.PbO$.hydraté, N1h; $Pb(NO_3)_2.2PbO$.hydraté, N2h; $3Pb(NO_3)_2.7PbO$.hydraté, N7/3h; $Pb(NO_3)_2.5PbO$.hydraté, N5h; $PbO.\frac{1}{3}H_2O$, PbO h.

Pour chacune des températures d'expérimentation, il est possible de tracer un graphique qui montre clairement les conditions optimales de

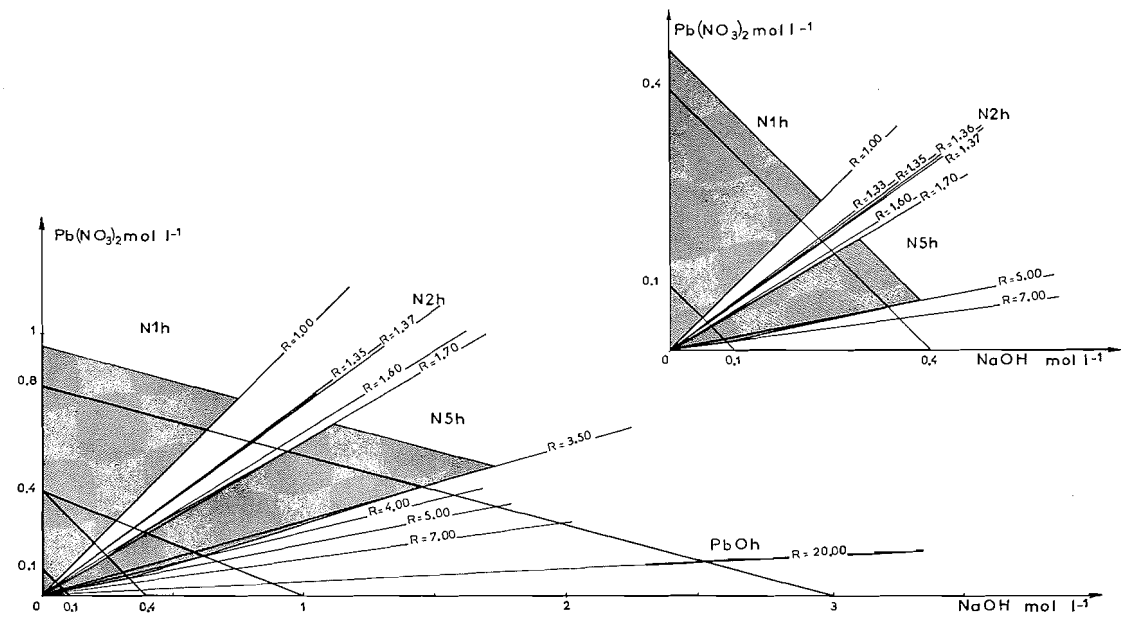

FIG. 9. Diagramme d'obtention à 3 ± 0.5 °C des oxynitrates de plomb hydratés et de l'oxyde de plomb hydraté.

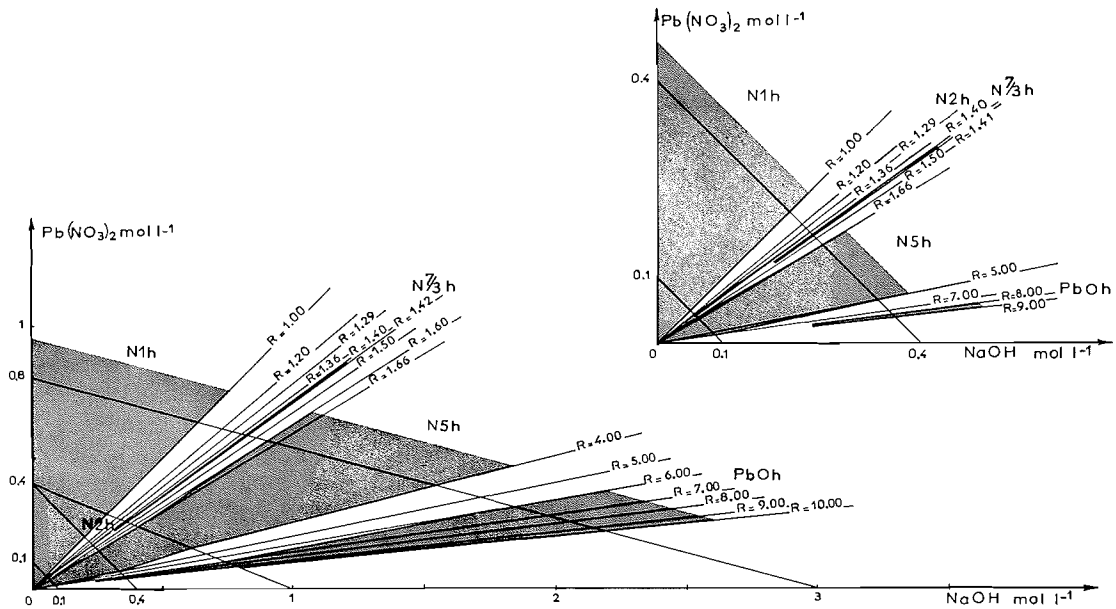

FIG. 10. Diagramme d'obtention à 27 ± 0.3 °C des oxynitrates de plomb hydratés et de l'oxyde de plomb hydraté.

synthèse de l'oxyde et des oxynitrates de plomb hydratés. Les zones colorées en gris dans les Figs. 9, 10 et 11 représentent les domaines d'obtention de ces solides purs aux températures suivantes: 3 ± 0.5, 27 ± 0.3 et 50 ± 0.3 °C.

La combinaison des relations [1] et [2] conduit à une relation linéaire entre (n) et (s):

$$[11] \qquad (n) = -(M_n.(s)/M_s) + M_n$$

La droite correspondant à cette équation est

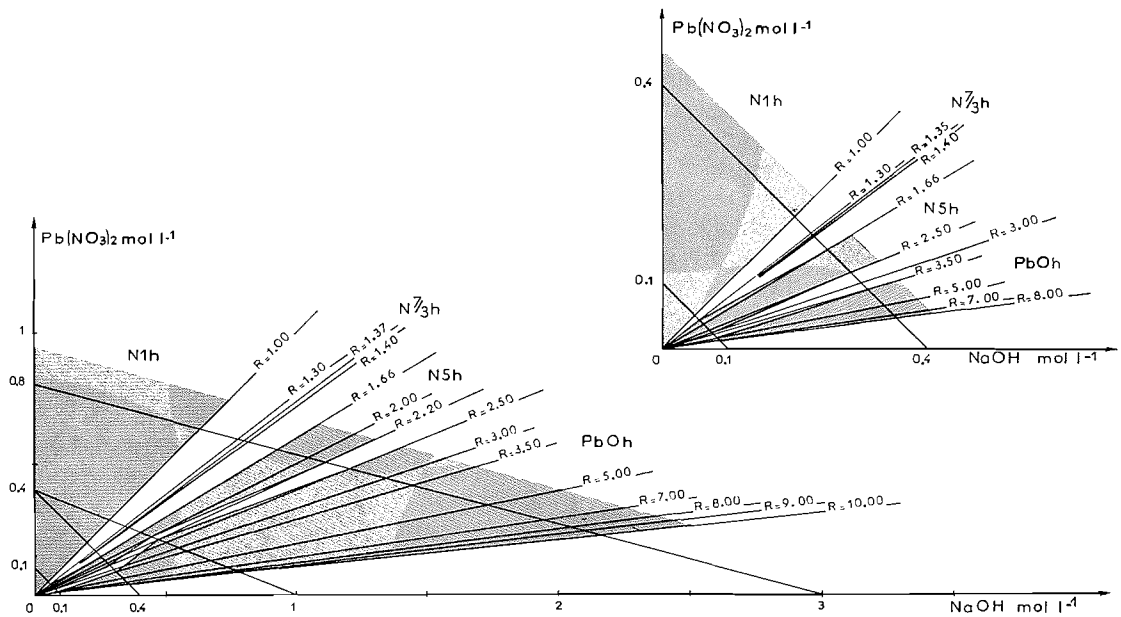

FIG. 11. Diagramme d'obtention à 50 ± 0.3 °C des oxynitrates de plomb hydratés et de l'oxyde de plomb hydraté.

Can. J. Chem. Downloaded from www.nrcresearchpress.com by 210.87.254.105 on 09/05/12
For personal use only.

Can. J. Chem. Downloaded from www.nrcresearchpress.com by 210.87.254.105 on 09/05/12
For personal use only.

le lieu des points représentatifs des mélanges d'une solution de soude de molarité M_s et d'une solution de nitrate de plomb de molarité M_n.

D'autre part, les points représentatifs des mélanges ayant même rapport R sont situés sur la droite correspondant à l'équation

$$[12] \qquad (n) = (s)/R$$

Ces expériences montrent qu'en choisissant convenablement la température et les concentrations des solutions de soude et de nitrate de plomb, on peut préparer facilement monoxynitrate, pentoxynitrate et oxyde de plomb hydratés. Par contre, la synthèse du dioxynitrate et de l'heptoxytrinitrate de plomb est plus délicate. Le dioxynitrate hydraté est obtenu à 3 °C, quelles que soient les concentrations des réactifs, pour des valeurs de R comprises entre 1.33 et 1.37. Cet oxynitrate ne se forme pas à 50 °C. Au contraire, l'heptoxytrinitrate hydraté ne se forme pas à 3 °C. A 50 °C, il peut être préparé, quelles que soient les concentrations des solutions de soude et de nitrate de plomb pour les valeurs de R comprises entre 1.37 et 1.40. Aux températures intermédiaires, l'un et l'autre de ces oxynitrates peuvent être obtenus.

Des expériences complémentaires ont montré que le lavage à l'eau distillée n'altère pas les préparations de ces solides purs. Le séchage nécessite certaines précautions pour éliminer toute trace d'humidité. Les précisions seront apportées dans une publication ultérieure.

Les dosages chimiques du monoxynitrate et du pentoxynitrate de plomb confirment ceux qui ont été signalés dans une autre étude (2). Cependant, l'incertitude sur la détermination de la valeur du rapport N_1/N_2 dans la formule générale des oxynitrates de plomb $Pb(NO_3)_2 \cdot N_1/N_2 PbO.x H_2O$ étant de l'ordre de 0.2, il est difficile de distinguer, par dosage chimique, $Pb(NO_3)_2.2PbO.y H_2O$ où $N_1/N_2 = 2$ et $Pb(NO_3)_2.\frac{7}{3}PbO.zH_2O$ où $N_1/N_2 = 2.33$. Cela, ajouté au fait qu'il est délicat de préparer l'un ou l'autre de ces oxynitrates à 20 °C, permet d'expliquer que dans une étude préliminaire (2), le dioxynitrate de plomb ait pu être confondu avec un trioxydinitrate et l'heptoxytrinitrate de plomb avec un dioxynitrate.

Préparation, à froid, de l'oxyde de plomb anhydre PbOβ

Il est connu que l'oxyde de plomb peut être préparé par voie humide, en faisant réagir une solution de soude ou de potasse sur la solution d'un sel de plomb tel que l'acétate, le perchlorate ou le nitrate mais il est spécifié que cette préparation doit être effectuée à l'ébullition (4). Or, en faisant réagir 140 cm^3 d'une solution de soude de concentration 1 mol l^{-1} et 50 cm^3 d'une solution de nitrate de plomb de concentration 0.4 mol l^{-1} (soit un rapport $R = 7$), à la température ambiante (21 ± 2 °C), nous avons abouti à des résultats différents selon que la solution de soude était préparée à partir de solutions concentrées livrées commercialement dans des récipients en verre ou préparée à partir de pastilles de soude. Dans le premier cas, nous obtenons toujours la formation de l'oxyde de plomb hydraté $PbO.\frac{1}{3}H_2O$. Dans le second cas, nous n'obtenons cet oxyde hydraté qu'après vieillissement pendant trois jours de la solution conservée en récipients de verre, sinon c'est un solide brun-jaune qui précipite. Son diffractogramme X est identique à celui de l'oxyde de plomb jaune PbOβ tel qu'il est consigné dans les fiches de l'A.S.T.M.

Il est connu que les solutions de soude attaquent faiblement et très lentement le verre, même à la température ambiante, cependant que d'autres matériaux tels que le polystyrène, le téflon offrent une bonne résistance aux solutions de soude concentrées même chaudes.

Nous avons donc comparé l'influence du vieillissement de solutions préparées à partir de pastilles de soude et conservées soit en récipients de polystyrène soit en récipients de verre. Dans le premier cas, les manipulations sont toutes effectuées en récipients de polystyrène; dans le second cas, elles sont effectuées en récipients de verre. Les expériences sont réalisées en faisant réagir 140 cm^3 de soude de concentration 1 mol l^{-1} et 50 cm^3 de solution de nitrate 0.4 mol l^{-1}. Nous avons observé que, lorsque les solutions sont préparées et conservées en récipients de polystyrène, on obtient toujours la formation de PbOβ quel que soit le temps de vieillissement (de un jour à quinze mois). Par contre, si les solutions sont préparées et conservées en récipients de verre, nous n'obtenons plus l'oxyde de plomb PbOβ après un vieillissement de trois jours; c'est l'oxyde hydraté $PbO.\frac{1}{3}H_2O$ qui se forme.

Nous avons recherché quel est, parmi les composants essentiels du verre, celui qui favorise la formation de $PbO.\frac{1}{3}H_2O$. A quatre solutions de soude de concentration 1 mol l^{-1} conservées

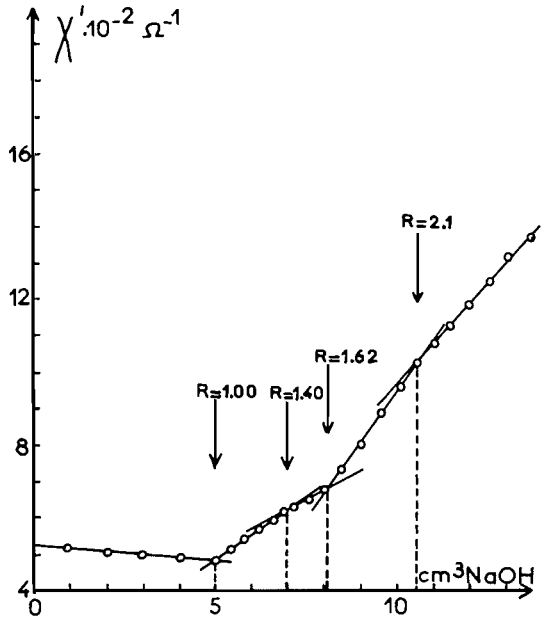

FIG. 12. Dosage conductimétrique de 50 cm^3 d'une solution de nitrate de plomb 0.4 mol l^{-1} par une solution de soude 4 mol l^{-1} (commentaires dans le texte).

en récipients de polystyrène, nous avons ajouté, dans la première, un gramme de silice en poudre; dans la seconde, des morceaux de silice vitreuse; dans la troisième, un gramme de borax; la quatrième est conservée comme témoin. Nous avons constaté qu'après un vieillissement de deux mois, la solution de soude pure et la solution de soude à laquelle on a ajouté du borax permettent encore d'obtenir l'oxyde de plomb PbOβ alors qu'après un mois de vieillissement seulement, les solutions de soude contenant de la silice conduisent à la formation de l'oxyde hydraté $PbO.\frac{1}{3}H_2O$.

En conclusion, la présence de silice, même à l'état de traces dans la solution de soude, inhibe la formation de l'oxyde PbOβ et favorise celle de l'oxyde hydraté $PbO.\frac{1}{3}H_2O$. Des expériences complémentaires, effectuées à partir de réactifs conservés en récipients de polystyrène, ont montré que la présence ou l'absence de traces de silice est sans influence sur les préparations des oxynitrates de plomb. Ainsi la courbe conductimétrique (Fig. 12) rend compte des résultats expérimentaux des dosages effectués en versant une solution de soude 4 mol l^{-1}, préparée et conservée en récipients de polystyrène, dans 50 cm^3 d'une solution de nitrate de plomb 0.4 mol l^{-1}. Les ruptures de pente correspondant aux valeurs $R = 1.00$, $R = 1.40$, $R = 1.62$ et $R = 2.1$ attestent la formation successive des monoxynitrate, heptoxytrinitrate, pentoxynitrate de plomb hydratés et de l'oxyde de plomb anhydre.

1. A. KIRRMANN et A. KRATTIGER. Bull. Soc. Chim. France, 225 (1953).
2. H. BRUSSET, J. J. P. MARTIN, et C. PELTIER. Bull. Soc. Chim. France, **4**, 1127 (1967).
3. H. R. OSWALD, J. R. GÜNTER, et W. STÄHLIN. Helv. Chim. Acta, **51**, 1389 (1968).
4. P. PASCAL. Nouveau traité de Chimie Minérale. Masson éditeur (France) Tome 7. 1963. p. 578.

Can. J. Chem. Downloaded from www.nrcresearchpress.com by 210.87.254.105 on 09/05/12
For personal use only.

Carboxylate Complexing of Iron(III). I. The Formation of Monoacetatoiron(III) in Aqueous Solution: Equilibria and Kinetics

R. N. PANDEY AND W. MACF. SMITH

Department of Chemistry, Queen's University, Kingston, Ontario

Received August 13, 1971

The kinetics and equilibria involved in the formation of monoacetatoiron(III) from iron(III) in aqueous solution has been investigated at ionic strength 0.50 *M* and temperatures ranging from 5.2 to 25 °C for kinetic studies and 5.2 to 41 °C for equilibria. The results support the view that the mechanism of the acid independent reaction involves the reactants $FeOH^{2+}$ and CH_3COOH in an interchange dissociative (I_d) mechanism with $\Delta H^{\ddagger} = 11.1 \pm 2.2$ kcal mol^{-1}. The nature of the acid dependent reactions remains unresolved.

Les cinétiques et les équilibres impliqués dans la formation du monoacétate de fer(III) à partir du fer(III) en solution aqueuse, ont été étudiés à force ionique de 0.50 *M* et sur une échelle de température allant de 5.2 à 25 °C pour les études cinétiques et de 5.2 à 41 °C pour les équilibres. Les résultats montrent que le mécanisme de la réaction, indépendant en acide, implique les réactifs $FeOH^{2+}$ et CH_3COOH dans un mécanisme d'échange et de dissociation (I_d) avec $\Delta H^{\ddagger} = 11.1 \pm 2.2$ kcal mol^{-1}. La nature des réactions qui dépendent de l'acide demeure non élucidée.

Canadian Journal of Chemistry, **50**, 194 (1972)

The acid independent term in the expression for the rate constant for the anation reactions of iron(III) has been interpreted as associated with reactions 1 and 2

[1] $$Fe(H_2O)_6^{3+} + L^- \rightarrow Fe(H_2O)_5L^{2+} + H_2O$$

[2] $$Fe(OH)(H_2O)_5^{2+} + HL \rightarrow Fe(H_2O)_5L^{2+} + H_2O$$

occurring with an interchange (I) mechanism. In such a mechanism an outer ion pair involving the two reactants with formation constant K_0 collapses to form the complex with a first-order rate constant k; and if this constant is much smaller than that for dissociation of the ion pair and if the concentration of ion pairs is substantially less than those of the reactants, the overall reaction is first order in each reactant (second order overall) and equal to kK_0 (2, 3). In the mechanism labelled I_d (dissociative interchange) k should be closely related to the rate constant for water exchange on the unassociated metal ion and this should be substantially greater for $Fe(OH)(H_2O)_5^{2+}$ than for $Fe(H_2O)_6^{3+}$ (4).

For ligands of low basicity such as Cl^- or Br^- the dominant contribution to the rate constant appears to be that associated with reaction 1 (5) with only a modest dependence of its magnitude on ligand type, but for reactions involving ligands of higher basicity it appears that reaction 2 proceeding by an essentially I_d mechanism is consistent with experimental data (6, 7). Assuming that reaction 1 is the dominant reaction results in a dependence of k on ligand basicity which was rationalized by Eigen by the hypothesis of inner hydrolysis (8). Assuming that reaction 2 is dominant yields values for k which are approximately constant and consistent with some estimates of the rate constant for water exchange on $Fe(OH)(H_2O)_5^{2+}$ (9). Recent work by Cavasino and Di Dio (7) on the reaction of the substituted phenols definitely rules out the possibility of reaction 1 being a dominant reaction for ligands of high basicity but some uncertainty remains about the nature of reactions involving ligands of modest basicity.

When we undertook the work reported in part in this paper there was a paucity of data on reactions involving iron(III) and ligands of similar structure but with basicities covering a range. We chose to study the characteristics of the reaction of the four monocarboxylato reactants: acetate, monochloroacetate, dichloroacetate, and trichloroacetate with basic ionization constants in water at 25 °C and ionic strength 0.5 ranging from 3.7×10^{-10} to 1.2×10^{-14}. Since then the work of Accascina, Cavasino, and Di Dio (6) on the reactions of iron(III) with various aliphatic acids including acetic and monochloroacetic and of Cavasino and Di Dio (7) on the substituted phenols has been published and has provided data for reactions involving ligands with a wide range

Can. J. Chem. Downloaded from www.nrcresearchpress.com by 210.87.254.5 on 09/05/12
For personal use only.

Can. J. Chem. Downloaded from www.nrcresearchpress.com by 210.87.254.5 on 09/05/12
For personal use only.

of basicities which support the assumption that the dominant process in the reactions studied is indeed reaction 2. However, their data are restricted to a single temperature. Their measurements were made with T jump relaxation techniques and for the aliphatic acids the data were interpreted using values obtained by Perrin for the association constants of the complexes.

Our kinetic investigation involved stopped flow techniques, covered the temperature range 5.2 to 25 °C, and also involved measurement of the association constants of the mono complex. This paper is restricted to the equilibria and kinetics of the acetate complex.

Experimental

Materials

Baker reagent grade acetic acid was purified by the method of Ritter and Simons (10). Sodium perchlorate was prepared by neutralization of reagent grade perchloric acid with Baker's analyzed reagent sodium hydroxide. Reagent grade iron(III) perchlorate from G. Frederick Smith was washed repeatedly with small amounts of 70% perchloric acid to remove traces of chloride prior to preparation of solutions. Sulfate estimated by the method of Fritz, Yamamura, and Richard (11) was found to be in negligible amount. The iron(III) and acid contents of the solutions were estimated by methods previously outlined (12).

Equilibrium Measurements

The acid ionization constant was assessed via electrometric measurement of the hydrogen ion concentration in buffer mixtures of sodium acetate and acetic acid with the ionic strength adjusted to 0.50 with sodium perchlorate. The electrometric cell involved calomel and hydrogen electrodes. The hydrogen was ultra pure quality from Matheson and was passed over platinized asbestos and platinum at ~200 °C and through a presaturator. The correlation between e.m.f. readings and hydrogen ion concentration was obtained with solutions of known concentrations of perchloric acid adjusted to ionic strength 0.50 with sodium perchlorate. The correction associated with variation in the partial pressure of the hydrogen between standardization and measurement was negligible compared with the reproducibility (±0.5 mV) and was ignored.

The data, from which the association constants of the complexes were estimated, were obtained spectrophotometrically with a Beckman DK1 spectrophotometer with a thermostatted cell holder with temperature control of ±0.15 °C and cells of 1, 10, and 50 mm path length. The total iron(III) concentration varied from 2.02×10^{-4} to 2.02×10^{-3}, the total concentration of acetic acid from 0.25 to 1.50 M, the hydrogen ion concentration was in the range 0.032 to 0.32 M. The difference in absorbances (ΔA) at λ320, 310, and 295 mμ and at temperatures 5.2, 15.2, 25.0, 35.2, 41.0 °C were determined for pairs of solutions identical in ionic strength, hydrogen ion concentration, and total iron(III) concentration but differing in that one contained acetic acid and the other did not.

Kinetic measurements involving the acetate complex were made with a Model D-150 Durrum stopped-flow spectrophotometer using λ310 mμ and an optical path length of 20 mm. The pertinent data involved the optical density as a function of time. As indicated below, the reactions were pseudo first order under the conditions used and it was not essential to determine the optical densities near zero time.

Interpretation of Experimental Data

Equilibria

The data upon which estimates of the association constant, K_{ass}, are based along with the parameters in the relations used in reducing the data are as follows:

T_m = the total molar concentration of iron(III) perchlorate added;

T_L = the total concentration of acetate added (as acetic acid);

h = the concentration of hydrogen ions;

K_h = the hydrolysis constant for iron(III);

Q_a = the acid ionization constant for acetic acid;

ΔA = the difference in absorbance of two solutions differing only in that $T_L = 0$ in one of them;

q = the concentration of perchloric acid;

c = the concentration of the mono complex FeL^{2+};

$V = Q_a/(K_h + h)$;

$[L^-]$ = the concentration of acetate ion;

ε_{FeL} = the molar absorptivity of the mono-acetato complex FeL^{2+};

ε_{Fe} = the molar absorptivity of ferric ion, Fe^{3+};

ε_{FeOH} = the molar absorptivity of $FeOH^{2+}$;

$\Delta\varepsilon = \varepsilon_{FeL} - \{\varepsilon_{FeOH} K_h/(K_h + h) + \varepsilon_{Fe} h/(K_h + h)\}$;

l = length of the optical path in the spectrophotometric measurements.

The values used for K_h were those determined by Connick and co-workers (13), those used for Q_a were determined as indicated above on the basis of knowledge of the concentrations of acetic acid and sodium acetate from make-up composition and the concentration of hydrogen ion from the electrometric measurement. Values so determined are shown on Table 1 and indicate a maximum in the range between 5.2 and 25.0 °C. Harned and Ehlers (14) measured the acid ionization constant conductometrically and found a maximum near 25 °C for the thermodynamic constant (zero ionic strength). Esti-

Can. J. Chem. Downloaded from www.nrcresearchpress.com by 210.87.254.5 on 09/05/12
For personal use only.

TABLE 1. Acid ionization constant (Q_a) of acetic acid at ionic strength 0.50 *M*

Temperature (°C)	$Q_a \times 10^5$ *M*
5.2	2.90±0.29
15.2	3.38±0.11
25.0	2.70±0.31
35.2	2.50±0.12
41.0	2.50±0.15

mates of ε_{FeOH} and ε_{Fe} were made on the basis of our measurements of the absorbance of solution of ferric perchlorate at ionic strength 0.50 and various acidities and Connick *et al.*'s values for K_h using the relationship

$$A_i = T_m l\left(\varepsilon_{FeOH}\frac{K_h}{K_h+h} + \varepsilon_{Fe}\frac{h}{K_h+h}\right)$$

where A_i is the contribution of iron(III) to the absorbance. Values obtained at 25 °C are shown in Table 2.

The method of Bent and French (15) was used to check the composition of the complexes formed. If only the mono complex is formed in significant amount, a plot of log ΔA against log $[L^-]$($[L^-] \sim Q_a T_L/h$) at constant T_m should have a slope of unity. The data covering the range of conditions of the equilibrium and kinetic studies yielded a line with slope 1.03 ± 0.03.

Association constants were obtained by interpreting the data by a Benesi–Hildebrand equation (16) of the form

$$[3] \quad \frac{T_m}{\Delta A} = \frac{1}{\Delta\varepsilon l} + \frac{1}{\Delta\varepsilon l}\frac{1}{K_{ass}[L^-]}\frac{K_h+h}{h}$$

The moderately low value of K_{ass} along with the smallness of the values of $[L^-]$ experimentally accessible, because of the weakness of acetic acid and the necessity of maintaining the value of h moderately high to minimize hydrolysis, led to groups of data which yielded very small intercepts with large relative dispersion in their values for the plot of $1/\Delta A$ *vs.* $1/[L^-]$ although the values for the slopes of the plots had much less dispersion. An iterative machine calculation was used to interpret the data starting with eq. 4 which derives directly from eq. 3

$$[4] \quad \frac{T_m}{\Delta A} = \frac{1}{\Delta\varepsilon l} + \frac{1}{\Delta\varepsilon l}\frac{1}{K_{ass}}\frac{1}{V(T_L - c - [L^-])}$$

and then using eq. 5 which relates the contribution A of the complex FeL^{2+} with molar extinction coefficient ε_{FeL} to the absorbance of the solution.

$$[5] \quad \frac{T_m}{A} = \frac{1}{\varepsilon_{FeL} l} + \frac{1}{\varepsilon_{FeL} l}\frac{1}{K_{ass}}\frac{1}{V(T_L - c - [L^-])}$$

$\Delta\varepsilon$ is dependent on the value of h if hydrolysis is significant particularly at lower values for λ and this implies that eq. 4 is not strictly linear, unless the data in a group are for one value of h or unless the optical densities are corrected to apply to a common reference acidity. To attain a useful range of concentrations for $[L^-]$ which would yield significant complexing of iron(III) without appreciably reducing the activity of the solvent water, h was varied in obtaining groups of data and allowance was made for the effect of hydrolysis.

First approximations for $\Delta\varepsilon$ and K_{ass} were obtained from data using a linear least mean squares treatment with eq. 4 assuming that $\Delta\varepsilon$ was independent of h, that $(T_L - c - [L^-]) = T_L$. Further cycles were carried out with values of c from $\Delta A/l\Delta\varepsilon$ and $[L^-]$ from $Q_a(T_L - c)/(h + Q_a)$. To allow for the effect of variation in the degree of hydrolysis on absorption, eq. 5 was used iteratively with values of A for each datum point estimated from $c.l\varepsilon_{FeL}$ where $\varepsilon_{FeL} = \Delta\varepsilon + \varepsilon_{Fe}\, h/(K_h + h) + \varepsilon_{FeOH}\, K_h/(K_h + h)$.

Allowance for the effect of hydrolysis of iron(III) and of complex formation as well as ionization of HL on h was written into the program using the relation

$$[6] \quad h = q + [L^-] + c\left(1 + \frac{K_h}{Q_a K_{ass}(T_L - c - [L^-])}\right)$$

TABLE 2. Values for the molar absorptivity of Fe^{3+} and $FeOH^{2+}$; temperature = 25 °C; ionic strength = 0.50 *M*

λ(mμ)	$\varepsilon_{Fe}(M^{-1}\,cm^{-1})$	$\varepsilon_{FeOH}(M^{-1}\,cm^{-1})$
290	3.52×10^2	2.25×10^3
295	2.88×10^2	1.33×10^3
310	0.56×10^2	1.98×10^3
320	0.13×10^2	1.16×10^2

TABLE 3. Association constants for the complex Fe $(CH_3.COO)^{2+}$; ionic strength = 0.50 M

Temperature (°C)	$K_{ass} \times 10^{-2}$ (M^{-1})
5.2	4.39±0.09
15.2	4.92±0.30
25.0	8.08±0.25
35.2	10.93±0.36
41.0	12.69±0.28

but values yielded for h are insignificantly greater than those for q for the acetate systems of this investigation and the allowance is not necessary.

The groups of data each characterized by a given value for T_L yielded slopes (eq. 5) with relative range of about ±8% but the range of the intercepts was ±50%. The difficulty of obtaining reliable intercepts under conditions similar to those in this work has been emphasized by several writers (17, 18). Rather than taking an average based on all data we have chosen the value for ε_{FeL} from a selected group of measurements where the precision in the measurements of ΔA was optimal and the relative error in the intercepts less than 15%. The values for ε_{FeL} so obtained were 2191 M^{-1} cm^{-1} at λ310 mμ, 1839 M^{-1} cm^{-1} at λ320 mμ and 3000 M^{-1} cm^{-1} at λ295 mμ. These values of ε_{FeL}, assumed to apply at all temperatures, were used with all data where the dispersion of slopes was within ±7.5% to yield the average values for K_{ass} summarized in Table 3.

A plot of log K_{ass} *vs.* $1/T$ indicated a close approximation to linearity for all data except those for 15.2 °C. If the value for 15.2 °C be omitted the data may be summarized by the relationship log $K_{ass} = A + B/T$ with $A = 6.68 \pm 0.04$ and $B = -1.13 \pm 0.01$. We have used this relationship to obtain a value for K_{ass} at 20 °C and an alternative value for K_{ass} at 15.2 °C. The values, 641 M^{-1} at 20 °C and 604 M^{-1} at 15.2 °C, were used in reducing the kinetic data.

Kinetics

Accascina, Cavasino, and Di Dio (6) have successfully interpreted the kinetic data relating to the monoacetato complex of iron(III) obtained by T jump relaxation methods by the following reaction scheme which also successfully accommodated our results.

$$Fe(H_2O)_6^{3+} + L^- \underset{k_{21}}{\overset{k_{12}}{\rightleftharpoons}} Fe(H_2O)_5L^{2+} + H_2O$$

$$Fe(H_2O)_5OH^{2+} + HL \underset{k_{46}}{\overset{k_{64}}{\rightleftharpoons}} Fe(H_2O)_5(OH)L^+ + H_2O + H^+$$

$$Fe(H_2O)_6^{3+} + HL \underset{k_{25}}{\overset{k_{52}}{\rightleftharpoons}} Fe(H_2O)_5L^{2+} + H_2O + H^+$$

$$Fe(H_2O)_5OH^{2+} + L^- \underset{k_{43}}{\overset{k_{34}}{\rightleftharpoons}} Fe(H_2O)_4(OH)L^+ + H_2O$$

The following reactions are relatively fast and the products and reactants are maintained close to equilibrium concentrations.

$$HL \rightleftharpoons H^+ + L^- \qquad Q_a$$

$$Fe(H_2O)_6^{3+} \rightleftharpoons Fe(H_2O)_5(OH)^{2+} + H^+ \qquad K_h$$

$$Fe(H_2O)_4(OH)L^+ + H^+ \rightleftharpoons Fe(H_2O)_5L^{2+}$$

On the basis of this scheme it follows that

$$\frac{dc}{dt} = k_f[Fe^{3+}][L^-] - k_b[FeL^{2+}]$$

where

$$[7] \quad k_f = k_{12} + k_{64}\frac{K_h}{Q_a} + k_{52}\frac{h}{Q_a} + k_{34}\frac{K_h}{h}$$

Noting that $k_f/k_b = K_{ass}$ and assuming that the concentrations of outer ion pairs

$$(Fe(H_2O)_6^{3+}.L)$$

is negligible relative to the concentration of reactants

$$\frac{dc}{dt} = k_f\frac{h}{K_h + h}T_m[L^-] - k_f\left(\frac{h}{K_h + h}[L^-] + \frac{1}{K_{ass}}\right)c$$

which on integration yields

$$-2.303 \log\frac{c_e - c}{c_e} = k_f\left(\frac{h}{K_h + h}[L^-] + \frac{1}{K_{ass}}\right)t$$

where c_e is the concentration of the complex at equilibrium. In terms of observables this becomes

$$[8] \quad -2.303 \log\frac{A_e - A_t}{A_e - A_0} = k_f\left(\frac{h}{K_h + h}[L^-] + \frac{1}{K_{ass}}\right)t$$

Can. J. Chem. Downloaded from www.nrcresearchpress.com by 210.87.254.5 on 09/05/12
For personal use only.

Can. J. Chem. Downloaded from www.nrcresearchpress.com by 210.87.254.5 on 09/05/12
For personal use only.

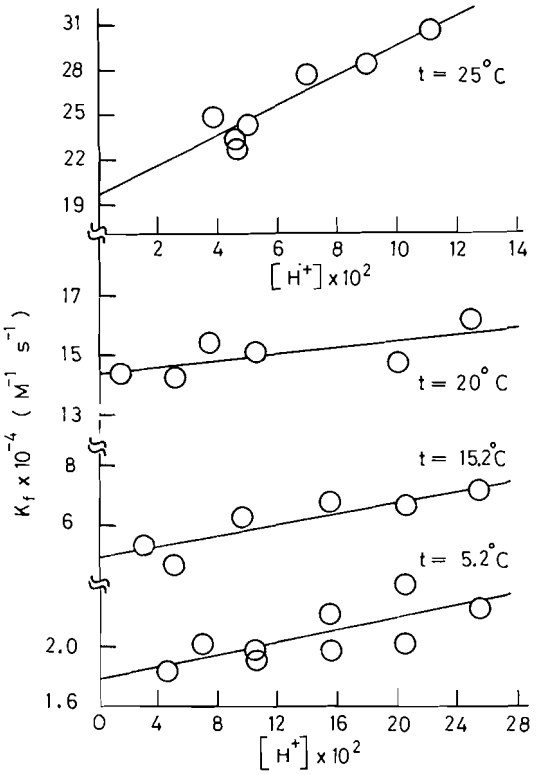

FIG. 1. Plot of forward rate constant k_f against hydrogen ion concentration.

where A_0 and A_e represent absorbances of the reacting solution initially and at equilibrium.

$$[L^-] = \frac{Q_a}{Q_a + h}(T_L - c) \sim \frac{Q_a}{Q_a + h} T_L$$

Consequently values for k_f may be estimated from the slope of the plot of $\log(A_e - A_t)$ against time.

From the exponential form of eq. 8, eq. 9 may be derived

$$[9] \quad A_t = A_e + (A_{t'} - A_e) \times \exp -k_f\left(\frac{h}{k_h + h} \cdot \frac{Q_a}{h} \cdot T_L + \frac{1}{K_{ass}}\right)(t - t')$$

where $A_{t'}$ and A_t are absorbances at times t' and t.

As has been pointed out by Guggenheim and Wiseman (19) it is statistically better to apply a least mean squares fit using the exponential relation rather than the logarithmic equation. Equation 9 is of the form $D = X + Ye^{-Zt}$ and we have used the procedure of Southworth and De Leeuw (20) to assess the values of Z and hence of k_f corresponding to a least mean squares fit of eq. 9 to the experimental data. The values of $h/(K_h + h)$ deviate from unity by at most 0.03 and were assigned a value of unity in all calculations.

A summary of the values of k_f is displayed in Fig. 1. The widest range of conditions were covered in the runs at 15.2 °C where T_m ranged from 0.505×10^{-3} to 6.88×10^{-3} M and T_L from 0.150 to 1.00 M. The data appear to show a linear dependence of k_f on h at each temperature, in consistency with the findings of Accascina, Cavasino, and Di Dio (which apply only to 20 °C) and we have therefore assumed that the term k_{34} in relation 7 is negligible, *i.e.* that

$$k_f = k_{12} + k_{64}\frac{K_h}{Q_a} + \frac{k_{52}}{Q_a} h = k_{intercept} + \frac{k_{52}}{Q_a} h$$

Table 4 contains values for $k_{intercept}$ ($= k_{12} + k_{64}K_h/Q_a$), values of k_{64} assuming that k_{12} is negligible and k_{52} estimated on the basis of the values of Q_a given in Table 1 with the value for 20 °C taken as 3.04×10^{-5} M and values for K_h of 0.67×10^{-3}, 1.18×10^{-3}, 1.51×10^{-3}, and 1.90×10^{-3} M at temperatures 5.2, 15.2, 20.0, and 25 °C, respectively. The values for K_h are based on the work of Connick and co-workers (13) with the values at 5.2 and 20 °C obtained by extrapolation and interpolation. Plots of $\log(k_{12}/T) - 1$ *vs.* $1/T$ (assuming $k_{12} = k_{intercept}$) and $\log(k_{64}/T)$ *vs.* $1/T$ (assuming k_{12} is negligible) are shown in Fig. 2. If the data for 20 °C be included, the deviation from linearity is considerable and the values for k_{64} for 20 and 25 °C show an anomalous temperature dependence. Values for the kinetic parameters obtained from lines of regression through the datum points for all four temperatures are: $\Delta H^{\ddagger}_{12} = 20.3 \pm 2.0$ kcal mol^{-1}, $\Delta S^{\ddagger}_{12} = 33.7 \pm 6.6$ cal deg^{-1} mol^{-1}, $\Delta H^{\ddagger}_{64} = 11.1 \pm 2.2$ kcal mol^{-1}, and $\Delta S^{\ddagger}_{64} = 5.4 \pm 7.0$ cal deg^{-1} mol^{-1}. The values of k_{52} also show considerable dispersion with the value applying to 20 °C deviating markedly from a moderately linear set for the other three datum points as if the intercept were too high and the slope too low. The line of regression through all four points yields a value for $\Delta H^{\ddagger}_{52}$ of 26 ± 12 kcal mol^{-1}.

TABLE 4. Formation rate constants for the complex $Fe(CH_3.COO)^{2+}$ (M^{-1} s^{-1}); ionic strength = 0.50 M

Temperature (°C)	$k_{intercept} \times 10^{-4}$ $(k_{12} + k_{64}K_h/Q_a)$ (M^{-1} s^{-1})	$k_{64} \times 10^{-3}$ (M^{-1} s^{-1})	k_{52} (M^{-1} s^{-1})
5.2	1.76±0.1	0.76±0.09	0.6±0.2
15.2	5.8 ±0.5	1.65±0.16	4.0±1.1
20.0	14.3 ±0.4	2.9 ±0.4	1.7±0.9
25.0	19.4 ±1.1	2.8 ±0.4	27 ±5

Discussion

Our data for acetic acid were obtained under conditions (ionic strength 0.50) different from those used by Accascina, Cavasino, and Di Dio (ionic strength 1.0) (6) but are consistent with those data and support the hypothesis that the dominant reaction for the acid independent path involves FeOH and HL reacting by an I_d mechanism. The magnitudes of $k_{intercept}$ at 20 and 25 °C (14×10^4 and 19×10^4 M^{-1} s^{-1}) are much greater than the values attributed to the reactions where the dominant path is assumed to involve Fe^{3+} and L^- (5) *e.g.* 9.4 M^{-1} s^{-1} for $Fe^{3+} + Cl^-$ at 25 °C and ionic strength 1.0 (21) and 20 M^{-1} s^{-1} for $Fe^{3+} + Br^-$ at 25 °C and ionic strength 1.7 (22). If the assumptions are made that $k_{intercept} = k_{12} + k_{64}K_h/Q_a$ and that k_{12} is of the same order of magnitude as k_{12} ($=k_{intercept}$) for the reactions of iron(III) with chloride and bromide, it is apparent that the term involving k_{64} is the dominant one.

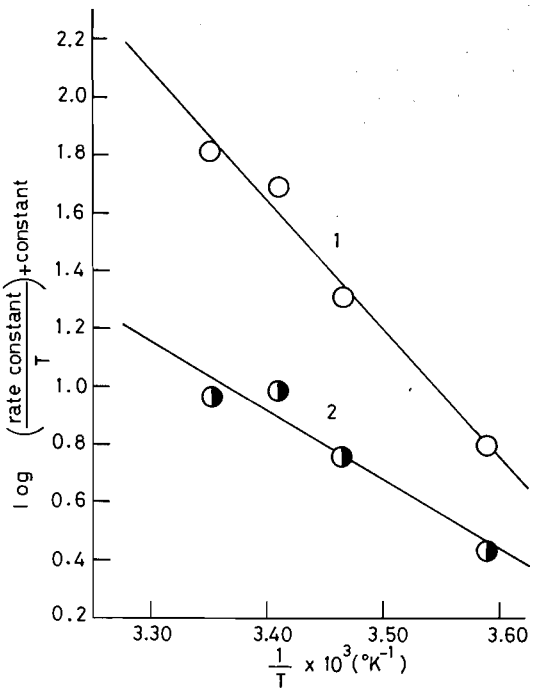

FIG. 2. Modified Arrhenius plots: (*1*) ○ plot of $\log (k_{12}/T) - 1$ against $1/T$ (values of ordinate displaced by 1 for clarity); (*2*) ◑ plot of $\log (k_{64}/T)$ against $1/T$.

The values of the first-order rate constants for collapse of the outer ion pairs (k_{012} and k_{064}) may be roughly estimated using the relations $k_{012} = k_{12}/K_{12}$ and $k_{064} = k_{64}/K_{64}$ and values $K_{12} \sim 2.3$ M^{-1} and $K_{64} \sim 0.3$ M^{-1} estimated from the Fuoss–Eigen relationships (23, 2). The value for k_{012} is substantially in excess of a recent value of 150 s^{-1} for the first-order rate constant for water exchange on $Fe(H_2O)_6^{3+}$ (9). The value for k_{064} (about 9×10^3 s^{-1}) is fairly close to the value to be anticipated for the rate constant for water exchange on $Fe(H_2O)_5OH^{2+}$ if one assumes as does Connick and Genser (4) that the rate constant for water exchange on $Fe(H_2O)_5(OH)^{2+}$ should be higher than that for water exchange on $Fe(H_2O)_6^{3+}$ by a factor of about 10^2.

Although the dispersion from linearity in the plot of $\log k_{52}$ *vs.* $1/T$ is large with the value for 20 °C anomalously low, the values of k_{52} are in the range of values for k_{12} associated with reactions of $Fe(H_2O)_6^{3+}$ with charged and uncharged ligands. The temperature coefficient for k_{52} and the associated value of $\Delta H^{\ddagger}_{52}$ (26 ± 12 kcal mol^{-1}) is, however, higher than would be anticipated for a reaction of such a nature (*i.e.* ~ 16 kcal mol^{-1}). A temperature coefficient for the slope of the plot of k_f *vs.* h, which is higher than that to be anticipated from any of the previously mentioned single mechanisms, could occur if with decrease in temperatures over the lower range of acidities there was increasing contribution to k_f from the

Can. J. Chem. Downloaded from www.nrcresearchpress.com by 210.87.254.5 on 09/05/12
For personal use only.

term involving k_{34}. Such a contribution should yield a curvature as well as a reduction in the slopes (24, 6) which if more marked at lower temperatures would yield abnormally high estimates for $\Delta H^{\ddagger}_{52}$. Such curvature is not clearly indicated by our data. However, the dispersion of the data along with the restricted range of hydrogen ion concentrations covered are such as to prevent adequate assessment of such a hypothesis or to attain acceptable precision in the estimates of the slopes.

In summary, our data support the assumption of Cavasino and co-workers (6) that the dominant component of the acid independent reaction yielding the mono acetato complex of iron(III) involves $FeOH^{2+}$ and CH_3COOH reacting by an I_d mechanism. However, data covering wider ranges of acidity and of higher precision are required to adequately assess the character of the acid dependent components.

We thank the National Research Council of Canada for financial support of this work.

1. C. H. Langford and H. B. Gray. Ligand substitution processes. W. A. Benjamin, New York, 1965. Chap. 1.
2. M. Eigen. Z. Electrochem. **64**, 115 (1960).
3. M. Eigen and R. G. Wilkins. Mechanisms of inorganic reactions. Advances in Chemistry Series, No. 49. American Chemical Society, Washington, D.C. 1965. p. 55.
4. R. E. Connick and E. E. Genser. Private communication. D. Seewald and N. Sutin. Inorg. Chem. **2**, 643 (1963).
5. F. Accasina, F. P. Cavasino, and S. D'Alessandro. J. Phys. Chem. **71**, 2474 (1967).
6. F. Accasina, F. P. Cavasino, and E. Di Dio. Trans. Faraday Soc. **65**, 489 (1969).
7. F. P. Cavasino and E. Di Dio. J. Chem. Soc. A, 1151 (1970).
8. M. Eigen. Advances in the chemistry of co-ordination compounds. MacMillan, New York. 1961. p. 371.
9. M. R. Judkins. Ph.D. Thesis, University of California, Berkeley, California. 1967. Available as Lawrence Radiation Laboratory Report UCRL 17561.
10. H. L. Ritter and J. H. Simons. J. Am. Chem. Soc. **67**, 757 (1945).
11. J. S. Fritz, S. S. Yamamura, and M. J. Richard. Anal. Chem. **29**, 158 (1957).
12. D. Pouli and W. MacF. Smith. Can. J. Chem. **38**, 567 (1960).
13. R. E. Connick, L. G. Hepler, Z. Z. Hugus Jr., J. W. Kury, W. M. Latimer, and Maak-Sang Tsao. J. Am. Chem. Soc. **78**, 1827 (1956).
14. H. S. Harned and R. W. Ehlers. J. Am. Chem. Soc. **55**, 652 (1933).
15. H. E. Bent and C. L. French. J. Am. Chem. Soc. **63**, 568 (1941).
16. H. A. Benesi and J. H. Hildebrand. J. Am. Chem. Soc. **71**, 2703 (1949).
17. W. B. Person. J. Am. Chem. Soc. **87**, 167 (1965).
18. K. Conrow, G. D. Johnson, and R. E. Bowen. J. Am. Chem. Soc. **86**, 1025 (1964).
19. E. A. Guggenheim and L. A. Wiseman. Proc. Roy. Soc. A**203**, 7 (1950).
20. R. W. Southworth and S. L. De Leeuw. Digital Computations and Numerical Analysis. McGraw-Hill, New York. p. 474.
21. R. E. Connick and C. P. Copel. J. Am. Chem. Soc. **81**, 6389 (1959).
22. P. Matthies and H. Wendt. Z. Phys. Chem. (Frankfurt) **30**, 137 (1961).
23. R. M. Fuoss. J. Am. Chem. Soc. **80**, 5059 (1958).
24. F. P. Cavasino. J. Phys. Chem. **72**, 1378 (1968).

Can. J. Chem. Downloaded from www.nrcresearchpress.com by 210.87.254.5 on 09/05/12
For personal use only.

Mössbauer and Infrared Spectra of Octahedral Complexes of Iron(II) Halides with Amides and Related Ligands

T. BIRCHALL AND M. F. MORRIS

Department of Chemistry, McMaster University, Hamilton, Ontario

Received July 26, 1971

A number of complexes of $FeCl_2$ and $FeBr_2$ with amides, ureas, aniline, and benzothiazole have been prepared and characterized by means of Mössbauer and i.r. spectroscopy, and magnetic measurements. The stoichiometries FeX_2L, FeX_2L_2, FeX_2L_3, FeX_2L_4, and FeX_2L_6 have been found in which the iron is six coordinate. With the exception of an isobutyramide complex which is formulated as $[Fe(BUA)_6][FeCl_4]$, complexes of the first three types are polymeric with bridging halogens, while FeX_2L_4 is monomeric and FeX_2L_6 is formulated as $[FeL_6]Cl_2$.

Certains complexes de $FeCl_2$ et $FeBr_2$ avec les amides, l'urée, l'aniline et le benzothiazole ont été préparés et caractérisés au moyen de la spectroscopie Mössbauer et infrarouge et par des mesures magnétiques. Les stoechiométries de FeX_2L, FeX_2L_2, FeX_2L_3, FeX_2L_4 et FeX_2L_6 ont été déterminées et il apparaît que le fer y est six fois coordonné. A l'exception d'un complexe avec l'isobutyramide qui est formulé comme $[Fe(BUA)_6][FeCl_4]$, les complexes des trois premiers types sont polymériques avec des ponts halogène, alors que FeX_2L_4 est monomérique et que FeX_2L_6 est formulé comme $[FeL_6]Cl_2$.

Canadian Journal of Chemistry, **50**, 201 (1972)

Introduction

Recent studies of iron(II) complexes FeX_2L_n show increasing evidence for polymeric halogen bridged structures, at least among 6-coordinate species. It has been shown (1) by X-ray diffraction methods that $FeCl_2 \cdot 2H_2O$ has the 6-coordinate polymeric chain structure **1**. $FeCl_2 \cdot 2NH_3$ and $FeBr_2 \cdot 2NH_3$ are also thought to have this structure (2), as are the $FeCl_2L_2$ complexes where L = methylcyanide (3), pyridine (4), and benzothiazole (5). It was suggested in a recent Mössbauer study (6) that the complexes $FeCl_2L_2$ (L = formamide, acetamide) also occur as the linear polymer **1**. A 1:1 pyridine complex $FeCl_2(py)$ is thought to be octahedral (7) with an extensively chlorine bridged structure such as **2**.

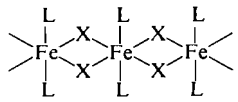

1

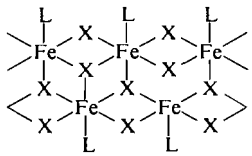

2

Polymers **1** and **2** may be thought of as derivatives of the anhydrous ferrous chloride structure in which iron is 6-coordinate and all chlorines are shared (8).

In this study a number of ferrous halide complexes with amide and urea ligands are investigated by means of Mössbauer, i.r. spectroscopy, and magnetic measurements. Complexes with aniline and benzothiazole are also investigated. Among these complexes a pronounced tendency to form halogen bridged polymers is found.

Experimental

Preparations

With the exception of $FeCl_2(BTH)_2$, $FeCl_2(UREA)_2$, $FeBr_2(DMU)_3$, and $FeCl_2(AN)_3$ all the complexes were prepared by the method of Singh and Rivest (9), alternate procedures for $FeCl_2(FA)_2$, $[Fe(MU)_6]Cl_2$, and $FeCl_2(DMU)_3$ were also used and are described below. $FeCl_2(BTH)_2$ was prepared by the method described by Chan *et al.* (5). Preparation of these samples, filtering, and washing of products, was carried out under nitrogen in a dry box. Products were white or colorless crystals except for the benzamide complex which was a white spongy material. Analytical data are presented in Table 1, where BTH = benzothiazole; FA = formamide; MFA = *N*-methylformamide; DMFA = *N,N'*-dimethylformamide; AM = acetamide; BM = benzamide; BUA = isobutyramide; MU = *N*-methylurea; DMU = *N,N'*-dimethylurea; AN = aniline.

Dichlorobisurea Iron(II)

A solution of 1.5 g ferrous chloride in 10 ml absolute ethanol was shaken with powdered iron until green. It was centrifuged, and the supernatant liquid poured into a solution of 2 g urea in ethanol. A precipitate formed in about 2 h, was filtered, washed with ether, and dried *in vacuo*.

Can. J. Chem. Downloaded from www.nrcresearchpress.com by 210.87.254.42 on 09/05/12
For personal use only.

TABLE 1. Iron and halogen analyses of complexes

Complex	Fe (%)		Halogen (%)	
	Calcd.	Obsd.	Calcd.	Obsd.
$[Fe(BUA)_6][FeCl_4]$	14.39	14.51	18.28	19.03
$[Fe(MU)_6]Cl_2$	9.78	9.56	12.42	11.95
		10.20		12.32
$FeCl_2(FA)_2$			32.70	31.50
$FeCl_2(FA)_4$	18.21	18.10	23.10	23.19
$FeCl_2(MFA)_2$	23.00	23.30	29.20	29.48
$FeCl_2(DMFA)_2$			25.99	23.42
$FeCl_2(AM)_2$	22.80	22.60	28.96	28.95
$FeCl_2(UREA)_2$	22.62	21.50	28.73	28.50
$FeCl_2(BM)$	22.55	21.30	28.61	26.72
$FeCl_2(AN)$			32.25	32.82
$FeCl_2(DMU)_3$	14.29	14.35	18.14	18.07
		14.10		17.89
$FeBr_2(DMU)_3$	11.64	11.77	33.20	33.58
$FeBr_2(AN)_3$	11.29	11.66		

Dichlorotetrakisformamide Iron(II)

A solution of 1.5 g anhydrous ferrous chloride in 10 ml absolute ethanol was prepared as above and poured into 2 g formamide. White crystals gradually formed and were filtered, washed with chloroform, and dried *in vacuo*.

Dichlorotris-N,N'-dimethylurea Iron(II)

A solution of 1.5 g anhydrous ferrous chloride in 10 ml acetone was prepared as above and poured into a solution of 3 g *N,N'*-dimethylurea in acetone. The mixture was then poured into 100 ml absolute ether. A white powder precipitated which was filtered, washed with chloroform and dried *in vacuo*.

Hexakis-N-methylurea Iron(II) Chloride

A solution of 1.24 g ferrous chlorine in 10 ml acetone was prepared as above and poured into a solution of 2 g *N,N'*-dimethylurea in acetone. A buff colored precipitate separated gradually, which was filtered, washed with acetone, and dried *in vacuo*.

Dibromotrisaniline Iron(II)

A solution of 1.25 g ferrous bromide in 20 ml absolute ethanol was shaken with powdered iron until green. It was filtered into 2.4 g aniline. A pale green precipitate formed which was filtered, washed with cold ethanol, and dried *in vacuo*.

Materials

All solvents were reagent grade which were dried and deoxygenated before use. Iron pentacarbonyl and tri-iron dodecacarbonyl were obtained from Alfa Inorganics and were used without further purification. All ligands were reagent grade and were used without further purification.

Mössbauer Spectra

Mössbauer spectra were recorded with an Austin Science Associates model S3 drive System used in conjunction with a Victoreen PIP400A multichannel analyzer operating in multiscalar mode. The source was ^{57}Co in a palladium matrix, obtained from the New England Nuclear Corporation. The strength of the source was approximately 5 mC. The 14.4 keV γ-ray was detected in the initial stages of the work by a thin 1/32 in. NaL(TL) activated crystal with matching photomultiplier tube manufactured by the Harshaw Chemical Company. In the later stages of the work a gas filled proportional counter was used: the filler gas was $Xe–CO_2$ at 1 atm pressure. Spectra with baselines of approximately 50 000 counts accumulated in about 6 h using the proportional counter. Samples generally contained 10 to 15 mg/cm^2 of iron. Complexes containing bromine showed very low count rates and small peak intensities. These were diluted to as little as 6 mg/cm^2 of iron in order to improve the spectra. Spectra were recorded at 295 and 77 °K.

The absorption envelopes were fitted to Lorentzian line shapes using an iterative least squares method. The velocity scale was calibrated with a sodium nitroprusside absorber and all isomer shifts are quoted with respect to the centroid of the sodium nitroprusside spectrum. The data are thought to be accurate to ± 0.02 mm/s.

Infrared Spectra

Infrared spectra in the 400–4000 cm^{-1} region were recorded on a Perkin–Elmer 521 Grating Infrared Spectrophotometer. Solid samples of ligands and complexes were recorded as Nujol or fluorolube mulls between KBr windows. Liquid samples of ligands, and solutions of ligands in dioxane, were also recorded between KBr windows in a normal i.r. cell.

Far i.r. spectra in the region 200–400 cm^{-1} were recorded as Nujol mulls between polyethylene windows on a Beckman IR 12 instrument.

Magnetic Measurements

Magnetic susceptibilities were measured by the Gouy balance method on equipment already described (10).

Results and Discussion

Mössbauer Spectra

Isomer Shift

The Mössbauer data are given in Table 2. The isomer shifts are, with one exception, greater than 1.35 mm/s, clearly in the range

Can. J. Chem. Downloaded from www.nrcresearchpress.com by 210.87.254.42 on 09/05/12
For personal use only.

TABLE 2. Mössbauer data for the amide, urea, and aniline complexes

Complex	Temperature (°K)	Isomer shift (mm/s)	Quadrupole splitting (mm/s)	Absorption (%)*	
				Low velocity	High velocity
$[Fe(BUA)_6][FeCl_4]$	295	1.51	0.88		
	195	1.31	1.28	(2.7, 2.8, 4.8)‡	
		1.54	0.82		
	77	1.31	2.02	(5.0, 5.0, 9.8)‡	
		1.62	1.40		
$[Fe(MU)_6]Cl_2$	295	1.51	1.60	2.5	2.3
	77	1.63	2.18	8.1	7.8
$FeCl_2(FA)_2$	295	1.43	2.66	4.0	4.0
	77	1.54	2.93	9.0	9.0
$FeCl_2(MFA)_2$	295	1.40	2.46	5.0	6.7
	77	1.51	2.76	9.3	11.3
$FeCl_2(DMFA)_2$	295	1.48	2.95	9.0	11.7
	77	1.59	3.20	15.5	15.8
$FeCl_2(AM)_2$†	295	1.39	2.64	5.4	5.4
	77	1.55	2.80	7.7	7.7
$FeCl_2(UREA)_2$	295	1.45	2.59	9.7	9.7
	77	1.57	2.65	15.0	15.0
$FeCl_2(BTH)_2$	295	1.36	1.46	10.0	9.0
	77	1.49	1.76	19.8	17.5
$FeCl_2(FA)_4$	295	1.46	0.66	8.0	8.0
	77	1.59	1.39	14.3	14.3
$FeCl_2(BM)$	295	1.40	2.53	3.3	3.3
	77	1.52	2.81	7.3	7.3
$FeCl_2(AN)$†	295	1.37	1.69	3.9	3.9
	77	1.49	2.18	7.1	7.1
$FeCl_2(DMU)_3$	295	1.41	2.20	2.2	3.4
	77	1.55	3.33	8.7	12.6
$FeBr_2(DMU)_3$	295	1.37	1.65	1.5	2.0
	77	1.48	2.09	3.9	4.4
$FeBr_2(AN)_3$	295	1.35	1.51	2.6	2.2
	77	1.47	1.98	7.5	6.4

*Uncorrected values.
†Reference 6.
‡See Fig. 1.

expected for complexes of iron(II) (6, 11). In addition to providing information about oxidation state, this parameter can also yield useful information about coordination number. For example a decrease in isomer shift on lowering the coordination number has been observed by several workers for iron(II) (12, 13). The effect is also evident in comparing isomer shifts of a number of tetrahedral (14–16) and octahedral iron(II) complexes (6, 17–20). These data show that shifts of 1.3 mm/s, or less, are usually characteristic of tetrahedral iron(II), while shifts greater than 1.3 mm/s are characteristic of octahedral iron(II). The benzothiazole complex (Table 2) is exemplary of this effect. It has been assigned a 6-coordinate polymeric structure on the basis of its electronic spectrum (5) and its isomer shift is 1.36 mm/s. The bromo analogue $FeBr_2(BTH)_2$ is tetrahedral (5) and has an isomer shift of 1.05 mm/s. Since the isomer shifts (Table 2) for the FeX_2L_n complexes are all greater than 1.35 mm/s, it seems reasonable to conclude that in these complexes the iron is 6-coordinate.

The isobutyramide complex differs somewhat from the rest in that it has two different iron environments. The three line Mössbauer spectrum (Fig. 1) is interpreted in terms of two

Can. J. Chem. Downloaded from www.nrcresearchpress.com by 210.87.254.42 on 09/05/12
For personal use only.

Can. J. Chem. Downloaded from www.nrcresearchpress.com by 210.87.254.42 on 09/05/12
For personal use only.

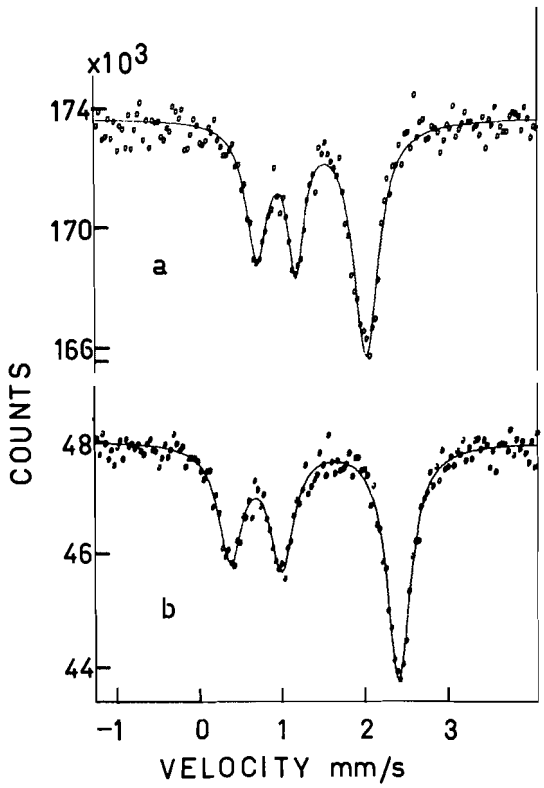

FIG. 1. Mössbauer spectrum of $[Fe(BUA)_6][FeCl_4]$ at (*a*) 195 °K (*b*) 77 °K.

iron sites each one giving rise to a quadrupole split doublet, with the high velocity lines of each doublet coincident. The relative peak intensities at 77 °K indicates that the two sites are of equal abundance. This complex has been formulated as $[Fe(BUA)_6^{2+}][FeCl_4^{2-}]$. The doublet with larger isomer shift (1.62 mm/s at 77 °K) is assigned to the 6-coordinate cation, while the doublet of lower isomer shift is assigned to the tetrachloroferrate(II) anion. This latter value agrees well with literature values for other tetrachloroferrate(II) complexes (11, 21). Absorption by the tetrahedral species is negligible at room temperature and explains why the spectrum apparently collapses to a doublet. The methylurea complex, like the 6-coordinate cation in the isobutyramide complex, has an isomer shift significantly larger than the other complexes. We have formulated this complex as $[Fe(MU)_6]Cl_2$. While the Mössbauer, and the i.r. evidence presented below, indicate an ionic formulation for these complexes, conductivity measurements could have provided the necessary confirmation. Unfortunately these, and the other complexes investigated, do not appear to be stable in solvents in which they are soluble and conductivity data are therefore not available.

With the two exceptions discussed above, the complexes investigated are believed to be non-ionic. Since the Mössbauer isomer shift data indicate that the iron atoms are 6-coordinate, it is necessary to postulate polymeric structures for the remainder, with the exception of $FeCl_2(FA)_4$. Such polymers can be visualised as having the $FeCl_2$ structure (8), in which halogens are successively replaced by ligand to achieve the required stoichiometry. The simplest of these would be the $FeCl_2L_2$ complexes in which two bridging chlorines are replaced by two ligands, *trans* to one another as in **1** (1–6). Addition of two more ligands would break the remaining halogen bridge bonds and give a $FeCl_2L_4$ monomeric complex in which the halogens are presumably *trans*. $FeCl_2(FA)_4$ would have this structure.

The 1 : 1 complexes $FeCl_2 \cdot BM$ and $FeCl_2 \cdot AN$ are believed to be cross-linked polymers such as **2** in which only one bridging chlorine in the $FeCl_2$ structure has been replaced. It has been suggested (6) that these complexes might be chlorine bridged dimers, containing 4-coordinate iron, but this now seems to be most unlikely because of the magnitude of the isomer shifts and the supporting evidence presented below.

The complexes $FeCl_2(DMU)_3$, $FeBr_2(DMU)_3$, and $FeBr_2(AN)_3$ have been assigned dimeric chlorine bridged structures such as **3**,

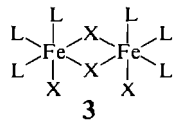

3

which is one of several possible isomers. The Mössbauer spectra show peaks attributable to only one kind of iron. However, the presence of more than one geometrical isomer in these compounds cannot be ruled out since the various possible arrangements may not have very different Mössbauer parameters. The ionic formulation $[FeL_6][FeX_4]$, analogous to the isobutyramide complex, can however be eliminated.

Can. J. Chem. Downloaded from www.nrcresearchpress.com by 210.87.254.42 on 09/05/12
For personal use only.

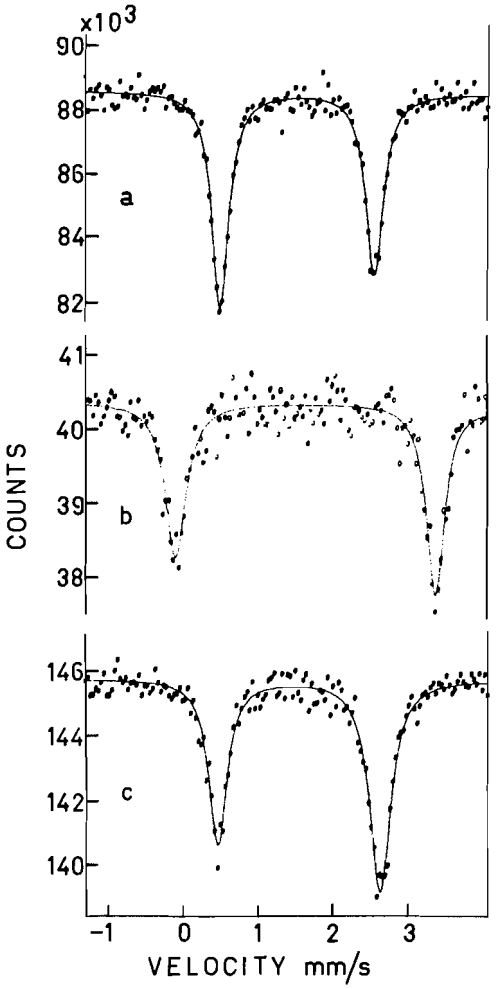

FIG. 2. Mössbauer spectrum at 77 °K of (*a*) $FeBr_2(AN)_3$ (*b*) $FeCl_2(DMU)_3$ (*c*) $FeBr_2(DMU)_3$.

No peaks attributable to the $[FeX_4]^{2-}$ anions could be detected in the spectra of these complexes (Fig. 2, Table 2) even at 77 °K at which temperature $[FeX_4]^{2-}$ peaks were clearly visible in the isobutyramide compound.

Edwards *et al.* (11) have noted an increase in isomer shift in the series $FeCl_2$, $FeCl_2 \cdot 2H_20$, $FeCl_2 \cdot 4H_2O$ in which H_2O replaces the bridging chlorine. They attributed this to the greater polarizability of the chlorine compared to the extra ligand. Allowing for the large variation in isomer shift for the $FeCl_2L_2$ complexes, we note a similar trend to more positive isomer shift as the six chlorines about the iron in $FeCl_2$ are successively replaced by amide ligands.

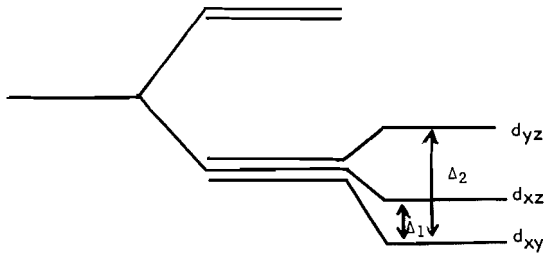

FIG. 3. Representation of the energy levels of the d orbitals in a distorted octahedral field.

Quadrupole Splitting

With the exception of the benzothiazole complex, the polymeric complexes $FeCl_2L_2$ all have room temperature quadrupole splittings in the range 2.5–3.0 mm/s and show small increases (Table 2) upon cooling to 77 °K. The fact that the splittings are all greater than 2 mm/s suggests that, in these complexes, if the *z*-axis is the O—Fe—O axis, then the d_{xy} orbital lies lowest (17). This is known to be so for $FeCl_2 \cdot 2H_2O$. Johnson (22) has studied the Mössbauer spectrum of a single crystal of this compound at 4.2 °K and 1.4 °K and concludes that the direction of maximum electric field gradient is the O—Fe—O axis. This is confirmed by the crystallographic data (1) which shows Fe—O bond lengths of 2.07 Å and Fe—Cl bond lengths of 2.49 and 2.54 Å. The observation of only a small temperature dependence in the quadrupole splittings of the $FeCl_2L_2$ complexes indicates that distortional splittings in the t_{2g} levels are of considerable size. The quadrupole splitting of $FeCl_2 \cdot 2H_2O$ shows similar behavior. Johnson (22) estimates $\Delta_1 = 520\ cm^{-1}$ and Δ_2 large with respect to the spin–orbit coupling constant of about 100 cm^{-1} (Fig. 3). The much smaller quadrupole splittings (1.46 and 1.76 mm/s at 295 °K and 77 °K, respectively) in the benzothiazole complex may be evidence for a d_{xz} or d_{yz} ground state in this compound.

The quadrupole splittings of the 1:4 formamide complex is unusually small. This, together with the large temperature dependence (Fig. 4) Table 2) points to a nearly regular octahedral structure with only small distortional splittings in the t_{2g} levels. The small value could also be due to a structure in which d_{xz} and d_{yz} lie lowest. This data suggests that the structure of

Can. J. Chem. Downloaded from www.nrcresearchpress.com by 210.87.254.42 on 09/05/12
For personal use only.

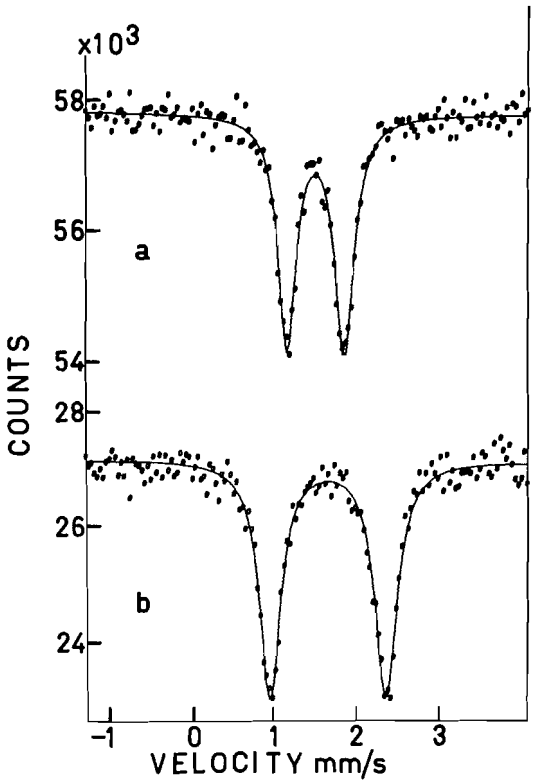

FIG. 4. Mössbauer spectrum of $FeCl_2(FA)_4$ at (*a*) 295 °K, (*b*) 77 °K.

the 1:4 formamide complex is indeed significantly different from that of $FeCl_2 \cdot 4H_2O$, for which Grant *et al.* (23) report a room temperature quadrupole splitting of 2.98 mm/s and almost negligible temperature dependence. The crystal structure (24) of $FeCl_2 \cdot 4H_2O$ shows it to have a distorted 6-coordinate *trans* structure in which Fe—Cl = 2.38, Fe—O = 2.09, and 2.59 Å, and the angle Cl—Fe—O = 81°.

The tetrachloroferrate(II) anion in the isobutyramide complex shows quadrupole splittings of 1.28 and 2.0 mm/s at 195 °K and 77 °K, respectively. The distortional splitting in the e_g levels, as calculated by the method of Edwards *et al.* (11) is 185 cm^{-1} for this complex. Presumably the bulky $Fe(BUA)_6^{2+}$ cation produces a greater distortion than do NMe_4^+ and NEt_4^+ (11, 21).

The octahedral cation $Fe(BUA)_6^{2+}$ shows quadrupole splittings of 0.82 and 1.40 mm/s at 195 °K and 77 °K, respectively. These values indicate a near cubic environment about iron and the possibility of a doublet ground state in the d-levels. The methylurea complex, suggested as containing the octahedral cation $Fe(MU)_6^{2+}$ has somewhat larger quadrupole splittings but is still within the region expected for a d_{xz} or d_{yz} ground state.

The 1:3 bromides show very similar quadrupole splittings which are smaller and less temperature dependent than those for the 1:3 chloride $FeCl_2(DMU)_3$. This may be due to a difference in d-orbital ground state or to increased covalency in Fe—Br bonds. In addition the quadrupole splitting in these complexes will depend upon η, the asymmetry parameter, which will now be none zero since these complexes are no longer axially symmetric.

One further point of interest from the data in Table 2 is that a number of the quadrupole split doublets have unequal intensities. This asymmetry could arise for one or more of the following reasons: (*i*) sample impurities, (*ii*) preferred crystal orientation, (*iii*) spin–lattice or spin–spin relaxation processes, and (*iv*) a Goldanskii–Karyagin effect. The first can be discounted on the basis of the analytical data and on the fact that the iron impurity would have to have quite unrealistic Mössbauer parameters in order to overlap only one of the doublet peaks. Asymmetry due to preferred crystal orientation is most unlikely since the compounds were extremely finely divided and the spectra are temperature dependent. Relaxation effects are discounted because of the sharpness of the lines < 0.3 mm/s. The most likely cause of the asymmetry would appear to be the Goldanskii–Karyagin effect (25) which is due to anisotropy of the recoil free fraction arising from a stiffening of the bonding in one direction compared to that in another. This is not unreasonable for compounds of this nature which are chain polymers. It is interesting to note that the most marked asymmetry occurs with the *N*-substituted ligands and is in the opposite sense (Fig. 2) to that for the $FeCl_2(BTH)_2$ and $FeBr_2(AN)_3$ complexes, in which the organic ligand is *N*-coordinating: the amides and ureas are O-coordinating (see i.r. data).

Infrared Spectra

The i.r. spectra in the region 1000–4000 cm^{-1} of the amide and urea ligands and their complexes have been set out in Tables 3–11 which

TABLE 12. Far infrared bands of the amide and urea complexes*

Complex	ν(Fe—X)	Bridged ν(Fe—X)		ν(Fe—O)		Ligand bands
$FeCl_2(FA)_2$	—	(262 s	220 m	195 s)		
$FeCl_2(MFA)_2$	—	(251 m 245 m	222 m	204 s 196 s	170 m)	392 s 377 s
$FeCl_2(DMFA)_2$	—	(—	227 s	200 s	180 m)	390 s 377 s
$FeCl_2(AM)_2$	—	(267 m	228 s	204 s	186 m) 174 m)	—
$FeCl_2(UREA)_2$	—	(266 s	222 s	200 s)		—
$FeCl_2(BTH)_2$	—	(251 m	220 sh	197 s)		363 m
$FeCl_2(BM)$	291 m	(252 m	225 m	—	179 m)	—
$FeCl_2(DMU)_3$	280 vs	(255 vs	—	203 m)		353 s
$FeBr_3(DMU)_3$	220 s				220 s	354 s
$[Fe(BUA)_6][FeCl_4]$	285 s				220 w	368 s
$[Fe(MU)_6]Cl_2$	—				234 m 196 m	360 s
$FeCl_2(FA)_4$	(200–275 cm^{-1} broad unresolved absorption)					

*Parentheses denote unassigned frequencies.

have been placed in the Depository of Unpublished Data.[1] Since the region from 400 to 1000 cm^{-1} provided little in the way of useful structural information the bands in this region have not been included. Significant shifts to lower frequency are seen, particularly in the N—H and C=O stretching bands, on going from a dilute solution of the ligand to the neat or mulled form, due to hydrogen bonding effects and comparisons have therefore been made between the complex and its ligand in dilute solution.

Bands arising from N—H, C=O, and C—N stretching, and NH_2 bending vibrations, which occur in the 1000–4000 cm^{-1} region, can all provide information about the mode of coordination of the ligand to the metal. If coordination were through the nitrogen one would expect a significant shift of the N—H band to lower frequency and this is not observed. In addition coordination through N would result, for the urea complexes, in two different kind of nitrogens and hence different N—H stretching bands. No change in overall peak pattern is observed and only one strong N—H stretching band is noted in this region. A further general observation regarding these N—H bands is that they often occur at lower frequency in the complex than when the ligand is in a dilute solution, but at higher frequency when in the pure or mulled form. This suggests that some hydrogen bonding is still effective in the coordinated ligand. Singh and Rivest (9) suggested that hydrogen bonding may occur between the amide hydrogens and the halogen.

That the carbonyl bands are in all cases shifted 30–60 cm^{-1} to lower frequency, provides firm evidence for coordination through oxygen in these complexes. Negative shifts in NH_2 bending frequencies are observable in all except the *N*-methylformamide case, and this gives additional support to coordination through oxygen.

Bands of C—N stretching character are expected to shift to higher frequency if coordination takes place through oxygen. This is the case for all but the *NN'*-dimethylformamide complex, where the peak at 1500 cm^{-1}, assigned as ν(C—N) in the ligand, appears at 1490 cm^{-1} in the complex. In view of the difficulties involved in unequivocally assigning bands in these complex systems the evidence presented above seems fairly conclusive of coordination through oxygen in all of these complexes.

An i.r. study of the aniline and benzothiazole complexes in the 400–4000 cm^{-1} region was not carried out. Aniline is a nitrogen coordinating ligand and it has been suggested by Chan *et al.* (5) that benzothiazole also coordinates through nitrogen.

The far i.r. bands of the amide and urea complexes are listed in Table 12. The similarity of

[1]Copies of Tables may be obtained, upon request, from the Depository of Unpublished Data, National Science Library, National Research Council of Canada, Ottawa, Canada K1A 0S2.

Can. J. Chem. Downloaded from www.nrcresearchpress.com by 210.87.254.42 on 09/05/12
For personal use only.

Can. J. Chem. Downloaded from www.nrcresearchpress.com by 210.87.254.42 on 09/05/12
For personal use only.

the spectra of the 1:2 complexes is evident. It is proposed that all of these are 6-coordinate chlorine bridged complexes. Four bands, generally poorly resolved, appear in most cases between 180 and 260 cm^{-1}. Gill *et al.* (4) have observed a similar far i.r. spectrum for the polymeric octahedral complex $FeCl_2(py)_2$ and report three poorly resolved peaks at 238, 227, and 219 cm^{-1}.

The spectra of these 1:2 complexes are strikingly different from tetrahedral 1:2 complexes which show strong, well resolved Fe—Cl stretching bands close to 300 cm^{-1} (16, 26). The shift of the ν(Fe—Cl) absorption region to lower frequency in the polymeric complexes is attributed to the weaker bridged chlorine bonds. Assignment of separate Fe—Cl of Fe—O stretching character to the peaks has not been attempted since it is expected that these vibrations will be strongly coupled.

It is noteworthy at this point to mention the ν(Fe—Cl) and ν(Fe—O) band assignments made by Singh and Rivest (9) for $FeCl_2(FA)_2$, $FeCl_2(MFA)_2$, and $FeCl_2(AM)_2$. These workers assign Fe—Cl stretches to bands between 350 and 380 cm^{-1}. Based on assignments made here and elsewhere (26–28), it is thought that this region is too high for Fe—Cl stretching in iron(II) complexes, even if these complexes were tetrahedral as claimed by Singh and Rivest (9). Rather Fe—Cl stretching in this region is indicative of iron(III), and it is possible that their complexes (9) may have been at least partially oxidized. Assignment of Fe—O stretching to bands between 400 and 475 cm^{-1} by these workers (9) is also questioned. Little information is available on iron(II) complexes with oxygen coordinating ligands. However, Kermarrec (29) reports Fe—O stretching at 357 cm^{-1} for $[Fe(H_2O)_6][SiF_6]$. Coordinated bonds with amides would be expected to be weaker than with water as a result of lower Lewis basicity, and (Fe—O) absorption should accordingly be at lower frequency (see below).

The 1:1 benzamide complex gives a spectrum very similar to those observed for the 1:2 complexes with an additional band at 291 cm^{-1}. The bands between 180 cm^{-1} are assigned as ν(Fe—O), bridged ν(Fe—O), and bridged ν(Fe—Cl) vibrations, as for the 1:2 complexes, in keeping with the polymeric structure **2** proposed for this complex. The band at 291 cm^{-1}, however, suggests that at least one of the Fe—Cl bonds is short and has essentially non-bridged character.

The complex $FeCl_2(DMU)_3$ shows a peak at 280 cm^{-1} which is attributable to free Fe—Cl stretching as well as peaks at 255 cm^{-1} and 203 cm^{-1} attributable to bridged Fe—Cl stretching and Fe—O stretching. This is consistent with the proposed structure **3** of this complex. The analogous bromide complex shows a single band at 220 cm^{-1} which is probably a strongly coupled Fe—Br and Fe—O stretching mode. Absorption due to bridged bromine bonds is expected to occur below 200 cm^{-1} (26).

The 1:4 formamide complex shows only broad, unresolved absorption between 200 and 275 cm^{-1} in the far i.r. Although Fe—Cl stretching is expected to occur in this region for monomeric octahedral complexes (26), no further interpretation was possible. $FeCl_2(MU)_6$ shows two peaks at 234 and 196 cm^{-1}. If this complex is $[Fe(MU)_6]Cl_2$, as proposed, then these must be Fe—O vibrations. The isobutyramide complex, formulated as $[Fe(BUA)_6][FeCl_4]$, shows a strong peak at 285 cm^{-1} assigned as ν(Fe—Cl) and a weak peak at 220 cm^{-1} assigned as ν(Fe—O). Clark and Dunn (29) observe ν(Fe—Cl) at 282 cm^{-1} in $[NEt_4]_2[FeCl_4]$.

Magnetic Moments

The magnetic moments of some of the amide and urea complexes are shown in Table 13. The room temperature moments are for the most part much larger than the spin only magnetic moment of 4.90 β. This indicates considerable orbital contribution, as is expected to occur in high spin octahedral iron(II) compounds in which the splitting in the t_{2g} levels is not large.

In all the complexes except $FeCl_2(AM)_2$ the magnetic moments show an abnormally large temperature dependence, dropping to values which are near the spin only values at 77 °K. Golding *et al.* (37) have calculated the temperature dependence of the magnetic moment of high spin iron(II) for various values of Δ, the distortional splitting in the t_{2g} levels, and λ, the spin–orbit coupling constant. Their calculation is based on the assumption that Δ and λ themselves do not vary with temperature. From

TABLE 13. Magnetic moments of amide and urea complexes

Complex	Temperature (°K)	$\mu_{eff}(\beta)$
$FeCl_2(AM)_2$	295	5.50
	77	5.32
$FeCl_2(UREA)_2$	295	5.45
	77	5.01
$FeCl_2(MFA)_2$	295	5.63
$FeCl_2(FA)_4$	295	5.46
	77	4.84
$FeCl_2(BM)$	295	5.34
	77	4.95
$FeCl_2(DMU)_3$	295	5.47
	77	5.04
$[Fe(MU)_6]Cl_2$	295	5.45
	77	4.93

their calculated curves it would appear that for moderate Δ values considerable orbital contribution to the magnetic moment should remain at 77 °K. It is therefore suggested that there may be some temperature dependence of Δ and/or λ in the present case.

Golding *et al.* (37) have also calculated a relationship between magnetic moment and quadrupole splitting for high spin iron(II) compounds in which d_{xy} lies lowest. Some of the data from this study have been compared with their calculated curve for the room temperature case in which λ is given its free ion value. Agreement with the curve, even when errors in the quadrupole splittings and magnetic moments are allowed, is not especially good, possibly indicating that the assumption of free ion spin–orbit coupling is a poor one. The 1:4 formamide and 1:6 *N*-methylurea complexes, in particular, show deviations from this curve, but as suggested earlier these complexes may have a d_{xz}, d_{yz} rather than a d_{xy} ground state.

The temperature variation of the magnetic moments could also be the result of some antiferromagnetic interaction between the iron atoms in these polymeric species, but a more comprehensive study would be needed to confirm this.

We thank the National Research Council of Canada for financial support.

1. B. MOROSIN and E. J. GRAEBER. J. Chem. Phys. **42**, 898 (1965).
2. R. J. H. CLARK and C. S. WILLIAMS. J. Chem. Soc. (A), 1425 (1966).
3. B. J. HATHAWAY and D. G. HOLAH. J. Chem. Soc. 2400 (1964).
4. N. S. GILL, R. S. NYHOLM, G. A. BARCLAY, T. I. CHRISTIE, and P. J. PAULING. J. Inorg. Nucl. Chem. **18**, 88 (1961).
5. N. N. Y. CHAN, M. GOODGAME, and M. J. WEEKS. J. Chem. Soc. (A). 2499 (1968).
6. T. BIRCHALL. Can. J. Chem. **47**, 1351 (1969).
7. D. M. L. GOODGAME, M. GOODGAME, M. HITCHMAN, and M. WEEKS. Inorg. Chem. **5**, 635 (1966).
8. A. F. WELLS. Structural inorganic chemistry. 3rd ed. Oxford University Press. London, England. 1967 p. 344.
9. P. P. SINGH and R. RIVEST. Can. J. Chem. **46**, 1773 (1968).
10. A. GUEST. Ph.D. Thesis. McMaster University, Hamilton, Ontario. 1968.
11. P. R. EDWARDS, C. E. JOHNSON, and R. J. P. WILLIAMS. J. Chem. Phys. **47**, 2074 (1967).
12. A. P. GINSBURG and M. B. ROBIN. Inorg. Chem. **2**, 817 (1963).
13. L. R. WALKER, G. K. WERTHEIM, and V. JACCARINO. Phys. Rev. Lett. **6**, 98 (1961).
14. C. D. BURBRIDGE and D. M. L. GOODGAME. J. Chem. Soc. (A), 1074 (1968).
15. C. D. BURBRIDGE and D. M. L. GOODGAME. J. Chem. Soc. (A), 694 (1967).
16. T. BIRCHALL and M. F. MORRIS. Can. J. Chem. This issue.
17. C. D. BURBRIDGE, D. M. L. GOODGAME, and M. GOODGAME. J. Chem. Soc. (A), 349 (1967).
18. J. F. DUNCAN, R. M. GOLDING, and K. F. MOK. J. Inorg. Nucl. Chem. **28**, 1114 (1966).
19. E. FLUCK. Adv. Inorg. Chem. Radiochem. **6**, 433 (1964).
20. V. I. GOLDANSKII. The Mössbauer effect and its applications in chemistry. Consultants Bureau, N.Y. 1964.
21. T. C. GIBB and N. N. GREENWOOD. J. Chem. Soc. 6989 (1965).
22. C. E. JOHNSON. Proc. Phys. Soc. (London), **88**, 943 (1966).
23. R. W. GRANT, H. WIEDERSICH, A. H. MUIR, JR., U. GONSER, and N. W. DELGASS. J. Chem. Phy. **45**, 1015 (1966).
24. B. R. PENFOLD and J. A. GRIGOR. Acta Cryst. **12**, 850 (1959).
25. V. I. GOLDANSKII, E. F. MAKAROV, and V. V. KHRAPOV. Phys. Lett. **3**, 344 (1963).
26. R. J. H. CLARK and C. S. WILLIAMS. Inorg. Chem. **4**, 350 (1965).
27. R. J. H. CLARK. Spectrochim. Acta, **21**, 955 (1965).
28. R. J. H. CLARK and T. M. DUNN. J. Chem. Soc. 1198 (1963).
29. Y. KERMARREC. Compte Rend. **258**, 5836 (1964).
30. J. C. EVANS. J. Chem. Phys. **22**, 1228 (1954).
31. T. MIYAZAWA, T. SHIMANOUCHI, and S. MIZUSHIMA. J. Chem. Phys. **24**, 408 (1956).
32. R. L. JONES. J. Mol. Spectrosc. **11**, 411 (1963); **2**, 581 (1958).

Can. J. Chem. Downloaded from www.nrcresearchpress.com by 210.87.254.42 on 09/05/12
For personal use only.

33. W. KUTZELNIGG and R. MECKE. Spectrochim. Acta. **18**, 549 (1962).
34. R. B. PENLAND, S. MIZUSHIMA, C. CURRAN, and J. V. QUAGLIANO. J. Amer. Chem. Soc. **79**, 1575 (1957).
35. T. J. LANE, A. YAMAGOUCHI, J. V. QUAGLIANO, J. A. RYAN, and S. MIZUSHIMA. J. Am. Chem. Soc. **81**, 3824 (1959).
36. T. MIYAZAWA, T. SHIMANOUCHI, and S. MIZUSHIMA. J. Chem. Phys. **29**, 611 (1958).
37. R. M. GOLDING, K. F. MOK, and J. F. DUNCAN. Inorg. Chem. **5**, 774 (1966).

Can. J. Chem. Downloaded from www.nrcresearchpress.com by 210.87.254.42 on 09/05/12
For personal use only.

Mössbauer and Infrared Spectra of Tetrahedral Complexes of Iron(II) Halides with Thioamides and Related Ligands

T. BIRCHALL AND M. F. MORRIS

Department of Chemistry, McMaster University, Hamilton, Ontario

Received August 27, 1971

A number of complexes of iron(II) halides with thioamides and ureas have been prepared and characterized by means of Mössbauer, infrared spectroscopy, and magnetic measurements. These complexes are shown to have distorted tetrahedral structures.

Un certain nombre de complexes d'halogénure de fer(II) avec les thioamides et les urées ont été préparés et caractérisés par spectroscopie Mössbauer, infrarouge et par des mesures magnétiques. Il est montré que ces complexes possèdent une structure tétrahédrique distordue.

Canadian Journal of Chemistry, **50**, 211 (1972)

Can. J. Chem. Downloaded from www.nrcresearchpress.com by 210.87.254.6 on 09/05/12
For personal use only.

Introduction

Tetrahedral complexes of iron(II) $[FeX_4]^{2-}$ where X = Cl, Br, NCS etc. have been characterized by means of their electronic spectra (1–6) and more recently by Mössbauer spectroscopy (7, 8). This latter technique has been invaluable in detecting Jahn Teller distortion Δ (Fig. 1) in these symmetrically substituted anions. The first estimate of the extent of distortion on $[FeCl_4]^{2-}$ was made by Gibb and Greenwood (7) and was obtained from an analysis of the temperature dependence of the quadrupole splitting parameter. Edwards *et al.* (8) have carried out similar studies on other tetrahedral Fe(II) salts and have shown that the ground state orbital in $[Me_4N]_2FeCl_4$ is the d_{z^2} orbital.

Complexes of the type FeX_2L_2 are also known where X = halogen and L = pyridine and substituted pyridines (1), triphenylphosphine (9, 10), triphenyl arsine (2), quinoline and 3-methylisoquinoline (11), benzothiazole (3), thioacetamide (12–14), and thiourea (15). With this stoichiometry (FeX_2L_2) it is, however, not necessary that the environment about the iron be tetrahedral. Polymerization can occur, via bridging halogen, to give an iron environment which is octahedral rather than tetrahedral. This has recently been demonstrated for a number of amide complexes of Fe(II) by means of Mössbauer spectroscopy (16, 17).

We wish to report here the preparation of some tetrahedral complexes of iron(II) with some thio-ligands and their characterization by means of Mössbauer, infrared, and magnetic measurements.

Experimental

Preparation of Complexes

A solution of 1.5 g ferrous chloride in 10 ml of either acetone, or ethanol, was shaken with powdered iron until green, centrifuged, and the supernatant liquid poured into a solution of ~3 g of the ligand in either acetone or ethanol. The complexes precipitated immediately, or on cooling in an ice bath, and were filtered, washed with solvent, and dried *in vacuo*.

All solvents were reagent grade and were dried and deoxygenated before use. All ligands were reagent grade and used without further purification. Thioacetamide (THA) and thiourea (THU) were obtained from Fisher Scientific Co., benzothiazole (BTH) from Eastman Organic Chemicals, *N,N*-dimethylthiourea (DMTHU) from Aldrich Chemical Co., and *N*-methylthiourea (MTHU) from K & K Laboratories. The preparation, filtering, washing of products and spectroscopic sample preparation were all carried out under nitrogen in a dry box.

Analysis

Chlorine was determined by the Volhard method, iron as

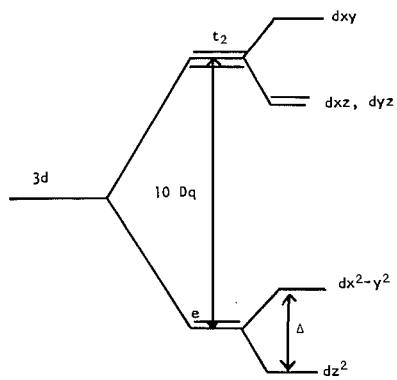

FIG. 1. Representation of the splittings of d orbitals energy levels in a distorted tetrahedral field.

TABLE 1. Analytical data for iron(II) halide complexes

Complex	Analysis (%)					
	Fe		Sulfur		Halogen	
	Found	Theor.	Found	Theor.	Found	Theor.
$FeBr_2(BTH)_2$	11.16	11.49	—	—	33.80	32.90
$FeCl_2(THA)_2$	20.00	20.65	23.05	23.15		
$FeBr_2(THA)_2$	15.20	15.28	17.05	17.54		
$FeCl_2(THU)_2$	19.38	20.02	22.90	23.00		
$FeCl_2(MTHU)_2$	18.39	18.20	19.08	20.90		
$FeCl_2(DMTHU)_2$	16.20	16.69	17.70	19.15		
$FeCl_2(THU)_4$	12.60	12.96	29.80	29.75		

ferric oxide and sulfur by the barium sulfate method. Analytical data are presented in Table 1.

Mössbauer spectra were recorded as previously described (16, 17). The drive system was calibrated by a standard sodium nitroprusside absorber and all shifts are relative to the center of the sodium nitroprusside doublet as zero velocity. Spectra were computer fitted to Lorentzian line shapes.

Infrared spectra were recorded on Perkin–Elmer 521 and Beckman IR 12 instruments. Magnetic susceptibilities were measured by the Gouy method.

Results and Discussion

Iron(II) halides form 1:2 complexes with many ligands in which the coordination number about the central iron may be either six or four. When the ligand is benzothiazole an octahedral complex is formed with $FeCl_2$, while $FeBr_2$ gives a tetrahedral complex (3). The structures of these complexes are based on an analysis of their electronic spectra. Dichlorbisbenzothiazoleiron-(II) has two low intensity bands at 9050 and 6600 cm^{-1} (3) similar to those found for $FeCl_2$-(pyridine)$_2$ which has an octahedral chlorine bridged polymeric structure (18). The analogous bromide, $FeBr_2(BTH)_2$, was found to have a quite different spectrum, with an intense absorption at 6330 cm^{-1} and a series of weak bands at higher energy (3). This is typical of iron(II) complexes in a tetrahedral environment, the intense absorption being due to the $^5E \rightarrow {}^5T_2$ transition. Similar electronic spectra have been observed for the tetrahedral species FeX_2L_2-(X = Cl, Br; L = quinoline, 3-methylisoquinoline) (11). Iron(II) halide complexes with thioacetamide, *i.e.* $FeX_2(TA)_2$ have been reported and concluded to have tetrahedral structures (12).

The structures assigned to the complexes reported here are based upon a comparison of the spectral data for $FeCl_2(BTH)_2$ and $FeBr_2$-$(BTH)_2$ which have octahedral and tetrahedral geometries about the iron, respectively. Mössbauer data for these complexes are presented in Table 2. It is immediately apparent that the $FeCl_2(BTH)_2$ has a significantly higher isomer shift, and hence a lower s electron density, than the bromo analogue. Some of this difference could be the result of a difference in covalent character of the Fe–Br and Fe–Cl bonds, but this effect is thought to be minor (19). A more satisfactory explanation is that the chloro complex being six coordinate (d^2sp^3 hybridized) has more d electrons which shield the s electrons from the nucleus and results in a lower s electron density at the nucleus than in the four coordinate (sp^3 hybridized) bromo complex.

One notes also the strong absorption at room temperature for the chloro complex but a weak absorption for the bromo. Furthermore there is a relatively greater temperature dependence of this absorption for the bromo than the chloro complex. Both of these observations suggest a lower Debye temperature for $FeBr_2(BTH)_2$ compared to $FeCl_2(BTH)_2$. Again this is expected behavior from tetrahedral and polymeric six coordinate structures, respectively. Other workers (7, 8, 16) have noted that tetrahedral compounds of iron exhibit weak or undetectable absorption at room temperature.

Far infrared data are given in Table 3 and spectra for $FeCl_2(BTH)_2$ and $FeBr_2(BTH)_2$ are shown in Fig. 2. The $FeBr_2(BTH)_2$ complex gives a relatively well resolved spectrum with two strong bands at 266 and 244 cm^{-1} assigned to Fe—Br stretches and a band at 205 cm^{-1} assigned to an iron–nitrogen vibration. Coordination of the benzothiazole is assumed to be through N rather than S, by analogy with

Can. J. Chem. Downloaded from www.nrcresearchpress.com by 210.87.254.6 on 09/05/12
For personal use only.

TABLE 2. Mössbauer data for the thioacetamide and thiourea complexes

Complex	Temperature (°K)	Isomer shift (mm/s)	Quadrupole splitting (mm/s)	Absorption (%)*	
				Low velocity	High velocity
$FeCl_2(BTH)_2$	295	1.36	1.46	10.0	9.0
	77	1.49	1.76	19.8	17.5
$FeBr_2(BTH)_2$	295	1.05	2.82	1.3	1.3
	77	1.17	3.02	2.9	3.5
$FeCl_2(THA)_2$	295	0.97	3.15	6.0	4.0
	77	1.09	3.28	17.5	14.0
$FeBr_2(THA)_2$†	77	1.07	3.49	1.7	1.3
$FeCl_2(THU)_2$	295	1.00	3.26	1.0	1.0
	77	1.10	3.41	3.4	4.2
$FeBr_2(THU)_2$	295	0.99	3.32	1.3	1.9
	77	1.09	3.45	3.7	4.8
$FeCl_2(MTHU)_2$	295	0.98	3.23	4.1	4.1
	77	1.11	3.33	12.6	12.2
$FeCl_2(DMTHU)_2$	295	1.01	3.29	3.8	3.6
	77	1.11	3.41	10.5	8.6
$FeCl_2(THU)_4$	295	1.27	3.46	4.0	4.0
	77	1.40	3.56	7.2	7.2

*Uncorrected values.
†No detectable absorption at 295 °K.

TABLE 3. Far infrared bands of the thioacetamide and thiourea complexes*

Complex	ν(Fe—X)	ν(Fe—L)	Ligand bands
$FeCl_2(BTH)_2$	(251 m, 220 sh, 197 s)		363 m
$FeBr_2(BTH)_2$	266 s, 244 s	205 m	363 m
$FeCl_2(THA)_2$	328 s, 304 s	235 s	385 w
$FeBr_2(THA)_2$	(260 sh, 253 s, 238 m, 235 sh)		387 w
$FeCl_2(THU)_2$	315 s, 293 s	248 s	—
$FeBr_2(THU)_2$	(270 w, 240 w, 212 m)		—
$FeCl_2(MTHU)_2$	325 sh, 300 vs	255 m	—
$FeCl_2(DMTHU)_2$	305 vs	278 s 215 mbr	—
$FeCl_2(THU)_4$	(227 m, 202 m)		—

*Parentheses denote unassigned frequencies.

$Co(BTH)_2(ClO_4)_2$ and $Ni(BTH)_2I_2$, where the evidence of Chan *et al.* (3) suggests coordination via nitrogen. This spectral pattern is typical of tetrahedral coordination (2, 20, 21). The spectrum of $FeCl_2(BTH)_2$ is less well resolved with only two prominent bands and a number of weak absorptions between 175 and 250 cm^{-1}. The absence of any Fe—Cl stretching vibrations at ~ 300 cm^{-1} is strong evidence in favor of the polymeric chlorine bridged structure (3, 17).

Mössbauer Data

Mössbauer data for all of the complexes are summarized in Table 2. With the exception of $FeCl_2(THU)_4$ the complexes with thio-ligands all have isomer shifts similar to the tetrahedral $FeBr_2(BTH)_2$ complex and less positive than the octahedral $FeCl_2(BTH)_2$ complex. This, together with the relatively weaker room temperature absorption than the $FeCl_2(BTH)_2$ complex, indicates that these thio-complexes have four coordinate tetrahedral geometries. Substitution of bromide for chloride, or variation of ligand L in these complexes, appears to have no detectable effect on the isomer shift. This is perhaps not too surprising since the σ character of the bonds is not likely to vary much with the ligand used and π bonding changes, which would

Can. J. Chem. Downloaded from www.nrcresearchpress.com by 210.87.254.6 on 09/05/12
For personal use only.

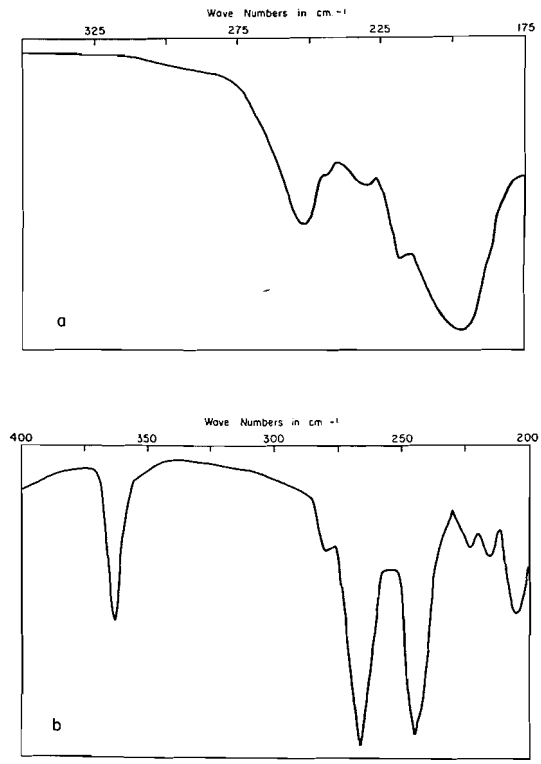

FIG. 2. Far infrared spectra of (*a*) $FeCl_2(BTH)_2$, (*b*) $FeBr_2(BTH)_2$.

remove d electrons and hence decrease δ, are likely to be small. There are variations in the magnitude of quadrupole splitting parameter but no obvious trends are apparent. These splittings are greater than ~ 3 mm/s and have only small temperature dependencies, indicating that the complexes are considerably distorted from a tetrahedral geometry. From the quadrupole splitting data one can estimate the degree of distortion Δ in the e levels (Fig. 1) in an analogous manner to that for the $FeCl_4^{2-}$ ion (7, 8). We estimate distortional splitting Δ of $\sim 800\ cm^{-1}$ in all of these tetrahedral complexes. Such highly distorted structures arise from the bulky nature of L and differences in covalent character of the Fe—X and Fe—L bonds.

The 1:4 thiourea complex $FeCl_2(THU)_4$ has a significantly more positive isomer shift than the tetrahedral complexes discussed above and is more consistent with six coordination about the iron. An alternate formulation would be $FeCl_2(THU)_2.2THU$, *i.e.*, with two lattice thiourea's. However, infrared evidence presented below favors the octahedral arrangement. Allowing a six coordinate iron(II) then the magnitude of the quadrupole splitting requires the complex to have the d_{xy} orbital lowest in energy (16). Complexes with the d_{xz}, d_{yz} orbitals lowest generally have splittings which are about one half those having the d_{xy} orbital lowest, and it has been suggested that this is the situation for $FeCl_2(BTH)_2$ (17) which has $\Delta E_Q = 1.76$ mm/s at 77 °K. The small temperature dependence of the quadrupole splitting for $FeCl_2(THU)_4$ indicates that the distortion in the t_{2g} levels is $\sim 1000\ cm^{-1}$. Spin–orbit coupling effects in such highly distorted structures are likely to be very small.

Infrared Spectra

Infrared spectral data of the complexes in the 400–4000 cm^{-1} range are summarized in Tables 4–7 which have been placed in the Depository of Unpublished Data.[1] No spectra were recorded for the benzothiazole complexes in this region. Flint and Goodgame (12) suggest that thioacetamide is coordinated through sulfur in the complex $CoCl_2(THA)_2$. The spectra of the iron–thioacetamide complexes are very similar to that of the cobalt complex, again supporting coordination through sulfur. In the N—H stretching region the iron complexes absorb at higher frequency than the ligand, in mull form, but at somewhat lower frequency than the ligand in dioxane solution, suggesting that the NH_2 group is still not as free as in dilute solutions of the ligand. Singh and Rivest (23) have suggested that some hydrogen bonding may occur between the NH_2 hydrogens and the halide in amide complexes. In neither of the iron complexes are there low lying N—H stretching bands which might result from coordination through nitrogen. The C—N stretching band at 1386 cm^{-1} is shifted to higher frequencies, as expected for coordination through sulfur. The bands at 973 and 719 cm^{-1}, which are of C=S stretching character, are shifted significantly to lower frequencies due to formation of S—Fe bonds.

The diagnostic vibrations for the thiourea complexes are the N—H stretching bands and the bands of C—N and C=S stretching charac-

[1]Copies may be obtained upon request from the Depository of Unpublished Data, National Science Library, National Research Council of Canada, Ottawa, Canada K1A 0S2.

Can. J. Chem. Downloaded from www.nrcresearchpress.com by 210.87.254.6 on 09/05/12
For personal use only.

Can. J. Chem. Downloaded from www.nrcresearchpress.com by 210.87.254.6 on 09/05/12
For personal use only.

ter. Bands in the ν(N—H) region are at significantly higher frequencies in the complexes than in the pure ligand. The absence of low lying absorption in this region again precludes the presence of N→Fe bonds. The N—C—N stretching band at 1472 cm^{-1} is found at higher frequencies in the complexes. The 1409 cm^{-1} band is split, presumably into a band of predominantly C—S stretching character, appearing at lower frequency, and one of predominantly N—C—N stretching character at higher frequency. The band at 730 cm^{-1}, which is largely of ν(C—S) character, is both split and lower in frequency. These effects have been noted by Swaminathan and Irving (25) in other thiourea complexes and are associated with coordination through sulfur.

The spectra of *N*-methylthiourea, *N,N'*-dimethylthiourea and their complexes with FeCl show no significant shifts to lower frequency of the bands in the ν(N—H) region. The dimethylthiourea complex shows only one strong N—H stretching band, supporting the presence of only one kind of nitrogen. The bands of mixed N—H bending and C—N stretching character at about 1550 cm^{-1} are shifted 20–25 cm^{-1} to higher frequencies, as are the bands of mixed C—N and C=S stretching character near 1500 cm^{-1}. It is thought that both these effects are due to an increase in C—N double bond character in the sulfur bonded ligand. *N,N'*-dimethylthiourea shows another band at 1355 cm^{-1} which has been tentatively assigned as mixed C—N and C=S stretching. This peak is also shifted to higher wave number on complex formation. The bands at 774 cm^{-1} in *N*-methylthiourea and 727 cm^{-1} in *N,N'*-dimethylthiourea are predominantly of C=S stretching character, and are shifted to lower frequency on coordination. The observation that none of the N—CH_3 stretching or deformation bands are significantly shifted also indirectly supports coordination through sulfur.

A comparison of the far infrared spectra of the thioacetamide and thiourea complexes with that of $FeBr_2(BTH)_2$ indicates clearly that all have the tetrahedral structure. Table 3 summarizes the data and a comparison of Fig. 2*b* and Fig. 3*a* shows the similarity, though the bands in the bromide complex are shifted to lower frequency as expected. The two bands in the 300 cm^{-1} region are assigned to the two expected Fe—Cl stretches. The analogous bromide complexes $FeBr_2(THA)_2$ and $FeBr_2(THU)_2$ show a similar, though less well resolved, pattern and individual assignments have not been made. It has been suggested in the case of $FeBr_2(THA)_2$ that ν(Fe—Br) and ν(Fe—S) vibrations are strongly coupled (12) and this may be the reason for the lack of resolution. The far infrared spectra of the methylthiourea and dimethylthiourea complexes are somewhat different from those of the thioacetamide and thiourea complexes. This difference is illustrated in Fig. 3*b* and one notes that while there are still two strong bands and a less intense absorption at lower frequency, the shapes and relative intensities have changed. The very strong band at 305 cm^{-1} in $FeCl_2(DMTHU)_2$ is broad, suggesting the presence of another band at ~315 cm^{-1}; in the MTHU complex this is somewhat better resolved with band at 300 cm^{-1} and a shoulder at 325 cm^{-1}. These have been assigned as Fe—Cl stretching vibrations while the bands to lower frequency are assigned to Fe—S vibrations. These assignments are again consistent with a tetrahedral geometry

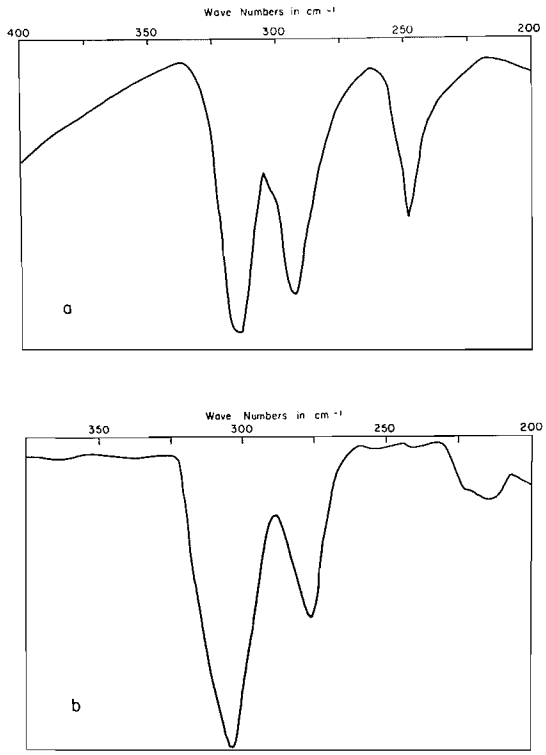

FIG. 3. Far infrared spectra of (*a*) $FeCl_2(THU)_2$, (*b*) $FeCl_2(DMTHU)_2$.

TABLE 8. Magnetic moments of thioacetamide and thiourea complexes

Complex	Temperature (°K)	μ_{eff} (β)
$FeCl_2(THA)_2$	295	5.27
$FeCl_2(THU)_2$	295	4.89
$FeCl_2(THU)_4$	295	5.25
$FeCl_2(MTHU)_2$	295	5.17
	77	4.83
$FeCl_2(DMTHU)_2$	295	5.09
	77	4.79

and the difference in spectral patterns is possibly the consequence of the bulkier ligand.

The 1:4 thiourea complex shows two bands at low frequency and by comparison with the far i.r. spectra of $FeCl_2(BTH)_2$ and related compounds (Table 3 and ref. 17) a *trans* octahedral structure is proposed. Both the ν(FeCl) and ν(Fe—S) vibrations are expected to be shifted to lower frequency as a result of longer, weaker bonds in the octahedral complex. The difference in Fe—Cl stretching frequency for the 1:2 and 1:4 thiourea complexes may be compared with that noted by Clark (27) for Co—Cl stretching in 1:2 and 1:4 pyridine complexes, where the tetrahedral complex has two ν(Co—Cl) bands at 344 and 304 cm^{-1}, but the octahedral species has only one ν(Co—Cl) band at 230 cm^{-1}.

Magnetic Moments

Magnetic data for some of the thioacetamide and thiourea complexes are summarized in Table 8. All of the data are consistent with magnetic moments expected for either tetrahedral or octahedral iron(II) in highly distorted environments.

We thank the National Research Council of Canada for financial support.

1. D. M. L. GOODGAME, M. GOODGAME, M. HITCHMAN, and M. WEEKS. Inorg. Chem. **5**, 635 (1966).
2. D. FORSTER and D. M. L. GOODGAME. J. Chem. Soc. 454 (1965).
3. N. N. Y. CHAN, M. GOODGAME, and M. J. WEEKS. J. Chem. Soc. (A), 2499 (1968).
4. C. FURLANI, E. CERVONE, and V. VALENTI. J. Inorg. Nucl. Chem. **25**, 159 (1963).
5. N. S. GILL. J. Chem. Soc. 3512 (1961).
6. D. FORSTER and D. M. L. GOODGAME. J. Chem. Soc. 268 (1965).
7. T. C. GIBB and N. N. GREENWOOD. J. Chem. Soc. 6989 (1965).
8. P. R. EDWARDS, C. E. JOHNSON, and R. J. P. WILLIAMS. J. Chem. Phys. **47**, 2074 (1967).
9. J. C. SHELDON and S. Y. TYREE. J. Am. Chem. Soc. **80**, 4775 (1958).
10. M. J. FRAZER, W. GERRARD, and R. TWAITS. J. Inorg. Nucl. Chem. **25**, 637 (1963).
11. C. D. BURBRIDGE and D. M. L. GOODGAME. J. Chem. Soc. (A), 1074 (1968).
12. C. D. FLINT and M. GOODGAME. J. Chem. Soc. (A), 750 (1968).
13. M. NARDELLI and I. CHIERICI. Gazzetta, **87**, 1478 (1957).
14. M. NARDELLI, G. F. GASPARRI, A. MUSOTTI, and A. MANFREDOTTI. Acta Cryst. **21**, 910 (1966).
15. M. NARDELLI, L. CAVALCA, and A. BRAIBANTI. Gazzetta, **86**, 867 (1957).
16. T. BIRCHALL. Can. J. Chem. **47**, 1351 (1969).
17. M. F. MORRIS. M.Sc. Thesis, McMaster University, Hamilton, Ontario. 1971. T. BIRCHALL and M. F. MORRIS. Can. J. Chem. This issue.
18. N. S. GILL, R. S. NYHOLM, G. A. BARCLAY, T. I. CHRISTIE, and P. J. PAULING. J. Inorg. Nucl. Chem. **18**, 88 (1961).
19. J. F. DUNCAN, R. M. GOLDING, and K. F. MOK. J. Inorg. Nucl. Chem. **28**, 1114 (1966).
20. C. D. BURBRIDGE and D. M. L. GOODGAME. J. Chem. Soc. (A), 694 (1967).
21. J. C. EVANS. J. Chem. Phys. **22**, 1228 (1954).
22. I. Suzuki. J. Chem. Soc. Jap. **35**, 1449 (1962).
23. P. P. SINGH and R. RIVEST. Can. J. Chem. **46**, 1773 (1968).
24. A. YAMAGOUCHI, R. PENLAND, S. MIZUSHIMA, J. LANE, C. CURRAN, and J. QUAGLIANO. J. Am. Chem. Soc., **80**, 527 (1958).
25. K. SWAMINATHAN and H. M. N. H. IRVING. J. Inorg. Nucl. Chem. **26**, 1291 (1964).
26. T. J. LANE, A. YAMAGOUCHI, J. V. QUAGLIANO, J. A. RYAN, and S. MIZUSHIMA. J. Amer. Chem. Soc., **81**, 3824 (1959).
27. R. J. H. CLARK. Spectrochim. Acta, **21**, 955 (1965).

Can. J. Chem. Downloaded from www.nrcresearchpress.com by 210.87.254.6 on 09/05/12
For personal use only.

Etude des mouvements de molécules linéaires en phase liquide par analyse du profil des bandes d'absorption infrarouge. II. Bande ν_3 du sulfure de carbonyle

A. M. BIZE, J. SOUSSEN-JACOB ET J. VINCENT-GEISSE
Laboratoire de Recherches Physiques, associé au C.N.R.S., Groupe infrarouge, 11 quai Saint Bernard, Paris (5°)

D. LEGAY ET J. P. PERCHARD
Laboratoire de Spectrochimie Moléculaire, 11 quai Saint Bernard, Paris (5°)

Reçu le 10 juin 1971

On a examiné la largeur et le profil de la bande ν_3 du sulfure de carbonyle (OCS) en solution dans une trentaine de solvants. L'étude de la variation de la largeur en fonction de la température permet de séparer les effets vibrationnel et rotationnel et de déterminer la barrière de potentiel s'opposant à la rotation. On a d'autre part tiré les fonctions de corrélation des résultats expérimentaux et calculé, à partir des deuxième et quatrième moments, la valeur du couple de rappel agissant sur le sulfure de carbonyle dans différents solvants. Les résultats obtenus mettent en évidence un effet rotationnel prépondérant dans les hydrocarbures saturés, tandis que, dans les autres solvants, l'élargissement vibrationnel se montre important.

The band width and profile of ν_3 mode of carbonyl sulfide (OCS) dissolved in about 30 solvents have been examined. The study of temperature broadening permits the separation of the vibrational and rotational effects and the determination of the potential barrier to rotation. Correlation functions have been plotted from the experimental results; the mean squared torques acting on carbonyl sulfide in various solvents have been calculated from the second and the fourth moments. The obtained results bear evidence of a dominant rotational effect for solutions in saturated hydrocarbons while, for the other solvents, vibrational broadening proves important.

Canadian Journal of Chemistry, **50**, 217 (1972)

Introduction

Une étude précédente, effectuée sur la molécule N_2O (1) a montré l'intérêt que présentait la détermination du profil des bandes d'absorption et des grandeurs que l'on peut en tirer, dans le cas des molécules triatomiques linéaires. Nous nous sommes proposé ici d'examiner la molécule OCS, elle aussi linéaire et dissymétrique, mais qui se distingue de N_2O, d'une part par l'existence d'un moment dipolaire non négligeable, égal à 0.71 D, et, d'autre part, par un moment d'inertie, sensiblement double de celui de N_2O, et égal à 141.2×10^{-40} g cm^2.

La molécule OCS possède, comme N_2O, trois modes fondamentaux de vibration dont deux, ν_1 et ν_3, parallèles à l'axe et un, ν_2, perpendiculaire à l'axe et dégénéré. L'étude des bandes parallèles conduisant à des résultats plus directement interprétables, nous nous limiterons dans le présent article à l'examen de la bande ν_3, la plus intense, et dont la fréquence se situe dans un domaine où de très nombreux solvants se montrent transparents.

Nous examinerons en premier lieu la largeur de bande à température ordinaire, puis sa variation en fonction de la température, dans tout le domaine de l'état liquide. Nous nous intéresserons en second lieu à la fonction de corrélation et aux moments des bandes.

Etude expérimentale

Le sulfure de carbonyle utilisé, de pureté 97%, provenait de la firme Matheson; les impuretés, principalement CO_2, CS_2 et CO, ne sont pas gênantes car elles n'absorbent pas dans le domaine spectral considéré.

Le spectre de OCS à l'état gazeux, dans la région de ν_3, est bien connu (2); la bande de vibration–rotation ν_3 a son centre à 2062.2 cm^{-1} et elle est accompagnée, du côté des basses fréquences, par une bande chaude parasite, $\nu_3 + \nu_2 - \nu_2$ située à 2054.9 cm^{-1}; en effet, le niveau ν_2, relativement bas (524 cm^{-1}), est peuplé à la température ordinaire par 18% des molécules. D'autre part un effet isotopique non négligeable peut se présenter, à cause, essentiellement, de l'isotope 34 du soufre, d'abondance naturelle 3%; le spectre de cette molécule isotopique n'a pas été examiné à notre connaissance, mais un calcul approché des fréquences de vibration nous a donné une différence de 1 cm^{-1} entre les nombres d'ondes des vibrations ν_3 correspondant aux deux espèces; compte tenu de l'ordre de grandeur de la largeur de ν_3, il est légitime de supposer que l'existence de cet isotope ne perturbe pas sensiblement le profil de la bande. Il en va tout autrement de la bande chaude, bien visible sur nos

Can. J. Chem. Downloaded from www.nrcresearchpress.com by 210.87.254.42 on 09/05/12
For personal use only.

Can. J. Chem. Downloaded from www.nrcresearchpress.com by 210.87.254.42 on 09/05/12
For personal use only.

TABLEAU 1. Largeur et fréquence de la bande ν_3 de OCS à $T = 313$ °K; $\nu_{gaz} = 2062.2\ cm^{-1}$*

N°	Solvants	ν_{sol} (cm^{-1})	$\Delta\nu_{1/2}$ (cm^{-1})	$\Delta\nu^s_{1/2}$ (cm^{-1})
1	Pentane	2048.0	14.3	12.7
2	Hexane	2047.3	12.6	11.4
3	Heptane	2047.0	11.6	10.5
4	Octane	2046.5	10.3	9.7
5	Cyclopentane	2046.2	11.2	10.2
6	Cyclohexane	2045.7	7.9	7.5
7	2-Méthylbutane	2048.8	11.9	11.1
8	2,2,4-Triméthylpentane	2047.3	11.1	10.3
9	2-Méthylpentane	2047.6	12.2	11.4
10	3-Méthylpentane	2047.7	12.0	10.7
11	Tétrachloréthylène	2044.2	9.2	8.8
12	Tétrachlorure de carbone	2045.0	10.4	9.6
13	Sulfure de carbone	2040.0	11.3	10.4
14	1,1,2-Trichlorotrifluoroéthane	2049.0	12.7	11.0
15	1-Hexène	2046.7	13.7	12.8
16	Benzène	2041.0	17.9	17.4
17	Dichlorométhane	2043.0	16.0	15.2
18	Dibromométhane	2039.2	16.0	15.6
19	Diiodométhane	2034.3	16.1	15.6
20	Chloroforme	2043.2	17.4	16.4
21	Bromoforme	2038.4	16.6	16.0
22	1,4-Dichlorobutane	2041.3	17.0	16.7
23	1,2-Dichloropropane	2042.3	17.5	17.2
24	Méthanol	$\simeq$2043.0	18.2	
25	Butanol	2044.1	18.0	15.2
26	Paradioxane	2041.5	18.0	17.9
27	Acétone	2043.2	20.7	20.6
28	Acétonitrile	2044.9	16.7	15.8
29	Pyridine	$\simeq$2039.0	19.4	
30	Tétrahydrofurane	2040.5	21.5	20.1

*Incertitude: solvants de 1 à 15: ν, $\pm 0.3\ cm^{-1}$; $\Delta\nu_{1/2}$, $\pm 0.2\ cm^{-1}$; $\Delta\nu^s_{1/2}$, $\pm 0.4\ cm^{-1}$; solvants de 16 à 30: ν, $\pm 0.5\ cm^{-1}$; $\Delta\nu_{1/2}$, $\pm 0.2\ cm^{-1}$; $\Delta\nu^s_{1/2}$, $\pm 1\ cm^{-1}$.

spectres (Fig. 2) et dont nous devrons tenir compte dans la suite.

Les solvants utilisés, au nombre d'une trentaine, sont des produits pour spectroscopie de Prolabo et Fluka dont la pureté a été considérée comme suffisante. Les solutions ont été préparées par barbotage à température ordinaire ou piégeage à 77 °K du sulfure de carbonyle dans les divers solvants; leur titre reste toujours inférieur à 0.1 mol/l.

Les spectres ont été enregistrés au moyen d'un spectromètre Perkin–Elmer 225; la largeur de fente spectrale est voisine de $0.7\ cm^{-1}$; un étalonnage en fréquences, obtenu à partir des raies d'absorption de l'oxyde de carbone, permet de fixer à $0.15\ cm^{-1}$ la précision des pointés. Les largeurs sont déterminées à $\pm 0.3\ cm^{-1}$ près. A la température ordinaire le rapport entre la largeur de fente spectrale et la largeur à mi-hauteur de la bande reste inférieur à 0.07 de sorte que la distorsion du profil par l'appareil peut être considérée comme négligeable. A très basse température il n'en va plus de même car le rapport précédent peut atteindre 0.25; les largeurs se montrent peu affectées mais le profil au centre de la bande davantage; nous n'en avons pas tenu compte dans ce qui suit.

Les spectres à température variable ont été obtenus, suivant le cas, de deux manières différentes. Dans un premier montage, la solution est placée dans une cellule thermostatée située dans une enceinte remplie en général d'un gaz sec (azote ou argon) et la température, mesurée au moyen d'un thermocouple fixé sur une face de la cellule, est stabilisée par circulation d'un fluide cryogénique de débit règlable; les mesures sont alors effectuées l'une à la suite de l'autre sur la solution et le solvant à même température, d'où la nécessité de ramener entre chaque mesure l'ensemble à la température ordinaire pour éviter les condensations d'eau et les chocs thermiques sur les fenêtres au moment du remplissage. Dans un deuxième montage, nous avons utilisé un cryostat de modèle RIIC, la cuve étant sous vide et le refroidissement effectué avec de l'azote liquide. Nous avons alors, dans une série de mesures, enregistré les spectres de la solution successivement à différentes températures et dans une autre série, ceux du solvant, ce qui nous a permis d'obtenir un plus grand nombre de points que dans le premier procédé.

Largeur de bande

(a) Température ordinaire

Nous avons rassemblé dans le Tableau 1 les résultats de nos mesures de largeur à la tempéra-

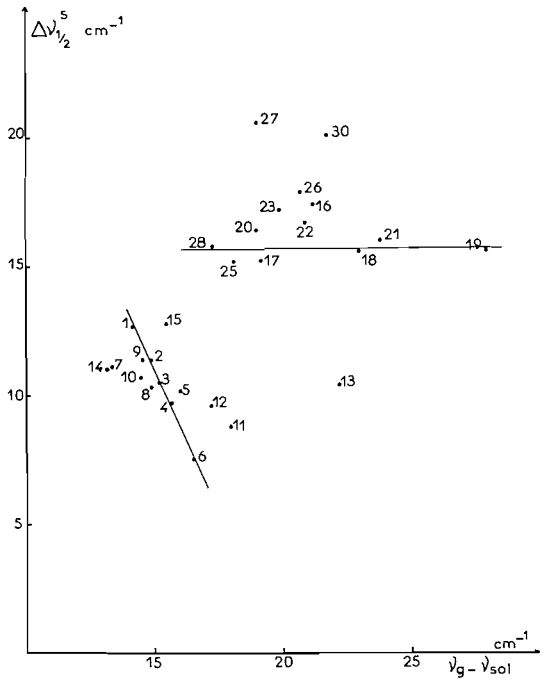

FIG. 1. Largeur de bande en fonction du déplacement de fréquence entre le gaz et la solution. Pour l'identification des solvants, se rapporter au Tableau 1.

TABLEAU 2. Constantes de diffusion rotationnelle calculées à partir des largeurs de bande

Solvant*	D (10^{12} s^{-1})
1	0.60
2	0.50
3	0.49
4	0.46
5	0.48
6	0.35
7	0.52
8	0.49
9	0.54
10	0.50
11	0.41
12	0.45
13	0.49
14	0.52
15	0.62

*Pour l'identification des solvants, se rapporter au Tableau 1.

ture ordinaire, soit 313 °K. La première colonne indique le nombre d'ondes du maximum d'absorption de la solution, la deuxième la largeur à mi-hauteur $\Delta\nu_{1/2}$ et la troisième la largeur symétrisée $\Delta\nu^s_{1/2}$, c'est-à-dire le double de la demi-largeur correspondant aux hautes fréquences; ces deux derniers chiffres se montrent assez nettement différents, dans le cas des faibles largeurs, à cause de l'existence, signalée plus haut, de la bande chaude. Dans ce qui suit nous discuterons les résultats relatifs à $\Delta\nu^s_{1/2}$, c'est-à-dire en supposant la bande symétrique. Cette hypothèse se justifie par le fait qu'à basse température la bande observée est effectivement symétrique en raison de la disparition de la bande chaude. Par ce procédé l'influence de cette dernière, qui varie selon la température, se trouve éliminée.

Nous avons porté, dans la Fig. 1, la largeur $\Delta\nu^s_{1/2}$ en fonction du déplacement $\nu_{gaz} - \nu_{sol}$, ce dernier facteur représentant, en quelque sorte, le degré d'activité du solvant. Les points représentatifs se classent nettement en deux groupes: Dans le premier, celui des solvants non polaires, ils se placent, excepté CS_2, au voisinage d'une droite de pente négative, assez forte, la largeur étant en première approximation d'autant plus grande que le solvant est plus inerte. Si nous émettons l'hypothèse, assez vraisemblable, que, dans ces solvants, la largeur est due principalement à la diffusion rotationnelle, nous voyons que celle-ci est la plus rapide pour le pentane, résultat en accord avec ce que nous avions observé pour N_2O (1). Les points correspondant aux solvants polaires, auxquels il faut ajouter le benzène, se situent tous nettement au-dessus des précédents et, si certains d'entre eux se placent au voisinage d'une droite horizontale, il ne semble plus y avoir de relation aussi nette entre largeur et déplacement. On peut en conclure que l'origine de l'élargissement n'est plus ici la diffusion rotationnelle, mais plutôt un effet vibrationnel dû à des actions intermoléculaires entre dipôles.

Nous avons porté, dans le Tableau 2, la valeur de la constante D de diffusion rotationnelle, calculée à partir de $\Delta\nu^s_{1/2}$ pour les solvants dans lesquels ce processus semble important.

$$[1] \qquad D = \tfrac{1}{2}\pi c \Delta\nu^s_{1/2}$$

Dans cette expression les effets vibrationnels sont négligés de sorte que la largeur entière de la bande est supposée provenir de la contribution rotationnelle. Par suite la valeur de D ainsi

Can. J. Chem. Downloaded from www.nrcresearchpress.com by 210.87.254.42 on 09/05/12
For personal use only.

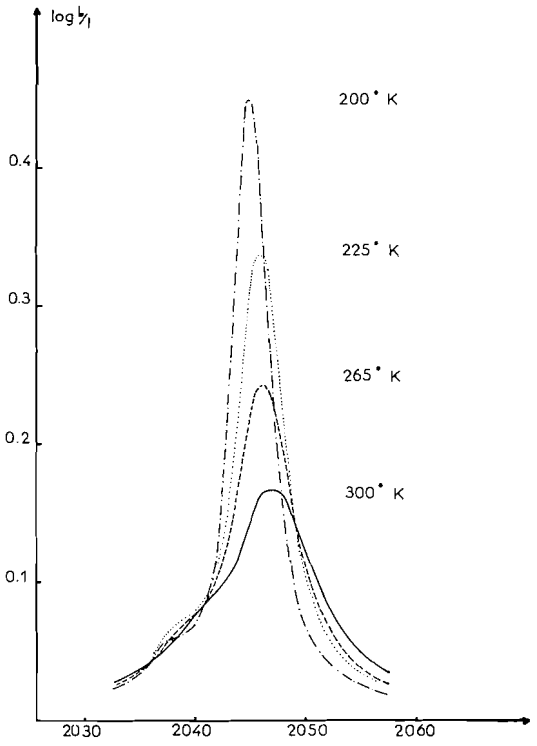

FIG. 2. Spectre de OCS dans l'heptane, à différentes températures.

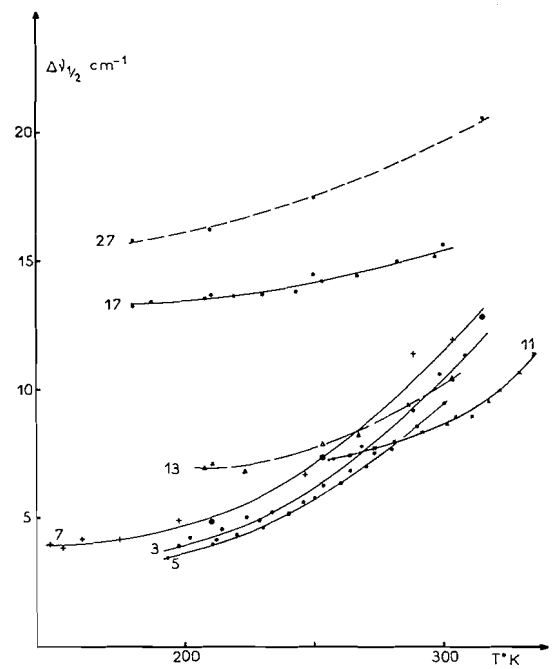

FIG. 3. Variation de la largeur en fonction de la température. Pour les numéros des courbes, se rapporter au Tableau 1. Courbe 7: les points ● sont ceux de l'hexane.

obtenue doit être considérée comme une limite supérieure. Si nous comparons les chiffres obtenus à ceux de N_2O dans les mêmes solvants (1), nous voyons qu'ils leur sont inférieurs, ce qui s'explique aisément par l'inertie plus grande de OCS.

(b) Variation en fonction de la température

Il est intéressant d'essayer de vérifier les conclusions précédentes par l'étude de la variation de largeur en fonction de la température. En effet, si celle-ci est due essentiellement à la diffusion rotationnelle, la largeur est donnée, d'après Rakov (3), par une formule de la forme:

$$[2] \qquad \Delta\nu_{1/2} = A\, e^{-U/RT} + \delta$$

dans laquelle le premier terme représente l'effet rotationnel et le second, δ, l'effet vibrationnel, petit par rapport au premier, et supposé, en première approximation, indépendant de T; U est la barrière de potentiel opposée à la rotation de la molécule. La Fig. 2 montre, à titre d'exemple, les spectres obtenus dans le cas de l'heptane; on voit que la variation du profil est très importante; la bande chaude, visible comme un épaulement à 300 °K, se montre nettement séparée à 200 °K alors que son intensité a considérablement diminué. Nous avons porté, dans la Fig. 3, la variation de la largeur $\Delta\nu_{1/2}$ en fonction de T ($\Delta\nu^s_{1/2}$ n'étant pas mesurable sur tous les spectres), dans le cas des solutions étudiées de manière continue; nous y avons ajouté les trois points relatifs à l'hexane et qui se placent sur la courbe du 2-méthylbutane (courbe 7), et ceux de l'acétone (courbe 27), bien qu'il n'y en ait que quatre; nous examinerons un peu plus loin, en prenant l'exemple de l'heptane, l'incidence du choix de $\Delta\nu_{1/2}$ ou $\Delta\nu^s_{1/2}$ sur la détermination des constantes. L'examen de la Fig. 3 suggère les commentaires suivants: les courbes 3, 5, 7 montrant la plus forte variation, correspondent à des points situés, sur la Fig. 1, dans le groupe auquel nous avons attribué un effet rotationnel prépondérant; les courbes 13 et 11, nettement différentes des autres sont celles, d'une part de CS_2, très distinct des autres solvants sur la Fig. 1, et, d'autre part de C_2Cl_4; enfin, et comme on pouvait s'y attendre, les courbes 17 et 27, correspondant à des solvants polaires, montrent une

Can. J. Chem. Downloaded from www.nrcresearchpress.com by 210.87.254.42 on 09/05/12
For personal use only.

TABLEAU 3. Constantes tirées de la formule de Rakov

	U (kcal/mole)	δ (cm^{-1})	A (cm^{-1})
Cyclopentane*	1.9∓0.2	2.3∓0.3	150∓ 30
Heptane *	2.2∓0.2	3.1∓0.1	300∓ 70
Heptane †	2.6∓0.2	3.2∓0.2	500∓150
2-Méthylbutane†	2.6	3.9	730
Sulfure de carbone*	2.8∓0.6	6.3∓0.5	450∓350
Tétrachloroéthylène*	3.7∓1.0	6.7∓0.5	(15∓10)10^3
Dichlorométhane*	4.3∓0.9	11.6∓0.6	(20∓9)10^4

*Calculées à partir de $\Delta\nu^s_{1/2}$.
†Calculées à partir de $\Delta\nu_{1/2}$.

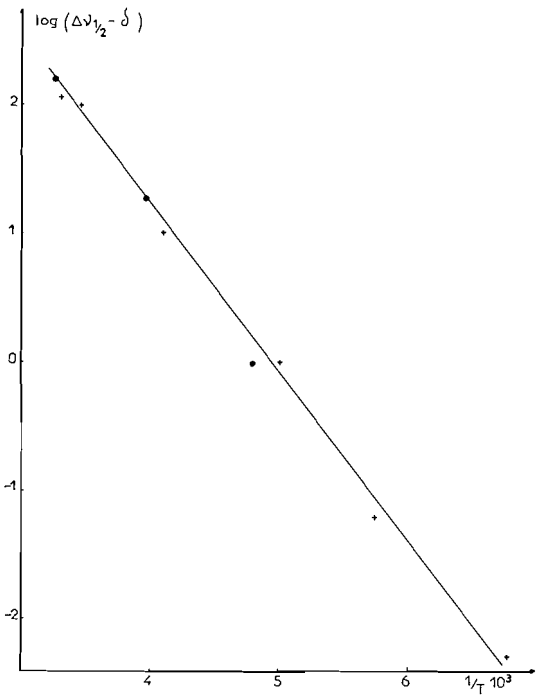

FIG. 4. ln ($\Delta\nu_{1/2} - \delta$) fonction de $1/T$: +, solution dans le 2-méthyl butane; ●, solution dans l'hexane.

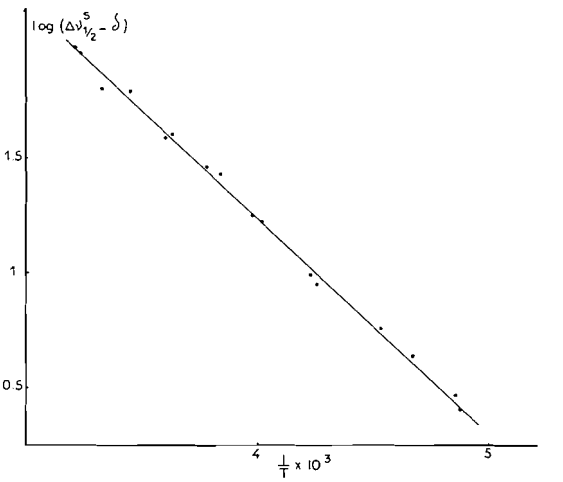

FIG. 5. ln ($\Delta\nu^s_{1/2} - \delta$) fonction de $1/T$. Solution dans le cyclopentane.

variation relative beaucoup plus faible que les précédentes.

A partir des courbes de la Fig. 3, nous avons calculé les constantes U, A et δ de la formule [2]. Tout d'abord, nous voyons que la solution dans le 2-méthylbutane (courbe 7) peut être étudiée jusqu'à une température suffisamment basse pour que $\Delta\nu_{1/2}$ tende vers une valeur constante qui nous fournit δ. Nous pouvons alors tracer le graphique donnant ln ($\Delta\nu_{1/2} - \delta$) en fonction de $1/T$ (Fig. 4); les points se placent bien sur une droite dont la pente nous permet de calculer la barrière de potentiel U et l'ordonnée à l'origine la constante A. Dans les autres cas nous déterminons les constantes en dérivant la formule [2] par rapport à $1/T$. En posant $y = \Delta\nu_{1/2}$ et $x = 1/T$ on obtient

$$[3] \qquad \frac{dy}{dx} = \frac{U}{R}(y - \delta)$$

L'incertitude entachant les résultats s'obtient en faisant varier systématiquement δ autour de la valeur approchée obtenue, de façon à connaître les valeurs extrêmes pour lesquelles la courbe semblable à celles des Figs. 4 et 5 est encore une droite. La Fig. 5 montre les résultats relatifs au cyclopentane; avec ce solvant, comme avec l'heptane, l'accord entre les résultats expérimentaux et la formule [2] est très bon.

Nous avons porté, dans le Tableau 3, les constantes U, A et δ de la formule [2], calculées dans tous les cas, sauf celui du 2-méthylbutane,

Can. J. Chem. Downloaded from www.nrcresearchpress.com by 210.87.254.42 on 09/05/12
For personal use only.

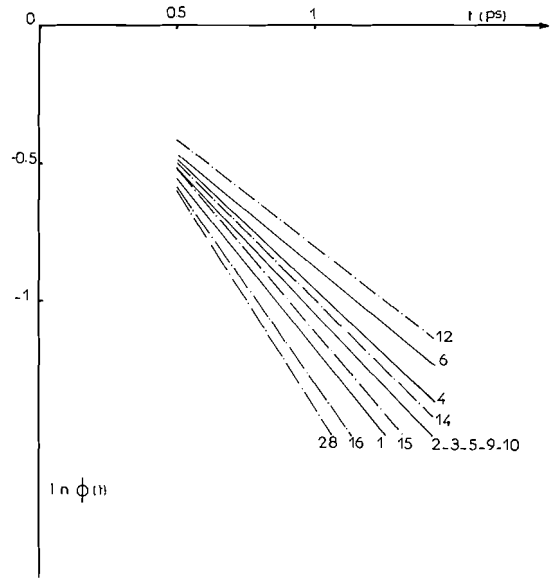

FIG. 6. Partie rectiligne de $\ln \Phi(t)$ dans différents solvants. Pour les numéros des courbes se rapporter au Tableau 1. — hydrocarbures saturés, -·-·- autres solvants.

avec la largeur symétrisée $\Delta\nu^s_{1/2}$. Afin de connaître l'incertitude due à l'emploi de $\Delta\nu_{1/2}$ au lieu de $\Delta\nu^s_{1/2}$, nous avons effectué les deux calculs pour l'heptane; nous voyons que l'utilisation de $\Delta\nu_{1/2}$ fournit une valeur plus grande pour U et pour A; la valeur de U pour le 2-méthylbutane est donc probablement surestimée et voisine en réalité de celle de l'heptane. Il est intéressant de comparer les valeurs obtenues pour δ aux largeurs totales de bandes (Tableau 1). Nous voyons que, dans le cas du cyclopentane, de l'heptane et du 2-méthylbutane, l'effet rotationnel fournit les deux tiers ou les trois quarts de la largeur totale à la température ambiante et nous estimons que la formule de Rakov nous donne une bonne approximation. Ailleurs il faut se montrer plus réservé: pour les trois derniers solvants du tableau, les points des graphiques semblables aux Figs. 4 et 5 s'alignent moins bien, et l'incertitude se montre beaucoup plus grande; ceci correspond au fait que l'élargissement rotationnel ne représente plus qu'une faible part de l'élargissement total. Il ne faut donc pas attacher trop d'importance aux chiffres des trois dernières lignes, particulièrement à ceux du dichlorométhane. Il existe dans ce cas un effet vibrationnel important et supposé indépendant de la température, ce qui n'est sans doute qu'une grossière approximation.

Fonctions de corrélation

Les fonctions de corrélation ont été calculées comme précédemment (1) pour la plus grande partie des spectres à température ordinaire et pour certains d'entre eux à température variable, mais, dans ce dernier cas, la précision avec laquelle elles sont connues, est moins bonne et nous n'en parlerons pas ici. Le calcul a été effectué dans un domaine d'intégration égal à environ 17 fois la largeur de la bande. Dans le cas des solutions en solvants inertes, on a pris les courbes symétrisées. On a cependant vérifié que l'utilisation de la bande entière ne modifiait que d'une façon négligeable la fonction de corrélation aux temps courts; par contre la pente de la partie linéaire varie approximativement dans le rapport des demi-largeurs $\Delta\nu_{1/2}/\Delta\nu^s_{1/2}$. Si nous traçons les courbes donnant $\ln \Phi$ en fonction du temps, celles-ci se classent en deux catégories: dans l'une d'elles correspondant à la plupart des solvants polaires, on n'obtient pas de partie rectiligne et ce fait se montre en accord avec l'hypothèse, faite plus haut, que, dans ces solvants, l'effet rotationnel est secondaire; il faut remarquer que ces courbes ne sont pas non plus des paraboles comme on s'y attendrait si l'élargissement était purement vibrationnel (4), mais se situent entre les deux. Dans le deuxième groupe, comprenant la plupart des solvants non polaires et l'acétonitrile, on observe une partie parabolique au voisinage de l'origine et ensuite une droite (Fig. 7); la Fig. 6 montre un certain nombre de ces droites. On voit que la corrélation diminue d'autant plus vite que la rotation est plus rapide ou les interactions moléculaires plus importantes.

Sur la Fig. 7 sont rassemblées quelques unes des fonctions de corrélation. La partie des courbes proche de l'origine, peut présenter deux allures différentes: ou bien elle suit d'abord la courbe du rotateur libre (R dans 7*a*, 7*b*, 7*c*) puis s'en écarte, passe par un point d'inflexion et devient rectiligne, la transition s'effectuant très rapidement, ou bien (7*d*, courbes 16 et 28) elle se place dès le départ au-dessous de R et ne présente plus de point d'inflexion. Les deux extrêmes sont la courbe du pentane (7*a*, courbe 1) qui se confond avec R jusqu'à $t = 0.3$ ps, l'angle de rotation correspondant étant 40°, et

Can. J. Chem. Downloaded from www.nrcresearchpress.com by 210.87.254.42 on 09/05/12
For personal use only.

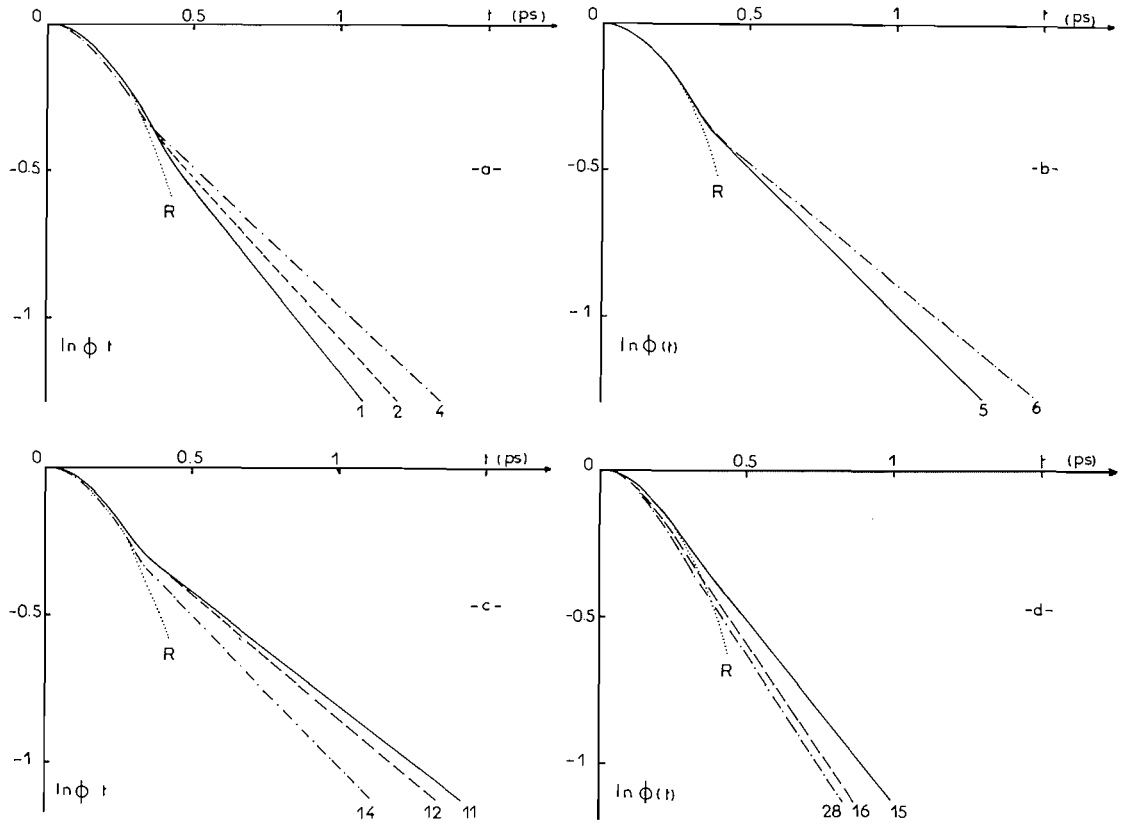

FIG. 7. ln $\Phi(t)$ dans différents solvants. R: courbe du rotateur libre. Pour les numéros des courbes, se rapporter au Tableau 1.

celle de l'acétonitrile (7*d*, courbe 28) pour laquelle la corrélation diminue plus rapidement, en accord avec le fait qu'il existe alors un effet vibrationnel supplémentaire important.

Nous avons porté dans le Tableau 4 diverses constantes tirées des graphiques précédents: τ_d est le temps correspondant au début de la diffusion rotationnelle; on remarque qu'il est le même, aux erreurs expérimentales près, pour tous les solvants de 1 à 15 et le même que pour N_2O (1). τ est le temps de corrélation calculé à partir de la pente des droites et D le coefficient de diffusion correspondant [4] $D = 1/2\,\tau$; nous pouvons comparer les chiffres de cette dernière colonne à ceux donnés dans le Tableau 2; l'accord se montre assez bon, bien que dans certains solvants (11 à 15) l'élargissement d'origine vibrationnelle ne soit pas négligeable.

TABLEAU 4. Constantes tirées des fonctions de corrélation présentant une partie linéaire

Solvant*	τ (ps)	D (ps)$^{-1}$	τ_d (ps)	φ_d
1	0.77	0.65	0.35	45°
2	0.91	0.55	0.40	47°
3	0.96	0.52	0.40	47°
4	1.00	0.49	0.35	44°
5	0.94	0.52	0.35	44°
6	1.13	0.44	0.30	40°
8	0.95	0.56	0.35	45°
9	0.86	0.58	0.40	47°
10	0.94	0.52	0.40	47°
11	1.39	0.36	0.30	52°
12	1.15	0.44	0.30	41°
14	0.94	0.51	0.36	46°
15	0.80	0.62	0.30	38°
16	0.67		0.20	32°
28	0.64		0.25	38°

*Pour l'identification des solvants, se rapporter au Tableau 1.

Can. J. Chem. Downloaded from www.nrcresearchpress.com by 210.87.254.42 on 09/05/12
For personal use only.

TABLEAU 5. Deuxième et quatrième moments

Solvant*	$M(2)$ 10^{24} (s^{-2})	$M(4)$ 10^{50} (s^{-4})	$\langle C^2\rangle^{1/2}$ (cm^{-1}/rad)
1	7.3	3.3	870
2	6.6	2.6	870
3	7.0	3.1	870
4	7.6	3.9	940
5	6.5	2.5	850
6	8.0	4.8	
8	7.2	3.4	
9	6.4	2.5	860
10	6.6	2.7	870
11	6.9	3.8	1050
12	6.8	3.7	1060
14	7.0	3.3	910
15	6.6	2.7	900
16	8.0	4.0	870
17	9.6	7.5	
18	9.3	6.6	
20	8.3	4.8	
24	8.4	4.6	
25	6.9	2.6	1060
27	9.5	7.9	
28	8.9	4.9	

*Pour l'identification des solvants, se rapporter au Tableau 1.

Enfin la dernière colonne du Tableau 4 donne un ordre de grandeur de l'angle moyen dont a tourné la molécule avant le début de la diffusion rotationnelle. Cet angle varie de 40 à 50°, alors qu'il était de 50 à 60° pour N_2O pour un temps sensiblement égal; la molécule OCS tourne moins vite en moyenne que N_2O, à cause de son plus grand moment d'inertie.

Deuxième et quatrième moments

Nous avons calculé, comme précédemment (1), dans tous les cas où le solvant ne présentait pas de bande d'absorption proche de ν_3, le deuxième et le quatrième moment. Les résultats obtenus sont loin de se montrer satisfaisants. En particulier nous avons observé quelquefois une croissance du deuxième moment en fonction de l'absorption maximale $\ln (I_0/I)_{max}$. On peut se demander s'il ne s'agit pas d'un effet dû à la concentration, bien que celle-ci reste toujours très faible. Une étude systématique entreprise sur OCS, en même temps que sur d'autres molécules linéaires non polaires, est en cours, et nous permettra peut-être d'expliquer les phénomènes observés. D'une manière générale les chiffres obtenus se montrent supérieurs à la valeur théorique: $6.2 \times 10^{24}\ s^{-2}$ (Tableau 5). Ce résultat pourrait peut-être s'interpréter par l'existence de l'élargissement vibrationnel qui devrait ajouter une contribution au second moment (6).

Dans ces conditions la détermination du couple de rappel, à partir de la valeur du quatrième moment, se montrait délicate; nous l'avons tout de même effectuée en nous limitant aux spectres donnant des valeurs de $M(2)$ assez proches de la valeur théorique et en appliquant la formule de Gordon (5),

$$[5] \qquad \frac{\langle C^2\rangle}{I^2} = M(4) - 2[M(2)]^2$$

espérant ainsi compenser, en prenant pour $M(2)$ la valeur expérimentale, les chiffres trop grands obtenus pour $M(2)$ et $M(4)$. Le Tableau 5 résume les résultats obtenus; les chiffres donnés pour le couple quadratique moyen, $\langle C^2\rangle^{1/2}$, fournissent au mieux un ordre de grandeur; celui-ci est de 870 cm^{-1}/rad (2.5 kcal/mol rad) pour un certain nombre de solvants et peut être comparé à la barrière de potentiel trouvée à partir de la variation de largeur en fonction de la température (Tableau 3); les valeurs sont voisines. Il est intéressant également de comparer ce chiffre à celui trouvé pour N_2O, $3kT$/rad, c'est-à-dire 1.9 kcal/mol rad. Le couple de rappel sur OCS serait plus important que celui agissant sur N_2O.

Can. J. Chem. Downloaded from www.nrcresearchpress.com by 210.87.254.42 on 09/05/12
For personal use only.

Conclusion

L'étude simultanée de la largeur et de la fonction de corrélation de la bande ν_3 de OCS en solution, à température ordinaire et à basse température, nous a permis de mettre en évidence un effet rotationnel prépondérant dans le cas des hydrocarbures saturés, et de calculer la constante de diffusion et la barrière de potentiel s'opposant à la rotation. Pour les autres solvants et, en particulier, les solvants polaires, on ne peut plus négliger l'élargissement vibrationnel et celui-ci, mal connu, masque en grande partie l'effet rotationnel.

1. J. VINCENT-GEISSE, J. SOUSSEN-JACOB, NGUYEN TAN TAI et D. DESCOUT. Can. J. Chem. **48**, 3918 (1970).
2. H. J. CALLOMON et H. W. THOMPSON. Proc. Roy. Soc. A **222**, 431 (1954).
3. A. V. RAKOV. Proc. of the P. N. Lebedev. Phys. Inst. 27 (1965). Optics and spectrosc. **13**, 203 (1962).
4. S. BRATOS, J. RIOS et Y. GUISSANI. J. Chem. Phys. **52**, 439 (1970).
5. R. G. GORDON. Advances in magnetic resonance. vol. 3. *Edited by* J. S. Waugh. Academic Press, Inc., New York. 1968.
6. R. G. GORDON. J. Chem. Phys. **41**, 1819 (1964).

Can. J. Chem. Downloaded from www.nrcresearchpress.com by 210.87.254.42 on 09/05/12
For personal use only.

Carbanions in Carbohydrate Chemistry: Novel Methods for Chain Extension and Branching[1]

S. HANESSIAN AND P. DEXTRAZE[2]

Department of Chemistry, University of Montreal, Montreal, Quebec

Received June 24, 1971

Methods are described for the introduction of two and three carbon units in carbohydrates by the reaction of suitable epoxides with sodio diethyl malonate. The reactions represent a means of branching and chain extension in the carbohydrate series and lead to the incorporation of highly functionalized carbon units at predetermined sites in the sugar molecule.

Des méthodes sont décrites pour l'introduction de fragments à deux ou trois atomes de carbone par l'action du sel de sodium du malonate de diéthyle sur l'époxyde approprié. Ces réactions représentent un moyen d'introduction d'une ramification et d'allongement d'une chaîne dans la série des hydrates de carbone et conduisent à l'incorporation en des sites prédéterminés sur la molécule de sucre de chaînes carbonées comportant de très nombreux groupes fonctionnels.

Canadian Journal of Chemistry, **50**, 226 (1972)

Can. J. Chem. Downloaded from www.nrcresearchpress.com by 210.87.254.6 on 09/05/12
For personal use only.

Branched-chain sugars (3) occupy a unique position among the various classes of carbohydrates, in that they are of considerable biological significance due to their occurrence as components of medicinally important antibiotics (4), and whose structural features still represent a challenge to the synthetic chemist. Unlike deoxy (5) and amino sugars (6) which occupy the uppermost ranks as biologically significant sugars, the methods of introduction of *C*-branching in carbohydrates are somewhat limited. The problem is further complicated when stereochemical considerations are taken into account. Quite fortuitously, those branched-chain sugars which occur as components of antibiotics are with few exceptions *C*-methyl hexoses containing a tertiary hydroxyl group at the branch site. Their syntheses by the reaction of appropriately substituted hexosuloses with organometallic or other reagents as the one-carbon source of the methyl group, has become relatively easy (4). Two preparatively significant routes to deoxy branched-chain sugars involve the opening of appropriate epoxides with organometallic reagents, which leads generally to a preponderance of one of two possible isomers, and the reaction of appropriately substituted hexosuloses with Wittig reagents (7, 8) followed by catalytic reduction which affords epimeric *C*-alkyl sugars. From a consideration of synthetic value and versatility, it would be desirable to introduce a *C*-chain that is functional, and not chemically inert as an alkyl group. Access to such functionalized substituents is somewhat scarce and it is this aspect of chain-branching reactions that is the subject matter of this paper. The application of the hydroformylation reactions of substituted glycals affords 2-*C*-hydroxymethyl sugars (9). In isolated examples, dimethylvinyl (10) and aldehyde (11, 12) chains have been introduced in the carbon skeleton by epoxide opening ring contraction and oxidation reactions respectively. Such groups as ($Me_2C{=}CH{-}$, $-CHO$, $-CH_2OH$, etc.), when attached to the carbohydrate skeleton represent functionally useful ramifications and they are amenable to further transformations.

Carbanions derived from malonic esters represent potentially interesting reactants as a means of introduction of highly functionalized substituents in carbohydrates. Despite the multitude of applications in other classes of organic compounds (13) carbanions of this type have been sparsely used in carbohydrate chemistry (14–17). We report in this paper our studies involving the stereoselective ring opening of carbohydrate epoxides with sodio diethyl malonate, as a means of branching and chain-extension.

To the best of our knowledge, the reaction of sodio diethyl malonate with methyl 2,3-anhydro-4,6-*O*-benzylidene-α-D-allopyranoside (**1**) represents the only recorded example of its kind in the carbohydrate series (Scheme 1). As reported by

[1]Part of a series on "Preparative and exploratory carbohydrate chemistry", see also refs. 1, 2.

[2]NRCC Predoctorate Fellow, 1969–1971.

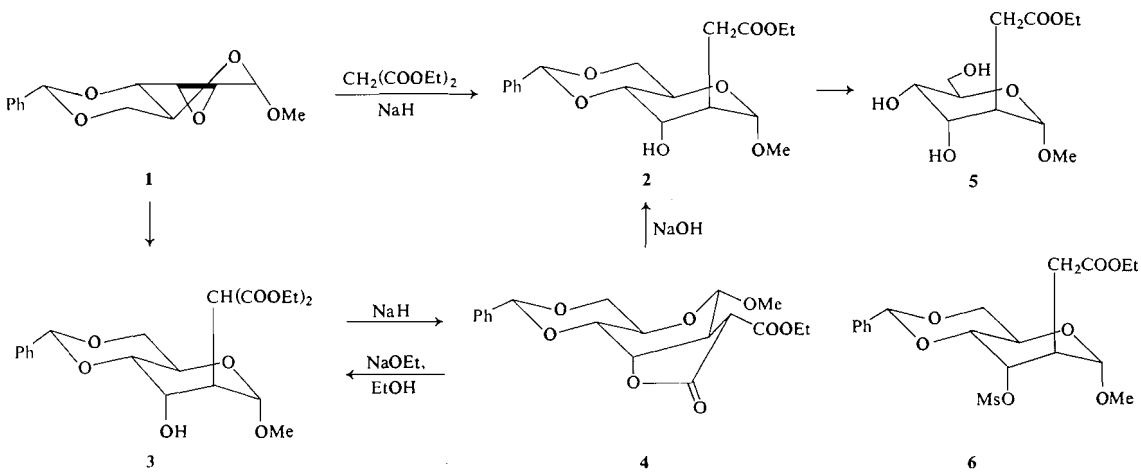

SCHEME 1

Kochetkov and coworkers (18), the reaction leads to a 25–30% yield of compound **2**. We reinvestigated this reaction with the objective of obtaining optimum and improved yields, searching for the possible formation of other products related to **2**, securing unambiguous proof of their structures and stereochemistry and shedding some light on the mechanism of the reaction.

At the outset, it was of interest to establish unambiguously the position of branching in the product **2** prepared according to the published procedure (18). Hydrolysis of the benzylidene group with dilute hydrochloric acid gave the crystalline product **5** in high yield. This compound was totally oxidized by periodate, as would be expected of its structure and the presence of the branching at C-2 was thus firmly established. Our efforts were then directed to the preparative and mechanistic aspects of the reaction of **1** with the carbanion.

After a detailed study of the effect of different solvents on the nature of the products, it appeared that benzene as used by the Russian workers (18), was the solvent of choice. It was more convenient however, to use sodium hydride instead of dispersed sodium to prepare the carbanion. The nature of the products between sodio diethyl malonate and **1** appeared to depend very strongly on the moisture content as well as on the temperature of the reaction. After prolonged periods at 40°, the reaction product was found to be the crystalline diester **3**, which was formed in 52% yield. Attempts to shorten the reaction time by raising the temperature led to mixtures of **2** and **3**. When the reaction was carried out in a strictly anhydrous medium, in refluxing benzene, a 74% yield of a new crystalline product was formed. Spectroscopic and chemical evidence permitted the assignment of the highly strained lactone structure **4** to this product. Treatment of **4** with sodium ethoxide in ethanol at room temperature afforded an almost quantitative yield of the diester **3**. On the other hand treatment of **3** with sodium hydride in benzene converted it into **4**, thus establishing the structural relationship between these products. Careful treatment of **4** with aqueous sodium hydroxide opened the lactone ring selectively to give an intermediate sodium salt (not isolated) which was decarboxylated upon heating, to give the monoester derivative **2** in quantitative yield. It is thus apparent that the initial reaction product in the reaction of sodio diethyl malonate with **1** is the diester **3** which cyclizes to the lactone **4** under the conditions of the reaction. In the presence of trace amounts of water, the lactone is hydrolyzed to the monoester **2**. These results explain the variable yields of **2** and its admixture with the diester **3**, when strict moisture control was not exercized. In fact, investigation of the mother liquors from such reactions invariably revealed the presence of lactone bands in the i.r. As a result of the present study, the

Can. J. Chem. Downloaded from www.nrcresearchpress.com by 210.87.254.6 on 09/05/12
For personal use only.

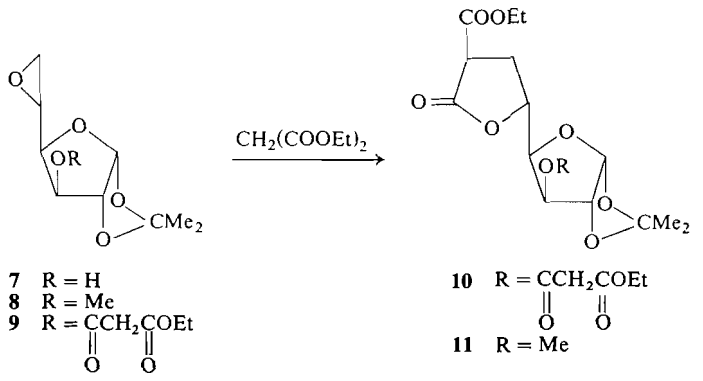

7 R = H
8 R = Me
9 R = CCH_2COEt (O, O)

10 R = CCH_2COEt (O, O)
11 R = Me

SCHEME 2

recommended procedure for the preparation of compound **2** appears to be through the lactone **4**.

Chain extension reactions through the terminal carbon atom of various carbohydrate derivatives have been done long before most of the *C*-methyl branched-chain sugars were found. The main reason for this was the availability of *aldehydo*-derivatives, which were suitable substrates for condensation reactions. Grignard reagents (19) organometallic reagents (20), nitromethane (21), and cyanohydrin condensation (22) have been used for this purpose. More recently, side chains of varying degrees of oxidation state have been introduced into carbohydrate structures (23), and these are amenable to a variety of transformations. The discovery of the antibiotic lincomycin (24–26) consisting of a C_8 amino dideoxy sugar (lincosamine) and more recently of the antibiotic polyoxin (27), a nucleoside of 5-amino-5-deoxy-D-alluronic acid has provided an added interest for the elaboration of newer methods of chain extension in the carbohydrate series.

We report herein the synthesis of sugar derivatives containing a highly functionalized C_3 unit, by the reaction of a terminal epoxide such as 5,6-anhydro-1,2-*O*-isopropylidene-α-D-glucofuranose (**7**) (28) with the carbanion derived from diethyl malonate (Scheme 2). Treatment of the epoxide **7** with 3 equiv of the carbanion in refluxing benzene gave a crystalline product (53%), to which we assign structure **10**. This assignment is substantiated by spectroscopic (n.m.r.) and mass spectral data as well as by an unambiguous independent synthesis. Thus, treatment of the epoxide with ethylmalonyl chloride in the presence of dimethylaniline in ether afforded the ester **9** as a syrup. Treatment of **9** with sodio diethyl malonate in refluxing benzene gave the product **10** in 44% yield. It should be noted that the opening of the epoxide in **9** was considerably faster than in **7**, which suggests that the transesterification step is slow. To obtain some measure of the reactivity of the C-3 hydroxyl group, sodio diethyl malonate was allowed to react with 1,2:5,6-di-*O*-isopropylidene-α-D-glucofuranose (**12**) (29) (Scheme 3). Even in the presence of a large excess of carbanion, the esterification was very slow compared to the reaction with **7**. Mild acid hydrolysis of the ester **13** afforded a product **14**, which on attempted purification on a column containing silica gel, was converted into the isomeric 6-*O*-(ethyl malonyl)-1,2-*O*-isopropylidene-α-D-glucofuranose (**15**). Such ester migrations from C-3 to C-6 in glucofuranose derivatives are not unprecedented but rare. The internal transesterification **14** → **15** presumably proceeds through a double migration, involving six- and five-membered orthoacid intermediates respectively (30).[3] The structure of compound **15** was proved by an independent route that involved the esterification of 3,5-*O*-benzylidene-1,2-*O*-isopropylidene-α-D-glucofuranose (32) with ethyl malonyl chloride followed by mild hydrolysis.

The reaction of 5,6-anhydro-1,2-*O*-isopropylidene-3-*O*-methyl-α-D-glucofuranose (**8**) (33)

[3]The possibility of a bicyclic orthoester involving C-3, -5, and -6 oxygen atoms as reported in some related cases cannot be eliminated (31).

Can. J. Chem. Downloaded from www.nrcresearchpress.com by 210.87.254.6 on 09/05/12
For personal use only.

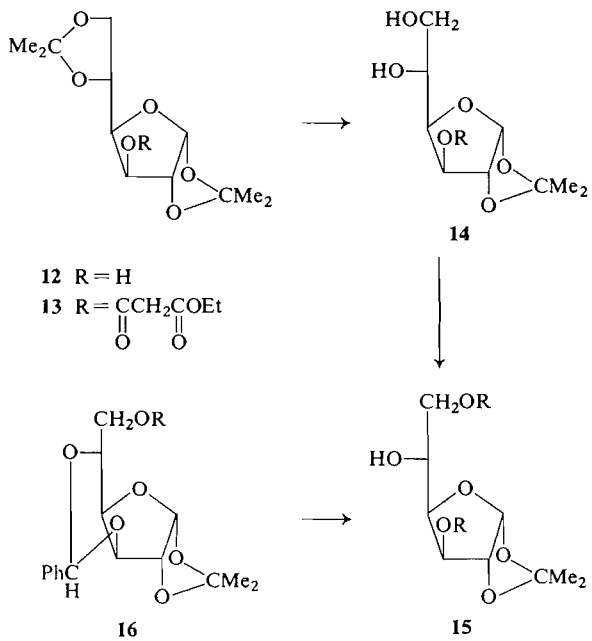

SCHEME 3

with sodio diethyl malonate was attempted in order to assess the role of a free hydroxyl group at C-3 in determining the type of product in such condensations. As in the case of **7**, the product of condensation was a cyclic lactone ester **11**, resulting from opening of the epoxide ring at C-6 and subsequent lactonization, with ejection of an ethoxide moiety.

Finally, it is of interest to note that in the products **4**, **10**, and **11**, a potential asymmetric center is created at the carbon bearing the carbethoxy group. Should the lactonization occur with some degree of chiral control, then these transformations would represent efficient procedures for asymmetric syntheses at a predetermined center in the molecule. These concepts are being actively studied in our laboratory.

Experimental

Melting points are uncorrected. The n.m.r. spectra were obtained in chloroform-*d* at 60 or 100 MHz, with tetramethylsilane as internal standard. The i.r. spectra (from Nujol) were recorded on a Beckman IR-8 instrument. Mass spectra were obtained on a Hitachi–Perkin–Elmer model RMU-6D instrument. The t.l.c. was performed on silica gel GF_{254} (Merck) and the spots were detected with a solution containing sulfuric acid in ethanol after heating the plates. Column chromatography on small scale (1–2 g) was done on short columns containing silica gel GF_{254} with moderate suction. Conventional processing signifies drying organic solutions over anhydrous sodium sulfate, filtration, and evaporation under diminished pressure.

Methyl 4,6-O-Benzylidene-2-(carboxymethyl)-2-deoxy α-D-altropyranoside Ethyl Ester (2)[4]

A solution containing 6 ml (39.1 mmol) of diethyl malonate and 0.72 g (30.0 mmol) of sodium hydride[5] in 75 ml of benzene (distilled from sodium hydride) was refluxed during 30 min. The solution was cooled and treated with 3.9 g (13.6 mmol) of **1** in 75 ml of benzene. After stirring at reflux temperature for 10–12 h, the mixture was cooled, excess base was neutralized with glacial acetic acid, and the insoluble salts were filtered. The filtrate was evaporated to a syrup and the residual diethyl malonate was removed by distillation under vacuum at 27°. The resulting syrup (5.5 g) was dissolved in absolute ethanol and a crystalline product (2.1 g, 44%) which proved to be a mixture of **2** and the diester **3**, was recovered. The mother liquors were chromatographed on a column containing silica gel GF_{254} and a further 1.37 g (27%) of mixed product was recovered. Recrystallization of the product from ethyl acetate afforded **2** as a chromatographically homogeneous product, in 50% yield (based on the mixture), m.p. 109–110°; recorded 109–110° (18); n.m.r. data ($CDCl_3$): τ 8.81 (CH_3CH_2—, t,

[4]The nomenclature adopted in this work is that suggested by Dr. K. Loening, Chemical Abstracts Service, Columbus, Ohio. We thank Dr. Loening for his assistance in naming these compounds.

[5]No precautions were taken to ensure the exclusion of moisture during the transfer and weighing of sodium hydride in this experiment.

Can. J. Chem. Downloaded from www.nrcresearchpress.com by 210.87.254.6 on 09/05/12
For personal use only.

Can. J. Chem. Downloaded from www.nrcresearchpress.com by 210.87.254.6 on 09/05/12
For personal use only.

$J = 7.2$ Hz), 7.50 (CH_2COO—, H_2, m), 6.64 (CH_3O—, s), 5.46 (H_1, s), 4.49 (C*H*Ph, s) etc.

Methyl 2-(Carboxymethyl)-2-deoxy-α-D-altropyranoside Ethyl Ester (5)

A solution containing **2** (0.15 g) in a mixture of ethanol (23 ml) and concentrated hydrochloric acid (0.06 ml) was stirred at room temperature for 2 h. The acid was neutralized with lead carbonate and the filtered suspension was processed as usual to give a syrup which was purified by preparative t.l.c. A syrup (0.11 g, 96%) was thus obtained that crystallized from cyclohexane to give the title compound, m.p. 78–79°, recorded, 80–82° (18).

Treatment of an aqueous solution of **5** with sodium periodate resulted in complete oxidation as evidenced by t.l.c.

Methyl 4,6-O-Benzylidene-2-deoxy-2-(dicarboxymethyl)-α-D-altropyranoside Diethyl Ester (3)

A solution containing 3.1 ml (20.2 mmol) of diethyl malonate and 0.37 g (15.3 mmol) of sodium hydride in 90 ml of benzene was refluxed in an atmosphere of nitrogen for 30 min. After cooling, 2 g (7.57 mmol) of **1** was added and the stirring was continued at 40° for 2 weeks, under nitrogen. Glacial acetic acid was cautiously added to the cooled solution, the salts were filtered, and the filtrate was evaporated to a syrup which crystallized upon trituration with ether. The crystals (0.39 g, 20%) were filtered and proved to be starting material. The filtrate was evaporated to a semi-crystalline syrup and traces of diethyl malonate were removed by distillation. The resulting residue was a mixture of the desired diester **3** and the lactone **4** which could be separated from each other by fractional crystallization from ethanol since the lactone is much less soluble. In this manner 1.1 g (35%) of the diester **3** was obtained. The mother liquors were chromatographed on a column containing silica gel to give additional product: total yield 1.24 g (52%, based on the reacted epoxide **1**) of **3**, m.p. 115–115.5°; $[\alpha]_D^{25}$ 69.1° (*c* 3.05, $CHCl_3$); n.m.r. data: τ 8.72 (CH_3CH_2—, t, $J = 7$ Hz), 7.00 (C*H*COO—, d, $J = 11.2$ Hz), 6.56 (CH_3O—, s), 5.35 (H_1, s), 4.37 (C*H*Ph, s), etc.

Anal. Calcd. for $C_{21}H_{28}O_9$: C, 59.43; H, 6.65. Found: C, 59.76; H, 6.78.

Methyl 4,6-O-Benzylidene-2-deoxy-2-(dicarboxymethyl)-α-D-altropyranoside γ-Lactone Ethyl Ester (4)

A solution containing 1.6 ml (10.54 mmol) of diethyl malonate and 0.24 g (10.0 mmol) of sodium hydride[6] in 70 ml of benzene was refluxed for 30 min. After cooling, 1 g (3.93 mmol of **1** was added and the solution was stirred under reflux, in an atmosphere of nitrogen for 13 h. Glacial acetic acid was added and the salts were filtered through a bed of Celite. The filtrate was evaporated to a syrup that crystallized slowly. The crystals were triturated with ether, filtered, and the filtrate was evaporated and the crystalline residue was treated again by the same process; yield 0.82 g (55%) of **4**. The mother liquors were freed from traces of diethyl malonate by distillation of the latter and an additional 0.29 (17%) of product was recovered from the residue; total yield 1.11 g (74%). Recrystallization from carbon tetrachloride afforded an analytical sample, m.p. 174–175°; $[\alpha]_D^{25}$ 92.0° (*c* 2.14, $CHCl_3$); λ_{max}: 1799 (lactone), 1738 cm^{-1} (ester); n.m.r. data: τ 8.71 (CH_3CH_2—, t, $J = 7.2$ Hz), 6.54 (CH_3O—, H_2, C*H*COO), 4.75 (H_1, d, $J_{12} = 7.9$ Hz), 4.38 (C*H*Ph, s), etc.

Anal. Calcd. for $C_{19}H_{22}O_8$: C, 60.13; H, 5.86. Found: C, 59.81; H, 5.86.

Methyl 4,6-O-Benzylidene-2-(carboxymethyl)-2-deoxy-3-O-methylsulfonyl-α-D-altropyranoside Ethyl Ester (6)

Mesylation of **2** (0.15 g) was done in the usual manner using mesyl chloride (0.3 ml) in pyridine (9 ml). After storing at 0° for 20 h and at room temperature for 3 h, the solution was poured into ice-water and the crystalline product was filtered and washed with cold water; yield 0.11 g (60%). Recrystallization was effected from toluene, m.p. 138.5–139.5° (dec.); $[\alpha]_D^{25}$ 61.5° (*c* 3.36, $CHCl_3$); n.m.r. data: τ 8.69 (CH_3CH_2—, t, $J = 7.1$ Hz), 7.36 (CH_2COO—, H_2, m), 7.16 (CH_3SO_3—, s), 6.56 (CH_3O—, s), 5.41 (H_1, s), 5.03 ($CHOSO_2$—, t), 4.36 (C*H*Ph), etc.

Anal. Calcd. for $C_{19}H_{26}O_9S$: C, 53.01; H, 6.09; S, 7.47. Found: C, 53.16; H, 6.09; S, 7.53.

Methyl 4,6-O-Benzylidene-2-deoxy-2-C-(hydroxyethyl)-α-D-altropyranoside

A solution of **2** (0.3 g) in 10 ml of tetrahydrofuran was added dropwise to a suspension of lithium aluminum hydride (0.1 g) in 15 ml of the same solvent. The suspension was stirred at room temperature for 15 min and excess reagent was destroyed with the cautious addition of water. The product was obtained as a chromatographically homogeneous syrup (0.25 g, 96%), after conventional processing. A sample of the syrup was further purified by preparative t.l.c. ($CHCl_3$: hexane: MeOH, 20:30:0.5) but the product did not crystallize.

Acetylation afforded a syrupy acetate that had the expected spectroscopic (i.r., n.m.r.) properties.

Alcoholysis of the Lactone 4

A solution containing 70 mg of **4** in 4 ml of ethanol was treated with 1 ml of a 0.182 *N* solution of sodium ethoxide. After stirring for 1 h at room temperature the solution was neutralized with Rexyn 102 (H^+), previously washed with ethanol, and the solution was filtered. Evaporation gave a syrup (72 mg, 96%) that crystallized from ethyl acetate to give a product identical with **3**, m.p. 113–114°.

Partial Hydrolysis and Decarboxylation of the Lactone 4

A solution containing 70 mg (0.183 mmol) of **4** in 6 ml of tetrahydrofuran was treated with 3 ml of water containing 15 mg (0.375 mmol) of sodium hydroxide. After 1 h at room temperature, the solution was acidified to p*H* 2 with 2 *N* hydrochloric acid and it was extracted with ether. The organic layer was dried and evaporated to a crystalline residue which was dissolved in 25 ml of dioxane and 3 ml of an aqueous solution saturated with sodium bicarbonate was added. The solution was refluxed for 1 h, the solvent removed under reduced pressure and the solution was diluted with dichloromethane. The latter was washed with water and processed in the usual way to give 62 mg (97%) of **2**, m.p. 109–110°.

7,7-Di-C-carboxy-6,7-dideoxy-1,2-O-isopropylidene-α-D-glucoheptofuranose γ-Lactone Ethyl Ester 3-(Ethyl Malonate) (10)

A solution containing 1.15 ml (7.57 mmol) of diethyl malonate and 0.18 g (7.3 mmol) of sodium hydride in 40 ml

[6]The weighing of sodium hydride and transfer to the reaction flask was done in a dry box in an atmosphere of nitrogen.

Can. J. Chem. Downloaded from www.nrcresearchpress.com by 210.87.254.6 on 09/05/12
For personal use only.

of benzene was refluxed for 30 min. The solution was cooled, 0.5 g (2.47 mmol) of **7** was added and the solution was refluxed for 6 h. After cooling, glacial acetic acid was added to neutralize excess reagent and the insoluble salts were filtered. The filtrate was evaporated to a syrup and the residual diethyl malonate was co-distilled with water. The residue was dissolved in chloroform, the solution was dried and processed in the usual manner to give a syrup. Purification on a column containing silica gel GF_{254} (CH_2Cl_2 developer) gave 0.56 g (53%) of a syrup which crystallized from ethanol. Recrystallization from ethanol gave pure material, m.p. 97.5–99°; $[\alpha]_D^{22}$ −47.3 (*c* 5.0, $CHCl_3$); λ_{max} 1783 (lactone), 1766, 1735, 1725 cm^{-1} (esters); n.m.r. data: τ 8.71, 8.58 (CH_3CH_2—, centers of triplets, $J = 7.2$ Hz); 8.67, 8.47 (CH_3—C); 6.56 (CH_2COOEt, s); 5.38 (H_2, d, $J_{21} = 3.6$ Hz); 5.16 (H_3, m); 4.05 (H_1, d, $J_{12} = 3.6$ Hz), etc.; *m/e* 415 (M^+-15); 273 (M^+-157,

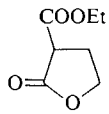

Anal. Calcd. for $C_{19}H_{26}O_{11}$: C, 53.02; H, 6.09. Found: C, 52.74; H, 6.11.

*7,7-Di-C-carboxy-6,7-dideoxy-1,2-O-isopropylidene-3-O-methyl-α-D-gluco-heptofuranose γ-Lactone Ethyl Ester (**11**)*

A solution containing 0.29 ml (1.89 mmol) of diethyl malonate and 44 mg (1.82 mmol) of sodium hydride in 10 ml of benzene was refluxed for 30 min then it was treated with 0.18 g (0.833 mmol) of **8** in 40 ml of benzene. The solution was refluxed for 9 h and processed as described for **10**. After removal of diethyl malonate by co-distillation with water, the product **11** was obtained as a chromatographically homogeneous syrup (0.2 g, 74%) (t.l.c., $CHCl_3$: hexane: MeOH, 4:6:0.1). Attempted purification of a portion by preparative t.l.c. failed to give a crystalline product; λ_{max} 1790 (lactone), 1737 cm^{-1} (ester); n.m.r. data were consistent with the expected structure; *m/e* 315 (M^+-15).

*3-O-(Ethyl Malonyl)-1,2:5,6-di-O-isopropylidene-α-D-glucofuranose (**13**)*

A solution containing 13.8 ml of diethyl malonate (90 mmol) and 2.1 g (88 mmol) of sodium hydride in 600 ml of benzene was refluxed for 30 min, it was then treated with 7.7 g (29.6 mmol) of **12**. The solution was refluxed for 30 h, the reagent was neutralized with glacial acetic acid, and the solution was processed as described before to give a syrup. Residual diethyl malonate was removed by distillation during which some **12** sublimed (1.5 g, 20%). The residual syrup was chromatographed on a column containing silica gel (CH_2Cl_2 developer) to give the title compound as a syrup which could not be crystallized; 4.4 g (57%); λ_{max} 1754, 1733 cm^{-1} (ester); n.m.r. data were consistent with the structure.

*6-O-(Ethyl Malonyl)-1,2-O-isopropylidene-α-D-glucofuranose (**15**)*

An amount of **13** (0.44 g) in 20 ml of 0.5 *N* hydrochloric acid was stirred at room temperature until the solution became clear and homogeneous (1.5–2 h). The acid was neutralized with lead carbonate, the solution was extracted with dichloromethane, and the organic phase was processed in the usual manner, to give a syrup (0.3 g, 79%). Spectroscopic (n.m.r.) and chromatographic analysis indicated that the product was the desired 3-*O*-(ethyl malonyl) derivative **14**. When the syrup was chromatographed on a column containing silica gel (CH_2Cl_2—MeOH, 97:3), a crystalline product **15** was obtained which had the same chromatographic properties as **14**. Recrystallization was effected from benzene to give **15**, m.p. 100–100.5°; $[\alpha]_D$ 0 ± 1° (*c* 2.70, $CHCl_3$); n.m.r. data indicated beyond doubt that the ester function was situated on C-6.

Anal. Calcd. for $C_{14}H_{22}O_9$: C, 50.30; H, 6.63. Found: C, 50.69; H, 6.68.

The same product was obtained from 3,5-*O*-benzylidene-1,2-*O*-isopropylidene-α-D-glucofuranose by sequential esterification (sodio diethyl malonate, benzene) to give a syrup **16** (75%), and partial hydrolysis (0.5 *N* HCl, 70°, 3h); m.p. 100–100.5° (undepressed upon admixture with **15**).

*Reaction of Sodio Diethyl Malonate with 5,6-Anhydro 3-O-(Ethyl Malonyl)-1,2-O-isopropylidene-α-D-glucofuranose (**9**)*

A solution containing 0.1 g (0.49 mmol) of **7** and 1 ml of dimethylaniline in 25 ml of ether was treated with 0.12 g (0.78 mmol) of ethyl malonyl chloride (34) at 0°. After stirring at room temperature for 15 min the solution was washed successively with dilute hydrochloric acid, aqueous sodium bicarbonate, and water. Processing the ethereal solution gave a syrup consisting of **9** (34%). The n.m.r. spectrum of a sample that was further purified by preparative t.l.c. was consistent with the structure.

Treatment of the product **9** (50 mg) with sodio diethyl malonate as described for the preparation of **10**, (reflux 2.5 h) gave the desired product **10** in 78% yield (chromatographically homogeneous syrup). Crystallization from ethanol afforded a product with m.p. 97–100° (44%), identical with a sample prepared from **9** and the carbanion.

The generous financial assistance from the National Research Council of Canada and an NRCC fellowship for P.D. are gratefully acknowledged.

1. S. HANESSIAN and P. DEXTRAZE. Chem. Ind. 958 (1971).
2. S. HANESSIAN and A. G. PERNET. Chem. Commun. 755 (1971).
3. F. SHAFIZADEH. Advan. Carbohydr. Chem. **11**, 263 (1956); W. G. OVEREND. Chem. Ind. 342 (1963).
4. S. HANESSIAN and T. H. HASKELL. The carbohydrates. Vol. IIA. Second ed. Academic Press, 1970. p. 139.
5. S. HANESSIAN. Advan. Carbohydr. Chem. **21**, 143 (1966).
6. D. HORTON. *In* The amino sugars. R. W. Jeanloz, *editor*. Volume 1A. Academic Press, New York, N.Y., 1969. p. 3.
7. A. MAERCKER. Org. Reactions, **14**, 270 (1965).
8. For some reports in the carbohydrate series, see A. ROSENTHAL and P. CATSOULACOS. Can. J. Chem. **46**, 2868 (1968); W. A. SZAREK, J. S. JEWELL, I. SZCZEREK, and J. K. N. JONES. Can. J. Chem. **47**, 4473 (1969); H. P. ALBRECHT, G. H. JONES, and J. G. MOFFATT. J. Am. Chem. Soc. **92**, 5511 (1970); J. M. J. TRONCHET and J. M. BOURGEOIS. Helv. Chim. Acta, **53**, 1463 (1970); and refs. cited therein.
9. A. ROSENTHAL. Advan. Carbohydr. Chem. **23**, 59 (1968).

10. A. A. J. FEAST, W. G. OVEREND, and N. R. WILLIAMS. J. Chem. Soc. C, 7378 (1965).
11. S. INOUE and H. OGAWA Bull. Chem. Soc. Japan, **8**, 79 (1960).
12. J. R. DYER, W. E. MCGONIGAL, and K. C. RICE. J. Am. Chem. Soc. **87**, 654 (1965).
13. A. ROSOWSKY. *In* Heterocyclic compounds with three and four membered rings. A. Weissberger, *editor*, Part 1. Interscience, New York, N.Y., 1964. p. 181–464.
14. J. V. KOŠTÍŘ and M. QUEISNEROVÁ. Chem. Listy, **43**, 277 (1949); Chem. Abstr. **45**, 553 (1951).
15. H. ZINNER, E. WITTENBURG, and G. REMBARZ. Chem. Ber. **92**, 1614 (1959).
16. E. J. REIST, P. A. HART, B. R. BAKER, and L. GOODMAN. J. Org. Chem. **27**, 1722 (1962).
17. H. H. BAER and K. S. ONG. Can. J. Chem. **46**, 2511 (1968).
18. N. K. KOCHETKOV, L. I. KUDRYASHOV, and A. P. KLYAGINA. J. Gen. Chem., U.S.S.R. Engl. Ed., **32**, 402 (1962).
19. See for example, W. A. BONNER. Advan. Carbohydr. Chem. **6**, 251 (1951); M. L. WOLFROM and S. HANESSIAN. J. Org. Chem. **27**, 1800, 2107 (1962); H. OHLE and C. DAMBERGIS. Ann. **481**, 255 (1930); E. WALTON, J. O. RODIN, C. H. STAMMER, F. W. HOLLY, and K. FOLKERS. J. Am. Chem. Soc. **80**, 5168 (1958).
20. J. E. ENGLISH, JR. and M. F. LEVY. J. Am. Chem. Soc. **78**, 2846 (1956).
21. H. H. BAER. Advan. Carbohydr. Chem. **24**, 67 (1969).
22. See for example, C. S. HUDSON. Advan. Carbohydr. Chem. **1**, 1 (1945); R. SCHAFFER and H. S. ISBELL. J. Am. Chem. Soc. **79**, 3867 (1957); H. PAULSEN and K. TODT. Chem. Ber. **99**, 3450 (1966).
23. See for example, N. K. KOCHETKOV and B. A. DMITRIEV. Tetrahedron, **21**, 803 (1965); D. HORTON, J. B. HUGHES, and J. M. J. TRONCHET. Chem. Commun. 481 (1965), and subsequent papers; J. M. J. TRONCHET, N. LE-HONG, and F. PERRET. Helv. Chim. Acta, **53**, 154 (1970); YU. A. ZHDANOV, YU. E. ALEKSEEV, and G. N. DOROFEENKO. J. Gen. Chem. U.S.S.R., Engl. Ed. **36**, 1737 (1966); G. B. HOWARTH, D. G. LANCE, W. A. SZAREK, and J. K. N. JONES. Chem. Commun. 1349 (1968); D. G. LANCE and W. A. SZAREK. Carbohydr. Res. **10**, 306 (1969); A. ROSENTHAL and J. N. C. WHYTE. Can. J. Chem., **46**, 2239 (1968).
24. D. J. MASON, A. DIETZ, and C. DEBOER. Antimicrobial agents and chemotherapy, 1962. American Society for Microbiology, Ann Arbor, Michigan, 1963. p. 554.
25. G. B. HOWARTH, W. A. SZAREK, and J. K. N. JONES. J. Chem. Soc. C, 2218 (1970).
26. B. J. MAGERLEIN. Tetrahedron Lett. 33 (1970).
27. K. ISONO, K. ASAHI, and S. SUZUKI. J. Am. Chem. Soc. **91**, 7490 (1969).
28. L. F. WIGGINS. Methods in carbohydrate chemistry. II, 190 (1963); H. OHLE and L. VARGHA. Ber. **62**, 2435 (1929).
29. O. TH. SCHMIDT. Methods in carbohydrate chemistry. II, 321 (1963).
30. E. J. HEDGLEY, and O. MERESZ. Proc. Chem. Soc. 399 (1964).
31. See also B. HELFERICH, and W. SCHUTTE-HÜRMANN. Chem. Ber. **87**, 977 (1954); R. K. NESS and H. G. FLETCHER JR. J. Org. Chem. **27**, 1465 (1957); N. K. KOCHETKOV, A. J. KHORLIN, A. B. BOCHKOV, and Z. G. YAZLOVETSKY. Carbohydrate Res., **2**, 84 (1966).
32. O. TH. SCHMIDT. Methods in carbohydrate chemistry. I, 199 (1962); P. BRIGL and H. GRUNER. Ber. **65**, 1428 (1932).
33. E. VISCHER and T. REICHSTEIN. Helv. Chim. Acta, **27**, 1332 (1944).
34. D. S. BRESLOW, E. BAUMGARTEN, and C. R. HAUSER. J. Am. Chem. Soc. **66**, 1286 (1944).

Can. J. Chem. Downloaded from www.nrcresearchpress.com by 210.87.254.6 on 09/05/12
For personal use only.

Chemistry and Synthetic Utility of α-(Dimethylamino)benzylidene and 1-(Dimethylamino)ethylidene Acetals[1,2]

S. HANESSIAN AND E. MORALIOGLU[3]

Department of Chemistry, University of Montreal, Montreal, Quebec

Received June 24, 1971

N,N-Dimethylbenzamide and *N,N*-dimethylacetamide dimethyl acetals react with vicinal *cis*-diols to give cyclic α-(dimethylamino)benzylidene and 1-(dimethylamino)ethylidene acetals respectively. In aqueous methanol, the acetals are hydrolyzed to the original diol. At p*H* 4–5, cleavage occurs to give benzoate and acetate esters, presumably by the sequential formation of acyloxonium and orthoacid intermediates. The acetals are thus useful as temporary protecting groups for vicinal diols and can be used for indirect, selective benzoylation and acetylation. They are compatible with the reaction conditions of acylation (acetylation, benzoylation, tosylation) and nucleophilic displacement (N_3^-).

Les acétals diméthyliques de la *N,N*-diméthylbenzamide et la *N,N*-diméthylacétamide réagissent avec les diols vicinaux *cis* pour donner les acétals cycliques α-(diméthylamino)benzylidénique et 1-(diméthylamino)-éthylidénique respectivement. Ces acétals sont hydrolysés dans le méthanol aqueux pour redonner le diol initial. A p*H* 4–5, le clivage conduit aux benzoates et acétates correspondants probablement par la formation successive d'un ion acyloxonium et d'un orthoacide comme intermédiaires. Ces acétals cycliques sont donc particulièrement utiles comme groupe protecteur momentané pour des diols vicinaux et peuvent être utilisés indirectement pour des benzoylations et acétylations sélectives. Ces acétals cycliques sont compatibles avec les réactions d'acylation (acétylation, benzoylation, tosylation) et de déplacements nucléophiles N_3^-).

Canadian Journal of Chemistry, **50**, 233 (1972)

The problem of temporary blocking of reactive functions, such as hydroxyl and amino groups, is one of primordial importance in synthetic organic chemistry. The utility of blocking groups is largely dependent on their compatibility with various reaction conditions and it is not surprising that an "all purpose" blocking group is still non-existent. There is at present a wide enough choice of protecting groups for isolated hydroxyl and amino functions and the design of a particular synthetic sequence using molecules containing such functions is relatively facile. The problem is somewhat different in the case of vicinal diols, as the number of possible modes of simultaneous blocking is limited. Acetals are among the most frequently utilized derivatives in the case of diols and they represent a distinct advantage in their ease of formation. A wide variety of syntheses in the area of carbohydrates (2), utilize acetals as intermediates, mainly because of their ease of formation and eventual hydrolysis.

Our interest in the reactions of amide halides and amide acetals with carbohydrates in general (3) and with nucleosides (4) in particular, prompted us to investigate the chemistry of (dimethylamino)benzylidene and ethylidene acetals of the 1,3-dioxolane type, as shown below, particularly with regard to their modes of preparation and cleavage, their stability and their utility as potential temporary blocking groups for 1,2- and 1,3-diols systems. In this paper, we report on our findings with α-(dimethylamino)benzylidene and 1-(dimethylamino)ethylidene acetals, utilizing selected carbohydrate derivatives as model substrates (1).

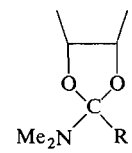

R = Me, Ph

Since their discovery by Meerwein and coworkers (5), amide acetals of the type

$$Me_2N{-}\overset{\overset{R}{|}}{C}(OMe)_2 \quad (R = H, \text{methyl})$$

have been known to be powerful electrophilic reagents. Their reactivity is due largely to the existence in solution of the corresponding imino

[1]Presented in part at the Sixth International Symposium on Carbohydrate Chemistry, Paris, France, August 19th, 1970. See also ref. 1.

[2]Part of a series on "Preparative and Exploratory Carbohydrate Chemistry".

[3]Taken from the M.Sc. thesis of Erkal Moralioglu, University of Montreal, 1971.

Can. J. Chem. Downloaded from www.nrcresearchpress.com by 210.87.254.40 on 09/05/12
For personal use only.

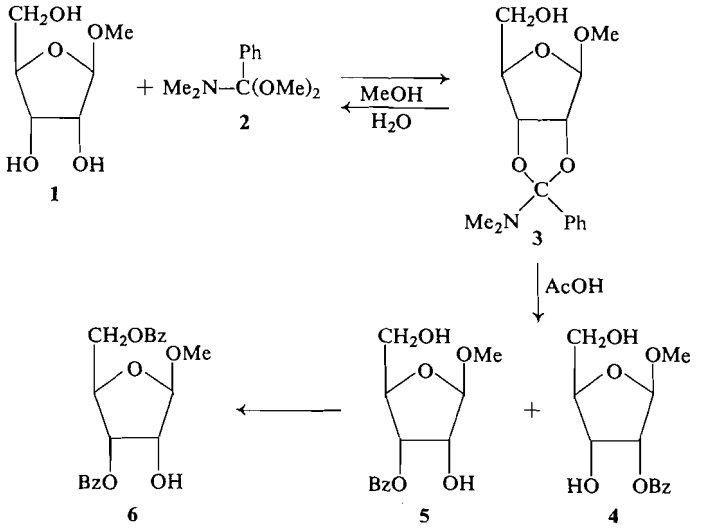

SCHEME 1

forms

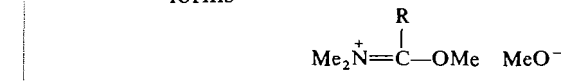

which are susceptible to attack by nucleophiles at the central carbon atom. For example, such amide acetals are excellent esterifying agents, even for hindered acids (6–8). With higher alcohols, the dimethyl acetal of *N*,*N*-dimethylformamide undergoes acetal exchange (5, 6) to give the corresponding dialkyl acetal. In the original work of Meerwein and coworkers (5), DMF and DMAC dimethyl acetals were reacted with ethylene glycol and the corresponding cyclic acetals were isolated, indicating the possibility of acetal exchange reactions with vicinal diols. Žemlička and Holý (9) have used DMF dimethyl acetal as a blocking group for amino groups in the heterocyclic moiety in various ribonucleosides, with simultaneous formation of 2′,3′-*O*-(dimethylamino)methylene acetals. The authors have pointed out, however, the extreme instability of this acetal. Employing methyl β-D-ribofuranoside **1** (10) as a model, we have also noted in our preliminary studies the particular lability of the corresponding 2,3-*O*-(dimethylamino)methylene acetal, obtained with DMF dimethyl acetal. While our work was in progress, a report appeared on the reactions of DMF dimethyl acetal with *cis* and *trans* cyclohexane 1,2-diols (11). We show in this paper that, in marked contrast to cyclic DMF acetals, those derived from *N*,*N*-dimethylbenzamide dimethyl acetal and *N*,*N*-dimethylacetamide dimethyl acetal, are of practical and preparative utility. In addition to their ease of formation and usefulness for the temporary protection of vicinal diols, they lend themselves to a variety of novel transformations, such as their cleavage to benzoate and acetate esters respectively. To the best of our knowledge, cyclic acetals of *N*,*N*-dimethylbenzamide have not been previously studied and the above-mentioned aspects may prove useful in synthetic organic chemistry.

Methyl β-D-ribofuranoside **1** was chosen as one of the model substrates, because it contains a vicinal diol system required for transacetalization, and a primary hydroxyl group which could serve to test the compatibility of the acetal with various transformations. The presence of the D-ribofuranose moiety in various biologically important molecules, such as nucleosides, was an added incentive for its choice as model substrate.

Reaction of **1** with a slight excess of *N*,*N*-dimethylbenzamide dimethyl acetal **2** (12) in 1,1,1-trichloroethane[4] was essentially complete at room temperature within 10–12 h. The product was isolated by rapid washing of the organic phase with water and processing to give methyl 2,3-*O*-[α-(dimethylamino)benzylidene]-β-D-ribofuranoside (**3**) as a syrup in high yield (Scheme 1). The n.m.r. spectral characteristics of **3** were those expected of its structure.

[4]This solvent was inadvertently termed 1,1,2-trichloroethane in ref. 1.

Can. J. Chem. Downloaded from www.nrcresearchpress.com by 210.87.254.40 on 09/05/12
For personal use only.

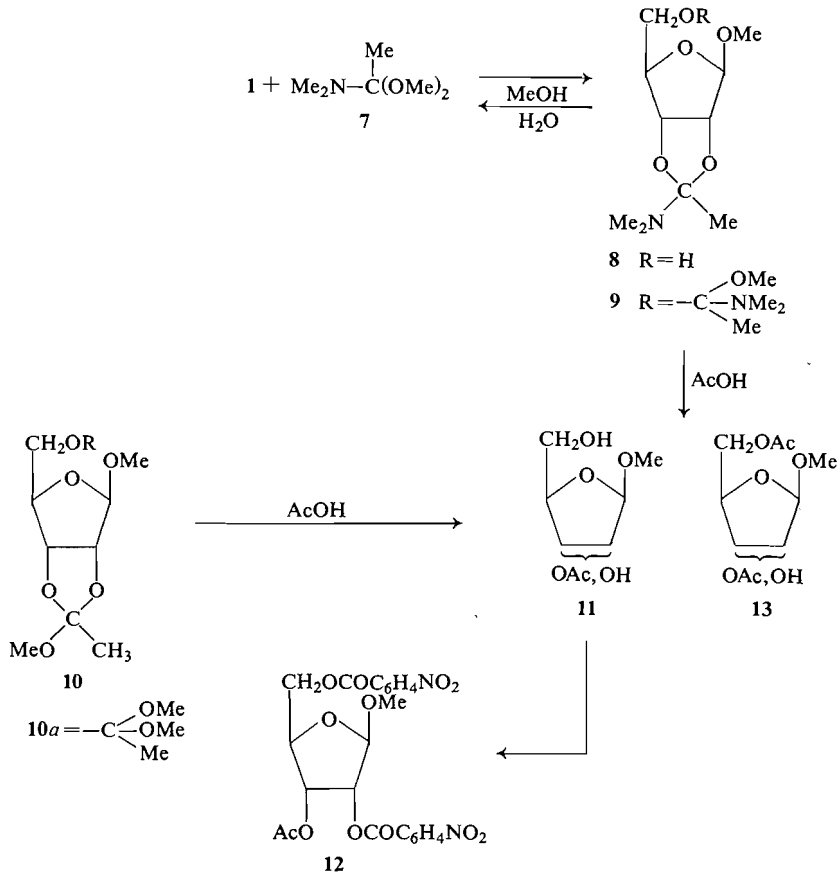

SCHEME 2

Reaction of **1** with *N*,*N*-dimethylacetamide dimethyl acetal **7** (5) in 1,1,1-trichloroethane for 1 h led to an almost quantitative conversion into the corresponding methyl 2,3-*O*-[1-(dimethylamino)ethylidene]-β-D-ribofuranoside (**8**) (Scheme 2). Processing the reaction mixture by direct evaporation, instead of a preliminary rapid washing with water to remove residual reagent, afforded, in addition to **8**, a second product of higher chromatographic mobility, which was proved to be the mixed acetal **9**.[5] The formation of this byproduct took place during the evaporation process, when the effective concentration of reagent (present in slight excess) became relatively high. The formation of such mixed acetals could be avoided by using equimolar amounts of reagent, or better yet, using a slight excess of reagent and rapid washing of the reaction mixture with water. This procedure afforded the acetal **8** as a relatively pure liquid in over 80% yield that was suitable for further transformations. Distillation at 103–108°/0.4 Torr afforded **8** as a 1:1 mixture of two diastereoisomers (see Fig. 1). This ratio was not always the same and varied with the time of reaction, the conditions of isolation and temperature. Attempts to separate the diastereoisomers by careful fractional distillation were unsuccessful although different cuts within a narrow temperature range showed different ratios as evidenced by n.m.r. In one instance, a fraction consisting predominantly of a single diastereoisomer was isolated (see Fig. 1). The acetal derivatives **3** and **8** were stable for prolonged periods, when kept under anhydrous conditions. When refluxed in 3% aqueous methanol, hydrolysis ensued, with the quantita-

[5]An alternative structure is one in which two molecules of **1** have condensed with **7** through the 5-hydroxyl group.

Can. J. Chem. Downloaded from www.nrcresearchpress.com by 210.87.254.40 on 09/05/12
For personal use only.

Can. J. Chem. Downloaded from www.nrcresearchpress.com by 210.87.254.40 on 09/05/12
For personal use only.

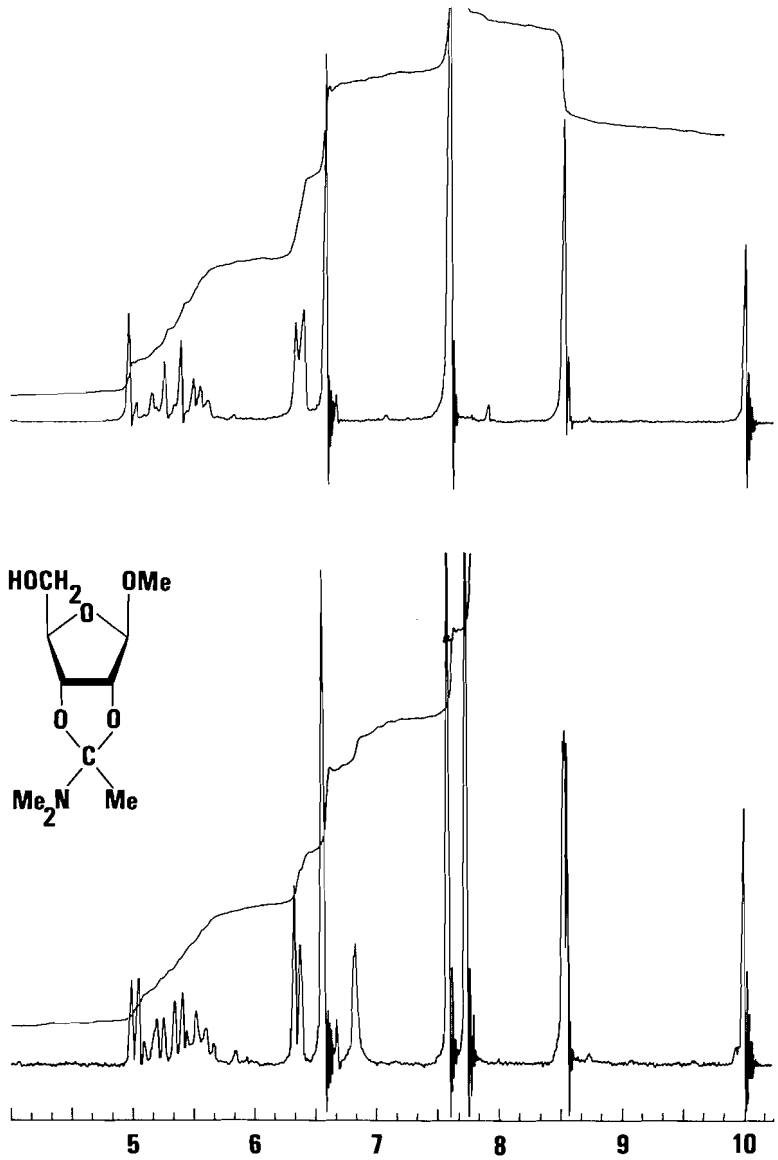

FIG. 1. The 60 MHz n.m.r. spectra of methyl 1-(dimethylamino)ethylidene-β-D-ribofuranoside: pure diastereoisomer (upper spectrum); mixture (lower spectrum).

tive recovery of the starting material **1**. Thus, both the formation and removal of cyclic α-(dimethylamino)benzylidene and 1-(dimethylamino)ethylidene acetals take place under very mild conditions. The facile regeneration procedure, which could be carried out at room temperature also, accentuates the role of acetals such as **2** and **7** as reagents for the temporary protection of vicinal diols, particularly when other substituents in the molecule are relatively base-stable.[6] The hydrolytic instability of these acetals in aqueous media is not unexpected in view of their orthoester structure. It should be pointed out however, that the instability is less

[6]Solutions of the reagents and the cyclic acetals are basic ($pH \simeq 10$).

Can. J. Chem. Downloaded from www.nrcresearchpress.com by 210.87.254.40 on 09/05/12
For personal use only.

pronounced than that of an alkoxy analog such as methyl 2,3-*O*-methoxyethylidene-β-D-ribofuranoside (**10**) (Scheme 2). The latter was prepared from trimethylorthoacetate in DMF containing *p*-toluenesulfonic acid as catalyst, and was isolated as a liquid that was slightly contaminated with the corresponding mixed acetal **10***a* arising from condensation of the primary hydroxyl group.

The possibility of controlled cleavage of the α-(dimethylamino)benzylidene and 1-(dimethylamino)ethylidene groups was investigated with the objective of preparing selectively acylated products. At p*H* 4–5 in aqueous acetic acid, cleavage of the acetal **3** took place within 1–2 h to give a syrup which consisted of methyl 2-*O*-benzoyl-β-D-ribofuranoside (**4**) and methyl 3-*O*-benzoyl-β-D-ribofuranoside (**5**) (predominant product) (Scheme 1). Catalytic debenzoylation of the mixture gave crystalline **1**, thus confirming the preservation of the D-*ribo* configuration in the acetal cleavage process. Selective benzoylation of the mixture containing **4** and **5** afforded a crystalline material from which a single product could be obtained by fractional crystallization. This product is designated as methyl 3,5-di-*O*-benzoyl-β-D-ribofuranoside (**6**), based on its n.m.r. spectral data and comparison with data for closely related compounds (13). The sequence leading to the dibenzoate **6** could also be effected without the isolation of the intermediate product **3**.

At p*H* 3–4 in 95% aqueous acetic acid, the acetal **8** was quantitatively cleaved to give a mixture of 2- and 3-monoacetates **11** and trimethylamine acetate (Scheme 2). A mixture of monoacetates was also formed in the presence of a variety of other aqueous acids at p*H* 3–4. Although the isomeric acetate derivatives could not be separated, their presence in approximately equal amounts in the product was ascertained by n.m.r. spectral studies. A crystalline di-*O*-*p*-nitrobenzoate was obtained from this syrupy mixture, which upon fractional crystallization from absolute ethanol afforded a single product, presumably methyl 3-*O*-acetyl-2,5-di-*O*-*p*-nitrobenzoyl-β-D-ribofuranoside(**12**). The mixture of monoacetates **11** could also be obtained by hydrolysis of the orthoester **10** in 10% aqueous acetic acid (p$H \simeq 5$) during 30 min. When samples containing both **8** and **9** were subjected to hydrolysis, the product consisted of the mixture of monoacetates **11** derived from **8** and a mixture of diacetates, corresponding to a 3,5- or a 2,5-diacetate **13**, resulting from hydrolysis of the minor component **9**. The isolation of these diacetates provides supporting evidence for the structure of **9**, which upon hydrolysis should give a diacetate, or a diacetate and a monoacetate if a dimeric structure for **9** is assumed. In order to assess the reactivity of the primary hydroxyl group in **8**, methyl 2,3-*O*-isopropylidene-β-D-ribofuranoside (14) was allowed to react with a large excess of **7**. After prolonged times, only a small amount of a new product was formed (t.l.c.). The reaction mixture was processed with aqueous acid and the less polar product was separated from unreacted starting material and proved to be methyl 5-*O*-acetyl-2,3-*O*-isopropylidene-β-D-ribofuranoside, thus providing conclusive proof that a transacetalization had taken place with the primary hydroxyl group. The much slower rate of the reaction compared to **8** may indicate a catalyzing effect of the 2,3-*O*-(dimethylamino)ethylidene group on the reactivity of the 5-hydroxyl group. The acetylated products **11**, **12**, and **13** were also converted into methyl β-D-ribofuranoside, upon treatment with sodium methoxide in methanol, indicating the absence of configurational inversions in the hydrolytic process.

Our exploratory experiments on acetal formation with model substances were continued with 1,2-*O*-isopropylidene-α-D-glucofuranose **14** as substrate. In this case, two aspects were to be considered, namely the type of acetal formed in view of the existence of two possibilities, and the direction of ring opening in weakly acidic media. Reaction of **14** with **2** revealed a selective acetal formation with the vicinal diol system and gave 5,6-*O*-[α-(dimethylamino)benzylidene]-1,2-*O*-isopropylidene-α-D-glucofuranose (**15**) (Scheme 3). Controlled cleavage of the 5,6-acetal function at p*H* 4–5 gave a good yield of crystalline 6-*O*-benzoyl-1,2-*O*-isopropylidene-α-D-glucofuranose (**16**). The latter was prepared in low yield by the controlled benzoylation of **14** according to a reported procedure (15).

The reaction of **14** with **7** was monitored by t.l.c. which indicated the formation of a product after stirring at room temperature for 20 h. Processing afforded a syrup which consisted of some starting material and 5,6-*O*-[1-(dimethylamino)ethylidene]-1,2-*O*-isopropylidene-

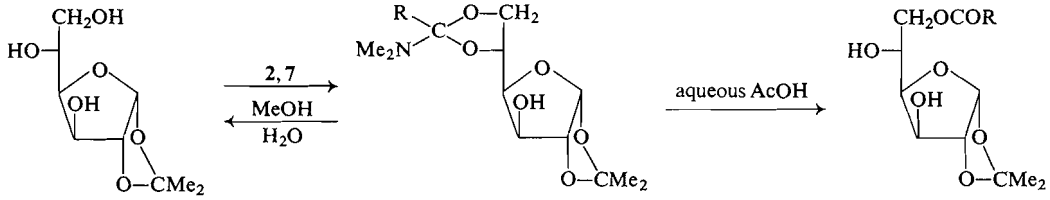

14

15 R=Ph
15*a* R=Me

16 R=Ph
16*a* R=Me

SCHEME 3

α-D-glucofuranose (**15***a*) as a mixture of diastereoisomers (Scheme 3). Unlike the acetal **8**, compound **15***a*, in which the acetal spans a primary and a secondary hydroxyl group, was much more sensitive to water and hydrolyzed to starting material. Treatment of the mixture with aqueous acetic acid gave an 88% yield of 6-*O*-acetyl-1,2-*O*-isopropylidene-α-D-glucofuranose (**16***a*) (16). Although optimum or forcing conditions were not explored, the yield of the acetal derivative **16***a* could be considerably improved by working under strictly anhydrous conditions.

From these results, it is evident that when polyhydroxy compounds containing vicinal diols, such as **14**, are treated with the acetals **2** or **7**, formation of a 1,3-dioxolane ring is clearly preferred under the conditions of the reaction. The directive influence in the acetal cleavage leads to a preparative method for the selective esterification of the primary hydroxyl group in such compounds.

The aforementioned reactions demonstrate some of the uses of α-(dimethylamino)benzylidene and 1-(dimethylamino)ethylidene acetals in preparative organic chemistry. The acid-catalyzed cleavage of these acetals to give monobenzoylated and monoacetylated diols is of synthetic and mechanistic significance. It is reasonable to assume the formation of benzoxonium, acetoxonium and/or iminium type intermediates such as **17**, **17***a*, **18**, **18***a* respectively, depending on the site of protonation (Scheme 4).

It is difficult at this stage to determine the underlying factors in the cleavage of the acetals **3** and **8**, which sometimes leads to a predominance of one isomer, since the initial products could conceivably equilibrate in the mildly acidic medium. The intermediacy of benzoxonium and acetoxonium ions of type **17** and **17***a* and orthoacids derived from them, rather than iminium ions of type **18** and **18***a* is suggested by the highly selective opening of acetals involving a primary alcohol group, such as **15** and **15***a*. The formation of a primary benzoate (and

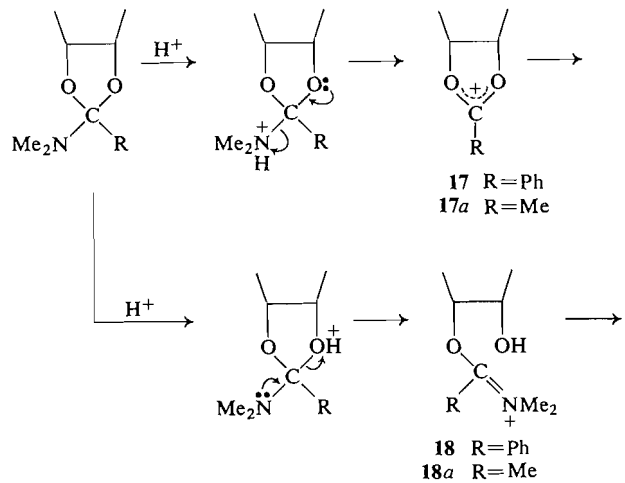

17 R=Ph
17*a* R=Me

18 R=Ph
18*a* R=Me

SCHEME 4

Can. J. Chem. Downloaded from www.nrcresearchpress.com by 210.87.254.40 on 09/05/12
For personal use only.

Can. J. Chem. Downloaded from www.nrcresearchpress.com by 210.87.254.40 on 09/05/12
For personal use only.

acetate) is in agreement with similar cleavage reactions involving benzoxonium ions spanning primary and secondary carbon atoms (17–22). In this respect, the presence of a (dialkylamino) group in these benzylidene and ethylidene acetals may offer some advantage over the analogous alkoxybenzylidene and alkoxyethylidene acetals. These aspects will be elaborated upon in future papers in this series. It has been reported (23–25) that equilibration of isomeric 2′- and 3′-acetates in certain ribonucleosides favors acetyl migration away from the glycosyl carbon atom, *i.e.* a predominance of the 3′-acetate isomer at equilibrium. Attempts to increase the proportion of one of the two isomers in **11** by equilibration have so far been unsuccessful in our hands. This aspect may be dependent on the nature of the aglycone. In contrast to **8**, the direction of ring opening of orthoesters spanning vicinal diols in conformationally rigid six-membered rings is such that a preponderance of one ester derivative is usually observed (26–28). In conformationally flexible systems, the selectivity is much less pronounced (29). Although the cleavage of acetals of type **8**, spanning two secondary hydroxyl groups in a pentofuranose system, proceeds in a non-selective manner, the reaction retains both preparative and interpretive significance. Except for the orthoester approach, there are no practical methods for effecting monoacetylation or monobenzoylation of the 2- and 3-positions in the ribofuranose series. The problem of selective acylation (25) is an important one, in connection with approaches to oligonucleotide syntheses as well as in understanding the mechanisms of aminoacylation and acyl migration in *t*-RNA.

In the interest of assessing the utility of α-(dimethylamino)benzylidene and 1-(dimethylamino)ethylidene acetals as temporary blocking groups, we investigated the possibilities of effecting various transformations at the primary hydroxyl groups in the presence of the acetal function as well as testing the compatibility of certain groups with the conditions of acetal formation.

Thus in an alternative approach to the dibenzoate **6**, the suitability of benzoate esters as *O*-protecting groups during cyclic acetal formation was explored. The reaction of methyl 5-*O*-benzoyl-β-D-ribofuranoside (**19**) (30) with **2** was carried out in 1,1,1-trichloroethane at 0° during

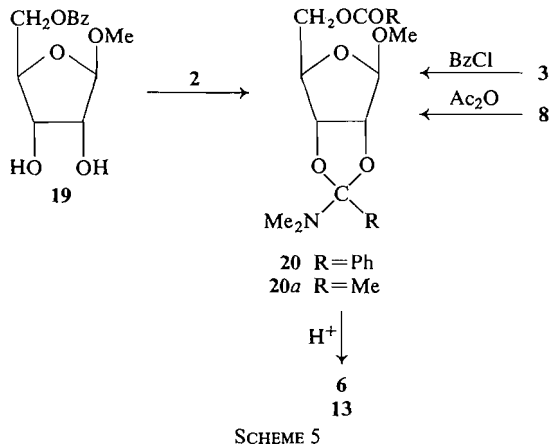

SCHEME 5

2 h and at room temperature for 5 h, to give methyl 5-*O*-benzoyl-2,3-*O*-[α-(dimethylamino)-benzylidene]-β-D-ribofuranoside (**20**) as a syrup in good yield (Scheme 5). The acetal **20**, probably a mixture of diastereoisomers, was sufficiently pure for further transformations. It is thus evident that benzoate esters are compatible with the conditions of acetal formation. Alternatively, compound **20** could be prepared from **3** by benzoylation with benzoyl chloride in pyridine. In order to avoid hydrolysis of the acetal group during the work-up process, a convenient procedure was to dilute the solution with 1,1,1-trichloroethane and to process by extraction with cold water. In this manner, the water-sensitive acetal remained in the organic phase during the work-up operation. Treatment of **20** prepared by the above methods with 95% aqueous acetic acid at p*H* 4–5 resulted in rapid cleavage of the acetal group to give a mixture of methyl β-D-ribofuranoside dibenzoates from which the pure 3,5-dibenzoate isomer **6** could be easily obtained by fractional crystallization (Scheme 5).

Methods of selective benzoylation of secondary hydroxyl groups in D-ribofuranose derivatives are scarce and somewhat tedious (31, 32). An indirect method of benzoylation of vicinal diols involves the acid-catalyzed cleavage of methoxybenzylidene derivatives, which are structurally related to the α-(dimethylamino)-benzylidene acetals. Selective benzoylations of uridine (33) and *N*,*N*-dimethyladenosine (34) have been effected by this method. Selective benzoylation with concomitant introduction of a bromine atom in the molecule can be effected

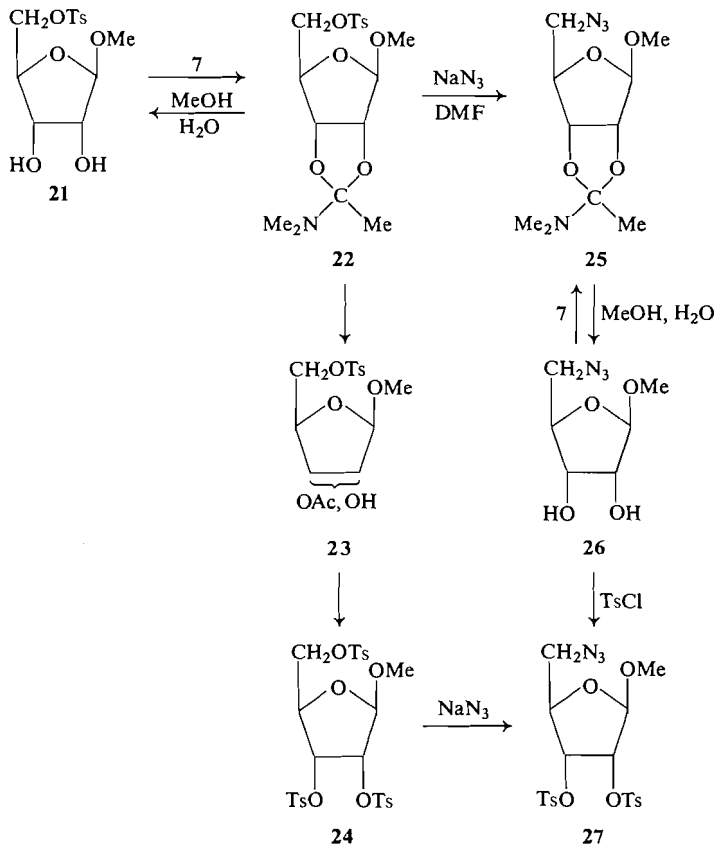

SCHEME 6

by the cleavage of *O*-benzylidene acetals with *N*-bromosuccinimide (17–20). Application of this reaction to *O*-benzylidene nucleosides has been demonstrated also (21). Furthermore, it has been shown that the presence of water in these reaction mixtures leads to the cleavage of the *O*-benzylidene acetals and the formation of benzoate esters (17, 22). Treatment of the acetal **8** with acetic anhydride in pyridine at room temperature overnight, followed by dilution with 1,1,1-trichloroethane and extraction with water, gave the corresponding 5-*O*-acetyl derivative **20***a* (92%) as a mixture of diastereoisomers (Scheme 5). The n.m.r. spectrum of **20***a* clearly showed the acetyl group to be in the primary position. Hydrolysis at p*H* 3–4 with 95% acetic acid gave a syrup in good yield which consisted of a mixture of 2,5- and 3,5-diacetates, **13**. Attempts to obtain a crystalline mono-*p*-nitrobenzoate were not unsuccessful. Treatment of **20***a* with 3% aqueous methanol afforded crystalline **1** in over 90% yield. The successful acylations of **3** and **8** point out the distinct advantages of α-(dimethylamino)benzylidene and 1-(dimethylamino)ethylidene acetals over the corresponding dimethylaminomethylene acetals derived from vicinal diols and DMF acetals. It has been reported that all attempts to acylate alcohol groups in such acetals have been unsuccessful, and led to acetal cleavage (9).

It was of interest to attempt nucleophilic displacement reactions in the presence of one of the acetal functions. The desired substrate, methyl 2,3-*O*-[1-(dimethylamino)ethylidene]-5-*O*-*p*-tolylsulfonyl-β-D-ribofuranoside (**22**) was prepared by acetalation of the corresponding methyl 5-*O*-*p*-tolylsulfonyl-β-D-ribofuranoside (**21**). The latter was obtained as a colorless syrup by controlled monotosylation of **1** and purification by column chromatography. Alternatively, the acetal **22** could also be prepared by tosylation of **8**, demonstrating another example of

Can. J. Chem. Downloaded from www.nrcresearchpress.com by 210.87.254.40 on 09/05/12
For personal use only.

Can. J. Chem. Downloaded from www.nrcresearchpress.com by 210.87.254.40 on 09/05/12
For personal use only.

acylation in the presence of the 1-(dimethylamino)ethylidene function (Scheme 6). Acid hydrolysis of **22** at p*H* 4–5 afforded methyl 5-*O*-*p*-tolylsulfonyl-β-D-ribofuranoside as a mixture of 2- and 3-monoacetates **23**. Deacetylation and tosylation afforded the known crystalline methyl 2,3,5-tri-*O*-*p*-tolylsulfonyl-β-D-ribofuranoside (**24**) (35). Treatment of **22** with aqueous methanol regenerated the tosylate **21** in good yield. As an example of displacement reaction we selected the system consisting of sodium azide in anhydrous DMF, which has become the classical and practical approach to amino sugar derivatives. Treatment of **22** at 90° during 6 h in the above system, followed by dilution with 1,1,1-trichloroethane and extraction with small portions of water afforded the desired methyl 5-azido-5-deoxy-2,3-*O*-[1-(dimethylamino)ethylidene]-β-D-ribofuranoside (**25**) as the major product. Traces of ring cleavage products could not be avoided in this case because of the difficulties with the complete removal of DMF and the necessity for repeated evaporation by codistillation with other solvents. Alternatively, the solvents could be lyophilyzed and work-up effected as usual. The syrupy **25** possessed the expected n.m.r. spectral characteristics and proved suitable for subsequent reactions. Hydrolysis with aqueous methanol afforded the known (35) methyl 5-azido-5-deoxy-β-D-ribofuranoside (**26**), that was also prepared from the corresponding 5-tosylate **21** for purposes of comparison. Reaction of **26** with **7** in the usual manner gave the corresponding acetal **25** in excellent yield. Both chromatographic and n.m.r. spectral properties of **25** were the same as those recorded in the alternate route described above. Cleavage of the acetal ring in **25** with aqueous acetic acid gave the expected mixture of 2- and 3-acetates as the sole products. Deacetylation and tosylation afforded the known crystalline methyl 5-azido-5-deoxy-2,3-di-*O*-*p*-tolylsulfonyl-β-D-ribofuranoside (**27**), prepared also from the corresponding tritosylate by selective displacement with azide ion (35).

Experimental

Melting points are uncorrected. The n.m.r. spectra were obtained in chloroform-*d* at 60 or 100 MHz, with tetramethylsilane as internal standard. The i.r. spectra were recorded on a Beckman IR-8 instrument. The t.l.c. was performed on silica gel GF_{250} (Merck) and the spots were detected with a solution containing sulfuric acid in ethanol after heating the plates. Column chromatography was done using Davidson silica gel.

Conventional processing signifies drying organic solutions over anhydrous sodium sulfate, filtration, and evaporation under diminished pressure. Optical rotations were measured with a Perkin–Elmer model 141 photoelectric spectropolarimeter.

N,N-Dimethylbenzamide Dimethyl Acetal (2)

A mixture of *N,N*-dimethylbenzamide (14.9 g, 0.1 mmol) and dimethylsulfate (12.6 g, 0.1 mmol) was heated at 90° for 4 h. The yellowish viscous solution was cooled and added dropwise and with stirring to a solution of sodium methoxide in methanol (prepared from 2.3 g of sodium in 35 ml of methanol). The desired product **2** was recovered by distillation, 8.6 g, 44%; b.p. 30–33°/0.1 Torr (12). The n.m.r. data: τ 1.48, 2.32 (aromatic protons); 6.64 (OCH_3); 7.80 ($—N(CH_3)_2$). The sample was contaminated with a small amount of *N,N*-dimethylbenzamide.

N,N-Dimethylacetamide Dimethyl Acetal (7)

A mixture of *N,N*-dimethylacetamide (43.6 g, 0.5 mmol) and dimethylsulfate (63.1 g, 0.5 mmol) was heated at 60–80° during 2 h. The viscous solution was then added dropwise to a solution of sodium methoxide (from 11.5 g sodium in 160 ml of methanol) with stirring at 0°. The resulting solution was heated gradually to 190° and the desired product 7 was obtained from a fraction with b.p. 103–112°/740 Torr (5). Redistillation gave 15 g, 23% of **7** as a colorless liquid which was stored in the dark at 0°. The n.m.r. data: τ 8.73 ($—CH_3$, singlet); 7.69 ($—N(CH_3)_2$, singlet); 6.76 ($—(OCH_3)_2$, singlet).

Methyl 2,3-O-[α-(Dimethylamino)benzylidene]-β-D-ribofuranoside (3)

A mixture of **1** (1 g, 6.1 mmol) and *N,N*-dimethylbenzamide dimethyl acetal **2** (2.2 g, 11 mmol) in 25 ml of chloroform was stirred in the dark at room temperature for 18 h. The solution was cooled, diluted with 1,1,1-trichloroethane (75 ml) and water (50 ml). The organic layer was separated, rapidly extracted with cold water, and processed to give the product as a syrupy mixture of diastereoisomers (82:18, by n.m.r.); yield 1.8 g, quant. The product exhibited a single spot by t.l.c. ($CHCl_3$–MeOH, 10:1) although a minor quantity of *N,N*-dimethylbenzamide was present. The n.m.r. data: 2.16, 2.80 (aromatic protons); 5.00, 5.03 (H_1, singlets); 5.38 (H_2–H_4, multiplet); 6.32 (OH, $H_{5,5'}$, multiplet); 6.48 (OCH_3); 7.42, 7.48 ($—N(CH_3)_2$, singlets).

Methyl 2,3-O-[1-(Dimethylamino)ethylidene]-β-D-ribofuranoside (8)

Method a

A solution containing 4 g (24 mmol) of **1** and 3.25 (24 mmol) of *N,N*-dimethylacetamide dimethyl acetal **7** in 100 ml of 1,1,1-trichloroethane was stirred at room temperature in the dark for 6 h. The solution was extracted with two 50 ml portions of cold water and the organic phase was dried and evaporated to a syrup (4.1 g, 80%) consisting essentially of the desired product as a mixture of diastereoisomers, b.p. 103–108°/0.4 Torr (t.l.c., $CHCl_3$–MeOH, 10:1). A portion was redistilled at 103–108°/0.4 Torr to give a small quantity of a pure diastereoisomer; n.m.r. data: τ 4.97 (H, singlet); 5.22 (H_2, doublet, $J_{2,3} = 6$ Hz); 5.41 (H_3, doublet, $J_{3,2} = 6$ Hz); 5.54 (H_4, triplet, $J_{4,5} = 4$ Hz);

Can. J. Chem. Downloaded from www.nrcresearchpress.com by 210.87.254.40 on 09/05/12
For personal use only.

6.35 ($H_{5,5'}$ and OH, multiplet); 6.57 (OMe, singlet); 7.54 (Me_2N—, singlet); 8.51 (CH_3—C, singlet).

Method b

The reaction was repeated as above in the presence of **2** equivalents of *N,N*-dimethylacetamide dimethyl acetal. Processing in the usual manner after a reaction period of 1 h afforded a syrup in quantitative yield, consisting predominantly of **8**. A minor product was the mixed acetal **9** which could be readily detected by t.l.c., ($CHCl_3$–MeOH, 10:1) as a component of higher chromatographic mobility.

Regeneration of Methyl β-D-Ribofuranoside from 3 and 8

Amounts of **3** (0.2 g) and **8** (0.5 g) were dissolved each in 10 ml of 3% aqueous methanol and the solutions were heated at reflux for 2 h. Evaporation of the respective solutions gave syrups which crystallized from ethyl acetate to give **1** (0.1 g, 90% and 0.26 g, 74% respectively), m.p. 78°, reported m.p. 79–80° (10). The mother liquors contained additional product in each case.

Acid Hydrolysis of Methyl 2,3-O-[α-(Dimethylamino)-benzylidene]-β-D-ribofuranoside (3)

A solution of **3** (0.6 g, 2 mmol) in 10 ml of 95% aqueous acetic acid (p*H* 3–4) was stirred at room temperature for 2 h. The solution was neutralized with sodium hydrogen carbonate and extracted with chloroform. Processing the organic phase afforded a syrup (0.25 g, 46%) consisting entirely of methyl 2-*O*-benzoyl-β-D-ribofuranoside **4** and the corresponding 3-benzoate **5** in an approximate ratio of 2:3; λ_{max} (film) 1740 cm^{-1} (benzoate); n.m.r. data; τ 2.09, 2.64 (aromatic protons); 4.64 (H_2, H_3, doublet, $J = 4$ Hz); 5.03, 5.12 (H_1, singlets); 5.64 (H_2, H_3, and H_4, multiplet); 6.32 ($H_{5,5'}$, multiplet); 6.64 (—OCH_3); 7.06 (OH).

Methyl 3,5-Di-O-benzoyl-β-D-ribofuranoside (6)

The mixture of esters **4** and **5** (0.13 g) was dissolved in 5 ml of dry pyridine and the solution was treated with 1 equiv of benzoyl chloride in pyridine at 0°. After standing at 4° overnight, and 1 h at room temperature, the solution was poured into ice-water and the mixture was extracted with chloroform. Processing of the organic layer gave a semi-crystalline syrup which was chromatographically homogeneous; yield 0.18 g (95%). Fractional crystallization from absolute ethanol gave the desired product (50 mg), m.p. 132–133°; $[\alpha]_D^{25}$ −8.77° (*c* 0.49, $CHCl_3$); λ_{max} 1740 cm^{-1} (benzoate); n.m.r. data: τ 2.06, 2.67 (aromatic protons); 4.70 (H_3, $J_{3,2} = 4$ Hz); 5.06 (H_1, singlet); 5.51 (H_2–$H_{5,5'}$, multiplet); 6.70 (—OCH_3); 7.32 (OH).

Anal. Calcd. for $C_{20}H_{20}O_7$: C, 64.69; H, 5.38. Found: C, 64.42; H, 5.44.

Methyl 5-O-Benzoyl-2,3-O-[α-(Dimethylamino)-benzylidene]-β-D-ribofuranoside (20)

(a) From Methyl 5-O-Benzoyl-β-D-ribofuranoside (19)

A solution containing **19** (0.5 g, 1.8 mmol) and *N,N*-dimethylbenzamide dimethyl acetal **2** (0.73 g, 3.7 mmol) in 12 ml of chloroform was stirred in the dark at 0° for 2 h and at room temperature for 4 h. The solution was processed as described for the preparation of **3** to give the product **20** as a syrup (0.74 g, quant.); λ_{max} (film) 1740 cm^{-1}. The n.m.r. data indicated a mixture of diastereoisomers in the ratio 3:1; τ 2.06, 2.64 (aromatic protons); 4.80, 4.83 (H_1, singlets); 5.06–5.80 (H_2–$H_{5,5'}$, multiplet); 6.48, 6.54 (—OCH_3, singlets); 7.64, 7.77 (—$N(CH_3)_3$, singlets).

(b) From 3 by Controlled Benzoylation

A solution of **3** (0.9 g, 2.5 mmol) in 20 ml of dry pyridine was cooled to 0° and treated dropwise with a solution of benzoyl chloride (0.43 g, 3 mmol). After standing overnight at 4° and at room temperature for 2 h, the solution was diluted with 1,1,1-trichloroethane, cooled, and extracted with cold water. The organic phase was separated and processed as usual to give the product **20** as a mixture of diastereoisomers; yield, 1.2 g, 98%; λ_{max} (film) 1740 cm^{-1}. The product was chromatographically homogeneous ($CHCl_3$–MeOH, 10:1) and was identical (i.r., n.m.r.) to that obtained by method *a*.

Acid Hydrolysis of Methyl 5-O-Benzoyl-2,3-O-[α-(Dimethylamino)benzylidene]-β-D-ribofuranoside (20)

A solution of **20** (0.735 g) in 10 ml of 95% acetic acid (p*H* 3–4) was stirred at room temperature for 1.5 h. The solution was neutralized with sodium hydrogen carbonate; it was extracted with chloroform and the extracts were processed in the usual manner to give a chromatographically homogeneous semi-crystalline residue (0.56 g, 81%). The n.m.r. data indicated the presence of a 1:1 mixture of the dibenzoate **6** and the isomeric 2,5-dibenzoate. Fractional crystallization from ethanol gave the pure dibenzoate **6** (0.27 g, 47%); m.p. 132–133°; identical in all respects with material prepared from **5**.

Acid Hydrolysis of Methyl 2,3-O-[1-(Dimethylamino)-ethylidene]-β-D-ribofuranoside (8)

An amount of **8** (0.5 g) was dissolved in 95% aqueous acetic acid (10 ml, p*H* 3–3.5), the solution was stirred at room temperature for 2 h and then it was lyophilyzed. The syrupy residue (0.36 g, 90%) was homogeneous by t.l.c. ($CHCl_3$–MeOH, 10:1) and consisted of a mixture (**11**) of methyl 2-*O*-acetyl-β-D-ribofuranoside and the corresponding 3-acetate in an approximate ratio of 1:1. The n.m.r. data: τ 4.74, 4.86 (pair of doublets, H_2, H_3, $J = 3.2$ Hz); 5.06 (H_1, singlet); 5.70 (H_4, H_2, or H_3, multiplet); 6.22 ($H_{5,5'}$, multiplet); 6.51, 6.52 (OCH_3, singlets); 7.22 (OH, broad); 7.80, 7.83 (—$COCH_3$, singlets).

A portion of the above mixture of acetates (0.3 g) was *p*-nitrobenzoylated in pyridine (room temperature, overnight) and processed by adding the solution to ice-water. The precipitated product was filtered, washed with aqueous sodium hydrogen carbonate, then with water to give 0.5 g (75%) of a chromatographically homogeneous product, m.p. 102–104°. Recrystallization from absolute ethanol afforded 0.1 g of pure *methyl 3-O-acetyl-2,5-di-O-p-nitrobenzoyl-β-D-ribofuranoside* (**12**) m.p. 147.5–148°; $[\alpha]_D^{25}$ 29.8° (*c* 0.5, $CHCl_3$);[7] λ_{max} 1600 cm^{-1} (carbonyl); n.m.r. data: τ 1.83 (aromatic protons, multiplet); 4.57 (H_2, H_3, multiplet); 4.89 (H_1, singlet); 5.41 (H_4, $H_{5,5'}$, multiplet); 6.64 (OCH_3, singlet); 8.06 (—$COCH_3$, singlet).

Anal. Calcd. for $C_{22}H_{20}N_2O_{12}$: C, 52.30; H, 4.00; N, 5.55. Found: C, 52.27; H, 4.02; N, 5.38.

Reaction of Methyl β-D-Ribofuranoside with Trimethylorthoacetate

A solution containing **1** (0.5 g), trimethylorthoacetate (2.1 ml), and 0.11 g of *p*-toluenesulfonic acid in 0.7 ml of DMF was stirred at room temperature for 3 h. The solution was neutralized with sodium methoxide in methanol and it was evaporated to dryness. Traces of DMF were removed

[7]The rotation value was previously reported as 37.5° (1).

Can. J. Chem. Downloaded from www.nrcresearchpress.com by 210.87.254.40 on 09/05/12
For personal use only.

by repeated evaporation from *n*-butanol to give *methyl 2,3-O-methoxyethylidene-β-D-ribofuranoside* (**10**), as a syrupy mixture of diastereoisomers (0.66 g, quant.) contaminated with a small quantity of the mixed acetal **10***a*, as evidenced by t.l.c. ($CHCl_3$–MeOH, 10:1). The product was particularly sensitive to moisture and was hydrolyzed to a mixture of monoacetates. Treatment of the acetal **10** (0.46 g) with 10% aqueous acetic acid (room temperature, 30 min), followed by lyophilization afforded a 76% yield of the mixture of acetates **11**. The crystalline di-*p*-nitrobenzoate derivative **12** could be obtained as in the previous case.

Acetylation of Methyl 2,3-O-[1-(Dimethylamino)-ethylidene]-β-D-ribofuranoside

An amount of **8** (0.7 g, 0.3 mmol) in 10 ml of dry pyridine was cooled and treated with acetic anhydride (0.46 g, 0.4 mmol). After standing overnight at room temperature, the solution was cooled, diluted with 1,1,1-trichloroethane and water. Extraction and processing of the organic phase afforded a syrup which was codistilled with toluene to remove residual pyridine. The resulting syrup (0.76 g, 92%) was homogeneous by t.l.c. ($CHCl_3$–MeOH, 10:1) and consisted approximately of a 3:2 mixture of diastereoisomers of *methyl 5-O-acetyl-2,3-O-[1-(dimethylamino)ethylidene]-β-D-ribofuranoside* (**20***a*); λ_{max} (film) 1740 cm^{-1} (acetate); n.m.r. data: 4.94, 5.00 (H_1, singlets); 5.32–6.00 (H_2–$H_{5,5'}$, multiplet); 6.64 (OCH_3, singlet); 7.64, 7.76 (—$N(CH_3)_2$, singlets); 7.89 (—$COCH_3$, singlet); 8.54, 8.57 (—CH_3, singlets).

Heating a solution of **20***a* in 3% aqueous methanol regenerated **1** in 90% yield.

Acid Hydrolysis of Methyl 5-O-Acetyl-2,3-O-[1-(Dimethylamino)ethylidene]-β-D-ribofuranoside (20a)

A solution containing **20***a* (0.76 g) in 10 ml of 95% aqueous acetic acid was kept at room temperature for 2 h and lyophilyzed. The residue was a homogeneous syrup (0.65 g, 94%), corresponding to 1:1 mixture (**13**) of methyl 2,5-di-*O*-acetyl-β-D-ribofuranoside and the corresponding 3,5-diacetate; n.m.r. data: 4.90, 5.00 (H_2, H_3, doublets, $J = 4$ Hz); 5.15 (H_1, singlet); 5.70 (H_4, $H_{5,5'}$, H_2, or H_3, multiplet); 6.50 (OH); 6.65 (OCH_3, singlet); 7.85, 7.92 (—$COCH_3$, singlets).

Treatment of the mixture with sodium methoxide in methanol gave a quantitative yield of **1**. The same mixture of **13** could be obtained by acid hydrolysis of fractions containing the mixed acetals corresponding to **9** and **10***a* respectively. The mixture of monoacetates **11** could then be separated from the diacetates **13** from such hydrolyses by extraction of the latter from an aqueous solution with chloroform.

5,6-O-[α-(Dimethylamino)benzylidene]-1,2-O-isopropylidene-α-D-glucofuranose (15)

A solution containing 1,2-*O*-isopropylidene-α-D-glucofuranose (**14**) (36) (0.5 g, 2.2 mmol) and **2** (0.88 g, 4.5 mmol) in 15 ml of chloroform was stirred in the dark at room temperature for 18 h. The solution was processed as described for the preparation of **3**, to give a syrup (0.8 g, quant.) which consisted of a major component (t.l.c., $CHCl_3$–MeOH, 10:1) and a minor component of lower mobility, in addition to traces of *N,N*-dimethylbenzamide; n.m.r. data indicated a 3:2 diastereoisomeric mixture: τ 2.22, 2.80 (aromatic protons); 4.32 (H_1, doublet $J_{1,2} = 4$ Hz); 5.80 (H_2–H_4, multiplet); 6.48 ($H_{6,6'}$, multiplet); 7.06 (OH); 7.70, 7.80 (—$(CH_3)_2$, singlets); 8.51, 8.67 (CH_3, singlets).

Heating a solution of **15** in 3% aqueous methanol regenerated **14** in high yield.

6-O-Benzoyl-1,2-O-isopropylidene-α-D-glucofuranose (16)

A solution of **15** (0.2 g) in 5 ml of 95% acetic acid was left at room temperature for 2 h. Neutralization with sodium hydrogen carbonate followed by extraction with chloroform and processing afforded a crystalline residue (0.1 g, 55%) which was chromatographically homogeneous ($CHCl_3$–MeOH, 10:1). Recrystallization from ethanol gave the product **16**, m.p. 193–194°, reported m.p. 196° (15); λ_{max} 1740 cm^{-1} (benzoate).

Compound **16** was also prepared by selective benzoylation of **14** with benzoyl chloride in pyridine (15); the yield was 7–10%.

5,6-O-[1-(Dimethylamino)ethylidene]-1,2-O-isopropylidene-α-D-glucofuranose (15a)

To a suspension of 1,2-*O*-isopropylidene-α-D-glucofuranose (**14**) (3 g, 13 mmol) in 30 ml of chloroform, was added 4.5 g (33 mol) of **7** and the resulting solution was stirred in the dark at room temperature for 4 h. Successive evaporation from toluene, petroleum ether (b.p. 30–60°) and diethyl ether gave a syrup (3.6 g, 90%) consisting predominantly of the desired product **15***a* (t.l.c., $CHCl_3$–MeOH, 10:1) and contaminated slightly with **16***a*. The n.m.r. data indicated the presence of diastereoisomers (3:2): τ 4.00 (H_1, doublet, $J_{1,2} = 4$ Hz); 5.43 (H_2, doublet, $J_{2,1} = 4$ Hz); 5.73 (H_3–H_5, multiplet); 7.00 ($H_{6,6'}$, multiplet); 7.56 (OH); 7.61, 7.63 (—$N(CH_3)_3$, singlets); 8.42, 8.51 (—$C(CH_3)_2$); 8.64 (—CH_3).

Heating **15***a* in 3% aqueous methanol regenerated **14** in 72% yield, m.p. 160°. The mother liquors contained additional product which was not recovered.

6-O-Acetyl-1,2-O-isopropylidene-α-D-glucofuranose (16a)

A solution containing **15***a* (0.125 g) in 6 ml of 95% aqueous acetic acid was stirred at room temperature for 1 h. The solution was neutralized with sodium hydrogen carbonate, it was extracted with chloroform, the extracts were processed as usual and evaporated to dryness. The crystalline residue was triturated with ether–pentane and the crystals were filtered to give **16***a* (0.1 g, 88%). Recrystallization was effected from ethanol, m.p. 145–147°, reported, 145–146° (16); n.m.r. data ($CDCl_3$ – pyridine-d_5): τ 3.64 (OH); 4.06 (H_1, doublet, $J_{1,2} = 4$ Hz); 5.48 (H_2, doublet, $J_{2,1} = 4$ Hz); 5.64 (H_3–$H_{6,6'}$, multiplet); 8.03 (—$COCH_3$); 8.48, 8.70 (—$C(CH_3)_2$).

Methyl 2,3-O-[1-(Dimethylamino)ethylidene]-5-O-p-toluenesulfonyl-β-D-ribofuranoside (22)

(a) From 8

To a solution containing 2 g (8 mmol) of **8** in 25 ml of dry pyridine was added *p*-toluenesulfonyl chloride (2.45 g, 1.2 mmol). After stirring at room temperature for 24 h, the solution was cooled and diluted with 1,1,1-trichloroethane and with water. The organic phase was processed as usual to give a syrup which was dissolved in toluene and evaporated several times. The final syrup (2.64 g, 80%), consisted of a 3:2 diastereoisomeric mixture of methyl 2,3-*O*-[1-(dimethylamino)ethylidene]-5-*O*-*p*-tolylsulfonyl-β-D-ribofuranoside (**22**); n.m.r. data: τ 2.32, 2.64 (aromatic protons); 5.06, 5.09 (H_1, singlets); 5.32–6.16 (H_2–$H_{5,5'}$, multiplet);

Can. J. Chem. Downloaded from www.nrcresearchpress.com by 210.87.254.40 on 09/05/12
For personal use only.

6.32 (OCH_3, singlet); 7.32 ($—C_6H_4CH_3$); 7.64, 7.73 ($—N(CH_3)_2$, singlets); 8.51, 8.54 ($—CH_3$, singlets).

(b) From Methyl 5-O-p-Tolylsulfonyl-β-D-ribofuranoside (21)

A solution containing 5 g (3 mmol) of **1** in 30 ml of pyridine was cooled and treated with 5.8 g (3 mmol) of *p*-toluenesulfonyl chloride in 15 ml of pyridine. After standing at 4° overnight, the solution was poured into ice-water and the resulting solution was extracted with chloroform. Processing the organic phase in the usual way afforded a syrup which consisted of a major product by t.l.c. ($CHCl_3$–MeOH, 10:1). Purification over a column containing silica gel afforded methyl 5-*O*-*p*-tolylsulfonyl-β-D-ribofuranoside (**21**) (3.85 g, 40%) as a syrup which had the expected spectral (i.r., n.m.r.) properties. A portion of **21** (0.37 g, 1 mmol) was treated with 0.38 g (2.8 mmol) of **7** in 13 ml of chloroform. After 26 h at room temperature in the dark, the solution was diluted with 1,1,1-trichloroethane, cold water, and chilled. Separation of the organic phase, drying and evaporation afforded a syrupy mixture of diastereoisomers of methyl 2,3-*O*-[1-(dimethylamino)ethylidene]-5-*O*-*p*-tolylsulfonyl-β-D-ribofuranoside (**22**) (0.45, quant.).

Acid hydrolysis of **22** in 95% aqueous acetic acid (p*H* 3–4, 1.5 h) followed by neutralization ($NaHCO_3$) and extraction with chloroform afforded a 66:44 mixture (**23**), of methyl 2-*O*-acetyl-5-*O*-*p*-tolylsulfonyl-β-D-ribofuranoside and its 3-*O*-acetyl analog, as a syrup (0.63 g, 84%); n.m.r. data: τ 2.48, 2.70 (aromatic protons); 5.16, 5.22 (H_2, H_3, two doublets, $J = 4$ Hz); 5.33 (H_1, singlet); 6.00 (H_4, $H_{5,5'}$, H_2, H_3, multiplet); 6.86 (OCH_3, singlet); 7.16 (OH); 7.64 ($—C_6H_4CH_3$); 7.74, 8.00 ($—\overset{O}{\overset{\|}{C}}CH_3$, singlets).

Heating a solution of **22** in 3% aqueous methanol at reflux for 1–2 h or treatment of **23** with sodium methoxide afforded the starting 5-tosylate as the sole product in both cases. Tosylation of the product so obtained afforded in each case the known methyl 2,3,5-tri-*O*-*p*-tolylsulfonyl-β-D-ribofuranoside (**24**) m.p. 124–125°; reported 126° (35).

Preparation of Methyl 5-Azido-5-deoxy-2,3-O-[1-(dimethylamino)ethylidene]-β-D-ribofuranoside (25)

(a) From Methyl 5-Azido-5-deoxy-β-D-ribofuranoside (16)

A solution containing **21** (0.6 g) and 0.6 g of sodium azide in 25 ml of *N*,*N*-dimethylformamide was heated with stirring at 90°. The solution was cooled, treated with 75 ml of diethyl ether, the solids were filtered, and the filtrate was evaporated to dryness (*n*-butanol azeotrope). The resulting chromatographically homogeneous syrup (0.35 g, 98%) consisted predominantly of the desired product **26**; λ_{max} (film) 2100 cm^{-1} (N_3). The syrup (0.35 g, 1.8 mmol) was dissolved in 15 ml of chloroform, 0.48 g (3.6 mmol) of **7** was added and the solution was stored in the dark at room temperature overnight. The solution was processed as described for the corresponding tosylate **22**, to give the desired product **25** as a syrupy mixture of diastereoisomers (0.2 g, 48%). Traces of ester were present (i.r.) due to some hydrolysis.

(b) From 22 by Displacement with Azide Ion

A solution containing **22** (0.8 g, 2 mmol), sodium azide (0.835 g, 18 mmol) in 40 ml of dry *N*,*N*-dimethylformamide was heated with stirring at 90° for 6 h. The solution was cooled to 0°, it was diluted with 100 ml of diethyl ether and the salts were filtered with minimum exposure to moisture. The filtrate was evaporated to dryness (*n*-butanol azeotrope) to give the desired **15** as a syrupy mixture of diastereoisomers (0.4 g, 75%) in a ratio of 64:36; n.m.r. data: τ 5.00, 5.16 (H_1, singlets); 5.19–6.00 (H_2–H_4, multiplet); 6.64–6.70 ($—OCH_3$, two singlets; $H_{5,5'}$, multiplet); 7.64, 7.80 ($—N(CH_3)_2$, singlets); 8.16, 8.32 ($—CH_3$, singlets).

Treatment of **25** with aqueous acetic acid as previously described afforded a mixture of methyl 5-azido-5-deoxy-β-D-ribofuranoside monoacetates in 52% yield. The n.m.r. data indicated a 4:1 mixture of 3- and 2-acetates.

Heating a solution of **25** in 3% aqueous methanol regenerated the starting 5-azido derivative **26** in quantitative yield. Tosylation of **26** afforded in good yield the known crystalline methyl 5-azido-5-deoxy-2,3-di-*O*-*p*-tolylsulfonyl-β-D-ribofuranoside (**27**), m.p. 116–117°; reported 122–123° (35); n.m.r. data: τ 2.35, 2.83 (aromatic protons); 5.19 (H_1, singlet); 5.32 (H_2, doublet, $J_{2,3} = 2$ Hz); 5.38 (H_3, doublet, $J_{3,2} = 2$ Hz); 5.70 (H_4, multiplet); 6.80 (OCH_3, $H_{5,5'}$); 7.54 ($—C_6H_4CH_3$, singlet).

Treatment of Methyl 2,3-O-Isopropylidene-β-D-ribofuranoside with 7

A solution of methyl 2,3-*O*-isopropylidene-β-D-ribofuranoside (14) (0.5 g) in 5 ml of dichloromethane containing 1 ml of **7** was stirred in the dark for 3 days. The solution was diluted with aqueous acetic acid and evaporated to dryness. Chromatographic examination revealed the presence of methyl 5-*O*-acetyl-2,3-*O*-isopropylidene-β-D-ribofuranoside, in addition to starting material. The acetate was separated by preparative t.l.c. and isolated as a syrup (80 mg). Its physical properties (i.r., n.m.r.) were identical with those of an authentic specimen, prepared by the acetylation of the starting material. Deacetylation (NaOMe, MeOH) of the acetate regenerated the initial substrate.

The financial assistance from the National Research Council of Canada is gratefully acknowledged.

1. S. Hanessian and E. Moralioglu. Tetrahedron Lett. 813 (1971).
2. A. N. DeBelder. Advan. Carbohydr. Chem., **20**, 220 (1965).
3. S. Hanessian and N. R. Plessas. J. Org. Chem. **34**, 2163 (1969); Chem. Commun. 1152 (1966).
4. S. Hanessian. Ger. Pat. 1 811 267 (1969); Chem. Abstr. **71**, 512 (1969).
5. H. Meerwein, W. Florian, N. Schön, and S. Stopp. Ann. **641**, 1 (1961).
6. H. Brechbühler, H. Büchi, E. Hatz, J. Schreiber, and A. Eschenmoser. Helv. Chim. Acta, **48**, 1746 (1965); Angew. Chemie, inter. ed. **2**, 212 (1963).
7. H. Vorbrüggen. Angew. Chemie, inter. ed. **2**, 211 (1963).
8. S. Hanessian. Unpublished observations in the carbohydrate series.
9. J. Žemlička and A. Holý. Coll. Czech. Chem. Commun. **32**, 3159 (1967); J. Žemlička. Coll. Czech. Chem. Commun. **28**, 1060 (1963).
10. R. Barker and H. G. Fletcher, Jr. J. Org. Chem. **28**, 4605 (1962).

11. H. NEUMANN. Chimia, **23**, 267 (1969).
12. M. BROWN. U.S. Pat. 3 092 637 (1963); Chem Abstr. **59**, 12764 (1963).
13. J. D. STEVENS and H. G. FLETCHER, JR. J. Org. Chem. **32**, 1399 (1968).
14. N. J. LEONARD and K. L. CARRAWAY. J. Heterocycl. Chem. **3**, 485 (1966); P. A. LEVENE and E. T. STILLER. J. Biol. Chem. **104**, 299 (1934).
15. L. VARGHA. Ber. **66**, 704 (1933).
16. G. H. COLEMAN, S. S. BRANDT, and C. M. MCCLOSKEY. J. Org. Chem. **22**, 1336 (1957).
17. S. HANESSIAN and N. R. PLESSAS. J. Org. Chem. **34**, 1035 (1969).
18. S. HANESSIAN and N. R. PLESSAS. J. Org. Chem. **34**, 1045 (1969).
19. S. HANESSIAN and N. R. PLESSAS. J. Org. Chem. **34**, 1053 (1969).
20. T. L. HULLAR and S. B. SISKIN. J. Org. Chem. **35**, 225 (1970).
21. M. M. PONPIPOM and S. HANESSIAN. Carbohydr. Res. **17**, 248 (1971).
22. G. N. BOLLENBACK and F. W. PARRISH. Carbohydr. Res. **17**, 431 (1971).
23. G. A. R. JOHNSTON. Tetrahedron, **24**, 6987 (1968).
24. C. B. REESE and D. R. TRENTHAM. Tetrahedron Lett. 2459 (1965).
25. B. E. GRIFFIN, M. JARMAN, C. B. REESE, J. E. SULSTON, and D. R. TRENTHAM. Biochem. **5**, 3638 (1966).
26. J. F. KING and A. D. ALLBUTT. Can. J. Chem. **48**, 1754 (1970) and references cited therein.
27. A. S. PERLIN. Can. J. Chem. **41**, 399 (1963); C. -S. GIAM, H. R. GOLDSCHMIDT, and A. S. PERLIN. Can. J. Chem. **41**, 3074 (1963).
28. R. U. LEMIEUX and A. R. MORGAN. Can. J. Chem. **43**, 2190 (1965).
29. H. PAULSEN, F. GARRIDO ESPINOSA, W. P. TRAUTWEIN, and K. HEYNS. Chem. Ber. **101**, 179 (1968).
30. J. A. MONTGOMERY and H. J. THOMAS. J. Am. Chem. Soc. **87**, 5442 (1965).
31. R. K. NESS, H. W. DIEHL, and H. G. FLETCHER, JR. J. Am. Chem. Soc. **76**, 763 (1954); R. K. NESS and H. G. FLETCHER, JR. J. Am. Chem. Soc. **76**, 1663 (1954).
32. D. H. RAMMLER and H. G. KHORANA. J. Am. Chem. Soc. **84**, 3112 (1962).
33. H. P. M. FROMAGEOT, B. E. GRIFFIN, C. B. REESE, and J. E. SULSTON. Tetrahedron, **23**, 2315 (1967).
34. D. P. L. GREEN and C. B. REESE. Chem. Commun. 729 (1968).
35. J. HILDESHEIM, J. CLEOPHAX, and S. D. GERO. Tetrahedron Lett. 5013 (1967).
36. O. TH. SCHMIDT. *In* Methods in carbohydrate chemistry **2**, 318 (1963).

Can. J. Chem. Downloaded from www.nrcresearchpress.com by 210.87.254.40 on 09/05/12
For personal use only.

The Reaction of *O*-Benzylidene Sugars with *N*-Bromosuccinimide. VI. A New Synthesis of 2′-Deoxyuridine and some of its Selectively Substituted Derivatives[1]

M. M. PONPIPOM[2] AND S. HANESSIAN

Department of Chemistry, University of Montreal, Montreal, Quebec

Received June 24, 1971

A new synthesis of 2′-deoxyuridine and its selectively substituted derivatives has been developed, based on the reaction of appropriately substituted 2′,3′-*O*-benzylideneuridines with *N*-bromosuccinimide (NBS). The preponderant products are uridines containing bromine and benzoate groups in the 2′- and 3′-positions respectively.

Une nouvelle synthèse de la 2′-déoxyuridine et de ses dérivés sélectivement substitués a été développée. Elle est basée sur la réaction des 2′,3′-*O*-benzylideneuridines substitués appropriées avec la *N*-bromosuccinimide (NBS). Les produits prépondérants sont les uridines contenant les substituants brome et benzoate respectivement en position 2′ et 3′.

Canadian Journal of Chemistry, **50**, 246 (1972).

Can. J. Chem. Downloaded from www.nrcresearchpress.com by 210.87.254.105 on 09/05/12
For personal use only.

In previous reports from this laboratory, the preparative and mechanistic aspects of the reaction of *O*-benzylidene acetals with *N*-bromosuccinimide (NBS), were adequately discussed (2, 3). The reaction provides easy access to selectively brominated and benzoylated derivatives which have been utilized in a number of synthetic sequences leading to deoxy, aminodeoxy, and other sugar derivatives. We now report on the successful application of the reaction to 2′,3′-*O*-benzylidene acetals of uridine and some of its derivatives, leading to the stereoselective bromination of these nucleosides in the sugar as well as in the heterocyclic ring (1). The incorporation of a halogen atom in the sugar ring, particularly in the 2′- and 3′-positions, provides compounds that are useful intermediates in the chemical modification of nucleosides. Halogenated pyrimidine nucleosides are compounds of considerable biochemical, medicinal, and chemical interest. The introduction of a halogen atom in the 5-position of the uracil ring, imparts biologically and therapeutically significant properties to the parent nucleoside, as in the case of 2′-deoxy-5-halouridines (4). Of the procedures available for the synthesis of 2′-deoxyuridine, those based on nucleoside interconversion, resulting in the ultimate placement at C-2′ of a reducible function such as halogen (5–10) or thioether (11) groups, are among the more practical. Under certain conditions, quasi-phosphonium halides (12–14), may lead to selective halogenation of pyrimidine nucleosides. Bromination and chlorination of uridine and some of its substituted derivatives with appropriate halomethylene (dimethylammonium) halides leads to selective substitution at the C-5′ position (15, 16). The direct substitution of a hydroxyl group by chlorine with the aforementioned reagents had been previously described from our laboratory (17). Catalytic reduction of these halogenonucleosides leads to the respective deoxynucleosides, including the biologically important 2′-deoxyuridine.

Uridine was allowed to react with benzaldehyde in the presence of zinc chloride, to give 2′,3′-*O*-benzylideneuridine (**1**) (18), which, based on its n.m.r. spectrum, appeared to consist of a pair of diastereoisomers. Treatment of **1** with 2.2 equiv of NBS in a mixture of 1,1,2,2-tetrachloroethane and carbon tetrachloride, in the presence of barium carbonate at 85–90°, afforded a crystalline product in 56% yield. Experiments described in this and the following paper (19), led to the unambiguous assignment of the structure as 3′-*O*-benzoyl-2′,5-dibromo-2′-deoxyuridine, (**2**) (1) (Scheme 1). The incorporation of two bromine atoms in the product was ascertained from its mass spectrum and the location of one of the bromine atoms at the 5-position of the uracil moiety was clearly evident from the n.m.r. spectrum. The sites and relative dispositions of

[1]For part V, see ref. 1.

[2]NRCC Postdoctorate Fellow, 1970–1971.

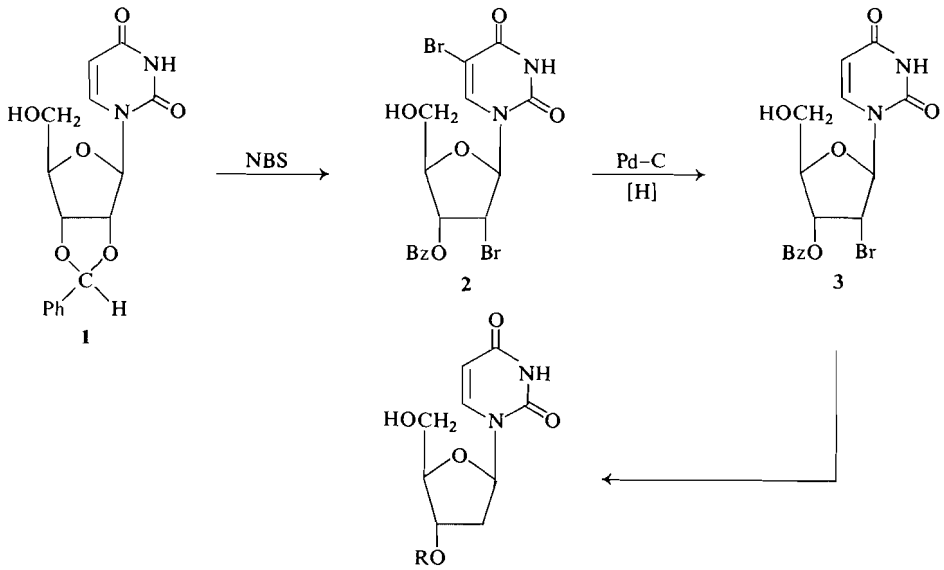

1 2 3

4, R = Bz
5, R = H

SCHEME 1

the second bromine atom and the benzoate group could not be conclusively derived from n.m.r. studies and independent chemical proof was sought. By a proper choice of catalyst (6% Pd–C), it was possible to effect a selective hydrogenolysis of the bromine atom attached at C-5, to give crystalline 3′-*O*-benzoyl-2′-bromo-2′-deoxyuridine (**3**) in 94% yield. Catalytic reduction of **2** or **3** in the presence of 20% Pd–C (20) afforded crystalline 3′-*O*-benzoyl-2′-deoxyuridine (**4**), in 80–85% yield. Debenzoylation in methanolic ammonia gave crystalline 2′-deoxyuridine (6, 9, 21) **5** in 80% yield. The synthesis of **5** can also be effected starting from **1**, without the isolation of intermediates. Another route (7, 22) to **5** consists in the reaction of 2,2′-anhydro-[1-(β-D-arabinofuranosyl)uracil] (**9**) (23, 24) with hydrogen bromide and subsequent reduction. Although the overall yields of **5** by this method are higher, the sequence **1**–**5** described in this paper is more versatile, since it incorporates in it, the feature of selective benzoylation at C-3′ and provides derivatives that could be useful in nucleoside interconversions and transformations.

Treatment of the 5′-*O*-acetyl derivative (**6**) (25) with NBS under essentially the same conditions as for **1**, afforded a crystalline product in 50% yield (Scheme 2). Based on mass spectral, n.m.r., and chemical data, the structure of this product was proved to be 2,2′-anhydro-[1-(5′-*O*-acetyl-3′-*O*-benzoyl-β-D-arabinofuranosyl) 5-bromouracil] (**7**) (1). Catalytic hydrogenation afforded the crystalline product (**8**) which upon de-esterification with methanolic ammonia at 0° gave, among other products, the known (23, 24) crystalline 2,2′-anhydro-[1-(β-D-arabinofuranosyl)uracil] (**9**). Alternatively, catalytic de-esterification of **7** under controlled conditions gave crystalline 2,2′-anhydro-[1-(β-D-arabinofuranosyl)-5-bromouracil] (**10**). Treatment of **9** with NBS led to a complex mixture of products, that contained minor amounts of **10**. Investigation of the mother liquors from the reaction product of **6** with NBS, revealed the presence of further quantities of **7** and at least three other products. The identities of some of these are discussed in the subsequent paper (19).

The somewhat unexpected behavior of **6**, compared to **1**, indicated a strong influence of substituents on the nature of products. Based on our previous experiences (26) with the effect of

Can. J. Chem. Downloaded from www.nrcresearchpress.com by 210.87.254.105 on 09/05/12
For personal use only.

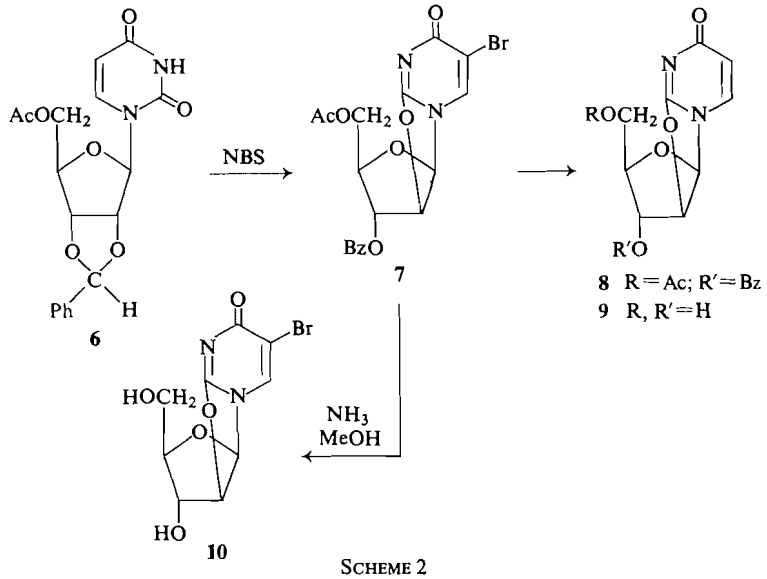

SCHEME 2

substituents, it was of interest to study the effect of a non-participating function at C-5′. Methylation of **1** with methyl iodide in *N*,*N*-dimethylformamide, in the presence of sodium hydride gave the corresponding *N*,*O*-dimethyl analog **11** as a chromatographically homogeneous syrup, having the expected n.m.r. spectral characteristics (Scheme 3).

Treatment of **11** with NBS in a mixture of carbon tetrachloride and 1,1,2,2-tetrachloroethane at 85–90° for 2.5 h afforded a crystalline product in 65% yield. Based on mass spectral

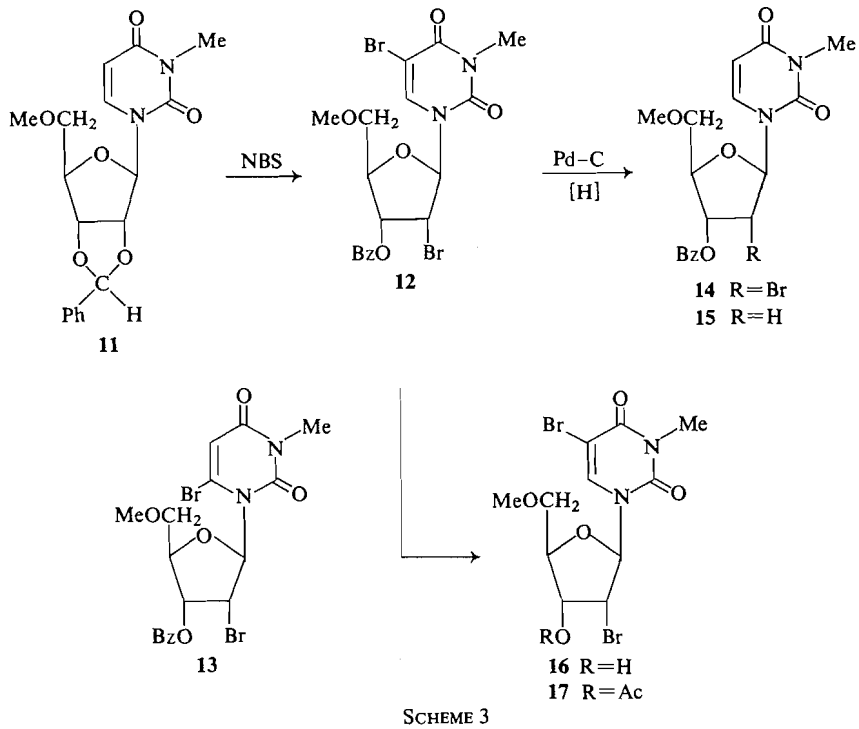

SCHEME 3

Can. J. Chem. Downloaded from www.nrcresearchpress.com by 210.87.254.105 on 09/05/12
For personal use only.

Can. J. Chem. Downloaded from www.nrcresearchpress.com by 210.87.254.105 on 09/05/12
For personal use only.

and n.m.r. data, the product was formulated as 3′-*O*-benzoyl-2′, 5-dibromo-2′-deoxy-3-*N*-methyl-5′-*O*-methyluridine (**12**) (1). This structure was also confirmed unambiguously by chemical means as shown here and in the following paper (19). Compound **12** could be obtained in two inconvertible crystalline forms, melting at 164–166° and 183–185°. Each form could be transformed into the other by recrystallization and nucleation. When equal amounts of each crystalline modification were co-crystallized, only the higher-melting form was obtained.

When the reaction of **11** with NBS was performed in the absence of 1,1,2,2-tetrachloroethane, or in concentrated solution, a second crystalline product, isomeric with **12**, was formed in low yield, in addition to **12**. Based on its mass spectrum and n.m.r. spectral data, its structure is assigned as 3′-*O*-benzoyl-2′,6-dibromo-2′-deoxy-3-*N*-methyl-5′-*O*-methyluridine (**13**). Halogenation of pyrimidines with *N*-halogenosuccinimides leads, in general, to the 5-halogeno derivatives and we are not aware of similar brominations in the 6-position of uridine derivatives. It appears that bromination in this position is a function of the effective concentration of bromine in the medium, since the formation of the 6-bromo derivative is observed principally in concentrated solutions or when the reaction is performed in carbon tetrachloride. In the latter solvent, the starting **11** is not very soluble and homogeneity is attained during the reaction. Attempts to increase the amount of **13** in the reaction of **11** with NBS were unsuccessful.

As in the other series, selective hydrogenolysis of the 5-bromo function was possible in the presence of 6% palladium-on-charcoal to give crystalline 3′-*O*-benzoyl-2′-bromo-2′-deoxy-3-*N*-methyl-5′-*O*-methyluridine (**14**) in 96% yield. Further hydrogenolysis in the presence of 20% palladium-on-charcoal afforded 3′-*O*-benzoyl-2′-deoxy-3-*N*-methyl-5′-*O*-methyluridine (**15**) as a chromatographically homogeneous syrup. Debenzoylation of **12** could be effected with methanolic ammonia or with sodium methoxide in methanol at 0° or higher temperature. A crystalline product **16** was obtained which upon benzoylation regenerated the starting benzoate **12**. Acetylation of **16** on the other hand, gave the crystalline acetate **17**. These experiments confirm the *cis*-relationship between the bromine and benzoate groups. A *trans*-relationship would have led to the formation of a 2′,3′-epoxide (or products derived from its opening). The formation of 2′-deoxy-3-*N*-methyl-5′-*O*-methyluridine derivatives, as shown by n.m.r. studies, combined with the indirect evidence for the disposition of the bromine atom in **12** and its transformation products, are in strong support of a D-*ribo* configuration. Conclusive proof and configurational interrelationships with other members of this series are discussed in the following paper (19).

Experimental

Melting points are uncorrected. The i.r. spectra were recorded with a Beckman IR-8 instrument. Optical rotations were measured with a Perkin–Elmer Model 141 polarimeter. The t.l.c. was performed on plates (20 cm length) coated with silica gel GF_{254} (Merck) and the spots were detected with a sulfuric acid spray and by u.v. visualization. Column chromatography was done on short columns containing silica gel GF_{254}, by application of a moderate suction. The n.m.r. spectra were measured on JEOL-4H-100 and 60 MHz instruments (s, singlet; d, doublet; t, triplet; m, multiplet; b, broad). Mass spectra were obtained on a Hitachi–Perkin–Elmer medium resolution mass spectrometer.

2′,3′-O-Benzylideneuridine (1)

A mixture of uridine (5.0 g) and anhydrous zinc chloride (7.5 g) in freshly distilled benzaldehyde (25 ml) was stirred at room temperature for 2 days. The clear mixture was diluted with ether. The precipitate was collected by decantation, it was dissolved in ethyl acetate, and washed with water. The organic layer was dried over anhydrous sodium sulfate and evaporated to a syrup which crystallized upon addition of ether. Recrystallization from ethyl acetate afforded pure material, 4.75 g (70%), m.p. 195–196°; reported m.p. 193–194°.

3′-O-Benzoyl-2′,5-dibromo-2′-deoxyuridine (2)

To a suspension of 2′,3′-*O*-benzylideneuridine (1.0 g) and barium carbonate (0.4 g) in 1,1,2,2-tetrachloroethane (50 ml) and carbon tetrachloride (10 ml) was added NBS (1.18 g). The mixture was stirred, while being heated at 85–90° (bath temperature), for 3 h. The hot solution was filtered and the filtrate was evaporated to dryness by co-distilling with toluene. The syrup (2.25 g) was dissolved in methylene chloride (70 ml) and washed with water (2 × 80 ml). The aqueous layer was re-extracted with ethyl acetate (70 ml). The methylene chloride layer was dried and evaporated to a small volume and allowed to crystallize in the refrigerator. The crystals were collected and the filtrate was evaporated to dryness. A minimum amount of chilled methylene chloride was added and, upon scratching, further crops of material were obtained. The combined crystals weighed 0.51 g and showed one spot on t.l.c. which moved slightly faster than the starting material (chloroform–methanol, 10:2, 20 cm plate). The mother liquor was evaporated to a syrup and triturated with ether and petroleum ether (b.p. 30–60°) to give a solid mass (0.88 g). The latter was passed through a column of silica gel and eluted with a mixture of methanol and chloroform (1:9). Fractions containing the desired compound were pooled together and evaporated to dryness. Crystallization from methylene chloride gave addi-

Can. J. Chem. Downloaded from www.nrcresearchpress.com by 210.87.254.105 on 09/05/12
For personal use only.

tional product (0.32 g). The total yield of **2** was 0.83 g (56%), m.p. 209–212°. Alternatively, the original methylene chloride extracts were evaporated to dryness and the resulting crystalline residue was suspended in 20 ml of chilled methylene chloride. The suspension was stirred with external cooling until the crystals were well dispersed. Filtration and washing gave an essentially chromatographically homogeneous product (0.56 g). Recrystallization from acetone afforded an analytical sample, m.p. 212–214°; $[\alpha]_D$ −85° (*c* 1.56, DMF); n.m.r. data (DMSO-d_6): τ −2.11 (NH, s); 1.43 (H-6, s); 3.65 (H-1′, d, $J_{1',2'} = 6.8$ Hz); 4.40 (H-3′, OH); 4.96 (H-2′, t, $J = 6.8$ Hz), etc.

Anal. Calcd. for $C_{16}H_{14}O_6N_2Br_2$: C, 39.30; H, 2.86; N, 5.71; Br, 32.65. Found: C, 39.31; H, 2.89; N, 5.86; Br, 32.83.

The ethyl acetate extract was evaporated to a syrup (0.16 g) which showed at least three spots on t.l.c. in addition to that corresponding to **2**. The major spot moved slower than the starting material. Owing to the low yields of these side products, their identities were not pursued.

*3′-O-Benzoyl-2′-bromo-2′-deoxyuridine (**3**)*

An amount of **2** (500 mg) was dissolved in warm methanol (90 ml) and the solution was allowed to cool before adding 6% palladium-on-charcoal (120 mg) and barium carbonate (300 mg). The stirred mixture was hydrogenated during 2 h at room temperature, it was then filtered and the filtrate was evaporated to a solid mass which was dissolved in methylene chloride. The solution was evaporated to a syrup (451 mg) which had a slightly slower chromatographic mobility than the starting material. Ethanol and ether were added and a trace of insoluble material was filtered. The filtrate was concentrated to dryness and triturated with ether to give crystals of **3** (395 mg, 94%), m.p. 175–178°. Recrystallization from absolute ethanol gave pure material, m.p. 179–181°; $[\alpha]_D$ −46.3° (*c* 1.43, DMF).

Anal. Calcd. for $C_{16}H_{15}O_6N_2Br$: C, 46.70; H, 3.65; N, 6.81; Br, 19.45. Found: C, 46.71; H, 3.70; N, 6.74; Br, 19.30.

*3′-O-Benzoyl-2′-deoxyuridine (**4**)*

The hydrogenation was carried out in the same manner as above using 20% palladium-on-charcoal. Conventional processing gave crystalline **4** (276 mg, 81.5%), m.p. 215–221°. Recrystallization from methanol–ethanol gave pure material, m.p. 225–226.5°; $[\alpha]_D$ −27.7° (*c* 0.75, DMF). The n.m.r. data (DMSO-d_6): τ −1.40 (N-H, b); 3.70 (H-1′, τ, $J \simeq 6.8$ Hz), etc.

Anal. Calcd. for $C_{16}H_{16}O_6N_2$: C, 57.80; H, 4.82; N, 8.43. Found: C, 57.39; H, 4.86; N, 8.26.

*2′-Deoxyuridine (**5**)*

3′-*O*-Benzoyl-2′-deoxyuridine (100 mg) was dissolved in anhydrous methanolic ammonia (7 ml) and the solution was allowed to stand in the cold overnight. Evaporation to dryness below 20° (bath temperature) followed by addition of methanol and repeated evaporation afforded a syrup. Crystallization and recrystallization from absolute ethanol gave the title compound (55 mg, 80%), m.p. 158–161°. The m.p. was not depressed upon admixture with authentic 2′-deoxyuridine.[3]

*5′-O-Acetyl-2′,3′-O-benzylideneuridine (**6**)*

A mixture of acetic anhydride (8 ml) and 2′,3′-*O*-benzylideneuridine (1.0 g) in dry pyridine (10 ml) was allowed to stand at room temperature for 5 h. The mixture was processed in the usual manner to give a syrup (1.1 g) which was relatively homogeneous on t.l.c. (chloroform–methanol, 10:1) and gave a satisfactory n.m.r. spectrum. It was used for subsequent steps without purification.

*2,2′-Anhydro-[1-(5′-O-acetyl-3′-O-benzoyl-β-D-arabinofuranosyl)-5-bromouracil] (**7**)*

To a suspension of 5′-*O*-acetyl-2′,3′-*O*-benzylideneuridine (1.1 g) and barium carbonate (0.4 g) in carbon tetrachloride (40 ml) and 1,1,2,2-tetrachloroethane (10 ml) was added NBS (1.2 g). The mixture was heated at reflux, with vigorous stirring, for 2.5 h. It was worked-up in the usual manner to give a syrup. Anhydrous ether was added and solids were collected (1.38 g). Crystallization from acetone–ether gave the title compound (0.42 g). Examination of the mother liquor on t.l.c. ($CHCl_3$—MeOH, 9:1) revealed two components, the anhydro derivative (**7**) and a faster-moving spot. Chromatographic separation (silica gel) gave additional material (0.25 g). The total isolated yield of the title product was 0.67 g (50%), m.p. 212–218°. Recrystallization from acetone afforded pure material, m.p. 220–220.5°; $[\alpha]_D$ −116° (*c* 2.27, DMF). The n.m.r. data (DMSO-d_6): τ 1.41 (H-6, s); 3.45 (H-1′, d, $J = 6$ Hz); (H-2′, d, $J_{2',1'} = 6.0$ Hz); 4.36 (H-3′, bs), etc; M^+ 450, 452 (bromine isotopes).

Anal. Calcd. for $C_{18}H_{15}O_7N_2Br$: C, 47.80; H, 3.32; N, 6.20; Br, 17.70. Found: C, 47.83; H, 3.35; N, 6.17; Br, 17.88. The faster-moving spot contained at least two compounds. One of the products was identified as 5′-*O*-acetyl-3′-*O*-benzoyl-2′,5-dibromo-2′-deoxyuridine, m.p. 198–203° by comparison with an authentic sample.

*2,2′-Anhydro-[1-(5′-O-acetyl-3′-O-benzoyl-β-D-arabinofuranosyl)uracil] (**8**)*

Compound **7** (0.5 g) was heated in methanol (90 ml) until solution was attained. The solution was allowed to cool before adding 20% palladium-on-charcoal (0.12 g) and barium carbonate (0.3 g) and the mixture was hydrogenated during 2.5 h at room temperature and processed in the usual way to give a syrup. Trituration with absolute ethanol gave crystalline **8** (0.39 g, 94.5%), m.p. 239–243°. Recrystallization from 50% ethanol afforded pure material, m.p. 240–243° (dec.); $[\alpha]_D$ −104.5° (*c* 1.34, DMF). The n.m.r. data (DMSO-d_6): τ 3.49 (H-1′, d, $J_{1',2'} = 6.0$ Hz); 4.10 (H-5, d, $J_{5,6} = 6.8$ Hz); 4.25 (H-2′, d, $J_{2',1'} = 6.0$ Hz); 4.4 (H-3′, bs), etc.

*2,2′-Anhydro-[1-(β-D-arabinofuranosyl)uracil] (**9**)*

Compound **8** (280 mg) was dissolved in anhydrous methanolic ammonia (25 ml) and the solution was allowed to stand at 3° overnight. The solution was processed as usual to give a syrup (272 mg). Addition of absolute ethanol and scratching gave colorless crystals which were recrystallized from the same solvent; yield 105 mg (62%), m.p. 235–238° (dec.). An authentic sample[4] melted at 238–241° (dec.), mixed m.p. 235–241° (dec.).

*2,2′-Anhydro-[1-(β-D-arabinofuranosyl)-5-bromouracil] (**10**)*

The anhydronucleoside derivative **7** (200 mg) was deacetylated with anhydrous methanolic ammonia (10 ml) in the usual manner to give a syrup. Crystallization from absolute ethanol yielded the title compound (80 mg, 59%), m.p. 166–175°. Recrystallization from absolute ethanol

[3]Purchased from Raylo Chemical Company, Edmonton, Alberta.

[4]We thank Dr. J. J. Fox for a sample of this compound.

Can. J. Chem. Downloaded from www.nrcresearchpress.com by 210.87.254.105 on 09/05/12
For personal use only.

afforded pure material, m.p. 195° (dec.); $[\alpha]_D$ 20.7° (*c* 1.17, DMF); M^+ 304, 306 (bromine isotopes).

*2',3'-O-Benzylidene-3-N-methyl-5'-O-methyluridine (**11**)*

Sodium hydride (1.0 g) was added to a cooled solution of 2',3'-*O*-benzylideneuridine (2.0 g) in DMF (30 ml) and the suspension was stirred for 10 min before the addition of methyl iodide (4 ml) at 0°. The reaction mixture was stirred at room temperature overnight and methanol was added gradually to destroy the excess sodium hydride. When the effervescence had ceased, the solution was concentrated to dryness, the residue was partitioned between methylene chloride (200 ml) and water (200 ml), the organic layer was separated and was washed with water (2 × 100 ml). The solution was dried, then it was evaporated to a syrup (2.12 g) which was homogeneous on t.l.c. and showed a satisfactory n.m.r. spectrum (in $CDCl_3$). This product was used for subsequent steps without purification.

*3'-O-Benzoyl-2'-deoxy-2',5-dibromo-3-N-methyl-5'-O-methyluridine (**12**)*

(a) Using 1,1,2,2-Tetrachloroethane and Carbon Tetrachloride as Solvents

To a solution of 2',3'-*O*-benzylidene-5'-*O*-methyl-N^3-methyluridine (2.12 g) in carbon tetrachloride (80 ml) and 1,1,2,2-tetrachloroethane (20 ml) was added barium carbonate (0.8 g) and NBS (2.36 g). The mixture was heated to reflux, while being vigorously stirred for 2.5 h. It was worked-up as usual to give a solid which was crystallized from anhydrous ether to give the title compound (1.87 g). The mother liquor (0.78 g) was chromatographed on a column containing silica gel. Fractions containing the desired product **12** were pooled together and evaporated to a syrup (0.25 g) which crystallized from anhydrous ether to give additional material (0.15 g). The total yield of **12** was 2.02 g (65%), m.p. 160–162°. Recrystallization from methanol with minimum heating afforded pure material, m.p. 164–166°; $[\alpha]_D$ −78° (*c* 2.02, $CHCl_3$). Recrystallization of this product from hot methanol gave the title product in another crystalline form, m.p. 183–185°; $[\alpha]_D$ −81° (*c* 1.86, $CHCl_3$). The lower melting form could be transformed into higher melting form and vice versa by recrystallization and seeding. When equal amounts of the two forms were mixed and crystallized, only the higher melting form was obtained. The n.m.r. data (in $CDCl_3$), τ 1.64 (H-6, s), 3.47 (H-1', d, $J_{1',2'} = 6.0$ Hz); 4.52 (H-3', $J_{3',4'} = 3.0$, $J_{3',2'} = 5.3$ Hz); 5.35 (H-2', $J_{2',3'} = 5.3$, $J_{2',1'} = 6.0$ Hz); 6.45, 6.56 (*O*,N^3-dimethyl protons); M^+ 518.

Anal. Calcd. for $C_{18}H_{18}O_6N_2Br_2$: C, 41.70; H, 3.48; N, 5.41; Br, 30.85. Found: C, 42.10; H, 3.55; N, 5.43; Br, 30.68.

(b) In the Absence of 1,1,2,2-Tetrachloroethane

This experiment was similar to that described in (*a*), except only 25 ml of carbon tetrachloride was used. The reaction was processed as usual to give a syrup which showed two major components on t.l.c. The n.m.r. spectrum of the crude mixture indicated the presence of the title compound and another isomeric compound. After crystallization and chromatographic separation of the mother liquors, the 5-bromo derivative **12** was obtained in 45% yield, m.p. 160–162°. Fractions containing the slower-moving component crystallized and the crystals were collected, washed with cold ether and dried. The n.m.r. spectrum was in accord with the structure of 3'-*O*-benzoyl-2'-bromo-2'-deoxy-2',-6-dibromo-3-*N*-methyl-5'-*O*-methyluridine (**13**), m.p. 159–162°; n.m.r. data: τ 3.62 (H-5, s); 3.79 (H-1', d, $J_{1',2'} = 7.2$ Hz); 4.52 (H-3', q, $J_{3',2'} = 7.0$, $J_{3',4'} = 4.5$ Hz); 5.23 (H-2', t, $J_{2',1'} = 7.2$, $J_{2',3'} = 7.0$ Hz); M^+ 518.

*3'-O-Benzoyl-2'-bromo-2'-deoxy-3-N-methyl-5'-O-methyluridine (**14**)*

The nucleoside derivative **12** (500 mg) was warmed in methanol (90 ml) until solution was attained. The solution was allowed to cool before adding 6% palladium-on-charcoal (120 mg) and barium carbonate (300 mg) and the mixture was hydrogenated during 2 h at room temperature, then it was processed as usual to give a syrup (478 mg) which crystallized upon standing. Trituration with cold absolute ethanol gave the title compound (401 mg, 96%), m.p. 117–122°. Recrystallization from the same solvent afforded pure material, m.p. 123–126°; $[\alpha]_D$ −59.2° (*c* 1.55, $CHCl_3$); n.m.r. ($CDCl_3$): τ 2.60 (H-6, d, $J_{6,5} = 8.0$ Hz); 3.73 (H-1', d, $J_{1',2'} = 7.0$ Hz); 4.40 (H-5, d, $J_{5,6} = 8.0$ Hz); 4.73 (H-3', t); 5.60 (H-2', d, $J_{2',1'} = 7.0$ Hz), etc.

Anal. Calcd. for $C_{18}H_{19}O_6N_2Br$: C, 49.25; H, 4.33; N, 6.38; Br, 18.22. Found: C, 48.84; H, 4.31; N, 6.21; Br, 18.11.

*3'-O-Benzoyl-2'-deoxy-3-N-methyl-5'-O-methyluridine (**15**)*

The hydrogenation was carried out in the same manner as above except using 20% palladium-on-charcoal. The solution was processed as usual to give a syrup which was relatively homogeneous on t.l.c. (chloroform–ethyl acetate, 4:1). Ethanol–ether was added, a trace of insoluble material was filtered, and the filtrate was evaporated to give a syrup (300 mg, 86%). A small sample was purified by preparative t.l.c., $[\alpha]_D$ −31.1° (*c* 3.39, $CHCl_3$); n.m.r. ($CDCl_3$): τ 2.23 (H-6, d, $J_{6,5} = 8.0$ Hz); 3.50 (H-1', $J = 6.0, 8.0$ Hz); 4.20 (H-5, d, $J_{5,6} = 8.0$ Hz); 7.60 (H-2', m), etc.

*Debenzoylation of 3'-O-benzoyl-2'-deoxy-2',-5-dibromo-3-N-methyl-5'-O-methyluridine (**12**)*

Compound **12** was stirred in anhydrous methanolic ammonia (10 ml) until a homogeneous solution was obtained. The resulting solution was allowed to stand at room temperature for 4 h, then it was worked-up in the usual manner to give a syrup (500 mg). A sample of the product was purified by preparative t.l.c. to give a syrup that crystallized upon standing. Cold absolute ethanol was added, the crystals were collected and recrystallized from the same solvent to afford 2'-bromo-2'-deoxy-5'-*O*-methyl-5-bromo-N^3-methyluridine (**16**), 135–136°; $[\alpha]_D$ −33° (*c* 1.44, $CHCl_3$). The same product was obtained when the debenzoylation was carried out with sodium methoxide in methanol.

*3'-O-Acetyl-2'-deoxy-2',5-dibromo-3-N-methyl-5'-O-methyluridine (**17**)*

A mixture of acetic anhydride (2 ml) and crude **16** (212 mg) in pyridine (2 ml) and methylene chloride (5 ml) was kept at 3° overnight. The solution was processed as usual to give a syrup which crystallized upon standing. Cold ethanol was added and crystals were collected (150 mg), m.p. 162–166°. Recrystallization from the same solvent afforded pure material, m.p. 167–168°; $[\alpha]_D$ −26.4° (*c* 1.65, $CHCl_3$).

Anal. Calcd. for $C_{13}H_{16}O_6N_2Br_2$: C, 34.20; H, 3.51; N, 6.14; Br, 35.10. Found: C, 34.42; H, 3.57; N, 6.25; Br, 34.54.

1. M. M. PONPIPOM and S. HANESSIAN. Carbohydr. Res. **17**, 248 (1971).

2. S. HANESSIAN and N. R. PLESSAS. J. Org. Chem. **34**, 1035 (1969) and earlier papers.
3. S. HANESSIAN and N. R. PLESSAS. J. Org. Chem. **34**, 1045 (1969).
4. H. E. KAUFMAN and E. D. MALONEY. Proc. Soc. Exptl. Biol. and Med. **112**, 4 (1963).
5. D. M. BROWN, D. B. PARIHAR, and A. R. TODD. J. Chem. Soc. 4242 (1958).
6. T. NAITO, M. HIRATA, Y. NAKAI, T. KOBAYASHI, and M. KANAO. Chem. Pharm. Bull. (Tokyo), **16**, 285 (1968).
7. J. F. CODINGTON, I. L. DOERR, and J. J. FOX. J. Org. Chem. **29**, 558 (1964); J. F. CODINGTON, I. DOERR, D. VAN PRAAG, A. BENDICH, and J. J. FOX. J. Am. Chem. Soc. **83**, 5030 (1961).
8. J. F. CODINGTON, I. L. DOERR, and J. J. FOX. J. Org. Chem. **29**, 564 (1964).
9. D. M. BROWN, D. B. PARIHAR, C. B. REESE, and A. R. TODD. J. Chem. Soc. 3035 (1958).
10. J. P. HORWITZ, J. CHUA, M. A. DAROOGE, M. NOEL, and J. L. LUNDT. J. Org. Chem. **31**, 205 (1966).
11. C. D. ANDERSON, L. GOODMAN, and B. R. BAKER. J. Am. Chem. Soc. **81**, 898 (1959).
12. J. P. H. VERHEYDEN and J. G. MOFFATT. J. Org. Chem. **35**, 2319, 2868 (1970); J. Am. Chem. Soc. **86**, 2093 (1964).
13. K. HAGA, M. YOSHIKAWA, and T. KATO. Bull. Chem. Soc. Jap. **43**, 3922 (1970).
14. M. M. PONPIPOM and S. HANESSIAN. Carbohydr. Res. **18**, 342 (1971).
15. R. F. DODS and J. S. ROTH. J. Org. Chem. **34**, 1627 (1969); Tetrahedron Lett. 165 (1969).
16. K. KIKUGAWA and M. ICHINO. Tetrahedron Lett. 87 (1970).
17. S. HANESSIAN and N. R. PLESSAS. J. Org. Chem. **34**, 2163 (1969); Chem. Commun. 1152 (1967).
18. N. BAGGETT, A. B. FOSTER, J. M. WEBBER, D. LIPKIN, and B. E. PHILLIPS. Chem. Ind. 136 (1965); J. M. GULLAND and H. SMITH. J. Chem. Soc. 338 (1947).
19. M. M. PONPIPOM and S. HANESSIAN. Can. J. Chem. This issue.
20. W. PEARLMAN. Tetrahedron Lett. 1663 (1967).
21. C. A. DEKKER and A. R. TODD. Nat. **166**, 157 (1960).
22. K. OKADA, M. ICHINO, Y. ARAKI, and S. FURUE. Jap. pat. 27, 809 (1969); Chem. Abstr. **72**, 448 (1970).
23. A. HAMPTON and A. W. NICHOL. Biochem. **5**, 2076 (1966).
24. J. J. FOX and I. WEMPEN. Tetrahedron Lett. 643 (1965).
25. A. M. MICHELSON and A. R. TODD. J. Chem. Soc. 2476 (1949).
26. S. HANESSIAN and N. R. PLESSAS. J. Org. Chem. **34**, 1053 (1969).

Can. J. Chem. Downloaded from www.nrcresearchpress.com by 210.87.254.105 on 09/05/12
For personal use only.

The Reaction of *O*-Benzylidene Sugars with *N*-Bromosuccinimide. VII. Stereochemical and Mechanistic Aspects in the Pyrimidine Nucleoside Series[1]

M. M. PONPIPOM[2] AND S. HANESSIAN

Department of Chemistry, University of Montreal, Montreal, Quebec

Received June 24, 1971

The reaction of 2′,3′-*O*-benzylideneuridine with *N*-bromosuccinimide (NBS) leads to 3′-*O*-benzoyl-2′,5-dibromouridine. The stereoselectivity of bromination in the sugar ring can be explained by invoking the sequential formation of benzoxonium ion and 2,2′-anhydronucleoside intermediates. Protonation of the appropriate 2,2′-anhydronucleoside, followed by treatment with NBS, recreates the conditions which prevail in the original reaction of the benzylidene acetal with NBS.

La réaction de la 2′,3′-*O*-benzylideneuridine avec la *N*-bromosuccinimide (NBS) conduit à la 3-*O*-benzoyl-2′,5-dibromouridine. La stéréosélectivité de la bromuration sur le reste hydrate de carbone peut être expliquée en invoquant la formation successive de l'ion benzoxonium et du 2,2′-anhydronucléoside comme intermédiaires. La protonation du 2,2′-anhydronucléoside approprié suivi du traitement par la NBS reconstituent les conditions existantes dans la réaction initiale de l'acétal benzylidénique sous la NBS.

Canadian Journal of Chemistry, **50**, 253 (1972)

Can. J. Chem. Downloaded from www.nrcresearchpress.com by 210.87.254.105 on 09/05/12
For personal use only.

In the preceding paper (1), it was shown that the reaction of 2′,3′-*O*-benzylideneuridine (**1**) (2) and the corresponding 3-*N*-5′-*O*-dimethyl analog (**2**) underwent bromination with *N*-bromosuccinimide (NBS), to give crystalline nucleoside derivatives, in which bromine atoms were incorporated in the 5- and 2′-positions stereoselectively (Scheme 1). Under essentially the same reaction conditions, the 5′-acetate derivative **5** afforded the 2,2′-anhydro analog **6**, with a bromine atom in the C-5 position only. Having established (1) that the bromine atom in the sugar portion of the nucleoside derivatives **3** and **4** was situated in the 2′-position, by catalytic reduction to the corresponding 2′-deoxyuridine derivatives, there remained to ascertain the stereochemical orientation of the bromine atom at this position in these products. The aim of this paper is to elucidate the stereochemistry of these halogenated nucleosides, to demonstrate their interrelations, and to discuss the mechanistic aspects involved in the stereoselective ring opening of the benzylidene acetal with concomitant bromination.

As part of their extensive researches on the chemical modification of pyrimidine nucleosides, Fox and coworkers (3, 4) have prepared several 2′-deoxy-2′-halogenouridines, by the opening of 2,2′-anhydro-[1-(β-D-arabinofuranosyl)uracil] (**7**) with the appropriate hydrogen halide (Scheme 2). Debenzoylation of the partially reduced derivative **8** (1) with methanolic ammonia, under controlled conditions, afforded

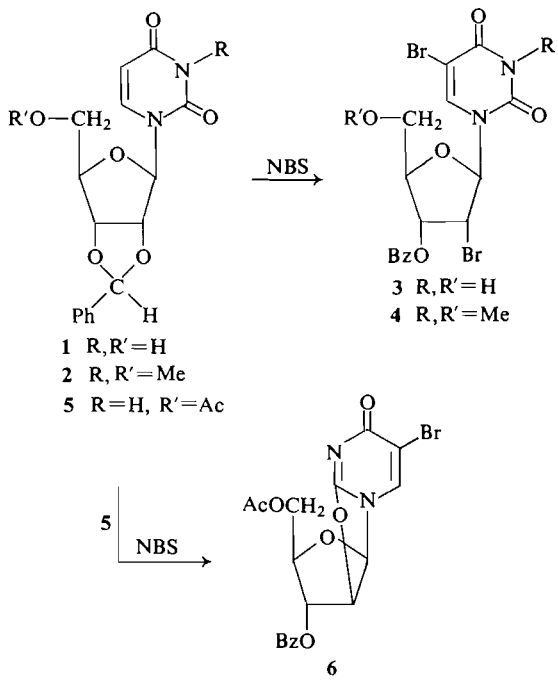

1 R,R′=H
2 R,R′=Me
3 R,R′=H
4 R,R′=Me
5 R=H, R′=Ac
6

SCHEME 1

[1]For Part VI, see preceding paper, ref. 1.
[2]NRCC Postdoctorate Fellow, 1970–1971.

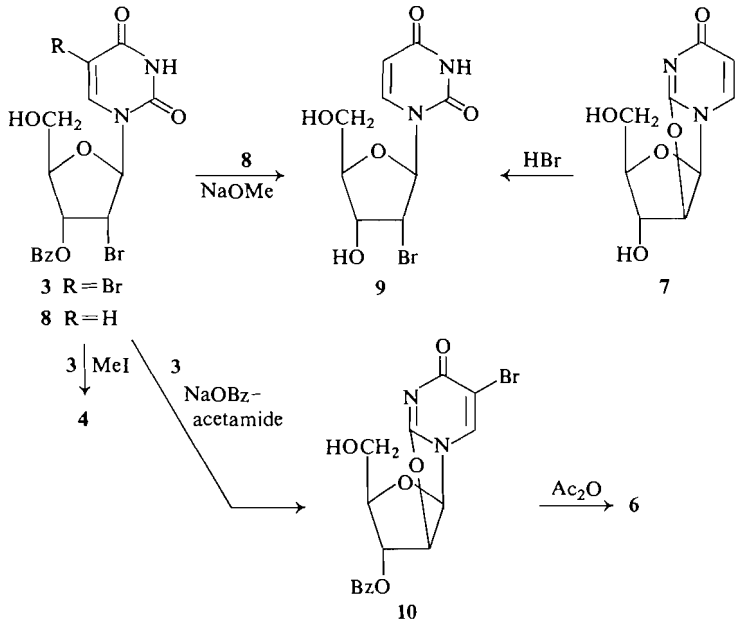

SCHEME 2

the known 2′-bromo-2′-deoxyuridine **9** (3). Since the conditions for the formation of **9** from **8** preclude any secondary transformations, it can be unambiguously established that the preponderant crystalline product isolated from the reaction of **1** with NBS (1) has the D-*ribo* configuration (structure **3**). The stereochemical assignment of the product resulting from the reaction of **2** with NBS was accomplished by controlled *N*,*O*-methylation of **3** (now of established configuration) with methyl iodide and sodium hydride in *N*,*N*-dimethylformamide. The reaction led to a mixture of products, from which the desired product was separated by preparative t.l.c., to give crystalline material identical with **4**, as obtained from the reaction of **2** with NBS. The stereochemical identity of compound **3**, hence that of **4**, was also confirmed by another route. It was shown in the preceding paper (1) that the 2,2′-anhydro derivative **6** could be transformed into **7**, thereby confirming its structure. Treatment of **3** with sodium benzoate in molten acetamide (5) gave a 67% yield of a crystalline product, that corresponded to the expected 2,2′-anhydro [1-(3′-*O*-benzoyl-β-D-arabinofuranosyl)-5-bromouracil] (**10**). Acetylation of this product afforded a crystalline product, identical with **6**. The transformation illustrated in Scheme 2 shows beyond doubt the stereochemical identities and interrelationships of compounds **3**, **4**, and **6**.

In previous papers in this series, the mechanism of the ring-opening reaction of *O*-benzylidene acetals with NBS was discussed in detail (6–8). The available data support the transformation of the benzylidene acetal, presumably via an α-bromo intermediate, into a benzoxonium ion and bromide ion. The latter attacks the oxonium ion at the two possible sites, depending on the nature of the positions involved, which leads to the attachment of a bromine atom and a benzoate group on the ring carbon atoms bearing the acetal function.

In the methyl 2,3-*O*-benzylidene-β-D-ribofuranoside series, which in our initial studies represented the simplest model for eventual applications to nucleoside analogs, the nature of the products resulting from the reaction with NBS was influenced by the type of substituent at C-5 (8). In the absence of a participating group, as in the case of the 5-*O*-methyl derivative, the products were a mixture of 2-bromo and 3-bromo derivatives, resulting from an attack of bromide ion on the intermediate 2,3-benzoxonium ion. In the presence of a participating group, as in the 5-*O*-benzoyl deriva-

Can. J. Chem. Downloaded from www.nrcresearchpress.com by 210.87.254.105 on 09/05/12
For personal use only.

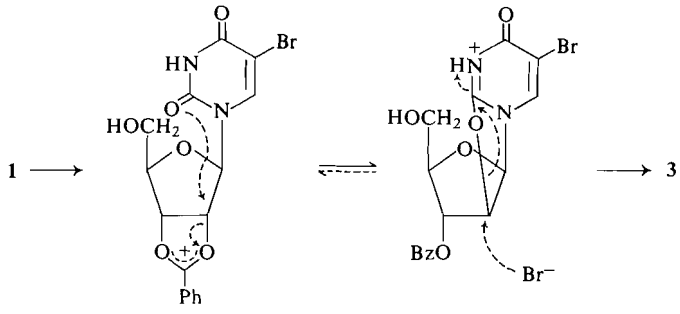

SCHEME 3

tive, the major product was a 5-bromo derivative, resulting from a participation by the C-5 benzoate group, to give a rearranged benzoxonium ion, spanning C-5 and -3, that was subsequently attacked by bromide ion.

The intermediacy of 2′,3′-benzoxonium ions in the reaction of 2′,3′-*O*-benzylidene nucleosides such as **1**, with NBS, presents some intriguing mechanistic implications (9) and important synthetic possibilities. In the intermediate benzoxonium ion **11** (Scheme 3), attack at C-2′ and/or C-3′ can occur by the external nucleophile in the medium, namely bromide ion, to give the corresponding products (D-*arabino*, D-*xylo* configurations). Since it was previously established (1) that the bromine atom was situated at the 2′-position, the mechanistic relevance of the reaction will be focused on the mode of formation of the 2′-bromonucleosides, and more explicitly compound **3**. Another mechanistic consideration is the internal attack on the benzoxonium ion **11** by the C-2 oxygen function, as has been shown in numerous cases involving solvolyses of C-2′ sulfonate esters and related nucleoside derivatives (9–11), which leads to the 2,2′-anhydro intermediate **12**. The preponderant formation of compound **3** can be satisfactorily explained by invoking a 2,2′-anhydro intermediate, that undergoes nucleophilic attack by bromide ion at C-2′. It is also possible that small amounts of the other products (D-*xylo*, D-*arabino* configurations) might be present in the crude reaction product. It is of interest that previously recorded examples, in which the transitory formation of benzoxonium ions was postulated, dealt with fully substituted nucleoside derivatives (9). The successful application of the acetal ring-opening reaction in the pyrimidine nucleoside series is perhaps reflective of the reactivity of the benzoxonium ion and the enhanced participating ability of the C-2 oxygen function, leading to conformationally rigid anhydro intermediates.

The researches of Fox and coworkers (5, 9) have shown that nucleophilic displacements of 2,2′-anhydronucleosides and 2-sulfonates of pyrimidine ribonucleosides are facilitated by adding to the reaction mixture 1 equiv of benzoic acid, which effects protonation of the 3-*N* atom, thus rendering the 2,2′-anhydro ring more labile. Displacement of such "primed" intermediates by nucleophiles in anhydrous media, occurs with overall retention of configuration at C-2′. From a consideration of the mechanistic pathways shown in Scheme 3, it can be seen that the 2,2′-anhydro intermediate **12** generated during the reaction is in fact protonated and the formation of a product having the D-*ribo* configuration as a result of an attack by bromide ion would be fully expected. Conclusive evidence for these mechanistic considerations was obtained in the following manner. Treatment of **3** with sodium benzoate in molten acetamide (9) gave crystalline 2,2′-anhydro-[1-(3′-*O*-benzoyl-β-D-arabinofuranosyl-5-bromouracil] (**10**). The latter was treated with 1 equiv of methane-

Can. J. Chem. Downloaded from www.nrcresearchpress.com by 210.87.254.105 on 09/05/12
For personal use only.

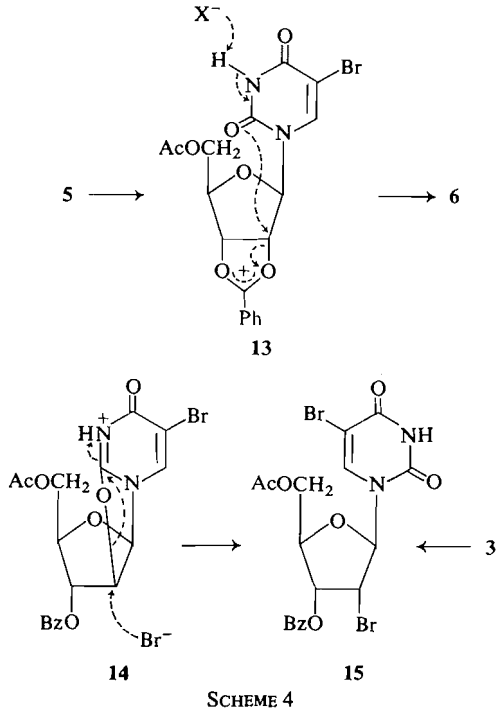

SCHEME 4

sulfonic acid (12) in a mixture of carbon tetrachloride and tetrachloroethane, followed by NBS and the mixture was heated at 80° as in the previous case. A 95% yield of compound **3** was obtained, with no trace of side-products. In the absence of added acid, negligible reaction took place (Scheme 3).

The formation of 2,2′-anhydro-[1-(5′-*O*-acetyl-3′-*O*-benzoyl-β-D-arabinofuranosyl)-5-bromouracil] (**6**), as a preponderant product in the reaction of **5** with NBS, accentuates the influence of subtle structural modifications, on the mechanistic pathway of the reaction (Scheme 4). It is evident that intramolecular attack of the carbonyl oxygen atom in the benzoxonium ion intermediate **13** is favored, but in this case, the protonated 2,2′-anhydro intermediate **14** is deprotonated to give the observed product. The operation of this process, in preference to an attack by bromide ion is particular to this derivative only, although the presence of a small amount of the expected D-*ribo* nucleoside **15** among the reaction products was ascertained from an investigation of the mother liquors of crystallization. The mechanistic aspects of its formation were verified by "priming" the 3-*N* position with methanesulfonic acid, then subjecting the protonated intermediate **14** to the conditions of the bromination reaction. This led to the formation of **15** in 90% yield. Although the "priming" experiment recreates the activated protonated intermediate that is presumably present in the original reaction, it can be seen that the product distribution is different in both cases (compare **6** and **15**). A plausible explanation can be offered at this time, although a detailed study involving appropriate substrates would be eventually desirable. It is conceivable that compound **13** is deprotonated by an anionic species X^- (X = Br, succinimidyl anion) *prior* to intramolecular participation by the carbonyl group, and that such a participation is done in a concerted fashion (Scheme 4). The results of the "priming" experiments clearly show that once the protonated 2,2′-anhydro intermediate **14** is formed, it will be attacked by bromide ion to give **15**, rather than being deprotonated to give **6**. Another aspect worthy of consideration is the relative concentrations of the intermediate **14** in solution, with respect to bromide ion when comparing the results of the transformation **5** → **6** (via NBS) and **6** → **15** (via $MeSO_3H$, NBS). In the latter case the substrate is available entirely in its activated form, while in the former case, the relative concentration of **14** in solution at any interval is low. To what extent the C-5 substituent influences the course of the reaction cannot be answered at the present time. The identity of compound **15** was also substantiated by an independent synthesis from **3** by simple acetylation.

The stereoselectivity of the bromination reaction in the series discussed in this paper is most pronounced in the case of the 3-*N*-5′-*O*-dimethyl analog **2**, as reflected in the isolation of the corresponding C-2′ bromo derivative **4** in 65% yield. The intermediate benzoxonium ion is presumably transformed into the 2,2′-anhydro intermediate which undergoes attack by bromide ion to give the observed product. The presence of the 3-*N*-methyl group thus provides only one possible pathway for termination. Any hindering effect by the C-5′ substituent, in preventing intramolecular participation in this case, is overcome by the highly activated nature of the benzoxonium ion intermediate and the enhanced participating ability of the C-2 oxygen function.

Can. J. Chem. Downloaded from www.nrcresearchpress.com by 210.87.254.105 on 09/05/12
For personal use only.

Can. J. Chem. Downloaded from www.nrcresearchpress.com by 210.87.254.105 on 09/05/12
For personal use only.

Experimental

Melting points are uncorrected. The i.r. spectra were recorded with a Beckman IR-8 instrument. Optical rotations were measured with a Perkin–Elmer Model 141 polarimeter. The t.l.c. was performed on plates (20 cm length) coated with silica gel GF_{254} (Merck) and the spots were detected with a sulfuric acid spray and by u.v. visualization. Column chromatography was done on short columns containing silica gel GF_{254}, by application of a moderate suction. The n.m.r. spectra were measured on a JEOL-4H-100 and 60 MHz instruments (s, singlet; d, doublet; t, triplet; m, multiplet; b, broad).

*2′-Bromo-2′-deoxyuridine (**3**)*

3′-*O*-Benzoyl-2′-bromo-2′-deoxyuridine (250 mg) (1) was dissolved in cold anhydrous methanolic ammonia (7 ml) and the solution was allowed to stand at 3° for 4 h. Examination of the reaction mixture on t.l.c. (chloroform–methanol, 10:3) revealed two major components in addition to two minor slow-moving components. The solution was concentrated *in vacuo* below 20° (bath temperature). Methanol was added and distilled off several times to remove all ammonia and the mixture was separated by preparative t.l.c. The spot having highest R_f was shown to be the starting material, m.p. 177–181°; mixed m.p. 175–181°. The second spot crystallized upon standing. Recrystallization from water gave pure material, m.p. 182–186°. The m.p. was not depressed on a mixture with authentic 2′-bromo-2′-deoxyuridine[3] (m.p. 186–190°) and the two products had identical n.m.r. spectra and chromatographic mobility.

3′,5′-Di-O-benzoyl-2′-bromo-2′-deoxy-3-N-benzoyluridine

*(a) From 2′-Bromo-2′-deoxyuridine (**9**)*

To a solution of 2′-bromo-2′-deoxyuridine (**9**, 0.5 g) in dry pyridine (8 ml) and dry methylene chloride (8 ml) was added benzoyl chloride (2.5 ml) dropwise at 0°. The mixture was allowed to stand at 3° overnight, and then poured into ice-water. The product was extracted with methylene chloride and washed successively with cold 5% sulfuric acid, aqueous sodium bicarbonate, and then water. The organic layer was dried and evaporated to dryness by co-distilling with toluene. The residue was washed several times with petroleum ether (b.p. 30–60°), cold ether, and then a small amount of cold methanol. The final residue was triturated with petroleum ether to give a solid (0.75 g) which was purified by chromatography on a column containing silica gel using ethyl acetate – chloroform (1:5) as irrigating solvent. The title compound was obtained as a colorless syrup, $[\alpha]_D$ −15° (*c* 1.45, $CHCl_3$); n.m.r. data: τ 3.54 (H-1′, $J_{1',2'} = 5.2$ Hz); 4.21 (H-5, $J_{5,6} = 8.2$ Hz); 4.35 (H-3′, multiplet), etc.

*(b) From 3′-O-Benzoyl-2′-bromo-2′-deoxyuridine (**8**)*

To a solution of 3′-*O*-benzoyl-2′-bromo-2′-deoxyuridine (0.19 g) (1) in pyridine (2 ml) and methylene chloride (2 ml) was added benzoyl chloride (1 ml) at 0°. The reaction mixture was allowed to stand at 3° overnight, and then poured into ice-water. It was worked-up in the usual manner to yield a solid (150 mg) after chromatography. The product was identical to that obtained by the above described method *a*.

[3]A sample was provided by Dr. J. J. Fox, see ref. 3.

*2,2′-Anhydro-[1-(3′-O-benzoyl-β-D-arabinofuranosyl) 5-bromouracil] (**10**)*

A mixture of 3′-*O*-benzoyl-2′,5-dibromo-2′-deoxyuridine (**3**, 0.5 g), sodium benzoate (0.5 g), and acetamide (9.0 g) was heated to a melt. The solution was vigorously stirred, while heating at 100–105° (bath temperature) for 20 min. The hot solution was poured into cold water (250 ml) with stirring and the solution was extracted with ethyl acetate. The extracts were concentrated to a syrup which crystallized upon standing (1 g). A minimum amount of cold ethanol was added and the crystals were collected. Recrystallization from aqueous methanol gave pure material (0.28 g, 67%), m.p. 208–211°; $[\alpha]_D$ −124° (*c* 0.90, $CHCl_3$). The mother liquor contained an appreciable amount of the starting material (t.l.c.).

Anal. Calcd. for $C_{16}H_{13}O_6N_2Br$: C, 47.0; H, 3.18; N, 6.85; Br, 19.55. Found: C, 47.04; H, 3.26; N, 6.81; Br, 19.36.

*Ring Opening of 2,2′-Anhydro-[1-(3′-O-benzoyl-β-D-arabinofuranosyl) 5-Bromouracil] (**10**) with NBS*

(a) In the Absence of an Acid

To a suspension of the title compound **10** (0.1 g) and barium carbonate (0.04 g) in 1,1,2,2-tetrachloroethane (5 ml) and carbon tetrachloride (1 ml) was added NBS (0.118 g). The mixture was stirred, while heating at 85–90° (bath temperature), for 3 h. It was worked-up in the normal way to give a syrup which showed the presence of the starting material, and a fast moving component which had the same chromatographic mobility (chloroform–methanol, 15:1, multiple developments) as 3′-*O*-benzoyl-2′,5-dibromo-2′-deoxyuridine (1).

(b) In the Presence of Methanesulfonic Acid

To a suspension of the title compound **10** (0.1 g) in 1,1,2,2-tetrachloroethane (5 ml) and carbon tetrachloride (1 ml) was added methanesulfonic acid (0.0159 ml, made up in anhydrous ether) followed by NBS (0.118 g). The reaction mixture was stirred, while heating at 85–90° (bath temperature), for 3 h. The cooled solution was neutralized by stirring with anhydrous sodium carbonate. The solids were filtered and the filtrate was evaporated to dryness by co-distilling with toluene. The resulting syrup (196 mg) which showed traces of starting material was dissolved in chloroform and washed with water. The chloroform layer was dried and concentrated to dryness. Chilled methylene chloride was added and crystals were collected (0.11 g, 92%), m.p. 204–207°. Recrystallization from acetone afforded pure material, m.p. 209–212°; mixed m.p. 210–213° (with a sample obtained from **1**).

*5′-O-Acetyl-3′-O-benzoyl-2′,5-dibromo-2′-deoxyuridine (**15**)*

A mixture of acetic anhydride (5 ml) and 3′-*O*-benzoyl-2′,5-dibromo-2′-deoxyuridine (**3**, 500 mg) in pyridine (5 ml) and methylene chloride (10 ml) was kept overnight at 5°. The reaction mixture was poured into ice-water and the solution was extracted with methylene chloride and washed successively with water, aqueous sodium bicarbonate, and then water. The organic layer was dried and evaporated to give a crystalline mass which was triturated with anhydrous ether and filtered to give the title compound (486 mg). Recrystallization from acetone–methanol afforded pure material, m.p. 199–202°; $[\alpha]_D$ −84° (*c* 2.49, $CHCl_3$).

Anal. Calcd. for $C_{18}H_{16}O_7N_2Br_2$: C, 40.6; H, 3.0; N, 5.27; Br, 30.0. Found: C, 40.38; H, 3.04; N, 5.18; Br, 29.69.

Ring Opening of 2,2'-Anhydro-[1-(5'-O-acetyl-3'-O-benzoyl-β-D-arabinofuranosyl) 5-Bromouracil] (6) with NBS

(a) In the Absence of an Acid

To a suspension of the title compound (100 mg) and barium carbonate (40 mg) in carbon tetrachloride (4 ml) and 1,1,2,2-tetrachloroethane (1 ml) was added NBS (47.3 mg). The mixture was heated to reflux, while stirring, for 4.5 h. It was processed as usual to give a syrup which showed the presence of starting material and traces of a faster moving component that had the same chromatographic mobility (chloroform–methanol, 10:3) as 5'-*O*-acetyl-3'-*O*-benzoyl-2',5-dibromo-2'-deoxyuridine (**15**).

(b) In the Presence of Methanesulfonic Acid

To a suspension of the title compound (100 mg) in carbon tetrachloride (4 ml) and 1,1,2,2-tetrachloroethane (1 ml) was added methanesulfonic acid (0.0144 ml, made up in anhydrous ether) followed by NBS (120 mg). The solution was heated to reflux, while stirring, for 2.5 h. The cooled solution was neutralized by stirring with anhydrous sodium carbonate and the mixture was worked-up in the normal way to give a syrup which showed traces of starting material. Addition of absolute ethanol gave a crystalline product (105 mg, 89%), m.p. 196–199°. Recrystallization from acetone–methanol afforded pure material, m.p. 198–201°, identical with the desired product **15**.

N,O-Methylation of 3-O-Benzoyl-2',5-dibromo-2'-deoxyuridine (3)

Sodium hydride (10 mg) was added to a cooled solution containing 100 mg of the title compound **3** in DMF (5 ml). The suspension was stirred at 0° for 10 min and methyl iodide (0.25 ml) was added slowly. After the mixture was stirred at room temperature for 5 h, methylene chloride was added and the solution was washed with water. The organic layer was processed as usual to give a syrup that showed at least five discernible spots on t.l.c. The desired component was separated by preparative t.l.c. and it was crystallized from ether to give pure material (5 mg) identical with authentic **4**, m.p. 157–160° (1).

It is a pleasure to acknowledge the financial support obtained from the National Research Council of Canada.

1. M. M. PONPIPOM and S. HANESSIAN. Can. J. Chem. This issue.
2. N. BAGGETT, A. B. FOSTER, J. M. WEBBER, D. LIPKIN, and B. F. PHILLIPS. Chem. Ind. 136 (1965); J. M. GULLAND and H. SMITH. J. Chem. Soc. 338 (1947).
3. J. F. CODINGTON, I. L. DOERR, and J. J. FOX. J. Org. Chem. **29**, 558 (1964); J. F. CODINGTON, J. DOERR, D. VAN PRAAG, A. BENDICH, and J. J. FOX. J. Am. Chem. Soc. **83**, 5030 (1961).
4. J. F. CODINGTON, I. L. DOERR, and J. J. FOX. J. Org. Chem. **29**, 564 (1964).
5. J. J. FOX and N. C. MILLER. J. Org. Chem. **28**, 936 (1963).
6. S. HANESSIAN and N. R. PLESSAS. J. Org. Chem. **34**, 1035 (1969).
7. S. HANESSIAN and N. R. PLESSAS. J. Org. Chem. **34**, 1045 (1969).
8. S. HANESSIAN and N. R. PLESSAS. J. Org. Chem. **34**, 1053 (1969).
9. J. J. FOX and K. A. WATANABE. Chem. Pharm. Bull. (Tokyo), **17**, 211 (1969).
10. D. M. BROWN, D. B. PARIHAR, and A. R. TODD. J. Chem. Soc. 4242 (1958).
11. T. NAITO, M. HIRATA, Y. NAKAI, T. KOBAYASHI, and M. KANAO. Chem. Pharm. Bull. (Tokyo), **10**, 285 (1968).
12. N. C. YUNG, J. H. BURCHENAL, R. FECHER, R. DUCHINSKY, and J. J. FOX. J. Am. Chem. Soc. **83**, 4060 (1961).
13. K. KIKUGAWA, M. ICHINO, and T. UKITA. Chem. Pharm. Bull. (Tokyo), **17**, 785 (1969).
14. K. OKADA, M. ICHINO, Y. ARAKI, and S. FURUE. Jap. Pat. 27 809 (1969); Chem. Abstr. **72**, 448 (1970).

Can. J. Chem. Downloaded from www.nrcresearchpress.com by 210.87.254.105 on 09/05/12
For personal use only.

Molecular Rearrangements. Part I. The Thermal Rearrangement of the Benzyl Naphthyl Ethers

M. ZARIF A. BADR[1] AND H. A. H. EL-SHERIEF

Department of Chemistry, Faculty of Science, University of Assiut, Assiut, Egypt, U.A.R.

Received July 27, 1971

Heating benzyl-β-naphthyl ether at 260° for some days causes benzylic migration to the α-position, together with the formation of β-naphthol, toluene, dibenzyl, and 9-phenyl-1,2,7,8-dibenzoxanthene.

Benzyl-α-naphthyl ether rearranges under similar conditions to give 2- and 4-benzyl-1-naphthol, toluene, dibenzyl, and 9-phenyl-3,4,5,6-dibenzoxanthene.

Rearrangement of the benzyl-α-naphthyl ether in quinoline gives the normal products of the rearrangement together with 2- and 4-benzylquinolines and 2-quinolyl-1-hydroxynaphthalene. In phenol and in anisole, the rearrangement is accompanied by benzylation of the solvent.

It is concluded that the thermal rearrangement of the benzyl naphthyl ethers depends on a homolytic fission of the ether to benzyl and naphthyloxy radicals.

En chauffant l'éther de benzyl-β-naphtyl à 260° pendant plusieurs jours, il se produit une migration benzylique vers la position α, en même temps que la formation de β-naphtol, toluène, dibenzyle et de 9-phényl-1,2,7,8-dibenzoxanthène.

L'éther de benzyl-α-naphtyl se transpose sous des conditions similaires pour donner le 2- et 4-benzyl-1-naphtol, le toluène, le dibenzyle et le 9-phényl-3,4,5,6-dibenzoxanthène.

La transposition de l'éther de benzyl-α-naphtyl dans la quinoléine donne les produits normaux de transposition avec en plus le 2- et 4-benzylquinoléines et le 2-quinolyl-1-hydroxynaphtalène. Dans le phénol et dans l'anisole, la transposition est accompagnée par une benzylation du solvant.

Il en a été conclu que la transposition thermique des éthers de benzyl-naphtyl est fonction de la rupture homolytique de l'éther en radicaux benzyl et naphtyloxy.

Canadian Journal of Chemistry, **50**, 259 (1972)

It was reported by Behagel and Friensehner (1), that benzyl-α-naphthyl ether gave 22% 4-benzyl-1-naphthol with 16% α-naphthol and unidentified higher boiling materials, when it was heated at 240° for 20 h. Benzyl-β-naphthyl ether and other aryl benzyl ethers also rearrange under similar conditions. However, the heating of ether in a sealed tube with 38% HCl, gave rearrangement products from which α-naphthol was identified as observed by Braun and Reich (2). It is not impossible that these results might be due to hydrolysis of benzyl chloride retained in the ether. The hydrochloric acid thus formed would catalyze the rearrangement. This explanation is not so improbable since it is found that benzyl chloride is persistently retained by benzyl ethers prepared from benzyl chloride and is not easily removed. Furthermore the observation that zinc accelerates such type of change (3) in other aryl ethers, can be explained as due to the formation of zinc chloride from the hydrochloric acid produced in the reaction.

[1]Present address; Department of Chemistry, University of Libya, Tripoli, P.O. Box 2558, Libya.

The object of the work described in this paper was to examine more closely the behavior of carefully purified benzyl naphthyl ethers on heating and if the thermal rearrangement did take place, to determine what products are formed and what bearing on the course of the change.

Benzyl-β-naphthyl ether, rigorously freed from all traces of benzyl chloride, changes on heating for some days in sealed tubes at about 260°. 1-Benzyl-2-naphthol is formed together with 9-phenyl-1,2,7,8-dibenzoxanthene, some toluene, dibenzyl, and β-naphthol. The ether, when heated at its boiling point under reflux gives the same products with the difference that some β-dinaphthol was isolated.

From benzyl-α-naphthyl ether, under similar conditions, 2- and 4-benzyl-1-naphthols are formed together with 9-phenyl-3,4,5,6-dibenzoxanthene, α-naphthol, and some toluene and water.

The products of these thermal rearrangements differ markedly, from those of the proton catalyzed rearrangements, from which neither

Can. J. Chem. Downloaded from www.nrcresearchpress.com by 210.87.254.105 on 09/05/12
For personal use only.

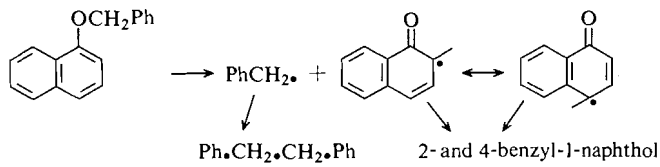

SCHEME 1

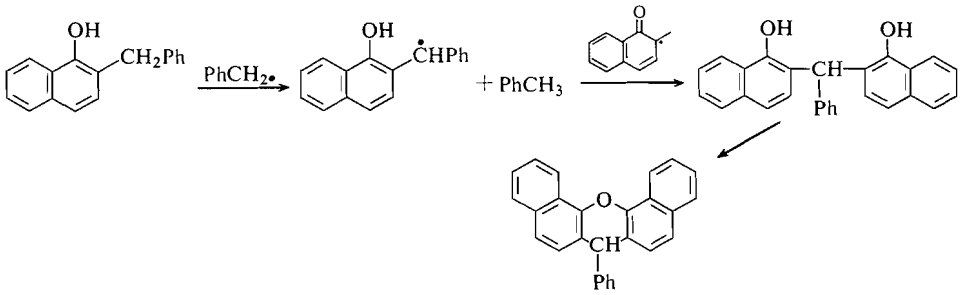

SCHEME 2

benzoxanthene, nor toluene nor dibenzyl have yet been reported (1, 2).

The formation of toluene and dibenzyl in the products of the thermal rearrangements is significant and suggests that the benzyl group takes part in the change as a free radical. If this is so, it should be possible to trap the benzyl group if the thermal rearrangement is carried out in a suitable solvent.

This has been realized, by heating benzyl-α-naphthyl ether in phenol. The normal products of rearrangement are accompanied by 2- and 4-benzylphenols. Similarly, in anisole, 2- and 4-benzylanisoles are formed.

Rearrangement of benzyl-α-naphthyl ether in quinoline gives the normal products of rearrangement together with those derived by substitution of quinoline; 2- and 4-benzylquinolines and an aminophenol provisionally identified as 2-quinolyl-1-naphthol. 2,2′-Biquinolyl is also isolated. A product is separated in all solvents and provisionally assigned as 4-benzyldi-α-naphthylene oxide from its elemental, i.r. and mass spectral analysis.

The simplest explanation of the rearrangement of the benzyl-α-naphthyl ether is to assume an initial homolytic fission to benzyl and naphthyloxy free radicals (see Scheme 1) and their substitution on the aromatic nuclei of the solvents used, through a mechanism analogous to that proposed by Williams and coworkers (4). However, subsequent recombination of both radicals is not excluded to give dibenzyl and some 2- and 4-benzyl-1-naphthols. Benzyl-β-naphthyl ether rearrangement is assumed to follow the same rule giving the corresponding products of its rearrangement.

The dibenzoxanthenes can be supposed to arise according to Scheme 2.

In quinoline, the formation of 2,2′-biquinolyl strongly suggests that (**1**) is also formed by reaction with a free radical (see Scheme 3). Combination of two such free radicals gives 2,2′-biquinolyl; with a benzyl radical, 2-benzylquinoline is formed; and a naphthyloxy radical gives 2-quinolyl-1-naphthol.

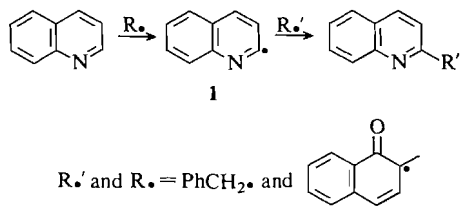

SCHEME 3

Experimental

Analysis

The lower boiling products of the rearrangement were analyzed by high-temperature g.l.c. of F. and M. scientific corporation Model 500, with flame ionization attachment and copper columns, 6 ft × 4 mm. The column used was 20% SE 30 on Chromosorb W (35–80 mesh) at 200° for the phenolic products and 215° for the neutral products. Infrared spectroscopic analysis was carried out on a Pye–Unicam I.R., Model SP200G.

Can. J. Chem. Downloaded from www.nrcresearchpress.com by 210.87.254.105 on 09/05/12
For personal use only.

Can. J. Chem. Downloaded from www.nrcresearchpress.com by 210.87.254.105 on 09/05/12
For personal use only.

Benzyl-α- and β-Naphthyl Ethers

These ethers were prepared by two methods: (*a*) By refluxing benzyl chloride for 5 h with a slight excess of the appropriate naphthol in acetone having finely powdered anhydrous potassium carbonate in suspension. (*b*) From the sodium naphthoxide and benzyl chloride in alcohol.

The crude ethers from these preparations persistently retained benzyl chloride, which was removed by refluxing with excess of pyridine for some time. The ether was recovered from this solution by dilution with water, adding ether and then washing the ethereal solution with dilute hydrochloric acid till freed from pyridine. Evaporation of this ether solution, after washing with alkali and drying, left the benzyl naphthyl ether. It was subjected to further treatment with pyridine until no trace of chloride could be detected in the redistilled ether. Only then were the benzyl naphthyl ethers considered pure enough for study of their rearrangement.

Benzyl-α-naphthyl ether was obtained, m.p. 74° from petroleum ether (60–80°).

Benzyl-β-naphthyl ether, m.p. 101–102° from ethyl alcohol.

Thermal Rearrangement of Benzyl Naphthyl Ethers

(a) Benzyl-β-naphthyl Ether

Benzyl-β-naphthyl ether (38 g) was boiled under reflux for 22 h. The first 2 h boiling caused the liquid temperature to drop from 257 to 235°, accompanied by a darkening from yellow to red–brown. The products of the change were the same as those detailed later with the exception that some β-dinaphthol (0.6 g) was isolated, m.p. and mixed m.p. 212–213°, dibenzoate, white needles m.p. and mixed m.p. 160°. Its i.r. spectrum was identical with that of an authentic specimen.

Better yields were achieved by heating the ether (38 g) in sealed tubes at 265° for 6 days. The ether was converted to a brown viscous mass with a green fluorescence. Distillation up to 200° removed toluene (1.8 g), (2,4-dinitro derivative m.p. and mixed m.p. 72°) and water (0.3 g).

The higher boiling material was separated into phenolic (*A*) and neutral products (*B*) by extraction with methyl alcoholic potassium hydroxide (Claisen's solution) after dilution with ether and benzene.

The neutral products (*B*) were separated by distillation into benzyl-β-naphthyl ether (6 g) b.p. 160–161°/1 mm, m.p. and mixed m.p. 101°, and 9-phenyl-1,2,7,8-dibenzoxanthene, as yellowish crystals from acetic acid, m.p. and mixed m.p. 189° (1 g).

From the neutral liquid fraction, b.p. 200–240°/13 mm, by its fractional crystallization from dilute ethanol, dibenzyl was separated (0.4 g), m.p. and mixed m.p. 52° (4,4′-dinitro derivative, m.p. and mixed m.p. 180°). It was further recognized by its i.r. spectrum and by its g.l.c. retention time.

The phenolic fraction (*A*) gave β-naphthol (5 g) and 1-benzyl-2-naphthol, m.p. and mixed m.p. 108–109°, benzoate, m.p. and mixed m.p. 96°. The yield estimated from g.l.c. was 8.4 g of 10.2 g of distillate.

(b) Benzyl-α-naphthyl Ether

The conditions were the same as those for the β-ether. The products were, toluene, water, dibenzyl, α-naphthol, 2-benzyl-1-naphthol, m.p. and mixed m.p. 74°, 4-benzyl-1-naphthol, m.p. and mixed m.p. 124°, and 9-phenyl-3,4,5,6-dibenzoxanthene, m.p. and mixed m.p. 248°. The i.r. spectra of these compounds were identical with those of authentic specimens.

Rearrangement of Benzyl-α-naphthyl Ether in Solvents

(a) Phenol

The ether (39 g) and phenol (11 g) were heated together in a sealed tube at 255° for 6 days. The product was worked up as described before where water (0.6 g) and toluene (2 g) were separated and identified. From the phenolic products, phenol and α-naphthol were isolated together with 2-benzyl-1-naphthol m.p. and mixed m.p. 73°, and 4-benzyl-1-naphthol m.p. and mixed m.p. 124°. From the liquid phenolic fractions, 2- and 4-benzylphenols were separated by fractional crystallization from benzene–petroleum ether (60–80°), where 4-benzylphenol separated, m.p. and mixed m.p. 84°, benzoate m.p. and mixed m.p. 87°. They were also recognized by their i.r. spectra and by g.l.c. analysis where they comprise 77% ortho-isomer and 23% para-benzylphenol.

A solid, m.p. 179–180° was isolated from the neutral fractions, b.p. 225–280°/11 mm provisionally identified as 4-benzyl-di-α-naphthylene oxide.

Anal. Calcd. for $C_{27}H_{18}O$ (mol. wt. 358): C, 90.1; H, 5.0. Found (358): C, 89.7; H, 5.3.

The i.r. spectrum had bands at 3010 and 3025 cm^{-1}, and showed the absence of OH. The m.p. was not changed by admixture with a sample of the same product separated in the following rearrangement.

From the neutral fraction, b.p. 310–320°/11 mm, 9-phenyl-3,4,5,6-dibenzoxanthene was isolated, m.p. and mixed m.p. 248–249°.

(b) Anisole

The ether (45 g) and anisole (11 g) heated together at about 260° for 10 days, gave water and toluene together with the same phenolic products as from the ether in absence of any solvent. The neutral fractions gave unchanged anisole, dibenzyl and 4-benzyl-di-α-naphthylene oxide. The remaining oil was recognized by g.l.c. as *o*-benzylanisole 40%, and *p*-benzylanisole 60%. They were further recognized by comparison of their i.r. spectra with those of the authentic specimens.

(c) Quinoline

The ether (70 g) and redistilled quinoline (40 g) were heated together at 260° for 14 days in sealed tube. Toluene (12 g) and water (1 g) were removed from the products by distilling up to 200°.

The higher boiling material was diluted with ether and extracted with Claisen's solution to remove phenols and aminophenols (*A*). Amines (*B*) were extracted from the ether solution by dilute hydrochloric acid. The remaining ether solution of neutral material (*C*) was distilled to give, 4-benzyl-di-α-naphthylene oxide, m.p. and mixed m.p. with the previously separated samples, 180–181°, and 9-phenyl-3,4,5,6-dibenzoxanthene, m.p. and mixed m.p. 248°. From the liquid fraction, b.p. 120–135°/10 mm, dibenzyl was separated, m.p. and mixed m.p. 52° (4,4′-dinitro derivative, m.p. and mixed m.p. 180°). It was further recognized by its i.r. spectrum and its retention time in g.l.c. analysis.

The amines liberated from the acid extract (*B*) were quinoline and a mixture of 2- and 4-benzylquinolines, b.p. 178–185°/8 mm which were separated by fractional crystallization of their picrates, into 4-benzylquinoline picrate m.p. and mixed m.p. 179°, and also 2-benzylquinoline picrate,

Can. J. Chem. Downloaded from www.nrcresearchpress.com by 210.87.254.105 on 09/05/12
For personal use only.

m.p. and mixed m.p. 158°. From the fraction b.p. 210–230°/8 mm, 2,2′-biquinolyl was separated (0.8 g), m.p. and mixed m.p. 194–195°, picrate, m.p. and mixed m.p. 210°. Its i.r. spectrum was identical to that of an authentic specimen.

The phenol and aminophenol extract was concentrated to remove the methyl alcohol and acidified with hydrochloric acid to liberate the phenolic products; α-naphthol and 2- and 4-benzyl-1-naphthols which were identified by their m.p. and mixed m.p. and the similarity of their i.r. spectra with that of authentic specimens.

The aminophenols in the acid extract of (*A*) were liberated by neutralizing with sodium carbonate. A quinolyl-1-naphthol, m.p. 262°, was isolated.

Anal. Calcd. for $C_{19}H_{14}NO$: C, 83.8; H, 5.2: N, 5.2. Found: C, 83.9; H, 5.0; N, 5.0.

(d) Heating Authentic Benzyl Naphthols in Sealed Tubes

Samples of 1-benzyl-2-naphthol (6 g) and 2-benzyl-1-naphthol (6 g) were heated separately in sealed tubes at 260° for 6 days. Identification of the reaction products by g.l.c., i.r. spectra and mixed m.p. method confirmed that the starting isomers were recovered unchanged in both cases, without formation of toluene or dibenzoxanthenes by-products.

Preparation of Reference Compounds

1-Benzyl-2-naphthol: prepared by the action of benzyl chloride, on a suspension of sodium-β-naphthoxide in toluene. On crystallization from benzene–petroleum ether (60–80°), white crystals separated, m.p. 109–110°, benzoate m.p. 96° (lit. 5*a*, m.p. 111–112°, benzoate m.p. 97°).

2-Benzyl-1-naphthol: prepared with a similar procedure as above. On crystallization from petroleum ether (60–80°), yellowish white crystals separated, m.p. 74° (lit. 5*b*, m.p. 74°).

4-Benzyl-1-naphthol: prepared by refluxing benzyl alcohol, α-naphthol in CS_2 and anhydrous $AlCl_3$. After extraction and crystallization from petroleum ether (60–80°), gave m.p. 125–126° (lit. 6, m.p. 125–126°).

2-Benzylanisole: prepared by methylation of 2-benzyl phenol. Its crystallization from ethanol gave white crystals, m.p. 27–28° (lit. 7, b.p. 123–124°/3 mm, m.p. 29–30°).

4-Benzylanisole (8): prepared from anisole, benzyl alcohol, and $AlCl_3$ by refluxing in petroleum ether (60–80°). It was collected by fractional distillation at 150–155°/7 mm, n_D^{20} 1.5781.

4-Benzylphenol: prepared from benzyl alcohol and phenol in CS_2, by the action of $AlCl_3$. From the oily fraction collected, on crystallization of the precipitated crystals from petroleum ether (60–80°) gave hairy needles, m.p. 84°, benzoate m.p. 87° (lit. 9, m.p. 84°).

4-Benzylquinoline: prepared by heating quinoline-1-oxide, and benzyl magnesium chloride in dry dioxane. On fractional distillation, it was collected at 228–235°/14 mm.

Anal. Calcd. for $C_{16}H_{13}N$: C, 87.6; H, 6.0; N, 6.4. Found: C, 87.5; H, 6.2; N, 6.3.

The picrate, m.p. 178–179° (lit. 10, b.p. 230°/17 mm, picrate, m.p. 178–179°).

2-Benzylquinoline picrate: separated from a mixture of 2- and 4-benzyl-quinolines obtained by treatment of quinoline with benzyl magnesium chloride in dry dioxane. Fractional crystallization of their picrates, separated 2-benzylquinoline picrate, m.p. 156–157° (lit. 10, b.p. 230°/14 mm, picrate m.p. 158–159°).

9-Phenyl-1,2,7,8-dibenzoxanthene: separated when boiling β-naphthol and benzaldehyde in glacial acetic acid saturated with HCl gas. On its crystallization from acetic acid gave rosy rhombic crystals, m.p. 189° (lit. 11, m.p. 189–190°).

9-Phenyl-3,4,5,6-dibenzoxanthene: prepared by reduction of 9-phenyl-3,4,5,6-dibenzoxanthenol with zinc dust and few crystals of platinum chloride in boiling acetic acid. On crystallization from acetic acid–acetic anhydride mixture, white crystals separated, m.p. 250° (lit. 12, m.p. 253°).

Anal. Calcd. for $C_{27}H_{18}O$: C, 90.5; H, 5.0. Found: C, 90.3; H, 5.3.

9-Phenyl-3,4,5,6-dibenzoxanthenol: prepared by reaction of phenyl magnesium bromide with dibenzoxanthenone. On crystallization from petroleum ether (60–80°), white crystals separated, m.p. 215°.

Anal. Calcd. for $C_{27}H_{18}O_2$: C, 86.6; H, 4.8. Found: C, 86.4; H, 5.0.

2,2′-Dihydroxy-1,1′-binaphthyl (β-dinaphthol): prepared by heating β-naphthol and copper sulfate in ammonium hydroxide solution. On extraction with chloroform and crystallization from toluene, it was separated as pale yellow crystals, m.p. 217–218°, dibenzoate, m.p. 160° (lit. 13, m.p. 218–219°).

Anal. Calcd. for $C_{20}H_{14}O_2$: C, 83.9; H, 4.9. Found: C, 83.7; H, 5.0.

2,2′-Biquinolyl: prepared by heating quinoline and 5% (w/w) iodine, in a sealed tube at 320° for 1 h. On crystallization from ethanol, white crystals separated, m.p. 195–196°, picrate, m.p. 210° (lit. 14, m.p. 196°, picrate m.p. 210°).

Dibenzyl: prepared by refluxing, for 15 h, a mixture of benzoin, zinc amalgam, and concentrated HCl. It was crystallized from ethanol as white crystals, m.p. 52°, 4,4′-dinitro derivative, m.p. 180°.

Anal. Calcd. for $C_{14}H_{14}$: C, 92.3; H, 7.7. Found: C, 92.1; H, 7.9.

1. O. Behagel and H. Friensehner. Ber. **67B**, 1368 (1934).
2. V. Braun and H. Reich. Ann. **445**, 225, 233 (1929).
3. Von Alphen. Rec. Trav. Chim. **46**, 804 (1927); F. Short. J. Chem. Soc. 528 (1928); W. F. Short and M. L. Steward. J. Chem. Soc. 553 (1929).
4. (*a*) Chang Shih, D. H. Hey, and G. H. Williams. J. Chem. Soc. 1871 (1959); (*b*) G. H. Williams. Homolytic aromatic substitution. Pergamon Press, Oxford, 1960; (*c*) G. B. Gill and G. H. Williams. J. Chem. Soc. 995 (1965).
5. (*a*) L. Claisen. Ann. **442**, 210 (1925); (*b*) Ann. **442**, 242 (1925).
6. M. Gomberg and C. C. Buchler. J. Am. Chem. Soc. **42**, 2059 (1920).
7. B. M. Dubinin. Zhur, Obshchei Khim **19**, 696 (1949); C.A. **44**, 1060 (1950).
8. J. Blackwell and W. J. Hickinbottom. J. Chem. Soc. 366 (1963).
9. J. Monacelli and G. F. Hinnion. J. Am. Chem. Soc. **63**, 1722 (1941).
10. F. M. Elkobaisi and W. J. Hickinbottom. J. Chem. Soc. 1286 (1960).
11. M. Zlokasaff and F. Ullman. Ber. **38**, 2111 (1905).
12. O. Dischendorfer, H. Hinrichs, and J. Schwetschenjo. Monatch, **75**, 31 (1944).
13. G. R. Clemo, J. G. Cockburn, and R. Spence. J. Chem. Soc. 1265 (1931).
14. A. P. Smirnoff. Helv. Chem. Acta, **4**, 802 (1921).

The Electroreduction of Substituted Benzofurazans

W. R. FAWCETT,[1] P. A. FORTE, R. O. LOUTFY, AND J. M. PROKIPCAK[1]

Department of Chemistry, University of Guelph, Guelph, Ontario

Received August 16, 1971

The electroreduction of 4- and 5-substituted benzofurazans was investigated at a platinum electrode in acetonitrile. Standard potentials for the reactions were linearly related to the energy of the lowest vacant molecular orbital as estimated by Hückel theory. Standard rate constants for electron transfer decreased as standard potentials in the series became more cathodic. This decrease is attributed to a double layer effect. No correlation was obtained between standard rate constants and observed hyperfine splitting constants for the anion radicals.

L'électroréduction des benzofurannes substitués en -4 et -5 a été étudiée dans l'acétonitrile au moyen d'une électrode en platine. Les potentiels standard pour les réactions ont été reliés d'une façon linéaire aux orbitales moléculaires vacantes les plus basses telles qu'estimées par la théorie d'Hückel. Les constantes de vitesse standard pour le transfert d'électrons décroissent au fur et à mesure que les potentiels standard dans les séries deviennent plus cathodiques. Cette diminution est attribuée à un effet de double couche. Aucune corrélation n'a été obtenue entre les constantes de vitesse standard et les constantes hyperfines de dédoublement observées pour les radicaux anioniques.

Canadian Journal of Chemistry, **50**, 263 (1972)

Can. J. Chem. Downloaded from www.nrcresearchpress.com by 210.87.254.6 on 09/05/12
For personal use only.

Introduction

It has been pointed out recently that, although substituent effects on the free energy of formation of radical ions are well documented (1), very few studies of substituent effects on the kinetics of electron transfer have been reported (2, 3). When organic electrode reactions are studied in aprotic solvents, one often observes a simple one electron transfer process with formation of a stable radical ion uncomplicated by adsorption on the electrode or accompanying proton transfer reactions. Atherton *et al.* (4) and Zhdanov *et al.* (5) have shown that benzofurazan (**1**) undergoes a one electron reduction to form

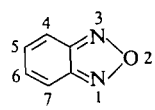

1

a stable anion radical at a dropping mercury electrode in dimethyl formamide and acetonitrile. The former authors, Strom and Russell (6), and Solodovnikov and Todres (7) investigated the e.s.r. spectrum of the anion radical, and demonstrated the applicability of the Hückel molecular orbital (HMO) model to interpreting the experimental results. In the present paper, the results of a study of the kinetics of electroreduction of 4- and 5-substituted benzofurazans, and of the e.s.r. spectra of their anion radicals are presented and discussed with respect to the corresponding HMO calculations.

[1]Authors to whom correspondence should be addressed.

Experimental

All experiments were carried out in acetonitrile (AN) solution containing 0.05 *M* tetraethylammonium perchlorate (TEAP). The solvent purification procedure was based on two previously described techniques (8, 9). Anhydrous Na_2CO_3 (20 g) and $KMnO_4$ (30 g) were added to 2 l of practical grade acetonitrile in a 3 l flask. Solvent was distilled from the mixture at a rate of 5 to 10 ml min^{-1} under atmospheric pressure with exclusion of water vapor. After adding 5 g P_2O_5 to each liter of product, it was fractionally distilled at a moderate rate. This product was stirred with CaH_2 (10 g l^{-1}) for 12 h and then fractionally distilled from fresh CaH_2 (5 g l^{-1}). The resulting distillate contained no detectable water (Karl Fischer titration and g.l.c.). In addition, the solvent's u.v. absorbance was similar to that prepared by the method of O'Donnell *et al.* (9), indicating that it was quite suitable for u.v. spectroscopy. TEAP was recrystallized twice from doubly distilled water and dried at 60 °C in a vacuum oven for 2 days. The accessible range on Pt in 0.05 *M* TEAP (+2.7 to −2.1 V *vs.* Ag/AgCl/0.1 *M* TEAP in AN//) was better than that obtained by either of the previous techniques (8, 9), indicating little or no water contamination from either the solvent or the salt.

Benzofurazan, 4- and 5-methoxy-, 4- and 5-methyl-, 5-chloro-, and 5,6-dimethylbenzofurazan were prepared as described previously (10). 4-Chloro- and 4- and 5-nitrobenzofurazan were supplied by Professor D. DalMonte, Universita di Bologna, Italy. All benzofurazans were purified by sublimation at 30 °C and 1 mm Hg.

The electrochemical cell, designed for use with a rotating disc electrode (RDE), was 6 cm in diameter and 9 cm high. The platinum working electrode (Pine Instrument Co.) was

Can. J. Chem. Downloaded from www.nrcresearchpress.com by 210.87.254.6 on 09/05/12
For personal use only.

embedded in a teflon cylinder (1.9 cm diameter) and had a circular area (0.76 cm diameter) exposed to the test solution. The counter electrode was a square of platinum (1.5 cm^2) opposite the working electrode on the bottom of the cell. The reference electrode (Ag/AgCl/0.1 *M* TEAP in AN//), placed close to and above the working electrode, was enclosed in a glass sleeve and joined to the system under investigation by a sintered glass disc.

The working electrode was cleaned before each run by immersing it in hot nitric acid for a few minutes, and rinsing several times with distilled water; it was then immersed in acidic ferrous ammonium sulfate and again rinsed repeatedly with distilled water. It was electrochemically pretreated in the base electrolyte solution by applying -1.5 V until the observed current decayed to a small constant value; the potential was then shifted anodically to $+0.05$ V in order to oxidize any adsorbed hydrogen. This cycle was repeated until the current at the potential limits was constant. The base electrolyte current–potential curves did not vary markedly from run to run, indicating that the above pretreatment technique resulted in reproducible surface conditions at the working electrode.

The thermodynamic and kinetic parameters of the reduction reactions were obtained by rotating disc voltammetry, cyclic voltammetry, and phase selective a.c. admittance measurements. Current–voltage curves were obtained with the above three electrode systems using a PAR Model 170 Electrochemistry System. In the case of RDE voltammetry, rotational speeds in the range 400–2500 r.p.m. were achieved using a Pine Instrument Rotator. For cyclic voltammetry, symmetrical triangular potential sweeps with slopes in the range 10–500 mV s^{-1} were applied to the stationary working electrode. In phase and out-of-phase a.c. admittances were measured in the frequency range 15–200 cycles s^{-1} with a 5 mV peak to peak a.c. signal superimposed on the d.c. potential of the working electrode. Depolarizer concentrations were in the range 1×10^{-4} to 1×10^{-3} *M*. All experiments were conducted in a dry box under a nitrogen atmosphere at 25.0 ± 0.5 °C.

The e.s.r. spectra were obtained using a Varian E3 spectrophotometer. The radical anions were generated electrochemically in a cell designed for use in the e.s.r. cavity. A quartz tube with 2 mm i.d. containing a concentric platinum cathode was sealed to the bottom of a simple Pyrex cell in which the anolyte and catholyte compartments were separated by sintered glass. The electrolyte solution was 0.05 *M* TEAP in AN with a depolarizer concentration in the catholyte of $\sim 1 \times 10^{-3}$ *M*.

Results and Discussion

Current–voltage curves for all the compounds except the nitro-substituted benzofurazans exhibited one reduction wave within the polarizable range of platinum in acetonitrile. For cyclic potential scan with rates up to 10 mV s^{-1}, reduction and oxidation peaks of equal height separated by 59 mV were observed on the cathodic and anodic sweeps respectively, indicating that a stable anion radical was formed in a one electron reduction process. As expected, the separation between the peaks increased at higher scan rates where the electrode process was no longer reversible (Fig. 1.). Two admittance peaks were obtained in the case of the nitro compounds. For cyclic potential scan at 20 mV s^{-1} in the region of the first peak, it was observed that the anodic peak current was considerably less than the cathodic, the peak potentials being separated by 59 mV. These results were interpreted as evidence that the first step involved formation of an ion radical in a one electron reduction. This radical then underwent a chemical reaction producing a species which was electroreducible at potentials cathodic of the first step (ECE mechanism).

Standard potentials for the one electron reduction reaction, determined in the usual manner from the a.c. admittance data and the peak potentials of cyclic voltagrams obtained at low scan rates, are recorded in Table 1. It is obvious that the standard potential continuously shifts in the cathodic direction as the substituent becomes more electron donating in character. The rate of electron transfer at this potential and the transfer coefficient were also determined from the current–potential data. The relationship derived by Gokhshtein and Gokhshtein (11) between peak currents and potentials was used in the case of cyclic voltagrams (Fig. 2). The standard rate constants were also determined from the frequency dependence of the in-phase and out-of-phase components of the faradaic admittance at low frequencies according to the procedure of Sluyters-Rehbach and Sluyters (12). Finally, the two kinetic parameters were obtained by analyzing current–voltage curves from RDE voltammetry at rotational speeds where the electrode process was both mass transfer and electron transfer controlled (13). Rate constants determined by the three methods agreed well with one another (Table 1), indicating that the assumption that the reactant is not adsorbed on the electrode is valid. This assumption was also confirmed by examining the frequency dependence of $\omega^{1/2}/Y'_{cl}$ at constant potential where ω is the angular velocity and Y'_{cl}, the in-phase component of the admittance. The fact that this function increased with frequency in all cases is an indication that reactant adsorption was non-existent or very weak (12). Furthermore, it should be noted that the range of the

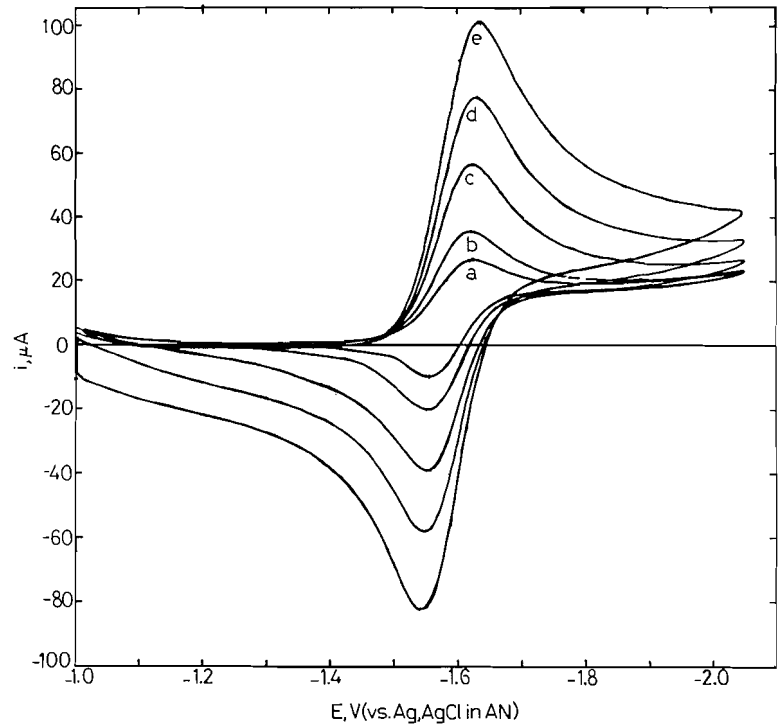

FIG. 1. Cyclic voltagrams for the electroreduction of 5-methyl benzofurazan at platinum in 0.05 *M* TEAP in AN at various scan rates: (*a*) 10, (*b*) 20, (*c*) 50, (*d*) 100, and (*e*) 200 mV s^{-1}.

observed faradaic current varied with the kinetic method, the largest current being obtained in RDE voltammetry. This fact considered together with the good agreement between rate constants determined by the three methods suggests that errors due to possible *IR* drop between the working and reference electrodes or non-uniform current distribution on the working electrode were negligible. Finally, it is apparent from the kinetic results that the rate of electron transfer decreased as the standard reduction potential became more cathodic.

The e.s.r. spectra were obtained for the anion radicals of all compounds except those with nitro substituents. In the case of benzofurazan, the hyperfine splitting constants (h.f.s.c.) were 5.40 G for the nitrogen atoms, and 3.37 and 2.00 G for the two pairs of equivalent hydrogen atoms. These results agree well with those reported earlier (4, 6, 7), the small differences being probably due to the fact that the spectra were obtained in different solvents and at several temperatures. The corresponding constants for the nitrogen atoms in substituted benzofurazans are recorded in Table 2. The HMO parameters for benzofurazan have been considered in detail by Atherton *et al.* (4). These authors concluded that the best parameters for the heteroatoms were $h_N = 0.75$, $h_O = 2.30$, $k_{CN} = 1.22$, and $k_{NO} = 0.80$ where h_x and k_{xy} are defined by eqs. 1 and 2,

$$[1] \qquad \alpha_x = \alpha_c + h_x\beta_{cc}$$

and

$$[2] \qquad \beta_{xy} = k_{xy}\beta_{cc}$$

α_c and β_{cc} being the coulomb and resonance integrals respectively, for the conjugated carbon atoms. Furthermore, they assumed that the proton and nitrogen h.f.s.c. were directly proportional to the spin densities at the contiguous ring carbon atoms and at the nitrogen atoms, respectively. They then pointed out that the energy of the lowest vacant molecular orbital (LVMO) in the Hückel approximation considering the symmetry properties of benzofurazan is given by $m = (a_4/a_5)^{1/2} - 1$ where m is the energy of the LVMO in units of β_{cc} above

Can. J. Chem. Downloaded from www.nrcresearchpress.com by 210.87.254.6 on 09/05/12
For personal use only.

Can. J. Chem. Downloaded from www.nrcresearchpress.com by 210.87.254.6 on 09/05/12
For personal use only.

TABLE 1. Electrochemical data for electroreduction of substituted benzofurazans and energy of the LVMO

	$E_{1/2}$ (V *vs.* Ag/AgCl in AN)	$k_0 \times 10^3$ (cm s^{-1})	Transfer coefficient α	m (units of β_{cc})
4-Nitro benzofurazan	−0.560			0.079
5-Nitro benzofurazan	−0.689			0.098
4-Chloro benzofurazan	−1.292	4.7*	0.38*	0.244
5-Chloro benzofurazan	−1.352	4.0* 4.9† 4.0‡	0.50* 0.50†	0.263
Benzofurazan	−1.523	3.5* 3.5† 3.9‡	0.38* 0.35†	0.296
4-Methyl benzofurazan	−1.590	3.2* 3.2† 2.5‡	0.38* 0.53†	0.340
5-Methyl benzofurazan	−1.594	2.5* 2.8† 2.4‡	0.43* 0.40†	0.321
4-Methoxy benzofurazan	−1.598	2.4* 2.2† 2.1‡	0.38* 0.40†	0.322
5-Methoxy benzofurazan	−1.650	2.5* 2.0† 2.1‡	0.36* 0.40†	0.311
5,6-Dimethyl benzofurazan	−1.664	1.8* 1.9† 1.8‡	0.38* 0.42†	0.329

*From cyclic voltammetry.
†From RDE voltammetry.
‡From ac admittance measurements.

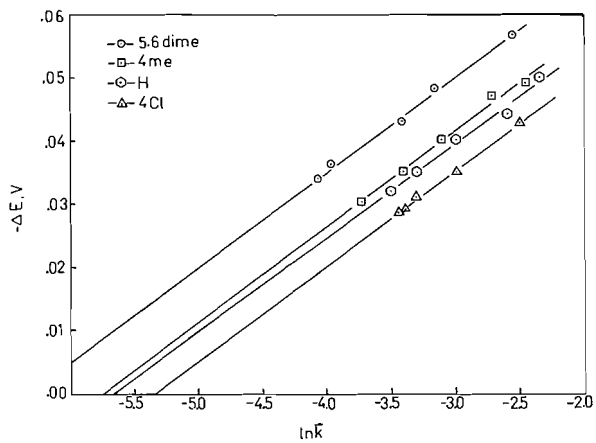

FIG. 2. Plot of the shift in peak potential from the half-wave potential, $\Delta E = E_p - E_{1/2}$ *vs.* the logarithm of the rate constant for reduction at E_p, ln $\boldsymbol{k}$ for typical data obtained from cyclic voltammetry. $\boldsymbol{k}$ was calculated from the peak current, i_p according to the equation $\boldsymbol{k} = i_p/(0.227\ FAc)$ where F is the Faraday, A, the area of the electrode, and c, the depolarizer concentration (11). The standard rate constant and transfer coefficient were calculated from the abscissa intercept and slope, respectively, of the best straight line through the points.

Can. J. Chem. Downloaded from www.nrcresearchpress.com by 210.87.254.6 on 09/05/12
For personal use only.

TABLE 2. Observed and calculated h.f.s.c. for N-1,3 in the anion radicals of substituted benzofurazans

	a_N(Gauss)			
	Observed		Calculated*	
	N-1	N-3	N-1	N-3
Benzofurazan	5.40	5.40	5.37	5.37
4-Chloro benzofurazan	5.88	4.96	5.27	4.41
5-Chloro benzofurazan	4.95	5.15	4.80	5.78
4-Methyl benzofurazan	4.50	6.36	5.34	5.76
5-Methyl benzofurazan	5.56	5.13	5.59	5.12
4-Methoxy benzofurazan	4.84	5.62	5.32	6.00
5-Methoxy benzofurazan	5.00	4.75	5.71	4.95
5,6-Methyl benzofurazan	5.40	5.40	5.32	5.32

*From spin densities for LVMO assuming $Q_N = 24.5$.

TABLE 3. Parameters for HMO calculations

>C—NO_2	$h_C = 0.20$ $h_N = 2.20$ $h_O = 1.40$	$k_{CN} = 1.20$ $k_{NO} = 1.45$
>C—Cl	$h_C = 0.50$ $h_{Cl} = 2.00$	$k_{C-Cl} = 0.40$
>C—CH_3	$h_{CH_3} = 2.00$	$k_{C-CH_3} = 0.70$
>C—OCH_3	$h_{OCH_3} = 2.00$	$k_{C-OCH_3} = 0.90$
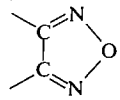	$h_N = 0.70$ $h_O = 2.00$	$k_{C-N} = 1.22$ $k_{N-O} = 0.80$

the reference energy level, α_c, and a_4 and a_5 are the h.f.s.c. at C-4,7 and C-5,6, respectively. A better fit to the present data was obtained assuming $h_N = 0.70$ and $h_O = 2.00$. The resulting spin densities were 0.219 at N-1,3, 0.125 at C-4,7, and 0.074 at C-5,6, and the calculated value of m, 0.296. The latter result is in excellent agreement with the value calculated from h.f.s.c. (0.298). Assuming McConnell constants, $Q_N = 24.5$ and $Q_H = 27$, the calculated h.f.s.c. are 5.37, 3.38, and 2.00.

The HMO calculations for the substituted molecules were carried out using the parameters listed in Table 3, the parameters for —Cl, —CH_3, and —CH_3O being taken from the tabulation of Purcell and Singer (14). The —NO_2 parameters were based on those used by Brodskii *et al.* (15) but were modified in order to obtain a better fit with the experimental data. A plot of the energy of the LVMO obtained in units of β_{cc} (Table 1) *vs.* the observed shift in half-wave potential for substituted benzofurazans is shown in Fig. 3. A good correlation was obtained by least squares (regression coefficient = 0.993), the equation of the straight line being

$$[3] \qquad \Delta E_{1/2} = 1.26 - 4.20\, m$$

If it is assumed that the half-wave potential is equal to the standard potential on the given potential scale, and that the difference in real solvation energies between an anion radical and the corresponding molecule does not depend on the nature of the substituent, then the slope

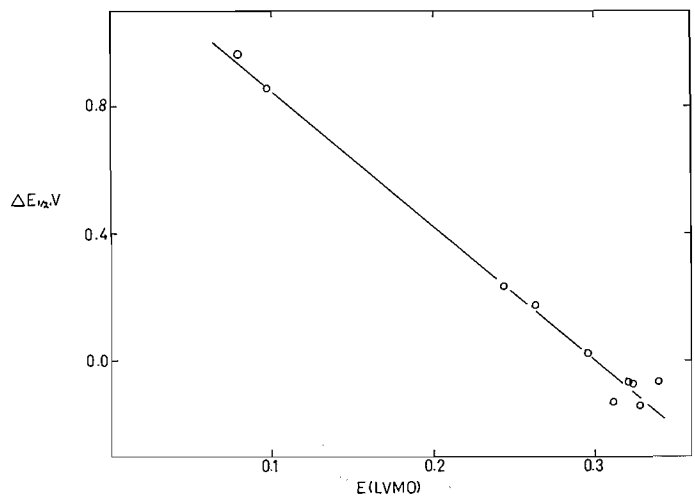

FIG. 3. Plot of the shift in the half-wave potential for substituted benzofurazans from that for benzofurazan, $\Delta E_{1/2}$ *vs.* the energy of LVMO in units of β_{cc} as calculated from HMO theory.

Can. J. Chem. Downloaded from www.nrcresearchpress.com by 210.87.254.6 on 09/05/12
For personal use only.

of the line gives β_{cc} in eV. The present result is higher than that observed for conjugated hydrocarbons and aromatic nitro-compounds but falls within the expected range (16). However, the assumption of a constant difference in real solvation energies is undoubtedly invalid for the present series since the charge distribution in both the neutral molecule and anion radical depends on the substituent (17, 18). The h.f.s.c. calculated from spin densities at the nitrogen atoms for the LVMO are recorded in Table 2. Agreement with observed h.f.s.c. is as good as can be expected considering the approximate nature of the calculation.

The variation in the rate of electron transfer with substituent can be partially attributed to a double layer effect (19). If it is assumed that the charge center of the activated complex is located at the outer Helmholtz plane in the transition state, then the true rate constant for transfer of one electron to a neutral species, k_t is given by eq. 4, where k_0 is the observed rate constant at the standard potential, ϕ_2, the

$$[4] \qquad k_t = k_0 \exp(-\alpha f \phi_2)$$

potential drop across the diffuse layer, and $f = F/RT$. Since ϕ_2 is negative at potentials cathodic of the point of zero charge in the absence of ionic adsorption, the double layer correction results in true rate constants which are larger than those calculated ignoring it. Unfortunately double layer data are not available for the Pt/AN interface; however, the magnitude in the change in the effect with potential may be estimated from diffuse layer theory from which it can be shown that, at cathodic potentials,

$$[5] \qquad d\phi_2/dE = -2C/fq$$

where C is the differential capacity of the interface per unit area, and q, the surface charge density. Assuming that $C \sim 20\ \mu F\ cm^{-2}$ and $q \leqslant -10\ \mu C\ cm^{-2}$, then $d\phi_2/dE \leqslant 0.1$. Thus the total change in $\alpha\phi_2$ in a 400 mV potential range is less than 16 mV. The assumption that the molecule is at the outer Helmholtz plane in the transition state is subject to some doubt (20), the double layer effect being greater if it is in fact closer to the electrode. The corresponding change in observed rate constants expressed as $(1nk_0)/f$ is 25 mV. Thus, it would appear that the majority of the observed decrease in rate constants can be attributed to a double layer effect if ionic specific adsorption is absent.

If the corrected or true rate constants vary with potential, then, according to current theories (21, 22), the change is mainly due to a corresponding change in the contributions to the free energy of activation from solvent reorientation (2). Assuming that free energies of solvation can be estimated by the Born model, and that the distance of the activated complex from the electrode in the transition state is constant, the change in free energy of solvation reorientation with substituent can be calculated from the spin densities at the component atoms in the molecule. Peover and Powell (2) applied the above model to kinetic data for the electroreduction of nitro-compounds and were able to correlate a decrease in rate of electron transfer to an increase in spin density at the nitrogen atom in the nitro-group. According to both the e.s.r. data and HMO calculations the nitrogen atoms in the anion radicals have the highest spin densities, so that a correlation might be expected between these spin densities and the observed rate constants. However, such a correlation is not apparent from the data in Tables 1 and 2. This is probably due to the fact that the total change in observed rate constants and spin densities is small so that any existing relationship is obscured by experimental error and by the fact that a correction could not be applied for the double layer effect.

Finally, it is interesting to note that the rate constants observed here are at the low end of the range of values reported for nitro compounds (2). In the latter case, the rate constant varied markedly with reactant structure, being lowest when the charge on the resultant anion radical was localized on the nitro group, that is, when a species of higher dipole moment was formed. Benzofurazan is similar to the nitro compounds in that it has a high dipole moment. The fact that the dipole moment of the benzofurazan anion radical is higher than that of the neutral molecule is probably the chief reason for the low rate constant for electron transfer. However, it should be noted that the kinetics for the two series were measured at different electrodes (Pt and Hg) and in different solvents (AN and dimethyl formamide). The correspond-

ing differences in double layer structure and solvation energies for reactants and products will affect the observed rate constants but these effects are not expected to be large (23, 24).

The authors wish to thank Dr. T. E. Gough for making available e.s.r. facilities at the University of Waterloo, Waterloo, Ontario, and for valuable assistance in analysis of the spectral data, and Professor D. DalMonte for supplying some of the compounds used. Financial assistance was received from the National Research Council of Canada and Defence Research Board of Canada, and from the Department of Chemistry, University of Guelph through an equipment grant.

1. P. ZUMAN. Substituent effects in organic polarography. Plenum Press, New York, N.Y. 1967.
2. M. E. PEOVER and J. S. POWELL. J. Electroanal. Chem. **20**, 427 (1969).
3. J. L. HUNTINGTON and D. G. DAVIS. J. Electrochem. Soc. **118**, 57 (1971).
4. N. M. ATHERTON, J. N. OCKWELL, and R. DIETZ. J. Chem. Soc. A, 771 (1967).
5. S. I. ZHDANOV, V. S. TSVENIASHVILI, and Z. V. TODRES. J. Polarograph. Soc. **13**, 100 (1967); Zhur. Obshch. Khim. **38**, 1888, 1894 (1968).
6. E. T. STROM and G. A. RUSSELL. J. Amer. Chem. Soc. **87**, 3326 (1965).
7. S. P. SOLODOVNIKOV and Z. V. TODRES. Khim. Geterotsikl. Soed. **3**, 811 (1967).
8. J. F. COETZEE, G. P. CUNNINGHAM, D. K. MCGUIRE, and G. R. PADMANABHAN. Anal. Chem. **34**, 1139 (1962).
9. J. F. O'DONNELL, J. T. AYRES, and C. K. MANN. Anal. Chem. **37**, 1161 (1965).
10. J. M. PROKIPCAK and P. A. FORTE. Can. J. Chem. **48**, 3059 (1970).
11. A. Y. GOKHSTEIN and Y. P. GOKHSTEIN. Dokl. Akad. Nauk SSSR, **131**, 601 (1960); R. S. NICHOLSON and I. SHAIN. Anal. Chem. **36**, 706 (1964).
12. M. SLUYTERS-REHBACH and J. H. SLUYTERS. Electroanalytical chemistry, A. J. Bard, *ed.* **4**, 1 (1970).
13. R. N. ADAMS. Electrochemistry at solid electrodes. Marcel Dekker. New York, N.Y. 1969. p. 240.
14. W. P. PURCELL and J. A. SINGER. J. Chem. Eng. Data, **12**, 235 (1967).
15. A. I. BRODSKII, L. L. GORDIENKO, and YU. A. KRUGLYAK. Teoret. Eksper. Khim. **3**, 98 (1967).
16. P. H. RIEGER and G. K. FRAENKEL. J. Chem. Physics, **39**, 609 (1963).
17. B. CASE, N. S. HUSH, R. PARSONS, and M. E. PEOVER. J. Electroanal. Chem. **10**, 360 (1965).
18. M. E. PEOVER. Electrochim. Acta, **13**, 1083 (1968).
19. P. DELAHAY. Double layer and electrode kinetics. Wiley-Interscience, New York, N.Y. 1965. Chapt. 7.
20. A. E. J. FORNO, M. E. PEOVER, and R. WILSON. Trans. Faraday Soc. **66**, 1322 (1970).
21. R. A. MARCUS. Ann. Rev. Phys. Chem. **15**, 155 (1964).
22. N. S. HUSH. Trans. Faraday Soc. **57**, 557 (1961).
23. R. PARSONS. Surface Science. **2**, 418 (1964); A. N. FRUMKIN. J. Electroanal. Chem. **9**, 173 (1965).
24. T. BIEGLER, E. R. GONZALEZ, and R. PARSONS. Coll. Czech. Chem. Commun. **36**, 414 (1971).

Can. J. Chem. Downloaded from www.nrcresearchpress.com by 210.87.254.6 on 09/05/12
For personal use only.

Flash Thermolysis: Quinones[1]

P. DE CHAMPLAIN[2] AND P. DE MAYO

Department of Chemistry, University of Western Ontario, London, Ontario

Received August 9, 1971

The flash thermolysis of a number of quinones is reported. *p*-Benzoquinone gives cyclopentadienone, isolated as the dimer. 2,5-Diphenylbenzoquinone gives 1- and 2-phenylnaphthalene together with benzo-[1,2-*b*:4,5-*b*']bisbenzofuran. Yields are very poor. Anthraquinone and phenanthraquinone give fluorenone, and the latter quinone gives small amounts of biphenylene.

La thermolyse-éclair d'un certain nombre de quinones est décrite. La *p*-benzoquinone donne la cyclopentadiénone qui est isolée sous la forme de son dimère. La diphényl-2,5 benzoquinone donne le phényl-1- et le phényl-2-naphthalène ainsi que le benzo-[1,2-*b*:4,5-*b*']bisbenzofuranne. Les rendements sont très faibles. L'anthraquinone et la phénanthraquinone donnent la fluorénone et cette dernière quinone donne de petites quantités de biphénylène.

Canadian Journal of Chemistry, **50**, 270 (1972)

The loss of carbon monoxide by the thermolysis of a variety of carbonyl compounds is a well-known process (for a review see ref. 1). Until recently, however, such a loss from quinones had only been observed in the mass spectrum (2). In 1967, DeJongh and his coworkers (3) showed that *o*-benzoquinone and some of its possible thermal progenitors (catechol sulfite and carbonate) lost one molecule of carbon monoxide to give, at 800°, cyclopentadienone which was isolated in good yield as its dimer (**2**). We considered that such decarbonylation might be a route to substituted cyclopentadienones, or, with more extravagant hopes, to cyclobutadiene derivatives.

For our initial experiments, we chose the readily available *p*-benzoquinone. The technique used has already been described and the apparatus was that represented in Fig. 1*b* of ref. 4. A platinum–rhodium resistor heater coil was used to reach the higher temperatures (above 1200°), but the coils had comparatively short life-times and could not be used at temperatures higher than 1350 °C. At 1310°, the maximum temperature at which the oven could be maintained for time enough to carry out 4–5 thermolyses before burning out the coil, *p*-benzoquinone gave the dimer of cyclopentadienone in 2.5% yield. At lower temperatures, down to 1150°, the yield of dimer progressively decreased.[3]

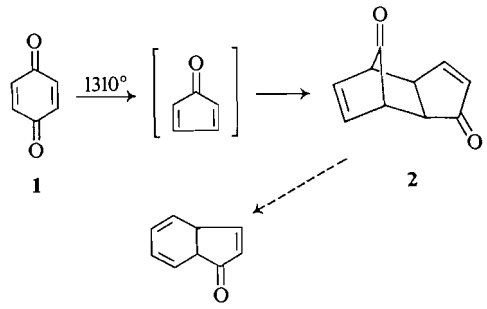

SCHEME 1

Since the completion of these experiments Suhr and Kruppa (5) have reported the obtention of **3** from **1** in the plasma glow discharge tube (see Scheme 1). DePuy and Lyons (6) have shown that **3** is easily derived from **2**.[3] In these experiments, we were unable to isolate any substance which could be derived from cyclobutadiene (*i.e.* the dimer, for instance). The high temperature required for the initial cleavage of the *p*-quinone was presumably responsible.

Substitution of the quinone should, in principle, lead to lowering of the bond strength of the vinyl–carbonyl linkage, and should, in addition, render the derived cyclopentadienone or other transformation product more easily isolable and identifiable (7). Thermolysis of **4**, indeed, proceeded at 1180° although in this case it was necessary to have a 100μ pressure flow

[1]Flash Thermolysis, Part 8.

[2]Holder of NRCC Scholarships 1969–1971.

[3]Professor O. L. Chapman and Dr. C. L. McIntosh have informed us that they have obtained cyclopentadienone from *o*-quinone, and measured its i.r. spectrum. We have also (with Dr. R. A. Marty) observed bands in the i.r. at 77 °K to be attributed to this substance.

Can. J. Chem. Downloaded from www.nrcresearchpress.com by 210.87.254.6 on 09/05/12
For personal use only.

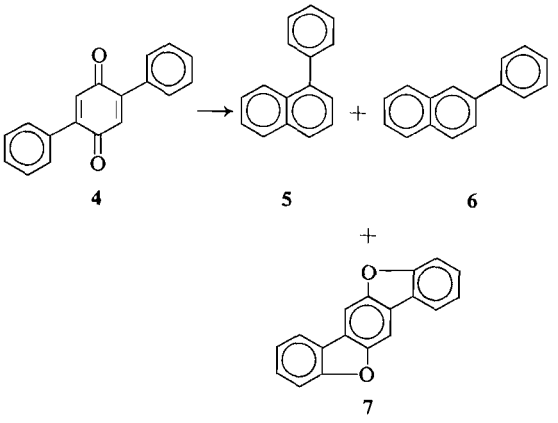

4 5 6 7

SCHEME 2

of nitrogen to ensure passage of the substance through the furnace. The products isolated were 1-phenylnaphthalene (**5**) (8%), 2-phenylnaphthalene (**6**) (8%), and benzo-[1,2-*b*:4,5-*b*']-bisbenzofuran (**7**) (6%) (see Scheme 2).

One possible product from such a reaction could be phenylacetylene, and the naphthalene could, in principle, have derived from the dimerization of this. Such a possibility was excluded by a control run using phenylacetylene: no naphthalenes were obtained. A second possibility which existed was that one isomer of the phenylnaphthalene was formed, by rearrangement, from the other (see Scheme 3). Since the formation of **6** may be more simply envisaged, the more likely rearrangement would be **6**→**5**. However, control runs with either isomer failed to show any isomerization. Only two general types of process appear to exist to allow for the formation of both isomers: either a phenyl migration occurs in an intermediate before formation of the naphthalenes, or the reaction pathway passes through a symmetrical

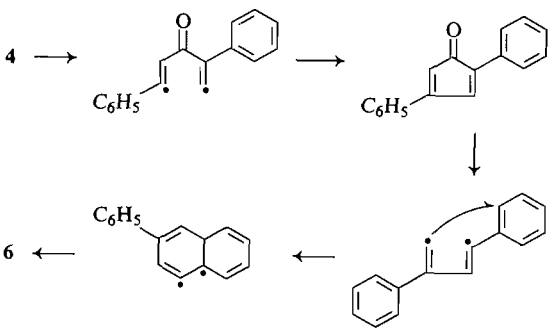

SCHEME 3

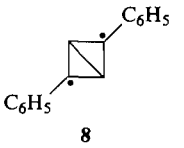

8

species having at least the symmetry of **8**. We have no data which could enable us to distinguish between these pathways. It is interesting that an equivalent transformation appears to have been recorded in the thermolysis of tetracyclone (8). Very recently Hageman and Wiersum (9) have reported the thermolysis of phenyl-*p*-benzoquinone (**9**) (see Scheme 4).

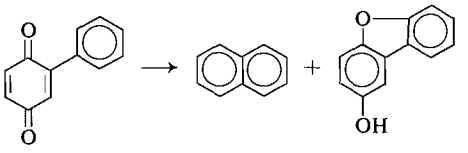

9 10

SCHEME 4

They obtained as products naphthalene and 4-hydroxydibenzofuran (**10**). It will be noted that the formation of **7** is essentially a cyclodehydrogenation very similar in nature to that obtained by Hay (10) in the thermolysis of 3,3',5,5'-tetraphenyldiphenoquinone.

Finally, we attempted the chemical verification of the best known mass spectrometric decarbonylations (2*c* and *d*); namely those of anthraquinone (**11**) and phenanthraquinone (**12**) to fluorenone (**14**) (see Scheme 5). Brown and Solly (11) had already succeeded in obtaining **14** from **12** in 76% yield at 800° in a packed silica tube and also identified traces of biphenylene (**13**) and biphenyl (**15**) as arising from fluorenone (**14**). Furthermore, they mention unsuccessful attempts (12) at obtaining fluorenone from anthraquinone (**11**). In our system, at 1180° and under 100 μ nitrogen carrier gas pressure, **11** and **12** yielded 40 and 53% fluorenone respectively. Furthermore, **12** yielded 2% biphenylene (**13**) and 1% each of biphenyl (**15**) and dibenzofuran (**16**). Under the same conditions, fluorenone gave only a trace of biphenylene. The presence of **13**, **15**, and **16** can be explained as occurring from the further decarbonylation of some intermediate species, presumably **17**, which is more readily generated from **12** than from **14**, the diradical **18** resulting from the

Can. J. Chem. Downloaded from www.nrcresearchpress.com by 210.87.254.6 on 09/05/12
For personal use only.

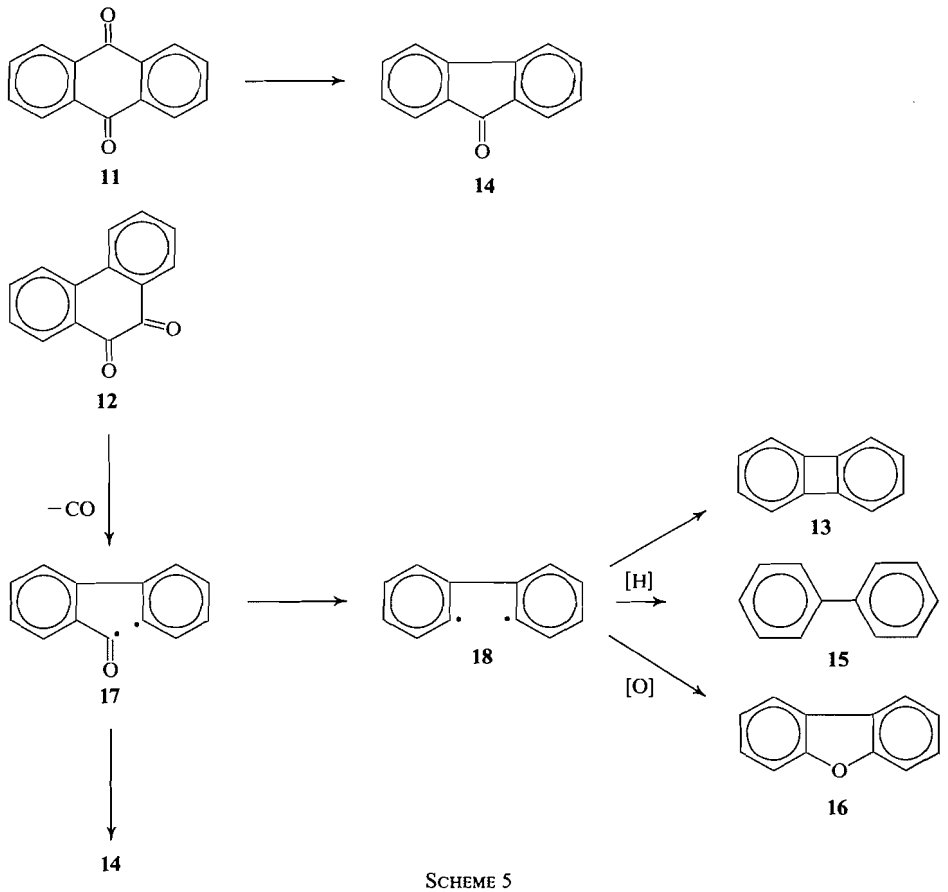

SCHEME 5

decarbonylation of **17** could close to form **13**, abstract hydrogen to give **15**, or react with a trace of oxygen contained in the carrier gas to yield **16**.

Experimental

Melting points were taken on a Kofler hot stage and are uncorrected. The i.r. spectra were determined on a Beckmann IR-10 spectrophotometer using sodium chloride cells. The n.m.r. spectra were taken on a Varian A-60. The t.l.c. was carried out on Merck GF-254 silica gel and the chromatographic columns were run on Merck PF-254 silica gel (with no binder). The u.v. spectra were run on a Carey 14 ultraviolet spectrophotometer. All yields expressed are based on the recovered starting material.

The thermolysis apparatus has been described previously (4).

Thermolysis of p-Benzoquinone (1)

p-Benzoquinone (220 mg; Matheson, resublimed) was sublimed through the oven under a pressure of 3 μ and thermolyzed at a temperature of 1310° (contact time: 1 ms.). After removal of the liquid nitrogen from the cold finger, the residual solid deposited was extracted with chloroform and transferred to a sublimation apparatus where the unreacted quinone (4%) was sublimed out. Preparative t.l.c. of the remaining solid ($CHCl_3$) yielded 2.5% of the cyclopentadienone dimer (**2**): ν_{max} 1705 and 1775–1785 cm^{-1} (lit. (13) 1705 and 1780 cm^{-1}), m.p. (hexane) 103–104.5° (lit. (13) 103–104°), the mass spectrum was identical to that of 1-indanone (see ref. 6).

Thermolysis of 2,5-Diphenyl-p-benzoquinone (4)

2,5-Diphenyl-*p*-benzoquinone (550 mg; Eastman Organic) was passed through the oven at 1180°, with 100 μ of nitrogen gas as carrier, over a period of 6 h. The solid left on the cold finger after pressurization and removal of liquid nitrogen was separated by preparative t.l.c. to yield 1-phenylnaphthalene (**5**) (8%), 2-phenylnaphthalene (**6**) (8%), benzo[1,2-*b*:4,5-*b*']bisbenzofuran (**7**) (6%), and 6% starting material.

1- and 2-phenylnaphthalenes were identified by comparison of i.r., n.m.r., and u.v. spectra with authentic specimens (Aldrich). The latter was also identified by mass spectrum and mixed m.p.

Benzo[1,2-*b*:4,5-*b*']bisbenzofuran (**7**) gave an m.p. (EtOAc) 269–270° (lit. (14) 265–266°) and had a u.v. spectrum identical to that recorded in the literature (15), λ_{max} (log ε):

Can. J. Chem. Downloaded from www.nrcresearchpress.com by 210.87.254.6 on 09/05/12
For personal use only.

328(4.52), 308(4.52), 260(4.18), and 247(3.94). The mass spectrum gave a parent peak at *m/e* 258.[4]

Thermolysis of Anthraquinone (11)

Anthraquinone (440 mg; Eastman Organic, resublimed) was thermolyzed in the same way as the diphenyl-*p*-benzoquinone (100 μ N_2, 1180 °C). The mixture of solids was chromatographed on a silica gel column to yield fluorenone (**14**; 40%)[5] identical with an authentic specimen.

Thermolysis of Phenanthrenequinone (12)

Phenanthrenequinone (350 mg; Eastman) was thermolyzed at 1180 °C with 100 μ pressure of N_2 carrier gas. The solid mixture was chromatographed on a silica gel column to give 53% of fluorenone, identical with an authentic sample, and a hydrocarbon fraction that was shown to contain biphenylene in 2% yield (from the u.v. spectrum of the crude mixture). Sublimation of the hydrocarbon fraction at 50°/0.1 mm afforded a yellow solid that was recrystallized from methanol to give biphenylene (**13**) m.p. 109–110.5°, mixed m.p. (Pflatz and Bauer) 110–111.5° (lit. (16) 110–111°).

Another run, performed under the same conditions and followed by sublimation of the solid residue at 100°/12 mm, afforded a mixture that was analyzed by v.p.c. (3% Poly A 103 on Gaschrom Q, $2\frac{1}{2}$ ft. × $\frac{1}{4}$ in., 60 cc He/min. 130 °C) and was shown to give yields of 2% biphenylene (**13**) and 1% each of biphenyl (**15**) and dibenzofuran (**16**) by integration of the peaks with an internal reference of 1-methylnaphthalene. The latter two reaction products were isolated by preparative v.p.c. (same column, 90 °C) and identified by mass and u.v. spectroscopy. No starting material was recovered.

[4]The authors would like to thank Prof. D. B. Maclean of McMaster University for kindly supplying them with the mass spectrum of this compound.

[5]Forty-five percent of the original anthraquinone was recovered.

This work was supported by the Petroleum Research Fund, administered by the American Chemical Society, and by the National Research Council of Canada.

1. B. P. Stark and A. J. Duke. Extrusion reactions. Pergamon Press, 1967.
2. (*a*) J. H. Bowie, D. W. Cameron, R. F. G. Giles, and D. H. Williams. J. Chem. Soc. B, 335 (1966). (*b*) T. A. Elwood and M. M. Bursey. Org. Mass Spectrom. **1**, 537 (1968). (*c*) J. H. Beynon, G. R. Lester, and A. E. Williams. J. Phys. Chem. **63**, 1861 (1959). (*d*) J. H. Beynon and A. E. Williams. Appl. Spectrosc. **14**, 156 (1960).
3. (*a*) D. C. DeJongh, R. Y. Van Fossen, and C. F. Bourgeois. Tetrahedron Lett. 271 (1967). (*b*) D. C. DeJongh and D. A. Brent. J. Org. Chem. **35**, 4204 (1970).
4. J. F. King, P. de Mayo, C. L. McIntosh, K. Piers, and D. J. H. Smith. Can. J. Chem. **48**, 3704 (1970).
5. H. Suhr and G. Kruppa. Ann. **744**, 1 (1971).
6. C. H. DePuy and C. E. Lyons. J. Am. Chem. Soc. **82**, 631 (1960).
7. M. A. Ogliaruso, M. G. Romanelli, and E. I. Becker. Chem. Rev. **65**, 261 (1965).
8. E. McNelis. J. Org. Chem. **30**, 4324 (1965).
9. H. J. Hageman and U. E. Wiersum. Chem. Commun. 497 (1971).
10. A. S. Hay. J. Org. Chem. **36**, 218 (1971).
11. R. F. C. Brown and R. K. Solly. Austr. J. Chem. **19**, 1045 (1966).
12. C. G. Macdonald and J. S. Shannon. As quoted in ref. 11.
13. K. Hafner and K. Goliasch. Chem. Ber. **94**, 2909 (1961).
14. K. Schimmelschmidt. Ann. **566**, 184 (1950).
15. J. Gripenberg. Tetrahedron, **10**, 135 (1960).
16. W. C. Lothrop. J. Am. Chem. Soc. **63**, 1187 (1941).

Can. J. Chem. Downloaded from www.nrcresearchpress.com by 210.87.254.6 on 09/05/12
For personal use only.

Proton Magnetic Resonance Spectra, Conformational Preferences, and Approximate Molecular Orbital Calculations for the *syn* and *anti* 2-Furanaldoximes

R. WASYLISHEN[1] AND T. SCHAEFER

Chemistry Department, University of Manitoba, Winnipeg, Manitoba

Received August 5, 1971

Evidence is adduced, mainly from proton chemical shift and long-range coupling constant data, that the *anti* isomer of 2-furanaldoxime exists almost exclusively in the *s-cis* form in solution, independently of the type of intermolecular association that occurs. Intramolecular hydrogen bonding apparently is absent in this isomer. Similarly, the *syn* isomer exists in roughly equal mixtures of *s-cis* and *s-trans* forms in solvents of widely different polarities. A variety of nuclear spin–spin coupling constants are calculated via the INDO and CNDO molecular orbital approximations, as are the dipole moments and conformational energies, for 2-furanaldehyde and its oximes. On the whole the experimental trends are well reproduced by the computations.

Les données relatives aux déplacements chimiques des protons et des constantes de couplage à longue distance constituent les preuves principales d'après lesquelles l'isomère *anti* du furanaldoxime-2 existe presque exclusivement en solution sous la forme *s-cis*; ceci indépendamment du type d'association intermoléculaire est apparemment absente dans cet isomère. D'une façon similaire, l'isomère *syn* est en gros constitué d'un égal mélange des formes *s-cis* et *s-trans* dans des solvants de polarités très différentes. De nombreuses constantes de couplage nucléaire spin–spin sont calculées au moyen des approximations d'orbitales moléculaires INDO et CNDO, et il en est de même pour les moments dipolaires et les énergies conformationnelles du furanaldéhyde-2 et de ses oximes. Dans l'ensemble, les données expérimentales sont bien reproduites par les calculs.

Canadian Journal of Chemistry, **50**, 274 (1972)

Introduction

The purpose of this paper is the investigation of the conformational preferences in solution of the *syn*, **1**, and *anti*, **2**, isomers of 2-furanaldoxime by means of solvent effects on the proton chemical shifts, stereospecific long-range proton–proton spin–spin coupling constants and by molecular orbital calculations in the INDO and CNDO approximations.

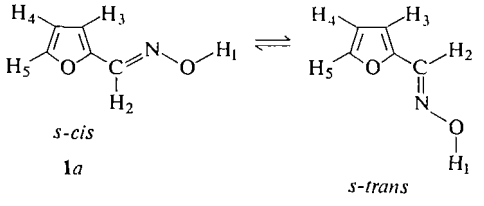

s-cis **1***a* ⇌ *s-trans* **1***b*

syn, m.p. 75 °C

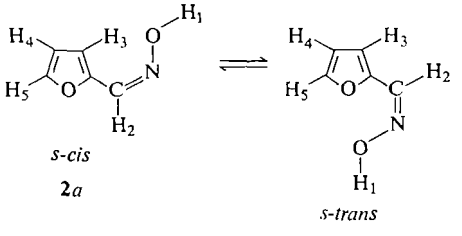

s-cis **2***a* ⇌ *s-trans* **2***b*

anti, m.p. 91 °C

[1]Holder of an NRCC Scholarship 1971-1972.

Some supplementary i.r. and shift reagent experiments are performed. 2-Furanaldehyde, **3**, is also discussed because it serves as a guide in the MO calculations and in the application of long-range coupling data in deducing conformational preferences for the oximes.

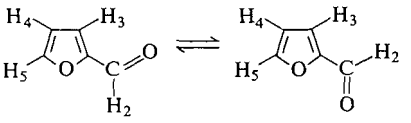

s-cis **3***a* ⇌ *s-trans* **3***b*

Experimental

The isomer of 2-furanaldoxime which melts at 75–76 °C was prepared by the method of Brady and Goldstein (1) and the isomer melting at 91–92 °C was obtained from Aldrich Chemical Co. The p.m.r. spectra of degassed solutions of these isomers in dry DMSO-d_6, 10 mol %, and in C_6D_6 and $CDCl_3$, both 3 mol %, were calibrated in the frequency sweep mode on an HA100-D spectrometer at a sweep rate of 0.02 Hz/s. A 7.7 mol % solution in acetone-d_6 of the isomer melting at 91–92 °C was studied at 60 MHz on a DA-60-I spectrometer in a similar way. The i. r. spectra of dilute solutions of both isomers in CCl_4 were recorded. Induced low-field shifts of H_2 to H_5 in each isomer were observed in $CDCl_3$ solution on the addition of 0.2 molar equivalents of 2,2,6,6-tetramethyl heptane dionate, europium (III), the latter obtained from Pierce Chemical Co. (Euro-shift). Rather severe broadening of peaks occurred on addition of the shift reagent.

Can. J. Chem. Downloaded from www.nrcresearchpress.com by 210.87.254.42 on 09/05/12
For personal use only.

Can. J. Chem. Downloaded from www.nrcresearchpress.com by 210.87.254.42 on 09/05/12
For personal use only.

TABLE 1. Spectral parameters at 100 MHz of the *syn* and *anti* isomers of 2-furanaldoxime in DMSO-d_6, C_6D_6, and $CDCl_3$ solutions

	syn (m.p. 75 °C)			*anti* (m.p. 91 °C)		
	DMSO*	$CDCl_3$†	C_6D_6†	DMSO*	$CDCl_3$†	C_6D_6†
$\nu(OH_1)$	869.260	—	—	923.360	—	—
ν_2	547.870	801.39	783.40	497.573	751.725	734.656
ν_3	414.279	662.581	616.736	466.442	734.235	738.324
ν_4	399.449	644.174	591.038	407.158	652.924	606.986
ν_5	515.957	747.322	692.562	518.777	746.611	690.430
$^4J(2,3)$	−0.418	−0.416	−0.404	−0.350	−0.350	−0.341
$^5J(2,4)$	0.252	0.254	0.295	0.711	0.691	0.694
$^5J(2,5)$	0.358	0.351	0.327	0.000	−0.001	−0.004
$^3J(3,4)$	3.386	3.450	3.423	3.442	3.476	3.476
$^4J(3,5)$	0.803	0.777	0.768	0.768	0.738	0.754
$^3J(4,5)$	1.825	1.825	1.819	1.793	1.790	1.789

*Chemical shifts in DMSO-d_6 are given in Hz to low field of the methyl signal of the undeuterated DMSO.

†Chemical shifts in $CDCl_3$ and C_6D_6 are given in Hz to low field of internal tetramethylsilane.

The coupling constants are probably accurate to 0.02 Hz; a first-order analysis of the 60 MHz spectrum of the *anti* isomer in acetone-d_6 yielding values within 0.01 to 0.03 Hz of those given above.

In the *anti* isomer in DMSO-d_6 the hydroxyl proton couples over four bonds to H_2 with magnitude of 0.35 Hz and also couples to H_3 on the ring by about 0.05 Hz. Similarly the hydroxyl proton of the *syn* isomer couples to H_2 with a magnitude of 0.35 Hz in DMSO-d_6.

Results and Discussion

(1) Spectral Analysis

All spectra were analyzed using the computer program LAME (2) and the results are given in Table 1. The spectra are not far from first order in appearance and are not reproduced here, their quality being similar to those recently published from this laboratory (3). The r.m.s. deviations between observed and calculated transition frequencies lie between 0.006 and 0.014 Hz for the various samples. The standard errors in the spectral parameters vary from 0.002 to 0.012 Hz, the average standard error being 0.006 Hz.

In addition to the tabulated data there exists a coupling over four bonds of ± 0.35 Hz between the hydroxyl proton and H_2 in both **1** and **2** in the DMSO-d_6 solutions. In **2** the hydroxyl proton also couples to H_3 on the ring by $\pm 0.05 \pm 0.01$ Hz, as determined by decoupling experiments.

(2) Assignment of Isomers

2-Furanaldoxime was the first aldoxime to be obtained in two forms (4). The assignment shown above is in agreement with dipole moment measurements (5), electronic absorption spectra (6), conductivity measurements (5), and chemical considerations (1, 7). In Table 1 there is a difference of 3.21 ppm between the OH and C—H_2 resonance positions in DMSO for the *syn* isomer, **1**, in excellent accord with the criterion established by Kleinspehn *et al.* (8). The analogous shift difference of 4.26 p.p.m. for the *anti* isomer also agrees with the criterion of these authors.

(3) Conformation about the Ring Carbon–Imino Carbon Bond

(a) Stereospecific Coupling over Five Bonds

The use of the zig–zag rule for coupling over five bonds between the aldehyde and ring protons in benzaldehyde derivatives is well-established (9–11). For a time it was thought (12) that the rule did not apply in 2-furanaldehyde. Correct assignments (13) have now shown that the rule holds in this compound as well: $^5J(2,5)$ is large in **3***b* and small in **3***a*. This fact encourages us to apply the zig–zag rule to the 2-furanaldoximes in an attempt to establish whether the *s-cis* or *s-trans* forms (see **1** and **2**) are more stable.

$^5J(2,5)$ is zero in the *anti* isomer, **2**, in all three solvents, which range in dielectric constant from 49 to 2. On the other hand, $^5J(2,4) = 0.70 \pm 0.01$ Hz in each of the solvents, suggesting that **2** exists in the *s-cis* form, **2***a*.

In the *syn* isomer, **1**, the sum of $^5J(2,4)$ and $^5J(2,5)$ is 0.61 ± 0.01 Hz in all three solvents. On the assumption that 0.61 Hz is the value of $^5J(2,4)$ in **1***a* and of $^5J(2,5)$ in **1***b* it follows that **1** exists 41% in the *s-cis* form. A 5% change in this number follows if a 0.1 Hz variation is assumed in the 0.61 Hz base value. The value of

TABLE 2. The aromatic solvent induced shift* $\Delta^{C_6D_6}_{CDCl_3}$ for four protons in the *anti* and *syn* isomers of 2-furanaldoxime

Proton†	$\Delta^{C_6D_6}_{CDCl_3}$ *syn*	*anti*
H_2	18.0	17.1
H_3	45.8	−4.1
H_4	53.1	45.9
H_5	54.8	56.2

*The solvent shift is found in Hz at 100 MHz by subtracting the shift in $CDCl_3$ to low field of internal TMS from the shift in C_6D_6 to low field of internal TMS.

†See structural formulae **1** and **2** for the numbering system used here.

41% is valid only if $^5J(2,5)$ in **1***a* and $^5J(2,4)$ in **1***b* are both zero.

(b) Aromatic Solvent Induced Shifts (ASIS)

It is known that benzene solvent molecules tend to avoid electron rich regions of solute molecules (14–16). In these oximes these regions are in the vicinity of the hydroxyl oxygen (see calculations below). Consequently the protons situated near the hydroxyl group are expected to display the smallest ASIS. In Table 2 the ASIS values are given for H_2, H_3, H_4, and H_5 of the two isomers.

In the *anti* form the ASIS value of H_3 is actually negative, strongly supporting the assignment of the *s-cis* form as the stable one in these solutions. H_3 lies very near the hydroxyl group in the *s-cis* form of the *anti* isomer. In both forms of the *syn* isomer H_3 does not approach the hydroxyl group as closely as it does in the *s-cis* form of the *anti* isomer (see **1** and **2**) and hence its ASIS value is now much larger and comparable to the ASIS values of the ring protons.

The ASIS numbers in Table 2 support the assignment of the *s-cis* form to the *anti* isomer and are qualitatively consistent with the proportions of *s-cis* and *s-trans* forms of the *syn* isomer deduced from the five-bond proton–proton couplings.

(c) Chemical Shifts of H_2 and H_3 in $CDCl_3$

The deshielding of nearby protons by the hydroxylimino group is thought to arise from the NOH anisotropy (15, 17). Thus in $CDCl_3$ proton 2 of the *syn* isomer lies to low field of H_2 in the *anti* isomer by 0.5 p.p.m. Again, in the same solvent H_3 in the *anti* isomer is deshielded by 0.7 p.p.m. compared to the *syn* isomer; constituting further support for the stability of the *s-cis* form of the *anti* isomer.

(d) Stretching Frequencies of the OH Group

Oximes can act as either proton donors or acceptors with various solvents (18–20). Perusal of the spectral data in Table 1 suggests that hydrogen bonding to the solvent does not alter the proportions of the *s-cis* and *s-trans* forms of the two isomers of 2-furanaldoxime. In CCl_4 the free OH stretching frequencies are found at 3600 cm^{-1} with equal intensities for both isomers. The hydrogen-bonded OH frequencies occur at 3250 cm^{-1} in the *anti* isomer and at 3300 cm^{-1} in the *syn* isomer, again with equal intensity. These results apparently rule out any *intra*molecular hydrogen-bonding in the *anti* isomer (18) while competition between self-association and hydrogen-bonding to the solvent does not affect the conformation about the ring carbon–imino carbon bond if the J data in Table 1 is to be believed. The i.r. data is therefore consistent with a stable *s-cis* form of the *anti* isomer.

(e) Use of the Shift Reagent, 2,2,6,6-Tetramethylheptane-dionate, Europium(III)

Wolkowski (21*a*) used tris(dipivalomethanato)europium as a shift reagent to distinguish between *syn* and *anti* isomers of some oximes. The magnitude of the induced proton shift varied as $r^{-2.3}$ where r was the proton to hydroxyl oxygen distance. Of course, for a pseudo contact shift a dependence on angle as well as on distance from the complexation site (actually the europium atom) is expected and the induced shift can be upfield or downfield from the shift positions in the uncomplexed molecule (21*b*).

For the experiments on the isomers of 2-furanaldoxime the observed downfield shifts at 100 MHz are as follows: $\Delta H_2 = 417$ (93), $\Delta H_3 = 265$ (96), $\Delta H_4 = 111$ (53), $\Delta H_5 = 60$ (39) Hz, where the shifts of the *syn* isomer are given in brackets.

The important point for our purposes is that in the *anti* isomer the *s-cis* form has H_3 relatively near the hydroxyl oxygen, assumed to be the site of complexation (21). Therefore a much larger shift is expected and observed for H_3 than for H_4 and H_5. If the *s-trans* form, **2***b*, were the

Can. J. Chem. Downloaded from www.nrcresearchpress.com by 210.87.254.42 on 09/05/12
For personal use only.

Can. J. Chem. Downloaded from www.nrcresearchpress.com by 210.87.254.42 on 09/05/12
For personal use only.

stable one the shifts of these three protons might well be much closer in magnitude. Hence the induced shifts are consistent with an *s-cis* form for the *anti* isomer.

The interpretation of the much smaller shifts observed for the *syn* isomer is ambiguous and examination of the geometry of the *s-cis* and *s-trans* forms, **1***a* and *b*, suggests that an angle dependence as well as a distance dependence is important (21*b*). At any rate, the induced shifts do not disprove the conformational deductions in previous sections.[2]

(4) INDO and CNDO Computations (22, 23)

(a) Dipole Moments and Relative Energies

These were calculated in an attempt at confirming the conformational deductions arrived at above. For the furan ring the atomic coordinates found by microwave work (24) were used. For furan itself we calculate $\mu = 0.72$ D, in exact agreement with experiment (25) while CNDO computes $\mu = 0.86$ D (26). For furanaldehyde standard geometries (22) were employed for the CHO fragment following the assumptions of Maciel *et al.* (27) in their calculations of the vicinal coupling constants on the ring.

The planar *s-cis* form of the aldehyde, **3***a*, was calculated to have $\mu = 2.79$ D by INDO and 2.64 D by CNDO while the planar *s-trans* form was calculated to have $\mu = 3.58$ D by INDO and 3.51 D by CNDO. The observed dipole moment is 3.6 D (5) suggesting the *s-trans* form as the predominant form at room temperature. From published $\Delta H°$ data (12) we calculate $P_t = 0.64$ and $P_c = 0.36$ at 30 °C. The calculated dipole moments of the two forms then predict a dipole moment of 3.3 D at 30 °C, in good agreement with experiment. Contrary to experiment (12) INDO calculates the *s-cis* form to be more stable than the *s-trans* by 1.2 kcal/mol.

For the planar *s-cis* form of the *anti* oxime, **2***a*, one finds $\mu = 0.67$ D by INDO while $\mu = 0.61$ D if the CHNOH group is twisted to lie 19° above the plane of the furan ring (this angle of twist occurring in the solid state for *anti p*-Cl-benzaldoxime (28, 29)). The observed dipole moment of the *monomeric* form of the *anti* isomer is 1.9 D in benzene (5). However, the calculated dipole moment of the oximes is very sensitive to the conformation of the O—H fragment. For example, if the OH bond in **2***a* is twisted 30° out of the plane of the CHNO group but pointing towards the ring the calculated dipole moment becomes 3.73 D. For this reason (the O—H bond being very polar, in agreement with the chemical properties), the calculated moment of 1.22 D of the *s-trans* form of the *anti* oxime, **2***b*, cannot be taken as evidence for the relative stability of this form. When, in **2***b*, the OH bond is turned through 180°, *i.e.* simulating an intramolecular hydrogen bond to the ring oxygen, the INDO dipole moment becomes 4.76 D and because this is so much larger than the observed value of 1.9 D, we tend to regard it as confirmatory evidence against such hydrogen bonding.

The *s-cis* form, **2***a*, is calculated by INDO to be 1.7 kcal/mol more stable than the *s-trans* form, **2***b*, of the *anti* isomer, in almost quantitative agreement with the available experimental evidence. However, INDO also finds the intramolecularly hydrogen bonded form of **2***b* (180° flip of the OH bond) to be 5.5 kcal/mol more stable than the *s-cis* form, **2***a*. Of course, intermolecular hydrogen bonding to solvent molecules in DMSO or to other solute molecules (cyclic dimers or trimers (18)) in $CDCl_3$ and C_6D_6 is not considered in the MO computations. The i.r. evidence (18) leaves little doubt about the occurrence of intermolecular hydrogen bonding but note that the coupling constant data in Table 1 almost certainly proves that the conformation about the C—C bond is independent of the type of intermolecular association.

The calculated dipole moments of the *syn* isomer are 1.28 D for the *s-cis* form, **1***a*, and 1.44 D for the *s-trans*, **1***b*. The monomer has a dipole moment of 1.2 D in C_6D_6 (5). The *s-trans* form is predicted to be 0.17 kcal/mol more stable than the *s-cis* form at room temperature; in close agreement with the deductions based on the long-range coupling constants in section 3. Again, the proportion of conformers is apparently independent of solvent and of the type of intermolecular association.

Intramolecular hydrogen bonding is most unlikely in the *syn* isomer for geometrical reasons. According to INDO the hydroxyl oxygen carries a negative charge of 0.24 electrons and the hydrogen a positive charge of 0.16

[2]One cannot rule out the possibility that complexation of the oximes to the shift reagent may affect the equilibrium between the *s-cis* and *s-trans* forms to some extent.

TABLE 3. Computed and observed proton–proton coupling constants in H_3 in the *s-cis* and *s-trans* forms of 2-furanaldehyde

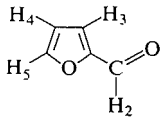

s-cis

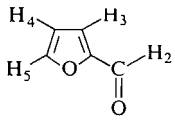

s-trans

	Observed	INDO	CNDO	Observed	INDO	CNDO
$^3J(3,4)$	3.70	2.80*	—	3.70	—	—
$^3J(4,5)$	1.75	1.26*	—	1.75	—	—
$^4J(3,5)$	0.80	—	—	0.80	—	—
$^4J(2,3)$	0.0†	−0.96	−0.05	0.0	−1.14	−0.20
$^5J(2,4)$	0.85	1.34	0.70	<0.2	0.20	0.01
$^5J(2,5)$	<0.2	−0.39	0.03	1.10	0.90	0.76

*Reference 27.
†In the isomer mixture near room temperature $^4J(2,3)$ has a magnitude of 0.06 Hz (33).

TABLE 4. Computed coupling constants in Hz involving H_2 and H_1 of the *s-cis* and *s-trans* forms of the *anti* isomer of 2-furanaldoxime

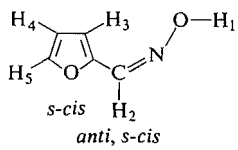

anti, s-cis

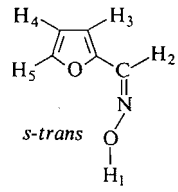

anti, s-trans

	INDO	CNDO	INDO	CNDO
$^2J(H_1, {}^{14}N)$	9.90	3.20	9.84	3.17
$^4J(H_1, H_2)$	−2.04	0.52	−1.75	0.63
$^6J(H_1, H_3)$	−0.01	−0.03	0.11	0.00
$^7J(H_1, H_4)$	−0.04	0.00	−0.02	0.02
$^7J(H_1, H_5)$	0.06	0.01	0.05	0.00
$^2J(H_2, {}^{14}N)$	10.15	9.80	8.83	9.40
$^1J(H_2, {}^{13}C)$	193.69	148.06	199.78	152.30
$^4J(H_2, H_3)$	−2.32	−0.08	−2.47	−0.19
$^5J(H_2, H_4)$	1.49	0.49	0.74	0.02
$^5J(H_2, H_5)$	−1.25	0.05	−0.39	0.56

electrons, in both isomers, values quite compatible with hydrogen bonding tendencies.

(b) Spin–Spin Coupling Constants

(i) Long-range to the Ring Protons

These were calculated using the finite perturbation technique (30). In Table 3 the calculated long-range couplings from the aldehydic to the ring protons in 2-furanaldehyde display stereospecificity for both methods, but CNDO is clearly in better overall agreement with experiment. Inasmuch as INDO considers one-center exchange integrals it includes the π electron contribution to the couplings but it apparently overestimates its magnitude somewhat. We have found a similar situation in benzaldehyde and its derivatives (3). Nevertheless, both INDO and CNDO are in semiquantitative agreement with the empirical zig–zag rule (10) of maximum coupling between protons over the "straightest" five-bond path and if the exact geometry of the sidechain were known the computational methods might even be exact (there is no evidence that solvents affect the long-range couplings).

In Table 4 (bottom) the CNDO results for $^5J(2,4)$, $^5J(2,5)$, and $^4J(2,3)$ are in best agreement with observations (Table 1) and agree with an *s-cis* form for the *anti* oxime isomer.

Can. J. Chem. Downloaded from www.nrcresearchpress.com by 210.87.254.42 on 09/05/12
For personal use only.

TABLE 5. Computed coupling constants in Hz involving H_1 and H_2 of the *s-cis* and *s-trans* forms of the *syn* isomer of 2-furanaldoxime

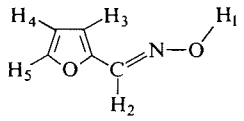

syn, s-cis

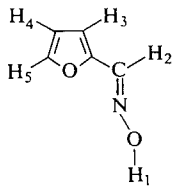

syn, s-trans

	INDO	CNDO	INDO	CNDO
$^4J(H_1, H_2)$	−2.95	−0.30	−2.85	−0.30
$^2J(H_2, ^{14}N)$	−1.87	2.07	−2.00	2.09
$^1J(H_2, ^{13}C)$	148.91	117.94	154.44	122.25
$^4J(H_2, H_3)$	−2.28	−0.11	−2.41	−0.24
$^5J(H_2, H_4)$	1.59	0.57	0.67	0.03
$^5J(H_2, H_5)$	−1.16	0.07	−0.11	0.63

Again, the CNDO results in Table 5 support our method of calculating the proportion of *s-cis* and *s-trans* forms of the *syn* isomer in solution.

(ii) Other Coupling Constants

A variety of coupling constants was calculated for the two oxime isomers (Tables 4 and 5).[3] The couplings over two bonds, $^2J(2,^{14}N)$, are not known for these oximes but are of interest because they are predicted to have a much larger magnitude in the *anti* than in the *syn* isomer, in agreement with the data available for some other oximes (31). The magnitudes of the calculated one-bond ^{13}C—H couplings in the sidechain are dependent on isomer type as is observed in the two isomers of acetaldoxime (32).

We are grateful to the National Research Council of Canada for financial support.

1. O. L. BRADY and R. F. GOLDSTEIN. J. Chem. Soc. 1959 (1927).
2. C. W. HAIGH and J. M. WILLIAMS. J. Mol. Spectrosc. **32**, 398 (1969).
3. R. WASYLISHEN and T. SCHAEFER. Can. J. Chem. **49**, 3216 (1971).
4. ODERNHEIMER. Ber. **16**, 2988 (1883) (referred to in ref. 1.
5. K. E. CALDERBANK and R. J. W. LE FÈVRE. J. Chem. Soc. 1462 (1949).
6. R. F. RAFFAUF. J. Am. Chem. Soc. **68**, 1765 (1946).
7. G. W. WHELAND. Advanced organic chemistry. 3rd ed. John Wiley and Sons, Inc., New York, N.Y., 1960.
8. G. G. KLEINSPEHN, J. A. JUNG, and S. A. STUDNIARZ. J. Org. Chem. **32**, 460 (1967).
9. S. FORSÉN, B. ÅKERMARK, and T. ALM. Acta Chem. Scand. **17**, 1712 (1963).
10. C. N. BANWELL and N. SHEPPARD. Discuss. Faraday Soc. **34**, 115 (1962).
11. S. FORSÉN and R. A. HOFFMAN. J. Mol. Spectrosc. **20**, 168 (1966).
12. K. DAHLQVIST and S. FORSÉN. J. Phys. Chem. **69**, 4062 (1965).
13. B. ROQUES, S. COMBRISSON, C. RICHE, and C. PASCARD-BILLY. Tetrahedron, **26**, 3555 (1970).
14. R. WASYLISHEN and T. SCHAEFER. Can. J. Chem. **48**, 2885 (1970).
15. Z. W. WOLKOWSKI, N. THOAI, and J. WIEMANN. Tetrahedron Lett. 93 (1970).
16. G. J. KARABATSOS and R. A. TALLER. Tetrahedron, **24**, 3347 (1968).
17. E. LUSTIG. J. Phys. Chem. **65**, 491 (1961).
18. D. HADŽI and L. PREMRU. Spectrochim. Acta, **23A**, 35 (1967).
19. D. S. JACKSON. J. Chem. Soc. B, 785 (1969).
20. P. C. CHERRY, W. R. T. COTTRELL, G. D. MEAKINS, and E. E. RICHARDS. J. Chem. Soc. C, 459 (1968).
21. (*a*) Z. W. WOLKOWSKI. Tetrahedron Lett. 825 (1971). (*b*) B. L. SHAPIRO, J. R. HLUBUCEK, G. R. SULLIVAN, and L. F. JOHNSON. J. Am. Chem. Soc. **93**, 3281 (1971).
22. J. A. POPLE and D. L. BEVERIDGE. Approximate molecular orbital theory. McGraw-Hill Book Co., New York, N.Y., 1970.
23. Program 141. QCPE. Indiana University, Bloomington, Indiana.
24. B. BAK, D. CHRISTENSEN, W. B. DIXON, L. HANSEN-NYGAARD, J. R. ANDERSON, and M. SCHOTTLÄNDER. J. Mol. Spectrosc. **9**, 124 (1962).
25. B. HARRIS, R. J. W. LE FÈVRE, and E. P. A. SULLIVAN. J. Chem. Soc. 1622 (1953).

[3]A smaller variety was calculated for the *syn* isomer, mainly for financial reasons: as many as 100 cycles of the SCF procedure were necessary to obtain convergence to 0.01 to 0.02 Hz in INDO; as few as 50 cycles sufficed for the CNDO computations.

Can. J. Chem. Downloaded from www.nrcresearchpress.com by 210.87.254.42 on 09/05/12
For personal use only.

26. N. S. HUSH and J. R. YANDLE. Chem. Phys. Lett. **1**, 493 (1967).
27. G. E. MACIEL, J. W. MCIVER, JR., N. S. OSTLUND, and J. A. POPLE. J. Am. Chem. Soc. **92**, 4497 (1970).
28. B. JERSLEV. Nature, **180**, 1410 (1957).
29. K. FOLTING, W. N. LIPSCOMB, and B. JERSLEV. Acta. Cryst. **17**, 1263 (1963).
30. J. A. POPLE, J. W. MCIVER, JR. and N. S. OSTLUND. Chem. Phys. Lett. **1**, 465, (1967).
31. D. CREPAUX, J. M. LEHN, and R. R. DEAN. Mol. Phys. **16**, 225 (1969).
32. T. YONEZAWA, I. MORISHIMA, K. FUKUTA, and Y. OHMORI. J. Mol. Spectrosc. **31**, 341 (1969).
33. R. FREEMAN and R. C. JONES. J. Chem. Phys. **52**, 465 (1970).

Can. J. Chem. Downloaded from www.nrcresearchpress.com by 210.87.254.42 on 09/05/12
For personal use only.

Sterically Hindered Aromatic Compounds. III.[1] Acid-catalyzed Reactions of 2,4,6-Tri-*t*-butyl- and 2-Methyl-4,6-di-*t*-butylbenzyl Alcohols and Chlorides

L. R. C. BARCLAY, H. R. SONAWANE,[2] AND M. C. MACDONALD
Department of Chemistry, Mount Allison University, Sackville, New Brunswick

Received August 30, 1971

Treatment of 2,4,6-tri-*t*-butylbenzyl alcohol (**2**), the corresponding benzyl chloride (**3**) and methyl ether (**5**) with strong acids gave high yields of 1,1-dimethyl-4,6-di-*t*-butylindane (**10**). On the other hand, acid-catalyzed reactions on 2-methyl-4,6-di-*t*-butylbenzyl alcohol (**13**), chloride (**16**), and methyl ether (**12**) yielded nucleophilic substitution products. According to comparative hydride transfer reactions between triethylsilane and carbonium ions generated from **2**, **3**, **13**, and **16** in trifluoroacetic acid, the 2,4,6-tri-*t*-butylbenzyl cation is very readily formed. A mechanism suggested for the formation of **10** involves this cation as an intermediate.

L'action des acides forts sur l'alcool tri-*t*-butyl-2,4,6 benzylique (**2**), sur le chlorure de benzyle (**3**) correspondant et sur l'éther méthylique (**5**) conduit au diméthyl-1,1 di-*t*-butyl-4,6 indane (**10**). D'un autre côté, les réactions acido-catalysées sur l'alcool méthyl-2 di-*t*-butyl-4,6 benzylique (**13**), sur le chlorure (**16**) correspondant, et sur l'éther méthylique (**12**) conduisent à des produits de substitution nucléophile. D'après des réactions comparables par transfert d'hydrure entre le triéthylsilane et les ions carboniums engendrés à partir de **2**, **3**, **13** et **16** et l'acide trifluoroacétique, le cation tri-*t*-butyl-2,4,6 benzyle se forme très rapidement. Un mécanisme est proposé pour la formation de **10** et celui-ci implique ce cation en tant qu'intermédiaire.

Canadian Journal of Chemistry, **50**, 281 (1972)

Introduction

Previous investigations in this laboratory established that two ortho *t*-butyl groups exert extreme steric hindrance on a carboxyl function. This was evident in the properties of 2,4,6-tri-*t*-butylbenzoic acid (1) and the unusual alkaline hydrolysis ($B_{AL}2$) of its methyl ester (2). The present investigation was undertaken to determine the effect of alkyl substituents, especially *o*-*t*-butyl, on reactions at an adjacent tetrahedral carbon function. Polyalkylated benzyl alcohols and chlorides were therefore required for solvolyses and related studies. A preliminary communication (3) reported unexpected high reactivity of 2,4,6-tri-*t*-butylbenzyl alcohol and -methyl ether. Under acid conditions, these compounds underwent a novel cyclization between the benzylic position and an ortho-*t*-butyl group. The purpose of the present paper is to report the details of these and related results. The nature of the side chain insertion reaction has been explored by the use of deuterium tracer in the benzylic group and by some carbonium ion–hydride transfer reactions.

[1]References 1 and 2 are considered as part I and II in this series.

[2]On leave of absence from the National Chemical Laboratory, Poona, India.

Results and Discussion

(a) Synthesis of Tri-t-butylbenzyl Compounds and the Cyclization Product 1,1-Dimethyl-4,6-di-t-butylindane

2,4,6-Tri-*t*-butylphenyllithium (**1**) prepared by bromine–lithium exchange on 2,4,6-tri-*t*-butylbromobenzene (1), was the starting point for synthesizing various 2,4,6-tri-*t*-butylbenzyl compounds (Scheme 1).

As reported earlier (4), reaction of **1** with formaldehyde yielded 2,4,6-tri-*t*-butylbenzyl alcohol (**2**) and reaction of the latter with thionyl chloride yielded the benzylchloride **3**. The reaction sequence **1**→**2**→**3** using dideutero formaldehyde proved very convenient for the synthesis of α,α-dideutero-2,4,6-tri-*t*-butylbenzyl chloride for tracer studies. The formation of **2** was accompanied by varying amounts of the ester 2,4,6-tri-*t*-butylbenzyl formate (**4**). This side reaction was not studied in detail. It is presumably a consequence of reaction of the intermediate 2,4,6-tri-*t*-butylbenzyloxy anion with formaldehyde followed by a hydride ion transfer analogous to the Cannizzaro reaction. Reaction of **1** with chloromethylmethyl ether yielded 2,4,6-tri-*t*-butylbenzylmethyl ether (**5**) and cleavage of **5** with boron chloride yielded **3** in high yield. The reaction sequence **1**→**5**→**3** was the preferred method for larger scale

Can. J. Chem. Downloaded from www.nrcresearchpress.com by 210.87.254.40 on 09/05/12
For personal use only.

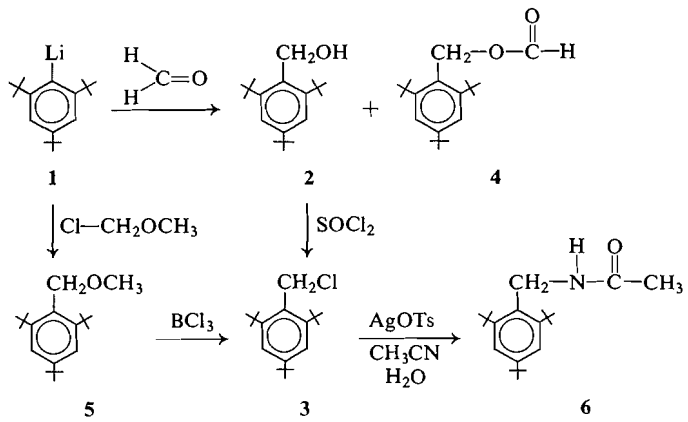

SCHEME 1

preparations of **3**. The intermediate ether (**5**) is readily purified and the side reaction involved in the conversion of **1** → **2** → **4** is avoided.

The alcohol **2** failed to react with toluenesulfonyl chloride. Steric hindrance afforded by the two *o*-*t*-butyl groups is evidently sufficient to prevent the alcohol **2** from attacking the sulfonyl chloride group. An attempt to prepare the tosylate from the chloride **3** by the action of silver tosylate in acetonitrile (5) resulted in the formation of the *N*-acetate (**6**) as the only identifiable product. The formation of **6** apparently results from attack of the carbonium ion derived from **3** on the solvent acetonitrile in a manner analogous to the Ritter reaction (6). This result was a preliminary indication of the reactivity of **3** under ionizing conditions.

Treatment of the alcohol **3** or the ether **5** was reported earlier (3) to yield a new hydrocarbon which was assigned the structure 1,1-dimethyl-4,6-di-*t*-butylindane (**10**) from spectroscopic evidence. It was desirable to have an independent synthesis of **10**. This was accomplished by Friedel–Crafts *t*-butylation of 1,1-dimethylindane (**7**) and of 1,1-dimethyl-6-*t*-butylindane (**8**) (see Scheme 2). It was necessary to carry out the *t*-butylations under mild conditions (below 0°, using pentane solvent which does not dissolve aluminum chloride) to avoid complex hydride transfers and dealkylation which may take place on compounds such as **7** (7). These mild conditions effected partial *t*-butylation of **7** to yield initially a mixture of approximately equal amounts of **8** and a new hydrocarbon. Comparison of its n.m.r. spectrum with that of **8** indicated that the structure is most probably 1,1-dimethyl-5-*t*-butylindane (**9**). On longer reaction time, **8** was converted into **10** (7%) while the relative amount of **9** increased. A separate partial *t*-butylation of **8** yielded **10** (25%) directly.

(b) Acid-catalyzed Reactions of the Trialkylbenzyl Compounds

The results from various acid-catalyzed reactions on 2,4,6-tri-*t*-butylbenzyl compounds are given in Table 3 (see Experimental) and outlined in Scheme 3. Reaction of methyl 2,4,6-tri-*t*-butylbenzyl ether (**5**) with hydriodic acid–acetic acid (Table 3, no. 1) yielded 1,1-dimethyl-4,6-di-*t*-butylindane (**10**). Reaction of 2,4,6-tri-*t*-butylbenzyl alcohol (**2**) with a variety of acids also yielded **10** as a major reaction product

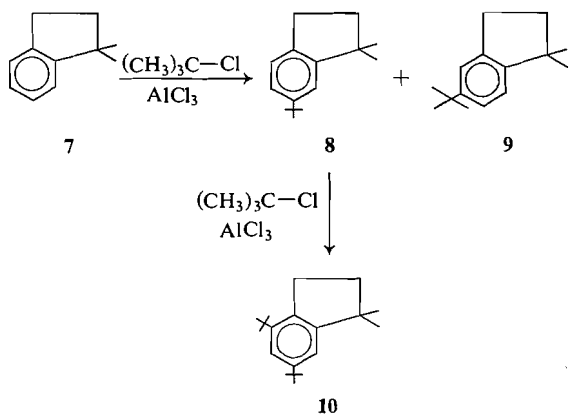

SCHEME 2

Can. J. Chem. Downloaded from www.nrcresearchpress.com by 210.87.254.40 on 09/05/12
For personal use only.

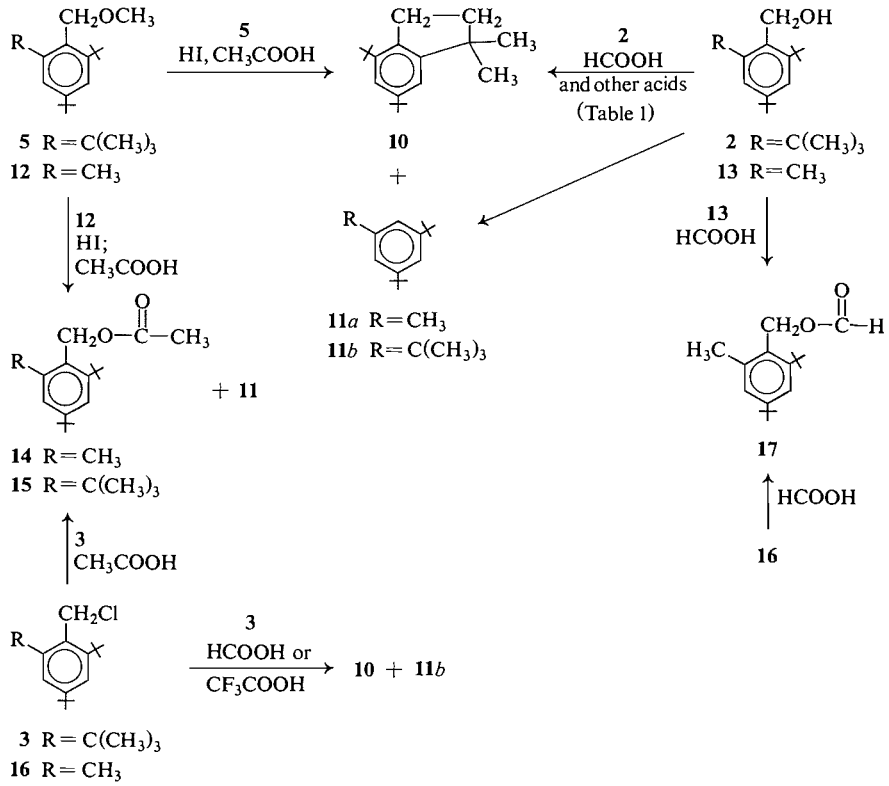

SCHEME 3

(nos. 2–6). Treatment of the chloride (**3**) with formic acid also gave a high yield of **10** (run 7*a*). The latter reaction apparently takes place by initial formation of 2,4,6-tri-*t*-butylbenzyl formate (**4**) (run 7*b*, *c*). On the other hand reaction of **2** with acetic acid stopped at formation of the corresponding acetate (run 8); there being no evidence for cyclization in this case.[3]

2-Methyl-4,6-di-*t*-butylbenzyl compounds were selected for a comparative study with the results on the tri-*t*-butylbenzyl series outlined above. The results are summarized in Table 4. (For structural formulas see Scheme 3.) Acid-catalyzed reactions on 2-methyl-4,6-di-*t*-butylbenzyl methyl ether (**12**) (Table 4, no. 1), corresponding alcohol (**13**) (nos. 2–5), and chloride (**16**) all led to the formation of expected nucleophilic substitution products (**14**, **16**, **17**) as the main reaction.

There was no evidence for the formation of cyclization products into the ortho-*t*-butyl group analogous to that found for the tri-*t*-butylbenzyl series.

(c) Carbonium Ion–Hydride Transfer Reactions of Alkyl Benzyl Chlorides and Alcohols

One mechanism considered (3) for the formation of the substituted indane **10** from the 2,4,6-tri-*t*-butylbenzyl compounds involved insertion of a hindered benzylic cation into a C—H bond of an ortho-*t*-butyl group. It was desirable therefore, to obtain some independent indication of the tendency of our trialkylbenzyl systems to form carbonium ions. Carey and Tremper (8) found that organosilanes such as triethylsilane will efficiently transfer hydride to free carbonium ions generated in acid medium from corresponding alcohols. Their studies in-

[3]A referee has suggested two explanations for the failure of acetic acid to produce the indane **10**: (*1*) acetic acid is a better nucleophile than the other acids used and (*2*) a more intimate ion pair is formed with the weaker acetic acid than the others acids. A shorter cation lifetime would be the result in either case with a resultant lower probability of indane formation.

Can. J. Chem. Downloaded from www.nrcresearchpress.com by 210.87.254.40 on 09/05/12
For personal use only.

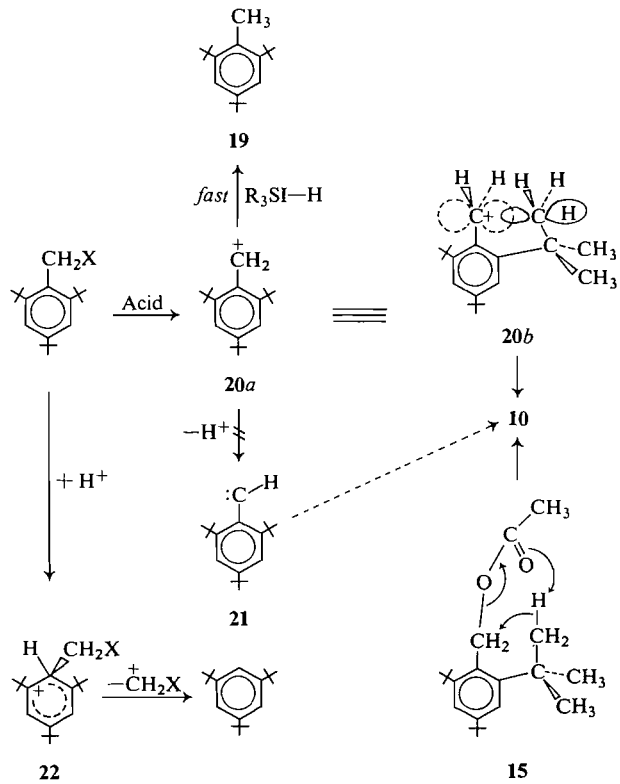

SCHEME 4

cluded hydride transfer to the 2,4,6-trimethyl cation to yield isodurene. We employed this technique as a probe for the behavior of the carbonium ions generated from trialkylbenzyl chlorides as well as alcohols. The results of our preliminary study are shown in Table 5. Benzyl chloride failed to undergo the hydride transfer in the presence of trifluoroacetic acid and triethylsilane even on prolonged treatment. This is in agreement with the behavior reported for benzyl alcohol (8). 2,4,6-Trimethylbenzyl chloride, like the corresponding alcohol (8), efficiently underwent the hydride transfer to yield isodurene (no. 2) and this shows that the method can be used to trap carbonium ions generated from chlorides as well as from alcohols. Both 2-methyl-4,6-di-*t*-butylbenzyl alcohol (**13**) and 2,4,6-tri-*t*-butylbenzyl alcohol (**2**) were readily converted (nos. 3 and 4) into the respective hydrocarbons, 2-methyl-4,6-di-*t*-butyltoluene (**18**) and 2,4,6-tri-*t*-butyltoluene (**19**) presumably via formation of intermediate substituted benzylic cations. An effort was made to determine the relative tendencies for carbonium ion formation from the corresponding trialkyl chlorides **16** and **3** (nos. 5 and 6) with some success. Direct n.m.r. observations showed that **16** was one half converted into the respective hydrocarbon (**18**) in 40 min. On the other hand the conversion of 2,4,6-tri-*t*-butylbenzyl chloride (**3**) was almost too fast to measure; being more than 80% converted into 2,4,6-tri-*t*-butyltoluene in 5 min. The results definitely establish the strong tendency for **3** (and **2**) to ionize to form the cation and indicate that the relative tendency for carbonium ion formation is -2,4,6-tri-*t*-butylbenzyl > 2-methyl-4,6-di-*t*-butylbenzyl > 2,4,6-trimethylbenzyl.

(d) A Mechanism for the Cyclization Reaction of 2,4,6-Tri-t-butylbenzyl Compounds

The very facile hydride transfer reactions observed for 2,4,6-tri-*t*-butylbenzyl chloride and alcohol in acid medium indicate ready formation of the carbonium ion (**20***a*, Scheme 4). Furthermore the cyclization reaction was observed under conditions (Table 3, no. 5) similar

Can. J. Chem. Downloaded from www.nrcresearchpress.com by 210.87.254.40 on 09/05/12
For personal use only.

Can. J. Chem. Downloaded from www.nrcresearchpress.com by 210.87.254.40 on 09/05/12
For personal use only.

to those used for the direct observation of the carbonium **20***a* by n.m.r. methods (4). These results indicate that the carbonium ion **20***a* is an intermediate in the cyclization leading to **10**. The detailed mechanism of this unique cyclization remains to be determined. Certain carbonium ions are known to form carbenes (9) by α-proton elimination and we considered that the cyclization might have taken place by insertion of the carbene **21** into a C—H bond of an *o*-*t*-butyl group. However, this possible mechanism must be excluded by the fact that there is no loss or rearrangement of deuterium during the cyclization of α,α-dideutero-2,4,6-tri-*t*-butyl chloride (Table 3, no. 9). This result also makes untenable complex mechanisms for cyclization which involve rearrangements, hydride shifts, and alkylations. We favor a mechanism involving insertion of the benzylic cation into an ortho-*t*-butyl group. Examination of space filling molecular models for the cation **20***a* shows strong steric congestion between the $\overset{+}{C}$—H bonds and the ortho-*t*-butyl groups when the —$\overset{+}{C}H_2$ group is coplanar with the aromatic ring. This congestion is relieved by rotation of the —$\overset{+}{C}H_2$ group out-of-plane. In the resulting conformer (**20***b*), the tail of an sp^3 orbital of a C—H in an ortho-*t*-butyl can line up in very close proximity to the —$\overset{+}{C}H_2$ group so as to overlap with the vacant p orbital. Steric congestion is not nearly so evident in the 2-methyl-4,6-di-*t*-butylbenzyl cation. This could explain why the latter undergoes intermolecular nucleophilic reactions rather than insertion into the ortho-*t*-butyl group.

There does not appear to be a very close analogy to this kind of carbonium ion insertion. On the other hand cyclizations into an ortho-*t*-butyl group are known. A comparison has been made (3) between our reaction forming the substituted indane (**10**) and the bond insertion by cationic nitrogen into an ortho-*t*-butyl group observed by Lansbury and co-workers (10). The formation of 1,1-dimethyl-4-carboxyl-6-nitrobenzocyclobutene from the diazonium salt of 3-amino-4-*t*-butyl-5-nitrobenzoic acid could be explained by an intramolecular electrophilic substitution of an aromatic cation into an ortho-*t*-butyl group (11) but a free radical mechanism was also considered. A mechanistic analogy was made by Baker and Davis (12) between our reaction and their reported cyclization into an aromatic methyl group by cationic oxygen during decomposition of the hypobromite of 1,5,8-trimethyl-1,2,3,4-tetrahydronaphth-1-ol. However, this analogy is probably not valid because Boido and Edwards have recently shown (13) that reactions of this kind are homolytic rather than ionic.

Trialkyl benzenes were formed in varying yields during various acid-catalyzed reactions of the trialkylbenzyl compounds. These hydrocarbons are most probably formed by protonation of the aromatic ring (*e.g.* **22**, Scheme 4) and elimination of the —CH_2—X group via a reverse Freidel–Crafts type reaction.

Examination of the fragmentation pattern in the mass spectrum of 2,4,6-tri-*t*-butylbenzyl acetate (**15**) indicated possible formation of the cyclic hydrocarbon **10** especially in the appearance of a peak at *m/e* 243, which is the most intense peak observed for the hydrocarbon **10**. This could result from a cyclic elimination on the acetate (**15**) (Scheme 4) similar to reactions observed in the pyrolysis of acetates and analogous to reactions recently observed in the mass spectrometer by Field (14). Vapor phase pyrolysis of the substituted benzyl acetates is now under investigation.

Experimental

The n.m.r. spectra were recorded on a Varian A-60 NMR Spectrometer using carbon tetrachloride solvent containing tetramethylsilane as internal standard. The i.r. spectra were recorded on a Perkin–Elmer model 337 Grating Spectrophotometer using potassium bromide pellets for solids and films for liquids. The u.v. spectra were recorded on a Beckmann DK-2 Spectrophotometer using cyclohexane solvent. The g.l.c. analyses were determined by means of F & M model 500 and model 700 programmed temperature gas chromatographs with dual columns. The columns were 1/4 in. by approximately 10 ft and packed with Apiezon grease (20%), unless noted otherwise, on Chromosorb W. Melting points were determined on a hot stage equipped with a microscope and are uncorrected. Elemental analyses were determined by C. Daesslé, Montreal and by A. Bernhardt, West Germany.

Preparations of Tri-t-butylbenzyl Compounds

(1) 2,4,6-Tri-t-butylbenzyl Alcohol (2)

2,4,6-Tri-*t*-butylbromobenzene was prepared as described previously (1). The crude product was always contaminated with a small amount of a yellow compound. The latter was separated readily due to its insolubility in cold carbon disulfide. Recrystallization from carbon disulfide yielded brilliant yellow needles, m.p. 165–166°.

Anal. Calcd. for $C_{14}H_{18}NO_4Br$ (mol. wt. 344): C, 48.85; H, 5.26; Br, 23.22. Found (344 (mass spectrum)): C, 48.82, 48.71; H, 5.47, 5.50; Br, 23.34, 22.92.

Can. J. Chem. Downloaded from www.nrcresearchpress.com by 210.87.254.40 on 09/05/12
For personal use only.

This yellow compound showed i.r. bands at 1675 and 1690 (s) (conjugated carbonyls), 1540 cm^{-1} (s) (NO_2 group); u.v. bands at λ_{max} 269 (ε 8800), 334 (ε 634), 415.5 (ε 103), and 555 mμ (ε 50.5); and n.m.r. bands at 8.66 and 8.51 τ (singlets) of equal intensity, assigned to two *t*-butyl groups.[4]

2,4,6-Tri-*t*-butylbromobenzene was converted into 2,4,6-tri-*t*-butylphenyllithium (1) and the latter reacted with formaldehyde as described (4) to prepare 2,4,6-tri-*t*-butylbenzyl alcohol (**2**). A mixture of the alcohol and a carbonyl compound (i.r.) was obtained. The latter compound was separated by chromatography on basic alumina and elution with petroleum ether. After sublimation the crystalline compound melted at 109–110°.

Anal. Calcd. for $C_{20}H_{32}O_2$: C, 78.89; H, 10.59. Found: C, 78.60; H, 10.57.

It showed an i.r. band at 1710 cm^{-1} (s) (carbonyl), n.m.r. bands at 8.66–8.56, 4.41, 2.61, and 0.02 τ (all singlets) with intensity ratios of 27:2:2:1 and assigned to the three *t*-butyls, benzylic methylene, aromatic hydrogens, and aldehydic hydrogen respectively.

(2) Methyl 2,4,6-Tri-t-butylbenzyl Ether (5)

2,4,6-Tri-*t*-butylbromobenzene (5.48 g, 0.016 mol) in 300 ml anhydrous ethyl ether was exchanged with *n*-butyllithium (13.2 ml hexane solution, 0.020 mol) under a dry nitrogen atmosphere for 1 h. Freshly distilled chloromethyl methyl ether (1.5 ml, 0.02 mol) in anhydrous ethyl ether was slowly added to the reaction at room temperature. The reaction was continued until g.l.c. analyses on aliquots indicated that the amount of desired ether (**5**) was optimized (12 h, 67% **5**). The reaction mixture was then shaken with diluted hydrochloric acid, water, dried over calcium chloride, and the solvent distilled. The residue was recrystallized from ethanol to yield colorless crystals, m.p. 79–80°.

Anal. Calcd. for $C_{20}H_{34}O$: C, 82.76; H, 11.72; OCH_3, 10.69. Found: C, 83.04; H, 11.82; OCH_3, 10.47.

It showed an i.r. band at 1050 cm^{-1} (s) (ether group) and n.m.r. bands at 8.72, 8.56, 6.76, 5.38, 2.72 τ (all singlets) in intensity ratios of 9:18:3:2:2 and assigned to *p*-*t*-butyl, *o*-*t*-butyls, -O-CH_3, benzylic methyl and aromatic hydrogens respectively.

(3) 2,4,6-Tri-t-butylbenzyl Chloride (3) and the α,α-Dideutero Chloride

Methyl 2,4,6-tri-*t*-butylbenzyl ether (1.53 g, 0.053 mol) was placed in a test tube cooled in an acetone–liquid nitrogen trap and 12 ml of boron trichloride was condensed in the test tube. After 30 min, the boron trichloride was allowed to evaporate, the crystalline residue dissolved in ethyl ether, the solution extracted with 1% sodium hydroxide, and the extract washed with water. Distillation of the ether left colorless crystals, m.p. 141–144° (lit. (4) 141.5–143.5°). The n.m.r. spectrum showed bands at 8.70, 8.47, 4.72, and 2.60 τ (singlets) in the intensity ratios of 9:18:2:2 and assigned to the *p*-*t*-butyl, *o*-*t*-butyls, methylene group, and aromatic hydrogens, respectively. This chloride proved identical by mixed m.p. and n.m.r. spectra to the chloride prepared from 2,4,6-tri-*t*-butylbenzyl alcohol (**2**) by the reaction of **2** with thionyl chloride (4).

α,α-Dideutero-2,4,6-tri-*t*-butylbenzyl alcohol was prepared by the reaction of 2,4,6-tri-*t*-butylphenyllithium with formaldehyde-d_2 (Merck, Sharp & Dohme) according to the procedure used for **2** above. The dideutero alcohol was converted into α,α-dideutero-2,4,6-tri-*t*-butylbenzyl chloride by the thionyl chloride method as before. The deuterium substitution at the methylene position of this chloride was found by comparative mass spectroscopic analysis to be essentially complete. The results for the major peaks are summarized in Table 1.

TABLE 1. Major mass spectral peaks 2,4,6-tri-*t*-butylbenzyl chloride and dideutero chloride

	Peak	Relative intensity	Assignment
Chloride **3**	294	58	M^+ (parent mass)
	279	46	M—CH_3
	259	100	M—Cl
	243	75	M—(CH_3, HCl)
α,α-Dideutero chloride	296	65	M^+ (parent mass)
	281	53	M—CH_3
	261	100	M—Cl
	245	75	M—(CH_3, HCl)

(4) Reaction of 2,4,6-Tri-t-butylbenzyl Chloride (3) with Silver Tosylate in Acetonitrile

The chloride (**3**) (0.294 g, 1.0 mmol) was added to a solution of silver tosylate (0.279 g, 1.0 mmol) in 2 ml of acetonitrile cooled to 0°. The precipitated silver chloride was removed by filtration and the solvent distilled to leave an amorphous residue which crystallized on adding water (yield 0.200 g, 63%). Recrystallization from petroleum ether yielded colorless crystals, m.p. 264–265°.

Anal. Calcd. for $C_{21}H_{35}ON$: C, 79.44; H, 11.11. Found: C, 79.96, 79.79; H, 11.20, 11.13.

This compound showed i.r. bands at 3280 cm^{-1} (m) (>N—H) and 1670 cm^{-1} (s) (carbonyl) and n.m.r. bands at 8.68, 8.55, 8.12, 5.17, and 2.55 τ (singlets) in intensity ratios of 9:18:3:2:2 assigned to *p*-*t*-butyl, *o*-*t*-butyls, —$COCH_3$, benzylic methylene, and aromatic hydrogens respectively.

(5) 2,4,6-Tri-t-butyltoluene (19)

(a) From 2,4,6-Tri-t-butylphenyllithium

2,4,6-Tri-*t*-butylphenyllithium was prepared from 2,4,6-tri-*t*-butylbromobenzene (2.5 g, 7.7 mol) and *n*-butyllithium (16 mmol) in ethyl ether. The solvent and butyl bromide formed were removed by distillation to dryness under reduced pressure at room temperature. Methyl iodide (2.8 g, 20 mmol) in ethyl ether was added to the residue and the mixture heated under reflux for 18 h. The reaction mixture was extracted with dilute hydrochloric acid, the solvent distilled and the residue sublimed at 70° and 0.7 mm. The colorless crystals obtained melted at 161–162° (0.95 g, 48%). This compound showed a broad u.v. band at λ_{max} 270 mμ (ε 204) and n.m.r. bands at 8.66, 8.51, 7.37 and 2.62 τ in intensity ratios of 9:18:3:2 and assigned to the *p*-*t*-butyl, *o*-*t*-butyls, arylmethyl, and aromatic hydrogens respectively.

[4]The structural formula

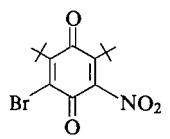

is assigned to this compound. Its mode or formation is not yet understood. It presumably involves nitration, bromination, and oxidation as well as di-*t*-butylation. The latter reaction is quite common under similar conditions (15).

Can. J. Chem. Downloaded from www.nrcresearchpress.com by 210.87.254.40 on 09/05/12
For personal use only.

TABLE 2. *t*-Butylation of 1,1-dimethylindane

Reaction time (h)		Products (%) in order of elution by g.l.c.
2	A	1,1-Dimethylindane (**7**) (88)
	B	6-*t*-Butyl-1,1-dimethylindane (**8**) (5.8)
	C	5-*t*-Butyl-1,1-dimethylindane (**9**) (6.1)
5.5	D	Trace of 1,1-dimethyl-4,6-di-*t*-butylindane (**10**) as well as A, B, and C
24*	A	**7** (18)
	B	**8** (29)
	C	**9** (45)
	D	**10** (7)

*More *t*-butyl chloride (3.80 g, 0.041 mol) and aluminum chloride (0.65 g) were added during this period

Mass spectroscopic analysis showed the expected parent mass of 260 with the base peak at 245 (M—CH_3). The above n.m.r. spectrum agrees with that reported in the literature (16) for **19** but there is a disparity between the melting points (lit. (16) m.p. for **19** is 149°). Therefore, we confirmed the identity of our **19** by an alternate synthesis below.

(b) From 2,4,6-Tri-t-butylbenzyl Chloride (3)

The chloride (3) (0.15 g, 0.51 mmol) was reduced by treatment with lithium aluminum hydride (0.5 g) in tetrahydrofuran at reflux temperature for 4 h followed by standing overnight. The excess hydride was destroyed with ethyl acetate, the product poured over ice, and extracted with ethyl ether. Distillation of the solvent yielded 0.12 g (92%) of crystalline product, m.p. 157°. Recrystallization from methanol raised the m.p. to 159°. It proved identical to the hydrocarbon from procedure *a* by mixed m.p. and n.m.r. spectra.

Synthesis of 1,1-Dimethyl-4,6-di-t-butylindane (10)

(1) t-Butylation of 1,1-Dimethylindane (7)

1,1-Dimethylindane (American Petroleum Institute) (17) (1.00 g, 6.8 mmol) was dissolved in 10 ml freshly distilled pentane and the mixture cooled to −5°. *t*-Butyl chloride (1.30 g, 13.6 mmol) in 10 ml of pentane and anhydrous aluminum chloride (0.266 g, 2.0 mmol) were slowly added to the reaction mixture over a period of 2 h, while the reaction course was monitored by g.l.c. analyses on aliquots. The results of the alkylation after 2 h, and after an extended period are summarized in Table 2.

The three products (g.l.c. components B, C, and D) were collected from the gas chromatograph. Components B and D were identified as 6-*t*-butyl-1,1-dimethylindane and 1,1-dimethyl-4,6-di-*t*-butylindane by comparison of their n.m.r. spectra and g.l.c. retention times with authentic samples. The main product (C) was a new liquid hydrocarbon.

Anal. Calcd. for $C_{15}H_{22}$: C, 89.04; H, 10.96. Found: C, 89.16, 89.07; H, 10.68, 10.67.

It showed n.m.r. bands at 8.79 (singlet), 8.74 (singlet), 8.14 (triplet $\Delta = 7$ Hz), 7.17 (triplet $\Delta = 7$ Hz), and 2.94 τ (multiplet) with intensity ratios of 6:9:2:2:3, assigned to the *gem*-dimethyls, *t*-butyl, β-methylene, α-methylene and aromatic hydrogens respectively. This spectrum was very similar to that of 6-*t*-butyl-1,1-dimethylindane (**8**) but they could be distinguished by slight differences in the aromatic hydrogen region.

(2) t-Butylation of 6-t-Butyl-1,1-dimethylindane (8)

6-*t*-Butyl-1,1-dimethylindane (American Petroleum Institute) (17) (1.00 g, 5.0 mmol) was alkylated with *t*-butyl chloride (1.38 g, 14.9 mmol) and anhydrous aluminum chloride (0.27 g, 2.0 mmol) using the above procedure. After a reaction time of 24 h, g.l.c. analysis and n.m.r. spectra on collected fractions showed 75% starting hydrocarbon (**8**) and 25% 1,1-dimethyl-4,6-di-*t*-butylindane (**10**).

Preparation of 2-Methyl-4,6-di-t-butyl Compounds

2-Methyl-4,6-di-*t*-butylbenzyl chloride (**16**), 2-methyl-4,6-di-*t*-butylbenzyl alcohol (**13**), and methyl 2-methyl-4,6-di-*t*-butylbenzyl ether (**12**) were prepared by procedures of Beets and co-workers (18).

(1) 2-Methyl-4,6-di-t-butylbenzyl Formate (17)

2-Methyl-4,6-di-*t*-butylbenzyl chloride (**16**) (0.253 g, 1 mmol) was added to a solution containing 0.7 ml of dioxane, 0.5 ml of formic acid, and 0.07 g of sodium formate. The mixture was heated on the steam cone until the n.m.r. spectrum showed that the benzylic methylene absorption of **16** (5.0 τ) had disappeared and was replaced by a new band at 4.5 τ (approximately 3/4 h). Solid sodium carbonate was added to neutralize excess acid and the solvent was distilled under reduced pressure. The crystalline residue was sublimed at 40°, 0.05 mm to give colorless crystals, m.p. 50–51.5°.

Anal. Calcd. for $C_{17}H_{26}O_2$: C, 77.81; H, 9.99. Found: C, 77.88, 78.00; H, 10.02, 10.18.

This compound had an i.r. band at 1725 cm^{-1} (carbonyl) and n.m.r. bands at 8.69 (singlet), 8.58 (singlet), 7.67 (singlet), 4.57 (singlet), 2.93 (doublet), 2.60 (doublet), and 1.92 (singlet) in intensity ratios of 9:9:3:2:1:1:1 and assigned to the *p*-*t*-butyl, *o*-*t*-butyl, aryl methyl, benzylic methylene, aromatic hydrogens, and aldehydic hydrogen respectively.

(2) 2-Methyl-4,6-di-t-butyltoluene (18)

2-Methyl-4,6-di-*t*-butyltoluene was prepared by hydride reduction of 2-methyl-4,6-di-*t*-butylbenzyl chloride according to the procedure under 5*b* (above). An analytical sample of the liquid hydrocarbon **18** was obtained by collection from g.l.c.

Anal. Calcd. for $C_{16}H_{26}$ (mol. wt. 218): C, 88.06; H, 11.94. Found (218 (mass spectrum)): C, 88.06, 87.92; H, 12.12, 12.11. The n.m.r. spectrum showed bands at 8.73, 8.59, 7.78, 7.68 (singlets), 3.04 (doublet), and 2.77 (doublet) in intensity ratios of 9:9:3:3:1:1, assigned to the *p*-*t*-butyl, *o*-*t*-butyl, two aryl methyls, and aromatic hydrogens respectively.

Acid-catalyzed Reactions of 2,4,6-Tri-t-butylbenzyl Compounds

Details on the conditions and yields of products from acid-catalyzed reactions of methyl 2,4,6-tri-*t*-butylbenzyl ether (**5**), alcohol (**2**), and chloride (**3**) are outlined in Table 3. Products from the reactions with thionyl chloride were obtained by distillation of the excess reagent under reduced pressure followed by g.l.c. analysis of the product (no. 2*a*) or crystallization (no. 2*b*). The other reactions were worked-up by pouring the reaction mixtures into crushed ice, followed by ether extraction, washing with dilute sodium carbonate and with water. The ether extracts were concentrated to a small volume for g.l.c. analyses. Compounds were identified by the use of known synthetic samples as internal standards on g.l.c. analyses and by collection of samples from the g.l.c. for spectral analyses.

Can. J. Chem. Downloaded from www.nrcresearchpress.com by 210.87.254.40 on 09/05/12
For personal use only.

TABLE 3. Acid-catalyzed reactions of 2,4,6-tri-*t*-butylbenzyl compounds

No.	Compound treated (mmol)	Reagent	Conditions (solvent; temperature; time)	Products (%)*
1	Methyl 2,4,6-tri-*t*-butylbenzyl ether (**5**) (0.69)	HI (1 ml)	CH_3COOH (10 ml); reflux; 1 h	1,1-Dimethyl-4,6-di-*t*-butylindane (**10**) (85); 1,3,5-tri-*t*-butylbenzene (**11***b*) (15)
2*a*	2,4,6-Tri-*t*-butylbenzyl alcohol (**2**) (0.54)	$SOCl_2$ (20 ml)	Reflux; 1 h	**10** (55); **11***b* (5); **2** (40)
2*b*	**2** (3.60)	$SOCl_2$ (4 ml)	25°; 24 h	2,4,6-Tri-*t*-butylbenzyl chloride (**3**) (79)
3	**2** (0.72)	HCl–$ZnCl_2$ (4 ml)	CH_3COOH; reflux; 3 h	**10** (86), **11***b* (14)
4	**2** (1.13)	HCOOH (10 ml)	100°; 2 h	**10** (>90)†
5	**2** (0.40)	SbF_5-FSO_3H (3 g)	SO_2; −78 to −40°; 1 h	**10** (81); **11***b* (3); **2** (16)
6	**2** (0.34)	CF_3COOH (0.25 ml)	$CHCl_2CHCl_2$; 95°; 3/4 h 4 h	**10** (25)‡ **10** (31); **11***b* (69)
7*a*	2,4,6-Tri-*t*-butylbenzyl chloride (**3**) (0.34)	HCOOH (10 ml)	100°; 3 h	**10** (90), **11***b* (10)
7*b*	**3** (0.22)	HCOOH (5 ml)	100°; 6 min	2,4,6-Tri-*t*-butylbenzyl formate (**4**) (67)†
7*c*	**4** (0.23)	HCOOH (10 ml)	100°; 1/2 h	**10** (54); **4** (46)‡
8	**3** (0.34)	CH_3COOH (10 ml)	100°; 3 h	2,4,6-Tri-*t*-butylbenzyl acetate (**15**) (76); **3** (24)
9	α,α-Dideutero-2,4,6-tri-*t*-butylbenzyl chloride (0.20)	HCOOH (5 ml)	100°; 3 h	3,3-Dideutero-1,1-dimethyl-4,6-di-*t*-butylindane (98), **11***b* (2)

*The percentages are relative amounts by gas chromatographic analyses, except where noted otherwise.
†Yields of runs 4 and 7*b* are actual amounts isolated.
‡The percentages here were determined by direct n.m.r. observations on the reaction.

Can. J. Chem. Downloaded from www.nrcresearchpress.com by 210.87.254.40 on 09/05/12
For personal use only.

TABLE 4. Acid-catalyzed reactions of 2-methyl-4,6-di-*t*-butylbenzyl compounds

No.	Compound treated (mmol)	Reagent	Conditions (solvent; temperature; time)	Products (%)*
1	Methyl 2-methyl-4,6-di-*t*-butylbenzyl ether (**12**) (2.0)	HI (1 ml)	CH_3COOH (10 ml); reflux, 3 h	2-Methyl-4,6-di-*t*-butylbenzyl acetate (**14**) (91); 3,5-di-*t*-butyltoluene (**11***a*) (9)
2	2-Methyl-4,6-di-*t*-butylbenzyl alcohol (**13**) (0.60)	$SOCl_2$ (3 ml)	Reflux; 3 h	2-Methyl-4,6-di-*t*-butylbenzyl chloride (**16**) (86)
3	**13** (0.90)	$HCl–ZnCl_2$ (4 ml)	CH_3COOH; reflux; 4 h	**13** (27); **16** (35); **11***a* (38).
4	**13** (0.62)	HCOOH (5 ml)	100°; 2 h	2-methyl-4,6-di-*t*-butylbenzyl formate (**17**) (100)
5	**13** (1.30)	$SbF_5–FSO_3H$ (9 g)	SO_2; −78 to −40°; 1/2 h	**13** (8.5); **11***a* (3); 2,2′-dimethyl-4,4′,6,6′-tetra-*t*-butyldibenzyl ether (88)
6	2-Methyl-4,6-di-*t*-butylbenzyl chloride (**16**) (0.60)	HCOOH (15 ml)	100°; 15 h	**17** (74); **11***a* (26)

*In nos. 1, 3, 5, and 6, percentages are relative amounts by gas chromatographic analyses; in nos. 2 and 4, percentages are amounts isolated.

TABLE 5. Carbonium ion–hydride transfer reactions of alkyl benzyl compounds

No.	Compound treated (mmol)	Reagents (mmol)	Conditions (solvent; temperature; time)	Products (%)*
1	Benzyl chloride (1.7)	TFA (2.7); Et_3SiH (1.3)	CH_2Cl_2; r.t.; 30 days	No reaction
2	2,4,6-Trimethylbenzyl chloride (0.89)	TFA (2.7); Et_3SiH (1.3)	CH_2Cl_2; r.t.; 2.5 h	Isodurene (79); 1,3,5-trimethylbenzene (9); starting chloride (12)
3	2-Methyl-4,6-di-*t*-butylbenzyl alcohol (**13**) (0.64)	TFA (4.1); Et_3SiH (2.0)	CH_2Cl_2; r.t.; 5 h	2-Methyl-4,6-di-*t*-butyltoluene (**18**) (85); 3,5-di-*t*-butyltoluene (**11***a*) (15)
4	2,4,6-Tri-*t*-butylbenzyl alcohol (**2**) (0.22)	TFA (1.3); Et_3SiH (0.70)	CD_2Cl_2; r.t.; 1 h	2,4,6-Tri-*t*-butyltoluene (**19**) (90)
5	2-Methyl-4,6-di-*t*-butylbenzyl chloride (**16**) (0.66)	TFA (1.3); Et_3SiH (1.3)	CH_2Cl_2; 40°; 40 min r.t.; 15 h	**18** (50); **16** (50) **16** (100)
6	2,4,6-Tri-*t*-butylbenzyl chloride (**3**) (0.22)	TFA (0.66); Et_3SiH (0.65)	CD_2Cl_2; 40°; 5 min 17 min	**19** (81); **3** (19) **19** (100)

*In nos. 1–4 percentages are relative amounts by gas chromatographic analyses. In nos. 5 and 6 percentages were determined by direct n.m.r. observations.

Can. J. Chem. Downloaded from www.nrcresearchpress.com by 210.87.254.40 on 09/05/12
For personal use only.

1,1-Dimethyl-4,6-di-*t*-butylindane (**10**) was first obtained from reaction no. 1 (Table 3) as colorless crystals, m.p. 129–130°.

Anal. Calcd. for $C_{19}H_{30}$: C, 88.37; H, 11.63. Found: C, 88.56, 88.61; H, 11.63, 11.69.

Its n.m.r. spectrum had singlets at 8.78, 8.72, and 8.65 τ of relative intensity ratios 6:9:9 assigned to the *gem*-dimethyls, 6-*t*-butyl, and 4-*t*-butyl. Two triplets centered at 8.15 ($\Delta = 7$ Hz) and 7.00 ($\Delta = 7$ Hz) τ were assigned to the β-methylene and α-methylene hydrogens respectively. Two doublets, at 3.12 and 2.92 τ ($\Delta = 1.8$ Hz) (intensity 1 H each) were assigned to the aromatic hydrogens. The mass spectrum showed the expected parent mass of 258 with the base peak at 243 (M—CH_3). The main product from treatment of α,α-dideutero-2,4,6-tri-*t*-butylbenzyl chloride with formic acid (no. 9) was identified as 3,3-dideutero-1,1-dimethyl-4,6-di-*t*-butylindane from comparison of its n.m.r. and mass spectra with those of **10**. The labelled hydrocarbon showed no absorption in the α-methylene region of the n.m.r. spectrum and as expected the β-methylene gave a broadened singlet. The mass spectrum of the labelled hydrocarbon showed the expected parent mass of 260 with the base peak at 245 (M—CH_3). There was no evidence of compounds that would result from loss or rearrangement of deuterium.

The acetate (**15**) from reaction no. 8 was purified by sublimation, m.p. 130–131.5°.

Anal. Calcd. for $C_{21}H_{34}O_2$: C, 79.19; H, 10.76. Found: C, 78.54; H, 10.60.

The mass spectrum showed the expected parent mass of 318 and an accurate mass determination agreed with the formula $C_{21}H_{34}O_2$. It showed an i.r. band at 1725 cm^{-1} (s) (carbonyl) and n.m.r. bands at 8.66, 8.56, 8.05, 4.55, and 2.60 τ (singlets) with intensity ratios of 9:18:3:2:2, assigned to the *p*-*t*-butyl, *o*-*t*-butyls, methyl, benzylic methylene, and aromatic hydrogens respectively.

Acid-catalyzed Reactions of 2-Methyl-4,6-di-t-butylbenzyl Compounds

Table 4 outlines the experimental details on the acid-catalyzed reactions of methyl 2-methyl-4,6-di-*t*-butylbenzyl ether (**12**), alcohol (**13**), and chloride (**16**). The products from the reactions were worked-up and identified by the same procedures used for the tri-*t*-butylbenzyl compounds previously. The main product from reaction no. 5 was separated by chromatography on alumina and elution with petroleum ether followed by ethyl ether. The latter eluted this compound (81% yield) as colorless crystals, m.p. 122–124°.

Anal. Calcd. for $C_{32}H_{50}O$: C, 85.33; H, 11.11. Found: C, 85.23, 85.54; H, 11.23, 11.36.

It showed a strong i.r. band at 1050 cm^{-1} (ether) and n.m.r. bands at 8.72, 8.53, 7.64 and 5.24 (singlets), and 3.07, 2.83 τ (doublets) of intensities ratios 18:18:6:4:2:2. These bands were assigned to the 4,4′-*t*-butyls, 6,6′-*t*-butyls, 2,2′-methyls, two benzylic methylenes and aromatic hydrogens of 2,2′-dimethyl-4,4′,6,6′-tetra-*t*-butyldibenzyl ether.

Carbonium Ion – Hydride Transfer Reactions of Alkyl Benzyl Compounds

Experimental details and product analyses for the reduction of various alkyl benzyl alcohols and chlorides with triethylsilane in the presence of trifluoroacetic acid (TFA) are summarized in Table 5. Each experiment was set up to monitor it directly by n.m.r. measurement of the loss of the benzylic methylene absorption and conversion into an aryl methyl group. The benzyl alcohol or chloride was dissolved in 0.5 ml of methylene chloride (in the case of alcohol **2** and chloride **3** CD_2Cl_2 was required for the n.m.r. measurements), triethylsilane was added and the n.m.r. spectrum was run. Then the trifluoroacetic acid was added and the spectrum was scanned repeatedly. In no case did reductions occur in the absence of trifluoroacetic acid. For example 2,4,6-tri-*t*-butylbenzyl chloride (**3**), the most reactive compound, was stable to triethylsilane alone even after prolonged treatment. Reactions were terminated by adding solid sodium carbonate. This was removed by filtration, the solvent distilled, and the residue dissolved in benzene for g.l.c. analyses using columns (10 ft × 1/4 in.) packed with 8% carbowax on Chromosorb W. The hydrocarbons were identified by the use of known synthetic samples as internal standards on the g.l.c. as well as by the n.m.r. spectra.

The financial support of this research provided by the National Research Council of Canada is gratefully acknowledged. We thank Dr. W. D. Jamieson of the Atlantic Regional Laboratory (NRCC), Halifax, for providing the mass spectroscopic analyses.

1. L. R. C. Barclay and E. E. Betts. Can. J. Chem. **33**, 1768 (1955).
2. L. R. C. Barclay, N. D. Hall, and G. A. Cooke. Can. J. Chem. **40**, 1981 (1962).
3. L. R. C. Barclay and M. C. MacDonald. Tetrahedron Lett. 881 (1968).
4. J. M. Bollinger, M. B. Comisarow, C. A. Cupas, and G. A. Olah. J. Am. Chem. Soc. **89**, 5687 (1967).
5. H. M. R. Hoffmann. J. Chem. Soc. 6748 (1965).
6. L. I. Krimen and D. J. Cota. Org. React. **17**, 213 (1969).
7. L. R. C. Barclay and E. C. Sanford. Can. J. Chem. **46**, 3325 (1968).
8. F. A. Carey and H. S. Tremper. J. Am. Chem. Soc. **90**, 2578 (1968); **91**, 2967 (1969).
9. R. A. Olofson, S. W. Walinsky, J. P. Marino, and J. L. Jernow. J. Am. Chem. Soc. **90**, 6554 (1968).
10. P. T. Lansbury and N. R. Mancuso. J. Am. Chem. Soc. **88**, 1205 (1966); P. T. Lansbury, J. G. Colson, and N. R. Mancuso. J. Am. Chem. Soc. **86**, 5225 (1964).
11. M. H. Knight, T. Putkey, and H. S. Mosher. J. Org. Chem. **36**, 1483 (1971).
12. K. M. Baker and B. R. Davis. Tetrahedron, **25**, 2487 (1969).
13. V. Boido and O. E. Edwards. Can. J. Chem. **49**, 2664 (1971).
14. F. H. Field. J. Am. Chem. Soc. **91**, 6334 (1969).
15. P. C. Myhre, G. S. Owen, and L. J. James. J. Am. Chem. Soc. **90**, 2115 (1968).
16. W. A. Gibbons and H. Fisher. Tetrahedron Lett. No. **1**, 43 (1964).
17. E. J. Eisenbraun, J. R. Mattox, R. C. Bansal, M. A. Wilhelm, P. W. K. Flanagan, A. B. Carel, R. E. Laramy, and M. C. Hamming. J. Org. Chem. **33**, 2000 (1968).
18. M. G. J. Beets, W. Meerburg, and H. Van Essen. Rec. trav. chim. **78**, 570 (1959).

Can. J. Chem. Downloaded from www.nrcresearchpress.com by 210.87.254.40 on 09/05/12
For personal use only.

Addition of ICl to Norbornene. The Preparation and Photochemical Isomerization of *syn*-7-Iodonorbornene

N. H. WERSTIUK, I. VANCAS, J. WARKENTIN, AND F. R. S. CLARK
Department of Chemistry, McMaster University, Hamilton, Ontario
Received August 16, 1971

The addition of ICl to norbornene in the presence of pyridine yields nortricyclyl iodide (**1***c*), *endo*-2-chloro-*exo*-3-iodonorbornane (**2***c*), and *syn*-7-iodo-*exo*-2-chloronorbornane (**3***b*) as the major products. Base-catalyzed elimination of HCl from **3***b* yields *syn*-7-iodonorbornene (**6***a*) which is isomerized photochemically to *anti*-7-iodonorbornene (**6***b*).

L'addition de ICl au norbornène en présence de pyridine conduit à l'iodure nortricyclyl (**1***c*), à l'*endo*-chloro-2 *exo*-iodo-3 norbornane (**2***c*), et au *syn*-iodo-7 *exo*-chloro-2 norbornane (**3***b*) en tant que produits majoritaires. L'élimination baso-catalysée de HCl à partir de **3***b* conduit au *syn*-iodo-7 norbornène (**6***a*) qui subit une isomérisation photochimique en *anti*-iodo-7 norbornène (**6***b*).

Canadian Journal of Chemistry, **50**, 291 (1972)

Introduction

The electrophilic addition of polar reagents to olefins and cycloolefins is of mechanistic (1–4) and theoretical interest (5). Studies have shown that product distribution, resulting from capture of the intermediate onium-3 ion, rearrangement and 1,3 elimination of a proton, as for example in the bicyclo[2.2.1]heptyl system, depends on the electrophile (1–4). Molecular orbital calculations on the system E^+ and ethylene by Bach and Henneike (5) indicate that the degree of double bond pertubation and therefore the extent of charge development on carbon also depends on the electrophile. That this would be important in directing the reactions of the intermediate onium ion is certain.

In this study ICl was added to norbornene to establish the behavior of I^+ and thereby provide data for a comparison of the results obtained with Cl^+ (2, 4) and Br^+ (2, 3). The synthesis of the previously unknown *syn*-7-iodonorbornene, via base-catalyzed elimination of HCl from *syn*-7-iodo-*exo*-2-chloronorbornane could be accomplished if the *syn-exo*-dihalide was a major product as in the bromination of norbornene (2, 3). The 7-iodonorbornene would then be a useful precursor for the 7-norbornenyl radical (6–8) and anion (9, 10) species in which there has been considerable interest.

Results

The addition of ICl in CH_2Cl_2 to norbornene in CH_2Cl_2 containing an equimolar quantity of pyridine gave nortricyclyl iodide (**1***c*), *endo*-2-chloro-*exo*-3-iodonorbornane (**2***c*), and *syn*-7-iodo-*exo*-2-chloronorbornane (**3***b*) as 85–90% of the reaction mixture (Fig. 1). Compound **1***c* was identified by its mass spectrum (M^+, *m/e* 220) and n.m.r. spectrum, the latter corresponding exactly to that reported for **1***c* by Diner and Lown (11). That **2***c* is *endo*-2-chloro-*exo*-3-iodonorbornane was established chemically and by n.m.r. spectroscopy. Treatment of **2***c* with KO*t*Bu–*t*BuOH gave the norbornenyl chloride **8** and established the 2,3 substitution. That the *endo*-2-*exo*-3-orientation was correct was established by several facts. The n.m.r. spectrum of **2***c* showed triplets at δ 4.75 and 3.85 for the C-3-*exo*- and C-2-*endo*-protons, respectively, exactly the pattern reported for the dibromide **2***b* by Marshall *et al.* (3). Treatment of **2***c* with *n*-$(Bu)_3SnH$ gave *endo*-norbornyl chloride **9***b*, the result of preferential reduction of iodine (12). The facile elimination of HI from **2***c* (reaction time less than 3 h) is further evidence that orientation of hydrogen and iodine is *cis-exo* at C-2, C-3 (13). That dihalide **3***b* is *syn-exo* was established by consideration of its n.m.r. spectrum and the results of several reactions. The

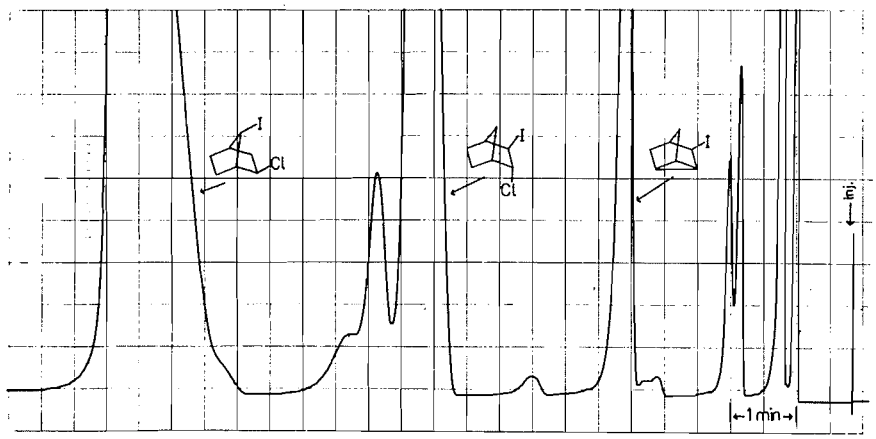

FIG. 1. The g.l.c. of products of ICl addition to norbornene.

n.m.r. of **3***b* which showed a multiplet at δ 4.08 (C-2-*endo*-H) which overlapped with a sharp multiplet at 3.90 (*anti*-7-H) was pattern-wise very similar to the corresponding absorptions for *syn*-7-bromo-*exo*-2-bromonorbornane reported by Marshall *et al.* (3). The assignment was corroborated by formation of **6***a*, **6***c*, and **7***a* when **3***b* was reacted with KO*t*Bu–*t*BuOH. That **6***a* was the *syn*-7-iodide was established by decoupling experiments and by photochemical isomerization to the *anti*-iodide **6***b*. Decoupling experiments on **6***b* as described in the experimental further supported the assignments. Reduction of **3***b* with *n*-$(Bu)_3SnH$ gave *exo*-norbornyl chloride by preferential reduction of iodine.

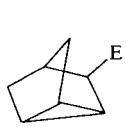

1

a E = Cl
b E = Br
c E = I

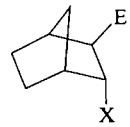

2

a X = E = Cl
b X = E = Br
c X = Cl; Y = E

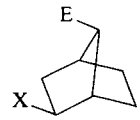

3

a X = E = Br
b X = Cl; E = I

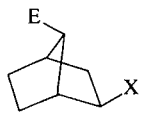

4

a X = E = Br
b X = Cl; E = I

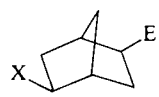

5

a X = E = Br
b X = Cl; E = I

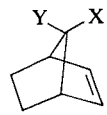

6

a X = I; Y = H
b X = H; Y = I
c X = H; Y = O*t*Bu
d X = H; Y = OMe
e X = H; Y = OCH_2Ph

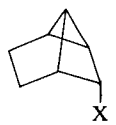

7

a X = O*t*Bu
b X = OMe
c X = OCH_2Ph

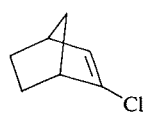

8

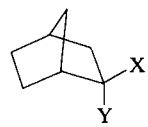

9

a X = Cl; Y = H
b X = H; Y = Cl

Can. J. Chem. Downloaded from www.nrcresearchpress.com by 210.87.254.40 on 09/05/12
For personal use only.

TABLE 1. Products of addition of polar reagents to norbornene

Reagent EX	Relative % yield							
	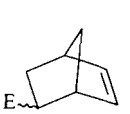	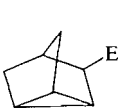	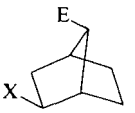	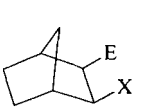	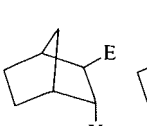	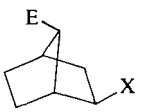	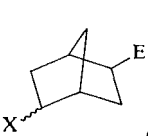	Other
Cl_2*,†	1	65	12	14		6		2
Br_2*,†	1	52	27	1	4	12	5	—
ICl†	1	12	40	1	35	5	2	7

*See refs. 13 and 14.
†EX (0.02 *M*) in CH_2Cl_2 was added dropwise to norbornene (0.02 *M*) and pyridine (0.02 *M*) in CH_2Cl_2.

The minor components of r_t 3.20, 7.35, and 7.70 min obtained in the addition are likely norbornenyl iodides and the *anti*-7-iodo-*exo*-2-chloro- and *exo*-3-iodo-*exo*-6-chloronorbornanes **4***b* and **5***b*, respectively, analogous to the dibromides **4***a* and **5***a* obtained in the bromination of norbornene (3, 4).

Discussion and Conclusions

The product distributions for the addition of Cl_2, Br_2, and ICl to norbornene in CH_2Cl_2 are listed in Table 1. Interestingly, the quantity of tricyclic component decreases from 65% in chlorination to 12% in the ICl addition, while the reverse trend is established for the *syn-exo*- and 2,3-*trans*-dihalides. Possibly, the 2,3-*trans*-trend reflects the degree of double bond pertubation ($Cl^+ > Br^+ > I^+$) and therefore the degree of bending of the olefinic C—H bonds, as suggested by Bach and Henneike (5), into an "*endo*-like" position. The greater the pertubation and thus distortion of the C—H bonds, the less favorable is nucleophilic attack by X^- on the onium ion. The minor amount of 2,3-*trans*-product in the bromination is accounted for by an increased pertubation by Br^+ over I^+, as well as the likely decreased nucleophilicity of Br^- over Cl^- in the aprotic solvent CH_2Cl_2 (15, 16). Certainly greater steric requirements of Br^- over Cl^- would also contribute to the effect. That the amount of 1,3 elimination and the stereochemistry of the process (2) leading to tricyclic product must be governed by the charge development at C-2, C-3 which occurs as E^+ attacks or as the onium ion opens or rearranges (2), is indicated by the decrease of relative percent yields of the nortricyclenes in the addition of Cl_2, Br_2, and ICl, respectively. It is attractive to postulate that E(Br or I) assists 1,2 Wagner–Meerwein rearrangement via partial Br-4 or I-4 participation by stabilizing the charge developed at C-1. This would account for the larger amounts of 2,7-dihalide formed when Br^+ and I^+ add and for the apparent *endo* and *exo* stereoselectivity observed for the 1,3 process in chlorination and bromination, respectively (2).

This work provides the first synthesis of the *syn*- and *anti*-7-iodonorbornenes, the latter via a previously unknown photochemical *syn–anti* isomerization. The formation of **6***c* and **7***a* during KO*t*Bu–*t*BuOH treatment of **3***b* has precedent since **6***d*, **7***b*, and **6***e*, **6***c* have been obtained previously by Brookhart *et al.* (17) and Tufariello *et al.* (18), respectively, from solvolysis of 7-substituted norbornenes. However, the preparation of *anti*-7-X-norbornenes and *endo*-6-X-tricyclo[3,2,0,0]^{2,7} heptanes is now possible directly in two steps from norbornene via ICl addition followed by elimination of HCl in a highly concentrated solution of the base M^+X^-.

The *syn–anti* isomerization of the 7-iodonorbornenes is the expected result of irradiating them at about 254 nm. Homolytic dissociation of the n–σ^* excited state of alkyl iodides is well known (19) and recombination of the 7-norbornenyl radical with iodine atoms in both stereochemical senses is in keeping with the non-stereospecific H-abstraction reactions of the 7-norbornenyl radical (7, 8). The photostationary state appears to favor the *anti*-iodide, the *syn*:*anti* ratio from photolysis at high dilution being about 1:1.5. However, one cannot conclude that the *anti*-iodide is thermodynami-

Can. J. Chem. Downloaded from www.nrcresearchpress.com by 210.87.254.40 on 09/05/12
For personal use only.

Can. J. Chem. Downloaded from www.nrcresearchpress.com by 210.87.254.40 on 09/05/12
For personal use only.

cally the more stable isomer in the absence of further information such as quantum yields.

The *syn*- and *anti*-7-iodonorbornenes will be useful precursors for preparation of the 7-norbornenyl radical (6–8) and perhaps the 7-norbornenyl anion (9) in that, for example, attempts to prepare the organolithium derivatives of 7-norbornenyl bromides and chlorides (20) and 7-benzonorbornenyl bromide (10) have failed.

Experimental

General

The n.m.r. spectra were recorded on Varian T-60 and HA-100 spectrometers in CCl_4 or $CDCl_3$ with tetramethylsilane as the internal standard. Ultraviolet spectra were obtained on a Carey Model 14 spectrophotometer. Preparative gas chromatographic isolations were done on a Varian-Aerograph 90-P-3 instrument with 5–10 ft × 1/4 in. 10–15% SE-30 on Chromosorb W glass and stainless steel columns with He as the carrier. Analytical chromatograms were obtained on a Varian-Areograph Model 204 chromatograph on a 10 ft × 1/8 in. 10% SE-30 on Chromosorb W column with He as the carrier. Pentane was stirred over fuming H_2SO_4, washed with bicarbonate solution, and distilled. All solutions were dried over anhydrous Na_2SO_4 and $MgSO_4$.

Addition of ICl to Norbornene in CH_2Cl_2–Pyridine

In a three-necked 1 l flask was added norbornene (44.5 g, 0.47 mol), pyridine (38.5 ml, 0.47 mol), and CH_2Cl_2 (290 ml). The mixture was cooled to 0° in an ice-bath and stirred magnetically as dry N_2 was bubbled through. ICl (75.8 g, 0.47 mol) in CH_2Cl_2 (140 ml) was added dropwise to the norbornene solution. After the mixture had stood for 20 min, the CH_2Cl_2 layer was washed three times with dilute thiosulfate solution, twice with dilute HCl, twice with distilled water, then dried. Most of the methylene dichloride was removed by distillation through a 1 ft Vigreux column. The g.l.c. on a 10 ft × 1/3 in. 5% SE-30 on Chromosorb W column at 150° (Fig. 1) showed products at r_t (flow rate ca. 25 ml/min) 1.8 min (6.8%) unknowns, 3.20 (<1%) norbornenyl iodides, 3.60 (15%) nortricyclyl iodide (**1***c*), 4.95 (<1%) unknown, 6.60 (35%) *endo*-2-chloro-*exo*-3-iodonorbornane (**2***c*), 7.35 (5%) and 7.80 (2%) chloroiodonorbornanes, 9.80 (<1%) unknown, 11.0 (40%) *syn*-7-iodo-*exo*-2-chloronorbornane (**3***b*). Vacuum distillation through a 1.5 ft vacuum jacketed Vigreux column gave fraction 1, b.p. 46–52° (3.8 mm), containing the first components including nortricyclyl iodide; fraction 2 (15 g), b.p. 56–58° (3.6 mm) nortricyclyl iodide, 90% pure by g.l.c.; fractions 3 and 4, b.p. 48–50° (2.5 mm) **2***c* and **3***b*; fraction 5 (20 g), b.p. 50–55° (4 mm) **2***c* (95% pure by g.l.c.); fraction 6 (30 g), b.p. 50–60° (2.5 mm) **3***b* (90% pure by g.l.c.).

The n.m.r., 60 MHz (CCl_4) **1***c*; δ 3.78 (1H, singlet, —C(H)—I), 2.10 (2H, singlet overlapping with doublet which was the low field portion of an AB quartet, C-4-H and C-7-H *syn* to the iodide) 1.7–0.9 (6H, multiplet, nortricyclyl envelope). The mass spectrum of **1***c* taken after preparative g.l.c. showed M^+ at *m/e* 220 corresponding to C_7H_9I. The n.m.r., 60 MHz (neat) **2***c*; δ 4.75 (1H, triplet; J = 2.5, 2.0 Hz, C-3-*exo*-H) 3.85 (1H, triplet; J = 1.5, 1.5 Hz, C-2-*endo*-H) 2.5 and 2.7 (2H, broad singlets, bridgehead-H's) 2.3–1.1 (norbornyl envelope). The n.m.r., 60 MHz (CCl_4) of **3***b*; δ 4.08 (1H, broad multiplet, C-2-*endo*-H), 3.90 (1H, sharp multiplet, *anti*-7-H), 2.7–1.1 (norbornyl envelope). After the first distillation the reddish-brown fractions 5 and 6 were dissolved in ether and washed with dilute thiosulfate. The ether was distilled off after drying and the remaining oil was distilled. In this way **2***c* and **3***b* were obtained as pale yellow-brown liquids.

*Reaction of **2***c* with Potassium t-Butoxide in t-Butyl Alcohol*

Compound **2***c* (2.1 g, 90% **2***c*, 5% **4***b*, 5% **3***b*) was dissolved in saturated KO*t*Bu–*t*BuOH solution (55 ml) in a 100 ml flask fitted with a condenser and a calcium chloride drying tube. The mixture was refluxed and stirred and after 3.5 h was 98% complete as determined by analytical g.l.c. The mixture was poured into water (100 ml) and extracted with pentane (3 × 50 ml). The pentane layer was washed with water (4 × 100 ml), dried, and the solvent was distilled off. The major peak (90%) was collected by preparative g.l.c. Mass spectrum, M^+ at *m/e* 128, 130 corresponded to C_7H_9Cl. The n.m.r., 60 MHz (CCl_4); δ 5.75 (1H, doublet, J = 3.5 Hz, olefinic-H), 2.85 (2H, broad multiplet, bridgehead-H's), 1.4–1.0 (6H, norbornenyl envelope).

*Reaction of **3***b* with KO*t*Bu in t*BuOH. Preparation of **6***a*

Run 1

Compound **3***b* (2.1 g, 95% **3***b*, 5% **2***c*) was refluxed in saturated KO*t*Bu–*t*BuOH solution (55 ml). Five aliquots were removed at 3.7, 14.3, 19.5, 25.0, and 35.0 h and analyzed by analytical g.l.c. Three products of r_t 2.0, 2.6, and 3.0 min were present as well as minor components (2%) of r_t 1–1.5 and 2.4 min relative to **3***b* of r_t 10.2. There was a gradual decrease in intensity of peaks r_t 10.2 and 3.0 min and an increase in the intensity of the peaks of r_t 2.0 and 2.6 min. After 35 h 10% of starting material remained and the ratio of the products of r_t 2.0, 2.6, and 3.0 was 2:1:1. The three components were isolated by preparative g.l.c. on a 10 ft × 3/8 in. 30% SE-30 Chromosorb W column maintained at 130°. The n.m.r., 60 MHz (CCl_4) of peak r_t 2.0 (**6***c*); δ 5.88 (2H, triplet, J = 1.5, 1.5 Hz, olefinic-H's), 3.25 (1H, broad singlet, —C(H)—O*t*Bu), 2.35 (2H, multiplet, bridgehead-H's), 1.80 (2H, multiplet, C-5, C-6-*exo*-C-H's), 1.10 (9H, singlet, —$C(CH_3)_3$), and 0.85 (2H, multiplet, C-5, C-6-*endo*-C-H's).

Anal. Calcd. for $C_{11}H_{18}O$: C, 79.52; H, 10.84. Found: C, 79.59; H, 10.97.

The n.m.r., 60 MHz (CS_2) of peak r_t 2.6 (**7***a*); δ 3.98 (1H, quartet, J = 8, 4 Hz, —C(H)—O—*t*Bu), 2.50 (1H, multiplet, bridgehead-H), 2.1–1.2 (7H, multiplet, norbornyl envelope including cyclopropyl-H's), 1.1 (9H, singlet, —$C(CH_3)_3$).

Anal. Calcd. for $C_{11}H_{18}O$: C, 79.52; H, 10.84. Found: C, 79.66; H, 10.72.

The n.m.r., 60 MHz (CS_2) of peak r_t 3.6; δ 6.15 (2H, multiplet, olefinic-H's), 3.82 (1H, multiplet, *anti*-C-7-H), 3.13 (2H, multiplet, bridgehead-H's), 1.83 (2H, multiplet, C-5,C-6-*exo*-H's), 1.13 (2H, multiplet, C-5,C-6-*endo*-H's). The n.m.r., 100 MHz (CCl_4); showed the band at δ 6.0 to be a triplet of doublets with J = 2.2, 1.8, 0.7 Hz. Irradiation of the *anti*-7-H collapsed the triplet of doublets to a triplet with J = 2.2 and 1.8 Hz. The u.v.; λ_{max} (hexane), 254 nm (ε 600).

Can. J. Chem. Downloaded from www.nrcresearchpress.com by 210.87.254.40 on 09/05/12
For personal use only.

Anal. Calcd. for C_7H_9I: C, 38.19; H, 4.09. Found: C, 38.50; H, 3.92.

Run 2

Compound **3***b* (5.8 g, 95% **3***b*, 5% **2***c*) was refluxed in saturated KO*t*Bu–*t*BuOH solution (150 ml) for 41.5 h. Work-up as described previously and analysis by analytical g.l.c. on 10 ft × 1/8 in. 5% SE-30 on Chromosorb W column showed the reaction to be 95% complete. The products **6***a*, **7***a*, and **6***c* were present in a ratio of 2:1:1.

Reaction of 2c with n-(Bu)$_3$SnH

To **2***c* (1.0 g, 90% **2***c*, 10% **4***b*) in pentane (25 ml) was added *n*-$(Bu)_3SnH$ (1.1 g, 3.8×10^{-3} mol) in pentane (30 ml) dropwise at 25°. After the addition was complete the pentane layer was washed with water (3 × 50 ml) and dried. The g.l.c. showed that the reaction was 95% complete. The pentane was distilled through a 6 in. Vigreux column and the major product (95%) was isolated by preparative g.l.c. The n.m.r. (CCl_4) showed the product to be a mixture of 90% of *endo*-norbornyl chloride and 10% *exo*-norbornyl chloride by comparison of the absorptions at δ 4.15 (C-2-*exo*-H) and 3.82 (C-2-*endo*-H), respectively, in accord with the percentage of **2***c* and **4***b* originally present in the starting material.

Reaction of 3b with n-(Bu)$_3$SnH

Compound **3***b* (1.3 g, 95% **3***b*, 5% **2***c*) in pentane (32 ml) was added dropwise to *n*-$(Bu)_3SnH$ (1.3 g, 4.6×10^{-3} mol) in pentane (37 ml) at 25°. The solution was washed with water (3 × 50 ml) and dried. The g.l.c. analysis showed one major product **9***a* (85%) and 10% of **3***b* and 5% of **2***c*. The major product was isolated by preparative g.l.c. after the pentane was removed by distillation through a 6 in. Vigreux column. The n.m.r., 60 MHz (neat); δ 3.9 (1H, triplet with

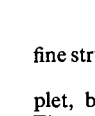

fine structure, $J = 6, 4.5$ Hz, —C—Cl), 2.3 (2H, broad multiplet, bridgehead-H's), 2.0–0.9 (8H, norbornyl envelope). There was less than 3% of absorption at δ 4.15 due to *endo*-norbornyl chloride.

Preparation of exo-Norbornyl chloride (9a)

exo-Norbornyl chloride (**9***a*) was prepared by treating norbornene with anhydrous HCl in pentane (21). The n.m.r., 60 MHz (neat); δ 3.92 (1H, triplet with fine structure, $J = 6$,

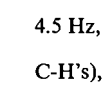

4.5 Hz, —C—Cl), 2.3 (2H, broad multiplet, bridgehead C-H's), 2.0–0.9 (8H, norbornyl envelope).

Irradiation of syn-7-Iodonorbornene (6a)

Run 1

Compound **6***a* (0.19 g, 8.7×10^{-5} mol, 99% pure) and iodine (0.0055 g, 2.0×10^{-5} mol, sublimed) were dissolved in *n*-hexane (0.7 ml, spectral grade) which contained a trace of methylene chloride as an internal standard. Irradiation (254 nm) of the solution in a quartz n.m.r. tube at 30° was carried out in a Rayonet reactor. After 30 min the C-7-H region of the n.m.r. showed two peaks of approximately equal intensity. A small amount of insoluble material accumulated in the tube and the vinyl absorption had decreased in intensity relative to CH_2Cl_2. After 6.8 h there was no change in the relative intensities of the peaks in the C-7-H region. The g.l.c. analysis on a 5 ft × 1/4 in. 20% SE-30 Chromosorb W column showed two products r_t 6.3 (55.6%) and 7.3 min (44.4%) amounting to 99% of the g.l.c. peak area. The peak of r_t 7.3 corresponded exactly to starting material **6***a*. The other product **6***b* was isolated by g.l.c. The n.m.r., 100 MHz (CCl_4); δ 6.0 (2H, triplet, $J = 2.0, 2.0$ Hz, olefinic-H's), 3.81 (1H, multiplet, *syn*-7-H), 2.86 (2H, multiplet, bridgehead-H's), 2.15 (2H, multiplet, C-5,C-6-*exo*-H's), and 1.12 (2H, multiplet, C-5, C-6-*endo*-H's). Irradiation of the *syn*-7-H did not change the olefinic absorption. The u.v.; λ_{max} (hexane) 251 nm (ε 892).

Run 2

Compound **6***a* (0.012 g) was dissolved in purified pentane (50 ml) and irradiated in a 1 in. diameter quartz tube for 3 h as described previously. The solution turned deep purple and some polymeric material accumulated. The mixture was shaken with aqueous KI to remove the free iodine, dried over anhydrous K_2CO_3, and the solvent was distilled off. The g.l.c. of the recovered oil (0.10 g, 83%) showed a *syn*:*anti*-iodide ratio of 1:1.7.

Run 3

Irradiation of **6***a* (0.0071 g) in purified pentane (50 ml) (degassed) for 15 min as described previously gave a *syn*:*anti* ratio of 1:1.4 as was determined by g.l.c.

1. T. G. Traylor. Acc. Chem. Res. **2**, 152 (1969).
2. N. H. Werstiuk and I. Vancas. Can. J. Chem. **48**, 3963 (1970) and references therein.
3. D. R. Marshall, J. R. Robinson, P. Reynolds-Warnhoff, and E. W. Warnhoff. Can. J. Chem. **49**, 885 (1971).
4. M. L. Poustma. J. Am. Chem. Soc. **87**, 4293 (1965).
5. R. D. Bach and H. F. Henneike. J. Am. Chem. Soc. **92**, 5589 (1970).
6. J. Warkentin and E. Sanford. J. Am. Chem. Soc. **90**, 1667 (1968).
7. G. A. Russell and G. W. Holland. J. Am. Chem. Soc. **91**, 3870 (1969).
8. P. Bakrizis, J. Kochi, and P. J. Krusic. J. Am. Chem. Soc. **92**, 1436 (1970).
9. R. Breslow, R. Pagni, and W. N. Washburn. Tetrahedron Lett., 547 (1970).
10. J. W. Wilt, G. Gutman, W. J. Ranus, Jr., and A. R. Zigman. J. Org. Chem. **32**, 893 (1967).
11. U. Diner and J. W. Lown. Can. J. Chem. **49**, 402 (1971).
12. D. J. Carlsson and K. U. Ingold. J. Am. Chem. Soc. **90**, 7047 (1968).
13. H. Kwart, T. Takeshita, and J. L. Nga. J. Am. Chem. Soc. **76**, 4072 (1954).
14. N. H. Werstiuk and I. Vancas. Unpublished results.
15. S. Winstein, L. G. Savedoff, S. Smith, I. D. R. Stevens, and J. S. Gall. Tetrahedron Lett. **9**, 24 (1960).
16. W. M. Weaver and I. D. Hutchinson. J. Am. Chem. Soc. **86**, 261 (1964).
17. M. Brookhart, A. Diaz, and S. Winstein. J. Am. Chem. Soc. **88**, 3133 (1966).
18. J. Tufariello, J. F. Mich, and R. J. Lorence. Chem. Commun., 1202 (1967).
19. C. E. McCauley, W. H. Hamell, and R. R. Williams, Jr. J. Am. Chem. Soc. **76**, 6263 (1954).
20. J. Warkentin and F. R. S. Clark. Unpublished results.
21. L. Schmerling. J. Am. Chem. Soc. **68**, 195 (1946).

Hydrogen Bonding in the case of Self-associated Fluoroalcohols

A. PLANCKAERT AND C. SANDORFY
Département de Chimie, Université de Montréal, Montréal, Québec
Received July 19, 1971

The OH stretching band of polymeric fluoroalcohols exhibits a much higher rate of shifting with temperature but it is less anharmonic than the corresponding band of ordinary alcohols. The degree of self-association in their solutions is discussed.

Les vibrations de valence des groupements OH des fluoroalcools polymères se déplacent avec la température beaucoup plus rapidement que les vibrations analogues des alcools correspondants mais elles sont moins anharmoniques. On examine le degré d'autoassociation dans leurs solutions.

Canadian Journal of Chemistry, **50**, 296 (1972)

Can. J. Chem. Downloaded from www.nrcresearchpress.com by 210.87.254.40 on 09/05/12
For personal use only.

Introduction

The changes with temperature of the frequency and width of the fundamental and first overtone of the OH stretching vibration of self-associated, polymeric alcohols were recently studied in solution down to liquid nitrogen temperature (1, 2). It has been found that both the fundamental and first overtone shift linearly and at about the same rate to lower frequencies with decreasing temperature. At the same time the anharmonicity constant

$$X_{12} = \nu_{01} - \frac{\nu_{02}}{2}$$

also decreases, by about half of the shift of the frequencies themselves. It seemed interesting to us to study the anharmonicity and temperature dependance of the OH stretching vibration of fluoroalcohols and compare these with the corresponding data for alcohols.

Results

n-Pentafluoropropanol and *n*-heptafluorobutanol were chosen because of their relatively good solubility in solvents which can be used for low temperature measurements. These were a 1:1 mixture of CCl_3F (freon-11) and $C_2F_4Br_2$ (freon 114-B-2) and a 1:1 mixture of decafluorocyclohexene and perfluoromethylcyclohexane (the abbreviated notation FR and DP will be used for these). Experimental details were given previously (1, 3). Poor solubility prevented us from going down to liquid nitrogen temperature. The results summarized in Table 1 relate to 173 °K. The data on unsubstituted alcohols are taken from Asselin and Sandorfy (1) and are given for comparison.

The following observations can be made:

(*1*) As in the case of alcohols the fundamental and first overtone of the fluoroalcohols shift at about the same rate with decreasing temperature (to lower frequencies).

(*2*) The rate of shift is much greater, by about a factor of two, for the fluoroalcohols.

(*3*) The OD deuterated fluoroalcohols have a lesser rate of temperature shift, just as OD deuterated alcohols (about half).

(*4*) The anharmonicity constants, X_{12}, are smaller for the fluoroalcohols than for the alcohols (82 and 91 cm^{-1} compared to 135 and 147 cm^{-1}).

(*5*) The free OH bands have a much greater relative intensity at the level of the first overtone than at the level of the fundamental at similar concentrations (Figs. 1 and 2).

(*6*) As in the case of alcohols, X_{12} varies by about half the shift of the frequencies when temperature decreases.

(*7*) The harmonic frequencies computed with the X_{12} given in Table 1 are significantly lower for the fluoroalcohols.

(*8*) The isotopic ratios show that the OH vibrations are of the same high degree of localizability for alcohols and fluoroalcohols.

(*9*) The half-width of the fundamental of dissolved fluoroalcohols is larger than that of dissolved alcohols.

Discussion

Fluoroalcohols are much more acidic than the related alcohols (4) and, with the same bases, form much stronger hydrogen bonds (HB) than do the corresponding alcohols. Purcell *et al.* (5–7 and earlier papers) measured the ΔH values

TABLE 1. The frequencies (in cm^{-1}) of the fundamental (ν_{01}) and first overtone (ν_{02}) of some dissolved alcohols and fluoroalcohols followed by the half width $(\nu_{1/2})_{01}$ of the fundamental, the rate of shift of ν_{01} and ν_{02} with temperature, the first anharmonicity constant X_{12}, the harmonic frequency, and isotopic ratios. The concentrations of the solutions was approximately 0.2 *M*.

Alcohols	T °K	ν_{01}	ν_{02}	$(\nu_{1/2})_{01}$	$\frac{d\nu_{01}}{dT}$	$\frac{d\nu_{02}}{dT}$	X_{12}	$\frac{dX_{12}}{dT}$	ω_{12}	$\frac{\nu_{01(OD)}}{\nu_{01(OH)}}$	Solvent
Isopropanol	173	3274	6280	167	0.59	0.59	135	0.28	3544	0.745	FR
Isopropanol-OD	173	2438	4702	95	0.48	0.44	87	0.17	2612		
t-Butanol	173	3285	6274	123	0.44	0.47	152	0.23	3573	0.746	FR
t-Butanol-OD	173	2451	4704	74	0.28	0.32	98	0.12	2647		
Pentafluoropropanol	173	3242	6318	210	0.96	0.86	82	0.53	3402	—	DP
Heptafluorobutanol	173	3246	6308	210	1.03	1.11	91	0.47	3426	0.748	FR
Heptafluorobutanol-OD	173	2435	—	—	0.57	—	—	—	—		
Heptafluorobutanol	173	3248	6328	208	0.94	0.85	81	0.51	3406	0.748	DP
Heptafluorobutanol-OD	173	2431	—		0.52	—	—	—	—		

for a number of these calorimetrically and found good linear relationships between ΔH and $\Delta\nu$ for HB between fluoroalcohols and a series of bases. Drago *et al.* (8) found linear relationships for series including alcohols and fluoroalcohols and a given base. Although the anharmonicities are not given in these papers it is clear that $\Delta\nu$ is a valid measure of HB energy for these acid–base pairs.

Conditions are less clear in the case of self-associated fluoroalcohols. Kivinen and Murto (9) investigated solutions of 2,2,2-trifluoroethanol and 1,1,1,3,3,3-hexafluoro-2-propanol. Fluoroalcohols are better proton-donors than ordinary alcohols but, for the same reasons, they are weaker proton-acceptors. The net result seems to be a lesser degree of self-association in fluoroalcohols than in alcohols (9, 10 and references 22–28 in ref. 9). The i.r. evidence for this is based on smaller values of association constants, the fact that polymer bands appear at higher concentrations for the fluoroalcohols than for alcohols and the greater intensity and persistence at higher concentrations of the free OH band in fluoroalcohols. The free OH band is well distinguished even in undiluted fluoroalcohols when it is completely absent from the spectra of the corresponding ordinary alcohols. Kivinen and Murto remark, however, that the intrinsic intensity of the free band is greater in the fluoroalcohols than in alcohols.

Now, the much higher temperature sensitivity

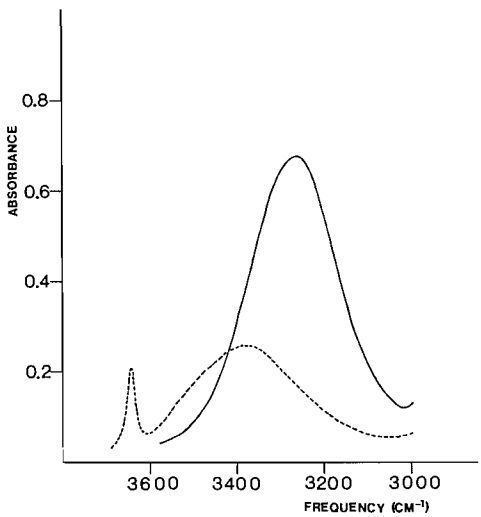

FIG. 1. The OH stretching fundamental of pentafluoropropanol in a 0.2 *M* solution of DP; --- at room temperature; — at −80 °C.

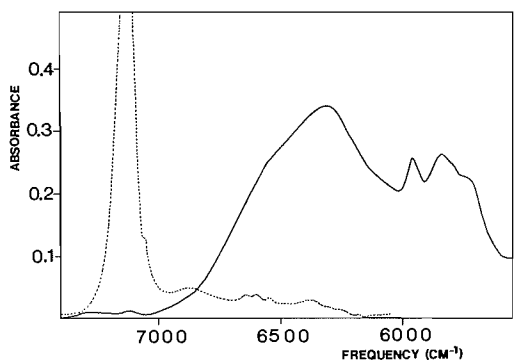

FIG. 2. The first overtone of the OH stretching vibration of pentafluoropropanol in a 0.16 *M* solution of DP; --- at room temperature; — at −100 °C. The absorbance of the 7125 cm^{-1} band at its maximum is 1.44.

Can. J. Chem. Downloaded from www.nrcresearchpress.com by 210.87.254.40 on 09/05/12
For personal use only.

of the OH frequency of the fluoroalcohols would seem to indicate stronger bonds. Since HB in solutions become shorter at lower temperatures (11, 1, 2) it is natural to think that a given decrease of temperature has more effect on the potential surface and the $\Delta\nu$ of a stronger bond which already has a shorter 0 --- 0 distance. The lower frequency of the fluoroalcohol polymers is in line with this (if there is at least a smooth relationship between ΔH and $\Delta\nu$).

The low mechanical anharmonicity of the OH vibration in the case of fluoroalcohols (meaning a steeper potential) together with the shorter HB length could contribute to explaining the high rate of temperature shift.

Normally, for hydrogen bonds formed by alcohols the OH stretching vibrations of stronger HB have higher anharmonicities. Anharmonicity diminishes, however, with decreasing temperature due probably to a shortening of the HB which becomes more symmetrical (*cf.* the $[FHF]^-$ ion). These observations show that when the 0 --- 0 distance is varied from infinite to near-zero the value of the mechanical anharmonicity must pass through a maximum. It is thus possible that a stronger HB has lower anharmonicity. The lower anharmonicity could also be a factor in making the relative intensities of the polymer bands lower (a lesser anharmonicity means lesser polarizability and weaker interactions with the surrounding medium) explaining that in the case of fluoroalcohols they start appearing at higher concentrations than in the case of ordinary alcohols. The low electrical anharmonicity of the polymers (12, 13) could be the cause of the much greater relative intensity of the free band at the level of the first overtone than at the level of the fundamental. A similar phenomenon is observed for alcohols except that there the mechanical anharmonicity of the polymer is higher than that of the monomer (13–15) and the electrical anharmonicity alone must be responsible for the decreased intensity of the polymer overtone (13). In the case of the fluoroalcohols mechanical anharmonicity would not oppose electrical anharmonicity and this could lead to very much weaker overtones, for the polymers, and this is observed.

It is also interesting to point out that the frequencies of the OH stretching fundamentals of fluoroalcohols are only about 40 cm^{-1} lower than those of ordinary alcohols but the differences between the harmonic frequencies (ω_{12}) are of the order of 100 cm^{-1}. Thus if the vibrations were entirely harmonic in both cases the fluoroalcohols would appear to form much stronger HB. Anharmonicity acts to diminish the difference in frequency between alcohol and fluoroalcohol polymers. This might perturb the $\Delta\nu - \Delta H$ relationship when alcohols and fluoroalcohols are considered together.

In conclusion we should like to make two points. First, we cannot give a definite answer to the important question: what are the factors determining the rate of temperature shift of bands affected by HB? Second, it is not yet known in our opinion if fluoroalcohols are more, or less associated than the corresponding ordinary alcohols.

We acknowledge financial help from the National Research Council of Canada.

1. M. Asselin and C. Sandorfy. J. Mol. Struct. **8**, 145 (1971).
2. M. Asselin and C. Sandorfy. Chem. Phys. Lett. **8**, 601 (1971).
3. G. Durocher and C. Sandorfy. J. Mol. Spectrosc. **20**, 410 (1966).
4. B. L. Dyatkin, E. P. Mochalina, and I. L. Knunyants. Tetrahedron, **21**, 2991 (1965).
5. K. F. Purcell, J. A. Stikeleater, and S. D. Brunk. J. Am. Chem. Soc. **91**, 4019 (1969).
6. K. F. Purcell, J. A. Stikeleater, and S. D. Brunk. J. Mol. Spectrosc. **32**, 202 (1969).
7. A. D. Sherry and K. F. Purcell. J. Phys. Chem. **74**, 3535 (1970).
8. R. S. Drago, N. O'Bryan, and G. C. Vogel. J. Am. Chem. Soc. **92**, 3924 (1970).
9. A. Kivinen and J. Murto. Suom Kemistil **B40**, 6, 14 (1967).
10. R. N. Haszeldine. J. Chem. Soc. 1757 (1953).
11. J. N. Finch and E. R. Lippincott. J. Chem. Phys. **24**, 908 (1956).
12. W. A. P. Luck and W. Ditter. J. Mol. Struct. **1**, 261 (1967–1968).
13. C. Bourdéron, J. J. Péron, and C. Sandorfy. In press.
14. M. Asselin, G. Bélanger, and C. Sandorfy. J. Mol. Spectrosc. **30**, 96 (1969).
15. M. Asselin and C. Sandorfy. J. Chem. Phys. **52**, 6130 (1970).

Can. J. Chem. Downloaded from www.nrcresearchpress.com by 210.87.254.40 on 09/05/12
For personal use only.

Use of *N*-Carboxyanhydrides in the Synthesis of Dipeptides. The Improvement of Isolated Yields by the Facile Removal of Buffer Components[1]

R. J. GAIT,[2] J. R. LANGLOIS, AND R. E. WILLIAMS[3]
Biochemistry Laboratory, National Research Council of Canada, Ottawa, Canada K1A 0R6

Received July 21, 1971

A modification of the *N*-carboxyanhydride synthesis of dipeptides is described. An improvement in the yield during dipeptide preparation is made possible by use of only organic acids and bases during the reaction to facilitate their removal before product isolation.

Une modification de la synthèse des dipeptides par l'emploi des *N*-carboxyanhydrides y est décrite. On obtient un meilleur rendement des produits isolés en employant les acides et bases organiques pendant la réaction; facilitant, ainsi, leur séparation du produit désiré.

Canadian Journal of Chemistry, **50**, 299 (1972)

Introduction

The preparative synthesis of peptides using *N*-carboxyanhydrides (NCA's) (Leuch's anhydrides) has had a long and varied history (1). In most cases, low yields were found and the method did not receive serious attention until a report that NCA's could be used to synthesize peptides under controlled conditions of temperature, concentration, and p*H*, appeared in 1967 (2). These experimental conditions and the reaction sequence are summarized in Scheme 1.

In general, to ensure adequate reaction, the method requires low temperatures, controlled p*H*, and rapid mixing. Even in the presence of an external buffer (borate) base addition was found necessary to achieve the p*H* control.

The general usefulness of the borate procedure and the fact that it is racemization free (3) has been illustrated by its use in the preparation of diasteriomeric dipeptides as a tool for the investigation of amino acid racemization (4) and in the preparation of fragments for the ultimate synthesis of a polypeptide having RNAase activity (5).

Several modifications of the original procedure have been made. The use of an external organic buffer whose basic component had a p*K* closer to the p*H* 10.2 normally used in the reaction was tried (6). Addition of a base (sodium hydroxide) was still found to be necessary to control the p*H* within the prescribed limits. Recently, another modification was made in which the reaction was run in 0.2 *M* sodium carbonate solution containing acetonitrile (7). No p*H* control was used in this case.

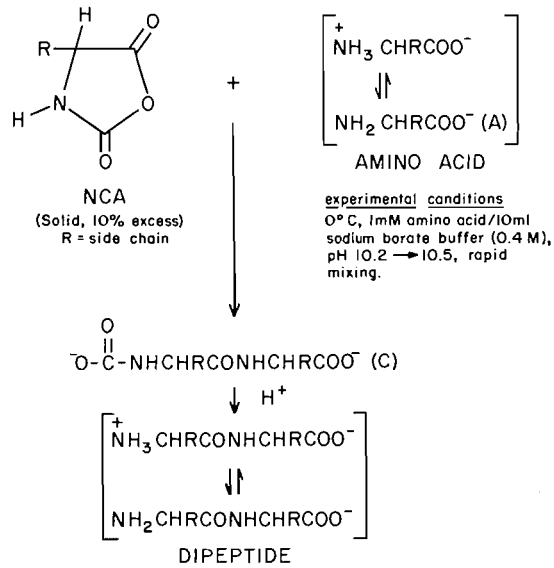

SCHEME 1. NCA dipeptide formation.

Each of these modifications has been used with success as evident in the high yields found in the preparation of di- and tripeptides. The resulting products have not, however, been easily isolated from the reaction mixture except in the cases where the product was insoluble and could be filtered off.

In view of the general usefulness of the NCA reaction we wish to report an additional modification of the original procedure which, for preparative purposes, will greatly aid in the isolation of the resulting products.

[1]NRCC No. 12232.
[2]NRCC Postdoctorate Fellow, 1969–1970.
[3]To whom all correspondence should be directed.

Can. J. Chem. Downloaded from www.nrcresearchpress.com by 210.87.254.40 on 09/05/12
For personal use only.

Can. J. Chem. Downloaded from www.nrcresearchpress.com by 210.87.254.40 on 09/05/12
For personal use only.

Experimental

Rotations were taken in a 1 dm tube on a Perkin–Elmer polarimeter, model 141. Melting points were taken either on a Fisher–Johns melting point apparatus or, where indicated, in a sealed capillary tube. They are uncorrected. Combustion analyses were performed by H. Seguin, Biochemistry Laboratories, NRCC, Ottawa. All chemicals were of reagent quality. Water was doubly distilled from glass. Phosgene C.P. was purchased from Matheson, Whitby, Ontario. The amino acids were obtained from Bion Biochemicals, Toronto, Ontario.

Thin-layer chromatography was performed on layers of silica gel (Camag Kieselgel, DF5) with a single solvent system (*n*-butanol, acetic acid, water, 4:1:1, v/v/v) being used. All R_f's reported are for this system. After development, the plates were developed with a ninhydrin spray (ninhydrin, *n*-butanol, acetic acid, 0.3:100:3 w/v/v).

Amino acid analyses were performed by A. E. Castagne on a Beckman amino acid analyzer, model 120C, using a standard amino acid elution programme on the 69 × 0.9 cm column (resin UR 30, sodium citrate buffers, 0.2 *N* in sodium ion, p*H* 3.25 and 4.30 (buffer change appearing at 130 min), temperature 55.5 °C, flow rate 68 ml/min). Amino acid and dipeptide elution times (in min) were as follows: asn, 54; gln, 57; gly, 86; met, 140; metasn, 161; metgln, 160; alagly, 141.5.

To ensure rapid mixing in all the NCA coupling experiments a Waring blendor was used. Analytical scale experiments were run on 40.0 ml of solution in a jacketed blendor of 125 ml capacity. After acidification at the end of the run, the contents of the blendor were diluted to 100.0 ml and 0.1 ml applied to the amino acid analyzer column. Preparative scale experiments were run on approximately 300 ml of solution in a jacketed blendor of 1000 ml capacity. The measurement of p*H* was made with a Radiometer Titrator, Model TTTlc, equipped with a Thomas combination electrode, Model 4858-L60 (1/4 in. × 6 in.), standardized to p*H* 7.0 at 20 °C.

The N-Carboxyanhydrides

These compounds were prepared in a *Hood* according to established procedures (1, 8, 10), L-methionine NCA, m.p. 34–35 °C dec. (lit. m.p. 42–44 °C dec. (8); 36–37° dec. (9)); L-alanine NCA, m.p. 89–90 °C dec. (lit. m.p. 90° dec. (10)).

Preparation of Methionylasparagine (metasn)

Methionylasparagine (m.p. 227–228 °C (sealed capillary); $[\alpha]_D$ + 12.7° (*c* 1.74, 10% NH_4OH); R_f 0.31) was prepared by each of the methods below.

Anal. Calcd. for $C_9H_{17}N_3O_4S$: C, 39.56; H, 6.23; N, 15.88: Found: C, 39.39; H, 6.29; N, 15.61.

(a) Borate Buffer.

Asparagine was dissolved in sodium borate buffer, p*H* 10.0, 0.4 *M* in borate, to give a solution containing 1 m*M* asparagine in 10 ml. The solution was cooled to 2 °C in the blendor and the p*H* adjusted to 10.2 with 4 *N* NaOH. Solid methionine NCA (10% excess) was added in one portion to the rapidly stirred solution while the p*H* was maintained at 10.2 with 4 *N* NaOH. At cessation of base uptake (approximately 3 min) the solution was rapidly acidified to p*H* 3–4 with concentrated HCl.

Isolation of the product was accomplished by evaporation of the filtered and acidified solution to dryness and extraction of the residue with hot methanol. Evaporation of the methanol gave a residue which was crystallized from ethanol–water to yield the pure dipeptide. A preparative experiment gave 4.4 gm dipeptide from 5.9 gm asparagine (37% yield).

(b) Triethylamine

Asparagine was dissolved in water to make a solution containing 1 m*M* asparagine in 10 ml. The solution was cooled to 2 °C in the blendor and the p*H* adjusted to 10.2 with neat triethylamine (approximately 0.2 ml per m*M* of amino acid). Solid methionine NCA (10% excess) was added in one portion to the rapidly stirring mixture while the p*H* was maintained at 10.2 by the syringe addition of triethylamine. At cessation of base uptake (approximately 3 min) the solution was rapidly acidified to p*H* 3–4 with concentrated formic acid.

Product isolation was accomplished as follows: the filtered and acidified solution was evaporated to remove the water. The oily residue was triturated several times with chloroform to yield a solid residue. This residue was crystallized from ethanol–water to give pure dipeptide. A preparative experiment gave 6.2 gm dipeptide from 5.9 gm asparagine (53% yield).

Methionylglutamine

Methionylglutamine (m.p. 215–216 °C (sealed capillary); $[\alpha]_D$ +13.80° (*c* 1.5, 10% NH_4OH); lit. m.p. 220–221 °C (12*a*), 232–233 °C (12*b*); $[\alpha]_D$ +14.1° (10% NH_4OH) (11*a*), $[\alpha]_D$ +17.3° (*c* 1.4 10% NH_4OH) (11*b*); R_f 0.33) was prepared by both the procedures above.

Anal. Calcd. for $C_{10}H_{19}N_3O_4S$: C, 43.32; H, 6.86; N, 15.16. Found: C, 43.57; H, 6.99; N, 15.29.

Work-up for the borate procedure (*a*) consisted of concentration of the filtered reaction mixture to about one half the original volume, cooling overnight, and filtering to remove the resulting crystals. Additional crystals could be obtained from the filtrate by addition of a small amount of ethanol and cooling. An analytical scale experiment gave 200 mg of dipeptide from 730 mg of glutamine (14.5% yield). Work-up for the triethylamine procedure (*b*) consisted of evaporation of the filtered reaction mixture to an oily residue, trituration with chloroform, and crystallization of the resulting solid from ethanol–water. A preparative scale experiment gave 7.8 gm dipeptide from 6.3 gm of glutamine (65% yield).

Alanylglycine

Alanylglycine ($[\alpha]_D$ +22.4° (*c* 1.9, 0.5 *N* HCl); (lit. $[\alpha]_D$ +22.6° (*c* 2.0, 0.5 *N* HCl) (12); R_f 0.21) was prepared by the triethylamine procedure (*b*) only.

Anal. Calcd. for $C_5H_{10}N_2O_3$: N, 19.15. Found: N, 18.98.

Work-up was essentially the same as for the methionyl dipeptides. Crystallization was from ethanol–water. A preparative experiment gave 5.7 gm of dipeptide from 3.8 gm of glycine (80% yield).

Results and Discussion

In general, product isolation from the reaction mixture after peptide formation by the NCA procedure implies the use of one or more of four general methods. For water insoluble products their isolation is achieved simply by filtering the mixture. For those compounds that are soluble

Can. J. Chem. Downloaded from www.nrcresearchpress.com by 210.87.254.40 on 09/05/12
For personal use only.

in water and insoluble in organic solvents addition of a water-miscible organic solvent, *e.g.* alcohol, usually results in the crystallization of the product from solution. For products that are soluble in organic solvents, evaporation of the water and extraction of the residue by the organic solvent usually suffices. Finally, for compounds not readily isolated by the above methods, chromatography of the reaction mixture has to be used. Carbon, silica gel, and ion exchange columns have been so far used (3).

In all cases the product must be isolated from the side products of the reaction including the starting amino acids and the buffer components. Since the reaction is run at a concentration of reactants of 0.01 *M* and a buffer concentration of 0.4 *M* the buffer components thus constitute a major portion of the residues and present a major separation problem.

In conjunction with other work going on in these laboratories (13) the preparation of two dipeptides, methionylasparagine (metasn) and methionylglutamine (metgln), became necessary. These two compounds served to illustrate to us the problems that are faced when product isolation after use of the NCA reaction is attempted. This led us to try to further simplify the procedure for product isolation.

The preparation of metasn from methionine NCA and asparagine by the borate procedure led to the production of a product which was soluble in both water and an organic solvent (methanol). It could be isolated by the complete evaporation of the reaction mixture and extraction of the residue with hot methanol. Subsequent crystallization of the extracted material from ethanol–water led to the isolation of pure product (37% yield).

The preparation of metgln led to a product that was slightly insoluble in water and almost completely insoluble in organic solvents. The isolation of adequate quantities of this compound proved very difficult. A small amount (15% yield) could be isolated either by concentration of the reaction mixture or by addition of a small amount of alcohol to the cooled solution. In both cases, as indicated by t.l.c., the major portion of the product remained in solution and could only be isolated along with large quantities of the buffer components.

The problems faced in the isolation of adequate quantities of the latter compound led us to consider the complete removal of the buffer components from the reaction mixture to aid in the product isolation.

Closer consideration of the reaction sequence (see Scheme 1) indicates that the reaction is simply the attack of an amino acid in the unprotonated form (A) on the NCA. The presence of an added buffer might not be absolutely necessary for the reaction to take place in adequate fashion. As long as the p*H* of the solution could be maintained above that corresponding to the pK_a of the α-amino group of the attacking amino acid the reaction should occur. It would be only necessary to use a base to establish and maintain the p*H* of the solution so that sufficient unprotonated α-amine would be present to react with the NCA. The base used could be either an inorganic one or a nonnucleophilic organic one. The amino acid being used as the nucleophile would be now serving as its own "buffer".

Use of an inorganic base, however, leads back to the same problem of removing it from the solution after the reaction. The use of an organic base would not necessarily suffer from this problem since it could be more easily removed from the evaporated mixture by trituration of the residue with an organic solvent in which the products were not soluble.

A series of analytical experiments were then run in order to see if the removal of the external buffer made any difference to the reaction yields. The preparation of metasn was attempted with no external buffer being used. The organic base selected was triethylamine. This liquid tertiary amine base is easily handled and is sufficiently strong as a base (pK_a 10.6) to allow the p*H* of the solution to be maintained above that of the pK_a of the α-amino group of most amino acids.

To allow a comparison with the borate procedure, metasn was prepared both ways under identical experimental conditions. The results are tabulated in Table 1. Under experimental conditions identical with those recommended for use with the borate buffer the per cent of asparagine consumed from solution was identical within experimental error for each procedure. The use of triethylamine did give a slightly better overall yield of dipeptide. This is attributable to the fact that conversion of the initial NCA/asparagine reaction product (Scheme 1, C) to metasn was beset by fewer side reactions.

TABLE 1. NCA preparation of methionylasparagine (metasn). Comparison of borate and triethylamine procedures*

Reaction medium	p*H*†	Temperature (°C)	% asparagine consumed‡, ‖	Overall yield§, ‖
Sodium borate	10.3	2	75	47
Triethylamine	10.3	2	80	63

*Analytical scale experiments (4 m*M*), 1 m*M* asn/10 ml of solution, rapid mixing, methionine NCA added as a solid (10% excess), RJG 1/79,83.
†Electrode standardized to p*H* 7.0, 20 °C.
‡Calculated as m*M* asn consumed from the solution/m*M* asn in solution at start × 100.
§Calculated as m*M* metasn formed/m*M* asn in solution at the start × 100.
‖Experimental errors, determined for at least three runs, amounted to approximately ±8% in each one of these calculated percentages. This variability can be attributed in part to the purity of the NCA used, the rate at which it was added, the variation of the p*H* from that desired during the reaction, as well as the time elapsed before the reaction was acidified in order to terminate it.

TABLE 2. NCA preparation of dipeptides. Comparison of borate and triethylamine procedures; isolated yields

Dipeptide	Dipeptide isolated yield (%)*	
	Borate	Triethylamine
Methionylasparagine	37	53
Methionylglutamine	15	65
Alanylglycine	—	80

*All yields are those isolated after purification by crystallization from a suitable solvent.

To be synthetically useful, any new modification should improve isolated yields. A few analytical scale runs might be necessary to ensure optimum conditions for most preparative scale experiments (approximately 30 m*M*, 5–10 g scale). For metasn and metgln, however, conditions approximating those recommended for the borate procedure, p*H* 10.2 and 2 °C, were chosen for the preparative runs since close p*H* control was possible and the overall reaction yields as determined by the analytical scale experiments were still synthetically acceptable. Methionylasparagine, methionylglutamine and, as an additional check on the procedure, alanylglycine were prepared using these conditions and the yields of pure product isolated are given in Table 2. These yields can be compared with those found for the preparative runs where borate was used as an added buffer. The advantage of using triethylamine to establish and maintain the p*H* is obvious. The higher yields resulted mainly from the simplification of the isolation procedure. After reaction, the p*H* of the solution was lowered to approximately 3.5 with an organic acid (*e.g.* formic acid) to form a completely organic acid/base salt (triethylamine formate). Trituration of the evaporated reaction mixture with chloroform to remove this acid/base salt gave a solid residue. The solid residue containing starting amino acids and product was finally crystallized from a suitable solvent to give the analytically pure dipeptides.

In summary, the use of an organic base to establish and maintain the p*H* during the reaction of an amino acid NCA with another amino acid is sufficient for the preparation of dipeptides in yields which are synthetically useful. The isolation of the resulting products is, in addition, aided since the added base (in this case, triethylamine), as an organic acid/base salt, can be easily removed by trituration of the evaporated reaction mixture with an organic solvent and the dipeptide can then be crystallized from a suitable solvent. Chromatography would have to be applied only where starting materials and side products were inseparable from the products by crystallization. Even here, prior removal of the large quantities of acid/base salt would be of benefit to the chromatographic separation.

1. J. P. GREENSTEIN and M. WINITZ. Chemistry of the amino acids. Vol. II. J. Wiley and Sons, Inc., New York, 1961. p. 860.
2. R. HIRSCHMANN, R. G. STRACHAN, H. SCHWAM, E. F. SCHOENEWALDT, H. JOSHUA, B. BARKENMEYER, D. F. VEBER, W. J. PALEVEDA, JR., T. A. JACOB, T. E. BEESLEY, and R. G. DENKEWALTER. J. Org. Chem. **32**, 3415 (1967).

Can. J. Chem. Downloaded from www.nrcresearchpress.com by 210.87.254.40 on 09/05/12
For personal use only.

3. R. G. DENKEWALTER, H. SCHWAM, R. G. STRACHAN, T. E. BEESLEY, D. F. VEBER, E. F. SCHOENWALDT, H. BARKENMEYER, W. J. PALEVEDA, JR., T. A. JACOB, and R. HIRSCHMANN. J. Am. Chem. Soc. **88**, 3163 (1963).
4. J. M. MANNING and S. MOORE. J. Biol. Chem. **243**, 5591 (1968).
5. R. HIRSCHMANN, R. F. NUTT, D. F. VEBER, R. A. VITALI, S. L. VARGA, T. A. JACOB, F. W. HOLLY, and R. G. DENKEWALTER. J. Am. Chem. Soc. **91**, 507 (1969).
6. K. D. KOPPLE, T. SAITO, and M. OHNISHI. J. Org. Chem. **34**, 1631 (1969).
7. Y. IWAKURA, K. UNO, M. OYA, and R. KATAKAI. Biopolym. **9**, 1419 (1970).
8. S. M. BLOOM, G. D. FASMAN, C. DE LOZÉ, and E. R. BLOUT. J. Am. Chem. Soc. **84**, 458 (1962).
9. R. HIRSCHMANN. Personal communication.
10. J. L. BAILEY. J. Chem. Soc. 3461 (1961).
11. (*a*) K. HOFMANN, T. A. THOMPSON, and E. T. SCHWARTZ. J. Am. Chem. Soc. **79**, 6087 (1957). (*b*) K. HOFMANN, T. A. THOMPSON, H. YAJIMA, E. T. SCHWARTZ, and H. INOUYE. J. Am. Chem. Soc. **82**, 3715 (1960).
12. B. F. ERLANGER and E. BRAND. J. Am. Chem. Soc. **73**, 3508 (1951).
13. (*a*) A. J. DICK, A. T. MATHESON, and J. H. WANG. Can. J. Biochem. **48**, 1182 (1970). (*b*) A. T. MATHESON, A. J. DICK, and F. ROLLIN. Can. J. Biochem. **48**, 1292 (1970). (*c*) A. T. MATHESON and A. J. DICK. FEBS Lett. **6**, 235 (1970).

Can. J. Chem. Downloaded from www.nrcresearchpress.com by 210.87.254.40 on 09/05/12
For personal use only.

Can. J. Chem. Downloaded from www.nrcresearchpress.com by 210.87.254.105 on 09/05/12
For personal use only.

Canadian Journal of Chemistry

Published by THE NATIONAL RESEARCH COUNCIL OF CANADA

VOLUME 50 FEBRUARY 1, 1972 NUMBER 3

Etude de propriétés hydrodynamiques de solutions de polymères en mauvais solvants

NGA HO-DUC ET H. DAOUST

Département de Chimie, Université de Montréal, Montréal, Québec

ET

F. BISSONNETTE

Département de Chimie, Collège Militaire Royal de St-Jean, St-Jean, Québec

Reçu le 14 juin 1971

Le coefficient de frottement d'une chaîne de polymère en solution peut être relié soit au coefficient de sédimentation soit à la viscosité de la solution. Plusieurs auteurs ont essayé de trouver des constantes universelles pour relier les mêmes valeurs déterminées par ultracentrifugation et par viscosimétrie. Il existe présentement certaines divergences dans l'interprétation des résultats, ces divergences venant surtout des points de vue différents sur le comportement des polymères en solvant thêta. Le présent travail étudie l'effet de concentration sur le coefficient de sédimentation au voisinage du point thêta pour des solutions de polystyrène dans le cyclohexane et de polyisobutylène dans le *n*-heptanoate d'éthyle. Pour fin d'interprétation, ce travail nécessite aussi des mesures de viscosité et de diffusion de la lumière dans les mêmes conditions. Les résultats sont interprétés à la lumière des théories de Wales et Van Holde, de Yamakawa, de Pyun et Fixman et d'Imai. Seule la théorie de Pyun et Fixman admet un effet de la concentration sur le coefficient de sédimentation au point thêta et les résultats expérimentaux rapportés dans ce travail appuient cette théorie.

Sedimentation coefficients (ultracentrifuge), second virial coefficients (light scattering) and intrinsic viscosities have been measured at various concentrations near the θ-point for solutions of polystyrene in cyclohexane and of polyisobutylene in ethyl heptanoate. The results have been analyzed in the light of several current theories, but are correlated satisfactorily only by the theory of Pyun and Fixman.

Canadian Journal of Chemistry, **50**, 305 (1972)

Introduction

Il est bien connu que le coefficient de sédimentation d'une macromolécule en solution varie avec la concentration. Cette variation peut être mathématiquement représentée par la relation

$$[1] \qquad \frac{1}{S_0} = \frac{1}{S_0^0}(1 + k_s c)$$

où S_0 et S_0^0 sont les coefficients de sédimentation sous une pression d'une atmosphère à la concentration c, exprimée en g/100 cc, et à dilution infinie respectivement. La constante k_s, en relation avec les propriétés thermodynamiques et hydrodynamiques des macromolécules en solution, a fait l'objet de plusieurs travaux théoriques. Ainsi, Wales et Van Holde (1), en admettant la définition du coefficient de frottement à dilution infinie donnée par

$$[2] \qquad f_0 = \eta_0 P \langle R_0^2 \rangle^{\frac{1}{2}}$$

où η_0 est la viscosité du solvant, P, une constante et $\langle R_0^2 \rangle$, la distance quadratique moyenne entre les bouts d'une chaîne non perturbée, en admettant également la théorie de Fox–Flory sur la viscosité des solutions de polymères et la relation de Burgers relative à la constante de sédimentation de particules sphériques en suspension, arrivent à la relation

$$[3] \qquad k_s/[\eta] = \Lambda N_A (\Phi^{\frac{1}{3}} P^{-1})^{-3}/16200\,\pi^2$$

où Λ est une constante venant de la théorie de Burgers, N_A, le nombre d'Avogadro, Φ, la

Can. J. Chem. Downloaded from www.nrcresearchpress.com by 210.87.254.105 on 09/05/12
For personal use only.

constante universelle de Fox–Flory et $[\eta]$, la viscosité intrinsèque. L'équation [3] montre que k_s est proportionnel à $[\eta]$ et que la constante de proportionalité (1.66) est indépendante de la nature du solvant, de la température et de la masse moléculaire du polymère. Par ailleurs, le traitement théorique de Yamakawa (2) veut que la valeur de k_s soit nulle à la température thêta, *i.e.* que S_0 soit indépendant de la concentration dans ces conditions. D'après sa théorie, $k_s/[\eta]$ est défini par

$$[4] \qquad k_s/[\eta] = \lambda(x)(A_2M/[\eta])$$

où $x = z/\alpha_0^3$, z étant le paramètre du volume exclu, α_0, le coefficient d'expansion linéaire à dilution infinie, A_2, le deuxième coefficient du viriel et M, la masse moléculaire du polymère. En bon solvant, $\lambda(x) \simeq 1.1$ et $(A_2M/[\eta]) \simeq 1.5$ et ainsi on se rapproche de la valeur constante de la relation [3]. Cependant, au point thêta, $A_2 = 0$ et $k_s/[\eta]$ s'annule. Un certain nombre de résultats expérimentaux (3–5) semblent confirmer les prédictions de la théorie de Yamakawa tandis que d'autres résultats la mettent en doute (6–13). Pyun et Fixman (14) ont relevé des faiblesses dans le développement théorique de Yamakawa; ce dernier a fait certaines approximations mathématiques discutables et il n'a pas tenu compte de l'effet de perturbation hydrodynamique sur la fonction de distribution intra et intermoléculaire dans les équations de base. Pyun et Fixman on traité le cas des sphères rigides et celui des sphères interpénétrables et ils ont trouvé pour k_s l'expression suivante

$$[5] \quad k_s = (4/300)(M/N_A\pi)^2 \times [(1 - \bar{v}\rho_0)/6\eta_0 S_0^0]^3[7.16 - \kappa(A)]$$

où $\bar{v}$ est le volume spécifique partiel du polymère, ρ_0, la densité du solvant et $\kappa(A)$ est une fonction où $A = 3n^2\ X/8\pi a^3$, n étant le nombre de segments par chaîne, a, le rayon de la sphère et X, le deuxième coefficient du viriel pour les intéractions segment–segment. Pour des petites valeurs de A, $\kappa(A)$ peut s'écrire (15)

$$[6] \qquad \kappa(A) = \kappa_0 - A\kappa_1 + A^2\kappa_2 + \ldots$$

Pour le cas de sphères interpénétrables, la valeur de $\kappa_0 = 4.2$ à 4.93 selon le modèle choisi pour décrire les intéractions hydrodynamiques entre les sphères. De plus, étant donné que $X \propto A_2$, $n^2 \propto M^2$ et que $a = (1 - \bar{v}\rho_0)M/6\pi\eta_0 N_A S_0^0$, l'équation [5] peut être réécrite sous la forme (14)

$$[7] \qquad k_s/[\eta] = C(7.16 - \kappa_0 + C'A_2M/[\eta])$$

où C et C' sont deux constantes. Au point thêta, $A = 0$, mais $\kappa(0) \neq 0$; il s'ensuit que $k_s \neq 0$ au point thêta contrairement à la théorie de Yamakawa. La constante k_s s'annule pour $A \simeq -1$, *i.e.* à une température inférieure à thêta pour le modèle des sphères interpénétrables. Plus récemment, Imai (16) a élaboré un long traitement mathématique à partir des relations de Fixman sur l'effet de la concentration sur la fonction de distribution des segments d'une chaîne de polymère et il a trouvé que k_s est relié au coefficient d'expansion linéaire viscosimétrique α_η de la façon suivante

$$[8] \qquad k_s = C_0M^{\frac{1}{2}}(\alpha_\eta - \alpha_\eta^{-1})$$

ou

$$[8a] \qquad k_s/[\eta] \simeq b(\alpha_\eta^{-2} - \alpha_\eta^{-4})$$

où C_0 et b sont des constantes dépendant des dimensions de la chaîne non-perturbée.

Ce présent travail rapporte les résultats obtenus sur l'étude de la variation de k_s avec la concentration au voisinage de la température thêta pour deux systèmes polymère-solvant différents et ses relations avec $[\eta]$ et A_2.

Partie expérimentale

Les échantillons de polystyrène (PS) utilisés dans ce travail proviennent de diverses sources; quatre fractions soient celle de $\bar{M}_p = 411\,000$ (Pressure Chemical Company), celle de 125 000 (Dr. McCormick, Dow Chemical of Canada) et celles de 2 380 000 et 1 590 000 (17) sont de très faible polydispersité ($\bar{M}_p/\bar{M}_n \leqslant 1.07$); les échantillons dont $\bar{M}_p = 7\,900\,000$ et 1 790 000 (17) et finalement, 243 000 (Lustrex, Monsanto) ne sont pas fractionnés. Les deux échantillons de polyisobutylène (PIB) proviennent d'un double fractionnement d'un polymère commercial Vistanex L-100 (Enjay Co. Inc.) et $\bar{M}_p = 920\,000$ et 1 750 000, respectivement (18). Les solvants utilisés sont de qualité réactif analytique.

Les mesures de sédimentation sont effectuées à l'aide d'une ultracentrifugeuse analytique Spinco modèle E-HT; les détails techniques et la façon de traiter les données expérimentales ont déjà été décrits ailleurs (19). Les viscosités intrinsèques sont obtenues à partir de mesures effectuées à l'aide d'un viscosimètre automatique Hewlett–Packard; la température du bain est maintenue à $\pm$ 0.05 °C. Les valeurs du second coefficient du viriel sont tirées de données expérimentales de diffusion de la lumière obtenues à l'aide d'un photo-gonio-diffusomètre Sofica; la technique expérimentale est décrite ailleurs (20). Les concentrations des solutions ne dépassent pas 0.5% (P/V) pour les différentes techniques utilisées.

TABLEAU 1. Résultats expérimentaux pour quatre systèmes polymère–solvant

Système	t (°C)	k_s (dl g^{-1})	$[\eta]$ (dl g^{-1})	$(\alpha_\eta^{-2} - \alpha_\eta^{-4})$	$A_2 \times 10^7$ (dl g^{-2} mol)
PS(411 000)–cyclohexane	28	~0	0.44_8	-0.13_7	-8.55
($\theta = 34.5$ °C)	34.5	0.36 ± 0.02	0.53_9	0	0
	40	0.50 ± 0.03	0.57_1	0.03_7	3.6_0
	50	0.81 ± 0.02	0.64_9	0.10_2	11.2_5
PS(125 000)–cyclohexane	28	0.10 ± 0.02	0.25_2	-0.06_0	
	34.5	0.18 ± 0.01	0.27_6	0	
	40	0.29 ± 0.02	0.29_0	0.03_3	
	50	0.38 ± 0.03	0.35_2	0.08_5	
PIB(1 750 000)–heptanoate	27	~0	1.12_2	-0.06_0	
d'éthyle ($\theta = 33$ °C)	33	0.74 ± 0.10	1.23_3	0	
	38	1.30 ± 0.15	1.35_0	0.05_4	
	50	2.20 ± 0.20	1.59_0	0.13_2	
PIB(920 000)–heptanoate	27	~0	0.89_2	-0.06_0	-2.9_0
d'éthyle	33	0.66 ± 0.08	0.97_2	0	0
	38	1.10 ± 0.08	1.03_3	0.03_8	1.5_0
	50	2.00 ± 0.20	1.17_2	0.10_6	6.0_0

Résultats et discussion

Les résultats pour quatre systèmes polymère–solvant sont donnés dans le Tableau 1. Les valeurs de α_η ont été calculées à partir de la relation

$$[9] \qquad [\eta] = [\eta]_\theta \alpha_\eta^3$$

où $[\eta]_\theta$ est la viscosité intrinsèque à la température thêta. Les valeurs de A_2 ont été calculées par la méthode graphique de Zimm. Dans tous les calculs où apparait la masse moléculaire du polymère, c'est la valeur moyenne en poids ($\bar{M}_p$) qui a été utilisée. La courbe de la Fig. 1 montre que $k_s/[\eta]$ est une fonction monotone de la température contrairement aux prédictions de la relation [3], et qu'elle ne s'annule pas au point thêta contrairement aux prédictions de la relation [4]. Cependant, il semble que $k_s/[\eta]$ tende lentement vers la valeur limite de 1.66 lorsqu'on s'éloigne au-dessus de la température thêta, en accord avec les théories de Wales et Van Holde et de Yamakawa.

La Fig. 2 montre que $k_s[\eta]$ est bien une fonction linéaire de $A_2M/[\eta]$ tel que prévu par les relations [4] et [7] sauf qu'elle ne passe pas par l'origine des coordonnées au point thêta comme prédit par la relation [4].

En ce qui concerne la variation de $k_s/[\eta]$ en fonction du coefficient d'expansion linéaire, la Fig. 3 montre que son allure correspond bien à celle prédite par l'équation [8*a*] sauf que les droites ne passent pas par l'origine des coordonnées à la température thêta. L'équation empirique est plutôt de la forme

$$[10] \qquad k_s/[\eta] \simeq (k_s/[\eta])_\theta + b(\alpha_\eta^{-2} - \alpha_\eta^{-4})$$

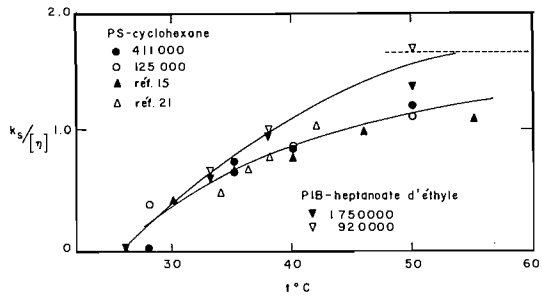

FIG. 1. Variation de $k_s/[\eta]$ en fonction de la température; la droite brisée représente la valeur limite 1.66.

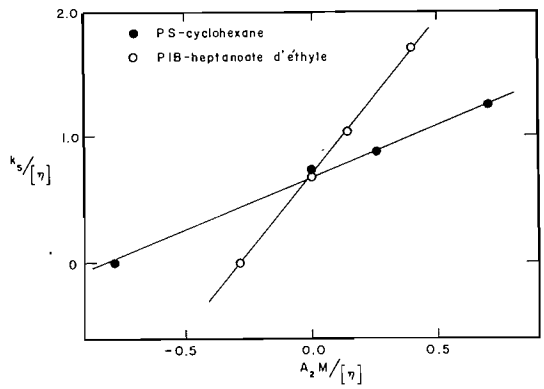

FIG. 2. Variation de $k_s/[\eta]$ en fonction de $A_2M/[\eta]$.

Can. J. Chem. Downloaded from www.nrcresearchpress.com by 210.87.254.105 on 09/05/12
For personal use only.

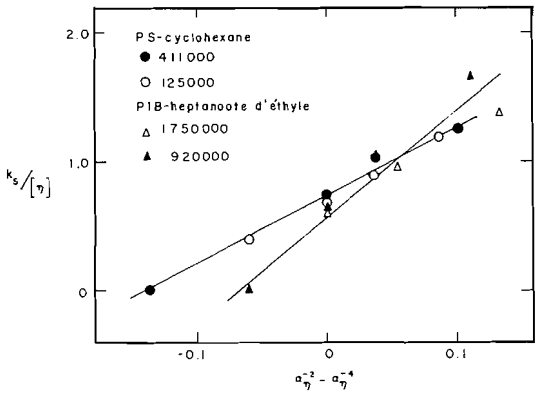

FIG. 3. Variation de $k_s/[\eta]$ en fonction de $(\alpha_\eta^{-2} - \alpha_\eta^{-4})$.

Dans le cas du système PS–cyclohexane, $b = 5.0$ tandis que Petrus et coll. rapportent une valeur de 4.5 pour le même système. Selon l'équation [10], la fonction $k_s/[\eta]$ dépend d'une part de la fonction de distribution des segments, contribution représentée par le deuxième terme tel que défini par Imai et d'autre part, de sa valeur propre au point thêta qui est due principalement à l'effet hydrodynamique décrit par Pyun et Fixman et à l'effet d'environnement décrit par Orofino (23), *i.e.* que $(k_s/[\eta])_0$ serait fonction de la nature du solvant thêta utilisé. En définitive, il semble bien que la théorie de Pyun et Fixman dans le cas de sphères interpénétrables soit celle qui se rapproche le plus des résultats expérimentaux présentés dans ce travail. Une petite remarque d'ordre pratique découle de ceci; il serait préférable de travailler à une température inférieure, à la température thêta lorsqu'on veut utiliser la méthode de la sédimentation à l'analyse de la polydispersité d'un échantillon de polymère afin d'éliminer toute correction due à l'effet de concentration. Cette température reste à déterminer empiriquement pour chaque cas car elle varie avec la masse moléculaire (15, 21).

Il existe, bien sûr, une relation entre k_s et $\bar{M}_p$ à une température donnée pour un système donné. A partir des relations [3] ou [7], il est possible de montrer que cette relation à la température thêta est de la forme (14)

$$[11] \qquad k_s = cte\ \bar{M}_p^{\frac{1}{2}}$$

Une telle relation est illustrée dans la Fig. 4 où sont groupés les résultats de ce travail et ceux de la littérature pour le système PS–cyclohexane à 34.5 °C. Dans le cas d'échantillons polydispersés, les résultats donnent une droite qui semble parallèle à celle obtenue pour les échantillons de faible polydispersité et la valeur moyenne des deux pentes est de 0.52×10^{-3} comparativement à 0.48×10^{-3} calculée par Pyun et Fixman.

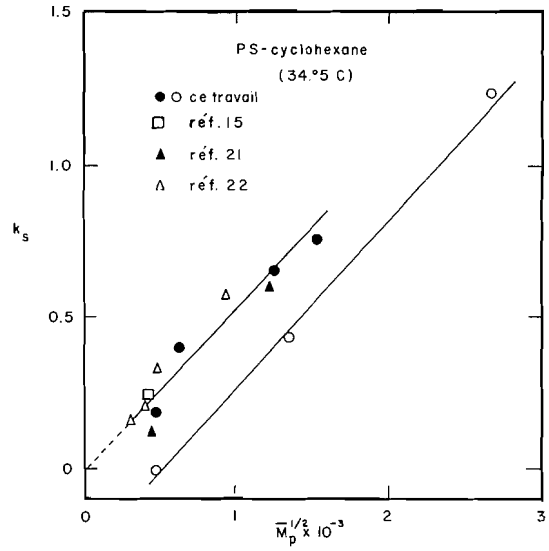

FIG. 4. Variation de k_s en fonction de $\bar{M}_p$ pour le polystyrène dans le cyclohexane à 34.5 °C. La droite supérieure est en relation avec les échantillons monodispersés et la droite inférieure, avec les échantillons polydispersés.

Nous remercions le Conseil National de Recherches du Canada et le Conseil de Recherche pour la Défense pour leurs aides financières au cours de ce travail.

1. M. WALES et K. E. VAN HOLDE. J. Polymer Sci. **14**, 81 (1954).
2. H. YAMAKAWA. J. Chem. Phys. **36**, 2995 (1962).
3. H. J. CANTOW. Makromol. Chem. **30**, 169 (1959).
4. A. HAUG et G. MEYERHOFF. Makromol. Chem. **53**, 91 (1962).
5. D. MCINTYRE et L. C. WILLIAMS. ACS Polymer Preprints **1**, No 2, 125 (1960).
6. M. WALES et S. J. REHFELD. J. Polymer Sci. **62**, 179 (1962).
7. D. MCINTYRE, A. WIMS, L. C. WILLIAMS et L. MENDELKERN. J. Phys. Chem. **66**, 1932 (1962).
8. I. H. BILLICK. J. Phys. Chem. **66**, 1941 (1962).
9. T. HOMMA, K. KAEAHARA, H. FUJITA et M. VEDA. Makromol. Chem. **67**, 132 (1963).
10. H. LÜTJE. Dissertation, Université de Mainz, Allemagne. 1962.
11. M. ABE, Y. MURAKAMI et H. FUJITA. J. App. Polymer Sci. **9**, 2549 (1965).
12. M. JACOB, R. VAROQUI, S. I. KLENINE et M. DAUNE. J. Chim. Phys. **59**, 865 (1962).

Can. J. Chem. Downloaded from www.nrcresearchpress.com by 210.87.254.105 on 09/05/12
For personal use only.

13. I. YA PODDUBNYI, V. A. GRECHANOVSKII et V. A. PODALINSKII. J. Polymer Sci. Part C, **16**, 3109 (1968).
14. C. W. PYUN et M. FIXMAN. J. Chem. Phys. **41**, 937 (1964).
15. I. H. BILLICK. ACS Polymer Preprints **5**, No 2, 855 (1964).
16. S. IMAI. J. Chem. Phys. **50**, 2116 (1968).
17. R. PRUD'HOMME. Thèse de maîtrise, Université de Montréal, Montréal, Québec. 1970.
18. J. DURANCEAU. Thèse de doctorat, Université de Montréal, Montréal, Québec. 1966.
19. N. HO-DUC et H. DAOUST. Can. J. Chem. **47**, 3299 (1969).
20. N. HO-DUC et H. DAOUST. Can. J. Chem. **46**, 2456 (1968).
21. V. PETRUS, I. DANIHEL et M. BOHDANECKÝ. European Polymer J. **7**, 143 (1971).
22. J. J. H. MULDERIJ. I.U.P.A.C. International Symposium on Macromolecules, Leiden, Abstracts Vol. 1, 343 (1970).
23. T. A. OROFINO. J. Chem. Phys. **45**, 4310 (1966).

Can. J. Chem. Downloaded from www.nrcresearchpress.com by 210.87.254.105 on 09/05/12
For personal use only.

The Dipole Moment Derivative of the Hydrogen Bond in Ice[1]

E. WHALLEY

Division of Chemistry, National Research Council of Canada, Ottawa, Canada

Received July 28, 1971

The dipole moment derivative of the hydrogen bond in ice has been calculated assuming that the molecules can be represented as non-overlapping polarizable charge distributions characterized by dipole and quadrupole moments. The value is 0.1 electron charges which is about one third of the experimental value obtained from the far-infrared spectrum. The model predicts therefore only about one tenth of the experimental integrated intensity from which the effective charge was derived. Most of the intensity must therefore be due to specific hydrogen-bond interactions.

On a calculé la dérivée du moment dipolaire de la liaison hydrogène dans la glace en supposant qu'on peut représenter les molécules par des distributions de charges polarisables et sans recouvrement, caractérisées par des moments dipolaires et quadrupolaires. La valeur est de 0.1 charge d'électron, ce qui représente environ le tiers de la valeur expérimentale obtenue du spectre d'infra-rouge lointain. Donc, le modèle prédit seulement environ le dixième de l'intensité expérimentale intégrée, à partir de laquelle on avait dérivé la charge effective. La plupart de l'intensité doit donc être due à des interactions spécifiques de liaison hydrogène.

Canadian Journal of Chemistry, **50**, 310 (1972)

Introduction

It is quite generally accepted on quantum theoretical grounds[2] that hydrogen bonds cannot be explained by the classical interaction of non-overlapping polarizable charge distributions, and that there is probably an intermolecular transfer of charge when a hydrogen bond is formed. One of the strongest experimental evidences for this conclusion is the large increase in the intensity of the X—H stretching vibration when a hydrogen bond is formed.

Nevertheless, the effects of hydrogen bonding in ice are frequently described in terms of the interaction of classically polarizable molecules with permanent electrostatic moments (2, 3). Indeed, for many purposes only this kind of model is reasonably tractable, and it is often used to describe the polarization of a molecule by its neighbors. The dielectric constant of ice, for example, indicates (see ref. 4 for a brief recent discussion) that the dipole moment of a water molecule is enhanced appreciably by intermolecular interaction. If Kirkwood's correlation parameter g is taken as 3.0, which is the value calculated from the geometry of ice (5, 6), the dielectric constant indicates that the dipole moment is enhanced by a factor 1.3, which can easily be accounted for by the polarization of a molecule by the electrostatic field of the multipole moments of its neighbors.

A quantitative measure of the polarization of water molecules by hydrogen bonding (strictly speaking the variation of the polarization with hydrogen bonding) has recently been obtained (7) from another source. The far-infrared spectrum of ice below 320 cm^{-1} is caused by the translational vibrations of the molecules. The intensity of absorption of this band can be interpreted in terms of the dipole moment derivative $\boldsymbol{M}$ with respect to the change of intermolecular distance r

$$\boldsymbol{M}_i = d\boldsymbol{\mu}/dr_i$$

where subscript i refers to the ith bond and $\boldsymbol{\mu}$ is the dipole moment of the crystal. $\boldsymbol{M}$ has the dimensions of charge and is also known as the effective charge. Because ice I is orientationally disordered, $\boldsymbol{M}$ can have several different values and directions, and the quantity obtained from experiment is the root-mean-square value, denoted e^*, and has the value

$$e^* = 0.3e$$

where e is the electronic charge. The question to be discussed in this paper is the origin of this effective charge.

Its value has been calculated for the model in which the water molecules are treated as non-overlapping polarizable charge distributions. The calculations indicate that the model is quite inadequate.

[1]NRCC No. 12216.

[2]For a theoretical review, see ref. 1*a*. Also see ref. 1*b* and references therein.

Can. J. Chem. Downloaded from www.nrcresearchpress.com by 210.87.254.105 on 09/05/12
For personal use only.

Can. J. Chem. Downloaded from www.nrcresearchpress.com by 210.87.254.105 on 09/05/12
For personal use only.

Calculation of Multipole-induced Dipole Moments

In ice I the distribution of molecules is, at least on the average, tetrahedral. The tetrahedron is not perfect because the ratio of the c and a axes of the hexagonal unit cell is 1.6280 ± 0.0002 (8), instead of the 1.633 it would be if the tetrahedron were perfect. Nevertheless, the assumption of a perfect tetrahedron is adequate for our purposes. The intermolecular distance is taken as 2.76 Å, the intermolecular distance in ice. The effects of both the dipole and quadrupole moment are taken account of.

The vapor dipole moment of 1.85 D is assumed although the actual moment of a molecule in the solid is undoubtedly enhanced by intermolecular interaction. There is no simple way of taking account of this enhancement. It can be done, as shown in the Appendix, for an isolated pair of molecules, and the dipole moment derivative can be written as a power series in α/r^3 where α is the polarizability of the molecule. Since α/r^3 has the value 0.0687 (see below), it is a reasonable approximation to take only the first term, which is of the first power.

The quadrupole moments were those calculated from the "c.i.7" wave function of McWeeny and Ohno (9) by Glaeser and Coulson (10). The moments used were defined as

$$\Theta_{\alpha\beta} = \tfrac{1}{2}\int \rho(3r_\alpha r_\beta - r^2\delta_{\alpha\beta})\,d\mathbf{r}$$

where ρ is the charge density at position $\mathbf{r}$, r_α are components of $\mathbf{r}$, $d\mathbf{r}$ is the element of volume at position $\mathbf{r}$, and $\delta_{\alpha\beta}$ is the Kronecker delta function, and were centered on the oxygen nucleus. The values were $\Theta_{xx} = -1.211$, $\Theta_{yy} = 0.853$, and $\Theta_{zz} = 0.358$, all $\times 10^{-26}$ e.s.u. cm^2, where the z axis coincides with the molecular axis, the y axis is in the plane of the molecule, and the system is right-handed. Intermolecular interaction will undoubtedly change the quadrupole moment of a molecule in ice, but nothing is known about the change, and it is ignored. The polarizability of a water molecule is assumed to be isotropic and equal to 1.444 Å^3 per molecule as calculated from the visible refractive index extrapolated to infinite wavelength and the Lorentz–Lorenz equation (11, 12).

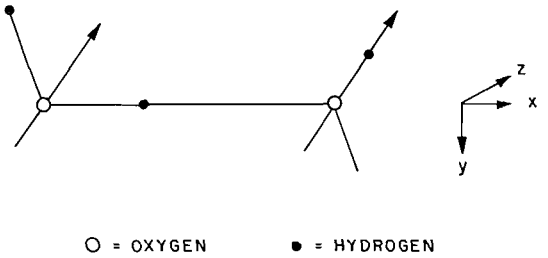

FIG. 1. The hydrogen-bonded water molecules. The left-hand molecule is in the plane of the paper. The plane of the right-hand molecule is perpendicular to the plane of the paper and in configuration S1 of Fig. 2.

For the calculations, the left-hand molecule was fixed in the position shown in Fig. 1, and the right-hand molecule rotated to the positions S1, S2, S2′, E1, E2, and E2′, shown in Fig. 2 in which Fig. 1 is viewed from the right. The dipole moment derivatives for settings S2 and S2′ and for E2 and E2′ differ of course only in direction but not in magnitude.

The effective charges of the pair of water molecules in the various settings, for a displacement along the lines of centers, is given in Table 1 where the coordinate system is that shown in Fig. 1.

The effective charge e^*/e does not differ more than 2% from the mean for any of the relative orientations of the molecules that occur in ice. It follows that its value for our model is 0.10 for both hexagonal and cubic ice.

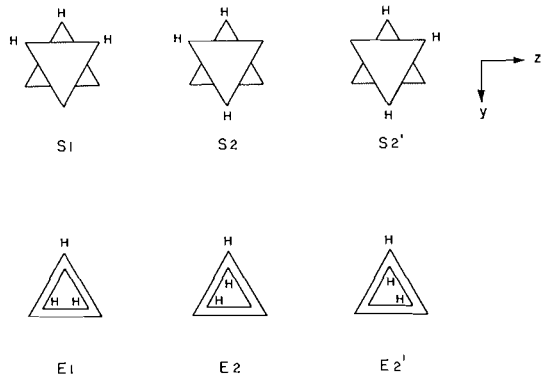

FIG. 2. Relative orientations of two water molecules in ice, viewed along the O---O bond from direction of the right-hand molecule in Fig. 1.

Can. J. Chem. Downloaded from www.nrcresearchpress.com by 210.87.254.105 on 09/05/12
For personal use only.

TABLE 1. Effective charge of a pair of water molecules caused by moments induced by the dipole and quadrupole moments

	Effective charge when orientation is											
	S1			S2			E1			E2		
Inducing moment	Dipole	Quad-rupole	Total	Dipole	Quad-rupole	Total	Dipole	Quad-rupole	Total	Dipole	Quad-rupole	Total
e_x^*/e	−0.0660	−0.0310	−0.0970	−0.0660	−0.0310	−0.0970	−0.0660	−0.0310	−0.0970	−0.0660	−0.0310	−0.0970
e_y^*/e	−0.0468	0.0147	−0.0321	−0.0116	−0.0021	−0.0137	−0.0234	−0.0077	−0.0311	−0.0342	0.0091	−0.0251
e_z^*/e	0	0	0	−0.0202	−0.0096	−0.0298	0.0234	0	0.0234	−0.0202	0.0096	−0.0106
$\lvert e^*/e \rvert$			0.102			0.102			0.105			0.101

Can. J. Chem. Downloaded from www.nrcresearchpress.com by 210.87.254.105 on 09/05/12
For personal use only.

Discussion

The effective charge calculated for the model of non-overlapping polarizable charge distributions is only about one third of the experimental value. The model therefore predicts only about one tenth of the experimental infrared integrated intensity from which the effective charge was derived.

The calculations have neglected the moments induced by the induced moments. The induced moment can be obtained in several ways. Coulson and Eisenberg (2) calculated the average field at a molecule due to its neighbors and calculated the induced moment from this field and the low-field polarizability. The total moment obtained in this way is 1.41 times the moment of the isolated molecule. The contribution of the orientation polarization to the dielectric constant yields the moment that reorients when a molecule reorients. According to Onsager's theory (13), the reorienting moment is greater than the moment μ_0 of the isolated molecule because of the effect of the reaction field. For substances of high dielectric constant like ice the enhancement factor is $(n^2 + 2)/3$, where n is well approximated by the visible refractive index. For ice it is 1.15. According to Kirkwood's theory (14), the difference between the limiting dielectric constants ε_0 and ε_∞ at low and high frequency of the orientation polarization region is, for substances of high dielectric constant,

$$\varepsilon_0 - \varepsilon_\infty = 2\pi N g \mu^2 / kT$$

where g is an orientation correlation parameter. The value of g calculated for ice from the known structure is 3.0 (5, 6) and this with the measured values (ref. 15 and many later workers) of ε_0 and ε_∞ leads to the value of μ of 1.3 times the vapor value. None of these moments is high enough to significantly reduce the discrepancy between theory and experiment. The relationship between them and the "effective moment" of a molecule for the translational vibrations is not at all clear. Nevertheless, it would seem impossible that the "effective moment" could be three times the moment of the isolated molecule which is what would be required to bring experiment and theory into agreement. It is concluded therefore that the model of non-overlapping polarizable dipolar and quadrupolar molecules fails by about an order of magnitude to explain the integrated far-infrared intensity of ice.

It follows therefore that there is a strong polarization caused by varying the O---O distance that is not accounted for on our model. Either the moment induced in each molecule by a small variation of the O---O distance is much greater than the simple model would imply, or there is a transfer of charge from one molecule to the other. Experiment can, at present, tell us no more.

Most quantum mechanical theories of hydrogen bonding discuss it in terms of charge transfer between molecules, but none has calculated the effective charge in the sense used in this paper. Kollman and Allen (16) on the other hand, using what are described as essentially Hartree–Fock-quality atomic orbitals as a basis, conclude that the enhancement of the O—H stretching intensity of water on hydrogen bonding is due more to charge redistribution within a molecule than to charge transfer. It appears that at present only theory can decide the relative importance of intermolecular charge transfer and intramolecular charge redistribution.

Appendix

We consider two molecules 1 and 2 carrying permanent dipoles $\boldsymbol{\mu}_{10}$ and $\boldsymbol{\mu}_{20}$ and dipoles $\boldsymbol{m}_{10}$ and $\boldsymbol{m}_{20}$ induced by their mutual interaction. The total moments of the molecules are therefore

$$\boldsymbol{\mu}_1 = \boldsymbol{\mu}_{10} + \boldsymbol{m}_{10} \quad [1]$$

$$\boldsymbol{\mu}_2 = \boldsymbol{\mu}_{20} + \boldsymbol{m}_{20} \quad [2]$$

The vector $\boldsymbol{r}$ joins the molecular centers. The moment induced in one molecule by the dipole of the other is the polarizability multiplied by the field. If the polarizability is isotropic, then

$$\boldsymbol{m}_{10} = \beta\left\{\frac{(3\boldsymbol{\mu}_2 \cdot \boldsymbol{r})\boldsymbol{r}}{r^2} - \boldsymbol{\mu}_2\right\} \quad [3]$$

$$\boldsymbol{m}_{20} = \beta\left\{\frac{3(\boldsymbol{\mu}_1 \cdot \boldsymbol{r})\boldsymbol{r}}{r^2} - \boldsymbol{\mu}_1\right\} \quad [4]$$

where

$$\beta = \alpha/r^3$$

Can. J. Chem. Downloaded from www.nrcresearchpress.com by 210.87.254.105 on 09/05/12
For personal use only.

By inserting eqs. 1 and 2 into eqs. 3 and 4

$$[5]\quad \boldsymbol{m}_{10} = \beta\left\{\frac{3(\boldsymbol{\mu}_{20}\cdot\boldsymbol{r})\boldsymbol{r}}{r^2} - \boldsymbol{\mu}_{20} + \frac{3(\boldsymbol{m}_{20}\cdot\boldsymbol{r})\boldsymbol{r}}{r^2} - \boldsymbol{m}_{20}\right\}$$

$$[6]\quad \boldsymbol{m}_{20} = \beta\left\{\frac{3(\boldsymbol{\mu}_{10}\cdot\boldsymbol{r})\boldsymbol{r}}{r^2} - \boldsymbol{\mu}_{10} + \frac{3(\boldsymbol{m}_{10}\cdot\boldsymbol{r})\boldsymbol{r}}{r^2} - \boldsymbol{m}_{10}\right\}$$

Then we find

$$[7]\quad \boldsymbol{m}_{10}\cdot\boldsymbol{r} = \beta(2\boldsymbol{\mu}_{20}\cdot\boldsymbol{r} + 2\boldsymbol{m}_{20}\cdot\boldsymbol{r})$$

$$[8]\quad \boldsymbol{m}_{20}\cdot\boldsymbol{r} = \beta(2\boldsymbol{\mu}_{10}\cdot\boldsymbol{r} + 2\boldsymbol{m}_{10}\cdot\boldsymbol{r})$$

$$[9]\quad \boldsymbol{m}_{10}\times\boldsymbol{r} = -\beta(\boldsymbol{\mu}_{20}\times\boldsymbol{r} - \boldsymbol{m}_{20}\times\boldsymbol{r})$$

$$[10]\quad \boldsymbol{m}_{20}\times\boldsymbol{r} = -\beta(\boldsymbol{\mu}_{10}\times\boldsymbol{r} - \boldsymbol{m}_{10}\times\boldsymbol{r})$$

By appropriate combinations from eqs. (7)–(10)

$$[11]\quad \boldsymbol{m}_{10}\cdot\boldsymbol{r} = \frac{2\beta}{1-4\beta^2}(\boldsymbol{\mu}_{20}\cdot\boldsymbol{r} - 2\beta\boldsymbol{\mu}_{10}\cdot\boldsymbol{r})$$

$$[12]\quad \boldsymbol{m}_{10}\times\boldsymbol{r} = -\frac{\beta}{1-\beta^2}(\boldsymbol{\mu}_{20}\times\boldsymbol{r} - \beta\boldsymbol{\mu}_{10}\times\boldsymbol{r})$$

and there are similar equations for the components of $\boldsymbol{m}_{20}$.

The terms in the first power of β in eqs. 11 and 12 describe the polarizations induced directly by the permanent moments of each molecule, and the terms of higher order in β describe the moments induced by the mutual induction. The value of β for ice is 0.069, and so no significant error is made if second and higher order terms are ignored.

The derivatives of the components of the moment with respect to the intermolecular distance is given by

$$r\frac{\partial}{\partial r}\left(\frac{\boldsymbol{m}_{10}\cdot\boldsymbol{r}}{r}\right) = -\frac{6\beta(1+4\beta^2)}{(1-4\beta^2)^2}\frac{\boldsymbol{\mu}_{20}\cdot\boldsymbol{r}}{r} - \frac{24\beta^2}{(1-4\beta^2)^2}\frac{\boldsymbol{\mu}_{10}\cdot\boldsymbol{r}}{r}$$

$$r\frac{\partial}{\partial r}\frac{\boldsymbol{m}_{10}\times\boldsymbol{r}}{r} = \frac{3\beta(1+\beta^2)}{(1-\beta^2)^2}\frac{\boldsymbol{\mu}_{20}\times\boldsymbol{r}}{r} + \frac{6\beta^2}{(1-\beta^2)^2}\frac{\boldsymbol{\mu}_{10}\times\boldsymbol{r}}{r}$$

I am indebted to Miss M. B. Howes for help with the calculations.

1. (*a*) S. Bratoz. Adv. Quant. Chem. **3**, 209 (1967). (*b*) G. C. Pimentel and A. L. McLellan. The hydrogen bond. W. H. Freeman and Co., San Francisco. 1960. p. 233.
2. C. A. Coulson and D. Eisenberg. Proc. R. Soc. A, **291**, 454 (1966).
3. E. S. Campbell, G. Gelertner, H. Heinen, and V. R. C. Moorty. J. Chem. Phys. **46**, 2690 (1967).
4. D. Eisenberg and W. Kauzmann. The structure and properties of water. Clarendon Press, Oxford. 1969. p. 105*ff*.
5. G. T. Hollins. Proc. Phys. Soc. **84**, 1001 (1964).
6. J. G. Powles. J. Chem. Phys. **20**, 1302 (1952).
7. J. E. Bertie, H. J. Labbé, and E. Whalley. J. Chem. Phys. **50**, 4501 (1969).
8. R. Brill and A. Tippe. Acta Cryst. **23**, 343 (1967).
9. R. McWeeny and K. A. Ohno. Proc. R. Soc. A, **255**, 367 (1960).
10. R. M. Glaeser and C. A. Coulson. Trans. Faraday Soc. **61**, 389 (1965).
11. W. H. Orrtung and J. A. Meyers. J. Phys. Chem. **67**, 1905 (1963).
12. E. A. Moelwyn-Hughes. Physical chemistry. 2nd ed. Pergamon Press, Oxford. 1961. p. 381.
13. L. Onsager. J. Am. Chem. Soc. **58**, 1486 (1936).
14. J. G. Kirkwood. J. Chem. Phys. **7**, 911 (1937).
15. R. P. Auty and R. H. Cole. J. Chem. Phys. **20**, 1309 (1952).
16. P. A. Kollman and L. C. Allen. J. Chem. Phys. **51**, 3286 (1969).

An X-Ray Structure Determination of the Twinned Crystals of Dinitrato-2,2′-dipyridylsilver(II)

G. W. BUSHNELL AND M. A. KHAN
Department of Chemistry, University of Victoria, Victoria, British Columbia

Received July 27, 1971

The crystal structure of dinitrato-2,2′-dipyridylsilver(II) has been solved and refined to an *R*-value of 0.070. Four circle diffractometer measurements were obtained from the twinned triclinic crystals. The unit cell dimensions at 22 °C are: $a = 697.5 \pm 0.2$ pm, $b = 999.4 \pm 0.2$ pm, $c = 1032.2 \pm 0.2$ pm, $\alpha = 113.46 \pm 0.02°$, $\beta = 100.71 \pm 0.02°$, $\gamma = 95.28 \pm 0.02°$. The space group is $P\bar{1}$ (No. 2) with two molecules per unit cell. The density is 2.06 ± 0.04 g cm^{-3} (measured), 2.02 g cm^{-3} (calculated). The four shortest bond lengths to silver are: Ag—O(1), 214.8 ± 1.5 pm; Ag—O(4), 213.6 ± 1.5 pm; Ag—N(1), 212.4 ± 1.6 pm; Ag—N(2), 220.7 ± 1.6 pm. These four bonds are distorted from square planar geometry with the silver atom lying 19.90 ± 0.17 pm out of the mean plane of the other four atoms. There are also long bonds to the nitrato groups of neighboring molecules: Ag—O(1′), 275.3 ± 1.3 pm; Ag—O(2″), 276.3 ± 1.6 pm. Inclusion of these bonds gives a distorted octahedral silver coordination. Though predominantly unidentate, there is a slight tendency toward bidentate bonding in both nitrato ligands: Ag—O(2), 305.8 ± 1.4 pm; Ag—O(5), 295.0 ± 1.7 pm. O(2) and O(5) approach the convex side of the distorted square planar coordination. The deviation from planarity of the closely bonded square, and angular distortions in the above mentioned octahedral coordination can be rationalized by considering the silver as eight coordinate. The bonds to silver may be grouped 4:2:2 by length or 4:3:1 by angular disposition.

Nous avons a déterminé la structure cristalline du dinitrato-2,2′-dipyridylargent(II) et l'avons raffinée pour obtenir une valeur de *R* de 0.070. Nous avons obtenu des mesures avec un diffractomètre à quatre cercles pour les cristaux tricliniques jumelés. Les dimensions de la maille à 22 °C sont $a = 697.5 \pm 0.2$ pm, $b = 999.4 \pm 0.2$ pm, $c = 1032.2 \pm 0.2$ pm, $\alpha = 113.46 \pm 0.02°$, $\beta = 100.71 \pm 0.02°$, $\gamma = 95.28 \pm 0.02°$. Le groupe spatial est $P\bar{1}$ (No. 2) avec deux molécules par maille. La densité est 2.06 ± 0.04 g cm^{-3} (mesuré), 2.02 g cm^{-3} (calculé). Les quatre liens les plus courts de l'argent sont: Ag—O(1), 214.8 ± 1.5 pm; Ag—O(4), 213.6 ± 1.5 pm; Ag—N(1), 212.4 ± 1.6 pm; Ag—N(2), 220.7 ± 1.6 pm. Ces quatre liens sont déformés à la géométrie du plan carré, l'atome d'argent se situant à 19.90 ± 0.17 pm en dehors du plan formé par les quatre autres atomes. Il y a aussi des liens longs entre l'argent et les groupes nitrato des molécules avoisinantes: Ag—O(1′), 275.3 ± 1.3 pm; Ag—O(2″), 276.3 ± 1.6 pm. L'inclusion de ces liens donne à l'argent une coordination octaédrique déformée. Même si les liens ont une prédominance à être monodentés, on remarque une légère tendance vers des liens bidentés pour les deux ligands nitrato: Ag—O(2), 305.8 ± 1.4 pm; Ag—O(5), 295.0 ± 1.7 pm. O(2) et O(5) approchent le côté convexe de la coordination du plan carré déformé. La deviation des quatre atomes liés de près à une structure planaire, ainsi que les déformations angulaires dans la coordination octaédrique ci-dessus mentionnée, peut-être rationnalisée en considerant l'argent comme ayant une coordination de huit. On peut grouper les liens à l'argent dans le rapport 4:2:2 pour la longueur ou 4:3:1 pour la disposition angulaire.

Canadian Journal of Chemistry, **50**, 315 (1972)

Introduction

There are many known crystal structures of copper(II) complexes and relatively few for silver(II) compounds. The difference in reduction potential between $e + Ag^{2+} \rightarrow Ag^{+}$ ($E^0 = +1.987$ *V* in 4 *M* $HClO_4$) and $e + Cu^{2+} \rightarrow Cu^{+}$ ($E^0 = +0.158$ *V*) greatly affects the chemical reactivity. Silver (II) species are strong oxidizing agents which react with water, decomposing quite rapidly with oxygen evolution. Copper(II) is a generally important oxidation state, but silver(II) is not. However, silver(II) compounds are theoretically and spectroscopically interesting, and it is fitting that a comparison of the structural aspects of Cu(II) and Ag(II) compounds should be attempted in the solid state where the silver(II) compounds may be long lived. In this way fresh information on the stereochemistry of d^9 species is obtainable, and the scarcity of suitable silver(II) compounds is compensated by the detail of the crystallographic results. The choice of a ligand or anion for the preparation of a silver(II) complex is limited to those species able to co-exist with a strong oxidizing agent. Pyridine and several related ligands meet this requirement and may also stabilize the silver(II) state. A number of pyridine, 2,2′-dipyridyl, and 1,10-phenanthroline complexes of silver(II) have been prepared (1). Nitrate, perchlorate, chlorate, hydrogen sulfate,

Can. J. Chem. Downloaded from www.nrcresearchpress.com by 210.87.254.40 on 09/05/12
For personal use only.

Can. J. Chem. Downloaded from www.nrcresearchpress.com by 210.87.254.40 on 09/05/12
For personal use only.

and persulfate have been successfully employed as anions (2). Synthetic methods have involved prior formation of $Ag(I)Ag(III)O_2$ (3), electrolytic oxidation (4), and the use of strong oxidizing agents such as ozone (5) or potassium persulfate (2).

Dinitratodipyridylsilver(II) was chosen for study after exploratory preparative work had shown that suitable crystals were obtainable. In addition to its intrinsic interest as a silver(II) complex, the bonding of the nitrato ligands was worth investigating and there was strong likelihood of meaningful comparison to copper(II) structures of a similar nature.

Experimental

Bisdipyridylsilver(I) nitrate was prepared according to the method of Morgan and Burstall (2). Dinitratodipyridylsilver(II) was prepared by ozone oxidation of bisdipyridylsilver(I) nitrate in 5 *M* nitric acid. Ozone was bubbled through a solution of 0.5 g of bisdipyridylsilver(I) nitrate in 10 mls of 5 *M* HNO_3 for 4 h. The dark brown crystals were filtered immediately, washed with small quantities of water and acetone, and dried *in vacuo*. Recrystallization was not practicable.

Anal. Calcd. for $C_{10}H_8AgN_4O_6$: C, 30.95; H, 2.08; Ag, 27.80; N, 14.44. Found: C, 31.25; H, 2.21; Ag, 27.94; N, 14.14.

Crystallographic Measurements

All the crystals were multiply twinned with no obvious reentrant angles visible under the microscope. Most of the crystals were too small for mounting convenience with a short columnar habit and an approximately hexagonal cross section difficult to observe on the microscope stage. The specimen used for intensity measurements had dimensions 0.10 × 0.08 × 0.24 mm. The column axis coincided with the axis *a*, the most convenient mounting direction. Most rotation photographs about *a* showed almost mirror symmetry across the zero layer in spot position, but not necessarily in spot intensity. On this axis the zero layer Weissenberg appeared like that of a single crystal, but each upper layer showed two triclinic patterns superimposed. The crystals were rotationally twinned with a two-fold twin axis along *a*. The angles β^* and γ^* were first obtained by indexing and then using the method of double offsets (6). The double offset was measured in the first layer between spots $1,k,l$ for twin 1 and $1,k,l$ for twin 2, with k and l selected so that both reflections have the same value of 2θ. All such pairs were found approximately on a line in the first layer passing through *a* and at 46° from the plane through *a* and b^*. The initial values of β^* and γ^* thus obtained made it possible to mount crystals for confirmatory precession photographs of the $h0l$ and $hk0$ planes of one of the twins. The crystal was set on a Picker 4-circle diffractometer mounted about *a*. The $0,k,l$ reflections of the two twins were superimposed. Further superimpositions, seen from the photographic results to be unlikely, were not observed. A set of 72 2θ measurements was obtained and the cell parameters were refined by the method of least squares. The crystal data are listed in Table 1. No piezoelectric effect was found using the Wooster Mark III piezoelectric test apparatus. Confirmation of space group $P\bar{1}$ was done solely by structure refinement. The density was measured by flotation in a solution of ethyl iodide and methyl iodide. Intensity measurements were obtained manually on a Picker 4-circle diffractometer using MoKα radiation ($\lambda = 71.069$ pm) and $\theta/2\theta$ scans for 1 min at a rate of 2°/min in 2θ. The diffractometer was operated in the bisecting position with $\omega = 0$. Background counts were measured for 30 s at each end of the scan. A set of three reflections was measured twice a day for orientation checking, and a standard reflection was examined after every batch of 50 scans. A total of 1275 reflections were measured up to a 2θ angle of 41°, 1019 of these were above background using the criterion that the net count must be $>3\sigma$, where σ is the standard deviation of the background count. Corresponding intensity measurements from the two twins were equal, the $0,k,l$ intensities were therefore halved. Apart from the $0,k,l$ set, all measurements were done on one of the twins. Lorentz and polarization factors were applied, but no absorption correction [$\mu t(\text{max}) = 0.38$, $\mu t(\text{min}) = 0.13$].

TABLE 1. Crystal data for dinitratodipyridylsilver(II)

System	Triclinic
Space group	$P\bar{1}$ (No. 2)
Molecular weight	388.07
Cell dimensions	$a = 697.5 \pm 0.2$ pm
	$b = 999.4 \pm 0.2$ pm
	$c = 1032.2 \pm 0.2$ pm
	$\alpha = 113.46 \pm 0.02°$
	$\beta = 100.71 \pm 0.02°$
	$\gamma = 95.28 \pm 0.02°$
Cell volume	637.5×10^{-24} cm^3
Density (measured)	2.06 ± 0.04 g cm^{-3}
Molecules per cell (calcd.)	2.04
Absorption coefficient (MoK$_\alpha$)	15.8 cm^{-1}

Structure Determination

The atomic scattering factor curve for silver was obtained from the work of Cromer and Waber (7). Atomic scattering factor curves for C, N, and O were obtained from the International Tables (8). All atoms were assumed to be uncharged, and a correction was made for the anomalous dispersion of silver (9). The calculations were done using a set of programs supplied by Penfold (10). The silver atom and the four most closely coordinated light atoms were positioned by interpretation of a three dimensional Patterson function. A Fourier synthesis phased with these five atoms treated as Ag + 4N, revealed the complete structure. The refinement was by minimization of $w(|F_o| - |F_c|)^2$ using full matrix least squares. The weights were derived from counting statistics and an experimentally determined instrument instability factor using the formulae given by Stout and Jensen (11). No systematic variations of $w(|F_o| - |F_c|)^2$ were found during refinement. The unobserved reflections were included in the structure factor calculations but excluded from the least squares sums. Conventional R values are given excluding the unobserved reflections. After one cycle of refinement the (Ag + 4N) model with isotropic temperature factors gave $R = 0.286$. The first structure factor calculation with all C, N, and O atoms included gave $R = 0.180$. The refinement was then continued with anisotropic temperature factors

Can. J. Chem. Downloaded from www.nrcresearchpress.com by 210.87.254.40 on 09/05/12
For personal use only.

TABLE 2. Fractional atomic coordinates*

Atom	X	Y	Z
Ag	0.2234(2)	−0.0978(2)	0.0527(2)
O(1)	0.1738(19)	0.0820(17)	−0.0057(14)
O(2)	0.3697(24)	0.0105(17)	−0.1565(16)
O(3)	0.2146(24)	0.1943(20)	−0.1429(16)
O(4)	0.1214(22)	−0.2574(17)	−0.1689(17)
O(5)	0.4192(29)	−0.3053(22)	−0.1511(20)
O(6)	0.2256(32)	−0.3719(20)	−0.3593(20)
N(1)	0.2563(22)	0.0429(20)	0.2761(17)
N(2)	0.2439(25)	−0.2494(20)	0.1603(19)
N(3)	0.2593(26)	0.0949(24)	−0.1067(20)
N(4)	0.2654(33)	−0.3123(21)	−0.2288(24)
C(1)	0.2745(32)	0.1889(30)	0.3265(23)
C(2)	0.2911(34)	0.2836(25)	0.4741(23)
C(3)	0.2767(34)	0.2176(28)	0.5652(26)
C(4)	0.2590(28)	0.0629(30)	0.5139(23)
C(5)	0.2447(28)	−0.0197(25)	0.3667(24)
C(6)	0.2344(28)	−0.1834(26)	0.3004(25)
C(7)	0.2002(31)	−0.2756(29)	0.3736(25)
C(8)	0.1923(34)	−0.4241(29)	0.3018(28)
C(9)	0.2183(33)	−0.4865(24)	0.1601(28)
C(10)	0.2437(35)	−0.3938(27)	0.0908(26)

*Estimated standard deviations in parentheses.

and the R-value sequence was 0.084, 0.071, 0.070, 0.070. Defining the weighted R value as $(\Sigma w\Delta^2/wF_o^2)^{1/2}$, the corresponding weighted R-value sequence was 0.359, 0.211, 0.101, 0.092, 0.088, 0.088. Including the un-observed reflections the final conventional $R = 0.103$, the final weighted $R = 0.104$. On the final cycle the maximum shift/error ratio was 0.02. A final difference synthesis gave no indication of any misplaced atoms. The maximum electron density was 1.35×10^{-6} e pm^{-3} attributable to a hydrogen atom on C(7). Similar but slightly lower peaks were found for the hydrogens on C(1), C(4), and C(9). Negative minima were found of the same order of magnitude. The estimated standard deviations of the parameters were calculated using the full variance-covariance matrix. The structure factor table is in the Depository for Unpublished Data.[1]

Results

The fractional atomic coordinates of dinitratodipyridylsilver(II) are listed in Table 2. The crystal structure is given in Fig. 1. The weaker coordinate bonds to silver are represented by single lines. If the single line bonding is ignored the structure is molecular. Fig. 1 shows one complete molecule and two other molecules in which the carbon atoms have been omitted for simplicity. The origin of the cell is at the lower right front and the axes are labelled. The central molecule with no primes on the atom labels has the fractional coordinates x, y, z given in Table 2. The right hand molecule with the single primes has coordinates $-x, -y, -z$, and the left hand molecule with double primes has coordinates $(1-x), -y, -z$. Table 3 gives the intramolecular bond lengths and also two intermolecular distances involving the silver atom. In Table 3(*a*) we list eight coordinate bonds to silver. Row 1 shows that the bonds from silver to the closest oxygens of the two nitrato groups are equal. The bond length indicates covalently bound nitrato ligands rather than nitrate ions. Row 2 contains distances of approximately 300 pm from the silver atom to the next nearest oxygen atom of each nitrato group. At this distance any bonding would be weak. Row 3 contains the silver to dipyridyl nitrogen distances and indicates that Ag—N(1) is not equal to Ag—N(2). This might be caused by the limited dipyridyl span. Row 4 contains two intermolecular coordinate bonds to silver which are equal in length at approximately 276 pm. Classified according to length there are four bonds at approximately 215 pm, two bonds at 276 pm, and two very long bonds at approximately 300 pm.

Table 3(*b*) contains the bond lengths for the two nitrato ligands. Differences between the two groups are hardly significant. A free nitrate ion has all three N—O bond lengths equal and close to 124.5 pm (12). We observe a marked lengthening of the N—O bonds to those oxygens which are strongly coordinated to the silver atom. The other N—O distances are shorter than 124.5 pm. Similar effects have been observed in other monodentate nitrato complexes (13, 14).

Table 3(*c*) gives the bond lengths of the dipyridyl ligand. There are no significant differences between the two pyridine rings as can be seen by comparing columns 1 and 2. The bond lengths are similar to those of the parent dipyridyl even though the free dipyridyl molecule is in the *trans* planar conformation (15).

Table 4 gives various least squares planes for the molecule. The orthogonal axis system used has x along a, y in the (a, b) plane, and z along c^*. The quantity minimized was $R = \sum_i W_i P_i^2$, where the weight W_i for atom i is given by $3/[\sigma^2(x_i) + \sigma^2(y_i) + \sigma^2(z_i)]$ and P_i is the perpendicular distance of atom i from the plane.

[1]Copies may be obtained upon request from the Depository of Unpublished Data, National Science Library, National Research Council of Canada, Ottawa, Canada K1A 0S2.

Can. J. Chem. Downloaded from www.nrcresearchpress.com by 210.87.254.40 on 09/05/12
For personal use only.

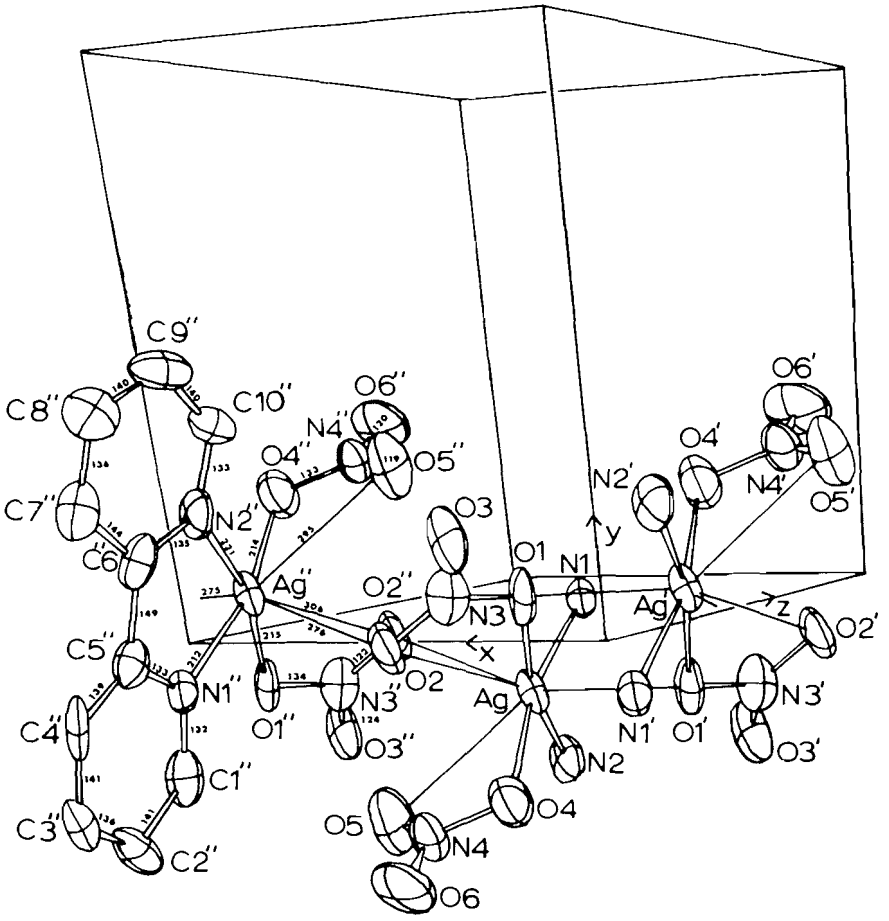

FIG. 1. The crystal structure of dinitratodipyridylsilver(II).

The quantity $\chi^2 = \sum_i [P_i^2/\sigma^2(P_i)]$, is calculated as an index of the planarity of the group. The perpendicular distance of the silver atom from the planes is denoted P_{Ag}, and the estimated standard deviations for this column are all 0.2 pm. Planes *1* and *2* are calculated in an attempt to find a central plane for the molecule. The set N(1)—N(4) is more planar than the set N(1), N(2), O(1), O(4) through the four most closely coordinated atoms. Plane *1* is only 1.12° from the crystallographic 1,0,0 plane. The nitrato ligands are definitely planar as shown by the results for planes *3* and *4*. The silver atom does not lie exactly in the plane of either nitrato ligand. The χ^2 values for planes *5* and *6* show that each pyridyl group is planar. The silver atom is much closer to plane *5* than to plane *6*, indicating that the first pyridyl group with the shorter Ag—N(1) bond maintains a more regular coordination position than the second pyridyl group with the longer Ag—N(2) distance. The results for plane *7* show that the dipyridyl ligand as a whole is significantly non-planar. The angle between planes *5* and *6* is 7.9°. This angle can be expressed in two components on an axis system natural to the ligand. To bring the second pyridyl group into the plane of the first pyridyl group requires a rotation of 6.7° about the C(5)—C(6) bond, and a bend of 4.2° about the midpoint of the same bond, perpendicular to the plane of the first group.

Table 5(*a*) is a list of the bond angles for the distorted silver octahedron obtained by consideration of bonds up to 276 pm. Row 1 gives the angles between ligands *trans* to each other, thereafter columns 1, 2, and 3 give angles ap-

Can. J. Chem. Downloaded from www.nrcresearchpress.com by 210.87.254.40 on 09/05/12
For personal use only.

TABLE 3. Interatomic distances*

(*a*) Coordinate bonds

Bond	Length (pm)	Bond	Length (pm)
Ag—O(1)	214.8(15)	Ag—O(4)	213.6(15)
Ag—O(2)	305.8(14)	Ag—O(5)	295.0(16)
Ag—N(1)	212.4(16)	Ag—N(2)	220.7(16)
Ag—O(1′)	275.3(13)	Ag—O(2″)	276.3(16)

(*b*) Nitrato ligand bonds

Bond	Length (pm)	Bond	Length (pm)
N(3)—O(1)	133.6(21)	N(4)—O(4)	132.5(22)
N(3)—O(2)	122.1(21)	N(4)—O(5)	119.2(23)
N(3)—O(3)	123.8(21)	N(4)—O(6)	120.0(22)

(*c*) 2,2′-Dipyridyl ligand bonds

Bond	Length (pm)	Bond	Length (pm)
N(1)—C(1)	132.4(27)	N(2)—C(10)	133.1(27)
N(1)—C(5)	132.5(25)	N(2)—C(6)	134.7(26)
C(1)—C(2)	141.3(29)	C(10)—C(9)	139.6(31)
C(2)—C(3)	135.9(30)	C(9)—C(8)	139.8(31)
C(3)—C(4)	140.5(31)	C(8)—C(7)	135.9(32)
C(4)—C(5)	139.0(29)	C(7)—C(6)	143.5(29)
C(5)—C(6)	149.0(29)		

*Estimated standard deviations are given in parentheses in tenths of a pm.

proximately in the three mutually perpendicular planes of the octahedron. The deviations from 90° or 180° are considerable. One element of the distortion is the angle N(1)—Ag—N(2) = 75.9 ± 0.7° caused by the limited span of the dipyridyl ligand. The shorter Ag—N(1) bond maintains a regular position relative to the nitrate ligands whereas the longer Ag—N(2) bond does not (O(1)—Ag—N(1) = 90.9° whereas N(2)—Ag—O(4) = 99.4°).

Table 5(*b*) gives the angles necessary to locate a second oxygen atom from each nitrato ligand in the coordination. Row 1 places O(2) in an octahedral quadrant, and row 2 similarly places O(5) in an adjacent quadrant. The single entry in row 3 is the angle between the two very long bonds. As may be seen in Fig. 1, the atoms surrounding the silver atom can be classified into groups of 4, 3, and 1 according to their angular distribution.

Table 5(*c*) gives the angles of the nitrato ligands. Comparison of row 1 with row 2 shows that both ligands are behaving identically. The angle facing the silver atom is close to 120°, but the remaining 240° is not bisected equally by Ag—O(3) or Ag—O(6). The reason for this probably lies in the similar way in which the nitrato ligands are bound to the silver atom. Both O(3) and O(6) are involved in intermolecular contacts but the involvement of the two atoms will be shown to be different. Intermolecular contacts therefore do not provide an explanation for the similarity of the angles in the two nitrato ligands. Rows 3 and 4 of Table 5(*c*) are comparable, and the difference between columns 1 and 2 for these rows emphasizes that the nitrato ligands are predominantly unidentate, and very far from being symmetrically bidentate.

Table 5(*d*) gives the angles of the dipyridyl ligand. Columns 1 and 2 are associated with pyridyl rings 1 and 2, respectively. Most of the angles in this table are close to 120°. The exceptions are C(6)—N(2)—Ag and N(1)—C(5)—C(6) at 112.4 ± 1.4° and 114.3 ± 1.9°. These values are reasonable considering the bonding and geometry of the pentagon Ag, N(1), C(5), C(6), N(2).

Table 6 is a compilation of intermolecular contacts. The molecules of dinitratodipyridylsilver(II) are shaped like disks which lie parallel

TABLE 4. Least squares planes: $k_1x + k_2y + k_3z = k_4$*

No.	Plane	k_1	k_2	k_3	k_4	χ^2	P_{Ag}
1	N(1)—N(4)	−0.9632	−0.0760	−0.2576	−1.740	13.39	+21.6
2	N(1), N(2), O(1), O(4)	−0.9932	−0.1156	−0.0112	−1.205	31.83	−19.9
3	N(3), O(1)—O(3)	−0.5894	−0.3743	−0.7158	−0.955	0.079	+14.6
4	N(4), O(4)—O(6)	+0.2551	+0.9669	−0.0004	−1.412	0.687	+64.6
5	N(1), C(1)—C(5)	−0.9788	+0.0087	−0.2044	−1.713	1.778	+9.0
6	N(2), C(6)—C(10)	−0.9415	+0.0033	−0.3371	−2.059	6.825	+43.6
7	N(1), N(2), C(1)—C(10)	−0.9635	+0.0001	−0.2677	−1.930	128.1	+31.0

*Angles between normals of planes *1,2* = 14.4°; *1,3* = 38.7°; *1,4* = 108.6°; *1,5* = 5.8°; *1,6* = 6.6°; *1,7* = 4.4°; *2,3* = 50.5°; *2,4* = 111.4°; *2,5* = 13.2°; *2,6* = 20.2°; *2.7* = 16.3°; *3,4* = 120.8°; *5,6* = 7.9°.

TABLE 5. Bond angles in dinitratodipyridylsilver(II)*

(*a*) Silver atom octahedron

Bonds	Angle (deg)	Bonds	Angle (deg)	Bonds	Angle (deg)
N(1)—Ag—O(4)	166.3(6)	N(2)—Ag—O(1)	165.3(5)	O(1′)—Ag—O(2″)	160.2(4)
N(1)—Ag—N(2)	75.9(7)	O(1′)—Ag—N(1)	88.5(5)	O(1′)—Ag—O(1)	69.8(5)
N(2)—Ag—O(4)	99.4(6)	N(1)—Ag—O(2″)	77.2(5)	O(1)—Ag—O(2″)	96.5(5)
O(4)—Ag—O(1)	91.9(5)	O(2″)—Ag—O(4)	115.8(5)	O(2″)—Ag—N(2)	87.1(5)
O(1)—Ag—N(1)	90.9(6)	O(4)—Ag—O(1′)	79.9(5)	N(2)—Ag—O(1′)	102.7(5)

(*b*) Other selected silver angles

Bonds	Angle (deg)	Bonds	Angle (deg)	Bonds	Angle (deg)
O(2)—Ag—O(2″)	73.6(5)	O(2)—Ag—O(4)	67.8(5)	O(2)—Ag—O(1)	46.3(4)
O(5)—Ag—O(2″)	70.7(5)	O(5)—Ag—N(2)	84.3(6)	O(5)—Ag—O(4)	47.1(5)
O(2)—Ag—O(5)	65.0(5)				

(*c*) Nitrato ligands

Bonds	Angle (deg)	Bonds	Angle (deg)	Bonds	Angle (deg)
O(1)—N(3)—O(2)	119.6(18)	O(2)—N(3)—O(3)	125.5(18)	O(3)—N(3)—O(1)	114.8(18)
O(4)—N(4)—O(5)	118.6(20)	O(5)—N(4)—O(6)	125.1(21)	O(6)—N(4)—O(4)	116.1(22)
Ag—O(1)—N(3)	117.7(13)	Ag—O(2)—N(3)	76.2(11)		
Ag—O(4)—N(4)	113.7(14)	Ag—O(5)—N(4)	77.4(13)		

(*d*) 2,2′-Dipyridyl ligand

Bonds	Angle (deg)	Bonds	Angle (deg)	Bonds	Angle (deg)
N(1)—C(1)—C(2)	123.6(20)	N(2)—C(10)—C(9)	119.8(20)	N(1)—C(5)—C(6)	114.3(19)
C(1)—C(2)—C(3)	116.8(22)	C(10)—C(9)—C(8)	118.5(21)	N(2)—C(6)—C(5)	117.8(19)
C(2)—C(3)—C(4)	120.3(21)	C(9)—C(8)—C(7)	121.1(22)	C(1)—N(1)—Ag	122.9(14)
C(3)—C(4)—C(5)	118.0(21)	C(8)—C(7)—C(6)	118.6(22)	C(10)—N(2)—Ag	123.7(15)
C(4)—C(5)—N(1)	122.4(20)	C(7)—C(6)—N(2)	118.3(21)	C(5)—N(1)—Ag	118.2(14)
C(1)—N(1)—C(5)	118.8(18)	C(10)—N(2)—C(6)	123.4(19)	C(6)—N(2)—Ag	112.4(14)
C(4)—C(5)—C(6)	123.1(21)	C(7)—C(6)—C(5)	123.7(21)		

*Estimated standard deviations are given in parentheses in tenths of a degree.

to the (1,0,0) planes of the crystal. The disks are stacked in the x direction so that the arrangement of each pile in the triclinic crystal resembles a slipping stack of coins. The molecules are assymmetric, as is a coin if the engraving is considered. In the space group $P\bar{1}$ there are centres of inversion between successive disks in each pile and also an equal number of such centres between the piles. Using the coin analogy still further, contacts in each stack must be head-to-head and tail-to-tail alternately. One side of the dinitratodipyridyl molecule is distinguished by the protrusion of the nitrato groups, particularly atoms O(2) and O(5). The other side is relatively flat. Figure 2 shows diagrammatically how the first nitrate group is involved in the face-to-face contacts, and may be compared with Fig. 1. The shorter and more relevant face-to-face contacts are listed in Table 6(*a*). Those involving the silver atom are particularly important. Column 1 contains the flat back-to-back intermolecular contacts and column 2 is concerned with contacts involving O(2) and O(5). Note that O(5) approaches the face of the nitrato group N(3″), O(1″), O(2″), O(3″). The shorter edge-to-edge contacts between different molecular stacks are given in Table 6(*b*). The peripheral atoms of the molecule are involved. These are O(3), O(6), and some of the carbon atoms.

The anisotropic temperature parameters are

Can. J. Chem. Downloaded from www.nrcresearchpress.com by 210.87.254.40 on 09/05/12
For personal use only.

Can. J. Chem. Downloaded from www.nrcresearchpress.com by 210.87.254.40 on 09/05/12
For personal use only.

TABLE 6. Intermolecular contacts*

(*a*) Face-to-face

Contact	Length (pm)	Contact	Length (pm)
Ag—O(1′)	275.3(13)	Ag—O(2″)	276.3(16)
O(1)—O(1′)	284.7(27)	O(5)—N(3″)	299.8(27)
O(1)—O(4′)	317.6(20)	O(5)—O(1″)	314.8(25)
O(3)—N(2′)	327.9(23)	O(5)—O(2″)	330.9(25)
O(3)—C(6′)	322.0(28)	O(5)—O(3″)	329.9(27)
O(4)—C(1′)	321.0(27)	O(2)—N(1″)	308.8(20)

(*b*) Edge-to-edge

Contact	Length (pm)	Contact	Length (pm)
O(3)—C(3)	321.6(28)	O(6)—C(7)	324.3(28)
O(3)—C(4)	333.8(25)	O(6)—C(8)	328.3(32)
		O(6)—C(2)	329.9(28)

*Estimated standard deviations are given in parentheses in tenths of a pm.

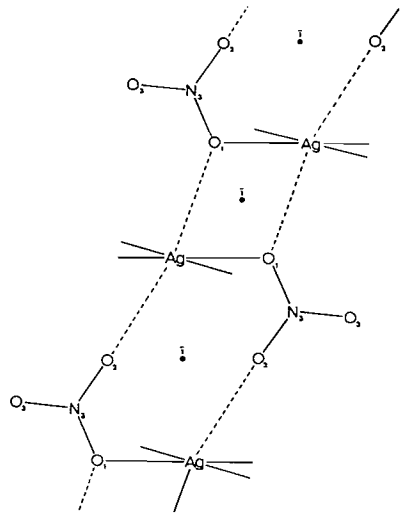

FIG. 2. The intermolecular bonding in dinitratodipyridylsilver(II).

given in Table 7. The corresponding thermal ellipsoids scaled to include 50% probability are shown in Fig. 1.

Discussion

In Table 8 we present the known coordinate bond lengths for Ag(II) in pyridine complexes. The values for dinitratodipyridylsilver(II) lie within the previously recorded ranges. Both bis(pyridine-2,3-dicarboxylate)silver(II) dihydrate (16), and dinitratodipyridylsilver(II) structures contain tetragonally lengthened and distorted octahedra. Bis(pyridine-2,6-dicarboxylate)silver(II) monohydrate has a very distorted octahedral coordination about the silver atom

TABLE 7. Anisotropic temperature parameters*

Atom	β_{11}	β_{22}	β_{33}	β_{12}	β_{13}	β_{23}
Ag	162(5)	124(3)	91(3)	66(3)	77(2)	44(2)
O(1)	133(37)	206(28)	68(19)	32(26)	65(23)	59(20)
O(2)	269(49)	149(26)	156(26)	103(31)	160(31)	62(22)
O(3)	320(53)	242(33)	140(26)	142(35)	162(30)	145(26)
O(4)	209(45)	160(27)	153(26)	71(29)	78(29)	43(22)
O(5)	246(55)	286(41)	178(32)	133(40)	94(35)	89(30)
O(6)	634(84)	164(32)	100(28)	49(39)	160(39)	1(25)
N(1)	128(44)	96(30)	94(26)	42(28)	53(27)	54(26)
N(2)	235(54)	140(35)	101(28)	47(32)	99(31)	81(26)
N(3)	164(53)	182(37)	112(30)	52(38)	31(34)	91(31)
N(4)	266(67)	131(33)	112(36)	56(40)	118(42)	41(29)
C(1)	191(64)	193(50)	90(36)	64(44)	57(36)	92(36)
C(2)	267(74)	128(39)	55(32)	66(42)	33(38)	−11(32)
C(3)	247(73)	139(47)	126(39)	78(44)	123(44)	34(37)
C(4)	91(52)	225(51)	67(32)	30(39)	51(33)	69(35)
C(5)	104(55)	122(40)	115(37)	34(35)	32(35)	66(34)
C(6)	100(55)	164(45)	120(38)	3(37)	19(36)	84(35)
C(7)	176(63)	181(47)	150(38)	63(42)	56(39)	119(38)
C(8)	228(72)	146(44)	140(42)	80(45)	21(43)	78(36)
C(9)	239(73)	82(36)	160(45)	65(41)	−9(45)	39(35)
C(10)	277(74)	86(37)	164(41)	77(41)	95(44)	45(35)

*$T = \exp[-(h^2\beta_{11} + k^2\beta_{22} + l^2\beta_{33} + 2hk\beta_{12} + 2hl\beta_{13} + 2kl\beta_{23})]$. The parameters have been multiplied by 10^4. Estimated standard deviations are given in parentheses.

TABLE 8. Bond lengths in Ag(II) complexes

Compound	Bond length (pm)			
	Ag—N (Square planar)	Ag—O		Reference
		Square planar	Extended	
Silver(II)-bis(pyridine-2,3-dicarboxylate) dihydrate	212	213	297	16
Silver(II)-bis(pyridine-2,6-dicarboxylate) monohydrate (anionic ligand)	209	220		17
Silver(II)-bis(pyridine-2,6-dicarboxylate) monohydrate (neutral ligand)	221		253	17
Dinitratodipyridylsilver(II)	212, 221	214, 215	275, 276	This work

(17), presumably due to ligand restraints. The electronic absorption spectrum is unlike those of other silver(II) species in tetragonally distorted octahedral environments, but as far as bond lengths are concerned we see a similarity. One ligand becomes ketonic and the other anionic and in this way the silver atom attains four short bonds in the range 209–221 pm and two longer bonds at 253 pm. The available evidence indicates that silver(II) complexes are structurally similar to those of copper(II). Since the structural chemistry of copper(II) is much better developed than that of silver(II), comparison of our results with some copper(II) structures is profitable.

Stephens determined the structure of bisnitrito-2,2′-dipyridylcopper(II) and found an approximately square planar complex (18). The 2,2′-dipyridyl ligand is twisted by only 3.2° about the 2,2′-bond and the two Cu—N lengths are the same. The mean Cu—O length in the square plane is 198.7 pm, but a second oxygen in each ligand approaches to give a mean Cu—O distance of 249.3 pm. This is interpreted as a compromise between purely monodentate or bidentate behavior. The more distant oxygen atoms of each nitrito ligand are on opposite sides of the square plane, tending to complete a very distorted octahedron. Comparing bis-nitrito-2,2′-dipyridylcopper(II) and dinitratodipyridylsilver(II) we find that the nitrito groups have more bidentate character, whereas one of the nitrato groups is heavily involved in intermolecular bridging. Thus six coordination is approached in different ways.

Procter and Stephens have determined the structure of nitritobis-2,2′-dipyridylcopper(II) nitrate (19). The copper atom is *cis*-distorted octahedral and the compound has unequally bound dipyridyl ligands (Cu—N = 199 and 208 pm). The 2,2′-dipyridyl ligands are nonplanar having planar pyridyl rings twisted by 10.8 and 11.6° about the 2,2′-bonds. Since the Cu—O bond distances are 224 and 233 pm, the nitrito group is considered to be bidentate. From our point of view it is interesting that this compound contains ionic nitrate and a bidentate nitrito ligand. Comparing the nitritobisdipyridylcopper(II) ion with the dinitratodipyridylsilver(II) molecule we find some similarity in the behavior of the dipyridyl ligands.

The crystal structure of nitrato-bis(2,2′-dipyridyl)copper(II) nitrate monohydrate has been determined by Nakai, Ooi, and Kuroya (20). The coordination about the copper atom is distorted trigonal bipyramidal and the monodentate nitrato ligand is in the equatorial plane. The Cu—O bond length is 230 pm, which is appreciably longer than the Ag—O bonds in dinitratodipyridylsilver(II).

Recently a small set of crystallographic results has accumulated for unidentate nitrato ligands. The compounds involved are nitratotris(methyldiphenylphosphine)copper(I) (21), nitratobisdipyridylcopper(II) nitrate monohydrate (20), *trans*-dinitratobis(methyl cyanide)copper(II) (22), potassium tetranitratoaurate(III) (13), nickel nitrate tetrahydrate (14), *cis*-dinitratobis(dimethylsulfoxide)palladium(II) (23). Our results on dinitratodipyridylsilver(II) make a significant addition since they fit into the series Cu(I), Cu(II), Ag(II), Au(III). It has been observed by Garner and Wallwork (13) that all unidentate nitrato ligands will probably have some weak interaction between the metal atom and a second oxygen atom more distant than the definitely bonded one. This seems to be inevitable considering the size, shape, and bonding of

Can. J. Chem. Downloaded from www.nrcresearchpress.com by 210.87.254.40 on 09/05/12
For personal use only.

Can. J. Chem. Downloaded from www.nrcresearchpress.com by 210.87.254.40 on 09/05/12
For personal use only.

a unidentate nitrato group. The results for dinitratodipyridylsilver(II) are in accord with this view, and also show some stereochemical consequences of the presence of the second oxygen atom.

The way in which the nitrato group N(3), O(1), O(2), O(3) in dinitratodipyridylsilver(II) is connected to form bridges is illustrated in Fig. 2. The assymmetric bridging through O(1), N(3), and O(2), for which the Ag—Ag″ distance is 466.4 ± 0.3 pm, is the same as that in *trans*-dinitratobis(methyl cyanide)copper(II) (22), and similar to the more symmetric bridging in solid $Cu(NO_3)_2$ and $Cu(NO_3)_2MeNO_2$ (24, 25). It is rather unusual and interesting that the same nitrato group is also involved in an assymmetric one atom bridge through O(1). This gives a Ag—Ag′ distance of 403.4 ± 0.3 pm and an O(1)—O(1′) distance of 284.7 ± 2.7 pm. The bridges involve bonds which are 276 pm in length.

Conclusion

Dinitratodipyridylsilver(II) may be regarded as a distorted square planar complex by considering coordinate bonds less than 221 pm only. If we consider bonds with lengths up to 277 pm, one nitrate group is monodentate and the other bridging, dinitratodipyridylsilver(II) becomes polymeric in the *x*-direction, and the geometry about the Ag(II) atom becomes that of an elongated octahedron with distortions. Finally we consider the distances Ag—O(2) at 305.8 pm and Ag—O(5) at 295.0 pm in order to provide some explanation for the angular distortions in the octahedral coordination. Figure 1 shows the even angular distribution of three oxygen atoms on the convex side of the primary square. Either over-crowding or weak bonding on this side of the molecule causes the silver atom to be 19.90 pm from the mean plane of O(1), O(4), N(1), and N(2).

Operating funds were obtained from the National Research Council of Canada and the Committee for Research, Leave and Travel of the University of Victoria. A major equipment grant and computing facilities were provided by the University of Victoria. Dr. A. Tweedale of the University of Victoria Computing Centre has generously given assistance. The authors gratefully acknowledge all these contributions.

1. J. A. McMillan. Chem. Rev. **62**, 65 (1962).
2. G. T. Morgan and F. H. Burstall. J. Chem. Soc. 2594 (1930).
3. B. M. Gordon, L. L. Williams, and N. Sutin. J. Am. Chem. Soc. **83**, 2061 (1961).
4. G. A. Barbieri. Atti. Accad. Lincei. **16**, 44 (1932).
5. A. Malaguti and T. Labianca. Gazz. Chim. Ital. **84**, 976 (1954).
6. M. J. Buerger. X-Ray crystallography. Wiley, New York. 1942.
7. D. T. Cromer and J. T. Waber. Acta Cryst. **18**, 104 (1965).
8. J. A. Ibers. International Tables for X-ray Crystallography. I.U.Cr. by the Kynoch Press, Birmingham. Vol. III, Table 3.3.1 A, 201 (1962).
9. D. T. Cromer. Acta Cryst. **18**, 17 (1965).
10. B. R. Penfold. University of Canterbury Crystallographic Programs, Christchurch, New Zealand.
11. G. H. Stout and L. H. Jensen. X-Ray structure determination. Macmillan, New York. 1968. p. 456.
12. C. C. Addison and D. Sutton. Progress in Inorganic Chemistry. Vol. 8. *Edited by* F. A. Cotton, Interscience Pub. 1967. p. 195. C. C. Addison, N. Logan, S. C. Wallwork, and C. D. Garner. Q. Rev. Chem. Soc. **25**, 289 (1971).
13. C. D. Garner and S. C. Wallwork. Chem. Commun. 108 (1969).
14. P. Gallezot, D. Weigel, and M. Prettre. Acta Cryst. **22**, 699 (1967).
15. L. L. Merritt and E. D. Schroeder. Acta Cryst. **9**, 801 (1956).
16. M. G. B. Drew, R. W. Matthews, and R. A. Walton. Inorg. Nucl. Chem. Lett. **6**, 277 (1970).
17. M. G. B. Drew, R. W. Matthews, and R. A. Walton. J. Chem. Soc. (A), 1405 (1970).
18. F. S. Stephens. J. Chem. Soc. (A), 2081 (1969).
19. I. M. Procter and F. S. Stephens. J. Chem. Soc. (A), 1248 (1969).
20. H. Nakai, S. Ooi, and H. Kuroya. Bull. Chem. Soc. Jap. **43**, 577 (1970).
21. W. A. Anderson, A. J. Carty, G. J. Palenik, and G. Schreiber. Can. J. Chem. **49**, 761 (1971).
22. B. Duffin. Acta Cryst. **B24**, 396 (1968).
23. D. A. Langs, C. R. Hare, and R. G. Little. Chem. Commun. 1080 (1967).
24. S. C. Wallwork and W. E. Addison. J. Chem. Soc. 2925 (1965).
25. B. Duffin and S. C. Wallwork. Acta Cryst. **20**, 210 (1966).

Can. J. Chem. Downloaded from www.nrcresearchpress.com by 210.87.254.5 on 09/05/12
For personal use only.

The Crystal and Molecular Structure of Two Thiathiophthen Nitrogen Isosteres

F. LEUNG[1] AND S. C. NYBURG

Lash Miller Chemical Laboratories, University of Toronto, Toronto 181, Ontario

Received May 27, 1971

Three dimensional crystal structure analyses have been carried out on two nitrogen isosteres (*a*) **5** and (*b*) **6** using diffractometer data. The crystal data are: (*a*) system: monoclinic, $P2_1/c$; $a = 7.350(3)$, $b = 12.309(5)$, $c = 23.268(8)$ Å, $\beta = 118.35(8)°$; (*b*) system: monoclinic, $P2_1/c$; $a = 9.34(1)$, $b = 9.58(1)$, $c = 25.65(3)$ Å, $\beta = 108.08(8)°$.

The S...S distances are 2.396(12) and 2.814(8) Å, respectively. This difference is an indication of the cleavage of the S—S "bond" in **5** when the terminal sulfur atom is methylated. The nature of the bonding of the outer sulfur atom in **6** is discussed.

Les analyses de structure d'un cristal tridimensionnel ont été menées à bien pour deux isostères de l'azote (*a*) **5** et (*b*) **6** en utilisant des données du diffractomètre. Les données du cristal sont: (*a*) système: monoclinique, $P2_1/c$; $a = 7.350(3)$, $b = 12.309(5)$, $c = 23.268(8)$ Å, $\beta = 118.35(8)°$; (*b*) système: monoclinique, $P2_1/c$; $a = 9.34(1)$, $b = 9.58(1)$ $c = 25.65(3)$ Å, $\beta = 108.08(8)°$.

Les distances S...S sont respectivement 2.396(12) et 2.814(8) Å. Cette différence est une indication du clivage de la liaison S—S dans **5** quand l'atome terminal de soufre est méthylé. On discute la nature de la liaison de l'atome de soufre extérieur dans **6**.

Canadian Journal of Chemistry, **50**, 324 (1972)

Introduction

Crystal structure analyses of thiathiophthen **1***a* (1), many of its derivatives **1***b* (2) and its isosteres **1***c* (3–6) have been reported. These

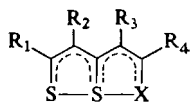

1*a* R1 = R2 = R3 = R4 = H; X = S
1*b* X = S
1*c* X = Se, O, N-3-quinolyl

investigations have revealed a wide variation in the S...S distance. As pointed out by Hordvik (7) and by Leung and Nyburg (6), the S...S distance seems to be dependent on the electronegativities of the terminal atom in the usually almost linear arrangements S...S...S and S...S...X. The "S—S bonding" in this type of compound is evidently very weak, and therefore one may expect a substantial difference in the S—S distance for different substituent groups attached to the thiathiophthen ring. This was in fact found to be the case when the S...S distances in 2,4-diphenylthiathiophthen **2** and in 2-*p*-dimethylanilino-4-phenyl-thiathiophthen **3** (7) were compared. The crystal structure of a

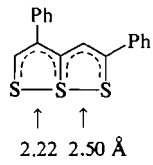

2.22 2.50 Å

2

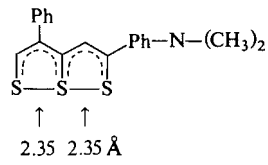

2.35 2.35 Å

3

thiathiophthen nitrogen isostere, 3,5-epidithio-2,5-diphenyl-2,4-pentadienylidene-3-aminoquinoline **4**, has been published (6). The purpose of the present work is to compare this structure with two other thiathiophthen nitrogen isosteres, 3,5-epidithio-2,5-diphenyl-2,4-pentadienylidene-aniline **5**, and its *S*-methylated derivative, 2,4-diphenyl-5-(3′-phenyl-2′-thiabutene-4′-yl)-isothiazolium iodide **6**. The relative importance of the resonance forms **6** and **6***a* is discussed below.

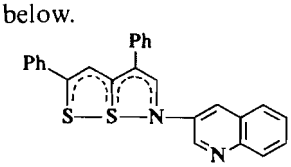

4

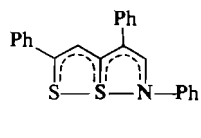

5

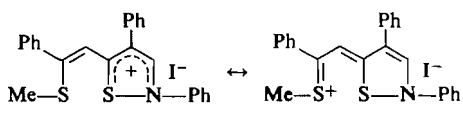

6 ↔ **6***a*

[1]Present address: Department of Chemistry, University of Montreal, Montreal, Quebec.

Can. J. Chem. Downloaded from www.nrcresearchpress.com by 210.87.254.5 on 09/05/12
For personal use only.

Experimental

(a) 3,5-Epidithio-2,5-diphenyl-2,4-pentadienylideneaniline **5**

This compound was crystallized from nitromethane giving orange plate-like crystals. The cell parameters were determined from diffractometer measurements and refined by a least squares procedure. The data were collected by 2θ scan at room temperature on a Picker four-circle automatic diffractometer using Cu$K\alpha$ radiation. A total of 2991 independent reflections were collected within $\sin\theta \leqslant 0.8918$, of which 614 were classified as unobserved. The crystal data are:

$C_{23}H_{17}NS_2$ f.w. = 371.5

Monoclinic, $a = 7.350(3)$, $b = 12.309(5)$, $c = 23.268(8)$ Å, $\beta = 118.35(8)°$, $V = 1852.6$ Å^3, $D_m = 1.32(2)$ g/cc, $D_c = 1.33$ g/cc, $Z = 4$, space group $P2_1/c$, $\mu = 25.4$ cm^{-1} (CuKα, $\lambda = 1.5418$ Å).

Structure Determination

The structure of **5** was determined by the symbolic addition procedure (8). After the normalized structure factor magnitudes had been generated, they were sorted into eight groups according to the parity of the indices *hkl*. The number of reflections with $|E| \geqslant 1.5$ in each of the parity groups is listed in Table 1 (g = even, u = odd). From Table 1 it is obvious that all reflections with large $|E|$'s are those with l = even. The reason for this is due to the fact that most atoms of the molecule lie near $y = 1/4$ and 3/4 thus making all reflections strong with l even and weak with l odd. From Table 4 it is clear that many of the nonhydrogen atoms lie near $y = \pm 1/4$.

From a total of 342 reflections with $|E| \geqslant 1.5$, the signs of 285 E's were determined using the Σ_2 equation. The starting set of reflections used in the application of the Σ_2 equation is shown in Table 2. There were numerous Σ_2 relationships indicating that the product *abc* is negative. Four different allocations of signs to the symbols are shown in Table 3. The sign combinations given in Table 3 were used successively to compute E-maps. (Computation of E-map 4 was not required.)

The peaks on both E-map 1 and E-map 2 could be interpreted as atomic sites for S(1), S(2), N, C(1), C(2), C(3), C(4), C(5), C(6), C(9), C(12), C(15), C(18), and C(21). All these peaks lay very close to $y = 1/4$, those lying elsewhere did not make chemical sense.

Structure factors were calculated based on the partial structures implied by E-maps 1 and 2 using the XFLS program (9). The R factors were 0.52 and 0.53, respectively. Fourier maps computed after the structure factors calculations contained no more information than the original E-maps. No further attempts were made to interpret E-maps 1 and 2.

TABLE 1. Compound **5**: the distribution of reflections with $|E| \geqslant 1.5$ among the parity groups

Parity Group	Number of Reflections $\lvert E\rvert \geqslant 1.50$
ggg	102
gug	74
ugg	72
uug	72
ggu	6
guu	6
ugu	8
uuu	2
Total	342

TABLE 2. The starting set of phases for compound **5**

Reflections	$\lvert E\rvert$	Phases
2 1 0	3.04	+
1 4 $\bar{2}$	3.19	+
3 6 $\bar{15}$	2.08	+
4 2 $\bar{18}$	4.15	*a*
9 3 $\bar{16}$	3.63	*b*
8 1 $\bar{24}$	3.48	*c*

Table 3. Allocation of signs to the symbols for compound **5**

E-maps	*a*	*b*	*c*
1	−	+	+
2	+	−	+
3	−	−	−
4	+	+	−

E-map 3 was then calculated, which showed the "thiathiophthen moiety" S(1), S(2), N, C(1), C(2), C(3), C(4), and C(5), the whole benzene ring attached to the nitrogen atom, C(9), and C(12), a total of 16 atoms. Refinement varying the atomic coordinates and the scale factor gave an R factor of 0.42, the Fourier synthesis computed subsequently revealed the whole structure.

Refinement

The atomic coordinates estimated from the final Fourier map were refined by full-matrix least squares using the XFLS program with the weighting scheme suggested by Abrahams and Bernstein (10). The atomic scattering factors used were calculated from the parameters given by Cromer and Mann (11). After anisotropic thermal refinement, an R factor of 0.09 was obtained and a difference Fourier computed at this stage revealed all the hydrogen-atom positions. Further refinement was carried out varying only positional parameters. The hydrogen atoms were assigned the same thermal parameters as the carbon atoms to which they were bonded and R finally converged to 0.07. The maximum shift calculated in the final cycle was 0.4σ of the parameter. The final positional and thermal parameters are listed in Table 4 and Table 5, respectively. The β_{ij} in Table 4 are the coefficients in the expression: $\exp(-(\beta_{11}h^2 + \beta_{22}k^2 + \beta_{33}l^2 + 2\beta_{13}hl + 2\beta_{12}hk + 2\beta_{23}kl))$. Final F_o and F_c values have been placed in the Depository for Unpublished Data.[2] Bond lengths and standard deviations from the ORFFE program (12) are given in Table 6; the lengths and angles are illustrated in Fig. 1. The largest standard deviation for the bond angles is 0.75°, and the average is 0.6°. Figure 2 shows the orientation and packing of the molecules in the

[2]Copies of table may be obtained, upon request, from the Depository of Unpublished Data, National Science Library, National Research Council of Canada, Ottawa, Canada K1A 0S2.

TABLE 4. Fractional atomic and thermal parameters × 10^5 for compound **5**

Atom	x	y	z	β_{11}	β_{22}	β_{33}	β_{12}	β_{13}	β_{23}
S(1)	0.80442(9)	0.28302(18)	0.34483(5)	626(18)	2363(56)	128(4)	−33(26)	152(7)	0(13)
S(2)	0.99312(9)	0.25717(17)	0.44535(5)	555(16)	1491(42)	147(4)	−29(26)	166(7)	−20(13)
N	1.13107(26)	0.23104(48)	0.52767(14)	502(50)	1588(144)	142(13)	82(78)	97(21)	17(43)
C(1)	0.71603(32)	0.25606(61)	0.38222(16)	601(64)	1359(160)	122(15)	28(99)	102(26)	−3(50)
C(2)	0.77356(33)	0.24602(63)	0.44837(17)	497(57)	1105(148)	142(15)	−53(92)	60(25)	−38(49)
C(3)	0.90448(33)	0.25095(59)	0.48602(17)	699(64)	1104(149)	130(15)	3(97)	168(26)	0(50)
C(4)	0.97593(31)	0.24356(61)	0.55421(16)	499(59)	1351(156)	136(15)	69(94)	128(25)	23(50)
C(5)	1.10202(33)	0.23203(61)	0.57586(18)	491(61)	1492(173)	190(17)	−26(92)	180(27)	−26(52)
C(6)	0.57900(32)	0.24885(63)	0.34268(17)	528(63)	1615(173)	137(16)	−126(102)	98(26)	−140(54)
C(7)	0.50996(38)	0.14216(66)	0.36274(19)	549(68)	2018(197)	161(19)	−187(95)	148(30)	−117(50)
C(8)	0.38229(41)	0.13771(74)	0.32621(22)	734(78)	2734(239)	202(21)	−32(112)	222(34)	7(59)
C(9)	0.32051(42)	0.24008(80)	0.27027(21)	894(79)	2179(213)	193(20)	60(121)	145(32)	−98(63)
C(10)	0.38967(42)	0.34786(71)	0.24997(21)	812(81)	1973(208)	162(19)	70(106)	49(32)	−66(53)
C(11)	0.51721(40)	0.34802(68)	0.28492(20)	710(73)	1958(200)	129(17)	31(99)	38(30)	3(50)
C(12)	0.92548(31)	0.25307(66)	0.60154(16)	473(57)	1826(167)	106(14)	−292(99)	98(23)	−144(52)
C(13)	0.96800(39)	0.13620(69)	0.65469(20)	668(72)	2378(216)	122(17)	−157(101)	82(29)	0(52)
C(14)	0.92622(46)	0.15339(77)	0.70042(21)	1022(90)	2580(236)	158(20)	−177(120)	186(36)	31(57)
C(15)	0.84004(43)	0.28548(75)	0.69252(21)	909(83)	2742(265)	196(21)	−392(122)	239(36)	−122(62)
C(16)	0.79867(40)	0.40177(72)	0.64071(23)	652(73)	2636(228)	200(21)	−463(108)	159(33)	−222(59)
C(17)	0.83958(37)	0.38682(68)	0.59434(20)	435(64)	2144(202)	186(19)	−111(92)	142(30)	−130(50)
C(18)	1.25272(31)	0.23782(62)	0.53455(17)	448(58)	1428(161)	169(17)	−37(92)	152(126)	−15(51)
C(19)	1.27078(39)	0.16691(65)	0.48402(20)	780(77)	1622(185)	211(20)	374(97)	236(33)	101(51)
C(20)	1.38721(41)	0.18490(70)	0.48833(23)	687(75)	2316(221)	243(22)	160(102)	249(34)	42(56)
C(21)	1.48086(41)	0.26685(75)	0.54073(23)	788(78)	2007(215)	300(24)	−39(114)	256(36)	−69(64)
C(22)	1.46297(40)	0.33223(67)	0.59109(25)	614(72)	1836(199)	282(24)	−22(98)	172(35)	−89(57)
C(23)	1.34743(36)	0.31797(58)	0.58787(20)	488(64)	1214(171)	232(20)	−30(82)	128(30)	−47(47)

unit cell as projected along the b-axis. The labelled molecule corresponds to the atomic coordinates listed in Table 4.

(b) 2,4-Diphenyl-5-(3'-phenyl-2'-thiabutene-4'-yl)-isothiazolium iodide **6**

The compound was crystallized from a mixture of ethanol and methanol giving crystals suitable for x-ray work as orange-red prisms. The cell parameters were determined as for (*a*) but using MoKα radiation. A total of 3930 independent reflections were collected in the same manner as for compound **5** within $\sin\theta \leqslant 0.4226$, of which 857 reflections were unobservably weak. The crystal data are:

$C_{24}H_{20}NS_2I$ f.w. = 513.5

Monoclinic, $a = 9.34(1)$, $b = 9.58(1)$, $c = 25.65(3)$ Å, $\beta = 108.08(8)°$, $V = 2182.7$ Å^3, $D_m = 1.57(2)$ g/cc, $D_c = 1.57$ g/cc, $Z = 4$, space group $P2_1/c$, $\mu = 17.0$ cm^{-1} (MoKα, $\lambda = 0.7071$ Å).

TABLE 5. Hydrogen fractional atomic coordinates for compound **5**

Atom	x	y	z
H(C2)	0.7268(34)	0.2352(59)	0.4741(18)
H(C5)	1.1785(34)	0.2247(59)	0.6297(19)
H(C7)	0.5567(35)	0.0784(60)	0.4042(19)
H(C8)	0.3384(37)	0.0568(65)	0.3387(20)
H(C9)	0.2315(39)	0.2369(66)	0.2418(19)
H(C10)	0.3426(37)	0.4187(64)	0.2084(19)
H(C11)	0.5661(36)	0.4305(63)	0.2716(19)
H(C13)	1.0353(37)	0.0409(63)	0.6625(19)
H(C14)	0.9596(38)	0.0600(66)	0.7394(21)
H(C15)	0.8118(38)	0.2988(66)	0.7283(20)
H(C16)	0.7386(36)	0.5031(65)	0.6351(21)
H(C17)	0.8062(36)	0.4688(67)	0.5576(20)
H(C19)	1.2074(38)	0.1155(61)	0.4449(21)
H(C20)	1.3936(37)	0.1382(66)	0.4517(20)
H(C21)	1.5660(38)	0.2814(63)	0.5414(20)
H(C22)	1.5321(37)	0.3834(60)	0.6332(21)
H(C23)	1.3319(35)	0.3748(58)	0.6252(20)

Structure Determination

The structure determination of **6** was straightforward. After the atomic coordinates of the iodine atom were deduced from the Patterson function, the structure was revealed by two successive Fourier syntheses.

The atomic coordinates estimated from the final electron density map were refined by full-matrix least squares in the same manner as in (*a*). All atoms except the I^- ion were assumed to be neutral, but the corresponding positive charge on the isothiazolium ion was not assigned. Isotropic temperature factors of 3.0 Å^2 were allocated to all the atoms as the initial thermal parameters. The refinement was continued with anisotropic thermal parameters, varying positional and thermal parameters in alternate cycles. An R factor of 0.071 was reached in the final cycle, the largest shift (in one of the carbon parameters) being 0.6 σ.

The sp^2 hydrogen positions were calculated from carbon atom positions obtained in the final cycle of refinement, assuming a C—H bond length of 1.00 Å. The difference Fourier map showed positive electron density in all the regions expected for sp^2 hydrogen atoms. Of the remaining three hydrogen atoms of the methyl group only one showed

Can. J. Chem. Downloaded from www.nrcresearchpress.com by 210.87.254.5 on 09/05/12
For personal use only.

Can. J. Chem. Downloaded from www.nrcresearchpress.com by 210.87.254.5 on 09/05/12
For personal use only.

TABLE 6. Bond lengths and their standard deviations for compound **5**

Bond	Length (Å)	σ (Å)
S(1)—S(2)	2.396	0.012
S(1)—C(1)	1.697	0.007
S(2)—N	1.871	0.010
S(2)—C(3)	1.752	0.007
N—C(5)	1.329	0.007
N—C(18)	1.429	0.007
C(1)—C(2)	1.357	0.009
C(1)—C(6)	1.490	0.010
C(2)—C(3)	1.423	0.010
C(3)—C(4)	1.403	0.009
C(4)—C(5)	1.388	0.009
C(4)—C(12)	1.501	0.008
C(6)—C(7)	1.390	0.010
C(6)—C(11)	1.395	0.009
C(7)—C(8)	1.387	0.010
C(8)—C(9)	1.378	0.010
C(9)—C(10)	1.399	0.010
C(10)—C(11)	1.383	0.010
C(12)—C(13)	1.388	0.009
C(12)—C(17)	1.394	0.009
C(13)—C(14)	1.390	0.009
C(14)—C(15)	1.384	0.010
C(15)—C(16)	1.364	0.010
C(16)—C(17)	1.395	0.009
C(18)—C(19)	1.397	0.008
C(18)—C(23)	1.368	0.010
C(19)—C(20)	1.395	0.009
C(20)—C(21)	1.358	0.010
C(21)—C(22)	1.378	0.009
C(22)—C(23)	1.392	0.009

clearly on the difference map; the positions of the other two hydrogen atoms were calculated from this. The hydrogen atoms were assigned the same thermal parameters as those of the carbon atoms to which they were bonded. Structure factor calculations, including the hydrogen atoms, showed a drop of 0.005 in R. The final F_o and F_c values have been placed in the Depository for Unpublished Data.[2] Further refinements varying all positional parameters, resulted in abnormal C—H bond lengths with negligible change in R value, hence no significance was attached to these shifts. The positional and thermal parameters are listed in Tables 7 and 8, respectively. The β_{ij}'s have the same meaning as in Part (*a*). Bond lengths and their standard deviations are given in Table 9, and the lengths and angles illustrated in Fig. 3. The maximum standard deviations for the bond angles is 0.7°. Figure 4 shows the orientations and packing of the molecules in the unit cell as viewed along the a^*-axis. The atomic coordinates listed in Table 7 correspond to the asymmetric molecule closest to (1/2, 0, 1/2).

Discussion

The bond lengths obtained for the system (S(1), S(2), N, C(1), C(2), C(3), C(4), and C(5)) in **5** are in good agreement with those obtained for the "thiathiophthen moiety" 3,5-epidithio-2,5-diphenyl-2,4-pentadienylidene-3-aminoquinoline **4**. The differences are about 1.0σ with the exception of the S...S distances, which differ by 2.7σ (σ is the standard deviation of the S...S distance listed in Table 6). The standard deviation, σ', in the S...S length estimated for **4** is 0.007 Å (6), and thus the

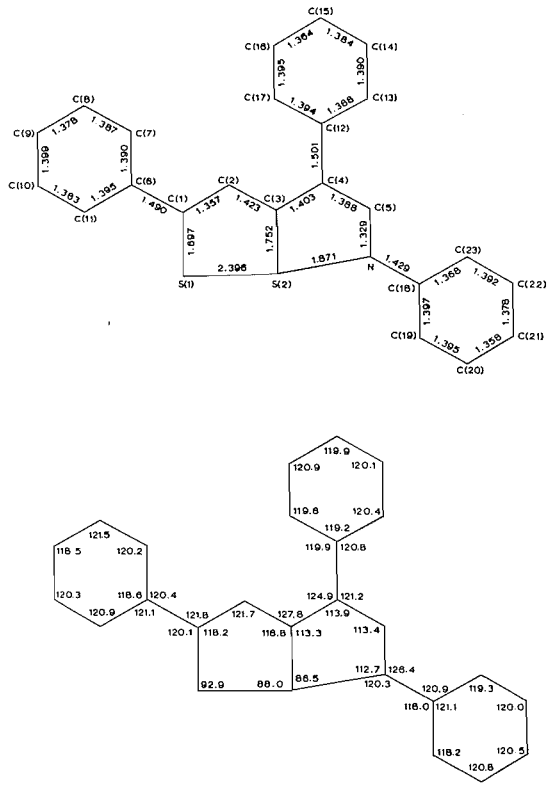

FIG. 1. Bond lengths and angles for compound **5**.

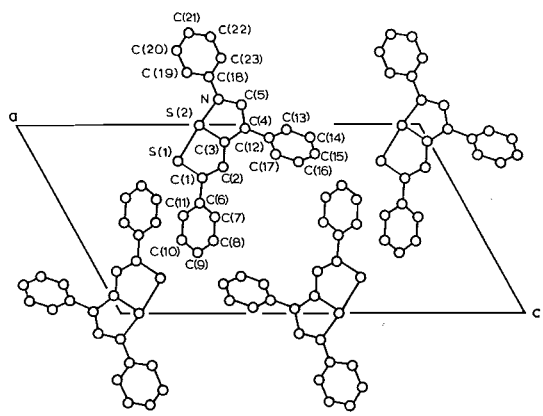

FIG. 2. Packing diagram for compound **5**.

TABLE 7. Fractional atomic coordinates and thermal parameters × 10^5 for compound **6**

Atom	x	y	z	β_{11}	β_{22}	β_{33}	β_{12}	β_{13}	β_{23}
I^-	0.25407(6)	0.12780(6)	0.06968(2)	1239(8)	1274(8)	217(1)	380(7)	232(2)	114(3)
S(1)	0.43349(22)	0.22511(21)	0.45085(8)	1252(29)	852(25)	132(4)	−215(22)	68(8)	60(8)
S(2)	0.27259(21)	0.01520(20)	0.48539(8)	1066(27)	722(22)	140(4)	−144(19)	131(8)	21(7)
N	0.17893(63)	−0.12724(61)	0.49928(24)	928(79)	765(73)	160(12)	−160(68)	133(25)	35(27)
C(Me)	0.36571(99)	0.40321(76)	0.43324(36)	1726(139)	677(96)	211(19)	208(91)	205(42)	47(35)
C(1)	0.38928(76)	0.13985(75)	0.38754(30)	859(94)	768(88)	157(15)	−8(78)	65(30)	45(32)
C(2)	0.32945(83)	0.00875(77)	0.38399(31)	1137(109)	813(94)	160(16)	−2(83)	179(34)	67(32)
C(3)	0.27770(73)	−0.06027(77)	0.42479(30)	711(97)	831(89)	163(16)	18(73)	81(31)	58(31)
C(4)	0.21093(70)	−0.19412(75)	0.41829(30)	552(90)	767(84)	174(16)	75(69)	80(30)	53(31)
C(5)	0.15481(78)	−0.22580(76)	0.46134(31)	982(105)	788(93)	173(16)	12(81)	186(33)	−8(32)
C(6)	0.13785(78)	−0.13134(76)	0.54953(30)	1019(99)	912(92)	144(14)	160(85)	154(31)	64(34)
C(7)	0.07385(85)	−0.25272(89)	0.56090(32)	1244(119)	1151(109)	170(17)	−180(97)	173(36)	93(36)
C(8)	0.03533(93)	−0.25784(97)	0.60894(33)	1497(133)	1391(125)	148(16)	−294(111)	122(37)	95(39)
C(9)	0.06086(98)	−0.14467(97)	0.64393(35)	1453(130)	1450(133)	181(18)	−75(109)	231(40)	20(41)
C(10)	0.12613(114)	−0.02613(98)	0.63140(39)	2252(178)	1230(125)	222(21)	−291(123)	381(51)	−125(43)
C(11)	0.16295(101)	−0.01900(87)	0.58266(35)	1884(155)	987(110)	203(19)	−288(106)	305(45)	−132(39)
C(12)	0.19025(77)	−0.28744(72)	0.37143(28)	1091(102)	691(86)	113(13)	−12(76)	131(30)	39(28)
C(13)	0.05473(87)	−0.35868(85)	0.35030(32)	1225(113)	1061(107)	159(16)	−7(93)	132(34)	71(36)
C(14)	0.03238(101)	−0.45425(84)	0.30766(35)	1837(148)	857(103)	158(17)	−8(99)	103(40)	−6(35)
C(15)	0.14714(112)	−0.47934(96)	0.28519(36)	2152(170)	1241(123)	165(18)	243(120)	261(47)	2(40)
C(16)	0.28304(105)	−0.40818(86)	0.30515(37)	1974(161)	941(109)	207(19)	178(104)	377(46)	4(37)
C(17)	0.30747(92)	−0.31374(85)	0.34837(34)	1470(129)	1004(103)	190(18)	79(93)	170(32)	49(31)
C(18)	0.42216(77)	0.20224(75)	0.34036(31)	869(96)	743(88)	175(16)	56(75)	170(32)	49(31)
C(19)	0.33082(97)	0.17135(83)	0.28719(33)	1664(138)	956(105)	148(16)	39(94)	163(38)	69(33)
C(20)	0.36399(105)	0.22655(89)	0.24241(36)	2057(156)	913(107)	211(19)	140(108)	328(45)	−28(39)
C(21)	0.48394(112)	0.31668(96)	0.24942(40)	2194(172)	1124(116)	240(21)	379(114)	528(52)	121(41)
C(22)	0.57274(101)	0.34997(90)	0.30207(88)	1680(143)	1161(122)	234(21)	216(105)	375(46)	129(41)
C(23)	0.54391(80)	0.29341(78)	0.34808(34)	944(103)	822(95)	227(19)	−6(81)	241(36)	29(35)

TABLE 8. Hydrogen fractional atomic coordinates for compound **6**

Atom	x	y	z
H(C2)	0.32306	−0.04032	0.34894
H(C5)	0.13086	−0.30297	0.43372
H(C7)	0.05603	−0.33406	0.53525
H(C8)	−0.01140	−0.03442	0.61845
H(C9)	0.03209	−0.14856	0.67835
H(C10)	0.14668	0.05429	0.65754
H(C11)	0.20732	0.06660	0.57149
H(C13)	−0.02875	−0.34074	0.36617
H(C14)	−0.06574	−0.50470	0.29323
H(C15)	0.13197	−0.54844	0.25474
H(C16)	0.36446	−0.42520	0.28818
H(C17)	0.40716	−0.26579	0.36256
H(C19)	0.24105	0.10928	0.28114
H(C20)	0.30046	0.20098	0.20449
H(C21)	0.50618	0.35726	0.21685
H(C22)	0.65898	0.41584	0.30694
H(C23)	0.60930	0.31776	0.38589
H1(Me)*	0.27500	0.40000	0.41000
H2(Me)	0.36380	0.45377	0.46713
H3(Me)	0.43412	0.45317	0.41625

*Coordinates were estimated from the difference map.

standard deviation of the difference ($\sigma_{diff} = \sigma^2 + \sigma'^2)^{1/2}$) in S...S lengths is 0.0139 Å. The actual difference in the S...S distances is thus 2.30 σ_{diff}. The probability that the difference occurs by chance is between 1 to 5%. According to Cruickshank (13), this difference is classified as of possible significance. The variation of the S...S distance from **4** to **5** is far less than that from **2** to **3**.

Of the three substituent phenyl groups in **5**, that attached at C(4) is most twisted out of coplanarity with the central ring (46.3°), a situation analogous to that found in compound **4**.

Since the S...S and the S...N distances lie between the sum of the corresponding van der Waals' radii and the normal single bond length, it is of interest to estimate the bond dissociation energies of these "bonds" using the Huggins' equation (14)

$$R_{AB} = r_A^* + r_B^* - \tfrac{1}{2} \log D_{A-B}$$

Can. J. Chem. Downloaded from www.nrcresearchpress.com by 210.87.254.5 on 09/05/12
For personal use only.

Can. J. Chem. Downloaded from www.nrcresearchpress.com by 210.87.254.5 on 09/05/12
For personal use only.

TABLE 9. Bond lengths and their standard deviations for compound **6**

Bond	Length (Å)	σ (Å)
S(1)—S(2)	2.814	0.008
S(1)—C(1)	1.749	0.009
S(1)—C(Me)	1.827	0.009
S(2)—N	1.717	0.007
S(2)—C(3)	1.728	0.008
N—C(5)	1.324	0.010
N—C(6)	1.455	0.009
C(1)—C(2)	1.366	0.010
C(1)—C(18)	1.465	0.010
C(2)—C(3)	1.443	0.010
C(3)—C(4)	1.413	0.011
C(4)—C(5)	1.395	0.010
C(4)—C(12)	1.462	0.010
C(6)—C(7)	1.380	0.010
C(6)—C(11)	1.346	0.011
C(7)—C(8)	1.388	0.011
C(8)—C(9)	1.380	0.012
C(9)—C(10)	1.374	0.012
C(10)—C(11)	1.397	0.012
C(12)—C(13)	1.391	0.011
C(12)—C(17)	1.420	0.010
C(13)—C(14)	1.392	0.012
C(14)—C(15)	1.387	0.013
C(15)—C(16)	1.391	0.013
C(16)—C(17)	1.394	0.012
C(18)—C(19)	1.398	0.012
C(18)—C(23)	1.399	0.010
C(19)—C(20)	1.384	0.011
C(20)—C(21)	1.382	0.013
C(21)—C(22)	1.385	0.013
C(22)—C(23)	1.399	0.011

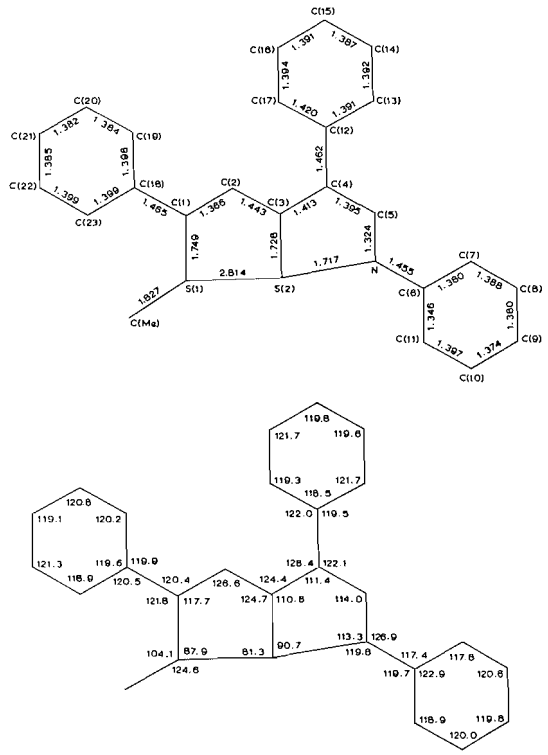

FIG. 3. Bond lengths and angles for compound **6**.

where R_{AB} is the bond distance of the bond A—B, D_{A-B} is the bond dissociation energy, r_A^* and r_B^* are constant energy radii for atoms A and B, respectively. Values of constant energy radii for various elements have been published by Huggins. The results of such calculations together with those calculated for some other thiathiophthen isosteres are shown in Table 11. The estimated dissociation energies for the S—S bond, the S—N bond, and the S—Se bond correspond approximately to 0.2, 0.5, and 0.5 of the respective single-bond energy. This suggests that any covalent bonding present is very weak. Similarly one may conclude that there is virtually no covalent bond ($D_{S-O} = 0.76$ kcal/mol) between the sulfur and oxygen atoms in **7** (15), in which the S...O distance (2.64 Å) is greater than the sum of the constant energy radii (2.58 Å), in spite of the fact that this

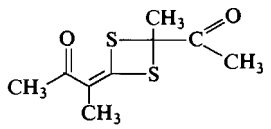

7

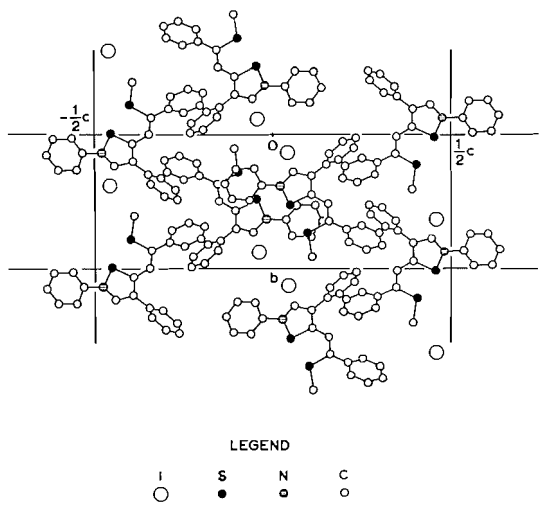

FIG. 4. Packing diagram for compound **6**.

TABLE 10. Best least squares planes for compound **5** of the form* $AX + BY + CZ = D$

(*a*) Coefficients

Plane	Atoms defining the plane	*A*	*B*	*C*	*D*	$\lvert\Delta^{max}\rvert$(Å)
1	S(1), S(2), C(1), C(2), C(3)	0.0411	−0.9962	−0.0773	−2.3281	0.042
2	S(2), N, C(3), C(4), C(5)	−0.0398	−0.9971	−0.0653	−2.7455	0.027
3	C(6), C(7), C(8), C(9), C(10), C(11)	0.3509	−0.7684	−0.5352	−3.9784	0.019
4	C(12), C(13), C(14), C(15), C(16), C(17)	−0.5594	−0.6352	−0.5325	−10.3934	0.008
5	C(18), C(19), C(20), C(21), C(22), C(23)	−0.0482	0.8849	−0.4633	−3.9934	0.009

X, Y, Z are real orthogonal coordinates, X along x, Z along z.

(*b*) Angles between normals to the planes (deg)

Plane	*1*	*2*	*3*	*4*	*5*
1		4.69	34.79	49.39	32.05
2			38.08	46.34	31.78
3				54.78	63.33
4					73.24

S...O distance is much shorter than the sum of the van der Waals' radii (3.25 Å). These results agree with the EHMO calculations performed by Kapecki and Baldwin (16), who concluded that the covalent bonding between S and O in these molecules is very weak or nonexistent.

The S...S distance observed in **6** (2.81 Å) is shorter than the "non-bonded" S...S distances in **8** (17), **9** (18), and **10** (19). The average "non-bonded" S...S distances for structures **6**, **8**, **9**, and **10** is 2.96 Å, which is longer than the sum of the constant energy radii of 2.92 Å (*i.e.*, D_{S-S}

TABLE 11. Dissociation energies estimated using the Huggins' equation

Molecule	Bond	Length (Å)	D_{A-B} (kcal/mol) (Huggins' equation)	Single-bond energy* (kcal/mol)	Reference
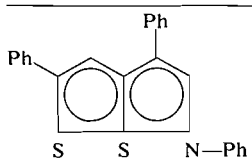	S—S	2.40	11.0	50.9	This work
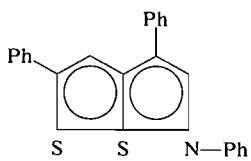	S—N	1.87	26.3	51.7	This work
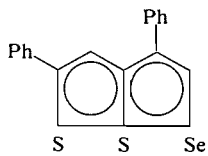	S—Se	2.33	26.3	47.6	3
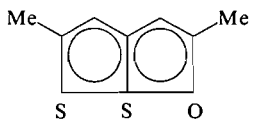	S—O	2.41	2.2	71.1	4

*The energy values for single bonds of like atoms, D(A—A), were taken from Pauling (20). The values for bonds of unlike atoms, D(A—B), were calculated using equation (20), $D(A—B) = \{D(A—A) \cdot D(B—B)\}^{1/2} + 30(x_A - x_B)^2$, where x_A and x_B are electronegativities for atoms A and B, respectively.

Can. J. Chem. Downloaded from www.nrcresearchpress.com by 210.87.254.5 on 09/05/12
For personal use only.

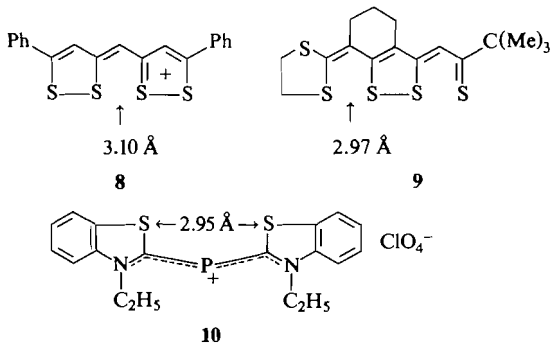

< 1 kcal/mol). In view of this, it appears more appropriate to consider the question of covalent bonding by comparing the interatomic distance with the sum of the constant energy radii rather than the sum of the van der Waals' radii.

The geometry of the molecule can be used as a guide as to which of the two resonance forms, **6** or **6***a*, predominates (20). First, a least squares plane analysis, Table 12, shows that whereas S(2), C(3), C(4), C(5), and N are strictly coplanar the atoms in the other five-membered ring S(1), C(1), C(2), C(3), and S(2) are not. (The angle between the two mean planes is 5.8°.) Moreover the methyl carbon atom is substantially out of the mean plane of this second ring. This geometry militates strongly against **6***a*. Secondly the C(Me)—S—C(1) angle is 104.1° (Fig. 3) whereas for **6***a* an angle closer to 120° would be expected. Lastly there is decidedly double bond character in the S(2)—C(3) and C(5)—N bonds. Thus this S—C bond is significantly shorter than S(1)—C(1), an unusual situation for a thiathiophthen isostere, and the C—N bond resembles the presumably partially double bond in formamide, length 1.322 Å (21).[3] All this geometric evidence implies that resonance hybrid **6** predominates. The phenyl group attached to nitrogen is virtually coplanar with the central molecular plane (4.2°) unlike the situation in compound **5** (31.8°, see Table 10).

In summary, therefore, we see that whereas changing one substituent in going from nitrogen isostere **4** to **5** seems to have had little effect on the geometry of the central part of the molecule, in **6**, methylation of the sulfur atom has had a profound effect. Rather than compare the distances between atoms doubtfully bonded together with the sum of their van der Waals radii, it is possibly more instructive to compare the distance with that calculated from Huggins' constant energy radii.

TABLE 12. Best least squares planes analysis for compound **6**

Atom	Deviations(Å)	
S(1)	−0.080	—
C(1)	+0.098	—
C(2)	−0.017	—
C(Me)*	+1.260	—
C(3)	−0.077	+0.012
S(2)	+0.076	−0.008
C(4)	—	−0.012
C(5)	—	0.004
N	—	0.003
C(6)*	—	−0.019

*Asterisked atoms are not included in the plane calculation.

This work constitutes partial fulfilment by Leung of the requirements for a Ph. D. degree.

We are grateful to Dr. Klingsberg for supplying crystalline specimens of the two compounds and to the National Research Council of Canada for financial support.

1. L. K. HANSEN and A. HORDVIK. Acta Chem. Scand. **24**, 2246 (1970).
2. S. BEZZI, M. MAMMI, and C. GARBUGLIO. Nature, **182**, 247 (1958). A. HORDVIK, E. SLETTEN, and J. SLETTEN. Acta Chem. Scand. **20**, 2001 (1966). A. HORDVIK. Acta Chem. Scand. **22**, 2397 (1968). F. LEUNG and S. C. NYBURG. Chem. Commun. 137 (1969). P. L. JOHNSON and I. C. PAUL. Chem. Commun. 1014 (1969). A. HORDVIK, E. SLETTEN, and J. SLETTEN. Acta Chem. Scand. **23**, 1852 (1969).
3. J. H. VAN DEN HENDE and E. KLINGSBERG. J. Am. Chem. Soc. **88**, 5045 (1966).
4. M. MAMMI, R. BARDI, S. TRAVERSO, and S. BEZZI. Nature, **192**, 1282 (1961).
5. A. HORDVIK, E. SLETTEN, and J. SLETTEN. Acta Chem. Scand. **23**, 1377 (1969).
6. F. LEUNG and S. C. NYBURG. Can. J. Chem. **49**, 167 (1971).
7. A. HORDVIK and L. J. SAETHRE. Acta Chem. Scand. **24**, 2261 (1970).
8. J. KARLE and I. L. KARLE. Acta Cryst. **21**, 849 (1966).
9. R. D. ELLISON. XFLS, an extensively modified version of ORFLS (Report ORNL-TM-305, Oak Ridge National Laboratory, 1962). Unpublished.
10. S. C. ABRAHAMS and J. L. BERNSTEIN. Acta Cryst. **18**, 926 (1965).
11. D. T. CROMER and J. B. MANN. Acta Cryst. **A24**, 321 (1968).

[3]Some S—N single bond lengths are also cited in ref. 6.

Can. J. Chem. Downloaded from www.nrcresearchpress.com by 210.87.254.5 on 09/05/12
For personal use only.

12. W. R. BUSING, K. O. MARTIN, and H. A. LEVY. ORFFE, a Fortran Crystallographic Function and Error Program (Report ORNL-TM-306, Oak Ridge National Laboratory, 1964).
13. D. W. J. CRUICKSHANK. Acta Cryst. **2**, 65 (1949).
14. M. L. HUGGINS. J. Am. Chem. Soc. **75**, 4126 (1953).
15. J. A. KAPECKI, J. E. BALDWIN, and I. C. PAUL. Tetrahedron Lett. 5307 (1967); J. Am. Chem. Soc. **90**, 5800 (1968).
16. J. A. KAPECKI and J. E. BALDWIN. J. Am. Chem. Soc. **91**, 1120 (1969).
17. A. HORDVIK. Acta Chem. Scand. **19**, 1253 (1965).
18. J. SLETTEN. Chem. Commun. 688 (1969).
19. R. ALLMANN. Ber. Chem. **99**, 1332 (1966).
20. E. KLINGSBERG. J. Org. Chem. **33**, 2915 (1968).
21. International Tables for X-Ray Crystallography, Vol. III. C. H. Macgillavry and G. D. Rieck, eds., Kynoch Press, Birmingham, England, 1962. L. Pauling. Nature of the Chemical Bond. 3rd ed. Cornell University Press, Ithaca, New York, 1960.

Can. J. Chem. Downloaded from www.nrcresearchpress.com by 210.87.254.5 on 09/05/12
For personal use only.

The Structure and Stereochemistry of Hydroxyachillin

F. W. BACHELOR AND A. B. PARALIKAR[1]
Department of Chemistry, University of Calgary, Calgary 44, Alberta
AND
SHÔ ITÔ
Department of Chemistry, Tohoku University, Sendai, Japan
Received July 13, 1971

The sesquiterpene lactone hydroxyachillin has been isolated from *Artemisia frigida* Wild. The position and stereochemistry of the free hydroxyl group has been established by n.m.r. examination as well as the conformation of the molecule using nuclear Overhauser effects.

L'hydroxyachilline lactone sesquiterpénique a été isolée à partir de *l'Artemisia frigida* Wild. La position et la stéréochimie des groupes hydroxyles libres ont été déterminés par r.m.n.; il en a été de même pour la conformation de la molécule en se servant de l'effet nucléaire Overhauser.
Canadian Journal of Chemistry, **50**, 333 (1972)

Although hydroxyachillin (**1***a*) has been previously isolated from *Achillea lanulosa* by White and Winter (1), its structure is based on its conversion to achillin (**1***d*) by removal of the free hydroxyl group. This was accomplished by preparing the nitrosylate (**1***b*), converting this to the

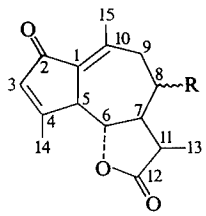

1

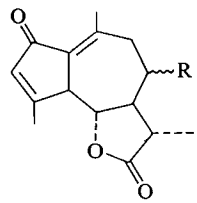

2

a R = OH
b R = *p*-$NO_2C_6H_4SO_2O$—
c R = I
d R = H
e R = CH_3CO_2—

a R = CH_3CO_2—
b R = H

iodide (**1***c*), and removing the iodine by reduction. This sequence still leaves the position of the hydroxyl group in doubt and although there are a sufficient number of analogies to suggest that the hydroxyl group is at C-8, including matricarin (**2***a*) (2), which is found in the same plant, this is not sufficient to prove its location.[2]

In our investigation of local *Artemisia* species we have found hydroxyachillin to be the principal sesquiterpene lactone present in *Artemisia frigida* Wild. Comparison of the i.r. spectrum of our compound with an authentic specimen showed them to be identical.[3] The recent stereospecific total syntheses of leukodin (**2***b*) and achillin (**1***d*) from α-santonin firmly establish the structures and stereochemistry of these molecules (4–6). There remains only the position and stereochemistry of the hydroxyl group of hydroxyachillin to be determined.

We have been able to complete the structure of hydroxyachillin by examination of the n.m.r. spectra of the free alcohol and its acetate. The n.m.r. data for these compounds are given in Table 1. Examination of these data shows that the hydroxyl group can only be located at C-8 or -9. As the new signal from the hydrogen on the alcohol carbon atom is found at 6.26 τ this places the hydroxyl group at C-8. If it were at C-9 it would be allylic and its position would be expected at lower field. For example the corresponding allylic hydrogen atom in geraniol is found at 5.85 τ (7). This hydrogen atom in hydroxyachillin is shifted to 5.24 τ in the acetate and is clearly seen as a triplet of doublets with

[1]Abstracted in part from the thesis of Mr. A. B. Paralikar submitted to the University of Calgary for the Ph.D. degree, 1970.

[2]A private communication from Prof. E. H. White informed us that the stability of the nitrosylate **1***b* and the formation of an impure cyclopropane derivative obtained on reduction of the iodide **1***c*, similar to that obtained from the corresponding compound in the matricarin series suggested to them that the hydroxyl was at C-8 (3).

[3]We wish to thank Dr. R. E. K. Winter for running the i.r. comparison of the two compounds.

Can. J. Chem. Downloaded from www.nrcresearchpress.com by 210.87.254.40 on 09/05/12
For personal use only.

TABLE 1. Proton chemical shifts of hydroxyachillin and related compounds

Compound	Position*							
	C-3	C-5	C-6	C-8	C-11	C-13	C-14	C-15
1*a*	3.85(s, broad)	6.60(d) $J = 10$	6.14(t) $J = 10$	6.26(dt) $J = 3, 10$		8.71(d) $J = 7$	7.69(d) $J = 1.5$	7.56(s)
1*e*†	3.83(c)	6.59(d) $J = 10$	6.10(t) $J = 10$	5.24(dt) $J = 3, 10$	7.18(quintet) $J = 7$	8.89(d) $J = 7$	7.70(d) $J = 1.5$	7.55(s)
1*d*‡	3.92(q) $J = 1.5, 1.5$	6.62(d, broad) $J = 10, 1.5$	6.21(t) $J = 10, 10$	8.88(c)	7.39(quintet) $J = 7.4$	8.90(d) $J = 7.4$	7.74(dd) $J = 1.5, 0.9$	7.60(d) $J = 0.9$
2*b*§	3.87	6.65	6.46			8.75	7.72	7.64

*All values are in τ relative to internal tetramethylsilane; s, singlet; d, doublet; t, triplet; q, quartet; dt, double triplet; c, complex.
†An additional signal appears at 7.91(s) for the acetyl methyl group.
‡See ref. 12.
§See ref. 5.

coupling constants of 10 and 3 Hz. This splitting is also only compatible with the location of the hydroxyl group at C-8 having three hydrogen atoms on the adjacent carbon atoms.

Spin–spin decoupling on the acetate **1***e* firmly established the relationship of a number of the proton signals. Irradiation of the vinyl hydrogen at 3.83 τ caused the allylic splitting to disappear in the methyl signal at 7.70 τ thus establishing it as the C-14 methyl group. Decoupling of the methyl doublet at 8.89 τ caused the quintet at 7.18 τ to collapse to a doublet ($J = 7$ Hz) for the hydrogen at C-11. A quintet of this type with similar stereochemistry has been observed in β-santonin (8). Although the complexity of the region did not allow us to locate exactly the position of the hydrogen at C-7, irradiation at 7.3 τ caused the signal at 5.24 τ to collapse to a broad unresolved peak and the triplet at 6.10 τ became a doublet. Finally, decoupling of the allylic hydrogen at 6.59 τ reduced the hydrogen signal at 6.10 τ to a doublet and the vinyl hydrogen signal which showed complex allylic coupling became a simple quartet ($J = 1.5$ Hz). This evidence firmly establishes the relationship of the hydrogen atoms at C-3, -5, -6, -7, -8, -11, -13, -14, and -15.

Guaianolide lactones with a *trans* lactone at C_6—C_7 and *trans* hydrogens at C-5 and -6 are capable of ring inversion. This leaves the possibility for the stereochemistry of the C-8 hydroxyl of being either α or β, each of which could exist in one of two conformations, unless the conformations are freely interconvertible. Examination of models of the four different possibilities showed that they could easily be distinguished from each other by determining the nuclear Overhauser effect (n.O.e.) of selected protons. Initially it must be remarked that there is a decided upfield shift of the C-13 methyl signal in the n.m.r. spectrum of hydroxyachillin acetate (**1***e*) from that of hydroxyachillin (**1***a*). This spatial interaction effect has been noted in the case of substituted tetralins (9). For example, in 1,4-dimethyl-5-hydroxydecalin (**3**), it was

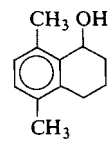

3

found that acetylation caused an upfield shift of the peri methyl group of 0.17 p.p.m. We observe an upfield shift of 0.18 p.p.m. in hydroxyachillin acetate. This shift is not observed if the two groups are *trans* diaxial or pseudo *trans* diaxial as they would be in one conformation of hydroxyachillin where the hydroxyl group is α. All of the other three conformations would allow for this spatial interaction.

Of the remaining conformations, one α and one β conformation could account for the observed coupling constants. In the case of the conformer with the oxygen substituent α, the hydrogen atom at C-8 approaches very closely to that at C-6.[4] Irradiation of either the hydrogen signal at C-6 or -8 of hydroxyachillin acetate (**1***e*) pro-

[4]From Dreiding models the internuclear distance is estimated to be 2.13 Å. For comparison of this n.O.e. with compounds showing similar signal enhancements and similar proton relationships see refs. 10 and 11.

Can. J. Chem. Downloaded from www.nrcresearchpress.com by 210.87.254.40 on 09/05/12
For personal use only.

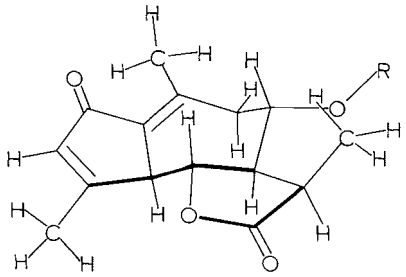

FIG. 1. The conformation of hydroxyachillin acetate ($R = COCH_3$).

duced a definite signal enhancement of approximately 10% in the other signal. This definitely establishes the hydrogen atom at C-8 as β and the conformation of the seven-membered ring such that the hydroxyl or acetate group is pseudo equatorial. This is in contrast to the oxygen functions at C-8 of the matricarin series which have been shown to have the α configuration (4). The complete conformational picture of hydroxyachillin acetate is given in Fig. 1. In addition to the n.O.e. at C-8 when radiating the C-6 proton signal, there was no observable enhancement of the signal due to the hydrogen atom at C-5. This verifies the *trans* relationship of these atoms.

The strong spatial interaction between the C-11 β-methyl group and the 8α-hydroxyl group is probably also responsible for the lack of reactivity of this hydroxyl group. Although it can be acetylated and the nitrosylate prepared, we have been unable to prepare the tosylate, brosylate, or iodoacetate. It is not oxidized to a ketone with the chromium trioxide – pyridine complex, but under more drastic conditions extensive oxidation takes place.

Experimental

The n.m.r. spectra were measured with a Varian HA-100 spectrometer with a frequency swept and tetramethylsilane-locked mode. Double and triple resonance experiments were performed by using the spectrometer in conjunction with two Hewlett–Packard HP-200ABR audio oscillators. The n.O.e. experiments were carried out by measuring the integrated intensities of a signal four times with and without irradiation at the resonance frequency of another signal at a sweep rate of 0.4 Hz/s. Samples were not degassed before carrying out n.O.e. measurements.

Extraction and Isolation of Hydroxyachillin

The aerial parts of *Artemisia frigida* Wild collected in the vicinity of Calgary, Alberta were dried and ground. The ground material (6 kg) was extracted successively with hexane and chloroform. The chloroform extract was concentrated to dryness and the residual gum dissolved in 3 l of ethanol. The ethanolic solution was mixed with a solution of 75 g of lead acetate in 3 l of water and 20 ml of acetic acid. After 4 days the clear supernatant was decanted through glass wool and the residue washed twice with ethanol. The ethanol–water mixture was concentrated to a small volume and extracted thoroughly with chloroform. The chloroform extract was dried (Na_2SO_4), filtered, and concentrated at reduced pressure. The residual gum (56 g) was taken up in benzene and chromatographed over 1500 g of alumina. The column was eluted with benzene, benzene–chloroform (1:1), chloroform, chloroform–methanol (1:1) and methanol. The benzene–chloroform fractions showed characteristic bands in the i.r. at 1775 cm^{-1} for a γ-lactone and these were combined and concentrated yielding a residue of 8.7 g. This material was again chromatographed on alumina (320 g). Elution with benzene–chloroform gave 6.5 g of a brown gum. This gum was crystallized first from benzene and the crystalline material then recrystallized from ethyl acetate to give 1.4 g of hydroxyachillin, m.p. 159.5–160 °C, $[\alpha]_D^{23}$ +112° (*c* 1.0 in CH_3OH); (lit. (4) m.p. 161–162°, $[\alpha]_D^{22}$ +110°).

Hydroxyachillin Acetate

A solution of 0.1 g of hydroxyachillin in 1 ml of pyridine was mixed with 2 ml of acetic anhydride. The solution was warmed for 3 h on a steam bath, then left overnight at room temperature. The reaction mixture was then poured over ice and the resulting crystalline solid collected by filtration. Crystallization and recrystallization gave 0.06 g of hydroxyachillin acetate, m.p. 194–195 °C, $[\alpha]_D^{25}$ + 110° (*c* 0.20 in $CHCl_3$) λ_{max} (MeOH) 255 mμ (ε 15 000); lit. (1) m.p. 193–194°, $[\alpha]_D^{22}$ + 116°).

We wish to thank the National Research Council of Canada for support of this work.

1. E. H. WHITE and R. E. K. WINTER. Tetrahedron Lett. **3**, 137 (1963).
2. W. HERZ and K. UEDA. J. Am. Chem. Soc. **83**, 1139 (1961).
3. R. E. K. WINTER. Ph.D. Thesis. The Johns Hopkins University, Baltimore, Maryland, 1963.
4. E. H. WHITE and J. N. MARX. J. Am. Chem. Soc. **89**, 5511 (1967).
5. E. H. WHITE, S. EGUCHI, and J. N. MARX. Tetrahedron, **25**, 2099 (1969).
6. J. N. MARX and E. H. WHITE. Tetrahedron, **25**, 2117 (1969).
7. NMR Spectra Catalog. Vol. 1. Varian Associates, Palo Alto, California. Spectrum No. 279.
8. J. T. PINHEY and S. STERNHELL. Aust. J. Chem. **18**, 543 (1965).
9. T. OKAMOTO and Y. KAWAZOE. Chem. and Pharm. Bull. (Japan), **11**, 643 (1963).
10. R. A. BELL and E. N. C. OSAKE. Chem. Commun. 1093 (1968).
11. K. TORI, M. OHTSURU, I. HORIBE, and K. TAKEDA. Chem. Commun. 943 (1968).
12. S. J. SMOLENSKI, C. L. BELL, and L. BAUER. Lloydia, **30**, 144 (1967).

Can. J. Chem. Downloaded from www.nrcresearchpress.com by 210.87.254.40 on 09/05/12
For personal use only.

Total Synthesis of (+)-Occidentalol[1]

M. SERGENT,[2] M. MONGRAIN,[3] AND P. DESLONGCHAMPS[4]

Laboratoire de synthèse organique, Département de chimie, Université de Sherbrooke, Sherbrooke, Québec

Received June 10, 1971

A synthesis of (+)-occidentalol (**1**) has been realized in six steps, starting from the readily available enone alcohol **3**.

La synthèse du sesquiterpène (+)-occidentalol (**1**) a été réalisée en six étapes en utilisant un produit de départ très facilement accessible, l'énone alcool **3**.

Canadian Journal of Chemistry, **50**, 336 (1972)

Can. J. Chem. Downloaded from www.nrcresearchpress.com by 210.87.254.40 on 09/05/12
For personal use only.

The structure of (+)-occidentalol, a sesquiterpene isolated (1) from the wood of Eastern white cedar (*Thuja occidentalis L.*) was first formulated as **2** (2) and later corrected to structure **1** (3).

We wish now to report a total synthesis of (+)-occidentalol which confirmed the proposed structure **1** for this sesquiterpene. A synthesis of (−)-occidentalol has recently appeared in the literature (4) and a synthesis of the naturally occuring (+)-occidentalol together with a chemical correlation have been completed by Heathcock and Amano (5).

The enone alcohol **3** is very readily available in large scale from (+)-dihydrocarvone in three steps (6). This compound (**3**) has served as key intermediate in a synthesis of α-agarofuran (6).

Structurally, compound **3** and (+)-occidentalol (**1**) have the same skeleton and both of which possess the same absolute stereochemistry at C-7 and -10. Thus, a specific reduction of the double bond of **3** to obtain a *cis*-decalone system (**4**), and the use of the remaining carbonyl group for the introduction of the diene chromophore in ring A, seemed to be a very logical approach. Consequently, the enone alcohol **3** appears to be an excellent precursor for (+)-occidentalol and it was therefore selected as starting material.

Catalytic hydrogenation of compound **3** in methanol in the presence of 10% palladium-on-charcoal gave directly the crystalline *cis*-ketol **4** in 65% yield. Treatment of the resulting mother liquor[5] with methanolic sodium hydroxide furnished a further crop of **4**, bringing up the total yield to 83%.

In order to confirm the *cis* juncture of **4**, a reduction of **3** with lithium in liquid ammonia was carried out and a mixture of two compounds was obtained. The minor product was found identical with **4**. Since, it is known that this reduction (7) generally affords the *trans* product, the major product must have the *trans* structure.[6]

The introduction of a double bond between C-1 and -2 was next considered and to realize such a transformation in a specific manner, ketol **4** was first converted into the corresponding hydroxy methylene derivative **5** in essentially quantitative yield. From this intermediate (**5**), we have developed two different routes to obtain the enone **6**.

Treatment of the sodium salt of **5** with bromine gave an unstable mixture of the two epimeric bromo-aldehydes **7** which was therefore directly subjected to dehydrobromination condition ($LiCl–Li_2CO_3$/DMF (8)) and the crystalline enone aldehyde **8** was readily isolated in 65% yield after column chromatography.

Deformylation of **8** to give the crystalline enone **6** was achieved in 80% yield with tris-triphenylphosphinerhodium chloride in boiling dichloromethane (9).

Alternatively, the transformation of bromo-aldehydes **7** to enone **6** can be accomplished by first performing a retro Claisen reaction (**7** → **9**)

[1]This paper has been presented at the "Congrès de l'Association Canadienne-Française pour l'Avancement des Sciences (ACFAS)", October 16–17, 1970 Québec.

[2]Holder of a "bourse France–Québec" 1969–1971.

[3]Holder of an NRCC Studentship, 1968–1971.

[4]A.P. Sloan Fellow, 1970–1972.

[5]The n.m.r. studies of the mother liquor before and after the basic treatment indicated the presence of C-4 epimers in the hydrogenated mixture. For a more detailed study of a similar reaction, see ref. 5.

[6]A systematic study of the metal ammonia reduction of **3** has been carried out, the result of which will be reported in a separate paper.

Can. J. Chem. Downloaded from www.nrcresearchpress.com by 210.87.254.40 on 09/05/12
For personal use only.

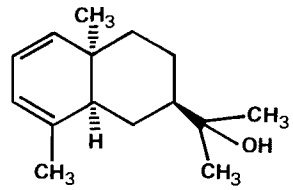

1

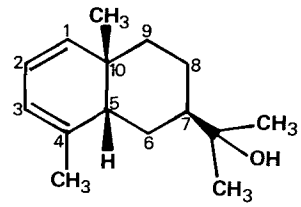

2

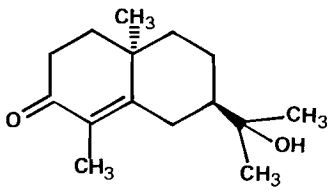

3

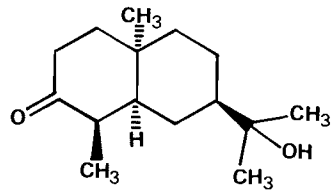

4

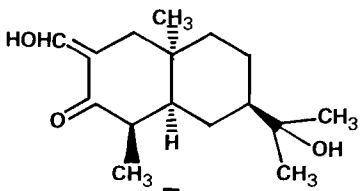

5

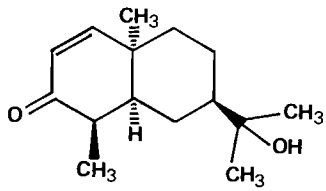

6

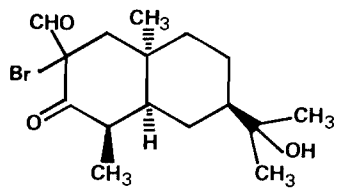

7

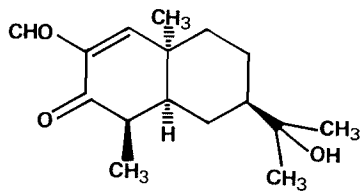

8

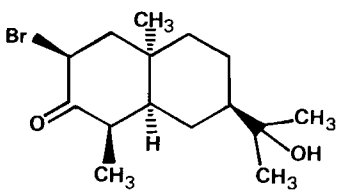

9

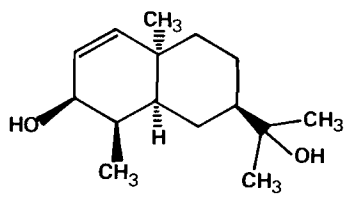

10

followed by dehydrobromination (**9** → **6**). This procedure (10) has the advantage of avoiding the use of the expensive rhodium complex.

In fact, we have carried out the bromination and the deformylation reaction in a single operation without the isolation of the unstable isomer **7**. Treatment of the hydroxymethylene **5** with bromine in the presence of an excess barium

hydroxide in ethanol gave directly the bromoketone **9**. Barium hydroxide served to generate the enolate salt of **5** necessary for bromination (→**7**) and to mediate *in situ* the retro Claisen reaction (**7** → **9**) (11).

Dehydrobromination of **9** proceeded smoothly to give the desired enone **6**. This sequence of reaction afforded **6** in 74% overall yield from **5**.

The enone **6** was then reduced in high yield with lithium aluminum hydride in ether to give the allylic alcohol **10**. The crude allylic alcohol dissolved in benzene containing *p*-toluenesulfonic acid at room temperature gave the alcohol **1** which was found to be completely identical with authentic (+)-occidentalol.

Experimental

Melting points are not corrected. The U.V. spectra (λ_{max}) were measured on a Cary model 14 spectrophotometer and i.r. spectra (ν_{max}) were recorded on a Perkin–Elmer spectrophotometer, model 257. The n.m.r. spectra (τ values) were taken on a Varian A60 spectrometer with tetramethylsilane as an internal standard. Anhydrous magnesium sulfate was used as the drying agent in working up reaction. Fisher Florisil 100–200 mesh was used for preparing all column chromatograms. Low boiling petroleum ether (b.p. 30–60 °C) was used.

(+)-Dihydrocarvone was prepared by the method of Malhotra *et al.* (12). The method of Hortmann *et al.* (13) was found superior to the one of Howe and McQuillin (14) to prepare (+)-5-α-hydroxy-4,7α*H*-eudesm-11-en-3-one which is the precursor of **3** (6).

cis-Ketol **4**

Enone alcohol **3** (9.45 g, 40 mmol) was hydrogenated in freshly distilled methanol (500 ml) with 10% palladium-on-charcoal (1 g) for 24 h. The catalyst was removed by filtration on Celite and the filtrate was evaporated to dryness to give a white solid (9.54 g). Crystallization from hexane afforded pure *cis*-ketol **4** (6.19 g, 65% yield).

The mother liquor (3.35 g) was dissolved in methanol (100 ml) and treated with 50% aqueous sodium hydroxide (10 ml) for 3 h at room temperature. After removal of the methanol and addition of water, the reaction mixture was extracted twice with ether. The combined extract was washed with brine, dried, and evaporated. Column chromatography yielded an additional quantity of the ketol **4** (1.72 g). Total yield 83%. The analytical sample was prepared by crystallization with petroleum ether, m.p. 87–88 °C; i.r. ν_{max} 3600, 3460, and 1710 cm^{-1}; n.m.r.: τ ($CDCl_3$) 8.69 (3H, s, CH_3), 8.83 (6H, s, *i*-propylol CH_3), and 9.02 (3H, d, $J = 6.5$ Hz, CH_3).

Anal. Calcd. for $C_{15}H_{26}O_2$: C, 75.58; H, 10.99. Found: C, 75.26; H, 10.96.

Hydroxy Methylene Derivative **5**

To sodium hydride (4 g, 50% suspension), which was previously washed with dry benzene to remove the oil, was added ketol **4** (2 g, 8.4 mmol), ethyl formate (50 ml), and anhydrous ether (400 ml). The mixture was refluxed for 5 h. After cooling, water was cautiously added and the aqueous phase was washed with ether, acidified to p*H* 5 with dilute hydrochloric acid and extracted with ether. The organic phase was washed with brine, dried, and evaporated to dryness to give crude **5** (2.24 g); i.r.: ν_{max} ($CHCl_3$) 3600, 3450, 1710, 1650, and 1580 cm^{-1}; n.m.r.: τ ($CDCl_3$) 1.52 and 2.08 (1H, s, hydroxymethylene hydrogen), 8.85 (6H, s, *i*-propylol CH_3) 8.85 (3H, d, $J = 7$ Hz, CH_3), and 9.00 (3H, s, CH_3).

Bromo-aldehydes **7**

Compound **5** (2.24 g, 8.4 mmol) dissolved in chloroform (100 ml) was mixed with an aqueous solution of sodium hydroxide (0.25 *N*, 33.6 ml). To the above mixture was added dropwise a solution of bromine in chloroform (1%, 44.8 ml) with stirring. After 45 min at room temperature, water was added and the phases were separated. The organic layer was washed with water, dried, and evaporated *in vacuo* at room temperature to give the crude bromo-aldehydes **7** (2.7 g) as an oil; i.r.: ν_{max} ($CHCl_3$) 3600, 3460, 1730, and 1710 cm^{-1}; n.m.r.: ($CDCl_3$) 0.33 and 0.67 (1H, 2s, (intensity ratio 4:1), aldehydic H). This unstable material was used immediately for the next step.

Enone Aldehyde **8**

The crude bromo-aldehydes **7** (2.7 g, 7.08 mmol) dissolved in dimethyl formamide (300 ml) containing lithium chloride (2.42 g, 55 mmol) and lithium carbonate (484 mg, 6.5 mmol) was heated at 125 °C (oil bath temperature) under nitrogen for 2.5 h. After cooling, water was added and the mixture was extracted with ether. The organic phase was washed with brine, dried, and evaporated to dryness. The resulting product was purified by column chromatography. Elution with ether–benzene (4:1) gave crystalline **8** (1.44 g, 65% yield from ketol **4**). The analytical sample was prepared by crystallization with ether–petroleum ether, m.p. 101.5 °C; $\alpha_{578}^{CHCl_3}$ −247°; i.r.: ν_{max}($CHCl_3$) 3600, 3500, 1730, 1705 and 1685 cm^{-1}; n.m.r.: τ ($CDCl_3$) 0.07 (1H, s, aldehydic H), 2.64 (1H, d, $J = 2$ Hz, olefinic H), 8.67 (3H, s, CH_3), 8.88 (3H, d, $J = 6$ Hz, CH_3), and 8.95 (6H, s, *i*-propylol CH_3); u.v.: λ_{max} (EtOH) 237 nm (ε 8100).

Anal. Calcd. for $C_{15}H_{24}O_3$: C, 72.69; H, 9.15. Found: C, 72.54, H, 8.91.

Bromo-ketone **9**

To a stirred mixture of the hydroxymethylene derivative **5** (266 mg, 1 mmol) and barium hydroxide (946 mg, 3 mmol) in ethanol (95%, 8 ml) was slowly added a solution of bromine (160 mg) in ethanol (5 ml). After 45 min at room temperature, water was added and the resulting mixture was extracted with ether. The organic phase was washed with dilute hydrochloric acid, brine, dried, and evaporated to dryness. The crude product (315 mg, 100% yield) was suitable for the next step. The analytical sample was purified by column chromatography (eluant: benzene–ether (7:3)) and crystallized from etherpetroleum ether, m.p. 88.5 °C (dec.), $\alpha_{578}^{CHCl_3}$ +206°; i.r.: ν_{max} ($CHCl_3$) 3590, 3440, and 1727 cm^{-1}; n.m.r.: τ ($CDCl_3$) 5.05 (1H, oct, $J = 1$, 6.5 and 12 Hz, H_2), 8.36 (3H, s, CH_3), 8.86 (6H, s, *i*-propylol CH_3), and 8.93 (3H, d, $J = 6.5$ Hz, CH_3).

Anal. Calcd. for $C_{15}H_{25}BrO_2$: C, 56.78; H, 7.94; Br, 25.19. Found: C, 56.92; H; 7.91; Br, 25.15.

Can. J. Chem. Downloaded from www.nrcresearchpress.com by 210.87.254.40 on 09/05/12
For personal use only.

Enone 6

(a) From Enone Aldehyde 8

The enone aldehyde **8** (83 mg, 0.3 mmol) and tris-triphenylphosphinerhodium chloride (335 mg, 0.36 mmol) in dichloromethane (12 ml) were kept at reflux for 16 h under nitrogen and 14 h at room temperature. The solvent was removed *in vacuo* and the residue was triturated with ethanol. After evaporation of the ethanolic extract the crude product was purified by chromatography. Elution with benzene–ether (7:3) gave crystalline **8** (66 mg, 83% yield). The analytical sample was prepared by crystallization from hexane, m.p. 84 °C, i.r.: ν_{max} ($CHCl_3$) 3600, 3450, 1675, and 1640 cm^{-1}; n.m.r.: τ (CCl_4) 3.65 (1H, quad, $J = 2$ and 10 Hz, H_1), 4.23 (1H, d, $J = 10$ Hz, H_2), 8.79 (3H, s, CH_3), 8.99 (6H, s, *i*-propylol CH_3), and 9.01 (3H, d, $J = 6.5$ Hz, CH_3); u.v.: λ_{max} (EtOH) 230 nm (ε 7950).

Anal. Calcd. for $C_{15}H_{24}O_2$: C, 76.22; H, 10.23. Found: C, 76.22; H, 10.08.

(b) From Bromo-ketone 9

The bromo-ketone **9** (3.1 g, 10 mmol) dissolved in dimethylformamide (150 ml) containing lithium bromide (3.1 g, 35 mmol) and lithium carbonate (2.6 g, 35 mmol) was heated at 130 °C (bath temperature) for 24 h. Water was added to the cooled reaction mixture which was then extracted with ether. The organic phase was washed with brine, dried, and evaporated to dryness (2.2 g). A portion of this crude material (812 mg) was purified by column chromatography with silica gel. Elution with benzene–ether (4:1) gave a pure sample (639 mg) which was identical to enone **6** obtained by the above procedure. The overall yield from the hydroxymethylene derivative **5** was 75%.

(+)-Occidentalol (1)

The enone **6** (371 mg, 1.7 mmol) dissolved in ether (25 ml) was slowly added to a suspension of lithium aluminum hydride (123 mg) in ether (25 ml) cooled in an ice bath. After 1 h at room temperature, the excess hydride was destroyed by addition of brine. The organic phase was separated, dried, and evaporated to dryness to give the crude allylic alcohol **10** (374 mg, 100% yield); i.r.: ν_{max} ($CHCl_3$) 3600, 3470, and 3450 cm^{-1}; n.m.r.: τ ($CDCl_3$) 4.17 (1H, quad, $J = 4$ and 10 Hz, H_2), 4.52 (1H, d with additional splitting, $J = 10$ Hz, H_1), 6.05 (H, t, $J = 4$ Hz), 8.86 (6H, s, *i*-propylol CH_3), 8.88 (3H, d, $J = 6$ Hz, CH_3), and 9.02 (3H, s, CH_3).

The above crude product dissolved in benzene (60 ml) was treated with *p*-toluenesulfonic acid (58 mg) for 3 h at room temperature. Water was added and the benzene layer was separated. The aqueous phase was extracted with ether and the combined organic solution was dried and evaporated to dryness. The crude product (345 mg) was purified by column chromatography. Elution with benzene gave (+)-occidentalol (214 mg, 62% yield from **6**). The allylic alcohol **10** (98 mg, 26%) was recovered from further elution with benzene–ether (1:1).

The (+)-occidentalol was further purified by sublimation and crystallization (petroleum ether), m.p. 95 °C; $\alpha_{578}^{CHCl_3}$ +369° (lit. (*2b*) m.p. 94–96.5 and 97.5–98 °C; $\alpha_{D}^{CHCl_3}$ +363.2°). The i.r. and n.m.r. spectra were identical with those of an authentic sample of (+)-occidentalol. Also, a mixed m.p. showed no depression.

Support for this work by the National Research Council of Canada and by the "Ministère de l'Education" (Québec) is gratefully acknowledged. We also thank Dr. E. von Rudloff for a generous gift of (+)-occidentalol.

1. T. NAKATSUKA and Y. HIROSE. Bull. Agric. Chem. Soc. Jap. **20**, 215 (1956).
2. (*a*) Y. HIROSE and T. NAKATSUKA. Bull. Agric. Chem. Soc. Jap. **23**, 140 (1959). (*b*) E. VON RUDLOFF and H. ERDTMANN. Tetrahedron, **18**, 1315 (1962). (*c*) K. MISLOW and A. MOSCOWITZ. Tetrahedron Lett. 699 (1963). (*d*) H. ZIFFER, T. J. BATTERHAM, U. WEISS, and E. VON RUDLOFF. Tetrahedron, **20**, 67 (1964).
3. A. G. HORTMANN and J. B. DE ROOS. J. Org. Chem. **34**, 732 (1969).
4. M. ANDO, K. NANAUMI, T. NAKAWAGA, T. ASAO, and K. TAKASE. Tetrahedron Lett. 3891 (1970).
5. C. H. HEATHCOCK and Y. AMANO. Can. J. Chem. This issue.
6. A. ASSELIN, M. MONGRAIN, and P. DESLONGCHAMPS. Can. J. Chem. **46**, 2817 (1968).
7. G. STORK and S. D. DARLING. J. Am. Chem. Soc. **86**, 1761 (1964).
8. (*a*) R. P. HOLYSZ. J. Am. Chem. Soc. **75**, 4432 (1953). (*b*) R. JOLY, J. WARNANT, G. NOMINÉ, and D. BERTIN. Bull. Chem. Soc. Fr. 366 (1958).
9. (*a*) J. TSUJI and K. OHNO. Tetrahedron Lett. 3969 (1965) (*b*) Y. SHIMIZU, H. MITSUHASHI and E. CASPI. Tetrahedron Lett. 4113 (1966).
10. K. MORI, M. SHIOZAKI, N. ITAYA, T. OGAWA, M. MATSUI, and Y. SUMIKI. Tetrahedron Lett. 2183 (1968).
11. W. S. JOHNSON, T. LI, D. J. FAULKNER, and S. F. CAMPBELL. J. Am. Chem. Soc. **90**, 6225 (1968).
12. S. K. MALHOTRA, D. F. MOAKLEY, and F. JOHNSON. J. Am. Chem. Soc. **89**, 2794 (1967).
13. A. G. HORTMANN, J. E. MARTINELLI, and Y. WANG. J. Org. Chem. **34**, 732 (1969).
14. R. HOWE and F. S. MCQUILLIN. J. Chem. Soc. 2423 (1955); 2670 (1956); 1194 (1958).

Can. J. Chem. Downloaded from www.nrcresearchpress.com by 210.87.254.40 on 09/05/12
For personal use only.

(+)-Occidentalol: Absolute Stereostructure and Total Synthesis[1]

YOUNG AMANO AND CLAYTON H. HEATHCOCK
Department of Chemistry, University of California, Berkeley, California 94720

Received June 10, 1971

Hydroxy ketone **7** has been prepared from both (+)-dihydrocarvone (**3**) and (+)-occidentalol (**2**), thus establishing the absolute stereostructure of the latter. The three-stage conversion of compound **7** into (+)-occidentalol constitutes a total synthesis of the sesquiterpene.

L'hydroxycétone **7** a été préparée à partir des deux produits (+)-dihydrocarvone (**3**) et (+)-occidentalol (**2**) établissant par le fait même la stéréostructure absolue de ce dernier. La conversion en trois étapes du composé **7** en (+)-occidentalol constitue une synthèse totale du sesquiterpène.

Canadian Journal of Chemistry, **50**, 340 (1972)

Can. J. Chem. Downloaded from www.nrcresearchpress.com by 210.87.254.6 on 09/05/12
For personal use only.

Introduction

The sesquiterpene alcohol (+)-occidentalol was first isolated from the wood of Eastern white cedar (*Thuja occidentalis* L.) by Nakatsuka and Hirose (1). Subsequent reports from various laboratories lead to the acceptance of structure **1** for this interesting sesquiterpene (2–5). In 1969, Hortmann and De Roos reported a careful analysis of the 100 MHz p.m.r. spectrum of (+)-occidentalol and suggested structure **2** (6).

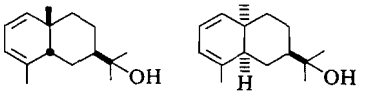

1 **2**

We have carried out a straightforward chemical correlation of (+)-occidentalol and (+)-dihydrocarvone (**3**) as well as a total synthesis of the sesquiterpene. Our results confirm Hortmann's structure, as well as the absolute configuration previously assigned to (+)-occidentalol on the basis of o.r.d. studies (3, 4). Since this work was completed, another synthesis of (+)-occidentalol (**7**) and one of its enantiomorph (8) have been reported.

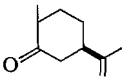

3

Natural (+)-occidentalol, generously provided by Professor H. Erdtmann, was selectively hydrogenated to obtain dihydrooccidentalol (**4**) (3) (see Scheme 1). Hydroboration of **4** yielded a mixture of diols, **5**, which was oxidized with bispyridinechromium(VI) oxide in methylene chloride (9). The initial product, which was mostly hydroxy ketone **6**, was converted to the more stable epimer **7** upon filtration through alumina. Compound **7**, m.p. 89–90°, had $[\alpha]_D^{CHCl_3}$ −18°.

Oxymercuration–demercuration (10) of (+)-

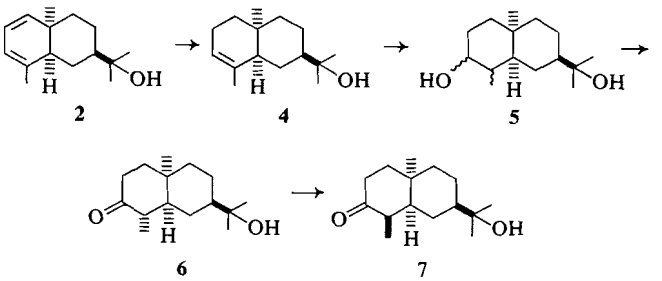

2 **4** **5** **6** **7**

SCHEME 1

[1]Presented at the Joint Meeting of the Chemical Institute of Canada and the American Chemical Society, Toronto, Ontario, May 26, 1970.

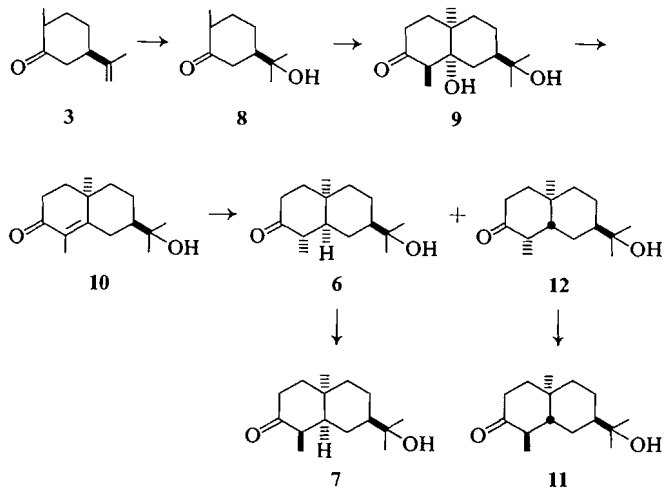

SCHEME 2

dihydrocarvone (**3**) yielded hydroxy ketone **8** (see Scheme 2). Base-catalyzed condensation of **8** with ethyl vinyl ketone gave the crystalline diol **9**, which was dehydrated to hydroxy-enone **10** by treatment with hydrogen chloride in refluxing tetrahydrofuran. The relative stereochemistry of this material, *epi*-carrisone, has been rigorously established as *trans* (11). Compound **10** was hydrogenated in methanol over palladized charcoal, yielding an oily mixture of dihydro derivatives. This crude product gave a poorly-resolved p.m.r. spectrum which was not identical to that of crystalline **7**. When a solution of the dihydro products was passed through a column of alumina, or simply stirred in contact with basic alumina, hydroxy ketone **7**, m.p. 88–89°, $[\alpha]_D^{CHCl_3}$ −16° was isolated in 32% yield.

The crude mother liquors remaining after the above treatment contained mainly *trans*-dihydro-*epi*-carrisone (**11**), an oil having $[\alpha]_D^{CHCl_3}$ +40°. Compound **11** was also obtained by reduction of *epi*-carrisone (**10**) with lithium in ammonia.

The dramatic transformation brought about by exposure to basic alumina of the oily mixture initially isolated after hydrogenation of *epi*-carrisone can be attributed to equilibration of the new axial, secondary methyl groups to their more stable epimeric positions.

The formation of the less stable *trans*-fused epimer **12** is expected, since this results from *cis*-delivery of hydrogen. However, the initial production of the less stable epimer **6** in the *cis*-series is at first sight surprising, since this stereochemistry implies *trans*-addition of hydrogen. Overall *trans*-addition can be achieved by initial 1,4-addition, followed by kinetic protonation of the resultant enol (see Scheme 3).

A more complicated mechanism for formation of **6**, involving prior double-bond isomerization, followed by hydrogenation, was ruled out by the following experiment. Catalytic *deuteration* of **10** yielded a mixture of hydroxy ketones which was stirred with methanolic sodium methoxide to epimerize the first formed products and also to assure exchange of the α-positions. Mass spectral analysis of the recrystallized, deuterated **7** showed the presence of only a single deuterium atom, presumably at the angular position.

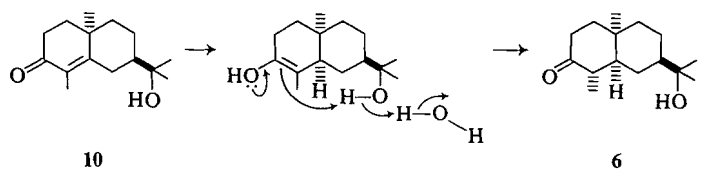

SCHEME 3

Can. J. Chem. Downloaded from www.nrcresearchpress.com by 210.87.254.6 on 09/05/12
For personal use only.

Can. J. Chem. Downloaded from www.nrcresearchpress.com by 210.87.254.6 on 09/05/12
For personal use only.

With the absolute stereostructure of (±)-occidentalol secured to our satisfaction, we set about to prepare the sesquiterpene by total synthesis. Our initial approach to the synthesis was based on a consideration of the stereochemistry of occidentalol (**2**) and its double-bond isomer **13**. Since occidentalol is a *cis*-fused decalin, it may exist in a conformation, **2***a*, in which the bulky isopropylol group occupies an equatorial position. Isomer **13**, on the other hand, is constrained to a single conformation, in which the isopropylol group is axial. From this consideration, it is clear that occidentalol

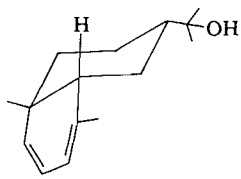

2*a*[2]

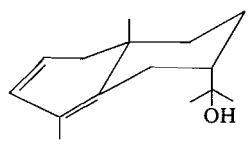

13[2]

should be more stable than isomer **13** (or the *trans*-fused isomer corresponding to **2**). It appeared attractive, therefore, to examine the isomerization of compound **13**, which was prepared in quantitative yield from *epi*-carrisone (**10**) by Shapiro's modification of the Bamford–Stevens reaction (12).

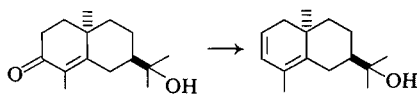

10 **13**

When diene **13** was treated under acidic conditions, only extensive degradation was observed. When **13** was treated with potassium *t*-butoxide in dimethylsulfoxide at 80°, there was no reaction. At 115°, some change occurred, but no occidentalol was formed (monitored by watching the δ 5.0–6.5 region in the p.m.r. spectrum, where occidentalol has a highly characteristic vinyl absorption pattern).

In order to test the stability of occidentalol itself under these conditions, it was heated with potassium *t*-butoxide in hexadeuteriodimethylsulfoxide at 80° for 50 h. After this period, the occidentalol was recovered in good yield, and extensive deuteration had occurred (20% d_3, 46% d_4, 30% d_5, and 4% d_6).

Having been thwarted in this attempt to prepare occidentalol from *epi*-carrisone, we turned to a less direct route. *cis*-Dihydro-*epi*-carrisone (**7**), prepared as outlined above, was subjected to the modified Bamford–Stevens reaction (12), to obtain the crystalline unsaturated alcohol **14** in 75% yield (see Scheme 4). This olefin reacted with bromine in CCl_4 to yield a dibromide (**15**, quantitative yield), which was dehydrobrominated by heating in 2,6-lutidine at 135° for 1 h. The product, obtained in 83% yield, was a mixture of (+)-occidentalol (**2**) and its isomer **16**, in a ratio of 55:45. The synthetic (+)-occidentalol, $[\alpha]_D^{CHCl_3}$ +313°, was indistinguishable from natural (+)-occidentalol by p.m.r., i.r., and v.p.c. mobility. The structure of isomer **16** was assigned on the basis of its spectra and empirical formula ($C_{15}H_{24}O$), determined by high resolution mass spectrometry.

The dehydrobromination of dibromide **15** was also accomplished with ethanolic KOH and with pyridine; similar ratios of **2** and **16** were obtained. Lithium dimethylpiperidide in hexane converted dibromide **15** back into olefin **14**.

Although the ratio of **2** to **16** was not changed

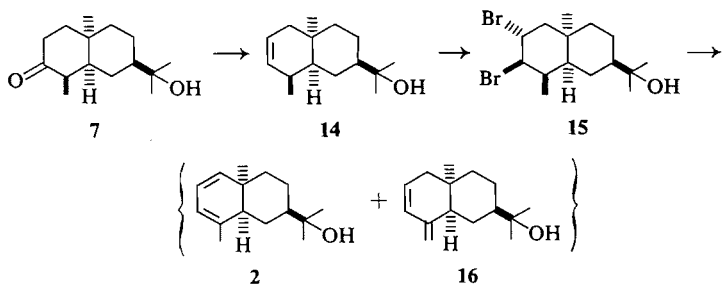

7 **14** **15**

2 **16**

SCHEME 4

[2]Enantiomeric projections have been used to more clearly illustrate the stereochemical point being made.

upon heating the mixture with potassium *t*-butoxide in dimethylsulfoxide, the percentage of occidentalol in the mixture did increase when it was treated in refluxing tetrahydrofuran with a trace of HCl. However, quantitative v.p.c. showed that this enhancement resulted from preferential destruction of **16**, rather than from conversion of **16** to **2**.

Experimental

All melting points are uncorrected. All p.m.r. spectra were measured on a Varian T-60 spectrophotometer.[3] Chemical shifts are given in p.p.m. downfield from internal tetramethylsilane. The i.r. spectra were measured on Perkin–Elmer 137 and 237 Infrared Spectrophotometers. Mass spectra were determined on a Consolidated 110 High Resolution Mass Spectrometer. Microanalyses were performed by the University of California Microanalytical Laboratory, Berkeley, California.

7β-(2-Hydroxy-2-propyl)-1,4aα-dimethyl-8aα-decahydronaphth-2-ol (5)

Dihydrooccidentalol (**4**) prepared by the method of von Rudloff and Erdtmann (3), was hydroborated by the method of Zweifel and Brown (13). From 1.9 g of unsaturated alcohol **4** was obtained 1.74 g of diol **5** (90% yield). The non-crystalline mixture was used directly in subsequent transformations.

7β-(2-Hydroxy-2-propyl)-1β,4aα-dimethyl-3,4,4a,5,6,7,8aα-octahydronaphthalen-2(1H)-one (7)

To a magnetically-stirred solution of 200 mg diol mixture **5** in 8.5 ml dry methylene chloride was added in one portion 430 mg red bispyridinechromium(VI) oxide (9). After stirring for 5 min, the supernatant liquid was decanted and the dark, tarry residue remaining was washed twice with 10 ml portions of ether. The combined organic fractions were washed successively with dilute, aqueous NaOH, dilute hydrochloric acid, and saturated brine. After drying over anhydrous $MgSO_4$, the solvent was removed to obtain 104 mg yellow oil, which gave a poorly resolved p.m.r. spectrum. Several rapid filtrations of a CCl_4 solution of this material through neutral alumina afforded 65 mg of a colorless oil which crystallized upon standing. The p.m.r. spectrum of this crystalline material was well resolved and completely different from that of the crude product. Recrystallization from hexane yielded material of analytical purity, m.p. 89–90°, $[\alpha]_D^{CHCl_3}$ −18°. The p.m.r. in CCl_4: δ 0.19 (C-1 Me, d, $J = 7$ Hz), 1.11 (*i*-propyl Me, s), 1.31 (angular Me, s); i.r. in CCl_4: 3400, 1700 cm^{-1}.

Anal. Calcd. for $C_{15}H_{26}O_2$: C, 75.58; H, 10.99. Found: C, 75.40; H, 11.11.

(+)-5β-(2-Hydroxy-2-propyl)-2α-methylcyclohexanone (8)

A 50 g sample of (+)-dihydrocarvone (**3**) was added in one portion to a stirred solution of 104 g mercuric acetate in 360 ml water and 360 ml THF (10). Characteristic decolorization occurred after 20 s. After 7 min, 360 ml of 3 *M* aqueous NaOH was added, followed by 360 ml 0.3 *M* $NaBH_4$ in 3 *M* aqueous NaOH.[4] The product was isolated in the normal way by extraction into ether. After stirring over 20 g basic alumina (to remove the residual, finely dispersed mercury), the solvent was removed to obtain 52 g (93%) of keto alcohol **8** as a colorless oil, which was used without further purification. The p.m.r. in CCl_4: δ 0.97 (Me, d, $J = 6$ Hz), 1.18 (*i*-propyl Me, s).

8aα-Hydroxy-7β-(2-hydroxy-2-propyl)-1β,4aα-dimethyl-octahydronaphthalen-2(1H)-one (9)

To a well-stirring solution of 52 g ketone **8** in 110 ml ether at 0°, under nitrogen, was added a solution of 3.8 g KOH in 12 ml 95% ethanol. After 10 min, 13 g ethyl vinyl ketone in 75 ether was added dropwise over a period of 1 h. Stirring was continued at 0° for an additional 1 h, then at 25° for 1.5 h, during which time considerable quantities of product **9** precipitated. The reaction mixture was concentrated to approximately one-half volume (vacuum) and the resulting precipitate isolated by filtration.[5] The solid was taken up in ethyl acetate, washed twice with water and once with brine. The aqueous washes were extracted once with ether and the organic portions were combined. The solvent was evaporated from the crude solution on a steam bath at atmospheric pressure until crystals began to appear. Compound **9** was obtained as colorless needles, m.p. 189–190°. The yield was 13.0 g (31%). The p.m.r. in CH_3OH: δ 0.99 (Me, s), 1.02 (Me, d, $J = 7$ Hz), 1.10 (Me, s); i.r. in KBr: 3500, 1690 cm^{-1}.

Anal. Calcd. for $C_{15}H_{26}O_3$: C, 70.83; H, 10.30. Found: C, 70.55; H, 10.15.

7β-(2-Hydroxy-2-propyl)-1β,4aα-dimethyl-4,4a,5,6,7,8-hexahydronaphthalen-2(3H)-one (epi-Carrisone (10))

A solution of 27 g keto-diol **9** in 600 ml THF was treated with 10 ml concentrated hydrochloric acid. After refluxing for 2 h, the solution was cooled and concentrated to 100 ml under reduced pressure. The concentrated solution was diluted with 400 ml ether and washed with 30% aqueous NaOH until the aqueous phase remained basic. After back-extraction of the aqueous washes with ether, the combined organic phases were washed with brine, dried, and evaporated under reduced pressure. The resultant oil was seeded with crystalline *epi*-carrisone, which had been previously obtained by chromatography of 6.5 g of the crude product (11). The solid obtained in this way was recrystallized from hexane – ethyl acetate to give 18.5 g (74% yield) of crystalline ketone **10**, m.p. 54–56° (lit. (13) m.p. 56°). The n.m.r. in CCl_4: δ 1.12 (angular Me, s), 1.22 (Me, s), 1.23 (Me, s), 1.74 (vinyl Me, s); i.r. in CCl_4: 3400, 1660 cm^{-1}.

[3]We thank the Dupont Company and the Research Committee, Berkeley Division, University of California, for the purchase of this instrument.

[4]Brown and Geohagen's procedure (10) calls for 0.5 *M* $NaBH_4$ in 3 *M* aqueous NaOH. However, some carbonyl reduction was observed when such a concentration was utilized in the present experiment.

[5]When these original mother liquors were washed several times with water and the volatile material evaporated under reduced pressure, a residue containing mostly ketone **8** was obtained. This oil could be resubmitted to the annelation reaction with ethyl vinyl ketone to give better yields of keto-diol **9** (greater than 50%) than were obtained using pure **8**.

Can. J. Chem. Downloaded from www.nrcresearchpress.com by 210.87.254.6 on 09/05/12
For personal use only.

TABLE 1. Catalytic hydrogenation of *epi*-carrisone

Run	Catalyst/solvent	Product ratio (7/11)	Method of analysis
(1)	10% Pd–C/95% ethanol	3:2	p.m.r.*
(2)	10% Pd–C/95% ethanol with a trace of KOH	1:1	p.m.r.*
(3)	10% Pd–C/ethyl acetate	2:1‡	p.m.r.;* v.p.c.†
(4)	10% Pd–C/acetic acid	4:1§	v.p.c.
(5)	10% Pd–C/95% ethanol with a trace of HCl	2:1	p.m.r.*
(6)	10% Pd–C/methanol	3:2	p.m.r.*
(7)	10% Pd–C/methanol with 5% (by weight) acidic Al_2O_3	3:1§	p.m.r.*
(8)	Rh–Al_2O_3/hexane	1:4§	p.m.r.*
(9)	Pt–C/95% ethanol	Complex mixture‖	p.m.r.*

*Estimates of *cis* to *trans* ratios were made by comparison of the relative areas of the isopropyl methyl peaks at δ 1.11 and 1.19, respectively.

†The v.p.c. analyses were made on the previously trimethylsilylated compounds.

‡This run gave 40% reduction of the carbonyl, which was not included in the *cis*/*trans* ratio.

§Although hydrogenation in acetic acid (run 4) gave the maximum *cis*/*trans* ratio, experience has shown that for ease of work-up and for optimum recovery of pure, crystalline *cis* isomer **7**, reduction in methanol with acidic alumina (run 7) is the method of preference.

‖This mixture probably includes products resulting from reduction of the carbonyl and hydrogenolysis.

7β-(2-Hydroxy-2-propyl)-1β,4aα-dimethyl-3,4,4a,5,6,7,-8,8aα-octahydronaphthalen-2(1H)-one (cis-Dihydro-epi-carrisone (7)) and 7β-(2-Hydroxy-2-propyl)-1β,4aα-dimethyl-3,4,4a,5,6,7,8,8aβ-octahydronaphthalen-2(1H)-one (trans-Dihydro-epi-carrisone (11))

A 4.79 g sample of *epi*-carrisone (**10**) in 100 ml absolute methanol was hydrogenated at atmospheric pressure over a mixture of 1.2 g acidic alumina and 0.2 g 10% palladium-on-carbon. Consumption of hydrogen ceased abruptly after the uptake of 1 *M* equiv. (500 ml hydrogen in 50 min). The reaction mixture was filtered and 2 ml water added to hydrolyze a small amount of methyl ketal (comprising about 5% of the product, as estimated by p.m.r.), which was observed to have formed in previous runs. After 2.5 h at room temperature, the reaction mixture was concentrated to 10 ml and partitioned between water and ether. The organic layer was washed with brine, dried, and evaporated. The crude crystalline product was obtained in quantitative yield. The crude material was shown by v.p.c. analysis to consist of a 3:1 mixture of *cis* and *trans*-dihydro-*epi*-carrisones (**7** and **11**, respectively). This conclusion was corroborated by comparison of the relative peak heights of the respective isopropylol methyl groups of **7** and **11** in the p.m.r. spectrum of the mixture (δ 1.11 for **7**, 1.19 for **11**).

By a combination of column chromatography (silica gel) and fractional crystallization, crystalline **7** was obtained; 2.09 g (43% yield), m.p. 88.5–89.5°, $[\alpha]_D^{CHCl_3}$ −18°. This material was identical by p.m.r., i.r., v.p.c. retention time, mixture m.p. and optical rotation with ketol prepared from (+)-occidentalol.

Anal. Calcd. for $C_{15}H_{26}O_2$: C, 75.58; H, 10.99. Found: C, 57.83; H, 10.98.

The structure assignment for the other product of this hydrogenation, **11**, was made on the basis of its p.m.r. spectrum, which was superimposable upon the p.m.r. spectrum of an authentic sample of **11** (see below), and its indistinguishability from authentic **11** by v.p.c.

Various other hydrogenation conditions were explored and are summarized in Table 1.

7β-(2-Hydroxy-2-propyl)-1β,4aα-dimethyl-3,4,4a,5,6,7,-8,8aβ-octahydronaphthalen-2(1H)-one (trans-Dihydro-epi-carrisone (11))

A solution of 0.4 g *epi*-carrisone (**10**) in 3 ml dry THF was added in one portion to 0.025 g lithium metal dissolved in 20 ml ammonia (freshly distilled from sodium). After 50 min, enough ammonium chloride was added to discharge the blue color, followed by enough dilute aqueous hydrochloric acid to acidify the solution to litmus. The mixture was extracted several times with ether and the combined ether extracts were washed with brine, dried, and evaporated under reduced pressure. *trans*-Dihydro-*epi*-carrisone was obtained as an oil; 0.353 g (88%). The analytical sample was obtained by preparative v.p.c. on a Carbowax column. The analytically pure material could not be crystallized from various proportions of ethyl acetate and hexane; $[\alpha]_D^{CHCl_3}$ +40°; p.m.r. in CCl_4: δ 0.95 (Me, d, J = 6 Hz), 1.08 (Me, s), 1.19 (*i*-propyl Me, s); i.r. in CCl_4: 3400, 1680 cm^{-1}.

Anal. Calcd. for $C_{15}H_{26}O_2$: C, 75.58; H, 10.99. Found: C, 75.85; H, 10.75.

7β-(2-Hydroxy-2-propyl)-1,4aα-dimethyl-4,4a,5,6,7,8-hexahydronaphthalene (13)

A 0.20 g sample of *epi*-carrisone (**10**) (11) 0.16 g *p*-toluenesulfonylhydrazide, and 1 drop concentrated hydrochloric acid was added to 10 ml tetrahydrofuran and the mixture was refluxed for 30 h. The mixture was then diluted with 10 ml benzene and distilled until all the tetrahydrofuran and benzene–water azcotrope had been collected and the b.p. had reached 80°. The remaining solution was cooled to 0°, under nitrogen, and diluted with 5 ml dry tetrahydrofuran. Ethereal methyllithium was added (1.8 ml of a 1.6 *M* solution), and the red reaction mixture was stirred for 2 h at room temperature. Excess methyllithium was de-

Can. J. Chem. Downloaded from www.nrcresearchpress.com by 210.87.254.6 on 09/05/12
For personal use only.

Can. J. Chem. Downloaded from www.nrcresearchpress.com by 210.87.254.6 on 09/05/12
For personal use only.

stroyed by the addition of 10 ml water, and the layers were separated. The aqueous layer was extracted several times with pentane. After drying, the combined organic solutions were evaporated to yield 0.19 g (99% yield) of diene **13**, as a slightly yellow oil, which was used directly without further purification. The p.m.r. in CCl_4: δ 0.91 (angular Me, s), 1.07 (Me, s), 1.13 (Me, s), 1.71 (vinyl Me, s); i.r. in CCl_4: 3400 cm^{-1}.

7β-(2-Hydroxy-2-propyl)-1β,4aα-dimethyl-1,4,4a,5,6,7,8,-8aα-octahydronaphthalene (14)

A 0.200 g sample of *cis*-dihydro-*epi*-carrisone (**7**) (1) in 20 ml tetrahydrofuran together with 0.147 g *p*-toluenesulfonylthydrazide and 2 drops concentrated hydrochloric acid was refluxed for 7 h on a steam bath. The nearly colorless reaction mixture was cooled and washed twice with 2 ml portions of saturated brine. The organic layer was diluted with 10 ml ether and 20 ml benzene and distilled until the b.p. reached 80°. The reaction flask was sealed with serum stoppers, cooled to 0°, and 5 ml of tetrahydrofuran was introduced. Ethereal methyllithium (3 ml of a 1.6 *M* solution) was added by syringe and the mixture was kept for 10 min at 0°. The cooling bath was then removed and the mixture was stirred at room temperature for 2.5 h, at which time gas evolution had ceased. The resultant brown mixture was treated cautiously with 5 ml water and then 3 ml pentane. The phases were then separated and the aqueous portion extracted twice with pentane. The combined organic phases were dried and evaporated to obtain 0.190 g of a lightly colored glass. Chromatography on 7 g silica gel yielded 0.138 g unsaturated alcohol **14** (75% yield) as a white solid, m.p. 75.5–76.5°, $[\alpha]_D^{CHCl_3}$ +54°; p.m.r. in CCl_4: δ 0.90 (Me, s), 0.95 (Me, d, J = 7 Hz), 1.08 (*i*-propyl Me, s), 5.25 (H-2 and -3, unresolved m); i.r. in CCl_4: 3400 cm^{-1}.

Anal. Calcd. for $C_{15}H_{26}O$: C, 81.02; H, 11.79. Found: C, 80.77; H, 11.84.

2β,3α-Dibromo-7β-(2-hydroxy-2-propyl)-1β,4aα-dimethyl-8aα-decahydronaphthalene (15)

To a 0.42 g sample of unsaturated alcohol **14** in 20 ml carbon tetrachloride at 0° was added a solution of 0.35 g bromine in 1 ml carbon tetrachloride. The reaction mixture was stirred for 2.5 h at 0°. The cooling bath was then removed and 0.5 ml water and sufficient sodium hydrogen sulfite to quench the excess bromine were added. The mixture was diluted with 50 ml pentane and washed with 5 ml portions of water, saturated aqueous sodium bicarbonate and brine. After drying and evaporation at reduced pressure, dibromide **15** was obtained in quantitative yield (0.75 g). The p.m.r. in CCl_4: δ 1.11 (*i*-propyl Me, s), 1.13 (Me, d, J = 7 Hz), 1.33 (Me, s), 4.58 (CBr—*H*, m, $w_{1/2}$ = 10 Hz), 4.97 (CBr—*H*, m, $w_{1/2}$ = 10 Hz); i.r. in CCl_4: 3300 cm^{-1}. This crude product was used in the succeeding transformation with further purification.

(+)-7β-(2-Hydroxy-2-propyl)-1,4aα-dimethyl-4a,5,6,7,8,-8aα-hexahydronaphthalene ((+)-occidentalol (2)) and 7β-(2-Hydroxy-2-propyl)-4aα-methyl-1-methylene-1,4,4a,5,6,7,8,8aα-octahydronaphthalene (16)

A solution of 0.626 g dibromide **15** in 9 ml freshly distilled 2,6-lutidine was heated in an oil bath at 133–135° for 1 h. During the heating period, the mixture darkened and lutidine hydrobromide precipitated. The reaction mixture was cooled to room temperature and decanted. After washing the solid residue with 40 ml of pentane, the combined organic solutions were diluted with more pentane to a total volume of 70 ml. The solution was washed with 15% aqueous hydrochloric acid until the wash remained acidic (five 10 ml portions), and the combined aqueous washes were extracted with pentane. The organic fractions were combined, washed with 5 ml 0.1 *M* aqueous NaOH, dried, and evaporated. The product was 0.298 g (82.5%) of pale yellow semi-solid, shown by v.p.c. analysis (3 ft × 1/4 in. Carbowax, 190°) to be a 55:45 mixture of (+)-occidentalol (**2**) and its isomer **16**. Analytical samples were obtained by preparative v.p.c. on the aforementioned column.

The synthetic (+)-occidentalol so obtained was identical to natural (+)-occidentalol by p.m.r. and i.r. spectroscopy and by v.p.c. and t.l.c. mobility. The synthetic material, collected by preparative v.p.c., melted over the range 86.5–92° (lit. (3) 97.5–98°, 95.2–95.6°). The m.p. of an authentic sample of (+)-occidentalol, generously supplied to us by Professor Erdtmann, m.p. 92–93°, was not depressed in admixture with the synthetic material. Our synthetic (+)-occidentalol had $[\alpha]_D^{CHCl_3}$ +313° (lit. (3) $[\alpha]_D^{CHCl_3}$ +361°). The authentic sample supplied us by Professor Erdtmann had $[\alpha]_D^{CHCl_3}$ +327°.

Anal. *m/e* for $C_{15}H_{24}O$: 220.1830.

The structural assignment for the isomeric product was made on the basis of its empirical formula, p.m.r. spectrum and i.r. spectrum; $[\alpha]_D^{CHCl_3}$ −67.7°; p.m.r. in CCl_4: δ 0.83 (Me, s), 1.14 (*i*-propyl Me, s), 4.71 (=CH_2, m); i.r. in CCl_4: 3400 cm^{-1}.

Anal. *m/e* for $C_{15}H_{24}O$: 220.1843.

We acknowledge financial support by the National Science Foundation, the Public Health Service, and the Alfred P. Sloan Foundation. We also thank Professor H. Erdtmann for a generous gift of (+)-occidentalol.

1. T. Nakatsuka and Y. Hirose. Bull. Agric. Chem. Soc. Jap. **20**, 215 (1956).
2. Y. Hirose and T. Nakatsuka. Bull. Agric. Chem. Jap. **23**, 140 (1959).
3. E. von Rudloff and H. Erdtmann. Tetrahedron, **18**, 1315 (1962).
4. K. Mislow and A. Moscowitz. Tetrahedron Lett. 699 (1963).
5. H. Ziffer, T. J. Batterham, U. Weiss, and E. von Rudloff. Tetrahedron, **20**, 67 (1964).
6. A. G. Hortmann and J. B. De Roos. J. Org. Chem. **34**, 736 (1969).
7. M. Sergent, M. Mongrain, and P. Deslongchamps. Can. J. Chem. This issue.
8. M. Ando, K. Nanaumi, T. Nakagawa, T. Asao, and K. Takase. Tetrahedron Lett. 3891 (1970).
9. J. C. Collins, W. W. Hess, and F. J. Frank. Tetrahedron Lett. 3363 (1968).
10. H. C. Brown and P. Geohagen. J. Am. Chem. Soc. **89**, 1522 (1967).
11. A. Asselin, M. Mongrain, and P. Deslongchamps. Can. J. Chem. **46**, 2817 (1968).
12. R. H. Shapiro. Tetrahedron Lett. 345 (1968).
13. G. Zweifel and H. C. Brown. Organic reactions. Vol. 13. Wiley. New York, N.Y., 1963. p. 31.

The Relative Rates of the Reaction of Active Nitrogen with Perfluoro-olefins and Perfluorobutyne-2[1]

M. RUJIMETHABHAS[2] AND W. E. JONES
Department of Chemistry, Dalhousie University, Halifax, Nova Scotia

Received March 12, 1971[3]

A formulation of the diffusion-kinetic model based on the spherical diffusion flame method is presented and discussed. The application of this technique has been made to obtain the relative rates of the reaction of active nitrogen with perfluoroethylene, perfluoropropene, perfluorobutadiene-1,3, and perfluorobutyne-2.

Une mise en formule du modèle de diffusion cinétique, fondé sur la méthode de la flamme à diffusion sphérique, est présentée et discutée. L'application de cette technique a servi à déterminer les vitesses relatives de la réaction entre l'azote actif et le perfluoroéthylène, le perfluoropropène, le perfluorobutadiène-1,3, et le perfluorobutyne-2.

Canadian Journal of Chemistry, **50**, 346 (1972)

Introduction

The reaction of active nitrogen with unsaturated perfluorocarbons has been found to produce a large number of products (1). Three of these, N_2O, probably produced by the action of N_2F_2 on the glass walls, FCN, and a polymer are the only products found to contain nitrogen. FCN and N_2O appear in negligibly small amounts. It is difficult in such a complicated system to study the kinetics by the usual methods. Since these reactions give very bright spherical flames with active nitrogen it was felt that the diffusion flame method could be applied to these reactions.

The spherical diffusion flame technique was first developed by Hartel and Polanyi (2). It has since been investigated by a number of workers and several reviews have been published (3–5) on the method. It has been applied to study the kinetics of the reaction of active nitrogen with ethylene by Greenblatt and Winkler (6) and later by Milton and Dunford (7). Both reports were based on the assumption that the rate constant obtained was due only to the primary reaction. Heller (8) has made a significant contribution by investigating the errors involved in the diffusion flame method and discussed many aspects of experimental conditions. The theory of the experimental method has also been studied by Reed and Rabinovitch (9, 10). The application has been extended by Garvin, Guinn, and Kistiakowsky (11, 12) to study the kinetics by mapping the steady state temperature pattern of the reaction zone, thereby providing a method for studying the kinetics of reactions which are not accompanied by a flame or other means of visual detection.

In applying the diffusion flame method, in which the visual boundaries of the flame are used to calculate the reaction rate, it is necessary that the chemical reaction follows the light emission. This is very likely true for the reactions of alkanes and alkenes with active nitrogen where the reactions proceed to complete consumption of the reactive species (13, 14). However, in certain reactions, for example active nitrogen $+C_2N_2$, reactive species have been found to be present after the light emitting reactions are complete (15). In the present study we have assumed that the flame produced in the reaction of active nitrogen with fluorocarbons is representative of the reaction.

Experimentally, one reactant (referred to here as the nozzle reactant) is carried by an inert gas and allowed to escape through a nozzle into the center of the reaction vessel containing a constant flow of the second reactant, normally known as the atmosphere reactant. The conditions of the experiment are adjusted so that the nozzle reactant reacts as it diffuses into the atmosphere reactant giving a reaction zone which has spherical symmetry.

In the treatment of Hartel and Polanyi the following simplifying assumptions were introduced: (*1*) There is a spherical symmetric dis-

[1]Presented at the 54th Annual Conference of the Chemical Institute of Canada, Halifax, Nova Scotia, 1971.
[2]Holder of Colombo Plan Scholarship.
[3]Revision received October 4, 1971.

Can. J. Chem. Downloaded from www.nrcresearchpress.com by 210.87.254.42 on 09/05/12
For personal use only.

Can. J. Chem. Downloaded from www.nrcresearchpress.com by 210.87.254.42 on 09/05/12
For personal use only.

tribution of the nozzle reactant in the reaction zone. (*2*) The effect of convective flow is negligible. (*3*) The concentration of the atmosphere reactant is constant throughout the reaction zone.

Reed and Rabinovitch observed that the flame was distorted from spherical to slightly oval in shape when seen from the direction perpendicular to the flow axis. They attributed this effect to convective flow. This effect has been estimated to be small and generally is considered negligible (10, 12).

The case involving only two reactive species where the concentration of one is assumed to be constant as in the third assumption above, has been studied by previous workers. This treatment leads to a single differential equation as obtained by Hartel and Polanyi. An attempt to eliminate the third assumption, *i.e.* taking into consideration the depletion of atmosphere reactant, has been made by Cvetanovic and Le Roy (16, 17). Two simultaneous second order nonlinear partial differential equations have been derived, which unfortunately cannot be solved analytically. An approximate solution was obtained by a trial and error numerical computation. Later, Smith (18) succeeded in solving a similar set of differential equations as derived by Cvetanovic and Le Roy, in terms of tabulated functions by successive approximations.

The reaction of atomic sodium with fluorinated methyl chlorides, where more than two reactive species are present has been discussed by Reed and Rabinovitch (9, 10). In this case they were able to obtain the overall rate constants for the reaction. The extent of the secondary reactions could be estimated by the ratio of NaCl:NaF formed as products. From this information corrections to the overall rate constants could be made, yielding the primary rate constants.

So far no attempt has been made to formulate a diffusion-kinetic model for the spherical diffusion flame for the case of more than two reactive species. In order to discuss the application of the diffusion flame method to the active nitrogen–fluorocarbon reactions, such formulation is necessary.

The derivation follows from the general equation of continuity for a chemical reaction in an isothermal system and an isotropic medium (19, 20, *cf.* 9–10):

$$[1]\quad \partial C/\partial t = D \text{ div grad } C - (\mathbf{v} \text{ grad } C) + q$$

where D = diffusion coefficient; $\mathbf{v}$, the convection velocity; C, the concentration of the diffusing substance as a function of time and space; q, the chemical source term (the amount of material changed through chemical reactions per unit volume per unit time). If the effect of convective flow is neglected, the equation takes the following form, *cf.* Crank (21) and Frank-Kamenetskii (20):

$$[2]\quad \partial C/\partial t = D\nabla^2 C + q$$

writing div grad $\equiv \nabla^2$ = Laplacian operator.

The reaction of active nitrogen with perfluoroethylene has been investigated and the following *principal* reaction steps have been proposed by Madhavan and Jones (1):

$$[3]\quad C_2F_4 + N \xrightarrow{k_3} CF_2N + CF_2$$

$$[4]\quad C_2F_4 + N \xrightarrow{k_4} FCN + CF_3$$

$$[5]\quad CF_2N \xrightarrow{k_5} FCN + F$$

$$[6]\quad CF_2 + N \xrightarrow{k_6} FCN + F$$

$$[7]\quad CF_3 + N \xrightarrow{k_7} FCN + 2F$$

$$[8]\quad C_2F_4 + FCN \xrightarrow{k_8} (C_3F_5N)\text{ polymer}$$

By application of [2], the diffusion-kinetic equations describing reactions 3 through 8 are given by [9], *cf.* (22) and its previous references,

$$[9]\quad \begin{cases} \partial P_{C_2F_4}/\partial t = D_{C_2F_4}\nabla^2 P_{C_2F_4} - k_3 P_{C_2F_4}P_N \\ \qquad - k_4 P_{C_2F_4}P_N - k_8 P_{C_2F_4}P_{FCN} \\ \partial P_N/\partial t = D_N\nabla^2 P_N - k_3 P_{C_2F_4}P_N \\ \qquad - k_4 P_{C_2F_4}P_N - k_6 P_N P_{CF_2} - k_7 P_N P_{CF_3} \\ \partial P_{CF_2N}/\partial t = D_{CF_2N}\nabla^2 P_{CF_2N} \\ \qquad + k_3 P_{C_2F_4}P_N - k_5 P_{CF_2N} \\ \partial P_{CF_2}/\partial t = D_{CF_2}\nabla^2 P_{CF_2} \\ \qquad + k_3 P_{C_2F_4}P_N - k_6 P_N P_{CF_2} \\ \partial P_{CF_3}/\partial t = D_{CF_3}\nabla^2 P_{CF_3} \\ \qquad + k_4 P_{C_2F_4}P_N - k_7 P_N P_{CF_3} \\ \partial P_{FCN}/\partial t = D_{FCN}\nabla^2 P_{FCN} + k_4 P_{C_2F_4}P_N \\ \qquad + k_5 P_{CF_2N} + k_6 P_N P_{CF_2} \\ \qquad + k_7 P_N P_{CF_3} - k_8 P_{C_2F_4}P_{FCN} \end{cases}$$

where P_i is the partial pressure of the ith species.

$$\nabla^2 \equiv \frac{\partial^2}{\partial r^2} + \frac{2}{r}\frac{\partial}{\partial r}$$

for spherical symmetry. This set of simultaneous second order non-linear partial differential eqs. 9 are representative of the species predicted in the overall mechanism. While [9] cannot be solved analytically, in principle, the numerical integration should be possible. However, the limitation has been set in the present study by inadequate knowledge of many of the parameters *e.g.* many unknown D's and k's. Without such information the model is too flexible and any number of sets of values might be substituted to reproduce the experimental data. This includes the variation of the k's which are normally constants. In addition, since a truly comprehensive mechanistic study has not been made for the active nitrogen–fluorocarbon reactions, other mechanistic interpretations might be possible and these would affect the flexibility of the model in the same manner as the unknown D's and k's. Because of these difficulties we have attempted to assume without loss of (mechanistic) generality, a simplified mechanism as follows:

[10] $$C_2F_4 + N \xrightarrow{k_{10}} FCN + CF_3$$

[11] $$CF_3 + N \xrightarrow{k_{11}} FCN + 2F$$

[12] $$C_2F_4 + FCN \xrightarrow{k_{12}} (C_3F_5N)\text{polymer}$$

The diffusion-kinetic equations corresponding to eqs. 10–12 are:

[13] $$\partial P_{C_2F_4}/\partial t = D_{C_2F_4}\nabla^2 P_{C_2F_4} - k_{10}P_{C_2F_4}P_N - k_{12}P_{C_2F_4}P_{FCN}$$

[14] $$\partial P_N/\partial t = D_N\nabla^2 P_N - k_{10}P_{C_2F_4}P_N - k_{11}P_{CF_3}P_N$$

[15] $$\partial P_{CF_3}/\partial t = D_{CF_3}\nabla^2 P_{CF_3} + k_{10}P_{C_2F_4}P_N - k_{11}P_{CF_3}P_N$$

[16] $$\partial P_{FCN}/\partial t = D_{FCN}\nabla^2 P_{FCN} + k_{10}P_{C_2F_4}P_N + k_{11}P_{CF_3}P_N - k_{12}P_{C_2F_4}P_{FCN}$$

Even with the simplified mechanism, these partial differential equations cannot be integrated analytically. Again there are many parameters which are not known. Since we know only the boundary conditions of the original reactants, *i.e.* $P_{C_2F_4}$ and P_N, it is only possible for us to further develop eqs. 13 and 14. For the steady reaction at any spatial position in the reaction volume, $\partial P_i/\partial t = 0$, so that at any instant it is possible to write:

$$k_{12}P_{C_2F_4}P_{FCN} = ak_{10}P_{C_2F_4}P_N$$

$$k_{11}P_{CF_3}P_N = bk_{10}P_{C_2F_4}P_N$$

where a and b are constants, and eqs. 13 and 14 take the following form:

$$D_{C_2F_4}\nabla^2 P_{C_2F_4} - (1+a)k_{10}P_{C_2F_4}P_N = 0$$

$$D_N\nabla^2 P_N - (1+b)k_{10}P_{C_2F_4}P_N = 0$$

Replacing $(1+a)\,k_{10}$ by k_a and $(1+b)\,k_{10}$ by k_b, where k_a and k_b are apparent rate constants, the above equations can be expressed as:

[17] $$D_{C_2F_4}\nabla^2 P_{C_2F_4} - k_aP_{C_2F_4}P_N = 0$$

[18] $$D_N\nabla^2 P_N - k_bP_{C_2F_4}P_N = 0$$

If it is assumed that the partial pressure of nitrogen atoms is constant throughout the reaction zone (*cf.* the third assumption of Hartel and Polanyi) which is a reasonable assumption in view of the experimental conditions that, in all cases, the spherical flame is photographed against the yellow background of active nitrogen, *i.e.* atomic nitrogen is always present in excess. To this approximation [18] will disappear and [17] could be written, in the case of spherical symmetry as:

[19] $$D_{C_2F_4}\left(\frac{d^2P_{C_2F_4}}{dr^2} + \frac{2}{r}\frac{dP_{C_2F_4}}{dr}\right) - k_aP_{C_2F_4}P_N = 0$$

the approximate solution to [19] similar to that obtained by Hartel and Polanyi is

[20] $$k_a = \frac{(\ln P_f/P_0)^2}{d^2/4}\cdot\frac{D}{P_N}$$

where k_a = the apparent rate constant; P_f, the partial pressure of fluorocarbon at the jet; P_0, the partial pressure of fluorocarbon at the edge of the flame; P_N, the partial pressure of nitrogen atoms; d, the diameter of the flame; D, the diffusion coefficient. Equation 20 has been used to obtain the apparent rate constants for the present work. In the derivation of this equation, which is strictly true for a point source nozzle, the finite nozzle size has been neglected. However, this approximation should not intro-

Can. J. Chem. Downloaded from www.nrcresearchpress.com by 210.87.254.42 on 09/05/12
For personal use only.

Can. J. Chem. Downloaded from www.nrcresearchpress.com by 210.87.254.42 on 09/05/12
For personal use only.

duce significant errors in the calculated rate constants.

The physical meaning of k_a may need further clarification, k_a as it is derived from [13] is equivalent to $(1 + a)k_{10}$, and thus not only represents k_{10}, the desired rate constant, but an added quantity ak_{10}. The value ak_{10} is related to k_{12} as follows

$$ak_{10}P_{C_2F_4}P_N = k_{12}P_{C_2F_4}P_{FCN}$$

It is impossible to know the size of a, but it is probable that it is small, since depletion of C_2F_4 by [12] is the second step of a consecutive reaction scheme. Provided, therefore, that a is small $(1 + a)k_{10}$ reduces to k_{10} the desired rate constant.

Experimental and Instrumental Method

Perfluoroethylene was obtained by the decomposition of Teflon at 450 °C, the product was purified by passing through a gas chromatographic column of silica gel coated with 3% squalane, only that fraction identified as perfluoroethylene by i.r. (23) was collected. Perfluoropropene and perfluorobutyne-2 were obtained from Peninsular Chemresearch Inc., and Pierce Chemical Company, respectively. These were purified by bulb-to-bulb distillation. Perfluorobutadiene-1,3 was obtained from Pierce Chemical Company and was used without further purification. Gas chromatographic analysis of these gases indicated no impurity. Nitric oxide was obtained from Matheson of Canada Ltd., purified by condensation in and evaporation from ascarite (8–20 mesh). Purified nitrogen from Canadian Liquid Air Corp. was further purified by passing through a column of heated copper at 425 °C and through a liquid nitrogen trap. It was activated either by a glow discharge excited by a 125 W microwave unit operating at 2450 MHz and at a power output of 85% or by a condensed electric discharge.

The reaction was studied in a fast flow system similar to that described by Madhavan and Jones (24).

The concentration of nitrogen atoms was measured by the NO gas titration technique (25, 26). Molecular diameters of the various gases necessary for the calculation of D (27), were taken as 3.75, 5.6, 6.6, 6.4, and 6.2 Å for nitrogen (28), perfluoroethylene, perfluoropropene, perfluorobutyne-2, and perfluorobutadiene-1,3, respectively. The diameter of molecular rather than atomic nitrogen was used, since the amount dissociated was only a small percentage of the total concentration. The diameters of perfluoropropene, perfluorobutyne-2, and perfluorobutadiene-1,3 were obtained from viscosity measurements (29), while the diameter of perfluoroethylene was calculated from the known viscosity (30).

Results and Discussion

Table 1 presents the data necessary for the calculation of the apparent rate constants for the reaction of active nitrogen with the perfluorocarbons. Columns P_f and P_0 denote the partial pressures of perfluorocarbon at the jet and at the edge of the flame respectively. P_N is the partial pressure of nitrogen atoms; d is the diameter of the flame, and D is the diffusion coefficient of fluorocarbon into the gas mixture. The data obtained by both the condensed and microwave discharges for each reaction are tabulated, except for the reaction of perfluorobutyne-2 with active nitrogen produced by microwave discharge in which case it was impossible to measure the extremely low flow rate of perfluorobutyne-2 necessary to produce a spherical flame.

The average apparent rate constants for the reactions of active nitrogen with, perfluoroethylene (C_2F_4), perfluoropropene (C_3F_6), *trans*-perfluorobutene-2 (t-C_4F_8-2), perfluorobutadiene-1,3 (C_4F_6-1,3), and perfluorobutyne-2 (C_4F_6-2) are collected in Table 2.

The use of the diffusion flame technique to obtain the absolute rate constant is rather difficult as has been pointed out by Benson (31). The normal sources of errors are the effect of the convective flow, the exact mathematical treatment of which is rather remote. The effect of pressure of the nozzle reactant and the problem associated with the boundary conditions at the flame edge. These effects have been investigated and discussed at length by Reed and Rabinovitch. They have applied different formula for the evaluation of k, the overall rate constants; from their results the major difference among k's are about a factor of 2. The photographs of the flame, see *e.g.* (24), taken in the direction perpendicular to the flow axis for the reaction of active nitrogen with perfluoro-olefins are seen to have a reasonably sharp flame edge. The flame is spherical rather than oval in shape as is usually observed for the reaction of atomic sodium with alkyl halides.

Cvetanovic and Le Roy (16) have estimated that the error created by neglecting the effect of atmosphere depletion is about 20% for the reaction of sodium atoms with CH_3CH_2Cl.

The difficulty in estimating the absolute rate constant for the primary reaction when the process is accompanied by the secondary reactions could be even more pronounced as evidenced by the previous workers (9, 10). The present work also encounters a somewhat similar difficulty; apart from the fact that there are many parameters which are presently unknown,

TABLE 1. Data for the calculation of k*

10^3P_f† (Torr)	10^3P_0 (Torr)	10^3P_N (Torr)	d (cm)	$10^{-3}k$ ($Torr^{-1}\,s^{-1}$)	$10^{-10}k$ ($cc\,mol^{-1}\,s^{-1}$)
	$N + C_2F_4$		Condensed discharge		
	(Temperature 313 °K,‡ $D = 42.2\ cm^2\ s^{-1}$)				
4.80	0.045	95.8	1.75	12.5	24.3
4.94	0.045	95.8	1.75	12.7	24.9
5.19	0.045	95.8	2.06	9.4	18.3
5.31	0.045	95.8	2.31	7.6	14.7
	$N + C_2F_4$		Microwave discharge		
	(Temperature 301 °K,‡ $D = 41.3\ cm^2\ s^{-1}$)				
0.95	0.055	14.8	2.18	19.0	35.7
1.29	0.055	14.8	2.57	16.7	31.4
1.42	0.055	14.8	2.79	15.1	28.4
1.81	0.055	14.8	3.10	12.8	26.6
	$N + C_3F_6$		Condensed discharge		
	(Temperature 313 °K,‡ $D = 34.3\ cm^2\ s^{-1}$)				
1.67	0.109	95.9	2.46	1.8	3.5
2.21	0.109	95.9	2.87	1.6	3.1
2.81	0.109	95.9	2.77	2.0	3.8
3.77	0.109	95.9	3.35	1.6	3.1
	$N + C_3F_6$		Microwave discharge		
	(Temperature 298 °K,‡ $D = 31.9\ cm^2\ s^{-1}$)				
1.16	0.043	14.8	3.07	9.9	18.3
1.38	0.043	14.8	3.23	9.9	18.3
2.04	0.043	14.8	3.78	8.9	16.5
1.47	0.043	14.8	3.23	10.4	19.3
	$N + C_4F_6$-1,3		Condensed discharge		
	(Temperature 313 °K,‡ $D = 36.9\ cm^2\ s^{-1}$)				
0.17	0.01	95.8	1.22	8.3	16.3
0.20	0.01	95.8	1.35	7.6	14.9
0.61	0.01	95.8	2.41	4.5	8.8
0.84	0.01	95.8	2.72	4.2	8.1
	$N + C_4F_6$-1,3		Microwave discharge		
	(Temperature 298 °K,‡ $D = 34.4\ cm^2\ s^{-1}$)				
0.06	0.003	14.8	3.53	6.6	12.4
0.08	0.003	14.8	3.84	6.8	12.5
0.11	0.003	14.8	4.45	6.1	11.4
	$N + C_4F_6$-2		Condensed discharge		
	(Temperature 313 °K,‡ $D = 35.4\ cm^2\ s^{-1}$)				
0.47	0.018	95.8	1.47	7.2	14.1
0.52	0.018	95.8	1.57	6.7	13.1
0.67	0.018	95.8	1.75	6.2	12.2
0.95	0.018	95.8	1.80	7.2	14.1

*N_2 flow rate 188×10^{-6} mol s^{-1}; N flow rate for condensed discharge 10.6×10^{-6} mol s^{-1}; N flow rate for microwave discharge 1.6×10^{-6} mol s^{-1}; total pressure 1.75 Torr.
†P_f indicates partial pressure of fluorocarbon.
‡All temperatures are ±3°.

the accuracy in estimating the rate constant for the primary process will depend upon how well the evaluation of the rates for many secondary reactions steps are carried out.

Although the simplified mechanism used as a model to derive the diffusion-kinetic equations leaves out some of the steps in the principal mechanism, it is considered that such a model

Can. J. Chem. Downloaded from www.nrcresearchpress.com by 210.87.254.42 on 09/05/12
For personal use only.

TABLE 2. Average and relative values of apparent k from the reaction of active nitrogen with perfluorocarbons

Reaction	$k_{Average} \times 10^{-10}$ (cc mol^{-1} s^{-1})		$k_{Relative}$*	
	Condensed	Microwave	Condensed	Microwave
$N + C_2F_4$	20.5±6	30.5±6	8.2	5.8
$N + C_3F_6$	3.4±0.4	18.1±2	1.4	3.4
$N + t\text{-}C_4F_8\text{-}2$†	2.5±1	5.3±2	1.0	1.0
$N + C_4F_6\text{-}1,3$	12.0±4	12.1±1	4.8	2.3
$N + C_4F_6\text{-}2$	13.4±1	‡	5.4	

*The rate of *trans*-perfluorobutene-2 has been taken as unity.
†See ref. 24.
‡Unobtainable due to the difficulty in measuring the extremely small flow rates necessary to produce a spherical flame.

should be sensitive to the secondary reactions. Evidence which may be used to support such a position comes from the work of Herron and Huie (32) who estimate by mass spectrometry the absolute rate constant for the reaction of active nitrogen with *trans*-C_4F_8-2 at 500 °K to be $\leqslant 4 \times 10^9$ cc mol^{-1} s^{-1} which is less than the value estimated by the diffusion flame method (24) of 2.5×10^{10} cc mol^{-1} s^{-1} at 313 °K.

It has not been possible for us to obtain the absolute rate constant for the reaction of active nitrogen with perfluorocarbons for the reason given earlier, however, since they produce very similar products (1), it is probable that the reaction of various fluorocarbons have very similar mechanisms, and the relative rates should yield useful information about the reactivities of these compounds. We, therefore, calculate the relative rate constants using the value of *trans*-perfluorobutene-2 as reference. These values are also presented in Table 2.

From Table 2 it is evident that the reactions of active nitrogen with perfluorocarbons could be arranged in order of increasing reactivity as follows: $t\text{-}C_4F_8\text{-}2 < C_3F_6 < C_4F_6\text{-}1,3 < C_4F_6\text{-}2 < C_2F_4$.

It has been suggested by Chesick (33) that the fluorine atoms in C_2F_4 exert a π-electron destabilization effect and that C_2F_4 is 16–18 kcal/mol less stable than ethylene. From the data obtained by his study, together with that of Schlag and Kaiser (34), Chesick has proposed as a working rule that it is the first substitution of a CF_3 group for a fluorine at the double bond which causes the principal stabilization of the π-electron system (to the extent of about 10 kcal/mol) and the effect of the second substitution of a CF_3 group is small relative to the first substitution. It is interesting to note that the relative rate constants for the reactions of active nitrogen with C_2F_4, C_3F_6 and $t\text{-}C_4F_8\text{-}2$ seem to indicate such a trend.

M.R. wishes to acknowledge his scholarship from the Canadian International Development Agency. We are also grateful for financial assistance from the National Research Council of Canada.

1. N. MADHAVAN and W. E. JONES. Can. J. Chem. **46**, 3824 (1968).
2. H. v HARTEL and M. POLANYI. Z. Phys. Chem. (Leipzig), **B11**, 97 (1930).
3. M. POLANYI. Atomic reactions. Williams and Norgate, Ltd., London, 1932.
4. C. E. H. BAWN. Annu. Rep. Chem. Soc. **39**, 36 (1942).
5. W. E. WARHURST. Q. Rev. (London), **5**, 44 (1951).
6. J. H. GREENBLATT and C. A. WINKLER. Can. J. Res. **B27**, 732 (1949).
7. E. R. V. MILTON and H. B. DUNFORD. J. Chem. Phys. **34**, 51 (1961).
8. W. HELLER. Trans. Faraday Soc. **33**, 1556 (1937).
9. J. F. REED and B. S. RABINOVITCH. J. Phys. Chem. **59**, 261 (1955).
10. J. F. REED and B. S. RABINOVITCH. J. Phys. Chem. **61**, 598 (1957).
11. D. GARVIN and G. B. KISTIAKOWSKY. J. Chem. Phys. **20**, 105 (1952).
12. D. GARVIN, V. P. GUINN, and G. B. KISTIAKOWSKY. Discuss. Faraday Soc. No. 17, 32 (1954).
13. H. G. V. EVANS, G. R. FREEMAN, and C. A. WINKLER. Can. J. Chem. **34**, 1271 (1956).
14. D. R. SAFRANY and W. JASTER. J. Phys. Chem. **72**, 518 (1968).
15. D. R. SAFRANY and W. JASTER. J. Phys. Chem. **72**, 3305 (1968).
16. R. J. CVETANOVIC and D. J. LE ROY. Can. J. Chem. **29**, 597 (1951).
17. R. J. CVETANOVIC. Can. J. Chem. **34**, 54 (1956).
18. F. T. SMITH. J. Chem. Phys. **22**, 1605 (1954).
19. W. JOST. Diffusion in solids, liquids, gases. Academic Press Inc., New York, 1960.
20. D. A. FRANK-KAMENETSKII. Diffusion and heat transfer in chemical kinetics. Plenum Press. New York, London, 1969. p. 47.

Can. J. Chem. Downloaded from www.nrcresearchpress.com by 210.87.254.42 on 09/05/12
For personal use only.

21. J. CRANK. The mathematics of diffusion. Oxford University Press, 1970. p. 145.
22. A. KUPPERMANN. J. Chem. Ed. **36**, 279 (1959).
23. J. R. NIELSON, H. CLAASSEN, and D. C. SMITH. J. Chem. Phys. **18**, 812 (1950).
24. N. MADHAVAN and W. E. JONES. J. Phys. Chem. **72**, 1812 (1968).
25. (*a*) A. A. WESTENBERG and N. DE HAAS. J. Chem. Phys. **40**, 3087 (1964). (*b*) L. ELIAS. J. Chem. Phys. **42**, 4311 (1965).
26. J. T. HERRON. J. Phys. Chem. **69**, 2736 (1965).
27. J. O. HIRSCHFELDER, C. F. CURTISS, and R. B. BIRD. Molecular theory of gases and liquids. 2nd ed. John Wiley and Sons, Inc., New York. p. 14.
28. See ref. 27, p. 545.
29. N. MADHAVAN and W. E. JONES. Rev. Sci. Inst. **40**, 1293 (1969).
30. J. C. MCCOUBREY and N. M. SINGH. Trans. Faraday Soc. **56**, 486 (1960).
31. S. W. BENSON. The foundations of chemical kinetics. McGraw-Hill Book Company, Inc., New York, 1960. p. 294.
32. J. T. HERRON and R. E. HUIE. J. Phys. Chem. **72**, 2538 (1968).
33. J. P. CHESICK. J. Am. Chem. Soc. **88**, 4800 (1966).
34. E. W. SCHLAG and E. W. KAISER, JR. J. Am. Chem. Soc. **87**, 1171 (1965).

Can. J. Chem. Downloaded from www.nrcresearchpress.com by 210.87.254.42 on 09/05/12
For personal use only.

A Study of the Barriers to Rotation in Some Highly Substituted Diphenyl Ethers[1]

J. J. BERGMAN[2] AND W. D. CHANDLER[3]

Department of Chemistry, University of Saskatchewan, Regina, Saskatchewan

Received July 27, 1971

Energy barriers to rotation about Ar–O bonds have been obtained from an analysis of the variable temperature n.m.r. spectra of a number of highly substituted diphenyl ethers. These barriers are explained on the basis of structural and conformational effects and their implication for the resolution of optical isomers is discussed.

Les barrières d'énergie de rotation autour des liaisons Ar—O ont été obtenues à partir des spectres r.m.n. à température variable d'un certain nombre de diphényl éthers fortement substitués. Ces barrières sont expliquées en fonction des effets structuraux et conformationnels; leur conséquence en vue de la résolution d'isomères optiques est discutée.

Canadian Journal of Chemistry, **50**, 353 (1972)

Can. J. Chem. Downloaded from www.nrcresearchpress.com by 210.87.254.42 on 09/05/12
For personal use only.

Introduction

It has been established that many triply ortho-substituted diphenyl ethers exist in solution preferentially in an H-inside conformation as shown in Fig. 1 (1, 2). Appropriately substituted ethers (*e.g.* 1) are dissymmetric (without reflection symmetry) in this conformation and could, in principle, be resolved into optical isomers. Several attempts to carry out resolution have, however, failed (3–7). Since rotation of either or both rings about the ether linkage would convert **1** to either an enantiomer or a diastereomer (see Discussion), it is of interest to determine the magnitude of the energy barriers for these rotational processes. This is especially important as these systems provide fundamental models to aid in the study of rotational barriers of ethers related to thyroxine and other medicinally important ethers which have been shown to exist in the same preferred conformation (8).

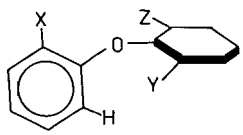

1

FIG. 1. H-Inside conformation of a triply ortho-substituted diphenyl ether.

[1]Abstracted from the Ph.D. Thesis of J. J. Bergman, University of Saskatchewan, Regina, June 1971.

[2]Present Address: Department of Chemistry, Saint Francis Xavier University, Antigonish, Nova Scotia.

[3]Author to whom correspondence should be addressed.

Nuclear magnetic resonance spectroscopy offers an excellent method for determining energy barriers if signal shapes or patterns are temperature dependent. Free energy barriers to rotation in diphenyl ethers may be calculated from coalescing signals by means of the Eyring equation, the logarithmic form of which is [1]

$$[1] \quad \Delta G^{\ddagger} = 4.57 T_c \,(10.32 + \log\,(T_c/k_c))$$

where T_c is the coalescence temperature and k_c is the rate constant for rotation at the coalescence temperature (9). Equation 1 will be applicable to rotation about Ar—O bonds if the protons whose signals are coalescing are exchanged by this rotation. The value of k_c may be calculated for the collapse of two singlets to one singlet from eq. 2, where $\Delta\nu$ is the chemical shift difference in Hz between the two singlets obtained from

$$[2] \quad k_c = \pi\Delta\nu/\sqrt{2}$$

the n.m.r. spectrum taken well below T_c (9). Equation 2 assumes equal concentrations of the equilibrating species and no coupling between the protons whose signals are coalescing. If $\Delta\nu$ is large compared with the natural line widths and coupling constants, coupling may be neglected but such coupling, when this is not the case, will result in an apparent k_c larger than the true one and too low a value for $\Delta G^{\ddagger}$ (10). There are other equations used to estimate k_c; the validity of these and [2] for different situations has been investigated recently by Kost *et al.* (11).

Since the spectra of ethers we studied pre-

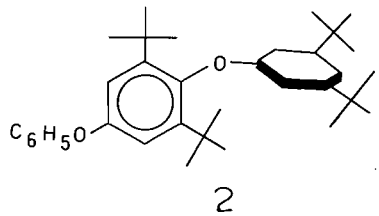

2

FIG. 2. H-Inside conformation suggested by Bolon (12).

viously (1, 2) indicated no temperature dependence, it seemed advisable to investigate ethers with larger ortho substituents. Bolan (12) has noted that the two *t*-butyl groups meta to the ether linkage in **2** appear to be non-equivalent from the n.m.r. spectrum, and this observation led him to suggest the H-inside conformation shown in Fig. 2. Kessler *et al.* (13) have calculated a free energy barrier to rotation of 17.8 kcal/mol for **3** based on the coalescence of the n.m.r. signals for the methyl groups within a given isopropyl group (henceforth referred to as the isopropyl methyl groups) at temperatures above 57°. This would appear to be the first direct measurement of the barrier in highly substituted diphenyl ethers although Lehmann (14) has argued that the coalescence phenomenon may be explained by hindered rotation about the Ar—isopropyl bond rather than about an Ar—O bond.

In this paper we report a study of rotation in other highly substituted diphenyl ethers using variable temperature spectroscopy. In some cases $\Delta G^{\ddagger}$ appears to be of suitable magnitude that optical resolution of the enantiomeric

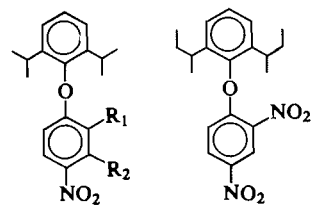

6

3 $R_1 = NO_2$; $R_2 = H$
4 $R_1 = R_2 = H$
5 $R_1 = H$; $R_2 = CH_3$

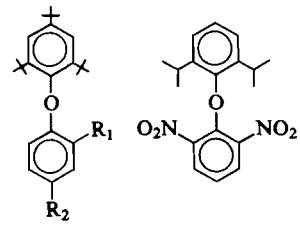

10

7 $R_1 = R_2 = H$
8 $R_1 = H$; $R_2 = Br$
9 $R_1 = R_2 = NO_2$

conformers of similar ethers containing the necessary dissymmetry may be possible.

Results

Variable temperature n.m.r. spectra of **3**, **4**, **5**, **6**, and **8** are reproduced in Figs. 3–7. Table 1 contains coalescence data (T_c and k_c) and $\Delta G^{\ddagger}$ determined at T_c for **3**, **4**, **5**, and **8**. The parameters k_c and $\Delta G^{\ddagger}$ were calculated from eqs. 1 and 2;[4] the estimated error in values of the latter is

TABLE 1. Coalescence data and $\Delta G^{\ddagger}$ values

Compound	Absorption measured	T_c (°C)	$\Delta\nu$ (Hz)[a]	$k_c(s^{-1})$[b]	$\Delta G^{\ddagger}$ (kcal/mol)[c]
3	Isopropyl methyls	57			17.8[d]
4	Isopropyl methyls	−70	7.0	15.6	10.6
	Ring protons	−60	107.0	238.0	10.1
5	Isopropyl methyls	−70	6.0	13.3	10.7
8	Ring protons	67	66.7	150.0	16.5

[a]The $\Delta\nu$ values for compounds **4** and **5** were obtained at 100 MHz. That for **8** was obtained at 60 MHz.
[b]From eq. 2.
[c]From eq. 1 at T_c.
[d]Reported by Kessler *et al.* (9, 13).

[4]Although the exchanging ring protons couple in these compounds, $\Delta\nu \gg J$ so that eq. 2 was used without correction for the coupling (9–11). It has been pointed out that the use of [2] for the isopropyl methyl absorptions is suspect. However, even if k_c were wrong by an order of magnitude, which is unlikely, $\Delta G^{\ddagger}$ would be wrong by less than 1 kcal/mol.

Can. J. Chem. Downloaded from www.nrcresearchpress.com by 210.87.254.42 on 09/05/12
For personal use only.

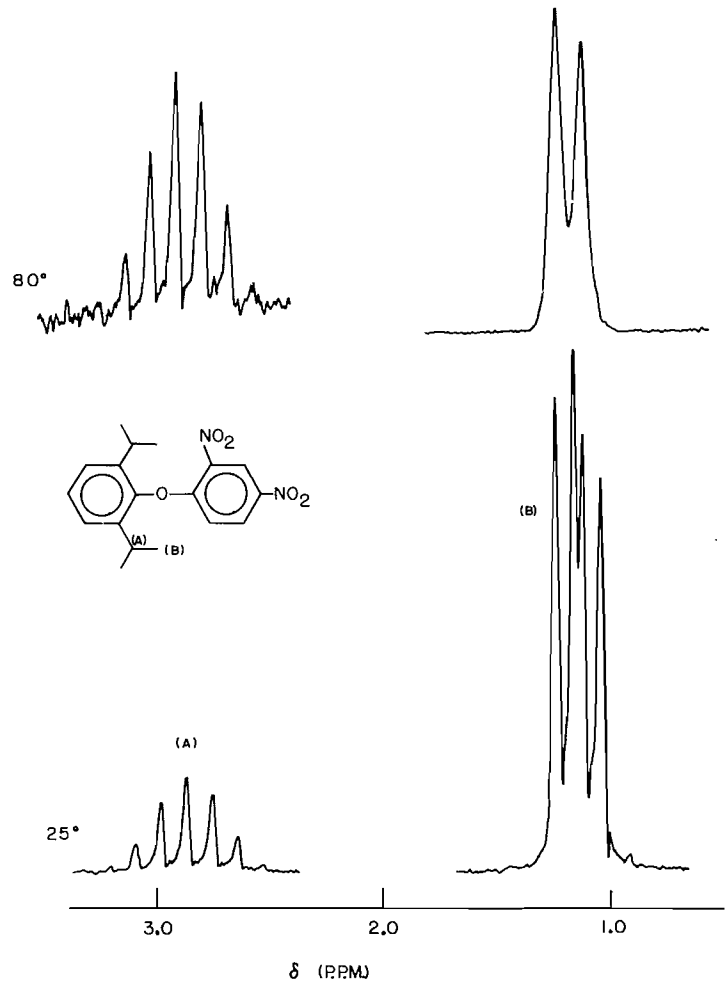

FIG. 3. Variable temperature n.m.r. spectra of **3**.

± 0.4 kcal/mol, based almost exclusively on uncertainties in T_c.

Compound **7** was found to undergo coalescence around ambient temperature at 60 MHz, having what appeared to be an AA′BB′C pattern for the protons of the non-alkylated ring above this temperature and an ABCDE pattern below it. No indication of n.m.r. changes were noted for **9** or **10** over a temperature range of -70 to 150° at 60 MHz.

Discussion

The basis for the observation of non-equivalence of the isopropyl methyl groups of an ether such as **3** (Fig. 3) is that in one H-inside conformer[5] the methyl groups within each isopropyl are anisochronous (15) although the two isopropyls are themselves enantiotopic[6] and are therefore normally equivalent in the n.m.r. spectrum. This non-equivalence of the methyl groups holds for all conditions of rotation about the Ar—isopropyl bond and is an example of a

[5]In this case there are two identical H-inside conformers, differing only by rotation of the di-isopropyl-substituted ring through 180°. If the alkyl-substituted ring had no plane of symmetry these two conformers would be enantiomers (see later discussion and Fig. 10). There is no spectral indication of any NO_2-inside conformers.

[6]Groups are enantiotopic if they can be interchanged by a rotation–reflection operation (S_n) to give a structure indistinguishable from the original (15).

Can. J. Chem. Downloaded from www.nrcresearchpress.com by 210.87.254.42 on 09/05/12
For personal use only.

Can. J. Chem. Downloaded from www.nrcresearchpress.com by 210.87.254.42 on 09/05/12
For personal use only.

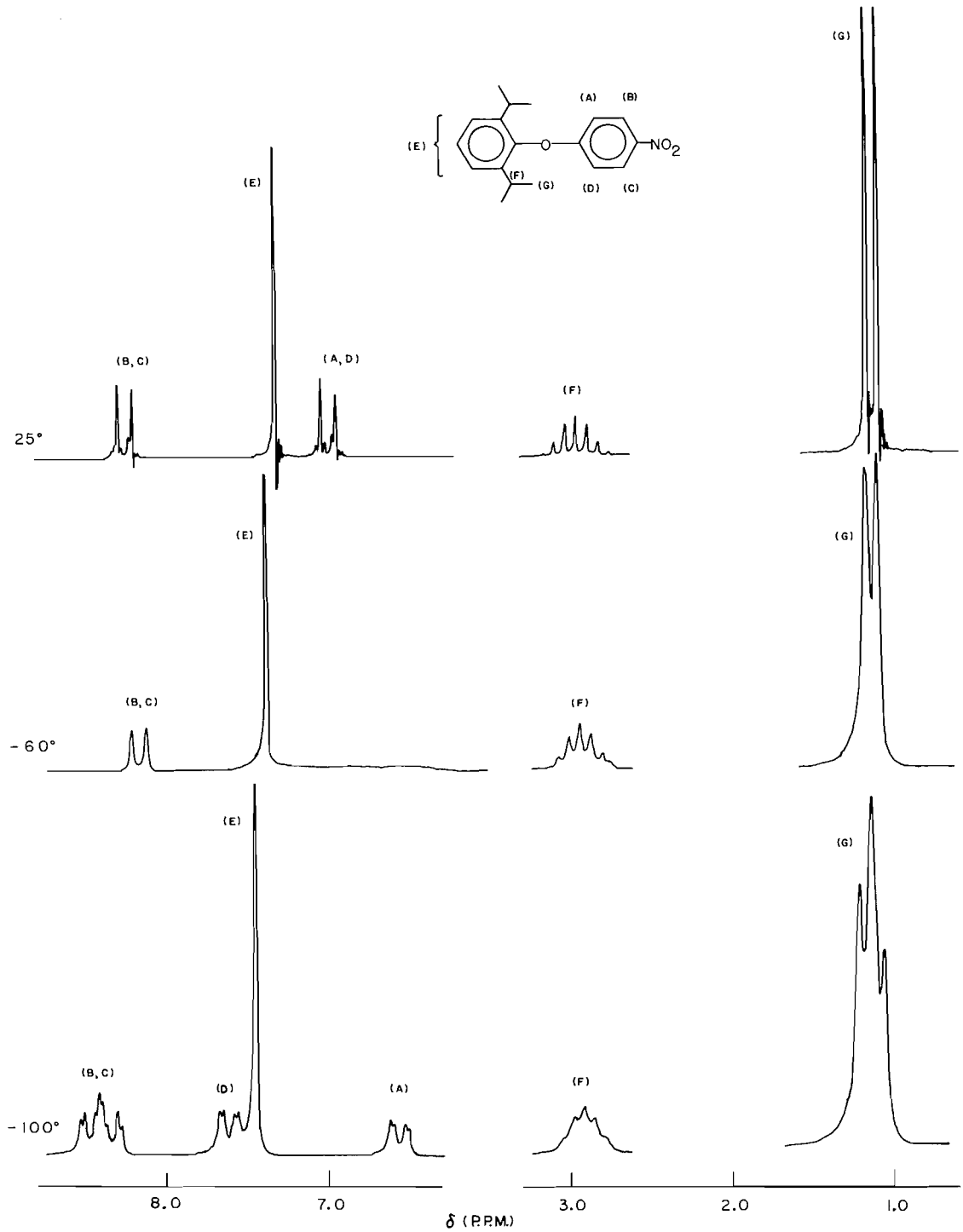

FIG. 4. Variable temperature n.m.r. spectra of **4**.

Can. J. Chem. Downloaded from www.nrcresearchpress.com by 210.87.254.42 on 09/05/12
For personal use only.

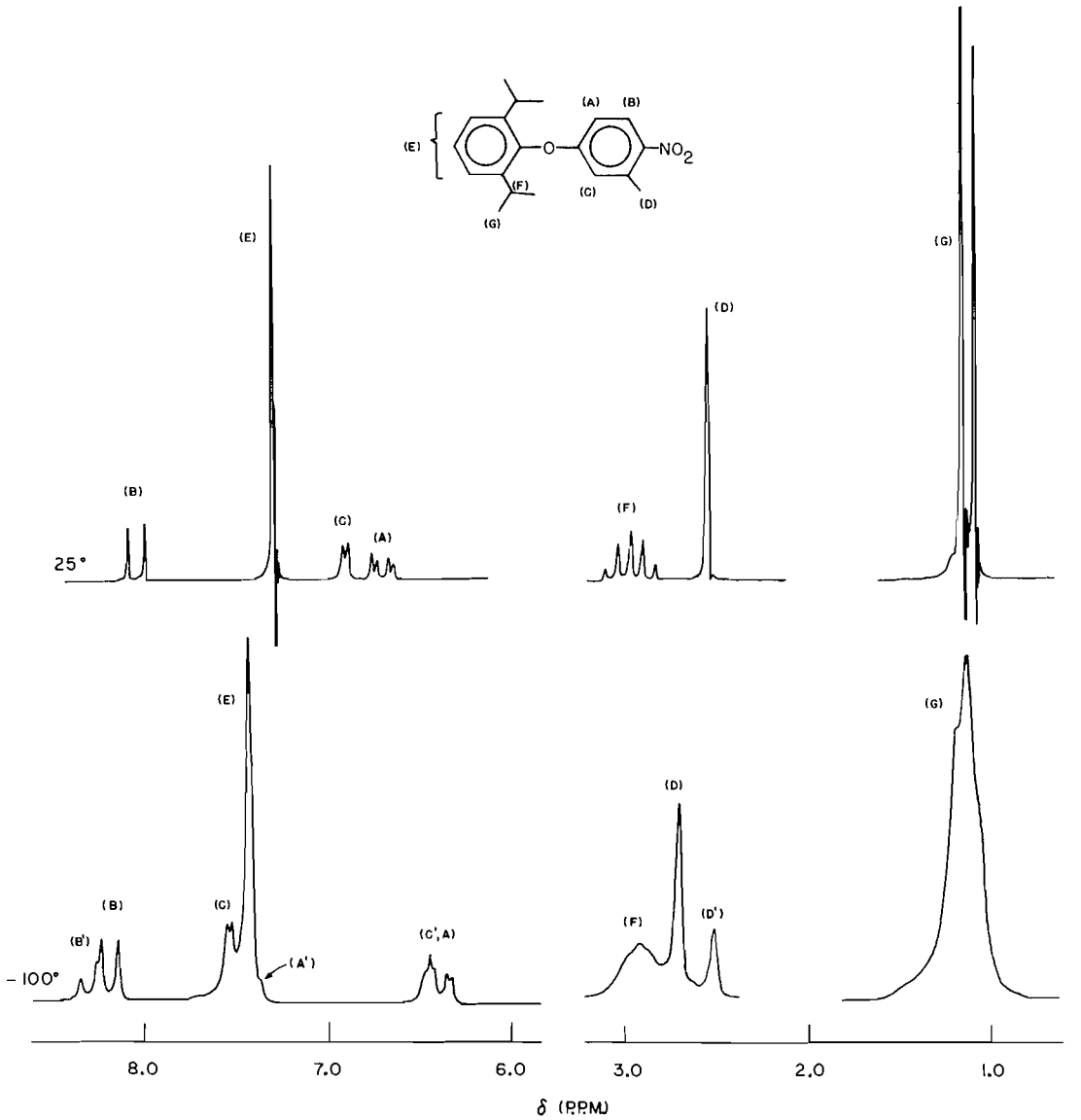

FIG. 5. Variable temperature n.m.r. spectra of **5**.

fairly well documented phenomenon (16–18) which produces non-equivalence of the X groups in any A-CX_2-B system where either A or B is asymmetric. Since the rate of rotation about the Ar—O bond increases with temperature, the n.m.r. spectrometer sees only a time average of the conformers above T_c (Fig. 8). The methyls in an isopropyl group exchange identity when the conformers are interconverted and are therefore seen as equivalent. At temperatures below T_c, interconversion of the conformers is slow enough for the spectrometer to be able to distinguish two different methyls. Thus, a study of the variable temperature behavior of isopropyl methyl signals is a study of rotation of the isopropyl-substituted ring about the Ar—O bond.

The spectrum of **6** (Fig. 6) shows one set of absorptions for the two sec-butyl groups at temperatures above 50° and two sets at lower

Can. J. Chem. Downloaded from www.nrcresearchpress.com by 210.87.254.42 on 09/05/12
For personal use only.

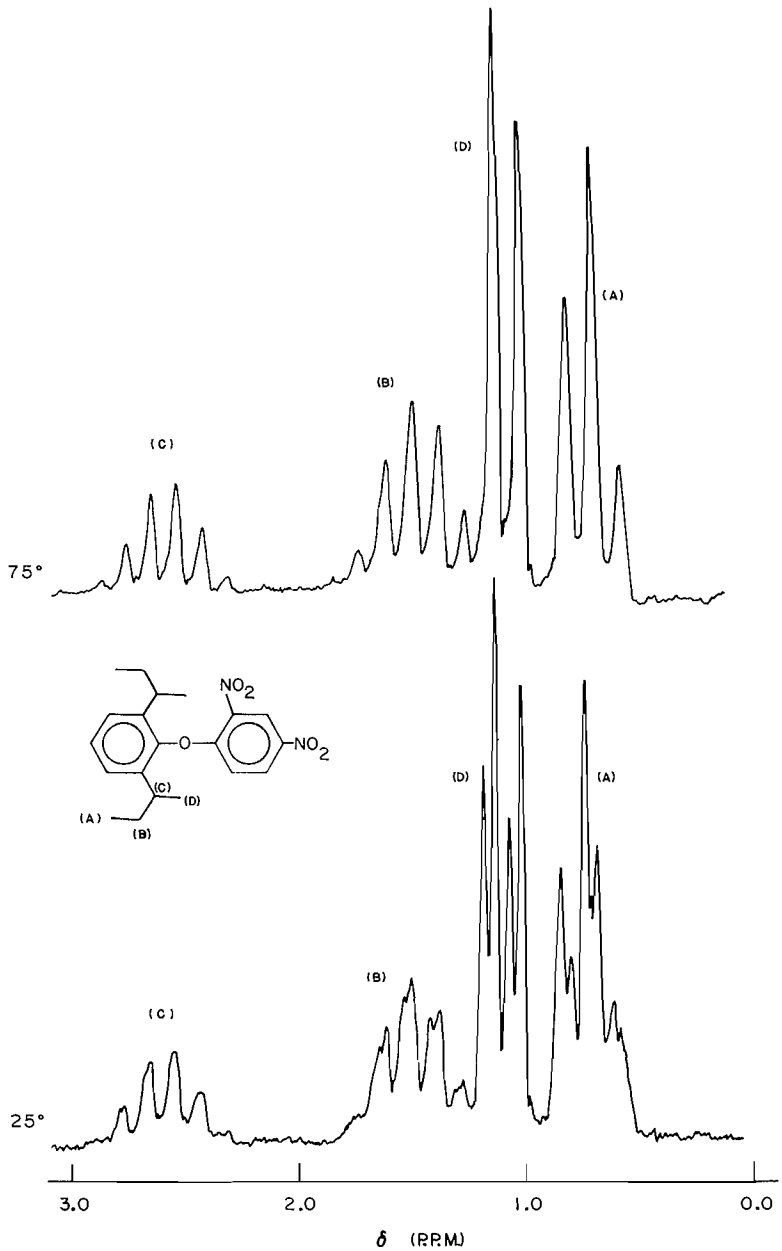

FIG. 6. Variable temperature n.m.r. spectra of **6**.

temperatures. Compound **6** possesses two asymmetric carbons in the sec-butyl substituents so the possibility of RR, SS, and RS combinations exists. Since in the meso RS form the sec-butyls are enantiotopic under all conditions of rotation about AR—O, it would be expected to show a temperature independent sec-butyl absorption provided that only the two identical H-inside conformers are equilibrating. If either the RR or SS form is *frozen into* one of the identical H-inside conformations, the two sec-butyl groups are diastereotopic (15) and are therefore magnetically non-equivalent. Rotation of the alkylated ring through 180° (see Fig. 8 for **3**)

Can. J. Chem. Downloaded from www.nrcresearchpress.com by 210.87.254.42 on 09/05/12
For personal use only.

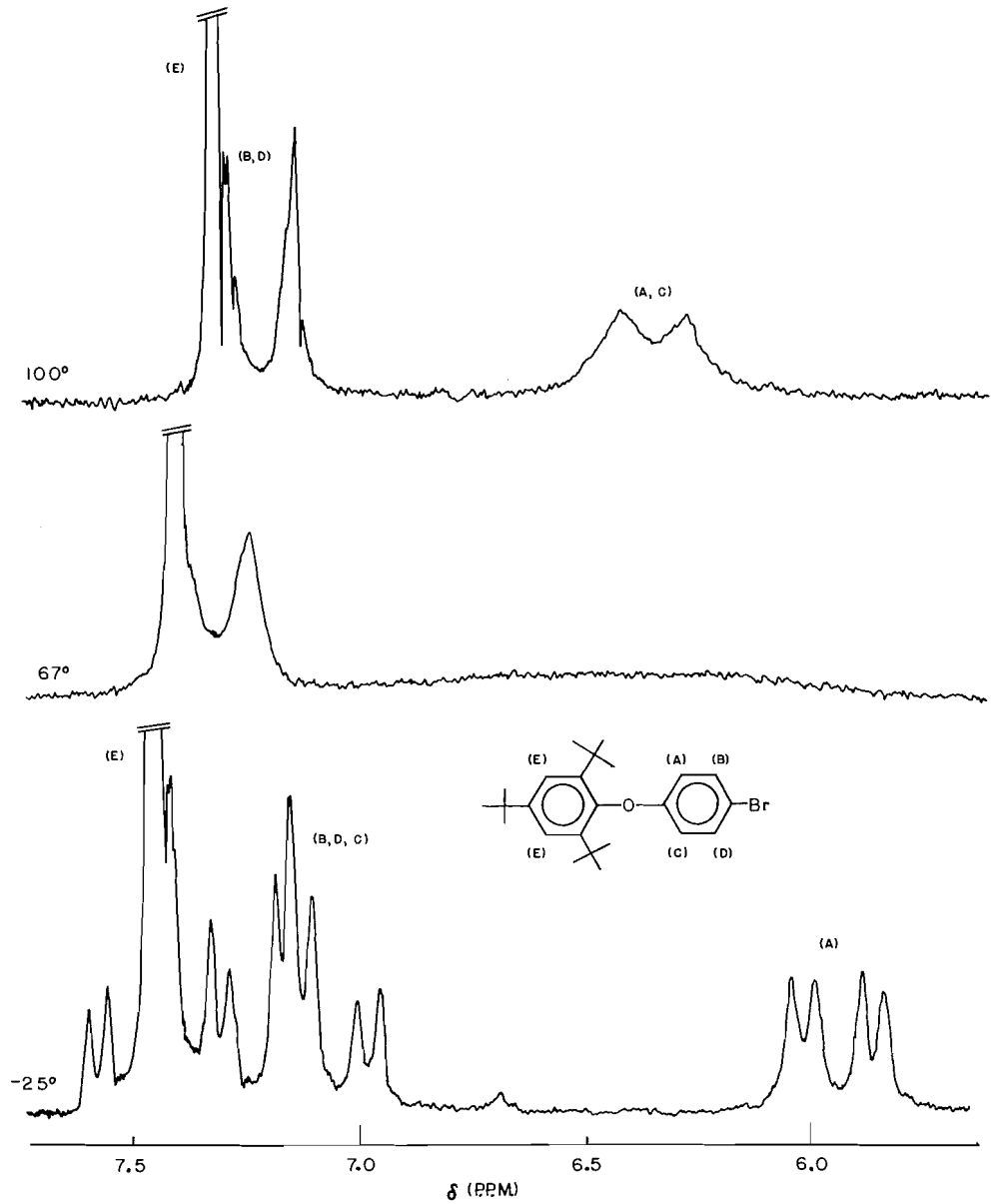

FIG. 7. Variable temperature n.m.r. spectra of **8**.

exchanges the identity of the two groups and they are seen as being equivalent in the high temperature spectrum.

The variable temperature n.m.r. spectra of **5** (Fig. 5) are quite revealing; in the high temperature extreme the meta-methyl appears as a slightly broadened singlet, the nitrated ring protons as an AMX pattern and the isopropyl methyl groups as a single doublet. All of this is consistent with fast exchange between two different H-inside conformations which, for convenience, we will refer to as the methyl-inside and the methyl-outside conformations[7]

[7]Each H-inside conformer is really two identical conformers differing by rotation of the alkylated ring (*cf.* footnote 5).

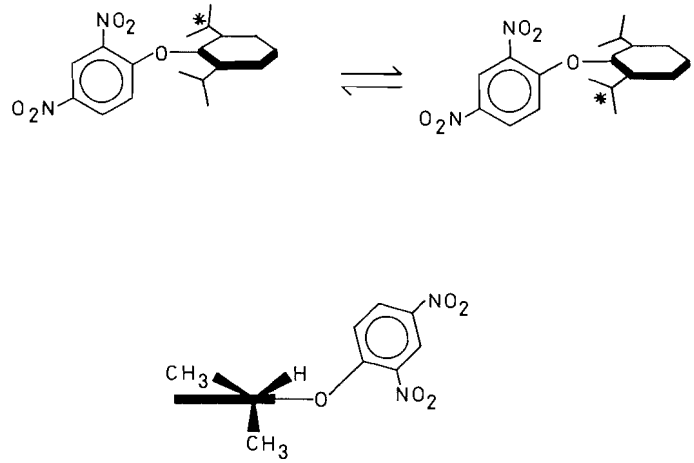

FIG. 8. Equilibration of conformers in **3**.

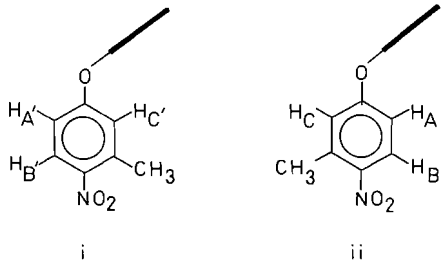

FIG. 9. (*i*) -ethyl-inside and (*ii*) Methyl-outside conformations of **5**.

(Fig. 9). At $-100°$ there are two sets of absorptions for all the protons including the isopropyls. This observation and the observed chemical shifts are consistent only with the *freezing out* of both conformations as well as the rotation of the di-isopropyl-substituted ring. The sets of signals for the two conformers are of unequal intensity since the methyl-outside conformer, in which there is less steric interaction between the methyl and the other ring is present in higher concentration.[8] The low intensity signals for the meta-methyl (D′) and for $H_{C'}$ (methyl-inside) appear at higher field than the corresponding high intensity signals (methyl-outside). This is due to the long-range shielding experienced in an H-inside conformation arising from the induced ring current of the other ring.[9] Similarly, the high intensity signals for H_A and H_B appear at higher field than the corresponding low intensity signals for $H_{A'}$ and $H_{B'}$.

The n.m.r. spectra of **4**, **7**, and **8** are also consistent with frequent interconversion between equivalent H-inside conformers at temperatures above T_c. Below T_c one observes ABCD or ABCDE patterns for the non-alkylated ring protons. Above T_c only the average resultant AA′BB′ or AA′BB′C patterns are observed.

That **9** showed no indication of hindered rotation is not surprising since there are only the two identical H-inside conformers resulting from rotation of the alkylated ring. Because the *t*-butyl groups, unlike isopropyls, are symmetric and are unable to be used as probes in the same way, one cannot observe the *freezing out* of the alkylated ring–O rotation even though it must occur.

In view of the results obtained by Kessler *et al.* (13) for **3**, the more hindered **10** might be expected to show similar results with an even higher coalescence temperature and $\Delta G^{\ddagger}$. That it does not may be explained in one of two ways: (*i*) free rotation occurs over the entire temperature range studied (-70 to $150°$) or, (*ii*) the compound is locked into some symmetrical conformation (or exchange occurs between two or more symmetrical conformations). In support of the former explanation is the fact that for **10**

[8]Although the two methyl signals overlap the isopropyl methine H signal at $-100°$, from their relative intensities the equilibrium constant was calculated to be about 3.5 leading to a value of 0.4 kcal/mol for ΔG. This appears to be the first experimental estimate of a conformational energy difference in diphenyl ethers.

[9]For a discussion of this effect in diphenyl ethers see ref. 2.

Can. J. Chem. Downloaded from www.nrcresearchpress.com by 210.87.254.42 on 09/05/12
For personal use only.

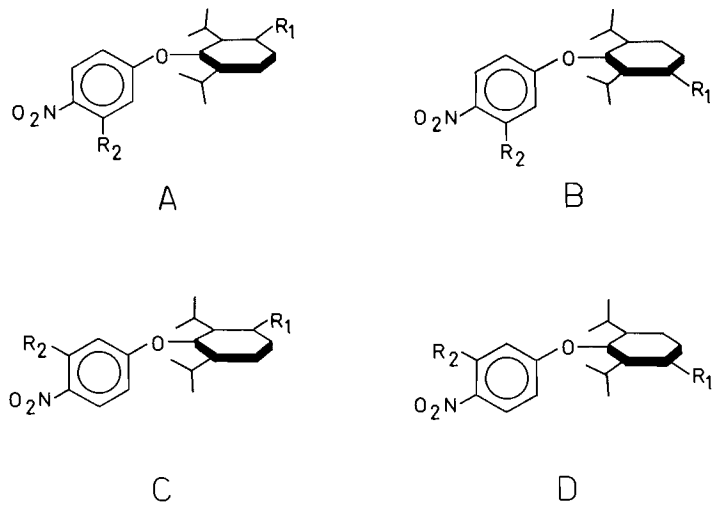

FIG. 10. The four stereoisomers of a dissymmetric, di-*ortho*-substituted diphenyl ether adopting H-inside conformations.

there can be no relatively low energy, H-inside conformation which the molecule can adopt. As a result, the conformer energies are high and the $\Delta G^{\ddagger}$ to rotation about the Ar—O bonds is low when compared with that of other molecules considered in this study.

It is worth mentioning again that calculation of an energy barrier using the data from ring proton coalescence is inherently more reliable than using data from the isopropyl methyl groups. In the former case $\Delta\nu$ is very large. Because of this it is possible to neglect coupling of the protons undergoing coalescence without introducing serious error into the calculated $\Delta G^{\ddagger}$ (see footnote 4). The major factor influencing the calculation of $\Delta G^{\ddagger}$ in either case is T_c.

The problem remains of assigning $\Delta G^{\ddagger}$ values to particular rotational processes. For a dissymmetric diphenyl ether with two vacant ortho positions on the same ring there may be four possible stereoisomeric H-inside conformers (Fig. 10, see also footnote 7 for the case when one ring has a plane of symmetry). This particular example was chosen because of its maximum lack of symmetry and the possibility of two enantiomeric pairs of H-inside conformers (the pair A and B and the pair C and D). Rotation about the alkylated ring—O bond alone interconverts enantiomers while rotation about the other Ar—O bond alone produces a diastereomer (A and C are interconverted as are B and D). A third rotational process that has been suggested (3) is the cogwheel rotation in which both rings rotate synchronously interconverting the pair A and D, and the pair B and C. Although a cogwheel mechanism will not by itself produce racemization of an optically active ether, the cogwheel rotation in concert with either or both of the other two processes can cause racemization. In order to isolate pure optical isomers, all of these rotational processes would have to be inhibited.

The variable temperature n.m.r. spectra of **4** could be accounted for by either the one-step, cogwheel rotation or by a two-step process in which rotation occurs first about one Ar—O bond and then the other. Inspection of molecular models suggests that rotation of the alkylated ring should be more hindered (should have a larger $\Delta G^{\ddagger}$) than rotation of the nitrated ring. The fact that, within experimental error, the values of $\Delta G^{\ddagger}$ determined from T_c and k_c for isopropyl and ring proton exchange are the same (Table 1) would seem to indicate that a one-step process occurs in ethers of this type (that would include **7** and **8** as well as **4**).

For triply ortho-substituted ethers (**3**, **6**, **9**) the cogwheel process would force the molecule into a high energy NO_2-inside conformation which is not observed by the n.m.r. spectrometer. It would seem unlikely that rotation of the alkyl-substituted ring occurs alone as that rotation would be highly hindered in the ethers studied. It would be possible for the two rings

Can. J. Chem. Downloaded from www.nrcresearchpress.com by 210.87.254.42 on 09/05/12
For personal use only.

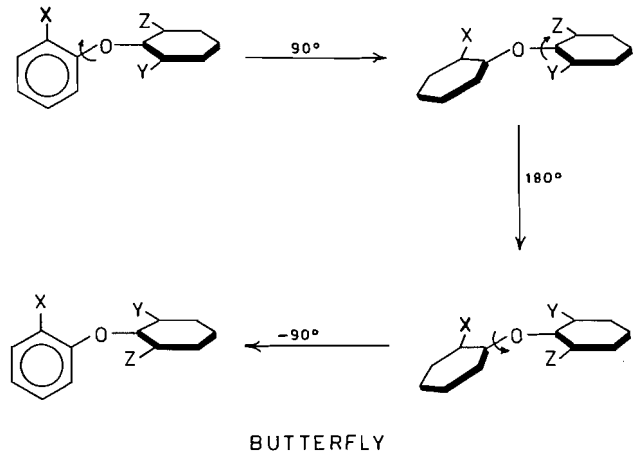

FIG. 11. Butterfly mechanism for rotation about an Ar—O bond in triply *ortho*-substituted diphenyl ethers.

to slip by one another through a *butterfly* intermediate (Fig. 11). This process could be envisaged as a three-step one involving both rings although not simultaneously as for the cogwheel mechanism. The butterfly mechanism could also account for the observations noted with the doubly ortho-substituted ethers as a single $\Delta G^{\ddagger}$ would be expected for both ring rotations; the final step could be rotation of the non-alkyl-substituted ring by 90° in either sense.

It appears likely, in the light of the experimental evidence, that a diphenyl ether such as **11** could be resolved into enantiomers. Comparing **3** and **4**, one sees that the introduction of an ortho-nitro group in **3** raises the T_c for rotation of the alkylated ring by about 130°.[10] A similar structural change in **8** would raise $\Delta G^{\ddagger}$ to around 23 kcal/mol, a barrier sufficient to allow separation of individual, enantiomeric H-inside conformers (9). Compound **11**, then should have a barrier to rotation sufficiently high and both rings are dissymmetric so that the two enantiomers could, in theory, be resolved at room temperature. It may be that the use of an ortho substituent such as CHO, CN or CO_2R which is less easily distorted from coplanarity with the ring than NO_2 might effect an even larger increment in the rotational barrier. The failure to observe hindered rotation in **10** indicates that one vacant ortho position should be maintained if diphenyl ethers for optical resolution studies are being synthesized.

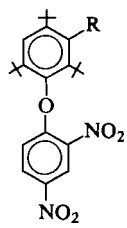

11

[10]It is interesting to note that a meta-methyl does not increase T_c or $\Delta G^{\ddagger}$ for this rotation (*cf.* values for **4** and **5**).

Experimental

The n.m.r. spectra were recorded on Varian A-60A and HA-100 spectrometers. For studies at low temperatures the samples were dissolved in acetone-d_6; otherwise chloroform-*d* was used as solvent. The chemical shifts of the aromatic protons on the brominated ring of **8**, in the low temperature spectrum, were reproduced to within ±0.1 Hz by means of an iterative computer calculation in order to estimate k_c.

Compounds **4** and **5** were prepared by the method of Wright and Jorgensen (19). Compounds **3** and **9** have been reported previously (20) while **6** and **10** were synthesized by the method of that reference. The properties of **6** and **10** are recorded in Table 2.

The n.m.r. and i.r. spectra of all compounds were consistent with the assigned structures.

2-Phenoxy-1,3,5-tri-t-butylbenzene (7)

2-(2′,4′-Dinitrophenoxy)-1,3,5,-tri-*t*-butylbenzene (**9**, 1.0 g) was dissolved in 95% ethanol (200 ml) and about 2 g of W-2 Raney Nickel added. Hydrogenation was performed in a Parr shaker apparatus for 12 h at a pressure of 40 lb/in.^{2} and the catalyst was removed by filtration. The resulting colorless solution was evaporated to give off-white crystals (0.8 g, 95%) of what, from n.m.r. and i.r. spectra, appeared to be 2-(2′,4′-diaminophenoxy)-1,3,5-tri-*t*-butylbenzene.

Without further purification, the crude diamine was dis-

Can. J. Chem. Downloaded from www.nrcresearchpress.com by 210.87.254.42 on 09/05/12
For personal use only.

TABLE 2. Properties of some new diphenyl ethers

Compound	m.p. or b.p. (°C/mm Hg)	Yield (%)	Analysis (%) Calculated C	H	N	Found C	H	N
6	213–216/0.4	28	64.50	6.50	7.52	64.22	6.36	7.41
10	113–115	24	62.78	5.85	8.14	62.67	5.74	7.97

solved in a mixture of concentrated sulfuric acid and glacial acetic acid (40 ml, 1:1). A solution of sodium nitrite (0.5 g) in concentrated sulfuric acid (20 ml) was prepared and both solutions were cooled to 5°. The nitrous acid solution was added to the amine over a period of 45 min and the deep red product was allowed to stand at 5° for a further 30 min. It was then added slowly to a mixture of hypophosphorus acid (75 ml, 50%) and crushed ice (300 g) and left for 24 h. At the end of this time, the contents were extracted with chloroform (100 ml) and the chloroform was evaporated to yield a red oil (0.66 g, 90%). A portion of this product was used without purification in the n.m.r. experiments then was recovered and combined with the remainder for use in the next synthetic step.

2-(4'-Bromophenoxy)-1,3,5-tri-t-butylbenzene (8)

Crude 2-phenoxy-1,3,5-tri-*t*-butylbenzene (0.6 g) was dissolved in glacial acetic acid (10 ml) and a solution of bromine (0.28 g) in acetic acid (10 ml) was added dropwise as described by Hamilton and Blanchard (21) for the bromination of other highly substituted diphenyl ethers. Even after standing for 15 h, the mixture did not appear to have reacted so that ferric chloride (0.01 g) was added and stirring was continued for another 24 h. During this time there was a slow evolution of HCl and/or HBr. The solution was poured into water (200 ml) and the precipitate collected by filtration. This solid could not be purified by recrystallization from common solvents but was obtained as white crystals after being eluted through an alumina column (neutral, Brockman activity 1, 80–200 mesh) with petroleum ether (b.p. 30–60). The pure product was obtained in 61% (0.42 g), m.p. 146–148°.

Anal. Calcd. for $C_{24}H_{33}BrO$: C, 69.05; H, 7.97; Br, 19.14. Found: C, 69.23; H, 7.90; Br, 19.30.

The authors wish to acknowledge the support of the National Research Council of Canada for a grant in aid of research and for a bursary to one of us (J.J.B.). The assistance of Mr. Mazurak and the National Research Council of Canada, Prairie Regional Laboratory, Saskatoon, Saskatchewan, in obtaining 100 MHz n.m.r. spectra is also gratefully acknowledged. In addition, the authors wish to thank Drs. R. Y. Moir and G. A. Neville for discussing and commenting upon the ideas and work presented in this paper.

1. W. D. CHANDLER, W. MACF. SMITH, and R. Y. MOIR. Can. J. Chem. **42**, 2549 (1964).
2. J. J. BERGMAN, W. D. CHANDLER, and R. Y. MOIR. Can. J. Chem. **49**, 225 (1971).
3. M. ALLEN and R. Y. MOIR. Can. J. Chem. **37**, 1799 (1959).
4. M. ALLEN and R. Y. MOIR. Can. J. Chem. **41**, 252 (1963).
5. G. A. NEVILLE and R. Y. MOIR. Can. J. Chem. **47**, 2787 (1969).
6. A. J. GORDON and J. P. GALLAGHER. Tetrahedron Lett. 2541 (1970).
7. P. A. LEHMANN. Rev. Soc. Quím. Méx. **14**, 122 (1970).
8. P. A. LEHMANN and E. C. JORGENSEN. Tetrahedron, **21**, 363 (1965).
9. H. KESSLER. Angew. Chem. Int. Ed. **9**, 219 (1970).
10. A. ALLERHAND, H. S. GUTOWSKY, J. JONES, and R. A. MEINZER. J. Am. Chem. Soc. **88**, 3185 (1966).
11. D. KOST, E. H. CARLSON, and M. RABAN. Chem. Commun. 656 (1971).
12. D. A. BOLON. J. Am. Chem. Soc. **88**, 3148 (1966).
13. H. KESSLER, A. RIEKER, and W. RUNDEL. Chem. Commun. 475 (1968).
14. P. A. LEHMANN. Org. Mag. Reson. **2**, 467 (1970).
15. K. MISLOW and M. RABAN. Topics in stereochemistry. Vol. 1. *Edited by* N. L. Allinger and E. L. Eliel. John Wiley and Sons, New York, N.Y. Chapt. 1.
16. M. VAN GORKOM and G. E. HALL. Quart. Rev. **22**, 14 (1968).
17. E. I. SNYDER. J. Am. Chem. Soc. **85**, 2624 (1963).
18. C. VAN DER VLIES. Rec. Trav. Chim. Pays-Bas, **84**, 1289 (1965).
19. J. WRIGHT and E. C. JORGENSEN. J. Org. Chem. **33**, 1245 (1968).
20. W. D. CHANDLER, J. J. BERGMAN, and G. H. HAAS. Can. J. Chem. **49**, 583 (1971).
21. J. B. HAMILTON and H. S. BLANCHARD. J. Org. Chem. **35**, 3342 (1970).

Can. J. Chem. Downloaded from www.nrcresearchpress.com by 210.87.254.42 on 09/05/12
For personal use only.

The Deamination of the 3α- and 3β-Aminocholestanes and their Amide Derivatives

F. W. BACHELOR
Department of Chemistry, The University of Calgary, Calgary 44, Alberta
AND
E. H. WHITE
Department of Chemistry, The Johns Hopkins University, Baltimore, Maryland 21218

Received July 30, 1971

The nitroso acetamides, naphthamides, and benzylcarbamates of 3α- and 3β-aminocholestanes were decomposed in various solvents and the nitrous acid deaminations of the free amines in acetic acid and aqueous acetic acid mixtures were studied. In these reactions the intramolecular process leads to products with high degrees of retention of configuration, whereas the intermolecular process leads to products which are predominantly equatorial. Diazoalkanes were shown not to be intermediates in these deaminations.

Les nitroso acétamides, les naphthamides, et les benzylcarbamates des amino-3α et 3β-cholestanes ont été décomposés dans plusieurs solvants. La désamination nitreuse des amines libres a été étudiée dans l'acide acétique et dans des mélanges acide-acétique – eau. Dans ces réactions, le processus intramoléculaire conduit à des produits où la rétention de configuration est très importante, alors que le processus intermoléculaire donne des produits surtout équatoriaux. Il est montré que les diazoalcanes ne sont pas des intermédiaires dans ces désaminations.

Canadian Journal of Chemistry, **50**, 364 (1972)

Can. J. Chem. Downloaded from www.nrcresearchpress.com by 210.87.254.6 on 09/05/12
For personal use only.

In recent years an increasing number of workers have reported on the deamination of cyclohexyl, decalyl, and steroidal amines (1–11) and have discussed the reaction paths and stereochemistry of these systems. Of these, however, only one (4) dealt with the deamination of nitrosoamides and this study was not concerned with the epimer ratios of the derived esters. It is apparent from these studies that in conformationally rigid systems few rearrangements take place with equatorial amines but are fairly common with the axial epimers. We wish to report the details of our work on the deaminations via the nitrosoacetamides, naphthamides, and benzylcarbamates of 3α- and 3β-aminocholestanes, as well as our studies of the deaminations of the free amines in acetic acid and acetic acid water mixtures. The latter studies were undertaken to reexamine the report of Shoppee *et al.* that deaminations of both isomers yielded essentially alcohols with complete retention of configuration (12).

On the basis of subsequent work (13, 14) where it has been shown that deaminations of substituted cyclohexylamines yield alcohols with retained and inverted configuration, Shoppee's results appear to be anomalous. Our results show that with both equatorial and axial amines, both alcohols are produced. This has been reported in a previous communication (15). Subsequently, Shoppee repeated his earlier work and has reported similar results (6).

The aminocholestanes were prepared by previously published procedures (16, 17) and purified by crystallization of their acetamides. The free amines were regenerated by prolonged hydrolysis in concentrated hydrochloric acid – acetic acid. The 3β-nitrosoamides (**1***a*, *b*, *c*) and the 3α-nitrosoamides (**1***a*, *c*) were prepared by the reaction of the parent amides with N_2O_4 in methylene chloride at −20 °C while the 3α-nitrosonaphthamide (**1***b*) was prepared by a low temperature modification (18). All the axial

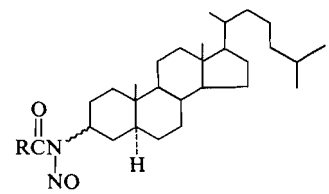

1

a R = CH_3
b R = 2-naphthyl
c R = $C_6H_5CH_2O$

TABLE 1. Decomposition of the nitrosoamides of 3α- and 3β-aminocholestanes

Compound **1**	Configuration	Solvent* + *M* equiv of addend	% olefins†	% esters†	Composition of esters 3α	3β
a	α	Ether + CH_2Cl_2	25	65	50	50
b	α	Ether‡	69	14	52	48
c	α	Hexane	84	16	83	17
c	α	Ether + 125 CH_2N_2	89	8	76	24
a	β	Cyclohexane	23	52	38	62
a	β	Cyclohexane + 42 CH_2N_2	45	44	35	65
a	β	$CHCl_3$	31	66	15	85
b	β	CH_2Cl_2 + 165 CH_3CO_2D	25	62‖	18	82
c	β	Heptane§	42	46	29	71

*All runs at room temperature unless otherwise noted.
†Corrected for recovered amide.
‡At −20 °C, $LiNO_3$ present.
§At 99 °C.
‖In addition, there was obtained 10% acetates, % composition: 25% 3α, 75% 3β.

α-nitrosoamides were unstable and decomposed at temperatures much lower than their corresponding β-epimers. The decomposition reaction mixtures were chromatographed on alumina and separated into alkene, ester, and alcohol fractions. The esters and alcohols were then analyzed by i.r. analysis, chromatographic analysis (19), gas chromatography, or by a combination of these methods. The naphthoates were converted to the alcohols via lithium aluminum hydride and analyzed as such. The reaction scheme is presented in eq. 1.

[1] $$RNHCR' \xrightarrow{N_2O_4} RN(NO)-C(=O)-R' \longrightarrow \begin{cases} ROCR' + N_2 \\ \text{Alkenes} + R'CO_2H + N_2 \end{cases}$$

The results shown in Table 1 indicate that retention of configuration predominates in all cases. The source of the inverted products is of some interest. Since these solvents are non-solvolytic, inversion must occur via an intramolecular reaction or by the reaction of some intermediate with the acid produced in the elimination reaction. The latter pathway can be checked in two ways: (*1*) by adding a scavenger for the freed carboxylic acid (in the present case diazomethane) or (*2*) by adding a large excess of a competing acid. Both of these methods were used. The addition of a large excess of diazomethane did not eliminate the inversion product. In the case of the decomposition of *N*-nitroso-3β-(2)-naphthoylamidocholestane (**1***b*) in the presence of a large excess of deuterioacetic acid, virtually no deuterium was incorporated in either the naphthoates or the acetates produced. Of these esters, only 10% was acetate and 18% of the naphthoates still had the inverted configuration. These results indicate clearly that an intramolecular inversion reaction is taking place. The mechanism of this reaction has been discussed in detail elsewhere (20). The absence of any significant deuterium incorporation in the acetates from the excess deuterioacetic acid experiment also precludes the possibility of a diazoalkane intermediate. Such intermediates are formed in non-polar solvents when the nitroso-amido group is attached to a primary carbon atom (21).

The relative unimportance of solvolysis as a source of product under these reaction conditions is shown by the low yield of acetates in the decomposition of *N*-nitroso-3β-(2)-naphthamidocholestane in the presence of a large excess of deuterioacetic acid. The ratio of acetates to naphthoates is approximately 1:6 although the ratio of acetic acid to starting nitrosonaphthamide is 165:1. Solvolysis becomes even less important when one considers that some of the

Can. J. Chem. Downloaded from www.nrcresearchpress.com by 210.87.254.6 on 09/05/12
For personal use only.

TABLE 2. The nitrous acid deamination of the 3α- and 3β-aminocholestranes

Configuration	Solvent	% olefins	% esters	% composition esters α	% composition esters β	% alcohol	% composition alcohols α	% composition alcohols β
α	Acetic acid	38	15	40	60	9	89	11
β	Acetic acid	5	53	34	66	41	10	90
α*	Acetic acid: H_2O, 1:1	45	19	—	—	13	61	39
β*	Acetic acid: H_2O:dioxane, 2:2:1	25	29	39	61	43	35	65

*Yields corrected for recovered amine.

acetate stems from frontside exchange (22), although the composition of the acetates approaches that of an equilibrium mixture with some net retention of configuration.[1]

We have found evidence for solvent bonding in runs performed in ether. A small amount (approximately 1%) of 3-ethoxycholestane of undetermined stereochemistry was found by gas chromatographic analysis of the cholestene fractions. This is in agreement with the results found by White and Billig (24) where the elements of tetrahydrofuran have been found in a nitrosoamide decomposition in this solvent. In addition to this, two other examples of solvent incorporation have been found resulting from the deamination of bridgehead amines. White *et al.* (25) have found the incorporation of the elements of benzene or chloroform during the deamination of *N*-nitroamides of norbornylamine, and Wilhelm and Curtin (26) found an 8% yield of 9-ethoxy-9,10-dihydro-9,10-ethanoanthracene from a nitrosyl chloride deamination of the corresponding amine.

We have also examined the nitrous acid deaminations of the 3α- and 3β-cholestanylamines in acetic acid and aqueous acetic acid solutions. The results are listed in Table 2. In all runs appreciable inversion is observed. The composition of the acetates does not change significantly regardless of which isomer one uses, nor over the solvent range used in our work. This data is in agreement with the revised results of Shoppee *et al.* (4, 6, 12) and with similar examples in the steroid field (5, 8, 10).

[1]An equilibrium mixture of the epimeric 4-*t*-butylcyclohexanols has been shown to consist of approximately 66% of the equatorial isomer (23). If we assume that the steric interactions involved at the 3-position of the cholestane nucleus are approximately the same, then the same equilibrium ratio should also apply here.

The source of the alcohols in anhydrous acetic acid is of some interest. Since water is produced in the reaction they could be the result of a bimolecular reaction. However, since there is such a high degree of retention of configuration in the deamination of both the 3α- and the 3β-amines it is more than likely that most of the alcohols result from an intramolecular process involving the hydroxyl group immediately associated with diazo hydroxide. In addition, deaminations in aqueous acetic acid do not significantly increase the amount of alcohols produced. These results are in agreement with those found by White and Stuber (18) and Cohen and Jankowski (3).

Products of solvolysis appear to favor the more stable 3β configuration. In all cases the acetates formed were predominantly equatorial. Also, as the concentration of water increased, the axial amine gave more of the equatorial alcohol. This is also seen in the work of Cohen and Jankowski (3) with their studies of the deamination of the axial 2-amino-*trans*-decalin in aqueous acetic acid at various concentrations. It is noteworthy in their studies as well as our own that the ratio of equatorial to axial acetate is fairly constant over a wide range of acetic acid – water mixtures. This is not true, however, in the case of the equatorial amines (27). In this case, as the water concentration increased, the ratio of equatorial to axial acetate increased, as did also the alcohol ratio to a smaller extent. From these results it is obvious that there are at least two mechanisms leading to solvolysis products. It has been suggested (3, 15) that specifically solvated ion pairs can lead to solvation products with a high degree of retention of configuration in acetic acid or in acetic acid rich aqueous reactions. In the case of the axial 2-amino-*trans*-decalin (3) and our work

Can. J. Chem. Downloaded from www.nrcresearchpress.com by 210.87.254.6 on 09/05/12
For personal use only.

Can. J. Chem. Downloaded from www.nrcresearchpress.com by 210.87.254.6 on 09/05/12
For personal use only.

this cannot apply completely since in all cases a predominance of inverted solvolysis product occurs.

Although we have examined our reactions for rearranged products, *i.e.* cholestanes substituted at the 2 and 4 positions, we have not been able to detect any significant amounts of these products. However, these rearrangements rarely exceed 5% and would not detract meaningfully from the results of this work.

Experimental

All melting points are corrected and were obtained with total immersion Anschutz thermometers. The i.r. spectra were recorded with a Perkin–Elmer model 21 spectrophotometer with scale expander. Deuterium was analyzed by combustion and i.r. comparisons. The g.l.c. measurements were performed on a Hewlett–Packard Biomedical Model 402 Gas Chromatograph.

3-Cholestanone Oxime

To a solution of 20 g of 3-cholestanone in 500 ml of refluxing ethanol was added 9.0 g of sodium acetate and 7.0 g of hydroxylamine hydrochloride. Refluxing was continued for 2 h. The solvent was then removed *in vacuo* and the residue taken up in ether, washed with water, and concentrated to dryness *in vacuo*. The residue was recrystallized from ethyl acetate. Yield 19.5 g (94%), m.p. 201–202 °C.

3α-Cholestanylamine

3α-Cholestanylamine was prepared by reduction of 3-cholestanone oxime in acetic acid over platinum according to the method of Shoppee *et al.* (16).

3β-Cholestanylamine

3β-Cholestanylamine was prepared by reduction of the oxime with sodium in refluxing amyl alcohol according to the method of Dodgson and Haworth (17).

3β-Acetamidocholestane

3β-Cholestanylamine (5.0 g) was dissolved in 150 ml of anhydrous ether and 2 ml of acetic anhydride added to the stirred solution. A precipitate formed almost immediately. The reaction was stirred for 1 h, ether then removed *in vacuo*, and the residue taken up in chloroform. The chloroform solution was washed with aqueous sodium bicarbonate and water, dried over sodium sulfate, and concentrated to dryness *in vacuo*. The amide was recrystallized from acetone to constant m.p.; m.p. 249–250°.

3α-Acetamidocholestane

This was prepared in the same manner as 3β-acetamidocholestane. Repeated recrystallization from acetone gave pure 3α-acetamidocholestane, m.p. 217–218° (lit. (28) 217–218°).

Hydrolysis of the α-Acetamidocholestane

The 3α-acetamidocholestane (1.0 g) was suspended in a mixture of 75 ml of glacial acetic acid and 30 ml of 6 *N* hydrochloric acid and refluxed for 8 days. On cooling the amine, hydrochloride precipitated as flakes. This was collected by filtration and dried *in vacuo* over P_2O_5 and KOH pellets; yield, 768 mg. Hydrolysis of 3β-acetamidocholestane was carried out in the same manner.

Benzyl-N-3α-cholestanyl Carbamate

3α-Cholestanylamine hydrochloride (1.0 g) was suspended between 40 ml of ether and 30 ml of 30% potassium hydroxide solution. The mixture was stirred until all the solid material had dissolved. Carbobenzyloxy chloride (0.41 ml) was added and stirring was continued for 2 h. The layers were then separated, the ether layer washed with water, 2*N* hydrochloric acid, water, and then dried over sodium sulfate. The ether was removed by concentration and the residue recrystallized from methanol; yield, 782 mg, m.p. 143.2–144.0 °C.

Anal. Calcd. for $C_{35}H_{55}O_2N$: C, 80.56; H, 10.62; N, 2.69. Found: C, 80.60; H, 10.39; N, 2.88.

Benzyl-N-3β-cholestanyl Carbamate

This was prepared in the same manner as the 3α-isomer. Recrystallized from ethanol; m.p. 145.0–145.5 °C.

Anal. Calcd. for $C_{35}H_{55}O_2N$: C, 80.56; H, 10.62; N, 2.69. Found: C, 80.38; H, 10.65; N, 2.85.

Benzyl-3α-cholestanyl Carbonate

3α-Cholestanol (201 mg) was dissolved in dry methylene dichloride (20 ml) and 1.0 ml of carbobenzyloxy chloride added. While stirring, a solution of 0.5 ml of dry pyridine in 12 ml of dry methylene chloride was added dropwise over a period of 2 h. The solution then stood overnight. The solution was poured into water and the organic layer washed twice with water, dried over sodium sulfate, and concentrated to dryness *in vacuo*. The residue was dissolved in a minimum amount of benzene–hexane and chromatographed on alumina (10.0 g Woelm, neutral, activity III). The carbonate (265 mg) was eluted with 5% benzene in hexane. Recrystallization from methanol–chloroform gave pure benzyl-3α-cholestanyl carbonate, m.p. 67.2–68.0 °C.

Anal. Calcd. for $C_{35}H_{54}O_3$: C, 80.41; H, 10.41. Found: C, 80.40; H, 10.56.

Benzyl-3β-cholestanyl Carbonate

This compound was prepared in the same manner as the 3α-isomer. Recrystallized from methanol, m.p. 95.2–96.2 °C.

Anal. Calcd. for $C_{35}H_{54}O_3$: C, 80.41; H, 10.41. Found: C, 80.61; H, 10.50.

3α-(2-Naphthamido)-cholestane

To 25 ml of dry pyridine was added 1.0 g of 3α-aminocholestane hydrochloride and 1.0 g of 2-naphthoyl chloride and the reaction stirred for 24 h. The reaction was then diluted with 100 ml of water and extracted with chloroform. The chloroform extract was washed with dilute sodium carbonate, water, 2 *N* hydrochloric acid, and water, then dried over sodium sulfate. Evaporation of the solvent left a residue which was recrystallized from acetone to yield the pure naphthamide; yield, 540 mg, m.p. 219.6–219.8 °C.

Anal. Calcd. for $C_{38}H_{55}ON$: C, 84.23; H, 10.23; N, 2.58. Found: C, 84.22; H, 9.97; N, 2.62.

3β-(2-Naphthamido)-cholestane

This compound was prepared in the same manner as the 3α-isomer. Recrystallized from acetone; m.p. 238.2–238.8 °C.

Anal. Calcd. for $C_{38}H_{55}ON$: C, 84.23; H, 10.23; N, 2.58. Found: C, 84.22; H, 10.12; N, 2.61.

Can. J. Chem. Downloaded from www.nrcresearchpress.com by 210.87.254.6 on 09/05/12
For personal use only.

Benzyl-N-nitroso-N-3β-cholestanyl Carbamate

Benzyl-*N*-3β-cholestanyl carbamate (398 mg) was dissolved in dry methylene chloride (10 ml) in a flask equipped with a drying tube. Anhydrous sodium acetate (300 mg) and anhydrous sodium sulfate (300 mg) were added to the solution and the mixture cooled to −20 °C in an ice-salt bath. To this was added, all at once, 10 ml of 0.325 *M* N_2O_4 in dry methylene chloride (1 ml liquid N_2O_4/50 ml CH_2Cl_2) with stirring, and the stirring continued for ½ h at −10 °C. The excess N_2O_4 was then removed *in vacuo* at 0 °C. The reaction was poured into 50 ml of ice cold concentrated sodium carbonate solution and the reaction flask washed with 50 ml of cold ether which was then added to the reaction mixture. The mixture was vigorously shaken and the layers separated. The organic layer was washed with ice cold concentrated sodium chloride solution and dried over sodium sulfate at 0 °C. After decantation the solvent was removed *in vacuo* at 0 °C. The solid yellow residue was dissolved in a minimum amount of pentane and cooled in a Dry Ice – acetone bath for several hours. The crystalline nitroso carbamate was collected by filtration–decantation and dried in hi-vac over P_2O_5; yield 372 mg, m.p. 113–114 °C (dec.).

Anal. Calcd. for $C_{35}H_{54}O_3N_2$: C, 76.32; H, 9.88; N, 5.09. Found: C, 76.45; H, 10.08; N, 5.24.

Benzyl-N-nitroso-N-3α-cholestanyl Carbamate

This compound was prepared in the same manner as the 3β-isomer. This compound could not be separated from unreacted amide and the crude nitroso-derivative was used in subsequent reactions.

N-Nitroso-3β-acetamidocholestane

This nitroso derivative was prepared in the same manner as benzyl-*N*-nitroso-3β-cholestanyl carbamate. It was recrystallized by dissolving in pentane, removing the unreacted amide by filtration, and cooling in a Dry Ice – acetone bath; yield (from 399 mg amide) 253 mg, m.p. 117.0° (dec.).

Anal. Calcd. for $C_{29}H_{50}O_2N_2$: C, 75.93; H, 10.99; N, 6.11. Found: C, 75.75; H, 10.92; N, 6.32.

N-nitroso-3β-(2-naphthamido)-cholestane

This nitroso derivative was prepared in the same manner as the nitroso carbamates. It was not possible to obtain this nitroso compound free from amide and the crude compound was used directly in decomposition reactions.

Preparation and Decomposition of N-Nitroso-3α-(2-naphthamido)-cholestane

A three-necked flask was fitted with two stopcock adapters, a rubber syringe cap, and a magnetic stirrer. One of the stopcock adapters was attached to a source of dry nitrogen. The other was alternately attached to a vacuum pump or opened when nitrogen was flowing through the system. A portion of 3α-(2-naphthamido)-cholestane (1.0 g) was dried in the flask under hy-vac for 2 h. The flask was then filled with dry nitrogen and 25 ml of ether freshly distilled from $LiAlH_4$ was added to the flask. A solution of *n*-butyllithium (1.4 ml, 1.64 *N* in hexane) was added with stirring via a syringe, after which time the solution was clear. The reaction was cooled to −60 °C in a Dry Ice – acetone bath and 50 ml of N_2O_4 gas (dried in the liquid state over P_2O_5) was added with a syringe. The solution rapidly turned yellow.

While continuing stirring, the temperature of the solution was allowed to slowly rise. At approximately −30 °C a small evolution of bubbles could be seen. At −20 °C the evolution of gas was quite evident, and a precipitate began to form. At 0 °C the evolution of gas was finished.

When the reaction had reached room temperature water was added and the layers separated. The non-aqueous layer was washed with concentrated sodium carbonate and water, dried over sodium sulfate, and concentrated to dryness *in vacuo*.

The naphthoates were isolated by chromatography on alumina and analyzed in the same manner as in the case of the decomposition of the 3β-isomer.

Preparation and Decomposition of N-Nitroso-3α-acetamidocholestane

N-Nitroso-3α-acetamidocholestane was prepared in the same manner as benzyl-*N*-nitroso-*N*-3β-cholestanyl carbamate. On the addition of ether during the work-up at 0 °C, the yellow color characteristic of the nitrosoamides disappeared completely and the reaction was then worked-up for the decomposition products. The organic layer was dried over sodium sulfate and concentrated to dryness *in vacuo*. The residue was then analyzed.

Decomposition of Nitrosoamides

The following are given as typical of the methods for decomposition of the nitrosoamides and nitrosocarbamates. All decompositions were performed at room temperature except as otherwise noted in Table 1.

Decomposition of N-Nitroso-3β-acetamidocholestane in Ether

N-Nitroso-3β-acetamidocholestane (175 mg) was dissolved in anhydrous ether (50 ml), 1 g of anhydrous sodium sulfate added, and the mixture was heated under reflux for 18 h. After this time the solution was completely colorless. The solvent was removed *in vacuo*, the residue dissolved in benzene and chromatographed on alumina (8.5 g, Woelm, neutral, activity I). Elution with benzene (45 ml) yielded 62 mg (44.0%) of mixed Δ^2- and Δ^3-cholestanes. Further elution with 2% ether in benzene (6 × 15 ml fractions) yielded 22 mg of pure 3β-cholestanyl acetate and 12 mg of mixed 3α- and 3β-cholestanyl acetates. Further elution with 20% ether in benzene eluted 18 mg of pure 3α-cholestanyl acetate; total acetates, 32.3%. Final stripping of the column with ether and 5% methanol in ether yielded 33 mg (20.2%) of material which was mostly denitrosated amide. The fractions were analyzed first by t.l.c. The composition of the mixed acetate fraction was estimated to be about 70% 3α-cholestanyl acetate by comparison with standard i.r. curves. Total recovery of material was 96.5%.

As a check the acetates were combined and analyzed by i.r. Comparison against standards showed the mixture to be 52% 3β-cholestanyl acetate and 48% 3α-cholestanyl acetate. Values from chromatography were 50% of each isomer.

Decomposition of Benzyl-N-nitroso-N-3α-cholestanyl Carbamate in Ether Containing Excess Diazomethane

Benzyl-*N*-nitroso-*N*-3α-cholestanyl carbamate (152 mg) was dissolved in a freshly prepared solution of diazomethane (approximately 1 g) in 50 ml of ether, which had been dried over KOH pellets. This stood for 48 h in the dark. The excess diazomethane and ether were then removed *in vacuo* and the residue dissolved in a minimum amount of hexane–benzene and chromatographed on alumina (15 g, Woelm,

Can. J. Chem. Downloaded from www.nrcresearchpress.com by 210.87.254.6 on 09/05/12
For personal use only.

neutral, activity III). Elution with hexane (75 ml) yielded 61 mg of mixed Δ^2- and Δ^3-cholestenes. Further elution with 2% benzene in hexane (150 ml) gave 6 mg of mixed benzyl-3α- and 3β-cholestanyl carbonates. Elution with 50% benzene–hexane yielded 54 mg of recovered carbamate. The carbonate mixture was analyzed by comparison with i.r. standards and was found to consist of 74% of benzyl-cholestan-3α-yl carbonate and 26% benzyl-cholestan-3β-yl carbonate.

Decomposition of N-Nitroso-3α-(2-naphthamido)-cholestane in O-Deuterioacetic Acid

N-Nitroso-3α-(2-naphthamido)-cholestane was prepared in the usual manner from 0.99 g of the amide. It was not isolated but was used directly. The nitroso amide was dissolved in a mixture of 40 ml of dry methylene chloride and 10 ml of 99+% *O*-deuterioacetic acid. The reaction was protected from moisture and stood for 3 days at room temperature. The solvents were then removed *in vacuo*. The residue was chromatographed on alumina (30 g, Woelm, neutral, activity II). Hexane (200 ml) eluted 131 mg of cholestenes. Further elution with 200 ml of 50% hexane–benzene gave 544 mg of mixed esters. Finally, elution with benzene yielded 203 mg of naphthamide. This amounts to a recovery of 96.5% based on starting amide.

The esters were separated by fractional sublimation at 0.06–0.03 mm Hg and 108 °C. After 3 days, all of the acetates had sublimed. The sublimation was followed by t.l.c. Analysis of the acetates (71.3 mg) was made by comparison with standards in the i.r. The mixture of acetates contained 25% 3α-cholestanyl acetate and 75% 3β-cholestanyl acetate.

The naphthoates (465 mg) were dissolved in 100 ml of dry ether and excess $LiAlH_4$ added. The reaction was heated at reflux overnight. The excess $LiAlH_4$ was decomposed with ethyl acetate, and then 6 *N* HCl added slowly until the solution was clear. The layers were separated and the ether layer washed twice with water. After drying over anhydrous sodium sulfate, the ether was removed *in vacuo*. The residue (456 mg) was then chromatographed on alumina (150 g, Alcoa F-20). Benzene eluted 59 mg of 3α-cholestanol and benzene–ether (8:1) eluted 355 mg of a mixture of 3β-cholestanol and 2-naphthyl carbinol. The naphthyl carbinol was removed by sublimation at 60° and 0.05 mm Hg. There remained 274 mg of 3β-cholestanol. Samples of the alcohols were crystallized for deuterium analysis. The acetates were used directly.

Thin-layer Chromatography Analyses

Analyses were made using silica gel G specially prepared for t.l.c. according to Stahl. Benzene was used for the moving phase and sulfuryl chloride vapors followed by steam and heating in an oven at 110° was found most satisfactory as a developing agent. Naphthoates could readily be seen with a u.v. lamp prior to sulfuryl chloride treatment. All isomeric pairs were clearly separated when sufficiently small spots of dilute solutions were applied. Only the two cholestenes did not separate. The amides did not move from the origin under these conditions but were readily analyzed by using ethyl acetate as the moving phase.

Analysis of Acetate Mixtures

(a) By Chromatography

The acetate mixture was dissolved in a small amount of benzene and placed on an alumina column (50 times the weight of acetate, Woelm, activity I, neutral). Careful elution with 5% ether in benzene separated the two acetates, the 3β-isomer being the first to come off the column. When no more 3β-isomer was present in the eluants, the remainder was eluted with ether. The composition of the fractions could be followed by t.l.c. The fractions containing each isomer were then combined and weighed.

(b) By Infrared Spectroscopy

A series of standard solutions of mixtures of 3α- and 3β-cholestanyl acetates was prepared varying in steps of 5%. The standards were dissolved in carbon tetrachloride to a final concentration of 30.0 mg/ml. The total acetate mixture from a reaction was also made up to the same concentration. Using a pair of matched 0.5 mm i.r. cells, a base line was recorded and then the reaction mixture recorded against this base line without changing any settings on the instrument. Immediately following this, standard solutions were recorded until the reaction spectrum was bracketed. The peaks used for analysis occur at 1160 and 1131 cm^{-1}. The former is characteristic of 3α-cholestanyl acetate whereas the latter is due to 3β-cholestanyl acetate. It was assumed that the absorption was linear in these small concentration variations and the value of the intermediate peaks of the reaction obtained by extrapolation.

(c) By Gas–Liquid Chromatography

Using a 4 ft × 3/8 in. pretested steroid column containing 3.8% SE-30 on AW-DMCS chromosorb W the acetates were clearly separated at 236 °C. Using an attached integrator the areas under the curves were readily calculated.

The three methods agreed very well.

Analysis of Carbonate Mixtures

A series of standards of mixed 3α- and 3β-benzylcholestanyl carbonates was prepared with a final concentration of 40 mg/ml in carbon disulfide. The spectra of these mixtures were recorded against a base line in matched 0.5 mm cells with the scale expander attachment to a Perkin–Elmer IR-21 set at 5X. Transmission *vs.* % composition was then plotted for five selected absorption peaks, 1389, 1163, 1001, 973, and 951 cm^{-1}. With the exception of the absorption at 1389 cm^{-1} the plots were essentially linear. The carbonate mixtures from the reactions were made up to the same concentration and the spectra recorded. The concentration was then estimated and the value of the 1389 cm^{-1} peak read from the graph for this concentration. The recorded 1389 cm^{-1} peak was then normalized and this factor used for the other peaks. The absorption bands at 1163 and 973 cm^{-1} were used for 3α-isomer rich solutions and those at 1001 and 951 cm^{-1} used for 3β-isomer rich solutions.

Analysis of Naphthoate Mixtures

Naphthoate mixtures were analyzed by reduction to the alcohols with $LiAlH_4$, removal of the 2-naphthyl alcohol by sublimation, and analyzing the residual cholestanols.

Analysis of 3-Cholestanol Mixtures

The cholestanol mixtures were analyzed by the chromatographic method of Vail and Wheeler (19).

Deamination of 3β-Aminocholestane in Glacial Acetic Acid

3β-Aminocholestane (prepared from 523 mg of amine hydrochloride) was dissolved in 50 ml of glacial acetic acid and 2.05 g of sodium nitrite added portionwise over a period of 2 h with stirring. The reaction was stirred overnight. Solvent was removed *in vacuo* and the residue treated

with water and ether. The layers were separated and the aqueous layer extracted twice more with ether. The combined ether layers were dried over sodium sulfate and concentrated to dryness. The residue was analyzed in the same manner as with the nitrosoacetamidocholestanes.

Deamination of 3α-Aminocholestane in Glacial Acetic Acid

The deamination of 3α-aminocholestane and the analysis of its products were similar to the method used for the 3β-isomer.

Deamination of 3β-Aminocholestane in Aqueous Acetic Acid

3β-Aminocholestane (from 433 mg of amine hydrochloride) was dissolved in a mixture of 30 ml H_2O, 40 ml acetic acid, and 20 ml of dioxane. A solution of 1.0 g of sodium nitrite in 10 ml of water was added portionwise over a period of ½ h with stirring, and stirring continued overnight. The insoluble amine nitrate (140 mg) was collected by filtration and the residue concentrated to dryness *in vacuo*. The residue was worked up as with the products from the acetic acid deamination.

Deamination of 3α-Aminocholestane in Aqueous Acetic Acid

The 3α-aminocholestane was deaminated in the same manner as the 3β-isomer except that it was dissolved in a mixture of 40 ml of water and 50 ml of acetic acid. The sodium nitrite was added in a solution of 1.0 g in 10 ml of water.

We wish to thank the National Research Council of Canada and the National Science Foundation (G 12311) for their support of this work.

1. T. N. SHATKINA, E. V. LEONT'VA, and O. A. REUTOV. Dokl. Akad. Nauk, SSSR, **177**, 143 (1967).
2. C. W. SHOPPEE, C. CULSHAW, and R. E. LACK. J. Chem. Soc. C, 506 (1969).
3. T. COHEN and E. JANKOWSKI. J. Am. Chem. Soc. **86**, 4217 (1964).
4. T. COHEN and A. DANIEWSKI. J. Am. Chem. Soc. **91**, 533 (1969).
5. K. SCHREIBER and H. RIPPERGER. Ann. **655**, 136 (1962).
6. C. W. SHOPPEE, R. E. LACK, and P. RAM. J. Chem. Soc. C, 1018 (1966).
7. C. W. SHOPPEE, J. K. HUMMER, R. E. LACK, and S. K. ROY. Tetrahedron Suppl. No. 7, 315 (1966).
8. C. W. SHOPPEE, J. G. FEHER, R. M. HALL, R. E. LACK, and L. TARASHOFF. J. Chem. Soc. C, 2211 (1968).
9. R. N. SEELYE and W. B. WATKINS. Tetrahedron, **25**, 447 (1969).
10. J. LAVISALLE and J. F. MOUCHARD. Bull. Soc. Chim. Fr. 678 (1970).
11. M. C. WHITING. Chem. Brit. **2**, 482 (1966).
12. C. W. SHOPPEE, P. J. W. CEMLYN, D. E. EVANS, and G. H. R. SUMMERS. J. Chem. Soc. 4364 (1957).
13. W. HÜCKEL and K. D. THOMAS. Ann. **645**, 177 (1961).
14. W. HÜCKEL. Ber. **96**, 220 (1963).
15. E. H. WHITE and F. W. BACHELOR. Tetrahedron Lett. **1**, 77 (1965).
16. C. W. SHOPPEE, D. E. EVANS, H. C. RICHARDS, and G. H. P. SUMMERS. J. Chem. Soc. 1649 (1956).
17. D. P. DODGSON and R. D. HAWORTH. J. Chem. Soc. 67 (1952).
18. E. H. WHITE and J. E. STUBER. J. Am. Chem. Soc. **85**, 2168 (1963).
19. O. R. VAIL and D. M. S. WHEELER. J. Org. Chem. **27**, 3803 (1962).
20. E. H. WHITE and D. J. WOODCOCK. *In* The chemistry of the amino group. *Edited by* S. Patai. Interscience Publishers, New York, 1968. p. 446.
21. (*a*) E. H. WHITE and C. A. AUFDERMARSH, JR. J. Am. Chem. Soc. **83**, 1174 (1961); (*b*) A. STREITWEISER and W. D. SCHAEFFER. J. Am. Chem. Soc. **79**, 2893 (1957).
22. E. H. WHITE. J. Am. Chem. Soc. **77**, 6014 (1955).
23. G. CHIURDOGLU and W. MASSCHELEIN. Bull. Soc. Chim. Belges, **70**, 767 (1961).
24. See ref. 20, p. 447.
25. E. H. WHITE, H. P. TIWARI, and M. J. TODD. J. Am. Chem. Soc. **90**, 4736 (1968).
26. M. WILHELM and D. Y. CURTIN. Helv. Chim. Acta, **40**, 2129 (1957).
27. See ref. 20, p. 479.
28. J. L. PINKUS, G. PINKUS, and T. COHEN. J. Org. Chem. **27**, 4356 (1962).

Can. J. Chem. Downloaded from www.nrcresearchpress.com by 210.87.254.6 on 09/05/12
For personal use only.

Synthesis and Isomerization of Adducts of Azodicarbonyl Compounds and Cyclopentadiene

J. A. CAMPBELL, DONALD MACKAY, AND T. D. SAUER
Department of Chemistry, University of Waterloo, Waterloo, Ontario

Received August 20, 1971

The synthesis of a range of bicyclic Diels–Alder adducts (structures *b*) of cyclopentadiene with symmetrical and unsymmetrical azodicarbonyl compounds is described. Thermal isomerization of these adducts to the bicyclic 1,3,4-oxadiazines (structures *c* and *d*) is especially rapid with bulky acyl groups. In unsymmetrical adducts with acyl groups of markedly different size, the larger group dictates completely the direction of isomerization. Adducts with two different aroyl groups give both isomers.

Spectroscopic properties of the adducts, the oxadiazines and the dihydro derivatives of the oxadiazines are described.

La synthèse d'une gamme de composés d'addition bicycliques du type Diels–Alder (structures *b*) du cyclopentadiène avec des composés azo-dicarbonyles symétriques et non symétriques est décrite. L'isomérisation thermique de ces composés d'addition en oxa-1,3,4 diazines bicycliques (structures *c* et *d*) est rapide spécialement avec des groupes acylés volumineux. Dans les composés d'addition non symétriques avec des groupes acyles de taille nettement différente, le groupe le plus gros impose complètement la direction d'isomérisation. Les composés d'addition avec deux groupes aroyles différents donnent à la fois des isomères.

Les propriétés spectroscopiques des composés d'addition, les oxadiazines et les dérivés dihydro des oxadiazines sont décrits.

Canadian Journal of Chemistry **50**, 371 (1972)

Can. J. Chem. Downloaded from www.nrcresearchpress.com by 210.87.254.105 on 09/05/12
For personal use only.

We have recently shown (1) that the thermal isomerization of the cyclopentadiene adduct **1***b* (2) gives, as suspected (3), the racemic 1,3,4-oxadiazine derivative **1***c,d*. The isomerization was cleanly first order, was relatively insensitive to solvent character, had a negative entropy of activation, and thus possessed all the features of a [3,3] sigmatropic process (4).

We now wish to describe the synthesis and properties of a range of adducts from cyclopentadiene and azodicarbonyl compounds and of their thermal isomers. These include the achiral[1] adducts **2***b*–**7***b* from symmetrically substituted azo compounds which give the racemates **2***c,d*–**7***c,d*[2] and the chiral ones (one enantiomer shown) **8***b*–**12***b* from unsymmetrically substituted azo compounds, and from each of which potentially two structural isomers, **8***c*–**12***c* and **8***d*–**12***d*, can be expected.

All of the azo compounds **2***a*–**12***a* required for the present study were obtained by oxidation of the appropriate dicarbonylhydrazine with *N*-bromosuccinimide (NBS) in the presence of pyridine (5) or by oxidation of the mercury(II) salt of the hydrazine with bromine (2). Only **3***a*, **7***a*, **9***a*, and **12***a* (6–9) have been previously prepared as pure substances.

The diaroyl azo compounds **2***a*, m.p. 155.5–157.5°, **4***a*, m.p. 157°, and **8***a*, m.p. 96–97° were all stable crystalline substances. None of the others could be isolated in crystalline form.

There have been several attempts (9–13) to synthesize azodiacetyl, the simplest aliphatic azodiacyl, but in no case has the product been adequately characterized. Stollé (10) described it as an unstable red oil, obtained by treating the mercury(II) salt of diacetylhydrazine with iodine, and Inhoffen *et al.* (11) prepared a solution of it by a similar method, and converted it into diacetyl by heating with cupric oxide. Curtin and Miller (13) measured its C=O stretching frequency in carbon tetrachloride but did not attempt to isolate it. We failed to obtain a satisfactory product using the mercury salt method but realized consistent, if modest, yields (30–35%) by stirring equimolar amounts of the hydrazine, NBS, and quinoline[3] in a suitable solvent (tetrachloroethylene, carbon tetrachloride, or benzene) and co-distilling the azo compound with the solvent. Azodiacetyl is a volatile red oil with a penetrating odor. Its solutions were in fact stable indefinitely at room tempera-

[1]On the basis of time-averaged conformational processes.
[2]Hereafter these will be designated simply as *e.g.* **2***c*.
[3]Preferred over pyridine (the more usual base in NBS oxidations) which also co-distilled with the solvent.

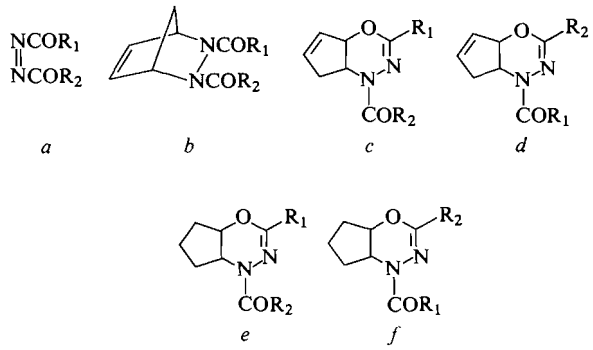

a *b* *c* *d* *e* *f*

1 $R_1 = R_2 = Ph$
2 $R_1 = R_2 = p\text{-}BrC_6H_4$
3 $R_1 = R_2 = p\text{-}MeOC_6H_4$
4 $R_1 = R_2 = p\text{-}O_2NC_6H_4$
5 $R_1 = R_2 = CMe_3$
6 $R_1 = R_2 = Me$
7 $R_1 = R_2 = OEt$
8 $R_1 = Ph$; $R_2 = p\text{-}BrC_6H_4$
9 $R_1 = p\text{-}O_2NC_6H_4$; $R_2 = p\text{-}MeOC_6H_4$
10 $R_1 = CMe_3$; $R_2 = Ph$
11 $R_1 = Ph$; $R_2 = Me$
12 $R_1 = Ph$; $R_2 = OEt$

ture and it had a half-life of 2 days in refluxing benzene.

Azodipivaloyl (**5***a*) has not been described It was obtained as a red oil by NBS oxidation of dipivaloylhydrazine (14) and was purified by vacuum distillation; it was stable only if stored below $-10°$. It was a rather unreactive dienophile, its condensation with cyclopentadiene taking 2 days at 10°.

NBS oxidation in carbon tetrachloride of 1-acetyl-2-benzoylhydrazine and of 1-benzoyl-2-pivaloylhydrazine (from benzoylhydrazine and pivaloyl chloride) gave the unsymmetrical azo compounds acetylazobenzoyl (**11***a*) and benzoylazopivaloyl (**10***a*), respectively. Both were unstable and were used directly in dilute solution; evaporation of the solvent caused rapid decomposition.

The azo compounds, except **5***a* and **10***a*, reacted rapidly at room temperature with cyclopentadiene, directly, or in solution in benzene or carbon tetrachloride, to give the adducts **2***b*–**12***b*, all of which were crystalline except **8***b*. Their melting points, spectroscopic data, and elementary analyses are shown in Table 1.

The i.r. spectra in the carbonyl region in general showed a doublet, even for the symmetrically substituted adducts. The appearance of the n.m.r. spectra of the latter closely resembled that of the related *N,N'*-dialkoxycarbonyl derivatives (*e.g.* **7***b*) (15), the vinyl and tertiary protons being an isochronous pair at room temperature and the methylene protons a very tight AB system, rarely (an example is **2***b*) discernible as a quartet. The unsymmetrical adducts **9***b*, **10***b*, and **11***b* showed non-equivalence in their tertiary protons.

The methyl group of the dianisoyl compound **3***b* absorbed sharply, but those of the dipivaloyl compound **5***b* and the diacetyl compound **6***b* showed slight broadening, which in the case of the latter sharpened by 55° (**5***b* was too labile to be examined at higher temperatures). These broadening effects are doubtless due to slow interconversion of planar rotamers involving the amide C—N bonds, and are strictly analogous to those found in their *N,N'*-dialkyoxycarbonyl counterparts (15) and in amides and urethanes in general (16).

As observed for **1***b* (1) the isomerization of the adducts **2***b*–**12***b* (except **7***b*, which was stable) could be achieved by heating neat or in solution and was quantitative in either case. Routinely they were refluxed in aqueous alcohol, isooctane, or (for the rather stable **6***b* and **12***b*) tetrachloroethylene, the residue from the solution after reflux being the pure oxadiazines. The adduct **5***b* was exceptionally labile, isomerizing slowly at room temperature and rapidly above its m.p. of 68°. (The m.p. had to be taken by insertion of the capillary tube into the apparatus just below this temperature. After melting the sample solidified and remelted at 74.5–75.5°, that of the pure oxadiazine **5***c*.) Table 2 lists properties of these oxadiazines.

The quantitative nature of the reaction with respect to oxadiazine formation was also revealed by u.v. analysis which was especially

Can. J. Chem. Downloaded from www.nrcresearchpress.com by 210.87.254.105 on 09/05/12
For personal use only.

Can. J. Chem. Downloaded from www.nrcresearchpress.com by 210.87.254.105 on 09/05/12
For personal use only.

TABLE 1. Properties of 2,3-diacyl-2,3-diazabicyclo[2.2.1.]hept-5-enes

Compound	The m.p. (°C)*	$\nu(CCl_4)$ (cm^{-1}) C=O		$\tau(CCl_4$ or $CDCl_3)$ $H_{5,6}$	$H_{1,4}$	H_7	Aryl or other‡	Analysis Calcd.: Found:	C	H	N
2*b*	150–151 (*a*)	1700	1673	3.55	4.81	8.00, 8.22	2.45	$C_{19}H_{14}Br_2N_2O_2$			34.6 (Br) 34.3 (Br)
3*b*	124–125 (*b*)	1690	1640	3.57	4.78	7.98, 8.16	1.7, 2.0 q 6.24 (OMe)	lit. (8)			
4*b*	220 (*c*)	1695	1663†	3.45	4.77	7.97, 8.15	1.7, 2.2 q	$C_{19}H_{14}N_4O_6$	57.9 58.1	3.6 3.7	14.2 14.2
5*b*	68 (*d*)	1703	1650	3.58	4.70	8.18	8.71 (*t*-Bu)	$C_{14}H_{24}N_2O_2$	68.2 68.4	9.2 9.1	10.6 10.6
6*b*	106–106.5 (*e*)	1705	1680	3.43	4.46	8.24	7.88 (Me)	$C_9H_{12}N_2O_2$	60.0 59.7	6.7 6.7	15.6 15.8
8*b*	Glass	1700	1675	3.72	4.96	8.14, 8.38	2.2–2.9				
9*b*	112–113 (*b*)	1690	1654	3.50	4.63 4.80	7.98, 8.18	2.3, 3.0 q 6.15 (OMe)	lit. (8)			
10*b*	87–88.5 (*d*)	1695	1650	3.65	4.67 5.00	8.4	2.3–2.8 8.87 (*t*-Bu)	$C_{17}H_{20}N_2O_2$	71.8 72.0	7.1 7.3	9.9 10.1
11*b*	100.5–101 (*e*)	1683		3.35 3.65	4.50 4.90	8.25	1.9–2.8 8.03 (Me)	$C_{14}H_{14}N_2O_2$	69.4 68.7	5.8 5.8	11.6 11.9
12*b*	68.5–70° (*e*)	1747 1695	1707 1655	3.53	4.90	8.30	2.2–2.9 5.97, 8.87 (Et)	$C_{15}H_{16}N_2O_3$	66.2 66.4	5.9 6.0	10.3 10.5

*Crystallization from: (*a*) benzene–hexane; (*b*) aqueous MeOH; (*c*) Me_2CO; (*d*) pentane; (*e*) CCl_4–hexane.
†Solvent: CH_2Cl_2.
‡τ-Values separated by a dash are at the extreme limits of the absorption; q, quartet.

Can. J. Chem. Downloaded from www.nrcresearchpress.com by 210.87.254.105 on 09/05/12
For personal use only.

TABLE 2. Properties of *cis*-4-acyl-4,4*a*,5,7*a*-tetrahydrocyclopenta-1,3,4-oxadiazines

Compound	The m.p. (°C)*	ν(Nujol) (cm^{-1})		τ(CCl_4 or $CDCl_3$)						Analysis			
		C=O	C=N	H_7	H_6	$H_{4a,7a}$	H_5		Aryl or other	Calcd.: Found:	C	H	N
2*c*	145–147 (*a*)	1656	1634	3.66	3.88	4.9–5.1‡	6.87	7.60	2.2–2.7	$C_{19}H_{14}Br_2N_2O_2$			34.6 (Br) 34.3 (Br)
3*c*	132 (*a*)	1638		3.68	3.89	4.8–5.3	6.90	7.59	2.1, 3.1 q 6.20 (OMe) 6.37 (OMe)	$C_{21}H_{20}N_2O_4$	69.2 69.2	5.5 5.7	7.7 7.5
4*c*	230.5–231.5 (*a*)	1661	1632	3.56	3.76	4.7–5.2	6.78	7.53	1.65, 2.0 q 1.8, 2.1 q	$C_{19}H_{14}N_4O_6$	57.9 58.0	3.6 3.4	14.2 14.1
5*c*	74.5–75.5 (*b*,*s*)	1650	1634	3.82	4.08	5.1–5.5	7.17	8.02	8.70 (*t*-Bu) 8.84 (*t*-Bu)	$C_{15}H_{24}N_2O_2$	68.2 68.3	9.2 9.0	10.6 10.6
6*c*	74–74.5 (*b*)	1673	1660	3.77	4.06	4.9–5.6	7.18	7.97	7.87 (OMe) 8.08 (OMe)	$C_9H_{12}N_2O_2$	60.0 60.1	6.7 6.8	15.6 15.3
9*c*	201–202 (*c*)	1651	1632†	3.60	3.80	4.8–5.1	6.83	7.62	1.8, 2.1 q 2.1, 3.0 q 6.08 (OMe)	$C_{20}H_{17}N_3O_5$	63.3 63.3	4.5 4.7	11.1 11.0
9*d*	134–135 (*c*)	1656	1639	3.62	3.83	4.8–5.1	6.92	7.58	1.7, 2.0 q 2.4, 3.2 q 6.18 (OMe)		63.3	4.7	11.0
10*c*	97–98 (*s*)	1650	1638	3.78	4.03	5.19, 5.33	7.00	7.72	2.2, 2.7 8.92 (*t*-Bu)	$C_{17}H_{20}N_2O_4$	71.8 71.7	7.1 7.1	9.9 10.0
11*c*	137–140 (*a*)	1657	1626	4.00	4.18	5.2–5.7	7.37	8.02	2.4, 2.9 7.87 (Me)	$C_{14}H_{14}N_2O_2$	69.4 69.4	5.8 5.9	11.6 11.8
12*c*	113.5–114 (*a*)	1733	1638	3.93		5.2–5.5	7.18	7.70	2.2, 2.8 5.72, 8.63 (Et)	$C_{15}H_{16}N_2O_3$	66.2 66.3	5.9 5.8	10.3 10.3

*Crystallization from: (*a*) aqueous MeOH; (*b*) pentane; (*c*) aqueous Me_2CO; (*s*) purified by sublimation.
†Solvent: CCl_4.
‡See footnote ‡ Table 1.

Can. J. Chem. Downloaded from www.nrcresearchpress.com by 210.87.254.105 on 09/05/12
For personal use only.

TABLE 3. Relative isomerization rates for symmetrical adducts in 71% aqueous ethanol at 77°

	$R_1 = R_2$	Relative rate
1*b*		1.00*
2*b*	*p*-BrC_6H_4	3.10
3*b*	*p*-$MeOC_6H_4$	1.12
4*b*	*p*-$O_2NC_6H_4$	7.15
5*b*	Me_3C	30.8
6*b*	Me	0.02†

*Actual value: 2.42×10^{-4} s^{-1}.
†Estimated from the value in refluxing tetrachloroethylene by assuming an E_a of 22 kcal mol^{-1}, a typical value for these adducts.

suitable for a kinetic study by following the development of the R—C(=N)— chromophore in the oxadiazine. This ranged between 280 and 350 nm for aromatic R groups and occurred around 240 nm for aliphatic ones. In all instances one or more isobestic points were observed. Detailed kinetic studies on the isomerization of these and related adducts have been carried out over a range of temperatures, and a discussion of the effect of structure and solvent on rates and thermodynamic activation parameters will be presented in a later publication. Relative rate constants for the isomerization of the symmetrical adducts at 77° in 71% aqueous ethanol are shown in Table 3, the value for **1***b* being taken as unity. Similar trends were found in iso-octane.

The remarkable rate enhancement for the dipivaloyl adduct **5***b* and retardation for the diacetyl adduct **6***b* suggest that the rearrangement is strongly subject to steric assistance. In line with this the adduct **10***b* from benzoylazopivaloyl isomerized rapidly to give only the oxadiazine **10***c* arising by participation of the pivaloyl group, while the adduct **11***b* gave only the oxadiazine **11***c* arising by participation of the benzoyl group. An inhibiting effect in carbonyloxy substituents is inferred by the fact that the adduct **7***b* from diethyl azodicarboxylate was stable indefinitely at 77°,[4] and the adduct **12***b* from ethyl benzoylazocarboxylate isomerized slowly, but by participation of the benzoyl group only, to the oxadiazine **12***c*.

In the isomerization of each of these three unsymmetrical adducts no trace of the isomeric oxadiazine, **10***d*, **11***d*, or **12***d* could be detected. All spectra of the total reaction product were superimposable on those of purified oxadiazine and samples of the adducts heated in sealed capillary tubes at 100° eventually (minutes for **10***b*, up to 2 days for **11***b* and **12***b*) gave the melting points of analytically pure products.

In the ensuing structure proofs of oxadiazines from unsymmetrical adducts great advantage was taken of the ease of removal by sulfuric acid of the *N*-acyl substituent on the dihydro derivative of an oxadiazine, first observed for the dihydro derivative **1***e* (1). The resulting base could then be converted into a range of *N*-acyl derivatives. Some properties of the dihydro oxadiazines obtained by this technique and by direct hydrogenation are shown in Table 4.

The structure of **10***c* follows from the absence of a u.v. band around 290 nm, required by the Ph—C(=N)— chromophore in the isomer **10***d*, and by its conversion into the dihydro derivative **5***e* as shown in Scheme 1. Hydrogenation (di-imide) of **10***c* to **10***e* and de-benzoylation gave a base (not isolated) which was converted by pivaloyl

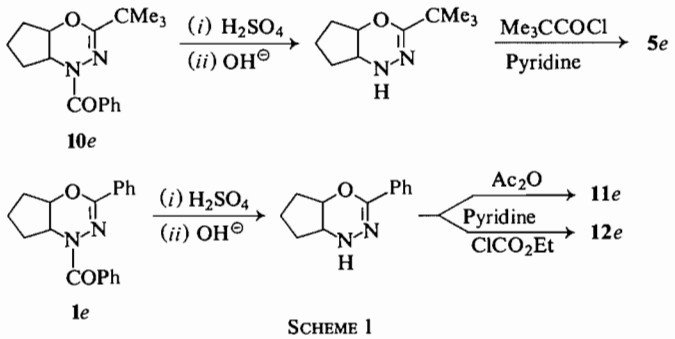

SCHEME 1

[4]At temperatures above 150° complex decomposition occurred.

TABLE 4. Properties of *cis*-4-acyl-4,4*a*,5,6,7,7*a*-hexahydrocyclopenta-1,3,4-oxadiazines (structures *e*, *f*)

Compound	The m.p. (°C)*	ν(Nujol) (cm^{-1}) C=O	ν(Nujol) (cm^{-1}) C=N	Analysis Calcd.: Found:	C	H	N
3*e*	102–104	1630		$C_{21}H_{22}N_2O_4$	68.8 68.6	6.1 6.2	7.7 7.7
5*e*	89–90 (*s*)	1705, 1700, 1693		$C_{15}H_{26}N_2O_2$	67.6 67.8	9.8 9.9	10.5 10.4
8*e*	176–177.5	1643, 1627		$C_{19}H_{17}N_2O_2Br$			20.7 (Br) 21.0 (Br)
9*f*	115–116.5	1659, 1630		$C_{20}H_{19}N_3O_4$	63.0 62.9	5.0 5.2	11.0 10.7
10*e*	102–103	1639, 1632		$C_{17}H_{22}N_2O_2$	71.3 71.3	7.7 7.7	9.8 9.7
11*e*	64–64.5	1675, 1656, 1624		$C_{14}H_{16}N_2O_2$	68.8 68.8	6.6 6.5	11.5 11.2
12*e*	105.5–106	1728, 1633		$C_{15}H_{18}N_2O_3$	65.7 65.5	6.6 6.5	10.2 10.2

*Crystallization from aqueous MeOH; (*s*), purified by sublimation.

chloride in pyridine into **5***e*, an authentic sample of which was obtained from **5***c* by catalytic hydrogenation with PtO_2.

The structure proof for the products **11***c* and **12***c* was obtained in a related manner as shown in Scheme 1, involving a rational synthesis of their dihydro derivatives.

As Table 3 shows, the rearrangement is evidently less sensitive to electronic than to steric effects. All para substituents appear to be rate enhancing, even when these have electronic effects as different as nitro and methoxy. The small spread in the rate values for the adducts **1***b*–**4***b* was reflected in the behavior of the two unsymmetrical adducts **8***a* and **9***a* from which both isomeric oxadiazines were produced in each case.

The adduct **8***b*, a glassy solid, was isomerized in 71% aqueous ethanol to give a crystalline product which showed only a single peak under a wide range of gas chromatographic conditions. The i.r., u.v., and n.m.r. spectra likewise failed to show whether one or both isomers had been produced; no major distinctions would indeed be expected in the spectra of these isomers. The proof of the formation and identities of both isomers, **8***c* and *d*, is outlined in Scheme 2.

Hydrogenation of the product with di-imide gave the dihydro derivatives **8***e* and *f*, again inseparable by g.l.c., which were de-aroylated with sulfuric acid to the mixture of non-isomeric bases. These were readily distinguished by analytical g.l.c. and had exactly equal peak areas. Assuming that the hydrogenation and de-aroylation steps were equally efficient (the yields were close to quantitative in each), and that the peak areas reflect molar ratios, the yields of the oxadiazines **8***c* and *d* were equal. A portion of the mixture of bases was treated with benzoyl chloride in pyridine to give the

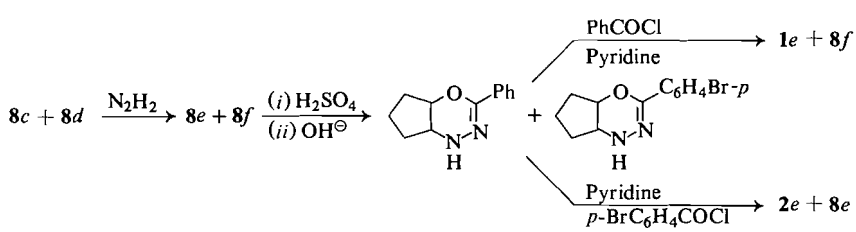

SCHEME 2

Can. J. Chem. Downloaded from www.nrcresearchpress.com by 210.87.254.105 on 09/05/12
For personal use only.

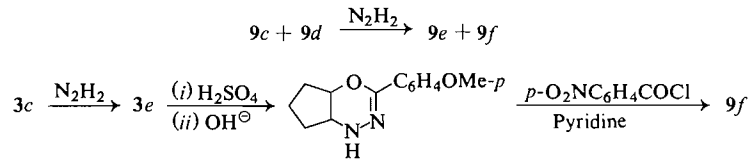

SCHEME 3

benzoyl derivatives separable by g.l.c. The more volatile had the same retention time as authentic **1***e* (by comparative g.l.c.) and the other the same retention time as the mixture of **8***e* and *f*, and was therefore **8***f*. *p*-Bromobenzoylation of the remainder of the basic mixture likewise gave two oxadiazines, the more volatile (**8***e*) in the g.l.c. having the retention time of the mixture of **8***e* and *f* and the other that of authentic **2***e*, obtained by hydrogenating **2***c*.

The analysis of the isomer mixture obtained from **9***b* in refluxing ethanol was more straightforward. The n.m.r. spectroscopy showed two methoxy singlets which were sufficiently shifted at 100 MHz to permit accurate integration, and were found to be in the ratio 60:40 (the ratio was identical when the isomerization was carried out in refluxing benzene). Separation of the isomers was partially achieved by chromatography on silica gel and completed by crystallization from aqueous methanol, giving an oxadiazine of m.p. 134–135°, λ_{max} 281 nm and one of m.p. 201–202°, λ_{max} 345 nm, the methoxy peak of the latter being coincident with the major peak in the spectrum of the mixture. The identities of these were inferred as **9***d* (40%) and **9***c* (60%), respectively, by the position of their ArC(=N)— chromophores (see later), and were proven more directly (Scheme 3) by reaction sequences analogous to those used for the brominated oxadiazines. Hydrogenation of the mixture gave dihydro derivatives **9***e* and *f* in which the ratio of the methoxy peak areas in the n.m.r. spectrum was unaltered: the minor peak was coincident with the methoxy peak of synthetic **9***f*, obtained by de-anisoylation of the dihydro-derivative of **3***b* and *p*-nitrobenzoylation of the resulting base.

The possibility has been recognized of a variety of structural types isomeric with the adducts *b*, all of which may be considered as formally arising by various cycloaddition modes of the azo compound to one double bond of the diene. These include [2 + 2] addition (to 1,2-diazetidines) and [2 + 4] addition (to dihydro-1,3,4-oxadiazines), as well as [2 + 3] and [2 + 6] addition (17).

The thermal isomers generated in the present series of reactions are indeed the bicyclic dihydro-oxadiazines; they are formed directly by the sigmatropic rearrangement of the parent adduct and not by a retro Diels–Alder reaction of the latter with recombination of the resulting diene and azo compound by reverse roles (heterodiene reaction). These conclusions follow from the similarity of spectra and properties of the isomers and their dihydro derivatives with those of **1***b* and *e*, respectively, (1), and by the quantitative nature of the isomerization reaction and its thermodynamic activation parameters.

The i.r. and n.m.r. spectra of the oxadiazines present a particularly uniform picture. Data from these are listed in Table 2.

The C=O and C=N stretching frequencies occurred between 1675 and 1625 cm^{-1} either as a broad band or as a doublet with the lower frequency peak being the less intense and presumably assignable to the C=N. The peak separation was more distinct in the solid phase (Nujol) than in carbon tetrachloride or chloroform solutions. A strong peak around 1090 cm^{-1} was also present; this has been attributed to the C—O—C stretching mode (18).

The key features of the n.m.r. absorptions of the cyclopentadiene derived protons in the oxadiazines were a well spaced strongly split methylene AB quartet (J_{AB} in the range 9–18 Hz), a complex overlapping pattern for the tertiary hydrogens, peaked towards the high field end, and a closely spaced vinyl AB quartet; both AB quartets showed additional fine structure.

The u.v. absorption data for the pyridazines, their isomeric oxadiazines, and the dihydro derivatives of the latter are listed in Table 5. As expected neither the position nor the intensity of the C=O and C=N bands in the oxadiazine was affected by hydrogenation of the olefinic

Can. J. Chem. Downloaded from www.nrcresearchpress.com by 210.87.254.105 on 09/05/12
For personal use only.

Can. J. Chem. Downloaded from www.nrcresearchpress.com by 210.87.254.105 on 09/05/12
For personal use only.

TABLE 5. The u.v. absorption data for the adducts *b*, oxadiazines *c*, *d*, and dihydro-oxadiazines *e*, *f* in ethanol

	λ_{max} (nm)	$\varepsilon \times 10^{-4}$
Pyridazines		
1*b*	255	1.28
3*b*	266*	1.98
4*b*	257	†
5*b*	‡	
6*b*	‡	
9*b*	268	2.56
10*b*	261	0.82
Oxadiazines		
1*c*	290	1.98
2*c*	300	2.29
3*c*	251, 301§	1.92, 2.12
4*c*	243, 333	†
5*c*	238	1.03
6*c*	239	1.43
9*c*	248, 345*	1.80, 1.27
9*d*	281*	2.03
10*c*	258	1.10
11*c*	281	1.25
12*c*	278	1.52
Dihydro-oxadiazines		
1*e*	290	1.33
3*e*	262, 299	1.87, 2.15
5*e*	239	1.43
9*f*	281	2.54
10*e*	260	1.02
11*e*	281	1.25

*71% aq EtOH.
†Saturated; very low solubility.
‡End absorption.
§Carbon tetrachloride.

bond. Examination of these spectra show them to be of unmistakeable diagnostic value.

The di-*p*-bromobenzoyl derivative **2***b* and the dianisoyl derivative **3***b* both absorb at longer wavelengths than the unsubstituted **1***b*, in keeping with the expected re-inforcing effect of two benzenoid substituents of opposite electronic character para to one another (19). The *p*-bromobenzoyl group and the anisoyl group in the unsymmetrical adducts **8***b* and **9***b*, respectively, likewise show this shift. By contrast the di-*p*-nitrobenzoyl derivative **4***b* shows little band shift.[5]

An electron releasing effect from the C=N group to the benzene ring is evident in the 3-aryloxadiazines since the band in the parent phenyl derivative **1***c* at 292 nm shifts to longer wavelengths (333 nm) in the dinitro compound **4***c*. There is also an interaction with the amide aroyl group since the *p*-nitrobenzimidoyl chromophores are even further shifted (to 345 nm) when the electron releasing, and hence stabilizing, *N*-anisoyl group is present (**9***c*). The isomer of **9***c* in which the substituent positions are exchanged, **9***d*, shows a dramatic reversal of these electronic effects: the *p*-methoxybenzimidoyl and *p*-nitrobenzoyl chromophores form a composite band at 281 nm.

The aliphatic imidoyl chromophores are evidently at longer wavelengths than the *N*-acyl chromophores. The *N*-acetyl and *N*-pivaloyl bands cannot be resolved from the end absorption (see the adducts **6***b* and **5***b*, or the oxadiazine **11***c* in which only the PhC=N band is detectable) and so the bands in the oxadiazines **6***c* and **5***c* at 239 and 238 nm are due to the acetimidoyl and pivalimidoyl chromophores, respectively.

The synthetic potential implicit in the sequence of isomerization, hydrogenation, dearoylation, and re-aroylation (see *e.g.* Schemes 1–3) points to the feasibility of a detailed study of these electronic effects with an almost unrestricted choice of substituents.

[5]The short wavelength bands in many of these adducts appeared as shoulders on the end absorption, and the absorption maximum was in some cases hard to estimate. The trends described, however, were clear.

Experimental

The i.r. spectra were taken on a Beckman IR 10 spectrophotometer. A Coleman EPS-3T Hitachi spectrophotometer or a Bausch and Lomb Spectronic 505 were used for measuring u.v. and visible spectra. The n.m.r. analyses were done on a Varian T-60 or HA-100 spectrometer and absorptions are quoted in τ values against tetramethylsilane as internal standard. For g.l.c. a Beckman GC4 instrument fitted with a dual flame ionization detector was used; the columns were 6 ft. × 1/8 in. 3% SE30 on Chromosorb W.

Solvents were purified by conventional means. Anhydrous magnesium sulfate was used as drying agent for solutions in organic solvents. Melting points are uncorrected.

Azo Compounds (2a–12a)

Compounds 3a, 7a, 9a, and 12a

Compounds **3***a* (m.p. 131–132° (6)), **9***a* (m.p. 131–132° (8)), and **12***a* (an oil (9)) were prepared by published procedures. Compound **7***a* was purchased from Aldrich Chemical Co.

Azo-di-p-bromobenzoyl (2a)

Compound **2***a* was obtained by oxidation of the mercury(II) salt of 1,2-di-*p*-bromobenzoylhydrazine (20) with bromine in carbon tetrachloride (2). It formed yellow crystals, m.p. 155.5–157.5° (dec.), from cyclohexane.

Anal. Calcd. for $C_{14}H_8Br_2N_2O_2$: Br, 40.5. Found: Br, 40.9.

p-Bromoazodibenzoyl (8a)

Compound **8***a* was prepared similarly from 1-benzoyl-2-*p*-bromobenzoylhydrazine (21). It was a pale orange solid, m.p. 96–97°, after crystallization from carbon tetrachloride.

Can. J. Chem. Downloaded from www.nrcresearchpress.com by 210.87.254.105 on 09/05/12
For personal use only.

Anal. Calcd. for $C_{14}H_9BrN_2O_2$: Br, 25.2. Found: Br, 25.5.

Azodi-p-nitrobenzoyl

Oxidation of the mercury salt of 1,2-di-*p*-nitrobenzoylhydrazine (22) with bromine in methylene chloride gave the sparingly soluble *azodi-p-nitrobenzoyl* which was precipitated from its solution by addition of pentane as a yellow solid, m.p. 157° (dec.).

Azodipivaloyl (5a)

A slurry of 1,2-dipivaloylhydrazine (4.0 g, 20 mmol) (14), *N*-bromosuccinimide (3.56 g, 20 mmol), and pyridine (1.61 ml, 20 mmol) in carbon tetrachloride (75 ml) was stirred for 45 min with exclusion of moisture. The whole was filtered and evaporated under reduced pressure and the residue taken up in pentane (20 ml) which caused the precipitation of some hydrazine. Filtration, evaporation, and distillation gave pure *azodipivaloyl* (2.0 g, 50%) as a red oil, b.p. 54°/1.3 mm; $\nu(CCl_4)$ 1752 cm^{-1} (C=O); $\tau(CCl_4)$ 8.73 p.p.m. (sharp singlet).

The azo compound decomposed slowly at room temperature but was stable at −10°.

Azodiacetyl (6a)

1,2-Diacetylhydrazine (Aldrich Chemical Co., recrystallized from benzene–methanol to m.p. 138.5–139.5°) (12.0 g, 105 mmol), *N*-bromosuccinimide (17.8 g, 100 mmol), and quinoline (12.9 g, 100 mmol) were stirred at room temperature for 3 h in tetrachloroethylene (120 ml). The mixture was filtered and the precipitate washed with further solvent (50 ml, in portions). The filtrate and washings were distilled through a 10 in. fractionating column under reduced pressure so that the temperature at the top of the column was in the range 30–35°. Towards the end of the distillation fresh solvent was added to the flask and the whole process continued till the distillate was almost colorless. The total red distillate (*ca.* 170 ml) contained 33 mmol (33%) of azodiacetyl, determined by n.m.r. analysis against the methyl peak in methyl benzoate added as an internal standard (analysis before distillation showed the yield to be 51%). The distillate was free of bromine (negative iodide test) and of quinoline (n.m.r.).

Benzene and carbon tetrachloride could also be used as solvents for the oxidation, but the final distillation then required the addition of fresh solvent several times to complete the co-distillation of the azo compound. Concentration of the solution at room pressure then gave a solution of any desired concentration.

Evaporation of a solution gave a red oily residue of azo compound which volatilized on standing and had a sharp penetrating odor. Solutions were stable indefinitely at room temperature, and in refluxing benzene (7×10^{-2} *M*) it had a half-life of 2 days.

The azo compound had $\nu(CCl_4)$ 1767 cm^{-1} (C=O) (lit. (13) 1765 cm^{-1}); λ_{max} (C_2Cl_4) 455 nm (ε 32); $\tau(CCl_4)$ 7.61, (C_2Cl_4) 7.75 p.p.m.

Benzoylazopivaloyl (10a)

Benzoylhydrazine (38.7 g, 282 mmol) and pivaloyl chloride (34.0 g, 282 mmol) were allowed to react in pyridine (200 ml) for 3 h at room temperature. The resulting slurry was added to water and the product recrystallized from aqueous ethanol (58%) or, more efficiently, sublimed at 200°/0.5 mm (85%) to give colorless 1-benzoyl-2-pivaloylhydrazine, m.p. 189–190°; $\nu(CCl_4)$ 3415, 3250 (NH), 1640 cm^{-1} (C=O); $\tau(CDCl_3)$ 0.13 (1 NH, doublet), 1.0 (1 NH, doublet, J = 5 Hz), 2.0–2.8 (5 phenyl H), 8.77 p.p.m. (9 *t*-Bu H, sharp singlet).

Anal. Calcd. for $C_{12}H_{16}N_2O_2$: C, 65.4; H, 7.3; N, 12.7. Found: C, 65.2; H, 7.2; N, 12.9.

The hydrazine was oxidized by the same method and on the same scale as in the preparation of azodipivaloyl. The carbon tetrachloride filtrate was concentrated and pentane added to precipitate out impurities. The red solution was used directly in synthesis since concentration to a small volume led to rapid evolution of nitrogen. The azo compound had $\nu(CCl_4)$ 1749, 1726 cm^{-1} (C=O); $\tau(CCl_4)$ 1.9–2.7 (5 phenyl H), 8.7 p.p.m. (9 *t*-Bu H, sharp).

Acetylazobenzoyl (11a)

Similar oxidation of 1-acetyl-2-benzoylhydrazine (from benzoylhydrazine and acetic anhydride with a trace of sulfuric acid) gave the azo compound which was also unstable (10) and was used in solution. The n.m.r. spectrum showed solutions so prepared to be slightly contaminated (pyridine and some aliphatic absorptions); the mercury salt method, though more troublesome, gave a cleaner product. The deep red carbon tetrachloride solution had ν 1767, 1727 cm^{-1} (MeC=O, PhC=O); τ 1.7–2.8 (5 phenyl H), 7.69 p.p.m. (3 methyl H, sharp).

2,3-Diaroyl-(or diacyl)-2,3-diazabicyclo[2.2.1]hept-5-enes (2b–12b)

The azo compounds were allowed to react with cyclopentadiene at room temperature, directly or in solution in benzene or carbon tetrachloride. Reaction was complete within minutes for azodiaroyls but was retarded by aliphatic acyl groups, azodiacetyl taking 1 h under the same conditions and azodipivaloyl 2 days at 10°. The n.m.r. analysis in all cases indicated the residue on evaporation to be essentially pure adduct. Solvents for crystallization, m.p.'s, i.r., and n.m.r. data and elementary analyses are shown in Table 1 and u.v. data in Table 5.

Sharp m.p.'s could not be obtained for **4***b*, **5***b*, or **10***b* by heating capillary tubes from room temperature in the conventional manner. The tube had to be inserted just below the m.p., found by trial and error; after melting the samples solidified and remelted at the m.p. of the pure oxadiazine.

cis-4-Aroyl-(or acyl)-4,4a,5,7a-tetrahydro-2-aryl-(or alkyl)-cyclopenta-1,3,4-oxadiazines (Structures c, d).

The isomerization of the adducts (**2***b*–**12***b*) was effected by heating neat or in solution as shown in Table 6.

The product in each case had spectra superimposable on those of purified oxadiazines or mixtures of isomeric oxadiazines. Most of the isomerizations were also followed in

TABLE 6. Reaction conditions for the isomerization of adducts **2***b*–**12***b*

Adduct	Reaction conditions	Time
2*b* and **8***b*	Refluxing EtOH:H_2O (4:1)	4 h
3*b* and **9***b*	Refluxing EtOH	8 h
4*b*	Refluxing EtOH	5 h
11*b*	Refluxing iso-octane	6 h
12*b*	Refluxing tetrachloroethylene	6 h
6*b*	Refluxing tetrachloroethylene	2 days
5*b*	Room temperature (or 70°)	1 day (or 5 min)
10*b*	Room temperature (or 70°)	3 days
(**7***b*	Stable indefinitely up to 150°)	

Can. J. Chem. Downloaded from www.nrcresearchpress.com by 210.87.254.105 on 09/05/12
For personal use only.

solution by repeated scanning u.v. spectrophotometry as part of a detailed kinetic study: one or more isobestic points were observed throughout.

Table 3 lists properties of these oxadiazines, analogous to those in Table 1; u.v. data are in Table 5.

cis-4-Aroyl-(or acyl)-4,4a,5,6,7,7a-hexahydro-2-aryl-(or alkyl)-cyclopenta-1,3,4-oxadiazines (Structures e, f)

(a) Direct Hydrogenation of Oxadiazines c, d

Di-imide was used in these reductions, generated from hydrazine and hydrogen peroxide for compounds **2***e*, **3***e*, **9***e* and *f*, and **12***e*, or from *p*-toluenesulfonylhydrazine in refluxing dioxane for **8***e* and *f* and for **11***e*; full details of reaction conditions and work-up have been described earlier (1). Compound **5***e* was obtained catalytically, with PtO_2 in ethanol.

(b) Acylation of cis-4,4a,5,6,7,7a-hexahydro-2-aryl-(or alkyl)-cyclopenta-1,3,4-oxadiazines

Brief treatment of the hydrogenated derivatives *e* and *f* with hot concentrated sulfuric acid, followed by neutralization with aq. sodium hydroxide and extraction with carbon tetrachloride (1) gave the title compounds which were not further purified. Acylation was performed in pyridine at room temperature over 18 h with the acid chloride (ethyl chloroformate for the synthesis of **12***e* and acetic anhydride for the synthesis of **11***e*). Work-up entailed neutralization with ice and dil. hydrochloric acid and extraction with ether and crystallization.

Compounds made by this method were **5***e* (debenzoylation of **10***e*, followed by pivaloylation), **9***f* (de-anisoylation of **3***e*, *p*-nitrobenzoylation), **11***e* (debenzoylation of **1***e*, acetylation) and **12***e* (debenzoylation of **1***e*, carbethoxylation). Taken in conjunction with the previous steps, *viz.* isomerization and hydrogenation, the above syntheses constitute unambiguous structure proofs of **10***e*, **9***f*, **11***e* and **12***e*, respectively.

Melting points, i.r. bands, and elementary analyses of the pure dihydro oxadiazine derivatives made by both of the above methods are listed in Table 4 and u.v. data for some of them in Table 5. The n.m.r. assignments are not included. They were of little interest, those for protons on the cyclopentane ring being very similar to those described for **1***e* (1).

Analysis of Isomer Mixture 8c and d from Isomerization of 8b

The mixture was crystalline and had ν(Nujol) 1650, 1630 cm^{-1} (C=O, C=N); $\tau(CDCl_3)$ 1.3–2.7 (9 aryl H) 3.55 (2 vinyl H, broad quartet), 4.95 (2 *t*-H, broad), 6.95, 7.55 p.p.m. (methylene AB quartet). The g.l.c. failed to separate the isomers under a wide range of conditions.

The dihydro derivatives **8***e* and *f*, obtained by refluxing with *p*-toluenesulfonylhydrazine in dioxane, were also inseparable by g.l.c. They were de-aroylated with sulfuric acid to the mixture of bases 2-phenyl- and 2-*p*-bromophenyl-*cis*-4,4*a*,5,6,7,7*a*-hexahydrocyclopenta-1,3,4-oxadiazine which were clearly separated and had equal peak areas in their gas–liquid chromatogram.

A portion of the bases was benzoylated as described above to give a mixture of oxadiazines. These were identified by g.l.c., in order of elution, as **2***e* and **8***f* by co-injection of authentic **2***e* (1) which increased the size of the first peak, and co-injection of the mixture **8***e* and *f* which increased the size of the second. Similarly the rest of the basic mixture was converted into the *p*-bromobenzoyl derivatives identified by g.l.c. as (in order) **8***e* and **4***e* by co-injection, respectively, of the mixture **8***e* and *f* and of authentic **4***e*.

Analysis of Isomer Mixture 9c and d from Isomerization of 9b

The composition of the crystalline mixture was determined by comparing the areas of the methoxy peaks in the 100 MHz spectrum of a solution of it in $CDCl_3$. The mean of a large number of determinations showed the ratio of **9***c*:**9***d* to be 60:40.

A portion of the mixture was chromatographed on silica gel with 1:1 ether:petroleum ether (b.p. 40–60°). Compound **9***d* was eluted first, followed by **9***c* which was contaminated with the end fractions of **9***d*; the latter could be removed by crystallization from aqueous methanol. Both oxadiazines formed yellow prisms from aqueous acetone, **9***d* having m.p. 134–135° and **9***c*, m.p. 201–202°.

Anal. Calcd. for $C_{20}H_{17}N_3O_5$: C, 63.3; H, 4.5; N, 11.1. Found for original mixture: C, 63.5; H, 4.5; N, 11.4.

We thank the National Research Council of Canada for financial assistance.

1. D. MACKAY, J. A. CAMPBELL, and C. P. R. JENNISON. Can. J. Chem. **48**, 81 (1970).
2. D. MACKAY, U. F. MARX, and W. A. WATERS. J. Chem. Soc. 4793 (1964).
3. L. A. CARPINO and E. S. RUNDBERG, Jr. Chem. Commun. 1431 (1968).
4. S. J. RHOADS. *In* Molecular rearrangements. *Edited by* P. de Mayo, Part 1. Rearrangement through "no mechanism" pathways. Interscience Publishers, Inc., New York, 1963, Chapt. 11.
5. L. A. CARPINO, P. H. TERRY, and P. J. CROWLEY. J. Org. Chem. **26**, 4336 (1961).
6. J. E. LEFFLER and W. B. BOND. J. Am. Chem. Soc. **78**, 335 (1956).
7. N. RABJOHN. *In* Organic syntheses. Coll. Vol. 3. *Edited by* E. C. Horning. John Wiley & Sons, Inc., New York, 1955. p. 375.
8. Y. SHABAROV, N. I. VASIL'EV, I. S. LEVINA, and R. Y. LEVINA. Zhur. Obshch. Khim. **32**, 2806 (1962).
9. H. BOCK and J. KRONER. Ber. **99**, 2039 (1966).
10. R. STOLLÉ. Ber. **45**, 273 (1912).
11. H. H. INHOFFEN, H. POMMER, and F. BOHLMANN. Ber. **81**, 507 (1948).
12. J. P. PICARD and J. L. BOIVIN. Can. J. Chem. **29**, 223 (1951).
13. D. Y. CURTIN and T. C. MILLER. J. Org. Chem. **25**, 885 (1960).
14. G. T. TISUE, S. LINKE, and W. LWOWSKI. J. Am. Chem. Soc. **89**, 6303 (1967).
15. J. E. ANDERSON and J. M. LEHN. Tetrahedron, **24**, 123 (1968).
16. W. E. STEWART and T. H. SIDDALL, III. Chem. Revs. **70**, 517 (1970).
17. E. K. VON GUSTORF, D. F. WHITE, B. KIM, D. HESS, and J. LEITICH. J. Org. Chem. **35**, 1155 (1970).
18. T. TAGUCHI, J. ISHIBASHI, T. MATSUO, and M. KOJIMA. J. Org. Chem. **29**, 1097 (1964).
19. H. H. JAFFÉ and M. ORCHIN. *In* Theory and applications of ultraviolet spectroscopy. John Wiley and Sons., Inc., New York, 1962. p. 259.
20. S. KUBOTA and T. AKITA. Chem. Abstr. **57**, 16471*i* (1962).
21. A. P. GREKOV, L. N. KULAKOVA, and O. P. SHVAIKA. Zhur. Obshch. Khim. **29**, 3054 (1959).
22. A. T. DANN and W. DAVIES. J. Chem. Soc. 1050 (1929).

Photolysis of Aqueous Solutions of 9,10-Anthraquinone-2-sulfonate. Part I. Dependence of Product Yields on Reaction Conditions

A. D. BROADBENT AND R. P. NEWTON

Department of Chemistry, Mount Allison University, Sackville, New Brunswick

Received June 30, 1971

The products of the photolysis of neutral aqueous solutions of 9,10-anthraquinone-2-sulfonate or of the action of Fenton's reagent on this quinone have been identified as 1- and 2-hydroxy- and dihydroxy-9,10-anthraquinone sulfonates. High quinone and low oxygen concentrations favor production of monohydroxy-anthraquinone sulfonates, while low quinone and high oxygen concentrations result in preferential formation of dihydroxylated derivatives of the quinone. Photolysis in aqueous NaOH solution gives essentially only 2-hydroxy-9,10-anthraquinone sulfonates.

Les produits de la photolyse de solutions aqueuses neutres de sulfonate-2 anthraquinone-9,10 ou de l'action du réactif de Fenton sur ce quinone ont été identifiés comme étant des sulfonates d'hydroxy-1 et -2 et de dihydroxy-anthraquinone-9,10. De fortes concentrations en quinone et faibles en oxygène favorisent la production de sulfonates d'anthraquinone monohydroxylée tandis que de faibles concentrations en quinone et fortes en oxygène conduisent préférentiellement à la formation de dérivés dihydroxylés de la quinone. La photolyse en solution aqueuse de soude ne donne essentiellement que des sulfonates d'hydroxy-2 anthraquinone-9,10.

Canadian Journal of Chemistry, **50**, 381 (1972)

Introduction

The crucial primary photochemical process in the photo-oxidation of alcohols sensitized by 9,10-anthraquinones is considered (1–5) to be hydrogen atom abstraction from the alcohol by the electronically excited quinone, according to eq. 1. The available evidence (4–6) indicates that the electronically excited 9,10-anthraquinone in reaction 1, A*, is a n,π^* triplet state molecule generated with high quantum efficiency.

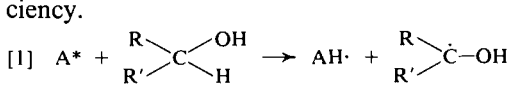

[1] $A^* + \begin{matrix} R \\ R' \end{matrix}\!\!>\!C\!<\!\begin{matrix} OH \\ H \end{matrix} \rightarrow AH\cdot + \begin{matrix} R \\ R' \end{matrix}\!\!>\!\dot{C}\!-\!OH$

Few studies have been conducted on the photolysis of 9,10-anthraquinones in purely aqueous solution, despite the fact that photo-oxidation of chloride and bromide ion sensitized by such quinones have been established (7), and that photoreduction of anthraquinones proceeds readily in aqueous solution in the absence of alcohols (8–11). Pfeilsticker (12) originally demonstrated that photolysis of sodium 9,10-anthraquinone-2-sulfonate (2-AS) in water caused reduction of the quinone and formation of what he incorrectly believed to be 2-hydroxy-9,10-anthraquinone. Subsequently, Mooney and Stonehill (13) indicated that at least four different hydroxyanthraquinone sulfonates are produced in this photolysis, by reaction of 2-AS with photochemically generated hydroxyl radicals. The formation of such colored hydroxy-anthraquinones had been observed in the 2-AS sensitized photo-oxidation of alcohols in aqueous solution (1, 3, 14, 15), particularly at low alcohol concentrations. A preliminary investigation (16) confirmed that the major products of the photolysis of 2-AS in aqueous solution were, in fact, 1- and 2-hydroxy-9,10-anthraquinone sulfonates and that the products of the primary photochemical reaction were hydroxyl radical and reduced 2-AS. Recent studies by Phillips *et al.* (17) have produced evidence, which suggests that the primary photochemical products are formed by reactions 2 and 3. However, Blyumenfel'd and coworkers

[2] $$A^* + A \rightarrow A^{\cdot -} + A^{\cdot +}$$

[3] $$A^{\cdot +} + HO^- \rightarrow A + HO\cdot$$

have also investigated this photolysis in alkaline solution (18–21). They conclude that reduction of 2-AS by hydroxide ion (reaction 4) occurs in the dark but is accelerated by light absorption resulting in electronic excitation of 2-AS.

[4] $$A + HO^- \rightarrow A^{\cdot -} + HO\cdot$$

This paper is concerned with the nature of the hydroxylated products from photolysis of 2-AS in aqueous solution and the dependence of the product distribution on the p*H* of the solution, its oxygen concentration and the initial 2-AS concentration. Such product distribution studies are a necessary prerequisite to elucidation of the

Can. J. Chem. Downloaded from www.nrcresearchpress.com by 210.87.254.105 on 09/05/12
For personal use only.

TABLE 1. Products from chromatography of photolyzed 2-AS solutions

Fraction*	Color on Al_2O_3	Relative yields		Identity
		p*H* 6	p*H* 13	
1	Colorless	Large	Large	2-AS
2	Red	Moderate	Large	2-Hydroxy-AQ† sulfonates
3	Orange	Large	Very small	1-Hydroxy-AQ sulfonates
4	Orange	Very small	Very small	Unknown
5	Blue	Moderate	Not detected	Dihydroxy-AQ sulfonates
6	Violet	Small	Small	

*In order of increasing adsorption on Al_2O_3.
†AQ = 9,10-anthraquinone.

TABLE 2. Infrared absorption frequencies (cm^{-1}) of fractions 1–3 and of various anthraquinones (solid state–Nujol and KBr)*

Compound	ν(C=O)	ν(O—H)	$\nu(SO_3^-)$
Fraction 1	1670	3530, 3420†	1180, 1050
AQ-2-$SO_3Na\cdot H_2O$	1670	3530, 3420†	1180, 1050
Fraction 2	1670, 1650(w)	3250	1190, 1040
2-HOAQ-6-SO_3Na	1675	3250	1170, 1045
2-HOAQ-7-SO_3Na	1675, 1650	3200	1180, 1040
2-HOAQ	1675, 1650(w)	3340	—
Fraction 3	1675, 1640	3400(w)	1190, 1050
1-HOAQ-6-SO_3Na	1675, 1635	3400(w)	1190, 1050
1-HOAQ-2-SO_3Na	1670, 1635	3300(w)	1050
1-HOAQ-4-SO_3Na	1675, 1640	3250(w)	1180, 1050
1-HOAQ	1675, 1640	3480(w)	—

*Weak absorption, (w).
†Water of crystallization.

primary photochemical process from rates of product formation on photolysis.

Results

Product Identification

Chromatography after photolysis of 2-AS in air-saturated water (p*H* 6) gave six fractions (Table 1). Fractions 4 and 6 obtained from photolyses at p*H* 13 appeared identical to the corresponding fractions from neutral photolysis. Although photolysis of 2-AS in water and NaOH solution yielded essentially the same products, the distribution of products was markedly p*H* dependent.

The u.v. and i.r. spectra of fraction 1 were superimposable on those of the original 2-AS (Tables 2 and 3).

Fraction 2 was readily soluble in water, being yellow in acidic and red in alkaline solution. Addition of $Na_2S_2O_4$ to the alkaline solution produced color changes characteristic of 2-hydroxy-9,10-anthraquinone sulfonates and confirmation of this was obtained by polarography (22). The i.r. and u.v. spectra of fraction 2 (Tables 2 and 3) were found to be composites of the essentially identical spectra of 2-hydroxy-9,10-anthraquinone-6-and-7-sulfonates. There was no indication of additional components in this fraction. Fraction 2 was converted into a mixture of 2,6- and 2,7-dihydroxy-9,10-anthraquinone (23), which were separated by fractional crystallisation of their calcium salts. However, the reaction gave poor yields, considerable amounts of polyhydroxyanthraquinones, and efficient separation was impractical. No further attempts to prepare derivatives were undertaken. Fraction 2, therefore, arises from hydroxylation of 2-AS at the 6- and 7-positions.

Fraction 3 was also water-soluble and gave similar color changes to those observed for fraction 2. However, reduction in alkaline solution with $Na_2S_2O_4$ gave an easily oxidized deep red product but no green anthrasemiquinone reduction intermediate was observed, indicating

Can. J. Chem. Downloaded from www.nrcresearchpress.com by 210.87.254.105 on 09/05/12
For personal use only.

TABLE 3. Visible and u.v. absorption maxima* of fractions 1–5 and of various 9,10-anthraquinones under different conditions

Compound	Acidic dilute aqueous HCl	Basic† 0.1 *M* aqueous NaOH	0.1 *M* aqueous NaOH + $Na_2S_2O_4$
Fraction 1	328, 275(sh), *256*		510, *432*
AQ-2-SO_3Na	328, 275(sh), *256*		520, *432*
Fraction 2	378, 330, *274*, *248*	472, *310*, *249*	526, 430
2-HOAQ-6-SO_3Na	376, 330, *275*, *246*	472, *309*, *248*	525, 436
2-HOAQ-7-SO_3Na	378, 330, *273*, *246*	472, *310*, *248*	530, *426*
2-HOAQ	374, 337, *270*, *248*‡	465, *310*, *246*	503, *413*, 394(sh)
Fraction 3	405, 328, 278(sh), *254*	492, 315, 272, *252*	491, *426*
1-HOAQ-6-SO_3Na	403, 327, 277(sh), *254*	492, 307, 274(sh), *252*	490, *426*
1-HOAQ-2-SO_3Na	395, 340, 282(sh), *258*	483, 310, 276, *246*	465(sh), *420*, 395
1-HOAQ-4-SO_3Na	400, 340, 280(sh), *257*	505, 312, 276, *246*	465(sh), *418*
1-HOAQ	415, 305, 277, *246*‡	486, 330, 275(sh), *255*	466, 414
Fraction 4	375, 331, *270*, 250	465, *310*, 290(sh), *247*	530, 423
2-HOAQ-3-SO_3Na	375, 330, *274*, *248*	473, *311*, 268(sh), *249*	550, 443
Fraction 5§		*610*, *569*	500(sh), *437*
1,2-diHOAQ-6-SO_3Na		620(sh), *581*, 550(sh)	542, *442*
1,2-diHOAQ-3-SO_3Na		*598*, *557*, 522(sh)	528, *428*
1,2-diHOAQ‖		*611*, *568*, 535(sh)	503, *421*
1,4-diHOAQ		*600*, *564*	
Photolyzed 2-AS soln.¶		*605*, *567*	

*Major absorptions are italicized; (sh), shoulder.
†Spectra of dihydroxyanthraquinones were recorded in 1.0 *M* aqueous NaOH to ensure complete ionization of hydroxy groups.
‡Recorded in CH_3OH.
§Recorded in 70% (v/v) aqueous ethanol.
‖Recorded in 50% (v/v) aqueous ethanol.
¶1×10^{-4} *M* aqueous 2-AS solution photolyzed at p*H* 6, O_2-saturated.

that fraction 3 was composed of 1-hydroxy-9,10-anthraquinone sulfonates (22). This conclusion was supported by the i.r. spectrum (Table 2) (24, 25). Both the u.v. and i.r. spectra of fraction 3 were almost identical with those of 1-hydroxy-9,10-anthraquinone-6-sulfonate and very similar to those of 1-hydroxy-9,10-anthraquinone-2-sulfonate but the i.r. spectra indicated that the latter compound is not a major component. Fraction 3 was, therefore, considered to be a mixture of 1-hydroxy-9,10-anthraquinone sulfonates, probably the 1,6- and 1,7-isomers, being formed by hydroxylation of 2-AS at the 5- and 8-positions.

The identity of fraction 4 was not established as only very small amounts of this minor component could be isolated. Treatment with $Na_2S_2O_4$ caused reduction, which was easily reversed on shaking the solution with air. Its u.v. spectrum was very similar to that of a 2-hydroxy-9,10-anthraquinone sulfonate but fraction 4 did not appear to be 2-hydroxy-9,10-anthraquinone-3-sulfonate.

Fraction 5 (blue on Al_2O_3) could be eluted with weakly alkaline ethanol containing 30% H_2O by volume but fraction 6 (violet on Al_2O_3) could not be eluted. The eluent containing fraction 5 contained considerable amounts of material dissolved from the Al_2O_3 column which prevented isolation of a pure product. Its visible absorption spectrum in strongly alkaline solution was very similar to that of alizarin and related dihydroxyanthraquinones. Fraction 5 gave yellow aqueous solutions, which became violet and then blue on addition of NaOH. The blue alkaline solutions turned orange on treatment with $Na_2S_2O_4$, the blue color being easily regenerated by shaking the solution with air.

Photolysis of 2-AS at low concentrations (1×10^{-4} *M*) in neutral, O_2-saturated solution gave almost exclusively fractions 5 and 6 alone (see later). This provided a convenient means of studying these products. Color changes and visible absorption spectra (Table 3) indicated that fractions 5 and 6 are apparently 1,2-, 2,3-, or 1,4-dihydroxy-9,10-anthraquinone derivatives (26, 27). The blue alkaline solutions slowly faded in the presence of air, supporting this

Can. J. Chem. Downloaded from www.nrcresearchpress.com by 210.87.254.105 on 09/05/12
For personal use only.

Can. J. Chem. Downloaded from www.nrcresearchpress.com by 210.87.254.105 on 09/05/12
For personal use only.

assignment (26, 27). Chromatography of the photolysis products under various conditions, and also the absence of fraction 5 in photolyses of 2-AS at p*H* 13, indicated that fractions 5 and 6 were not different forms of the same substance.

Both the reaction products and the synthesized anthraquinone derivatives were difficult to purify so that molar absorptivities could not be determined. The recovery of substance on recrystallization was often low and removal of residual inorganic salts such as sodium chloride and sulfate is difficult. The hydroxyanthraquinone sulfonates are also hygroscopic. In addition to these problems, the identification of the photolysis products is further complicated because more conveniently handled derivatives, in which the sulfonate group has been replaced, cannot be prepared in high yield and also because each fraction from chromatography of the photolyzed solutions is probably a mixture of closely related isomers. Unambiguous identification of the reaction products was therefore not possible. Nevertheless, in many instances, the almost exact superimposition of the u.v. and i.r. spectra of the chromatographic fraction and of the appropriate model compounds strongly suggests that the reaction products are 1- and 2-hydroxy- and dihydroxy-9,10-anthraquinone sulfonates, the sulfonate group being at its original site but mainly in the non-hydroxylated ring.

Dependence of Product Yields on pH

On increasing the p*H* of the solution from 6 to 13, the striking change in product distribution (see Table 1) was accompanied by a fourfold increase in the rate of formation of hydroxylated derivatives of 2-AS. The pronounced change in product distribution and the increase in hydroxylation rate both occurred as the HO^- concentration was increased above 1×10^{-3} *M*.

Fractions 2 and 3 were separated by column chromatography and their relative yields measured by absorption spectrophotometry assuming identical molar absorptivities for the two species at the wavelengths of their absorption maxima.

Photolysis of neutral 3×10^{-3} *M* aqueous 2-AS solutions for 1 h gave yield (3)/yield (2) $= 3.5 \pm 0.8$ for both air- and O_2-saturated solutions. Similar photolyses in 0.4 *M* aqueous NaOH gave a ratio <0.01. The molar absorptivity ratio probably differs from unity, *e.g.* in aqueous NaOH for 2,7-$HOAQSO_3Na$, $\varepsilon_{472} = 5400$ and for 1,4-$HOAQSO_3H$, $\varepsilon_{492} = 7140$ (28). In addition, some tailing of fraction 2 may have resulted in contamination of fraction 3 during chromatography. Therefore, the above values of the ratio of yields should be considered as upper limits.

The change in the pattern of monohydroxylation on changing the p*H* of the photolyzed solution appeared related to the changes in the yields of dihydroxyanthraquinones (fractions 5 and 6). The striking decrease in the value of the ratio of yields above p*H* 11 was accompanied by the total disappearance of fraction 5 and a reduced yield of fraction 6.

Dependence of Product Yields on the Initial Concentrations of Oxygen and 2-AS

Photolyses of 2-AS at various initial concentrations in neutral and alkaline aqueous solutions saturated with air or oxygen showed that the formation of monohydroxyanthraquinones is favored at high quinone and low oxygen concentrations, whereas dihydroxyanthraquinones are the major products at low quinone and high oxygen concentrations. Some typical spectra of photolyzed 2-AS solutions are shown in Fig. 1, and data on the effects of O_2 and 2-AS concentrations on the relative yields of mono- and dihydroxylated derivatives are given in Table 4.

Reactions with Fenton's Reagent

In previous investigations (13, 16) it was established that reaction of 2-AS with Fenton's reagent (aqueous $FeSO_4 + H_2O_2$) gave deeply colored solutions, which after precipitation of $Fe(OH)_3$ and column chromatography on Al_2O_3, gave fractions whose u.v. spectra were identical with those of the photolysis products. This supports the proposal that hydroxyl radicals, generated by photolysis of 2-AS in water, are responsible for the observed hydroxylation of this quinone.

Because of the dependence of product yields on the conditions of photolysis, reactions of 2-AS with equimolar quantities of $FeSO_4$ and H_2O_2 were conducted in aqueous solution in the dark at various O_2 and 2-AS concentrations. In solutions containing O_2, decreasing its concentration reduced only the yield of dihydroxyanthraquinones but even under N_2 substantial

Can. J. Chem. Downloaded from www.nrcresearchpress.com by 210.87.254.105 on 09/05/12
For personal use only.

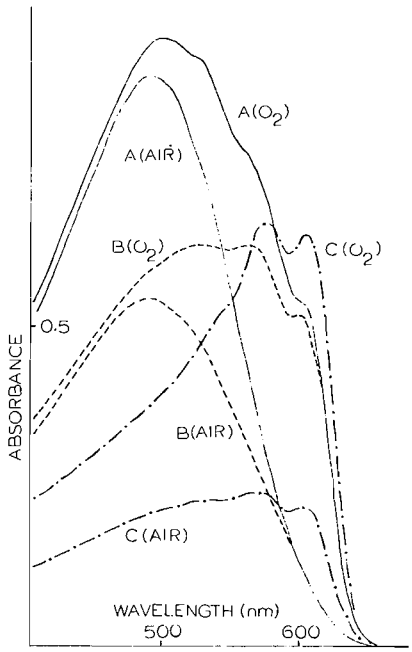

FIG. 1. Absorption spectra of photolyzed aqueous 2-AS solutions. Neutral O_2- or air-saturated aqueous solutions of 2-AS, at various initial concentrations, were photolyzed for 6 min at 366 nm, NaOH added to give a concentration of 1.0 *M*, and absorption spectra recorded in 1.0 cm (A and B) or 5.0 cm (C) optical cells. Initial 2-AS concentrations were: (A) 1.0×10^{-3} *M*, (B) 5.0×10^{-4} *M*, and (C) 5.0×10^{-5} *M*.

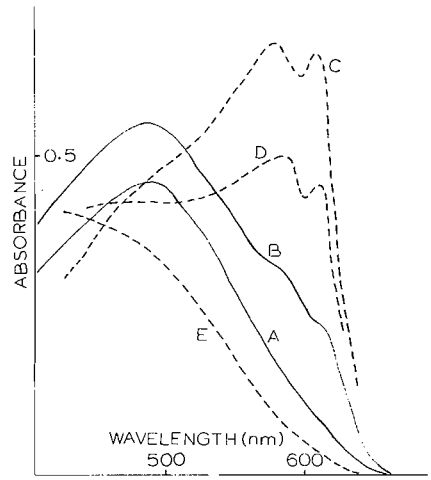

FIG. 2. Absorption spectra of 2-AS solutions. Solutions of 2-AS, $FeSO_4$, and H_2O_2 (all 2×10^{-3} *M*) reacted 10 min and then made alkaline with NaOH and oxygenated (A) or oxygenated and made alkaline (B). Neutral, oxygen-saturated solutions of 2-AS (5×10^{-5} *M*) photolyzed in the presence of zero (C), 5×10^{-5} *M* (D), and 1×10^{-4} *M* $K_3Fe(CN)_6$ (E) and subsequently made alkaline.

quantities of these products still resulted. However, the distribution of products from reactions in O_2-free solution was dependent on the treatment of the solution after reaction. Even after 15 min reaction under N_2, it was possible to influence the product distribution by treatment of samples of the reaction mixture with NaOH or O_2 (see Fig. 2). The formation of dihydroxylated products ($\lambda_{max} = 610$ nm) on introducing O_2 in such reactions was also suppressed by addition of excess 2-AS (as saturated aqueous solution) and completely prevented by addition of an equimolar amount of $K_3Fe(CN)_6$ shortly after the initial mixing. Therefore, in reactions with Fenton's reagent, the product distribution could be influenced by the concentrations of

TABLE 4. Effects of initial oxygen and 2-AS concentrations on the relative yields of mono- and dihydroxyanthraquinones in the photolysis of aqueous 2-AS solutions and in reactions of 2-AS with Fenton's reagent*

		AQOH/AQ(OH)$_2$†		
[2-AS] *M*	O_2-Content	p*H* 6	p*H* 13	Fenton's reagent*
1×10^{-2}	O_2-saturated	9.8		
1×10^{-3}	O_2-saturated	1.4	8.5	0.7
1×10^{-3}	Air-saturated	10.5	8.3	5.5
2.5×10^{-4}	O_2-saturated			1.1
2.5×10^{-4}	Air-saturated			2.0
1×10^{-4}	O_2-saturated	0.2	1.5	
1×10^{-4}	Air-saturated	0.6	1.4	

*Reaction of 2-AS with $FeSO_4 + H_2O_2$ in aqueous H_2SO_4.
†Yield ratio for mono- and dihydroxy derivatives of 2-AS calculated as outlined in the Experimental section.

Can. J. Chem. Downloaded from www.nrcresearchpress.com by 210.87.254.105 on 09/05/12
For personal use only.

O_2, HO^-, and 2-AS in solution, as well as by addition of $K_3Fe(CN)_6$, just as in photolysis (see later).

Photolysis in the Presence of Ferricyanide Ion

Photolysis of neutral, O_2-saturated solutions of 2-AS at a concentration of 5×10^{-5} *M* gave products which are violet or blue in alkaline solution, exhibiting absorption maxima at about 570 and 610 nm characteristic of dihydroxyanthraquinones. Potassium ferricyanide has no absorption above 475 nm and did not interfere with product analysis. Although $K_3Fe(CN)_6$ absorbed some of the incident light at 366 nm, its addition to the solution being photolyzed efficiently suppressed the formation of dihydroxylated products and significantly increased the relative yields of monohydroxyanthraquinones (see Fig. 2).

Discussion

The variations in product distribution in the reactions of 2-AS with $HO^{\cdot}$, generated either by photolysis of 2-AS or from Fenton's reagent, can be explained in terms of the reactions of the intermediate radical produced by addition of $HO^{\cdot}$ to 2-AS. Hydroxyl radical is known to be electrophilic (29) and the available evidence suggests that it reacts with benzene derivatives by addition, generating hydroxycyclohexadienyl radicals, rather than by abstraction of a hydrogen atom from the benzene ring. The addition of $HO^{\cdot}$ to 2-AS can produce several adducts. Product analysis indicated that hydroxylation of 2-AS occurred mainly in the non-sulfonated ring, in agreement with the known electrophilic character of $HO^{\cdot}$ and the electronic and steric effects of sulfonate groups.

Land and coworkers (30) have observed a transient intermediate in pulse radiolysis of oxygen-free aqueous solutions of 2-AS, which is believed to be the product of the addition of hydroxyl radical to the quinone. They have measured the rate constant for the addition and also established that the adduct disappears by a second order process in dilute 2-AS solutions. Clark and Stonehill (31) find that this transient disappears very rapidly in the presence of oxygen. Phillips *et al.* (17) postulated that monohydroxyanthraquinone sulfonates result from the coupling of the quinone–hydroxyl radical adduct with O_2, followed by elimination of $HO_2^{\cdot}$. Our results have shown that this is not so, since monohydroxylation occurs exclusively on photolysis in the absence of oxygen.

In the reactions of 2-AS with Fenton's reagent, the product distribution could be varied by addition of O_2, HO^-, $K_3Fe(CN)_6$, or excess 2-AS. This can be explained by postulating reactions of these species with the quinone–hydroxyl radical adduct. Reaction with O_2 would generate dihydroxyanthraquinones while reaction with HO^- would result in monohydroxylation. In the presence of $K_3Fe(CN)_6$, or excess 2-AS, oxidation of the adduct to monohydroxyanthraquinones is proposed.

Detailed kinetic studies are now in progress to confirm these proposals, particularly since the effects of quinone concentration on rate of hydroxylation reported by Phillips *et al.* (17) as confirming reactions 2 and 3 may well arise from the effects of 2-AS concentration on the relative rates of the secondary reactions producing hydroxylated derivatives rather than from the proposed reaction 2.

Experimental

Anthraquinone Derivatives

Sodium 9,10-anthraquinone-2-sulfonate monohydrate was purified by repeated recrystallization from hot water in the dark. Prolonged heating of the solutions was avoided to prevent hydrolysis to 2-hydroxy-9,10-anthraquinone.

Sodium 2-hydroxy-9,10-anthraquinone-6- and 7-sulfonates, and 1-hydroxy-9,10-anthraquinone-4-sulfonic acid were available from previous studies (22). 1-Hydroxy-, 2-hydroxy-, and 1,2-dihydroxy-9,10-anthraquinone and sodium 1,2-dihydroxy-9,10-anthraquinone-3-sulfonate were purified by recrystallization of commercial samples.

Sodium 1-hydroxy-9,10-anthraquinone-2-sulfonate was prepared by sulfonation of 1-hydroxy-9,10-anthraquinone with 20% oleum at 80 °C for 1.5 h. Higher temperatures give the 2,4-disulfonate. 2-Hydroxy-9,10-anthraquinone was sulfonated with 65% oleum for 8 h on the steam bath to yield after neutralization, sodium 2-hydroxy-9,10-anthraquinone-3-sulfonate. Sodium 1,2-dihydroxy-9,10-anthraquinone-6-sulfonate was prepared by refluxing the 2,6-disulfonate with NaOH solution (26). It was separated from 2-hydroxy-9,10-anthraquinone-6-sulfonate by chromatography on Al_2O_3, but required 5% aqueous HCl for elution.

The literature method of preparing 1-hydroxy-9,10-anthraquinone-6-sulfonate (26) based on reaction of the 1,6-nitro sulfonate with CH_3OH/NaOH and subsequent hydrolysis of the methyl ether gave several products. Sodium 1-nitro-9,10-anthraquinone-6-sulfonate (32) (ν (Nujol) 1673, 1543, 1375 cm^{-1}) was reduced with $Na_2S_2O_4$ in 2 *M* aqueous NaOH at room temperature. Subsequent air oxidation gave sodium 1-amino-9,10-anthraquinone-6-sulfonate, (ν (Nujol) 3280, 3170, 1670, 1640, 1620 cm^{-1}) which was diazotized at 0 °C with $NaNO_2$/HCl and gave N_2 and the sodium 1-hydroxy-9,10-anthraquinone-6-sulfonate on warming.

All the anthraquinone sulfonates were recrystallized from water.

Can. J. Chem. Downloaded from www.nrcresearchpress.com by 210.87.254.105 on 09/05/12
For personal use only.

Photolysis

All photolyses were conducted in a Rayonet Photochemical Reactor, using lamps with strong emission at 365 nm.

For product identification studies sodium 9,10-anthraquinone-2-sulfonate ($1–5 \times 10^{-3}$ *M*) was photolyzed in water or 0.1–0.5 *M* aqueous NaOH saturated with air and contained in a Pyrex vessel. The neutralized solution was evaporated under vacuum below 50 °C and 95% ethanol and a small amount of dilute aqueous NaOH were added to give a solution containing 80% ethanol by volume. Any unreacted 2-sulfonate and NaCl which crystallized out were removed and the resulting solution run through a column of basic activated Al_2O_3, using 80% ethanol as eluent and subsequently diluting this with water containing a little NaOH. The collected fractions were neutralized and evaporated to dryness under vacuum and the solid products recrystallized from water. During all photolyses, the solutions were stirred by bubbling with O_2, air, or N_2. Rates of formation of hydroxyanthraquinones were sufficiently low, that depletion of oxygen was assumed negligible.

Estimation of product yields

In addition to chromatographic examination, the following procedure was used to obtain information about the relative yields of mono- and dihydroxyanthraquinone sulfonates. After reaction, NaOH was added to the solution to give a solution of 1.0 *M* hydroxide ion. In the case of reactions with Fenton's reagent, precipitated iron hydroxides were removed by centrifugation. The yield of dihydroxyanthraquinone sulfonates was determined from measurements of the absorbance of the alkaline solution at 610 nm; that of monohydroxy derivatives being related to absorbance at the wavelength of maximum absorbance in the region 470–500 nm. Examination of the spectra of the model compounds showed that eq. 5 gave a suitable measure of the relative yields of products.

$$[5] \quad \frac{\text{Yield AQOH}}{\text{Yield AQ(OH)}_2} = \frac{A_{470-500} - 0.45\,A_{610}}{A_{610} - 0.03\,A_{470-500}}$$

The yield ratio was partially corrected to account for the absorbance of the other products at the particular wavelength. Equation 5 should actually contain three absorbance values in the numerator and in the denominator. The equation was derived assuming that 45% of the contribution to the total absorbance at 610 nm by AQOH and 3% of the contribution to the total absorbance at 470–500 nm by $AQ(OH)_2$ were negligible. Because these terms could not be experimentally determined and were also minor corrections, they were not considered. In addition, the unknown ratio of the molar absorptivities of the mono- and dihydroxylated products was taken as unity, although it is probably somewhat higher.

Despite the qualitative nature of the procedure, it proved exceedingly useful in providing new information about product distributions under different conditions.

The authors gratefully acknowledge the award of a Queen Elizabeth Research Fellowship (A.D.B. 1965–1967), the generous hospitality of the Department of Organic Chemistry, University of Adelaide, where this study was initiated, and recent financial support from the National Research Council of Canada.

1. J. L. Bolland and H. R. Cooper. Proc. Roy. Soc. (London), Ser. A. **225**, 405 (1954).
2. C. F. Wells. Nature, **177**, 483 (1956).
3. C. F. Wells. Trans. Faraday Soc. **57**, 1703, 1719 (1961).
4. F. Wilkinson. J. Phys. Chem. **66**, 2569 (1962).
5. K. Tickle and F. Wilkinson. Trans. Faraday Soc. **61**, 1981 (1965).
6. H. H. Dearman and A. Chan. J. Chem. Phys. **44**, 416 (1966).
7. A. Eckert. Chem. Ber. **58**, 313 (1925); **60**, 1691 (1927).
8. H. Berg and H. E. Jacob. Z. Naturforsch. **17B**, 306 (1962); Photochem. Photobiol. **4**, 55 (1965).
9. E. W. Abrahamson and I. Panik. Adv. Mol. Spectrosc. **1**, 354 (1962).
10. P. J. Baugh, G. O. Phillips, and J. C. Arthur. J. Phys. Chem. **70**, 3061 (1966).
11. D. Tresselt. Studia Biophys. **3**, 35 (1967).
12. K. Pfeilsticker. Biochem. Z. **199**, 8 (1928).
13. B. Mooney and H. I. Stonehill. Chem. Ind. 1309 (1961).
14. C. F. Wells. Discuss. Faraday Soc. **29**, 219 (1960).
15. G. O. Phillips, P. Barber, and T. Rickards. J. Chem. Soc. 3443 (1964).
16. A. D. Broadbent. Chem. Commun. 382 (1967).
17. G. O. Phillips, N. W. Worthington, J. F. McKellar, and R. R. Sharpe. Chem. Commun. 835 (1967); J. Chem. Soc. A, 767 (1969).
18. L. A. Blyumenfel'd, A. V. Karyakin, V. A. Kuz'min, G. V. Fomin, A. K. Chibisov, and S. I. Sholina. Izv. Akad. Nauk SSSR, 2615 (1969).
19. S. I. Sholina, G. V. Fomin, and L. A. Blyumenfel'd. Zh. Fiz. Khim. **43**, 800 (1969).
20. G. V. Fomin, L. M. Gurdzhiyan, and L. A. Blyumenfel'd. Dokl. Akad. Nauk SSSR, **191**, 151 (1970).
21. L. I. Korshunov, Y. M. Zolotovitskii, and V. A. Benderskii. Chem. Abst. **71**, 118319 (1969).
22. A. D. Broadbent and H. Zollinger. Helv. Chim. Acta, **47**, 2140 (1964); **49**, 1729 (1966).
23. J. Hall and A. G. Perkin. J. Chem. Soc. 2029 (1923).
24. M. St. C. Flett. J. Chem. Soc. 1441 (1948).
25. H. Bloom, L. H. Briggs, and B. Cleverley. J. Chem. Soc. 178 (1959).
26. Beilsteins Handbuch der Organischen Chemie. 4th ed. Springer Verlag, Berlin, 1925. Vol. 8.
27. Elsevier's encyclopedia of organic chemistry. Ser. III, Elsevier Pub. Co. Inc., Amsterdam, 1948. Vol. 13.
28. A. D. Broadbent. Dissertation, ETH Zurich, 1963.
29. E. J. Fendler and J. H. Fendler. Progress in physical organic chemistry. Vol. 7. J. Wiley and Sons, Inc. New York, 1970. p. 229.
30. B. E. Hulme, E. J. Land, and G. O. Phillips. Chem. Commun. 518 (1969).
31. K. Clark and H. I. Stonehill. Reported in ref. 17.
32. H. E. Fierz-David. Helv. Chim. Acta, **10**, 197 (1927).

Deuterium Isotope Effects in the Reduction of Cyclohexanones. The Concepts of Steric Approach Control and Product Development Control[1]

DONALD C. WIGFIELD AND DAVID J. PHELPS
Department of Chemistry, Carleton University, Ottawa, Canada K1S 5B6

Received June 30, 1971

Definitions for the terms *steric approach control* and *product development control* in relation to the degree of bonding in the transition state are put forward. Kinetic deuterium isotope effects in the reduction of a graded series of ketones by $NaBH_4$ and $NaBD_4$ have been measured. These effects are inverse, and show no systematic dependence on the degree of steric hindrance of the ketone. This evidence appears to invalidate the steric approach control–product development control explanation of the axial to equatorial product ratios (1). The primary isotope effect is very small, which is consistent with an early transition state in these reductions, as demanded by other explanations of product ratios, but since several other factors causing small isotope effects may be applicable, the evidence does not constitute proof of an early transition state.

The main conclusions of this work have already been published in preliminary form (2).

Les notions de *"steric approach control"* et *"product development control"* en relation avec le degré de liaison dans l'état de transition, sont précisées. Les effets isotopiques du deutérium sur la cinétique de réduction d'une série de cétones par $NaBH_4$ et $NaBD_4$, ont été mesurés. Ces effets sont inverses et ne montrent aucune dépendance systématique avec le degré d'empêchement stérique de la cétone. Cette mise en évidence montre que l'explication des rapports du produit axial et équatorial par le "steric approach control" et "product development control", n'est pas valable (1). L'effet isotopique primaire, très faible, est compatible avec un début d'état de transition dans ces réductions. Ce résultat, déjà mentionné dans d'autres études, ne constitue pas une preuve puisque de nombreux autres facteurs peuvent être la cause de ces faibles effets isotopiques. Les conclusions principales de ce travail ont déjà été publiées dans une note préliminaire (2).

Canadian Journal of Chemistry, **50**, 388 (1972)

Introduction

It has been well known for many years that the stereochemical outcome of reducing cyclic ketones with complex metal hydrides depends crucially on the degree of steric hindrance around the carbonyl group. In the case of simple cyclohexanones a predominance of equatorial alcohol arises from non-hindered ketones, whereas more axial alcohol is formed from more hindered ketones (1) (see Fig. 1). Various suggestions as to the basis of this striking stereochemical dependence have been offered (1, 3–5). Fifteen years ago, in a paper which has now become a classic in this area of hydride reductions, Dauben *et al.* (1) put forward the first explanation and introduced the terms steric approach control and product development control. Since that time, confusion has reigned over precisely what these terms mean, and it is clear that today, although the terms are used widely, there is no uniformity of meaning. We regard this situation as very unfortunate, since the terms are extremely useful when used uniformly, but of no value if they have no definite signification. It is this confusion that has prompted our work in this area and this paper will be concerned primarily with clarifying these terms and evaluating the correctness of the Dauben explanation.

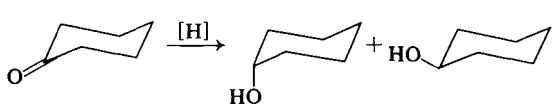

FIG. 1. Reduction of cyclic ketones.

[1]Transition State Analysis III.

Discussion and Results

The Terms Steric Approach Control and Product Development Control

The definition of steric approach control given by Dauben *et al.* is "a steric postulate involving competitive attacks from a favoured (unhindered) or an unfavoured (hindered) side"; that of product development control "an energy consideration involving the relative stability of the possible products" (1). In attempting to produce a more uniform and precise definition of these terms it must be remembered that these reductions of ketones are purely kinetically controlled. The axial to equatorial product ratio must therefore depend on, and only on, the

Can. J. Chem. Downloaded from www.nrcresearchpress.com by 210.87.254.5 on 09/05/12
For personal use only.

Can. J. Chem. Downloaded from www.nrcresearchpress.com by 210.87.254.5 on 09/05/12
For personal use only.

relative free energies of the two transition states leading to the two diastereomeric products. Thus, in a reaction where the product ratio is being controlled by (steric) ease of approach of the attacking reagent (steric approach control), the transition states in question must be at an early stage of bond breakage and bond formation. Similarly, in reactions where factors controlling the relative energies of the transition states are similar to those controlling the relative energies of the products (product development control), the structures and geometries of transition state and product must be similar and thus a "late" transition state is involved. Therefore a convenient redefinition[2] of the terms steric approach control and product development control may be made purely in terms of the degree of bonding in the transition state. The need for this type of thinking has been pointed out by Brown and Deck (6), and probably the most general interpretation of these terms has been in relation to transition states, many workers in the field having concerned themselves with "early" or "late" transition states (6–16). Using this type of definition, the Dauben explanation of product ratios simplifies to the hypothesis (*a*) that a late transition state is involved in reduction of unhindered ketones and thus the lower energy alcohol (equatorial hydroxyl) is produced since the transition state leading to formation of the equatorial alcohol is of lower energy than the transition state leading to formation of the axial alcohol; and (*b*) that an early transition state pertains to reduction of hindered ketones, the transition state energy being controlled by such factors as ease of approach of the hydride, which thus attacks from the equatorial side to yield the axial alcohol. In contrast to this type of definition, Eliel and Senda (7) have defined the expressions in terms of individual steric interactions. In this particular reaction we feel that the transition state definitions and the steric interaction definitions are equivalent, the steric interaction definition being precise and restricted to this reaction, and the transition state definition being more general. We prefer the transition state definition because of its ready applicability to reactions besides reductions of ketones.

In order to try to clarify this situation, we put forward for consideration the following definitions, which we believe will be of general utility to reactions besides the one under present consideration. We suggest that *the terms approach control and product development control refer in a relative sense to the position of the transition state along the reaction coordinate, approach control inferring a reactant-like or early transition state, and product development control a product-like or late transition state.* The term *steric approach control* then becomes a special case of approach control where the factors involved are steric.[3]

The Validity of the Steric Approach Control–Product Development Control Concept

Having defined the above terms, it becomes clear that the explanation of product ratios rests on the concept of different transition states for reduction of hindered and unhindered ketones, with the transition state being later with less steric hindrance. It is precisely this point which sets this explanation apart from others, which postulates an early transition state for all cases (3–5). The test of the Dauben hypothesis thus becomes one of evaluating the extent of bond breaking and bond making in the transition states of reduction of ketones with varying steric hindrance and determining whether or not there is a transition state shift. In the past few years, the majority of workers engaged in rationalizing axial:equatorial product ratios have lent their support to explanations involving early transition states (3–5, 7, 8, 10, 16), and in particular have regarded product development control as "an unnecessary concept" (10). However, these conclusions have rarely rested on any experimental evidence other than the product ratios they are supposed to explain. It is interesting that workers using other approaches to the nature of the transition state have often arrived at an opposing conclusion: Lamaty and coworkers (12), on the basis of Hammett relationships (18, 19) have concluded that the borohydride reductions of ketones pass through product-like transition states, and Karabatsos and Althuis have argued

[2]It should be stressed that this redefinition is considered to be a logical extension of the original definition. It does not necessarily imply that the original authors (1) had this type of definition in mind.

[3]See ref. 17 for a case of regiospecificity where the factors involved in approach control are electronic.

Can. J. Chem. Downloaded from www.nrcresearchpress.com by 210.87.254.5 on 09/05/12
For personal use only.

on the basis of the breakdown of a model for carbonyl additions that the transition state for borohydride and aluminohydride reduction of aldehydes is also product-like (11). From the point of view of the Dauben explanation it is particularly fascinating, although not very relevant to the reaction under consideration, that a Hammett plot of borohydride reductions of aromatic acid chlorides was non-linear, indicating a change in mechanism or transition state (20).

Finally, one recent publication deserves comment. Lamaty and his coworkers have published evidence which "prove beyond any reasonable doubt that the transition state is product-like" in borohydride reduction of ketones (13). This evidence is a comparison of rates of attack on 4-*t*-butylcyclohexanone and adamantanone by borohydride and by the sulfite anion. It is found that $k_{\text{adamantanone}} \simeq 2k_a$ for sulfite attack and $k_{\text{adamantanone}} \simeq 2k_e$ for borohydride attack, where k_a and k_e are axial and equatorial rate constants of attack by the appropriate species on 4-*t*-butylcyclohexanone, respectively. This is interpreted in terms of a reactant-like transition state for sulfite addition, and a product-like transition state for borohydride reduction. We feel that there is an alternative explanation of these data. As the authors point out, attack from either side of the carbonyl group in adamantanone is equivalent, being equatorial to one ring and axial to another. Attack at this center on either side, therefore, is equivalent to attack at the least favored side of 4-*t*-butylcyclohexanone, regardless of whether this happens to be axial or equatorial. Since there are two equivalent sides to attack, one would then immediately predict that $k_{\text{adamantanone}} \simeq 2k_u$, where k_u is the rate constant for attack at the least favored side of 4-*t*-butylcyclohexanone by the appropriate nucleophile. This is the result observed in both cases, and thus it would seem that the evidence put forward by these authors does not constitute unambiguous evidence for a late transition state in the borohydride reduction of ketones.

In view of these conflicting data, and the lack of a systematic study involving *both* product ratios and an independent indication of transition state structure, we have investigated the borohydride reduction of a graded series of cyclohexanones with various degrees of steric hindrance. The experimental parameter selected to indicate transition state structure was the magnitude of the kinetic deuterium isotope effect, which, despite recent controversy (21), has long been accepted to be sensitive to the degree of bond breaking in the transition state (22). Axial-equatorial alcohol product ratios were determined independently by gas chromatography and n.m.r. spectroscopy, giving results in close accord. The rate constants for reduction by sodium borohydride and sodium borodeuteride were determined spectrophotometrically by following the disappearance of the n–π^* ketone band at around 285 nm. The data were treated by standard second-order kinetics and gave satisfactorily reproducible plots. Two such typical plots are shown in Figs. 2 and 3. It was found that an $x\%$ error in the ketone extinction coefficient caused an approximately $x\%$ error in the rate constant and the extinction coefficients were therefore determined with sufficient accuracy ($<2\%$) to make this contribution to the error of the rate constant insignificant. The overall reproducibility of the rate constants was generally found to be around 5%. Product ratios and kinetic data obtained are summarized in Table 1.

A number of features of the values of the isotope effects deserve comment. The most obvious feature is that they are all inverse. This feature is not surprising since hydrolysis of sodium borohydride (27), hydrolysis of pyridine alkylboranes (28), and the methanolysis of lithium borohydride (29) all have inverse isotope effects. In the reduction of ketones by borohydride, it has been shown (30, 46) that the rate determining step is transfer of the first hydrogen (Fig. 4).

Thus the observed isotope effect is the composite of the primary isotope effects of the hydrogen being transferred superimposed on the secondary isotope effects of the three hydrogens not being transferred. It is probable that the inverse effect arises from the three secondary effects outweighing the primary effect (27, 31, 32) and this view is substantiated by the observation that reduction of methyl alkyl ketones with morpholine-borane (33) shows a small normal isotope effect.

The second, and most important feature of the values of the isotope effects is that, regardless of whether the isotope effects are normal or inverse, there is no systematic relationship

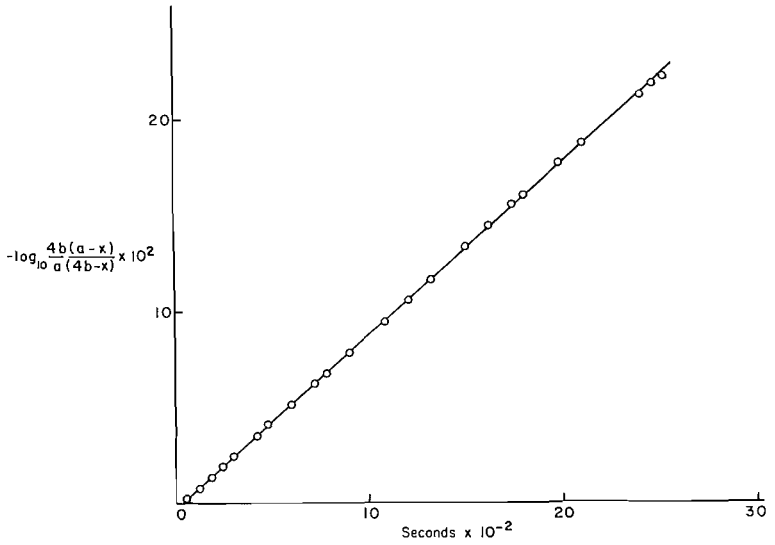

FIG. 2. Typical kinetic plot of the reduction of 2-methylcyclohexanone by sodium borohydride.

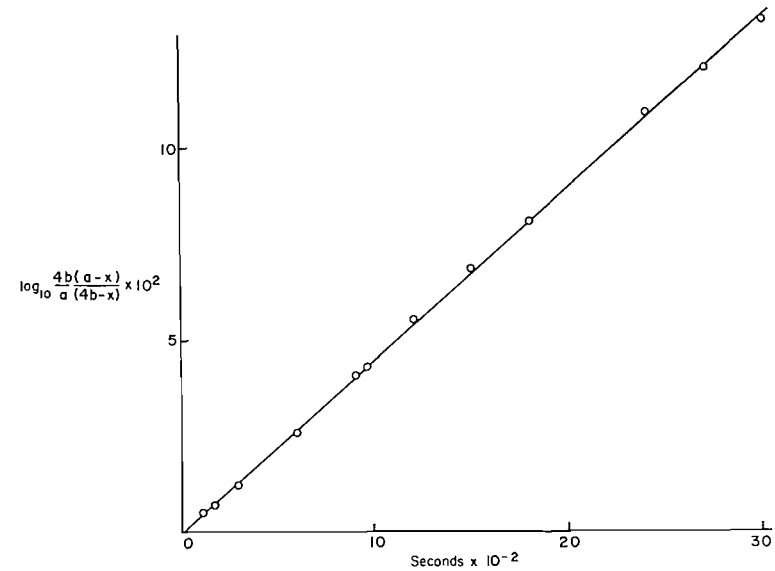

FIG. 3. Typical kinetic plot of the reduction of 2-methylcyclohexanone by sodium borodeuteride.

between product ratio and magnitude of the isotope effect. The product ratios vary from essentially 100% equatorial alcohol through 3,3,5-trimethylcyclohexanone with an excess of axial alcohol and to 3,3,5,5-tetramethylcyclohexanone with presumably an even greater amount of initial equatorial hydride attack but for which no "product ratio" is obtainable. Although the question of whether transfer of the first hydrogen gives the same product ratio as transfer of subsequent hydrogens has been ignored, the results of Rickborn and Wuesthoff (47) indicate that this change in product ratio, although significant, would be far overshadowed by the differences due to the varying steric hindrances of the ketones themselves. Clearly there is no trend towards lower isotope effect with formation of a greater proportion of axial isomer as would be anticipated if the steric approach control–product development control

Can. J. Chem. Downloaded from www.nrcresearchpress.com by 210.87.254.5 on 09/05/12
For personal use only.

TABLE 1. Stereochemical product ratios and rate constants for reduction of ketones by sodium borohydride and sodium borodeuteride in 2-propanol at 25°

Ketone	Axial:equatorial product ratio			Rate constants $\times 10^4$ ($l\ mol^{-1}\ s^{-1}$)		
	g.l.p.c.	n.m.r.	lit.	k_H	k_D	k_H/k_D
Cyclohexanone				765±31	1290±41	0.59
Cholestan-3-one	1:99*	0:100	15:85(23) 7:93(24)	456±4§	590±10§	0.77§
3-Methylcyclohexanone	25:75†	24:76	13:87(25)	605±12	939±34	0.64
2-Methylcyclohexanone	31:69‡	32:68	31:69(9)	149±3	198±7	0.75
3,3,5-Trimethylcyclohexanone	55:45†	51:49	58:52(19) 55:45(26)	21.8±0.4	31.5±1.6	0.69
3,3,5,5-Tetramethylcyclohexanone				1.92±0.21	2.72±0.15	0.71

*α-OH:β-OH.
†*trans:cis*.
‡*cis:trans*.
§Revised Beer's Law data caused a significant change in these results from those previously reported (2).

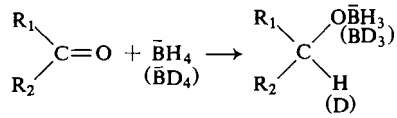

FIG. 4. Rate determining step in the borohydride reduction of ketones.

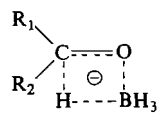

FIG. 5. Four-center transition state for borohydride reduction of ketones.

were operative. *This evidence appears to invalidate the steric approach control–product development control* (as redefined) *explanation of stereo-chemical product ratios*, for the reduction of ketones by sodium borohydride. It does not, however, detract from the value of the concepts (1) themselves which may well be operative in other reactions.

A third feature is concerned with the absolute magnitude of the *primary* isotope effect. Although masked by the secondary isotope effects, it is clear that if the secondary effects are able to overshadow the primary effect, then the primary effect itself must be very small, probably less than 2. This small value is certainly consistent with an early transition state as required by other explanations of product ratios (3–5); it is also equally consistent with a very late transition state, where the hydrogen has been substantially transferred. Other possible reasons for a very small isotope effect concern the nature of the reaction and the geometry of the transition state itself. Isotope effects in hydride transfers as opposed to proton transfers have been the subject of some discussion (34, 35) and in general, on both theoretical and experimental grounds, the magnitude of isotope effects in hydride transfers appears to be considerably smaller than in proton transfers, rarely exceeding 2.5 (34). Additionally, the transition state for hydride reductions has frequently been considered to be four-centered (15, 24) as shown in Fig. 5, which suggests a B.....H.....C angle in the neighborhood of 90°.

Recently More O'Ferrall (36) has calculated that isotope effects where such an angle deviates significantly from 180° can drastically diminish from 6–8 down to 1–2. As mentioned above, the weight of current opinion of those workers concerned with explaining product ratios favors an early transition state, and thus *the magnitudes of the isotope effects, while not constituting unambiguous evidence for this opinion, do not contradict it*. We have experiments currently in progress which we hope will shed further light on the primary isotope effect and on the geometry of the transition state in hydride reduction of ketones.

Experimental

General

Melting points were taken on a Fisher–Johns melting point apparatus and are uncorrected. The i.r. spectra

Can. J. Chem. Downloaded from www.nrcresearchpress.com by 210.87.254.5 on 09/05/12
For personal use only.

TABLE 2. Physical data of ketones

Ketone	n_D^{22}	b.p. (°C/mm)	lit. n_D^{20}; b.p. (°C/mm)	λ_{max}* (nm)	ε*
Cyclohexanone	1.4495	149–150/755	1.4505; 155/760(41)	283	17.2±0.1
2-Methylcyclohexanone	1.4478	80/20	1.4475; 162–163/760(42)	285	18.7±0.2
3-Methylcyclohexanone	1.4444	86/70	1.4440; 53.5–54/2.2(43)	285	18.3±0.4
3,3,5-Trimethylcyclohexanone	1.4441	90/26	1.4461; 73–74/14(37)	287	19.0±0.2
3,3,5,5-Tetramethyl-cyclohexanone	1.4504	127/60	1.4520; 196–197/760(44)	289	19.5±0.1
Cholestan-3-one		127.5–128 (m.p.)	129–130 (m.p.) (24)	277	20.5±0.0

*In 2-propanol at 25°.

were measured on a Perkin–Elmer 237B Grating Infrared Spectrophotometer, and u.v. spectra on a Perkin–Elmer 202 Ultraviolet–Visible Spectrophotometer. The n.m.r. spectra were obtained on a Varian T60 NMR spectrometer using deuteriochloroform as solvent and tetramethylsilane as internal standard. A Hewlett–Packard F and M Scientific 402 High Efficiency Gas Chromatograph was employed for all g.l.p.c. measurements.

Reagents

Sodium borohydride (98%, Fisher Scientific) and sodium borodeuteride (Merck, Sharpe and Dohme) were used without further purification, care being taken to keep them dry. 2-Propanol (Fisher, spectral grade) was passed through a neutral alumina column, dried over anhydrous calcium sulfate, and distilled before use. All ketones except 3,3,5-trimethylcyclohexanone and cholestan-3-one were commercial samples purified by distillation. 3,3,5-trimethylcyclohexanone was prepared from 3,3,5-trimethylcyclohexanol by dichromate oxidation (37) and was purified by distillation. Cholestan-3-one (K and K Laboratories) was used without further purification. Gas chromatography showed all ketones to have a purity greater than 99%. The appropriate physical data are summarized in Table 2.

Product Ratios

The following procedure is typical. To a solution of sodium borohydride (0.47 g; 12.4 mmol) in 2-propanol (50 ml) was added the ketone solution (12.4 mmol) in 2-propanol (10 ml). The mixture was stirred overnight. Concentrated hydrochloric acid (5 ml) was added to destroy excess borohydride and hydrolyze the borate esters, 2-propanol was removed by rotary evaporation, and the alcohol products extracted into ether (2 × 10 ml). The combined ether extracts were dried (Na_2SO_4) and injected into g.l.p.c. For the cyclohexanols the following conditions were used: 6 ft QF-1 column; flash heater 120°; column oven 50–75°; carrier gas flow 3.1 ml/min: for cholestanols: 6 ft OV-210 column; flash heater 290°; column oven 250°; carrier gas flow 3.1 ml/min. Peak areas were determined either by mechanical integration or by the peak height–half-width product.

For n.m.r. determination of product ratios, the dried ether extract was evaporated and the n.m.r. spectrum measured. The chemical shift (38, 39) and the splitting (40) of the methine proton on the hydroxyl-bearing carbon depends on the axial–equatorial nature of the proton, the axial protons appearing in the range δ 3.2-3.7 p.p.m. and the equatorial protons in the range 3.6–4.2 p.p.m. Integration of the signals due to these protons gave the product ratio.

Kinetic Method[4]

A spectrophotometric method employing a Gilford 240 spectrophotometer, equipped with a Haake constant temperature device to maintain the temperature at 25.0 ± 0.02°, was used. The wavelength used was the appropriate absorption maximum for each ketone (see Table 2). The reference cell consisted of 2.0 ml of 2-propanol and 1.0 ml of standardized sodium borohydride solution in 2-propanol (45) in a 3.0 ml, 1.0 cm quartz cuvette. The sample cell contained 1.0 ml of the standardized sodium borohydride solution to which 2.0 ml of a 2-propanol solution of the ketone was added. Zero time was taken as the half-time of addition. Mixing was achieved by inversion of the cuvette three times. Beer's law plots were used to calculate ketone concentration from absorptions at appropriate time intervals. The data were treated by plotting $\log_{10} 4b(a-x)/a(4b-x)$ against t where a is the initial ketone concentration, b, initial borohydride concentration, and x, concentration of reacted ketone at time t. The slope, equal to $k(a-4b)/2.303$, where k[5] is the second-order rate constant, was computed with a least-squares programme[6] on an Olivetti–Underwood Programma 101 desk computer. Figures 2 and 3 show typical plots for reduction of 2-methylcyclohexanone by sodium borohydride and sodium borodeuteride, respectively. Initial concentrations of ketone ranged from 1.36×10^{-2} to 6.84×10^{-2} M, and those of sodium borohydride from 0.44×10^{-2} to 1.71×10^{-2} M, giving a [ketone]/[hydride] ratio ranging from 1.05 to 6.48. In the case of 3-cholestanone, owing to solubility problems, the ketone concentration was kept in the range 0.17×10^{-2} to 0.28×10^{-2} M, giving a [ketone]/[hydride] ratio of 0.24 to 0.59. Satisfactorily

[4]The titration method (46) was found to be less consistent than the spectrophotometric method.

[5] The rates of disappearance of ketone and borohydride obviously differ by a factor of 4. Previous rate constants (46) refer to borohydride and, in order that direct comparisons may be made, our values also refer to this rate, despite the fact that our measurements are based on ketone concentrations.

[6]We are very grateful to Dr. M. Parris for this programme.

Can. J. Chem. Downloaded from www.nrcresearchpress.com by 210.87.254.5 on 09/05/12
For personal use only.

reproducible rate constants were obtained, the values being found to be independent of the initial concentrations chosen, in agreement with the findings of Brown *et al.* (46) and in confirmation of the assumption of second-order kinetics. The values of k_H and k_D are summarized in Table 1 and represent the results of at least three independent kinetic runs for each determination.

The generous financial support of the National Research Council of Canada and of the President's Research Fund, Carleton University is much appreciated. The award of a National Research Council of Canada Scholarship to D. J. Phelps is gratefully acknowledged.

1. W. G. Dauben, G. J. Fonken, and D. S. Noyce. J. Am. Chem. Soc. **78**, 2579 (1956).
2. D. C. Wigfield and D. J. Phelps. Chem. Commun. 1152 (1970).
3. J. C. Richer. J. Org. Chem. **30**, 324 (1965).
4. M. Cherest, H. Felkin, and N. Prudent. Tetrahedron Lett. 2199 (1968).
5. M. Cherest and H. Felkin. Tetrahedron Lett. 2205 (1968).
6. H. C. Brown and H. R. Deck. J. Am. Chem. Soc. **87**, 5620 (1965).
7. E. L. Eliel and Y. Senda. Tetrahedron, **26**, 2411 (1970).
8. D. C. Ayres, D. N. Kirk, and R. Sawdaye. J. Chem. Soc. B, 505 (1970).
9. H. C. Brown and J. Muzzio. J. Am. Chem. Soc. **88**, 2811 (1966).
10. D. N. Kirk. Tetrahedron Lett. 1727 (1969).
11. G. J. Karabatsos and T. H. Althuis. Tetrahedron Lett. 4911 (1967).
12. P. Geneste, G. Lamaty, and J. P. Roque. Tetrahedron Lett. 5007 (1970).
13. P. Geneste, G. Lamaty, C. Moreau, and J. P. Roque. Tetrahedron Lett. 5011 (1970).
14. P. Geneste, G. Lamaty, and J. P. Roque. Tetrahedron Lett. 5015 (1970).
15. P. Geneste and G. Lamaty. Bull. Soc. Chim. Fr. 669 (1968).
16. J. Klein and D. Lichtenberg. J. Org. Chem. **35**, 2654 (1970).
17. D. C. Wigfield. Can. J. Chem. **48**, 2120 (1970).
18. K. Bowden and M. Hardy. Tetrahedron, **22**, 1169 (1966).
19. P. T. Lansbury and R. E. MacLeay. J. Am. Chem. Soc. **87**, 831 (1965).
20. S. F. Sun and N. O. del Rosario. J. Org. Chem. **35**, 4025 (1970).
21. F. G. Bordwell and W. J. Boyle, Jr. J. Am. Chem. Soc. **93**, 512 (1971); K. Kwart and M. C. Latimore. J. Am. Chem. Soc. **93**, 3770 (1971).
22. F. H. Westheimer. Chem. Revs. **61**, 265 (1961).
23. O. H. Wheeler and J. L. Mateos. Can. J. Chem. **36**, 1049 (1958).
24. O. R. Vail and D. M. S. Wheeler. J. Org. Chem. **27**, 3803 (1962).
25. H. B. Henbest and M. G. Combe. Tetrahedron Lett. 404 (1961).
26. H. Haubenstock and E. L. Eliel. J. Am. Chem. Soc. **84**, 2368 (1962).
27. R. E. Davis, E. Bromels, and C. L. Kibby. J. Am. Chem. Soc. **84**, 885 (1962).
28. R. E. Davis and R. E. Kenson. J. Am. Chem. Soc. **89**, 1384 (1967).
29. R. E. Dessy and E. Grannen, Jr. J. Am. Chem. Soc. **83**, 3953 (1961).
30. R. E. Davis and J. A. Gottbrath. J. Am. Chem. Soc. **84**, 895 (1962).
31. R. E. Davis, C. L. Kibby, and C. G. Swain. J. Am. Chem. Soc. **82**, 5950 (1960).
32. R. E. Davis, R. E. Kenson, C. L. Kibby, and H. H. Lloyd. Chem. Commun. 593 (1965).
33. S. S. White and H. C. Kelly. J. Am. Chem. Soc. **92**, 4203 (1970).
34. C. G. Swain, R. A. Wiles, and R. F. W. Bader. J. Am. Chem. Soc. **83**, 1945 (1961) and references therein.
35. B. Belleau and J. Moran. Ann. N.Y. Acad. Sci. **107**, 822 (1963).
36. R. A. More O'Ferrall. J. Chem. Soc. B, 785 (1970).
37. E. L. Eliel and H. Haubenstock. J. Org. Chem. **26**, 3504 (1961).
38. R. U. LeMieux, R. K. Kullnig, H. J. Bernstein, and W. G. Schneider. J. Am. Chem. Soc. **80**, 6098 (1958).
39. E. L. Eliel, M. H. Gianni, Th. H. Williams, and J. B. Stothers. Tetrahedron Lett. 741 (1962).
40. D. H. Williams and N. S. Bhacca. J. Am. Chem. Soc. **86**, 2742 (1964).
41. M. S. Kharasch, J. Kuderna, and W. Nadenberg. J. Org. Chem. **18**, 1225 (1953).
42. H. Hopff. Ber. **65B**, 482 (1932).
43. Y. R. Naves. Helv. Chim. Acta, **31**, 932 (1948).
44. M. S. Kharasch and P. O. Tawney. J. Am. Chem. Soc. **63**, 2308 (1941).
45. D. A. Lyttle, E. H. Jensen, and W. A. Struck. Anal. Chem. **24**, 1843 (1952).
46. H. C. Brown, O. H. Wheeler, and K. Ichikawa. Tetrahedron, **1**, 214 (1957).
47. B. Rickborn and M. T. Wuesthoff. J. Am. Chem. Soc. **92**, 6894 (1970).

Can. J. Chem. Downloaded from www.nrcresearchpress.com by 210.87.254.5 on 09/05/12
For personal use only.

The Photochemistry of 1-Methoxy-1,4-dihydro-1,4-enthenoanthracene

C. O. BENDER, J. L. M. ELDER,[1] A. J. HERBST,[1] AND L. E. MILLER[1]

Department of Chemistry, University of Lethbridge, Lethbridge, Alberta

Received August 5, 1971

The primary photoproducts of direct and benzophenone sensitized irradiation of the barrelene 1-methoxy-1,4-dihydro-1,4-ethenoanthracene are the semibullvalenes 2- and 5-methoxynaphtho[2,3-*c*]tricyclo[3.3.0.0^{2,8}]-octa-3,6-diene (**6** and **7**), formed with quantum efficiencies of $\Phi_6 \simeq 0.23$ and $\Phi_7 \simeq 0.31$ in each case. Whereas **6** is inert to further direct irradiation, **7** photoisomerizes to 6-methoxycycloocta[*b*]naphthalene (**4**) ($\Phi = 0.40$); **4** photoisomerizes to 10*b*-methoxy-2*a*, 10*a*-dihydrocyclobut[*a*]anthracene upon direct ($\Phi = 0.11$) or benzophenone-sensitized irradiation ($\Phi = 0.05$).

Les produits primaires issus de l'irradiation directe et de l'irradiation photosensibilisée par la benzophénone, du barrelène méthoxy-1 dihydro-1,4 étheno-1,4 anthracène sont les semi-bullvalènes méthoxy-2 et -5 naphto[2,3-*c*] tricyclo[3.3.0.0.^{2,8}] octadiène-3,6 (**6** et **7**) obtenus avec des rendements quantiques de $\Phi_6 \simeq 0.31$ respectivement. Tandis que **6** est inerte à une irradiation ultérieure directe, **7** s'isomérise en méthoxy-6 cycloocta[*b*] naphtalène (**4**) ($\Phi = 0.40$); **4** s'isomérise en méthoxy-10*b* dihydro-2*a*,10*a* cyclobuta[*a*] anthracène par irradiation directe ($\Phi = 0.11$) ou photosensibilisée par la benzophénone ($\Phi = 0.05$).

Canadian Journal of Chemistry, **50**, 395 (1972)

Can. J. Chem. Downloaded from www.nrcresearchpress.com by 210.87.254.40 on 09/05/12
For personal use only.

Introduction

In a recent study, the photochemistry of 2,3-naphthobarrelene (**1**) was shown to be strikingly different from that of barrelene (1), benzobarrelene (2), 1,2-naphthobarrelene (3), and other barrelenes (4), in that cyclooctatetraene product was not observed to result from direct irradiation (3). Instead, 2,3-naphthosemibullvalene (**2**), from di-π-methane rearrangement, was found to be the exclusive product (see Scheme 1), and was formed with the same efficiency ($\Phi = 0.46$) as when derived from triplet sensitization. In order to examine the further generality of this behavior, the photochemistry of the bridgehead methoxyl derivative **3** was investigated.

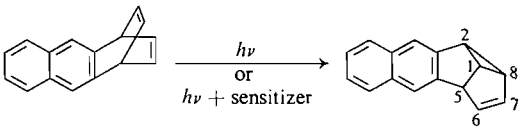

1 2

SCHEME 1

Results

1-Methoxy-1,4-dihydro-1,4-ethenoanthracene (**3**) was obtained in 12% yield from the addition of 2,3-naphthyne to anisole. The structural assignment follows from the n.m.r. spectrum: the aromatic protons appear as a multiplet centered at τ 2.54, the vinyl protons as a multiplet at 3.25, the bridgehead proton as a multiplet at 5.36, and the methoxyl protons as a singlet at 6.34.

During exploratory runs, the direct irradiations of **3** at 313 nm were monitored by n.m.r. spectroscopy, which indicated the formation of four products (see Scheme 2): 6-methoxycycloocta[*b*]naphthalene (**4**), 10*b*-methoxy-2*a*,10*a*-dihydrocyclobut[*a*]anthracene (**5**), and 2- and 5-methoxynaphtho[2,3-*c*]tricyclo[3.3.0.0^{2,8}]octa-3,6-diene (**6** and **7**), in time-dependent proportions as shown in Fig. 1.

The methoxycyclooctatetraene structure for **4** was suggested by its 60 MHz n.m.r. spectrum which besides a 6H aromatic multiplet centered at τ 2.57 and a methoxyl singlet at 6.33, showed only complex absorption for five protons in the vinylic region between τ 3.20 and 4.88. Treatment of **4** with acid led to the formation of a ketonic product **8** (see Scheme 3) ($\nu_{C=O}$ (KBr) 1670 cm^{-1}), the u.v. spectrum of which showed extensive conjugation: λ_{max} (MeOH) 261 (44 000), 323 inf (5300), and 367 nm (2400) [*cf.* the long-wavelength band of 2-naphthaldehyde (MeOH) at 344 nm (2000) (5)]. Since the 60 MHz n.m.r. spectrum of **8** contains, besides a 5H aromatic multiplet centered at

[1]Undergraduate Research Assistants, 1970.

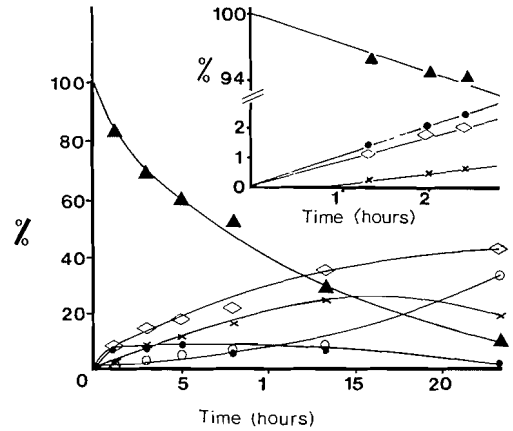

FIG. 1. Plot of extended conversions of barrelene **3** (▲) and the appearance of cyclooctatetraene **4** (×), cyclobutene **5** (○), and semibullvalenes **6** and **7** (◇ and ●) *vs.* time of irradiation. The insert is a plot of low conversion runs *vs.* time of irradiation.

τ 2.28 and complex absorption for four vinylic protons between 2.88 and 4.32, a methylene doublet at 6.46 ($J = 8$ Hz), and a strongly deshielded 1H aromatic singlet (H-5) at 1.09, the position of the carbonyl in **8** and hence the position of the methoxyl group in **4** is tentatively established as being alpha to the aromatic ring.

The structure of cyclobutene **5** was also deduced mainly from n.m.r. spectral data. The aromatic protons appear as a multiplet centered at τ 2.46 and the methoxyl as a singlet at 6.97; the methine proton, H-2*a*, is coupled to three of the four vinylic protons, forming the X part of two ABX spin systems, one comprising H-4 (τ 3.50, d, $J_{AB} = 10$, $J_{AX} = 0$ Hz), H-3 (τ 4.04,

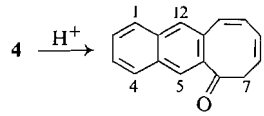

8

SCHEME 3

d of d, $J_{BA} = 10$, $J_{BX} = 4.8$ Hz), and H-2*a* (τ 6.60, br d, $J_{XB} = 4.8$ Hz), and the other H-2 (τ 3.88, d of d, $J_{AB} = 2.8$, $J_{AX} = 1.3$ Hz), H-1 (τ 4.12, d of d, $J_{BA} = 2.8$, $J_{BX} = 0.8$ Hz), and H-2*a*. These designations were confirmed by spin decoupling techniques: irradiation of the methine proton simplified the vinylic region to two AB quartets. Thus, whereas H-4 was unchanged, H-3 was collapsed to a doublet ($J = 10$ Hz), H-2 to a doublet ($J = 2.8$ Hz), and H-1 to a doublet ($J = 2.8$ Hz). The 2.8 Hz coupling constant between H-1 and -2 is characteristic of cyclobutene vinylic protons (6).

The semibullvalene structures assigned to the photoproducts **6** and **7** follow straightforwardly from comparison of their n.m.r. spectral parameters with those of 2,3-naphthosemibullvalene (**2**) (Table 1). Chemical evidence for structure **6** derives from its protolysis, typical of methoxycyclopropanes, to the ketonic compound **9** during chromatography on silicic acid[2] (7) (see Scheme 4). 3,3*a*,4,10*b*-Tetrahydro-4-oxonaphtho[2,3-*a*]pentalene (**9**) shows a u.v. (cyclohexane) long-wavelength band at 352 nm (1600) and an i.r. carbonyl band at 1700 cm^{-1}. The n.m.r. spectrum contains no methoxyl protons, a singlet at τ 1.75 (H-5), a multiplet at 2.35 (remaining aromatics), a doublet of doublets at

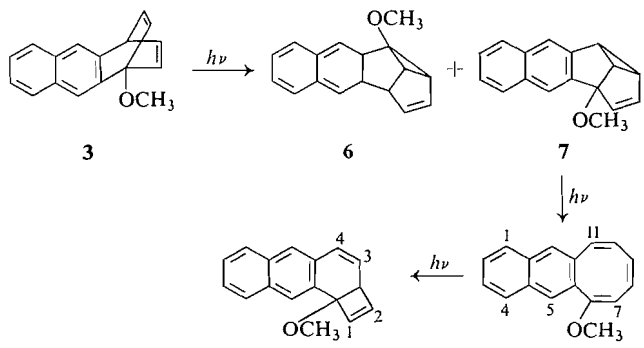

SCHEME 2

[2]In order to limit this reaction when isolation of **6** was desired, chromatography columns were eluted rapidly under reduced pressure (see Experimental).

Can. J. Chem. Downloaded from www.nrcresearchpress.com by 210.87.254.40 on 09/05/12
For personal use only.

TABLE 1. The n.m.r. spectra of semibullvalenes*,†

Assignment	Description and signal position, τ		
	2‡	**6**	**7**
Aromatic	2.36–2.93, m	2.24–2.78, m	2.25–2.84, m
H-6	4.51, *A*BM q	4.50, *A*BM q	4.53, AB d
H-7	4.84, A*BZ* q	4.75, A*BZ* q	4.93, A*BZ* q
H-5	5.99, A*MX* q	6.01, A*MX* q	—
H-1	6.71, M*X*YZ q	6.67§, M*X*Z t	6.67§, *X*YZ t
H-2	7.01, X*Y*Z t	—	6.93, X*Y*Z t
H-8	7.41, BXY*Z* d of t	7.13, BX*Z* q	7.35, BXY*Z* d of t
OCH_3	—	6.67, s	6.67, s

*Run on 100 MHz n.m.r. in CCl_4 with TMS as internal standard.
†Corresponding coupling constants, where applicable, were within 0.5 Hz: typically $J_{12} = J_{15} = J_{18} = J_{28} = 6.5$, $J_{56} = J_{78} = 2.0$, and $J_{67} = 5.0$ Hz.
‡The aliphatic-olefinic region comprises an ABMXYZ spin system.
§Center limb obscured by methoxyl signal.

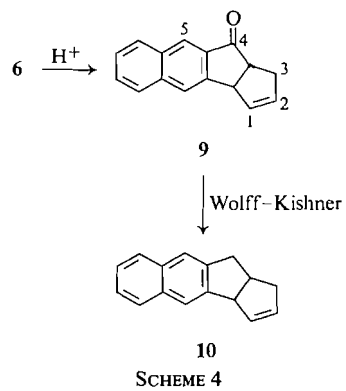

SCHEME 4

4.18 (H-1, $J = 2$ and 5.5 Hz), another doublet of doublets at 4.42 (H-2, $J = 2$ and 5.5 Hz), a broad doublet at 5.46 (H-10*b*, $J = 5.5$ Hz), a multiplet at 6.63 (H-3*a*), and another multiplet at 7.28 (methylene). The structure of ketone **9** is supported by its reduction under Wolff–Kishner conditions to give the alkene **10**. The i.r. spectrum of 3,3*a*,4,10*b*-tetrahydronaphtho-[2,3-*a*]pentalene (**10**) shows no carbonyl band and the u.v. spectrum shows no absorption maxima above 323 nm. In the n.m.r. spectrum, the aromatic protons appear as a multiplet at τ 2.58, the vinylic protons as a multiplet at 4.34, the allylic methine (H-10*b*) as a broad singlet at 5.73 (H-10*b*), the C-4-methylene as a multiplet at 6.77, the C-3 methylene as a multiplet at 7.27, and the remaining methine (H-3*a*) as a multiplet at 7.80.

The photoproducts **4**–**7** were irradiated separately at 313 nm in order to examine for the occurrence of secondary photochemical processes. It was revealed that cyclooctatetraene **4** yields cyclobutene **5** with a quantum yield of $\Phi = 0.11$ [ferrioxalate actinometry], a photocyclization reaction also observed with cyclooctatetraene (8), while semibullvalene **7** affords **4** ($\Phi = 0.40$), a transformation unknown with 2,3-naphthosemibullvalene (**2**) (3). Cyclobutene **5** was photochemically inactive as was, surprisingly, semibullvalene **6**.

It was of interest to determine the multiplicities of the excited state species involved in the above reactions, thus sensitization runs with benzophenone at 343 nm, with the sensitizer capturing more than 95% of the light, were investigated. Whereas cyclooctatetraene **4** readily gave cyclobutene **5** ($\Phi = 0.05$), semibullvalene **7** was found to be unreactive. Since the photoreduction of benzophenone was efficiently quenched in the presence of **7**, it seems certain that triplet energy transfer to the semibullvalene had been successful. In the case of barrelene **3**, triplet sensitization led cleanly to the formation of **6** and **7** with appearance quantum yields of $\Phi = 0.24$ and 0.30, respectively.

Thus far, two processes can account for the formation of cyclooctatetraene **4** during direct irradiations of barrelene **3**. Either it arises from a $(2 + 2)\pi$-cycloaddition, or it derives from photoisomerization of initially formed semibullvalene **7**. In order to distinguish between these two pathways, runs to low conversion were carried out. Extrapolation of the cyclooctatetraene (**4**) product concentration to zero time did not pass through the origin (insert to Fig. 1): thus **4** is not a primary photoproduct and must arise exclusively from semibullvalene **7**. The fact that the extinction coefficient of **7**

Can. J. Chem. Downloaded from www.nrcresearchpress.com by 210.87.254.40 on 09/05/12
For personal use only.

TABLE 2. Quantum yield data*

Reactant	Reactant concentration (mM)†	Sensitizer concentration (mM)‡,§	Products	Quantum yields‖
3	4.14	—	**6** and **7**	0.22 and 0.32¶
3	0.94	2.72	**6** and **7**	0.24 and 0.30
7	0.50	—	**4**	0.40
7	0.51	2.42	—	0
4	0.43	—	**5**	0.11
4	0.30	2.26	**5**	0.05

*Cyclohexane solvent.
†313 nm light was used for direct runs.
‡343 nm light was used for sensitized runs.
§Sensitizer absorbing >95% of light.
‖Based on product appearance from runs to ⩽17% conversion.
¶Obtained from 2.5% conversion run and corrected for formation of small amount of **4**.

is approximately six times that of barrelene **3** at 313 nm and that the quantum yield for its conversion to **4** is $\Phi = 0.40$, readily explains how the cyclooctatetraene appears so early on during the direct irradiation of **3**.

The low conversion runs also enabled values of $\Phi = 0.22$ and 0.32 to be calculated for the unsensitized appearance quantum yields of **6** and **7**, after correcting for light utilized to form small amounts of cyclooctatetraene **4**. Summarized in Table 2 are the quantitative data for the observed photochemistry.

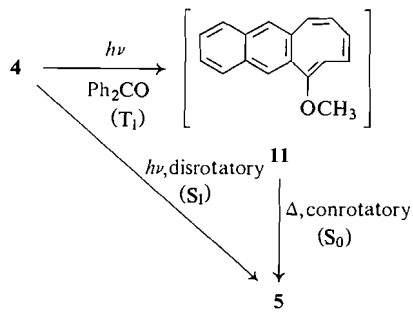

SCHEME 5

Discussion

The primary photoproducts of both direct and sensitized irradiations of methoxybarrelene **3** are the semibullvalenes **6** and **7**. Their dual formation is consistent with their arising from a di-π-methane rearrangement which proceeds with almost equal facility from both modes of initial vinyl–vinyl bridging. Because the quantum yields for the direct and sensitized formations of the semibullvalenes are the same, within experimental error, it is feasible that they derive from the same excited state, providing we assume an intersystem crossing efficiency of almost unity. Such an assumption seems to be reasonable in view of the small fluorescence quantum yield ($\Phi_f = 0.08$) noted for 2,3-naphthobarrelene (3). The introduction of a methoxy group into the bridgehead position is seen therefore, not to alter the course of the excited state reaction of the 2,3-naphthobarrelene system.

With regard to the cyclooctatetraene transformation, the quantum yield data indicate cyclobutene **5** to be attainable both from an excited singlet and, less efficiently, from an excited triplet pathway (see Scheme 5). By analogy with Lui's work on 1,3-cyclooctadiene (9) it is possible that the singlet pathway involves a concerted disrotatory closure (10), while the triplet pathway involves a two step mechanism, with initial isomerization of the all *cis* isomer **4** to a highly strained mono *trans* isomer[3] such as **11**, which then undergoes symmetry allowed thermal conrotatory closure to **5**. We have not obtained evidence for the formation of an intermediate such as **11** during sensitized runs, but this may simply be due to the rate of closure to **5** being much greater than the rate of formation of **11** at the photolysis temperature employed ($\sim 20°$). Whichever pathway is utilized, the cyclization of the methoxyl

[3]White *et al.* have recently shown that the all *cis* isomer of 1,2,4,7-tetraphenylcyclooctatetraene can be converted to the mono *trans* isomer during photolysis (11).

Can. J. Chem. Downloaded from www.nrcresearchpress.com by 210.87.254.40 on 09/05/12
For personal use only.

Can. J. Chem. Downloaded from www.nrcresearchpress.com by 210.87.254.40 on 09/05/12
For personal use only.

substituted diene moiety appears to be totally selective, and we attribute this to the ability of the methoxy group to localize excitation into the attached vinyl (12, 13). Chapman and coworkers have noted a similar exclusive selectivity to operate in the photoisomerization of 1-methoxycycloheptatriene to 1-methoxybicyclo[3.2.0]hepta-3,6-diene (12).

Examination of the photochemistry of semibullvalenes **6** and **7** has revealed the formation of **4** to be subject to a dramatic positional substituent effect. We are presently investigating the photolysis of other semibullvalenes to determine whether this effect is uniquely associated with the methoxy group and its attachment at C-5, and hence if its origin is steric or electronic in nature. Finally, the singlet excited state seems to be responsible for the highly efficient formation of **4** since the reaction occurs only during direct irradiations.

Experimental

The n.m.r. spectra were run on Varian A-60 and HA-100 instruments with TMS as internal standard. The i.r. spectra were recorded on a Perkin–Elmer Model 337 spectrophotometer and the u.v. spectra on a Cary 15 spectrophotometer. All m.p. are uncorrected. Elemental analyses were performed by Galbraith Labs. Inc., Knoxville, Tennessee. Cyclohexane solvent for photolyses was stirred with 30% fuming sulfuric acid for 6 h, washed with 10% aq sodium hydroxide, dried ($MgSO_4$), and distilled from calcium hydride. Benzophenone sensitizer was recrystallized twice from ethanol, m.p. 47–49°.

1-Methoxy-1,4-dihydro-1,4-ethenoanthracene (3)

A mixture of 6.0 g of 3-diazonium-naphthalene-2-carboxylate (3) and 300 ml of anisole was heated with stirring at 90° for 4 h in a nitrogen atmosphere. The mixture was concentrated *in vacuo* and the oily residue column chromatographed on silicic acid. Elution with 0.5% ether/hexane gave 833.5 mg (12%) of colorless **3**, m.p. 84–86°, from early fractions. Crystallization from hexane raised the m.p. to 95–97°: u.v. max (cyclohexane) 233 (68 000), 237 (65 000), 255 (9500), 263 (10 000), 273 (9000), 283 (5 000), 296 (330), 299 inf (260), 305 (260), 309 (400), 318 (200), and 323 nm (310); n.m.r. (100 MHz, CCl_4) τ 2.54 (m, 6H, arom) 3.25 (m, 4H, vinyl), 5.36 (m, 1H, bridgehead), and 6.34 (s, 3H, methoxyl).

Anal. Calcd. for $C_{17}H_{14}O$: C, 87.15; H, 6.02. Found: C, 87.08; H, 5.89.

Direct Irradiation of 3: Preparation of 4, 5, 6, and 9

A nitrogen-flushed solution of 250.5 mg (1.07 mmol) of **3** in 250 ml of cyclohexane was irradiated for 250 min with a quartz-jacketed Hanovia 450 W water-cooled, medium pressure immersion lamp fitted with a Pyrex filter sleeve. The solvent was evaporated *in vacuo* and the residue chromatographed on a 2 × 18 cm silicic acid column with 3 l of hexane and then 500 ml of 5% ether/hexane as eluting agent. The flow-rate was maintained at 50 ml/min with the aid of an aspirator; 100 ml fractions were collected. Fractions 8–13 gave 9.4 mg (4%) of **4**. Crystallization from ethanol gave colorless crystals, m.p. 85–87°: u.v. max (cyclohexane) 225 (55 000), 246 inf (24 500), 280 (12 000), 291 inf (10 500), and 304 nm inf (6300); n.m.r. (60 MHz, $CDCl_3$) τ 2.57 (m, 6H, arom), 3.23 (br d, 1H, H-11, $J = 12$ Hz), 3.78–4.30 (m, 3H, H-8, -9, -10), 4.88 (m, 1H, H-7), and 6.33 (s, 3H, methoxyl).

Anal. Found: C, 87.10; H, 6.24.

Fractions 18–28, after crystallization from hexane and sublimation (80°/0.1 mm), gave 45.2 mg (18%) of colorless **6**, m.p. 94–96°: u.v. max (cyclohexane) 237 (65 000), 264 (5200), 273 (6000), 283 (5700), 294 inf (3400), 313 (840), 319 (420), and 327 nm (1000); n.m.r., see Table 1.

Anal. Found: C, 86.85; H, 6.31.

Fractions 29–34 contained a mixture of **5**, **6**, and **9**. The mixture was applied to a 2 × 35 cm silicic acid column slurry-packed with hexane and left for 24 h without elution, to ensure complete protolysis of **6** to **9**. After this time the column was eluted with 1% ether/hexane; 100 ml fractions were collected. Fractions 8–14 contained 87.8 mg (35%) of **5** as an oil. Crystallization from hexane and sublimation (85°/0.1 mm) gave colorless crystals, m.p. 92–94°: u.v. max (cyclohexane) 252 (57 000), 266 (24 000), 285 (11 000), 295 (14 000), and 306 nm (10 800); n.m.r. (100 MHz, CCl_4) τ 2.46 (m, 6H, arom), 3.50 (d, 1H, H-4, $J = 10$ Hz), 3.88 (d of d, 1H, H-2, $J = 2.8$, 1.3 Hz), 4.04 (d of d, 1H, H-3, $J = 10$, 4.8 Hz), 4.12 (d of d, 1H, H-1, $J = 2.8$, 0.8 Hz), 6.60 (br d, 1H, H-2*a*, $J = 4.8$ Hz), and 6.97 (s, 3H, methoxyl). Double resonance was performed on the HA-100 MHz n.m.r. Irradiation of H-2*a* collapsed H-1 to a d ($J = 2.8$ Hz), H-2 to a d ($J = 2.8$ Hz), and H-3 to a d ($J = 10$ Hz).

Anal. Found: C, 87.37; 6.08.

Fractions 18–27 yielded 11.8 mg (5%) of colorless **9**, m.p. 145–147°, after crystallization from hexane: i.r. (KBr) 1700 cm^{-1}, C=O; u.v. max (cyclohexane) 245 inf (45 000), 248 (50 000), 272 inf (2500), 281 (4500), 293 (8000), 306 (10 000), 321 (1000), 336 (1500), and 352 nm (1600); n.m.r. (100 MHz, $CDCl_3$) τ 1.75 (s, 1H, H-5), 2.35 (m, 5H, remaining aromatics), 4.18 (d of d, 1H, H-1, $J = 5.5$, 2.0 Hz), 4.42 (d of d, 1H, H-2, $J = 5.5$, 2.0 Hz), 5.46 (br d, 1H, H-10*b*, $J = 5.5$ Hz), 6.63 (m, 1H, H-3*a*), and 7.28 (m, 2H, methylene).

Anal. Calcd. for $C_{16}H_{12}O$: C, 87.24; H, 5.49. Found: C, 86.96; H, 5.60.

Acetophenone Sensitized Irradiation of 3: Preparation of 7

A solution of 233.2 mg (1.0 mmol) of **3** and 10 ml of acetophenone in 250 ml of cyclohexane was photolyzed under nitrogen for 14 min with a quartz-jacketed Hanovia 450 W water-cooled, medium pressure immersion lamp fitted with a Pyrex filter sleeve. The solvent and acetophenone were removed *in vacuo* and the residue, diluted with 10 ml of hexane, was loaded onto a 2 × 40 cm silicic acid chromatography column, slurry-packed in hexane, and left to stand for 24 h. The column was then eluted with 3 l of 1% ether/hexane followed by 1 l of 3% ether/hexane; 100 ml fractions were collected. Fractions 11–13 contained 32.6

Can. J. Chem. Downloaded from www.nrcresearchpress.com by 210.87.254.40 on 09/05/12
For personal use only.

mg (14%) of **3**; 16–23, 119.1 mg (51%) of **7**; and 30–39, 48.9 mg (22%) of the ketone **9**.

Fractions 16–23, after crystallization from hexane, gave colorless **7**, m.p. 63–65°: u.v. max (cyclohexane) 240 (80 000), 281 inf (6000), 286 (6300), 297 inf (4600), 313 (1100), 320 (600), and 328 nm (1200); n.m.r., see Table 1.

Anal. Found: C, 87.46; H, 6.09.

6,7-Dihydro-6-oxocycloocta[b]naphthalene (8)

A solution of 150.1 mg (0.64 mmol) of cyclooctatetraene **4** in 5 ml of glacial acetic acid was heated at 90° for 4 h. After cooling, the solution was basified (aqueous NaOH) and extracted with benzene (2 × 50 ml). The extracts were dried ($MgSO_4$), concentrated *in vacuo*, and the residue chromatographed on a silicic acid column. Elution with 1% ether/hexane gave, after crystallization from benzene/hexane and sublimation (120°/0.1 mm), 119.0 mg (84%) of pale-yellow **8**, m.p. 120–122°: i.r. (KBr) 1670 cm^{-1}, C=O; u.v. max (methanol) 261 (44 000), 323 inf (5300), and 367 nm (2400); n.m.r. (60 MHz, $CDCl_3$) τ 1.09 (s, 1H, H-5), 2.28 (m, 5H, remaining aromatics), 2.95 (br d, 1H, H-11, $J = 13$ Hz), 3.55–4.32 (m, 3H, H-8, 9, 10), and 6.46 (d, 2H, methylene, $J = 8$ Hz).

Anal. Found: C, 87.27; H, 5.39.

*Protolysis of Semibullvalene **6** to Ketone **9***

A solution of 29.9 mg (0.13 mmol) of **6** in 20 ml of hexane was loaded onto a silicic acid chromatography column slurry-packed in hexane, and allowed to stand for 24 h. Elution with 3% ether/hexane gave 28.2 mg (100%) of ketone **9**, m.p. 142–144°; sublimation (130°/0.1 mm) gave 27.9 mg (99%), m.p. 145–147°.

3,3a,4,10b-Tetrahydronaphtho[2,3-a]pentalene (10)

A solution of 113.3 mg (0.51 mmol) of ketone **9**, 2 g (0.36 mol) of potassium hydroxide, 2 ml (2.1 g, 0.04 mol) of hydrazine hydrate, and 10 ml of triethylene glycol was refluxed for 46 h, cooled, diluted with 100 ml of 20% aqueous HCl, and extracted with ether. The extracts were washed with water, dried ($MgSO_4$), concentrated *in vacuo*, and the residue chromatographed on a 2 × 120 cm silicic acid column. Elution was with hexane; 50 ml fractions were collected. Fractions 11–12 contained 8.4 mg of an unidentified colorless solid; 13–17 gave, after crystallization from hexane, 75.4 mg (71%) of colorless **10**, m.p. 61–63°, which was raised to 64–66° after sublimation (75°/0.1 mm): u.v. max (cyclohexane) 219 (84 000), 254 (3600), 264 (4600), 273 (5600), 283 (6200), 294 (4300), 302 (1300), 309 (1500), 313 (700), 315 (800), 318 (600), and 323 nm (2100); n.m.r. (100 MHz, CCl_4) τ 2.58 (m, 6H, arom), 4.34 (m, 2H, H-1 and -2), 5.73 (br s, 1H, H-10*b*), 6.77 (m, 2H, C-4 methylene), 7.27 (m, 2H, C-3 methylene), and 7.80 (m, 1H, H-3*a*).

Anal. Calcd. for $C_{16}H_{14}$: C, 93.16; H, 6.84. Found: C, 93.02; H, 6.95.

Quantum Yield Apparatus

This consisted of a "merry-go-round" apparatus fitted with a 450 W Hanovia medium-pressure mercury arc and surrounded by a water-cooled quartz immersion well and filter solutions. For direct irradiations, 313 nm light was isolated by a two compartment filter consisting of a 1.5 cm path length of a solution of 28 g of cobaltous sulfate heptahydrate per 100 ml of water, and a 0.6 cm path length of a solution of 0.252 g of potassium carbonate; transmittance was 300–332 nm with a maximum at 313 nm (13%). For benzophenone sensitized irradiations, 343 nm light was isolated by a one compartment filter consisting of a 2.0 cm path length of a solution of 450 g of cobaltous chloride hexahydrate, 60 g of stannous chloride dihydrate, and 150 g of nickel chloride hexahydrate per 1.2 l of 20% aqueous HCl; transmittance was 319–382 nm with a maximum at 343 nm (5%).

Quantum Yield Irradiations

Prior to irradiations, solutions of the sample ($3–41 \times 10^{-4}$ *M*) and benzophenone ($2.3–2.7 \times 10^{-3}$ *M*, if any) in 35 ml of cyclohexane, contained in 25 × 150 mm constricted Pyrex test-tubes, were degassed by two freeze–pump–thaw cycles (1.5×10^{-3} mm minimum pressure) and sealed under vacuum. During sample runs, the lamp output was measured by potassium ferrioxalate actinometry (14). After irradiation, the solvent was removed *in vacuo*, a known amount of para-xylene was added to serve as internal standard, and the mixture analyzed by n.m.r. spectroscopy. The peak areas in the spectra were calibrated against authentic reactant and product mixtures of closely similar constitution. Quantum yields for the observed processes are given in Table 2 and were obtained from runs to $\leqslant 17\%$ conversion; the estimated probable errors are $\pm 10\%$.

*Monitored Direct Irradiations of Barrelene **3***

Extended Conversions

Six sample solutions of **3** (~ 0.43 m*M*) in 35 ml of cyclohexane, and prepared as for quantum yield runs, were irradiated in the "merry-go-round" apparatus at 313 nm. Samples were removed periodically and component concentrations were determined by n.m.r. spectroscopy as before. The results are plotted in Fig. 1.

Low Conversions

Three sample solutions of **3** in 35 ml of cyclohexane, prepared as for quantum yield runs, were irradiated in the "merry-go-round" apparatus at 313 nm to $<6\%$ conversions. Component concentrations of the photolysates were obtained from column chromatography; samples were removed periodically, loaded onto a silicic acid column slurry-packed in hexane, left to stand for 24 h, and then eluted as before to give **3**, **4**, **7**, and **9**. The conversion of **6** to **9** was assumed to be quantitative in each case. The results of the low conversion runs are plotted in the insert to Fig. 1.

The authors thank Mr. David Gifford of the Spectroscopic Services Laboratory, University of Alberta, for the 100 MHz n.m.r. spectra and interpretative discussions, and gratefully acknowledge the financial support of the National Research Council of Canada, and the University of Lethbridge Research Committee.

1. H. E. ZIMMERMAN and G. L. GRUNEWALD. J. Am. Chem. Soc. **88**, 183 (1966).
2. H. E. ZIMMERMAN, R. S. GIVENS, and R. M. PAGNI. J. Am. Chem. Soc. **90**, 6096 (1968).
3. H. E. ZIMMERMAN and C. O. BENDER. J. Am. Chem. Soc. **92**, 4366 (1970).

4. (*a*) J. P. N. BREWER and H. HEANEY. Chem. Commun. 811 (1967); (*b*) R. S. H. LIU. J. Am. Chem. Soc. **90**, 215 (1968).
5. The UV atlas of organic compounds. Vol. III. Butterworths, London, 1967. Spectrum E1/11.
6. O. L. CHAPMAN. J. Am. Chem. Soc. **85**, 2014 (1963).
7. E. WENKERT and D. A. BERGES. J. Am. Chem. Soc. **89**, 2507 (1967).
8 E. MIGIRDICYAN and S. LEACH. Bull. Soc. Chim. Belges, **71**, 845 (1962).
9. R. S. H. LIU. J. Am. Chem. Soc. **89**, 112 (1967).
10. R. B. WOODWARD and R. HOFFMANN. J. Am. Chem. Soc. **87**, 395 (1965).
11. E. H. WHITE, E. W. FRIEND, JR., R. L. STERN, and H. MASKILL. J. Am. Chem. Soc. **91**, 523 (1969).
12. G. W. BORDEN, O. L. CHAPMAN, R. SWINDELL, and T. TEZUKA. J. Am. Chem. Soc. **89**, 2979 (1967).
13. S. P. PAPPAS and N. A. PORTNOY. Chem. Commun. 1126 (1970).
14. C. G. HATCHARD and C. A. PARKER. Proc. R. Soc. (London). A**235**, 518 (1956).

Can. J. Chem. Downloaded from www.nrcresearchpress.com by 210.87.254.40 on 09/05/12
For personal use only.

Rates of Reaction of Nickel(II) with Terpyridine in Dimethyl Sulfoxide

PATRICIA A. COCK, C. E. COTTRELL, AND R. K. BOYD
Department of Chemistry, University of Guelph, Guelph, Ontario

Received August 4, 1971

The rates at which 2,2′,2″-terpyridine reacts with nickel(II) ion to form the monoligand–nickel(II) and the bisligand–nickel(II) complexes were determined in DMSO solution. $Ni(terpy)Cl_2$ was isolated, and used to study the rate of formation of bis complex. The second-order rate constants were found to parallel the rates of DMSO exchange, determined using n.m.r. techniques, from the respective paramagnetic nickel species. Attempts were made to relate the results to the generally accepted "dissociative" pathways for this class of substitution reactions.

On a déterminé les vitesses auxquelles réagit la terpyridine-2,2′,2″ avec l'ion nickel(II) pour former les complexes monoligand–nickel(II) et biligand–nickel(II) dans une solution de DMSO. On a isolé le complexe $Ni(terpy)Cl_2$ et on l'a utilisé pour étudier la vitesse de formation du complexe bis. Les constantes de vitesse de second ordre vont de pair avec les vitesses d'échange de DMSO, ce qu'on a déterminé en utilisant les techniques de r.m.n., à partir des espèces paramagnétiques respectives de nickel. On a tenté de relier les résultats aux mécanismes "dissociatifs" qui sont généralement acceptés pour cette classe de réactions de substitution.

Canadian Journal of Chemistry, **50**, 402 (1972)

I. Introduction

The kinetics of replacement reactions of complexes of certain aquated transition metal ions with 2,2′,2″-terpyridine were studied by Holyer *et al.* (1). The rates of formation of the $M(terpy)(H_2O)_n^{2+}$ species (mono complex) were found (1) to fall into the general pattern of such ligand substitution reactions, usually described (2) in terms of the dissociative interchange model [1]:

$$[1] \qquad NiS_6^{2+} + L \overset{K_E}{\rightleftharpoons} NiS_6^{2+} \cdot L$$

$$NiS_6^{2+} \cdot L \overset{k_s}{\rightarrow} NiS_5L^{2+} + S$$

Reaction 1 has been written for the special case of an electrically neutral, monodentate ligand L; the solvent molecules are represented by S. For the present case of the tridentate ligand terpyridine, it is believed (1) that the first attachment to the metal ion is rate-determining, the subsequent completion of the chelate being extremely rapid. The encounter complex $NiS_6^{2+} \cdot L$ is assumed to be in equilibrium with NiS_6^{2+} and L; the rate constant k_s is then the rate constant for solvent exchange k_{ex}, modified by a statistical factor accounting for the probability of L occupying an outer sphere site close to the inner sphere solvent molecule in the process of exchange (3). The second-order rate constant k_f is thus interpreted as k_sK_E.

For the cases M = Fe, Co, and Ni, the solid mono complexes may be isolated in the pure state, as the bromide, chloride, or thiocyanate (4, 5). The kinetics of the reaction of mono complex with terpyridine to form the bis complex, $M(terpy)_2^{2-}$, could thus be studied unambiguously (1). The observed rate constants in aqueous solution were reported to be some 200 times greater than the corresponding values for the formation of mono complex although, from stereochemical and statistical considerations, it might be expected that the rate constants for bis formation should be significantly smaller (1).

The present work was undertaken with the hope that some light might be thrown on this problem by studying the reaction using dimethylsulfoxide (DMSO) as solvent, instead of water; it was hoped that comparison of the two systems might offer some clue to the correct explanation of the discrepancy. In addition, puzzling features exist in results obtained for ligand replacement reactions of $Ni(DMSO)_6^{2+}$ in DMSO as solvent (6, 7). The present work was also undertaken to provide further documentation of these features.

II. Experimental

Materials

$Ni(DMSO)_6^{2+}(ClO_4^-)_2$ was prepared by keeping a saturated DMSO solution of the corresponding hexahydrate over concentrated sulfuric acid, under vacuum, until crystallization occurred. Stock solutions of $Ni(DMSO)_6^{2+}$ in DMSO were analyzed by EDTA titration using murexide indicator; 1 ml of the stock solution was added to 50 ml of

water, and titrated with EDTA according to standard procedures. $Ni(terpy)_2^{2+}(ClO_4^-)_2$ was prepared according to the method of Harris and Lockyer (4); both of these perchlorate salts were found to be extremely explosive when dry.

$Ni(terpy)Cl_2$ (the mono complex chloride) was prepared by the method of Harris and Lockyer (4); attempts to use the method of Hogg and Wilkins (5), starting from the bis complex dichloride, were unsuccessful.

Anal. Calcd. for $Ni(terpy)Cl_2$: C, 49.5; H, 3.05; N, 11.55. Found: C, 49.04; H, 3.17; N, 11.45.

The DMSO used was spectroanalytical grade, obtained from Fisher Scientific Co.; other chemicals were reagent grade.

Spectroscopic and Conductance Measurements

All u.v.–visible spectra (room temperature) were recorded on a Unicam SP-800 spectrophotometer; the wavelength calibration was checked, before each spectrum, using the calibration standards supplied with the instrument. Nuclear magnetic resonance spectra were obtained using a Varian A-60-A spectrometer. Conductances were measured on a Beckman RC-18A conductivity bridge, at room temperature.

Kinetic Experiments

Slower reactions were followed spectrophotometrically using the Unicam SP-800 instrument, either at fixed wavelength or by repetitive scans over a small wavelength range. Faster reactions were studied using an all-glass stopped-flow apparatus designed to permit the use of non-aqueous solvents (8). The basic design of this apparatus followed that used by Holyer *et al.* (1), with certain modifications (9). The light source used was a Bausch and Lomb xenon lamp and monochromator, with a specially designed stabilized power supply. The mixing and observation chambers, plus the long glass capillary coils used to connect the chambers to the syringes, were all contained in a thermostatted tank (± 0.1 °C). This arrangement permitted full thermal equilibration of the solutions before mixing, and also minimized mechanical disturbance of the quartz observation chamber while operating the syringes (9).

Treatment of Data

Treatment of kinetic data was straightforward in all cases except those in which the rate of formation of the bis complex, from $Ni(terpy)Cl_2$ plus terpyridine, was studied. The two complexes have such similar u.v. absorption spectra that it was not possible to follow the reaction at a wavelength such that only one species absorbed. However, it may be readily shown that the standard kinetic equations, in terms of absorbances, also apply to pseudo-first order cases like the present one, in which

$$[\text{product}] + [\text{reactant}] = [\text{reactant}]_{t=0}$$

the effective extinction coefficient is the difference of the extinction coefficients of the two absorbing species (reactant and product) (8).

III. Results

(a) Characterization of Species in Solution

Formation of complexes from terpyridine plus $Ni(DMSO)_6^{2+}(ClO_4^-)_2$ in DMSO solution may be inferred from the appearance of a double peak in the region 320 to 350 mμ, where neither component alone absorbs. If the Ni(II) concentration is at least 40 times greater than that of terpyridine, the peaks are observed at 323 and 337 mμ, with $\varepsilon_{323} = 1.9 \times 10^4$ and $\varepsilon_{337} = 1.8 \times 10^4$ mol^{-1} cm^2. For Ni(II): terpy ratios much less than 40, the two peaks shifted to 327 and 341 mμ, with $\varepsilon_{327} = 3.5 \times 10^4$ and $\varepsilon_{341} = 3.4 \times 10^4$ mol^{-1} cm^2. It seems reasonable to identify the first spectrum as that of the mono complex, and the latter as that of the bis complex. The bis complex in water was reported (1) as having very similar extinction coefficients, though the reported peak wavelengths (1) are about 5 mμ less than those reported here for DMSO solution.

As a check on our present techniques, spectra were run on an aqueous solution of $Ni(H_2O)_6^{2+}$ perchlorate, in 50-fold excess over terpyridine. It was found that the spectrum changed with time, reaching its final form over approximately 24 h. The results obtained were as follows:

(*i*) Immediately after mixing, peaks at 333 and 321 mμ. $\varepsilon_{333} = 2.3 \times 10^4$ and $\varepsilon_{321} = 2.4 \times 10^4$ mol^{-1} cm^2.

(*ii*) After 24 h, peaks at 331 and 319 mμ. $\varepsilon_{331} = 2.4 \times 10^4$ and $\varepsilon_{319} = 1.9 \times 10^4$ mol^{-1} cm^2. The final spectrum (*ii*) appears entirely consistent with that reported by Holyer *et al.* (1) for the mono complex in aqueous solution.

The u.v. spectra of $Ni(terpy)Cl_2$ were also obtained, in both DMSO and water as solvents. In DMSO, peaks were observed at 334 and 321 mμ, with $\varepsilon_{334} = 0.9 \times 10^4$ and $\varepsilon_{321} = 1.1 \times 10^4$ mol^{-1} cm^2; these peak wavelengths are about 2 mμ lower than those quoted above for excess $Ni(DMSO)_6^{2+}(ClO_4^-)_2$ plus terpyridine in DMSO, and the extinction coefficients are about a factor of two lower. In water, $Ni(terpy)Cl_2$ gave peaks at 332 and 320 mμ, with $\varepsilon_{332} = 1.6 \times 10^4$ and $\varepsilon_{320} = 1.7 \times 10^4$ mol^{-1} cm^2. No change occurred in this spectrum over a period of days; the same was true of all the DMSO solutions.

The nickel(II) perchlorate–terpyridine system thus does not appear to be at all well defined in aqueous solution. In particular, the species formed in the initial fast reaction, the kinetics of which were studied previously (1), is different from both the fully equilibrated species, and from the species formed by $Ni(terpy)Cl_2$ in aqueous solution.

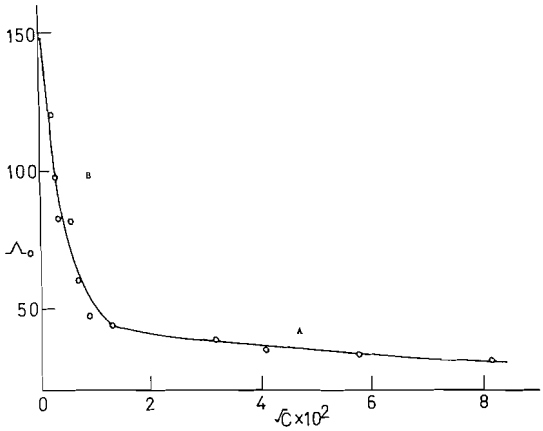

FIG. 1. Molar conductance of solutions of $Ni(terpy)Cl_2$ in DMSO, at 25 °C. Region A, species mainly $[Ni(terpy)Cl(DMSO)_2]^+$; Region B, dissociation of second chloride.

In view of the latter discrepancy, also observed in DMSO solution, conductivity data were obtained for the $Ni(terpy)Cl_2$ species in both solvents, in an attempt to further characterize the solutions. The results obtained in DMSO solution are shown in Fig. 1, and are typical of the behavior of a weak electrolyte, which approaches complete dissociation at infinite dilution. The limiting value at high concentration appears typical of that for a 1:1 electrolyte in DMSO at 25 °C, (*e.g.* for LiCl, Λ_0 in DMSO is 35.5 ohm^{-1} $mmol^{-1}$ cm^{-1} (10)), while the extrapolated value at zero concentration seems consistent with that of a 2:1 electrolyte. Since no extra chloride was present in the system, the most probable interpretation would appear to be the simplest one, whereby the predominant species in solution, at higher concentrations, are $[Ni(terpy)Cl(DMSO)_2]^+$ and Cl^-; at concentrations below about 10^{-4} *M*, the dissociation of the second chloride becomes increasingly important. This explanation in terms of coordinated chloride offers a reasonable explanation of the discrepancies in the u.v. spectra obtained for mono complexes in DMSO, and is also consistent with n.m.r. results described below. The data of Fig. 1 were treated by a non-linear least squares procedure, on the above assumption. A value of K_{diss}, for the dissociation of the second chloride, of $(2.1 \pm 0.4) \times 10^{-5}$ *M* was obtained, using the additional erroneous assumption that activity coefficients and ionic mobilities are independent of ionic strength; the quoted uncertainty in K_{diss} thus refers only to the random error in the measurements, and takes no account of such systematic errors in the interpretation.

In aqueous solution, $Ni(terpy)Cl_2$ gave a molar conductivity typical of a 2:1 electrolyte over the entire concentration range. The chloride thus appears to be completely dissociated in aqueous solution, and the discrepancies observed in the u.v. spectra thus remain unexplained in this case.

(b) Kinetics of Complex Formation

The rate at which terpyridine reacts with $Ni(DMSO)_6^{2+}$ perchlorate to form the mono complex $[Ni(terpy)(DMSO)_3]^{2+}$ in DMSO solution was investigated on the stopped-flow apparatus, at the peak absorption wavelength of the mono complex. The initial terpyridine concentration was always 2.5×10^{-5} mol l^{-1}, and the Ni(II) was in at least 40-fold excess; excellent pseudo-first order behavior was obtained, and the plot (Fig. 2) of the pseudo-first order rate constant k_{obs} *vs.* [Ni(II)] extrapolated through the origin, to within experimental uncertainty. Thus, under the conditions used, formation of mono complex perchlorate is essentially irreversible. The slope of such a plot gives the second-order rate constant for complex formation, k_f. The variation of k_f with temperature was studied over the range 25 to

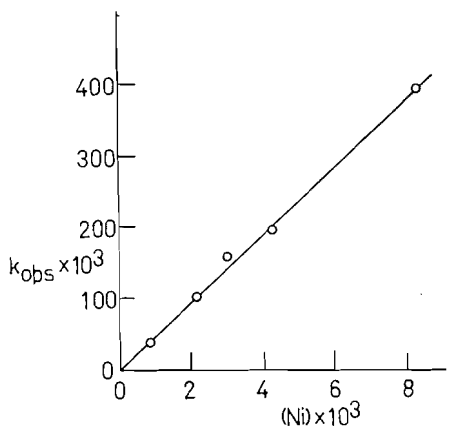

FIG. 2. Pseudo-first-order rate constants for reaction of terpyridine plus $[Ni(DMSO)_6]^{2+}$ perchlorate (excess) in DMSO, at 25 °C.

TABLE 1. Variation of k_f with temperature, for reaction $[Ni(DMSO)_6]^{2+}(ClO_4^-)_2$ + terpy $\rightarrow [Ni(terpy)(DMSO)_3]^{2+}$*

Temperature (°C)	k_f ($mol^{-1}\,l\,s^{-1}$)
25	33
30	47
35	69
40	94
45	138
50	171

*Uncertainty in k_f values = ± 1 $mol^{-1}\,l\,s^{-1}$; enthalpy of activation = 11.9 ± 0.2 kcal mol^{-1}; entropy of activation = -11.6 ± 0.5 cal deg^{-1} mol^{-1} for solute standard state of 1 mol l^{-1}.

TABLE 2. Variation of k_f with temperature, for reaction of mono complex chloride with terpyridine in DMSO, to form bis complex

(*a*) Excess terpyridine plus $Ni(terpy)Cl_2$ (10^{-5} mol l^{-1})

Temperature (°C)	k_f ($mol^{-1}\,l\,s^{-1}$)
25	338
30	491
35	602
40	893

(*b*) Excess $Ni(terpy)Cl_2$ plus terpyridine (10^{-5} mol l^{-1})

Temperature (°C)	k_f (± 15 $mol^{-1}\,l\,s^{-1}$)
25	1275
30	1405
35	1555
40	1710
45	2030

50 °C, and the results are summarized in Table 1, which also lists the derived activation parameters.

Attempts were made to study the kinetics of the reaction between $[Ni(DMSO)_6]^{2+}$ and terpyridine, under conditions such that both mono and bis complexes were expected to be formed (*i.e.* Ni(II):terpy < 40:1). The reaction was followed using the peak wavelength of both the reactant ligand and the complex product. Unfortunately, we were unable to interpret these data in any self-consistent fashion, and they will not be presented here. The negative conclusion is in marked contrast to the findings of Holyer *et al.* (1) who, from the analogous data obtained in aqueous solution, extracted a rate constant identified as that controlling the rate of formation of mono complex.

Since pure $[Ni(terpy)(DMSO)_3]^{2+}(ClO_4^-)_2$ could not be isolated, the rate of formation of the bis complex from terpyridine plus mono complex in DMSO solution was studied using the mono complex chloride, which in the solid state exists as $Ni(terpy)Cl_2$. In this case, pseudo-first-order behavior was obtained when either terpyridine or $Ni(terpy)Cl_2$ was in excess; again, the back (dissociation) reaction was immeasurably slow. The results obtained are summarized in Table 2, and are plotted in Arrhenius form in Fig. 3.

It is clear from these results that, even though good pseudo-first-order behavior was obtained in each case, the second-order rate constants differ in the two cases, both in absolute magnitude and in temperature dependence. A more complete discussion of these findings is given below; however, it seems clear that this effect must be connected with the partial dissociation of coordinated chloride on the nickel, discussed in section III(*a*) above.

Finally, it seemed useful to study the kinetics of formation of the mono complex perchlorate in mixed DMSO–water solvent; this reaction is free of the complicating effects associated with the chloride ion. The results obtained are shown

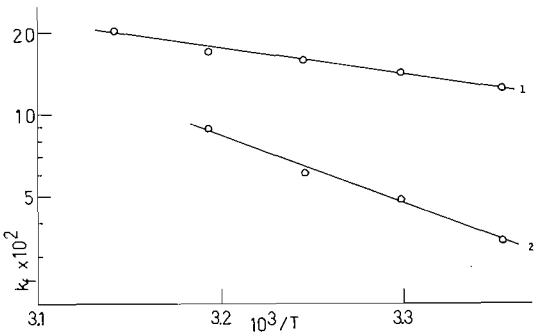

FIG. 3. Arrhenius plots of second-order rate constants for reaction of DMSO solutions of $Ni(terpy)Cl_2$, plus terpyridine to give bis complex. (*1*) Excess $Ni(terpy)Cl_2$; (*2*) excess terpyridine.

in Fig. 4; the dramatically slower rate observed in pure DMSO, compared with that in H_2O, is apparent (6, 7). In addition, the effect on the rate of adding water to DMSO is not significant until the mole fraction of water is about 0.4. This undoubtedly reflects the greater basicity of DMSO.

(c) Solvent Exchange Rates from Nuclear Magnetic Resonance Line Broadening

The solvent exchange rate constant k_{ex} for $[Ni(DMSO)_6]^{2+}(ClO_4^-)_2$ in DMSO solution has been studied previously (11–14). Present experiments confirmed the findings that the exchange rate is rapid on the n.m.r. timescale (15). At 25 °C, the value obtained for k_{ex}, calculated from the relevant solution of the Bloch equations for the system (16), is $7.4 \pm 0.7 \times 10^3$ s^{-1}, with an activation enthalpy of 6.2 ± 0.7 kcal mol^{-1} and an entropy of activation of -20 ± 2 cal deg^{-1} mol^{-1}, measured over the range 20 to 100 °C.

Over the same temperature range, a solution of $Ni(terpy)Cl_2$ in DMSO yielded no significant broadening of the DMSO line. The characteristic terpyridine pattern, between 4.31 and 7.38 p.p.m. downfield from DMSO, was not present, so that it seems clear that the species in solution was paramagnetic. It seemed likely that the exchange at room temperature was sufficiently fast, on the n.m.r. timescale, to be unobservable. Since DMSO freezes at 18 °C, it was not possible to lower the temperature sufficiently to slow the exchange rate to match the n.m.r. timescale. However, a 1:1 mixture of DMSO and nitromethane could be cooled at −40 °C without freezing; over the range −40 to +40 °C, neither broadening nor contact shift of the nitromethane peak was observed, within the precision of our measurements, when $Ni(terpy)Cl_2$ was dissolved. Only slight broadening was observed previously (3) using the nitrate salt of $[Ni(DMSO)_6]^{2+}$.

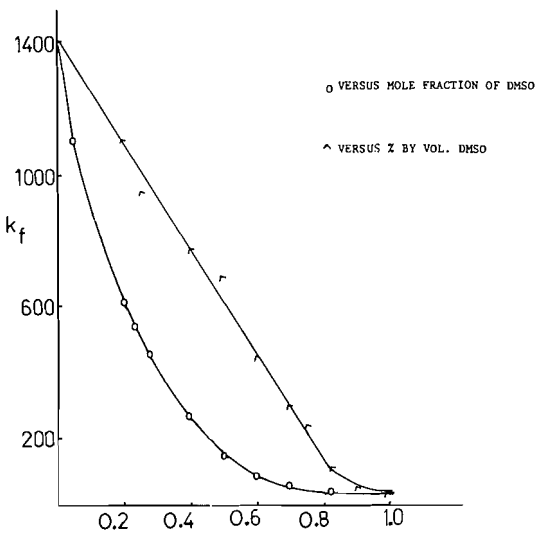

FIG. 4. Variation of second-order rate constant for mono complex formation with solvent composition, in DMSO–water mixtures, at 25 °C.

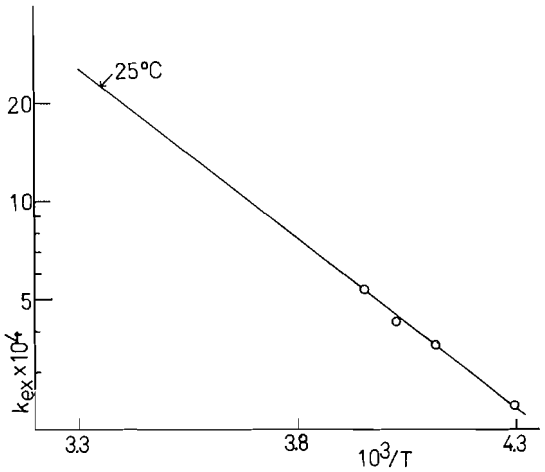

FIG. 5. Arrhenius plot of rate constant for DMSO exchange in concentrated solutions of $Ni(terpy)Cl_2$ in mixed DMSO–nitromethane solvent.

When $Ni(terpy)Cl_2$ was dissolved in this mixed solvent, the DMSO exchange rate fell in the fast-exchange region, over the range −40 to −20 °C. The Arrhenius plot of the derived values for k_{ex} is shown in Fig. 5, which also makes clear the extent of the extrapolation necessary to estimate k_{ex} at 25 °C as $3 \pm 2 \times 10^5$ s^{-1}; the activation enthalpy is 4 ± 2 kcal mol^{-1}, and $\Delta S^{\ddagger} = 20 \pm 9$ cal deg^{-1} mol^{-1}. The solvent exchange rate is thus about 40 times faster if the solute used is $Ni(terpy)Cl_2$, instead of $[Ni(DMSO)_6]^{2+}$.

IV. Discussion

The differences observed, between the u.v. spectra of various preparations of the mono complex in DMSO solution, may be satisfactorily explained in terms of coordinated chloride

TABLE 3. Rate parameters for ligand substitution reactions of Ni(II)

Reaction	k_f(mol^{-1} l s^{-1})	$\Delta H^{\ddagger}$ (kcal mol^{-1})	$\Delta S^{\ddagger}$ (cal deg^{-1} mol^{-1})	Reference
$Ni(DMSO)_6^{2+}$ (excess) + terpy, in DMSO	33	11.9±0.2	−11.6±0.5	Present work
	26	11.6±0.2	−13.1±0.5	19
$[Ni(terpy)Cl(DMSO)_2]^+$ + terpy	1275	3.7±0.2	−32.0±0.5	Present work
Excess terpy, in DMSO, + $Ni(terpy)Cl_2$	339	11±2	−10±6	Present work

Reaction	k_{ex} at 25 °C (s^{-1})	$\Delta H^{\ddagger}$ (kcal mol^{-1})	$\Delta S^{\ddagger}$ (cal deg^{-1} mol^{-1})	Reference
$Ni(DMSO)_6^{2+}$ in DMSO	7.5×10^3	8±0.7	−14±7	11
	9.3×10^3	7.3±0.5	−16±2	12
	5.2×10^3	12.1±0.3	−1.2±0.5	13
	3.2×10^3	13.0	+3.2	14
	$7.4(\pm0.7)\times10^3$	6.2±0.7	−20±2	Present work
$[Ni(terpy)Cl(DMSO)_2]^+$ in DMSO–nitromethane	$3(\pm2)\times10^5$	4±2	−20±9	Present work
$Ni(H_2O)_6^{2+}$ in H_2O	3.4×10^3	12.7	+2.9	22
$Ni(terpy)Br_2$ in H_2O	5.2×10^3	11.3	−1.0	22

ion. Thus, at concentrations of $Ni(terpy)Cl_2$ in DMSO greater than 10^{-4} mol l^{-1}, the predominant species present is probably $[Ni(terpy)Cl(DMSO)_2]^+$; addition of terpyridine to excess Ni(II) perchlorate, on the other hand, is expected to give $[Ni(terpy)(DMSO)_3]^{2+}$ in solution. No such explanation is available for the corresponding discrepancies observed in aqueous solution, in view of the conductance data. In addition, the time-dependence of the spectra observed on mixing excess Ni(II) perchlorate with terpyridine, in aqueous solution, is not readily explained. A slow partial disproportionation to the bis complex is one possibility (5); another related possibility involves the initial formation, in a large excess of Ni(II), of bridged species such as $^{2+}Ni(H_2O)_5$—(terpy)—$^{2+}Ni(H_2O)_5$, which slowly disproportionate to give the more stable mono species $[Ni(terpy)(H_2O)_3]^{2+}$. Either possibility is consistent with the fact that the absorbance peak due to $Ni(H_2O)_6^{2+}$ was invariably observed to *increase* slightly, concurrently with the more extreme changes in the complex spectrum.

Kinetic parameters of interest for the present discussion have, for convenience, been collected in Table 3. The activation parameters were obtained by fitting the rate constants, as functions of temperature, to the usual Eyring equation (17) using a non-linear least squares procedure (18). The value and standard deviation quoted for k_{ex} at 25 °C, for DMSO on $[Ni(terpy)Cl(DMSO)_2]^+$, were obtained from the values quoted for $\Delta H^{\ddagger}$ and $\Delta S^{\ddagger}$ and from the covariance matrix, including the cross-correlation coefficients (18).

The solvent exchange data, for DMSO on $[Ni(DMSO)_6]^{2+}$ perchlorate, show a wide spread; the present results agree well with those of two of the previous investigations (11, 12); the other two measurements (13, 14) differ, while agreeing with each other. The activation parameters for DMSO exchange, listed in Table 3, are those quoted in the original work (11–14), since insufficient information was available to use the present fitting procedure (18).

Although the enthalpies and entropies of activation for DMSO exchange on $[Ni(DMSO)_6]^{2+}$ vary markedly (Table 3), the $\Delta G^{\ddagger}$ values (*i.e.* the actual rate constants) are in reasonable agreement, with respect to the usual uncertainties in work of this type. It seems likely that the spreads in $\Delta H^{\ddagger}$ (7 kcal) and $\Delta S^{\ddagger}$ (23 cal deg^{-1}) may be attributed (20) to systematic errors; these arise, in some cases, from the use of approximate formulae, as well as from the fact that dynamic n.m.r. parameters are susceptible to spurious effects such as field in-

homogeneities (20). In principle, the spin-echo method, used by Blackstaffe and Dwek (12) is more accurate than line-shape analysis, since T_2 is measured directly, and a wider temperature range can be studied. However, in practice, this method does not appear to have proven superior (21).

We are indebted to a referee for drawing to our attention the work of Bennetto and Caldin (19), on the (terpy + Ni^{2+}) reaction, which appeared while the present work was in the process of being refereed; the activation parameters from this work (19), quoted in Table 3, were for comparison purposes computed from the original data (19) using the present procedure (18). The rate constants obtained in the present work are some 30% higher than the comparable data of Bennetto and Caldin (19), the activation enthalpies being in good agreement.

The second-order rate constant for the reaction of terpyridine with $[Ni(terpy)Cl(DMSO)_2]^+$ (*i.e.* with excess $[Ni(terpy)Cl_2] > 10^{-4}$ *M*, in DMSO), is about 40 times greater than that for the reaction with excess $[Ni(DMSO)_6]^{2+}$, at 25 °C; this is also the ratio of the corresponding solvent-exchange rate constants. In spite of this excellent agreement, it should be borne in mind that the long extrapolation necessary to obtain k_{ex} at 25 °C for $[Ni(terpy)Cl(DMSO)_2]^+$ necessarily involves a large uncertainty (Table 3). In addition, although these latter data were obtained in DMSO–nitromethane mixtures, it has been shown (14) that the DMSO exchange rates of $[Ni(DMSO)_6]^{2+}$, in mixed DMSO–nitromethane solvents, are independent of solvent composition. Unfortunately, it was not possible to make a similar test for $[Ni(terpy)Cl(DMSO)_2]^+$, in the present work, due to the problem of keeping the temperature sufficiently low. However, if arguments by analogy have any validity here, the present results indicate that variations in the overall rate constant k_f parallel those in the solvent exchange rate constant, associated with the coordinated chloride; this conclusion lends support to a dissociative mechanism for the reaction (7). Labilization of coordinated solvent by coordinated chloride has been previously observed (23) for the Co(II) ion in methanol.

The rate constant obtained for the reaction of excess terpyridine with an initial concentration of 10^{-5} mol l^{-1} of $Ni(terpy)Cl_2$ in DMSO, may be interpreted in terms of reaction scheme [2]

[2]
$$\begin{array}{ccc} [Ni(terpy)Cl(DMSO)_2]^+ + Cl^- & \underset{}{\overset{K_{diss}}{\rightleftharpoons}} & [Ni(terpy)(DMSO)_3]^{2+} + 2Cl^- \\ \searrow^{+\,terpy,\ k_{2x}} & & \swarrow^{+\,terpy,\ k_{2y}} \\ & [Ni(terpy)_2]^{2+} & \end{array}$$

In scheme [2], k_{2x} corresponds to k_f measured using excess $Ni(terpy)Cl_2$, at concentrations such that $[Ni(terpy)Cl(DMSO)_2]^+$ is the predominant species. However, when the concentration is only 10^{-5} mol l^{-1}, the degree of dissociation, α, of the second chloride, is only about 50%, as calculated from K_{diss} obtained from the conductance data. The simple mechanistic scheme [2] then leads to the following rate expression

[3] $$dC_B/dt = k_{2x}[terpy](C_x + C_y) \times [1 - \alpha(1 - k_{2y}/k_{2x})]$$

where C_B, C_x, and C_y are the concentrations of $[Ni(terpy)_2]^{2+}$, $[Ni(terpy)Cl(DMSO)_2]^+$, and $[Ni(terpy)(DMSO)_3]^{2+}$, respectively. Equation 3 predicts pseudo-first-order behavior, in excess terpyridine, only if α is constant. In fact, for the initial $(C_x + C_y) = 10^{-5}$ mol l^{-1}, the value of K_{diss} derived from the conductance data predicts that α varies only over the range 0.54 to 0.60, over three half-lives; the derivation of eq. 3, and the computations of α, are outlined in the Appendix.

The ratio of the two second-order rate constants, for formation of bis complex from $Ni(terpy)Cl_2$ in DMSO, should thus be $[1 - \alpha(1 - k_{2y}/k_{2x})]$, where α and k_{2x} are known. The resulting value of k_{2y} turns out to be negative. If, however, k_{2y}/k_{2x} is set to its minimum possible value of zero, and an effective value of α is then calculated, the resulting value of K_{diss}

TABLE 4. Substitution rates on nickel ion in DMSO at 25 °C

Reactants	Product	Solvent exchange rate constant (s^{-1})	k_f (mol^{-1} l s^{-1})
$[Ni(DMSO)_6]^{2+}$ + SCN^-	Probably 1:1 complex†	7.4×10^3*§	29†
$[Ni(DMSO)_6]^{2+}$ + murexide$^-$	1:1 complex	7.4×10^3	77†
$[Ni(DMSO)_6]^{2+}$ + bipyridine	Probably 1:1 complex‡	7.4×10^3	69‡
$[Ni(DMSO)_6]^{2+}$ + terpyridine	1:1 complex	7.4×10^3	33§
$[Ni(terpy)Cl(DMSO)_2]^+$ + terpyridine	$[Ni(terpy)_2]^{2+}$	230×10^3§	1275§

*Reference 11.
†Reference 7.
‡References 6 and 19.
§Present work.

at 25 °C is 4×10^5, a factor of two greater than that obtained from the conductance data. In view of the approximations used in the interpretations of both sets of data, it seems likely that this agreement is acceptable, and that mechanism [2] accounts satisfactorily for the differences observed; k_{2y} is unlikely to be *exactly* zero, but appears to be much smaller than k_{2x}. The reaction system in DMSO solution thus appears to be susceptible to a self-consistent interpretation.

The present work offers no such rationale for the same reaction system in aqueous solution. The solvent exchange rates are practically identical (22) for $[Ni(H_2O)_6]^{2+}$ and for $[Ni(terpy)(H_2O)_3]^{2+}$, formed by dissociation of $Ni(terpy)Br_2$ in solution (5); on the other hand, the rates of reaction of these species with terpyridine differ by a factor of 155 (1). The only clue, offered by the present work, to the resolution of this dilemma, arises from the rather indeterminate characterization of the actual species present in solution, as shown by the u.v. spectra.

The present kinetic results fall into the pattern observed previously (6, 7, 19) for substitution reactions of Ni(II) ion in DMSO solution; these results are, for convenience, collected together in Table 4. Activation parameters are available only for the present systems (Table 3), plus a value of 12.6 kcal mol^{-1} for the activation enthalpy, and -7.7 cal deg^{-1} mol^{-1} for the activation entropy, for the bipyridine reaction. As pointed out previously (7), these data are not readily correlated in terms of the I_d (dissociative interchange) mechanism [1]; either K_E or k_{ex}, (or both) would be required to be much smaller than theoretically acceptable values. In addition, K_E would require to have a temperature coefficient corresponding to an enthalpy change of 4–5 kcal mol^{-1}, which seems very large (6). The mechanism is, however, believed to be of a dissociative nature (7); this conclusion is supported by the present observation that the solvent exchange rates parallel the rates of complex formation, although this evidence is not entirely unequivocal.

It has been suggested (7) that these reactions in DMSO solution might proceed via a pathway involving a five-coordinate intermediate $[Ni(DMSO)_5]^{2+}$, of lifetime sufficient to discriminate between different ligands in reaction. This proposed scheme is shown below

$$[4] \quad [Ni(DMSO)_6]^{2+} \underset{k_{-ex}}{\overset{k_{ex}}{\rightleftharpoons}} [Ni(DMSO)_5]^{2+} + DMSO$$
$$+ L \Big\downarrow k_2$$
$$[Ni(DMSO)_5L]^{2+}$$

As in scheme [1] the mechanism has been written for the special case of a monodentate neutral ligand L. Assuming the initial step to be essentially at equilibrium, the overall second-order rate constant is now identified as $k_f = k_{ex}k_2/k_{-ex}$. As pointed out by Langford and Tsiang (7), if the competition ratio $k_2[L]/k_{-ex}[S]$ is very small, relative to K_E of mechanism [1] the values of k_f will indeed be smaller than expected on the basis of the latter. In addition, mechanism [4] readily accounts for results obtained on the broadening of the n.m.r. line of nitromethane in mixed

CH_3NO_2–DMSO solvents (7) containing Ni(II) ion.

However, it does not appear that this suggestion can be the complete explanation. In particular, it is not at all clear why mechanism [4] should predominate over mechanism [1] in the present case; in view of the correlation between solvent exchange rate and overall reaction rate in DMSO solution found in the present work it seems unlikely that k_s is vastly different from k_{ex}, the rate constant for solvent exchange. If this conclusion is valid, the effective value of K_E must be much smaller than that predicted by the Fuoss equation (24); for neutral ligands, this equation gives:

$$[5] \qquad K_E = (N_0(4/3)\pi a^3)/(1000)$$

where a is the distance of closest approach of the two species. The numerator of this expression is the volume surrounding one mole of one of the species (say the metal ion), available to an added ligand molecule for formation of an encounter complex; the denominator (1 liter) is the volume available to the added ligand if it is to remain in solution as "free" ligand. These considerations apply, as they must, to the standard state of 1 mol l^{-1}. Since K_E is taken as the ratio of these volumes, with no account taken of any solvent–solute interactions or solvent structuring etc., it is clear that the Fuoss equation (24) is based upon the assumption of an ideal solution, for which the probability of finding a neutral molecule, at *any* location in the solution, is a constant. The only solvent property taken into account in the Fuoss equation (24) is the bulk dielectric constant. Thus, deviations from the *absolute* values predicted by the Fuoss equation (24) are to be expected, though the relative effects of charges on the species, and of dielectric constant of solvent, are taken into account. Indeed, it is a matter of surprise that the Fuoss equation, in conjunction with the I_d mechanism (1), accounts so well for the data obtained in such a highly structured solvent as water.

It seems entirely possible that the effect of solvent structure is reflected in the activation parameters listed in Table 3. The slower rates observed in DMSO, relative to those in water, are entirely due to the entropy term; indeed, the activation energies are higher in water than in DMSO. The release of structured solvent in the bulk liquid during the activation process will increase both the entropy and energy of activation, due to the break-up of the solvation shells. These effects will be largest in solvents like water, which are known to form rigid solvation structures. Thus, the mere fact that the absolute value of K_E, required for the reaction to be interpreted in terms of the I_d mechanism [1], is lower than that calculated from the Fuoss equation (24), seems to be no reason for discarding the I_d mechanism.

An even more problematical aspect concerns the effect of the charge of the entering ligand L, on the reaction rate. As may be seen from Table 4, this parameter has absolutely no effect on the rate of reaction in DMSO solution, in marked contrast to the situation in aqueous solution. This is not easily reconciled with the I_d mechanism [1], but this is also true of mechanism [4], since regardless of the precise nature of the second slower step, it is not obvious how k_2 might fail to be affected by the charge on L. Thus, if the five-coordinate intermediate $[Ni(DMSO_5]^{2+}$ can, indeed, react discriminately with incoming ligands (7), it is difficult to imagine how such discrimination might stop short at the nature of the charge on L.

It appears, then, that no completely self-consistent explanation of the results listed in Tables 3 and 4 has yet been given. The present authors believe (8) that the almost complete disavowal of specific solvent effects, in previous interpretations, is at least partly to blame for this situation; somewhat similar views have been expressed previously (6). Speculative interpretations of the present observations, in terms of solvent structuring, have been presented elsewhere (8). More data, for a wider variety of ligands in DMSO and other solvents, seem necessary.

Appendix

Rate Equation Derived from Mechanism [2]

Let the concentrations of $[Ni(terpy)Cl(DMSO)_2]^+$, $[Ni(terpy)(DMSO)_3]^{2+}$, $[Ni(terpy)_2]^{2+}$, and Cl^-, be denoted by C_x, C_y, C_B, and C_{Cl}, respectively. If $C^0 = (C_x + C_y)$ at time $t = 0$, then in excess terpyridine, $C^0 = C_B^\infty$ (the infinite time concentration of bis complex), since the reaction is essentially irreversible.

Then

[A1] $$C_B^\infty = C_x + C_y + C_B$$

[A2] $$C_y C_{Cl^-} / C_x = K_{diss}$$

[A3] $$C_{Cl^-} = C_B^\infty + C_B + C_y$$

Equation [A3] takes account of the fact that one chloride is always completely dissociated (C_B^∞ term), while one additional chloride ion is in solution for every molecule of bis complex formed (C_B term) and for every molecule of the x species which dissociates to give a y molecule (C_y term).

According to mechanism [2]

[A4] $$dC_B/dt = k_{2x} C_L C_x + k_{2y} C_L C_y$$

Combining eqs. [A1] and [A4] gives

[A5] $$dC_B/dt = k_{2x} C_L (C_B^\infty - C_B) \times [1 + C_y/(C_B^\infty - C_B)(k_{2y}/k_{2x} - 1)]$$

Since $C_B^\infty - C_B = C_x + C_y$ (eq. [A1]), and since the degree of dissociation α is given by:

[A6] $$\alpha = C_y/(C_x + C_y)$$

the final equation is:

[A7] $$dC_B/dt = k_{2x}[1 + \alpha(k_{2y}/k_{2x} - 1)] \times C_L(C_x + C_y)$$

To evaluate α, eliminate (C_y/C_x) from eqs. [A2] and [A6], to give:

[A8] $$\alpha = K_{diss}/(K_{diss} + C_{Cl})$$

Now rewrite eq. [A3] as

[A9] $$C_{Cl} = C_B^\infty + C_B + \alpha(C_B^\infty - C_B)$$

so that equation [A8] becomes

[A10] $$\alpha^2(C_B^\infty - C_B) + \alpha(C_B^\infty + C_B + K_{diss}) - K_{diss} = 0$$

Thus, α may be calculated for any C_B^∞ and C_B. Qualitatively, the reason why α varies so slowly as reaction proceeds is that, although $(C_x + C_y) = (C_B^\infty - C_B)$ decreases as reaction proceeds, thus tending to increase α (Ostwald dilution law), the remaining $(C_x + C_y)$ is present in an ever-increasing excess of free Cl^-, which tends to suppress the dissociative equilibrium.

Note added in proof

While the present work was being refereed, the extensive work of Bennetto and Caldin (19), together with their interesting discussion (25) of the effects of solvent structure on these reactions, was published.

It is a pleasure to acknowledge the assistance and advice offered by Dr. R. H. Holyer in the earlier stages of this work. Financial support by the National Research Council of Canada and the Ontario Department of University Affairs is also gratefully acknowledged.

1. R. H. Holyer, C. D. Hubbard, S. F. A. Kettle, and R. G. Wilkins. Inorg. Chem. **5**, 622 (1966).
2. M. Eigen. Proceeding of VIIth International Conference on Coordination Chemistry. Butterworth and Co. Ltd., London. 1963.
3. C. H. Langford and W. R. Muir. J. Am. Chem. Soc. **89**, 3141 (1967).
4. C. M. Harris and T. N. Lockyer. Aust. J. Chem. **23**, 1703 (1970).
5. R. Hogg and R. G. Wilkins. J. Chem. Soc. 341 (1962).
6. H. P. Bennetto and E. F. Caldin. Chem. Commun. 599 (1969).
7. C. H. Langford and H. G. Tsiang. Inorg. Chem. **9**, 2346 (1970).
8. P. A. Cock. M.Sc. Thesis, University of Guelph, Guelph, Ontario. 1971.
9. E. F. Caldin. Private communication.
10. J. N. Butler. J. Electroanal. Chem. **14**, 89 (1967).
11. S. Thomas and W. L. Reynolds. J. Chem. Phys. **46**, 4164 (1967).
12. S. Blackstaffe and R. D. Dwek. Mol. Phys. **15**, 279 (1968).
13. N. S. Angerman and R. B. Jordan. Inorg. Chem. **5**, 1362 (1966).
14. L. S. Frankel. Chem. Commun. 1264 (1969).
15. F. Basolo and R. G. Pearson. Mechanisms of inorganic reactions. Wiley, New York. 1967. p. 156.
16. T. J. Swift and R. E. Connick. J. Chem. Phys. **37**, 307 (1962).
17. I. Amdur and G. C. Hammes. Chemical kinetics. McGraw-Hill, New York. 1966. p. 56.
18. W. E. Wentworth. J. Chem. Ed. **42**, 96 (1965).
19. H. P. Bennetto and E. F. Caldin. J. Chem. Soc. A. 2191 (1971).
20. A. Allerhand, H. S. Gutowsky, J. Jonas, and R. A. Meinzer. J. Am. Chem. Soc. **88**, 3185 (1966).
21. G. Binsch. *In* Topics in stereochemistry. Vol. 3. *Edited by* E. L. Eliel and N. L. Allinger. Interscience, New York. 1968. p. 97.
22. D. Rablen and G. Gordon. Inorg. Chem. **8**, 395 (1969).
23. Z. Luz. J. Chem. Phys. **41**, 1748 (1964).
24. R. M. Foss. J. Am. Chem. Soc. **80**, 5059 (1958).
25. H. P. Bennetto and E. F. Caldin. J. Chem. Soc. A. 2198 (1971).

Nuclear Magnetic Resonance Experiments on Acetals. 35. Proton Magnetic Resonance Spectra and Quantitative Conformational Analysis of 4-Fluoromethylated-6-Me-1,3-dioxanes[1]

P. DIRINCK AND M. ANTEUNIS

State University of Gent, Department of Organic Chemistry, Laboratory for NMR Spectroscopy, Krijgslaan, 271, S.4, B-9000 Gent, Belgium

Received July 12, 1971

4-Substituted (CF_3-, CHF_2-, and CH_2F)-6-Me-1,3-dioxanes together with model derivatives (*cis*- and *trans*-4-CH_nF_{3-n}-6-*t*.Bu-1,3-dioxane, and 2-Me-4,6-disubstituted 1,3-dioxanes) were prepared and their p.m.r. spectra analyzed, using i.a. INDOR techniques. Special features which correlate configuration and p.m.r. data are discussed and especially the fluorine–hydrogen (long-range) couplings have been studied. From vicinal (ring) coupling data (using appropriate models), from the vicinal *exo*-couplings $^3J(H4,CF_{3-n}H_n)$ and from absolute shift values, the equilibria were obtained in the conformational heterogenous *trans*-4-CH_nF_{3-n}-6-Me-1,3-dioxanes ($n = 0 \rightarrow 2$). The results, according to the different methods, are mutually in excellent agreement, as is also the case for $\Delta G^0(CF_3)$, obtained approximately from dipole moment measurements. The anomeric effect is pronounced, and the conformer with the axial fluoromethylated substituent is the preferred one (CF_3: 76%; CF_2H: 62%) at room temperature in CS_2. For CH_2F the contrary seems to be the case (presumably for entropy reasons also). Finally ΔH^0(chair–twist) was evaluated at 3.7 kcal/mol (ΔS^0(ch$\rightleftarrows$ tw) = 6.1 e.u.) using ^2J(H2) criteria in *trans*-4-CF_3-6-*t*.Bu-1,3-dioxane.

On a préparé les 4-(CF_3-, CHF_2-, et CH_2F)-6-Me-1,3-dioxannes de même que des dérivés modèles (*cis*- et *trans*-4-CH_nF_{3-n}-6-*t*.Bu-1,3-dioxanne, et 2-Me-1,3-dioxannes 4,6-disubstitués) et analysé leurs spectres r.p.m., utilisant les techniques INDOR. On discute des aspects spéciaux qui établissent la correlation entre la configuration et les données de r.p.m. et spécialement des couplages fluor–hydrogène (à longue portée). A partir des données de couplage vicinal (anneau) (utilisant les modèles appropriés), des couplages vicinaux "*exo*" $^3J(H4,CF_{3-n}H_n)$ et des valeurs de déplacement absolues, on a obtenu les équilibres dans le cas des molécules *trans*-4-CH_nF_{3-n}-6-Me-1,3 dioxannes ($n = 0 \rightarrow 2$) de conformation hétérogène. Les résultats, selon les différentes méthodes, sont mutuellement en excellent accord, comme c'est le cas pour $\Delta G^0(CF_3)$, obtenu approximativement des mesures de moment dipolaire. L'effet anomérique est prononcé, et le conformère avec le substituant fluorométhylé en position axiale est le plus abondant (CF_3: 76%; CF_2H: 62%) dans du CS_2 à température ambiante. Le cas contraire semble se produire pour le CH_2F (vraisemblablement du pour des raisons d'entropie). On a évalué finalement ΔH^0 (chaise–bateau croisé) comme étant de 3.7 kcal/mol (ΔS^0(ch.$\rightleftarrows$ bat.cr.) = 6.1 e.u.) utilisant le critère ^2J(H2) dans le cas du *trans*-4-CF_3-6-*t*.Bu-1,3-dioxanne.

Canadian Journal of Chemistry, **50**, 412 (1972)

As part of a wider project of conformational studies on 1,3-dioxanes possessing polar groups, we report in this paper some results of fluoromethylated derivatives of the 1,3-dioxane system. Our choice for F is inspired by several considerations *e.g.* (*a*) the increasing importance (in n.m.r.) of fluorinated compounds enabling ^{19}F-n.m.r. investigations where necessary, and/or allowing studies of ^{19}F-H interactions; (*b*) its relative and acceptable bulkiness with respect to H or other halogens, and (*c*) its expected pronounced electrical influence on conformation, as the result of the large C—F dipole.

1,3-Dioxanes with fluorinated methyl groups in different positions (C-4 and -5) were prepared, the substituents ranging from CH_2F, CHF_2, to CF_3. In order to obtain eventually non-anancomeric (biased) systems, additional methyl groups were introduced as a counterbalance in adequate positions. For comparative purposes, and in order to obtain suitable reference p.m.r. parameters, a *t*.Bu-group (*e.g.* in C-6 position) or a methyl group in C-2 position was also introduced (Chart 1). The C-2 substituted fluoromethyl derivatives will be investigated in the future.

(1) Nuclear Magnetic Resonance Spectroscopic Features

Because the *trans*-4-fluoromethyl-6-Me-1,3-dioxane (**2***a* $\rightleftarrows$ **3***a*; **2***b* $\rightleftarrows$ **3***b*) could not be frozen out, conformational data could not be obtained

[1]Presented at the IUPAC congress (Section OC-5) July, 1971; Boston, Mass.

Can. J. Chem. Downloaded from www.nrcresearchpress.com by 210.87.254.42 on 09/05/12
For personal use only.

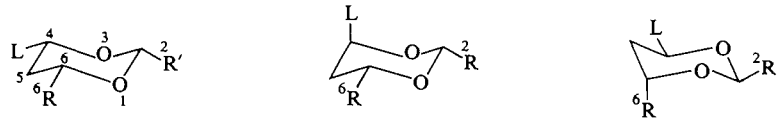

1 2 3

a L = CFH_2; R = Me; ^{2}R = H
b L = CF_2H; R = Me; ^{2}R = H
c L = CF_3; R = Me; ^{2}R = H
d L = CFH_2; ^{6}R = *t*.Bu
e L = CF_2H; ^{6}R = *t*.Bu
f L = CF_3; ^{6}R = *t*.Bu
g L = CFH_2; R = Me; ^{2}R = Me
h L = CF_2H; R = Me; ^{2}R = Me
i L = CF_3; R = Me; ^{2}R = Me

CHART 1

from parameters extracted from low temperature studies. One must rely instead upon model compounds to obtain suitable reference parameters. These model compounds can be divided into two series: (*a*) the *cis*-4-fluoromethyl-6-Me-1,3-dioxanes, as well as *cis*- and *trans*-4-CF_nH_{3-n}-6-*t*.Bu-1,3-dioxanes; (*b*) the 2-Me-substituted derivatives. In the latter series theoretically four configurations are possible, but through g.c. separation only three could be isolated (*e.g.*, 2-Me-4-CF_3-6-Me-1,3-dioxanes: **1***i*, **2***i*; **3***i*).

The assignation of configurations can easily be done on basis of n.m.r. criteria.

(i) Shift Criteria (Table 1)

(*a*) The shift difference between H-2a and H-2e (δ(2a → 2e) for the AB spin system of H-2) is >30 Hz in all *cis*-derivatives, but it is only 0–10 Hz in the corresponding *trans* derivatives.

(*b*) A deshielding of H-2a in the 2-Me-substituted series is observed when a *syn-axial* substituent is present.

(*c*) In the *cis* derivatives H-2a resonates at higher field, while in the *trans*-series this situation is reversed (1). This is easily ascertained by inspection of proton–proton long-range phenomena (n.m.d.r.) (*e.g.*, *J*(2e,5e), *J*(2e,4e) (2)).

(*d*) The shifts of the H-atoms of the CF_nH_{3-n}-substituents are characteristic of the substituent in axial or equatorial position (*vide infra*).

(ii) Fluorine–Proton and CF_nH_{3-n}-Coupling (Table 2)

These data afforded several possibilities for the determination of the axial or equatorial character of the fluoromethyl substituents, distinguishing the two possible *cis–trans* configurations in the 2-Me-substituted compounds.

(*a*) The $^3J^{exo}$(4aCF_3,H4e) is larger than $^3J^{exo}$(4eCF_3,H4a). This is useful for the determination of the equilibrium constant in *trans*-4-CF_3-6-Me-1,3-dioxane.

(*b*) ^{19}F–^{1}H long-range coupling: in the derivatives with axial 4-fluoromethyl groups, pronounced fluorine–proton long-range couplings were found with H-5a, H-2a, and H-2e. ^5J(F,H-2) is larger with Ha than with He. A non-classical long-range ^5J(4aCF_3,H6a) was also observed. Figures 1 and 2 are typical for *trans*-4-CF_3-6-*t*.Bu-1,3-dioxane.

(*c*) Coupling non-equivalency: in the (CF_2H-a) derivatives, there is a coupling non-equivalency for CHF_2 in ^2J(H,F) and ^5J(2a,F), only visible by extended sweeps, which is not observed in the derivatives with an equatorial CF_2H group. This is the result of the diastereotopicity of these fluoratoms and this is clearly enhanced for axial substitution by unequivalent rotamer distribution. Also the *exo*-couplings ^3J(H4,CHF_2) are different in axial and equatorial difluoromethyl. Figures 3 and 4 represent typical examples.

Due to the diastereotopicity of the CFH_2 protons in these compounds, the pattern is also quite different for the axial and equatorial position. In both cases there is no coupling non-equivalency in ^2J(H,F). From Fig. 5 one can conclude that the two diastereotopic atoms are isochronous, resulting in a doublet of doublets for the monofluormethyl H-atoms in axial position. For the CFH_2 in equatorial position the situation is more complicated (Fig. 6). Neglecting the ^2J(H,F) the CFH_2 protons form the AB part of an ABX system (X = H4), almost an ABC. We can, however, evaluate the necessary parameters quite accurately by the subspectral procedure (3), showing a different ^3J(CH_2F,H_4) with both hydrogens.

(2) Quantitative Conformational Data for trans-4-Fluoromethyl-6-Me-1,3-dioxanes

As stated, the 4,6-disubstituted compounds could not be frozen out down to −110 °C, a situation which parallels the 4,6-dialkyl series

Can. J. Chem. Downloaded from www.nrcresearchpress.com by 210.87.254.42 on 09/05/12
For personal use only.

Can. J. Chem. Downloaded from www.nrcresearchpress.com by 210.87.254.42 on 09/05/12
For personal use only.

TABLE 1. Shift values in p.p.m. from TMS int. of (2-Me)-4-fluoromethyl-6-alkyl-1,3-dioxanes*

^{2}R	^{4}R	^{6}R	Configuration	H-2	H-5	H-4	H-6	CF_nH_{3-n}	Me-4	Me-2	δ(2a → 2e) (Hz)†	δ(5a → 5e) (Hz)†
—	CF_3	Me	*trans* (**2***c*)	4.84	1.79	4.09	3.96		1.29		8.11	−13.97
—	CF_3	*t*.Bu	*trans* (**2***f*)	4.92	1.84	4.16	3.39		0.91		9.91	30.03
—	CF_3	Me	*cis* (**1***c*)	4.77	1.65	3.85	3.60		1.22		−38.02	− 7.40
—	CF_3	*t*.Bu	*cis* (**1***f*)	4.81	1.57	3.83	3.12		0.91		−44.90	4.72
—	CF_2H	Me	*trans* (**2***b*)	4.79	1.72			5.76	1.23		≃0	−25.97
—	CF_2H	*t*.Bu	*trans* (**2***e*)	4.82	1.74	3.89	3.30	5.91	0.88		6.88	21.94
—	CF_2H	Me	*cis* (**1***b*)		1.48			5.51	1.22		−35.82	− 8.47
—	CF_2H	*t*.Bu	*cis* (**1***e*)	4.76	1.47	3.61	3.10	5.48	0.90		−41.05	
—	CFH_2	Me	*trans* (**2***a*)	4.75	1.62			4.38	1.23		≃0	−17.57
—	CFH_2	Me	*cis* (**1***a*)	4.71				4.21	1.17		−32.73	
Me	CF_3	Me	*r*-2-Me-*trans*-4-*cis*-6 (**2***i*)	4.94	1.71	4.08	3.83		1.16	1.20		+37.49
Me	CF_3	Me	*r*-2-Me-*cis*-4-*cis*-6 (**1***i*)	4.60	1.48	3.86	3.63		1.22	1.27		− 9.90
Me	CF_3	Me	*r*-2-Me-*cis*-4-*trans*-6 (**3***i*)	4.92	1.70	4.07	4.21		1.34	1.22		+67.32
Me	CF_2H	Me	*r*-2-Me-*trans*-4-*cis*-6 (**2***h*)	4.86				5.51				
Me	CF_2H	Me	*r*-2-Me-*cis*-4-*cis*-6 (**1***h*)	4.54				5.91				
Me	CF_2H	Me	*r*-2-Me-*cis*-4-*trans*-6 (**3***h*)	4.86		3.86	4.17	5.51	1.32	1.16		
Me	CFH_2	Me	*r*-2-Me-*cis*-4-*cis*-6 (**1***g*)	4.55				4.20	1.16	1.21		
Me	CFH_2	Me	*r*-2-Me-*trans*-4-*cis*-6 (**2***g*)	4.86	1.59			4.52	1.13	1.14		+17.15
Me	CFH_2	Me	*r*-2-Me-*cis*-4-*trans*-6 (**3***g*)	4.89	1.50			4.20	1.30	1.13		+56.96

*The 100 MHz p.m.r. spectra were run at room temperature in carbon disulfide solutions (40 μl dioxane/400 μl CS_2 for 4-fluoromethyl-6-Me-1,3-dioxanes; the amount of 6-*t*.Bu- and 2-Me-substituted derivatives was corrected to obtain the same molar concentrations).

†Values are positive if He is upfield.

TABLE 2. Fluorine–proton couplings in Hz, $^3J(CF_n^{exo}H_{3-n},H4)$ and $^2J(CF_nH_{3-n})$*

Compound	^3J(H4,^{exo}F)	^2J(H,F)	^{19}F–^{1}H long-range couplings‡				^3J(H4,H$_F$)	^2J(CH$_2$-4′)
			^4J(5a,F)	^5J(6a,F)	^5J(2a,F)	^5J(2e,F)		
2*c*	8.71		0.71		1.57	≃1		
2*f*	9.62		0.96	1.68	1.91	≃1.1		
1*c*	6.27		— †	—	—	—		
1*f*	6.27		—	—	—	—		
2*b*		55.21	—		1.6		3.81	
		55.75			0.9			
2*e*		54.51	—	3	2.5	1.5	3.41	
		55.75			1.3			
1*b*		55.6	—	—	—	—	4.26	
1*e*		55.5	—	—	—	—	4.26	
2*a*		46.71	0.6		0.8		5.86	9.39
							3.98	
1*a*		46.56	—	—	—	—	5.05	9.39
							4.00	
2*i*	9.62		—		1.84			
1*i*	6.27		—	—	—			
3*i*	6.27		—	—	—			
2*h*		55.38					3.36	
		56.71						
1*h*		56.36	—	—	—		4.34	
3*h*		54.72	—	—	—		4.34	
1*g*		46.46	—	—	—		5.86	9.09
							3.76	
2*g*		46.66	1.25		1.62		5.05	
3*g*			—	—	—		5.80	9.09
							3.41	

*The 100 MHz p.m.r. spectra were run at room temperature in carbon disulfide (standard conditions).
†All dashes indicate that no fluorine–proton long-range coupling was observed.
‡Two values indicate coupling non-equivalency.

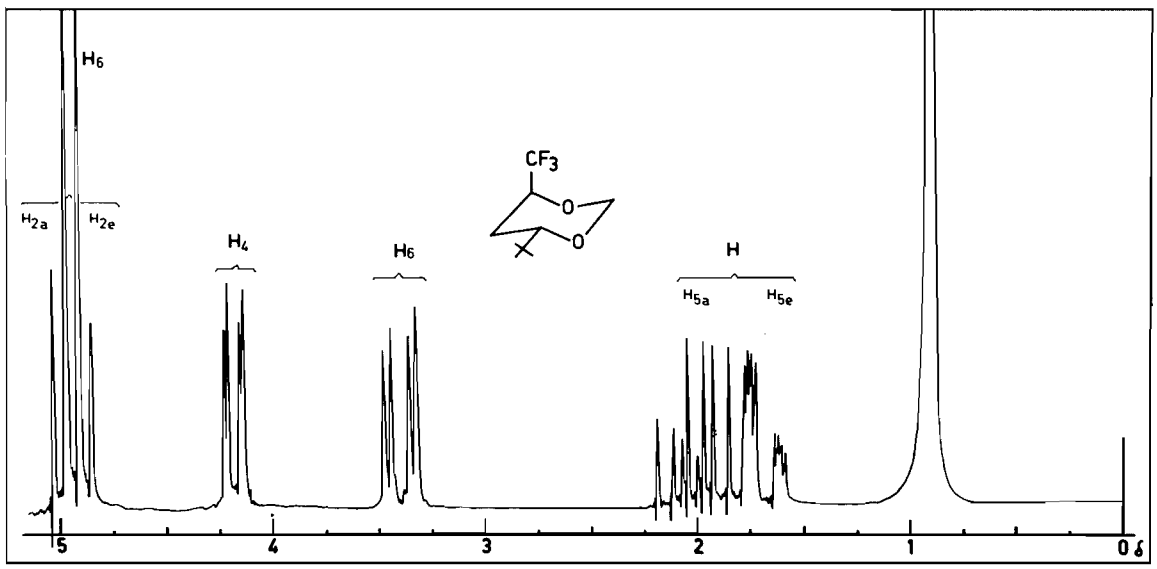

FIG. 1. The 100 MHz spectrum (CS_2, TMS int.) for *trans*-4-CF_3-6-*t*.Bu-1,3-dioxane (**2***f*).

Can. J. Chem. Downloaded from www.nrcresearchpress.com by 210.87.254.42 on 09/05/12
For personal use only.

Can. J. Chem. Downloaded from www.nrcresearchpress.com by 210.87.254.42 on 09/05/12
For personal use only.

(4). This is understandable if one takes into account *syn-axial* no-bond strain in the ground state, which lowers the barrier for inversion (5). Thus, conformational data cannot be obtained from line-shape analysis and one must rely upon criteria, such as coupling and shift values. Although in most instances (as for example in phenyl-substituted derivatives (5–7)) these criteria are untrustworthy, in the actual compounds and in other 4,6-dialkyl-substituted derivatives (3), the results obtained are consistent and independent methods such as dipole moment measurements indicate that they are reliable.

Data from Vicinal (Ring) Coupling Values

Vicinal (ring) coupling values are obtained from subspectral procedures (3) for the ABXY spin system, formed by H5, H4, and H6. The AB (H5) consists of four subspectral ab systems, defining eight subspectral shifts from which the vicinal coupling values are obtained.

The "axial" and "equatorial" parts in the AB part may be identified (n.m.d.r.) from long-range considerations (see section *1*, parts *ic* and *iib*). Subspectral parts could easily be relayed by appropriate INDOR experiments. The X- and Y-part, is well separated in the spectrum for the *t*.Bu derivatives (see Fig. 1) but not in the Me-substituted derivatives. Here ^{19}F-decoupled spectra obtained with a Heteronuclear Spindecoupler (NMR-Specialities) were very useful. It is relatively easy to obtain directly $\Sigma^3 J(X) = {}^3J(AX) + {}^3J(BX)$ of the X-part, $\Sigma^3 J(Y) = {}^3J(AY) + {}^3J(BY)$ for the Y-part. Furthermore semi-quantitative considerations of the Karplus relation allow unambiguous assignation in the anancomeric derivatives. The results are gathered in Table 3.

Once the vicinal couplings are extracted from the spectra one can interpolate values for the conformational mobile systems using the equations shown in Chart 2.

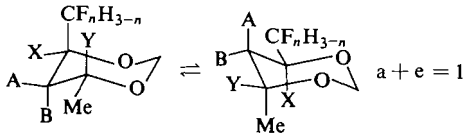

a e

$J(A,X) = a.J(5e,4e) + e.J(5a,4e)$....I
$J(B,X) = a.J(5a,4e) + e.J(5e,4a)$....II
$J(A,Y) = a.J(5e,6a) + e.J(5a,6e)$....III
$J(B,Y) = a.J(5a,6a) + e.J(5e,6e)$....IV

CHART 2

(i) trans-4-Fluoromethyl-6-t.Bu-1,3-dioxanes and cis-4,6-Disubstituted-1,3-dioxanes as Model Compounds

It will be remarked (Tables 4 and 5) that values obtained from anancomeric *cis*-Me- and *cis-t*.Bu-4,6-substituted derivatives differ somewhat. Therefore we have gathered the results separately in Table 4. Equations III and IV, Chart 2 may only be used for CF_3-substituted derivatives, because only the necessary values

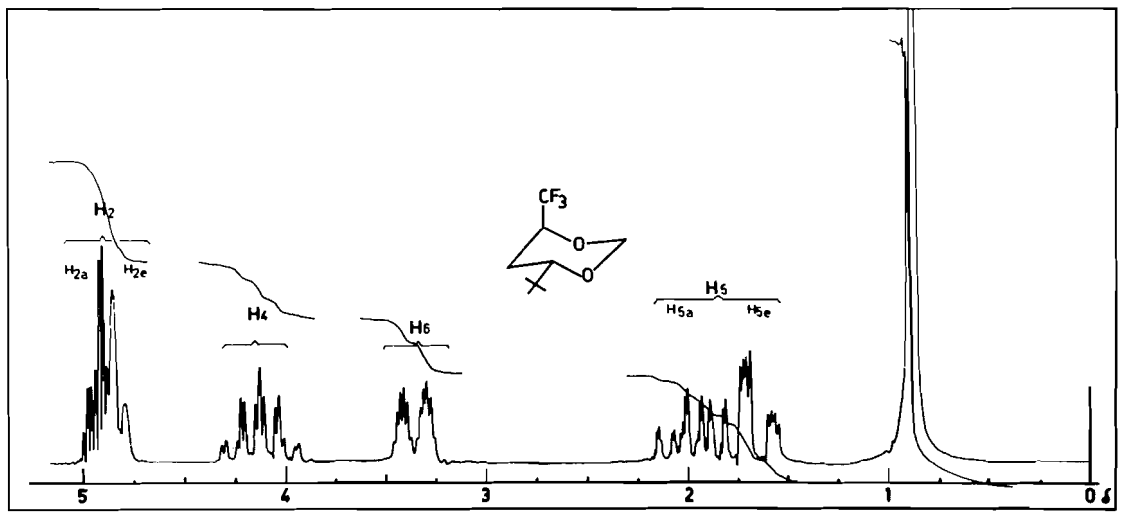

FIG. 2. The F-decoupled 100 MHz spectrum (CS_2, TMS int.) for *trans*-4-CF_3-6-*t*.Bu-1,3-dioxane (*2f*).

TABLE 3. Coupling values in Hz for (2-Me)-4-fluoromethyl-6-alkyl-1,3-dioxanes

Compound	$^2J2$	$^2J5$	^3J(4e,5a)	^3J(4a,5a)	^3J(4e,5e)	^3J(4a,5e)	^3J(6e,5a)	^3J(6a,5a)	^3J(6e,5a)	^3J(6a,5e)
2*c**	6.32	13.97	6.46		4.01			9.05		3.66
2*f*	5.73†	14.07	7.43		1.49			11.97		3.06
1*c*	6.27	12.95		10.03		4.54		11.38		2.07
1*f*	6.30	12.44		11.14		3.58		12.34		1.51
2*b**	‡	13.68	5.92		4.71			8.09		4.71
2*e*	5.60†	13.81	7.20		2.00			11.86		3.02
1*b*	6.36	12.98		10.09		4.18		12.94		1.85
1*e*	6.16	‡		‡		‡		‡		‡
2*a**	‡	13.05	4.85		6.26			6.48		4.70
1*a*	6.10	‡		‡		‡		‡		‡
2*i*		14.18	7.68		1.11			11.55		2.87
1*i*		12.52		11.25		2.24		11.25		2.24
3*i*		13.00		12.82		2.55	6.38		1.12	
2*h*		‡	‡		‡			‡		‡
1*h*		‡		‡		‡		‡		‡
3*h*		‡		‡		‡	‡		‡	
1*g*		‡		‡		‡		‡		‡
2*g*		13.24	6.48		1.38			11.14		2.99
3*g*		12.68		11.62		3.60	5.96		1.39	

*For the conformationally heterogeneous compounds (**2***a*, *b*, *c*) averages are given, identified with the left conformer (conventionally the one with axial fluoromethyl group).
†Remarkable low value.
‡Could not be analyzed.

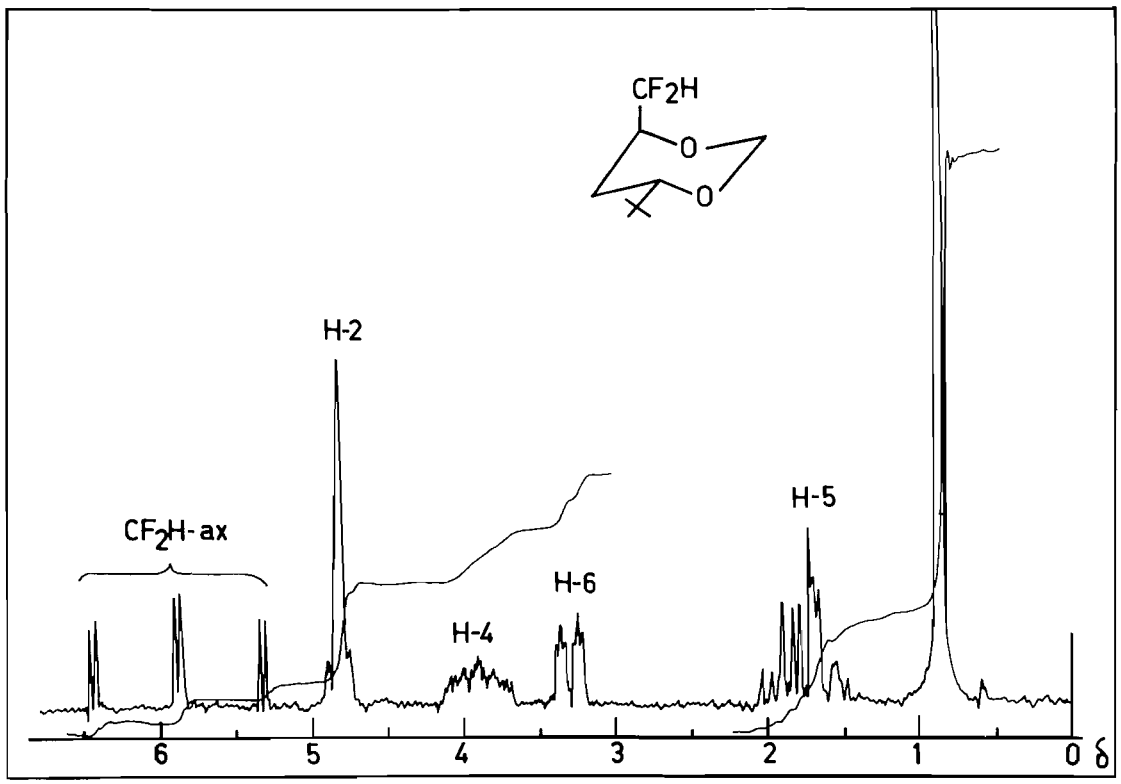

FIG. 3. The 100 MHz spectrum (CS_2, TMS int.) for *trans*-4-CF_2H-6-*t*.Bu-1,3-dioxane (**2***e*). Coupling non-equivalency for CF_2H not visible in non-extended registrations; these for H-2 and H-4 are clearly visible.

Can. J. Chem. Downloaded from www.nrcresearchpress.com by 210.87.254.42 on 09/05/12
For personal use only.

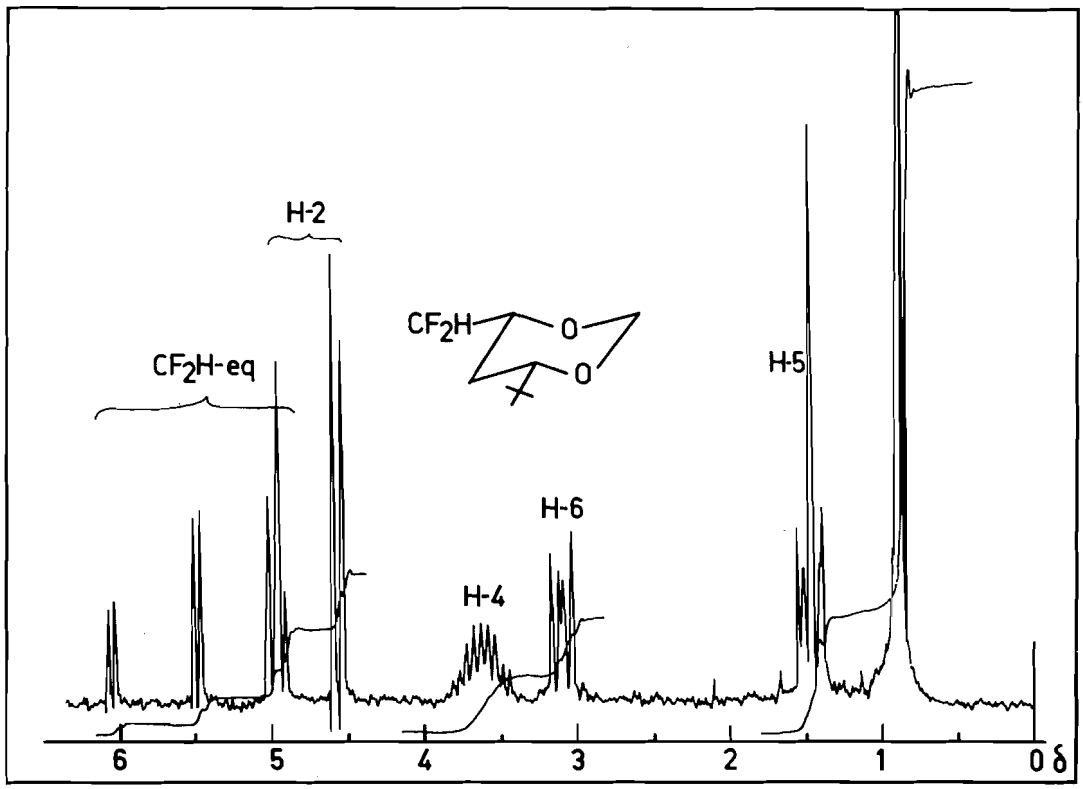

FIG. 4. The 100 MHz spectrum (CS_2, TMS int.) for *cis*-4-CF_2H-6-*t*.Bu-1,3-dioxane (**1***e*).

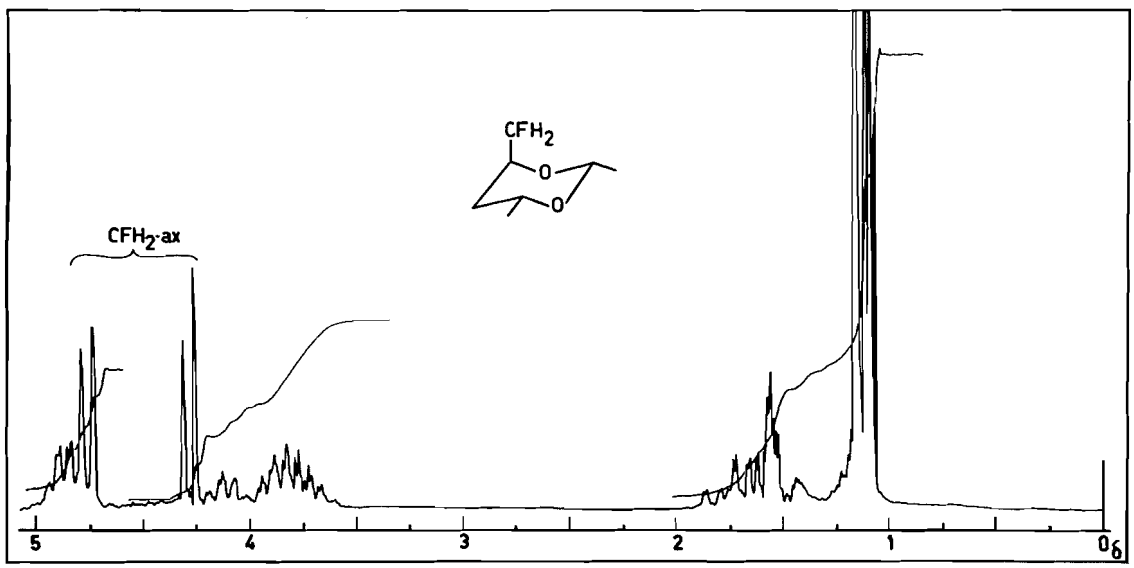

FIG. 5. The 100 MHz spectrum (CS_2, TMS int.) for *r*-2-Me-*trans*-4-CF_2H-*cis*-6-Me-1,3-dioxane (**2***h*).

Can. J. Chem. Downloaded from www.nrcresearchpress.com by 210.87.254.42 on 09/05/12
For personal use only.

TABLE 4. Conformational data in 4-fluoromethyl-6-Me-1,3-dioxane from vicinal (ring) coupling values

Model values (models indicated)*					
2*c*	**2***f*		*a*%	$\Delta\Delta G^0_{300}$ (cal/mol)	$\Delta G°(CF_3\text{-}4)$† (kcal/mol)
$^3J(A,X) = 4.01$	$^3J(5e,4e) = 1.49$	$^3J(5a,4a) = 10.03$ (**1***c*)	70.5	519	2.48
		$= 11.34$ (**1***f*)	73.9	619	2.38
		$= 11.66$ (**1***k*)	75.2	662	2.34
$^3J(B,X) = 6.46$	$^3J(5a,4e) = 7.43$	$^3J(5e,4a) = 4.54$ (**1***c*)	66.4	407	2.59
		$= 3.58$ (**1***f*)	74.8	648	2.35
		$= 3.20$ (**1***k*)	77.1	723	2.28
$^3J(A,Y) = 3.66$	$^3J(5e,6a) = 3.06$	$^3J(5a,6e) = 5.26$ (**1***k*)	72.7	584	2.42
$^3J(B,Y) = 9.05$	$^3J(5a,6a) = 11.97$	$^3J(5e,6e) = 2.08$ (**1***k*)	70.5	518	2.48
2*b*	**2***e*	**1***b*			$\Delta G^0(CF_2H\text{-}4)$
$^3J(A,X) = 4.71$	$^3J(5e,4e) = 2.00$	$^3J(5a,4a) = 10.09$	66.5	408	2.59
$^3J(B,X) = 5.92$	$^3J(5a,4e) = 7.20$	$^3J(5e,4a) = 4.18$	57.6	183	2.82

*1*k*: 4-CF_3-1,3-dioxane (CF_3 100% equatorial).
†ΔG^0(Me-4) = 3.0 kcal/mol (8, 15). Only approximate values (principle of additivity).

for ^3J are known from the anancomeric 4-CF_3-1,3-dioxane (CF_3 100% equatorial (8, 9)).

The results obtained in Table 4 in general are mutually consistent. Fluctuations are easily explained by considerations of (*a*) difficulties encountered in analyses of overlapping resonance lines, as the result of the small differences in shifts of H-5a and H-5e (see $\delta(5a \rightarrow 5e)$, Table 1); especially for the *cis* derivatives, where often the subspectral ab systems are greatly degenerated; (*b*) the possibility of the occurrence of a certain amount of flexible forms. This is suggested by the low (absolute) values of ^2J(H2) in *trans*-4-CF_3-6-*t*.Bu- and *trans*-4-CF_2H-6-*t*.Bu-1,3-dioxane (-5.73 and -5.60 Hz, respectively, where it is normally -6.30 Hz (in solution)). It was shown that ^2J(H2) is a sensible criterium for the presence of flexible forms (10, 11). We will show later, however, that the amount of flexible forms at room

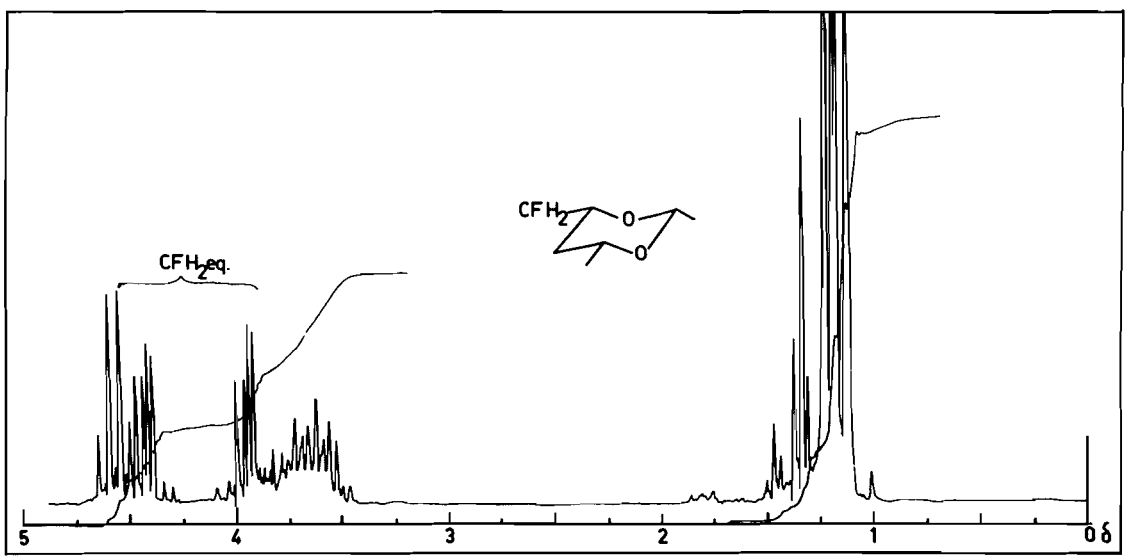

FIG. 6. The 100 MHz spectrum (CS_2, TMS int.) for *r*-2-Me-*cis*-4-CF_2H-*cis*-6-Me-1,3-dioxane (**1***h*).

Can. J. Chem. Downloaded from www.nrcresearchpress.com by 210.87.254.42 on 09/05/12
For personal use only.

TABLE 5. Conformational data in 2-Me-substituted-1,3-dioxanes as model compounds from vicinal (ring) coupling values

Model values (models indicated)					
2*c*	**2***i*	**3***i*	*a*%	$\Delta\Delta G^0_{300}$ (cal/mol)	$\Delta G^0(CF_3\text{-}4)$ (kcal/mol)
$^3J(A,X) = 4.01$	$^3J(5e,4e) = 1.11$	$^3J(5a,4a) = 12.82$	75.2	663	2.34
$^3J(B,X) = 6.46$	$^3J(5a,4e) = 7.68$	$^3J(5e,4a) = 2.55$	76.2	695	2.31
$^3J(A,Y) = 3.66$	$^3J(5e,6a) = 2.87$	$^3J(5a,6e) = 6.38$	77.5	737	2.26
$^3J(B,Y) = 6.26$	$^3J(5a,6a) = 11.55$	$^3J(5e,6e) = 1.12$	76.0	689	2.31
2*a*	**2***g*	**3***g*			$\Delta G^0(CFH_2\text{-}4)$
$^3J(A,X) = 6.26$	$^3J(5e,4e) = 1.38$	$^3J(5a,4a) = 11.62$	52.3	56	2.94
$^3J(B,X) = 4.85$	$^3J(5a,4e) = 6.48$	$^3J(5e,4a) = 3.60$	43.4	−158	3.16
$^3J(A,Y) = 4.70$	$^3J(5e,6a) = 2.99$	$^3J(5a,6e) = 5.96$	42.4	−182	3.18
$^3J(B,Y) = 6.48$	$^3J(5a,6a) = 11.14$	$^3J(5e,6e) = 1.39$	52.2	53	2.95

TABLE 6. Conformational data and sums of vicinal (ring) coupling values from H(4)-patterns for CF_3 derivatives (in Hz)*

$\sum^3J(4e,5a) + {}^3J(4e,5e)$	$\sum^3J(4a,5e) + {}^3J(4a,5a)$	*a*%	$\Delta\Delta G^0(CF_3\text{-}4)$ (cal/mol)
8.75 (**2***f*)	13.97 (**1***c*)	74.1	628
	13.37 (**1***f*)	70.8	527
	14.07 (**1***i*)	74.6	643
8.58 (**2***i*)	14.80 (**3***i*)	77.7	743

*Interpolating value for **2***c* = 10.10 Hz.

temperature cannot greatly influence the reference values for vicinal coupling, as it is only 4% for the CF_3 derivative; and (*c*) possible ring shape deformation caused by typical substitution in these model compounds.

(ii) r-2-Me-trans-4-Fluoromethyl-cis-6-Me-1,3- and r-2-Me-cis-4-Fluoromethyl-trans-6-Me-1,3-dioxanes as Model Compounds

In spite of several attempts, we did not succeed in preparing the 4-CFH_2-6-*t*.Bu-1,3-dioxanes. Therefore we considered the use of the 2-Me-substituted derivatives in order to obtain the necessary reference ring coupling values. In some of these cases the AB parts of the ABXY spin systems were partly hidden under the Me protons, and could only be analyzed by INDOR experiments (12). The 2-Me-4-CF_2H-6-Me-1,3-dioxanes could not be used because g.c. separations of the configurations failed. In Table 5 results are collected.

The accuracy of the coupling constant method is determined by the wisdom of the model-choice. Ring deformations have an important influence on ^3J(ring). We think that the 2-Me-substituted derivatives are, in that respect, superior, and therefore the data of Table 6 somewhat more trustworthy than those of Table 5. This is confirmed by inspecting Table 6 where the summarized values $\sum^3J$ of the vicinal (ring) coupling constants are collected, as they can be extracted directly from the H-4 pattern after ^{19}F-decoupling (separation of outer peaks).

The introduction of a *t*.Bu group or the taking of a *cis* configuration as model compound for the conformer with equatorial fluoromethyl group (as is the case in the first series of model compounds) is clearly illustrated.

We may conclude therefore, that the coupling constant method supplies with good approximation the energy differences for the equilibrium in *trans*-4-CF_2H-6-Me-1,3- and *trans*-4-CFH_2-6-Me-1,3-dioxanes. We estimate even more accurately the mean value for the equilibrium in *trans*-4-CF_3-6-Me-1,3-dioxane, as obtained from the second series of model compounds. These mean values are summarized in Table 7.

Can. J. Chem. Downloaded from www.nrcresearchpress.com by 210.87.254.42 on 09/05/12
For personal use only.

Can. J. Chem. Downloaded from www.nrcresearchpress.com by 210.87.254.42 on 09/05/12
For personal use only.

TABLE 7. Mean conformational values from vicinal coupling data

Compound	a% (room temperature)*	ΔG^0_{300} (cal/mol)	$\Delta G^0(CF_nH_{3-n}$-4) (kcal/mol)
2*c*	76.2	695	$\Delta G^0(CF_3\text{-}4) = 2.31$
2*b*	62.1	294	$\Delta G^0(CF_2H\text{-}4) = 2.71$
2*a*	47.6	−57	$\Delta G^0(CFH_2\text{-}4) = 3.06$

*With axial fluoromethyl group. See Chart 2.

Data from Vicinal exo-Coupling Values

In agreement with earlier published data, there is a general trend that *exo*-coupling values are larger where axial, rather than equatorial, substituents are involved (13). This is also found here. The *exo*-coupling value can be obtained from inspection of the H-4 pattern, which, however, is also coupled with H-5a (and in the *trans* derivative additionally with H-2e). It was found that $^3J^{exo}$ does not depend on additional alkyl substitution. As the result of the diastereotopicity the situation for CF_2H is too complicated, and the *exo* values are not obtainable with enough accuracy. The method was therefore checked only for the CF_3-substituted derivative (**2***c*). From $^3J^{exo}$(4aCF$_3$,H4e) = 9.62 Hz (**2***f* and *i*) and $^3J^{exo}$(4eCF$_3$,H4a) = 6.27 Hz (**1***f*, *i*, and *c*) it follows from the value of 8.71 Hz in (**2***c*) that $a = 72.8\%$ at equilibrium and at room temperature ($\Delta\Delta G^0 = 588$ cal/mol), in satisfactory agreement with the mean value obtained from ring coupling constants (Table 7).

Data from Absolute Shift Values

Precise absolute shift values (TMS internal) were obtained for the 4-CF_2H-6-R-1,3-dioxanes (Hewlett Packard 5512A Electronic Counter), and it was found that $\delta(CF_2H)$ is characteristic for the position of the substituent: $\delta(CF_2H$-ax) = 5.906 (from **2***e*) and $\delta(CF_2H$-eq) = 5.511 from (**1***b* and *e*). For the conformational mixture (**2***b*) a value of 5.757 is found, and from this it follows $a = 62.28\%$ ($\Delta\Delta G^0 = 299$ cal/mol), again in excellent agreement with the data obtained from ring coupling values.

Data from Dipole Moments

Calculations of dipole moments for both conformers of the *trans*-4-fluoromethyl-6-Me-1,3-dioxanes show that the difference between the dipole moment of the conformer with an axial fluoromethyl and equatorial fluoromethyl group, respectively, is largest for the CF_3 derivative. In continuation of the n.m.r. method, the conformational equilibrium in *trans*-4-CF_3-6-Me-1,3-dioxane (**2***c*) may be calculated using the expression for the mean square moment of the equilibrium mixture:

$$\mu^2 = a\mu_a^2 + e\mu_e^2$$

in which a and e denote the molar fractions of both conformers. Here *cis*-4-CF_3-6-Me-1,3-dioxane (**1***c*) and *trans*-4-CF_3-6-*t*.Bu-1,3-dioxane (**2***f*) may serve as model compounds for the evaluation (17, 18) of μ_e and μ_a which were found to be 3.07 and 1.26 D, respectively. *trans*-4-CF_3-6-Me-1,3-Dioxane has $\mu = 1.80$ D, therefore $\%a = 78.9\%$ ($\Delta\Delta G^0_{298} = 782$ cal/mol), a value which is somewhat higher than obtained in previous methods.

Due to the electric nature of the system, especially accentuated in the equatorial conformer, we may expect that in cyclohexane the less polar conformation (axial CF_3) will tend to be more highly represented. Therefore, the method based upon dipole moment interpolation (in cyclohexane) entirely confirms the n.m.r. findings obtained in carbon disulfide, the latter method being by far superior.

*(3) Chair–Twist Interconversion in trans-4-CF_3-6-t.Bu-1,3-Dioxane (**2***f*)*

As mentioned above, the too positive values for $^2J(2)$ in **2***f* and *e* (see Table 3), led us to suppose (10) that some flexible forms may occur here. If that is the case, one should find a temperature dependency for $^2J(2)$, from which, with the aid of appropriate limit values for the chair and the twist forms respectively, the thermodynamic properties for chair–twist interconversion may be calculated (10). As for other 4,6-disubstituted dioxanes we have supposed that the limiting forms are the classical chair ($^2J2 = -6.19$ Hz for the pure liquid compounds as follows from spectra at −25 °C) and the twist–boat with alternating two-fold axes through C2–C5 for which the 4-(1′-adamantyl)-6-*t*.Bu-1,3-dioxane serves as a model having $^2J2 = 2.8$ Hz (10).

From the variation of $^2J2$ with temperature (Table 8) for the pure *trans*-4-CF_3-6-*t*.Bu-1,3-dioxane we can calculate ΔH^0(twist ⇄ chair **2***f*) = 3.72 kcal/mol and ΔS^0(twist ⇄ chair **2***f*) = 6.1 e.u. ($r = 0.895$).

We have previously found (10) that ΔH^0(tw ⇄

TABLE 8. $^2J(2)$-values for *trans*-4-CF_3-6-*t*.Bu-1,3-dioxane (**2***f*) as a function of temperature

T °K	$^2J(2)$	% twist	ΔG (ch ⇌ tw)
247	6.19		
257	6.18	0.2	2857
268	6.13	1.8	2139
279	6.11	2.4	2061
289	6.06	3.8	1852
301	6.05	4.1	1883
313	5.98	6.2	1691
308	5.95	7.1	1573
319	5.93	7.7	1578
331	5.87	9.4	1486
342	5.87	9.4	1538
354	5.82	10.9	1476
366	5.82	10.9	1524
377	5.72	13.9	1368
389	5.65	15.9	1284
400	5.61	17.1	1255
412	5.57	18.3	1224
423	5.52	19.8	1177
435	5.49	20.6	1162
446	5.45	21.8	1131
458	5.43	22.4	1128

ch) for 1,3-dioxane amounts to 6.2 ± 0.3 kcal/mol (see also ref. 14; $\Delta H^0 = 6.8 \pm 0.7$ kcal/mol). Therefore with the actual value in *trans*-4-CF_3-6-*t*.Bu-1,3-dioxane we come to the conclusion that $\Delta H^0(CF_3\text{-}4) \simeq 2.5$ kcal/mol. Accepting that the additivity principle can be applied, a value of $\Delta G^0(CF_3\text{-}4) = 2.3$ kcal/mol was deduced from the previously described equilibria data (see Table 7). In view of the totally different approach, and the fact that ΔS^0 has been neglected, this is an unexpected conformity.

(4) Conclusion

Although a CF_3 group is a "larger" group for a carbocyclic ring ($\Delta G^0(CF_3) = 2.1$ kcal/mol; $\Delta G^0(Me) = 1.7$ kcal/mol (16)), this is not the case in heterocyclic compounds, at least when substituted next to oxygen. The influence of the mutual dipole interaction (*cf.* anomeric effect) is well illustrated, when one knows that $\Delta G^0(Me4) = 3.1$ kcal/mol for Me4 in dioxane (15) and that we, therefore, expect a still higher value *e.g. ca.* 3.8 kcal/mol, merely on the basis of pure steric interactions.

Instead the axial CF_3 group is preferred. The "anomeric" effect (19) is thus evaluated at 3.8–2.3 = 1.5 kcal/mol. Similar behavior is found for less fluorinated methyl groups. Unfortunately no thermodynamic data such as ΔH^0 and ΔS^0 could be obtained, due to the lack of accurate temperature dependent criteria. It would be interesting to obtain such data and also the dependency on polarity of the medium, in order to obtain more insight into the nature and operation of the different effects which determine the conformational behavior of polar substituents (on polar substrates).

1. D. TAVERNIER and M. ANTEUNIS. Bull. Soc. Chim. Belges, **76**, 157 (1967).
2. M. ANTEUNIS, D. TAVERNIER, and F. BORREMANS. Bull. Soc. Chim. Belges, **75**, 396 (1966).
3. P. DIEHL, R. K. HARRIS, and R. G. JONES. *In* Progress in NMR spectroscopy. Vol. 3. *Edited by* J. Emsley, J. FEENEY, and L. SUTCLIFFE. Pergamon Press, 1967. p. 1–62. *cf.* P. DIEHL. Helv. Chim. Acta, **48** (3), 567 (1965).
4. D. TAVERNIER. Ph.D. Thesis. State University of Gent, Gent, Belgium, 1971.
5. H. FRIEBOLIN, H. SCHMID, S. KABUSS, and W. FAISST. Org. Magn. Res. **1**, 67 (1969); E. COENE and M. ANTEUNIS. Bull. Soc. Chim. Belges, **79**, 37 (1970).
6. M. ANTEUNIS. Sympos. Brussels, September, 1969; Conformational analysis. *Edited by* G. Chiurdoglu. Academic Press Inc., New York, 1971. p. 31–50.
7. D. TAVERNIER, M. ANTEUNIS, and G. SWAELENS. In preparation.
8. G. SWAELENS. Ph.D. Thesis. State University of Gent, Gent, Belgium, 1970.
9. G. SWAELENS, M. ANTEUNIS, and D. TAVERNIER. Bull. Soc. Chim. Belges, **79**, 441 (1970).
10. M. ANTEUNIS and G. SWAELENS. Org. Magn. Res. **2**, 389 (1970).
11. M. ANTEUNIS, G. SWAELENS, and F. ANTEUNIS-DE KETELAENE. Bull. Soc. Chim. Belges, **80**, 409 (1971).
12. E. B. BACKER. J. Chem. Phys. **37**, 911 (1962). For an extensive and excellent treatment see W. Van Deursen. Org. Magn. Res. **3**, 221 (1971).
13. M. ANTEUNIS. Bull. Soc. Chim. Belges, **80**, 3 (1971).
14. K. PIHLAJA and S. LUOMA. Acta Chem. Scand. **22**, 716 (1968).
15. E. ELIEL and M. KNOEBER, SR. J. Am. Chem. Soc. **88**, 5347 (1966).
16. E. ELIEL, N. ALLINGER, S. ANGYAL, and S. MORRISON. Conformational analysis. Interscience Publishers, 1965; E. DELLA. Tetrahedron Lett. 3347 (1966); Topics in stereochemistry. *Edited by* E. Eliel and N. Allinger. Vol. I. Interscience Publishers, 1967. p. 199.
17. I. F. HALVERSTADT and W. D. KUMLER. J. Am. Chem. Soc. **64**, 2988 (1942).
18. G. HEDESTRAND. Z. Physik Chem. **2B**, 428 (1929).
19. E. L. ELIEL. Svensk Kemisk Tidskrift, **81**, 7 (1969), and references cited herein.

Can. J. Chem. Downloaded from www.nrcresearchpress.com by 210.87.254.42 on 09/05/12
For personal use only.

Nuclear Magnetic Resonance Experiments on Acetals. 36. Proton Magnetic Resonance Spectra and Quantitative Conformational Data in 5-Fluoromethylated-5′-Me-1,3-Dioxanes[1]

M. ANTEUNIS AND P. DIRINCK

State University of Gent, Department of Organic Chemistry, Laboratory for NMR Spectroscopy, Krijgslaan 271 (S4) Gent; Belgium B-9000

Received July 12, 1971

A proton magnetic resonance study of 5-CHF_2- and 5-CH_2F-5′-Me-1,3-dioxanes and the corresponding 2-Me-substituted derivatives enables approximate conformational insights. The system prefers an equatorial polar substitutent at C-5. This is very pronounced for CHF_2, and to a lesser but still important extent for CH_2F ($\Delta\Delta H^0 = 488$ cal/mol; $\Delta\Delta S^0 = -3.0$ e.u.).

L'étude r.m.n. des CHF_2-5 et CH_2F-5 CH_3-5′ dioxannes-1,3 et des dérivés correspondants méthyl-2 substitués, donne un aperçu approximatif de leurs conformations. Le système adopte préférentiellement la conformation où le substituant polaire en C-5 est équatorial. Cet effet, très prononcé pour CHF_2, l'est moins dans le cas de CH_2F ($\Delta\Delta H^0 = 488$ cal/mol; $\Delta\Delta S^0 = -3.0$ e.u.).

Canadian Journal of Chemistry, **50**, 423 (1972)

Introduction

We have discussed in the preceding paper (1) the spectra and conformational features of the parent 4,6-disubstituted-1,3-dioxanes. We wish to report in this paper, the data obtained in 5-CF_nH_{3-n}-5′-Me-1,3-dioxanes ($n = 1, 2$) (Chart 1).

In contrast with the 4,6-disubstituted compounds in this series (1), conformational data can usually be obtained by a variable temperature study because at *ca.* −65 °C mixed spectra of both conformations (CF_nH_{3-n} axial and equatorial) are observed. However, due to the anancomeric (biased) nature of the equilibrium in 5-CF_2H-5′-Me-1,3-dioxane, suitable reference parameters could not be obtained by low temperature measurements and for this derivative, one must again rely upon anancomeric model compounds. They can easily be obtained by introducing a supplementary methyl group on C-2, which is a "blocking" group (2).

Proton Magnetic Resonance Spectroscopic Data

Shift and coupling values for (2-Me)-5-fluoromethyl-5′-Me-1,3-dioxanes are collected in Table 1. In contrast with a fluoromethyl group on C-4 (1), inspection of Table 1 reveals ^{19}F–H long-range coupling occurring when the fluoromethyl on C-5 is in equatorial position. This ^4J(H4,F) is more important with H-4a than with H-4e. Furthermore, pronounced down- and upfield shifts are observed for the CF_2H and Me-5 protons, respectively, in the conformer with equatorial fluoromethyl group, in contrast with the conformer with CF_2H in axial position (Figs. 1 and 2).

Conformational Data for 5-CF_2H-5′-Me-1,3-Dioxane (1b)

This derivative is not soluble enough in CS_2 to allow low temperature measurements (it crystallizes out at $\leqslant -50$ °C). In Freon-12 ($CFHCl_2$) however, spectra can be obtained down to −100 °C. Although a certain broaden-

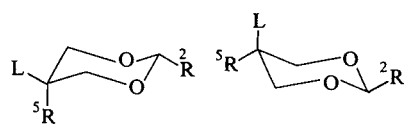

1 2

a	L = CFH_2; R = Me; ^{2}R = H	*d*	L = CFH_2; R = *t*.Bu	*g*	L = CFH_2; R = Me; ^{2}R = Me
b	L = CF_2H; R = Me; ^{2}R = H	*e*	L = CF_2H; R = *t*.Bu	*h*	L = CF_2H; R = Me; ^{2}R = Me
c	L = CF_3; R = Me; ^{2}R = H	*f*	L = CF_3; R = *t*.Bu	*i*	L = CF^3; R = Me; ^{2}R = Me

CHART 1

[1]Presented at the IUPAC congress (section OC-5), July, 1971, Boston, Mass.

Can. J. Chem. Downloaded from www.nrcresearchpress.com by 210.87.254.6 on 09/05/12
For personal use only.

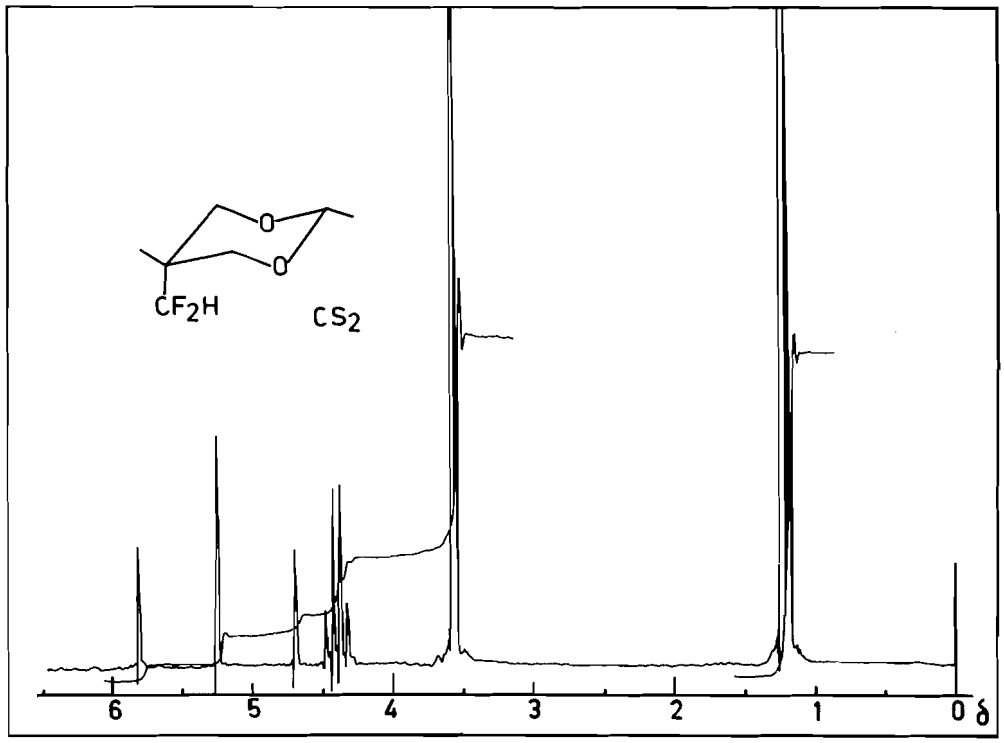

FIG. 1. The 100 MHz spectrum (CS_2, TMS int.) for *r*-2-Me-*cis*-5-CF_2H-*trans*-5′-Me-1,3-dioxane (2*h*).

ing at *ca* −65 °C is observed, the conformational equilibrium is too one-sided to compute any reasonable equilibrium value (with the aid of line-shape analysis or interpolation of shift values). Therefore we tried to estimate the equilibrium at room temperature from shift data. Shifts (in CS_2 and $CFHCl_2$) were measured in (1*b*) for CHF_2 and *Me*-5, and they were compared with the respective values in anancomeric model compounds such as *r*-2-Me-*trans*-5-CF_2H-*cis*-5′-Me-1,3-dioxane (1*h*) and *r*-2-Me-*cis*-5-CF_2H-*trans*-5′-Me-1,3-dioxane (2h). To keep the results uniform fluorodichloromethane, which is an excellent low temperature solvent, was also so used for 5-CFH_2-5′-Me-1,3-dioxane. It also enables us in that case to observe the influence of dielectric constant on the conformational equilibrium. In Table 2 results are gathered.

Table 2 shows that $\Delta\Delta G^0$ values differ a lot, whether the equilibrium determination is assessed from absolute shift measurement of CF_2H or of Me-5. However, we estimate the free energy difference as found from shift interpolation of CF_2H proton to be more trustworthy because: (*a*) in the 4-fluoromethyl-6-alkyl-1,3-dioxane series it is proved that characteristic absolute shifts of protons geminal to fluor (whether we deal with equatorial or axial fluoromethyl groups) are independent of other ring substituents; (*b*) for the equilibrium under investigation the conformer with CF_2H equatorial is the less polar one.[2] On changing from carbon disulfide to fluorodichloromethane we expect an equilibrium shift to the side of the more polar conformer, *e.g.* the one with axial difluoromethyl group. This is confirmed by the calculations from CF_2H which show the more polar conformer to become stabilized with an additional $\simeq$200 cal/mol, on changing from carbon disulfide to fluorodichloromethane.

From this we estimate $\Delta\Delta G^0$ (Me5, CF_2H5) $\simeq$ 1.87 kcal/mol, suggesting from additivity calcultation and with ΔG^0 (Me-5) = 0.9 kcal/mol (2, 3), that ΔG^0 (CF_2H5; CS_2) $\simeq$ 2.77 kcal/mol. No data concerning ΔH^0 and ΔS^0 however, could be obtained.

[2]This contrasts with the 4-substituted series, as is easily understood from considerations of dipole–dipole interactions between C-CF_nH_{3-n} and the dioxanic ring.

Can. J. Chem. Downloaded from www.nrcresearchpress.com by 210.87.254.6 on 09/05/12
For personal use only.

Can. J. Chem. Downloaded from www.nrcresearchpress.com by 210.87.254.6 on 09/05/12
For personal use only.

TABLE 1. The p.m.r. parameters (J in Hz and shifts in p.p.m.) for (2-Me)-5-fluoromethyl-5′-Me-1,3-dioxanes

^{5}R	^{5}′R	^{2}R	Configuration	Solvent	H2	δ(2a → 2e)*	H4,6	δ(4a → 4e)*	Me5	Me2	CFH_2 and CF_2H	^2J2	^2J4	^2J(H,F)	^4J(4a,CF_nH_{3-n}-5)	^4J(4e,CF_nH_{3-n}-5)
CFH_2	Me	—	**1***a*	$CFHCl_2$	4.78	−31.34	3.56	−42.99	0.82		4.47	6.08	11.51	48.23	4.81	
CF_2H	Me	—	**1***b*	CS_2	4.66	−35.79	3.58	−58.01	0.77		6.08	5.90	11.76	55.43	3.36	1.38
CF_2H	Me	—	**1***b*	$CFHCl_2$	4.75	−34.76	3.68	−57.85	0.81		6.23	6.08	11.92	55.67		
CF_2H	Me	Me	*r*-2-Me-*trans*-5-*cis*-5′ (**1***h*)	CS_2	4.48		3.60	−58.05	0.70	1.23	6.12		11.68	56.34	3.72	1.35
CF_2H	Me	Me	*r*-2-Me-*trans*-5-*cis*-5′ (**1***h*)	$CFHCl_2$	4.57		3.69		0.74	1.29	6.28			56.14		
CF_2H	Me	Me	*r*-2-Me-*cis*-5-*trans*-5′ (**2***h*)	CS_2	4.39		3.58	0	1.24	1.23	5.30			55.95	—	—
CF_2H	Me	Me	*r*-2-Me-*cis*-5-*trans*-5′ (**2***h*)	$CFHCl_2$	4.50		3.71	0	1.32	1.31	5.40			55.02		

*Positive if He is upfield with respect to Ha. This is determined by n.m.d.r. and ^{19}F–H long-range couplings.

TABLE 2. Shift (in p.p.m. from TMS internal) and conformational data for 5-CF_2H-5′-Me-1,3-dioxane

Solvent	Substituent	5-CF_2H-5′-Me-1,3-dioxane (**1***b*)	*r*-2-Me-*trans*-5-CF_2H-*cis*-5′-Me-1,3-dioxane (**1***h*)	*r*-2-Me-*cis*-5-CF_2H-*trans*-5′-Me-1,3-dioxane (**2***h*)	% **1**	$\Delta\Delta G^0_{300}$ (cal/mol)
CS_2	Me-5′	0.770	0.699	1.239	86.85	1125
	CF_2H-5	6.084	6.118	5.296	95.86	1873
$CFHCl_2$	Me-5′	0.813	0.738	1.323	87.18	1143
	CF_2H-5	6.277	6.276	5.393	94.45	1690

Can. J. Chem. Downloaded from www.nrcresearchpress.com by 210.87.254.6 on 09/05/12
For personal use only.

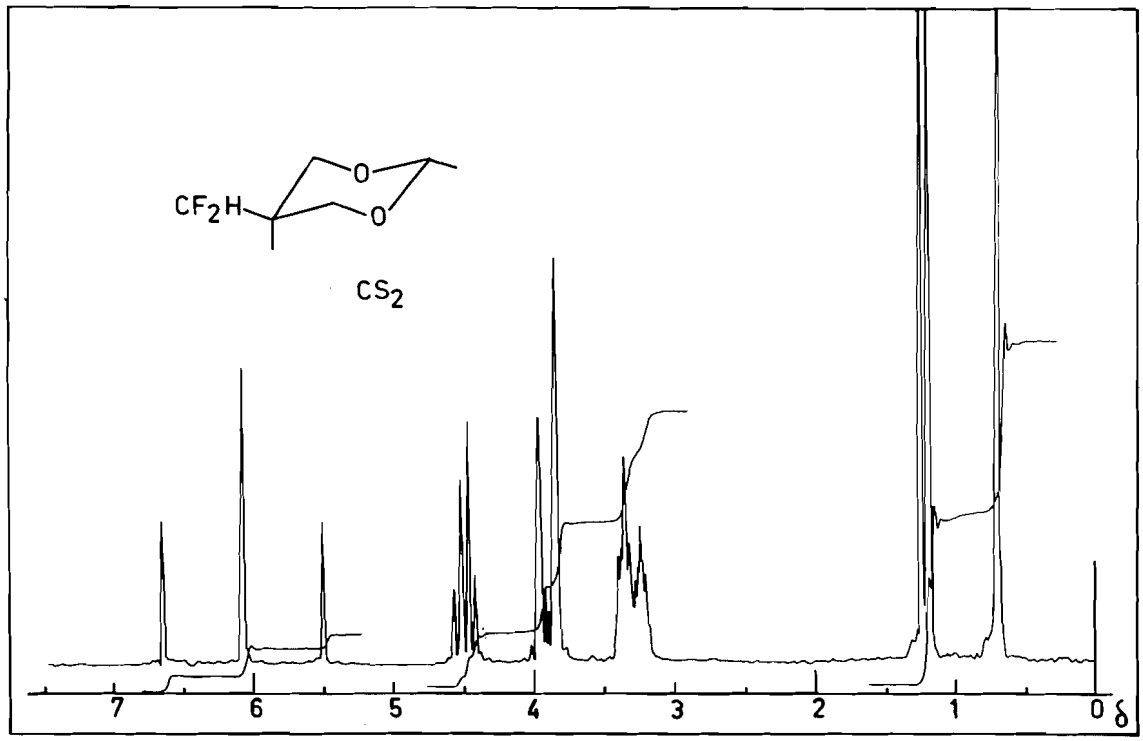

FIG. 2. The 100 MHz spectrum (CS_2, TMS int.) for *r*-2-Me-*trans*-5-CF_2H-*cis*-5′-Me-1,3-dioxane (1*h*).

Conformational Data for
5-CFH_2-5′-Me-1,3-Dioxane (1a)

This compound could be "frozen out" (T_c = 207.3 °K) and the appearance of a second Me peak shows the conformational system not to be biased. The AB spin system for H-2 however, remains unique (in $CHFCl_2$), showing accidental shift equivalency (isochronism) for both conformers. Table 3 gives us the variation of $\delta(2a \rightarrow 2e)$ in function of the temperature (173–300 °K). With the aid of a PDP-8/1 computer program (4), and following the procedure discussed in earlier papers (5), we obtain the data for $\Delta\Delta G^0$ gathered in Table 4.

It follows that $\Delta\Delta G^0{}_{300}$ (**1***a*) = 1.4 kcal/mol in favor of the axial Me conformer with $\Delta\Delta H^0$ (**1***a*) = 488 cal/mol and $\Delta\Delta S^0$ (**1***a*) = −3.0 e.u. It is interesting to note that we do not expect a large difference in $\Delta\Delta G^0$ on steric grounds (ΔG^0 (Me-5) = 0.9 kcal/mol and ΔG^0 (*t*.Bu-5) = 1.7 kcal/mol (2, 3). The observed difference is thus mainly due to electric contributions, disfavoring by mutual dipole–dipole orientation, the conformer with the axial CF_2H-substituent. Furthermore, again for electric (and presumably also steric) reasons the latter conformer is restricted in rotamers with respect to population as is depicted in Chart 2. This is the more plausible because it is in general difficult to locate the exact origin of the dipole vector (6).

Conclusion

Unfortunately we were unable to synthesize the 5-CF_3-5′-Me-1,3-dioxane. In view of the biased situation for the (less polar) CHF_2 derivative however, we may predict the compound to be anancomeric. It would be interesting

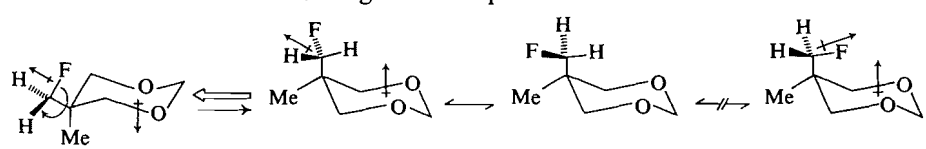

CHART 2

Can. J. Chem. Downloaded from www.nrcresearchpress.com by 210.87.254.6 on 09/05/12
For personal use only.

TABLE 3. Variation of $\delta(2a \rightarrow 2e)$ at 100 MHz in $CFHCl_2$ for 5-CFH_2-5′-Me-1,3-dioxane (1*a*) as a function of temperature

T^0	$\Delta\nu$ (Hz)
300	25.10
298	25.97
277.5	26.43
267	27.20
256	27.93
245	28.83
240	29.14
235	29.50
230	30.05
225	30.47
220	30.89
216	31.45
211	32.59
208	33.83
206	35.95
204	36.92
201	37.66
199	38.29
198	38.14
196	38.43
194	38.74
192	38.93
189.5	38.58
183	38.58
177	38.81
173	38.80

therefore to study the parent 5′-*t*.Bu derivative, but even the introduction of a 5-CF_2H together with a 5′-*t*.Bu group has failed until now. The conformational results for 5-CFH_2-5′-Me-1,3-dioxane show a pronounced preference for equatorial population of the polar substituent, both for ethalpy and entropy reasons. Undoubtedly entropy participation comes from the exclusions of rotamers, where the F atom is orientated over the ring, *e.g.* in close approach with the axial p-orbitals of the ring-oxygen atoms. Even some deformation (flattening) of the ring is suggested by the somewhat lowered (absolute) value observed for $^2J2$ (7).

TABLE 4. Thermodynamic parameters for the conformational equilibrium in 5-CFH_2-5′-Me-1,3-dioxane in favor of CFH_2 equatorial

T^0	$\Delta\Delta G^0$ (cal/mol)
200	1092
210	1136
220	1160
230	1292
240	1224
250	1254
260	1284
270	1314
280	1342
290	1370
300	1397

One of us (P.D) thanks the "Instituut voor Wetenschappelijk Onderzoek in Nijverheid en Landbouw (IWONL)" for a scholarship. The authors are indebted to the "Fonds voor Kollektief Wetenschappelijk Onderzoek" for financing their research.

1. P. DIRINCK and M. ANTEUNIS. Can. J. Chem. This issue.
2. E. L. ELIEL and M. KNOEBER, SR. J. Am. Chem. Soc. **88**, 5347 (1966).
3. F. RIDDELL. Tetrahedron, **23**, 3471 (1967).
4. J. GELAN. Ph.D. Thesis. State University of Gent, Gent, Belgium, 1971. *cf.* M. ANTEUNIS. *In* Conformational analysis. *Edited by* F. Chiurdoglu. Academic Press, N.Y. 1971. pp. 31–50.
5. J. GELAN and M. ANTEUNIS. Bull. Soc. Chim. Belges, **79**, 313 (1970); J. GELAN and M. ANTEUNIS. Bull. Soc. Chim. Belges, **78**, 599 (1969); E. COENE and M. ANTEUNIS. Bull. Soc. Chim. Belges, **79**, 25 (1970); W. VANDENBROUCKE and M. ANTEUNIS. J. Chem. Soc. In press.
6. *cf.* E. L. ELIEL. Svensk Kemisk Tidskrift, **81**, 7 (1969).
7. M. ANTEUNIS, G. SWAELENS, and J. GELAN. Tetrahedron, **27**, 1917 (1971).

The Racemization and Geometrical Isomerization of Oxiranes

HELEN H. J. MACDONALD AND ROBERT J. CRAWFORD
Department of Chemistry, University of Alberta, Edmonton 7, Alberta

Received August 4, 1971

Optically active *trans*-2-phenyl-3-*p*-tolyloxirane and *cis*-2-phenyl-3-*p*-tolyloxirane were synthesized and the kinetics of their racemization and geometrical isomerization were studied.

The slower rate of racemization of the *cis*-isomer compared with that of the *trans* is attributed to the con-rotatory opening of the oxirane ring.

Le *trans*-2-phényl-3-*p*-tolyloxiranne et le *cis*-2-phényl-3-*p*-tolyloxiranne optiquement actifs ont été synthétisés et les cinétiques de leur racémisation et isomérisation géométrique ont été étudiées.

La vitesse de racémisation plus lente de l'isomère *cis*, par rapport à celle de l'isomère *trans*, est attribuée à une ouverture con-rotatoire du cycle oxirannique.

Canadian Journal of Chemistry, **50**, 428 (1972)

Can. J. Chem. Downloaded from www.nrcresearchpress.com by 210.87.254.5 on 09/05/12
For personal use only.

Introduction

Convincing evidence for the cleavage of the carbon–carbon bond in an oxirane ring has been demonstrated by the addition of tetracyanoethylene oxide (TCNEO) to olefins (1). It has been shown that the reaction takes place in two steps, the first being the cleavage of the carbon–carbon bond with the formation of an intermediate. The intermediate was found to have little ionic character as ascertained by a study of solvent polarity and olefin substituent changes. Additional evidence of a reversible ring opening and closing at the carbon–carbon bond was provided by the observation that the racemization of *trans*-stilbene oxide proceeds 172 times faster at 220° than does the *trans* to *cis* isomerization (2).

The ring open form of oxiranes is a 4π electron system since the lone pair electrons on the oxygen mix with the p-orbitals on the terminal carbons. This system, with its highest occupied molecular orbital antisymmetric, resembles the allyl anion (3). Orbital symmetry considerations (4) suggest that a conrotatory mode of ring close is preferred, see Fig. 1.

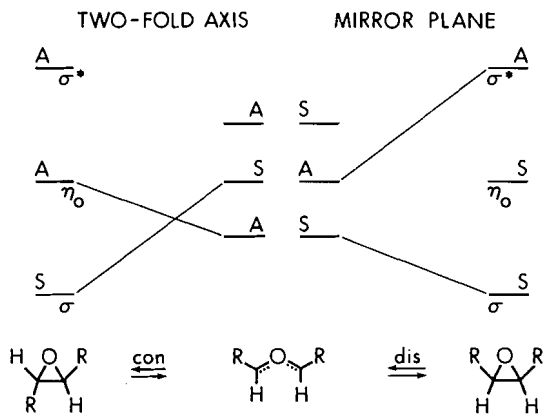

FIG. 1. Correlation diagram for the oxatrimethylene ring closure.

Recently a nonempirical self-consistent-field and configuration-interaction study of ethylene oxide, and other three-membered ring systems, has shown the open form to be essentially a linear combination of the resonance system, $C{=}\overset{+}{O}{-}\overline{C}\leftrightarrow\overline{C}{-}\overset{+}{O}{=}C$ and a diradical $\dot{C}{-}O{-}\dot{C}$ (5).

That the conrotatory mode is preferred in the ring opening of aziridines has been convincingly demonstrated by Huisgen *et al.* with the stereospecific conversion and trapping of the azomethine ylides (6). In the absence of a trapping agent some geometrical isomerization has been observed (7).

Arnold and coworkers (8) have elegantly demonstrated the existence of the open form of the oxirane ring in both the thermal and photochemical reactions of the 5-oxabicyclo[2.1.0]-pentane system. They were able to trap the intermediate by a 1,3-dipolar addition with benzonitrile. Such a ring opening is constrained to occur in a disrotatory mode. The driving force for Arnold and Karnischky's reaction is provided by the two phenyl groups and the ring strain of the 1,2-diphenyl-3,3,4,4-tetramethyl-5-oxabicyclo[2.1.0]pentane. The oxatrimethylene, or carbonyl ylide, intermediate has also been postulated in photochemical processes by Do-Minh *et al.* (9).

The preference of a conrotatory or dis-

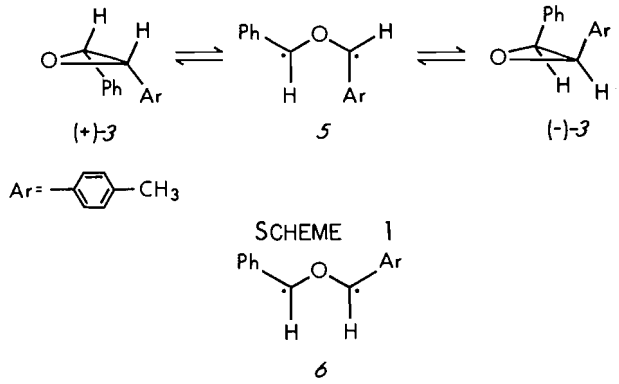

rotatory mode of ring opening and closing has not been demonstrated experimentally for oxiranes. Trapping agents are not as successful in competing with the ring closure in the oxirane–oxatrimethylene system as is the case in the aziridine system (2).[1] An alternative way to approach the problem is to note that in the oxatrimethylene species (**2**) the four ring substituents of the oxirane (**1**) have been rotated into the C—O—C plane and thus starting from a chiral oxirane we can detect the rate at which this isomerization proceeds by measuring the rate of loss of chirality by the oxirane. We have undertaken such a study choosing as our model compounds, *cis*-2-phenyl-3-*p*-tolyloxirane (**3**) and *trans*-2-phenyl-3-*p*-tolyloxirane (**4**).

If the conrotatory mode of ring opening is the reaction path then (+)-**3** will open to **5** and reclose to (±)-**3**, see Scheme 1. If however the disrotatory mode prevails then (+)-**3** would open to the more stable intermediate **6** and would reclose to (±)-**3**. The converse is true for (+)-**4**. Thus orbital symmetry considerations predict that the rate constant for the racemization of the *trans*-oxirane (**4**), k_t^a, will be larger than the rate constant for the racemization of the *cis*-oxirane (**3**), k_c^a.

Results

(a) Synthesis

The *trans*-oxirane ((−)-**4**) was obtained by treating the quaternary ammonium salt of (*1S*:*2R*)-(+)-2-amino-2-phenyl-1-*p*-tolylethanol (**7**) with silver oxide. The alcohol (+)-**7** was obtained using (+)-glutamic acid in 50% ethanol and the configurations assigned by comparison

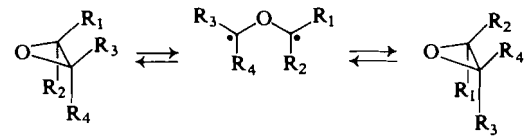

with the assignments of configuration to 2-amino-1,2-diphenylethanol (**10**). The *cis*-oxirane (**3**) was obtained by inversion of the hydroxyl group of (+)-**7** to give (−)-**8** by the oxazoline method (11). The synthesis of (+)-**3** is outlined in Scheme 2.

(b) Kinetic Studies

Of the several solvent systems investigated chlorobenzene was found to be the most suitable over the temperature range required. One factor in its choice was its lack of absorption in the region of the n.m.r. spectrum of the oxiranes ring hydrogen. Initially some erratic rates were observed with the intervention of other products in the higher temperature runs. These products were also produced if a small amount of hydrogen chloride was added. This side reaction was prevented by carefully distilling the solvent immediately before it was used, and by adding a small amount of anhydrous sodium carbonate to each tube. The rate of disappearance of the n.m.r. absorption attributed to the ring protons of **3**, and the appearance and increase in the absorption of the signal attributed to the ring protons of **4** were carefully measured. The reaction was found to follow first order kinetics and the slope of $\ln (P_t - P_\infty)/P_0 - P_\infty)$ *vs.* time gave k_{obs}, where P_t is the percentage of **3** present at time t, P_0 is the percentage of **3** at $t = 0$, and P_∞ is the percentage of **3** at equilibrium.

The kinetic data for the *cis–trans* equilibration are presented in Table 1. The value of K_{eq}

[1]NOTE ADDED IN PROOF: Huisgen *et al.* (16) have now provided evidence for the conrotatory ring opening of oxiranes.

Can. J. Chem. Downloaded from www.nrcresearchpress.com by 210.87.254.5 on 09/05/12
For personal use only.

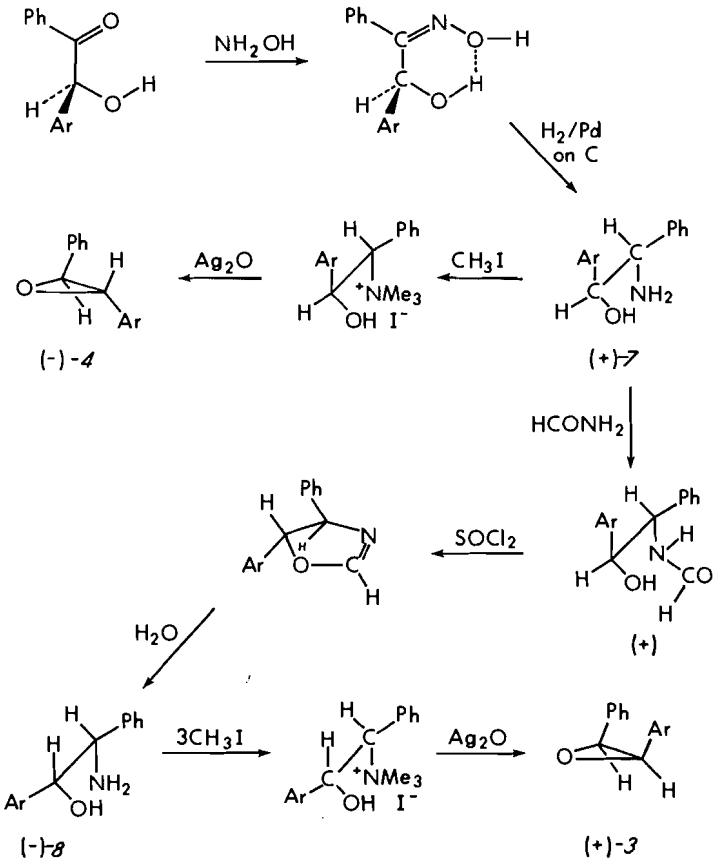

SCHEME 2

TABLE 1. Kinetic data for the interconversion of **3** and 4

Temperature (±0.05°)	$-10^5 k_{obs}$ (s^{-1})	$10^5 k_{tc}$	$10^5 k_{ct}$
229.14	3.16±0.08	0.301*	2.86*
239.69	6.89±0.06	0.657	6.26
246.15	11.6 ±0.2	1.22	10.5
	E_a kcal mol^{-1}	39.6±0.8	39.6±0.5
	log A	11.72	12.68
	$\Delta S^{\ddagger}$ cal deg^{-1} mol^{-1}	−8±3	−3±2

*Obtained from $K_{eq} = 9.52$ and that $k_{obs} = k_{tc} + k_{ct}$; where k_{tc} and k_{ct} are the rate constants for *trans* to *cis* and *cis* to *trans* isomerization.

TABLE 2. Kinetic data for the racemization of **3***

Temperature (±0.05°)	$-10^5 k^a_{obs}$ (s^{-1})	k^a_c (s^{-1})	E_a (kcal mol^{-1})	log A	$\Delta S^{\ddagger}$
225.32	2.96±0.03	0.86†	41.1±0.6	12.96	−2±2
247.59	16.7 ±0.2	5.10			

*Because of scarcity of sample, kinetic data were only obtained at two temperatures.
†Obtained by subtracting k_{ct} from k^a_{obs}.

Can. J. Chem. Downloaded from www.nrcresearchpress.com by 210.87.254.5 on 09/05/12
For personal use only.

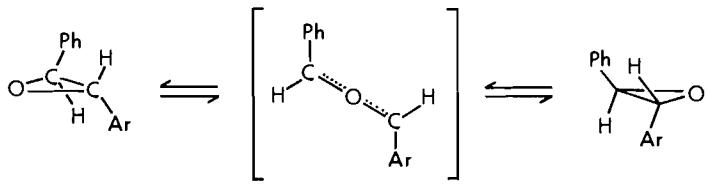

SCHEME 3

was found to be essentially constant over the temperature range examined ($K_{eq} = [trans]/[cis] = 9.52$).

The racemization of **3** was conveniently measurable in the temperature range 225–250°. At these temperatures the conversion of **3** to **4** is also occurring and so the observed rate must be corrected to account for the formation of **4**. Several samples from the racemization studies were checked using n.m.r. to see that the geometrical isomerization was proceeding in the normal fashion. In each instance excellent agreement between the calculated percentage of **3** and the observed percentage of **3** was obtained. The rate constants, k_c^a, and activation parameters for the racemization of **3** are given in Table 2.

The racemization of **4** was found to be considerably more facile than the other processes studied and was found to be conveniently measurable in the temperature range of 180–210°. The rate constants for the racemization of the *trans*-isomer **4**, k_t^a, are listed in Table 3 along with the activation parameters.

Discussion

At 207.2° the *trans*-oxirane (**4**) racemizes sixty times faster than the *cis*-oxirane (**3**). This may be rationalized by the conrotatory ring opening of **3** producing the oxatrimethylene intermediate (**5**) wherein one of the bulky aryl groups is in a sterically crowded configuration, whereas **4** racemizes via **6**. Although the ground state for the racemization of the *cis*-isomer is 2.2 kcal mol^{-1} higher than that of the *trans*-isomer, the bulky aryl group on the inside of the C—O—C angle in **5** causes sufficient destablization to increase the barrier to its formation by 6 kcal mol^{-1}. This is consistent with, and best explained by, the conrotatory mode of oxirane ring opening. There are few other methods by which simultaneous inversion of two asymmetric centers can occur. One alternative route would be to force the oxygen of the oxirane through a point between the two carbons to the opposite side as per Scheme 3. It is difficult to see how the *cis*-oxirane (**3**) would be at such a disadvantage relative to the *trans*-isomer in the racemization process in such a scheme.

Huisgen *et al.* (7) have recently presented a reaction scheme to explain both the geometrical and optical isomerization of aziridines. The analogous route for the oxiranes is presented in Scheme 4 with the corresponding reaction coordinate as Fig. 2. This implies that *cis* to *trans* isomerization proceeds by going through both intermediates. The possibility also exists that a non-allowed disrotatory ring closure converts **5** to **4** and **6** to **3**. Such a process would be controlled by the splitting between the highest occupied molecular orbital and the lowest unoccupied molecular orbital. There also exists the possibility that the *cis–trans* isomerization

TABLE 3. Kinetic data for the racemization of **4**

Temperature (±0.05°)	$-10^5 k_t^a$ (s^{-1})	E_a (kcal mol^{-1})	log A
179.82	1.09±0.01		
197.22	4.75±0.03	35.9±0.5	12.34
207.21	10.5 ±0.5		

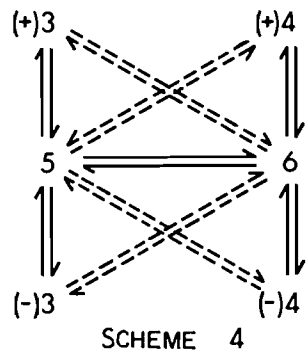

SCHEME 4

Can. J. Chem. Downloaded from www.nrcresearchpress.com by 210.87.254.5 on 09/05/12
For personal use only.

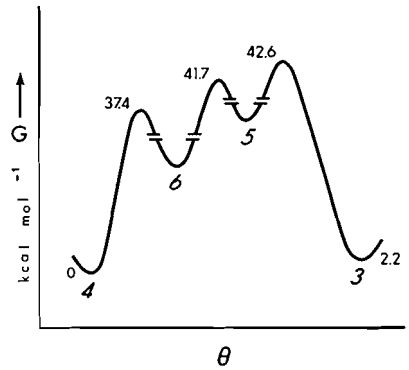

FIG. 2. Reaction coordinate wherein **5** and **6** are intermediates on the reaction path. Numbers indicate energies in kcal mol^{-1} relative to **4** being zero.

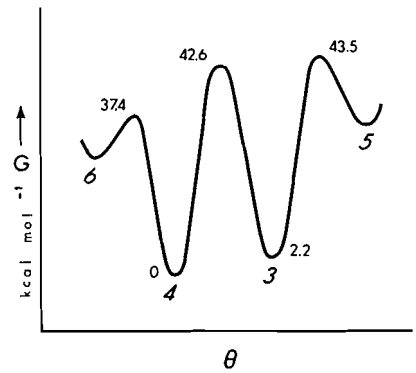

FIG. 3. Reaction coordinate wherein **5** and **6** are formed independently of the geometrical isomerism **4**⇌**3**. The numbers indicate energies in kcal mol^{-1} relative to **4** being zero.

is independent of the racemization processes as indicated in the reaction coordinate in Fig. 3. While the oxatrimethylene species are useful in rationalizing the TCNEO cycloaddition and other reactions (7) as well as the racemization process, a more subtle probe may be required to define the mode of geometrical isomerization.

Experimental

Microanalyses were performed by the Microanalytical Laboratory, Department of Chemistry, University of Alberta. Mass spectra were measured using an A.E.I. MS-2 spectrometer at an ionization potential of 70 eV. The n.m.r. spectra were recorded on a Varian Associates A-60, A-56-60-A, and A-60D using TMS as internal standard and $CDCl_3$ as solvent unless otherwise stated.

4-Methylbenzoin

The procedure used was similar to that of Fuson *et al.* (12) except toluene was used as the solvent. Yield of white needle-like crystals was 59%, m.p. 119–129°; i.r. (KBr discs) ν_{max} 3400 (O—H) and 1670 cm^{-1} (C=O); n.m.r. τ 7.7 (s, 3, methyl), 5.55 (S, 1H, OH), 4.1 (S, 1H, methine), 2.5 (m, 9H, aromatics).

Anal. calcd. for $C_{15}H_{14}O_2$: C, 79.62; H, 6.24. Found: C, 79.52; H, 6.31.

4-Methylbenzoin Oxime

The method used was essentially that of Goldschmidt and Polonowska (13). The yield of white crystals was 87.6%, m.p. 139–139.5°; i.r. (Nujol) ν_{max} 1675 cm^{-1} (C=N); n.m.r. τ 7.92 (s, 3H, methyl), 4.42 (q, 2H methine and OH), 2.98 (d, 9H, aromatics), 0.5 (s, 1H, NOH) with D_2O exchange of NOH and OH hydrogens was observed.

Anal. Calcd. for $C_{15}H_{15}O_2N$: C, 74.66; H, 6.27; N, 5.81. Found: C, 74.41; H, 6.06; N, 5.83.

erythro-2-Amino-2-phenyl-1-p-tolylethanol (7)

The hydrogenation of 4-methylbenzoin oxime using Pd-on-charcoal in ethanol was analogous to the procedure of Huffman and Elliot (14). Needle-like crystals were obtained in a 96% yield, m.p. 142–143°; i.r. (KBr discs) ν_{max} 3410 (O—H), 3360, and 3295 cm^{-1} (NH_2); n.m.r. τ 7.99 (s, 3H, NH_2 and OH), 7.68 (s, 3H, methyl), 5.62 (2d, chemical shift difference 35 cps, 2H methines), 2.89 (s, 4H, aromatics), 2.72 (s, 5H, aromatics) with D_2O the NH_2 and OH protons exchanged; M (mass spectrometry), 227.

Anal. Calcd. for $C_{15}H_{17}ON$: C, 79.26; H, 7.54; N, 6.16. Found: C, 79.26; H, 7.44; N, 6.16.

The hydrochloride was prepared by adding **7** to a 1:1 ether–ethanol solution containing excess hydrochloric acid.

The method of resolution of **7** was essentially that of Tishler *et al.* (10*d*) using L-(+)-glutamic acid in 50% ethanol. $[\alpha]_D^{20}$ + 5° (*c*, 1.0, ethanol).

(2S:3S)-(−)-2-Phenyl-3-p-tolyloxirane (4)

The quaternary ammonium salt of (+)-**7** (3.6 g, 9 mmol) was treated with silver oxide (about 3 g, 9.6 mmol) in water and the solution was steam distilled, as described by Read and Campbell (15), yielding 1.47 g of **4** (7 mmol, 7690), m.p. 76–76.5°, $[\alpha]_D^{20}$ −380° (*c*, 0.16, ethanol); n.m.r. τ 7.65 (s, 3H, methyl), 6.18 (s, 2H, methines), 2.78 (s, 4H, aromatics), and 2.65 (s, 5H, aromatics); M (mass spectrometry), 210.

Anal. Calcd. for $C_{15}H_{14}O$: C, 85.67; H, 6.71. Found: C, 85.56; H, 6.62.

(1R:2R)-(−)-2-Amino-2-phenyl-1-p-tolylethanol (8)

The hydrochloride of (+)-**7** was treated with formamide to give the *N*-formyl derivative and this in turn was treated with thionyl chloride as described by Attenburrow *et al.* (11). Care was taken to purify **10** by several recrystallizations from 60% ethanol; $[\alpha]_D^{20}$ −141° (*c*, 1.7, ethanol), m.p. 116–118°; n.m.r. τ 7.72 (s, 6H, methyl, NH_2 and OH), 5.72 (2d, chemical shift difference 40 Hz, 2H, methines), 2.98 (s, 4H, aromatics), 2.82 (s, 5H, aromatics) with D_2O the NH_2 and OH protons exchanged.

Anal. Calcd. for $C_{15}H_{17}NO$: C, 79.26; H, 7.54; N, 6.16. Found: C, 78.98; H, 7.46; N, 6.24.

(2S:3R)-(+)-2-Phenyl-3-p-tolyloxirane (3)

The quaternary ammonium salt of (−)-**8** was prepared by heating (−)-**8** to reflux in the presence of iodomethane, anhydrous sodium carbonate and anhydrous methanol for 3–4 days. The oxirane (**3**) was prepared in a similar manner to **4**. The yield of pale yellow oil was 70%; $[\alpha]_D^{20}$ +12.8° (*c*,

Can. J. Chem. Downloaded from www.nrcresearchpress.com by 210.87.254.5 on 09/05/12
For personal use only.

1.7, ethanol); n.m.r. τ 7.8 (s, 3H, methyl), 5.72 (s, 2H, methines), 3.02 (s, 4H, aromatics), and 2.88 (s, 5H, aromatics); M (mass spectrometry), 210.

Anal. Calcd. for $C_{15}H_{14}O$: C, 85.67; H, 6.71. Found: C, 85.46; H, 6.74.

Kinetic Studies

The racemization studies were carried out using 1.00 ml aliquots of the respective solutions which were placed in ampoules of 2 mm walled glass tubing with an inner diameter of 0.5 cm and about 1.5 cm long. Each sample was degassed on a vacuum rack with liquid nitrogen cooling during evacuation. Three freeze–degas–thaw cycles were performed on each ampoule. After the appropriate times in the constant temperature bath the samples were immediately quenched in an ice-water bath. Each ampoule contained about 15 mg anhydrous potassium carbonate to prevent any acid-catalyzed reactions. Infinity tubes were checked by n.m.r. and the only products observed were **3** and **4**.

The authors wish to acknowledge the support of the National Research Council of Canada. They also wish to thank Prof. T. R. Lynch for some early exploratory work and Mr. Utz Liebe for some technical assistance.

1. W. J. LINN AND R. E. BENSON. J. Am. Chem. Soc. **87**, 3657 (1965).
2. T. R. LYNCH. Unpublished data from this laboratory.
3. R. HOFFMANN. J. Am. Chem. Soc. **90**, 1475 (1968).
4. R. B. WOODWARD and R. HOFFMANN. Angew. Chem. *Int. Ed.* **8**, 1475 (1969).
5. E. F. HAYES and A. K. Q. SIU. J. Am. Chem. Soc. **93**, 2090 (1971).
6. R. HUISGEN, W. SCHEER, and H. HUBER. J. Am. Chem. Soc. **89**, 1753 (1967).
7. R. HUISGEN, H. MADER, and H. HERMANN. J. Am. Chem. Soc. **93**, 1779 (1971).
8. D. R. ARNOLD and L. A. KARNISCHKY. J. Am. Chem. Soc. **92**, 1404 (1970); D. R. ARNOLD, A. B. EVNIN, and P. H. KASAI. J. Am. Chem. Soc. **91**, 784 (1969).
9. T. DO-MINH, A. M. TROZZOLO, and G. W. GRIFFIN. J. Am. Chem. Soc. **92**, 1402 (1970).
10. (*a*) J. WEIJLAND, K. PFISTER, E. F. SWANZEY, C. A. ROBINSON, and M. TISHLER. J. Am. Chem. Soc. **73**, 1216 (1951); (*b*) A. WEISBERGER and H. BACK. Ber. **64**, 1094 (1934); **65**, 63 (1935); (*c*) A. MACKENZIE and D. J. C. PIRIE. Ber. **69**, 876 (1936).
11. J. ATTENBURROW, D. F. ELLIOT, and G. F. PENNY. J. Chem. Soc. 310 (1948); C. PFISTER, C. A. ROBINSON, A. C. SHABICA, and M. TISHLER. J. Am. Chem. Soc. **70**, 2297 (1948); **71**, 1101 (1949).
12. R. C. FUSON, W. S. EMERSON, and H. H. WEINSTOCK. J. Am. Chem. Soc. **61**, 412 (1939).
13. H. GOLDSCHMIDT and N. POLONOWSKA. Ber. **20**, 492 (1889).
14. J. W. HUFFMANN and R. P. ELLIOT. J. Org. Chem. **30**, 365 (1965).
15. J. READ and I. G. CAMPBELL. J. Chem. Soc. 412 (1939).
16. H. HAMBEIGER and R. HUISGEN. Chem. Commun. 1190 (1971); A. DAHMEN, H. HAMBEIGER, R. HUISGEN, and V. MARKOWSKI. 1192 (1971).

Can. J. Chem. Downloaded from www.nrcresearchpress.com by 210.87.254.5 on 09/05/12
For personal use only.

The Mechanism for Hydrolysis of Primary Alkyl Chlorosulfates in Water. The Kinetic Solvent Isotope Effect and the Secondary Deuterium Isotope Effect

E. C. F. Ko[1] AND R. E. ROBERTSON

Department of Chemistry, University of Calgary, Calgary 44, Alberta

Received September 17, 1971

The temperature coefficients of the enthalpy of activation ($\Delta C_p^{\ddagger}$) for the hydrolysis of the three chlorosulfates, methyl, ethyl, and β-chloro, are shown to have values of -50, -55, and -60 cal deg^{-1} mol^{-1}; values in the same range as previously reported for the hydrolysis of the sulfonyl chlorides. The corresponding value for the β-methoxy isomer was -40 cal deg^{-1} mol^{-1}, about the same as found for the *p*-methoxybenzenesulfonyl chloride. The kinetic solvent isotope effect, however, was significantly lower than reported for the sulfonyl chloride series, being about the same as found for the hydrolysis of the alkyl halides. While some degree of nucleophilic overlap is probably required in the activation process, the requirement here is reduced to about the same level as that for the primary halides, and there is no need to postulate a different mechanism on passing from the methyl to the ethyl member of the series, confirming the earlier conclusion of Buncel and Millington.

On montre que les coefficients de température de l'enthalpie d'activation ($\Delta C_p^{\ddagger}$) pour l'hydrolyse des trois chlorosulfates, méthyle, éthyle, et β-chloro, ont les valeurs de -50, -55, et -60 cal deg^{-1} mol^{-1}; valeurs se situant dans le même domaine que celle rapportées précédemment pour l'hydrolyse des chlorures de sulfonyl. La valeur correspondante pour l'isomère β-méthoxy était de -40 cal deg^{-1} mol^{-}, environ la même que celle trouvée pour le chlorure de *p*-méthoxybenzènesulfonyl. L'effet cinétique de solvant isotopique était toutefois largement plus faible que celui rapporté pour la série des chlorures de sulfonyl et ressemblait à celui qu'on avait trouvé pour l'hydrolyse des halogénures d'alkyles. Alors que le procédé d'activation demande un certain degré de recouvrement nucléophilique, le recouvrement dans le cas qui nous concerne est réduit environ au même niveau que dans le cas des halogénures primaires, sans besoin de postuler un mécanisme de passage différent du méthyle à l'éthyle dans la série, confirmant une conclusion précédente de Buncel et Millington.

Canadian Journal of Chemistry, **50**, 434 (1972)

Introduction

Three possible mechanistic pathways have been proposed (1–6) for nucleophilic displacement reactions involving alkyl chlorosulfates. These proposals are summarized in eqs. 1–3.

Pathway 2 would lead to an alkylhydrogen sulfate which is stable under our reaction conditions and is not found among the reaction products. The final products for paths 1 and 3 are the same and can be represented by the overall equation:

[4] $ROSO_2Cl + 2H_2O \rightarrow ROH + 3H^+ + SO_4^{2-} + Cl^-$

Current opinions (3, 4) favor the mechanism

(1) Nucleophilic displacement at carbon

$$\overset{\delta+}{R}\ \ldots\overset{\delta-}{O}SO_2Cl \xrightarrow[H_2O]{S_N2} \text{Products} \qquad [a]$$

[1] $ROSO_2Cl \rightleftarrows$

$$\overset{\delta+}{ROSO_2}\ \ldots\ \overset{\delta-}{Cl} \xrightarrow{S_N1} R^+ \,\|\, OSO_2Cl$$

$$\text{or} \longrightarrow \text{Products} \qquad [b]$$

$$\overset{\delta+}{ROSO_2} \,\|\, \overset{\delta-}{Cl}$$

(2) Nucleophilic displacement at sulfur

[2] $ROSO_2Cl + H_2O \rightarrow \langle ROSO_2 \ldots Cl\rangle \rightarrow ROSO_2OH + Cl^- + H^+$

(3) Fragmentation

[3] $ROSO_2Cl \rightarrow \langle R^+ \ldots OSO_2 \ldots Cl^-\rangle \rightarrow R^+ + SO_3 + Cl^- \rightarrow \text{Products}$

[1]Postdoctoral Fellow 1970–1972.

Can. J. Chem. Downloaded from www.nrcresearchpress.com by 84.22.46.98 on 09/08/12
For personal use only.

TABLE 1. Empirical constants for eq. 5

Chlorosulfate	A_1	$-A_2$	$-A_3$	$n_{T_1}^{T_2}$*
Methyl	83.16664	7456.099	24.22491	$29_{0.1}^{20}$
Ethyl	91.09558	7998.382	26.63965	$39_{0.3}^{20}$
β-Methoxyethyl	67.89214	7076.117	18.99437	$26_{1.0}^{43}$
β-Chloroethyl	99.32613	8598.823	29.83195	$25_{1.5}^{55}$

*n is number of rate constants with a temperature range from T_1 to T_2.

represented by eq. 1. However, if the R group is neopentyl, Buncel and Millington suggest (4, 5) that mechanism 3 is probable.

While direct attack of water on the methyl carbon of methyl chlorosulfate is acceptable, a rate determining ionization of the sulfur–chlorine bond was suggested for the ethyl chlorosulfate followed by a rapid reaction of the nucleophile with the ethoxysulfonylium ion at carbon.[2] If the ethyl compound reacts by a rate controlling ionization [1*b*], this fact should be evident by the contrast between the value of $\Delta C_p^{\ddagger}$ for the hydrolysis of this compound in water and that for the hydrolysis of the methyl isomer (6).

There is always the possibility that no one mechanism is dominant resulting in "mixed kinetics". If such a complexity is present, this too will be apparent in the value of $\Delta C_p^{\ddagger}$. Accordingly, to determine whether significant differences exist in charge development at the transition state for the hydrolysis of methyl and ethyl chlorosulfates and two related compounds, we have determined the temperature dependency of the rate for hydrolysis in water over a sufficient range of temperature to permit an estimate of the temperature coefficient of $\Delta H^{\ddagger}$.

Results and Discussion

Rate constants[3] for the hydrolysis of methyl, ethyl, β-methoxyethyl, and β-chloroethyl chlorosulfates were measured over a temperature range of at least 20°. These rate data were fitted to the usual empirical three constant equation

[5] $$\log_{10} k = A_1 + A_2/T + A_3 \log_{10} T$$

The corresponding values of the empirical constants, A_1, A_2, and A_3 are given in Table 1 and provide a convenient means for calculating the rate of hydrolysis at temperatures within the experimental range and for short extrapolations outside that range. Pseudo-thermodynamic parameters for the activation processes have been calculated from eq. 5 according to the method of Clarke and Glew (7) and making the usual assumptions regarding the attenuation of the rate–temperature relation (6). The values of $\Delta H^{\ddagger}$, $\Delta S^{\ddagger}$, and $\Delta C_p^{\ddagger}$ are given in Table 2. Rate constants calculated for 25 °C and corresponding relative rates are given in Table 3.

Rossal and Robertson have shown from a consideration of kinetic solvent isotope effects (k.s.i.e.) that there is good evidence for nucleophilic interaction at the transition state in the hydrolysis of a series of benzenesulfonyl chlorides (8) in contrast to the rather small to negligible effect in the hydrolysis of the alkyl halides (6) and the even smaller effect for the hydrolysis of alkylbenzenesulfonic esters (9). This rate ratio thus provides an indication of the presence or absence of nucleophilic interaction in excess of interactions present in bulk solvent. According to this criteria, it is apparent (Table 3) that nucleophilic interaction up to the transition state is small or absent in the hydrolysis of the four chlorosulfates studied here.

Initial State Interaction

Interpretation of $\Delta C_p^{\ddagger}$ and k.s.i.e. values for ionogenic reactions in water depend largely on changes in water structure in the activation process either as a consequence of change of temperature, or of isotopic substitution. The conclusions are suggestive rather than final. These effects depend to an important degree on the nature of solvation of the reactants in the initial state (6), the dominant feature of the solution of many non-electrolytes in water being the fact that water–water interaction > water solute interaction. The alkyl chlorosulfates are relatively insoluble, the tendency of the sulfonyl oxygens to hydrogen bond with water being

[2]For a review of other possibilities under varying conditions see Buncel (5).

[3]Individual values of rates are available from the Depository of Unpublished Data, National Science Library, National Research Council of Canada, Ottawa, Canada K1A 0S2.

Can. J. Chem. Downloaded from www.nrcresearchpress.com by 84.22.46.98 on 09/08/12
For personal use only.

TABLE 2. Pseudothermodynamic activation parameters for the hydrolysis of chlorosulfates

Chlorosulfates	$\Delta H^{\ddagger}$ (cal mol^{-1})	$\Delta S^{\ddagger}$ (cal mol^{-1} deg^{-1})	$-\Delta C_p^{\ddagger}$ (cal mol^{-1} deg^{-1})
Methyl	19923.5 ± 3.8	0.19 ± 0.02	50 ± 1
Ethyl	21046.0 ± 4.5	4.58 ± 0.02	55 ± 1
β-Methoxyethyl	20531.8 ± 16.5	−2.68 ± 0.05	40 ± 4
β-Chloroethyl	20465.5 ± 6.1	−5.11 ± 0.02	61 ± 1

TABLE 3. The kinetic solvent isotope effect (k_{H_2O}/k_{D_2O}) and the secondary deuterium isotope effect (k_H/k_D) for the hydrolysis of chlorosulfates

Chlorosulfate	Temperature (°C)	Solvent	$10^3\,k(s^{-1})$	k_{H_2O}/k_{D_2O}
Methyl	10.087	H_2O	2.751*	1.23
		D_2O	2.236	
Ethyl	10.083	H_2O	3.405*	1.20
		D_2O	2.830	
				k_H/k_D
Methyl-d_3	10.087	H_2O	2.894	0.951

*Calculated from eq. 5.

TABLE 4. Rate constants at 25° and their relative rate for the hydrolysis of chlorosulfates

Chlorosulfate	$10^3k(s^{-1})$*	Relative rate
Methyl	16.44	35
Ethyl	22.46	48
β-Methoxyethyl	1.442	3
β-Chloroethyl	0.4666	1

*Calculated from eq. 5.

somewhat less than that of the oxygens in the sulfonyl chlorides according to the test used by Kartha and co-workers (10), Table 5. This tendency is significantly less than the interaction found for the alkyl sulfonic esters according to the same test (10). The greater value of $\Delta\nu$ for the 2-methoxyethylchlorosulfate is attributed to interaction of water with the ether oxygen rather than with the sulfonyl oxygens, rate comparison (Table 4) showing the electronic effect of MeO and Cl are similar. Hence, the effect of the methoxy group on the hydrogen bonding of the sulfonyl oxygens is in the direction of reduced interaction in the initial state solvation shell. This is the opposite effect to that required to account for the change in $\Delta C_p^{\ddagger}$.

The k.s.i.e. for the four chlorosulfates are in the narrow range 1.2–1.25 (Table 3) about the same as found for the hydrolysis of the alkyl halides (6); significantly higher than recorded for the hydrolysis of the alkyl benzenesulfonates and significantly less than the corresponding values found for the substituted benzenesulfonyl chlorides (1.3–1.9). That the ratio k_{H_2O}/k_{D_2O} is higher than that for the sulfonic esters may be attributed to the greater degree of interaction of the latter with water in the initial state and the more diffused charge in the leaving group. That the value of k.s.i.e. for the chlorosulfates is significantly less than found for the sulfonyl chlorides and about the same as found for the halides, does not necessarily imply the absence of nucleophilic interaction at the transition state but rather that if such interaction is required, it is similar to that required in the hydrolysis of a primary halide. The inverse secondary deuterium isotope effect ($k_H/k_D = 0.95$), Table 3, is similar to that found in the hydrolysis of the methyl halides (11) and is at least consistent with the above hypothesis. The same conclusion is supported by the values of $\Delta C_p^{\ddagger}$.

Heat Capacity of Activation

The values of the temperature coefficient of the enthalpy of activation for three of the chlorosulfates (Table 5) are about the same as reported for the sulfonyl chlorides (8). It is probable that the initial state interaction of the chlorosulfates is, if anything, less than that of the sulfonyl

Can. J. Chem. Downloaded from www.nrcresearchpress.com by 84.22.46.98 on 09/08/12
For personal use only.

TABLE 5. Relative tendency of sulfonyl oxygens to hydrogen bond

Compound	$\Delta\nu(cm^{-1})$	$-\Delta C_p^{\ddagger}$ (cal mol^{-1} deg^{-1})	Reference
ClC_6H_4OH	0		This work
CH_3OSO_2Cl	38	50	"
$CH_3CH_2OSO_2Cl$	48	55	"
$CH_3OCH_2CH_2OSO_2Cl$	88	40	"
$ClCH_2CH_2OSO_2Cl$	30	61	"
$MeOSO_2Me$	118	38	10
$MeOSO_2C_6H_5$	111	36	10
$MeSO_2Cl$	60	55	10
p-$CH_3C_6H_5SO_2Cl$	65	72	10

chlorides (Table 5), hence the charge distribution on the chloride at the transition state is similar. Were the product forming step to occur subsequent to the transition state, we would have expected a much more negative value of $\Delta C_p^{\ddagger}$. Thus the value of this coefficient for the hydrolysis of dimethylsulfamoyl chloride is -76 cal deg^{-1} mol^{-1} (12) an example of a sulfonyl chloride where structural considerations predicate an S_N1 mechanism. Such steric hindrance to nucleophilic interaction is absent in the chlorosulfate series.

The value of $\Delta C_p^{\ddagger}$ is somewhat lower for the β-methoxyethyl isomer, an effect which was also observed for the hydrolysis of p-methoxybenzenesulfonyl chloride (13) and was attributed in the latter case to the effect of temperature on the interaction of the methoxy group with adjacent water molecules. We have advanced arguments why similar effect will account for the abnormal values of ΔC_p found for the ionization of benzoic acids substituted with the methoxy group (13). We do not regard the more positive value of $\Delta C_p^{\ddagger}$ found for this member of the series reflects a breakdown of water structure about the sulfonyl group in the initial state since the effect of the methoxy group on the rate is similar to that of the β-chloro substituent.

From the above evidence we conclude that there is no substantial difference in mechanism between the four members of the chlorosulfate series reported here. This conclusion confirms the earlier conclusion reached by Buncel and Millington on other evidence (3, 4). From a consideration of isotope effects and a comparison of $\Delta C_p^{\ddagger}$ values with the corresponding values found for the sulfonyl chloride series, some small degree of bonding between water and carbon is required in the activation process for the examples studied.

Experimental

Alkyl chlorosulfates were made by the reaction of sulfuryl chloride and the appropriate alcohol at low temperature as outlined by several workers (14–16). Two to three vacuum distillations on a spinning band column furnished the pure product on basis of the homogeneous absorption on a 5% silicone–gum–rubber column on an analytical v.p.c. and on n.m.r., b.p. methyl, 24–25/~2.5 (lit. 48/29, (14)); methyl-d_3, 22–23/~2.5; ethyl, 23/~2 (lit. 42/10, (14)); β-methoxy, 72/~15; and β-chloroethyl, 58/~3.

The purification of solvents and the procedures of kinetic measurements were as reported in the previous paper (17).

The hydrolyses gave cleanly reaction products analyzed by titration and v.p.c. as summarized in eq. 4.

1. J. GUGOT and L. J. SIMMON. Compt. Rend. **170**, 326 (1920).
2. H. K. HALL, JR. J. Am. Chem. Soc. **78**, 1450 (1956).
3. E. BUNCEL and J. P. MILLINGTON. Can. J. Chem. **43**, 547 (1965).
4. E. BUNCEL and J. P. MILLINGTON. Can. J. Chem. **43**, 556 (1965).
5. E. BUNCEL. Chem. Revs. **70**, 323 (1970).
6. R. E. ROBERTSON. Progr. Phys. Org. Chem. **5**, 121 (1967).
7. E. C. W. CLARKE and D. N. GLEW. Trans. Faraday Soc. **62**, 539 (1966).
8. B. ROSSALL and R. E. ROBERTSON. Can. J. Chem. **49**, 1451 (1971).
9. P. M. LAUGHTON and R. E. ROBERTSON. Can. J. Chem. **34**, 1714 (1956); **35**, 1319 (1957).
10. V. KARTHA, R. N. JONES, and R. E. ROBERTSON. Proc. Indian Acad. Sci. **58A**, 216 (1963).
11. K. T. LEFFEK, J. A. LLEWELLYN, and R. E. ROBERTSON. Can. J. Chem. **38**, 2171 (1960).
12. E. C. F. KO and R. E. ROBERTSON. J. Am. Chem. Soc. In press.
13. B. ROSSALL and R. E. ROBERTSON. Can. J. Chem. **49**, 1441 (1971).
14. W. W. BRINKLEY and E. F. DEGERING. J. Am. Chem. Soc. **60**, 2810 (1938).
15. J. CHARALAMBOUS, H. J. DAVIES, M. J. FRAZER, and W. GERRARD. J. Chem. Soc. 1505 (1962).
16. J. CHARALAMBOUS, M. J. FRAZER, and W. GERRARD. J. Chem. Soc. 5480 (1964).
17. R. E. ROBERTSON, B. ROSSALL, S. E. SUGAMORI. Can. J. Chem. **47**, 4199 (1969).

Can. J. Chem. Downloaded from www.nrcresearchpress.com by 84.22.46.98 on 09/08/12
For personal use only.

Sur la réduction par les hydrures complexes de quelques benzylidène-3 camphres

JEAN-CLAUDE RICHER ET ARMAND ROSSI[1]

Département de chimie, Université de Montréal, B.P. 6128, Montréal, Québec

Reçu le 10 mai 1971

L'action de $LiAlH_4$, $LiAlH(OtBu)_3$, le tétrakis-(*N*-déhydropyridil) aluminate de lithium (LDPA), et $NaBH_4$ sur quelques benzylidène-3 camphres a été examinée. Les quantités relatives d'addition 1:2 *vs.* 1:4 sur ces dérivés sont déterminées; les résultats obtenus sont discutés en fonction de la nature de l'agent réducteur, du solvant et du caractère électroaffinitaire ou électrorépulsif des substituants portés par le noyau benzénique.

Reduction by $LiAlH_4$, $LiAlH(OtBu)_3$, lithium tetrakis-(*N*-dehydropyridil)aluminate (LDPA), and $NaBH_4$ of several 3-benzylidene camphors have been studied. The relative amounts of the 1:2 *vs.* 1:4 addition are determined. The results obtained are discussed with respect to the nature of reductive species, solvents, and withdrawing and repulsive effects of the aromatic ring substituents.

Canadian Journal of Chemistry, **50**, 438 (1972)

Introduction

Il a été établi antérieurement (1–3) que la réduction par les hydrures complexes de méthylène-3 camphres substitués **1** peut conduire à des quantités variables d'addition 1:2 et 1:4 des hydrures sur le groupement carbonyle conjugué. Afin d'évaluer avec plus de précision la nature des facteurs pouvant influencer le cours de ces réactions, le benzylidène-3 camphre (**1***a*), ses homologues *p*-méthylé (**1***b*), *p*-méthoxylé (**1***c*), et *m*-fluoré (**1***d*) sur le noyau benzénique, et pour lesquels le noyau aromatique occupe une position figée dans le plan du système conjugué (4), ont été réduits par $LiAlH_4$ et $NaBH_4$ dans différents solvants, $LiAlH(OtBu)_3$ dans la pyridine. Les résultats de cette étude font l'objet de la présente communication.

Résultats et discussion

Pour fins de comparaison tous les produits de réduction des benzylidène-3 camphres (**1**) ont déjà été préparés, leurs constantes physiques et leurs caractéristiques spectrales rapportées (5).

Les pourcentages d'addition 1:4 des hydrures sur le système conjugué des benzylidène-3 camphres (**1**) peuvent être résumés dans le tableau 1. Il ressort de ces résultats que le caractère électroaffinitaire ou électrorépulsif influence peu sur les quantités relatives d'addition 1:2 *vs.* 1:4 pour les réductions effectuées dans cette série en milieu aprotique. Parallèlement afin d'évaluer la réactivité relative des composés **1**, la réduction compétitive par $LiAlH(OtBu)_3$ dans le THF à 70 °C et le LDPA dans la pyridine à 35° du *p*-méthoxy benzylidène-3 camphre (**1***c*) et de chacun de ses homologues différemment substitués **1***a*, *b*, ou *d*, de mélanges prélevés, à différents intervalles de temps, sur les milieux réactionnels, permet de constater que les quantités relatives d'addition 1:2 *vs.* 1:4 sont constantes à tous les stades de la réduction (schéma 1). Les lois de vitesse sont donc du même ordre en cétone et en hydrure pour les deux modes d'addition, 1:2 et 1:4. Il a été rapporté

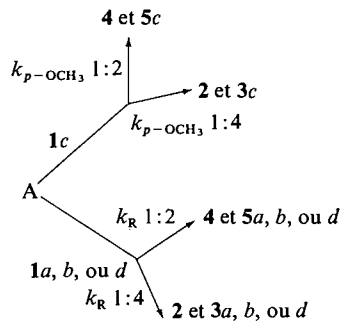

INDICES: p-OCH_3 = *p*-méthoxy benzylidène-3 camphre
R = benzylidène-3 camphres autrement substitués (R = H, p-CH_3, *m*-F)
1:2 = addition 1:2
1:4 = addition 1:4

SCHÉMA 1. Réduction compétitive de mélanges équimoléculaires (A) de cétones **1** par $LiAlH(OtBu)_3$ dans le THF à 70 °C et le LDPA dans la pyridine à 35 °C.

[1]Les résultats rapportés dans cette communication sont extraits en partie de la thèse soumise par M. Armand Rossi en vue de l'obtention du grade de Ph.D. (Faculté des Sciences, Université de Montréal, janvier, 1971).

Can. J. Chem. Downloaded from www.nrcresearchpress.com by 210.87.254.6 on 09/05/12
For personal use only.

TABLEAU 1. Pourcentages† d'addition 1:4 des hydrures complexes sur les benzylidène-3 camphres (**1**)*

Cétones réduites **1**	$LiAlH_4$ Et_2O	$LiAlH_4$ THF	$LiAlH_4$ diglyme	$LiAlH(OtBu)_3$ THF	LDPA pyridine	$NaBH_4$ iso-PrOH	$NaBH_4$ diglyme + 2% d'eau
a	4.4±2.0	15.2±3.0	16.8±3.0	23.7±1.1	56.4±3.0	45.2±2.0	40.3±3.0
b	3.7±2.0	11.0±3.0	15.5±3.0	25.1±1.8	55.3±3.0	43.4±2.0	33.5±3.0
c	4.4±2.0	12.3±3.0	16.8±3.0	26.3±3.0	57.3±3.0	42.4±2.0	25.4±3.0
d	2.3±2.0	17.6±3.0	21.3±3.0	21.6±1.4	60.3±2.0	50.3±1.5	52.6±3.0

*Les conditions et les modes expérimentaux utilisés pour ces réactions sont identiques à ceux rapportés pour la réduction des *p*-méthyl benzyl-3 camphres (**2** et **3**), réf. 5.

†Les valeurs données dans ce tableau sont les moyennes effectuées sur les résultats de trois expériences au minimum.

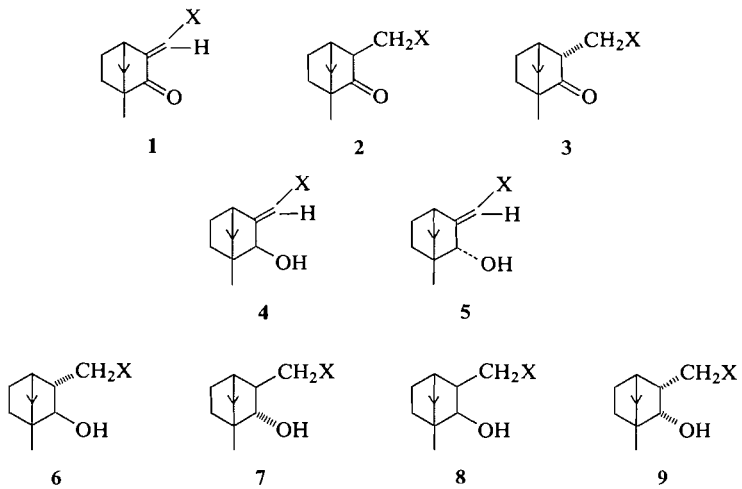

1 **2** **3** **4** **5** **6** **7** **8** **9**

a X = C_6H_5—
b X = *p*-$CH_3C_6H_4$—
c X = *p*-$OCH_3C_6H_4$—
d X = *m*-FC_6H_4—

d'autre part, que la réduction de cétones saturées par $LiAlH(OtBu)_3$ dans le THF (6) et le LDPA dans la pyridine (7) est du premier ordre en cétone et en hydrure. Dans le cadre de ce travail, il paraît logique d'admettre que l'ordre en cétone est le même pour la réduction du groupe carbonyle d'une cétone α,β insaturée et d'une cétone saturée.[2]

A partir de ces données et en accord avec le schéma réactionnel 1, l'éq. 1 donnant $\log b_0/b$ *vs.* $\log b_0/b'$ a été établie pour l'addition 1:2; b_0 représente la concentration initiale des deux cétones dans les mélanges de réduction, b et b' les concentrations respectives en *p*-méthoxy benzylidène-3 camphre (**1***c*) et ses homologues différemment substitués (**1***a*, *b*, ou *d*) à un instant donné.

$$[1]\quad \log\frac{b_0}{b} = \frac{k_{p\text{-}OCH_3}\,1:2}{k_R\,1:2} \times \left[\frac{1+\dfrac{k_{p\text{-}OCH_3}\,1:4}{k_{p\text{-}OCH_3}\,1:2}}{1+\dfrac{k_R\,1:4}{k_R\,1:2}}\right] \times \log\frac{b_0}{b'}$$

$$\frac{k_{p\text{-}OCH_3}\,1:2}{k_R\,1:2}$$

Les résultats obtenus pour les deux réactions étudiées sont résumés par les courbes (fig. 1).

Les rapports des constantes de vitesse donnés par la pente des droites, sont déterminés par la méthode des moindres carrés. Les valeurs calculées et les coefficients de corrélations *r* sont rapportés dans le tableau 2. Ces résultats nous ont permis d'établir une corrélation de Ham-

[2]Des mesures cinétiques directes sur la réduction du benzylidène-3 camphre ont été effectuées et elles ont permis de mettre en évidence que ces réactions étaient du premier ordre en cétone. Toutefois les valeurs obtenues pour les constantes de vitesse n'ont pu être retenues à cause du manque de précision sur les mesures des concentrations initiales en hydrure.

Can. J. Chem. Downloaded from www.nrcresearchpress.com by 210.87.254.6 on 09/05/12
For personal use only.

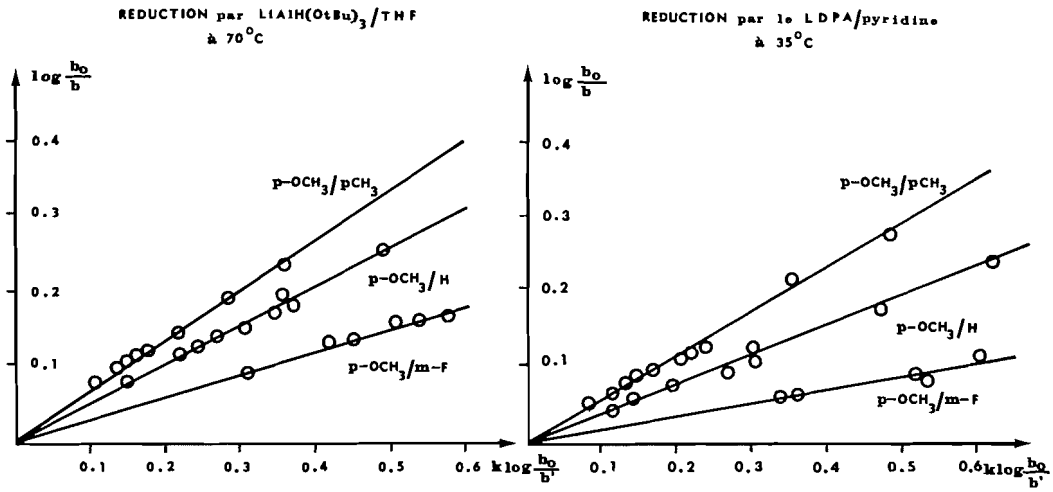

FIG. 1. Variation de log b_0/b en fonction de log b_0/b' pour l'addition 1:2.

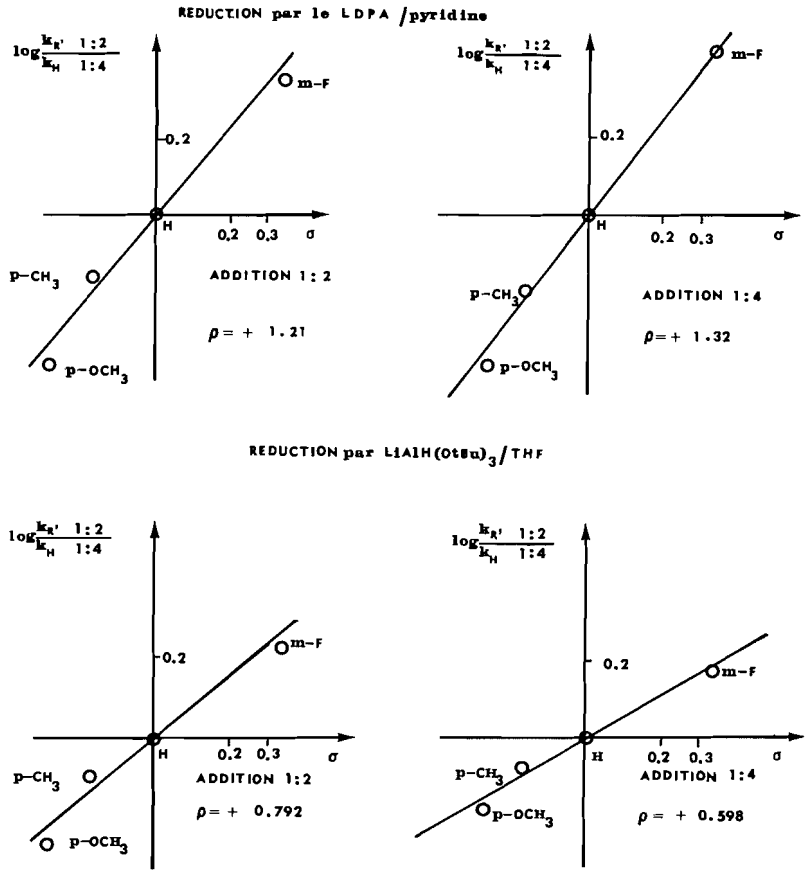

FIG. 2. Corrélations de Hammett pour les deux modes d'addition de l'hydrure (1:2 et 1:4) intervenant dans les réactions étudiées.

Can. J. Chem. Downloaded from www.nrcresearchpress.com by 210.87.254.6 on 09/05/12
For personal use only.

Can. J. Chem. Downloaded from www.nrcresearchpress.com by 210.87.254.6 on 09/05/12
For personal use only.

TABLEAU 2. Mode de réduction

	LiAlH (O*t*Bu)$_3$/THF		LDPA/pyridine	
R	$k_{p\text{-}OCH_3}$ 1:2 / k_R 1:2	r	$k_{p\text{-}OCH_3}$ 1:2 / k_R 1:2	r
H	0.536	0.996	0.382	0.996
p-CH_3	0.662	0.998	0.582	0.994
m-F	0.302	0.998	0.166	0.990

mett, $\log k_H = \log k_{R'} + \rho\sigma$ ($R' = OCH_3$, *p*-CH_3, *m*-F) pour les deux modes d'addition de l'hydrure (1:2 et 1:4) intervenant dans les réactions étudiées. Les courbes (fig. 2) résument les résultats obtenus.

Les valeurs de ρ positives, obtenues pour les additions 1:2 et 1:4 d'hydrure sur les composés **1**, confirment que ces réactions sont favorisées par des substituants à constantes σ positives, c'est à dire attracteurs d'électrons. De plus la différence des valeurs ρ 1:2 − ρ 1:4, faible, est en accord avec le fait que la différence d'énergie libre d'activation pour les deux modes d'addition concurentiels (1:2 et 1:4) reste sensiblement constante et est indépendante du substituant porté par le noyau aromatique. Il semble donc qu'en milieu aprotique la densité de charge répartie sur le système conjugué (groupe carbonyle–double liaison éthylénique) est différente pour chacun des composés **1**; cependant les résultats des réductions semblent indiquer que le rapport des densités de charge des deux sites réagissant est constant et indépendant de la nature des substituants.

Une solvatation spécifique du groupe carbonyle avec formation de liaison hydrogène (8) entre le solvant et l'oxygène du groupe carbonyle peut expliquer les résultats des réductions des benzylidène-3 camphres (**1**) par $NaBH_4$ dans le propanol-2 et le diglyme contenant 2% d'eau. Dans ce cas la conjugaison du groupe aryle avec le groupe carbonyle sera plus importante que dans la cétone libre. La contribution à la résonance allant en décroissant dans le sens: *p*-OCH_3, *p*-CH_3, H, *m*-F et une addition 1:4 détruisant entièrement la conjugaison du système, l'énergie nécessaire pour atteindre l'état de transition diminuera dans le même sens.

Les valeurs rapportées dans le tableau 3 expriment les pourcentages normalisés des benzylidène-3 isobornéols (**4**) par rapport aux isomères *endo* **1** obtenus en cours de l'addition

TABLEAU 3. Quantité d'isomère *exo* obtenu au cours de l'addition 1:2 d'hydrure sur le groupe carbonyle des benzylidène-3 camphres (**1**) et du camphre

Mode de réaction	**1**	Camphre (5)
$LiAlH_4$/éther	84.0	92.0
$LiAlH_4$/THF	96.0–88.0	—
$LiAlH_4$/diglyme	96.0–87.0	—
LiAlH (O*t*Bu)$_3$/THF	94.0	93.0
LDPA/pyridine	67.0	62.5
$NaBH_4$/iso-PrOH	84.0	86.0
$NaBH_4$/diglyme/2% H_2O	82.0	—

1:2 d'hydrure sur le groupe carbonyle des benzylidène-3 camphres (**1**); pour fins de comparaisons les résultats obtenus pour la réduction du camphre (**5**) sont inclus. De ces données, il ressort que l'introduction des groupes benzylidènes en position 3 des cétones **1** influence peu sur la stéréochimie de la réduction du groupe carbonyle comparée aux résultats obtenus pour la réduction du camphre. Au cours de ce travail il a été vérifié également que les alcools **4** et **5** ne réagissent pas dans les conditions utilisées pour la réduction des benzylidène-3 camphres (**1**).

Un autre aspect des résultats obtenus mérite des commentaires. Alors que l'action de LiAlH (O*t*Bu)$_3$ et le LDPA sur les cétones **1** conduit principalement aux cétones saturées **2** et **3** et aux alcools allyliques **4** et **5** (dans tous les cas moins de 3% d'alcools saturés sont formés); en général des quantités plus importantes d'alcools saturés **6**–**9** sont obtenus lors des réductions par $LiAlH_4$ et sont dûes à des traces d'humidité ou à l'addition d'eau utilisée pour décomposer l'hydrure en excès, en accord avec les résultats déjà mentionnés dans la littérature (3). Les pourcentages relatifs des alcools saturés présents dans les mélanges de réduction des cétones **1** par $NaBH_4$ dans le propanol-2 et le diglyme renfermant 2% d'eau sont comparables à ceux qui seraient obtenus en réduisant dans les mêmes conditions, un mélange des cétones saturées (**2** et **3**) dans les proportions *exo*:*endo* de l'ordre de 7:93 [proportions obtenues pour la mise à l'équilibre des deux cétones **2** et **3** (5)] (voir tableau 4).

Les alcools saturés (**6**, **8**, et **9**) présents en fin de réaction proviennent donc, pour les deux derniers cas cités, de la réduction des cétones saturées **2** et **3** correspondantes, obtenus après hydrolyse du borate intermédiaire, produit

TABLEAU 4. Pourcentages relatifs pour la réduction des cétones **1**

	-2 *exo* -3 *endo* **6**	-2 *endo* -3 *exo* **7**	-2 *exo* -3 *exo* **8**	-2 *endo* -3 *endo* **9**
$NaBH_4$/iso-PrOH	41.0	—	18.8	40.2
$NaBH_4$/diglyme/2% eau	42.5	—	12.8	44.7

d'addition 1:4, en accord avec le mécanisme classique proposé déjà par plusieurs auteurs (9, 10), cette réduction se faisant probablement avec une épimérisation du groupe benzyle en position 3 (5).

Partie expérimentale

Pour fins de comparaison tous les produits de réduction des benzylidène-3 camphres (**1**) ont déjà été préparés, leurs constantes physiques et leurs caractéristiques spectrales rapportés (**5**). Les conditions de réduction des benzylidène-3 camphres **1** sont celles décrites pour la réduction des benzyl-3 camphres **2** et **3** (5).

Les temps de rétention de chacun des produits et les conditions expérimentales permettant de faire une analyse complète, en c.p.g. de tous les produits de chaque série sont résumés dans une publication précédente (5).

*(1) Réduction compétitive des benzylidènes-3 camphres **1** par $LiAlH(OtBu)_3$ dans le THF*

On ajoute 20 ml de THF anhydre fraîchement distillé sur $LiAlH_4$, à 0.5 mmol de chaque cétone pesée dans un Erlenmeyer de 50 ml. Le récipient est bouché soigneusement et placé dans un bain à 70 °C pendant 1 h. Cette solution est ajoutée à 20 ml de THF contenant 2 à 4 mmol de $LiAlH(OtBu)_3$, maintenue sous azote et à la même température. Des prélèvements de 10 ml sont effectués à des intervalles de temps différents et hydrolysés dans 30 ml d'une solution de soude à 5%. Après extraction à la manière habituelle, les produits de la réaction sont analysés par c.p.g.

*(2) Réduction compétitive des benzylidène-3 camphres **1** par le LDPA dans la pyridine*

On ajoute 20 ml de pyridine anhydre à 0.5 mmol de chaque cétone pesée dans un Erlenmeyer de 100 ml. Le récipient est fermé hermétiquement à l'aide d'un septum en caoutchouc et placé dans un bain à 35 °C. Un récipient identique contenant une solution de LDPA préparée d'après la méthode décrite par Lansbury et Peterson (11) (1 g de $LiAlH_4$ pour 100 ml de pyridine), est maintenu à la même température. Après 1 h, 20 ml (environ 3 mmol) de la solution de LDPA sont ajoutés à la solution cétonique à l'aide d'une seringue. Le mélange est agité vigoureusement et replacé dans le bain. Des prélèvements sont effectués à différents intervalles de temps à l'aide d'une seringue. Après hydrolyse dans 50 ml d'une solution d'HCl très diluée (2%) et extraction des produits à la manière habituelle, les mélanges réactionnels sont analysés par c.p.g.

1. J.-C. RICHER et R. CLARKE. Tetrahedron Lett. 935 (1964).
2. J.-C. RICHER et C. LAMARRE. Can. J. Chem. **45**, 1581 (1967).
3. J.-C. RICHER et Y. PÉPIN. Can. J. Chem. **48**, 1226 (1970).
4. J. SOTIROPOULOS. Thèse de Doctorat. Faculté des Sciences, Toulouse, France, 1968.
5. J.-C. RICHER et A. ROSSI. Can. J. Chem. Sous presse.
6. J. KLEIN et E. DUNKELBLUM. E. L. ELIEL et Y. SENDA. Tetrahedron Lett. **58**, 6127 (1968).
7. P. T. LANSBURY et R. E. MACLEAY. J. Am. Chem. Soc. **87**, 831 (1965).
8. W. W. BRANDT. J. Am. Chem. Soc. **85**, 2628 (1963).
9. K. IQBAL et W. R. JACKSON. J. Chem. Soc. 616 (1968).
10. P. I. SCHUSTER, J. M. PALMER, et S. O. DICKERMAN. J. Org. Chem. **31**, 4281 (1966).
11. P. T. LANSBURY et J. O. PETERSON. J. Am. Chem. Soc. **85**, 2236 (1963).

Can. J. Chem. Downloaded from www.nrcresearchpress.com by 210.87.254.6 on 09/05/12
For personal use only.

Can. J. Chem. Downloaded from www.nrcresearchpress.com by 210.87.254.40 on 09/05/12
For personal use only.

Paniculatin, a New Coumarin from *Murraya paniculata* (L.) Jack[1]

WARREN STECK

Prairie Regional Laboratory, National Research Council of Canada, Saskatoon, Saskatchewan

Received August 16, 1971

The coumarin derivatives osthol and coumurrayin were isolated from foliage of *Murraya paniculata* (Rutaceae). In addition, a new coumarin, *paniculatin*, was obtained. By means of chemical degradation and u.v., n.m.r., and mass spectroscopy, the new compound was identified as 7-methoxy-8-(isovaleryloxy-2-keto-3-methylbutyl)coumarin.

L'osthol et la coumurrayine des dérivés de la coumarine, ont été isolés à partir du *Murraya paniculata* (Rutaceae). En plus, une nouvelle coumarine, la *paniculatine*, a été obtenue. En utilisant la dégradation chimique et la spectroscopie u.v., r.m.n., et de masse, le nouveau composé a été identifié comme étant le méthoxy-7 (isovaléryloxycéto-2 méthyl-3 butyl)-8 coumarine.

Canadian Journal of Chemistry, **50**, 443 (1972)

The plant *Murraya paniculata* (L.) Jack (*M. exotica* L.), family Rutaceae, is known to contain coumarin derivatives. Bose and Mookerjee (1) isolated scopoletin glucoside from the petals, while from other organs Ramstad *et al.* (2) and Dreyer (3) obtained 5,7-dimethoxy-8-(3-methyl-2-butenyl)coumarin (coumurrayin), and Chakraborty *et al.* (4) 5,7-dimethyoxy-8-(2,3-dihydroxy-3-methylbutyl)coumarin (mexoticin).

Gas chromatographic examination of foliage extracts of this plant have now revealed the presence of coumurrayin and several other coumarins. Osthol (7-methoxy-8-(3-methyl-2-butenyl)coumarin) was identified by u.v. and n.m.r. spectroscopy (5) and by co-chromatography with an authentic standard, and two other 8-isopentenyl-type derivatives present only in trace amounts were partly characterized. These, isolated by gas chromatography, had the same fluorescence and u.v. absorption characteristics as osthol. In their n.m.r. spectra doublets could be discerned at δ 6.2, 7.7, 6.9, and 7.4, indicating they were 8-alkyl coumarins (5). Both showed 7-methoxyl at δ 3.9 but the aliphatic end of the spectrum was obscured by instrument noise: in one derivative signals (3H?) could be seen at δ 1.23, 1.31 and 1.70, in the other at δ 1.78 and 2.42. In addition, a new coumarin for which the name *paniculatin* is suggested, was isolated in reasonable quantities and identified as 7-methoxy-8-(1-isovaleryloxy-2-keto-3-methylbutyl)coumarin (**1**) on the basis of the following evidence. The compound had a molecular formula $C_{20}H_{24}O_6$, determined by mass spectroscopy (calcd. and found *m/e* 360.1573), and fluoresced violet under u.v. excitation in the same way as osthol. The u.v. spectrum, λ_{max} (EtOH) 247, 256, and 320 nm, unchanged by the addition of NaOH or $AlCl_3$, was typical of 7-alkoxycoumarins. This was confirmed by the [^{1}H]n.m.r. spectrum in $DCCl_3$ (Fig. 1), in which the characteristic coumarin H-3/H-4 and H-5/H-6 doublet pairs appeared. The position of the H-4 doublet at δ 7.66 showed clearly that no oxygen function was present at C-5, a possibility not excluded by the u.v. spectrum. An oxygen function at C-5 would require the H-4 doublet to be located at $\delta > 7.9$ (6). The H-6 doublet was not meta-coupled, so C-8 must bear a carbon chain. At δ 6.94 was a sharp one-proton singlet with an extremely low field which was reminiscent of the benzylic protons of the coumarins athamantin and archangelicin (7), which resonated at δ 6.97 and 7.12, respectively, under the same conditions. The septet at δ 2.88 was shown by spin decoupling to be coupled ($J = 6.7$ Hz) to the methyl doublets at 1.03 and 1.17, forming an isopropyl group which must be adjacent to a carbon lacking protons entirely. The multiplet at 2.0–2.3 and the coupled doublet at 0.95 indicated the presence of an isovalerate residue.

Mild alkaline hydrolysis of paniculatin gave

[1]NRCC No. 12275.

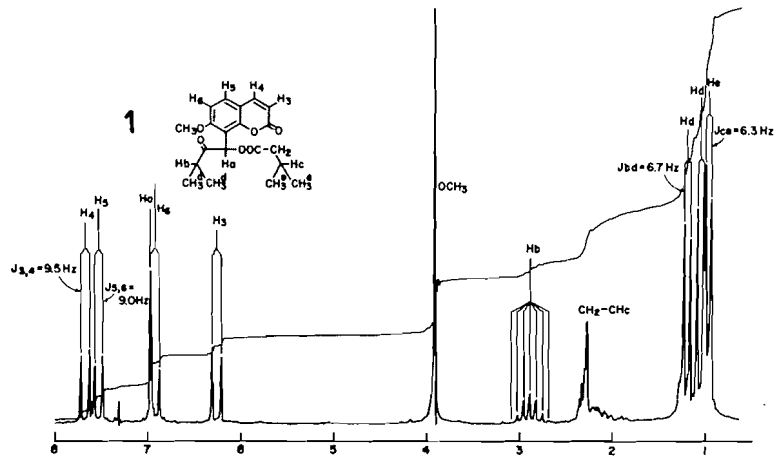

FIG. 1. The 100 MHz[^{1}H]n.m.r. spectrum of paniculatin; solvent, $DCCl_3$; TMS internal standard.

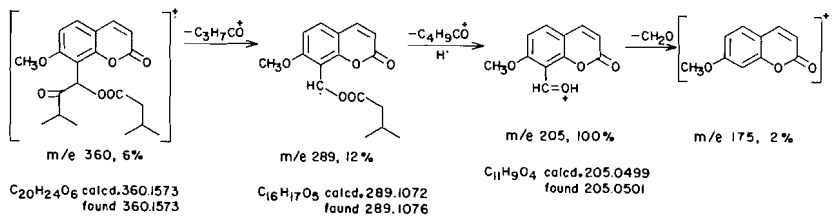

FIG. 2. Fragmentation of paniculatin, from the mass spectrum.

isovaleric acid, a coumarin identified as 7-methoxy-8-(1-hydroxy-2-keto-3-methylbutyl)-coumarin (**2**) and a trace of a compound with the same fluorescence, u.v. absorption, and chromatographic characteristics as authentic 7-methoxy-8-(2-keto-3-methylbutyl)coumarin synthesized from osthol (8). Acid hydrolysis gave a somewhat larger proportion of this last compound along with the same two major products. Isovaleric acid was identified by gas co-chromatography with authentic material on UC-W98 and FFAP columns, and on UC-W98 and 1.5% SE-52 after methylation with diazomethane. A strong odor of isovaleric acid was also apparent in the acidified hydrolyzate. Compound **2** was isolated by g.l.c. and identified by its u.v. and n.m.r. spectra; the absorption spectrum was identical with that of the parent ester. The n.m.r. spectrum was similar except for the absence of isovalerate signals, the appearance of a hydroxyl proton at δ 4.2 and the shift from δ 6.94 to 5.89 of the benzylic proton signal, thus confirming the position of the ester group.

The only structure for paniculatin in harmony with the above spectral, chromatographic, and hydrolytic data is **1**, optical configuration unknown. The mass spectrum of the coumarin supported this assignment, showing major peaks at *m/e* 360 (M) and 289 (M-71, loss of C_3H_7CO), further fragmenting with rearrangement to a very strong base peak at 205 (loss of C_4H_9CO and hydrogen transfer), then to 7-methoxycoumarin ion at *m/e* 175 (loss of CH_2O). Fragment *m/e* peaks at 43 ($C_3H_7^+$), 57 ($C_4H_9^+$), 71 ($C_3H_7CO^+$) and 85 ($C_4H_9CO^+$) corroborated this scheme; the expected metastable peaks were present at *m/e* 232.0 (360 → 289), 145.3 (289 → 205), and 149.3 (205 → 175). High resolution measurements showed the fragment formulas were $C_{16}H_{17}O_5$ at *m/e* 289 and $C_{11}H_9O_4$ at 205, consistent with the scheme shown in Fig. 2.

Paniculatin represents a novel type of coumarin in having an α-keto ester moiety, and is of some biosynthetic interest. It is doubtless derived from 7-hydroxycoumarin, probably via osthol; the subsequent stages in its formation may involve benzylic hydroxylation and esterification of meranzin (osthol epoxide) or meran-

Can. J. Chem. Downloaded from www.nrcresearchpress.com by 210.87.254.40 on 09/05/12
For personal use only.

zin hydrate (the corresponding diol). The natural occurrence of compounds very similar to these hypothetical ester intermediates (9, 10), and the common existence of benzylic esters in other classes of coumarins (7) provide some support for this idea.

Thanks are extended to Dr. W. D. Jamieson (NRCC Atlantic Regional Laboratories, Halifax, Nova Scotia) for mass spectral measurements, and to Mr. B. K. Bailey for technical assistance.

1. P. K. Bose and A. Mookerjee. J. Indian Chem. Soc. **14**, 489 (1937).
2. E. Ramstad, W. C. Lin, T. Lin, and W. Koo. Tetrahedron Lett. 811 (1968).
3. D. L. Dreyer. J. Org. Chem. **33**, 3574 (1968).
4. D. P. Chakraborty, B. K. Chowdhury, and B. C. Das. Tetrahedron Lett. 3471 (1967).
5. W. Steck and B. K. Bailey. Can. J. Chem. **47**, 3577 (1969).
6. J. Reisch, I. Novak, K. Szendrei, and E. Minker. Die Pharm. **22**, 205 (1967).
7. B. E. Nielsen. Coumarins of umbelliferous plants. The Royal Danish School of Pharmacy, Copenhagen, 1970.
8. G. A. Kuznetsova and A. B. Abyshev. Khim. Prir. Soed. **1**, 283 (1965).
9. K. Hata and M. Kozawa. Tetrahedron Lett. 4557 (1965).
10. J. P. Kutney, R. N. Young, and A. K. Verma. Tetrahedron Lett. 1845 (1969).

The Basicity of Aliphatic Ethers

Donald G. Lee and Ronald Cameron

Department of Chemistry, University of Saskatchewan, Regina Campus, Regina, Saskatchewan

Received October 1, 1971

The pK_{BH^+} values of aliphatic ethers have been calculated from n.m.r. chemical shift data to be approximately -6.4.

Les valeurs des pK_{BH^+} d'éthers aliphatiques ont été calculées à partir des données r.m.n. des déplacements chimiques. Ces valeurs sont voisines de -6.4.

Canadian Journal of Chemistry, **50**, 445 (1972)

Introduction

The basicities of aliphatic ethers is a topic of current interest and debate (1). The results of distribution studies which indicate that the pK_{BH^+}[1] values for these compounds are approximately -3 to -4 were at one time widely accepted (2, 3). However, more recent work has shown that aliphatic ethers may be less basic than the distribution studies suggested. Edward and coworkers (4, 5), on the basis of indicator measurements and n.m.r. studies, found the pK_{BH^+} of diethyl ether to be about -6, while Arnett *et al.* (6), using heats of protonation data, calculated it to be -5.1. Estimated basicity constants obtained by other methods have been tabulated elsewhere (2, 6).

We recently reported an n.m.r. method which gave reliable pK_{BH^+} values for aliphatic ketones (7) and we wish now to report results obtained when the protonation of aliphatic ethers was studied in a similar manner. Although the earlier literature (2, 4) seemed to indicate that n.m.r. chemical shifts were not suitable physical properties to use for protonation studies, later reports have shown that this procedure can be successfully employed with a wide variety of functional groups (7–13).

Edward's most recent results indicate that the chemical shifts of cations are influenced by the solvent through hydrogen bonding; hence the use of ammonium ions as internal standards introduces a potential error into the analysis (14). To overcome this we have used the difference (Δ) between the chemical shifts of α- and β-hydrogens as a measure of the extent of protonation (7). Since the α-hydrogens are closer to the site of protonation they are subject to greater shifts and consequently Δ increases with the extent of protonation. Thus when weak organic bases are dissolved in H_2SO_4 solutions

[1]In this context, pK_{BH^+} is taken to be the H_0 (15) of the solution in which the ether is one-half protonated.

Can. J. Chem. Downloaded from www.nrcresearchpress.com by 210.87.254.40 on 09/05/12
For personal use only.

zin hydrate (the corresponding diol). The natural occurrence of compounds very similar to these hypothetical ester intermediates (9, 10), and the common existence of benzylic esters in other classes of coumarins (7) provide some support for this idea.

Thanks are extended to Dr. W. D. Jamieson (NRCC Atlantic Regional Laboratories, Halifax, Nova Scotia) for mass spectral measurements, and to Mr. B. K. Bailey for technical assistance.

1. P. K. Bose and A. Mookerjee. J. Indian Chem. Soc. **14**, 489 (1937).
2. E. Ramstad, W. C. Lin, T. Lin, and W. Koo. Tetrahedron Lett. 811 (1968).
3. D. L. Dreyer. J. Org. Chem. **33**, 3574 (1968).
4. D. P. Chakraborty, B. K. Chowdhury, and B. C. Das. Tetrahedron Lett. 3471 (1967).
5. W. Steck and B. K. Bailey. Can. J. Chem. **47**, 3577 (1969).
6. J. Reisch, I. Novak, K. Szendrei, and E. Minker. Die Pharm. **22**, 205 (1967).
7. B. E. Nielsen. Coumarins of umbelliferous plants. The Royal Danish School of Pharmacy, Copenhagen, 1970.
8. G. A. Kuznetsova and A. B. Abyshev. Khim. Prir. Soed. **1**, 283 (1965).
9. K. Hata and M. Kozawa. Tetrahedron Lett. 4557 (1965).
10. J. P. Kutney, R. N. Young, and A. K. Verma. Tetrahedron Lett. 1845 (1969).

The Basicity of Aliphatic Ethers

Donald G. Lee and Ronald Cameron

Department of Chemistry, University of Saskatchewan, Regina Campus, Regina, Saskatchewan

Received October 1, 1971

The pK_{BH^+} values of aliphatic ethers have been calculated from n.m.r. chemical shift data to be approximately −6.4.

Les valeurs des pK_{BH^+} d'éthers aliphatiques ont été calculées à partir des données r.m.n. des déplacements chimiques. Ces valeurs sont voisines de −6.4.

Canadian Journal of Chemistry, **50**, 445 (1972)

Introduction

The basicities of aliphatic ethers is a topic of current interest and debate (1). The results of distribution studies which indicate that the pK_{BH^+}[1] values for these compounds are approximately −3 to −4 were at one time widely accepted (2, 3). However, more recent work has shown that aliphatic ethers may be less basic than the distribution studies suggested. Edward and coworkers (4, 5), on the basis of indicator measurements and n.m.r. studies, found the pK_{BH^+} of diethyl ether to be about −6, while Arnett *et al.* (6), using heats of protonation data, calculated it to be −5.1. Estimated basicity constants obtained by other methods have been tabulated elsewhere (2, 6).

We recently reported an n.m.r. method which gave reliable pK_{BH^+} values for aliphatic ketones (7) and we wish now to report results obtained when the protonation of aliphatic ethers was studied in a similar manner. Although the earlier literature (2, 4) seemed to indicate that n.m.r. chemical shifts were not suitable physical properties to use for protonation studies, later reports have shown that this procedure can be successfully employed with a wide variety of functional groups (7–13).

Edward's most recent results indicate that the chemical shifts of cations are influenced by the solvent through hydrogen bonding; hence the use of ammonium ions as internal standards introduces a potential error into the analysis (14). To overcome this we have used the difference (Δ) between the chemical shifts of α- and β-hydrogens as a measure of the extent of protonation (7). Since the α-hydrogens are closer to the site of protonation they are subject to greater shifts and consequently Δ increases with the extent of protonation. Thus when weak organic bases are dissolved in H_2SO_4 solutions

[1]In this context, pK_{BH^+} is taken to be the H_0 (15) of the solution in which the ether is one-half protonated.

Can. J. Chem. Downloaded from www.nrcresearchpress.com by 210.87.254.5 on 09/05/12
For personal use only.

TABLE 1. Protonation data

H_2SO_4		Diethyl ether		Tetrahydrofuran		Diisopropyl ether	
%	H_0	Δ	log I	Δ	log I	Δ	log I
0	7	143.3		112.3			
7.62	−0.1	143.7		112.4		161.6	
29.6	−1.68	145.1		113.2		163.0	
37.8	−2.26	145.9	−1.52	113.7	−1.53	163.2	
48.0	−3.17					165.9	−1.07
53.3	−3.73					168.5	−0.83
56.3	−4.05	149.5	−0.77	117.0	−0.71	169.5	−0.72
61.0	−4.57	151.2	−0.60	118.4	−0.47	172.2	−0.58
64.0	−4.95			120.1	−0.39		
64.1	−4.96					175.6	−0.40
66.4	−5.26	154.6	−0.35				
68.9	−5.64	155.4	−0.30	121.6	−0.27	179.0	−0.26
72.0	−6.10	157.4	−0.18	123.2	−0.15	182.8	−0.11
73.7	−6.37			125.9	0.04		
74.7	−6.52					188.4	0.11
75.3	−6.60	162.2	0.10				
76.9	−6.85			126.4	0.08	192.0	0.25
77.4	−6.93	164.3	0.22	128.5	0.23		
79.7	−7.29	165.0	0.26	129.0	0.26		
81.2	−7.53					194.9	0.37
82.8	−7.78					195.7	0.41
83.3	−7.86	168.2	0.47	131.5	0.47		
84.5	−8.05	169.6	0.59	132.7	0.60	195.6	0.40
86.4	−8.35					197.5	0.50
88.7	−8.72	171.5	0.77	134.2	0.78		
91.0	−9.10	172.7	0.92	135.2	0.95	204.6	1.02
97.0	−10.21	174.8		136.8		207.7	
98.5	−10.55					208.5	
100.1	−12.45	176.4		138.1		208.7	

of various concentrations and the difference in chemical shift between the α- and β-hydrogens is plotted against H_0 (15) sigmoidal curves are obtained, with the inflection points occurring at the position of one-half protonation. Since the α- and β-hydrogens are both in approximately the same chemical environment medium effects are minimized by this procedure.

Experimental

The experimental procedures used were identical to those previously reported (7). The spectra of the unprotonated ethers were all consistent with an approximately first order analysis and with published spectra (16). Diethyl ether exhibited a well defined quartet and triplet under all conditions, while diisopropyl ether gave a doublet and a septet. With the latter compound an additional signal, probably due to cleavage products, was observed in concentrations of H_2SO_4 greater than 80%. However, the presence of this signal did not interfere seriously with the measurement of Δ. The spectrum of tetrahydrofuran consisted of two multiplets both with prominent spikes near their centers. The values of Δ for this compound were consequently measured using the points of these spikes as an estimation of the chemical shifts for α- and β-hydrogens.

Results and Discussion

When the Δ values (Table 1) were plotted against H_0, well defined titration curves were obtained as indicated in Fig. 1. The inflection points of these curves then correspond to the acidity at which the ethers are one-half protonated; *i.e.* the apparent pK_{BH^+} values. A more accurate estimation of the pK_{BH^+} can, however, be obtained from the relationship, $\log [BH^+]/[B] = -mH_0 + pK_{BH^+}$, where [B] is the concentration of unprotonated ether and $[BH^+]$ is the concentration of the protonated species (7). Plots of $\log [BH^+]/[B]$ against H_0 should thus be linear with the intercept equal to the pK_{BH^+} of the compound. Least-squares statistical methods can then be applied to these plots and the apparent pK_{BH^+} values can consequently be defined more precisely. The ratio $[BH^+]/[B]$, which we have designated as I, is equal to $(\Delta - \Delta_B)/(\Delta_{BH^+} - \Delta)$ where Δ_B is the difference between the chemical shifts of the α- and β-hydrogens of the unprotonated ether, Δ_{BH^+} is

Can. J. Chem. Downloaded from www.nrcresearchpress.com by 210.87.254.5 on 09/05/12
For personal use only.

TABLE 2. Statistical data for plots of log I *vs.* $-H_0$

Compound	Intercept (pK_{BH^+})	Slope (m)	n*	r†
Diethyl ether	-6.4 ± 0.1	0.35	13	0.995
Tetrahydrofuran	-6.3 ± 0.2	0.32	13	0.987
Diisopropyl ether	-6.4 ± 0.3	0.32	14	0.983

*Number of points.
†Correlation coefficient.

the same parameter for the protonated ether, and Δ is the chemical shift when the ether is partly protonated.

The calculated values of log I are given in Table 1 and the statistical data obtained from plots of log I against H_0 are summarized in Table 2. These results clearly indicate that the apparent pK_{BH^+} values for these compounds are approximately -6.4, in reasonably good agreement with the most recent results reported by Arnett *et al.* (6) and Edward (5). Hence it can be concluded that aliphatic ethers are one-half protonated in about 80% H_2SO_4.

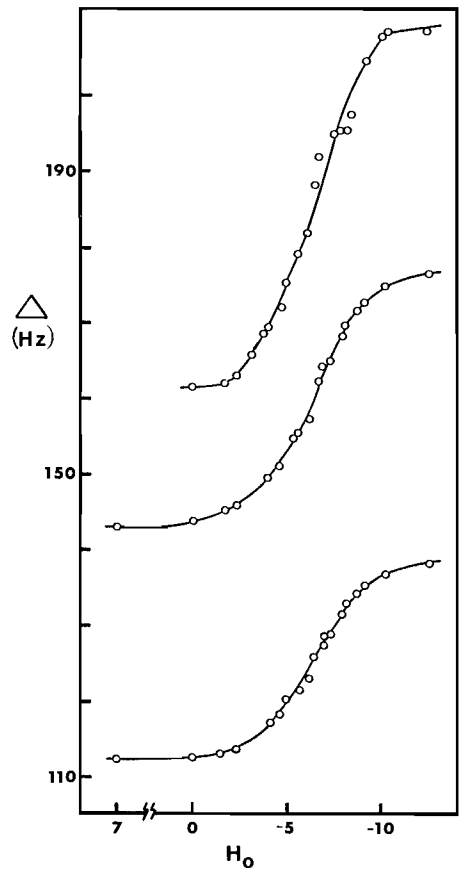

FIG. 1. Titration curves for the protonation of diisopropyl ether, diethyl ether, and tetrahydrofuran (top to bottom).

However, the fact that none of the slopes reported in Table 2 are close to unity indicates that the H_0 acidity function does not correctly define the protonation equilibria for aliphatic ethers. This is not too surprising since it is likely that aromatic amine indicators (on which the H_0 function is based) have different solvation requirements than the aliphatic ethers. Similar observations have previously been made when comparing the protonation of other oxygen bases with this function (9, 11, 13, 17–21).

It should be noted that Edward *et al.* (4) and Arnett (2) have both reported previous attempts to study the protonation of aliphatic ethers in this way. It would appear that their failure to obtain good sigmoidal curves was probably associated with the limited range over which they studied the reaction. Since the slopes of the log I vs. H_0 plots are much less than unity it is necessary to study the behavior of the ethers over a very wide range of acidities.

The authors are grateful to the National Research Council of Canada for financial support.

1. S. SEARLES and M. TAMRES. *In* The Chemistry of the ether linkage. S. Patai, Editor. Interscience. 1967. p. 243–308. G. A. OLAH, A. M. WHITE, and D. H. O'BRIEN. Chem. Rev. **70**, 561 (1970).
2. E. M. ARNETT and C. Y. WU. J. Am. Chem. Soc. **82**, 4999 (1960); **84**, 1680, 1684 (1962). E. M. ARNETT. Prog. Phys. Org. Chem. **1**, 223 (1963).
3. N. C. DENO and M. J. WISOTSKY. J. Am. Chem. Soc. **85**, 1735 (1963). N. C. DENO and J. O. TURNER. J. Org. Chem. **31**, 1969 (1966).
4. J. T. EDWARD, J. B. LEANE, and I. C. WANG. Can. J. Chem. **40**, 1521 (1962).
5. J. T. EDWARD. Chem. and Ind. 489 (1963).
6. E. M. ARNETT, R. P. QUIRK, and J. J. BURKE. J. Am. Chem. Soc. **92**, 1260 (1970).
7. D. G. LEE. Can. J. Chem. **48**, 1919 (1970).
8. E. GRUNWALD, A. LOEWENSTEIN, and S. MEIBOOM. J. Chem. Phys. **27**, 641 (1957).

Can. J. Chem. Downloaded from www.nrcresearchpress.com by 210.87.254.5 on 09/05/12
For personal use only.

9. P. HAAKE, R. D. COOK, and G. H. HURST. J. Am. Chem. Soc. **89**, 2650 (1967).
10. P. HAAKE and R. D. COOK. Tetrahedron Lett. 427 (1968).
11. D. LANDINI, G. MODENA, G. SCORRANO, and F. TADDEI. J. Am. Chem. Soc. **91**, 6703 (1969).
12. N. C. DENO, C. U. PITMAN, and M. J. WISOTSKY. J. Am. Chem. Soc. **86**, 4370 (1964).
13. J. SIIGUR, T. PEHK, U. HALDNA, and E. LIPPMAA. Reakts. Sposobnost Org. Soedin, 7, 179 (1970).
14. J. T. EDWARD. Can. J. Chem. **49**, 2364 (1971).
15. M. J. JORGENSON and D. R. HARTTER. J. Am. Chem. Soc. **85**, 878 (1963).
16. N. S. BHACCA, L. F. JOHNSON, and J. N. SHOOLERY. High resolution n.m.r. catalog. Varian Associates (1962). G. A. OLAH and D. H. O'BRIEN. J. Am. Chem. Soc. **89**, 1725 (1967).
17. D. G. LEE and R. CAMERON. J. Am. Chem. Soc. **93**, 4724 (1971).
18. K. YATES, J. B. STEVENS, and A. R. KATRITZKY. Can. J. Chem. **42**, 1957 (1964).
19. T. G. BONNER and J. PHILLIPS. J. Chem. Soc. B, 650 (1966).
20. C. C. CREIG and C. D. JOHNSON. J. Am. Chem. Soc. **90**, 6453 (1968). A. A. EL-ANANI, C. C. CREIG, and C. D. JOHNSON. Chem. Commun. 1024 (1970).
21. G. C. LEVY, J. D. CARGIOLI, and W. RACELA. J. Am. Chem. Soc. **92**, 6238 (1970).

Application of Factor Analysis to Gas–Liquid Chromatography

PAUL H. WEINER[1] AND DARRYL G. HOWERY[2]

Department of Chemistry, Brooklyn College of the City University of New York, Brooklyn, N.Y. 11210

Received August 12, 1971

The mathematical method of factor analysis is applied to a data matrix of retention indices for 30 solutes on 23 stationary liquid phases. Eight abstract eigenvectors are required to reproduce the data within experimental error. A gas phase imperfection term based on the van der Waals equation of state tests successfully as a fundamental factor of the space. A test vector termed the uniqueness test is used to determine the extent to which molecules possess a particular property. The uniqueness test is applied to rank solutes in terms of (*1*) alcohol-like character and (*2*) electron-donor ability.

La méthode mathématique d'analyse des facteurs est appliquée à une matrice de données d'indices de rétention pour 30 solutés sur 23 phases liquides stationnaires. Huit eigenvecteurs abstraits sont nécessaires pour reproduire les données dans le domaine de l'erreur expérimentale. Un terme d'imperfection de la phase gazeuse fondé sur l'équation d'état de van der Waals se comporte avec succès comme un facteur fondamental de l'espace. Un vecteur test exprime comme par un test d'unicité est utilisé pour déterminer le domaine dans lequel les molécules possèdent une propriété particulière. Le test d'unicité est appliqué pour ranger les solutés en termes du (*1*) caractère d'alcool et (*2*) de possibilité de donneur d'électrons.

Canadian Journal of Chemistry, **50**, 448 (1972)

Recently the mathematical technique of factor analysis has been applied to studies of the determination of activity coefficients in gas–liquid chromatography (1) and of the effect of solvent on proton magnetic resonance spectra (2–5). We report here the use of factor analysis to determine the number and the nature of some of the fundamental factors which govern retention indices in gas–liquid chromatography (g.l.c.).

The mathematical development of factor analysis is presented elsewhere (2, 5). Here it is sufficient to point out that we must be able to express the quantity being factor analyzed as a linear sum of factors each of which is a product function. For retention indices measured in g.l.c., we look for a solution of the form

$$[1] \qquad I_{i,\alpha} = \sum_j U_{ij} V_{j\alpha}$$

where $I_{i,\alpha}$ is the retention index of solute i on stationary liquid solvent α; U_{ij} is the jth solute factor of the ith solute; and $V_{j\alpha}$ is the jth solvent factor of the αth solvent. The sum is taken over the number of controlling factors or eigenvectors, j, necessary to span the factor space. Factor analysis allows us to determine the number of controlling factors, and, by using a least squares mathematical rotational scheme, to test physically significant parameters for possible identification with the abstract eigenvectors of the space.

[1]Present address: Chemistry Department, University of Mississippi, University, Mississippi 38677.

[2]To whom correspondence should be addressed.

Can. J. Chem. Downloaded from www.nrcresearchpress.com by 210.87.254.5 on 09/05/12
For personal use only.

9. P. HAAKE, R. D. COOK, and G. H. HURST. J. Am. Chem. Soc. **89**, 2650 (1967).
10. P. HAAKE and R. D. COOK. Tetrahedron Lett. 427 (1968).
11. D. LANDINI, G. MODENA, G. SCORRANO, and F. TADDEI. J. Am. Chem. Soc. **91**, 6703 (1969).
12. N. C. DENO, C. U. PITMAN, and M. J. WISOTSKY. J. Am. Chem. Soc. **86**, 4370 (1964).
13. J. SIIGUR, T. PEHK, U. HALDNA, and E. LIPPMAA. Reakts. Sposobnost Org. Soedin, 7, 179 (1970).
14. J. T. EDWARD. Can. J. Chem. **49**, 2364 (1971).
15. M. J. JORGENSON and D. R. HARTTER. J. Am. Chem. Soc. **85**, 878 (1963).
16. N. S. BHACCA, L. F. JOHNSON, and J. N. SHOOLERY. High resolution n.m.r. catalog. Varian Associates (1962). G. A. OLAH and D. H. O'BRIEN. J. Am. Chem. Soc. **89**, 1725 (1967).
17. D. G. LEE and R. CAMERON. J. Am. Chem. Soc. **93**, 4724 (1971).
18. K. YATES, J. B. STEVENS, and A. R. KATRITZKY. Can. J. Chem. **42**, 1957 (1964).
19. T. G. BONNER and J. PHILLIPS. J. Chem. Soc. B, 650 (1966).
20. C. C. CREIG and C. D. JOHNSON. J. Am. Chem. Soc. **90**, 6453 (1968). A. A. EL-ANANI, C. C. CREIG, and C. D. JOHNSON. Chem. Commun. 1024 (1970).
21. G. C. LEVY, J. D. CARGIOLI, and W. RACELA. J. Am. Chem. Soc. **92**, 6238 (1970).

Application of Factor Analysis to Gas–Liquid Chromatography

PAUL H. WEINER[1] AND DARRYL G. HOWERY[2]

Department of Chemistry, Brooklyn College of the City University of New York, Brooklyn, N.Y. 11210

Received August 12, 1971

The mathematical method of factor analysis is applied to a data matrix of retention indices for 30 solutes on 23 stationary liquid phases. Eight abstract eigenvectors are required to reproduce the data within experimental error. A gas phase imperfection term based on the van der Waals equation of state tests successfully as a fundamental factor of the space. A test vector termed the uniqueness test is used to determine the extent to which molecules possess a particular property. The uniqueness test is applied to rank solutes in terms of (*1*) alcohol-like character and (*2*) electron-donor ability.

La méthode mathématique d'analyse des facteurs est appliquée à une matrice de données d'indices de rétention pour 30 solutés sur 23 phases liquides stationnaires. Huit eigenvecteurs abstraits sont nécessaires pour reproduire les données dans le domaine de l'erreur expérimentale. Un terme d'imperfection de la phase gazeuse fondé sur l'équation d'état de van der Waals se comporte avec succès comme un facteur fondamental de l'espace. Un vecteur test exprime comme par un test d'unicité est utilisé pour déterminer le domaine dans lequel les molécules possèdent une propriété particulière. Le test d'unicité est appliqué pour ranger les solutés en termes du (*1*) caractère d'alcool et (*2*) de possibilité de donneur d'électrons.

Canadian Journal of Chemistry, **50**, 448 (1972)

Recently the mathematical technique of factor analysis has been applied to studies of the determination of activity coefficients in gas–liquid chromatography (1) and of the effect of solvent on proton magnetic resonance spectra (2–5). We report here the use of factor analysis to determine the number and the nature of some of the fundamental factors which govern retention indices in gas–liquid chromatography (g.l.c.).

The mathematical development of factor analysis is presented elsewhere (2, 5). Here it is sufficient to point out that we must be able to express the quantity being factor analyzed as a linear sum of factors each of which is a product function. For retention indices measured in g.l.c., we look for a solution of the form

$$[1] \qquad I_{i,\alpha} = \sum_j U_{ij} V_{j\alpha}$$

where $I_{i,\alpha}$ is the retention index of solute i on stationary liquid solvent α; U_{ij} is the jth solute factor of the ith solute; and $V_{j\alpha}$ is the jth solvent factor of the αth solvent. The sum is taken over the number of controlling factors or eigenvectors, j, necessary to span the factor space. Factor analysis allows us to determine the number of controlling factors, and, by using a least squares mathematical rotational scheme, to test physically significant parameters for possible identification with the abstract eigenvectors of the space.

[1]Present address: Chemistry Department, University of Mississippi, University, Mississippi 38677.

[2]To whom correspondence should be addressed.

Can. J. Chem. Downloaded from www.nrcresearchpress.com by 210.87.254.105 on 09/05/12
For personal use only.

Can. J. Chem. Downloaded from www.nrcresearchpress.com by 210.87.254.105 on 09/05/12
For personal use only.

In g.l.c. the free energy of evaporation of a solute from a stationary liquid solvent in principle can be expressed as a sum of terms representing the free energies of the different types of interactions between the solute and the environment. Rohrschneider (6) states that the retention index also can be given as a sum of terms associated with the different types of solute-stationary phase interactions. He further assumes that each term in the sum can be expressed as a product of solute and solvent parameters. Thus we anticipate that a solution to the retention index problem in the form of eq. 1 does exist and therefore that factor analysis should yield useful information when applied to a matrix of retention index data.

The matrix of experimental data used in the present study was taken from the careful work of Rohrschneider (6) who measured the retention indices of 30 nonpolar and polar solutes on 23 stationary liquid solvents. With the data matrix having rows corresponding to solutes and columns corresponding to solvents, we find by applying the factor analysis technique (2) that a minimum of eight eigenvectors ($j = 8$) are sufficient to span the retention index factor space such that all data are reproduced to better than 1%, *i.e.*, within experimental error. All calculations were performed on a PDP 10 or an IBM 360-40 digital computer, using a Fortran IV program (2).

Now let us see the results of attempts to rotate physically significant parameters of the solutes into the abstract eigenvectors. A major advantage of the factor analysis technique is that each suspected factor can be tested individually by a purely mathematical route without any knowledge of the other factors.

Gas Imperfection Test

One interaction which might lead to variations in retention indices is gas non-ideality. As pointed out by Littlewood (7), several authors have treated this effect using second virial coefficients to estimate gas imperfections. However, reliable values of the second virial coefficients for most of the polar solutes contained in our scheme are not available. We therefore proceeded to evaluate the gas imperfection term using the van der Waals equation of state which holds for both nonpolar and polar solutes.

We can consider the evaporation of a solute to occur in two steps: (*1*) evaporation of the solute from the sorbed state to form an ideal gas and (*2*) transformation of the ideal gas to the real gas at the same pressure. If we assume that the van der Waals equation of state holds for a gaseous solute and that the fugacity of a solute–carrier gas mixture can be evaluated by treating the mixture as ideal even though the components are non-ideal, then the change in free energy per mole for the gas-phase transformation is

$$[2]\quad \Delta G = RT\left\{\left(\ln\frac{RT}{\bar{V}-b}+\frac{b}{\bar{V}-b}-\frac{2a}{RT\bar{V}}\right)-\ln P\right\}$$

$$\approx \frac{RTb}{\bar{V}}-\frac{2a}{\bar{V}}$$

where $\bar{V}$ is the gaseous molar volume, and a and b are the van der Waals constants of the solute. A solute test vector having the form of eq. 2 can be checked for possible rotation into one of the abstract eigenvectors. Fortunately, all the a's and b's need not be available in order to test a given factor; factor analysis predicts values for the missing data if a successful rotation is made (2).

The test for eq. 2 at 373 °K using critical constant data to calculate the a's and b's is shown in Table 1. If each of the test points on the test vector is rotated to a nearly equivalent value on the abstract eigenvector, we have indeed identified a physically significant parameter with an abstract factor. The reasonable agreement between the theoretical free energy test term calculated from eq. 2 and the complete rotated vector clearly indicates that gas imperfection is a factor of the retention index space and does have a measurable effect on retention index. Unfortunately, the magnitude of the effect cannot be predicted by factor analysis unless all eight factors (2) are identified. The form of eq. 2 is consistent with the form required for the product-type terms in eq. 1, with the solute term being evaluated by eq. 2 and the solvent part being unity. Predicted values of the non-ideality term for those gases for which van der Waal constants were missing are also included in Table 1.

Uniqueness Test

The rotation part of the factor analysis scheme has considerable potential for determining on a qualitative scale the extent to which a molecule

Can. J. Chem. Downloaded from www.nrcresearchpress.com by 210.87.254.105 on 09/05/12
For personal use only.

TABLE 1. Comparison between suspected solute test factors and those generated by factor analysis*

	Test factor											
			Uniqueness ‡									
	Gas imperfection†		Alcohol		Pyridine		Nitrile		Nitrile		Nitrile–Nitro	
Solute	Test	Predicted	Test	Predicted	Test	Predicted	Test	Predicted	Test	Predicted	Test	Predicted
2,4-Dimethylpentane	2.26	2.20	0	0.00	0	0.00	0	−0.04	0	0.01	0	0.04
2-Ethylhexene-1		2.48	0	0.00	0	−0.05	0	−0.05	0	0.00	0	−0.01
Cyclohexane		1.71	0	0.00	0	0.15	0	0.00	0	−0.06	0	−0.05
Toluene	1.95	1.91	0	0.00	0	−0.04	0	−0.06	0	−0.04	0	−0.02
Styrene	2.45	2.16	0	0.00	0	−0.04	0	−0.04	0	0.00	0	−0.01
Phenylacetylene		2.09		0.05	0	−0.03	0	0.05		0.28		0.21
Acetone	1.24	1.35		−0.13	0	0.04	0	0.07		0.55		0.77
Propionaldehyde		1.27		−0.10	0	0.00	0	0.08		0.44		0.58
Crotonaldehyde		1.67		−0.15	0	0.03	0	0.15		0.64		0.79
n-Butylacetate		2.44		−0.18	0	−0.01	0	0.06		0.60		0.70
Acetonitrile	1.43	1.11		−0.20	0	−0.01	1	0.29	1	0.97	1	1.01
Nitroethane		1.74		−0.14	0	−0.04	0	0.20		0.84	1	0.93
Dioxane	1.54	1.54		0.14	0	0.19	0	−0.03		0.25		0.39
n-Dibutylether		2.78		0.03	0	−0.19	0	−0.06		0.11		0.04
Thiophene	1.37	1.36		0.00	0	0.03	0	0.01		0.10		0.08
Chloroform	1.21	1.40		0.37	0	−0.06	0	0.04	0	−0.01	0	0.00
Carbon tetrachloride	1.56	1.56	0	0.00	0	−0.05	0	0.01	0	0.03	0	0.00
Methyl iodide	0.87	0.88		0.10	0	0.09	0	0.07	0	0.00	0	−0.02
Ethyl bromide	0.93	1.20		0.00	0	0.06	0	0.05	0	0.13	0	0.15
Difluro tetrachloroethane		2.10		−0.08	0	−0.02	0	0.02		0.34		0.34
n-Propanol	1.28	1.29	1	1.00	0	0.13	0	0.01		−0.13		0.24
Isopropanol	1.24	1.19		0.94	0	−0.01	0	−0.05		−0.19		0.25
Allylalcohol	1.22	1.23		1.02	0	0.08	0	0.04		−0.04		0.25
t-Butanol	1.48	1.46		0.74	0	−0.14	0	−0.14		−0.24		0.21
Cyclopentanol		1.74		0.95	0	0.14	0	0.02		−0.17		0.21
Benzene	1.48	1.57	0	0.00	0	0.09	0	−0.04	0	0.00	0	0.01
Ethanol	0.95	0.89	1	1.00	0	0.04	0	0.01		−0.15		0.25
Methylethylketone	1.58	1.70		−0.11	0	−0.02	0	0.06		0.48		0.67
Nitromethane	1.27	1.41		−0.03	0	0.00	0	0.25		0.93	1	1.01
Pyridine		1.19		0.69	1	0.73	0	−0.03		−0.17		0.43

*Blanks represent free floating points on test vectors.
†Test vector for gas imperfection was calculated from eq. 2 using critical constant data to estimate van der Waals constants. Critical constant data were taken from ref. 8. All values are negative.
‡Uniqueness test vectors for functional groups.

Can. J. Chem. Downloaded from www.nrcresearchpress.com by 210.87.254.105 on 09/05/12
For personal use only.

or group of molecules possesses a property which would lead to a unique type of interaction. For this "uniqueness" test, a crude test factor is created in which those solutes felt to possess this unique factor are assigned a value of unity and those solutes which are felt not to have the attribute are assigned a value of zero. If one is in doubt about the value to assign a particular solute in the test vector, that solute can be allowed to free float, *i.e.*, left blank, to avoid biasing the test vector. We recall that factor analysis yields values for the missing points if the test vector is rotated into an eigenvector of the factor space.

A uniqueness test of this kind was tried for the alcohols, which should be unique among the 30 solutes in their potential for hydrogen bonding. Since Rohrschneider speculated that chloroform also exhibits hydrogen-bonding characteristics (6), the value for chloroform in particular was allowed to free float. The uniqueness test for alcohols given in Table 1 indicates that alcohols definitely have a unique property since the predicted value for each of the alcohols is quite near one whereas nearly all the other solute terms are near zero. The value predicted for chloroform shows that chloroform does exhibit some alcohol-like character. The quite high value predicted for pyridine suggests that pyridine (which cannot be a hydrogen-bond donor) might be a unique solute. A pyridine uniqueness test (Table 1) shows that pyridine is truly unique, as suggested by Rohrschneider (6).

Rohrschneider also postulated that the nitro group and the nitrile group each shows distinctive properties (6). A uniqueness test for acetonitrile in which all the other solutes are assigned values of zero predicted a low value for acetonitrile, implying that the nitrile group is not unique. If the nitro-containing solutes and other solutes which might have properties similar to those of the nitrile group are allowed to free float during the nitrile uniqueness test, we find that the nitro- and nitrile-containing solutes have rotated values quite near one while several of the free floated solutes have relatively large values. Essentially the same results were obtained from a uniqueness test for nitro compounds in which acetonitrile and several other solutes were free floated and from a combined test for nitro-nitrile solutes. The results of three illustrative rotations are presented in Table 1. We conclude that individually the nitro and nitrile groups do not have unique behavior, but that the nitro-nitrile combined test defines an upper limit to a test vector. This uniqueness test may furnish an estimate of the combined ability of a solute to function as an electron donor and as a hydrogen-bond acceptor (6).

We express our appreciation to Edmund R. Malinowski for helpful discussions and to the Computer Centers at Stevens Institute of Technology and Brooklyn College. This work was supported by a grant from the City University of New York Faculty Research Award Program.

1. P. T. Funke, E. R. Malinowski, D. E. Martire, and L. Z. Pollara. Separation Sci. **1**, 661 (1966).
2. P. H. Weiner, E. R. Malinowski, and A. R. Levinstone. J. Phys. Chem. **74**, 4537 (1970).
3. P. H. Weiner and E. R. Malinowski. J. Phys. Chem. **75**, 1207 (1971).
4. P. H. Weiner and E. R. Malinowski. J. Phys. Chem. **75**, 3160 (1971).
5. P. H. Weiner. Ph.D. Thesis, Stevens Institute of Technology, Hoboken, N.J. 1971.
6. L. Rohrschneider. J. Chromatogr. **22**, 6 (1966).
7. A. B. Littlewood. Gas chromatography. 2nd ed. Academic Press, New York. 1970. p. 32.
8. R. C. Weast (*Editor*). Handbook of Chemistry and and Physics. Chemical Rubber Co., Cleveland. 1970. p. F63.

Gallium(III)-trisfluorosulfate

A. STORR, P. A. YEATS, AND F. AUBKE[1]

Department of Chemistry, The University of British Columbia, Vancouver 8, British Columbia

Received July 19, 1971

Gallium(III)-trisfluorosulfate is prepared by the reaction of gallium(III)-trichloride with either $S_2O_6F_2$ or $BrOSO_2F$. The i.r. spectrum is interpreted in terms of a polymeric compound containing bridging bidentate fluorosulfate groups only, thus resulting in hexacoordination around gallium. Gallium(III)–trisfluorosulfate is found to react with trimethylamine, however adducts of variable composition are formed.

Le trifluorosulfate de gallium(III) a été préparé par action du trichlorure de gallium sur $S_2O_6F_2$ ou sur $BrOSO_2F$. Le spectre infrarouge est interprété en fonction d'un composé polymérique contenant uniquement des groupes fluorosulfates bidentates servant de ponts; il en résulte ainsi une hexacoordination autour du gallium. Le trifluorosulfate de gallium(III) réagit avec la triméthylamine en donnant des produits de composition variable.

Canadian Journal of Chemistry, **50**, 452 (1972)

Introduction

We became interested in the synthesis and the structural characterisation of anhydrous gallium(III)-trisfluorosulfate $Ga(SO_3F)_3$ for a number of reasons. Only very few stable binary metal trisfluorosulfates are reported (1). Aluminum(III)-trisfluorosulfate appears to be obtainable only as a 1:3 complex with acetonitrile (2) and only for the recently reported $Fe(SO_3F)_3$ (3), an i.r. spectrum and magnetic susceptibility measurements are reported.

On the other hand, of the gallium(III) salts with oxyanions only $Ga_2(SO_4)_3$ (4) is said to exist in its anhydrous form, whereas $Ga(ClO_4)_3$ (5) and $Ga(NO_3)_3$ (6) are known as hydrates with all dehydration attempts resulting in the formation of basic salts (7).

Gallium(III)-fluorosulfate could feasibly act in the HSO_3F solvent system as an acid, that is as an SO_3F^- ion acceptor, and could play a similar role as $B(SO_4H)_3$ in the sulfuric acid system (8). Not many solutes are known to act as acids in the HSO_3F system (9).

Suitable fluorosulfonating agents can be seen in peroxydisulfuryl difluoride (10) ($S_2O_6F_2$) and in bromine(I)-fluorosulfate (11) ($BrOSO_2F$). Both have been found to replace chlorine quite readily (12, 13), so that $GaCl_3$ could be used as the substrate resulting hopefully in the formation of anhydrous $Ga(SO_3F)_3$.

The compound should also be a suitable Lewis acid and is expected to form addition compounds with trimethylamine.

[1]To whom all correspondence should be addressed.

Experimental

Chemicals

Gallium(III)-chloride was prepared and purified as previously described (14). Peroxydisulfuryl difluoride was obtained in a flow reaction of F_2 (Allied Chem. Corp.) with SO_3 (Baker and Adamson) over AgF_2 according to Cady and Shreeve (15). Bromine(I)-fluorosulfate was synthesized from Br_2 (British Drug House Corp. Ltd.) and $S_2O_6F_2$ as reported before (16). Trimethylamine was obtained from Matheson of Canada and HSO_3F was purified by double distillation according to Barr *et al.* (17).

Instrumentation

The i.r. spectra were obtained on a Perkin–Elmer 457 spectrophotometer. Silver chloride and bromide as well as KRS-5 (all from Harshaw Chemicals) were used. All manipulations were carried out either in a standard high vacuum line, fitted with greaseless Teflon stem stopcocks for the transfer of $S_2O_6F_2$ or $BrOSO_2F$, or in a glove box, filled with dry nitrogen.

Preparation

(a) $Ga(SO_3F)_3$

The reaction between $S_2O_6F_2$ (present in an approximately 10-fold excess) and $GaCl_3$ is performed in a 100 ml Pyrex reactor with a flat bottom. Gallium trichloride is introduced in the drybox through an attached side arm fitted with B14 ground-glass joint from a small storage ampule via sublimation. The side arm is sealed off after addition, the amount of $GaCl_3$ added can be determined by weighing the ampule before and after addition. $S_2O_6F_2$ is introduced through a Teflon stem stopcock via distillation. The reaction mixture is allowed to warm up to room temperature where immediate exothermic reaction and the release of Cl_2 is noted. A fine white powder is formed. The reaction mixture is stirred externally, in order to complete the reaction, for about 1 h. The volatile reaction product and the excess $S_2O_6F_2$ are removed under vacuum, $Ga(SO_3F)_3$ is left behind as a hygroscopic white powder. In a typical reaction 1.318 g $GaCl_3$ are converted into 2.733 g $Ga(SO_3F)_3$, indicating complete conversion.

The reaction of $GaCl_3$ with $BrOSO_2F$ is carried out in the

Can. J. Chem. Downloaded from www.nrcresearchpress.com by 210.87.254.5 on 09/05/12
For personal use only.

TABLE 1. Vibrational modes of $Ga(SO_3F)_3$ and some related compounds*

$Ga(SO_3F)_3$ (s)	$Fe(SO_3F)_3$ (3) (s)	$(CH_3)_2Sn(SO_3F)_2$ (s)	$SnCl_2(SO_3F)_2$ (18) (s)	$KBr(SO_3F)_4$ (19) (s)	KSO_3F (20) (s)	Assignment
1398 s	1360	1350	1385	1416†	1285	SO_3 stretch, as
1177 vs	1137	1180	1130	1229†		SO_3 stretch
1090 ms	1090	1072	1087	970	1079	SO_3 stretch, sym
868 s	850	827	864	834	745	SF stretch
636 m	630	620	628	615		SO_3 bend sym
591 m	579	590	586	578	590	SO_3 bend as
555 s	551	554	555	553	570†	SO_3 bend sym
445 w,b						Ga—O stretch?
417 mw	419	417	420	406	407	SO_2F rock
328 m	318	304	312	239		SO_3F torsion

*vs = very strong, s = strong, m = medium, w = weak, vw = very weak, b = broad, sym = symmetric, as = asymmetric.
†Average value.

same way. The reaction proceeds less vigorously and a slightly yellowish powder is left behind.

(b) $Ga(SO_3F)_3.xN(CH_3)_3$

When an excess of trimethylamine is condensed onto samples of $Ga(SO_3F)_3$, ranging in amounts from 150 to about 400 mg, solid white products are formed which exhibit $Ga(SO_3F)_3:N(CH_3)_3$ ratios of 1:1.2 to 1:1.7. A typical analysis is given below. All products were found to be thermally stable up to 230 °C. Analysis: Gallium was determined gravimetrically as the 8-hydroxyquinolate. Microanalysis for carbon was done by Mr. P. Borda of this department and analysis for S and F was carried out by A. Bernhardt, microanalytical laboratory in Elbach, West Germany.

Anal. Calcd. for $Ga(SO_3F)_3$: Ga, 19.01; S, 26.20; F, 15.50. Found: Ga, 19.16; S, 26.08; F, 15.65.

Anal. Calcd. for $Ga(SO_3F)_3.N(CH_3)_3$: Ga, 16.38; C, 8.46. Found: Ga, 15.80; C, 9.95.

Discussion

Gallium(III)-trisfluorosulfate is formed in a fast and clean reaction from $GaCl_3$ and $S_2O_6F_2$ or $BrOSO_2F$, according to

$$2GaCl_3 + 3S_2O_6F_2 \xrightarrow{25\ °C} 2Ga(SO_3F)_3 + 3Cl_2$$

or

$$2GaCl_3 + 6BrOSO_2F \xrightarrow{25\ °C} 2Ga(SO_3F)_3 + 3Cl_2 + 3Br_2$$

Since $BrOSO_2F$ is obtained from $S_2O_6F_2$ the first route is less circuitous and therefore preferable. The obtained product is thermally stable without melting up to 320 °C at atmospheric pressure. The thermal decomposition under vacuum starts at 240 °C and proceeds rather slowly under the release of sulfur trioxide only. Disulfuryl difluoride ($S_2O_5F_2$) and sulfuryl fluoride, the two other likely products in a pyrolysis of metal fluorosulfates (3) are not observed. Attempts to study the solution behavior of $Ga(SO_3F)_3$ in HSO_3F failed. Addition of the solute to the acid did not result in any change of the specific conductance, it must therefore be concluded that the compound is completely insoluble in this medium as is visually apparent. Addition of KSO_3F did not increase the solubility of $Ga(SO_3F)_3$. This observation may possibly be interpreted in terms of a polymeric structure for gallium(III)-trisfluorosulfate.

All attempts to synthesize other group III fluorosulfates with either $S_2O_6F_2$ or $BrOSO_2F$ as fluorosulfonating agents were unsuccessful. Neither $AlCl_3$, $InCl_3$, nor indium metal were found to react even at temperatures up to +100 °C.

The i.r. spectrum of $Ga(SO_3F)_3$ is rather uncomplicated, indicating the presence of only one type of SO_3F group in the molecule. The vibrational frequencies are listed in Table 1 together with the corresponding modes for some related compounds and a proposed assignment.

It has been pointed out before (3, 18, 19) that the symmetry of the free SO_3F^- ion will be reduced from C_{3v} to C_s where the SO_3F group acts as a covalently bonded mono- or bidentate group. As a consequence the number of fundamentals will increase from 6 to 9, all i.r. and Raman active.

A decision, whether a monodentate or a bidentate fluorosulfate group is present can be made when considering the position of the three SO stretching modes. These three modes are produced from the 2 SO_3 modes in ionic SO_3F^-, an A_1 mode found at 1080 cm^{-1} and an E mode

Can. J. Chem. Downloaded from www.nrcresearchpress.com by 210.87.254.5 on 09/05/12
For personal use only.

Can. J. Chem. Downloaded from www.nrcresearchpress.com by 210.87.254.5 on 09/05/12
For personal use only.

at 1285 cm^{-1} (20), when the degeneracy of the latter is lifted and the band splits up.

For $(CH_3)_2Sn(SO_3F)_2$ (21), where the existence of bidentate bridging SO_3F group is demonstrated by X-ray diffraction (22), and for $SnCl_2(SO_3F)_2$ (18), where a similar configuration is postulated based on the ^{119}Sn Mössbauer spectrum, the two higher SO stretching modes are found at 1355–1385 and 1130–1180 with the position of the last SO mode virtually unchanged in respect to its position for KSO_3F.

For monodentate SO_3F groups, as found in solids of the type $K[Hal(OSO_2F)_4]$ (19) with Hal = Br and I, the three SO modes are found at ~1410, ~1240, and ~985 cm^{-1}, respectively.

As seen in the table, not only the stretching but also the deformation modes of the SO_3F group in $Ga(SO_3F)_3$ compare well to the identical modes in the two tin(IV) derivatives. It is on this evidence that we prefer to interpret the i.r. spectrum in terms of a bidentate bridging SO_3F group in $Ga(SO_3F)_3$, with bridging occurring over two oxygen atoms. This will result in hexacoordination for gallium, GaF_3 and most modifications of Ga_2O_3 (23, 7) are precedents for this coordination among simple binary gallium(III) compounds, and in a polymeric structure, consistent with our previous observations.

The relatively close resemblance of the i.r. spectra of $Ga(SO_3F)_3$ and $Fe(SO_3F)_3$ (3) suggests a similar conformation of the SO_3F group in both compounds.

In addition to the discussed absorption bands, attributed to the SO_3F group, a broad and rather weak band is found at 445 cm^{-1}. We interpret this absorption as being due to gallium–oxygen stretching. Attempts to obtain a Raman spectrum on the solid were unsuccessful.

The interaction of $Ga(SO_3F)_3$ with trimethylamine proceeds spontaneously at room temperature under formation of white, thermally stable solids. However, in contrast to observations in the $GaCl_3$–$N(CH_3)_3$ system (24), where 1:1 adducts are obtained under these conditions, the uptake of amine was higher resulting in composition between 1:1 and 1:2 stoichiometry. The amine uptake was found to be highest where finely powdered samples of $Ga(SO_3F)_3$ were used. Similar observations were made by us (25) in reaction of a large range of N-donor ligands with a number of methyltin(IV)-fluorosulfate compounds where also bridging bidentate SO_3F groups are present (12, 21, 22). The observations reported here again suggest a polymeric structure for $Ga(SO_3F)_3$.

This study was financially supported by the National Research Council of Canada.

1. A. A. Woolf in E. A. V. Ebsworth, A. G. Maddock and A. G. Sharpe. New pathways in inorganic chemistry. Cambridge University Press, Cambridge. 1968. p. 327.
2. E. Hayek, A. Czaloun, and B. Krismer. Mh. Chem. **87**, 742 (1956).
3. J. Goubeau and J. B. Milne. Can. J. Chem. **45**, 2321 (1967).
4. P. E. Lecoq de Boisboudran. Ann. Chim. Phys. [5], **10**, 100 (1877).
5. L. S. Foster. J. Am. Chem. Soc. **61**, 3122 (1939).
6. E. Einecke. Angew. Chem. **55**, 43 (1942).
7. I. A. Sheka, I. S. Chaus, and T. T. Mityureva. The chemistry of gallium. Elsevier Publishing Company, Amsterdam. 1966.
8. R. J. Gillespie and E. A. Robinson. *In* T. C. Waddington Non-aqueous solvent systems. Academic Press, London. 1965.
9. R. C. Thompson. *In* Inorganic sulphur chemistry. *Edited by* G. Nickless, Elsevier Publ. Co. Inc., Amsterdam. 1968. p. 587.
10. F. B. Dudley and G. H. Cady. J. Am. Chem. Soc. **79**, 513 (1957).
11. J. E. Roberts and G. H. Cady. J. Am. Chem. Soc. **82**, 352 (1960).
12. J. M. Shreeve and G. H. Cady. J. Am. Chem. Soc. **83**, 452 (1961).
13. D. D. Des Marteau. Inorg. Chem. **7**, 434 (1968).
14. N. N. Greenwood and K. Wade. J. Chem. Soc. 1527 (1956).
15. G. H. Cady and J. M. Shreeve. Inorg. Syn. **7**, 124 (1953).
16. F. Aubke and R. J. Gillespie. Inorg. Chem. **7**, 599 (1968).
17. J. Barr, R. J. Gillespie, and R. C. Thompson. Inorg. Chem. **3**, 1149 (1964).
18. P. A. Yeats, B. L. Poh, B. F. E. Ford, J. R. Sams, and F. Aubke. J. Chem. Soc. (A), 2188 (1970).
19. H. A. Carter, S. P. L. Jones, and F. Aubke. Inorg. Chem. **9**, 2485 (1970).
20. A. M. Qureshi, H. A. Carter, and F. Aubke. Can. J. Chem. **49**, 35 (1971).
21. P. A. Yeats, B. F. E. Ford, J. R. Sams, and F. Aubke. Chem. Commun. 791 (1969).
22. F. A. Allen, J. Lerbscher, and J. Trotter. J. Chem. Soc. In press.
23. A. F. Wells. Structural inorganic chemistry. Oxford Press, Oxford. 1962, p. 456.
24. N. N. Greenwood and A. Storr. J. Chem. Soc. 3426 (1965).
25. D. Klett and F. Aubke. Unpublished results.

Erratum: Isomérisation des époxydes

KRYZSZTOF JANKOWSKI ET JEAN-YVES DAIGLE
Département de Chimie, Université de Moncton, Moncton, Nouveau-Brunswick
Received October 22, 1971
(Ref. Can. J. Chem. **49**, 2594 (1971))

Canadian Journal of Chemistry, **50**, 455 (1972)

Page 2594, paragraphe 3, colonne 1, au lieu de
"L'époxydation de l'hydroxy-2-cyclohexene (**3**) avec même peracide donne principalement l'époxyde *trans* **4***a* . . . . . "
doit être
". . . . . principalement l'époxyde *cis* **4***b* . . . . . ".

Can. J. Chem. Downloaded from www.nrcresearchpress.com by 210.87.254.40 on 09/05/12
For personal use only.

Can. J. Chem. Downloaded from www.nrcresearchpress.com by 210.87.254.42 on 09/05/12
For personal use only.

A Novel Phosphate Protecting Group for Oligonucleotide Synthesis

R. H. WIGHTMAN

Department of Chemistry, Carleton University, Ottawa, Canada K1S 5B6

AND

S. A. NARANG[1] AND K. ITAKURA[2]

Biochemistry Laboratory,[3] National Research Council of Canada, Ottawa, Canada K1A 0R6

Received November 10, 1971

2-Phenylmercaptoethanol is found to be a very stable phosphate protecting group during oligonucleotide synthesis. However, when necessary it can be easily removed, after activation.

Le phényl-2 mercaptoéthanol apparaît comme étant un groupe phosphate protecteur très stable pendant la synthèse d'oligonucléotides. Il est cependant facile à enlever, après activation, lorsque c'est nécessaire.

Canadian Journal of Chemistry, **50**, 456 (1972)

Protection of the terminal phosphomonoester group is a necessary step in any chemical synthesis of oligonucleotides. We wish to report 2-phenylmercaptoethanol (**1**) (1) as a new phosphate protecting group which is easily introduced and stable to conditions normally encountered in oligonucleotide manipulations, such as (*i*) 1 *N* aqueous sodium hydroxide at room temperature for 8 h, (*ii*) concentrated ammonium hydroxide at 50° for 2 h, (*iii*) aqueous pyridine at room temperature for 1 week, (*iv*) mesitylene sulfonyl chloride in anhydrous pyridine at room temperature for 3 h, (*v*) aqueous hydrochloric acid (p*H* 2) at room temperature for 3 days. However, when "activated" this group is readily removed. Additionally, it incorporates one benzene ring to take advantage of the absorptive property of benzoylated DEAE Sephadex for purification of products (2).

Protection of the deoxymononucleotide 5′-phosphate **2** was completed in 24 h by treating its pyridinium salt with 2-phenylmercaptoethanol and dicyclohexylcarbodiimide (both in 10 *M* excess). Unused DCC was then decomposed with aqueous pyridine, the urea filtered off, and excess reagent removed by extraction with ethyl acetate. The aqueous phase was concentrated and a final purification was achieved by gel-filtration on a Sephadex G-25 (superfine) column, using 0.1 *M* triethylammoniumbicarbonate buffer, (p*H* 7.5) as eluant.

Each of the protected mononucleotides **3** was condensed with 3′-*O*-acetyl thymidine 5′-phosphate **4**. Work-up with aqueous pyridine and 2 *N* aqueous sodium hydroxide followed by sequential chromatography on benzoylated DEAE Sephadex and Sephadex G-25 superfine (2) gave the desired protected dinucleotides **5** (see Scheme 1). The 2-phenylmercaptoethyl group was removed by treating the protected nucleotide in aqueous solution (or in 0.1 *M* triethylammoniumbicarbonate) with sodium metaperiodate (approximately 5 *M* excess, as a freshly prepared 0.1 *M* aqueous solution) at room temperature for 1 h. It was apparently oxidized to the corresponding sulfoxide derivative **6** (3). After decomposition of the excess periodate with ethylene glycol and precipitation of inorganic residues with 90% aqueous pyridine, the free dinucleotide **7** was liberated by treatment with 2 *N* aqueous sodium hydroxide at room temperature for 30 min. A similar approach has been reported (4) for peptide synthesis.

Since some *N*-acetyl groups were labile to alkali, we found it more convenient for this initial investigation to deblock any amino func-

[1]Author to whom correspondence should be addressed.
[2]NRCC Postdoctorate Fellow, 1971–present.
[3]NRCC No. 12342.

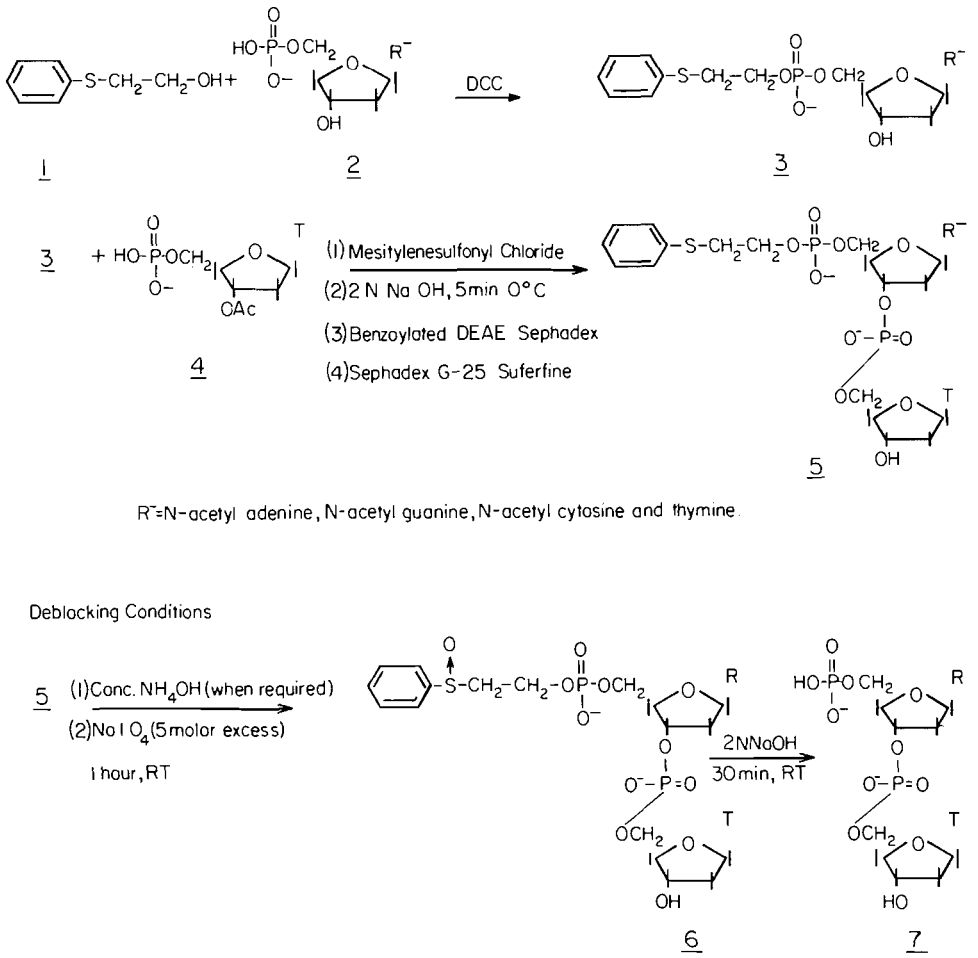

SCHEME 1

tions before activating the 2-phenylmercaptoethyl group for removal. Consequently each of the four 5′-mononucleotides (*i.e.* d-pA, d-pC, d-pG, and pT) obtained from **3** via a complete deblocking sequence were fully characterized by t.l.c. in three solvent systems (5) and u.v. spectroscopy to ensure that the periodate treatment in no way affected the heterocyclic bases. Indeed all the dinucleotides **7** were characterized by t.l.c. as well as u.v. spectra of the components obtained by enzymic degradations. We feel the properties of this protecting group, make it more generally applicable than 2-cyanoethanol (6) for many aspects of oligonucleotide synthesis.

We wish to acknowledge helpful suggestions by Dr. T. Durst, Department of Chemistry, University of Ottawa.

1. A. H. FORD-MOORE, R. A. PETERS, and R. W. WAKELIN. J. Chem. Soc. 1754 (1949).
2. (*a*) S. A. NARANG, O. S. BHANOT, J. GOODCHILD, and R. H. WIGHTMAN. Chem. Commun. 91, 516 (1970). (*b*) J. J. MICHNIEWICZ, O. S. BHANOT, J. GOODCHILD, S. K. DHEER, R. H. WIGHTMAN, and S. A. NARANG. Biochem. Biophys. Acta, **224**, 626 (1970).
3. N. J. LEONARD and C. R. JOHNSON. J. Org. Chem. **27**, 282 (1962).
4. P. M. HARDY, H. N. RYDON, and R. C. THOMPSON. Tetrahedron Lett. 2525 (1968).
5. S. A. NARANG, O. S. BHANOT, S. K. DHEER, J. GOODCHILD, and J. J. MICHNIEWICZ. Biochem. Biophys. Res. Commun. **41**, 1248 (1970).
6. G. M. TENER. J. Am. Chem. Soc. **83**, 159 (1961).

Can. J. Chem. Downloaded from www.nrcresearchpress.com by 210.87.254.42 on 09/05/12
For personal use only.

Can. J. Chem. Downloaded from www.nrcresearchpress.com by 210.87.254.40 on 09/05/12
For personal use only.

Canadian Journal of Chemistry

Published by THE NATIONAL RESEARCH COUNCIL OF CANADA

VOLUME 50 FEBRUARY 15, 1972 NUMBER 4

Reactions of Unsaturated Compounds with Silicon Difluoride. Part I. Acetylene

C. S. LIU
Department of Chemistry, University of Toronto, Toronto 181, Ontario

J. L. MARGRAVE
Department of Chemistry, Rice University, Houston, Texas

J. C. THOMPSON[1]
Department of Chemistry, University of Toronto, Toronto 181, Ontario
and
Department of Chemistry, Rice University, Houston, Texas

AND

P. L. TIMMS[2]
Department of Chemistry, Rice University, Houston, Texas

Received September 16, 1971

The reaction of acetylene with silicon difluoride at low temperatures has been studied. Three products have been identified as volatile species after the reaction: tetrafluorodisilacyclobutene, 3,4-tetrafluorodisilahex-1-yne-5-ene, and 5,6,7-hexafluorotrisilanorborn-2-ene. Spectroscopic data for the compounds are presented, together with a possible mechanism to account for the formation of the observed products.

La réaction de l'acétylène avec le difluorure de silicium a été étudiée à basse température. Trois produits ont été identifiés comme des espèces volatiles après la réaction: le tétrafluorodisilacyclobutène, le 3,4-tétrafluorodisilahex-1-yne-5-ène et le 5,6,7-hexafluorotrisilanorborn-2-ène. Les données spectroscopiques des composés sont présentées en même temps qu'un mécanisme possible pour rendre compte de la formation des produits observés.

Canadian Journal of Chemistry, **50**, 459 (1972)

Introduction

The low-temperature reaction chemistry of silicon difluoride (SiF_2) has been the subject of a number of recent studies, and has resulted in the formation of a variety of new silicon–fluorine derivatives (1). Of considerable interest has been the reactivity of SiF_2 with unsaturated organic compounds such as ethylene (2), benzene (3), and trifluoropropyne (4). We have studied the reactions of SiF_2 with a range of alkyne and alkene derivatives, and shall report the products from these reactions in this and subsequent papers.[3]

Experimental

A greaseless vacuum system was used for the reactions and for the manipulation of volatile compounds which were studied by mass spectrometry, n.m.r. spectroscopy, and i.r. spectroscopy.

SiF_2 (gas) was prepared, as has been described previously (5), by reduction of silicon tetrafluoride with silicon metal at 1150 °C. The gaseous mixture of SiF_2 and SiF_4 was co-condensed at −196 °C with an approximately 2:1 excess of

[1]Author to whom correspondence should be addressed (Toronto).

[2]Present address: Department of Chemistry, University of Bristol, Bristol, United Kingdom.

[3]Part 2. Reactions with alkyl substituted acetylenes. Can. J. Chem. This issue.

TABLE 1. Nuclear magnetic resonance data for compounds **1**, **2**, **3**

Compound	Nucleus	Chemical shifts*	Coupling constants†	
1, $C_2H_4Si_2F_4$	H	1.67	J_{HF}	16.2
	F	129.2	$J_{HF'}$	5.0
2, $C_4H_4Si_2F_4$	H	7.25(1)	J_{HF}	2.2
	H′	~3.6(3)		
	F	135.3(1)	$J_{FF'}$	11.8
	F′	140.1(1)		
3, $C_4H_4Si_3F_6$	H(1, 4)	7.95(1)		
	H(2, 3)	3.72(1)		
	F(5, 6 or 5′, 6′)	128.5(2)	$J_F(5, 5')$	31.0
	F(5, 6 or 5′, 6′)	145.9(2)	$J_F(5, 6')$	15.0
	F(7 or 7′)	131.2(1)	$J_F(7, 7')$	56.0
	F(7 or 7′)	150.4(1)		

*In p.p.m., τ (tau) scale for ^1H, positive values upfield from CCl_3F for ^{19}F; integrated intensities in parentheses.
†In Hz, estimated from multiplet patterns.

acetylene. Such conditions led to the largest quantities of volatile products, which, however, were only formed in up to 5% yield based on acetylene consumed in the reaction.

Results

(i) Reaction between SiF_2 and $HC{\equiv}CH$

Co-condensation of the reagents at −196 °C produced a reddish-brown condensate, which, on warming slowly to room temperature, evolved volatile material and left a brown residue.

(ii) Involatile Residue

The residue was spontaneously inflammable in moist air, the heat evolved during combustion being sufficient to melt Pyrex glass, and also dissolved violently in dilute HF or KOH solutions. Heating in vacuo at 250–300 °C led to the formation of only small quantities of volatile material, insufficient for further investigation, while a small quantity of the residue exploded in the vacuum line at about 350 °C. The solid was insoluble in all solvents with which it did not react, and hence little is known of its composition or structure.

(iii) Volatile Material

SiF_4 and $HC{\equiv}CH$ were removed by distillation at −120 °C, after which the remaining volatile species were further separated by trap-to-trap distillation into two main fractions.

(a) Fraction Held at −80 °C, Volatile at −55 °C

At room temperature this was a colorless liquid and was shown mass spectrometrically to contain two species of *m/e* 158 and 184, corresponding to molecular formulae $C_2H_2Si_2F_4$ (**1**) and $C_4H_4Si_2F_4$ (**2**). Due to their similar volatilities and to the ready decomposition of (**1**), the two compounds could not be separated by distillation and **1** was never obtained in a pure state. However, by allowing the mixture to stand at room temperature for 3 h, it was found that no **1** remained as a volatile species, but that a spontaneously inflammable solid residue remained. Thus **2** could be obtained in a relatively pure form, but attempts to remove all traces of impurities (such as Si_3F_8, detected by n.m.r. and mass spectrometry) by gas chromatography failed due to its ready decomposition on the columns used. The gas phase molecular weight of **2** was 187 ± 5, which is further support for the molecular formula suggested from the mass spectrum. Nuclear magnetic resonance spectra were obtained from mixtures of **1** and **2** and from **2** alone, thus allowing some of the details of the spectra of **1** to be deduced. The results are shown in Fig. 1 and Table 1. Gas phase i.r. spectra of the mixture and of **2** showed only minor differences, which did not permit assignment of specific absorptions to **1**. However, **2** showed characteristic bands at (cm^{-1}) 3315(m) (νH—C≡), 3016(m) (νH—C=), 2165(w) (νC≡C), 1599(w) (νC=C), and 920(vs) (νSiF). Hydrolysis of **2** with dilute HF yielded approximately equal amounts of acetylene and ethylene.

On the basis of all these results the structures shown in Fig. 1 are assigned to **1** and **2**.

A planar four-membered ring for **1** would in

Can. J. Chem. Downloaded from www.nrcresearchpress.com by 210.87.254.40 on 09/05/12
For personal use only.

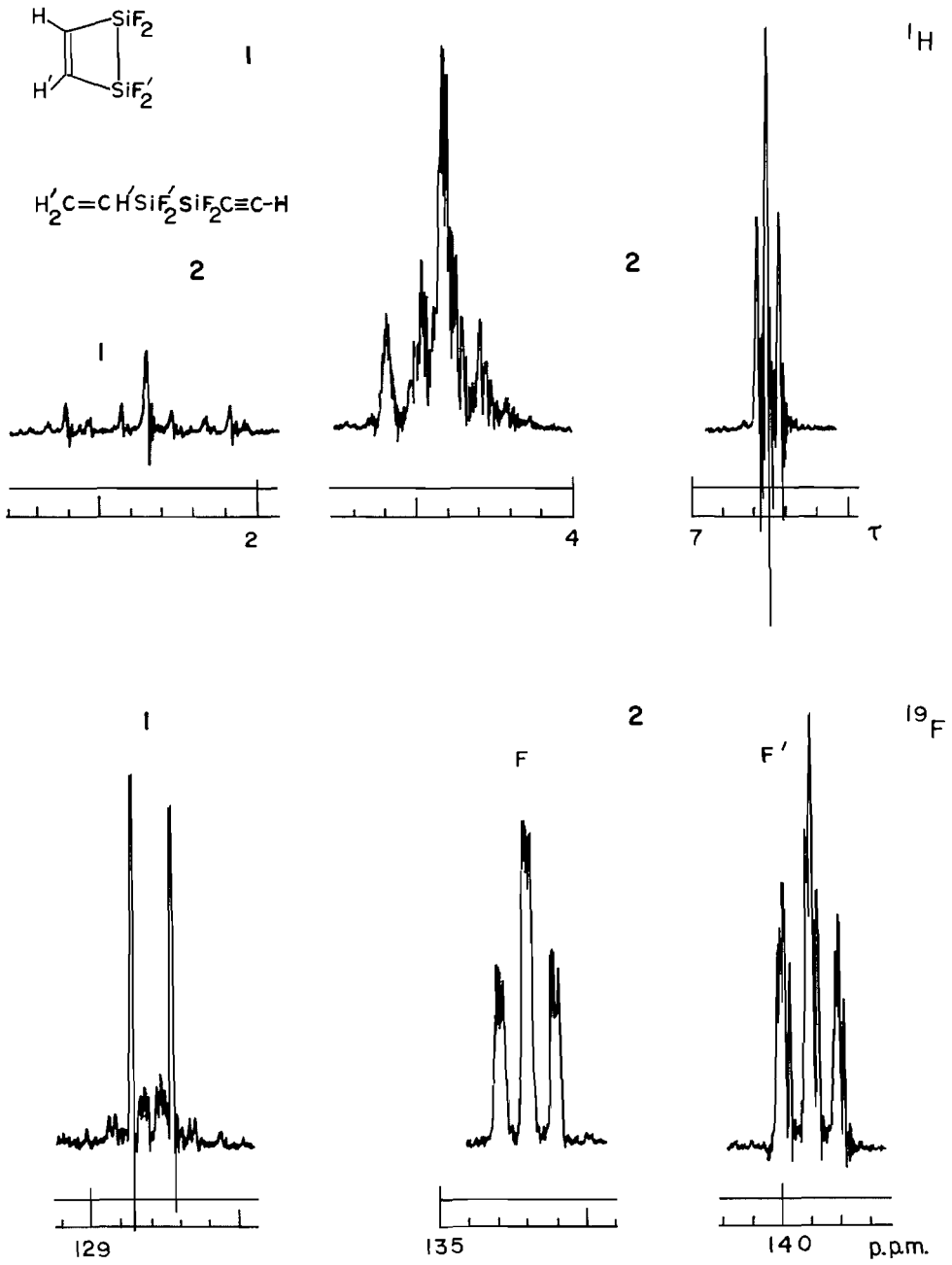

FIG. 1. Nuclear magnetic resonance spectra and structures of **1** and **2**.

theory show n.m.r. patterns corresponding to the $A_2A_2'XX'$ spin-system. No full analysis of our spectra has yet been attempted, but it is noted that the observed patterns are quite similar in appearance, for both the A and X parts, to those observed and analyzed for the analogous spin-system in perfluorocyclobutene (6). The highly strained ring, with a comparatively weak silicon–silicon bond, might be expected to result in an unstable compound as we

Can. J. Chem. Downloaded from www.nrcresearchpress.com by 210.87.254.40 on 09/05/12
For personal use only.

Can. J. Chem. Downloaded from www.nrcresearchpress.com by 210.87.254.40 on 09/05/12
For personal use only.

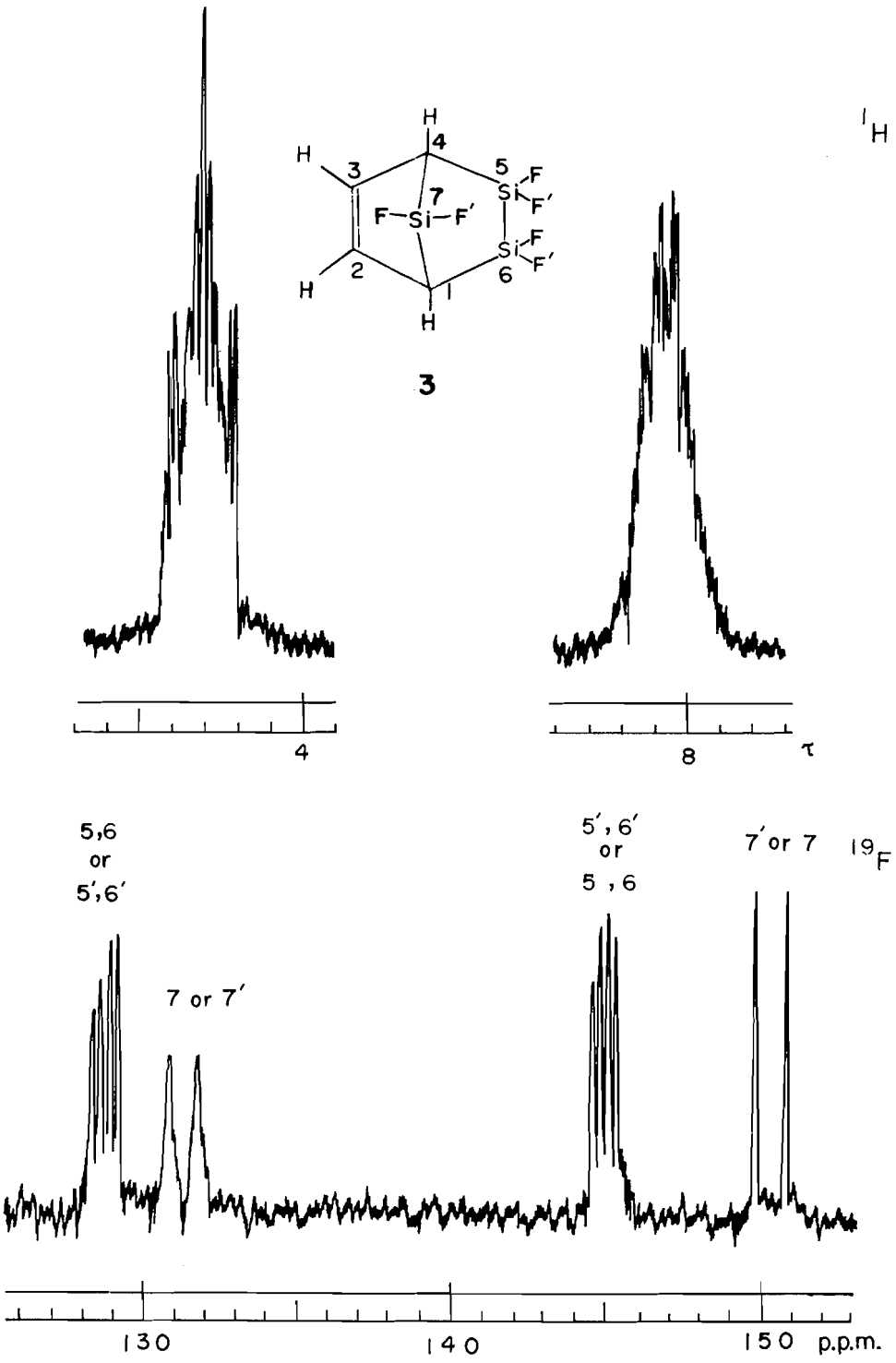

FIG. 2. Nuclear magnetic resonance spectra and structure of **3**.

Can. J. Chem. Downloaded from www.nrcresearchpress.com by 210.87.254.40 on 09/05/12
For personal use only.

observed. No information has yet been obtained as to the mode of decomposition or the nature of the eventual pyrophoric products.

The asymmetric open-chain structure of **2** is assigned from the n.m.r. and i.r. spectra. As has been found in other vinyl-substituted silicon fluorides (7), the three protons in the vinyl group have similar chemical shifts and are highly coupled amongst themselves and to two pairs of fluorine atoms resulting in the very complex multiplet observed in the proton spectrum.

(b) Fraction Held at −35 °C, Volatile at −10 °C

This contained colorless needle-like crystals (m.p. 34°) which sublimed in the vacuum system. The mass spectrum showed the heaviest ion at *m/e* 250, which corresponds to a formula $C_4H_4Si_3F_6$ **3**, with an important fragment at *m/e* 52 ($C_4H_4^+$). Elemental analysis (Crobaugh Laboratories) confirmed the molecular formula.

Anal. Calcd. for $C_4H_4Si_3F_8$: H, 1.6; C, 19.2; Si, 33.6; F, 45.6. Found: H, 1.68; C, 19.31; Si, 32.88; F, 46.14.

3 was not very soluble in common organic solvents, but satisfactory n.m.r. spectra were eventually obtained from dilute solutions in $CDCl_3$. The spectra (Table 1 and Fig. 2) showed several important differences from those obtained from **2** and indicated that **3** was not a simple homologue of **2** with the additional SiF_2 unit in the chain. The fluorine spectrum indicates single non-equivalent fluorine atoms coupled in pairs, while the equal relative intensities of the two resonances in the proton spectrum show equal numbers of hydrogen atoms. On the basis of this n.m.r. data the structure shown in Fig. 2 is indicated. The rigid skeleton of this trisilanorbornene derivative leads to four types of chemically non-equivalent fluorine atoms (5 or 6, 5′ or 6′, 7 and 7′) and the spin-coupling of, for example 5 with 5′ and 6′, accounts for the observed n.m.r. spectra. The chemical shift differences between the geminal fluorine atoms of 17.4 (5′ and 6′) and 19.2 (7′) p.p.m. are similar to those found in some norbornene derivatives with CF_2 in the 7-position, where typical chemical shift differences ranged between 16 and 20 p.p.m. (8). However the *gem F*—Si—*F* coupling of 56.0 Hz in the 7-position is considerably lower than J_{F-C-F} of around 175 Hz found previously (8, 9). Since **3** represents the first silicon fluorine compound for which $J_{FF(gem)}$ can be determined, it is not yet possible to say whether the smaller value may be characteristic of SiF_2 compounds or whether it is associated with the structure of this particular compound.

Preliminary results from a single crystal X-ray structure determination have confirmed the structure of **3** as shown in Fig. 2. Full details of the structure will be reported when refinement of the data is completed (11).

Discussion

With the exception of **3**, which has in addition a single bridging SiF_2 unit, each of these compounds is apparently formed by attack of Si_2F_4 radicals on the acetylenic triple bond. Such disilicon-compounds are apparently the general type of product formed in SiF_2 reactions with unsaturated carbon compounds, except when there is a fluorine atom directly bound to unsaturated carbon (2, 3). It thus seems likely that the initial stages of the reaction proceed via

$$HC{\equiv}CH + \cdot Si_2F_4 \cdot \rightarrow \underset{a}{H\dot{C}{=}CH{-}SiF_2{-}\dot{S}iF_2}$$

The intermediate species *a* may then undergo either ring closure to form **1**, or reaction with further SiF_2 units probably forming polymers, or reaction with acetylene to form a second possible intermediate

$$\underset{b}{H\dot{C}{=}CH{-}SiF_2{-}SiF_2{-}CH{=}\dot{C}H}$$

We do not isolate the ring closure product of (*b*), which would be a 5,6-disilacyclohexa-1,3-diene, however **3** might be regarded as being formed from reaction of SiF_2 with the cyclic diene. The reason for the formation of the single silicon bridge is not at all clear, since no other monosilicon units have been found in this type of reaction, and it is known that this disilacyclohexadiene system is not inherently unstable (ref. 4, and part 2 of this series). **2** may be formed from (*b*) through a 1,5-hydrogen migration to form the unsymmetrical chain compound. Such migrations involving vinyl-type radicals have been previously postulated to explain the range of products found in other free radical addition reactions to substituted acetylenes (10).

A proposed reaction scheme for SiF_2–acetylene reaction is shown in Scheme 1.

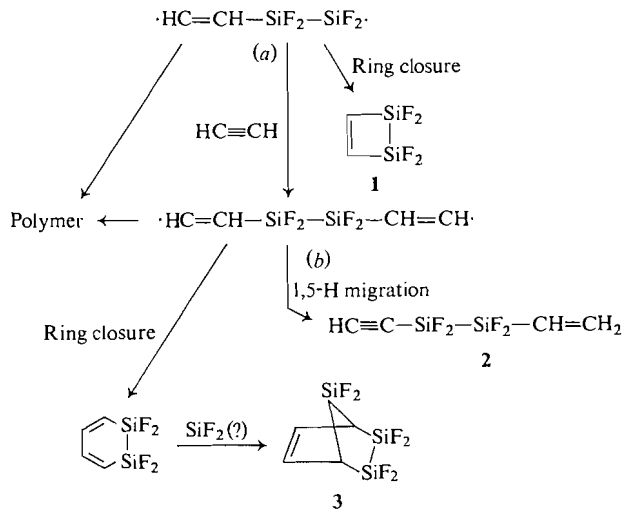

SCHEME 1

This work was supported at Rice University by the U.S. Army Research Office (Durham) and at the University of Toronto by the National Research Council of Canada. One of us (C.S.L.) thanks the Ontario Department of University Affairs for a Post-Graduate Fellowship.

1. J. L. MARGRAVE and P. W. WILSON. Acc. Chem. Res. **4**, 145 (1971).
2. J. C. THOMPSON, J. L. MARGRAVE, and P. L. TIMMS. Chem. Commun. 566 (1966).
3. P. L. TIMMS, D. D. STUMP, R. A. KENT, and J. L. MARGRAVE. J. Am. Chem. Soc. **88**, 940 (1966).
4. C. S. LIU and J. C. THOMPSON. Inorg. Chem. **10**, 1100 (1971).
5. P. L. TIMMS, R. A. KENT, T. C. EHLERT, and J. L. MARGRAVE. J. Am. Chem. Soc. **87**, 824 (1965).
6. R. K. HARRIS and C. R. DITCHFIELD. Spectrochim. Acta (A), **24**, 2089 (1968).
7. *a* E. SCHNELL and E. G. ROCHOW. J. Inorg. Nucl. Chem. **6**, 303 (1958). *b* A. ORLANDO and J. C. THOMPSON. To be published.
8. K. L. WILLIAMSON and J. C. FENSTERMAKER. J. Am. Chem. Soc. **90**, 342 (1968).
9. R. E. BANKS, A. C. HARRISON, R. N. HASZELDINE, and K. G. ORRELL. J. Chem. Soc. (C), 1608 (1967).
10. E. A. I. HEIBA and R. M. DESSAU. J. Am. Chem. Soc. **89**, 3772 (1967).
11. C. S. LIU, S. C. NYBURG, J. T. SYSMANSKI, and J. C. THOMPSON. J. Chem. Soc. (Dalton). In press.

Can. J. Chem. Downloaded from www.nrcresearchpress.com by 210.87.254.40 on 09/05/12
For personal use only.

Reactions of Silicon Difluoride with Unsaturated Organic Compounds. Part II. Alkyl Substituted Alkynes

C. S. LIU
Department of Chemistry, University of Toronto, Toronto 181, Ontario

J. L. MARGRAVE
Department of Chemistry, Rice University, Houston, Texas

AND

J. C. THOMPSON[1]
Department of Chemistry, University of Toronto, Toronto 181, Ontario
and
Department of Chemistry, Rice University, Houston, Texas

Received September 16, 1971

The reactions between silicon difluoride and propyne, propyne-d_1, 1-butyne, 2-butyne, and 3,3-dimethyl-1-butyne were studied. In each case products resulting from combining ratios (SiF_2:alkyne) of 2:1 and 2:2 were isolated and identified. The 2:1 compounds were shown to be derivatives of disilacyclobutene, while three types of 2:2 compounds were identified. These either had an open chain structure, resulting from migration of either α (to C≡C)—CH or acetylenic H, or were derivatives of disilacyclohexadiene. Rationalizations of the types of products found and of the conditions which affect the reaction mechanism are discussed.

On a étudié les réactions entre le difluorure de silicium et le propyne, le propyne-d_1, le butyne-1, le butyne-2 et le diméthyl-3,3 butyne-1. Dans chaque cas, on a isolé et identifié les produits résultant des rapports de combinaison (SiF_2:alcyne) de 2:1 et 2:2. On constate que les composés 2:1 sont des dérivés du disilacyclobutène, alors que trois types de composés 2:2 ont été identifiés. Ceux-ci avaient, soit une structure à chaîne ouverte, résultant de la migration du H acétylénique ou celui en α du CH (en C≡C), ou étaient des dérivés du disilacyclohexadiène. On discute des rationalisations des types de produits isolés et des conditions qui affectent le mécanisme de réaction.

Canadian Journal of Chemistry, **50**, 465 (1972)

Introduction

We have recently reported the reactions of silicon difluoride (SiF_2) with acetylene (1) and with 3,3,3-trifluoropropyne (2). In both of these systems we identified derivatives of disilacyclobutene formed by combination of two SiF_2 units with one molecule of the alkyne. In addition we also found products resulting from 2:2 combination of the reagent molecules. In the case of acetylene this product was a straight chain compound resulting from migration of an acetylenic hydrogen atom during the reaction. However, from trifluoropropyne this was not observed and we identified the 2:2 product as a derivative of disilacyclohexadiene. We now report our results from studies of the reactions of SiF_2 with a number of alkyl-substituted alkynes, which give products similar to those mentioned above, but also show that a further hydrogen migration may occur in specific cases.

[1]To whom correspondence should be addressed (Toronto).

Experimental

All volatile products were manipulated in a greaseless vacuum system. SiF_2 was prepared as previously described (3) and co-condensed with approximately equimolar quantities of the alkyne reagants. The latter were either commercially available or were prepared ($CH_3C{\equiv}CD$ (4) and $(CH_3)_3CC{\equiv}CH$ (5)) by standard methods. Reaction products were separated by trap-to-trap distillation and examined by n.m.r., i.r., and mass spectroscopy.

Results

Each alkyne formed a brownish-yellow deposit on co-condensation with the SiF_2/SiF_4 mixture at −196 °C. On gently warming to room temperature, volatile material was evolved and a yellow involatile residue remained. Except in the reaction of $(CH_3)_3CC{\equiv}CH$ (see below), no further products were obtained from heating the solid residues. Each was spontaneously inflammable in air and dissolved vigorously in dilute HF or KOH solutions.

In addition to SiF_4 and excess unreacted alkyne, the volatile products also contained

Can. J. Chem. Downloaded from www.nrcresearchpress.com by 210.87.254.5 on 09/05/12
For personal use only.

TABLE 1. Distillation data for SiF_2–alkyne products

Reagent	Trapping temperature/distillation temperature (°C) 2:1 compound	2:2 compound	% Yield of volatile products
$CH_3C{\equiv}CH$	−78/−45	−45/−22	5
$CH_3C{\equiv}CD$*	−64/−22	−64/−22	—
$CH_3CH_2C{\equiv}CH$	−64/−45	−45/−22	8
$CH_3{-}C{\equiv}CCH_3$	−45/−22	−22/0	5
$(CH_3)_3CC{\equiv}CH$	−22/0	0/*RT*	5

*Only one fraction which contained both 2:1 and 2:2 compounds was collected.

TABLE 2. Mass spectrometric data for SiF_2:alkyne products

		Ion abundance (% of base peak)								
m/e	Assignment	**1**	**3**	**4**	**5**	**6**	**8**	**9**	**10**	**11**
296	$C_{12}H_{20}Si_2F_4^+$	—	—	—	—	—	—	—	10.0	7.0
281	$C_{11}H_{17}Si_2F_4^+$	—	—	—	—	—	—	—	3.0	10.7
253	$C_9H_{13}Si_2F_4^+$	—	—	—	—	—	—	—	1.3	3.0
240	$C_8H_{12}Si_2F_4^+$	—	—	—	—	—	0.9	1.0	2.0	—
239	$C_8H_{11}Si_2F_4^+$	—	—	—	—	—	—	—	2.1	5.6
230	?	—	—	—	5.4	—	—	—	—	—
225	$C_7H_9Si_2F_4^+$	—	—	—	—	—	—	—	—	2.7
224	$C_7H_8Si_2F_4^+$	—	—	—	—	—	—	40.0	—	—
214	$C_6H_{10}Si_2F_4^+$	—	—	—	63.5	—	—	—	2.8	2.8
212	$C_6H_8Si_2F_4^+$	—	—	—	—	1.0	—	—	—	—
205	$C_4H_6Si_2F_5^+$	—	—	3.1	—	—	1.5	63.0	—	—
204	$C_4H_5Si_2F_5^+$	—	4.2	—	—	—	1.0	—	—	—
199	$C_5H_7Si_2F_4^+$	—	—	—	35.2	—	—	—	—	—
197	$C_5H_5Si_2F_4^+$	—	—	—	—	9.0	—	—	—	—
188	$C_4H_8Si_2F_4^+$	—	—	—	—	—	—	—	—	—
187	$C_4H_7Si_2F_4^+$	—	—	—	—	—	2.0	—	—	—
186	$C_4H_6Si_2F_4^+$	—	1.0	10.2	—	—	—	—	—	—
185	$C_4H_5Si_2F_4^+$	—	1.0	—	—	—	2.8	—	—	—
173	$C_3H_5Si_2F_4^+$	—	—	—	13.5	—	—	—		
173	$C_8H_{11}SiF_2^+$	—	—	—	—	—	—	—	1.7	3.2
172	$C_3H_4Si_2F_4$	0.5	—	—	—	—	—	—	—	—
156	$C_7H_6SiF_2^+$	—	—	—	—	—	—	—	—	4.0
153	$C_3H_4Si_2F_3^+$	0.5	—	—	—	—	—	—	—	—
148	$C_6H_{10}SiF_2^+$	—	—	—	58.5	—	—	—	2.4	—
146	$C_6H_8SiF_2^+$	—	—	—	—	29.8	—	—	—	—
140	$C_4H_7SiF_3^+$	—	—	—	—	—	4.0	—	—	—
139	$C_4H_6SiF_3^+$	—	—	71.7	—	—	—	52.0	—	—
138	$C_4H_5SiF_3^+$	—	15.5	—	—	—	24.2	—	—	—
133	$C_5H_7SiF_2^+$	—	—	—	75.2	—	—	—	2.5	—
129	$C_6H_{10}SiF^+$	—	—	—	37.8	—	—	—	2.5	3.9
126	$C_3H_5SiF_3^+$	—	—	—	—	21.2	—	—	—	—
124	$C_3H_3SiF_3^+$	—	—	—	—	23.5	—	—	—	—
121	$C_4H_7SiF_2^+$	—	—	—	—	—	5.0	—	—	—
120	$C_4H_6SiF_2^+$	—	—	26.3	—	—	10.0	15.0	—	—
119	$C_4H_5SiF_2^+$	—	26.1	—	—	—	6.2	—	—	—
112	$C_2H_3SiF_3^+$	—	—	—	—	14.7	—	—	—	—
107	$C_3H_5SiF_2^+$	—	—	—	—	33.5	—	—	—	—
105	$C_3H_3SiF_2^+$ / $C_4H_{10}SiF^+$	—	12.0	100.0	—	22.9	—	67.0	3.8	3.2
104	$C_3H_2SiF_2^+$ / SiF_4	12.1	—	—	—	—	—	—	—	—

(Continued)

Can. J. Chem. Downloaded from www.nrcresearchpress.com by 210.87.254.5 on 09/05/12
For personal use only.

TABLE 2. (*Concluded*)

		Ion abundance (% of base peak)								
m/e	Assignment	**1**	**3**	**4**	**5**	**6**	**8**	**9**	**10**	**11**
93	$C_2H_3SiF_2^+$	—	6.0	16.2	—	—	12.0	8.7	—	—
91	$C_2HSiF_2^+$	—	16.7	20.4	—	—	13.6	14.0	—	7.2
85	SiF_3^+	100.0	100.0	62.0	9.5	100.0	100.0	100.0	7.6	1.0
83	$C_6H_{11}^+$	—	—	—	37.8	—	—	—	100.0	1.0
82	$C_6H_{10}^+$	—	—	—	37.8	—	—	—	9.4	1.0
81	$CH_3SiF_2^+$									
	$C_6H_9^+$	—	—	12.3	26.0	—	—	6.3	5.1	1.0
67	$HSiF_2^+$	5.0	6.0	10.8	100.0	14.7	22.7	6.3	7.6	4.0
66	SiF_2^+	3.5	2.5	4.0	2.0	10.1	5.0	3.8	2.5	2.0
57	$C_4H_9^+$	—	—	—	99.0	—	—	—	39.8	100.0
55	$C_4H_7^+$	—	4.8	12.4	4.2	—	24.1	28.0	12.1	3.3
54	$C_4H_6^+$	—	50.1	71.8	—	—	15.1	38.0	—	—
53	$C_4H_5^+$	—	12.0	31.9	—	—	27.3	24.0	—	—
52	$C_4H_4^+$	—	—	8.1	—	—	7.5	7.6	—	—
51	$C_4H_3^+$	—	—	9.2	—	—	14.0	11.0	—	—
50	$C_4H_2^+$	—	—	8.0	—	—	—	6.3	—	—
47	SiF^+	13.5	9.0	17.2	39.0	29.5	30.3	10.0	11.4	5.6
43	$C_3H_7^+$	1.0	11.9	3.0	1.5	6.0	15.1	1.0	7.6	1.0
41	$C_3H_5^+$	—	14.3	7.4	75.7	35.5	6.1	6.3	22.3	19.2
40	$C_3H_4^+$	10.8	—	—	—	1.0	—	—	—	—
39	$C_3H_3^+$	1.0	16.6	29.2	33.5	38.2	12.0	19.0	7.1	4.8

compounds formed from combination of SiF_2 and alkyne in the ratios 2:1 and 2:2. Distillation temperatures are given in Table 1.

*(i) 2:1 Compounds (**1–5**)*

The molecular formulae were established by mass spectrometry (Table 2) and structural evidence obtained from the i.r. (Table 3) and n.m.r. (Table 4) spectra. All the evidence supports the assignment of the structure of each of these compounds as a derivative of disilacyclobutene. Such was also the case in the reactions of acetylene and trifluoropropyne, whose n.m.r. data are also given in Table 4 for comparison.

None of these compounds is very stable at room temperature, turning yellow within a few minutes and subsequently forming involatile residues. This process is thought to be polymerization. In the product from propyne (**1**) it was observed that the n.m.r. signal due to the vinylic proton decreased in intensity while a new broad peak at τ 7.90 increased in intensity. Thus the polymerization probably involves reaction at the C=C bond perhaps being preceded by cleavage of Si—C or Si—Si bonds.

The i.r. and Raman data for the product from butyne-2 (**4**) are consistent with a molecule of C_{2v} symmetry and agree with the supposition of a planar ring indicated by the n.m.r. data.

(ii) 2:2 Compounds

*(a) From Propyne (**6**), Propyne-d_1 (**7**), 1-Butyne (**8**), 2-Butyne (**9**)*

The mass spectrometric, i.r., and n.m.r. data are given in Tables 2, 3, and 5, respectively, and the proton n.m.r. spectra shown schematically in Fig. 1. All the evidence points to open chain compounds of the type shown in Table 5. The assignment of specific groups *trans* to each other at R_4 and R_6 is based on the magnitude of the H–H coupling constants of about 19 Hz when $R_4 = R_6 = H$.

Each of these products results from H-migration when there is the CH—C≡C grouping in the starting alkyne, and when this condition is met, this particular mode of reaction appears to be the favored one since we have no evidence in these reactions for the types of compounds (to be discussed below) found in reactions with the remaining alkynes.

Alcoholysis of **6** with methanolic KOH in a vacuum sealed tube yielded allene as the most volatile product, a small amount of oily liquid tentatively identified from its n.m.r. and mass spectra as $H_2C{=}C{=}CH{-}Si(OCH_3)_2{-}Si(OCH_3)_2{-}CH{=}CHCH_3$, a series of compounds, probably $(CH_3O)_nSi_2F(5-n)CH{=}CHCH_3$, mixed with excess methanol and an

Can. J. Chem. Downloaded from www.nrcresearchpress.com by 210.87.254.5 on 09/05/12
For personal use only.

Can. J. Chem. Downloaded from www.nrcresearchpress.com by 210.87.254.5 on 09/05/12
For personal use only.

TABLE 3. Vibrational spectra of SiF_2: alkyne products*

	Vibrational frequency (cm^{-1})									
			4							
Assignment	1	3	Infrared	Raman	5	6	8	9	10	11†
νC—H	2975 w 2890 w 2832 w	2950 w 2845 w	2920 w 2860 w	2929 m 2863 m(p)	2965 w 2878 w	2995 w 2910 w 2835 w	3005 w 2925 w 2900 w 2845 w	2975 w 2850 w	2970 w 2905 w 2872 w	2980 w 2920 w 2800 w
νC≡C									2150 s	
νC=C=C						1935 m	1935 m	1930 m		
νC=C	1580 m	1610 m	1558 m	1560 m(p)	1560 m	1615 m	1620 m	1540 m	1550 m	1570 w
δC—H	1450 w 1315 w	1435 w	1440 w 1374 w	1443 m 1375 m(p)	1420 w 1365 w	1450 m	1435 w		1475 m 1360 m 1250 m	
νC—C	1154 m	1160 w	1165 w	1160 m(p)	1213 w	1180 s 1090 m	1170 m	1200 m	1150 m	
δC=C=C(?)						1018 m				
νSi—F	960 s	972 s	995 s	960 w 898 w	986 s	970 s	984 s	984 s	950 s	1000
	850 s	910 m	885 m	882 w	947 m	928 s	942 s	915 s	908 s	800
	815 s	834 s	846 s	850 m(p)	832 s	874 s	887 m	885 s	855 s	vs b

*s = strong, m = medium, w = weak, b = broad, (p) = polarized.
†All gas phase except **11** in $CDCl_3$ solution.

Can. J. Chem. Downloaded from www.nrcresearchpress.com by 210.87.254.5 on 09/05/12
For personal use only.

TABLE 4. Nuclear magnetic resonance data for $2(SiF_2):1$(alkyne) compounds

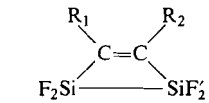

Compound	Chemical shifts*				Coupling constants†				
	R_1	R_2	F	F′	$J_{R_1,F}$	$J_{R_1,F'}$	$J_{R_2,F}$	$J_{R_2,F'}$	J_{R_1,R_2}
‡	(H) 1.67 c	(H) 1.67 c	129.2 c	129.2 c	16.2	5.0	5.0	16.2	—
1	(CH_3) 7.70 q	(H) 2.36 t of m	129.2 c	or 130.3 c	1.6	—	3.2	18.5	1.6
2	(CH_3) 7.70 t	(D) —	129.2 c	or 130.3 c	1.6	—	—	—	—
3	(CH_3) 8.83 t (CH_2) 7.37 q of m	(H) 2.25 t of m	129.8 c	or 130.9 c	1.5	—	3.0	19.7	$J_{CH_2,H}$ 1.5 J_{CH_2,CH_3} 7.5
4	(CH_3) 7.95 q^n	(CH_3) 7.95 q^n	130.2 sp	130.2 sp	0.6	0.6	0.6	0.6	—
5	((CH_3)$_3$C) 8.97 s	(H) 2.38 t of t	125.0 c	or 129.7 c	—	—	3.0	19.5	—
§	(CF_3) 65.7 m	(H) 1.69 t of m	131.3	or 132.7 c	2.4	0.8	1.6	16.5	1.6

*c = complex, s = singlet, t = triplet, q = quartet, q^n = quintet, m = multiplet, sp = septet. τ units for ^1H; p.p.m. upfield of CCl_3F for ^{19}F.
†Measured from multiplet patterns (Hz).
‡Reference 1.
§Reference 2.

Can. J. Chem. Downloaded from www.nrcresearchpress.com by 210.87.254.5 on 09/05/12
For personal use only.

TABLE 5. Nuclear magnetic resonance data for $2(SiF_2):2(alkyne)$ compounds **6**, **7**, **8**, **9**

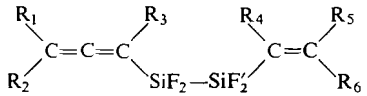

Compound	Chemical shifts*							
	R_1	R_2	R_3	R_4	R_5	R_6	F	F′
6	(H) 5.27 c	(H) 5.27 c	(H) 4.93 c	(H) 4.33 d of m	(CH_3) 8.07 d of q	(H) 3.29 d of q	132.6 or 135.2 c	
7	(H) 5.28 c	(H) 5.28 c	(D) —	(D) —	(CH_3) 8.07 d of t (CH_3) 8.96 t	(H) 3.30 q	132.6 or 135.2 c	
8	(CH_3) 8.33 d of d	(H) 4.95 c	(H) 4.87 c	(H) 4.37 c	(CH_2) 7.76 q of m	(H) 3.29 d of t	131.9 or 135.0 c	
9	(H) 5.32 m	(H) 5.32 m	(CH_3) 8.27 c	(CH_3) 8.27 c	(CH_3) 8.27 c	(H) 3.62 q of q	133.1 or 135.9 c	

*c = complex, s = singlet, d = doublet, t = triplet, q = quartet, m = multiplet; τ units for ^1H, p.p.m. upfield of CCl_3F for ^{19}F.

Compound	Coupling constants*													
	$J_{FF'}$	$J_{R_1R_2}$	$J_{R_1R_3}$	J_{R_1F}	$J_{R_2R_3}$	J_{R_2F}	J_{R_3F}	$J_{R_4F'}$	J_{R_4F}	$J_{R_4R_5}$	$J_{R_4R_6}$	$J_{R_5R_6}$	$J_{R_5F'}$	$J_{CH_2CH_3}$
6	11.5	—	7.8	2.2	7.8	2.2	0.9	2.8	1.0	1.5	19.1	6.0	1.6	—
7	11.5	—	—	2.2	—	2.2	—	—	—	—	—	6.0 $J_{R_5CH_2}$	1.6 $J_{CH_2F'}$	—
8	11.0	7.0	4.7	—	7.0	—	—	3.6	0.9	1.8	19.5	5.8	1.8	7.5
9	11.5	—	3.3	2.1	3.3	2.1	—	—	—	—	2.2	7.2	0.5	—

*Estimated from multiplet pattern (Hz).

Can. J. Chem. Downloaded from www.nrcresearchpress.com by 210.87.254.5 on 09/05/12
For personal use only.

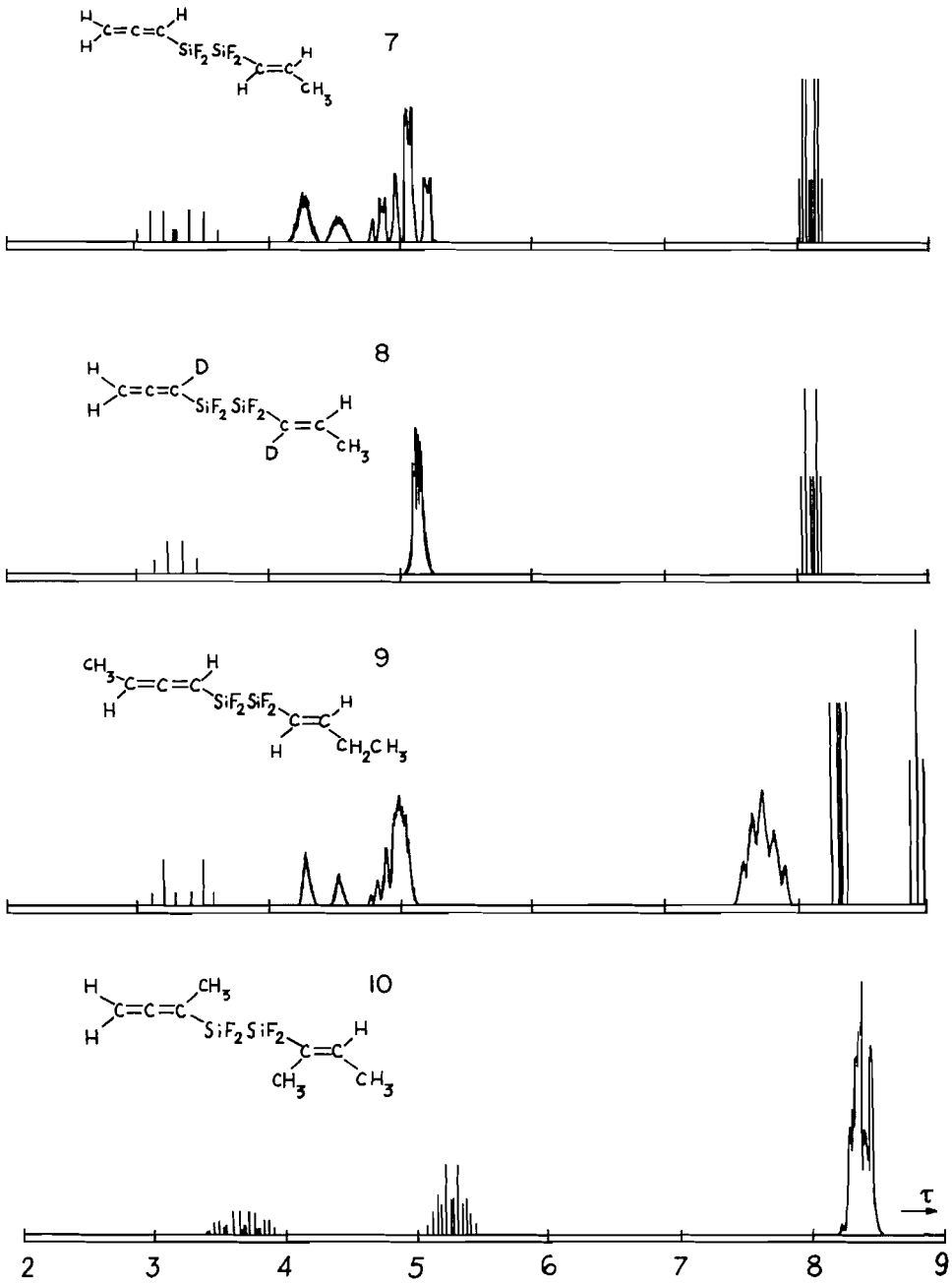

FIG. 1. Schematic proton n.m.r. spectra for compounds **6**, **7**, **8**, and **9**.

TABLE 6. Nuclear magnetic resonance data for $2(SiF_2):2$(alkyne) compounds **10** and **11**

(*a*)

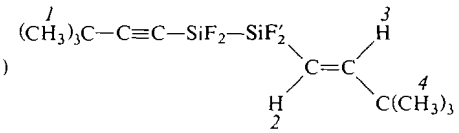

Proton	Chemical shift*	Fluorine	Chemical shift*	Coupling constants†	
1	8.95 s	F	132.90 c	$J_{2,3}$	19.5
2	4.46 d of m	F′	137.11 c	$J_{2F'}$	2.3
3	3.29 d of m			J_{2F}	1.2
4	8.75 s			$J_{3F'} \simeq J_{3F}$	0.5
				$J_{FF'}$	11.0

(*b*)

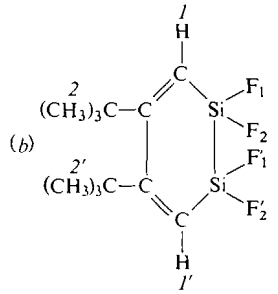

Proton	Chemical shift*	Fluorine	Chemical shift*	Coupling constants†	
1	3.86 m	F or F′	140.96 c	J_{1F_1}	4.0
2	8.77 s	F′ or F	152.34 c	J_{1F_2}	1.6
				$J_{1F_1'} \simeq J_{1F_2'}$	1.2

*c = complex, s = singlet, d = doublet, m = multiplet; τ units for ^1H; p.p.m. upfield of CCl_3F for ^{19}F.
†Measured from multiplet patterns (Hz).

unidentified white solid. The liberation of allene is further evidence for the proposed structure. Similar results and the formation of methylallene were obtained from **8** and **9**.

*(b) From 3,3-Dimethyl-1-butyne (**10** and **11**)*

Two isomers of a 2:2 compound were obtained: one liquid which was volatile at room temperature in the vacuum system, and a second compound which was sublimed as colorless crystals from the reaction residue at 60 °C. Mass spectrometric, i.r., and n.m.r. data are given in Tables 2, 3, 6. On the basis of this evidence we assign the structures also shown in Table 6.

The open chain compound (**10**) is similar to that obtained from the reaction of SiF_2 with acetylene, and results from the migration of acetylenic-H during the reaction, while the derivative of disilacyclohexadiene (**11**) is analogous to the compound formed in the trifluoropropyne reaction. The positions of the two *t*-butyl groups in the latter compound are assigned on the basis of the number of areas of resonance in the proton spectrum and on the coupling constants between magnetic nuclei. No volatile organic products were obtained from HF, KOH, or CH_3OH/KOH hydrolysis of this material.

The two complex sets of peaks observed in the fluorine n.m.r. spectra of (**11**) are not immediately consistent with the structural assignment. However, if there are two adjacent *t*-butyl groups on the ring, one might anticipate a rigid "half-chair" conformation which would give one "axial" and one "equatorial" fluorine atom on each silicon atom, with a significant chemical shift difference. No change was observed in the ^{19}F n.m.r. spectrum up to 75 °C

Can. J. Chem. Downloaded from www.nrcresearchpress.com by 210.87.254.5 on 09/05/12
For personal use only.

Can. J. Chem. Downloaded from www.nrcresearchpress.com by 210.87.254.5 on 09/05/12
For personal use only.

when decomposition of the compound occurred. With a rigid ring structure the compound should exhibit optical isomerism. No separation of the two forms has yet been achieved, but work is continuing on this aspect and on an X-ray crystal structure determination.

Discussion

Since we do not observe silacyclopropene derivatives, analogous to the cyclopropenes produced in carbene chemistry, in any of these reactions, it seems clear that the dimeric radical $\cdot SiF_2—SiF_2\cdot$ is the most reactive species towards alkyne reagents, as all the products found here are based on the Si_2F_4-unit. Also, since the type of compound formed appears to be fairly specifically related to the structure of the starting alkyne one can make some observations as to a possible mechanism for these reactions.

Diradical $\cdot SiF_2—SiF_2\cdot$ initially adds to an alkyne $RC{\equiv}CR'$ to form an intermediate $R\dot{C}{=}CR'SiF_2SiF_2\cdot$ which may either undergo ring closure to form a 2:1 compound, or react with further SiF_2 units (probably leading to polymers) or react with another molecule of alkyne to give $R\dot{C}{=}CR'SiF_2SiF_2R'C{=}\dot{C}R$. The latter intermediate then has at least three possibilities in addition to further reactions with either SiF_2 or alkyne units: ring closure to give a disilacyclohexadiene, H-migration from R or from R′. Sterically, because of the length of Si—Si and Si—C bonds it appears that the 8-membered transition state required for a migration of H from R is likely to be the most favored, and this is indeed what we found in the alkynes with the CH—C≡C grouping.

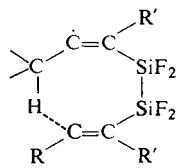

For migration of R′ (when R′ = H) or for ring closure a six-membered ring interaction is required and this is less favored on steric grounds, but the expected types of products are found when there is no CHC≡C group in the alkyne. Electronic and steric factors may explain why both processes occur in the $(CH_3)_3CC{\equiv}CH$ and $HC{\equiv}CH$ (1) reactions, while only ring closure is observed when $CF_3C{\equiv}CH$ is the starting alkyne (1, 6).

The ring compound **11** formed from $(CH_3)_3$-$CC{\equiv}CH$ is unusual in that 2,3-di(*t*-Bu)-cyclohexa-1,3-dienes are apparently unknown. Some of the strain between the two *t*-butyl groups is probably relieved by the greater puckering of the ring allowed by the longer (than C—C)Si—C and Si—Si bonds. Estimates of the strain energy in *o*-di(*t*-bu)benzenes are of the order of 22 kcal/mol (7), which would correspond very roughly to an n.m.r. coalescence temperature for the ^{19}F resonances 210 °C (8). Thus the limited stability of the compound did not permit study of the n.m.r. spectra at temperatures high enough to cause any significant changes.

The non-appearance of more complex (than 2:2) species in any of these reactions is probably due to their being less volatile and also less stable than the identified compounds. Heating of some of the polymeric residues directly into the mass spectrometer leads to very extensive ranges of mass peaks $(acetylene)_m(SiF_2)_n$, but apart from those discussed here none have been isolated in sufficient quantities for identification.

This work was initiated at Rice University under a grant from the U.S. Army Research Office (Durham). It has been continued at the University of Toronto with support from the National Research Council of Canada and the Ontario Department of University Affairs. One of us (C.S.L.) thanks the Ontario Department of University Affairs for a Postgraduate fellowship.

1. C. S. Liu, J. L. Margrave, P. L. Timms, and J. C. Thompson. Can. J. Chem. This issue.
2. C. S. Liu and J. C. Thompson. Inorg. Chem. **10**, 1100 (1971).
3. P. L. Timms, R. A. Kent, T. C. Ehlert, and J. L. Margrave. J. Am. Chem. Soc. **87**, 824 (1965).
4. R. J. Grisenthwaite and H. W. Thompson. Trans. Faraday Soc. **50**, 212 (1954).
5. P. D. Bartlett and L. J. Rosen. J. Am. Chem. Soc. **64**, 543 (1942).
6. N. L. Allinger and V. Zalkow. J. Org. Chem. **25**, 701 (1960).
7. E. M. Arnett, J. C. Sanda, J. M. Bellinger, and M. Barber. J. Am. Chem. Soc. **89**, 5389 (1967).
8. J. A. Pople, W. G. Schneider, and H. J. Berstein. High resolution NMR. McGraw-Hill, New York. 1959. p. 223.

The Dissociation of Anilinium Ions in Aqueous Dimethylsulfoxide

KEITH YATES AND GRAEME WELCH[1]

Department of Chemistry, University of Toronto, Toronto 181, Ontario

Received September 15, 1971

The pK_a values of ten substituted primary anilines and six substituted tertiary anilines have been determined in 70% DMSO–water. The ΔpK_a values relative to those in aqueous solution indicate that DMSO is about 2 log units stronger as a base than H_2O. The normal order of basicity (tertiary > primary) is inverted in this solvent system and the Hammett ρ values for the two series provide evidence for a different ionization mechanism than that in water.

Les valeurs des pK_a de dix anilines primaires substituées et de six anilines tertiaires substituées ont été déterminées dans une solution aqueuse de DMSO à 70%. Les valeurs de ΔpK_a, correspondant à celles en solution aqueuse, indiquent que le DMSO est une base plus forte que H_2O par environ 2 log unités. L'ordre normal de basicité (tertiaire > primaire) se trouve inversé dans ce système de solvant et les valeurs ρ de Hammett pour les deux séries constituent une preuve d'un mécanisme d'ionisation différent que dans l'eau.

Canadian Journal of Chemistry, **50**, 474 (1972)

Introduction

The changes in pK_a of organic acids and bases on transfer from water to DMSO solutions is often very large (1). This variation is thought to arise from DMSO's inability to solvate anions effectively, whereas the opposite is true for cations (2). The consequent high activity of anions has excited considerable interest in the behavior of basic DMSO solutions (3) but little attention has been given to the behavior of its acidic solutions. The behavior of cation acids is nonetheless of considerable interest and Kolthoff and Chantooni (4) have commented on the "puzzling" nature of the pK_a changes of primary and tertiary alkylammonium ions between water and DMSO solution.

In connection with a study of the acidity of aqueous-DMSO solutions we have found it necessary to measure the pK_a values of a number of anilinium and dimethylanilinium ions in 70% DMSO–water. We now wish to report these data since the observed ΔpK_a values offer evidence that the mechanism of proton transfer of anilinium ions in DMSO is quite different from that reported by Grunwald and Yu (5) for purely aqueous solutions.

Results and Discussion

The pK_a values of a series of primary and tertiary aromatic amines, determined in 70% (w/w) DMSO–H_2O[2] are listed in Table 1 and compared with the values reported for aqueous solution (8). These were measured by standard potentiometric methods, except for *N*,*N*-dimethyl-4-nitroaniline, *N*,*N*-dimethyl-3-nitroaniline, 4-nitroaniline, and 3-nitroaniline which were too weakly basic in DMSO–H_2O. The values for these four compounds were obtained spectrophotometrically by the standard acidity function approach, as described by Rochester (9).

The pK_a values of the primary anilinium ions are about 1–2 units smaller in DMSO–H_2O than in aqueous solution, whereas those for the tertiary anilinium ions are the order of 2–3 units smaller. Both these differences qualitatively reflect the greater basicity of DMSO relative to water. The relationship between the pK_a's of a species BH^+ in two different solvents is given by the equation

$$(pK_a)_s - (pK_a)_w = \log {}^mf_{H^+} + \log \frac{{}^mf_B}{{}^mf_{BH^+}}$$

where the ${}^mf$ terms are the medium activity coefficients (10), representing the differences in standard chemical potential of each solute in the two solvents. For solvents of similar dielectric

[1]Present address: Department of Chemistry, McGill University, Montreal, Quebec.

[2]This particular composition, which corresponds to a mole ratio DMSO:H_2O of 1:2, was selected because its physical properties (6) suggest minimal structural resemblance to either pure H_2O or pure DMSO. However, both pK_a values and acidity function behavior in this system resemble those in pure DMSO (7) much more closely than those in pure H_2O.

Can. J. Chem. Downloaded from www.nrcresearchpress.com by 210.87.254.105 on 09/05/12
For personal use only.

Can. J. Chem. Downloaded from www.nrcresearchpress.com by 210.87.254.105 on 09/05/12
For personal use only.

TABLE 1. pK_a values of substituted anilinium ions in 70% DMSO–H_2O and water at 25 °C

Substituents	$pK_a(H_2O)$*	pK_a(DMSO/H_2O)	ΔpK_a
4-Hydroxy	5.60	4.90	0.70
4-Methoxy	5.34	4.47	0.87
4-Methyl	5.12	4.00	1.12
3-Methyl	4.69	3.65	1.04
—	4.58	3.41	1.17
3-Methoxy	4.20	3.09	1.11
4-Chloro	3.98	2.43	1.55
3-Nitro	2.50	0.78	1.72
4-Nitro	1.00	−1.09	2.09
N,*N*,4-Trimethyl	5.63	3.57	2.06
N,*N*-Dimethyl	5.06	2.99	2.07
N,*N*,3-Trimethyl	5.34	3.26	2.08
N,*N*-Dimethyl-4-bromo	4.23	1.80	2.43
N,*N*-Dimethyl-3-nitro	2.63	0.16	2.47
N,*N*-Dimethyl-4-nitro	0.66	−1.96	2.62
N-Methyl	4.85	3.06	1.79
2,6-Dimethyl	3.90	2.80	1.10

*Reference 8.

constant, as is the case with 70% DMSO–H_2O (61) and water (78.4) (11), the difference in the electrostatic contribution to the standard chemical potential of the proton should be small and ${}^mf_{H^+}$ should mainly reflect the difference in solvent basicity.[3] However, unless ${}^mf_B \approx {}^mf_{BH^+}$ it is not possible to obtain an exact value of the difference in solvent basicity from such ΔpK_a values. For DMSO solutions this can be a serious problem because of the large differentiation between DMSO's ability to solvate cationic, anionic, and neutral species. As a result $(pK_a)_{H_2O} - (pK_a)_{DMSO}$ is of the order of −7 for carboxylic acids (1) but is about +2 for alkylammonium ions. However, solubility measurements on tertiary anilines and their pentacyanopropenide salts (13) show very similar degrees of "salting in" to DMSO–water, which suggests ${}^mf_B \approx {}^mf_{BH^+}$ in this system, lending support to a basicity difference between water and DMSO of about 2 log units, based on the values in Table 1. Various attempts to measure the pK_{BH^+} of both DMSO (14) and H_2O (15) have yielded little unanimity; however, an average value of $\Delta pK = pK_{H_3O^+} - pK_{DMSOH^+} = 2$ does not seem unreasonable. Kolthoff *et al.* (4) have estimated a difference of 1.5 ± 0.5 on the basis of comparison of their basicities in acetonitrile.

The problem of estimating solvent basicities from indicator measurements is clearly illustrated by the ΔpK_a values in Table 1. These ΔpK_a values are not only dependent on the basicity of individual indicators, but the relative basicity of the primary and tertiary aniline series has been inverted with respect to that in aqueous solution (in which the tertiary anilines are the stronger bases). These points are illustrated by means of linear free energy relationships of the $\rho\sigma$ type in Fig. 1.

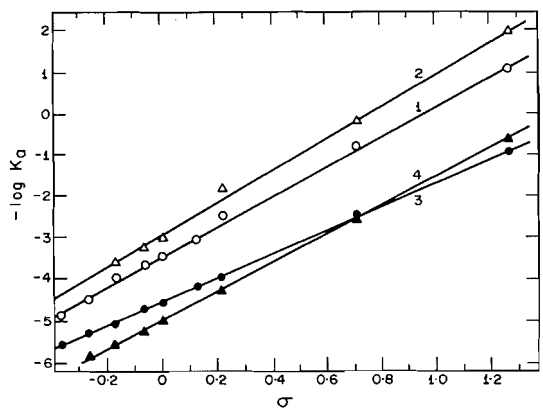

FIG. 1. Plots of pK_a *vs.* σ for (*1*) primary anilines in DMSO–H_2O, (*2*) tertiary anilines in DMSO–H_2O, (*3*) primary anilines in H_2O, (*4*) tertiary anilines in H_2O.

[3]Schaal and co-workers (12) have estimated a value of ${}^mf_{H^+}$ in 70% DMSO–H_2O of 0.85 p*H* units based on potentiometric measurements in dilute solutions. The same value was obtained in the present work. However, such estimates are made uncertain by unknown junction potentials.

[1] 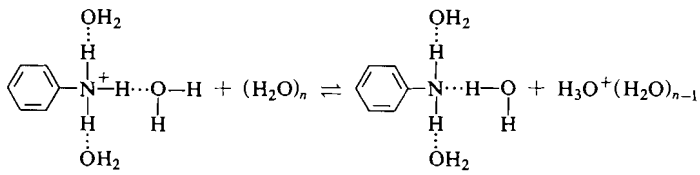

[2] 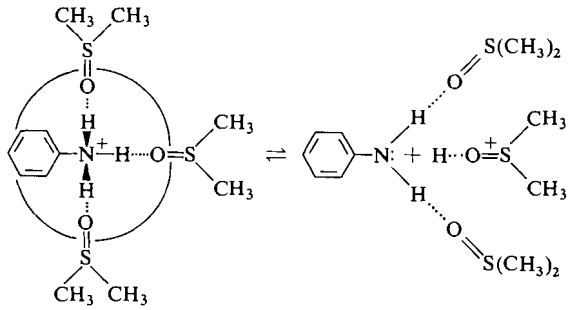

Although solvate complexes between primary and tertiary anilines and DMSO have been reported not to involve hydrogen-bonding (16), it seems more reasonable in the present case to conclude that the above reversal in basicity must arise from the ability of DMSO to act as a strong hydrogen bond acceptor. At least one stable complex of ammonia and DMSO has been reported (17) and the strong interaction of aniline protons with DMSO has been demonstrated by n.m.r. measurements (18). Interaction of DMSO with the anilinium cation would be expected to be even stronger.

One way of assessing such interactions is through the medium dependence of the ρ values, which for the present type of dissociation reaction should represent a measure of the balance between external charge dispersal (through solvation interactions) and internal charge delocalization (via the aromatic ring substituents).[4] This must be considered in terms of the detailed mechanisms for proton transfer in the two media. In purely aqueous solution, Grunwald and Yu (5) have demonstrated that for the dissociation equilibria of amines the mechanism is as shown in reaction 1. The proton is not lost directly from the nitrogen atom but is removed by the basic solvent from the periphery of a hydrated anilinium ion. Since the proton is transferred from the periphery of a hydrated cation, the sensitivity of its dissociation to ring substituents should be reduced. When the equilibrium is shifted to an aprotic (or predominantly aprotic[5]) medium such as DMSO the corresponding solvated anilinium ion would be as shown if the cation were solvated only by DMSO molecules, reaction 2. In this case the solvate would present an essentially lyophobic face to the solvent, and no peripheral proton transfer mechanism such as that described for purely aqueous solutions would seem possible. Thus dissociation would be more likely to take place by a completely different mechanism, that is, by loss of a protonated DMSO molecule. Since the proton is lost directly from nitrogen, and the charge on the cation is more shielded from the solvent, the internal charge dispersal should be relatively more important than in aqueous solution. Therefore the sensitivity of the dissociation to ring substituents should be increased.[6] The medium dependence of ρ for each series is fully consistent with the above description.

[4]Ritchie and Uschold (1) have suggested that the ρ value for ionization of carboxylic acids reflects the ability of the solvent to form hydrogen bonds to the carboxylate ion; hence the very high value (2.8) obtained in DMSO (poor anion solvation) compared with ρ in water (1.0).

[5]Although the present medium is not strictly aprotic, both the pK_a values and their substituent dependence closely resemble the values reported for anilinium ions in pure DMSO acid solutions ($\rho = 3.3$) (7).

[6]In this discussion the pK_a variations and hence the ρ values are considered to be predominantly controlled by the effect of substituents on the "uphill" dissociation step, in the sense described in the extensive investigations of Eigen (19).

Can. J. Chem. Downloaded from www.nrcresearchpress.com by 210.87.254.105 on 09/05/12
For personal use only.

Can. J. Chem. Downloaded from www.nrcresearchpress.com by 210.87.254.105 on 09/05/12
For personal use only.

For the primary anilines ρ changes from 2.77 (20) in water to 3.64 in DMSO–water, and for the tertiary anilines from 3.43 (21) in water to 3.87 in DMSO–water. The effect of stabilizing the anilinium ion with an aprotic solvent molecule such as DMSO would be very similar to the effect of introducing alkyl substituents on nitrogen. Thus the ρ value for *N*,*N*-dimethylanilinium ion dissociation in water is higher than that for the anilinium series. In addition the medium effect on this ρ in changing from water to DMSO solution would be expected to be less pronounced, as observed.

Experimental

The compounds used for potentiometric pK_a measurements are shown in Table 1. They were all commercial samples, purified either by recrystallization or by distillation at reduced pressure where appropriate.

DMSO was carefully purified by fractional distillation in a specially designed still similar to that described by Schlafer and Schaffernicht (22), under a dry nitrogen atmosphere at reduced pressure (b.p. 35–40 °C/1–2 mm Hg). Standard HCl solutions were prepared by diluting constant boiling (aqueous) HCl with the appropriate quantities of DMSO and doubly distilled water to give 0.1 *M* HCl in 70% (w/w) DMSO–H_2O. The concentration was checked by potentiometric titration and the less concentrated acids prepared by dilution with 70% DMSO–H_2O.

The pK_a's of the aniline indicators were determined by standard techniques. However, it was first necessary to define a "pH" scale in 70% DMSO–H_2O, as follows. A Leeds and Northrup 7405 p*H* meter was standardized with aqueous buffers (KH phthalate, 0.05 *m*, p*H* = 4.01; KH_2PO_4, 0.025 *m*/Na_2HPO_4 0.025 *m*, p*H* = 6.86) and shown to give good linear response in the range p*H* 3–7. The electrodes were an L and N STD.1190-30 glass electrode with calomel internal and an L and N 117208 calomel reference (saturated KCl) incorporating a diffusion junction. The meter p*H* readings for a series of standard HCl solutions of known concentration in 70% w/w DMSO–H_2O were determined with respect to the aqueous buffer standards. Each p*H* value was determined by the following procedure. The electrodes were placed in the aqueous buffer and the meter corrected to the buffer p*H*. The buffer solution was removed and the electrodes were rinsed with distilled water, wiped with tissue, and placed in the DMSO–H_2O solution. The meter response was immediate and there was no evidence of drift in the p*H* value. The p*H* value was recorded and the electrodes again rinsed and dried, and replaced in the aqueous buffer. In all cases, the original aqueous buffer value was reproduced, without evidence of slow response or drift. Successive measurements on identical solutions were reproducible within the readability error of the meter.

The concentrations of the HCl solutions were converted to activities by use of the empirical (Debye-Hückel) expression:

$$-\log a_{H^+} = -\log c_{H^+} - \frac{0.5\sqrt{I}}{1 - 1.5\sqrt{I}}$$

where *I* is the ionic strength. The constant terms were those used for aqueous solution; the small correction for the difference in dielectric constant (70% w/w DMSO–H_2O, 60.5; H_2O, 78.30) was not considered warranted.

When the calculated $pa^S_{H^+}$ ($-\log a_{H^+}$) and measured p*H* values for the solutions were plotted against each other (Fig. 2) a straight line of unit slope (error of fit ±0.025) could be drawn demonstrating that the term = $(-\bar{E}_j - \log {}^m f_{SH^+})$[7]

TABLE 2. Calculation of pK_a of acetic acid in 70% (w/w) DMSO–H_2O

$V_{titrant}$	V_{total}	p*H*	pa_{H^+}	log *I*	p*K*′
0	50.0	10.42			
0.5	50.5	8.75	7.90	−0.99	6.90
1.0	51.0	8.40	7.55	−0.64	6.91
1.5	51.5	8.17	7.32	−0.41	6.91
2.0	52.0	7.98	7.13	−0.22	6.91
2.5	52.5	7.80	6.95	−0.05	6.90
3.0	53.0	7.62	6.77	0.11	6.88
3.5	53.5	7.43	6.58	0.28	6.86
4.0	54.0	7.22	6.37	0.48	6.85
4.5	54.5	6.96	6.11	0.74	6.85

$$pK_a = pa_{H^+} - \log \frac{c_{HOAc}}{c_{OAc}} - \log f_{OAc^-}$$

Temperature = 25.00 ± 0.05 °C
Titrant = 0.102 *m* HCl
Volume at half-ionization = 52.5 ml
Concentration of NaOAc = 0.0187 *m*
Mean* value of p*K*′ = 6.89 ± 0.04
At half-ionization, $-\log f_{OAc^-} = 0.12$
$pK_a = pK'_a + 0.12$
$= 7.01 \pm 0.04$

*Calculated as arithmetic mean of antilog ($-pK'_a$).

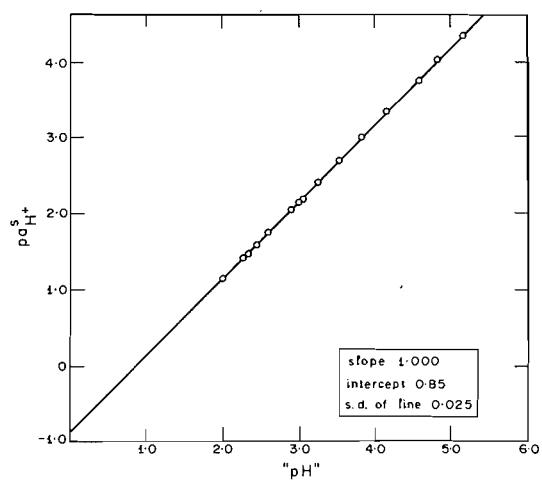

FIG. 2. Plot of $pa^S_{H^+}$ *vs.* "p*H*" determined potentiometrically in the DMSO–H_2O system.

[7] $\bar{E}_j$ is the junction potential and ${}^m f_{SH^+}$ is the medium activity coefficient for the proton.

is essentially constant over the range of activity studied. The value of $pa^{S}_{SH^+}$, referred to a standard state of 70% w/w DMSO–H_2O, could therefore be obtained from the pH meter (standardized against aqueous buffers) simply by subtracting 0.85 pH units from the meter reading. In order to verify the validity of the calibration, the pK_a of acetic acid was measured by the standard titrimetric method (see Table 2). The value of 7.01 $\pm$ 0.04 obtained for its pK_a is in excellent agreement with the value of 6.99 obtained from an exact potentiometric determination in this solvent system by Morel (23).

The $pa^{S}_{H^+}$ scale defined above was used to determine the pK's of the anilines from the data given in Table 3.[8] The pH values of the indicator buffer solutions were determined by the same technique described for the calibration of the meter. No corrections were made for the activity coefficient of the protonated aniline.

The continued financial support of the National Research Council of Canada and awards of Ontario Graduate Fellowships to G.W. are gratefully acknowledged.

1. C. D. RITCHIE and R. W. USCHOLD. J. Am. Chem. Soc. **90**, 2821 (1968).
2. A. J. PARKER. Quart. Rev. **16**, 163 (1962).
3. C. H. ROCHESTER. Quart. Rev. **20**, 511 (1966); J. R. JONES. Chem. in Britain, **7**, 336 (1971).
4. I. M. KOLTHOFF, M. K. CHANTOONI, JR., and S. BHOWMIK. J. Am. Chem. Soc. **90**, 23 (1968).
5. E. GRUNWALD and A. K. YU. J. Am. Chem. Soc. **90**, 29 (1968).
6. J. M. G. COWIE and P. M. TOPOROWSKI. Can. J. Chem. **39**, 2240 (1961); R. G. LEBEL and D. A. I. GORING. J. Chem. Eng. Data, **1**, 100 (1962); J. KENTAMAA and J. J. LINDBERG. Suomen Kemi, **33B**, 32, 98, 104 (1960).
7. A. G. COOK and G. W. MASON. J. Inorg. Nucl. Chem. **28**, 2579 (1966).
8. D. D. PERRIN. Dissociation constants of organic bases in aqueous solution. Butterworths, London. 1965.
9. C. H. ROCHESTER. Acidity functions. Academic Press, London. 1970. Chap. 1.
10. R. G. BATES. *In* The chemistry of non-aqueous solvents. *Edited by* J. J. Lagowski. Academic Press, New York. 1966. Chap. 3.
11. Y. DOUCET, F. CALMES-PERRAULT, and M. T. DURAND. Compt. Rend. **260**, 1878 (1965).
12. J. C. HALLÉ, R. GABORIAUD, and R. SCHAAL. Bull. Soc. Chim. Fr. 1851 (1969).
13. K. YATES and G. J. WELCH. Unpublished results; G. J. Welch. Ph.D. Thesis, University of Toronto, Toronto, Ontario. 1969.
14. R. HAAKE and R. D. COOK. Tetrahedron Lett. 427 (1968); P. OLAVI, I. VIRTANEN, and J. KORPELA. Suomen Kemi, **B41**, 326 (1968).
15. E. M. ARNETT. *In* Progress in physical organic chemistry. Interscience, New York. 1963. Vol. 1. p. 283.
16. J. KENTAMAA and J. J. LINDBERG. Suomen Kami, **34**, 117 (1961).
17. E. M. ARNETT and R. D. BUSHICK. J. Am. Chem. Soc. **86**, 1564 (1964).
18. G. FRAENKEL and J. P. KIM. J. Am. Chem. Soc. **88**, 4203 (1966).
19. M. EIGEN. Angew Chemie. Int. Ed. **3**, 1 (1964).
20. H. H. JAFFE. Chem. Rev. **53**, 191 (1950).
21. M. M. FICKLING, A. FISCHER, B. R. MANN, J. PACKER, and J. VAUGHN. J. Am. Chem. Soc. **81**, 4226 (1959).
22. H. L. SCHLAFER and W. SCHAFFERNICHT. Angew. Chem. **72**, 618 (1960).
23. J. P. MOREL. Bull. Soc. Chim. Fr. 1405 (1967).

[8]Table 3 is available from the Depository of Unpublished Data, National Science Library, National Research Council of Canada, Ottawa, Canada K1A 0S2.

Can. J. Chem. Downloaded from www.nrcresearchpress.com by 210.87.254.105 on 09/05/12
For personal use only.

Phase Equilibria in the Systems Acetone–Methanol, Acetone–Cyclohexane, Methanol–Cyclohexane, and Acetone–Methanol–Cyclohexane

A. N. CAMPBELL AND S. C. ANAND

Department of Chemistry, University of Manitoba, Winnipeg 19, Manitoba

Received July 27, 1971

The vapor pressure and vapor composition of the methanol–cyclohexane system were investigated at temperatures ranging from 25 to 50°. The same properties of the binary systems: acetone–methanol and acetone–cyclohexane, as well as those of the ternary system: methanol–cyclohexane–acetone, were determined experimentally at 25°. The total pressures and compositions of the vapor for solutions lying close to the critical solution temperature of the binary system or close to the plait point of the ternary system are constant within the range of experimental accuracy. All these systems show azeotropic behavior. The methanol–cyclohexane system has an equimolar excess Gibbs free energy, G^E, at 25° of 384.7 cal/mol, while the corresponding equimolar value of G^E for the acetone–methanol system at 25° is 102.6 and for the acetone–cyclohexane system, at 25°, it is 274.5 cal/mol.

La pression de vapeur et la composition de vapeur du système méthanol–cyclohexane ont été étudiées sur une échelle de température allant de 25 à 50°. Les mêmes propriétés des systèmes binaires: acétone–méthanol et acétone–cyclohexane, ainsi que celles des systèmes ternaires: méthanol–cyclohexane–acétone, ont été déterminées expérimentalement à 25°. Les pressions totales et les compositions de la vapeur pour des solutions proches de la température critique de la solution du système binaire ou proches du point de plissement du système ternaire, sont constantes dans l'intervalle d'exactitude expérimental. Tous ces systèmes montrent un comportement azéotropique. Le système méthanol–cyclohexane a un excès d'énergie libre équimolaire de Gibbs, G^E, de 384.7 cal/mol à 25°, alors que les valeurs équimolaires correspondantes de G^E pour le système acétone–méthanol est de 102.6 à 25° et pour le système acétone–cyclohexane de 274.5 cal/mol à 25°.

Canadian Journal of Chemistry, **50**, 479 (1972)

Introduction

Because of our interest in the critical phenomena, liquid ⇄ gas (1–3), and in the analogous critical phenomena, liquid$_1$ ⇄ liquid$_2$ (4–7), which has continued for several years, it was decided to extend our study to still another partially miscible system, *viz.* methanol–cyclohexane. By the addition of a third component, acetone, this system becomes homogeneous and it is then possible to study critical phenomena isothermally, in the ternary system methanol–cyclohexane–acetone. The complete study of the ternary system also involves that of the binary systems acetone–methanol and acetone–cyclohexane.

The methanol–cyclohexane system was chosen for the following reasons: (*a*) This system has a low critical solution temperature, *viz.* 45.87°. It was easily possible to work at temperatures above the critical solution temperature. (*b*) Both components, methanol and cyclohexane, have high vapor pressures, and it is therefore possible to investigate the partial pressures of both. (*c*) The difference in density of cyclohexane and methanol is slight and hence the effect of gravity in altering the shape of the coexistence curve in the neighborhood of the critical solution temperature, is almost negligible (8, 9). Previous work on the binary systems is summarized in Table 1. The equilibrium diagram of the ternary system methanol–cyclohexane–acetone has not been investigated previously.

Experimental Procedures

Purification of Materials

All three reagents were purified with great care; the details are to be found in ref. 22. Some physical properties of the products are given in Table 2.

Determination of Vapor Pressures and Equilibrium Vapor Compositions

The vapor pressures were measured directly with a manometer in the static manner, and the vapor compositions by means of isothermal distillation, using the air displacement method. Theoretically, at least, the latter method should give partial pressures directly, but this requires an exact knowledge of the volume of dry air passed through the apparatus and this is not easy to obtain. The combination of the two methods obviates the necessity for any knowledge of the volume of air passed through.

The Static Method: The method is well known and needs no specific mention here (23).

The Differential Method: The differential manometric method was employed to measure the difference in vapor pressure of solutions lying in the critical region and for measuring the difference in vapor pressure between pure solvent and solutions low in the other component. The

Can. J. Chem. Downloaded from www.nrcresearchpress.com by 210.87.254.5 on 09/05/12
For personal use only.

Can. J. Chem. Downloaded from www.nrcresearchpress.com by 210.87.254.5 on 09/05/12
For personal use only.

TABLE 1. Previous work on the binary systems

System	Investigators	Property measured	Numerical Value of Result
Methanol–cyclohexane	Mondain-Monval (10)	CST	49.1°
	Jones and Amstall (11)	CST	45.60° (72 wt.% cyclohexane)
	Eckfeldt and Lucasse (12)	CST	45.14°
	Debye, Chu, and Kaufman (13)	CST	45.14°
	Campbell and Kartzmark (4)	CST	45.87°
	Marinichev and Susarev (14)	$l \rightleftarrows v$ equilibrium at 35°, 45°, and 55°	Azeotrope at 35° contains 58.4 mol% methanol: at 55°, 61.2 mol% methanol
	Storonkin, Morachevskii, and Belousov (15)	$l \rightleftarrows v$ equilibrium	Azeotrope at 35° contains 55.7 mol% methanol
	Morachevskii and Komarova (16)	$l \rightleftarrows v$ equilibrium	Azeotrope at 55° contains 60.6 mol% methanol Azeotrope under 760 mm Hg pressure contains 60.4 mol% methanol
	Madhavan and Murti (17)	$l \rightleftarrows v$ equilibrium	Azeotrope under 760 mm pressure contains 60.4 mol% methanol
	Wood (18)	Excess thermodynamic functions (calculated)	G^E and H^E positive throughout TS^E positive except in solutions very rich in methanol
Acetone–methanol	Marinichev and Susarev (14)	$l \rightleftarrows v$ equilibrium, at 35°, 45°, and 55°, and under constant pressure (760 mm)	Exhibits azeotropic behavior
	Bushmakin, Molodenko, and Lyzlova (19)	$l \rightleftarrows v$ equilibrium	Confirm result of ref. 14
	Lang (20)	$l \rightleftarrows v$ equilibrium	Confirm result of ref. 14
Acetone–cyclohexane	Marinichev and Susarev (14)	$l \rightleftarrows v$ equilibrium	Exhibits azeotropic behavior
	Kurmanadharao and Vendata-Rao (21)	$l \rightleftarrows v$ equilibrium	Confirm results of ref. 14 but differ as to numerical results.

TABLE 2. Physical properties of pure reagents

Reagent	Density ($d_4^{25°}$) (g/ml)	Refractive index (n_{25}^{D})	Viscosity (cp)	Freezing point (°C)
Acetone	0.78425	1.35615	0.302	—
Methanol	0.78655	1.32693	0.545	—
Cyclohexane	0.77384	1.42355	—	6.55

apparatus used was that of Campbell, Kartzmark, and Oliver (24) who modified that of Gibson and Adams (25). Since vacuum pump oil, diethylphthalate, *n*-butyl phthalate, and other manometric liquids are soluble in one or other of the organic liquids of this research, it was necessary to use mercury as the manometric fluid. The diameter of the manometer tube was 22 mm, so that no meniscus correction was necessary.

Degassing was accomplished by freezing the liquid either in liquid nitrogen or in a mixture of Dry Ice and acetone, then evacuating until the residual pressure was less than 0.001 mm Hg. The liquid was then melted and the freezing and evacuating procedure repeated four or five times. The manometer was evacuated to about 1 μ and placed in a bath at the required temperature.

Determination of Vapor Composition

The composition of mixed vapor in equilibrium with mixed liquid of known composition was determined by isothermal distillation in a current of air. The apparatus of Bichowsky and Storch (26) was used. Nitrogen from a cylinder was passed into a pre-saturator whose temperature was kept 5° above that of the saturator. The nitrogen then passed through a heated tube to the saturator, whose temperature was controlled to $\pm 0.005°$. After leaving the last unit of the saturator, the nitrogen was led to a trap through a heated tube. After the vapor had condensed, the nitrogen was passed out of the system through a drying tube, to prevent condensation of water vapor from the air.

Methods of Analysis

The binary and ternary systems were analyzed as follows:

Methanol–Cyclohexane System. The refractive index method was used here, as the refractive indices of methanol and cyclohexane are 1.32693 and 1.42355 at 25°, respectively. The refractive index was measured with an old Zeiss–Pulfrich refractometer (it must be at least sixty years old) which is extremely accurate and has one great advantage, from our point of view, *viz.* the refractomer cell holds 2 ml of solution. This meant that evaporation from so large a quantity of solution during the short time required for a determination produced no appreciable change in composition, as was shown by the constancy of the reading. A volatile mixture in an Abbé refractomer changes continuously, as shown by the drift in the reading. Our thermostated Pulfrich instrument gave an accuracy of ± 0.0001 in the refractive index which corresponds to an analytical accuracy of about 1 in 1000 or somewhat less if the dilution effect consequent on the addition of excess pure liquid is taken into account. It was sometimes necessary to do this, because at temperatures above room temperature, mixtures of certain compositions became heterogeneous on cooling to room temperature. Therefore, a weighed excess of the appropriate pure component (methanol) was added to a known weight of solution. The composition of the homogeneous solution produced was determined from a calibration curve of refractive index *vs.* wt. % methanol.

Acetone–Cyclohexane System. This system was also analyzed by the refractive index method, since the refractive indices of acetone and cyclohexane are 1.35615 and 1.42355, respectively, at 25°.

Acetone–Methanol System. The compositions of the solutions were determined by viscosity, using a viscometer of the Cannon and Fenske type. Compositions were further checked by dielectric constant. The two methods gave an overall accuracy of $\pm 0.5\%$.

Methanol–Cyclohexane–Acetone System. Theoretically, the composition of a ternary mixture may be obtained from a knowledge of any two physical properties. It is necessary first to prepare calibration curves of the physical properties for all compositions and to express the results on a triangular diagram in the form of curves of equal values. The choice of physical properties is determined by the following considerations: they must (*a*) be easily and accurately determinable; (*b*) vary largely for small changes in composition; and (*c*) exhibit a graphical behavior such that curves of the different properties intersect at a steep angle. Viscosity and dielectric constant were found to satisfy these conditions for this system. The overal accuracy of determination was about $\pm 0.75\%$.

Results

We record here only such numerical results as are necessary for the understanding of the paper by the general reader. The numerical results "in toto" are to be found in the Depository of Unpublished Data.[1]

Vapor Pressure

We have used the Antoine equation (27)

$$\log P = A - \frac{B}{C + t}$$

to express our results for the vapor pressures of pure cyclohexane and of pure methanol. The constants A, B, and C were calculated by the

[1]Tables may be obtained, upon request, from the Depository of Unpublished Data, National Science Library, National Research Council of Canada, Ottawa, Canada K1A 0S2.

Can. J. Chem. Downloaded from www.nrcresearchpress.com by 210.87.254.5 on 09/05/12
For personal use only.

TABLE 3. Values of the constants of Antoine equation

Compound	*A*	*B*	*C*	Standard deviation
Cyclohexane	6.85852	1212.008	223.942	0.019
Methanol	8.07248	1574.990	238.860	0.014

TABLE 4. Binodal curve data for the ternary system methanol–cyclohexane–acetone at 25 °C

Upper layer		Bottom layer	
Mole fraction methanol	Mole fraction cyclohexane	Mole fraction methanol	Mole fraction cyclohexane
0.1857	0.8035	0.7995	0.1870
0.1926	0.7952	0.7928	0.1917
0.2014	0.7792	0.7533	0.2102
0.2110	0.7643	0.7255	0.2298
0.2165	0.7551	0.7129	0.2383
0.2176	0.7525	0.7049	0.2417
0.2215	0.7423	0.6893	0.2553
0.2291	0.7286	0.6629	0.2725
0.3042	0.6300	0.6162	0.3097
0.3290	0.5937	0.4888	0.4174

method of weighted least squares (28), using the non-linear formulae (29). The values of the constants are listed in Table 3.

Liquid–Vapor Equilibria

(a) Cyclohexane–Methanol. These equilibria were investigated, for liquid mixtures of different original compositions, at the temperatures 25, 40, 46, 48, and 50°. From these data[1] the relative volatility of methanol (y_1x_2/y_2x_1) and the ratio of the activity coefficients ($\log \gamma_1/\gamma_2$) were calculated, using the equation

$$[1] \qquad \log \frac{\gamma_1}{\gamma_2} = \log \frac{y_1 x_2}{y_2 x_1} - \log \frac{p_1^0}{p_2^0}$$

where p_1^0 and p_2^0 are the vapor pressures of pure methanol and of pure cyclohexane, respectively, x_1 is the mole fraction of methanol in the liquid ($x_2 = 1 - x_1$), y_1 the mole fraction of methanol in the vapor ($y_2 = 1 - y_1$). Similar calculations were done for the following systems:

(b) Acetone–Methanol. Investigated at 25° only, for 11 different liquid mixtures, covering the entire composition range.

(c) Acetone–Cyclohexane. Investigated at 25° only, for 10 different liquid mixtures.

(d) Methanol–Cyclohexane–Acetone. Investigated at 25° only, for 10 different liquid mixtures.

Total Vapor Pressures

(a) Methanol–Cyclohexane. These were determined for 15 different liquid mixtures, covering the whole composition range, at the temperatures of 25.0, 40.0, 45.0, 45.8, 45.9, 46.0, 46.1, 46.2, 46.3, 46.4, 47.0, 48.0, and 50.0°.

(b) Acetone–Methanol. These were determined for 12 different liquid mixtures at 25° only.

(c) Acetone–Cyclohexane. These were determined for 11 different mixtures at 25° only.

(d) Methanol–Cyclohexane–Acetone. Determined for 10 different mixtures at 25° only.

Difference in Pressure between Solutions lying close to the Heterogeneous Region of the Methanol–Cyclohexane System

Three sets of solutions, whose compositions lay on opposite sides of the critical composition but not far from it, were prepared and the difference in vapor pressure of the solutions determined with the differential manometer at temperatures just above the critical solution temperature, *viz.* 45.8, 45.9, 46.0, 46.1, 46.2, 47.0, 48.0, and 50.0°. Only at 50.0° was a difference in vapor pressure amounting to 0.01 mm Hg observed. This indicates that the equality of vapor pressure, which is thermodynamically necessary for congruent solutions, also persists

Can. J. Chem. Downloaded from www.nrcresearchpress.com by 210.87.254.5 on 09/05/12
For personal use only.

Can. J. Chem. Downloaded from www.nrcresearchpress.com by 210.87.254.5 on 09/05/12
For personal use only.

for several degrees above the critical solution temperature, for solutions whose compositions are not far from the critical. The same effect was observed (isothermally) for the ternary system methanol–cyclohexane–acetone, at 25°, for solutions of compositions lying near the critical.

Congruent Compositions for the System: Methanol–Cyclohexane–Acetone at 25°

See Table 4.

Partial Pressures

(a) Methanol–Cyclohexane. From the total pressures of this system, and the equilibrium vapor compositions, the partial pressures of both components were calculated, using Dalton's law; that is, assuming that the vapors behaved ideally. This no doubt produces some error in the values of the partial pressures but, when calculating the excess free energy of mixing, G^E, the error in G^E due to our error in determining the exact composition of the solution (liquid phase) is greater than that due to errors in partial pressure. The calculation was made for mixtures of various composition, at 25.0, 40.0, 46.0, 48.0, 50.0°.

(b) Acetone–Methanol. Similar calculations were made for 25° only.

(c) Acetone–Cyclohexane. Similar calculations for 25° only.

(d) Methanol–Cyclohexane–Acetone. Similar calculations for 25° only.

Discussion

Vapor Pressure of Pure Components

The agreement between our values for the vapor pressure of cyclohexane and those of Cruikshank and Cutler (30) is excellent, while the agreement with the results of Brown and Ewald (31) and of Willingham (32) is satisfactory. Our values for the vapor pressure of methanol at different temperatures are in excellent agreement with those of Scatchard and Ticknor (33) and Harper and Moore (34) but differ slightly from those of Singh and Benson (35). Our value for the vapor pressure of acetone at 25.0° (230.40 mm Hg) agrees well with the literature values (36, 37).

Thermodynamic Analysis

Consistency Tests

Numerous forms of consistency tests exist (38–43), most of which are based directly on the Gibbs–Duhem equation. When the thermodynamic data satisfy the Gibbs–Duhem equation, it is likely, but by no means certain, that they are correct but, if they do not satisfy this equation, it is certain that they are incorrect.

The vapor–liquid equilibrium data for the methanol–cyclohexane system could not be fitted to the van Laar (44), Margules (45), Wilson (46), or Scatchard and Hamer equations (47). This, however, does not necessarily mean that the vapor–liquid equilibrium data for this system are thermodynamically inconsistent, because the above equations may not apply to partially miscible liquid mixtures (48). The liquid–vapor equilibrium data of the acetone–methanol and acetone–cyclohexane systems can be fitted to the van Laar equation of the third order.

The consistency of the vapor–liquid equilibrium data was tested by the equal area test proposed independently by Coulson and Herington (38) and by Redlich and Kister (39). Figure 1 shows a plot of $\log \gamma_1/\gamma_2$ *vs.* mole fraction methanol for the system methanol–cyclohexane at 46°. Similar plots for the systems acetone–methanol and acetone–cyclohexane, respectively, were made. By graphical integration, the two areas, one above and the other below the zero axis, were found to be equal within 1.25 to 1.75% for these systems. The smallness of the deviations indicates that the vapor–liquid equilibrium data of all these systems are thermodynamically

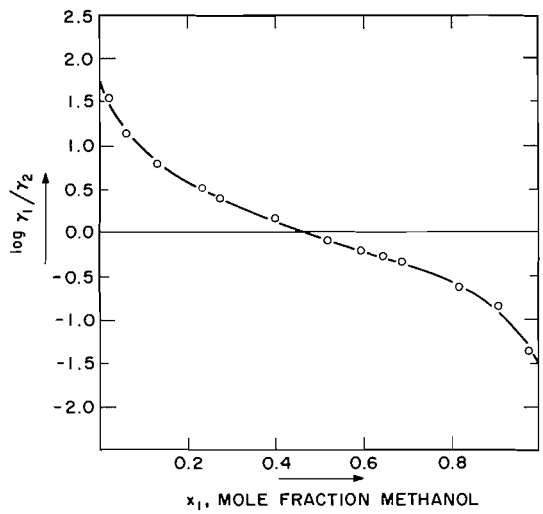

FIG. 1. $\log \gamma_1/\gamma_2$ for the methanol–cyclohexane system at 46°.

Can. J. Chem. Downloaded from www.nrcresearchpress.com by 210.87.254.5 on 09/05/12
For personal use only.

consistent. The equal area test could not be applied to the methanol–cyclohexane system, at 25 and 40°, because the two components are not miscible in all proportions at these temperatures.

The consistency of the vapor–liquid equilibrium data was also tested by a unified method described by Tao (43). This method requires a knowledge of the total vapor pressures of solutions, in order to calculate activity coefficients. As we measured total vapor pressures at solution concentrations different from those used in the vapor–liquid experiments, we were obliged to obtain the total vapor pressures by graphical interpolation. The method of Tao showed our data to be thermodynamically consistent within the limits of experimental error (maximum error in vapor pressure = 0.2 mm, in temperature control = 0.01°, and in composition = 0.3%).

Vapor–Liquid Equilibria

(a) Methanol–Cyclohexane System. The experimental results for this system are to be found in Depository.[1] Representation of the experimental data in the form of relative volatility as a function of solution composition reveals the main features of the interaction between the components of the system. This system is characterized by positive deviations from ideal solution behavior as shown by the decrease in the magnitude of the relative volatility of methanol with increase in mole fraction of methanol in the solution (Fig. 2). The relative volatility of methanol increases with increase in temperature. The influence of temperature on relative volatility can be described by Vrevskii's first law (49), which can be written in the form

$$[2] \qquad \frac{d}{dT}\ln \alpha_{12} = \frac{\bar{L}_1 - \bar{L}_2}{RT}$$

where α_{12} is the relative volatility of methanol in the methanol–cyclohexane system and $\bar{L}_1$, $\bar{L}_2$ are the partial molar heats of volatilization of methanol and of cyclohexane, respectively. From the fact that the isotherms of relative volatility of methanol have no points of intersection, it follows that the difference in $\bar{L}_1$ and $\bar{L}_2$ has the same sign throughout the whole concentration.

(b) Acetone–Methanol System. This system is also characterized by positive deviations from Raoult's law, the magnitude of the relative volatility of acetone decreasing with increase in mole fraction of acetone. The vapor–liquid equilibrium data of this system can be fitted to van Laar's equation of the third order (50). A straight line is obtained when $\sqrt{\log \gamma_2}$ is plotted *vs.* $\sqrt{\log \gamma_1}$, as shown in Fig. 3. The constants A and B of the van Laar equations

$$[3] \qquad \log \gamma_1 = \frac{A}{(1 + Ax_1/Bx_2)^2} \qquad \log \gamma_2 = \frac{B}{(1 + Bx_2/Ax_1)^2}$$

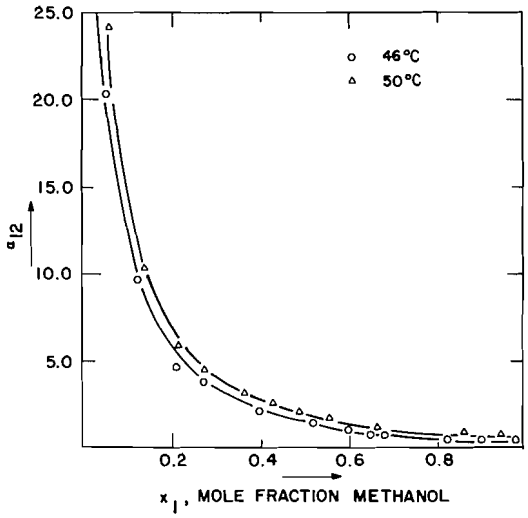

FIG. 2. Relative volatility of methanol in the methanol–cyclohexane system at different temperatures.

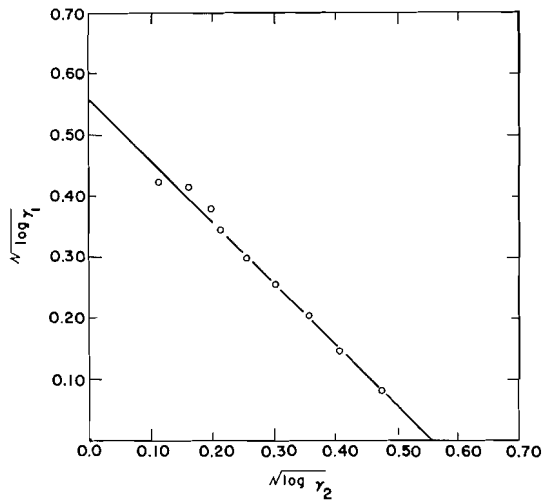

FIG. 3. Plot of $\sqrt{\log \gamma_1}$ *vs.* $\sqrt{\log \gamma_2}$ for the acetone–methanol system at 25°.

TABLE 5. Activity coefficients and excess Gibbs free energy (cal/mol) for the acetone(3)–methanol(1) system at 25 °C

					G^E		
						Calculated, using the van Laar equation	
x_3	$\log \gamma_1$	$\sqrt{\log \gamma_1}$	$\log \gamma_3$	$\sqrt{\log \gamma_3}$	Experimental	$A = B = 0.310$	$A = 0.306, B = 0.314$
0.10	0.0068	0.0824	0.2206	0.4697	38.45	38.07	37.65
0.20	0.0212	0.1456	0.1626	0.4032	67.51	67.68	67.13
0.30	0.0422	0.2054	0.1268	0.3561	92.21	88.83	88.42
0.40	0.0641	0.2532	0.0892	0.2987	101.16	101.52	101.24
0.50	0.0874	0.2956	0.0630	0.2510	102.61	105.74	105.72
0.60	0.1196	0.3458	0.0483	0.2198	104.82	101.52	101.76
0.70	0.1472	0.3837	0.0382	0.1954	96.39	88.83	89.28
0.80	0.1724	0.4152	0.0249	0.1578	74.23	67.68	68.10
0.90	0.1761	0.4196	0.0123	0.1109	39.13	38.07	38.45

were obtained from the intercepts which this line makes with the axis. A close look at the data[1] and Fig. 3 reveals that there are some points in the region of 0.7 to 1.0 mole fraction acetone which do not lie on a straight line. This is because the van Laar equation does not give constant values of A and B throughout the whole range of concentration, when the solutions show azeotropic behavior (51).

The methods of Carlson and Colburn (52) and of Prigogine (53) could not be used to calculate the azeotropic composition of this system at different temperatures because the vapor pressures of the components differ appreciably.

From Fig. 3, the values of A and B were found to be 0.306 and 0.314, respectively, *i.e.*, the value of A is almost equal to the value of B; in other words the vapor–liquid equilibrium data for this system can also be represented by the equation

$$[4] \qquad G^E = 2.303\ RTAx_1x_2$$

Thus G^E for the acetone–methanol system can be represented by eq. 4 with $A = B = 0.310$. Both the Margules and van Laar equations reduce to eq. 4 when $A = B$. Table 5 gives the results of these calculations. The agreement between the calculated and the experimental values of the excess Gibbs free energy is not good for concentrations lying close to the azeotrope.

The variation in the values of A and B with composition is especially large in this system, as the azeotrope occurs near an extreme range of concentration (51) at 25° (greater than 0.918 mole fraction acetone).

(c) Acetone–Cyclohexane System. This system is again characterized by positive deviation from Raoult's law; the magnitude of the relative volatility of acetone decreases with increase in the mole fraction of acetone. Of various equations tried for this system, the van Laar equation (44) was found to be the best. Again, the scattering of points from the straight line can be explained in a similar manner as due to the occurrence of an azeotrope. The values of the constants A and B of the van Laar equation were found to be 1.156 and 0.656. As seen from Table 6, the van Laar equation reproduces only qualitatively the behavior of the excess Gibbs free energy for this system, because it fails to give satisfactory values for azeotropic solutions (51).

Activity Coefficients and Excess Gibbs Free Energy

All systems of this study, both binary and ternary, show large positive deviations from Raoult's law, since the activity coefficients in all these systems are greater than unity. It is to be expected that the activity coefficients will be largest in the methanol–cyclohexane system, as this is a partially miscible mixture. Actually, as our data show, the activity coefficients for the methanol–cyclohexane system are greater than those of the acetone–cyclohexane system and these again greater than those of the acetone–methanol system. The plots of the logarithms of the activity coefficients of the various constituents of the systems and their form (48, 51) suggest that the data, as a whole, are thermodynamically consistent.

Can. J. Chem. Downloaded from www.nrcresearchpress.com by 210.87.254.5 on 09/05/12
For personal use only.

TABLE 6. Activity coefficients and excess Gibbs free energy (cal/mol) for the acetone(3)–cyclohexane(2) system at 25°C

					G^E	
x_3	$\log \gamma_2$	$\sqrt{\log \gamma_2}$	$\log \gamma_3$	$\sqrt{\log \gamma_3}$	Experimental	Calculated, using the van Laar eq. $A = 1.156$, $B = 0.656$
0.10	0.0362	0.1903	0.5790	0.7609	123.21	132.14
0.20	0.0844	0.3072	0.4896	0.6997	236.66	219.07
0.30	0.1220	0.3493	0.3489	0.5907	259.35	269.85
0.40	0.1769	0.4206	0.2457	0.4957	278.93	290.33
0.50	0.2293	0.4789	0.1730	0.4159	274.46	285.61
0.60	0.2943	0.5425	0.1183	0.3439	257.48	260.07
0.70	0.3870	0.6221	0.0675	0.2598	222.89	215.41
0.80	0.5015	0.7082	0.0233	0.1526	162.29	156.60
0.90	0.6200	0.7874	0.0008	0.0283	84.60	83.80

TABLE 7. Activity coefficients and excess Gibbs free energy (cal/mol) for the methanol–cyclohexane system at 25 °C*

			G^E		
				Calculated	
Mole fraction of methanol in liquid	$\log \gamma_1$	$\log \gamma_2$	Experimental	Scatchard–Hamer eq.	van Laar eq.
0.05	1.2021	0.0161	102.88	59.28	69.29
0.10	0.9646	0.0334	172.61	113.59	131.15
0.15	0.8081	0.0351	206.03	162.74	185.37
0.85	0.0637	0.7761	233.33	100.75	180.32
0.90	0.0599	0.8981	196.08	52.23	126.94
0.95	0.0511	1.0454	137.54	13.94	66.86

*Subscript 1 for methanol, 2 for cyclohexane.

(a) Methanol–Cyclohexane System. The magnitude of the activity coefficients in this system decreases with increase of temperature. The temperature dependence of the activity coefficients can be represented by the following equation (51)

$$[5] \qquad \left(\frac{\partial \ln \gamma_i}{\partial T}\right)_{P,x} = -\frac{(\bar{H}_i - H_i^0)}{RT^2}$$

where the term $(\bar{H}_i - H_i^0)$ gives the difference between the partial molar enthalpy of the ith constituent in the solution and the molar enthalpy of the pure constituent. As the values of the activity coefficients of this system fall with rising temperature, $(\bar{H}_i - H_i^0)$ must be positive, that is, heat is absorbed on mixing and this agrees with the data of Campbell and Kartzmark, who found the partial molar heat of mixing of both constituents to be positive in this system.

An important question arises as to the magnitude of the activity coefficients for solutions showing a miscibility gap. A thermodynamic argument, which need not be gone into here, applied to eq. 4, yields the results:

$$[6] \qquad \log \gamma_1 \geqslant 0.868 x_2^2$$
$$\log \gamma_2 \geqslant 0.868 x_1^2$$

Thus, for a partially miscible liquid mixture whose excess Gibbs free energy varies in a symmetrical manner, the values of the activity coefficients γ_1 and γ_2 should be greater than 5.047 and 1.221, respectively, for $x_1 = 0.1$, and so on for other proportions. This argument may be taken to mean that if a system shows partial miscibility, it will exhibit very large positive activity coefficients for both constituents or conversely, if a system exhibits very large positive activity coefficients, it will be partially miscible.

In Tables 7 and 8, the excess Gibbs free energy calculated from the liquid–liquid equilibrium data of Campbell and Kartzmark is compared

Can. J. Chem. Downloaded from www.nrcresearchpress.com by 210.87.254.5 on 09/05/12
For personal use only.

TABLE 8. Activity coefficients and excess Gibbs free energy (cal/mol) for the methanol–cyclohexane system at 40 °C*

Mole fraction of methanol in liquid	log γ_1	log γ_2	G^E Experimental	G^E Calculated: Scatchard–Hamer eq.	G^E Calculated: van Laar eq.	Wood's calcd. value
0.10	0.9351	0.0296	172.19	98.07	130.10	122.0
0.20	0.6610	0.0799	281.06	180.28	228.59	216.0
0.80	0.0792	0.6739	283.90	78.30	213.94	213.0
0.90	0.0526	0.8840	194.53	1.27	169.52	119.0

*Subscript 1 for methanol, 2 for cyclohexane.

with the experimental value. The lack of agreement is due to the failure of the van Laar and Scatchard and Hamer equations to apply to this partially miscible system. Wood (18) calculated the excess Gibbs free energy, for this system at 31 and 40° from the solubility data of Eckfeldt and Lucasse (12), using certain empirical equations. Again, the agreement is not good. There are several reasons for this, the most important being that he used an incorrect equation, on the basis of his own reasoning, unless this is a printer's error.

(b) Acetone–Methanol System. As already stated, the excess Gibbs free energy of this system was expressed by eq. 4. Table 5 shows that the agreement between the calculated and experimental G^E is good, despite the fact that an azeotrope exists in this system. The activity coefficients of this system are greater than unity and hence there is a possibility that this system may exhibit partial miscibility at some lower temperature. Campbell and Kartzmark (unpublished data) have recently measured the heats of mixing for this system at 25° and find the heat of mixing to be positive at all concentrations. It therefore follows that the activity coefficients increase with falling temperature. In other words, the region of partial miscibility will be approached by lowering the temperature.

Other Excess Thermodynamic Functions

(a) Methanol–Cyclohexane System. The excess thermodynamic functions of this system at 50°, are given in Table 9 and shown graphically in Fig. 4. The general shape of all the curves is the same at temperatures ranging from 46 to 50°. The methanol–benzene system (54) and other systems containing a polar and a non-polar component (55) show a similar type of behavior.

TABLE 9. Excess thermodynamic functions for the methanol–cyclohexane system at 50 °C

Mole fraction methanol	G^E (cal/mol)	H^{E*} (cal/mol)	V^E (ml/mol)	TS^E (cal/mol)
0.10	158.5	201.0	0.115	42.5
0.20	272.4	290.2	0.210	17.8
0.30	336.6	313.1	0.295	−23.5
0.40	375.5	303.5	0.365	−72.0
0.50	384.7	283.5	0.415	−101.2
0.60	372.4	264.0	0.420	−108.4
0.70	335.0	244.0	0.410	−91.0
0.80	273.0	211.3	0.335	−61.7
0.90	182.1	141.8	0.190	−40.3

*Reference 7.

The positive values of G^E and H^E lead to an upper critical solution temperature, as suggested by Rice (56), Hasse (57), Munster (58), Tompa (59) and Barker *et al.* (60).

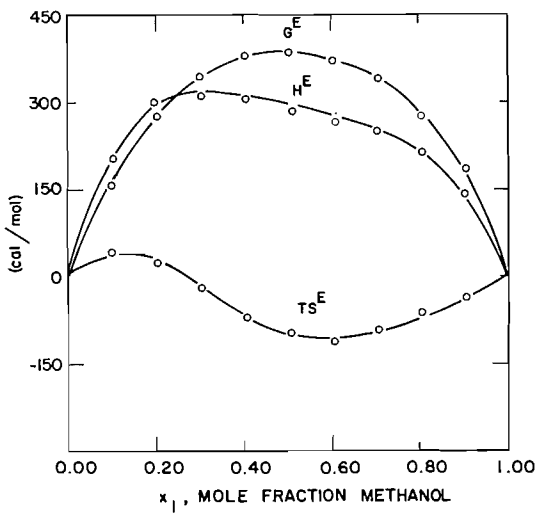

FIG. 4. Excess thermodynamic functions for the methanol–cyclohexane system at 50°.

Can. J. Chem. Downloaded from www.nrcresearchpress.com by 210.87.254.5 on 09/05/12
For personal use only.

TABLE 10. Excess thermodynamic functions for the acetone–methanol system at 25 °C

Mole fraction acetone	G^E (cal/mol)	H^E (cal/mol) Experimental*	H^E (cal/mol) Calculated from eq. 8	V^E (ml/mol)	TS^E (cal/mol)
0.10	38.5	62.4	62.3	−0.13	23.9
0.20	67.5	110.2	110.4	−0.21	42.7
0.30	92.2	145.1	144.8	−0.27	52.9
0.40	101.2	168.7	165.5	−0.32	67.5
0.50	102.6	185.1	172.2	−0.33	82.5
0.60	104.8	190.8	165.5	−0.32	86.0
0.70	96.4	162.6	144.8	−0.28	66.2
0.80	74.2	118.5	110.4	−0.20	44.3
0.90	39.1	61.4	62.3	−0.11	22.3

*A. N. Campbell and E. M. Kartzmark, unpublished data.

The excess entropy is negative for all mixtures containing more than 0.23 mole fraction methanol but the values differ greatly from those calculated by Wood (18). A possible source of error lies in the value of the heat of mixing which Wood calculates to be 800 cal/mol at the maximum. Wood admits, however, that due to uncertainties in the heat of mixing, too great emphasis should not be placed on his numerical value of the excess entropy.

(b) Acetone–Methanol System. The excess free energy of this system can be represented by eq. 4. From this equation, the other excess thermodynamic functions can be derived as follows:

$$[7] \quad S^E = \left(\frac{-\partial G^E}{\partial T}\right)_p = -2.303 x_1 x_2 R \left[A + T\left(\frac{\partial A}{\partial T}\right)_p\right]$$

$$[8] \quad H^E = G^E + TS^E = -2.303 x_1 x_2 R T^2 \left(\frac{\partial A}{\partial T}\right)_p$$

The excess heats of mixing, H^E, calculated from eq. 8, using $(\partial A/\partial T)_p = -0.00169$, are compared with the experimental values of H^E of Campbell and Kartzmark in Table 10. The agreement between the calculated and experimental values of H^E is good for solutions having less than 0.50 mole fraction acetone. Again, the difference between the calculated and experimental values of H^E is to be explained as due to the failure of the van Laar equation, when applied to azeotropic solutions.

TABLE 11. Excess thermodynamic functions for the acetone–cyclohexane system at 25 °C

Mole fraction acetone	G^E (cal/mol)	H^E* (cal/mol)	V^E (ml/mol)	TS^E (cal/mol)
0.10	123.2	170.2	0.46	47.0
0.20	236.7	290.3	0.76	53.6
0.30	259.4	350.4	0.97	91.0
0.40	278.9	395.1	1.03	116.2
0.50	274.5	405.2	1.08	130.7
0.60	257.5	380.1	1.06	122.6
0.70	222.9	340.3	0.95	117.4
0.80	162.3	260.1	0.73	97.8
0.90	84.6	152.2	0.42	67.6

*A. N. Campbell and E. M. Kartzmark, unpublished data.

(c) Acetone–Cyclohexane System. The excess thermodynamic functions for this system are given in Table 11 for 25°. All the excess thermodynamic functions are positive in this system. Again, the positive excess heat is small in mixtures rich in acetone, since the addition of a small amount of an inert solvent like cyclohexane to a large amount of acetone breaks few bonds in acetone. This heat is large in mixtures weak in acetone, as the addition of a small amount of it to a large amount of cyclohexane must break most of the bonds in acetone. The excess entropy is positive, owing to the loss of orientation order consequent on the breaking of the bonds.

1. A. N. CAMPBELL and R. M. CHATTERJEE. Can. J. Chem. **46**, 575 (1968).
2. A. N. CAMPBELL and R. M. CHATTERJEE. Can. J. Chem. **47**, 3893 (1969).

Can. J. Chem. Downloaded from www.nrcresearchpress.com by 210.87.254.5 on 09/05/12
For personal use only.

Can. J. Chem. Downloaded from www.nrcresearchpress.com by 210.87.254.5 on 09/05/12
For personal use only.

3. A. N. CAMPBELL and R. M. CHATTERJEE. Can. J. Chem. **48**, 277 (1970).
4. A. N. CAMPBELL and E. M. KARTZMARK. Can. J. Chem. **45**, 2433 (1967).
5. A. N. CAMPBELL, E. M. KARTZMARK, S. C. ANAND, Y. CHENG, H. P. DZIKOWSKI, and S. M. SKRYNYK. Can. J. Chem. **46**, 2399 (1968).
6. A. N. CAMPBELL, E. M. KARTZMARK, and S. C. ANAND. Can. J. Chem. **48**, 1579 (1970).
7. A. N. CAMPBELL and E. M. KARTZMARK. Can. J. Chem. **48**, 904 (1970).
8. M. A. WEINBERGER and W. G. SCHNEIDER. Can. J. Chem. **30**, 422 (1952).
9. M. FIXMAN. Advances in chemical physics. Vol. VI. Interscience Publishers, John Wiley and Sons Ltd., London. 1964. p. 175.
10. P. MONDAIN-MONVAL. Compt. Rend. **183**, 1104 (1926).
11. D. C. JONES and S. AMSTALL. J. Chem. Soc. 1316 (1930).
12. E. L. ECKFELDT and W. L. LUCASSE. J. Phys. Chem. **47**, 164 (1943).
13. P. DEBYE, B. CHU, and H. KAUFMANN. J. Chem. Phys. **36**, 3378 (1962).
14. A. N. MARINICHEV and M. P. SUSAREV. Zh. Prikladnoi Khimii, **38**, 1619 (1965).
15. A. V. STORONKIN, A. G. MORACHEVSKII, and V. P. BELOUSOV. Vestn. L.G.V. **10**, 94 (1958).
16. A. G. MORACHEVSKII and E. G. KOMAROVA. Vestn. L.G.V. **4**, 118 (1957).
17. S. MADHAVAN and P. S. MURTI. Chem. Eng., Sci. **21**, 465 (1966).
18. S. E. WOOD. J. Am. Chem. Soc. **68**, 1963 (1946).
19. I. N. BUSHMAKIN, YA P. MOLODENKO, and R. V. LYZLOVA. Zh. Prikladnoi Khimii, **26**, 1268 (1953).
20. H. LANG. Z. Phys. Chem. **196**, 278 (1950).
21. K. V. KURMANADHARAO and C. VENDATA-RAO. Chem. Eng. Sci. **7**, 97 (1957).
22. S. C. ANAND. Ph.D. Thesis. University of Manitoba, Winnipeg, Manitoba. 1970.
23. G. S. PARKS and C. S. CHAFFEE. J. Phys. Chem. **31**, 439 (1927).
24. A. N. CAMPBELL, E. M. KARTZMARK, and B. G. OLIVER. Can. J. Chem. **44**, 925 (1966).
25. R. E. GIBSON and L. M. ADAMS. J. Am. Chem. Soc. **55**, 2679 (1933).
26. F. R. BICHOWSKY and H. STORCH. J. Am. Chem. Soc. **37**, 2696 (1915).
27. C. ANTOINE. Cr hebd. Seanc. Acad. Sci., Paris, **107**, 681 (1888); **107**, 778 (1888).
28. A. F. FORZIATI, W. R. NORRIS, and F. D. ROSSINI. J. Res. Nat. Bur. Std. **43**, 555 (1949).
29. J. MANDEL. The statistic analysis of experimental data, Wiley, New York, 1964.
30. A. J. B. CRUIKSHANK and A. J. B. CUTLER. J. Chem. Eng. Data, **12**, 326 (1967).
31. I. BROWN and A. H. EWALD. Aust. J. Sci. **3**, 306 (1950).
32. C. B. WILLINGHAM, W. G. TAYLOR, J. M. PIGNOCCO, and F. D. ROSSINI. J. Res. Natl. Bur. Std. **35**, 219 (1945).
33. G. SCATCHARD and L. B. TICKNOR. J. Am. Chem. Soc. **74**, 3724 (1952).
34. B. G. HARPER and J. C. MOORE. Ind. Eng. Chem. **49**, 1249 (1968).
35. J. SINGH and G. C. BENSON. Can. J. Chem. **46**, 1249 (1968).
36. J. A. TALLMADGE and L. N. CANJAR. Ind. Eng. Chem. **49**, 411 (1957).
37. H. H. AMER, R. PAXTON, and M. VAN WINKLE. Ind. Eng. Chem. **48**, 142 (1956).
38. E. A. COULSON and E. F. G. HERINGTON. Trans. Faraday Soc. **44**, 629 (1948).
39. O. REDLICH and A. T. KISTER. Ind. Eng. Chem. **40**, 341 (1948).
40. E. F. G. HERINGTON. J. Inst. Petrol. **37**, 332 (1951).
41. N. V. IBL and B. F. DODGE. Chem. Eng. Sci. **2**, 120 (1953).
42. F. D. STEVENSON and V. E. SATER. A.I.Ch.E.J. 586 (1966).
43. L. C. TAO. Ind. Eng. Chem. **56(2)**, 36 (1964).
44. J. J. VAN LAAR. Z. Phys. Chem. Leipzig, **185**, 35 (1929).
45. M. MARGULES. Sitzb. Akad. Wiss. Wien, Abt. II, **104**, 1243 (1895).
46. G. M. WILSON. J. Am. Chem. Soc. **86**, 127 (1964).
47. G. SCATCHARD and W. J. HAMER. J. Am. Chem. Soc. **57**, 1805 (1935).
48. M. B. KING. Phase equilibrium in mixtures. Pergamon Press, London. 1969.
49. M. S. VREVSKII. Papers on the theory of solutions. Izd. AN SSR (1953).
50. C. BLACK. Ind. Eng. Chem. **50**, 403 (1958).
51. E. HALA, J. PICK, V. FRIED, and O. VILIM. Vapour–liquid equilibrium. Pergamon Press, London. 1968.
52. H. L. CARLSON and A. P. COLBURN. Ind. Eng. Chem. **34**, 581 (1942).
53. I. PRIGOGINE. J. Phys. Radium, **5**, 185 (1944).
54. G. SCATCHARD and F. G. SATKIEWICZ. J. Am. Chem. Soc. **86**, 130 (1964).
55. J. S. ROWLINSON. Liquids and liquid mixtures. Butterworth, London. 1969.
56. O. K. RICE. Chem. Rev. **44**, 69 (1949).
57. R. HAASE. Thermodynamik der Mischphasen. Springer, Berlin. 1956. p. 329.
58. A. MUNSTER. Trans. Faraday Soc. **46**, 165 (1950).
59. H. TOMPA. J. Chem. Phys. **21**, 250 (1953).
60. J. A. BARKER, I. BROWN, and F. SMITH. Discuss. Faraday Soc. **15**, 142 (1953).

The Hydrogen–Oxygen Reaction on Lanthanide Oxides. I. Hydrogen and Oxygen Adsorption on Some Lanthanide Oxides

JOHN F. READ

Department of Chemistry, Mount Allison University, Sackville, New Brunswick

Received June 28, 1971

Hydrogen and oxygen adsorption have been measured on neodymium oxide and dysprosium oxide from 77 to 771 °K up to equilibrium pressures of approximately 6 Torr. In addition, hydrogen adsorption measurements have been made on samarium oxide and gadolinium oxide from 77 °K to approximately 100 °K. The adsorption is effectively instantaneous in all cases except for oxygen adsorption on neodymium oxide at 491 and 541 °K. Adsorption appears to be dissociative for all cases studied except for hydrogen adsorption on neodymium oxide at all temperatures and for hydrogen adsorption on dysprosium oxide at high temperatures. For neodymium oxide and dysprosium oxide three types of adsorption are observed in different temperature ranges. At low temperatures, the adsorption is probably physical; at intermediate temperatures, it is either physical, or chemical on isolated double sites; and at high temperatures it is chemical. In general, the Freundlich isotherm gives the highest correlation between calculated and experimental data. The isosteric heat of adsorption and the equilibrium uptake of hydrogen increase as the ionic radius of the metal ion decreases.

L'adsorption d'hydrogène et d'oxygène sur l'oxyde de néodyme et l'oxyde de dysprosium ont été mesurées de 77 °K jusqu'à 771 °K avec une pression à l'équilibre d'approximativement 6 Torr. En supplément, les mesures d'adsorption de l'hydrogène sur l'oxyde de samarium et l'oxyde de gadolinium ont été faites de 77 °K jusqu'à environ 100 °K. L'adsorption est effectivement instantanée dans tous les cas excepté pour l'adsorption d'oxygène sur l'oxyde de néodyme à 491 °K et 541 °K. L'adsorption paraît être dissociative pour tous les cas étudiés excepté pour l'adsorption d'hydrogène sur l'oxyde de néodyme à toutes températures et pour l'adsorption d'hydrogène sur l'oxyde de dysprosium à hautes températures. Pour l'oxyde de néodyme et l'oxyde de dysprosium, trois types d'adsorption sont observés dans différents intervalles de températures. A basses températures, l'adsorption est probablement physique; à températures intermédiaires, elle est soit physique, soit chimique sur les sites doubles isolés; et à hautes températures elle est chimique. En général, l'isotherme de Freundlich donne une corrélation maximum entre les données calculées et expérimentales. La chaleur isostérique d'adsorption et la fixation à l'équilibre de l'hydrogène augmentent comme le rayon ionique de l'ion métallique diminue.

Canadian Journal of Chemistry, **50**, 490 (1972)

Introduction

There is evidence in the literature that the lanthanide oxides can act as either Lewis acids or Lewis bases, making them effective catalysts for reactions which involve the adsorption of either hydrogen or oxygen. The elementary reactions that have been studied include para-hydrogen conversion (1–4), hydrogen–deuterium equilibration (2, 3), hydrogen–oxygen reaction (5–8), isotopic oxygen exchange, *e.g.* (9–12). Preliminary studies have also been made of the adsorptive properties of the lanthanide oxides (13, 14).

The purpose of this contribution is to present data on the adsorption of hydrogen and oxygen on some of the lanthanide oxides, as a basis for further detailed studies of the hydrogen–oxygen reaction.

Experimental

The apparatus comprised a conventional high-vacuum system. Spectroscopically pure oxygen was supplied by the British Oxygen Company and the hydrogen was purified by passage through a palladium thimble. The adsorption was carried out by admitting a known amount of gas onto the sample. The pressure was then measured every few minutes for at least 30 min using a McLeod gauge, the stopcock between the sample and the gauge always being closed before a reading was taken. Further doses of the gas were added until a final equilibrium pressure of approximately 6 Torr was obtained. A trap, surrounded by liquid nitrogen, protected the sample from contamination by grease or mercury vapors.

The adsorption was studied over the temperature range 77 to 771 °K. Low temperatures were obtained by using coolant baths of liquid nitrogen (77 °K), liquid oxygen (90 °K), or solid carbon dioxide in acetone (195 °K). A specially constructed cryostat (15) was used to obtain temperatures in the range 90 to 193 °K. The volume of the system was measured at each temperature.

The four oxides used in the adsorption studies were neodymium oxide, samarium oxide, gadolinium oxide, and dysprosium oxide. They were of "Specpure" grade supplied by Johnson Matthey. X-Ray and i.r. analysis confirmed that all four oxides possessed the C-type structure (16) and that there was no change in structure during the experiments. The C-type structure is derived by the ordered absence of the oxygen ions from a quarter of the lattice positions of the

Can. J. Chem. Downloaded from www.nrcresearchpress.com by 210.87.254.40 on 09/05/12
For personal use only.

TABLE 1. Summary of results

Oxide	Specific surface area ($m^2\ g^{-1}$)	Total surface area (m^2)	Temperature range studied (°K)	
			Hydrogen adsorption	Oxygen adsorption
Nd_2O_3	6.38	20.3	77–689	273–677
Sm_2O_3	4.04	20.8	77–99	—
Gd_2O_3	7.55	36.5	77–97	—
Dy_2O_3	2.73	9.0	77–689	333–771

face-centered cubic fluorite structure, space group *Ia*3. There was no change in the powder diffraction patterns or the i.r. spectra for any of the oxides after heating in vacuum at various temperatures in the range 650 to 800 °K. Structural changes occurred at much higher temperatures, for example neodymium oxide changed from C-type to A-type after prolonged heating at 1300 °K. It is possible that neodymium oxide is hydrated. Infrared analysis showed that water was present and the cubic lattice dimension of 11.16 Å, calculated from the powder diffraction pattern, compared favorably with the value of 11.518 Å found by Glushkova *et al.* (17) for cubic $3Nd_2O_3.2H_2O$. The powder pattern changed slightly after the neodymium oxide had been stored in a desiccator for nine months.

The oxides were specifically chosen because of their relative structural and stoichiometric stability at the pressures and temperatures used in this investigation (18). Surface areas were measured by the B.E.T. method using krypton.

The oxides were conditioned by heating for seven days at 700 °K and $<10^{-6}$ Torr pressure. The system was evacuated overnight for experiments at different temperatures. The hydrogen adsorption measurements were performed first and then the oxide was left in contact with 15 Torr of oxygen for 10 h. The oxide was then baked out for two days at 700 °K and $<10^{-6}$ Torr pressure before proceeding with the oxygen adsorption experiments.

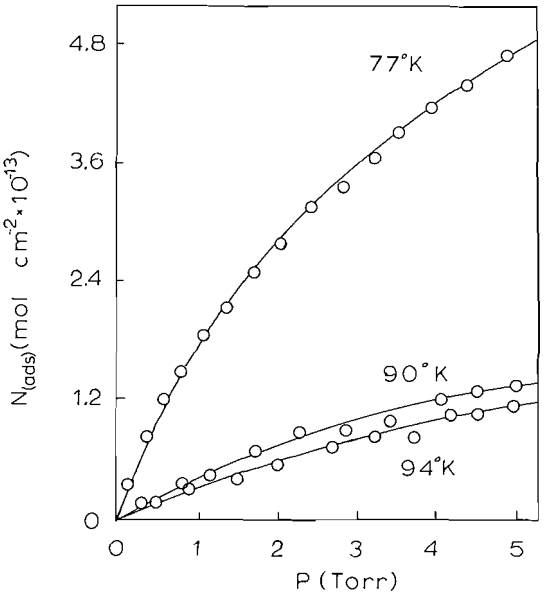

FIG. 1. Hydrogen isotherms on neodymium oxide.

Results

Hydrogen and oxygen adsorption were studied over neodymium oxide, samarium oxide, gadolinium oxide, and dysprosium oxide in the temperature ranges indicated in Table 1 at about twelve different equilibrium pressures up to 6 Torr. The adsorption was effectively instantaneous in all cases except for oxygen adsorption on neodymium oxide at 491 and 541 °K.[1]

The isotherms for the three lowest temperatures on each oxide are shown in Figs. 1–4,

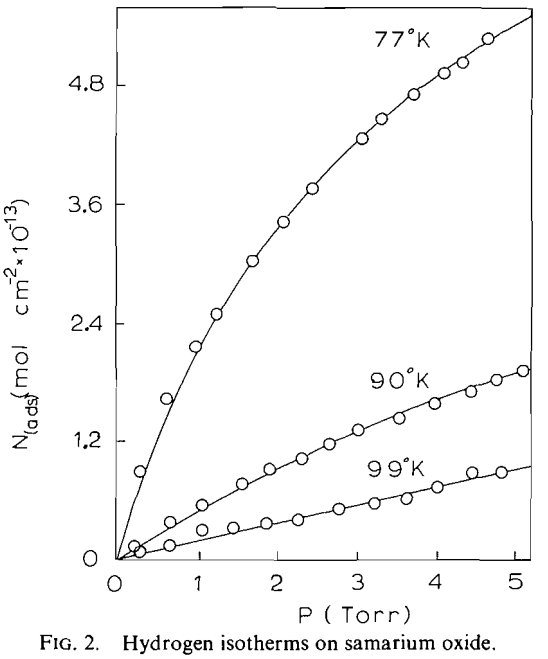

FIG. 2. Hydrogen isotherms on samarium oxide.

[1]Complete tables of results are available from the Depository of Unpublished Data, National Science Library, National Research Council of Canada, Ottawa, Canada K1A 0S2.

Can. J. Chem. Downloaded from www.nrcresearchpress.com by 210.87.254.40 on 09/05/12
For personal use only.

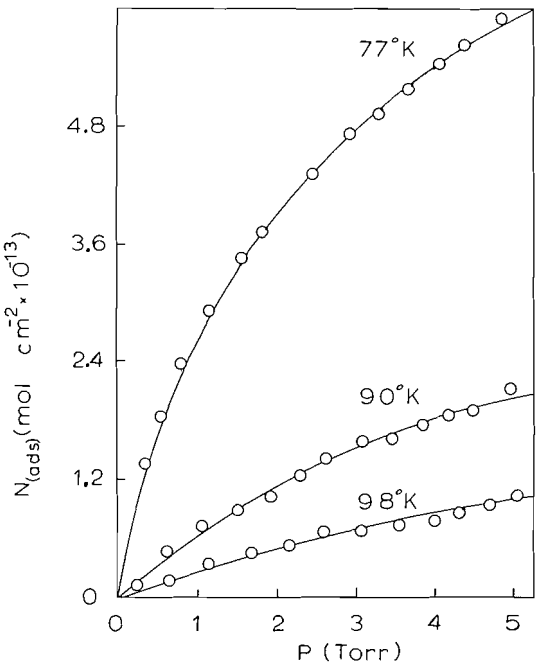

FIG. 3. Hydrogen isotherms on gadolinium oxide.

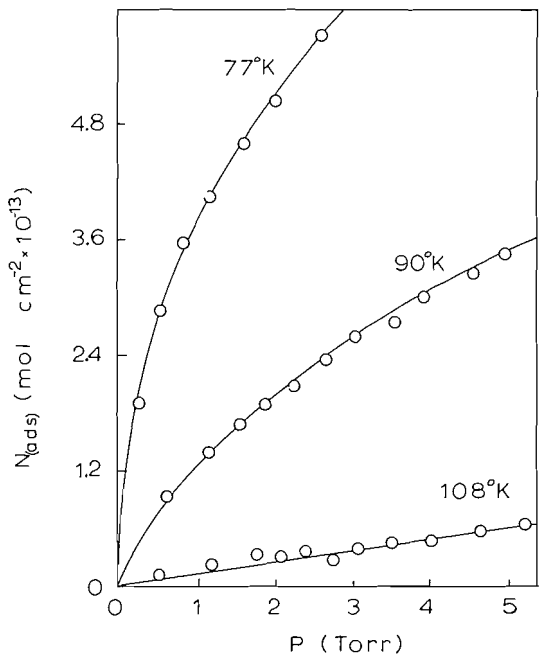

FIG. 4. Hydrogen isotherms on dysprosium oxide.

where P is the equilibrium pressure in Torr and $N_{(ads)}$ is the total number of molecules adsorbed per unit surface area standardized to the value at S.T.P. Isobars for hydrogen and oxygen adsorption on neodymium oxide and dysprosium oxide are shown in Figs. 5 and 6. These are shown for an equilibrium pressure of 4 Torr except for oxygen adsorption on neodymium oxide which is for an equilibrium pressure of 0.2 Torr.

Discussion

(A) Hydrogen Adsorption

Isobars

(a) Neodymium Oxide

The isobar at an equilibrium pressure of 4 Torr is shown in Fig. 5. Maximum adsorption occurs at the three lowest temperatures with a decrease in the amount of adsorption as the temperature increases from 77 to 94 °K. The amount of adsorption in the range 195 to 491 °K is negligible or very small, with an indication of a slight increase at 359 °K. The amount of adsorption then increases as the temperature increases from 548 to 689 °K.

In Fig. 5, the isobar is compared with the graphs obtained by Ashmead, Eley, and Rudham (2, 3) of log (rate of parahydrogen conversion), at a pressure of 4 Torr, against the reciprocal of the absolute temperature (log k_m *vs* $1/T$), and of log (rate of hydrogen–deuterium equilibration), at a pressure of 4 Torr, against the reciprocal of the absolute temperature (log k_m *vs.* $1/T$). All three plots have a similar shape at high temperatures and the isobar and the parahydrogen conversion plots are similar at all temperatures.

By comparing the parahydrogen conversion and the hydrogen–deuterium equilibration reaction, Ashmead *et al.* considered that the parahydrogen conversion proceeded by a paramagnetic physical mechanism at low temperatures, and by a chemical mechanism at high temperatures. It follows that the adsorption is probably physical at low temperatures and chemical at high temperatures.

At intermediate temperatures, a peak occurs in both the isobar, and the rate of conversion against temperature graph, whereas the equilibration reaction is immeasurably slow. Ashmead *et al.* considered that the conversion proceeded by a physical mechanism in this temperature range, on sites associated with an energy of accessibility. The rate of conversion increases

Can. J. Chem. Downloaded from www.nrcresearchpress.com by 210.87.254.40 on 09/05/12
For personal use only.

Can. J. Chem. Downloaded from www.nrcresearchpress.com by 210.87.254.40 on 09/05/12
For personal use only.

with temperature up to a maximum, after which the desorption of hydrogen is favored, and the rate decreases. An alternative mechanism in this intermediate temperature range is a chemical mechanism on isolated double sites with no surface migration. Either mechanism can be adopted to explain the adsorption results. Within this temperature range (290 °K), the system was partially evacuated and a Tesla discharge was passed through the remaining hydrogen. Negligible hydrogen adsorption occurred. The discharge would not be expected to affect the amount of physical adsorption, or the amount of chemisorption, unless dissociative hydrogen adsorption was a slow, rate determining step.

(b) Dysprosium Oxide

In Fig. 6 the isobar at an equilibrium pressure of 4 Torr is shown together with the parahydrogen conversion and hydrogen–deuterium equilibration graphs obtained by Ashmead *et al.* (2, 3). A comparison of these plots indicates that adsorption is probably physical at low temperatures and chemical at high temperatures.

Form of the Isotherms

The data obtained at the three lowest temperatures on each of the oxides were used to determine the form of the isotherms. The results for the Freundlich isotherm,

$$N_{(ads)} = kP^n$$

where k and n are temperature dependent constants, are shown in Table 2 (C is the correlation coefficient).

TABLE 2. Values for k and n with the correlation coefficient using the Freundlich isotherm

Oxide	Temperature (°K)	k	n	C
Nd_2O_3	77	1.6	0.70	0.998
	90	0.37	0.81	0.996
	94	0.30	0.79	0.996
Sm_2O_3	77	2.1	0.61	0.997
	90	0.52	0.79	0.999
	99	0.23	0.77	0.991
Gd_2O_3	77	2.6	0.53	0.998
	90	0.66	0.72	0.999
	98	0.28	0.75	0.995
Dy_2O_3	77	3.7	0.42	0.998
	90	1.3	0.61	0.999
	108	0.20	0.60	0.947

For all the oxides, the results fit the Freundlich isotherm although the correlation is lowest at

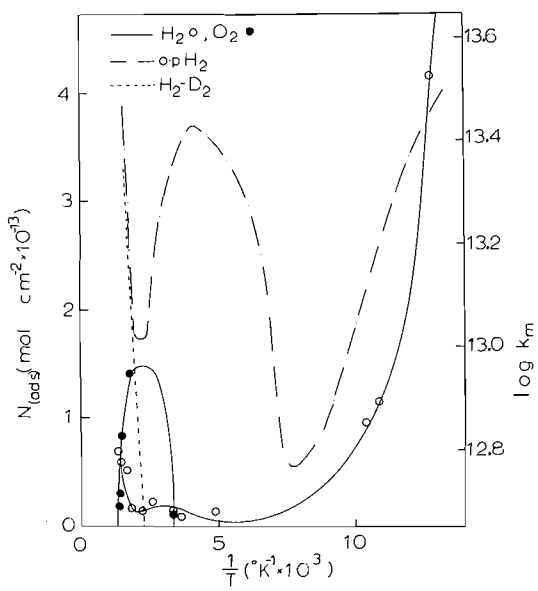

FIG. 5. Comparison of the oxygen isobar, the hydrogen isobar, the rate of the parahydrogen conversion and the rate of the hydrogen–deuterium equilibration on neodymium oxide.

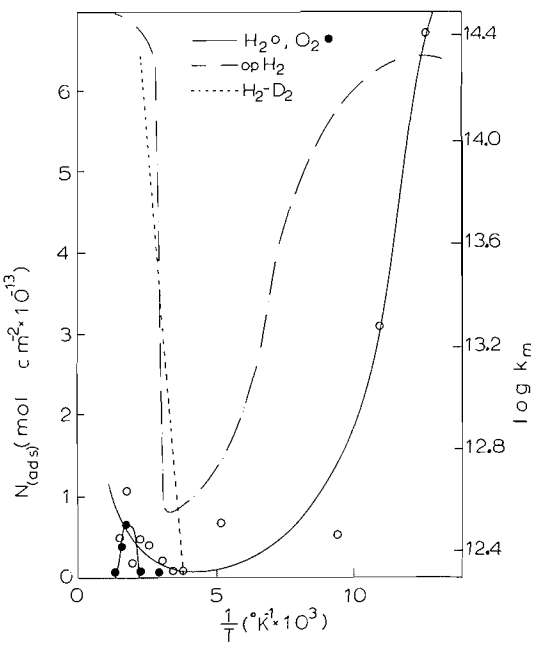

FIG. 6. Comparison of the oxygen isobar, the hydrogen isobar, the rate of the parahydrogen conversion and the rate of the hydrogen–deuterium equilibration on dysprosium oxide.

TABLE 3. Heat of adsorption and equilibrium uptake for hydrogen

Oxide	Ionic radius of metal ion, Me^{3+} (Å)	Hydrogen uptake at an equilibrium pressure of 4 Torr (molecules $cm^{-2} \times 10^{-13}$)		Isosteric heat of adsorption (kcal mol^{-1})
		77 °K	90 °K	
Nd_2O_3	1.15	4.15	1.14	1.85
Sm_2O_3	1.13	4.87	1.56	2.06
Gd_2O_3	1.11	5.37	1.81	2.13
Dy_2O_3	1.07	6.55	3.03	2.26

the highest temperature. This may be due to the fact that the cryostat was used to obtain the highest temperature resulting in a lower temperature stability. The expected trend of increasing n and decreasing k with increasing temperature is seen for all the oxides. In addition, n decreases and k increases as the ionic radius of the metal decreases. Using the model for the Freundlich isotherm that the heat of adsorption decreases exponentially with coverage, values for the heat of adsorption can be calculated from the constants given in Table 2. The heats are 0.9, 1.0, 1.1, and 1.3 kcal mol^{-1} for neodymium oxide, samarium oxide, gadolinium oxide, and dysprosium oxide, respectively. These values agree to within 1 kcal mol^{-1} with the isosteric heats of adsorption calculated from the Clausius–Clapeyron equation (see Table 3).

As expected for the low coverages studied, the data also fitted the Langmuir isotherm, although the correlation was usually slightly lower than for the Freundlich isotherm. For samarium oxide, gadolinium oxide, and dysprosium oxide the results indicated dissociative adsorption whereas non-dissociative adsorption was indicated for neodymium oxide. This is in accord with the results of Bakumenko and co-worker (5, 7) for the hydrogen–oxygen reaction where the order with respect to hydrogen was higher for neodymium oxide than for the other oxides studied.

The results from the adsorption on neodymium oxide at 548, 618, and 689 °K, and on dysprosium oxide at 594 and 689 °K were also analyzed. Again, the highest correlations were obtained using the Freundlich isotherm. The results from the Langmuir isotherm indicated that non-dissociative adsorption was occurring on both oxides, though the correlation was very low in all cases. The similarity between the rates of parahydrogen conversion and hydrogen–deuterium equilibration at high temperatures (2, 3) suggest that dissociative adsorption is occurring. Therefore, it is not possible to state conclusively which type of adsorption is occurring at high temperatures though it appears to be non-dissociative.

Heat of Adsorption and Surface Coverage

The isosteric heat of adsorption was determined from the results at the three lowest temperatures on each of the oxides studied by plotting log (equilibrium pressure) at a particular coverage *vs.* the reciprocal of the absolute temperature. This plot is shown in Fig. 7 for

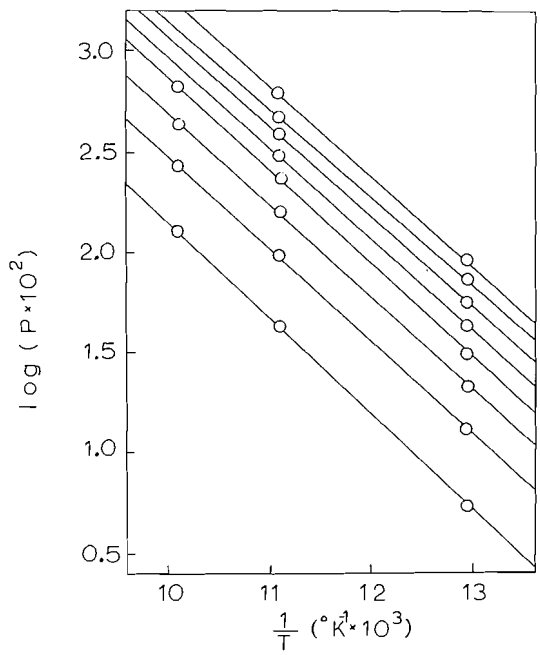

FIG. 7. Clausius–Clapeyron plot for hydrogen adsorption on samarium oxide.

Can. J. Chem. Downloaded from www.nrcresearchpress.com by 210.87.254.40 on 09/05/12
For personal use only.

Can. J. Chem. Downloaded from www.nrcresearchpress.com by 210.87.254.40 on 09/05/12
For personal use only.

samarium oxide at coverages from 0.25×10^{13} molecules cm^{-2} to 2.50×10^{13} molecules cm^{-2} at intervals of 0.25×10^{13} molecules cm^{-2}. The resulting plot of heat of adsorption *vs.* coverage is shown for all four oxides in Fig. 8. The average heats of adsorption are shown in Table 3. No systematic change in heat of adsorption with coverage could be detected. The magnitude of the heat is suggestive of a physical process.

The surface coverage of hydrogen at an equilibrium pressure of 4 Torr at 77 and 90 °K is shown for the four oxides in Table 3. The calculated value for a monolayer coverage of physically adsorbed hydrogen is 2.6×10^{15} molecules cm^{-2} (assuming a totally accessible surface and a value for the molecular diameter of hydrogen of 2.2×10^{-8} cm). The coverage at an equilibrium pressure of 4 Torr on neodymium oxide, at 77 and 90 °K is, therefore, 0.016 and 0.004 of a monolayer, respectively. For physical adsorption, the low coverage would be expected because of the very high value for the vapor pressure of hydrogen at these temperatures. For chemisorption, it must be assumed that only a small fraction of the surface is active. It is possible that most of the surface is poisoned by irreversibly adsorbed gases, the most likely contaminant being water. Anderson and Gallagher (13) have found that praseodymium oxide adsorbs carbon dioxide very strongly but it must be noted that praseodymium oxide has a much stronger tendency to become non-stoichiometric than do the oxides presently being studied. An alternate explanation for the low coverages is that adsorption only occurs on specially active sites. The C-type oxides contain anion vacancies. Assuming a surface containing equal areas of the (100), (110), and (111) planes, the number of anion vacancies for neodymium oxide is 2.49×10^{14} cm^{-2}. The amount of gas adsorbed is less than the number of anion vacancies but it is possible that clusters of these vacancies form the active sites. These same active sites may be responsible for the high temperature adsorption and the coverage agrees well with the value of 0.001 calculated by Ashmead *et al.* (2, 3). The low coverages are also in line with experimental results indicating that the lanthanide oxides are insulators (8).

In Table 3, the equilibrium uptake of hydrogen at 77 and 90 °K is shown with the isosteric heat of adsorption and the ionic radius of the

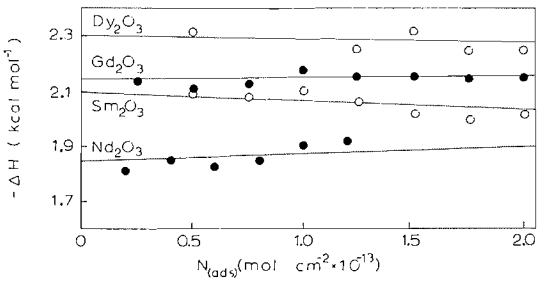

FIG. 8. Heat of adsorption for hydrogen *vs.* coverage.

metal ion for each of the four oxides studied. It can be seen that both the equilibrium uptake and the heat of adsorption increase as the ionic radius of the metal ion decreases. The increase in uptake can be explained by an increase in the number of anion vacancies per cm^2. The increase in heat of adsorption parallels the increase in the bond energy between hydrogen and the surface calculated by Balandin and Tolstopiatova (19).

(B) Oxygen Adsorption

Isobars

For both neodymium oxide and dysprosium oxide, adsorption was measurable over only a small temperature range. At an equilibrium pressure of 0.2 Torr, there is a maximum adsorption of 1.31 molecules cm^{-2} at 500 °K for neodymium oxide and 0.15 molecules cm^{-2} at 600 °K for dysprosium oxide. Barrett and Barry (14) observed a similar maximum in the isobar on A-type neodymium oxide and explained this by noting that below about 600 °K, adsorption is dominant over incorporation, whereas above this temperature incorporation becomes dominant. The relatively large uptake of oxygen for neodymium oxide is in line with the anomalously high activity reported for this oxide towards hydrogen oxidation (5, 7). The insulator character of these oxides is illustrated by the similarity between the amounts of hydrogen and oxygen adsorbed at high temperatures.

Form of the Isotherms

The data obtained from the isotherms at 677 °K on neodymium oxide and 591 °K on dysprosium oxide was used to determine the form of the isotherms. For both oxides, the results fitted the Freundlich isotherm and the Langmuir dissociative adsorption isotherm. The correlation was much higher for neodymium

oxide than for dysprosium oxide. The dissociative adsorption is to be expected in view of the activity of these oxides towards oxygen exchange reactions and the fact that adsorption increased considerably when a discharge was passed through the oxygen gas.

Kinetics of Adsorption

The adsorption was effectively instantaneous for all measurements except at 491 and 541 °K on neodymium oxide. The change in the kinetics of adsorption above 600 °K may result from the change in mechanism suggested by Barrett and Barry (14). The results at 491 °K were analyzed according to the integrated form of the Elovich equation:

$$N_{ads} = \frac{1}{\alpha}[\log_e (t + t_0) - \log_e t_0]$$

where α and t_0 are constants during any one run. A linear plot was obtained with a value of $t_0 = 15$ min.

In general, the data presented in this paper confirm the conclusions reached by Ashmead, Eley, and Rudham (2, 3) on the type of hydrogen adsorption occurring on neodymium oxide and dysprosium oxide. The results also show that, at high temperatures, hydrogen and oxygen adsorption occurs to similar extents, indicating that these oxides should be effective catalysts for the hydrogen–oxygen reaction. Comparison of the results over the four oxides show that there is a steady increase in both the equilibrium uptake and the heat of adsorption of hydrogen as the ionic radius of the metal ion decreases.

Appreciation is expressed for considerable help given by Dr. R. Rudham of Chemistry Department, Nottingham University, England.

1. H. S. TAYLOR and H. DIAMOND. J. Am. Chem. Soc. **57**, 1251 (1935).
2. D. R. ASHMEAD, D. D. ELEY, and R. RUDHAM. Trans. Faraday Soc. **59**, 207 (1963).
3. D. R. ASHMEAD, D. D. ELEY, and R. RUDHAM. J. Catal. **3**, 280 (1964).
4. P. W. SELWOOD. J. Catal. **19**, 353 (1970).
5. T. T. BAKUMENKO. Kinet. Katal. **6**, 74 (1965).
6. G. V. ANTOSHIN, KH. M. MINACHEV, and R. V. DMITRIEV. IZV. Akad. Nauk. SSSR, Ser. Khim. **8**, 1864 (1967).
7. T. T. BAKUMENKO and I. T. CHASHECHNIKOVA. Kinet. Katal. **10**, 796 (1969).
8. J. F. READ. Ph.D. Thesis, Nottingham University, Nottingham, England. 1964.
9. KH. M. MINACHEV and G. V. ANTOSHIN. Dokl. Akad. Nauk. SSSR, **161**, 122 (1965).
10. L. A. SAZONOV, A. N. PATOV, and T. G. RATOVA. Kinet. Katal. **6**, 836 (1965).
11. G. V. ANTOSHIN, KH. M. MINACHEV, and R. V. DMITRIEV. Kinet. Katal. **9**, 816 (1968).
12. E. R. S. WINTER. J. Chem. Soc. A, 2889 (1968).
13. J. S. ANDERSON and K. J. GALLAGHER. J. Chem. Soc. 52, (1963).
14. M. F. BARRETT and T. I. BARRY. J. Inorg. Nucl. Chem. **27**, 1483 (1965).
15. D. R. ASHMEAD and R. RUDHAM. Chem. Ind. 401 (1962).
16. H. R. HOEKSTRA. Inorg. Chem. **5**, 754 (1966).
17. V. B. GLUSHKOVA, E. K. KELER, and YU. G. SOKOLOV. Dokl. Akad. Nauk. SSSR, **158**, 151 (1964).
18. R. S. ROTH and S. J. SCHNEIDER. J. Res. Nat. Bur. Std. A, **64A**, 309 (1960).
19. A. A. BALANDIN and A. A. TOLSTOPIATOVA. Int. Congr. Catal. 3rd. **1**, 533 (1965).

Can. J. Chem. Downloaded from www.nrcresearchpress.com by 210.87.254.40 on 09/05/12
For personal use only.

A Selective Determination of the Proton Nuclear Relaxation Times of the Alkaloid Vindoline[1]

R. BURTON, C. W. M. GRANT,[2] AND L. D. HALL[3]

Department of Chemistry, The University of British Columbia, Vancouver 8, British Columbia

Received August 9, 1971

An audiofrequency-pulse n.m.r. spectrometer has been used to measure the nuclear relaxation times of individual protons of the alkaloid, vindoline. For this substance in deuterochloroform solution the spin–lattice relaxation times (T_1) vary between 1.15 and 1.50 s and the spin–spin relaxation times (T_2) are between 0.90 and 1.40 s. The *N*-methyl group has the shortest relaxation time of those resonances which were measured. A discussion of the apparatus and methodology is given.

On a utilisé un spectromètre à pulsations audiofréquences r.m.n. pour mesurer les temps de relaxation nucléaire des protons individuels de l'alcaloïde vindoline. Si on met cette substance en solution dans le deutérochloroforme, les temps de relaxation spin–réseau (T_1) se situent entre 1.15 et 1.50 s. Les temps de relaxation spin–spin (T_2) varient entre 0.90 et 1.40 s. Le groupe *N*-méthyle possède le temps de relaxation le plus court parmi les résonances qui ont été mesurées. On donne une discussion sur l'appareillage et la méthode utilisés.

Canadian Journal of Chemistry, **50**, 497 (1972)

Introduction

The high resolution proton n.m.r. spectrum of a chemical substance may be characterized by four sets of parameters, namely: (*i*) the relative areas of the individual resonance bands or multiplets; (*ii*) the chemical shifts of the individual resonances; (*iii*) the coupling constants of each spin-multiplet; and (*iv*) the characteristic nuclear relaxation times T_1 and T_2 of each resonance or of each individual transition of a resonance multiplet.

The many, varied ways in which the first three sets of data can be used as the basis of structural, configurational, and conformational assignments are too well known to require discussion here. However, the diagnostic potential of the fourth set of parameters remains to be established and although experiments with simple chemical substances have been described (1), applications to more complex systems have remained unexplored.

The principal reason why measurements of proton relaxation times have, in the past, been confined to comparatively simple substances is that suitable instrumentation for selective measurements with complex molecules *on a routine basis* has not been available until very recently. The major instrumental breakthrough in this area is the audiofrequency pulse technique described by Freeman and Wittekoek in 1969 (2). Prior to that development the methods available, which included the so-called saturation recovery (3), multiple resonance (4), progressive saturation (5), and $(T_1)_\rho$ (6) techniques all suffered from a variety of limitations as far as larger molecules were concerned. Furthermore, the conventional types of radiofrequency-pulse experiments lacked the selectivity necessary for studies of complex systems.

In the present paper we shall show that the audiofrequency-pulse technique is suitable for relaxation-time measurements with substances having the molecular complexity commonly associated with "natural products". Specifically, we shall discuss measurements made with vindoline, a substance which is of interest because of its relation with the anti-tumour principles obtained from *Vinca rosea lin* (7). The important point which we wished to establish was whether the individual protons of a substance of this complexity would still have differing nuclear relaxation times: as will be seen a differential does exist, although all of the relaxation times are rather short.

It is inappropriate to give a detailed discussion here of the principles and of the limitations of the audiofrequency pulse technique since Freeman and Wittekoek (2) have already given an excellent account. Suffice for the present discussion to comment that since all of the radiofrequency fields of a Varian HA-100 n.m.r.

[1]Part 1 of a series "Applications of pulsed nuclear magnetic resonance spectroscopy".

[2]Recipient of an NRCC 1967 Science Scholarship, 1968–1971.

[3]Alfred P. Sloan Foundation Research Fellow.

Can. J. Chem. Downloaded from www.nrcresearchpress.com by 210.87.254.42 on 09/05/12
For personal use only.

Can. J. Chem. Downloaded from www.nrcresearchpress.com by 210.87.254.42 on 09/05/12
For personal use only.

spectrometer are produced by audio-modulation techniques, the pulsed radiofrequency field required for nuclear-relaxation studies may be conveniently obtained by "gating" (switching) of the audio-modulation signal. In like fashion, the required radiofrequency phase-shifts are also conveniently obtained by introducing a phase change in the audio-modulation circuitry. It is important to note that these audio-frequency-pulse experiments have extremely stringent requirements as regards frequency stability; following Freeman and Wittekoek (2), we find it convenient to use a frequency synthesiser as the source of the audio-frequencies used for both the "lock" and the "observing" channels of the spectrometer.

Experimental

The basic format of the spectrometer used for nuclear relaxation experiments follows that of Freeman and Wittekoek (2). Because we were uncertain as to which pulse-durations would be most suitable for studies of complex organic substances we chose to use a small digital computer to control all pulse durations and intervals. It should be emphasized that the components which we used as the basis for the gate and other circuits were selected solely because they were already available in our laboratory at the time we started these experiments; more versatile, and cheaper, components are now available from a variety of manufacturers.

A block diagram of the instrument, together with the intersystem connections required for interface with a Varian HA-100 spectrometer, is given in Fig. 1. The two major components of the system are a JEOLCO computer (model JRA-5) and a Hewlett–Packard Frequency Synthesiser (model 5110B), which is driven by a "master oscillator" (Hewlett–Packard, model 5105B). For the convenience of these initial experiments a commercially available lock-in amplifier (Princeton Applied Research, model 121) was used for the detection of resonances in the observation channel in preference to the unit which is included in the Varian lock-box (V-4354).

The principal components of the pulse-unit are summarized in Fig. 2. Briefly, the circuitry used here serves the following functions:

(*a*) In the lock-channel, it takes a 1 MHz signal from the master oscillator and reduces it by digital division to a 2.5 KHz square wave. This signal (at 1 V p.p) is then used in the Varian lock-box (V-4354) instead of the signal normally provided by the manual oscillator (card 910868). We have made this interchange switchable so that it does not require physical removal of the manual oscillator card. All subsequent operations of the lock-circuitry are unaltered

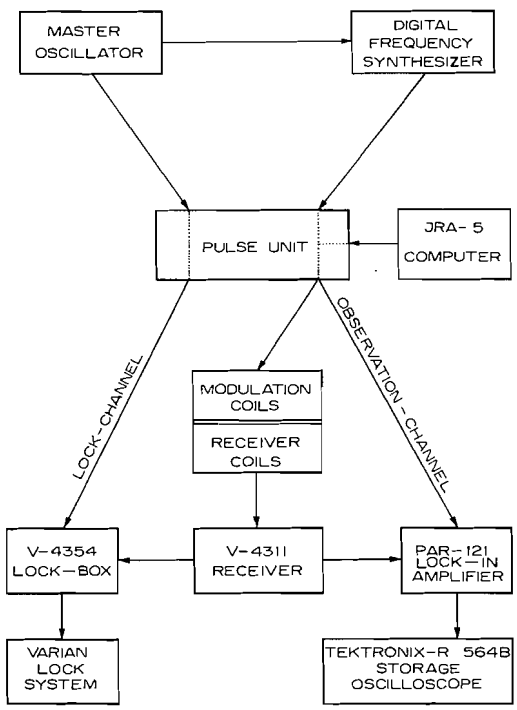

FIG. 1. Block diagram of the components used in the audiofrequency-pulse spectrometer.

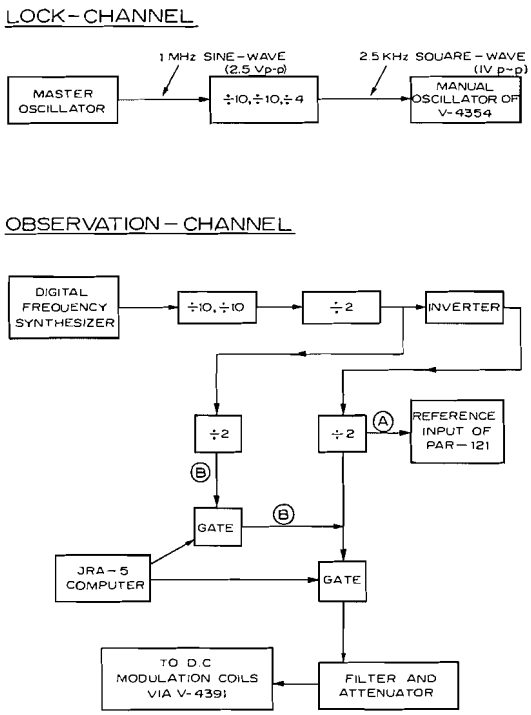

FIG. 2. Block diagram of the components used in the pulse-unit.

Can. J. Chem. Downloaded from www.nrcresearchpress.com by 210.87.254.42 on 09/05/12
For personal use only.

by this interchange except that lock-offsets are not possible.

(*b*) In the observation channel the circuitry provides the audio-modulation frequency required for the detection of resonances. At the same time this channel requires provision for switching, phase shifting, and filtering. In order to obtain a sufficiently fine (± 0.01 Hz) control of the frequency of the observation side-band, the digital frequency synthesizer is generally run at *ca.* 1 MHz and the required audiofrequency (*ca.* 2.5 KHz) is obtained by digital division as for the lock-channel. Since the phase-shifts required in pulse experiments are integral units of 90° these are conveniently obtained during the above division. Sequential division $\div 10$, $\div 10$, $\div 2$, invert, $\div 2$ gives the required audiofrequency square-wave which is used in line A (Fig. 2) as the reference signal to the PAR lock-in amplifier and to the gate. Using the first three stages of the above sequence ($\div 10$, $\div 10$, $\div 2$) followed by a separate $\div 2$ stage gives a second audiofrequency square-wave in line B. This square wave has precisely the *same frequency* as that of line A but differs from it and the signal in the lock-in amplifier by a *precisely 90° phase-shift*. Either of these two audiofrequencies can then be connected to the modulation coils via a filter and an attenuator. The latter is 10-turn, 200 ohm helipot.

The switching of both line A and line B is controlled by the JEOLCO JRA-5 computer which is programmed to perform the following:

(*a*) To accept positive integers ($<32\,000$) from the teletype; nine of these integers may be used. Each of these controls a specific switching operation.

(*b*) To turn on, or off, either line A or line B of the observation channel. When line A of Fig. 2 is "on" pulse, the phase-shift of the irradiating field is zero and when line B is "on" the phase-shift[4] is 90°.

(*c*) To pause for a time-interval which is numerically equal to the integer selected in (*a*) above, multiplied by 10 ms.

It is of course a trivial matter to vary the pulse-lengths, pulse-intervals, and phase sequences in any of a wide variety of ways.

The spectra obtained from the pulse spectrometer are conveniently recorded on a storage oscilloscope (Tektronix, model R564 B) and a permanent record obtained with a homemade scope camera[5] using Polaroid film. For very long relaxation-times it should be possible to use a highly responsive chart recorder; that of our Varian HA-100 is too slow.

Each individual relaxation measurement requires the sequential adjustment of the correct observing frequency, of the amount of power contained in a single pulse, and of the phase of the irradiating field. In general it is convenient to set up these parameters in the order: (*1*) pulse phasing, (*2*) exact frequency determination, (*3*) pulse power.

With the apparatus available to us at this juncture we have found it convenient to correctly adjust the phase of the observing field in the fashion generally used in high resolution n.m.r. experiments: by using the sweep-oscillator of the frequency synthesizer it is convenient to sweep repeatedly in both directions through the resonance of interest and to make adjustments of the phasing control of the PAR lock-in amplifier. Freeman and Wittekoek (2) have described previously how $(T_1)_\rho$ experiments can be used for optimizing the phasing controls. We have used their method and find it to be quite convenient providing that a $(T_1)_\rho$ experiment can be meaningfully performed on the particular sample: however, we have found such experiments to be difficult to perform in the presence of near-neighbor transitions (*vide infra*) and this seriously limits their generality.

The precise frequency required for a particular experiment can be obtained either of two ways. Either by direct measurement and calibration of the high resolution spectrum or by observation of the decay occuring after a pulse of 90° or less. In the latter case the line position is quickly measured to within 0.5 Hz and the frequency is adjusted in small increments to achieve a smooth exponential decay to baseline after each pulse. The off-resonance condition is marked by the trace of the magnetization vector either continuing through the baseline before returning to its equilibrium position or by a hump in the otherwise smooth decay curve. This method is very fast and quite general, and can give the frequency to within ± 0.02 Hz (depending on the linewidth).

The amount of power required to produce a particular pulse is conveniently ascertained by setting up the condition for a π-pulse; it is then a simple matter to halve the power for a $\pi/2$ pulse.

The set of spectra shown in Fig. 3 were obtained during the initial "debugging" of the instrument and serve to show the type of spectra which are readily obtained. In this regard they may be regarded as being truly "typical" results. These experiments are unexceptional. It is of interest to note in Fig. 3*e* the close superimposition of the T_2 and $(T_1)_\rho$ curves, which accords well with prediction (3*a*, 8).

It is convenient to obtain the numerical values of T_1 and T_2 from the scope photograph by graphical methods as follows.

Evaluation of T_1

The outline of the overall exponential decay curve, which is exemplified in Fig. 4*f* is given by

$$M_t = M_0(1 - 2\,e^{-t/T_1})$$

$$\therefore \qquad \ln (M_0 - M_t) = \ln (2M_0) - \left(\frac{1}{T_1}\right)t$$

where M_0 is the initial magnetization, M_t is the magnetization at some time t. Thus a plot of $\ln (M_0 - M_t)$ *vs.* t has slope $-(1/T_1)$ and intercept $\ln (2M_0)$.

Evaluation of T_2

The exponential decay of either a $(T_1)_\rho$ or a modified Carr–Purcell experiment is represented by the relationship

$$M_t = M_0 . e^{-t/T_2}$$

$$\therefore \qquad \ln M_t = \ln M_0 - \left(\frac{1}{T_2}\right)t$$

It follows from this that a plot of $\ln M_t$ against t has a slope of $-1/T_2$ and an intercept of $\ln M_0$.

[4]More accurately, the phase-shift between the reference signal going to the PAR-121 lock-in amplifier and the signal going to the modulation coil.

[5]Derived from a Polaroid camera (model 210). It is necessary to divide the original camera into two parts, the back-film holder and the lens-shutter mechanism. The two parts are then remounted approximately twice as far apart as in the original camera. The total cost of our camera was less than $50.

Can. J. Chem. Downloaded from www.nrcresearchpress.com by 210.87.254.42 on 09/05/12
For personal use only.

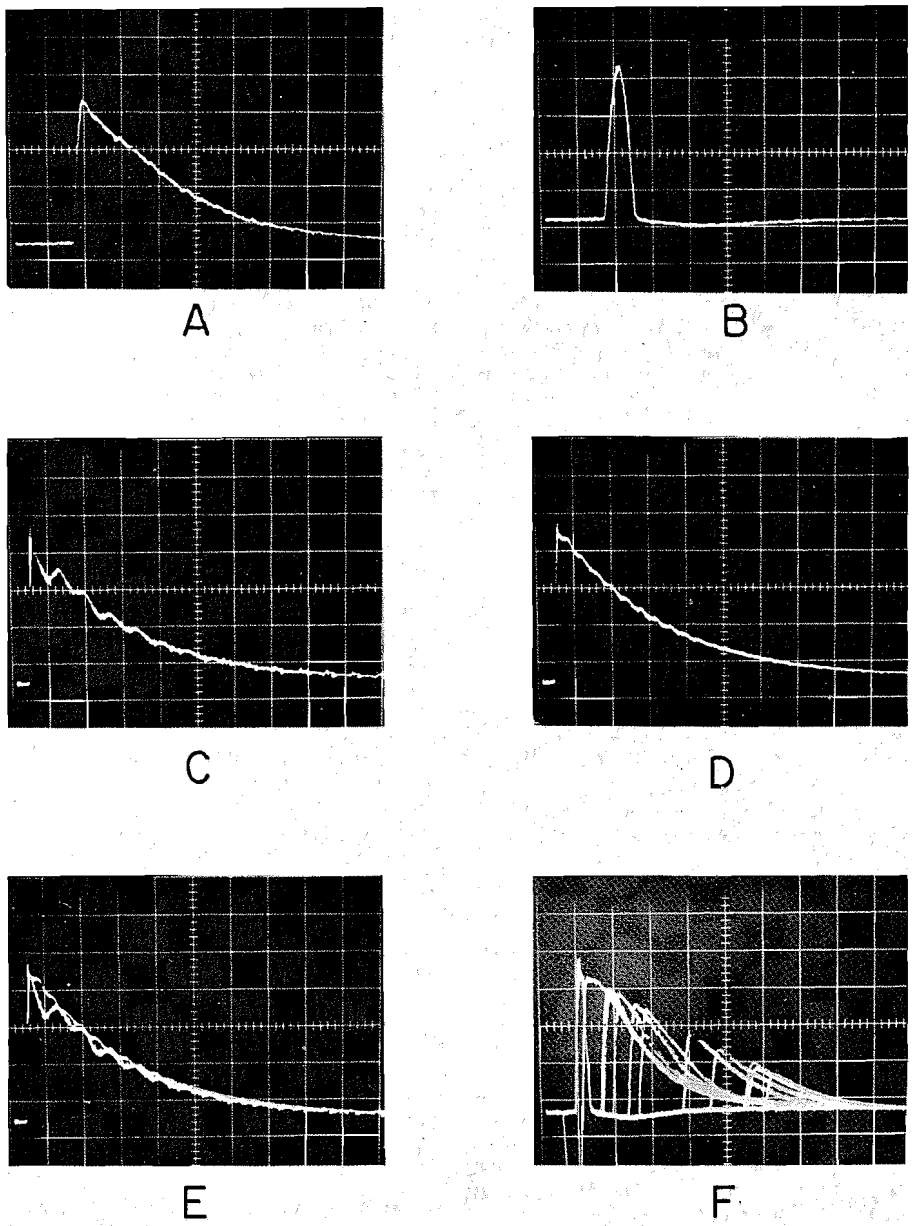

FIG. 3. Typical audiofrequency pulse spectra of an 0.5 M solution of $CHCl_3$ in $CDCl_3$. [A], A $\pi/2$-pulse duration 0.1 s, scale 0.5 s/cm. [B], A π-pulse duration 0.4 s, scale 0.5 s/cm. [C], A T_2 measurement by the Carr–Purcell method with the Meiboom–Gill modification; $\pi/2$-pulse duration 0.2 s, scale 2 s/cm. [D], A $(T_1)_\rho$ measurement, $\pi/2$-pulse duration 0.2 s, scale 2 s/cm. [E], Superimposition of the traces shown in [C] and [D]. [F], first section of a T_1 measurement using repeated π-,$|\pi/2$-pulses; $\pi/2$-pulse duration 0.2 s, scale 1 s/cm; the phase of the $\pi/2$-pulses is inverted 180° from the more conventional orientation.

Discussion

The normal ^1H n.m.r. spectra of vindoline in deuterochloroform solution is shown in Fig. 4. Initially, the relaxation times of the acetate-methyl and N-methyl singlets were determined.

The measurement of the spin–spin relaxation times (T_2) for these two resonances followed the usual Meiboom–Gill modification (9) of

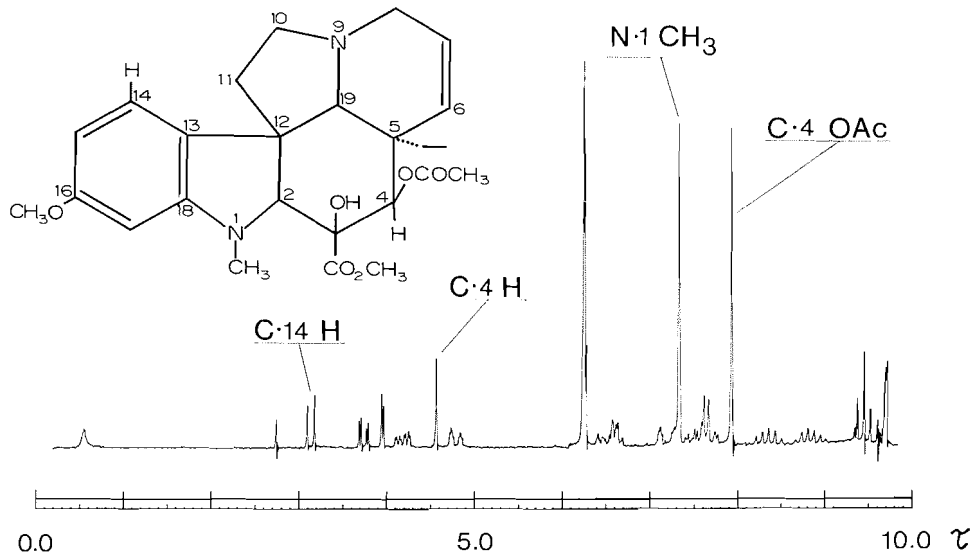

FIG. 4. The ^{1}H n.m.r. spectrum (100 MHz) of vindoline (0.100 g) in deuterochloroform (1.00 ml).

the Carr–Purcell experiment (10). A typical experiment is shown in Fig. 5. Because of the rather short relaxation time of these protons, the spin-echo trace falls to zero rather rapidly and only the first few echoes can be used for measurement purposes. The plot required for the estimation of the T_2 of this transition is shown in Fig. 6. It can be seen that even though the oscilloscope trace is not "elegant" the data it contains are internally consistent.

The determination of the spin–lattice relaxation time (T_1) is, in principle, possible via a single pulse sequence consisting of an initial π-pulse followed by a series of 2π-pulses at regular intervals. However, this technique can have a number of drawbacks: (*a*) errors in setting the length of the 2π-pulse are cumulative; (*b*) for transitions having short relaxation times the total time required by even the first few pulses may be prohibitive; indeed in the case of very short T_1 values the time required for application of a single 2π-pulse may be an appreciable fraction of the total T_1; (*c*) in the same context, the selectivity required for a particular experiment may be incompatible with the power needed to apply a series of 2π-pulses.

An alternative approach which is more time consuming but which is less influenced by the presence of near-neighbor lines, involves a

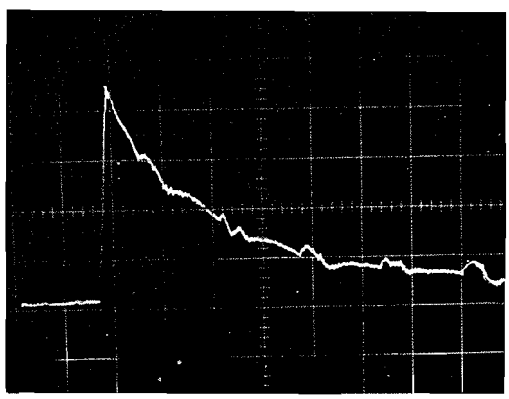

FIG. 5. Measurements of T_2 of the C-4 acetate resonance of vindoline, using a modified Carr–Purcell sequence. $\pi/2$-Pulse duration 0.1 s, scale 0.5 s/cm.

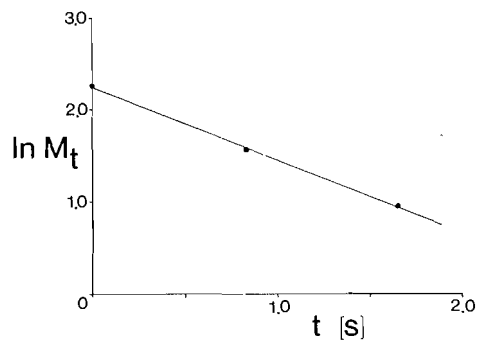

FIG. 6. Plot for measurement of T_2 of the C-4 acetate resonance of vindoline based on data derived from Fig. 5. For each measurement several runs were recorded at different pulse intervals and were averaged.

Can. J. Chem. Downloaded from www.nrcresearchpress.com by 210.87.254.42 on 09/05/12
For personal use only.

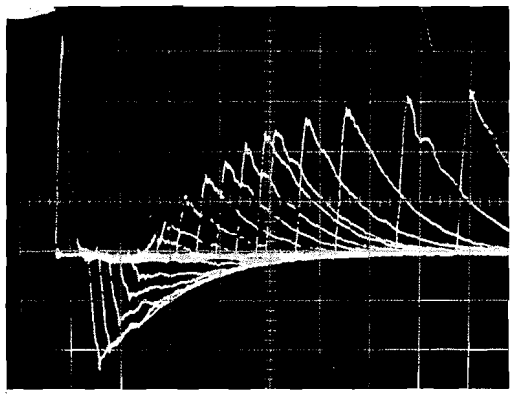

FIG. 7. The T_1 measurement on the C-4 acetate resonance of vindoline. $\pi/2$-Pulse duration, 0.10 s, scale 0.5 s/cm.

repeated series of two-pulse experiments. Initially a π-pulse is applied to tip the magnetization vector along the $-z$-axis and then after a specified delay-time, during which the magnetization vector undergoes some decay, the remaining magnetization is assayed by application of a $\pi/2$-pulse which then tips the vector along the observation axis. After a suitable resting period the whole process is repeated using a different delay-time. A sequence of such experiments gives the entire T_1-decay envelope including the zero-point, as is illustrated in Fig. 7.

Instrumentally, the measurement of $(T_1)_\rho$ values is particularly straightforward by the audiofrequency-pulse method. Thus, the initial $\pi/2$-pulse is readily phase-shifted by precisely 90° and the $(T_1)_\rho$ decay detected. Unfortunately, these particular measurements appear to be sufficiently prone to interference from neighboring lines that their general application to complex organic substances would appear to be somewhat limited. For example, the $(T_1)_\rho$ measurement shown in Fig. 8 clearly fails to return to the baseline as it should.

Following these comparatively simple experiments on the intense singlet resonances, attention was next directed to the other resonances. The two methoxyl groups gave two resonances which were only separated by *ca.* 1 Hz and it proved impossible to effect any recognizable experiments with them. On the other hand, the singlet due to the single C-4 proton was readily amenable to measurements of both T_1 and T_2. Of the many spin-multiplets only the sharp doublet due to the C-14 proton proved suitable for relaxation measurements. This doublet has a splitting of 8.0 Hz and it was possible to perform measurements on both of the transitions. We were disappointed that it was impossible to make measurements on the other well-resolved multiplets: unfortunately the small peak-separations and the rather short relaxation times effectively precluded meaningful experiments. Indeed we were so concerned by the lack of success that extensive efforts were made to degass a solution of vindoline: no appreciable lengthening of relaxation times was observed.

It does not seem appropriate to make any lengthy discussion of the values of the relaxation times obtained, beyond a brief comment that even though they are all quite short, some differential still remains. As can be seen from the data summarized below the *N*-methyl group has the shortest relaxation time as might have been expected. The experiments on vindoline give values which are probably accurate to $\pm 10\%$ in terms of reproducibility.

In conclusion then, it seems that selective

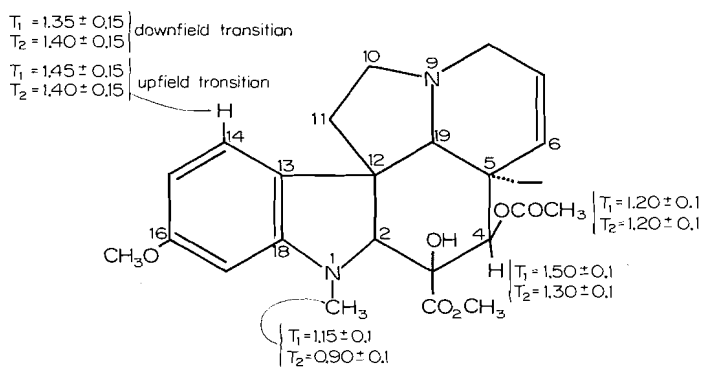

Can. J. Chem. Downloaded from www.nrcresearchpress.com by 210.87.254.42 on 09/05/12
For personal use only.

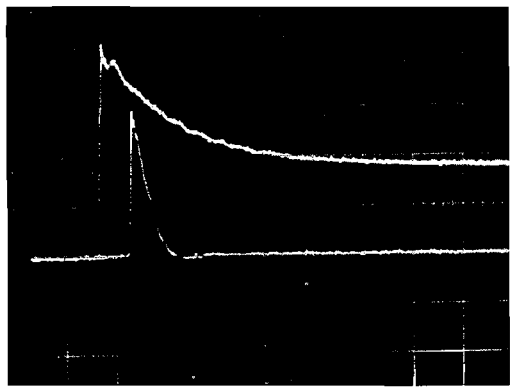

FIG. 8. Traces arising from application of a $\pi/2$-pulse (lower trace) and a $(T_1)_\rho$-pulse (upper trace) to the resonance of the C-4 proton. $\pi/2$-Pulse duration 0.10 s, scale 1.0 s/cm. Note the extra height of the $(T_1)_\rho$-pulse and the fact that its trace does not return to the baseline.

measurements of the individual relaxation times of the protons of reasonably complex organic substances are feasible. The audiofrequency-pulse technique is compatible with measurements for transitions separated by 5 Hz or more from a neighboring resonance, providing that the monitored transition is sharp, *i.e.* $T_2 > 3$ s: for broader transitions a separation of 8–10 Hz is a more realistic one. Providing these limitations are satisfied these measurements can be performed by rather modest modifications to many commercially available high resolution n.m.r. spectrometers.[6] Although relaxation times may in principle be used as the basis for a variety of structural assignments, it is clearly necessary for a systematic catalogue of data to be accumulated before this potential can be realized. If more complete relaxation determinations are to be made for complex organic molecules then techniques having a greater degree of selectivity than those discussed in this paper will be required.

It is also noteworthy that Fourier Transform (F.T.) techniques are being developed (12–14) which should shorten considerably the amount of time required for the routine measurement of selective relaxation times. In this context it is interesting to note that the measurement of T_1 by the F.T. method may involve the repeated application of two-pulse sequences and is thus somewhat analogous to the two-pulse experiments described in this paper. The principal limitations of the F.T. method at this time are associated with measurements of T_2.

[6]Two other laboratories have recently reported the development of audiofrequency-pulse accessories; see ref. 11.

It is a pleasure to thank Dr. Ray Freeman of Varian Associates for his advice and encouragement in the early stages of this project. This work was supported by equipment grants (E-1338 and E-I854) and by an operating grant (A-1905) from the National Research Council of Canada. The sample of vindoline was provided by Dr. J. P. Kutney of this Department.

1. (*a*) J. G. POWLES and D. J. NEALE. Proc. Phys. Soc. (London), **77**, 737 (1961). (*b*) T. E. BURKE and S. I. CHAN. J. Mag. Res. **3**, 55 (1970) and references therein.
2. R. FREEMAN and S. WITTEKOEK. J. Mag. Res. **1**, 238 (1969). For a variant on that paper see, R. FREEMAN, S. WITTEKOEK, and R. R. ERNEST. J. Chem. Phys. **52**, 1529 (1970).
3. (*a*) W. A. ANDERSON. *In* N.M.R. and E.P.R. spectroscopy. Pergamon Press. New York, N.Y. 1960. (*b*) J. H. NOGGLE. J. Chem. Phys. **43**, 3304 (1965).
4. (*a*) W. A. ANDERSON and R. FREEMAN. J. Chem. Phys. **37**, 85 (1962). (*b*) R. A. HOFFMAN and S. FORSEN. J. Chem. Phys. **45**, 2049 (1966).
5. (*a*) E. G. FINER and R. K. HARRIS. Chem. Commun. 42 (1969). (*b*) R. A. HOFFMAN. *In* Advances in magnetic resonance. Vol. 4. Academic Press. New York, N.Y. 1970.
6. B. D. SYKES and J. M. WRIGHT. Rev. Sci. Inst. **41**, 876 (1970).
7. M. GORMAN, N. NEUSS, and K. BIEMANN. J. Am. Chem. Soc. **84**, 1058 (1962).
8. I. SOLOMON. Compte Rend. **248**, 92 (1959).
9. S. MEIBOOM and D. GILL. Rev. Sci. Inst. **29**, 688 (1958).
10. H. Y. CARR and E. M. PURCELL. Phys. Rev. **94**, 630 (1954).
11. (*a*) P. LALANNE and S. ELETR. Rev. Sci. Inst. **41**, 71 (1970). (*b*) A. R. MUIR and D. W. TURNER. Chem. Commun. 286 (1971).
12. R. L. VOLD, J. S. WAUGH, M. P. KLEIN, and D. E. PHELPS. J. Chem. Phys. **48**, 3831 (1968).
13. R. FREEMAN and H. D. W. HILL. J. Chem. Phys. **51**, 3140 (1969); **53**, 4103 (1970); **54**, 301 (1971); **54**, 3367 (1971).
14. A. ALLERHAND and D. W. COCHRAN. J. Am. Chem. Soc. **92**, 4482 (1970).

Can. J. Chem. Downloaded from www.nrcresearchpress.com by 210.87.254.42 on 09/05/12
For personal use only.

Measurements of Deuterium Chemical Shifts by $^1H-\{^2H\}$ INDOR Spectroscopy[1]

J. R. CAMPBELL,[2] L. D. HALL, AND P. R. STEINER[3]

Department of Chemistry, The University of British Columbia, Vancouver 8, British Columbia

Received July 13, 1971

Heteronuclear $^1H-\{^2H\}$ INDOR spectroscopy has been used to measure the deuterium chemical shifts of acetone-d_5, dimethylsulfoxide-d_5, and of 1,2:5,6-di-*O*-isopropylidene-α-D-allofuranose-3-*d*.

La spectroscopie hétéronucléaire $^1H-\{^2H\}$ INDOR a été utilisée pour mesurer les déplacements chimiques du deutérium dans l'acétone-d_5, le diméthylsulfoxyde-d_5, et dans le 1,2:5,6-di-*O*-isopropylidène-α-D-allofuranose-3-*d*.

Canadian Journal of Chemistry, **50**, 504 (1972)

Introduction

With the ever increasing availability of reagents for introducing deuterium substituents into organic systems the need for information concerning deuterium chemical shifts has become more pressing. Direct detection of a deuterium (^2H) resonance is possible, but is complicated somewhat by the comparatively low relative intrinsic sensitivity of deuterium compared (1) with that of protons (9.65×10^{-3}:1). The present paper demonstrates that the measurement of deuterium chemical shifts by the INDOR[4] technique is facile. Since there appears to be a general paucity of absolute deuterium chemical shift data we have included measurements with several simple substances which are commonly used as solvents for n.m.r. studies; these latter data are of particular importance because of the development of n.m.r. instruments[5] which rely on a deuterium resonance as the basis for a heteronuclear lock. Surprisingly, we could find no previous record of this application of INDOR spectroscopy.

Experimental

All n.m.r. measurements were made with an extensively modified Varian HA-100 spectrometer operating in the frequency-swept mode, and using tetramethylsilane as internal reference for the field-frequency lock. The transmitter coil of the V-4332 probe was double-tuned to accept the 100 and the 15 MHz frequencies, as described elsewhere (3). The components used for the heteronuclear INDOR accessory have been described previously (4).

The samples of deuteroacetone, deuterobenzene, and deuterodimethylsulfoxide were commercially available[6] solvents. 1,2:5,6-Di-*O*-isopropylidene-α-D-allofuranose-3-d was kindly provided by Mr. Bruce Donaldson of this laboratory.

The experimental values of the deuterium resonance frequencies, measured in Hz, were converted to a scale on which the ^1H resonance of tetramethylsilane occurs at precisely 100 MHz, using the formula (5),

$$X_{TMS} = \frac{10^8 . X_{obs}}{10^8 + \text{lock sideband frequency}}$$

where X_{TMS} is the chemical shift relative to the protons of tetramethylsilane resonating at exactly 100 000 000 Hz and X_{obs} is the resonance frequency actually recorded (TMS is the the lock signal).

Results and Discussion

In order to ascertain the feasibility of this project, and also the power levels at which the deuterium resonance might be best detected, a detailed study was made of a sample of commercially available acetone-d_6. This material contained a small amount of acetone-d_5 as an isotopic impurity. The ^1H resonance of this "impurity" is shown in Fig. 1A; it is a 1:2:3:2:1 quintet due to the coupling of the lone proton with two equivalent deuterium nuclei, each having spin of unity. The geminal hydrogen–deuterium coupling is 2.2 Hz. INDOR measurements were made in which these five transitions were sequentially monitored while the frequency synthesizer was digitally swept through the appropriate frequency range.

The traces shown in Figs. 1B, C, D, E, and F indicate the observed INDOR responses; the

[1]This paper may be regarded as Part VII of a series entitled, "Studies of carbohydrate derivative by nuclear magnetic double resonance".

[2]NRCC Postdoctorate Fellow, 1969–1971.

[3]Recipient of an NRCC Scholarship, 1969–1970.

[4]An acronym coined by Baker (2) for Inter Nuclear DOuble Resonance.

[5]Such as the Varian XL-100 system.

[6]From Merck, Sharp and Dohme, Montreal.

Can. J. Chem. Downloaded from www.nrcresearchpress.com by 210.87.254.42 on 09/05/12
For personal use only.

Can. J. Chem. Downloaded from www.nrcresearchpress.com by 210.87.254.42 on 09/05/12
For personal use only.

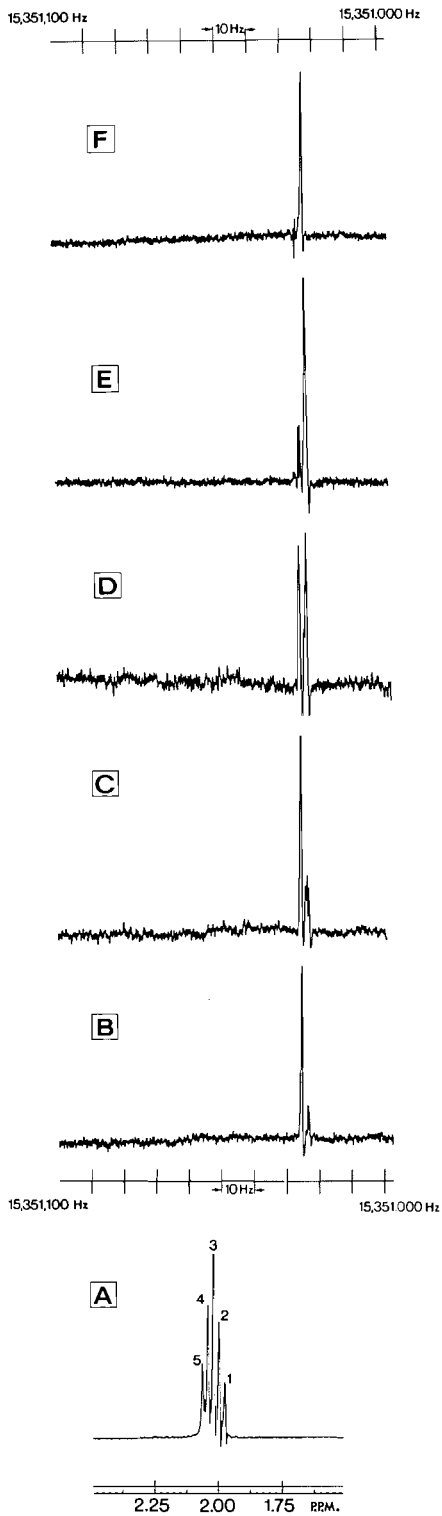

FIG. 1. A, The ^1H n.m.r. spectrum (100 MHz) of the acetone-d_5 "impurity" present in deuteroacetone. The traces shown in B, C, D, E, and F are the INDOR responses obtained by monitoring sequentially transitions 1 through 5 while scanning a radio frequency through the deuterium resonance region.

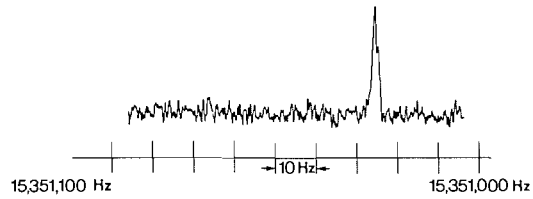

FIG. 2. The response observed during a $^1H-\{^2H\}$ INDOR experiment in which the central transition of the resonance of the acetone-d_5 "impurity" of a solution of deuteroacetone–tetrachloromethane (10% v/v) was monitored. The power level of the deuterium radio frequency field was chosen to give the optimal signal-to-noise ratio.

power level of the radio frequency used to irradiate the deuterium spectrum was chosen such that the doublet shown in Fig. 1D had the optimal resolution (the line width at half-height is 0.5 Hz). The splitting of the observed doublet (2.2 Hz) is, as expected, identical with that of the proton resonance shown in Fig. 1A. A singlet response is observed in the other four traces because the monitored lines correspond to a single deuterium spin state: only transition 3 is degenerate in this regard.

Subsequent experiments with the same sample of deuteroacetone showed that an increase in the radio frequency power caused an enormous improvement in the effective signal-to-noise ratio of the measurement, albeit with some increase in half-height width (to 2.0 Hz). The spectrum shown in Fig. 2 of a solution of deuteroacetone in tetrachloromethane (10% v/v), gives some indication of the sensitivity available.

With these experiments completed it was a simple matter to measure the chemical shifts of the isotopic impurities of deuterobenzene (benzene-d_5) and of deuterodimethylsulfoxide (dimethylsulfoxide-d_5). The chemical shift data, corrected as described in the experimental section are given in Table 1. It must be emphasized that these values are slightly different from those of the related perdeutero derivatives

TABLE 1. Deuterium chemical shifts

Compound	Deuterium chemical shifts	
	Observed frequency (Hz)	Calculated value* (Hz)
$CD_3C(O)CD_2H$	15 351 026	15 350 641
C_6D_5H	15 351 103	15 350 718
$CD_3S(O)CD_2H$	15 351 031	15 350 646
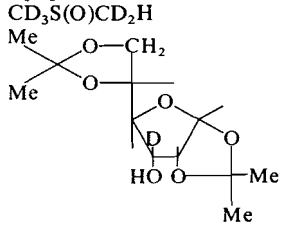	15 351 056	15 350 671

*Using the formula given in the Experimental section.

because of a small isotope shift.[7] Strictly, the value for benzene is that of the deuterium substituents which are ortho to the proton substituent.

In order to demonstrate the feasibility of measuring the deuterium shifts of a specifically deuterated substance having somewhat higher molecular weight, measurements were made with a sample of 1,2:5,6-di-*O*-isopropylidene-α-D-allofuranose-3-d. The spectrum obtained by monitoring an H-2 transition is shown in Fig. 3

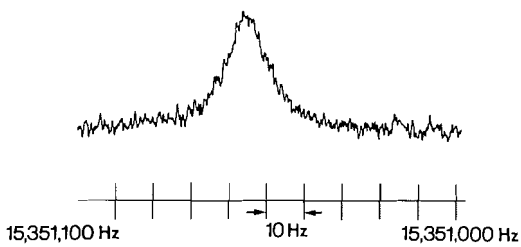

FIG. 3. Response obtained from a $^1H-\{^2H\}$ INDOR experiment on 1,2:5,6-di-*O*-isopropylidene-α-D-allofuranose-3-*d* in deuterochloroform solution (20% w/v). The high field transition of the H-2 resonance was monitored.

[7]We do not wish to discuss such isotope effects here although two referees requested that we should. For a paper on the isotope effects of deuterium substituents on ^1H *shifts* see ref. 6.

and the chemical shift is listed in Table 1. Although the resolution of this resonance is poorer than that observed for the traces shown in Fig. 1 the accuracy of the chemical shift is entirely adequate for most chemical purposes.

In summary then, it is possible to measure deuterium chemical shifts *via* the $^1H-\{^2H\}$ INDOR method for compounds having a deuterium substituent which is coupled with a proton; however, the shifts obtained will not be the same as those of the perdeutero-derivative.

It is a pleasure to thank the National Research Council of Canada for their generous financial support, via both equipment and operating grants.

1. Nuclear Magnetic Resonance Table. Varian Associates, Palo Alto, California, 1968.
2. E. B. BAKER. J. Chem. Phys. **37**, 911 (1962).
3. R. BURTON and L. D. HALL. Can. J. Chem. **48**, 59 (1970).
4. R. BURTON, L. D. HALL, and P. R. STEINER. Can. J. Chem. **49**, 588 (1971).
5. W. MCFARLAN. Annual reviews in N.M.R. spectroscopy. Vol. 1. *Editor*, E. F. Mooney. Academic Press, 1968. p. 135–163, and references therein.
6. W. SAUR, H. L. CRESPI, and J. J. KATZ. J. Mag. Res. 2, 47 (1970).

Can. J. Chem. Downloaded from www.nrcresearchpress.com by 210.87.254.42 on 09/05/12
For personal use only.

Addition of Pseudohalogens to Unsaturated Carbohydrates. V. Addition of Iodine Trifluoroacetate[1]

R. G. S. RITCHIE AND W. A. SZAREK
Department of Chemistry, Queen's University, Kingston, Ontario

Received August 20, 1971

Treatment of 5,6-dideoxy-1,2-*O*-isopropylidene-α-D-*xylo*-hex-5-enofuranose (**1**) with silver trifluoroacetate and iodine in acetonitrile gave 3,6-anhydro-5-deoxy-5-iodo-1,2-*O*-isopropylidene-α-D-gluco(and β-L-ido)-furanose (**2**) and 5-deoxy-5-iodo-1,2-*O*-isopropylidene-6-*O*-trifluoroacetyl-α-D-gluco(and/or β-L-ido)furanose (**3**). Component **2** was converted into 3,6-anhydro-5-deoxy-1,2-*O*-isopropylidene-α-D-*xylo*-hexofuranose (**5**) by hydrogenation over Raney nickel, and component **3** was converted into 5-deoxy-1,2-*O*-isopropylidene-α-D-*xylo*-hexofuranose (**6**) by treatment with methanol, followed by hydrogenation. Treatment of 5,6-dideoxy-1,2-*O*-isopropylidene-3-*O*-trifluoroacetyl-α-D-*xylo*-hex-5-enofuranose (**7**) with silver trifluoroacetate and iodine in acetonitrile gave the addition product **8**, but no 3,6-anhydro derivative; **8** was converted into the iodohydrin **4** by treatment with methanol. The preparation of the 5-deoxy derivative **6** by way of the iodohydrin **4** represents an overall anti-Markovnikov hydration of the olefin **1**; the reactions described are a convenient alternative to the hydroboration–oxidation procedure for the preparation of **6**.

Le traitement du 5,6-didéoxy-1,2-*O*-isopropylidène-α-D-*xylo*-hex-5-énofuranose (**1**) par le trifluoracétate d'argent et l'iode dans l'acétonitrile conduit aux 3,6-anhydro-5-déoxy-5-iodo-1,2-*O*-isopropylidène-α-D-gluco(et β-L-ido)furanose (**2**) et 5-déoxy-5-iodo-1,2-*O*-isopropylidène-6-*O*-trifluoroacétyl-α-D-gluco(et/ou β-L-ido)furanose (**3**). Le composé **2** a été transformé en 3,6-anhydro-5-déoxy-1,2-*O*-isopropylidène-α-D-*xylo*-hexafuranose (**5**) par hydrogénation sur nickel de Raney et le composé **3** a été transformé en 5-déoxy-1,2-*O*-isopropylidène-α-D-*xylo*-hexofuranose (**6**) par traitement avec le méthanol puis par hydrogénation. Le traitement du 5,6-didéoxy-1,2-*O*-isopropylidène-3-*O*-trifluoroacétyl-α-D-*xylo*-hex-5-énofuranose (**7**) par le trifluoroacétate d'argent et l'iode dans l'acétonitrile conduit au produit d'addition **8**, mais pas au dérivé 3,6-anhydro; le composé **8** a été transformé en iodohydrine **4** par traitement dans le méthanol. La préparation du dérivé 5-déoxy **6** au moyen de l'iodohydrine **4** représente une hydratation anti-Markovnikov de l'oléfine **1**; les réactions décrites représentent un autre moyen possible d'hydroboration-oxydation pour la préparation de **6**.

Canadian Journal of Chemistry, **50**, 507 (1972)

Introduction

The addition of pseudohalogens to unsaturated carbohydrates, as a method of introducing nitrogen-containing functional groups, has been the subject of several recent publications (1–6). In connection with a study (7) of the addition of iodine nitrate, it was necessary to prepare some carbohydrate iodohydrins. Such compounds have been obtained mainly from sugar epoxides (8). Recently, the preparation of iodohydrins directly from olefins, by reaction with iodine in the presence of water and a suitable oxidizing agent, was described by Cornforth and Green (9). Here we report some results of an investigation of the synthesis of carbohydrate iodohydrins by way of the addition of iodine trifluoroacetate to unsaturated carbohydrates. The trifluoroacetyl group has been used in carbohydrate chemistry as a blocking group, particularly, because of its ease of hydrolysis; removal of the group has been achieved under extremely mild conditions at room temperature with anhydrous methanol, aqueous acetone, or aqueous pyridine (10).

Iodine trifluoroacetate is produced by the reaction of iodine and silver trifluoroacetate; the positive iodine generated in this way has been shown (11) to be very reactive in electrophilic aromatic substitution. Henbest (12) first reported the addition of iodine trifluoroacetate to ethylenic compounds, although in that work, the adducts were not isolated. In 1966 Hey *et al.* (13) showed that iodine trifluoroacetate adds stereospecifically to 5α-cholest-2-ene to give 3α-iodo-5α-cholestan-2β-yl trifluoroacetate in high yield. In the present work the reaction of iodine trifluoroacetate with 5,6-dideoxy-1,2-*O*-isopropylidene-α-D-*xylo*-hex-5-enofuranose (**1**) (14) and a 3-*O*-substituted derivative (**7**) has been studied.

[1]For part IV in this series, see ref. 6.

Can. J. Chem. Downloaded from www.nrcresearchpress.com by 210.87.254.40 on 09/05/12
For personal use only.

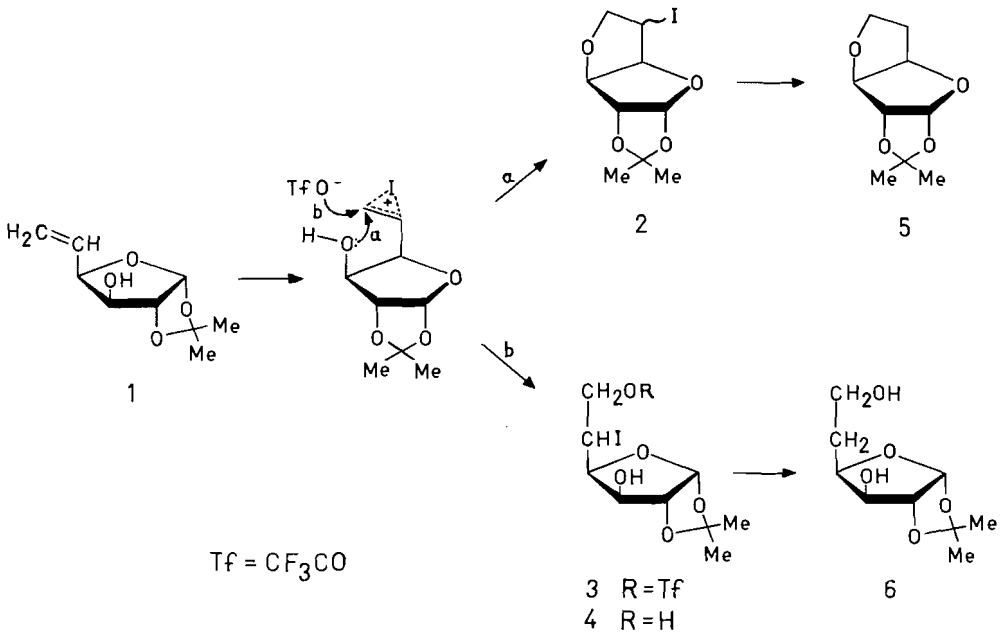

SCHEME 1

Results and Discussion

Addition of silver trifluoroacetate and olefin **1** to a solution of iodine in acetonitrile[2] at room temperature gave in 5 min a syrupy mixture of two components; the i.r. spectrum showed absorptions at 3460 and 1790 cm^{-1} attributable to the presence of hydroxyl and trifluoroacetate groups, respectively. The isolation of a compound containing a trifluoroacetate group could not, however, be achieved by column chromatography on silica gel, because of the lability of this group. Instead, the mixture was briefly treated with methanol, and the resultant syrupy material was fractionated on silica gel. Two components were obtained, which were assigned the structures **2** and **4** (Scheme 1). The first component was a crystalline solid with a 5° m.p. range; its i.r. spectrum and elemental analysis were consistent with the assigned structure (**2**). However, the presence in the n.m.r. spectrum of two doublets with equal spacings (3.7 Hz) at τ 3.76 and 4.06, attributable to H-1, indicated that this component was a mixture of two compounds; the ratio of peak areas was 2:15, respectively. Hydrogenation over a Raney nickel catalyst gave only one compound, which was assigned the structure of 3,6-anhydro-5-deoxy-1,2-*O*-isopropylidene-α-D-*xylo*-hexofuranose (**5**) on the basis of its n.m.r. spectrum. The first component was, therefore, a 2:15 mixture of epimers: 3,6-anhydro-5-deoxy-5-iodo-1,2-*O*-isopropylidene-α-D-glucofuranose and the β-L-*ido* isomer. The isomer distribution was assigned on the basis of the chemical shifts of the H-1 signals in the n.m.r. spectrum. In the L-*ido* compound, the iodine is *exo* in the bicyclic system formed by the furanose and 3,6-anhydro rings, whereas, in the D-*gluco* compound, it is *endo*, and relatively close to H-1. The H-1 signal in the former compound should, therefore, be less affected by the iodine at C-5, and it is reasonable to expect that its chemical shift would be very close to that of the H-1 signal in the 5-deoxy compound **5** (τ 4.08). Thus, the preponderant isomer, whose H-1 signal is at τ 4.06, has been assigned the L-*ido* structure.

The second component (**4**) was isolated as a syrup in 37% yield. Its i.r. spectrum showed a very strong hydroxyl absorption at 3460 cm^{-1}, but no absorption attributable to a trifluoroacetate group. The assignation of the iodine to

[2]The use of acetonitrile for the *in situ* generation of iodine trifluoroacetate gave satisfactory results with equimolar amounts of silver trifluoroacetate and iodine; other workers used an excess of the silver salt with nitrobenzene (11) or methylene chloride (13).

Can. J. Chem. Downloaded from www.nrcresearchpress.com by 210.87.254.40 on 09/05/12
For personal use only.

Can. J. Chem. Downloaded from www.nrcresearchpress.com by 210.87.254.40 on 09/05/12
For personal use only.

C-5 was established by the conversion of **4** into 5-deoxy-1,2-*O*-isopropylidene-α-D-*xylo*-hexofuranose (**6**) by hydrogenation over a Raney nickel catalyst. The preparation, in the present work, of the 5-deoxy derivative **6** by way of the iodohydrin **4** represents an overall anti-Markovnikov hydration of the unsaturated sugar **1**. An improved protocol for the conversion of **1** into **6** is described later in this paper. A synthesis of **6** from **1** has been reported previously (15), namely, by hydroboration. A number of other syntheses of compound **6** have also been achieved (16).

Component **4** was unstable on standing, and an iodine-colored syrup was formed even in the dark at 5°. The structure proposed for **4** was supported by its mass spectrum, which shows many of the features of the spectra of monosaccharide isopropylidene derivatives (17). A weak molecular ion was observed at *m/e* 330 ($C_9H_{15}O_5I$), and a more intense peak at *m/e* 315 (M-15) owing to the ion formed from the molecular ion by elimination of one of the methyl groups; the most intense peak was at *m/e* 59, attributable to protonated acetone.

The reaction of 5,6-dideoxy-1,2-*O*-isopropylidene-α-D-*xylo*-hex-5-enofuranose (**1**) with silver trifluoroacetate and iodine in acetonitrile is considered to proceed by way of an intermediate cationic species such as that shown in Scheme 1. Attack by the C-3 hydroxyl group at the less-hindered C-6 position (route *a*) would then yield a 3,6-anhydro derivative (**2**), whereas attack by trifluoroacetate ion (route *b*) would give a 5-deoxy-5-iodo-6-*O*-trifluoroacetyl derivative (**3**). Treatment of **3** with methanol afforded the iodohydrin **4**. The possibility of the formation of **2** from the adduct **3** in the reaction mixture was excluded by the observation that the proportion of the products remained unchanged when the time of the reaction was extended from 5 to 40 min. Moreover, the formation of **2** was not observed, within 40 min, when olefin **1** was treated with only iodine in acetonitrile; a decomposition of **1**, involving elimination of acetone, was observed with longer reaction times. Since the two faces of the double bond in **1** are diastereotopic, the addition of iodine trifluoroacetate by the mechanism suggested above would be expected to yield two diastereoisomers. Although the presence of two isomers of **2** was clearly discernible in its n.m.r. spectrum by the observation of two anomeric signals, such was not the case for **4**. The spectrum of **4** showed what appeared to be only one anomeric signal. It is interesting that, in the reaction of the pseudohalogen iodine azide (IN_3) with olefin **1**, the formation of a 3,6-anhydro derivative was not reported (4); the product isolated was the adduct 6-azido-5,6-dideoxy-5-iodo-1,2-*O*-isopropylidene-β-L-idofuranose. The addition of iodine azide presumably also occurs by way of the cyclic iodonium ion intermediate shown in Scheme 1. In the present work, the formation of the 3,6-anhydro component **2** as the preponderant product is probably attributable to the trifluoroacetate anion's low nucleophilicity.

In order to obviate the formation of a 3,6-anhydro derivative, it was clearly necessary to block the hydroxyl group at C-3 in the olefin **1** with a non-participating group. For this purpose, the highly electronegative trifluoroacetyl group was selected. Thus, treatment of olefin **1** with trifluoroacetic anhydride – sodium trifluoroacetate gave an almost quantitative yield of the 3-*O*-trifluoroacetyl derivative **7** (Scheme 2). The reaction of **7** with silver trifluoroacetate and iodine in acetonitrile then gave the adduct **8** in high yield without the formation of a 3,6-anhydro derivative. A brief treatment of **8** with methanol afforded the iodohydrin **4**. The preceding reactions constitute a convenient procedure for the preparation of **4**, and hence of

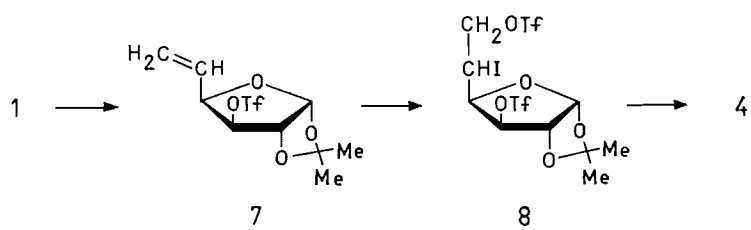

SCHEME 2

Can. J. Chem. Downloaded from www.nrcresearchpress.com by 210.87.254.40 on 09/05/12
For personal use only.

the 5-deoxy sugar derivative **6** with subsequent hydrogenation.

Hey *et al.* (13) have reported that heating 3α-iodo-5α-cholestan-2β-yl trifluoroacetate, the adduct from the reaction of 5α-cholest-2-ene and iodine trifluoroacetate, with silver trifluoroacetate and hydrolyzing the intermediate (presumably the 2β,3β-diester) gave the 2β,3β-diol. In the present work, an attempted displacement of an iodo group by trifluoroacetate in **8**, using silver trifluoroacetate in acetonitrile, gave only an intractable material. With dichloromethane–toluene as the solvent, even after refluxing for 24 h, no change in the starting material was observed.

Experimental

Melting points were determined with a Fisher–Johns apparatus and are uncorrected. Microdistillations were performed with a Gallenkamp heating block. Optical rotations were measured using a Perkin–Elmer Model 141 automatic polarimeter at 23 ± 2°. The i.r. spectra were recorded on a Unicam SP 1000 or a Perkin–Elmer 180 spectrophotometer. The n.m.r. spectra were obtained on a Varian A-60 spectrometer in chloroform-*d* with tetramethylsilane (τ 10.00) as internal standard; coupling constants were measured at a 250 Hz sweep width. High resolution mass spectra were determined with a JEOLCO double focusing spectrometer, Model JMS-01SC, equipped with a heated, direct sample-injection system operated at 83°, and fitted to record data by a photoplate; ionizing potential 75 eV. The t.l.c. was performed with silica gel G as the adsorbent in the following solvent systems (v/v): (A) petroleum ether (b.p. 60–80°) – ethyl acetate, 3:2; (B) 3:1; (C) 2:3. The developed plates were air-dried, sprayed with 5% ethanolic sulfuric acid, and heated at about 150°. Column chromatography was performed on Brinkmann silica gel (70–325 mesh) with the following eluants (v/v): (D) carbon tetrachloride – ethyl acetate, 3:1; (E) 1:1; the glass columns were covered with aluminum foil to exclude light. Carbon tetrachloride was freshly distilled, and acetonitrile was kept over Type 3A molecular sieves for at least 1 week prior to its use. Solvents were evaporated under reduced pressure below 35°. Silver trifluoroacetate was prepared as described by Janssen and Wilson (18).

Reaction of 5,6-Dideoxy-1,2-O-isopropylidene-α-D-xylo-hex-5-enofuranose (1) with Silver Trifluoroacetate and Iodine

Olefin **1** (395 mg, 2.1 mmol) and silver trifluoroacetate (563 mg, 1.2 equiv) in dry acetonitrile (15 ml) were added, in one portion, to a stirred solution of iodine (647 mg, 1.2 equiv) in dry acetonitrile (25 ml) in a flask covered with aluminum foil. After 5 min, the reaction mixture was filtered, and the filtrate was concentrated to a dark red syrup. The syrupy residue was extracted with carbon tetrachloride (50 ml), and the extract was washed with aqueous sodium thiosulfate solution, dried over anhydrous sodium sulfate in the presence of decolorizing charcoal, and filtered through Celite. The clear, colorless filtrate was concentrated to a syrup (761 mg). The t.l.c. (solvent A) showed that all of the starting olefin (R_F 0.5) had been consumed and revealed the presence of two new components, one as a well defined spot (R_F 0.8) and the other as a tailing spot (R_F 0.6). The i.r. spectrum (film) showed absorptions at 3460 (OH) and 1790 cm^{-1} ($CF_3C{=}O$). The syrup was dissolved in methanol; after 1 min, t.l.c. (solvent A) showed the presence of two components having R_F values of 0.8 and 0.2. The solvent was evaporated to leave a pale yellow syrup (633 mg), which was fractionated on silica gel, with solvent D as eluant, to yield the two components **2** and **4**.

Component **2** was obtained from ethanol as a crystalline solid (295 mg, 45%), m.p. 105–110°, $[\alpha]_D$ +4° (*c*, 1.0 in chloroform); ν_{max} ($CHCl_3$) 1380, 1390 cm^{-1} (CMe_2), no absorption attributable to OH or $CF_3C{=}O$; n.m.r. data: τ 3.76, 4.06 (1-proton, two doublets with a ratio of peak areas of 2:15, respectively, $J_{1,2} = 3.7$ Hz, H-1 of two isomers), 5.15 (1-proton quartet, $J_{3,4} = 3.4$ Hz, $J_{4,5} = 2.4$ Hz, H-4), 5.25 (1-proton doublet, $J_{2,3} < 0.5$ Hz, H-2), 5.45 (1-proton doublet, H-3), 5.7–6.3 (3-proton multiplets, H-5, 2H-6's), 8.50, 8.67 (3-proton singlets, CMe_2).

Anal. Calcd. for $C_9H_{13}O_4I$: C, 34.6; H, 4.2; I, 40.7. Found: C, 34.8; H, 4.2; I, 40.4.

Component **4** was obtained as a syrup (260 mg, 37%), $[\alpha]_D$ −2°, $[\alpha]_{365}$ +10° (*c*, 0.9 in chloroform), ν_{max} (film) 1380, 1390 (CMe_2), 3440 cm^{-1} (very strong, OH), no absorption attributable to $CF_3C{=}O$; n.m.r. data: τ 4.04 (1-proton doublet, $J_{1,2} = 3.6$ Hz, H-1), 5.32 (1-proton doublet, $J_{2,3} <$ 0.5 Hz, H-2), 5.68 (3-proton broad singlet), 5.88 (2-proton singlet, disappeared on deuteration, 2OH's), 6.03 (2-proton multiplet), 8.48, 8.64 (3-proton singlets, CMe_2).

Anal. Calcd. for $C_9H_{15}O_5I$: C, 32.7; H, 4.6. Found: C, 32.4; H, 4.7.

Syrupy **4** was unstable on standing, and a satisfactory analysis for iodine could not be obtained. The molecular formula was confirmed by mass spectrometry: M^+ 329.994, M^+-Me 314.970 (Calcd. for $C_9H_{15}O_5I$: 329.996; M^+-Me: 314.973).

3,6-Anhydro-5-deoxy-1,2-O-isopropylidene-α-D-xylo-hexofuranose (5)

A solution of component **2** (168 mg, 0.54 mmol) in ethanol containing W-4 Raney nickel catalyst and triethylamine (1 ml) was subjected to a hydrogen pressure of 40 p.s.i.g. The t.l.c. (solvent B) showed that the reaction was complete in 80 min. The catalyst was removed by filtration and extracted with boiling ethanol. The combined filtrate and extract were concentrated, and the residue was partitioned between ether and water. The dried (sodium sulfate) ether solution was decolorized with charcoal and then concentrated to give **5** as an oil (79 mg, 79%), b.p. 56–60°/0.06 Torr, $[\alpha]_D$ +15.5° (*c*, 2.0 in chloroform); n.m.r. data: τ 4.08 (1-proton doublet, $J_{1,2} = 3.9$ Hz, H-1), 5.02 (1-proton multiplet, H-4), 5.39 (1-proton doublet, $J_{2,3} <$ 0.5 Hz, H-2), 5.58 (1-proton doublet, $J_{3,4} = 3.4$ Hz, H-3), 5.86–6.34 (2-proton multiplet, 2H-6's), 7.75–8.18 (2-proton multiplet, 2H-5's), 8.49, 8.67 (3-proton singlets, CMe_2). The i.r. spectrum did not show any absorptions attributable to OH or $CF_3C{=}O$.

Anal. Calcd. for $C_9H_{14}O_4$: C, 58.0; H, 7.6. Found: C, 57.9; H, 7.7.

Can. J. Chem. Downloaded from www.nrcresearchpress.com by 210.87.254.40 on 09/05/12
For personal use only.

5-Deoxy-1,2-O-isopropylidene-α-D-xylo-hexofuranose (6)

A solution of freshly prepared component **4** (264 mg, 0.8 mmol) in ethanol containing W-4 Raney nickel catalyst and triethylamine (1 ml) was subjected to a hydrogen pressure of 40 p.s.i.g. for 3 h; the progress of the reaction was followed by t.l.c. (solvent C). The catalyst was removed by filtration and extracted with boiling ethanol. The combined filtrate and extract were concentrated to a crystalline residue, which was extracted with ether. The ether was evaporated, and the residue was chromatographed on silica gel (60–120 mesh), with, initially, 1:2 carbon tetrachloride–ethyl acetate and, finally, ethyl acetate as eluants, to yield compound **6** (104 mg, 64%). After recrystallization from ether–petroleum ether (b.p. 60–80°), the compound had m.p. 93–94.5° and $[\alpha]_D$ −10.5° (*c*, 1.7 in chloroform). These physical constants are in agreement with those reported for compound **6** by other workers (15, 16); its n.m.r. spectrum was identical with that published by Wolfrom *et al.* (15).

5,6-Dideoxy-1,2-O-isopropylidene-3-O-trifluoroacetyl-α-D-xylo-hex-5-enofuranose (7)

5,6-Dideoxy-1,2-*O*-isopropylidene-α-D-*xylo*-hex-5-enofuranose (**1**) (312 mg, 1.68 mmol) and sodium trifluoroacetate (77 mg) were treated with ice-cold trifluoroacetic anhydride (1 ml). The vigorous, exothermic reaction subsided in 5 min, and the mixture was then concentrated to dryness, under reduced pressure and a bath temperature of less than 35°, three times with 50 ml portions of carbon tetrachloride. The residue was extracted with hot carbon tetrachloride, and the solvent was evaporated to give **7** as a colorless oil (450 mg, 95%), b.p. 40–43°/0.008 Torr, $[\alpha]_D$ +24.4° (*c*, 3.0 in carbon tetrachloride); ν_{max} (film) 1385, 1390 (CMe_2), 1790 cm^{-1} (strong, $CF_3C{=}O$), no absorption attributable to OH; n.m.r. data: τ 3.95 (1-proton doublet, $J_{1,2}$ = 3.8 Hz, H-1), 3.9–4.8 (4-protons, H-3, H-5, 2H-6's), 5.13 (1-proton multiplet, H-4), 5.34 (1-proton doublet, $J_{2,3}$ < 0.5 Hz, H-2), 8.45, 8.65 (3-proton singlets, CMe_2). As would be expected, the n.m.r. spectrum of **7** showed an "acylation shift" compared with the spectrum of olefin **1**; the magnitudes of the shifts were even greater than those observed with the 3-*O*-acetate of **1** (19).

Anal. Calcd. for $C_{11}H_{13}O_5F_3$: C, 46.8; H, 4.6; F, 20.2. Found: C, 46.3; H, 4.6; F, 20.4.

Reaction of 5,6-Dideoxy-1,2-O-isopropylidene-3-O-trifluoroacetyl-α-D-xylo-hex-5-enofuranose (7) with Silver Trifluoroacetate and Iodine

Olefin **7** (300 mg, 1.06 mmol) and silver trifluoroacetate (277 mg, 1.2 equiv) in dry acetonitrile (8 ml) were added to a stirred solution of iodine (319 mg, 1.2 equiv) in dry acetonitrile (10 ml) in a flask covered with aluminum foil. After 10 min, the reaction mixture was filtered through Celite, and the filtrate was concentrated to dryness. The residue was extracted with hot carbon tetrachloride, and the extract was washed with aqueous sodium thiosulfate solution and dried over anhydrous sodium sulfate. The solvent was evaporated to leave an oil (498 mg) from which **8** was obtained by distillation, b.p. 88–92°/0.008 Torr, $[\alpha]_D$ −5°, $[\alpha]_{365}$ −9° (*c*, 1.2 in carbon tetrachloride); ν_{max} (film) 1378, 1385 (CMe_2), 1790 cm^{-1} (very strong, $CF_3C{=}O$), no absorption attributable to OH; n.m.r. data: τ 3.98 (1-proton doublet, $J_{1,2}$ = 3.7 Hz, H-1), 4.55 (1-proton doublet, $J_{3,4}$ = 1.5 Hz, H-3), 5.1–5.7 (5-protons, H-2, H-4, H-5, 2H-6's), 8.45, 8.66 (3-proton singlets, CMe_2).

Anal. Calcd. for $C_{13}H_{13}O_7IF_6$: C, 29.9; H, 2.5. Found: C, 30.4; H, 2.6.

A portion (470 mg) of the crude oil obtained above was dissolved in methanol (15 ml), and the solvent was subsequently evaporated to leave a syrup (274 mg). Chromatography of this material on silica gel, with solvent E as eluant, gave the expected **4** (190 mg) and some 5,6-dideoxy-1,2-*O*-isopropylidene-α-D-*xylo*-hex-5-enofuranose (**1**) (21 mg). The presence of **1** was probably the result of incomplete addition of iodine trifluoroacetate to olefin 7.

The authors thank Professor J. K. N. Jones for his interest and encouragement, and the National Research Council of Canada for financial support of this work.

1. W. A. Szarek, D. G. Lance, and R. L. Beach. Chem. Commun. 356 (1968); Carbohydr. Res. **13**, 75 (1970).
2. W. A. Szarek, J. S. Jewell, I. Szczerek, and J. K. N. Jones. Can. J. Chem. **47**, 4473 (1969).
3. E. L. Albano, D. Horton, and J. H. Lauterbach. Carbohydr. Res. **9**, 149 (1969).
4. J. S. Brimacombe, J. G. H. Bryan, and T. A. Hamor. J. Chem. Soc. B, 514 (1970).
5. J. S. Brimacombe, F. Hunedy, and M. Stacey. Carbohydr. Res. **13**, 447 (1970).
6. R. G. S. Ritchie and W. A. Szarek. Carbohydr. Res. **18**, 443 (1971).
7. J. S. Jewell, R. G. S. Ritchie, W. A. Szarek, and J. K. N. Jones. To be published.
8. F. H. Newth. Quart. Rev. (London), **13**, 30 (1959); R. U. Lemieux, E. Fraga, and K. A. Watanabe. Can. J. Chem. **46**, 61 (1968).
9. J. W. Cornforth and D. T. Green. J. Chem. Soc. C, 846 (1970).
10. T. G. Bonner. Advan. Carbohydr. Chem. **16**, 59 (1961).
11. R. N. Haszeldine. J. Chem. Soc. 584 (1951); R. N. Haszeldine and A. G. Sharpe. J. Chem. Soc. 993 (1952).
12. H. B. Henbest. Proc. Chem. Soc. 159 (1963).
13. D. G. Hey, G. D. Meakins, and M. W. Pemberton. J. Chem. Soc. C, 1331 (1966).
14. J. K. N. Jones and J. L. Thompson. Can. J. Chem. **35**, 955 (1957).
15. M. L. Wolfrom, K. Matsuda, F. Komitsky, Jr., and T. E. Whiteley. J. Org. Chem. **28**, 3551 (1963).
16. E. J. Hedgley, O. Mérész, and W. G. Overend. J. Chem. Soc. C, 888 (1967); H. Paulsen and D. Stoye. Ber. **99**, 908 (1966); J. G. Buchanan and E. M. Oakes. Tetrahedron Lett. 2013 (1964); R. E. Gramera, T. R. Ingle, and R. L. Whistler. J. Org. Chem. **29**, 878, 2074 (1964).
17. D. C. De Jongh and K. Biemann. J. Am. Chem. Soc. **86**, 67 (1964); N. K. Kochetkov and O. S. Chizhov. Advan. Carbohydr. Chem. **21**, 39 (1966).
18. D. E. Janssen and C. V. Wilson. Inorg. Syn. Coll. Vol. IV, 547 (1963).
19. D. G. Lance and W. A. Szarek. Carbohydr. Res. **10**, 306 (1969).

Studies on Fluorinated Vinylic and Aromatic Alcohols and Esters[1]

I. S. CHANG, J. T. PRICE, A. J. TOMLINSON, AND C. J. WILLIS[2]

Department of Chemistry, University of Western Ontario, London 72, Ontario

Received September 2, 1971

Synthetic studies and pK_a measurements are reported on a number of highly fluorinated tertiary alcohols and diols, namely $(CF_2CF)C(CF_3)_2OH$, $(CF_2CF)_2C(CF_3)OH$, $(C_6F_5)C(CF_3)_2OH$, $(C_6F_5)_2C(CF_3)OH$, $(C_6F_5)_3COH$, $(C_6H_5)C(CF_3)_2OH$, $[(CF_3)_2COH]_2$, and $[(C_6F_5)C(CF_3)OH]_2$. General agreement is found with earlier work reporting a correlation between pK_a values and differences between free and H-bonded O—H stretching frequencies.

The reaction of C_6F_5Li with the acyl halides CF_3COCl and C_6F_5COCl in appropriate molar ratio gives the esters $(C_6F_5)_2C(CF_3)OCOC_6F_5$ and $(C_6F_5)_3COCOC_6F_5$, respectively; this constitutes a useful preparative route to fully fluorinated esters.

On rapporte des études synthétiques et des mesures de pK_a sur certains alcools et diols tertiaires fortement fluorés, notamment $(CF_2CF)C(CF_3)_2OH$, $(CF_2CF)_2C(CF_3)OH$, $(C_6F_5)C(CF_3)_2OH$, $(C_6F_5)_2C(CF_3)OH$, $(C_6F_5)_3COH$, $(C_6H_5)C(CF_3)_2OH$, $[(CF_3)_2COH]_2$, et $[(C_6F_5)C(CF_3)OH]_2$. On est généralement d'accord avec les travaux précédents rapportant une correlation entre les valeurs de pK_a et les différences entre les fréquences d'élongation du groupement O—H libre et relié à un proton.

La réaction de C_6F_5Li avec les halogénures d'acyle CF_3COCl et C_6F_5COCl dans les rapports molaires appropriés donne les esters $(C_6F_5)_2C(CF_3)OCOC_6F_5$ et $(C_6F_5)_3COCOC_6F_5$ respectivement; cela constitue une voie de préparation utile vers les esters totalement fluorés.

Canadian Journal of Chemistry, **50**, 512 (1972)

Introduction

Reported studies on fully fluorinated alcohols have been largely confined to tertiary species, because of the limited stability of primary and secondary fluorinated alcohols with respect to elimination of hydrogen fluoride. Knunyants and coworkers (1) reported the first authentic fluorinated tertiary alcohol, nitroperfluoro-*t*-butanol (**1**), and subsequently (2) prepared perfluoro-*t*-butanol (**2**) itself via *t*-nitroso-perfluoroisobutane. Other workers have since reported alternative routes to perfluoro-*t*-butanol (3–5).

The pronounced acidic character of perfluoro tertiary alcohols has been investigated by several workers. Knunyants and Dyatkin found a pK_a of 3.9 for **1** and 5.4 for **2**, while pK_a's for the alcohols CF_3CH_2OH and $(CF_3)_2CHOH$ were 12.8 and 9.3, respectively (2). Using these data, pK_a values were related to the sum of the Taft polar substituent constants, σ^*, by the equation

$$[1] \qquad pK_a = -1.44 \sum \sigma^* + 16.67$$

and $\sigma^*(CF_3)$ was found to be 2.6, on a scale where $\sigma^*(H) = 0$.

The general validity of this equation was confirmed by Filler and Schure (3), who also discovered that the acidity of the alcohol could be related linearly to the difference, $\Delta\lambda$, between the free O—H stretching frequency (in carbon tetrachloride solution) and the hydrogen-bonded O—H frequency (in tetrahydrofuran). Middleton and Lindsey (6) had previously observed that this difference correlated roughly with the relative order of hydrogen-bond strength between the alcohol and tetrahydrofuran. They also noted that tenacious hydrogen-bonded complexes, stable to distillation, are formed between the alcohols and various donor solvents.

Perfluoropinacol (PFP) and the hydrates of several perfluoroketones (*i.e. gem*-diols) are also strongly acidic, and can be regarded as monobasic acids obeying eq. 1 [PFP, p$K_a = 5.95$; $(CF_3)_2C(OH)_2$, p$K_a = 6.58$ (6)].

Hydrogen-bonding and acidity studies on perfluorotertiary alcohols have so far been confined to those containing only perfluoroalkyl groups, and it was the object of the present study to extend this to include those containing trifluorovinyl and pentafluorophenyl groups.

Trifluorovinyl Alcohols

Considerable work in this area has been re-

[1]Presented in part at the Sixth International Symposium on Fluorine Chemistry, Durham, England, 1971.

[2]To whom inquiries should be addressed.

Can. J. Chem. Downloaded from www.nrcresearchpress.com by 210.87.254.6 on 09/05/12
For personal use only.

TABLE 1. The ^{19}F n.m.r. spectra of trifluorovinyl alcohols

Chemical shift*	**3** $(CF_2CF)C(CF_3)_2OH$	**4** $(CF_2CF)_2C(CF_3)OH$
CF_3	76.9	78.2
F_a	90.9	93.5
F_b	107.3	108.5
F_x	184.9	183.4
Coupling constant (*J*, Hz)		
a–b	62.0	63.5
a–x	40.1	38.8
b–x	114.6	115.6
a–CF_3	0.9	—
b–CF_3	4.6	6.2
x–CF_3	8.2	9.4
a–b′	—	—
a–x′	—	—
b–x′	—	4.4

*All chemical shifts are in p.p.m. from $CFCl_3$.

ported by Tarrant *et al.* They have prepared trifluorovinyl-lithium from bromotrifluoroethylene (7) or trifluoroethylene (8) or the Grignard reagent from C_2F_3Br (8) and obtained alcohols by reaction with various carbonyl-containing compounds. When the carbonyl compound contained no perfluoroalkyl substituents, the alcohols produced were generally unstable, rearranging with elimination of HF to give α-fluoroalkenyl carboxylic acids. With partially fluorinated compounds, such as trifluoroacetone, both alcohol and acid were obtained (8), while hexafluoroacetone gave only perfluoro(2-methyl-3-buten-2-ol), $CF_2{:}CFC(CF_3)_2OH$ (**3**). Recently, reaction of trifluorovinyl-lithium with trifluoroacetyl chloride has been reported (9) to give perfluoro(3-methyl-1,4-pentadien-3-ol), $(CF_2{:}CF)_2C(CF_3)OH$ (**4**), with b.p. 91°, in close agreement with that found in our work (92–94°). With alcohol **3**, however, we find b.p. 65–66°, the reported b.p. of 86° being that of the ether complex. The pure alcohol, which we isolated from the ether adduct by distillation from sulfuric acid, had C=C absorption at 1780 cm^{-1} in its i.r. spectrum and was further characterized by preparation of its trimethylsilyl ether derivative.

We have unsuccessfully attempted to prepare the third member of this series, tris(trifluorovinyl)carbinol, by the reaction of trifluorovinyl-lithium or -Grignard with dimethyl carbonate, but in each case a black oil was obtained, which eliminated HF on attempted distillation. This is in accord with the reported failure to prepare the unfluorinated analogue, $(CH_2{:}CH)_3COH$, when only polymeric material was obtained (10).

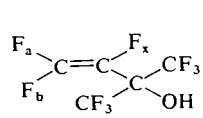

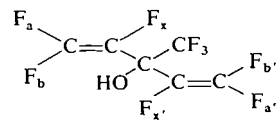

The ^{19}F n.m.r. spectrum of alcohol **3** (Table 1) showed the expected four peaks, ratio 6:1:1:1 (field increasing). The chemical shifts are very similar to those reported for $CF_2CFC(CF_3)$-$(CH_3)OH$ (11). The three vinylic fluorine peaks each appear as doublets of doublets of septuplets ($J_{a\text{-}CF_3} = 0.9$, $J_{b\text{-}CF_3} = 4.6$, $J_{x\text{-}CF_3} = 8.2$ Hz), while the CF_3 peak is a doublet of doublets of doublets. These long-range couplings have been observed previously, though of lower magnitude, in several trifluorovinyl compounds (11).

Alcohol **4** also has four peaks, ratio 3:2:2:2, the chemical shifts being very similar to the equivalent ones in **3**. The CF_3 group in this case is coupled only to b ($J = 6.2$ Hz) and x ($J = 9.4$ Hz), but an extra inter-vinyl coupling ($J_{x\text{-}b'} = 4.4$ Hz) is present. Couplings between two vinyl groups have been previously observed in several trifluorovinyl derivatives of metals and metalloids (12).

Can. J. Chem. Downloaded from www.nrcresearchpress.com by 210.87.254.6 on 09/05/12
For personal use only.

TABLE 2. The ^{19}F n.m.r. spectra of pentafluorophenyl alcohols

Chemical shift	**5** $C_6F_5C(CF_3)_2OH$	**6** $(C_6F_5)_2C(CF_3)OH$	**7** $(C_6F_5)_3COH$
CF_3	76.2	79.3	—
ortho-F	135.3	139.0	139.7
meta-F	160.6	160.9	162.9
para-F	149.5	151.0	154.3
Coupling constant			
CF_3-ortho	14.6	15.0	—

Attempts were made to prepare metal complexes of alcohols **3** and **4**. Alcohol **3** could possibly act as a bidentate ligand, coordinating via both the double bond and the oxygen atom. Reactions in basic aqueous solution with the metal ions Ag(I), Pd(II), Fe(III), Ni(II), Zn(II), VO(II), Hg(II), Co(II), Cu(II), and Cr(III) were carried out, but in no case was any evidence of complex formation observed. Likewise, alcohol **4** could complex via a double bond and the oxygen atom, or via both double bonds. No complexes were obtained with the above metals nor with low valent carbonyls of Fe, Mn, or Ni.

The reported (13) addition of perfluoroketones to tetrafluoroethylene in the presence of cesium fluoride to give saturated perfluoro alcohols offered a possible means of converting alcohol **3** to perfluoro tertiary diols, which would be potentially useful ligands, but reactions of this type carried out in either diglyme or acetonitrile gave, on hydrolysis, none of the desired diols, the only identifiable products being unchanged alcohol **3** and hexafluoroacetone hydrate.

Pentafluorophenyl Alcohols

Several primary, secondary, and tertiary alcohols containing the C_6F_5-group are known. Pentafluorobenzyl alcohol and bis(pentafluorophenyl)methanol were both prepared from pentafluorobenzaldehyde by Tatlow and coworkers (14), and tris(pentafluorophenyl)carbinol (**7**) has been made through the reaction of pentafluorophenyl-lithium with decafluorobenzophenone by two groups of workers (15, 16). Tamborski *et al.* (17) prepared several tertiary arylalkyl perfluoroalcohols, including perfluoro-α,α-dimethylbenzyl alcohol (**5**), from reactions of fluoroaryl lithium reagents with hexafluoroacetone. None of these alcohols showed any tendency to form stable isolable complexes with tetrahydrofuran or other solvents, although i.r. studies suggested that hydrogen bonding between the alcohols and tetrahydrofuran was present in solution.

In the present work, alcohols **5** and **7** were prepared by the above methods. Perfluoro(1,1-diphenylethanol) (**6**), which was not previously reported, was made by reaction between pentafluorophenyl-lithium and trifluoroacetyl chloride. It was obtained as a viscous oily liquid, b.p. 108–112°/0.01 mm, which did not solidify neat but formed white crystals, m.p. 34–36°, from cold pentane solution. The ^{19}F n.m.r. spectra of the aromatic alcohols were, as expected, considerably more complex. Principal data for these spectra are given in Table 2.

Alcohol **5** showed the expected four peaks, ratio 6:2:1:2. The aliphatic fluorine peak, at 76.2 p.p.m. from $CFCl_3$, appeared as a triplet ($J = 14.6$ Hz) by coupling with the two aromatic ortho-fluorines. The para- and meta-fluorine peaks, at 149.5 and 160.6 p.p.m., had typical chemical shifts and general shapes, while the ortho-fluorine peak appeared as a broad, unresolved multiplet centered on 135.3 p.p.m.

The ^{19}F n.m.r. spectrum of alcohol **6** also contained four peaks, ratio 3:4:2:4. The CF_3 peak appeared as a pentuplet ($J = 15.0$ Hz) by coupling with four ortho-fluorines. The para- and meta-fluorines gave multiplets slightly broadened as compared to those in alcohol **5**; this may be ascribed to inter-ring coupling between the two pentafluorophenyl groups. The peak due to the ortho-fluorine atoms appeared as a broad triplet (or pentuplet), width 85 Hz. Prediction of this multiplet from the other data in the spectrum gave an 80-line multiplet in good agreement with the observed peak.

Alcohol **7** had three peaks in its spectrum, 2:1:2, all of which were considerably broadened,

Can. J. Chem. Downloaded from www.nrcresearchpress.com by 210.87.254.6 on 09/05/12
For personal use only.

Can. J. Chem. Downloaded from www.nrcresearchpress.com by 210.87.254.6 on 09/05/12
For personal use only.

presumably by inter-ring coupling. However, an alternative explanation, based on steric hindrance, had been advanced (18) to account for similar broadenings in the spectra of the compounds $(C_6F_5)_nMX_{(4-n)}$ (X = Me, Ph).

Tertiary Perfluoro-1,2-diols

The only previously known compound of this type, perfluoropinacol (**8**), may be synthesized by several methods. Knunyants and coworkers (19) used the reaction between hexafluoroacetone and triethyl phosphite, giving a cyclic phosphorane which can be hydrolyzed to perfluoropinacol. The diol has also been prepared by Middleton and Lindsey (6) by reductive dimerization of hexafluoroacetone, either with magnesium amalgam or photolytically with isopropanol. We have previously reported (20) preparation of the dilithium and disodium salts in solution by reaction of hexafluoroacetone with the metal in tetrahydrofuran or diglyme, the pinacol being given on hydrolysis. Perfluoropinacol is a fairly strong monobasic acid, but attempts to form the dianion in aqueous solution lead to hydrolysis and decomposition. Stable derivatives of complexes with main-group elements and transition metals can readily be made. (20–22).

The mixed C_6F_5-, CF_3-substituted diol **9** was prepared by the photolytic route from octafluoroacetophenone.

$$2CF_3COC_6F_5 \xrightarrow[h\nu]{\text{2-PrOH}} C_6F_5-\underset{HO}{\overset{CF_3}{C}}-\underset{OH}{\overset{CF_3}{C}}-C_6F_5$$

Attempted synthesis via the triethyl phosphorane intermediate failed to give any product, possibly because of unfavorable (eclipsed) steric requirements in the cyclic phosphorane. It was, however, possible to prepare metal complexes of the diol (23). Like perfluoropinacol (19) and 2,3-diphenylhexafluorobutane-2,3-diol (which was also prepared photolytically) (24), diol **9** did not undergo a pinacol–pinacolone rearrangement in conditions much more acidic than those normally required (concentrated H_2SO_4/100°). The presence of the electrophilic CF_3 and C_6F_5 groups apparently precludes the development of the carbonium ion character necessary for the rearrangement to take place (24).

The diol **9**, containing two asymmetric carbon atoms, can exist in three isomeric forms; a *meso*-isomer and two optically active enantiomers. It was purified by sublimation and recrystallization to give a white solid (m.p. 123–125°) which had a satisfactory analysis. However, the complex appearance of the n.m.r. spectra and other properties of the compound suggested that more than one isomer was present, and work is continuing in an attempt to separate and characterize these completely, when a fuller account of this interesting alcohol will be published.

Acidity Studies

Ballinger and Long (25) have related the acidities of a series of primary alcohols, RCH_2OH, to the polar substituent constants, σ^*, for the groups R by the equation

$$[2] \qquad pK_a = -1.42\,\sigma^* + 15.9$$

This is very similar to eq. 1, given above, which Knunyants and co-workers developed for fluorinated alcohols. It was hoped that the numerical values of the polar substituent constants for the pentafluorophenyl and trifluorovinyl groups, which have not been reported, could be obtained by measuring the acidities of various alcohols containing these groups.

Only two of the five alcohols studied were freely soluble in water, so in all cases the pK_a was measured in a range of ethanol/water mixtures using the half end-point method. Values obtained are shown in Table 3.

Both the trifluorovinyl-containing alcohols were soluble in water. Alcohol **3** had a pK_a of 6.82, measured in water, while a plot of pK_a values against mole fraction (*mf*) of ethanol gave a curve corresponding to the quadratic relationship

$$[3] \qquad pK_a = 19.6(mf)^2 + 1.7mf + 6.80$$

For alcohol **4**, the pK_a value found in water was 7.71, while measurements in ethanol/water mixtures gave the linear relationship

$$[4] \qquad pK_a = 5.95mf + 7.70$$

Application of these values to Knunyant's equation (eq. 1), using $\sigma^*(CF_3) = 2.6$, gives values of $\sigma^*(CF_2{=}CF)$ as 1.65 (alcohol **3**) and 1.82 (alcohol **4**) for an average σ^* value of 1.7_3.

For the pentafluorophenyl-containing alcohols and the diol, the limited solubility in water necessitated extrapolation from ethanol/water mixtures to obtain aqueous pK_a values. The

TABLE 3. The pK_a values for fluorinated alcohols and diols

Ethanol in Water							
Vol. %	Mole fraction	3	4	5	6	9	12
0	0	6.82	7.71	i.s.*	i.s.	i.s.	i.s.
10	0.033	6.90	7.91	i.s.	i.s.	i.s.	9.04
20	0.072	7.02	8.16	i.s.	i.s.	i.s.	9.27
30	0.117	7.27	8.39	8.65	i.s.	i.s.	9.50
40	0.171	7.66	8.75	9.00	10.08	9.17	9.98
50	0.236	8.29	9.11	9.26	10.36	9.34	10.35
60	0.317			9.53	10.66	9.47	
70	0.419			9.82	10.97	9.69	

*i.s. = insufficiently soluble for readings to be obtained.

accuracy of the values obtained was further reduced by the very weakly acidic nature of the alcohols.

Alcohol **5**, $C_6F_5C(CF_3)_2OH$, was soluble only in mixtures containing at least 30% ethanol. The plot of pK_a against mole fraction of ethanol gave a quadratic dependence

$$[5] \qquad pK_a = -6.4(mf)^2 + 7.25mf + 7.90$$

from which the extrapolated pK_a value is 7.90.

Alcohol **6**, $CF_3C(C_6F_5)_2OH$, required at least 40% ethanol for adequate solubility and gave the relationship

$$[6] \qquad pK_a = -3.65(mf)^2 + 5.7mf + 9.2$$

giving an extrapolated pK_a value of 9.2.

The completely aromatic alcohol **7**, $(C_6F_5)_3COH$, was only soluble in 60% ethanol, and no end-point could be detected in titration. From data obtained from the other alcohols, a pK_a of at least 11 would be expected.

The diol **9** dissolved in a minimum of 40% ethanol, and the linear equation found was

$$[7] \qquad pK_a = 2.0mf + 8.85$$

giving an extrapolated pK_a of 8.85.

The pK_a values for alcohols **5** and **6** were then used to calculate the substituent constant σ^* for the pentafluorophenyl group, again using $\sigma^*(CF_3) = 2.6$. Values found were 0.9 and 1.3 from the pK_a's of **5** and **6**, respectively, giving an average of 1.1.

In the case of the diols perfluoropinacol (**8**, $pK_a = 5.95$) and $[CF_3C(C_6F_5)OH]_2$ (**9**), the σ^* values for the R_2COH groups can be estimated from the pK_a values for the first ionization, leading to $\sigma^*[(CF_3)_2COH] = 2.3$ and $\sigma^*[CF_3C(C_6F_5)OH] = 1.8$.

Filler and Schure (3) related the pK_a of several fluorinated alcohols to the difference, $\Delta\lambda$, in O—H stretching frequencies between solutions in CCl_4 (free O—H) and THF (H-bonded O—H), obtaining a linear relationship. In the present work, we have extended this to include all new alcohols and diols prepared (except alcohol **7**), together with the known compound $C_6H_5C(CF_3)_2OH$ (**12**) (Fig. 1). For the majority of the alcohols, pK_a and $\Delta\lambda$ values fitted well to the straight line obtained by Filler and Schure, which has the equation

$$[8] \qquad pK_a = -25.7\Delta\lambda + 18.15$$

However, the alcohols containing pentafluorophenyl groups (*i.e.* alcohols **5** and **6** and diol **9**) each showed slightly higher pK_a values than would be consistent with this relationship, indicating a limitation to its general applicability.

Esters of Perfluoro Tertiary Alcohols

The published method (14) for the preparation of octafluoroacetophenone, which was required for the synthesis of diol **9**, makes use of the reaction between pentafluorophenyl Grignard reagents and lithium trifluoroacetate. This method gives only moderate yields (20–50%) and reactions between lithium reagents and acid chlorides were therefore investigated as possible routes to octafluoroacetophenone and other perfluoroarylketones.

Using trifluoroacetyl chloride, an oily liquid was obtained which had a C=O stretch in its i.r. spectrum. It boiled at 160°, whereas octafluoroacetophenone has b.p. 130°. Elemental

Can. J. Chem. Downloaded from www.nrcresearchpress.com by 210.87.254.6 on 09/05/12
For personal use only.

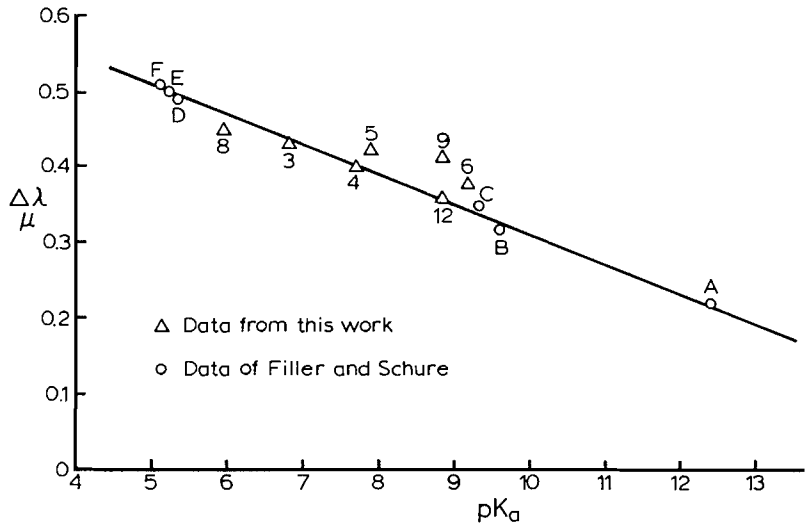

FIG. 1. Plot of difference between free and H-bonded O—H stretching frequency, $\Delta\lambda$, against pK_a of fluorinated alcohols. (A) CF_3CH_2OH; (B) $(CF_3)_2C(CH_3)OH$; (C) $(CF_3)_2CHOH$; (D) $(CF_3)_2C(CClF_2)OH$; (E) $(CF_3)_3COH$; (F) $(CF_3)_2C(CCl_3)OH$; (3) $(CF_2CF)C(CF_3)_2OH$; (4) $(CF_2CF)_2C(CF_3)OH$; (5) $(C_6F_5)C(CF_3)_2OH$; (6) $(C_6F_5)_2C(CF_3)OH$; (8) $[(CF_3)_2COH]_2$; (9) $[(C_6F_5)C(CF_3)OH]_2$; (12) $(C_6H_5)C(CF_3)_2OH$.

$$C_6F_5Li + CF_3COCl \longrightarrow C_6F_5COCF_3 \xrightarrow{C_6F_5Li} (C_6F_5)_2C(CF_3)OLi \xrightarrow{CF_3COCl} (C_6F_5)_2C(CF_3)OCOCF_3$$

SCHEME 1

analysis showed it had the same empirical formulation as octafluoroacetophenone, but its mass spectrum showed a molecular weight twice that of the ketone. The ^{19}F n.m.r. spectrum (Table 4) confirmed that it was ester **10**, produced in the sequence shown by Scheme 1.

This spectrum contained five peaks, three aromatic and two aliphatic, ratio 3:3:4:2:4

TABLE 4. The ^{19}F n.m.r. spectra of esters

Chemical shift*	**10** $(C_6F_5)_2C(CF_3)OCOCF_3$	**11** $(C_6F_5)_3COCOC_6F_5$
CF_3(a)	73.4	—
CF_3(b)	75.5	—
ortho-F(a)	135.9	138.0
ortho-F(b)	—	137.3
meta-F(a)	160.6	161.3
meta-F(b)	—	160.5
para-F(a)	149.1	151.4
para-F(b)	—	146.7
Coupling constants		
CF_3(a)–ortho-F(a)	15.3	—
CF_3(b)–ortho-F(a)	1.0	—

*(a) and (b) refer to fluorine atoms in the alcoholic and acidic groups, respectively.

Can. J. Chem. Downloaded from www.nrcresearchpress.com by 210.87.254.6 on 09/05/12
For personal use only.

Can. J. Chem. Downloaded from www.nrcresearchpress.com by 210.87.254.6 on 09/05/12
For personal use only.

field increasing. The aliphatic peaks consisted of a high field peak (acidic CF_3, triplet or pentuplet, $J = 1.0$ Hz) and a low field pentuplet (alcoholic CF_3, $J_{CF_3\text{-ortho}} = 15.3$ Hz). The aromatic peaks consisted of a broad low field pentuplet (ortho-F), a triplet of triplets (para-F, $J_{p-m} = 19.9$; $J_{p-o} = 5.8$ Hz), and a complex multiplet at high field (meta-F). The latter four peaks were almost identical to those found in the spectrum of alcohol **6**, $CF_3C(C_6F_5)_2OH$. The aliphatic-ortho coupling of 15.3 Hz is very similar to those observed in alcohols **5** and **6**, and the splitting observed in the acidic CF_3 part of the spectrum indicates that even these fluorines may be slightly coupled to the aromatic ortho-fluorines.

Formation of the ester in this reaction, but not in the published preparation using C_6F_5MgBr, presumably arises from the much greater reactivity of C_6F_5Li.

In the attempted preparation of decafluorobenzophenone by this method, reaction followed a similar route, yielding a white solid (96% yield) formulated as the ester $(C_6F_5)_3COCOC_6F_5$ (**11**) by elemental analysis and ^{19}F n.m.r. and mass spectroscopy. The ^{19}F n.m.r. spectrum contained six peaks, two in each region; ortho-, para-, and meta- as deduced from chemical shifts. In each case the higher field peak (alcoholic C_6F_5) was three times as intense as, and also considerably broader than, the lower field peaks, indicating considerable inter-ring couplings. The broadness precluded any attempt to measure these inter-ring couplings. The alcoholic C_6F_5 peaks were very similar in chemical shift and shape to those observed in the alcohol $(C_6F_5)_3COH$ (**7**).

The i.r. spectra of the esters showed carbonyl stretching vibrations at 1805 and 1740 cm^{-1} for **10** and **11**, respectively.

This reaction scheme forms a possibly useful method for formation of appropriate fully fluorinated esters, in view of the known difficulties (3, 4) in preparation and purification of esters when both acid and alcohol contain polyfluoro groups.

Experimental

General Techniques

Volatile compounds were manipulated in the absence of air in a conventional vacuum manifold. Hexafluoroacetone, bromotrifluoroethylene, and trifluoroacetyl chloride were commercial samples purified by fractional condensation *in vacuo*. The i.r. spectra were recorded on a Beckman IR-10 instrument and fluorine n.m.r. spectra on a Varian HA-100 (94.1 MHz). Titrations were followed with a Corning model 12 p*H* meter. Microanalyses were performed by Alfred Bernhardt Laboratories.

Mass spectra (Varian M-66 instrument) were used in characterization, a molecular ion peak being observed in all cases except for alcohol **4**, $(CF_2CF)_2C(CF_3)OH$, this presumably reflecting the lesser stability of poly(trifluorovinyl) compounds.

Perfluoro(2-methyl-3-buten-2-ol) (Alcohol 3) (8)

A solution of trifluorovinyl-lithium was prepared by passing bromotrifluoroethylene (20.5 g, 0.127 mol) into a solution of methyl-lithium (0.679 g, 0.127 mol) in ether (150 ml) at −78°. After 0.5 h, when the solution had become dark-colored, hexafluoroacetone (21.1 g, 0.127 mol) was bubbled in and the solution allowed to warm to 20°. The light-brown solution remaining was hydrolyzed (dilute HCl), ether-extracted, the organic layer dried ($MgSO_4$), and fractionated to give alcohol **3** as its ether complex, b.p. 80–86° (lit. b.p. (8), given for pure alcohol, 85°). Distillation from sulfuric acid gave the pure alcohol, b.p. 65–66° (lit. b.p. (26), 67°) (16.9 g, 54%).

Anal. Calcd. for C_5HF_9O: C, 24.2; H, 0.4; F, 68.9. Found: C, 24.1; H, 0.5; F, 69.2.

The trimethylsilyl ether derived from **3** was prepared by refluxing the alcohol with hexamethyldisilazane, followed by distillation (b.p. 106–110°).

Anal. Calcd. for $C_8H_9F_9OSi$: C, 30.0; H, 2.8; F, 53.4. Found: C, 30.0; H, 3.2; F, 53.0.

Attempted Reaction of Alcohol 3 with Cesium Fluoride and Hexafluoroacetone

Alcohol **3** (6.75 g, 27.2 mmol) and dry cesium fluoride (4.14 g, 27.4 mmol) were added to acetonitrile (20 ml, dried over P_2O_5) in a Carius tube. Hexafluoroacetone (4.52 g, 27.2 mmol) was condensed into the tube, which was sealed and heated to 70° for 3 days, by which time most of the cesium fluoride had dissolved. The mixture was then hydrolyzed, ether-extracted, and distilled to give only two fractions. The first, b.p. 90–105° (5 g) was mainly the trihydrate of hexafluoroacetone (lit. b.p. (27), 105°) as shown by i.r., n.m.r., and mass spectrum. A further reaction, using diglyme as solvent, likewise gave none of the desired product.

Perfluoro(3-methyl-1,4-butadien-3-ol) (Alcohol 4)

This alcohol was prepared by the same procedure as alcohol **3** by the reaction of trifluorovinyl-lithium with trifluoroacetyl chloride in a 2:1 mol ratio. The ether complex, b.p. 102–104° was converted to the pure alcohol, b.p. 92–94° (lit. b.p. (9), 91°) by sulfuric acid distillation.

Anal. Calcd. for C_6HF_9O: C, 27.7; H, 0.4; F, 65.7. Found: C, 27.9; H, 0.5; F, 65.2.

Attempted Preparation of Tris(trifluorovinyl)carbinol

(*a*) Trifluorovinyl-lithium (0.164 mol), prepared as described above, was kept in ether (150 ml) at −78° and dimethyl carbonate (4.92 g, 0.055 mol) in ether was added dropwise. The solution was allowed to warm to 20°, hydrolyzed, and worked-up as before, when the product was a black oil which evolved hydrogen fluoride on attempted distillation.

(*b*) The above procedure was repeated using trifluorovinyl magnesium bromide, with the same result.

Can. J. Chem. Downloaded from www.nrcresearchpress.com by 210.87.254.6 on 09/05/12
For personal use only.

Perfluoro(2-phenylpropan-2-ol) (Alcohol 5) (17)

Pentafluorophenyl-lithium was prepared from *n*-butyllithium (31.5 ml, 23.1% in hexane, 0.075 mol) and bromopentafluorobenzene (18.53 g, 0.075 mol) in ether (100 ml) at −30°. After 10 min, hexafluoroacetone (12.5 g, 0.075 mol) was bubbled in and the mixture allowed to warm to 20°. The solution was hydrolyzed (dilute HCl), ether-extracted, dried ($MgSO_4$), and fractionated to give alcohol **5**, b.p. 156–162° (lit. b.p. (17), 158–160°; 22.9 g, 91%). Further purification was effected by distillation from sulfuric acid (b.p. 101–102°/150 mm).

Perfluoro(1,1-diphenylethanol) (Alcohol 6)

Pentafluorophenyl-lithium (0.0875 mol) was prepared as described above and trifluoroacetyl chloride (5.8 g, 0.044 mol) bubbled in. Work-up as before gave 13.5 g (71%) of a viscous oil, b.p. 108–112°/0.01 mm, which formed white crystals from cold pentane, m.p. 34–36°.

Anal. Calcd. for $C_{14}HF_{13}O$: C, 38.9; H, 0.2; F, 57.1. Found: C, 39.0; H, 0.3; F, 57.4.

Perfluoro(triphenylcarbinol) (Alcohol 7) (15, 16)

The compound was prepared as previously reported from pentafluorophenyl-lithium and decafluorobenzophenone. Residual ketone could not be separated by recrystallization, but sublimed out slowly at 45°/0.01 mm. Further sublimation gave alcohol **7**, m.p. 113–115° (lit. m.p. (15), 117°).

Perfluoro(2,3-diphenyl-butane-2,3-diol) (Alcohol 9)

Octafluoroacetophenone (12 g), prepared from lithium trifluoroacetate and pentafluorophenylmagnesium bromide (14), in 2-propanol (75 ml) with a few drops of hydrochloric acid, was irradiated (Hg lamp) for 5 days. Removal of volatile materials gave a yellow solid which was sublimed at 100°/0.01 mm and recrystallized from ethanol/hexane to give the diol **9**, m.p. 123–125°.

Anal. Calcd. for $C_{16}H_2F_{16}O_2$: C, 36.2; H, 0.4; F, 57.3. Found: C, 36.0; H, 0.3; F, 57.1.

Perfluoro(1,1-biphenylethyl Acetate) (Ester 10)

Pentafluorophenyl-lithium (0.104 mol) in ether (150 ml) was held at −78° and trifluoroacetyl chloride (13.7 g, 0.103 mol) bubbled in. A white solid formed as the solution was allowed to warm to 20°. Filtration and solvent removal gave a pale-yellow oil, fractionally distilled to give ester **10** (b.p. 160–163°/60 mm, 19.0 g, 70%).

Anal. Calcd. for $C_{16}F_{16}O_2$: C, 36.4; H, 0.0; F, 57.5. Found: C, 36.4; H, 0.1; F, 57.6.

The ester was also produced in a similar experiment in which the lithium reagent was added to the acid chloride. Hydrolysis (KOH in ethanol/water for 2 h) followed by ether extraction and work-up gave alcohol **6**, identified by i.r. spectroscopy.

Perfluoro(triphenylmethyl Benzoate) (Ester 11)

Pentafluorophenyl-lithium (0.2 mol) was held at −78° and carbon dioxide (1.7 mol) bubbled through. Lithium pentafluorobenzoate, which precipitated immediately, was hydrolyzed (dilute H_2SO_4) and the acidified solution extracted with ether to give pentafluorobenzoic acid (31 g, 0.142 mol, 73%) m.p. 99–101° (lit. m.p. 103°). Thionyl chloride (17.4 g, 0.146 mol) was added to this acid and the mixture gently refluxed until evolution of acid vapors ceased (4 h). Distillation gave 21.0 g (62%) of pentafluorobenzoyl chloride, b.p. 157–160° (lit. b.p. 158–159°). Pentafluorophenyl-lithium (0.061 mol) in ether (100 ml) was held at −78° and pentafluorobenzoyl chloride (14.1 g, 0.061 mol) in ether (15 ml) added dropwise, when an immediate precipitate formed. The mixture was allowed to warm to 20°, filtered, and volatile materials removed to give a white solid (21.3 g, 96%) recrystallized from cyclohexane/ether to give the pure ester **11**, m.p. 132-134°.

Anal. Calcd. for $C_{26}F_{20}O_2$: C, 43.1; H, 0.0; F, 52.5. Found: C, 43.2; H, 0.15; F, 52.6.

Hydrolysis as before gave a yellow solid, shown by i.r. spectroscopy to be a mixture of perfluoro(triphenylcarbinol) (7) and pentafluorobenzoic acid.

α,α-Bis(trifluoromethyl)benzyl Alcohol (Alcohol 12)

This compound was prepared by the reaction of hexafluoroacetone with phenylmagnesium bromide according to Knunyants *et al.* (28) and had b.p. 152–155°. Its identity was confirmed by i.r. and mass spectrum. For pK_a measurements, it was found to be sufficiently soluble only in solutions containing at least 10% ethanol in water: the extrapolated pK_a value in aqueous solution was 8.80.

Financial support from the National Research Council of Canada is gratefully acknowledged. We thank Dr. M. C. Woods for helpful discussions concerning the ^{19}F n.m.r. spectra.

1. I. L. KNUNYANTS, A. V. FOKIN, B. L. DYATKIN, and V. A. KOMAROV. Izv. Akad. Nauk SSSR, Ser. Khim. 1425 (1964).
2. I. L. KNUNYANTS and B. L. DYATKIN. Izv. Akad. Nauk SSSR, Ser. Khim. 923 (1964).
3. R. FILLER and R. M. SCHURE. J. Org. Chem. **32**, 1217 (1967).
4. F. J. PAVLIK and P. E. TOREN. J. Org. Chem. **35**, 2055 (1970).
5. R. E. A. DEAR. Synth. 361 (1970).
6. W. J. MIDDLETON and R. V. LINDSEY. J. Am. Chem. Soc. **86**, 4948 (1964).
7. P. TARRANT, P. JOHNCOCK, and J. SAVORY. J. Org. Chem. **28**, 839 (1963).
8. F. G. DRAKESMITH, R. D. RICHARDSON, O. J. STEWART, and P. TARRANT. J. Org. Chem. **33**, 286 (1968).
9. P. TARRANT, R. H. SUMMERVILLE, and R. W. WHITFIELD. J. Org. Chem. **35**, 2742 (1970).
10. T. S. SORENSON. Can. J. Chem. **43**, 2744 (1965).
11. C. G. MORELAND and W. S. BREY. J. Chem. Phys. **45**, 803 (1966).
12. T. D. COYLE, S. L. STAFFORD, and F. G. A. STONE. Spectrochim. Acta, **17**, 968 (1961).
13. D. P. GRAHAM and V. WEINMAYR. J. Org. Chem. **31**, 957 (1966).
14. A. K. BARBOUR, M. W. BUXTON, P. L. COE, R. STEPHENS, and J. C. TATLOW. J. Chem. Soc. 808 (1961).
15. N. N. VOROZHTSOV, V. A. BARKHASH, T. N. GERASIMOVA, E. G. LOKSHINA, and N. G. IVANOVA. Zhur. Obshch. Khim. **37**, 1293 (1967).
16. R. FILLER, C. S. WANG, M. A. MCKINNEY, and F. N. MILLER. J. Am. Chem. Soc. **89**, 1026 (1967).
17. C. TAMBORSKI, W. H. BURTON, and L. W. BREED. J. Org. Chem. **31**, 4229 (1966).
18. D. E. FENTON, A. G. MASSEY, K. W. JOLLEY, and L. H. SUTCLIFFE. Chem. Commun. 1097 (1967).

19. N. P. GAMBARYAN, Y. A. CHEBURKOV, and I. L. KNUNYANTS. Izv. Akad. Nauk SSSR, Ser. Khim. 1526 (1964).
20. M. ALLAN, A. F. JANZEN, and C. J. WILLIS. Can. J. Chem. **46**, 3671 (1968).
21. M. ALLAN and C. J. WILLIS. J. Am. Chem. Soc. **90**, 5343 (1968).
22. A. P. CONROY and R. D. DRESDNER. Inorg. Chem. **9**, 2739 (1970).
23. W. S. CRIPPS and C. J. WILLIS. Unpublished observations.
24. W. A. MOSHER and N. D. HEINDEL. J. Am. Chem. Soc. **85**, 1548 (1963).
25. P. BALLINGER and F. A. LONG. J. Am. Chem. Soc. **81**, 1050 (1959).
26. E. E. GILBERT and B. VELDHUIS. U.S. Pat. 3 362 985, 1968.
27. Allied Chemical Co. French Pat. 1 385 110, 1965.
28. I. L. KNUNYANTS, N. P. GAMBARYAN, C. Y. CH'EN, and E. M. ROKHLIN. Izv. Akad. Nauk SSSR, Otd. Khim. Nauk, 684 (1962).

Can. J. Chem. Downloaded from www.nrcresearchpress.com by 210.87.254.6 on 09/05/12
For personal use only.

Conformational Studies of Substituted Trimethylene Sulfites by Proton Magnetic Resonance[1]

GORDON WOOD, G. W. BUCHANAN,[2] AND M. H. MISKOW[3]
Department of Chemistry, University of Windsor, Windsor, Ontario
Received June 15, 1971

Proton n.m.r. chemical shifts and coupling constants are reported for trimethylene sulfite and 10 alkyl derivatives in CCl_4. Data are discussed in terms of possible chair and non-chair conformations and results are compared with those from dipole moment studies. The shift reagent $Eu(dpm)_3$ is used to aid configurational assignments. Conclusions from n.m.r. and dipole moments are consistent and indicate that several of the sulfites exist to a considerable degree in non-chair conformations.

Les déplacements chimiques des protons en r.m.n. et les constantes de couplage sont données dans CCl_4 pour le triméthylène sulfite et pour dix dérivés alkylés. Les données sont discutées en fonction des conformations possibles chaise et non-chaise et les résultats comparés à ceux des études de moment dipolaire. Le réactif de déplacement $Eu(dpm)_3$ est utilisé pour faciliter les assignations de configuration. Les conclusions tirées de la r.m.n. et des moments dipolaires sont importantes et indiquent que plusieurs des sulfites existent pour une part importante sous des conformations non-chaise.
Canadian Journal of Chemistry, **50**, 521 (1972)

Introduction

Although much effort has been directed toward elucidating the conformations of trimethylene sulfites, a clear picture of the shapes of these molecules has been slow to develop. The bulk of the published data comes from dipole moment measurements, i.r. spectroscopy, and ultrasonic relaxation studies (1–7). Recently (5) we reported dipole moments for a series of alkyl-substituted sulfites and emphasized the importance of vicinal electron pairs in determining their conformations (8). It was concluded that chair⇌chair interconversion barriers must be high[4] in these molecules and the existence of non-chair forms for several sulfites was suggested.

Herein, we present proton n.m.r. results for the above sulfites. Some of the parameters are particularly sensitive to conformational change, permitting a somewhat more confident appraisal of the observed trends than do the dipole moments. Chemical shifts of methine, methylene, and methyl protons are discussed in detail and shielding trends can be explained on the basis of various contributions from chair and non-chair forms. Coupling constants are compared with values for chair and twist forms of the related trimethylene phosphites to gain information regarding sulfite geometry. The proton shift reagent, tris(dipivaloylmethanato)-europium, $Eu(dpm)_3$ has been used to aid the configurational assignments since the magnitudes of the shifts are primarily dependent on the individual proton–Eu distances.

Results and Discussion

To facilitate comparison with the n.m.r. data, the previously determined dipole moments (5) are listed in Table 1.

Proton Chemical Shifts

Table 2 contains the proton shieldings for trimethylene sulfite and 10 alkyl derivatives. In general, the spectra are first order and assignments are straightforward. An exception is that of compound **3** where the only precise shift obtained is for the methyl group. It should be noted that in compounds **4** and **5**, the overlap of resonances for the C-5 protons in CCl_4 can

[1]Taken in part from the Ph.D. thesis of M. H. Miskow, University of Windsor, 1971.

[2]Present address: Department of Chemistry, Carleton University, Ottawa 1, Canada.

[3]Recipient of NRCC Scholarships, 1966–1970. Present address: Department of Chemistry, University of Ottawa, Ottawa, Canada.

[4]The barrier in 5,5-dimethyltrimethylene sulfate is 8.3 kcal/mol (9). Recently, the barrier for the molecule with no exocyclic oxygens, 5,5-dimethyl-1,3,2-dioxathiane was found to be 12.5 kcal/mol (10). Accordingly, the chair⇌chair barrier for the sulfites is likely in the accessible n.m.r. range. The lack of observed coalescence phenomena for compounds thought to be chairs with axial S=O functions can be attributed to the low population of the higher energy form with equatorial S=O ($-\Delta G^{\circ}_{S=O} = 2.1 \pm 0.5$ kcal/mol) (5, 13).

Can. J. Chem. Downloaded from www.nrcresearchpress.com by 210.87.254.42 on 09/05/12
For personal use only.

TABLE 1. Dipole moments for compounds of general structure:

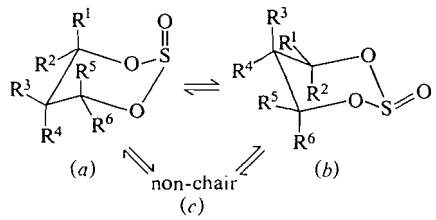

Compound	Conformation	Substituent*	Dipole moment (D) C_6H_{12}	CCl_4	C_6H_6	Dioxane
1	*a*			3.34		
2	*a*	$R^2 = CH_3$		3.35	3.41	
3	*b,c*	$R^1 = CH_3$		4.66	4.75	
4	*a*	$R^2 = R^6 = CH_3$	3.44	3.51	3.60	
5	*a,c*	$R^2 = R^5 = CH_3$	3.97	3.93	3.93	
6	*b*	$R^1 = R^5 = CH_3$		5.31	5.37	
7	*a,c*	$R^1 = R^2 = R^6 = CH_3$	3.91		3.86	
8	*b,c*	$R^1 = R^2 = R^5 = CH_3$	4.53		4.71	
9	*c*	$R^1 = R^2 = R^5 = R^6 = CH_3$	4.22		4.30	
10	*a*	$R^3 = (CH_3)_3C$	3.50	3.54	3.60	3.66
11	*a,c*	$R^4 = (CH_3)_3C$	3.54	3.63	3.90	4.15

*All R's not specified = H.

be removed in DMSO. Bracketed values in Table 2 denote tentative assignments.

Data for **1**, **4**, **5**, and **6** agree well with those recently reported by Wucherpfennig (11). From double resonance experiments we have verified in compound **5** that the CH_3 group at $\delta = 1.27$ p.p.m. is coupled to the proton at $\delta = 4.97$ p.p.m.

On examination of the data and comparison with the dipole moments, several trends are apparent. (*a*) For compounds whose moments correspond to a chair conformation with axial S=O (**1**, **2**, **4**, and **10**), the shifts for protons in the "*syn*-diaxial" orientation relative to the S=O group are nearly identical (4.91 ± 0.03 p.p.m.). The deshielding influence of the axial S=O group in trimethylene sulfite on the 1,3-diaxial protons is now well documented (11, 12). A close similarity in the equatorial proton shifts at C-4 and -6 of **1**, **2**, and **10** is also apparent. (*b*) Compounds **2** and **4** have nearly identical shifts for their equatorial CH_3 groups. The 0.1 p.p.m. downfield shift in compound **3** sug-

TABLE 2. ^1H n.m.r. shieldings δ(p.p.m. from TMS)* ± 0.01

Compound	Substituent R^1	R^2	R^3	R^4	R^5	R^6
1	4.88	3.75	1.65	2.50	4.88	3.75
2	4.88	1.30	1.63	2.40	4.88	3.80
3	1.40	(4.4)	(1.8)	(1.8)	(4.4)	(4.4)
4	4.94	1.27	1.73	1.73	4.94	1.27
5	4.97	1.27	1.98	1.98	1.58	4.35
6	1.39	4.54	1.75	1.54	1.39	4.54
7	1.70	1.28	1.65	1.92	5.07	1.32
8	1.45	1.50	2.45	1.73	1.38	4.50
9	1.55	1.42	1.85	2.75	1.55	1.42
10	4.88	3.85	0.97	2.09	4.85	3.85
11	4.75	3.91	1.72	1.06	4.75	3.91

*20% by weight in CCl_4.

Can. J. Chem. Downloaded from www.nrcresearchpress.com by 210.87.254.42 on 09/05/12
For personal use only.

Can. J. Chem. Downloaded from www.nrcresearchpress.com by 210.87.254.42 on 09/05/12
For personal use only.

gests a small contribution from the diaxial form. This is consistent with the high dipole moment for **3**, which indicates that it exists predominantly (but not exclusively) in some form with an equatorial S=O (be it a chair or a non-chair with a similar geometry at the sulfite end of the molecule). Compound **8**, with a moment near that of **3** shows a like behavior in the shifts of its R^1 and R^5 methyl groups. (*c*) For compound **6**, the observed moment is interpreted in terms of a chair form with equatorial S=O (5). Calculations[5] of van Woerden are in accord with this (13). The C-4 and -6 methine protons of **6** are now shifted upfield by *ca.* 0.35 p.p.m. relative to **4**, as expected for an equatorial S=O orientation. (*d*) Moments for **5** and **7** are thought to imply either a distortion of the S=O axial chair or a non-chair form (5, 11). The downfield shifts of the R^5 and R^1 CH_3 groups in **5** and **7**, respectively, are indicative of a quasi 1,3-diaxial $CH_3 \cdots S{=}O$ interaction. It is interesting that the R^5 methine proton in **7** and its R^1 counterpart in **5** are at even lower field than when the S=O is pure axial (*i.e.* in **1**, **2**, **4**, and **10**). This can be attributed to an extra Van der Waals deshielding of the methine protons by the *syn*-axial CH_3 functions (14). (*e*) The tetramethyl derivative **9** has a moment of intermediate value (independent of solvent polarity) and accordingly was postulated to be almost exclusively in a non-chair form. In agreement with this, the ^1H methyl group shifts of **9** are at lower field than those observed for "pure" equatorial methyls and at higher field than for axial or quasi-axial (R^1 in **7**) substituents. (*f*) For compound **11**, dipole moment behavior indicates a mixture of interconverting conformations with that of higher moment being favored in the more polar solvent. In CCl_4, the deshielding of the *t*-butyl methyl protons of **11** relative to **10** coincides with the trends observed for 1.3 dioxanes (15) and cyclic phosphites (16) with axial *t*-butyl functions. However, the 0.1 p.p.m. upfield shift of the R^1 and R^5 methine protons of **11** relative to **10** does suggest some contribution from an equatorial or pseudo-equatorial S=O moiety. In more polar solvents (*i.e.* acetone) this shift difference does not increase noticeably. Association factors are known to be operative in these systems (17, 18) and thus preclude any meaningful discussion of solvent shifts in terms of conformational changes. (*g*) In most of the sulfites, axial protons at C-5 appear at lower field than their equatorial counterparts, as is true for 1,3 dioxanes and phosphites. The positive end of the dipole in the sulfites is at C-5 and accordingly this position is the most susceptible to association phenomena. The overlap of some C-5 proton resonances in CCl_4 and their resolution in DMSO reflect this property. Previously reported results from this laboratory (18) show that in benzene solution, the equatorial proton at C-5 of **1** is shifted to the greatest extent. Recently, a model for benzene–sulfite association at the C-5 end of the molecule has been proposed (11).

[5]van Woerden has recently measured moments for the two isomers of *trans*-1,3,2-dioxathiadecalin-2-oxide (13). Values are 3.85 and 5.15 D. These structures are assigned as chairs having axial and equatorial S=O groups, respectively.

Proton Nuclear Magnetic Resonance Coupling Constants

Table 3 lists the couplings measured for trimethylene sulfite and its alkyl derivatives. In all cases the numbers represent absolute values, although the geminal couplings can be assumed to be negative. Generally, the geminal couplings between methylene protons at C-5 are *ca.* 2 Hz larger than for protons on C-4 and -6.

Most of the discussion to follow will deal with vicinal couplings and their relation to molecular conformation. It is of interest to note, however, that in compound **10** both the equatorial and axial C-4 and -6 protons are split into triplets by a ^4J coupling of *ca.* 1 Hz. The existence of an equatorial–equatorial coupling is not surprising since the geometry is close to the most suitable planar "W" arrangement (19). Anderson (20) has reported a ^4J axial–axial coupling of 0.8 Hz between protons at C-4 and -6 of 1,3 dioxanes. Apparently, the axial–axial coupling in sulfite **10** is of similar magnitude.

^3J couplings between methine and methyl protons are the same in all the sulfites, *ca.* 6.5 Hz.

It is useful to compare the vicinal methine–methylene couplings for **10**, believed from dipole moments to be a chair having an equatorial *t*-butyl group and an axial S=O, with the recently studied *cis*-5-*t*-butyl-2-methoxyl-1,3,2-dioxaphosphorinane (16). Bentrude and Hargis

TABLE 3. ^{1}H n.m.r. coupling constants (Hz)* ±0.2

	Compound										
J	**1**	**2**	**3**	**4**	**5**	**6**	**7**	**8**	**9**	**10**	**11**
R^1R^2	12.4	6.5	6.5	6.5	6.6	6.5				11.9	11.5
R^1R^3	3.0	3.0		3.3	6.8	3.0					5.3
R^1R^4	11.4	11.5		10.8	6.8					12.0	
R^1R^5										1.2	
R^2R^3	3.0					10.8					5.3
R^2R^4	4.5	4.5								4.5	
R^2R^6										1.2	
R^3R^4	14.4	14.0		14.4†	‡	14.4	14.4	14.4	14.4		
R^3R^5	3.0	3.0		3.3		3.0	6.6				5.3
R^3R^6	3.0	2.5			5.7	10.8		11.8			5.3
R^4R^5	11.4	11.5		10.8			6.6			12.0	
R^4R^6	4.5	4.5			5.7			3.2		4.5	
R^5R^6	12.4	11.5		6.5	6.6	6.5	6.5	6.5		11.9	11.5

*20 weight % solutions in CCl_4.
†DMSO solution.
‡Due to overlap of resonances, this geminal coupling could not be determined.

have pointed out the striking similarity in the equilibration behavior of these compounds and assign a chair conformation with equatorial *t*-butyl and an axial methoxyl on phosphorus to the above phosphite. From a computer analysis, $J_{4a,5e} = 3.8$ and $J_{4a,5a} = 11.9$ Hz for this *cis*-phosphite. Corresponding values for the sulfite **10** are in reasonable agreement with these and accordingly the assignment of a "rigid" chair for **10** is supported. From Table 3, it can be seen that couplings for the other compounds expected to be chairs with axial S=O functions (*i.e.* **1**, **2**, and **4**) closely coincide with those for **10**.

For compound **6**, the couplings indicate a chair conformation in accord with the dipole moment studies. The 11.8 Hz coupling in **8** is characteristic of an axial–axial interaction and thus a large contribution from a chair form is suggested in this molecule.

Intermediate values for the vicinal methine–methylene coupling are noted for compounds **5**, **7**, and **11**. These data can be interpreted in terms of chair⇌chair equilibria (21) or by the existence of non-chair or twist forms (11). Cazaux and Maroni (22) have postulated twist conformations for a series of racemic 4,6-diisopropyl-5,5-dimethyl trimethylene sulfites as has Wucherpfennig (11) for compound **5**. Both **5** and **7** have axial methyl–axial S=O interactions in their chair forms and it is highly likely that twist forms or distorted chairs predominate in these molecules. The constancy of the dipole moments for **5** and **7** in various solvents support this, as a chair⇌chair equilibrium should produce a large dipole moment change with solvent polarity. Recently, Bentrude and Hargis (16) have estimated couplings for a twist form of *trans*-5-*t*-butyl-2-methoxy-1,3,2-dioxaphosphorine. With the assumption that the twist conformation of the sulfites has a similar geometry to that of the above phosphite, a comparison of results is valid. For the twist phosphite, estimated values of $J_{4e,5e}$ and $J_{4a,5e}$ are 5.12 and 7.0 Hz, respectively. The couplings of 5.7 for R^3R^6 in **5**, 6.8 for R^1R^3 in **5**, and 6.6 for R^3R^5 in **7**, are consistent with twist geometries in these sulfites. Although compound **11** has been assumed to be a mixture of chair conformers (23, 24) because of its dipole moment variation with solvent, alternative explanations involving non-chair forms seem more attractive. The single small coupling (5.3 Hz) points either to a mixture of non-chair forms (12, 22, 25) with near equal couplings but different dipole moments or to a mixture of chair and non-chair forms (which should have different dipole moments) (11), including the chair with an axial *t*-butyl group. We tend to favor the latter possibility as does Bentrude for the corresponding *trans*-5-*t*-butyl phosphite. Using the predicted values of 4.0 and 2.0 for $J_{4a,5e}$ and $J_{4e,5e}$ of the *trans*-diaxial chair phosphite (16) along with the above values for the twist form,

Can. J. Chem. Downloaded from www.nrcresearchpress.com by 210.87.254.42 on 09/05/12
For personal use only.

TABLE 4. Downfield shifts (p.p.m.) induced by 0.48 equiv of $Eu(dpm)_3$*,†

Compound	R^1	R^2	R^3	R^4	R^5	R^6
1	5.73 (1.00)	2.50 (1.23)	1.92 (1.35)	2.48 (1.26)	5.73 (1.00)	2.50 (1.23)
2	5.70 (1.00)	1.30 (1.42)	1.90 (1.35)	2.50 (1.26)	5.70 (1.00)	2.40 (1.23)
4	5.78 (1.00)	1.35 (1.42)	1.90 (1.35)	2.50 (1.26)	5.78 (1.00)	1.35 (1.42)
10	5.90 (1.00)	2.35 (1.23)	1.01 (1.61)	2.59 (1.26)	5.90 (1.00)	2.35 (1.23)
6	1.36 (1.35)	2.80 (1.12)	1.40 (1.26)	1.02 (1.35)	1.36 (1.35)	2.80 (1.12)
5	5.21	1.30	2.20	2.41	3.00	2.45
7	3.45	1.30	2.10	2.35	5.40	1.55
11	4.95	2.30	2.00	1.04	4.95	2.30
3	3.05					
8	2.25	3.00	7.75	2.70	2.10	3.31
9	2.70	1.80	2.5	5.50	2.70	1.80

*CCl_4 Solutions (2 mol %).
†Distance factors are given in parentheses.

one can approximate the 5.3 Hz coupling in the sulfite **11** by a 25% contribution from the *trans*-diaxial chair and 75% from the twist conformation.

Eu(dpm)$_3$ Shift Studies

In recent months many reports of the application of lanthanide complexes to spread out and simplify proton spectra have appeared in the literature (26, 27). The origin of the induced effects is thought to involve a pseudocontact interaction (28). Accordingly the magnitudes of the observed shifts in fixed systems are found to be proportional to $1/r_i^3$ where r_i is the lanthanide–proton distance.

Fraser and Wigfield (29) have used $Eu(dpm)_3$ induced shifts for the configurational assignment of several sulfoxides, however, no studies on sulfites have been published to date.

The effects of addition of 0.48 equiv of $Eu(dpm)_3$ on the spectra of the 11 sulfites are listed in Table 4. All shifts were essentially linear with complex concentration up to *ca.* 0.5 equiv where solubility problems prevented further study. To ensure correct assignments, the shift changes for individual protons were monitored at four concentrations of $Eu(dpm)_3$ up to the maximum. Included in Table 4 in parentheses are the relative distance factors for each proton as measured from models, assuming 3.5 Å as the europium–oxygen distance (29).

Shift values for compounds **1**, **2**, **4**, and **10** in Table 4 are remarkably similar. Assuming that the europium atom complexes on the exocyclic oxygen of the chair conformation with axial S=O, the expected distance–shift relationship is obtained. Compound **10** having an equatorial *t*-butyl function, and compound **4**, with two equatorial methyls, can be considered to be essentially locked into chair forms with axial S=O. Apparently, complexing with $Eu(dpm)_3$ does not appreciably alter the geometries of **1** and **2** relative to **4** and **10**, although **1** and **2** lack definite "locking" substituents. Clearly, the protons closest to the axial S=O group, namely the axial protons at C-4 and -6 are most affected by the shift reagent (5.8 ± 0.1 p.p.m.) in all compounds thought to exist in chair confirmations on the basis of dipole moments.

Compound **6**, deemed a chair with equatorial S=O shows a similar distance–shift relationship. Axial C-4 and -6 protons are again affected the most by the complex, but to a much smaller extent (2.8 p.p.m.) than when the S=O is axial. Equatorial methyl groups, be they in chairs with axial S=O (**2**, **4**) or equatorial S=O (**6**) are shifted downfield to nearly the same extent (1.35 p.p.m.).

For all other sulfites the existence of chair $\rightleftharpoons$ non-chair equilibria are postulated (with the exception of **9**, which may be exclusively a twist form). The question of preferential conformational biasing due to the $Eu(dpm)_3$ now arises, precluding estimation of meaningful distance factors since weighted averages must now be considered.

Nevertheless, several qualitative trends are clear. Compounds **5** and **7** again exhibit behavior consistent with their dipole moments. The *ca.* 5.3 p.p.m. shifts of the axial protons at

Can. J. Chem. Downloaded from www.nrcresearchpress.com by 210.87.254.42 on 09/05/12
For personal use only.

Can. J. Chem. Downloaded from www.nrcresearchpress.com by 210.87.254.42 on 09/05/12
For personal use only.

C-4 and -6 (R^1 in **5** and R^5 in **7**) denote a high contribution from a form with a pseudo-axial S=O. Also, the much larger downfield shift for the R^5 and R^1 methyls of **5** and **7** (*ca.* 3.2 p.p.m.) *vs.* 1.3 p.p.m. for equatorial methyls denote at least a quasi-axial orientation for these groups.

For **11**, the 4.95 p.p.m. shift for the axial C-4 and -6 protons (R^1 and R^5) indicates a mixture of forms including that with an axial S=O chair.

In compound **3**, the only reliable shift is 3.05 p.p.m. for the methyl group, again indicative of a quasi-axial substituent. This is not entirely consistent with the dipole moment results and probably reflects the difficulty in predicting conformer populations for $Eu(dpm)_3$ complexes of conformationally mobile molecules.

The axial C-6 proton in **8** (R^6) shows the expected behavior for a molecule having a large contribution from a chair form with equatorial S=O. In contrast, the 7.75 p.p.m. shift for R^3 clearly does not correlate with the expected distance from the metal.

In compound **9**, deemed to be a twist form, the CH_3 group shifts of 2.70 and 1.80 p.p.m. are intermediate between those for axial and equatorial methyls as expected on the basis of a twist configuration. The 5.50 p.p.m. shift for R^4, however, again shows that $Eu(dpm)_3$ induced shifts at C-5 are unreliable for assigning conformations to mobile sulfites.

A parallel thus is evident between the proton n.m.r. shieldings in CCl_4 and the $Eu(dpm)_3$ induced values. Using shifts of substituents at the C-4 and -6 ring positions one can seemingly obtain valuable information regarding sulfite conformation. It is abundantly clear that association phenomena in any form most strongly perturbs the C-5 ring carbon. Consequently, parameters for substituents at this position must be viewed with caution.

Summary and Conclusions

A comprehensive treatment of the proton n.m.r. data for an extensive series of related sulfites has been presented for the first time. The applicability of shift reagents for studying sulfite conformation has been critically tested. The data provided supporting evidence for previous conclusions based on dipole moments.

The results are consistent with a large free energy difference between the two chair conformations and lower free energy differences between chair and boat conformations. Also, the high preference for axial S=O orientation is seen from the observed $Eu(dpm)_3$ shifts.

Like trimethylene sulfite **1**, compounds **2**, **4**, and **10** can be regarded as chair forms with axial S=O functions. Increased steric interactions between the *syn*-axial methyl groups and the exocyclic oxygen atom lead to the adoption of non-chair forms for **3**, **5**, **7**, **8**, and **9**. For **6**, the presence of the alternative chair form with equatorial S=O is verified. It appears in **11**, that the 5-*t*-butyl group cannot "anchor" the ring into a diequatorial chair, but rather the molecule probably exists as a mixture of the diaxial chair and non-chair conformations.

Further studies on these and related molecules using ^{13}C n.m.r. spectroscopy are presently in progress.

Experimental

The syntheses of the sulfites have been described elsewhere (5). The proton n.m.r. spectra were obtained on a JEOL JNM-C60S or C60HL using TMS as internal standard. Chemical shifts were measured by interpolation. $Eu(dpm)_3$ was purchased from the Pierce Chemical Company.

The financial assistance of the National Research Council of Canada is gratefully acknowledged. We thank Dr. H. F. van Woerden for providing preprints.

1. D. G. Hellier, J. G. Tillett, H. F. van Woerden, and R. F. M. White. Chem. Ind. (London), 1956 (1963).
2. H. F. van Woerden. Ph.D. Thesis, Leiden, 1964.
3. B. A. Arbouzov, O. D. Zolova, and L. K. Yulbasheva. Zh. Strukt. Khim. **8**, 291 (1967).
4. H. F. van Woerden and E. Havinga. Rec. Trav. Chim. Pays-Bas, **86**, 341, 353 (1967).
5. G. Wood, J. M. McIntosh, and M. H. Miskow. Can. J. Chem. **49**, 1202 (1971).
6. R. A. Pethrick and E. Wyn-Jones. Quart. Revs. **23**, 304 (1969).
7. G. Eccleston, R. A. Pethrick, E. Wyn-Jones, P. C. Hamblin, and R. F. M. White. Trans. Faraday Soc. **66**, 310 (1970).
8. S. Wolfe, A. Rauk, L. M. Tel, and I. G. Csizmadia. J. Chem. Soc. B, 136 (1971).
9. G. Wood, J. M. McIntosh, and M. H. Miskow. Tetrahedron Lett. 4895 (1970).
10. G. Wood and R. M. Srivastava. Tetrahedron Lett. 2937 (1971).
11. W. Wucherpfennig. Ann. Chem. **737**, 144 (1970).
12. D. G. Hellier. Thesis. University of London, 1966.
13. H. F. van Woerden. Private communication.
14. V. M. S. Gil and W. A. Gibbons. Mol. Phys. **8**, 199 (1964).

15. E. L. Eliel and D. Railenu. Chem. Commun. 291 (1970).
16. W. G. Bentrude and J. H. Hargis. J. Am. Chem. Soc. **92**, 7136 (1970).
17. G. Wood and M. H. Miskow. Tetrahedron Lett. 1775 (1970).
18. G. Wood and M. H. Miskow. Tetrahedron Lett. 4433 (1966).
19. S. Sternbell. Rev. Pure Appl. Chem. **14**, 15 (1964).
20. J. E. Anderson. J. Chem. Soc. B. 712 (1967).
21. C. G. Overberger, T. Kurtz, and S. Yaroslavsky. J. Org. Chem. **30**, 4363 (1965).
22. L. Cazaux and P. Maroni. Tetrahedron Lett. 3667 (1969).
23. H. F. van Woerden, H. Cerfontain, C. H. Grain, and R. J. Reijerkerk. Rec. Trav. Chim. Pays-Bas, **87**, 6107 (1968).
24. R. Pethrick, E. Wyn-Jones, P. Hamblin, and R. White. J. Mol. Struct. **1**, 333 (1967).
25. E. L. Eliel and M. C. Knoeber. J. Am. Chem. Soc. **90**, 3444 (1968) and references therein.
26. C. C. Hinckley. J. Am. Chem. Soc. **91**, 5160 (1969).
27. J. K. M. Sanders and D. H. Williams. Chem. Commun. 422 (1970).
28. J. Briggs, G. H. Frost, F. A. Hart, G. P. Moss, and M. L. Staniforth. Chem. Commun. 749 (1970).
29. R. R. Fraser and Y. Y. Wigfield. Chem. Commun. 1471 (1970).

Can. J. Chem. Downloaded from www.nrcresearchpress.com by 210.87.254.42 on 09/05/12
For personal use only.

Photocyclization Reactions of Aryl Polyenes. V.[1] Photochemical Synthesis of Substituted Chrysenes[2]

CLIFFORD C. LEZNOFF AND ROGER J. HAYWARD
Department of Chemistry, York University, Downsview, Ontario

Received September 14, 1971

The photocyclization-oxidation reaction of 1,6-di-*p*-substituted-phenyl-1,3,5-hexatrienes gave 3,9-disubstituted-chrysenes. Similarly, irradiation of 1-*p*-substituted-phenyl-6-phenyl-1,3,5-hexatrienes yielded 3-substituted-chrysenes. The 3-substituted-chrysenes were independently prepared in a high yield by the photocyclization-oxidation of 1-α-naphthyl-2-*p*-substituted-phenylethylenes.

La réaction d'oxydation-photocyclisation des di-(phényl *p*-substitué)-1,6 hexatriènes-1,3,5 conduit aux chrysènes disubstitués-3,9. D'une façon similaire, l'irradiation des (phényl *p*-substitué)-1 phényl-6 hexatriènes-1,3,5 conduit aux chrysènes substitués-3. Les chrysènes substitués-3 ont été préparés d'une façon indépendante avec un haut rendement par l'oxydation-photocyclisation des α-naphtyl-1 (phényl *p*-substitué)-2 éthylènes.

Canadian Journal of Chemistry, **50**, 528 (1972)

Can. J. Chem. Downloaded from www.nrcresearchpress.com by 210.87.254.105 on 09/05/12
For personal use only.

Although chrysene itself is commercially available, substituted chrysenes are little known and can be obtained only by tedious synthetic pathways (1–3). Chrysenes substituted in the 6 and 12 positions are readily obtained by electrophilic substitution reactions (4), but other substituted chrysenes are rare and many polysubstituted chrysenes are completely unknown. Chrysenes are interesting polyaromatic compounds in that the 6-methylchrysene is known to be carcinogenic (5), but 6-aminochrysene is carcinostatic (6). Although chrysenes have been obtained directly from steroids by catalytic dehydrogenation (7), the formation of steroids from substituted chrysenes has not been attempted, probably due to the lack of available substituted chrysenes.

In 1962 Fonken (8) described the formation of chrysene by the photochemical-oxidation of 1,6-diphenyl-1,3,5-hexatriene. In this paper, we present a general synthesis of 3-substituted- and 3,9-disubstituted-chrysenes using the photochemical method of Fonken (Scheme 1).

The 1,6-di-*p*-substituted-phenyl-1,3,5-hexatrienes (**1***a–e*) were prepared in moderate yield (Table 1) by reacting 2-butene-1,4-bis(tri-*n*-butylphosphonium chloride) (9) with the appropriate *p*-substituted-benzaldehyde in a Wittig reaction (10). The 1-*p*-substituted-phenyl-6-phenyl-1,3,5-hexatrienes (**2***a–e*) were prepared in moderate yield (Table 1) by reaction of *p*-substituted-benzylphosphonium chlorides with 5-phenylpenta-2,4-dien-1-al in a Wittig reaction (10).

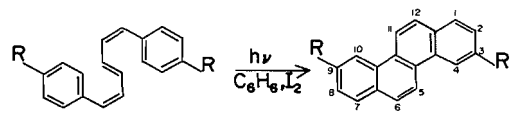

a R = MeO
b R = Me
c R = Cl
d R = F
e R = CN

SCHEME 1

The hexatrienes, **1***a–e* and **2***a–e*, were readily characterized by their spectral data (Table 2) and by comparison with known 1,6-diaryl-1,3,5-hexatrienes. Mass spectroscopy revealed the presence of strong parent ions for **1***a–e* and **2***a–e*. The u.v. and i.r. spectra clearly showed the presence of the hexatriene moiety.[3]

Irradiation of 8.0×10^{-4} *M* solutions of 1,6-di-*p*-substituted-phenyl-1,3,5-hexatrienes (**1***a–d*) in dry benzene, containing 3.2×10^{-3} *M* iodine, gave after 24 h 3,9-disubstituted-chrysenes (**3***a–*

[1]For Part IV, see Leznoff and Hayward (17).

[2]Taken in part from the thesis submitted by Roger J. Hayward in partial fulfilment of the requirements for the Ph.D. degree.

[3]It is assumed that the all-*trans* hexatrienes are formed from the method of preparation and the i.r. spectral data of **1***a–e* and **2***a–e*, which show absorption peaks for *trans* double bonds.

TABLE 1. 1,6-Di-*p*-substituted-phenyl-1,3,5-hexatrienes (**1***a–e*) and 1-*p*-substituted-phenyl-6-phenyl-1,3,5-hextrienes (**2***a–e*)

Compound	Substituent	Melting point (°C)	Yield* %	Molecular formula	Analysis (%) Calculated C	H		Found C	H	
1*a*	MeO	249–250†	26	—	—	—		—	—	
1*b*	Me	233–234‡	24	—	—	—		—	—	
1*c*	Cl	220–221§	29	—	—	—		—	—	
1*d*	F	181–182	8.5	$C_{18}H_{14}F_2$	80.58	5.22		80.35	5.20	
1*e*	CN	210–212	30.1	$C_{20}H_{14}N_2$	85.01	5.06	9.92 (N)	84.57	5.06	10.24 (N)
2*a*	MeO	198–199	58	$C_{19}H_{18}O$	86.97	6.87		87.26	6.53	
2*b*	Me	195–196	71	$C_{19}H_{18}$	92.65	7.32		93.01	7.46	
2*c*	Cl	202–203	47.5	$C_{18}H_{15}Cl$	81.03	5.63	13.3 (Cl)	80.80	5.23	12.93 (Cl)
2*d*	F	182–183	57	$C_{18}H_{15}F$	86.37	5.99		86.21	5.62	
2*e*	CN	194.5–195.5	33.5	$C_{19}H_{15}N$	88.68	5.83	5.44 (N)	88.76	5.49	5.21 (N)

*Obtained by direct crystallization from the reaction media. Further amounts could be obtained from the mother liquors by chromatographic methods.
†Literature 9, m.p. 250–251.
‡Literature 9, m.p. 233–234.
§Literature 9, m.p. 220–221.

TABLE 2. Spectral characteristics of 1,6-di-*p*-substituted-phenyl-1,3,5-hexatrienes (**1***a–e*) and 1-*p*-substituted-phenyl-6-phenyl-1,3,5-hexatrienes (**2***a–e*)

Compound	Substituent	u.v. spectra (benzene) λ_{max}(nm) (ε)	i.r. spectra ν (cm^{-1})	Mass spectra *m/e*, M^+ (% of base peak)
1*a*	MeO	393 (48 300), 372 (68 300), 355 (53 900)	1633, 1610, 1172, 989	292 (15.4)
1*b*	Me	384 (50 000), 363 (69 100), 346 (51 700)	1572, 999	260 (23.7)
1*c*	Cl	386.5 (56 900), 366 (78 100), 343 (59 200)	1597, 991	300 (56.4)
1*d*	F	371 (44 600), 353 (62 800), 338 (48 700)	1628, 1598, 1168, 991	268 (100)
1*e*	CN	400.5 (29 100), 378 (42 700), 361 (36 600)	2205, 1588, 998	282 (100)
2*a*	MeO	381 (37 100), 365 (57 700), 351 (52 000)	1612, 1600, 1171, 990	262 (100)
2*b*	Me	386 (50 900), 366 (74 000), 348 (54 100)	1590, 992	246 (100)
2*c*	Cl	382 (49 000), 362.5 (67 600), 344.5 (51 300)	1600, 988	266 (100)
2*d*	F	377 (53 600), 357 (73 200), 340.5 (54 900)	1610, 1600, 1229, 988	250 (100)
2*e*	CN	387.5 (29 200), 371 (44 000), 357 (42 300)	2214, 1604, 990	257 (100)

d) in 12–14% yield. The 1,6-di-*p*-cyanophenyl-1,3,5-hexatriene (**1***e*) gave 3,9-dicyanochrysene (**3***e*) in 60% yield. Compound **3***e* was very insoluble in benzene and precipitated from solution as it was formed, and this fact may account for the relatively high yield of **3***e*.

Similarly, irradiation of 1-*p*-substituted-phenyl-6-phenyl-1,3,5-hexatrienes (**2***a–e*) gave 3 substituted-chrysenes (**4***a–e*) in 12–15% yield (Scheme 2).

The stilbene-like photocyclization-oxidation of 1-α-naphthyl-2-phenylethylene yields chrysene (11) and it is highly likely that the irradiation of **2***a–e* (and **1***a–e*) goes through 1-α-naphthyl-2-*p*-substituted-phenylethylene inter-

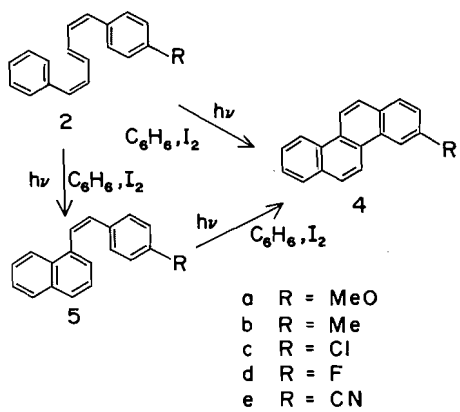

SCHEME 2

Can. J. Chem. Downloaded from www.nrcresearchpress.com by 210.87.254.105 on 09/05/12
For personal use only.

TABLE 3. 3,9-Disubstituted-chrysenes (**3***a–e*) and 3-substituted-chrysenes (**4***a–e*)

Compound	Substituent	Melting point (°C)	Yield (%) photo-product	Molecular formula	Analyses % Calculated C	H		Found C	H	
3*a*	MeO	220–221	12*	$C_{20}H_{16}O_2$	83.17	5.48		83.28	5.56	
3*b*	Me	233–235	13.8*	$C_{20}H_{16}$	93.71	6.25		93.62	6.20	
3*c*	Cl	208–209	12*	$C_{18}H_{10}Cl_2$	72.74	3.37	23.91 (Cl)	72.53	3.28	23.54 (Cl)
3*d*	F	239–241	11*	$C_{18}H_{10}F_2$	81.80	3.79		81.64	3.52	
3*e*	CN	238–239	60*	$C_{20}H_{10}N_2$	86.29	3.60	10.08 (N)	85.94	3.59	9.87 (N)
4*a*	MeO	145–146§	13† (51)‡	$C_{19}H_{14}O$	88.38	5.44		88.19	5.46	
4*b*	Me	173–174‖	13† (69.2)‡	$C_{19}H_{14}$	94.18	5.78		94.42	5.96	
4*c*	Cl	180–181	13† (70)‡	$C_{18}H_{11}Cl$	82.26	4.19	13.53 (Cl)	82.01	4.12	13.26 (Cl)
4*d*	F	218–219	14† (82)‡	$C_{18}H_{11}F$	87.78	4.47		87.58	4.46	
4*e*	CN	200–201	12† (80)‡	$C_{19}H_{11}N$	90.09	4.43	5.53 (N)	90.39	4.07	5.58 (N)

*Photo-product from **1***a–e*.
†Photo-products from **2***a–e*.
‡Photo-product from **5***a–e*.
§Literature (14), m.p. 147.5–148.5°.
‖Literature (14), m.p. 170–170.5.

mediates. To test this possibility, a series of 1-α-naphthyl-2-*p*-substituted-phenylethylenes (**5***a–e*) were prepared by the Wittig reaction of 1-*p*-substituted-benzylphosphonium chlorides and 1-naphthaldehyde and irradiated under conditions identical to those for **1***a–e* and **2***a–e*. The physical and spectral properties of **5***a–e* were consistent with the assigned structures (see Experimental).

Irradiation of **5***a–e* gave **4***a–e* in 30–60% yield. The 3-substituted-chrysenes (**4***a–e*), obtained from **5***a–e*, showed identical physical and spectral properties to **4***a–e* obtained by the irradiation of **2***a–e* (Tables 3 and 4). It is thus highly likely that **5***a–e* are intermediates in the photocyclization-oxidation reactions of **2***a–e* to **4***a–e*.[4]

In an experiment designed to show that all the 1,6-diaryl-1,3,5-hexatrienes underwent an identical type of photocyclization-oxidation reaction, an attempt was made to convert the photoproducts, 3,9-dichlorochrysene (**3***c*) and 3-chlorochrysene (**4***c*), obtained from **1***c* and **2***c*, respectively, into the photoproducts 3,9-dicyanochrysene (**3***e*) and 3-cyanochrysene (**4***e*), obtained from **1***e* and **2***e*, respectively. When **3***c* and **4***c* were heated under reflux in pyridine with cuprous cyanide for 24 h, **3***e* and **4***e* were obtained in 25 and 33% yield, respectively.

The structures of the previously unknown 3,9-substituted-chrysenes (**3***a–e*) and 3-substituted-chrysenes (**4***a–e*) were determined from their method of preparation and spectral data (Table 4). Mass spectroscopy revealed the presence of strong parent ions for **3***a–e* and **4***a–e*. The u.v. (12) and i.r. spectra of **3***a–e* and **4***a–e* were characteristic of chrysenes. The n.m.r. spectra of **3***a–e* and **4***a–e* were typical of chrysene itself (13). Martin *et al.* and Memory and Cobb (13) found that protons at H-4, -5, -10, and -11 in chrysene itself were abnormally deshielded and occurred downfield by approximately 0.65 p.p.m. compared to the other eight protons in the molecule. The n.m.r. spectra of **3***a–b* and **4***a–e* showed the same deshielding effect for the four protons, which emphasize that the substituents could not be at C-4, -5, -10, and -11 of chrysene and support the assigned structures. Compounds **3***a* and *b* were identical to compounds previously synthesized by a totally unambiguous route (14) and thus the structure of these compounds is confirmed. It is very unlikely that any functional group or skeletal migrations have occurred during irradiation.

It has been demonstrated that substituted chrysenes can be synthesized in reasonable yield by a simple one-step photocyclization-oxidation reaction from readily available precursors.

[4]The intermediacy of 1-styryl-7-substituted-naphthalenes is equally likely, especially in light of the fact that a substituent on a phenyl ring of the related 1,4-diphenyl-1,3-butadiene does not appreciably affect the direction of photocyclization (16).

Can. J. Chem. Downloaded from www.nrcresearchpress.com by 210.87.254.105 on 09/05/12
For personal use only.

Can. J. Chem. Downloaded from www.nrcresearchpress.com by 210.87.254.105 on 09/05/12
For personal use only.

TABLE 4. Spectral characteristics of 3,9-disubstituted-chrysenes (**3***a–e*) and 3-substituted-chrysenes (**4***a–e*)

Compound	Substituent	u.v. spectra (95% EtOH) λ_{max}(nm)*	n.m.r. spectra† (p.p.m.)	Mass spectra m/e, M^+ (% for base peak)
3*a*	MeO	323, 309, 295, 274, 254, 247, 228	8.68–8.52 (4H, m), 8.2–7.30 (6H, m), 4.03 (6H, s)	288 (100)
3*b*	Me	322.5, 308.5, 297, 285, 271.5, 262, 243.5, 224	8.8–8.63 (4H, m),8.1–7.42 (6H, m) 2.65 (6H, s)	256 (100)
3*c*	Cl‡	323, 310, 297, 286, 272, 262, 244, 226	— — —	297 (100)
3*d*	F‡	315, 302, 291.5, 279, 268, 258.5, 241, 219	— — —	264 (100)
3*e*	CN‡	352, 276, 270.5, 266, 243, 237	— — —	278 (100)
4*a*	MeO	351, 322, 307.5, 267, 258, 222	8.95–8.62 (4H, m), 8.23–7.34 (7H, m) 3.97 (3H, s)	258 (100)
4*b*	Me	320, 307, 296, 259, 259.5, 242.5, 221	8.98–8.72 (4H, m), 8.24–7.60 (7H, m), 2.63 (3H, s)	242 (100)
4*c*	Cl	321.5, 308, 304, 291, 279, 280, 260.5, 243.5, 226.5	8.81–8.46 (4H, m), 8.05–7.58 (7H, m)	262 (100)
4*d*	F	318.5, 207, 302, 293, 283.5, 268, 258, 241.5, 219	9.0–8.64 (4H, m), 8.26–7.54 (7H, m)	246 (100)
4*e*	CN	330, 304, 290, 267.5, 240, 231	9.2–8.65 (4H, m), 8.3–7.85 (7H, m)	253 (100)

*Quantitative spectra were not possible because of the very low solubility of **3***a–e* and **4***a–e* in a suitable organic solvent.
†Solvent $AsCl_3$.
‡Due to the very low solubility of these compounds in organic solvents including $AsCl_3$ n.m.r. spectra could not be taken.

TABLE 5. 1-(α-Naphthyl)-2-*p*-substituted-phenylethylenes (**5***a–e*)

Compound	Substituent	Melting Point (°C)	Yield (%)	Molecular formula	Analysis (%) Calculated C	H		Found C	H	
5*a*	MeO	104–105	34	$C_{19}H_{16}O$	87.63	6.15		87.26	5.79	
5*b*	Me	82–83	51	$C_{19}H_{16}$	93.46	6.56		93.44	6.20	
5*c*	Cl	99–100	43	$C_{18}H_{13}Cl$	81.60	4.91	13.42 (Cl)	81.61	4.71	13.40 (Cl)
5*d*	F	b.p. 171–173 (0.1 mm)	22.5	$C_{18}H_{13}F$	87.05	5.24		86.98	5.18	
5*e*	CN	131–132	63	$C_{19}H_{13}N$	89.38	5.11	5.49 (N)	89.18	5.02	5.46 (N)

TABLE 6. Spectral characteristics of 1-(α-naphthyl)-2-*p*-substituted-phenylethylenes (**5***a–e*)

Compound	Substituent	u.v. spectra (95% EtOH) λ_{max} (nm) (ε)	i.r. spectra ν (cm^{-1})	Mass spectra *m/e*, M^+ (% of base peak)
5*a*	MeO	318 (19 800), 221.5 (33 800)	1608, 1170, 1022, 960	260 (100%)
5*b*	Me	317.5 (8 900), 224 (31 100)	1592, 961	244 (100%)
5*c*	Cl	324 (20 100), 227.5 (30 100)	1591, 1004, 954	264 (100%)
5*d*	F	319 (16 000), 226.5 (32 100)	1638, 1225, 1154, 1010	248 (100%)
5*e*	CN	325 (15 500), 221.5 (44 000)	2212, 1589, 995	255 (100%)

Experimental

All m.p.s. were determined on a Kofler hot stage and are uncorrected. The i.r. spectra were recorded on a Perkin–Elmer 257 spectrometer using KBr discs. The u.v. spectra were measured using a Cary 14 u.v. spectrometer and benzene as a solvent. The n.m.r. spectra were measured on a Varian A60 spectrometer using tetramethylsilane as an internal standard ($\delta = 0$ p.p.m.) and deuterochloroform as solvent. Mass spectra were recorded on a Hitachi–Perkin–Elmer RMU-6 mass spectrometer. Silica gel was used for thin- and thick-layer chromatography. All photochemical reactions were carried out in a Rayonet photochemical reactor using RPR 3500 °A lamps. Microanalyses were performed by A. B. Gygli of Toronto.

Synthesis of 1,6-Di-p-substituted-phenyl-1,3,5-hexatrienes

All the 1,6-di-*p*-substituted-phenyl-1,3,5-hexatrienes were synthesized in a manner identical to that of *1,6-di-p-chlorophenyl-1,3,5-hexatriene* (**1***c*). To a mixture of 5 g (0.035 mol) of *p*-chlorobenzaldehyde and 9.0 g (0.017 mol) of 2-butene-1,4-bis(tri-*n*-butylphosphonium chloride) (9) in 50 ml of methanol was added 80 ml of 0.4 *M* lithium methoxide. The mixture was allowed to crystallize overnight after which crystals of 1,6-di-*p*-chlorophenyl-1,3,5-hexatriene were filtered off.

Synthesis of 1-p-Substituted-phenyl-6-phenyl-1,3,5-hexatrienes

A typical example is given for the preparation of *1-p-methoxy-phenyl-6-phenyl-1,3,5-hexatriene* (**2***a*). To a mixture of 2.0 g (0.0126 mol) of 5-phenylpenta-2,4-dien-1-al (15) and 5.83 g (0.012 mol) of *p*-methoxybenzyltriphenylphosphonium bromide in 30 ml of methanol was added 50 ml of 0.4 *M* lithium methoxide. The mixture was allowed to crystallize overnight after which the product was filtered off.

*Physical and Spectral Properties of the 1,6-Di-p-substituted-phenyl-1,3,5-hexatrienes (**1***a–e*) and 1-p-Substituted-phenyl-6-phenyl-1,3,5-hexatrienes (**2***a–e*)*

The physical and spectral properties of these compounds are given in Tables 1 and 2, respectively.

Synthesis of 1-(α-Naphthyl)-2-p-substituted-phenylethylenes

A typical example is given for the preparation of *1-(-α-naphthyl)-2-p-methylphenylethylene* (**5***a–e*). To a mixture of 3 g (0.0193 mol) of 1-naphthaldehyde and 7.75 g (0.0193 mol) *p*-methylbenzyltriphenylphosphonium chloride in 20 ml of methanol was added 25 ml of 1.2 *M* lithium methoxide. The mixture was allowed to crystallize overnight after which the product was filtered off.

*Preparation of 1-(α-Naphthyl)-2-p-fluorophenylethylene (**5***d*)*

This compound was made by a Grignard reaction. To the ice cold Grignard-reagent from 5 g (0.035 mol) *p*-fluorobenzylchloride and 0.8 g (0.035 mol) of magnesium in 50 ml of dry ether was added 5.0 g (0.032 mol) of 1-naphthaldehyde in 10 ml of ether. After the addition was completed the mixture was stirred for 2 h at room temperature, then cooled with ice. To this mixture was added 100 ml of ice-cold saturated ammonium chloride solution. The mixture was then boiled under reflux, cooled, and extracted with ether. The ether solution was dried with anhydrous magnesium sulfate and evaporated. The remaining crude product was distilled at a reduced pressure; the fraction boiling at 171–173 °C (0.1 mm) was found to be 1-(α-naphthyl)-2-*p*-fluorophenylethylene.

*Physical and Spectral Properties of the 1-(α-Naphthyl)-2-p-substituted-phenylethylenes (**5***a–e*)*

The physical and spectral properties of these compounds are given in Tables 5 and 6, respectively.

Can. J. Chem. Downloaded from www.nrcresearchpress.com by 210.87.254.105 on 09/05/12
For personal use only.

TABLE 7. *p*-Substituted-benzyltriphenylphosphonium halides

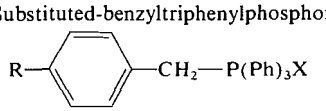

Substituents		Melting point	Yield	Analysis (%) Found		Calculated	
R	X	(C°)	(%)	C	H	C	H
MeO	Br	242–243	97.5	69.02	5.87	68.97	5.64
Cl	Cl	307–308	95	64.42	4.97	64.26	5.20
F	Cl	315–316	75	73.62	5.86	73.30	5.56

Preparation of p-Substituted-benzyltriphenylphosphonium halides

The *p*-substituted-benzylphosphonium halides were synthesized in a manner identical to that described before (16). Physical properties of phosphonium halides are given in Table 7.

Irradiation of Starting Materials

The general techniques of irradiation on a preparative scale have been described previously (16). The photocyclization-oxidation reaction products were isolated by preparative t.l.c. using hexane:benzene (3:1) as eluant. All photocyclization-oxidation monomeric products moved faster than the starting materials on t.l.c. Compounds moving slower than the starting material invariably turned out to be dimeric products.

Since the starting materials **1***a*, **1***b*, and **2***a* were so insoluble in organic solvents a different technique was used to irradiate them. An example is given for 1,6-di-*p*-methoxyphenyl-1,3,5-hexatriene (**1***a*). A slurry of 100 mg of **1***a* in 500 ml of benzene containing 3.2×10^{-3} *M* iodine was irradiated for 3 days in the usual way. The mixture was subjected to vigorous agitation by passing through it a dry stream of nitrogen. After 3 days no starting material could be detected by t.l.c. The mixture was then worked-up in the usual way (16).

The physical and spectral properties of the substituted chrysenes are given in Tables 3 and 4, respectively.

Preparation of Cyanochrysenes from Chlorochrysenes

The procedure given previously for the preparation of cyano-1-phenylnaphthalenes from chloro-1-phenylnaphthalenes was followed exactly.

The authors wish to thank the National Research Council of Canada for a grant in aid of this research and a referee for helpful comments.

1. H. L. LEWIS, G. R. RAMAGE, and R. ROBINSON. J. Chem. Soc. 1412 (1935); G.R. RAMAGE and R. ROBINSON. J. Chem. Soc. 607 (1933).
2. L. GOLDBERG and R. ROBINSON. J. Chem. Soc. 575 (1941).
3. S. M. MUKHERJI, K. S. DABAS, and K. S. SHARMA. Tetrahedron, **24**, 4373 (1968).
4. N. P. BUI-HOI, J. P. HOEFFINGER, and P. JACQUIGNON. Bull. Chem. Soc. France, 3808 (1968).
5. M. J. SHEAR and J. LEITER. J. Nat. Cancer Inst. **2**, 241 (1941).
6. J. GELZER and P. LOUSTALOT. Eur. J. Cancer, **3**, 79 (1967).
7. L. RUZICKA and H. F. MELDAHL. Helv. Chim. Acta, **23**, 364 (1940).
8. G. J. FONKEN. Chem. Ind. 1327 (1962).
9. H. HEITMAN. Synthesis of symmetrical polyenes by Wittig reactions. Ph.D. Thesis. Amsterdam, Holland, 29 (1965).
10. R. N. MCDONALD and T. W. CAMPBELL. J. Org. Chem. **24**, 1969 (1959).
11. C. S. WOOD and F. B. MALLORY. J. Org. Chem. **29**, 3373 (1964).
12. M. BADGER, R. S. PEARCE, and R. PETTIT. J. Chem. Soc. 3199 (1951).
13. R. H. MARTIN, N. DEFAY, F. GEERTS-EVRARD, and S. DELAVARENNE. Tetrahedron, **20**, 1073 (1964); J. D. MEMORY and T. B. COBB. J. Chem. Phys. **39**, 2316 (1963).
14. W. E. BACHMANN and W. S. STRUVE. J. Org. Chem. **5**, 416 (1940).
15. A. LUTTRINGHAUS and G. SCHILL. Chem. Ber. **93**, 3048 (1960).
16. C. C. LEZNOFF and R. J. HAYWARD. Can. J. Chem. **48**, 1842 (1970).
17. C. C. LEZNOFF and R. J. HAYWARD. Can. J. Chem. **49**, 3596 (1971).

Can. J. Chem. Downloaded from www.nrcresearchpress.com by 210.87.254.105 on 09/05/12
For personal use only.

Reactions of Tetrasubstituted Azomethine Ylides Generated from Tetracyanoethylene Oxide

J. W. LOWN AND K. MATSUMOTO[1]

Department of Chemistry, University of Alberta, Edmonton 7, Alberta

Received September 2, 1971

Reaction of a series of Schiff bases (bearing substituents which effect electron release in either the benzal or aniline moieties), with tetracyanoethylene oxide generates several tetra-substituted azomethine ylides which may be trapped in the presence of dipolarophiles both heteromultiple and homomultiple. The methine n.m.r. assignments in the adducts are obtained by using benzal-$[^2H]_1$-2,4,6$[^2H]_3$-aniline in the reactions which results in >98% deuterium incorporation. Diphenylcyclopropenone reacts preferentially with tetracyanoethylene oxide to give 3,4-diphenyl-5,5,6,6-tetracyano-5,6-dihydropyran-2-one while diphenylcyclopropenethione reacts with tetracyanoethylene oxide to give 1,2-diphenyl-3-dicyanomethylenecyclopropene in a 67% yield superior to that of existing preparations.

La réaction d'une série de bases de Schiff (substituants porteurs avec perte d'effet électronique dans une partie du benzylidène ou de l'aniline) avec l'oxyde de tétracyanoéthylène produit plusieurs ylides d'azométhine substitués qui peuvent être piégés en présence de dipolarophiles à la fois hétéromultiple et homomultiple. Les attributions du groupe méthinique en r.m.n. dans les composés d'addition sont obtenus par l'utilisation du benzylidène $[^2H_1]$-2,4,6$[^2H_3]$-aniline dans les réactions qui résultent d'une deutération 98%. Le diphénylcyclopropenone réagit préférentiellement avec l'oxyde de tétracyanoéthylène pour donner la diphényl-3,4-tétracyanoéthylène-5,5,6,6-dihydropyrane-5,6-one-2 tandis que la diphénylcyclopropènethione réagit avec l'oxyde de tétracyanoéthylène pour donner le diphényl-1,2-dicyano-méthylène cyclopropène-3 dans un rendement de 67%, supérieur aux préparations existantes.

Canadian Journal of Chemistry, **50**, 534 (1972)

The orbital symmetry-controlled thermal and photochemical cleavage of aziridines to azomethine ylides (1) and subsequent 1,3-dipolar cycloaddition of the latter species to a variety of homomultiple and heteromultiple bonds leads to several useful synthetic routes to many heterocyclic systems (2). In the monocyclic aziridine series the systems that have been examined from this viewpoint are limited to the examples **1***a–g*. In examples of type **1***h* substituents of the type $R_3 = R_4 = X$ where X is a strongly electron-withdrawing group *e.g.* CN, would be expected to confer increased stability and longer lifetimes on the azomethine ylides which otherwise enjoy only transient existence. Since such aziridines of the type **1***h* are inaccessible synthetically we have reexamined the generation of tetrasubstituted azomethine ylides produced from tetracyanoethylene oxide reported by Linn and Ciganek (14). Tetracyanoethylene oxide (**2**) reacts with benzalaniline in benzene to give species **3** and **4** which can react

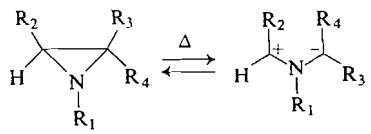

1

a	R_1 = Ar;	$R_2 = CO_2CH_3$;	R_3 = H;	$R_4 = CO_2CH_3$ (1)
b	R_1 = Alkyl;	R_2 = Ar;	R_3 = H;	R_4 = COAr (3–6)
c	R_1 = Alkyl;	R_2 = Ar;	R_3 = H;	$R_4 = CO_2R$ (7, 8)
d	R_1 = Ar;	R_2 = Ar;	R_3 = H;	R_4 = Ar (9)
e	R_1 = Alkyl;	R_2 = Ar;	R_3 = H;	R_4 = CN (8)
f	R_1 = Ar;	R_2 = R;	$R_3 = CO_2CH_3$;	$R_4 = CO_2CH_3$,CN (10–12)
g	R_1 = Ar;	R_2 = Ar;	R_3 = H;	$R_4 = CO_2Et$,$CONEt_2$ (13)
h	R_1 = Ar;	R_2 = Ar;	R_3 = X;	R_4 = X

[1]NRCC Postdoctorate Fellow, 1969–1971.

Can. J. Chem. Downloaded from www.nrcresearchpress.com by 210.87.254.40 on 09/05/12
For personal use only.

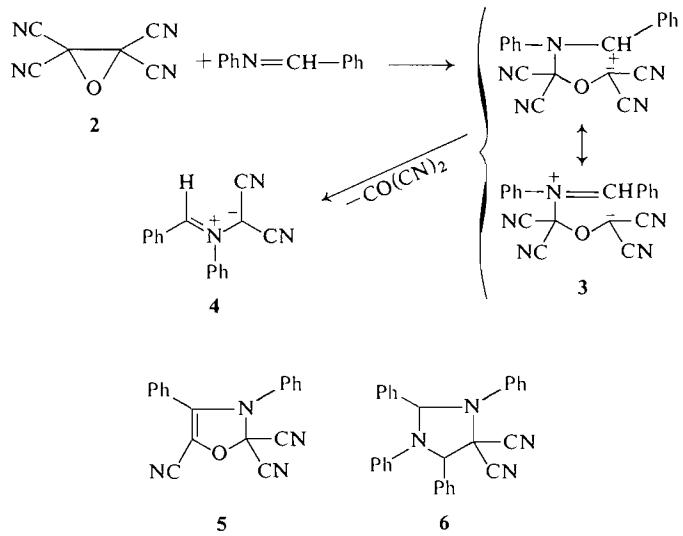

SCHEME 1

with dipolarophiles to give products of 1,3-dipolar addition (14). In the absence of other dipolarophiles the 4-oxazoline **5** is formed (by ring closure of **3** and elimination of a molecule of hydrogen cyanide) together with the imidazolidine **6** (formed by 1,3-dipolar addition of benzalaniline to the azomethine ylide **4** in a regiospecific manner), see Scheme 1.

It seemed worthwhile to extend the synthetic usefulness of the reaction by introducing more reactive dipolarophiles into the reaction to take advantage of the relatively low dipolarophilic activity of benzal aniline and other simple imines. Therefore reaction of tetracyanoethylene oxide and benzal aniline in the presence of *N*-phenylmaleimide gave the substituted pyrrolidine **7***a* in 51% yield. The pyrrolidine **7***a* exhibited an AMX spectrum for the methine protons. All the chemical shifts and corresponding coupling constants were obtained unambiguously by a parallel experiment employing benzal-*d*-2,4-6-trideuteroaniline (prepared by the condensation of formyl-*d*-benzaldehyde (99.5% *d*) with 2,4,6-*N*,*N*-pentadeuteroaniline) with tetracyanoethylene oxide and *N*-phenylmaleimide. Examination of the n.m.r. spectrum of the deuterated pyrrolidine showed >98% deuterium incorporation implying little or no proton exchange from intermediate **3** or **4** into the reaction medium. By comparison of the spectra of the protium and deuterium compounds values for the vicinal coupling constants of $J_{2,3} = 6$ and $J_{3,4} = 10$ Hz were derived, which favor the configuration shown (see Scheme 2).

Reactions of several benzal anilines (bearing different substituents in both the benzal and aniline moieties) and tetracyanoethylene oxide in the presence of an equivalent of *N*-phenylmaleimide were now examined. The effects of the substituents on production of the pyrrolidine are summarized in the legend in Scheme 2.

Substituents which effect electron release by resonance mechanisms in either the benzal or aniline moieties and increase the basicity of the nitrogen promote the reaction leading to the trapping of the azomethine ylide. These results are consistent with, on the one hand, increased nucleophilicity of the imine nitrogen promoting the ring cleavage of the oxirane, and on the other hand, with the enhanced resonance stabilization afforded intermediate **3**. Conversely, electron-withdrawing substituents in either moiety of the imine preclude the reaction.

Electron-releasing substituents in the aniline moiety, are only effective provided their influence is not countermanded by electron-withdrawing substituents in the benzal moiety (contrast **7***d* with **7***k* and *l*).

Dimethyl fumarate reacted readily with **2** and benzal aniline to form the pyrrolidine **8***a* which consisted of one stereoisomer only. The assignments of the chemical shifts and coupling con-

Can. J. Chem. Downloaded from www.nrcresearchpress.com by 210.87.254.40 on 09/05/12
For personal use only.

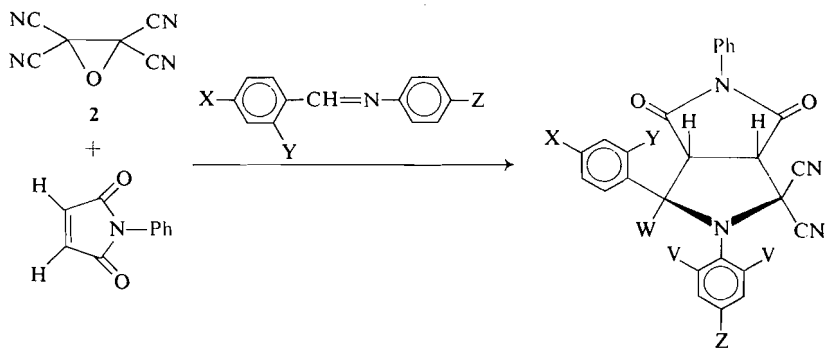

Adducts formed		No adduct formed	
7a	X = H; Y = H; Z = H; W = H	*g*	X = NO_2; Y = H; Z = H
b	X = H; Y = H; Z = H; W = D	*h*	X = H; Y = H; Z = NO_2
c	X = OCH_3; Y = H; Z = H; W = H	*i*	X = Cl; Y = H; Z = H
d	X = H; Y = H; Z = OCH_3; W = H	*j*	X = Cl; Y = Cl; Z = H
e	X = H; Y = H; Z = Cl; W = H	*k*	X = Cl; Y = Cl; Z = OCH_3
f	X = H; Y = H; Z = Br; W = H	*l*	X = Cl; Y = H; Z = OCH_3
	(V = D for **7***b* only, otherwise = H)		

SCHEME 2

stants were made by comparison with the n.m.r. spectrum of the deuterated analog **8***b*, prepared using benzal-*d*-2,4,6-trideuteroaniline, which demonstrated values for the coupling constants of $J_{2,3} = 9$ and $J_{3,4} = 11.5$ Hz. The flexibility of the five-membered pyrrolidine ring precludes rigorous assignment of the relative configuration of the 2- and 3-groups, in the absence of the stereoisomer for comparison.

Dimethyl maleate proved insufficiently reactive under these conditions to form the isomeric pyrrolidine. While the lower reactivity of dimethyl maleate than dimethyl fumarate in 1,3-dipolar additions is well documented (15) the former reacts readily and retains its configuration during the addition to 3-benzoyl-1-cyclohexyl-2-(2′-thienyl)aziridine (16). The failure of dimethyl maleate to react with **4** in the present reaction may indicate the enhanced stability afforded the latter by two nitrile groups and hence the lower reactivity of **4**.

trans-Dibenzoylethylene reacted readily with tetracyanoethylene oxide in the presence of benzal aniline to give a single pyrrolidine **9**. The methine protons exhibited a strongly coupled ABC spectrum in the n.m.r. from which an $H_{2,3}$ coupling of 10 Hz could be estimated. This was confirmed when, upon standing in chloroform for 1 week at room temperature, **9** underwent spontaneous *trans*-4,5 elimination of hydrogen cyanide to give the 2-pyrroline **10** quantitatively. The latter exhibited a clean AB quartet $J_{2,3} =$ 10 Hz for the methine proton n.m.r. signals.

Reaction of *N*-phenylmaleimide and maleimide, respectively, with tetracyanoethylene oxide in the presence of benzal aniline gave pyrrolidines **7***a* and **11***a*. Each exhibited an AMX spectrum for the methine protons. All the

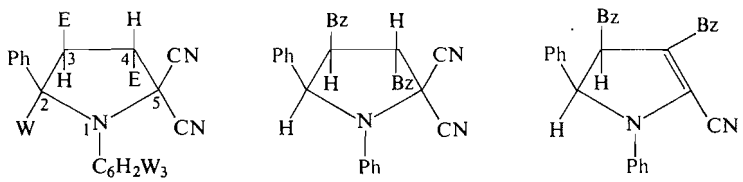

8

a E = CO_2CH_3; W = H
b E = CO_2CH_3; W = D

9 Bz = COPh

10

Can. J. Chem. Downloaded from www.nrcresearchpress.com by 210.87.254.40 on 09/05/12
For personal use only.

Can. J. Chem. Downloaded from www.nrcresearchpress.com by 210.87.254.40 on 09/05/12
For personal use only.

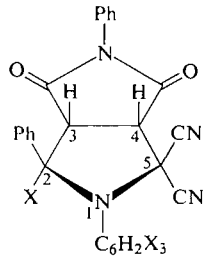

7
a X = H
b X = D

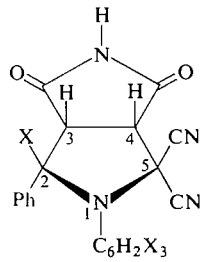

11
a X = H
b X = D

chemical shifts and coupling constants were obtained, as before, by comparison with the 2-deuterated analogs giving values of $J_{2,3} = 6$ and $J_{3,4} = 10$ Hz for **7***a* and $J_{2,3} = 9.2$ and $J_{3,4} = 8$ Hz for **11***a*. Comparison of the relative magnitudes of $J_{2,3}$ vicinal coupling constants in such structurally similar compounds as **7***a* and **11***a* seems reasonable. Therefore it appears that **7***a* and **11***a* have opposite configurations of the phenyl groups at the 2-positions.

Heteromultiple bonds in dipolarophiles react readily with **4**. Thus dimethyl azodicarboxylate affords the triazolidine **12***a* in 28% yield. Similarly diethyl azodicarboxylate gives **12***b* in 40% yield.

The highly polarized carbonyl bond in chloral reacts readily with tetracyanoethylene oxide and substituted benzalanilines in a regiospecific manner to give the oxazolidines **13***a–c*. The orientation of addition is evident from the n.m.r. spectra of **13** which show clean singlets for the methine protons. Cycloaddition of polarized carbonyl compounds to azomethine ylides with the above regiospecificity to give oxazolidines is well documented (6, 12, 17).

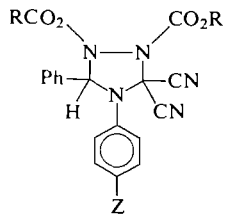

12
a R = CH_3; Z = H
b R = CH_2CH_3; Z = H
c R = CH_3; Z = OCH_3

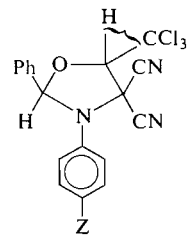

13
a Z = H
b Z = OCH_3
c Z = Cl

The highly polarized and dipolarophilic carbonyl group of diphenylcyclopropenone (8) might have been expected to behave similarly to that of chloral. However, a rapid prior competing reaction between the tetracyanoethylene oxide and the cyclopropenone ensued giving **14** or **15**. The product shows strong nitrile and carbonyl absorption in the i.r. spectrum which is not sufficiently characteristic to distinguish **14** and **15**. Chemical precedents (*e.g.* the reaction of tetracyanoethylene oxide with benzaldehyde to form **16** (14)) and mechanistic considerations however, favor structure **14**.

In contrast diphenylcyclopropenethione **17** reacted readily with tetracyanoethylene oxide to form the known 1,2-diphenyl-3-dicyanomethylenecyclopropene **18** in good yield. By analogy with the reported reaction of thiobenzophenone with tetracyanoethylene oxide (14) this plausibly proceeds as follows (see Scheme 3). The yield of **18** obtained here (67%) is superior to that obtained in previously reported syntheses of **18**, 19.5 (18), 23 (19), and 4.8% (20) and now represents the method of choice.

The present study supports the findings of Linn and Ciganek and extends them by showing that nucleophilic opening of tetracyanoethylene oxide by a variety of substituted Schiff bases provides a convenient route to tetrasubstituted azomethine ylides, and thus widens the scope of azomethine ylides presently available.

Experimental

Melting points were determined on a Fisher–Johns apparatus and are uncorrected. The i.r. spectra were recorded on a Perkin–Elmer model 421 spectrophotometer, and only the principal, sharply defined peaks are reported. The n.m.r. spectra were recorded on Varian A-60 and A-100

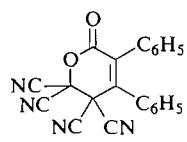

14

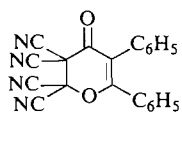

15

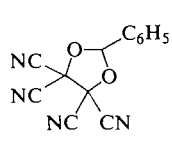

16

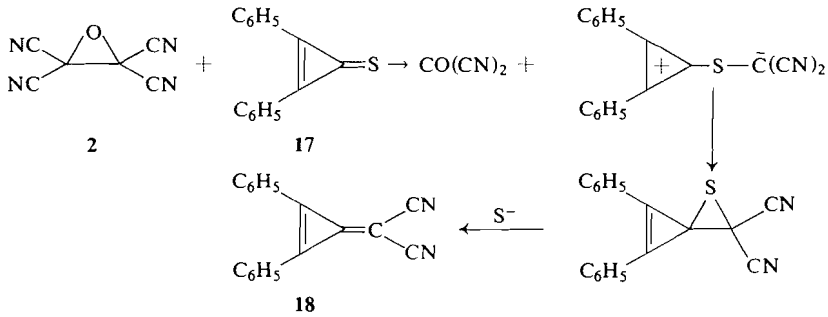

SCHEME 3

analytical spectrometers. The spectra were measured on approximately 10–15% (w/v) solutions in $CDCl_3$, with tetramethylsilane as a standard. Line positions are reported in p.p.m. from the reference. Mass spectra were determined on an Associated Electrical Industries MS-9 double focusing high resolution mass spectrometer. The ionization energy, in general, was 70 eV. Peak measurements were made by comparison with perfluorotributylamine at a resolving power of 15 000. Kieselgel DF-5 (Camag, Switzerland) and Eastman Kodak precoated sheets were used for t.l.c. Microanalyses were carried out by Dr. C. Daesslé, Organic Microanalysis Ltd., Montreal, Quebec and by Mrs. D. Mahlow of this Department.

Preparation of Starting Materials

Tetracyanoethylenoxide was prepared according to the method of Linn *et al.* (21).

The Schiff bases required in this study were readily obtained by the condensation of an aromatic aldehyde with an equimolar quantity of the substituted aniline by heating briefly on the steam bath and were purified by recrystallization from 95% ethanol.

Generation of Tetrasubstituted Azomethine Ylides and 1,3-Dipolar Cycloadditions

The general reaction conditions and purification procedures are exemplified by the following three examples. Thereafter the analytical and spectral data on adducts prepared by similar procedures are summarized in Tables 1 and 2.

(a) Reaction of Tetracyanoethylene Oxide and Benzylidene Aniline in the Presence of N-Phenylmaleimide

To a refluxing solution of 3.2 g (22 mmol) of tetracyanoethylene oxide and 7.6 g (44 mmol) of *N*-phenylmaleimide in 50 ml of dry benzene under nitrogen, there was added dropwise a solution of 4.0 g (22 mmol) of *N*-benzylidene aniline in 50 ml of dry benzene. After completed addition some solvent was distilled out (*ca.* 50 ml) under a continuous stream of nitrogen. A further 50 ml of benzene was added and the distillation under nitrogen was continued until the volume of the solution was *ca.* 50 ml. Cooling of this solution resulted in the precipitation of 0.83 g of excess *N*-phenylmaleimide. The filtrate was made up to 100 ml with benzene and 40 ml of this solution was subjected to chromatography on Florisil. Successive elution with 100 ml fractions of (*i*) hexane, (*ii*) hexane:benzene (9:1), (*iii*) hexane:benzene (4:1), (*iv*) hexane:benzene (3:2), (*vi*) benzene (200 ml) afforded one main fraction. Evaporation of the solvent gave a pale yellow solid, recrystallization of which from chloroform: 95% ethanol gave the pyrrolidine **7***a* as a colorless solid, 2.23 g (60% yield overall), m.p. 253–254°.

Anal. Calcd. for $C_{26}H_{18}N_4O_2$ (mol. wt. 418.1430): C, 74.64; H, 4.34; N, 13.39. Found (418.1426 (mass spectrum)): C, 74.39; H, 4.57; N, 13.13.

The n.m.r. spectrum δ_{TMS} ($CDCl_3$): 3.69 (q, 1H, $J_{2,3}$ = 6 Hz), $J_{3,4}$ = 10 Hz, H_3); 4.39 (d, 1H, $J_{3,4}$ = 10 Hz, H_4); 5.14 (d, 1H, $J_{2,3}$ = 6 Hz, H_2), 7.0–7.6 (m, 15H, aromatic protons). The i.r. spectrum ν (KBr disc) 1785, 1718 cm^{-1} (C=O).

(b) Reaction of Tetracyanoethylene Oxide and Benzylidene Aniline in the Presence of Dimethyl Fumarate

To a refluxing solution of 3.2 g (22 mmol) of tetracyanoethylene oxide and 6.5 g (44 mmol) of dimethyl fumarate in 50 ml of dry benzene under nitrogen was added dropwise (more slowly than in the case of *N*-phenylmaleimide) a solution of 40 g (22 mmol) of benzylidene aniline in 50 ml of dry benzene. Some of the benzene was distilled out (50 ml) and replaced as before. The reaction mixture when cooled deposited excess of dimethyl fumarate 0.88 g as a colorless solid. The filtrate was made up to 100 ml with benzene and 40 ml of the solution was subjected to chromatography on Florisil. Successive elution with 100 ml portions of hexane, hexane:benzene (9:1), hexane:benzene (4:1), hexane:benzene (3:2) then benzene and evaporation of the solvent gave as the main product a solid consisting of a mixture of adduct **8***a* and unreacted dimethyl fumarate. Two recrystallizations of the solid from chloroform: 95% ethanol afforded pure **8***a*, 1.06 (32% yield overall), m.p. 111–113°.

Anal. Calcd. for $C_{22}H_{19}N_3O_4$ (mol. wt. 389.1376): C, 67.86; H, 4.92; N, 10.79. Found (389.1370 (mass spectrum)): C, 67.98; H, 4.97; N, 10.44.

The n.m.r. spectrum δ_{TMS} ($CDCl_3$): 3.57 (q. 1H, $J_{2,3}$ = 9, $J_{3,4}$ = 11.5 Hz, H_3); 4.38 (d, 1H, $J_{3,4}$ = 11.5 Hz, H_4); 5.10 (d, 1H, $J_{2,3}$ = 9 Hz, H_2), 6.7–7.5 (m, 15H, aromatic protons). The i.r. spectrum ν ($CHCl_3$) 1750 cm^{-1} (C=O).

(c) Reaction of Tetracyanoethylene Oxide with Benzal-p-chloroaniline in the Presence of Chloral

To a refluxing solution of 1.7 g (12 mmol) of tetracyanoethylene oxide and 5 ml of chloral in 25 ml of dry benzene there was added dropwise under nitrogen a solution of 5.18 g (22 mmol) of benzal-*p*-chloroaniline in 25 ml of

Can. J. Chem. Downloaded from www.nrcresearchpress.com by 210.87.254.40 on 09/05/12
For personal use only.

Can. J. Chem. Downloaded from www.nrcresearchpress.com by 210.87.254.40 on 09/05/12
For personal use only.

TABLE 1. Adducts obtained from tetrasubstituted azomethine ylides generated from TCNEO

Adduct number	Dipolarophile	X*	Z*	Yield† (%)	Melting point (°C)‡	Found C	Found H	Found N	Found Molecular ion (mass spectrum)	Calcd. C	Calcd. H	Calcd. N	Calcd. Molecular ion (mass spectrum)
7*a*	*N*-Phenylmaleimide	H	H	51	253–254	74.39	4.57	13.13	418.1426	74.64	4.34	13.39	418.1430
7*b*									422.1748				422.1742
8*a*	Dimethylfumarate	H	H	29	111–113	67.98	4.97	10.44	389.1370	67.86	4.92	10.79	389.1376
8*b*									393.1680				393.1688
9	*t*-Dibenzoylethylene	H	H	50	215–217	79.93	4.82	8.55	481.1784	79.82	4.81	8.73	481.1790
11*a*	Maleimide	H	H	13	253–257	—	—	16.42	342.1117	—	—	16.36	342.1111
12*a*	Dimethyl azodicarboxylate	H	H	28	148–149	61.18	4.45	17.69	391.1276	61.37	4.38	17.90	391.1281
12*b*	Diethyl azodicarboxylate	H	H	40	140–142	63.12	5.15	16.57	419.1590	63.00	5.05	16.70	419.1594
13	Chloral	H	H	34	140–142	57.04	3.35	11.15 (Cl:25.50)	391.0044	57.39	3.21	10.40 (Cl:28.24)	391.0047
7*d*	*N*-Phenylmaleimide	H	OCH_3	37	223–225	72.56	5.04	12.54	448.1530	72.30	4.50	12.50	448.1535
7*e*	*N*-Phenylmaleimide	H	Cl	33	187–189	68.86	4.33	12.25 (Cl:8.07)	452.1035	68.95	3.78	12.37 (Cl:7.83)	452.1041
7*c*	*N*-Phenylmaleimide	OCH_3	H	33	208–210	72.15	4.55	12.32	448.1506	72.30	4.50	12.50	448.1535
7*f*	*N*-Phenylmaleimide	H	Br	13	188–190	62.93	3.77	11.06 (Br:16.37)	496.0525	62.76	3.45	11.25 (Br:16.06)	496.0535
13*b*	Chloral	H	OCH_3	18		§—			421.071				421.0153
13*c*	Chloral	H	Cl	29	140–142	51.80	2.91	10.42 (Cl:32.21)	424.9682	52.58	2.70	10.22 (Cl:34.50)	424.9658
12*c*	Dimethyl azodicarboxylate	H	OCH_3	26	oil				421.1738				421.1786

*Refer to Scheme 2.
†Yield not optimized.
‡The m.p.'s depend on rate of heating.
§Too hygroscopic for satisfactory microanalysis.

Can. J. Chem. Downloaded from www.nrcresearchpress.com by 210.87.254.40 on 09/05/12
For personal use only.

TABLE 2. The n.m.r. spectroscopic data on adducts§

Adduct number	Dipolarophile	X*	Z*	n.m.r. δ_{TMS} ($CDCl_3$) Aromatic-H	H_2†	H_4	H_3	Methyl-H
7*a*	*N*-Phenylmaleimide	H	H	7.0–7.6 (15H)m	5.14 (1H)d $J_{2,3}$ = 6 Hz	4.39 (1H)d $J_{3,4}$ = 10 Hz	3.69 (1H)q $J_{2,3}$ = 6 Hz $J_{3,4}$ = 10 Hz	
7*b*	(from D-anil >98% *d*)	H	H	7.0–7.6 (15H)m	(0.0H)	4.39 (1H)d $J_{3,4}$ = 10 Hz	3.69 (1H)d	
8*a*	Dimethylfumarate†‡	H	H	6.7–7.5 (15H)m	5.10 (1H)d $J_{2,3}$ = 9 Hz	4.38 (1H)d $J_{3,4}$ = 11.5 Hz	3.57 (1H)q $J_{2,3}$ = 9 Hz, $J_{3,4}$ = 11.5 Hz	3.90 (3H)s, 3.68 (3H)s
8*b*	(from D-anil *ca.* 50% *d*)	H	H	6.7–7.5 (15H)m	5.10 (0.5H)	4.38 (1H)d	3.57 (1H)d	3.90 (3H)s, 3.68 (3H)s
11*a*	Maleimide†‡	H	H	6.8–8.0 (10H)m	5.35 (1H)d $J_{2,3}$ = 9.2 Hz	(11.84 (1H)s D_2O exchangeable (NH)) 4.48 (1H)d $J_{3,4}$ = 8 Hz	3.89 (1H)q $J_{2,3}$ = 9.2 Hz, $J_{3,4}$ = 8 Hz	
12*a*	Dimethylazodicarboxylate	H	H	6.9–7.7 (10H)m	6.83 (1H)s			3.94 (3H)s, 3.86 (3H)s
12*b*	Diethylazodicarboxylate	H	H	6.9–7.7 (10H)m	6.86 (1H)s		4.36 (2H)q‖ 4.32 (2H)q‖	1.34 (3H)t 1.28 (3H)t
13	Chloral	H	H	6.6–7.7 (10H)m	6.48 (1H)s	5.35 (1H)s		
7*d*	*N*-Phenylmaleimide	H	OCH_3	6.6–7.8 (14H)m	4.93 (1H)d $J_{2,3}$ = 6 Hz	4.23 (1H)d $J_{3,4}$ = 10 Hz	3.50 (1H)q $J_{2,3}$ = 6 Hz, $J_{3,4}$ = 10 Hz	3.58 (3H)s
7*e*	*N*-Phenylmaleimide	H	Cl	7.1–7.8 (14H)m	5.03 (1H)d $J_{2,3}$ = 6.0 Hz	4.30 (1H)d $J_{3,4}$ = 10 Hz	3.59 (1H)q $J_{2,3}$ = 6.0 Hz, $J_{3,4}$ = 10 Hz	
7*c*	*N*-Phenylmaleimide	OCH_3	H	6.6–7.8 (14H)m	4.95 (1H)d $J_{2,3}$ = 6 Hz	4.26 (1H)d $J_{3,4}$ = 10 Hz	3.53 (1H)q $J_{2,3}$ = 6 Hz, $J_{3,4}$ = 10 Hz	3.59 (3H)s
7*f*	*N*-Phenylmaleimide	H	Br	7.0–7.8 (14H)m	5.04 (1H)d $J_{2,3}$ = 6 Hz	4.28 (1H)d $J_{3,4}$ = 10 Hz	3.60 (1H)q $J_{2,3}$ = 6 Hz $J_{3,4}$ = 10 Hz	
13*c*	Chloral	H	Cl	7.0–7.7 (9H)	6.48 (1H)s	5.40 (1H)s	—	—
12*c*	Dimethyl azodicarboxylate	H	OCH_3	6.8–7.8 (9H)	6.68 (1H)s	—	—	3.96 (3H)s 3.80 (3H)s 3.91 (3H)s

*Refer to Scheme 2.
†Refer to formulas **12** and **13**.
‡$(CD_3)_2SO$ as solvent.
§The adducts exhibited i.r. spectra consistent with the proposed structures.
‖Methylene protons of CH_3CH_2 groups.

Can. J. Chem. Downloaded from www.nrcresearchpress.com by 210.87.254.40 on 09/05/12
For personal use only.

dry benzene. After the addition was completed the reaction mixture assumed a dark red color and a continuous stream of nitrogen was passed through the solution to remove some of the benzene. When the volume of the mixture was about 20 ml, a further 25 ml of dry benzene was added, and distillation continued to a total volume of reaction mixture of about 20 ml. After cooling the solution excess of solvent and unreacted chloral was removed under reduced pressure. Benzene (20 ml) was added and a grey precipitate collected 0.45 g which proved to be a mixture of unreacted tetracyanoethylene oxide and benzal *p*-chloroaniline. The filtrate was chromatographed on Florisil with elution by benzene which gave one main yellow fraction. Evaporation of the solvent gave a yellow oil, trituration of which with cold 95% ethanol afforded the adduct **13***c* as a yellow solid, 1.50 g (29% yield), m.p. 140–142°.

Anal. Calcd. for $C_{18}H_{11}Cl_4ON_3$ (mol. wt. 424.9658): C, 52.58; H, 2.70; N, 10.22; Cl, 34.50. Found (424.9682): C, 51.80; H, 2.91; N, 10.42; Cl, 32.21.

The n.m.r. spectrum: 5.35 (s, 1H, H_5), 6.48 (s, 1H, H_2), 6.6–7.7 (m, 10H, aromatic protons).

Preparation of 2-Cyano-3,4-dibenzoyl-1,5-diphenyl-2-pyrroline

A dilute chloroform solution of adduct **9** was set aside at room temperature for 1 week during which time the progress of the elimination of hydrogen cyanide was monitored by the n.m.r. spectrum. At the end of this period the original methine ABC spectrum of **9** had been replaced by a clean AB quartet $J_{4,5} = 10$ Hz of **10**. Evaporation of the solvent gave a white solid of **10**, 2-cyano-3,4-dibenzoyl-1,5-diphenyl-2-pyrroline in quantitative yield, m.p. 124–126°.

Anal. Calcd. for $C_{30}H_{22}N_2O_2$ (mol. wt. 454.1672): N, 6.50. Found (454.1681 (mass spectrum)): N, 6.87.

The n.m.r. spectrum δ_{TMS} ($CDCl_3$): 5.38, 5.62 (ABq, 2H, $J = 10$ Hz, methine protons); 6.88–8.18 (m, 20H, aromatic protons). The i.r. spectrum ν ($CHCl_3$): 1670, 1731 cm^{-1} (C—O).

Preparation of Benzal-[^2H]-2,4,6-[^2H]$_3$-aniline

(i) 2,4,6-N,N-Pentadeuteroaniline

A mixture of 13 g (0.1 mol) of aniline hydrochloride and 20 ml of deuterium oxide (Merck, Sharp and Dohme, Montreal, Canada, 99.7%) was sealed in a pressure bottle and heated on the steam bath for 24 h. After removal of excess of deuterium oxide *in vacuo* the residue was treated with a further 20 ml of fresh deuterium oxide and the sealed mixture heated for a further 24 h. This procedure was repeated four times. The pentadeuteroaniline deuterochloride was neutralized in deuterium oxide with anhydrous potassium carbonate, extracted with anhydrous ether, and the extract dried ($CaSO_4$). After removal of the solvent, distillation under reduced pressure afforded aniline-d_5, 9.0 g (93% yield).

Mass spectrum: parent peak at 98. $C_6H_2D_5N$ requires 98. The n.m.r. spectrum confirmed complete replacement of the amine protons.

(*ii*) A mixture of 1 g (10 mmol) of benz [^{2}H]aldehyde (99.5% deuteration, Merck, Sharp and Dohme, Montreal, Canada) was heated on a steam bath for a few minutes. The resulting solid was recrystallized from 95% ethanol affording benzal-[^{2}H]-2,4,6-[^{2}H]$_3$-aniline, 1.8 g (90% yield), m.p. 51–52°.

The n.m.r. spectrum confirmed virtually complete isotopic replacement of the benzal proton (>98% incorporation).

Reaction of Tetracyanoethylene Oxide and Benzal-[^2H]-2,4,6-[^2H]$_3$-aniline in the Presence of N-Phenylmaleimide

To a boiling solution of 0.72 g (5 mmol) of tetracyanoethylene oxide and 1.73 g (10 mmol) of *N*-phenylmaleimide in 13 ml of dry benzene under nitrogen there was added dropwise a solution of 0.91 g (5 mmol) of benzal-[^{2}H]-2,4,6-[^{2}H]$_3$-aniline in 13 ml of dry benzene. After the addition was completed some of the benzene was distilled out in a stream of nitrogen. When the volume of the reaction mixture was about 15 ml, a further 20 ml of dry benzene was added and distillation was continued to a final volume of about 15 ml. The resulting dark green solution was subjected to chromatography on Florisil. Elution with benzene gave one band, evaporation of which gave a yellow oil which upon trituration with cold 95% ethanol gave a pale yellow solid of **7***b*. The product was purified by recrystallization from chloroform–95% ethanol as a colorless solid, 0.85 g (40% yield), m.p. 252–254°.

The n.m.r. spectrum confirmed the complete disappearance (±2%) of the H_2 signal while the H_3 resonance became a doublet $J_{3,4} = 10$ Hz.

Reaction of Diphenylcyclopropenone with Tetracyanoethylene Oxide

Initially the reaction was carried out as described previously in the presence of benzal aniline. However, the only isolable product was a 1:1 adduct between tetracyanoethylene oxide and diphenylcyclopropenone (22) in 59% yield. This was confirmed by an independent reaction carried out in the absence of benzal aniline. A mixture of 0.90 g (6 mmol) of tetracyanoethylene oxide and 1.24 g (6 mmol) of diphenylcyclopropenone in 25 ml of dry benzene was heated under reflux for 2 h. When cooled a colorless solid deposited, 1.53 g (71% yield), m.p. 165° **14**.

Anal. Calcd. for $C_{20}H_{10}N_4O_2$ (mol. wt. 350.0804): C, 71.99; H, 2.88; N, 16.00. Found (350.0800): C, 72.21; H, 2.76; N, 15.87.

The n.m.r. spectrum δ_{TMS} ($CDCl_3$) 7.1–8.1 (m, aromatic protons). The i.r. spectrum ν ($CHCl_3$): 1787, 1843 (C=O), 2250 cm^{-1} (C=N).

Reaction of Diphenylcyclopropenethione with Tetracyanoethylene Oxide

To a stirred solution of 1.11 g (5 mmol) of diphenylcyclopropenethione (23, 24) in 25 ml of dry benzene, there was added 0.72 g (5 mmol) of tetracyanoethylene oxide in portions. Stirring was continued for about 4 h. A pale grey solid which had precipitated was collected, 0.48 g. The filtrate on setting aside at room temperature for 3 days deposited a further 0.37 g of the product, representing a total yield of 0.87 g (67% yield) of 1,2-diphenyl-3-dicyanomethylenecyclopropene m.p. 295–298° (from tetrahydrofuran) (lit. m.p. 299° (18)).

The i.r. spectrum of this material was superimposable with an authentic sample.

This research was supported by a National Research Council of Canada grant to J. W. Lown and by the University of Alberta. We thank Mr. R. Swindlehurst and Dr. A. Hogg for the n.m.r. and mass spectra.

1. R. HUISGEN, W. SCHEER, and M. HUBER. J. Am. Chem. Soc. **89**, 1753 (1967).
2. J. W. LOWN. Rec. Chem. Prog. **32**[2], 51 (1971).
3. A. PADWA and L. HAMILTON. Tetrahedron Lett. 4363 (1965).
4. J. W. LOWN, G. DALLAS, and T. W. MALONEY. Can. J. Chem. **47**, 3557 (1969).
5. J. W. LOWN, J. P. MOSER, and R. WESTWOOD. Can. J. Chem. **47**, 4335 (1969).
6. G. DALLAS, J. W. LOWN, and J. P. MOSER. J. Chem. Soc. C, 2383 (1970).
7. P. B. WOLLER and N. H. CROMWELL. J. Org. Chem. **35**, 889 (1970).
8. J. W. LOWN, T. W. MALONEY, and G. DALLAS. Can. J. Chem. **48**, 584 (1970).
9. H. W. HEINE and R. PEAVY. Tetrahedron Lett. 3123 (1965).
10. F. TEXIER, J. JAZ, and R. CARRIE. Compt. Rend. Acad. Sci. (Paris), C**269**, 646 (1969).
11. F. TEXIER and R. CARRIE. Compt. Rend. Acad. Sci. (Paris) C**268**, 1396 (1969).
12. F. TEXIER and R. CARRIE. Compt. Rend. Acad. Sci. C**269**, 709 (1969).
13. J. A. DEYRUP. J. Org. Chem. **34**, 2724 (1969).
14. W. J. LINN and E. CIGANEK. J. Org. Chem. **34**, 2146 (1969).
15. R. HUISGEN. Angew. Chem. Int. Ed. **2**, 640 (1963).
16. J. W. LOWN and K. MATSUMOTO. Can. J. Chem. **48**, 2215 (1970).
17. J. W. LOWN and K. MATSUMOTO. Can. J. Chem. **48**, 3399 (1970).
18. S. ANDREADES. J. Am. Chem. Soc. **87**, 3941 (1965).
19. Y. KITAHARA and M. FUNAMIZU. Bull. Chem. Soc. Jap. **37**, 1897 (1964).
20. E. D. BERGMAN and I. AGRANAT. J. Am. Chem. Soc. **86**, 3587 (1964).
21. W. J. LINN, O. W. WEBSTER, and R. E. BENSON. J. Am. Chem. Soc. **87**, 3651 (1965).
22. R. BRESLOW, T. EICHER, A. KREBS, R. A. PETERSON, and J. POSNER. J. Am. Chem. Soc. **87**, 1320 (1965).
23. T. EICHER and G. FRENZEL. Z. Naturforsch, **20***b* (3), 274 (1965).
24. J. W. LOWN and T. W. MALONEY. J. Org. Chem. **35**, 1716 (1970).

Can. J. Chem. Downloaded from www.nrcresearchpress.com by 210.87.254.40 on 09/05/12
For personal use only.

Valence-shell Transitions in the Vacuum-Ultraviolet Spectra of Fluorobenzenes[1]

R. GILBERT, P. SAUVAGEAU, AND C. SANDORFY
Département de Chimie, Université de Montréal, Montréal, Québec

Received August 12, 1971

The vacuum–ultraviolet spectra of a nearly complete series of fluorinated benzene derivatives were measured. The assignments of $\pi^* \leftarrow \pi$ and $\sigma^* \leftarrow \sigma$ valence-shell type transitions are discussed as well as the influence that the fluorine substituents exert on these.

Les spectres dans le lointain ultraviolet de la série presque complète des dérivés fluorés du benzène sont présentés. On discute l'attribution des transitions du type $\pi^* \leftarrow \pi$ et $\sigma^* \leftarrow \sigma$ et l'influence du nombre et des positions des fluors sur ces transitions.

Canadian Journal of Chemistry, **50**, 543 (1972)

Can. J. Chem. Downloaded from www.nrcresearchpress.com by 210.87.254.42 on 09/05/12
For personal use only.

Introduction

The near-ultraviolet spectra of the fluoroderivatives of benzene are well known. The α-band ($^1B_{2u} \leftarrow {}^1A_{1g}$ in benzene) is in all cases similar to that of benzene. Sponer (1) correlated its shifting with the number of fluorine atoms and the geometry of the molecule, and a thorough theoretical study has been carried out by Petruska (2).

We shall not be concerned with this band. The p and β bands ($^1B_{1u} \leftarrow {}^1A_{1g}$ and $^1E_{1u} \leftarrow {}^1A_{1g}$, respectively, in benzene) have received less attention but Kimura and Nagakura (3) measured the spectra of fluorobenzene down to 1600 Å, and Hammond, Price, Teegan, and Walsh (4) down to 1350 Å. Petruska also considered these bands in his perturbation treatment (2).

Recently we published our new results on monofluorobenzene (5) for both the valence-shell and Rydberg transitions. In the present paper we communicate results concerning the $\pi^* \leftarrow \pi$ and (presumably) $\sigma^* \leftarrow \sigma$ transitions found in the 2100–1200 Å part of the u.v. spectrum for a nearly complete series of di-, tri-, tetra-, penta-, and hexafluorobenzenes in the vapor phase. In all these spectra we find numerous Rydberg transitions. These will be dealt with in subsequent publications. Here we shall discuss the assignment of the bands having valence-shell characteristics. These are expected to be the p and β bands, higher $\pi^* \leftarrow \pi$ transitions, and transitions of the bonding σ electrons at the high frequency end of the given spectral range.

The photoelectron spectra of several fluorobenzene derivatives are known (6–10). The lone pairs of the fluorine atoms have ionization potentials of 16–17 eV and their electronic transitions are expected to appear at wavelengths shorter than 1200 Å. The fluorine atoms should influence the spectrum mainly by their inductive effect which is expected to affect the σ orbitals much more than the π orbitals (6, 11–13).

The following abbreviations will be used: B, benzene; FB, fluorobenzene; (1,2), 1,2-difluorobenzene and so on.

Figures 1, 3, and 5 give the spectra of (1,2,4), (1,2,3,5), and (6) from 2100–1200 Å as typical examples. Figures 2, 4, and 6 give the 1600–1200 Å part of the same spectra with an extended scale for the extinction coefficients.

Experimental

The spectra were measured with a McPherson model 225 monochromator with a hydrogen discharge tube as the light source, a double beam attachment, and photoelectric recording. Instrumental details were given in previous publications from this laboratory (14, 15).

The samples were commercial products from the Pierce Chemical Co. They were purified by gas chromatography using a 20 ft column containing CHROMOSORB-W with 30% of KEL-F oil no. 3 as adsorbent. Mass spectrographic analysis yielded purities higher than 99.9%.

Vapor pressures in the absorption cell varied from 0.02–0.5 Torr.

Results and Discussion

Table 1 lists the p and β bands. No clear cor-

[1]The research for this paper was supported by the Defence Research Board of Canada; Grant No. 9530-63.

TABLE 1. Frequency at the band maximum and molecular extinction coefficient of the p and β bands of the fluorobenzenes

Compound	p band		β band		1350–1200 Å*
	ν_{max} (cm^{-1})	ε_{max}	ν_{max} (cm^{-1})	ε_{max}	
B	50125	6600	57066	59000	0.082
FB	50378	5200	55463	51600	0.071
(1,2)	50150	5700	54494	40000	
(1,3)	50251	4700	54501	39000	0.046
(1,4)	50352	5100	54967	39000	
(1,2,4)	50201	5600	53882	40000	
(1,3,5)	50075	5800	54273	44000	0.034
(1,2,3,4)	51921	6300	52266	52000	
(1,2,3,5)	49900 (52600)	4300	52930	47500	
(5)	51282	6400	51726	44000	0.030
(6)	51493	5200	51578	41000	0.020

*Approximate overall oscillator strength of the 1350–1200 Å region (integrated over the whole area).

relation is found between the number and location of the F atoms and the frequency of the broad p band except that in the tetra-, penta-, and hexafluorobenzenes, they are shifted to higher frequencies by about a thousand wavenumbers. In the case of the (1,2,3,5) derivative we find two bands in this part of the spectrum. We are not trying to interpret this since contamination by another tetrasubstituted isomer cannot be excluded. The oscillator strength of the p band is of the order of $f = 0.075$.

The β bands shift much more (1600–3200 cm^{-1}) and again the tetra-, penta-, and hexa compounds shift significantly more than the others (4000–5500 cm^{-1}). The oscillator strength is of the order of $f = 1.10$.

What other $\pi^* \leftarrow \pi$ transitions can we expect? As is well known, B and (6) have only one allowed transition, $^1E_{1u} \leftarrow {}^1A_{1g}$. In particular, all transitions originating from the a_{2u} level or arriving

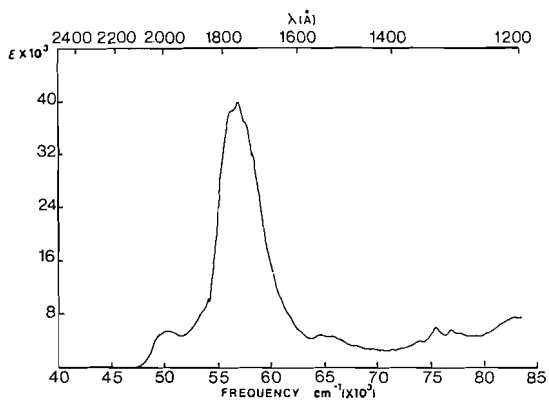

FIG. 1. The ultraviolet spectrum of (1,2,4) from 2100–1200 Å.

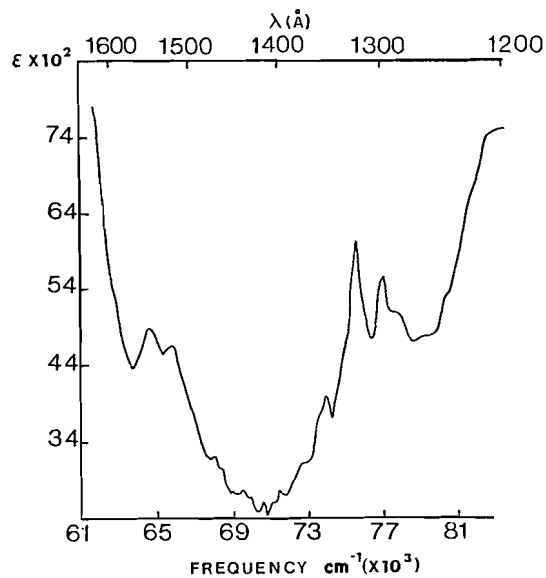

FIG. 2. The ultraviolet spectrum of (1,2,4) from 1600–1200 Å (magnified).

Can. J. Chem. Downloaded from www.nrcresearchpress.com by 210.87.254.42 on 09/05/12
For personal use only.

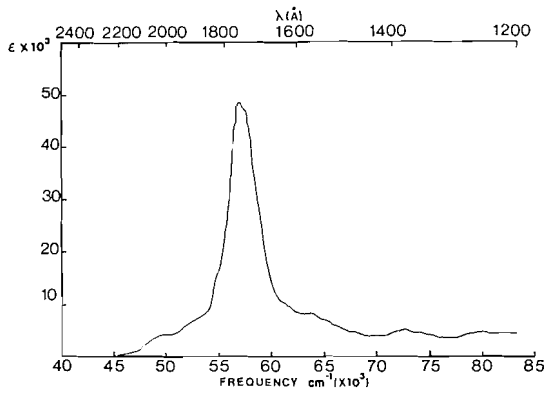

FIG. 3. The ultraviolet spectrum of (1,2,3,5) from 2100–1200 Å.

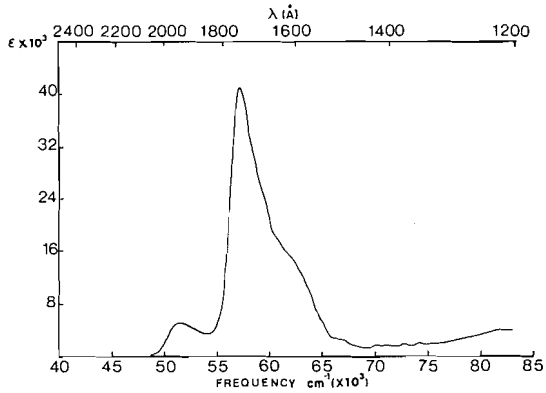

FIG. 5. The ultraviolet spectrum of (6) from 2100–1200 Å.

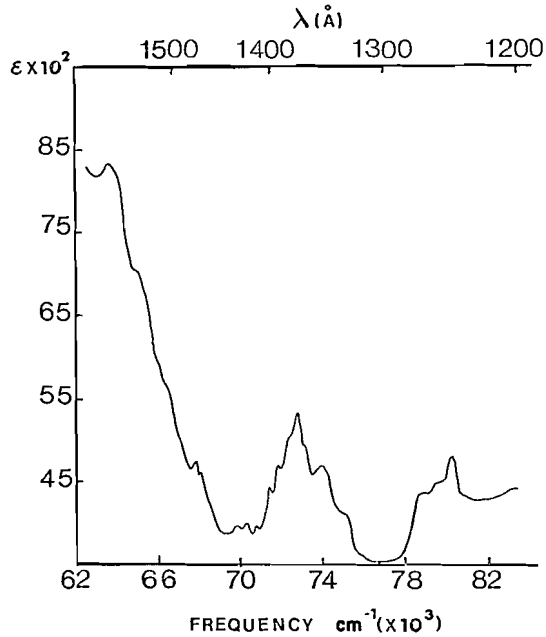

FIG. 4. The ultraviolet spectrum of (1,2,3,5) from 1600–1200 Å (magnified).

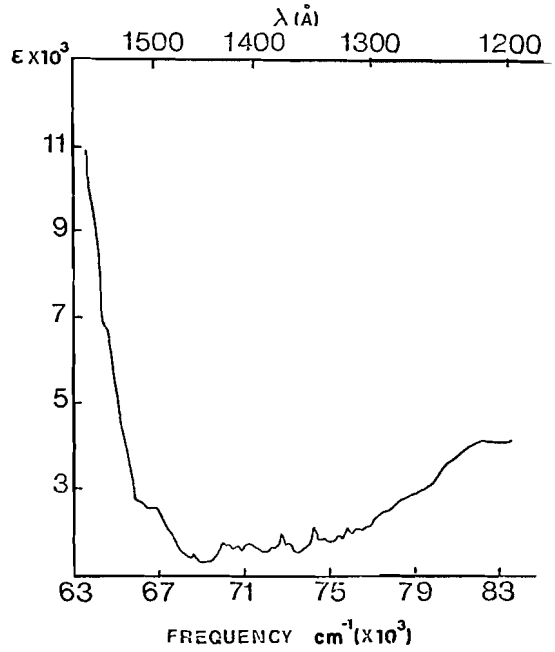

FIG. 6. The ultraviolet spectrum of (6) from 1600–1200 Å (magnified).

at the b_{2g} level are electronically forbidden. Under D_{3h} symmetry (1, 3, 5) only $^1E' \leftarrow {}^1A_1'$ is allowed but in this case there are three such transitions: one resulting from a transition between the two degenerate levels and two others corresponding to transitions between one non-degenerate a_2'' and one degenerate level (e''). The spectra of the D_{6h} and D_{3h} derivatives are not very different, however, and this is the first indication of the fact that in the case of fluorine substituted benzenes, the transitions between π levels are not profoundly affected by the substituents.

Under D_{2h}, C_{2v}, and C_s symmetries the β bands should be split and a number of other

Can. J. Chem. Downloaded from www.nrcresearchpress.com by 210.87.254.42 on 09/05/12
For personal use only.

Can. J. Chem. Downloaded from www.nrcresearchpress.com by 210.87.254.42 on 09/05/12
For personal use only.

transitions should become possible. If we compare the spectra, however, we find that they are all of the same general type. The β band is by far the most intense in all of them. In all the spectra we find a broad band at the high frequency side having about the same intensity as the p band (between 65000 and 63000 cm^{-1}; the sharp bands superimposed on it are Rydberg bands). Ironically it is strongest in (6) which has D_{6h} symmetry. In benzene this could correspond to one of the forbidden $^1E_{2g} \leftarrow {}^1A_{1g}$ transitions. The fact that its intensity is about the same in all our molecules, regardless of their symmetry, seems to show that this band does not result from the splitting of the β band. Vibronic coupling with the allowed β band is probably a more important factor in providing intensity to the other bands; the lowering of the symmetry of benzene by fluorine substitution being of secondary importance.

It is surprising that no clear indication is found for the splitting of the β band. According to available photoelectron ionization potential data (6), (7) the splitting between π_2 and π_3 amounts to 0.2–0.6 eV for the different derivatives.

One more $\pi^* \leftarrow \pi$ transition remains to be located, the one corresponding to $b_{2g} \leftarrow a_{2u}$ in benzene. It is impossible to do it, however, with any degree of certainty, although some weak and broad features are observed in some of the spectra around 1500 Å.

There are two other areas of broad absorption, one between 1400 and 1300 Å and another between 1300 and 1200 Å which are, in most cases, overlapped by Rydberg bands. These could possibly be $\sigma^* \leftarrow \sigma$.

There has been some controversy relating to the highest σ levels in benzene (13, 16, 17). One of these should lie between (π_2,π_3) and π_1 or slightly below π_1. Large deviations from Koopmans' theorem are likely to occur (18). This makes any attempt of ordering the orbitals on the basis of photoelectron spectra difficult. Even less is known about the σ^* levels. We know, however, that in ethane the first band due to σ electrons is located between 1400 and 1300 Å (15). In ethylene there is no evidence for σ transitions down to 1200 Å (18).

In benzene it is expected to appear again at somewhat longer wavelengths, quite possibly in the 1300–1200 Å region, where we observe broad bands. Now, we know that in paraffins, fluorine substitution stabilizes the σ levels and shifts the $\sigma^* \leftarrow \sigma$ bands to higher frequencies, while decreasing their intensity (19). The data of Table 1 (last column) are significant in this respect. They show that the intensity in the 1300–1200 Å region decreases by a large factor for the highly substituted derivatives. This we take as an indication that most of the intensity in that part of the spectrum comes from $\sigma^* \leftarrow \sigma$ transitions. Usually two weaker bands remain, one closer to 1300 Å, the other to 1200 Å. These might be due to Rydberg transitions which could be first members of series converging toward the higher π ionization potential.

$\pi \leftrightarrow \sigma$ transitions are possible, but are expected to be very weak. They are likely to contribute to background absorption.

Conclusion

In conclusion we should like to point out that the number of fluorine substituents appears to be more important in determining the characteristics of these spectra than their location, or the symmetry of the corresponding molecules. Their influence on the $\pi^* \leftarrow \pi$ transitions is moderate, but it is stronger on the σ transitions which appear at wavelengths shorter than 1400 Å.

1. H. Sponer. J. Chem. Phys. **22**, 234 (1954).
2. J. Petruska. J. Chem. Phys. **34**, 1111, 1120 (1961).
3. K. Kimura and S. Nagakura. Mol. Phys. **9**, 117 (1965).
4. V. J. Hammond, W. C. Price, J. P. Teegan, and A. D. Walsh. Discuss. Faraday Soc. **9**, 53 (1950).
5. R. Gilbert and C. Sandorfy. Chem. Phys. Lett. **9**, 121 (1971).
6. I. D. Clark and D. C. Frost. J. Am. Chem. Soc. **89**, 244 (1967).
7. B. Narayan and J. N. Murrell. Mol. Phys. **19**, 169 (1970).
8. D. W. Turner, C. Baker, A. O. Baker, and C. R. Brundle. Molecular photoelectron spectroscopy. Wiley–Interscience, London and New York. (1970).
9. D. W. Davies. Chem. Phys. Lett. **2**, 173 (1968).
10. L. Burnelle and M. J. Kranepool. J. Mol. Struct. **2**, 331 (1968).
11. D. W. Turner. Tetrahedron Lett. 3419 (1967).
12. G. Bélanger and C. Sandorfy. Chem. Phys. Lett. **3**, 661 (1969).
13. C. R. Brundle, M. B. Robin, and N. A. Kuebler. In press.

14. B. A. LOMBOS and P. SAUVAGEAU. Can. Spectrosc. **13**, 46 (1962).
15. B. A. LOMBOS, P. SAUVAGEAU, and C. SANDORFY. J. Mol. Spectrosc. **24**, 253 (1967).
16. A. D. BAKER, C. R. BRUNDLE, and D. W. TURNER. Int. J. Mass Spectrosc. Ion Phys. **1**, 443 (1968).
17. A. D. BAKER and D. W. TURNER. Philos. Trans. Roy. Soc. Lond. A, **268**, 131 (1970).
18. A. J. MERER and R. S. MULLIKEN. Chem. Rev. **69**, 639 (1969).
19. G. BÉLANGER, P. SAUVAGEAU, and C. SANDORFY. Chem. Phys. Lett. **3**, 649 (1969).

Can. J. Chem. Downloaded from www.nrcresearchpress.com by 210.87.254.42 on 09/05/12
For personal use only.

Dipole Moments and Conformation of Sultones, Thiosultones, and Sultines

O. EXNER

J. Heyrovský Institute of Polarography, Czechoslovak Academy of Sciences, Prague 1, Czechoslovakia

AND

DAVID N. HARPP AND JOHN G. GLEASON[1]

Department of Chemistry, McGill University, Montreal, Quebec

Received July 23, 1971

Dipole moments of five- and six-membered sultones and thiosultones have been used to establish the values of bond moments used in conformational studies of open-chain analogues. Hence, the gauche conformation of acyclic sulfonic esters has been confirmed and the same conformation deduced from published data for thiolsulfonate esters. The dipole moment of a five-membered sultine has been interpreted similarly, while in the case of the six-membered derivative, the axial sulfinyl conformation has been determined in agreement with n.m.r. data.

On a utilisé les moments dipolaires des sultones et thiosultones en cycles à cinq ou à six dans le but de déterminer les valeurs des moments des liens utilisés dans des études conformationnelles d'analogues à chaîne ouverte. On a ainsi confirmé la conformation gauche des esters sulfoniques acycliques et déduit la même conformation à partir des résultats publiés pour les esters thiolsulfonates. On a interprété le moment dipolaire d'une sultine dans un cycle à cinq de façon similaire, alors que dans le cas du cycle à six, on a déterminé la conformation du sulfinyl axial en accord avec les résultats de la r.m.n.

Canadian Journal of Chemistry, **50**, 548 (1972)

Introduction

In the course of our recent interest in the conformation of simple functional groups, we have measured dipole moments of acyclic sulfonates (1) and sulfinates (2) and attributed them the *a priori* unexpected gauche conformations **1** and **2**, respectively (Newman projection viewed along the O—S bond). As usual with this method, several assumptions had to be made concerning the values of bond moments since suitable model compounds of rigid cyclic structure were not available to us.

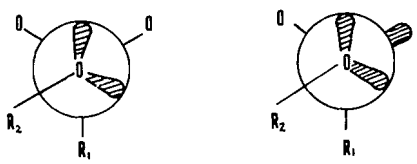

1 2

Recent syntheses furnished some missing members of this class of compounds (3) and enabled us to study dipole moments of the cyclic derivatives **3**–**8**. Slight deviations from planarity in the five-membered derivatives (**3**, **5**, **7**) will not seriously affect the resulting moments, thus these compounds can serve well to check the bond moments used previously (1, 2). In addi-

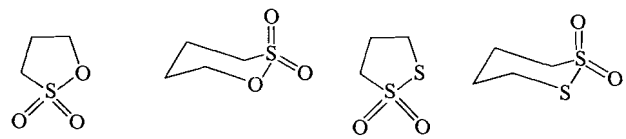

3 4 5 6

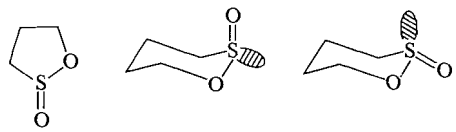

7 8*a* 8*b*

[1]NRCC Scholarship recipient, 1968–1970.

Can. J. Chem. Downloaded from www.nrcresearchpress.com by 210.87.254.40 on 09/05/12
For personal use only.

TABLE 1. Polarization data of sultones, thiosultones, and sultines **3–8** (Benzene, 25°)

No.	Compound	n_D^{20}	d^{20}	R_D^{20} (cm^3)	${}_{\infty}P_2$ (cm^3)	μ(5%)* (D)	μ(15%)* (D)
3	1,2-Oxathiolane 2,2-dioxide			25.2†	574.1	5.17	5.16
4	1,2-Oxathiane 2,2-dioxide	1.4625	1.3347	28.07	591.8	5.24	5.23
5	1,2-Dithiolane 1,1-dioxide			31.4†	568.3	5.11	5.10
6	1,2-Dithiane 1,1-dioxide			34.2†	563.3	5.08	5.06
7	1,2-Oxathiolane 2-oxide	1.4902	1.2236	25.19	336.6	3.89	3.88
8	1,2-Oxathiane 2-oxide	1.4808	1.2364	27.64	279.1	3.50	3.48

*Correction for the atomic polarization 5 or 15% of the R_D value, respectively.
†Estimated values, see Experimental.

tion, the conformation of thiolsulfonates may now be estimated on the basis of published dipole moment data (4). The six-membered sultone **4** and thiosultone **6** likely exist in one conformation only, while for sultine **8**, the axial (**8***a*) and equatorial (**8***b*) forms are theoretically possible. On the basis of experimental dipole moment measurements, results of a prior n.m.r. study (5) can now be compared.

Experimental

Materials

Compounds **3–8** were prepared as previously described (3, 5).

Measurements of Dipole Moments

The same technique was used as in previous work (1, 2), based on the method of Halverstadt and Kumler (6). Molar refractions (R_D) of liquid compounds **4**, **7**, and **8** were determined experimentally, the values at 20° being preferred enabling comparison with most reported values. The value found for **4** is only 0.2 cm^3 lower than the sum of Vogel's additive increments (7) while those of **7** and **8** show somewhat greater deviations; the former is 1.3 cm^3 higher and the latter 0.8 cm^3 lower than values computed with the increment (2) 10.02 cm^3 for the S(O)O group. This makes the estimation of R_D for the remaining compounds rather difficult. We took the same R_D for **3** as for **7**, relying on similar increments of the SO and SO_2 groups (2, 7), and calculated R_D values for **5** and **6** from those of **3** and **4**, respectively, by adding 6.16 cm^3 (*i.e.* the difference between increments (7) of bivalent S and O). The inaccuracy in the whole procedure does not markedly affect dipole moment values.

Experimental polarization, dipole moments, and refractions are collected in Table 1. The values of dipole moments with 5 and 15% correction are to be viewed as formerly, but in the particular case under consideration the differences are unimportant.

Calculation of Theoretical Dipole Moments

In the case of the five-membered rings, calculations were performed graphically with the accuracy of *ca.* 0.03 D. For six-membered rings, Dreiding models were used; the accuracy achieved is significantly lower.

Results and Discussion

The molecule 1,2-oxathiolane 2,2-dioxide (**3**) can exist in a planar form with common bond lengths and with angles of 114° on O, 100° on S, and 106, 108, and 112° on C_{1-3}, respectively. These angles agree reasonably with values measured in crystals of similar compounds (8, 9). The deviation from planarity cannot be of such an extent to markedly influence the calculated moments. With bond moments used in our previous papers (1, 2) (H—C_{a1}, 0.3; C—O, 0.74; C—S, 0.7; S—O, 0.2 D) and with the moment of the SO_2 group as a vector of 3.0 D bisecting the angle O—S—O, we obtain a moment of 4.70 D, distinctly lower than the experimental value. Using the higher value of 3.7 D for SO_2 (which was found necessary for chlorosulfonates (2)) the final result is somewhat high (5.38 D). (See Table 2 for a comparison of calculated and experimental values of μ.) The general applicability of five-membered heterocycles as true models for open-chain compounds has been questioned, since the computed results were usually too high (10). For this reason we considered that 3.2 D is a reasonable estimate of the SO_2 group moment in sulfonate esters, and will use it for subsequent calculations although it yields only 4.89 D for **3**.

For 1,2-oxathiane 2,2-dioxide (**4**), the calculated moment was 4.70 D, using the mentioned bond moments (3.2 D for SO_2) and the geometry given by Dreiding models. The agreement with experiment is still somewhat worse than previous, the apparent reason being an imperfect knowledge of the geometry of the molecule. However, the molecule in the chair conformation[2] should be stable since it has the

[2]It should be noted that the calculated moment for a twist conformation is only slightly different: 4.79 D.

Can. J. Chem. Downloaded from www.nrcresearchpress.com by 210.87.254.40 on 09/05/12
For personal use only.

TABLE 2. Comparison of calculated and experimental dipole moments

Compound no.	Group moments (D) used for SO	Group moments (D) used for SO_2	μ calculated (D)	μ observed (D)	$\Delta\mu$ (D)
3	—	3.0	4.70	—	
	—	3.2	4.89	5.16	−0.27
	—	3.7	5.38	—	
4	—	3.2	4.70	5.23	−0.53
5	—	3.2	4.91	5.10	−0.19
6	—	3.2	4.74	5.06	−0.32
7	2.8 (37°)	—	4.40	—	
	2.6 (37°)	—	4.20	3.88	+0.32
8*a*	2.6 (37°)	—	3.58	3.48	+0.10
8*b*	2.6 (37°)	—	4.27	—	(+0.69)*
$PhSO_2SPh$ (g)	—	3.2	5.06	5.06†	0.00
(t)	—	3.2	3.64	—	(−1.42)*
4-$BrC_6H_4SO_2Ph$ (g)	—	3.2	3.88	4.01†	−0.13
(t)	—	3.2	2.67	—	(−1.34)*

*With an incorrect assignment of conformation.
†According to ref. 4, with a 15% correction applied for P_A.

same conformation (**1**) of the functional group as open-chain analogues.[3]

For purposes of calculation, 1,2-dithiolane 1,1-dioxide (**5**) may also be considered planar with the required bond lengths (8, 9) and with angles of 98° on the two sulfur atoms and 114, 114, and 116° on C_{1-3}, respectively. The necessary deformation of bond angles is larger than in the case of compound **3**. The expected moment calculated with the previously mentioned bond moments (4.91 D) meets better with experiment than in the case of **3**. It seems that the SO_2 group moment is effectively somewhat smaller in **5**. In the calculation, the S—S bond was taken with a zero moment although it is likely appreciably polarized. However, this polarization is of little effect on the resulting moment.

For 1,2-dithiane 1,1-dioxide (**6**), the calculation yields 4.74 D, so that in all cyclic derivatives the calculated values are somewhat low. The deviations could be compensated in a formal manner by raising the SO_2 group moment. However, we feel this would not be fully substantiated with respect to dipole moments of open-chain derivatives and to general reservations (10) against cyclic derivatives as model compounds in the quantitative sense.

With these bond moments, the conformation of thiolsulfonates in solution can be solved on the basis of experimental moments of Grishko and Guryanova[4] (4). The calculated values for various conformations are plotted as μ^2 in a graph (Fig. 1) according to our original method (11) on the x-axis for ethyl benzenethiolsulfonate and on the y-axis for its para-bromo derivative. The experimental point (showing approximately the inaccuracy inherent in the whole procedure) coincides unambiguously with that one for the gauche conformation (as in **1** with S instead of O). Similar graphs can be constructed for phenyl benzenethiolsulfonate and its 4,4′-dichloro derivative, however, it is still necessary to account for higher experimental moments (4) of phenyl esters. Probably polarization of the phenyl group effectively enhanced the SO_2 moment by some 0.3 D.

[3]When the determination of the conformation of sulfonic esters (1) is now repeated with the SO_2 moment 3.2 D instead of 3.0 D, the conclusions are not appreciably changed. The agreement is better in some instances, worse in the others, but the gauche form **1** remains the best possible solution.

[4]In ref. 4 no correction to atomic polarization was taken. Hence we have recalculated the results to $P_A = 15\%$, P_E to be comparable with our data; however, the correction is unimportant.

Can. J. Chem. Downloaded from www.nrcresearchpress.com by 210.87.254.40 on 09/05/12
For personal use only.

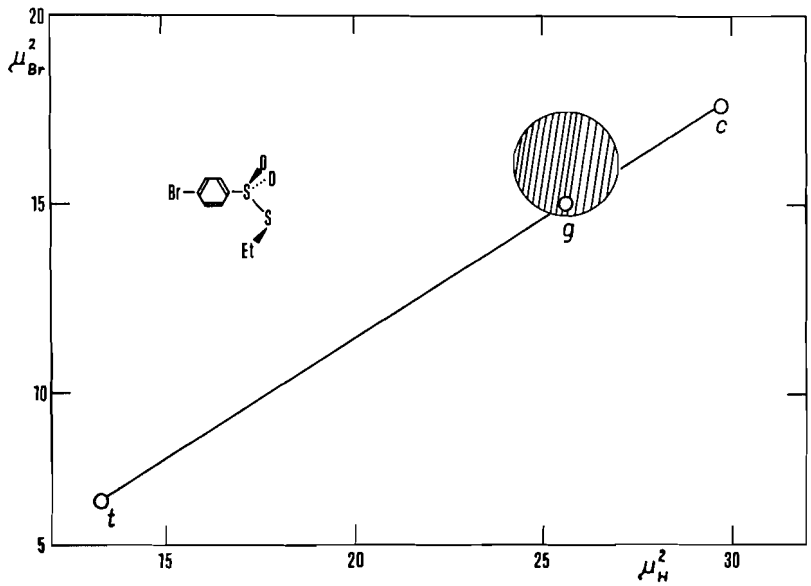

FIG. 1. Determination of conformation of aromatic thiolsulfonates by comparison of computed and experimental (4) dipole moments (*x*-axis ethyl benzenethiolsulfonate, *y*-axis its 4-bromo derivative, the experimental point hatched): t, *trans*; c, *cis*; g, *gauche*.

The gauche conformation of thiolsulfonates in solution (the same as in the crystalline state (8)) agrees with that of sulfonates in solution (1) and *N*-monosubstituted sulfonamides in the crystal (12). In the latter case one of the lone electron pairs in conformation **1** is replaced by a hydrogen atom, however, the decision between **9** and **10** does not follow from X-ray crystallography (12). In a dipole moment study of sulfonanilides, only eclipsed forms were considered (13); in the other one free rotation around the S—N bond was claimed (14). In our opinion, the conformation of sulfonamides in solution is probably similar as in the crystal, *i.e.* either **9** or **10**.

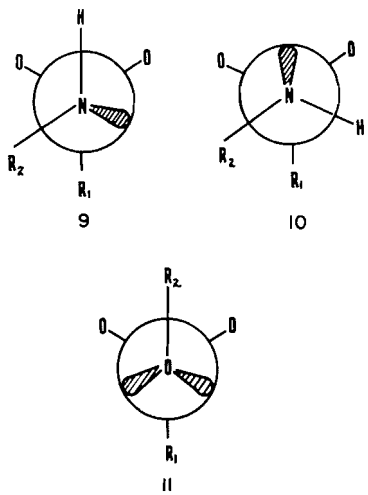

The *a priori* unexpected stability of gauche forms **1**, **9**, or **10** is to be discussed as a part of the general problem of the conformation of molecules with lone electron pairs and strongly polar bonds. Recent calculations accounting for various kinds of attractive and repulsive forces lead to the following simplifying rules (15): gauche interactions between polar bonds and/or lone electron pairs are preferred except the conformation which places a polar bond between two electron pairs; this is disfavored (the so-called Edward–Lemieux effect (15)). In the gauche form **1** as well as in the alternative *trans* form **11** there are four bond–lone pair interactions, two bond–bond interactions, and one Edward–Lemieux effect; in the former, the S—O bond, and in the latter the S—C bond is situated between two electron pairs. If only the strongly polar S—O bonds were considered, form **11** would be preferred. Apparently the simplified rules cannot cover all possibilities: *e.g.* in sulfinates the direction of the σ S—O bond moment is not accounted for since the conformation (C—C bond) is considered (15) such that all polar bonds are oriented with the

Can. J. Chem. Downloaded from www.nrcresearchpress.com by 210.87.254.40 on 09/05/12
For personal use only.

negative end outside. Nevertheless, these rules meet with experiment in a number of cases (10).

To compute the dipole moment of 1,2-oxathiolane 2-oxide (**7**) it is either necessary to attribute a partial moment to the lone electron pair, or to account for it by giving the S—O group a moment non-collinear with the S—O bond. Taking the S—O value applied for chlorosulfinates (2.80 D, with an angle of 37° to the S—O bond (16)) we obtain a predicted moment of 4.40 D, *i.e.* significantly larger than the experimental value. When the supposed contribution of the lone pair is reduced, the final result is not much altered. Apparently this group moment is too high for simple sulfinates. With a non-collinear bond moment of 2.6 D for S—O, a calculation of 4.20 D results.[5]

Nevertheless, the accuracy of computation (using 2.6 D for S—O) seems sufficient to decide between the axial (**8***a*) and equatorial (**8***b*) forms of 1,2-oxathiane 2-oxide (**8**). Using Dreiding models, the calculated values are 3.58 and 4.27 D, respectively,[6] and confirm unambiguously the axial form **8***a* deduced previously from an n.m.r. study (5).[7] The unusual conformational stability of these compounds was discussed in terms of dipole–dipole interactions (5). However, since the axial conformation **8***a* corresponds to **2** in open-chain compounds, (**8***b* would correspond to **12**), a similar explanation is formally possible as for sulfonates. A strong Edward–Lemieux effect (15) clearly disfavors form **12**. Pure electrostatic considerations in terms of dipole–dipole interactions lead to the same result (5) and would be thus satisfactory in this case. However, with conformations **1** and **11** they would yield a false prediction. We thus feel that complex factors controlling conformation may not necessarily be reduced to simple electrostatic forces.

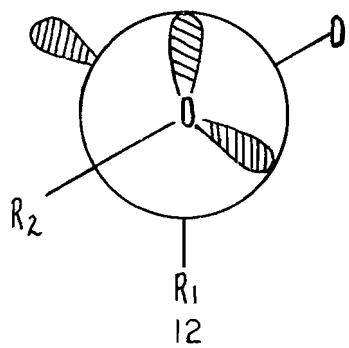

12

[5]Our determination of the conformation of sulfinates (2) was carried out simply with a group moment collinear with the S—O bond. However, the qualitative conclusions leading to form **2** remain unchanged whether the non-collinear bond moment of 2.80 or 2.60 D is employed; the latter value cannot be further significantly lowered with respect to moments of simple aliphatic sulfoxides.

[6]Theoretical calculations (CNDO with Prof. James P. Snyder) also predict the axial form to have a dipole moment of about 1 D less than the equatorial isomer although the absolute values are higher.

[7]Both axial (17–19) and twist (20, 21) conformations have been attributed to the structurally similar sulfites.

The measurements of dielectric constants and densities have been carried out by Mrs. M. Kuthanova under the supervision of Dr. V. Jehlicka; the aid of both is gratefully acknowledged.

1. O. Exner, Z. Fidlerova, and V. Jehlicka. Collect. Czech. Chem. Commun. **33**, 2019 (1968).
2. O. Exner, P. Dembech, and P. Vivarelli. J. Chem. Soc. B, 278 (1970).
3. D. N. Harpp and J. G. Gleason. Tetrahedron Lett. 1447 (1969); D. N. Harpp, J. G. Gleason, and D. K. Ash. J. Org. Chem. **36**, 322 (1971).
4. N. I. Grishko and E. N. Guryanova. Zh. Fiz. Khim. **32**, 2725 (1958).
5. D. N. Harpp and J. G. Gleason. J. Org. Chem. **36**, 1314 (1971).
6. I. F. Halverstadt and W. D. Kumler. J. Am. Chem. Soc. **64**, 2988 (1942).
7. A. I. Vogel. J. Chem. Soc. 1842 (1948).
8. J. H. Nordik and A. Vos. Rec. Trav. Chim. **86**, 156 (1967).
9. H. Sorum. Acta Chem. Scand. **6**, 1 (1953).
10. O. Exner, V. Jehlicka, and J. Firl. Collect. Czech. Chem. Commun. In press.
11. O. Exner and V. Jehlicka. Collect. Czech. Chem. Commun. **30**, 639 (1965).
12. B. Rerat. Acta Crystallogr. B, **25**, 1392 (1969).
13. E. Szczucki and K. Okon. Bull. Acad. Pol. Sci., Ser. Sci. Chim. Geol. Geogr. **7**, 75 (1959).
14. N. P. Lushina, B. L. Levashova, and E. N. Guryanova. Zh. Strukt. Khim. **10**, 490 (1969).
15. S. Wolfe, A. Rauk, L. M. Tel, and I. G. Csizmadia. J. Chem. Soc. B, 136 (1971).
16. O. Exner, P. Dembech, and P. Vivarelli. J. Chem. Soc. B, 620 (1971).
17. N. de Wolf, C. Romers, and C. Altona. Acta Crystallogr. **22**, 715 (1967).
18. V. A. Naumov, N. M. Zarinov, and L. F. Shatrukov. Zh. Strukt. Khim. **11**, 579 (1970).
19. G. Eccleston, R. A. Pethrick, E. Wyn-Jones, P. C. Hamblin, and R. F. M. White. Trans. Faraday Soc. **66**, 310 (1970).
20. V. A. Arbuzov, O. D. Zolova, and D. K. Yuldasheva. Zh. Strukt. Khim. **8**, 291 (1967).
21. G. Wood, J. M. McIntosh, and M. H. Miskow. Can. J. Chem. **49**, 1202 (1971).

Can. J. Chem. Downloaded from www.nrcresearchpress.com by 210.87.254.40 on 09/05/12
For personal use only.

Synthesis and Properties of Substituted Germylhydrazines

L. K. PETERSON AND K. I. THÉ

Department of Chemistry, Simon Fraser University, Burnaby 2, British Columbia

Received June 18, 1971

By using reactions between Me_3GeBr or Me_2GeCl_2 and appropriate lithium hydrazide salts, the following new compounds were prepared: $Me_2NN(R)GeMe_3$ (R = H, **1**; Me, **2**; $GeMe_3$, **3**; $SiMe_3$, **4**), $Me_3GeN(Me)NHGeMe_3$, **5***a*, $MeNHN(GeMe_3)_2$, **5***b*, $(Me_3Ge)_2NN(Me)GeMe_3$, **6**, $Me_3GeNHNHGeMe_3$, **7***a*, $(Me_3Ge)_2NNH_2$, **7***b*, $(Me)_{11}Ge_4N_6H$, **11**, $(Me_2GeNNMe_2)_3$, **12**, $Me_2Ge[N(R')NMe_2]_2$ (R′ = Me, **13**; $SiMe_3$, **14**). Thus the reaction of Me_3GeBr with $Li(MeN_2H_2)$ and with LiN_2H_3 gave mixtures of disubstituted isomers, **5***a* and *b*, and **7***a* and *b*, respectively, rather than mono-substituted derivatives. Reactions of Me_2GeCl_2 gave (*i*) an unresolvable, highly condensed product with LiN_2H_3; (*ii*) the high molecular weight compound **11**, with $Li(MeN_2H_2)$; and (*iii*) the cyclic trigermazane **12** with Me_2NNHLi; the extent of self-condensation is a function of the degree of substitution of the hydrazine moiety. Reactions with protic reagents (H_2O, MeOH, anhydrous HCl) effect cleavage of the Ge—N bond in germylhydrazines. New compounds were characterized on the basis of i.r., n.m.r., and mass spectral measurements.

Par utilisation de réactions entre Me_3GeBr ou Me_2GeCl_2 et les sels d'hydrazide de lithium appropriés, les nouveaux composés suivants furent préparés: $Me_2NN(R)GeM_3$ (R = H, **1**; Me, **2**; $GeMe_3$, **3**; $SiMe_3$, **4**), $Me_3GeN(Me)NHGeMe_3$, **5***a*, $MeNHN(GeMe_3)_2$, **5***b*, $(Me_3Ge)_2NN(Me)GeMe_3$, **6**, $Me_3GeNHNHGeMe_3$, **7***a*, $(Me_3Ge)_2NNH_2$, **7***b*, $(Me)_{11}Ge_4N_6H$, **11**, $(Me_2GeNNMe_2)_3$, **12**, $Me_2Ge[N(R')NMe_2]_2$ (R′ = Me, **13**; $SiMe_3$, **14**). Ainsi la réaction de Me_3GeBr avec $Li(MeN_2H_2)$ et avec LiN_2H_3 donna des mélanges d'isomères disubstitués, **5***a* et *b*, et **7***a* et *b* respectivement, plutôt que les dérivés monosubstitués. Les réactions de Me_2GeCl_2 donnèrent (*i*) un produit, hautement condensé, indéterminable, avec LiN_2H_3; (*ii*) un composé à haut poids moléculaire **11** avec $Li(MeN_2H_2)$; et (*iii*) le trigermazane cyclique **12** avec Me_2NNHLi; le développement de l'auto-condensation est fonction du degré de substitution d'une partie de l'hydrazine. Les réactions avec les réactifs protiques (H_2O, MeOH, HCl anhydre) provoque le clivage de liaisons Ge—N dans les germylhydrazines. Les nouveaux composés furent caractérisés sur la base des spectres: i.r., de r.m.n., et de masse.

Canadian Journal of Chemistry, **50**, 553 (1972)

Results and Discussion

Aminogermanes (1), aminosilanes (2), and silylhydrazines (2) may be prepared by the aminolysis and hydrazinolysis of the appropriate metalloid–halogen bond, the halogen displacement reaction being favored by the simultaneous formation of an ionic, poorly soluble hydrohalide salt; an added strong base may be used for the latter purpose (2, 3), in cases where the amine or hydrazine is very weakly basic. The hydrazinolysis of the Ge—X bond is difficult to effect, even in the presence of strong base, in contrast to the facile reactions of the Si—X bond (2). Both halo-silanes (4) and halo-germanes (5) form donor–acceptor complexes with nucleophiles, hence no mechanistic barrier to the formation of an intermediate complex is apparent, but because of uncertainties in M—N bond energy data (M = Si, Ge), comparisons of the enthalpies of conversion of M—Br to M—N are inconclusive (E_{Si-Br} 74 (6); E_{Si-N} 73–79 (6, 7); E_{Ge-Br} 66 (6, 8); E_{Ge-N} 55–64 kcal/bond (8)). The use of lithium amide (9, 10) or hydrazide (11), however, is generally effective in the synthesis of metalloid-nitrogen systems. In the synthesis of a lithium hydrazide salt via the reaction of butyllithium with an appropriate hydrazine (11), an excess of hydrazine must be used to preclude formation of di-lithio salt, and the excess must be removed from the product before adding bromogermane and solvent (ether); without this latter precaution, much hexamethyldigermane is found. Using appropriate lithium hydrazide salts and Me_3GeBr or Me_2GeCl_2, all of the compounds **1**–**14** (Table 1) were obtained, except for **8**–**10** (eqs. 1 and 2).

$$[1]\quad [RR'R''N_2]Li + Me_3GeX \rightarrow LiX + RR'R''N_2GeMe_3$$

$$[2]\quad [RR'R''N_2]Li + Me_2GeX_2 \rightarrow LiX + Me_2Ge(N_2RR'R'')_2$$

(R groups = H, Me, $SiMe_3$, $GeMe_3$)

Compounds **8** and **10** were made according to the method of Wannagat and Höfler (11). Compound **9**, previously prepared by the action of methyl iodide on $Me_2NN(Li)SiMe_3$ (12), was obtained in improved yield from the reaction

TABLE 1. The p.m.r. spectra of germyl and silyl derivatives of hydrazines*

No.	Compound	$\tau(NMMe_3)$† / $\tau(NMMe_2)$	τ(NH)	τ(NMe)	$\tau(NMe_2)$
1	$Me_2NNHGeMe_3$	9.75	8.30	—	7.66
2	$Me_2NN(Me)GeMe_3$	9.83	—	7.58	7.68
3	$Me_2NN(GeMe_3)_2$	9.67	—	—	7.40
4	$Me_2NN(SiMe_3)GeMe_3$	9.97($SiMe_3$) 9.62($GeMe_3$)	—	—	7.42
5*a*	$Me_3GeN(Me)NHGeMe_3$	9.83(Me_3GeNMe) 9.78($NHGeMe_3$)	8.42	7.46	—
5*b*	$MeNHN(GeMe_3)_2$	9.75	7.16	7.55 7.66	—
6	$Me_3GeN(Me)N(GeMe_3)_2$	9.80(Me_3GeNMe) 9.78[$N(GeMe_3)_2$]	—	7.36	—
7*a*	$Me_3GeNHNHGeMe_3$	9.72	7.52	—	—
7*b*	$(Me_3Ge)_2NNH_2$	9.67	7.00	—	—
8	$Me_2NNHSiMe_3$	10.02	8.29	—	7.73
9	$Me_2NN(Me)SiMe_3$	10.00	—	7.57	7.65
10	$Me_2NN(SiMe_3)_2$	9.99	—	—	7.48
11	$Me_{11}Ge_4N_6H$				
12	$(Me_2GeNNMe_2)_3$	9.38	—	—	7.35
13	$Me_2Ge[N(Me)NMe_2]_2$	9.63	—	7.43	7.55
14	$Me_2Ge[N(SiMe_3)NMe_2]_2$	9.47($GeMe_3$) 9.93($SiMe_3$)	—	—	7.42

*Measured, using ~10% solutions in $CDCl_3$, relative to TMS at τ = 10.00.
†M = Si or Ge.

of Me_2NNHMe with Me_3SiCl in the presence of triethylamine. The end-products of the reaction of lithium hydrazide with Me_3GeBr are hydrazine and a mixture of the isomers of bis(trimethylgermyl)hydrazine, **7***a* and *b*; the analogous reaction of lithium methylhydrazide yields methylhydrazine and a mixture of the isomers of bis(trimethylgermyl)methylhydrazine, **5***a* and *b*. It may be assumed that one or both of the monosubstituted isomers $Me_3GeN(R)NH_2$ (*a*) and $Me_3GeNHNHR$ (*b*) are initially formed, followed by disproportionation via four-center intermediate transition states, as in the case of silylhydrazines (12, 13), thus giving the parent hydrazine and both isomers of the bis(trimethylgermyl)hydrazine (eq. 3*a*–c); then isomerization may occur via a mechanism involving intramolecular migration of organogermyl groups between the two nitrogen atoms, and catalyzed by the presence of the basic hydrazide ion (base B, eq. 4), in the manner postulated by West *et al.* (14) for the isomeriza-

[3*a*]

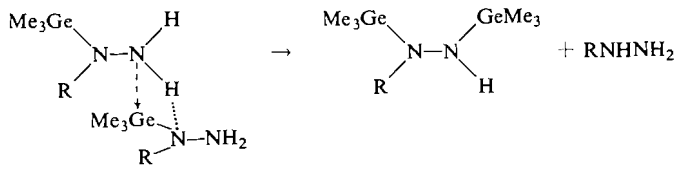

Isomer *a*

[3*b*]

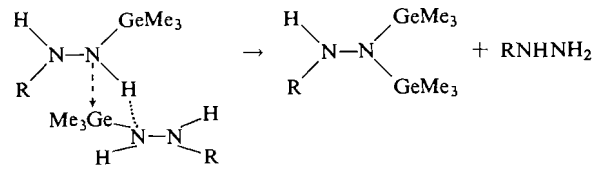

Isomer *b*

[3c] 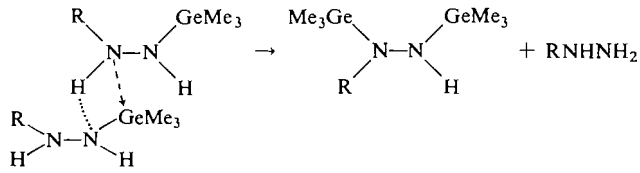

Isomer *b*

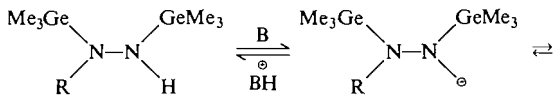

[4] 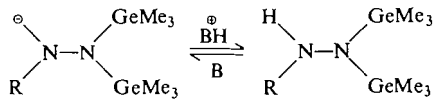

tion of bis(organosilyl)hydrazines. A similar isomerization mechanism is possible for the monosubstituted germylhydrazines.

The bis(alkylhydrazine)germanes are even less stable than the germylhydrazines with respect to self-condensation; thus, the derivative, $Me_2Ge(NHNMe_2)_2$, rapidly evolves Me_2NNH_2, ultimately yielding compound **12** (eq. 5). By contrast, the dimethylsilyl analogue $Me_2Si(NHNMe_2)_2$ is stable against self condensation (15).

[5] $3Me_2Ge(NHNMe_2)_2 \rightarrow (Me_2GeNNMe_2)_3 + 3Me_2NNH_2$

In the reactions of Me_2GeCl_2 with lithium methylhydrazide or lithium hydrazide, the possible intermediates $Me_2Ge(NHNHMe)_2$ and $Me_2Ge(NHNH_2)_2$ were not detected; in the former case, one of the ultimate products, the high molecular weight compound **11**, was formulated as $Me_{11}Ge_3N_6H$ on the basis of mass spectral observations; a possible bicyclic structure is shown in Fig. 1.

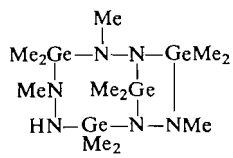

FIG. 1. A possible bicyclic structure: compound **11**.

Mass Spectral Measurements

The polyisotopic mass spectral fragmentation patterns of the germylhydrazines (Table 2) were of particular value in the identification of species containing more than one germanium atom. The relative intensities of the isotopic lines were calculated, using the method of Carrick and Glockling (16); the discrepancies between calculated and observed intensities are due to the fact that the loss of small neutral fragments (mostly H atoms) gives rise to overlapping patterns. The spectra show that facile cleavage occurs at the Ge—N bond, giving Me_3Ge and hydrazino fragments; a characteristic feature of the bis(trimethylgermyl) derivatives **3**, **5***a*, **6**, and **7**, was the formation of large amounts of hexamethyldigermane. The mixed silylgermyl derivative, $Me_2NN(SiMe_3)GeMe_3$, **4**, however, gave $Me_3SiGeMe_3$ in very small amounts; in this case, and for compound **14**, the preferential cleavage of the Ge—N, rather than the Si—N bond is noted.

Proton Magnetic Resonance Spectra

The p.m.r. spectra of compounds **1**–**14**, given in Table 1, were consistent with the given formulations; in most cases, assignments were readily made on the basis of the positions and relative intensities of bands. Two mixtures of isomers, however, were encountered: the mixture of **5***a* and *b* could not be completely separated by fractionation, and gave absorption bands in the Me_3Ge region at τ 9.75, 9.78, and 9.83. The last two bands, of equal intensity, were assigned to germyl-methyl protons of the $NHGeMe_3$ and $MeNGeMe_3$, respectively, in compound **5***a*, on the basis of the inductive, and

TABLE 2. Mass spectral data for germyl derivatives of hydrazines*

No.	Compound	Parent peak multiplet	Other major fragments
1	$Me_2NNHGeMe_3$	174(59)(56) 176(80)(75) 177(32)(21) 178(100)(100) 180(23)(21)	Me_3Ge, Me_2Ge, Me_2NNH
2	$Me_2NN(Me)GeMe_3$	188(64)(56) 190(85)(75) 191(30)(21) 192(100)(100) 194(24)(21)	Me_3Ge, Me_2Ge, Me_2NNMe
3	$Me_2NN(GeMe_3)_2$	288(13)(18) 290(48)(47) 291(13)(13) 292(95)(95) 293(30)(18) 294(100)(100) 295(30)(24) 296(73)(74) 297(22)(5) 298(25)(25)	$(Me_3Ge)_2$, Me_3Ge, $Me_2NNGeMe_3$, Me_2NGeMe_3 or $Me_2NNGeHMe_2$
4	$Me_2NN(SiMe_3)GeMe_3$	246(59)(56) 247(10)(0) 248(82)(75) 249(33)(21) 250(100)(100) 251(18)(0) 252(27)(21)	Me_3Ge, Me_3Si, $Me_2NNSiMe_3$
5*a*	$Me_3GeN(Me)NHGeMe_3$	274(20)(18) 276(47)(48) 277(25)(13) 278(95)(95) 279(33)(18) 280(100)(100) 281(38)(24) 282(74)(74) 283(15)(5) 284(25)(25)	$(Me_3Ge)_2$, $MeNHNGeMe_3$, Me_3Ge
6	$Me_3GeN(Me)N(GeMe_3)_2$	390(21)(18) 391(11)(5) 392(50)(47) 393(23)(13) 394(83)(81) 395(40)(27) 396(100)(100) 397(39)(28) 398(87)(86) 399(34)(21) 400(44)(51) 401(16)(7) 402 (23)(18)	$Me_3GeN(Me)NGeMe_3$, $(Me_3Ge)_2$, Me_3Ge, MeNN
7	$(Me_3Ge)_2N_2H_2$	260(20)(18) 262(48)(47) 263(22)(13) 264(94)(95) 265(34)(18) 266(100)(100) 267(40)(24) 268(77)(74) 269(18)(5) 270(27)(25)	$(Me_3Ge)_2$, Me_3Ge
11	$Me_{11}N_6Ge_4H$	532(15)(6) 533(13)(2) 534(30)(20) 535(17)(7) 536(51)(14) 537(34)(18) 538(77)(78) 539(47)(31) 540(100)(100) 541(53)(18) 542(96)(98) 543(49)(33) 544(72)(73) 545(34)(20) 546(43)(39) 547(18)(7) 548(19)(15)	$Me_4Ge_3N_4H$, $Me_3Ge_2N_4H$, $Me_2Ge_2N_4$, Me_4GeN_4, Me_3Ge, Me_2Ge
12	$(Me_2GeNNMe_2)_3$	474(5)(4) 476(20)(18) 477(8)(5) 478(49)(47) 479(23)(13) 480(78)(81) 481(38)(27) 482(100)(100) 483(42)(28) 484(85)(86) 485(34)(21) 486(53)(51) 487(16)(6) 488(22)(18) 489(4)(1) 490(5)(3)	$Me_{10}Ge_2N_6$, $Me_9Ge_2N_6$, $Me_2NNGeMe_2$
13	$Me_2Ge[N(Me)NMe_2]_2$	246(55)(56) 247(5)(0) 248(76)(75) 249(31)(21) 250(100)(100) 252(23)(21)	$Me_2GeN(Me)NMe_2$, Me_2Ge
14	$Me_2Ge[N(SiMe_3)NMe_2]_2$	362(55)(56) 363(18)(0) 364(72)(75) 365(36)(21) 366(100)(100) 367(35)(0) 368(34)(21)	$Me_2GeN(SiMe_3)NMe_2$, $Me_2NNSiMe_3$, Me_2Ge

*The numbers in parentheses refer to observed and calculated relative intensities, respectively. Calculated values were obtained using the method of Carrick and Glockling (16).

TABLE 3. The p.m.r. data for compounds **1–4** and **8–10***

$Me_2N—N(R)GeMe_3$	H(1)	Me(2)	$GeMe_3$(3)	$SiMe_3$(4)
$\tau(Me_2N)$	7.66	7.68	7.40	7.42
$\tau(Me_3Ge)$	9.75	9.83	9.67	9.62
τ(R)	8.30	7.58	(9.67)	9.97
$Me_2N—N(R)SiMe_3$	H(8)	Me(9)	$GeMe_3$(4)	$SiMe_3$(10)
$\tau(Me_2N)$	7.73	7.65	7.42	7.48
$\tau(Me_3Si)$	10.02	10.00	9.97	9.99
τ(R)	8.29	7.57	9.62	(9.99)

*τ(TMS) = 10.00; $\tau(Me_4Ge)$ = 9.87 (18).

TABLE 4. The p.m.r. data for substituted hydrazines, Me_2NNHR and $Me_2NN(Me)R$

R	H*	Me*	$(CF_3)_2P$†	$(CF_3)_2As$‡	$(C_6H_5)_2P$§	Me_3Si‖	Me_3Ge‖
(a) Me_2NNHR							
τ(NH)	6.77	—	5.95	5.73	5.93	8.29	8.30
$\tau(Me_2N)$	7.67	7.70	7.50	7.50	6.71	7.73	7.66
(b) $Me_2NN(Me)R$							
τ(NMe)	7.59	—	7.15	7.11	—	7.57	7.58
$\tau(Me_2N)$	7.70	—	7.50	7.51	—	7.65	7.68

*G. L. Wilson, unpublished results.
†Reference 25.
‡Reference 26.
§Reference 27.
‖This work.

hence shielding, effect of the methyl group on N. The NH and MeN bands of appropriate intensities occur at τ 8.42 and 7.46, respectively. The remaining bands were consistent for compound **5***b*, $MeNHN(GeMe_3)_2$, the groups being $(Me_3Ge)_2$ (τ 9.75) NH(7.16), and MeN (two peaks, at 7.55 and 7.66, in a 2:1 ratio). A similar splitting pattern is reported for the MeN protons of $MeNHN(SiMe_3)_2$ (12). In compound **12**, a cyclotrigermazane (Fig. 2), the chemical shifts for the MeGe and MeN protons have the lowest values in the series **1–14** studied; this may mean that delocalization of the lone pairs on nitrogen into the vacant 4d orbitals of germanium occurs, such that σ-electron density is withdrawn from the ring-Ge and exocyclic-Me_2N groups; however, changes in hybridization resulting from bond angle requirements at germanium could equally well explain the observed spectral features. Substituent effects, summarized in Tables 3 and 4, have been discussed in terms of inductive and π-bonding effects (17–21).

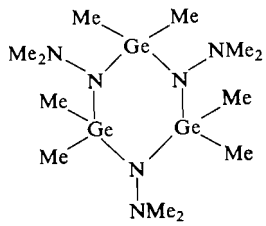

FIG. 2. A cyclotrigermazane: compound **12**.

Chemical Characteristics

Since typical reactions of aminogermanes with nucleophiles and with electrophiles involve cleavage of the Ge—N bond (9), we were particularly interested in the possibility of forming stable adducts, or salts, between hydrazino germanes and Lewis acids, a mode of reaction

which would demonstrate the overriding basicity of the terminal N atom, relative to the central N atom. A study of reactions involving BX_3 (X = Me, F, Cl) and CY_2 (Y = O, S) is described elsewhere (22), while reactions with protic reagents HX (X = Cl, OH, OMe) are described here, since cleavage patterns demonstrated the composition and corroborated our formulations of new compounds.

Representative reactions involving protic reagents HX (X = Cl) were carried out with compounds **1**—**4** and **13**, while for X = OH and OMe, *i.e.* with water and methanol, compound **2** was used. In all cases cleavage of N–metalloid bonds was indicated, according to eqs. 6–9.

[6] $$RR'NNR''GeMe_3 + 2HCl \rightarrow Me_3GeCl + RR'NNHR''HCl$$

[7] $$2RR'NNR''GeMe_3 + H_2O \rightarrow (Me_3Ge)_2O + 2Me_2NNHMe$$

[8] $$RR'NNR''GeMe_3 + MeOH \rightarrow Me_3GeOMe + Me_2NNHMe$$

[9] $$Me_2Ge[N(SiMe_3)NMe_2]_2 + 6HCl \rightarrow Me_2GeCl_2 + 2Me_3SiCl + 2Me_2NNH_2HCl$$

On the basis that the above cleavage reactions proceed quantitatively, the nitrogen atoms are not of sufficiently different basicity to give rise to stable salts

$$Me_2N—N(R)MMe_3$$
$$\quad\quad\downarrow$$
$$\quad\quad H—X$$

instead, the cleavage reaction may proceed via an unstable intermediate of the type

$$[Me_2N—N(R)MMe_3]$$
$$\quad\quad\quad\downarrow$$
$$\quad\quad\quad H—X$$

Experimental

Standard high vacuum methods were used to handle volatile, air-sensitive compounds, while inert atmosphere systems were used for involatile materials. Sealed, all-glass reaction vessels were used for most reactions; wherever filtration operations were required, a sintered filter disc was incorporated in the design of the reaction vessel. Solvents were dried before use. Mass spectra were measured with a double focussing RMU-6E Hitachi Perkin–Elmer instrument, n.m.r. spectra with a Varian A56/60, and i.r. spectra with a Beckmann I.R. 12 spectrophotometer. A Bendix Series 2200 instrument was used for gas phase chromatographic separations. Saturated vapor pressure measurements were obtained using mercury tensimeters.

Hydrazine, methylhydrazine, and *N,N*-dimethylhydrazine, purchased from Fisher Scientific Co., were dried over anhydrous barium hydroxide, and were distilled from calcium hydride. Trimethylamine (Matheson) and triethylamine (K & K) were dried in a similar way, and fractionated. Triethylhydrazine was prepared according to the method of Class, *et al.* (23). Trimethylchlorosilane and dimethyldichlorogermane (Alfa Inorganics) were fractionated through a suitable train of cold traps. Butyllithium (Alfa) was obtained as a 2 *M* solution in hexane.

Trimethylsilyltrimethylhydrazine (**9**), was obtained in high yield from the reaction of Me_3SiCl and trimethylhydrazine, in ether solution, using Et_3N as hydrogen halide acceptor. An alternative method, using $Me_2NN(Li)SiMe_3$ and methyl iodide, gives poor yields (12). *N,N*-dimethyl-*N'*-(trimethylsilyl)hydrazine (**8**) and *N,N*-dimethyl-*N',N'*-bis(trimethylsilyl)hydrazine (**10**) were prepared according to methods of Wannagat and Höfler (11). Trimethylbromogermane was made from Me_4Ge (Alfa), using the method of Brown and Fowles (24).

(1) Preparation of Lithium Hydrazide Salts

The following general procedure, described in detail for the synthesis of $Me_2NN(Li)Me$, was used to make Me_2NNHLi, $MeNHNHLi$ (or $MeN(Li)NH_2$), $MeN(Li)N(GeMe_3)_2$, $Me_3GeN(Me)N(Li)GeMe_3$, N_2H_3Li, $Me_2NN(Li)GeMe_3$, and $Me_2NN(Li)SiMe_3$.

Lithium trimethylhydrazide was prepared according to the method of Wannagat and Höfler (11), by treating Me_2NNHMe (14.5 mmol) in solution in hexane with a slight deficiency of butyllithium (13 mmol) in the same solvent. The reaction vessel was sealed and heated at 85–90° for 12–16 h, with the upper part of the vessel at room temperature, thus effecting reflux action. The evolved butane was estimated, and solvent and unreacted Me_2NNHMe were removed from the flask; to remove final traces of the hydrazine from the lithium salt, the flask was immersed in an oil bath at 85–90° for 12–24 h while still connected to the high vacuum pumping system. The yield of lithium trimethylhydrazide was calculated on the basis of the evolved butane.

(2) Reaction of Me_2NNHLi with Me_3GeBr

Preliminary experiments with Me_2NNH_2 and Me_3GeBr indicated the formation of the 1:1 adduct, $Me_2NNH_2 \cdot Me_3GeBr$, together with small quantities of $Me_2NN(H)GeMe_3$ and $(Me_3Ge)_2$.

The salt Me_2NNHLi (15 mmol) was treated with ether and Me_3GeBr (12 mmol); the only volatile reaction product was $Me_2NNHGeMe_3$ (**1**) (11.3 mmol, 99%), identified by mass spectral ($P_{obsd.}$ 178; $P_{calcd.}$ 178), p.m.r. and i.r. measurements; the saturated vapor pressure was 4.40 mm/0.0°.

The i.r. spectrum of $Me_2NNHGeMe_3$ (**1**) (gas phase):[1] 450(6), 530(6), 575(16), 610(82), 680(15), 720(11), 760(46), 825(100), 855(89), 899(48), 910(54), 1010(33), 1035(26), 1050(26), 1155(28), 1245(66), 1440(sh), 1460(59), 1590(23), 1610(sh), 2770(89), 2820(85), 2850(72), 2920(69), 2960(74), 3000(97), 3220(21).

(3a) Reaction of Me_2NNHMe with Me_3GeBr, with Et_3N Present

An exploratory experiment indicated the absence of reaction between Me_2NNHMe (4.52 mmol) and Me_3GeBr

[1]The i.r. bands are given in cm^{-1}. The numbers in parentheses denote relative intensities, with an arbitrary value of 100 assigned to the most intense band.

(4.41 mmol) in solution in diethylether (4.8370 g). Triethylamine (4.37 mmol) was added to the mixture, causing immediate formation of white precipitate. The most volatile reaction products, separated by gas chromatography (column, 30% SE-52 on chromosorb W, 45–60 mesh) into $(Me_3Ge)_2$ and $Me_2NN(Me)GeMe_3$ (**2**) were identified by p.m.r. and mass spectral measurements ($P_{obsd.}$ 237 and 192; $P_{calcd.}$ for $(Me_3Ge)_2$ 237; $P_{calcd.}$ for $Me_2NN(Me)GeMe_3$ 192); a solid product, obtained in small quantity, was believed to be $Me_3GeGe(Me)_2N(Me)NMe_2$ ($P_{obsd.}$ 292; $P_{calcd.}$ 294; isotope pattern indicative of two Ge atoms in the molecule).

(3b) Reaction of $Me_2NN(Li)Me$ with Me_3GeBr

Lithium trimethylhydrazide (~12 mmol), ether (7.69 g), and Me_3GeBr (10.4 mmol) were heated together in a sealed flask for 16 h at 65–70°, the upper walls of the flask being sufficiently cool to maintain reflux action. The only volatile product, other than solvent, was $Me_2NN(Me)GeMe_3$ (9.1 mmol, 90% yield), identified by p.m.r. and mass spectral analysis ($P_{obsd.}$ 192; $P_{calcd.}$ 192); the vapor phase molecular weight was 195 ($M_{calcd.}$ 192), and the saturated vapor pressure was 8.00 mm/24.20°.

The i.r. spectrum of $Me_2NN(Me)GeMe_3$ (**2**) (gas phase): 560(70), 600(77), 750(38), 820(100), 880(34), 960(5), 1010(13), 1085(43), 1150(19), 1245(68), 1410(sh), 1455(32), 1465(30), 1480(30), 2780(68), 2830(79), 2850(79), 2890(78), 2920(79), 2950(89), 2990(96).

(4) Reaction of $Me_2NN(Li)GeMe_3$ with Me_3GeBr

$Me_2NN(Li)GeMe_3$, (5.8 mmol) prepared from $Me_2NNHGeMe_3$ by the method described above, and Me_3GeBr (5.8 mmol) in solution in ether, were heated together for 14 h at 90°. The product, separated from the LiBr residue by heating and pumping, was $Me_2NN(GeMe_3)_2$ (**3**) (4.6 mmol, 80%; $P_{obsd.}$ 294; $P_{calcd.}$ 294; for p.m.r. spectrum, see Table 1). Saturated vapor pressure readings were 2.75 mm/20.0° and 6.55 mm/50.0°.

The i.r. spectrum of $Me_3NN(GeMe_3)_2$ (**3**) (pure liquid film): 460(34), 480(sh), 570(59), 600(87), 750(70), 810(100), 860(sh), 1010(29), 1085(14), 1150(10), 1235(89), 1400(43), 1430(31), 1450(40), 1470(26), 2770(49), 2820(59), 2850(65), 2870(54), 2910(83), 2930(83), 2980(89).

(5) Reaction of $Me_2NN(Li)SiMe_3$ with Me_3GeBr

A mixture of $Me_2NN(Li)SiMe_3$ (~20 mmol), ether, and Me_3GeBr (10 mmol) was heated together to yield $Me_2NN(SiMe_3)GeMe_3$ (8.0 mmol, 80%), liberated from the LiBr precipitate by pumping and heating (90°, 4 h). The product was identified as $Me_2NN(SiMe_3)GeMe_3$ by mass ($P_{obsd.}$ 250; $P_{calcd.}$ 250) and p.m.r. spectral measurements. The saturated vapor pressure at 50° was 5.05 mm.

The i.r. spectrum of $Me_2NN(SiMe_3)GeMe_3$ (**4**) (pure liquid film): 470(44), 495(47), 570(59), 600(84), 625(40), 680(46), 750(66), 830(100), 920(sh), 950(96), 1015(39), 1085(16), 1150(6), 1225(sh), 1240(86), 1260(sh), 1300(6), 1410(23), 1440(26), 1450(27), 1465(sh), 2780(37), 2820(43), 2850(56), 2880(49), 2910(60), 2940(73), 2980(70).

(6a) Reaction of Lithium Methylhydrazide with Me_3GeBr

Lithium methylhydrazide (~12 mmol) was treated with ether and Me_3GeBr (5.7 mmol); the volatile products were methylhydrazine (2.5 mmol) and a liquid, held at −33°, with a parent peak indicative of $(Me_3Ge)_2(Me)N_2H$ ($P_{obsd.}$ 280; $P_{calcd.}$ 280). The presence of the two isomeric species, $Me_3GeN(Me)NHGeMe_3$ (**5***a*) and $MeNHN(GeMe_3)_2$ (**5***b*) was indicated by the p.m.r. spectra. The overall yield was 80%.

(6b) Reaction of the Two Isomers of Bis(trimethylgermyl)-methylhydrazine with Butyllithium and Me_3GeBr

A mixture of $Me_3GeN(Me)NHGeMe_3$ and $MeNHN(GeMe_3)_2$ (6.0 mmol) in hexane was treated with butyllithium according to the method described above, the resulting salt was treated with ether and Me_3GeBr (6.5 mmol). The products were $(Me_3Ge)_2$ (3.0 mmol) and tris(trimethylgermyl)methylhydrazine $(Me_3Ge)_2NN(Me)GeMe_3$ (**6**) (0.9 mmol); the latter product, obtained only after pumping and heating the reaction vessel, with its residue of LiBr, for 4 h at 90° was identified by its mass spectrum ($P_{obsd.}$ 397; $P_{calcd.}$ 397) and by its p.m.r. spectra.

The i.r. spectrum of $Me_3GeN(Me)N(GeMe_3)_2$ (**6**) (pure liquid film): 400(69), 560(97), 595(97), 620(sh), 750(100), 800(100), 850(sh), 970(66), 1120(55), 1200(55), 1235(90), 1400(67), 1425(sh), 1465(34), 2770(72), 2820(sh), 2840(76), 2910(86), 2970(86), 3020(sh).

(7) Reaction of Lithium Hydrazide with Me_3GeBr

A mixture of lithium hydrazide (~10 mmol), ether, and Me_3GeBr (9.2 mmol) were heated together at 65° for 12 h. The products were (*a*) a small quantity of nitrogen, (*b*) a small quantity of ammonia, (*c*) hexamethyldigermane, (*d*) hydrazine, (*e*) a mixture of the isomers *N,N'*- and *N,N*-bis(trimethylgermyl)hydrazine, (*7a* and *b*, respectively), from which a pure sample of *N,N*-bis(trimethylgermyl)-hydrazine, $(Me_3Ge)_2NNH_2$ was obtained on repeated fractionation. The i.r., p.m.r., and mass spectral measurements were used in the identification of these products.

The i.r. spectrum of $(Me_3Ge)_2NNH_2$ (*7b*) (pure liquid film): 510(49), 570(82), 600(99), 660(45), 750(87), 800(100), 860(sh), 1010(sh), 1070(28), 1100(sh), 1150(5), 1240(89), 1320(16), 1400(53), 1430(sh), 2800(28), 2860(sh), 2910(83), 2980(91), 3020(sh), 3290(16).

(8) Reaction of Lithium Hydrazide, LiN_2H_3, with Me_2GeCl_2

A mixture of lithium hydrazide (~20 mmol) was heated at 90° for 12 h; on removing the solvent, an involatile white solid residue remained in the flask. Attempts to release products of low volatility, by heating the flask to 100°, led to the evolution of hydrazine. The residue was partly soluble in THF; the soluble fraction showed a "parent" peak of 458, believed to be a fragment of a larger polymeric structure.

(9) Reaction of MeN_2H_2Li with Me_2GeCl_2

A mixture of lithium methylhydrazide (~16 mmol), ether, and Me_2GeCl_2 (8.1 mmol) was heated at 90° for 12 h, yielding $MeNHNH_2$ (8.5 mmol) and a colorless, oily liquid, held at 20°, believed, from its mass and p.m.r. spectra, to be $Me_{11}Ge_4N_6H$ (**11**) (see Fig. 1) ($P_{obsd.}$ 540; $P_{calcd.}$ 540).

(10) Reaction of Me_2NNHLi with Me_2GeCl_2

A mixture of Me_2NNHLi (~30 mmol), ether, and Me_2GeCl_2 (8.6 mmol) was heated at 90° for 12 h, to yield Me_2NNH_2, and a liquid held at −16°; the latter product decomposed into Me_2NNH_2 (total recovery, 7.6 mmol) and an involatile yellow oil during subsequent fractionation. The p.m.r. and mass spectra ($P_{obsd.}$ 482; $P_{calcd.}$ 482) of the

yellow oil were consistent for $(Me_2GeNNMe_2)_3$ (**12**) yield, 65%.

The i.r. spectrum of $(Me_2GeNNMe_2)_3$ (**12**) (pure liquid film): 470(64), 570(sh), 590(78), 620(83), 750(100), 790(sh), 820(87), 865(86), 1010(53), 1030(sh), 1085(40), 1150(36), 1215(sh), 1235(74), 1410(56), 1435(53), 1445(54), 1460(49), 2760(59), 2800(42), 2040(64), 2910(71), 2930(71), 2980(67).

(11) Reaction of $Me_2NN(Li)Me$ with Me_2GeCl_2

A mixture of $Me_2NN(Li)Me$ (~8 mmol), ether, and Me_2GeCl_2 (4.5 mmol) was heated together, yielding unreacted Me_2GeCl_2 (0.6 mmol), and $Me_2Ge[N(Me)NMe_2]_2$ (**13**) held at −33°, and identified by its mass ($P_{obsd.}$ 250; $P_{calcd.}$ 250) and p.m.r. spectra. The saturated vapor pressure at 50° was 5.85 mm; yield, ~90%.

The i.r. spectrum of $Me_2Ge[N(Me)NMe_2]_2$, (**13**) (pure liquid film): 425(28), 480(33), 575(27), 610(45), 745(30), 810(sh), 820(100), 850(sh), 980(17), 1010(38), 1085(67), 1150(30), 1215(sh), 1240(55), 1435(sh), 1455(55), 1470(50), 2770(73), 2820(91), 2850(95), 2870(89), 2940(63), 2980(85).

(12) Reaction of $Me_2NN(Li)SiMe_3$ with Me_2GeCl_2

A mixture of $Me_2NN(Li)SiMe_3$ (~19 mmol), ether, and Me_2GeCl_2 (7.5 mmol) was heated at 90° for 12 h; upon recovering the solvent, a white residue remained, which released the desired product, $Me_2Ge[N(SiMe_3)NMe_2]_2$ (**14**) (3.4 mmol, 45%) only after heating at 125–160° for 14 h. The p.m.r. and mass ($P_{obsd.}$ 366; $P_{calcd.}$ 366) spectra established the given formulation. The saturated vapor pressure at 100° was 3.45 mm; yield, 45%.

The i.r. spectrum of $Me_2Ge[N(SiMe_3)NMe_2]_2$, (**14**), (pure liquid film): 470(56), 500(51), 570(48), 590(51), 630(33), 680(55), 750(71), 800(88), 830(100), 910(sh), 950(92), 1020(59), 1090(21), 1230(sh), 1250(92), 1310(7), 1410(29), 1450(41), 1460(44), 1470(33), 2790(52), 2830(59), 2860(71), 2890(62), 2920(69), 2950(82), 2970(78), 2990(sh).

(13) Reactions Involving Anhydrous Hydrogen Chloride

(a) With $Me_2NNHGeMe_3$

In a typical procedure, a mixture of $Me_2NNHGeMe_3$ (0.82 mmol), ether (0.7996 g), and anhydrous HCl (1.70 mmol) was kept in a sealed tube for 3 h. The recovered products were: Me_3GeCl (0.74 mmol) Me_2NNH_2HCl (0.81 mmol), and an "ether fraction" (0.8178 g); products were characterized by m.p., molecular weight, i.r. and mass spectral measurements, as appropriate. Thus the stoichiometry of the reaction is

$$\underset{\text{obsd. } 0.82}{Me_2NNHGeMe_3} + \underset{1.70}{2HCl} \rightarrow \underset{0.74}{Me_3GeCl} + \underset{0.81 \text{ mmol}}{Me_2NNH_2\cdot HCl}$$

Using similar procedures with other compounds the following cleavage reactions were observed:

(b) With $Me_2N(N)MeGeMe_3$

$$\underset{\text{obsd. } 0.80}{Me_2NNMeGeMe_3} + \underset{1.76}{2HCl} \rightarrow \underset{0.78}{Me_3GeCl} + \underset{0.81 \text{ mmol}}{Me_2NNHMe\cdot HCl}$$

(c) With $Me_2NN(GeMe_3)_2$

$$\underset{0.45}{Me_2NN(GeMe_3)_2} + \underset{1.55}{3HCl} \rightarrow \underset{0.82}{2Me_3GeCl} + \underset{0.41 \text{ mmol}}{Me_2NNH_2HCl}$$

(d) With $Me_2NN(SiMe_3)GeMe_3$

$$\underset{0.74}{Me_2NN(SiMe_3)GeMe_3} + \underset{2.60}{3HCl} \rightarrow \underset{0.76}{Me_3GeCl} + \underset{0.72}{Me_3SiCl} + \underset{0.77 \text{ mmol}}{Me_2NNH_2\cdot HCl}$$

(e) With $Me_2Ge(NMeNMe_2)_2$

$$\underset{0.43}{Me_2Ge(NMeNMe_2)_2} + \underset{\text{excess}}{HCl} \rightarrow \underset{0.45 \text{ mmol}}{Me_2GeCl_2} + Me_2NNHMe$$

(14) Reactions with Hydroxylic Protic Reagents

(a) With Methanol

A mixture of $Me_2NN(Me)GeMe_3$ (0.60 mmol) and methanol (0.60 mmol) yielded, after 12 h at room temperature the products Me_2NNHMe (0.62 mmol) and Me_3GeOMe, identified by i.r. and mass spectroscopic methods. The stoichiometry of the reaction is:

$$\underset{\text{obsd. } 0.60}{Me_2NN(Me)GeMe_3} + \underset{0.60}{MeOH} \rightarrow \underset{0.62}{Me_2NNHMe} + \underset{0.59 \text{ mmol}}{Me_3GeOMe}$$

(b) With Water

After 2 days at room temperature, a mixture of $Me_2NN(Me)GeMe_3$ (0.77 mmol) and water (0.97 mmol) yielded Me_2NNHMe (0.78 mmol), $(Me_3Ge)_2O$ (0.25 mmol), and a small amount of a mixture of H_2O and $(Me_3Ge)_2O$ that could not be separated by fractionation. The stoichiometry approximates to the equation

$$2Me_2NN(Me)GeMe_3 + H_2O \rightarrow 2Me_2NNHMe + (Me_3Ge)_2O$$

the deficiency in $(Me_3Ge)_2O$ (0.25 *vs.* 0.38 mmol) being due to experimental difficulties.

The authors acknowledge the financial assistance of the National Research Council of Canada, and Miss E. Cheah and Mr. G. Owen for n.m.r. and mass spectral measurements.

1. H. H. Anderson. J. Am. Chem. Soc. **74**, 1421 (1952). I. Ruidisch and B. Mebert. J. Organometal. Chem. **11**, 77 (1968).
2. U. Wannagat. Advan. Inorg. Chem. Radiochem. **6**, 225 (1964).
3. M. Wieber and C. D. Frohning. J. Organometal. Chem. **8**, 459 (1967).
4. I. R. Beattie. Quart. Rev. London, **17**, 382 (1963). H. J. Campbell-Ferguson and E. A. V. Ebsorth. J. Chem. Soc. A, 1508 (1966).
5. J. G. A. Luijten, F. Rijkens, and G. J. M. van der Kerk. Advan. Organometal. Chem. **3**, 397 (1965).
6. E. A. V. Ebsworth. Volatile silicon compounds. Pergamon Press Book, The Macmillan Co., New York, 1963.
7. J. C. Baldwin, M. F. Lappert, J. B. Pedley, and J. A. Treverton. J. Chem. Soc. A, 1980 (1967).
8. J. S. Poland. Ph.D. Thesis. University of Sussex, U.K., 1969.

9. J. SATGE, M. BESBRE, and M. BAUDET. Compt. Rend. **259**, 4733 (1964).
10. K. JONES and M. F. LAPPERT. J. Chem. Soc. 1944 (1965).
11. U. WANNAGAT and F. HÖFLER. Monatsh. Chem. **97**, 976 (1966).
12. F. HÖFLER and U. WANNAGAT. Monatsh. Chem. **97**, 1598 (1966).
13. U. WANNAGAT, C. KRÜGER, and H. NIEDERPRÜM. Z. Anorg. Allg. Chem. **321**, 198 (1963).
14. R. WEST, M. ISHIKAWA, and R. E. BAILEY. J. Am. Chem. Soc. **89**, 4072 (1967).
15. U. WANNAGAT, G. SCHREINER, O. BRANDSTÄTTER, and M. PEACH. Monatsh. Chem. **96**, 1902 (1965).
16. A. CARRICK and F. GLOCKLING. J. Chem. Soc. A, 623 (1966).
17. A. L. ALLRED and E. G. ROCHOW. J. Inorg. Nucl. Chem. **5**, 269 (1958).
18. M. P. BROWN and D. E. WEBSTER. J. Am. Chem. Soc. **64**, 698 (1960).
19. H. SCHMIDBAUR. J. Am. Chem. Soc. **85**, 2336 (1963).
20. C. W. N. CUMPER, A. MELNIKOFF, E. F. MOONEY, and A. I. VOGEL. J. Chem. Soc. B, 874 (1966).
21. J. MACK and C. H. YODER. Inorg. Chem. **8**, 278 (1969).
22. L. K. PETERSON and K. I. THÉ. Can. J. Chem. This issue.
23. J. B. CLASS, J. G. ASTON, and J. OAKWOOD. J. Am. Chem. Soc. **75**, 2937 (1953).
24. M. P. BROWN and G. W. A. FOWLES. J. Chem. Soc. 2811 (1958).
25. L. K. PETERSON and G. L. WILSON. Can. J. Chem. **46**, 685 (1968).
26. L. K. PETERSON and K. I. THÉ. Chem. Commun. 1056 (1967).
27. R. P. NIELSEN and H. H. SISLER. Inorg. Chem. **2**, 753 (1963).

The Reactions of Substituted Germyl- and Silylhydrazines with BX_3 and CY_2 Acceptor Species

L. K. PETERSON AND K. I. THÉ

Department of Chemistry, Simon Fraser University, Burnaby 2, British Columbia

Received June 18, 1971

Boron trimethyl reacts with each of the organometalloid-hydrazine derivatives $Me_2NN(R)GeMe_3$ (R = H, Me, $SiMe_3$) except $Me_2NN(SiMe_3)GeMe_3$, and with $Me_2NNHSiMe_3$, forming 1:1 adducts. With $Me_2NN(SiMe_3)GeMe_3$ and BMe_3, no adduct was formed even at low temperatures. On the basis of p.m.r. spectra, the metalloid-substituted nitrogen atom rather than the terminal nitrogen, is indicated as the basic center at which adduct formation occurs. With BF_3, the Si—N and Ge—N bonds of the hydrazine derivatives were cleaved, again indicating attack at the central nitrogen atom. In a series of experiments involving CY_2 (Y = O, S) and $Me_2NN(R)MMe_3$ (R = H, Me, $SiMe_3$; M = Si, Ge), reaction occurred readily for R = H, but less readily for R = Me and for the compound $Me_2NN(GeMe_3)_2$, while no reaction was observed for the compounds $Me_2NN(SiMe_3)_2$ and $Me_2NN(SiMe_3)GeMe_3$, even when heat or basic catalysts were employed. Reaction products, carbamate and thiocarbamate derivatives, $Me_2NN(R)C(Y)YMMe_3$, were characterized on the basis molecular weight, i.r., p.m.r., and mass spectroscopy, and m.p. data. Ease of formation is discussed in terms of electronic and steric effects.

Le bore triméthyle réagit avec les dérivés organométalliques de l'hydrazine $Me_2NN(R)GeMe_3$ (R = H, Me, $SiMe_3$) sauf $Me_2NN(SiMe_3)GeMe_3$ et $Me_2NNHSiMe_3$, en donnant des composés d'addition 1:1. Aucune réaction n'est obtenue avec $Me_2NN(SiMe_3)GeMe_3$ et BMe_3, même à basse température. Le spectre r.m.n. montre que le site de l'addition est l'atome d'azote substitué par le métalloide plutôt que l'atome d'azote terminal. Avec BF_3, les liaisons Si—N et Ge—N des dérivés de l'hydrazine sont coupées, indiquant là encore une attaque sur l'atome d'azote central. Dans une série d'expériences entre CY_2 (Y = O, S) et $Me_2NN(R)MMe_3$ (R = H, Me, $SiMe_3$; M = Si, Ge); la réaction est facile pour R = H, moins facile pour R = Me et pour le composé $Me_2NN(GeMe_3)_2$, tandis qu'aucune réaction n'est observée pour les composés $Me_2NN(SiMe_3)_2$ et $Me_2NN(SiMe_3)GeMe_3$ même avec l'emploi de la chaleur et des catalyseurs basiques. Les produits de réactions, dérivés de carbamate et de thiocarbamate, sont caractérisés par leur masse moléculaire, leurs spectres i.r. et r.m.n., leur spectre de masse et leur points de fusion. La facilité de réaction est discutée en fonction des facteurs électronique et stérique.

Canadian Journal of Chemistry, **50**, 562 (1972)

Results and Discussion

In organometalloid-hydrazine systems

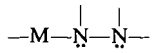

the lone pairs of electrons may occupy distinct valence bond orbitals, or, alternatively, they may occupy delocalized molecular orbitals associated with the whole or part of the skeleton. This paper describes a study of the structural features of adduct formation by such systems, as an attempt to distinguish between the two different electron density models. On steric and electronic grounds, the central nitrogen atom is expected to be least basic, thus allowing for the possibility of salt or adduct formation between Lewis acids and the terminal nitrogen site of metalloid-hydrazines; such mode of reaction would contrast with the typical cleavage of metalloid–nitrogen bonds by many electrophiles (1).

A series of reactions between germylhydrazines and protic Lewis acids led exclusively to cleavage of the Ge—N bond (2). With acids of the type BX_3, however, a range of acceptor power is available, thus permitting a selective study of the differing basicities of the hydrazino nitrogen atoms. The use of n.m.r. methods for this purpose has been described (3, 4).

With trimethylboron, the only adducts stable at room temperature were $Me_2NNHMMe_3 \cdot BMe_3$ (M = Si, Ge), both distillable under vacuum. Contrary to expectations, a comparison of the p.m.r. spectra of the adducts, and of the parent hydrazines, indicate 1:1 complexation at the metalloid–N site, even for $Me_2NNHSiMe_3$, where the silyl group might be expected to diminish the basicity of the adjacent nitrogen atom. While the p.m.r. bands for the Me_2N and Me_3M groups show fine structure, resolution into a 6:2:1 intensity pattern was effected only for the latter.

The 1:1 adduct $Me_2NN(Me)GeMe_3 \cdot BMe_3$ is stable only at $-78°$, being fully dissociated at

Can. J. Chem. Downloaded from www.nrcresearchpress.com by 210.87.254.42 on 09/05/12
For personal use only.

Can. J. Chem. Downloaded from www.nrcresearchpress.com by 210.87.254.42 on 09/05/12
For personal use only.

$-45°$. Attempts to construct molecular models of the adduct revealed severe steric congestion, obviously compensating the enhanced basicity expected from the additional methyl group. Similarly, the basic centres in $Me_2NN(SiMe_3)$-$GeMe_3$ are even more crowded, precluding adduct formation even at low temperatures.

Reactions involving BF_3 resulted in the cleavage of M—N bonds (M = Si, Ge), with formation of Me_3MF, as is generally the case with aminosilanes (5, 6). With $Me_2NN(SiMe_3)$-$GeMe_3$, it appears that one of the M—N bonds is cleaved initially, and, from the relative amounts of Me_3SiF and Me_3GeF produced, the difluoroborane intermediate $Me_2NN(BF_2)$-$SiMe_3$ readily undergoes further self-condensation (eqs. 1*a* and 1*b*).

$$[1a]\quad 2Me_2NN(SiMe_3)GeMe_3 + 2BF_3 \rightarrow Me_2NN(BF_2)GeMe_3 + Me_3SiF + Me_2NN(BF_2)SiMe_3 + Me_3GeF$$

$$[1b]\quad xMe_2NN(BF_2)SiMe_3 \rightarrow (Me_2NNBF)_x + xMe_3SiF$$

Analogous studies of adduct formation between phosphinohydrazines $RR'NNR''P(CF_3)_2$-(R, R′, R″ = H, Me) and BX_3 Lewis acids have shown that BMe_3 does not form an adduct with the trifluoromethylphosphino derivative of trimethylhydrazine, as observed for the trimethylgermyl and trimethylsilyl derivatives; but stable adducts are obtained with BF_3, without cleavage of the P—N bond. In one case, *viz.* $(CF_3)_2$-$PNMeNH_2BX_3$, n.m.r. evidence indicated that complexation occurred at the terminal, least substituted N atom (3).

Insertion Reactions with CO_2 and CS_2

While CS_2 forms simple 1:1 adducts with bases such as Et_2NH (7), the reaction with metalloid-substituted amines, such as trialkylstannyl- (8), germyl- (1), and silyl- (7) dialkylamines, proceeds further to yield thiocarbamate derivatives (1, 8, 9). Similar reactions occur with CO_2 (1, 8, 10) and COS (10). With trialkylmetalloid-hydrazines $Me_2NN(R)MMe_3$ (R = H, Me, $GeMe_3$; M = Si, Ge) two modes of reaction with CS_2 are possible, the insertion mode, described above, or the formation of 1:1 adducts, utilizing the terminal nitrogen atom. With CO_2, the trisubstituted hydrazines (R = H) readily reacted, forming carbamate derivatives $Me_2NNHC(O)OMMe_3$ (M = Ge, Si). The fully substituted sterically hindered compounds (R = Me, $GeMe_3$) required forcing conditions (heating at 90° for several hours) to yield $Me_2NN(Me)C(O)OMMe_3$. The behavior of the bis-organometalloid derivatives Me_2NN-$(MMe_3)M'Me_3$(M, M′ = Si, Ge) is of interest in that reaction could be effected in only one case, *viz.* the conversion of $Me_2NN(GeMe_3)_2$ into $Me_2NN(GeMe_3)C(O)OGeMe_3$. Prolonged heating, and the use of basic catalysts (7), such as Et_2NH and Me_2NNH_2 failed to induce reaction by $Me_2NN(SiMe_3)GeMe_3$ and Me_2NN-$(SiMe_3)_2$ with CO_2. The steric resistance to reaction, due to two organometalloid groups, must be approximately the same for all three molecules, hence the electronic reduction in the basicity of the central nitrogen atom of Me_2NN-$(SiMe_3)GeMe_3$ and $Me_2NN(SiMe_3)_2$ by Me_3Si groups is an important factor in preventing reaction. With CS_2, similar results were obtained, in that thiocarbamate derivatives Me_2NN-$(R)C(S)SMMe_3$ (R = H, Me; M = Si, Ge) and $Me_2NN(GeMe_3)C(S)SGeMe_3$ were formed from the appropriate organometalloid-hydrazine, while the compounds $Me_2NN(SiMe_3)$-$GeMe_3$ and $Me_2NN(SiMe_3)_2$ again failed to react. The reaction of $Me_2NNHSiMe_3$ with CS_2 was noticeably slower than the corresponding reaction of the trimethylgermyl analogue, presumably due to the lower basicity of the former substance. The reaction of $Me_2NN(GeMe_3)_2$ with CS_2 gave rise to some hexamethyldigermane, a product not observed in the corresponding reaction with CO_2.

Mass Spectra of Carbamate and Thiocarbamate Derivatives

Parent ions appropriate to the given formulations were observed in all cases except Me_2-$NNHC(O)OGeMe_3$ and $Me_2NN(GeMe_3)C(S)$-$GeMe_3$, as were small fragments such as CY_2 (Y = O, S), MMe_3 (M = Si, Ge), and Me_2NNR (R = H, Me, $GeMe_3$). The fragments Me_3SiO, Me_3SiS, Me_3SiOCO and $Me_3SiSCSMe$ were observed for the trimethylsilylhydrazines; the corresponding trimethylgermyl fragments were not observed, presumably reflecting the weaker Ge—Y, relative to Si—Y, bond energies (E_{Ge-O} 82 (11); E_{Si-O} 103 (12); E_{Ge-S} 59 (11); E_{Si-S} 79 kcal (12)). Hexamethyldigermane was eliminated from $Me_2NN(GeMe_3)C(O)OGeMe_3$, as was also observed with the bis(trimethylgermyl)-hydrazines of the type $MeN(R)N(GeMe_3)_2$ (R = H, Me, $GeMe_3$), $Me_3GeNHNHGeMe_3$, and $(Me_3Ge)_2NNH_2$ (2). The facile formation

TABLE 1. The p.m.r. data for carbamate and thiocarbamate derivatives.*

Compound	τ (MMe_3)	τ (NH)	τ (NMe)	τ (Me_2N)
$Me_2NNHC(O)OGeMe_3$	9.38	4.40	—	7.41
$Me_2NNHC(s)SGeMe_3$	9.19	—†	—	7.28
$Me_2NN(Me)C(O)OGeMe_3$	9.35	—	7.02	7.35
$Me_2NN(Me)C(S)GeMe_3$	9.25	—	6.60	7.36
$Me_2NN(GeMe_3)C(O)OGeMe_3$	9.40‡ 9.57§	—	—	7.28
$Me_2NN(GeMe_3)C(S)SGeMe_3$	9.30‡ 9.35§	—	—	7.43
$Me_2NNHC(O)OSiMe_3$	9.67	4.22	—	7.36
$Me_2NNHC(s)SSiMe_3$	9.35	—†	—	7.25
$Me_2NN(Me)C(O)OSiMe_3$	9.67	—	7.02	7.35
$Me_2NN(Me)C(S)SSiMe_3$	9.48	—	6.66	7.41

*Measured in solution (5–10%) in $CDCl_3$, relative to TMS, with $\tau = 10.00$.
†Insufficiently soluble to show the NH absorption.
‡$YMMe_3$ protons (Y = O, S).
§$NMMe_3$ protons.

of the Ge—Ge bond, with elimination of $(Me_3Ge)_2$, appears to be a common transition for parent ions containing two Me_3Ge groups. Both $Me_2NNHC(O)OGeMe_3$ and $Me_2NN(GeMe_3)C(S)SGeMe_3$ decomposed in the heated inlet system of the mass spectrometer. A study of the thermal decomposition of the former indicated the formation of $Me_2NN(GeMe_3)C(O)OGeMe_3$, Me_2NNH_2, and CO_2, rationalized according to eq. 2. The decomposition products of $Me_2NN(GeMe_3)C(S)SGeMe_3$ were $(Me_3Ge)_2$, $(Me_3Ge)_2S$, and brown residues. It is puzzling that $Me_2NNHC(S)SGeMe_3$ is more stable than the corresponding carbamate, $Me_2NNHC(O)OGeMe_3$, whereas $Me_2NN(GeMe_3)C(O)OGeMe_3$ is more stable than the thiocarbamate $Me_2NN(GeMe_3)C(S)GeMe_3$.

[2] $2Me_2NNHC(O)OGeMe_3 \rightarrow Me_2NN(GeMe_3)C(O)OGeMe_3 + Me_2NNH_2 + CO_2$

Proton Magnetic Resonance Spectra of Carbamate and Thiocarbamate Derivatives

The p.m.r. data for the compounds $Me_2NN(R)C(Y)YMMe_3$ (R = H, Me, $GeMe_3$; M = Si, Ge) are given in Table 1. The methyl protons of the groups $YMMe_3$ (Y = O, S; M = Si, Ge) are more shielded in the carbamate derivatives than in the thiocarbamate derivatives, i.e. greater shielding occurs with Y = O than with Y = S, the converse of what is expected simply on the basis of the relative electronegativities of oxygen and sulfur. This apparent anomaly has been interpreted in terms of greater dative π-bonding between O and Si or Ge, an effect which compensates the σ-electron withdrawal (13). In the conversions $Me_2NN(R)MMe_3 \rightarrow Me_2NN(R)C(Y)YMMe_3$, the $—C(Y)YMMe_3$ substituent causes a deshielding of both the central RN and terminal Me_2N protons. In the corresponding pairs $Me_2NNHC(Y)YGeMe_3$ and $Me_2NNHC(Y)YSiMe_3$ (Y = O, S), the deshielding effect of thiocarbamate is greater than that of carbamate, whereas in the fully substituted derivatives $Me_2NN(R)C(Y)YMMe_3$, the deshielding effects are quite similar for the two cases. These observations may be interpreted in terms of varying contributions among the resonance structures shown in Fig. 1.

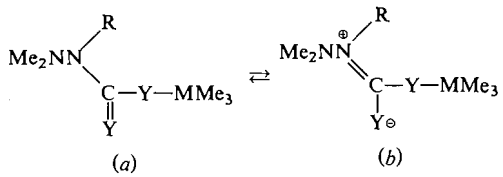

FIG. 1. Resonance structures for carbamate and thiocarbamate derivatives.

Infrared Spectra of Carbamate and Thiocarbamate Derivatives

The carbonyl stretching vibration (10) occurs at 1690–1700 cm^{-1} in the trimethylsilyl derivatives $Me_2NN(R)C(O)OSiMe_3$ (R = H, Me), and at 1660–1680 in the corresponding trimethylgermyl compounds. These observations are consistent if the imine form is dominant for the trimethylgermyl derivatives (Fig. 1*b*), while the π-bonded structure (Fig. 1*a*) is of

Can. J. Chem. Downloaded from www.nrcresearchpress.com by 210.87.254.42 on 09/05/12
For personal use only.

TABLE 2. The i.r. spectra* of $Me_2NN(R)C(O)OMMe_3$; R = H, Me, $GeMe_3$; M = Ge, Si

$Me_2NNHC(O)OGeMe_3$ (Nujol and "Halo-oil" mull):
620(60), 680(54), 720(54), 780(20), 800(20), 830(60), 890(28), 1000(12), 1020(32), 1100(68), 1170(32), 1250(100), 1270(64), 1470(60), 1520(60), 1680(60), 2780(24), 2820(20), 2860(32), 2880(36), 2920(40), 2960(56), 2990(60), 3200(10)

$Me_2NNHC(O)OSiMe_3$ (KBr disc):
460 (broad), 650 (broad), 750(18), 770(7), 840(100), 900(27), 1000(16), 1015(18), 1050(28), 1090(68), 1150(89), 1250(98), 1270(77), 1420(29), 1450(30), 1500(32), 1650(sh), 1690(80), 1700(sh), 2780(9), 2820(14), 2860(23), 2960(32), 2980(14), 3200(45)

$Me_2NN(Me)C(O)OGeMe_3$ (pure liquid film):
460(13), 510(4), 560(15), 620(76), 640(11), 680(15), 710(26), 730(54), 750(41), 800(100), 820(80), 860(43), 920(28), 970(4), 1025(10), 1060(sh), 1090(7), 1140(sh), 1160(33), 1190(35), 1220(26), 1240(59), 1280(39), 1360(48), 1425(50), 1460(33), 1660(76), 2780(17), 2820(30), 2880(48), 2910(59), 2940(59), 2970(74)

$Me_2NN(Me)C(O)OSiMe_3$ (gas phase):
450(10), 600(21), 680(6), 750(17), 800(sh), 830(sh), 855(100), 920(19), 1000(13), 1030(17), 1070(65), 1140(29), 1160(38), 1180(sh), 1260(60), 1330(sh), 1360(42), 1440(25), 1700(50), 2770(21), 2840(25), 2870(29), 2900(38), 2960(63), 2990(sh)

$Me_2NN(GeMe_3)C(O)OGeMe_3$ (pure liquid film):
460(26), 590(22), 570(51), 610(90), 680(61), 735(51), 755(47), 795(78), 825(96), 900(48), 920(26), 1020(32), 1060(65), 1090(66), 1160(17), 1240(83), 1300(100), 1330(82), 1410(43), 1440(52), 1470(25), 1590(25), 1630(sh), 1660(96), 2780(13), 2820(12), 2860(38), 2880(52), 2910(55), 2940(58), 2980(62)

*The i.r. bands are given in cm^{-1}. The numbers in parentheses denote relative intensities, with an arbitrary value of 100 assigned to the most intense band.

TABLE 3. The i.r. spectra* of $Me_3NN(R)C(S)SMMe_3$; R = H, Me, $GeMe_3$; M = Ge, Si

$Me_2NNHC(S)SGeMe_3$ (KBr disc):
380(38), 400(25), 445(28), 470(42), 570(48), 610(61), 690(38), 750(19), 820(78), 915(63), 1000(89), 1160(41), 1180(86), 1235(68), 1335(84), 1385(sh), 1400(sh), 1430(100), 1460(sh), 2700(51), 2840(52), 2900(56), 2940(51), 2980(48), 3200(38)

$Me_2NNHC(S)SSiMe_3$ (KBr disc):
440(15), 460(30), 470(45), 670(45), 810(sh), 840(83), 950(sh), 965(80), 1030(94), 1160(100), 1180(sh), 1250(sh), 1280(73), 1430(42), 1500(23), 2700(sh), 2740(64), 2860(82), 3050(61), 3180(sh)

$Me_2NN(Ne)C(S)SGeMe_3$ (KBr disc):
280(32), 310(49), 460(66), 470(58), 565(89), 590(99), 610(sh), 750(61), 820(100), 920(92), 1010(95), 1080(99), 1140(92), 1180(89), 1230(84), 1250(sh), 1350(99), 1400(sh), 1920(89), 2700(68), 2820(76), 2860(76), 2900(74), 2940(71), 2980(59)

$Me_2NN(Me)C(S)SSiMe_3$ (KBr disc):
460(28), 590(76), 900(83), 940(69), 1020(80), 1110(100), 1150(96), 1180(65), 1220(20), 1250(30), 1330(41), 1370(87), 1430(sh), 1440(96), 1470(94), 1510(48), 2780(30), 2820(37), 2900(39), 2990(20)

$Me_2NN(GeMe_3)C(S)SGeMe_3$ (pure liquid film):
415(86), 520(16), 550(17), 565(60), 610(86), 645(26), 735(100), 760(sh), 820(90), 845(88), 915(60), 1020(7), 1040(12), 1070(7), 1160(10), 1210(16), 1235(53), 1320(36), 1355(19), 1390(38), 1440(28), 1485(26), 1600(14), 2800(10), 2860(17), 2900(40), 2940(26), 2980(48)

*See footnote, Table 2.

major importance in the trimethylsilyl compounds. In the thiocarbamate series, ν(C=S) (10) occurs at 1180 cm^{-1} in $Me_2NNHC(S)SMMe_3$, and at 1220–1230 cm^{-1} in $Me_2NN(Me)C(S)SMMe_3$ (M = Si, Ge); in these compounds, π-bonding between S and the metalloid does not appear to play a significant role. The i.r. data for carbamate and thiocarbamate derivatives are collected in Tables 2 and 3, respectively.

Can. J. Chem. Downloaded from www.nrcresearchpress.com by 210.87.254.42 on 09/05/12
For personal use only.

Can. J. Chem. Downloaded from www.nrcresearchpress.com by 210.87.254.42 on 09/05/12
For personal use only.

Experimental

Apparatus, instrumentation, and experimental procedures for the synthesis of trimethylsilyl and trimethylgermyl derivatives of hydrazines have been described (2, 14, 15). Boron trifluoride, boron trichloride, trimethyl boron, and anhydrous hydrogen chloride, obtained from Matheson, were fractionated through a suitable train of cold traps. Solvents were dried and distilled before use.

In a typical procedure, the substituted hydrazine and BX_3 were mixed, either in a 1:1 molar ratio, or with BX_3 in known excess. After 1 h at room temperature, the products were separated by fractionation, and estimated, thus giving the stoichiometry of the reaction. If necessary, the reaction tube was cooled (not lower than $-78°$) in order to check for adduct formation at low temperatures; in other cases, solutions of the hydrazine and BX_3 were prepared, and their p.m.r. spectra were recorded at various temperatures. With BMe_3, 1:1 adducts were obtained according to eq. 3,

[3] $Me_2NN(R)MMe_3 + BMe_3 \rightarrow Me_2NN(R)MMe_3 \cdot BMe_3$

for R = Me, H and M = Ge, and for $Me_2NNHSiMe_3$. The compound $Me_2NN(Me)GeMe_3BMe_3$, stable at $-78°$, was fully dissociated at $-45°$. With BF_3, cleavage of metalloid–nitrogen bonds was observed in all cases; typically, the products of the reaction of $Me_2NN(Me)GeMe_3$ (0.69 mmol) and BF_3 (0.71) were: BF_3 (trace), Me_3GeF (0.67 mmol), and a white solid residue.

Reactions between organometalloid-hydrazines and CO_2 or CS_2 were carried out according to modified procedures of Lappert and coworkers (8). The following compounds, characterized on the basis of m.p., molecular weight, and mass, i.r., and p.m.r. spectral measurements, were obtained: $Me_2NNHC(O)OGeMe_3$, m.p. 60–61°; $Me_2NN(Me)C(O)OGeMe_3$, m.p. $-18.5°$ ($P_{obsd.}$ 236, $P_{calcd.}$ 236, plus the fragments CO_2, Me_2NNMe, Me_3Ge); $Me_2NN(GeMe_3)C(O)OGeMe_3$, liquid at room temperatures, glassy solid ($P_{obsd.}$ 338, $P_{calcd.}$ 338, plus CO_2, $Me_2NNGeMe_3$, $(Me_3Ge)_2$); $Me_2NNHC(O)OSiMe_3$, m.p. 76.6–77.0° ($P_{obsd.}$ 176, $P_{calcd.}$ 176; plus CO_2, Me_3SiOCO, Me_3SiO, Me_3Si); $Me_2NN(Me)C(O)SiMe_3$, m.p. $-12.5°$ ($P_{obsd.}$ 190, $P_{calcd.}$ 190; plus CO_2, Me_3SiOCO, Me_3SiO, Me_3Si); no reaction was observed for $Me_2NN(SiMe_3)_2$ and $Me_2NN(SiMe_3)GeMe_3$ with CO_2. $Me_2NNHC(S)SGeMe_3$, m.p. 103–104° ($P_{obsd.}$ 253, $P_{calcd.}$ 254; plus CS_2, Me_3Ge); $Me_2NN(Me)C(S)SGeMe_3$, m.p. 72–73° ($P_{obsd.}$ 268, $P_{calcd.}$ 268; plus CS_2, Me_3Ge); $Me_2NN(GeMe_3)C(S)SGeMe_3$, liquid at room temperature, glassy solid; $Me_2NNHC(S)SSiMe_3$, white solid ($P_{obsd.}$ 209, $P_{calcd.}$ 208; plus CS_2, Me_2NNH, Me_3SiS, Me_3Si); $Me_2NN(Me)C(S)SSiMe_3$, m.p. 58–59° ($P_{obsd.}$ 222, $P_{calcd.}$ 222; plus CS_2, Me_2NNMe, $Me_3SiC(S)SMe$, Me_3Si); no reaction was observed for $Me_2NN(SiMe_3)_2$ and $Me_2NN(SiMe_3)GeMe_3$ with CS_2. The observed reactions with CO_2 and CS_2 corresponded to eq. 4.

[4] $Me_2NN(R)MMe_3 + CY_2 \rightarrow Me_2NN(R)C(Y)YMMe_3$

The authors acknowledge the financial assistance of the National Research Council of Canada.

1. J. SATGE, M. LESBRE, and M. BAUDET. Compt. Rend. **259**, 4733 (1964).
2. L. K. PETERSON and K. I. THÉ. Can. J. Chem. This issue.
3. L. K. PETERSON and G. L. WILSON. Can. J. Chem. **49**, 3171 (1971).
4. C. W. HEITSCH. Inorg. Chem. **4**, 1019 (1965).
5. S. SUJISHI and S. WITZ. J. Am. Chem. Soc. **79**, 2447 (1957).
6. H. GROSSE-RUYKEN and R. KLEESAAT. Z. Anorg. Chem. **308**, 122 (1961).
7. H. BREEDERVELD. Rec. Trav. Chim. **81**, 276 (1962).
8. (*a*) K. JONES and M. F. LAPPERT. J. Chem. Soc. 1944 (1965). (*b*) T. A. GEORGE, K. JONES, and M. F. LAPPERT. J. Chem. Soc. 2157 (1965).
9. E. W. ABEL and J. P. CROW. J. Chem. Soc. A, 1361 (1968).
10. R. F. DALTON and K. JONES. J. Chem. Soc. A, 590 (1970).
11. J. S. POLAND. Ph.D. Thesis. University of Sussex, U.K., 1969.
12. J. C. BALDWIN, M. F. LAPPERT, J. B. PEDLEY, and J. A. TREVERTON. J. Chem. Soc. A, 1980 (1967).
13. H. SCHMIDBAUR. J. Am. Chem. Soc. **85**, 2336 (1963).
14. U. WANNAGAT and F. HÖFLER. Monatsh. Chem. **97**, 976 (1966).
15. F. HÖFLER and U. WANNAGAT. Monash. Chem. **97**, 1598 (1966).

Metal Halide Ammines. II.[1] Thermal Analyses, Calorimetry and Infrared Spectra of Fluoride Ammines and Hydrates of Bivalent Metals

K. C. PATIL AND E. A. SECCO

Chemistry Department, St. Francis Xavier University, Antigonish, Nova Scotia

Received August 13, 1971

Thermal analyses of bivalent metal fluoride ammines reveal that decomposition occurs in two or more steps. Calorimetric measurements along with related enthalpic values of the various decomposition steps are given. The infrared spectral data of the ammines and hydrates are compared with theoretical and some experimental values already in the literature.

Les analyses thermiques d'ammines de métaux fluorés bivalents indiquent que la décomposition se fait en deux étapes ou plus. Des mesures calorimétriques ainsi que les valeurs d'enthalpie correspondantes sont données pour les différentes étapes de décomposition.

Les données infrarouges des amines et des hydrates sont comparées avec les valeurs théoriques et quelques valeurs expérimentales déjà dans la littérature.

Canadian Journal of Chemistry, **50**, 567 (1972)

Introduction

Although metal chloride, bromide, and iodide ammines (1, 2) have attracted the interest of chemists for some time, surprisingly little effort has been directed towards the metal fluoride ammines.

Alkali and alkaline earth metal fluorides are not known to form ammines with ammonia gas or liquid since such a reaction is expected to be highly endothermic with a large amount of energy required to expand the fluoride lattice (3). Fluorides of Ag(I) and the bivalent metals Cu, Mn, Fe, Co, and Ni add NH_3 to form ammoniate complexes (4); these complexes are explained in terms of the large coordination energy released in surrounding the strongly polarizing cation with the polarizable ammonia molecules (5).

Recently, Cavell and Clark (6, 7) have reported the preparation of V, Nb, and W fluoride ammines. In this laboratory, we have prepared a number of bivalent metal fluoride ammines by reacting the fluoride hydrate with liquid ammonia. The purpose of this work was to study the mode of decomposition, heat of decomposition, relative thermal stability, and infrared spectra of fluoride ammines of some bivalent transition metals; the analogous hydrates were also studied and included for comparison purposes.

[1]For Part I, see ref. 22.

Experimental

$ZnF_2.4H_2O$ and $CdF_2.2H_2O$ were obtained by treating ZnO and CdO, respectively, with aqueous HF in plastic ware. $CuF_2.2H_2O$ was obtained by following a known procedure (8). $CoF_2.4H_2O$ and $NiF_2.4H_2O$, used in this work were obtained by recrystallization in aqueous HF of the commercially available compounds.

The fluoride tetra- and hexa-ammines were prepared by refluxing the freshly prepared fluoride hydrate with anhydrous liquid ammonia as previously described in Part I of this series. No color change was noticed with ZnF_2 and CdF_2 for the hydrate → ammine conversion whereas distinct color changes were observed for the following:

$$CuF_2.2H_2O \text{ (blue)} \rightarrow CuF_2.6NH_3 \text{ (deep blue)}$$

$$CoF_2.4H_2O \text{ (pink)} \rightarrow CoF_2.4NH_3 \text{ (red)}$$

$$NiF_2.4H_2O \text{ (green)} \rightarrow NiF_2.6NH_3 \text{ (blue-violet)}$$

The monoammines of ZnF_2 and CdF_2 were prepared by heating ZnO and CdO, respectively, with NH_4F thoroughly mixed in 1:4 molar ratio for 8–10 h at 150 °C and eliminating the excess NH_4F by washing with methanol.

The composition, and purity, of the hydrates and ammines was assessed by their infrared spectra and thermal analyses along with identification of their decomposition products.

The heating curves recorded for differential thermal analysis, thermogravimetry, and calorimetry were obtained using the instrumentation and following the procedure described (9, 10). The electrical thermal analyzer, ETA-960, a plug-in accessory to the duPont 900 console, was used according to supplier's instruction manual to monitor the electrical conductivity as a function of temperature. The sample material was packed in a holder between two Pt electrodes. A d.c. potential of 10 V was applied across the sample and the current developed, from a low current limit of 10^{-10} A, was recorded as a function of temperature at a constant heating rate.

The infrared spectra of the compounds were recorded on a

Can. J. Chem. Downloaded from www.nrcresearchpress.com by 210.87.254.5 on 09/05/12
For personal use only.

TABLE 1.
(*a*) Thermogravimetric analysis of fluoride hydrates

Compound	Step number	Temperature range* (°C)	% of total weight lost	
			Observed	Calculated
$ZnF_2.4H_2O$	1	60–200	41.40	41.10
$CdF_2.2H_2O$	1	40–120	20.40	19.30
$FeF_2.4H_2O$	1	60–350	43.50	43.44
$CoF_2.4H_2O$	1	90–300	41.80	42.62
$NiF_2.6H_2O$	1	100–350	42.80	43.08

*Onset and terminal temperatures.

(*b*) Differential thermal analysis of fluoride hydrates

Compound	Peak number*	Peak temperature (°C)	Reaction
$ZnF_2.4H_2O$	1	110	[1]
	2	845	Fusion ZnF_2
$CdF_2.2H_2O$	1	90	[1]
	2	980	Fusion CdF_2
$FeF_2.4H_2O$	1	90	[1]
	2	250	$FeF_2 + O_2 \rightarrow$ oxyfluoride mixed?
$CoF_2.4H_2O$	1	152	[1]
$NiF_2.4H_2O$	1	175	[1]

*All endotherms.

Perkin–Elmer Model-180 Spectrophotometer using the standard pellet technique with KBr as the matrix material.

X-Ray diffraction patterns of solid specimens were recorded on a Norelco X-ray diffractometer unit using Cu K_α radiation with Ni filter or Mo K_α radiation with Zr filter as previously described (11).

Results and Discussion

A. Thermal Analyses of Hydrates

The results of thermogravimetry presented in Table 1 show that all the fluoride hydrates studied, except $CuF_2.2H_2O$ which was reported earlier, undergo dehydration in a single step represented by the general equation

$$[1] \qquad MeF_2.xH_2O_{(s)} \rightarrow MeF_{2(s)} + xH_2O_{(g)}$$

The DTA heating curves show two endotherms in the case of Zn, Cd, and Fe but a single endotherm for Co and Ni. The first endotherm is identified with dehydration while the second endotherm in Zn and Cd compounds is due to melting of the anhydrous fluoride. Dehydration of $FeF_2.4H_2O$ yields a mixture of oxide, fluoride, and/or oxyfluoride in the solid residue as reported earlier by Ostrovskaya and Amirova (12).

The heats of dehydration are presented in Table 2. The column of values for ΔH per mole of H_2O liberated shows a constant value of 12–13 kcal for the tetrahydrates and a higher value of 16 kcal for the dihydrate.

B. Thermal Analyses of the Ammines

The results of thermogravimetry and DTA measurements are presented in Tables 2 and 3, respectively. The proposed reactions for each compound are those which best fit the observed weight loss in TG and correlated with DTA heating curves along with identification of the intermediate and final products by X-ray diffraction. Each compound is discussed in sequence.

Zinc Fluoride Ammines

According to TG the hexammine decomposed to zinc fluoride in two steps:

$$[2] \qquad ZnF_2.6NH_{3(s)} \rightarrow ZnF_2.2NH_3 + 4NH_{3(g)}$$

$$[3] \qquad ZnF_2.2NH_{3(s)} \rightarrow ZnF_{2(s)} + 2NH_{3(g)}$$

The DTA heating curve showed the two endotherms corresponding to reactions 2 and 3 along with an exotherm at 580 °C and an additional endotherm at 640 °C. The exotherm

Can. J. Chem. Downloaded from www.nrcresearchpress.com by 210.87.254.5 on 09/05/12
For personal use only.

TABLE 2. Thermogravimetric analysis of fluoride ammines

Compound	Step number	Temperature range* (°C)	% of total weight lost		Reaction
			Observed	Calculated	
$ZnF_2.6NH_3$	1	50–150	33.26	33.11	[2]
	2	175–280	50.00	49.66	[3]
$ZnF_2.NH_3$	1	120–300	13.22	14.17	Deammoniation
$CdF_2.6NH_3$	1	50–140	33.10	33.68	[4]
	2	140–250	40.50	40.41	[5]
$CdF_2.NH_3$	1	50–275	9.10	10.18	[5]
$CuF_2.6NH_3$	1	50–150	32.63	33.44	[6]
	2	150–200	41.77	41.77	[7]
	3	200–290	49.59	50.12	[8]
	4	>800			[9]
$CuF_2.8NH_3$*	1	25–120	41.77	42.95	[10]
	2	180–220	48.83	50.11	[11]
	3	240–320	70.38	71.30	[12]
	4	400–450	72.94	73.26	[13]
$CoF_2.4NH_3$	1	50–200	34.10	34.20	[14]
	2	200–300	42.60	41.33	[15]
$NiF_2.6NH_3$	1	60–175	31.81	32.57	[16]
	2	175–400	48.34	48.87	[18]

*TG of $CuF_2.6NH_3$ exposed to flowing NH_3 initially formed $CuF_2.8NH_3$.

TABLE 3. Differential thermal analysis of fluoride ammines

Compound	Peak number*	Peak temperature (°C)	Reaction
$ZnF_2.6NH_3$	1	145	[2]
	2	255	[3]
	3†	580	Formation Zn_3N_2
	4	640	Decomposition Zn_3N_2
$ZnF_2.NH_3$	1	270	Deammoniation
	2	875	Fusion ZnF_2
$CdF_2.6NH_3$	1	155	[4]
	2	250	[5]
	3†	430	Formation Cd_3N_2
	4	580	Decomposition Cd_3N_2
$CdF_2.NH_3$	1	155	[5]
	2	985	Fusion CdF_2
$CuF_2.6NH_3$	1	130	[6]
	2	190	[7]
	3	270	[8]
	4	340	[12*a*]
	5	640	[13]
$CoF_2.4HN_3$	1	170	[14]
	2	280	[15]
$NiF_2.6NH_3$	1	165	[16]
	2	225	[17]
	3	290	[18]

*All endotherms except those marked with †.

Can. J. Chem. Downloaded from www.nrcresearchpress.com by 210.87.254.5 on 09/05/12
For personal use only.

Can. J. Chem. Downloaded from www.nrcresearchpress.com by 210.87.254.5 on 09/05/12
For personal use only.

is assigned to the formation of the nitride Zn_3N_2, a product of the reaction between ZnF_2 and NH_3 during the decomposition of diammine. The X-ray diffraction pattern of the DTA residue halted at 580 °C displays the lines characteristic of both ZnF_2 and Zn_3N_2. The endotherm at 640 °C is then identified with the dissociation of Zn_3N_2 (13). The endotherm expected from the melting of ZnF_2 *ca.* 850 °C was not observed; however, the DTA heating curve of the residue from TG arrested at 350 °C showed the 850 °C endotherm due to ZnF_2 fusion. The apparent disparity between the presence of Zn_3N_2 and absence of ZnF_2 in DTA and *vice versa* in TG is accounted for in terms of the dynamic conditions prevailing in TG relative to the static conditions in DTA where NH_3 is accumulated and interacts with the metal fluoride.

The monoammine decomposed to ZnF_2 in one step as shown by TG and DTA; the melting endotherm of ZnF_2 also appeared in the DTA heating curve.

Cadmium Fluoride Ammines

The hexammine decomposed to CdF_2 via reactions 4 and 5

$$[4] \quad CdF_2.6NH_{3(s)} \rightarrow CdF_2.NH_{3(s)} + 5NH_{3(g)}$$

$$[5] \quad CdF_2.NH_{3(s)} \rightarrow CdF_{2(s)} + NH_{3(g)}$$

The DTA heating trace showed two endotherms consistent with reactions 4 and 5 in addition to an exotherm at 430 °C and another endotherm at 580 °C. Parallel to the zinc fluoride hexammine DTA features assignment, the 430 °C exotherm represents the formation of Cd_3N_2 with its subsequent decomposition giving rise to the 580 °C endotherm. The formation of Cd_3N_2 was confirmed by X-ray diffraction of the DTA residue obtained at 450 °C and by reaction of CdF_2 in NH_3 atmosphere under simulated DTA conditions.

The monoammine decomposed in one step to yield CdF_2. In addition to the decomposition endotherm, the melting endotherm of CdF_2 was also evident in the DTA trace.

Copper Fluoride Ammine

The decomposition pattern of copper fluoride hexammine was observed to be influenced by the nature of the atmosphere in contact with the ammine. The decomposition sequence under a static atmosphere or an atmosphere of flowing N_2 is represented as follows

$$[6] \quad CuF_2.6NH_{3(s)} \rightarrow CuF_2.2NH_{3(s)} + 4NH_{3(s)}$$

$$[7] \quad CuF_2.2NH_{3(s)} \rightarrow CuF_2.NH_{3(s)} + NH_{3(g)}$$

$$[8] \quad CuF_2.NH_{3(s)} \rightarrow CuF_{2(s)} + NH_{3(g)}$$

$$[9] \quad CuF_{2(s)} \rightarrow \text{volatilization } (>800\ ^\circ C)$$

Under an atmosphere of flowing NH_3, there is a rapid initial uptake of NH_3 by the hexammine with the quantitative data of the subsequent decomposition steps indicating the initial formation of the octaammine and its breakdown as follows

$$[10] \quad CuF_2.8NH_{3(l)} \rightarrow CuF_2.2NH_{3(s)} + 6NH_{3(g)}$$

$$[11] \quad CuF_2.2NH_{3(s)} \rightarrow CuF_2.NH_{3(s)} + NH_{3(g)}$$

$$[12] \quad 6CuF_2.NH_{3(s)} \rightarrow 2Cu_3N_{(s)} + 2NH_{3(g)} + 12HF_{(g)} + N_{2(g)}$$

$$[13] \quad Cu_3N_{(s)} \rightarrow 3Cu_{(s)} + \tfrac{1}{2}N_{2(g)}$$

The DTA heating curve displayed four endotherms assigned to reactions 6, 7, 8, 12*a*,

$$[12a] \quad 3CuF_{2(s)} + 2NH_{3(g)} \rightarrow Cu_3N_{(s)} + 6HF + \tfrac{1}{2}N_{2(g)}$$

along with one exotherm identified with reaction 13. As mentioned above, *viz.* zinc fluoride ammine, the conditions in DTA allow NH_3 to accumulate and, in the final stage, to interact with the fluoride to form the nitride paralleling the TG experiment under ammonia atmosphere. Copper nitride is reported to form when anhydrous copper fluoride is heated in the presence of NH_3 gas (14). A sharp rise in the ETA conductivity trace at 350 °C supports the transition of CuF_2 to Cu_3N via reaction 12*a*.

The intermediates from thermogravimetry and differential thermal analysis were identified by their characteristic X-ray diffraction patterns and infrared spectra.

Cobalt Fluoride Ammine

The thermogravimetry of the tetraammine showed the mode of decomposition to occur via the monoammine,

$$[14] \quad CoF_2.4NH_{3(s)} \rightarrow CoF_2.NH_{3(s)} + NH_{3(g)}$$

$$[15] \quad CoF_2.NH_{3(s)} \rightarrow CoF_{2(s)} + NH_{3(g)}$$

The DTA trace exhibited two endotherms interpreted in terms of reactions 14 and 15.

The residue from TG and DTA, CoF_2, was confirmed by its X-ray diffraction patterns.

Nickel Fluoride Ammine

According to TG data the hexammine decomposed to NiF_2 through the diammine intermediate. The DTA curve exhibited three endo-

TABLE 4. Heats of decomposition of hydrates and ammines

Compound	Reaction*	Heat of decomposition† (kcal/mol) ΔH of compound decomposed	ΔH per mole of NH_3 or H_2O formed
$ZnF_2.4H_2O$	$ZnF_2.4H_2O_{(s)} \xrightarrow{80-160} ZnF_{2(s)} + 4H_2O_{(g)}$	52.00±0.25	13.00±0.06
$CdF_2.2H_2O$	$CdF_2.2H_2O_{(s)} \xrightarrow{50-125} CdF_{2(s)} + 2H_2O_{(g)}$	32.00±0.50	16.00±0.25
$CoF_2.4H_2O$	$CoF_2.4H_2O_{(s)} \xrightarrow{110-195} CoF_{2(s)} + 4H_2O_{(g)}$	52.20±0.25	13.05±0.06
$NiF_2.4H_2O$	$NiF_2.4H_2O_{(s)} \xrightarrow{110-220} NiF_{2(s)} + 4H_2O_{(g)}$	49.00±0.10	12.25±0.03
$ZnF_2.NH_3$	$ZnF_2.6NH_{3(s)} \xrightarrow{215-265} ZnF_{2(s)} + 6NH_{3(g)}$	10.89±0.02	10.89±0.02
$ZnF_2.6NH_3$	$ZnF_2.6NH_{3(s)} \xrightarrow{60-300} ZnF_{2(s)} + 6NH_{3(g)}$	56.52±0.27	9.42±0.07
$CdF_2.NH_3$	$CdF_2.NH_{3(s)} \xrightarrow{165-260} CdF_{2(s)} + NH_{3(g)}$	10.81±0.02	10.81±0.02
$CdF_2.6NH_3$	$CdF_2.6NH_{3(s)} \xrightarrow{25-235} CdF_{2(s)} + 6NH_{3(g)}$	60.75±0.25	10.12±0.04
$CuF_2.6NH_3$	$CuF_2.6NH_{3(s)} \xrightarrow{50-260} CuF_{2(s)} + 6NH_{3(g)}$	63.58±0.52	10.59±0.08
$CoF_2.4NH_3$	$CoF_2.4NH_{3(s)} \xrightarrow{100-300} CoF_{2(s)} + 4NH_{3(g)}$	43.83±0.02	10.95±0.01
$NiF_2.6NH_3$	$NiF_2.6NH_{3(s)} \xrightarrow{65-225} NiF_{2(s)} + 6NH_{3(g)}$	69.28±0.50	11.54±0.08

*Over temperature range in °C.
†All determinations were done in duplicate; ΔH values accompanied by average deviations.

therms, none was reversible, which prompts us to suggest the following reaction sequences:

[16] $NiF_6.6NH_{3(s)} \rightarrow NiF_2.2NH_{3(s)} + 4NH_{3(g)}$

[17] $NiF_2.2NH_{3(s)} \rightarrow NiF_2.NH_{3(s)} + NH_{3(g)}$

[18] $NiF_2.NH_{3(s)} \rightarrow NiF_{2(s)} + NH_{3(g)}$

C. Calorimetric Results

The heats of decomposition of both the hydrates and the ammines are presented in Table 4. The last column shows the values of ΔH per mole of H_2O liberated to be slightly higher (by 2–5 kcal) than the ΔH per mole of NH_3 liberated for the same metal fluoride. This fact suggests that the water molecule is more strongly bound to the fluoride lattice relative to the ammonia molecule; most likely due to the stronger H-bonding in the hydrates than in the ammines taking into account oxygen to be more electronegative than nitrogen. It must be noted that the reactivity of the metal fluoride is much greater towards H_2O than towards NH_3; evident by hydrolysis of the fluoride to yield basic fluorides on storage whereas ammonolysis of the fluoride was undetectable over the same time interval.

It may be worth noting that the observed ΔH per mole of H_2O formed *ca.* 13.6 kcal/mol is consistent with the assigned bond energy of 13 kcal/mol for each O—H...F^- bond assumed for hydrogen bonds between F^- and ligated water molecules (21).

D. Infrared Spectral Data

The infrared absorption frequencies of metal fluoride hydrates and ammines, with their assignments, in the 4000–180 cm^{-1} region are presented in Tables 5 and 6, respectively. The vibrational assignments for the ammines are made on the basis that the site symmetry of the complex ion in the compound of formula $[Me(NH_3)_6]F_2$ is O_h (18); the assignments for the hydrates are given in accordance with the model considered by Fujita *et al.* (15).

Our data show a high degree of internal consistency for the various assignments; the data are also in agreement with the existing literature values, both theoretical and experimental, for other metal halide hexammines.

The infrared spectra of metal halide complexes serve as a useful means to assess the nature of bonding of the ligands to the metals. In the case of the fluoride hydrates where one considers Me—OH_2 and O—H...X (X = halogen) distances as a measure of the strength of coordination and of H-bonding, respectively, one

Can. J. Chem. Downloaded from www.nrcresearchpress.com by 210.87.254.5 on 09/05/12
For personal use only.

TABLE 5. Infrared absorption band frequencies of fluoride hydrates

Compound	Frequency* (cm^{-1})					
	$\nu_{(OH)}$	$\delta_{(H_2O)} + \nu_{(H_2O)_R}$	$\delta_{(H_2O)}$	$\nu_{(H_2O)_R}$	$\nu_{(H_2O)_{wag}}$	$\nu_{(M-F)}$
$[Fe(OH_2)_4]F_2$	3450(s) 3180(s)	2460(w)	1650(m)	810(m)	690(w)	465(s)
$[Co(OH_2)_4]F_2$	3450(s) 3180(s)	2330(w)	1650(m)	865(w) 760(m)	635(w)	485(s) 400(s) 280(w)
$[Ni(OH)_2]_4F_2$	3430(s) 3180(s)	2340(w)	1660(m)	905(w) 775(m)	660(w) 640(w)	500(s) 400(s) 360(w) 290(w)
$[Cd(OH_2)_4]F_2$	3440(s) 3170(s)	2350(w)	1655(m)	865(w) 740(m)	640(w)	485(w) 400(s)
$ZnF_2.4H_2O$	3540(s) 3160(s)		1600(m)	750(m)		480(w) 430(s)
$CuF_2.2H_2O$	3500(s) 3150(s)		1625(m) 1525(w)	745(m)		490(s)

*s = strong; m = medium; w = weak.

can expect the rocking frequency of H_2O in aquo complexes to shift to higher frequency with increasing coordination as is evident for metal–ammine complexes (15–17). The $\nu_{(H_2O)_R}$ of medium intensity in Table 5 increases in the order Fe > Ni > Co > Cd indicating a decrease in the O—H...X distance in the direction Fe < Ni < Co < Cd. The absorption band in the 2450–2350 cm^{-1} region is assigned to a combination of $\delta_{(H_2O)}$ and $\nu_{(H_2O)_R}$. In contrast to the above aquo complexes, the infrared spectra of Zn and Cu fluoride hydrates are interpreted in terms of simple hydrates and not aquo complexes.

The metal fluoride ammines in Table 6 show the characteristic frequencies of coordinated ammonia; characteristic frequencies of analogous halide ammines are included for com-

TABLE 6. Infrared absorption band frequencies of fluoride ammines

Compound	Frequency* (cm^{-1})							
	$\nu_{(NH)_{as}}$	$\nu_{(NH)_s}$	$\delta_{(NH_3)_d}$	$\delta_{(NH_3)_s}$	$\rho_{(NH_3)_\gamma}$	$\nu_{(M-F)}$	$\nu_{(M-N)}$	$\delta_{(N-M-N)}$
$[Co(NH_3)_6]F_2$	3350(s)	3170(s,b)	1620(m,b)	1175(s,sp)	650(s)	440(s)	320(s,sp)	—
$[Co(NH_3)_6]Cl_2$†	3330 (3330)	3250 (3250)	1605 (1605)	1160 (1171)	634 (625)	— —	318 (323)	— (184)
$[Ni(NH_3)_6]F_2$	3350(s)	3170(s,b)	1610(m,b)	1185(s,sp)	670(s)	440(s)	325(s)	—
$[Ni(NH_3)_6Cl_2$†	(3393)	3370(vb) (3310)	1610 (1606)	1175 (1197)	678 (625)	— —	330 (335)	215 (214)
$[Zn(NH_3)_6]F_2$	3310(s)	3190(s) 3145(s)	1620(m,b)	1260(s,sp)	705(s,sp)	420(s)	—	—
$[Cu(NH_3)_6]F_2$	3300(s)	3240(s) 3160(s)	1600(m,b)	1270(s) 1250(s,sp)	700(m)	470(s)	—	—
$[Cd(NH_3)_6]F_2$	3350(s)	3200(s) 3080(s)	1620(m,b)	1260(s,sp)	985(w) 860(m)	400(s)	—	—

*s = strong; m = medium; w = weak; b = broad; sp = sharp; v = very.
†Taken from ref. 19 and included for comparison purposes. Frequencies enclosed in parentheses are calculated values.

Can. J. Chem. Downloaded from www.nrcresearchpress.com by 210.87.254.5 on 09/05/12
For personal use only.

parison purposes (18–20). The observed frequency *ca.* 320 cm^{-1} for Co and Ni ammines is assigned to $\nu_{(M-N)}$ mode while the bands in the 400–470 cm^{-1} region are assigned to $\nu_{(M-F)}$.

Grateful acknowledgement for financial support of this work is made to the National Research Council of Canada and the University Council for Research.

1. G. W. A. Fowles and D. Nicholls. Quart. Rev. **16**, 19 (1962).
2. G. W. A. Fowles. Prog. in Inorg. Chem. **6**, 1 (1964).
3. W. Biltz and H. G. Grimm. Z. anorg. allgem. Chem. **145**, 63 (1925).
4. W. Biltz and E. Rahys. Z. anorg. allgem. Chem. **166**, 351 (1927).
5. J. C. Bailer. Chemistry of coordination compounds ACS monograph. No. 131. Reinhold Publishing Corp. 1956. p. 142.
6. R. G. Cavell and H. C. Clark. J. Inorg. Nucl. Chem. **17**, 257 (1961).
7. H. C. Clark and H. J. Emeleus. J. Chem. Soc. 4778 (1957).
8. P. Ramamurthy and E. A. Secco. Can. J. Chem. **47**, 2185 (1969).
9. O. K. Srivastava and E. A. Secco. Can. J. Chem. **45**, 579 (1967).
10. P. Ramamurthy and E. A. Secco. Can. J. Chem. **46**, 3605 (1968).
11. E. A. Secco. Can. J. Chem. **42**, 2143 (1964).
12. T. V. Ostrovskaya and S. A. Amirova. Russ. J. Inorg. Chem. **14**, 755 (1969).
13. R. Juza and H. Hahn. Z. anorg. allgem. Chem. **239**, 273 (1938).
14. R. Juza and H. Hahn. Z. anorg. allgem. Chem. **241**, 172 (1939).
15. J. Fujita, K. Nakamoto, and M. Kobayashi. J. Am. Chem. Soc. **78**, 3963 (1956).
16. J. Fujita, K. Nakamoto, and M. Kobayashi. J. Am. Chem. Soc. **78**, 3925 (1956).
17. S. Mizushima, I. Nagakawa, and J. Quagliano. J. Chem. Phys. **23**, 1367 (1955).
18. L. Sacconi, A. Sabatini, and P. Gans. Inorg. Chem. **3**, 1772 (1964).
19. T. Shimanouchi and I. Nagakawa. Inorg. Chem. **3**, 1805 (1964).
20. D. M. Adams. Metal-Ligand and related vibrations. Edward Arnold Ltd., London. 1967.
21. L. Pauling. The nature of the chemical bond. 3rd Ed. Cornell University Press, Ithaca, New York. 1960. p. 461.
22. K. C. Patil and E. A. Secco. Can. J. Chem. **49**, 3831 (1971).

Can. J. Chem. Downloaded from www.nrcresearchpress.com by 210.87.254.5 on 09/05/12
For personal use only.

Theory of Ionic Conduction in Solids

L. YOUNG

Department of Electrical Engineering, The University of British Columbia, Vancouver 8, British Columbia

Received July 20, 1971

When a constant field in the 10^6 V cm^{-1} range is applied to annealed anodic oxide films the ion current builds up in accelerating fashion. It is shown that a model in which the ions move through channels in the oxide and in which the moving ions clear the initially blocked channels reproduces the general form of the ion current *vs.* time behavior. Dignam's theory of this process is discussed. A recent claim that considerations of mean free path render inapplicable to these films models in which the concentration of ions changes with field due to homogeneous generation of Frenkel defects is shown to be unjustified.

A further observed phenomenon in which the latent ionic conductivity of the films decays at zero field is also discussed in terms of the competing models.

Quand un champ constant dans le domaine de 10^6 V cm^{-1} est appliqué à des films d'oxyde anodique après traitment thermique, le courant ionique s'établit d'une façon accélérée. On montre qu'un modèle dans lequel les ions se déplacent à travers les canaux de l'oxyde tout en dégageant les canaux initialement bloqués, reproduit la forme générale d'un courant ionique dans le temps. La théorie de Dignam sur ce processus est discutée. Récemment, on a déclaré que à partir de considérations sur le libre parcous moyen on ne peut appliquer a ces films les modèles dans lesquels la concentration des ions change avec le champ en raison de la génération homogène des défauts de Frenkel. On montre que ceci est injustifié. Un phénomène observé plus avant dans lequel la conductivité ionique latente des films décroît à champ nul, est aussi discuté en termes de modèles mis en compétition.

Canadian Journal of Chemistry, **50**, 574 (1972)

Models Consistent with Constant-field Transients

The correct model for the ionic conduction process involved in the growth of anodic films is uncertain (1). It has been suggested by Bean, Fisher, and Vermilyea (2) that the concentration of mobile ions is field-dependent. The model proposed by these authors involved the removal of metal ions from network-forming sites in the amorphous oxide by ordinary field-assisted thermal activation. Each such event would create an interstitial metal ion and a vacant cation site, *i.e.*, a Frenkel defect. The vacancies were supposed to be negatively charged. This was expected since the oxide was supposed to be neutral before the creation of the vacancy–interstitial pair. The interstitial ions were supposed to be mobile and the vacancies not. Bean *et al.* tacitly assumed that the two components of the Frenkel defects would remain in equal concentrations. Dewald (3) showed explicitly that this would occur due to assuming electroneutrality and equal charges on the two components of the Frenkel defects. Interstitial ions were supposed to be destroyed by capture by vacancies. A steady state concentration of mobile ions would hence exist for any given electrostatic field. When the field was changed the concentration of the mobile interstitials would not immediately jump to its new value and, consequently, various transient phenomena would be expected for step changes in either field or current. Dewald showed that this model explained his experimental data on transients. However, it was later found by Young (4) that if a relatively large and constant field is applied to films prepared in such a way that, if the theory is correct, they would contain a low concentration of defects, the ion current increases in accelerating fashion (Fig. 1). Since the rate of production of defects is, in this model, a function of the field only, whereas the rate of destruction is supposed to be given by σJn (where σ is a capture cross-section, J is the ionic current density (in units of (ions/area × time)), and n is the defect concentration); n and hence J should build up rapidly at first and then more slowly. The result was first observed for tantalum but similar experiments on aluminum by Dignam and Ryan (5) gave similar results. However, these experiments by no means offer unique support to Dignam's model (to be outlined below). The experiment certainly shows that if the transients are due to the changes in concentration of carriers, then the rate of generation of carriers cannot be

Can. J. Chem. Downloaded from www.nrcresearchpress.com by 210.87.254.105 on 09/05/12
For personal use only.

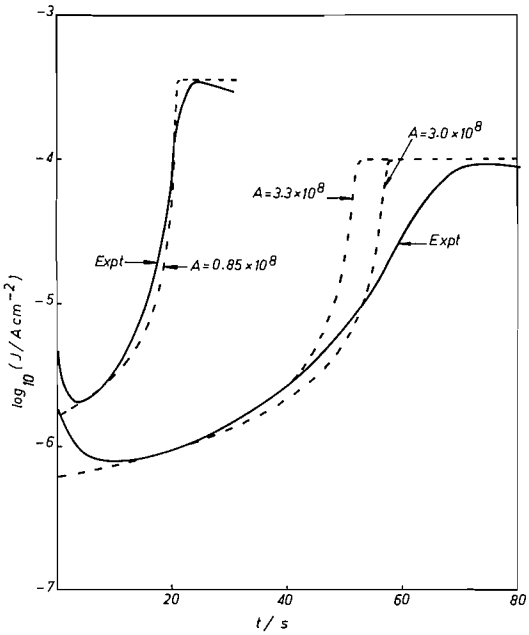

FIG. 1. Computed curves from channel model and experimental data from Fig. 6 of ref. 4 on ionic current density after application at 0 °C of 131 and 126 V to 2040 Å film annealed at 100 °C.

controlled by the field only (4). It was suggested (4) that a momentum transfer process causes moving ions to generate further Frenkel defects (a sort of ionic avalanche effect) and a speculation about a detailed mechanism leading to agreement with the rate of acceleration was suggested.[1] The model proposed by Dignam (6) involves the concept (7, 8) that an effective field (*i.e.* a field containing a contribution from the dielectric polarization of the oxide) causes ionic motion. The central new assumption was that the rate of build-up of one part of the polarization towards its equilibrium value at a given field was taken to be dependent on the current density, again due to a momentum-transfer process involving the moving ions.

Channel Model

A rather simple and apparently physically realistic model of these glassy oxides leads to the type of non-linearity in log $J-E$ which is found with these films (9). It has been suggested that the mobile ions pass through channels in the rather open atomic structures. Due to the randomness of the structure some parts will contain deeper potential energy wells which may act as traps. If these traps may be represented as coulombic, then following the well-known derivation for field-assisted thermally activated release of electrons from traps (Poole–Frenkel law) we expect a steady state current density

$$J = J_0 \exp(-(W - \gamma E^{1/2})/kT$$

where J_0, W, and γ are constants. This form of equation was shown to represent the experimental data quite well for so simple a model. However, it has since been shown (10) that the duplex nature of the films contributes to non-linearity in the steady-state dependence of log J on E. The overall situation on the non-linearity is therefore unclear. The model was not discussed in relation to the transients.

Even if the ions do not move freely through most of their path it seems clear that each metal ion entering the oxide will find a path of least resistance, so that channels exist in a formal sense. Also some potential wells along the path will be deeper than others and will therefore be more effective as traps.[2]

Whether or not the above explanation of non-linearity in log $J-E$ is correct, the model appears to offer a means of explaining some of the transient effects since it naturally evokes the idea that the build-up of current in the constant-field transients is due to the unblocking of the channels (9). The unblocking process must again be postulated to involve momentum transfer from moving ions, perhaps in neighboring channels. As a crude treatment of this channel model, we may assume that the current density is proportional to the fraction θ of unblocked channels

$$J = B(E,T)\theta$$

and that

$$\frac{d\theta}{dt} = AJ^2(1-\theta)$$

[1]The momentum transfer process need not supply the full activation energy.

[2]As supporting evidence for the reasonableness of this model it is noted that in α-quartz dielectric losses are observed corresponding to impurity ions moving along the spiral channels (along the *c*-axis) for distances much greater than single atomic jumps before being blocked by obstructions in the channel; presumably larger impurity ions (11).

Can. J. Chem. Downloaded from www.nrcresearchpress.com by 210.87.254.105 on 09/05/12
For personal use only.

This gives

$$t(J) = (1/AB)(1/J_0 - 1/J) + (1/AB^2)\log((B/J_0 - 1)/(B/J - 1))$$

where $J = J_0$

at $t = 0$

This scheme reproduces the main feature of the transient, as shown in Fig. 1. The initial excess current observed in experiments may be a polarization current or current due to cracks in the film which become sealed. The fall-off in the experimental current is due to a decrease in field as the film starts to grow at appreciable rates: the experiments were done at constant voltage. To obtain a better fit a re-blocking term would be needed which increased more rapidly with current. It is notable (and unsatisfactory) that A has to be chosen smaller for larger fields. A distribution of channel parameters could be used to improve the fit.

Dignam's model, in the simplified form with which it was tested by Dignam and Ryan, is represented by the following equations

$$J = \alpha \exp \beta E^*$$

where E^* is an effective field which is taken to be proportional to the electric displacement D

$$D = \varepsilon_0 E + P$$

and the polarization

$$P = P_0 + P_s$$

where P_0 is ordinary dielectric polarization (time dependence neglected) and P_s is a special polarization and obeys

$$\frac{dP_s}{dt} = BJ(\varepsilon_0 \chi_s E - P_s)$$

where B is a constant and χ_s is the susceptibility for this special polarization. This equation is the same as for Debye-type losses except BJ replaces $1/\tau$, where τ is the relaxation time. The first equation would give a linear dependence of log J on E which is not observed. In this system we again have

$$\frac{dJ}{dt} \propto J^2$$

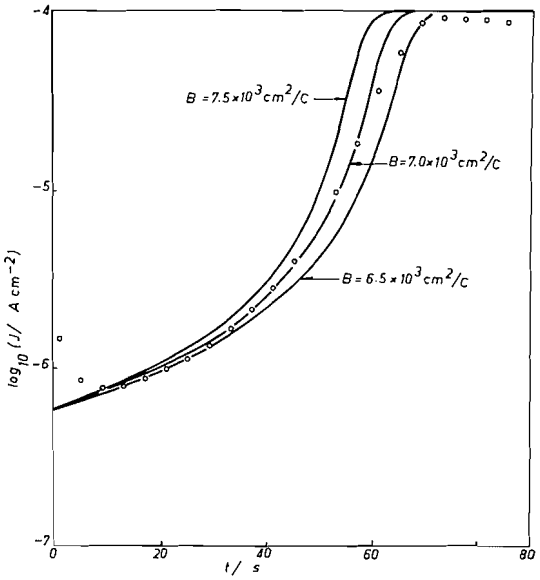

FIG. 2. Computed curves on Dignam's model and experimental data as Fig. 1 at 126 V.

for the initial stages of the transient. The saturation of J arises from the saturation of P_s.

By straightforward manipulation, as shown by Dignam and Ryan (eq. 9, ref. 5), for the constant field transients

$$\frac{dJ}{dt} = J^2 B \log(J_s/J)$$

where J_s is the final steady ionic state current density for this field. Dignam and Ryan apparently integrated experimental data for Al and Ta and plotted $1/J$ *vs.* $\int_0^t \log(J_s/J)dt$ obtaining a straight line as required.

Figures 2 and 3 show computed curves for various values of B and experimental data for tantalum at two fields (experimental details in ref. 4). Values for the initial and final current densities were assumed to fit the experimental data making three adjustable parameters in all (as for the channel model). The calculated curves were obtained by 4th-order Runge–Kutta method on the U.B.C. Computing Centre's IBM 360. These figures show that a good fit is obtained except (*cf.* Fig. 2) in the later stage of the transient where the current density is noticeably low for a value of B which gives a good fit in the early stages. A very noteworthy point in favor of Dignam's equations as they

Can. J. Chem. Downloaded from www.nrcresearchpress.com by 210.87.254.105 on 09/05/12
For personal use only.

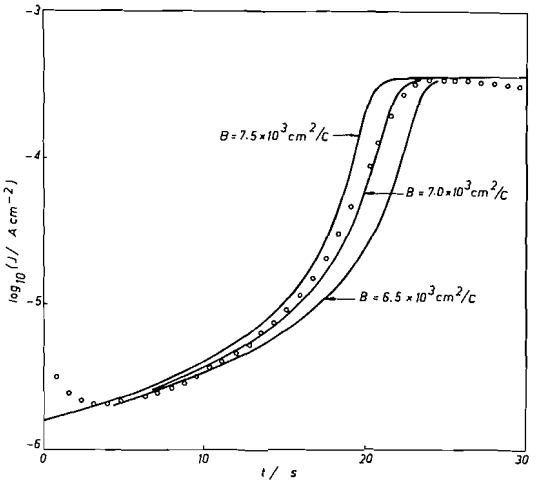

FIG. 3. Computed curves on Dignam's model and experimental data as Fig. 1 at 131 V.

stand is that the same value of B (0.70×10^4 cm^2/C) gives the best fit for both transients (*i.e.*, for two fields). This point was not noted in the paper by Dignam and Ryan who tested their data on Al and the present author's data for tantalum at only one field and did not test the later stage of the transient (Fig. 4, ref. 5). Actually, however, one might expect τ to depend on E as well as on J and T.

To sum up, it is clear that Dignam's equations do give a remarkably good description of the available data. However, it may be considered that the nature of the special polarization mechanism and the way in which moving ions tend to accelerate its approach to equilibrium are not very clearly specified in atomic terms. It is quite possible that a physically simpler model could lead to equally good agreement with the data. More experimental data are certainly required, *e.g.*, for different temperatures. It should be mentioned that the constant field transients are slower with films formed in dilute phosphoric acid (19).

As regards other possibilities, it is possible that a model could be devised in terms of space charge effects due to oxygen ion motion.

As regards Dignam's claim that the model explains the comparable mobility of both ions, the argument presented would not seem specific to the polarization model. Any model involving momentum transfer could be supported by the same arguments. An electronic activation step preceding ion hopping is suggested as an alternative to a momentum transfer mechanism. Charge transfer from metal to oxygen would increase the force on both species. Such an effect is suggested by the u.v. stimulation of ion current.

Mean Free Path

Dignam and Taylor (12) have recently claimed to eliminate all theories involving homogeneous production of defects in the films. This would include the original and the modified Bean, Fisher, and Vermilyea models. Their argument involves the mean free path or, more accurately, the schubweg defined as the distance travelled by a newly-freed ion before capture by a vacant lattice site. It is claimed (12, p. 420) that "for any conduction model in which the mobile defects are generated within the transport medium, motion in the direction of the field can be characterized by a mean free path, λ. The net flux of defects is simply the product of their rate of formation and the mean distance travelled by each defect in the field direction before annihilation". In Dignam and Taylor's notation $J = \lambda(dn_+/dt)$ where dn_+/dt is the rate of creation of defects. On p. 421 the second leg of the argument is introduced (2): "from a consideration of the physical system, λ_s (*i.e.*, the steady state value of λ) cannot be smaller than one jump distance, nor as large as one-half of film thickness". This is elaborated on p. 422 ref. 12: "the steady state mean free path must be in fact substantially less than $X/2$, otherwise it will not be controlled entirely by kinetic phenomena in the film but will be greatly influenced by film thickness". The argument proceeds by evaluating λ_s using

$$J = \lambda(dn_+/dt)$$

plus the equations of the Frenkel defect theory and showing that λ_s varies by too much with experimental conditions to obey $X/2 > \lambda_s \gtrsim 3$ Å. The deduction, of course, is that this model would not give the observed independence of thickness of $J(E,T)$ in the steady state.

This argument seems incorrect. Thus, if λ is the actual schubweg defined as the mean resolved path before the ion is destroyed or leaves the film, then the first quoted statement and the equation

$$J = \lambda(dn_+/dt)$$

Can. J. Chem. Downloaded from www.nrcresearchpress.com by 210.87.254.105 on 09/05/12
For personal use only.

Can. J. Chem. Downloaded from www.nrcresearchpress.com by 210.87.254.105 on 09/05/12
For personal use only.

are only true if $\lambda \ll X$. For each ion that leaves the film (or rather reacts at the oxide/solution interface in this model), another must enter the film from the metal to preserve electrical neutrality. The total distance covered by the original ion and its replacements until the given vacancy is destroyed might be equated to an effective λ. Alternatively, if the equation is taken as defining λ in terms of the current density and the rate of production of defects (which are given by known expressions in this model) then λ is by definition the mean free path which an ion would have if X was big enough. So long as the film thickness X is such that electroneutrality may be assumed, and the film has properties independent of thickness, then the equations given by Bean *et al.* (2) for the volume rates of creation and destruction of Frenkel defects should be good for their model independent of thickness, and hence their expression for J in terms of film parameters should be good. The schubweg does not enter the picture. For each ion that leaves the film in the steady state, another enters; for each vacancy destroyed another is created. It is the concentration of interstitials that is controlled by the competing processes of Frenkel defect creation and annihilation.[3]

It should be noted that the assumption that the bulk of the film is free from space charge must theoretically breakdown for thin enough films. The arguments have been reviewed at length elsewhere (17). It has generally been supposed that one has the typical macroscopic situation in which relatively narrow space charge layers exist at the interfaces and adjust the field so that current continuity occurs between the interfaces and the neutral bulk of the film. In most of the film the field is constant and is independent of the interfaces. The reason for this assumption is that existing experimental evidence points to an (average) field at a given current independent of thickness. This could be Mott and Gurney's (13) case in which space charge is negligible and the interface controls the field, but if so a dependence on, say, crystal face would be expected. More usually it has been assumed that one has Verwey's case of essentially macroscopic conduction. For thin enough films such a situation can no longer hold: the space charge layers would occupy a significant fraction of the thickness of the film or would be incomplete. Experimentally, this effect has not been detected. However, Dignam did not show that mean free path was involved in this situation.

A.C. Response

Some comment should perhaps be made on Dignam and Taylor's rebuttal (15) of a recent note (16) on a.c. response during constant field transients. Our point was that it is known that the losses in the audio range require a wide distribution of relaxation type processes: not just one or two relaxation times. The distribution presumably arises from the amorphous nature of the material, *i.e.*, the processes are all basically the same but with a range of parameters. If these same dielectric processes are identified as those involved in Dignam's model then if one such process behaves as Dignam claims, all should. Hence the capacitative response at 1 kHz should increase with J during constant-field transients. Naturally a single process which builds up over 60 seconds will not respond to a 1 kHz signal. Our argument thus referred to a modified version of Dignam's model and not to the original model. It should also be noted that no change in *a.c.* response at 1 kHz was observed which correlated with the large change in d.c. current during the transient. This justifies the neglect of out-of-phase ionic current.

Decay of Latent Conductivity at Zero Field

As a further test of the theory it is of interest to examine the following experimentally-observed phenomenon which has not previously been used to test Dignam's model. A film is grown at constant ionic current density J_1 (and hence at constant field) till a certain voltage is reached. The film is then held at zero voltage (*i.e.*, field) for time t; the same voltage is then re-applied and the "instantaneously" observed ionic current density $J_2(t)$ is obtained by backwards extrapolation of a current *vs.* time recording.

[3]Dignam and Taylor's argument is analogous to the effect of the schubweg on the primary photo currents observed with blocking cathodes as discussed by Mott and Gurney (13). In the present case of Bean *et al.*'s (2) model and the modifications of it a more relevant analogy is the Bube model of the effect of trapped holes on photoconduction in CdS in which the electron concentration maintains the value giving electroneutrality in the presence of a variable space charge due to the trapped holes (14). The above correction is agreed by Dignam and Taylor (20).

Can. J. Chem. Downloaded from www.nrcresearchpress.com by 210.87.254.105 on 09/05/12
For personal use only.

It is found that $J_2(t)$ is less than J_1. The latent ionic conductivity may be said to have decayed during the period t at $E = 0$. This effect is expected on any Frenkel defect theory since the interstitial ions and vacant lattice sites will recombine due to thermally activated jumps assisted by the local electric field acting on a given interstitial vacancy by a neighboring vacancy. Experimental data and a discussion on the basis of the Frenkel defect model have been published some time ago (18).

In terms of Dignam's model, the decay of the latent conductivity has to be due to the decay of the special polarization process. The decay of this process occurs, despite $E = 0$, since $J \neq 0$: the ionic current continues to flow since the effective field goes to zero only when P_s is zero.

$$J = \alpha \exp \beta E^* = \alpha \exp \beta\gamma P_s(t)$$

where

$$E^* = \gamma D$$

$$dP_s/dt = BJ(0 - P_s(t))$$

or, putting

$$\beta\gamma P_s(t) = y$$

$$[1] \qquad \frac{dy}{dt} = -BJy = -B\alpha\,(\exp y)y$$

On reapplying E at t

$$J_2(t) = \alpha \exp \beta\gamma(\varepsilon_0 E + P_o + P_s(t))$$

whereas before putting $E = 0$

$$J_1 = \alpha \exp \beta\gamma(\varepsilon_0 E + P_o + P_{s,o})$$

where $P_{s,o}$ is the steady state value of P_s. Hence

$$[2] \quad R(t) = J_2(t)/J_1 = \exp \beta\gamma(P_s(t) - P_{s,o}) = \exp\,(y(t) - y(0))$$

To obtain $y(0)$, the fact is used that, on this model, the minimum value of $R = R(\infty)$ is the ratio of initial and final currents in a constant field transient, if it can be assumed that the film is initially "fully annealed" as regards P_s. For the conditions of one of the curves in Fig. 1,

$$R(\infty) = \exp\,(-y(0)) = (6 \times 10^{-7})/(1 \times 10^{-4})$$

or

$$y(0) = 2.303 \ln (1.67 \times 10^2) = 5.1$$

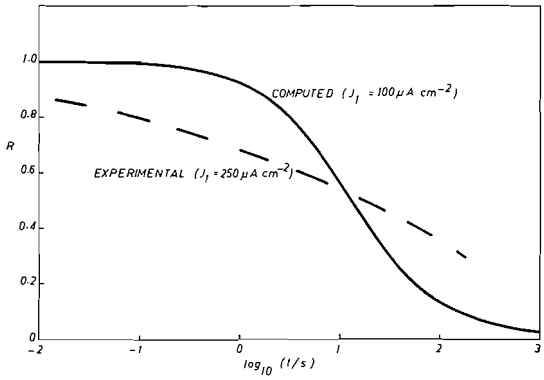

FIG. 4. Computed curve on Dignam's model and experimental curve from ref. 18 of decay of latent conductivity.

With a value of $B\alpha = 10^{-4}$, chosen purely to obtain a reasonable time scale, we obtain the data in Fig. 4 which may be compared with the experimental data in ref. 18. The difference is chiefly in the S-shaped nature of the calculated curve. On the Frenkel defect theory the curve has to be considered (essentially) as a superposition of a wide range of exponential decays corresponding to the different spacings of the components of the defects. The decay of R is faster if J_1 is larger. This is expected on the Frenkel defect theory since the average spacing is smaller. On Dignam's theory it is also expected since P_s and hence $y(0)$ is larger for larger initial E. Thus, Dignam's model shows the required effects here but some form of Frenkel defect theory seems more likely to give the observed wide distribution of relaxation times.

1. C. J. DELL'OCA, D. L. PULFREY, and L. YOUNG. Anodic oxide films. *In* Physics of thin films. Vol. 6. Academic Press, London and New York. 1971. p. 1.
2. D. P. BEAN, J. C. FISHER, and D. A. VERMILYEA. Phys. Rev. **101**, 551 (1956).
3. J. F. DEWALD. J. Phys. Chem. Solids, **2**, 55 (1957).
4. L. Young. Proc. Roy. Soc. A, **263**, 395 (1961).
5. M. J. DIGNAM and P. J. RYAN. Can. J. Chem. **46**, 449 (1968).
6. M. J. DIGNAM. J. Electrochem. Soc. **112**, 722 (1965).
7. L. Young. Trans. Faraday Soc. **52**, 502 (1955). C. J. DELL'OCA and D. L. PULFREY. Anodic oxide films, Academic Press, London and New York. 1961. p. 17.
8. R. J. MAURER. J. Chem. Phys. **9**, 579 (1941).
9. L. YOUNG and F. G. R. ZOBEL. J. Electrochem. Soc. **113**, 277 (1966).
10. C. J. DELL'OCA and L. YOUNG. J. Electrochem. Soc. **117**, 1545, 1172 (1970).

11. E. H. SNOW and P. GIBBS. J. Appl. Phys. **35**, 2368 (1964).
12. M. J. DIGNAM and D. F. TAYLOR. Can. J. Chem. **49**, 416, 1971 (1971).
13. N. F. MOTT and R. W. GURNEY. Electronic processes in ionic crystals. Clarendon Press. Oxford. 1940. p. 118.
14. R. H. BUBE. Photoconductivity. *In* Phys. and Chem. of II–VI Compds. *Edited by* M. Aven and J. S. Prener. American Elsevier Co., New York. 1967.
15. M. J. DIGNAM and D. F. TAYLOR. Appl. Phys. Lett. **15**, 198 (1969).
16. C. J. DELL'OCA and L. YOUNG. Appl. Phys. Lett. **13**, 228 (1968).
17. L. YOUNG. Anodic oxide films. Academic Press, London and New York. 1961. p. 18.
18. L. YOUNG. J. Electrochem. Soc. **111**, 1289 (1964).
19. C. J. DELL'OCA and L. YOUNG. Unpublished results.
20. M. J. DIGNAM and D. F. TAYLOR. Private communication.

Can. J. Chem. Downloaded from www.nrcresearchpress.com by 210.87.254.105 on 09/05/12
For personal use only.

Can. J. Chem. Downloaded from www.nrcresearchpress.com by 210.87.254.5 on 09/05/12
For personal use only.

A Critical Test of the Hammett Acidity Function

KEITH YATES AND STANLEY A. SHAPIRO
Department of Chemistry, University of Toronto, Toronto 181, Ontario

Received September 15, 1971

The applicability of the H_0 acidity function to primary aromatic amines in general has been tested by using a set of five aniline indicators bearing no nitro-substituents. Up to 45% sulfuric acid the scale generated by these bases is the same (within experimental uncertainty) as that based entirely on nitro-anilines.

La possibilité d'application de la fonction d'acidité H_0 aux amines aromatiques primaires en général a été testée en utilisant une série de cinq indicateurs aniline ne portant pas de substituants nitro jusqu'à 45% d'acide sulfurique, l'échelle produite par ces bases est la même (dans les limites de l'incertitude expérimentale) que celle fondée uniquement sur les nitro-anilines.

Canadian Journal of Chemistry, **50**, 581 (1972)

It is now clear that the applicability of any acidity function is largely restricted to a particular class of organic base. In the case of the original acidity function H_0, this class is the primary aromatic amine series. However, in order to establish the H_0 scale of acidity it was necessary to employ nitro-substituents to produce indicators of progressively weaker basicity in order to extend measurements over a wide range of acidity. In fact every indicator used by Hammett and Deyrup (1), and subsequently those used by Jorgenson and Hartter (2), contained at least one such group; even the primary reference indicator used to anchor the scale to the dilute aqueous standard state was *p*-nitroaniline.

From what is currently known of the medium variation of activity coefficients for typical organic bases and their cations (3), it is evident that substituent groups such as nitro- can produce as marked variations in individual f_B and f_{BH^+} values as changing the nature of the basic group itself (4). Thus, if the contributions to the ratio f_{BH^+}/f_B (which determines different acidity function behavior) by nitro-substituents were atypical of substituents in general, the H_0 function would not be generally applicable even to primary amine bases. It is therefore very important to test this possibility, since it is a necessary condition for the establishment of any acidity function that the medium variation of the ratio f_{BH^+}/f_B be the same (or very similar) for each member of the particular class of base which defines it, *i.e.*, that it be independent of the nature of the other substituent groups.

We have therefore investigated a set of primary anilines of differing basicity, which contain no nitro groups, to determine whether the H_0 function generated by these bases coincides with that reported for nitroanilines.[1]

Results and Discussion

Nitro groups are strongly electron withdrawing oxygen-containing groups which would be expected to interact strongly and specifically with the solvent through formation of strong O^-—H—O type hydrogen bonds. This is particularly true of the free base forms, since the nitro- and amino- group are directly conjugated in *o*- and *p*-substituted nitroanilines. We have therefore chosen anilines substituted only by such groups as —F, —Cl, —Br, —CF_3; which although electron withdrawing, would be expected to produce weaker and less specific solute–solvent interactions. The set of indicators chosen and their pK_{BH^+} values are listed in Table 1. The pK_{BH^+} values of the primary

[1]Note that it is not a sufficient test merely to plot ionization curves for individual non-nitro-substituted anilines against H_0. This would only investigate their approximate obedience to this function in terms of an indicator slope near unity.

TABLE 1. pK_{BH^+} values of substituted aniline indicators

Substituted aniline	pK_{BH^+}	% H_2SO_4 at $\frac{1}{2}$ ionization
2-Chloro-5-trifluoromethyl-	+1.195 ±0.004	0.4
2,5-Bis(trifluoromethyl)-	+0.38 ±0.005	2.4
Pentafluoro-	−0.36 ±0.016	9.3
4-Bromo-2,3,5,6-tetrafluoro-	−0.93 ±0.020	18.4
2,4-Dichloro-3,5,6-trifluoro-	−1.28 ±0.028	25.2

indicator 2-chloro-5-trifluoromethylaniline was determined spectrophotometrically in dilute hydrochloric acid and values of $K = C_B C_{H^+}/C_{BH^+}$ extrapolated to infinite dilution (see Fig. 1) in the usual procedure (5), so that the pK_{BH^+} reported in Table 1 is a thermodynamic pK value. This is important since any subsequently derived H_0 scale depends strongly on both the nature and the pK of the first indicator. The remaining pK values were obtained by the standard overlap method (6) using spectrophotometrically determined log I values (I = ionization ratio = $[BH^+]/[B]$).[2] The overlap and parallelism between successive indicator curves was excellent.

Acidity function values were calculated from the equation $H_0 = pK_{BH^+} - \log I$ using all pK and log I data available for any given acid, using the method given by Katritzky (7). These are listed in Table 2, with two sets of reported values for H_2SO_4 at 25° based on nitroaniline indicators, for comparison. It can be seen that the present H_0 values, entirely based on non-nitro-substituted anilines, are in very good agreement with the previously reported values. The maximum difference, at the highest acidity available for comparison, is only of the order of 0.1 logarithmic unit.[3] This demonstrates that the H_0 scale is independent of the number and type of non-basic substituents, at least up to 45% acid. It seems unlikely that extension of the scale by the present approach would produce variations significantly outside the normally accepted range of uncertainty of acidity function values in more concentrated acids. In any

[2]Tabulated values can be obtained from the authors on request.

[3]It is noteworthy that differences of this magnitude arise between independently determined H_0 scales even using essentially the same indicator set of nitro-substituted anilines. See, for example, the data of Ryabova and co-workers (8).

TABLE 2. Comparison of H_0 values generated by non-nitro- and nitro-substituted anilines for aqueous H_2SO_4 at 25 °C

	H_0 values		
% H_2SO_4	This work	Reference 7	Reference 2*
2	0.51	0.53	0.55
4	0.15	0.20	0.23
6	−0.07	−0.02	0.03
8	−0.27	−0.20	−0.14
10	−0.44	−0.35	−0.31
12	−0.59	−0.50	−0.45
14	−0.72	−0.65	−0.60
16	−0.83	−0.78	−0.72
18	−0.94	−0.92	−0.86
20	−1.06	−1.06	−1.01
22	−1.16	−1.20	−1.15
24	−1.28	−1.34	−1.30
26	−1.39	−1.47	−1.44
28	−1.52	−1.60	−1.58
30	−1.64	−1.73	−1.72
32	−1.76	−1.85	−1.85
34	−1.90	−1.99	−1.99
36	−2.05	−2.12	−2.12
38	−2.20	−2.27	−2.27
40	−2.35	−2.42	−2.41
42	−2.50	−2.60	−2.53
44	−2.63	−2.77	−2.73

*Taken from values reported by Hammett and Deyrup (1) and incorporated into Jorgenson and Harter's revised H_0 scale.

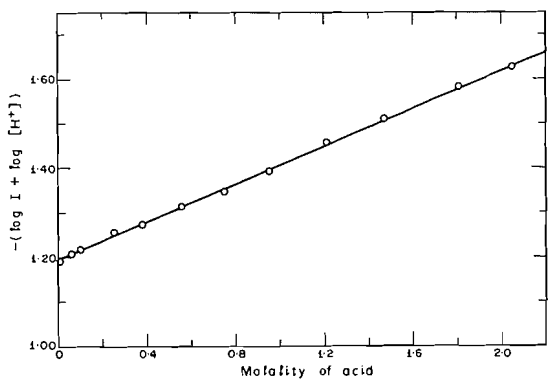

FIG. 1. Extrapolation of ionization data for primary reference indicator (2-chloro-5-trifluoromethylaniline) to obtain pK_a value at infinite dilution.

Can. J. Chem. Downloaded from www.nrcresearchpress.com by 210.87.254.5 on 09/05/12
For personal use only.

event, further extension would be difficult to accomplish experimentally since there are few suitable substituent groups which could achieve the necessary diminutions in base strength comparable with those of dinitro- or trinitroanilines.

It is very reassuring that the H_0 function meets the above test adequately, since if it had not, the damage to the Hammett acidity function concept (even with its presently recognized limited generality) would have been irreparable. It would be of interest to determine whether other acidity functions meet the same critical test as adequately as H_0.

Experimental

2-Chloro-5-trifluoromethylaniline and pentafluoroaniline were commercial samples and were purified by repeated distillation.

2,5-Bis(trifluoromethyl)aniline

1,4-Bis(trifluoromethyl)benzene was nitrated by the method of Ross (9) to yield 2,5-bis(trifluoromethyl)nitrobenzene. The nitro compound was dissolved in ethanol and reduced with hydrogen using Raney nickel as a catalyst. The amine was purified by distillation. Boiling point 50–51 °C (5 mm). Melting point of acetyl derivative, 143–145 °C; literature (9): b.p., 70.5 °C (145 mm). Melting point of acetyl derivative 146.5–147 °C.

4-Bromo-2,3,5,6-tetrafluoroaniline

This compound was obtained by the bromination of 2,3,5,6-tetrafluoroaniline according to the method of Castellano and co-workers (10), and purified by recrystallization and sublimation. Melting point, 60–61 °C; literature (11): 60–61 °C.

2,4-Dichloro-3,5,6-trifluoroaniline

1,3-Dichlorotetrafluorobenzene (supplied by I.C.I. of England) and a slight excess of concentrated aqueous ammonia were added to ethanol to give a homogeneous solution. This was then heated in a sealed autoclave at 140 °C for 24 h. The solution was diluted with water and extracted with methylene chloride. The methylene chloride extract was treated with 60% sulfuric acid and the acid layer diluted with water yielding a white solid. After washing well and drying, the solid was purified by repeated sublimation: m.p. 73–74 °C.

Anal. Calcd. for $C_6H_2Cl_2F_3N$: C, 33.37; H, 0.93; N, 6.48; Cl, 32.83. Found: C, 33.39; H, 0.96; N, 6.29; Cl, 32.68.

The continued financial assistance of the National Research Council of Canada is gratefully acknowledged.

1. L. P. Hammett and A. J. Deyrup. J. Am. Chem. Soc. **54**, 272 (1932).
2. M. J. Jorgenson and D. R. Hartter. J. Am. Chem. Soc. **85**, 878 (1963).
3. R. H. Boyd. *In* Solvent–solute interactions. *Edited by* Coetzee and Ritchie. Marcel Dekker, New York. 1969.
4. L. M. Sweeting and K. Yates. Can. J. Chem. **44**, 2395 (1966); L. P. Hammett and R. P. Chapman. J. Am. Chem. Soc. **56**, 1282 (1943).
5. M. A. Paul and F. A. Long. Chem. Rev. **57**, 1 (1957).
6. C. H. Rochester. Acidity functions. Academic Press, New York. 1970. Chap. 1.
7. C. D. Johnson, A. R. Katritzky, and S. A. Shapiro. J. Am. Chem. Soc. **91**, 6654 (1969).
8. R. S. Ryabova, I. M. Medvetskaya, and M. I. Vinnik. Russ. J. Phys. Chem. **40**, 182 (1966).
9. S. D. Ross, M. Markarian, and M. Schwarz. J. Am. Chem. Soc. **75**, 4967 (1953).
10. J. A. Castellano, J. Green, and J. M. Kauffman. J. Org. Chem. **31**, 821 (1966).
11. G. G. Yakobson, G. G. Furin, L. S. Kobrina, and N. N. Vorozhtsov. Zh. Obshch. Khim. **37**, 1289 (1967).

Can. J. Chem. Downloaded from www.nrcresearchpress.com by 210.87.254.5 on 09/05/12
For personal use only.

Reaction of Diphenylcyclopropenethione with Pyridinium Imines

J. W. LOWN AND K. MATSUMOTO[1]

Department of Chemistry, University of Alberta, Edmonton 7, Alberta

Received August 31, 1971

Reaction of diphenylcyclopropenethione with a variety of *N*-substituted pyridinium imines in refluxing benzene gives 2,4,5-trisubstituted-6*H*-1,3-oxazin-6-thiones in good to excellent yields. The structure of 2,4,5-triphenyl-6*H*-1,3-oxazin-6-thione prepared in this manner was proven by oxidation and by hydrolysis to the known 2,4,5-triphenyl-6*H*-1,3-oxazin-6-one. In the preparation of 4,5-diphenyl-2-ethoxy-6*H*-1,3-oxazin-6-thione changing the heteroaromatic residue in the imine from pyridine to 3-picoline to 3,5-lutidine had little effect on the yield (about 60%).

La réaction de la diphénylcyclopropènethione avec une variété d'imines de pyridinium *N*-substituées dans le benzène à reflux donne des trisubstituées-2,4,5-6*H*-1, oxazine-3-thione-6 avec un excellent rendement. La structure de la triphényl-2,4,5-6*H*-1, oxanine-3-thione-6 préparée de cette manière est prouvée par oxydation et par hydrolyse jusqu'à la triphényl-2,4,5-6*H*-1, oxazine-3-one-6 qui est connue. Dans la préparation de la diphényl-4,5-éthoxy-2-6*H*-1, oxanine-3-thione-6, le changement du résidu hétéroatomique dans l'imine de la pyridine à la picoline-3 et à la lutidine-3,5 a un faible effet sur le rendement (autour de 60%).

Canadian Journal of Chemistry, **50**, 584 (1972)

Since its initial preparation by Breslow *et al.* (1) and Vol'pin *et al.* (2) diphenylcyclopropenone **1** has proven to be a versatile synthetic intermediate leading to *e.g.* 3,4,6-triaryl-2*H*-pyran-2-ones (3), indolizine derivatives (1,4), cyclic dienones (5,6), a 4-pyridazone (7), aziridinyl enamides (8), methylene cyclopropenes (9), pyrroles (10), pyrrolines (10), furans (11–13), 4-oxazolines (11–13), a 3,4-benzotropone (10), and pyrrolo[1,2-*b*]pyridazines (4), 2,3,6-triphenylphenol, and esters of 3,5-hexadienoic acid (14). Its sulfur analog diphenyl-

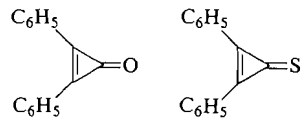

1 2

cyclopropenethione **2** might be expected to exhibit similar synthetic potential but to date relatively little success has been obtained with this compound which is thermally less stable than its oxygen counterpart. Compound **2** reacts with pyridinium ylides to give 3,4,6-triaryl-2*H*-pyran-2-thiones (3), and with 1-(*N*-pyrrolidino)-1-propene to form 2,3-diphenyl-5-methyl-4-(*N*-pyrrolidino)-2-cyclopentenethione (15), while reaction with heteroaromatic nitrogen compounds provides thionpyrazolo[1,2-*a*]pyridazine, 2,3-diphenyl-1-thionpyrazolo[1,2-*a*]benzo[*c*]cinnoline, di-(7,8-diphenylpyrrolo[1,2-*a*]-pyrazinyl)-6-sulfide, and related structures (16).

We report the reaction of diphenylcyclopropenethione with pyridinium imines which yields a variety of 6*H*-1,3-oxazin-6-thiones in good to excellent yields.

For example treatment of a suspension of pyridinium-*N*-(benzoyl)-imine (**3**) with an equimolar quantity of diphenylcyclopropenethione (**2**) in dry benzene under reflux for 12 h afforded 2,4,5-triphenyl-6*H*-1,3-oxazin-6-thione (**4**) in 88% yield as a deep orange crystalline solid (Scheme 1). The spectral characteristics of **4** and similar structures are very similar to

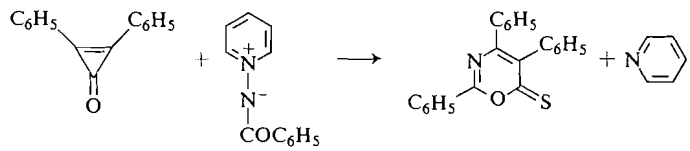

2 3 4

SCHEME 1

[1]NRCC Postdoctorate Fellow 1969–1971.

Can. J. Chem. Downloaded from www.nrcresearchpress.com by 210.87.254.42 on 09/05/12
For personal use only.

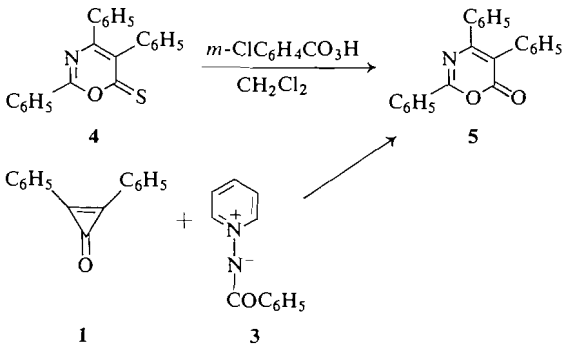

SCHEME 2

those of the 3,4,6-triaryl-2*H*-pyran-2-thiones formed in the analogous reaction of pyridinium ylides on **2** (3). The structure of **4** was proven conclusively by conversion with *m*-chloroperbenzoic acid (17) to the known 2,4,5-triphenyl-6*H*-1,3-oxazin-6-one (**5**) which was also prepared independently by the reaction of the pyridinium imine **3** on diphenylcyclopropenone (Scheme 2).

After this paper was submitted for publication, Sasaki *et al.* reported the similar formation of 2,4,5-trisubstituted-6*H*-1,3-oxazin-6-ones by the reaction of pyridinium imines on diphenylcyclopropenone (18).

Compound **5** had previously been synthesized by Sprio by the oxidation of 2,4,5-triphenylpyrrole with peracetic acid (19).

Hydrolysis of **4** with sodium methoxide in methanol followed by acidification with hydrochloric acid also gave the 6*H*-1,3-oxazin-6-one (**5**) (Scheme 3). Since the intermediate stage after alkaline hydrolysis is soluble in water, from which the orange solid **5** is precipitated upon acidification, it is plausibly represented by the salt **6**.

The generality of this preparation of 2,4,5-trisubstituted-6*H*-1,3-oxazin-6-thiones is demonstrated by the variety of substituted pyridinium imines which react with **2**. The analytical and spectral data on the new compounds are summarized in Tables 1 and 2.

In the preparation of 4,5-diphenyl-2-ethoxy-6*H*-1,3-oxazin-6-thiones, changing the heteroaromatic residue in the imine, and therefore the leaving group in the cyclization step from pyridine to 3-picoline to 3,5-lutidine had a minimal effect on the yield. The range of 6*H*-1,3-oxazin-6-thiones made available by this procedure is evident from the 2-substituents which include aryl, alkoxy, arenoyl, and heterocyclic groups. This preparation of 6*H*-1,3-oxazin-6-thiones represents an extension of the apparently general principal of the ring expansion of triafulvenes (20) with pyridinium betaines, phosphonium ylides, and sulfonium ylides (14).

The mechanism of such processes has been examined by Eicher and his coworkers (14). Three alternative pathways have been considered and recent evidence favors that involving initial attack by the α carbon of the betaine or ylide on C-1 position of the triafulvene followed by formation of a ketene with cyclization of the latter to the products. The latter intramolecular process is evidently rapid in this case compared with possible intermolecular reaction of the ketene with a protic solvent since reaction of diphenylcyclopropenethione with *N*-benzoylpyridinium imine in methanol–benzene gave **4** in 80% yield with no trace of an ester byproduct.

Experimental

Melting points were determined on a Fisher-Johns apparatus and are uncorrected. The i.r. spectra were recorded on a Perkin–Elmer model 421 spectrophotometer, and only the principal sharply defined peaks are reported. The n.m.r. spectra were recorded on Varian A-60 and A-100 analytical spectrometers. The spectra were measured on approximately 10–15% (w/v) solutions in $CDCl_3$, with tetramethylsilane as a standard. Line positions are reported in p.p.m. from the reference. Mass spectra were determined on an Associated Electrical Industries MS-9 double focusing high resolution mass spectrometer. The ionization energy, in general, was 70 eV. Peak measurements were made by

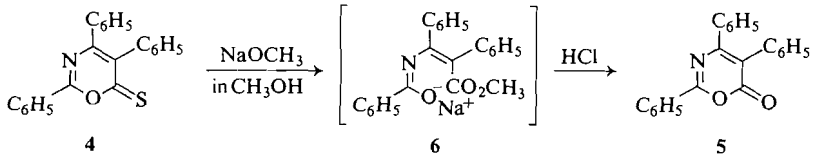

SCHEME 3

Can. J. Chem. Downloaded from www.nrcresearchpress.com by 210.87.254.42 on 09/05/12
For personal use only.

Can. J. Chem. Downloaded from www.nrcresearchpress.com by 210.87.254.42 on 09/05/12
For personal use only.

TABLE 1. 2,4,5-Trisubstituted-6*H*-1,3-oxazin-6-thiones

R*	Yield (%)	Melting point (°C)	Found					Calculated				
			C	H	N	S	Molecular ion (mass spectrum)	C	H	N	S	Molecular ion (mass spectrum)
C_2H_5	63	135	69.69	5.10	4.57	10.63	309.0816	69.85	4.89	4.53	10.36	309.0823
p-$CH_3OC_6H_4$	90	175–177	———		3.81	8.52	371.0980	———		3.77	8.63	371.0942
p-$CH_3C_6H_4$	94	180–181	77.88	4.71	3.98	9.11	355.1030	77.71	4.82	3.94	9.02	355.1031
m-$CH_3C_6H_4$	83	138–140	———		3.77	8.62	355.1026	———		3.94	9.02	355.1031
o-$CH_3C_6H_4$	50	154–156	77.89	5.01	4.12	8.99	355.1025	77.71	4.82	3.94	9.02	355.1031
p-ClC_6H_4	74	136–138	———		3.65	8.20	375.0480	———		3.73	8.53	375.0485
C_6H_5	88	180	77.54	4.58	4.10	9.19	341.0868	77.40	4.43	4.10	9.39	341.0874
$C_6H_5CH{=}CH$	61	185	78.13	4.82	3.98	9.07	367.1030	78.44	4.66	3.81	8.73	367.1031
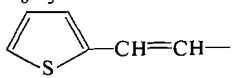	48	170–171	70.54	4.10	3.55	1.75	373.0590	70.75	4.05	3.75	17.17	373.0596
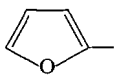	50	129–133	———		4.20	9.80	331.0662	———		4.23	9.68	331.0667
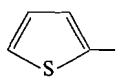	47	123–125	———		4.35	18.01	347.0435	———		4.03	18.46	347.0439

*Refers to formula 7:

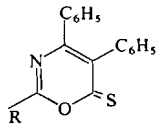

TABLE 2. Spectroscopic data on 2,4,5-trisubstituted-6*H*-1,3-oxazin-6-thiones

R*	n.m.r. spectrum δ_{TMS} ($CDCl_3$)			i.r. spectrum ν (KBr disc)			
	Vinyl and aromatic protons		Methyl protons				
C_2H_5O	6.9–7.6 (10H)m	4.60 (2H)q (methylene-H)	1.48 (3H)t	950	1052	1300	1483
p-$MeOC_6H_4$	8.31, 6.99 (4H)ABq $J = 9$ Hz	7.0–7.6 (10H)m	3.87 (3H)s	954	1126	1257	1477
p-MeC_6H_4	7.30, 8.24 (4H)ABq $J = 8$ Hz	7.1–7.55 (10H)m	2.42 (3H)s	953	1115	1278	1477
m-MeC_6H_4	8.05–8.3 (2H)m	7.1–7.6 (12H)m	2.43 (3H)s	950	1116	1287	1472
o-MeC_6H_4	8.1–8.4 (1H)m	7.0–7.6 (13H)m	2.80 (3H)s		1110	1285	1472
p-ClC_6H_4	8.36–7.53 (2H)ABq	7.1–7.5 (12H)m		952	1120	1290	1475
C_6H_5	8.2–8.6 (2H)m	6.9–7.7 (13H)m		953	1120	1276	1478
C_6H_5—CH=CH—	8.04, 6.86 (2H)ABq $J = 16.5$ Hz	7.05–7.8 (15H)m		950	1120	1278	1475
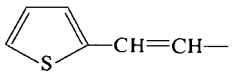	8.10, 6.64 (2H)ABq $J = 15.5$ Hz	6.9–7.6 (13H)m			1114	1273	1470
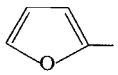		7.0–8.2 (13H)m			1110		1490
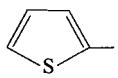		7.0–8.3 (13H)m		950	1110	1270	1473

*Refers to formula 7.

comparison with perfluorotributylamine at a resolving power of 15 000. Kieselgel DF-5 (Camag, Switzerland) and Eastman Kodak precoated sheets were used for t.l.c. Microanalyses were carried out by Dr. C. Daesslé, Organic Microanalysis Ltd., Montreal, Quebec and by Mrs. D. Mahlow of this Department.

Preparation of Pyridinium Imines

The pyridinium imines required in this study were prepared and purified by the general procedures given by Sasaki *et al.* (21) and Snieckus and coworkers (22). New imines prepared by these procedures are summarized in Tables 3 and 4.

Diphenylcyclopropenethione

This compound was prepared by the method of Eicher and Frenzel (23), see also (17).

Reactions of Diphenylcyclopropenethione with Pyridinium Imines

The reaction conditions and purification procedures are illustrated by the following three examples. The analytical and spectral properties of other compounds similarly prepared are summarized in Tables 1 and 2.

(a) Reaction of N-(p-Toluoyl)pyridinium Imine with Diphenylcyclopropenethione

A suspension of 1.06 g (5 mmol) of *N*-(*p*-toluoyl)pyridinium imine and 1.11 g (5 mmol) of diphenylcyclopropenethione in 25 ml of dry benzene was refluxed for 12 h during which time the solution became dark red. Removal of the solvent *in vacuo* and trituration of the residual oil with cold methanol afforded the 4,5-diphenyl-2-(*p*-tolyl)-6*H*-1,3-oxazin-6-thione as a bright orange solid m.p. 180–181°, 1.68 g (94% yield).

Anal. Calcd. for $C_{23}H_{17}NOS$ (mol. wt. 355.1031): C, 77.71; H, 4.82; N, 3.94; S, 9.02. Found (355.1030 (mass spectrum)): C, 77.88; H, 4.71; N, 3.98; S, 9.11.

The n.m.r. spectrum δ_{TMS}($CDCl_3$): 2.42 (s, 3H, aromatic CH_3); 7.1–7.43 (ABq, 4H, tolyl protons); 7.1–7.55 (m, 10H, aromatic protons). The i.r. spectrum ν (KBr disc) 953, 1115, 1278, 1477 cm^{-1}.

(b) Reaction of N-(Carboethoxy)pyridinium Imine with Diphenylcyclopropenethione

A suspension of 0.84 g (5 mmol) of *N*-(carboethoxy)pyridinium imine and 1.11 g (5 mmol) of diphenylcyclopropenethione in 25 ml of dry benzene was heated under reflux for 12 h. Removal of the solvent *in vacuo* and trituration of the residual oil with methanol afforded 4,5-diphenyl-2-ethoxy-6*H*-1,3-oxazin-6-thione as orange crystals, m.p. 135°, 0.95 g (63% yield).

Anal. Calcd. for $C_{18}H_{15}NO_2S$ (mol. wt. 309.0823): C, 69.85; H, 4.89; N, 4.53; S, 10.36. Found (309.0816 (mass spectrum)): C, 69.69; H, 5.10; N, 4.57; S, 10.63.

The n.m.r. spectrum δ_{TMS}($CDCl_3$): 1.48 (t, 3H, CH_3CH_2) 4.60 (q, 2H, CH_3CH_2); 6.9–7.6 (m, 10H, aromatic protons). The i.r. spectrum (KBr disc), 950, 1052, 1300, 1483 cm^{-1}.

The identical product was obtained by the reaction of diphenylcyclopropenethione with (*i*) *N*-(carboethoxy)-3-methylpyridinium imine, (*ii*) *N*-(carboethoxy)-4-methylpyridinium imine, and (*iii*) *N*-(carboethoxy)-3,4-dimethylpyridinium imine in 60, 58, and 54% yields, respectively.

Can. J. Chem. Downloaded from www.nrcresearchpress.com by 210.87.254.42 on 09/05/12
For personal use only.

Can. J. Chem. Downloaded from www.nrcresearchpress.com by 210.87.254.42 on 09/05/12
For personal use only.

TABLE 3. *N*-Substituted pyridinium imines

R*	Yield (%)	Melting point (°C)	Found				Calculated			
			C	H	N	Molecular ion (mass spectrum)	C	H	N	Molecular ion (mass spectrum)
p-$CH_3OC_6H_4$	86	145	68.47	5.03	11.19	228.0894	68.39	5.30	12.27	228.0899
p-CH_3—C_6H_4	81	164–166	73.36	5.78	13.36	212.0944	73.55	5.70	13.20	212.0949
m-$CH_3C_6H_4$	88	87–88	—	—	13.06	212.0946	—	—	13.20	212.0949
o-$CH_3C_6H_4$	82	104	73.31	5.64	12.85	212.0947	73.55	5.70	13.20	212.0949
p-Cl—C_6H_4	80	186–187	61.82	3.90	11.71	232.0400	61.92	3.90	12.05	232.0404
C_6H_5—CH=CH	90	149–150	75.14	5.63	12.61	224.0948	74.96	5.46	12.50	224.0950
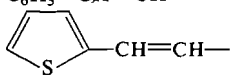	87	125–126	62.07	4.53	12.21 (S:13.72)	230.0516	61.84	4.33	12.03 (S:13.73)	230.0515
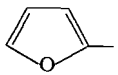	78	223–224	63.56	4.27	14.57	188.0583	63.80	4.29	14.88	188.0586
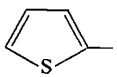	91	208–209	58.83	4.38	13.64 (S:15.99)	204.0354	58.79	3.95	13.72 (S:15.70)	204.0358

*Refers to formula **8**:

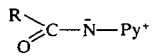

TABLE 4. Spectroscopic data on *N*-substituted pyridinium imines

R*	n.m.r. spectrum δ_{TMS} ($CDCl_3$)				i.r. spectrum ν (KBr disc)
	Vinyl and Aromatic Protons			Methyl Protons	
p-$CH_3OC_6H_4$	8.75–9.0 (2H)m	6.96, 8.18 (4H)ABq $J = 9$ Hz	7.2–8.0 (3H)m	3.95 (3H)s	1630 (w)
p-CH_3—C_6H_4	8.75–9.0 (2H)m	7.26, 8.11 (4H)ABq $J = 8$ Hz	7.4–7.9 (3H)m	2.38 (3H)s	1610 (w)
m-CH_3—C_6H_4	8.75–9.0 (2H)m	7.15–8.15 (7H)m		2.41 (3H)s	1613 (w)
o-CH_3—C_6H_4	8.65–8.90(2H)m	7.10–7.9 (7H)m		2.58 (3H)s	1610 (w)
p-Cl—C_6H_4	8.8–9.0 (2H)m	7.2–8.2 (7H)m			1607 (w)
C_6H_5—CH=CH	8.65–8.95(2H)m	6.6–8.0 (10H)m			1634 (s)
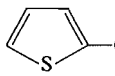	8.6–9.0 (2H)m	6.3–8.0 (8H)m			1633 (s)
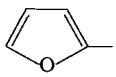	8.7–9.0 (2H)m	6.8–8.2 (6H)m			1619 (w)

*Refers to formula **8**.

(c) Reaction of N-(Cinnamoyl)pyridinium Imine with Diphenylcyclopropenethione

A mixture of 1.12 g (5 mmol) of *N*-(cinnamoyl)pyridinium imine and 1.11 g (5 mmol) of diphenylcyclopropenethione in 25 ml of dry benzene was heated at 100° under nitrogen in a sealed tube for 24 h. Evaporation of the solvent gave a dark red oil, trituration of which with cold methanol gave 4,5-diphenyl-2-*trans*-styryl-6*H*-1,3-oxazin-6-thione 1.08 g, (61% yield), m.p. 185–186° (from benzene–methanol).

Anal. Calcd. for $C_{24}H_{17}NOS$ (mol. wt. 367.1031): C, 78.44; H, 4.66; N, 3.81; S, 8.73. Found (367.1030 (mass spectrum)): C, 78.97; H, 14.82; N, 3.98; S, 8.82.

The n.m.r. spectrum δ_{TMS}($CDCl_3$): 6.86, 8.04 (ABq, $J = 16.5$ Hz, 2H, *trans*-styryl protons); 7.05–7.8 (m, 15H, aromatic protons). The i.r. spectrum ν(KBr disc): 950, 1120, 1278, 1475 cm^{-1}.

Reaction of 2,4,5-Triphenyl-6H-1,3-oxazin-6-thione with m-Chloroperbenzoic Acid

To a stirred solution of 0.68 g (2 mmol) of 2,4,5-triphenyl-1,3-oxazin-6-thione in 20 ml of dichloromethane was added dropwise a solution of 0.43 g (2 mmol) of 80% *m*-chloroperbenzoic acid in 20 ml of dichloromethane over 10 min. A 10% aqueous solution of sodium sulfite was added to decompose the unreacted *m*-chloroperbenzoic acid and the organic layer was washed successively with 5% sodium hydrogen carbonate solution and water and then dried ($CaSO_4$). Removal of the solvent *in vacuo* gave 2,4,5-triphenyl-6*H*-1,3-oxazin-6-one 0.52 g (80% yield) which was purified by recrystallization from dichloromethane–methanol, m.p. 205–207° (lit. m.p. 207° (19)) as a pale green solid. The i.r. spectrum ν(KBr) C=O 1725 cm^{-1}. The mass spectrum: 325, $C_{22}H_{15}NO_2$ requires M, 325.

Reaction of Diphenylcyclopropenone with N-Benzoyl Pyridinium Imine

A suspension of 1.03 g (5 mmol) of diphenylcyclopropenone and 1.0 g (5 mmol) of *N*-benzoyl pyridinium imine in 30 ml of dry benzene was heated under reflux for 12 h during which time the solution turned dark green. The excess of solvent was removed *in vacuo* and trituration of the residue with cold methanol afforded 2,4,5-triphenyl-6*H*-1,3-oxazin-6-one as a light green solid which was purified by recrystallization from benzene–methanol 1.16 g (71% yield) m.p. 205–207°.

The i.r. spectrum of this compound was superimposable with that obtained in the oxidation reaction described above.

Reaction of Diphenylcyclopropenethione with N-Benzoyl Pyridinium Imine in Benzene–Methanol

A solution of 1.11 g (5 mmol) of diphenylcyclopropenethione and 1.0 g (5 mmol) of *N*-benzoyl pyridinium imine in 30 ml of 1:1 benzene–methanol was heated at 90° in a sealed tube for 12 h, during which time the solution became dark red. The solvent was removed *in vacuo* and trituration of the residual oil with cold methanol afforded 2,4,5-triphenyl-6*H*-1,3-oxazin-6-thione (**4**) as a bright orange solid 1.36 g (80% yield), m.p. 178–180°. The product was identical with that obtained in the absence of methanol.

Hydrolysis of 2,4,5-Triphenyl-6H-1,3-oxazin-6-thione with Sodium Methoxide in Methanol

A mixture of 0.34 g (1 mmol) of 2,4,5-triphenyl-1,3-oxazin-6-thione and 25 ml of a methanol solution of sodium methoxide (prepared from 1.0 g of sodium in 100 ml of methanol) was refluxed for 3 h during which time the orange solution became light green in color. The excess of methanol was removed *in vacuo*, the residue diluted with water and the solution extracted with ether (3 × 20 ml). The organic layer was dried ($CaSO_4$) and the solvent evaporated to give a trace of a green oil. Acidification of the aqueous layer resulted in the precipitation of 2,4,5-triphenyl-6*H*-1,3-oxazin-6-one (**5**) as a light orange solid, m.p. 207°. The i.r. spectrum of this compound was superimposable with that of the authentic material.

Can. J. Chem. Downloaded from www.nrcresearchpress.com by 210.87.254.42 on 09/05/12
For personal use only.

This research was supported by a National Research Council of Canada grant to J. W. Lown and by the University of Alberta. We thank Mr. R. Swindlehurst and Dr. A. Hogg for the n.m.r. and mass spectra.

1. R. Breslow, T. Eicher, A. Krebs, R. A. Peterson, and J. Posner. J. Am. Chem. Soc. **87**, 1320 (1965).
2. (*a*) M. E. Vol'pin, Yu. D. Koreshkov, and D. N. Kursanov. Izv. Akad. Nauk. SSSR, Otd. Khim. Nauk, **3**, 560 (1959). (*b*) D. N. Kursanov, M. E. Vol'pin, and Yu. D. Koreshkov. J. Gen. Chem. USSR, **30**, 2855 (1960).
3. T. Eicher and A. Hansen. Tetrahedron Lett. 1169 (1967).
4. J. W. Lown and K. Matsumoto. Can. J. Chem. **49**, 1165 (1971).
5. J. Ciabattoni and G. A. Berchtold. J. Org. Chem. **31**, 1336 (1966).
6. J. W. Lown and K. Matsumoto. J. Org. Chem. **36**, 1405 (1971).
7. P. T. Izzo and A. S. Kende. Chem. Ind. (London), 839 (1964).
8. E. V. Dehmlow. Tetrahedron Lett. 5177 (1967).
9. (*a*) M. A. Battiste. J. Am. Chem. Soc. **86**, 942 (1964). (*b*) W. M. Jones and J. M. Denham. J. Am. Chem. Soc. **86**, 944 (1964). (*c*) E. D. Bergmann and I. Agranat. J. Am. Chem. Soc. **86**, 3587 (1964). (*d*) S. Andreades. J. Am. Chem. Soc. **87**, 3941 (1965). (*e*) T. Eicher and K. Eiglmeier. Chem. Ber. **104**, 605 (1971).
10. J. W. Lown, T. W. Maloney, and G. Dallas. Can. J. Chem. **48**, 584 (1970).
11. J. W. Lown, R. K. Smalley, G. Dallas, and T. W. Maloney. Can. J. Chem. **48**, 89 (1970).
12. J. W. Lown, R. K. Smalley, G. Dallas, and T. W. Maloney. Can. J. Chem. **48**, 103 (1970).
13. J. W. Lown and K. Matsumoto. Can. J. Chem. **48**, 3399 (1970).
14. (*a*) T. Eicher, E. von Angerer, and A. M. Hansen. Ann. **746**, 102 (1971). (*b*) T. Eicher and E. von Angerer Ann. **746**, 120 (1971).
15. J. W. Lown and T. W. Maloney. Chem. Ind. (London), 870 (1970).
16. J. W. Lown and K. Matsumoto. Can. J. Chem. **49**, 3119 (1971).
17. J. W. Lown and T. W. Maloney. J. Org. Chem. **35**, 1716 (1970).
18. T. Sasaki, K. Kanematsu, and A. Kakehi. J. Org. Chem. **36**, 2451 (1971).
19. V. Spiro. Gazz. Chim. Ital. **85**, 569 (1955). Chem. Abstr. **50**, 4910*c* (1956).
20. I. Agranat and E. D. Bergmann. Tetrahedron Lett. 2373 (1966).
21. T. Sasaki, K. Kanematsu, A. Kakehi, I. Ichikawa, and K. Hayakawa. J. Org. Chem. **35**, 426 (1970).
22. A. Balasubramanian, J. M. McIntosh, and V. Snieckus. J. Org. Chem. **35**, 433 (1970).
23. T. Eicher and G. Frenzel. Z. Naturforsch, **20***b* (3), 274 (1955), Chem. Abstr. **63**, 8215*a* (1965).

An Electron Spin Resonance Study of a Rhodium(I) Molecular Oxygen Complex in Solution

B. R. James, F. T. T. Ng, and Ei. Ochiai

Department of Chemistry, University of British Columbia, Vancouver 8, British Columbia

Received July 9, 1971

Electron spin resonance studies on the oxygenation of the rhodium(I) cyclooctene complex $[RhCl(C_8H_{14})_2]_2$, in *N*,*N*-dimethylacetamide (DMA) solution containing chloride show the presence of a paramagnetic species. This is thought to involve a rhodium(II)–superoxide (O_2^-) species which is likely responsible for some previously reported autoxidation reactions.

Les études e.s.r. sur l'oxygénation du complexe rhodium(I) cyclooctène $[RhCl(C_8H_{14})_2]_2$, dans une solution de *N*,*N*-diméthylacétamide (DMA) contenant du chlore, indiquent la présence d'espèces paramagnétiques. Il est supposé qu'une espèce rhodium(II)–superoxyde (O_2^-) est impliquée et que celle-ci est probablement responsable des réactions d'auto-oxydation précédemment rapportées.

Canadian Journal of Chemistry, **50**, 590 (1972)

In recent communications from this laboratory (1, 2), we have reported on the catalytic activity of $[RhCl(C_8H_{14})_2]_2$ for the oxidation by molecular oxygen of DMA, cyclooctene, and cumene under mild conditions. The complex initially forms a molecular oxygen complex (one O_2 per Rh atom) in benzene, 1,2-dichloroethane, *etc.*, and also in DMA containing lithium chloride; the dimer initially dissociates to an active monomeric species. Gas uptake kinetic

Can. J. Chem. Downloaded from www.nrcresearchpress.com by 210.87.254.42 on 09/05/12
For personal use only.

This research was supported by a National Research Council of Canada grant to J. W. Lown and by the University of Alberta. We thank Mr. R. Swindlehurst and Dr. A. Hogg for the n.m.r. and mass spectra.

1. R. Breslow, T. Eicher, A. Krebs, R. A. Peterson, and J. Posner. J. Am. Chem. Soc. **87**, 1320 (1965).
2. (*a*) M. E. Vol'pin, Yu. D. Koreshkov, and D. N. Kursanov. Izv. Akad. Nauk. SSSR, Otd. Khim. Nauk, **3**, 560 (1959). (*b*) D. N. Kursanov, M. E. Vol'pin, and Yu. D. Koreshkov. J. Gen. Chem. USSR, **30**, 2855 (1960).
3. T. Eicher and A. Hansen. Tetrahedron Lett. 1169 (1967).
4. J. W. Lown and K. Matsumoto. Can. J. Chem. **49**, 1165 (1971).
5. J. Ciabattoni and G. A. Berchtold. J. Org. Chem. **31**, 1336 (1966).
6. J. W. Lown and K. Matsumoto. J. Org. Chem. **36**, 1405 (1971).
7. P. T. Izzo and A. S. Kende. Chem. Ind. (London), 839 (1964).
8. E. V. Dehmlow. Tetrahedron Lett. 5177 (1967).
9. (*a*) M. A. Battiste. J. Am. Chem. Soc. **86**, 942 (1964). (*b*) W. M. Jones and J. M. Denham. J. Am. Chem. Soc. **86**, 944 (1964). (*c*) E. D. Bergmann and I. Agranat. J. Am. Chem. Soc. **86**, 3587 (1964). (*d*) S. Andreades. J. Am. Chem. Soc. **87**, 3941 (1965). (*e*) T. Eicher and K. Eiglmeier. Chem. Ber. **104**, 605 (1971).
10. J. W. Lown, T. W. Maloney, and G. Dallas. Can. J. Chem. **48**, 584 (1970).
11. J. W. Lown, R. K. Smalley, G. Dallas, and T. W. Maloney. Can. J. Chem. **48**, 89 (1970).
12. J. W. Lown, R. K. Smalley, G. Dallas, and T. W. Maloney. Can. J. Chem. **48**, 103 (1970).
13. J. W. Lown and K. Matsumoto. Can. J. Chem. **48**, 3399 (1970).
14. (*a*) T. Eicher, E. von Angerer, and A. M. Hansen. Ann. **746**, 102 (1971). (*b*) T. Eicher and E. von Angerer Ann. **746**, 120 (1971).
15. J. W. Lown and T. W. Maloney. Chem. Ind. (London), 870 (1970).
16. J. W. Lown and K. Matsumoto. Can. J. Chem. **49**, 3119 (1971).
17. J. W. Lown and T. W. Maloney. J. Org. Chem. **35**, 1716 (1970).
18. T. Sasaki, K. Kanematsu, and A. Kakehi. J. Org. Chem. **36**, 2451 (1971).
19. V. Spiro. Gazz. Chim. Ital. **85**, 569 (1955). Chem. Abstr. **50**, 4910*c* (1956).
20. I. Agranat and E. D. Bergmann. Tetrahedron Lett. 2373 (1966).
21. T. Sasaki, K. Kanematsu, A. Kakehi, I. Ichikawa, and K. Hayakawa. J. Org. Chem. **35**, 426 (1970).
22. A. Balasubramanian, J. M. McIntosh, and V. Snieckus. J. Org. Chem. **35**, 433 (1970).
23. T. Eicher and G. Frenzel. Z. Naturforsch, **20***b* (3), 274 (1955), Chem. Abstr. **63**, 8215*a* (1965).

An Electron Spin Resonance Study of a Rhodium(I) Molecular Oxygen Complex in Solution

B. R. James, F. T. T. Ng, and Ei. Ochiai

Department of Chemistry, University of British Columbia, Vancouver 8, British Columbia

Received July 9, 1971

Electron spin resonance studies on the oxygenation of the rhodium(I) cyclooctene complex $[RhCl(C_8H_{14})_2]_2$, in *N*,*N*-dimethylacetamide (DMA) solution containing chloride show the presence of a paramagnetic species. This is thought to involve a rhodium(II)–superoxide (O_2^-) species which is likely responsible for some previously reported autoxidation reactions.

Les études e.s.r. sur l'oxygénation du complexe rhodium(I) cyclooctène $[RhCl(C_8H_{14})_2]_2$, dans une solution de *N*,*N*-diméthylacétamide (DMA) contenant du chlore, indiquent la présence d'espèces paramagnétiques. Il est supposé qu'une espèce rhodium(II)–superoxyde (O_2^-) est impliquée et que celle-ci est probablement responsable des réactions d'auto-oxydation précédemment rapportées.

Canadian Journal of Chemistry, **50**, 590 (1972)

In recent communications from this laboratory (1, 2), we have reported on the catalytic activity of $[RhCl(C_8H_{14})_2]_2$ for the oxidation by molecular oxygen of DMA, cyclooctene, and cumene under mild conditions. The complex initially forms a molecular oxygen complex (one O_2 per Rh atom) in benzene, 1,2-dichloroethane, *etc.*, and also in DMA containing lithium chloride; the dimer initially dissociates to an active monomeric species. Gas uptake kinetic

Can. J. Chem. Downloaded from www.nrcresearchpress.com by 210.87.254.105 on 09/05/12
For personal use only.

data in DMA (1–3) established the overall mechanism shown in reactions 1–3.

$$[1] \quad [RhCl(C_8H_{14})_2]_2 \xrightarrow{LiCl} 2RhCl_x(DMA)_y$$

$$[2] \quad RhCl_x(DMA)_y + O_2 \rightleftharpoons O_2RhCl_x(DMA)_y$$

$$[3] \quad O_2RhCl_x(DMA)_y + \text{substrate} \rightarrow RhCl_x(DMA)_y + \text{oxidation products}$$

Reaction 2 is complete within a minute at 1 atm O_2 at 35–80°, and reaction 3 is rate determining.

An i.r. study of the system in dichloroethane or benzene (2) for the oxidation of cyclooctene showed the presence of a hydroperoxide intermediate, likely formed by hydrogen abstraction from the substrate by the oxygen complex; this mechanism suggests a free radical nature for the oxygen complex, although, except for one recently reported ruthenium(II) system (4), all such isolated and characterized species of d^6, d^8, and d^{10} complexes have been found to be diamagnetic (5). An e.s.r. signal had been observed in the DMA–LiCl media (1), and this paper reports on more detailed e.s.r. studies in DMA containing 0.2 *M* LiCl and in benzene solution. Measurements were made on a Varian Associates E3 spectrometer.

The e.s.r. data are summarized in Fig. 1. Spectrum A ($g_{\|}$, $g_{\perp}$, g'_1, g'_2, g'_3) appears to be a composite one consisting of two components: one component with $g_{\|} = 2.10$ and $g_{\perp} = 2.00$ ($g_{av} = 2.03$) is very similar to the spectra reported for the O_2^- ion (6–8); the second component appears very similar to spectrum B (g_1, g_2, g_3). This spectrum, which builds up to about twice the intensity after a further 2 days, collapses into a single broad peak at room temperature which indicates rhombic symmetry associated with the three different g values ($g_{(r.m.s.)} = 2.04$). B is attributed to a rhodium(II) species.

During catalytic oxidations at 80°, the activity slowly decreases with time and this appears to be due to a slow oxidation to a higher rhodium valency state; this is accompanied by the appearance of a greenish tinge to the orange rhodium(I)–oxygen solutions. The solutions do not contain rhodium(III) species (9), and since the active rhodium(I) species can be regenerated by hydrogen reduction, the presence of paramagnetic rhodium(II) species is indicated (3). Previously reported $g_{(r.m.s.)}$ values for rhodium(II) complexes are between 2.03 and 2.21 (10 and references therein).

The e.s.r. data fit into our previously suggested (1–3) oxidation mechanism, which can now be presented in further detail (Scheme 1).

Spectrum A is thought to represent species **1** which is in equilibrium with the diamagnetic oxygen complex. Spectrum B is attributed to species **2**.

Approximate concentrations of the paramagnetic species were estimated by using standard solutions of diphenylpicrylhydrazol and comparing areas of integrated spectra. After 1 min, spectrum A indicates the presence of *ca.* 7×10^{-5} *M* paramagnetic species; significant amounts of **2** are absent and hence the K_2 value is estimated as *ca.* 3×10^2. The intensity of the spectra increases with time but this results from a build up of **2**, and the concentration of **1** remains essentially constant at least up to the stage at which it can readily be estimated (~90 min); the concentration of **1** is governed by K_2 and the concentration of $O_2RhCl_x(DMA)_y$ which decreases by only 5% after 2 days.

Relatively weak interaction between the Rh^{II} and O_2^- centers in A would give a spectrum essentially the superimposition of those of O_2^- and Rh^{II}. The g_3 value of the latter appears to be

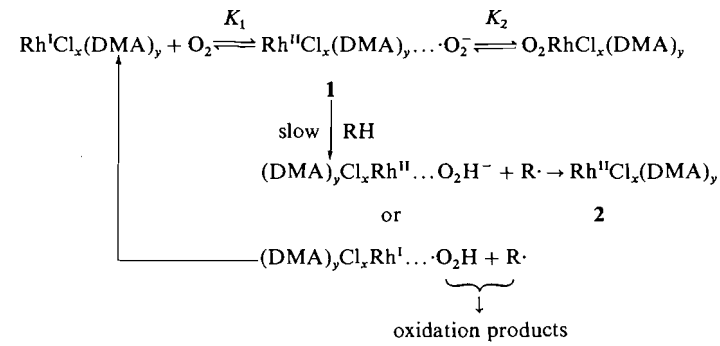

SCHEME 1

Can. J. Chem. Downloaded from www.nrcresearchpress.com by 210.87.254.105 on 09/05/12
For personal use only.

Can. J. Chem. Downloaded from www.nrcresearchpress.com by 210.87.254.105 on 09/05/12
For personal use only.

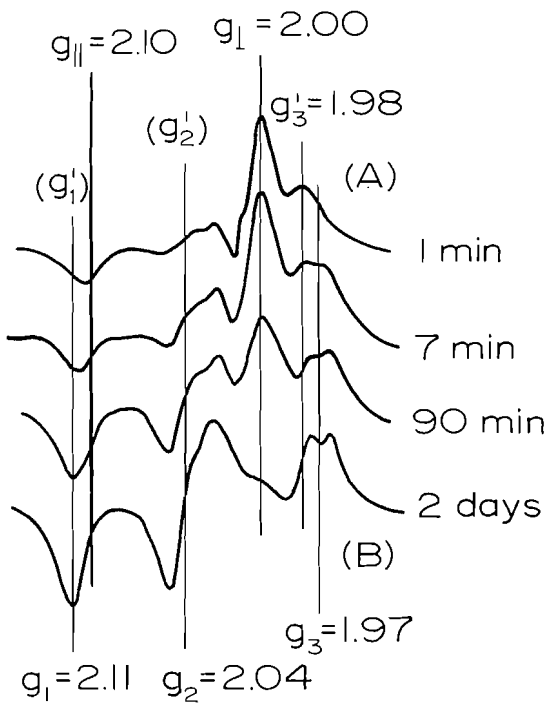

FIG. 1. Electron spin resonance spectra of [RhCl-$(C_8H_{14})_2]_2$ + O_2 in DMA (0.2 *M* LiCl), measured at 77 °K. The reaction time is the exposure time to air at room temperature (23°); $[O_2RhCl_xDMA_y] = 2.0 \times 10^{-2}$ *M*. The estimated concentrations are: $[1] \approx 7 \times 10^{-5}$ *M* at 1 min, $[1] \approx 7 \times 10^{-5}$ *M* at 7 min, $[1] \approx [2]$ at 90 min, and $[2] \approx 1 \times 10^{-3}$ *M* at 2 days. (The relative intensities are not drawn to scale.)

somewhat modified in the $Rh^{II}O_2^-$ species, and is labelled g_3' in the A spectrum; the g_1' and g_2' values for the Rh^{II} component in A appear almost indistinguishable from g_1 and g_2. The weak interaction may arise due to the relatively strong donor properties of the solvent, since the corresponding system in benzene gives an unresolved broad peak centered around $g \sim 2.5$, which may be indicative of greater interaction and a more complex spectrum. The intensity of this broad peak decreases with time at a rate paralleling that of the ν_{0-0} band observed by i.r. spectroscopy (2).

Hydrogen abstraction from the RH substrate by $[Rh^{II}\ldots\cdot O_2^-]$ is thought to constitute the catalytic effect. Stern (11) has suggested that the autoxidation of cumene catalyzed by palladium(0) phosphine complexes could proceed via a hydroperoxide free radical reaction initiated by hydrogen abstraction by a molecular oxygen complex. Whether or not electron transfer equilibria, as exemplified by K_2, are necessary requirements of such catalyzed oxidations remains to be established more fully. Catalytic ability could depend on the value of K_2. If K_2 is 10^2 times greater than the value estimated above, the catalytic activity would not be appreciable, and this corresponds to a free energy difference of only about 3 kcal mol^{-1} at 30°. Slight changes in the coordinated ligands could be significant, and it is of interest to note that while $Pd[P(p\text{-}CH_3C_6H_4)_3]_2$ is active, $Pd[P(p\text{-}ClC_6H_4)_3]_2$ is inactive.

The suggested mechanism is not the same as the Haber–Weiss type mechanism proposed by Kurkov and co-workers (12) for the autoxidation of hydrocarbons catalyzed by rhodium(I) complexes, although both involve formation of free radicals.

The mechanism outlined in Scheme 1 may be applicable to other molecular oxygen systems with d^6, d^8, and d^{10} transition metals. A theoretical discussion on this aspect will be published elsewhere.

We thank the National Research Council of Canada and the University of British Columbia for support of this research, and Johnson Matthey Ltd. for loan of the rhodium.

1. B. R. JAMES and F. T. T. NG. Chem. Commun. 908 (1970).
2. B. R. JAMES and EI. OCHIAI. Can. J. Chem. **49**, 975 (1971).
3. F. T. T. NG. Ph.D. Thesis, University of British Columbia, Vancouver, British Columbia. 1970.
4. M. M. TAQUI KHAN, R. K. ANDAL, and P. T. MANOHARAN. Chem. Commun. 561 (1971).
5. D. M. P. MINGOS. Nature (Physical Science Sect.), **230**, 154 (1971).
6. B. M. HOFFMAN, D. L. DIEMENTE, and F. BASOLO. J. Am. Chem. Soc. **92**, 61 (1970).
7. G. N. SCHRAUZER and L. P. LEE. J. Am. Chem. Soc. **92**, 1551 (1970).
8. K. M. WANG and J. H. LUNSFORD. J. Phys. Chem. **75**, 1165 (1971).
9. B. R. JAMES and G. L. REMPEL. Discuss. Faraday Soc. **46**, 48 (1968).
10. M. A. BENNETT and P. A. LONGSTAFF. J. Am. Chem. Soc. **91**, 6266 (1969).
11. G. E. STERN. Chem. Commun. 736 (1970).
12. V. P. KURKOV, J. Z. PASKY, and J. B. LAVIGNE. J. Am. Chem. Soc. **90**, 4743 (1968).

Rearrangement Studies with ^{14}C. XXXV. The Absence of Isotopic Scrambling in the Photolysis of 2-^{14}C-3-Phenylpropionaldehyde.

C. C. LEE AND D. UNGER

Department of Chemistry and Chemical Engineering, University of Saskatchewan, Saskatoon, Saskatchewan

Received September 3, 1971

The photolytic decarbonylation of 2-^{14}C-3-phenylpropionaldehyde gave isotopically unrearranged β-^{14}C-ethylbenzene, indicating that under the experimental conditions employed, there was no detectable amount of 1,2-phenyl shift in the reaction.

La décarbonylation du 2-^{14}C-3-phénylpropionaldéhyde conduit au β-^{14}C-éthylène isotopiquement non transposé. Il en résulte que dans les conditions expérimentales utilisées, il n'y a aucun déplacement-1,2 de phényle dans la réaction.

Canadian Journal of Chemistry, **50**, 593 (1972)

Slaugh (1) has reported that the peroxide catalyzed decarbonylation of 2-^{14}C-3-phenylpropionaldehyde (**1**-CHO-2-^{14}C) gave rise to 2.3–5.1% rearrangement of the ^{14}C-label from C-β to C-α in the resulting ^{14}C-ethylbenzene (**2**-^{14}C). This isotopic scrambling was attributed to a 1,2-phenyl shift of the 1-^{14}C-2-phenylethyl to the 2-^{14}C-2-phenylethyl radical. On the other hand, the report of about 20% rearrangement in the reaction of 1-^{14}C-2-phenylethyl bromide (**1**-Br-1-^{14}C) with magnesium and cobaltous bromide in refluxing ether (2), also originally attributed to a 1,2-phenyl shift in the 2-phenylethyl radical, has been shown to be incorrect (3). Subsequently, the cobaltous bromide catalyzed radical reaction between **1**-Br-1-^{14}C and phenylmagnesium bromide was found to give only 0.5% isotope position rearrangement in the mixture of ethylbenzene and styrene that was obtained (4). Similarly, prolonged irradiation with ^{60}Co-γ rays of various 1-^{14}C-2-phenylethyl halides (**1**-X-1-^{14}C) resulted in the formation of small amounts of 2-^{14}C-2-phenylethyl halides (**1**-X-2-^{14}C) (5–7). It would be of interest to ascertain whether 1,2-phenyl shifts would take place in a photochemically generated 2-phenylethyl radical. The photolysis of **1**-CHO has been reported by Cohen and coworkers (8, 9) in connection with a study on the sensitization by certain ketones and mercaptans on the light-induced decarbonylation of a number of aldehydes. Radical mechanisms were proposed to explain the results, and from **1**-CHO, the liquid product was found to be ethylbenzene (**2**). In the present work, the photolytic decarbonylation of **1**-CHO-2-^{14}C was investigated in order to find out whether any isotopic scrambling has occurred in the resulting **2**-^{14}C.

1-CHO-2-^{14}C was prepared as described by Slaugh (1). After irradiation at ambient temperature for the desired length of time, ordinary **2** was added as carrier and this product was then recovered by preparative v.p.c. Isotope dilution calculations gave the yield of the **2**-^{14}C, and the results are summarized in Table 1. In all the experiments, alkaline permanganate oxidation of the recovered **2**-^{14}C (1, 3) gave benzoic acid containing no detectable ^{14}C-activity ($0.0 \pm 0.2\%$), indicating that the product was **2**-β-^{14}C with essentially no scrambling to **2**-α-^{14}C.

In the peroxide catalyzed decarbonylation of **1**-CHO-2-^{14}C, Slaugh (1) has noted that the extent of isotopic scrambling in the recovered **2**-^{14}C increased significantly with higher temperature, suggesting that the energy of activation for the 1,2-phenyl shift in the 2-phenylethyl radical was greater than that for the abstraction of hydrogen to give **2**-^{14}C. Moreover, the presence of added thiophenol was found to decrease the extent of rearrangement in the **2**-^{14}C. Since the thiol was a good hydrogen-donor, it was suggested that the presence of the thiol would allow the hydrogen abstraction step to compete more favorably with the 1,2-phenyl shift, thus in effect decreasing the lifetime of the 2-phenylethyl radical and consequently decreasing the extent of 1,2-phenyl shift. From the present work, the data in Table 1 indicated that hydrogen abstraction by the 1-^{14}C-2-phenylethyl radical would play an important role since greater yields of **2**-β-^{14}C were observed in solvents that could more readily donate hydro-

Can. J. Chem. Downloaded from www.nrcresearchpress.com by 210.87.254.105 on 09/05/12
For personal use only.

TABLE 1. Yields of β-^{14}C-ethylbenzene (**2**-β-^{14}C) from the photolytic decarbonylation of 2-^{14}C-3-phenylpropionaldehyde (**1**-CHO-2-^{14}C)

Weight **1**-CHO-2-^{14}C (g)	Solvent*	Irradiation time (h)	Yield of **2**-β-^{14}C (%)†
1.850	None	115	3.3
2.125‡	CCl_4	120	None
1.759	Benzene	119	6.8
2.081	Cyclohexane	111	17.8
2.061	Cyclohexane	111	17.7
1.700§	Cyclohexane	67	30.2

*Enough solvent was added to the **1**-CHO-2-^{14}C to give a total volume of 25 ml.
†Obtained by isotope dilution calculations.
‡Inactive **1**-CHO was used and no ethylbenzene as product was detectable by v.p.c.
§Containing an equimolar amount of benzophenone as photosensitizer.

gen. Apparently, 1,2-phenyl shifts in the 1-^{14}C-2-phenylethyl radical generated under the conditions of the present experiments could not compete appreciably with hydrogen abstraction, hence only isotopically unrearranged **2**-β-^{14}C was formed without any detectable amount of **2**-α-^{14}C.

Experimental

The u.v. spectrum of **1**-CHO showed a weak absorption at 290 mμ, $\varepsilon = 33$, due to the carbonyl chromophore, and aromatic bands at 265 and about 200 mμ. The u.v. source used in the present experiments was a utility model, 100 W, Hanovia high-pressure quartz mercury-vapor arc lamp fitted with a pyrex filter which did not transmit radiations below 280 mμ. The 25-ml pyrex reaction vessel, about 2 cm diameter × 11 cm, was joined at the open end to a narrower tubing which was fitted to a reflux condenser. About 2 g of **1**-CHO-2-^{14}C was weighted in the vessel and solvent was added to make up a total volume of 25 ml. The sample was flushed with nitrogen for 2 h and an atmosphere of nitrogen was maintained above the sample throughout the irradiation. The material was irradiated at ambient temperature at a fixed distance (7.5 cm) from the u.v. source for the desired length of time. Ordinary ethylbenzene (**2**) (1–2 g) was then added as carrier and the volatile material was removed at 30° and 5 mm pressure and collected in a receiver cooled in liquid nitrogen. In preliminary trials with inactive material without any added carrier, v.p.c. analysis (25 ft × 1/8 in. copper column packed with silicone DC 710 on 60/80 mesh chromosorb W using an Aerograph 200 chromatograph with flame ionization detector) showed that in the volatile product so obtained, only **2** and traces of unreacted **1**-CHO were present besides the solvent. In the experiments with **1**-CHO-2-^{14}C, the **2**-^{14}C, diluted by the inactive carrier, was recovered by preparative v.c.p. using a Pye Automatic Preparative chromatograph with a 12 ft × 3/8 in. copper column containing the same silicone packing as described above.

On oxidation with alkaline $KMNO_4$ (1, 3), the recovered **2**-^{14}C gave inactive benzoic acid, indicating no scrambling of the ^{14}C-label from C-β to C-α for the **2**-^{14}C. In some of the experiments, the unreacted **1**-CHO-2-^{14}C was recovered by vacuum distillation, b.p. 57–58° at 2 mm, and then oxidized to benzoic acid which was also inactive, indicating no scrambling of the ^{14}C from C-2 to -3 in the recovered aldehyde.

The financial support given by the National Research Council of Canada is gratefully acknowledged.

1. L. H. SLAUGH. J. Am. Chem. Soc. **81**, 2262 (1959).
2. W. B. SMITH and J. D. ANDERSON. J. Am. Chem. Soc. **82**, 656 (1960).
3. D. P. THORNHILL and C. C. LEE. Can. J. Chem. **41**, 2861 (1963).
4. C. C. LEE and D. P. THORNHILL. Can. J. Chem. **42**, 1502 (1964).
5. C. C. LEE, D. G. LEE, and I. S. BHARDWAJ. Radiation Res. **17**, 536 (1962).
6. D. P. THORNHILL and C. C. LEE. Can. J. Chem. **41**, 2482 (1963).
7. C. C. LEE and D. J. KROEGER. Can. J. Chem. **42**, 976 (1964).
8. S. G. COHEN, J. D. BERMAN, and S. ORMAN. Tetrahedron Lett. 43 (1962).
9. J. D. BERMAN, J. H. STANLEY, W. V. SHERMAN, and S. G. COHEN. J. Am. Chem. Soc. **85**, 4010 (1963).

Can. J. Chem. Downloaded from www.nrcresearchpress.com by 210.87.254.105 on 09/05/12
For personal use only.

Can. J. Chem. Downloaded from www.nrcresearchpress.com by 210.87.254.105 on 09/05/12
For personal use only.

The Role of HgH in the $Hg(6^3P_0)$ Photosensitized Decomposition of the Alkanes and Hydrogen

A. C. VIKIS AND D. J. LE ROY

Lash Miller Chemical Laboratories, University of Toronto, Toronto 181, Ontario

Received November 29, 1971

Mercury hydride, arising from the $Hg(6^3P_0)$ photosensitized decomposition of hydrogen containing molecules, has been detected in the presence of H_2, D_2, CH_4, C_2H_6, C_3H_8, and n-C_4H_{10}. For the alkanes, this is the first experimental evidence that HgH is formed in the primary process $Hg(6^3P_0) + RH \rightarrow HgH + R$.

L'hydrure de mercure, provenant de la décomposition photosensibilisée au mercure $Hg(6^3P_0)$ de molécules contenant de l'hydrogène, a été détectée en présence de H_2, D_2, CH_4, C_2H_6, C_3H_8, et n-C_4H_{10}. Dans le cas des alcanes, c'est la première preuve expérimentale que HgH est formé au cours d'un procédé primaire: $Hg(6^3P_0) + RH \rightarrow HgH + R$.

Canadian Journal of Chemistry, **50**, 595 (1972)

The primary formation of HgH in the $Hg(6^3P_{1,0})$ photosensitized decomposition of the alkanes and hydrogen

[1] $$Hg(6^3P_{1,0}) + RH \rightarrow HgH + R$$

rather than the alternative primary process

[2] $$Hg(6^3P_{1,0}) + RH \rightarrow Hg(6^1S_0) + R + H$$

has been proposed in a number of publications (1–3). However, no experimental evidence of reaction 1 has been obtained except when the quencher was H_2 or D_2 (4–7), in which cases the quantum yields of reaction 1 were found to be close to unity (7). In particular, Masson and Steacie (6), and recently Callear and Hedges (7), were unsuccessful in attempts to detect HgH in any alkane system.

The lack of evidence for HgH formation in the alkanes contrasted with the results for the analogous reactions with $Cd(5^3P_{1,0})$ atoms, where CdH is formed with both H_2 and the alkanes (8, 9). For $Cd(5^3P_{1,0})$ atoms, reaction via CdH formation is the only energetically feasible reaction channel. The higher reaction exothermicity in the $Hg(6^3P_{1,0})$ reactions with RH was suggested as an explanation (6), but the results of ref. 7 obtained at $\sim$1 atm pressure seem to contradict this proposition. An alternative explanation based on HgR formation was also proposed in ref. 7.

It seemed reasonable to us to expect that even if HgH is formed by reaction 1, it could be consumed by reactions with the parent molecule RH or with a reaction product (olefin or alkyl radical). If so, the unsuccessful attempts to observe it (6, 7) may have been due to not having used the most favorable conditions for detection, and in particular, to having used too high partial pressures of RH. The strong RH pressure dependence found in this work shows that this was definitely the case in Masson and Steacie's (6) system.

The method employed in this work utilized electronic excitation of the HgH by collisions of the second kind with $Hg(6^3P_0)$, and observation of the HgH emission (4–6). A Hilger and Watts model E-517 quartz spectrograph and Kodak 103-O spectrographic plates were used for monitoring the HgH sensitized emission. The dispersion of the spectrograph was $\sim$80 Å/mm at 3500 Å. The spectrograph slit was varied in the range of 0.05 to 0.2 mm and the exposure times were of the order of 10 min to an hour. The reaction was studied in the flow system described in ref. 10 at a nitrogen flow rate of 20 std cc/min and a total pressure of 20 to 50 Torr.

The results are presented in Figs. 1 and 2. The 0,0 band of the HgH $^2\Pi_{3/2} \rightarrow {}^2\Sigma^+$ transition at 3500 Å was detected in all systems. The 0,0 band for $^2\Pi_{1/2} \rightarrow {}^2\Sigma^+$ at 4017 Å is not as evident because of interference in this region from quartz

Can. J. Chem. Downloaded from www.nrcresearchpress.com by 210.87.254.105 on 09/05/12
For personal use only.

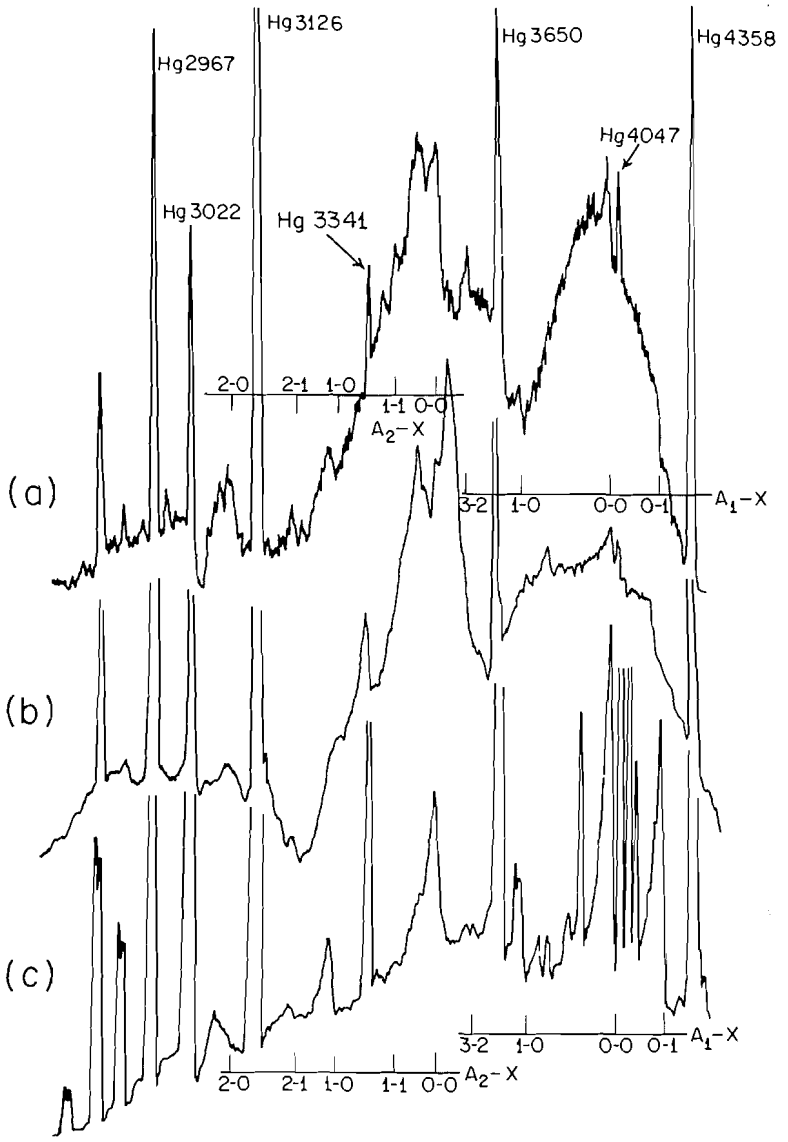

FIG. 1. HgH $^2\Pi_{3/2} \rightarrow {}^2\Sigma^+$ and $^2\Pi_{1/2} \rightarrow {}^2\Sigma^+$ band emission excited by (*a*) Hg(6^3P_0) in the presence of 0.004 Torr of H_2, 20 Torr of N_2; (*b*) Hg(6^3P_0) in the presence of 0.005 Torr of D_2, 20 Torr of N_2; (*c*) microwave discharge in a continuous flow Hg–H_2 lamp at ~2 Torr of H_2.

fluorescence. Other HgH transitions were observed at long exposures in H_2. All were identified on the basis of literature data (11) and the microwave discharge spectrum of HgH obtained in this laboratory, Fig. 1*c*.

The HgH emission intensity was found to be very sensitive to the pressure of H_2 or RH, apparently due to HgH and (HgH)* depletion processes and the depopulation of the Hg(6^3P_0), which excites the emission. The RH pressures for maximum emission were approximately 0.4, 0.2, 0.007, <0.01, and <0.002 Torr for CH_4, C_2H_6, H_2, C_3H_8, and *n*-C_4H_{10}, respectively. They represent the composite efficiency of HgH formation and decay in the presence of each RH. At higher or lower pressures the emission dropped sharply to unobservable intensities. This is the most likely explanation for the lack

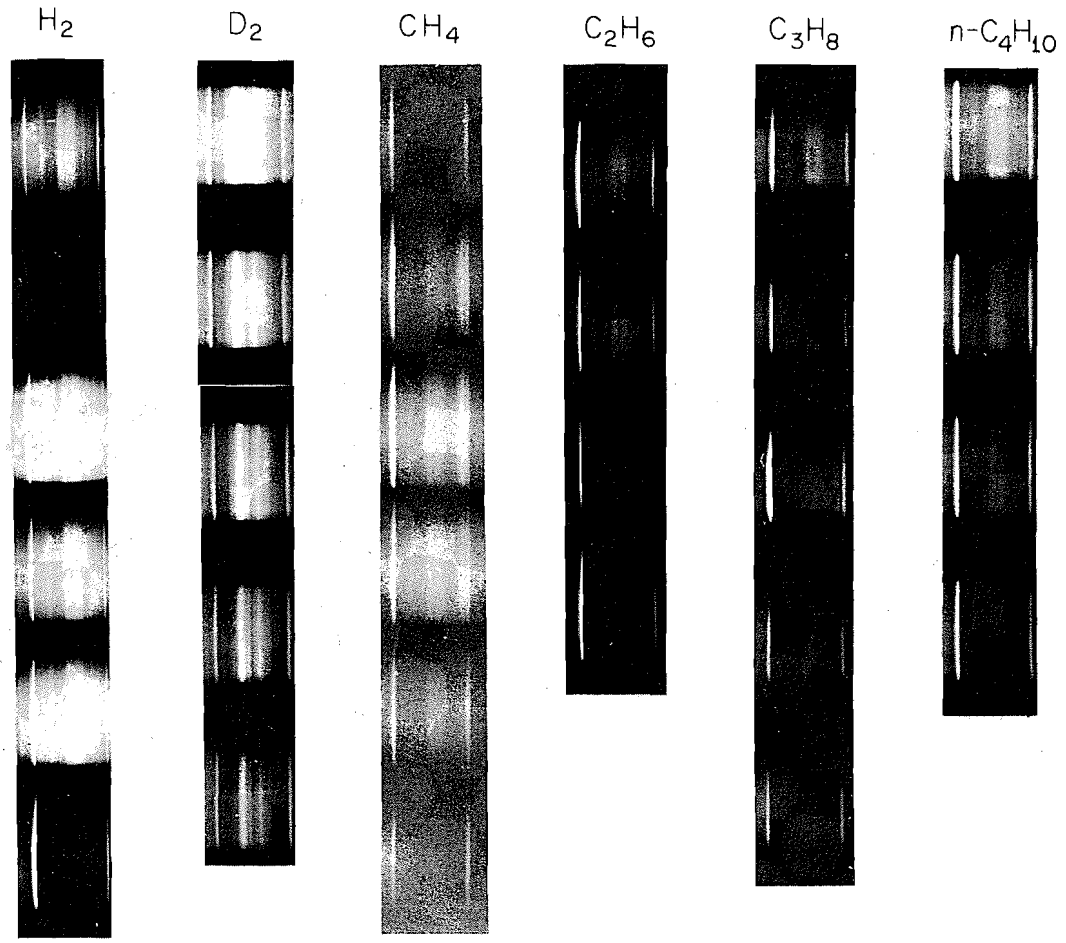

FIG. 2. Mercury hydride 3500 Å band emission excited by $Hg(6^3P_0)$ in the presence of various pressures of H_2, D_2, RH, and N_2. The atomic lines to the left and right of each of the thirty spectra are Hg 3650 Å and Hg 3341 Å, respectively. (Read from top to bottom, pressures in Torr; N_2 was added to raise the total pressure to the value given in parentheses, H_2(50): 0.010, 0.000; H_2(20): 0.006, 0.004, 0.002, 0.000; D_2(20): 0.005, 0.008, 0.009, 0.017, 0.028; CH_4(53): 0.10, 0.22, 0.38, 0.80, 1.6, 3.3; C_2H_6(20): 0.11, 0.22, 0.41, 0.00; C_3H_8(20): 0.011, 0.026, 0.0, 0.054, 0.12; n-C_4H_{10}(20): 0.002, 0.006, 0.010, 0.016. Note that only intensities in the same column and at the same N_2 pressure are directly comparable. The transition adjacent to the 3341 Å Hg line which appears in some cases was identified with the 3357 Å NH $A^3\Pi_i \rightarrow X^3\Sigma^-$ 0,0 band. Its origin is uncertain (4), although in the present work it may be due to the system's previous exposure to NH_3.)

of evidence for HgH formation with alkanes in previous work (6, 7).

The intensity of the 3500 Å band was studied as a function of the intensity of the primary lamps for H_2 and n-C_4H_{10}, and found to obey the expected second power dependence. Also a comparison of rough intensity calculations of rotational distributions with observed intensities indicated that high rotational temperatures (2000–3000 °K) prevail in the 3500 Å band. A similar conclusion can also be reached by comparison with the microwave discharge HgH spectrum. This is in agreement with Rieke's (5) work on the 4017 Å HgH band studied in H_2 with the same method. This high rotational temperature undoubtedly arises from the secondary excitation process and the subsequent vibrational cascading of excited HgH rather than from the primary HgH formation process (5).

The possible formation of HgH in an equilibrium process

[3] $$Hg + H + N_2 \rightleftarrows HgH + N_2$$

Can. J. Chem. Downloaded from www.nrcresearchpress.com by 210.87.254.105 on 09/05/12
For personal use only.

is excluded in the present system because of low Hg ($\sim 10^{-4}$ Torr) and N_2 pressures. Approximate calculations showed that if both reactions 1 and 2 are occurring equally fast, reaction 3 would be less favored as a source of HgH than reaction 1 by a factor of ~ 100 in our experiments. This, in combination with Callear and Hedge's (7) quantum yield of near unity in the case of H_2, and the comparable emission intensity yields observed with H_2 and the alkanes in our system, indicate that the equilibrium reaction [3] is not significant.[1]

In conclusion, the present results indicate that primary HgH formation is an important reaction channel in the $Hg(6^3P_0)$ photosensitized decomposition of the alkanes. Accurate quantum yields of HgH formation for the various alkanes would be of significant value in elucidating the role of the exothermicity in these reactions. Such studies are anticipated in this laboratory and we expect to present the results in this journal as they become available.

The authors gratefully acknowledge the financial support received from the National Research Council of Canada.

1. K. S. LAIDLER. The chemical kinetics of excited states. Oxford at the Clarendon Press. 1955.
2. R. J. CVETANOVIĆ. Progr. Reaction Kinet. **2**, 41 (1964).
3. A. C. VIKIS and H. C. MOSER. J. Chem. Phys. **53**, 2333 (1970).
4. E. GAVIOLA and R. W. WOOD. Phil. Mag. (7) **6**, 1191 (1928).
5. F. F. RIEKE. J. Chem. Phys. **4**, 513 (1936).
6. C. R. MASSON and E. W. R. STEACIE. J. Chem. Phys. **18**, 210 (1950).
7. A. B. CALLEAR and R. E. M. HEDGES. Trans. Faraday Soc. **66**, 615 (1970).
8. E. W. R. STEACIE and D. J. LE ROY. J. Chem. Phys. **12**, 34 (1944).
9. W. H. BRECKENRIDGE and A. B. CALLEAR. Trans. Faraday Soc. **67**, 2009 (1971).
10. A. C. VIKIS, G. TORRIE and D. J. LE ROY. Can. J. Chem. **50**, 176 (1972).
11. J. G. PHILLIPS and S. P. DAVIS. The spectrum of the HgH molecule. University of California Press, Berkeley and Los Angeles. 1968.

[1]A referee has pointed out that if electronically excited $(HgH)^*$ were formed by the reaction

[4] $$Hg(6^3P_0) + H + M \rightleftarrows (HgH)^* + M$$

it would be difficult to distinguish it kinetically from reaction 1 followed by

[5] $$Hg(6^3P_0) + HgH \rightarrow (HgH)^* + Hg$$

However, if one assumes normal rate constants for reactions 4 and 5 (*ca.* $10^9\ M^{-2}\ s^{-1}$ and $10^{10}\ M^{-1}\ s^{-1}$, respectively), it can be shown that formation of $(HgH)^*$ by reaction 4 is not favored in our system.

π-Cyclopentadienylmanganese Thiocarbonyl Complexes

A. E. FENSTER AND I. S. BUTLER
Department of Chemistry, McGill University, Montreal 101, Quebec

Received November 15, 1971

The complete series of thiocarbonyl complexes, π-$C_5H_5Mn(CO)_{3-x}(CS)_x$ ($x = 1, 2, 3$), have been prepared by reaction of the appropriate *cis*-cyclooctene derivative, π-$C_5H_5Mn(CO)_{3-x}(CS)_{x-1}(C_8H_{14})$, with CS_2 in the presence of triphenylphosphine.

La série complète de complexe thiocarbonyl, π-$C_5H_5Mn(CO)_{3-x}(CS)_x$ ($x = 1,2,3$), a été preparée par la réaction de CS_2 avec les composés de *cis*-cyclooctene appropriés, π-$C_5H_5Mn(CO)_{3-x}(CS)_{x-1}(C_8H_{14})$, en présence de triphenylphosphine.

Canadian Journal of Chemistry, **50**, 598 (1972)

Recently, we reported the isolation in low yield ($< 10\%$) of π-$C_5H_5Mn(CO)_2(CS)$ (**1**), the first thiocarbonyl complex of manganese, from the reaction of π-$C_5H_5Mn(CO)_2$ (*cis*-cyclooctene) with carbon disulfide (1). We have now succeeded in obtaining **1** in about 85% yield by carrying out the same reaction under reflux conditions for 24 h in the presence of a stoichiometric amount of triphenylphosphine. In contrast to the reaction in the absence of ϕ_3P, there are no carbonyl- or thiocarbonyl-containing side-products formed. The only other products

Can. J. Chem. Downloaded from www.nrcresearchpress.com by 210.87.254.105 on 09/05/12
For personal use only.

is excluded in the present system because of low Hg ($\sim 10^{-4}$ Torr) and N_2 pressures. Approximate calculations showed that if both reactions 1 and 2 are occurring equally fast, reaction 3 would be less favored as a source of HgH than reaction 1 by a factor of ~ 100 in our experiments. This, in combination with Callear and Hedge's (7) quantum yield of near unity in the case of H_2, and the comparable emission intensity yields observed with H_2 and the alkanes in our system, indicate that the equilibrium reaction [3] is not significant.[1]

In conclusion, the present results indicate that primary HgH formation is an important reaction channel in the $Hg(6^3P_0)$ photosensitized decomposition of the alkanes. Accurate quantum yields of HgH formation for the various alkanes would be of significant value in elucidating the role of the exothermicity in these reactions. Such studies are anticipated in this laboratory and we expect to present the results in this journal as they become available.

The authors gratefully acknowledge the financial support received from the National Research Council of Canada.

1. K. S. LAIDLER. The chemical kinetics of excited states. Oxford at the Clarendon Press. 1955.
2. R. J. CVETANOVIĆ. Progr. Reaction Kinet. **2**, 41 (1964).
3. A. C. VIKIS and H. C. MOSER. J. Chem. Phys. **53**, 2333 (1970).
4. E. GAVIOLA and R. W. WOOD. Phil. Mag. (7) **6**, 1191 (1928).
5. F. F. RIEKE. J. Chem. Phys. **4**, 513 (1936).
6. C. R. MASSON and E. W. R. STEACIE. J. Chem. Phys. **18**, 210 (1950).
7. A. B. CALLEAR and R. E. M. HEDGES. Trans. Faraday Soc. **66**, 615 (1970).
8. E. W. R. STEACIE and D. J. LE ROY. J. Chem. Phys. **12**, 34 (1944).
9. W. H. BRECKENRIDGE and A. B. CALLEAR. Trans. Faraday Soc. **67**, 2009 (1971).
10. A. C. VIKIS, G. TORRIE and D. J. LE ROY. Can. J. Chem. **50**, 176 (1972).
11. J. G. PHILLIPS and S. P. DAVIS. The spectrum of the HgH molecule. University of California Press, Berkeley and Los Angeles. 1968.

[1]A referee has pointed out that if electronically excited $(HgH)^*$ were formed by the reaction

[4] $$Hg(6^3P_0) + H + M \rightleftarrows (HgH)^* + M$$

it would be difficult to distinguish it kinetically from reaction 1 followed by

[5] $$Hg(6^3P_0) + HgH \rightarrow (HgH)^* + Hg$$

However, if one assumes normal rate constants for reactions 4 and 5 (*ca.* $10^9\ M^{-2}\ s^{-1}$ and $10^{10}\ M^{-1}\ s^{-1}$, respectively), it can be shown that formation of $(HgH)^*$ by reaction 4 is not favored in our system.

π-Cyclopentadienylmanganese Thiocarbonyl Complexes

A. E. FENSTER AND I. S. BUTLER
Department of Chemistry, McGill University, Montreal 101, Quebec

Received November 15, 1971

The complete series of thiocarbonyl complexes, π-$C_5H_5Mn(CO)_{3-x}(CS)_x$ ($x = 1, 2, 3$), have been prepared by reaction of the appropriate *cis*-cyclooctene derivative, π-$C_5H_5Mn(CO)_{3-x}(CS)_{x-1}(C_8H_{14})$, with CS_2 in the presence of triphenylphosphine.

La série complète de complexe thiocarbonyl, π-$C_5H_5Mn(CO)_{3-x}(CS)_x$ ($x = 1,2,3$), a été preparée par la réaction de CS_2 avec les composés de *cis*-cyclooctene appropriés, π-$C_5H_5Mn(CO)_{3-x}(CS)_{x-1}(C_8H_{14})$, en présence de triphenylphosphine.

Canadian Journal of Chemistry, **50**, 598 (1972)

Recently, we reported the isolation in low yield ($< 10\%$) of π-$C_5H_5Mn(CO)_2(CS)$ (**1**), the first thiocarbonyl complex of manganese, from the reaction of π-$C_5H_5Mn(CO)_2$ (*cis*-cyclooctene) with carbon disulfide (1). We have now succeeded in obtaining **1** in about 85% yield by carrying out the same reaction under reflux conditions for 24 h in the presence of a stoichiometric amount of triphenylphosphine. In contrast to the reaction in the absence of ϕ_3P, there are no carbonyl- or thiocarbonyl-containing side-products formed. The only other products

Can. J. Chem. Downloaded from www.nrcresearchpress.com by 210.87.254.105 on 09/05/12
For personal use only.

TABLE 1. Infrared spectra of the new π-cyclopentadienylmanganese thiocarbonyl complexes

Compound	Medium	Frequency (cm^{-1})† ν_{CO}	ν_{CS}
2, π-$C_5H_5Mn(CO)(CS)_2$	CS_2	1991 s	1305 s, 1235 vs
	Nujol	1966 s	1308 s, 1240 s
3, π-$C_5H_5Mn(CS)_3$*	CS_2		1338 m, 1240 vs

*This complex has as yet only been characterized by its i.r. spectrum.
†s = strong, vs = very strong, m = medium.

that are present in any significant amount in the reaction mixture are triphenylphosphine sulfide and *cis*-cyclooctene.

It appears that the method used here to prepare complex **1** may well prove to be a general method for the synthesis of transition metal thiocarbonyl complexes because we have managed to complete the series of π-cyclopentadienylmanganese thiocarbonyl complexes by preparing π-$C_5H_5Mn(CO)(CS)_2$ (**2**) and π-$C_5H_5Mn(CS)_3$ (**3**) using the same method. The starting materials in the preparation of complexes **2** and **3** are π-$C_5H_5Mn(CO)(CS)$ (*cis*-cyclooctene) and π-$C_5H_5Mn(CS)_2$ (*cis*-cyclooctene), respectively. These olefin complexes are obtained from the photochemical reactions of **1** and **2**, respectively, with excess *cis*-cyclooctene in *n*-hexane solution.

The dithiocarbonyl complex **2** (yellow crystals, m.p. 71–72°) has been characterized by elemental analysis, i.r., n.m.r., and mass spectroscopy. Owing to extensive decomposition in the preparation of π-$C_5H_5Mn(CS)_2$ (*cis*-cyclooctene), we have as yet only obtained the trithiocarbonyl complex **3** in minute quantities. Consequently, this complex has been only characterized by its i.r. spectrum.

The i.r. spectra of complexes **2** and **3** exhibit the anticipated number of CO and CS stretching absorptions (Table 1) and the out-of-plane C—H mode at around 825 cm^{-1} characteristic of the π-cyclopentadienyl moiety.

The isolation of the new thiocarbonyl complexes indicates that such complexes may be far more widespread than is currently believed. Furthermore, it is of interest to note that the di- and trithiocarbonyl complexes reported here are the first examples of thiocarbonyl complexes having more than one CS group attached to a metal atom.

We thank the Canada Council for a scholarship (A.E.F.) and the National Research Council of Canada for financial support of this research.

1. I. S. BUTLER and A. E. FENSTER. Chem. Commun. 933 (1970).

Can. J. Chem. Downloaded from www.nrcresearchpress.com by 210.87.254.105 on 09/05/12
For personal use only.

Can. J. Chem. Downloaded from www.nrcresearchpress.com by 210.87.254.5 on 09/05/12
For personal use only.

Canadian Journal of Chemistry

Published by THE NATIONAL RESEARCH COUNCIL OF CANADA

VOLUME 50 MARCH 1, 1972 NUMBER 5

^{13}C Nuclear Magnetic Resonance Studies. XVI. ^{13}C Spectra of some Substituted Acrylic Acids and their Methyl Esters. A Correlation of Olefinic Shieldings in α,β-Unsaturated Carbonyl Systems[1]

H. BROUWER[2] AND J. B. STOTHERS

Department of Chemistry, University of Western Ontario, London, Ontario

Received August 18, 1971

The carbon-13 n.m.r. spectra of 26 α,β-unsaturated methyl esters and 16 substituted acrylic acids have been determined and the ^{13}C shieldings are discussed. These data are compared with the recently reported values for several α,β-unsaturated carboxylic acids. Linear regression analysis of the olefinic shielding data for several α,β-unsaturated carbonyl derivatives yields a set of parameters which correlate the results with reasonable precision. The solvent dependence of the ^{13}C shieldings of acrylic acid and methyl acrylate has been examined briefly. The proton results for the methyl esters are discussed briefly.

Les spectres r.m.n. du carbone 13 de 26 méthyl esters α,β-insaturés et de 16 acides acryliques substitués ont été déterminés et les effets d'écran ^{13}C sont discutés. Ces données sont comparées aux valeurs récemment rapportées pour quelques acides carboxyliques α,β-insaturés. Une analyse de la régression linéaire des données de l'effet d'écran oléfinique pour quelques dérivés carbonylés α,β-insaturés permet d'obtenir une série de paramètres qui sont en corrélation, avec une précision raisonnable avec les résultats. La dépendance entre le solvant et les effets d'écran de ^{13}C pour l'acide acrylique et l'acrylate de méthyle a été examinée brièvement. Les résultats concernant les protons pour les esters méthylés sont discutés brièvement.

Canadian Journal of Chemistry, **50**, 601 (1972)

Introduction

The geometrical dependence of aliphatic ^{13}C shieldings has been recognized for several years in both unsaturated (1–7) and alicyclic systems (8–14) and, in general, it has been found that ^{13}C shieldings are much more sensitive to molecular geometry than those of the corresponding protons. Consequently ^{13}C n.m.r. spectroscopy constitutes a new and powerful tool for the investigation of stereochemistry. In alicyclic systems it is observed that carbons separated by three bonds are shielded in the *gauche* orientation relative to those in an *anti* relationship. For example, an axial carbon bonded to a cyclohexane ring absorbs at higher field than its equatorial counterpart (9, 10, 12, 14); furthermore, the C-3 and -5 cyclohexyl carbons are similarly shielded in the former orientation (9, 14). This tendency, termed a γ-effect, has been ascribed to sterically induced polarization arising from nonbonded interactions of the hydrogen atoms bonded to the γ-carbons (15). It has also been established that carbon shieldings are similarly affected by other atoms in the γ-position (8, 13) and such γ-effects have proved to be useful in the analysis of the ^{13}C spectra of steroids (16), inositols (17), and several carbohydrates (18). Because of the rigidity of the double bond it follows that the α-carbons in *cis*-olefins will be shielded relative to those in the *trans*-isomers since the former are held in an eclipsed orientation; this is found to be the case. In addition, the magnitude of the difference is comparable to the γ-effect found for alicyclic systems (*ca.* 5 p.p.m.).

As part of a detailed investigation of the geometrical dependence of ^{13}C shieldings in relative-

[1]Part XV, Stothers *et al.* (32).

[2]Holder of NRCC Scholarships 1966–1970.

Can. J. Chem. Downloaded from www.nrcresearchpress.com by 210.87.254.5 on 09/05/12
For personal use only.

ly simple systems, the ^{13}C spectra of several methyl α,β-unsaturated carboxylates have been determined as well as the spectra of a number of the corresponding carboxylic acids. Recently, however, the results for an extensive series of the latter were reported by Lippmaa and coworkers (19). These data together with the earlier results for several α,β-unsaturated aldehydes and ketones (4) permit one to examine the general trends exhibited by the ^{13}C shieldings of aliphatic conjugated carbonyl derivatives as a function of substituent geometry. In this paper, these trends are discussed and a correlation of the olefinic shieldings, obtained by linear regression analysis, is presented. It has been found that the olefinic shieldings can be correlated with a set of substituent parameters comparable to those developed by Grant and Paul for saturated hydrocarbons (20). Although much of the available data for these carbonyl derivatives is less precise than that obtained from current spectrometers the quality of the correlation indicates that these parameters may be useful for the prediction of shieldings in related systems. In any event, the existence of the correlation is of theoretical interest since it offers further proof of the additivity of the factors affecting ^{13}C shieldings in aliphatic systems.

The proton spectra of the methyl esters were obtained in the course of this study and these data are recorded with a brief comment on the general trends.

Experimental

Materials

Several of the methyl esters and carboxylic acids employed in this study were obtained commercially while the others were prepared by standard methods. The halogenated compounds were formed by the addition of hydrogen halide to propynoic and butynoic acids and, in general, separation of the isomers was accomplished by conversion to the methyl esters, followed by fractional distillation. For the latter purpose an 18-inch platinum, spinning-band column was employed; in each case, the proton spectra provided a straightforward method for assessing the purity of each fraction. Subsequent hydrolysis to the solid carboxylic acid afforded an unequivocal characterization. In most cases, essentially pure samples (>99%) of each isomer were obtained. One notable exception, however, was methyl *Z*-3-methoxybutenoate which could only be obtained as the minor component in a mixture with the *E*-ester. In our hands the most favorable mixture was obtained by pyrolysis of the dimethyl ketal of methylacetoacetate at 350°. Initially the product, obtained by dropping the ketal onto an electrically-heated column of porcelain beads under a slow stream of nitrogen, was found to be a 3 : 2 mixture of *Z*- and *E*-isomers which after rapid distillation contained approximately equal quantities of each ester and some ketal. In contrast, the corresponding methyl 3-methoxypropenoates are readily separable by fractional distillation: *E*-isomer, b.p. 99–100°/85 mm and *Z*-isomer, b.p. 120–123°/85 mm; in contrast to the reported values of 80°/16 mm for each (21). Their proton and i.r. spectra are consistent with the assigned structures as was an elemental analysis.

Anal. Calcd. for $C_5H_8O_3$: C, 51.72; H, 6.94. Found: C, 51.44; H, 6.82.

Spectra

Most of the ^{13}C spectra were determined by rapid-passage dispersion-mode operation at 15.1 MHz. The samples were contained in a 15 mm concentric cell with a spherical reference cavity containing enriched methyl iodide as a standard. Calibration was accomplished by generating side bands of the reference signals with a GR1300A audio oscillator; the frequencies were monitored with a HP5245L counter. In certain cases, proton decoupling with a NMR Specialties SD60 decoupler was employed to increase the observed S/N. Each value represents the average of at least five scans in each field direction. The precision of the data obtained in this way is judged to be *ca* ± 0.3 p.p.m.

Some of the spectra were obtained under field-frequency lock conditions in which the signals are observed in the absorption mode, with noise-modulated decoupling to eliminate all proton–^{13}C coupling interactions. In these cases, the decoupled solvent signal was used as a "lock" and each spectrum repetitively scanned several times to obtain a suitable S/N. The instrument operated at 15.1 MHz and spectral accumulation was accomplished with a Varian 620i computer which also controlled the sweep unit, a Wave Tek Model 111 voltage-controlled oscillator. Decoupling was accomplished with a HP608F signal generator and HP8708A VHF synchronizer combination[3] the output of which was modulated with a HP3722A noise generator and amplified with a class C amplifier (the final stages of the NMRS SD60 decoupler). A Varian V4336 probe[4], double-tuned at 15.1 and 60 MHz, was employed in which 12 mm spinning sample tubes are used. In some cases a lock signal was obtained from a 3 mm capillary, containing 60%-enriched CS_2, which was held in the center of the sample tube with Teflon plugs. Operation with this instrument permitted measurements having a precision better than 0.1 p.p.m.

The proton spectra were obtained with a Varian HA-100 instrument; the analysis was straightforward in each case. Assignments for specific protons were checked, where necessary, by nuclear Overhauser enhancement measurements.

Results

The shielding results for the propenoic acids and methyl esters are collected in Tables 1 and 2, respectively. Since the precision of the two techniques employed to obtain these data differ

[3]We gratefully acknowledge the assistance of the Centre for Radio Science, University of Western Ontario for the loan of this VHF source.

[4]We wish to thank Varian Associates, Palo Alto, California for generously providing this probe for these studies.

TABLE 1. ^{13}C shieldings in some substituted propenoic acids, RC(X)=C(Y)COOH

			δ_C (p.p.m. from TMS)*											
			C-1			C-2			C-3			Other		
R	X	Y	*Z*		*E*	*Z*		*E*	*Z*		*E*	*Z*		*E*
H	H	H		168.9†			129.2†			130.8†				
Me	H	H	169.*8*		169.*3*	121.*0*		122.*8*	146.2‡		146.*0*	15.*0*		17.*3*
H	H	Me		170.*8*			136.*3*			126.*2*			17.5	
Me	Me	H		169.*4*			116.*1*			157.*5*			19.4†	
													26.5†	
Me	H	Me	171.*3*		170.*9*	127.*4*		128.*2*	136.*6*		137.*9*	15.*2*		11.1†
												19.*9*		13.5†
H	Cl	H	166.*2*		166.*4*	121.*4*		125.*2*	133.*2*		137.*0*			
Me	Cl	H	166.*2*		167.*0*	117.*1*		119.*5*	146.*4*		153.*1*	27.*3*		22.*9*
H	Br	H	166.*5*		166.*1*	124.7‡		129.*1*‡	122.*0*‡		128.*3*			
H	I	H	167.*2*		166.*5*	130.*6*		137.*4*	97.*4*		100.*3*			
Me	I	H	168.*5*			128.*5*			115.*4*			37.*2*		

*Methanolic solutions (25% v/v); unless otherwise noted, data obtained by rapid-passage operation.
†Slow-passage, absorption-mode measurements.
‡Data differ >2 p.p.m. from those reported in ref. 19.

appreciably, the less precise results (±0.3 p.p.m.), measured under rapid-passage conditions, are distinguished from the high-resolution data (±0.1 p.p.m.) by italicizing the last figure in the former, *i.e.* 166.5 *vs.* 166.5 p.p.m. The rapid-passage data were measured relative to external methyl iodide and converted to the δ_C scale (TMS = 0) using the shielding value of CH_3I, −20.5 p.p.m. The high-resolution data for cyclohexane solutions, measured initially from C_6H_{12}, were converted using $\delta_C(C_6H_{12})27.7$. In other cases the following conversion factors were employed: δ_C (CS_2 (ext)) 193.7; δ_C (dioxane) 67.4; δ_C (C_6H_6) 128.7. Lippmaa's data (19) were converted to the δ_C scale using the factor 193.7 p.p.m. To examine the solvent dependence of these shieldings, methyl acrylate and acrylic acid were measured in a few solvents, using the high-resolution method; these data are listed in Table 3 together with the results reported by Lippmaa *et al.* (19*b*) for acrylic acid.

The assignment of individual absorption patterns to specific carbons in this series of compounds presented no difficulties. The carboxyl carbons are readily identified as the lowest field signals (24) while the methoxyl carbons of the COOMe groups absorb near δ_C 51. The olefinic methyl carbons were also easily identified since their signals appear at highest field. Although the signal for one of the olefinic carbons in methyl β-cyanoacrylate is near that of the cyano carbon in the decoupled spectrum, these are readily distinguished in the coupled spectrum. From these shieldings, 111.7 and 114.7 p.p.m., respectively, the assignments of the singlets arising from C-3 and C≡N in the methyl β-cyanocrotonate spectra follow because of the downfield shift of *ca.* 13 p.p.m. expected for the olefinic absorption upon methyl substitution (2).

For those compounds in which the olefinic carbons are bonded to different numbers of hydrogen atoms, the multiplicities of the patterns in the coupled spectra serve to identify the α- and β-nuclei directly. For those cases in which each olefinic carbon bears a single hydrogen atom, the relative magnitudes of the $^{13}C-^{1}H$ coupling constants provide the necessary information to complete the assignments since J_{CH} increases with increasing electronegativity of X in the fragment X—C—H (25). In the present series the β-carbons bearing halogens or a methoxyl group have J_{CH} values which are 15–40 Hz larger than those of the α-carbons. The J_{CH} values were measured in the coupled ^{13}C spectra.

The proton parameters for the methyl esters, obtained by first-order analysis are listed in Table 4.

Discussion

It is apparent that, with the exception of the methoxyl group, the configuration of β-substituents has virtually no effect on the carboxyl

Can. J. Chem. Downloaded from www.nrcresearchpress.com by 210.87.254.5 on 09/05/12
For personal use only.

Can. J. Chem. Downloaded from www.nrcresearchpress.com by 210.87.254.5 on 09/05/12
For personal use only.

TABLE 2. ^{13}C shieldings in some α,β-unsaturated methyl esters RCX=C(Y)COOMe*

			δ_C (p.p.m. from TMS)†												
			OMe		C-1		C-2		C-3		Other				
R	X	Y	*Z*	*E*	*Z*	*E*	*Z*	*E*	*Z*	*E*	*Z*	*E*	*Z*	*E*	Solvent
H	H	H		50.9		166.0		128.7		129.9					
H	H	Me		51.*3*		166.*7*		136.*2*		125.*0*				17.*9*	
Me	H	H	50.*6*	50.*3*	166.*2*	166.*0*	120.*4*	122.*3*	144.*5*	144.*1*	15.*6*			17.*1*	CS_2(Z)
Me	Me	H		49.*9*		166.*3*		114.*8*		155.*9*			18.*9*	27.*0*	
Me	H	Me	50.3	50.*9*	167.*1*	167.*4*	128.*3*	128.*6*	137.*9*	136.*4*			20.5	11.8	
													20.5	13.9	
H	Cl	H	51.*5*	51.*8*	163.*9*	164.*1*	121.*5*	125.*0*	133.*3*	137.*5*					
Me	Cl	H	50.7	50.9	163.5	164.5	117.2	119.2	145.7	152.5	27.9		23.2		C_6H_{12}
H	Br	H	51.*4*	51.*7*	163.*6*	163.*9*	124.*1*	128.*4*	121.*4*	127.*0*					
Me	Br	H	51.6	51.0	163.6	164.2	120.4	120.0	135.8	143.6	30.9		26.0		C_6H_{12}
H	I	H	51.*3*	52.*5*	164.*5*	163.*5*	129.*9*	136.*2*	95.*9*	100.*0*					CS_2(Z)
															CCl_4(E)
Me	I	H	51.1	50.9	163.9	164.0	126.1	131.6	112.0	119.7	36.6		31.0		C_6H_{12}
H	OMe	H	50.*3*	50.*4*	164.*9*	167.*4*	95.*1*	95.*7*	160.*9*	163.*3*	61.*9*		57.*2*		
Me	OMe	H		50.*0*		167.*4*		90.*2*		172.*5*				17.*9*(Me)	
														55.*0*(OMe)	
H	OMe	Me		50.*4*		167.*9*		105.*3*		158.*3*				8.*5*(Me)	
														60.*1*(OMe)	
H	CN	H	52.*8*		163.*3*		111.*7*		138.*3*				114.7		$CHCl_3$
Me	CN	H	51.*8*	52.*0*	163.*5*	164.*4*	132.*7*	132.*4*	123.*8*	126.*8*			116.*8*(CN)	119.*1*(CN)	
													21.*5*(Me)	17.*0*(Me)	

*The relative orientation of substituents is indicated by the Blackwood convention (22) in which (*Z*) denotes the isomer having the highest priority groups (23) on the same side of the double bond.

†Measured using either (A) rapid-passage dispersion mode operation or (B) in slow-passage, absorption mode with time-averaging. With A, the precision is *ca.* ±0.3 p.p.m. denoted as 51.*3*; with B the precision is *ca.* 0.1 p.p.m. denoted as 51.3.

TABLE 3. Solvent effects on the ^{13}C shieldings of acrylic acid and methyl acrylate

Solute	Solvent*	δ_C (p.p.m. from TMS) C-1	C-2	C-3	OMe
Methyl acrylate	nil	166.0	128.7	129.9	50.9
	C_6H_{12}	165.9	129.2	129.4	51.0
	C_6H_6	166.1	128.7	129.9	51.2
	p-Dioxane	166.3	129.0	130.2	51.2
	MeOH	167.1	128.6	130.3	51.2
Acrylic acid	nil	171.2	128.3	132.9	
		171.6†	128.4†	133.1†	
	H_2O†‡	170.6	128.9	133.4	
	MeOH	168.9	129.2	130.8	
	DMSO†‡	168.4	130.7	131.6	
	p-Dioxane	167.8	129.1	131.2	
	C_6H_6	172.1	128.3	132.9	

*Unless otherwise noted, results were obtained for 25% (v/v) solutions.
†Reference 19*b*.
‡50% solutions.

carbon shieldings in either the carboxylic acids or their methyl esters. Although there is a small shift toward higher field (*ca.* 3 p.p.m.) in the case of the halo- and cyano-substituted systems the observed difference between carboxyl shieldings in the *Z*- and *E*-isomers is less than 1 p.p.m. Similarly these carbons are essentially unaffected by β-methyl groups while α-methyl substitution tends to deshield the carboxyl carbons by *ca.* 1 p.p.m. The shielding of the methoxyl carbon of the ester group is also unaffected by these β-substituents, lying in the narrow range of *ca.* 2 p.p.m. for this series. The upfield shifts of 3–4 p.p.m. observed for the carboxyl carbon signals upon esterification are qualitatively comparable to those found for saturated systems (26–28) presumably because of a decrease in the polarization caused by hydrogen bonding in the acid (see below), but it may be noted that the change is approximately 50% of that observed for saturated systems.

The shieldings of the olefinic carbons as well as those of the β-methyl and β-methoxyl carbons, however, depend markedly on the orientation of the β-substituent. In general, the olefinic carbons of the *Z*-isomers absorb at higher field than their *E*-analogs, whereas β-methyl carbons *cis* to the carboxyl function are shielded relative to those in the *trans*-orientation. For example, the β-methyl shieldings of the *E*-isomers of the 3-substituted crotonates differ from those of the *Z*-isomer by *ca.* −4 p.p.m. It is to be noted, however, that the upfield trend associated with the *cis*-orientation of the β-methyl carbon is more pronounced for *cis*-vicinal methyl groups. This is most clearly illustrated by the results for methyl angelate and methyl tiglate. In the former, the C-methyl carbons are equivalent, δ_C 20.5, while for the latter, in which these carbons are *cis*, the signals appear at δ_C 11.8 and 13.9. Presumably the major factor contributing to the upfield shifts observed for *cis*-methyl carbons arises from steric interactions between the closely-lying groups. These γ-effects, attributed to sterically induced polarization (15), are generally found for carbons in gauche or eclipsed orientations. On the basis of steric interactions it seems reasonable that a greater shift will be observed for *cis*-vicinal methyls than for a methyl carbon *cis* to a carboxyl or carbomethoxyl function.

The effects of methyl substitution on the olefinic shieldings are comparable to those found for related α,β-unsaturated carbonyl derivatives (4). Upon replacement of an olefinic hydrogen atom by a methyl group the absorption of the substituted carbon undergoes a downfield shift of 10–15 p.p.m. while the neighboring olefinic carbon is shielded (5–10 p.p.m.). Similar changes are found upon introduction of a chlorine atom but the shifts are reversed for bromine and iodine substitution. Furthermore, while the shifts exhibited by the olefinic carbons in the methyl substituted derivatives are almost in-

Can. J. Chem. Downloaded from www.nrcresearchpress.com by 210.87.254.5 on 09/05/12
For personal use only.

Can. J. Chem. Downloaded from www.nrcresearchpress.com by 210.87.254.5 on 09/05/12
For personal use only.

TABLE 4. Proton parameters for some α,β-unsaturated methyl esters, R(X)C=C(Y)COOMe

			Shieldings (p.p.m. from TMS)								Coupling constants (Hz)				
			Olefinic												
			α		β		Methoxyl		Methyl		Vicinal		Allylic		
R	X	Y	*Z*	*E*	*Z*	*E*	*Z*	*E*	*Z*	*E*	*Z*	*E*	*Z*	*E*	Other
H	H	H	6.982		6.674(*trans*) 7.230(*cis*)		3.72				17.34(*trans*) 10.55(*cis*)				1.51(J_{gem})
H	H	Me	—		5.481(*trans*) 6.017(*cis*)		3.70		1.90				−1.00(*trans*) −1.61(*cis*)		1.93(J_{gem})
Me	H	H	5.723		6.253		3.65		2.125		11.41		−1.75		7.12($J^{vic}_{Me,H}$)
Me	Me	H	5.585		—		3.60		1.88(*trans*) 2.14(*cis*)				−1.35 −1.35		
Me	H	Me	—	—	5.978	6.745	3.68	3.66	1.96 1.85	1.77 1.80			−1.30 −1.45		7.15($J^{vic}_{Me,H}$)
H	Cl	H	6.123	6.199	6.661	7.321	3.73	3.72			8.26	13.50			
Me	Cl	H	5.934	6.017	—	—	3.67	3.67	2.25	2.58			−1.25	−1.20	
H	Br	H	6.557	6.480	6.944	7.545	3.73	3.60			8.24	13.77			
Me	Br	H	6.208	6.271	—	—	3.68	3.65	2.46	2.78			−1.30	−1.35	
H	Br	Me		—		7.459		3.72		1.99				−1.47	
H	I	H	6.852	6.820	7.423	7.800	3.75	3.70			8.92	14.60			
Me	I	H	6.223	6.568	—	—	3.70	3.65	2.74	2.99			−1.47	−1.52	
H	OMe	H	4.680	5.089	6.366	7.517	3.59 3.83*	3.62 3.68*			7.00	12.66			0.45† 0.27†
Me	OMe	H		4.910		—		3.57 3.61*						−0.53	0.45†
H	OMe	Me		—		7.143		3.61 3.80*		1.66				−1.38	
Me	CN	H	6.270	6.357	—	—	3.79	3.74	2.17	2.35			−1.68	−1.71	

*C-3 methoxyl signals.
†*J* MeO, H in *E*-isomers, the corresponding values for *Z*-isomers are ←0.1 Hz.

TABLE 5. Substituent parameters for alkyl substitution in α,β-unsaturated carbonyl compounds, $>C^{\beta}=C^{\alpha}COX$ (in p.p.m.)*

Parameter† A_j	α-C	No. of examples	β-C	No. of examples
α	7.5±0.4	13	13.7±0.6	26
β^{π}	−5.4±0.4	26	−5.6±0.6	13
β^{σ}	(5.8±0.8)	1	5.5±0.9	4
γ^{π}	−1.7±0.6	4		
β^{gem}			−2.2±1.0	5
cis alkyl	−1.3±0.6	8	−0.5±0.7	8
carbonyl	−2.3±0.6	9		
X = Me	−1.5±0.6	11	−10.3±0.9	11
=OH	−10.1±0.6	7	−7.6±0.9	7
=OMe	−10.2±0.6	7	−9.1±0.9	7
Constant, K	138.3		139.2	
Standard error	±0.7		±1.0	
Multiple correlation coefficient	0.998		0.996	

*A positive value indicates a downfield shift.
†The symbol indicates the position of substitution relative to the carbon of interest while the superscript denotes the bonding pathway to that carbon.

dependent of the stereochemistry of the methyl group this is not the case for the halogens. In one of the first discussions of the effects of polar substituents on olefinic ^{13}C shieldings (1) it was proposed that alterations in the electron density arising from steric inhibition of resonance in *cis*-isomers were the primary source of the geometrical dependence of the olefinic shieldings but this view was subsequently modified (6). It was suggested that the tendency toward charge separation and a reduced bond-order in the olefinic bond of the *cis*-isomers may be the principal factor governing the differential shifts. Although application of the Pople–Karplus treatment (29) gave results consistent with the observations for unsymmetrically substituted ethylenes this approach fails with the symmetrical systems indicating that the apparent agreement for the former cases may be fortuitous since the possible effect of variations in excitation energies and contributions from the *d*-electrons of the halogens were neglected.

It is interesting that the olefinic shieldings in a variety of alkyl-substituted α,β-unsaturated carbonyl derivatives may be correlated reasonably well with a linear expression of the form

$$[1] \qquad \delta^{i}_{C} = K + \sum_{j} A_j n_{ij}$$

where δ^{i}_{C} represents the shielding of either the α- or β-olefinic carbon, A_j is an additive shift parameter for a specific substitution j, n_{ij} the number of such substitutions, and K is a constant. Linear regression analysis of the α- and β-carbon shieldings, separately, led to the generation of the parameters listed in Table 5. This approach is exactly analogous to that employed by Grant and Paul (20) to correlate their saturated hydrocarbon shieldings with the additional feature that two types of substituent parameters are required to differentiate between effects transmitted entirely through σ-networks and those which act through the π-bond. In addition, it was found necessary to include geometrical parameters denoted "*cis* (alkyl)" and "*cis* (carbonyl)" to achieve a fit for the data. In the light of the standard error of this analysis it would appear that these parameters may be useful for predicting ^{13}C shieldings in other closely-related systems but, in any event, the existence of the correlation emphasizes the remarkable additivity of substituent effects on ^{13}C shieldings. This analysis should provide constants, K, which correspond to the shieldings of acrolein, the observed shieldings (4) for which, after conversion to the TMS scale, are 136.*4* and 136.*0* p.p.m., *i.e.* somewhat more shielded than the calculated values. A similar analysis was attempted for the 3-halo substituted examples but the results were less satisfactory; since some interesting trends emerge, however, these data are collected in Table 6 for comparison. In this case, the constant terms, K, correspond closely

Can. J. Chem. Downloaded from www.nrcresearchpress.com by 210.87.254.5 on 09/05/12
For personal use only.

TABLE 6. Substituent parameters for some β-substituents on the olefinic ^{13}C shieldings of α,β-unsaturated carboxylic acids and esters, $>C^{\beta}=C^{\alpha}HCOOR$ (in p.p.m.)*

Substituent parameters	α-C		β-C	
	This work	Ref. 19†	This work	Ref. 19†
Me	−5.6±0.7	−4	13.6±1.2	10
Cl	−3.1±0.7	−4	5.8±1.2	4
Br	−0.4±0.7	1	−3.3±1.2	−1
I	8.8±0.7	11	−29.6±1.2	−35
cis-Me	−2.3±0.5	−2	1.4±0.9	2
cis-Cl	−4.1±0.6	−2	−4.7±1.0	−5
cis-Br	−3.5±0.6	−6	−6.1±1.1	−12
cis-I	−6.5±0.6	−9	−3.7±1.0	−4
gem Me,X	1.8±0.7		1.7±1.3	
R = H	0.6±0.3		1.0±0.5	
= Me	0.0		0.0	
Constant, *K*	128.1		130.4	
Standard error	0.8		1.3	

*A positive value indicates a downfield shift.
†See text.

to the shieldings of methyl acrylate. The methyl group was included in the regression analysis as a check with the data in Table 5 and the agreement is satisfactory. The values of the geometric parameters found for the halogens emphasize the difficulty in interpretation of the effects of these substituents. While the "direct" effects change monotonically to judge from the second, third, and fourth parameters, the geometrical effects exhibit a different trend for the series: Cl, Br, I. The results for an extensive series of polysubstituted acrylic acids have recently been analyzed to test for the existence of an additive relationship and a series of parameters has been derived in a somewhat different manner (19). Lippmaa *et al.* following an approach analogous to that originally employed by Savitsky and Namikawa (1) generated two sets of parameters for the α- and β-olefinic carbons, in each of which there are three parameters for each substituent depending on its position with respect to the carboxyl group, *i.e. gem, cis,* and *trans.* Thus, their *trans* parameters and the difference between the *cis* and *trans* parameters may be compared with the values obtained by our linear regression analysis; these data are included in Table 6. Since the latter parameters were derived from shieldings for the acids only and these were examined either as neat liquids or in DMSO solutions, it is not surprising that these values differ somewhat from our values. Lippmaa and coworkers (19) found that their parameters give predicted shieldings which are generally within 4 p.p.m. of the observed values and they pointed out that this is equivalent to an error of *ca.* 0.13 p.p.m. for ^{1}H shieldings since the ^{13}C shielding range is *ca.* 30-fold larger. Clearly these parameters should be useful for approximate estimates of the ^{13}C shieldings in related systems. As Grant and Paul (20) found in their analysis of the results for the saturated hydrocarbons, it is necessary to include additional factors for geminal substituents. In the present series, a parameter for geminal methyl and halogen was generated while Lippmaa *et al.* derived factors for geminal halogen atoms.

To examine the effect of medium on these shieldings, the spectra of acrylic acid and methyl acrylate were obtained in a few different solvents. These data together with the earlier results reported by Lippmaa *et al.* (19*b*) show (Table 3) that each carbon in the acid is affected by the solvent but the ester shieldings are virtually independent of the medium. The solvent dependencies of the carbons in acrylic acid appear to be explicable in terms of hydrogen bonding. In the neat liquid, the acid exists predominantly as a dimeric species, **1**, in which the carboxyl group is strongly polarized by hydrogen bonding. Since water and methanol can act both as donors and acceptors in hydrogen-bonded complexes, however, species such as **2** and **3** enter the equilibrium in these solvents such that the relative dimer concentration is reduced

Can. J. Chem. Downloaded from www.nrcresearchpress.com by 210.87.254.5 on 09/05/12
For personal use only.

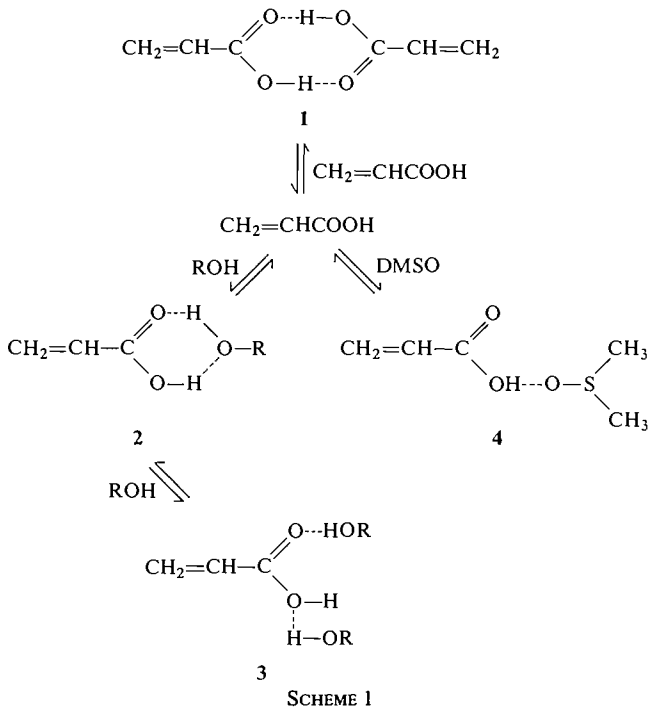

SCHEME 1

(see Scheme 1). The fact that the shieldings in water and methanol differ, with the aqueous values close to those for the pure liquid, indicates that water is the more strongly hydrogen-bonded and the polarization of the conjugated system in **2** and **3** (R = H) is comparable to that in **1**. Dioxane and dimethylsulfoxide, on the other hand, act only as acceptors and species such as **4** would be expected to be less polarized; the upfield shifts of the carboxyl and β-carbon signals in these solvents relative to the shieldings of the pure liquid are consistent with this view.

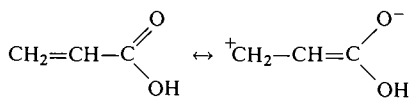

In effect, hydrogen-bonding should enhance the contribution of forms such as **5** to the overall electron distribution in the conjugated systems. To test the concentration dependence of these shieldings in a hydrogen-bonding medium, the ^{13}C shieldings of acrylic acid were measured as a function of increasing amounts of methanol. These results are illustrated in Fig. 1 from which it is apparent that the carboxyl and β-carbon nuclei are more strongly affected. It is interesting that most of the solvent shift occurs with less than 2 *M* equiv of methanol indicating that both **2** and **3** indeed are formed. These relatively small

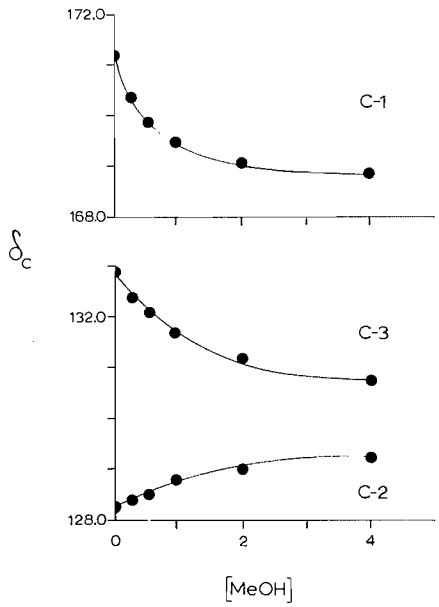

FIG. 1. Variation of acrylic acid ^{13}C shieldings (δ_C) in methanolic solutions (*M* equiv).

Can. J. Chem. Downloaded from www.nrcresearchpress.com by 210.87.254.5 on 09/05/12
For personal use only.

Can. J. Chem. Downloaded from www.nrcresearchpress.com by 210.87.254.5 on 09/05/12
For personal use only.

shifts of *ca.* 2 p.p.m., however, are much smaller than the 7 p.p.m. difference found for the carboxyl carbon of acetic acid upon dilution in acetone (30); this is consistent with the notion that **3** is reasonably strongly polarized although less so than the dimer, **1**. In summary, these results are comparable to those found by Maciel and Traficante (30) in their detailed examination of the solvent dependence of the acetic acid carboxyl shielding and may be interpreted in a similar manner. There is the additional feature that the β-olefinic carbon shieldings are also expected (4, 25) to reflect variations in the polarization of the carboxyl function as observed.

The proton shielding results for the methyl esters (Table 4) follow the usual trends in that the β-protons absorb at lower fields than the α-protons and β-protons or β-methyl protons *cis* to the ester grouping are consistently deshielded relative to their *trans*-counterparts. The values for the majority of the coupling constants are also unexceptional and require no specific comments. The long-range interactions between the methoxyl and olefinic protons, however, are interesting. The *E*-isomers (*i.e.* those having the methoxyl and carbomethoxyl function *trans*) exhibit readily measurable four- and five-bond couplings whereas in the corresponding *Z*-isomers these interactions are not resolved. Presumably the magnitude of these long-range coupling constants depends on the conformation of the methoxyl methyl group as proposed by Feeney and Sutcliffe (31). According to these authors coupling between the nearest olefinic proton and those on the methoxyl carbon will be greater in the rotamer **6**, having the methoxyl group close to the double bond, rather than **7**.

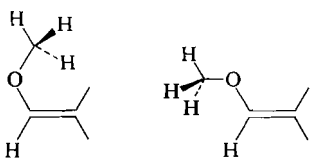

6 7

In **6** the olefinic and one of the methyl protons is in the familiar W arrangement known to favor long-range coupling. Since there will be steric interference with the carbomethoxyl and methoxyl groups in the *Z*-isomers, however, rotamer **7** will be the preferred form in these systems and the long-range couplings may be expected to be smaller, as is observed. Similar results were obtained for the *Z*- and *E*-isomers of 1-methoxy-1-propene. Although no long-range coupling involving the methoxyl protons is evident in the spectrum of the former, the four- and five-bond interactions are 0.28 and $\sim$0.1 Hz, respectively, in the latter. On the basis of these results it is not surprising that comparable long-range coupling was not resolved in the spectrum of 1-methoxy-2-methyl-1-propene.

We wish to acknowledge the financial support of the National Research Council of Canada through an operating grant and scholarships. We also wish to thank Varian Associates, Palo Alto, California for the loan of the V4336 probe and the Centre for Radio Science, University of Western Ontario, Dr. P. A. Forsyth, Director, for the use of the r.f. generator employed in the proton decoupler.

1. G. B. SAVITSKY and K. NAMIKAWA. J. Phys. Chem. **67**, 2754 (1963).
2. R. A. FRIEDEL and H. L. RETCOFSKY. J. Am. Chem. Soc. **85**, 1300 (1963).
3. G. E. MACIEL. J. Chem. Phys. **42**, 2746 (1965).
4. D. H. MARR and J. B. STOTHERS. Can. J. Chem. **43**, 596 (1965).
5. E. LIPPMAA, S. RANG, O. EISEN, and T. PEHK. Eesti NSV Tead. Akad. Toim Fuus-Matem, **16**, 351 (1967).
6. G. B. SAVITSKY, P. D. ELLIS, K. NAMIKAWA, and G. E. MACIEL. J. Chem. Phys. **49**, 2391 (1968).
7. S. RANG, E. LIPPMAA, T. PEHK, and O. EISEN. Eesti NSV Tead. Akad. Toim Keem-Geol. **17**, 294 (1968).
8. G. W. BUCHANAN, D. A. ROSS, and J. B. STOTHERS. J. Am. Chem. Soc. **88**, 4301 (1966).
9. D. K. DALLING and D. M. GRANT. J. Am. Chem. Soc. **89**, 6612 (1967).
10. G. W. BUCHANAN and J. B. STOTHERS. Chem. Commun. 1250 (1967).
11. E. LIPPMAA and T. PEHK. Kem. Teollisuus, **24**, 1001 (1967); Eesti NSV Tead. Akad. Toim. Keem-Geol. **17**, 287 (1968).
12. G. W. BUCHANAN, J. B. STOTHERS, and SIU-TZYY WU. Can. J. Chem. **47**, 3113 (1969).
13. G. W. BUCHANAN and J. B. STOTHERS. Can. J. Chem. **47**, 3605 (1969).
14. F. A. L. ANET, C. H. BRADLEY, and G. W. BUCHANAN. J. Am. Chem. Soc. **93**, 258 (1971).
15. D. M. GRANT and B. V. CHENEY. J. Am. Chem. Soc. **89**, 5315 (1967).
16. H. J. REICH, M. JAUTELAT, M. T. MESSE, F. J. WEIGERT, and J. D. ROBERTS. J. Am. Chem. Soc. **91**, 7445 (1969).
17. D. E. DORMAN, S. T. ANGYAL, and J. D. ROBERTS. Proc. Nat. Acad. Sci. **63**, 612 (1969); J. Am. Chem. Soc. **92**, 1351 (1970).
18. D. E. DORMAN and J. D. ROBERTS. J. Am. Chem. Soc. **92**, 1355 (1970); A. S. PERLIN, B. CASU, and H. J. KOCH. Can. J. Chem. **48**, 2596 (1970).

19. (*a*) C. RAPPE, E. LIPPMAA, T. PEHK, and K. ANDERSSON. Acta Chem. Scand. **23**, 1447 (1969). (*b*) E. LIPPMAA, T. PEHK, K. ANDERSSON, and C. RAPPE. Org. Mag. Res. **2**, 109 (1970).
20. D. M. GRANT and E. G. PAUL. J. Am. Chem. Soc. **86**, 2984 (1964).
21. E. WINTERFELT and H. PREASS. Chem. Ber. **99**, 450 (1966).
22. J. E. BLACKWOOD, C. L. GLADYS, A. E. PETRARCA, W. H. POWELL, and J. E. RUSH. J. Chem. Doc. **8**, 30 (1968).
23. R. S. CAHN, C. K. INGOLD, and V. PRELOG. Angew Chem. Int. Ed. **5**, 385 (1966).
24. P. C. LAUTERBUR and J. B. STOTHERS. Can. J. Chem. **42**, 1563 (1964).
25. W. MCFARLANE. Quart. Rev. **23**, 187 (1969).
26. D. H. MARR and J. B. STOTHERS. Can. J. Chem. **45**, 225 (1967).
27. R. HAGEN and J. D. ROBERTS. J. Am. Chem. Soc. **91**, 4504 (1969).
28. E. LIPPMAA and T. PEHK. Eesti NSV Tead. Akad. Toim Keem-Geol. **17**, 210 (1968).
29. M. KARPLUS and J. A. POPLE. J. Chem. Phys. **38**, 2803 (1963).
30. G. E. MACIEL and D. D. TRAFICANTE. J. Am. Chem. Soc. **88**, 220 (1966).
31. J. FEENEY and L. H. SUTCLIFFE. Spectrochim. Acta, **24A**, 1135 (1968).
32. J. B. STOTHERS, L. J. DANKS, and J. F. KING. Tetrahedron Lett. 2551 (1971).

Can. J. Chem. Downloaded from www.nrcresearchpress.com by 210.87.254.5 on 09/05/12
For personal use only.

The Nature of the Tricyclic Dimer Formed from Acetonylacetone and Hydrazine: An Application of ^{13}C Nuclear Magnetic Resonance[1]

P. DE MAYO, J. B. STOTHERS, AND M. C. USSELMAN
Chemistry Department, University of Western Ontario, London, Ontario

Received August 27, 1971

The structure of the dimer formed from acetonylacetone and hydrazine has been re-examined. On the basis of chemical and spectroscopic data, a covalent tricyclic structure is proposed.

La structure du dimère formé à partir de l'acétylacétone et de l'hydrazine a été réexaminée. Sur la base de données chimiques et spectroscopiques, une structure covalente tricyclique est proposée.

Canadian Journal of Chemistry, **50**, 612 (1972)

Can. J. Chem. Downloaded from www.nrcresearchpress.com by 210.87.254.42 on 09/05/12
For personal use only.

Introduction

For another purpose we had need of the substance **2***a* (3,6-dimethyl-6-*n*-butyl-1,4,5,6-tetrahydropyridazine) and sought to prepare it by the method used by Overberger and Kesslin (1) for the preparation of the phenyl derivative **2***b*. This drew our attention to the nature of the intermediate dimeric substance **1**, to which no adequate structure had been assigned (2). The substance **1** was formed by the action of acetonylacetone on hydrazine, and on arylation gave **2***b*. Earlier workers (3–5) had attributed a structure **3** to this substance, but this was discarded by Overberger. Work is described below, both chemical and spectroscopic, which leads to the conclusion that this substance is best represented by structure **4**.

Results and Discussion

Compound **1**, a colorless solid m.p. 52–53°, was shown by Overberger *et al.* (2) to react as if it were the monomeric 3,6-dimethyl-4,5-dihydropyridazine (**5**). Under a variety of conditions, therefore, the dimer **1** must have a facile route for reversion to monomer. In confirmation of this our synthesis of the monomeric *n*-butyl adduct **2***a* proceeded cleanly and in good yield (eq. 1). It has been equally clear, however, to those who have worked with **1** that a simple monomeric structure is not possible. The earliest workers based their conclusions principally on molecular weight determinations, which gave values of *ca.* 220, corresponding to the molecular weight of a dimer. Overberger *et al.* (2), on the basis of its cryoscopic molecular weight in water, which varied with concentration, concluded that **1** existed as an associated dimer. The i.r. spectrum (2) contained NH absorption, which is not present in **5**, and yet **1** reacted with a variety of reagents, such as hydrogen cyanide and hydrogen peroxide (2), as a simple monomer. All of these facts are readily explained if **1** indeed exists as an associated dimer.

The proton spectrum of **1** clearly indicated a dimer which contained 20 protons, including one exchangeable amine hydrogen (at 5.35 p.p.m.) and four nonequivalent methyl groups (1.85, 1.70, 1.40, and 0.97 p.p.m.). The spectra were identical for samples of **1** purified by fractional distillation, recrystallization, or sub-

[1]

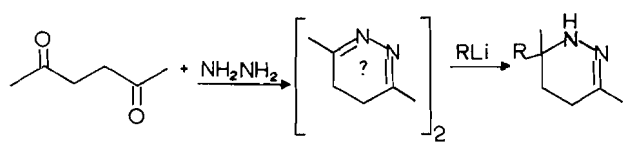

1 **2a** R=n Bu
2b R=Ph

[1]Part XVII in the series ^{13}C Nuclear Magnetic Resonance Studies. For Part XVI see ref. 14.

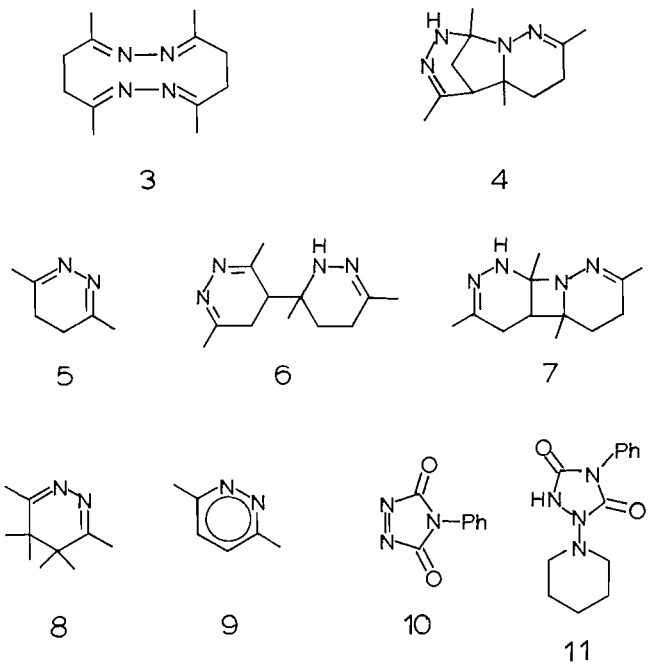

Can. J. Chem. Downloaded from www.nrcresearchpress.com by 210.87.254.42 on 09/05/12
For personal use only.

limation. The four methyl absorptions were singlets and no identifiable coupling patterns could be discerned for the methylene protons.

Since the proton spectra indicated the existence of a stable dimer, even in very dilute solution, the molecular weight of **1** was determined by osmometry in CCl_4 at various concentrations and found to be independent of concentration, contrary to the result reported for the aqueous solution (2). Thus, it appears that **1** is a covalent, stable dimer in neutral solution, but under basic or acidic conditions, the dimer dissociates wholly, or in part, to monomer (**5** or one of its tautomers): reactions then proceed from the monomer. Not surprisingly, the mass spectrum showed no signal at *m/e* 220, the signal of greatest *m/e* being at 110.

If **1** be stable in neutral media it should be possible to anchor the molecule in its dimeric form by acetylating the amine function. Reaction of **1** with acetic anhydride in pyridine resulted in a nearly quantitative conversion to the *N*-acetyl derivative, which was stable in polar solvents, as expected, although, like the dimer **1**, it slowly decomposed on exposure to air. Its proton spectrum in carbon tetrachloride contained three separate methyl absorptions at 2.1, 1.9, and 1.1 p.p.m. in a ratio of 2:2:1, respectively; five resolved methyl singlets appeared in benzene solution at 2.50, 2.35, 1.80, 1.60, and 0.78 p.p.m.

The u.v. spectrum of **1** in cyclohexane solution was recorded over a concentration range of 10^4 and was found to follow Beer's law over the entire concentration span, thus indicating that the dimer was unaffected by dilution, in agreement with the osmometry result. In addition, the u.v. spectrum of **1** in carbon tetrachloride (the solvent used for i.r., n.m.r., and osmometry) was identical to that in hexane, at least in the region in which carbon tetrachloride was transparent. The species examined by n.m.r., i.r., and osmometry is hence the same as that studied by u.v. spectroscopy.

From these facts it appears that **1** exists as a covalent dimer, and the first step in many of its chemical reactions is dissociation to the monomer, or tautomers thereof, which subsequently reacts to give product.

Of the possible dimeric structures, only those in which the six-membered ring of the monomer is intact were considered seriously, since all reactions of the dimer lead to substituted pyridazines as products. The formation of structures **4**, **6**, or **7** may be envisaged to arise

[2] 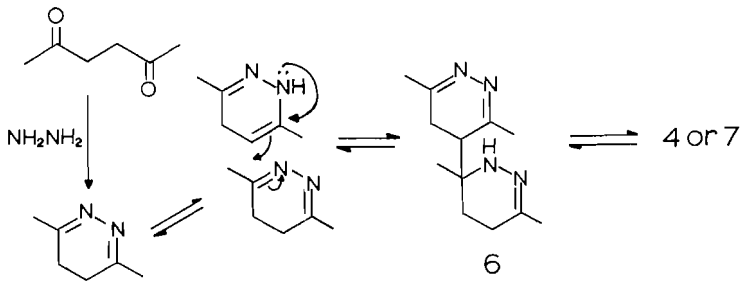

as shown in eq. 2. Structures **4** and **7** are easily obtained from **6** by addition of the amino nitrogen to one or the other of the imine bonds.

Structures **4** and **7** are expected to have very similar spectral properties but **6** should give distinctly different spectra. If **6** were the correct structure, its u.v. spectrum should approximate a composite of the spectra of **2***a* (λ_{max} 230 nm (4700)) and hexamethyl-4,5-dihydropyridazine[2] (**8**) (λ_{max} 250 nm (2800)) but the dimer exhibits a single maximum at 250 nm (7200) which is much more intense than that of **8**. Although red-shifted 20 nm, the shape of the dimer spectrum is similar to that of **2***a* (**4** and **7** are approximated by two such chromophores) suggesting that **4** and **7** are more likely formulations.

Structure **6** was judged even more unlikely in light of the proton spectrum. One would expect the two methyl groups of the dihydro ring to have very similar chemical shifts but this was not observed. This discrepancy may be explained if the dimer is intramolecularly hydrogen-bonded preventing free rotation about the bond joining the two rings. To this end, i.r. spectra of the dimer in chloroform were recorded over a concentration range of 20 (the amount of dimer between the plates was held constant through the use of cells of varying path length). In the most dilute solution a sharp NH absorption at 3350 cm^{-1} appeared. With increasing concentration, the NH band broadened considerably until it extended to 3200 cm^{-1} in the most concentrated solution. This change is indicative of intermolecular rather than intramolecular hydrogen-bonding, since the latter is expected to be concentration independent. The proton spectrum was compatible with structures **4** and **7**, however, since the four methyl groups in each structure are in different environments.

We next attempted to distinguish between **6** and structures **4** and **7** by chemical means, and used two approaches, both of which were intended to demonstrate the correctness of structure **6**. The first of these was oxidation of the dihydro ring, and the second Diels–Alder addition to that ring.

As shown initially by Overberger *et al.* (2), oxidation of the dimer itself gives only dimethylpyridazine (**9**). In addition, the *N*-acetyl dimer was stable to hydrogen peroxide in refluxing 50% aqueous isopropanol and to palladium-on-carbon in *o*-xylene at 150°. Thus, structure **6** seems unlikely since its dihydro ring should be easily oxidized. Oxidation with Pd/C in refluxing *p*-cymene (180°) gave seven products, none of which was that expected. On the basis of these results structures **4** and **7** are strongly favored.

Although Diels–Alder additions of the *N*-acetyl dimer with *N*-phenyl maleimide, tetracyanoethylene, and 4-phenyl-1,2,4-triazoline-3,5-dione (**10**) were unsuccessful,[3] **10** reacted instantaneously with dimer **1** in cold benzene to produce dimethylpyridazine **9** and *N*-phenylurazole. The urazole precipitated out of solution as a fine white powder. With the addition of 2 mol of triazolinedione, 1 mol of the dimer was oxidized quantitatively to 2 mol of dimethylpyridazine, with the production of 2 mol of the urazole.

The reaction of triazolinedione with compounds containing an active hydrogen is well known. Pirkle and Stickler isolated a 1:1

[2]We thank Dr. D. A. Arnold for a generous sample of this compound.

[3]Arnold and coworkers have shown (6, 7) that triazolinedione reacts rapidly with five-membered ring isopyrazoles to give Diels–Alder adducts. However, he has found that **8** does not react with triazolinedione (8).

Can. J. Chem. Downloaded from www.nrcresearchpress.com by 210.87.254.42 on 09/05/12
For personal use only.

Can. J. Chem. Downloaded from www.nrcresearchpress.com by 210.87.254.42 on 09/05/12
For personal use only.

[3]

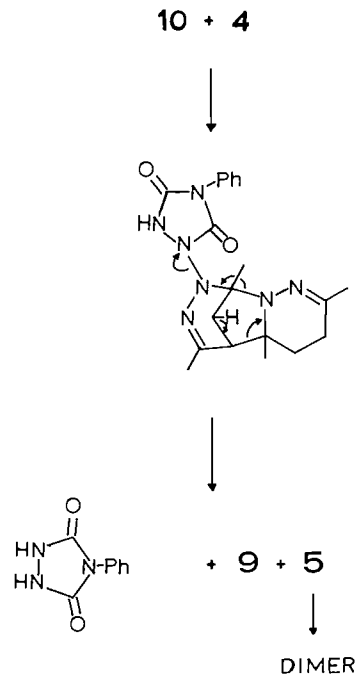

addition product from reaction of triazolinedione with olefins bearing an allylic hydrogen (9), and Cookson *et al.* were able to oxidize alcohols to ketones in high yield with triazolinedione (10). It is possible that oxidation of **1** proceeds via an addition–elimination step as illustrated in eq. 3 for structure **4**.

We propose addition to NH as the first step for two reasons. First, the *N*-acetyl derivative is stable to triazolinedione, and thus the NH function of the dimer must be responsible for overall reaction. Secondly, it was possible to isolate a similar 1:1 adduct from the reaction of triazolinedione with piperidine. The addition of triazolinedione to a benzene solution of piperidine gave an instantaneous reaction and a light yellow compound formed as the sole product. Its spectra were compatible with the 1:1 adduct **11**. It was stable at room temperature under nitrogen for about 12 h.

On the basis of the accumulated data, **4** and **7** appeared to be the most probable structures for the dimer. To reach an unambiguous conclusion, the ^{13}C n.m.r. spectra of the dimer and related compounds were examined.

The proton decoupled ^{13}C spectrum of **1** in acetone-d_6 solution contained 12 separate resonances, with two at significantly lower field (139.9 and 146.5 p.p.m.) than the others. This observation conclusively ruled out **6** as a possible structure since it contains three sp^2-hybridized carbons which are expected to absorb at $\delta_C >$ 100. Three signals at intermediate fields (47.5, 62.9, and 75.4 p.p.m.) were shown by off-resonance decoupling to arise from a tertiary and two quaternary carbons, respectively. Of the remaining seven signals, four were readily assigned to methyl carbons (22.2, 24.5, 24.7, and 27.4 p.p.m.) and three to methylene carbons (23.9, 25.0, and 31.2 p.p.m.) by off-resonance decoupling. Tentative assignments for each signal are indicated in **12**. Although these are

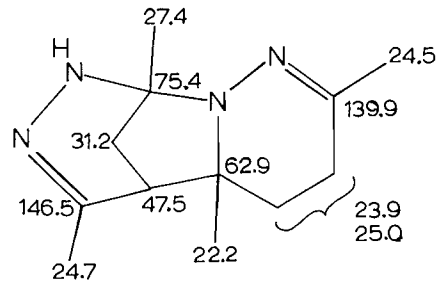

12

difficult to confirm because of a lack of suitable model systems, some supporting evidence is provided by the spectra of **1**-NAc, and **2***a*. The low field signals in the spectrum of the *N*-acetyl derivative appeared at 47.3, 63.0, 80.4, 141.0, and 151.4 p.p.m. and, with the exception of the first, were shown to arise from quaternary carbons. Thus, only one of the doubly-bonded carbons and the carbon absorbing at 75.4 p.p.m. in the dimer are significantly affected by acetylation, as expected for the tricyclic structures. Since the methine signal (47.5 p.p.m.) and that for one of the saturated quaternary centers (62.9 p.p.m.) are unaffected by *N*-acetylation these carbons must be more than three bonds from the N—H group in the dimer. One methylene signal, however, is shifted 4 p.p.m. upfield upon acetylation which may be expected for structure **4** but not **7** since the *N*-acetyl group is three bonds from C-12 in **4**. In general, substitution of a hydrogen three bonds from a given carbon tends to increase the shielding of that carbon because of the so-called "γ-effect";

Can. J. Chem. Downloaded from www.nrcresearchpress.com by 210.87.254.42 on 09/05/12
For personal use only.

several examples of this tendency have been reported (11). The imine carbon in **2***a* absorbed at 141.7 p.p.m., supporting the assignments for the corresponding carbon in **4** and the *N*-acetyl derivative. In addition to the four signals of the *n*-butyl group, two methylene carbons absorbed at 24.8 and 26.1 p.p.m. corresponding to the 23.9 and 25.0 p.p.m. signals for the dimer. The *n*-butyl signals (14.7 (CH_3), 24.1, 30.8, and 39.1 p.p.m.) were assigned by comparison with the spectra of *n*-butylcyclohexane (12) 1-, 3-, and 4-*n*-butylcyclohexanes (13). Thus, the ^{13}C spectral data unequivocally eliminate **6** from consideration and appear to favor **4** over **7** although the latter cannot be rigorously excluded. In addition, since the reaction is readily reversible and the formation of **4** is mechanistically equivalent to the formation of **7**, the product of thermodynamic control **4**, is expected.

Experimental

Preparation of Dimer (1)

The dimer was prepared and purified by the method of Overberger *et al.* (2). Recrystallization from petroleum ether (30–60°) gave transparent square crystals, m.p. 52–53°; ν_{max} (CCl_4) 3360, 2940, 1620 cm^{-1}; δ (CCl_4) 5.35 (1H, broad singlet), 2.40–1.90 (5H, multiplet), 1.85 (3H, singlet), 1.70 (3H, singlet), 1.60–1.45 (2H, multiplet), 1.40 (3H, singlet), and 0.97 (3H, singlet); *m/e* (70 eV) 43, 58, 83, 85, 95, 97, 109, and 110.

3,6-Dimethyl-3-n-butyl-2,3,4,5-tetrahydropyridazine (2a)

Compound **2***a* was prepared by a method similar to Overberger and Kesslin's synthesis (1) of the phenyl analogue (**2***b*). The crude product was a yellow oil which was fractionally distilled (N_2) through a 6 in. Vigreux column. A first fraction b.p. 30–50°/0.2 mm was collected in 20% yield, mainly dimethylpyridazine, the second, b.p. 50–70°/0.2 mm, was crude butylpyridazine (50% yield), and the remainder was mainly unreacted starting material. The crude product was purified by distillation (N_2) on a 2 ft spinning band under reduced pressure and pure **2***a* (35%) was obtained as a colorless liquid b.p. 52°/0.2 mm; λ_{max} (cyclohexane) 230 nm (ε 4700); ν_{max} (CCl_4) 3300, 2930, 1640, 1440, and 1375 cm^{-1}; δ (CCl_4) 5.00 (1H, broad singlet), 2.20–1.50 (7H, multiplet containing a methyl singlet), 1.40–1.10 (6H, multiplet), and 1.10–0.80 (6H, multiplet); *m/e* (70 eV) 28, 43, 108, 111, 153, and 168.

Anal. Calcd. for $C_{10}H_{20}N_2$: C, 71.37; H, 11.98; N, 16.65. Found: C, 71.11; H, 11.67; N, 16.70.

Preparation of the N-Acetyl Dimer

Equimolar amounts of the dimer **1** and acetic anhydride were dissolved in 5 ml of dry pyridine and let stand under nitrogen at room temperature for 24 h. The solvent was then removed under vacuum at room temperature to yield a pale yellow solid in 80–90% yield. The solid was recrystallized three times from petroleum ether (60–80°), to yield colorless, rectangular crystals, m.p. 153–153.5°; λ_{max} (cyclohexane) 235 nm (ε 11 000); ν_{max} (CCl_4) 2940, 1690, 1630, 1435, 1390, and 1360 cm^{-1}; δ (CCl_4) 2.30–2.00 (9H, multiplet containing a sharp singlet), 2.00–1.80 (8H, multiplet containing sharp singlet), 1.80–1.30 (2H, multiplet), and 1.10 (3H, singlet); δ (C_6H_6), 2.50 (3H, singlet), 2.35 (3H, singlet), 2.00–1.60 (10H, multiplet containing two sharp singlets), 1.50–0.90 (multiplet, 3H), and 0.78 (3H, singlet).

Anal. Calcd. for $C_{14}H_{22}N_4O$; C, 64.09; H, 8.45; N, 21.36. Found: C, 64.27; H, 8.45; N, 21.31.

Piperidine/4-Phenyl-1,2,4-triazoline-3,5-dione Adduct (11)

Freshly distilled piperidine was dissolved in benzene and an equimolar amount of dione in benzene was added dropwise. The red color disappeared immediately and the solution turned pale yellow. The piperidine was removed under pressure (20 mm) leaving a bright yellow oil which t.l.c. showed to be the only product. The yellow oil was purified by preparative t.l.c. (50% ether/benzene as eluent). The yellow color darkened rapidly upon exposure to air but was stable for up to 12 h under nitrogen; λ_{max} (EtOH) 240, 325 nm; ν_{max} ($CHCl_3$) 3000, 2940, 2860, 1650, 1600, 1500, and 1440 cm^{-1}; δ ($CDCl_3$) 7.4–7.0 (5H, multiplet), 6.5 (1H, broad singlet), 3.4 (4H, multiplet), and 1.6 (6H, multiplet).

Oxidation of Dimer with Triazolinedione

To 102 mg of dimer **1** in benzene at 6° was added dropwise a solution of 200 mg dione in benzene. The addition was stopped when the red color of the dione failed to disappear within 1 min, at which point 170 mg of dione (2.07 mol) had been added. The *N*-phenyl urazole which had precipitated as a fine white powder was filtered off and the solvent removed under vacuum. The residue which remained was greater than 90% dimethylpyridazine identified by comparison with an authentic sample.

Attempted Oxidations of N-Acetyl Dimer

(a) With Hydrogen Peroxide

The dimer (300 mg) was refluxed for 15 min in water/isopropanol solution with an equimolar amount of peroxide. Thin-layer chromatography showed only unreacted starting material.

(b) With 5% Palladium-on-carbon

Equal weights (300 mg) of **1** and Pd/C were heated to 150° under nitrogen in *o*-xylene for 3 days with no reaction. When repeated in refluxing *p*-cymene (180°), seven products were formed after 20 h. The n.m.r. of the crude concentrated reaction mixture showed no new peaks in the aromatic region.

Molecular Weight Determination of Dimer in CCl_4

Four solutions of the dimer in CCl_4 were made up from 0.003–0.06 *M*, and the molecular weight determined on a Hewlett-Packard 301A vapor pressure osmometer. Recrystallized acenaphthene was used as a calibrating compound. The experimentally determined molecular weight for each of the four concentrations was 208 ± 2.

Ultraviolet of the Dimer in Cyclohexane

The absorption coefficients at 225, 250, and 270 nm of the dimer absorption in cyclohexane were determined for dimer concentrations ranging from 1.37×10^{-1} to 1.37×10^{-5} *M*. The molar extinction coefficient at the wavelengths

chosen was constant over the concentration range of 10^{-4}, following Beer's law.

Effect of Dilution on NH Absorption of Dimer

The i.r. spectrum of the dimer in $CHCl_3$ was taken in 0.1, 1, and 2 mm cells with the amount of dimer between the plates held constant. In the most concentrated solution, the NH absorption was broad and extended from 3350 (free NH) to 3200 cm^{-1} (hydrogen-bonded NH). In the more dilute sample the NH absorption was sharper, and in the most dilute sample the NH absorption was very sharp at 3350 cm^{-1}.

Nuclear Magnetic Resonance Spectra

The ^{13}C spectra were obtained using a Varian XL-100-15 system operating at 25.2 MHz with proton noise decoupling at 100 MHz; the deuterium signal from the acetone-d_6 solvent served as the lock. The peak positions were measured from internal TMS (δ_C 0) with a precision better than 0.1 p.p.m. Proton spectra were obtained with Varian T-60 and HA-100 spectrometers.

1. C. G. OVERBERGER and G. KESSLIN. J. Org. Chem. **27**, 3898 (1962).
2. C. G. OVERBERGER, N. R. BYRD, and R. B. MESROBIAN. J. Am. Chem. Soc. **78**, 1961 (1956).
3. T. GRAY. J. Chem. Soc. **79**, 682 (1901).
4. E. E. BLAISE. Compt. Rend. **170**, 1324 (1920).
5. B. G. ZIMMERMAN and H. L. LOCHTE. J. Am. Chem. Soc. **60**, 2456 (1938).
6. A. B. EVNIN and D. R. ARNOLD. J. Am. Chem. Soc. **90**, 5330 (1968).
7. A. B. EVNIN, D. R. ARNOLD, L. A. KARNISCHKY, and E. STROM. J. Am. Chem. Soc. **92**, 6218 (1970).
8. D. R. ARNOLD. Private communication.
9. W. H. PIRKLE and J. C. STICKLER. Chem. Commun. 760 (1967).
10. R. C. COOKSON, I. D. R. STEVENS, and C. T. WATTS. Chem. Commun. 744 (1966).
11. J. B. STOTHERS. Carbon-13 NMR spectroscopy. Academic Press, New York, 1972. Chapt. 5.
12. T. PEHK and E. LIPPMAA. Eesti NSV Tead. Akad. Toim. keem.-geol. **17**, 291 (1968).
13. T. PEHK, S. RANG, O. EISEN, and E. LIPPMAA. Eesti NSV Tead. Akad. keem.-geol. **17**, 296 (1968).
14. H. BROUWER and J. B. STOTHERS. Can. J. Chem. This issue.

Can. J. Chem. Downloaded from www.nrcresearchpress.com by 210.87.254.42 on 09/05/12
For personal use only.

The Preparation and Acetolyses of 5-Deuteriated *exo*-2-Norbornyl-*p*-bromobenzenesulfonates[1]

N. H. WERSTIUK, R. R. MACDONALD,[2] R. W. OUWEHAND,[2] W. L. CHAN,[2]
F. P. CAPPELLI,[3] J. G. BALLARD,[3] R. E. YOUNG,[3] R. E. MASSEY,[3] G. TIMMINS, I. GOODWIN,[4]
A. WALLING,[4] AND MISS Y. TERUTA[4]

Department of Chemistry, McMaster University, Hamilton, Ontario

Received August 16, 1971

The deuterionorborneols **2***a*, *b*, *c*, and *e* have been prepared and converted to the brosylates **1***a*, *b*, *c*, and *e*. The deuterium isotope effects determined spectrophotometrically for solvolysis in HOAc–KOAc are 1.00 ± 0.01, 1.01 ± 0.01, 0.99 ± 0.01, and 1.11 ± 0.01, respectively. These data establish that: (*a*) a steric deuterium isotope effect does not operate at C-5 and therefore probably not at C-6; (*b*) hyperconjugative stabilization of the norbornonium ion to the C-5 hydrogens is confirmed to be not important, and (*c*) provides the first experimental evidence that the hydrogen (deuterium) shift – internal return pathway contribution to the γ-deuterium isotope effects observed for **1***d* and *e* is minor.

Les norbornéols deutérés **2***a*, *b*, *c*, et *e* ont été préparés et transformés en brosylates **1***a*, *b*, *c*, et *e*. Les effets isotopiques du deutérium ont été déterminés par spectrophotométrie pour la solvolyse dans HOAc–KOAc et sont respectivement de 1.00 ± 0.01, 1.01 ± 0.01, 0.99 ± 0.01 et 1.11 ± 0.01. Ces données mettent en relief les faits suivants, (*a*) un effet isotopique stérique du deutérium ne se produit pas sur C-5 et par conséquent, probablement pas non plus sur C-6; (*b*) la stabilisation par hyperconjugaison de l'ion norbornium aux hydrogènes en C-5 est confirmée comme étant de peu d'importance, et (*c*) apporte la première preuve expérimentale du fait que la contribution du mécanisme de retour, par déplacement interne d'hydrogène (deutérium), aux effets isotopiques du γ-deutérium, observés pour **1***d* et *e*, est de peu d'importance.

Canadian Journal of Chemistry, **50**, 618 (1972)

Introduction

α-, β-, and γ-deuterium isotope effects have been used extensively to probe the nature of the norbornyl cation generated solvolytically (2*a*–*i*). Of special interest has been the work of Murr *et al.* (2*c*) and Jerkunica *et al.* (2*d*), which showed that the isotope effects for *exo*-norbornyl and *endo*-norbonyl brosylates-6-*d* were 1.10 and 1.00, respectively. The γ-deuterium isotope effects obtained for the *endo*-brosylates were consistent with those expected for a classical ion transition state. However, the unusually large γ-effects for the *exo*-brosylates contrast with those observed in the solvolysis of deuteriated 3-methyl-2-butyl tosylate (3) (1.00), deuterio-*n*-propyl halides and tosylates (0.93) (4*a*), deuteriocyclopropyl-methyl benzenesulfonates (0.95) (4*b*), and 6-deuteriated-1,2-dimethyl norbornyl-*p*-nitrobenzoates (1.02) (2*g*).

In this study, the 5-deuteriated-*exo*-2-norbornyl brosylates **1***a*, *b*, and *c* were prepared and solvolyzed in KOAc buffered glacial acetic acid, to determine the δ-deuterium isotope effect in the solvolysis of *exo*-norbornyl brosylate. The work was designed to (*a*) determine the possible contribution of a "steric" isotope effect of deuterium at C-5; (*b*) check for hyperconjugative stabilization of the norbornonium ion **3** via the C-5 hydrogens, and (*c*) ascertain whether or not the 6,2–6,1 hydrogen(deuterium) shift – internal return mechanism is important in the solvolysis of *exo*-norbornyl brosylate and therefore contributes to the deuterium isotope effect of 1.10 observed by Murr *et al.* (2*c*) in the solvolysis of **1***d* and *e*. That this study would give information on (*c*) is seen from a consideration of Scheme 2. If the hydrogen shift – internal return pathway is important, then **8***a*, and especially **8***c*, would be converted to deuterio brosylate **14***a*, and **14***c* in which deuterium is situated *exo* at C-3. Since the k_H/k_D values for **14***a* and *c* are 1.07 as determined by Murr *et al.* (2*i*), the conversion of the brosylates **8***a* or *c* to **14***a* and *c* would then result in a contribution of >1 to the isotope effect for **8***a* and *c*.

This study would give information on whether or not a steric isotope effect arising via inter-

[1]For a preliminary report of this work see N. H. Werstiuk *et al.* (1).
[2]McMaster Undergraduate Summer Student, 1968–1969.
[3]McMaster Undergraduate Student, 1969–1970.
[4]McMaster Undergraduate Student, 1970–1971.

Can. J. Chem. Downloaded from www.nrcresearchpress.com by 210.87.254.6 on 09/05/12
For personal use only.

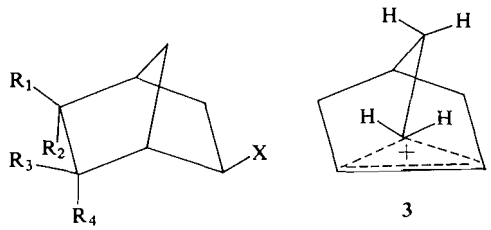

3

1 X = OBs
2 X = OH

a $R_1 = D; R_2 = R_3 = R_4 = H$
b $R_1 = H; R_2 = D; R_3 = R_4 = H$
c $R_1 = R_2 = D; R_3 = R_4 = H$
d $R_1 = R_2 = R_3 = D; R_4 = H$
e $R_1 = R_2 = R_3 = H; R_4 = D$
f $R_1 = D; R_2 = H; R_3 = D; R_4 = H$
g $R_1 = R_2 = R_3 = R_4 = H$

actions between the 6-*exo*-D, 5-*exo*-H, and 7-*anti*-H contributes to the k_H/k_D of 1.10 observed for **1***d* and *e*. The *exo*-5- and *exo*-6-hydrogens(deuteriums) are identical sterically at least in the ground state. Confidence in observing a large effect was minimal, since the torsional energy of the major interactions arising from the eclipsed hydrogens in the partial butane structure, including C-1, -6, -5, and, -4 in the [2.2.1.] system, would probably not be affected by deuterium as shown by Weiss and LeRoi from a study of deuterioethanes (5). Furthermore, Jewett and Dunlap (6) have shown that the effect for nine deuteriums in the solvolysis of the non-rigid system nonadeuteriodimethylneopentylcarbinyl chloride is inverse and small (0.983). Although hyperconjugative stabilization of the norbornonium ion **3** via the C-5 hydrogens would not be expected to be important in that C-6 is essentially sp^3 hybridized (7) and bears little positive charge (8), the study would serve to confirm this premise.

To calibrate our technique *exo*-norbornyl brosylate-6-*endo*-*d* was prepared and k_H/k_D was obtained. The value of 1.11 ± 0.01 corresponds exactly to that reported by Murr *et al.* (2*c*).

Results

The 5-deuteriated brosylates were prepared via a sequence of reactions outlined in Scheme 1. The keto-acetate **4** was converted to the previously unknown 5-deuteriated-*exo*-2-norborneols by a reduction–brosylation–reduction sequence which involved the reducing agents $NaBH_4$–$LiAlD_4$ for **2***a*, $NaBD_4$–$LiAlH_4$ for **2***b*, and $NaBD_4$–$LiAlD_4$ for **2***c*. The i.r. fingerprint regions and the partial n.m.r. spectra of *exo*-norborneol, **2***a* and *b* which were isolated by preparative g.l.c. and are at least 98–99% *exo*, 1–2% *endo*, are included in Figs. 1 and 2, respectively. The d.m.r. spectroscopy of **2***a* and *b* showed the *exo*-5- and *endo*-5-deuteriums as

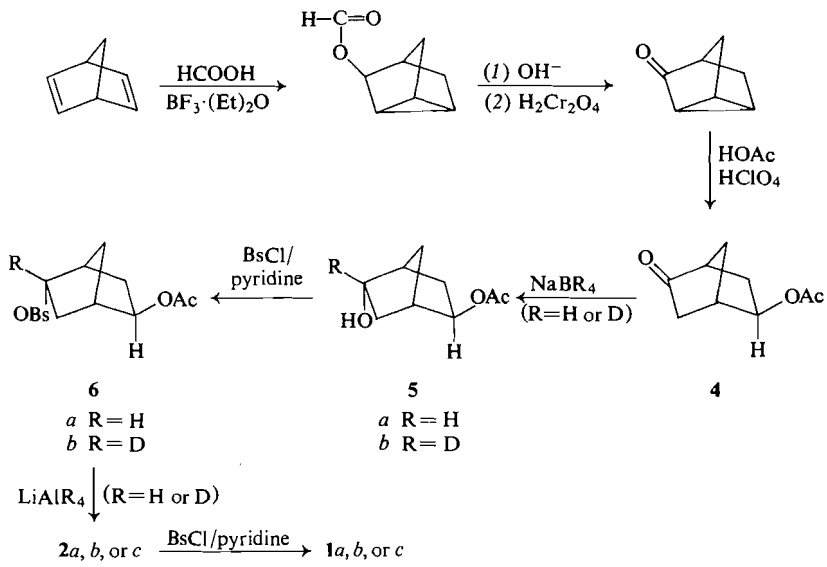

SCHEME 1

Can. J. Chem. Downloaded from www.nrcresearchpress.com by 210.87.254.6 on 09/05/12
For personal use only.

Can. J. Chem. Downloaded from www.nrcresearchpress.com by 210.87.254.6 on 09/05/12
For personal use only.

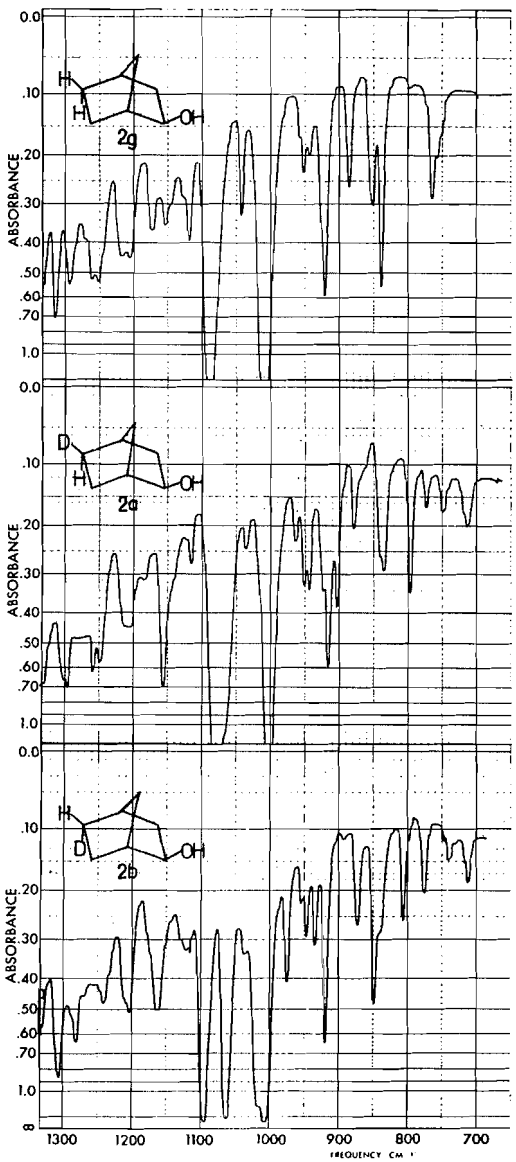

FIG. 1. The i.r. (CS_2) fingerprint regions of *exo*-norborneol (**2***g*), *exo*-norborneol-5-*exo*-*d* (**2***a*), and *exo*-norborneol-5-*endo*-*d* (**2***b*).

broad singlets at 141 and 148 Hz respectively, upfield from $CDCl_3$ in accord with the relative chemical shifts of the *exo*- and *endo*-hydrogens in norbornyl systems (9*a* and *b*). The spectra showed that **2***a* and *b* were composed of at least 95% of only one specifically deuteriated species and that the deuterium was at least 85–95% stereochemically pure in each case.

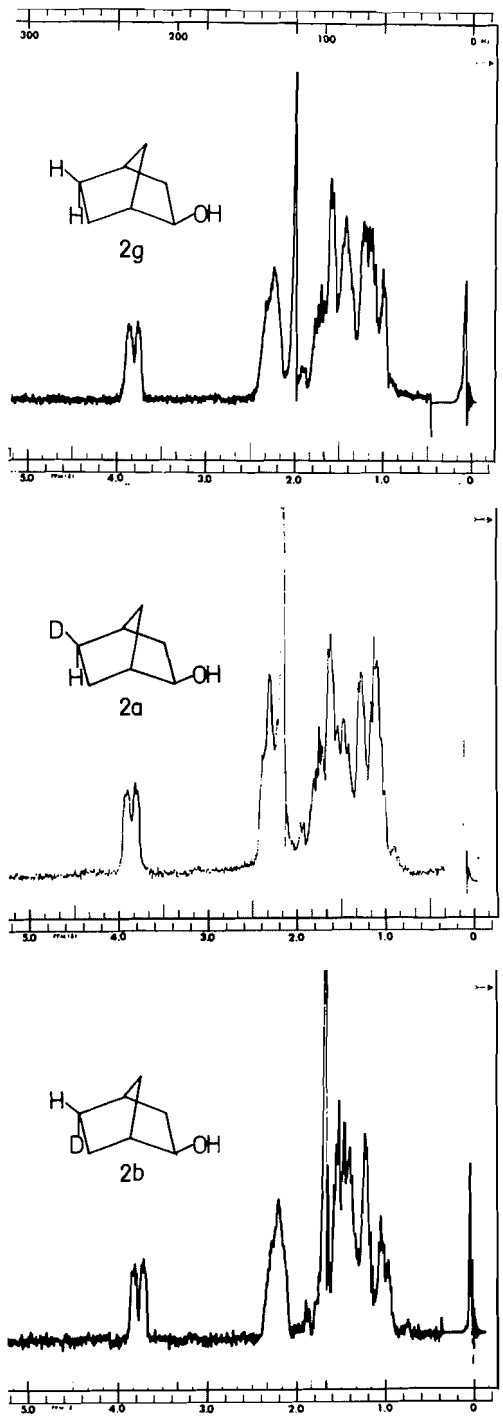

FIG. 2. The 60 MHz n.m.r. spectra ($CDCl_3$) of *exo*-norborneol (**2***g*), *exo*-norborneol-5-*exo*-*d* (**2***a*), and *exo*-norborneol-5-*endo*-*d* (**2***b*).

TABLE 1. Solvolysis of norbornyl brosylates in HOAc–KOAc at 29.40 ± 0.02°

	Substrate **1**				
Run no.	*g*	*a*	*b*	*c*	*e*
1	0.98±0.01*	0.99±0.01	1.01±0.01	1.00±0.01	1.11±0.01†
2	1.00±0.01	1.00±0.01	1.01±0.01	0.98±0.01	1.11±0.01
3	0.99±0.01	0.99±0.01	1.01±0.01	0.99±0.01	
4	1.00±0.01	1.01±0.01		0.99±0.01	
Mean	0.99±0.01	1.00±0.01	1.01±0.01	0.99±0.01	1.11±0.01

*Errors expressed as the standard deviation of the points from the least squares slope. For example, the data from the computer for run 3 of **1***a* was: slope for **1***g* $10.473 \times 10^{-3} \pm 8.339 \times 10^{-5}$, and for **1***a* $10.602 \times 10^{-3} \pm 6.148 \times 10^{-5}$.

†81.2% d_1 and 8.8% d_0 species; k_H/k_D (+0.02) corrected for incomplete deuteration.

The preparation of **1***e*, required for the calibration work, began with the opening of the cyclopropane ring in 3-nortricyclyl bromide with D_2SO_4–DOAc[5] to yield as the major products the *anti*-7-bromo-*exo*-2-norbornyl-6-*endo*-*d*- (49%) and *syn*-7-bromo-*exo*-2-norbornyl-6-*endo*-*d*-acetates (26%). The deuterium was shown to be at least 95% stereochemically pure *endo* in the two major products by reducing each to the *exo*-norborneol-*d* and comparing its i.r. fingerprint region to that of an authentic sample of **1***e*.[6] The minor products of the reaction were 5-*exo*-bromo-*exo*-2-norbornyl-deuterio-acetate (10%) in which 10% of the deuterium was in the *endo*-2-position and at least 70–90% at C-6, 5-*endo*-bromo-*exo*-2-norbornyl-deuterio-acetate (8%) of which 6% of the deuterium was in the *endo*-2-position and at least 70–80% at C-6, as well as 2–3% of unidentified material. Compound **2***e* used to prepare **1***e* was obtained by reduction of the mixture of deuteriobromoacetates with $LiAlH_4$ to give *exo*-norborneol-6-*endo*-*d* which contained 2–2.5% *exo*-norborneol-2-*endo*-*d*. That the *exo*-norborneol-6-*d* was at least 85–95% stereochemically pure *endo* was supported by comparison of its i.r. fingerprint region to that of authentic sample.[6]

The deuterio-*exo*-norborneols **2***a*, *b*, *c*, *e*, were isolated by preparative g.l.c. and analyzed on a 200 ft × 0.01 in. UCON HB capillary column, and were at least 98–99% *exo* and 1–2% *endo*. Treatment of the deuterionorborneols with brosyl chloride in pyridine gave the brosylates which were recrystallized 1–2 times prior to use in the kinetic studies, and once prior to each successive run. The k_H/k_D values listed in Table 1 were obtained from the solvolysis of **1***a*, *b*, *c*, and *e* simultaneously with **1***g* in the thermostatted compartment of a Carey Model 14 U.V. spectrophotometer.

Importantly, the results for **1***a*, *b*, and *c* show that 1–2% of *endo*-norborneol initially present in the deuterio-*exo*-norborneols had no effect on the rate data, since there is no significant change in k_H/k_D through the runs 1–4 as the brosylate was recrystallized prior to each run. That this would be expected is seen from an analysis of the contribution of up to 2% of deuterio-*endo*-brosylate to the absorbance change during a kinetic run. The half-life of **1***g* is *ca.* 1 h. Since runs were typically carried on for 13–14 h or to 99.99% completion, and $k_{exo} = 300k_{endo}$, then (13/300)(0.5)(0.02) of the *endo*-brosylate solvolyzes in 13–14 h. Since $A_t - A_\infty$ in the kinetic runs was typically *ca.* 0.7, (0.04)(0.5)(0.02)(0.7) or 0.0003 of an absorbance unit change would result from 2% *endo*-brosylate. This is insignificant in that the estimated error for determination of A for any one point is ±0.002–0.003. A typical plot, *i.e.* run 3 for **1***c*, given in Fig. 3, indicates the quality of the results.

Discussion and Conclusions

The possible contributions to the δ-deuterium isotope effect in **1***a*, *b*, and *c* and the expected effects of each on k_H/k_D are listed in Table 2.

That a steric effect of deuterium does not make a significant contribution >1 to the δ-k_H/k_D is established by the values of 1.00 ± 0.01, 1.01 ±

[5]Presented in part at the 54th Annual Meeting of the Chemical Institute of Canada, Halifax, Nova Scotia, June, 1971.

[6]We thank Professor A. Nickon for the i.r. spectrum of *exo*-norborneol-6-*endo*-*d*.

Can. J. Chem. Downloaded from www.nrcresearchpress.com by 210.87.254.6 on 09/05/12
For personal use only.

TABLE 2. Possible contributions to δ deuterium isotope effect

Entry	Contribution by	Expected effect on k_H/k_D
1	Steric effect	(*a*) < 1 if steric requirement of D > H (*b*) > 1 if steric requirement of D < H
2	Hyperconjugation	(*a*) > 1
3	H shift followed by internal return to 3*a*, *b*, or *c*	(*a*) > 1

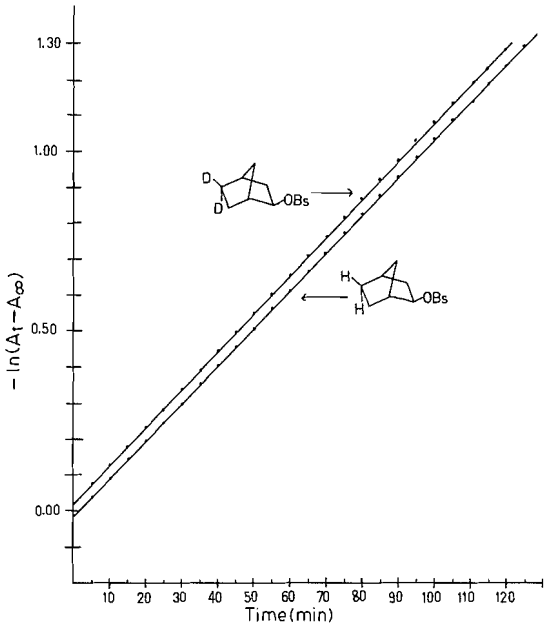

FIG. 3. First order plots for solvolysis of *exo*-norbornyl brosylate (**1***a*) and *exo*-2-norbornyl brosylate-*exo*-5-*endo*-5-d_2 (**1***d*).

0.01, and 0.99 ± 0.01, observed for **1***a*, *b*, and *c*, respectively, since the other effects (entries 2 and 3) must total > 1. Since the *exo*-5- and *exo*-6-hydrogens(deuteriums) are in the same environment sterically, with respect to the *exo*-5, *exo*-6, and-*syn*-7-interactions, at least in the ground state, the data therefore strongly suggest that there is no significant steric isotope effect contribution > 1 to the γ-k_H/k_D of 1.10 observed for **1***d* and *e* by Murr *et al.* (2*c*). The results do not give information about steric isotope effects which might result from differential interactions between *exo*- and *endo*-6-D and C-1-H and *endo*-2-H in the *exo*-brosylate. However, the effects would be expected to be small, since the γ-isotope effects for *exo*-brosylate-6-*endo*-*d* and *exo*-brosylate-6-*exo*-*d* are equal (1.10) within experimental error (2*c*).

These data provide the first experimental evidence that the hydrogen shift – internal return pathway (hs–irp) (Scheme 2) does not contribute significantly, by formation of **14***d* and **15***d*, to the k_H/k_D of 1.10 for **8***d* observed by Murr *et al.* (2*c*). This conclusion is warranted when Scheme 2 and Table 1 are considered. Attention is directed to **8***c*, since **8***a* yields equal quantities of **14***a* (k_H/k_D 1.07) and **13***a* (k_H/k_D 1.02) through **10** and **11** via equally likely 6,1- and 6,2-hydrogen(deuterium) shifts, thereby lowering the magnitude of the contribution of the hs–irp to k_H/k_D for **8***a*. Since k_H/k_D for solvolysis of **14***c* in HOAc–KOAc is 1.07 (2*i*) and the method used detects isotope effects of 1%, the results for **8***c* show that a maximum of 2 × 1/7 or 25–30% of the hs–irp may operate. The factor of 2 is included on the assumption that internal return to C-2 and -6 in **10** and **11** is equally likely to yield **12** and **15**, as well as **13** and **14**.

Since the k_H/k_D for *exo*-norbornyl brosylate-*endo*-2-*d*, **14***d* in HOAc-KOAc is 1.12 (2*h*), its contributions to k_H/k_D of 1.10 for **8***d* (2*i*), via the hs–irp would be (0.25)(0.30)(0.12) or 0.01. Furthermore, since k_H/k_D for *exo*-norbornyl brosylate-1-*d* should be a maximum of 1.12 (*c.f.* 2*c*), the hs–irp contributions a maximum of 0.02, via **14***d* and **15***d*, to the k_H/k_D of 1.10 observed for **1***d*.

The data also show that the C-5 hydrogens are not involved in the stabilization of **3** via hyperconjugation. This removes the possibility that loss of hyperconjugative stabilization contributes significantly to the rate retardation observed by Greever and Gwynn (10) in the solvolysis of *exo*-norbornyl-5-keto-brosylate. This

Can. J. Chem. Downloaded from www.nrcresearchpress.com by 210.87.254.6 on 09/05/12
For personal use only.

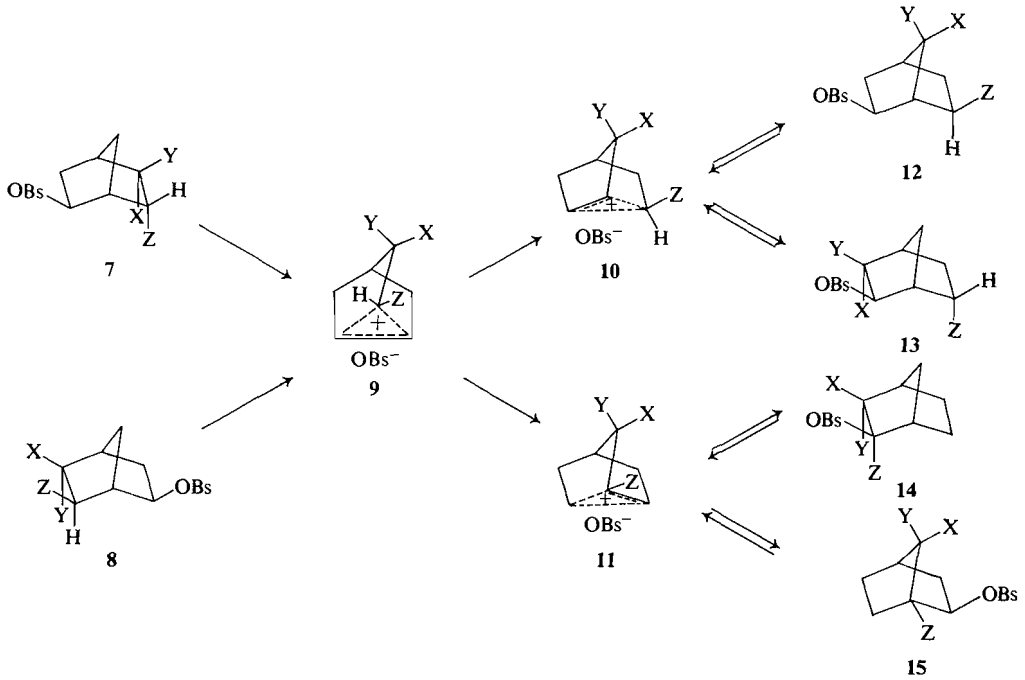

7–15*a* X = D; Y = H; Z = H
b X = H; Y = D; Z = H
c X = Y = D; Z = H
d X = Y = H; Z = D

SCHEME 2

work also provides a general route to the previously unknown 5-deuterionorbornyl systems.

Experimental

General

Melting points were taken on a Kofler hot-stage melting point apparatus and are uncorrected. The i.r. spectra were recorded on Perkin–Elmer Model 337 and 521 spectrometers. The n.m.r. spectra were taken on Varian A-60 and HA-100 spectrometers in CCl_4 or $CDCl_3$ with tetramethylsilane as the internal standard. Pentane was stirred over fuming H_2SO_4, washed with bicarbonate solution and distilled. Preparative gas chromatographic isolations were done on a Varian-Areograph 90-P-3 instrument with 5 ft × 1/4 in., 20% Carbowax and 10 ft × 3/8 in., 15% Carbowax on Chromosorb W columns with He as the carrier. Analytical chromatograms were obtained on Varian-Areograph Model 204 and 1200 chromatographs on 10 ft × 1/8 in., 10% Carbowax, and 10% SE-30, on Chromosorb W and 200 ft × 0.01 in. UCON HB capillary columns with He as the carrier. All solutions were dried over anhydrous Na_2SO_4 and $MgSO_4$. Kinetic runs were carried out on a Carey Model 14 u.v. spectrophotometer. A Haake Model NBe constant temperature bath was used to thermostat the cell compartment to within ±0.02°.

Nortricyclyl Formate

Nortricyclyl formate (270 g, b.p. 64° (10 mm)) was prepared from 325 g of norbornadiene according to the procedure of Schmerling *et al.* (11). The g.l.c. analysis on a 10 ft × 1/3 in. 10% SE-30 on Chromosorb W column showed the mixture to be composed of 85–90% nortricyclyl formate and two other components (10–15%) of shorter retention time.

Nortricyclanol

Base-catalyzed hydrolysis of the formate mixture (260 g) was carried out as described by Schmerling *et al.* (11) to yield 180 g of nortricyclanol m.p. 106–107° (lit. m.p. 108–109° (12)) after two recrystallizations from pentane. The g.l.c. on a 10 ft × 1/3 in., 10% Carbowax on Chromosorb W column showed the nortricyclanol to be 90% pure with one component (10%) of shorter retention time.

Nortricyclanone

Nortricyclanone (46 g, b.p. 113° (88 mm)) 90% pure, was prepared from (72.0 g, 90% purity) nortricyclanol by chromic acid oxidation according to the procedure of Meinwald *et al.* (13).

exo-5-Acetoxynorboran-2-one (4)

Compound **4** (48.0 g, 90% purity by g.l.c.) was prepared from nortricyclanone (46 g, 90% purity) with acetic acid–perchloric acid according to the procedure of Meinwald

Can. J. Chem. Downloaded from www.nrcresearchpress.com by 210.87.254.6 on 09/05/12
For personal use only.

Can. J. Chem. Downloaded from www.nrcresearchpress.com by 210.87.254.6 on 09/05/12
For personal use only.

et al. (14). The n.m.r. (CCl_4); δ 4.74 (1H, doublet of doublets, $J = 7$ and 3 Hz, *endo*-5-C-H), 2.72 (1H, broad multiplet, bridgehead—C—H), 2.50 (1H, doublet, bridgehead—C—H), 2.0 (3H, singlet, CH_3COO—), and the norbornyl envelope ranging from 2.2–1.4.

endo-5-Hydroxy-exo-2-norbornyl Acetate (5a)

The ketoacetate **4** (7.2 g, 90% purity) was dissolved in absolute ethanol (50 ml). $NaBH_4$ (0.68 g) was added portion-wise to the solution over 2–3 min. The mixture was heated on the steam bath for 3–5 min then poured onto ice. The solution was saturated with NaCl and extracted with ether (1 × 100, 3 × 50 ml). Evaporation of the ether gave 6.7 g of the hydroxyacetate **5***a* (95% pure) a mixture of *ca.* 90% of the *endo* and 10% *exo* stereoisomers respectively, as was shown by gas chromatography on a 10 ft × 1/3 in. 10% SE-30 on Chromosorb W at 150°. Vacuum distillation of the mixture at 0.3 mm gave fraction 1, b.p. 106–108°, 0.8 g; fraction 2, b.p. 108–110°, 4.3 g; fraction 3, b.p. 108–110°, 0.5 g. Gas chromatography showed a new peak (10–15%) of lower retention time than the hydroxy acetates. Apparently some decomposition occurred during distillation even at 110°. This material was used for the next step without further purification. The n.m.r. (CCl_4); δ 4.60 (1H, doublet with fine structure, $J = 7$ Hz, *endo*-5-C-H), 4.08 (1H, quarter, $J = 8$, 5,4 Hz, *exo*-2-C—H), 3.00 (1H, singlet, —O—H), 1.95 (3H, singlet, CH_3—COO—), and the norbornyl envelope ranging from 2.6–1.4.

endo-5-Hydroxy-exo-5-deuterio-exo-2-norbornyl Acetate (5b)

The ketoacetate **4** (15.0 g, 90% purity) was dissolved in absolute ethanol (55 ml) and the solution was cooled in ice. To the chilled solution was added $NaBD_4$ (1.0 g, 95–98% isotopically pure) in small portions. The mixture was heated on the steam bath for 1 min and the mixture was cooled in ice. An aliquot worked-up and analyzed by g.l.c. showed unreacted ketoacetate. An additional portion of $NaBD_4$ (0.95 g) was added and the solution was heated on the steam bath 2–3 min. The hot solution was poured onto crushed ice (400 g) and extracted with ether (4 × 100, 4 × 50 ml). The ethereal layer was washed with water (1 × 100 ml) and the water layer was extracted with ether (5 × 25 ml). Evaporation of the solvent gave 16.6 g of an oil. Vacuum distillation gave 9.5 g of the deuteriohydroxyacetate **5***b* of 95% purity as was shown by g.l.c. analysis on 10 ft × 1/3 in. 10% SE-30 on Chromosorb W column at 150°. The g.l.c. showed that the ratio of *endo*:*exo*-OH at C-2 was 9:1. The n.m.r. (CCl_4); δ 4.60 (1H, doublet with fine structure, $J = 7$ Hz, *endo*-5-C—H), 3.60 (singlet, —O—H), 1.98 (3H, singlet CH_3—COO—), and the norbornyl envelope ranging from 2.6–1.7. The multiplet which corresponded to the *exo*-2-C—H in **5***a* was absent.

exo-5-Acetoxy-endo-2-norbornyl Brosylate (6a)

The hydroxyacetate **5***a* (3.0 g, 90–95% pure) and brosyl chloride (4.5 g) were dissolved in pyridine. After 10 days in the refrigerator the mixture was poured into ice-water (250 ml) and extracted with ether (150 ml). The ether layer was washed with water (5 × 50 ml) and dilute aqueous HCl (100 ml). Evaporation of the solvent gave an oil which crystallized when washed with pentane–ether. Recrystallization from pentane–ether gave 4.0 g of the brosylate acetate **6***a*, m.p. 78–81°. Repeated recrystallization from pentane–ether gave 1.0 g of the brosylate acetate, m.p. 78–81°. An analytical sample m.p. 80–81.5° was obtained by two additional recrystallizations from ether–pentane.

Anal. Calcd. for $C_{15}H_{17}O_5BrS$: C, 46.27%; H, 4.37%. Found: C, 46.37%; H, 4.37%.

The n.m.r. ($CDCl_3$); δ 7.75 (4H, singlet, aromatic C—H), 4.75 (2H, multiplet, BsO—C—H and AcO—C—H overlapping), 2.00 (3H, singlet, CH_3COO—), norbornyl envelope centered at 1.6.

exo-5-Acetoxy-exo-2-deuterio-endo-2-norbornyl Brosylate (6b)

The deuteriohydroxyacetate **5***b* (0.34 g, 95% purity) and freshly recrystallized brosyl chloride (0.51 g) were dissolved in pyridine (4 ml). After 13 days several ice crystals were added to the pyridine solution. The mixture was kept at room temperature for 10 min and poured into ice-water and extracted with an ether–pentane mixture (2 × 25 ml). The ethereal layer was washed with ice-water (4 × 50 ml), dried, and evaporated to yield a viscous oil which crystallized when placed under vacuum. The solid (0.68 g) was recrystallized twice from ether–pentane to give 0.39 g of the deuteriobrosylate acetate, m.p. 79–81°. A third recrystallization gave 0.18 g, m.p. 79–81°. The n.m.r. ($CDCl_3$); δ 7.72 (4H, singlet, aromatic C—H), 4.70 (1H, doublet with fine structure; $J = 8$ Hz, AcO—C—H), 2.00 (3H, singlet, CH_3COO—), and norbornyl envelope centered at 1.6. The *exo*-2-H in the spectrum of **6***a* which contributed to the multiplet centered at 2.75 was absent.

Interestingly, when deuteriobrosylate acetate, which was prepared in a previous experiment and which had remained in the refrigerator for 8 months was recrystallized, a m.p. of 92–93° was observed. The n.m.r. of this material was identical in overall appearance to the deuteriobrosylate which had an m.p. 78–81° except for an increase in sharpness of the absorption in the norbornyl envelope. Possibly the small amount of *exo*-brosylate, a contaminant, had slowly decomposed over the 8 month period.

$LiAlH_4$ Reduction of the Deuteriobrosylate Acetate (6b)

The deuteriobrosylate acetate (0.18 g, m.p. 92–93°) was dissolved in dry ether (25 ml) and added to a slurry of $LiAlH_4$ (0.85 g) in dry ether (50 ml). The solution was refluxed for 14 days. Water (0.9 ml), 15% NaOH (0.9 ml), water (2 ml), and ether (20 ml) were then added consecutively to the vigorously stirred solution. The granular salts were filtered off and washed with ether. The g.l.c. analysis on a 10 ft × 1/3 in., 10% Carbowax on Chromosorb W column showed that the mixture was 90–95% *exo*-norborneol, by comparison with a standard sample. The solution was concentrated to 2 ml by distillation through a 1.5 ft glass helices-packed column and the norborneol-*d* (**2***a*) (0.025 g) was isolated by preparative gas chromatography on a 5 ft, 15% Carbowax on Chromosorb W column at 140°. The norborneol-*d* was at least 99% pure and at least 98–99% *exo* as determined by g.l.c. The n.m.r. (CCl_4); δ 3.63 (1H, doublet with fine structure; $J = 8$ Hz, HO—C—H), 2.80 (1H, singlet, —O—H), 2.14 (2H, broad multiplet, bridgehead C—H's) and norbornyl envelope centered at 1.35 (7.2 H). The d.m.r. ($CDCl_3$) spectrum showed a broad absorption at 148 Hz upfield from $CDCl_3$ and indicated that the alcohol was composed of at least 85–95% of only one specifically deuteriated species.

Can. J. Chem. Downloaded from www.nrcresearchpress.com by 210.87.254.6 on 09/05/12
For personal use only.

$LiAlD_4$ Reduction of Deuteriobrosylate Acetate (6b)

The deuteriobrosylate acetate (**6b**) (0.28g, m.p. 78–82°) was dissolved in dry ether (50 ml). $LiAlD_4$ (0.9 g) was added and the mixture was stirred and refluxed for 14 days. Work-up with water (1.0 ml), 15% aqueous NaOH (1.0 ml), and water (2 ml) gave an ether solution which was concentrated to 2 ml. The dideuterionorborneol **2c** (0.027g) was isolated by preparative g.l.c. and was shown to be at least 98–99% pure and at least 98–99% *exo* by analytical g.l.c.

Chromic Acid Oxidation of exo-2-Norborneol-5,5-d_2

The dideuterionorborneol **2c** (0.003 g) was dissolved in preoxidized ether (3 ml) and Brown's reagent was added (0.01 ml). The mixture was stirred at room temperature for 24 h. An additional 0.005 ml of oxidizing reagent was added and the mixture was stirred for 2 h. Water (1 ml) was added and the ether layer was withdrawn and dried. The solution was concentrated to 1 ml and the dideuterionorcamphor was isolated by preparative g.l.c. on a 5 ft × 1/4 in., 20% Carbowax on Chromosorb W column at 120°. Mass spectral analysis showed the ketone to be a composite of 91.6% d_2, 6.4% d_1, and 2.0% d_0 species.

$LiAlD_4$ Reduction of exo-2-Acetoxy-endo-5-norbornyl Brosylate (6a)

The brosylate acetate **6a** (1.0 g, m.p. 79–81°) was dissolved in dry ether (50 ml) and $LiAlD_4$ (1.6 g) was added. The mixture was refluxed for 14 days and worked-up as described previously. Preparative g.l.c. gave *exo*-2-norborneol-*exo*-5-*d* (**2a**) (0.14 g) at least 98–99% pure and 98–99% *exo* as determined by analytical g.l.c. Approximately 1–2% of *endo*-norborneol was present. The n.m.r. ($CDCl_3$); δ 3.75 (1H, doublet with fine structure; $J = 8$ Hz, >CH—O—), 2.20 (2H, broad multiplet, bridgehead C—H's), 2.08 (1H, singlet, —O—H), and the norbornyl envelope centered at 1.3 (7.1 H). The d.m.r. ($CDCl_3$) spectrum showed a broad absorption 141 Hz upfield from $CDCl_3$ and indicated that the compound was composed of at least 95% of one specifically deuteriated species. Chromic acid oxidation as described previously gave deuterionorcamphor which was 99% d_1 and 1.0% d_0 as determined mass spectrometrically.

D_2SO_4–DOAc Opening of 3-Bromonortricyclene

3-Bromonortricyclene (2.1 g), CH_3CO_2D (30 ml, prepared from freshly distilled acetic anhydride and D_2O, 95–98% d_1) and D_2SO_4 (0.28 g) were mixed and stirred magnetically at 70° for 50 h. The mixture was added to a saturated $NaHCO_3$ solution to neutralize the acid and extracted with ether (3 × 25 ml) to give a mixture of deuteriobromonorbornyl acetates after the solution was dried and evaporated. The g.l.c. analysis showed two major components to be present. The first compound isolated by preparative gas chromatography from a previous non-deuteriated run was a bromonorbornyl acetate as deduced from consideration of spectral data (n.m.r. and i.r.). Reduction to the bromohydrin and oxidation gave a ketone which yielded a 2,4-dinitrophenylhydrazone m.p. 116–118° (lit. 116.5–117.5° and 151.5–152.5° (15) for the 2,4-DNP of *anti*-7-bromonorcamphor) identified the major product as *anti*-7-bromo-*exo*-2-norbornyl acetate (47%). When the total bromoacetate mixture was reduced with $LiAlH_4$ in ether and the reaction was closely monitored, the *syn*-7-bromo-*exo*-2-norborneol (35%) was isolated and identified by preparation of the corresponding 2,4-DNP of the *syn*-7-bromonorcamphor, m.p. 202.5–203.5° (lit. 201.5–202.5° (16)). Preliminary experiments[5] have also shown that there are at least three other components (15–20% total).

$LiAlH_4$ Reduction of the Deuteriobromonorbornyl Acetate Mixture

The deuteriobromoacetate mixture (1.1 g) prepared previously was dissolved in ether and added dropwise to a slurry of $LiAlH_4$ (1.1 g) in ether (60 ml). The mixture was stirred and refluxed for 24 h. Additional quantities of $LiAlH_4$ (1 g and 1 g) were added consecutively after 12 h intervals. Six hours after the last portion was added, 1/4 of the mixture was worked-up by the addition of H_2O (1.5 ml), 10% NaOH (2 ml), water (2 ml), and ether (50 ml). The *exo*-norborneol-*d* (0.030 g) was isolated from ether extract by preparative g.l.c. The i.r.; ν_{max} (CS_2) 952 w, 920 w, 880 w, 865 m, 840 m, 805 w, 775 w, 785 w, 710 w was identical to the spectrum of *exo*-2-norborneol-*endo*-6-*d*, 90–95% stereochemically pure *endo*, prepared by Nickon *et al.* (17). The remainder of the reaction mixture was worked-up after 2 days to give additional deuterio-*exo*-norborneol-*d* (0.091 g).

Chromic acid oxidation of the norborneol-*d* (0.0036 g) with Brown's reagent in preoxidized ether as described previously gave norcamphor-*d* which was isolated by preparative g.l.c. Mass spectroscopic analysis showed the mixture to be a composite of 1.0% d_2, 80.6% d_1, and 18.4% d_0 species.

Chromic acid oxidation of the *exo*-2-norborneol-*endo*-6-*d* (0.015 g) gave norcamphor-*endo*-6-*d*. The i.r.; ν_{max} (CS_2), 1065 m, 1028 w, 966 w, 940 m, 870 m, 775 m was essentially identical to that of *endo*-6-*d*-norcamphor (90–95% stereochemically pure) prepared by Nickon *et al.* (17) except for minor changes in weak bands at 900, 850, and 760. The norcamphor-*endo*-6-*d* is estimated to be at least 85–95% stereochemically pure *endo*.

exo-Norborneol

exo-Norborneol (>99% stereochemically pure) was prepared from norbornene and formic acid according to the procedure of Kleinfelter and Schleyer (18).

exo-2-Norbornyl Brosylate

exo-Norborneol (0.11 g) and brosyl chloride (0.27 g) were dissolved in pyridine and kept in the refrigerator for 7 days. A crystal of ice was added to the pyridine solution and after 10 min at room temperature the mixture was poured into ice-water and extracted with purified pentane (100 ml). The pentane layer was washed with ice-water (2 × 50 ml), dried, and the solvent was removed on the rotatory evaporator. The oily residue crystallized when placed under vacuum. Two recrystallizations from pentane gave *exo*-norbornyl brosylate m.p. 55.5–57.0° (lit. 55.5–56.5° (19)).

exo-Norbornyl Brosylate-endo-5-d

exo-2-Norborneol-*endo*-5-*d* (0.021 g) and brosyl chloride (0.048 g) gave *exo*-2-norbornyl brosylate-*endo*-5-*d*, m.p. 56.0–57.5°, after two recrystallizations from pentane as described previously. The n.m.r. ($CDCl_3$); δ 7.70 (4H, multiplet, aromatic C—H), 4.49 (1H, triplet; $J = 8,5$, Hz, H—C—OBs), 2.33 (2H, broad multiplet, bridgehead C—H's), norbornyl envelope centered at 1.3 (*ca.* 7.4 H). Comparison of the spectrum to that of norbornyl brosylate showed major simplification in the spectrum in the δ 1.3–0.8 region, what would be expected when an *endo*-H is replaced by deuterium.

exo-Norbornyl Brosylate-exo-5-d

Dideuterionorborneol **2***c* (0.023 g) and brosyl chloride (0.52 g) were converted to the brosylate, m.p. 55.5–57.0°, after two recrystallizations as described previously. The n.m.r. ($CDCl_3$); δ 7.74 (4H, multiplet, aromatic C—H's), 4.50 (1H, triplet with fine structure, $J = 8{,}3$ Hz, H—C—OBs), 2.35 (2H, multiplet, bridgehead C—H's), 1.70–0.9 (7H, norbornyl envelope centered at 1.3).

Kinetic Procedure

Kinetic runs were carried out spectrophotometrically using a Carey Model 14 u.v. spectrophotometer. The runs were carried out in freshly distilled glacial acetic acid which was 0.04 *M* in KOAc (anhydrous). The nondeuteriated and deuteriated brosylates were run simultaneously in the sample compartment of the spectrophotometer which was thermostatted with a Haake Model NBe constant temperature bath maintained at 29.40 ± 0.02°. The brosylates, recrystallized from pentane prior to run, were weighed (*ca.* 0.002–0.003 g) into 2 ml volumetric flasks and placed in the constant temperature bath for *ca.* 10 min. The acetic acid solution (2 ml) which was equilibrated in the bath for at least 12 h was added with a pipette insulated with several layers of kimwipes. The insulated pipette had previously been equilibrated in the cell compartment, along with the two 1 cm u.v. cells, for at least 12 h. The brosylates were dissolved, and the 2 ml volumetrics were placed back into the constant temperature bath for *ca.* 10 min. The solvolysis solutions were transferred, with thermostatted pipettes, to the equilibrated cells in the cell compartment. After 20 min the spectrum was scanned in the region of 270 nm to obtain a maximum absorbance. The slit controls were then shut off to avoid fluctuations of the slit opening. Absorbance readings were obtained at the position of the maximum (around 270 nm) at 5, 10, and 20 min intervals, by running the pen and chart paper from 10 s before to 10 s after the minute. The absorbance readings for at least three half-lives were obtained by taking the reading at the mid-point of this line and averaging out the pen fluctuations. The zero, checked on the instrument after the infinity reading was taken (12–14 h), varied less than ±0.003 of an absorbance unit from the original zero. The data, $-\ln(A_t - A_\infty)$ and t in min, were analyzed on IBM 1604 and CDC 6400 computers for slopes and standard deviations in the slopes by a least squares program.

A typical first order plot for the solvolysis of *exo*-norbornyl and *exo*-2-norbornyl brosylate-*exo*-5-*endo*-5-d_2 is given in Fig. 3.

Control experiments with nondeuteriated norbornyl brosylate in both cells showed that a ratio of the slopes of 0.99 ± 0.01 to 1.00 ± 0.01 were routinely obtainable (see Table 2).

Financial support by the National Research Council of Canada and the Department of University Affairs (Ontario) is very gratefully acknowledged.

1. N. H. Werstiuk, R. R. MacDonald, R. W. Ouwehand, W. L. Chan, F. P. Cappelli, J. G. Ballard, R. E. Young, R. E. Massey, and G. Timmins. Tetrahedron Lett. **49**, 4363 (1970).
2. (*a*) S. Borčić, V. Belanie-Lipovac, and D. E. Sunko. Croat. Chem. Acta, **33**, 35 (1961). (*b*) C. C. Lee and E. W. Wong. J. Am. Chem. Soc. **86**, 2753 (1964). (*c*) B. L. Murr, A. Nickon, T. Swartz, and N. H. Werstiuk. J. Am. Chem. Soc. **89**, 1730 (1967). (*d*) J. M. Jerkunica, S. Borčić, and D. E. Sunko. J. Am. Chem. Soc. **89**, 1732 (1967). (*e*) J. M. Jerkunica, S. Borčić, and D. E. Sunko. Chem. Commun. 1302 (1967). (*f*) J. P. Schaefer, M. J. Dagauri, and D. S. Weinberg. J. Am. Chem. Soc. **89**, 6938 (1967). (*g*) H. L. Goering and K. Humski. J. Am. Chem. Soc. **91**, 4594 (1969). (*h*) B. L. Murr and J. A. Conkling. J. Am. Chem. Soc. **92**, 3462 (1970). (*i*) B. L. Murr and J. A. Conkling. J. Am. Chem. Soc. **92**, 3464 (1970).
3. S. Winstein and J. Takahashi. Tetrahedron Lett. **2**, 316 (1958).
4. (*a*) K. T. Leffek, J. A. Llewellyn, and R. E. Robertson. J. Am. Chem. Soc. **82**, 6315 (1960). (*b*) S. Borčič, M. Nikoletic, and D. E. Sunko. J. Am. Chem. Soc. **84**, 1615 (1962).
5. S. Weiss and G. E. LeRoi. J. Chem. Phys. **48**, 962 (1968).
6. J. G. Jewett and R. P. Dunlap. J. Am. Chem. Soc. **90**, 809 (1968).
7. M. Simonetta and S. Winstein. J. Am. Chem. Soc. **76**, 18 (1954).
8. P. v. R. Schleyer, P. J. Stang, and D. J. Raber. J. Am. Chem. Soc. **92**, 4725 (1970).
9. (*a*) P. Laszlo and P. v. R. Schleyer. J. Am. Chem. Soc. **86**, 1171 (1964). (*b*) N. H. Werstiuk and T. Kadai. Unpublished results.
10. J. C. Greever and D. E. Gwynn. Tetrahedron Lett. **10**, 813 (1969).
11. L. Schmerling, J. P. Luvisi, and R. W. Welch. J. Am. Chem. Soc. **78**, 2819 (1956).
12. J. D. Roberts, E. R. Turnbull, Jr., W. Bennett, and R. Armstrong. J. Am. Chem. Soc. **72**, 3116 (1950).
13. J. Meinwald, J. Crandall, and W. E. Hymans. Org. Syn. **45**, 77 (1965).
14. J. Meinwald, J. Crandall, and P. G. Gassman. Tetrahedron, **18**, 815 (1962).
15. A. C. Oehlschlager, C. D. Kennedy, and L. H. Zalkow. J. Org. Chem. **31**, 1682 (1966).
16. L. H. Zalkow and A. C. Oehlschlager. J. Org. Chem. **29**, 1625 (1964).
17. A. Nickon, J. L. Lambert, S. J., R. D. Williams, and N. H. Werstiuk. J. Am. Chem. Soc. **88**, 3354 (1966).
18. D. C. Kleinfelter and P. v. R. Schleyer. Org. Syn. **42**, 79 (1962).
19. S. Winstein and D. Trifan. J. Am. Chem. Soc. **74**, 1154 (1952).

Can. J. Chem. Downloaded from www.nrcresearchpress.com by 210.87.254.6 on 09/05/12
For personal use only.

The Infrared and Raman Spectra of 3-Chloro-1,2,5-thiadiazole

A. W. RICHARDSON
Bishop's University, Lennoxville, Quebec
Received July 12, 1971

The i.r. and Raman spectra of 3-chloro-1,2,5-thiadiazole have been recorded. Assignments have been made for all 15 fundamental vibrations on the basis of these observations plus some data from the vapor-phase u.v. absorption spectrum.

Les spectres i.r. et Raman du chloro-3 thiadiazole-1,2,5 ont été enregistrés. L'attribution des 15 vibrations fondamentales a été faite en se fondant sur ces observations et sur quelques données obtenues à partir des spectres u.v. d'absorption en phase vapeur.

Canadian Journal of Chemistry, **50**, 627 (1972)

Can. J. Chem. Downloaded from www.nrcresearchpress.com by 210.87.254.6 on 09/05/12
For personal use only.

Introduction

We are currently studying the electronic absorption spectra of 1,2,5-thiadiazole (**1**) and some of its 3-mono- and 3,4-di-substituted derivatives. In particular, 3-chloro-1,2,5-thiadiazole (**2**) is under investigation. Since a knowledge of the ground state vibrational frequencies and descriptions of the normal modes of vibration are needed for complete interpretation of an electronic absorption spectrum, the i.r. and Raman spectra of **2** have been recorded and the analysis of these spectra is presented here.

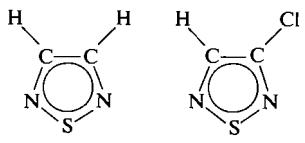

1 **2**

Experimental

Compound **2** was prepared by the reaction of α-aminoacetonitrile bisulfate with sulfur monochloride in dimethylformamide (1). The product was purified by g.l.c. using a 20 ft × 3/8 in. column of 30% SE30 on 45/60 Chrom W with a Varian Aerograph autoprep 700 gas chromatograph. Analytical g.l.c. on polar and non-polar columns showed the sample purity to be in excess of 99%.

The i.r. spectra were recorded on a Perkin–Elmer model 621 i.r. spectrophotometer. Spectra of the gas were recorded with the sample at its vapor pressure around room temperature in a 10 cm cell with KBr or CsI windows while those of the liquid were recorded for a capillary film between KBr plates or sheets of polyethylene. The Raman spectrum of the liquid sealed in a melting point tube was excited by an argon ion laser and measured on a Spex double monochromator with a rotatable analyzer to measure depolarization ratios ρ.

Results and Discussion

The i.r. spectra of **2** in the gas and liquid phases are shown in Figs. 1 and 2,[1] respectively, and the Raman spectrum of the liquid is shown in Fig. 3.[1] The frequencies of all observed bands together with other information such as estimated relative intensities, band types, depolarization ratios, etc. are presented in Table 1. The accuracy of the measured frequencies is estimated to be ± 2 cm^{-1} except for weak bands where it is, of course, not as good.

Compound **2** is assumed to be planar like **1** (2) and thus belongs to the C_s point group and has $11A'$ and $4A''$ normal modes of vibration (3). The assignments of the normal modes were made using the following guides.

(i) Band Contours

In the vapor, the $11A'$ modes will have type A, B, or AB-hybrid band contours whereas the $4A''$ modes will have type C band contours. To facilitate making assignments, type A, B, and C band contours were calculated for **2** in the rigid asymmetric rotor approximation (4) using a computer program written by Pierce. The calculated contours are shown in Fig. 4 and were obtained using the rotational constants $A = 0.25903$, $B = 0.05418$, and $C = 0.04481$ cm^{-1} for both the lower and upper states. These rotational constants were calculated by assuming the structure of **2** to be exactly the same as **1** (2) and r(C—Cl) = 1.70 Å (5). Band contours calculated for rotational constants differ-

[1]Photocopies of Figs. 2 and 3 are available from the Depository of Unpublished Data, National Science Library, National Research Council of Canada, Ottawa, Canada K1A 0S2.

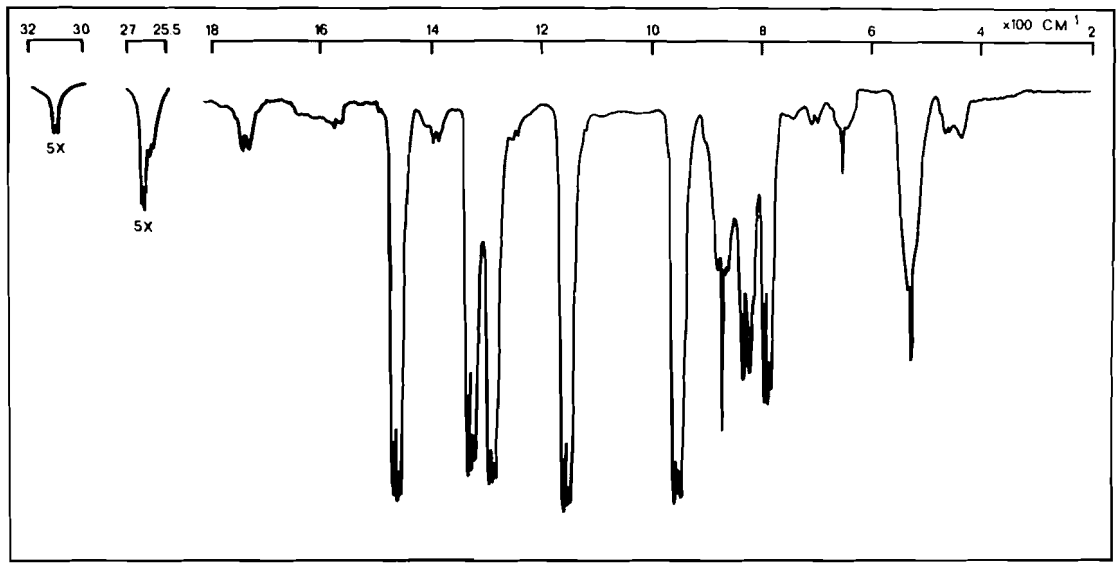

FIG. 1. The i.r. spectrum of 3-chloro-1,2,5-thiadiazole in the gas phase. The bands at the left of the diagram were recorded using an ordinate expansion of five.

ing somewhat from those above were found to differ very little from those in Fig. 4.

(ii) Depolarization Ratios

From theory, the $11A'$ modes will be polarized ($\rho < 0.75$) and the $4A''$ modes depolarized ($\rho = 0.75$) in the laser Raman spectrum. ρ values calculated from the observed spectra may differ somewhat from the theoretical values due to the experimental errors in measuring intensities.

(iii) Assignments for 1,2,5-Thiadiazole

The i.r. and Raman spectra of **1** have been studied and assignments made for all 15 fundamental vibrational frequencies and approximate descriptions of the normal modes given (6, 7). Several assignments for **2** follow directly from those made for **1**.

(iv) Assignments for the X-Sensitive Fundamental Vibrations of Chlorobenzene

Since **1** has been shown to have aromatic character (2, 8), it is reasonable to expect that the effect on the vibrational frequencies of replacing H by Cl might be similar to that in benzene. Therefore, the X-sensitive fundamentals of chlorobenzene (9, 10) were used as a guide to some low frequency assignments of **2**.

A″ Vibrations

These are discussed first since there are only four vibrations in this class. From the observed strong type C band contours, it is clear that the bands at 868, 647, and 518 cm^{-1} are due to A'' modes. The 868 cm^{-1} band is clearly the C—H out-of-plane mode since the average of the symmetric and antisymmetric C—H out-of-plane modes for **1** is 873 cm^{-1} and these modes are normally observed in the 750–950 cm^{-1} range for substituted benzenes (9), and various diazines (11). The 518 cm^{-1} band is clearly a ring-out-of-plane mode corresponding to the 520 cm^{-1} band of **1**. The 647 cm^{-1} band is also assigned as a ring out-of-plane mode.

Of the remaining bands, only the 233 and 297 cm^{-1} bands could possibly be the fourth A'' mode. The band at 233 cm^{-1} is assigned as the C—Cl out-of-plane bending mode because of its higher depolarization ratio, the assignment of certain combination bands (*vide infra*), and the observed C—Cl out-of-plane bending mode at 196 cm^{-1} in chlorobenzene (9). There is also evidence, as discussed later, for the assignment of 297 cm^{-1} as an A' mode.

A′ Vibrations

From the observed band contours, depolarization ratios, and intensities, the following bands are taken to be fundamental vibrations of A' symmetry: 3111, 1460, 1325, 1287, 1150,

Can. J. Chem. Downloaded from www.nrcresearchpress.com by 210.87.254.6 on 09/05/12
For personal use only.

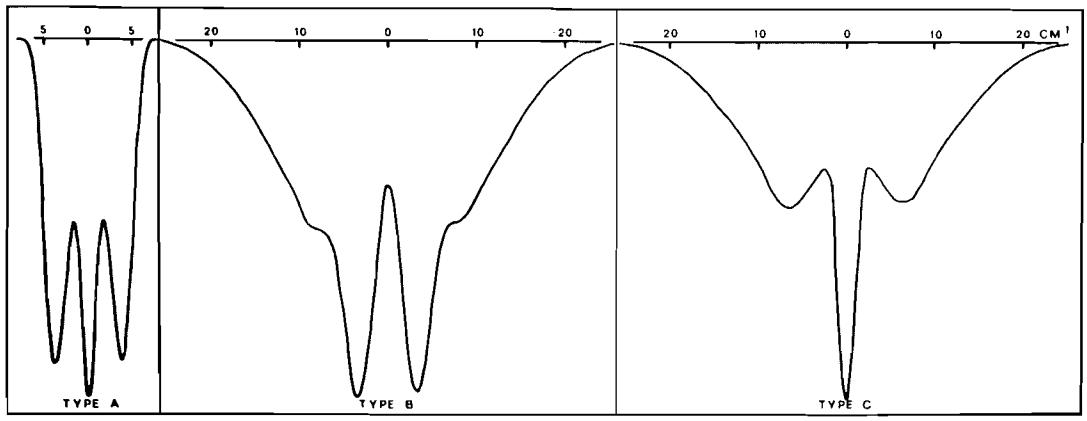

FIG. 4. Calculated type A, B, and C band contours for 3-chloro-1,2,5-thiadiazole.

949, 825, 786, 701, 430 cm^{-1}. The eleventh A' mode is chosen as 297 cm^{-1} as explained below.

Clearly, 3111 cm^{-1} is the C—H stretching mode. By comparison with the fundamentals of **1**, the bands at 1460, 1325, and 1287 can be assigned as ring-stretching modes. 1150 is close to the average value 1134 cm^{-1} for the symmetric and antisymmetric C—H in-plane bending modes for **1** and so can be assigned to the C—H in-plane bending mode. In chlorobenzene, the C—Cl stretch is at 701 and the C—Cl in-plane bend at 297 cm^{-1} (9, 10). This leads to the assignment of bands observed also at 701 and 297 cm^{-1} for **2** as the C—Cl stretch and C—Cl in-plane bend, respectively. The depolarization ratio of 0.80 for the 297 cm^{-1} band is higher than it should be; however, the assignment given for the 297 cm^{-1} band is further supported by some observations in the u.v. spectrum as discussed below.

Overtone and Combination Bands

All the stronger bands not assigned as fundamentals can be accounted for as first overtones or as binary combinations. In some cases more than one assignment is possible. For some rather weak bands no simple assignment was found. These assignments are listed in Table 1.

The assignments for some overtone and combination bands support the assignments given for the fundamentals. In particular, $2 \times 233(A'') = 466(A')$ and $233(A'') + 515(A'') = 748(A')$ agree with the bands observed at 463 and 751 cm^{-1} in the liquid while $949(A') + 296(A') = 1245(A')$ agrees with $1245(A')$. These support the assignments made for the 233 and 296 cm^{-1} bands.

Ultraviolet Data

As stated previously, this analysis was undertaken in order to determine the ground state fundamental vibrational frequencies of **2** so that they can be used in the interpretation of the electronic absorption spectrum. From the preliminary investigation of the gas phase u.v. absorption spectrum in the region 2875–2550 Å, bands have been observed at intervals of 300 ± 4, 433 ± 2, 704 ± 3, and 788 ± 3 cm^{-1} to long wavelengths of a common band at several places.[2] Since the electronic transition in **2** must be allowed and there is good agreement between the last three intervals and frequencies assigned as ground state A' fundamentals on the basis of i.r. and Raman data, the common band in each case must be acting as an origin (or pseudo-origin) for "hot" bands (12). The 300 cm^{-1} interval from the common origin band must also be due to an A' fundamental vibration (12), thus providing conclusive evidence for the assignment given for the band observed at 297 cm^{-1} in the i.r. and Raman.

[2]The figures given are the average value and standard deviation for 6, 6, 8, and 8 intervals, respectively, determined from the u.v. absorption spectrum of the vapor.

Can. J. Chem. Downloaded from www.nrcresearchpress.com by 210.87.254.6 on 09/05/12
For personal use only.

TABLE 1. The i.r. and Raman spectra of 3-chloro-1,2,5-thiadiazole

Liquid		Vapor			Raman				
ν	Intensity	ν*	Intensity	Band type	ν	Intensity	ρ	Symmetry	Assignment†
		3115							
3095	10	3111	1	B	3093	10	0.25	A'	C—H stretch
		3107							
		2650							
2642	2	2644	2	B				A'	$2 \times 1325(1) = 2650(A')$
		2640							
2608	1								$\begin{cases} 1325(1) + 1282(1) = 2607(A') \\ 1151(1) + 1455(1) = 2606(A') \end{cases}$
2356	1								
		2152							
2147	1	2145	1	B				A'	$1325 + 825 = 2150(A')$
		2140							
2094	1	2103	1	A?					$1287 + 825 = 2112(A')$
		1740							
		1735	5	B				A'	$\begin{cases} 2 \times 868 = 1736(A') \\ 949 + 768 = 1735(A') \end{cases}$
		1728							
1685	1								$868(1) + 820(1) = 1688(A'')$
1652	1	1648	1	C?					$868 + 786 = 1654(A'')$
1635	2								
1617	1								$1325(1) + 296(1) = 1621(A')$
1595	2								$820(1) + 782(1) = 1602(A')$
1559	2								$\begin{cases} 2 \times 782(1) = 1564(A') \\ 697(1) + 868(1) = 1565(A'') \end{cases}$
1540	1								
1521	1				1517	1			$\begin{cases} 820(1) + 697(1) = 1517(A') \\ 868(1) + 647(1) = 1515(A') \end{cases}$
1506	1								
		1465							
1455	78	1460	96	A	1452	8	0.79	A'	Ring stretch
		1454							
		1408							
		1405	2	B				A'	$2 \times 701 = 1402(A')$
		1402							
		1394							
1394	1	1389	3	B				A'	$868 + 518 = 1386(A')$
		1384							
		1330							
1325	77	1325	71	A	1322	20	0.53	A'	Ring stretch
		1319							
1302	21				1299	36	0.01	A'	$2 \times 647(1) = 1294(A')$
		1292							
1282	84	1287	78	A	1280	80	0.03	A'	Ring stretch
		1280							

Can. J. Chem. Downloaded from www.nrcresearchpress.com by 210.87.254.6 on 09/05/12
For personal use only.

TABLE 1. (*Concluded*)

Liquid		Vapor			Raman				
ν	Intensity	ν*	Intensity	Band type	ν	Intensity	ρ	Symmetry	Assignment†
1244	2	1250 1245 1240	3	B	1243	2		A'	944(1) + 296(1) = 1240(A')
1180	5								944(1) + 233(1) = 1177(A'')
1151	88	1155 1150 1144	100	A	1149	4	0.23	A'	C—H in-plane bend
1023	1								2 × 515(1) = 1030(A')
944	100	953 949 942	86	A	943	30	0.03	A'	Ring in-plane bend
868	25	876 868 863‡ 859	53	C				A''	C—H out-of-plane bend
820	51	830 825 818	38	B	820	67	0.04	A'	Ring in-plane bend
782	51	791 786 780	45	A	783	100	0.03	A'	Ring in-plane bend
751	2	742	1	A?					515(1) + 233(1) = 748(A')
697	4	706 701 696	2	B	696	55	0.22	A'	C—Cl stretch
647	10	660 649 640	7	C	647	1		A''	Ring out-of-plane bend
515	69	525 518 512	48	C	514	4	0.66	A''	Ring out-of-plane bend
463	2	462 456 453	2	B	467	7	0.08	A'	2 × 233(1) = 466(A')
438	8	430	3,b§	A?	440	62	0.16	A'	Ring in-plane bend
296	1				297	27	0.80	A'	C—Cl in-plane bend
					233	23	0.87	A''	C—Cl out-of-plane bend

*For type B bands, the middle number listed is the frequency of the central minimum.
†Liquid frequencies are designated by (1) after the frequency.
‡Small peak beside 868 cm^{-1} maximum.
§b = broad.

Can. J. Chem. Downloaded from www.nrcresearchpress.com by 210.87.254.6 on 09/05/12
For personal use only.

TABLE 2. Frequencies (cm^{-1}) of normal vibrations of 3-chloro-1,2,5-thiadiazole

Symmetry		Frequency (cm^{-1})	Approximate description
A'	ν_1	3111	C—H stretch
	ν_2	1460	Ring stretch
	ν_3	1325	Ring stretch
	ν_4	1287	Ring stretch
	ν_5	1150	C—H in-plane bend
	ν_6	949	Ring in-plane bend
	ν_7	825	Ring in-plane bend
	ν_8	786	Ring in-plane bend
	ν_9	701	C—Cl stretch
	ν_{10}	430	Ring in-plane bend
	ν_{11}	297	C—Cl in-plane bend
A''	ν_{12}	868	C—H out-of-plane bend
	ν_{13}	649	Ring out-of-plane bend
	ν_{14}	518	Ring out-of-plane bend
	ν_{15}	233	C—Cl out-of-plane bend

Conclusions

The assignments of the fundamental vibrational frequencies which have been made for 3-chloro-1,2,5-thiadiazole are summarized in Table 2. The i.r. and Raman spectra are consistent with the molecule being planar as expected. The majority of the fundamental vibrational frequencies are very similar to those of the parent compound 1,2,5-thiadiazole. The few which differ significantly involve the chlorine substituent and correlate very well with similar vibrational frequencies observed for chlorobenzene.

The author thanks the National Research Council of Canada for providing financial assistance for this work. Thanks are also due Dr. A. Canana of l'Université de Sherbrooke, Sherbrooke, Quebec for use of the Perkin–Elmer model 621 spectrophotometer, to Dr. G. W. King of McMaster University, Hamilton, Ontario for having the Raman spectra recorded, to Dr. L. Pierce of the University of Notre Dame, South Bend, Indiana for use of the asymmetric rotor band contour program, and to the Department of Education of Quebec for the use of computing facilities.

1. L. M. WEINSTOCK, P. DAVIS, B. HANDELSMAN, and R. TULL. J. Org. Chem. **32**, 2823 (1967).
2. V. DOBYNS and L. PIERCE. J. Am. Chem. Soc. **85**, 3553 (1963).
3. G. HERZBERG. Molecular spectra and molecular structure. Vol. II. Infrared and Raman spectra of polyatomic molecules. Van Nostrand, Princeton, N.J., 1945. p. 134.
4. H. C. ALLEN, JR. and P. C. CROSS. Molecular vibrotors. John Wiley and Son, Inc., New York, N.Y., 1963.
5. Interatomic distances. Special Publication No. 11. The Chemical Society, London, 1958.
6. B. SOPTRAJANOV and G. E. EWING. Spectrochim. Acta, **22**, 1417 (1966).
7. E. BENEDETTI, G. SBRANA, and V. BERTINI. Gazz. Chim. Ital. **97**, 379 (1967).
8. L. M. WEINSTOCK and P. I. POLLAK. *In* Advances in heterocyclic chemistry. Vol. 9. *Edited by* A. Katritzky and A. J. Bonlton. Academic Press, New York, N.Y., 1968.
9. D. H. WHIFFEN. J. Chem. Soc. 1350 (1956).
10. J. R. SCHERER. Planar vibrations of chlorinated benzenes. The Dow Chemical Co., Midland, Michigan, 1963.
11. K. K. INNES, J. P. BYRNE, and I. G. ROSS. J. Mol. Spectrosc. **22**, 125 (1967).
12. G. HERZBERG. Molecular spectra and molecular structure. Vol. III. Electronic spectra and electronic structure of polyatomic molecules. Van Nostrand, Princeton, N.J., 1967. p. 150.

Can. J. Chem. Downloaded from www.nrcresearchpress.com by 210.87.254.6 on 09/05/12
For personal use only.

Energy Distributions of Reaction Product by Statistical Phase Space Theory

W. H. WONG[1]

Noyes Chemical Laboratory, University of Illinois, Urbana, Illinois

Received August 27, 1971

The phase space theory of chemical reaction in which all accessible channels are uniformly weighted was shown to be inappropriate for describing exothermic reactions. Modification to the theory was introduced by a concept of partial statisticity in which only that portion of the phase space available to each vibrational level was treated statistically. The product rotational and translational distributions of the reaction, Cl + HI, and its isotopic variant, Cl + DI, were computed by this modified formulation and compared with that obtained from a straight application of the phase space theory. The implication of the profound differences found from these two formulations was discussed in light of experimental data.

La théorie spatiale de la phase d'une réaction chimique dans laquelle tous les voies accessibles sont uniformément envisagées s'avère n'être pas appropriée pour la description de réactions exothermiques. Une modification à cette théorie a été introduite en envisageant une statistique partielle dans laquelle seulement chaque portion de l'espace de phase convenable à chaque niveau de vibration a été traitée statistiquement. Les distributions rotationnelles et de translation dans le produit de la réaction, Cl + HI et de sa variante, Cl + DI, ont été programmées avec cette formulation modifiée et comparées à celles obtenues à partir de l'application stricte de la théorie spatiale de la phase. L'implication des profondes différences trouvées à partir de ces deux formulations a été discutée à la lumière des données expérimentales.

Canadian Journal of Chemistry, **50**, 633 (1972)

I. Introduction

During the last decade or so, advances in experimental techniques for studying gas-phase reactions have provided significant information on the dynamics of reactive collision. The crossed molecular-beam method (see, for example, ref. 1) not only reveals the reaction cross-section as a function of collisional energy, but it can also determine the translational energy as well as the scattering angle of the product. Complementary to this, the spectroscopic technique (2), which involves direct observation of radiation from excited states, is capable of establishing the nascent distribution of internal energies before its collisional degradation. All these data are extremely valuable in unravelling the fundamental dynamics of the collision and in inferring the precise interaction between the collision partners. Stimulated by these experimental achievements, a large amount of theoretical work has appeared. One of the theories designed to predict the outcome of reactive collisions is the statistical phase space theory put forward by Light and co-workers (3). In this theory, the reactant species pass through a strong-coupling configuration which subsequently decomposes into various channels with a probability proportional to the volume of phase space available to that channel. In terms of quantum scattering theory, this is equivalent to assuming that all the non-zero elements of the **S** matrix are replaced by an average value and hence all are equal in magnitude (4, 5). Even though the formation of a long-lived reaction intermediate which has sufficient time for randomizing its energy among various degrees of freedom undoubtedly gives physical interpretation to this assumption, it is perhaps significant to emphasize that a very impulsive collision such as a hard-sphere type will also display statistical behavior. A good example for the latter justification is the success of the random phase approximation for rotational energy transfer (6). This statistical theory is particularly attractive because of its simplicity. Thus no detailed information on the potential energy surface other than the regions around the asymptotic reactant and product configurations is required and the very difficult dynamical calculation is avoided. The application of this theory to various types of reactions has been reviewed by Light and co-workers (3), and more recent works have been presented by Trular and Kuppermann (*7a*), Wolf and Haller (*7b*), Trular (*7c*), and White and Light (*7d*).

[1]Present address: Chemistry Department, University of Toronto, Toronto 181, Ontario.

Can. J. Chem. Downloaded from www.nrcresearchpress.com by 210.87.254.40 on 09/05/12
For personal use only.

Can. J. Chem. Downloaded from www.nrcresearchpress.com by 210.87.254.40 on 09/05/12
For personal use only.

Despite the various extent of success of this theory to certain types of reaction, it consistently failed to account for the product vibrational distribution of all exothermic reactions studied so far. Since there are always more states available from a lower vibrational level than from a higher one, simply because of energy constraint, the phase space theory invariably predicts a decreasing product population with increasing vibrational quantum number. In sharp contrast to this, the chemiluminescent experiments (8) as well as trajectory calculations (9) indicated that a significant amount of the released exothermicity appeared in vibration of the newly-formed molecule and hence the product vibrational distribution peaked at higher quantum numbers. This vibrational population inversion provides, of course, the basis of chemical laser action (10). Although this statistical theory fails to account for the product vibrational distribution of exothermic reactions, it is still interesting to investigate its applicability to rotational distribution, particularly in view of the fact that the energy difference between rotational states is usually small and hence the distribution will more likely be statistical. However, in those cases in which this theory fails to predict the vibrational distribution, one can no longer uniformly treat the whole phase space available to the product. Instead, one should weigh the subspace available to the product in each vibrational level in such a way as to reflect the probability of product being formed in that level. The statistical treatment can be applied only within each subspace and thus the statistical calculation of the rotational distribution should be performed on each vibrational level separately. The overall rotational distribution can then be obtained by summing over all vibrational levels each of which carries the prescribed weight. This weighting factor can either be obtained from some simplified dynamical models, such as the non-adiabatic sudden-switch model (11), or from experimental data (8). It is interesting to note that all previously published work on the phase space theory assumed uniform weighting of the whole phase space, even in those cases in which its prediction of vibrational distribution was contrary to the observed data. From the above argument, it is obvious that the overall rotational distribution thus predicted could no longer be compared meaningfully with experiment.

In this paper we try to investigate the rotational distribution of highly exothermic reaction. We follow closely the quantum mechanical version of the phase space theory (3*a*, *c*), but modify it in such a way that the relative probability (obtained from dynamical calculation or from experimental data) of product being formed at each vibrational level could be incorporated. The weighting factors used in this paper were obtained from chemiluminescence data. The overall rotational and translational distributions were computed with this modification and were compared with those obtained by straight application of Light's (3) formulation. The systems chosen for specific consideration are Cl + HI and its isotopic variant Cl + DI. Accurate product vibrational distribution of these two reactions is available (8), and the dynamics of these two reactions has been investigated by Monte Carlo calculation (9*a*, *b*).

II. Theory

The cross-section for the formation of a strong-coupling complex (not necessarily long-lived) is given by (see for example, ref. 12)

$$[1] \qquad \sigma = \sum_{l=0}^{l_{max}} (2l+1)\,\frac{\pi\hbar}{2\mu E_t}$$

where μ, E_t, and l are the reduced mass, the relative translational energy, and the orbital angular momentum quantum number, respectively, of the collision system in the incoming channel. The upper limit of the summation, l_{max}, is the quantum number specifying the largest partial wave that could lead to the formation of a strong-coupling complex. Following the work of Light and co-workers (3), we define the boundary of the strong-coupling region as the barrier of the effective potential of the form

$$V_e(r) = -\frac{c}{r^6} + \frac{l(l+1)\hbar}{2\mu r}$$

where c is the coefficient of the long range attraction, and r is the separation between the collision partners. The requirement that the system should have sufficient energy to surmount the barrier to form the complex sets an upper limit

Can. J. Chem. Downloaded from www.nrcresearchpress.com by 210.87.254.40 on 09/05/12
For personal use only.

to l, which is (3*b*)

$$[2a] \qquad l_{max}(l_{max}+1)\hbar^2 = 6\mu c^{1/3}\left(\frac{E_t}{2}\right)^{2/3}$$

The maximum impact parameter is then related to l_{max} by

$$[2b] \qquad 2\mu E_t b_{max}^2 = l_{max}(l_{max}+1)\hbar^2$$

If the probability of this complex decomposing into product channels is denoted by k, the total reaction cross-section is

$$[3] \qquad \sigma_R = \sum_{l=0}^{l_{max}} (2l+1)k\,\frac{\pi\hbar}{2\mu E_t}$$

where k should be understood to be a function of l, and its value is between zero and unity. In the original formulation of the phase space theory by Light and co-workers (3), the probability k is just the ratio of the number of states available in the product channels to the total number of states (reactive and non-reactive) accessible from the complex with specified total energy (E), and total angular momentum ($J\hbar$). Since the original theory is known to overestimate the reaction cross-section, we choose to leave this factor k in the formulation, and calculate the relative values. For the purpose of studying rotational distribution, we decompose the total reaction cross-section into more detailed quantities. The probabilities $P(v')$ and $P_{v'}(j')$ are defined in such a way that the cross-section for the formation of product at rotational state j' in a specified vibrational level v' is given by

$$[4] \qquad \sigma(v',j') = \sigma_R \cdot P(v') \cdot P_{v'}(j')$$

where v' and j' are product vibrational and rotational quantum numbers, respectively. Since

$$\sum_{v'} \sum_{j'(v')} \sigma(v',j') = \sigma_R$$

we have

$$\sum_{v'} P(v') \sum_{j'(v')} P_{v'}(j') = 1$$

and since

$$\sum_{j'(v')} \sigma(v',j') = \sigma(v')$$

we must have

$$\sum_{j'(v')} P_{v'}(j') = 1$$

and

$$\sum_{v'} P(v') = 1$$

Thus $P(v')$ is the normalized probability of product being formed at vibrational level v', and $P_{v'}(j')$ is the normalized probability of product being formed at state j' of the vibrational level v'. As discussed in section I, we apply statistical treatment to the rotational distribution of each vibrational level separately. From the usual argument of the statistical theory (3), the probability of product being formed at state j' is proportional to the number of quantum states, $N_{v'}(j')$, available to that j', subject to conservation of total energy and total angular momentum. That is

$$[5] \qquad P_{v'}(j') = \frac{N_{v'}(j')}{\sum_{j'} N_{v'}(j')}$$

The conservation of energy can be expressed as

$$[6] \qquad E = E_t + E_v + E_r + Q = E_t' + E_v' + \frac{j'(j'+1)\hbar^2}{2I'}$$

where E_t, E_v, and E_r are translational, vibrational, and rotational energies, respectively, of the reactant, and the primed quantities refer to product. The quantity I' is the moment of inertia of the product molecule (we only consider diatomic), and the exothermicity, Q, is taken to be positive when energy is released. From eq. 6, the upper limit of j' on a given v' level is

$$[6a] \qquad j'_{max}(j'_{max}+1)\hbar^2 = 2I'(E - E_v')$$

The conservation of total angular momentum requires that the set of orbital angular momentum quantum numbers in the exit channel (l') to be associated with each j' should obey

$$[7] \qquad |J - j'| \leqslant l' \leqslant (j + j')$$

On the other hand, the requirement that the complex should have sufficient energy to over-

Can. J. Chem. Downloaded from www.nrcresearchpress.com by 210.87.254.40 on 09/05/12
For personal use only.

come the centrifugal barrier at the exit channel, sets an upper limit to l'. That is

$$[7a] \qquad l' \leqslant l'_{\max}$$

This maximum is again determined by eq. 2*a*, but with quantities relevant to the outgoing channel. Thus the number of states available to j' from a complex of angular momentum J, is given by

$$[8] \quad N_{v'}(J \to j') = (2J+1)(2j'+1) \times \sum_{l'_{\min}}^{l'_{\max}} H\left(E - E'_v - \frac{j'(j'+1)\hbar^2}{2I} - V_e^*(r')\right)$$

where the upper limit of the summation obeys eqs. 7 and 7*a* simultaneously, while the lower limit observes constraint eq. 7.

The Heaviside function in eq. 8 is

$$H(x) = 1, \quad x \geq 0$$
$$= 0, \quad x < 0$$

and $V_e^*(r')$ is the exit centrifugal barrier. Since at room temperature, the rotational angular momentum of the reactant molecule is small compared to the orbital angular momentum of the collision, we simply neglect its contribution to the total angular momentum of the complex. Thus $J\hbar$ is simply taken to be the orbital angular momentum of the incoming partial waves and the summing over all J is equivalent to summing over all l. The total number of states associated with j' is then

$$[9] \quad N_{v'}(j') = \sum_J N_{v'}(J \to j') = \sum_{l=0}^{l\max} (2l+1)(2j'+1) \times \sum_{l'_{\min}}^{l'_{\max}} H\left(E - E'_v - \frac{j'(j'+1)\hbar^2}{2I'} - V_e^*(r')\right)$$

The cross-section of product being formed at j' on vibrational level v' is

$$[10] \qquad \sigma(v',j') = \sigma_R P(v') \frac{N_{v'}(j')}{\sum_{j'} N_{v'}(j')}$$

The overall rotational distribution is

$$[11] \qquad \sigma(j') = \sigma_R \sum_{v'} P(v') \cdot \frac{N_{v'}(j')}{\sum_{j'} N_{v'}(j')}$$

Since the translational energy is just the difference between the total energy and the sum of rotational and vibrational energies, its distribution can readily be deduced from eqs. 10 and 11. When the cross-section is expressed as a function of energy rather than quantum numbers, we can simply write

$$[12] \qquad \sigma(E'_t) = \sigma(E - E'_v - E'_r)$$

III. Computations and Discussion

Calculations were performed on two reactions, Cl + HI and its isotopic variant Cl + DI, at a relative translational energy of 1.2 kcal. This energy was chosen to simulate the experiment at room temperature (8*b*). Both the original version of the phase space theory (3) in which the whole phase space is uniformly weighted and the modified version as expressed in eqs. 10 and 11 were employed.

The coefficient of the attractive potential for the interaction between A and BC was calculated from the well-known Landon's dispersion energy formula

$$C = \frac{3}{2} \frac{\varepsilon_A \varepsilon_{BC}}{\varepsilon_A + \varepsilon_{BC}} \alpha_A \alpha_{BC} + D_{BC}{}^2 \alpha_A$$

where ε, α, and D are the transition energy of dipole excitation, the polarizability, and the dipole moment, respectively. The vibrational energy of the diatomic molecule was calculated by the expression

$$E_v = \omega_e(v + \tfrac{1}{2}) - \omega_e\chi_e(v + \tfrac{1}{2})^2$$

These and other molecular data used in the computation were summarized in Table 1.

It is interesting to note that a relative translational energy of 1.2 kcal, the maximum impact parameter for the formation of the complex as defined by eq. 2 is 4.8 Å for both reactions, only slightly larger than the corresponding value of 4.3 Å obtained from Monte Carlo calculation (9*a*). However, the total reaction cross-section obtained from Light's formulation is 72 Å^2 for Cl + HI and 73 Å^2 for Cl + DI. The corresponding values obtained from Monte Carlo calculations are 6.8 Å^2 and 6.5 Å^2, respectively. For this type of co-valent reaction, it is very unlikely that the cross-section would far exceed 10 Å^2. This is perhaps another evidence that the phase

Can. J. Chem. Downloaded from www.nrcresearchpress.com by 210.87.254.40 on 09/05/12
For personal use only.

TABLE 1. Molecular data*

Molecule	Dipole moment, D (Debye)	Polarizability, α (Å^3)	Resonance energy, ε (eV)	Dissociation energy, D_e (eV)	Vibrational frequency, ω_e (cm^{-1})	Equilibrium separation, γ_e (Å)
Cl		2.14	13.01			
HI	0.38	5.44	10.38	3.198	2309.5	1.604
DI	0.38	5.44	10.38	3.198	1640.09	1.604
I		4.96	10.44			
HCl	1.03	2.63	13.4	4.614	2989.74	1.274
DCl	1.03	2.63	13.4	4.614	2090.78	1.274

*These molecular data are extracted from Table IV of ref. 7*a*.

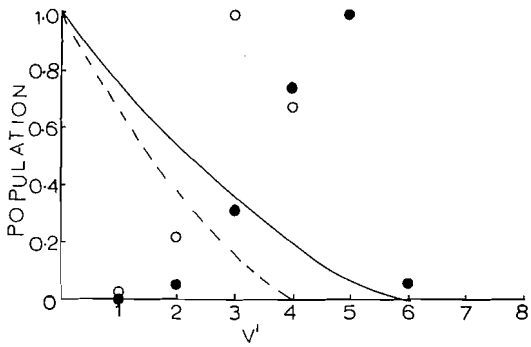

FIG. 1. Product vibrational energy distribution. The solid circles denote the experimental data for DCl and the open circles for HCl. The trends predicted by Light's formulation are shown as solid (DCl) and dashed (HCl) lines. Distribution normalized to unity at maximum.

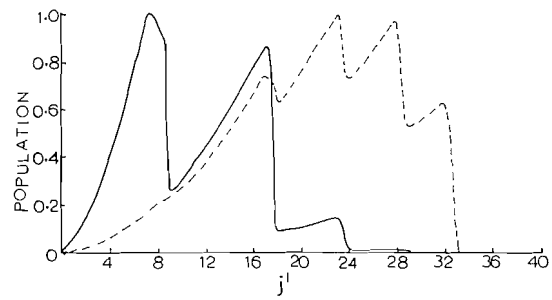

FIG. 2. Overall rotational energy distribution of HCl. Solid line computed from the modified formulation eq. 11; dashed line computed from Light's formulation.

space theory overestimates the reaction cross-section for an exothermic reaction. In fact, it is generally recognized (*7a*, *3c*) that this theory only gives an upper limit to the reaction cross-section, since the sole criterion determining the probability of reaction is the number of states accessible and the steric effect is completely ignored. Thus, with the uniform weighting of the whole phase space, the ratio of the number of accessible states for reaction to that of non-reactive collision is found to be around 1.3×10^2 for both reactions. But from Monte Carlo calculation, the average reaction probability of an encounter with an impact parameter less than the maximum value is only about 16%. It is apparent from the steric factor revealed in the Monte Carlo calculation that the uniform weighting of the whole phase space is inappropriate.

The relative vibrational distribution of the two isotopic reactions obtained from Light's formulation is displayed in Fig. 1. Also shown in the figure are the chemiluminescence data of Polanyi and co-workers (*8b*). The monotonic decrease of population with increasing quantum number is in strong contrast to the experimental trend. Similar failure of this theory for other exothermic reactions has already been pointed out by other workers (3). This, of course, supports the contention put forward in section I, that the whole phase space accessible to the product should not be equally weighted.

The relative rotational distribution on *each* vibrational level computed from eq. 10 of course is the same as that obtained from Pechukas and Light's formulation (3). All of these distributions peak at the highest j' consistent with energy conservation. Since we are mainly interested in the effect of introducing the correct weighting factors on the *overall* rotational and translational distributions, we refrain from displaying the distributions on individual levels.

The overall rotational distribution from our modified formulation was calculated from eq. 11, with the weighting factors, $P_{v'}$'s, obtained from chemiluminescent experiment (*8b*). The results are shown in Figs. 2 and 3. Also shown in these two plots are the distributions obtained from straight application of Light's formulation. Both sets of distributions are normalized to unity at the maximum. It is obvious that the two formulations give entirely different trend. For both reactions, Cl + HI and Cl + DI, Light's formulation not only predicts the maximum of the distribution at a much higher j', but also that the main body of the distribution shifts to much higher quantum numbers. Thus the average rotational energies of products HCl and DCl are 13.9 kcal and 13.6 kcal, respectively. The corresponding values from our modified formulation are 4.4 kcal and 5.1 kcal. It is interesting to note that the experimental values are around 4 kcal (13). This profound difference arises, of course, from the different weighting of the phase space. From Light's version, the most probable product vibrational state is the ground level, and on this level, the product can reach very high j' without violating energy conservation. In our modified formulation, on the other hand, we have readjusted the weighting of the phase space such that the most probable vibra-

Can. J. Chem. Downloaded from www.nrcresearchpress.com by 210.87.254.40 on 09/05/12
For personal use only.

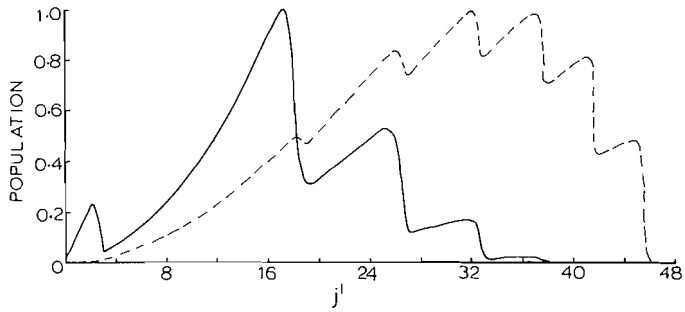

FIG. 3. Overall rotational energy distribution of DCl. Solid line computed from the modified formulation eq. 11, and dashed line from Light's formulation.

tional level is at high v', as was observed in experiment. On these higher vibrational levels, the product molecule would have insufficient energy to populate very high j' states. Thus the higher fraction of available energy being absorbed by the vibrational motion decreases proportionally the share for the rotational motion. Another feature that is worth noting in these plots is that the peaks of the distribution are better resolved in the modified version than that from Light's formulation. Thus for the product HCl (Fig. 2), our modified version predicts only two sharp peaks with their maxima separated by ten quantum numbers. Each of these two peaks can be clearly identified with the population of the two most probable vibrational levels. In Light's formulation, however, due to the overlap of the rotational populations of different vibrational levels, the peaks are much less prominent and much less resolved. The better resolution of the modified version is again evident for the product DCl, as shown in Fig. 3. Since the separation between the peaks in our modified version is well within the resolution power of chemiluminescent experiments, it seems likely that the features of the overall rotational distribution could be fruitfully applied to diagnose whether the dynamics exhibit complete or only partial statistical behavior. It would be extremely interesting to compare with accurate experimental data when available.

For convenience of comparison with crossed molecular-beam data, we have also computed the relative distribution of product translational energy of these two reactions. The translational energy was obtained by subtracting the sum of the quantized vibrational and rotational energies from the specified total energy, and the distribution was computed by eq. 12. These distributions are displayed in Figs. 4 and 5. The abscissas are in fraction of total available energy of the reaction (33.9 kcal for Cl + HI and 34.0 kcal for Cl + DI). Since the rotational energy is not a linear function of rotational quantum number, it introduces some scattering of data on the translational energy distribution plotted against a linear energy scale. To capture the essential feature and to avoid the unnecessary complications, the curves have been smoothed out. It is apparent from Figs. 4 and 5 that Light's

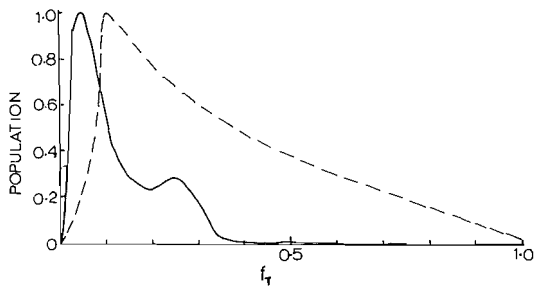

FIG. 4. Translational energy distribution of HCl. Solid line computed from the modified formulation eq. 12, and dashed line from Light's formulation.

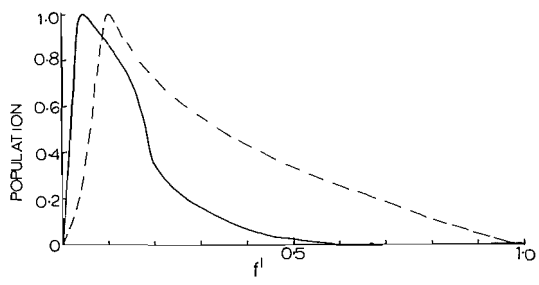

Fig. 5. Translational energy distribution of DCl. Solid line computed from the modified formulation eq. 12, and dashed line from Light's formulation.

Can. J. Chem. Downloaded from www.nrcresearchpress.com by 210.87.254.40 on 09/05/12
For personal use only.

formulation again predicts a higher product translational energy. The average value is 11.3 kcal for Cl + HI, and 11.0 kcal for Cl + DI as compared with the corresponding 3.7 kcal and 4.0 kcal obtained from our modification. Although the maxima of the distributions are quite close in these two formulations, our modified version predicts a much sharper peak centered around low energy region while Light's version predicts a very broad distribution with a substantial population at the high energy end of the spectrum. This broad energy distribution seems to be the characteristic of a completely statistical theory.

IV. Summary

The phase space theory of chemical reaction was applied to study two exothermic reactions, Cl + HI and Cl + DI. It was found that this theory in which the whole phase space was uniformly weighted overestimated the reaction cross-section and predicted a reverse trend of product vibrational distribution as was observed in chemiluminescent experiments. A modified version of the theory was formulated by introducing a weighting factor to the subspace accessible to each product vibrational level. This modification as well as the original version of the phase space theory was used to compute the rotational and translational energy distributions of these two exothermic reactions. It was found that the two formulations predicted drastically different trends. The original version predicted much higher rotational and translational energies and much broader distributions. It seems that the average product rotational and translational energies obtained from our modified version are in better agreement with experimental data, although a rigorous test of its applicability can only be done when an accurate rotational energy distribution from chemiluminescent experiments and an accurate translational energy distribution from molecular-beam experiments are available. Nevertheless, if this partially statistical formulation (statistical only within that portion of the phase space corresponding to a vibrational level) still fails to agree with experiment, we may conclude that none of the motions in an exothermic reaction can be described statistically.

I am indebted to Professor R. A. Marcus for many incisive discussions.

1. D. R. HERSCHBACH. Adv. Chem. Phys. **10**, 319 (1966).
2. J. C. POLANYI. J. Quant. Spectrosc. Radiat. Transfer, **3**, 471 (1963).
3. (*a*) P. PECHUKAS and J. C. LIGHT. J. Chem. Phys. **42**, 1281 (1965). (*b*) P. PECHUKAS, J. C. LIGHT, and C. RANKIN. J. Chem. Phys. **44**, 794 (1966). (*c*) J. C. LIGHT. Discuss. Faraday Soc. **44**, 14 (1967).
4. W. H. MILLER. J. Chem. Phys. **52**, 543 (1970).
5. R. D. LEVINE. Quantum mechanics of molecular rate processes. Oxford University Press, London. 1969. Chap. 3-5.
6. R. B. BERNSTEIN, A. DALGARNO, H. MASSEY, and I. C. PERCIVAL. Proc. Roy. Soc. London, A, **274**, 427 (1963).
7. (*a*) D. G. TRULAR and A. KUPPERMANN. J. Phys. Chem. **73**, 1722 (1969). (*b*) F. A. WOLF and J. L. HALLER. J. Chem. Phys. **52**, 4910 (1970). (*c*) D. G. TRULAR. J. Chem. Phys. **54**, 2635 (1971). (*d*) R. A. WHITE and J. C. LIGHT. J. Chem. Phys. **55**, 379 (1971).
8. (*a*) K. G. ANLAUF, P. J. KUNTZ, D. H. MAYLOTTE, P. D. PACEY, and J. C. POLANYI. Discuss. Faraday Soc. **44**, 183 (1967). (*b*) K. G. ANLAUF, J. C. POLANYI, K. B. WOODALL, and W. H. WONG. J. Chem. Phys. **49**, 5189 (1968).
9. (*a*) W. H. WONG. Ph.D. Thesis, University of Toronto, Toronto, Ontario. 1969. (*b*) J. C. POLANYI and W. H. WONG. J. Chem. Phys. To be published. (*c*) J. C. POLANYI and W. H. WONG. J. Chem. Phys. **51**, 1439 (1969). (*d*) P. J. KUNTZ, E. M. NEMETH, J. C. POLANYI, S. D. ROSNER, and C. E. YOUNG. J. Chem. Phys. **44**, 1168 (1966).
10. J. C. POLANYI. Appar. Opt. Suppl. No. 2. 109 (1965).
11. W. H. WONG. Can. J. Chem. To be published.
12. L. D. LANDAU and E. M. LIFSHITZ. Quantum mechanics. Pergamon Press, Oxford. 1958. p. 118.
13. D. H. MAYLOTTE. Ph.D. Thesis, University of Toronto, Toronto, Ontario. 1968.

Can. J. Chem. Downloaded from www.nrcresearchpress.com by 210.87.254.40 on 09/05/12
For personal use only.

Anomalous Ratios of Formation Constants: Possible Invalidity in the Successive Constants[1]

H. F. STEGER[1]

Mineral Sciences Division, Department of Energy, Mines and Resources, Ottawa, Canada

Received September 24, 1971

The causes of inaccuracy in the values of the successive formation constants for 1:2 metal:ligand complex systems for which $K_1 \leqslant K_2$ are discussed. The experimental error in the $\bar{n}$,pL data has been shown to become increasingly important as K_1/K_2 decreases. It has been concluded that the successive constants cannot be determined if $K_1/K_2 < 10^{-2.4}$. Their product, K_1K_2, can, however, be determined. It is also shown that the value of K_2 cannot be determined for the iron complexes with bipyridyl and 1,10-phenanthroline.

On discute des causes d'inexactitude quant aux valeurs obtenues pour les constantes de formation successive des complexes 1:2 métal:ligand pour lesquels $K_1 \leqslant K_2$. L'erreur expérimentale dans la donnée $\bar{n}$,pL devient d'autant plus importante que le rapport K_1/K_2 décroit. Il en a été conclu que les constantes successives ne peuvent être déterminées si $K_1/K_2 < 10^{-2.4}$. Cependant, leur produit, K_1K_2, peut être déterminé. Il a également été montré que la valeur de K_2 ne peut être déterminée pour les complexes du fer avec le bipyridyle et la 1,10-phénanthroline.

Canadian Journal of Chemistry, **50**, 641 (1972)

Introduction

Small values of the ratio K_1/K_2 where, $K_1 \leqslant K_2$ have been found for the Cu(II) complex with 2,9-dimethyl-1,10-phenanthroline (1) and some transition metal complexes of 2-thienyl-8-hydroxyquinoline (2). These anomalous ratios of K_1/K_2 have been attributed to changes in the stereochemistry of the metal ion caused by steric interaction between the incoming first molecule of ligand and coordinated water resulting in a decrease in K_1(1, 3). The second molecule of ligand coordinates to the distorted structure in the usual fashion without a decrease in K_2.

There is no question that the experimentally determined values of K_1 and K_2 signify the presence of a factor not usually operative in metal complex formation. However, to impart any special significance to their magnitudes other than indicating an anomalous stability effect must be done with caution for certain factors which affect the accuracy of K_1 and K_2 become increasingly important as K_1/K_2 decreases. The aim of this study is to discuss the difficulties in the calculation of accurate values of K_1 and K_2 for $K_1 \leqslant K_2$.

The discussion is extended to the iron complex systems with bipyridyl and 1,10-phenanthroline (4) for which $K_3 > K_1,K_2$. In these systems the calculation of accurate values of the successive formation constants is also shown to be subject to the same difficulties.

Discussion

Several methods are known for the calculation of metal complex formation constants by the use of $\bar{n}$, the average number of ligands bound to the metal, and [L], the concentration of free ligand anion (5). The formation constants for 1:2 metal:ligand complexes are, in general, calculated by a linear least-squares fit of $\bar{n}$,[L] data to

$$[1] \qquad K_1 = \frac{\bar{n}}{(1-\bar{n})[\mathrm{L}]} - \frac{(2-\bar{n})[\mathrm{L}]K_1K_2}{(1-\bar{n})}$$

In metal complex systems in which $K_1 \leqslant K_2$, special consideration concerning the accuracy of the values of K_1 and K_2 calculated thusly must be undertaken for two reasons. First, the experimental errors, both random and systematic, become increasingly important as the ratio of K_1/K_2 decreases. Second, the possibility of an insensitivity of the experimental $\bar{n}$,[L] data to both ligand addition reactions cannot be eliminated completely.

Due to the extraordinary nature of the systems for which $K_1 \leqslant K_2$, few such examples have been

[1]Crown copyrights reserved. Mineral Sciences Division, Division Report MS-PP 71-27.

Can. J. Chem. Downloaded from www.nrcresearchpress.com by 210.87.254.5 on 09/05/12
For personal use only.

Can. J. Chem. Downloaded from www.nrcresearchpress.com by 210.87.254.5 on 09/05/12
For personal use only.

reported. The equilibrium data for some metal 2-thienyl-8-hydroxyquinolinates (2) and the Cu(II) complex with 2,9-dimethyl-1,10-phenanthroline (1) are summarized in Table 1. Also shown are the values of log K_1, log K_2, and the corresponding standard deviation, σ, as calculated by eq. 1. The values of log K_1 at the individual data points were calculated by the back-substitution of log K_1K_2 into eq. 1 from which it had been calculated. The column "Dev" gives the values of the individual K_1's as a percentage of the terms $\bar{n}/(1-\bar{n})[L]$ and $(2-\bar{n})[L]K_1K_2/(1-\bar{n})$, whichever is the greater.

At first glance, the low standard deviation found for the metal 2-thienyl-8-hydroxyquinolinates would suggest that eq. 1 renders a more than satisfactory fit of the equilibrium data. An examination of the values of log K_1 at the individual data points, however, clearly demonstrates that this is somewhat misleading. There is appreciable scatter in the value of log K_1. The precision of log K_1 is approximately ± 0.3 units for all the metal 2-thienyl-8-hydroxyquinolinates, and is much greater than is desirable.

The cause of this large scatter in K_1 is random experimental error. The values in the column "Dev" illustrate that the value of K_1 is considerably less than either term on the right-hand side of eq. 1, *e.g.*, K_1 varies from $\sim 1\%$ to a maximum of 22, 34, 10, 12, and 38% of the larger of the terms for the Co, Ni, Cu, Zn, and Cd complex, respectively. It can readily be seen that because K_1, the difference between the terms $\bar{n}/(1-\bar{n})[L]$ and $(2-\bar{n})[L]K_1K_2/(1-\bar{n})$, is appreciably smaller than these terms, the precision of the values of log K_1 will be greatly dependent on the errors in the terms on the right-hand side of eq. 1, which, in turn, are determined by the random experimental error in the $\bar{n}$,[L] data.

The experimental error in pL, Log K_1, and log K_2 for metal complex systems in which $K_1 > K_2$ has been calculated to be ± 0.02 units (6, 7). On the assumption that this estimation of the error also applies to metal complex systems in which $K_1 \leqslant K_2$, the fractional error in pL is approximately 0.4% for the 2-thienyl-8-hydroxyquinolinates. The fractional errors in the terms $\bar{n}/(1-\bar{n})[L]$ and $(2-\bar{n})[L]K_1K_2/(1-\bar{n})$ can be calculated to be approximately 0.4% if the errors in the components containing $\bar{n}$ are assumed to be self-cancelling (8). Since the actual value of K_1 is less than either term, its fractional error must be larger than 0.4%. Indeed, the variation in log K_1 of ± 0.3 units suggests that the fractional error in K_1 has increased to approximately 5% for the metal 2-thienyl-8-hydroxyquinolinates. Since formation constants are, in general, determined with much greater precision, the increased importance of experimental error in systems in which $K_1 \leqslant K_2$ must be considered in reporting the values of the formation constants.

The question arises, however, if there is a lower limit to the value of the ratio K_1/K_2 below which the evaluation of K_1 is not possible by the use of the available equilibrium data. The answer, of course, is that such a lower limit does exist and that it is related directly to the error in experimentally determined quantities such as pL, $\bar{n}$, *etc.* The calculation of a value of K_1 which is less than the error in the terms $\bar{n}/(1-\bar{n})[L]$ and $(2-\bar{n})[L]K_1K_2/(1-\bar{n})$ cannot be justified, *i.e.*, eq. 1 will yield values of K_1 which are in fact, reflections of the experimental error instead of mono-ligand complex formation. Therefore, if K_1 is less than 0.4% of both terms above, its value cannot be calculated. For such a situation, both positive and negative values of K_1 will be obtained because of random experimental error. Herein lies a test for the reliability of the value of K_1. If all of the values of K_1 at the individual data points are positive, then $K_1 \geqslant$ experimental error and its value can be determined. It must be noted, however, that the reproducibility of the value of K_1 will decrease as its value approaches that of the experimental error.

An estimate of the value of the lower limit of the value of the ratio K_1/K_2 was made as follows. A value of log K_1K_2 was selected arbitrarily. Values of $\bar{n}$ for a given series of values of pL were then calculated for several values of the ratio K_1/K_2. These values of $\bar{n}$ and the corresponding pL, to which an error of 0.02 units was added or subtracted alternately, were used to calculate the values of K_1 at the individual data points. It was observed that for $K_1/K_2 \leqslant 10^{-2.4}$, one half of the values of K_1 at the individual data points were negative, as expected, *i.e.*, the applied error in pL is of greater significance than is the contribution made by K_1 to eq. 1. At $K_1/K_2 > 10^{-2.4}$, positive values of K_1 are obtained for those values of pL which gave negative values above, with the exception of data points for which $\bar{n}$ is close to unity and which, in general, would be omitted in the calculation of formation constants (5). Hence, the contribution of K_1 to eq. 1 has become greater than the applied error in pL.

TABLE 1. Metal complex equilibrium data*

$\bar{n}$	pL	log K_1	Dev.	$\frac{1}{2}$ log K_1K_2	$\bar{n}$	pL	log K_1	Dev.	$\frac{1}{2}$ log K_1K_2
Co(TQ)					*Ni(TQ)*				
0.376	6.830	5.969	22.839	6.512	0.379	6.749	6.078	34.966	6.455
0.477	6.748	5.933	16.789	6.496	0.481	6.650	6.002	24.245	6.400
0.579	6.682	5.945	13.321	6.487	0.584	6.582	6.040	20.448	6.390
0.680	6.620	5.891	8.785	6.476	0.686	6.512	5.974	13.250	6.371
0.782	6.567	5.940	6.580	6.471	0.788	6.455	6.000	9.432	6.362
0.883	6.510	5.518	1.351	6.459	0.891	6.393	5.701	2.489	6.345
1.188	6.363	5.853	4.663	6.446	1.198	6.236	5.925	7.470	6.323
1.289	6.309	5.890	7.874	6.438	1.300	6.173	6.019	13.931	6.307
1.391	6.259	5.738	7.804	6.438	1.402	6.131	5.741	10.454	6.316
1.492	6.198	5.748	10.483	6.432	1.505	6.059	5.834	16.645	6.300
1.593	6.139	5.568	9.088	6.435	1.607	5.992	5.746	17.658	6.298
1.694	6.045	5.731	16.595	6.417	1.709	5.898	5.762	23.290	6.282
1.795	5.951	5.532	14.432	6.422	1.810	5.795	5.609	22.567	6.284
1.896	5.802	5.187	10.297	6.432					
log K_1 = 5.82					log K_1 = 5.93				
log K_2 = 7.10					log K_2 = 6.75				
σ = 0.02					σ = 0.02				
Cu(TQ)					*Zn(TQ)*				
0.316	10.301	8.781	6.534	9.938	0.381	7.835	6.719	12.437	7.521
0.394	10.240	8.779	5.322	9.935	0.484	7.758	6.633	7.986	7.510
0.478	10.187	8.897	5.597	9.936	0.586	7.703	6.793	8.683	7.512
0.563	10.132	8.642	2.513	9.929	0.689	7.641	6.609	4.196	7.501
0.653	10.090	9.008	4.401	9.933	0.792	7.591	6.693	3.319	7.499
0.743	10.042	8.845	2.198	9.928	0.895	7.537	†	†	7.491
0.836	10.000	9.075	2.333	9.928	1.100	7.447	6.307	0.654	7.491
1.117	9.869	8.985	1.351	9.920	1.203	7.401	6.042	0.732	7.490
1.213	9.826	8.733	1.398	9.920	1.306	7.347	6.535	3.487	7.484
1.308	9.776	9.018	3.949	9.914	1.408	7.299	6.192	2.213	7.487
1.405	9.729	8.810	3.359	9.916	1.511	7.231	6.586	7.113	7.476
1.501	9.669	8.996	6.614	9.908	1.614	7.170	6.319	5.089	7.481
1.599	9.609	8.847	6.092	9.909	1.717	7.072	6.598	12.303	7.463
1.695	9.525	9.009	11.107	9.897	1.819	6.964	6.431	11.661	7.465
1.793	9.431	8.837	10.131	9.900					
log K_1 = 8.91					log K_1 = 6.51				
log K_2 = 10.94					log K_2 = 8.48				
σ = 0.01					σ = 0.01				
Cd(TQ)					*Cu(Phe)*‡				
0.311	7.071	6.306	38.075	6.704	0.460	5.815	†	†	5.553
0.405	6.969	6.252	28.170	6.671	0.480	5.810	3.667	0.779	5.560
0.499	6.889	6.203	20.699	6.650	0.600	5.720	†	†	5.536
0.594	6.826	6.211	16.594	6.639	0.900	5.605	4.754	1.565	5.561
0.688	6.766	6.167	11.418	6.626	1.300	5.420	4.277	1.634	5.554
0.782	6.715	6.199	8.496	6.619	1.330	5.300	5.720	39.497	5.449
0.877	6.657	5.750	1.739	6.603	1.700	4.940	5.635	67.090	5.317
1.159	6.518	6.130	5.314	6.588	1.710	4.870	5.733	75.192	5.255
1.254	6.463	6.219	10.348	6.576	1.900	4.480	5.620	86.734	5.119
1.348	6.418	6.070	10.372	6.576					
1.442	6.362	6.067	13.437	6.568					
1.536	6.306	5.986	14.321	6.566					
1.630	6.233	6.003	18.532	6.555					
1.724	6.155	5.912	19.346	6.553					
1.818	6.042	5.873	23.348	6.542					
log K_1 = 6.14					log K_1 = 5.35				
log K_2 = 7.06					log K_2 = 5.72				
σ = 0.02					σ = 0.08				

*TQ = 2-thienyl-8-hydroxyquinoline.
†Negative values of K_1 in eq. 1.
‡Phe = 2,9-Dimethyl-1,10-phenanthroline.

Can. J. Chem. Downloaded from www.nrcresearchpress.com by 210.87.254.5 on 09/05/12
For personal use only.

Can. J. Chem. Downloaded from www.nrcresearchpress.com by 210.87.254.5 on 09/05/12
For personal use only.

Since the experimental error in pL can, in fact, be intermediate between 0.02 and -0.02 units, the true lower limit for K_1/K_2 for which the successive constants can be evaluated will be somewhat less than $10^{-2.4}$.

The inability to calculate the successive formation constants may also be described as an insensitivity of the equilibrium data to both ligand addition reactions. In metal complex systems for which $K_1/K_2 < 10^{-2.4}$, the formation of the 1:2 metal:ligand complex must ensue immediately upon that of the mono-ligand complex such that both addition reactions appear to act as one:

$$M^{2+} + 2HL \xrightarrow{K_1} [ML^+ + HL + H^+] \xrightarrow{\text{immediate}} ML_2 + 2H^+$$

The equilibrium equation describing this reaction is easily derived from the mathematics for 1:2 metal complex systems for which $K_1 > K_2$ by equating [ML] to zero and is

$$[2] \qquad K_1K_2 = \frac{\bar{n}}{(2-\bar{n})[L]^2}$$

Equation 2 is a convenient method of determining if the successive formation constants can be calculated for a metal complex system. It is easily seen that this equation must fail for those systems in which [ML] is significant. The values of $\frac{1}{2}\log K_1K_2$ as calculated with eq. 2 are shown in Table 1.

The data in Table 1 indicate that eq. 2 does not explain the equilibrium data for the metal 2-thienyl-8-hydroxyquinolinates satisfactorily. A decrease in the $\frac{1}{2}\log K_1K_2$ is observed with increasing $\bar{n}$. For both the Cu and Zn 2-thienyl-8-hydroxyquinolinates, however, this decrease is small (*i.e.*, 0.02 units) and suggests that, perhaps, too great a significance should not be placed on the calculated values of K_1 for these complexes. These K_1 values should be accepted as good approximations only. The greater range in $\frac{1}{2}\log K_1K_2$ for the Co, Ni, and Cd complexes suggests that their calculated K_1 values can be accepted with more confidence.

The Cu(II) complex with 2,9-dimethyl-1,10-phenanthroline is an excellent example of eq. 1 yielding erroneous values of the successive formation constants. It is readily noted that the equilibrium data are distinctly separable into those at $\bar{n} \leqslant 1.3$ for which $K_1/K_2 < 10^{-2.4}$ and those at $\bar{n} > 1.3$ for which normal behavior is observed. Of special importance is the observation that $\log K_1$ for the individual data points at $\bar{n} > 1.3$ is equal to $\frac{1}{2}\log K_1K_2$ at $\bar{n} < 1.3$ which is possible only if $K_1 = K_2$. Such is not the case. It is evident that the inclusion of all the data in the calculation of the successive formation constants by the use of eq. 1 yields erroneous results. The values of the successive formation constants reported for the Cu(II) complex with 2,9-dimethyl-1,10-phenanthroline (1) are incorrect and further study is required. Hawkins and Perrin have previously pointed out several of the difficulties encountered in this complex system (9).

The results of this study clearly illustrate that the calculation of successive formation constants for systems for which $K_1 \leqslant K_2$ requires special precautions due to the increased importance of the experimental error and to the possible insensitivity of the data to both ligand addition reactions. These precautions must also be undertaken in higher ligand:metal complex systems such as the iron complexes with bipyridyl and 1,10-phenanthroline (4) for which $K_3 > K_1, K_2$. For these complexes, $\log K_1$, $\log K_2$, and $\log K_3$ were found to be 4.3, 3.7, and 9.5 and 5.8, 5.2, and 10.0, respectively. The very small ratio of $K_2/K_3 \simeq 10^{-4.8}$ strongly suggests the "instantaneous" formation of the tris-complex upon that of the bi-complex such that the equilibrium data may be insensitive to the second ligand addition reaction. Indeed, an insensitivity of the data to both the first and second ligand addition reactions was found for the 1,10-phenanthroline complex. Furthermore only the overall formation constant β_3 (where $\beta_3 = K_1K_2K_3$) had been reported previously (4).

The value of K_1 was obtained from measurements on solutions containing a large excess of iron (4). The values of $\log K_1K_2$ at the individual data points calculated using the values of K_1 and β_3 above in the equation

$$[3] \qquad \frac{\bar{n}}{(1-\bar{n})[L]} = K_1 + \frac{(2-\bar{n})[L]}{(1-\bar{n})} K_1K_2 + \frac{(3-\bar{n})[L]^2}{(1-\bar{n})} \beta_3$$

are summarized in Table 2. The great frequency with which negative values of K_1K_2 are obtained clearly demonstrates that the value of this

TABLE 2. Iron complex equilibrium data

$\bar{n}$	pL	$\log K_1K_2$	$\bar{n}$	pL	$\log K_1K_2$
*Fe(Bip)**			*Fe(Phe)†*		
0.253	6.143	‡	0.243	7.380	‡
0.315	6.072	‡	0.323	7.340	‡
0.525	6.022	‡	0.480	7.280	‡
0.630	5.959	‡	0.640	7.240	12.01
0.780	5.934	‡	0.760	7.200	‡
1.250	5.882	9.680	1.170	7.120	13.20
1.390	6.860	10.72	1.310	7.050	‡
1.560	5.838	11.29	1.540	7.040	13.08
1.650	5.788	‡	1.800	6.980	‡
1.780	5.818	11.94	1.810	6.970	13.74
1.830	5.770	10.97	2.200	6.870	14.04
2.240	5.680	‡	2.460	6.830	‡
2.450	5.631	‡	2.730	6.720	‡
2.540	5.585	‡	2.840	6.550	13.53
2.740	5.488	‡			
2.850	5.460	‡			

*Bip = Bipyridyl.
†Phe = 1,10-Phenanthroline.
‡Negative values of K_1K_2 in eq. 3.

product cannot be gleaned from the equilibrium data available. Although the results are not shown herein, the values of $\bar{n}$ calculated with the use of the values of the formation constants obtained by Irving and Mellor (4) were unaffected by any terms containing the product K_1K_2. It is quite clear, therefore, that the value of K_2 for the iron complexes with bipyridyl and 1,10-phenanthroline are not obtainable with the data available.

The author wishes to express his thanks to Dr. A. Corsini of Department of Chemistry, McMaster University, for the use of the equilibrium data for the metal 2-thienyl-8-hydroxyquinolinates and to Dr. P. G. Manning of Department of the Environment, for reviewing this manuscript.

1. H. IRVING and D. H. MELLOR. J. Chem. Soc. 5237 (1962).
2. A. CORSINI and E. J. BILLO. Can. J. Chem. **47**, 4655 (1969).
3. F. J. C. ROSSOTTI. Modern coordination chemistry. *Edited by* J. Lewis and R. G. Wilkins. Interscience, New York. 1960, Chapt. 1.
4. H. IRVING and D. H. MELLOR. J. Chem. Soc. 5222 (1962).
5. F. J. C. ROSSOTTI and H. ROSSOTTI. The determination of stability constants. McGraw-Hill, New York. 1961.
6. K. E. JABALPURWALA, K. A. VENKATACHALAM, and M. B. KABADI. J. Inorg. Nucl. Chem. **26**, 1011 (1964).
7. D. G. VARTAK and K. R. MENON. J. Inorg. Nucl. Chem. **33**, 1003 (1971).
8. J. TOPPING. Errors of observations and their treatment. 3rd. ed. Reinhold, New York. 1963.
9. C. J. HAWKINS and D. D. PERRIN. J. Chem. Soc. 1351 (1962).

Can. J. Chem. Downloaded from www.nrcresearchpress.com by 210.87.254.5 on 09/05/12
For personal use only.

A Semi-empirical Analysis of the Electronic Spectrum and Molecular Structure of Formaldehyde

I. ABSAR,[1] C. S. LIN,[2] AND K. L. MCEWEN

Department of Chemistry and Chemical Engineering, University of Saskatchewan, Saskatoon, Saskatchewan

Received July 26, 1971

The electronic transition energies and ionization potentials of formaldehyde have been calculated by a semi-empirical molecular orbital method, using several different ways of evaluating the diagonal matrix elements, in an attempt to adapt the Pariser–Parr–Pople method to the calculation of σ electron properties. The use of theoretically computed penetration integrals in this semi-empirical calculation lead to incorrect relative separation of the π-, σ-, and nonbonding molecular orbital energies, and hence to failure in predicting $n \rightarrow \pi^*$ and $n \rightarrow \sigma^*$ transition energies. A method is developed which reproduces the spectrum of formaldehyde (which includes n–π^*, π–π^*, and n–σ^* electronic transitions) satisfactorily. In paper II of this series, this method is applied to study the spectrum of HCN and CO_2.

Les énergies de transition électronique et les potentiels d'ionisation du formaldéhyde ont été calculés par la méthode semi-empirique des oribitales moléculaires en utilisant diverses méthodes permettant d'évaluer les éléments diagonaux de la matrice, en vue d'adapter la méthode de Pariser–Parr–Pople au calcul des propriétés des électrons σ.

L'utilisation, dans ce calcul semi-empirique, des intégrales de pénétration obtenues par des calculs théoriques, conduit à une séparation incorrecte entre les énergies des orbitales moléculaires π, σ et non-liante et par conséquent à un échec dans la prévision des énergies de transition $n \rightarrow \pi^*$ et $n \rightarrow \sigma^*$.

Une méthode est développée et reproduit de façon satisfaisante le spectre du formaldéhyde, qui comprend les transitions électroniques n–π^*, π–π^* et n–σ^*. Dans le mémoire suivant, cette méthode est appliquée à l'étude du spectre de HCN et de CO_2.

Canadian Journal of Chemistry, **50**, 646 (1972)

Introduction

In order to better understand the spectra of certain compounds of interest to spectroscopists, we have concerned ourselves with the problem of finding suitable molecular wave-functions, so that the various molecular electronic transition energies may be calculated. Theoretical as well as semi-empirical calculations have been done by various workers in attempts to tackle this problem. Theoretically computed transition energies have generally not been in agreement with the observed spectra, the n–π^* transition energies being calculated too low while the π–π^* transition energies being sometimes twice as much as the observed value. In many semi-empirical calculations, on the other hand, the σ electrons have usually been neglected by the use of the Π-approximation. In the few cases where σ electrons have been included in semi-empirical calculations, with the possible exception of the work of Del Bene and Jaffe (1) using a modified CNDO approximation, the results have generally failed to show the correct energy separation between the σ, π, and n (nonbonding) systems of electrons, even though these calculations have proved very successful in the evaluation of π–π^* transition energies. Also, while interpreting results most workers neglect to take into account the fact that the calculated values are for Franck–Condon transitions, and the experimental values quoted are those of the 0–0 transition.

In order to investigate several questions that arise in an application of the semi-empirical method, we have carried out a series of studies on formaldehyde, a compound which has been studied extensively both by theoretical calculations (2–7) and semi-empirical workers (1,8–14) and for which there are ultraviolet spectral and ionization potential data involving σ, π, and nonbonding electrons. We have tried to extend to the σ electron systems, the method developed by Pariser–Parr (15) and Pople (16), and have attempted to achieve the correct relative energy

[1]Present address: Department of Chemistry, Vanderbilt University, Nashville, Tennessee 37203.

[2]Present address: Department of Chemistry, University of Windsor, Windsor, Ontario.

Can. J. Chem. Downloaded from www.nrcresearchpress.com by 210.87.254.6 on 09/05/12
For personal use only.

Can. J. Chem. Downloaded from www.nrcresearchpress.com by 210.87.254.6 on 09/05/12
For personal use only.

separation between the σ, π, and nonbonding molecular orbitals.

Method

Starting from the molecular orbital formulation due to Roothaan (17) and using the LCAO form for the molecular orbitals; *i.e.*

$$[1] \qquad \psi_i = \sum_{\mu=1}^{\infty} \phi_\mu c_{\mu i}$$

where the ϕ_μ are atomic orbital wave-functions, one can write the following secular equations

$$[2] \qquad \sum_{\mu=1}^{\alpha} c_{\mu i}(H_{\mu\nu} - S_{\mu\nu}E_i) = 0,\ \nu = 1, 2, \cdots, \alpha$$

where

$$[3] \qquad S_{\mu\nu} = \int \phi_\mu^* \phi_\nu \, d\tau$$

and

$$[4] \qquad H_{\mu\nu} = \int \phi_\mu^* H \phi_\nu \, d\tau$$

H being the Hamiltonian operator. Neglecting spin–orbit, spin–spin, and relativistic effects one may write out the Hamiltonian for an n-electron system as $H^{\text{core}} + \frac{1}{2}\sum_i^n \sum_j^n 1/r_{ij}$, where H^{core} is the sum of the kinetic and potential energies of all electrons in the field of the core

$$[5] \qquad H^{\text{core}} = \sum_{i=1}^{n} [T(i) + V_{(i)}^{\text{core}}] = \sum_{i=1}^{n} H_{(i)}^{\text{core}}$$

Defining

$$[6] \qquad P_{\eta\delta} = 2\sum_i C_{\eta i}^* C_{\delta i}$$

where i refers to all filled orbitals, and

$$[7] \qquad H_{\rho\sigma}^{\text{core}} = \int \phi_\rho^* \left[\sum_i H_{(i)}^{\text{core}}\right] \phi_\sigma \, d\tau$$

one may write

$$[8] \qquad H_{\rho\sigma} = H_{\rho\sigma}^{\text{core}} + \sum_\eta \sum_\delta P_{\eta\delta}[(\rho\sigma|\eta\delta) - \tfrac{1}{2}(\rho\delta|\eta\sigma)]$$

where

$$[9] \qquad (\rho\sigma|\eta\delta) = \iint \phi_\rho^*(1)\phi_\sigma(1) \frac{e^2}{r_{12}} \phi_\eta^*(2)\phi_\delta(2) \, d\tau_1 \, d\tau_2$$

Adopting the notation that, if ϕ_μ is the atomic orbital under consideration on atom A and is denoted by μ, μ' indicates any atomic orbital on atom A other than ϕ_μ, and ν indicates any atomic orbital on any other atom (ν' is related to ν in the same manner as μ' is to μ) assuming zero overlap and zero diatomic differential overlap (16, 18), one arrives at the following matrix elements from eq. 8

$$[10] \qquad H_{\mu\mu} = H_{\mu\mu}^{\text{core}} + \tfrac{1}{2}P_{\mu\mu}(\mu\mu|\mu\mu) + \sum_{\substack{\mu' \\ (\mu' \neq \mu)}} \{P_{\mu'\mu'}[(\mu\mu|\mu'\mu') - \tfrac{1}{2}(\mu\mu'|\mu\mu')] + P_{\mu\mu'}(\mu\mu|\mu\mu')\} + \sum_\nu \left[P_{\nu\nu}(\mu\mu|\nu\nu) + \sum_{\substack{\nu' \\ (\nu' \neq \nu)}} P_{\nu\nu'}(\mu\mu|\nu\nu')\right]$$

$$[11] \qquad H_{\mu\nu} = H_{\mu\nu}^{\text{core}} - \tfrac{1}{2}P_{\mu\nu}(\mu\mu|\nu\nu)$$

and

$$[12] \qquad H_{\mu\mu'} = H_{\mu\mu'}^{\text{core}} - \tfrac{1}{2}P_{\mu\mu'}[(\mu\mu|\mu'\mu') - 3(\mu\mu'|\mu\mu')]$$

$$[13] \qquad H_{\mu\mu}^{\text{core}} = \int \phi_\mu^* \left[\sum_i \left(\frac{h^2}{8\pi^2 m} V_i^2 + V_{\text{A}}(i) + \sum_{\text{B} \neq \text{A}} V_{\text{B}}(i)\right)\right] \phi_\mu \, d\tau$$

To a first approximation

$$V_{\text{B}}(1) = Z_{\text{B}} \cdot \frac{e^2}{\bar{r}_{1\text{B}}}$$

where Z_{B} is the number of electrons contributed by atom B to the molecular orbital system being calculated; therefore

$$[14] \qquad \int \phi_\mu^* \sum_i V_{\text{B}}(i)\phi_\mu \, d\tau = -\sum_\nu Z_\nu(\mu\mu|\nu\nu)$$

where Z_ν denotes the number of electrons contributed by the atomic orbital ϕ_ν on atom B. More accurately one should add the penetration integral (B:$\mu\mu$) to the right-hand side of eq. 14 in order to take into account the interaction between an electron in ϕ_μ and the neutral atom B.

The penetration integral (B:$\mu\mu$) may be defined by

Can. J. Chem. Downloaded from www.nrcresearchpress.com by 210.87.254.6 on 09/05/12
For personal use only.

[15] $$(\mathrm{B}:\mu\mu) = [b|\mu\mu] + \sum_{\nu} Z_{\nu}(\mu\mu|\nu\nu)$$

where $[b|\mu\mu]$ stands for the nuclear (or atomic core) attraction of atom B for an electron in ϕ_μ.

The rest of the terms in eq. 13 may be defined as

[16] $$\int \phi_\mu^* \left(-\frac{h^2}{8\pi^2 m}\nabla^2 + V_{\mathrm{A}}\right)\phi_\mu \, d\tau = -W_\mu - \sum_{\mu'} z_{\mu'}[(\mu\mu|\mu'\mu') - \tfrac{1}{2}(\mu\mu'|\mu\mu')]$$

where W_μ is the energy of an electron in orbital ϕ_μ of atom A, and as suggested by Pariser and Parr (15), may be approximated by the ionization potential for ϕ_μ of the free atom A.

Calculation

The calculations reported in this paper are all valence electron SCF-LCAO-MO calculations using minimum basis Slater-type orbitals to represent the atomic wave functions.

In the present calculations, the W_μ of eq. 16 were approximated in each case by the appropriate valence state ionization potential involving an electron in the relevant atomic orbital of the free atom.

One-center Coulomb repulsion integrals of the type $(\mu\mu|\mu\mu)$ were evaluated using the Pariser approximation (19)

[17] $$(\mu\mu|\mu\mu) = I_\mu - A_\mu$$

where the relevant ionization potential, I_μ, and electron affinity, A_μ, are determined using atomic data (20). Theoretical values of all two-center electron repulsion integrals were computed from Roothaan's formulae (21). Semi-empirical values of two-center electron repulsion integrals of the type $(\mu\mu|\nu\nu)$ were evaluated by the Parr–Pariser type formula (15).

[18] $$(\mu\mu|\nu\nu) = \tfrac{1}{2}[(\mu\mu|\mu\mu) + (\nu\nu|\nu\nu)] - aR - bR^2$$

in which the parameters a and b are determined for any particular atomic pair by substituting into eq. 18 semi-empirical one-center integrals obtained from eq. 17, and theoretical values for $(\mu\mu|\nu\nu)$ computed for two large internuclear distances.

Penetration integrals were calculated using values of the quantities $[b|\mu\mu]$ and $(\mu\mu|\nu\nu)$ obtained from formulas given by Roothaan (21), and overlap integrals were obtained from the tables of Mulliken *et al.* (22). Since the values of penetration integrals and integrals of the form $(\mu\mu|\nu\nu')$ are relatively small, they were not semi-empirically readjusted, and the effect of neglecting these integrals altogether was investigated.

$H_{\mu\nu}^{\mathrm{core}}$ was equated to the resonance integral $\beta_{\mu\nu}$, and assumed to be directly proportional to the corresponding overlap integral. A value of $\beta_{\mu\nu} = -3.00$ eV was assigned to the resonance integral between π-atomic orbitals of a "standard double bond". This assignment is based on previous experience with ethylene (15) and formaldehyde (9), where the approximate value $\beta_{\mu\nu} = -3.00$ eV gave a satisfactory π–π^* transition energy. For resonance integrals

$$\beta_{\mathrm{XH}} = \tfrac{1}{2}(\beta_{\mathrm{X_2}} + \beta_{\mathrm{H_2}})$$

was used, $\beta_{\mathrm{X_2}}$ and $\beta_{\mathrm{H_2}}$ being evaluated at the internuclear distance R_{XH}.

McLachlan (23) has shown that corrections for the neglect of overlap can be introduced into eq. 10 by using modified core integral $\mathscr{H}_{\mu\mu}^{\mathrm{core}}$ instead of $H_{\mu\mu}^{\mathrm{core}}$, *i.e.*

[19] $$\mathscr{H}_{\mu\mu}^{\mathrm{core}} = H_{\mu\mu}^{\mathrm{core}} - \sum_{\nu} S_{\mu\nu}\beta_{\mu\nu} + \tfrac{1}{4}\sum_{\nu} H_{\nu\nu}^{\mathrm{core}} S_{\mu\nu}^2 + \tfrac{3}{4}\sum_{\nu,\delta} \beta_{\mu\nu} S_{\nu\delta} S_{\mu\delta}$$

where $\mathscr{H}_{\mu\mu}^{\mathrm{core}}$ as defined by eq. 19 implies a change of orbital basis to orthogonalized atomic orbitals (12), whereas $H_{\mu\mu}^{\mathrm{core}}$ is the same integral evaluated in terms of non-orthogonalized atomic orbitals. The effect of including this overlap correction in the diagonal matrix element was investigated.

The basic integrals over atomic orbitals required for formaldehyde are tabulated in Table 1. The molecular geometry for formaldehyde (24) and the coordinate system used are shown in Fig. 1. The z-axis is taken perpendicular to the plane of the paper.

In order to study the objectives as outlined in the introduction several calculations were done using different approximations for the matrix elements. In each calculation the secular equations were set up for both σ and π electron systems, and were brought to self-consistency considering the effect of π-polarity on the σ system and σ-polarity on the π system after each iteration. For this purpose a Fortran IV program was developed to run on the IBM 360-50 computer.

TABLE 1. Basic integrals over atomic orbitals for formaldehyde (eV)*†

Integral	Value	Integral	Value	Integral	Value
$I(s_O)$	32.28	$\beta(x_O c_O)$	−4.33	$(sp\|sp)_C$	2.421
$I(x_O,z_O)$	17.28	$\beta(y_O y_C), \beta(z_O z_C)$	−3.00	$(p\bar{p}\|p\bar{p})_C$	0.636
$I(y_O)$	14.77	$\beta(s_C s_H)$	−5.18	$(ss\|ss)_O$	15.450
$I(s_C)$	21.43	$\beta(x_C s_H)$	+1.43	$(pp\|pp)_O$	14.580
$I(x_C,y_C,z_C)$	11.42	$\beta(y_C s_H)$	−2.79	$(ss\|pp)_O$	15.450
$I(s_H)$	13.595	$(ss\|ss)_C$	12.17	$(pp\|\bar{p}\bar{p})_O$	12.812
$\beta(s_O s_C)$	−5.26	$(pp\|pp)_C$	10.84	$(sp\|sp)_O$	3.365
$\beta(s_C x_O)$	−4.31	$(ss\|pp)_C$	12.17	$(p\bar{p}\|p\bar{p})_O$	0.884
$\beta(s_O x_C)$	−6.46	$(pp\|\bar{p}\bar{p})_C$	9.568	$(ss\|ss)_H$	12.848

*All ionization potentials and electron affinities were obtained from ref. 25.
†2s atomic orbitals on atom A are denoted by the symbol s, and 2p atomic orbitals by the symbol p unless their direction is to be specified, in which case they are denoted by x, y, or z. A bar over p indicates an orbital at right angles to the 2p orbital without a bar.

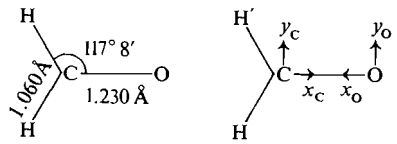

FIG. 1. Molecular geometry (22) and coordinate system for formaldehyde.

Discussion

Using eqs. 10, 11, and 12 as starting points for evaluating the various matrix elements, and employing values of one-center Coulomb repulsion integrals obtained semi-empirically from spectral data (25), several calculations were conducted in order to investigate: (*i*) the relative adequacy of the use of theoretical and semi-empirically adjusted two-center Coulomb repulsion integrals; (*ii*) the effect of neglecting penetration integrals and integrals of the form $(\mu\mu|\nu\nu')$; (*iii*) the effect of including the overlap correction to the diagonal matrix elements; (*iv*) the effect of neglecting resonance integrals for non-adjacent atoms.

It was found that exclusion of penetration integrals resulted in an improvement in the n–π^* transition energy, while inclusion of overlap correction led to a worsening of this number. This may be attributed to the theoretical values of penetration integrals being too large, and if they are to be included, the values should be scaled down semi-empirically. The inclusion of overlap correction implies a re-definition of the basis orbitals used, and it is then no longer consistent to calculate the electron repulsion integrals and penetration integrals using a Slater basis.

The Coulomb repulsion integrals of the type $(\mu\mu|\nu\nu')$ may be neglected without any drastic effects on the n–π^* or n–σ^* transition energies, but the neglect of resonance integrals for non-adjacent atoms improves the values of these transition energies appreciably. This is probably due to the reason that resonance integrals occur in the off-diagonal elements.

When theoretically calculated values are used for all the two-center Coulomb repulsion integrals, the values of n–π^* transition energies are greater than the observed value, while when all of these integrals are semi-empirically adjusted the n–π^* transition energies as well as the n–σ^* transition energies become too low. Good agreement with observed transition energies of all types is obtained when theoretical values of all σ–σ two-center Coulomb repulsion integrals and semi-empirically adjusted values for π–π and σ–π two-center Coulomb repulsion integrals are used. The results of a calculation with Coulomb repulsion integrals so evaluated, and neglecting penetration integrals, resonance integrals between non-adjacent atoms and integrals of the type $(\mu\mu|\nu\nu')$ are given in Tables 2 and 3.

Table 2 compares our orbital energies with those from an *ab initio* study (3) using a similar basis set, and those obtained from the CNDO and INDO methods. The negative of an orbital energy is an approximation to the vertical ionization energy needed to remove an electron from that orbital. Therefore, in the last column of Table 2, we have listed the negative of photoelectron ionization potentials (33). All our predicted ionization potentials on this basis are

Can. J. Chem. Downloaded from www.nrcresearchpress.com by 210.87.254.6 on 09/05/12
For personal use only.

TABLE 2. Orbital energies (eV) and dipole moment (D) for formaldehyde

Symmetry	Molecular orbital	Orbital energy				
		*Ab initio**	CNDO	INDO	This work	Observed†
$3a_1$	σ_1	−38.03	−43.95	−44.81	−35.59	
$4a_1$	σ_2	−22.62	−28.72	−28.31	−25.33	~ −21
$1b_2$	σ_3	−18.39	−24.98	−24.40	−17.98	−16.9
$5a_1$	σ_4	−16.14	−20.32	−18.72	−17.76	−16.0
$1b_1$	π_5	−13.53	−18.55	−18.43	−15.27	−14.4
$2b_2$	σ_6‡	−10.76	−14.53	−13.69	−13.03	−10.86
$2b_1$	π_7	+6.12	+4.22	+4.40	−0.03	
$6a_1$	σ_8	+10.75	+6.23	+5.89	+2.27	
$3b_2$	σ_9	+14.80	+8.67	+8.88	+3.05	
$7a_1$	σ_{10}	+21.89	+12.95	+12.26	+6.75	
Dipole moment		0.554	1.897	1.897	2.347	2.34

*See ref. 3.
†Observed values of orbital energies are photoelectron ionization potentials (33) with negative sign. For observed dipole moment see ref. 26.
‡σ_6 is the nonbonding orbital sometimes indicated by n.

TABLE 3. Electronic spectrum of formaldehyde

State*	Electronic transition energy (eV)		Transition	After configuration interaction between $^1A_1$ states	Oscillator strength		References
	Observed value	Best calculated value			Observed	Calculated	
$^3A_2$	3.6	3.694	$(\sigma_6-\pi_7)$		10^{-5}	0	3, 4, 27
$^1A_2$	4.26	4.104	$(\sigma_6-\pi_7)$		10^{-4}	0	4, 16, 27, 31
$^3B_2$	—	6.437	$(\sigma_6-\sigma_8)$				
$^1B_2$	7.1	7.275	$(\sigma_6-\sigma_8)$		2×10^{-2}	8×10^{-2}	27, 16, 31, 1
$^3A_1$	—	4.796	$(\pi_5-\pi_7)$				
$^1A_1$	8.0	8.174	$(\pi_5-\pi_7)$		0.1–0.5	0.23	32, 31, 1
$^3B_2$	—	—					
$^1B_2$	8.14	—					1
^3C	—	—					
^1C	8.88	—					1
^3D	—	—					
^1D	9.26	—					1
$^3A_1$	—	—					
$^1A_1$	9.58	—	$^1A_1+{}^1A_1^1={}^1A_1^+$	9.597 eV	strong	0.3	1
$^3B_2$	—	—					
$^1B_2$	9.63	—					1
$^3A_1^1$	—	6.681	$(\sigma_6-\sigma_9)$				
$^1A_1^1$	8.0	8.155	$(\sigma_6-\sigma_9)$		0.1–0.5	0.15	31, 1
			$^1A_1-{}^1A_1^1={}^1A_1^-$	6.733 eV	0		
		$^1A_1^+=0.7095{}^1A_1+0.7048{}^1A_1^1$					
		$^1A_1^-=0.7048{}^1A_1-0.7095{}^1A_1^1$					

*The symmetry of states C and D is not yet known.

in fairly good agreement with experiment, and consistently better than those predicted by CNDO and INDO methods. Also, our values are consistently slightly larger in magnitude than the experimental value, as opposed to the *ab initio* values which are sometimes larger and sometimes smaller. Table 2 also shows the dipole moment of formaldehyde. Our calculated value corresponds surprisingly well with the observed value, but this good agreement is probably accidental. However, it does seem safe to conclude that the σ contribution to the dipole moment of formaldehyde (0.104 D) is small as compared to the π-contribution (2.243 D). The

Can. J. Chem. Downloaded from www.nrcresearchpress.com by 210.87.254.6 on 09/05/12
For personal use only.

Can. J. Chem. Downloaded from www.nrcresearchpress.com by 210.87.254.6 on 09/05/12
For personal use only.

main feature which distinguishes our wave functions from the *ab initio*, or CNDO or INDO wave-functions is that our wave-function shows the expected high polarity C^+—O^- of the π-molecular orbital.

Table 3 compares our calculated transition energies with the observed spectrum of formaldehyde. The observed 0–0 bands of the $^1A_1$–$^3A_2$ transition (26, 27) and the $^1A_1$–$^1A_2$ transition 26, 28, 29) have been reported at about 3.12 and 3.5 eV, respectively, while the maximum intensity bands corresponding to the vertical transitions have been estimated to be at 3.6 and 4.26 eV, respectively (30). Our calculated values of 3.694 eV for the $^1A_1$–$^3A_2$ transition and 4.104 eV for the $^1A_1$–$^1A_2$ transition are therefore in very good agreement with the experimental values; much better than those calculated by previous workers. These transitions are forbidden by symmetry but may be made allowed by changes in the geometry of the molecule; they are, however, expected to be weak in intensity. This is confirmed from both the observed and calculated intensities. As these are the n–π^* transitions, we may conclude that we have been able to satisfactorily fix the relative energy separation of the σ system and the π system of electrons.

Most previous workers (2, 6, 9, 12, 30) have assigned the $^1A_1$–$^1B_2$ transition (7.1 eV) to a n–σ^* excitation, and the $^1A_1$–$^1A_1$ transition (8.0 eV) to a π–π^* excitation. Our calculations show a n–σ^* transition at 7.275 eV which has the correct symmetry and the correct order of calculated intensity. Moreover, we have calculated a π–π^* configuration at 8.174 eV and a n–σ^* configuration at 8.155 eV. Both of these configurations have $^1A_1$ symmetry and will therefore mix. A configuration interaction calculation gives a $^1A_1^+$ state at 9.597 eV, which might correspond to the observed $^1A_1$–$^1A_1$ transition observed at 9.58 eV, and a $^1A_1^-$ state at 6.733 eV, which may be obscured by other transitions in the region, since it will be very weak due to cancellation of intensity.

Herzberg (31), following on the lines of Allison and Walsh (32), has assigned all transitions 7.1 eV and above to Rydberg series. This brings us to an interesting question: to what extent may the distinction between Rydberg states and non-Rydberg states be somewhat artificial? It seems from the present work that there could easily be states that from the "united atom" point of view must clearly be considered as Rydberg states, while from the present point of view of the separated atoms, they would not be considered as such.

Conclusion

We have shown that for formaldehyde molecule a semi-empirical calculation of π, σ, and nonbonded electron properties, including electronic spectra, ionization potentials, and dipole moment, can be made using essentially the Pariser–Parr–Pople approach. If penetration integrals are included in the calculation then the σ and π molecular orbitals are stabilized too much relative to the energy of the nonbonding orbital. If corrections to the diagonal matrix elements for neglect of overlap are included as well as penetration integrals, then the results are slightly better than if penetration integrals alone are included. The best results, however, are obtained if neither penetration integrals nor corrections for overlap are included, and the σ–σ Coulomb repulsion integrals are theoretical while the π–π, and σ–π Coulomb repulsion integrals are semi-empirically adjusted.

1. J. Del Bene and H. H. Jaffe. J. Chem. Phys. **48**, 1807 (1968); **48**, 4050 (1968); **49**, 1221 (1968); **50**, 1126 (1969).
2. J. M. Foster and S. F. Boys. Rev. Mod. Phys. **32**, 303 (1960).
3. M. D. Newton and W. E. Palke. J. Chem. Phys. **45**, 2329 (1966).
4. S. Aung, R. M. Pitzer, and S. I. Chan. J. Chem. Phys. **45**, 3457 (1966).
5. N. W. Winter, T. H. Dunning, and J. H. Letcher. J. Chem. Phys. **49**, 1871 (1968).
6. P. L. Goodfriend, F. W. Birss, and A. F. B. Duncan. Rev. Mod. Phys. **32**, 307 (1960).
7. B. Levy. Chem. Phys. Lett. **4**, 17 (1969).
8. T. Anno and A. Sado. J. Chem. Phys. **26**, 1759 (1957).
9. J. W. Sidman. J. Chem. Phys. **27**, 429 (1957).
10. J. A. Pople and J. W. Sidman. J. Chem. Phys. **27**, 1270 (1957).
11. R. D. Brown and M. L. Hefferman. Trans. Faraday Soc. **54**, 757 (1958).
12. J. M. Park and R. G. Parr. J. Chem. Phys. **32**, 1657 (1960).
13. F. L. Pilar. J. Chem. Phys. **47**, 884 (1967).
14. J. A. Pople and G. A. Segal. J. Chem. Phys. **43**, S136 (1965).
15. R. Pariser and R. G. Parr. J. Chem. Phys. **21**, 466 (1953); **21**, 767 (1953).

16. J. A. POPLE. Trans. Faraday Soc. **49**, 1375 (1953).
17. C. C. J. ROOTHAAN. Rev. Mod. Phys. **23**, 69 (1951).
18. K. L. MCEWEN. J. Chem. Phys. **34**, 547 (1961).
19. R. PARISER. J. Chem. Phys. **21**, 568 (1953).
20. H. A. SKINNER and H. O. PRITCHARD. Chem. Rev. **55**, 745 (1955).
21. C. C. J. ROOTHAAN. J. Chem. Phys. **19**, 1445 (1951).
22. R. S. MULLIKEN, C. A. RIEKE, D. ORLOFF, and H. ORLOFF. J. Chem. Phys. **17**, 1248 (1949).
23. A. D. MCLACHLAN. Mol. Phys. **4**, 49 (1961).
24. D. W. DAVIDSON, B. P. STOICHEFF, and H. J. BERNSTEIN. J. Chem. Phys. **22**, 289 (1954).
25. H. A. SKINNER and H. O. PRITCHARD. Chem. Rev. **55**, 745 (1955).
26. J. C. D. BRAND. J. Chem. Soc. 858 (1956).
27. A. D. COHEN and C. REID. J. Chem. Phys. **24**, 85 (1956).
28. H. L. MCMURRAY. J. Chem. Phys. **9**, 231 (1941).
29. H. SPONER and E. TELLER. Rev. Mod. Phys. **13**, 75 (1941).
30. J. W. SIDMAN. J. Chem. Phys. **29**, 644 (1958).
31. G. HERZBERG. Molecular spectra and molecular structure. Vol. 3. Van Nostrand Company, Inc. (1966).
32. K. ALLISON and A. D. WALSH. Chemical Institute of Canada Symposium, Ottawa, 1957.
33. C. R. BRUNDLE and D. W. TURNER. Chem. Commun. 1957. p. 314.

Can. J. Chem. Downloaded from www.nrcresearchpress.com by 210.87.254.6 on 09/05/12
For personal use only.

A Semi-empirical Analysis of the Electronic Spectra and Molecular Structures of Hydrogen Cyanide and Carbon Dioxide

I. ABSAR[1] AND K. L. MCEWEN

Department of Chemistry and Chemical Engineering, University of Saskatchewan, Saskatoon, Saskatchewan

Received July 26, 1971

All valence electron molecular orbital calculations have been carried out on hydrogen cyanide and carbon dioxide using a minimum basis set of Slater-type orbitals by a semi-empirical SCF-LCAO-MO method described earlier for formaldehyde. Since many of the excited states of these molecules are bent, a series of calculations is carried out on hydrogen cyanide in the linear configuration and in bent configurations with H—C—N angles of 150°, 120°, and 90°, and on carbon dioxide in the linear configuration and bent configuration with O—C—O angle of 90°. The binding energy changes in various molecular orbitals on bending are used to interpret electronic spectra and are also compared with Walsh's curves.

Tous les calculs d'orbitales moléculaires d'électrons de valence ont été effectués sur l'acide cyanhydrique et le dioxyde de carbone en utilisant comme base minimum le système d'orbitales du type Slater par une méthode semi-empirique SCF-LCAO-MO décrite précédemment pour le formaldéhyde. Puisque plusieurs des états excités de ces molécules sont courbés, une série de calculs est effectués sur l'acide cyanhydrique dans la configuration linéaire et dans les configurations courbées avec des angles H—C—N de 150°, 120°, et 90° et sur le dioxyde de carbone dans la configuration linéaire et dans la configuration courbée avec un angle O—C—O de 90°. L'énergie de liaison varie suivant la courbure dans les différentes orbitales moléculaires qui sont utilisées pour interpréter les spectres électroniques et sont aussi comparées aux courbes de Walsh.

Canadian Journal of Chemistry, **50**, 653 (1972)

Introduction

Hydrogen cyanide and carbon dioxide are molecules for which there is available a fair amount of spectroscopic data, but there is only limited theoretical work. As many of the excited states of these molecules are highly bent (1–6), and as much of the experimental data are in the form of energies for 0–0 transitions, and also because by the presently available methods it is possible to calculate vertical transition energies only, a series of calculations has been conducted by varying the H—C—N and O—C—O angles in order to get a more comprehensive picture.

The calculations reported in this paper are all valence electron SCF-LCAO-MO calculations using minimum basis set of Slater-type orbitals to represent the atomic wave-functions. The method of calculation is the same as the best method described in the earlier paper on formaldehyde (7). For this method, the diagonal matrix elements $H_{\mu\mu}$ and the off-diagonal elements $H_{\mu\mu'}$ and $H_{\mu\nu}$ of the secular determinant may be represented by:

[1] $$H_{\mu\mu} = -W_\mu + \tfrac{1}{2}P_{\mu\mu}(\mu\mu|\mu\mu) + \sum_{\mu\neq\mu'}(P_{\mu'\mu'} - Z_{\mu'})[(\mu\mu|\mu'\mu') - \tfrac{1}{2}(\mu\mu'|\mu\mu')] + \sum_{\substack{\nu\neq\mu \\ \nu\neq\mu'}}[(P_{\nu\nu} - Z_\nu)(\mu\mu|\nu\nu)]$$

[2] $$H_{\mu\mu'} = -\tfrac{1}{2}P_{\mu\mu'}[(\mu\mu|\mu'\mu') - 3(\mu\mu'|\mu\mu')]$$

and

[3] $$H_{\mu\nu} = \beta_{\mu\nu} - \tfrac{1}{2}P_{\mu\nu}(\mu\mu|\nu\nu)$$

where $P_{\mu\nu}$ provide a description of electron distribution, $(\mu\eta|\nu\delta)$ represent Coulombic integrals of the type

$$\int \mu(1)\eta(1)\frac{e^2}{r_{12}}\nu(2)\delta(2)\,d\tau_1\,d\tau_2$$

The Greek letters μ and ν denote atomic orbitals on Atom A and any other atom B, respectively. The atomic orbitals with a prime, *e.g.*, μ', indicate any atomic orbitals of atom A, other than μ. W_μ is the ionization potential for orbital μ of the free atom A, Z_μ the number of electrons provided by orbital μ, and $\beta_{\mu\nu}$ is the resonance integral.

The basic integrals over atomic orbitals re-

[1]Present address: Department of Chemistry, Vanderbilt University, Nashville, Tennessee 37203.

Can. J. Chem. Downloaded from www.nrcresearchpress.com by 210.87.254.5 on 09/05/12
For personal use only.

TABLE 1. Basic integrals over atomic orbitals* for hydrogen cyanide and carbon dioxide (eV)

Parameter	Value	Parameter	Value	Parameter	Value
I_{s_O}	32.28	$\beta_{\sigma C s_H}$	+3.14	$(sp\|sp)_C$	2.421
$I_{y_O} = I_{z_O}$	17.28	β_{sCs_H}	−5.18	$(ss\|ss)_O = (ss\|pp)_O$	15.450
I_{x_O}	14.77	β_{sCs_N}	−6.60	$(pp\|pp)_O$	14.580
I_{s_C}	21.43	$\beta_{sC\sigma_N}$	−5.50	$(pp\|\bar{p}\bar{p})_O$	12.812
$I_{x_C} = I_{y_C} = I_{z_C}$	11.42	$\beta_{\sigma Cs_N}$	−7.08	$(p\bar{p}\|p\bar{p})_O$	0.884
I_{s_N}	27.50	$\beta_{\sigma C\sigma_N}$	−4.19	$(sp\|sp)_O$	3.365
$I_{x_N} = I_{y_N} = I_{z_N}$	13.83	$\beta_{\pi C\pi_N}$	−4.19	$(ss\|ss)_N = (ss\|pp)_N$	13.710
$\beta_{s_O s_C}$	−5.77	$(ss\|ss)_C = (ss\|pp)_C$	12.17	$(pp\|pp)_N$	12.980
$\beta_{s_O \sigma_C}$	−6.91	$(pp\|pp)_C$	10.84	$(pp\|\bar{p}\bar{p})_N$	11.548
$\beta_{\sigma_O s_C}$	−4.73	$(pp\|\bar{p}\bar{p})_C$	9.568	$(p\bar{p}\|p\bar{p})_N$	0.716
$\beta_{\sigma_O \sigma_C}$	−4.27	$(p\bar{p}\|p\bar{p})_C$	0.636	$(sp\|sp)_N$	2.726
$\beta_{\pi_O \pi_C}$	−3.43			$(ss\|ss)_H$	12.848

*2s atomic orbitals on atom A are denoted by the symbol s, and 2p atomic orbitals by the symbol p unless their direction is to be specified, in which case they are denoted by x, y, z, σ, or π. A bar over p indicates an orbital at right angles to the 2p orbital without a bar.

quired for hydrogen cyanide and carbon dioxide are shown in Table 1. The basic molecular geometry and coordinate system for hydrogen cyanide is shown in Fig. 1 and that for carbon dioxide in Fig. 2; the z axis is perpendicular to the plane of paper in each case.

Discussion

A. Electronic Spectrum of Hydrogen Cyanide

Studies on the ultraviolet spectrum of hydrogen cyanide by Herzberg and Innes (1, 6, 8) and by Bancroft, Hollas, and Ramsay (9) show that the ground state of hydrogen cyanide is linear, and that there are three bent excited states, the

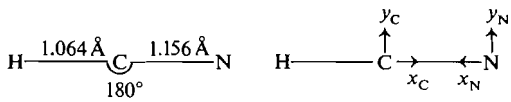

FIG. 1. Molecular geometry (21) and coordinate system for hydrogen cyanide.

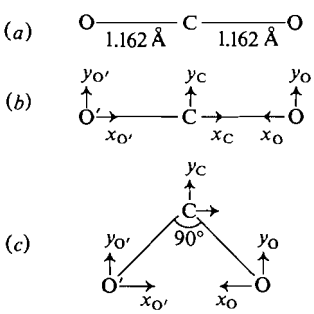

FIG. 2. (*a*) Molecular geometry (22) for CO_2; (*b*) coordinate system for linear CO_2; (*c*) coordinate system for CO_2, hypothetical case with O—C—O angle of 90°.

α state which has symmetry A'' at about 6.5 eV, the β state with symmetry A'' at about 6.8 eV, and the γ state with symmetry A' at about 8.1 eV. Using the orbital diagram given by Walsh (10), the above five workers have identified the α state with the $^1A''$ state which arises from the bending of a linear $^1\Delta$ state (resulting from the π–π^* transition), and the γ state with the $^1A'$ state which arises from the bending of a linear $^1\Pi$ state (resulting from a n–π^* transition); however, they encountered difficulties in assigning the β state because according to Walsh's diagram (Fig. 3) all the other expected bent states have A' symmetry.

Herzberg and Innes (6, 8) have also reported a fourth excited state of hydrogen cyanide at about 8.9 eV, which we shall call the δ state. There is no indication as to whether this δ state is linear or bent and whether it is electronically of A' or A'' symmetry.

From the molecular orbitals for the linear molecule, and the hypothetical bent molecules with HCN bond angles of 150°, 120°, and 90° we have constructed an orbital diagram (Fig. 4) for hydrogen cyanide similar to that of Walsh (Fig. 3) for HAB molecules. The main difference between our results and Walsh's predictions is that the binding energy of the nonbonding orbital σ_3 actually increases with decrease in bond angle instead of decreasing as predicted by Walsh. Moreover, the binding energy of orbital σ_1, instead of remaining constant, also increases slightly with bending; and in the light of our results Walsh's prediction that there would be a large increase in binding energy on bending

Can. J. Chem. Downloaded from www.nrcresearchpress.com by 210.87.254.5 on 09/05/12
For personal use only.

TABLE 2. Electronic spectrum of hydrogen cyanide[a]

Transition	Electronic transition energy (eV) when ∠ HCN = 180°	150°	120°	90°	Symmetry		
$\pi \rightarrow \pi^*$ $^1\Sigma^-$	8.03	8.43	8.15	7.53	(Bent)	A''	β
$\pi \rightarrow \pi^*$ $^1\Delta^\pm$	8.34	7.32	6.15	5.18	(Bent)	A''	α
$\pi \rightarrow \pi^*$ $^1\Sigma^+$	8.34	7.66	5.63	4.23	(Bent)	A'	
	11.80	10.09	10.10	10.10	(Bent)	A'	
$n \rightarrow \pi^*$ $^1\Pi^\pm$	9.29	8.93	8.44	7.60	(Bent)	A'	γ
	9.29	9.40	9.64	9.94	(Linear)	A''	δ?
$\pi \rightarrow \sigma_4^*$ $^1\Pi^\pm$	9.65	10.43	10.14	8.69	(Bent)	A'	δ?
	9.65	9.94	10.49	10.11	(Linear)	A''	
$n \rightarrow \sigma_4^*$ $^1\Sigma^+$	9.39	9.57	10.15	10.45	(Linear)	A'	δ?

[a]The nonbonding orbital denoted in this table by n is σ_3.

of one of the anti-bonding π orbitals seems to be somewhat exaggerated. These differences lead to the conclusion that all four excited states arising from π–π^* excitations are actually stabilized on bending (Table 2), so that there is another bent A'' state arising from the linear π–π^* excitation ($^1\Sigma^+$–$^1\Sigma^-$), which can perhaps be identified with the β state.

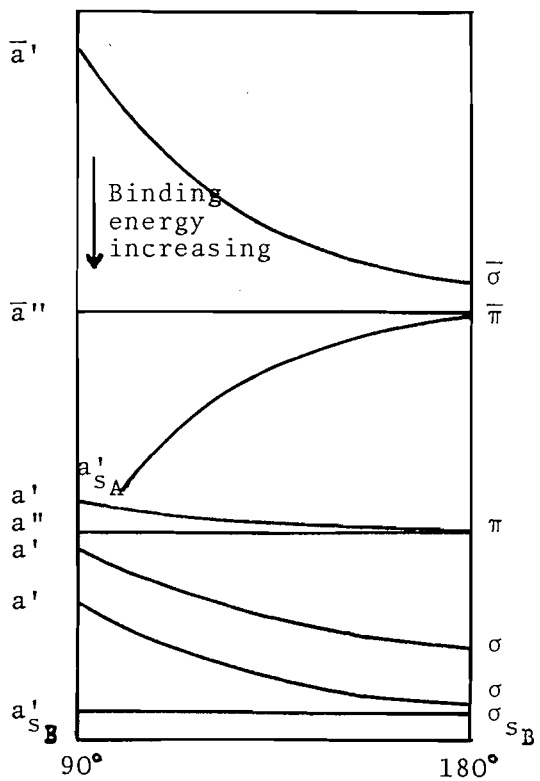

FIG. 3. Orbital diagram for HAB type molecules (from ref. 10).

The calculations for the electronic spectrum of hydrogen cyanide are summarized in Table 2. Note that all observed values of transition energies are for the 0–0 transitions from a linear ground state to a bent excited state, while the calculated values are either from a linear ground state to a linear excited state or from a hypothetical bent ground state to the corresponding bent excited state. This means that the reported

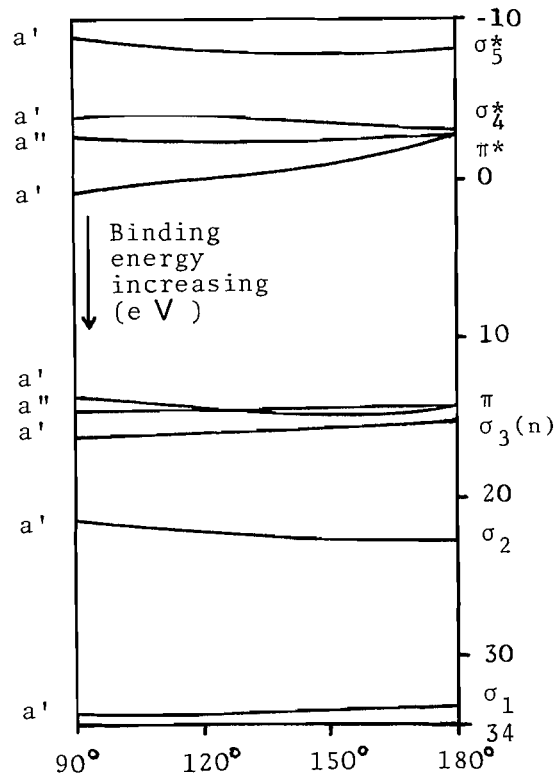

FIG. 4. Orbital diagram for hydrogen cyanide.

Can. J. Chem. Downloaded from www.nrcresearchpress.com by 210.87.254.5 on 09/05/12
For personal use only.

observed values contain an energy contribution equivalent to the energy difference between the linear ground state and the hypothetical bent ground state with the HCN angle corresponding to that of the equilibrium configuration of the excited state, in addition to the energy of transition from the hypothetical bent ground state to the corresponding excited state. Hence the lowest of the calculated values of a certain excitation energy should be slightly lower than the observed 0–0 value. The energies of the α and γ states fit very well with this expectation. The value given for the β state is for DCN, as the data for the corresponding system observed in HCN are rather fragmentary. The correct 0–0 value for the transition energy to the β state of HCN may possibly be slightly higher than for DCN, since the same trend is observed for the α states of HCN and DCN. Furthermore, the calculated value of 7.53 eV, which is higher than the observed 0–0 value for DCN, takes no account of stretching of the CH and CN bonds.

The δ state, if it should be bent and electronically of A' symmetry, could well be accounted for by the $^1A'$ state which results from the bending of the $^1\Pi$ state arising from the π–σ^* transition. If, on the other hand, the δ state is linear, it might arise from either the n–σ^* transition or the n–π^* transition depending on whether it is electronically A' or A'' (Table 2).

We may conclude, therefore, that this procedure of calculation can explain satisfactorily the observed spectral states of hydrogen cyanide to the extent that data are available.

B. Electronic Spectrum of Carbon Dioxide

The orbital diagram constructed from the molecular orbitals for the linear molecule and the hypothetical molecule bent to 90° is shown in Fig. 6 and compared with the general orbital diagram for BAB type molecules drawn by Walsh (11) and reproduced in Fig. 5. In the light of our calculation it appears that Walsh's view of the various changes in the orbital energies upon bending may be rather exaggerated. The main difference between our results and Walsh's predictions is that orbital $4\sigma_g$-a_1 favors a bent conformation instead of highly favoring the linear conformation as predicted by Walsh. Our results indicate that the $2\sigma_u$, $3\sigma_u$, ($1\pi_u$-b_1), $1\pi_g$, $5\sigma_g$ and $4\sigma_u$ orbitals favor the

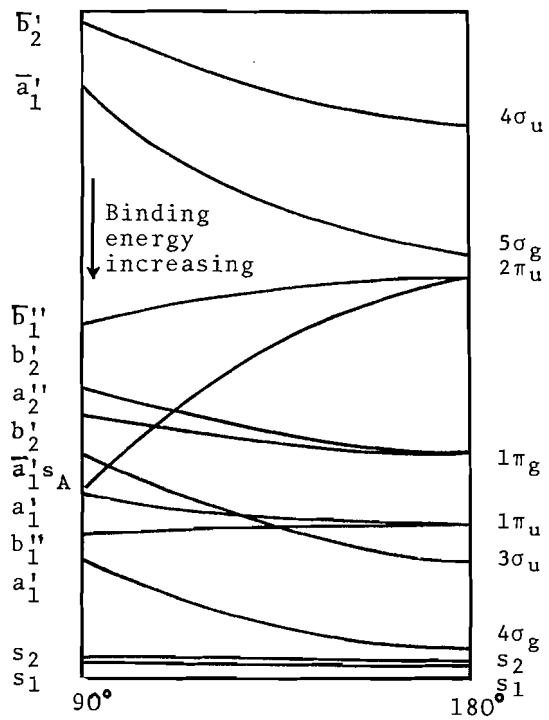

FIG. 5. Orbital diagram for BAB type molecules (from ref. 11).

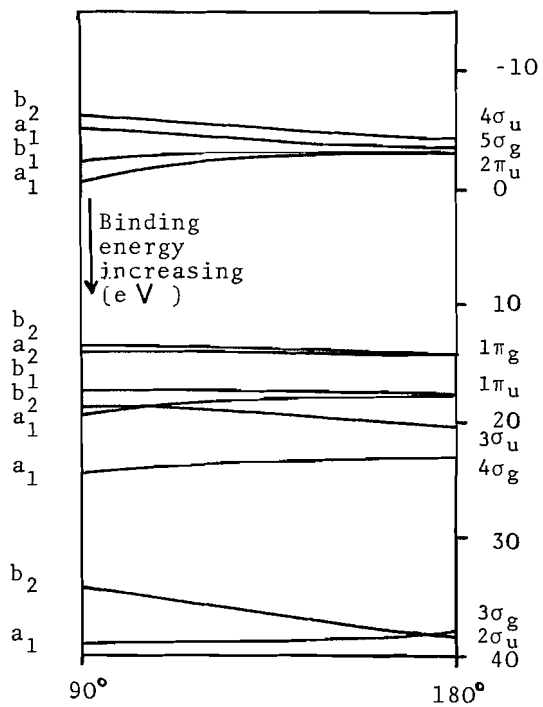

FIG. 6. Orbital diagram for carbon dioxide.

Can. J. Chem. Downloaded from www.nrcresearchpress.com by 210.87.254.5 on 09/05/12
For personal use only.

linear conformation while $3\sigma_g$, $4\sigma_g$, $(1\pi_u\text{-}a_1)$ and $2\pi_u$ orbitals favor the bent conformation. These differences lead to differences between our predictions about the stability of the linear or bent conformations of various states of the molecule and those made according to Walsh's scheme.

Carbon dioxide has been studied theoretically by Mulliken (12–15) and Mulligan (16). Mulliken's approach was to use a rough LCAO approximation coupled with experimental data and semi-empirical evidence. On this basis he predicted the various orbital energies for carbon dioxide (13). Mulligan (16) has conducted a more comprehensive and purely theoretical SCF-LCAO-MO calculation for linear carbon dioxide. The orbital energies obtained by Mulligan and the ones predicted by Mulliken are compared in Fig. 7 with the experimental values and the values obtained by the present semi-empirical SCF-LCAO-MO approach. Our calculation apparently gives the correct order for the orbital energies, in contrast with Mulligan's work where the order of $1\pi_u$ and $3\sigma_u$ orbitals is reversed. Experimental values have been reported by Tanaka, Jursa, and Le Blanc (17) and Tanaka and Ogawa (18).

Carbon dioxide does not show any absorption in the visible and near ultraviolet regions, but in emission, a group of bands is observed between 5000 and 3500 Å. Gaydon (2) suggested that the absence of any absorption bands in the visible and near ultraviolet regions may be due to the fact that the molecule is highly bent in its excited state. A detailed analysis of emission spectrum by Dixon (3) indicates a $^1B_2$ excited state with an O—C—O angle of about 122°; Dixon reports the 0–0 transition to this excited state to be at about 5.7 eV.

Price and Simpson (5) and Inn *et al.* (4) report two 0–0 transitions for the absorption systems between 1390 and 1220 Å to be at 8.99 and 9.06 eV and a vertical transition at about 9.3 eV. All of the bands in this region are weak and probably correspond to forbidden transitions becoming allowed upon bending.

There is a series of bands in the region starting at about 1750 Å and reaching a maximum at 1475 Å (4, 19, 20). The intensities and spacings of the bands are quite irregular. This system of bands is thought to contain a vertical transition at about 8.4 eV. Dixon (3) suggests that the upper state of this vertical transition may be the same as the upper state of the 0–0 transition at 5.7 eV.

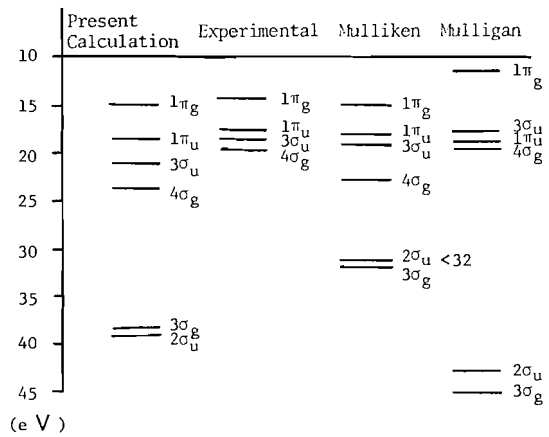

FIG. 7. Ionization energies for the ground state of carbon dioxide molecule. The values from the present calculation are compared with experimental values (17, 18), and those predicted by Mulliken (13), and by Mulligan (16).

Tanaka and Ogawa (18) and Tanaka *et al.* (17) have studied the short wavelength part of the spectrum and have classified transitions in Rydberg series starting at about 11.0 eV and converging to the various ionization potentials of carbon dioxide, and non-Rydberg series with 0–0 transitions at 10.6, 12.0 eV, and others at even higher energy.

Before we proceed to compare our results with the experimental spectrum, it may be of interest to contrast them with those obtained by the purely theoretical calculation of Mulligan (16) (Table 3).

All of our energy values are lower than those obtained by Mulligan for the corresponding transitions. This is what might be expected, since, as was seen for formaldehyde (7) and as is generally found to be the case, purely theoretical calculations give too high energy values for π–π^* and n–π^* transitions, sometimes as much as twice the observed value.

The results of the present calculations for the electronic spectrum of carbon dioxide are summarized in Table 4. The $1\pi_g \rightarrow 2\pi_u$ transition ($^1\Delta$–$^1B_2$) may correspond to the 0–0 transition at 5.7 eV, designated here as the α transition, and which has a bent upper state with $^1B_2$ symmetry, and the transition designated γ at 8.4 eV may correspond to the corresponding forbidden vertical transition; *i.e.*, as predicted by Gaydon

Can. J. Chem. Downloaded from www.nrcresearchpress.com by 210.87.254.5 on 09/05/12
For personal use only.

TABLE 3. Carbon dioxide states: Mulligan's values *vs.* results of this work

Transition and state	Mulligan Energy (eV)	Mulligan Probable form	This work Energy (eV)	This work Probable form	Symmetry in bent form
$1\pi_g \rightarrow 2\pi_u$ $^1\Delta_u^{\pm}$	9.5	Linear	8.72	Bent	$^1A_2$
	9.5	Bent	8.72	Bent	$^1B_2$
$^1\Sigma_u^-$	9.2	Linear	8.87	Bent	$^1A_2$
$^1\Sigma_u^+$	22.1	Linear	11.22	Bent	$^1B_2$
$1\pi_g \rightarrow 5\sigma_g$ $^1\Pi_g^{\pm}$	14.6	Linear	9.10	Linear	$^1A_2$
	14.6	Linear	9.10	Bent	$^1B_2$

TABLE 4. The electronic spectrum of carbon dioxide*

Transition and state	Electronic transition energy (eV) when LOCO = 180°	90°	Symmetry and probable form	Assignment
$1\pi_g \rightarrow 2\pi_u$ $^1\Delta_u^{\pm}$	8.72	6.04	$^1B_2$ (Bent)	γ, α
	8.72	4.87	$^1A_2$ (Bent)	
$^1\Sigma_u^-$	8.87	7.36	$^1A_2$ (Bent)	β?
$^1\Sigma_u^+$	11.22	8.64	$^1B_2$ (Bent)	β?
$1\pi_u \rightarrow 2\pi_u$ $^1\Delta_g^{\pm}$	11.83	8.47	$^1B_1$ (Bent)	β?
	11.83	9.94	$^1A_1$ (Bent)	
$^1\Sigma_g^-$	12.06	12.95	$^1B_1$ (Linear)	
$^1\Sigma_g^+$	12.53	11.64	$^1A_1$ (Bent)	
$3\sigma_u \rightarrow 2\pi_u$ $^1\Pi_g^{\pm}$	14.80	9.33	$^1B_2$ (Bent)	β?
	14.80	12.49	$^1A_2$ (Bent)	
$1\pi_g \rightarrow 5\sigma_g$ $^1\Pi_g^{\pm}$	9.10	8.70	$^1B_2$ (Bent)	δ, β?
	9.10	10.09	$^1A_2$ (Linear)	δ
$1\pi_u \rightarrow 5\sigma_g$ $^1\Pi_u^{\pm}$	12.43	13.49	$^1B_1$ (Linear)	
	12.43	13.48	$^1A_1$ (Linear)	
$3\sigma_u \rightarrow 5\sigma_g$ $^1\Sigma_u^+$	14.07	15.31	$^1B_2$ (Linear)	

*The experimental spectrum contains the following transitions: 0–0 transitions at about 5.7 (designated α), 8.99 (designated β), 9.06 (designated β), 10.56, 10.64, and 11.98 eV; vertical transitions at about 8.4 (designated γ) and 9.3 eV (designated δ); Rydberg transitions at 10.98, 11.05, 11.38, 11.45, 12.31 eV and higher. A series of bands at 7.34, 7.41, 7.46, and 7.53 eV.

(2) and Dixon (3), the upper state of this transition is the same as the upper state of the 0–0 transition at 5.7 eV.

It should be noted that the 0–0 transition energy contains an energy contribution equivalent to the energy difference between the linear ground state and the hypothetical bent ground state, in addition to the energy of the transition from the hypothetical bent ground state to the corresponding excited state. On this basis then, two of the five configurations marked β should correspond to the upper state of the 0–0 transitions observed at 8.99 and 9.06 eV. Assignment with more certainty is not possible at the moment because the symmetry and geometry of the upper bent states of the observed transitions are not known. Three of the states marked β have $^1B_2$ symmetry.

The assignment of the α transition is in accord with the predictions of Walsh (11) and Mulliken (15). Mulliken (15) has assigned the 0–0 bands at 8.99 and 9.06 eV to the π_u–π_u^* transitions with upper states $^1\Delta_g$–$^1A_1$ and $^1\Sigma_g^-$–$^1B_1$; he has rejected Walsh's prediction that either corresponds to the $^1\Sigma_u^+$–$^1B_2$ state of the Π_g–Π_u^* transition on grounds of Mulligan's calculation and also because it is an allowed transition and thus should be intense.

Three of the states marked β, namely $^1\Sigma_u^+$, $^1\Pi_g^+$, and $^1\Pi_g^+$ resulting from $1\pi_g \rightarrow 2\pi_u$, $3\sigma_g \rightarrow$

Can. J. Chem. Downloaded from www.nrcresearchpress.com by 210.87.254.5 on 09/05/12
For personal use only.

$2\pi_u$, and $1\pi_g \rightarrow 5\sigma_g$ transitions, respectively, have $^1B_2$ symmetry in the bent form. Of the other two, $^1\Sigma_u^-$ resulting from $1\pi_g \rightarrow 2\pi_u$ has $^1A_2$ symmetry in the bent form and $^1\Delta_g$ resulting from $1\pi_u \rightarrow 2\pi_u$ has $^1B_1$ symmetry in the bent configuration. Since $^1\Sigma_u^+$ state of the $1\pi_g \rightarrow 2\pi_u$ transitions is an allowed transition and should be strong in intensity and since the observed bands are of weak intensity, it is safe to count this configuration out. However, more exact assignment has to await work on the symmetry of the upper states of these transitions.

The vertical transition designated δ at 9.3 eV may, however, be assigned with some confidence to the $^1\Pi_g^+$ states resulting from the $1\pi_g \rightarrow 5\sigma_g$ transition. If the upper state of this transition is the same as that of one of the transitions marked β, at least one of them may be assigned to the $^1B_2$ state from this transition.

The other higher transition energies calculated by us may correspond with some of the higher energy non-Rydberg series (17, 18) mentioned earlier.

Conclusion

We have shown that the spectra of HCN and CO_2 may be explained, using the same approach as was used earlier for CH_2O(7). The energies of the observed spectral states were explained satisfactorily, and some new assignments proposed. Further spectroscopic work needs to be done to show the reliability of our results. Two general conclusions that may be drawn from our work are that in any meaningful calculation of electronic spectra, it is not safe to ignore the σ electrons, and that in interpretation of spectra using Walsh's diagrams, it should be recognized that some of the predicted trends may be exaggerated.

1. G. HERZBERG and K. K. INNES. Can. J. Phys. **35**, 842 (1957).
2. A. G. GAYDON. Proc. Roy. Soc. **176A**, 505 (1940).
3. R. N. DIXON. Proc. Roy. Soc. **275A**, 431 (1963); Discuss. Faraday Soc. **35**, 105 (1963).
4. E. C. Y. INN, K. WATANABE, and M. ZELIKOFF. J. Chem. Phys. **21**, 1648 (1953).
5. W. C. PRICE and D. M. SIMPSON. Proc. Roy. Soc. **169A**, 501 (1939).
6. G. HERZBERG. Molecular spectra and molecular structure. Vol. 3. Van Nostrand Company, Inc.
7. I. ABSAR, C. S. LIN, and K. L. McEWEN. Can. J. Chem. This issue.
8. G. HERZBERG and K. K. INNES. To be published.
9. J. L. BANCROFT, J. M. HOLLAS, and D. A. RAMSAY. Can. J. Phys. **40**, 322 (1962).
10. A. D. WALSH. J. Chem. Soc. 2290 (1953).
11. A. D. WALSH. J. Chem. Soc. 2268 (1953).
12. R. S. MULLIKEN. Phys. Rev. **40**, 60 (1932).
13. R. S. MULLIKEN. J. Chem. Phys. **3**, 720 (1935).
14. R. S. MULLIKEN. Rev. Mod. Phys. **14**, 204 (1942).
15. R. S. MULLIKEN. Can. J. Chem. **36**, 10 (1958).
16. J. F. MULLIGAN. J. Chem. Phys. **19**, 347 (1951).
17. Y. TANAKA, A. S. JURSA, and F. J. LE BLANC. J. Chem. Phys. **32**, 1199 (1960).
18. Y. TANAKA and M. OGAWA. Can. J. Phys. **40**, 879 (1962).
19. S. W. LIEFSON. Astrophys. J. **63**, 73 (1926).
20. P. G. WILKINSON and H. L. JOHNSTON. J. Chem. Phys. **18**, 190 (1950).

Can. J. Chem. Downloaded from www.nrcresearchpress.com by 210.87.254.5 on 09/05/12
For personal use only.

Second Cross Virial Coefficients of Carbon Tetrachloride – Gas Mixtures Determined from Solubility Measurements at High Pressures[1]

S. K. GUPTA AND A. D. KING, JR.

Department of Chemistry, University of Georgia, Athens, Georgia 30601

Received August 31, 1971

The solubility of carbon tetrachloride in compressed helium, hydrogen, nitrogen, argon, methane, carbon dioxide, and ethylene has been measured over pressure ranges of 1–60 atm at temperatures ranging from −10 to 75 °C. Second cross virial coefficients representing carbon tetrachloride – gas interactions are evaluated from the data. It is shown that when allowance is made for the effects of quantum deviations and quadrupolar interaction on the critical temperatures and volumes of helium, hydrogen, and carbon dioxide, respectively, ordinary combining rules produce pseudocritical parameters which reduce all of the measured cross virial coefficients to a single function of reduced temperature. When reduced on a Boyle point basis, it is found that the data are best represented by virial coefficients corresponding to a 7-28 Mie type potential or a Kihara core potential having a core radius somewhat smaller than the carbon–chlorine bond length in carbon tetrachloride.

La solubilité du tétrachlorure du carbone dans l'hélium, l'hydrogène, l'azote, l'argon, le méthane, le dioxyde de carbone et dans l'éthylène comprimés a été mesurée, dans des domaines de pressions situés entre 1 et 60 atm, à des températures entre −10 à 75 °C. On a évalué les seconds coefficients croisés du viriel, qui représentent les interactions entre le tétrachlorure de carbone et le gaz, à partir des données. On démontre que, lorsque sont permis les effets de déviations quantiques et d'interaction quadrupolaire sur les volumes et températures critiques de l'hélium, de l'hydrogène et du dioxyde de carbone, respectivement, les règles ordinaires de combinaison produisent des paramètres pseudo-critiques qui réduisent tous les coefficients croisés du viriel en une fonction simple de température réduite. Quand on les réduit en se basant sur un point de Boyle, on trouve que les données sont mieux représentées par des coefficients du viriel correspondant à un type de potentiel 7-28 de Mie ou à un potentiel de noyau de Kihara ayant comme rayon du noyau une valeur sensiblement plus faible que la longueur de liaison chlore-carbone dans le tétrachlorure de carbone.

Canadian Journal of Chemistry, **50**, 660 (1972)

Introduction

Second cross virial coefficients are a potentially valuable source of information about the nature of intermolecular forces, both physical and chemical, that exist between molecules of different species in the gas phase.[1] They offer a considerable advantage over pure component virial coefficients as a means for studying intermolecular forces in that they allow one to investigate changes in potential energy brought about by selectively varying one member of a pair of interacting molecules while holding the other constant. This advantage is offset to some extent by the increased experimental difficulties encountered in making accurate determinations of cross virial coefficients of gaseous mixtures. In addition, second cross virial coefficients share a weakness common to all virial coefficients in that there is a wide range of temperature, encompassing the Boyle point, over which these coefficients are almost totally insensitive to the shape of the potential energy function describing the intermolecular interaction (2). Unfortunately, these temperature ranges often coincide with temperatures readily accessible in the laboratory.

Mixtures involving globular molecules such as the carbon tetrahalides, neopentane, etc., with simple gases are particularly attractive systems for studying intermolecular interactions between dissimilar molecules by virtue of the simple geometries involved. In a recent study of such a system, Douslin and co-workers determined very accurate values for the second cross virial coefficients of the tetrafluoromethane–methane system over temperatures spanning the Boyle point (3). They found that when reduced using pseudocritical constants derived from combining rules first propounded by Guggenheim and McGlashan (4), the cross virial coefficients did not satisfy the principle of corresponding states but rather deviated in a manner similar to that found for mixtures of neopentane, tetramethylsilane, and sulfur hexafluoride with methane (5). When the CF_4–CH_4 data were reduced on a Boyle point basis, however, the reduced cross virial coefficients followed the same corresponding states curve as

[1] An excellent review on this subject can be found in ref. 1.

Can. J. Chem. Downloaded from www.nrcresearchpress.com by 210.87.254.42 on 09/05/12
For personal use only.

Can. J. Chem. Downloaded from www.nrcresearchpress.com by 210.87.254.42 on 09/05/12
For personal use only.

those of the respective pure components. The Boyle point parameters of the CF_4–CH_4 system differed from the pseudo-Boyle point parameters generated using simple combining rules in a manner predicted by Hamann, who interpreted this as resulting from difference in shape of the potential functions describing the interaction between globular molecules and that for the small gas molecules (5).

In order to examine the nature of mixed interactions more fully, second cross virial coefficients of a related compound, carbon tetrachloride, with a series of light gases, have been determined from solubility measurements of CCl_4 in the respective gases. By limiting these measurements to systems involving one large globular molecule with a series of small gas molecules, geometric factors affecting the intermolecular potential can be expected to be reasonably constant, thus providing a more detailed picture regarding the role the smaller molecule plays in such interactions.

The experiments themselves are based upon the fact that the solubility of a liquid in a compressed gas is determined by two factors: variations in the fugacity of the liquid phase caused by hydrostatic pressure and dissolved gas, and deviations from ideal behavior in the fugacity of the liquid component in the gas phase. At the pressures of these experiments, concentrations of dissolved gas in the liquid phase are quite low so that the liquid phase exhibits ideal solution behavior. However, in the gas phase, deviations from ideality caused mainly by pair interactions between molecules of the liquid component and those of the gas are often quite significant. As a consequence, measurements of solubilities of liquids in compressed gases can be used to provide accurate values of second cross virial coefficients representing such deviations from ideality.

Experimental

The experimental technique used here for determining the solubility of CCl_4 in compressed gases is a modification of the method used by Prausnitz and Benson (6) and is described in detail in ref. 7. The method entails saturating the gas to be studied with CCl_4 vapor under pressure and subsequently expanding the high pressure vapor–gas mixture into a low pressure system where the CCl_4 vapor is removed from the gas stream by a series of cold traps maintained at -80 to -70 °C depending on the gas studied. The volume of the gas accompanying the vapor is measured with a wet test meter. In these experiments, the amounts of CCl_4 collected were relatively large, ranging from 0.5 to 8 g depending upon the temperature and duration of each run. The weights of CCl_4 collected in each cold trap were routinely examined to monitor the efficiency of the traps. The amount found in the last of the three traps averaged 0.4% and never exceeded 2% of the total weight collected. Before calculating mole fractions, each value for total weight recorded was corrected for losses of CCl_4 vapor under the assumption that the gas exiting the last trap was in equilibrium with solid CCl_4. These corrections seldom exceeded 1% except for the lowest temperature measurements (-10 °C) with hydrogen and helium where the calculated losses ranged up to 15% of the total CCl_4 trapped. In the lowest temperature runs with hydrogen, small but measurable amounts of water, as an impurity, were trapped out along with the CCl_4. Rather than prepurifying the hydrogen, impurity levels of water in the hydrogen were measured by passing large samples of the gas alone through the trapping section and the low temperature data for CCl_4 with hydrogen were corrected accordingly. The maximum correction occurred at -10 °C where it was estimated that 7% of the total weight collected was due to water vapor impurities in the hydrogen. At temperatures greater than 0 °C, the larger mole fractions of CCl_4 vapor made such corrections unnecessary. If each of these corrections is assumed correct to within 10%, the combined error in measured mole fraction amounts to about 2% for hydrogen at -10 °C. This has the effect of approximately doubling the error in second cross virial coefficient values over that found at higher temperatures.

Initial data taken at each temperature were examined for variations of measured CCl_4 concentration with flow rate indicating incomplete saturation. It was found that three equilibrium cells in series were necessary to insure saturation up to 25 °C, while two cells were sufficient for higher temperatures. Similarly, no trends with pressure were found in the cross virial coefficients calculated from the mole fraction data taken at different pressures.

The hydrocarbon gases used in these experiments (CP grade) were obtained from Matheson Co. Inc. The other gases, helium, hydrogen, nitrogen, and argon, were obtained from Selox Corp., having quoted purities of 99.995, 99.9, 99.9, and 99.995%, respectively. Reagent grade carbon tetrachloride was used in all experiments.

Results and Discussion

Under conditions where the concentration of gas dissolved in liquid carbon tetrachloride, X_1, is low, the vapor concentration of CCl_4, expressed as mole fraction Y_2, in equilibrium with the liquid phase is related to the total pressure P, by (6, 7)

$$[1] \quad Y_2 = \frac{(1 - X_1)P_2^0}{P}\left(\frac{\phi_2^0}{\phi_2}\right)\exp\left[\frac{V_2^{0(L)}(P - P_2^0)}{RT}\right]$$

Here $V_2^{0(L)}$ and P_2^0 are the molar volume and saturated vapor pressure of liquid CCl_4 at temperature T while ϕ_2^0 and ϕ_2 represent the fugacity coefficients of pure CCl_4 vapor and

Can. J. Chem. Downloaded from www.nrcresearchpress.com by 210.87.254.42 on 09/05/12
For personal use only.

CCl_4 vapor in the dense gas, respectively. If contributions from third and higher virial coefficients are neglected, the fugacity coefficient of CCl_4 in a gaseous mixture can be expressed as

$$[2] \quad \ln \phi_2 = 2/V[Y_2 B_{22}(T) + Y_1 B_{12}(T)] - \ln Z$$

where Y_1 represents the mole fraction of diluent gas in the gas phase, V is the molar volume of the gas mixture, and the symbols $B(T)$ denote second virial coefficients representing deviations from ideality caused by pair interactions between species designated by the subscripts. Z is the compressibility factor for the gaseous mixture.

It is seen from eq. 1 that any given experimental measurement of the mole fraction of carbon tetrachloride vapor in some diluent gas at a known temperature and pressure and a knowledge of the liquid phase composition under these conditions are sufficient to evaluate the ratio of fugacity coefficients ϕ_2^0/ϕ_2. The second cross virial coefficient for this particular CCl_4–gas system can then be determined from this ratio through an iterative procedure using eq. 2 and a trial value of $B_{12}(T)$ in the appropriate virial expansions for V and Z to make initial estimates of these quantities. In the computations used here, gas fugacities along with

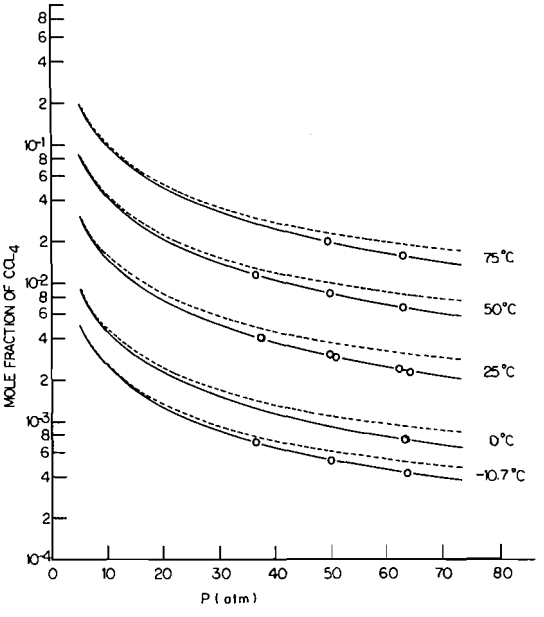

FIG. 1. Mole fraction of CCl_4 in helium as a function of pressure.

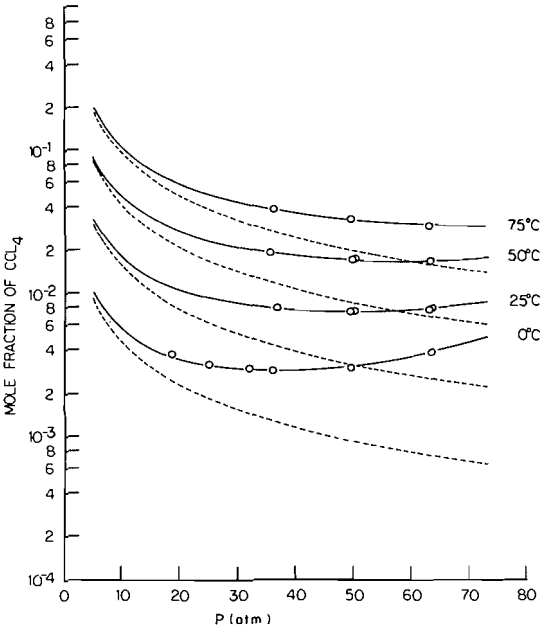

FIG. 2. Mole fraction of CCl_4 in methane as a function of pressure.

Henry's law constants obtained from data found in refs. 8 and 9 were used to calculate the mole fractions of dissolved gas, X_1 of eq. 1, as a function of pressure for the various gases used. In the case of helium for which no such data are available, it was assumed that the solubility of He in CCl_4 is the same as that in the physically similar liquid benzene (9). Because of the exceedingly low solubility of helium in these solvents, this approximation does not introduce any significant error in values of $B_{12}(T)$ derived from the experimental data. Values of pure component second virial coefficients used in eq. 2 are found in refs. 10–17.

The experimentally determined mole fractions of carbon tetrachloride vapor with the various gases studied are not tabulated here for the sake of brevity.[2] However, the data for two CCl_4–gas systems are shown graphically in Figs. 1 and 2. These systems were chosen because they illustrate the two limiting types of behavior exhibited by gaseous mixtures at high pressures. In Fig. 1, measured mole fractions of CCl_4 in He are compared with the hypothetical concentration of

[2]Tabular data are available from the Depository of Unpublished Data, National Science Library, National Research Council of Canada, Ottawa, Canada K1A 0S2.

Can. J. Chem. Downloaded from www.nrcresearchpress.com by 210.87.254.42 on 09/05/12
For personal use only.

TABLE 1. Second cross virial coefficients for CCl_4 with various gases

Gas	Temperature (°C)	$B_{12}(T)$*
He	−10.7	+37±5
	0	+46±4
	25	+61±4
	50	+56±2
	75	+59±2
H_2	−10.7	−20±5
	0	−8±5
	25	−6±4
	50	+9±5
	75	+27±5
N_2	0	−132±4
	25	−102±4
	50	−91±2
	75	−64±2
Ar	0	−155±3
	25	−124±2
	50	−100±2
	75	−77±2
CH_4	0	−252±8
	25	−205±4
	50	−174±3
	75	−129±5
C_2H_4	0	−457±10
	25	−384±7
	50	−299±5
	75	−248±3
CO_2	25	−287±7
	50	−213±5
	75	−185±7

*Error expressed as average deviation from mean.

CCl_4 that would exist if intermolecular forces were absent (calculated from eq. 1 letting $\phi_2^0/\phi_2 = 1$). It is seen that helium suppresses the vapor concentration, indicating that repulsive interactions exert a dominant role at these temperatures. In the case of CCl_4 with methane, Fig. 2, the opposite is true. Here attractive forces prevail, resulting in a significant enhancement of CCl_4 vapor concentration.

Second cross virial coefficients for the various carbon tetrachloride – gas mixtures have been calculated from the experimental mole fraction data and average values of these $B_{12}(T)$ are listed in column 3 of Table 1. With the exception of the −10 °C data discussed previously, the error limits quoted represent the average deviation from the mean. The cross coefficients are shown graphically in Fig. 3 along with values obtained previously by Prausnitz and Benson (6) for CCl_4 with H_2, N_2, and CO_2 at the higher temperatures. With the exception of nitrogen, the agreement between the data is seen to be reasonably good.

When compared with the data of Table 2, it is seen that with the exception of CO_2, the cross virial coefficients become more negative as the critical temperature and molecular polarizability of the gas increase as might be expected for mixed systems in which dispersion forces represent the dominant mode of attraction. The fact that CO_2 seems to have an unusually high critical temperature in comparison with the other gases, particularly ethylene, in Table 2, has been noted previously (18). This stems from the fact that carbon dioxide differs from the other gases of Table 2 in that its molecules, while not highly polarizable, possess a large quadrupole moment, so that angle dependent quadrupolar interactions play a significant role in determining its critical properties. As a result, experimental critical constants of CO_2 do not accurately reflect the extent to which carbon dioxide interacts with other molecules of systems in which dispersion forces predominate. It is possible, however, to make estimates of the critical temperature and volume that carbon

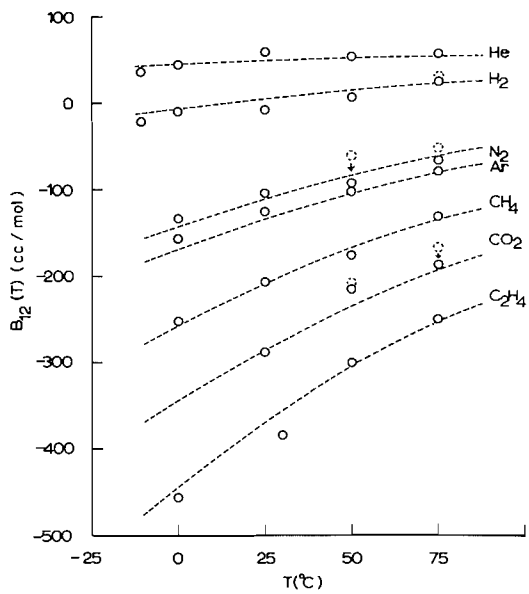

FIG. 3. Second cross virial coefficients of CCl_4 with He, H_2, N_2, Ar, CH_4, CO_2, and C_2H_4. Dashed lines correspond to curve described by reduced cross virial coefficients in Fig. 4. Broken circles denote values from ref. 6.

TABLE 2. Critical constants and molecular parameters

Substance	T^c (°K)*	V^c (cc/mol)	$\frac{P^cV^c}{RT^c}$	Average polarizability ($\alpha \times 10^{25}$ cm^3)†	Quadrupole Moment ($\theta \times 10^{26}$ e.s.u. cm^2)‡
He	5.25(13.0)§	57.8(31.2)	0.300	2.16	—
H_2	34.15(47.7)§	65.0(47.0)	0.304	7.9	+0.662
N_2	126.15	90.1	0.292	17.6	−1.52
Ar	151.15	75.3	0.291	16.3	—
CH_4	190.05	99.0	0.290	26.0	—
CO_2	304.15(241)‖	94.0(108)	0.287	26.5	−4.3±0.3
C_2H_4	283.05	123.6	0.291	42.6	+1.5
CCl_4	556.35	276	0.272	105	—

*Critical constant data are taken from ref. 33.
†Data taken from ref. 34.
‡Recommended values from ref. 35. Ethylene is assumed to be axially symmetric.
§Critical constants in parentheses for He, H_2, are "classical" values derived from reduced critical constants found in ref. 23.
‖Critical constants in parentheses for CO_2 reflecting dispersion contributions only from ref. 36.

dioxide would exhibit if quadrupolar interactions were absent using equations developed by Rowlinson and Cook (19, 20):

$$[3] \qquad T_e^c = T_0^c(1 + 2\delta^c)$$

$$[4] \qquad V_e^c = V_0^c(1 - \delta^c)$$

These equations relate the hypothetical critical temperature T_0^c, and volume V_0^c, that CO_2 would possess if dispersion forces alone were operative, to the corresponding experimentally determined properties T_e^c and V_c^c. The parameter δ^c, which serves as a measure of the importance of quadrupole–quadrupole forces relative to dispersion forces at the critical point has been assigned a value of 0.13 on the basis of independent thermodynamic data (18, 20). This value has been shown to be consistent with the directly measured value of the molecular quadrupole moment of carbon dioxide (21). Values for the hypothetical critical constants T_0^c and V_0^c, estimated from eqs. 3 and 4 with $\delta^c = 0.13$, are listed in parentheses after the experimental values for carbon dioxide. It is seen that they are intermediate with the values for methane and those of ethylene, as are the cross virial coefficients for this system.

A similar situation exists in the case of hydrogen and helium in that quantum effects significantly influence the physical properties of these substances at their critical points. For this reason, the experimental critical constants of these substances are inappropriate for correlating intermolecular interactions at higher temperatures where classical statistics prevail. "Classical" values for the critical constants of these compounds which do not reflect quantum effects can be readily derived by requiring that "classical" and experimental values for each critical constant be proportionate to the corresponding reduced quantities listed by de Boer (22). This procedure has an advantage over that used by Prausnitz *et al.* (23) for the purposes here in that no assumption is made regarding the critical compressibility factor in arriving at a classical estimate for the critical volume, although the values derived by each method are substantially the same. Classical values for critical temperatures and volumes of hydrogen and helium obtained in this manner are listed in parentheses in Table 2.

Figure 4 shows the graph that results when the data of Table 1 are plotted in reduced form using pseudocritical temperatures T_{12}^c, and volumes V_{12}^c, constructed according to the simple combining rules:

$$[5] \qquad T_{12}^c = (T_1^c T_2^c)^{1/2}$$

and

$$[6] \qquad V_{12}^c = \tfrac{1}{8}[(V_1^c)^{1/3} + (V_2^c)^{1/3}]^3$$

using quadrupole and quantum corrected critical constants for CO_2, He, and H_2. It is seen that the reduced cross virial coefficients correlate well in describing a single function of reduced temperature. The fact that the CO_2 data fall on this curve when the quadrupole corrected critical constants are used indicates that angle dependent interactions between CO_2 and CCl_4 make no

Can. J. Chem. Downloaded from www.nrcresearchpress.com by 210.87.254.42 on 09/05/12
For personal use only.

Can. J. Chem. Downloaded from www.nrcresearchpress.com by 210.87.254.42 on 09/05/12
For personal use only.

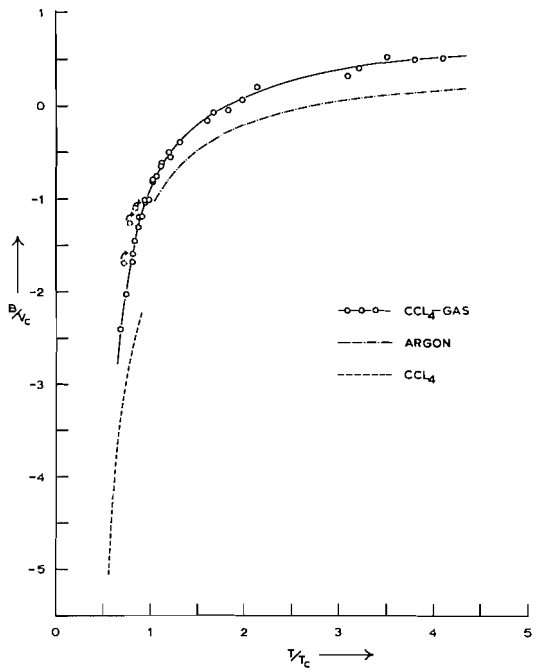

FIG. 4. Reduced virial coefficients as a function of reduced temperature. Broken circles denote CCl_4–CO_2 data reduced with uncorrected critical constants for CO_2.

significant contribution to the intermolecular potential energy. This is to be expected considering the weakness and short range nature of quadrupole – induced dipole and quadrupole–octupole forces. The broken lines shown in Fig. 4 represent the curves described by reduced pure component virial coefficients of CCl_4 and argon (taken as typical of the gases). Values recommended by Dymond and Smith (24) were used to generate these curves. It is apparent, as found by Hamann, Douslin, and co-workers (5, 3), that the virial coefficients for the mixed systems do not satisfy the principle of corresponding states but rather are displaced towards lower reduced temperatures from the pure component data.

Combining rules other than eqs. 5 and 6 were tested with these data under the assumption that a constant proportionality exists between the critical constants T^c and V^c and the respective molecular parameters ε and r^{*3} for all the pure substances involved; ε and r^* being the energy and distance parameters characterizing the interaction potentials of these pure substances. No improvement in the correlation among reduced cross virial coefficients resulted from using the Hudson and McCoubrey combining rule (25)

$$T_{12}^c = (T_1^c T_2^c)^{1/2} \frac{2(I_1 I_2)^{1/2}}{I_1 + I_2} \frac{2^6 V_1^c V_2^c}{[(V_1^c)^{1/3} + (V_2^c)^{1/3}]^6}$$

where I_i is the ionization potential of component i, and a decidedly poorer correlation resulted when the Fender and Halsey rule (26)

$$T_{12}^c = \frac{2T_1^c T_2^c}{T_1^c + T_2^c}$$

was used. Likewise, the use of a geometric mean combining rule for V_{12}^c (27) did not affect the scatter of data. The fact that neither the Hudson and McCoubrey combining rule nor the geometric mean combining rule for V_{12}^c affect the correlation among the reduced cross virial coefficients of the various CCl_4–gas pairs is not surprising considering the ratio of V_{12}^c calculated from a geometric mean to V_{12}^c of eq. 6 varies by only 15% in going from helium to ethylene.

Since the reduced virial coefficient data of Fig. 4 extend through the Boyle point, one can recast these data on a Boyle point reduction basis. In Fig. 5, the second cross virial coefficients

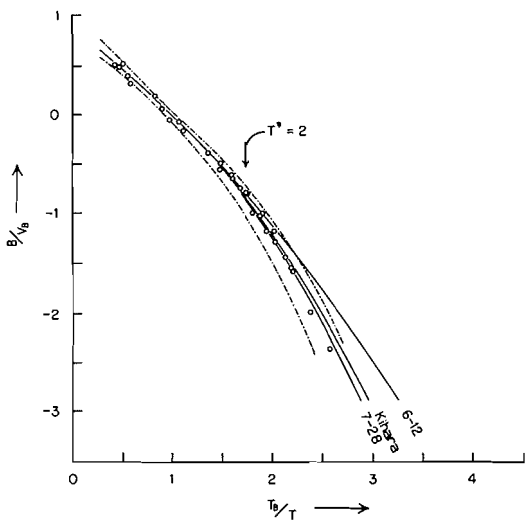

FIG. 5. Experimental data and virial coefficients calculated from various potentials reduced on a Boyle point basis. Dashed lines represent error bounds for the experimental data estimated from the standard error in the ratios relating Boyle point parameters to pseudocritical constants.

Can. J. Chem. Downloaded from www.nrcresearchpress.com by 210.87.254.42 on 09/05/12
For personal use only.

reduced with the Boyle volume, $B_{12}(T)/V^{B}_{12}$, are shown plotted as a function of reciprocal reduced temperature. The transformation from Fig. 4 to Fig. 5 requires knowledge of the ratios V^{B}_{12}/V^{c}_{12} and T^{B}_{12}/T^{c}_{12}, where the Boyle temperature, T^{B}_{12}, is defined to be the temperature at which $B_{12}(T) = 0$ for a mixed system and the Boyle volume, V^{B}_{12}, is defined as

$$V^{B}_{12} = T\frac{dB_{12}(T)}{dT}\bigg|_{T=T_B}$$

These ratios were obtained through a least squares fit of a second degree polynomial to $B_{12}(T)/V^{c}_{12}$ data expressed as a function of T^{c}_{12}/T, yielding values of

$$T^{B}_{12}/T^{c}_{12} = 1.78 \pm 0.06$$

and

$$V^{B}_{12}/V^{c}_{12} = -(T^{c}_{12}/T)\frac{d(B_{12}(T)/V^{c}_{12})}{d(T^{c}_{12}/T)}\bigg|_{B_{12}(T)/V^{c}_{12}=0}$$

$$= 1.02 \pm 0.11$$

The family of curves in Fig. 5 represents the temperature dependence of reduced virial coefficients generated by various spherically symmetric potential functions. These curves clearly illustrate the point made by Klein (2) that second virial coefficients offer little discrimination between potential functions at temperatures greater than

$$T^* = T/(\varepsilon/k)_{6-12} = 2$$

The combining rules, eqs. 5 and 6, used to reduce the cross virial coefficients in Figs. 4 and 5 are, of course, empirical in nature. However, the fact that the reduced cross virial coefficients correlate well with the calculated curves over the entire range in the insensitive region ($T^* > 2$) of Fig. 5, gives one some confidence that they, in particular the combining rule for temperature, are appropriate for generating pseudoconstants representative of the energy and distance parameters of the interaction potential for dissimilar pairs. Outside the region of insensitivity (at temperatures lower than $T^* = 2$), the reduced cross virial coefficients describe a curve which approximates that generated by a 7-28 potential more closely than that of the more traditional 6-12 potential. Cross virial coefficients reduced using the Hudson–McCoubrey combining rule and those reduced using eq. 5 are indistinguishable within experimental error when recast on a Boyle point basis.

According to Pitzer's interpretation of the principle of corresponding states (28) in order for virial coefficients of a given class of compounds to correlate as a function of temperature: (*a*) the interactions between molecules must be described by a two-parameter potential function of the form

[7] $$\phi_{12}(r) = \varepsilon f(r^*/r)$$

with r^* and ε being distance and energy parameters characterizing the minimum of the potential well and, (*b*) the function, $f(r^*/r)$, must be the same for all members of a particular class. Since the data of Fig. 5 correlate well outside as well as inside the region of insensitivity, it can be inferred that carbon tetrachloride – gas interactions are adequately described by a single potential function of the form above and that a constant proportionality exists between the pseudocritical constants T^{c}_{12}, V^{c}_{12} of eqs. 5 and 6 and the corresponding molecular parameters ε, r^{*}[3], independent of the nature of the gas.

In previous studies concerning the properties of gaseous systems containing globular molecules, Hamann and co-workers (5, 29) proposed a specific potential function which is applicable, in principle, to these CCl_4–gas systems. According to this model, it is assumed that the overall interaction of two quasi-spherical molecules, or one such molecule and a small gas molecule, can be approximated by summing individual atom–atom interaction energies (assumed to be 6-12) and averaging the resulting potential over all orientations of the respective molecules. If it is assumed that the carbon tetrachloride and gas molecules differ in size to the extent that the polyatomic gases can be treated as being effectively monatomic in nature,[3] then according to the Hamann model, the potential function for the CCl_4–gas pairs becomes

[8] $$\frac{\phi_{12}(r)}{\varepsilon} = \left[C_1 + \frac{1}{5}\left(\frac{r^*}{\rho}\right)F_{10}\left(\frac{r^*}{r}\right)\right]\left(\frac{r^*}{r}\right)^{12} - \left[2C_1 + \left(\frac{r^*}{\rho}\right)F_4\left(\frac{r^*}{r}\right)\right]\left(\frac{r^*}{r}\right)^{6}$$

[3]This assumption is supported by the nearly identical values of the critical compressibility factors of the non-quadrupolar heavier gases; C_2H_4, CH_4, N_2, and Ar listed in Table 2.

Can. J. Chem. Downloaded from www.nrcresearchpress.com by 210.87.254.42 on 09/05/12
For personal use only.

where

$$F_n\left(\frac{r^*}{r}\right) \equiv \left\{ \frac{\left[1 - C_2\left(\frac{r^*}{r}\right)\right]^{-n}}{\left(\frac{r^*}{r}\right)} - \frac{\left[1 + C_2\left(\frac{r^*}{r}\right)\right]^{-n}}{\left(\frac{r^*}{r}\right)} \right\}$$

and

$$C_1 = \frac{\varepsilon'}{\varepsilon} \qquad C_2 = \frac{\rho}{r^*}$$

Here ρ is the carbon–chlorine bond distance in CCl_4 (taken to be 1.77 Å), r^* and ε are the force constants describing the interaction of gas molecules with the peripheral chlorine atoms of CCl_4, with ε' being the force constant characterizing interactions involving the central carbon atom and the gases.

Equation 8 satisfies the conditions outlined by Pitzer provided, (*a*) C_1 and C_2 are independent of the nature of the gas and (*b*) ε and r^{*3} are proportional to T^c_{12} and V^c_{12}, respectively. The London formulation of dispersion forces suggests that it is reasonable to expect C_1 to be constant; furthermore for values of C_1 ranging between 0 and 2, the overall potential function is almost totally insensitive to the value assigned to C_1. Thus, according to this model, CCl_4 molecules behave as if they consist only of chlorine atoms distributed symmetrically about the center of mass so that only parameters characterizing the chlorine atoms and their distribution in space are significant in determining the shape of the overall potential. The ratio, C_2, is just such a parameter and, as expected, the shape of the potential well of eq. 8 is considerably more sensitive to changes in this parameter. It is difficult to see how C_2 can remain constant independent of the gas involved since estimates of r^* based on collision radii listed in ref. 30 suggest that C_2 might be expected to vary some 30% in going from helium to ethylene. Nevertheless it will be assumed on the basis of the correlations in Figs. 4 and 5 that r^* takes on a constant value, taken to be 3.3 Å, the arithmetic mean of the van der Waals radius of the chlorine atom listed by Hildebrand (31) and that for argon found in ref. 30. It is seen in Fig. 6 that the potential function of eq. 8, calculated with

$$C_2 = \frac{1.77 \text{ Å}}{3.3 \text{ Å}} = 0.54$$

and C_1 equal to unity, indeed more nearly approximates the 7-28 potential than the broader well of the 6-12 potential. It is also seen in Fig. 6 that a Kihara core potential of the form

$$[9] \qquad \phi(r) = \varepsilon\left[\left(\frac{r^*}{r-a}\right)^{12} - 2\left(\frac{r^*}{r-a}\right)^{6}\right]$$

where a denotes the core radius of CCl_4, also approximates the 7-28 and Hamann potentials when the ratio $a/r^* = 0.413$. A comparison of this ratio to the ratio $\rho/r^* = 0.54$ of eq. 8 taken as typical for these CCl_4–gas systems indicates that a core radius 25% shorter than the C—Cl bond length is appropriate for describing these mixed interactions. This "shrinkage" reflects the effect of multiple attractions by peripheral chlorine atoms which are absorbed by the core radius when the Kihara core model is used to represent carbon tetrachloride–gas interactions. This decrease in core radius is virtually identical to that predicted (28) and later found (32) by Pitzer and Danon for interactions between globular molecules themselves. This suggests

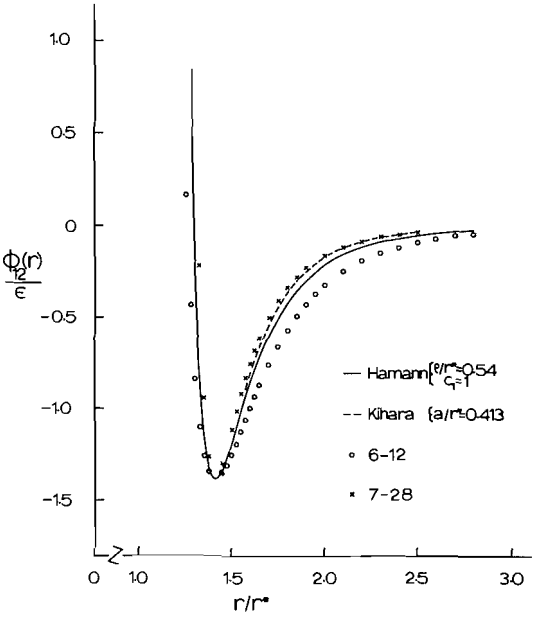

FIG. 6. Potential functions generating reduced second virial coefficients denoted by solid lines in Fig. 5.

that while less shrinkage occurs in globular molecule – gas interactions than when two globular molecules interact, it is accommodated by one rather than two cores, with the result that the core radii characterizing the globular molecule in these two types of systems are the same. Thus, through such cancellation effects, core radii take on the role of a true molecular parameter for the types of systems considered here.

This work was supported by the National Science Foundation

1. E. A. MASON and T. H. SPURLING. The virial equation of state. The international encyclopedia of physical chemistry and chemical physics. Topic 10, Vol. 2. Pergamon Press, New York. 1969.
2. M. KLEIN. J. Res. Natl. Bur. Stand. A, **70**, 259 (1966).
3. D. R. DOUSLIN, R. H. HARRISON, and R. T. MOORE. J. Phys. Chem. **71**, 3477 (1967).
4. E. A. GUGGENHEIM and M. L. MCGLASHAN. Proc. Roy. Soc. London, A, **206**, 448 (1951).
5. S. D. HAMANN, J. A. LAMBERT, and R. B. THOMAS. Aust. J. Chem. **8**, 149 (1955).
6. J. M. PRAUSNITZ and P. R. BENSON. A.I.Ch.E.J. **5**, 161, (1959).
7. C. R. COAN and A. D. KING, JR. J. Chromatogr. **44**, 429 (1969).
8. G. JUST. Z. Phys. Chem. **37**, 342 (1901).
9. J. HORIUTI. Sci. Pap. Inst. Phys. Chem. Res. Tokyo, **17**(341), 125 (1931).
10. J. D. LAMBERT, G. A. H. ROBERTS, J. S. ROWLINSON, and V. J. WILKINSON. Proc. Roy. Soc. A, **196**, 113 (1949).
11. W. G. SCHNEIDER and J. A. H. DUFFIE. J. Chem. Phys. **17**, 751 (1949).
12. A. MICHELS and M. GOUDEKET. Physica, **8**, 347 (1941).
13. A. MICHELS, H. WOUTERS, and J. DE BOER. Physics, **1**, 587 (1934).
14. D. R. DOUSLIN, R. H. HARRISON, R. T. MOORE, and J. P. MCCULLOUGH. J. Chem. Eng. Data, **9**, 358 (1964).
15. A. MICHELS and M. GELDERMANS. Physica, **9**, 967 (1942).
16. A. MICHELS, HUB. WIJKER, and HK. WIJKER. Physica, **15**, 627 (1949).
17. A. MICHELS and C. MICHELS. Proc. Roy. Soc. A, **153**, 201 (1935).
18. A. D. KING, JR. J. Chem. Phys. **49**, 4083 (1968).
19. D. COOK and J. S. ROWLINSON. Proc. Roy. Soc. London, A, **219**, 405 (1951).
20. J. S. ROWLINSON. Trans. Faraday Soc. **50**, 647 (1954).
21. A. D. KING, JR. J. Chem. Phys. **51**, 1262 (1969).
22. J. DE BOER. Physica, **14**, 139 (1948).
23. R. D. GUNN, P. L. CHUEH, and J. M. PRAUSNITZ. A.I.Ch.E.J. **12**, 937 (1966).
24. J. H. DYMOND and E. B. SMITH. The virial coefficients of gases. Clarendon Press, Oxford. 1969.
25. G. H. HUDSON and J. C. MCCOUBREY. Trans. Faraday Soc. **56**, 761 (1960).
26. B. E. F. FENDER and G. D. HALSEY, JR. J. Chem. Phys. **36**, 1881 (1962).
27. R. J. GOOD and C. J. HOPE. J. Chem. Phys. **53**, 540 (1970).
28. K. S. PITZER. J. Am. Chem. Soc. **77**, 3427 (1955).
29. S. D. HAMANN and J. A. LAMBERT. Aust. J. Chem. **7**, 1 (1954).
30. J. O. HIRSCHFELDER, C. F. CURTISS, and R. B. BIRD. Molecular theory of gases and liquids. John Wiley and Sons, Inc., New York. 1934. Append. 1-A.
31. J. H. HILDEBRAND. J. Chem. Phys. **15**, 727 (1947).
32. F. DANON and K. S. PITZER. J. Chem. Phys. **36**, 425 (1962).
33. K. A. KOBE and R. E. LYNN. Chem. Rev. **52**, 117 (1953).
34. H. A. LANDOLT and R. BÖRNSTEIN. Zahlenwerte und Functionen. 6th ed. Springer, Berlin. 1951. Vol. 1, Pt. 1, p. 401; Pt. 2, p. 509.
35. D. E. STOGRYN and A. P. STOGRYN. Mol. Phys. **24**, 1002 (1956).
36. H. BRADLEY, JR. and A. D. KING, JR. J. Chem. Phys. **52** (6), 2851 (1970).

Can. J. Chem. Downloaded from www.nrcresearchpress.com by 210.87.254.42 on 09/05/12
For personal use only.

2,4-Diazapentadienes. I. Prototropy, Cyclization, and Addition–Elimination

D. H. HUNTER AND S. K. SIM
Department of Chemistry, University of Western Ontario, London, Ontario

Received August 26, 1971

The preparations and reactions of a series of 1,3,5-triaryl-2,4-diaza-1,3-pentadienes (**1**) have been investigated. Products of cyclization (**2** and **4**), prototropy **3** and addition–elimination (**5**, **6**, and **7**) have been characterized. Also, the preparations and reactions of **3**, a new isomer of **1**, have been studied.

Les préparations et les réactions d'une série de triaryl-1,3,5 diazo-2,4 pentadiènes-1,3 (**1**) ont été étudiées. Les produits de cyclisation (**2** et **4**) de prototropie **3** et d'addition–élimination (**5**, **6**, et **7**) ont été caractérisés. On a également étudié les préparations et les réactions de **3**, un nouvel isomère de **1**.

Canadian Journal of Chemistry, **50**, 669 (1972)

Introduction

It was noted as early as 1837 (1) that benzaldehyde reacts with ammonia to produce the unique trimeric product, hydrobenzamide **1***a*. The observation of the isomerization of hydrobenzamide upon heating to form amarine **2***a* was reported in 1844 (2). While benzaldehyde was the first material studied, the generality to aromatic aldehydes of both these reactions was soon established.[1] A third isomer, isoamarine **4***a*, obtained by treatment of amarine under basic conditions was recognized in 1859 (4). The structural assignments came later (5). Since early investigations, hydrobenzamides **1** have been studied as gasoline antioxidant agents (6), as chelating agents (7), and for chemiluminescence properties (8). Similarly amarines **2** and isoamarines **4** have been studied for chemiluminescence (9), as precursors to the *d*-, *l*-, and *meso*-stilbene-diamines (10) and to the lophines (11).

The mechanism of formation of the hydrobenzamides **1** has received some attention (12), but the conversion of the hydrobenzamides **1** to amarines **2** has been essentially neglected (13). During the course of an investigation of this latter process, it has been possible to extend our understanding of the structures and reactions of these and related compounds. It is this aspect which is presented here and the mechanistic details of the hydrobenzamide **1** to amarine **2** interconversion are in the following article (14).

[1]For example, one of the earliest *chemical* works of Alexander Borodin reported on the reactions of the "cuminols" to form the isopropyl substituted hydrobenzamide and amarine. (3)

Results and Discussion

The preparations, structures, and reactions of the 1,3,5-triaryl-2,4-diaza-1,4-pentadienes (**1**) and of its isomers will be discussed and will be presented under separate headings for each isomer. Details of n.m.r. and i.r. spectra are to be found in the Experimental.

1,3,5-Triaryl-2,4-diaza-1,4-pentadienes (1)

Preparative procedures for **1** with various substituents have been numerous but all involve in essence the reaction of an aromatic aldehyde with ammonia with yields in the 50–80% region. As a complicating feature, **1** is prone to base-catalyzed reactions and thus the more acidic derivatives (*e.g.* **1***c* and *d*) must be generated under buffered conditions.

A rigorous structure assignment for **1** has not been made but only one geometric isomer of **1** has been obtained for each. Since the n.m.r. spectrum shows but one type of azomethine proton (15), the most likely configuration for **1** is the *anti,anti* form; *syn–anti* interconversions should be slow (16).

The reactions of **1** are summarized in Scheme 1 and can be placed in three categories: prototropy, addition–elimination, and cyclization. The cyclization reaction of **1**, as mentioned in the Introduction, was one of the first reactions observed but had long been considered a thermal reaction. The catalytic effect of amide ion had been noted but only in passing (17). We have found that there is indeed a relationship between reagent base strength and reaction rate consistent with base-catalysis. Thus the following provide preparative conditions for

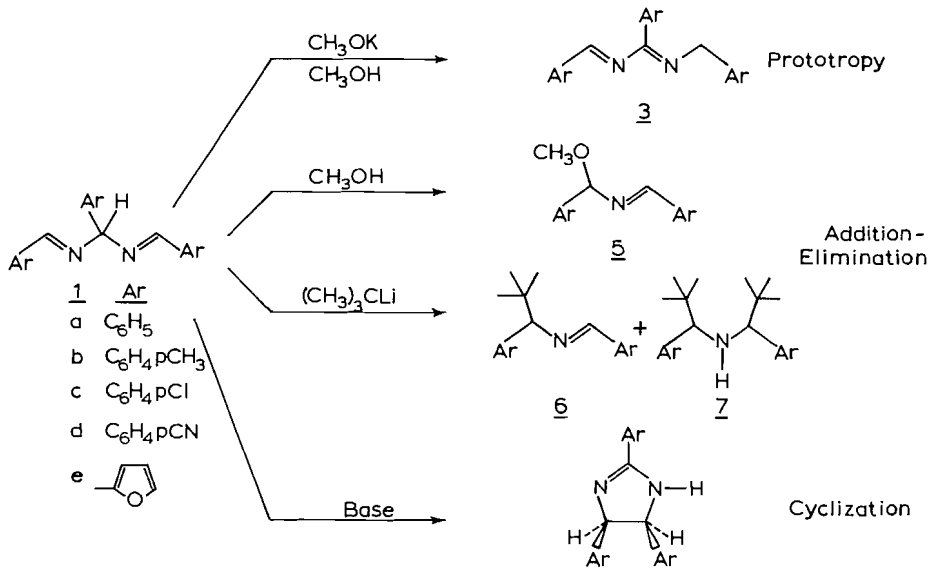

SCHEME 1

2*a*: 0.5 *M* potassium *t*-butoxide–*t*-butanol at 25°, 0.1 *M* potassium amide–ammonia at −30°, and 0.8 *M* phenyllithium–THF at −80°.

The effect of substituents on **1** is also indicative of base-catalysis. Whereas the phenyl compound **1***a* reacts slowly at −80° with phenyllithium–THF, the *p*-cyanophenyl compound **1***d* reacts rapidly at −130°. The sensitivity of **1** to base is important preparatively; the *p*-chlorophenyl **1***c* and *p*-cyanophenyl **1***d* compounds are prepared under buffered conditions to avoid subsequent cyclization of the products.

A unique feature of the reaction of **1***a* with potassium methoxide–methanol was the observation of a fourth and new isomer of **1** produced in significant amounts (~50%). This compound **3** apparently arises from a base-catalyzed 1,3-proton shift and the chemistry of **3** will be discussed further under a separate heading.

In contrast to the reaction in potassium methoxide–methanol, when **1***a* is refluxed in methanol for moderate periods of time, good yields (~70%) of *N*-benzylidene-α-methoxybenzylamine (**5**) are obtained. This would appear to be an acid-catalyzed reaction since **5** is not observed under basic conditions even when the base-catalyzed reactions are proceeding slowly. The overall reaction can be viewed as addition of methanol and elimination of benzaldehyde imine although the detailed process is probably more complicated.

Another marked change in reaction pathway occurs when comparing the reactions of phenyllithium and *t*-butyllithium. When **1***a* is treated with phenyllithium in THF at −80°, the only observable[2] product is **2***a*. However, with *t*-butyllithium in threefold excess in THF at −80° an 88% yield of *N*,*N*-di-(α-*t*-butylbenzyl)-amine **7** was obtained. The mixture of diastereomers was in the ratio of 12 to 1 as judged by n.m.r. With 1 equiv of *t*-butyllithium, 60% of *N*-benzylidene-α-*t*-butylbenzylamine (**6**) could be observed by n.m.r. and a 22% yield of α-*t*-butylbenzylamine could be isolated after hydrolysis. Thus the relative rates of the proton abstraction and addition reactions of **1***a* change by a factor of about 10^3 when changing from phenyllithium to *t*-butyllithium.

Complicated structure–reactivity relationships are observed for the addition reactions of organolithiums to carbon–carbon double bonds and have been interpreted in terms of varying states of aggregation and varying reactivity of the reagent (18). The ability of the nitrogen lone pair in **1** to act as a Lewis base towards the organolithium aggregates may well enhance the addition reactions relative to the proton abstraction reaction of the more agglomerated *t*-butyllithium and result in the observed changes.

[2]As much as 0.5% of the addition–elimination product analogous to **6** may be produced.

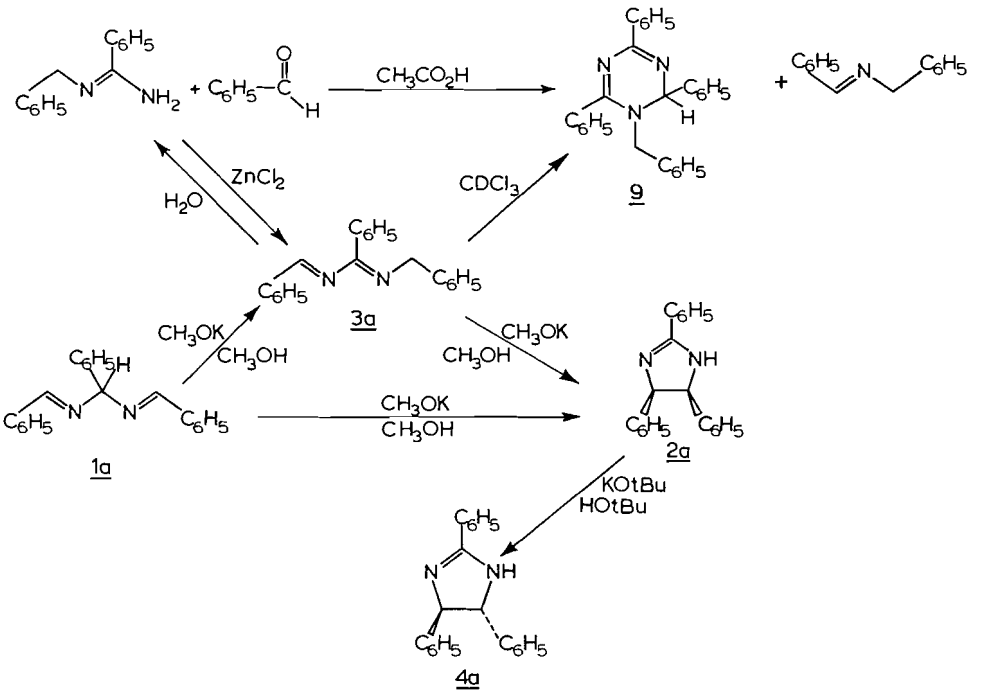

SCHEME 2

1,3,5-Triaryl-2,4-diaza-1,3-pentadienes (3)

Examples of the C=N—C=N system are rare (19) and the observation of the base-catalyzed interconversion of **1***a* to **3***a* is the first example of prototropy in a 2,4-diazapentadiene system. The cyclization and prototropy of **1***a* are in close competition in CH_3OK–CH_3OH at 60° and **3***a*/**2***a* are produced in a ratio of 0.9. Both **3***b* and *c* have also been observed by n.m.r. when **1***b* and *c* were reacted in methanol–methoxide and the ratio of prototropy to cyclization proved to depend upon the substituent. Thus **3***b*/**2***b* were produced in a ratio of 1.2 and **3***c*/**2***c* in 0.5. While both **2** and **3** are also isomerized by base (Scheme 2) the conditions required are more severe than for the isomerization of **1**. Thus **3***a* reacts about 10^3 slower than **1***a* in CH_3OK—CH_3OH at 60° and **2***a* requires refluxing KO*t*Bu–HO*t*Bu.

The structure of **3***a* was deduced by i.r., n.m.r., mass spectrum, combustion analysis, and was verified by an independent synthesis. The structures of **3***b* and *c* were assigned on the basis of their n.m.r. spectra and by isolation of the *p*-substituted *N*-benzylbenzamidines after hydrolysis. The configuration is presumably *anti,anti*.

Distinctly different reactions are observed for **3***a* when it is treated with acid or with base. Base leads to cyclization with exclusive formation of **2***a*, whereas under apparently acidic conditions **3***a* appears to be converted to a triazine derivative **9** and *N*-benzylidenebenzylamine. The structure of **9** was verified by an independent synthesis. Experimentally **9** was observed as the decomposition product of **3***a* when n.m.r. samples were allowed to stand (*e.g.* $CDCl_3$ for three days) and **3***a* is the probable intermediate in the conversion of N-benzylidenebenzylamine and benzaldehyde into **9** when refluxed with acetic acid in benzene (Scheme 3).

2,4,5-Triarylimidazolines (2 and 4)

The preparative reactions for the *cis*-4,5-diarylcompounds (**2**, amarines) and the *trans*-4,5-diarylcompounds (**4**, isoamarines) are interesting from both a synthetic and a mechanistic point of view since each is formed quite selectively (<1 and <5% of the other cyclic isomer, respectively). Thus each diastereomer is obtained cleanly and in reasonable yield even though the preparations of both involve base-catalysis. The preparation of **2** from **1** requires

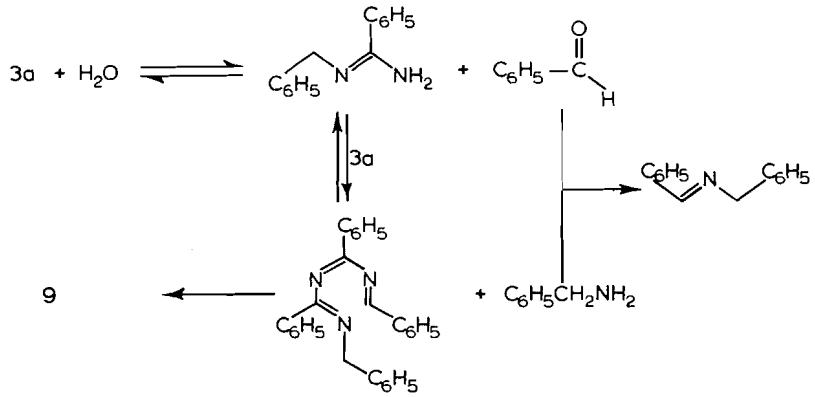

SCHEME 3

mildly basic conditions which depend upon the nature of the aromatic substituent while **4** is produced from **2** using considerably more vigorous conditions (*e.g.* KO*t*Bu–HO*t*Bu at reflux). Both **2** and **4** are sensitive to air oxidation which results in the production of lophines and thus the reactions must be carried out in an inert atmosphere.

The conversion of **2** to **4** by equilibration with base possibly involves the carbanion generated by abstraction of the benzylic proton. As expected **4** (*trans*-aryl groups) is greatly favored in the equilibrium mixture. Solutions of either **2** or **4** in 0.41 *N* potassium *t*-butoxide–*t*-butyl alcohol were heated to 100° for 18 and 30 h respectively, and then analyzed by n.m.r. The same mixture was obtained from either; 4% of **2** and 96% of **4**. The mechanism of the conversion of **1** to **2** is the subject of the following article.

The assignment of the configurations of **2** and **4** has been most rigorously demonstrated for amarine **2***a* and isoamarine **4***a*. The structure proofs have involved degradation to the stilbenediamines (10), synthesis from the stilbenediamines (5*a*) and, most convincingly, resolution of **4***a* (5*b*). As the results in Table 1 show, the methine–methine proton coupling constants for the *N*-benzoyl derivatives of **2***a* and **4***a* strongly support the assigned structures (20) and thus provide a basis for assignments to the other examples of **2** and **4**. A satisfying consistency between preparative procedure and coupling constants is observed for the *p*-chlorophenyl and α-furanyl compounds supporting both.

TABLE 1. Methine–methine coupling constants for the derivatives of **2** and **4**

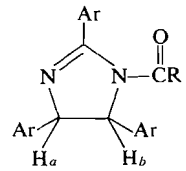

Compound	J_{AB}
2*a*	8.4
2*c*	8.6
2*e*	8.6
4*a*	3.4
4*c*	3.9
4*e*	2.6

Experimental

The i.r. spectra were obtained with a Beckman IR-10. The n.m.r. spectra ($CDCl_3$ or CCl_4) were run on Varian HA-100, T-60, or A-60 spectrometers using internal TMS. Mass spectra were obtained using a Varian M-66 mass spectrometer. Melting points and boiling points are uncorrected. Microanalyses were run by A. B. Gygli, Toronto and Chemalytics, Inc., Tempe, Arizona.

1,3,5-Triaryl-2,4-diaza-1,4-pentadienes (1)

A variety of procedures has been used to prepare the various substituted hydrobenzamides **1**. Hydrobenzamide **1***a* was obtained in 84% yield (m.p. 101–102; lit. (10) 101–102°) from benzaldehyde in liquid ammonia. The i.r. (CCl_4) showed C=N at 1640 cm^{-1}. Concentrated ammonium hydroxide was used with *p*-tolualdehyde to yield 66% of material **1***b* (m.p. 88–90; lit. (21) 91°; i.r. C=N at 1630 cm^{-1}) and with furfuraldehyde to yield 46% of product **1***e* (m.p. 116–117; lit. (17) 115°). The i.r. showed C=N at 1635 cm^{-1}.

TABLE 2. The n.m.r. parameters for 1,3,5-triaryl-2,4-diaza-1,4-pentadienes

	Proton shift δ			
Aryl group	Aromatic	Azomethine	Methine	Methyl
Phenyl	7.7 (4H,m) 7.3 (11H,m)	8.4 (1H,s)	5.9 (1H,s)	
p-Tolyl	7.7 (4H,d) 7.4 (2H,d) 7.1 (6H,m)	8.4 (1H,s)	5.9 (1H,s)	2.3 (9H,s)
p-Chlorophenyl	7.8 (4H,d) 7.4 (8H,m)	8.4 (1H,s)	5.9 (1H,s)	
p-Cyanophenyl	8.0 (2H,d) 7.8 (4H,d) 7.7 (4H,s)	8.5 (1H,s)	6.1 (1H,s)	
α-Furanyl	7.5 (2H,m) 7.4 (1H,m) 6.9 (2H,d) 6.4 (2H,m) 6.3 (2H,m)	8.4 (1H,s)	6.1 (1H,s)	

Buffered solutions of ammonium hydroxide with ammonium chloride were used for *p*-chlorobenzaldehyde to produce **1***c* (50% yield; m.p. 84.5–85.5; lit. (12) 87–90°; i.r. C=N at 1635 cm^{-1}) and *p*-cyanobenzaldehyde to produce **1***d* (54% yield; m.p. 116.5–117; lit. (12) 130–132°). The i.r. showed C≡N at 2240 cm^{-1} and C=N at 1640 cm^{-1}.

The n.m.r. parameters for the hydrobenzamides **1** are given in Table 2.

2-cis-4,5-Triarylimidazolines (Amarines, 2)

(a) Phenyllithium in Tetrahydrofuran

The reaction of **1***a* typifies this procedure. A sample of **1***a* (2.5 g, 8.4 mmol) in 45 ml of freshly distilled THF at −78° under an argon atmosphere was reacted with 20 ml of 0.82 *M* phenyllithium in THF (16.4 mmol). The reaction mixture was allowed to warm to room temperature (*ca.* 2 h) and then 1.0 g (16.6 mmol) of acetic acid was added. After solvent evaporation, the residue was dissolved in ether and washed three times with water. After drying, the amarine **2***a* was precipitated as the hydrochloride by bubbling in excess dry hydrochloric acid. The precipitate was washed and dried to yield 99% of material m.p. 260–265°.

Compound **2***a* was recovered by reacting the hydrochloride with excess sodium hydroxide in aqueous THF. After the usual ether–water extraction process, the residue was recrystallized from ether to yield 80% of material m.p. 127–128° (lit. (10) 129–130°).

In this manner, the *p*-tolyl compound **2***b* (m.p. 126–128, lit. (21) 127°) was obtained in 42% yield upon recrystallization from 1:1 carbon tetrachloride–petroleum ether. The *p*-chlorophenyl **2***c*, compound upon recrystallization from carbon tetrachloride, was obtained in 78% yield (m.p. 176–177°).

The n.m.r. parameters for the amarines, **2**, are given in Table 3.

Anal. Calcd. for $C_{21}H_{15}N_2Cl_3$: C, 62.78; H, 3.78; N, 6.97. Found: C, 62.83; H, 3.66; N, 6.92.

(b) Potassium Amide in Liquid Ammonia

The phenyl **2***a* and α-furanyl **2***e* derivatives were prepared using the following procedure. A sample of **1***a* (3 g, 10 mmol) was added gradually to a refluxing solution of 150 ml of 0.1 *N* potassium amide in liquid ammonia. After stirring at reflux for 1 h, the ammonia was allowed to evaporate and the residue was dissolved in ether which was washed with water, dried, and solvent evaporated. The residue was recrystallized from petroleum ether to give a 63% yield.

Analogously the α-furanyl **2***e* compound was obtained in 60% yield (m.p. 115–116, lit. (17) 116°) upon recrystallization from benzene.

(c) Ammonium Hydroxide

The more acidic derivatives of **1** such as the *p*-chlorophenyl compound **1***c* could be cyclized with concentrated ammonium hydroxide by proceeding directly from the aldehyde to the imidazoline **2***c* without isolating the intermediate. Thus *p*-chlorobenzaldehyde (215 g, 1.5 mol) was heated at 50° for 10 h with 400 ml of concentrated NH_4OH. The resulting oil was dissolved in ether. The ether layer was extracted with 10% KH_2PO_4 solution (3 × 200 ml), then washed with water, dried, and evaporated to dryness. The product was recrystallized from carbon tetrachloride to give 92 g (45% yield) of product.

(d) Dimethylsulfoxide

A solution of **1***d* (7.2 g, 19 mmol) in 50 ml of dimethylsulfoxide was heated for 0.5 h on the steam bath and then poured into water. The precipitate was filtered and recrystallized from 95% ethanol to yield 59% of product which melted at 222–224° with decomposition.

Although a satisfactory combustion analysis was not obtained, the mass spectrum showed a parent peak at *m/e* of 373.

TABLE 3. The n.m.r. parameters for the 2-cis-4,5-triarylimidazolines (**2**)

Aryl group	Proton shift δ			
	Aromatic	Methine	Amine	Methyl
Phenyl	8.0 (2H,m) 7.4 (3H,m) 7.3 (10H,s)	4.9 (2H,s)	5.3 (1H, broad)	
p-Tolyl	7.8 (2H,d) 7.2 (2H,d) 7.1 (8H,s)	5.3 (2H,s)	4.0 (1H, broad)	2.4 (3H,s) 2.1 (6H,s)
p-Chlorophenyl	7.8 (2H,d) 7.3 (2H,d) 7.0 (4H,d) 6.8 (4H,d)	5.3 (2H,s)	4.6 (1H, broad)	
p-Cyanophenyl	8.0 (2H,d) 7.7 (2H,d) 7.3 (4H,d) 7.0 (4H,d)	5.6 (2H,s)	6.0 (1H, broad)	
α-Furanyl	7.4 (1H,m) 7.1 (3H,m) 6.5 (1H,m) 6.1 (4H,m)	4.4 (2H,s)	5.0 (1H, broad)	

*1,3,5-Triphenyl-2,4-diaza-1,3-pentadiene (**3**)*

(a) Isolation

A sample of **1***a* (20 g, 67 mmol) was stirred 20 h at room temperature in 200 ml of 0.5 *N* potassium methoxide–methanol. After solvent removal the residue was dissolved in 150 ml of ether and extracted ten times with 100 ml of 1 *M* KH_2PO_4 to remove the imidazoline **2***a*. The residue, after drying and solvent removal, was recrystallized from petroleum ether to yield 20% of product **3** (m.p. 82–84°).

Anal. Calcd. for $C_{21}H_{18}N_2$: C, 84.53; H, 6.08. Found: C, 84.51; H, 6.09.

The n.m.r. spectrum ($CDCl_3$) showed the azomethine proton as a singlet $\delta = 8.2$ (1H), the aromatic protons as multiplets (4H at 7.9 and 11H at 7.5), and the methylene protons as a singlet at $\delta = 4.7$ (2H). The i.r. spectrum showed the C=N stretches at 1635 and 1615 cm^{-1}.

(b) Synthesis

Benzaldehyde (5 g, 48 mmol) and *N*-benzylbenzamidine (22) (10 g, 48 mmol) and 0.2 g of a zinc chloride–*N*-benzylbenzamidine complex were refluxed for 8 h in 50 ml of toluene using a Dean–Stark water trap. After filtration and solvent removal the residue was recrystallized from about 100 ml of petroleum ether (60–80) to yield 40% of crude product m.p. 65–70°. Repeated recrystallization from pentane yielded material of m.p. 82–84°. Admixture with the material isolated previously showed no m.p. depression.

The zinc chloride complex was prepared by precipitation with water from a solution of 1 g *N*-benzylbenzamidine in 5 ml of ethanol and 5 ml of saturated aqueous zinc chloride.

(c) Hydrolysis

The reaction mixtures obtained by treating **1** with methanol–potassium methoxide were hydrolyzed by adding a large excess of water to the methanol solution and stirring for an additional 60 h at room temperature. The product mixture which contained **2**, the aromatic aldehyde, and the substituted *N*-benzylbenzamidine was extracted with ether which was washed twice with water and then with saturated $NaHCO_3$ to selectively remove the *N*-benzylbenzamidine. Treatment with base and extraction with ether yielded material of m.p. 72–73° (lit. (23) 77–78°) for the phenyl compound, material of m.p. 130–132° for the *p*-tolyl-compound and material of m.p. 123–124° for the *p*-chlorophenyl compound.

Anal. Calcd. for $C_{15}H_{18}N_2$: C, 80.61; H, 7.40. Found: C, 80.63; H, 7.61.

Anal. Calcd. for $C_{14}H_{12}N_2Cl_2$: C, 60.23; H, 4.33; N, 10.04. Found: C, 60.51; H, 4.15; N, 10.04.

*2-trans-4,5-Triarylimidazolines (Isoamarines, **4**)*

Except for the tricyano compound all the substituted imidazolines were prepared by approximately the same procedure. To a degassed solution of about 0.2 *N* potassium *t*-butoxide in *t*-butyl alcohol under an argon atmosphere was added an imidazoline to produce about a 0.1 to 1 *M* solution. After reflux for up to 13 h with t.l.c. monitoring, the reaction mixture was extracted with ether–water, the organic layer dried and evaporated.

The *p*-tolyl compound was obtained in 48% yield on recrystallization from 75% ethanol (m.p. 168–169°). The i.r. ($CHCl_3$) showed NH at 3400 and C=N at 1610 cm^{-1}.

Anal. Calcd. for $C_{24}H_{24}N_2$: C, 84.67; H, 7.11. Found: C, 84.83; H, 7.02.

Isoamarine (the phenyl compound) was obtained in 59% yield on recrystallization from 70% ethanol (m.p. 194–196°, lit. (10) 198–201°). The i.r. ($CHCl_3$) showed NH at 3420 and C=N at 1620 cm^{-1}.

The *p*-chlorophenyl compound was obtained in 69% yield on recrystallization from benzene (m.p. 193–194°).

TABLE 4. The n.m.r. parameters for the 2-*trans*-4,5-triarylimidazolines

Aryl group	Proton shift δ			
	Aromatic	Methine	Amine	Methyl
Phenyl	8.0 (2H,m) 7.4 (3H,m) 7.3 (10H,s)	4.9 (2H,s)	5.3 (1H)	
p-Tolyl	7.8 (2H,d) 7.2 (2H,d) 7.1 (8H,s)	4.8 (2H,s)	5.1 (1H)	3.4 (3H,s) 3.3 (6H,s)
p-Chlorophenyl	7.8 (2H,d) 7.4 (6H,d) 7.1 (4H,d)	4.7 (2H,s)	4.2 (1H)	
p-Cyanophenyl	8.2 (2H,d) 8.0 (2H,d) 7.8 (4H,d) 7.5 (4H,d)	5.1 (2H,s)	4.5 (1H)	
α-Furanyl	7.5 (1H,m) 7.4 (2H,m) 7.1 (1H,d) 6.5 (1H,m) 6.3 (4H,s)	5.2 (2H,s)	5.0 (1H)	

TABLE 5. Properties of *N*-benzoyl- and acetylimidazolines

Parent compound	Melting point (°C)	Analysis								C=N cm^{-1}
		Calculated				Found				
		C	H	N	O	C	H	N	O	
2*a*	179	83.58	5.47	6.97	3.93	83.76	5.49	7.07	4.12	1620
4*a*	177–178	83.58	5.47	6.97	3.93	83.72	5.50	6.95	4.16	1620
2*c*	151–152	66.48	3.79	5.54		66.28	3.93	5.57		1620
4*c*	88–90	66.48	3.79	5.54		65.47	4.15	5.51		1620
2*e**	140–142	65.79	4.55	9.03		65.69	4.65	9.02		1630
4*e**	114–116	65.79	4.55	9.03		65.53	4.69	8.79		1630

*These are the *N*-acetyl derivatives; other results are the *N*-benzoyl derivatives.

The i.r. ($CHCl_3$) showed NH at 3400 and C=N at 1620 cm^{-1}.

Anal. Calcd. for $C_{21}H_{15}N_2Cl_3$: C, 62.78; H, 3.78; N, 6.97. Found: C, 62.55; H, 3.71; N, 6.86.

Isofurfurine (the α-furanyl compound) was obtained in 56% yield on recrystallization from 70% ethanol (m.p. 138–139°, lit. (24) 143°). The i.r. ($CHCl_3$) showed NH at 3410 and C=N at 1630 cm^{-1}. The *p*-cyanophenyl compound was prepared in an analogous procedure from tricyanoamarine except methanol – 0.34 *N* potassium methoxide was used with a 2 h reflux period. After the usual work-up a 30% yield of material m.p. 222–223° was obtained after recrystallization from 95% ethanol. A mass spectrum gave a parent ion peak at 373 *m/e* although a satisfactory combustion analysis was not obtained. The i.r. (Nujol) showed NH at 3360, C≡N at 2240, and C=N at 1605 cm^{-1}.

The n.m.r. parameters for the isoamarines **4** are given in Table 4.

N-Benzoylimidazolines

A mixture of 1 equiv of benzoyl chloride with 2 equiv of the substituted imidazoline in benzene (*ca.* 0.1 *M* solutions) was refluxed 1 h and then cooled. The precipitated hydrochloride was removed by filtration and the solvent evaporated. Petroleum ether was used for recrystallization and yields in the 70–90% range were obtained. Acetyl derivatives were prepared using acetyl chloride. The properties of both the benzoyl- and acetylimidazolines are given in Table 5. The n.m.r. parameters for the *N*-benzoylimidazolines are given in Table 6.

N-Benzylidene-α-methoxybenzylamine (5)

Compound **1***a* (10 g, 33 mmol) was refluxed in 100 ml of methanol for 2.5 h and the excess methanol was then film evaporated. Distillation of the residue yielded 5.2 g (70% yield) of product of b.p. 120° at 0.025 mm of Hg.

Anal. Calcd. for $C_{15}H_{15}NO$: C, 79.97; H, 6.71; N, 6.22. Found: C, 80.33; H, 6.77; N, 6.27.

TABLE 6. The n.m.r. parameters for *N*-benzoylimidazolines

	Proton shift δ			
		Methine		
Aryl group	Aromatics	A	B	J_{AB}
cis-Phenyl	7.80 (2H,m) 7.20 (18H,m)	5.74	5.56	8.4
trans-Phenyl	7.70 (2H,m) 7.30 (18,m)	5.30	5.24	3.4
cis-p-Chlorophenyl	7.70 (2H,d) 7.20 (15H,m)	5.63	5.57	8.6
trans-p-Chlorophenyl	7.70 (2H,d) 7.30 (15H,m)	5.15	5.07	3.9
cis-α-Furanyl	7.59 (1H,d) 7.21 (2H,m) 7.08 (1H,d) 6.55 (1H,m) 6.19 (4H,m)	5.67	5.51	8.6
trans-α-Furanyl	7.56 (1H,m) 7.40 (2H,m) 7.10 (1H,m) 6.52 (1H,m) 6.34 (4H,m)	5.54	5.31	2.6

In the n.m.r. spectrum ($CDCl_3$) the azomethine proton appeared as a singlet at δ 7.4 (1H), the aromatic protons as a multiplet 7.8 (2H) and as a multiplet 7.3 (8H), the methoxy protons as a singlet 2.3 (3H), and the benzyl proton as a singlet 5.5 (1H).

The i.r. spectrum (neat liquid) showed the C=N stretch at 1640 cm^{-1}.

α-t-Butylbenzylamine

To a degassed solution at −78° of **1***a* (3 g, 10 mmol) in 100 ml of THF, under an argon atmosphere was added slowly 5.5 ml (1.82 *M*, 10 mmol) of commercial *t*-butyllithium solution. The reaction mixture was quenched with excess water after being stirred 1 h at −78° and warming to room temperature. After solvent removal the residue was dissolved in ether, washed twice with water, the solution was dried and solvent evaporated. At this stage n.m.r. indicated the following mol %: 14% **1***a*, 10% **2***a*, 59% **6**, and 17% **7**.

Chromatography of this mixture on silica gel using 5% ether–pentane as eluent yielded a sample of the *N*-benzylidene-α-*t*-butylbenzylamine; m.p. 69–70° (lit. (25) m.p. 70.5 °C).

Anal. Calcd. for $C_{18}H_{21}N$: C, 86.01; H, 8.42. Found: C, 86.15; H, 8.31.

In the n.m.r. spectrum ($CDCl_3$) the azomethine proton appeared as a singlet δ 8.3 (1H), the aromatic protons as a multiplet (2H at 7.9 and 8H at 7.5), the benzyl proton as a singlet 4.0 (1H), and the *t*-butyl protons as a singlet 1.0 (9H).

The i.r. spectrum ($CHCl_3$) showed the C=N stretch at 1645 cm^{-1}.

The original reaction mixture also was hydrolyzed by stirring for 12 h in 10% hydrochloric acid and the acid solution was extracted with ether and again with ether after neutralization. This latter ether solution was dried, solvent evaporated, and the residue vacuum distilled to yield 22% of product (b.p. 40° at 0.025 mm lit. (26) 110–112 at 11 mm).

N,N-Di(α-t-butylbenzyl)amine (7)

Following the procedure reported above for α-*t*-butylbenzylamine, **1***a* (1 g, 3.3 mmol) was reacted with *t*-butyllithium (1.82 *M*, 5.5 ml, 10 mmol). The product was separated from the reaction mixture by chromatography with silica gel (50 g) using 2% ether in pentane. Vacuum distillation (b.p. 110° at 0.05 mm Hg) yielded 88% of product which was apparently about 12:1 mixture. In the n.m.r. of the major component of the diastereomers, the phenyl protons appeared as a broad singlet δ 7.2 (10H), the benzyl protons as a singlet 3.9 (2H), the amine proton as a broad singlet 2.0 (variable; 1H), and the *t*-butyl protons as a singlet at 0.90 (18H). The minor component showed a signal at δ 3.2 (benzyl proton) and at 0.95 (*t*-butyl protons).

The i.r. spectrum showed a very weak band at 3380 cm^{-1} for the N—H stretch (27).

Anal. Calcd. for $C_{22}H_{31}N$: C, 85.38; H, 10.10. Found: C, 85.54; H, 10.17.

1-Benzyl-2-hydro-2,4,6-triphenyl-s-triazine (9)

(a) Isolation

N-Benzylbenzamidine (10 g, 48 mmol), benzaldehyde (5 g, 48 mmol), and 2 ml of acetic acid were refluxed in 30 ml of benzene for 72 h. After a work-up involving ether–water extraction the residue contained *N*-benzylidenebenzylamine and **9**. Distillation under reduced pressure yielded 54%

of *N*-benzylidene-benzylamine (b.p. 100° at 0.025 mm, lit. (28) b.p. 122 at 0.5 mm) whose n.m.r. spectrum (CCl_4) showed the azomethine proton as a singlet at δ 8.30 (1H), the aromatic protons as multiplets at 7.70 (2H) and 7.30 (8H), and the methylene protons as a singlet 4.77 (2H). The distillation residue was recrystallized from 50% ethanol to yield 62% of material m.p. 135–136°.

The n.m.r. spectrum ($CDCl_3$) showed the aromatic protons as multiplets at δ 8.3 (2H) and 7.4 (18H), the methine proton as a singlet at 6.0 (1H), and the methylene protons as an AB quarter (δ_A 5.0, δ_B 4.1, and J_{AB} = 14 Hz).

The i.r. spectrum showed CH stretch at 3080, 2980 and C=N at 1610 cm^{-1}.

(b) Synthesis

2,4,6-Triphenyl-*s*-triazine was obtained in 88% yield from benzonitrile with chlorosulfonic acid (29). Upon recrystallization from toluene, material of m.p. 230–232° (lit. (29) m.p. 232°) was obtained.

1,2-Dihydro-2,4,6-triphenyl-*s*-triazine was prepared by lithium aluminum hydride reduction of 2,4,6-triphenyl-*s*-triazine (30). A 12% yield of material m.p. 170–172° (lit. (30) m.p. 175–177°).

The title compound was prepared by adding benzyl-chloride (0.58 ml, 5 mmol) to a degassed tetrahydrofuran solution (20 ml) of 1,2-dihydro-2,4,6-triphenyl-*s*-triazine (1.55 g, 5 mmol) that had been reacted with 1 equiv of 0.62 *N* phenyllithium–THF. Stirring for 12 h at room temperature showed incomplete reaction and the reaction mixture was then refluxed for 4 h. The solvent was evaporated and the reaction mixture extracted with ether–water, dried, and solvent evaporated. Chromatography on silica gel with 1:1 ether–pentane and recrystallization yielded 40% of material m.p. 142–143°.

Anal. Calcd. for $C_{28}H_{23}N_3$: C, 83.76; H, 5.59; N, 10.47. Found: C, 84.24; H, 5.59; N, 10.01.

Admixture of this material with the previously isolated material showed no m.p. depression.

The authors wish to thank the National Research Council of Canada for their financial assistance.

1. M. A. LAURENT. Ann. **21**, 130 (1937).
2. M. A. LAURENT. C. R. Acad. Sci. Paris, **19**, 353 (1844).
3. (*a*) A. BORODIN. St. Petersburg Acad. Sci. Bull. **17**, 38 (1858). (*b*) A. BORODIN. Ann. **110**, 78 (1859).
4. (*a*) EKMAN. Ann. **112**, 151 (1859). (*b*) H. L. SNAPE and A. BROOKE. Trans. Chem. Soc. (London), **77**, 208 (1899).
5. (*a*) F. R. JAPP and J. MOIR. Trans. Chem. Soc. (London), **77**, 608 (1900). (*b*) H. L. SNAPE. Trans. Chem. Soc. (London), **77**, 778 (1900).
6. J. A. CHENICEK. (to Universal Oil Products Co.) U.S.Pat. 2 533 205. December 12, 1950.
7. M. WRONSKI. Chem. Anal. (Warsaw), **4**, 641–642 (1959).
8. I. NICHOLSON and R. PORETZ. J. Chem. Soc. 3067 (1965).
9. F. MCCAPRA, D. G. RICHARDSON, and Y. C. CHANG. Photochem. and Photobiol. **4**, 1111–1121 (1965).
10. O. F. WILLIAMS and J. C. BAILAR. J. Am. Chem. Soc. **81**, 4466 (1959).
11. T. HAYASHI. Bull. Chem. Soc. Jap. **37**(11), 1702 (1964).
12. Y. OGATA, A. KAWASAKI, and N. OKUMURA. J. Org. Chem. **29**, 1985 (1962).
13. D. H. HUNTER and S. K. SIM. J. Am. Chem. Soc. **91**, 6202 (1969).
14. D. H. HUNTER and S. K. SIM. Can. J. Chem. This issue.
15. C. G. MCCARTY. *In* The chemistry of the carbon–nitrogen double bond. Interscience. New York, N. Y., 1970. Chapt. 9–11.
16. M. SAUNDERS and F. YAMADA. J. Am. Chem. Soc. **85**, 1882 (1963).
17. H. H. STRAIN. J. Am. Chem. Soc. **52**, 1217 (1930).
18. (*a*) M. SZWARC. Carbanions, living polymers, and electron-transfer processes. Interscience. New York, N. Y., 1968. Chapt. 8–4. (*b*) R. WAACK and M. A. DORAN. J. Org. Chem. **32**, 3395 (1967).
19. J. P. ANSELME. The chemistry of the carbon–nitrogen double bond. Interscience, New York, N.Y., 1970. p. 321.
20. S. STERNHELL. Quart. Rev. **23**, 236 (1969).
21. A FURTH. Monatsh, **17**, 839 (1906).
22. P. OXLEY and M. W. PARTRIDGE. J. Chem. Soc. 1110 (1947).
23. F. L. PYMAN. J. Chem. Soc. 3373 (1923).
24. J. P. MILLINGTON and H. HIBBERT. Chem. Soc. Lond. Proc. **16**, 161 (1900).
25. R. P. OSSORIO and F. G. HERRERA. Anales Real. Soc. Españ. fis. y quim. 50B, **86**, 875 (1954).
26. S. H. GRAHAM and A. J. S. WILLIAMS. Tetrahedron, **21**, 3263 (1965).
27. R. A. RUSSEL and H. W. THOMPSON. J. Chem. Soc. 1955, 483.
28. T. G. BONNER. Chem. Ind. (London). 267 (1965).
29. A. COOK and D. JONES. J. Chem. Soc. 281, (1941).
30. H. L. NYQUIST. J. Org. Chem. **31**, 784 (1966).

2,4-Diazapentadienes. II. A Carbanion Cyclization

D. H. HUNTER AND S. K. SIM
Department of Chemistry, University of Western Ontario, London, Ontario

Received August 26, 1971

The mechanism of the cyclization and 1,3-proton shift of 1,3,5-triaryl-2,4-diaza-1,3-pentadienes (**1**) catalyzed by phenyllithium and by potassium methoxide–methanol has been studied. On the basis of substituent effects, hydrogen–deuterium exchange, isotope effects, and solvent effects, it was deduced that both the cyclization and prototropy involve a common W-shaped carbanion which rapidly cyclizes. A kinetic deuterium isotope effect of 2 was calculated for protonation of this intermediate carbanion in methanol.

On étudie le mécanisme de cyclisation et de migration-1,3 de proton dans les triaryl-1,3,5 diaza-2,4 pentadiènes-1,3 (**1**) catalysées par le phényllithium et par le méthylate de potassium-méthanol. En se fondant sur les effets des substituants, de l'échange hydrogène–deutérium, des effets isotopiques et des effets de solvant, il en a été conclu que la cyclisation ainsi que la prototropie impliquent un carbanion commun en forme de W qui se cyclise rapidement. Un effet isotopique cinétique du deutérium d'une valeur de 2 a été calculé pour la protonation dans le méthanol de ce carbanion intermédiaire.

Canadian Journal of Chemistry, **50**, 678 (1972)

Introduction

The reaction of benzaldehyde with ammonia to form hydrobenzamide **1** and the 'thermal' isomerization of **1** to amarine **2** must stand among the first organic reactions studied (1). Yet surprisingly little attention has been paid to these and related molecules especially from a mechanistic point of view (2). Particularly intriguing to us was the highly stereoselective cyclization of **1** to form **2**, the cyclic isomer with the phenyl rings *cis* to each other. Since the preliminary report (3) which noted that this reaction was base-catalyzed and in which orbital symmetry was invoked, the study of this reaction using phenyllithium in THF has been further elaborated. Also the study has been extended using methanol–methoxide and examples of **1** substituted *p*, *p'*, *p''* in an attempt to obtain a more complete understanding of this reaction. The preparations, reactions, and structural assignments for **1** and related compounds have been described in the preceding article (4). As an example of the nomenclature to be used in the following sections, *p*-CH_3-**1** will refer to the tris-*p*-methyl substituted hydrobenzamide (1).

Results and Discussion

As indicated in Scheme 1, the cyclization of **1** to **2** is catalyzed by a variety of bases (4) (e.g. KO*t*Bu–HO*t*Bu at room temperature) and produces **2** highly selectively (< 1% of **4**). The *cis–trans* interconversion of **2** to **4** requires more vigorous conditions (*e.g.* KO*t*Bu–HO*t*Bu at reflux) thereby allowing a study of the base-catalyzed reactions of **1** under conditions where **2** is not reactive. The equilibrium mixture of **2** and **4** in *t*-butyl-alcohol at 100° contains 96% of **4** and 4% of **2** as might be expected.

Reactions with Phenyllithium

The results of treating **1** and its derivatives with phenyllithium in tetrahydrofuran are gathered in Table 1. As run 3 indicates, when **1** is reacted with an equivalent of phenyllithium at −78° and then warmed to room temperature, only **2** is observed by t.l.c. and n.m.r. in the reaction mixture and an 80% yield of **2** can be

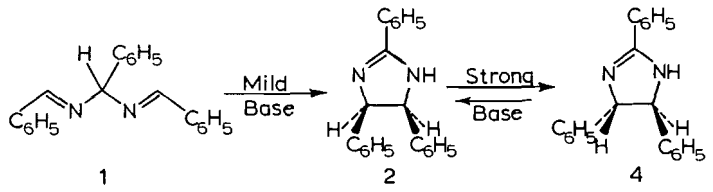

SCHEME 1

Can. J. Chem. Downloaded from www.nrcresearchpress.com by 210.87.254.40 on 09/05/12
For personal use only.

Can. J. Chem. Downloaded from www.nrcresearchpress.com by 210.87.254.40 on 09/05/12
For personal use only.

TABLE 1. Reactions of *p*-substituted hydrobenzamides **1** with phenyllithium* in THF

Run	Substrate		T (°C)†	Time (min)‡	Quencher nature§	Products (%)		
	p-X	Concentration (*M*)				**1**	**2**	**4**
1	H	0.05	−78	360	H	44	56	0.8
2	H	0.075	−78	850	H	66	34	0.7
3	H	0.13	−78 to 25	270	H	<0.2	100¶	<0.5
4	CH_3	0.13	−78 to 25	1000	H	<0.2	100	<0.5
5	Cl	0.024	−78	30	H	26	74	<0.5
6	CN	0.026	−78	~1	D	<0.2	100	<0.5
7	H	0.016	−78	90	D	88 (<0.15 atoms D)‖	12	
8	Cl	0.024	−78	15	D	34 (<0.15 atoms D)‖	66	
9	CN	0.026	−130	~1	D	49 (<0.10 atoms D)‖	51	
10	H	0.07	−65	*360*	H	84	13	3
11	H	0.08	−78	*1050*	H	71	26	2.5
12	H	0.05	−40	*375*	H	<0.2	93	7
13	H	0.07	−20	*360*	H	<0.2	99	0.8
14	Cl	0.11	−130 to −90	5	H	26	73	**
15	**2**	0.08	−78	*1080*	H	—	97	3
16	**4**	0.08	−78	*695*	H	—	<0.7	99

*One equivalent of 0.5 or 0.72 *M* phenyllithium in THF was used except for run 3 (a two-fold excess of base).
†Dry Ice–acetone temperature is reported as −78°; −78 to 25 refers to reaction begun at −78° and allowed to warm to room temperature.
‡Times reported in italics are for runs involving irradiation (see Experimental).
§H refers to CH_3CO_2H and D to CH_3CO_2D.
‖Upper limit on atoms of D/molecule of starting material (n.m.r.).
¶Amarine was isolated in 80% yield.
** <0.5% *p*-Cl-**4** but 1% of *p*-Cl-**3** was observed.

Can. J. Chem. Downloaded from www.nrcresearchpress.com by 210.87.254.40 on 09/05/12
For personal use only.

isolated. As seen in runs 1 and 2, where the entire reaction was run at $-78°$ and quenched with excess acetic acid at the times indicated, the reaction is proceeding slowly and the rates are not highly reproducible except that not more than 1% of **4** is produced.

These observations can be generalized to *p*-CH_3, *p*-Cl, and *p*-CN-**1** (runs 4, 5, and 6) although there is a definite substituent effect upon the observed rate of reaction. This is exemplified by run 6 where *p*-CN-**1** is completely consumed in 1 min. The apparent order of reactivity is *p*-CN-**1** > *p*-Cl-**1** > **1** > *p*-CH_3-**1**.

The singular feature of all these reactions was the appearance of an intense color when the phenyllithium reagent was added. The color varied with the substituent and the visible spectrum obtained for **1** showed a long wavelength absorption maximum at 592 nm. The color faded to a light yellow when the reaction mixture was warmed to ambient temperature. It is tempting to ascribe the color to an anionic intermediate in the cyclization reaction and in an attempt to assess this hypothesis three experimental approaches were used: (*a*) quenching with CH_3CO_2D; (*b*) quenching with CH_3CO_2H with careful product analysis; and (*c*) irradiation of the colored solution. These are summarized in Scheme 2.

Runs 7, 8, and 9 report on the results obtained when the colored solutions obtained from **1**, *p*-Cl-**1**, and *p*-CN-**1** were quenched with CH_3CO_2D before complete conversion had occurred. Again the accelerating effect of the cyano grouping is observed (run 9), for even at $-130°$, with immediate quenching (at 1 min) about 50% reaction had occurred. The reaction mixtures were analyzed for deuterium incorporation into **1** and surprisingly none could be detected (<0.15 atoms D/molecule). These results require that the rate of proton abstraction from **1** by phenyllithium be slow at these temperatures and also if significant quantities of anionic intermediate are generated that quenching does not lead back to **1**.

In an attempt to obtain further information on the character of the possible carbanionic intermediate, the colored solutions obtained from **1** and *p*-Cl-**1** were quenched while cold after a short reaction period (run 14 for *p*-Cl-**1**) with excess acetic acid. An examination of the reaction product by n.m.r. revealed that about 1% of *p*-Cl-**3** was present and on work-up a sample of *N*-*p*-chlorobenzyl-*p*-chlorobenzamidine was isolated. The n.m.r. spectrum of the reaction mixture from **1** did not show **3** but a trace of *N*-benzylbenzamidine was observed upon hydrolysis.

The base-catalysis, the substituent effect, the color, and the quenching results with CH_3CO_2H all support the intermediacy of an anion generated by proton abstraction from **1**. However, from the small amounts of **3** and *p*-Cl-**3** isolated and from the lack of deuterium incorporation into **1** upon quenching with CH_3CO_2D, the concentration of anion must be small but still large enough to give an intense color. Assuming an extinction coefficient of about 10^5 (5), amounts of anion in the 1 to 0.001% range are suggested.

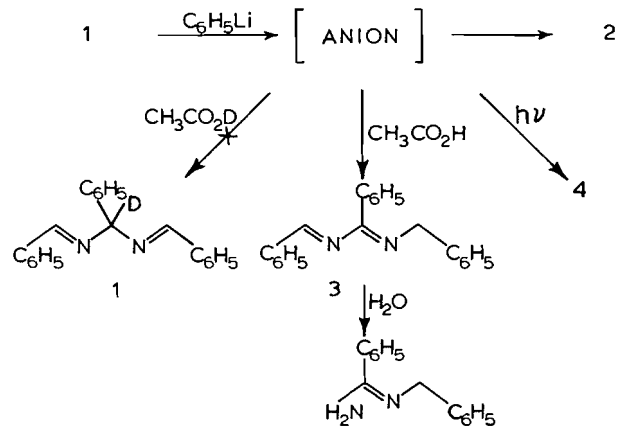

SCHEME 2

TABLE 2. Kinetic runs in CH_3OH*–CH_3OK at 60 °C

Run	Substrate	[Base] (M)	3/2‡	Rate constants†	
				k_1 ($s^{-1} \times 10^5$)	k_2 ($M^{-1}\,s^{-1} \times 10^4$)§
17	*p*-CH_3-**1**	0.23	1.2±0.1	6.4	2.8
18	**1**	0.23	0.8±0.1	34	15
19	**1**	0.21	0.9±0.1	26	12
20	**1**	0.097	0.75±0.05	13	13
21	**1**	0.14‖	0.7±0.1	31	22
22	*p*-Cl-**1**	0.023	0.5±0.1	73	320
23	**3**	0.21		0.046	0.022

*0.6 M in THF.
†Based upon three points for run 17, five for run 18, six for run 19, five for run 20, three for run 21, four for run 22, and five for run 23; $k \pm 10\%$ k.
‡Average value for all points.
§Assuming first order in added base (6).
‖Contains 1 equiv of dibenzo-18-crown-6-ether.

As further evidence of an anionic intermediate, the colored solution due to the reaction of **1** was irradiated with appropriate filters to isolate the long wavelength absorption band (runs 10, 11, 12, and 13). For the first time significant amounts of **4** now appeared and up to 10% of **4** in the cyclized products could be obtained by extended irradiation at −78°. The relative amount of **4** obtained was temperature dependent and by −20° the thermal cyclization of the anionic intermediate was sufficiently facile to exclude significant photochemical reaction. As reported in runs 15 and 16, both **2** and **4** are largely unaffected by irradiation under these conditions.

In summary, the reactions with phenyllithium suggest that the cyclization of **1** to **2** can occur through a carbanionic intermediate whose concentration is never large. This intermediate is formed by proton abstraction and can be trapped by protonation or irradiation. These results are summarized in Scheme 2.

Reactions with Methanol–Methoxide

A study of the reactions of **1** and substituted-**1** in methanol–potassium methoxide (0.02–0.2 M) mostly at 60° was made primarily in an attempt to further characterize any intermediates in the **1** to **2** conversion. As shown in Scheme 3, **3** was now observed as well as **2** and, as indicated by runs 17, 18, 19, 20, 21, and 22 of Table 2, **3** and **2** were produced in similar amounts although the ratio did depend upon the substituent.

The reaction proved to be first order in **1** over the range of concentrations studied, and as runs 18, 19, and 20 show both the ratio of **3** to **2** and the second order rate constant were reproducible within experimental error. From runs 17, 22 and runs 24 and 25 of Table 3, it is clear that electron-withdrawing substituents

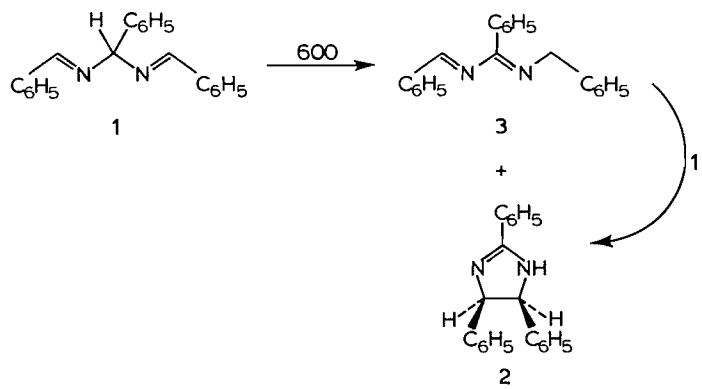

SCHEME 3

Can. J. Chem. Downloaded from www.nrcresearchpress.com by 210.87.254.40 on 09/05/12
For personal use only.

Can. J. Chem. Downloaded from www.nrcresearchpress.com by 210.87.254.40 on 09/05/12
For personal use only.

TABLE 3. Reactions in methanol and methanol-*O*-*d* with potassium methoxide

Run	Substrate		Solvent	Base concentration (*M*)	*T* (°C)	Time (min)	Products %		
	Nature	Concentration (*M*)					**1**	**3**§	**2**
24	*p*-CN-**1**	0.008	CH_3OH	0.02	27	5	<0.5	<0.5	100
25	*p*-CN-**1**	0.007	CH_3OH	0.39*	24	30	40	<0.5	60
26	**1**	0.13	CH_3OD	0.19	60	15	59†	12	29
27	**1**	0.13	CH_3OD	0.19	60	45	25	21	54
28	**1**	0.13	CH_3OD	0.19	60	65	18	23	59
29	**1**	0.10	CH_3OD	0.25	60	60	5	28‡	67
30	**3**	0.20	CH_3OD	0.25	60	6870	<0.5	70‡	30
31	**3**	0.19	CH_3OD	0.25	60	11235	<0.5	70‡	30
32	**3**-*d*¶	0.17	CH_3OH	0.22	60	1715	<0.5	87‡	13||
33	**3**-*d*¶	0.14	CH_3OH	0.22	60	3110	<0.5	84‡	16||
34	**3**-*d*¶	0.15	CH_3OH	0.22	60	4610	<0.5	78‡	22||
35	*p*-CH_3-**1**	0.08	CH_3OD	0.25	60	180	26†	27	47
36	*p*-CH_3-**1**	0.08	CH_3OD	0.25	60	420	<0.5	31	69
37	*p*-Cl-**1**	0.07	CH_3OD	0.25	60	45	14†	19	67

*Triethylenediamine was the added base.
†Contained <0.05 atoms D/molecule at the methine position (HA-100 n.m.r.).
‡*N*-Benzylbenzamidine obtained upon hydrolysis contained, for run 29, 0.86 atoms D/molecule; run 30, 0.08 atoms D/molecule; run 31, 0.10 atoms D/molecule; run 32, 0.65 atoms D/molecule; run 33, 0.64 atoms D/molecule; run 34, 0.62 atoms D/molecule by mass spectral analysis.
§For those reactions of **1** in CH_3OD, the percentage of **3** was calculated from n.m.r. assuming 0.84 atoms D/molecule.
||Products showed for run 32, 65% d_1; for run 33, 66% d_1; and for run 34, 65% d_1 by mass spectral analysis.
¶Starting material showed 77% d_1 by mass spectral analysis.

Can. J. Chem. Downloaded from www.nrcresearchpress.com by 210.87.254.40 on 09/05/12
For personal use only.

have an accelerating effect upon the rate of reaction. Using the data of runs 17–22 and σ values, a ρ of 3.8 is calculated for the trisubstituted molecule.

Treatment of **3** under the reaction conditions results in production of **2** but at a rate about 600 times slower than **1**. Thus for most reactions of **1** reported here, any **3** produced should not react further to any significant extent.

By analogy with the extensive studies on allylic, pentadienyl (7), and particularly the azallylic systems (8), the conversion of **1** to **3** must certainly involve an intermediate carbanion. The behavior of this intermediate was investigated using methanol-*O*-*d* and these results are included in Table 3. Of particular interest are runs 29, 35, and 37, for analysis of the recovered **1** for deuterium incorporation showed no observable uptake (<0.05 atom *D*/molecule) at >40% conversion. When **3** was analyzed for deuterium (run 29), only 0.86 atoms *D*/molecule were present showing that the isomerization had occurred with a low degree of intramolecularity (9). These results are consistent with an anionic intermediate(s) which protonates preferentially at the end carbon to yield **3** over **1**. Once formed, **3** returns to the anion considerably more slowly as evidenced by slow deuterium uptake and cyclization (runs 30 and 31). Thus the reaction of **1** can be studied under conditions where the products **2** and **3** are not significantly reactive.

Reaction Schemes 4 and 5

One of the mechanisms considered, Scheme 4, has **1** lead only into a carbanion or carbanions which competitively reprotonate or cyclize. Since reprotonation (k_{-2}) should be occurring with rate constants of about 10^6 s^{-1} or greater in methanol (10), this scheme requires the cyclization rate constant (k_{-3}) to also be of this order of magnitude. This is several orders of magnitude greater than the rate constants which have been observed for electrocyclizations of other carbanions (*e.g.* heptatrienyllithium, 10^{-3} s^{-1} at $-30°$ (11); cyclooctadienylpotassium or -lithium, 10^{-5} s^{-1} at 30° (12); and pentadienyl not at all (13)) and thus the second mechanism was considered carefully.

In Scheme 5, the carbanions serve merely to

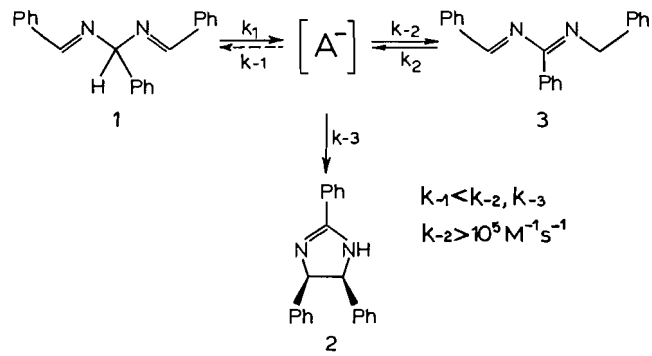

SCHEME 4

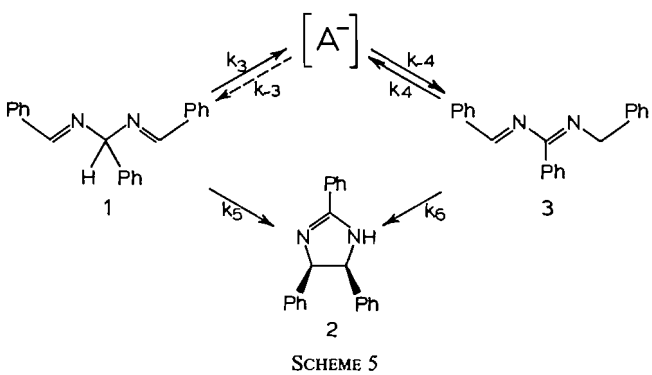

SCHEME 5

Can. J. Chem. Downloaded from www.nrcresearchpress.com by 210.87.254.40 on 09/05/12
For personal use only.

interconnect **1** and **3**, and **2** arises from **1** not through an intermediate but a transition state. Thus possibly certain conformations of **1** would be more appropriate for cyclization with a bonding interaction across the 1 and 5 carbons occurring as the methine proton is being abstracted.

In an attempt to differentiate between these seemingly feasible mechanisms, the following results were obtained and analyzed.

Substituent Effects on the 3/2 Ratio

As the results of runs 17–22 and 25[1] indicate, the ratio of **3/2** depends upon the substituents in a systematic fashion with the more electron-withdrawing substituents resulting in a lower **3** to **2** ratio. Considering Scheme 5 first, the rate constants that determine the **3** to **2** ratio are k_3 and k_5. It would seem unlikely that both k_3 and k_5 would respond to the same degree to changes in the substituent. Delocalization at the 1, 3, and 5 positions should stabilize the full charge that is developing in the anion more than in the transition state leading to **2** which has bonding developing across the terminal carbons. Thus this scheme would predict that the **3** to **2** ratio should increase with more electron-withdrawing groups contrary to the observation.

In Scheme 4, the ratio of **3** to **2** is determined by k_{-2} and k_{-3}. How k_{-3} would respond to substituent is uncertain but it does not seem unreasonable that k_{-2} would decrease as the anion becomes more stabilized. Thus Scheme 4 does not seem inconsistent with the observations and the substituent effects favor the mechanism in which both the prototropy and cyclization proceed through carbanionic intermediates (Scheme 4).

Solvent Isotope Effect on the 3/2 Ratio

As summarized in Table 4, when methanol is replaced by methanol-*O*-*d*, the ratio **3/2** drops by about a factor of 2 for *p*-CH_3-**1**, **1**, and *p*-Cl-**1**. Returning to Scheme 5, the ratio of **3** to **2** is determined by k_3 and k_5 of which neither should be directly affected by the solvent isotope. In Scheme 4, k_{-2} and k_{-3} are the important kinetic parameters and while the solvent is not directly involved in k_{-3}, the step which determines k_{-2} is reprotonation in which the OH or OD bond of solvent is being broken. In going from CH_3OH to CH_3OD, k_{-2} should be reduced to the extent of the primary isotope effect. Thus Scheme 4 is consistent with the results of Table 4 and a solvent isotope effect of about 2 is observed.

TABLE 4. Ratio of **3/2** obtained in methanol and methanol-*O*-*d* at 60°

Runs	Substrate	Solvent	**3/2**
17	*p*-CH_3-**1**	CH_3OH	1.2
35, 36	*p*-CH_3-**1**	CH_3OD	0.5
18–20	**1**	CH_3OH	0.8
26–29	**1**	CH_3OD	0.4
22	*p*-Cl-**1**	CH_3OH	0.5
37	*p*-Cl-**1**	CH_3OD	0.3

Effect of Methanol Concentration on the 3/2 Ratio

In a further attempt to distinguish between Schemes 4 and 5, the effect of diluting the methanol solvent with dimethylsulfoxide was observed and these results are collected in Table 5. As can be seen from runs 20, 38, 39, and 40, as the percentage of dimethylsulfoxide is increased from zero to 80 weight %, the ratio **3/2** drops to about zero. Runs 41 and 42 demonstrate that with 80 weight % dimethylsulfoxide, **3** is being rapidly converted to **2** but at a rate sufficiently slow to indicate that in run 40, the amount of **3** produced must still be quite small.

The effect of added dimethylsulfoxide in methanol should be twofold: the concentration of methanol is reduced and also the ΔpK_a between the methanol and substrate should be reduced, resulting in a reduced rate of reprotonation (10). Applying this reasoning to Scheme 5 where k_3 and k_5 are product determining suggests that both should be increased similarly by the enhanced basicity of the methoxide. However, in Scheme 4, while k_{-3} should be unaffected, k_{-2} should be systematically reduced as dimethylsulfoxide is introduced.

Again the experimental results are in accord with Scheme 4. Important, however, is the observation that **2** is produced to the exclusion of **4** and thus, any anionic intermediates generated must find their way to **2** alone.

Exchange and Cyclization of 3

If Scheme 4 is obeyed and there is a common anionic intermediate for cyclization and reprotonation, then the same k_{-2} and k_{-3} should be observed starting from either **1** or **3**. Since $k_{-1} < k_{-2}$, k_{-3}, the ratio k_{-2}/k_{-3} can be

[1]As run 24 indicates, *p*-CN-**1** is so reactive that triethylenediamine was used as base. Controls were not run on *p*-CN-**3** but presumably it is still less reactive than *p*-CN-**1**.

Can. J. Chem. Downloaded from www.nrcresearchpress.com by 210.87.254.40 on 09/05/12
For personal use only.

TABLE 5. Reactions in CH_3OH–CH_3SOCH_3–CH_3OK at 60°

Run	Substrate		Solvent weight % DMSO*	Base concentration (*M*)	Time (min)	Products	
	Nature	Concentration (*M*)				% Substrate	**3**/**2**‖
20	**1**	0.067	0	0.097		†	0.75±0.05
38	**1**	0.073	25	0.097		‡	0.55±0.05
39	**1**	0.04	50	0.067		§	0.3 ±0.05
40	**1**	0.04	80	0.030	8	<0.5	<0.5
41	**3**	0.03	80	0.030	5	60	
42	**3**	0.03	80	0.030	15	33	

*Solutions were 0.5–1.0 M in THF.
†Aliquots were removed at **14**, 27, 39, **46**, and 55% reaction.
‡Aliquots were removed at 25, 40, 61, and 83% reaction.
§Aliquots were removed at 57 and 97% reaction.
‖Average ratio is reported.

calculated directly from the **3**/**2** ratio when **1** is the reactant. When **3** is the reactant k_{-2}/k_{-3} must be estimated from the rate of exchange of **3** relative to the rate of cyclization. The details of this calculation are included in the Appendix but in essence the results of runs 30 and 31 where **3** was reacted in CH_3OD were used to calculate the k_{-2}/k_{-3} ratio.

Beginning with **1** in CH_3OD, the k_{-2}/k_{-3} ratio is 0.4 and with **3** as substrate the ratio is 0.3 ± 0.1. The agreement is sufficiently good to again support Scheme 4. Scheme 5 is not inconsistent with these results but would require the fortuitous equality $k_3/k_5 = k_4/k_6$.

Carbanion Geometries

Having apparently established that Scheme 4 best represents the reactions of **1**, it is interesting to consider the possible character of the anionic intermediate or intermediates. Three basic skeletal geometries are available to a near planar carbanion, U, W and sickle, and each of these is shown in Scheme 6 with the phenyls arranged to give the most stable form.

If orbital symmetry restraints (14) are dominant, any concerted cyclization should occur in a disrotatory manner. Thus since only **2** is produced, the 'sickle' shape would not be the intermediate responsible for cyclization since it should lead to **4**. This leaves the U and W shapes as candidates. While the U-shaped carbanion would seem to be ideal for cyclization, the W-shaped anion is undoubtedly much more favored energetically and should be formed in great preference to the U shape.

Whatever anion is generated in methanol, its lifetime must be quite short ($<10^{-6}$ s) since reprotonation must be rapid (10). This brings into doubt the likelihood of geometric interconversions occurring prior to cyclization if the configurationally stable carbanions phenylallyllithium (15), 1-phenylbutenylpotassium (16), and pentadienyllithium (13) can be used as analogies. Life-times for rotational isomers in these molecules are of the order of 10^2–10^{-2} s near room temperature; considerably longer than the 10^{-8} s which might be needed to interconvert the W- and U-shaped anions. However, the rotational barrier around the 2,3-bond in this system might well be lower[2] since the two isolated parts are relatively stable.

[2]As emphasized by a referee.

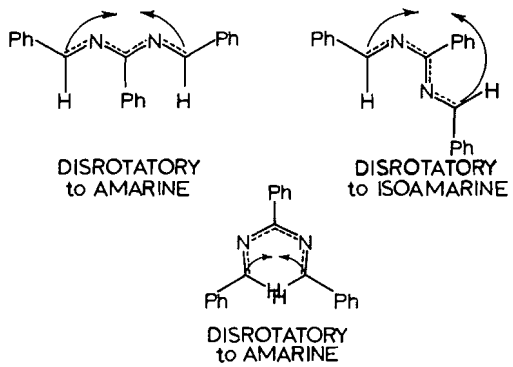

SCHEME 6

A second factor bears on the question of initial formation of the thermodynamically more stable W-shaped carbanion followed by conversion to the U-shaped carbanion which cyclizes. The pathways from the W-shaped anion to the U-shaped anion or from the sickle-shaped anion to the U-shaped anion and from the U-shaped anion to the cyclized product were analyzed using molecular models. It is apparent that the energy surfaces for these processes cross and that the W-shaped anion or sickle-shaped anion could be diverted to cyclized products before reaching the U-shaped species.

Thus consideration of the possible geometries leads to the conclusion that the W-shaped anion is the one produced and rapid cyclization occurs either directly from this form or perhaps with prior conversion to the 'sickle' and then the U shape.

A complicating feature of direct cyclization from either the W or sickle shape is the recognition that the one or both nitrogen atoms rotate through 180° during the cyclization process. Orbital symmetry selects an initial disrotatory motion but if 1,5-bonding has not progressed to an important extent by the time the π-system is destroyed, symmetry rules need no longer apply. The possible involvement of a lone pair on nitrogen might complicate this simple picture.

Ion-pairing

Carbanions of different selectivity in their relative rates of cyclization and reprotonation are possible if ion pairs and dissociated carbanions were both being generated. In order to test whether the counterion might be affecting the relative amounts of cyclization and repro-

Can. J. Chem. Downloaded from www.nrcresearchpress.com by 210.87.254.40 on 09/05/12
For personal use only.

Can. J. Chem. Downloaded from www.nrcresearchpress.com by 210.87.254.40 on 09/05/12
For personal use only.

tonation, two experiments were run. In runs 18, 19, and 20 the base concentration was varied by a factor of 2.4 and resulted in no change in the ratio **3**/**2**. In run 21, the potassium ion was complexed with dibenzo-18-crown-6-ether (17) and again no change in **3**/**2** was observed. Again one carbanion is favored for both reprotonation and cyclization.

Reactivity of the Intermediate

If as has been considered above, the W-shaped anion is responsible for cyclization then the rate for this process must be high and the barrier to deformation must be low. In fact as discussed before, the barrier must be considerably lower than that observed for rotation around partial double bonds in other delocalized carbanions. The factor responsible for enhanced rotation in this system might well be thermodynamic, for rotational interconversions in phenylallyllithium and related compounds lead to products of the same or similar energy. The cyclization reaction of the carbanionic intermediate from **1** is undoubtedly highly exothermic. As a result 1,5-bonding interaction might account for the reduced barrier to cyclization.

Isotope Effects on Protonation and Deprotonation

The conversion of **1** to **2** and **3** provides one of the few opportunities to estimate a solvent isotope effect on the protonation of a short-lived carbanion in protic solvent. As was shown in Table 4 and discussed in the Solvent Isotope Effect section, the change in the ratio **3**/**2** should directly measure the primary isotope effect on k_{-2}. Within the accuracy of the **3**/**2** ratio a k_H/k_D of 2 ± 0.3 is observed.

The primary isotope effect for the conversion of **3** to carbanion has also been estimated from the results of runs 32, 33, and 34 of Table 3 (Appendix) and is k_H/k_D is $\geqslant 5$. In summary then the primary deuterium kinetic isotope effect on k_2 is ≥ 5 and on k_{-2} is 2.[3]

[3]The authors wish to thank R. D. Guthrie, University of Kentucky, for providing a preprint of electron-transfer results which also yielded a primary deuterium kinetic isotope for reprotonation of a carbanion. For the anion of 9-methoxyfluorene in methanol at 30°, $k_H/k_D = 5.3$. Although the reasons for the difference between the two systems are not established there may be a solvent isotope effect on the cyclization reaction.

Experimental

Solvents and Bases

Phenyllithium in tetrahydrofuran (THF) was prepared (19) as 0.7–0.8 *M* solutions. Methanol-*O*-*d* (0.99 atoms *D*/molecule) as analyzed by n.m.r. was prepared from dimethyl carbonate (20). Methanol was dried (<0.001 *M* in H_2O) and purified by distillation from magnesium (21). Dimethyl sulfoxide was distilled from lithium amide onto Molecular Sieves (freshly baked 4A). Tetrahydrofuran was freshly distilled from lithium aluminum hydride before use (<0.001 *M* in H_2O). The n.m.r. spectra were obtained in chloroform-*d* with TMS internal standard. Potassium methoxide in methanol (methanol-*O*-*d*) was prepared by reaction of freshly cleaned potassium with the alcohol and was stored under an argon atmosphere (<0.001 *M* in H_2O). All solvents and base solutions were analyzed for water using an Aquatest automatic Karl-Fisher titrator.

Compounds

The preparation and characterization of the substituted **1**, **2**, **3**, and **4** are to be found in the preceding paper (4).

Isomerization with Phenyllithium

To a degassed solution of **1** (0.1–0.05 *M*) in THF under an argon atmosphere at the indicated temperature was added dropwise the THF solution of phenyllithium. The characteristic blue color formed on addition of the first drop of base to the stirred solution. After complete addition (~2 min) the reaction mixture was stirred for the time indicated and then quenched by adding ~1.1 equiv of a 10 volume % solution of acetic acid in THF.

The THF was removed with a rotary evaporator and the residue worked-up with ether–water, extracting the ether layer twice with water. Drying and solvent evaporation yielded the crude reaction mixture. Products were analyzed by n.m.r. and t.l.c.

Samples for irradiation were treated in a similar manner, except the reactions were run in a cell with provision for cooling. A Hanovia 1000 W high pressure mercury lamp was used for irradiation. The long wavelength absorption band was isolated using a soft glass plate for primary filtering and either a Corning glass filter (type 2-62) or a combination of solution filters (cupric chloride and potassium dichromate (22)).

Isomerization and Exchange with Methanol–Methoxide

To the stirred, degassed methanol – potassium methoxide solution held at a constant temperature and under an argon atmosphere was added a THF solution of the substrate. The resulting solutions were 2–4 mol % in THF. At the time indicated, aliquots were removed and treated with ether–water. The ether layer was washed twice with water, dried, and solvent evaporated. The residual oils were analyzed by n.m.r. and t.l.c.

Mixtures of **2** and **3** could be separated by multiple extraction of **2** from the ether solution using 1 *M* potassium dihydrogen phosphate solution.

Samples of **3** were converted to *N*-benzoyl-*N'*-benzylbenzamidines for isotopic analysis by mass spectrometry. The procedure involved basic hydrolysis of **3** to *N*-benzylbenzamidine by treatment of the reaction mixture or isolated **3** with excess water. The *N*-benzylbenzamidine could be extracted from ether using saturated sodium bicar-

bonate. The aqueous layer was made basic with 6 *N* sodium hydroxide and extracted with ether. After washing, drying, and solvent removal the *N*-benzylbenzamidine was isolated. This product was reacted with 1 equiv of benzoyl chloride in benzene. Ether, saturated sodium bicarbonate, and water were used for extraction. The product was recrystallized from (1:1) benzene–hexane (m.p. 139–142°).

Analytical Procedures

The composition of mixtures of the hydrobenzamides, amarines, and *N*-benzylidene-*N*-benzylbenzamidines was normally determined by n.m.r. from the average of five integrations of the benzyl protons of each molecule. The complicating N—H protons were exchanged for deuterons where necessary.

Deuterium analyses of the isolated products or their derivatives were by mass spectrometry (Varian M-66) under conditions where P-1 peaks were absent. Usually the average of three scans of maximum scale expansion was obtained. In some cases n.m.r. integration was used for deuterium analysis again with maximum scale expansion.

The authors wish to thank the National Research Council of Canada for their financial assistance.

Appendix

Calculation of the ratio k_{-2}/k_{-3} of Scheme 4 using **3** as the substrate requires three separate pieces of evidence.

(a) Intramolecularity

Since **1** can be converted to **3** in CH_3OD without complete exchange occurring (run 29), the use of hydrogen–deuterium exchange as a quantitative measure of carbanion formation probably results in an underestimation of the extent of carbanion formation. One simplifying assumption is that the observed 14% intramolecularity (run 29) is a feature common to the carbanion whether formed from **1** or **3**. Thus in the following calculations it was assumed that exchange measured only 86% of the reacted material.

(b) Kinetic Deuterium Isotope Effect

In order to estimate the primary kinetic deuterium isotope effect, a sample of monodeuterio-**3** was employed (runs 32, 33, and 34) which had been isolated from a run similar to run 29. By deuterium analysis of the **2** generated at low conversion, the isotope effect could be estimated (see Scheme 7).

As expected the isolated **2** contained primarily d_1 material, but to make a more accurate determination of the isotope effect, it was necessary to correct for the fact that the

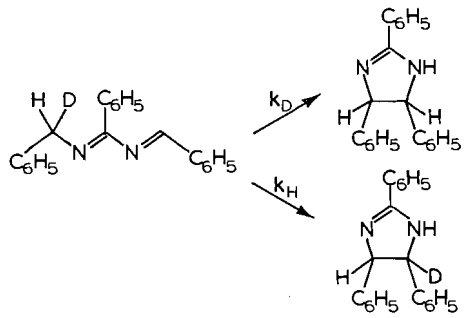

SCHEME 7

starting material (**3**) was only 77% d_1 and its composition changed to 66% d_1 during the reaction. This correction was applied crudely as follows: To obtain **2** of the observed isotopic composition ($\sim$65% d_1) from **3** of the composition of the starting material, an isotope effect of about 5 would be required; **3** of the composition observed at the end of the reaction ($\sim$66% d_1) would require a very large isotope effect. Thus the actual isotope effect is described as $k_H/k_D > 5$.

(c) Relative Rates of Exchange and Cyclization

The method employed to estimate k_{-2}/k_{-3} used the results of runs 30 and 31 to compare the relative amounts of cyclization and exchange. The results were fit to a scheme which allowed for the isotope effect and the further reaction of exchanged **3**. The technique is essentially that employed in an earlier study (18) and will not be described further. A ratio of 0.3 ± 0.1 for k_{-2}/k_{-3} fit the data best and proved to be insensitive to isotope effect.

1. (*a*) M. A. LAURENT. Ann. **21**, 130 (1837). (*b*) M. A. LAURENT. C. R. Acad. Sci. Paris, **19**, 353 (1844).
2. H. H. STRAIN. J. Am. Chem. Soc. **49**, 1558 (1927).
3. D. H. HUNTER and S. K. SIM. J. Am. Chem. Soc. **91**, 6202 (1969).
4. D. H. HUNTER and S. K. SIM. Can. J. Chem. This issue.
5. R. KUHN and D. REWICKI. Liebigs Ann. Chem. **690**, 50 (1965).
6. D. J. CRAM, B. RICKBORN, C. A. KINGSBERY, and P. HABERFIELD. J. Am. Chem. Soc. **83**, 3678 (1961).
7. D. J. CRAM. Fundamentals of carbanion chemistry. Academic Press, Inc., New York, 1965. Chapt. 5.
8. D. J. CRAM and R. D. GUTHRIE. J. Am. Chem. Soc. **88**, 5760 (1966).
9. J. ALMY, D. C. GARWOOD, and D. J. CRAM. J. Am. Chem. Soc. **92**, 4321 (1970).

Can. J. Chem. Downloaded from www.nrcresearchpress.com by 210.87.254.40 on 09/05/12
For personal use only.

10. C. D. RITCHIE and R. E. USCHOLD. J. Am. Chem. Soc. **90**, 3415 (1968).
11. (*a*) R. B. BATES, W. H. DIENES, D. A. MCCOMBS, and D. E. POTTER. J. Am. Chem. Soc. **91**, 4608 (1969). (*b*) H. KLOOSTERZIEL and J. A. A. VAN DRUNEN. Rec. Trav. Chim. **88**, 1084 (1969).
12. (*a*) P. R. STAPP and R. F. KLEINSCHMIDT. J. Org. Chem. **30**, 3006 (1965). (*b*) L. H. SLAUGH. J. Org. Chem. **32**, 108 (1967). (*c*) R. B. BATES and D. A. MCCOMBS. Tetrahedron Lett. 977 (1969). (*d*) H. KLOOSTERZIEL and J. A. A. VAN DRUNEN. Rec. Trav. Chim. **89**, 368 (1970).
13. R. B. BATES, D. W. GOSSELINK, and J. A. KACZYNSKI. Tetrahedron Lett. 205 (1967).
14. R. B. WOODWARD and R. HOFFMANN. The conservation of orbital symmetry. Academic Press, Wienheim, 1971.
15. V. R. SANDEL, S. V. MCKINLEY, and H. H. FREEDMAN. J. Am. Chem. Soc. **90**, 495 (1968).
16. H. KLOOSTERZIEL and J. A. A. VAN DRUNEN. Rec. Trav. Chim. **87**, 1025 (1968).
17. C. J. PEDERSEN. J. Am. Chem. Soc. **89**, 7017 (1967).
18. D. H. HUNTER and R. W. MAIR. Can. J. Chem. **47**, 2361 (1969).
19. H. GILMAN and B. J. GAJ. J. Org. Chem. **22**, 1165 (1957).
20. A. E. STREITWIESER, L. VERBIT, and P. STANG. J. Org. Chem. **29**, 3706 (1969).
21. A. I. VOGEL. Practical organic chemistry. Longmans, Greene and Co., New York, 1948.
22. J. G. CALVERT and J. N. PITTS. Photochemistry. Wiley, New York, 1967. p. 740.

Can. J. Chem. Downloaded from www.nrcresearchpress.com by 210.87.254.40 on 09/05/12
For personal use only.

Pyrochlores. VII. The Oxides of Antimony: an X-Ray and Mössbauer Study[1]

DAVID J. STEWART, OSVALD KNOP, AND CONRAD AYASSE[2]
Department of Chemistry, Dalhousie University, Halifax, Nova Scotia

AND

F. W. D. WOODHAMS
Department of Natural Philosophy, University of Aberdeen, Aberdeen, Scotland

Received September 23, 1971

Antimonic acid cannot be dehydrated by heating in air to give products of constant and reproducible weight without simultaneous reduction of some of the Sb^{V} to Sb^{III}. Neither anhydrous Sb_2O_5 nor the hydroxy oxide Sb_3O_6OH postulated by Dihlström and Westgren can be obtained by this method. Two well-defined products of the dehydration/decomposition are $Sb_2O_{4.35(5)} = Sb_6O_{13}$, which forms between 650 and 850°, and β-Sb_2O_4. The latter, and *not* Sb_2O_3, results on heating Sb_6O_{13} to 935°. Sb_6O_{13} has a cubic structure of the defect pyrochlore type, $a_0 = 10.303(1)$ Å, $x(O_2) = 0.4304(14)$. Combined evidence from X-ray diffractometry, density determination, and Mössbauer spectroscopy leads to $Sb^{3+}Sb^{5+}{}_2O_6O_{0.5}$ as the most probable structural formula.

The Mössbauer parameters of β-Sb_2O_4 are closely similar to those reported for α-Sb_2O_4, but the isomer shifts (relative to InSb at 77 °K) for Sb^{V} in antimonic acid and Sb_6O_{13} are significantly larger than those in α- and β-Sb_2O_4.

L'acide antimonique ne peut être déshydraté par chauffage à l'air pour donner des produits de poids constants et reproductibles sans produire une réduction simultanée d'un peu de Sb^{V} en Sb^{III}. On ne peut obtenir par cette méthode ni Sb_2O_5 anhydre ni l'hydroxyoxyde Sb_3O_6OH postulé par Dihlström et Westgren. Deux produits de la déshydratation/décomposition bien characterisés sont $Sb_2O_{4.35(5)} = Sb_6O_{13}$, qui se forme entre 650 et 850°, et β-Sb_2O_4. C'est ce dernier, et non pas Sb_2O_3, qui résulte du chauffage de Sb_6O_{13} à 935°. Sb_6O_{13} possède une structure cubique du type pyrochlore défectueux, $a_0 = 10.303(1)$ Å, $x(O_2) = 0.4304(14)$. Les données combinées de la diffraction aux rayons X, de la détermination de densité et de l'effet Mössbauer mènent à $Sb^{3+}Sb^{5+}_2O_6O_{0.5}$ comme formule structurale la plus probable.

Les paramètres Mössbauer du β-Sb_2O_4 sont très semblables à ceux rapportés pour α-Sb_2O_4, mais les déplacements isomères (relatifs à InSb à 77 °K) pour Sb^{V} dans l'acide antimonique et Sb_6O_{13} sont plus grands que ceux dans α- et β-Sb_2O_4.

Canadian Journal of Chemistry, **50**, 690 (1972)

Antimony has been reported to form oxides of formulae Sb_2O_3 (cubic, senarmontite; orthorhombic, valentinite), α-Sb_2O_4 (orthorhombic, cervantite), (1), β-Sb_2O_4 (monoclinic) (2), Sb_6O_{13} (3, 4), and Sb_2O_5 (5–13). In addition, an hydroxy oxide, Sb_3O_6OH, has been claimed to exist (14), and hydrated forms of Sb_2O_3 and Sb_2O_5 are known as antimonious and antimonic acids, respectively.

The existence of the two forms of Sb_2O_3 is unquestionable, and both the Sb_2O_4 dimorphs have been well characterized by single-crystal X-ray studies (1, 2). Both antimonious and antimonic acid may be readily prepared, although it is doubtful that their water content can be defined, as many authors have tried to do (9, 10, 15–18).

No conclusive evidence is available in the literature for the existence of Sb_6O_{13} and Sb_3O_6OH, which are claimed to form during the dehydration/decomposition of antimonic acid. The formula Sb_6O_{13} appears to have been assigned to an apparent "plateau" (~500–700°) on the isobaric (10 Torr) "equilibration" curve for antimonic acid (Fig. 1*a*) merely because it was the nearest "whole number formula" to the observed MW. The second plateau (~700–900°) on the curve was originally assigned to Sb_2O_4 (3). However, the material corresponding to this plateau gave an X-ray powder pattern of the cubic *pyrochlore* (*P*) type rather than that of Sb_2O_4, which prompted Dihlström and Westgren (14) to reassign the 700–900° plateau to the composition Sb_3O_6OH. This interpretation was based entirely on circumstantial evidence and no direct attempt was made to

[1]For Part VI see ref. 19.
[2]Holder of a Killam Graduate Scholarship, 1969–1971.

Can. J. Chem. Downloaded from www.nrcresearchpress.com by 210.87.254.105 on 09/05/12
For personal use only.

Can. J. Chem. Downloaded from www.nrcresearchpress.com by 210.87.254.105 on 09/05/12
For personal use only.

verify the presence of the postulated OH group. The formula Sb_3O_6OH was chosen by analogy with the reported "ideal" formulae of minerals having the *P* structure such as pyrochlore itself ($NaCaNb_2O_6F$) and romeite ($NaCaSb_2O_6OH$); it was considered proven by the synthesis of the compound $BiTa_2O_6F$, which turned out to have a cubic structure of the *P* type (14). Since the presence of an OH group in the dehydration product obtained at 700° requires that either OH or water be present in all precursors, the formula Sb_6O_{13} assigned to the 500–700° product is not compatible with the formula Sb_3O_6OH claimed for the 700–900° material. Nevertheless, both these compounds are accepted by many present-day texts, as is anhydrous Sb_2O_5, whose formation by dehydrating antimonic acid was questioned as long ago as 1927 (4, 18).

The considerable age of most of the literature quoted in the foregoing, and our interest in compounds with the *P* structure (19), have prompted us to re-investigate the products of thermal dehydration/decomposition of antimonic acid. The minimum information required to establish the nature and identity of these products is reliable knowledge of their composition. Chemical analysis presents, however, numerous difficulties. The material is practically insoluble; its content of hydrogenic species may be very small, or it may depend on the exact conditions of sample preparation; and the difference between the formulae Sb_2O_4 and Sb_6O_{13}, for example, corresponds to a difference of only about 2 wt.% in the Sb content. Direct and indirect evidence from other methods is therefore desirable. In particular, since the Mössbauer effect in ^{121}Sb has been shown to yield useful information about the valency state *in situ* of antimony in compounds such as Sb_2O_3 (20–22), α-Sb_2O_4 (22), and a material referred to as Sb_2O_5 (21–23), it appeared that it should be useful in this study. The method is well suited for demonstrating the simultaneous presence of Sb^{III} and Sb^V as the absorption peaks for these valency states are well separated, having isomer shifts (relative to InSb) of about -3 to -6 mm/s and around $+9$ mm/s, respectively. In α-Sb_2O_4 the two absorption peaks have been reported to have equal areas (22). This suggests that measurement of Sb^{III}:Sb^V area ratios should enable Sb_2O_4 to be distinguished from, say, Sb_6O_{13} or Sb_3O_6OH, for which area ratios of 1:2 would be expected, or from products with intermediate Sb^{III}:Sb^V contents.

Experimental

Antimonic acid was prepared by hydrolysis of $SbCl_5$ (Baker & Adamson, 99%) in a mixture of ice and 30% H_2O_2. The white precipitate obtained was boiled for several hours and then washed by decantation, filtered, and dried to constant weight in air at room temperature; the drying process was followed by plotting a drying curve. The time taken to achieve constant weight was usually about 5 days. Preparations made in glass apparatus contained Na as an impurity. However, the use of Teflon vessels enabled a sample to be prepared whose spectrographic analysis was: Na, 0.01%; Bi, Pb, Cu, Al, Fe, 0.001%; all other elements, less than 0.001%.

All the antimonic acid preparations were only very sparingly soluble in all reagents tried, unless first the oxide was reduced in H_2 to the metal. Unfortunately, the temperature required to reduce the antimonic acid was also sufficient to cause some of the metal to vaporize. The following procedure was therefore used instead. All samples were first fired to constant weight at either 700 or 950° in air in a muffle furnace and the loss of weight noted. Infrared spectra of these products showed them to contain no detectable OH or H_2O. Next the products were fired for 8 h in a stream of H_2 at 635(5)° followed by cooling in H_2. If the X-ray powder photograph of this product showed lines other than those of Sb_2O_3 (either senarmontite or a mixture of senarmontite and valentinite) the sample was ground in an agate mortar and the firing repeated. When complete reduction to Sb_2O_3 had been accomplished, the weight loss, after correction for losses on grinding, could be used to calculate the MW of the initial material and also of the 700 and 950° intermediates. Knowing from the Mössbauer spectra that only Sb^V was present in antimonic acid,[3] the formula of the initial material could be calculated as $Sb_2O_5.nH_2O$. Since the infrared spectra showed the 700 and 950° products to contain no hydrogenic species, the formulae of these materials could also be derived. In each firing under H_2 a control sample of Sb_2O_3 was included to check that no reduction occurred beyond Sb_2O_3. There was no evidence of this taking place at 635(5)° on any firing. The method gave excellent reproducibility, with a maximum variation, on a formula of Sb_2O_4, of ± 0.05 on the oxygen figure.

Mössbauer Spectra

The Mössbauer spectrometer and computer fitting technique used have been described elsewhere (24). The source was 0.5 mCi ^{121}Sn in $BaSnO_3$ (New England Nuclear Corp.). Both source and absorber were maintained at liquid-nitrogen

[3]For the Sb^{III} absorption to be visible, the Sb^{III} content of the sample must be greater than about 5–10% of the Sb^V content, so that there is a possibility that a small amount of Sb^{III} could have been present. Its presence would mean only very slight changes in the formulae calculated for the antimonic acid samples (Table 1).

TABLE 1. Antimonic acid preparations

No.	Method	Formula	a_0, Å
180	Hydrolysis of $SbCl_5$ in ice	$Sb_2O_5.3.55H_2O$	10.338(5)
8*a*	Hydrolysis of $SbCl_5$ in ice and H_2O_2	$Sb_2O_5.3.67H_2O$	10.337(2)
61	Excess HNO_3 added to a solution of $KSb(OH)_6$	$Sb_2O_5.3.51H_2O$	10.378(2)

temperature whilst collecting the spectra. Isomer shift values are quoted with respect to InSb at 77 °K. Absorbers were prepared by dispersing the sample powder in acrylic disks, each disk containing about 10 mg/cm^2 of natural Sb. When asymmetry of a resonance peak was evident (*e.g.*, the Sb^{III} peak of sample 180*a*, Fig. 3*c*), the peak was treated as being due to an unresolved electric field gradient and fitted by an 8-line program similar to that described by Ruby *et al.* (20). The ratio of the quadrupole moments of the excited and the ground states was taken as 1.34 (25); the asymmetry parameter, which has only a small effect on the spectrum, was taken as zero.

If it is assumed that at 77 °K the recoil-free fractions for Sb^{III} and Sb^{V} atoms in non-equivalent crystallographic sites are essentially equal, the Sb^{III}:Sb^{V} area ratios of the absorption peaks can be equated with the corresponding ratios in mixed-valency samples. While in general this assumption can by no means be taken for granted, there are grounds for believing that for the compounds investigated here it cannot be far wrong and leads to reasonably realistic independent estimates of the Sb^{III}:Sb^{V} ratios.[4]

X-Ray Diffraction

Integrated X-ray intensities were obtained on a Philips powder diffractometer fitted with a focussing monochromator after the rotating specimen. Details of the wavelengths (Cu Kα), sample preparation, counting procedure, and powder photography have been described elsewhere (26, 27).

F-Refinements of the structure of Sb_6O_{13} (individual isotropic temperature factors) were carried out using atomic scattering factors for O^{2-} (28) and Sb^{3+}, Sb^{5+} (29), the latter corrected for dispersion (both parts, ref. 30). Full-matrix *ad hoc* programs and the weighting scheme $1/\sigma(I_0)$ were employed.

[4]For α-Sb_2O_4, in which Sb^{III} and Sb^{V} atoms occupy each its own type of site in a ratio 1:1 (1), Long *et al.* (22) under experimental conditions similar to ours obtained an area ratio which was at first stated to be close to unity but later (31) specified as 0.91(3). The ratio observed in the present work for β-Sb_2O_4 was 0.98(4), and for Sb_6O_{13} the ratio agreed reasonably well with the ratio obtained from chemical analysis (Tables 2 and 4). It seems that the observed area ratios tend to be smaller than ratios obtained from chemical analysis or from crystallographic considerations. However, the errors associated with the peak areas are sufficiently large that any small differences in the recoil-free fractions would not significantly alter the Sb^{III}:Sb^{V} ratio. It is of interest to note that in a recent investigation of non-stoichiometric pyrochlores resembling Sb_6O_{13} and containing simultaneously Sn^{2+} and Sn^{4+}, the recoil-free fractions of these two valency species have been shown to differ by less than 10% (35).

Other Methods

Infrared spectra were recorded with a Perkin–Elmer model 521 spectrophotometer. Specimens were prepared and examined both in the form of KBr pellets and as mulls in Nujol.

Thermogravimetric analysis curves were obtained on a Stanton model HT thermobalance in stagnant air with a linear heating rate of 6°/min. Densities of sample powders were determined by a method described in ref. 24.

Results and Discussion

Table 1 shows the formulae and the dimensions of the cubic unit cell of three preparations of antimonic acid after drying to constant weight at room temperature. The preparations had slightly different water contents, even though closely similar preparative procedures were used in each case.

Products Obtained by Firing Antimonic Acid below 900°

Figure 1*b* shows the t.g.a. curve obtained for preparation 8a.[5] The MWs at the "plateaus" are assigned from the chemical analysis of the products resulting at the corresponding temperatures. Allowing for different experimental conditions, the general shape of the curves in Fig. 1 *a* and *b* is much the same.[6]

The t.g.a. curves between room temperature and *ca.* 700° correspond to dehydration/decomposition of antimonic acid. Despite the apparent inflexion in the t.g.a. curve at about 400°, which might be interpreted as indicating the formation of Sb_2O_5, it was not possible to obtain under isothermal firing conditions any material of constant and reproducible weight other than the final 700° product, $Sb_2O_{4.35}$ (*vide*

[5]All preparations gave the same t.g.a. curves except for different initial MWs and hence longer, or shorter, dehydration/decomposition regions.

[6]Curve 1*a* represents, schematically, the average *oxygen* contents of the three sample runs reported in ref. 4. The water contents of the samples must be allowed for when comparing 1*a* with the t.g.a. curve 1*b*. At 200° this would increase the MW by an amount corresponding to 1.49–1.77H_2O.

Can. J. Chem. Downloaded from www.nrcresearchpress.com by 210.87.254.105 on 09/05/12
For personal use only.

Can. J. Chem. Downloaded from www.nrcresearchpress.com by 210.87.254.105 on 09/05/12
For personal use only.

infra). It must thus be concluded that the inflexion arises from a change in dehydration/-decomposition rate rather than from the formation of a discrete compound. The loss of water from antimonic acid was accompanied by reduction of some of the Sb^{V} to Sb^{III}, as noted already by Simon and Thaler (4) and by Natta and Baccaredda (18).

Direct evidence that all the antimony in the antimonic acid was pentavalent (Fig. 3*a*) and that reduction of Sb^{V} occurred during the firing was provided by the Mössbauer spectra. This evidence was especially valuable because the chemical analysis could not distinguish whether a weight loss corresponded to loss of water, OH, oxygen, or a combination of these species, and was therefore ineffective. The Mössbauer parameters for the various spectra are listed in Table 2.

The X-ray powder patterns of antimonic acid and of the products of isothermal firing were all well defined and of the cubic *P* type (space group *Fd3m*).[7] However, the relative intensities of the reflections changed with the firing temperature (Fig. 2). A structural rearrangement must therefore occur during firing. The large changes in intensities indicate that it is the cations that must undergo redistribution, since loss, or rearrangement, of the anions could not cause variations of this magnitude. The dependence of diffraction intensity on firing temperature supports the conclusion from the Mössbauer spectra, *viz.*, that firing antimonic acid does not merely cause a loss of adsorbed water.

Existence of Sb_2O_5

These results also explain the poor correlation of the X-ray powder patterns for "Sb_2O_5" compiled by Swanson *et al.* (12), who considered all the reported samples to be identical, whether hydrated or not. In fact some samples were antimonic acid, some were material dried at 100° or higher, and Swanson's own preparation, which had been fired to 780°, was in reality $Sb_2O_{4.35}$ (*vide infra*). This is the material whose powder pattern is listed in the 1966 edition of the ASTM X-ray powder data card file (No. 11-690) erroneously as Sb_2O_5. Our results also

[7]The similarity of the X-ray powder patterns of the dehydration products was pointed out already in refs. 3, 4, and 18.

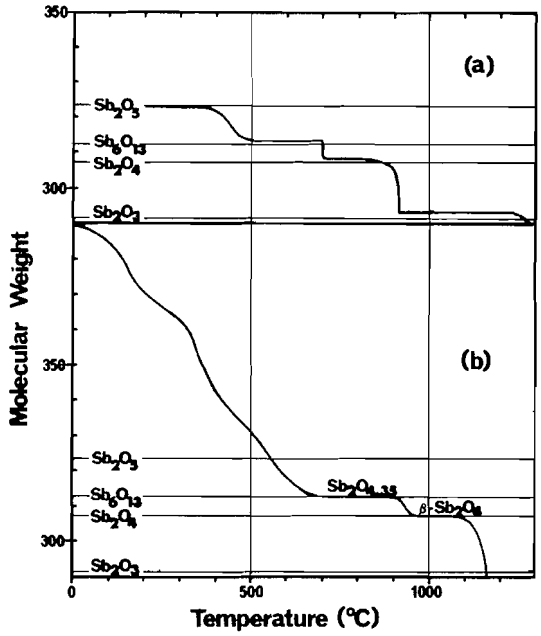

FIG. 1. Comparison of dehydration/decomposition curves of antimonic acid. (*a*) Isobaric "equilibrium" conditions (10 Torr; composite curve from data of ref. 4, see text). (*b*) Thermogravimetric analysis, this work (No. 8*a*; heating rate, 6°/min in stagnant air). Curve *a* represents, schematically, only the oxygen content of the solid.

explain the fact that some authors have found "Sb_2O_5" to be yellow, while others reported it to be white. We found, in agreement with ref. 18, that firing antimonic acid (which is white) to temperatures of 150 to 450° induced the development of a yellow color which intensified with increasing temperature. Firing to 650° produced $Sb_2O_{4.35}$ which was again white. Table 3 compares our preparations with those reported in the literature and shows the correlation possible if the above factors are taken into consideration.

A survey of "Sb_2O_5" samples used for previous Mössbauer studies also reveals that the authors did not in fact have samples of anhydrous antimony pentoxide. The material examined by Long *et al.* (22) was a commercial product marketed by the Research Organic/-Inorganic Chemical Co., Sun Valley, Calif., as "99.5% Sb_2O_5". Supposedly the same material was supplied to us; our analysis indicated a formula of $Sb_2O_5.3.61H_2O$. Whilst the difference in formulation does not invalidate those authors' assignment of the isomer shift for the observed absorption peak as being for Sb^{V}, it

Can. J. Chem. Downloaded from www.nrcresearchpress.com by 210.87.254.105 on 09/05/12
For personal use only.

TABLE 2. Mössbauer parameters (in mm/s) of antimony oxides at 77 °K*

Compound	Sb^{III} IS	Sb^{III} QS	Sb^{III} Γ	Sb^{V} IS	Sb^{V} QS	Sb^{V} Γ	Area ratio Sb^{III}:Sb^{V}	Reference
Sb_2O_3 (cubic)	−3.17(12)†	18.3(4)	3.14(10)	—	—	—	—	22
	−3.30(7)	18.2(5)	3.07(8)	—	—	—	—	This work
Sb_2O_3 (orthorhombic)	−3.18(9)†	17.0(2)	2.89(11)	—	—	—	—	22
α-Sb_2O_4	−6.21(12)†	16.4(6)	3.13(14)	8.76(9)	−6.1(10)	3.31(15)	‡	22
β-Sb_2O_4 (No. 180*a*, 935°)	−6.30(15)	17.0(14)	3.2(2)	8.79(6)	§	3.47(10)	0.98(4)	This work
Antimonic acid (No. 180)	—	—	—	9.31(12)	§	3.6(2)	—	This work
$Sb_2O_{4.35}$ (=Sb_6O_{13}) (No. 180*f*)	−6.6(4)	17(6)	3.4(6)	9.27(6)	§	3.17(10)	0.42(6)	This work
(No. 117*a*)	−5.8(4)	§	5(1)	9.35(6)	§	3.7(2)	0.36(7)	This work
"Sb_2O_5" (see text)	—	—	—	9.21(6)	−4.3(11)	3.49(13)	—	22

*IS, isomer shift relative to InSb at 77 °K; QS, quadrupole splitting (e^2qQ); Γ, line width (full-width at half-height). The standard deviations are in units of the last decimal place; those for this work are quoted with 90% confidence limits.

†Converted to InSb as reference by adding 8.15(6) mm/s to the IS figures quoted in ref. 22.

‡The areas of the Sb^{III} and Sb^{V} absorptions were quoted as being equal, but no figure was given for their ratio. However, in a later publication Bowen *et al.* (31) refer back to ref. 22 and quote the Sb^{III}:Sb^{V} ratio as 0.91(3).

§It did not appear warranted to fit the 8-line quadrupole model to these spectra, as there was no visible asymmetry.

TABLE 3. Correlation of reported "Sb_2O_5" X-ray powder patterns with those of dehydration/decomposition products of antimonic acid investigated in this work

ASTM Card	Reference	Material	*a*, Å	Intensity of reflection 111	311	222	400	331	422	511 + 333	Radiation	Corresponds to (Fig. 2)
1-0154	13	Yellow	10.3	100	80	80	16	4	—	16	Mo Kα	*b*
2-1386†	18	"Antimonic anhydride" (Kahlbaum commercial reagent); yellow	10.2	40	40	60	40	—	20	50	Mo Kα	*a* to *b**
2-1383‡	18	$KSb(OH)_6 + HNO_3$; yellow	10.2	—	40	60	50	—	—	20	Mo Kα	?*
2-1385	18	Kahlbaum material dehydrated at 390°; yellow	10.3	20	—	60	20	—	—	50	Mo Kα	*d* to *e**
11-690	12	$Sb + HCl + HNO_3$; product fired at 780° for ½ h; white	10.305	27	22	100	30	4	2	6	Cu Kα	*e*
16-938§	14	White	10.30	—	60	100	80	20	20	60	Cr Kα	*e**

*The observed photographic intensities were originally estimated visually as "strong", "weak", etc. For inclusion in the ASTM file they were assigned the above numerical values. Comparison with our diffractometer intensities is therefore only very approximate, which makes a unique correlation of the material difficult. The standard ASTM conversion method gives a particularly bad agreement for card No. 16-938 (*cf.* the original table of intensities, ref. 14).

†At least 10 years old; stated to be $Sb_2O_5.H_2O$.

‡Five years old, dehydrated at 360°; stated to be $Sb_2O_5.3H_2O$.

§Listed as Sb_3O_6OH.

TABLE 4. Comparison of $Sb_2O_{4.35}$ preparations

Preparation	Method	Formula*	a_0, Å	Density, g/cm^3	Reference
117*a*	Hydrolysis of $SbCl_5$ in ice, Teflon apparatus; 735°/24 h	$Sb_2O_{4.40}$, $Sb_2O_{4.38}$	10.303(1)	5.62(1)	This work
180*f*	Hydrolysis of $SbCl_5$ in ice and H_2O_2; 500°/240 h, 580°/24 h, 590°/48 h, 680°/17 h, 720°/17 h	$Sb_2O_{4.35}$, $Sb_2O_{4.29}$	10.307(3)		This work
204*b*	Hydrolysis of $SbCl_5$ in ice and H_2O_2; 730°/5 h, 700°/20 h	$Sb_2O_{4.31}$, $Sb_2O_{4.35}$	10.304(3)		This work
"Sb_2O_5"	Sb + HCl + HNO_3; 780°/½ h		10.305		12
"Sb_3O_6OH"	Sb + HNO_3; 780°/3 h		10.30†	5.78	14

*Duplicate results of chemical analysis. For method, see text.
†Converted from kX.

again discounts the claim that an oxide of formula Sb_2O_5 was examined. Other commercial products listed by the suppliers as "Sb_2O_5" have been found from our analysis to be either α-Sb_2O_4 (Fisher Certified Reagent), amorphous $Sb_2O_{4.3}$ (Baker Analyzed Reagent), or again, antimonic acid.

The Oxide $Sb_2O_{4.35}$ or Sb_6O_{13}

The first isothermally reproducible product obtained from firing antimonic acid appears at the plateau at 700–900° on the t.g.a. curve (Fig. 1*b*). It retains the cubic *P* structure (Fig. 2*e*) and was reproducible in composition from one preparation to another (Table 4). The MW obtained was 313.1(8), which corresponds to $Sb_2O_{4.35(5)}$ and could therefore be as well represented as being Sb_3O_6OH. However, its infrared spectra showed no sign of any OH or H_2O absorption peaks. Furthermore, the MW for Sb_3O_6OH (318.9 per 2 Sb) is outside the error margin of the chemical analysis. The Mössbauer spectrum of the $Sb_2O_{4.35}$ (Fig. 3*b*) contained two peaks corresponding to Sb^{III} and Sb^V, respectively, whose area ratio was 0.42(6) (Table 2). This compares to the ratio of Sb^{III}:Sb^V = 0.48(4) indicated by chemical analysis. From this combined evidence it must be concluded that antimony forms an oxide of formula $Sb_2O_{4.35(5)}$ which is thermally and chemically stable, and which is reproducible from one preparation to another. A material prepared by thermal decomposition of antimonic acid and having the formula proposed by Dihlström and Westgren on the basis of circumstantial evidence, does not exist.

Firing above 900°

When the oxide $Sb_2O_{4.35}$ is fired above 935° in air, a small loss in weight occurs. The product is β-Sb_2O_4. Its lattice parameters agree satisfactorily with those reported by Skapski and Rogers (1). These authors give 933(10)° as the temperature of formation of β-Sb_2O_4, in close agreement with the temperature observed by us.

The Mössbauer spectrum of the 935° product (Fig. 3*c*) showed two peaks of Sb^{III}:Sb^V area ratio 0.98(4) and thus supported our assignment of the identity of the product. The isomer shifts of the Sb^{III} and Sb^V absorptions were close to those obtained by Long *et al.* (22) for α-Sb_2O_4 (Table 2). This is not surprising when the similarity of the α and β structures is considered.

On the other hand, the isomer shift of the Sb^V absorption in β-Sb_2O_4 (No. 180*a*, Table 2) is significantly lower than that in $Sb_2O_{4.35}$ (Nos. 180*f* and 117*a*), indicating an increase in the s-electron density at the ^{121}Sb nucleus as compared with that in $Sb_2O_{4.35}$. This variation is not unexpected, as the Sb^V coordinations are slightly different in the two structures. In $Sb_2O_{4.35}$ the six nearest oxygen neighbors (at 1.957(18) Å)[8] are equidistant from the Sb^V atom, whereas in the monoclinic β-Sb_2O_4 the six Sb^V—O distances vary between 1.956(9) and 1.990(9) Å (2). Although the Sb^V environments in both these oxides are not of cubic symmetry, the electric field gradient produced is not sufficient to give an asymmetric quadrupole spectrum. It merely leads to a slight in-

[8]Owing to the incomplete occupation of the 16(*c*) equipoint in the structure of $Sb_2O_{4.35}$ the randomly distributed cation vacancies in 16(*c*) will affect the positions of their nearest oxygen neighbors in 48(*f*), thereby indirectly distorting the coordination octahedron about Sb^V in 16(*d*). The distance 1.957(18) Å determined from X-ray diffraction must thus be viewed as a mean of the (randomly) unequal Sb^V–O distances in the defect *P* structure (*cf.* also next section).

Can. J. Chem. Downloaded from www.nrcresearchpress.com by 210.87.254.105 on 09/05/12
For personal use only.

crease in the line width relative to that observed in InSb, 2.7(2) mm/s, for example.

Once formed, the β-Sb_2O_4 was thermally stable up to 1050°, and after being identified as such could be used as a reference standard in any subsequent gravimetric analysis of less reduced Sb oxides. The analytical figures obtained on this basis were always in excellent agreement with those obtained by the chemical analysis method described earlier.

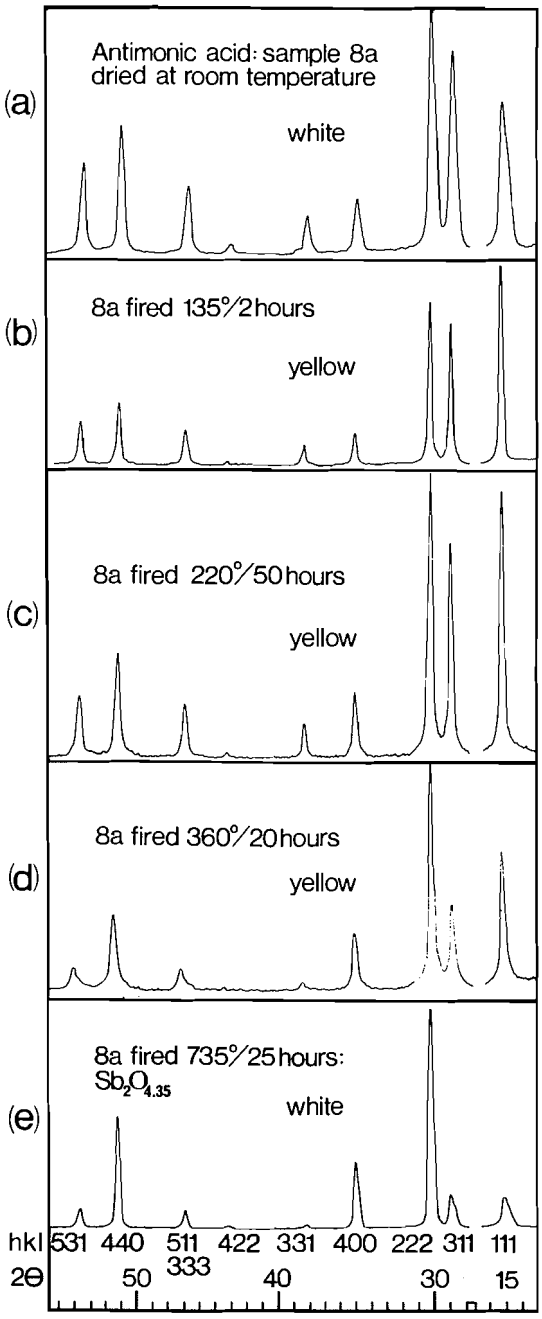

FIG. 2. X-Ray powder diffraction patterns of antimonic acid (No. 8*a*) fired to different temperatures in air (Cu Kα radiation).

Finally, at temperatures above 1050°, β-Sb_2O_4 vaporized without transforming first to Sb_2O_3. When firing was discontinued before all of the β-Sb_2O_4 had vaporized, no weight gain occurred on cooling the remaining material. This indicated that no oxidation took place on cooling. Powder photographs showed only β-Sb_2O_4 to be present. However, crystals of both Sb_2O_4 and Sb_2O_3 could be collected from the walls of the t.g.a. furnace, where they had been deposited as the result of the vaporization process.

Crystal Structure of $Sb_2O_{4.35} = Sb_6O_{13}$

A crystal-structure refinement from powder diffractometer intensities was carried out on $Sb_2O_{4.35}$ (No. 117*a*) to define the material further. The measured density of this sample along with its chemical analysis (Table 4) indicated an occupancy of the *P* unit cell which was very close to $8\ Sb^{III} + 16\ Sb^{V} + 52\ O = 4\ Sb_6O_{13}$. The most likely distribution amongst the *P* sites should then be

16(*c*)	16(*d*)	48(*f*)	8(*a*)
$8\ Sb^{3+}$	$16\ Sb^{5+}$	$48\ O^{2-}$	$4\ O^{2-}$

This model refined to a low value of *R* and gave small or very small correlation coefficients (Tables 5 and 6). Refinements allowing for simultaneous variation in the occupancies of 16(*c*) and 8(*a*) according to the formula $Sb_u^{3+}Sb_2^{5+}O_6^{2-}O_{(3u/2)-1}^{2-}$ showed that this model ($u = 1$) in fact gives the minimum *R* value (Fig. 4). When the statistical validity of models with other values of *u* was tested against $u = 1$ as the best model,[9] it was found that $u = 0.9$ could be rejected at significance levels between 50 and 5%, while $u = 1.1$ could be rejected at the 50% but not at the 25% significance level. All the other *u* values could be rejected at levels down to $\frac{1}{2}$% with the possible exception of $u = 1.2$, which was barely acceptable at the $\frac{1}{2}$% level. Probable occupancies of 16(*c*) between, approximately, 7.2 and 9.6 Sb could therefore also account for the observed diffraction intensities. A wide range of other conceivable ionic distri-

[9]The generalized discrepancy factor $R_w(u)$ was compared with R_w (1) as discussed by Hamilton (32).

Can. J. Chem. Downloaded from www.nrcresearchpress.com by 210.87.254.105 on 09/05/12
For personal use only.

Can. J. Chem. Downloaded from www.nrcresearchpress.com by 210.87.254.105 on 09/05/12
For personal use only.

TABLE 5. Refinement of the crystal structure of $Sb_2O_{4.35} = Sb_6O_{13}$ ($= Sb^{3+}Sb_2^{5+}O_6^{2-}O_{0.5}^{2-}$)

Parameter	Initial values	After 10 cycles
$x(O_2)$	0.4330	0.4304(14)
$B(16c)$, Å^2	0.9	6.2(4)
$B(16d)$, Å^2	0.9	0.9(1)
$B(48f)$, Å^2	1.5	1.7(7)
$B(8a)$, Å^2	1.5	11.8(63)
R, %		1.68
R_w, %		1.95

TABLE 6. Observed and calculated intensities (Cu Kα) for $Sb_2O_{4.35} = Sb_6O_{13}$*

hkl	I_0	I_c	I_0'
111	31.9	31.8	32.3
220	0.5	0.4	0.5
311	16.2	16.8	16.1
222	100.9	100	100.0
400	28.4	28.0	27.8
331	1.1	1.7	1.1
422	1.1	1.4	1.0
511, 333		6.5	
440	40.4	40.0	38.0
531	7.8	8.2	7.3
620	—	0.2	—
533	4.0	3.7	3.6
622	33.9	33.8	30.9
444	8.8	8.6	8.0
711, 551		6.3	
642	—	0.0	—
731, 553		6.3	
800	4.6	4.5	4.0
733	—	0.6	—
822, 660		0.5	
751, 555		2.2	
662	10.5	10.8	8.9
840	9.7	9.4	8.2
911, 753		3.2	
664	—	0.1	—
931	2.3	2.3	2.0
844	6.7	6.5	5.7
933, 771, 755		2.5	
10.2.0, 862		0.1	
951, 773		2.6	
10.2.2, 666		7.7	
953	2.1	1.7	1.8
10.4.2	—	0.0	—
11.1.1, 775		1.5	
880	2.2	2.2	2.0
11.3.1, 971, 955		4.3	
10.6.0, 866		0.1	
11.3.3, 973		3.3	
10.6.2	11.5†	9.8	10.7†

*Only intensities corresponding to unique reflections were measured. The intensities have been normalized to $I_c(222)$. These normalized monochromatized integrated intensities are converted to conventional integrated intensities I_0' by multiplying by the ratio of the polarization factors, $(1 + \cos^2 2\theta)/(1 + 0.66 \cos^2 2\theta)$.

†Slight overlap with 11.3.3 + 973.

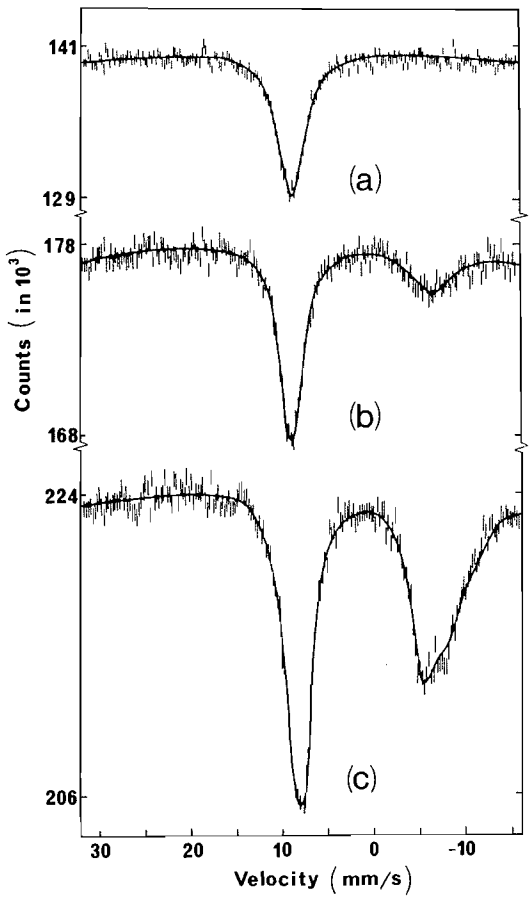

Fig. 3. Mössbauer ^{121}Sb spectra at 77 °K. (*a*) Antimonic acid (No. 180); (*b*) $Sb_2O_{4.35} = Sb_6O_{13}$ (No. 180*f*); β-Sb_2O_4 (No. 180*a*). The zero of the velocity scale refers to InSb at 77 °K.

butions was also tested and found to be unacceptable.

The value of the positional parameter $x(O_2)$ of the oxygen atom in 48(*f*), 0.4304(14), falls in the range expected for *2–5* oxide pyrochlores, from *ca.* 0.425 to 0.4375 (33).[10] The high values of the isotropic temperature factors $B(16c)$ and $B(8a)$ very likely have their origin in the incomplete occupancies of the two equipoints. In a stoichiometric *P* structure each oxygen atom O_1 in 8(*a*) is surrounded by four *A* cations in 16(*c*) at the corners of a regular tetrahedron. With the occupancies of 8(*a*) and 16(*c*) reduced by half there will be a high incidence of local situations where an O_1 atom will have only two Sb^{3+} atoms as nearest neighbors, and an Sb^{3+}

[10]Origin taken at center in 16(*c*) (*cf.* ref. 26).

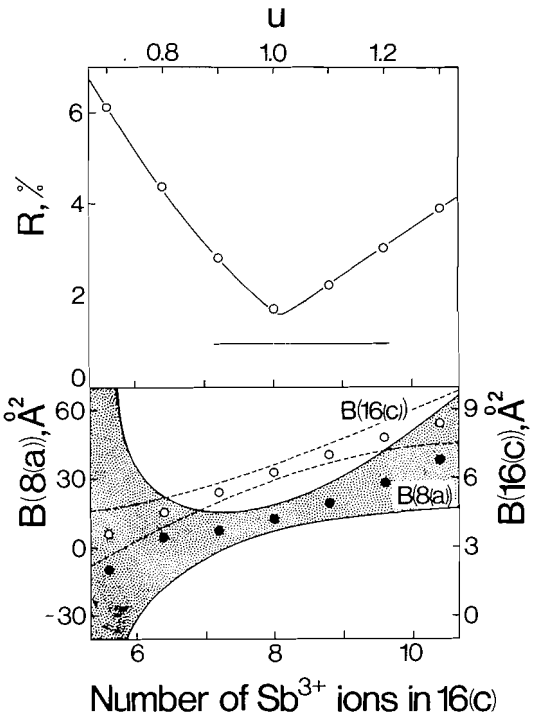

FIG. 4. Variation of the discrepancy factor R, and of the isotropic temperature factor $B(16c)$, with the assumed occupancy of the 16(c) equipoint in $Sb_u^{3+}Sb_2^{5+}O_6^{2-}O_{(3u/2)-1}^{2+}$ for the pyrochlore-structure model

16(c)	16(d)	48(f)	8(a)
$8u$ Sb^{3+}	16 Sb^{5+}	48 O^{2-}	$(12u-8)$ O^{2-}

The vertical width of the two B fields corresponds to the estimated standard deviation. The horizontal arrow indicates the 95% confidence limits of u.

atom will have only one instead of two O_1 atoms as its nearest oxygen neighbors. The adjacent vacancies will make the potential field in the immediate vicinity of an O_1 or an Sb^{3+} atom strongly asymmetric, and the resulting effective displacement of the scattering-charge centroids from the ideal parameter-free positions 8(a) and 16(c) will manifest itself by a decreased contribution to the diffraction intensity by charge at these sites. To compensate for the excess scattering charge introduced into the model through atomic scattering factors appropriate to the particular degree of random occupancy, the refinement leads to an abnormal increase in the temperature factors.

The above ionic distribution is similar to that assumed by Dihlström and Westgren for their hypothesized Sb_3O_6OH. The only difference is that for their formulation the 8(a) site would contain 8 OH^- instead of 4 O^{2-} ions. A refinement of our intensities using their model yielded, after 5 cycles, an R of 4.8% and an unacceptably high $B(8a)$ factor, 21.8(129) Å^2. This may again be taken as a confirmation that the oxide obtained from antimonic acid by firing at 700° is $Sb_2O_{4.35} = Sb_6O_{13}$ and not Sb_3O_6OH.

The apparent non-existence of Sb_2O_5 can be explained from an examination of the characteristics of the P structure. It has long been considered that the structure requires for its existence a basic network of filled 16(d) and 48(f) sites. Occupancy of the 16(c) sites is not essential, nor is that of the 8(a) sites. However, if ions are to occupy the 16(c) sites, they must be larger than those in the 16(d) sites, and the radius ratio of the 16(c) to 16(d) ions must fall within certain limits (33, 34). If antimonic acid is to conform to the above considerations, it must have a structure of the type

16(d)	48(f)
16 Sb^{5+}	32 O^{2-} + 16 OH^-

which corresponds to an overall formula of $Sb_2O_5.H_2O$.[11] Other structures are possible, however, with a greater proportion of OH^- ions in 48(f) and with OH^- also in 8(a). Dehydration of such material would lead to a decrease in the number of ions in 48(f) until for the formula Sb_2O_5 there would be only 40 O^{2-} ions left. The P structure could not support this deficiency in the 48(f) sites, so that either the material would convert to a structure of a different type, or else a rearrangement would occur in which some of the Sb^{5+} ions move into the 16(c) sites until the 48(f) sites become filled. However, if Sb^{5+} is to move into 16(c) it must become reduced to Sb^{3+} in order to satisfy the size requirement for this site. The structure that would result from the minimum amount of such rearrangement would have the ionic distribution

16(c)	16(d)	48(f)
$5\frac{1}{3}$ Sb^{3+}	16 Sb^{5+}	48 O^{2-}

or, for an integral number of ions in 16(c),

16(c)	16(d)	48(f)	8(a)
6 Sb^{3+}	16 Sb^{5+}	48 O^{2-}	1 O^{2-}

[11] This model (C) gave the best agreement, with visually estimated intensities, of the three models considered by Natta and Baccaredda (18).

Can. J. Chem. Downloaded from www.nrcresearchpress.com by 210.87.254.105 on 09/05/12
For personal use only.

This last arrangement corresponds to an occupancy of 37.5% in 16(*c*) or $u = 0.75$ (Fig. 4), which does not agree as well with the X-ray intensities as does the arrangement with 8 Sb^{3+} ($u = 1$). It therefore seems that rearrangement on firing continues beyond the minimum required to fill the 48(*f*) sites, probably owing to such requirements as attainment of minimum lattice energy, etc.

Conclusions

1. There is no satisfactory evidence to-date for the existence of an anhydrous oxide of antimony having the formula Sb_2O_5. All references to this material in the literature can be shown to refer rather to hydrated Sb_2O_5 (antimonic acid) or to an oxide containing some Sb^{III}. Anhydrous Sb_2O_5 cannot be obtained from dehydration of antimonic acid by firing in air.

2. An oxide of formula $Sb_2O_{4.35(5)}$ is obtained by firing antimonic acid in air to 650–850°; the composition is equivalent to the formula Sb_6O_{13} within the stated experimental analysis error. This oxide has a cubic *P*-type structure, $a_0 = 10.303(1)$ Å. The X-ray powder diffractometer intensities observed for this material are best accounted for by the following arrangement of atoms in the unit cell:

16(*c*)	16(*d*)	48(*f*)	8(*a*)
8 Sb^{3+}	16 Sb^{5+}	48 O^{2-}	4 O^{2-}

The mean value of the positional parameter $x(O_2)$ of the oxygen atom in 48(*f*), 0.4304(14), is in the range expected for *2–5* oxide pyrochlores.

3. The hydroxy oxide Sb_3O_6OH proposed by Dihlström and Westgren (14) does not exist. The material investigated by these authors appears to be identical with the oxide Sb_6O_{13} described in the present work.

4. Sb_6O_{13} loses oxygen on firing to 935° and forms β-Sb_2O_4, *not* Sb_2O_3. β-Sb_2O_4 vaporizes above 1050° without first transforming into Sb_2O_3.

5. The Mössbauer parameters of β-Sb_2O_4 are closely similar to those reported for α-Sb_2O_4 by Long *et al.* (22). However, the isomer shifts observed for Sb^V in antimonic acid and its dehydration/decomposition products are significantly larger than those for α- and β-Sb_2O_4.

Note added in proof

The oxygen content of sample 180*f* was recently determined by neutron activation analysis using an Sb_2O_3 standard of 99.99% purity. The average of ten determinations (total counts accumulated, 10^6) was 22.01(9)%. This is in excellent agreement with the theoretical oxygen content of 22.11(20)% for the composition $Sb_2O_{4.32(5)}$ established by chemical analysis (Table 4). However, the Sb^{III}:Sb^V ratio corresponding to this analysis, 0.54(4), is higher than the Mössbauer area ratio for this material, 0.42(6).

We are indebted to Dr. M. Falk for placing at our disposal the infrared spectrophotometer. Financial support of this investigation by the National Research Council of Canada is hereby acknowledged. The neutron activation analysis was carried out by Mr. R. Dayal of the Department of Geology, Dalhousie University, to whom we wish to express our appreciation.

1. A. C. Skapski and D. Rogers. Chem. Commun. **23**, 611 (1965).
2. D. Rogers and A. C. Skapski. Proc. Chem. Soc. 400 (1964).
3. A. Simon. Z. Anorg. Allg. Chem. **165**, 31 (1927).
4. A. Simon and E. Thaler. Z. Anorg. Allg. Chem. **161**, 113 (1927).
5. J. J. Berzelius. Ann. Chim. Phys. **86** (1), 225 (1813).
6. J. Clarke. Chem. News, **67**, 249 (1893).
7. Zambelli and Luzzatto. Ann. Pharm. Chim. **3** (4), 229 (1886).
8. Hampe. Chem. Ztg. **18**, 1899 (1895).
9. A. Geuther. J. Prakt. Chem. **4** (2), 438 (1871).
10. H. Daubrawa. Liebigs Ann. **186**, 110 (1877).
11. G. Jander and A. Simon. Z. Anorg. Allg. Chem. **127**, 68 (1923).
12. H. E. Swanson, M. I. Cook, E. H. Evans, and J. H. de Groot. Natl. Bur. Stand. U.S. Circ. 539, **10**, 10 (1969).
13. J. D. Hanawalt, H. W. Rinn, and L. K. Frevel. Ind. Eng. Chem. Anal. Ed. **10**, 457 (1938).
14. K. Dihlström and A. Westgren. Z. Anorg. Allg. Chem. **235**, 153 (1937).
15. E. Fremy. Ann. Chim. Phys. **23** (3), 385 (1848).
16. A. E. Delacroix. Bull. Soc. Chim. Fr. **21** (3), 1049 (1899).
17. J. B. Senderens. Bull. Soc. Chim. Fr. **21** (3), 47 (1899).
18. G. Natta and M. Baccaredda. Gaz. Chim. Ital. **66**, 308 (1936).
19. D. J. Stewart and O. Knop. Can. J. Chem. **48**, 1323 (1970).
20. S. L. Ruby, G. M. Kalvius, R. E. Snyder, and G. B. Beard. Phys. Rev. **148**, 176 (1966).
21. V. A. Bryukhanov, B. Z. Iofa, V. Kotkhekar, S. I. Semenov, and V. S. Shpinel'. Sov. Phys. JETP **26**, 912 (1968).
22. G. G. Long, J. G. Stevens, and L. H. Bowen. Inorg. Nucl. Chem. Lett. **5**, 799 (1969).

Can. J. Chem. Downloaded from www.nrcresearchpress.com by 210.87.254.105 on 09/05/12
For personal use only.

23. S. L. RUBY, G. M. KALVIUS, G. B. BEARD, and R. E. SNYDER. Phys. Rev. **159**, 239 (1967).
24. C.-H. HUANG, O. KNOP, and F. W. D. WOODHAMS. Am. Miner. **55**, 1115 (1970).
25. J. G. STEVENS and S. L. RUBY. Phys. Lett. A**32**, 91 (1970).
26. O. KNOP, F. BRISSE, L. CASTELLIZ, and SUTARNO. Can. J. Chem. **43**, 2812 (1965).
27. F. BRISSE and O. KNOP. Can. J. Chem. **46**, 859 (1968).
28. M. TOKONAMI. Acta Cryst. **19**, 486 (1965).
29. D. T. CROMER and J. T. WABER. Acta Cryst. **18**, 104 (1965).
30. D. T. CROMER. Acta Cryst. **18**, 17 (1965).
31. L. H. BOWEN, P. E. GARROU, and G. G. LONG. Inorg. Nucl. Chem. Lett. **33**, 953 (1971).
32. W. C. HAMILTON. Acta Cryst. **18**, 502 (1965).
33. F. BRISSE, D. J. STEWART, V. SEIDL, and O. KNOP. To be published.
34. W. W. BARKER, J. GRAHAM, O. KNOP, and F. BRISSE. Crystal chemistry of oxide pyrochlores. *In* The chemistry of extended defects in non-metallic solids. *Edited by* L. Eyring and M. O'Keeffe. North-Holland Publ. Co., Amsterdam, London. 1970. pp. 198–206.
35. D. J. STEWART, O. KNOP, R. E. MEADS, and W. G. PARKER. To be published.

Can. J. Chem. Downloaded from www.nrcresearchpress.com by 210.87.254.105 on 09/05/12
For personal use only.

Influence of Surface Area Variation on the Kinetics of Hydration of Tricalcium Silicate

K. G. McCurdy and B. P. Erno

Department of Chemistry, University of Lethbridge, Lethbridge, Alberta

Received June 7, 1971

Tricalcium silicate reacts initially with aqueous solutions according to a rate law that is first order with respect to the mass of the solid. A kinetic investigation of the hydration of tricalcium silicate for fixed solid to solution, w/w, ratio has been conducted using samples of tricalcium silicate of different total surface area to volume ratios. Consideration of the p*H* independent rate constants indicates that the rate for the initial step in the hydration process is proportional to the surface area of the solid. Subsequent p*H* independent rate constants in the overall hydration process are surface area independent.

Le silicate tricalcique réagit en solution aqueuse, dans l'étape initiale, selon une cinétique du premier ordre par rapport à la masse du solide. La cinétique d'hydration du silicate tricalcique a été étudiée pour des poids fixes de solide et de solution, en utilisant des échantillons de silicate dont les rapports surface: volume varient. La vitesse d'hydration, indépendante du p*H*, indique qu'elle est proportionnelle à la surface du solide dans l'étape initiale. La non dépendance, au stade ultérieur, des constantes de vitesse du processus global de l'hydration vis-à-vis du p*H* montre qu'elles sont indépendantes de la surface.

Canadian Journal of Chemistry, **50**, 701 (1972)

Can. J. Chem. Downloaded from www.nrcresearchpress.com by 210.87.254.5 on 09/05/12
For personal use only.

Introduction

The heterogeneous chemical reaction of crystalline tricalcium silicate, Ca_3SiO_5, in aqueous systems has been investigated many times (1, 2). Recently some progress has been made in understanding the kinetics of the reaction (3–5). A previous publication from this laboratory (6) proposed a reaction mechanism for the hydration of tricalcium silicate in excess water at constant p*H*. The mechanism proposed was

[1] $$3CaO\cdot SiO_2(s) + nH_2O(l) \xrightarrow{k_1} 1.5Ca^{2+}(aq) + 3OH^-(aq) + 1.5CaO\cdot SiO_2(s)$$

[2] $$1.5CaO\cdot SiO_2(s) + nH_2O(l) \xrightarrow{k_2} 1.5Ca^{2+}(aq) + 3OH^-(aq) + SiO_2(aq)$$

[3] $$1.5CaO\cdot SiO_2(s) + SiO_2(aq) \underset{}{\overset{K_3}{\rightleftharpoons}} 1.5CaO\cdot SiO_2\cdot SiO_2(s)$$

[4] $$1.5CaO\cdot SiO_2\cdot SiO_2(s) + nH_2O(l) \xrightarrow{k_4} 1.5Ca^{2+}(aq) + 3OH^-(aq) + 2SiO_2(aq)$$

Here $SiO_2(aq)$ denote the total silica in solution, with the realization that it is distributed in solution among the species H_4SiO_4, $H_3SiO_4^-$, and $H_2SiO_4^{2-}$ as a function of the p*H* of the solution.

A subsequent investigation (7) reported results of the influence of p*H* on the various reactions in the sequence and led to the proposal that the rate constants are proportional to the hydrogen ion activity adsorbed, $(a_{H+})_{ads.}$, on the solid surface. The equilibrium written as reaction 3 was observed to be p*H* independent. The Langmuir adsorption isotherm was used to correlate the hydrogen ion activity on the surface with the hydrogen ion activity in the liquid phase.

Few previous investigations of the effect of particle size on the rates of hydration have been published. None of these have been conducted at constant p*H*.

According to Brunauer and Greenburg (1), Anderegg and Hubbel (8) found no difference in the rates of hydration of tricalcium silicate for fractions of solid with mean dimensions of 19, 22, and 25 μ. Brunauer and Greenburg (1) also describe a study by Sloan *et al.* (9) in which three fractions, 65–100, 100–200, and 200–300 mesh, tricalcium silicate were investi-

TABLE 1. Size characteristics of tricalcium silicate samples

Sample number	Passed through		Did not pass through	
	U.S.B.S. Sieve number	Sieve opening U.S.B.S. spec. mm	U.S.B.S. Sieve number	Sieve opening U.S.B.S. spec. mm
1	—	—	50	0.297
2	50	0.297	100	0.149
3	100	0.149	140	0.105
4	140	0.105	170	0.088
5	170	0.088	230	0.062
6	230	0.062	270	0.053
7	270	0.053	325	0.044
8	325	0.044	400	0.037
9	400	0.037	—	—

gated and no difference in the rates of hydration was observed.

Particle size or the surface area of powder has been proposed as having an effect on the hydration rate of tricalcium silicate (3, 10).

Surface area effects have been proposed for heterogeneous solid liquid reactions (11, 12).

The present investigation using tricalcium silicate with samples of particles of different diameters was undertaken to investigate the effect of the surface area of the tricalcium silicate on the kinetics of the reaction.

Experimental

Materials

The tricalcium silicate used in the present investigation has been previously described (7). The various particle size ranges were obtained by sieving the tricalcium silicate for thirty minutes on stacks of Endicott N.B.S. sieves. The particle sizes obtained are described in Table 1.

All solutions were prepared using double distilled water. All experiments were duplicated.

Equipment

The p*H* stat used was a Radiometer titrigraph SBR2C/-SBU1 composed of a TTT1 automatic titrator, SBR2C recorder, and SBU1 syringe burette. The titrant was delivered from a calibrated 0.5 ml syringe. A Radiometer G202C glass electrode and a K401 calomel reference electrode were used to monitor the p*H*.

Procedure

The reactions were carried out in 10 ml of solution in a reaction vessel in which an access port above the level of the solution was available for the introduction of the tricalcium silicate, 10 mg in all experiments in the present paper.

The solution was stirred and thermostated at 25 ± 0.05 °C. A stream of nitrogen was passed through water and then through the reaction solution to avoid carbonation.

An experiment was carried out by placing 10 ml of a 0.2 m*M* $Ca(OH)_2$ solution in the reaction cell. The p*H* of the solution was adjusted with a concentrated solution of HCl to the desired value. Chloride ion had previously been shown to not have an effect on the reaction under these conditions (6). The p*H* stat was set to maintain the p*H* of the solution at the preset value.

When thermal equilibrium had been attained the tricalcium silicate was introduced rapidly by means of a small funnel through the access port. The stat then recorded the volume of standardized HCl solution required to maintain the p*H* of the solution at the preset value.

The reaction was followed until no further addition of HCl was required for a period of 5 min.

Results and Discussion

Table 2 lists the experiments performed at the indicated p*H* and involving the specified sample of tricalcium silicate. The mathematical analysis for the rate constants involved the use of the differential form of the rate law for the formation of base (6).

$$[5]\quad \frac{d\,[OH^-]_T}{dt} = 3k_1([OH^-_{01}] - [OH^-_{t1}])$$

$$+ 3k_2(1.5CaO\cdot SiO_2) + 3k_4(1.5CaO\cdot SiO_2\cdot SiO_2)$$

In this equation OH^-_{t1} is the hydroxide liberated by the first reaction at time t and OH^-_{01} is the total amount of hydroxide that would be generated by completion of the first reaction. Parentheses denote concentrations of suspended solids in moles per liter and square brackets denote solute concentrations in moles per liter. In eq. 5 we have used the symbol $1.5CaO\cdot SiO_2$ to denote the amount of intermediate formed from eq. 1 that is free. The expression $1.5CaO\cdot SiO_2\cdot SiO_2$ denotes the

Can. J. Chem. Downloaded from www.nrcresearchpress.com by 210.87.254.5 on 09/05/12
For personal use only.

TABLE 2. Experimental conditions for the hydration of tricalcium silicate in dilute calcium hydroxide solution

Series	Sample number	k_1 (min^{-1})	k_2 (min^{-1})	K_3 (l/mol)	k_4 (min^{-1})	Tricalcium silicate reacted (μmol)
				pH = 10.1		
85	1	0.052	0.106	2583	0.255	37.59
86	2	0.069	0.078	815	0.195	38.25
87	3	0.112	0.051	1837	0.080	39.69
88	4	0.216	0.036	1011	0.078	39.49
89	5	0.166	0.053	1327	0.082	39.95
90	6	0.223	0.045	1116	0.080	38.08
91	7	0.188	0.065	998	0.085	36.75
92	8	0.266	0.061	841	0.096	36.09
93	9	0.552	0.089	327	0.167	38.19
				pH = 9.1		
94	1	0.072	0.082	685	0.210	40.85
95	2	0.079	0.091	980	0.210	40.48
96	3	0.114	0.075	734	0.167	43.37
97	4	0.251	0.061	760	0.120	40.88
98	5	0.179	0.084	1226	0.139	42.21
99	6	0.272	0.100	929	0.142	40.08
100	7	0.207	0.112	1005	0.141	45.71
101	8	0.340	0.105	726	0.177	40.56
102	9	0.700	0.190	589	0.308	42.92
				pH = 8.5		
103	1	0.087	0.083	558	0.183	41.76
104	2	0.088	0.090	543	0.235	43.76
105	3	0.120	0.089	655	0.181	43.66
106	4	0.255	0.051	983	0.119	43.04
107	5	0.199	0.067	917	0.143	42.17
108	6	0.233	0.081	983	0.139	39.00
109	7	0.223	0.108	972	0.145	40.86
110	8	0.320	0.114	1059	0.171	40.06
111	9	0.715	0.262	1076	0.349	41.98
				pH = 7.5		
112	2	0.091	0.110	598	0.241	41.62
113	3	0.128	0.071	648	0.130	39.42
114	5	0.196	0.087	589	0.157	42.08
115	6	0.285	0.082	882	0.150	41.82
116	7	0.235	0.111	992	0.161	39.75
117	8	0.328	0.099	1870	0.196	42.28
118	9	0.589	0.246	1517	0.354	42.18

amount of intermediate formed from the reaction given by eq. 1 that is complexed. Introducing the symbol θ which denotes the fraction of the total intermediate that is complexed at any time gives

$$[6]\quad \theta = \frac{1.5\text{CaO}\cdot\text{SiO}_2\cdot\text{SiO}_2}{(1.5\text{CaO}\cdot\text{SiO}_2)_T} = \frac{K_3[\text{SiO}_2]}{1 + K_3[\text{SiO}_2]}$$

if the equilibrium denoted by reaction 3 is rapid and one silica is adsorbed per 1.5CaO·SiO_2. Equation 5 may be rewritten as

$$[7]\quad \frac{\text{d}[\text{OH}^-]_T/\text{d}t - 3k_1([\text{OH}^-_{01}] - [\text{OH}_{t1}])}{3(1.5\text{CaO}\cdot\text{SiO}_2)_T} = k_2(1-\theta) + k_4\theta$$

Graphical analysis of eq. 7 as described by McCurdy and Erno (7) yields the results reported in Table 2.

Further examination (7) of the hydration of

Can. J. Chem. Downloaded from www.nrcresearchpress.com by 210.87.254.5 on 09/05/12
For personal use only.

Can. J. Chem. Downloaded from www.nrcresearchpress.com by 210.87.254.5 on 09/05/12
For personal use only.

TABLE 3. Reciprocals of the slope of the plot of k_n/H^+ *vs.* H^+

Sample	k_1^1 (min^{-1})	k_2^1 (min^{-1})	k_4^1 (min^{-1})
1	0.088	0.083	0.181
2	0.091	0.111	0.241
3	0.128	0.071	0.129
4	0.256	0.051	0.120
5	0.196	0.088	0.155
6	0.287	0.082	0.150
7	0.236	0.111	0.161
8	0.329	0.098	0.197
9	0.588	0.246	0.355

tricalcium silicate at various p*H* values indicated a p*H* dependence of rate constants k_1, k_2, and k_4 as determined by the previous method. McCurdy and Erno (7) reported that this p*H* dependence could be removed from the rate constants by proposing that they are proportional to the hydrogen ion activity adsorbed, $(a_{H+})_{ads.}$, on the solid surface.

The Langmuir adsorption isotherm (13) was used in the form

$$\bar{\theta} = \frac{\alpha\mu}{\alpha\mu + \upsilon}$$

Here α is the fraction of hydrogen ions striking the surface which adhere, μ is the number striking 1 cm^2 per unit of time, and υ is a constant for adsorption of hydrogen ions on the surface, $\bar{\theta}$ is the fraction of total surface covered at any time by hydrogen ions. If μ is proportional to $(a_{H+})_{aq}$ with proportionality constant, c, and the rate constants are proportional to the fraction of total surface covered by hydrogen ions, we have the following equation

$$k_n = k_n^1 \frac{\alpha[a_{H+}]_{aq}}{\alpha[a_{H+}]_{aq} + \upsilon/c}$$

where k_n^1 is the p*H* independent rate constant. The numerical value of n denotes a particular reaction step. A method was presented (7) for determining the value of k_n^1. The values of k_n^1 for the present investigation are reported in Table 3. The data in this table indicate a surface area effect in k_1^1 but k_2^1 and k_4^1 appear constant over the various surface area samples studied.

Surface Area Dependence of k_1^1

The numerical value of k_1^1 for the samples investigated in the present work reflects the effect of changing the ratio of the surface area of the solid to the volume of the solution with a constant mass of tricalcium silicate. Table 3 indicates an increase of the value of k_1^1 as the ratio of surface area of solid to volume of solution increases. The rate constant k_1^1 is by previous definition (7) the rate constant when the surface is completely covered with hydrogen ions. It would be anticipated then that k_1^1 should increase as the surface area increases. The following derivation is based on spherical particles although it applies as well to cylindrical particles in which end effects are neglected. If k_1^1 is proportional to A_s then

$$[8] \qquad k_1^1 = A_s k_1^{11}$$

where k_1^{11} is the proportionality constant. This can be written as

$$[9] \qquad k_1^1 = k_1^{11}\, 4\pi r^2 n$$

for spherical particles where r is the radius of a particle and n is the number of such particles. The value of n can be determined from the initial weight of the sample W_I and the density of the solid ρ as

$$[10] \qquad n = \frac{W_I}{\frac{4}{3}\pi r^3 \rho}$$

Then substituting for n in eq. 9 gives

$$[11] \qquad k_1^1 = k_1^{11} \frac{W_I^3}{\rho}\left(\frac{1}{r}\right)$$

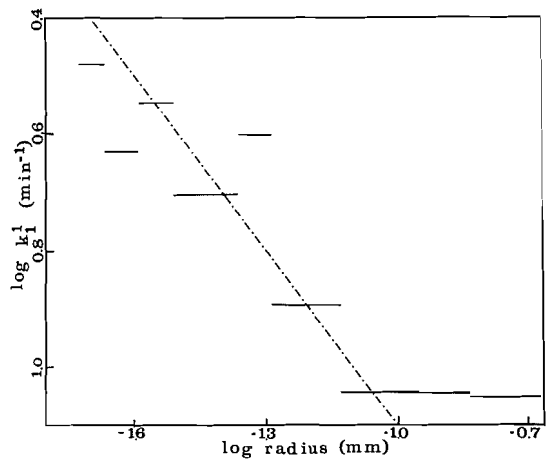

FIG. 1. Plot of log k_1^1 *vs.* log r. A line of slope minus one is drawn for reference-·-·.

Can. J. Chem. Downloaded from www.nrcresearchpress.com by 210.87.254.5 on 09/05/12
For personal use only.

Plots of $\log k_1^1$ *vs.* $\log r$ (obtained from Table 1) should be a straight line with a negative slope of unity. Figure 1 is a graphical representation of the data in Table 3 using the samples given in Table 1. A line of slope -1 is drawn for reference. The lengths of the horizontal lines indicate the range of particle radii in the various samples.

This dependence of k_1^1 on the surface area of the solid is in agreement with the results of the ball mill hydration (14) in which unhydrated solid is continually exposed to the solution by the grinding action. The ball mill hydration is much more rapid than paste hydration, and faster than bottle hydration.

Surface Area Dependence of the Reaction Rate Law for the Initial Step in the Reaction Sequence

The initial reaction in the hydration of tricalcium silicate has been shown to be first order with respect to the mass of the solid. A first order mechanism suggests a two dimensional attack with adsorption (15, 16). A cylindrical model for the solid particles in which end effects are neglected and adsorption included accounts for the observed first order kinetics. This model leads to a rate law that is second order in surface area.

There is a considerable amount of microscopic evidence to suggest that the particles of tricalcium silicate are approximately equidimensional. A spherical model would therefore seem to be more realistic. A rate law that is first order in mass of solid leads to a reaction that is 3/2 order in surface area for spherical particles. There is some evidence (11, 12) that dissolution reactions are second order in surface area. This second order effect is attributed to the fact that both reactants (lattice components in the surface and adsorbed H^+) depend on the surface area. If the hydration of spherical particles of tricalcium silicate was second order in surface area we should have observed a reaction that was 4/3 order in mass of tricalcium silicate. We were, however, unable to satisfactorily reproduce the rate of production of base using a 4/3 order reaction if, as was the case, the rate constant for reaction 1 was calculated from the integrated rate law and the amount of base generated at a short period of time (6). The rate of generation of base by the 4/3 order reaction using the integrated rate law was not fast enough in the later stages of the reaction to match the experimentally determined base.

Many explanations are possible for this observation, one is however in accord with a previously proposed mechanism. Stein and Stevels (17) proposed that tricalcium silicate reacts rapidly in aqueous media to form a first hydrate (F.H.). This hydrate has a molar ratio of lime to silica of approximately 3. Base would not liberate during its formation and therefore would not be detected by our method of analysis. Stein and Stevels suggest that this F.H. is converted into a second hydrate (S.H.) of approximate formula $(0.8–1.5)CaO \cdot SiO_2 \cdot nH_2O$. This second hydrate catalyzes the decomposition of first hydrate. We calculate a considerable amount of $1.5CaO \cdot SiO_2$ at short times by our mechanism (6). The suggestion that this hydrate is capable of catalyzing the conversion of F.H. into S.H. would lead to an order for the F.H. to S.H. conversion lower than that expected on the basis of a spherical model with adsorption. This appears to be the case in the present investigation. A spherical model with adsorption should lead to 4/3 order kinetics. We actually observe first order kinetics with respect to the mass of the solid.

We are indebted to the National Research Council of Canada for financial support. The continuing financial support of the University of Lethbridge Research Committee is greatly appreciated. The authors wish to thank the Departments of Physics and Mathematics for the use of their computing facilities.

1. S. BRUNAUER and S. A. GREENBURG. Proceedings of the 4th International Symposium on the Chemistry of Cements, Washington, D.C., 1960.
2. L. E. COPELAND and D. L. KANTRO. Proceedings of the 5th International Symposium on the Chemistry of Cements, Tokyo, Japan, 1968.
3. R. KONDO and S. UEDA. Proceedings of the 5th International Symposium on the Chemistry of Cements, Tokyo, Japan, 1968.
4. S. A. GREENBURG and T. N. CHANG. J. Phys. Chem. **69**, 533 (1965).
5. H. N. STEIN and J. M. STEVELS. J. Appl. Chem. **14**, 338 (1964).
6. K. G. McCURDY and B. P. ERNO. Can. J. Chem. **48**, 3291 (1970).
7. K. G. McCURDY and B. P. ERNO. Can. J. Chem. **49**, 833 (1971).
8. F. O. ANDEREGG and D. S. HUBBELL. Proc. Am. Soc. Test. Mater. **29**, Part I, 554 (1929); **30**, Part II, 572 (1930).

9. R. C. SLOAN, W. J. MCCAUGHEY, W. D. FOSTER, and C. SHREVE. Eng. Expt. Stn. Bull. **61**, (1931).
10. J. H. TAPLIN. Proceedings of the 5th International Symposium on the Chemistry of Cements, Tokyo, Japan, 1968. p. 337.
11. W. T. GRANQUIST and G. F. SUMNER. Proc. 6th Natl. Conf. Clay. Minerals, 1959. p. 292.
12. A. PACKTER and H. S. DHILLON. J. Chem. Soc. (A) 2588 (1969).
13. S. GLASSTONE. Textbook of physical chemistry. 2nd ed. D. Van Nostrand Co., Inc., New Jersey. 1946. Chap. XIII.
14. S. BRUNAUER and D. L. KANTRO. The chemistry of cement. Vol. I. *Edited by* H. F. W. Taylor. Academic Press, London. 1964.
15. E. A. MOELYWN-HUGHES. Physical chemistry. Pergamon Press, Oxford. 1961.
16. J. C. JUNGERS and J. C. BALACEANU. Technique of organic chemistry. Vol. VIII, Part I. *Edited by* S. L. Friess, E. A. Lewis, and A. Weissberger. Interscience Publishers Inc., N.Y. 1961.
17. H. N. STEIN and J. M. STEVELS. J. Appl. Chem. **14**, 338 (1964).

Can. J. Chem. Downloaded from www.nrcresearchpress.com by 210.87.254.5 on 09/05/12
For personal use only.

Dielectric Studies. Part XXXII. Detection of High Frequency Absorption from Microwave Data

G. D. MARTIN AND S. WALKER[1]

Department of Chemistry, Lakehead University, Thunder Bay, Ontario

Received August 26, 1971

The dielectric constants and losses have been determined for solutions of *o*-hydroxyacetophenone, 1-chloro- and 1-bromonaphthalene and 2-chloro- and 2-bromonaphthalene in dilute solutions of 15 °C involving a nonpolar solvent. Either seven or eight microwave frequencies were employed over a wide range from about 1 to 145 GHz, and the relaxation times of the molecules were such that the high frequency side of the Cole–Cole plot near the dielectric constant at high frequencies (ε_∞) was well defined. For these polar solutes in nonpolar solvents no high frequency deviations from the Cole–Cole plot are apparent in the plot itself based solely on microwave data. In a few cases the distribution parameter was negligible (less than 0.03) and in one case it was zero. In all cases a Cole linear plot and also a Brot plot revealed the existence of additional absorption to that contributed by molecular relaxation. Such additional absorption would have been difficult to be certain of from the Cole–Cole plot alone when the distribution parameter was either negligible or very small. The frequency points at about 70 and 145 GHz are invaluable in detecting such additional high frequency absorption contributions.

Les constantes diélectriques et les pertes ont été déterminées pour des solutions d'*o*-hydroxyacétophénone, de chloro-1 et bromo-1 naphtalène, en solutions diluées à 15 °C avec un solvant non polaire. Sept à huit fréquences micro-ondes ont été employées dans un intervalle de 1 à 145 GHz et les temps de relaxation des molécules étaient tels que la haute fréquence du tracé de Cole–Cole proche de la constante diélectrique à haute fréquence (ε_∞), était bien définie. Pour ces solutés polaires dans des solvants non polaires, il n'y a pas de déviations apparentes de hautes fréquences obtenues à partir du tracé de Cole–Cole, basées uniquement sur des données micro-ondes. Dans certains cas, le paramètre de distribution était négligeable (inférieur à 0.3) et nul dans un cas. Dans tous les cas, un tracé linéaire de Cole et de Brot, révélait l'existence d'une absorption additionnelle à celle contribuée par la relaxation moléculaire. Une telle absorption additionnelle aurait été difficile à identifier à partir du seul tracé de Cole–Cole où le paramètre de distribution était soit négligeable soit très petit. Les points de fréquences entre 70 et 145 GHz sont d'une valeur inestimable dans la détection d'une telle contribution à l'absorption des hautes fréquences.

Canadian Journal of Chemistry, **50**, 707 (1972)

Can. J. Chem. Downloaded from www.nrcresearchpress.com by 210.87.254.5 on 09/05/12
For personal use only.

Introduction

When the loss factor (ε'') is plotted against the dielectric constant (ε') for a wide range of frequency at a fixed temperature for a system characterized by one relaxation time a semi-circle results with its center on the ε' axis and intercepts of ε_0 and ε_∞ on this axis where the former corresponds with the low frequency side of the plot and the latter with the high frequency side. This plot is sometimes termed the Debye semi-circle (1). For systems with more than one relaxation time the ε'' against ε' plot leads to a semi-circle with its inclination to the ε' axis depressed by the angle $\alpha\pi/2$, where α is termed the distribution parameter and measures the width of the distribution of relaxation times about a most probable (mean) relaxation time (τ_0). This representation of ε'' against ε' has been termed the Cole–Cole plot (2). The equation from which the equation of the Debye semi-circle may be derived is (3)

$$[1] \qquad \varepsilon^* = \varepsilon_\infty + \frac{\varepsilon_0 - \varepsilon_\infty}{1 + i\omega\tau} = \varepsilon' - i\varepsilon''$$

The Cole–Cole equation, however, which assumes a continuous distribution of relaxation times about the mean relaxation is

$$[2] \qquad \varepsilon^* = \varepsilon_\infty + \frac{\varepsilon_0 - \varepsilon_\infty}{1 + (i\omega\tau_0)^{1-\alpha}}$$

Thus, when $\alpha = 0$, then the system is characterized by one relaxation time, and the Cole–Cole equation reduces to the Debye equation, and the system is said to exhibit Debye behavior. When $\alpha \neq 0$ the system would be described as deviating from Debye behavior.

Often no distinction in terminology is made between the Cole–Cole plot and the Debye semi-circle, and this procedure will be followed

[1]To whom correspondence should be addressed.

TABLE 1. Dielectric constant (ε') and dielectric loss (ε'') data for o-hydroxyacetophenone, 1-chloro-, 1-bromo-, 2-chloro-, and 2-bromonaphthalenes in specified nonpolar solvents at 15 °C at specified weight fractions (ω_2)

Solution	Frequency (GHz)	ε'		ε''	
		Observed	Calculated*	Observed	Calculated*
o-Hydroxyacetophenone in CCl_4	1.51	2.35_5	2.35_6	0.019	0.019
$\omega_2 = 0.007$	1.95	2.35_6	2.35_4	0.024	0.023
	9.313	2.30_6	2.30_4	0.050	0.051
	16.10	2.28_4	2.27_9	0.046	0.043
	23.98	2.27_2	2.26_8	0.043	0.033
	34.86	2.26_4	2.26_2	0.024	0.025
	70.60	2.26_0	2.25_7	0.019	0.013
	144.9	2.25_8	2.25_5	0.010	0.006
1-Chloronaphthalene in CCl_4	1.45	2.47_2	2.46_9	0.042	0.041
$\omega_2 = 0.069$	1.96	2.46_2	2.46_2	0.053	0.052
	9.313	2.35_7	2.35_9	0.082	0.082
	16.20	2.33_1	2.32_6	0.062	0.062
	23.98	2.31_5	2.31_2	0.046	0.047
	34.86	2.30_7	2.30_5	0.034	0.034
	70.60	2.30_1	2.29_8	0.024	0.017
	144.9	2.29_7	2.29_6	0.016	0.008
1-Bromonaphthalene in CCl_4	1.51	2.50_0	2.49_9	0.056	0.055
$\omega_2 = 0.098$	1.96	2.49_8	2.48_9	0.067	0.066
	9.313	2.36_7	2.36_7	0.086	0.087
	16.20	2.34_1	2.33_5	0.066	0.063
	23.98	2.32_8	2.32_3	0.046	0.047
	34.86	2.31_9	2.31_6	0.033	0.034
	70.60	2.31_5	2.30_9	0.023	0.016
	144.9	2.31_1	2.30_8	0.014	0.008
2-Chloronaphthalene in CCl_4	0.95	2.44_5	2.43_9	0.039	0.037
$\omega_2 = 0.049$	1.53	2.43_2	2.42_7	0.055	0.054
	2.47	2.41_4	2.40_4	0.072	0.071
	9.313	2.31_7	2.31_3	0.058	0.061
	16.20	2.30_6	2.29_6	0.045	0.041
	23.98	2.29_3	2.29_0	0.028	0.029
	34.86	2.29_0	2.28_7	0.022	0.020
	70.60	2.28_7	2.28_4	0.014	0.010
	144.9	2.28_6	2.78_3	0.009	0.005
2-Bromonaphthalene in CCl_4	1.96	2.39_8	2.39_7	0.063	0.062
$\omega_2 = 0.056$	2.47	2.38_9	2.38_4	0.069	0.068
	9.313	2.31_1	2.30_4	0.048	0.048
	16.20	2.30_0	2.29_3	0.031	0.030
	23.98	2.29_0	2.28_9	0.021	0.021
	34.86	2.29_0	2.28_7	0.015	0.015
	70.60	2.29_0	2.28_6	0.012	0.007
	144.9	2.28_7	2.28_6	0.008	0.004
1-Chloronaphthalene in cyclohexane	2.45	2.14_7	2.14_5	0.025	0.025
$\omega_2 = 0.072$	9.313	2.10_5	2.10_5	0.043	0.043
	16.20	2.09_2	2.08_5	0.036	0.037
	23.98	2.07_5	2.07_5	0.030	0.029
	34.86	2.06_5	2.06_9	0.022	0.022
	70.60	2.06_3	2.06_2	0.013	0.011
	144.9	2.06_1	2.06_1	0.009	0.006
1-Bromonaphthalene in cyclohexane	1.55	2.16_2	2.16_4	0.021	0.020
$\omega_2 = 0.098$	9.313	2.10_5	2.10_9	0.045	0.047
	16.20	2.09_3	2.08_9	0.042	0.038
	23.98	2.07_8	2.08_0	0.027	0.029
	34.86	2.07_7	2.07_5	0.020	0.021
	70.60	2.07_3	2.07_0	0.014	0.012
	144.9	2.07_0	2.06_9	0.008	0.005

*The ε'_{calc} and ε''_{calc} values have been estimated from the parameters ε_0, ε_∞, α, and τ_0 listed in Table 2.

Can. J. Chem. Downloaded from www.nrcresearchpress.com by 210.87.254.5 on 09/05/12
For personal use only.

TABLE 2. Static dielectric constant (ε_0), dielectric constant at very high frequency (ε_∞), refractive index squared for the sodium-D line, the distribution parameter (α) and the observed relaxation time (τ_0) for the solutions at 15 °C listed in Table 1

Solution	ε_0	ε_∞	n_D^2	α	τ_0 (ps)
o-Hydroxyacetophenone in CCl_4	2.360	2.25_5	2.140	0.01_8	$18._4$
1-Chloronaphthalene in CCl_4	2.482	2.29_6	2.190	0.04_2	$25._0$
1-Bromonaphthalene in CCl_4	2.519	2.30_8	2.208	0.04_6	$29._3$
2-Chloronaphthalene in CCl_4	2.450	2.28_3	2.179	0.02_9	$38._5$
2-Bromonaphthalene in CCl_4	2.431	2.28_6	2.179	0.0	$45._0$
1-Chloronaphthalene in cyclohexane	2.154	2.06_1	2.065	0.05_4	$18._3$
1-Bromonaphthalene in cyclohexane	2.169	2.06_9	2.074	0.02_7	$21._0$

here. For cases though where $\alpha = 0$ it should be noted that the Cole–Cole plot could be termed the Debye semi-circle.

Much interest has centered on such plots, and one of the most recent developments is due to Leroy *et al.* (4) who have found deviations from the semi-circular Cole–Cole plot (2) at far infrared frequencies. It was thought worthwhile to determine whether deviations from the Cole–Cole plot could be detected for rigid polar molecules in dilute solution of a nonpolar solvent from microwave data. In addition it seemed desirable to find out which were the best procedures for detecting deviations from Debye behavior or indicating the existence of additional absorption processes other than that of molecular relaxation. If appreciable deviations do occur then false estimates of the dielectric constant at infinite frequency (ε_∞) would result since this is frequently obtained from the Cole–Cole plot. The consequences of this would be that data (5) derived from ε_∞, such as the dipole moment, would be inaccurate.

Clearly, the most useful frequencies in this type of study, apart from the most accurate static dielectric constant point, are the ones which lead to points on the ε_∞ side of the Cole–Cole plot and as close to ε_∞ as feasible. This object would be served by selecting polar molecules which have a long relaxation time. However, if the dielectric loss of the solutions becomes too low the accuracy of the measurement decreases, and thus the solutes selected for study and the concentration of their solutions were chosen bearing this in mind. As far as possible, the solutes were selected for examination in as dilute a solution as feasible in a nonpolar solvent with a view to minimizing internal field effects and complications due to molecular interaction.

Experimental

The dielectric constants and losses of the solutions were measured at microwave frequencies by methods which have been described previously (6, 7). The values at 8.313, 16.2, 23.98, and 34.86 GHz (X, P, K, and Q bands, respectively) were measured using a bridge technique (6), the accuracy of which has been discussed previously (7). The data at 1, 1.5, 2, and 2.5 GHz were obtained with a coaxial line method (8), and the data at 70.6 and 144.9 GHz were obtained using two very similar types of Michelson interferometer (9, 10). In order to examine the accuracy of the results from the higher frequency interferometer a plot was made of ε' and ε'' against mole fraction by C. S. Stewart in this laboratory for six solutions of chlorobenzene in benzene at 20 °C and 2.1 mm wavelength. Good linear plots were obtained and the results favorably compared with those obtained by Garg, Kilp, and Smyth (10). The ε' values of *n*-heptane and cyclohexane were also measured at (*a*) this wavelength and temperature and yielded values of 1.920 and 2.024, respectively, which is in excellent agreement with the values of 1.921 and 2.024 reported by these authors (10) and (*b*) at 70.6 GHz where the values were 1.921 and 2.024, respectively, which is to be expected since the dispersion in each case is negligible. The static dielectric constant of each solution was measured on a WTW Dipolmeter DM01 at a frequency of 2 MHz. The values of the refractive indices of the solutions for the sodium D lines were measured on a Carl Zeiss refractometer. All values of dielectric constant and loss were calculated from the experimental measurements by an IBM 360-40 computer.

In Table 1 are shown the observed and calculated values of dielectric constant and loss of the solutions, while in Table 2 the values of ε_0, n_D^2, ε_∞, the (mean) relaxation time (τ_0), and the distribution parameter (α) are given. The evaluation of the parameters ε_∞, τ_0, and α has been described previously (11). The values of the dielectric constant and losses at 70.6 and 144.9 GHz were not used in the calculation of ε_∞, τ_0, and α, since these two frequencies would be affected most if there was some abnormal dispersion in this region. The values of ε' and ε'' at 70.6 and 144.9 GHz were calculated from these parameters and then compared with the observed values (Table 1).

Can. J. Chem. Downloaded from www.nrcresearchpress.com by 210.87.254.5 on 09/05/12
For personal use only.

Can. J. Chem. Downloaded from www.nrcresearchpress.com by 210.87.254.5 on 09/05/12
For personal use only.

Discussion

Leroy *et al.* (4) give Cole–Cole plots (2) of trichloroethane in hexane, of pure trichloromethane, and of tribromomethane. In all three cases there is a marked deviation from a semi-circle at the high frequency end. For the trichloroethane in hexane the semi-circle curves in, corresponding to an "inertial effect", and for the other two it curves out, corresponding to an "excess absorption" (4). The experimental points which indicated these phenomena were obtained by interferometric methods in the far infrared region. As illustrated in Fig. 1 the present results, within experimental error, lie on a semi-circle. The highest frequency used for the present results was 144.9 GHz and that used by Leroy *et al.* was 6000 GHz. Both our 70.6 and 144.9 GHz points do not indicate any significant visual deviation from the Cole–Cole plot (Fig. 1).

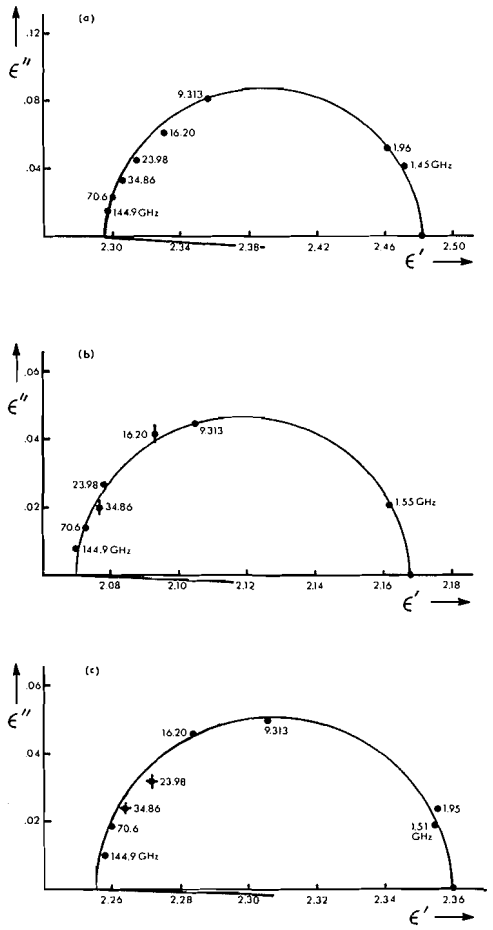

FIG. 1. Cole–Cole plots of (*a*) 1-chloronaphthalene in carbon tetrachloride; (*b*) 1-bromonaphthalene in cyclohexane; (*c*) *o*-hydroxyacetophenone in carbon tetrachloride at 15 °C.

Previous work by Antony and Smyth (12) indicated that for a dilute solution of *o*-hydroxyacetophenone in cyclohexane the distribution parameter (α) was zero. Our value of 0.01_8 for this solute in carbon tetrachloride cannot be regarded as a significant deviation from zero. In fact, the α values for 2-chloro- and 2-bromonaphthalene in carbon tetrachloride and 1-bromonaphthalene in cyclohexane are negligible, while the variation in α of 1-bromonaphthalene from 0.02_7 in cyclohexane to 0.04_6 in carbon tetrachloride must be ascribed to a solvent effect and not to a modification of the relaxation processes of the solute molecule. Thus, in almost all cases, α is either zero or tends to zero and the systems can almost be represented by Debye behavior. Hence, from a Cole–Cole plot type of representation, in the majority of these cases, it might seem that the molecular relaxation time contribution was either adequate or almost so to describe the absorption.

Plots other than the Cole–Cole exist for detecting the presence of an additional relaxation process(es). Two plots which have found frequent use and are attributable to Cole (13) are based on the equations

$$[3] \qquad \varepsilon' = -\tau(\omega\varepsilon'') + \varepsilon_0$$

$$[4] \qquad \varepsilon' = (1/\tau)(\varepsilon''/\omega) + \varepsilon_\infty$$

From eq. 3 a plot of ε' against $\varepsilon''\omega$ yields a straight line of slope $-\tau$ for one relaxation process while a plot of ε' *vs.* ε''/ω has a slope of $1/\tau$. These plots are shown for the present data in Fig. 2. For all solutions in Fig. 2*a* it can be seen that two intersecting straight lines are obtained and not one. In each case it is the 70.6 and 144.9 GHz points which define the second straight line, suggesting at least one other dispersion process is occurring. In the ε' *vs.* $\varepsilon''\omega$ plot it can also be seen that the slopes of the lines given by these two high frequency points are very much less steep than for the main relaxation processes (*i.e.* the second possible relaxation time, τ_2, is much shorter than

Can. J. Chem. Downloaded from www.nrcresearchpress.com by 210.87.254.5 on 09/05/12
For personal use only.

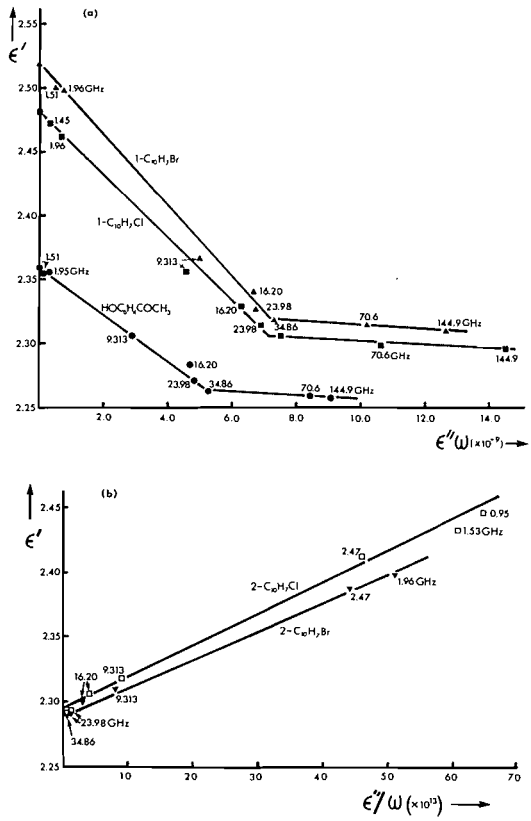

FIG. 2. Cole plots of (*a*) ε' *vs.* $\varepsilon''\omega$ for *o*-hydroxyacetophenone, 1-chloro- and 1-bromonaphthalene in carbon tetrachloride at 15 °C; (*b*) ε' *vs.* ε''/ω for 2-chloro-, and 2-bromonaphthalene in carbon tetrachloride at 15 °C.

the main relaxation process τ_1). For all solutions τ_2 values estimated from the slopes are shorter than 2 ps. Such a plot is therefore valuable in indicating that mm absorption cannot be accounted for in terms of the molecular relaxation time alone. However, it does not prove that the τ_2 relaxation time is meaningful in relation to a specific molecular motion and that the τ_2 process is of the Debye type, or that it is permissible to apply eq. 3 to estimate an additional relaxation time associated with the additional absorption.

It should be noted that for an ε' *vs.* ε''/ω plot in Fig. 2*b* a straight line appears to represent the data adequately. In this type of plot the high frequency points bunch together near the ordinate axis and the additional relaxation process(es) cannot be distinguished in these cases by the mm data.

Brot (14) deduced a useful equation relating the parameters ε', ε'', ε_0, ε_∞, ω, and τ which yields a straight line from the appropriate plot. This equation is

$$[5] \quad \omega/\varepsilon'' = [\tau/(\varepsilon_0 - \varepsilon_\infty)]\omega^2 + [(\varepsilon_0 - \varepsilon_\infty)\tau]^{-1}$$

From eq. 5 a plot of ω/ε'' *vs.* ω^2 spreads out the high frequency points, and two such plots are given in Fig. 3 which reveals that the absorption cannot be characterized solely by a molecular relaxation time.

The slope of the straight line through the experimental points in the 1.5 to 34.86 GHz region in Figs. 2*a* and *b*, based on eqs. 3 and 4, respectively, leads to a relaxation time value in agreement with the τ_0 values listed in Table 2 to better than 9%. Figure 3, however, which compresses these low frequency points is not a suitable plot for such a determination. The fact that the τ_0 and the value from the low frequency slope are in fairly close agreement (the error in τ_0 could amount to at least 5%) indicates that there is, at most, only a small contribution to the dielectric absorption at these frequencies from any higher frequency absorption processes.

Thus the plots based on eqs. 3 and 5 have indicated that the dielectric data cannot be characterized solely by a molecular relaxation time, and it has been the 70.6 and 144.9 GHz points which have been the critical ones. In

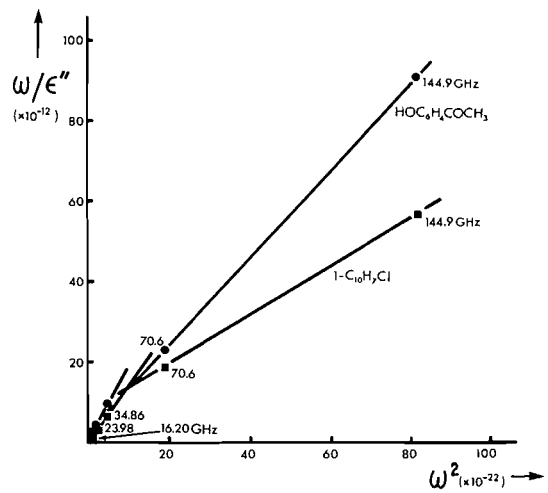

FIG. 3. Brot plot of ω/ε'' *vs.* ω^2 for *o*-hydroxyacetophenone and 1-chloronaphthalene in carbon tetrachloride at 15 °C.

particular the variation of ε'' at these frequencies has been critical in detecting deviations from Debye behavior, that is, the absorption cannot be accounted for in terms of one relaxation time. From Table 1 a comparison can be made between ε''_{obs} and ε''_{calc} for the 70.6 and also the 144.9 GHz points where their difference is seen to be between $+0.002$ to $+0.007$ for the 70.6 GHz and $+0.003$ to $+0.008$ for the 144.9 GHz points for all solutions; this is to be contrasted with all the 0.95 to 34.86 GHz points where the difference between the calculated and observed values of ε'', is, in general, of the order of ± 0.001 to ± 0.002. The observed losses at 70.6 and 144.9 GHz are therefore larger than the ones calculated based on the appropriate parameters in Table 2 indicating that the Debye and the Cole–Cole approach cannot account for all the absorption at these high frequencies; that is, some additional absorption remains to be explained.

Recent studies now have indicated that the far infrared absorption in polar and weakly polar liquids is not of the Debye type (15). It would then be reasonable to conclude that for the solutions studied here the value of τ_2 which may be deduced from Cole and Brot types of plots is not a satisfactory value in relation to a particular molecular motion since the corresponding process is not of the Debye type. From the plots in Figs. 2*a* and 3 it can be concluded though that for these systems there are not less than two absorption processes detectable in the frequency range examined and this is also true of the other systems examined here but not plotted.

Conclusions

The present results indicate that for current microwave data of a simple rigid polar solute molecule in a nonpolar solvent, no high frequency deviations from the Cole–Cole plot are apparent in the plot itself. When the distribution parameter is small (*e.g.* less than 0.03) it is difficult to distinguish by the Cole–Cole plot between this value and zero. In such a case, a better procedure to establish the presence of absorption in addition to that due to molecular relaxation is (*i*) to employ linear types of plots such as those due to Cole or Brot based on eqs. 3 and 5, (*ii*) to determine τ_0, ε_∞, and α from the microwave frequencies other than the 70 and 145 GHz points and use the estimated parameters to calculate the loss factor at these two frequencies. If $\varepsilon''_{obs} - \varepsilon''_{calc}$ emerges as a positive quantity significantly greater than the experimental error, then this indicates additional absorption. It should be noted that for these two frequencies the difference $\varepsilon'_{obs} - \varepsilon'_{calc}$, for the solutions studied here, was of the order of the experimental error and thus it is understandable that these points appear to fall on the Cole–Cole plot.

We wish to thank the National Research Council of Canada for the support which made this work possible and Mr. B. K. Morgan for invaluable technical assistance.

1. N. H. Hill, W. E. Vaughan, A. H. Price, and M. Davies. Dielectric Properties and Molecular Behaviour. Van Nostrand Reinhold Co., London. 1969.
2. K. S. Cole and R. H. Cole. J. Chem. Phys. **9**, 341 (1941).
3. P. Debye. Polar Molecules. Chemical Catalog Co. Inc., New York. 1929.
4. Y. Leroy, E. Constant, C. Abbar, and P. Desplanques. Adv. Mol. Relax. Processes. **1**, 273 (1967).
5. W. F. Hassell and S. Walker. Trans. Faraday Soc. **62**, 861 (1966).
6. W. F. Hassell, M. D. Magee, S. W. Tucker, and S. Walker. Tetrahedron, **20**, 2136 (1964).
7. M. D. Magee and S. Walker. Trans. Faraday Soc. **62**, 3093 (1966).
8. S. E. Keefe and E. H. Grant. Rev. Sci. Instrum. **39**, 800 (1962).
9. W. E. Vaughan, W. S. Lovell, and C. P. Smyth. J. Chem. Phys. **36**, 535 (1962).
10. S. K. Garg, H. Kilp, and C. P. Smyth. J. Chem. Phys. **43**, 2341 (1965).
11. W. F. Hassell, A. Jarvie, and S. Walker. J. Chem. Phys. **46**, 3159 (1967).
12. A. A. Antony and C. P. Smyth. J. Am. Chem. Soc. **86**, 156 (1964).
13. R. H. Cole. J. Chem. Phys. **23**, 493 (1955).
14. C. Brot. Comput. Rend. **19**, 397 (1959).
15. M. Davies, G. W. F. Pardoe, J. E. Chamberlain, and H. A. Gebbie. Trans. Faraday Soc. **64**, 847 (1968).

Can. J. Chem. Downloaded from www.nrcresearchpress.com by 210.87.254.5 on 09/05/12
For personal use only.

Urea–Boron Trihalide Adducts. I. The Boron Trifluoride Adduct of Tetramethylurea

J. S. HARTMAN AND G. J. SCHROBILGEN[1]

Department of Chemistry, Brock University, St. Catharines, Ontario

Received September 8, 1971

Evidence is presented that oxygen is the donor atom in the 1:1 adduct of tetramethylurea and boron trifluoride ($TMU.BF_3$). Hydrogen fluoride, a common impurity in boron trifluoride, leads to the formation of $TMU.H^+BF_4^-$ as well as $TMU.BF_3$. Exchange reactions among TMU, $TMU.H^+BF_4^-$ and $TMU.BF_3$ are investigated briefly. The results of the present investigation are compared with the results of a previous study which indicated that nitrogen is the donor atom in BF_3 adducts of some partially alkylated ureas.

Il est prouvé que l'oxygène est l'atome donneur dans le produit d'addition 1:1 de la tétraméthylurée avec le trifluorure de bore ($TMU.BF_3$). Le fluorure d'hydrogène, une impureté commune dans le trifluorure de bore, conduit à la formation de $TMU.H^+BF_4^-$ ainsi qu'à $TMU.BF_3$. Les réactions d'échange entre TMU, $TMU.H^+BF_4^-$ et $TMU.BF_3$ ont été brièvement étudiées. Les résultats de cette étude ont été comparés avec ceux d'une étude précédente dans laquelle il apparaît que l'azote est l'atome donneur dans les produits d'addition de BF_3 avec des urées partiellement alkylés.

Canadian Journal of Chemistry, **50**, 713 (1972)

Introduction

Ureas are well known to form 1:1 donor–acceptor adducts with boron trifluoride (1, 2), in which nitrogen and oxygen are possible donor atoms. Although oxygen has been shown to be the donor in closely related 1:1 adducts of amides with BF_3 and BCl_3 (3–5), Greenwood and Robinson have interpreted their n.m.r., i.r., and u.v. studies of BF_3 adducts of a number of partially-alkylated ureas as indicating that nitrogen is the donor atom (1). However, these studies were complicated by effects such as association of the adducts, probably as a result of N–H hydrogen bonding, and the results were not conclusive.

Although a comparison of the simple nitrogen and oxygen donors R_3N and R_2O shows that nitrogen is a better donor atom than oxygen toward BF_3 (6, 7), the effects of the donor atom can be greatly outweighed by the effects of adjacent groups in the donor molecule. Electron-withdrawing substituents or bulky substituents can greatly decrease the base strength of a potential donor atom. Thus in ureas, if canonical forms such as **1***b* and **1***c* are important enough sufficient electron density would be removed from the nitrogens and added to the oxygen that oxygen would become the preferred donor. As discussed by Greenwood and Robinson (1), a number of structural and chemical studies have shown that oxygen is the preferred donor atom in many urea complexes of a number of different elements, although a few complexes appear to be nitrogen-coordinated. In very strong acid solutions diprotonation of TMU occurs, with oxygen and one of the nitrogens being donor atoms (8). Although two donor sites of TMU are available to protons, only the 1:1 adduct with BF_3 has been reported. In the present paper we report variable-temperature n.m.r. studies which were undertaken to provide new evidence concerning the donor site in $TMU.BF_3$.

Experimental

Methylene chloride, used as the solvent in all of this work, was dried over P_2O_5 and vacuum distilled before use. Boron trifluoride (Matheson) was allowed to stand over sodium fluoride to remove hydrogen fluoride, then triply distilled under vacuum from a trap at $-78°$ to a trap at liquid nitrogen temperature, the initial and final cuts being rejected

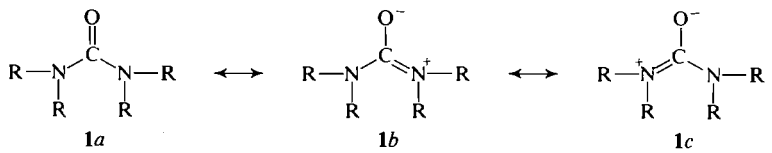

1*a* **1***b* **1***c*

[1]Present address: Department of Chemistry, McMaster University, Hamilton, Ontario.

Can. J. Chem. Downloaded from www.nrcresearchpress.com by 210.87.254.42 on 09/05/12
For personal use only.

TABLE 1. Nuclear magnetic resonance data of $TMU.BF_3$ and related compounds

Compound	Chemical shifts*		Coupling constants (Hz)		Isotope shift (p.p.m.)
	^1H	^{19}F	$J_{^1H-^{13}C}$	$J_{^{11}B-^{19}F}$	
TMU	2.75	—	136.8	—	—
$TMU.BF_3$	3.02	149.2	140.0	— †	0.064
$TMU.H^+BF_4^-$	3.12‡	151.2		0.97	0.055
$(n\text{-}C_4H_9)_4N^+BF_4^-$§		151.3		1.0	0.050

*^1H, p.p.m. to low field of TMS; ^{19}F, p.p.m. to high field of $CFCl_3$.
†Broadened resonance; isotope shift visible but no splittings due to boron–fluorine coupling.
‡Methyl resonance; the added proton absorbed at 11.4 δ.
§Reference 12.

each time. Tetramethylurea (Aldrich) and hydrogen fluoride (Matheson) were used without further purification.

Pure $TMU.BF_3$ was prepared on a vacuum line by condensing an excess of BF_3 onto a solution of TMU in CH_2Cl_2. The solvent was removed and the viscous residue dried at 80° under vacuum for 3 h. The low melting, extremely hygroscopic adduct was stored under vacuum over P_2O_5 until used. The adduct gave single ^1H and ^{19}F n.m.r. peaks. When the adduct was prepared by the procedure of Greenwood and Robinson (1), using commercial BF_3 direct from the cylinder, additional ^1H and ^{19}F peaks were observed.

$TMU.H^+.BF_4^-$ was prepared by treatment of a CH_2Cl_2 solution of pure $TMU.BF_3$ with hydrogen fluoride in a polyethylene vessel. Upon standing, colorless monoclinic crystals (m.p. 113–115°), moderately soluble in CH_2Cl_2, were obtained.

On standing for a month over calcium sulfate in a desiccator, a methylene chloride solution of $TMU.BF_3$ precipitated boric acid (m.p. 168.0–168.5°; lit. $169 \pm 1°$). The filtered solution gave a moderately soluble solid, m.p. 110–112°, which had the same ^1H and ^{19}F spectra as $TMU.H^+BF_4^-$.

Proton n.m.r. spectra were recorded at 60 MHz on a Varian Associates A-60 spectrometer equipped with a V-6040 variable temperature controller and variable temperature probe. ^{19}F spectra were recorded at 56.4 MHz on a Varian Associates DA-60IL spectrometer operating in HR sideband mode. The spectra were calibrated by the usual audio sideband method. Large ^{19}F chemical shifts (from $CFCl_3$) were calibrated by using 2500 Hz sidebands arising from a Hewlett–Packard 200 CDR audio oscillator. A Varian V-4540 variable temperature controller and variable temperature probe were used. Chemical shifts are given in p.p.m. to low field of TMS (^1H) and p.p.m. to high field of $CFCl_3$ (^{19}F).

Infrared spectra were obtained on a Perkin–Elmer Model 237B grating spectrophotometer. Spectra were recorded in CH_2Cl_2 solutions against a solvent blank using 0.1 mm solution cells with potassium bromide windows.

Results

The n.m.r. parameters of $TMU.BF_3$ and related compounds are listed in Table 1. Like free TMU (9), $TMU.BF_3$ and $TMU.H^+BF_4^-$ each give a single sharp methyl resonance at temperatures down to $-100°$, with no evidence for an amide-like *cis–trans* nonequivalence of methyl groups. Complexation of TMU with BF_3 shifts the ^1H n.m.r. peak 0.27 p.p.m. to low field and increases the ^{13}C–^1H coupling constant of the *N*-methyl groups by 3.2 Hz. At low temperatures the single room temperature ^{19}F peak at 149.2 p.p.m. is split into two peaks of relative areas 1:4 and relative chemical shift 0.064 p.p.m. This splitting can be attributed to a ^{10}B–^{11}B isotope shift, and its collapse at higher temperatures indicates rapid redistribution of fluorine among boron atoms (10, 11). In the presence of excess TMU the room temperature ^1H spectrum contained separate sharp singlets corresponding to TMU and $TMU.BF_3$. The ^{19}F spectrum contained the $TMU.BF_3$ peak as the only major peak; in some samples a second small peak could be detected at 151.2 p.p.m. In the presence of excess BF_3 the ^1H spectrum showed only the $TMU.BF_3$ peak, and the room temperature ^{19}F spectrum showed a single peak of chemical shift intermediate between BF_3 and $TMU.BF_3$, which indicated rapid fluorine exchange between free BF_3 and $TMU.BF_3$.

The ^1H spectrum of $TMU.H^+BF_4^-$ consisted of a sharp methyl singlet (3.12δ) and a broadened singlet with concentration-dependent chemical shift (about 11.4δ) arising from the added proton. The relative peak intensities were approximately 12:1. The ^{19}F spectrum consisted of a broadened singlet (peak width at half-height, 3.4 Hz) at 151.2 p.p.m. No fine structure could be observed, but in the presence of TMU (0.5 M) the signal was resolved to show an isotope shift, with the F-on-^{11}B portion split into a 1:1:1:1 quartet. These ^{19}F param-

Can. J. Chem. Downloaded from www.nrcresearchpress.com by 210.87.254.42 on 09/05/12
For personal use only.

TABLE 2. Some i.r. absorption frequencies in TMU and $TMU.BF_3$

Assignment*	Frequency (cm^{-1}) TMU	Frequency (cm^{-1}) $TMU.BF_3$	Complexation shift (cm^{-1})
Amide I (predominantly C—O stretch)	1636	1605	−31
Partially C—N stretch	1497	1550	+53

*Discussed in refs. 1 and 3.

eters agree closely with those observed for $(n\text{-}C_4H_9)_4N^+BF_4^-$ in CH_2Cl_2 (12).

Addition of $TMU.BF_3$ did not affect the ^1H or ^{19}F n.m.r. peaks of $TMU.H^+BF_4^-$. In contrast, addition of free TMU to $TMU.H^+BF_4^-$ had striking effects on the ^1H spectrum, as well as sharpening the ^{19}F signal as described above. Separate methyl resonances for TMU and $TMU.H^+$ could not be observed at any temperature down to −95°, indicating a rapid chemical exchange process. Titration of CH_2Cl_2 solutions of $TMU.H^+BF_4^-$ with free TMU led first to a down-field shift of the low-field proton absorption, followed by a reversal in the trend as more TMU was added (Fig. 1*a*). The single exchange averaged methyl peak shifted to higher field with increasing proportions of TMU (Fig. 1*b*).

When $TMU.BF_3$ was prepared directly from commercial BF_3, the ^1H and ^{19}F spectra were a superposition of the spectra of $TMU.BF_3$ and $TMU.H^+BF_4^-$. The $TMU.H^+BF_4^-$ peaks varied in size in different samples but always remained smaller than the $TMU.BF_3$ peaks. The chemical exchange behavior is that expected for a mixture of the two species. Thus on addition of free TMU the $TMU.BF_3$ ^1H peak is unaffected, but only a single averaged methyl resonance is observed for TMU and $TMU.H^+$. The assignment of the smaller ^{19}F resonance at 151.2 p.p.m. to BF_4^- was confirmed by a pronounced increase in its size, with no observable change in the isotope shift or the boron–fluorine coupling, when $(n\text{-}C_4H_9)_4N^+BF_4^-$ was added to the sample.

Infrared frequencies and BF_3 complexation shifts for two prominent bands of TMU and $TMU.BF_3$ are given in Table 2.

Discussion

The Donor Site in $TMU.BF_3$

(i) ^1H Nuclear Magnetic Resonance Evidence: Chemical Exchange

The single ^1H n.m.r. peak which is observed at temperatures as low as −100° is strong evidence that a rapid chemical exchange process is occurring in $TMU.BF_3$. In the slow-exchange

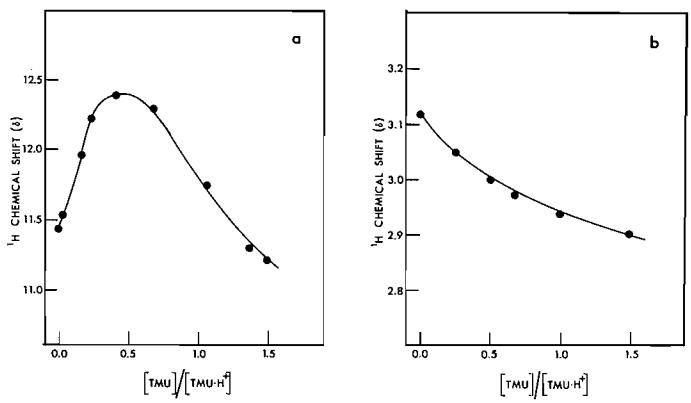

FIG. 1. Variation of the ^1H chemical shift of (*a*) the oxygen proton, (*b*) the CH_3 protons, of $TMU.H^+BF_4^-$ on titration with TMU.

Can. J. Chem. Downloaded from www.nrcresearchpress.com by 210.87.254.42 on 09/05/12
For personal use only.

Can. J. Chem. Downloaded from www.nrcresearchpress.com by 210.87.254.42 on 09/05/12
For personal use only.

limit, either oxygen donation or nitrogen donation should give more than one ^1H peak. Oxygen donation would give separate peaks due to the methyl groups *cis* and *trans* to the carbonyl group (**2**), with the added possibility that *cis-trans* isomerism about the C=O bond (13) would result in unique environments for all four methyl groups. Nitrogen donation should

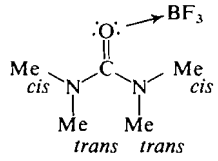

2

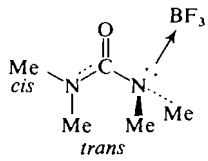

3

give separate resonances due to the free and complexed NMe_2 groups, with the uncomplexed NMe_2 group showing amide-like nonequivalence of methyls *cis* and *trans* to the carbonyl group (**3**). The observation of separate peaks for TMU and TMU.BF_3 when excess TMU is present rules out an averaging of methyl environments *via* rapid *inter*molecular exchange. Rapid *intra*molecular exchange of BF_3 between the two nitrogens or between nitrogen and oxygen cannot be excluded. However, in other BF_3 complexes with both oxygen (2, 10) and nitrogen (14) donors, breaking and reforming of donor–acceptor bonds is slow on the n.m.r. time scale at temperatures well above $-100°$. If nitrogen is the donor, an especially rapid transfer of BF_3 between the two nitrogens must be invoked to explain the single ^1H peak. If oxygen is the donor, rapid rotation about the "amide" C—N bonds can account for the averaging of the methyl environments without the need to invoke bond breaking. As in amides (15), the barrier to rotation about the C—N bond should increase on complex formation due to enhancement of the contribution of the resonance forms **1***b* and **1***c*. However, rotation could still be rapid in TMU.BF_3 at $-100°$. The inability to observe an amide type of *cis–trans* nonequivalence of *N*-alkyl groups in ureas has been discussed in terms of competitive conjugation of the two "amide" systems (16) and in terms of steric repulsion in TMU which prevents the C_2NCONC_2 skeleton from being completely planar (17). Both of these factors would remain effective in the complex and would lower the barrier to rotation about the C—N bond. Thus the single low-temperature ^1H resonance of TMU.BF_3 seems more consistent with oxygen donation.

(ii) ^{13}C–^1H Coupling in N-Methyl Groups

Henneike and Drago have used changes in ^{13}C–^1H coupling constants of *N*-methyl groups on complexation with BF_3 as an empirical test for the donor site in dimethylcyanamide (18). Complexation direct to the nitrogen of the *N*-methyl group was shown to cause large increases in $J_{^{13}C-^1H}$ (8–11 Hz in aliphatic amines), whereas complexation at a site two bonds farther removed, as in dimethylacetamide, causes much smaller increases (<1 Hz). According to this criterion, the increase in $J_{^{13}C-^1H}$ in TMU on complexation (3.2 Hz) is larger than that expected for oxygen donation but smaller than that expected for nitrogen donation. It appears to be somewhat more consistent with nitrogen donation than with oxygen donation, since a rapid chemical exchange of BF_3 between the two nitrogens could average a change in $J_{^{13}C-^1H}$ of 6.4 Hz to the observed value. However, the criterion of changes in $J_{^{13}C-^1H}$ has been applied to only a limited number of compounds (18) and may have limited applicability. Thus the ^{13}C–^1H coupling constant data do not exclude oxygen donation in TMU.BF_3.

(iii) ^{19}F Nuclear Magnetic Resonance Evidence

Table 3 gives the ^{19}F chemical shifts of a number of BF_3 adducts of simple oxygen and nitrogen donors. Whereas the nitrogen-donor adducts absorb over a range of 22 p.p.m. and the oxygen-donor adducts absorb over a range of 10 p.p.m., the adducts of the four simple aliphatic carbonyl donors in Table 3 absorb over a range of only 3.3 p.p.m. Since TMU.BF_3 absorbs in this same range, very close to the absorption of the closely related dimethylacetamide adduct, donation from the carbonyl oxygen is indicated. However, the wide range of chemical shifts for nitrogen donation covers the narrow range for carbonyl donation, so that nitrogen donation in TMU.BF_3 cannot be excluded on the basis of the ^{19}F chemical shift.

If nitrogen were the donor we would expect TMU.BF_3 to have some of the characteristics of amine adducts, such as splittings due to

TABLE 3. ^{19}F Chemical shifts of some BF_3 adducts*

Class of donor	BF_3 Adduct of	^{19}F chemical shift
	TMU	149.2
Carbonyl donors	Acetone	148.2
	Dimethylacetamide	148.6
	Methyl acetate	149.4
	Dimethylformamide	151.5
Ether donors	Diethyl ether	153.7
	Ethyl methyl ether	156.2
	Dimethyl ether	158.2
Nitrogen donors	Acetonitrile	142.3
	4-Methylpyridine	142.4
	Triethylamine	149.7
	Trimethylamine	164.1

*Methylene chloride solution, −80°, p.p.m. to high field of $CFCl_3$. The chemical shifts of some of these adducts have been reported (19), but a variety of solvents and reference compounds were used in the previous studies.

boron–fluorine coupling and boron–proton coupling in the ^{19}F and ^{1}H spectra, respectively (20). The absence of such splittings and the appearance of a ^{10}B–^{11}B isotope shift in the ^{19}F spectrum has been characteristic of oxygen donation in BF_3 complexes (10), and by these criteria oxygen should be the donor in TMU.BF_3, but again the evidence is not conclusive. The absence of splittings due to boron–fluorine coupling may be merely a characteristic of weak donation. Thus $CH_3CN.BF_3$, a weak nitrogen–donor complex, does not show such splittings.

(iv) Infrared Evidence

As discussed by Greenwood and Robinson (1), nitrogen coordination in ureas should cause an increase in the C—O stretching frequency because loss of resonance involving the coordinated nitrogen should give greater double bond character to the C—O bond. Conversely, oxygen coordination is known to decrease the vibrational frequency of this bond. In urea itself and in its adducts the principal modes of vibration are strongly coupled, and similar effects are operative in alkylated ureas (1). Since ureas can be considered to have two "amide" linkages to the carbonyl bond, the interpretation of their i.r. spectra is similar to that of amides. The complexities of amide i.r. spectra, and the effects of complexation to boron trihalides, have been discussed (3). In amides, the so-called Amide I band, which occurs in the 1600–1700 cm^{-1} region, arises mainly (>80%) from the carbonyl stretch. Following Greenwood and Robinson we assume that the band at highest frequency in TMU in this region is analogous to the Amide I band and is predominantly a C—O stretching mode. The shift of this band to lower frequency on complexation with BF_3 (Table 2) contrasts with the shifts of the analogous band in partially alkylated ureas to higher frequency (1) and indicates oxygen coordination rather than nitrogen coordination in TMU.BF_3.

The shift to lower frequency of the Amide I band of TMU on BF_3 complexation is much less (31 cm^{-1}) than the analogous shifts of the carbonyl stretching frequency in other bases (BF_3 complexation shifts: acetone, 70 cm^{-1} (21); acetophenone, 107 cm^{-1} (21); ethyl acetate, 119 cm^{-1} (22)). This can be attributed to contributions to the Amide I band by factors other than the C—O stretch. This is in line with related results for dimethylamides. When dimethylformamide and dimethylacetamide are complexed with BCl_3 the Amide I bands undergo negligible complexation shifts, although donation is known to be from oxygen (3). Because of the coupling of vibrations this result is still consistent with oxygen donation; nitrogen donation would require a pronounced shift to higher frequencies (3).

Assignment of the absorption at lower frequency (1497 cm^{-1} in TMU, Table 2), is not clear-cut, but by analogy with amides it should have a large component of C—N stretch. If so, the increase in the frequency of this peak on adduct formation is consistent with the greater contribution from structures **1***b* and **1***c* expected in the adduct.

The BF_3 complexation shifts of the Amide I band in partially alkylated ureas were consistently to higher frequencies, in both solution and solid state spectra (1). This does suggest nitrogen coordination, and it is possible that nitrogen coordination occurs in the less sterically hindered di- and trialkylureas but that a change to oxygen coordination occurs in TMU.BF_3. However, Greenwood and Robinson have presented evidence for association of the adducts in non-polar solvents, and there is i.r. evidence that uncomplexed partially alkylated ureas are themselves associated in non-polar solvents (23). Association could take place via strong inter-

Can. J. Chem. Downloaded from www.nrcresearchpress.com by 210.87.254.42 on 09/05/12
For personal use only.

Can. J. Chem. Downloaded from www.nrcresearchpress.com by 210.87.254.42 on 09/05/12
For personal use only.

molecular hydrogen bonding and would affect the i.r. frequencies. In view of these complicating factors the suggestion of nitrogen donation in the BF_3 adducts of partially alkylated ureas does not seem to be too strongly based. Hydrogen bonding is not possible in TMU or TMU.BF_3 and thus the results should be easier to interpret. Our results support oxygen donation in TMU.BF_3.

(v) Summary

No single one of the above lines of evidence is sufficient to establish oxygen as the donor site in TMU.BF_3. However, the different lines of evidence taken as a whole do establish oxygen donation with a fairly high degree of certainty.

Hydrogen Fluoride Contamination of Urea–BF_3 Adducts

Boron trifluoride is capable of increasing the Bronsted acidity of hydrogen fluoride so that the pair HF–BF_3 is a very strong acid (24), capable of protonating ureas:

$$[1] \qquad HF + BF_3 + \text{urea} \rightarrow \text{urea}.H^+BF_4^-$$

Our results demonstrate the ease with which TMU.BF_3 becomes contaminated with TMU.$H^+BF_4^-$. When sufficient precautions are taken to avoid HF contamination a single ^{19}F peak is observed for TMU.BF_3. A second ^{19}F peak, 2 p.p.m. to higher field, is diagnostic of the presence of BF_4^-. We find that commercial BF_3 may contain up to 20 mol% HF, if the BF_3 is taken from nearly-empty gas cylinders in which the less volatile HF has become concentrated. A brief study has shown that the effects of hydrogen fluoride on the ^{19}F spectra of dialkylamide-BF_3 and dialkylurea-BF_3 systems are similar to the effects in the TMU-BF_3 system.

Greenwood and Robinson reported that their BF_3 adducts of di- and trialkylated ureas gave two ^{19}F signals, a broad resonance at 148.5 ± 1 p.p.m. and a sharp peak at 150.5 ± 1 p.p.m. (1). No fine structure was reported. We can assign their smaller high-field peak to BF_4^-. Since good analyses were reported for the crystalline adducts, the impurity may have been formed on solution. If the solvent were not dry, traces of water might have given urea.$H^+BF_4^-$:

$$[2] \qquad \text{urea}.BF_3 + 3H_2O \rightarrow B(OH)_3 + 3HF + \text{urea}$$
$$HF + \text{urea}.BF_3 \rightarrow \text{urea}.H^+BF_4^-$$

This could explain the observation that the relative areas of the ^{19}F peaks depended on the solvent. In accord with a process such as [2], we have isolated boric acid and TMU.$H^+BF_4^-$ from a methylene chloride solution of TMU.BF_3 which have been allowed to stand in a desiccator for a month. The water required may have been abstracted from the calcium sulfate desiccant.

Exchange Processes Involving Protonated TMU

In TMU.H^+ the added proton is probably attached to the carbonyl oxygen, as indicated by previous work (25). Its ^1H chemical shift (11.4δ) is similar to that of protonated amides and esters which are known to be carbonyl donors. (8). The peculiar variation of the chemical shift of this proton on titration with free TMU (Fig. 1*a*) is apparently a result of hydrogen bonding effects. The observation of a single methyl resonance down to $-100°$ for TMU.$H^+BF_4^-$ indicates a low barrier to rotation about the "amide" C—N bonds, as in TMU and TMU.BF_3. This contrasts with *di*protonated TMU which has a very high barrier to rotation about the single remaining "amide" bond (8).

Whereas TMU and TMU.BF_3 give separate room temperature ^1H signals, only a single averaged methyl resonance is observed for TMU and TMU.H^+, even at $-100°$. On titration of TMU.$H^+BF_4^-$ with TMU the single methyl peak shifts to higher field and approaches the value for free TMU (Fig. 1*b*). Proton exchange among TMU molecules is fast on the n.m.r. time scale even at $-100°$, whereas BF_3 exchange is slow at room temperature. A similar difference of several orders of magnitude for H^+ and BF_3 exchange rates has been reported previously in the methanol–BF_3 system (26).

The occurrence of rapid proton exchange between base molecules can easily lead to difficulties in interpretation of ^1H n.m.r. spectra of BF_3 adducts. Such difficulties are especially likely to arise when the study is being carried out in the presence of excess base, and it is not recognized that varying amounts of the protonated base may be present in different samples. It is then difficult to account for the low-field shifts of "free base" peaks, with respect to their positions in the absence of the BF_3 adduct. It is also difficult to account for the presence of a second ^{19}F peak. Such a second peak has been observed in a number of studies of BF_3 adducts.

We thank the National Research Council for financial support, Dr. J. M. Miller for helpful discussions, and the Department of Chemistry, McMaster University, for the use of ^{19}F n.m.r. facilities.

1. N. N. GREENWOOD and B. H. ROBINSON. J. Chem. Soc. A, 511 (1967).
2. A. FRATIELLO and R. E. SCHUSTER. Inorg. Chem. **8**, 480 (1969).
3. W. GERRARD, M. F. LAPPERT, H. PYSZORA, and J. W. WALLIS. J. Chem. Soc. 2144 (1960).
4. S. J. KUHN and J. S. MCINTYRE. Can. J. Chem. **43**, 375, 995 (1965).
5. W. E. STEWART and T. H. SIDDALL, III. Chem. Rev. **70**, 517 (1970).
6. A. G. MASSEY. Adv. Inorg. Chem. Radiochem. **10**, 1 (1967).
7. N. N. GREENWOOD and R. L. MARTIN. Quart. Rev. London, **8**, 1 (1954).
8. G. A. OLAH and A. M. WHITE. J. Am. Chem. Soc. **90**, 6087 (1968); G. A. OLAH, A. M. WHITE, and D. H. O'BRIEN. Chem. Rev. **70**, 561 (1970).
9. R. G. KOSTYANOVSKII, I. I. CHERVIN, and T. Z. PAPOYAN. Bull. Acad. Sci. USSR, Div. Chem. Sci. 1834 (1968).
10. R. J. GILLESPIE and J. S. HARTMAN. Can. J. Chem. **46**, 2147 (1968).
11. R. J. GILLESPIE, J. S. HARTMAN, and M. PAREKH. Can. J. Chem. **46**, 1601 (1968).
12. J. S. HARTMAN and G. J. SCHROBILGEN. Inorg. Chem. In press.
13. U. HENRIKSSON and S. FORSÉN. Chem. Commun. 1229 (1970).
14. A. FRATIELLO and R. E. SCHUSTER. Inorg. Chem. **7**, 1581 (1968); Org. Mag. Res. **1**, 139 (1969).
15. E. S. GORE, D. J. BLEARS, and S. S. DANYLUK. Can. J. Chem. **43**, 2135 (1965).
16. T. H. SIDDALL and W. E. STEWART. J. Org. Chem. **32**, 3261 (1967).
17. R. L. MIDDAUGH, R. S. DRAGO, and R. J. NIEDZIELSKI. J. Am. Chem. Soc. **86**, 388 (1964).
18. H. F. HENNEIKE and R. S. DRAGO. Inorg. Chem. **7**, 1908 (1968).
19. C. H. DUNGAN and J. R. VAN WAZER. Compilation of reported F^{19} NMR chemical shifts. Wiley-Interscience, New York. 1970.
20. C. W. HEITSCH. Inorg. Chem. **4**, 1019 (1965).
21. B. P. SUSZ and P. CHALANDON. Helv. Chim. Acta, **41**, 1332 (1958).
22. M. F. LAPPERT. J. Chem. Soc. **542** (1962).
23. R. L. WERNER, V. F. DUCKWORTH, and H. J. SCHNITZERLING. Aust. J. Chem. **18**, 1751 (1965).
24. D. A. MCCAULAY and A. P. LIEN. J. Am. Chem. Soc. **73**, 2013 (1951); E. L. MACKOR, A. HOFSTRA, and J. H. VAN DER WAALS. Trans. Faraday Soc. **54**, 66 (1958).
25. T. BIRCHALL and R. J. GILLESPIE. Can. J. Chem. **41**, 2642 (1963).
26. R. J. GILLESPIE and J. S. HARTMAN. Can. J. Chem. **45**, 2243 (1967).

Can. J. Chem. Downloaded from www.nrcresearchpress.com by 210.87.254.42 on 09/05/12
For personal use only.

Tricarbonylchromium π-Complexes of αβγδ-Tetraphenylporphin and its Metal Chelates

NIALL J. GOGAN AND ZAHIR U. SIDDIQUI
Memorial University of Newfoundland, St. John's, Newfoundland

Received September 24, 1971

Tricarbonylchromium π-complexes of αβγδ-tetraphenylporphin and its Cr(II), Mn(III), Ni(II), Cu(II), and Zn(II) chelates have been prepared. The complexes vary in stability with the Zn compound being the most stable. The complexes have been studied by their visible and i.r. spectra and their n.m.r. spectra where applicable. A study of the CO stretching vibrations in the i.r. shows no appreciable interaction between the two metals and arguments are made to show that this lack of interaction is due to absence of π interactions between the porphin and phenyl ring systems.

Les complexes π tricarbonylchrome des tétraphénylporphines αβγδ et de ses chélates avec le Cr(II), Mn(III), Ni(II), Cu(II), et Zn(II) ont été préparés. Ces complexes, de stabilité variable (ceux de Zn étant les plus stables), ont été étudiés par spectroscopie visible, i.r. et r.m.n. quand ce dernier était applicable. L'étude de la vibration de valence du CO à l'i.r. ne montre aucune interaction notable entre les deux métaux et les arguments avancés pour expliquer ce fait s'appuient sur l'absence des interactions π entre la porphine et les systèmes aromatiques.

Canadian Journal of Chemistry, **50**, 720 (1972)

Introduction

Many complexes containing two different transition metals have been prepared and studied. Most of these have the two metals either directly bonded or joined by simple bridges[1] and relatively few have the metals arranged in such a way that the two metals can interact only through the ligand system.[2] In this paper we wish to report the synthesis and study of complexes in this latter category. These consist of complexes of αβγδ-tetraphenylporphin (TPP) in which one transition metal is σ-bonded to the four central nitrogen atoms while a tricarbonylchromium group is π-bonded to a phenyl ring.[3] The general structure of these complexes is shown in Fig. 1.

The choice of TPP as a ligand in this study is particularly appropriate because porphyrins are perhaps the most important class of ligands which occur in nature. The study of these double metal complexes could help elucidate the electron distribution in porphyrins. Porphyrin metal chelates have been extensively studied and a good account of many of these studies is given in the book by Falk (1). Much work has been done on the metal chelates of TPP. These studies include their visible spectra (2), their i.r. spectra (3), as well as some work on their n.m.r. (4) and e.s.r. (5) spectra, and crystal structure determinations (6). There is some evidence from the i.r. studies (3) that electronic effects are transmitted from the central metal to the phenyl ring. Apart from the preparation of these complexes, the purpose of this study is to probe these effects.

A large number of tricarbonylchromium complexes of substituted benzenes have been prepared and studied. This work has been reviewed by Dobson *et al.* (7). A particularly interesting aspect of these complexes is that the positions of the carbonyl stretching vibrations are sensitive to changes in electron distribution

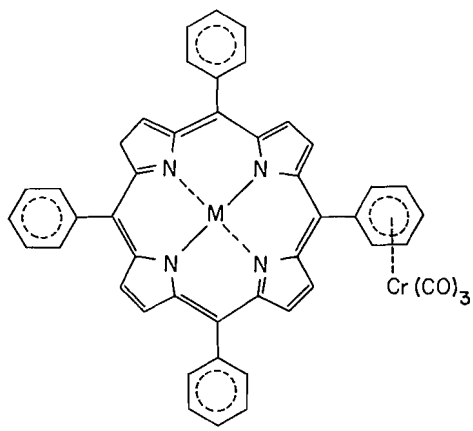

FIG. 1. Structures of the double metal complexes M-TPPCr(CO)$_3$.

[1]A selection of these are tabulated in Table 5 of the review by Abel and Stone (13).

[2]Most of the complexes in this category are tabulated in the review by Cais and Lupin (14).

[3]A preliminary communication of the preparation of the Zn complexes has been made previously (15).

Can. J. Chem. Downloaded from www.nrcresearchpress.com by 210.87.254.6 on 09/05/12
For personal use only.

Can. J. Chem. Downloaded from www.nrcresearchpress.com by 210.87.254.6 on 09/05/12
For personal use only.

in the benzene ring (8). In this study we use the carbonyl stretching vibrations to see if electronic effects are transmitted from the central σ-bonded metal to the tricarbonylchromium group.

Experimental

General

Visible spectra were recorded on a Perkin–Elmer 202 spectrometer, i.r. spectra on a Perkin–Elmer 457 spectrometer, and n.m.r. spectra on a Varian HA-100 spectrometer. Elemental analyses were determined by Schwarzkopf analytical labs., New York. Solution spectra were determined in spectroscopic grade solvents which had been deoxygenated before use by refluxing in a stream of pure nitrogen. Other solvents and chemicals were purified, if necessary, before use.

Preparations

TPP

TPP was prepared by the method of Adler *et al.* (9) by the reaction of pyrrole and benzaldehyde in refluxing propionic acid. It was purified by chromatography and recrystallized from benzene. Its visible spectrum agreed with the literature (2).

Co(II), Ni(II), Cu(II), and Zn(II) Chelates of TPP

The relevant metal acetate and TPP were refluxed in a mixture of chloroform and acetic acid (usually 1:5). The solvent was evaporated off *in vacuo*. The solid product was washed with water to remove any unreacted metal acetate. If any free TPP was present it was extracted in a Soxhlet apparatus with a mixture of methanol and ether (1:2). The product obtained was then recrystallized from suitable solvents. The visible spectra agreed with the literature (2).

Mn(III)TPPCl

TPP (2 g) and manganese acetate hydrate (1 g) were refluxed in 100 ml glacial acetic acid, for 4 h. Unreacted TPP and manganese acetate were removed from the solid product as described above. The resulting product (0.5 g) was refluxed in a mixture of 250 ml glacial acetic acid, 50 ml chloroform, and 2.5 ml concentrated hydrochloric acid for 3 h in a stream of air. The solvents were removed *in vacuo*. The solid product was washed with water and extracted with methanol in a Soxhlet apparatus. The product was recrystallized from benzene. Its visible spectrum was the same as that reported by Boucher (10).

Co(III)(TPP)(Pyridine)Cl

This compound was prepared by the method of Yamamoto and Tonomura (11) by the reaction of TPP, Co(II) acetate, pyridine, and hydrochloric acid in the presence of air. Its visible spectrum agreed with the literature (11).

Cr(II)TPP

TPP (0.5 g) and hexacarbonylchromium(0) (0.5 g) were refluxed in di-*n*-butyl ether for 6 h in an atmosphere of nitrogen containing small quantities of air. The solvent was evaporated *in vacuo* leaving a green solid. Its visible spectrum showed almost complete conversion to the metal chelate. The product was then purified by extraction into methanol to give a blue solid (visible maxima 398, 450, 568, and 607 nm). The analysis agreed with the formula $CrTPP{\cdot}4H_2O$. Its magnetic susceptibility obtained by the Faraday method gave 4.9 BM in keeping with a high spin d^4 system;[4] yield, 540 mg, 90%.

Anal. Calcd. for $C_{44}H_{36}N_4O_4Cr$: C, 71.73; H, 4.93; N, 7.60. Found: C, 70.96; H, 5.00; N, 7.62.

The Reaction of Hexacarbonylchromium(0) and Zn(II)TPP

Hexacarbonylchromium(0) (0.5 g) and Zn(II)TPP (0.5 g) were reacted together in 500 ml of di-*n*-butyl ether for 9 h in an atmosphere of nitrogen. The solvent was removed *in vacuo*. The resulting solid was chromatographed on Florisil to give two tricarbonylchromium(0) complexes and recovered Zn(II)TPP. $Zn(II)TPPCr(CO)_3{\cdot}2H_2O$; yield, 300 mg, 47%.

Anal. Calcd. for $C_{47}H_{32}N_4O_5CrZn$: C, 66.40; H, 3.79; N, 6.59. Found: C, 66.11; H, 4.06; N, 6.56.

The Reaction of Hexacarbonylchromium(0) and M-TPP (M = Mn(III)Cl, Co(II), Ni(II), and Cu(II))

The reaction was carried out in a manner similar to the reaction of Zn(II)TPP. In each case the solid product before chromatography showed two strong absorptions in the carbonyl stretching region of the i.r. After chromatography the tricarbonylchromium complex had either decomposed completely or the elemental analysis showed it to be partially decomposed.

The Reaction of Hexacarbonylchromium(0) and TPP

Hexacarbonylchromium(0) (0.5 g) and TPP (0.5 g) were refluxed in di-*n*-butyl ether for 6 h in an atmosphere of pure nitrogen. The solvent was removed *in vacuo*. The dry product showed four bands in the carbonyl stretching region of the i.r. Their relative intensities indicated them to be two sets of two bands with one set having maxima at 1990 and 1930 cm^{-1} and the other set, with about 10% of the intensity of the first, having maxima at 1970 and 1900 cm^{-1}. These latter bands disappeared when the solid was dissolved in $CHCl_3$ or CCl_4. Chromatography on Florisil yielded two bands. One has maxima in the carbonyl stretching region of the i.r. at 1990 and 1930 cm^{-1} and proved to be $TPPCr(CO)_3$. The second band was CrTPP.

The Reaction of Hexacarbonylchromium(0) and Co(III)TPP(pyridine)Cl

This reaction was carried out in a manner similar to the reaction with the other chelates. No tricarbonylchromium complex was formed and Co(II)TPP was recovered from the reaction.

Results and Discussion

Synthesis

All the metal chelates, M-TPP, have been reported previously with the exception of the chromium chelate.[4] Reaction of the metal chelates with hexacarbonylchromium(0) produced the tricarbonylchromium derivatives. In

[4]Recently, Fleischer and Srivastava (16) have reported the preparation of Cr(III)(OMe)TPP·2MeOH. They did not report the characterization of a Cr(II) compound but did observe an intermediate $Cr(CO)_3$ complex but apparently did not isolate it.

TABLE 1. The n.m.r. spectra of Zn complexes (τ)($CDCl_3$)

Complex	β-Pyrrole	Uncomplexed phenyl	Complexed phenyl
ZnTPP	1.17	1.80, 2.23	
$ZnTPPCr(CO)_3$	1.11	1.81, 2.25(3)*	3.33, 4.21(1)
$ZnTPP[Cr(CO)_3]_2$	1.09	1.83, 2.26(1)	3.44, 4.20(1)

*Numbers in parentheses denote relative intensities.

TABLE 2. Visible spectra of Zn complexes

Complex	nm ($\varepsilon \times 10^{-3}$)		
Zn-TPP	420 (600)	550 (22)	595 (6.0)
$Zn\text{-}TPPCr(CO)_3$	422 (230)	562 (13)	612 (6.3)
$ZN\text{-}TPP[Cr(CO)_3]_2$	424 (200)	570 (12)	621 (6.9)

the case of Zn(II)TPP a reasonably stable tricarbonylchromium complex was obtained with the structure shown in Fig. 1. A second complex was recovered with two phenyl rings complexed with tricarbonylchromium groups. Attempts to recrystallize these complexes slowly resulted in decomposition with Zn(II)TPP recovered. The other complexes could not be obtained pure due to decomposition. Thus satisfactory elemental analysis could not be obtained. The Mn(III)TPPCl tricarbonylchromium complex was particularly unstable and decomposed when attempts were made to isolate it. The Co(III)-TPPCl pyridine did not form a tricarbonylchromium complex. The reaction of TPP with hexacarbonylchromium(0) in refluxing di-*n*-butyl ether with rigorous exclusion of air resulted in the isolation of the tricarbonylchromium π-complex of TPP itself, Fig. 2. The tricarbonylchromium π-complex of CrTPP was also formed in this reaction but it decomposed when attempts were made to isolate it.

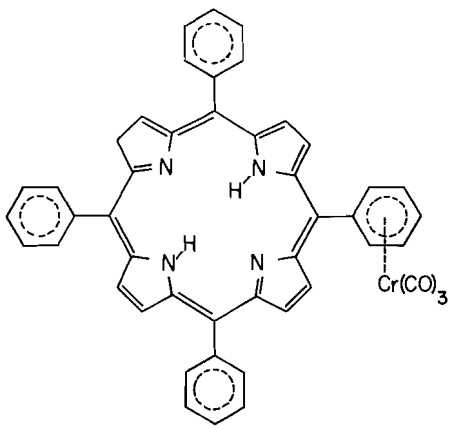

FIG. 2. Structure of the free base complex $TPPCr(CO)_3$.

Structure

Both complexes obtained from Zn(II)TPP showed strong carbonyl stretching absorptions in the i.r. at 1972 and 1902 cm^{-1} ($CHCl_3$) as expected for the tricarbonylchromium grouping. The n.m.r. spectrum of the Zn(II)TPPCr-$(CO)_3$ is shown in Fig. 3. The spin–spin splittings could not be resolved as in the case of TPP (4). The n.m.r. of the complex with two tricarbonylchromium groups attached is similar to Fig. 3 except the two groups of phenyl resonances are of equal intensity. The n.m.r. results are given in Table 1. The protons of the uncomplexed phenyl rings and the β-pyrrole proton are almost unchanged from those in Zn(II)TPP. The shift in phenyl proton resonance on attachment of a tricarbonylchromium group is comparable to that found between benzene and tricarbonylbenzenechromium(0). The relative intensities of the phenyl proton resonances are given in parentheses in Table 1 and agree with the assigned composition.

The visible spectra maxima of the Zn compounds (Table 2) show shifts to higher wavelength on addition of tricarbonylchromium groups. This was useful for determining whether the π-complex or the parent metal chelate was present. When the solid complexes were heated above 110 °C they decomposed giving the parent Zn(II)TPP. Similar decomposition also occur-

Can. J. Chem. Downloaded from www.nrcresearchpress.com by 210.87.254.6 on 09/05/12
For personal use only.

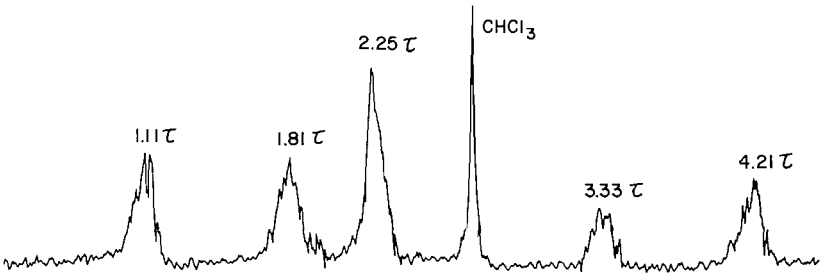

FIG. 3. The n.m.r. of Zn-TPPCr(CO)$_3$.

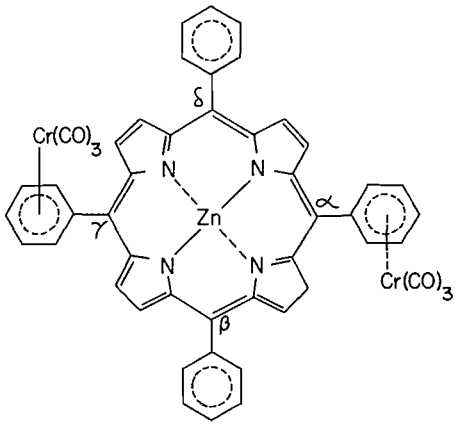

FIG. 4. One possible structure of Zn-TPP[Cr(CO)$_3$]$_2$.

red when solutions of the complexes in chloroform were left standing for several hours. This behavior is typical of tricarbonylarenechromium compounds. The above data, together with the elemental analysis, show that the structure given in Fig. 1 is correct for Zn(II)-TPPCr(CO)$_3$ and that the second Zn complex has a second phenyl ring with a tricarbonylchromium group attached. This latter compound could exist in several isomeric forms

TABLE 3. Visible spectra nm ($CHCl_3$)

M	M-TPP			M-TPPCr(CO)$_3$		
Co(II)	411	530		410	531	
Ni(II)	417	528		417	534	
Cu(II)	416	542		440	565	606
Zn(II)	420	550	595	422	562	612
H_2	417	514	550	418	517	552
		591	647		594	636

with the substituted *trans* α,γ-form (Fig. 4) being the most likely on steric grounds.

The general structural features of the other mixed transition metal complexes were deduced mainly by analogy to the zinc compounds. All showed two strong carbonyl stretching absorptions in the i.r. The visible spectra maxima are listed in Table 3. All the complexes showed the same general shift in the positions of their maxima to higher wavelength. All the complexes decomposed on standing in solution to the parent metal chelate, and some decomposed in the solid phase. The tricarbonylchromium complex of TPP gave an n.m.r. spectrum (Fig. 5). It also shows a shift in phenyl proton resonance due to complexation. However, the shift is not as great as that for the Zn complex and there is

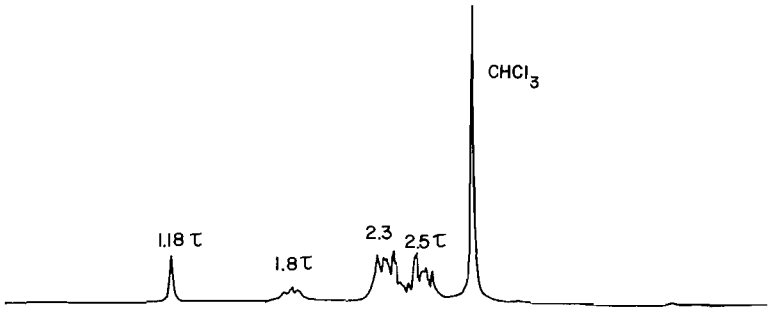

FIG. 5. The n.m.r. of TPPCr(CO)$_3$.

Can. J. Chem. Downloaded from www.nrcresearchpress.com by 210.87.254.6 on 09/05/12
For personal use only.

TABLE 4. The i.r. CO stretching region for M-TPPCr(CO)$_3$, cm^{-1}(CHCl$_3$)

M = Cr(II)	Mn(III)Cl	Co(II)	Ni(II)	Zn(II)	H_2
1970*	1972†	1972	1973	1972	1990
1900	1904	1904	1903	1902	1930

*The Cr compound decomposed in both $CHCl_3$ and CCl_4; these figures are the Nujol mull values.

†The Mn compound's i.r. could not be obtained in CCl_4; these values are obtained from the CCl_4 values (1978, 1906 cm^{-1}) with reference to the Zn compounds.

overlap between the proton resonances of the complexed and uncomplexed phenyl rings.

Infrared Spectra and Electronic Effects

The striking feature of the i.r. spectra of the double metal complexes, MTPPCr(CO)$_3$ (Table 4) is the similarity in the positions of the carbonyl stretching vibrations. These occur at the same frequency within the experimental error. The free base complex TPPCr(CO)$_3$ was the only tricarbonylchromium complex in the series to show any significant difference in this respect. The higher wavelength (1990, 1930 cm^{-1}) in this complex means that there is less π-electron density on the carbonyl group's antibonding orbitals than in the metal complexes.

Figure 6 shows a qualitative molecular orbital scheme for the higher bonding orbitals of the metalloporphin system. The scheme is based on the work of Zerner and Gouterman (12). The variation in the number of σ and π electrons, indicated in Fig. 6, means that if there was either a σ or π effect or both, transmitted from the central metal to the carbonyl groups, it should be observable in a variation in the position of the carbonyl stretching vibrations. However, no variation was observed. If there was significant interaction between the π-systems of the porphin ring and the phenyl rings one would expect an appreciable effect on the tricarbonylchromium group. On the other hand, if the systems could interact only through the σ framework, the effect would be very small as the σ orbitals are localized on pairs of atoms. This interpretation is consistent with the X-ray work of Fleischer *et al.* (6) who showed that the phenyl rings in ZnTPP are perpendicular to the plane of the porphin system. This configuration would not allow any π interaction between the porphin and the phenyl rings. The present work, therefore, would suggest that the mutual configuration of the porphin and phenyl systems are perpendicular in solution, as well as in the solid. The results of Thomas and Martel (3) showed a variation of 5 cm^{-1} in the C—Cl stretching vibration position of *p*-chlorotetraphenylporphinmetals on changing the metals. This effect is rather small and is consistent with the above interpretation.

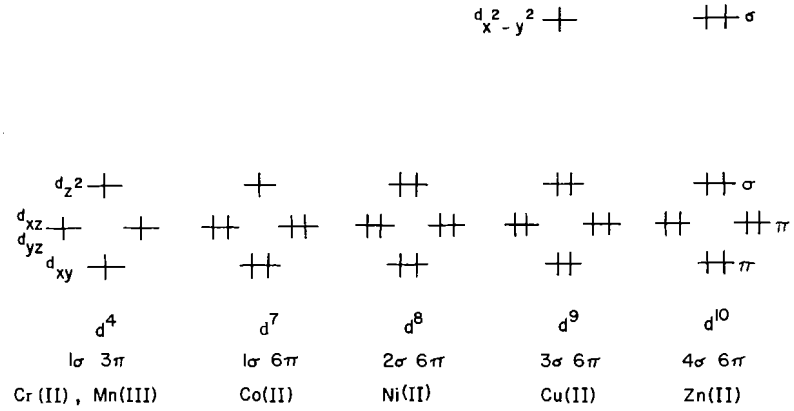

FIG. 6. Qualitative molecular orbital diagram for the central metal–porphin interaction.

Can. J. Chem. Downloaded from www.nrcresearchpress.com by 210.87.254.6 on 09/05/12
For personal use only.

The authors wish to thank the National Research Council of Canada for financial support.

1. J. E. FALK. Porphyrins and metalloporphyrins. Elsevier, 1964.
2. G. D. DOROUGH, J. R. MILLER, and M. HUENNEKENS. J. Am. Chem. Soc. **73**, 4315 (1951); D. W. THOMAS and A. E. MARTELL. Arch. Biochem. Biophys. **76**, 286 (1958).
3. D. W. THOMAS and A. E. MARTELL. J. Am. Chem. Soc. **81**, 5111 (1959).
4. L. E. WEBB and E. B. FLEISCHER. J. Chem. Phys. **43**, 3100 (1965).
5. A. MACCRAGH, C. B. STORM, and W. S. KOSKI. J. Am. Chem. Soc. **87**, 1470 (1965); G. L. CLOSS and L. E. CLOSS. J. Am. Chem. Soc. **85**, 818 (1963).
6. E. B. FLEISCHER, C. K. MILLER, and L. E. WEBB. J. Am. Chem. Soc. **86**, 2342 (1964).
7. G. R. DOBSON, I. W. STOLZ, and R. K. SHELINE. Adv. Inorg. Chem. and Radiochem. **8**, 1 (1966).
8. D. A. BROWN and H. SLOAN. J. Chem. Soc. 3849 (1962).
9. A. D. ADLER, F. R. LONGO, J. D. FINARELLI, J. GOLDMACHER, J. ASSOUR, and L. KARSAKOFF. J. Org. Chem. **32**, 476 (1967).
10. L. J. BOUCHER. J. Am. Chem. Soc. **92**, 2725 (1970).
11. K. YAMAMATO and S. TONOMURA. Sci. Papers I.P.C.R. **58**, 122 (1964).
12. M. ZERNER and M. GOUTERMAN. Theoret. Chim. Acta, **4**, 44 (1966).
13. E. W. ABEL and F. G. A. STONE. Quart. Revs. **23**, 325 (1969).
14. M. CAIS and M. S. LUPIN. Organomet. Chem. Revs. **8**, 211 (1970).
15. N. J. GOGAN and Z. U. SIDDIQUI. Chem. Commun. 284 (1970).
16. E. B. FLEISCHER and T. S. SRIVASTAVA. Inorg. Chim. Acta, **5**, 151 (1971).

Can. J. Chem. Downloaded from www.nrcresearchpress.com by 210.87.254.6 on 09/05/12
For personal use only.

A Synthetic Study in the Tricyclovetivene Series

A. DELJAC, W. D. MACKAY, CONNIE S. J. PAN, KAREL J. WIESNER, AND K. WIESNER
Natural Products Research Center, University of New Brunswick, Fredericton, New Brunswick

Received September 29, 1971

The total synthesis of racemic tricyclovetivene (**1***a*) and isomers (**1***b* and **26**) is described. The crucial reaction of the synthesis is a cyclization (**iii**) developed in this laboratory.

La synthèse totale du tricyclovetivène (**1***a*) racémique et de ses isomères (**1***b* et **26**) est décrite. L'étape cruciale de la synthèse est une cyclisation (**iii**) mise au point dans ce laboratoire.

Canadian Journal of Chemistry, **50**, 726 (1972)

Can. J. Chem. Downloaded from www.nrcresearchpress.com by 210.87.254.6 on 09/05/12
For personal use only.

In the course of model studies conducted in preparation to a total synthesis of songorine (**i**), we have discovered (1) a novel route to the C,D ring system of this alkaloid. The synthetic route involved the cyclization of compound **ii** in a basic or compound **iii** in an acidic medium. Both reactions were stereospecific and gave the products **iv** or **v** respectively. In order to explore further the scope and applicability of our method and also in order to ascertain the stereospecificity of the reaction in compounds not including a preformed bicycloheptane system as **ii** or **iii**, we decided to use the method in the synthesis of some sesquiterpene.

It appeared to us that the hydrocarbon tricyclovetivene (2) (**1***a*) might serve as a useful and, at the same time, profitable model for our synthetic scheme.

The readily available starting material, 1-methyl-indan-5-ol (**2**) (3) was converted to its allyl ether (**3**) by alkylation with allyl chloride in the presence of potassium carbonate and potassium iodide. A Claisen rearrangement of compound **3** at 185 °C gave the phenol (**4**) (i.r. hydroxyl at 3615 cm^{-1}; n.m.r., vinyl protons τ 3.96–5.16).[1] Since the rearrangement was expected to prefer the less hindered ortho position and since only one product was observed, it was preliminarily assumed that the product must indeed have the structure **4** (for proof, *vide infra*).

The phenol (**4**) was methylated with dimethyl sulfate and alkali to give the methoxy derivative (**5**). The unsaturated side chain was modified by a series of standard reactions (**6**–**8**) to prepare it for eventual cyclization. Treatment of **5** with sodium chlorate and a catalytic amount of osmium tetroxide gave the diol (**6**) which in turn underwent oxidative cleavage with sodium periodate to furnish directly the aldehyde (**7**) (i.r., aldehyde at 1725 cm^{-1}). Ketalization with ethylene glycol and *p*-toluenesulfonic acid gave the corresponding acetal (**8**).

Modification of the bicyclic system of **8** in preparation for cyclization was accomplished in the following two steps. The acetal (**8**) was subjected to a Birch reduction and the resulting dienol ether (**9**) was immediately hydrolyzed in aqueous methanolic oxalic acid to furnish the β,γ-unsaturated ketone (**10**) (i.r., ketone at 1720 cm^{-1}; n.m.r., no vinyl protons).

Cyclization of the β,γ-unsaturated ketone (**10**) was accomplished by heating in 80% acetic acid to furnish a mixture of tricyclic epimers (**11***a* and *b*) in a ratio of 2:3.[2] The stereochemistry of the hydroxyl in **11***a* and *b* remains undefined. This is unimportant since the asymmetry of the carbon carrying the hydroxyl will be subsequently removed by its reduction to a methylene. However, only two sharply melting diastereoisomers, **11***a*, m.p. 68–69 °C (ether–hexane) and **11***b*, m.p. 167–168 °C (ether) were isolated by fractional crystallization and thus it was clear that in each case the hydroxyl has a unique configuration. The i.r. spectra of the two epimers (**11***a* and *b*) both showed absorption maxima for the α,β-unsaturated ketone, 1685 cm^{-1} for **11***a* and 1680 cm^{-1} for **11***b* and the hydroxyl, 3625 cm^{-1} for **11***a* and 3615 cm^{-1} for **11***b*, with only minor differences in the fingerprint region. The n.m.r. spectrum showed a distinct difference for position of the methyl

[1]Only relevant spectral data are mentioned in the theoretical; for full spectral and characterization data see Experimental.

[2]Base-catalyzed cyclization of a corresponding β,γ-unsaturated keto aldehyde gave in this case no result.

Can. J. Chem. Downloaded from www.nrcresearchpress.com by 210.87.254.6 on 09/05/12
For personal use only.

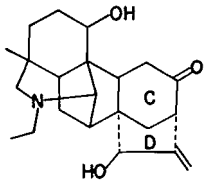

i

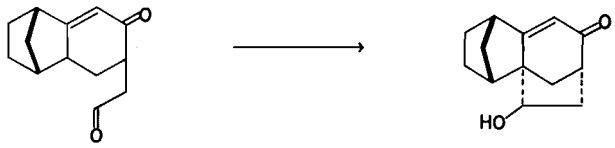

ii iv

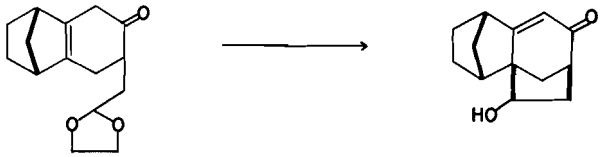

iii v

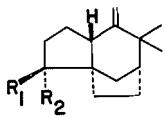

1a R_1 = Me R_2 = H

1b R_1 = H R_2 = Me

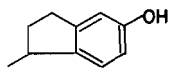

2

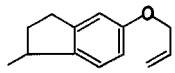

3

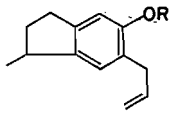

4 R = H

5 R = Me

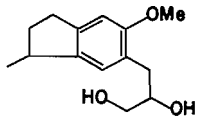

6

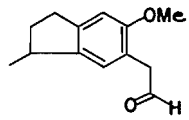

7

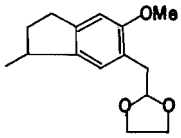

8

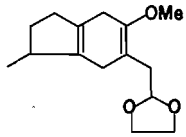

9

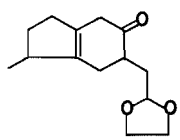

10

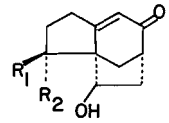

11a R_1 = Me R_2 = H

11b R_1 = H R_2 = Me

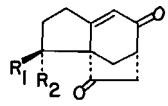

12a R_1 = Me R_2 = H

12b R_1 = H R_2 = Me

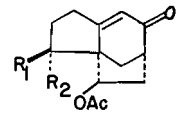

13a R_1 = Me R_2 = H

13b R_1 = H R_2 = Me

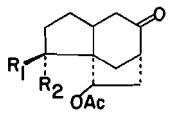

14a R_1 = Me R_2 = H

14b R_1 = H R_2 = Me

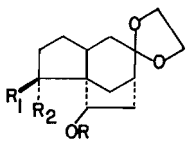

15a R = Ac R_1 = Me R_2 = H

15b R = Ac R_1 = H R_2 = Me

16a R = H R_1 = Me R_2 = H

16b R = H R_1 = H R_2 = Me

17a R = Xa R_1 = Me R_2 = H

17b R = Xa R_1 = H R_2 = Me

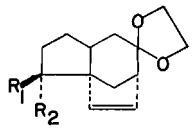

18a R_1 = Me R_2 = H

18b R_1 = H R_2 = Me

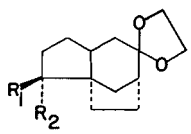

19a R_1 = Me R_2 = H

19b R_1 = H R_2 = Me

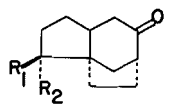

20a R_1 = Me R_2 = H

20b R_1 = H R_2 = Me

doublet, τ 9.04, $J = 7$ Hz for **11***a* and τ 8.85, $J = 7$ Hz for **11***b*.

The configurational assignments of the epimers (**11***a* and *b*) were made by comparing models and spectral data of the diketones (**12***a* and *b*) obtained via Jones' oxidation of the ketones (**11***a* and *b*). Models of these compounds showed that in epimer **12***a* the methyl group was directed away from the ketone while in epimer **12***b* the methyl group lay directly in the deshielding zone of the ketone. Accordingly, the n.m.r. spectra showed the methyl doublet of the ketone (**12***b*), τ 8.82, $J = 7$ Hz, definitely deshielded relative to the methyl doublet of ketone (**12***a*), τ 9.05, $J = 7$ Hz. The i.r. showed absorption maxima for the five-membered ketones, 1748 cm^{-1} for **12***a* and 1745 cm^{-1} for **12***b*. It is thus clear that the cyclization reaction with compound **10** is not stereospecific and that the stereospecificity previously encountered with **iii** must be due to the well known preference of the bicycloheptene system for exo attack by electrophillic reagents. Compounds **12***a* and *b* also provide conclusive evidence for our initial assumption about the course of the Claisen rearrangement, **3** → **4**. The presence in **12***a* and *b* of an α,β-unsaturated ketone (i.r., 1685 cm^{-1} for both) with one vinylic hydrogen which gives a singlet in the n.m.r. spectrum (τ 4.13 for both) does not allow any alternative structures for these two diastereoisomers. Although the alcohol (**11***b*) which has the undesired stereochemistry (for a tricyclovetivene synthesis) comprises 60% of the cyclized product mixture, it was, nevertheless, put to good use to find a possible synthetic pathway to convert the alcohol (**11***a*) to tricyclovetivene.

Acetylation of the alcohol (**11***b*) with acetic

Can. J. Chem. Downloaded from www.nrcresearchpress.com by 210.87.254.6 on 09/05/12
For personal use only.

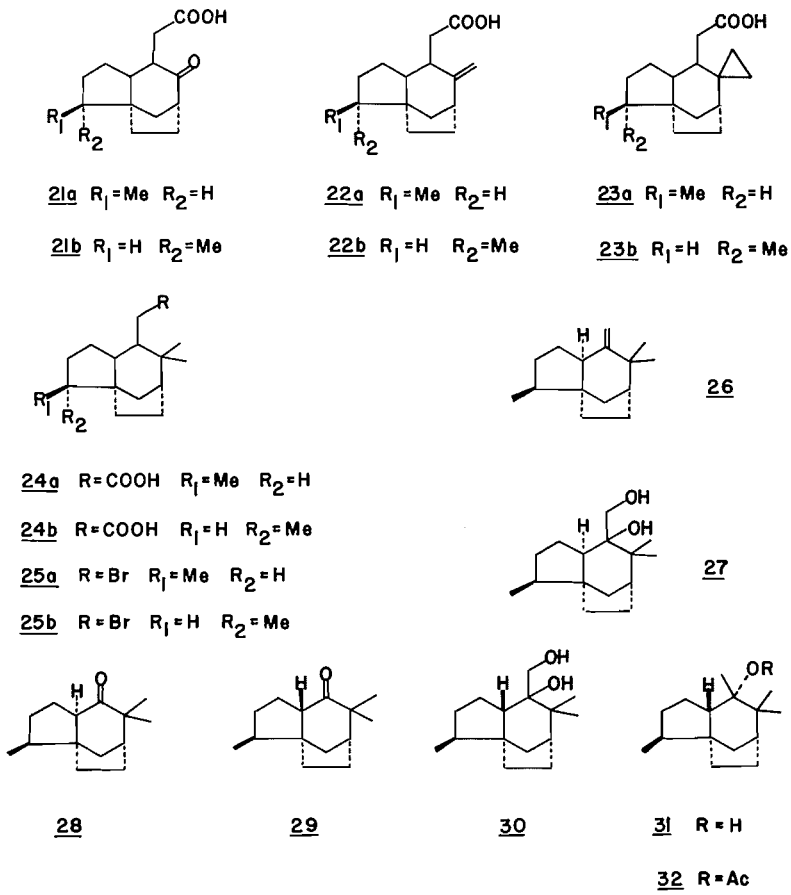

anhydride and pyridine gave the acetate (**13***b*), which easily underwent hydrogenation in ethanol with palladium-on-charcoal to furnish the keto acetate (**14***b*) (m.p. 79–81 °C from hexane). It will be clear from the sequel that the hydrogenation was stereospecific and the hydrogens were added *trans* to the methyl group. Ketalization with ethylene glycol and *p*-toluenesulfonic acid gave the ketal (**15***b*), followed by hydrolysis in aqueous methanolic potassium hydroxide to yield the ketal alcohol (**16***b*). Treatment with carbon disulfide and methyl iodide resulted in formation of the ketal xanthate (**17***b*), which when pyrolyzed at 250 °C gave the unsaturated ketal (**18***b*). Hydrogenation over an excess of Raney nickel and deketalization in 80% acetic acid produced the tricyclic ketone (**20***b*) (DNP; m.p. 148–149 °C).

Stork alkylation of the ketone (**20***b*) with pyrolidine and ethyl bromoacetate followed by hydrolysis in methanolic potassium hydroxide yielded the keto acid (**21***b*). A Wittig reaction with methylidene-phosphorane was performed on the sodium salt of the carboxylic acid to give the unsaturated carboxylic acid (**22***b*), (n.m.r., vinyl protons at τ 5.47, $J = 14$ Hz). Simmons–Smith cyclopropanation of the olefin (**22***b*) with zinc–copper couple and diiodomethane produced the tetracyclic carboxylic acid (**23***b*), (n.m.r., cyclopropane methylenes at τ 9.67–9.87) which on hydrogenation over Adams catalyst gave the *gem*-dimethyl carboxylic acid (**24***b*) (n.m.r., *gem*-dimethyl singlets at τ 9.08 and 9.15).

Bromodecarboxylation using the modified Hunsdiecker method (4) with bromine and red mercuric oxide gave the tricyclic bromide (**25***b*) which when dehydrobrominated with lithium bromide and lithium carbonate in dimethylformamide produced the tricyclic hydrocarbon (**1***b*).

Can. J. Chem. Downloaded from www.nrcresearchpress.com by 210.87.254.6 on 09/05/12
For personal use only.

Can. J. Chem. Downloaded from www.nrcresearchpress.com by 210.87.254.6 on 09/05/12
For personal use only.

The second epimeric series possessing the natural tricyclovetivene methyl configuration (**11***a* to **25***a*) was processed by steps identical to those just discussed. (See Experimental for yield and physical properties of the compounds.)

Dehydrobromination of the tricyclic bromide (**25***a*) in the same manner used for **25***b* produced the tricyclic hydrocarbon (**26**).

By means of comparing the hydrocarbons **1***b* and **26** to natural tricyclovetivene (**1***a*) (2) it was now possible to establish the stereochemistry of the hydrogenated products (**14***a* and *b*) obtained from hydrogenation of the unsaturated ketones (**13***a* and *b*). The synthetic hydrocarbon (**26**) is not identical with tricyclovetivene (**1***a*) and must differ from it by the stereochemistry of the allylic proton. This is borne out by the fact that in the n.m.r. spectrum the doublets of the vinylic protons for **26** and tricyclovetivene (**1***a*) are significantly different (τ 5.17, $J = 5$ Hz; τ 5.33, $J = 8$ Hz respectively). It appears from models, that the vinylic protons in **26** and **1***a* must be strongly influenced by the configuration of the adjacent asymmetric center.

The synthetic hydrocarbon (**1***b*) is also not identical with tricyclovetivene (**1***a*) but the reason for this nonidentity must be only the configuration of the methyl group. This is borne out by the fact that the vinylic doublet in the n.m.r. spectrum of **1***b* is almost identical (τ 5.33, $J = 11$ Hz) with the same doublet in tricyclovetivene (**1***a*). It is thus clear that the methyl group influences the stereochemistry of the hydrogenation of the acetates (**13***a* and *b*) in such a manner that the hydrogenation proceeds always trans to this group.

Natural tricyclovetivene (**1***a*) and the synthetic epi-tricyclovetivene (**26**) were individually treated with osmium tetroxide to give the diols **30** and **27** respectively and these compounds were in turn cleaved with periodate to furnish the nor-ketones **29** and **28**, respectively. The "natural"[3] nor-ketone (**29**) (2) was epimerized in methanolic sodium methoxide to the "natural" nor-ketone (**28**) and the synthetic nor-ketone (**28**) was epimerized to the synthetic nor-ketone (**29**). The spectral data (i.r. and n.m.r.) of "natural" and synthetic nor-ketones (**28**) were completely superimposable as were the spectral data of "natural" and synthetic nor-ketones (**29**).

Since the Wittig reaction on the nor-ketones (**29**) gave a poor yield, the compounds were treated with methyl lithium yielding the synthetic and "natural" alcohols (**31**). Treatment with acetic anhydride in pyridine gave the unstable synthetic and "natural" acetates (**32**) which pyrolized *in situ* to give respectively synthetic racemic and "natural" tricyclovetivene (**1***a*), both with spectral data completely superimposable with those of natural tricyclovetivene (2). The reason why we have been able to cause elimination of the acetate (**32**) practically exclusively to form an exocyclic methylenic group must be its stereochemistry. The alcohol (**31**) has been produced by the action of methyl lithium on the nor-ketone (**29**) and very probably has the stereochemistry shown. As a consequence of this, a cyclic pyrolytic elimination of the acetate (**32**) to produce an endocyclic olefin is sterically impossible.

Experimental

Preparation of the Allyl Ether (3)

A solution of 1-methyl-indan-5-ol (**2**) (3) (14.6 g) in acetone (66 ml) was treated with potassium carbonate (14 g), potassium iodide (8.4 g), allyl chloride (9.6 g) and the mixture refluxed for 20 h. The resulting mixture was diluted with acetone, filtered, stripped of solvent to yield a residue which was dissolved in diethyl ether. The ethereal solution was washed twice with water, dried, and evaporated to yield 18.5 g of oil which was purified by silica gel (600 g, 20% benzene–light petroleum) column chromatography to furnish the allyl ether (**3**) (16.53 g, 88%) as a mobile oil, homogeneous in t.l.c.

Mol. Wt. Calcd. for $C_{13}H_{16}O$: 188.1201. Found (mass spectroscopy): 188.1200.

The i.r. (CCl_4): 3080, 3012, 2955, 2860, 1640 (olefinic), 1610 cm^{-1} (aromatic). The n.m.r. (CCl_4): τ 3.07–3.51 (m, 3H, aromatic protons), 3.71–5.00 (m, 3H, vinyl protons), 5.60 (d, 2H, allyl ether methylenes), 8.75 (d, $J = 7$ Hz, 3H, methyl).

Rearrangement of 3 to 4

Allyl ether (**3**) (67 g) divided equally among four Pyrex ampoules, evacuated and sealed, was heated in an oil bath at 180–185 °C for 5 h. The combined contents were purified by silica gel (2 kg, 20% benzene in light petroleum) column chromatography to furnish the phenol (**4**) (38 g, 84%) as an oil homogeneous in t.l.c.

Mol. Wt. Calcd. for $C_{13}H_{16}O$: 188. Found (mass spectroscopy): 188.

The i.r. (CCl_4): 3615 (hydroxyl), 3540, 3080, 3010, 2955, 2860, 1630, 1615 cm^{-1}. The n.m.r. (CCl_4): τ 3.96–5.16 (m, 3H, vinyl protons), 6.71 (d, $J = 6$ Hz, 2H, allyl protons), 8.80 (d, $J = 7$ Hz, 3H, methyl).

[3]"Natural" should be understood to mean "obtained from natural tricyclovetivene".

Can. J. Chem. Downloaded from www.nrcresearchpress.com by 210.87.254.6 on 09/05/12
For personal use only.

Preparation of Methyl Ether (5)

A solution of the phenol (**4**) (37 g), sodium hydroxide (12 g), and dimethyl sulfate (22 ml) in water (80 ml) was stirred at room temperature for 1 h followed by addition of sodium hydroxide (2.4 g) in water (20 ml) and dimethyl sulfate (5 ml) and the total stirred of an addition 1 h. The mixture was diluted with diethyl ether and extracted twice with 10% aqueous sodium hydroxide which was in turn back extracted once with diethyl ether. The combined ethereal phases were dried and evaporated to give a residue which was purified on silica gel (1 kg, 20% benzene in light petroleum) column chromatography to yield the allyl methoxy compound (**5**) (33 g, 91%) as an oil homogeneous in t.l.c.

Mol. Wt. Calcd. for $C_{14}H_{18}O$: 202.1358. Found (mass spectroscopy): 202.1352.

The i.r. (CCl_4): 3075, 2990, 2955, 2860, 2845, 1670 (olefinic), 1610 cm^{-1} (aromatic). The n.m.r. (CCl_4): τ 3.92–5.36 (m, 3H, vinyl protons), 6.36 (s, 3H, methoxyl), 6.72 (d, $J = 6$ Hz, 2H, allyl protons), 8.81 (d, $J = 7$ Hz, 3H, methyl).

Preparation of the Diol (6)

A homogeneous solution of the methyl ether (**5**) (2.02 g), tetrahydrofuran (25 ml), sodium chlorate (1.6 g), and water was treated with a solution of osmium tetroxide in tetrahydrofuran (1.0 ml, 80 mg/ml) and the total stirred at room temperature for 3 h. The solution was diluted with water and extracted with ether which in turn was dried and evaporated. The resulting residue was purified by silica gel (100 g, diethyl ether) column chromatography to yield the diol (**6**) (1.80 g, 76%) as an oil homogeneous in t.l.c.

Mol. Wt. for $C_{14}H_{20}O_3$: 236.1413. Found (mass spectroscopy): 236.1408.

The i.r. ($CHCl_3$): 3580 (hydroxyl), 3490, 2995, 2955, 2860, 1612 cm^{-1} (aromatic).

The n.m.r. ($CDCl_3$): τ 2.86–3.34 (m, 2H, aromatic protons), 6.26 (s, methoxyl), 8.80 (d, $J = 7$ Hz, 3H, methyl).

*Cleavage of **6** to the Aldehyde (7)*

A solution of the diol (**6**) (1.55 g) in tetrahydrofuran (20 ml) was treated with a solution of sodium periodate (15 g) in water (20 ml) and the total stirred at room temperature for 20 min. The mixture was filtered, diluted with diethyl ether, washed three times with water, dried, and evaporated to yield pure aldehyde (**7**) (1.32 g, 99%) as an oil, homogeneous in t.l.c.

Mol. Wt. for $C_{13}H_{16}O_2$: 204.1150. Found (mass spectroscopy): 204.1145.

The i.r. (CCl_4): 3000, 2955, 2860, 2840, 2720, 1725 (aldehyde), 1610 cm^{-1} (aromatic). The n.m.r. ($CDCl_3$): τ 0.40 (bs, 1H, aldehydic proton), 2.96–3.44 (m, 2H, aromatic protons), 6.24 (s, 3H, methoxyl), 8.76 (d, $J = 7$ Hz, 3H, methyl).

Preparation of the Acetal (8)

A solution of the aldehyde (**7**) (18 g), ethylene glycol (6.5 g), *p*-toluenesulfonic acid (0.5 g) all in benzene (600 ml) was refluxed over a water separator for 30 min. The cooled solution was washed with saturated sodium bicarbonate solution and water, dried, and evaporated to yield the acetal (**8**) (20.5 g, 100%) as an oil, homogeneous in t.l.c.

Mol. Wt. Calcd. for $C_{15}H_{20}O_3$: 248.1413. Found (mass spectroscopy): 248.1406.

The i.r. (CCl_4): 2955, 2875, 1610 cm^{-1} (aromatic). The n.m.r. ($CDCl_3$): τ 2.90–3.34 (m, 2H, aromatic protons), 4.93 (t, 1H, acetal proton), 6.22 (s, 7H, methoxyl and acetal methylenes), 8.77 (d, $J = 7$ Hz, 3H, methyl).

Preparation of the Diene (9)

A solution of the ketal (**8**) (10 g) in diethyl ether (250 ml) and tertiary butanol (10 ml) was added dropwise over a period of 1/2 h to a stirred solution of lithium metal (20.7 g) in dry liquid ammonia (1000 ml) and the total stirred for 5 min, whereupon a solution of diethyl ether (20 ml) and tertiary butanol (250 ml) was added dropwise and the total stirred for an additional 24 h. Absolute ethanol (300 ml) was added until the blue color disappeared and the mixture was allowed to stand to evaporate the ammonia. The residue was taken up in ether, washed with saturated sodium chloride solution, dried, and evaporated. The resulting residue was purified by silica gel (500 g, benezene–ether) column chromatography to yield the diene (**9**) (6.5 g, 65%), homogeneous in t.l.c.

Mol. Wt. for $C_{15}H_{22}O_3$: 250. Found (mass spectroscopy): 250.

The i.r. (CCl_4): 2955, 2875, 1665 (olefinic), 1650 cm^{-1} (olefinic). The n.m.r. ($CDCl_3$): τ 5.08 (t, $J = 5$ Hz, 1H, acetal proton), 6.16 (s, acetal methylenes), 6.48 (s, 3H, methoxyl), 8.98 (d, $J = 7$ Hz, 3H, methyl).

Preparation of the β,γ-Unsaturated Ketone (10)

A solution of the diene (**9**) (1.0 g) in methanol (50 ml) was treated with a solution of oxalic acid (1.0 g) in water (10 ml) and the total stirred at room temperature for 45 min, followed by dilution with water and extraction with diethyl ether. The ethereal extract was washed with aqueous sodium bicarbonate solution and water, dried, and evaporated to give the ketone (**10**) (0.91 g, 100%) as an oil, homogeneous in t.l.c.

Mol. Wt. for $C_{14}H_{20}O_3$: 236. Found (mass spectroscopy): 236.

The i.r. (CCl_4): 2955, 2925, 2875, 2840, 1720 cm^{-1}, (ketone). The n.m.r. ($CDCl_3$): τ 5.02 (t, $J = 5$ Hz, 1H, acetal proton), 6.17 (s, 4H, acetal methylenes), 8.88 (d, $J = 7$ Hz, 3H, methyl).

Cyclization to the Alcohols (11a and b)

A solution of the ketone (**10**) (300 mg) in 80% acetic acid (3 ml) was heated in an oil bath at 80 °C for 3 h followed by evaporation of the solvent in high vacuum. The residue was purified by silica gel (20 g, benzene–ether) column chromatography to give the epimeric alcohols (**11***a* and *b*) (90 mg, 35%) as a semi-crystalline oil, appearing homogeneous in t.l.c. Dissolution of the mixture of epimeric alcohols in ether resulted in immediate crystallization of the alcohol (**11***b*), m.p. 167–168 °C. Repeated crystallizations succeeded in removing all this epimer from the mother liquors.

Anal. Calcd. for $C_{12}H_{16}O_2$ (mol. wt. 192) (alcohol **11***b*): C, 74.96; H, 8.39. Found (192 (mass spectroscopy)): C, 74.60; H, 8.32.

The i.r. (CCl_4): 3615, 3450, 2955, 2860, 1680 (α,β-unsaturated ketone), 1630 cm^{-1} (olefin). The n.m.r. ($CDCl_3$): τ 4.14 (s, 1H, vinyl proton), 5.51 (m, 1H, adjacent to OH), 8.85 (d, $J = 7$ Hz, 3H, methyl), λ_{max} (EtOH): 244.5 nm (11 700).

The oily residue from the mother liquors cyrstallized from ether–hexane to give the alcohol (**11***a*) m.p. 68–69 °C. Ratio of alcohols (**11***a* and *b*) was 2:3.

Can. J. Chem. Downloaded from www.nrcresearchpress.com by 210.87.254.6 on 09/05/12
For personal use only.

Anal. Calcd. for $C_{12}H_{16}O_2$ (mol. wt. 192) (alcohol **11***a*): C, 74.96; H, 8.39. Found (192 (mass spectroscopy)): C, 75.57; H, 8.35.

The i.r. (CCl_4): 3625, 3425, 2955, 2860, 1685 (α,β-unsaturated ketone), 1630 cm^{-1} (olefin). The n.m.r. ($CDCl_3$): τ 4.34 (s, 1H, vinyl proton), 6.09 (m, 1H, adjacent to OH), 9.04 (d, $J = 7$ Hz, 3H, methyl), λ_{max} (EtOH): 244.5 nm (11 100).

*Formation of the Diketones (**12***a and b)*

A solution of the alcohol (**11***b*) (150 mg) in acetone at 0 °C was treated dropwise with Jones' reagent to a slight excess followed by evaporation of the solvent. The residue was taken up in water extracted with ether, dried, and evaporated to give an oil which was purified by silica gel (20 g, benzene–ether) column chromatography to furnish the diketone (**12***b*) (99 mg, 66%), homogeneous in t.l.c.

Mol. Wt. Calcd. for $C_{12}H_{14}O_2$ (diketone **12***b*): 190.0994. Found (mass spectroscopy): 190.0990.

The i.r. (CCl_4): 2955, 2925, 2860, 1745 (five-membered ketone), 1685 (conjugated ketone), 1625 cm^{-1} (olefin). The n.m.r. ($CDCl_3$): τ 4.13 (s, 1H, vinyl proton), 8.82 (d, $J = 7$ Hz, 3H, methyl), λ_{max} (EtOH): 228.5 (10 000), 253 nm (7300).

The epimeric diketone (**12***a*) was obtained in the same manner.

Mol. Wt. Calcd. for $C_{12}H_{14}O_2$ (diketone **12***a*): 190.0994 Found (mass spectroscopy): 190.0990.

The i.r. (CCl_4): 2955, 2925, 2860, 1748 (five-membered ketone), 1685 (conjugated ketone), 1630 cm^{-1} (olefin). The n.m.r. ($CDCl_3$): τ 4.13 (s, 1H, vinyl proton), 9.05 (d, $J = 7$ Hz, 3H, methyl), λ_{max} (EtOH): 226 (9800), 251 nm (7400).

*Preparation of the Acetates (**13***a and b)*

A solution of the alcohol (**11***a*) (1.0 g) in acetic anhydride (4 ml) and pyridine (3 ml) was allowed to stand overnight followed by evaporation under high vacuum to give a thick oil which was purified by silica gel (40 g, 30% diethyl ether in benzene) column chromatography to yield the acetate (**13***a*) (1.22 g, 100%), homogeneous in t.l.c.

Mol. Wt. Calcd. for $C_{14}H_{18}O_3$: 234.1256. Found (mass spectroscopy): 234.1250.

The i.r. (CCl_4): 2955, 2855, 1742 (acetate), 1685 (conjugated ketone), 1630 cm^{-1} (olefin). The n.m.r. ($CDCl_3$): τ 4.31 (s, 1H, vinyl proton), 5.11 (m, 1H, adjacent to acetate), 7.91 (s, 3H, acetate methyl), 9.01 (d, $J = 7$ Hz, 3H, methyl), λ_{max}(EtOH): 234 nm (13 100).

By the same method, acetylation of alcohol (**11***b*) (3.45 g) gave the acetate (**13***b*) (4.20 g, 100%) as an oil, homogeneous in t.l.c.

Mol. Wt. Calcd. for $C_{14}H_{18}O_3$: 234.1256. Found (mass spectroscopy): 234.1250.

The i.r. (CCl_4): 2955, 2860, 1750 (acetate), 1685 (conjugated ketone), 1630 cm^{-1} (olefin). The n.m.r. ($CDCl_3$): τ 4.09 (bs, 1H, vinyl proton), 4.70 (m, 1H, proton adjacent to acetate), 8.00 (s, 3H, acetate methyl), 8.91 (d, $J = 6$ Hz, 3H, methyl), λ_{max} (EtOH): 238 nm (12 600).

*Preparation of Keto Acetates (**14***a and b)*

A mixture of the acetate (**13***a*) (1.0 g) and 10% palladium-on-charcoal (0.1 g) all in ethanol (30 ml) was hydrogenated for 3 h followed by filtration and evaporation. The resulting oil was immediately dissolved in acetone (20 ml) and treated with an excess of Jones' reagent followed by dilution with water and extraction with ether. The ethereal extract was dried, evaporated, and the residue purified by silica gel (35 g, 10% ether–benzene) column chromatography to yield the keto acetate (**14***a*) (758 mg, 75%) as a clear oil, homogeneous in t.l.c.

Mol. Wt. Calcd. for $C_{14}H_{20}O_3$: 236.1413. Found (mass spectroscopy): 236.1407.

The i.r. (CCl_4): 2955, 2860, 1740 (acetate), 1715 cm^{-1} (ketone). The n.m.r. ($CDCl_3$): τ 5.03 (m, 1H, adjacent to acetate), 7.95 (s, acetate methyl), 8.95 (d, $J = 6$ Hz, 3H, methyl).

By the same method, reduction of the acetate (**13***b*) (2.23 g) gave the acetate (**14***b*) (1.57 g, 70%) as an oil which crystallized from hexane, m.p. 79–81 °C.

Anal. Calcd. for $C_{14}H_{20}O_3$ (mol. wt. 236): C, 71.15; H, 8.51. Found (236 (mass spectroscopy)): C, 70.97; H, 8.35.

The i.r. (CCl_4): 2955, 2905, 2870, 1740 (acetate), 1715 cm^{-1} (ketone). The n.m.r. ($CDCl_3$): τ 4.60 (m, 1H, proton adjacent to acetate), 7.94 (s, 3H, acetate methyl), 9.01 (d, $J = 6$ Hz, 3H, methyl).

*Preparation of the Ketal Acetates (**15***a and b)*

A solution of the keto acetate (**14***a*) (1.0 g), ethylene glycol (620 mg), and *p*-toluenesulfonic acid (50 mg) all in dry benzene (25 ml) was refluxed over a water separator for 2 h. The solution was cooled, washed with saturated sodium bicarbonate solution and water, dried, and evaporated to give the ketal acetate (**15***a*) (1.2 g, 100%) homogeneous in t.l.c.

Mol. Wt. Calcd. for $C_{16}H_{24}O_4$: 280.1675. Found (mass spectroscopy): 280.1668.

The i.r. (CCl_4): 2955, 2875, 1737 cm^{-1} (acetate). The n.m.r. ($CDCl_3$): τ 5.12 (m, 1H, adjacent to acetate), 6.12 (s, 4H, ketal methylenes), 7.94 (s, acetate methyl), 9.05 (d, $J = 6$ Hz, 3H, methyl).

By the same method, ketalization of the keto acetate (**14***b*) (580 mg) gave the ketal acetate (**15***b*) (678 mg, 97%) as an oil, homogeneous in t.l.c.

Mol. Wt. Calcd. for $C_{16}H_{24}O_4$: 280.1675. Found (mass spectroscopy): 280.1670.

The i.r. (CCl_4): 2955, 2905, 2870, 1740 (acetate), 1245, 1045 cm^{-1}. The n.m.r. ($CDCl_3$): τ 4.87 (m, 1H, proton adjacent to acetate), 6.15 (s, 4H, ketal methylenes), 8.00 (s, 3H, acetate methyl), 9.10 (d, $J = 6$ Hz, 3H, methyl).

*Preparation of the Ketal Alcohols (**16***a and b)*

A solution of the ketal acetate (**15***a*) (560 mg) in 5% methanolic potassium hydroxide (10 ml) was refluxed for 3 h. The solution was cooled, diluted with water, extracted with diethyl ether, dried, and evaporated to furnish the ketal alcohol (**16***a*) (480 mg, 100%) as an oil, homogeneous in t.l.c.

Mol. Wt. Calcd. for $C_{14}H_{22}O_3$: 238. Found (mass spectroscopy): 238.

The i.r. (CCl_4): 3620 (hydroxyl), 3495, 2950, 2875 cm^{-1}. The n.m.r. ($CDCl_3$): τ 6.14 (s, 4H, ketal methylenes), 8.95 (d, $J = 6$ Hz, 3H, methyl).

By the same method, hydrolysis of the ketal acetate (**15***b*) (572 mg) gave the ketal alcohol (**16***b*) (480 mg, 100%) as an oil homogeneous in t.l.c.

Mol. Wt. Calcd. for $C_{14}H_{22}O_3$: 238.1569. Found (mass spectroscopy): 238.1567.

The i.r. (CCl_4): 3625 (hydroxyl), 3500, 2955, 2905, 2870,

Can. J. Chem. Downloaded from www.nrcresearchpress.com by 210.87.254.6 on 09/05/12
For personal use only.

1455, 1050 cm^{-1}. The n.m.r. ($CDCl_3$): τ 5.73 (m, 1H, proton adjacent to alcohol), 6.13 (s, 4H, ketal methylenes), 9.05 (d, $J = 6$ Hz, 3H, methyl).

*Preparation of Xanthates (**17a** and **b**)*

A mixture of ketal alcohol (**16***a*) (480 mg), 75% sodium hydride in mineral oil (100 mg) all in tetrahydrofuran (25 ml) was refluxed for 1 h followed by cooling and addition of carbon disulfide (4 ml) with the total being heated for an additional $1\frac{1}{2}$ h. The mixture was again cooled and treated with methyl iodide (4 ml) followed by reflux for 1 h. The solvent was distilled off and the residue dissolved in benzene which in turn was washed with water, dried, and evaporated. Chromatography of the residue on silica gel (25 g, 10% ether–benzene) furnished the xanthate (**17***a*) (560 mg, 85%) as a yellow oil which crystallized from hexane, m.p. 108–109 °C.

Anal. Calcd. for $C_{16}H_{24}O_3S_2$ (mol. wt. 328): C, 58.51; H, 7.37; S, 19.53. Found (328 (mass spectroscopy)): C, 58.66; H, 7.40; S, 19.18.

The i.r. (CCl_4): 2950, 2875, 1230 cm^{-1} (xanthate). The n.m.r. ($CDCl_3$): τ 4.34 (m, 1H, proton adjacent to xanthate), 6.10 (s, 4H, ketal methylenes), 7.44 (s, 3H, xanthate methyl), 8.95 (d, $J = 6$ Hz, 3H, methyl).

By the same method, addition to the ketal alcohol (**16***b*) (770 mg) gave the xanthate (**17***b*) (890 mg, 84%) as an oil, homogeneous in t.l.c.

Mol. Wt. Calcd. for $C_{16}H_{24}O_3S_2$: 328. Found (mass spectroscopy): 328.

The i.r. (CCl_4): 2950, 2870, 1220, 1060 cm^{-1}. The n.m.r. ($CDCl_3$): τ 4.13 (m, 1H, proton adjacent to xanthate), 6.10 (s, 4H, ketal methylenes), 7.40 (s, 3H, xanthate methyl), 9.07 (d, $J = 6$ Hz, 3H, methyl).

*Formation of the Olefins (**18a** and **b**)*

The xanthate (**17***a*) (328 mg) was pyrolyzed in an open Pyrex tube at 190 °C for 30 min followed by distillation to yield the olefin (**18***a*) (170 mg, 95%) as an oil b.p. 150 °C/1 mm, appearing homogeneous in t.l.c.

Mol. Wt. Calcd. for $C_{14}H_{20}O_2$: 220. Found (mass spectroscopy): 220.

The i.r. (CCl_4): 3050 (olefin), 2950, 2875, 1650 (olefin), 1120 cm^{-1}. The n.m.r. ($CDCl_3$): τ 4.20 (m, 2H, vinyl protons), 6.10 (s, 4H, ketal methylenes), 9.12 (d, $J = 6$ Hz, 3H, methyl).

By the same method, the xanthate (**17***b*) (730 mg) was pyrolyzed to give the olefin (**18***b*) (502 mg) as a liquid, b.p. 250 °C/16 mm, homogeneous in t.l.c.

Mol. Wt. Calcd. for $C_{14}H_{20}O_2$: 220.1463. Found (mass spectroscopy): 220.1458.

The i.r. (CCl_4): 3050 (olefin), 2950, 2860, 1640 cm^{-1} (olefin). The n.m.r. ($CDCl_3$): τ 3.83–4.27 (m, 2H, vinyl protons), 6.10 (s, 4H, ketal methylenes), 9.10 (d, $J = 6$ Hz, 3H, methyl).

*Hydrogenation of the Olefins, **18a** and **b** to **19a** and **b***

A mixture of the olefin (**18***a*) (1.0 g) in ethanol (150 ml) and Raney nickel (40 g) was hydrogenated for 4 h followed by filtration and evaporation to yield the saturated ketal (**19***a*) (953 mg, 95%), homogeneous in t.l.c.

Mol. Wt. Calcd. for $C_{14}H_{22}O_2$: 222. Found (mass spectroscopy): 222.

The i.r. (CCl_4): 2950, 2875, 1110 cm^{-1} (ketal). The n.m.r. ($CDCl_3$): τ 6.11 (s, 4H, ketal methylenes), 9.18 (d, $J = 6$ Hz, 3H, methyl).

By the same method, hydrogenation of the olefin (**18***b*) (502 mg) gave the saturated ketal (**19***b*) (408 mg) as an oil, homogeneous in t.l.c.

Mol. Wt. Calcd. for $C_{14}H_{22}O_2$: 222. Found (mass spectroscopy): 222.

The i.r. (CCl_4): 2950, 2860, 1102 cm^{-1} (ketal). The n.m.r. ($CDCl_3$): τ 6.09 (s, 4H, ketal methylenes), 9.13 (d, $J = 6$ Hz, 3H, methyl).

*Preparation of the Tricyclic Ketones (**20a** and **b**)*

A solution of the ketal (**19***a*) (1.0 g) in 80% acetic acid was heated at 80 °C for 30 min followed by dilution with water and extraction with chloroform. The chloroform extract was dried and evaporated to furnish the tricyclic ketone (**20***a*) (802 mg, 100%) as an oil, homogeneous in t.l.c.

Mol. Wt. Calcd. for $C_{12}H_{18}O$ (the ketone): 178. Found (mass spectroscopy): 178.

The i.r. (CCl_4): 2955, 2875, 1715 cm^{-1} (ketone). The n.m.r. ($CDCl_3$): τ 7.34, 7.84, 8.07, 8.47, 9.08 (d, $J = 6$ Hz, 3H, methyl).

Anal. Calcd. for $C_{18}H_{22}N_4O_4$ (dinitrophenylhydrazone, m.p. 156–157 °C): C, 60.32; H, 6.18; N, 15.64. Found: C, 59.45; H, 6.09; N, 15.93.

By the same method, deketalization of the ketal (**19***b*) (408 mg) gave the tricyclic ketone (**20***b*) (324 mg, 82% based on the xanthate (**17***b*)) as an oil, homogeneous in t.l.c.

Mol. Wt. Calcd. for $C_{12}H_{18}O$: 178. Found (mass spectroscopy): 178.

The i.r. (CCl_4): 2955, 2875, 1715 cm^{-1} (ketone). The n.m.r. ($CDCl_3$): τ 7.33, 7.80, 8.33, 8.47, 9.06 (d, $J = 6$ Hz, 3H, methyl).

Anal. Calcd. for $C_{18}H_{22}N_4O_4$ (dinitrophenylhydrazone, m.p. 148–149 °C): C, 60.32; H, 6.18; N, 15.65. Found: C, 60.50; H, 6.12; N, 15.72.

*Preparation of the Keto Acids (**21a** and **b**)*

A solution of the tricyclic ketone (**20***a*) (600 mg) and pyrrolidine (1.19 g) in dry benzene (20 ml) was refluxed under nitrogen and a water separator for 15 h followed by replacement of the solvent with dry dioxane (15 ml). Ethyl bromoacetate (1.11 g) in dioxane (5 ml) was added dropwise over a period of 1/4 h and the mixture heated at 100 °C under nitrogen for 24 h, followed by evaporation of the solvent and treatment of the residue with water (20 ml) at reflux for 2 h. The cooled aqueous solution was extracted with diethyl ether and in turn washed with water, saturated sodium chloride solution, dried, and evaporated to give a residue (710 mg) which was saponified by refluxing in 1 *N* methanolic potassium hydroxide solution (15 ml) for 2 h. The reaction was stripped of solvent and the residue taken up in water, followed by extraction with diethyl ether which on drying and evaporation yielded starting ketone (**20**) (232 mg). The aqueous solution was acidified with 5% hydrochloric acid and extracted with diethyl ether and in turn washed with water, saturated sodium chloride solution, dried, and evaporated to give the keto acid (**21**) (266 mg, 72% with recovery) as a thick oil, homogeneous in t.l.c. Recycling furnished a 54% overall yield.

Anal. Calcd. for $C_{14}H_{20}O_3$ (mol. wt. 236): C, 71.16; H, 8.53; O, 20.31. Found (236 (mass spectroscopy)): C, 70.95; H, 8.55; O, 20.39.

The i.r. (CCl_4): 3525, 2950, 2860, 1715 (ketone), 1710 cm^{-1} (carboxylic acid). The n.m.r. ($CDCl_3$): τ 0.53 (bs. 1H, carboxylic acid proton), 9.05 (d, $J = 6$ Hz, 3H, methyl).

Can. J. Chem. Downloaded from www.nrcresearchpress.com by 210.87.254.6 on 09/05/12
For personal use only.

By the same method, the tricyclic ketone (**20***b*) (340 mg) was alkylated to give the keto acid (**21***b*) (79 mg, 81% with recovery) as an oil, homogeneous in t.l.c. Recycling furnished a total of 225 mg (50%).

Mol. Wt. Calcd. for $C_{14}H_{20}O_3$: 236. Found (mass spectroscopy): 236.

The i.r. (CCl_4): 3530, 2960, 2875, 1715 cm^{-1} (carboxylic acid and ketone). The n.m.r. ($CDCl_3$): τ −0.17 (bs, 1H, carboxylic acid proton), 9.05 (d, $J = 6$ Hz, 3H, methyl).

*Preparation of the Tricyclic Olefins (**22***a and b)*

A stirred suspension of oil-free sodium hydride (197 mg) in dimethylsulfoxide (20 ml) under nitrogen was treated with methyl triphenylphosphonium iodide (1.26 g) and stirred for 2 h followed by addition of a solution of the keto acid (**21***a*) (369 mg) in dimethylsulfoxide (5 ml) and the total stirred at room temperature for 4 h and at 75 °C for 24 h. The solution, cooled well, was acidified dropwise with 5% hydrochloric solution and in turn taken up in chloroform. The chloroform was washed with water and evaporated to give a residue which was taken up in 5% sodium hydroxide solution, washed with diethyl ether, and acidified with 5% hydrochloric acid. The aqueous mixture was extracted with diethyl ether, washed with water and saturated sodium chloride solution, dried, and evaporated to give the tricyclic olefin (**22***a*) (327 mg, 89%) as a thick oil, homogeneous in t.l.c.

Anal. Calcd. for $C_{15}H_{22}O_2$ (mol. wt. 234): C, 76.88; H, 9.46; O, 13.66. Found (234 (mass spectroscopy)): C, 76.58; H, 9.25; O, 13.71.

The i.r. (CCl_4): 3530, 2950, 2860, 1705 (carboxylic acid), 1640 cm^{-1} (olefin). The n.m.r. ($CDCl_3$): τ + 0.57 (bs, 1H, carboxylic acid proton), 5.42 (d, $J = 20$ Hz, 2H, vinyl protons), 9.18 (d, $J = 6$ Hz, 3H, methyl).

By the same method, the Wittig reaction on the keto acid (**21***b*) (235 mg) gave the tricyclic olefin (**22***b*) (181 mg, 78%) as a thick oil, homogeneous in t.l.c.

Mol. Wt. Calcd. for $C_{15}H_{22}O_2$: 234.1620. Found (mass spectroscopy): 234.1616.

The i.r. (CCl_4): 3530, 3080, 2950, 2875, 1705 (carboxylic acid), 1635 cm^{-1} (olefin). The n.m.r. ($CDCl_3$): τ −0.83 (bs, 1H, carboxylic acid proton), 5.47 (d, $J = 14$ Hz, 2H, vinyl protons), 9.15 (d, $J = 6$ Hz, 3H, methyl).

*Preparation of the Tetracyclic Carboxylic Acids (**23***a and b)*

A suspension of zinc–copper couple (338 mg), a few crystals of iodine, and a few drops of diiodomethane all in dry diethyl ether (5 ml) was stirred until the iodine color was absent followed by addition of diiodomethane (1.98 g) and the total refluxed for 1/2 h. The mixture was cooled and treated with a solution of the tricyclic olefin (**22***a*) (290 mg) in dry diethyl ether (5 ml) and the total refluxed for 4 days. The mixture was filtered, diluted with diethyl ether, washed with 5% hydrochloric acid and water followed by extraction with 5% sodium hydroxide solution which was in turn washed with diethyl ether, acidified with 5% hydrochloric acid, and extracted with diethyl ether. The ethereal extract was washed with water, saturated sodium chloride solution, dried, and evaporated to give the tetracyclic carboxylic acid (**23***a*) (214 mg, 70%) as a thick oil, homogeneous in t.l.c.

Anal. Calcd. for $C_{16}H_{24}O_2$ (mol. wt. 248): C, 77.37; H, 9.74; O, 12.88. Found (248 (mass spectroscopy)): C, 76.82; H, 9.61; O, 13.75.

The i.r. (CCl_4): 3525, 2945, 2865, 1705 cm^{-1} (carboxylic acid). The n.m.r. ($CDCl_3$): τ −1.10 (bs, 1H, carboxylic acid proton), 9.15 (d, $J = 6$ Hz, 3H, methyl), 9.65–9.87 (m, 4H, cyclopropane methylenes).

By the same method, from the tricyclic olefin (**22***b*) (152 mg) was prepared the tetracyclic carboxylic acid (**23***b*) (138 mg, 72%) as a thick oil, homogeneous in t.l.c.

Mol. Wt. Calcd. for $C_{16}H_{24}O_2$: 248. Found (mass spectroscopy): 248.

The i.r. (CCl_4): 3530, 3075, 3005, 2955, 2875, 1705 cm^{-1} (carboxylic acid). The n.m.r. ($CDCl_3$): τ −0.73 (bs, 1H, carboxylic acid proton), 9.15 (d, $J = 6$ Hz, 3H, methyl), 9.67–9.87 (m, 4H, cyclopropane methylenes).

*Hydrogenation of **23***a and b to the Tricyclic Carboxylic Acids (**24***a and b)*

A mixture of the tetracyclic carboxylic acid (**23***a*) (660 mg) and Adams catalyst (660 mg) all in glacial acetic acid (20 ml) was hydrogenated at 2000 p.s.i. for 24 days at room temperature. The mixture was filtered and evaporated to furnish the tricyclic carboxylic acid (**24***a*) (562 mg, 84%) as a clear, colorless, thick oil, homogeneous in t.l.c.

Mol. Wt. Calcd. for $C_{16}H_{26}O_2$: 250.1933. Found (mass spectroscopy): 250.1924.

The i.r. (CCl_4): 2950, 2865, 1705 cm^{-1} (carboxylic acid). The n.m.r. ($CDCl_3$): τ −0.20 (bs, 1H, carboxylic acid proton), 9.10 (s, 6H, two methyls), 9.15 (d, $J = 6$ Hz, 3H, methyl).

By the same method, hydrogenation of the tetracyclic carboxylic acid (**23***b*) (288 mg) gave the tricyclic carboxylic acid (**24***b*) (261 mg, 90%) as a thick oil, homogeneous in t.l.c.

Mol. Wt. Calcd. for $C_{16}H_{26}O_2$: 250.1933. Found (mass spectroscopy): 250.1928.

The i.r. (CCl_4): 3530, 2950, 2870, 1705 cm^{-1} (carboxylic acid). The n.m.r. ($CDCl_3$): τ −1.30 (bs, 1H, carboxylic acid proton), 9.08 (s, 3H, methyl), 9.15 (s, 3H, methyl), 9.15 (d, $J = 6$ Hz, 3H, methyl).

*Preparation of the Tricyclic Bromides (**25***a and b)*

A refluxing mixture of the tricyclic carboxylic acid (**24***a*) (550 mg) and red mercuric oxide (570 mg) in dry carbon tetrachloride (8 ml) was treated dropwise with a solution of bromine (422 mg) in dry carbon tetrachloride (2 ml) and the total refluxed for an additional 1 h. The mixture was filtered, diluted with carbon tetrachloride, washed with 5% sodium hydroxide solution, water, saturated sodium chloride solution, dried, and evaporated. The labile residue (594 mg) was immediately purified by preparative silica gel t.l.c. (light petroleum) to furnish the tricyclic bromide (**25***a*) (156 mg, 25%) as a clear colorless oil, homogeneous in t.l.c.

Mol. Wt. Calcd. for $C_{15}H_{25}Br$: 285. Found (mass spectroscopy): m/e 286, 284.

The i.r. (film): 2950, 2865, 1470, 1235, 760 cm^{-1}. The n.m.r. ($CDCl_3$): τ 6.50 (m, 2H, protons α to bromine), 9.07 (s, 3H, methyl), 9.10 (s, 3H, methyl), 9.15 (d, $J = 6$ Hz, 3H, methyl).

By the same method, bromodecarboxylation of the tricyclic carboxylic acid (**24***b*) (260 mg) gave the tricyclic bromide (**25***b*) (103 mg, 36%) as a clear colorless liquid, homogeneous in t.l.c.

Mol. Wt. Calcd. for $C_{15}H_{25}Br$: 285. Found (mass spectroscopy): 284, 286.

The i.r. (film): 2950, 2875, 1460, 1230 cm^{-1}. The n.m.r.

Can. J. Chem. Downloaded from www.nrcresearchpress.com by 210.87.254.6 on 09/05/12
For personal use only.

($CDCl_3$): τ 6.33–6.87 (m, 2H, protons α to bromine), 8.97 (s, 3H, methyl), 9.10 (s, 3H, methyl), 9.15 (d, $J = 6$ Hz, 3H, methyl).

*Preparation of epi-Tricyclovetivene (**26**)*

A mixture of the tricyclic bromide (**25**) (150 mg), lithium bromide (277 mg), and lithium carbonate (235 mg) all in dimethylformamide (3 ml) was refluxed under nitrogen for 90 min. The mixture was diluted with ice-cold 5% hydrochloric acid until solution occurred, followed by extraction with diethyl ether. The ethereal extract was washed with 5% hydrochloric acid, water, saturated sodium chloride solution, and the ether fractionally distilled off. The residual liquid was purified by preparative silica gel t.l.c. (light petroleum) to furnish epi-tricyclovetivene (**26**) (92 mg, 85%) as a clear colorless liquid, homogeneous in t.l.c.

Mol. Wt. Calcd. for $C_{15}H_{24}$: 204.1878. Found (mass spectroscopy): 204.1872.

The i.r. (film): 3075 (olefin), 2950, 2860, 1630 (olefin), 890 cm^{-1}. The n.m.r. ($CDCl_3$): τ 5.17 (d, $J = 4$ Hz, 2H, vinyl protons), 7.77 (bt, 1H, allyl proton), 8.85 (s, 3H, methyl), 8.92 (s, 3H, methyl), 9.15 (d, $J = 6$ Hz, 3H, methyl).

*Preparation of the Methyl Epimer (**1b**) of Tricyclovetivene*

A mixture of the tricyclic bromide (**25***b*) (100 mg), lithium bromide (183 mg), and lithium carbonate (155 mg) all in dimethylformamide (2 ml) was refluxed under nitrogen for 90 min. The reaction mixture was cooled, diluted with ice-cold 5% hydrochloric acid until solution occurred, and extracted with ether. The ethereal extract was washed with 5% hydrochloric acid, water, dried, and the solvent fractionally distilled off. The residual liquid was purified by preparative silica gel t.l.c. (light petroleum) to furnish the methyl epimer (**1***b*) (35 mg, 49%) of tricyclovetivene as a clear colorless liquid, homogeneous in t.l.c.

Mol. Wt. Calcd. for $C_{15}H_{24}$: 204.1878. Found (mass spectroscopy): 204.1875.

The i.r. (film): 3080 (olefin), 2940, 2860, 1635 (olefin), 1455, 1375, 890, 735 cm^{-1}. The n.m.r. ($CDCl_3$): τ 5.33 (d, $J = 11$ Hz, 2H, vinyl protons), 7.60 (bt, 1H, allyl proton), 8.45, 8.92 (s, 6H, 2 methyls), 9.15 (d, $J = 6$ Hz, 3H, methyl).

*Spectra of Natural Tricyclovetivene (**1a**)*

The i.r. (film): 3080 (olefin), 2940, 2860, 1635 (olefin), 1460, 1375, 890 cm^{-1}. The n.m.r. ($CDCl_3$): τ 5.33 (d, $J = 8$ Hz, 2H, vinyl protons), 7.47 (bt, 1H, allylic proton), 8.23, 8.57, 8.90 (s, 3H, methyl), 8.93 (s, 3H, methyl), 9.05 (d, $J = 6$ Hz, 3H, methyl).

*Preparation of the Tricyclic Diol (**27**)*

A solution of epi-tricyclovetivene (**26**) (59 mg) in dry pyridine (1.1 ml) was treated with a tetrahydrofuran solution (1 g OsO_4/4 ml) of osmium tetroxide (0.32 ml) and the total stirred at room temperature for 3 h. The resulting black mixture was treated with a solution of sodium bisulfite (134 mg) in water (2.5 ml) and pyridine (1.5 ml) and the total stirred for 30 min at room temperature. The solution was extracted with methylene chloride, washed with saturated sodium chloride solution, dried, and evaporated. The residue was purified by preparative silica gel t.l.c. (chloroform) to give the tricyclic diol (**27**) 56 mg, 81% as a clear, colorless, thick oil, homogeneous in t.l.c.

Mol. Wt. Calcd. for $C_{15}H_{26}O_2$: 238.1933. Found (mass spectroscopy): 238.1938.

The i.r. (film): 3400 (hydroxyl), 2950, 2865, 1465, 1025 cm^{-1}. The n.m.r. ($CDCl_3$): τ 6.50 (s, 2H, methylenes of primary alcohol), 7.83 (bs, 2H, exchanges with D_2O), 8.97 (s, 3H, methyl), 9.07 (s, 3H, methyl) 9.15 (d, $J = 6$ Hz, 3H, methyl).

*Cleavage of **27** to epi-Tricyclovetivene Nor-ketone (**28**)*

A homogeneous solution of the tricyclic diol (**27**) (56 mg) in tetrahydrofuran (1.5 ml) and water (1 ml) was treated with powdered sodium meta periodate (500 mg) and the total stirred at room temperature for 30 min. The mixture was filtered, diluted with diethyl ether, washed with water, saturated sodium chloride solution, dried, and evaporated to give epi-tricyclovetivene nor-ketone (**28**) (43 mg, 90%) as a clear colorless liquid, homogeneous on t.l.c.

Mol. Wt. Calcd. for $C_{14}H_{22}O$: 206.1671. Found (mass spectroscopy): 206.1670.

The i.r. (film): 2950, 2860, 1695 cm^{-1} (ketone). The n.m.r. ($CDCl_3$): τ 7.70 (bt, 1H, proton α to ketone), 8.85 (s, 3H, methyl), 8.92 (s, 3H, methyl), 9.08 (d, $J = 6$ Hz, 3H, methyl).

*Epimerization of **28** to Tricyclovetivene Nor-ketone (**29**)*

A solution of epi-tricyclovetivene nor-ketone (**28**) (30 mg) in 1% methanolic sodium methoxide (1 ml) was refluxed for 15 h followed by evaporation of the solvent. The residue was diluted with water and extracted with diethyl ether which in turn was washed with water, saturated sodium chloride solution, dried, and evaporated. The residual liquid consisting of a 1:1 mixture of epimers (**28** and **29**) was purified and the epimers separated by preparative silica gel t.l.c. (10% diethyl ether–light petroleum). The unepimerized epimer (**28**) was exhaustively epimerized to yield a total of tricyclovetivene nor-ketone (**29**) (19 mg, 63%) as a clear colorless liquid, homogeneous in t.l.c.

Mol. Wt. Calcd. for $C_{14}H_{22}O$: 206.1671. Found (mass spectroscopy): 206.1670.

The i.r. (film): 2950, 2860, 1705 cm^{-1} (ketone). The n.m.r. ($CDCl_3$): τ 7.07 (bt, 1H, proton α to ketone), 8.80 (s, 3H, methyl), 8.95 (s, 3H, methyl), 9.01 (d, $J = 6$ Hz, 3H, methyl).

*Preparation of the "Natural"[3] Tricyclic Diol (**30**)*

A solution of natural tricyclovetivene (**1***a*) (102 mg) in dry pyridine (2 ml) was treated with a solution (0.52 ml) of osmium tetroxide (1 g OsO_4/4 ml tetrahydrofuran) and the total stirred at room temperature for 3 h. The mixture was treated with a solution of sodium bisulfite (230 mg) in water (4 ml) and pyridine (2.5 ml) and stirred for 30 min at room temperature. The solution was extracted with methylene chloride, washed with saturated sodium chloride solution, dried, and evaporated. The residual oil was purified by preparative silica gel chromatography (chloroform) and crystallized from light petroleum to furnish the "natural" tricyclic diol (**30**) (100 mg, 84%) as white prisims, m.p. 86.5–87.0 °C (lit. (2) 84–84.5).

Anal. Calcd. for $C_{15}H_{26}O_2$ (mol. wt. 238: C, 75.58; H, 11.00; O, 13.42. Found (238 (mass spectroscopy)): C, 75.93; H, 10.84; O, 13.33.

The i.r. (film): 3500 (hydroxyl), 2950, 2865, 1465, 1025 cm^{-1}. The n.m.r. ($CDCl_3$): τ 6.20 (d, $J = 5$ Hz, 2H, methylene of primary alcohol), 7.27 (s, 1H, exchanges with D_2O), 7.67 (t, $J = 5$ Hz, 1H, exchanges with D_2O), 8.93 (s, 3H, methyl), 9.03 (s, 3H, methyl), 9.08 (d, $J = 6$ Hz, 3H, methyl).

*Cleavage of **30** to "Natural" Tricyclovetivene Nor-ketone (**29**)*

A homogeneous solution of the tricyclic diol (**30**) (90 mg) in tetrahydrofuran (2 ml) and water (1.5 ml) was treated with powdered sodium meta periodate (813 mg) and the total stirred at room temperature for 30 min. The mixture was filtered, diluted with diethyl ether, washed with water, saturated sodium chloride solution, dried, and evaporated to give "natural" tricyclovetivene nor-ketone (**29**) (77 mg, 99%) as a clear colorless liquid, homogeneous in t.l.c.

Mol. Wt. Calcd. for $C_{14}H_{22}O$: 206.1671. Found (mass spectroscopy): 206.1670.

The i.r. (film): 2950, 2860, 1705 cm^{-1} (ketone). The n.m.r. ($CDCl_3$): τ 7.07 (t, 1H, proton α to ketone), 8.80 (s, 3H, methyl), 8.95 (s, 3H, methyl), 9.01 (d, $J = 6$ Hz, 3H, methyl).

*Epimerization of "Natural" **29** to "Natural" epi-Tricyclovetivene Nor-ketone (**28**)*

A solution of the "natural" tricyclovetivene nor-ketone (**29**) (77 mg) in 1% methanolic sodium ethoxide solution (5 ml) was refluxed for 15 h followed by evaporation of the solvent. The residue was diluted with water, extracted with ether, washed with water, saturated sodium chloride solution, dried, and evaporated to give a 1:1 mixture of the epimers (**28** and **29**). The epimers were separated by preparative silica gel t.l.c. (10% diethyl ether–light petroleum). The unepimerized "natural" nor-ketone (**28**) was recycled to give a total of "natural" epi-tricyclovetivene nor-ketone (**28**) (39 mg, 50%) as a clear colorless oil, homogeneous in t.l.c.

Mol. Wt. Calcd. for $C_{14}H_{22}O$: 206.1671. Found (mass spectroscopy): 206.1670.

The i.r. (film): 2950, 2860, 1695 cm^{-1} (ketone). The n.m.r. ($CDCl_3$): τ 7.70 (bt, 1H, proton α to ketone), 8.85 (s, 3H, methyl), 8.92 (s, 3H, methyl), 9.08 (d, $J = 6$ Hz, 3H, methyl).

*Preparation of the Tricyclic Alcohol (**31**)*

A solution of the "natural" nor-ketone (**29**) (60 mg) in anhydrous ether (1 ml) was treated dropwise with an ethereal solution of methyl lithium (excess) and the total refluxed for 1 h. The reaction mixture was diluted with wet ether and in turn washed with water. The ethereal extract was dried and evaporated to yield the "natural" tricyclic alcohol (**31**) (60 mg, 93%) as an oil, homogeneous in t.l.c.

Mol. Wt. Calcd. for $C_{15}H_{26}O$: 222.1984. Found (mass spectroscopy): 222.1977.

The i.r. (CCl_4): 3605 (hydroxyl), 2950, 2860, 1460, 1390, 1370 cm^{-1}. The n.m.r. ($CDCl_3$): τ 8.97 (s, 3H, methyl), 9.02 (s, 3H, methyl), 9.07 (s, 3H, methyl), 9.12 (d, $J = 6$ Hz, 3H, methyl).

By the same method, synthetic nor-ketone (**29**) (5.2 mg) was converted to the synthetic alcohol (**31**) (5.6 mg, 100%).

Analysis: all analytical data (i.r., n.m.r., mass, and t.l.c.) for synthetic alcohol (**31**) were superimposable with that shown above for "natural" alcohol (**31**).

*Conversion of the Alcohol (**31**) to Tricyclovetivene (**1a**)*

A solution of the "natural" alcohol (**31**) (90 mg) in anhydrous acetic anhydride (0.7 ml) and anhydrous pyridine (0.7 ml) was heated at 120 °C for 60 h. After cooling, the reaction mixture was chromatographed on a silica gel column (light petroleum) yielding a mixture of exocyclic and endocyclic olefins which was purified by gas–liquid phase chromatography (15 ft × 1/4 in. column of 30% SE-30 at 225 °C) to give the "natural" tricyclovetivene (**1a**) (7.5 mg) as an oil, homogeneous in t.l.c.

Analysis: all analytical data (i.r., n.m.r., mass, and t.l.c.) for "natural" tricyclovetivene were superimposable with that of natural tricyclovetivene.

By the same method, synthetic alcohol (**31**) (5.6 mg) was converted to racemic tricyclovetivene (**1a**) (1.5 mg).

Mol. Wt. Calcd. for $C_{15}H_{24}$: 204.1878. Found (mass spectroscopy): 204.1876.

The remaining recorded spectral data (i.r. and g.l.c.) were completely identical to that of natural tricyclovetivene.

We wish to thank the National Research Council of Canada, Ottawa, Canada, and Hoffmann-La Roche, Nutley, New Jersey, for financial support of these studies.

1. K. Wiesner, A. Deljac, and T. Y. R. Tsai. Tetrahedron Lett. **14**, 1145 (1970).
2. For structure determination see R. Sakuma and A. Yoshikoshi. Chem. Commun. **1**, 41 (1968); for previous syntheses see F. Kido, H. Uda, and A. Yoshikoshi. Chem. Commun. 1335 (1969) and D. F. MacSweeney and R. Ramage. Tetrahedron **27**, 1481 (1971).
3. R. E. Dean, A. Midgley, E. N. White, and D. McNeil. J. Chem. Soc. 2773 (1961).
4. J. A. Davis, J. Herynk, S. Carroll, J. Bunds, and D. Johnson. J. Org. Chem. **30**, 415 (1965).

Can. J. Chem. Downloaded from www.nrcresearchpress.com by 210.87.254.6 on 09/05/12
For personal use only.

Photoelectron Spectra of Phosgene and Thiophosgene

DAVID CHADWICK[1]

Department of Chemistry, University of British Columbia, Vancouver 8, British Columbia

Received September 1, 1971

The high resolution photoelectron spectra of phosgene and thiophosgene have been obtained and, in each case, all ionization potentials up to 21.2 eV determined. The spectra are interpreted in terms of the molecular orbital structures and it is concluded that there is a strong interaction between the chlorine p_π "lone pair" electrons and those in the C=O or C=S π bond. The measured ionization potentials are compared with those calculated by the CNDO/2 method and with those obtained for similar molecules.

On a obtenu le spectre photoélectronique à haute résolution du phosgène et du thiophosgène et dans chaque cas, on a déterminé tous les potentiels d'ionisation jusqu'à 21.2 eV. On a interprété les spectres en termes de structures d'orbitales moléculaires et on a conclu qu'il existe une forte interaction entre la paire d'électrons libres du chlore p_π et ceux de la liaison π du C=O ou du C=S. On a comparé les potentiels d'ionisation mesurés à ceux calculés par la méthode CNDO/2 et ceux obtenus pour des molécules semblables.

Canadian Journal of Chemistry, **50**, 737 (1972)

Introduction

The electronic structures of molecules containing chromophores such as the carbonyl or thiocarbonyl group have been the subject of extensive research, much of which has been devoted to studies of the electronic spectra of these molecules. Photoelectron spectroscopy (p.e.s.) is a direct method for obtaining the orbital structures of molecules. Detailed studies of the photoelectron spectra of simple carbonyl compounds, such as formaldehyde (1) and carbonyl fluoride (2), have been carried out, but the spectra of similar thiocarbonyl compounds have not been reported. In this paper the high-resolution HeI photoelectron spectra of phosgene (**1**) and thiophosgene (**2**) are presented.

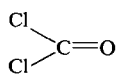

1

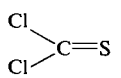

2

Both spectra are interpreted in terms of nine ionization potentials (I.P.'s) below the 21.2 eV cutoff, with some bands overlapping in the phosgene spectrum. In each case, several of the bands exhibit resolvable fine structure due to vibrational excitation of the ion in the ionization process. For ionization from a non-degenerate orbital, only totally symmetric ionic vibrational modes can be excited. The measured vibrational frequencies may be compared with the known vibrational frequencies of the ground-state molecule. Such a comparison often indicates the bonding characteristics of the molecular orbital responsible for a particular ionization potential.

The overall agreement between the observed I.P.'s and values calculated by the CNDO/2 method is usually not good. However, it is often adequate and, in such cases, the calculations can be said to provide a reasonable description of the electronic structure of the particular molecule. In this work CNDO/2 calculations have been performed on both phosgene and thiophosgene and are found to predict some essential features of the p.e. spectra.

Experimental

The sample of phosgene was obtained from the Matheson Company and was used without further purification. Thiophosgene was obtained from K and K Laboratories. The initial photoelectron spectrum of thiophosgene revealed CS_2 as an impurity. This was eliminated by careful fractionation of the thiophosgene sample.

The spectra were recorded using the 584 Å (21.22 eV) helium I resonance line from a 2450 MHz microwave discharge. The spectrometer used employs a hemispherical electrostatic analyzer, the whole apparatus being similar in design and operation to the one described previously (3). The resolution (f.w.h.m.) of the instrument, as measured by the argon doublet, was 22 mV. Both the phosgene and thiophosgene spectra were calibrated by flowing a small quantity of xenon through the spectrometer simultaneously with the sample gas.

The Lyman β line was an apparent impurity in the light source, thereby causing the spectra to be unreliable around

[1]Present address: Central Electricity Research Laboratories, Kelvin Avenue, Leatherhead, Surrey, United Kingdom.

Can. J. Chem. Downloaded from www.nrcresearchpress.com by 210.87.254.105 on 09/05/12
For personal use only.

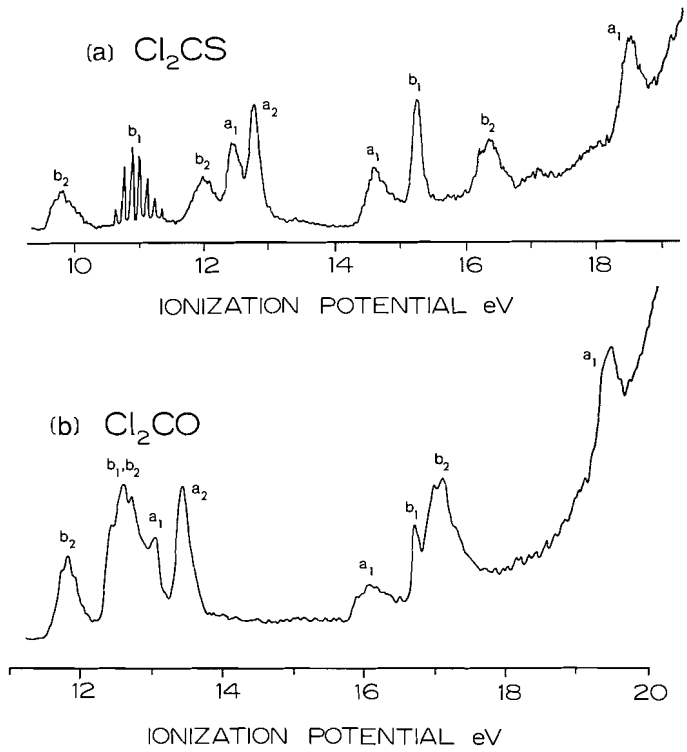

FIG. 1. Photoelectron spectra of (*a*) thiophosgene (*b*) phosgene.

20–21.2 eV. For this reason, the affected portions of the spectra are not reproduced in the figures.

Results and Discussion

The p.e. spectra of thiophosgene and phosgene are reproduced in Fig. 1*a* and *b*, respectively. In the case of Cl_2CS, nine I.P.'s are clearly observed below the 21.2 eV limit. Only seven bands are visible in the Cl_2CO spectrum, but the complex second band can be shown to be due to three I.P.'s. There are some noticeable similarities between the two spectra, particularly at higher binding energies. It would be more "natural" to consider the details of the Cl_2CO spectrum before that of Cl_2CS. However, it is convenient to discuss the Cl_2CS spectrum first, since the interpretation is facilitated by its straightforward appearance.

The theoretical I.P.'s have been calculated using the CNDO/2 method devised by Pople and co-workers (4). The 4 eV correction factor, which has been suggested (5) for molecules containing only first-row elements, has been used in this work. The geometry of phosgene was that obtained from a study of its microwave spectrum (6). In the case of thiophosgene, the C=S bond length assumed in the early electron diffraction work (7) has been used together with the same CCl_2 parameters as the phosgene molecule. This structure was assumed by Brand *et al.* in a study of the electronic spectrum of thiophosgene (8).

Thiophosgene

The measured adiabatic and vertical I.P.'s of Cl_2CS are given in Table 1. The observed vibrational spacings are also included. In assigning these vibrational frequencies to normal modes of the ion it has been assumed that the ion retains C_{2v} symmetry in all of the observed states. The vibrational frequencies of the ground-state molecule have been reported by Frenzel *et al.* (9) and are compared to the observed ionic frequencies in this work.

It is useful to consider briefly the features which can be expected in the $Cl_2C{=}S$ p.e.

Can. J. Chem. Downloaded from www.nrcresearchpress.com by 210.87.254.105 on 09/05/12
For personal use only.

TABLE 1. Observed and calculated photoelectron spectrum of thiophosgene

I.P. number	Observed			Calculated	
	Adiabatic* (eV)	Vertical* (eV)	Vibrational† spacing (cm^{-1})	I.P. (eV)	Orbital symmetry
1	9.61‡	9.84	1060,265	8.8	$9b_2$
2	10.65	10.88	905	8.9	$4b_1$
3	11.67	11.96	—	10.3	$13a_1$
4	—	12.38	—	10.4	$8b_2$
5	—	12.69	(260)	11.1	$2a_2$
6	14.23	14.47	380	14.4	$12a_1$
7	14.99	15.11	—	14.9	$3b_1$
8	15.99	16.19	—	15.3	$7b_2$
9	18.09	18.25	—	17.7	$11a_1$

* ± 0.02.
† $\pm 40\ cm^{-1}$.
‡See text.

spectrum. The p.e. spectrum of a thiocarbonyl compound similar to thiophosgene has not been reported, but results derived from the p.e. spectra of several organic sulfides (10) indicate that the first I.P. of $Cl_2C{=}S$ is from a sulfur "lone pair" orbital. Higher I.P.'s should arise from chlorine "lone pair" orbitals and a C=S π (b_1) orbital. The symmetry of the molecule (C_{2v}) results in four chlorine non-bonding orbitals, namely b_2, a_2, b_1, and a_1. A consideration of the dichlorethylenes (11, 12) and methylene chloride (13, 14) p.e. spectra leads one to anticipate I.P's arising from these four orbitals in the 11–13 eV range for Cl_2CS.

CNDO/2 calculations give the following orbital structure for Cl_2CS:

$$^1A_1,$$
$$\ldots(11a_1)^2(7b_2)^2(3b_1)^2(12a_1)^2(2a_2)^2(8b_2)^2(13a_1)^2(4b_1)^2(9b_2)^2$$

The calculated I.P.'s and orbital symmetries are included in Table 1 for comparison with the observed values. Agreement between the observed and calculated I.P.'s is not good, though it is significantly better at higher binding energies. The calculation appears to overestimate the separation between the non-bonding "lone pair" orbitals and the σ bonding orbitals.

First Band

The complex structure of the first p.e. band can be seen in Fig. 2*a*. The vertical I.P. at 9.84 eV is well defined, but the adiabatic I.P. and the ionic vibrational frequencies are dependent on the interpretation of the fine structure. Clearly, two or more normal modes are excited in the ion, one of which has a fairly high frequency (measured as $1060\ cm^{-1}$). This frequency is assigned to $\nu_1(a_1)$, the C=S stretching vibration, which has a value of $1135\ cm^{-1}$ in the groundstate molecule (9). If we take 9.68 eV to be the adiabatic I.P. (the first strong peak) and attribute the weak onset to "hot bands" of $\nu_3(a_1)$, the CCl_2 bending vibration, the secondary fine structure may be assigned to excitation of $\nu_2(a_1)$, the CCl_2 stretching vibration, and $\nu_3(a_1)$, or excitation of $\nu_3(a_1)$ only. This ambiguity arises because of the fact that in the groundstate molecule ν_2 is approximately twice ν_3. However, it is preferable to include the weak onset in a single progression in $\nu_3(a_1)$. The poor resolution at the onset may be due to the superimposition of a ν_3 "hot band" of the first strong peak. This interpretation results in an adiabatic I.P. of 9.61 eV and a vibrational interval of $265\ cm^{-1}$, which may be compared to the groundstate value of $295\ cm^{-1}$ for $\nu_3(a_1)$. The apparent loss of vibrational structure about 10.05 eV may be due to dissociation of the ion. No appearance potential data are available to confirm this interpretation.

This first band is readily assigned to ionization from the $9b_2$ sulfur "lone pair" orbital, because of its low binding energy. However, excitation of ν_1 and ν_3, plus the width of the band, points to significant delocalization. No doubt the excitation of ν_3 occurs because of some interaction between the $9b_2$ orbital and

Can. J. Chem. Downloaded from www.nrcresearchpress.com by 210.87.254.105 on 09/05/12
For personal use only.

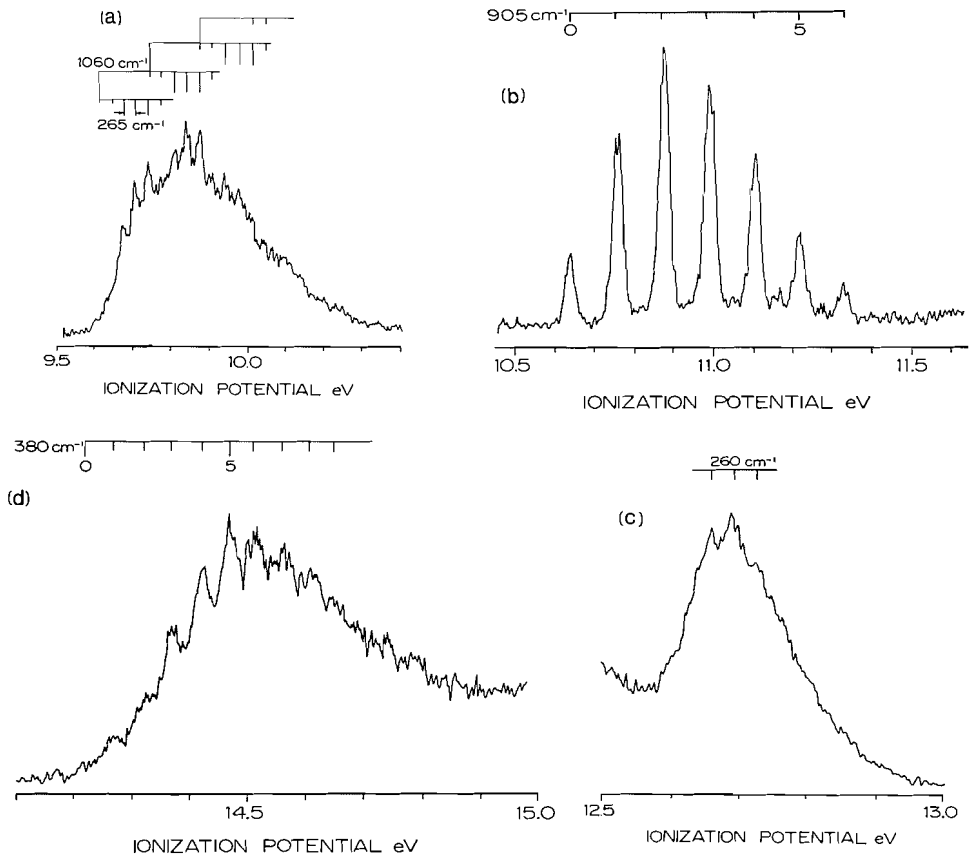

FIG. 2. Individual p.e. bands of thiophosgene.

the $8b_2$ chlorine "lone pair" orbital. Qualitatively, the CNDO/2 calculations are in agreement, as the highest orbital is predicted to be essentially a sulfur "lone pair" orbital with some 20% delocalization onto the chlorine atoms.

Second Band

The second p.e. band consists of a single vibrational progression of frequency 905 cm^{-1} from an adiabatic I.P. of 10.65 eV, Fig. 2*b*. The vibrational structure is attributed to $\nu_1(a_1)$, the C=S stretching frequency, which is considerably reduced from its groundstate value of 1135 cm^{-1} (9). Assignment of this band is straightforward. Excitation of $\nu_1(a_1)$ only and with reduced frequency suggests that the orbital responsible is mainly C–S bonding in character. At such binding energies, only the $4b_1$ C=S π orbital fits this description. However, the appearance of this p.e. band is deceptively simple since a consideration of the higher I.P.'s indicates that there is a large interaction between the C=S π orbital and the $3b_1$ chlorine "lone pair" orbital (see below).

Higher Ionization Potentials

The three bands occurring at vertical I.P.'s of 11.96, 12.38, and 12.69 eV are undoubtedly due to ionization from chlorine "lone pair" orbitals. Only on the fifth band, shown in Fig. 2*c*, is there any indication of resolvable vibrational structure. The tentatively measured frequency of 260 cm^{-1} probably corresponds to $\nu_3(a_1)$ which has a value of 295 cm^{-1} in the groundstate molecule (9). The integrated intensities of the three bands are approximately equal, indicating that only three orbitals are responsible, whereas four chlorine "lone pair" ionizations are excepted at these binding ener-

Can. J. Chem. Downloaded from www.nrcresearchpress.com by 210.87.254.105 on 09/05/12
For personal use only.

Can. J. Chem. Downloaded from www.nrcresearchpress.com by 210.87.254.105 on 09/05/12
For personal use only.

gies. In the order of increasing overlap these are $8b_2$, $2a_2$, $3b_1$, and $13a_1$, with the a_1 orbital at highest binding energy. Recently, Dixon *et al.* (14) have pointed out the importance of interactions between these and other orbitals in modifying this order for CH_2Cl_2. In view of the "conjugative" interaction between the π orbital and chlorine p_π "lone pair" orbitals in various chloroethylenes (11, 12), which include $Cl_2C{=}CH_2$, and the binding energy of the C=S π orbital ($4b_1$), it is reasonable to assume that the b_1 chlorine "lone pair" orbital in $Cl_2C{=}S$ has been lowered considerably in energy. Simple consideration of the band envelopes of the four higher I.P.'s assigns the sharp seventh band at a vertical I.P. of 15.11 eV to the $3b_1$ chlorine non-bonding orbital. Thus, the third, fourth, and fifth I.P.'s are due to the $8b_2$, $2a_2$, and $13a_1$ chlorine "lone pair" orbitals. The $2a_2$ orbital is the only valence orbital of that symmetry (excluding d orbitals) and, therefore, cannot interact with any other valence orbitals. On this basis, it should appear as the sharpest p.e. band arising from the chlorine "lone pair" orbitals. An interpretation of the p.e. spectrum of Cl_2O places the a_1 chlorine non-bonding level above the a_2 (15, 16). This inversion of the order on the basis of overlap considerations is attributed to a small interaction of the chlorine a_1 orbital with an a_1 σ bonding orbital at higher binding energy (16). In $Cl_2C{=}S$, the I.P.'s arising from σ bonding orbitals occur at much lower binding energy than those of Cl_2O. Hence, the $13a_1$ chlorine orbital should be above the $2a_2$ and, possibly the $8b_2$, since the first σ ionization is at 14.47 eV, only 2 eV higher than the chlorine non-bonding I.P.'s. Therefore, the I.P. at 12.69 eV is assigned to the $2a_2$ orbital. The narrow profile of the band and the excitation of ν_3, the CCl_2 bend, are consistent with the assignment. Experimentally there is no evidence for any particular ordering of the $13a_1$ and $8b_2$ orbitals since both should give rise to broad p.e. bands. The CNDO/2 calculations place the $13a_1$ above the $8b_2$. Despite this, the reverse order, expected on chlorine–chlorine overlap grounds, is preferable since this assignment is more consistent with the orbital structures of the dichloroethylenes (16). Summarizing, the third, fourth, and fifth ionizations are assigned to the $8b_2$, $13a_1$, and $2a_2$ chlorine "lone pair" orbitals, respectively.

Of the remaining four higher I.P.'s, only in the case of the sixth at 14.47 eV was any vibrational structure resolved. This consists of a single progression of frequency 380 cm^{-1} (Fig. 2*d*) and could be due to either $\nu_3(a_1)$ or $\nu_2(a_1)$, the CCl_2 stretching mode. The loss of vibrational structure at 14.7 eV may be due to dissociation of the ion. The I.P.'s at 14.47, 16.19, and 18.25 eV appear as broad photoelectron bands, which clearly demonstrates the bonding character of the parent orbitals. These three I.P.'s may be assigned to ionization from the $12a_1$, $7b_2$, and $11a_1$ σ bonding molecular orbitals which are predicted by the calculations to be at similar binding energies to the observed. On this basis the vibrational structure on the sixth band is due to $\nu_2(a_1)$ reduced from its groundstate value of 500 cm^{-1} (9).

The fact that the seventh band at 15.11 eV, attributed to the $3b_1$ ionization, is strikingly similar in appearance to the $2a_2$ band at 12.69 eV, supports these assignments. The large shift to higher binding energy of the $3b_1$ "lone pair" orbital is due to its interaction with the $4b_1$ C=S π orbital. An unperturbed value for the $3b_1$ chlorine I.P. must be approximately the same as the $2a_2$ I.P. (12.69 eV). Thus the interaction shifts the $3b_1$ orbital by about 2.5 eV. This places the unperturbed C=S π ionization at approximately 13 eV, which compares with the Π_u ionization in CS_2 at 12.83 eV (1).

The preferred assignment of the thiophosgene p.e. spectrum is indicated in Fig. 1*a* and in the orbital correlation diagram to be discussed later (Fig. 4). The orbital structure differs from that predicted by the calculations only in the inverse ordering of the $13a_1$ and $8b_2$ chlorine orbitals.

Phosgene

Table 2 contains the measured adiabatic and vertical I.P.'s of Cl_2CO and vibrational frequencies, where particular p.e. bands have been resolved. The following discussion concerning the assignment of the observed vibrational spacings to normal modes of the ion again assumes that the ion retains C_{2v} symmetry in all of the observed states. In support of this assumption, the molecule F_2BO, which is similar to Cl_2CO^+, possesses C_{2v} symmetry in both the ground and first-excited states (17).

Ionization potentials arising from an oxygen

TABLE 2. Observed and calculated photoelectron spectrum of phosgene

I.P. number	Observed: Adiabatic* (eV)	Observed: Vertical* (eV)	Observed: Vibrational† spacing (cm^{-1})	Calculated: I.P. (eV)	Calculated: Orbital symmetry
1	11.55	11.83	285	9.5	$8b_2$
2	—}	12.6±0.1	—	11.3	$3b_1$
3	—}			11.4	$7b_2$
4	—	13.05±0.05	—	11.5	$2a_2$
5	13.39	13.50	290	11.7	$11a_1$
6	15.80	16.15±0.1	(540; 260)	16.8	$10a_1$
7	16.66	16.73	280	18.4	$2b_1$
8	—	17.11	(~1000)	19.3	$6b_2$
9	19.29	19.48	—	20.5	$9a_1$

*±0.02 except where stated otherwise.
†±40 cm^{-1}.

"lone pair" orbital (b_2), four chlorine "lone pair" orbitals (b_2, a_2, b_1, a_1), and a C=O π orbital (b_1) can be expected in the Cl_2C=O p.e. spectrum. As in the case of Cl_2C=S, some mixing of the two b_1 orbitals must occur. The orbital structure predicted by the CNDO/2 calculations on Cl_2C=O is:

$$^1A_1, \ldots(9a_1)^2(6b_2)^2(2b_1)^2(10a_1)^2(11a_1)^2(2a_2)^2(7b_2)^2(3b_1)^2(8b_2)^2$$

For convenience the theoretical I.P.'s and corresponding orbital symmetries are contained with the measured values in Table 2. Agreement is poor, although the correct number of I.P.'s is predicted.

First Band

Figure 3*a* shows the first p.e. band which occurs over 11.5–12.4 eV and consists of a long progression in an ionic vibrational mode of frequency 285 cm^{-1}. This measured frequency most probably corresponds to $\nu_3(a_1)$, the CCl_2 deformation, which has the same frequency in the groundstate molecule (18). The possibility that the observed ionic vibration is $\nu_2(a_1)$, the CCl_2 stretch, which has been greatly reduced from its groundstate value of 567 cm^{-1} (18), cannot be excluded. The measured adiabatic I.P. is in good agreement with the 11.77 eV value obtained by electron impact (19).

The broad nature of the band is indicative of a significant change in structure upon ionization and, therefore, it seems likely that the parent orbital has considerable bonding properties. In contrast, the first band in the p.e. spectrum of formaldehyde (1) is quite different in appearance and occurs at lower binding energies (10.88 eV). The strong 0–0 component demonstrates the non-bonding character of the orbital which is clearly the "lone pair" orbital localized on oxygen (b_2). The substitution of two chlorine atoms for the two hydrogens in H_2C=O would result in a stabilization of the b_2 oxygen "lone pair" orbital. The upper limit for this stabilization would be expected in F_2CO, where the first I.P. is a broad band in the 13–14 eV range (2). These considerations place the unperturbed oxygen b_2 ionization in fairly close proximity to the b_2 chlorine non-bonding I.P. Some ambiguity arises since it is possible that the unperturbed oxygen b_2 orbital would be more stable than the chlorine non-bonding b_2 orbital. In either case, any interaction would result in the highest orbital having b_2 symmetry. The I.P. of the b_2 oxygen "lone pair" in Cl_2CO may be estimated in the following way: the first I.P.'s of CH_3CHO, CH_3CFO, and CH_3CClO at 10.2, 11.8, and 11.1 eV, respectively, are all assigned to the removal of an electron from the oxygen "lone pair" orbital (20). Therefore, replacement of a hydrogen by a chlorine stabilizes the oxygen "lone pair" by 0.9 eV. Thus, two chlorines would be expected to produce a stabilization of about 1.8 eV. The corresponding I.P. in Cl_2CO may then be calculated to be 12.0 eV in reasonable agreement with the measured value of 11.83 eV. The reliability of this calculation may be tested by following the same procedure for the fluorides. The predicted

Can. J. Chem. Downloaded from www.nrcresearchpress.com by 210.87.254.105 on 09/05/12
For personal use only.

Can. J. Chem. Downloaded from www.nrcresearchpress.com by 210.87.254.105 on 09/05/12
For personal use only.

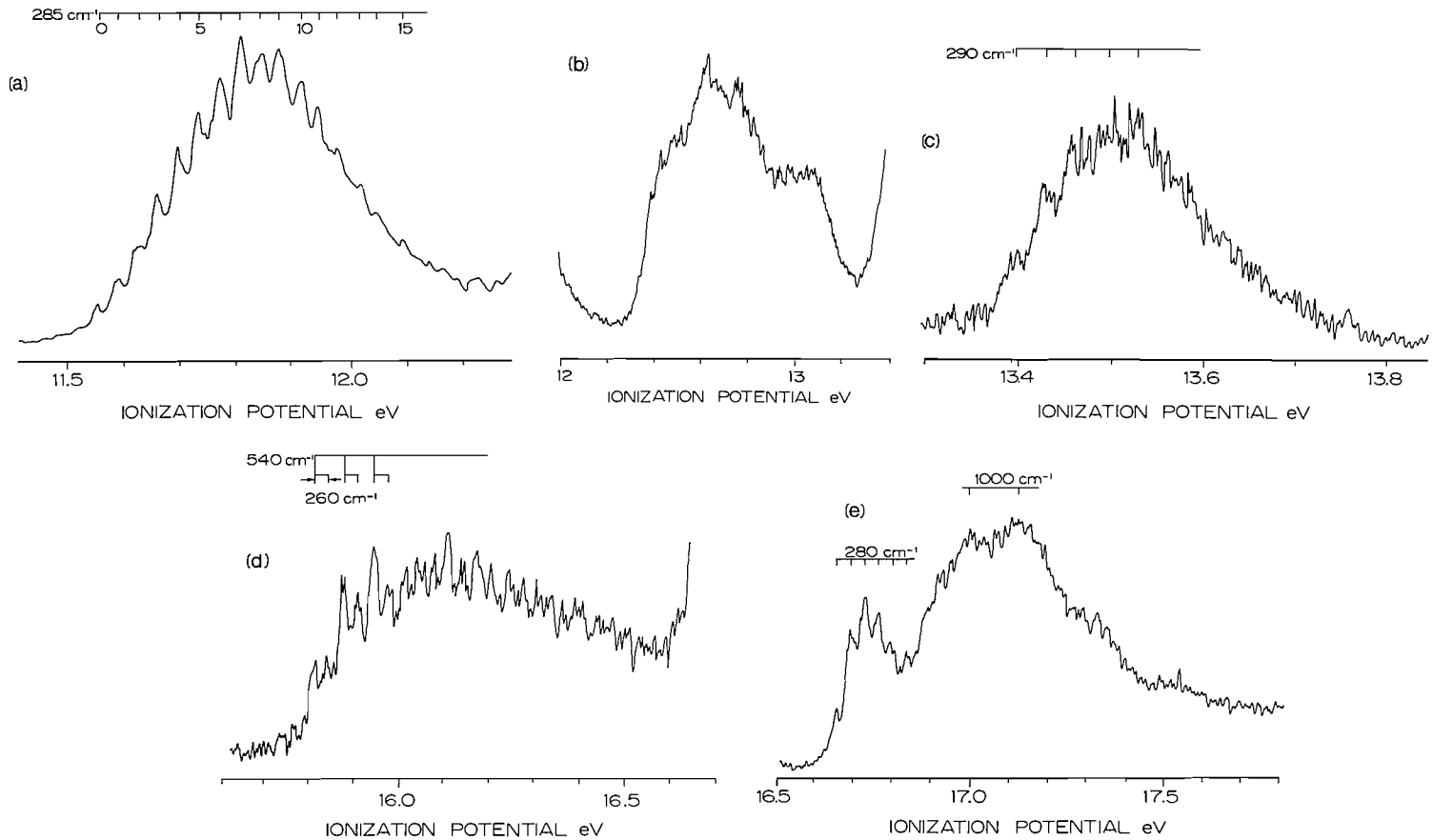

FIG. 3. Individual p.e. bands of phosgene.

Can. J. Chem. Downloaded from www.nrcresearchpress.com by 210.87.254.105 on 09/05/12
For personal use only.

value for F_2CO is thus $10.2 + 2 \times 1.6 = 13.4$ eV compared to the observed binding energy of 13.6 eV (2). The agreement is not really surprising, since any halogen "lone pair" – oxygen "lone pair" interaction has been taken into account by the above method. Thus, the view is taken here that the highest orbital is derived from an oxygen "lone pair" with some delocalization onto the chlorine atoms (*i.e.* mixing of the two b_2 orbitals). The CNDO/2 calculations predict that the first I.P. arises from the $8b_2$ orbital which is strongly delocalized but has only O–Cl bonding character. This would explain the extensive excitation of ν_3. Comparing the first I.P.'s of Cl_2CS and Cl_2CO it may be noted that both are 0.5–1.0 eV lower than the corresponding I.P.'s of H_2O (12.61 eV) and H_2S (10.48 eV) (1). The greater excitation ν_3 in the case of Cl_2CO suggests that there is more delocalization of the oxygen "lone pair" than the corresponding orbital in Cl_2CS. No doubt this reflects the closer proximity in energy of the unperturbed b_2 "lone pair" of chlorine to that of oxygen than that of sulfur. The CNDO/2 calculations support this interpretation since the $9b_2$ orbital in Cl_2CS is predicted to be 80% localized on sulfur.

Photoelectron spectroscopy bands are often similar in profile to transitions in a Rydberg series converging to the corresponding I.P. In the vacuum u.v. spectrum of phosgene (21) several observed electronic transitions consist of long progressions with a vibrational interval of $\sim 280\ cm^{-1}$. It may be that these transitions form a part of a Rydberg series to the first I.P.

Second and Third Bands

The complex second band is reproduced in Fig. 3*b* and is clearly the result of three overlapping ionizations. It is not possible to determine accurately the vertical I.P.'s of the first two components so that both are assigned the value 12.6 ± 0.1 eV. A vibrational progression of frequency $290\ cm^{-1}$ is apparent on the third band at 13.50 eV (Fig. 3*c*), which probably corresponds to the CCl_2 deformation, $\nu_3(a_1)$.

The four I.P.'s observed in this region of the spectrum (12–14 eV) are assigned to the chlorine non-bonding orbitals, $7b_2$, $2a_2$, $3b_1$, and $11a_1$. In formaldehyde, the C=O π (b_1) ionization occurs in the 14–15 eV range (1) in close proximity to the highest binding energy chlorine "lone pair" ionization observed here (13.50 eV). It is likely that the $3b_1$ orbital is pushed to higher energy by interaction with the $2b_1$ C=O π orbital (see below). When this is taken into account the following order is obtained: $3b_1$, $7b_2$, $2a_2$, $11a_1$, which is also that predicted by the CNDO/2 calculations. However, since the a_2 orbital was concluded to be the highest binding energy chlorine non-bonding level in Cl_2CS and Cl_2O (15, 16), this must be true of Cl_2CO where the σ ionizations are at slightly lower binding energies than in Cl_2O. The observed progression in ν_3 is consistent with the assignment of 13.50 eV I.P. to be the $2a_2$.

Higher Ionization Potentials

Three bands occur in the 16–18 eV region of the spectrum. The fourth band is reproduced in Fig. 3*d* and the overlapping fifth and sixth bands are shown in Fig. 3*e*. Apart from the fifth band, the existence of vibrational structure is tentative. There is an indication of two vibrational modes of frequency $540\ cm^{-1}$ and $260\ cm^{-1}$ on the fourth band, the former being the more strongly excited, which may be assigned to $\nu_2(a_1)$ and $\nu_3(a_1)$ by comparison with the groundstate values of 567 and $285\ cm^{-1}$, respectively (18). The fifth band is comparatively narrow in appearance with a vibrational spacing of $280\ cm^{-1}$, which is attributed to $\nu_3(a_1)$. The overlapping sixth band is very broad and may have a highly anharmonic vibrational progression with an interval of approximately $1000\ cm^{-1}$. This would probably correspond to $\nu_1(a_1)$, the C=O stretching mode, greatly reduced from its ground state value of 1827 cm^{-1}. The broad nature of the individual peaks may be due to the short lifetime of the ion in this state or to excitation of a second vibration of frequency too small to be resolved. The ninth I.P. at 19.48 eV appears as a broad structureless band.

This portion of the Cl_2CO p.e. spectrum is similar to that of Cl_2CS and it is likely that the three broad bands arise from similar σ bonding molecular orbitals in the two molecules. The sharp band at 16.73 eV must be due to ionization from the $2b_1$ C=O π orbital. The calculated ordering for these higher binding energy orbitals is $10a_1$, $2b_1$, $6b_2$, and $9a_1$ in agreement with the above assignments. If H_2CO is taken as a model

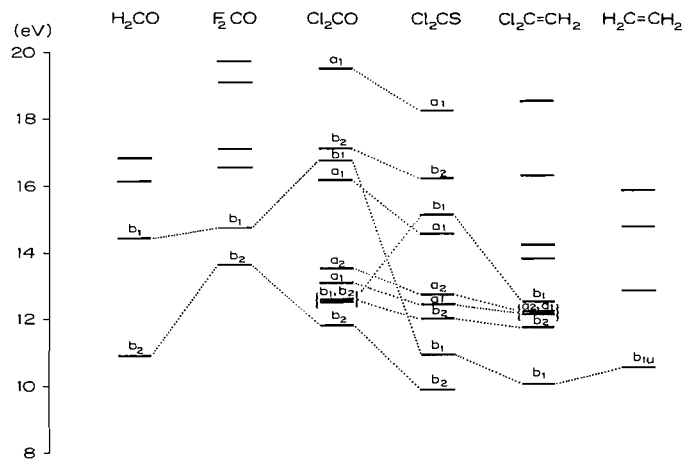

FIG. 4. Orbital correlation diagram.

for the unperturbed C=O π orbital (14.4 eV) (1), then the $2b_1$ orbital in Cl_2CO has been shifted to lower energy by 2.3 eV due to interaction with the $3b_1$ chlorine "lone pair" orbital. Presumably this interaction is responsible for the excitation of the CCl_2 deformation mode on ionization from the $2b_1$ orbital. The fact that the $3b_1$ orbital does not appear to shift to higher energy by a similar amount, infers that there is some interaction with the C=O π^* orbital which is also of b_1 symmetry and is the first excited state of the molecule (22).

The complete assignment is given in Fig. 1*b* and Fig. 4 and differs from that calculated by the reverse order of the $2a_2$ and $11a_1$ chlorine non-bonding orbitals.

General Comments

The orbital structures concluded for Cl_2CS and Cl_2CO may be conveniently compared with those derived for similar molecules by means of an orbital correlation diagram (Fig. 4). Photoelectron results for H_2CO (1), F_2CO (2), $CCl_2{=}CH_2$ (11, 12), and $CH_2{=}CH_2$ (3) have been included in Fig. 4. An important feature of the diagram is the marked variation in the binding energy of the b_1 chlorine "lone pair" orbital in Cl_2CS, Cl_2CO, and $Cl_2C{=}CH_2$. This reflects the changes in the unperturbed energies of the various π bonds. In contrast to the large π interaction in the chlorocompounds, the binding energy of the π orbital in F_2CO is virtually unchanged from the value for H_2CO. These results concerning the mixing of the two b_1 orbitals indicate that, in the chlorocompounds, the C—Cl bonds have considerable "π character". In view of the larger interaction in Cl_2CO and Cl_2CS than in $Cl_2C{=}CH_2$ (only 0.5 eV if ethylene is taken as a model for the unperturbed π orbital energy), the "π character" should be greater for the former two molecules. Evidence for this may be obtained from the chlorine nuclear quadrupole coupling constants in the groundstate molecules. These have been derived from the microwave spectra of Cl_2CO (6) and $Cl_2C{=}CH_2$ (23) and show that the extent of π contribution to the C—Cl bond is significantly greater in the former molecule.

Another noteworthy feature is the higher binding energy of the chlorine "lone pair" orbitals (neglecting interactions with bonding orbitals) in Cl_2CO than in Cl_2CS and $Cl_2C{=}CH_2$ due to the stronger inductive effect of the oxygen atom. As might be expected, all the σ levels in Cl_2CS are destabilized relative to corresponding orbitals in Cl_2CO.

I am grateful to the Research Council of Great Britain for the award of a NATO Fellowship. I wish to thank Professor C. A. McDowell and Professor D. C. Frost for encouragement throughout the course of this work and for kindly extending to me the facilities of their laboratories at the University of British Columbia. I am also indebted to Dr. F. G. Herring for the generous loan of a CNDO/2 computer program and to Dr. J. P. Crow for purifying the thiophosgene sample.

Can. J. Chem. Downloaded from www.nrcresearchpress.com by 210.87.254.105 on 09/05/12
For personal use only.

1. D. W. TURNER, C. BAKER, A. D. BAKER, and C. R. BRUNDLE. Molecular photoelectron spectroscopy. Wiley–Interscience, New York, 1970.
2. C. R. BRUNDLE and M. B. ROBIN. Private communication.
3. G. R. BRANTON, D. C. FROST, T. MAKITA, C. A. MCDOWELL, and I. A. STENHOUSE. J. Chem. Phys. **52**, 802 (1970).
4. J. A. POPLE, D. L. SANTRY, and G. A. SEGAL. J. Chem. Phys. Suppl. **43**, 129 (1965); **43**, 136 (1965).
5. D. W. DAVIES. Chem. Phys. Lett. **2**, 173 (1968).
6. G. W. ROBINSON. J. Chem. Phys. **21**, 1741 (1953).
7. L. PAULING, L. O. BROCKWAY, and J. Y. BEACH. J. Am. Chem. Soc. **57**, 2705 (1935).
8. J. C. D. BRAND, J. H. CALLOMON, D. C. MOULE, J. TYRELL, and T. H. GOODWIN. Trans. Faraday Soc. **61**, 236 (1965).
9. C. A. FRENZEL, K. E. BLICK, C. R. BENNETT, and K. NIEDENZU. J. Chem. Phys. **53**, 198 (1970).
10. F. G. HERRING, D. C. FROST, A. KATRIB, C. A. MCDOWELL, and R. A. N. MCLEAN. To be published.
11. R. F. LAKE and H. W. THOMPSON. Proc. Roy. Soc. Lond. A, **314**, 323 (1970).
12. N. JONATHAN, K. ROSS, and V. TOMLINSON. Inter. J. Mass Spectry. Ion Phys. **1**, 111 (1968).
13. A. W. POTTS, H. J. LEMPKA, D. G. STREETS, and W. C. PRICE. Philos. Trans. Roy. Soc. Lond. A, **268**, 59 (1970).
14. R. N. DIXON, J. N. MURRELL, and B. NARAYAN. Mol. Phys. **20**, 611 (1970).
15. A. B. CORNFORD, D. C. FROST, F. G. HERRING, and C. A. MCDOWELL. J. Chem. Phys. **55**, 2820 (1971).
16. D. CHADWICK, A. B. CORNFORD, D. C. FROST, F. G. HERRING, A. KATRIB, C. A. MCDOWELL, and R. A. N. MCLEAN. Submitted to the International Conference on Electron Spectroscopy. Asilomar, Calif. 1971.
17. C. W. MATHEWS and K. K. INNES. J. Mol. Spectry. **15**, 199 (1965).
18. E. CATALANO and K. S. PITZER. J. Am. Chem. Soc. **80**, 1054 (1958).
19. J. D. MORRISON and A. J. NICHOLSON. J. Chem. Phys. **20**, 1021 (1952).
20. D. CHADWICK, D. C. FROST, A. KATRIB, and C. A. MCDOWELL. Unpublished results.
21. S. R. LA PAGLIA and A. B. F. DUNCAN. J. Chem. Phys. **34**, 125 (1961).
22. V. HENRI and O. R. HOWELL. Proc. Roy. Soc. Lond. A, **128**, 192 (1930). D. C. MOULE and P. D. FOO. J. Chem. Phys. **55**, 1262 (1971).
23. S. SEKINO and T. NISHIKAWA. J. Phys. Soc. Jap. **12**, 43 (1957).

Can. J. Chem. Downloaded from www.nrcresearchpress.com by 210.87.254.105 on 09/05/12
For personal use only.

Infrared and Nuclear Magnetic Resonance Spectra of Methyl Titanium Halides

J. F. HANLAN[1] AND J. D. MCCOWAN[2]

Central Research Laboratory, DuPont of Canada, Kingston, Ontario

Received June 24, 1971

Nuclear magnetic resonance and infrared spectra have been obtained for CH_3TiCl_3, $(CH_3)_2TiCl_2$, and some related materials. The rather unusual n.m.r. data for these compounds and for $C_2H_5TiCl_3$ are compared with the results for related species involving Group IVA elements and the variations are discussed in terms of n.m.r. and bonding parameters. Exchange of methyl groups between CH_3TiCl_3 and $(CH_3)_2TiCl_2$ and between each of these compounds and $(CH_3)_2Zn$ has been studied by this means. Infrared data remain difficult to interpret, and unambiguous assignment of bands has not been achieved.

Les spectres r.m.n. et infrarouges de CH_3TiCl_3, $(CH_3)_2TiCl_2$ et de quelques substances apparentées, ont été obtenues. Les données r.m.n. inhabituelles obtenues pour ces composés et pour $C_2H_5TiCl_3$ sont comparées avec les résultats obtenus pour des espèces apparentées impliquant les éléments du groupe IVa; les variations observées sont discutées en termes de paramètres de liaison et r.m.n. L'échange des groupes méthyles entre CH_3TiCl_3 et $(CH_3)_2TiCl_2$ et entre chacun de ces composés et $(CH_3)_2Zn$, a été étudié par ces moyens. Les données infrarouges demeurent difficiles à interpréter et une attribution définitive des bandes n'a pas été effectuée.

Canadian Journal of Chemistry, **50**, 747 (1972)

Can. J. Chem. Downloaded from www.nrcresearchpress.com by 210.87.254.40 on 09/05/12
For personal use only.

The recent interest in both organometallic and transition metal chemistry has resulted in a rapid growth of knowledge of the preparation and characteristics of alkyl transition metal halides. Although attempts to prepare these materials date from the nineteenth century (1, 2), success was achieved only within recent years (3–5).

Because of the instability of alkyl titanium halides, spectroscopic studies have been difficult. Infrared spectra of CH_3TiCl_3 have been obtained under varied conditions (3, 6–9) but have been inadequate to permit an unequivocal assignment of bands. Although the existence of more highly methylated titanium halides has been established (10, 11), little is known of their i.r. spectra (7). Nuclear magnetic resonance spectra of these materials have not been previously published.

In the present work, n.m.r. was found to be the technique of choice to study formation and decomposition of methyl titanium trichloride and dimethyl titanium dichloride (12) since the starting material and decomposition products all display well resolved, single line resonances. Nuclear magnetic resonance data on the related species reported herein were obtained to assist us in our assignment and to provide additional insight into the rather unexpected line positions and shifts which were observed and possibly to assist in the explanation of the unusual chemistry of these species. A few new i.r. data were obtained to the same end.

[1]Present address: N.C.R.L., The National Gallery of Canada, Ottawa, Canada.

[2]Present address: Department of Chemistry, Queen's University, Kingston, Ontario.

Experimental

(i) Preparation of Materials

Solvents were purchased in pure grades, and sparged with dry nitrogen to remove oxygen and, in some cases, unacceptable stabilizers. All manipulations, including sparging of solvent, were performed in a chamber containing an atmosphere of dry nitrogen. $TiCl_4$ was similarly handled, except for the $TiCl_4$ enriched to 40% in ^{47}Ti, which was used as obtained from Orgmet Industries, Hampstead, N.H. This material, used in the preparation of enriched CH_3TiCl_3, had itself been prepared from enriched TiO_2 obtained from Oak Ridge National Laboratory, Oak Ridge, Tennessee.

$(CH_3)_3Al$ was used as obtained from the supplier, Texas Alkyls Incorporated, Pasadena, Texas. $(CH_3)_2Zn$ was prepared by the method of Elston as reported by Gray *et al.* (7).

$(CH_3)_2TiCl_2$ was prepared by adding approximately 50 ml of *n*-hexane and 2.2 ml of $TiCl_4$ to a dry, nitrogen filled vessel illustrated in Fig. 1. The vessel was then cooled by liquid nitrogen to -195 °C and 3.8 ml of $(CH_3)_3Al$ were added. The contents were brought slowly to room temperature with constant stirring.

The vessel was then cooled by dry ice/trichloroethylene to -80 °C, where $(CH_3)_2TiCl_2$ precipitated. The liquid phase was then withdrawn through the filter as were two subsequent washes with CCl_3F. The last traces of CCl_3F were removed by pumping the vessel to 10^{-3} Torr at -80 °C. The working solvent was then added, the vessel heated to room temperature, and the solution withdrawn through the filter.

Can. J. Chem. Downloaded from www.nrcresearchpress.com by 210.87.254.40 on 09/05/12
For personal use only.

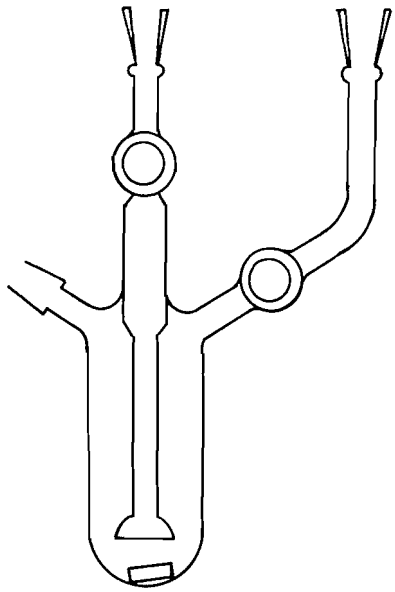

FIG. 1. Sample vessel used for preparations.

At first, CH_3TiCl_3 was prepared by a variation of the method by Karapinka *et al.* (6). The only change was omission of the vanadium binders during the second distillation. Subsequently it was found that mixing hexane solutions of $(CH_3)_2Zn$ and $TiCl_4$ maintaining a ratio of zinc-to-titanium of 0.49 produced a product of excellent quality. Solutions were mixed in the vessel shown in Fig. 1, and the liquid transferred through the filter in order to separate the zinc chloride precipitate. Precipitation and distillation were then carried out as before.

$C_2H_5TiCl_3$ was prepared by mixing $(C_2H_5)_2AlCl$ and $TiCl_4$ in CCl_3F solution at -60 °C with an Al/Ti ratio of 0.4. Solution was slowly warmed to room temperature, where it slowly turned a deep red color. It was then cooled to -60 °C. This material was used only to obtain a spectrum and was not isolated from the solution in which it was prepared.

For the i.r. spectral study, suitable mixtures of deuterated dimethyl zinc and titanium tetrachloride were prepared in hexane solution and run immediately. Time studies were made to assure us that species studied were as claimed.

Attempts to isolate ether-free tetramethyl titanium, which was expected to be of great spectroscopic interest, were totally unsuccessful.

(ii) Equipment and Techniques

Samples were prepared in a glove box under an atmosphere of dry nitrogen. Storage bottles, syringes, and other handling equipment were dried under vacuum and placed in the dry box in sealed vessels. Samples were sealed in n.m.r. tubes or in i.r. cells in the box. The complete absence of methoxy titanium or methoxy zinc resonances, the positions of which had been determined previously, was taken as evidence that oxygen had been excluded.

Nuclear magnetic resonance spectra were obtained using a Varian A60 spectrometer equipped with a low temperature probe. Peak positions were measured accurately using standard audio sideband techniques. Samples could be run within 3 min of preparation. Negligible temperature and concentration shifts were found over the ranges dictated by sample stability and equipment performance.

Infrared spectra were obtained in polyethylene cells on a Perkin–Elmer 621 spectrometer.[3]

Results

The n.m.r. data for methyl titanium trichloride, dimethyl titanium dichloride, and ethyl titanium trichloride are given in Table 1 for solutions in tetrachloroethylene and benzene. Included for comparison are the data for the corresponding carbon compounds, for biscyclopentadienyl titanium dimethyl, and for dimethyl zinc. Chemical shifts are reported in p.p.m. relative to tetramethylsilane (TMS) with minus or plus signs indicating downfield and upfield shifts, respectively. Since, in much of our work, TMS was in an interfering position and there was the possibility of methyl group exchange, cyclohexane and methylene chloride were used as internal standards. Separate experiments established the validity of conversion of chemical shift so obtained to values relative to TMS. Methyl titanium trichloride was also studied in solution in CCl_4 and CCl_3F with results the same as for the C_2Cl_4 solutions. We believe therefore that the reported results for C_2Cl_4 solutions can be compared with data for similar species in CCl_4 without confusion from solvent effects.

The data reported in Table 1 for ethyl titanium trichloride are based on a simple first order analysis. Diethyl titanium dichloride was found to be too unstable even at -60 °C to permit observation.

Early stages of the work were made difficult by the line breadth of the dimethyl titanium dichloride resonance. We found that a rapid exchange of methyl groups between $(CH_3)_2TiCl_2$ and $(CH_3)_2Zn$ broadens the n.m.r. spectra of these materials at ambient temperatures when both are present. In equimolar (10^{-1} *M*) solutions of $(CH_3)_2Zn$ and $(CH_3)_2TiCl_2$ in C_2Cl_4 the line widths at half-height (less the width in the absence of exchange) range from 1.4 Hz at -20 °C to 24.5 Hz at 40 °C. Using the

[3]Courtesy of Dr. A. J. Dahl, Elastomers Division, Experimental Station, E. I. DuPont de Nemours, Wilmington, Delaware.

TABLE 1. Proton chemical shift in p.p.m. relative to TMS and C^{13}—H coupling constant in Hz; data for methyl and ethyl titanium chlorides and related compounds in C_2Cl_4 and C_6H_6 solutions

Compound	Proton chemical shift (p.p.m.)			$J^{13C-H}_{CH_3}$ (C_2Cl_4)
	$CH_3(C_2Cl_4)$	$CH_2(C_2Cl_4)$	CH_3 (C_6H_6)	
CH_3TiCl_3	−2.78		−2.20	134
$(CH_3)_2TiCl_2$	−2.47		−2.00	?
$C_2H_5TiCl_3$	−2.08	−3.33		¶
CH_3CCl_3	−2.70*		−2.18	134
$(CH_3)_2CCl_2$	−2.15*		−1.78	130
$C_2H_5CCl_3$	−1.30*	−2.70		
$(C_5H_5)_2Ti(CH_3)_2$	−0.18†		−0.07‡	122
$(CH_3)_2Zn$	+0.52§		+0.67	122

*In substantial agreement with previous results obtained in CCl_4 (14).
†For solutions in CCl_4 the value −0.06 p.p.m. has been reported (15).
‡The observed resonance position could be shifted nearly 0.16 p.p.m. downfield by increasing the amount of TMS reference added.
§In substantial agreement with previous results obtained in CCl_4 (16).
¶ $J^{H-H}_{C_2H_5} = 7.5$ Hz.

analysis for slow exchange (17) this gives pre-exchange lifetimes, τ, ranging from 13 to 0.23 ms.

An Arrhenius plot of these data yields an activation energy, E_a, *i.e.*:

$$k = \frac{p}{\tau} = k_0 \exp\left(\frac{-E_a}{RT}\right)$$

where k is the rate constant and p is the mole fraction of the components. Figure 2 portrays the best straight line, on a least squares basis, for these data and similar data for benzene solutions. Fewer points are obtainable in the latter case since benzene freezes at 4 °C and the upper temperature limit is determined by the onset of decay of $(CH_3)_2TiCl_2$ in both solutions. For C_2Cl_4 solutions an activation energy for CH_3 group exchange of 7.5 kcal/mol is obtained. The value for benzene is approximately the same but with a reduction of the frequency factor, k_0. This is consistent with the solvation of the titanium compound by the aromatic solvent that is indicated by the large chemical shift difference observed in the n.m.r. spectra (Table 1).

Experiments were carried out using $(CD_3)_2Zn$ to establish whether the methyl groups of CH_3TiCl_3 are also labile. A quantity of $(CD_3)_2$-Zn, in tetrachloroethylene solution, was added to slightly more than twice the amount of $TiCl_4$ in a n.m.r. tube thus creating a solution of CD_3TiCl_3 with a very small excess of $TiCl_4$ and a precipitate of $ZnCl_2$. To this was added a solution of $(CH_3)_2TiCl_2$. The known concentration of each species was compared with the integrated methyl group intensity of that species. A spectrum obtained 5 min after mixing showed that exchange was complete and deuterated

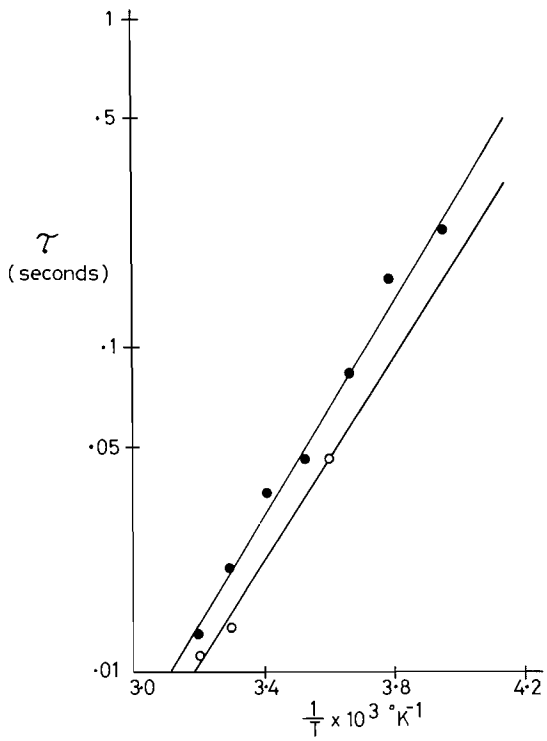

FIG. 2. Variation of pre-exchange lifetime, τ, with reciprocal temperature. ● C_2Cl_4 ○ C_6H_6.

Can. J. Chem. Downloaded from www.nrcresearchpress.com by 210.87.254.40 on 09/05/12
For personal use only.

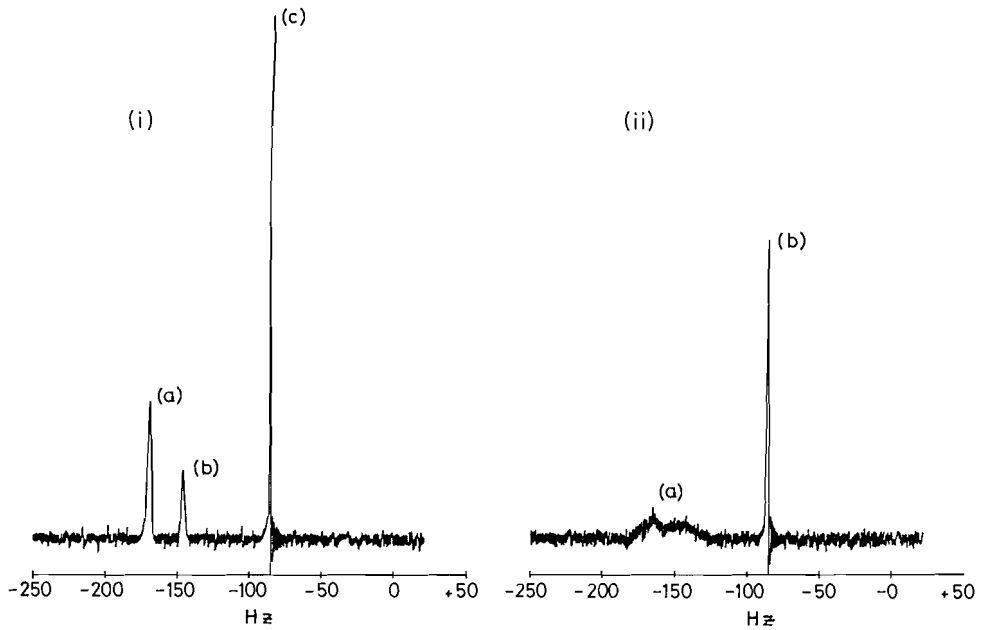

FIG. 3. Proton n.m.r. spectra of (*i*) CH_3TiCl_3 (*a*) and $(CH_3)_2TiCl_2$ (*b*) in C_2Cl_4 solution at 35 °C. Reference (*c*) is C_6H_{12}. (*ii*) Same species at 115 °C, showing CH_3TiCl_3 and $(CH_3)_2TiCl_2$ at (*a*) and C_6H_{12} at (*b*). All spectra are at 60 MHz.

methyls were found to be distributed proportionally between the two species. This exchange is not rapid on the n.m.r. time scale and little or no broadening is observed at ambient temperature. The n.m.r. spectra of a mixture of CH_3TiCl_3 and $(CH_3)_2TiCl_2$ at 35 °C and 115 °C, shown in Fig. 3 *a* and *b*, indicate a rapid exchange between the two species at elevated temperature. The broadening is not affected by the onset or progress of decomposition. These experiments provided proof that methyl group exchange was occurring and that the broadening was not due to complex formation or the presence of paramagnetic impurities.

The possibility of the methyl group protons coupling with the high spin titanium isotopes, ^{47}Ti (7.28%, $I = 5/2$) and ^{49}Ti (5.51%, $I = 7/2$), while remote, was important to us for quantitative accuracy. Also knowledge of any Ti–C–H coupling constant would be valuable for an understanding of the bonding in these species. We, therefore, prepared methyl titanium trichloride from $TiCl_4$ enriched to 40% in ^{47}Ti. No sidebands were observed and the integrated methyl group intensity was in complete stoichiometric agreement with the concentration of titanium analyzed chemically. Evidently quadrupolar relaxation completely decouples the proton spin from the titanium spin. It should be pointed out that in the symmetric environment of the probably tetrahedral tetramethyl titanium, this coupling might be observed as it has been for ^{27}Al ($I = 5/2$) in $Al(CH_3)_4^-$ (18). The data reported by Tabacchi and Jacot-Guillarmod are for $(CH_3)_4Ti$ in ethereal solution, $\delta = -0.68$, (19) and attached to strong complexing agents (20).

In Table 2 we list our *i.r.* results for $(CH_3)_2TiCl_2$, CD_3TiCl_3, and $(CD_3)_2TiCl_2$ along with those of Gray (8) and of van Looy *et al.* (9). Due to the lack of a suitable spectrometer on the site of this work and to the instability and sensitivity of the materials, our experimental work in this area is very limited. The data must therefore be regarded as incomplete and will not be discussed extensively.

Discussion

(i) Infrared

The only species for which satisfactory agreement exists is $(CH_3)_2TiCl_2$. The published spectrum of Gray *et al.* (7) shows a relatively greater intensity for the band at 462 cm^{-1} than we observed. This is probably due to the

Can. J. Chem. Downloaded from www.nrcresearchpress.com by 210.87.254.40 on 09/05/12
For personal use only.

TABLE 2. Observed i.r. frequencies in cm^{-1}

CH_3TiCl_3	CD_3TiCl_3*			$(CH_3)_2TiCl_2$†		$(CD_3)_2TiCl_2$‡
Gray (7)	Gray (8)	van Looy (9)	This work	Gray (7)	This work	this work
391			370	396	393	370
464			385	427	422	385
550	405		(398) very weak	462	457	400
		488	490	550	550	495
		518	515			512
	530					

*$(CD_3)_2Zn/TiCl_4$ in a mole ratio of 0.5. $ZnCl_2$ separated.
†Prepared and isolated in Kingston and transported at 77 °K to Wilmington.
‡$(CD_3)_2Zn/TiCl_4$ in a mole ratio of 1.4. $ZnCl_2$ separated.

presence in his sample of some CH_3TiCl_3 which has a strong band at 464 cm^{-1}. It is interesting to note that no sign of unreacted $(CD_3)_2Zn$ appears in our spectrum for $(CD_3)_2$-$TiCl_2$ although we know from our other work (12) that at this ratio excess $(CH_3)_2Zn$ appears in the n.m.r. spectra of such mixtures. Introduction of chloride causes the hydrogen resonance from CH_3—Zn to shift from +41 to +25 Hz. This was observed both in $(CH_3)_2Zn/TiCl_4$ systems and in experiments where HCl or $ZnCl_2$ were introduced into solutions of $(CH_3)_2Zn$. The complexing thus indicated would explain the absence of an *i.r.* band at 543 cm^{-1} from excess $(CD_3)_2Zn$, since this band assigned by van Looy (9) to the methyl rock would probably undergo a major shift. Attempts to investigate this phenomenon further by the preparation and isolation of a definite complex were unsuccessful although our work (unpublished) and that of others (21) on the system $(C_2H_5)_2Zn$ plus $ZnCl_2$ clearly demonstrate a progressive downfield shift of the n.m.r. resonances with increasing $ZnCl_2$, indicating a species such as "C_2H_5ZnCl".

It is, we feel, clear from the discrepancies in Table 2 for the deuterated species that the assignments for the i.r. spectra of CH_3TiCl_3 and $(CH_3)_2TiCl_2$ are far from settled. Reliance cannot be placed on the existing data for the deuterated species. In particular, *in situ* preparation of CD_3TiCl_3 is not satisfactory. The band at about 515 cm^{-1} observed by van Looy (9) and ourselves, both of whom used $(CD_3)_2Zn$ as a reagent, was not observed by Gray (7) who used $(CD_3)_6Al_2$ and is most probably a Zn—Cl stretch (*cf*: ν_3 of 516 cm^{-1} for $ZnCl_2$ vapor (22)). Study of purified, authentic samples of CD_3TiCl_3 and $(CD_3)_2TiCl_2$ should permit resolution of the problem since well characterized samples are certainly possible as is indicated by the good agreement for $(CH_3)_2$-$TiCl_2$ prepared quite differently by Gray and ourselves. Isolation of the bromide or iodide analogs in an effort to obtain additional information was attempted but not achieved. Preliminary n.m.r. evidence suggests that this is due to their insolubility in our conditions rather than their instability. The preparation of CH_3TiBr_3 reported by Thiele *et al.* (23) using somewhat different reaction conditions supports this suggestion.

(ii) Nuclear Magnetic Resonance

Nuclear magnetic resonance data on the alkyl derivatives of other transition metals are even more rare than the instances of the preparation of materials in this category (24, 25). Thus we have little prior information upon which to base comparisons. The alkyl derivatives of group IIB, IIIA, and IVA have been extensively studied. However, with the exception of the study by Beachell and Butter (15) of bis-cyclopentadienyl titanium derivatives, with their rather different bonding, and that of Burger and Neese (26) of the tris(dialkylamino) titanium alkyls, there is no other instance of n.m.r. data for species with presumed largely empty d orbitals. In the bidentate ligand adducts of CH_3TiCl_3 examined by Clark and McAlees (27) or tetramethyl titanium complexed (20) and in polar solvents (19), titanium will have acquired considerable electron density in its d orbitals. Since it is the

Can. J. Chem. Downloaded from www.nrcresearchpress.com by 210.87.254.40 on 09/05/12
For personal use only.

TABLE 3. Nuclear magnetic resonance chemical shifts in p.p.m. downfield from TMS for methyl and ethyl chlorides of titanium and group IVA elements

Element or compound	$\delta(CH_3)_4M$	$\delta(CH_3)_3MCl$	$\delta(CH_3)_2MCl_2$	$\delta\ CH_3MCl_3$	δ/n	$\Delta\ C_2H_5MCl_3$ ¶
C*	0.98	1.60	2.17	2.74	0.60‖	1.4
Si*	0.0	0.42	0.80	1.44	0.36	0.195§
Ge	0.12†	0.59‡	1.14‡	1.58‡	0.46	—
Sn*	0.07	0.63	1.16	1.65	0.51	—
$Ti(C_2Cl_4)$	1.85	—	2.47	2.78	0.31	1.25
$Ti(C_6H_6)$	—	—	2.00	2.20	0.20	—

*Reference 15 (in CCl_4 solution).
†Reference 16 (converted to CCl_4 solution).
‡Reference 36 (internal standard).
§Reference 35.
‖Extrapolated.
¶$\Delta = \delta CH_3 - \delta CH_2$.

presence of unfilled d orbitals which probably provides the low energy path for the reaction which is suggested by the high reactivity of our compounds, it is useful to attempt to understand the implications of the rather unexpected chemical shifts found for the methyl and ethyl titanium chlorides.

While there is, of course, no reason to expect any great correspondence between n.m.r. results for titanium in Group IVB with the elements of Group IVA, the latter have been extensively studied and do provide a set of data for molecules of similar geometry and substitution. Further, it is interesting and perhaps valuable to consider the nature of the variations between titanium and Group IVA elements. It is immediately apparent from the data of Table 1 that the near identity of resonance positions for CH_3TiCl_3 and CH_3CCl_3 in spite of the difference in electronegativity of the central atom (1.6 for Ti and 2.5 for C (28)) indicates that other than inductive effects and simple bonding effects are operative. However, the value of 134 Hz for $J_{^{13}C-H}$ is typical for sp^3 hybridized C with a strongly electronegative substituent (29) and yields an s character, a_H^2 of 0.268 from the equation $J_{CH} = 500a_H^2$ and a Juan and Gutowsky substituent parameter, ΔX, of 0.072 (30). The coupling constant of 122 Hz of $(C_5H_5)_2Ti(CH_3)_2$ provides the corresponding values of $a_H^2 = 0.244$ and $\Delta X = -0.024$ which may reflect a relatively small inductive effect due to the cyclopentadienyl groups and hence more nearly equal C—Ti and C—H bonding for the methyl group.

Spiesecke and Schneider (31) have pointed out the pitfalls in attempts to provide simple correlations between chemical shifts and electronegativities. However, within similar series such correlations have proven satisfactory for methyl (16, 31–34) and ethyl (31, 35) derivatives. Table 3 presents the relevant data for the titanium and Group IVA derivatives. Chemical shifts of the methyl group plotted *vs.* n for the series $(CH_3)_nMCl_{4-n}$ provide good straight lines from which the shift per chlorine, δ/n, were obtained. Brown and Webster (14) have pointed out that the smaller value for the change of chemical shift with substitution of a Cl for a CH_3 group in the silicon series can be taken to imply an increased electron density at the silicon due to double bond character in the Si—Cl bond. This back donation of electron density via $d\pi$—$p\pi$ bonding is evidently even greater in the Ti—Cl bond and is consistent with the availability of empty d orbitals of titanium(IV). The even smaller value of δ/n and increased shielding for CH_3TiCl_3 and $(CH_3)_2TiCl_2$ in benzene solution suggests either that the solvation further augments the electron density at titanium or that the paramagnetic shift due to the benzene ring current is stronger in the trichloride than the dichloride due to more effective solvation. It is interesting to note that for $(C_5H_5)_2CH_3TiCl$ and $(C_5H_5)_2(CH_3)_2Ti$, δ/n is 0.62 (15) similar to that for C in Table 3. If this can be taken as the normal inductive effect for a Cl atom replacing a methyl group it suggests that no novel Ti—Cl or Ti—CH_3 bonding is present in the cyclopentadienyl derivatives.

The chemical shifts and electronegativities of

Can. J. Chem. Downloaded from www.nrcresearchpress.com by 210.87.254.40 on 09/05/12
For personal use only.

TABLE 4. Effective electronegativities for $—MCl_3$

Compound	Effective electronegativity when M = C	Si	Ge	Sn	Ti
CH_3MCl_3*	3.3	2.6	2.7	2.7	3.3
CH_3MCl_3†	3.0	2.0	2.1	2.1	3.0
$C_2H_5MCl_3$‡	2.9	2.2	—	—	2.8
E_x§	2.6	1.9	2.0	1.93	1.6‖

*Using non-halogen curve, ref. 31, p. 727.
†Using halogen curve, ref. 31, p. 727.
‡Reference 35.
§Reference 32, p. 288, electronegativities calculated from n.m.r. and n.q.r. data.
‖Reference 28, "best value" electronegativity.

Si, Ge, and Sn are very similar. Hence, a plot of these two parameters for the series CH_3MCl_3 where M = C, Si, Ge, Sn, does not cover a sufficient range to make comparisons with the data for CH_3TiCl_3 very meaningful. However, one can obtain approximate effective electronegativities for the MCl_3 group from the data given by Spiesecke and Schneider (31) for a variety of compounds of the type CH_3X. These are given on Table 4 where the first line is the effective electronegativity from their data X ≠ halogen and the second line that for X = halogen. The electronegativities in the third line are calculated from the equation $E_x = 0.62\Delta + 2.07$ where $\Delta = \delta CH_3 - \delta CH_2$ given by Narasimhan and Rogers (35) for metal ethyl derivatives. The rather good agreement for the effective electronegativities $—CCl_3$, $—SiCl_3$, and $—TiCl_3$ between lines 2 and 3 of Table 4 is, we feel, largely fortuitous. Spiesecke and Schneider have indicated the important effect of magnetic anisotropy due to the X group in C_2H_5X compounds on the chemical shift of β-hydrogen. This effect is evident in the large downfield shift of the CH_3 group $C_2H_5TiCl_3$ (Table 1). The above authors provide a graphical presentation of the chemical shift of the CH_3 and CH_2 groups in C_2H_5X compounds. Our data for $C_2H_5CCl_3$ fit their lines for X ≠ halogen near an electronegativity of 3. However, the data for $C_2H_5TiCl_3$ do not even come close to fitting either the lines for X ≠ halogen or X = halogen and the implication is that the magnetic effect on the β-hydrogen is even greater for $—TiCl_3$ than for the strongly anisotropic iodine derivatives. Alternatively, the known instability toward alkene elimination of alkyltitanium derivatives having a β-hydrogen (37) may imply the origin of these unusual chemical shifts arises from an unusual electronic configuration, although the quite typical value of $J^{H-H} = 7.5$ Hz for the C_2H_5 group in $C_2H_5TiCl_3$ (Table 1) would not support this. Additional experimental data would be needed to permit the detailed analysis necessary to answer this question.

If the extrapolated value for $(CH_3)_4Ti$ of $\delta = 1.85$ is correct we would conclude from the data of Table 3 also that there is a major variation from accepted values indicated for the electronegativity of titanium, that is, Ti is apparently more electronegative than C. Alternatively a hybridization with substantial d character as proposed by Dijkgraaf and Rousseau (38) for titanium with novel effects on the shielding for the methyl groups may be the explanation. However, the orbital electronegativities calculated by Hinze and Jaffé (39) decrease markedly with increasing d character. Burger and Neese (26) calculate an electronegativity of 1.25 for Ti from their chemical shift data on tris(dialkylamino) titanium ethyl. It may be that the bonding is different for these species but we would prefer to suggest that, for transition elements, one must consider the group and cannot discuss a central atom alone. It is clear that the unusual chemical behavior of these species is reflected in the equally novel spectral properties.

Much of the work of this paper was done while the authors were members of the Central Research Laboratory of DuPont of Canada Limited. The interest and encouragement of Dr. M. Phibbs and the technical assistance of Messrs. M. Hughson and B. Landon are gratefully acknowledged.

Can. J. Chem. Downloaded from www.nrcresearchpress.com by 210.87.254.40 on 09/05/12
For personal use only.

The authors thank Mr. N. Vanstone for producing recent n.m.r. spectra and the National Research Council and the Ontario Department of University Affairs for supporting grants for one of us (J.D.M.).

1. A. CAHOURS. Ann. **122**, 48 (1862).
2. F. A. COTTON. Chem. Rev. **55**, 551 (1955).
3. Farbwerke Hoechst A. G. Belg. Patent No. 553,477.
4. M. P. GROENEWEGE. Zeit. Phys. Chem. **18**, 147 (1958).
5. C. E. H. BAWN and J. GLADSTONE. Proc. Chem. Soc. 227 (1959).
6. G. L. KARAPINKA, J. J. SMITH, and W. L. CARRICK. J. Poly. Sci. **50**, 143 (1961).
7. A. P. GRAY, A. B. CALLEAR, and F. H. C. EDGECOMBE. Can. J. Chem. **41**, 1502 (1963).
8. A. P. GRAY. Can. J. Chem. **41**, 1511 (1963).
9. H. M. VAN LOOY, L. A. M. RODRIGUEZ, and J. A. GABANT. J. Poly. Sci. A, **4**, 1927 (1966).
10. C. BEERMANN and H. BESTIAN. Angew. Chem. **71**, 618 (1959).
11. H. J. BERTHOLD and G. GROH. Z. Anorg. and Allg. Chem. **319**, 230 (1963).
12. J. D. MCCOWAN and J. F. HANLAN. Can. J. Chem. This issue.
13. C. BEERMANN and H. BESTIAN. Ger. Patent No. 1,037,446 (1958).
14. M. P. BROWN and D. E. WEBSTER. J. Phys. Chem. **64**, 698 (1960).
15. H. C. BEACHELL and S. A. BUTTER. Inorg. Chem. **4**, 1133 (1965).
16. C. R. MCCOY and A. L. ALLRED. J. Inorg. Nucl. Chem. **25**, 1219 (1963).
17. J. A. POPLE, W. G. SCHNEIDER, and H. J. BERNSTEIN. High resolution nuclear magnetic resonance. McGraw-Hill Book Co. Inc., New York. 1959. pp. 221, 367.
18. J. P. OLIVER and C. A. WILKE. J. Am. Chem. Soc. **89**, 163 (1967).
19. R. TABACCHI and A. JACOT-GUILLARMOD. Helv. Chim. Acta, **53**, 1977 (1970).
20. R. TABACCHI and A. JACOT-GUILLARMOD. Chim. **24**, 271 (1970).
21. J. BOERSMA and J. G. NOLTE. J. Organomet. Chem. **8**, 551 (1967).
22. A. BUCHLER, W. KLEMPERER, and A. G. EMSLIE. J. Chem. Phys. **36**, 2499 (1962).
23. K.-H. THIELE, P. ZDUNNECK, and D. BAUMGART. Z. Anorg. Allg. Chem. **378**, 62 (1970).
24. G. W. PARSHALL and J. J. MROWCA. Adv. in Organomet. Chem. **7**, 157 (1968).
25. M. L. MADDOX, S. L. STAFFORD, and H. D. KAESZ. *Ibid.* **3**, 1 (1964).
26. H. BURGER and H. J. NEESE. J. Organoment. Chem. **20**, 129 (1969).
27. R. J. H. CLARK and A. J. MCALEES. J. Chem. Soc. A, 2026 (1970).
28. H. O. PRITCHARD and H. A. SKINNER. Chem. Rev. **55**, 745 (1955).
29. N. MULLER and D. E. PRITCHARD. J. Chem. Phys. **31**, 738, 1471 (1959).
30. C. JUAN and H. S. GUTOWSKY. J. Chem. Phys. **37**, 2198 (1962).
31. H. SPIESECKE and W. G. SCHNEIDER. J. Chem. Phys. **35**, 722 (1961).
32. A. L. ALLRED and E. G. ROCHOW. J. Inorg. Nucl. Chem. **5**, 269 (1958).
33. A. L. ALLRED and E. G. ROCHOW. J. Am. Chem. Soc. **79**, 5361 (1957).
34. A. N. EGOROCHKIN, V. F. MIROHOV, and M. G. VORNOKOV. J. Struct. Chem. USSR, 7, 425 (1966).
35. P. T. NARASIMHAN and M. T. ROGERS. J. Am. Chem. Soc. **82**, 5983 (1960).
36. A. N. EGOROCHKIN *et al.* Izv. Akad. Nauk. USSR, Ser. Khim. 1964 (2) 373 CA **60** 15318 c.
37. H. DEVRIES. Rec. Trav. Chim., **80**, 866 (1961).
38. C. DIJKGRAAF and J. P. G. ROUSSEAU. Spectrochim. Acta, **25** A, 1455 (1969).
39. J. HINZE and H. H. JAFFÉ. Can. J. Chem. **41**, 1315 (1963).

Can. J. Chem. Downloaded from www.nrcresearchpress.com by 210.87.254.40 on 09/05/12
For personal use only.

Thermal Decomposition of Methyl Titanium Chlorides

J. D. McCowan[1] and J. F. Hanlan[2]

Central Research Laboratory, DuPont of Canada Limited, Kingston, Ontario

Received June 24, 1971

The thermal decomposition of CH_3TiCl_3 and $(CH_3)_2TiCl_2$ in C_2Cl_4 and C_6H_6 has been examined over the range 20 to 110 °C under a nitrogen atmosphere utilizing n.m.r. spectroscopy, mass spectroscopy, and elemental analysis. The reaction products are found to be the result of at least four separate, simultaneous, and competing reactions.

La décomposition thermique de CH_3TiCl_3 et de $(CH_3)_2TiCl_2$ dans C_2Cl_4 et C_6H_6 a été examinée sur une échelle de température allant de 20 à 110 °C, sous une atmosphère d'azote, et en utilisant la spectroscopie et RMN et de masse ainsi que l'analyse élémentaire. Les produits de la réaction sont le résultat d'au moins quatre réactions isolées, simultanées, et compétitives.

Canadian Journal of Chemistry, **50**, 755 (1972)

Can. J. Chem. Downloaded from www.nrcresearchpress.com by 210.87.254.42 on 09/05/12
For personal use only.

Introduction

Studies of the decomposition of alkyl titanium chlorides have yielded a diversity of views on the mechanism involved. The proposition that decomposition involved a radical attack upon the solvent (1, 2) has been effectively disproven as a general theory by de Vries (3), although radical attack may occur under special conditions (4). However the theory of de Vries leads to awkward explanations for the decomposition of methyl titanium halides, particularly the postulated existence of either CH_2 or CH_2TiCl_3 without supporting evidence.

The present work was designed to inquire into the decomposition of methyl titanium chlorides, with a view to either producing evidence to support one of the existing theories or uncovering an alternative.

Experimental

(i) Use of Nuclear Magnetic Resonance Spectroscopy

The decomposition of both methyl titanium trichloride and dimethyl titanium dichloride and the corresponding production of soluble hydrogen-bearing products such as methane, were conveniently followed by n.m.r. spectroscopy. Samples were made up in n.m.r. tubes to known concentrations and component ratios. Spectra were obtained periodically as required on a Varian A-60 spectrometer equipped with a variable temperature probe.

Samples were prepared in a dry nitrogen atmosphere using syringes of from 0.1 ml to 1.0 ml capacity. Samples involving study of more than a few hours duration were made up in tubes having a constriction near the top at which a flame seal was made after filling. Liquid volumes were chosen to minimize vapor volume. This decreased the proportion of volatile products which was in the gaseous phase and which was, consequently, not in the n.m.r. sample region.

Samples were stored, between spectral measurements, in a rotating drum which ensured continuous mixing by turning the samples end over end in a period of about 1 min. The drum for ambient temperature was constructed by boring holes in a polyethylene block. A second mixing drum, constructed from aluminum, was mounted in a modified laboratory oven. Light was excluded totally in storage and as much as possible during handling. Just prior to each n.m.r. determination, any solids were centrifuged to the top of the tube so as not to interfere with the homogeneity of the liquid phase. The solid was redispersed before returning the sample to the mixer.

Peak positions, and quantitative measurements of the concentration of each species, were obtained by comparison of spectra and integrated peak heights with those of a reference material of known concentration. This reference was usually cyclohexane, but cyclopentane, benzene, and dichloromethane were used on occasions when a search for some special phenomenon was made. Integral values used were the average of five or more consecutive runs.

Studies were made of the path of decomposition at 20, 50, 80, and 110 °C and in a variety of solvents. A few specialized experiments, such as continuous centrifuging to compact the solid or removal of the solid initially formed, were also performed.

(ii) Elemental Analyses

Elemental analyses were carried out by both chemical means (A. Bernhardt)[3] and by neutron activation analysis (General Atomic).[4] The first was used for carbon, hydrogen, and chlorine, and the second for zinc, chlorine, and titanium.

Solid decomposition products were isolated using fine porosity ground glass filter crucibles, dried by pumping to 10^{-4} Torr or better, sealed in glass and sent for analysis. A

[1]Present address: Department of Chemistry, Queen's University, Kingston, Ontario.

[2]Present address: N.C.R.L., The National Gallery of Canada, Ottawa, Canada.

[3]A. Bernhardt. Mikroanalytisches Laboratorium, Mulheim, West Germany.

[4]General Dynamics Corp. General Atomic Div., San Diego, California.

Can. J. Chem. Downloaded from www.nrcresearchpress.com by 210.87.254.42 on 09/05/12
For personal use only.

few samples were sent in a moist condition as a test for volatile products.

Analysis of solids initially precipitated on mixing dimethyl zinc with titanium tetrachloride in a solvent were also carried out by methods analogous to those above. In this case speed was important and tests were made to ensure that filter porosity did not effect either the weight or nature of the product.

(iii) Mass Spectrometric Studies of the Nature of the Alkyl Content of the Solid Decomposition Products

Solid decomposition products were isolated as for elemental analysis, and sealed in a glass vessel designed for the purpose. D_2O was introduced and the resulting gaseous products analyzed by mass spectrometry.

(iv) Consideration of Errors

In the quantitative study of decomposition using n.m.r. spectroscopy, errors were introduced by syringe accuracy and handling, and by the reproducibility of the integrations by the spectrometer. Syringes of the most suitable size were used to minimize errors. Tests indicated that syringe errors are approximately 2 to 3% for any one measurement, giving a cumulative error of 5% from the double step of making the solution and drawing from it.

Errors in integration were minimized by running five integrals on each spectrum. Reproducibility of successive integrals was within 30%. This poor reproducibility arose since the spectra and integrals were obtained at low temperatures and the heater-sensor insert is subject to fluctuations in its position within the insert of the probe. Reproducibility of the average of successive sets of five integrals was within 10%.

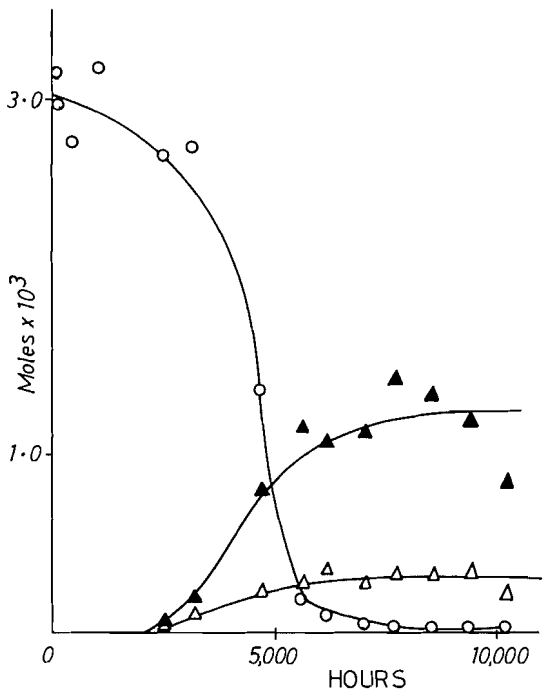

FIG. 1. Thermal decomposition at ambient temperature of initially 1.5 *M* CH_3TiCl_3 in C_2Cl_4. Symbols are: ○, CH_3TiCl_3; △, CH_4; ▲, C_2H_6.

(v) Materials

Trimethyl aluminum was used as obtained from Texas Alkyls.[5] Dimethyl zinc was prepared by the method of Elston (6). Analysis indicated a high degree of purity in both cases. Dimethyl titanium dichloride and methyl titanium trichloride were prepared by the methods described previously (5).

Tetrachloroethylene, benzene, cyclohexane, and titanium tetrachloride were bought in the purest available grades and sparged with dry nitrogen. Batches of tetrachloroethylene, containing a non-volatile inhibitor (*t*-butyl phenol) which was not removed by sparging, were found to give anomalous results. Air distillation of tetrachloroethylene led to formation of traces of Cl_3CCOCl which likewise interfered. Care had to be taken in the storage of tetrachloroethylene from which the inhibitor had been removed in order to prevent formation of interfering oxidation products.

All light sensitive materials were stored in darkened storage bottles. Thermally unstable materials were stored at −195 °C in the short period before use. Air and water sensitive materials were stored in glass vessels with double ground-glass stoppers. The vessels were kept in a nitrogen atmosphere.

Results

Soluble Decomposition Products

Almost two hundred samples, mainly $(CH_3)_2Zn/TiCl_4$ systems, were studied. Table 1 summarizes the effect on decomposition product distribution of variations in solvent, temperature, and means of preparation of CH_3TiCl_3 and $(CH_3)_2TiCl_2$. The eight representative runs in Figs. 1 to 8 illustrate the rates under varying conditions, as well as showing exact values of product distribution for their particular cases. The amounts of each species are plotted as calculated from the n.m.r. integrals, except for a 6% addition for CH_4 corresponding to the amount of CH_4 in the vapor phase. This correction is based on known solubility data and is constant because the volumes of reagent solution were chosen always to total 95% of the 1.95 ml total volume of the sealed n.m.r. tube. Figure 9 illustrates the reproducibility to be expected and the hydrogen balance obtained. The latter assumes, for reasons to be discussed, that one CH_2 exists in the solid decomposition products for each CH_4 formed.

In all $(CH_3)_2Zn/TiCl_4$ systems (*e.g.* Figs. 5, 7, and 8), the observed initial concentrations of CH_3TiCl_3 and of $(CH_3)_2TiCl_2$ are less than

[5]Stauffer Chemical Company, 6910 Fannin St., Houston, Texas.

Can. J. Chem. Downloaded from www.nrcresearchpress.com by 210.87.254.42 on 09/05/12
For personal use only.

TABLE 1. Decomposition products

System	Solvent	Soluble products by proton n.m.r.	
		At 25 °C	At 80 °C
CH_3TiCl_3	C_2Cl_4	CH_4, C_2H_6 both important, C_2H_6 being more abundant above initial CH_3TiCl_3 concentrations of ~ 1 *M*; traces of 1,1,2-trichloropropene-1, especially for very low initial concentrations*; traces of CH_3Cl	CH_4, C_2H_6, CH_3Cl, and 1,1,2-trichloropropene-1 are all abundant
CH_3TiCl_3	C_6H_6	CH_4, C_2H_6 both important, with abundance of C_2H_6 again favored by high initial concentrations of CH_3TiCl_3	
$(CH_3)_2Zn/TiCl_4$ ($Zn/Ti < 0.5$)†	C_2Cl_4	CH_4, C_2H_6, CH_3Cl all important. CH_3Cl abundance increases as Zn/Ti ratio decreases;‡ traces of 1,1,2-trichloropropene-1	CH_4, C_2H_6, 1,1,2-trichloropropene-1 all abundant, with relative amounts dependent on initial concentrations, and Zn/Ti ratio. CH_3Cl depends on Zn/Ti ratio as at 20 °C. 1,1,2-trichloropropene-1 favored by low initial concentrations of CH_3TiCl_3
$(CH_3)_2Zn/TiCl_4$ ($Zn/Ti < 0.5$)†	C_6H_6	CH_4 and C_2H_6 are abundant. Traces of toluene are found	CH_4, C_2H_6, and toluene are all abundant
$(CH_3)_3Al/TiCl_4$ ($Al/Ti < 0.33$)†	C_2Cl_4 or C_6H_6	Products closely parallel those in $(CH_3)_2Zn/TiCl_4$ systems of $Zn/Ti < 0.5$	1,1,2-trichloropropene-1 very abundant. CH_4, C_2H_6, and CH_3Cl all abundant, with CH_3Cl showing usual inverse dependence on ratio
$(CH_3)_2TiCl_2/CH_3TiCl_3$	C_2Cl_4	CH_4	
$(CH_3)_2Zn/TiCl_4$ ($Zn/Ti > 0.5$)	C_2Cl_4	CH_4, $(CH_3)_2Zn$§	CH_4, $(CH_3)_2Zn$§ and considerable 1,1,2-trichloropropene-1
$(CH_3)_2Zn/TiCl_4$ ($Zn/Ti > 0.5$)	C_6H_6	CH_4, $(CH_3)_2Zn$§	CH_4, $(CH_3)_2Zn$§ and traces of toluene, particularly at ratios near 0.5
$(CH_3)_3Al/TiCl_4$ ($0.33 < Al/Ti < 1.0$)‖	C_2Cl_4	CH_4, considerable 1,1,2-trichloropropene-1, and traces of C_2H_6	
$(CH_3)_2TiCl_2$	C_2Cl_4	CH_4	
$(CH_3)_3Al/TiCl_4$ ($Al/Ti > 1.0$)	C_2Cl_4	CH_4 and traces of 1,1,2-trichloropropene-1 and C_2H_6	

*No sign of products of further exchange, such as 1,1-dichloro-2-methylpropene-1 or 2,2-dichlorobutene-2 were observed in any of this work.
†At these ratios, CH_3TiCl_3 is observed and $(CH_3)_2TiCl_2$ is not.
‡For three samples all of identical initial CH_3TiCl_3 concentration but of Zn/Ti ratios of 0.15, 0.30, and 0.45, the CH_3Cl produced corresponded to 32, 15, and 5%, respectively, of the total soluble products observable by proton n.m.r.
§See Figs. 7 and 8.
‖At these ratios, both CH_3TiCl_3 and $(CH_3)_2TiCl_2$ are present, at least during part of the decomposition.

Can. J. Chem. Downloaded from www.nrcresearchpress.com by 210.87.254.42 on 09/05/12
For personal use only.

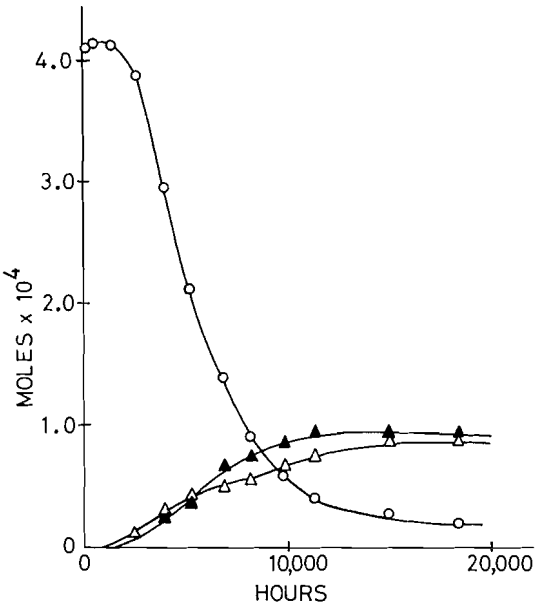

FIG. 2. Thermal decomposition at ambient temperature of initially 0.22 *M* CH_3TiCl_3 in C_6H_6. Symbols are: ○, CH_3TiCl_3; △, CH_4; ▲, C_2H_6.

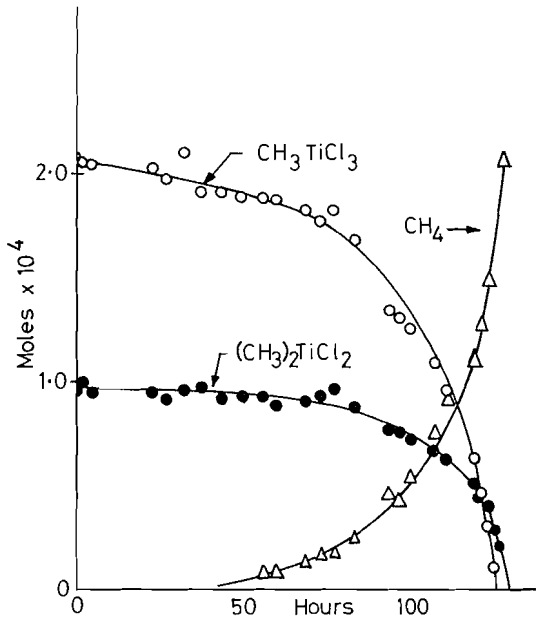

FIG. 4. Thermal decomposition at ambient temperature of initially 0.11 *M* CH_3TiCl_3 and 0.051 *M* $(CH_3)_2TiCl_2$ in C_2Cl_4. Symbols are: ○, CH_3TiCl_3; ●, $(CH_3)_2TiCl_2$; △, CH_4.

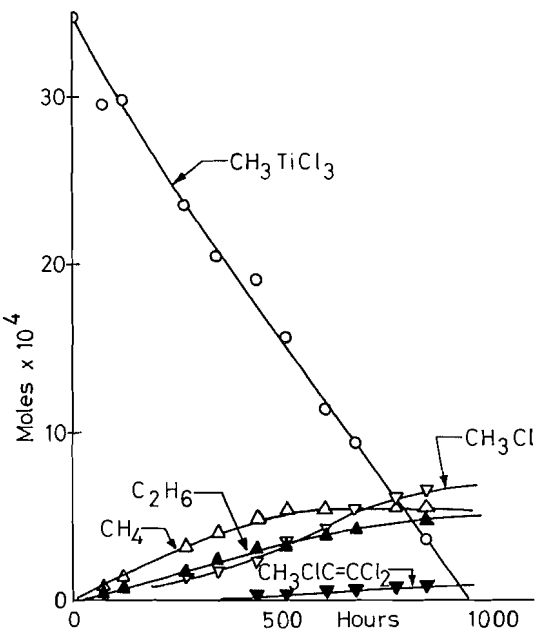

FIG. 3. Thermal decomposition at 80 °C of initially 1.5 *M* CH_3TiCl_3 in C_2Cl_4. Symbols are: ○, CH_3TiCl_3; △, CH_4; ▲, C_2H_6; ▽, CH_3Cl; ▼, $CH_3ClC{=}CCl_2$.

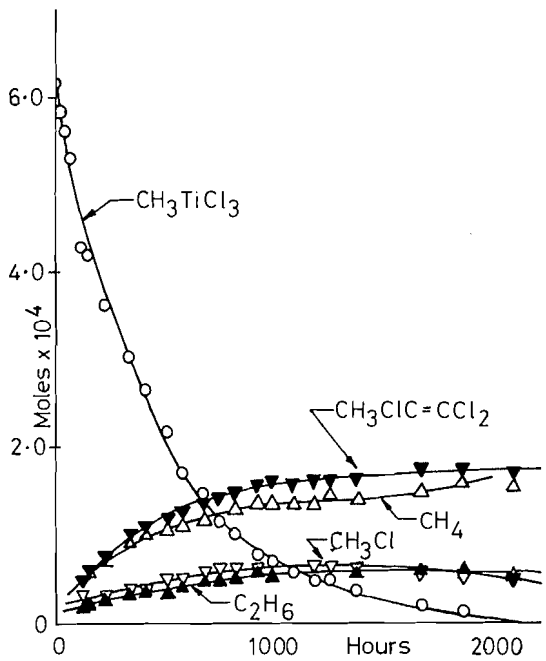

FIG. 5. Thermal decomposition at 80 °C of materials formed from 0.17 *M* $(CH_3)_2Zn$ and 0.56 *M* $TiCl_4$ in C_2Cl_4. Symbols are: ○, CH_3TiCl_3; △, CH_4; ▲, C_2H_6; ▽, CH_3Cl; ▼, $CH_3ClC{=}CCl_2$.

TABLE 2. Elemental analyses of solid decomposition products*

Components as added			Solid composition by analysis					Liquid phase by difference		
			Cl							
Cl	Zn	Ti	G.A.	A.B.	Ave	Zn	Ti	Cl	Zn	Ti
1.82	0.72	0.46	1.69	1.77	1.72	0.33	0.42	0.10	0.39	0.04
1.82	0.72	0.46	1.83	1.84	1.84	0.37	0.48	−0.02	0.35	−0.02
1.82	2.16	0.46	1.55	1.47	1.52	0.15	0.31	0.30	2.01	0.15
1.82	2.16	0.46	1.55	1.48	1.52	0.17	0.53	0.30	1.99	−0.07
1.82	0.72	0.46	1.62	1.66	1.64	0.28	0.37	0.18	0.44	0.09
3.64	0.72	0.91	3.56	3.60	3.58	0.57	0.92	0.06	0.15	−0.01

*All elements are given in equivalents $\times 10^2$. Total volume of solvent was 60 ml. No carbon and hydrogen measurements were made. Original components were measured by analysis. The number of equivalents of each element remaining in solution is determined by the difference of the component and product solid measurements.

would be expected from the stoichiometry. This is attributed to CH_3TiCl_3 complexing with solid $ZnCl_2$.

The role of the precipitated $ZnCl_2$ in realkylation of zinc (Figs. 7, 8) was explored by preparation of two identical n.m.r. samples, each containing 2.14×10^{-4} mol of $(CH_3)_2Zn$ and 1.45×10^{-4} mol of $TiCl_4$ in 1.85 ml of C_2Cl_4. One was mixed constantly so as to maintain a distribution of finely divided $ZnCl_2$ throughout the solution. The other was centrifuged constantly, to compact the $ZnCl_2$ and reduce its available surface area. In the latter, titanium chlorides formed by decomposition were deposited on the $ZnCl_2$ as they formed, further reducing the available area of $ZnCl_2$. In the mixed tube, 4.5×10^{-5} mol of $(CH_3)_2Zn$ and 7.2×10^{-5} mol of CH_4 were formed. In the centrifuged tube, 2.8×10^{-5} mol of $(CH_3)_2Zn$ and 1.12×10^{-4} mol of CH_4 were produced. In both cases, the quoted amount of $(CH_3)_2Zn$ is that formed in addition to the residual $(CH_3)_2Zn$ observed immediately after the formation of $(CH_3)_2TiCl_2$.

Rates of Decomposition

The shape of the n.m.r. tubes precluded good mixing. Coagulation and disintegration of solid products periodically occurred. Consequently, kinetic data obtained from these experiments are too unreliable to permit unequivocal assignment of particular rate laws. Nevertheless, as Fig. 9 illustrates, accuracy and reproducibility are sufficient to yield considerable information.

CH_3TiCl_3 in solution, even in $(CH_3)_2Zn/TiCl_4$ systems, decomposes unexpectedly slowly. Much more rapid is the decomposition of $(CH_3)_2TiCl_2$ and of CH_3TiCl_3 in the presence of $(CH_3)_2TiCl_2$. See Figs. 1–8.

An induction time exists for the decomposition of CH_3TiCl_3 at 20 °C, the formation of CH_4 and of C_2H_6 being associated with autocatalysis (Figs. 1, 2, 4).

Rates of formation of CH_3Cl, of 1,1,2-trichloropropene-1, and of toluene increase more rapidly with temperature than do those of CH_4 and C_2H_6.

Insoluble Decomposition Products

Elemental analyses of the solid decomposition products were obtained by both chemical methods and neutron activation analysis. Results obtained from both techniques had failings. Chemical methods indicated hydrogen contents in hydrogen-free test samples almost as great as those in the study samples. Chlorine analyses proved very accurate by chemical methods, but were more erratic in neutron activation data.

Despite these errors, some characteristics of the solids emerged clearly. The solids produced in CH_3TiCl_3 systems and in $(CH_3)_2Zn/TiCl_4$ systems of $Zn/Ti < 0.5$, have a Cl/Ti ratio very close to three, with virtually no non-volatile hydrocarbon content.

Solids produced by the thermal decomposition of $(CH_3)_2TiCl_2$ alone in solution have a Cl/Ti ratio close to 2, and a large hydrocarbon content, the nature of which is described subsequently. Solids produced by $(CH_3)_2Zn/TiCl_4$ systems of $Zn/Ti > 0.5$ have a Cl/Ti ratio intermediate between 2 and 3, and a moderate hydrocarbon content. Table 2 shows the results of the most self consistent set of analyses carried out on $(CH_3)_2Zn/TiCl_4$ systems.

A preliminary study of the nature of the hydrocarbon content of the solid was made by mass

Can. J. Chem. Downloaded from www.nrcresearchpress.com by 210.87.254.42 on 09/05/12
For personal use only.

Can. J. Chem. Downloaded from www.nrcresearchpress.com by 210.87.254.42 on 09/05/12
For personal use only.

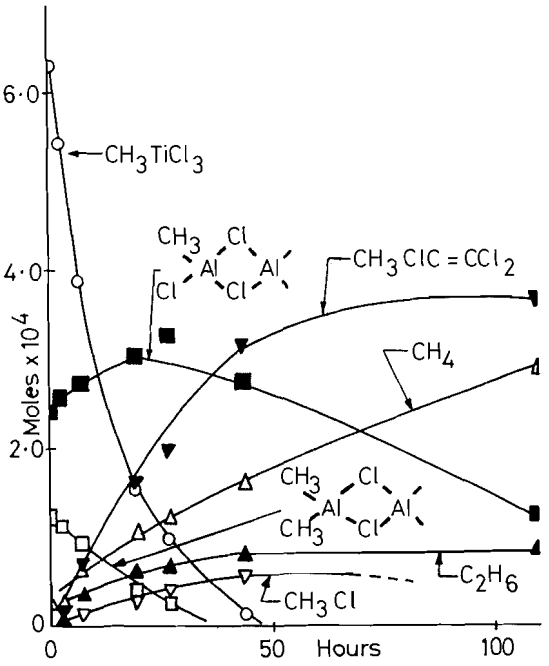

FIG. 6. Thermal decomposition at 80 °C of materials formed from 0.17 *M* $(CH_3)_3Al$ and 0.56 *M* $TiCl_4$ in C_2Cl_4. Symbols are: ○, CH_3TiCl_3; △, CH_4; ▲, C_2H_6; ▽, CH_3Cl; ▼, $CH_3ClC{=}CCl_2$.

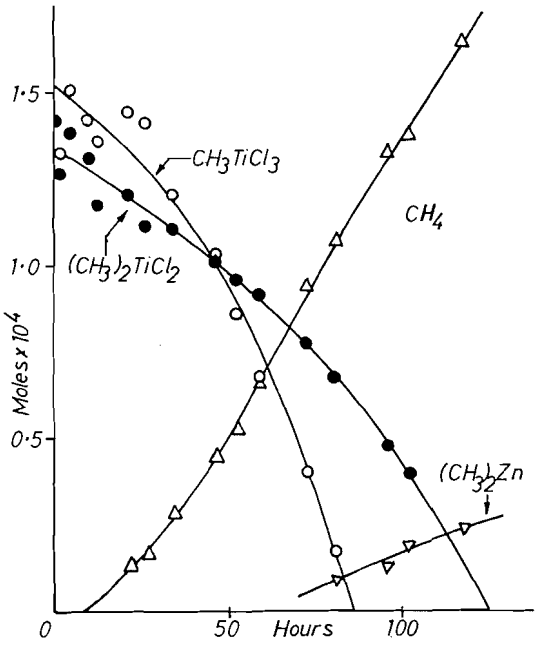

FIG. 7. Thermal decomposition at ambient temperature of materials formed from 0.11 *M* $(CH_3)_2Zn$ and 0.15 *M* $TiCl_4$ in C_2Cl_4. Symbols are: ○, CH_3TiCl_3; ●, $(CH_3)_2TiCl_2$; △, CH_4; ▽, CH_3Cl.

spectrometric analysis of the gases produced on adding D_2O or H_2O to the solids. Solids obtained from the thermal decomposition of *n*-hexane or C_2Cl_4 solutions of $(CH_3)_2TiCl_2$, and from *n*-hexane solutions of $(CH_3)_2Zn/TiCl_4$ systems were studied.

In deuterated systems, the relative abundance of the products observed decreased as CH_3D, CH_4, $C_2H_4D_2$, and C_2H_5D. Small amounts of higher alkyls observed in some samples appeared to arise from residual *n*-hexane. Slight amounts of more highly deuterated ethanes were observed. In the case of products from $(CH_3)_2TiCl_2$ solutions, the amounts of methane were from two to six times the amounts of ethanes. In the case of products of $(CH_3)_2Zn/TiCl_4$ systems of Zn/Ti ratios greater than one, the methanes to ethanes ratio was ten or more.

Discussion

The complexity of these reactions can lead to false conclusions if data from different systems are compared without knowledge of, or consideration of, the effects of different solvents, different temperatures, or different means of preparation. The experiments in this paper were carried out to provide a background of such knowledge against which more detailed and specific experiments could be judged. As such, they permit, when considered with the data of others (3, 4), postulation of a set of reactions which, while not entirely proven, provides a consistent explanation of both kinetic and polymerization observations.

(i) $(CH_3)_2TiCl_2$

It is our hypothesis that some unknown, otherwise unimportant mechanism produces traces of $TiCl_2$ in $(CH_3)_2TiCl_2$ systems. Reaction 1 then occurs on the crystal surface.[6]

[1] $$(CH_3)_2TiCl_2 + TiCl_2(s) \rightarrow 2CH_3{-}TiCl_2(s)$$

The solid so formed would have a valency intermediate between 2 and 3, depending on the extent to which reaction 1 occurs. Such an intermediate and variable valency explains the

[6]The notation R—$TiCl_n$(s) implies a surface R group on a titanium chloride lattice. It does not imply stoichiometric replacement of $1/(n+1)$ of the chlorines by alkyls.

Can. J. Chem. Downloaded from www.nrcresearchpress.com by 210.87.254.42 on 09/05/12
For personal use only.

range of valencies reported for related systems (7, 8, 9, 10). A speculation that further alkylation of the surface may occur by the exchange reaction 2 is reasonable but unsupported.

[2] $(CH_3)_2TiCl_2 + Cl—TiCl_x(s) \rightarrow CH_3—TiCl_x(s) + CH_3TiCl_3$

Since CH_4 is formed without hydrogen contribution by the solvent, a minimum of two methyl groups in near proximity on the surface are therefore required. Reactions 1 and 2 continuously regenerate the required methyl population on the surface.

The preliminary mass spectrometric data do not unequivocally determine the nature of that portion of the carbon and hydrogen which is incorporated in the solid. The large amount of CH_3D produced on adding D_2O implies the existence of methyl groups attached to the metal atoms in the solid in keeping with the equation postulated. As did Rodriguez *et al.* (15, 16), we found small amounts of more highly deuterated methanes. Unlike Rodriguez *et al.*, we are reluctant to interpret these as other than the products of deuterium–hydrogen exchange either on the solid or on the inlet of the mass spectrometer. The former possibility would in itself be of interest. Isotopic exchange is well known for heavier transition metals (11, 12) and can occur quite rapidly for temperatures at least as low as 80 °C (13).

Small amounts of low molecular weight alkanes were observed in solution and rather larger amounts were produced by deuterolysis of the solid. The latter was principally $C_2H_4D_2$,

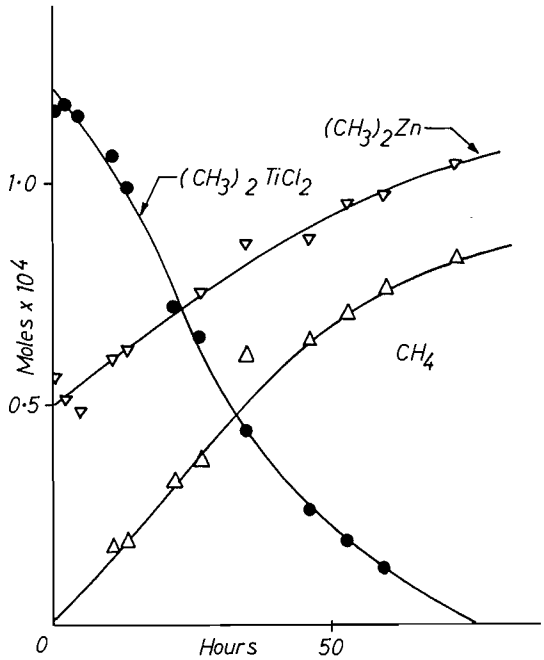

FIG. 8. Thermal decomposition at ambient temperature of materials formed from 0.11 *M* $(CH_3)_2Zn$ and 0.077 *M* $TiCl_4$ in C_2Cl_4. Symbols are: ●, $(CH_3)TiCl_2$; △, CH_4; ▽, CH_3Cl.

with significant amounts of C_2H_5D (14). Although no careful measurements of quantities were made, such material is not sufficient to complete the mass balance.

The configuration of the important solid state precursor of $C_2H_4D_2$ is uncertain. It is geometrically possible for a dimethylene group to "bridge" two adjacent titanium atoms along the

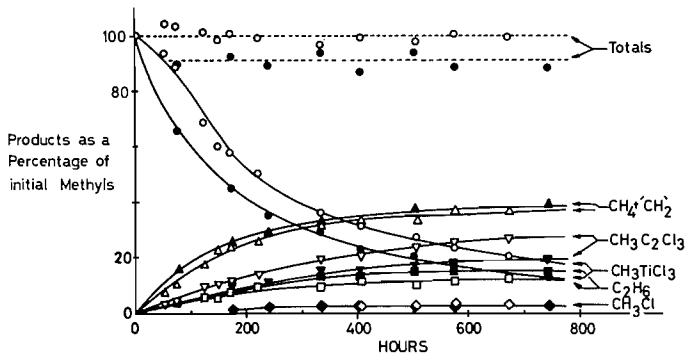

FIG. 9. Reproducibility test showing (*a*) amounts measured in two identical runs, one designated by open symbols and one by black symbols and (*b*) comparison of amounts of carbon and hydrogen in the products, assuming that one methylene exists as polymer or in the solid for each methane, with the amounts in the initial material.

Can. J. Chem. Downloaded from www.nrcresearchpress.com by 210.87.254.42 on 09/05/12
For personal use only.

c-axis of a β-$TiCl_3$ structure. The C—C axis would be skewed relative to the *c*-axis if the carbons occupied Cl vacancies and considerable strain would be expected. However, such a species would explain the origin of both the $C_2H_4D_2$ and the small amounts of low molecular weight alkanes, since it could be released as ethylene and subsequently incorporated in polymer at some Ziegler site.

$(CH_3)_2Zn$ is regenerated where $(CH_3)_2TiCl_2$ is formed *in situ* in $(CH_3)_2Zn/TiCl_4$ systems. While this phenomenon is not essential to thermal decomposition, it is associated with it and must be explained concurrently. We believe that soluble CH_3ZnCl reacts with surface methyls according to reaction 3

[3] $$CH_3ZnCl + CH_3—TiCl_x(s) \rightarrow (CH_3)_2Zn + Cl—TiCl_x(s)$$

and that both CH_3ZnCl and $(CH_3)_2Zn$ are absorbed, to some extent, on the solid titanium chloride. $(CH_3)_2Zn$ formed by reaction 3 can then react with precipitated $ZnCl_2$ to generate more CH_3ZnCl. This is consistent with our experimental evidence that increasing the area of $ZnCl_2$ both retards CH_4 formation (by reducing the surface concentration of methyl groups through reaction 3) and accelerates $(CH_3)_2Zn$ formation (through permitting more rapid regeneration of CH_3ZnCl). This is consistent with n.m.r. mass balance data and with the high CH_3D content in the deuterolysis of $(CH_3)_2Zn/TiCl_4$ systems.

By contrast, $(CH_3)_3Al_2Cl_3$ produced in $(CH_3)_6Al_2/TiCl_4$ and $(CH_3)_4Al_2Cl_2/TiCl_4$ systems continues to methylate the solid, although slowly, and CH_4 continues to form (Fig. 6). Aluminum based systems therefore have a high surface concentration of methyl groups whereas with zinc based systems it is very low. If, as in Cossee's model (17), an active Ziegler site requires an alkyl bonded to a transition metal atom, such observations suggest an alternative to the explanation offered by Rodriguez and van Looy (18) for the difference in catalytic activity between $(CH_3)_3Al/TiCl_4$ systems and $(CH_3)_2Zn/TiCl_4$ systems.

(ii) CH_3TiCl_3

It is apparent from the diversity of products that the decomposition of CH_3TiCl_3 is more complicated than that of $(CH_3)_2TiCl_2$.

In C_2Cl_4, one obtains CH_4, C_2H_6, 1,1,2-trichloropropene-1, and CH_3Cl. In C_6H_6, the last two products are missing. In alkanes, CH_4, C_2H_6, and CH_3Cl occur (3, 4).

It is suggested that CH_4 formation is, at least in part, the product of $(CH_3)_2TiCl_2$ which has been formed through the equilibrium [4].

[4] $$2CH_3TiCl_3 \rightleftharpoons (CH_3)_2TiCl_2 + TiCl_4$$

Such a route is supported by the slight reduction in CH_4 production observed at low Zn/Ti ratios (where $TiCl_4$ is present in excess) and by the observation (3) that CH_4 is reduced relative to C_2H_6 and CH_3Cl by addition of $TiCl_4$ to CH_3TiCl_3 in *n*-heptane. Formation of $TiCl_2$ by decomposition can be expected to constantly increase the formation of $(CH_3)_2TiCl_2$ through removal of $TiCl_4$ according to reaction 5

[5] $$TiCl_2(s) + TiCl_4 \rightarrow 2TiCl_3(s)$$

and contributes to the observed autocatalysis.

In contrast to the high alkyl content in the solid produced in $(CH_3)_2TiCl_2$ systems through the operation of reactions 1 and 2, CH_3TiCl_3 systems show low alkyl contents. This is to be expected on the basis of the unimportance of reaction 1 (due to low $(CH_3)_2TiCl_2$ concentrations) relative to reactions 5 and 6.

[6] $$TiCl_2(s) + CH_3TiCl_3 \rightarrow CH_3TiCl_2 \cdot TiCl_3(s)$$

The highly methylated solid produced by reaction 1 leads to CH_4 formation, reduction of titanium and residual hydrocarbon in the solid. The solid produced by reactions 5 and 6 is trivalent with a small methyl content.

Ethane formation is also autocatalytic. Unlike de Vries (3), we did not observe that the decrease in CH_4 associated with excess $TiCl_4$ was paralleled by an increase in C_2H_6. However, excess $TiCl_4$ was present only in our $(CH_3)_2Zn/TiCl_4$ and $(CH_3)_3Al/TiCl_4$ systems, so the data are not strictly comparable.

The autocatalysis suggests that adsorption of CH_3TiCl_3 is a necessary step in C_2H_6 formation. It is reasonable to suppose that adsorbed CH_3TiCl_3 has a configuration and energy quite different from the solution species. Chlorine and titanium atoms are likely to enter lattice positions appropriate to the underlying β-$TiCl_3$ lattice. Such epitaxially induced changes are consistent with the observed increase in Ziegler

Can. J. Chem. Downloaded from www.nrcresearchpress.com by 210.87.254.42 on 09/05/12
For personal use only.

catalytic activity (3, 4) when $TiCl_3$ is introduced into a CH_3TiCl_3 solution.

CH_3Cl is believed to form according to reaction 7

[7] $CH_3TiCl_3 + TiCl_4 \rightarrow CH_3Cl + 2TiCl_3(s)$

Whether this reaction is influenced by the solid is not certain from the reaction rates. CH_3Cl is abundant only where $TiCl_4$ is present in excess. The low yields of CH_3Cl in CH_3TiCl_3 systems are attributed to the low $TiCl_4$ concentrations resulting from reactions 4 and 5. Direct reaction of two CH_3TiCl_3 to give CH_3Cl cannot be excluded.

Although in the work reported, CH_3Cl is produced in C_2Cl_4 and not in C_6H_6, reaction with the solvent is not believed to be important. Both de Vries (3) and Beermann and Bestian (4) have shown it to be produced in alkanes where no solvent chlorine atoms are available. The lack of CH_3Cl in C_6H_6 is attributed to solvation of CH_3TiCl_3 by benzene inhibiting the reaction. Benzene solvation is supported by n.m.r. data on the pre-exchange lifetime of methyl groups on titaniums in the two solvents.

As to the formation of 1,1,2-trichloropropene, it is known from separate studies that this product forms by simple ligand exchange for other alkyl metal/halogenated solvent systems, such as those shown in reactions 8 and 9.

[8] $(CH_3)_2Zn + 2C_2Cl_4 \rightarrow ZnCl_2 + 2CH_3C_2Cl_3$

[9] $2(CH_3)_3Al + 2C_2Cl_4 \rightarrow (CH_3)_4Al_2Cl_2 + 2CH_3C_2Cl_3$

Production of $CH_3C_2Cl_3$ in CH_3TiCl_3 systems is presumably by a similar route [10]. Toluene production in benzene systems may be analogous.

[10] $CH_3TiCl_3 + C_2Cl_4 \rightarrow TiCl_4 + CH_3C_2Cl_3$

It should be noted that $CH_3C_2Cl_3$ is produced much more abundantly in $(CH_3)_2Zn/TiCl_4$ systems than in CH_3TiCl_3 systems, presumably through the action of residual CH_3ZnCl or $(CH_3)_2Zn$ in the solid according to reaction 8.

(iii) Solutions Containing both $(CH_3)_2TiCl_2$ and CH_3TiCl_3

The case of the decomposition of mixtures of CH_3TiCl_3 and $(CH_3)_2TiCl_2$ in solution is of special interest because of the abrupt change in decomposition rate and product distribution that occurs. Addition of a trace of $(CH_3)_2TiCl_2$ to a solution of CH_3TiCl_3, or elevation of the Zn/Ti ratio to 0.55 from 0.45 in a $(CH_3)_2Zn/TiCl_4/C_2Cl_4$ system, results in relatively rapid decomposition of the methyl titanium trichloride and virtual disappearance of ethane and 1,1,2-trichloropropene-1 from among the products.

Figure 4 illustrates the extraordinary autocatalysis exhibited by CH_3TiCl_3 systems. It is invariably found that, notwithstanding the much greater thermal "stability" of CH_3TiCl_3, it is the first to disappear when mixed in solution with $(CH_3)_2TiCl_2$.

The rapid decomposition of CH_3TiCl_3 in these mixtures could be explained for $(CH_3)_2Zn/TiCl_4$ systems by reactions 4 and 11.

[11] $(CH_3)_2Zn + ZnCl_2 \rightleftharpoons 2CH_3ZnCl$

[11*a*] $(CH_3)_2Zn + ZnCl_2 \rightleftharpoons (CH_3)_2Zn{:}ZnCl_2$

$(CH_3)_2Zn$ thus formed would in turn alkylate the CH_3TiCl_3 to yield more $(CH_3)_2TiCl_2$. Such a system is illustrated in Fig. 7. However, Fig. 4 illustrates the decomposition of a $CH_3TiCl_3/(CH_3)_2TiCl_2$ system containing no zinc chloride, and consequently the rapid decomposition of the CH_3TiCl_3 in this case cannot be explained by introducing an alkyl zinc intermediate.

Moreover, the data shown in Figs. 1–3 indicate that the equilibrium constant for reaction 4 is very small. Consequently, the rapid decline in CH_3TiCl_3 concentration cannot be explained on the basis of the equilibrium [4] operating to replace decomposed $(CH_3)_2TiCl_2$, since the latter is at all times in much greater concentration than in the cases shown in Figs. 1–3. It is therefore concluded that CH_3TiCl_3 reacts directly with adsorbed $(CH_3)_2TiCl_2$ to form CH_4 or with a product of $(CH_3)_2TiCl_2$ decomposition, perhaps simply as in reaction 6.

Summary

CH_3TiCl_3 decomposes by several routes, including a free radical route in polar solvents (4, 20) not observed in our systems. In addition, alkyl analogues having a hydrogen on a carbon β to the metal may decompose by the path proposed by de Vries (3). Other alkyl titanium systems offer additional possibilities, such as intramolecular formation of CH_4 by abstrac-

tion of hydrogen from the amino group in $[(C_2H_5)_2N]_3TiCH_3$ (21).

For σ-bonded alkyl transition metal compounds, comparisons of "relative stabilities" are actually comparisons of "relative rates of decomposition" (19). Where there are many paths of decomposition, each affected differently by various parameters, predictions of "relative stabilities" based on data from different conditions are of dubious value. Moreover, any general explanation of thermal instability of σ-bonded organotransition metal compounds is likely to be more complex than those so far put forward (3, 22) if it is to account for all paths of decomposition.

The authors wish to acknowledge their debts to Dr. J. A. Stone, for assistance in interpreting mass spectrometric data, to Dr. M. K. Phibbs and other colleagues for useful discussions, and to Messrs. M. Hughson and B. Landon for their skillful technical assistance.

1. M. L. Cooper and J. B. Rose. J. Chem. Soc. 795 (1959).
2. E. J. Arlman and J. R. de Jong. Rec. Trav. Chim. **79**, 1319 (1960).
3. H. de Vries. Rec. Trav. Chim. **80**, 866 (1961).
4. C. Beermann and H. Bestian. Angew. Chem. **71**, 618 (1959).
5. J. F. Hanlan and J. D. McCowan. Can. J. Chem. This issue.
6. A. P. Gray, A. B. Callear, and F. H. C. Edgecombe. Can. J. Chem. **41**, 1502 (1963).
7. K. Ziegler. Suomen Kemistilehti **30**, 109 (1957).
8. A. Simon, L. Kovacs, L. Kollar, and G. Dezsenyi. Monatsh. Chem. **90**, 443 (1959).
9. K. Ziegler, H. Martin, and J. Stedefeder. Tetrahedron Lett. **20**, 12 (1959).
10. A. Simon, L. Kollar, and L. Borocz. Monatsh. Chem. **95**, 842 (1964).
11. M. M. Wright and H. S. Taylor. Can. J. Res. **27**, 303 (1949).
12. C. Kemball. Proc. Roy. Soc. A **217**, 376 (1953).
13. D. W. McKee and F. J. Norton. J. Phys. Chem. **68**, 481 (1964).
14. Y. Amenomiya and R. F. Pottie. Can. J. Chem. **46**, 1735 (1968).
15. L. A. M. Rodriguez, J. Gabant, and B. Hargitay. Tetrahedron Lett. **17**, 7 (1959).
16. L. A. M. Rodriguez and J. Gabant. J. Poly. Sci. **57**, 881 (1962).
17. P. Cossee. J. Catal. **3**, 80 (1964).
18. L. A. M. Rodriguez and H. M. van Looy. J. Poly. Sci. A **4**, 1971 (1966).
19. M. L. H. Green. Organometallic compounds. Vol. 2, 3rd ed. Methuen, London. 1968.
20. F. S. D'yachkovskii, N. E. Khrushch, and A. E. Shilov. Kin. i Kataliz, **9**, 1006 (1968).
21. H. Burger and H.-J. Neese. J. Organomet. Chem. **21**, 381 (1970).
22. J. Chatt and B. L. Shaw. J. Chem. Soc. 705 (1959).

Can. J. Chem. Downloaded from www.nrcresearchpress.com by 210.87.254.42 on 09/05/12
For personal use only.

Can. J. Chem. Downloaded from www.nrcresearchpress.com by 210.87.254.42 on 09/05/12
For personal use only.

Erratum: Normal Coordinate Calculations of the Vibrations of Methylene Cyclopropane-h_6 and -d_6

J. E. BERTIE AND S. SUNDER

Department of Chemistry, The University of Alberta, Edmonton, Alberta

Received December 3, 1971

(Ref.: Can. J. Chem. **49**, 2229 (1971))

Canadian Journal of Chemistry, **50**, 765 (1972)

In Table 8 of a previous paper from this laboratory (1) the thermodynamic functions for C_4H_6 and C_4D_6 are presented. Due to a card punching error, which set the degeneracy of one of the modes in each molecule as 10 instead of 1, these thermodynamic properties are in error. The corrected properties are presented in Table 1, using the observed fundamental frequencies of assignment II and the A_2 mode frequencies from Model I (1).

When the A_2 mode frequencies from Model II (1) are used, the calculated values differ from those given in Table 1 in the following way for C_4H_6 and C_4D_6 (in parentheses): $(H_0 - E_0^0)/T$ is the same (greater by 0.02) at 150 °K; is greater by 0.1 (0.12) at 300 °K, and by 0.17 (0.20) at 500 °K; $-(G_0 - E_0^0)/T$ is the same at 150 °K, greater by 0.03 (0.05) at 300 °K, and by 0.09 (0.14) at 500 °K; S_0 is the same (greater by 0.02) at 150 °K, greater by 0.10 (0.18) at 300 °K, and by 0.27 (0.34) at 500 °K; C_p is greater by 0.03 (0.10) at 150 °K, by 0.28 (0.31) at 300 °K, and by 0.32 (0.25) at 500 °K.

TABLE 1. Thermodynamic functions for C_4H_6 and C_4D_6 at 1 atm pressure and for the ideal gaseous state*

T	$(H_0 - E_0^0)/T$		$-(G_0 - E_0^0)/T$		S_0		C_p	
(°K)	C_4H_6	C_4D_6	C_4H_6	C_4D_6	C_4H_6	C_4D_6	C_4H_6	C_4D_6
150	8.61	8.99	46.88	48.16	55.50	57.16	10.24	11.53
200	9.23	9.98	49.44	50.88	58.68	60.85	12.03	14.44
250	10.02	11.20	51.58	53.23	61.60	64.43	14.34	17.72
300	10.95	12.56	53.49	55.39	64.45	67.95	16.96	20.99
350	12.00	13.98	55.26	57.43	67.26	71.42	19.64	24.02
400	13.12	15.41	56.93	59.39	70.05	74.81	22.21	26.75
450	14.27	16.81	58.54	61.29	72.81	78.10	24.60	29.20
500	15.41	18.16	60.11	63.13	75.51	81.29	26.77	31.39

*Using the observed frequencies of assignment II and the A_2 mode frequencies of Model I; units are cal mol^{-1} deg^{-1}.

1. J. E. BERTIE and M. G. NORTON. Can. J. Chem. **49**, 2229 (1971).

Optical Activities of Two Steroids Containing a Chiral Cyclopentene Ring

J. T. EDWARD, N. E. LAWSON,[1] AND (in part) DAPHNE L'ANGLAIS[2]
Department of Chemistry, McGill University, Montreal, Quebec
Received December 22, 1970[3]

The direction of the optical rotation of the steroid **3** can be reconciled with Brewster's rules, if account is taken of "bond fixation", but the direction of the optical rotation of **2** cannot be.

La direction de la rotation optique de la steroide **3** est en accord avec les reglements de Brewster, si on considère la "fixation des bondes", mais la direction de la rotation de **2** est en desaccord.
Canadian Journal of Chemistry, **50**, 766 (1972)

As part of a study (*cf.* ref. 1) of the Bamford–Stevens reaction (2–5), the *p*-toluenesulfonylhydrazone of equilenin methyl ether (**1**) was thermally decomposed in ethylene glycol in the presence of the sodium alkoxide. The product (m.p. 121–122°, $[\alpha]_D$ +24.3°) could be assigned the structure **2**[4] on the basis of its n.m.r. spectrum, which showed a doublet at δ 1.1 (methyl group at C-17) and no peaks due to olefinic protons. Further support for the structure **2** came from the u.v. absorption spectrum of the compound (Fig. 1), which showed a striking similarity to that of 2-vinylnaphthalene (7*b*) when the presence of the methoxyl group was taken into account, and from its dehydrogenation over 5% palladium-on-charcoal in boiling xylene to the phenanthrene derivative **3**. The properties of **3** agreed with those reported for this compound by Cohen *et al.* (8). These authors do not report the u.v. absorption characteristics of their compound; however, we found the spectrum of our compound **3** very similar to that reported for 2-methoxyphenanthrene (9).

The formation of **2** is to be expected; Johns (6) obtained similar rearrangement products from the Bamford–Stevens reaction of estrone

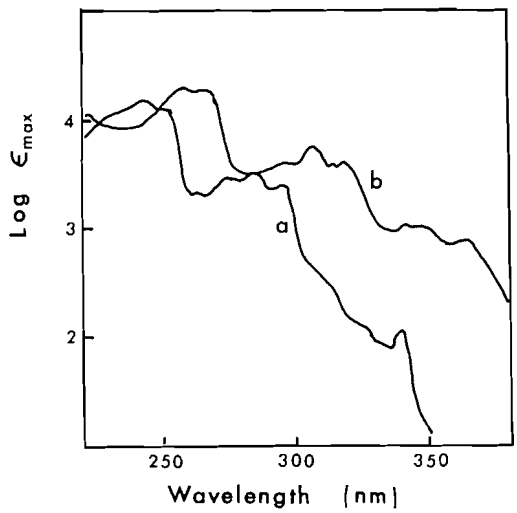

FIG. 1. The u.v. absorption spectra of 2-vinylnaphthalene (*a*) and of steroid **2** (*b*).

derivatives. These and other reactions (8, 10–12) in which a C-17 carbonium ion is formed at temperatures above 100° lead to a 1,2-shift of the 18-methyl group. In contrast, the C-17 carbonium ion formed at 0° in the nitrous acid deamination of 17-androstanylamine gives only the product of solvent attack at C-17 and no rearrangement (13).

Compounds **2** and **3** contain only one asymmetric carbon atom, and offer an opportunity to test Brewster's empirical rules (14, 16), by which the molecular rotation of a compound is calculated by addition of terms for chiral atoms and for chiral conformations. The molecular rotations found for solutions of **2** and **3** in chloroform are shown in Scheme 1, along with rotations taken from the literature for the model compounds **4** and **5**. Brewster (14) has shown

[1]Holder of a University Graduate Scholarship, 1966–1967.
[2]Holder of NRCC Studentships, 1961–1963.
[3]Revision received November 8, 1971.
[4]Johns (6) assigned this structure to a compound, m.p. 84–85°, $[\alpha]_D$ −1°, obtained by heating 17α-chloro-3-methoxyestra-1,3,5(10)-triene with potassium iodide and sodium acetate in ethanol at 125°, or by heating estradiol-3-methyl ether in boric acid at 280° or treating it with phosphorus pentachloride. Johns' assignment was based on elemental analysis and n.m.r. and u.v. absorption spectra λ_{max} 280 nm, log ε 3.41, in methanol). The last is more compatible with a compound having a methoxybenzene chromophore (7*a*), and suggests that possibly the elemental analysis was slightly in error.

Can. J. Chem. Downloaded from www.nrcresearchpress.com by 210.87.254.40 on 09/05/12
For personal use only.

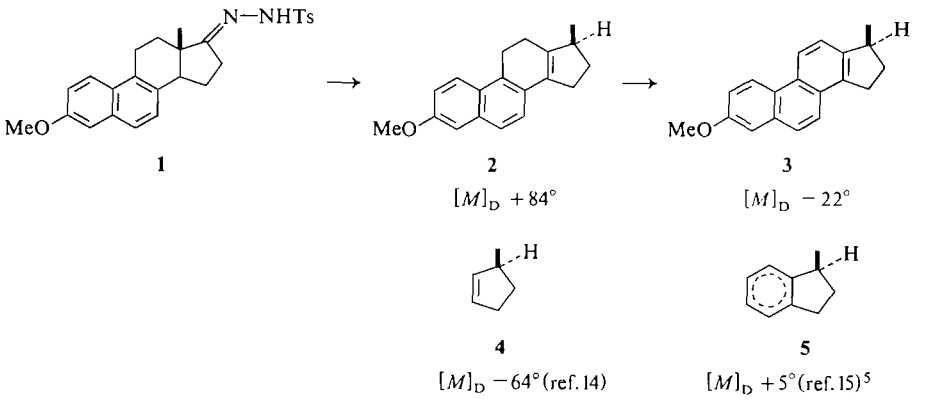

SCHEME 1

that the rotation of **4** is largely determined by the "conformational unit" (16) **6**, which is more important than the other conformational units in this molecule because vinyl carbon is more polarizable than the other groups present (14).

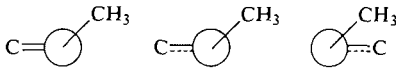

On the other hand, all of the bonds of the aromatic ring of the indan **5** are equivalent (contrary to early ideas of Mills and Nixon (17)), and in this molecule the two most important conformational units are **7** (negative contribution) and **8** (positive contribution). Consequently, the rotation of **5** is close to zero. If all the aromatic bonds in the phenanthrene **3** were equivalent, its rotation would also approximate zero; if the double bonds were "fixed" in the positions shown in **3**, its rotation would approximate that of **4**. In the event, its rotation is negative but smaller than that of **4**, showing some "fixation" of the double bonds. This accords with molecular orbital calculations and chemical evidence for such fixation (17).

The rotation of **2** would be expected, like that of **4**, to be negative as long as there is not also a contribution from the skewed vinylnaphthalene chromophore (18). Examination of Dreiding models of **2** shows two skewed vinylnaphthalene conformations of opposite chirality to be possible; neither conformation is notably disfavored over the other by non-bonded interactions. Measurements of the optical rotary dispersion of a dilute solution of **2** in dioxane showed no Cotton effect at wavelengths down to 240 nm, indicating possibly equal populations of the two conformations, and hence no contribution from a skewed vinylnaphthalene chromophore. The positive rotation of this compound consequently remains anomalous.

[5]Optical rotations in ref. 15 are reported for (*R*)-1-methylindan only up to a wavelength of 556 nm; the value for (*S*)-1-methylindan (**5**) was obtained by extrapolation and reversal of sign.

Experimental

For general experimental details, see ref. 19.

Equilenin Methyl Ether p-Toluenesulfonylhydrazone (1)

A solution of 0.94 g of equilenin methyl ether (20) and 1.2 g of *p*-toluenesulfonylhydrazine in 100 ml of 1:1 ether–ethanol containing one drop of concentrated hydrochloric acid was refluxed for 3 h. The solvent was evaporated under reduced pressure, and the solid residue was recrystallized from ethanol to give 1.4 g (93%) of **1**, m.p. 201°, ν_{max} (KBr) 1385 and 1170 cm^{-1}.

Anal. Calcd. for $C_{26}H_{28}N_2O_3S$: C, 69.66; H, 6.25; N, 6.24. Found: C, 69.97; H, 6.01; N, 6.06.

3-Methoxy-18-nor-17β-methylestra-1,3,5(10),6,8,13-hexaene (2)

Sodium (1.2 g) was dissolved in 60 ml of ethylene glycol and 1.2 g of **1** was added. The temperature of the mixture was raised to 170° over 1 h and held there for 30 min. The cooled solution was diluted with water and extracted repeatedly with ether. The ether extracts were combined, washed with water and with saturated sodium chloride, dried, and evaporated under reduced pressure. The residue was crystallized from ethanol to give 0.69 g of **2** containing one molecule of water of crystallization. Chromatography of the mother liquors on Woelm neutral alumina, grade III, raised the yield to 0.76 g (89%) of **2** m.p. 121–122°, $[\alpha]_D^{25}$ +24.3° (*c*, 0.10), δ 1.1 (doublet, J = 6.6 Hz, C-17 methyl), 2.1 (singlet, water of crystallization, disappeared on D_2O

Can. J. Chem. Downloaded from www.nrcresearchpress.com by 210.87.254.40 on 09/05/12
For personal use only.

exchange), 3.9 (singlet, OCH_3), and 7.0–8.0 (multiplet, aromatic protons).

Anal. Calcd. for $C_{19}H_{20}O.H_2O$: C, 80.81; H, 7.85. Found: C, 80.80; 7.72.

Anal. Calcd. for $C_{19}H_{20}O$: C, 86.32; H, 7.63. Found (after drying at 80° over P_2O_5): C, 85.97; H, 7.80.

3-Methoxy-18-nor-17β-methylestra-1,3,5(10),6,8,11,13-heptaene (3)

A mixture of **2** (27 mg) and 5% palladium-on-charcoal (180 mg) in xylene (3 ml) was refluxed for 3 h while a slow stream of nitrogen bubbled through it. The solution was cooled, filtered, concentrated under reduced pressure, and the residue was crystallized from ethanol to give a virtually quantitative yield of **3**, m.p. 149–151° (lit. (8) m.p. 146.5–148.5°), $[\alpha]_D^{25} -7.4°$ (*c*, 0.14), λ_{max} (EtOH) (log ε_{max}) 263 (5.0), 282 (4.5), 291 (4.35), 303 (4.25), 308 (3.35), 325 (3.15), 332 (3.1), 342 (3.3), and 375 nm (2.25).

The *sym*-trinitrobenzene complex had m.p. 133–133.5° (lit. (8) m.p. 135.5–136.5°).

We are grateful to Professor Peter Morand for the o.r.d. curve, to Ayerst, McKenna, and Harrison Ltd. for generous gifts of starting materials, and to the Medical Research Council and National Research Council of Canada for financial support.

1. J. T. EDWARD, D. L'ANGLAIS, and S. MEYERSON. Can. J. Chem. **44**, 1866 (1966).
2. W. R. BAMFORD and T. S. STEVENS. J. Chem. Soc. 4735 (1952).
3. L. FRIEDMAN and H. SCHECTER. J. Am. Chem. Soc. **81**, 5512 (1959).
4. J. W. POWELL and M. C. WHITING. Tetrahedron **7**, 305 (1959).
5. C. H. DEPUY and D. H. FROEMSDORF. J. Am. Chem. Soc. **82**, 634 (1960).
6. W. F. JOHNS. J. Org. Chem. **26**, 4583 (1961).
7. R. A. FRIEDEL and M. ORCHIN. Ultraviolet spectra of aromatic compounds. John Wiley and Sons Inc., New York, N.Y., 1951. (*a*) No. 57; (*b*) No. 229.
8. A. COHEN, J. W. COOK, and C. L. HEWETT. J. Chem. Soc. 445 (1935); see also M. KIMURA, K. AKIYAMA, K. HARITA, T. MIURA, and M. KAWARA. Tetrahedron Lett. 377 (1970).
9. G. N. WALKER. J. Am. Chem. Soc. **79**, 1772 (1957).
10. K. MIESCHER and H. KAGI. Helv. Chim. Acta, **32**, 761 (1949).
11. K. HEUSLER and A. WETTSTEIN. Ber. **87**, 1301 (1954).
12. M. TANABE and D. F. CROWE. J. Org. Chem. **28**, 3197 (1963).
13. C. W. SHOPPEE and J. C. P. SLY. J. Chem. Soc. 345 (1959).
14. J. H. BREWSTER. J. Am. Chem. Soc. **81**, 5493 (1959).
15. J. H. BREWSTER and J. G. BUTA. J. Am. Chem. Soc. **88**, 2233 (1966).
16. J. H. BREWSTER. J. Am. Chem. Soc. **81**, 5475, 5483 (1959); Tetrahedron **13**, 106 (1961).
17. G. M. BADGER. Quart. Rev. **5**, 147 (1951).
18. P. CRABBE. Optical rotatory dispersion and circular dichroism in organic chemistry. Holden-Day Co., San Francisco, 1965. p. 253.
19. J. T. EDWARD and N. E. LAWSON. J. Org. Chem. **35**, 1426 (1970).
20. G. SANDULESCO, W. W. TCHUNG, and A. GIRARD. Compt. rend. **196**, 137 (1933).

Erratum: Stereochemistry of Dehydrogenation by *D*-Galactose Oxidase

A. MARADUFU, G. M. CREE, AND A. S. PERLIN
Department of Chemistry, McGill University, Montreal, Quebec

Received December 6, 1971
(Ref.: Can. J. Chem. **49**, 3429 (1971))

Canadian Journal of Chemistry, **50**, 768 (1972)

On p. 3429, right-hand column, lines 5 and 6, the numbers **2** and **3** should be interchanged, *i.e.* the lines should read:

"... upon the carbinol group as in **3**) and H_R, the *pro-R* hydrogen as in the *R* diastereomer **2**. From ..."

On. p. 3430, left-hand column, lines 10 and 11, Scheme 1 should read Scheme 2, *i.e.*:

"... configurational correlations illustrated on Scheme 2."

Can. J. Chem. Downloaded from www.nrcresearchpress.com by 210.87.254.40 on 09/05/12
For personal use only.

Can. J. Chem. Downloaded from www.nrcresearchpress.com by 210.87.254.6 on 09/05/12
For personal use only.

A Simplification in the Synthesis of Deoxyribooligonucleotides

S. A. NARANG,[1] K. ITAKURA,[2] AND R. H. WIGHTMAN[3]

Biochemistry Laboratory, National Research Council of Canada,[4] Ottawa, Canada K1A 0R6

Received December 29, 1971

The synthesis of oligonucleotides can be accomplished with no "protection" of the amino function in the case of adenine and guanine bases under the usual reaction conditions.

La synthèse d'oligonucléotides peut s'accomplir sans qu'on ait besoin de "protéger" la fonction amine dans le cas des bases adénine et guanine sous les conditions habituelles de réaction.

Canadian Journal of Chemistry, **50**, 769 (1972)

For the synthesis of oligonucleotides, it is generally conceded that the primary amino group of the heterocyclic bases must be protected ostensibly to prevent any reaction which might form complicating side-products (1). A number of blocking groups have been introduced for this purpose: acetyl (2), benzoyl or anisoyl (2), isobutyloxycarbonyl (3), and dimethylaminomethylene (4). However, there were scattered reports in the literature which inferred that blocking of the amino groups might not be necessary under the usual condensation conditions (5, 6).

This communication reports our preliminary findings that the synthesis of oligonucleotides can indeed be accomplished with no "protection" of the amino function in the case of adenine and guanine bases but not with cytosine. Our general procedure for synthesis and purification is outlined in Scheme 1. For example, 2-phenylmercaptoethyl 5′-phosphate deoxyadenosine or deoxyguanosine (**1**) was condensed with 3′-*O*-acetylthymidine 5′-phosphate (**2**) under the usual conditions (7). The composition of the crude reaction mixtures as well as yields[5] and purity of the desired products[6] were substantially the same whether the nucleotides involved had "protected" or free amino groups. In fact, we have noticed that chromatographic resolution of the unprotected nucleotides is generally better than those with protected amino groups. On the other hand, the condensation of phosphate protected deoxycytosine with 3′-*O*-acetylthymidine 5′-phosphate under the same conditions gave two components. The fast-moving component on t.l.c. (*ca.* 20% minor product) was identified as the desired 3′–5′ phosphodiester compound (by their u.v. spectra, mobility on t.l.c. in three solvent systems, bacterial alkaline phosphatase, spleen and snake venom phosphodiester treatments). Whereas the slow-moving component on t.l.c. (*ca.* 42% major product) was sensitive to bacterial alkaline phosphatase and snake venom phosphodiesterase enzymes but completely resistant to action of spleen phosphodiesterase. From this we inferred that this component might be a *N*-phosphorylated compound.

These observations show that the two units, adenine and guanine out of three basic units which have a primary amino group can be used in the synthesis of oligonucleotides without protecting their amino function. Application of these important observations should be a general asset in the long range synthesis of polynucleotides.

[1]Author to whom correspondence should be sent.

[2]NRCC Postdoctorate Fellow, 1971–present.

[3]Visiting Professor from Carleton University, Ottawa, Canada.

[4]NRCC No. 12401.

[5]Usually the products were isolated in 50–70% yield.

[6]The desired compounds were checked for their purity on Avicel–Cellulose plate (0.1 mm thickness) in the usual three-solvent systems (8). Final characterization was carried out by their complete digestion with spleen and snake venom phosphodiesterase enzyme after bacterial alkaline phosphatase treatment.

1. (*a*) P. T. GILHAM and H. G. KHORANA. J. Am. Chem. Soc. **81**, 4647 (1959); (*b*) M. SMITH, D. H. RAMMLER, I. H. GOLDBERG, and H. G. KHORANA. J. Am. Chem. Soc. **84**, 430 (1962); (*c*) H. SCHALLER, G. WEISMAN, B. LERCH, and H. G. KHORANA. J. Am. Chem. Soc. **85**, 3821 (1963).

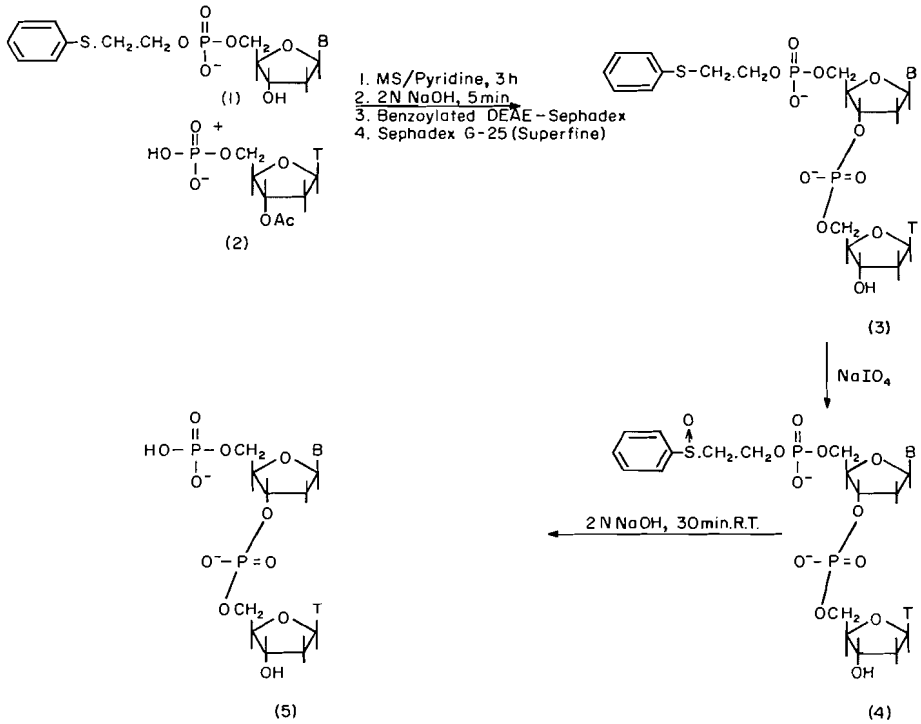

SCHEME 1

2. (*a*) R. K. RALPH and H. G. KHORANA. J. Am. Chem. Soc. **83**, 2926 (1961); (*b*) R. K. RALPH, W. J. CONNORS, H. SCHALLER, and H. G. KHORANA. J. Am. Chem. Soc. **85**, 1983 (1963); (*c*) H. G. KHORANA, A. F. TURNER, and J. P. VIZSOLYI. J. Am. Chem. Soc. **83**, 686 (1961).
3. R. L. LESTINGER and P. S. MILLER. J. Am. Chem. Soc. **91**, 3556 (1969).
4. J. ZEMLICKA and J. SMRT. Coll. Czech. Chem. Commun. **32**, 3159 (1967).
5. A. M. MICHELSON. J. Chem. Soc. 1371 (1959).
6. B. E. GRIFFIN, M. JARMAN, and C. B. REESE. Tetrahedron, **24**, 639 (1968).
7. R. H. WIGHTMAN, S. A. NARANG, and K. ITAKURA. Can. J. Chem. In press.
8. S. A. NARANG, O. S. BHANOT, S. K. DHEER, J. GOODCHILD, and J. J. MICHNIEWICZ. Biochem. Biophys. Res. Commun. **41**, 1248 (1970).

Can. J. Chem. Downloaded from www.nrcresearchpress.com by 210.87.254.6 on 09/05/12
For personal use only.

Kinetic Evidence for Predominant Oxygen Protonation of Amides

CLINTON R. SMITH AND KEITH YATES
Department of Chemistry, University of Toronto, Toronto 5, Ontario

Received November 3, 1971

Comparison of rate data for the acid-catalyzed hydrolysis of amides, and model compounds for *O*- and *N*-protonated amides, provides strong evidence that amides protonate predominantly on oxygen in dilute as well as in concentrated aqueous acids, contrary to a recent proposal that the protonation sites are different in the two media.

La comparaison des données de vitesse dans le cas de l'hydrolyse des amides catalysée par les acides et des composés modèles pour les amides protonées en *O*- et *N*- fournit une preuve irréfutable que les amides sont protonées de façon prédominante sur l'oxygène dans les solutions d'acide, autant diluées que concentrées, contrairement à ce qu'on avait proposé quelques temps auparavant, soit que les sites de protonation soient différents dans ces deux milieux.

Canadian Journal of Chemistry, **50**, 771 (1972)

The fact that amides protonate predominantly on oxygen (**1**) in strongly acidic media has been established for some time (1, 2). Liler (3) has recently confirmed this from a study of the n.m.r. spectra of ^{15}N amides, but has also proposed that in dilute acid predominant protonation is on nitrogen (**2**). We now wish to present kinetic data on the acid-catalyzed hydrolyses of benzamide, methyl benzimidate, and benzoylimidazole, which along with other available kinetic data, can be used to test this proposal.

It has been suggested that acyl ammonium (**3**) (4) and acyl pyridinium salts (**5**) (5) would be reasonable models for the estimation of the reactivity of *N*-protonated amides. Although acetyl ammonium (6) and acetyl pyridinium salts (7) can be prepared, benzoylammonium (8) and benzoylpyridinium (7) salts are thermally unstable at room temperature. However, acylimidazole compounds (9) are readily available. Unlike in an *N*-protonated amide or in the acylammonium and pyridinium salts, the positive charge on nitrogen in a protonated acyl imidazole (**5**) is delocalized, and thus these cations would be expected to be less reactive than those with a full localized charge on nitrogen. Therefore their reactivity should represent a lower limit for the reactivity of an *N*-protonated amide. *N*-Acylimidazolium compounds are in fact known to be less reactive than acyl pyridinium ions (10). Edward and Meacock (11) have suggested that imidate salts (**6**) would be good models for oxygen protonated amides.

Thus we have the models shown in Scheme 1 for *N*- and *O*-protonated amides acting as substrates in hydrolysis reactions.

Rate data for the hydrolysis of acetamide, benzamide, and the corresponding *N*- and *O*-protonated models are given in Table 1. The rate data in 8 *M* HCl were available directly from the literature. The values in dilute and moderately concentrated H_2SO_4 were determined recently in our laboratories. Data for methyl acetimidate are not available. However,

O-Protonated amide and model ion

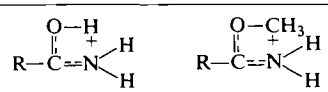

1 **6**

N-Protonated amide and model ions

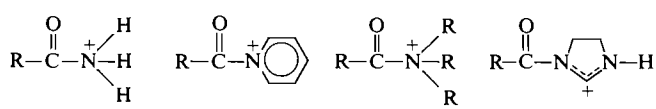

2 **4** **3** **5**

SCHEME 1

Can. J. Chem. Downloaded from www.nrcresearchpress.com by 210.87.254.5 on 09/05/12
For personal use only.

TABLE 1. Relative rate of hydrolysis of amide and model compounds

Substrate	k_p^{rel}[a] (25 °C)			
	$[H_2SO_4] = 1.4$	$[H_2SO_4] = 8.9$	[HCl] = 0	[HCl] = 8
Benzamide[l,m]	1.0[d,k]	1.0[e,k]	1[b,f]	1[c,f]
Methyl benzimidate	9.6[k]	3.7[k]	6[f]	3[f]
Benzoyl imidazole	3.9×10^3 [k]	4.9×10^5 [k]	2×10^3 [g]	7×10^3 [g]
Acetamide[l,n]			2[h]	6[h]
N-Ethyl methyl acetimidate			4[i]	
Acetyl imidazole			3×10^3 [g]	4×10^3 [g]
Acetyl pyridinium chloride			1×10^6 [j]	

[a]Rate of hydrolysis relative to rate of hydrolysis of benzamide.
[b]k_p (benzamide) = 1.6×10^{-5} s^{-1}.
[c]k_p (benzamide) = 3.4×10^{-7} s^{-1}.
[d]k_p (benzamide) = 5.3×10^{-6} s^{-1}.
[e]k_p (benzamide) = 1.0×10^{-9} s^{-1}.
[f]Reference 11.
[g]Reference 9.
[h]Reference 17.
[i]Reference 18.
[j]Reference 10.
[k]This work.
[l]$k_p = k_{obs}(h_A + K_{SH}^+)/h_A$.
[m]$pk_{SH^+} = -1.7$, ref. 12.
[n]$pk_{SH^+} = -0.6$, ref. 12.

we have found (12) that one *N*-alkyl group has little effect on the rate constant for acid-catalyzed methyl benzimidate hydrolysis and it is assumed therefore that *N*-ethyl methyl acetimidate is a reasonable model for an oxygen protonated acetamide.

The rate constants listed in Table 1 are for the process:

$$SH^+ + H_2O \xrightarrow{k_p} \text{Products}$$

The observed rate constants for these moderately weakly basic amides have therefore been corrected for the extent of protonation of the substrate. To enable direct comparisons, the amide and imidate data in dilute HCl solution have been extrapolated to unit water activity (for the imidates this corresponds closely to the maximum rate of hydrolysis for water acting as a nucleophile). The values for the *N*-protonated models in dilute HCl are as reported by Marburg and Jencks (9) for unit water activity. It can be seen from Table 1 that in both the acetyl and benzoyl series the imidazole *N*-protonated models react at least 10^3 times as fast as the *O*-protonated models at both high and low acidity. In the acetyl series, the pyridinium compound reacts 10^6 times as fast as the *O*-protonated model. Therefore, it is reasonable that an *N*-protonated amide would react at least 10^3 times as rapidly as the *O*-protonated form. The imidates however, react at a very similar rate to amides. This fact has been established previously for the benzoyl series (11).

Thus if amides protonated exclusively on nitrogen in dilute acid, as Liler suggests, hydrolysis would occur through the very reactive *N*-protonated form, and the p*K*'s observed by the u.v. (13) and n.m.r. (14) would be those arising from *N*-protonation. However, this postulate is inconsistent with the rate data in Table 1 since the k_p values show that amides are about 10^3 to 10^6 times *less* reactive than would be expected from an exclusively *N*-protonated amide.

Two alternative possibilities are consistent with the rate data; firstly, that amides are predominantly oxygen protonated in dilute solution and react through a minor *N*-protonated form in very low concentration; secondly, that amides are predominantly oxygen protonated and also react through this form.[1] In both of these cases the rate data require that the extent of *N*-protonation be at least 10^5 times *less* than the extent of *O*-protonation in dilute acid and that this be the upper limit of *N*-protonation. A recent

[1]Neither of these possibilities is inconsistent with the n.m.r. evidence from dilute acid solution. A minor amount of rapid *N*-protonation would be sufficient to explain the n.m.r. equivalence of the groups attached to nitrogen observed in dilute acid (15, 16).

Can. J. Chem. Downloaded from www.nrcresearchpress.com by 210.87.254.5 on 09/05/12
For personal use only.

estimate of the relative pK's for O- and N-protonation of an amide by Fersht (5) yields a factor of 10^7 in favor of the former.

The continued financial assistance of the National Research Council of Canada is gratefully acknowledged.

1. R. B. HOMER and C. D. JOHNSON. The chemistry of amides. J. Zabicky, Editor. Interscience Publishers, 1970. p. 187.
2. C. J. O'CONNOR. Quart. Rev. **24**, 553 (1970).
3. M. LILER. Chem. Commun. 115 (1971).
4. C. A. BUNTON, C. J. O'CONNOR, and T. A. TURNEY. Chem. and Ind. 1835 (1967).
5. A. R. FERSHT. J. Am. Chem. Soc. **93**, 3504 (1971).
6. F. KLAGES and E. ZANGE. Liebigs. Ann. **607**, 35 (1957).
7. A. K. SHINKMAN, S. L. PORTNOVA, Y. N. SHEINKER, and A. N. KOST. Dockl. Akad. Nauk SSSR. **157**, 1416 (1964); Dokl. Chem. 817 (1964).
8. R. GOMPPER and P. ALTREUTHER. Zs. Anal. Chem. **170**, 205 (1959).
9. S. MARBURG and W. P. JENCKS. J. Am. Chem. Soc. **84**, 232 (1962).
10. A. R. FERSHT and W. P. JENCKS. J. Am. Chem. Soc. **92**, 5432 (1970).
11. J. T. EDWARD and S. C. R. MEACOCK. J. Chem. Soc. 2000, 2009 (1957).
12. C. R. SMITH and K. YATES. Unpublished results.
13. K. YATES and J. B. STEVENS. Can. J. Chem. **43**, 529 (1965).
14. (*a*) M. LILER. J. Chem. Soc. B, 334 (1969). (*b*) D. W. FARLOW and R. B. MOODIE. J. Chem. Soc. B, 334 (1970).
15. A. BERGER, A. LOEWENSTEIN, and S. MEIBOOM. J. Am. Chem. Soc. **81**, 62 (1959).
16. G. FRAENKEL and C. FRANCONI. J. Am. Chem. Soc. **82**, 4478 (1960).
17. H. J. CAMPBELL. Ph.D. Thesis. McGill University, Montreal, Quebec, 1961.
18. T. C. PLETCHER, S. KOEHLER, and E. H. CORDES. J. Am. Chem. Soc. **90**, 7072 (1969).

Relationship of ^{13}C to Vicinal ^1H Coupling to the Torsion Angle in Uridine and Related Structures[1]

R. U. LEMIEUX, T. L. NAGABHUSHAN,[2] AND B. PAUL[3]
Department of Chemistry, University of Alberta, Edmonton, Alberta

Received December 29, 1971

Uracil was prepared enriched at C2 with carbon-13 and converted into uridine from which 2,5′-anhydro-1-β-D-*ribo*-furanosyl and 2,2′-anhydro-1-β-D-*arabino*-furanosyl uracil were prepared. The $^{13}C2$ to vicinal proton coupling constants for these compounds were measured and are compared in terms of the expected torsion angles defined by the two atoms. The evidence suggests the existence of a Karplus-type relationship as is found for vicinal proton coupling. The data establish the *anti* conformation for uridine in solution.

On a préparé l'uracile enrichi au C2 avec le carbone-13 et on l'a converti en uridine à partir duquel le 2,5′-anhydro-1-β-D-*ribo*-furanosyl et le 2,2′-anhydro-1-β-D-*arabino*-furanosyl uracile ont été préparés. Les constantes de couplage entre $^{13}C2$ et le proton vicinal pour ces composés ont été mesurées et comparées en termes des angles de torsion définis par les deux atomes. L'évidence suggère l'existence d'une relation de type Karplus telle qu'on en trouve dans le cas de couplage de protons vicinaux. Les résultats établissent la conformation *anti* pour l'uridine en solution.

Canadian Journal of Chemistry, **50**, 773 (1972)

The relationship between the torsion angle defined by vicinal hydrogens and their coupling constant (1–4) has had a profound influence on elucidation of configuration and conformational analysis. That a similar stereochemical – coupling constant relationship may exist for ^{13}C-atoms vicinal to hydrogen atoms is an obvious extension of n.m.r. to problems of stereochemistry. The availability of ^{13}C-enriched compounds has made possible in many cases the detection of such vicinal coupling constants using high resolution proton magnetic resonance (5–8) and more recently ^{13}C-magnetic resonance (9). Should it prove possible to establish a relationship between these coupling constants and

[1]Presented in part by R.U.L. at the McGill University Sesquicentennial Chemistry Symposium, Montreal, Quebec, May 27–28, 1971.
[2]Professional Research Associate.
[3]Postdoctorate Fellow, 1970.

Can. J. Chem. Downloaded from www.nrcresearchpress.com by 210.87.254.5 on 09/05/12
For personal use only.

estimate of the relative pK's for O- and N-protonation of an amide by Fersht (5) yields a factor of 10^7 in favor of the former.

The continued financial assistance of the National Research Council of Canada is gratefully acknowledged.

1. R. B. HOMER and C. D. JOHNSON. The chemistry of amides. J. Zabicky, Editor. Interscience Publishers, 1970. p. 187.
2. C. J. O'CONNOR. Quart. Rev. **24**, 553 (1970).
3. M. LILER. Chem. Commun. 115 (1971).
4. C. A. BUNTON, C. J. O'CONNOR, and T. A. TURNEY. Chem. and Ind. 1835 (1967).
5. A. R. FERSHT. J. Am. Chem. Soc. **93**, 3504 (1971).
6. F. KLAGES and E. ZANGE. Liebigs. Ann. **607**, 35 (1957).
7. A. K. SHINKMAN, S. L. PORTNOVA, Y. N. SHEINKER, and A. N. KOST. Dockl. Akad. Nauk SSSR. **157**, 1416 (1964); Dokl. Chem. 817 (1964).
8. R. GOMPPER and P. ALTREUTHER. Zs. Anal. Chem. **170**, 205 (1959).
9. S. MARBURG and W. P. JENCKS. J. Am. Chem. Soc. **84**, 232 (1962).
10. A. R. FERSHT and W. P. JENCKS. J. Am. Chem. Soc. **92**, 5432 (1970).
11. J. T. EDWARD and S. C. R. MEACOCK. J. Chem. Soc. 2000, 2009 (1957).
12. C. R. SMITH and K. YATES. Unpublished results.
13. K. YATES and J. B. STEVENS. Can. J. Chem. **43**, 529 (1965).
14. (*a*) M. LILER. J. Chem. Soc. B, 334 (1969). (*b*) D. W. FARLOW and R. B. MOODIE. J. Chem. Soc. B, 334 (1970).
15. A. BERGER, A. LOEWENSTEIN, and S. MEIBOOM. J. Am. Chem. Soc. **81**, 62 (1959).
16. G. FRAENKEL and C. FRANCONI. J. Am. Chem. Soc. **82**, 4478 (1960).
17. H. J. CAMPBELL. Ph.D. Thesis. McGill University, Montreal, Quebec, 1961.
18. T. C. PLETCHER, S. KOEHLER, and E. H. CORDES. J. Am. Chem. Soc. **90**, 7072 (1969).

Relationship of ^{13}C to Vicinal ^1H Coupling to the Torsion Angle in Uridine and Related Structures[1]

R. U. LEMIEUX, T. L. NAGABHUSHAN,[2] AND B. PAUL[3]
Department of Chemistry, University of Alberta, Edmonton, Alberta

Received December 29, 1971

Uracil was prepared enriched at C2 with carbon-13 and converted into uridine from which 2,5′-anhydro-1-β-D-*ribo*-furanosyl and 2,2′-anhydro-1-β-D-*arabino*-furanosyl uracil were prepared. The $^{13}C2$ to vicinal proton coupling constants for these compounds were measured and are compared in terms of the expected torsion angles defined by the two atoms. The evidence suggests the existence of a Karplus-type relationship as is found for vicinal proton coupling. The data establish the *anti* conformation for uridine in solution.

On a préparé l'uracile enrichi au C2 avec le carbone-13 et on l'a converti en uridine à partir duquel le 2,5′-anhydro-1-β-D-*ribo*-furanosyl et le 2,2′-anhydro-1-β-D-*arabino*-furanosyl uracile ont été préparés. Les constantes de couplage entre $^{13}C2$ et le proton vicinal pour ces composés ont été mesurées et comparées en termes des angles de torsion définis par les deux atomes. L'évidence suggère l'existence d'une relation de type Karplus telle qu'on en trouve dans le cas de couplage de protons vicinaux. Les résultats établissent la conformation *anti* pour l'uridine en solution.

Canadian Journal of Chemistry, **50**, 773 (1972)

The relationship between the torsion angle defined by vicinal hydrogens and their coupling constant (1–4) has had a profound influence on elucidation of configuration and conformational analysis. That a similar stereochemical – coupling constant relationship may exist for ^{13}C-atoms vicinal to hydrogen atoms is an obvious extension of n.m.r. to problems of stereochemistry. The availability of ^{13}C-enriched compounds has made possible in many cases the detection of such vicinal coupling constants using high resolution proton magnetic resonance (5–8) and more recently ^{13}C-magnetic resonance (9). Should it prove possible to establish a relationship between these coupling constants and

[1]Presented in part by R.U.L. at the McGill University Sesquicentennial Chemistry Symposium, Montreal, Quebec, May 27–28, 1971.
[2]Professional Research Associate.
[3]Postdoctorate Fellow, 1970.

Can. J. Chem. Downloaded from www.nrcresearchpress.com by 210.87.254.6 on 09/05/12
For personal use only.

TABLE 1. Relationship of vicinal ^{13}C–^{1}H coupling constants to torsion angle

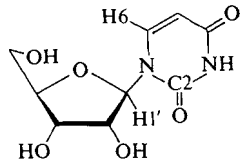

4

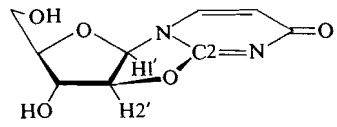

5

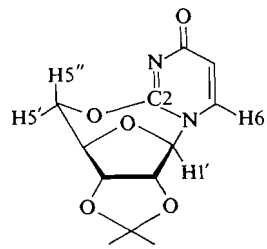

6

Vicinal atoms	$J_{^{13}C,^{1}H}$ (Hz)	Torsion angle(ϕ°)	Solvent
C2—H6	8.0 (uracil)	180	D_2O
	8.0 (**4**)	180	$(CD_3)_2CO$
	7.2 (**6**)	~175	$CDCl_3$
C2—H1′	2.4 (**4**)	−45	D_2O
	3.6 (**5**)	−125	D_2O
	6.6 (**6**)	170	$CDCl_3$
C2—H2′	2.0 (**5**)	120	D_2O
C2—H5′	8.7 (**6**)	175	$CDCl_3$
C2—H5″	2.0 (**6**)	50	$CDCl_3$

conformational features, then these developments would be of especially great interest to studies of the conformational properties of such important classes of compounds as the nucleic acids **1**, peptides **2** (10), and glycosides **3** (11) by providing estimates of the average torsion angle ϕ for the vicinal C* and H* atoms.

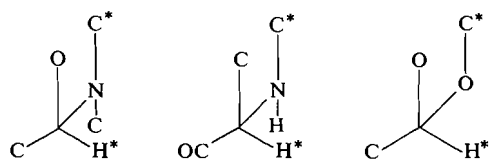

1 2 3

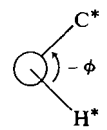

Karabatsos and coworkers (5–7) realized the possibilities of this coupling to study rotational isomerism and later showed (12) that, as expected from vicinal H–H coupling, vicinal ^{13}C–H coupling is much stronger for the atoms in *trans* than in *cis*-relationship. More recently, Perlin and Casu (8) found this situation present in the spectra of ^{13}C-enriched α-D-glucopyranose. However, it has become clearly apparent that, in contrast to H–H coupling constants, vicinal ^{13}C–H coupling constants are much more sensitive to structural parameters (electronegativity, heteroatom, carbon hybridization) other than steric relationships (7, 9). Nevertheless, the hope remained that useful empirical torsion angle – coupling constant relationships may exist for chemically closely related structures and perhaps especially when the ^{13}C and H atoms are bridged only through sigma bonds. This communication reports such results for nucleoside-

Can. J. Chem. Downloaded from www.nrcresearchpress.com by 210.87.254.6 on 09/05/12
For personal use only.

Can. J. Chem. Downloaded from www.nrcresearchpress.com by 210.87.254.6 on 09/05/12
For personal use only.

type bicyclic structures for which torsion angles can be roughly estimated from molecular models.

Uridine (**4**) was synthesized enriched (about 60%) with ^{13}C at the 2-position of the uracil residue using essentially published procedures (13, 14). The compound was then converted to the cyclonucleoside structures **5** (15) and **6** (16) following established methods. The coupling constants for this isotopically enriched carbon with the vicinal protons in these compounds (**4**, **5**, and **6**) were then determined as indicated in Table 1. The dihedral angles considered most probable in compounds **5** and **6** are also listed. Clearly, a Karplus-type relationship (3) is apparent. Furthermore, near zero coupling was found (17) for both H1 and H2 with the orthoester carbon of α-D-glucopyranose 3,4,6-triacetate 1,2-(methyl 1-^{13}C-orthoacetate). For this compound, the molecular model indicates that these atoms define near 90° torsion angles.

Uridine in aqueous solution is considered (18, 19) to exist extensively in the *anti*-conformation ($\phi_{C2,H1'} \simeq -30°$)[4] and that no change in the ribose–uracil torsion angle takes place over the temperature range 28–78°. The small change in $J_{C2,H1'}$ found for uridine at 26 and 67° in D_2O, namely, 2.3 and 2.4 Hz, respectively, confirms the latter conclusion and these coupling constants together with the data plotted in Fig. 1 suggest either $\phi_{C2,H1'}$ is about ±45° (*anti* conformation) or $\phi_{C2,H1'}$ is about ±120° (*syn* conformation). The latter conformation is highly implausible since the uracil residue would be strongly eclipsed with either the Cl—O4 or Cl—C2 bonds. The conformation of uridine was recently determined in the crystalline state (22). The compound was found to exist in two conformers per asymmetric crystal unit with $\phi_{C2,H1'} = -36$ and $-43°$. Thus it is apparent that the *anti*-conformation adopted by uridine in the crystal field is maintained in solution. It is noteworthy that esters (23, 24) and amides (10) tend to have the C=O and a vicinal C—H bond in opposition and defining a torsion angle of less than 60° and that the *anti*-conformation for uridine also possesses this conformational feature.

[4]The ϕ_{CN} designation (20) for defining sugar-base conformational relationships does not give a true torsion angle. Sundaralingam, (21) provides the designation χ for glycosidic torsion angles which for pyrimidine nucleosides correspond to $\phi_{C6,O4'}$ (O4′ is referred to as O1′).

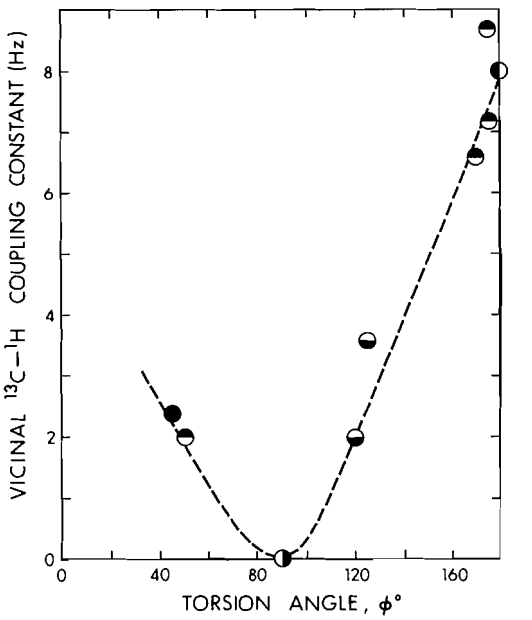

FIG. 1. Plot of the coupling constants *vs.* torsion angles defined by ^{13}C and vicinal protons in compounds **4** (●), **5** (◒), **6** (◓) (see Table 1), uracil (◐), and α-D-glucopyranose triacetate 1,2-(methyl orthoacetate) (◑).

Although the conversion of uridine into its 2′,3′-*O*-isopropylidine derivative did not alter $J_{C2,H1'}$, this coupling constant for 5′-deoxy-5′-iodo-2′,3′-*O*-isopropylidene 2-^{13}C-uridine in $CDCl_3$ was 5.0 Hz. Removal of the *O*-isopropylidene group caused the coupling constant to decrease to 2.9 Hz (acetone-d_6 – D_2O as solvent). It is therefore apparent that substitutional changes on the ribose portion of uridine can substantially influence the ribose-base torsion angle.

In conclusion, the results obtained indicate that measurement of vicinal ^{13}C to H couplings can be expected to provide information on conformational preferences for structural units as depicted in partial structures, **1**, **2**, and **3** and these matters are under active investigation in this laboratory.

We wish to thank the National Research Council of Canada for the support of this research through a grant-in-aid of research to R. U. Lemieux (A-172) and Dr. M. J. Robins for valuable discussions. Thanks are also expressed to G. Bigam, D. Gifford, and T. Brisbane for measurements of spectra.

1. R. U. LEMIEUX, R. K. KULLNIG, and R. Y. MOIR. J. Am. Chem. Soc. **80**, 2237 (1958).

2. R. U. LEMIEUX, R. K. KULLNIG, H. J. BERNSTEIN, and W. G. SCHNEIDER. J. Am. Chem. Soc. **79**, 1005 (1957); **80**, 2237 (1958).
3. M. KARPLUS. J. Chem. Phys. **30**, 11 (1959); J. Am. Chem. Soc. **85**, 2870 (1963).
4. F. A. L. ANET. Can. J. Chem. **39**, 789 (1961).
5. G. J. KARABATSOS. J. Am. Chem. Soc. **83**, 1230 (1961).
6. G. J. KARABATSOS, J. D. GRAHAM, and F. M. KANE. J. Am. Chem. Soc. **84**, 37 (1962).
7. G. J. KARABATSOS and C. F. ORZECH, JR. J. Am. Chem. Soc. **87**, 560 (1965).
8. A. S. PERLIN and B. CASU. Tetrahedron Lett. 2921 (1969).
9. F. J. WEIGERT and J. D. ROBERTS. J. Am. Chem. Soc. **90**, 3543 (1968).
10. R. U. LEMIEUX and M. A. BARTON Can. J. Chem. **49**, 767 (1971).
11. R. U. LEMIEUX and J. C. MARTIN. Carbohydr. Res. **13**, 139 (1970).
12. G. J. KARABATSOS, C. E. ORZECH, JR., and N. HSI J. Am. Chem. Soc. **88**, 1817 (1966).
13. H. G. MANDEL and C. L. BROWN. J. Am. Chem. Soc. **74**, 2439 (1952).
14. K. A. WATANABE and J. J. FOX. J. Heterocycl. Chem. **6**, 109 (1969).
15. A. HAMPTON and A. W. NICHOL. Biochem. **5**, 2076 (1966).
16. BARBARA F. WEST. *In* Synthetic procedures in nucleic acid chemistry. W. W. Zorbach and R. S. Tipson, Eds. Interscience Publishers, New York, N.Y., 1968. p. 313.
17. R. U. LEMIEUX and R. BRUCE. Unpublished results.
18. B. J. BLACKBURN, A. A. GREY, I. C. P. SMITH, and F. E. HRUSKA. Can. J. Chem. **48**, 2866 (1970).
19. P. A. HART and J. P. DAVIS. J. Am. Chem. Soc. **93**, 753 (1971).
20. J. DONAHUE and K. N. TRUEBLOOD. J. Mol. Biol. **2**, 363 (1966).
21. M. SUNDARALINGAM. Biopolym. **7**, 821 (1969).
22. E. A. GREEN, R. SHIONG, R. D. ROSENSTEIN, and D. J. ABRAHAM. Chem. Commun. 53 (1971).
23. A. M. MATHIESON. Tetrahedron Lett. **46**, 4137 (1965).
24. J. S. MARTIN, JUN-ICHI HAYAMI, and R. U. LEMIEUX. Can. J. Chem. **46**, 3263 (1968).

Can. J. Chem. Downloaded from www.nrcresearchpress.com by 210.87.254.6 on 09/05/12
For personal use only.

Can. J. Chem. Downloaded from www.nrcresearchpress.com by 210.87.254.42 on 09/05/12
For personal use only.

Canadian Journal of Chemistry

Published by THE NATIONAL RESEARCH COUNCIL OF CANADA

VOLUME 50 MARCH 15, 1972 NUMBER 6

Thermal Reactions of Sodium Azide in the Presence of Nitric Oxide and Hydrogen[1]

R. A. BACK AND W. NIP[2]

Division of Chemistry, National Research Council of Canada, Ottawa

Received October 12, 1971

Nitric oxide (120 Torr) strongly suppressed the thermal decomposition of NaN_3 at 350 °C. A relatively slow and complex reaction occurred instead, yielding N_2, N_2O, $NaNO_2$, and Na_2O. Isotopic experiments revealed that most of the N_2 (60–80%) came from the azide alone, some from NO alone (10–28%), and a small proportion (5–8%) was mixed, with one atom derived from each reagent. Nitrous oxide initially was derived entirely from NO.

Hydrogen (12–75 Torr) also suppressed the normal azide decomposition at 350 °C. In its place, a rapid reaction occurred, consuming H_2 and NaN_3 and producing N_2, NH_3, Na, and probably $NaNH_2$.

Both systems were complex and probably best described as concerted reactions between the azide and the added gas rather than reactions of NO or H_2 with transient nitrogen species formed in the thermal decomposition of the azide.

L'oxyde nitrique (120 Torr) supprime fortement la décomposition de NaN_3 à 350 °C. Une réaction, relativement lente et complexe se produit plutôt, résultant en N_2, N_2O, $NaNO_2$, et Na_2O. Les expériences isotopiques révèlent que la plus grande partie de N_2 (60–80%) vient de l'azide seul, un peu vient seulement de NO (10–28%), et une petite partie (5–8%) est mélangée, avec un atome venant de chacun des réactifs. L'oxyde nitreux, initialement, est dérivé entièrement de NO.

L'hydrogène (12–75 Torr) supprime aussi la décomposition normale de l'azide à 350 °C. Il se produit plutôt une réaction rapide consommant H_2 et NaN_3 et donnant lieu à N_2, NH_3, Na et probablement $NaNH_2$.

Les deux systèmes sont complexes et probablement mieux décrits comme étant des réactions concertées entre l'azide et le gaz ajouté plutôt que des réactions de NO ou H_2 avec des dérivés d'azote transitoires formés pendant la décomposition thermique de l'azide.

Canadian Journal of Chemistry, **50**, 777 (1972)

Introduction

Current theories of the decomposition of metal azides postulate a reaction between two N_3 species at a surface site, forming three N_2 molecules and leaving behind neutral metal atoms (1–6). This process is highly exothermic, and it has been suggested that electronically excited N_2 might be formed (7, 8). In a long series of experiments, Audubert and his collaborators observed emission of light from decomposing azides, which they attributed to excited N_2 molecules (8–14). Formation of free N_3 or N atoms in the decomposition has also been postulated.

A brief and unsuccessful search was made by Back *et al.* (15) for possible chemical reactions in decomposing azides similar to those of "active nitrogen" produced in an electric discharge. Several metal azides, decomposed in the presence of ethylene, yielded no HCN, and no NH_3 could be detected when barium azide was decomposed at 160 °C in the presence of H_2. The chemistry of possible reactive nitrogen species is now much better understood, and it appeared worthwhile to look again for evidence of their reactions in an azide decomposition. The present paper describes a brief study of the thermal reactions of sodium azide in the

[1]NRCC No. 12321.

[2]NRCC summer student, 1967. Present address: Chemistry Department, University of Toronto, Toronto, Ontario.

Can. J. Chem. Downloaded from www.nrcresearchpress.com by 210.87.254.42 on 09/05/12
For personal use only.

presence of NO and H_2, using ^{15}NO in the former system to determine unambiguously the source of nitrogenous products.

Experimental

Weighed samples of NaN_3 (~50 mg) were placed on a shallow Pyrex dish 1 cm in diameter which rested on the bottom of a 100 ml spherical Pyrex flask attached to a vacuum line. Samples were heated under vacuum at about 200 °C for several hours to remove traces of water. The decomposition was begun by quickly raising a preheated fluidized sand bath around the flask, and stopped by removing it. Between experiments, sodium was removed from the dish and flask by washing with water and dilute acid. The course of the decomposition was followed by pressure measurements with a mercury manometer.

After an experiment with NO present, N_2 was removed through traps at −210 °C and measured in a gas burette. Nitric oxide was then removed at −184 °C, and condensible products remaining were measured in a gas burette. Gas chromatography and mass spectrometry were used to identify and analyse products. When NO was absent, non-condensible gases were removed at −196 °C. In the experiments with H_2, NH_3 was removed and measured in a gas burette or by titration with standard HCL.

Reagent-grade sodium azide (B.D.H.) in the form of a crystalline powder was used without further treatment. Hydrogen of high purity was taken from sealed Pyrex flasks (Airco). Nitric oxide (Matheson) was repeatedly fractionated by bulb-to-bulb distillation to remove other oxides of nitrogen present in small amounts. Nitric oxide and nitrogen containing about 95% N–15 were obtained from Biorad.

Results and Discussion

Preliminary experiments

Sodium azide was decomposed at 330, 340, and 350 °C, initially under vacuum, and in the presence of nitrogen and helium, to test the effect of inert gases on the decomposition. The usual S-shaped pressure–time curves were obtained (Fig. 1); the added gases affected both the induction periods and the maximum rates in much the same way as has been observed previously (2, 3, 6), but had no gross effect on the decomposition. If gross effects are observed with other gases, simple physical causes can thus be ruled out. In all these experiments, the final yield of N_2 was quantitative, leaving no undecomposed azide as has been observed under some conditions below 350 °C (4, 5).

Isotopically natural sodium azide was decomposed at 350 °C in the presence of 20 Torr of $^{15}N_2$, and no isotopic mixing was observed. This ensured that N_2 once produced did not undergo further exchange.

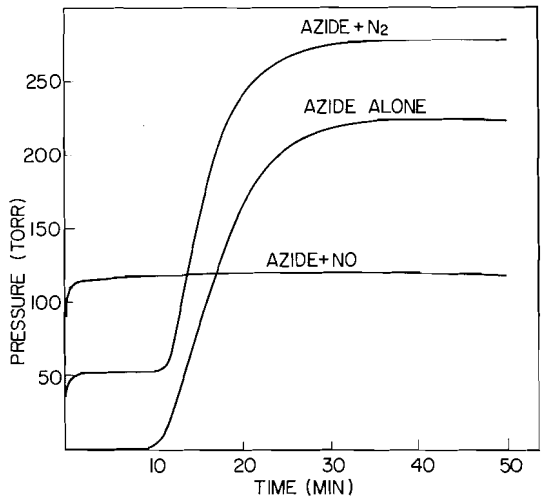

FIG. 1. The effect of N_2 and NO on the thermal decomposition of NaN_3 at 350 °C.

Sodium Azide–Nitric Oxide System

NaN_3 was heated at 350 °C with about 120 Torr of NO for times ranging from 7 to 75 min. The pressure remained virtually constant after the initial thermal equilibration (Fig. 1). Azide and NO were consumed while N_2 and N_2O were evolved in amounts roughly proportional to time, with $[N_2O]$ = about $\frac{2}{3}$ $[N_2]$. The rate of disappearance of azide was very much slower than that in the absence of NO, with typically about 5% decomposition after 75 min and no acceleration with time (*cf.* Fig. 1). If the reaction was stopped by cooling, the NO pumped away, and the residue reheated, for reaction times up to 30 min the residue decomposed exactly like pure NaN_3 under vacuum; for longer times, the residue decomposed more slowly than normal and showed longer induction periods (decomposition of the residue to completion in this way was used to estimate the undercomposed azide).

The NaN_3–NO system was complicated by secondary reaction of sodium with NO. This was studied by first pyrolyzing NaN_3 to completion, then cooling and pumping off the N_2, admitting NO (about 120 Torr), and reheating to 350 °C. A fairly fast reaction occurred, with a drop in pressure, which was complete within 2 or 3 min. NO was consumed, N_2 was evolved, and $NaNO_2$ and Na_2O were produced in very approximately equal amounts. These reactions were apparently complete in 2 or 3 min; at longer times there was a slow steady production

TABLE 1. Isotopic composition of N_2 from $Na^{14}N_3$–^{15}NO reaction

Reaction time (min)	% $^{14}N_2$	% $^{14}N^{15}N$	% $^{15}N_2$	% mixed* N_2
7	61.5	10.4	28.1	7.6
15	74.8	8.3	17.0	6.3
30	79.3	8.1	12.6	6.3
45	80.8	8.5	10.7	6.8
60	80.9	8.2	10.9	6.5
75	78.1	7.3	14.5	5.4

*Mixed N_2 contains one atom from the azide and one from NO and is calculated by correcting the $^{14}N^{15}N$ for isotopic impurity of both reagents.

of N_2O. The speed of reaction of sodium with NO at 350 °C probably ensures that in the decomposition of NaN_3 in the presence of NO, any Na formed would have reacted with NO almost as fast as it was produced. Some of the N_2 and N_2O formed thus probably came from this secondary reaction, as is borne out by the isotopic composition of the products (Table 1). Rapid removal of Na nuclei by reaction with NO probably also accounts for the marked retardation of the azide decomposition.

The isotopic composition of the N_2 formed in the reaction of $Na^{14}N_3$ and ^{15}NO is shown in Table 1 for a range of reaction times. The $^{15}N_2$ presumably came from the reaction of ^{15}NO with sodium or the thermal decomposition of the NO; there is relatively somewhat more at shorter times. In the last column it is seen that significant amounts of "mixed" N_2 were formed, with one atom from the azide and one from the NO.

The composition of the nitrous oxide formed also showed some evidence for isotopic mixing. In this case, however, the trend with reaction time indicated that initially, N_2O was derived almost entirely from the NO alone, suggesting that the mixed N_2O came from a secondary reaction of a product.

The reaction yielding mixed N_2 may be formally written as

$$Na^{14}N_3 + {}^{15}NO \rightarrow {}^{14}N_2 + {}^{14}N^{15}N + (NaO)$$

where (NaO) is a precursor of some more stable oxide of sodium. The amount of $^{14}N_2$ observed was not equal to the mixed N_2, however, but about 10 times larger, the excess representing presumably a more or less simple thermal decomposition of the azide alone. This may have been similar in mechanism to the normal azide decomposition, but strongly retarded by reaction of NO with the sodium nuclei which are thought to be involved in the rapid acceleration of the normal decomposition. The reaction yielding mixed nitrogen may correspond to the occasional interaction of NO with a transient N_3 species produced in the normal decomposition, but could equally well be a quite separate concurrent process. The NaN_3–NO system is clearly too complex to permit detailed conclusions about the mechanism from the present brief study.

Sodium Azide–Hydrogen System

This system was studied at 350 °C with initial pressures of H_2 ranging from about 12 to 75 Torr. Pressure–time plots are shown in Fig. 2.

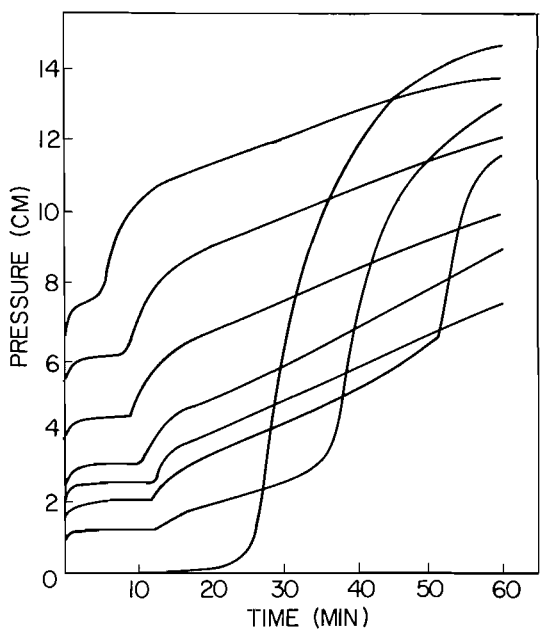

FIG. 2. Pressure changes during the reaction of NaN_3 in the presence of H_2 at 350 °C.

Can. J. Chem. Downloaded from www.nrcresearchpress.com by 210.87.254.42 on 09/05/12
For personal use only.

Can. J. Chem. Downloaded from www.nrcresearchpress.com by 210.87.254.42 on 09/05/12
For personal use only.

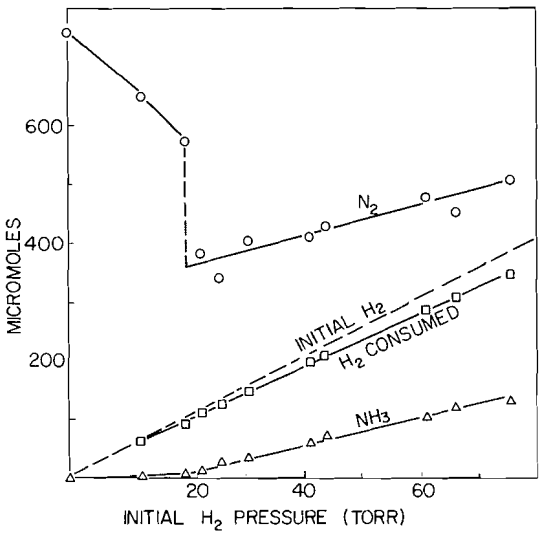

FIG. 3. Gaseous products and H_2 consumption in the reaction of NaN_3 with H_2 at 350 °C after 60 min reaction time.

After 60 min the vessel was cooled and the gases present (N_2, H_2, and NH_3) were removed, measured, and analyzed. Yields of N_2 and NH_3, together with H_2 consumed, are shown in Fig. 3 plotted against initial pressure of H_2, for a constant reaction time of 60 min.

Hydrogen consumption was virtually complete at low pressures, and even at the highest pressure of hydrogen, was almost 90% of that initially present. The NH_3 produced did not correspond to the loss of H_2. Hofmann and Hofmann (16) reported that sodamide, $NaNH_2$, was a major product in the thermal reaction of NaN_3 and H_2, and it very probably accounts for the rest of the hydrogen consumed in the present system. Sodium hydride, which seems to be the only other possible product, can be ruled out by its equilibrium dissociation pressure at 350 °C of about 62 Torr (17, 18), well in excess of the final H_2 pressure in all our experiments. No attempt was made to analyze for $NaNH_2$ or NaH. If it is assumed that NH_3 and $NaNH_2$ account for all the hydrogen consumed, and that no other undetected nitrogenous products were formed, then from the elemental ballances, $NaNH_2 = H_2$ consumed $-\frac{3}{2}NH_3$, and NaN_3 consumed $=\frac{2}{3}N_2 + \frac{1}{3}NaNH_2$. Plots of $NaNH_2$ yields and [NaN_3] consumed calculated from these relations are shown in Fig. 4. Finally, in Fig. 5, yields of NH_3 and $NaNH_2$ are shown as percentages of the azide consumed.

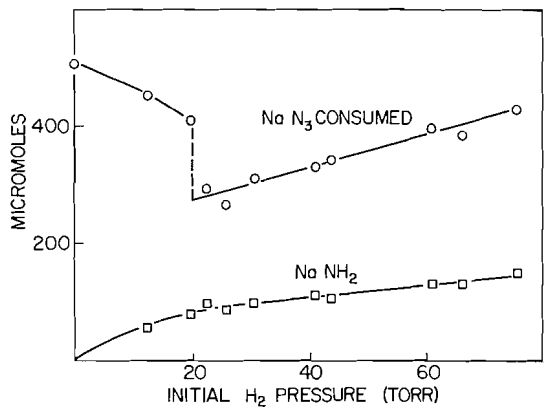

FIG. 4. Calculated amounts of $NaNH_2$ produced and NaN_3 consumed in the reaction of NaN_3 with H_2 at 350 °C after 60 min reaction time.

The pressure–time plots (Fig. 2) show a complex but systematic change with increasing pressure of H_2. After an induction period, a pressure rise ensued which was almost linear at the lowest H_2 pressure; at higher pressures it became resolved into a steep initial increase followed by a slower linear portion. With increasing H_2 pressure, the induction period became progressively shorter and the initial increase more rapid, while the slope of the linear portion remained almost constant. At the two lowest pressures of H_2, the linear increase was terminated by a sharp pressure rise very similar to that of the normal azide decomposition in the absence of hydrogen, but delayed in time. This,

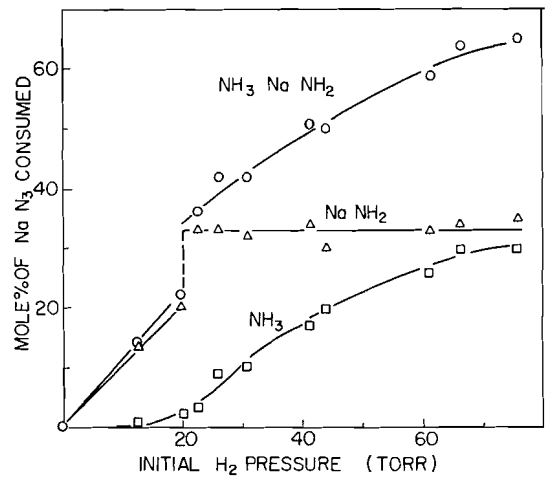

FIG. 5. Yields of NH_3 and $NaNH_2$ expressed as percentage of NaN_3 consumed in the reaction of NaN_3 with H_2 at 350 °C after 60 min reaction time.

Can. J. Chem. Downloaded from www.nrcresearchpress.com by 210.87.254.42 on 09/05/12
For personal use only.

very probably, was in fact the normal azide decomposition, setting in after complete or nearly complete consumption of hydrogen (see Fig. 3). At higher pressures of H_2 this did not occur before the arbitrary termination of the reaction after 60 min, and it is this that accounts for the abrupt changes in some of the product yields between 20 and 30 Torr initial pressures of H_2 (Figs. 3–5).

The processes occurring in the NaN_3–H_2 system may be considered, formally at least, as the sum of the 3 reactions,

$$[1] \qquad NaN_3 \rightarrow Na + \tfrac{3}{2} N_2$$

$$[2] \qquad NaN_3 + H_2 \rightarrow NaNH_2 + N_2$$

$$[3] \qquad NaNH_2 + \tfrac{1}{2} H_2 \rightarrow Na + NH_3$$

In interpreting the pressure–time plots, note that reaction 2 causes no change in pressure. Thus the changes observed can be attributed to reaction 1, augmented by reaction 3 at higher pressures of H_2 as NH_3 becomes an important product. Measured pressure changes after 60 min are in close agreement with those calculated from product analysis and the assumption that reactions 1, 2, and 3 completely describe the system, which suggests that no other reactions of importance were occurring. Some tentative conclusions about the mechanisms of reactions 1, 2, and 3 can be drawn:

(*i*) Reaction 2 is probably a primary reaction occurring at the azide–gas interface.

(*ii*) Reaction 3 appears to be a secondary reaction between H_2 and $NaNH_2$. Sakurazawa and Hara (18) suggested the reaction $NaNH_2 + H_2 \rightarrow NaH + NH_3$, which under our conditions with NaH decomposing rapidly would be equivalent to reaction 3. Reaction of $NaNH_2$ with the Pyrex vessel is also a possible source of NH_3 (18).

(*iii*) Reactions 1 and 2 proceeded concurrently and competitively. The steady increase in the combined yields of $NaNH_2$ and NH_3 with increasing H_2 pressure (Fig. 5) suggests such a competition, and it appears that conversion of the azide to $NaNH_2$ or NH_3 via reactions 2 and 3 would become quantitative at sufficiently high pressure of hydrogen. An alternative to reaction 1 is the thermal decomposition of $NaNH_2$ to give $Na + \frac{1}{2}N_2 + H_2$, but the results do not support a secondary reaction of this sort.

(*iv*) The evidence suggests that reaction 1 is *not* simply the normal azide decomposition, and that reaction 2 is *not* a reaction of H_2 with a transient nitrogen species released in such a decomposition, nor a simple elementary reaction of H_2 with NaN_3, but rather that reactions 1 and 2 occur together in a concerted interdependent manner. The pressure–time plots indicate that an initial nucleation phenomenon is involved, and the mechanism could be quite similar to that of the azide decomposition, but with H_2 participating actively at the reaction sites.

Summary

The present work was undertaken to look for chemical reactions of possible transients generated in the thermal decomposition of NaN_3. Chemical interactions of the azide nitrogen with the reagent gas were indeed observed in both systems, which *could* have proceeded through such transient species. However, the course of the azide decomposition was so modified by both gases that it is difficult to distinguish between reaction of a transient from the decomposing azide and an actual concerted reaction between the azide and the reagent gas. Use of one of the less stable azides, perhaps $Ba(N_3)_2$ or AgN_3, which decomposes at lower temperatures and yields a less reactive metal would probably avoid some of these problems.

1. P. GRAY. Quart. Rev. **17**, 441 (1963).
2. K. TORKAR and A. ISENBERG. Monatsh. Chem. **95**, 1129 (1964).
3. K. TORKAR, O. HEISS, A. ISENBERG, and G. HERZOG. Intern. Symp. React. Solids, 5th, Munich, 1964. 1965. p. 519.
4. R. F. WALKER, N. GANE, and F. P. BOWDEN. Proc. Roy. Soc. A, **294**, 417 (1966).
5. E. A. SECCO. Can. J. Chem. **40**, 2191 (1962).
6. P. W. M. JACOBS and A. R. TARIQ KUREISHY. J. Chem. Soc. 4718 (1964).
7. R. W. NICHOLLS. J. Phys. Chem. **64**, 1760 (1960).
8. R. AUDUBERT. Trans. Faraday Soc. **35**, 197 (1939).
9. R. AUDUBERT and H. MURAUER. C.R. Acad. Sci. Paris, **204**, 431 (1937).
10. R. AUDUBERT. C.R. Acad. Sci. Paris, **204**, 1192 (1937).
11. R. AUDUBERT. C.R. Acad. Sci. Paris, **206**, 748 (1938).
12. R. AUDUBERT and J. MATTLER. C.R. Acad. Sci. Paris, **206**, 1639 (1938).
13. R. AUDUBERT and G. CALMAR. J. Chim. Phys. **54**, 324 (1957).
14. M. A. FINKELSTEIN. J. Chim. Phys. **49**, 185 (1952).
15. R. A. BACK, M. MENZIES, and C. A. WINKLER. Can. J. Chem. **32**, 399 (1954).
16. K. A. HOFMANN and U. HOFMANN. Ber. **59 B**, 2574 (1926).
17. F. G. KEYES. J. Am. Chem. Soc. **34**, 779 (1912).
18. K. SAKURAZAWA and R. HARA. J. Soc. Chem. Ind. Jap. Supp. Bind. **40**, 10 B (1937).

Trapped Electrons and Radicals in γ-Irradiated Propylene Carbonate Glasses[1]

ERIC A. SHAEDE[2]

Chemistry Department, The University of British Columbia, Vancouver 8, British Columbia

Received February 8, 1971[3]

Radicals formed by γ-irradiation of propylene carbonate (PC) glasses at 77 °K were studied by e.s.r. and optical spectroscopy. Trapped electrons were identified by their narrow ($\Delta H_{ms} = 4.5$ G) Gaussian e.s.r. line at $g = 2.0028$ which was completely resolved from the radical spectrum. The trapped electrons were unstable at 77 °K. They decayed fairly rapidly via a process exhibiting non-homogeneous kinetics believed to be reaction with positive ions. The temperature dependence of the e.s.r. spectra of the other radicals formed is discussed although conclusive assignment of the lines could not be made.

Ultraviolet photolysis of the radicals in the irradiated PC glasses produced new species identified as HCO, CO_3^-, and CH_3 by their characteristic e.s.r. spectra. In addition, a complex optical absorption band in the 500–750 nm region was assigned to a combination of the absorption bands of the CO_3^- radical anion and the HCO radical.

Les radicaux issus de l'irradiation γ des verres de carbonate de propylène (CP) à 77 °K, ont été étudiés par r.p.e. et spectroscopie optique. Les électrons piégés ont été identifiés en r.p.e. par leur courbe de gausse fine à $g = 2.0028$ complètement résolue à partir du spectre du radical. Les électrons ainsi piégés sont instables à 77 °K et disparaissent assez rapidement selon un mécanisme laissant supposer une réaction avec des ions positifs, d'après les cinétiques non homogènes observées. La variation en fonction de la température du spectre r.p.e. des autres radicaux formés est discutée bien que l'attribution définitive de ces courbes ne puisse être faite. La photolyse u.v. des radicaux issus de l'irradiation des verres en CP produit de nouvelles espèces identifiées à HCO, CO_3^- et CH_3 par leur spectre r.p.e. caractéristique. De plus, une bande d'absorption complexe dans la région de 500 à 750 nm est attribuée à une combinaison des bandes d'absorption du radical anion CO_3^- et du radical HCO.

Canadian Journal of Chemistry, **50**, 782 (1972)

Introduction

Cyclic organic carbonates are an unusual and interesting group of compounds whose radiation chemistry is virtually unexplored.[4] Propylene carbonate (4-methyl-2-dioxolone, to be referred to as PC for brevity) is the five-membered heterocyclic ring compound illustrated in Fig. 1. It is a very polar aprotic solvent with some extraordinary physical and chemical properties (1). These include a very large liquid range from less than −70 to +240 °C (1*a*), a high dielectric constant of 65 at room temperature (1*b*), a corresponding large permanent dipole moment of 4.94×10^{-18} e.s.u. cm (1*d*), and chemical stability towards strong reducing agents such as the alkali metals (1*g*). Like many other organic compounds with low freezing points, PC forms a glassy solid when rapidly cooled to 77 °K.

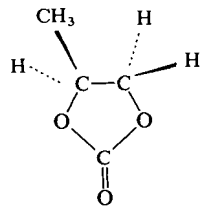

FIG. 1. One of the stereoisomers of propylene carbonate.

Studies of the radiolysis of frozen polar systems have been mainly concerned with water, its solutions, and the alcohols,[5] although ketones and ethers have been examined[6] and the very polar acetonitriles have been investigated (4). The weakly polar frozen systems which have been most extensively studied are the glassy ethers (5).

[1]Prepared from the author's Ph.D. thesis, University of British Columbia, Vancouver, British Columbia, 1971.

[2]Present address: Department of Chemistry, The Ohio State University, 140 W. 18th Avenue, Columbus, Ohio 43210.

[3]Revision received November 8, 1971.

[4]The effects of large doses of high energy radiation on ethylene carbonate and its tetraphenyl derivative have been reported (24). The pulse radiolytic determination of the free-ion yield in PC was recently reported, see ref. 6.

[5]For a recent review on irradiated frozen polar systems, see, for example, ref. 2.

[6]For a recent review on irradiated frozen ketones and ethers, see, for example, ref. 3.

Can. J. Chem. Downloaded from www.nrcresearchpress.com by 210.87.254.40 on 09/05/12
For personal use only.

Can. J. Chem. Downloaded from www.nrcresearchpress.com by 210.87.254.40 on 09/05/12
For personal use only.

In virtually every saturated organic compound which forms a glassy solid, radiolytically generated species identified as trapped electrons have been discovered.[7] These entities are characterized by intense, near-infrared or visible optical absorption spectra and single, narrow, Gaussian-shaped e.s.r. lines near the free-spin g-value. The e.s.r. line is normally quite easily power-saturated (8). Photobleaching of the trapped electrons with light in the region corresponding to their optical absorption also occurs (9). The species may also be eliminated by added solutes of high electron affinity, such as naphthalene (10). Though normally stable for long periods of time in the very polar glasses at 77 °K (2), trapped electrons in the weakly polar systems (such as methyl tetrahydrofuran) are not stable and they decay via processes at least partially attributable to recombination with their parent ions (11).

By analogy with other highly polar compounds, propylene carbonate glasses should also trap electrons with a significant yield. In order to determine whether such trapping occurs, an investigation of the e.s.r. and optical spectra of irradiated PC glasses was undertaken.

Experimental

(i) Materials

Eastman Kodak practical grade propylene carbonate was dried for several days over molecular sieve. The dried solvent was then vacuum fractionated twice using a 4 ft glass column packed with glass helices; the middle 50% was collected each time and the purified solvent was stored under dry helium in a Pyrex dispensing flask. Conventional analyses (*i.e.*, mass spectrum, u.v., n.m.r., and i.r.) indicated that the purified PC was >99% pure.

Methanol was Fisher certified 99.9 mol% grade.

All other chemicals were analytical grade or equivalent.

(ii) Radiation Source

A 4000 C, ^{60}Co Gammacell was used for the irradiations. Doses ranged from 0.1 to 2 Mrads at a dose rate of about 0.3 Mrad/h.

(iii) Glass Preparation

Electron spin resonance measurements were made on glassy balls of PC, 2–3 mm in diameter, prepared by dropping the deoxygenated liquid into a Dewar of liquid nitrogen as described by Alger (12). The balls made in this manner were nearly perfect spheres, completely transparent, free from bubbles and cracks, and mechanically sound.[8]

For the optical studies, the sample of PC was sealed in a 1 cm^2 quartz spectrophotometer cell after thorough degassing by multiple freeze–pump–thaw cycles. When immersed in liquid nitrogen these samples usually became partially polycrystalline. On occasion, however, a reasonably transparent "glass" was formed with relatively few cracks and these samples were used.

(iv) Electron Spin Resonance Measurements

A Varian Associates E-3 spectrometer (x-band) was used for all measurements. The spectra were usually recorded with the sample balls in a quartz Dewar filled with liquid nitrogen. A custom-made quartz variable temperature Dewar cooled by gas flowing from a copper coil immersed in a liquid nitrogen bath was used for temperatures above 77 °K. The sample ball was supported in the center of this Dewar on the tip of a thin evacuated quartz tube which also contained the thermocouple. In practice, the Dewar was first cooled to the minimum possible temperature (about 85 °K) and the gas flow was then momentarily interrupted while a sample ball was quickly transferred from a liquid nitrogen bath and dropped into the top of the Dewar. (Continuous monitoring of the Dewar temperature indicated that during the transfer process the samples were probably warmed to about 95 °K before the gas flow was restarted.)

The magnetic field strength and field scan linearity were calibrated with a proton-probe gaussmeter and the microwave frequency was checked with a Hewlett–Packard model 5255A digital frequency counter. Microwave power levels were not calibrated and the values quoted herein are those read directly from the power attenuator control of the spectrometer.

g-Values were determined using a finely powdered sample of DPPH as the standard, taking $g = 2.0036$.

(v) Optical Measurements

Optical absorption spectra were recorded using a Cary 14 spectrophotometer. The sample cell was maintained at liquid nitrogen temperature in a quartz Dewar with optical windows. Nitrogen bubbling in the Dewar caused some "noise" problems but by using a slow scan rate and maximum pen damping, it was possible to obtain a reasonable signal-to-noise ratio. For measurements in the infrared region, the sample was protected from bleaching by the tungsten i.r. lamp source by placing a thick u.v.–visible cutoff filter (Corning #2-61) between the source and the sample.

Results

(i) Electron Spin Resonance Observations

The e.s.r. derivative spectra measured at 77 °K immediately following irradiation of the PC glasses are shown in Fig. 2. At the lowest power level available (~0.5 mW) a nine-line spectrum was observed (Fig. 2*a*) spread over a region some 130 G wide and centered at the free-spin g-value. Increasing the microwave power level caused the center line, A, to rapidly decrease in intensity until it was completely saturated at ~10 mW (Fig. 2*b*). The broad doublet signal labeled C was also saturated at

[7]For recent reviews on solvated and trapped electrons, see, for example, ref. 7.

[8]Attempts to prepare a glass in small bore quartz tubing always gave partially polycrystalline samples.

Can. J. Chem. Downloaded from www.nrcresearchpress.com by 210.87.254.40 on 09/05/12
For personal use only.

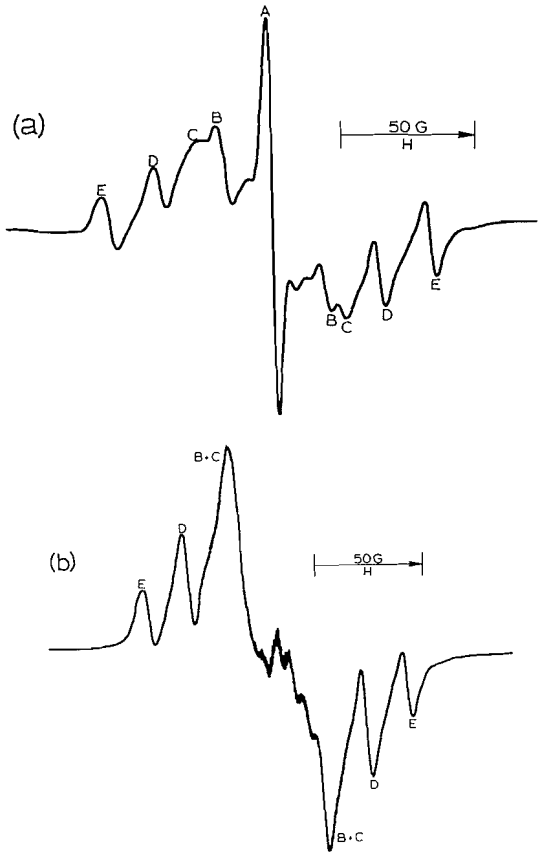

FIG. 2. Electron spin resonance derivative spectra of γ-irradiated glassy propylene carbonate at 77 °K immediately following irradiation. Dose ~0.8 Mrad (*a*) at low microwave power (~0.5 mW), (*b*) at higher microwave power (~10 mW).

this power level. A higher resolution scan of the central resonance line A is shown in Fig. 3 where the line-shape can be seen to be nearly Gaussian. The line-width, as measured between points of maximum slope, was found to be 4.5 ± 0.1 G and the *g*-value of the resonance was determined to be 2.0028 ± 0.0002.

Addition of carbon dioxide at atmospheric pressure to the PC samples did not measurably affect the e.s.r. spectra. However, both iodine and naphthalene removed the central line A as shown in Fig. 4. Iodine also eliminated some of the other paramagnetic species as can be seen in Fig. 4*a*. The naphthalene containing sample appeared dark green in color following radiolysis, indicating the presence of the naphthalene radical anion.

The intensity of the central resonance line A

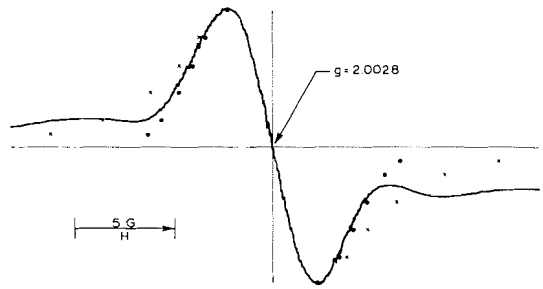

FIG. 3. High resolution e.s.r. scan of line A from Fig. 2*a*. ● = Gaussian, *x* = Lorentzian line-shape.

decreased fairly rapidly with time. Figure 5 shows this isothermal decay at 77 °K for several different initial irradiation times. Here the amplitude of the e.s.r. derivative signal is plotted on a logarithmic scale as a function of time following the end of the irradiation period. Since the line-width remained essentially constant, the amplitude of the derivative signal is a

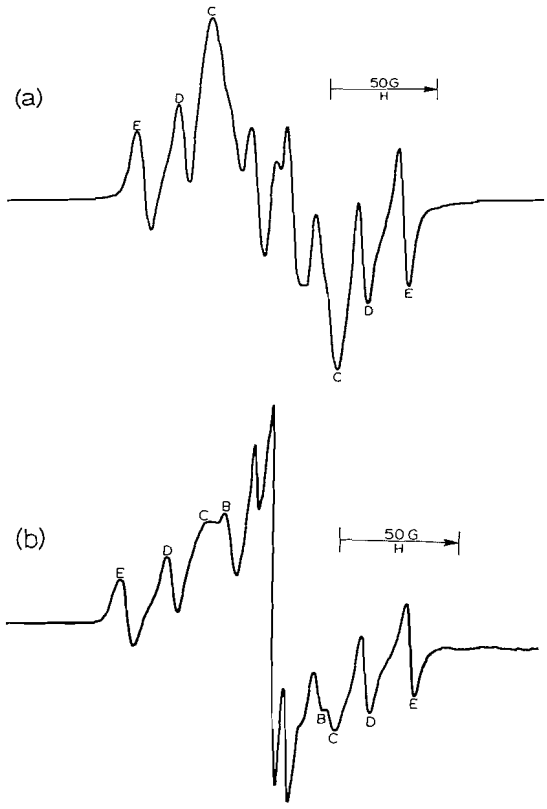

FIG. 4. Electron spin resonance derivative spectra of γ-irradiated glassy propylene carbonate at 77 °K (*a*) containing 0.02 M iodine, (*b*) containing 0.1 *M* naphthalene.

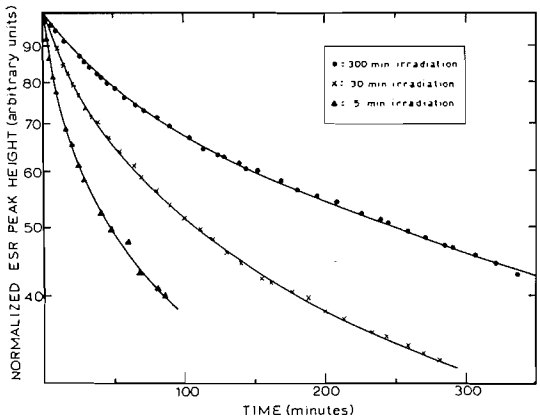

FIG. 5. Natural decay at 77 °K of the intensity of e.s.r. line A of Fig. 2*a* plotted on a logarithmic scale as a function of time after the irradiation. Dose rate ~5000 rads min^{-1}. Data are arbitarily normalized at 0 time.

reasonably good measure of spin concentration. (Note, however, that the sample sizes and cavity positions were not identical for the individual experiments and, therefore, the three sets of data are not inter-comparable on an *absolute* spin concentration basis.) The decay of resonance line A did not result in the production of any new paramagnetic species nor was there any noticeable change in the intensity of the other e.s.r. spectra.

Photolysis experiments performed using a filtered 100 W tungsten lamp showed that the e.s.r. spectra were unaffected by light with $\lambda > 500$ nm. However, the decay of the central resonance line A was significantly accelerated by light in the wavelength range below 500 nm.

Ultraviolet photolysis of unirradiated PC glasses at 77 °K with light from an unfiltered low pressure mercury lamp produced no paramagnetic species. Ultraviolet photolysis of the γ-irradiated sample, however, resulted in a dramatic color change with the samples becoming dark blue. The e.s.r. spectrum observed for the samples exposed only very briefly to the u.v. light is shown in Fig. 6*a*. A new, intense, asymmetric single line, labeled G, appeared downfield at $g \sim 2.015$ and a new asymmetric doublet, labeled H, was generated centered at the free-spin g-value and with hyperfine splitting of about 130 G. After prolonged exposure to the u.v. light, the samples became nearly colorless accompanied by the virtually complete disappearance of the asymmetric singlet G. The intensity of the doublet H was

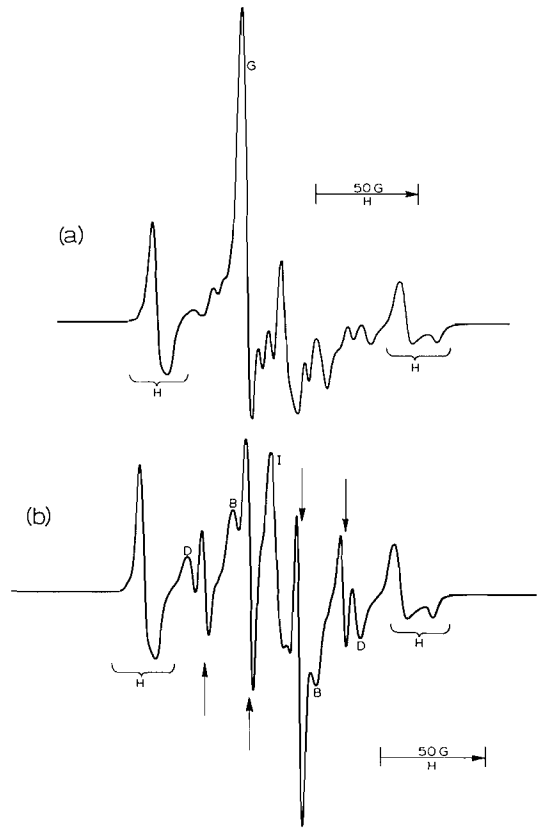

FIG. 6. Electron spin resonance derivative spectra of the γ-irradiated PC glasses at 77 °K (*a*) after brief u.v. photolysis, (*b*) after prolonged, intense u.v. photolysis; arrows indicate methyl radical quartet.

considerably diminished and a new quartet signal was produced as shown by the arrows in Fig. 6*b*. This new resonance was centered at $g = 2.0023$ with hyperfine splitting of 21 ± 2 G and a 1:3:3:1 relative line intensity. (Both signals G and H in Fig. 6*a* could also be bleached using red light from a He/Ne laser.)

When the PC glasses were warmed above 77 °K the central line A disappeared very rapidly apparently by the same mechanism as at 77 °K. At 110 °K the resolution of the remaining e.s.r. lines (B, D, E) improved due to the decay of the broad overlapping signal C. A new paramagnetic species characterized by a multiple line e.s.r. signal was formed as shown in Fig. 7*a*. The e.s.r. parameters of signals B, D, E, as measured from Fig. 7*a* were $g = 2.0023 \pm 0.0003$ and the hyperfine splittings were 42 ± 2, 83 ± 3, and 124 ± 4 G, respectively. All remaining paramagnetic species decayed rapidly above

Can. J. Chem. Downloaded from www.nrcresearchpress.com by 210.87.254.40 on 09/05/12
For personal use only.

Can. J. Chem. Downloaded from www.nrcresearchpress.com by 210.87.254.40 on 09/05/12
For personal use only.

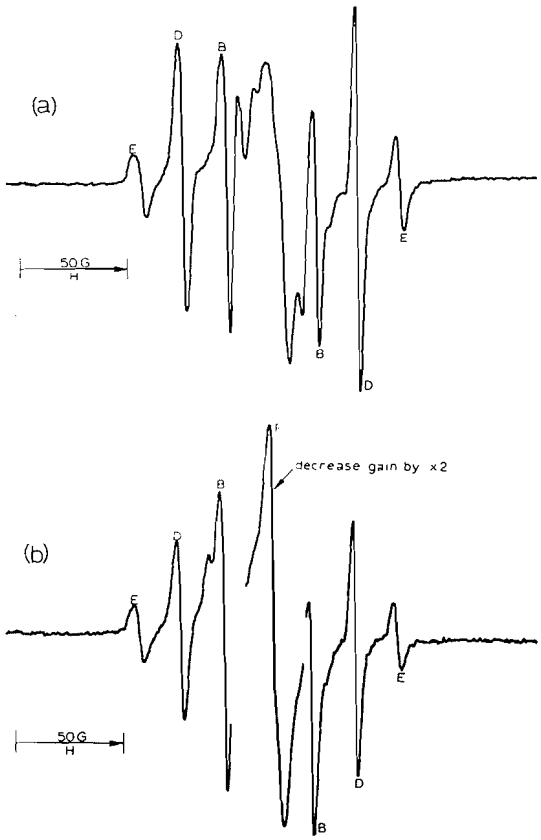

FIG. 7. Electron spin resonance derivative spectra of the γ-irradiated PC glasses (*a*) at ~110 °K after the thermal decay of some radicals, (*b*) at ~110 °K after exposure to u.v. light.

150 °K. Ultraviolet photolysis of the samples at 110 °K, after the disappearance of species C, did not produce the blue coloration or the e.s.r. signals observed after photolysis at 77 °K. Instead, the doublet signal D was observed to decrease in intensity with a concomitant production of a new resonance in the center of the spectrum as shown in Fig. 7*b*.

(ii) Optical Absorption Spectra

γ-Irradiation of the glassy PC at 77 °K imparted only a pale greenish color to the samples. This is in contrast to most other glassy materials which become intensely colored when irradiated at low temperatures (13).

The optical absorption spectrum recorded immediately after irradiation is represented by curve *1* of Fig. 8. There was a strong absorption band in the u.v. with λ_{max} below 280 nm, a

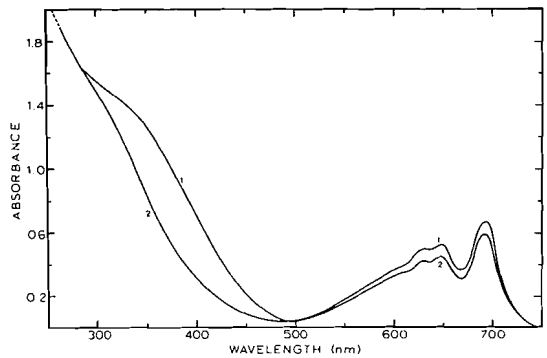

FIG. 8. Optical absorption spectra of γ-irradiated PC at 77 °K (sample partially crystalline) in a 1 cm cell. Curve *1* is the spectrum obtained immediately after the irradiation, curve *2* was obtained 24 h later. Dose ~1.3 Mrad.

shoulder on the u.v. band in the 300–500 nm region, and a complex band showing fine structure between 500 and 750 nm. No evidence was found for any absorption beyond 750 nm into the infrared. After a sample has remained in the dark at 77 °K for 24 h following irradiation, the magnitude of the absorption in the 300–500 nm region was greatly reduced as illustrated by curve *2* in Fig. 8. The intensity of the complex band between 500–750 nm, however, had only slightly decreased during this time.

Ultraviolet photolysis of the γ-irradiated samples caused them to become a deep blue color as noted above. The coloration was due to a very large increase in the intensity of the 500–750 nm absorption band, which is shown in more detail in Fig. 9.

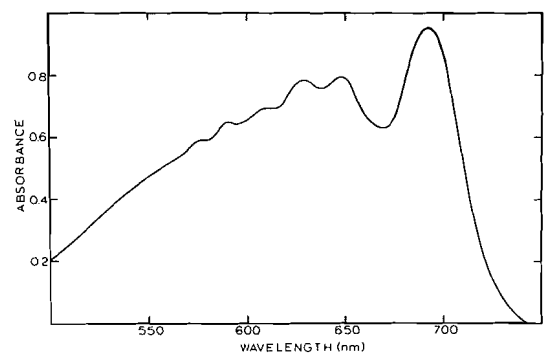

FIG. 9. Absorption spectrum in the 500–750 nm region for γ-irradiated PC after brief u.v. photolysis at 77 °K. The spectrum is attributed to a combination of the HCO and CO_3^- radical absorption bands.

Can. J. Chem. Downloaded from www.nrcresearchpress.com by 210.87.254.40 on 09/05/12
For personal use only.

Discussion

There are three different species which could give rise to the central narrow e.s.r. line A shown in Figs. 2*a* and 3. These are (*i*) trapped electrons, (*ii*) CO_2^- radical ions formed either from traces of CO_2 impurity or via molecular decomposition processes, and (*iii*) molecular anions of propylene carbonate (PC^-) produced by electron attachment to the carbonyl group. The latter two possibilities may be eliminated on the basis of the following arguments.

The CO_2^- radical ion has been observed in a number of irradiated crystalline systems (14) and it has been shown to be the species responsible for a narrow e.s.r. line observed in 3-methyl pentane (15). The narrow, easily saturated e.s.r. line in the irradiated PC glasses and its photobleaching characteristics are in fact similar to those observed by Johnson and Albrecht for CO_2^- in the 3-methyl pentane glasses (15). However, stringent precautions were taken in the preparation of the PC samples to avoid CO_2 contamination. In addition, CO_2 added to the samples at atmospheric pressure did not affect the e.s.r. spectrum, whereas Johnson and Albrecht found a very substantial increase in the relative intensity of the e.s.r. line. This leaves the possibility that CO_2^- may have been formed as a product of the radiation decomposition processes, most probably via a molecular anion such as PC^-. Although this is conceivable, there are two additional arguments against the involvement of CO_2^- in this system. The *g*-value of 2.0028 ± 0.0002 and the isotropic Gaussian line-shape of the narrow resonance in γ-irradiated PC are substantially different to those reported for the CO_2^- resonance in crystalline systems where an anisotropic line-shape is observed with $g_{av} \sim 2.001$ (14). (Unfortunately, Johnson and Albrecht did not report this information for CO_2^- in the glassy 3-methyl pentane.) In addition, the relatively fast spontaneous decay of the species is inconsistent with it being a molecular anion since molecular mobility should be very limited in the low temperature glass.

A molecular anion of PC might be formed in the irradiated glass by electron attachment to the carbonyl group. Indeed, such electron attachment is commonly observed in irradiated ketones (16). However, there is evidence that the carbonyl group in PC is not a typical "ketone type" $\rangle C{=}O$, but rather the double bond character should be considered as partially delocalized over the entire carbonate group. This is evident in the fact that PC does not show the characteristic $n \rightarrow \pi^*$ carbonyl band in its u.v. absorption spectrum. In addition, PC is unreactive with the alkali metals (1*g*) which suggests that electron attachment to the $\rangle C{=}O$ is not favored.

The observed properties of the e.s.r. line A clearly discount the possibility of it being due to a species such as PC^-. The small γ-proton hyperfine interactions and anisotropy due to confining the unpaired electron to a molecular orbital should result in a line-width much greater than the 4.5 G observed. In addition, one would expect the resonance of a large molecular anion to not saturate at such low power levels since it would be more effectively coupled to the environment. The natural decay of the species (which, as will be shown later, is characterized by non-homogeneous second-order kinetics) is also inconsistent with a large molecular anion.

The observed e.s.r. signal is, however, exactly that expected for trapped electrons in an organic glass. Trapped electrons produced in other organic glasses at liquid nitrogen temperature are characterized by narrow Gaussian e.s.r. lines near $g = 2.0023$ which are easily power saturated (7, 8). Thus, having eliminated the other likely candidates, it seems reasonable to assign the narrow line at $g = 2.0028$ to trapped electrons in the PC glasses.

Iodine and naphthalene are both known to be good electron scavengers (10) and thus they removed the trapped electron resonance as shown in Fig. 4. The absence of any e.s.r. resonance due to the expected product I_2^- (17) may be explained on the basis of a fast dissociation reaction to form an iodine atom and I^-. The iodine atom may then react with other radicals to cause the observed additional modifications to the e.s.r. spectrum. Naphthalene has been used as a trapped electron scavenger in other systems (10*b*) where the reaction produces the naphthalene radical anion (or its protonated form). In the present case the observed green color and the multiplet e.s.r. signal (Fig. 4*b*) indicate the presence of the naphthalene anion.

Having established that trapped electrons are formed in the irradiated PC glasses, the question of their optical absorption spectrum then arises.

Can. J. Chem. Downloaded from www.nrcresearchpress.com by 210.87.254.40 on 09/05/12
For personal use only.

In all other systems studied to date, trapped and solvated electrons are observed to have a broad asymmetric optical absorption band in the visible or near infrared (7). As will be shown later, the complex absorption band observed in the 500–750 nm region in PC (Figs. 8 and 9) can be attributed to a combination of the absorption bands of the CO_3^- and HCO radicals. Since no absorption was observed in the infrared region, the only remaining alternative for the trapped electron band is the absorption in the 300–500 nm region. The spectrum obtained by subtracting curve *2* from curve *1* of Fig. 8 is a broad band with a maximum at about 370 nm (3.4 eV) and a half width of approximately 0.9 eV. Because light in this wavelength range caused accelerated decay of the trapped electrons, it is reasonable to assign the absorption band to trapped electrons. Unfortunately, experimental difficulties prevented a detailed study of the decay of the optical band at 370 nm. Thus, confirmation of the assignment by a correlation of the optical decay with that observed by e.s.r. was not possible. While a trapped electron absorption band with λ_{max} in the violet region is unusual, it is not inconsistent with the physical properties of the solvent. On the basis of the high dielectric constant of PC (65 at room temperature, increasing to >90 below −60 °C (*1b*)) one would predict an absorption band for a solvated electron in the visible region and the trapped electron band should be blue shifted relative to that of the solvated species. Ekstrom (*7a*) has presented some data for trapped electrons in a glass composed of formamide +15% water at 77 °K where an absorption with a λ_{max} near 400 nm was apparently observed. (Pure formamide has a dielectric constant of 109.) In addition, if the rough correlation between room temperature dielectric constant and the optical absorption maxima observed for trapped electrons in a variety of organic glasses at 77 °K (*7a*) is extended, then a λ_{max} in the vicinity of 400 nm may be expected for trapped electrons in PC.

The apparent instability of the trapped electrons in the PC glasses is particularly surprising since electrons in most other polar glasses, for example the alcohols, are indefinitely stable (2). As shown in Fig. 5, the electrons decay rapidly with the *apparent* rate decreasing

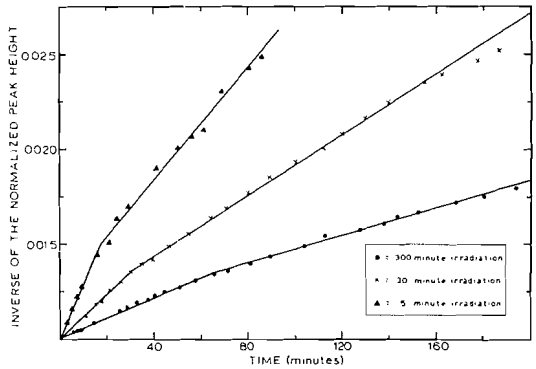

FIG. 10. Second-order kinetic analyses of the decay data from Fig. 5.

with increasing absorbed dose. The decay process is obviously not a simple electron attachment reaction with one of the solvent molecules surrounding the trapping site (as might be expected) since the decay curves are not linear on the logarithmic plot in Fig. 5, nor is any new paramagnetic species formed. The spontaneous decay is best rationalized on the basis of a non-homogeneous second-order reaction between the trapped electrons and positive ions. Second-order analyses of the data from Fig. 5 are presented in Fig. 10 where the inverse of the e.s.r. derivative signal amplitude is plotted as a function of time. The three sets of data all show two linear portions; an initial short period of faster decay, followed by a region of slower decay which is maintained for several half lives. From the results of the 5 min irradiation experiment, it is seen that nearly 50% of the electrons have decayed within 15 min after the end of the irradiation. Therefore, a large fraction of those produced during the early stages of the 30 and 300 min irradiations had already reacted before the irradiation was completed. Thus, the initial transient features indicated in the second-order plots (Fig. 10) are likely caused by the fast reaction of "short-lived" species formed during the latter stages of the irradiation period. These electrons may be those trapped so close to a positive ion that they are already effectively "captured" and thus, have no choice but to recombine. The remainder of the electrons are sufficiently distant from a positive ion that the trap energy is comparable to, or greater than,

Can. J. Chem. Downloaded from www.nrcresearchpress.com by 210.87.254.40 on 09/05/12
For personal use only.

the Coulombic forces and therefore they have a relatively long lifetime governed mainly by diffusion.

It is difficult to determine whether the initial fast decay of the majority of the electrons occurs by the recombination process discussed above. In some of the glassy ethers, the trapped electrons also appear to be predestined to react with a particular positive ion (11) and thus, the decay rate is independent of the total number of positive charges present in the system. As a result the normalized decay curves for samples irradiated with different doses are superimposable over a considerable time range and dose variation. In the present system, it was not possible to compare the data in this manner since absolute spin concentrations could not be determined. In addition, the decay "half-lives" were shorter than the irradiation periods so that a clear interpretation of the kinetics of the fast decay was not possible.

One important implication of the instability of the electrons was to prevent an accurate measurement of their yield. In an early attempt to estimate $G(e_t^-)$, the intensity of the e.s.r. signals of the trapped electron in PC and CH_2OH radicals produced in irradiated methanol glasses were compared under carefully controlled conditions to eliminate sample size and cavity position factors. This crude comparison indicated a yield of trapped electrons of approximately $G(e_t^-) = 0.3$. However, because a long irradiation time was necessary to obtain a reasonable signal level in the small samples, the G value obtained is undoubtedly much smaller than the primary yield of electrons (perhaps by as much as a factor of 10) since a large fraction of them would have decayed during the irradiation period. In addition, the intensity of the e.s.r. line in PC may be substantially less than the "true" value because of partial microwave power saturation. In comparison with trapped electrons in other systems, 0.5 mW is a high power level and this could be causing some decrease in line intensity. γ-Radiolysis scavenger experiments (18) and pulse radiolysis studies (6) on liquid propylene carbonate have indicated that the yield of solvated electrons (or possibly reactive molecular anions) is about $G = 2$. One would expect an even higher total yield of trapped electrons in the glassy solid.

The other radicals produced by the radiolysis with significant yields could not be identified. As was shown in Fig. 2*a*, these radicals gave rise to an eight-line e.s.r. spectrum centered at the free-spin *g*-value. The relative ease of power saturation and the thermal instability of the broad doublet labeled C suggest that this resonance is due to a separate species. The hyperfine splitting of 58 ± 3 G implies the strong interaction of a single proton and the free-spin *g*-value suggests an electron excess radical.[9] The other six lines, labeled B, D, E in the spectrum illustrated in Fig. 2*a*, were shown to be associated with three independent radicals. Species B was removed by iodine as illustrated in Fig. 4*a* and it also decayed slowly over a period of several hundred hours. Ultraviolet photolysis of the irradiated samples at 110 °K preferentially removed species D and produced a new radical giving a single e.s.r. line as illustrated in Fig. 7*b*. Because of the apparent large doublet hyperfine splittings (42 ± 2, 83 ± 3, and 124 ± 4 *G* for B, D, E, respectively), the free-spin *g*-value and the isotropic line-shapes, these e.s.r. signals cannot be attributed to simple radicals such as HCO, HCO_2, OH, etc. In fact, it is difficult to even speculate as to their identity. The total radical yield as estimated by comparison with the CH_2OH radical generated in irradiated methanol was $G(R) \sim 4$.

Ultraviolet photolysis of the irradiated glasses at 77 °K did, however, produce radicals which could be identified. The e.s.r. spectrum shown in Fig. 6*a* may be interpreted as follows. The intense asymmetric line labeled G appeared to be formed as a result of the photolysis of the radical responsible for the broad doublet labeled C in Fig. 2*a*. In addition, this new radical was at least partially responsible for the blue coloration of the photolyzed sample. These inferences were supported by the fact that neither the e.s.r. line nor the blue color could be generated by u.v. photolysis of the samples at 110 °K when the broad doublet had been thermally removed. The blue coloration was due to a very large increase in the intensity of the 500–750 nm absorption

[9]The radical $CH_3\dot{C}OCH_2OC{=}O$, as suggested by one of the referees, could account for the observed broad doublet since in the rigid planar structure one of the β-protons could have a strong interaction with the unpaired electron.

band which was shown in Fig. 9. On the basis of the e.s.r. line at $g \sim 2.015$ and the position of the absorption band, the presence of the CO_3^- radical ion was indicated. CO_3^- has been observed spectroscopically in aqueous solution where a broad asymmetric optical absorption with $\lambda_{max} \sim 600$ nm was observed on flash photolysis or pulse radiolysis of carbonate solutions (19). Ershov *et al.* (20) reported essentially the same optical spectrum for CO_3^- produced in frozen aqueous carbonate glasses at 77 °K and also attributed an asymmetric e.s.r. line at $g_{av} = 2.011$ to the species.

It is therefore evident that the fine structure on the 500–750 nm band is really absorption due to a separate species superimposed on the broad structureless band of CO_3^-. The species believed responsible for these narrow bands is the HCO radical. The presence of HCO was confirmed by the asymmetric doublet e.s.r. signal, labeled H in Fig. 6*a*. This doublet was identical to that reported for HCO in other media (21) and to that observed for HCO radicals generated by u.v. photolysis of γ-irradiated methanol glasses (22). The HCO is also known to show at least seven narrow optical absorption bands in the region between 500 and 700 nm when trapped in a carbon monoxide matrix at 20 °K (23). Although the positions of the bands observed in PC at 77 °K (~690, ~650, ~630, ~610, ~590, and ~575 nm) do not agree precisely with those reported for the CO matrix (670, 635, 605, 579, 555, 533, and 510 nm) the differences are probably caused by the overlapping of the CO_3^- spectrum and rather poor resolution.

The presence of the weak optical absorption due to the CO_3^- and HCO radicals in the irradiated samples before u.v. photolysis (Fig. 8) indicates that these radicals may be formed with a small yield during the primary radiolysis processes. (The initial yield must be relatively small since the e.s.r. signals of these species are not observed in the original samples (Fig. 2*a*).) Alternatively, the small yield of the radicals may be the result of photolysis caused by Cerenkov radiation generated in the sample and liquid nitrogen.

If the samples were exposed to intense u.v. light for a long period of time, the CO_3^- radical was eventually bleached out and a new radical characterized by a quartet e.s.r. signal centered at the free-spin g-value with 21 ± 2 G hyperfine splitting was formed as indicated in Fig. 6*b*. This new e.s.r. signal can be assigned to the methyl radical (2, 22). This assignment is supported by the observation that these radicals were relatively unstable in the matrix at 77 °K and decayed rapidly over a period of a few hours.

Financial support of the National Research Council of Canada is gratefully acknowledged. The author is indebted to Professors D. C. Walker and F. G. Herring for helpful discussions and, in particular, thanks Mr. N. S. Dalal for assistance in the operation of the e.s.r. spectrometer and in the interpretation of the spectra.

1. (*a*) Propylene carbonate, Technical bulletin. Jefferson Chemical Company, Inc., Houston, Texas, U.S.A. (*b*) L. SIMERAL and R. L. AMEY. J. Phys. Chem. **74**, 1443 (1970). (*c*) H. FINEGOLD. J. Phys. Chem., **72**, 3244 (1969). (*d*) R. KEMPA and W. H. LEE. J. Chem. Soc. 1963 (1958). (*e*) J. P. GOSSE and B. ROSE. Compt. Rend. Acad. Sci. Paris, Ser. C, **267**, 927 (1968). (*f*) R. F. NELSON and R. N. ADAMS. J. Electroanal. Chem. **13**, 184 (1967). (*g*) W. S. HARRIS. Ph.D. Thesis, University of California, Los Angeles, California, 1958; Report #UCRL-8381.
2. L. KEVAN. Actions Chimiques et Biologigues des Radiations, **13**, 57 (1969).
3. J. TEPLY. Radiat. Res. Rev. **1**, 361 (1969).
4. (*a*) M. A. BONIN, K. TAKEDA, K. TSUJI, and F. WILLIAMS. Chem. Phys. Lett. **2**, 263 (1968). (*b*) M. A. BONIN. Ph.D. Thesis, University of Tennessee, Knoxville, Tennessee, 1969. (*c*) R. J. EGLAND and M. C. R. SYMONS. J. Chem. Soc. A, 1326 (1970).
5. W. H. HAMILL. *In* Radical ions. Edited by E. T. Kaiser and L. Kevan, Interscience, New York, N.Y. 1968.
6. E. HAYON. J. Chem. Phys. **53**, 2353 (1970).
7. (*a*) A. EKSTROM. Radiat. Res. Rev. **2**, 381 (1970). (*b*) K. EIBEN. Angew. Chem. Int. Engl. Ed. **9**, 619 (1970).
8. D. R. SMITH and J. J. PIERONI. Can. J. Chem. **43**, 876 (1965).
9. P. J. DYNE and O. A. MILLER. Can. J. Chem. **43**, 2696 (1965).
10. (*a*) C. CHACHTY and E. HAYON. Nature, **200**, 59 (1963). (*b*) F. S. DAINTON, J. P. KEENE, T. J. KEMP, G. A. SALMON, and J. TEPLY. Proc. Chem. Soc. 265 (1964).
11. J. E. WILLARD. *In* Fundamental processes in radiation chemistry. Edited by P. Ausloos. Interscience, New York, N.Y. 1968.
12. R. S. ALGER. Electron paramagnetic resonance—techniques and applications. Interscience, New York, N.Y. 1969.
13. R. S. ALGER, T. H. ANDERSON, and L. A. WEBB. J. Chem. Phys. **30**, 695 (1959).
14. (*a*) P. W. ATKINS and M. C. R. SYMONS. The structure of inorganic radicals. Elseview, Amsterdam. 1967. (*b*) R. A. NAZHAT, N. B. NAZHAT, P. N. MOORTHY, and J. J. WEISS. J. Phys. Chem. **74**, 1901 (1970).

Can. J. Chem. Downloaded from www.nrcresearchpress.com by 210.87.254.40 on 09/05/12
For personal use only.

15. P. M. JOHNSON and A. C. ALBRECHT. J. Chem. Phys. **44**, 1845 (1966).
16. T. SHIDA and W. H. HAMILL. J. Am. Chem. Soc. **88**, 3683 (1966).
17. E. BOESMAN and D. SCHOEMAKER. J. Chem. Phys. **37**, 671 (1962).
18. E. A. SHAEDE. Ph.D. Thesis. University of British Columbia, Vancouver, British Columbia. 1971.
19. (*a*) G. E. ADAMS, J. W. BOAG, and B. D. MICHAEL. Proc. Chem. Soc. 411 (1964). (*b*) D. BEHAR, G. CZAPSKI, and I. DUCHOVNY. J. Phys. Chem. **74**, 2206 (1970).
20. B. G. ERSHOV, O. F. KHODZHAEV, and A. K. PIKAEV. High energy chemistry, **2**, 29 (1968). (A translation of Khimiya Vysokikh Energii, **2**, 35 (1968).)
21. (*a*) J. A. BRIVATI, N. KEEN, and M. C. R. SYMONS. J. Chem. Soc. 237 (1962). (*b*) F. J. ADRIAN, E. L. COCHRAN, and W. A. BOWERS. J. Chem. Phys. **36**, 1661 (1962).
22. P. J. SULLIVAN and W. S. KOSKI. J. Am. Chem. Soc. **85**, 384 (1963).
23. G. E. EWING, W. E. THOMPSON, and G. C. PIMENTEL. J. Chem. Phys. **32**, 927 (1960).
24. U.S. Atomic Energy Report No. NYO-3410-2.

Can. J. Chem. Downloaded from www.nrcresearchpress.com by 210.87.254.40 on 09/05/12
For personal use only.

Conformational Terminology for Crystalline Cellulose

P. R. SUNDARARAJAN[1] AND R. H. MARCHESSAULT

Département de Chimie, Université de Montréal, C.P. 6128, Montréal

Received August 26, 1971

Two different crystalline models of cellulose have received attention from crystallographers: the "straight chain" model of Meyer and Misch and the "bent chain" model of P. H. Hermans. We have examined these models and have given a mathematical interpretation of each in terms of the conformational angles ϕ and ψ and the glycosidic angle τ. For a given geometry of the glucose residue, the "straight chain" corresponds to a unique value of τ; for a value of τ greater than the unique value, two "bent chains" are possible, one allowing an intramolecular hydrogen bond (O-3...O-5′) and the other not. It is suggested that the former only be referred to as the Hermans conformation.

Au cours des années, les cristallographes ont proposé deux modèles différents pour la chaîne cellulosique: un modèle à chaîne "droite" et un modèle à chaîne "plissée". On a maintenant donné une interprétation mathématisée à ces deux modèles en se référant aux angles conformationnels: ϕ et ψ et l'angle glycosidique τ. Pour une géométrie fixe du résidu glucosidique, la chaîne "droite" correspond à une valeur unique de τ; pour un τ plus élevé que cette valeur unique, on retrouve deux chaînes "plissées" mais seulement une d'elle permet une liaison hydrogène intramoléculaire (O-3...O-5′). On propose que seulement cette dernière soit appelée la conformation de Hermans.

Canadian Journal of Chemistry, **50**, 792 (1972)

In the crystalline state (1) the β,D $(1 \rightarrow 4')$ glucan, cellulose, has an axial repeat of 10.3 Å. In 1937, Meyer and Misch (2) proposed a crystal structure based on the stereochemical knowledge of that time wherein a twofold screw axis ran along the cellulose chain and all glycosidic oxygens were coplanar. However, it was eventually realized (3) that this structure implied too close a contact between the C-6 and O-2′ atoms of contiguous residues. For this reason the "bent" chain conformation for the cellulose molecule, originally proposed by Hermans (4), because it allowed a favorable hydrogen bond between the O-3 hydroxyl of one residue and the O-5′ ring oxygen of the next, was favored by contemporary workers. The presence of this type of hydrogen bond is in keeping with the most straightforward interpretation of the polarized infrared spectra of cellulose (5).

Modern workers in the field of cellulose structure have had the benefit of accurate crystallographic data on simple organic molecules in general and carbohydrates in particular (6). This has provided information on bond lengths and bond angles of a kind which was not available to early workers. In addition, high speed computers have permitted a model building approach wherein the whole of conformational space is explored by rigid body transformation methods (7). This involves the assumption of rigid glucopyranose residues joined by a suitable β-glucoside bond angle with two rotational angles ϕ and ψ (rotation about C-1—O and O—C-4, respectively) which define all possible conformations for two contiguous glucose residues (8–9). When a chain is generated with ϕ,ψ constant for all pairs of neighboring glucose residues then a regular conformation is obtained. Thus each point in ϕ,ψ space defines a conformation where glucose residues occupy equivalent positions about an axis.

Various workers have reported conformational analyses of this type and Fig. 1 shows the contours of iso-n and iso-h for cellulose where n is the number of residues per turn of the helix and h is the advance per residue projected along the helix axis.

From this figure, it is seen that there are two positions on the (ϕ,ψ) map, where the chain with parameters $n = 2$ and $h = 5.15$ Å occurs. Of these, the position C_1 has been associated (8, 9) with the Hermans type of conformation since the C_1 position on the (ϕ,ψ) map allows the intramolecular hydrogen bond mentioned above. The position C_2 was claimed (8, 9) to be similar to the Meyer–Misch type of chain

[1]Present address: Department of Chemistry, Stanford University, Stanford, Calif. 94305.

Can. J. Chem. Downloaded from www.nrcresearchpress.com by 210.87.254.42 on 09/05/12
For personal use only.

Can. J. Chem. Downloaded from www.nrcresearchpress.com by 210.87.254.42 on 09/05/12
For personal use only.

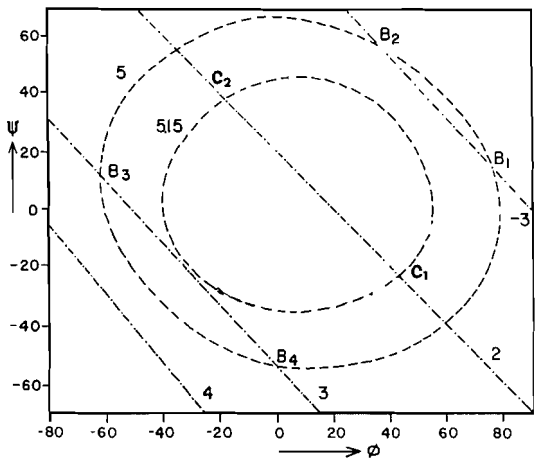

FIG. 1. Curves of *iso-n* (·-·-·) and *iso-h* (---) for the β,D(1→4′)glucan. C_1,C_2: positions of the chain with two-fold screw axis and a repeat of 10.3 Å. B_1,B_2: positions of the chain with threefold screw axis and a repeat of 14.85 Å (left-handed). B_3,B_4: same as B_1,B_2 but right-handed (taken in part from ref. 10).

(M.M. chain hereafter) due to the close contact between C-6 and O-2′ atoms, in position C_2 on the (ϕ,ψ) map. We have now examined the M.M. type of chain and deduced a few conclusions regarding the role of the angle (τ) at the bridge oxygen atom in the conformations of the cellulose chain.

The analysis of the coordinates given by M.M. shows that a value of 105° was used for the angle C—O—C at the bridge oxygen atom, which is close to the value of the angle H—O—H in water. The C-6 and O-2′ atoms are 2.68 Å apart, which according to the contact distance criterion (7) is only 0.02 Å less than the extreme limit. Further, in terms of the convention used in Fig. 1 for the conformational angles (ϕ,ψ), this structure corresponds to (ϕ,ψ) = (0°,0°). Fig. 2*a* shows the curve of $n = 2$ obtained using the M.M. coordinates and a value of 105° for τ. It is to be noted that while in Fig. 1 there are two positions (C_1 and C_2) where $n = 2$ and $h = 5.15$ Å are possible, in Fig. 2*a*, there is only one position where such a chain can be built mathematically. Using the M.M. coordinates, and a value of 112° for τ (Fig. 2*b*) there are two solutions possible for the chain, as observed in Fig. 1. Thus it is clear that while for $\tau = 112°$, there are two solutions of (ϕ,ψ) with $n = 2$, $h = 5.15$ Å they reduce to a unique solution as τ is reduced to a value of 105°. Among the two solutions for $\tau = 112°$, the position C_1 favors the O-3...O-5′ type of hydrogen bonding while the position C_2 gives rise to a close contact between C-6 and O-2′ atoms. For τ below the critical value of 105°, it would be impossible to construct a chain with the parameters $n = 2$, $h = 5.15$ Å. For the atomic parameters used for Fig. 1, the critical value of τ (τ_c) (below which $n = 2$, $h = 5.15$ Å would be impossible) turns out to be 109.5°.

Figure 3 shows the cellulose chain conformations in projection. Figure 3*a*, with $\tau_c = 105°$, depicts the straight chain conformation. The

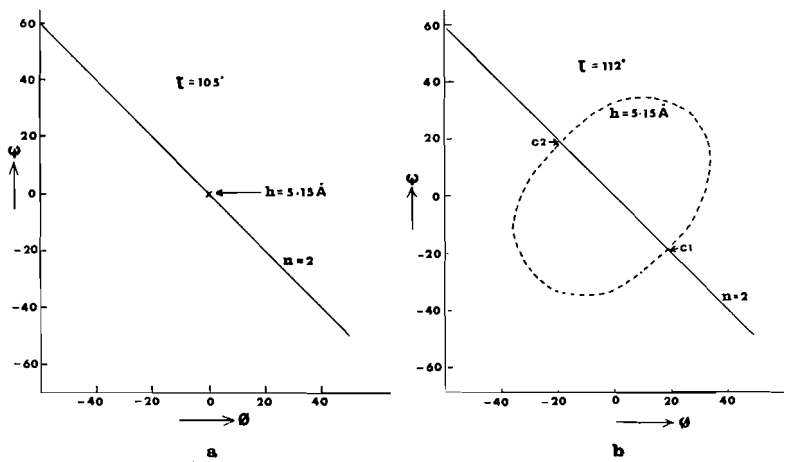

FIG. 2. Curves of *iso-n* = 2 (—) and *iso-h* = 5.15 Å (---) with the M.M. geometry for the glucose residue. (*a*) With $\tau = 105°$, as in the original M.M. structure. (*b*) With $\tau = 112°$.

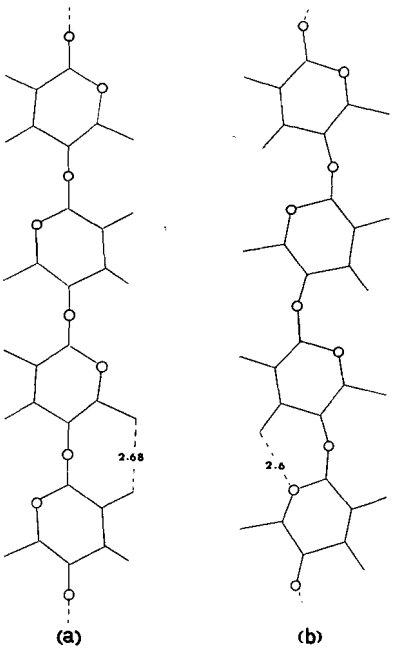

FIG. 3. Projection of the cellulose conformations: (*a*) "Straight chain" conformation, with $(\tau,\phi,\psi) = (105°,0°,0°)$ with M.M. geometry for the glucose residue. (*b*) "Hermans type" of bent chain conformation with $(\tau,\phi,\psi) = (117.5°,-40°,-20°)$ with the geometry of the glucose residue as in ref. 9.

straight chain appearance is due to the fact that $(\phi,\psi) = (0°,0°)$ and the atoms C-1, O-1, O-4, and C-4 of all the residues are coplanar. However, the bridge oxygens do not lie on the chain axis, as is obvious from Fig. 4*b* of ref. 2. Figure 3*b* shows the conformation C_1, which is similar to the Hermans bent chain conformation. The bent chain appearance is due to the slight rotation of the residues around the bonds C-1—O and O—C-4′ away from $(\phi,\psi) = (0°,0°)$ which is required by the fact that the bridge oxygen angle is not equal to τ_c. Thus the term straight chain conformation applies only to that conformation of the cellulose chain in which the τ is equal to τ_c and $(\phi,\psi) = (0°,0°)$. The position C_1 may be said to correspond to a "Hermans type of bent chain" conformation (Hermans conformation) and the position C_2 may be termed the "alternate bent chain" conformation. Only if C_1 and C_2 merge at $(\phi,\psi) = (0°,0°)$ can the chain be said to have the "straight chain" conformation.

The value of τ_c for a given n and h depends on the atomic parameters chosen for the monomer. While τ_c is 105° for the geometry used by Meyer and Misch, it turns out to be 109.5° for the geometry of the residue used by Gabbay *et al.* (10). Figure 1 also shows that for the chain with $n = 3$ and $h = 5$ Å, like the β,D $(1 \rightarrow 4')$ xylan, there are two positions B_3 and B_4 which represent right-handed helices and two positions B_1 and B_2 for left-handed. It was observed that on reducing the angle τ from 117.5° to $\tau = 115°$, B_1 and B_2 merge and give rise to a unique left-handed chain. Below the value of 115°, the curves of $n = 3$ and $h = 5$ Å do not meet, implying that such a chain would not be mathematically feasible for the given geometry of the pyranose residue.

1. R. H. MARCHESSAULT and A. SARKO. Adv. Carbohyd. Chem. **22**, 421 (1967).
2. K. H. MEYER and L. MISCH. Helv. Chim. Acta, **20**, 232 (1937).
3. D. CARLSTRÖM. Biochim. Biophys. Acta, **59**, 361 (1962).
4. P. H. HERMANS. Kolloid-Z. **102**, 169 (1943).
5. C. Y. LIANG and R. H. MARCHESSAULT. J. Polymer Sci. **37**, 385 (1959).
6. G. A. JEFFREY and R. D. ROSENSTEIN. Adv. Carbohyd. Chem. **19**, 7 (1964).
7. G. N. RAMACHANDRAN, C. RAMAKRISHNAN, and V. SASISEKHARAN. *In* Aspects of protein structure. *Edited by* G. N. Ramachandran. Academic Press, London. 1963. p. 121.
8. D. A. REES and R. J. SKERRETT. Carbohyd. Res. **7**, 334 (1968).
9. P. R. SUNDARARAJAN. Ph.D. Thesis, University of Madras, India. 1969.
10. S. M. GABBAY, P. R. SUNDARARAJAN, and R. H. MARCHESSAULT. Biopolymers. In press.

Can. J. Chem. Downloaded from www.nrcresearchpress.com by 210.87.254.42 on 09/05/12
For personal use only.

Chemistry of Proximal π-Bond Systems. Part I. Synthesis of Vicinal Exocyclic Dimethylene Hydrocarbons

D. N. Butler and R. A. Snow
Chemistry Department, York University, Toronto, Ontario

Received June 14, 1971

Thirteen new bi- or polycyclic vicinal exocyclic dimethylene hydrocarbons (**10**–**22**) have been synthesized and some of their spectral properties recorded. The generally most useful synthetic route to such compounds utilizes base-catalyzed double elimination from *trans*-1,2-bis(hydroxymethyl)alkyl *p*-toluenesulfonates as the final step in the production of the conjugated diene.

Treize nouveaux hydrocarbures (**10**–**22**), bi ou polycycliques, ayant des groupements diméthylènes exocycliques et vicinaux ont été synthétisés et quelques unes de leurs propriétés spectrales sont rapportées. La méthode de synthèse la plus efficace pour de tels composés consiste en une double élimination baso-catalysée à partir des *trans* bis(hydroxyméthyl)-1,2 alkyl *p*-toluènesulfonates; ceci constitue l'étape finale en vue de la formation des diènes conjugués.

Canadian Journal of Chemistry, **50**, 795 (1972)

Introduction

Interest in the chemistry of organic molecules containing proximal π-bonds is widespread in contemporary chemical literature (1). Perhaps the most interesting of this class of compounds are those in which the π-bonds are constrained in bi- and polycyclic hydrocarbons of known or predictable proximities by virtue of the fixed geometries of the ring systems involved, *e.g.* norbornadiene (2), barrelene (3), and bullvalene (4).

Most of the systematic work done, however, has been associated with endocyclic π-bonds. The synthesis of hydrocarbons of types **1** and **2** (where -X- represents any bridge) incorporating a vicinal exocyclic dimethylene bridge would allow a comparison of the effects of the possible mixing of the *cis*-diene π-orbitals with the endocyclic π-system of compounds **1** in the ground or first excited states with the situation as presented in compounds **2** where such mixing is not possible. Also, comparative chemistry (*e.g.* Diels–Alder additions) of **1** and **2** should reveal insights into the influence of ring size, state of hybridization, and -X-bridge geometric parameters on the transition states leading to the respective products. Such chemistry also generates many novel polycyclic systems, themselves potentially capable of further addition, thermal, or photochemical reactions. Accordingly, a synthetic program designed to provide a general high-yielding route to compounds of the type **1** and **2** was undertaken.

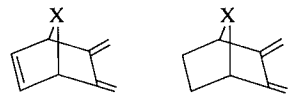

1 **2**

Of the compounds **3**–**22** below, **3**–**9** are known (5–8). The remainder (**10**–**22**) represent those of the many possible structures of (or related to) **1** and **2** which we have prepared to date. This paper describes their synthesis and offers general comments on the various methods available for the preparation of bridged vicinal dimethylene hydrocarbons.

Results and Discussion

The majority of the published syntheses of mono- and bicyclic vicinal exocyclic dimethylene hydrocarbons involves either acetate pyrolysis (route *i*, Scheme 1) (7, 9) or quaternary amine hydroxide (Hofmann elimination) pyrolysis (route *ii*, Scheme 1) (5) as the final diene producing step. The acetate route suffers from the high temperatures (400–500°) necessary to effect elimination and cannot be considered when the possibility of retro-Diels–Alder reaction exists.

In this present work, route *ii* was modified to employ pyrolysis under vacuum of the bis-(dimethylamine-*N*-oxides) (Cope reaction (10)). The temperatures used were a little lower than in the Hofmann procedure, but it was found that with large scale preparations (up to 0.5 mol) uncontrolled decomposition of the *N*-oxide sometimes took place.

Can. J. Chem. Downloaded from www.nrcresearchpress.com by 210.87.254.6 on 09/05/12
For personal use only.

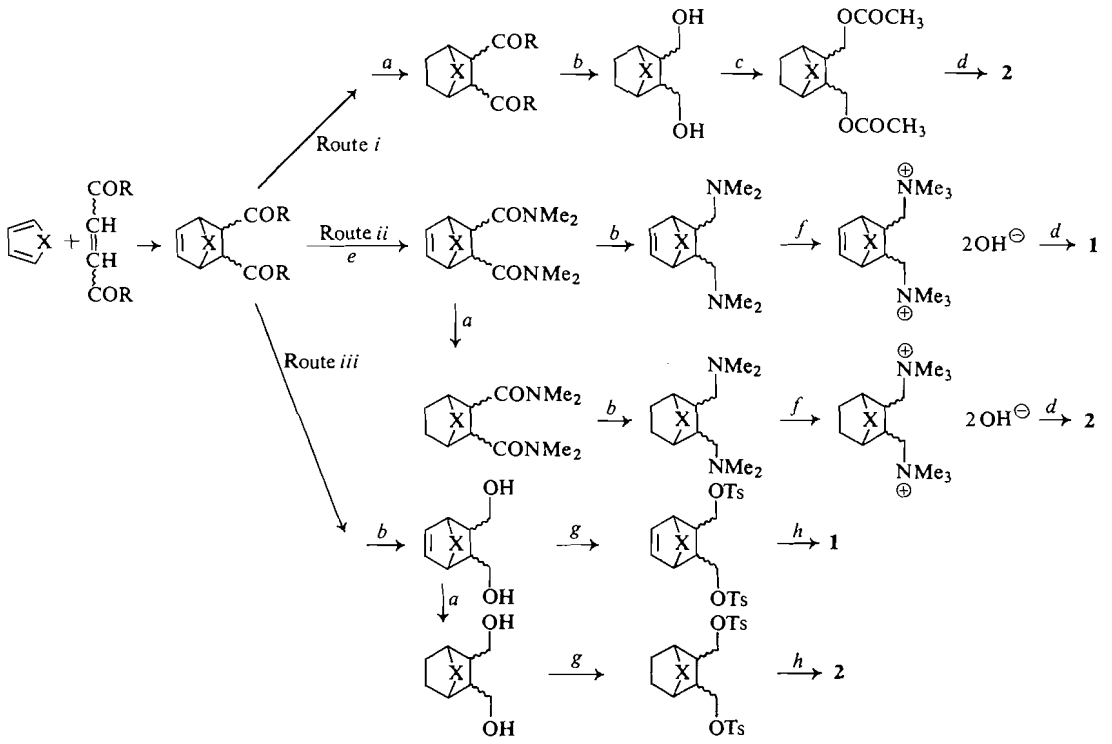

SCHEME 1. General routes to vicinal exocyclic dimethylene hydrocarbons.

After the tosylation/base-catalyzed elimination sequence (route *iii*, Scheme 1) had been developed in this laboratory, the synthesis of **23** (11) was published using exactly this method. This route proved to be the best in terms of overall yields, lack of hazard, and purity of product.

Compound **9** has been prepared using a modification of route *iii*, Scheme 1 (8) (as step *h*: sodium hydroxide/refluxing ethanol). However, the use of potassium *t*-butoxide in dimethyl sulfoxide at room temperature facilitated reaction and increased yields to *ca.* 95% from the *trans*-di-*p*-toluenesulfonate precursor.

Several other individual syntheses of vicinal exocyclic dienes have been published (12) but these are not considered to be generally useful.

The ten hydrocarbons **3–8**, **10**, **11**, **16**, and **17** were all prepared via the Cope reaction modification as the final step of route *ii*, Scheme 1. The starting materials for all these compounds were the known, respective Diels–Alder adducts of fumaryl chloride and the cyclic diene necessary to construct the ring system. Thus, the corresponding intermediate bisamides, bisamines, and bisamine oxides all have *trans* stereochemistry.

The remaining ten hydrocarbons **9**, **12–15**, and **18–22** were all obtained from the di-*p*-toluenesulfonate esters of the corresponding

Can. J. Chem. Downloaded from www.nrcresearchpress.com by 210.87.254.6 on 09/05/12
For personal use only.

Can. J. Chem. Downloaded from www.nrcresearchpress.com by 210.87.254.6 on 09/05/12
For personal use only.

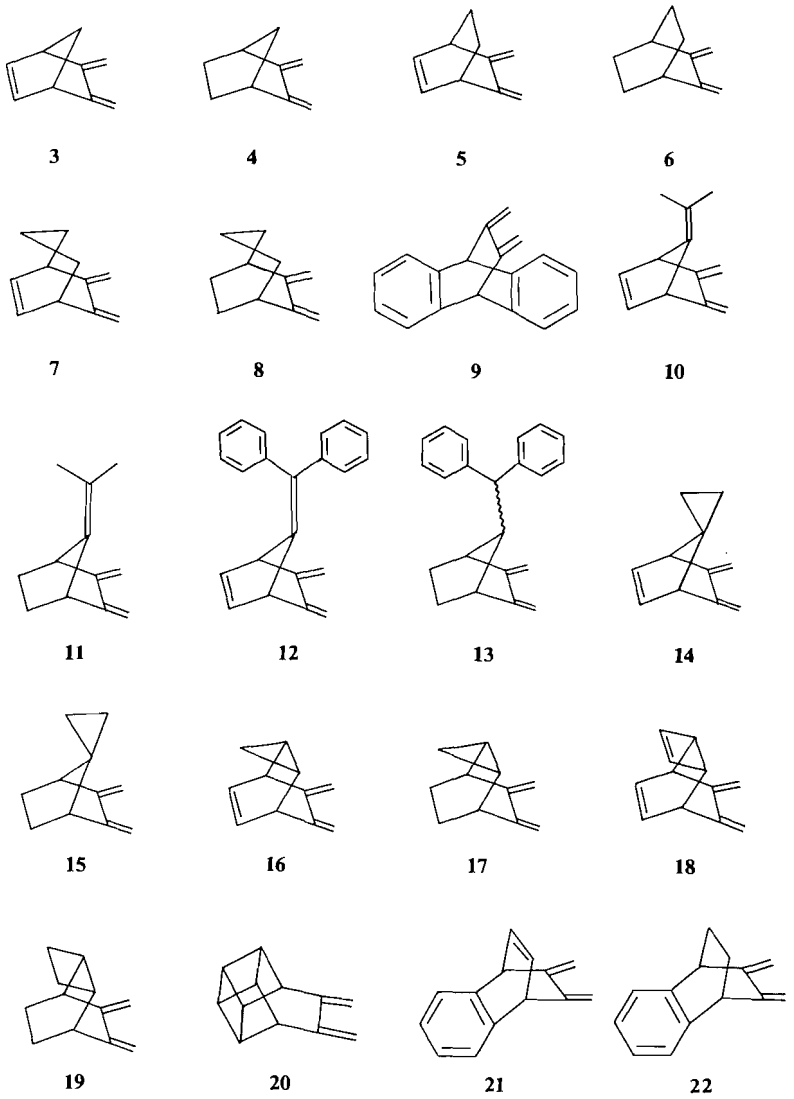

bis-primary alcohols by treatment in dimethyl sulfoxide with potassium *t*-butoxide (route *iii*, Scheme 1). The starting compounds for the syntheses of hydrocarbons **9**, **12**–**15**, and **18** were again the fumaryl chloride adducts of the respective, necessary cyclic dienes. Catalytic hydrogenation reduced both double bonds of the diol intermediate from lithium aluminum hydride reduction of the cyclooctatetraene–fumaryl chloride adduct and thus furnished the necessary diol for compound **19**.

The known 1,4-etheno-1,2,3,4-tetrahydronaphthalene-(*trans*)-2,3-dicarboxylic acid dimethyl ester **24** (13) was reduced in lithium aluminum hydride/tetrahydrofuran to provide the necessary diol intermediate for hydrocarbon **21**, and after catalytic reduction, that for hydrocarbon **22**. The advisability for having a *trans* disposition of the vicinal hydroxymethyl functions in these syntheses was revealed when attempted *p*-toluenesulfonation of the *cis*-diol **25** from lithium aluminum hydride reduction of the anthracene–maleic anhydride adduct produced the known cyclic ether **26** (14).

Can. J. Chem. Downloaded from www.nrcresearchpress.com by 210.87.254.6 on 09/05/12
For personal use only.

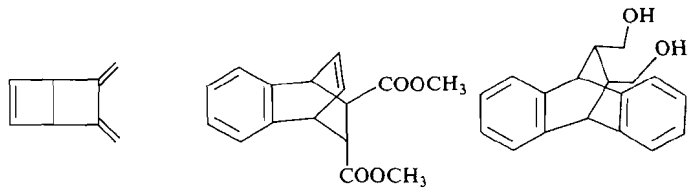

23 24 25

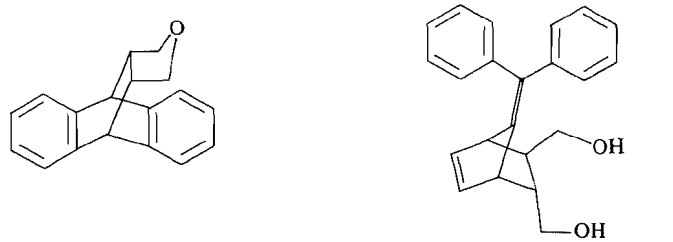

26 27

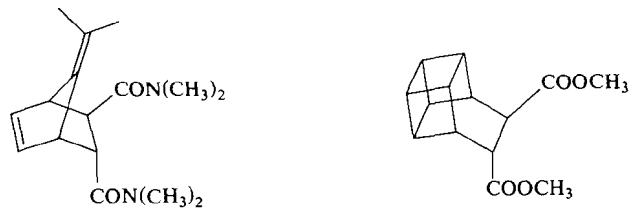

28 29

Somewhat unexpectedly, the catalytic hydrogenation of the diol **27** reduced both double bonds, whereas the corresponding reduction of intermediate **28** (en route to **11**) hydrogenated only the disubstituted olefin. The stereochemistry of **13** and its preceding intermediates are not known but they presumably are the *syn* isomers if reduction proceeded to the least hindered side of **27**. The known *trans*-dimethyl ester **29** (15) provided the required intermediates for hydrocarbon **20** via the route *iii*, Scheme 1 sequence.

The physical, analytical, and spectroscopic data for the 13 new hydrocarbons (**10–22**) supporting the structural assignments are collected along with the unpublished spectra of the seven known compounds **3–9** in Tables 1 and 2. The exocyclic methylene absorption in the p.m.r. spectra all occur as two singlets or very narrow doublets between δ 5.25 and 4.60 p.p.m. and represent the "inside" and the "outside" vinyl protons. From the observed anisotropic effects of the olefinic bond (16) it is likely that the "inside" proton would be the more deshielded. The chemical shift difference in these two protons varies regularly with the size of the -X- bridge in the series **4**, **6**, and **8** and inversely to the carbon–carbon double bond stretching frequency in the i.r. spectra suggesting a systematic influence of geometrical parameters on these spectroscopic measurements. The u.v. spectra of those hydrocarbons not containing any aromatic rings easily divide into the two structure types **1** and **2** and clearly indicate the *cisoid* conformation of the diene moiety (17). We are investigating these geometric–spectroscopic relationships further as well as the Diels–Alder reactivity and electrocyclic chemistry of this series of related hydrocarbons.

Experimental

All melting points are uncorrected. The i.r. spectra were determined on a Unicam SP1000 spectrophotometer as liquid films or as KBr discs. The p.m.r. spectra were recorded on Varian HA100 or A60 instruments in carbon tetrachloride or deuteriochloroform using tetramethylsilane as the internal standard. Mass spectra were taken at 70 eV using a

Can. J. Chem. Downloaded from www.nrcresearchpress.com by 210.87.254.6 on 09/05/12
For personal use only.

TABLE 1. Hydrocarbons (**3–22**), physical, analytical, i.r., and u.v. data

Compound	Melting point or boiling point (°C or °C/mm)	Molecular formula	Observed parent ion *m/e*	Analytical data (%) Calculated C	Calculated H	Found C	Found H	Strong infrared‡ absorptions (cm^{-1})	Ultraviolet spectra λ_{max}‖ mμ (log ε)
3	142/760	C_9H_{10}	118	—	—	—	—	670, 756, 784, 876, 1312, 1646, 2986, 3076	206 (3.88), 222 (3.86) s, 228.5 (3.92), 240 (3.95) b
4	67/50	C_9H_{12}	120	—	—	—	—	877, 1113, 1636, 2870, 2966, 3080	205 (3.35), 241 (3.92) s, 248 (3.95)
5	68/12	$C_{10}H_{12}$	132	—	—	—	—	677, 741, 875, 1610, 2865, 2955, 3055	205 (3.92), 214 (3.50) s, 219.5 (3.56), 226 (3.63) s, 246 (3.91), 252 (3.91)
6	93/50	$C_{10}H_{14}$	134	—	—	—	—	880, 1455, 1614, 2858, 2935, 3078	205 (3.31), 247 (3.88), 252 (3.88)
7	88/20	$C_{11}H_{14}$	146	—	—	—	—	701, 881, 1441, 1606, 2857, 2930, 3040	206 (3.70), 246.5 (3.83) b, 252 (3.82)
8	103/30	$C_{11}H_{16}$	148	—	—	—	—	884, 1453, 1602, 2862, 2930, 3082	205 (3.29) s, 247 (3.87) b
9	157–157.5*	$C_{18}H_{14}$	230	—	—	—	—	720, 727, 738, 758, 875, 889, 1624, 2965, 3020, 3070	208 (4.17), 240.5 (3.54) s, 252 (3.47), 261 (3.37) s, 268.5 (3.31) s, 276 (3.18)
10	74.5– 75.5	$C_{12}H_{14}$	158	91.08	8.92	91.31	8.91	672, 780, 868, 1646, 1653, 2930, 2982, 3010, 3070	205.5 (3.88), 230 (4.04) s, 246 (4.11) b
11	66.5–67	$C_{12}H_{16}$	160	89.94	10.06	90.02	10.10	737, 809, 881, 1620, 1639, 2860, 2980, 3085	204.5 (3.67), 250 (4.07) b
12	95–96	$C_{22}H_{18}$	282	93.58	6.42	93.34	6.40	690, 734, 744, 790, 874, 883, 1595, 1641, 2985, 3010, 3025, 3035	206.5 (4.45), 225 (4.23) b, 267 (4.10) b
13	103.5–104.5	$C_{22}H_{22}$	286	92.26	7.74	92.19	7.77	697, 870, 880, 1585, 1595, 1633, 2960, 3020, 3050, 3080	207 (4.28), 222 (4.10), 241 (3.86) s, 249 (3.91), 259 (3.74) s
14	†	$C_{11}H_{12}$	144	91.61	8.39	91.50	8.61	671, 777, 877, 1005, 1308, 1428, 1658, 2985, 3075	205 (3.93), 229 (3.95) s, 241.5 (3.98)
15	†	$C_{11}H_{14}$	146	90.35	9.65	90.54	9.41	804, 876, 1003, 1636, 2872, 2968, 3076	205 (3.38), 242.5 (3.93) s, 247.5 (3.97), 257 (3.77) s
16	†	$C_{11}H_{12}$	144	91.61	8.39	91.63	8.20	681, 739, 811, 837, 880, 1628, 2955, 3020, 3050, 3080	205 (3.77), 225 (3.74) s, 242 (3.91), 247 (3.90)
17	†	$C_{11}H_{14}$	146	90.35	9.65	90.11	9.73	835, 880, 1620, 2875, 2948, 3008, 3079	206 (3.43) s, 243.5 (3.91), 249.5 (3.92)
18	†	$C_{12}H_{12}$	156	92.26	7.74	92.31	7.89	679, 727, 778, 878, 1297, 1615, 2950, 3050	206 (3.72), 243.5 (3.91), 249 (3.90)
19	15†	$C_{12}H_{16}$	160	89.94	10.06	89.68	10.20	882, 1616, 2950, 3080	207 (3.33), 247.5 (3.91), 253 (3.91) s
20	45†§	$C_{12}H_{12}$	156	92.26	7.74	91.99	7.89	680, 780, 882, 1266, 1601, 1619, 2980, 3075	205 (3.40), 254 (3.77), 262 (3.74) s
21	47–48	$C_{14}H_{12}$	180	93.29	6.71	93.48	6.77	660, 708, 745, 765, 809, 882, 1614, 2980, 3075	208.5 (4.50), 234 (4.34) s, 243 (4.32), 277 (3.74)
22	93.5–94	$C_{14}H_{14}$	182	92.26	7.74	92.46	7.67	707, 763, 883, 1608, 2865, 2950, 3020, 3075	208.5 (4.17), 251.5 (4.03), 263.5 (3.84) s, 271.5 (3.48)

*Literature m.p. 151–153° (8).
†Sample transferred under vacuum (0.01 mm); bath temperature 40–120° as appropriate.
‡Infrared spectra taken as liquid films and KBr discs.
§Vacuum transfer at 80°/0.01 mm caused partial thermal reversion to **18**.
‖Taken in ethanol solution; s, shoulder; b, broad.

TABLE 2. The 100 MHz p.m.r. data for hydrocarbons **3–22***†

Compound	Vicinal vinyl —C=C— H H	Exomethylene vinyl =C(H)(H) ‡		Bridgehead C—H	Other proton assignments
3	6.10 (2H)	5.06 (2H)	4.86 (2H)	3.22 (2H)	1.47–1.78 (2H)§
4	—	5.02 (2H)	4.73 (2H)	2.76 (2H)	1.16–1.80 (6H)§
5	6.17 (2H)	5.03 (2H)	4.67 (2H)	3.12 (2H)	1.22–1.72 (4H)§
6	—	5.14 (2H)	4.62 (2H)	2.26 (2H)	1.58 (8H)§
7	6.02 (2H)	5.25 (2H)	4.68 (2H)	2.92 (2H)	1.36–1.80 (6H)§
8	—	5.21 (2H)	4.62 (2H)	2.56 (2H)	1.42–1.82 (10H)§
9	—	5.16 (2H)	5.01 (2H)	4.71 (2H)	6.92–7.24 (8H) aromatic
10	6.22 (2H)	4.98 (2H)	4.81 (2H)	3.63 (2H)	1.52 (6H) *gem* dimethyl
11	—	4.95 (2H)	4.67 (2H)	3.12 (2H)	1.61 (6H) *gem* dimethyl; 1.35–1.78 (4H)§
12	6.35 (2H)	5.12 (2H)	4.91 (2H)	3.75 (2H)	6.96–7.30 (10H) aromatic
13	—	4.98 (2H)	4.64 (2H)	2.39 (2H)	7.02–7.24 (10H) aromatic; 3.60 (1H) benzylic; 1.28–2.04 (5H)§
14	6.16 (2H)	5.07 (2H)	4.80 (2H)	2.57 (2H)	0.22–0.59 (4H) cyclopropyl
15	—	5.04 (2H)	4.66 (2H)	1.96 (2H)	1.32–1.95 (4H)§; 0.28–0.50 (4H) cyclopropyl
16	5.71 (2H)	5.09 (2H)	4.73 (2H)	3.22 (2H)	0.96 (2H), 0.12–0.32 (2H) cyclopropyl
17	—	5.21 (2H)	4.69 (2H)	2.48 (2H)	0.06–1.02 (4H) cyclopropyl; 1.18–1.50 (4H)§
18	5.89 (2H), 5.83 (2H)	5.16 (2H)	4.75 (2H)	3.07 (2H)	2.72 (2H) cyclobutenyl
19	—	5.15 (2H)	4.60 (2H)	2.39 (2H)	1.99–2.26 and 1.33–1.59 (10H)§
20	—	5.22 (2H)	4.71 (2H)	—	3.02–3.43 (8H) bridgehead and cyclobutyl
21	6.47 (2H)	5.07 (2H)	4.87 (2H)	4.35 (2H)	6.90–7.15 (4H) aromatic
22	—	5.12 (2H)	4.81 (2H)	3.56 (2H)	7.03 (4H) aromatic; 1.40–1.92 (4H)§

*δ-Value determined in CCl_4 solution using TMS as internal standard.
†Unless otherwise shown, the centers of multiplets are indicated.
‡Singlets or narrow doublets ($J \leq 1.0$ Hz).
§Protons in saturated bridge or bridges.

Hitachi–Perkin Elmer RMU-6E instrument. Microanalyses were obtained from A. B. Gygli, Toronto.

Starting Materials — Diels–Alder Adducts

(*anti*)-Tricyclo[3.2.2.$0^{2,4}$]non-8-ene-(*trans*)-6,7-dicarbonyl chloride(18); (*anti*)-tricyclo[4.2.2.$0^{2,5}$]deca-3,9-diene-(*trans*)-7,8-dicarbonyl chloride (19); 7-isopropylidenebicyclo[2.2.1]-hept-5-ene-(*trans*)-2,3-dicarbonyl chloride (20); 7-diphenylmethylenebicyclo[2.2.1]hept-5-ene-(*trans*)-2,3-dicarbonyl chloride (21); 1,4-etheno-1,2,3,4-tetrahydronaphthalene-(*trans*)-2,3-dicarboxylic acid dimethyl ester (**24**) (13); pentacyclo[4.2.2.$0^{2,5}$.$0^{3,8}$.$0^{4,7}$]decane-(*trans*)-9,10-dicarboxylic acid dimethyl ester (**29**) (15).

Spiro[cyclopropane-1,7′-[5]norbornene]-(trans)-2′,3′-dicarbonyl Chloride

Fumaryl chloride (36 g) in dry ether (50 ml) was added dropwise over 1 h to an ice-cooled solution of spiro[2.4]-hepta-4,6-diene (22) (19 g) in dry ether (250 ml). The resulting solution was evaporated to a yellow–green oil which showed p.m.r. absorptions (CCl_4) at δ 6.18, m (2H); 3.93, m (1H); 3.16, d ($J = 5.5$ Hz) (1H); 2.90, m (2H); and 0.41 p.p.m., s (4H) consistent with the adduct structure. This oily dichloride was directly reduced to the corresponding diol without further identification (see below).

Preparation of Bis(N,N-dimethylamides)

The diacid chloride (0.1 mol) was dissolved in dry diethyl ether (70 ml) and slowly dropped into an ice-cooled solution of dimethylamine (0.5 mol) in dry diethyl ether (200 ml). After allowing the reaction mixture to come to room temperature, the dimethylammonium chloride was filtered off, washed with ether, and the filtrate evaporated to afford the crude bisamide. This was dissolved in benzene (100 ml) and passed through a bed of neutral alumina (Woelm: activity grade 1; 20 × 2.5 cm). A further 400 ml of benzene were passed through the column and the total eluate evaporated to leave the pure amides. The yields were almost quantitative. The analytical samples were either recrystallized from ether or sublimed.

The following new compounds were prepared by this method. (*anti*)-Tricyclo[3.2.2.$0^{2,4}$]non-8-ene-(*trans*)-6,7-bis-(*N,N*-dimethylcarboxamide), m.p. 122–123.5°.

Anal. Calcd. for $C_{15}H_{22}N_2O_2$: C, 68.67; H, 8.45; N, 10.68. Found: C, 68.42; H, 8.58; N, 10.46.

7-Isopropylidenebicyclo[2.2.1]hept-5-ene-(*trans*)-2,3-bis-(*N,N*-dimethylcarboxamide), m.p. 93.5–94.5°.

Anal. Calcd. for $C_{16}H_{24}N_2O_2$: C, 69.53; H, 8.75; N, 10.14. Found: C, 69.20; H, 8.59; N, 10.28.

The above two bisamides were subjected to catalytic hydrogenation in methanol using 10% palladium-on-charcoal as catalyst. After 1 mol of hydrogen had been absorbed, the catalyst was filtered off and the solvent removed under vacuum. The remaining dihydrobisamides were essentially pure. Analytical samples were recrystallized from ether. (*anti*)-Tricyclo[3.2.2.$0^{2,4}$]nonane-(*trans*)-6,7-bis-(*N,N*-dimethylcarboxamide), m.p. 135–136.5°.

Anal. Calcd. for $C_{15}H_{24}N_2O_2$: C, 68.15; H, 9.15; N, 10.60. Found: C, 68.14; H, 9.33; N, 10.34.

Can. J. Chem. Downloaded from www.nrcresearchpress.com by 210.87.254.6 on 09/05/12
For personal use only.

Can. J. Chem. Downloaded from www.nrcresearchpress.com by 210.87.254.6 on 09/05/12
For personal use only.

7-Isopropylidenebicyclo[2.2.1]heptane-(*trans*)-2,3-bis-(*N*,*N*-dimethylcarboxamide), m.p. 114–115.5°.

Anal. Calcd. for $C_{16}H_{26}N_2O_2$: C, 69.03; H, 9.41; N, 10.06. Found: C, 69.32; H, 9.37; N, 9.68.

Preparation of the Bisamines

The above amides were individually reduced in diethyl ether using lithium aluminum hydride (1.2 mol/mol bisamide) by refluxing for 10 h. After this time a volume of 20% KOH solution (equal to the weight in grams of bisamide taken) was added dropwise, followed by an equal volume of water. After stirring for 2 h, this mixture was filtered, the precipitate washed well with ether, and the filtrate evaporated to give the crude bisamines as yellow oils. The yields were variable (50–85%) and these products were oxidized directly to the bisamine oxides.

Oxidation of Bisamines

The above bisamines were individually taken up in methanol (500 ml/mol) and 30% H_2O_2 (60 ml) added in 5 ml batches over 1 h. Further 60 ml portions of 30% H_2O_2 were added after 2 and after 6 h and the mixture allowed to stand overnight. The excess H_2O_2 was decomposed by the cautious addition of a small quantity of platinum black, and when no more oxygen was seen to be forming, the mixture was filtered and evaporated under vacuum to give the crude bis(amine-*N*-oxides) as viscous oils. They were directly pyrolyzed without further purification.

Pyrolysis of Bis(amine-N-oxides)

The bis(amine-*N*-oxides) (0.1–0.5 mol), contained in a 1 l round bottom flask connected to a liquid air cooled vacuum trap, were separately heated under vacuum (0.1 mm) using a free flame. Decomposition began from about 80° and heating was continued until all the contents of the flask had decomposed. Considerable charring occurred in most cases. The contents of the trap were extracted with petrol ether (30–60°) and washed three times with water. The combined extracts were dried over anhydrous magnesium sulfate, filtered, and evaporated at 25° (water pump pressure). The residue was taken up in petrol (10 ml) and passed through a short column of alumina (10 × 1.0 cm) using further solvent to wash the column. The total eluate was evaporated and the residue either vacuum transferred or recrystallized from methanol to afford the pure hydrocarbons (see Tables 1 and 2). The yields were 20–40% based on the bisamine taken.

Preparation of Diols and Di-p-toluenesulfonates

The diacid chloride (0.1 mol) in dry diethyl ether (70 ml) was slowly dropped into a stirred suspension of lithium aluminum hydride (0.2 mol) in 1:1 dry diethyl ether/dry tetrahydrofuran (300 ml). After the initial reaction had subsided, the mixture was subjected to reflux for 16 h and the excess hydride decomposed by the addition of a volume of 20% aqueous KOH solution (equal to the weight in grams of dichloride taken) followed by an equal volume of water. After stirring a further 2 h at room temperature, the precipitate was filtered, washed well with ether, and the total filtrate evaporated to afford the crude diol. In some of these reductions, the diol remained complexed to the precipitated alumina and was extracted therefrom with ethanol. If the diol crystallized, analytical samples were prepared by recrystallization from benzene or carbon tetrachloride. If it did not crystallize, it was converted to the di-*p*-toluenesulfonate directly. The yields varied from 50–80%.

In the case of the *trans*-dimethyl esters **24** and **29**, the above reduction was carried out in dry tetrahydrofuran rather than the mixed ether solvent.

The following pure diols were prepared by this method. They all exhibited strong hydroxyl absorption near 3350 cm^{-1} in their i.r. spectra. The di-*p*-toluenesulfonates were prepared by the standard method (*p*-toluenesulfonyl chloride/pyridine, 0 °C, overnight).

trans-7,8-Bis(hydroxymethyl)-(*anti*)-tricyclo[4.2.2.$0^{2,5}$]-deca-3,9-diene, m.p. 93–93.5°.

Anal. Calcd. for $C_{12}H_{16}O_2$: C, 74.97; H, 8.39. Found: C, 74.80; H, 8.13.

Di-*p*-toluenesulfonate, m.p. 159–160° (methanol).

Anal. Calcd. for $C_{26}H_{28}O_6S_2$: C, 62.38; H, 5.64. Found: C, 62.42; H, 5.73.

trans-2,3-Bis(hydroxymethyl)-1,4-etheno-1,2,3,4-tetrahydronaphthalene, m.p. 142–143°.

Anal. Calcd. for $C_{14}H_{16}O_2$: C, 77.75; H, 7.46. Found: C, 77.57; H, 7.54.

Di-*p*-toluenesulfonate, m.p. 133–134° (methanol).

Anal. Calcd. for $C_{28}H_{28}O_6S_2$: C, 64.10; H, 5.38. Found: C, 64.12; H, 5.46.

The following diols were prepared by the above route but analytical samples were not secured. All showed consistent i.r. and p.m.r. spectra for the structures indicated:

trans-2′,3′-Bis(hydroxymethyl)spiro[cyclopropane-1,7′-[5]norbornene]. Di-*p*-toluenesulfonate, m.p. 120.5–121.5° (methanol).

Anal. Calcd. for $C_{25}H_{28}O_6S_2$: C, 61.45; H, 5.78. Found: C, 61.51; H, 5.88.

trans-9,10-Bis(hydroxymethyl)pentacyclo[4.2.2.$0^{2,5}$.$0^{3,8}$-.$0^{4,7}$]decane. Di-*p*-toluenesulfonate, m.p. 177–178° (methanol).

Anal. Calcd. for $C_{26}H_{28}O_6S_2$: C, 62.38; H, 5.64. Found: C, 62.55; H, 5.85.

trans-2,3-Bis(hydroxymethyl)-7-diphenylmethylenebicyclo[2.2.1]hept-5-ene. Di-*p*-toluenesulfonate failed to crystallize.

Catalytic Reduction of the Diols

The diols were reduced in methanol using 10% Pd-on-C as catalyst and isolated in the usual way. If they did not crystallize they were directly converted to the *p*-toluenesulfonates as above. The following pure diols and di-*p*-toluenesulfonates were obtained. All showed consistent i.r. and p.m.r. data for the structures indicated.

trans-7,8-Bis(hydroxymethyl)-(*anti*)-tricyclo[4.2.2.$0^{2,5}$]-decane, m.p. 82–83°.

Anal. Calcd. for $C_{12}H_{20}O_2$: C, 73.43; H, 10.27. Found: C, 73.41; H, 9.97.

Di-*p*-toluenesulfonate, m.p. 178.5–179.5° (methanol).

Anal. Calcd. for $C_{20}H_{32}O_6S_2$: C, 61.88; H, 6.39. Found: C, 61.75; H, 6.51.

trans-2,3-Bis(hydroxymethyl)-1,4-ethano-1,2,3,4-tetrahydronaphthalene, m.p. 129–130°.

Anal. Calcd. for $C_{14}H_{18}O_2$: C, 77.03; H, 8.31. Found: C, 76.96; H, 8.31.

Di-*p*-toluenesulfonate, m.p. 132.5–133° (methanol).

Anal. Calcd. for $C_{28}H_{30}O_6S_2$: C, 63.85; H, 5.74. Found: C, 63.93; H, 5.77.

trans-2,3-Bis(hydroxymethyl)-7-(diphenylmethyl)bicyclo-

[2.2.1]heptane di-*p*-toluenesulfonate, m.p. 110–110.5° (methanol).

Anal. Calcd. for $C_{36}H_{38}O_6S_2$: C, 68.54; H, 6.07. Found: C, 68.73; H, 6.27.

trans-2′,3′-Bis(hydroxymethyl)spiro[cyclopropane-1,7′-norbornane] di-*p*-toluenesulfonate, m.p. 110–111° (methanol).

Anal. Calcd. for $C_{25}H_{30}O_6S_2$: C, 61.20; H, 6.16. Found: C, 61.35; H, 6.08.

General p-Toluenesulfonate Elimination Procedure

To the di-*p*-toluenesulfonate (0.01 mol) dissolved in dimethyl sulfoxide (60 ml) was added powdered potassium *t*-butoxide (0.025 mol). The mixture darkened rapidly to deep green–brown and was stirred at room temperature for 5 h. The mixture was poured onto ice-water (200 g) and extracted with petroleum ether (30–60°) (4 × 30 ml). The combined extracts were washed with saturated sodium chloride solution (3 × 100 ml) to remove the dimethyl sulfoxide, dried over anhydrous magnesium sulfate, and evaporated to yield the crude hydrocarbon. The yields varied from 80–95%. The pure hydrocarbons were secured by chromatography in petroleum ether (30–60°) over alumina (Woelm: activity grade 1; 20 × 1 cm column), evaporation of the solvent under vacuum and sublimation or vacuum transfer at 40–140° and 0.01 mm depending on the melting or boiling point of the sample. The physical, analytical, and spectroscopic data are collected in Tables 1 and 2.

The authors wish to thank the National Research Council of Canada and the Department of University Affairs of the Province of Ontario for their financial assistance. Thanks are also due to Dr. B. H. Khouw for the measurement of mass spectra, and to Dr. C. E. Holloway for the measurement of the p.m.r. spectra.

1. R. B. WOODWARD and R. HOFFMANN. The conservation of orbital symmetry. Academic Press, New York, N.Y., 1969.
2. C. F. WILCOX, S. WINSTEIN, and W. G. MCMILLAN. J. Am. Chem. Soc. **82**, 5450 (1960).
3. H. E. ZIMMERMAN and G. L. GRUNEWALD. J. Am. Chem. Soc. **88**, 183 (1966).
4. G. SCHROËDER. Angew. Chem. Int. Ed. **2**, 481 (1963).
5. Compounds **3**, **5**, and **7**: K. ALDER, S. HARTUNG, and O. NETZ. Chem. Ber. **90**, 1 (1957).
6. Compound **4**: (*a*) K. ALDER and W. ROTH. Chem. Ber. **88**, 407 (1955). (*b*) W. J. BAILEY and W. B. LAWSON. J. Am. Chem. Soc. **77**, 1606 (1955). (*c*) M. A. P. BOWE, R. G. T. MILLER, J. B. ROSE, and D. G. M. WOOD. J. Chem. Soc. 1541 (1960).
7. Compounds **6** and **8**: K. ALDER and H. MÖLLS. Chem. Ber. **89**, 1960 (1956).
8. Compound **9**: J. S. MEEK and R. C. STACY. J. Org. Chem. **26**, 300 (1961).
9. W. J. BAILEY and S. S. MILLER. J. Org. Chem. **28**, 802 (1963) and the preceding papers in this series.
10. (*a*) A. T. BLOMQUIST and Y. C. MEINWALD. J. Am. Chem. Soc. **82**, 3619 (1960). (*b*) P. D. BARTLETT, A. S. WINGROVE, and R. OWYANG. J. Am. Chem. Soc. **90**, 6067 (1968).
11. (*a*) F. R. FARR and N. L. BAULD. J. Am. Chem. Soc. **92**, 6695 (1970). (*b*) J. G. KUDERNA and G. R. HAYNES. U.S. Pat. 3 265 721. Chem. Abstr. **65**, 20 033*e* (1966).
12. (*a*) C. K. ALDEN, J. A. CLAISSE, and D. I. DAVIES. J. Chem. Soc. C, 1228 (1968). (*b*) P. E. HOCH. J. Org. Chem. **26**, 2066 (1961). (*c*) K. B. WIBERG, G. J. BURGMAIER, and P. WARNER. J. Am. Chem. Soc. **93**, 246 (1971). (*d*) F. BOBERG and H. KHALAF. Ann. **741**, 153 (1970). (*e*) M. P. CAVA and A. A. DEANA. J. Am. Chem. Soc. **81**, 4266 (1959). (*f*) J. A. ELIX, M. V. SARGENT, and F. SONDHEIMER. J. Am. Chem. Soc. **92**, 962, 969 (1970).
13. K. TAKEDA, K. KITAHONOKI, M. SUGIURA, and Y. TAKANO. Chem. Ber. **95**, 2344 (1962).
14. H. M. WALBORSKY. Helv. Chim. Acta, **36**, 1251 (1953).
15. (*a*) S. MASAMUNE, H. CUTS, and M. G. HOGBEN. Tetrahedron Lett. 1017 (1966). (*b*) W. G. DAUBEN and D. L. WHALEN. Tetrahedron Lett. 3743 (1966).
16. N. S. BHACCA and D. H. WILLIAMS. *In* Applications of n.m.r. spectroscopy in organic chemistry. Holden-Day, San Francisco, 1964. p. 88.
17. H. SUZUKI. *In* Electronic absorption spectra and geometry of organic molecules. Academic Press, Inc., New York, N.Y., 1967. p. 360.
18. K. ALDER and G. JACOBS. Chem. Ber. **86**, 1528 (1953).
19. M. AVRAM, G. MATEESCU, and C. D. NENITZESCU. Ann. **636**, 174 (1960).
20. K. ALDER and R. RÜHMANN. Ann. **566**, 1 (1950).
21. K. ALDER, F. W. CHAMBERS, and W. TRIMBORN. Ann. **566**, 27 (1950).
22. K. ALDER, H. J. ACHE, and F. H. FLOCK. Chem. Ber. **93**, 1888 (1960).

Can. J. Chem. Downloaded from www.nrcresearchpress.com by 210.87.254.6 on 09/05/12
For personal use only.

Synthesis and Stereochemistry of Diastereoisomeric 1,3-Dimethylpiperidin-4-ols and Related Compounds

A. F. CASY AND W. K. JEFFERY

Faculty of Pharmacy and Pharmaceutical Sciences, University of Alberta, Edmonton, Alberta

Received October 8, 1971

The synthesis of *cis* and *trans* 1,3-dimethylpiperidin-4-ols and derived acetate, benzilate, and diphenylacetate esters is described. Configurations and preferred conformations of these derivatives are assigned on the basis of 4-methine and 4-hydroxyl p.m.r. characteristics. Conformational studies of esters of 1-methylpiperidin-3-ol and isomeric 3-tropanols are also described. Epimeric conjugate acids are well defined in 3-acetoxy-1-methylpiperidine hydrochloride as solute in $CDCl_3$.

La synthèse des *cis* et *trans* diméthyl-1,3 pipéridinols-4 et des esters qui en dérivent, acétates, benzylates, et diphénylacétates, est décrite. Les configurations et les conformations privilégiées de ces dérivés sont attribuées en se fondant sur les caractéristiques p.m.r. du méthine-4 et de l'hydroxyl-4. Les études conformationnelles des esters du méthyl-1 pipéridinol-3 et des tropanols-3 isomères, sont également décrites. Les acides conjugués épimères sont bien définis dans le chlorhydrate d'acétoxy-3 méthyl-1 pipéridine dissous dans le $CDCl_3$.

Canadian Journal of Chemistry, **50**, 803 (1972)

Can. J. Chem. Downloaded from www.nrcresearchpress.com by 210.87.254.42 on 09/05/12
For personal use only.

The *cis* and *trans* 1,3-dimethyl-4-piperidyl esters described in this paper were prepared as the steric analogs of cholinolytic esters of tropine and pseudotropine for use in structure-activity studies of drugs related to atropine. The parent piperidinols **1** were obtained by

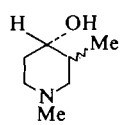

1

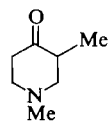

2

reduction of 1,3-dimethyl-4-piperidone (**2**) under various conditions. These reactions were first reported by Mistryukov (1) who separated the two alcohols by g.l.c. and column chromatography. He assigned configurations *cis* and

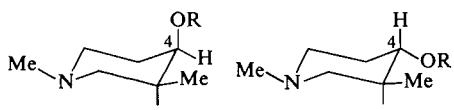

cis **3** *trans* **4**

a R=H
b R=COMe

trans to the initially and finally displaced isomers respectively, on the assumption of the *cis* isomer **3***a* having an axial (hindered), and the *trans* **4***a* an equatorial (accessible) hydroxyl function. These assignments are now confirmed by p.m.r. data, as shown later. We sought to achieve separation of the piperidinols **1** in bulk by crystallization of the base hydrochlorides. In this way only the *trans* salt could be separated from a total base mixture obtained from the piperidone **2** and LAH; treatment of the base recovered from the mother liquors with acetyl chloride in hot ethyl acetate, however, gave the *cis* acetate **5** hydrochloride from which

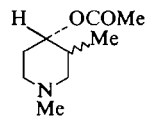

5

the alcohol could be derived after treatment of the free ester with LAH. It was later found that the *trans* ester **5** separated quantitatively during the reaction when the total piperidinols **1** were acetylated leaving the almost pure *cis* isomer in the mother liquors. Isomeric purity of the products was confirmed from their p.m.r. spectra (see below). This procedure was adopted as the best route to the pure *cis* and *trans* piperidinols **1**; it also enabled isomer ratios in the total products of various reductions of **2** to be calculated. The *trans*/*cis* ratio after LAH (2.3) was reasonably close to the reported (1) value of 1.7, while that after aluminum iso-

TABLE 1. 4-Methine p.m.r. characteristics of isomeric 1,3-dimethylpiperidin-4-ols and derived acetates

Structure	Isomer	Form	Solvent	4-H p.m.r. characteristics* Chemical shift (δ)	Base width (b.w. Hz)	Width at half height ($w_{1/2}$ Hz)
1	*trans*	Base	$CDCl_3$	<3.3†	—	—
1	*cis*	Base	$CDCl_3$	3.73	16	7.5
1	*trans*	Base	Pyridine	3.25	31	17
1	*cis*	Base	Pyridine	3.86	18	8.5
1	*trans*	HCl	DMSO-d_6	<3.5†	—	—
1	*cis*	HCl	DMSO-d_6	3.5	16	7.5
5	*trans*	Base	$CDCl_3$	4.4	31.5	17
5	*cis*	Base	$CDCl_3$	4.93	17	6.5
5	*trans*	HCl	$CDCl_3$	4.65	32	16.5
5	*cis*	HCl	$CDCl_3$	5.03	16	7.0
1	*cis*	MeI	DMSO-d_6	3.65	16	8.0
5	*trans*	MeI	DMSO-d_6	4.61	34	16
5	*cis*	MeI	DMSO-d_6	4.85	13	6.0

*When signals were broad (> 25 Hz) measurements were only accurate to about ±2 Hz because of difficulty in judging terminal limits of the bands while shallowness of the signal also prevented accurate measurement of $w_{1/2}$ values; greater degrees of accuracy were possible when signals were narrower as in spectra of *cis* derivatives.
†Signal within ring proton band.

propoxide (1.2, reported 0.56) reflects the operation of an equilibration process (2) which the modified procedure adopted here allows (reaction period increased from 3.5 to 9 h). Hydrogenation of **2** in ethanol at atmospheric pressure with platinum dioxide as catalyst gave the *cis* piperidinol **1** exclusively. This result was unexpected since Mistryukov (1) obtained a mixture (*trans*/*cis* ratio 2.2) after reduction under the same conditions but at high pressure. Reduction of the corresponding *N*-benzyl analog of **2** gave a mixture of piperidinols which could not be separated as their hydrochlorides; the *N*-benzyl acetate **6** hydrochlorides, however, could be separated readily by fractional crystallization of the total product derived from 1-benzyl-3-methyl-4-piperidone. The *cis* acetate was converted to the corresponding *N*-methyl-

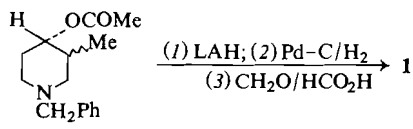

6

piperidinol **1** in three steps as shown above. Diphenylacetates of the piperidinols **1** were obtained by use of diphenylacetyl chloride–benzene or, in better yield, by a transesterification procedure using methyl diphenylacetate (3). Benzilates of **1** were also made by a transesterification reaction.

The p.m.r. characteristics of the piperidinols **1** and derivatives which confirm **3** and **4** as the preferred conformations, respectively, of *cis* and *trans* isomers are as follows (details in Table 1).

4-Methine Signals. The *cis* signals[1] were about 0.5 p.p.m. lower field of the *trans* resonances in accord with an equatorial 4-H in **3** and an axial proton in **4** (4, 5). In most spectra of the piperidinols **1**, only the *cis* signal was resolvable but both isomeric signals could be identified in pyridine, a solvent which induces downfield shifts in protons adjacent to hydroxyl functions (6).[2] *cis* and *trans* 4-methine signals were well resolved in the spectra of esters in $CDCl_3$ as a result of downfield acylation shifts (7).

Further verification of preferred conformation follows from the broader base widths

[1]Here, "*cis* signals" refers to the resonance of the 4-methine proton in spectra of *cis* **3***a*; this and like abbreviations are used throughout this paper for brevity.

[2]In spectra of total piperidinols **1** in pyridine the two methine signals did not overlap and could be integrated separately; isomer ratios so derived agreed well with those calculated from yields of acetate hydrochlorides.

Can. J. Chem. Downloaded from www.nrcresearchpress.com by 210.87.254.42 on 09/05/12
For personal use only.

Can. J. Chem. Downloaded from www.nrcresearchpress.com by 210.87.254.42 on 09/05/12
For personal use only.

(b.w.) and widths at half height ($w_{1/2}$) of the *trans* methine signals, only the axial signal as in **4** receiving two large $^3J_{a/a}$ coupling contributions. Closest models for **3** and **4** are the 2,6-diphenylpiperidinols, **7** and **8** respectively, whose conformations are fixed by the bulky phenyl substituents (8).

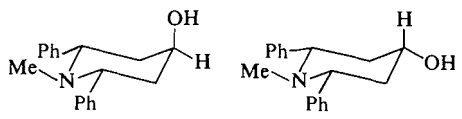

7 4-H b.w. in $CDCl_3$ = 16.4 Hz

8 = 32.4 Hz

In **7** and **8**, methine protons are coupled to 4 vicinal protons whereas only three are involved in the 3-methylpiperidine derivatives. Hence 4-H signal dimensions observed (Table 1) are larger than those anticipated from the model values. In *cis* examples this result is evidence for significant contributions from inverted chair forms such as **9** in which an axial–axial coupling

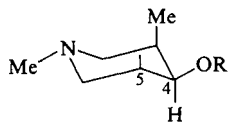

9
(R=H or COMe)

operates between 4-H and 5-H. In *cis* methiodides, populations of such chair forms will be very low as a result of 1,3 diaxial 1-Me/3-Me interactions, and 4-H signal dimensions are significantly reduced in the spectrum of the quaternary salt of *cis* **5**. In the spectrum of *cis* **1** methiodide recorded in DMSO-d_6 allowance needs to be made for HCOH coupling (see below), and the corrected b.w. (16–3.5 = 13.5 Hz) is consistent with that of the equatorial 4-H model **7**.

4-OH Signals. The p.m.r. parameters of hydroxyl proton signals are not normally characteristic because of their sensitivity to solvent, concentration, temperature, and other factors. However, when the OH group is strongly hydrogen bound as in solvent DMSO-d_6, the O*H* resonance position is relatively unaffected by small changes in the factors mentioned above, while ^3J coupling to α-protons may be detected and have stereochemical utility (9, 10). Coupling of this nature is not observed in aminoalcohols except when the basicity of nitrogen is eliminated as in methiodide salts (11).[3] In spectra of isomeric methiodides the *trans* OH signal (doublet δ 4.96) did not differ significantly in chemical shift from the *cis* (doublet δ 4.93) but the assignments **3***a* and **4***a* are confirmed by the larger ^3J values of the *trans* OH doublet (*trans* 5.5, *cis* 4.2 Hz) (10).

The conformation of 1-methylpiperidin-3-ol and its derivatives is of special interest. Evidence for a significant population of the axial conformer **10** is provided by (*i*) the fact that the

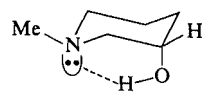

10

width of the 3-H resonance (b.w. 25 Hz, $w_{1/2}$ 14 Hz in CCl_4) is intermediate between that of the methine signals of the axial- and equatorial-OH models **7** and **8** respectively, and (*ii*) demonstration of an intramolecular N--HO bond in dilute solutions of the piperidinol (12). The 3-H signal b.w. of the acetate of 1-methylpiperidin-3-ol was close to that of the piperidinol, but that of the acetate hydrochloride in $CDCl_3$ was distinctly narrower. On closer inspection the signal near δ 5 was seen to be composed of overlapping broad and narrow multiplets typical of axial and equatorial methine signals respectively, a fact which was clearer in the 100 MHz spectrum (Fig. 1.).

In addition, the spectrum showed duplicate *N*-methyl doublets ($H\overset{+}{N}Me$ coupling) and OCO*Me* singlets, of about equal intensities. The results are evidence that epimeric conjugate acids (13*a*) arise when the basic ester is protonated, represented by structures **11** and **12** in their most probable conformations. The narrowness

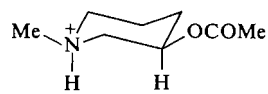

11 (*cis*)

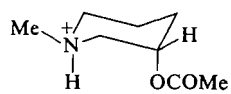

12 (*trans*)

[3]The HCOH coupling was not seen in the DMSO-d_6 spectra of hydrochloride salts of **1**, hence sufficient base must be present in equilibrium with the conjugate acid to catalyze proton exchange.

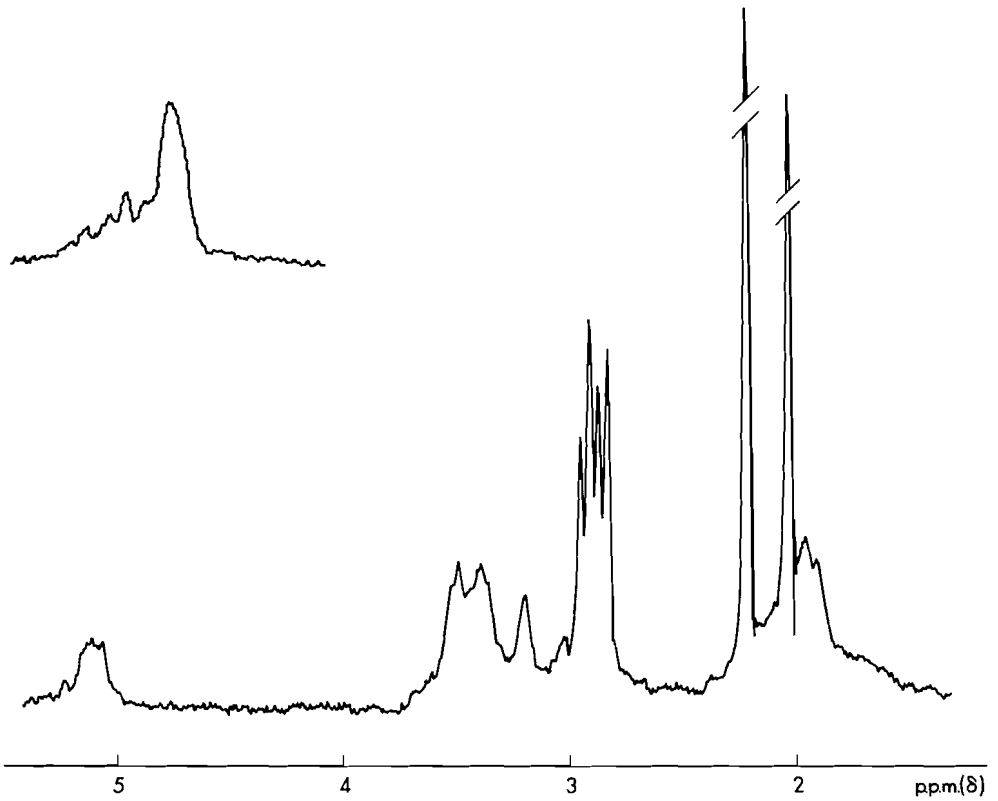

FIG. 1. The 60 MHz p.m.r. spectrum of 3-acetoxy-1-methyl-piperidine hydrochloride in $CDCl_3$. Insert is the 3-methine signal recorded at 100 MHz.

of one of the 3-H resonance bands ($w_{1/2}$ 8 Hz) is evidence against a high population of inverted forms of the *trans* isomer **12** which would have an axial 3-H proton. The lower field OCO*Me* signal (δ 2.23) is assigned to the *trans* isomer since the ester function is close to and will be deshielded by the charged $^+$NH group (13*b*); the *cis* OCOMe resonance (δ 2.03) is close to that of *trans* **4***b* hydrochloride (δ 2.06 in $CDCl_3$), a compound in which the ester substituent is equatorial and removed from the charged basic center. The higher field NMe signal is assigned to **12** on the basis of intensity comparisons and the probability, from studies of pyranose acetates (14), of the *N*-methyl protons being shielded more by an axial than equatorial acetoxy function. Axial and equatorial methine (*H*CO) signals are normally resolved in isomeric piperidinol acetates (see above) and the unusually low field position of the axial proton in the present case (Fig. 1), leading to signal overlap, must be due to its proximity to the deshielding $^+$NH group (see **11**). The relative peak heights of NMe and OCOMe signals in Fig. 1 reveal a small preference for the *trans* isomer **12** which may be stabilized by an

$$^+\text{NH}\text{----}\text{O}=\text{C}\begin{matrix}\diagup\text{O}\\ \diagdown\text{Me}\end{matrix}$$

bond[4] or by transannular interactions between the unit positive charge on nitrogen and the ether oxygen atom (15). The spectrum of the 3-piperidyl acetate salt in DMSO-d_6 showed a 3-H resonance more characteristic of an axial proton (b.w. 28 Hz) and single NMe and OCOMe resonances, hence the *trans* isomer **12** is less favored in this solvent. Evidence for favored axial OCOR conformers was also

[4]The i.r. evidence on this point was inconclusive since (in $CHCl_3$) $\nu_{C=O}$ of both *N*-methyl-3- and -4-piperidyl acetates increased by 15 cm^{-1} when hydrochlorides were examined over the concentration range 0.1–3%.

Can. J. Chem. Downloaded from www.nrcresearchpress.com by 210.87.254.42 on 09/05/12
For personal use only.

obtained from the spectrum of 1-methyl-3-piperidyl benzilate hydrochloride (3-H b.w. 21 Hz) in spite of the solvent being DMSO-d_6.

Proton magnetic resonance studies of tropine and pseudotropine have established their preferred conformation in solution as **13** and **14** respec-

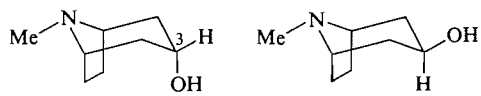

13 **14**

tively, the piperidine ring being flattened at the C-3 end as a result of the bimethylene bridge linkage (16). It was of importance to determine whether esterification would affect these conformational preferences in view of the pronounced antimuscarinic properties of certain tropyl esters. The 3-H p.m.r. signal dimensions of acetate and benzilate salts of tropine in various solvents and of tropyl (±)-tropate (atropine) in D_2O fell in the range 15–16.5 Hz (b.w.) and 9.5–11 Hz ($w_{1/2}$), and did not differ significantly from those of tropine itself, *e.g.* atropine sulfate in D_2O, b.w. 16.5, $w_{1/2}$ 9.5 Hz. A bulky ester function does not therefore alter the preference of the piperidine ring of tropine for a chair conformation, thus the acyl moiety must be directed away from the bimethylene bridge. As anticipated, 3-methine p.m.r. characteristics of pseudotropyl acetate and benzilate (b.w. ~40 Hz) were very similar to those of pseudotropine itself. Duplication of N—Me signals in the spectra of tropyl and pseudotropyl acetate hydrochlorides in $CDCl_3$ gave evidence of the separate existence of epimeric conjugate acids in this solvent; as Closs found for pseudotropine (17), the minor N—Me signals fell to lower field of the major resonances, *e.g.* pseudotropyl acetate hydrochloride, ν_{NMe} δ 2.8 (major doublet), 2.97 (minor).

The spasmolytic and mydriatic activities of certain basic esters described here will be reported elsewhere.

Experimental

The p.m.r. spectra were recorded on a Varian A-60D spectrometer operating at 40 ± 1° with TMS as internal standard. Bases were recovered from hydrochloride salts by adding excess of aqueous ammonia and extracting with ether (extracts dried with Na_2SO_4). Salts were crystallized from ethanol–ether unless otherwise stated. Melting points were determined using a Thomas Hoover Capillary apparatus and are uncorrected.

Reduction of 1,3-Dimethyl-4-piperidone

The piperidone **2** (25.4 g) in ether (75 ml) was added to a stirred suspension of LAH (8 g) in ether (75 ml) at a rate which maintained gentle refluxing. The mixture was kept at the reflux temperature for 8 h, then cooled and decomposed with ice-water. The ether was decanted, dried (Na_2SO_4), and evaporated to leave the isomeric mixture **1** (21.5 g), b.p. 78°/1 mm, lit. 64°/0.25 mm (18). The base (4.3 g) in ethanol (50 ml) was acidified with hydrogen chloride and diluted with ether when *trans* **1** hydrochloride (2.7 g) separated, m.p. 184–186°, lit. 183–184° (1).

Anal. Calcd. for $C_7H_{16}ClNO$: C, 50.8; H, 9.7; N, 8.45. Found: C, 50.7; H, 9.9; N, 8.7.

The base (2 g) recovered from the mother liquors was heated under reflux with acetyl chloride (3.1 g) in ethyl acetate (105 ml) for 24 h. The mixture, on cooling and storage at 5°, deposited *cis* **5** *hydrochloride* (2.7 g), m.p. 145–146°.

Anal. Calcd. for $C_9H_{18}ClNO_2$: C, 52.1; H, 8.7; N, 6.7. Found: C, 51.9; H, 8.3; N, 7.05.

trans **1** was acetylated in the same way to give *trans* **5** *hydrochloride*, m.p. 208–210°.

Anal. Found: C, 52.2; H, 8.9; N, 6.95.

The *cis* acetate **5** (4 g) was reduced with LAH (1 g) as described above for **2** to give *cis* **1** (2.4 g), isolated as a *hydrochloride*, m.p. 110–111°.

Anal. Found: C, 50.7; H, 9.6; N, 8.1.

The total alcohols **1** (5 g) (derived from **2** and LAH) were acetylated with acetyl chloride (6.4 g) in ethyl acetate (150 ml) in the manner described above. The solution on cooling to room temperature deposited *trans* **5** hydrochloride (5.8 g), m.p. 208–210°. The *cis* salt (2.5 g), m.p. 143–145°, separated from the mother liquors after storage at 5° for 48 h. This procedure was adopted for the separation of isomers from all reduction experiments.

Reduction of **2** with aluminum isopropoxide was carried out by adding the piperidone (10 g) in isopropanol (180 ml) to a solution of the reagent (16 g) in isopropanol (100 ml) contained in a flask fitted with a Vigreaux column. The mixture was heated under reflux for 9 h at a rate to maintain slow distillation; the distillate gave a negative test for acetone (19) after 2–3 h. Most of the solvent was evaporated, the residue hydrolyzed with cold aqueous ammonia and the bases **1** (10 g) recovered by continuous extraction with ether. Catalytic hydrogenation of **2** was achieved by stirring a mixture of the piperidone (1 g), ethanol (150 ml), and platinum dioxide (150 mg) with hydrogen at room temperature and pressure. When uptake of hydrogen ceased the product was filtered and the filtrate evaporated to yield the piperidinols **1** (1 g). No reduction occurred when 10% palladium-on-charcoal was used as catalyst.

The following *methiodides* were prepared (all recrystallized from ethanol):

trans **1**, m.p. 161–163°.

Anal. Calcd. for $C_8H_{18}INO$: C, 35.45; H, 6.6; N, 5.2. Found: C, 35.6; H, 6.7; N, 5.05.

cis **1**, m.p. 208–210°.

Anal. Found: C, 35.5; H, 6.8; N, 5.4.

trans **5**, m.p. 192–193°.

Anal. Calcd. for $C_{10}H_{20}INO_2$: C, 38.4; H, 6.4; N, 4.5. Found: C, 38.4; H, 6.4; N, 4.1.

Can. J. Chem. Downloaded from www.nrcresearchpress.com by 210.87.254.42 on 09/05/12
For personal use only.

cis **5**, m.p. 184–185°.
Anal. Found: C, 38.3; H, 6.4.

1-Benzyl-3-methyl-4-piperidyl Acetates
(by M. M. A. Hassan)

The 1-benzylpiperidinol mixture (3 g) from 1-benzyl-3-methyl-4-piperidone and LAH was heated under reflux with acetyl chloride (2 g) and ethyl acetate (20 ml) for 8 h. On cooling the *trans acetate* **6** *hydrochloride* (1.0 g) separated, m.p. 255–256°.

Anal. Calcd. for $C_{15}H_{22}ClNO_2$: C, 63.5; H, 7.8; N, 4.9. Found: C, 63.8; H, 7.8; N, 4.95.

The mother liquors on storage at 5° gave *cis* **6** *hydrochloride* (1.8 g), m.p. 180–182°.

Anal. Found: C, 63.25; H, 7.65; N, 5.1.

cis 1-Benzyl-3-methylpiperidin-4-ol (3.9 g), derived as usual from *cis* **6** and LAH, was shaken with 10% palladium-on-charcoal (390 mg), ethanol (25 ml), and hydrogen at atmospheric pressure. When gas absorption ceased the mixture was filtered and the filtrate evaporated to yield oily *cis* 3-methylpiperidin-4-ol (1.9 g). This base was heated under reflux with formalin (5 ml), formic acid (5 g, 97%), and ethanol (100 ml) for 24 h. The solvents were then evaporated and an ethereal solution of the residue dried (Na_2SO_4). The dry base gave *cis* **1** hydrochloride (2.2 g), m.p. and mixed m.p. 109–111°.

Aromatic Esters of the Piperidinols **1**

The diphenylacetate of *cis* **1** was prepared using diphenylacetyl chloride by the method of Coan *et al.* (20), and was isolated as a *hydrobromide*, m.p. 202–204°.

Anal. Calcd. for $C_{21}H_{26}BrNO_2$: C, 62.4; H, 6.4. Found: C, 62.7; H, 6.4.

It gave a *methiodide*, m.p. 187–188° from ethanol.

Anal. Calcd. for $C_{22}H_{28}INO_2$: C, 56.8; H, 6.0. Found: C, 57.1; H, 6.0.

The diphenylacetate of *trans* **1** was obtained by ester exchange with methyl diphenylacetate following the method of Cannon (3), and was isolated as a *hydrochloride*, m.p. 122–124°.

Anal. Calcd. for $C_{21}H_{26}ClNO_2$: C, 70.1; H, 7.2; N, 3.9. Found: C, 70.0; H, 7.25; N, 4.0.

It gave a *methiodide*, m.p. 243–245° from ethanol.

Anal. Found: C, 57.2; H, 6.15.

Benzilates of **1** were obtained by the tranesterification procedure using methylbenzilate, and the following salts prepared:

trans **1** *Benzilate hydrochloride*, m.p. 183–184°.

Anal. Calcd. for $C_{21}H_{26}ClNO_3$: C, 67.2; H, 6.9; N, 3.9. Found: C, 66.9; H, 7.1; N, 3.6.

cis **1** *Benzilate hydrochloride*, m.p. 266–267°.

Anal. Found: C, 67.1; H, 7.0.

trans **1** *Benzilate methiodide*, m.p. 209–211° from ethanol.

Anal. Calcd. for $C_{22}H_{28}INO_3$: C, 54.8; H, 5.8. Found: C, 55.3; H, 6.1.

cis **1** Benzilate *methiodide*, m.p. 189–190° from ethanol.

Anal. Found: C, 54.9; H, 5.8.

Esters of 1-methylpiperidin-3-ol were prepared by methods described above. The acetate formed a *hydrochloride*, m.p. 143–144°.

Anal. Calcd. for $C_8H_{11}ClNO_2$: C, 49.6; H, 8.3; N, 7.2. Found: C, 49.7; H, 8.2; N, 7.45.

The benzilate gave a hydrochloride, m.p. 217–218° from acetone, lit. 221–223° (21).

Anal. Calcd. for $C_{20}H_{24}ClNO_3$: C, 66.4; H, 6.6. Found: C, 66.45; H, 6.5.

Esters of Tropine and Pseudotropine

Acetates and benzilates of isomeric 3-tropanols were obtained by the described methods. Salts isolated were as follows:

Tropyl acetate hydrochloride, m.p. 209–210°.

Anal. Calcd. for $C_{10}H_{18}ClNO_2$: C, 54.95, H, 8.2. Found: C, 54.6; H, 8.25.

Pseudotropyl acetate hydrochloride, m.p. 218–219° from ethanol.

Anal. Found: C, 54.95; H, 8.24; N, 6.6 (Calcd. 6.4).

Tropyl benzilate hydrochloride, m.p. 242–243°, lit. 239–240° (22).

Anal. Calcd. for $C_{22}H_{26}ClNO_3$: C, 68.15; H, 6.7; N, 3.6. Found: C, 67.95; H, 6.7; N, 3.8.

Pseudotropyl benzilate hydrochloride, m.p. 226–228°, lit. 232° (23).

Anal. Found: C, 67.9; H, 6.6; N, 3.6.

The authors thank the Defence Research Board of Canada for financial support and Dr. M. M. A. Hassan for carrying out reduction experiments on 1-benzyl-3-methyl-4-piperidone.

1. E. A. Mistryukov. Bull Acad. Sci. U.S.S.R. 1788, 1793 (1965).
2. M. Balasubramanian and N. Padma. Tetrahedron, **19**, 2135 (1963).
3. J. G. Cannon. J. Org. Chem. **25**, 959 (1960).
4. L. M. Jackman and S. Sternhell. Applications of nuclear magnetic resonances spectroscopy in organic chemistry. 2nd ed. Pergamon, Oxford. 1969.
5. J. W. ApSimon, W. G. Craig, P. V. Demarco, D. W. Mathieson, L. Saunders, and W. B. Whalley. Tetrahedron **23**, 2339 (1967).
6. P. V. Demarco, E. Farkas, D. Doddrell, B. L. Mylava, and E. Wenkert. J. Am. Chem. Soc. **90**, 5480 (1968).
7. C. C. J. Culvenor. Tetrahedron Lett. 1091 (1966).
8. C. Y. Chen and R. J. W. Le Fèvre. J. Chem. Soc. 3467 (1965).
9. O. L. Chapman and R. W. King. J. Am. Chem. Soc. **86**, 1256 (1964).
10. C. P. Rader. J. Am. Chem. Soc. **88**, 1713 (1966); **91**, 3248 (1969).
11. R. J. Bass and M. J. Sewell. Tetrahedron Lett. 1941 (1969).
12. G. Hite, E. E. Smissman, and R. West. J. Am. Chem. Soc. **82**, 1207 (1960).
13. A. F. Casy. Proton magnetic resonance spectroscopy in medicinal and biological chemistry. Academic Press, London. 1971. (*a*) p. 145, (*b*) p. 203.
14. R. U. Lemieux and J. D. Stevens. Can. J. Chem. **44**, 249 (1966).
15. R. D. Stolow, D. I. Lewis, and P. A. D'Angelo. Tetrahedron, **26**, 5831 (1970).
16. C. Y. Chen and R. J. W. Le Fèvre. J. Chem. Soc. 3473 (1965); R. J. Bishop, G. Fodor, A. R. Katritzky, E. Soti, L. E. Sutton, and F. J. Swinbourne. J. Chem. Soc. C, 74 (1966); M. Ohashi, I. Morishima, K. Okada, and T. Yonezawa. Chem. Commun. 34 (1971).

Can. J. Chem. Downloaded from www.nrcresearchpress.com by 210.87.254.42 on 09/05/12
For personal use only.

17. G. L. CLOSS. J. Am. Chem. Soc. **81**, 5456 (1961).
18. C. R. GANELLIN and R. G. W. SPICKETT. J. Med. Chem. **8**, 619 (1965).
19. A. L. WILDS. Org. React. **2**, 178 (1944).
20. S. B. COAN, B. JAFFE, and D. PAPA. J. Am. Chem. Soc. **78**, 3701 (1956).
21. J. H. BIEL, E. P. SPRENGLER, H. A. LEISER, J. HORNER, A. DRUKKER, and K. L. FRIEDMAN. J. Am. Chem. Soc. **77**, 2250 (1955).
22. O. HROMATKA, C. CSOKLICH, and I. HOFBAUER. Montash. Chem. **83**, 134 (1956).
23. H. KREITMAIR. Klin. Woch. **19**, 676 (1936).

Can. J. Chem. Downloaded from www.nrcresearchpress.com by 210.87.254.42 on 09/05/12
For personal use only.

Steroids and Steroidases. XIII.[1] Illustrations of the Potential of Lithiodithiane–Epoxide Reactions for the Stereospecific Introduction of Substituents into the Steroid Nucleus

J. Bryan Jones and Roger Grayshan

Lash Miller Chemical Laboratories, Department of Chemistry, University of Toronto, Toronto 181, Ontario

Received August 30, 1971

The reactions of 2-lithio-1,3-dithiane with both 2α,3α- and 2β,3β-oxiranyl-5α-cholestane have been used to prepare both epimers of 2-methyl-3-oxo- and 3-methyl-2-oxo-5α-cholestane. The results obtained illustrate the potential of the dithiane-epoxide route as an attractive and versatile general procedure for the stereospecific introduction of substituents into alicyclic compounds. Furthermore, since for six-membered ring compounds the epoxide ring is opened in a *trans*-diaxial manner, the substituent is introduced into the thermodynamically less stable orientation. Subsequent isomerization to the preferred equatorial isomer is thus possible and accordingly, both epimers are obtainable from the same synthetic sequence.

On a utilisé les réactions du 2-lithio-1,3-dithiane avec le 2α,3α- et le 2β,3β-oxyranyl-5α-cholestane pour préparer les épimères du 2-méthyl-3-oxo- et du 3-méthyl-2-oxo-5α-cholestane. Les résultats obtenus illustrent le potentiel du dithiane-époxyde comme étant une procédure générale attractive et versatile pour l'introduction stéréospécifique de substituants dans les composés alicycliques. De plus, puisque le noyau époxyde, de façon *trans*-diaxiale pour les composés possédant un cycle à six, le substituant est introduit dans l'orientation la moins stable au point de vue thermodynamique. L'isomérisation subséquente en isomère équatorial plus stable est alors possible et à partir de cela, les deux épimères peuvent être obtenus à partir de la même séquence de synthèse.

Canadian Journal of Chemistry, **50**, 810 (1972)

As a result of our interest in the mechanism of action of the $\Delta^5 \rightarrow \Delta^4$-3-ketoisomerase of *P. testosteroni* (1*a*, *b*) we became interested in developing convenient and versatile routes to stereospecifically substituted steroids suitable for "mapping" the active site of the enzyme. Of the general routes surveyed those based on a lithiodithiane–epoxide reaction appeared the most attractive and examples of the feasibility and advantages of this approach have been reported in communication form (1*c*). This note records the experimental and other details omitted from the preliminary communication since it is now apparent that the human resources required to continue the project as originally planned are unlikely to become available in the foreseeable future.

The possibilities of achieving a satisfactory general method for introducing substituents into the steroid nucleus by exploiting the properties of epoxides was drawn to our attention by the previous application of the reactions of Δ^5-epoxides with Grignard reagents (2–5). Disappointingly, this approach to the stereospecific introduction of alkyl groups did not prove to be universally applicable since when the epoxide was not located at a ring junction, ring contraction predominated with both steroidal (6) and cyclohexene oxide (7) reactions.[2] However, the fact that the latter compound underwent the expected ring opening with 2-lithio-1,3-dithiane (9*a*, *b*) indicated that similar reactions could be expected in the steroid field, and accordingly the representative synthetic pathways outlined in Scheme 1 were investigated.

Conversion of 5α-cholestan-3β-ol to its tosylate followed by alumina-catalyzed elimination gave 5α-cholest-2-ene in 60% yield. Epoxidation with peracetic acid proceeded smoothly and a 90% yield of 2α,3α-oxiranyl-5α-cholestane (**1**) was obtained exclusively (10). None of the isomeric 2β,3β-epoxide was detectable in the reaction mixture. On treatment of the 2α,3α-epoxide **1** with 2-lithio-1,3-dithiane in dry tetrahydrofuran for 1 week, *trans*-diaxial opening of the oxirane ring occurred to give 80% of the 2β-dithianyl-3α-hydroxy derivative **2**. Desulfurization of **2** to 2β-methyl-5α-cholestan-3α-ol

[1] For part XII see ref. 1*a*.

[2] This complication can now be overcome by using organocopper analogues of the Grignard reagents (8).

Can. J. Chem. Downloaded from www.nrcresearchpress.com by 210.87.254.105 on 09/05/12
For personal use only.

Can. J. Chem. Downloaded from www.nrcresearchpress.com by 210.87.254.105 on 09/05/12
For personal use only.

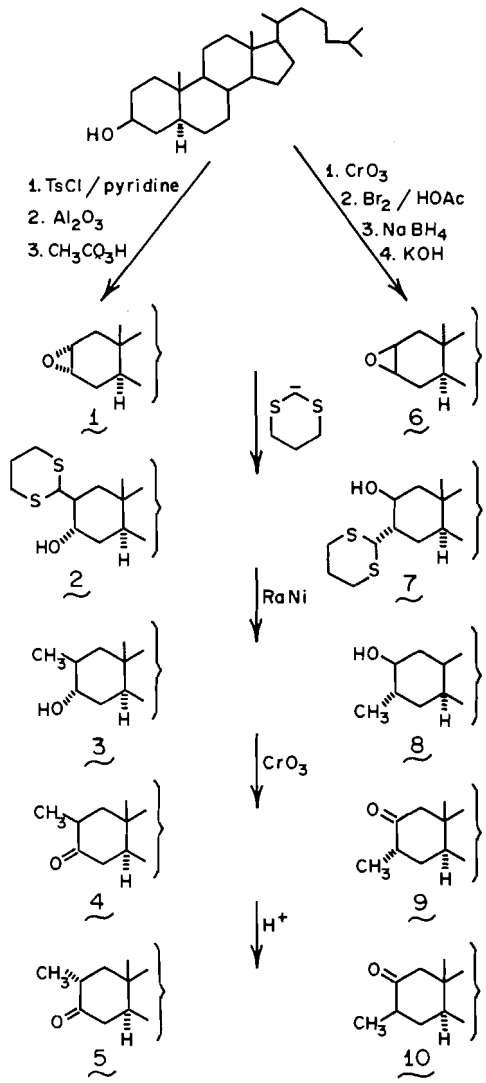

SCHEME 1

(**3**) with Raney nickel in ethanol was readily accomplished (85% yield).

Problems had been anticipated in achieving controlled oxidation of **3** to the axial-methyl ketone **4** without some epimerization occurring during the reaction or work-up procedures. However, the transformation proved surprisingly simple to accomplish and oxidation of the precursor alcohol **3** with Jones' reagent at 0° for 3 min afforded the thermodynamically unstable 2β-methyl-5α-cholestan-3-one (**4**) in quantitative yield. Under these conditions only a trace of the energetically preferred epimer **5** was detectable by t.l.c. analysis. As expected, subsequent isomerization of **4** to the equatorial 2α-methyl epimer **5** was readily effected (also in quantitative yield) by treatment with ethanolic sulfuric acid.

The corresponding reactions in the 2β,3β-epoxide series were equally facile. 2β,3β-Oxiranyl-5α-cholestane (**6**) was obtained in 35% overall yield from 5α-cholestan-3β-ol via the sequence of reactions indicated in Scheme 1 (9*c*). On treatment of **6** with lithiodithiane anion in dry tetrahydrofuran at 0° for 2 days, the β-epoxide ring opened smoothly, again in a *trans*-diaxial manner, to give 3α-dithianyl-5α-cholestan-2β-ol (**7**, 80%). Raney nickel desulfurization of **7** afforded a 70% yield of the 3α-methyl-2β-hydroxy compound **8**. Oxidation of the latter compound without incurring any epimerization at C-3 was effected with Jones' reagent at 0° for 1 min and the thermodynamically less favored 3α-methyl-2-ketone **9** was obtained in quantitative yield. Acid-catalyzed epimerization of **9** to its isomer **10**, in which the methyl group is in the more stable equatorial orientation, presented no problems and the 3β-methyl isomer was again isolated in quantitative yield.

Although pure samples of each **4**, **5**, **9**, and **10** have been obtained previously by other methods (11, 12), the routes to these types of compounds outlined in Scheme 1 represent a significant improvement over any of the synthetic pathways developed earlier. The facility with which reactions were achieved, and the excellent yields obtained at every stage, indicate that the dithiane-epoxide procedure has considerable potential for effecting the stereospecific introduction of a range of substituents into the steroid nucleus. The approach is an attractive one from several points of view. For example, the fact that cleavage of the epoxide ring by dithiane occurs in a *trans*-diaxial fashion ensures the introduction of the substituent into the thermodynamically less stable axial orientation. Subsequent isomerization to the corresponding equatorial compounds will then often be possible thereby enabling both epimers to be obtained from the same synthetic scheme. Furthermore, conversions of the dithiane group into other functions have been well documented (9*a*, *b*) and thus a variety of substitution pat-

terns can be elaborated from a single dithianyl intermediate.

Experimental

The i.r. and n.m.r. data were obtained on CCl_4 and $CDCl_3$ solutions, respectively. All compounds were purified until no impurities could be detected at least by g.l.c. analyses. The t.l.c. analyses were performed with silica gel G and the spots were visualized with iodine vapor or with a ceric sulfate in sulfuric acid spray. The p.l.c. separations were effected on plates up to 20 × 100 cm in size coated with 0.5 mm of silica gel G. All other analytical methods, the instrumentation used, criteria of purity, *etc.* were as described previously (1).

2β-(2-(1,3-Dithianyl))-5α-cholestan-3α-ol (2)

2α,3α-Oxiranyl-5α-cholestane (**1**) m.p. 104–105° (lit. m.p. 105–106° (10)) was obtained in 54% overall yield from 5α-cholestan-3β-ol according to the method of Fürst and Plattner (10). A solution of 2-lithio-1,3-dithiane was then prepared by the slow addition of *n*-butyl lithium (13.8 ml of a 1.6 *M* hexane solution, 22 mmol) to 1,3-dithiane (2.59 g, 22 mmol) in dry tetrahydrofuran (55 ml) at −20° under nitrogen (9*b*). After stirring for a further 1 h, a −20° solution of the 2α,3α-epoxide **1** (1.12 g, 2.9 mmol) in dry tetrahydrofuran (10 ml) was added and the mixture was kept at 0° for 1 week. The reaction solution was then poured into water (500 ml) and extracted with ether (4 × 50 ml). The combined ether extracts were washed with water (2 × 25 ml) and then dried ($MgSO_4$) and evaporated. The yellow gum obtained was purified by p.l.c. using firstly benzene, and then benzene–ether (5:1) as developing solvents. The 2β-(2-(1,3-dithianyl))-5α-cholestan-3α-ol (**2**) obtained was recrystallized from ether–methanol to give plates (1.24 g) m.p. 73–77°; i.r. 1278 and 915 cm^{-1} (dithianyl); n.m.r. δ 0.64 (C-18 CH_3), 0.85 (C-19 CH_3), 4.32 (1H, d, $J = 7$ Hz, $HCS_2C_3H_6$), and 4.26 p.p.m. (1H, m, C-3 H).

2β-Methyl-5α-cholestan-3α-ol (3)

2β-Dithianyl-5α-cholestan-3α-ol (**2**, 320 mg, 0.63 mmol) in ethanol (60 ml) was heated under reflux for 4 h with freshly prepared Raney nickel (3.5 g). The mixture was then filtered and the ethanolic filtrate evaporated. The several component crude product obtained was purified by p.l.c. using benzene as the developing solvent and recrystallization of the major fraction from ether–methanol gave 2β-methyl-5α-cholestan-3α-ol (**3**) as needles (140 mg), m.p. 117–118°;[3] n.m.r. δ 0.64 (C-18 CH_3), 0.82 (C-19 CH_3), 1.03 (3H, d, $J = 7$ Hz, C-2β CH_3), and 3.74 p.p.m. (1H, m, C-3β H).

Anal. Calcd. for $C_{28}H_{50}O$: C, 83.5; H, 12.5. Found: C, 83.2; H, 12.5.

2β-Methyl-5α-cholestan-3-one (4)

2β-Methyl-5α-cholestan-3α-ol (**3**, 70 mg, 0.17 mmol) in acetone (10 ml) was stirred at 0° for 3 min with Jones' reagent (containing 0.05 ml of 8 *N* chromic acid) and the mixture was then immediately poured into water (100 ml). Extraction with ether (3 × 50 ml) followed by evaporation of the dried ($MgSO_4$) extracts yielded 2α-methyl-5α-cholestan-3-one (**4**, 69 mg) containing only a trace (by t.l.c.) of its epimer **5**. Recrystallization of **4** from ether–methanol gave the pure compound as needles m.p. 97.5–98.5° (lit. m.p. 85–92°[3] (13), 96–97° (6)); n.m.r. δ 0.66 (C-18 CH_3), 0.76 (C-19 CH_3), and 1.04 p.p.m. (3H, d, $J = 7$ Hz, C-2 CH_3).

2α-Methyl-5α-cholestan-3-one (5)

Epimerization of 2β-methyl-5α-cholestan-3-one (**4**, 40 mg, 0.1 mmol) was effected by refluxing in ethanol (5 ml) containing 20% aqueous sulfuric acid (0.1 ml) for 2 h. The mixture was diluted with water (200 ml), extracted with ether (3 × 50 ml), and the dried ($MgSO_4$) ether extracts evaporated to give 2α-methyl-5α-cholestan-3-one (**5**, 39 mg). Recrystallization from ether–methanol afforded needles m.p. 118–120° (lit. m.p. 119–120° (11)); n.m.r. δ 0.68 (C-18 CH_3), 1.00 (3H, d, $J = 7$ Hz, C-2α CH_3), and 1.06 p.p.m. (C-19 CH_3).

3α-(2-(1,3-Dithianyl))-5α-cholestan-2β-ol (7)

2β,3β-Oxiranyl-5α-cholestane (**6**) m.p. 87–88° (lit. m.p. 90–91° (9*c*)) was prepared from 5α-cholestan-3-one in 30% overall yield by the method of Corey (9*c*). The 2β,3β-epoxide **6** (200 mg, 0.52 mmol) in dry tetrahydrofuran (2 ml) was then added to a solution of 2-lithio-1,3-dithiane (2 mmol, prepared as described above from 1,3-dithiane (235 mg, 2 mmol)) in dry tetrahydrofuran (5 ml) at −20° under nitrogen. After keeping for 2 days at 0° the reaction mixture was poured into water (100 ml) and extracted with ether (3 × 25 ml). The gum obtained on evaporation of the $MgSO_4$ dried ether solution was purified by p.l.c. using benzene, followed by benzene–ether (9:1) development. The 3α-(2-(1,3-dithianyl))-5α-cholestan-2β-ol (**7**) obtained was recrystallized from ether–methanol to give plates (218 mg) m.p. 158–159°; i.r. 1278 and 915 cm^{-1} (dithianyl); n.m.r. δ 0.64 (C-18 CH_3), 0.99 (C-19 CH_3), 4.21 (1H, d, $J = 8$ Hz, $HCS_2C_3H_6$), and 4.32 p.p.m. (1H, m, C-3α H).

Anal. Calcd. for $C_{31}H_{54}OS_2$: C, 73.4; H, 10.7; S, 12.7. Found: C, 73.7; H, 10.9; S, 12.7.

3α-Methyl-5α-cholestan-2β-ol (8)

3α-Dithianyl-5α-cholestan-2β-ol (**7**, 187 mg, 0.37 mmol) in ethanol (50 ml) was refluxed for 4 h with freshly prepared Raney nickel (2.5 g). Following removal of the nickel by filtration, the ethanolic solution was evaporated and the residual gum was purified by p.l.c. with benzene–ether (9:1) as the developing solvent. The 3α-methyl-5α-cholestan-2β-ol (**8**) obtained (102 mg) was recrystallized from ether–methanol as needles, m.p. 158–159°, n.m.r. δ 0.65 (C-18 CH_3), 0.93 (3H, d, $J = 8$ Hz, C-3α CH_3), 1.00 (C-19 CH_3), and 3.75 p.p.m. (1H, broad s, C-2α H).

Anal. Calcd. for $C_{28}H_{50}O$: C, 83.5; H, 12.5. Found: C, 83.8; H, 12.3

3α-Methyl-5α-cholestan-2-one (9)

3α-Methyl-5α-cholestan-2β-ol (**9**, 83 mg, 0.2 mmol) in acetone (10 ml) was stirred at 0° for 1 min with Jones' reagent (containing 0.059 ml of 8 *N* chromic acid). The mixture was then poured immediately into water (100 ml) and extracted with ether (3 × 50 ml). Evaporation of the dried ($MgSO_4$) ether solution gave 3α-methyl-5α-cholestan-2-one (**9**, 82 mg) which contained none (by t.l.c.) of the 3β-methyl

[3]The m.p. of this compound has previously been reported as 122–128° (13). However, the relatively broad melting range suggests that impurities were present in the latter sample. The ketone m.p. 85–92° derived from this material also appears to have been impure.

Can. J. Chem. Downloaded from www.nrcresearchpress.com by 210.87.254.105 on 09/05/12
For personal use only.

epimer. Recrystallization from ether–methanol afforded needles m.p. 127.5–128° (lit. m.p. 127–128° (12)); n.m.r. δ 0.65 (C-18 CH_3), 0.75 (C-19 CH_3), and 1.20 p.p.m. (3H, d, $J = 8$ Hz, C-3α CH_3).

Anal. Calcd. for $C_{28}H_{48}O$: C, 83.9; H, 12.1. Found: C, 83.7; H, 11.9.

*3β-Methyl-5α-cholestan-2-one (**10**)*

3α-Methyl-5α-cholestan-2-one (**9**, 25 mg, 0.06 mmol) in ethanol (5 ml) containing 10% aqueous sulfuric acid (0.1 ml) was heated under reflux for 2 h and was then poured into water (200 ml). Extraction with ether (3 × 50 ml) and evaporation of the $MgSO_4$ dried ether solution yielded 3β-methyl-5α-cholestan-2-one (**10**, 24 mg) containing a trace (by t.l.c.) of the starting material **9**. Purification by p.l.c. with benzene development followed by recrystallization from ether–methanol gave microcrystals of the pure compound m.p. 150–151° (lit. m.p. 151–153° (12)); n.m.r. δ 0.65 (C-18 CH_3), 0.70 (C-19 CH_3), and 0.90 p.p.m. (3H, d, $J = 7$ Hz, C-3β CH_3).

This work was supported by the National Research Council of Canada. The award of a postdoctoral fellowship (to R.G.) by the School of Graduate Studies, University of Toronto, is gratefully acknowledged.

1. (*a*) J. B. Jones and S. Ship. Biochim. Biophys. Acta, In press; (*b*) J. B. Jones and D. C. Wigfield. Can. J. Chem. **47**, 4459 (1969); (*c*) J. B. Jones and R. Grayshan. Chem. Commun. 141 (1970).
2. H. J. Ringold, E. Batres, and G. Rosenkranz. J. Org. Chem. **22**, 99 (1957).
3. (*a*) D. N. Kirk and V. Petrow. J. Chem. Soc. 1091 (1962); (*b*) G. Cooley, B. Ellis, D. N. Kirk, and V. Petrow. J. Chem. Soc. 4112 (1957).
4. J. A. Campbell, J. C. Babcock, and J. A. Hogg. J. Am. Chem. Soc. **80**, 4717 (1958) and references therein.
5. J. C. Gasc and L. Nedelec. Tetrahedron Lett. 2005 (1971); Bull. Soc. Chem. Fr. 2556 (1970).
6. P. N. Rao and J. C. Uroda. Tetrahedron Lett. 1117 (1964).
7. B. G. Christensen, R. G. Strachan, N. R. Trenner, B. H. Arison, R. Hirshman, and J. M. Chemerda. J. Am. Chem. Soc. **82**, 3995 (1960).
8. R. W. Herr, D. M. Wieland, and C. R. Johnson. J. Am. Chem. Soc. **92**, 3813 (1970).
9. (*a*) E. J. Corey and D. Crouse. J. Org. Chem. **33**, 298 (1968); D. Seebach, N. R. Jones, and E. J. Corey. J. Org. Chem. **33**, 300 (1968); (*b*) E. J. Corey and D. Seebach. Angew. Chem. Internat. Edn. **4**, 1075, 1134 (1965); D. Seebach. Syn. 17 (1969); (*c*) E. J. Corey. J. Am. Chem. Soc. **75**, 4832 (1953).
10. A. Fürst and P. Plattner. Helv. Chem. Acta, **32**, 275 (1949).
11. Y. Mazur and F. Sondheimer. J. Am. Chem. Soc. **79**, 2906 (1957); **80**, 5220 (1958).
12. V. Dovinola and L. Mangoni. Gazz. Chim. Ital. **99**, 206 (1969); Chimica e Industria, **49**, 166 (1967).
13. C. Djerassi, N. Finch, R. C. Cookson, and C. W. Bird. J. Am. Chem. Soc. **82**, 5488 (1960).

Can. J. Chem. Downloaded from www.nrcresearchpress.com by 210.87.254.105 on 09/05/12
For personal use only.

Carbon-13 Chemical Shifts of Methylcyclohexanes, Cyclohexanols, α- and β-D-Glucose and their Relation to Carbon Electron Densities from the Extended Hückel and Del Re Theories

N. CYR, A. S. PERLIN, AND M. A. WHITEHEAD
Chemistry Department, McGill University, Montreal 110, Quebec

Received July 28, 1971

An evaluation is made of the extent to which ^{13}C chemical shifts of diastereoisomeric cyclohexane derivatives and pyranoses are related to electron density. Values of the latter for carbon atoms in cyclohexane, methylcyclohexanes, cyclohexanols, and D-glucose are calculated using the Extended Hückel Theory (EHT), with and without iteration, and the Del Re theory. It is shown that when electronegativities of all of the atoms are similar then the theories do not give electron densities which correlate with the ^{13}C chemical shifts; when a strongly electronegative atom, such as oxygen, is present, the electron density differences are greater than the inaccuracy in the calculated individual densities and a fair correlation with ^{13}C chemical shifts is obtained. Iteration is shown to give lower carbon electron densities and a better correlation.

L'importance de la relation entre la densité électronique et les déplacements chimiques du ^{13}C est évaluée dans les dérivés diastéréoisomériques du cyclohexane et les pyranoses. Les densités électroniques sur les atomes de carbone dans le cyclohexane, les méthylcyclohexanes, les cyclohexanols et le D-glucose sont calculées par la "théorie de Hückel étendue" (THE) avec et sans iteration et par la théorie de Del Re. On montre que lorsque les électronégativités de tous les atomes sont semblables, les théories ne donnent pas les densités électroniques qui correspondent aux déplacements chimiques du ^{13}C; par contre lorsqu'un atome fortement électronique, tel l'oxygène, est présent, les différences dans les densités électroniques sont plus élevées que l'imprécision sur les densités individuelles calculées de sorte qu'une bonne corrélation avec les déplacements chimiques du ^{13}C est obtenue. On montre que l'iteration donne les densités électroniques plus faibles pour le carbone ainsi qu'une meilleure corrélation.

Canadian Journal of Chemistry, **50**, 814 (1972)

Can. J. Chem. Downloaded from www.nrcresearchpress.com by 210.87.254.6 on 09/05/12
For personal use only.

Introduction

Carbon-13 n.m.r. chemical shifts in cyclic compounds are influenced strongly by configurational and conformational factors. For example, in the cyclohexane series, most of the ^{13}C chemical shifts of isomers containing an axial group are found at higher fields than the shifts for the corresponding stereoisomers containing only equatorial groups (1–3). Similarly, higher chemical shifts are observed for aldohexopyranoses and aldohexopyranosides when one or more of the substituent groups is axially oriented (4, 5). Furthermore, the interaction energies of substituent groups in both series appear to be substantially reflected in the ^{13}C chemical shifts (3, 5).

In order to explain the ^{13}C chemical shifts, the total electronic structure of the molecule must be determined. Although ^{13}C chemical shifts depend on factors other than charge distributions on the carbon nuclei, it has been shown in a number of instances that charge density is the dominant factor (6–11). Thus, correlations of n.m.r. chemical shifts with charge distributions calculated by the Extended Hückel Theory (12), have been demonstrated for alkanes, halogenated alkanes, and alkenes. However, similar data are not available for alicyclic compounds and the sugars, nor for a comparison of geometric isomers.

Two relatively simple and dependable semi-empirical methods, the Del Re method (13), and the Extended Hückel M.O. method, have been employed in the current study to calculate the electronic structures of such compounds, the latter method being used both with and without iteration.

Calculations

The Extended Hückel Theory

The complete overlap matrix **S** is computed using overlap integral formulae (14) for Slater orbitals. The coulomb integral, H_{rr}, for each atomic orbital is taken to be the Valence State Ionization Potential (VSIP) of that orbital in the molecule, using Cusach's values (15), which

Can. J. Chem. Downloaded from www.nrcresearchpress.com by 210.87.254.6 on 09/05/12
For personal use only.

are dependent on the charge at the nucleus and on the orbital populations of the nucleus considered. The resonance integral, H_{rs}, is given by (16):

$$[1] \qquad H_{rs} = \frac{(2 - S_{rs})(H_{rr} + H_{ss})S_{rs}}{2}$$

where S_{rs} is the overlap between the r-th and s-th atomic orbitals. The variational matrix equation is:

$$[2] \qquad \boldsymbol{HC = SCE}$$

solved by Lowdin's method (17). The solution of this equation provides orbital energies and the LCAO coefficients of the MO, subject to the Hückel approximations (18).

When the theory is made iterative, the second charge input density is corrected using the first input and first output charge densities according to the equation (19):

$$[3] \quad \text{Input } II = \text{Input } I - 0.1\,(\text{Input } I - \text{Output } I)$$

Calculations were carried out until the output charge density and the previous input charge density differed by less than 0.01.

The Del Re Theory

The Del Re method (13) for calculating charge densities has been employed without modification.

Geometries of the Molecules

(a) Cyclohexane and Methylcyclohexanes

The C—C and C—H distances used were 1.53 and 1.09 Å, respectively. All the bond angles were assumed to be regular tetrahedral. The methyl hydrogens were so arranged that the C—H bonds in the methyl groups were gauche to the ring C—C and C—H bonds.

(b) Cyclohexanol and Cyclohexanediols

The bond distances and bond angles used were: C—C = 1.53; C—H = 1.09; C—O = 1.43; O—H = 0.97 Å; ∠CCC = ∠CCH = regular tetrahedral; ∠COH = 107; ∠CCO = 112.5°; and the OH bonds were gauche to the ring C—H bonds.

(c) D-Glucoses

Although accurate X-ray data for the β-D-glucose structure in the crystal are known (20), the geometry was simplified slightly for the present calculations. The coordinates used for the carbons and ring oxygen were as shown in Table 1, whereas the atomic distances were: C—C = 1.53; C—O = 1.43; C—H = 1.06; O—H = 0.97 Å. All of the required interatomic distances were calculated from the atomic coordinates.

TABLE 1. Coordinates used for the carbons and ring oxygen of β-D-glucose in the EHT calculation β

	x(Å)	y(Å)	z(Å)
C(1)	1.17586	2.14776	0.0
C(2)	1.24086	0.71641	0.50739
C(3)	0.0	0.0	0.0
C(4)	−1.24086	0.71641	0.50739
C(5)	−1.17586	2.14776	0.0
C(6)	−2.41672	2.86417	0.50739
O(5)	0.0	2.80676	0.47735

Results

(a) Methylcyclohexanes

The charge distributions of the following 15 compounds were calculated by the Extended Hückel method without iterating: cyclohexane; *e*- and *a*-methylcyclohexane; 1,1(*e*,*a*), 1,2(*e*,*e*), 1,2(*e*,*a*), 1,3(*e*,*e*), 1,3(*e*,*a*), 1,4(*e*,*e*), and 1,4(*e*,*a*) dimethylcyclohexane; 1,2,4(*e*,*e*,*e*), 1,2,4(*e*,*e*,*a*), 1,3,5(*e*,*e*,*e*), 1,1,2(*e*,*a*,*e*), and 1,1,3(*e*,*a*,*e*) trimethylcyclohexane.

The plot of charge densities against the observed ^{13}C chemical shifts for each of these compounds showed that there was no consistently close correlation between $\delta_{\text{p.p.m.}}$ and q. Since the second order paramagnetic term, which seems to be the most dominant in the ^{13}C chemical shifts, arises from the unbalance of electrons in orbitals with non-zero angular momentum (21), the carbon p orbital charge densities were also plotted against ^{13}C chemical shifts. Again, however, there was no satisfactory correlation between the carbon 2p orbital populations and the chemical shifts. The Del Re method (13) was also used to calculate charge densities for several of these methylcyclohexanes, but correlation with the chemical shifts was as poor as obtained by the non-iterative EHT.

Cyclohexane, *e*-methylcyclohexane and *trans*-(*e*,*e*)1,2-dimethylcyclohexane were then selected and their charge distributions were calculated by the EHT *with the iterative procedure*. After 8 ~ 10 iterations, the values became consistent

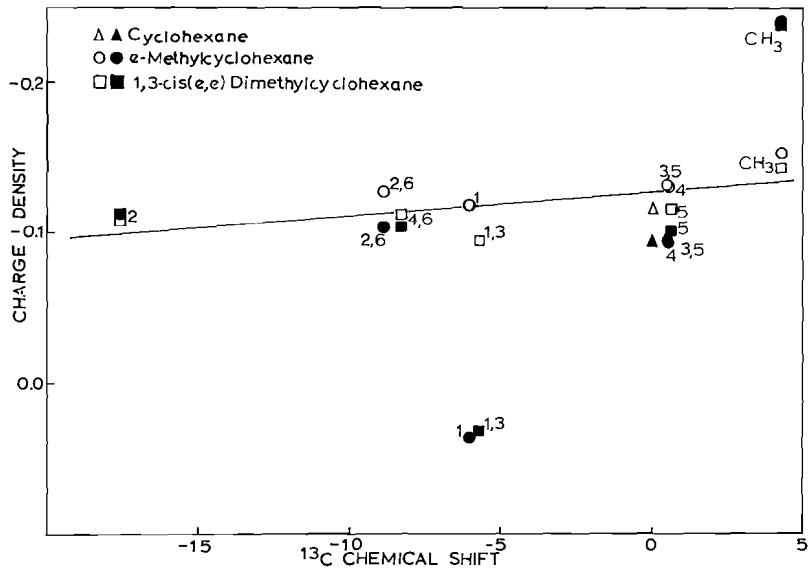

FIG. 1. A plot of ^{13}C chemical shifts (in p.p.m. from cyclohexane) against charge density obtained by the iterative (white) and non-iterative (black) EHT, for cyclohexane, *e*-methylcyclohexane, and *cis*-1,3-dimethylcyclohexane. (No correction has been made to account for *a*-methylcyclohexane to the ^{13}C chemical shift.) The straight line applies to the iterative data.

TABLE 2. Calculated charge densities and observed ^{13}C chemical shifts for 1,3(*a*,*e*) dimethylcyclohexane

	EHT			
Carbon	Non-iterative	Iterative	Del Re	^{13}C δ (p.p.m.) (2)*
1,3	0.0318	−0.0948	−0.0317	−5.76
2	−0.1144	−0.1074	−0.0765	−17.54
4,6	−0.1043	−0.1112	−0.0758	−8.31
5	−0.0994	−0.1137	−0.0754	0.61
Methyl	−0.2413	−0.1414	−0.1187	4.25

*From cyclohexane.

within the set limit (+0.01), and the overall charge differences between atoms in a molecule became much smaller. Calculated charges on carbons of the 1,3-dimethyl derivative are given in Table 2 together with their observed ^{13}C chemical shifts and the calculated empirical charge densities obtained by the Del Re method. A comparison of plots of charge densities with and without iteration for all three compounds is shown in Fig. 1. After several iterations a definite improvement in correlation between charge density and ^{13}C chemical shift is seen, although it is still not adequate to differentiate between stereoisomers. However, the iterative EHT is more successful than the Del Re theory in approaching a satisfactory correlation of $\delta_{p.p.m.}$ and q.

(b) Cyclohexanol and Cyclohexanediols

Another cyclohexane system, with one or two oxygen atoms, *i.e.*, cyclohexanol and cyclohexanediols, was then studied. The introduction of oxygen atoms should result in larger charge density differences, therefore decreasing the importance of any uncertainty in the calculation. A plot of calculated charge densities by the iterative EHT method against ^{13}C chemical shifts is shown in Fig. 2, and the values are tabulated in Table 3, together with the results of the non-iterative EHT method,[1] and the results from a Del Re calculation.

As seen from Fig. 2, the general correlation between charge densities and ^{13}C chemical shifts is good. However, the small high field shifts observed for 1,2-*cis*-(*e*,*a*) cyclohexanediol with respect to 1,2-*trans*-(*e*,*e*) cyclohexanediol are not reflected in the results of the present

[1]Iteration not only reduces the overall charge differences between atoms but, in several instances (Table 3), it produces a reversal in the order of charge densities, resulting in the much better correlation that is observed (Fig. 2).

Can. J. Chem. Downloaded from www.nrcresearchpress.com by 210.87.254.6 on 09/05/12
For personal use only.

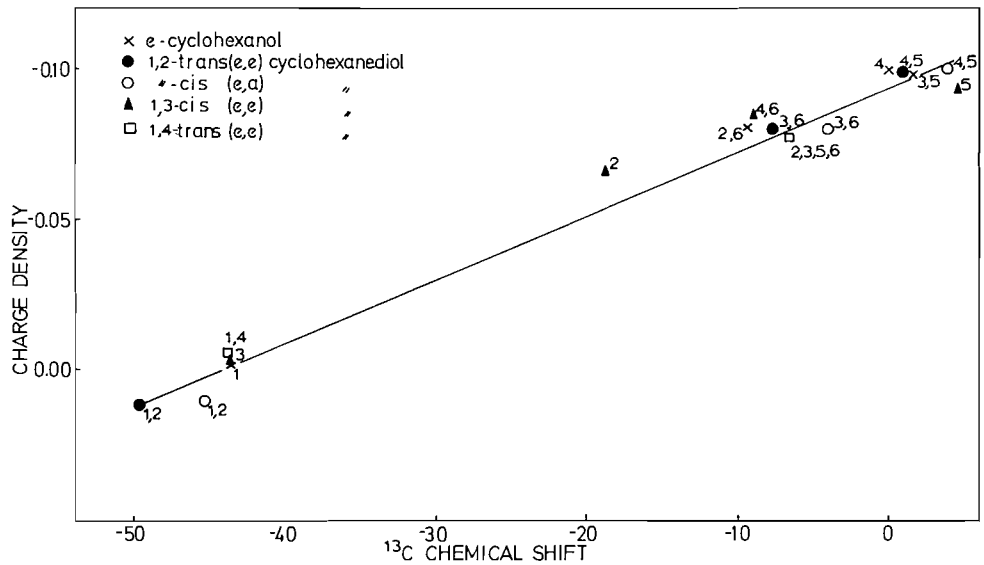

FIG. 2. A plot of charge density against ^{13}C chemical shift (in p.p.m. from cyclohexane) for cyclohexanol and cyclohexanediols by iterative EHT.

TABLE 3. Calculated charge densities* and observed ^{13}C chemical shifts for cyclohexanol and cyclohexanediols

Compound (carbon)	EHT		Del Re	^{13}C δ (p.p.m.) (3)‡
	Non-iterative	Iterative		
e-Cyclohexanol				
(1)	0.1531	−0.0042	0.0816	−43.5
(2,6)	−0.6193	−0.0815	−0.0638	−9.3
(3,5)	−0.4581	−0.0979	−0.0665	+1.6
(4)	−0.5779	−0.0995	−0.0746	0.0
1,2(*e*,*e*) Diol				
(1,2)	0.1105	0.0103	0.0746	−49.5
(3,6)	−0.6172	−0.0812	−0.0623	−7.4
(4,5)	−0.5890	−0.0981	−0.0738	+1.1
1,2,(*e*,*a*) Diol†				
(1,2)	0.1107	0.0106	0.0746	−45.2
3,6	−0.6217	−0.0801	−0.0623	−4.0
4,5	−0.5926	−0.0989	−0.0738	+4.1
1,3(*e*,*e*) Diol				
(1,3)	0.1497	−0.0019	0.0832	−43.2
(2)	0.6526	−0.0664	−0.0697	−18.7
(4,6)	0.6269	−0.0836	−0.0635	−8.9
(5)	0.5811	−0.0922	−0.0720	+4.7
1,4(*e*,*e*) Diol				
(1,4)	0.1424	−0.0062	0.0821	−43.8
(2,3,5,6)	−0.6166	−0.0784	−0.0623	−6.6

*These densities are based on a value of zero for a carbon having 4.0000 valence electrons.
†Average of (*e*,*a*) and (*a*,*e*) isomers.
‡From cyclohexane.

Can. J. Chem. Downloaded from www.nrcresearchpress.com by 210.87.254.6 on 09/05/12
For personal use only.

TABLE 4. Calculated charge densities and observed ^{13}C chemical shifts for α- and β-D-glucose

Compound (carbon)	EHT		Del Re	^{13}C δ (p.p.m.) (5)*
	Non-iterative	Iterative		
α-D-Glucose				
(1)	0.4835	0.0955	0.1896	100.4
(2)	0.0640	0.0595	0.1161	120.9
(3)	0.0865	0.0542	0.1086	119.5
(4)	0.0840	0.0437	0.1051	122.8
(5)	0.1119	0.0454	0.0962	121.2
(6)	−0.3021	0.0000	0.0468	131.4
β-D-Glucose				
(1)	0.4872	0.0859		96.5
(2)	0.0650	0.0570	Same	118.2
(3)	0.0943	0.0550	as	116.6
(4)	0.0839	0.0441	above	122.8
(5)	0.1173	0.0452		116.6
(6)	−0.3024	0.0000		131.4

*From CS_2.

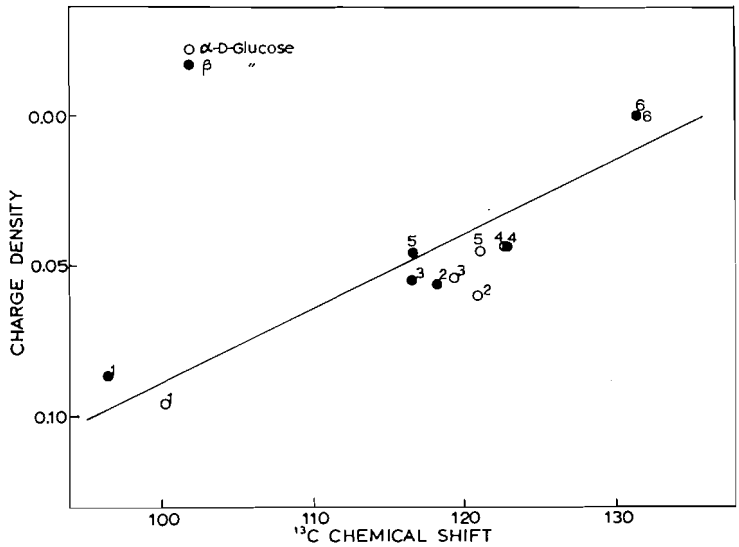

FIG. 3. A plot of charge density against ^{13}C chemical shift (in p.p.m. from CS_2) for α- and β-D-glucose by iterative EHT. The straight line applies to the data for β-D-glucose.

method of calculation; the charge distributions in these two isomers are practically identical.

(c) α- and β-D-Glucose

Another system in which charge distributions were calculated includes α-D-glucose and β-D-glucose. The results are shown in Table 4 and in Fig. 3.

As in the cyclohexanediol series, each carbon charge density is well correlated with its ^{13}C chemical shift (5) within a given molecule as expected from previous calculation by the Del Re method (22, 23). However, the high field shift caused by introduction of the anomeric axial —OH group is not reflected in the calculations.

Conclusions and Discussion

The following conclusions can be drawn from the charge density calculations by the EHT and the Del Re methods:

Can. J. Chem. Downloaded from www.nrcresearchpress.com by 210.87.254.6 on 09/05/12
For personal use only.

Can. J. Chem. Downloaded from www.nrcresearchpress.com by 210.87.254.6 on 09/05/12
For personal use only.

(*1*) The calculated charge densities by the EHT on atoms in the cyclohexanol system and in D-glucopyranoses, show an approximately linear correlation with observed ^{13}C chemical shifts.

(*2*) For the methylcyclohexane system where only carbon and hydrogen atoms are involved, the correlation is poor both by the EHT and the Del Re methods.

(*3*) The EHT results show no differentiation between small geometrical variations, such as changing a hydroxyl group from the equatorial orientation to the axial orientation, whereas the change in shielding is clearly detected by the high field shifts of ^{13}C signals.

The failure of the EHT method to differentiate between stereoisomers in which a group changes from equatorial to axial is probably due, at least in part, to the neglect of intratomic repulsion terms, both inter- and intraorbital, in the coulomb integrals H_{rr} making up the basis set of the calculation (24). The neglect of the intraorbital terms gives rise to the large charge density values and consequently high polarities in the C—H bonds when the non-iterative EHT is used, which are only partly offset in the interative EHT, whereas the interorbital repulsions would help to correct inaccuracies in the magnitude of the inductive effects (24). It is to be hoped that semi-empirical all valence electron methods such as the CNDO/BW (25, 26), which include electron–electron repulsion terms will be capable of differentiating between structural isomers.

(*4*) As seen from Tables 3 and 4, the Del Re method gives charge densities comparable with those of the iterative EHT and, unlike the non-iterative EHT, does not overestimate the charge densities. However, those charge densities for the cyclohexanol carbon atoms to which hydroxyl groups are bonded do not correlate with the observed ^{13}C chemical shifts, and this method is not applicable to stereoisomers.

Since EHT calculations generate energy criteria (12), energies for several of the molecules examined here were readily obtained. Particularly pertinent are values for the anomeric D-glucoses, for which some data are already available. Thus, Neely (27) has reported that the non-iterative EHT gives a value of 9 kcal/mol higher energy for α-D-glucose than for the β-anomer. In fact, the α-anomer is the less stable by 0.35 kcal/mol (28). By contrast we find a difference of only 0.5 kcal/mol by the non-iterative procedure and as much as 11 kcal/mol higher after 10 iterative procedures, although in favor of the β-anomer. Since the geometry of the molecules and the values for the matrix elements in Neely's calculation are slightly different from the present ones, *the parameters used in the EHT clearly have a large effect on the calculated energy values.* Among the methylcyclohexanes, the data obtained by non-iterative EHT imply that the introduction of an axial methyl group causes an increase in energy of ~10 kcal/mol over that of its equatorial counterpart, which is at least five times the accepted values (28, 29). Those large discrepancies indicate therefore that energy values derived from EHT data must be appraised with utmost care.

The authors express their thanks to the National Research Council of Canada for financial support, and Mr. E. Koller of the Pulp and Paper Research Institute of Canada for solving sets of linear equations.

1. G. W. BUCHANAN, D. A. ROSS, and J. B. STOTHERS. J. Am. Chem. Soc. **88**, 4301 (1966).
2. D. K. DALLING and D. M. GRANT. J. Am. Chem. Soc. **89**, 6612 (1967).
3. A. S. PERLIN and H. J. KOCH. Can. J. Chem. **48**, 2639 (1970).
4. D. E. DORMAN and J. D. ROBERTS. J. Am. Chem. Soc. **92**, 1355 (1970).
5. A. S. PERLIN, B. CASU, and H. J. KOCH. Can. J. Chem. **48**, 2597 (1970).
6. J. M. SICHEL and M. A. WHITEHEAD. Theoret. chim. Acta. **5**, 35 (1966).
7. N. C. BAIRD and M. A. WHITEHEAD. Theoret. chim. Acta, **6**, 167 (1966).
8. P. C. LAUTERBUR. J. Chem. Phys. **43**, 360 (1965).
9. T. YONEZAWA, I. MORISHIMA, and H. KATO. Bull. Chem. Soc. Jap. **39**, 1398 (1966).
10. R. J. PUGMIRE and D. M. GRANT. J. Am. Chem. Soc. **90**, 697, 4232 (1968).
11. T. TOKUHIRO and G. FRAENKEL. J. Am. Chem. Soc. **91**, 5005 (1969).
12. R. HOFFMANN. J. Chem. Phys. **39**, 1397 (1963); **40**, 2745, 2474, 2480 (1964).
13. G. DEL RE. J. Chem. Soc. 4031 (1958).
14. R. S. MULLIKEN, C. A. RIEKE, D. ORLOFF, and H. ORLOFF. J. Chem. Phys. **17**, 1248 (1949).
15. L. C. CUSACHS and J. W. REYNOLDS. J. Chem. Phys. **43**, S160 (1965).
16. L. C. CUSACHS. J. Chem. Phys. **43**, S157 (1965).
17. P. O. LOWDIN. J. Chem. Phys. **18**, 365 (1950).
18. R. G. PARR. Quantum theory of molecular electronic structure. Benjamin, 1964.
19. D. G. CARROL, A. T. ARMSTRONG, and S. P. MCGLYNN. J. Chem. Phys. **44**, 1865 (1966).

20. S. S. C. CHU and G. A. JEFFREY. Acta Cryst. B**24**, 830 (1968).
21. C. J. JAMESON and H. S. GUTOWSKY. J. Chem. Phys. **40**, 1714 (1964).
22. Y. A. ZHDAVOV, V. I. MINKIN, Y. A. OSTROUMOV, and G. A. DOROFEENKO. Carbohyd. Res. **7**, 156 (1968).
23. A. SALINAS and J. F. SPROVIERO. Carbohyd. Res. **16**, 243 (1971).
24. J. M. SICHEL and M. A. WHITEHEAD. Theoret. chim. Acta, **3**, 135 (1965).
25. R. J. BOYD and M. A. WHITEHEAD. J. Chem. Soc. A, 3579 (1971).
26. R. J. BOYD, J. P. SNYDER, and M. A. WHITEHEAD. J. Am. Chem. Soc. Submitted.
27. W. B. NEELY. J. Med. Chem. **12**, 16 (1969).
28. E. L. ELIEL, N. L. ALLINGER, S. J. ANGYAL, and G. A. MORRISON. Conformational analysis. Interscience, 1967.
29. F. A. L. ANET, C. H. BRADLEY, and G. W. BUCHANAN. J. Am. Chem. Soc. **93**, 258 (1971).

Can. J. Chem. Downloaded from www.nrcresearchpress.com by 210.87.254.6 on 09/05/12
For personal use only.

Mass Spectra of Some Tropolones and Tropolone Methyl Ethers[1]

J. L. C. WRIGHT,[2] W. D. JAMIESON, S. SAFE, AND L. C. VINING

Atlantic Regional Laboratory, National Research Council of Canada, Halifax, Nova Scotia

Received July 13, 1971

The mass spectra and fragmentation patterns of several tropolones and tropolone methyl ethers are reported. Deuteration studies confirmed that elimination of a formyl radical from 2-methoxytropone upon electron impact involves a specific rearrangement of the methoxyl group but sequential loss of carbon monoxide and a hydrogen radical from the ring are competing reactions. They also showed that in a dimethyl ether of anhydrosepedonin elimination of a formyl radical is completely suppressed. In the methyl ether of stipatatonic acid elimination of carbon monoxide is followed by expulsion of carbon dioxide with no loss of 29 mass units. The mass spectrum of [8-^{13}C]-anhydrosepedonin as well as the energy spectrum for sepedonin have been investigated. These results not only provide a plausible account of the fragmentation of tropolones following electron impact but also illustrate the effect of product ion stability in determining which among a number of alternative modes of fragmentation will be more probable.

La spectrométrie de masse et les types de fragmentation de plusieurs tropolones et de tropolones méthyléthers sont rapportés. Les études sur des composés deutérés confirment que l'élimination d'un radical formyl de la méthoxy-2 tropone par l'impact d'électrons implique un réarrangement spécifique du groupe méthoxy mais la perte ultérieure du monoxyde de carbone et d'un radical hydrogène du cycle sont des réactions compétitives. Elles montrent également que dans un éther diméthylé de l'anhydrosepedonine l'élimination d'un radical formyl est complètement supprimée. Dans l'éther méthylé de l'acide stipatatonique, l'élimination du monoxyde de carbone est suivie par l'expulsion de dioxyde de carbone sans perte de 29 unités de masse. Le spectre de masse de la [8-^{13}C]anhydrosepedonine aussi bien que le spectre des énergies pour la sepedonine ont été examinés. Ces résultats non seulement apportent une interprétation plausible de la fragmentation des tropolones suivant l'impact des électrons mais illustrent aussi l'influence de la stabilité des ions produits pour l'identification desquels un certain nombre de modes de fragmentation possibles seraient les plus probables.

Canadian Journal of Chemistry, **50**, 821 (1972)

Can. J. Chem. Downloaded from www.nrcresearchpress.com by 210.87.254.40 on 09/05/12
For personal use only.

The mass spectra of tropone, tropolone, and several derivatives have been examined by Wilson *et al.* (1) who reported that carbon monoxide was eliminated preferentially, leaving a fragment which decomposed as expected for the appropriate phenyl ion-radical. An apparent exception was tropolone methyl ether which gave a relatively intense fragment ion corresponding to the loss of 29 mass units. Budzikiewicz *et al.* (2) suggested that hydrogen transfer in the molecular ion *a* might give the species *b* which would then yield the stable oxonium ion *c* (Scheme 1). While investigating the fungal tropolone sepedonin (**1***a*), which is readily dehydrated (3) and gave a mass spectrum closely resembling that of anhydrosepedonin (**2***a*), we observed fragment ions at *m/e* 178 and 177 which could be attributed to the elimination of carbon monoxide and a formyl radical, respectively. The spectra showed a metastable ion at *m/e* 153.8 for the reaction (*d*, *m/e* 206) → (*e*, *m/e* 178) (Scheme 2) but none corresponding to the loss of 29 mass units from *d*. Instead, a metastable ion at *m/e* 176 accounted for *m/e* 177 as the product of H ejection from *m/e* 178.

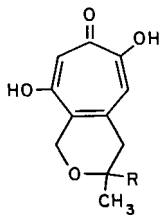

1a, R = OH
1b, R = H

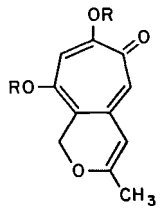

2a, R = H
2b, R = CD_3

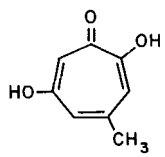

3

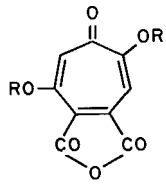

4, R = H
5, R = CH_3

[1]Issued as NRCC No. 12325.

[2]NRCC Postdoctorate Fellow 1967–1968.

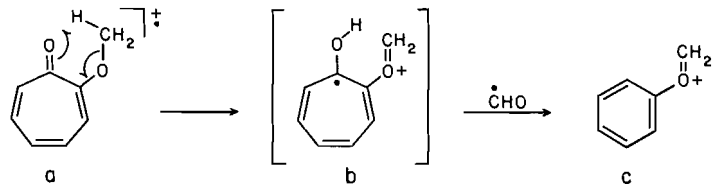

SCHEME 1

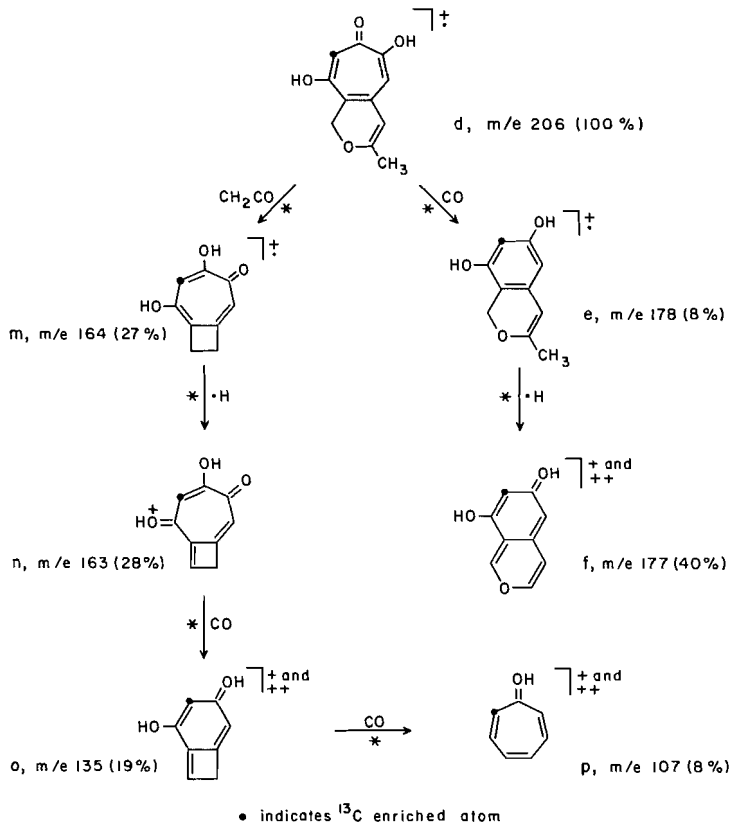

SCHEME 2

Mass spectra of the three anhydrosepedonin dimethyl ethers (4) all showed abundant molecular ions at *m/e* 234. In each spectrum the M − 29 peak at *m/e* 205 was substantial (in dimethyl ethers A and B it was the base peak) whereas the M − 28 peak was smaller. However, a strong metastable ion at *m/e* 204 again showed that M − 29 was formed, at least in part, by expulsion of H from M − 28.

To investigate whether loss of 29 mass units in tropolone methyl ethers does, in fact, proceed by the mechanism suggested by Budzikiewicz *et al.* we first reexamined the mass spectrum of 2-methoxytropone. As reported (1) the ion *c* at *m/e* 107 formed by expulsion of CHO from *a* was more intense (27% of base peak) than that of the M-CO ion at *m/e* 108 (11%). Metastable ions for these reactions were observed at *m/e* 84.5 and 85.8, respectively. No change occurred in the relative intensity of peaks in the *m/e* 105–108 region as the electron beam energy was lowered from 70 to 15 eV. To determine the origin of hydrogen in the formyl radical, 2-methoxytropone-d_3 was prepared. Its mass spectrum

Can. J. Chem. Downloaded from www.nrcresearchpress.com by 210.87.254.40 on 09/05/12
For personal use only.

showed a relatively small M-28 peak (*m/e* 111, 9%); the largest peak in the *m/e* 106–111 range corresponded to loss of CDO (*m/e* 109, 23%). Intense metastable ions were observed for both reactions (peaks at *m/e* 88.6 and 85.5, respectively) but none was found at *m/e* 87.1, the value expected for expulsion of CHO from the molecular ion. On the other hand, metastable ions were observed at *m/e* 137 and 109, corresponding to the reactions M → (M − 1) and (M-CO) → (M-CO − 1) respectively, while there was no evidence for similar expulsion of a deuterium atom.

We conclude that the M − 29 ion from 2-methoxytropone can be formed in three ways: (*i*) by loss of a tropolone H, then a CO radical, (*ii*) the reverse of (*i*), and (*iii*) by expulsion of a CHO radical where the H is derived from the methoxyl substituent as suggested by Budzikiewicz *et al.* (2). In each case the reactions are not accompanied by prior H/D equilibration.

The M − 29 ion from the anhydrosepedonin methyl ethers appears to be formed exclusively by successive loss of CO and then a hydrogen radical. The mass spectrum of anhydrosepedonin dimethyl ether A methoxy-d_6 (**2***b*) displayed a molecular ion at *m/e* 240 as well as intense ions at *m/e* 212 (M-CO, base peak) and *m/e* 211 (M-CHO, 36%). In contrast to 2-methoxytropone-d_3 it showed no ion at *m/e* 210 corresponding to loss of CDO. Metastable ions at *m/e* 187.3 and 210 indicated that the molecular ion (*g*, Scheme 3) first expelled CO to give an intermediate (*h*) which ejected H. However, it is unlikely that this H was lost from the tropolone ring, as in the fragmentation of 2-methoxytropone, since aromatization of the dihydropyran moiety would give the stable oxonium ion, *i*. Presumably because this more favorable path to an even electron ion is available the specific H transfer reaction (*a* → *b*) found with 2-methoxytropone is suppressed.

The mass spectrum of the parent anhydrosepedonin (**2***a*) can be accounted for similarly. Elimination of CO and a hydrogen radical produces the abundant ion at *m/e* 177, which was also present as the double ion at *m/e* 88.5. The resorcinol system is relatively stable (5) and again the most likely site of hydrogen elimination is from C-1 in the pyran moiety, giving the oxonium ion (*f*, Scheme 2) in which delocalization of charge among the three oxygens would lead to enhanced stability. Two additional tropolones **1***b* and **3**, derived from sepedonin (3) showed pairs of peaks in their mass spectra corresponding to the loss of 28 and 29 mass units from their molecular ions. In **3** these were similar in intensity, but in **1***b* the fragment at M − 29 was about 4 times as abundant as that at M − 28. Stipatatonic acid (**4**) and its dimethyl ether (**5**), which possess no hydrogens or hydrogen-bearing substituents at C-4 and -5, gave substantial M − 28 but no M − 29 peaks. Instead an intense ion was observed at M − 72, corresponding to loss of CO_2 from the M − 28 fragment. Again formation of a stable oxonium ion is probably responsible for channelling fragmentation of the tropolone ions into a single pathway.

Techniques have been described (6) for operating double-focussing mass spectrometers in a defocussed mode so ion products of "metastable" reactions can be observed directly and with greater sensitivity. They yield data which often establish unambiguously the occurrence of ion decompositions even where these may not

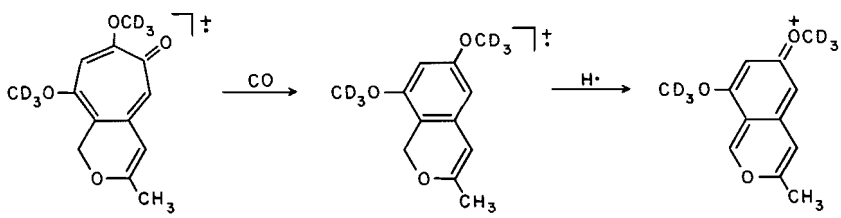

m/e 240 g — m/e 212 h — m/e 211 i

SCHEME 3

Can. J. Chem. Downloaded from www.nrcresearchpress.com by 210.87.254.40 on 09/05/12
For personal use only.

TABLE 1. Transitions detected in the energy spectrum of sepedonin

Voltage at ion current maxima (kV)	Daughter ions detected		Probable parent
	m/e	mass	*m/e*
4.96	67.5	135	163
5.15	164	164	206
"	53.5	107	135
"	53	106	135
5.56	39.5	79	107
"	39	78	107

have led to the usual "metastable-peaks" in the normal mass spectrum of the focussed ion beam. With a mass spectrometer of Mattauch–Herzog geometry, the photographic plate detector can yield high resolution data about daughter ions produced by ion decompositions in that part of the drift tube preceding the energy-focussing sector. Transitions detected by this means in the energy spectrum of sepedonin (Table 1) indicate that expulsion of ketene from the pyran moiety opens an alternative fragmentation pathway. The initial product ion *m/e* 164 is tentatively represented as *m* (Fig. 2). A large peak at *m/e* 43, established by a high resolution study to be mainly the CH_3CO ion, suggests that the C_2H_2O fragment can also be lost as an acetyl ion after H transfer. A metastable ion at *m/e* 162.1 indicates that the ion formed by loss of ketene eliminates a hydrogen radical to yield the ion *m/e* 163 which we represent as *n* although no definitive evidence for this structure was obtained. A group of ions at *m/e* 106–109 is probably similar to that observed by Shannon (7) in the mass spectrum of benzyl alcohol. They generate comparable series of daughter ions and, although depicted as cyclic structures, are likely to be highly unsaturated linear compounds (8).

In support of the fragmentation pathways postulated, the mass spectrum of [8-^{13}C] anhydrosepedonin (9) showed equally enhanced P + 1 peaks for all of the ions described except that at *m/e* 43. Loss of ketene during fragmentation after electron impact was also found to occur with two other natural products, fusarubin (10) and fulvic acid (11), which contain a dihydropyran moiety similar to that of sepedonin.

Experimental

Mass Spectra

Samples were vaporized directly into the ion source of a DuPont/CEC model 21-110B double-focussing mass spectrometer. The accelerating voltage was 8 kV, electron beam energy 70 eV (except as noted otherwise) and resolving power approximately 1:1500. The source temperature, initially below that required to volatilize the sample, was increased rapidly to 170° for sepedonin and anhydrosepedonin, or to 120° for the anhydrosepedonin dimethyl ethers. The spectra of 2-methoxytropone and its deuterated analogue were recorded between 0–25° using a controlled temperature probe (12).

Ion kinetic energy spectral data were obtained by variation of the ion accelerating voltage while the voltage applied to the plates of the energy-focussing sector (and, hence, the energy band passed) remained constant. Photographic plate (Ilford Q2) detection was used to record high resolution data concerning daughter ion species. Separate photoplate records were made for each band in the ion kinetic energy spectrum. For high resolution operation the object slit was adjusted to yield a resolving power of about 1:15 000.

2-Methoxytropone-d_3

Tropolone (122 mg) in dioxane (1 ml) was treated with deuterium oxide (1 ml) for 2 h and evaporated. An ethereal solution of diazomethane-d_2 was prepared by reacting *N*-methyl-d_3 *N*-nitroso-*p*-toluenesulfonamide (500 mg) in a mixture of ether (25 ml) and methanol-*d* (5 ml) with a solution prepared by dissolving clean sodium (200 mg) in deuterium oxide (0.5 ml). Diazomethane was distilled from the mixture and added to the tropolone. After 2 h at 4°, solvent and excess reagent were removed by evaporation.

Anhydrosepedonin Dimethyl Ether A-d_6

Anhydrosepedonin (40 mg) was gently boiled with a suspension of potassium carbonate (60 mg) in dry acetone (4 ml). Methyl iodide-d_3 (200 mg, 99 atom % excess) was introduced, with stirring, in four portions while heating was continued for 5 h. The filtered reaction mixture was evaporated to a yellow gum which, by preparative t.l.c. on silica gel HF_{254} (E. Merck, Darmstadt) with methanol–chloroform (1:20), showed a main component at R_f 0.63. This was extracted from the zone with ethyl acetate and crystallized from benzene as yellow needles (16 mg) identified by m.p. and u.v. absorption spectrum as anhydrosepedonin dimethyl ether A (3).

We are grateful to Mr. J. C. Berrigan and Mr. D. J. Embree for expert technical assistance.

1. J. M. WILSON, M. OHASHI, H. BUDZIKIEWICZ, C. DJERASSI, S. ITO, and T. NOZOE. Tetrahedron, **19**, 2247 (1963).
2. H. BUDZIKIEWICZ, C. DJERASSI, and D. H. WILLIAMS. Mass spectrometry of organic compounds. Holden-Day Inc., San Francisco. 1967. p. 542.
3. P. V. DIVEKAR, H. RAISTRICK, T. A. DOBSON, and L. C. VINING. Can. J. Chem. **43**, 1835 (1965).

Can. J. Chem. Downloaded from www.nrcresearchpress.com by 210.87.254.40 on 09/05/12
For personal use only.

4. J. L. C. WRIGHT, A. G. MCINNES, D. G. SMITH, and L. C. VINING. Can. J. Chem. **48**, 2702 (1970).
5. T. ACZEL and H. E. LUMPKIN. Anal. Chem. **32**, 1819 (1960).
6. E. M. CHAIT and W. B. ASKEW. Org. Mass Spectrom. **5**, 147 (1971) and references cited therein.
7. J. S. SHANNON. Aust. J. Chem. **15**, 265 (1962).
8. K. R. JENNINGS. Z. Naturforsch. **229**, 454 (1967).
9. J. L. C. WRIGHT, D. G. SMITH, A. G. MCINNES, L. C. VINING, and D. W. S. WESTLAKE. Can. J. Biochem. **47**, 945 (1969).
10. H. W. RUELIUS and A. GAUHE. Ann. **569**, 38 (1950).
11. F. M. DEAN, R. A. EADE, R. MOUBASHER, and A. ROBERTSON. J. Chem. Soc. 3497 (1957).
12. W. D. JAMIESON and F. G. MASON. Rev. Sci. Instrum. **41**, 778 (1970).

Can. J. Chem. Downloaded from www.nrcresearchpress.com by 210.87.254.40 on 09/05/12
For personal use only.

3-Ketoglutarates: Compounds with Mn(II), Co(II), Ni(II), Cu(II), Zn(II), Mg, and Na[1]

F. W. YERHOFF[2] AND D. W. LARSON

Department of Chemistry, University of Saskatchewan, Regina, Saskatchewan

Received September 9, 1971

Where A designates the dinegative 3-ketoglutarate ion and L indicates a trinegative species (likely the enolate ion), the following compounds have been obtained: Na_2A, $NaCuL.XH_2O$, $MgA.XH_2O$, $MnA.XH_2O$, $CoA.XH_2O$, $NiA.XH_2O$. Hydration numbers are uncertain. Stoichiometry of Cu(II) and Zn(II) compounds could not be established. Structures have been assigned on the basis of the infrared spectra. Na_2A appears to be a simple ionic carboxylate. MgA, MnA, CoA, and NiA are assigned a similar structure, with unidentate carboxylate coordination and hydrogen-bonded coordination between the metal and the second carboxylate oxygen (through water). NaCuL is assigned a metal-bridged polymer structure. There is not significant metal interaction with the carbonyl oxygen in any of the proposed structures.

Où A désigne l'ion dinégatif cétoglutarate 3 et L indique une espèce trinégative (probablement l'ion énolate), les composés suivants ont été obtenus: Na_2A, $NaCuL.XH_2O$, $MgA.XH_2O$, $MnA.XH_2O$, $CoA.XH_2O$, $NiA.XH_2O$. Les nombres de molécules d'eau d'hydration sont incertains. La stoéchiométrie des composés Cu(II) et Zn(II) n'a pas pu être établie. Les structures ont été attribuées sur la base des spectres infrarouges. Na_2A paraît être un carboxylate ionique simple. Une structure similaire est attribuée à MgA, MnA, CoA et NiA avec une coordination carboxylate unidentate et une coordination liaison hydrogène entre le métal et le deuxième oxygène carboxylate (à travers l'eau). Une structure polymère pont métallique est attribuée à NaCuL. Il n'y a pas d'interactions métalliques significatives avec l'oxygène carbonyle dans aucune des structures proposées.

Canadian Journal of Chemistry, **50**, 826 (1972)

Introduction

Studies of the decomposition of 3-ketoglutaric acid (acetonedicarboxylic acid) in aqueous solutions, and the observed enhancement of the rate of decarboxylation in the presence of multivalent cations, have led a number of investigators to propose complexes in solution (1, 2). Several structures have been proposed through consideration of reaction mechanisms or by analogy with similar systems. Prue (1) and Hay and Leong (3) have suggested a ketonic chelate structure, involving coordination to the ketone carbonyl and one carboxylate. A bicyclic ketonic chelate, with coordination by both carboxylates and the ketone carbonyl, has been suggested for the Sr(II) complex in solution (4). It has been proposed (5) that the Cu(II) complex in aqueous media is markedly different in character from the complexes with divalent Co, Ni, and Zn.

Few solid 3-ketoglutarates have been reported, and little information on structure is available. Schroeter (6) describes two barium salts, with 1:1 and 3:2 metal-to-ligand ratios; to the latter, he assigns an enolic structure (without giving the basis for his suggestion):

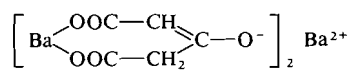

There have been reports of a 2:3 salt with La^{3+} (7), a 1:1 salt with UO_2^{2+} (8), and a light-green crystalline Cu^{2+} salt (9). Larson and Lister (5) prepared compounds with Co^{2+}, Ni^{2+}, Cu^{2+}, Zn^{2+}, and Na^+; but these were not studied extensively. In the present work, these five latter compounds have been studied, as well as those of Mn^{2+} and Mg^{2+}.

Experimental

Reagents and Apparatus

3-Ketoglutaric acid was obtained from Koch-Light Laboratories. A Bendix Model MA-1 (time of flight) mass spectrometer was used for studies of decomposition products. X-Ray diffraction patterns were obtained with a Philips powder camera, using glass capillaries and nickel filtered CuKα radiation.

Infrared spectra were run on KBr discs, containing 0.4–1.0 mg compound and 100–300 mg KBr. Comparison spectra

[1]From M.Sc. Thesis presented by F.W.Y., August, 1971.

[2]Present address: Department of Chemistry, University of Western Ontario, London, Ontario.

Can. J. Chem. Downloaded from www.nrcresearchpress.com by 210.87.254.5 on 09/05/12
For personal use only.

TABLE 1. Composition of 3-ketoglutarates

Stoichiometry	Calculated				Observed			
	C	H	M	Na	C	H	M	Na
$Na_2C_5H_4O_5.3H_2O$*‖	24.6	4.1		18.8	25.2	3.5	—	17.3
$Na_2C_5H_4O_5.0.3H_2O$†	30.7	2.4		23.5	30.8	2.4	—	23.5
$NaCuC_5H_3O_5.2H_2O$‡	22.6	2.7	23.9	8.7	23.2	2.3	24.1	8.5
Cu compound§‖					21.1	2.2	33.8	—
Zn compound§‖					22.3	2.2	33.5	
$MgC_5H_4O_5.2H_2O$§	29.4	3.9	11.9		28.2	3.5	12.3	
$MnC_5H_4O_5.2H_2O$§	25.3	3.4	23.2		24.9	2.6	24.4	
$CoC_5H_4O_5.2H_2O$‡	25.1	3.4	24.7		22.7	3.0	24.3	
§					22.7	2.8	24.9	
$NiC_5H_4O_5.2H_2O$‡	25.2	3.4	24.6		22.5	3.3	25.0	
§					21.0	2.8	24.8	

*Aqueous preparation.
†Non-aqueous preparation.
‡Metal chloride synthesis.
§Metal carbonate synthesis.
‖Analysis variable.

were obtained with a Beckman IR8 spectrophotometer; the wavenumber data in Table 4 were taken from spectra obtained (for the same KBr discs) with a Beckman IR-12 spectrophotometer.

Synthesis

Divalent metal 3-ketoglutarates were prepared from the metal chloride and/or carbonate. In the chloride synthesis, a cold concentrated solution of 3-ketoglutaric acid (3 *M*) was partially neutralized with NaOH and mixed with a cold concentrated solution of the metal chloride. In the case of copper, precipitation of a bright-green solid occurred immediately; for Co, Ni, Mn, and Zn, the mixture was added to a large excess of cold, well stirred absolute ethanol, which caused precipitation of a solid. (Similar addition to ethanol of the filtrate from the Cu preparation produced a precipitate which, as judged by infrared spectrum and analysis, was identical to the initial aqueous phase product.) In the alternative preparation, powdered metal carbonate was added to a cold aqueous solution of 3-ketoglutaric acid; the mixture was stirred for about 20 min and filtered by suction, the clear filtrate falling directly into excess cold absolute ethanol. As with the chloride preparation, the solid precipitate was filtered off, washed with absolute ethanol and ether, and dried *in vacuo*. The products were purified by preparing a saturated solution in cold dilute (0.05 *M*) 3-ketoglutaric acid and reprecipitating the solid in ethanol.

A non-aqueous preparation was used for the sodium compound: when solutions of sodium and 3-ketoglutaric acid were mixed, a white solid was precipitated from ethanol.

Decomposition Studies

Gases evolved during thermal decomposition of the sodium, nickel, and sodium copper compounds were examined by mass spectrometry. Samples were heated in a glass vacuum apparatus in steps (35 °C in 30 min); accumulated gas pressure was noted for each heating interval, and a sample of the collected gas was admitted to the mass spectrometer. Composition of the gases was determined by comparison of the mass spectra to published standard fragmentation patterns (10, 11). A separate thermogravimetric study was carried out on some of the compounds; samples were heated at rates between 2.5 deg min^{-1} and 5.0 deg min^{-1}.

Results

A noteworthy phenomenon was observed during development of the preparative procedures. Reversal of the solvent change procedure (*i.e.* addition of ethanol to the chloride or carbonate preparative solution) in the cases of Mn, Co, Ni, Zn, and Mg normally produced a liquid product. This second liquid phase varied from a mobile fluid near room temperature to a firm gum near 0 °C. The infrared spectra of these oils (taken of films between salt plates) were markedly similar to those of the solid compounds. The Mn, Co, and Ni oils were intensely colored in the same hue as the corresponding solid. No such liquid phase product was ever observed with copper. It was impossible to obtain a solid sodium compound directly from aqueous solutions by solvent change; however, a viscous yellow fluid, washed several times with absolute ethanol and ether and stored at low temperature, became crystalline.

Analysis and Properties

Elemental composition data are presented in Table 1. Expected values for certain stoichiometric compounds are given for reference. Hydration numbers could not be established; best fit to analytical results varied from $1.4H_2O$ to $2.6H_2O$ for the divalent metal compounds. Stoichiometry of the zinc and copper com-

Can. J. Chem. Downloaded from www.nrcresearchpress.com by 210.87.254.5 on 09/05/12
For personal use only.

Can. J. Chem. Downloaded from www.nrcresearchpress.com by 210.87.254.5 on 09/05/12
For personal use only.

TABLE 2. X-Ray powder patterns

$Na_2A.XH_2O$		Na_2A (anhyd)		$NaCuL.XH_2O$	
D	I/I_1*	*D*	I/I_1*	*D*	I/I_1*
8.77	30	10.31	100	10.55	60
7.91	30	6.55		5.41	100
7.12	30	5.15		5.05	
6.64		4.75	40	4.42	
6.18	100	3.69		4.18	
5.46		3.43		3.73	
5.01		3.35		3.50	30
4.30		3.04	50	3.42	30
4.11	30	2.842	70	3.25	80
3.92	80	2.673		3.19	
3.78	30	2.569	60	3.09	
3.54		2.425		2.966	
3.21	30	2.322		2.896	
3.11	60	2.221		2.833	
3.02		2.050		2.782	
2.877	40	2.011	15	2.712	
2.811		1.874	15	2.631	
2.715		1.699	15	2.565	30
2.664		1.677		2.450	
2.612	70	1.581		2.412	
2.519	60	1.508		2.375	
2.450		1.466		2.308	
2.402	25	1.418		2.213	20
2.290		1.357		2.155	
2.223	50			2.112	
2.182				2.059	
2.128				2.005	
2.074				1.964	
2.037				1.915	
1.976	20			1.854	25

*Relative intensities visually estimated for most prominent lines.

pounds could not be assigned. The sodium compound prepared in absolute ethanol was observed to be extremely hygroscopic.

The Mg, both Na and NaCu compounds are apparently stable at room temperature; all of the others show evidence of decomposition (gas evolution, and progressive changes in composition with time, consistent with decarboxylation).

Clear X-ray powder diffraction patterns were obtained for the NaCu and both Na compounds; three markedly dissimilar patterns occurred. Attempts to index the lines (Table 2) have only demonstrated that the structures are not likely simple ones of high symmetry. No diffraction lines were observed for the remaining compounds, even after they had been subjected to a variety of grinding and annealing procedures.

Decomposition Studies

All major peaks in the mass spectra of the gaseous decomposition products of the Ni, NaCu, and Na (non-aqueous preparation) compounds heated to 300 °C could be accounted for by the presence of CO_2, $(CH_3)_2CO$, and H_2O. The following mass peaks were used as quantitative measures of the amount of each component in an accumulated sample (12); as determined from standard disintegration patterns (10, 11), they represented approximately equal proportions of the total peak sum for each compound: for CO_2, 44; H_2O, 18; $(CH_3)_2CO$, 43 + 58. The fraction of a component in a collected gas sample (peak height ratio) multiplied by the observed gas pressure yields a semi-quantitative partial pressure (Table 3).

Infrared spectra of the solid residues of the Mg, Mn, Co, and Ni compounds heated to 75, 200, and 300 °C showed similar changes: appearance of broad metal carbonate bands; spectra of residues heated above 350 °C for several hours showed no absorptions in the range 4000–700 cm^{-1}. Residues of the Na and NaCu compounds heated at 300 °C for several hours showed only absorptions corresponding to those of sodium carbonate.

In the thermogravimetric studies the Co and Ni compounds showed similar patterns: a gradual weight loss from room temperature to 150 °C; a sloping plateau between 150 and 230 °C (23–27% weight loss for Co; 25–32% for Ni); sudden rapid weight loss at 235 °C; and constant weight to 300 °C (57% weight loss for Co; 62% for Ni). The NaCu compound samples showed: only slight loss to 135 °C (5%); rapid loss between 140 and 170 °C; a little further weight change when heated above 200 °C (plateau at 49% weight loss).

Discussion

Thermal Decomposition

The thermal decomposition data are consistent with the following decomposition reactions

[1] $Na_2C_5H_4O_5.H_2O \rightarrow CO_2 + (CH_3)_2CO + Na_2CO_3$

Release of equal volumes of CO_2 and $(CH_3)_2CO$ was shown in the mass spectra; the residue was apparently Na_2CO_3. (The sample used was from a non-aqueous preparation; however, water was present in the sample initially, and further hydration occurred on storage.)

TABLE 3. Gaseous products of thermal decomposition

Median temperature (°C)	Partial pressure of the products of decomposition of (TORR)								
	$NaCuC_5H_3O_5.XH_2O$			$Na_2C_5H_4O_5.XH_2O$			$NiC_5H_4O_5.XH_2O$		
	CO_2	Acetone	H_2O	CO_2	Acetone	H_2O	CO_2	Acetone	H_2O
45	—	—	1	1	1	1	3	TR†	2
80	2	—	6	3	3	1	23	26	3
115	3	—	7	4	3	TR†	49	50	3
150	96*	100*	17*	15	12	—	34	27	1
185	101*	110*	—	100*	91*	—	25	17	TR†
220	24	3	2	9	12	—	18	9	1
255	30	1	6	1	6	—	14	10	—
290	3	TR†	1	8	9	—	87	26	—
325	1	TR†	TR†	13	2	—	88	31	—
360				9	2		95	11	7
395				18	3		24	—	1
430				14	3	2	2	—	3

*Absolute magnitude not accurate.
†TR: trace.

[2] $2NaCuC_5H_3O_5.2H_2O \rightarrow 2CuO + CO_2 + 2(CH_3)_2CO + H_2O + Na_2CO_3$

Expected weight loss would be 50%; observed, 49%. There is a discrepancy between the two decomposition studies of $NaCuL.XH_2O$; whereas the thermogravimetry showed a rather narrow temperature range of decomposition in one step below 175 °C, the mass spectra suggest two stages, with additional CO_2 being released above 205 °C, after release of $(CH_3)_2CO$ has virtually ceased. It may be that the slower heating in the latter study allowed transient formation of $NaHCO_3$ or a cupric carbonate, which subsequently decomposed, releasing additional CO_2.

[3] $2NiC_5H_4O_5.2H_2O \rightarrow$ "$NiCO_3.Ni(C_4H_5O_3)OH.2H_2O$" $+ 2CO_2 + (CH_3)_2CO$

[4] "$NiCO_3.Ni(C_4H_5O_3)OH.2H_2O$" $\rightarrow$ $2CO_2 + (CH_3)_2CO$ + residue (Ni oxides, hydroxides)

For the nickel 3-ketoglutarate, both thermogravimetry and mass spectra of gaseous decomposition products suggest a two stage decomposition. While the second-stage evolution of CO_2 (see Table 3) could be explained by the intermediate formation of a nickel carbonate, this would not account for the pause in $(CH_3)_2CO$ evolution. This latter phenomenon could have arisen, as suggested in reaction 3, from the transient formation of a nickel acetoacetate compound (the product formulated is intended to present only the gross stoichiometry of the intermediate solids, not the structure). Predicted weight loss for reaction 3, 31%; observed in thermogravimetry, plateau, 25–32%. Predicted weight loss for reactions 3 and 4, 61%; observed, 62%. Thermogravimetry indicates a similar two stage decomposition of cobalt 3-ketoglutarate.

Infrared Data and Structures

Some information on structure can be obtained from an examination of the carboxylate and carbonyl absorptions of the ligand. Carboxylate groups have been shown by X-ray diffraction studies to coordinate with cations in four ways (13): (*1*) ionic, (*2*) unidentate, (*3*) bidentate, (*4*) bridging.

Sodium 3-Ketoglutarate

The spectrum of Na_2A shows a strong absorption at 1709 cm^{-1}, which corresponds to that expected for an uncoordinated ketonic carbonyl group. A very strong absorption at 1602 cm^{-1} can be attributed to a carboxylate antisymmetric stretch. Two strong peaks at 1387 and 1407 cm^{-1} may be due to a split carboxylate symmetric stretch, or the latter may be due to active methylene bending. This spectrum corresponds well in peak positions and relative intensities to that of sodium pyruvate (14), which has been shown by X-ray diffraction to have an ionic structure (15). Correspondence of carboxylate stretching and bending modes with

Can. J. Chem. Downloaded from www.nrcresearchpress.com by 210.87.254.5 on 09/05/12
For personal use only.

Can. J. Chem. Downloaded from www.nrcresearchpress.com by 210.87.254.5 on 09/05/12
For personal use only.

TABLE 4. Infrared absorption frequencies for 3-ketoglutaric acid and metal 3-ketoglutarates*

H_2A	Na_2A (anhyd)	Na compound (hyd)	$NaCuL.XH_2O$	Cu compound	$CoA.XH_2O$	$NiA.XH_2O$	$MnA.XH_2O$	$MgA.XH_2O$	Zn compound
442 w			401 s	402 m	397 m	399 m	397 m	405 m	
486 w	523 vw			465 w					
548 w					674 w	669 w	664 w	674 w	677 w
617 m	639 vw	644 vw	626 w						
704 w			689 m	686 w	817 w	822 w	822 w	825 w	820 w
	765 vw								
			834 m	819 w	(951 sh)	(948 sh)	(956 sh)	(961 sh)	955 m
927 m, br	905 w	905 w			970 m, br	975 m	970 m	980 m	974 m
			948 m	(953 sh)					
977 w	959 vw	(961 vw)	970 s	972 m	1030 w	1033 w	1032 w	(1032 vw)	(1034 w)
								(1049 vw)	
			1020 vw					(1091 vw)	
			1032 vw				(1114 vw)	(1114 vw)	
1077 m	(1082 w)					(1177 w)		(1166 vw)	(1171 w)
1126 w	1102 w		1168 w	(1176 w)				(1210 vw)	
1209 m		1210 vw			(1287 sh)	1292 w	1286 w	1291 w	1297 w
1276 m	(1250 vw)	1264 vw		1287 w					
1295 m			1301 m		1331 m	1333 m	1331 m	1342 m	1331 s
(1315 sh)									
1342 m	1325 vw	1325 vw	1334 m	1328 s	1387 s	1390 s	1390 s	1402 s	1405 s
1389 m	1387 s	1383 s	1385 m	(1387 sh)	(1408 sh)	(1412 sh)	(1412 sh)	(1432 sh)	(1448 sh)
					(1447 sh)	1450 w	(1447 sh)		
(1423 w)	1407 m	1414 m	1404 m	(1410 sh)			(1465 sh)	1476 w	
1440 m			1448 s	1448 m	1504 w	1504 w	1505 w	1499 w	1499 w
1460 w				1485 w	1587 vs	1588 vs	1593 vs	1595 vs	1595 vs
			1525 m	(1555 sh)	(1630 sh)	(1630 sh)	(1625 sh)	(1645 sh)	(1630 sh)
	1602 vs	1601 vs	1591 s	1595 vs	1704 w	1703 w	1712 w	1713 m	1715 w
			1610 s						
							2833 w		
1704 s	1709 s	1711 s	(1700 sh)		2929 w		2929 m		2939 w
1742 s					(2956 sh)		2958 w		(2965 sh)
2586 w	(2857 vw)		2864 w		(3260 sh)		(3260 sh)	(3274 sh)	
2688 w	2930 w	(2941 vw)	2921 w	2929 w	3403 s, br	3404 s, br	3409 s, br	3400 s, br	3428 s, br
2940 w	(2979 vw)	2980 w	2966 w						
3085 s, br									
(3370 sh)	3430 m, br	3428 s, br	3350 s, br	3422 s, br					

*w = weak; m = medium; s = strong; v = very; br = broad; sh = shoulder; anhyd = anhydrous preparation; hyd = hydrated; comp = compound; parentheses denote position uncertain due to weak, broad absorption or poorly defined shoulder.

Can. J. Chem. Downloaded from www.nrcresearchpress.com by 210.87.254.5 on 09/05/12
For personal use only.

other ionic structures such as sodium malonate (16) is also good. Since the carbonyl seems not to be involved in coordination, a linear configuration is probable:

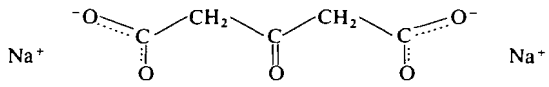

3-Ketoglutarates of Mg, Mn, Co, and Ni

The similarity of the spectra of these four compounds suggests that they may have the same type of structure; and consideration of the spectra as a group is useful, as trends over a series of metal ions may yield structural information. Peaks in the range 1386 to 1402 cm^{-1} (Table 4) may be assigned empirically to the symmetric carboxylate stretch; and peaks in the range 1587 to 1595 cm^{-1} to the corresponding antisymmetric mode. Peaks between 1703 and 1713 cm^{-1} are likely due to uncoordinated or very weakly coordinated ketonic carbonyls.

With change of metal ion in these four 3-ketoglutarates, symmetric and antisymmetric carboxylate absorptions are observed to shift in the same direction, with a shift to higher frequencies in the order: Co (1387, 1587 cm^{-1}) $\simeq$ Ni (1390, 1588 cm^{-1}) < Mn (1390, 1593 cm^{-1}) < Mg (1402, 1595 cm^{-1}). It has been shown (17) that for unidentate coordination antisymmetric and symmetric frequencies tend to move in opposite directions with change in metal, and that the increase in the antisymmetric frequency appears to follow the Irving–Williams order. Since the increase in frequency noted above is the opposite of the Irving–Williams order, and carboxylate frequencies shift in the same direction, it appears that unidentate coordination (which has been suggested in the proposed structures of the metal complexes in solution) does not occur in the solid state. This conclusion is supported by the persistence of a ketonic carbonyl absorption, which suggests that metal–carbonyl coordination is of little importance.

The small changes in carboxylate frequencies with change of cation suggest ionic coordination (as would be expected for the Mg compound); the spectra also indicate approximately equal C—O bonds. Bidentate and bridging structures would give such spectra; but these structures are not found in carboxylates of Mg, Mn, Co, and Ni. A more likely possibility is a structure similar to that of cobalt and nickel acetate tetrahydrates; these have been shown by X-ray diffraction (18) to have approximately equal carboxylate bond lengths (1.29, 1.31 Å). Although only one carboxylate oxygen is coordinated to the metal ion, the other is strongly hydrogen bonded to a water molecule coordinated to the same metal ion. While no comparative infrared studies of these acetates are available, the metal–oxygen distances (2.12 Å) suggest an essentially ionic interaction.

Below is a proposed structure, where M represents Mg, Mn, Co, or Ni. One could speculate on the possibility of a polymeric form for such compounds; it has been noted that these 3-ketoglutarates form apparently amorphous solids, and that unusual liquid phase products can be obtained in their preparation.

Sodium Copper 3-Ketoglutarate

In this spectrum, an absorption at 1448 cm^{-1} and a doublet at 1591 and 1610 cm^{-1} can be assigned to the symmetric and antisymmetric modes for the carboxylate. No ketonic carbonyl absorption is noted, confirming stoichiometric results which indicate a trivalent (enolic) form. This premise is further supported by the presence of a moderately strong absorption at 834 cm^{-1}, which can be attributed to an olefinic C—H in plane deformation, and an absorption at 1525 cm^{-1}, which may be due to the enolic C=C stretch absorption.

A bidentate chelate (with unidentate carboxylate coordination) would be expected to exhibit carboxylate stretch absorptions at frequencies similar to those for copper glycinate (1593, 1387 cm^{-1}) and copper α-alinate (1606, 1386 cm^{-1}) (17). The symmetric absorption frequencies are considerably lower than that

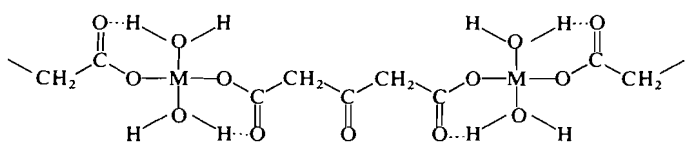

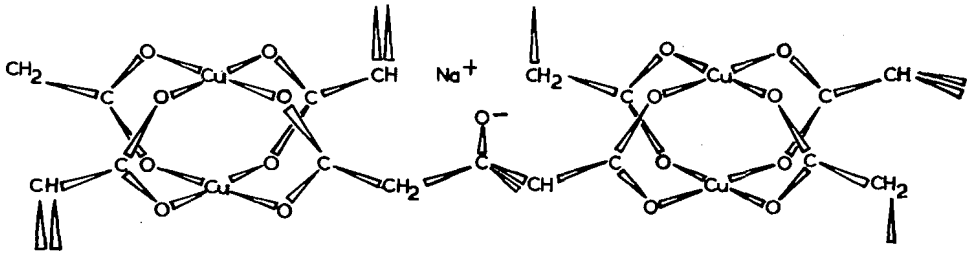

FIG. 1. Metal-bridged structure for NaCu 3-ketoglutarate.

assigned here (1448 cm^{-1}) for the NaCu compound. In copper malonate the symmetric absorption appears at an even lower frequency, 1371 cm^{-1} (19). There is much better agreement with frequencies noted in copper carboxylates known to have bridged structures; two examples are copper succinate (1608, 1432 cm^{-1}) (19), and levulinate (1600, 1450 cm^{-1}) (20).

Coordination between copper and the enol oxygen would be unlikely in a bridged structure (for steric reasons). The metal-bridged polymer structure in Fig. 1 suggests a free enolate. Assignments of free enolate absorptions in sodium (1360 cm^{-1}) and potassium (1408 cm^{-1}) acetylacetonates (21) are matched here by absorptions at 1385 or 1404 cm^{-1} (although the intensity of these peaks is rather low).

If the proposed structure for sodium copper 3-ketoglutarate is accepted, there remains the question of the driving force toward enolization. Perhaps an enolic form in the solid arises from enolization in solution. Although no structural work is available, it has been suggested (5) that the enolic form of the ligand is the primary complexing species with copper in aqueous solution. This could be due to preferential complexing of the enolic form of the ligand (with a subsequent shift in the keto–enol equilibrium), or to a direct interaction of copper with the ligand in a way which favours enolization.

It is interesting to note that a compound $CuA.XH_2O$ does not seem to occur, nor was it possible to prepare Na_3L; the occurrence of a trivalent 3-ketoglutarate species appears to be associated only with Cu(II). (Stoichiometry has not been assigned for the Cu and Zn compounds (see Table 1); the difficulty lies in the very low carbon-to-metal ratios, which preclude a simple formula $MA.XH_2O$. The infrared spectra are presented only for comparison.)

Summary

Compounds of 3-ketoglutaric acid with Mg, Na, and a number of divalent transition metals have been prepared. Where A designates the dinegative 3-ketoglutarate ion and L indicates a trinegative species, the following stoichiometries are indicated: $NaCuL.XH_2O$, $MgA.XH_2O$, $MnA.XH_2O$, $CoA.XH_2O$, $NiA.XH_2O$; hydration numbers are uncertain, but $X \simeq 2$.

The infrared spectra have been used to assign structures. A simple ionic structure is proposed for Na_2A. A modified ionic structure is proposed for the Mg, Mn, Co, and Ni compounds with a water molecule linking the metal ion to one of the carboxylate oxygens. $NaCuL.XH_2O$ is assigned a metal-bridged structure with a free enolate group.

This work was supported by the National Research Council of Canada and by the University of Saskatchewan.

1. J. E. PRUE. J. Chem. Soc. 2331 (1952).
2. O. TOYAMA, Y. KEBOKAWA, and Y. YOSHIDA. J. Chem. Soc. Jap. **74**, 955 (1954).
3. R. W. HAY and K. N. LEONG. Chem. Commun. 800 (1967).
4. I. E. BUKOLOV, K. V. ASTAKHOV, V. I. ZIMIN, and V. S. TAIROV. Russ. J. Inorg. Chem. (Zh. Neorg. Khem. Eng. transl.) **7**, 816 (1962).
5. D. W. LARSON and M. W. LISTER. Can. J. Chem. **46**, 823 (1968).
6. G. SCHROETER. Ber. **59B**, 973 (1926).
7. E. C. C. AMARAL and R. A. GUEDES DE CARVALHO. J. Inorg. Nucl. Chem. **31**, 2695 (1969).
8. A. MULLER. C.A. **35**, 3969 (1940); J. Prakt. Chem. **157**, 89 (1940).
9. J. V. DUBSKY, FR. BRYCHTA, and M. KURAS. Pub. Faculte Sci. Univ. Masaryk **129**, 1 (1931).
10. J. ROBOZ. Introduction to mass spectrometry. Wiley and Sons, New York, N.Y. 1968. p. 282.
11. F. W. MCLAFFERTY. Interpretation of mass spectra. Benjamin, New York, N.Y. 1966. p. 115.
12. T. B. JOYNER and F. H. VERHOEK. J. Am. Chem. Soc. **83**, 1069 (1961).

Can. J. Chem. Downloaded from www.nrcresearchpress.com by 210.87.254.5 on 09/05/12
For personal use only.

13. K. NAKAMOTO. Infrared spectra of inorganic and coordination compounds. Wiley and Sons, New York, N.Y. 1963. p. 201.
14. W. J. JENKS and J. CARRIULO. Nature, **182**, 598 (1958).
15. S. S. TAVALE, L. M. PANT, and A. B. BISWAS. Acta Cryst. **14**, 1281 (1961).
16. M. J. SCHMETZ, I. NAKAGAWA, S. MIZUSIMA, and J. V. QUAGLIANO. J. Am. Chem. Soc. **81**, 287 (1959).
17. K. NAKAMOTO, Y. MORIMOTO, and A. E. MARTELL. J. Am. Chem. Soc. **83**, 4528 (1961).
18. J. N. VAN NIEKERK and F. R. L. SCHOENING. Acta Cryst. **6**, 609 (1953).
19. Y. KURODA and M. KUBO. J. Phys., Chem. **64**, 759 (1960).
20. J. GOPALAKRISHNAN and C. C. PATEL. Inorg. Chem. **6**, 2111 (1967).
21. R. WEST and R. RILEY. J. Inorg. Nucl. Chem. **5**, 295 (1958).

Can. J. Chem. Downloaded from www.nrcresearchpress.com by 210.87.254.5 on 09/05/12
For personal use only.

Studies in Solubility Parameter Theory for Mixed Solvent Systems[1]

AVIJIT PURKAYASTHA AND JOHN WALKLEY[2]

Department of Chemistry, Simon Fraser University, Burnaby 2, British Columbia

Received August 9, 1971

Data are presented for the saturation solubility and partial molal volume of iodine in a mixed benzene–cyclohexane solvent and for the saturation solubility of stannic iodide in the same solvent mixture. A successful interpretation of these data in terms of solubility parameter theory is possible if we define an effective volume fraction term. This term reflects the immediate solvent environment of the solute molecule with the preferential solvation of the solute by one of the solvent molecules. Data for iodine in a mixed carbon tetrachloride–benzene solvent mixture and for iodine in a carbon tetrachloride–perfluoroheptane mixture are also interpreted in terms of the proposed theory.

Les résultats relatifs à la solubilité à saturation et au volume molaire partiel de l'iode dans un solvant mixte benzène–cyclohexane, ainsi que ceux relatifs à la solubilité à saturation de l'iodure stannique dans le même mélange de solvants, sont présentés. En fonction d'une théorie de paramètres de solubilité, une bonne interprétation de ces données est possible à condition de définir un terme de fraction de volume réel. Ce terme réflète l'environnement immédiat des molécules du soluté par le solvant ainsi que la solvatation préférentielle du soluté par l'une des molécules de solvant. Les résultats relatifs à l'iode dans un mélange de solvants tétrachlorure de carbone–benzène et ceux de l'iode dans un mélange de solvants tétrachlorure de carbone–perfluoroheptane, sont également interprétés en fonction de la théorie proposée.

Canadian Journal of Chemistry, **50**, 834 (1972)

Introduction

Many studies have been done on the correlation of the behavior of non-electrolyte solutions with the molecular parameters of the pure components and, in general, the theories developed have been of reasonable predictive value (1). Few studies have been done on systems of more than two components though the extension of present theories appears fairly simple. A particularly useful field of study is that of a dilute solute in a two component non-polar solvent mixture. Such systems, however, appear complicated by the preferential solvation of the solute molecule by one of the solvent species. To explain the dependence of the equilibrium constant for the iodine–pyridine charge transfer complex upon the solvent used, Christian was required to assume some degree of preferential solvation (2). A similar assumption is required to explain the diffusion coefficient values of iodine in various alcohol–hydrocarbon mixed solvents. Nakanishi *et al.* (3) proposed a mechanism that assumed the solute iodine molecule to spend more time in an environment preferentially composed of the energetically favored solvent molecule. An earlier study of the partial molal volume of bromine in mixed CCl_4–*c*-$C_4Cl_2F_6$ solvent by Smith and Walkley (4) showed the preferential solvation of the bromine by the CCl_4. This was such that at even a very low mole-fraction composition of CCl_4 in the solvent mixture the partial molal volume of the dissolved solute fell from its value in the pure chloro–fluorocarbon to a value similar to that in pure CCl_4. Our present study is concerned with the interpretation of the saturation solubility and partial molal volume of simple dilute solutes in two component non-polar solvents. Data are measured over the complete range of solvent composition. Recognizing the success of Hildebrand's solubility parameter theory in interpreting the saturation solubility behavior of dilute solutes in single component solvents we have chosen to extend his theory (5) to our two component solvent data. We have extended the theory by attempting to take into account the "preferential" nearest neighbor environment of the solute molecules. The theory is remarkably successful and offers an approach to the nearest neighbor environment which is necessary to the further interpretation of the diffusion and spectroscopic studies of these systems.

[1]Presented at C.I.C. Conference, May 1971.

[2]To whom correspondence should be addressed.

Can. J. Chem. Downloaded from www.nrcresearchpress.com by 210.87.254.6 on 09/05/12
For personal use only.

Can. J. Chem. Downloaded from www.nrcresearchpress.com by 210.87.254.6 on 09/05/12
For personal use only.

TABLE 1. Saturation solubility of iodine in a mixed benzene–cyclohexane solvent at 25 °C

Volume fraction of benzene Φ_1	Saturation solubility $-\ln x_2^M$	δ_M		
		Experimental (eq. 2)	Calculated	
			Eq. 3, from Φ_1	Eq. 5, from Φ_1^*
0.0	4.7396	8.2	—	—
0.2551	4.0345	8.92	8.46	8.92
0.5093	3.6052	9.41	9.12	9.41
0.6211	3.4239	9.57	9.32	9.57
0.6804	3.2589	9.66	9.42	9.66
0.7604	3.2571	9.75	9.56	9.75
0.8451	3.1688	9.84	9.71	9.84
0.8657	3.1566	9.86	9.75	9.86
1.000	3.0464	9.99	—	—

TABLE 2. Saturation solubility of stannic iodide in a mixed benzene–cyclohexane solvent at 25 °C

Volume fraction of benzene Φ_1	Saturation solubility $-\ln x_2^M$	δ_M		
		Experimental	Calculated	
			From Φ_1	From Φ_1^*
0.0	4.9236	8.5	—	—
0.1648	4.6166	8.68	8.62	8.69
0.2602	4.9991	8.76	8.72	8.77
0.3778	4.3078	8.99	8.83	8.87
0.5853	4.1311	9.01	8.93	9.02
0.7604	3.9878	9.12	9.05	9.12
1.000	3.8259	9.24	—	—

TABLE 3. Solubility parameter values used in calculations $(cal/cc)^{1/2}$

System	δ_1	δ_2	δ_3
$C_6H_6 - I_2 - c\text{-}C_6H_{12}$	9.99	14.1	8.24
$C_6H_6 - I_2 - c\text{-}C_6H_{12}$	9.99	14.1	8.60
$n\text{-}C_7F_{16} - I_2 - CCl_4$	6.00	14.1	8.60
$C_6H_6 - SnI_4 - c\text{-}C_6H_{12}$	9.24	11.6	8.50

Experimental

The solvents (C_6H_6 and $c\text{-}C_6H_{12}$) were spectroscopic grade solvents and were used without further purification. The preparation of saturated iodine and stannic iodide solutions was by the same technique as described earlier by Walkley and Vittoria (6). The iodine concentration in the saturated solution was determined spectroscopically at 520 mμ and that of stannic iodide at 360 mμ. Aliquots from the saturated solution were diluted in the ratio 1:250 with cyclohexane before optical density measurements were made. Saturation solubility measurements were made over the complete range of composition of the solvent mixture. All data were measured at 25.00 ± 0.01 °C. For those experiments involving stannic iodide, photochemical decomposition of SnI_4 in solution was avoided by using black-painted dissolution cells.

The partial molal volume of iodine in the mixed solvent was measured using the dilatometric technique described by Hildebrand and Glew (7). The dilatometer was of 150 ml capacity and the capillary of 2 mm internal diameter. No temperature fluctuation of the liquid level in the capillary arm was observed and the scatter of individual experimental data allowed the partial molal volumes to be measured to a precision of 0.8%.

Results

Saturation solubility (mole fraction x_2^M) and partial molal volume ($\bar{V}_2$ cc mol^{-1}) of iodine in the mixed $C_6H_6 - c\text{-}C_6H_{12}$ solvent over the complete range of composition are given in Tables 1 and 3. In Table 2 saturation solubility

Can. J. Chem. Downloaded from www.nrcresearchpress.com by 210.87.254.6 on 09/05/12
For personal use only.

data for SnI_4 in mixed $C_6H_6-c\text{-}C_6H_{12}$ solvent are presented.

Discussion

The solubility parameter theory equation expressing the saturation solubility of a solute (x_2) in terms of its ideal solubility (a_2^i) and the δ-parameters of the solvent and the solute (δ_1 and δ_2) has been well tested (5). With the usual notation this equation is

$$[1] \qquad \ln a_2^i = \ln x_2 + \frac{\Phi_1^2 V_2^0}{RT}(\delta_2 - \delta_1)^2$$

Generally, for any chosen solute (of known δ_2 value) the equation is tested by comparing the experimental δ_1 value (for a range of solvents) to the thermodynamic value ((molar energy of vaporization/molar volume)$^{1/2}$). For a wide range of solute–solvent systems this self-consistency has been shown to exist (8).

For systems in which a solute is dissolved in a binary solvent mixture (of components *1* and *3*), it has been suggested (5) that eq. 1 could be rewritten as

$$[2] \qquad \ln a_2^i = \ln x_2^M + \frac{\Phi_M^2 V_2^0}{RT}(\delta_2 - \delta_M)^2$$

where

$$[3] \qquad \delta_M = \Phi_1\delta_1 + \Phi_3\delta_3$$

and Φ_M the volume fraction of the solvent mixture, *i.e.* $\Phi_1 + \Phi_3 \to 1$, $\Phi_2 \to 0$. In Tables 1 and 2 we make a comparison of δ_M(experimental) and the δ_M value given by eq. 3. It is seen that the comparison is bad. The experimental data allow δ_M, δ_1, and δ_3 to be calculated to an accuracy of 0.1% for a given value of δ_2. To better emphasize the role of δ_M we derive from eq. 1 and 2 the relationship

$$[4] \quad [\ln a_2^i - \ln x_2^M]^{1/2} = (\ln a_1^i - \ln x_2^3)^{1/2} - (\ln a_1^i - \ln x_2^3)^{1/2}\Phi_1\left(\frac{\delta_1 - \delta_3}{\delta_2 - \delta_3}\right)$$

where x_2^3 is the saturation solubility of solute (*2*) in the pure solvent component (*3*). We use eq. 4 for those systems for which $\Phi_2 \to 0$, *i.e.* $\Phi_1 + \Phi_3 = 1$. In the derivation of eq. 4 the dependence upon the solvent composition, Φ_1, arises solely through the definition of δ_M by eq. 3. The linear relationship expected between Φ_1 and the experimental quantity $(\ln a_2^i - \ln x_2^M)^{1/2}$ does not, however, depend upon the assumption of actual δ_i values. From the linear relationship expected of eq. 4 the intercept at $\Phi_1 = 0$ and the ratio of slope/intercept may be compared to experimental values. In Figs. 1 and 2 we plot $(\ln a_2^i - \ln x_2^M)^{1/2}$ *vs.* Φ_1 using our data for the systems $I_2-C_6H_6-c\text{-}C_6H_{12}$ and $SnI_4-C_6H_6-$

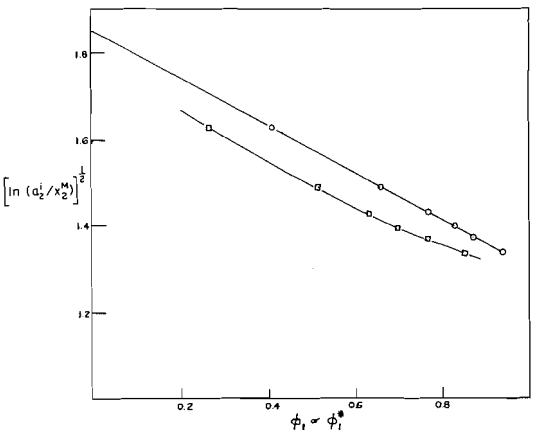

FIG. 1. Iodine in benzene–cyclohexane solvent, $[\ln (a_2^i/x_2^M)]^{1/2}$ plotted as a function of benzene volume fraction (□) and as a function of benzene "effective volume fraction" (○). Data at 25.0 °C.

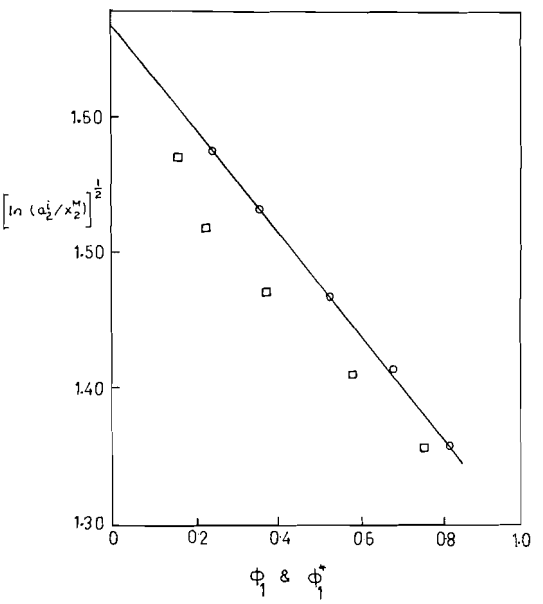

FIG. 2. Stannic iodide in mixed benzene–cyclohexane solvent; $[\ln (a_2^i/x_2^M)]^{1/2}$ plotted as a function of benzene volume fraction (□) and as a function of the benzene effective volume fraction (○). Data at 25 °C.

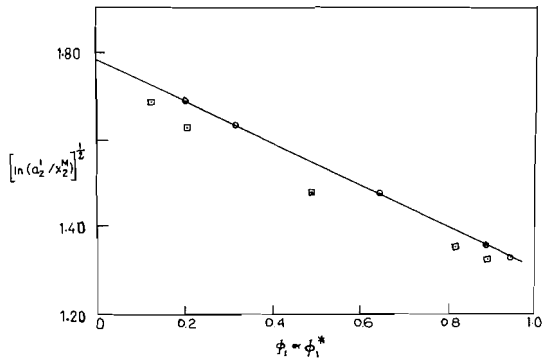

FIG. 3. Iodine in a mixed benzene carbon tetrachloride solvent; $[\ln (a_2^i/x_2^M)]^{1/2}$ plotted as a function of benzene volume fraction (□) and as a function of the benzene effective volume fraction (○). All data at 25 °C.

c-C_6H_{12} and in Fig. 3 using the data of Wood *et al.* (9) for the I_2–C_6H_6–CCl_4 system. It is seen that for all three systems the expected linearity is not observed.

From the graphical dependence discussed above and from the direct comparison of δ_M values it would appear that the definition of δ_M by eq. 3 is not acceptable. Following the suggestion that the immediate solvent environment is not reflected by the bulk solvent composition but requires the assumption of the preferential "solvation" by one of the solvent components we have attempted to define an "effective volume fraction", Φ_1^*, reflecting this solvation, and so define

$$[5] \qquad \delta_M = \Phi_1^*\delta_1 + \Phi_3^*\delta_3$$

Christian (2) suggested that the relative number of each of the two solvent molecules in the solute nearest neighbor environment could be regarded as a Boltzmann weighting term involving the heat of solution of the solute in each of the pure solvents. If we use this approach to calculate an "effective volume fraction" term then the comparison of experimental and theoretical δ_M values is no better than that found assuming the immediate solute environment to be represented by bulk solvent mixture composition.

The solvent environment of a solute molecule can be discussed in a simplistic way using the arguments of the quasi-lattice theory (5). For very dilute solutions Hildebrand has shown that this model leads to an expression for the heat of solution of the solute identical to that found from solubility parameter theory. Following this approach for those systems in which the solubility of the solute in the binary solvent mixture is small the nearest neighbor environment may be defined as

$$[6] \qquad \frac{\Phi_1^*}{\Phi_3^*} = \frac{\Phi_1(\delta_2 - \delta_3)^2}{\Phi_3(\delta_2 - \delta_1)^2} \qquad (\text{where } \Phi_1^* + \Phi_3^* = 1)$$

In eq. 6 the effective volume fraction terms are related to the bulk volume fraction terms by the inverse of the heats of mixing of the solute in each of the pure solvents. Using eq. 6 to define Φ_1^* and using eq. 5 to define δ_M it is easily shown that eq. 4 can be reformulated to require a linear relationship to exist between $(\ln a_2^i - \ln x_2^M)^{1/2}$ and Φ_1^*. In Figs. 1–3 such a linearity is seen to exist for each of the systems considered. The intercept values at $\Phi_1^* = 0$ and the expected values of $(\ln a_2^i - \ln x_2^3)^{1/2}$ are 1.663, 1.655; 1.840, 1.835; 1.785, 1.80; respectively for the three systems considered. Furthermore the ratio of slope/intercept for each of the three systems is found self-consistent with those δ values used in evaluating the Φ_1^* terms and satisfying the saturation solubility of the solute in each of the pure solvents (Table 3).

Benzene was chosen as one of the solvent components for the iodine solute study as it was anticipated that the well known charge transfer (10) interaction between them should make benzene the energetically preferred nearest neighbor. It is seen that the preferential solvation still exists when stannic iodide is made the solute and for this system no specific solute–solvent interaction occurs. As a final test of our $(\ln a_2^i - \ln x_2^M)^{1/2}$ *vs.* Φ_1 (or Φ_1^*) relation we plot in Fig. 4 the theoretical lines for the system iodine–CCl_4–n-C_7F_{16} (4). Only two data points exist for this system and we compare them to the theoretical lines calculated from the known solubility of iodine in the pure perfluorocarbon and the accepted δ values (5). The wide difference in the solute parameter (14.1) and that of one of the solvent pairs (6.0) puts a considerable strain upon the proposed theory. As may be seen, however, the data points lie on that line drawn using the effective volume fraction (Φ_i^*) term.

As a further test of the acceptability of the proposed "effective volume fraction" term we examine the partial molal volume data for

Can. J. Chem. Downloaded from www.nrcresearchpress.com by 210.87.254.6 on 09/05/12
For personal use only.

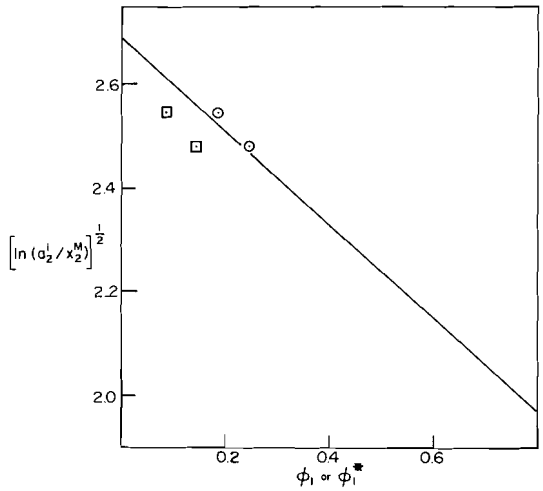

FIG. 4. Iodine in mixed carbon tetrachloride – perfluoroheptane solvent. Data points plotted against simple volume fraction of carbon tetrachloride in mixed solvent (□) and against "effective volume fraction" of carbon tetrachloride (○). Solid line represents the theoretical $[\ln (a_2^1/x_2^M)]^{1/2}$ *vs.* Φ_1 or Φ_1^* relationship. Data at 25.0 °C.

iodine in the mixed benzene–cyclohexane solvent. In terms of the mixed solvent δ_M parameter we may reformulate the usual equation relating the partial molal volume of the solute ($\bar{V}_2^M$) to the isothermal compressibility of the solvent β_M and the solubility parameters of solute and solvent as

$$[7] \qquad \bar{V}_2^M - \bar{V}_2^0 = n_M \beta_M V_2^0 (\delta_2 - \delta_M)^2$$

where V_2^0 is the reference volume of the solute (5). We can assume a value of unity for n_M (the ratio of the internal pressure to the cohesive energy density (5)) and define β_M in terms of the isothermal compressibility of the pure solvents without any loss in the predictive value of eq. 7 as, $\beta_M = \Phi_1\beta_1 + \Phi_3\beta_3$. Since eq. 7 cannot be rearranged allowing $\bar{V}_2^M$ to be directly analyzed in a manner emphasizing the dependence on Φ_1 or Φ_1^* we compare in Table 4 the experimental $\bar{V}_2^M$ values with those calculated from eq. 7 using either the bulk volume fraction or effective volume fraction definition of δ_M. It is obvious that an acceptable comparison with experiment is found only with the use of the effective volume fraction terms.

We have made experimental studies for systems for which in eq. 2 the approximation that $\Phi_M \rightarrow 1$ cannot be made, *e.g.* the naphthalene–CCl_4 – *c*-C_6H_{12} system as reported by Heric and Yeh (11). For these systems the "effective volume fraction" approach is again found necessary for the interpretation of the data. These systems often involve a maximum in the saturation solubility value (*i.e.* those for which $\delta_1 < \delta_2 < \delta_3$) but as the formulation of the saturation solubility equation is more complex they will be dealt with in another paper. It is clear that within its limitations solubility parameter theory may be extended so that the solubility thermodynamic properties of dilute solutes in two component solvent mixtures can be predicted.

TABLE 4. The partial molal volume of iodine in a mixed benzene–cyclohexane solvent at 25 °C

Volume fraction of benzene Φ_1	Partial molal volume (cc mol^{-1})		
	$\bar{V}_2$ (expt.)	$\bar{V}_2$ (calc.)	$\bar{V}_2$ (calc.)*
0.0	68.2		—
0.2551	65.5	66.8	65.4
0.5693	64.4	64.9	64.2
0.6927	63.3	64.2	63.2
0.7604	63.1	63.8	62.8
0.8657	62.9	63.2	62.6
1.000	62.4		—

*Calculated using $\delta_M = \Phi_1^*\delta_1 + \Phi_3^*\delta_3$.

We wish to thank the National Research Council of Canada for their support of this project.

1. R. L. SCOTT and D. V. FENBY. Ann. Rev. Phys. Chem. **20**, 11 (1969).
2. S. CHRISTIAN. J. Am. Chem. Soc. **91**, 6514 (1969).
3. K. NAKANISHI, T. OZASA, and K. ASHITANI. J. Phys. Chem. **75**, 963 (1971).
4. E. B. SMITH, J. Walkley, and J. H. HILDEBRAND. J. Phys. Chem. **63**, 703 (1959).
5. J. H. HILDEBRAND and R. L. SCOTT. The solubility of non-electrolytes. 3rd Ed. Dover Publications Inc., New York. (1964).
6. M. VITTORIA and J. WALKLEY. Trans. Faraday Soc. **65**, 57, 62 (1969).
7. J. H. HILDEBRAND and D. N. GLEW. J. Phys. Chem. **60**, 616 (1956).
8. E. B. SMITH and J. WALKLEY. Trans. Faraday Soc. **56**, 220 (1960).
9. S. E. WOOD, B. D. FINE, and L. M. ISAACSON. J. Phys. Chem. **61**, 1605 (1957).
10. R. S. MULLIKEN. J. Am. Chem. Soc. **70**, 600 (1950); J. Phys. Chem. **56**, 801 (1952).
11. E. L. HERIC and K. N. YEH. J. Chem. Eng. Data, **15**, 13 (1970).

Can. J. Chem. Downloaded from www.nrcresearchpress.com by 210.87.254.6 on 09/05/12
For personal use only.

Phase Relationships in the Calcium Chloride – Calcium Carbide System

J. F. MAILLOT

Department of Engineering, University of Moncton, Moncton, New Brunswick

AND

D. R. MORRIS

Department of Chemical Engineering, University of New Brunswick, Fredericton, New Brunswick

Received July 19, 1971

The system calcium chloride – calcium carbide has been examined by thermal analysis. The depression of the freezing point of $CaCl_2$ by CaC_2 is ideal. The system is a eutectic one, with a eutectic point at 90 mol% $CaCl_2$ at 740 °C. Carbon is believed to be present in the electrolyte as the so called acetylide ion C_2^{2-}. The melting point of pure $CaCl_2$ was found to be 775.2 ± 0.6 °C.

Le système chlorure de calcium – carbure de calcium a été examiné par analyse thermique. La dépression du point de congélation de $CaCl_2$ par CaC_2 est idéale. Le système est un eutectique, avec un point eutectique correspondant à 90% de moles de $CaCl_2$ à 740 °C. Le carbone est présent dans l'électrolyte sous forme d'ion acétylure C_2^{2-}. Le point de fusion de $CaCl_2$ pur est de 775.2 ± 0.6 °C.

Canadian Journal of Chemistry, **50**, 839 (1972)

Can. J. Chem. Downloaded from www.nrcresearchpress.com by 210.87.254.42 on 09/05/12
For personal use only.

Introduction

The solubility of calcium carbide in a number of fused salts was examined for the first time by Barber and Sloan (1) in 1961. Using the technique of equilibration and quenching they reported the solubility of CaC_2 in $CaCl_2$ to be 0.103 mole fraction at a temperature of 820 °C.

This system was used more recently by Hawkes and Morris (2) as an electrolyte in a galvanic cell designed to establish the activity of carbon in solid iron–carbon alloys.

In view of the importance of the $CaCl_2$–CaC_2 system in many of the projects derived from the above study it has been necessary to determine the relative solubility of these compounds. In this paper we present a partial phase diagram of the system determined by thermal analysis.

Experimental

Materials

The calcium carbide was prepared by direct synthesis from calcium and carbon following a technique developed by Aksaranan (3). After synthesis the purity level was 96–99 weight %; the principal impurity was calcium oxide. Dried reagent grade calcium chloride from Fisher Scientific Company was used in the experiments. The bulk of the water (about 25 weight %) was removed in a premelting stage while the purification stage was used to remove the calcium oxide hydrolysis product, according to the reaction

$$CaO + 2HCl \rightarrow CaCl_2 + H_2O$$

Apparatus and Procedures

The purification furnace and the operating procedure for the purification of $CaCl_2$ have been previously described by Kojima, Whiteway, and Masson (4) for the purification of inorganic fluorides. Anhydrous hydrogen chloride gas was bubbled through the molten chloride for 2 to 7 h, followed by dry argon. The freezing points of the mixtures were determined by the method of thermal arrests with the apparatus described previously by Bell and Masson (5), modified to enable evacuation of the furnace envelope. Melts were held in steel crucibles, 1 in. in diameter and 1.5 in. deep, equipped with a re-entrant well, which housed the junction of the thermocouple. Approximately 11 g of mixture were used in each experiment. The temperature was measured with a Pt/Pt – 13% Rh thermocouple calibrated periodically against copper, aluminum, and zinc, supplied by the U.S. National Bureau of Standards. A Texas potentiometric recorder with a full chart range of 2 mV was used to measure the electromotive force (e.m.f.). The recorder was calibrated after each series of measurements by a Leeds and Northrup potentiometer. The temperature of the furnace was controlled by a Honeywell program controller, actuated by a second thermocouple located close to the furnace winding. A linear cooling rate of 1 °C/min was used.

The use of steel crucibles and the blending of the anhydrous salts prior to melting gave homogeneous melts. Reproducibility of the melting points determination was ± 1.5 °C. Some experiments were conducted in graphite crucibles; these were unsatisfactory due to leakage of the melt through the pores of the graphite.

Analysis

The analytical procedure to determine the concentration of the principal constituents of the solution has been described by Aksaranan *et al.* (6). This is a development of the method proposed by Edwards (7) and used later by Morris and Harry (8). A weighed sample of the solidified calcium carbide – calcium chloride solution was hydrolyzed in a closed system. A sample of the gases thus liberated was analyzed using a gas partitioner which was calibrated previously with hydrogen–acetylene mixtures. This method permitted the direct analysis of the calcium metal content

Can. J. Chem. Downloaded from www.nrcresearchpress.com by 210.87.254.42 on 09/05/12
For personal use only.

TABLE 1. Chemical composition of the cryoscopic melts and temperatures of the thermal arrests

Experiment No.	Mol % as per analysis, carbon-free basis*				Observed thermal arrests (±1.5 °C)†					Temperature span covered in experiment (°C)
	CaC_2 (±3%)	CaO (±10%)	Ca (±3%)	$CaCl_2$ (±1%)	t_1	t_2	t_3	t_4	t_5	
195‡	—	—	—	100	774.0	—	—	—	670.9	822–647
171	—	0.50	—	99.5	773.0	—	—	—	—	790–711
193	—	0.50	—	99.5	774.5	—	—	—	677.2	790–638
194	—	0.50	—	99.5	773.5	—	—	—	673.9	814–664
173‡	0.80	—	—	99.2	772.0	745.5	—	—	675.5	795–643
177	0.073	0.96	0.01	99.0	772.5	743.1	—	—	672.2	798–660
192	0.15	1.46	0.01	98.4	769.0	746.0	—	688.1	671.5	798–655
191	1.21	0.50	0.04	98.3	766.1	—	723.1	685.2	670.5	806–647
159‡	2.40	—	—	97.6	766.0	—	—	—	—	807–760
172	0.20	2.92	0.10	96.8	768.0	743.0	—	690.0	670.0	798–621
190	2.16	1.46	0.05	96.3	764.0	731.0	719.2	688.1	670.9	798–655
176‡	4.50	—	—	95.5	761.5	—	720.0	692.0	672.0	786–660
187	2.60	1.96	0.04	95.4	759.0	—	725.0	689.2	669.8	794–639
175	1.19	3.51	0.10	95.4	763.0	728.0	718.5	690.0	672.0	786–639
169	0.89	5.05	0.27	93.8	753.0	740.5	722.0	—	—	810–629
181	5.90	0.90	0.27	92.9	748.0	733.0	713.7	690.0	669.6	798–660
174	4.86	3.20	0.19	91.8	745.6	734.5	719.0	692.5	676.0	765–657
160‡	8.40	—	—	91.6	747.6	740.0	717.5	695.5	667.0	798–657
179	5.87	2.94	0.05	91.1	743.2	731.2	721.8	690.3	675.9	773–647
182	6.91	3.46	0.06	89.6	736.9	732.0	709.4	691.0	677.0	790–665
168‡	10.7	—	—	89.3	—	733.5	710.5	694.5	674.0	790–631
183	9.16	2.12	0.08	88.6	—	736.1	716.1	690.1	671.2	794–655
185	8.87	3.00	0.08	88.0	—	737.1	719.1	691.1	675.0	765–630
170‡	14.0	—	—	86.0	—	734.0	712.5	691.5	—	757–678
184	11.5	2.56	0.11	85.8	—	739.6	717.4	692.3	669.7	790–630
161‡	15.8	—	—	84.2	—	730.6	—	—	—	766–715
186‡	16.0	—	—	84.0	—	738.0	713.0	687.5	669.8	806–650
162‡	19.6	—	—	80.4	—	732.1	—	—	—	750–724
178‡	20.1	—	—	79.9	—	728.0	715.9	692.7	669.8	797–656
196	Steel crucible packed with graphite powder					—	—	—	671.5	798–660
198	Steel crucible packed with steel turnings					—	—	—	670.5	790–660

*Free carbon contents not reported; carbon assumed insoluble in melt. Uncertainty levels estimated from errors arising from analytical procedure (6).
†Uncertainty of temperature arrests determined from replicated cooling curves. Uncertainty on melting point of purified $CaCl_2$: ± 0.6 °C.
‡Chemical analysis not performed. Analysis figures as per initial inventory.

Can. J. Chem. Downloaded from www.nrcresearchpress.com by 210.87.254.42 on 09/05/12
For personal use only.

and the calcium carbide. Total chloride and free oxide were determined by conventional analysis of the hydrolyzed sample.

Results and Discussion

Equilibrium between a pure solid A_rX_s (component 1) and a liquid mixture is described by the equation (9),

$$[1]\quad \frac{d \ln a_1}{d(1/T)} = \frac{d \ln N_A^r N_X^s}{d(1/T)} + \frac{d \ln \gamma_1}{d(1/T)} = \frac{-\Delta H_f}{R}$$

where a_1 and γ_1 are, respectively, the activity and activity coefficient of the solid A_rX_s in solution at equilibrium with the pure solid at temperature T. N_A and N_X are the Temkin ion fractions and ΔH_f is the heat of fusion of the pure A_rX_s.

Assuming the salts used in the present investigation to be fully ionized, $N_A \equiv N_{Ca^{2+}} = 1$, and $r = 1$. In the low concentration region the activity coefficient is unity and over the small temperature span involved, ΔH_f may be taken to be independent of temperature. Equation 1 then becomes, with $X \equiv Cl^-$ and $s = 2(CaCl_2)$,

$$[2]\quad 2 \ln N_{Cl^-} = \frac{\Delta H_f}{R}\left(\frac{1}{T_m} - \frac{1}{T}\right)$$

where T_m is the melting point of pure $CaCl_2$.

By definition, $N_{Cl^-} = (1 - N_Y)$ where N_Y is the total ion fraction of foreign anions and if N_Y is small relative to unity, $\ln (1 - N_Y) \simeq -N_Y$. Equation 2 becomes

$$[3]\quad -2N_Y = \frac{\Delta H_f}{R}\left(\frac{1}{T_m} - \frac{1}{T}\right)$$

Identifying Y as the divalent anion of a calcium salt, *e.g.* O^{2-} or $(C_2)^{2-}$, it is easily shown that $N_{CaY} = 2N_Y$ when N_Y is small, whence

$$[4]\quad N_{CaY} = \frac{\Delta H_f}{R}\left(\frac{1}{T} - \frac{1}{T_m}\right)$$

In the more general case and by further approximation, the van't Hoff relation is obtained

$$[5]\quad T_m - T = \Delta T \simeq \frac{RT_m^2}{\Delta H_f} \nu N_2$$

where ν is the number of foreign particles introduced into the solution per molecule of solute 2.

It follows from the above that measurement of the equilibrium temperature T for a system of known composition gives information regarding the species in solution and thermodynamic data in respect of the solution.

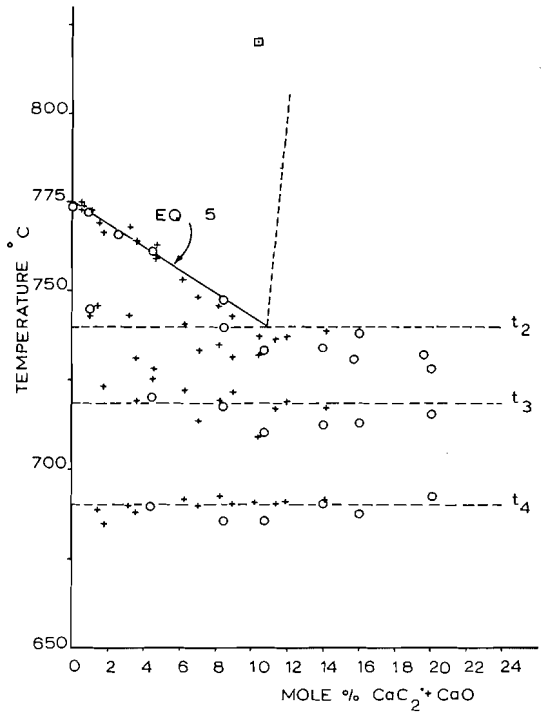

FIG. 1. Partial phase diagram of the pseudo binary system: $CaCl_2$ – (CaC_2 + CaO): ×, Observed thermal arrest temperatures; ○, ditto (melts not analyzed); ⊡, solubility datum point, ref. 1.

The temperatures associated with each thermal arrest are shown in Table 1. Also reported in the same table are the chemical analyses of the melts. Five constituents were found: $CaCl_2$, CaC_2, CaO, C, and Ca. The average mass balance percentage was 101.6%. The carbon contents are not reported; carbon was assumed to be insoluble in the melt.

Pseudo Binary System $CaCl_2$ – (CaC_2 + CaO)

It is evident from the chemical analysis of each sample that the depression of freezing point of the solvent, $CaCl_2$, may be attributed to the combined effects of calcium carbide, calcium oxide, and calcium, though the last may be neglected in view of the low concentration. A plot of the thermal arrests as a function of the system composition, on a carbon free basis is presented in Fig. 1. Included in this figure is the theoretical liquidus line corresponding to eq. 5. Using $T_m = 1048.2$ °K, $\Delta H_f = 6780$ cal/mol,

$v = 1$, the liquidus temperature t_l °C is given by

[6] $$t_l = 775.2 - 320\ N_{CaY}$$

From the experimental data, the following equation was derived

[7] $$t_l = 775.2 - (300 \pm 70)\ N_{CaY}$$

The close agreement between the theoretical line and the experimental data points suggests that no solid solution is formed. This absence of solid solution could be attributed to the difference of crystalline structures; calcium carbide has a cubic structure (10) while calcium chloride is tetragonal (11).

Ternary System $CaCl_2$–CaO–CaC_2

The results of the chemical analysis of the cryoscopic melts (Table 1) and the extensive scatter of the sub-liquidus thermal arrests observed (Fig. 1) suggested interpretation of these data in terms of the additive ternary system $CaCl_2$–CaO–CaC_2.

In general, the incorporation of a third component to a binary system lowers the binary eutectic temperature until with further addition the ternary eutectic point is reached. At this point the saturated liquid is in equilibrium with the three pure solids, assuming no solid solution. The four condensed phase, three component, system is then invariant. Thermal arrests would then be observed at the liquidus, the boundary curve (both variable with composition), and the ternary eutectic (invariant) (12).

It is evident from the thermal arrest data that the situation is more complex. Thus in general, the first arrest observed at (CaC_2 + CaO) concentrations less than about 10 mol% corresponds well to the liquidus, the second (not always observed) may be identified as the boundary curve temperature, and the third should then correspond to the ternary eutectic (invariant) temperature. However, the third (not always observed) arrest is not invariant, 718.0 ± 4.9 °C, but the fourth arrest is invariant within the limits of experimental error, 690.6 ± 2.4 °C.

The fourth arrest was observed in most melts as was also a fifth arrest, also invariant within the limits of experimental error, 672.1 ± 2.6 °C. Tests conducted in which the steel crucible used for containing the melts was charged with graphite powder or steel scrap also showed the last arrest; it should therefore not be considered in relation to the system under discussion.

An attempt has been made to construct the polythermal projection of the temperature–composition prism (the phase diagram) for the ternary system assuming the liquidus line to be straight. The boundary curve, representing the locus of points of three phase equilibrium may then be determined by graphical construction, since at the boundary curve temperature (t_2) for a given composition, the ratio of liquid to solid is given by the ratio $(t_m - t_1)/(t_1 - t_2)$. A short extrapolation of the boundary curve to the CaO-free axis of the phase diagram gives 10.0 mol % CaC_2, 740 °C for the eutectic of the CaC_2–$CaCl_2$ binary system. However, due to the relatively large uncertainties in the Δt terms of the above expression the boundary curve cannot be located with certainty at the present time.

Furthermore, neither t_3 nor t_4 can be regarded as the ternary eutectic of the system as defined above in view of the eutectic for the CaO–$CaCl_2$ binary system given by Threadgill (13), 30 mol % CaO, 597 °C. It is clear that resolution of these phenomena must await a more complete study of the phase equilibria in this ternary system.

Conclusions

(*1*) Aksaranan *et al.* (6) have established, from a thermodynamic argument that the heterogeneous equilibrium,

[8] $$CaC_{2(soln)} \leftrightharpoons Ca_{(soln)} + 2[C]$$

where [C] represents carbon in solid solution in the crucible, exists in the system CaC_2–$CaCl_2$. The presence of Ca is confirmed by the analytical data of Table 1. The liquidus line of Fig. 1 is consistent with a model in which the CaC_2 is ionized in the solution according to

[9] $$CaC_{2(soln)} \leftrightharpoons Ca^{2+} + C_2^{2-}$$

and in which no solid solution of CaC_2 in $CaCl_2$ occurs. Mitchell (14) reached similar conclusions in respect of the CaC_2–CaF_2 system.

(*2*) Interpretation of the sub liquidus thermal arrest data is complicated by contamination of the melt with O^{2-} ion, a consequence of the high reactivity of calcium carbide to oxygen. An attempt to construct a ternary phase diagram from the available data was unsatisfactory.

Can. J. Chem. Downloaded from www.nrcresearchpress.com by 210.87.254.42 on 09/05/12
For personal use only.

The authors wish to thank the National Research Council of Canada for the permission to carry out the experiments in their laboratory in Halifax. These thanks are extended to Dr. A. C. Neish, Dr. C. R. Masson, Dr. S. G. Whiteway, and Dr. I. B. Smith.

Thanks are due to the American Iron and Steel Institute for financial support, and to the Université de Moncton for the grant of a year of study leave to J.F.M.

Thanks are also due to Mr. C. Aksaranan for the preparation of calcium carbide.

1. W. A. Barber and C. L. Sloan. J. Am. Chem. Soc. **65**, 2026 (1961).
2. G. L. Hawkes and D. R. Morris. Trans. Met. Soc. AIME **242**, 1083 (1968).
3. C. Aksaranan. M.Sc. Thesis. University of New Brunswick, Fredericton, New Brunswick. 1969.
4. H. Kojima, S. G. Whiteway, and C. R. Masson. Can. J. Chem. **46**, 2968 (1968).
5. H. B. Bell and C. R. Masson. J. Sci. Inst. **41**, 389 (1964).
6. C. Aksaranan, V. Dosaj, D. R. Morris, and S. H. White. Can. J. Chem. **49**, 2014 (1971).
7. A. H. Edwards. Anal. **71**, 521 (1946).
8. D. R. Morris and J. R. Harry. Proc. Inter. Conf. Ind. Carbon and Graphite, Soc. Chem. Ind. London. 1965. p. 36.
9. M. Blander. Molten salt chemistry. Interscience, 1964. p. 139.
10. N. C. Vannerberg. Acta Chem. Scand. **15**, 769 (1961).
11. O. Kubaschewski and E. Evans. La thermochimie en métallurgie. Gauthier Villars, Paris. 1964.
12. J. E. Ricci. *In* Molten salt chemistry. *Edited by* M. Blander. Interscience, John Wiley and Sons, Inc., New York. 1964. p. 239.
13. W. D. Threadgill. J. Electrochem. Soc. **112**, 632 (1965).
14. A. Mitchell. Trans. Met. Soc. AIME, **242**, 2507 (1968).

Can. J. Chem. Downloaded from www.nrcresearchpress.com by 210.87.254.42 on 09/05/12
For personal use only.

Reactions of Thiyl Radicals. VII. Photolysis of Methyl Sulfide Vapor[1]

P. M. RAO[2] AND A. R. KNIGHT

Department of Chemistry and Chemical Engineering, University of Saskatchewan, Saskatoon, Saskatchewan

Received August 19, 1971

The photolysis of methyl sulfide vapor has been investigated as a function of substrate pressure, exposure time, and temperature in the wavelength range 2000 to 2300 Å. The effects of added propane, sulfur hexafluoride, and 2-methylpentane have been studied. The principal products of the decomposition are CH_4, C_2H_6, CH_3SSCH_3, and CH_3SH. The data indicate direct C—S bond scission in the primary process giving rise to "hot" CH_3 and CH_3S radicals. A mechanism in which disproportionation of methylthiyl radicals is a very minor process is proposed.

The reactions of CH_3 and CH_3S radicals with methyl sulfide have been examined also by photolyzing CH_3SSCH_3 and CH_3COCH_3 in the presence of CH_3SCH_3. Quantum yields at 2288 Å have been determined as a function of several variables. A number of rate parameters for the reactions of methyl radicals and methylthiyl radicals have been calculated.

On effectue la photolyse des vapeurs de sulfure de méthyle en fonction de la pression de substrat, du temps d'exposition et de la température dans un domaine de longueur d'onde de 2000 à 2300 Å. On étudie les effets de l'addition de propane, d'hexafluorure de soufre, et de 2-méthylpentane. Les principaux produits de décomposition sont CH_4, C_2H_6, CH_3SSCH_3, et CH_3SH. Les données indiquent une scission directe du lien C—S dans le procédé primaire donnant lieu à des radicaux CH_3 et CH_3S "chauds". On propose alors un mécanisme dans lequel la disproportionation des radicaux méthylthiyl est un procédé très secondaire.

Les réactions des radicaux CH_3 et CH_3S avec le sulfure de méthyle sont aussi examinées en photolysant CH_3SSCH_3 et CH_3COCH_3 en présence de CH_3SCH_3. Les rendements quantiques à 2288 Å sont aussi déterminés en fonction de plusieurs variables. On calcule aussi un certain nombre de paramètres de vitesse pour les réactions des radicaux méthyl et méthylthiyl.

Canadian Journal of Chemistry, **50**, 844 (1972)

Introduction

Some aspects of the photolysis of methyl sulfide have been investigated previously. Haines *et al.* (1) photolyzed liquid CH_3SCH_3 for 65 h and reported H_2 and CH_4 as products. Milligan *et al.* (2) found CH_4 and C_2H_6 along with methyl disulfide as products from the 2537 Å photolysis. Inaba and Ogoro (3) studied the gross features of the gas phase photolysis. They found CH_4, C_2H_6, CH_3SH, and CH_3SSCH_3 among the products. All yields, except that of the disulfide were reduced by addition of argon. Recently, Callear and Dickson (4) investigated the flash photolysis of CH_3SCH_3 at 1950 Å and established that the primary process was C—S bond scission producing CH_3 and CH_3S radicals. CH_2S was observed spectroscopically and was found to be quenched by the addition of nitric oxide.

Lossing and co-workers (5) examined the mercury photosensitized decomposition in a flow system coupled to a mass spectrometer. Relatively large yields of CH_3SH were detected and on the basis of that work a disproportionation/recombination ratio of 0.4 ± 0.1 was suggested. The photolysis of disulfides in a glass at 77 °K (6) has also yielded spectroscopic evidence of significant disproportionation of RS radicals.

The detailed investigation of the vapor phase photolysis of methyl sulfide reported here was undertaken to obtain further information about the nature of the reactions that occur in the system and kinetic data on CH_3S radical reactions, particularly the role of disproportionation of that species. Results obtained in this laboratory have indicated a maximum value of *ca.* 0.05 for the disproportionation/recombination ratio for thiyl radicals formed in the direct photolysis of thiols (7, 8) and disulfides (9, 10) in the vapor phase. In the liquid phase, disproportionation is virtually negligible (11).

Experimental

The photolysis was carried out in a conventional grease-free vacuum system previously described (9). The light

[1]From the thesis submitted by P. M. Rao in partial fulfilment of the requirements of the Ph.D. degree, University of Saskatchewan, Saskatoon, Saskatchewan.

[2]Present address, Department of Chemistry, University of Alberta, Edmonton, Alberta.

Can. J. Chem. Downloaded from www.nrcresearchpress.com by 210.87.254.5 on 09/05/12
For personal use only.

Can. J. Chem. Downloaded from www.nrcresearchpress.com by 210.87.254.5 on 09/05/12
For personal use only.

sources were a Hanovia type 30620 medium pressure mercury lamp filtered to remove wavelengths less than 2000 Å or, in one series of experiments, wavelengths less than 2300 Å; and a Phillips 93107 Cd-spectral lamp used in conjunction with a Baird-Atomic interference filter passing only the 2288 Å cadmium resonance line. Reaction cells were plane end quartz cylinders 5 cm in diameter with path length of 16 cm or 1 m. Methyl sulfide (Eastman) was purified by triple distillation at atmospheric pressure, degassing, and a further low temperature fractionation in the vacuum line. Impurities detected by g.c. were less than 0.01%. Methyl disulfide (Eastman) was purified in the same manner. Baker reagent acetone was used after degassing and trap-to-trap distillation at reduced pressure. Eastman 2-methylpentane was distilled in the vacuum system and the fraction condensable between −160 and −84 °C used.

At the conclusion of each reaction involving CH_3SCH_3, CH_4 was removed at −196 °C; C_2H_6 at −160 °C, and the remaining condensable products, including the substrate, analyzed by g.c. using a 6 ft tricresyl phosphate column. In experiments with addends, the addend was removed by trap-to-trap distillation prior to g.c. analysis.

Light intensities at 2288 Å for quantum yield determinations were found using the photolysis of acetone at 155 °C. The extinction coefficient for acetone at this wavelength was determined and a Beer–Lambert law calculation of the fraction absorbed by the actinometer at an acetone pressure of 200 Torr carried out. Φ(CO) was assumed to be unity and rate of carbon monoxide formation were determined by g.c. analysis using a molecular sieve column.

Results

In the photolysis of the substrate at 25 °C with effective radiation between 2000 and 2300 Å, CH_4, C_2H_6, CH_3SSCH_3, and CH_3SH accounted for 91–98% of the volatile products. No hydrogen was detected. The expected mass balance among the products, $[CH_3S] = [CH_3]$, where each term represents the total yield of products containing the indicated group, is not obtained. Although there are variations under different reaction conditions, products determined quantitatively showed in general a deficiency in sulfur containing compounds.

Irradiation of the substrate for periods of 24 h or more gives rise to a non-volatile oil that forms as droplets on the walls of the reaction vessel. Mass spectral analysis of the residue of evaporated $CHCl_3$ solutions of this material indicated a relatively high molecular weight (at least 258) mixture of compounds containing the CH_2S and CH_3S groups. Although it was not possible to identify definitively the components of the mixture, the presence of sulfur in the residue was confirmed by comparison of calculated and observed $^{34}S/^{32}S$ peak ratios. This aspect of the decomposition was not investigated further since during the long exposure times required to form sufficient non-volatile material for analysis, there would be significant secondary decomposition of initially formed higher molecular weight products.

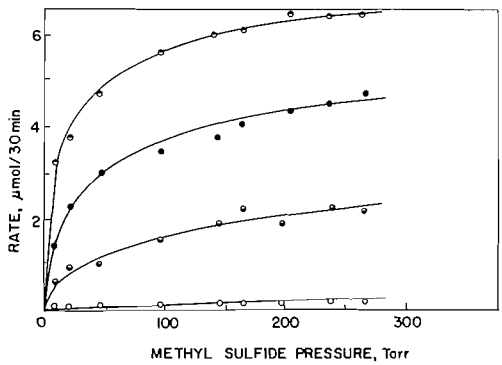

FIG. 1. Rate of formation of C_2H_6, ◓; CH_3SSCH_3, ●; CH_4, ◒; and CH_3SH, 0; as a function of methyl sulfide pressure at 25 °C for an exposure time of 30 min.

Figure 1 shows the rate of production of the principal products as a function of methyl sulfide pressure. The yield of CH_3SH is quite small, increasing more or less regularly from 0.045 μmol/30 min at $P(CH_3SCH_3) = 50$ Torr to 0.12 μmol/30 min when the substrate pressure was 282 Torr. It should be noted, however, that because of the minute CH_3SH yields, the experimental error in mercaptan rates is relatively large and it is therefore difficult to assess quantitatively the pressure dependence of this rate at low substrate pressures. The rate data actually obtained indicate that $R_{CH_3SH}/R_{CH_3SSCH_3}$ is less than *ca.* 0.03 for substrate pressures up to about 300 Torr.

Two series of experiments were carried out in a 1 m pathlength cell to permit small percent conversions but with sufficient absolute amounts of products for analysis. The results of the series at 20 Torr sulfide pressure are shown in Fig. 2. CH_3SH was not analyzed for in this series. The rate of formation of methyl disulfide is evidently very much less dependent on exposure time than that of either methane or ethane. In the second set of experiments carried out at 5 and at 20 Torr substrate pressure, the yields of both the thiol and disulfide were determined. The results, shown as the ratio of the rate of formation of CH_3SH and CH_3SSCH_3, are given in Fig. 3. They demonstrate that the relative amount of these products is dependent on both exposure

TABLE 1. Effect of addends on the photolysis of methyl sulfide*

Pressure (Torr)			Rate (μmol/30 min)		
CH_3SCH_3	C_3H_8	SF_6	CH_4	C_2H_6	CH_3SSCH_3
25	0	0	1.34	4.41	2.92
25	60	0	0.45	†	2.61
25	138	0	0.28	†	2.75
25	325	0	0.20	†	2.72
250	0	0	2.21	6.35	4.49
250	0	300	1.31	2.5	4.78
250	0	695	1.03	1.9	4.11

*Exposure time = 30 min; $T = 27$ °C.
†Not determined.

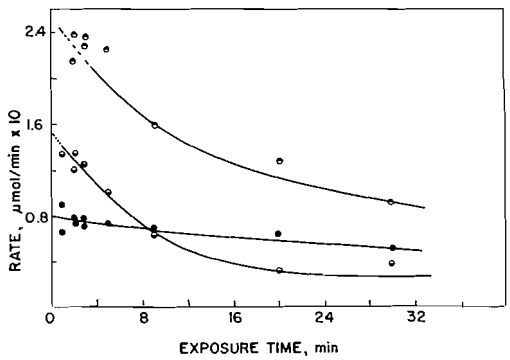

Fig. 2. Rate of formation of CH_4, ◒; C_2H_6, ◓; and CH_3SSCH_3, ●; as a function of exposure time for the photolysis of 20 Torr methyl sulfide at 25 °C.

time and on substrate pressure. To establish the possible effects of surface reactions two sets of experiments were conducted in which the rates of CH_4, C_2H_6, and CH_3SSCH_3 formation were determined in a cylindrical cell of 172 cm^3 volume and compared with rates observed when the cell was filled with glass beads. The effective volume in the packed cell was 72 cm^3 and the surface volume ratio increased from 0.72 cm^{-1} in the unpacked cell to 18.4 cm^{-1} when the packing was present. The ratio of rates for the packed and unpacked vessel, R_P/R_U, observed were 0.31 for CH_4, 0.30 for C_2H_6, and 0.36 for CH_3SSCH_3 when the methyl sulfide pressure was 25 Torr and 0.47, 0.33, and 0.47 respectively, when 100 Torr substrate was photolyzed.

The effects of inert addends, propane and sulfur hexafluoride, were examined and the results are given in Table 1. As is apparent from the data, the rate of disulfide formation is virtually independent of addend pressure, while the yields of CH_4 and C_2H_6 are significantly pressure dependent. The ethane rates determined in the presence of added gases are likely accurate to no more than ±10% because of the difficulties in separating this product from the large amount of addend.

A series of experiments was carried out at each of four temperatures and yields measured as a function of 2-methylpentane pressure for the photolysis of 25 Torr CH_3SCH_3. Figure 4

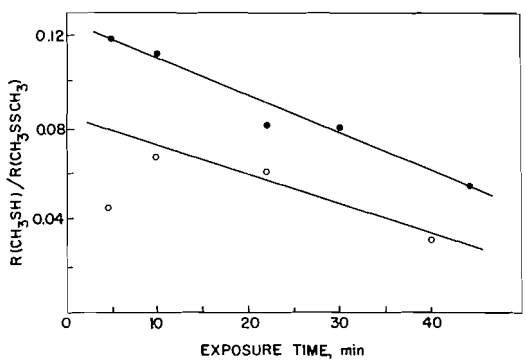

FIG. 3. $R_{CH_3SH}/R_{CH_3SSCH_3}$ as a function of exposure time for the photolysis of 5 Torr, ●; and 20 Torr, 0, of methyl sulfide in a 1 m cell at 25 °C.

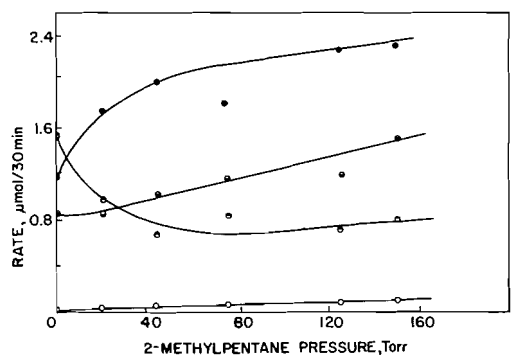

FIG. 4. Rate of formation of CH_4, ◒; C_2H_6, ◓; CH_3SSCH_3, ●; and CH_3SH, 0; as a function of pressure of 2-methylpentane in the photolysis of 25 Torr methyl sulfide at 25 °C for 30 min.

Can. J. Chem. Downloaded from www.nrcresearchpress.com by 210.87.254.5 on 09/05/12
For personal use only.

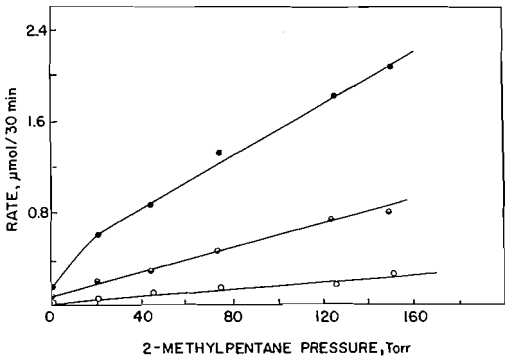

FIG. 5. Rate of formation of CH_3SH as a function of pressure of 2-methylpentane in the photolysis of 25 Torr methyl sulfide at 57 °C, 0; 104 °C, ◒; and 154 °C, ●.

shows the rates of formation of CH_4, C_2H_6, CH_3SSCH_3, and CH_3SH at 25 °C. The same measurements were made at 57, 104, and 154 °C and Fig. 5 shows the rates of CH_3SH formation at these temperatures. The rates for the other products were determined as well but the only aspect of these data relevant to the purpose of this series of experiments is the fact that at 154 °C the rate of CH_3SH formation exceeds that of all other products for P(2-methylpentane) > 75 Torr. The addend was chosen as a source of labile H-atoms because the vapor pressure characteristics of 2-methylpentane permitted its facile separation from reaction products. Furthermore, it would be expected to act as a rather efficient deactivator for vibrationally excited species in the system.

The most important feature of these results is the linear dependence of methanethiol rate on 2-methylpentane pressure and the fact that this rate increases significantly with temperature to the extent that CH_3SH is the major product of the reaction at 154 °C.

In comparing the rates for 30 min exposures at the four temperatures studied, it is to be noted that the effect of exposure time was determined only at room temperature. The relation between initial rates and those at 30 min may change with temperature, although the data in Fig. 2 indicate that the rates are strongly dependent on time primarily in the early stages of the reaction.

The role of CH_3S radicals in this system was further investigated by producing this species from the photolysis of CH_3SSCH_3. Mixtures of the disulfide and sulfide were photolyzed at 27 and 154 °C at wavelengths greater than

TABLE 2. Photolysis of methyl disulfide in the presence of methyl sulfide*

$P_{CH_3SCH_3}$ (Torr)	T (°C)	Reaction time (min)	Rate (μmol/min) CH_4	C_2H_6	CH_3SH
0	27	30	0.029	0.009	0.13
20	27	30	.061	.018	0.13
75	27	30	.043	.014	0.11
0	154	10	.007	.002	0.041
20	154	10	.006	.003	0.171
40	154	10	.006	.003	0.272
60	154	10	†	†	0.304
75	154	10	†	†	0.414

*Disulfide pressure = 20 Torr; $\lambda > 2300$ Å.
†Not determined.

2300 Å where the sulfide is transparent (12, 13). It is well established that the primary process in the disulfide is S—S bond cleavage (9–11). Thus under the conditions of this experiment the photolysis produced CH_3S radicals in the presence of CH_3SCH_3. The data are listed in Table 2. CH_3SH formation accounts for about 5% of thiyl radicals from the disulfide photolysis (9). At the higher temperature there is a significant increase in the rate of thiol formation, while production of CH_4 and C_2H_6 (likely originating from the disulfide decomposition) is not altered appreciably. The absolute yields of these two products is hardly above the limits of detection. If it is assumed that CH_3SH arises by abstraction of an H-atom by CH_3S, simple kinetic analysis of R_{CH_3SH} in the presence and absence of sulfide indicates that the ratio of rate for thiyl radical attack on CH_3SCH_3 and CH_3SSCH_3 is 0.4 ± 0.1.

Using the same effective wavelengths, acetone was photolyzed in another series of experiments in the presence of CH_3SCH_3 to obtain data on the attack of CH_3 radicals on the substrate. The results are listed in Table 3.

Finally, quantum yields at 2288 Å were de-

TABLE 3. Photolysis of acetone in the presence of methyl sulfide*

$P_{CH_3SCH_3}$ (Torr)	CH_4 (μmol)
0	3.20
25	3.83
50	3.66
100	4.16

*$P(CH_3COCH_3) = 142$ Torr, $T = 154$ °C, exposure time = 5 min, $\lambda > 2300$ Å.

Can. J. Chem. Downloaded from www.nrcresearchpress.com by 210.87.254.5 on 09/05/12
For personal use only.

TABLE 4. Quantum yields in the photolysis of methyl sulfide at 2288 Å*

$P(CH_3SCH_3)$ (Torr)	T (°C)	I_8†	Quantum yield			
			CH_4	C_2H_6	CH_3SH	CH_3SSCH_3
25	25	3.42	0.025	‡	‡	0.103
25	156	3.42	0.293	‡	0.014	0.016
87	156	3.42	0.296	‡	0.014	0.040
150	156	3.42	0.377	‡	0.015	0.108
200	156	3.42	0.392	‡	0.022	0.276
150	25	3.42	0.135	‡	0.016	0.041
10	25	3.33	< .01	0.074	< .01	0.012
10§	25	3.33	< .01	0.020	< .01	0.014
25	25	3.33	0.021	0.074	< .01	0.102
25§	25	3.33	0.015	0.034	‡	0.014
25‖	25	3.33	0.114	‡	‡	0.023
25	61	3.33	0.053	0.044	‡	‡
25	156	3.33	0.199	< .01	‡	0.012
150	25	3.33	0.104	0.050	0.022	0.049
150	61	3.33	0.161	0.007	‡	‡
150	83.5	3.33	0.197	< .01	‡	‡
150	107.5	3.33	0.266	< .01	0.027	0.043
150	156	3.33	0.289	< .01	0.028	0.048
25	156	0.66	0.335	< .01	< .01	0.017
150	25	0.66	0.216	< .01	< .01	0.052
150	156	0.66	0.575	< .01	< .01	0.087

*Exposure time = 1000 min.
†μEinsteins/min × 10^3, from R_{CO} measurements in photolysis of acetone at 154 °C.
‡Not determined.
§150 Torr SF_6 added.
‖150 Torr 2-methylpentane added.

termined under a variety of pressure, temperature, and addend pressure conditions at two different light intensities. The results are given in Table 4. Because of the low effective intensity in the actinometry apparatus the exposure time was 1000 min, but percent conversions were comparable to those involved in the mercury lamp photolyses.

Discussion

The results obtained indicate C—S bond scission in the primary process, and the formation of the principal reaction products can be rationalized readily on that basis. It has been suggested previously that this primary process characterizes the liquid phase photolysis (1, 2), the Hg-sensitized decomposition (5), and the gas phase photolysis in both a conventional system (3) and in flash photolysis (4).

Ogoro and Inaba (3) proposed the initial formation of CH_3SCH_3* excited molecule which gives rise to CH_3 and CH_3S radicals in the absence of collisional deactivation. It appears, however, that the primary process can best be described in terms of direct C—S bond cleavage since the formation of CH_3SCH_3* in the primary process should be manifested by a decrease in the yields of *all* products in the presence of deactivating addends, an effect not found here.

The dependence of product yields on the pressure of the substrate itself, shown in Fig. 1, is most probably associated with light absorption characteristics. Absorption by CH_3SCH_3 in the wavelength region used here is comprised of two bands, one structureless band centered around 2040 Å and a system lying between 2150 and 2300 Å. The vibrational structure of the spectrum has been analyzed in detail (13) and the bands assigned to transitions involving excitation of a non-bonding electron from the S-atom to an antibonding orbital associated with the C—S bond. These workers suggest that the lower-energy excited states of CH_3SCH_3 are best described as initial members of a Rydberg series. At 2288 Å light absorption in the 16 cm path length cell should be complete at a sulfide pressure of 8 Torr. The initial sharp rise in yields as the substrate pressure is raised would correspond to increasing absorption. With the

Can. J. Chem. Downloaded from www.nrcresearchpress.com by 210.87.254.5 on 09/05/12
For personal use only.

Can. J. Chem. Downloaded from www.nrcresearchpress.com by 210.87.254.5 on 09/05/12
For personal use only.

incident irradiation in the 2000–2300 Å range, the more gradual increase in rates at pressures above *ca.* 50 Torr may be due to increasing absorption of wavelengths where the extinction coefficient is relatively small. Methane, ethane, and methyl disulfide all show the same variation with substrate pressure. Because of the error in thiol rates at low substrate pressure it is not clear whether that product follows the same trend.

The main products and the principal features of the photolysis may be explained in terms of the mechanism shown by eqs. 1–12.

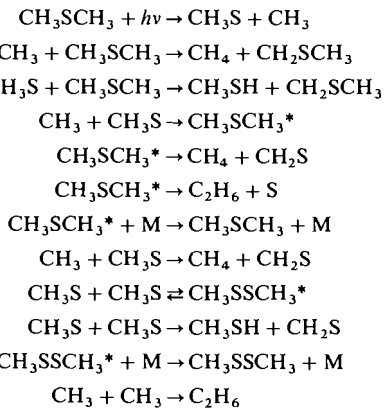

[1] $CH_3SCH_3 + h\nu \rightarrow CH_3S + CH_3$

[2] $CH_3 + CH_3SCH_3 \rightarrow CH_4 + CH_2SCH_3$

[3] $CH_3S + CH_3SCH_3 \rightarrow CH_3SH + CH_2SCH_3$

[4] $CH_3 + CH_3S \rightarrow CH_3SCH_3^*$

[5] $CH_3SCH_3^* \rightarrow CH_4 + CH_2S$

[6] $CH_3SCH_3^* \rightarrow C_2H_6 + S$

[7] $CH_3SCH_3^* + M \rightarrow CH_3SCH_3 + M$

[8] $CH_3 + CH_3S \rightarrow CH_4 + CH_2S$

[9] $CH_3S + CH_3S \rightleftarrows CH_3SSCH_3^*$

[10] $CH_3S + CH_3S \rightarrow CH_3SH + CH_2S$

[11] $CH_3SSCH_3^* + M \rightarrow CH_3SSCH_3 + M$

[12] $CH_3 + CH_3 \rightarrow C_2H_6$

On the basis of this reaction sequence the observed value for $R_{CH_3SH}/R_{CH_3SSCH_3}$ would be indicative of the *upper limit* for k_{10}/k_9. The actual rate constant ratio would be lower depending on the contribution of reaction 3 and the possible formation of some CH_3SH from $CH_3SCH_3^*$ to be discussed below. The graphs in Fig. 3 indicate that the ratio decreases from 0.12 to 0.08 as the CH_3SCH_3 pressure is increased from 5 to 20 Torr. The relatively minor importance of disproportionation is consistent with the thermochemical data for the process involved. Both reactions are exothermic, $\Delta H_9 = -78 \pm 2$ and $\Delta H_{10} = -42 \pm 8$ kcal (14). In the case of alkoxy radicals the exothermicities for CH_3O disproportionation and recombination are -78 ± 2 and -36.1 ± 1 kcal and there the disproportionation dominates completely (14). It is important to note, however, that the data for the CH_3SCH_3 photolysis points in general to H-atom abstraction as an important CH_3SH source, reaction 3. Disproportionation of CH_3S radicals is thus likely less important than indicated by the upper limit values of k_{10}/k_9.

Considering now the fate of radicals produced in the primary process, if 2288 Å, where there is a maximum in the absorption by CH_3SCH_3, is taken as a reference wavelength, the quantum energy is 126 kcal/mol. This is 54 kcal/mol in excess of the carbon–sulfur bond energy of 72 kcal/mol. Assuming that the excess energy is carried over by the two radicals in inverse proportion to their masses, the calculated excess energies are $E_{CH_3^*} = 41$ and $E_{CH_3S^*} = 13$ kcal/mol. These values, however, represent only approximate upper limits for excess energies. The pronounced vibrational structure in the CH_3SCH_3 spectrum (13) suggests there may be significant vibrational equipartition in the excited state and thus the calculation based on a simple mass effect may not be appropriate. The excess energy effect will nevertheless be present and should be manifested in CH_3 and CH_3S reaction rates characteristic of "hot" species.

In other systems, for example the photolysis of methyl iodide (15–17), "hot" methyl radicals have been shown to produce inordinately large yields of CH_4 via abstraction reactions that show little or no temperature dependence.

An Arrhenius plot for the formation of methane in this system, utilizing $\Phi(CH_4)$ values from Table 4, is linear and gives a value of 2.3 kcal/mol for the apparent activation energy. Thus although the CH_3^* abstraction reaction is not temperature independent, the apparent E_a value is appreciably lower than that for many other hydrogen atom abstraction reactions involving CH_3 radicals.

Further evidence for the participation of CH_3^* radicals comes from the results obtained in the photolysis of CH_3COCH_3 as CH_3 source in the presence of CH_3SCH_3 at 154 °C (Table 3). Assuming in the absence of the required data that the pre-exponential factors for reaction 2 and H-atom abstraction reaction from acetone are the same and taking E_a for the latter reaction as 9.5 kcal/mol, the rate constant ratio at 25 Torr sulfide indicates $E_{a2} = 9.3$ kcal/mol. In comparing this value to the 2.3 kcal/mol found when CH_3SCH_3 is the source of methyl radicals, it is to be noted that the apparent activation energy for reaction 2 represents an upper limit since CH_4 production from reaction 5, to be discussed below, would be expected to increase with temperature. The other possible source of methane, reaction 8, would not be expected to exhibit a temperature dependence.

Can. J. Chem. Downloaded from www.nrcresearchpress.com by 210.87.254.5 on 09/05/12
For personal use only.

The other characteristic that should be exhibited by CH_3* radicals is susceptibility to collision deactivation. The data in Table 1 show that C_3H_8 can effect such deactivation resulting in a decline in methane yields.

The energy carryover calculations indicate that methylthiyl radicals formed initially in this system are also hot. The rate data obtained permit determination of the activation energy of CH_3S hydrogen atom abstraction. An Arrhenius plot of R_{CH_3SH} values at zero addend pressure from Figs. 4 and 5 is linear and gives a value of 5.4 kcal/mol for the apparent activation energy of abstraction by CH_3S from the substrate. Any possible contribution from CH_3S disproportionation in reaction 10 would not be expected to change with temperature. Although the same comparison between hot and thermalized species carried out above for methyl radicals is not possible for CH_3S (methylthiyl radicals from the selective photolysis of CH_3SSCH_3 are themselves hot and thus the data in Table 2 do not apply to thermalized species), the value of the apparent activation energy is somewhat lower than might be expected for thermalized radicals.

The results can be used to exclude from consideration a number of possible reactions of CH_3S* radicals which might otherwise have to be included in a kinetic treatment of the system. The data in Table 2 show that when CH_3S* radicals are formed (from the CH_3SSCH_3 photolysis) in the presence of non-absorbing CH_3SCH_3, there is no significant production of C_2H_6 or CH_4 that might arise if either of the possible reactions,

[13] $CH_3S + CH_3SCH_3 \rightarrow CH_3SSCH_3 + CH_3$

[14] $CH_3S + CH_3SCH_3 \rightarrow CH_3SS + C_2H_6$

were occurring. Furthermore, CH_3SS radicals would lead to the formation of H_2S (16, 18) which was not detected here. This observation would also rule out another possible source of CH_3SS and CH_3 radicals,

[15] $CH_3S + CH_3S \rightarrow CH_3SS + CH_3$

Finally, unimolecular decomposition of methylthiyl radicals by either of

[16] $CH_3S \rightarrow CH_3 + S$

[17] $CH_3S \rightarrow CH_2S + H$

is not significant. Reaction 16 has an activation energy of at least 30 kcal/mol (3) while reaction 17 is endothermic to the extent of 45.5 kcal/mol (19).

It is instructive to consider the energetics of the two possible reactions between CH_3 and CH_3S radicals. Disproportionation, reaction 8, is exothermic by 56 kcal/mol, while $\Delta H = 72$ kcal/mol for reaction 4 if both species are thermalized. Carryover energies of one or both radicals would increase the exothermicity. Although the occurrence of the recombination process is indicated by the reactions that can be ascribed to subsequent decomposition of the CH_3SCH_3* molecule formed, it is not possible to assess quantitatively the importance of disproportionation. The formation of small amounts of C_2H_5SH and $C_2H_5SSC_2H_5$ which could come from reaction 8 followed by

[18] $CH_3 + CH_2S \rightarrow C_2H_5S$

and H-atom abstraction by C_2H_5S, as well as the possible formation of trithiane as a nonvolatile product, indicate that disproportionation may be occurring to some extent.

The two reactions of CH_3SCH_3* that may be occurring in this system are [5] and [6]. Both are exothermic, 66 and 26 kcal/mol respectively, but the reaction forming methane and thioformaldehyde is more favored energetically. Furthermore, the absence of S_2 in the flash photolysis of CH_3SCH_3 (4) suggests that reaction 6 is not an important mode of decomposition of excited methyl sulfide molecules.

The combination of two CH_3S radicals in process 9 yields CH_3SSCH_3* with minimum energy of the sulfur–sulfur bond and maximum energy given by the sum of the bond strength and the excess energy of the two CH_3S* radicals. The evidence in this system, and in the photolysis of the disulfide itself (8), indicates that an important reaction of CH_3SSCH_3* is the formation of two CH_3S radicals in the reverse of reaction 9. The stationary state concentration of CH_3S radicals is controlled in part by stabilization of CH_3SCH_3*. As the pressure is increased, $[CH_3S]$ is reduced via the deactivation process involving CH_3SCH_3*, but simultaneously there is increased stabilization of CH_3SSCH_3*, shifting the thiyl radical–disulfide equilibrium in favor of the latter. The observed results, which in general show an apparent insensitivity of disulfide yields to addend pressure, suggest that the enhancement of $R_{CH_3SSCH_3}$ due to stabilization of

Can. J. Chem. Downloaded from www.nrcresearchpress.com by 210.87.254.5 on 09/05/12
For personal use only.

TABLE 5. Rate constant ratios for the reaction of methylthiyl radicals with methyl sulfide and 2-methylpentane*

		k_{19}/k_3				
T (°C)	P_{2MP}, (Torr):	20	44	74	125	150
57		1.9	1.7	1.8	0.9	1.4
104		2.7	1.9	2.1	2.0	1.6
154		3.2	2.2	2.1	1.8	1.8

*Data from Fig. 5.

hot disulfide molecules balances the decline to be expected if $[CH_3S]$ is reduced by stabilization of CH_3SCH_3*.

The results with 2-methylpentane as H-atom source indicate that abstraction by CH_3S radicals can be an important process at high addend pressure and increasing temperature.[3] Kinetic treatment of the results from this series of experiments can be used to obtain a rate parameter for CH_3S reactions.

At constant temperature, the alteration in R_{CH_3SH} with 2-methylpentane pressure may be employed to determine the ratio of rate constants for reaction 3 and abstraction from the addend

[19] $$CH_3S + 2MP \rightarrow CH_3SH + \dot{R}$$

(where 2MP represents the addend and $\dot{R}$, the alkyl radical resulting from the abstraction) assuming that reaction 3 is the sole source of CH_3SH in the photolysis of the pure substrate at higher temperatures. The calculated values of k_{19}/k_3 at 57, 104, and 154 °C, utilizing values of R_{CH_3SH} from Fig. 5, are listed in Table 5. Although these data suggest there may be a pressure dependence of the ratio that would be consistent with a contribution to CH_3SH formation from

[20] $$CH_3SSCH_3^* \rightarrow CH_3SH + CH_2S$$

the effect is not sufficiently large to indicate definitively an important role for this process.[4] Since the bond energies in the two H-atom

[3]Pryor and co-workers (20, 21) consider that the abstraction reaction RS + QH → RSH + Q, where QH is the hydrogen donor, is important with QH compounds having C—H bonds weaker than the RS—H bond (see also ref. 22).

[4]If reaction 20 is considered, the kinetic treatment of CH_3SH rates must then include reactions 3, 9, 11, and 19. A least squares analysis of the appropriate kinetic plot using data at 154 °C leads to a k_{19}/k_3 value of 1.85 at that temperature.

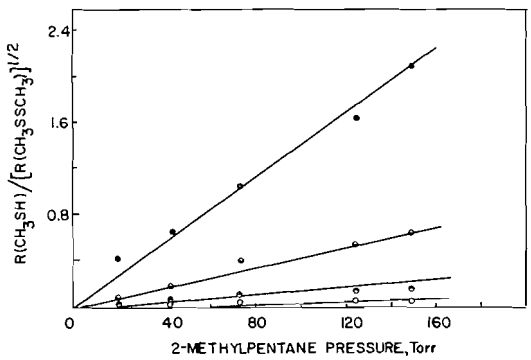

FIG. 6. $R_{CH_3SH}/(R_{CH_3SSCH_3})^{\frac{1}{2}}$ as a function of 2-methylpentane pressure in the photolysis of 25 Torr methyl sulfide at 25 °C, 0; 57 °C, ◓; 104 °C, ◒; and 154 °C, ●, at an exposure time of 30 min.

donors involved are quite different, the fact that k_{19} and k_3 are comparable over the temperature range investigated is further evidence for the participation of hot CH_3S radicals whose energy apparently attenuates the true activation energy difference that must surely exist between the reactions 3 and 19 and that would give rise to significantly different rate constants were only thermalized thiyl radicals involved.

Finally the variation of R_{CH_3SH} with addend pressure at each of the four temperatures investigated may be utilized to obtain the energy of activation for abstraction from 2-methylpentane. At each temperature it is assumed that CH_3SH production through reaction 3 will be independent of addend pressure and thus the mercaptan rate, $R^a_{CH_3SH}$ can be computed from $R^a_{CH_3SH} = R_{CH_3SH} - R^0_{CH_3SH}$ where $R^a_{CH_3SH}$ represents the amount of mercaptan formed via the abstraction process 19. If the recombination of CH_3S radicals, reaction 9, is used as reference

[21] $$R^a_{CH_3SH}/(R_{CH_3SSCH_3})^{\frac{1}{2}} = k_{19}/k_9(P_{2MP})$$

A plot of the left hand side of equation 21 as a function of addend pressure is given in Fig. 6. A plot of the slopes of these lines k_{19}/k_9 against $1/T$ is linear and gives $E_{a19} = \frac{1}{2}E_{a9} = 7.5$ kcal/mol which, making the usual assumption that the recombination has zero activation energy, represents the activation energy for abstraction from 2-methylpentane.

The study of methyl sulfide has yielded considerably more information about CH_3S radical reactions than previous investigations of the disulfide where thiyl radical recombina-

tion regenerates the substrate. Because of this advantage of the sulfides as substrate, studies are currently underway in this laboratory on the photolysis of methyl ethyl sulfide and diethyl sulfide.

The authors gratefully acknowledge the financial support of the National Research Council of Canada for this work.

1. W. E. HAINES, B. L. COOK, and J. S. BALL. J. Am. Chem. Soc. **78**, 5213 (1936).
2. B. MILLIGAN, D. E. RIVETT, and W. E. SAVIGE. Aust. J. Chem. **16**, 1029 (1960).
3. T. INABA and H. OGORO. Kogyo Kogaku Zasshi, **72**, 114 (1969).
4. A. B. CALLEAR and D. R. DICKSON. Trans. Faraday Soc. **67**, 1987 (1970).
5. A. JONES, S. YAMASHITA, and F. P. LOSSING. Can. J. Chem. **46**, 833 (1968).
6. K. J. ROSENSREN. Acta Chem. Scand. **16**, 1418 (1962).
7. R. P. STEER and A. R. KNIGHT. J. Phys. Chem. **72**, 2143 (1968).
8. R. P. STEER and A. R. KNIGHT. Can. J. Chem. **47**, 1335 (1969).
9. P. M. RAO, J. A. COPECK, and A. R. KNIGHT. Can. J. Chem. **45**, 1369 (1967).
10. P. M. RAO and A. R. KNIGHT. Can. J. Chem. **46**, 2642 (1968).
11. K. SAYAMOL and A. R. KNIGHT. Can. J. Chem. **46**, 999 (1968).
12. L. B. CLARK and W. T. SIMPSON. J. Chem. Phys. **43**, 3666 (1965).
13. S. D. THOMPSON, D. G. CARROLL, F. WATSON, M. O'CONNELL, and S. P. MCGLYNN. J. Chem. Phys. **45**, 1367 (1966).
14. A. JONES and F. P. LOSSING. J. Phys. Chem. **71**, 4111 (1967).
15. W. WEST and L. SHLESSINGER. J. Am. Chem. Soc. **60**, 961 (1938).
16. R. D. SOUFFIE. J. Am. Chem. Soc. **78**, 917 (1956).
17. R. SCHULTZ and H. A. TAYLOR. J. Chem. Phys. **18**, 194 (1950).
18. H. BOHME and G. ZINNER. Annal. der Chem. **585**, 142 (1954).
19. D. R. DICKSON. Ph.D. Thesis. Cambridge, 1969.
20. W. A. PRYOR and J. P. STANLEY. J. Am. Chem. Soc. **93**, 1412 (1971).
21. W. A. PRYOR, J. P. STANLEY, and M. G. GRIFFITH. Sci. **169**, 181 (1970).
22. C. WALLING and W. HELMREICH. J. Am. Chem. Soc. **81**, 1144 (1959).

Can. J. Chem. Downloaded from www.nrcresearchpress.com by 210.87.254.5 on 09/05/12
For personal use only.

Cancentrine. II.[1] The Structure of Cancentrine

R. RODRIGO AND R. H. F. MANSKE
Department of Chemistry, University of Waterloo, Waterloo, Ontario
AND
D. B. MACLEAN, L. BACZYNSKYJ, AND J. K. SAUNDERS
Department of Chemistry, McMaster University, Hamilton, Ontario

Received August 24, 1971

The structure of cancentrine (F_{22}), an alkaloid of *Dicentra canadensis* (Goldie) Walp., is reported. Some reactions of the base are described and an analysis of the p.m.r. and mass spectra of cancentrine and several derivatives is made.

On rapporte la structure de la cancentrine (F_{22}), un alkaloide du *Dicentra canadensis* (Goldie) Walp. Certaines réactions de la base sont décrites et une analyse par r.m.n. et par spectrométrie de masse de la cancentrine et de quelques dérivés, a été effectuée.

Canadian Journal of Chemistry, **50**, 853 (1972)

Can. J. Chem. Downloaded from www.nrcresearchpress.com by 210.87.254.105 on 09/05/12
For personal use only.

In 1932 an investigation of the alkaloids of *Dicentra canadensis* (Goldie) Walp. was reported (1). It was found that this plant contained five major alkaloids. Four of them were easily separated, purified, and characterized, namely bulbocapnine, corydine, isocorydine, and protopine. A fifth alkaloid, designated later (2) as F_{22}, was also present. It had an intense yellow–orange color and unusual chemical behavior. A preliminary characterization and elemental analysis showed, however, that it was a very complex alkaloid and the elucidation of its structure was postponed.

We have reinvestigated the yellow alkaloid, F_{22}, and found it to be a mixture of at least five components. Structure **1** has been proposed (3) for the major component, now called cancentrine, and structures **2** and **3** for two minor components called dehydrocancentrine-A and -B, respectively (4). We report here an account of some of the chemical and spectroscopic data which led to the structure of cancentrine.

The physical and spectroscopic properties[2] of the alkaloid suggested the presence of three methoxyl groups, one *N*-methyl group, one phenolic —OH group, one conjugated carbonyl group, and three pairs of aromatic protons in an ortho relationship to each other. Of the two nitrogen atoms in the molecule, one, not bearing a methyl group, was apparently non-basic. The presence of a phenolic hydroxyl group was confirmed by conversion of the alkaloid to an *O*-methyl ether (**4**) and an *O*-acetate (**5**). The mass spectra[3] though of great value later on, bore no similarity to that of any known dimeric benzylisoquinoline alkaloid. The u.v. spectra, too, were not characteristic of any known class of isoquinoline alkaloids and indicated the presence of a novel chromophore which imparted to the alkaloid its bright yellow color.

In an attempt to obtain structural information concerning its skeletal structure several chemical degradations were attempted. The alkaloid was stable to sodium borohydride but was reduced by both lithium aluminum hydride and zinc–hydrochloric acid with loss of its characteristic yellow color, but stable reduction products could not be isolated. The initial products decomposed rapidly to yield complex mixtures of intractable oils. Attempted cleavage of the molecule by sodium–liquid ammonia gave like results. An attempt at reductive acetylation (zinc–acetic anhydride–acetic acid) however, yielded two stable crystalline products very different from cancentrine. The spectral data on one of these products showed that extensive aromatization had taken place and that the

[1]Reference 3 is to be considered as part 1 in this series.

[2]A preliminary account of the spectroscopic properties of cancentrine has been presented (3). The p.m.r. data of cancentrine and its derivatives and the u.v. and i.r. data are reported in detail in the Experimental section.

[3]A complete listing of mass spectral peaks of **1**, 7, and **8** down to 5% intensity is available at the Depository of Unpublished Data, National Science Library, National Research Council of Canada, Ottawa, Canada K1A 0S2.

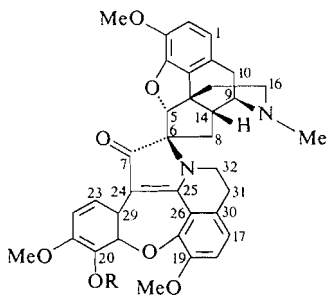

1 R = H
2 8,14-dehydro **1**
3 31,32-dehydro **1**
4 R = $COCH_3$
5 R = Me

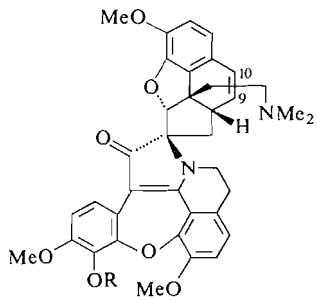

6 R = H
7 R = Me
8 9,10-dihydro **7**
9 9,10-dihydro **6**

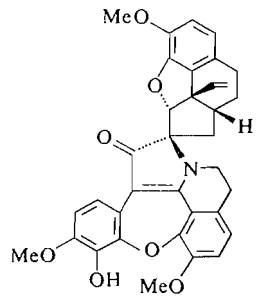

10

elements of C_3H_9NO had been lost from the original molecule including the oxygen atom of the original carbonyl group (as H_2O) and the *N*-methyl group (as C_3H_7N). The latter fragment corresponds exactly to the ethanamine bridge of the morphine alkaloids and thus constituted the first piece of structural information obtained. The existence of a morphine-like moiety in cancentrine was then quickly confirmed. Cancentrine methiodide was refluxed with acetic anhydride–sodium acetate, the expelled ethanamine bridge was isolated and characterized as *N*-methylethanolamine aurichloride. The sharp singlet at 4.88 δ in the p.m.r. spectrum of cancentrine could now be assigned to the proton at C-5 by analogy with the morphine alkaloids (5). All significant ions in the mass spectrum below *m/e* 243 could be similarly rationalized (6). The structures and properties of the products formed on acetolysis and the syntheses of their new ring systems will be published later.

The Hofmann degradation of cancentrine was then undertaken in order to effect a similar aromatization characteristic of most morphine alkaloids. Cancentrine methiodide was heated under reflux with 50% aqueous methanolic potassium hydroxide to give the methine **6** ($C_{37}H_{36}N_2O_7$). The i.r., u.v., and p.m.r. spectra of the methine were similar to that of cancentrine except that it now showed a broad singlet at 2.1 δ (6H) assigned to the *N*,*N*-dimethyl group and two olefinic protons due to the new double bond introduced. One of these is present in the same region as the aromatic protons while the other proton, H_9, appears at higher field as four lines coupled as it is to the olefinic proton at C-10 and the methine proton at C-14. The pattern is characteristic of the B part of an ABX system. It suggests the following structural feature in the molecule.

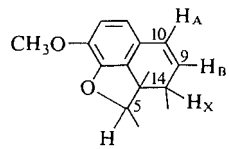

Methine **6** was converted to its *O*-methyl ether **7** by treatment with diazomethane and then by hydrogenation (H_2/Pt) to the dihydromethine *O*-methylether **8**. Compound **8** was also obtained by carrying out the hydrogenation first to give the dihydromethine **9** followed by methylation to the ether. Compounds **6** and **7** have a similar vinylic H_9 pattern in their p.m.r. spectra and are readily differentiated from **8** and **9** which lack the 9,10 double bond. All four compounds have the singlet attributed to the hydrogen at C-5 at 5.1–5.2 δ. Surprisingly, when **6** was converted to its methiodide and refluxed with alcoholic potassium hydroxide as before, the starting material was recovered unchanged even after 36 h. Only when the methiodide was refluxed with potassium *t*-butoxide in anhydrous tertiary butyl alcohol could the bis-methine **10** be obtained. Again, the expected aromatization had not occurred; simple elimination had taken place instead and the product obtained in high yield showed the presence of an extra vinylic unit and the absence of a *N*,*N*-dimethyl group in its p.m.r. spectrum.

Can. J. Chem. Downloaded from www.nrcresearchpress.com by 210.87.254.105 on 09/05/12
For personal use only.

Can. J. Chem. Downloaded from www.nrcresearchpress.com by 210.87.254.105 on 09/05/12
For personal use only.

Cancentrine, its simple derivatives **4** and **5**, and the Hofmann products, **6**–**10**, are all bright yellow compounds with very similar u.v. spectra and an i.r. band at 1660 ± 5 cm^{-1} associated with the carbonyl function. It would appear therefore that the two Hofmann degradations had achieved only simple, superficial changes and left intact the still unknown chromophoric system which must be associated with the carbonyl group. It must mean that the aromatization characteristic of morphine-like systems already demonstrated by the acetolysis experiment was blocked, in basic media, by some structural feature of the molecule. Several structures involving a morphine moiety linked through nitrogen and oxygen to an aporphine system were considered and discarded and several schemes devised to test these hypotheses were carried out. None of them was informative in a structural sense but some interesting products were isolated and characterized. As our supplies of cancentrine were not inexhaustible a search was begun for a suitable derivative for X-ray crystallographic analysis. The tendency of cancentrine and most of its derivatives to solvate made this much more difficult than expected and after about a dozen crystalline derivatives had been rejected we found that **8** as its hydrobromide was satisfactory. The results of the X-ray study have been reported briefly (3) and the structure of **8** which resulted is shown in the accompanying formula.

The novel *cis-s-trans-β*-amino-enone system which forms part of a modified cularine (7) system was now identified as the chromophore responsible for the long-wavelength absorption (8) and the non-basicity of the second nitrogen atom. Furthermore, the 'spiro' carbon atom, C-6, is clearly the structural feature that blocks aromatization by basic reagents whereas cationic attack at the carbonyl oxygen can be followed by ring expansion of the five-membered ring leading ultimately to phenanthrenoid systems. Reactions of this type will be discussed in detail in a subsequent publication.

The u.v., i.r., and p.m.r. data of **4**–**10** already referred to, unambiguously indicate that they retain the basic framework of cancentrine. Thus only two problems remained in order to deduce the structure of cancentrine from **8**. The position of the phenolic hydroxyl group had to be ascertained and the *N*-terminus of the ethanamine bridge had to be established. Both problems were solved by further consideration of the p.m.r. spectra.

A comparison of the mass spectra of cancentrine and its *O*-methyl ether (see later) showed that the phenolic function was located in the cularine system while a comparison of the p.m.r. spectra of cancentrine and its *O*-acetate led to the conclusion that the phenolic function is para to the aromatic proton appearing at lowest field (9). It follows that the phenolic —OH group must be located at C-20 in cancentrine. This placement of the —OH group has been substantiated by nuclear Overhauser effect (n.O.e.) studies (10) which are discussed subsequently.

The second problem was resolved in the following way. Upon examination of a molecular model, it is apparent that the nitrogen of the ethanamine bridge may be attached to carbon atoms 5, 9, 10, or 14; carbon atom 8 is excluded on the basis that attachment at this site would cause too much strain in the system. Examination of the p.m.r. spectrum of **6** precludes C-5 and -14 as possible sites of attachment since the spectrum of **6** has an absorption at 5.18 δ typical of the hydrogen at C-5 in morphine systems and has two olefinic protons. Barring rearrangement in the formation of **6**, the nitrogen atom of cancentrine must be attached at C-9 or -10 with the former preferred on biogenetic grounds. That the nitrogen atom is indeed attached to C-9 was apparent (3) on careful comparison of the spectrum of cancentrine with that of codeine (5).

From a combination of decoupling and n.O.e. studies it is possible to assign many of the signals in the p.m.r. spectrum of **5**. The signal centered at 3.18 δ (one-half of an AB quartet) assigned to $H_{10\beta}$ was used as the point of reference. Irradiation of this signal causes a sharpening of the aromatic doublet centered at 6.65 δ which is therefore assigned to H_1. Irradiation of H_1 defines H_2 since an ortho coupling is removed at the doublet centered at 6.83 δ. An n.O.e. of 25% is observed at H_2 when the methoxyl signal 3.91 δ is saturated, thus defining the methoxyl resonance at C-3.

From chemical shift studies it was concluded that the low field proton of **5** at 7.88 δ was para to the acetoxy group and double irradiation has shown that this proton is ortho to a proton responsible for the doublet centered at 6.68 δ.

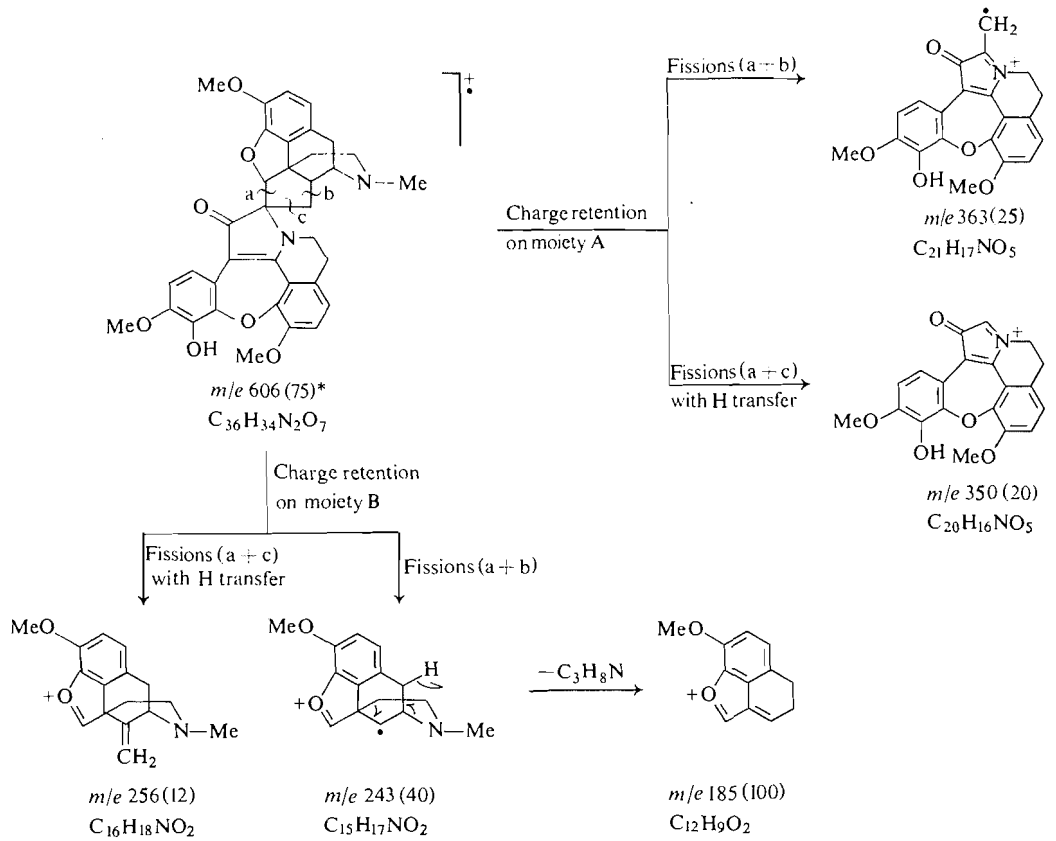

*Ion intensity as in parenthesis

SCHEME 1

An n.O.e. of 24% was observed for the latter when the methoxyl signal at 3.76 was irradiated. This defines the substitution pattern at positions 20–23. When the third methoxyl resonance at 3.85 δ was saturated an n.O.e. of 25% was observed for the proton centered at 6.98. Thus the following assignments could be made $H_1 = 6.65$, $H_2 = 6.83\ \delta$, $J_{1,2} = 9.0$ Hz; $H_{17} = 6.85$, $H_{18} = 6.98\ \delta$, $J_{17,18} = 8.5$ Hz; $H_{22} = 6.68$, $H_{23} = 7.88\ \delta$, $J_{22,23} = 8.0$ Hz. The resonances of the three methoxyls are also defined by the study.

The mass spectrum of cancentrine[4] provides a great deal of structural information and its interpretation is of value in solving future structural problems in the area (4). The molecular ion readily loses a methyl and a methoxyl radical but does not lose any other small fragments. Peaks of diagnostic value occur at *m/e* 363 and 350 with compositions $C_{21}H_{17}NO_5$ and $C_{20}H_{16}NO_5$. Further important ions occur at *m/e* 256, 243, and 185 with compositions $C_{16}H_{18}NO_2$, $C_{15}H_{17}NO_2$, and $C_{12}H_9O_2$, respectively. The latter ion is the base peak in the spectrum. The formation of these ions can be rationalized according to the sequence shown in Scheme 1. The molecule has a tendency to break into two parts: a 'cularine part' (moiety A) and a 'morphine part' (moiety B). Ions with the charge on moiety A appear at *m/e* 363 and 350 resulting from fission of bonds 'a' and 'b', and 'a' and 'c', respectively. The latter process is accompanied by hydrogen transfer. The same fissions can lead to ions with charge on moiety 'B' at *m/e* 243 and 256 respectively. The ion at *m/e* 243 through loss

[4]Cancentrine and its derivatives show strong molecular ions and weaker ions 14 mass units above M^+, a behavior similar to that of dimeric indole alkaloids (see Thomas and Biemann (18)).

Can. J. Chem. Downloaded from www.nrcresearchpress.com by 210.87.254.105 on 09/05/12
For personal use only.

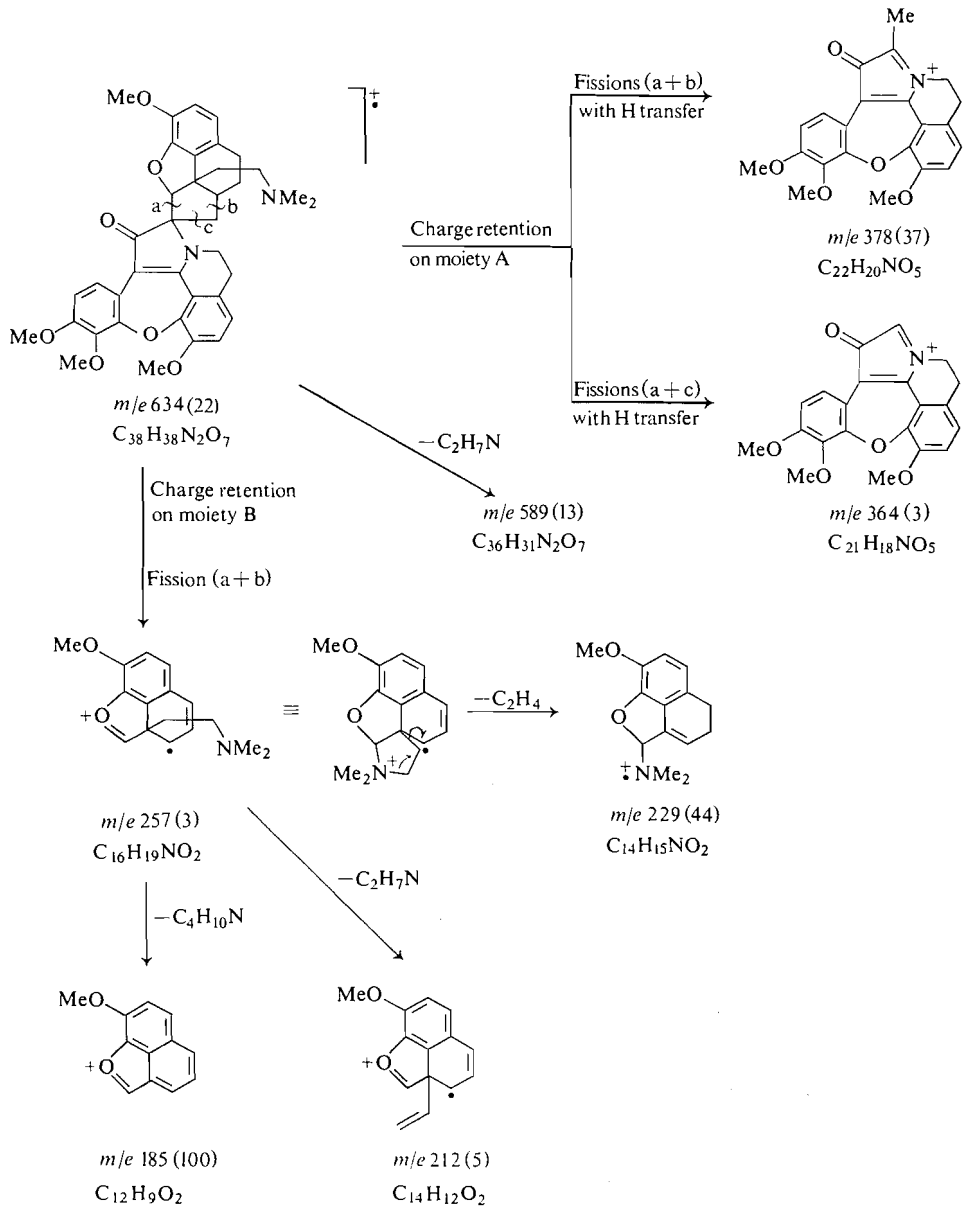

SCHEME 2

of C_3H_8N gives rise to the ion at *m/e* 185, the most intense in the spectrum. The ion at *m/e* 363 is accompanied by ions one mass unit higher and one and two mass units lower which differ in composition from *m/e* 363 by one or two hydrogen atoms. The same applies to the ions at *m/e* 350, 256, and 243. A cluster of ions centered at *m/e* 229 ($C_{14}H_{15}NO_2$) is apparently derived from moiety B of the molecule. The ion at *m/e* 226 ($C_{15}H_{16}NO$) may form from *m/e* 256 through loss of CH_2O. The spectrum of cancentrine also has a relatively intense ion at *m/e* 303 resulting from a doubly charged molecular ion.

The spectra of the *O*-methyl ether and the *O*-acetate of cancentrine show the shifts expected from methylation and acetylation of the

Can. J. Chem. Downloaded from www.nrcresearchpress.com by 210.87.254.105 on 09/05/12
For personal use only.

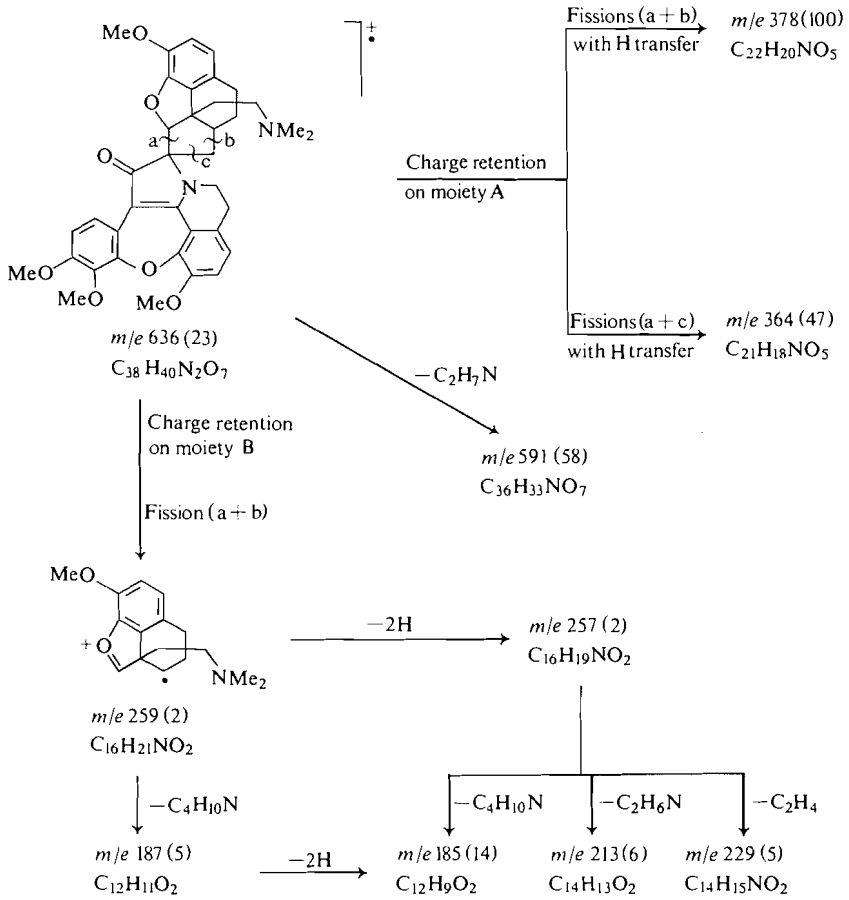

SCHEME 3

phenolic hydroxyl group. The shifts allow the —OH group to be placed in moiety A of the molecule since only these ions are affected. For example in the case of *O*-methyl cancentrine ions at *m/e* 243 and 256 remained the same whereas the ions at *m/e* 350 and 363 had moved upwards by 14 mass units to *m/e* 364 ($C_{21}H_{18}NO_5$) and 377 ($C_{22}H_{19}NO_5$). The *O*-acetate shows a pronounced tendency to eliminate ketene so that the spectrum of the acetate has all the peaks associated with cancentrine itself as well as ions 42 mass units greater in those ions involving moiety A.

In Scheme 2 a fragmentation scheme for the methine-*O*-methyl ether **7** is proposed. This system breaks down in much the same way as cancentrine. The ions at *m/e* 378 and 364 are homologues of the corresponding ions in cancentrine. There appears to be only one mode of fission, (a + b) which produces an ion at *m/e* 257, leading to ions from moiety **B**. This ion can fragment in a straightforward way to *m/e* 185 and 212 as shown. The relatively intense ion at *m/e* 229 deserves comment. Its composition demands that it come from moiety **B**. A scheme for its formation is shown in which it is postulated that a new carbon–nitrogen bond is formed followed by expulsion of C_2H_4 from *m/e* 257.

The fragmentation of the dihydromethine-*O*-methyl ether **8** is shown in Scheme 3. The same ions from moiety A are found at *m/e* 378 and 364 as are found in the spectrum of **7**. Fission at 'a' and 'b' with charge retention of moiety **B** gives the ion at *m/e* 259. This ion may lose $C_4H_{10}N$ directly to give *m/e* 187, a relatively weak ion, or it may lose two hydrogen atoms to give *m/e* 257 and fragment in the same manner as the comparable ion derived from **7**. The lack of a 9,10

Can. J. Chem. Downloaded from www.nrcresearchpress.com by 210.87.254.105 on 09/05/12
For personal use only.

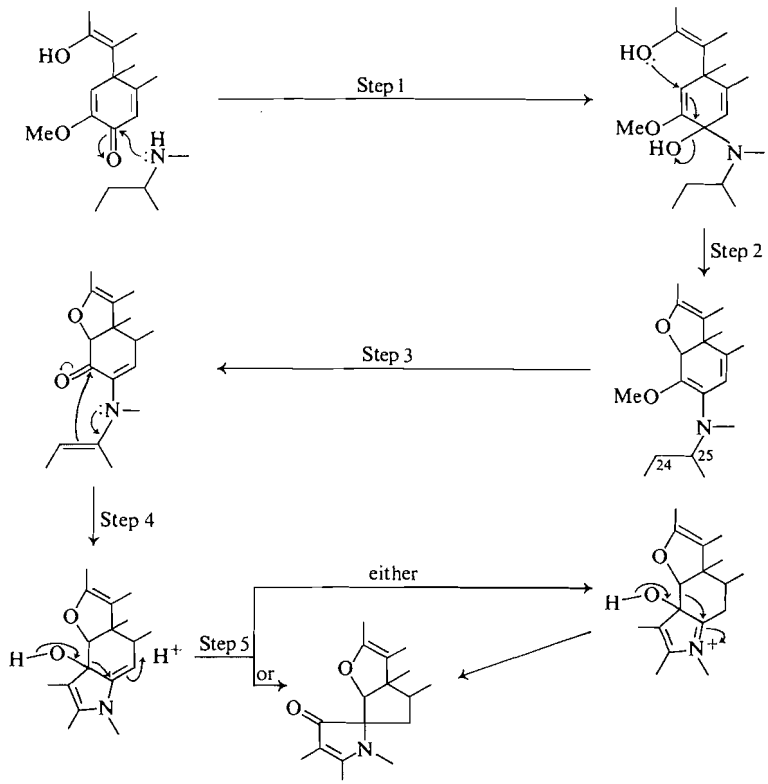

SCHEME 4

double bond in **8** results in a greatly reduced intensity of the ion at *m/e* 185 and of all of the ions of moiety B. Because of the low intensities of *m/e* 257 and 259 it is possible that the ions at *m/e* 213 and 185 may in fact be derived from *m/e* 591.

A morphinandienone alkaloid, pallidine has recently been isolated (11) from *Corydalis pallida* a genus closely allied to *Dicentra*. The cularine alkaloids have been found only in these two genera. Neither type of alkaloid has hitherto been found naturally in a dimeric form and the substitution pattern of the known cularine alkaloids is different from that of the cularine half of cancentrine (12). However, the outstanding feature of cancentrine from a biogenetic point of view is the mode of linkage of the two constituent units.

In Scheme 4 we suggest a possible route to the spiro system based on known chemical and biosynthetic analogies. Step 1 represents the formation of the C_6—N bond by a nucleophilic addition similar to that in the *Erythrina* (13) alkaloids. This is followed in step 2, by closure of the furan ring and expulsion of the OH substituent in the generally accepted manner of morphine biogenesis. In step 3 we postulate hydrolysis of the enol ether and oxidation to produce a C_{24}—C_{25} dehydro derivative now set up for ring closure by enamine condensation in step 4 in a manner analogous to that postulated for the formation of chelidonine (14). Step 5 involves the formation of the spiro system by the rearrangement shown. A similar rearrangement with the same type of ring contraction has been demonstrated (15) in a morphine derivative. In this case it may involve the intermediacy of an immonium ion in a process reminiscent of the rearrangement of hydroxy and acyloxyindolenines to pseudoindoxyls (16).

Experimental

Methods

Melting points were determined on a Fischer Mel-Temp apparatus and are uncorrected. Mass spectra were recorded on a CEC 21-110 B double focussing mass spectrometer.

Can. J. Chem. Downloaded from www.nrcresearchpress.com by 210.87.254.105 on 09/05/12
For personal use only.

Can. J. Chem. Downloaded from www.nrcresearchpress.com by 210.87.254.105 on 09/05/12
For personal use only.

For high resolution work spectra were recorded on plates and accurate mass measurements were made using perfluorokerosene as a marker (17). The composition of all ions discussed in the paper have been checked by h.r.m.s. The p.m.r. spectra were recorded using the frequency sweep mode of a Varian HA-100 spectrometer. Samples were dissolved in $CDCl_3$ using added TMS as the internal locking signal. Chemical shifts were measured relative to TMS using a V315 frequency counter incorporated in the instrument and are reported in p.p.m. (δ) from TMS. Double irradiation was achieved by employing a Hewlett–Packard 201 C audiogenerator at the desired frequency. A Beckmann IR10 spectrometer was used to record the i.r. spectra and a Coleman-Hitachi EPS-3T spectrometer was used for the u.v. spectra.

Cancentrine (1)

The isolation (1) of cancentrine and its purification (4) have already been described.

The u.v. spectrum: λ_{max}^{EtOH} 213, 230 (sh), 268, 291 (sh), 330 (sh), and 435 nm, log ε_{max} 4.80, 4.63, 4.32, 4.22, 3.62, and 3.82 respectively.

The i.r. spectrum: $\nu_{max}^{CHCl_3}$ 3450 and 1665 cm^{-1}.

The p.m.r. spectrum: 1.6–3.8 14H, aliphatic protons partially assigned; see (3); 2.51 (s) 3H, N—CH_3; 3.86 (s), 3H(OCH_3); 3.95 (s) 3H(OCH_3); 4.00 (s) 3H, OMe; 4.88 (s) 1H, C_5H; 6.5–7.2 (m) 5H, aromatic protons; 7.51 (d) 1H, $C_{23}H$.

Anal. Calcd. for $C_{36}H_{34}N_2O_7.3H_2O$: C, 65.42; H, 6.11; N, 4.24; 3 × OMe, 14.08. Found: C, 65.97; H, 5.78; N, 4.22; OMe, 13.87.

The molecular formula was confirmed by high resolution mass spectrometry (h.r.m.s.).

Calcd. for $C_{36}H_{34}N_2O_7$: 606.237. Found: 606.240.

Cancentrine Hydrochloride

The preparation has been described (2).

Anal. Calcd. for $C_{36}H_{34}N_2O_7.HCl.2H_2O$: C, 63.66; H, 5.78; N, 4.12; Cl, 5.23; 3 × OMe, 13.70. Found: C, 64.43; H, 5.77; N, 3.95; Cl, 5.69; OMe, 13.77.

Cancentrine-O-methyl Ether (4)

Cancentrine (200 mg) was dissolved in hot methanolic sodium hydroxide (30 ml, 1.0 g). Trimethylanilinium tosylate (250 mg) was added and the sodium salt which precipitated on cooling was filtered and washed with a little methanol. The filtrate was evaporated to dryness and heated in dimethyl sulfoxide (10 ml) at 120–125° for 2–3 h. The solution was cooled, poured into water, and extracted with chloroform several times. The chloroform extracts were dried and the solvent removed under reduced pressure. The residue was chromatographed on silica gel in benzene–methanol (9:1) and the first few fractions of the main yellow band collected. These were rechromatographed to remove the substantial amounts of unchanged cancentrine which ran only very slightly slower than the ether. Several variations of this procedure were tried with respect to solvent, period of heating, temperature, etc. Always significant amounts of cancentrine remained. When pure, the *O*-methyl ether crystallized from methanol–cyclohexane (32 mg, best yield), m.p. 269°.

The u.v. spectrum: λ_{max}^{EtOH} 210, 230 (sh), 269, 330 (sh), and 433 nm, log ε_{max} 4.83, 4.66, 4.22, 3.56, and 3.71 respectively.

The i.r. spectrum: $\nu_{max}^{CHCl_3}$ 1660 cm^{-1}.

The p.m.r. spectrum: 1.5–3.8, 14H, aliphatic protons; 2.52 (s) 3H, N–CH_3; 3.84 (s) 3H, OCH_3; 3.94 (s) 3H, OCH_3; 3.96 (s) 3H, OCH_3; 4.01 (s) 3H, OCH_3; 4.88 (s) 1H, C_5H; 6.5–7.2 (m) 5H, aromatic protons; 7.70 (d) 1H, $C_{23}H$.

Anal. Calcd. for $C_{37}H_{36}N_2O_7$: C, 71.60; H, 5.85; N, 4.51. Found: C, 71.70; H, 5.75; N, 4.46.

The molecular formula was confirmed by h.r.m.s.

Calcd. for $C_{37}H_{36}N_2O_7$: 620.252. Found: 620.253.

Cancentrine-O-acetate (5)

Cancentrine (100 mg) was refluxed with acetic anhydride (5 ml) in pyridine (10 ml) for ½ h. Most of the liquids were removed under reduced pressure, water (50 ml) added, and the aqueous mixture neutralized with sodium bicarbonate and extracted with chloroform. The chloroform extracts were dried, the solvent removed, and the residue chromatographed as before. The main yellow band was collected and the solvents removed. The residue was pure (t.l.c.) but resisted crystallization.

The i.r. spectrum: $\nu_{max}^{CHCl_3}$ 1770 and 1600 cm^{-1}.

The p.m.r. spectrum: 1.5–3.8, 14H, aliphatic protons; 2.46 (s) 3H, O=C—CH_3; 2.53 (s) 3H, N—CH_3; 3.76 (s) 3H, OCH_3; 3.85 (s) 3H, OCH_3; 3.91 (s) 3H, OCH_3; 4.85 (s) 1H, C_5H; 6.5–7.1 (m) 5H, aromatic protons; see text for analysis; 7.88 (d) 1H, $C_{23}H$.

The molecular formula was determined by h.r.m.s.

Calcd. for $C_{38}H_{36}N_2O_8$: 648.247. Found: 648.243.

Cancentrine Methine (6)

Cancentrine (400 mg) was dissolved in chloroform (50 ml) and methanol (10 ml) was added. Methyl iodide (20 ml) was added and the solution allowed to stand for 48 h at room temperature. The solvents were removed under reduced pressure and the residual methiodide crystallized from methanol (440 mg).

Cancentrine methiodide (400 mg), without further purification, was refluxed with 50% aqueous-methanolic potassium hydroxide (50 ml, 5 g KOH) for 24 h. Carbon dioxide was passed through the hot solution and the methanol evaporated, the solution cooled, and filtered. The solid was dried and chromatographed as before and the main yellow band collected. The solvents were removed and the residue was crystallized from methanol (240 mg), m.p. 230°.

The u.v. spectrum: λ_{max}^{EtOH} 227, 270, and 435 nm, log ε_{max} 4.61, 4.38, and 3.75 respectively.

The i.r. spectrum: $\nu_{max}^{CHCl_3}$ 3450 and 1660 cm^{-1}.

The p.m.r. spectrum: 1.6–3.8 11H aliphatic protons; 2.22 (s) 6H, 2 × N—CH_3; 3.87 (s) 3H, OCH_3; 3.99 (s) 3H, OCH_3; 4.00 (s) 3H, OCH_3; 5.18 (s) 1H, C_5H; 5.85 (q) 1H, C_9H; 6.35–7.40 6H, aromatic protons + $C_{10}H$; 7.52 (d) 1H, $C_{23}H$.

Anal. Calcd. for $C_{37}H_{36}N_2O_7$: C, 71.60; H, 5.85. Found: C, 71.45, 71.67; H, 5.76, 5.74.

The molecular formula was confirmed by h.r.m.s.

Calcd. for $C_{37}H_{36}N_2O_7$: 620.252. Found: 620.255.

Dihydrocancentrine Methine (9)

Cancentrine methine (100 mg) was dissolved in methanol (50 ml) and hydrogenated overnight at room temperature and pressure in the presence of Adams catalyst (20 mg). The catalyst was filtered off, the filtrate taken to dryness, and the residue crystallized from aqueous methanol (90 mg), m.p. 215°.

Can. J. Chem. Downloaded from www.nrcresearchpress.com by 210.87.254.105 on 09/05/12
For personal use only.

The u.v. spectrum: λ_{max}^{EtOH} 227, 270, and 438 nm, log ε_{max} 4.56, 4.25, and 3.69 respectively.

The i.r. spectrum: $\nu_{max}^{CHCl_3}$ 3450 and 1660 cm^{-1}.

The p.m.r. spectrum: 1.6–3.8 15H, aliphatic protons; 2.21 (s) 6H, 2 × N—CH_3; 3.88 (s) 3H, OCH_3; 3.97 (s) 3H, OCH_3; 4.00 (s) 3H, OCH_3; 5.12 (s) 1H, C_5H; 6.5–7.4 5H, aromatic protons; 7.52 (d) 1H, $C_{23}H$.

Anal. Calcd. for $C_{37}H_{38}N_2O_7$: C, 71.37; H, 6.15. Found: C, 71.57; H, 6.45.

The molecular formula was confirmed by h.r.m.s.

Calcd. for $C_{37}H_{38}N_2O_7$: 622.268. Found: 622.270.

*Dihydrocancentrine Methine-O-methyl Ether (**8**)*

Dihydrocancentrine methine **9** (100 mg) was dissolved in methanol (30 ml) and treated with excess ethereal diazomethane. The mixture was allowed to stand in the refrigerator for 2 days and the excess diazomethane and solvents allowed to evaporate overnight at room temperature. The residue was chromatographed as before and the main yellow band collected. The solvents were removed and the residue crystallized from aqueous methanol (80 mg), m.p. 189°.

The u.v. spectrum: λ_{max}^{EtOH} 208, 230 (sh), 270, 330 (sh), and 433 nm, log ε_{max} 4.57, 4.37, 4.28, 3.61, and 3.77 respectively.

The i.r. spectrum: $\nu_{max}^{CHCl_3}$ 1660 cm^{-1}.

The p.m.r. spectrum: 1.6–3.7 15H, aliphatic protons; 2.22 (s) 6H, 2 × N—CH_3; 3.82 (s) 3H, OCH_3; 3.96 (s) 6H, OCH_3; 4.01 (s) 3H, OCH_3; 5.10 (s) 1H, C_5H; 6.5–7.1 5H, aromatic protons; 7.70 (d) 1H, $C_{23}H$.

Anal. Calcd. for $C_{38}H_{40}N_2O_7$: C, 71.68; H, 6.33; N, 4.40. Found: C, 71.98; H, 6.61; N, 4.72.

The molecular formula was confirmed by h.r.m.s.

Calcd. for $C_{38}H_{40}N_2O_7$: 636.284. Found: 636.289.

*Cancentrine Methine-O-methyl Ether (**7**)*

Cancentrine methine (100 mg) was dissolved in methanol (50 ml) and excess ethereal diazomethane added. The mixture was allowed to stand in the refrigerator for 3 days and the excess diazomethane and solvents were then allowed to evaporate overnight at room temperature. The residue was chromatographed as before and the main yellow band collected. The solvents were removed and the residue crystallized from methanol (60 mg), m.p. 138°.

The u.v. spectrum: λ_{max}^{EtOH} 228, 273, and 436 nm, log ε_{max} 4.54, 4.37, and 3.69 respectively.

The i.r. spectrum: $\nu_{max}^{CHCl_3}$ 1660 cm^{-1}.

The p.m.r. spectrum: 1.6–3.7 13H, aliphatic protons; 2.22 (s) 6H, 2 × N—CH_3; 3.82 (s) 3H, OCH_3; 3.94 (s) 6H, 2 × OCH_3; 3.98 (s) 3H, OCH_3; 5.18 (s) 1H, C_5H; 5.87 (q) 1H, C_9H; 6.4–7.2 6H, aromatic protons + $C_{10}H$; 7.72 (d) 1H, $C_{23}H$.

Anal. Calcd. for $C_{38}H_{38}N_2O_7$: C, 71.91; H, 6.03. Found: C, 71.67; H, 5.84.

The molecular formula was confirmed by h.r.m.s.

Calcd. for $C_{38}H_{38}N_2O_7$: 634.268. Found: 634.267.

*Cancentrine Bis-methine (**10**)*

Cancentrine methine (200 mg) was dissolved in methanol (50 ml) and methyl iodide (5 ml) added. The solution was allowed to stand overnight at room temperature and the methine–methiodide which had crystallized out was filtered, washed with some methanol, and dried (220 mg). It was then refluxed in anhydrous tertiary butyl alcohol (50 ml) with potassium *t*-butoxide (200 mg). A strong fishy smell (probably trimethylamine) developed as the reaction proceeded. After 4 h the refluxing was stopped, the solvent removed under reduced pressure, water (50 ml) added, the mixture saturated with carbon dioxide. The precipitated yellow solid was filtered, washed, and dried and recrystallized from methanol (120 mg), m.p. 192°.

The u.v. spectrum: λ_{max}^{EtOH} 229, 270, and 438 nm, log ε_{max} 4.75, 4.52, and 3.84 respectively.

The i.r. spectrum: $\nu_{max}^{CHCl_3}$ 3440 and 1665 cm^{-1}.

Anal. Calcd. for $C_{35}H_{29}NO_7$: C, 73.03; H, 5.08; N, 2.43. Found: C, 73.20; H, 5.05; N, 2.80.

The molecular formula was confirmed by h.r.m.s.

Calcd. for $C_{35}H_{29}NO_7$: 575.201. Found: 575.198.

We thank the National Research Council of Canada for financial support of this work.

1. R. H. F. MANSKE. Can. J. Res. B**7**, 258 (1932).
2. R. H. F. MANSKE. Can. J. Res. **B16**, 81 (1938).
3. G. R. CLARK, R. H. F. MANSKE, G. J. PALENIK, R. RODRIGO, D. B. MACLEAN, L. BACZYNSKYJ, D. E. F. GRACEY, and J. K. SAUNDERS. J. Am. Chem. Soc. **92**, 4998 (1970).
4. D. B. MACLEAN, L. BACZYNSKYJ, R. RODRIGO, and R. H. F. MANSKE. Can. J. Chem. This issue.
5. (*a*) T. RÜLL. Bull. Soc. Chim. Fr. 568 (1963). (*b*) T. RÜLL and D. GAZNAIRE. Bull. Soc. Chim. Fr. 2189 (1963). (*c*) S. OKUDA, S. YAMAGUCHI, Y. KAWAZOE, and K. TSUDA. Chem. Pharm. Bull. (Tokyo), **12**, 104 (1964). (*d*) T. J. BATTERHAM, K. H. BELL, and U. WEISS. Aust. J. Chem. **18**, 1799 (1966).
6. H. AUDIER, M. FETIZON, D. GINSBURG, A. MENDELBAUM, and T. RÜLL. Tetrahedron Lett. 12 (1965).
7. R. H. F. MANSKE. Alkaloids, **4**, 249 (1954).
8. C. KASHIMA, M. YAMAMOTO, and N. SUGIYAMA. J. Chem. Soc. C, 111 (1970).
9. R. J. HIGHET and P. F. HIGHET. J. Org. Chem. **30**, 902 (1965).
10. F. A. L. ANET and A. J. R. BOURN. J. Am. Chem. Soc. **87**, 5250 (1965).
11. T. KAMETANI, M. IHARA, and T. HONDA. Chem. Commun. 1301 (1969).
12. T. KAMETANI, K. FUKUMOTO, and M. FUJIHARA. Chem. Commun. 352 (1971).
13. R. K. HILL. Alkaloids, **9**, 511–512 (1967).
14. A. R. BATTERSBY, R. J. FRANCIS, M. HIRST, R. SOUTHGATE, and J. STAUNTON. Chem. Commun. 602 (1967).
15. K. W. BENTLEY, D. G. HARDY, and B. MEEK. J. Am. Chem. Soc. **89**, 3293 (1967).
16. N. FINCH, C. W. GEMENDEN, I. HSIU-CHU HSU, A. KERR, G. A. SIM, and W. I. TAYLOR. J. Am. Chem. Soc. **87**, 2229 (1965).
17. K. BIEMANN. Pure Appl. Chem. **9**, 95 (1964).
18. D. THOMAS and K. BIEMANN. J. Am. Chem. Soc. **87**, 5477 (1965).

Can. J. Chem. Downloaded from www.nrcresearchpress.com by 210.87.254.105 on 09/05/12
For personal use only.

Cancentrine. III.[1] Dehydroderivatives

D. B. MacLean and L. Baczynskyj
Department of Chemistry, McMaster University, Hamilton, Ontario
AND
R. Rodrigo and R. H. F. Manske
Department of Chemistry, University of Waterloo, Waterloo, Ontario

Received August 24, 1971

The structures of dehydrocancentrine-A and -B are elucidated by a combination of physical and chemical methods.

Les structures des déhydrocancentrines-A et -B ont été élucidées au moyen de méthodes physiques et chimiques.

Canadian Journal of Chemistry, **50**, 862 (1972)

Recently we reported the characterization and structural elucidation of a new dimeric benzylisoquinoline alkaloid, cancentrine (1, 2). Here we describe two new alkaloids, dehydrocancentrine-A (**2**) and dehydrocancentrine-B (**3**), closely related in structure to cancentrine (**1**). Both alkaloids are found in *Dicentra canadensis* (Goldie) Walp. in very small amounts and were separated from cancentrine by chromatography.

Dehydrocancentrine-B is a red alkaloid with the following u.v. spectrum: λ_{max}^{EtOH} 216 (sh), 242, 270 (sh), 310 (sh), 370, 446, 492, and 525 (sh) nm; log ε_{max} 4.86, 4.78, 4.23, 4.16, 3.90, 4.00, 3.95, and 3.85, respectively. It has i.r. bands at 3450 (OH), 1660 (C=O), and 1630 (C=C) cm^{-1}. In its mass spectrum the molecular ion appeared at *m/e* 604 corresponding to an elemental composition of $C_{36}H_{32}N_2O_7$. The fragmentation pattern is very similar to that of cancentrine (2), with the exception that the ions due to the 'cularine' part (moiety A) appear two mass units lower than in the case of cancentrine, indicating that the double bond must be located in the cularine part of the molecule. The only available position is at C_{31}—C_{32} and the fragmentation pattern is rationalized accordingly (Scheme 1). Only the formation of the most abundant ions is represented. The elemental compositions in parentheses were determined by high resolution mass spectrometry. Fissions 'a' and 'b' (2) taking place as indicated lead to two fragment ions, one corresponding to the morphine part (moiety B) which fragments further in exactly the same manner as in cancentrine, and the other corresponding to the cularine part, now two mass units lower (at *m/e* 361) than the corresponding ion in cancentrine. Fissions a and b also proceed with H transfer to give an ion at *m/e* 362. Alternatively, fragmentation at 'a' and 'c' with hydrogen transfer from the 'morphine' to the 'cularine' moiety leads to ions at *m/e* 256 and 348, the latter again being two mass units

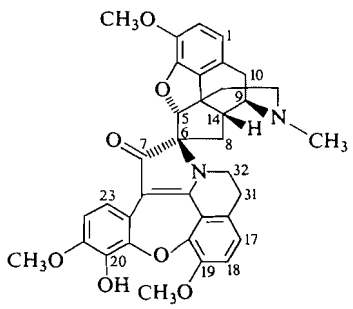

1

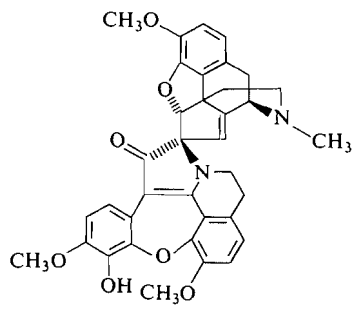

2

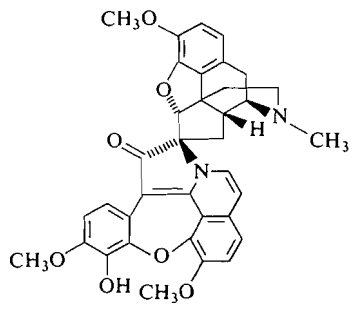

3

[1]For Part II, see ref. 2.

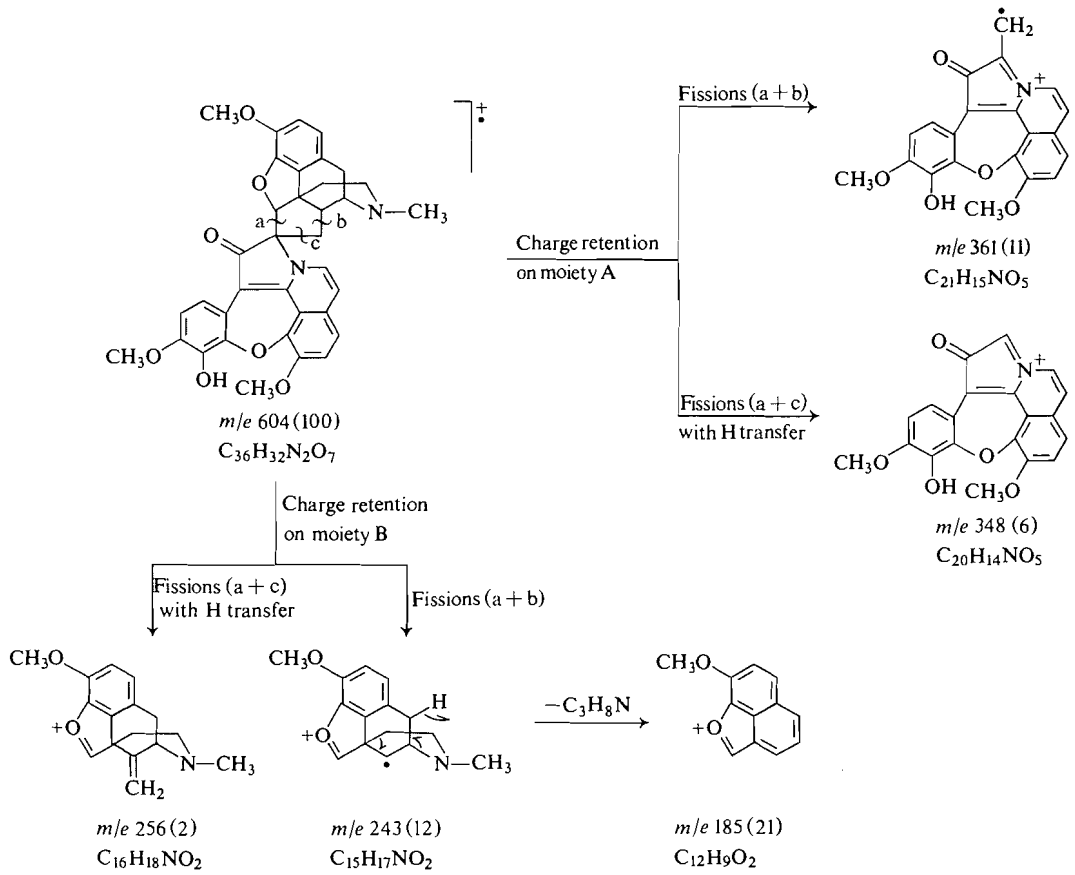

SCHEME 1

lower than the corresponding ion in cancentrine. These ions do not appear to fragment further.

The p.m.r. spectrum confirms this placement of the double bond at C_{31}—C_{32}. The spectrum displays a sharp singlet at 2.50 δ (3H) corresponding to one *N*-methyl group, three sharp singlets at 3.84 (3H), 3.90 (3H), and 3.99 δ (3H) due to the three aromatic methoxyls, a sharp singlet at 4.84 δ (1H) attributed to the 5β proton, and the three aromatic AB systems (6H). A fourth new AB system due to the double bond at C_{31}—C_{32} is partly masked by the aromatic hydrogens but one half of it is clearly seen at 6.25 δ (1H) with a coupling constant $J_{AB} = 7.0$ Hz.

Dehydrocancentrine-A is a yellow alkaloid with the following u.v. spectrum: λ_{max}^{EtOH} 216, 269, 296 (sh), and 445 nm; log ε_{max} 4.77, 4.36, 4.29, and 3.87, respectively. It has i.r. bands at 3440 (OH), 1660 (C=O), and 1620 (C=C) cm^{-1}. Its high resolution mass spectrum has a molecular ion at *m/e* 604 corresponding in composition to $C_{36}H_{32}N_2O_7$. The 100 MHz p.m.r. spectrum of dehydrocancentrine-A (in $CDCl_3$) has all the characteristic peaks of cancentrine (2), namely, three aromatic methoxyls at 3.80 (6H) and 3.93 δ (3H), one *N*-methyl singlet at 2.53 δ (3H), and six aromatic hydrogens forming three AB systems. There is also a sharp singlet at 5.04 δ as in the case of cancentrine but integrating for more than one proton. The spectrum was therefore recorded in DMSO-d_6 where it showed two sharp singlets at 5.05 and 5.26 δ integrating for one proton each and attributed to the 5β hydrogen and a vinylic hydrogen, respectively. The vinylic proton is not coupled to any other proton in the spectrum and, therefore, the double bond in **2** must be

Can. J. Chem. Downloaded from www.nrcresearchpress.com by 210.87.254.105 on 09/05/12
For personal use only.

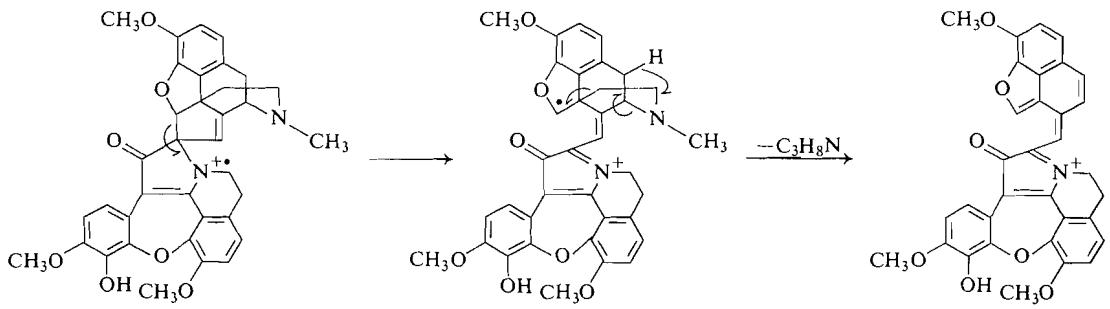

SCHEME 2

located at C_9—C_{10} or C_8—C_{14}. A double bond at C_9—C_{10} would be at a bridgehead position, and therefore the structure of dehydrocancentrine-A is represented as in formula **2**.

This structure is in accord with the fragmentation pattern revealed in the mass spectrum. The only important fragment ion is formed by loss of the nitrogen bridge from the molecular ion giving rise to the ion at *m/e* 546 (Scheme 2). This is typical of the morphine alkaloids (3). The ion at *m/e* 546 has no tendency to fragment further because of its aromatic character. This behavior of **2** is strikingly different from that of cancentrine and its derivatives, and constitutes a good example of how a small structural change in a molecule can have a dramatic effect upon its fragmentation pattern. Both the molecular ion, *m/e* 604, and the fragment ion, *m/e* 546, have homologous ions 14 mass units above and below, apparently resulting from *trans* methylation processes at the high source temperatures required for volatilization of these high molecular weight compounds. Dehydrocancentrine-B behaved similarly but to a lesser degree.

Finally, the position of the hydroxyl group in **2** and **3** was shown to be identical with that in cancentrine by catalytic hydrogenation of the alkaloids to the latter compound. In the case of **2** a small amount of another yellow compound probably the C-14 epimer, was also formed and detected by t.l.c. Dehydrogenation of cancentrine over 5% palladium–charcoal in boiling naphthalene gave *inter alia* **2** and **3** in low yield and only detectable by t.l.c. Since the relative stereochemistry of cancentrine is known (1), these results support the stereochemical assignments made for the alkaloids in structures **2** and **3**.

Experimental

Methods

Melting points were determined on a Fisher Mel-Temp apparatus and are uncorrected. Mass spectra[2] were recorded on a CEC 21-110B double focussing mass spectrometer. For high resolution work, spectra were recorded on plates and accurate mass measurements were made using perfluorokerosene as marker (4). The p.m.r. spectra were recorded using the frequency sweep mode of a Varian HA-100 spectrometer. Samples were dissolved in $CDCl_3$ (unless otherwise specified) using added TMS as the internal locking signal. Chemical shifts were measured relative to TMS using a V315 frequency counter incorporated in the instrument. A Beckmann IR 10 spectrometer was used to record the i.r. spectra and a Coleman-Hitachi EPS-3T spectrometer was used for the u.v. spectra.

The Purification of Cancentrine and Isolation of Dehydrocancentrine-A and -B

Crude cancentrine (5) when chromatographed on a t.l.c. plate (silica gel) in benzene–methanol (4:1) proved to be a mixture of several compounds. The major component cancentrine (90%) had a R_f of about 0.35 in the system, while dehydrocancentrine-A ran about 20% faster and dehydrocancentrine-B almost overlapped with cancentrine (*ca.* 2% faster).

Cancentrine (10 g) was chromatographed on a large column of silica gel (85 × 3 cm; 70–325 mesh ASTM; E. Merck) in benzene–methanol, 9:1. The column was eluted slowly over several days and the relevant fractions collected.

The solvents were removed and the residues crystallized from methanol. Dehydrocancentrine-A (40 mg), m.p. 194°. Dehydrocancentrine-B could only be induced to crystallize after repeated chromatography to separate it completely from cancentrine (25 mg), m.p. 206°. The molecular formulae were determined by high resolution mass spectrometry.

Dehydrocancentrine-A: Calcd. for $C_{36}H_{32}N_2O_7$: 604.221. Found: 604.224.

Dehydrocancentrine-B: Calcd. for $C_{36}H_{32}N_2O_7$: 604.221. Found: 604.221.

[2]A complete listing of mass spectral data may be found in the Depository of Unpublished Data, National Science Library, National Research Council, Ottawa, Canada K1A 0S2.

Can. J. Chem. Downloaded from www.nrcresearchpress.com by 210.87.254.105 on 09/05/12
For personal use only.

Hydrogenation of Dehydrocancentrine-A and -B

Dehydrocancentrine-A (20 mg) in methanol (25 ml) was hydrogenated overnight at room temperature and pressure in the presence of Adams catalyst (10 mg). The solution was filtered and the methanol removed from the filtrate under reduced pressure. A small specimen of the residue when tested by t.l.c. (silica gel; benzene–methanol, 4:1) showed the presence of cancentrine (*ca.* 90%) and another yellow compound (*ca.* 10%) with R_f about half that of cancentrine. The bulk of the crude product was therefore purified by column chromatography and crystallized from $CHCl_3$–MeOH (12 mg), m.p. 235°. The i.r. spectrum of the product and its behavior on t.l.c. were identical with that of cancentrine.

Dehydrocancentrine-B (5 mg) was similarly hydrogenated, in this case, a single product was obtained. Its. i.r. spectrum and t.l.c. behavior were identical with that of cancentrine.

Dehydrogenation of Cancentrine

Cancentrine (1 g) was refluxed in naphthalene (5 g) with 5% palladium–charcoal (100 mg) for 3 h. Most of the naphthalene was sublimed out on a steam bath under reduced pressure and a small specimen of the residue was then examined by t.l.c. using the same system as before. It proved to be a very complex mixture containing a large proportion of unchanged cancentrine but the presence of both dehydrocancentrine-A and -B was clearly evident. The bulk of the dehydrogenation product was then chromatographed on a column of silica gel as before and the relevant fractions taken. These fractions when examined by t.l.c. in comparison with authentic samples, confirmed the presence of dehydrocancentrines-A and -B, but it was not possible to obtain these small amounts of material sufficiently pure to induce crystallization.

We thank the National Research Council of Canada for financial support of this work.

1. G. R. CLARK, R. H. MANSKE, G. J. PALENIK, R. RODRIGO, D. B. MACLEAN, L. BACZYNSKYJ, D. E. F. GRACEY, and J. K. SAUNDERS. J. Am. Chem. Soc. **92**, 4998 (1970).
2. R. RODRIGO, R. H. F. MANSKE, D. B. MACLEAN, L. BACZYNSKYJ, and J. K. SAUNDERS. Can. J. Chem. This issue.
3. (*a*) H. AUDIER, M. FETIZON, D. GINSBURG, A. MANDELBAUM, and T. RULL. Tetrahedron Lett. 13 (1965). (*b*) D. S. WHEELER, T. H. KINSTLE, and K. L. RINEHART, JR. J. Am. Chem. Soc. **89**, 4494 (1967).
4. K. BIEMANN. Pure Appl. Chem. **9**, 95 (1964).
5. R. H. F. MANSKE. Can. J. Res. **B7**, 258 (1932).

Can. J. Chem. Downloaded from www.nrcresearchpress.com by 210.87.254.105 on 09/05/12
For personal use only.

Organic Sulfur Mechanisms. 12. Reaction of Sulfenes with Triphenylphosphine[1]

J. F. KING, E. G. LEWARS, AND L. J. DANKS

Department of Chemistry, University of Western Ontario, London 72, Ontario

Received September 16, 1971

Phenylmethanesulfonyl chloride (**1***a*) and 2,4-dinitrophenyl phenylmethanesulfonate (**1***b*) react with a mixture of triphenylphosphine and triethylamine to give the benzyltriphenylphosphonium salts (**2**) in 32 and 87% yields, respectively. Methanesulfonic anhydride (**1***c*) similarly gives the methyltriphenylphosphonium salt. These reactions evidently constitute the first illustrations of the reaction of a sulfene with a trivalent phosphorus compound.

Le chlorure de phénylméthanesulfonyle (**1***a*) et le dinitrophényl-2,4 phénylméthanesulfonate (**1***b*) réagissent avec un mélange de triphénylphosphine et de triéthylamine pour donner des sels de benzyltriphénylphosphonium avec respectivement des rendements de 32 et 87%. L'anhydride méthanesulfonique (**1***c*) conduit d'une façon similaire au sel de méthyltriphénylphosphonium. Ces réactions constituent les premiers exemples de la réaction d'un sulfène avec un composé trivalent du phosphore.

Canadian Journal of Chemistry, **50**, 866 (1972)

Addition of nucleophilic reagents to sulfenes ($RR'C{=}SO_2$) is probably the most important reaction of these useful and highly reactive intermediates. There are no reports, however, on the reaction of sulfenes with trivalent phosphorus compounds, and, as part of our general study of the reactions of sulfenes (ref. 1 and earlier work cited), we decided to look into the possibility of reaction between a sulfene and a tertiary phosphine.

Accordingly phenylmethanesulfonyl chloride (**1***a*) was treated with a mixture of triethylamine and triphenylphosphine in the hope that the sulfonyl chloride would be attacked by the amine to give the sulfene faster than it is reduced by the triphenylphosphine (2). The reaction gave benzyltriphenylphosphonium chloride (**2***a*) (see eq. 1) mixed with the corresponding phosphonium phenylmethanesulfonate (**2***d*) (the total yield of the phosphonium ion was 32%).

[1] $$RCH_2SO_2Z + Ph_3P \xrightarrow{Et_3N} RCH_2\overset{+}{P}Ph_3\ Z^-$$

1 **2**

a R = Ph; Z = Cl

b R = Ph; Z = 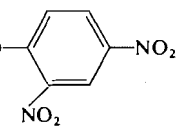

c R = H; Z = OSO_2CH_3

d R = Ph; Z = OSO_2CH_2Ph

Triphenylphosphine oxide and triphenylphosphine sulfide were also isolated but these probably arose by the direct reduction of the sulfonyl chloride by the phosphine, since they are also obtained when triethylamine is left out of the reaction; the phosphonium salts are not formed under the latter conditions. Horner and Nickel (2) have reported the formation of triphenylphosphine oxide on reaction of triphenylphosphine and benzenesulfonyl chloride. Theirs is clearly a reaction which cannot involve a sulfene, and presumably takes place by attack of the phosphine on the chlorine with displacement of the sulfinate anion. Pearson's "hard-soft-acid-base" (HSAB) theory (3) suggested that the direct reaction of the phosphine and the sulfene precursor **1** might be slowed if the chlorine were replaced by a "harder" function capable of acting as a leaving group. Singh in these laboratories (4) had shown that 2,4-dinitrophenyl phenylmethanesulfonate (**1***b*) and related esters give products evidently derived from phenylsulfene. When **1***b* was treated with triphenylphosphine alone for 3 h little reaction was observed, but with a mixture of triethylamine (1 mol) and triphenylphosphine (3 mol), benzyltriphenylphosphonium 2,4-dinitrophenoxide (**2***b*) was isolated in good (87%) yield. Sulfur dioxide was also generated in the reaction, which is apparently complete in less than 1 min. The salt **2***b* was not obtained crystalline; it was characterized by conversion to and formation from benzyltriphenylphosphonium

[1]For part 11 see ref. 1.

Can. J. Chem. Downloaded from www.nrcresearchpress.com by 210.87.254.40 on 09/05/12
For personal use only.

Can. J. Chem. Downloaded from www.nrcresearchpress.com by 210.87.254.40 on 09/05/12
For personal use only.

[2] $$\underset{\mathbf{3}}{RCH{=}SO_2} \xrightarrow{Ph_3P} \underset{\mathbf{4}}{RCH\underset{PPh_3}{\diagdown\!\!\diagup}SO_2} \xrightarrow{-SO_2} \underset{\mathbf{5}}{RCH{=}PPh_3} \xrightarrow{Et_3\overset{+}{N}H\ Z^-} \underset{\mathbf{2}}{RCH_2\overset{+}{P}Ph_3\ Z^-}$$

chloride (**2***a*). Essentially the same result was obtained with equimolar amounts of **1***b*, the amine and the phosphine.

Methanesulfonyl chloride with triethylamine and triphenylphosphine gave no sign of any methyltriphenylphosphonium species. This is not very surprising since sulfene formation with triethylamine is about 1000 times slower with methanesulfonyl chloride than with phenylmethanesulfonyl chloride (5). It is unlikely that the corresponding change in the rate of the triphenylphosphine reduction is as large, and hence it would be expected that the reduction would be relatively much faster than sulfene formation from methanesulfonyl chloride. 2,4-Dinitrophenyl methanesulfonate also gave no phosphonium salt. It was found that 2,4-dinitrophenyl methanesulfonate did not react with triethylamine even on standing for a number of hours, and it is therefore likely that again, sulfene formation was not sufficiently fast to compete with other reactions. Methanesulfonic anhydride (**1***c*), however, gave a moderate yield of the methyltriphenylphosphonium ion, characterized as the bromide (41% yield). No systematic study varying either the sulfonyl chloride or phosphine was attempted, though our results suggest a somewhat limited generality for this reaction. The reaction of tributylphosphine and triethylamine with **1***b* showed no sign of the phosphonium salt.

To account for the formation of the phosphonium salts **2** we suggest the mechanism summarized in eq. 2 as a reasonable possibility. The cyclic intermediate **4** could conceivably be formed by a direct cycloaddition onto the sulfene **3**, or perhaps via the zwitterionic species **6** and **7**. The intermediacy of **4** is, of course, not required by the available data; the ylide **5** could arise directly from either of the zwitterions, such a process being particularly simple from **7**, the zwitterion deriving from "abnormal attack" (6) on the sulfene. The ylide **5** would be expected to pick up a proton very rapidly from the triethylammonium ion formed as a by-product from the original sulfene generation. In the present system in which sulfene is formed by removal of HZ (in eq. 1) with base, the presence of a conjugate acid capable of protonating the ylide cannot be avoided without introducing further complications. We tried to carry out the reaction with triphenylphosphine using the Staudinger–Pfenninger diazoalkane and sulfur dioxide procedure for forming sulfenes (7). No sign of any ylide was found, though this could be due merely to preclusion of the sulfene formation by a faster reaction between the phenyldiazomethane and triphenylphosphine (*cf.* ref. 8).

$$\underset{\mathbf{6}}{\overset{-}{R}CH{-}SO_2\overset{+}{P}Ph_3} \qquad \underset{\mathbf{7}}{\begin{array}{c} RCH{-}SO_2^- \\ | \\ {}^+PPh_3 \end{array}}$$

Experimental

Melting points were determined in capillary tubes with a Gallenkamp apparatus and are uncorrected.

The i.r. spectra were recorded in CH_2Cl_2 solutions, unless stated otherwise, with a Beckman IR-20A or IR-10 instrument.

The n.m.r. spectra were recorded in $CDCl_3$ solutions, unless stated otherwise, with a Varian T-60 spectrometer. The band positions are reported in p.p.m. downfield from TMS as internal reference (δ scale).

Analytical t.l.c. was carried out with silica gel (Camag DF5, containing u.v. indicator) on microscope slides. Preparative t.l.c. was carried out with *ca.* 1.0 mm thick layers of silica gel (Camag DF5, containing u.v. indicator) on 20 × 20 cm glass plates. Unless stated otherwise, t.l.c. chromatograms were developed with CH_2Cl_2–MeOH, 100:15 (v/v), analytical chromatograms were made visible with iodine vapor, and preparative chromatograms by the quenching of the u.v. phosphor.

Solvents were removed from solutions with a Büchi rotary evaporator in conjunction with a water aspirator. Dichloromethane solutions were dried by passing them through a small plug of cotton wool before evaporation.

The term "separation into polar and nonpolar fraction with silica gel" as used here means that the CH_2Cl_2 solution was swirled with about 10 times its weight of t.l.c. silica gel, filtered through a sintered glass funnel, and the filtrate again treated with silica gel and filtered. The CH_2Cl_2 filtrates then contained the "nonpolar" material. Extraction of the silica gel with CH_2Cl_2–MeOH (100:15, v/v) gave a solution of the "polar" material. Unless otherwise stated, recrystallization was effected from dichloromethane–hexane.

2,4-Dinitrophenyl Phenylmethanesulfonate (1b)

Triethylamine (4.37 ml, 3.19 g, 31.5 mmol) was added

Can. J. Chem. Downloaded from www.nrcresearchpress.com by 210.87.254.40 on 09/05/12
For personal use only.

with stirring to a solution of phenylmethanesulfonyl chloride (6.0 g, 31.4 mmol) and 2,4-dinitrophenol (27.8 g, 151 mmol) in dichloromethane (400 ml). After stirring for 30 min, the solution was washed repeatedly with aqueous sodium bicarbonate until the aqueous layer was pale yellow, then passed through a small plug of cotton wool and concentrated to *ca.* 40 ml. Enough hexane was added to the bright red solution to make it slightly cloudy, then dichloromethane was added till the solution was again clear; crystallization began at once. The product consisted of light yellow prisms, m.p. 111–114.5°; yield 7.1 g (67%). The n.m.r. spectrum showed absorption at δ 8.87 (d, $J = 2.4$ Hz, 1H), 8.45 (d of d, $J = 2.4$ and 6.0 Hz, 1H), 7.3–7.7 (m dominated by spike at 7.50, 6H), 4.80 (s, 2H).

Anal. Calcd. for $C_{13}H_{10}N_2O_7S$: C, 46.15; H, 2.98; N, 8.28; S, 9.48. Found: C, 46.10; H, 3.06; N, 8.32; S, 9.34.

Reaction of 2,4-Dinitrophenyl Phenylmethanesulfonate with Triethylamine and Triphenylphosphine

(1) Identification of Benzyltriphenylphosphonium 2,4-Dinitrophenoxide

2,4-Dinitrophenyl phenylmethanesulfonate (169 mg, 0.50 mmol) in dichloromethane (10 ml) was added from a syringe over 50 min under nitrogen to a stirred solution of triethylamine (71 μl, 52 mg, 0.51 mmol) and triphenylphosphine (394 mg, 1.50 mmol) in dichloromethane (5 ml). The bright golden-yellow solution was stirred a further 3 h, at the end of which time t.l.c. showed the absence of 2,4-dinitrophenyl phenylmethanesulfonate. The dichloromethane solution was washed once with an equal volume of water. Evaporation of the pale yellow aqueous layer gave a slightly sticky yellow solid, 17 mg, the n.m.r. spectrum of which showed it to be essentially triethylammonium 2,4-dinitrophenoxide. Evaporation of the bright golden yellow dichloromethane layer gave a slightly sticky orange solid, 543 mg. This was separated into polar and nonpolar fractions with silica gel. The nonpolar fraction, 276 mg, was shown to be triphenylphosphine by direct comparison with an authentic sample. The polar material was a bright yellow foam, 233 mg. Comparison with authentic triphenylphosphonium 2,4-dinitrophenoxide by n.m.r., i.r., and t.l.c. indicated that this material was essentially triphenylphosphonium 2,4-dinitrophenoxide (yield *ca.* 87%). This material (the foam could be broken up to give a non-crystalline solid) failed to crystallize, but its identity was firmly established by conversion to benzyltriphenylphosphonium chloride and 2,4-dinitrophenol as follows. A 1.7 × 22 cm Dowex 1-X2 resin column was washed successively with saturated aqueous potassium chloride, water, and methanol. A methanolic solution of the phosphonium salt from the reaction was passed through the column, eluting with methanol. Evaporation of the eluate and recrystallization gave very pale yellow microprisms, m.p. 317–322°, 167 mg (89% based on the phosphonium dinitrophenoxide, 77% from 2,4-dinitrophenyl phenylmethanesulfonate); mixed t.l.c. of this with authentic benzyltriphenylphosphonium chloride (see below) gave one spot. Recrystallization gave colorless prisms, m.p. 326.5–329.5°, mixed m.p. with authentic benzyltriphenylphosphonium chloride of m.p. 325–329°, 325.5–328.5° (9). The i.r. spectrum was identical with that of the authentic phosphonium chloride. Further elution of the column with methanolic hydrogen chloride (*ca.* 2 *N*) and evaporation of the eluate gave 2,4-dinitrophenol as a pale yellowish solid, 81 mg (101%). Mixed t.l.c. with authentic 2,4-dinitrophenol gave one spot. Recrystallization gave yellowish-brown platelets, m.p. 111–112°, mixed m.p. with authentic 2,4-dinitrophenol (m.p. 112–113°), 111–113°. The i.r. spectrum was identical with that of authentic 2,4-dinitrophenol.

(2) Identification of SO_2

In another experiment, the reaction solution was slowly swept with nitrogen and the gases passed through a trap cooled in Dry Ice–acetone. The dichloromethane in the trap was shown to contain sulfur dioxide (*ca.* 17%) by its smell and by i.r. and u.v. spectrometry.

(3) Use of One Equivalent of each Reactant

When 1 equiv of each of the three reactants was used, the yield of benzyltriphenylphosphonium 2,4-dinitrophenoxide was *ca.* 85%.

When a dichloromethane solution of 2,4-dinitrophenyl phenylmethanesulfonate was added all at once to a dichloromethane solution of triethylamine and triphenylphosphine (1 equiv of each reactant), a transient red color was seen; in *ca.* 1 s this faded, giving an orange solution. The t.l.c. of the reaction solution, performed within 1 min of addition of the 2,4-dinitrophenyl phenylmethanesulfonate, was identical to that after 3 h, indicating that the reaction was complete within 1 min.

Treatment of 2,4-Dinitrophenyl Phenylmethanesulfonate with Triphenylphosphine in the Absence of Triethylamine

When the reaction was carried out as described above but omitting the triethylamine, after 3 h t.l.c. showed mainly the starting materials, and no trace of the phosphonium salt. Preparative t.l.c. (dichloromethane) led to the recovery of most of the starting materials.

Benzyltriphenylphosphonium 2,4-Dinitrophenoxide (2b)

An anionic resin column was made up by washing a 7 × 2 cm Dowex 1-X2 column successively with aqueous methanolic potassium 2,4-dinitrophenoxide (prepared by adding a saturated methanolic solution of 4.4 g (24 mmol) of the phenol to an aqueous solution of 1.62 g (11.7 mmol) of potassium carbonate), water, and methanol. Benzyltriphenylphosphonium chloride (**2a**) (9) (388 mg, 1.0 mmol) in methanol was passed through the column, eluting with methanol. Evaporation of the eluate gave a bright yellow foam, 484 mg (90%), which did not crystallize, ν_{max} 1603, 1552, 1310, 1126 cm^{-1}; δ 8.70 (d, $J = 3.6$ Hz, 1H), 7.4–8.1 (m, strong spike at 7.75, *ca.* 17H), 6.9–7.4 p.p.m. (m, *ca.* 5H).

Reaction of Phenylmethanesulfonyl Chloride (1a) with Triethylamine and Triphenylphosphine

A solution of phenylmethanesulfonyl chloride (188 mg, 0.98 mmol) in dichloromethane (10 ml) was added under nitrogen over 1 h to a stirred solution of triethylamine (141 μl, 103 mg, 1.02 mmol) and triphenylphosphine (800 mg, 3.05 mmol) in dichloromethane (6 ml); the bright yellow solution was stirred for another 3 h. After this time, the solution was washed once with an equal volume of water, and the aqueous and organic layers were examined.

Evaporation of the aqueous layer gave a white solid, 149 mg, which was shown by t.l.c. and i.r. and n.m.r. spectrometry to be largely triethylammonium chloride.

Can. J. Chem. Downloaded from www.nrcresearchpress.com by 210.87.254.40 on 09/05/12
For personal use only.

Evaporation of the dichloromethane layer gave a yellow solid, 929 mg, which was separated into polar and nonpolar fractions with silica gel. The nonpolar material, 573 mg, was shown by t.l.c. and i.r. spectrometry to be triphenylphosphine contaminated with a modest amount of triphenylphosphine sulfide and a trace of triphenylphosphine oxide. The polar fraction was a white foam, 303 mg. This was subjected to preparative t.l.c. (dichloromethane–methanol, 100:10, v/v, two developments), which gave essentially three bands.

The most polar band represented a white solid, 138 mg. This was shown by direct comparison (t.l.c., i.r., n.m.r.) with an authentic mixture to be a *ca.* 60:40 (mol basis) mixture of benzyltriphenylphosphonium chloride and phenylmethanesulfonate. The yield of phosphonium salts was thus 0.31 mmol (32%).

The band of intermediate polarity corresponded to a white solid, 114 mg, shown by i.r. and n.m.r. spectrometry and t.l.c. to be triphenylphosphine oxide. The least polar material was a white solid, 28 mg, ν_{max} 1117 cm^{-1} which was not investigated further.

Benzyltriphenylphosphonium Phenylmethanesulfonate

(1) Preparation of Benzyl Phenylmethanesulfonate

Triethylamine (2.19 ml, 1.60 g, 15.8 mmol) was added over 6 min to a stirred solution of phenylmethanesulfonyl chloride (3.09, 15.7 mmol) and benzyl alcohol (1.70 g, 15.7 mmol) in dichloromethane (50 ml). The reaction mixture was stirred for 20 min, then washed once with an equal volume of water, passed through cotton wool, and concentrated until crystallization started. Hexane was then added and the solid filtered off and washed with hexane. The product was a colorless microcrystalline solid, 1.3 g, m.p. 80.5–81.5°. The mother liquors yielded 0.5 g of colorless microcrystalline solid, m.p. 93–94°. The i.r. and n.m.r. spectra of the two crops were identical, they were indistinguishable on t.l.c., and the mixed m.p. was 80–81°, showing that benzyl phenylmethanesulfonate is dimorphic. The total yield was 1.8 g (44%). The n.m.r. spectrum showed singlets at 7.35 (10H), 5.07 (2H), and 4.30 p.p.m. (2H); the i.r. had very strong bands at 1357, 1169, and 936 and 916 cm^{-1}.

(2) Conversion of Benzyl Phenylmethanesulfonate to Benzyltriphenylphosphonium Phenylmethanesulfonate

Benzyl phenylmethanesulfonate (262 mg, 1.0 mmol) and triphenylphosphine (262 mg, 1.0 mmol) were refluxed for 9 h in ethanol-free chloroform. The solution was concentrated and hexane was added until cloudiness was seen. Colorless prisms were deposited, 461 mg (88%), m.p. 182–185°; δ 7.3–7.9 (m, *ca.* 15H), 6.8–7.3 (m, *ca.* 10H), 4.87 (d, $J = 14$ Hz, 2H), 4.03 (s, 2H); ν_{max} 1178, 1107, 1031 cm^{-1}.

Anal. Calcd. for $C_{32}H_{29}O_3SP$: C, 73.26; H, 5.57. Found: C, 73.19; H, 5.12.

Reaction of Phenylmethanesulfonyl Chloride with Triphenylphosphine in the Absence of Triethylamine

A solution of triphenylphosphine (280 mg, 1.07 mmol) in dichloromethane (10 ml) was added dropwise to a stirred solution of phenylmethanesulfonyl chloride (200 mg, 1.05 mmol) in dichloromethane (2 ml). After 15 min, t.l.c. showed triphenylphosphine and a trace of starting material, together with a third component. More triphenylphosphine (37 mg) in dichloromethane (1 ml) was added, and after a further 20 min the solution was evaporated and subjected to preparative t.l.c. The most mobile band afforded a solid, 215 mg, which was recrystallized to give 50 mg of triphenylphosphine sulfide, the identity of which was established by direct comparison (m.p., i.r.) with an authentic sample. The mother liquors gave material of m.p. 82–89°, the i.r. spectrum of which showed it to be largely phenylmethanesulfonyl chloride. The least mobile band afforded triphenylphosphine oxide (258 mg), as shown by the i.r. spectrum of the material.

Another reaction, using sufficient triphenylphosphine to react with all the phenylmethanesulfonyl chloride, gave a reaction mixture in which no products containing the benzyl moiety were detected (n.m.r.).

Reaction of 2,4-Dinitrophenyl Phenylmethanesulfonate with Triethylamine and Tri-n-butylphosphine

2,4-Dinitrophenyl phenylmethanesulfonate (84.5 mg, 0.25 mmol) in dichloromethane (2.0 ml) was added under nitrogen over 7 min to a stirred solution of triethylamine (35 μl, 36 mg, 0.25 mmol) and tri-*n*-butylphosphine (59 μl, 50 mg, 0.25 mmol) in dichloromethane. The solution was stirred for a further 2.5 h, then the dichloromethane was replaced by deuteriochloroform and the n.m.r. spectrum of the reaction mixture was taken. This showed that benzyltri-*n*-butylphosphonium ion was absent and indicated the presence of a little starting **1***b*; t.l.c. (benzene) showed that tri-*n*-butylphosphine was absent. Authentic benzyltri-*n*-butylphosphonium chloride was prepared essentially as described by Smith and Winbush (10) except that chloroform rather than ethanol was used as the reaction solvent.

Reaction of Methanesulfonic Anhydride with Triethylamine and Triphenylphosphine

Methanesulfonic anhydride (11) (348 mg, 2.0 mmol) in dichloromethane (10 ml) was added under nitrogen to a stirred solution of triethylamine (0.282 ml, 2.04 mmol) and triphenylphosphine (1.57 g, 6.0 mmol) in dichloromethane (10 ml). The yellow solution was stirred for a further 20 min, then the reaction mixture was separated into nonpolar and polar fractions with silica gel. A methanol solution of the polar material was passed through an anionic resin column (Rexyn 203, bromide form, 7 × 2 cm), eluting with methanol. The methanol was removed, affording a yellow solid, 758 mg, the n.m.r. spectrum of which indicated it to be a mixture of triethylammonium bromide, methyltriphenylphosphine bromide, and a little triphenylphosphine oxide; t.l.c. was consistent with this. Preparative t.l.c. led to the isolation of triethylammonium bromide (80 mg), methyltriphenylphosphonium bromide (295 mg, recrystallized to give colorless prisms, m.p. 226–227°, mixed m.p. with authentic phosphonium bromide (12) (of m.p. 226.5–229°) 226.5–229; identity further confirmed by n.m.r. and i.r. spectra and by t.l.c.), and triphenylphosphine oxide (257 mg).

Reaction of Methanesulfonyl Chloride with Triethylamine and Triphenylphosphine

Methanesulfonyl chloride (0.156 ml, 2.0 mmol) was treated with triethylamine in the same way as was methanesulfonic anhydride. Separation into polar and nonpolar fractions and t.l.c. led to the isolation of triphenylphosphine oxide (282 mg) and triethylammonium chloride (148 mg) in addition to unidentified material (67 mg) which from its

n.m.r. spectrum could not contain more than 35 mg (yield <6%) of methyltriphenylphosphonium chloride (if any at all).

Reaction of 2,4-Dinitrophenyl Methanesulfonate with Triethylamine and Triphenylphosphine

2,4-Dinitrophenyl methanesulfonate (13) (65.5 mg, 0.25 mmol) was mixed with equimolar amounts of both triethylamine and triphenylphosphine in dichloromethane (2 ml total), and allowed to react for 1⅔ h; the mixture was then washed with water. The aqueous layer gave 25 mg of material identical in i.r. spectrum with triethylammonium 2,4-dinitrophenoxide. The organic phase gave 105 mg of material which after work-up yielded triphenylphosphine oxide (70 mg), identified by t.l.c. and n.m.r.; there was no sign of any methyltriphenylphosphonium ion.

In a separate experiment it was found that 2,4-dinitrophenyl methanesulfonate underwent little reaction with triethylamine under these conditions even after *ca.* 24 h.

Reaction of Phenyldiazomethane with Sulfur Dioxide, Triphenylphosphine, and Triethylammonium Chloride

Triphenylphosphine (262 mg, 1.0 mmol) and triethylammonium chloride (138 mg, 1.0 mmol) were dissolved, under nitrogen, in sulfur dioxide (*ca.* 10 ml) at −10°. The mixture was stirred under nitrogen and a solution of phenyldiazomethane (**14**) (118 mg, 1.0 mmol) in ethyl ether (7.7 ml) was added over *ca.* 1 min. The mixture was allowed to stand at room temperature for 1 h with exclusion of moisture, then the ether was removed to give a yellow solid, 601 mg, the n.m.r. spectrum of which showed the absence of benzyltriphenylphosphonium chloride.

We gratefully acknowledge the support of the National Research Council of Canada and of the Petroleum Research Fund (administered by the American Chemical Society).

1. J. F. KING, R. A. MARTY, P. DE MAYO, and D. L. VERDUN. J. Am. Chem. Soc. **93**, 6304 (1971).
2. L. HORNER and H. NICKEL. Ann. **597**, 20 (1955).
3. R. G. PEARSON. *In* Survey of progress in chemistry. *Edited by* A. F. Scott. Vol. 5. Academic Press, New York, 1969. p. 1. and references cited.
4. J. R. SINGH. M.Sc. Thesis. University of Western Ontario, London, Ontario, 1971.
5. T. W. S. LEE. Ph.D. Thesis. University of Western Ontario, London, Ontario, 1969.
6. J. F. KING and R. P. BEATSON. Chem. Commun. 663 (1970) and references cited.
7. H. STAUDINGER and F. PFENNINGER. Ber. **49**, 1941 (1916).
8. H. STAUDINGER and J. MEYER. Helv. Chim. Acta, **2**, 619 (1919).
9. J. GRIMSHAW and J. S. RAMSEY. J. Chem. Soc. B, 63 (1968).
10. G. P. SMITH and S. V. WINBRUSH. J. Am. Chem. Soc. **88**, 2127 (1966).
11. L. N. OWEN and S. P. WHITELAW. J. Chem. Soc. 3723 (1953).
12. G. WITTIG and U. SCHÖLLKOPF. Org. Syn. **40**, 66 (1960).
13. J. H. LOOKER. J. Org. Chem. **17**, 510 (1952).
14. P. YATES and B. L. SHAPIRO. J. Org. Chem. **23**, 759 (1958).

Can. J. Chem. Downloaded from www.nrcresearchpress.com by 210.87.254.40 on 09/05/12
For personal use only.

Mass Spectrometry of some Nuclear Substituted Styryl Ketones

P. J. SMITH[1]

Department of Chemistry and Chemical Engineering, University of Saskatchewan, Saskatoon, Saskatchewan

AND

J. R. DIMMOCK AND W. G. TAYLOR[2]

College of Pharmacy, University of Saskatchewan, Saskatoon, Saskatchewan

Received August 31, 1971

The mass spectra of a series of nuclear substituted styryl ketones with the structure

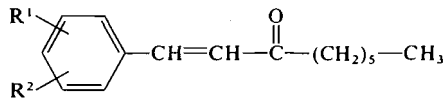

and several related compounds have been determined. The major fragmentation pathways include such processes as an aromatic substitution reaction occurring in the molecular ion as well as the McLafferty rearrangement. Only one of the two possible α-cleavages at the carbonyl function was observed. The major decomposition processes are outlined and compared with the recent results of a study on α,β-unsaturated aliphatic ketones. Mechanistic pathways are suggested for the formation of the major fragment ions.

Les spectres de masse d'une série de styryle cétones, substituées sur le noyau aromatique de structure

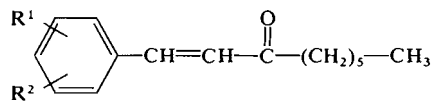

et de quelques composés apparentés, ont été déterminés. Les processus majeurs de la fragmentation incluent aussi bien des réactions de substitution aromatique se faisant sur l'ion moléculaire, que des transpositions du type McLafferty. Seul un des deux clivages possibles en α de la fonction carbonyle a été observé. Les processus majeurs de décomposition sont esquissés et comparés avec les résultats récents obtenus avec des cétones aliphatiques α,β-insaturées. Des mécanismes sont proposés pour rationaliser les principaux ions fragments.

Canadian Journal of Chemistry, **50**, 871 (1972)

Introduction

The mass spectrometry of α,β-unsaturated cyclic ketones have been reported previously (1, 2). It is only recently that the modes of fragmentation of α,β-unsaturated acyclic ketones have been studied in detail (3, 4).

α,β-Unsaturated ketones are alkylating agents and react with nucleophiles including thiols (5, 6). We have been interested in some nuclear substituted styryl ketones (7, 8) for this reason. The results of the mass spectral study of these compounds are reported in this paper and compared with those obtained from the study of the α,β-unsaturated aliphatic ketones (4).

[1]Author to whom all correspondence should be addressed.

[2]Holder of a Medical Research Council Studentship, 1969–1971.

Results and Discussion

The compounds which have been investigated are those shown in series 1 as well as several related derivatives as shown in series 2. The mass spectra are reproduced in Figs. 1–10.

The olefinic double bond in compounds **1–9** were shown from their n.m.r. spectra to have the *trans* arrangement.

A feature of particular interest in the spectra of compounds **1–9** is the presence of an M-H and/or an M-Cl peak. In all cases the process resulting in the loss of chlorine from the parent ion was confirmed by the observation of the appropriate metastable ions. It has been suggested (9, 10) that the species corresponding to these peaks arises from an intramolecular aromatic substitution reaction occurring in the

Can. J. Chem. Downloaded from www.nrcresearchpress.com by 210.87.254.40 on 09/05/12
For personal use only.

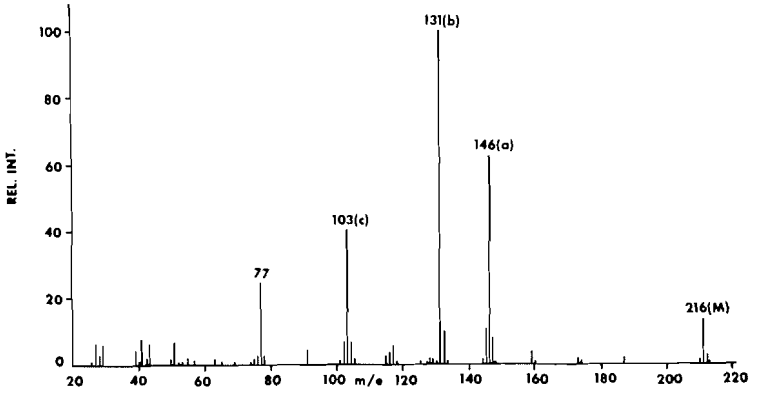

FIG. 1. Mass spectrum (70 eV) of **1**.

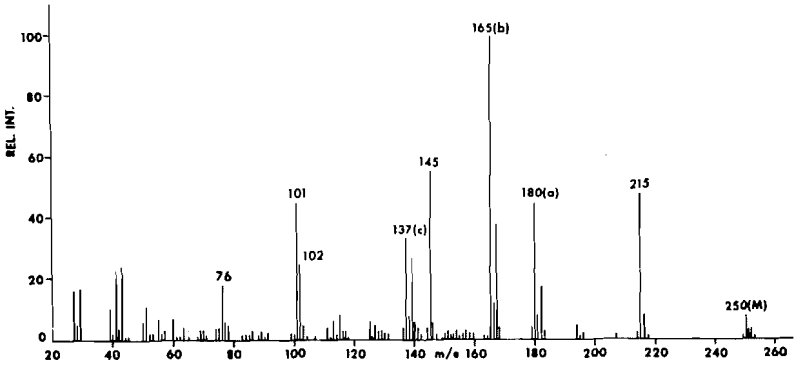

FIG. 2. Mass spectrum (70 eV) of **2**.

molecular ions with the formation of a relatively stable benzopyrylium ion. For this process to be operative a prior *trans* to *cis* isomerization in the molecular ion is necessary.

We suggest that attack of the carbonyl oxygen occurs only at the positions ortho to the styryl double bond since only when a chlorine is in this position is a peak observed for the loss of halogen from the molecular ion (see Scheme 1). In fact, the spectrum of the 2,6-dichloro compound, **5**, Fig. 5, has the M-Cl peak as the base peak, *m/e* 249, and does not exhibit an M-H peak. Compounds such as the 4-Cl, **3**, and the 3,4-dichloro, **6**, however, do not exhibit an M-Cl peak but only M-1 peaks corresponding to the loss of a hydrogen atom.

The relative intensity of the M-H and the M-Cl peaks in the spectrum of the 2-chloro substrate, Fig. 2, is noteworthy. The formation

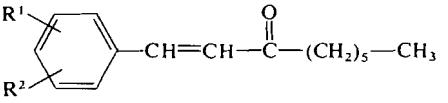

Series 1

1 $R^1 = R^2 = H$
2 R^1 = 2-Cl; $R^2 = H$
3 R^1 = 4-Cl; $R^2 = H$
4 R^1 = 2-Cl; R^2 = 4-Cl
5 R^1 = 2-Cl; R^2 = 6-Cl
6 R^1 = 3-Cl; R^2 = 4-Cl
7 R^1 = 4-$N(CH_3)_2$; $R^2 = H$

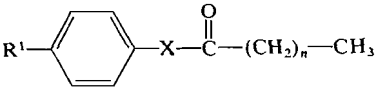

Series 2

8 $R^1 = H$; X = (CH = CH); $n = 1$
9 R^1 = Cl; X = (CH = CH); $n = 1$
10 $R^1 = H$; X = $(CH = CH)_2$; $n = 5$

Can. J. Chem. Downloaded from www.nrcresearchpress.com by 210.87.254.40 on 09/05/12
For personal use only.

Can. J. Chem. Downloaded from www.nrcresearchpress.com by 210.87.254.40 on 09/05/12
For personal use only.

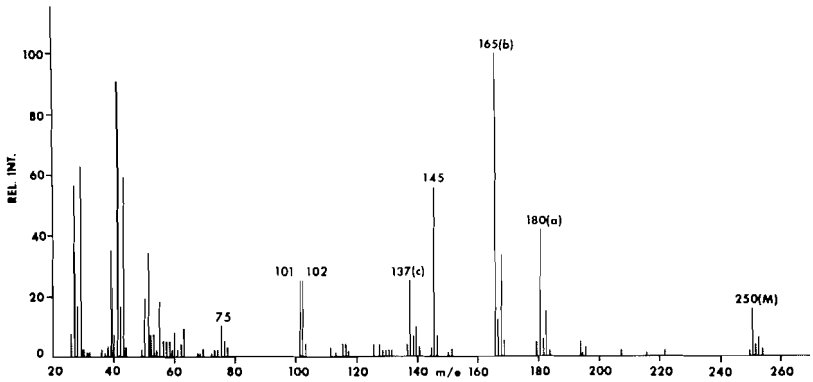

FIG. 3. Mass spectrum (70 eV) of **3**.

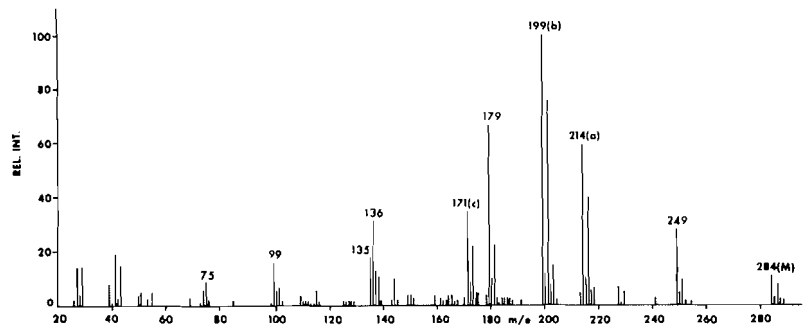

FIG. 4. Mass spectrum (70 eV) of **4**.

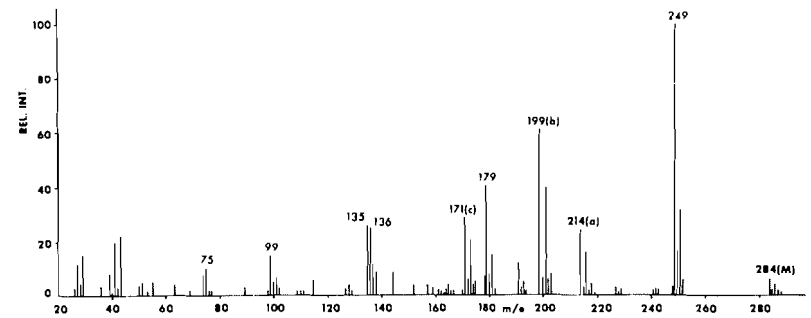

FIG. 5. Mass spectrum (70 eV) of **5**.

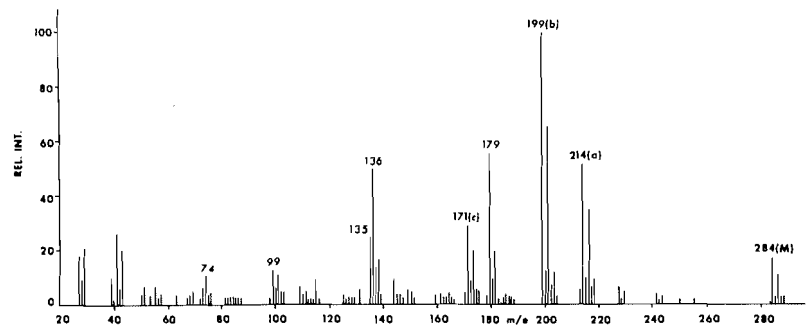

FIG. 6. Mass spectrum (70 eV) of **6**.

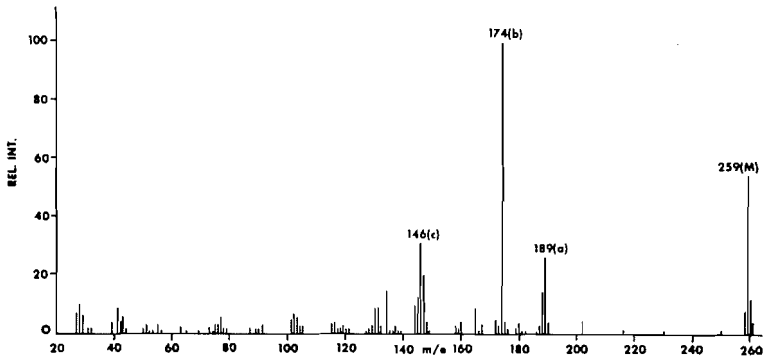

FIG. 7. Mass spectrum (70 eV) of **7**.

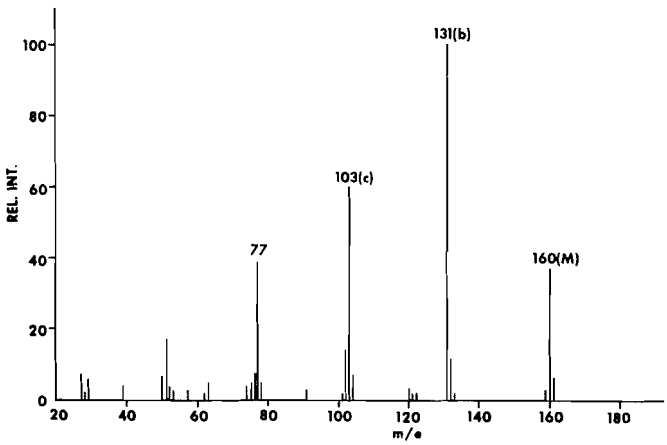

FIG. 8. Mass spectrum (70 eV) of **8**.

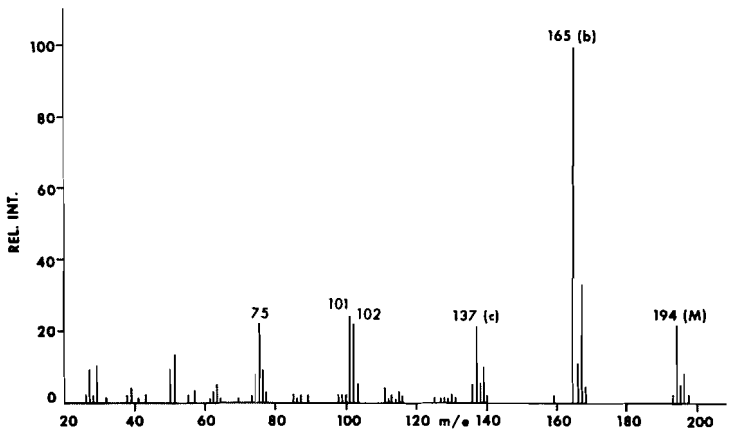

FIG. 9. Mass spectrum (70 eV) of **9**.

Can. J. Chem. Downloaded from www.nrcresearchpress.com by 210.87.254.40 on 09/05/12
For personal use only.

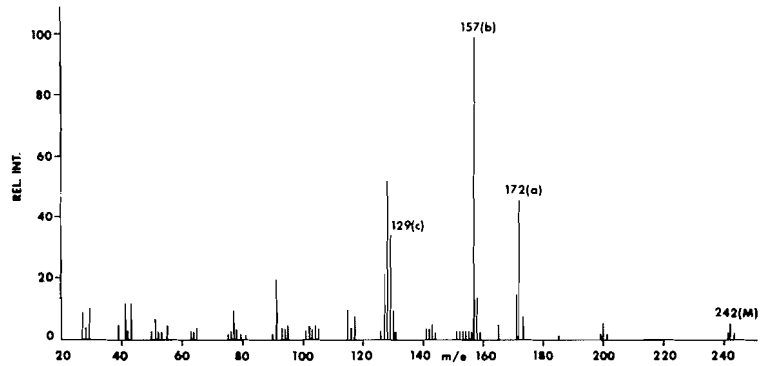

FIG. 10. Mass spectrum (70 eV) of **10**.

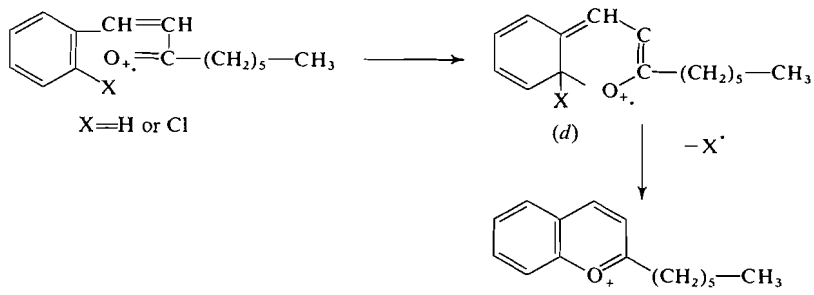

SCHEME 1

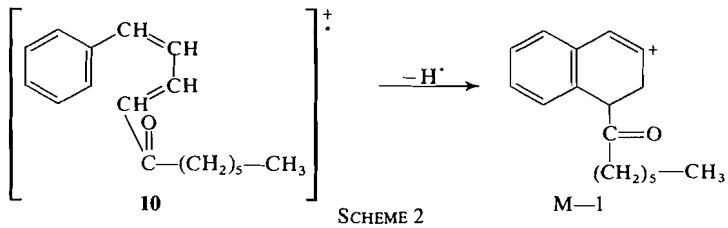

SCHEME 2

of the intermediate (*d*) might be expected to be retarded when attack occurs at the carbon bearing the chlorine for steric reasons and thus result in a greater peak intensity from the M-H process as compared with the loss of chlorine from the molecular ion. The fact that the loss of chlorine is much more favored than the loss of hydrogen, [M-Cl]/[M-H] is approximately 36:1, suggests that the steric factors are relatively unimportant compared to the leaving ability of the ortho substituent.

The spectrum of compound **10**, $C_6H_5CH{=}CH{-}CH{=}CH{-}\overset{\overset{O}{\|}}{C}{-}(CH_2)_5{-}CH_3$, Fig. 10, also exhibits an M-1 peak. By analogy to the styryl ketones the ion corresponding to this peak might arise via a similar intramolecular aromatic substitution reaction (Scheme 2).

A very prominent peak in all the spectra, except for compounds **8** and **9** where the alkyl side chain is less than three carbon atoms in length, corresponds to the McLafferty rearrangement product, ion (*a*). The appropriate

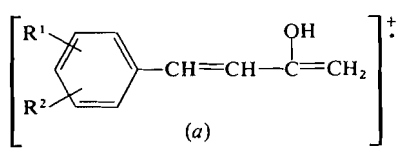

Can. J. Chem. Downloaded from www.nrcresearchpress.com by 210.87.254.40 on 09/05/12
For personal use only.

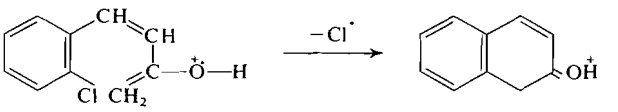

(*a*) (*a*) − Cl·

SCHEME 3

metastable peak was observed in all cases. Only the McLafferty product along with the molecular ion and the M-Cl ion from the ortho-substituted compounds was observed when the spectra were recorded at 15 eV.

Sheikh *et al.* (4), in the detailed study of α,β-unsaturated aliphatic ketones, found that the McLafferty rearrangement product, from such ketones as $CH_3(CH_2)_3CH{=}CH{-}\overset{O}{\overset{\|}{C}}{-}C_5H_{11}^n$, lost a methyl radical as shown by a strong metastable peak. It was proposed that this loss might proceed via a resonance form of the McLafferty product rather than through the keto form.[3] We have not found any evidence of a metastable peak corresponding to this loss of methyl in the present series of compounds. The chloro substituted compounds, **2**–**6**, however, all showed an intense metastable peak corresponding to the loss of a halogen atom from the McLafferty rearrangement product to give an ion at *m/e* 145 for **2** and **3** and an ion at *m/e* 179 for compounds **4**–**6**. This loss of halogen appears to be independent of the position of chlorine on the ring relative to the styryl double bond contrary to the results observed for the loss of halogen from the molecular ion. As expected, there was not a peak in the mass spectrum of **7**, corresponding to the loss of $N(CH_3)_2$ from the rearrangement product.

The loss of halogen from the McLafferty rearrangement ion, (*a*), could presumably proceed via a combination of either a simple bond cleavage process or via a cyclization similar to that represented for the loss of an ortho chlorine from the parent ion in the case of those substrates with a 2-chloro substituent (Scheme 3). That the latter pathway is followed to some extent is shown by the fact that the rearrangement product from all the compounds studied lost a hydrogen atom except the 2,6-dichloro substrate where an ortho hydrogen is not available.

In the study of the α,β-unsaturated aliphatic ketones, $R^1{-}CH{=}CH{-}\overset{O}{\overset{\|}{C}}{-}R$, Sheikh *et al.* (4) found that a general fragmentation was the cleavage of the vinylic double bond leading to the loss of R^1, C_4H_9, from the molecular ion. This *a priori* unfavorable vinylic bond rupture with loss of a substituted phenyl radical was not observed in the spectra of the present series of compounds. This presumably is a result of the conjugation in the molecular ion of the styryl ketones which would make such a bond cleavage unfavorable.

Contrary to the observation in the aliphatic series (4), where both product ions resulting from cleavage α to the carbonyl were noted, the present investigation revealed only one α-cleavage product, (*b*) (Scheme 4). The preferred α-cleavage to give ion (*b*) is probably due to

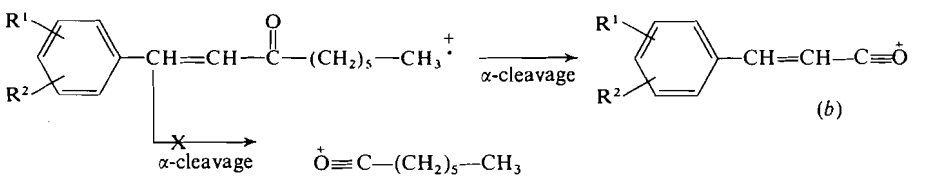

m/e 113

SCHEME 4

[3]It has been shown that the McLafferty product does not ketonize in cyclic ketones (11), malonic esters (11), and substituted barbituric acids (12).

Can. J. Chem. Downloaded from www.nrcresearchpress.com by 210.87.254.40 on 09/05/12
For personal use only.

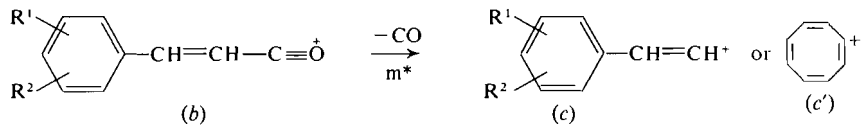

SCHEME 5

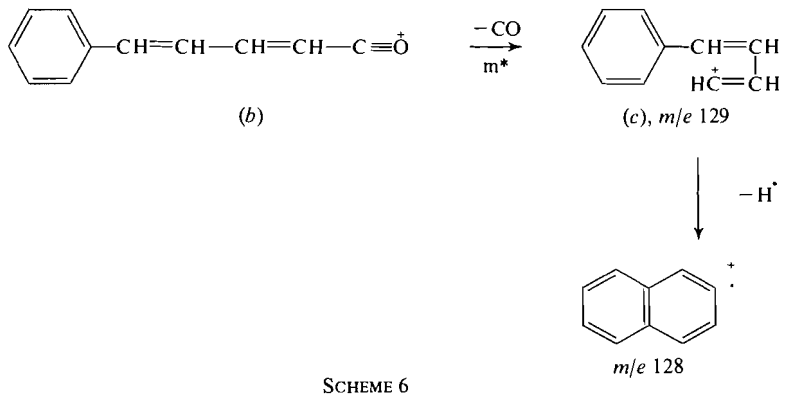

SCHEME 6

the fact that (*b*) is considerably more stable than the ion at *m/e* 113. In fact, ion (*b*) represented the base peak in all the spectra determined except for substrate **5**, the 2,6-dichloro compound which had as its base peak, the M-Cl ion. A metastable ion was observed for the above α-cleavage process only in the spectra of compounds **8**–**10**.

A fragmentation pathway common to all of the compounds studied, as confirmed by the appropriate metastable peaks, was the conversion of ion (*b*) to ion (*c*) or (c^1) (Scheme 5). Such a process leading to a vinylic cation, (*c*), was expected to be unfavorable. The results can be rationalized in terms of the structure (c^1) and as well by the favorable loss of the neutral molecule, carbon monoxide.

The formation of an ion of structure (*c*), *m/e* 129, in the case of compound **10** resulted in the facile loss of a hydrogen atom to form an ion at *m/e* 128, probably possessing a naphthalene structure (Scheme 6).

Ion (*c*), *m/e* 103, formed during the fragmentation of compounds **1** and **8**, confirmed by the appropriate metastable ions, lost C_2H_2 to give the relatively intense ion, $C_6H_5^+$. The corresponding ions, (*c*) *m/e* 137, however, from the mono chloro substrates; *i.e.*, **2**, **3**, and **9**, decomposed by first losing Cl· or HCl followed by a subsequent loss of acetylene. Both steps of this fragmentation route were confirmed by metastable ions. It is noteworthy that the ion (*c*), derived from **7**, the dimethylamino compound, is reasonably stable as evidenced by very little subsequent fragmentation from this ion. This could be due to the electron-donating power of the para-dimethylamino function.

Ion (*c*), *m/e* 171, derived from the dichloro substituted compounds, first lost a chlorine atom to give an ion at *m/e* 136 as confirmed by a metastable ion. Loss of a hydrogen from *m/e* 136 yields an ion at *m/e* 135 which subsequently loses HCl to give an ion at *m/e* 99 as shown by a metastable peak. The ion at *m/e* 101 resulting from the loss of the two halogens from (*c*), *m/e* 171, decomposed by loss of C_2H_2 to give $C_6H_5^+$.

As expected for those compounds with six carbon atom side chains, compounds **1**–**7** and compound **10**, an ion produced by γ-cleavage was observed, M-C_3H_7, as well as the appropriate metastable peak. Peaks observed in all the spectra except for compounds **8** and **9** at *m/e* 43 and 41 probably arise from the hydrocarbon side chain. Such peaks are absent in

Can. J. Chem. Downloaded from www.nrcresearchpress.com by 210.87.254.40 on 09/05/12
For personal use only.

TABLE 1. Substituted 1-phenyl-1-nonen-3-ones

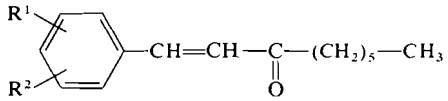

Compound	R^1	R^2	b.p. (°/mm)	Recrystallization solvent	m.p. (°C)	Yield (%)	Found (%) C	Found (%) H	Calcd. (%) C	Calcd. (%) H
1*	H	H	133–134/0.8	MeOH	34	29	83.19	9.31	83.28	9.32
2†	2-Cl	H	122/0.15	—	—	65	71.59	7.70	71.84	7.64
3	4-Cl	H		Me_2CO	59–60	39	71.99	7.51	71.84	7.64
4	2-Cl	4-Cl		MeOH	47	50	63.42	6.40	63.17	6.36
5‡	2-Cl	6-Cl	139/0.35	—	—	60	63.18	6.50	63.17	6.36
6	3-Cl	4-Cl		Petroleum ether (b.p. 40–60°)	39–41	38	63.30	6.31	63.17	6.36
7§	4-$N(CH_3)_2$	H		EtOH	75.5–76	48	78.52	9.86	78.72	9.72

*Literature (13) m.p. 34°.

†The yield of 1-(*o*-chlorophenyl)-1-nonen-3-one was determined by g.l.c. on the crude product mixture. Two distillations under reduced pressure followed by distillation of the purest fractions through an air condenser packed with 10 cm of Raschig rings furnished the analytical sample.

‡The yield of 1-(2,6-dichlorophenyl)-1-nonen-3-one was determined as for **2**. A second distillation of the purest fraction through a 10 cm Vigreaux column gave pure **5**.

§Compound **7** was prepared by the literature method. Reported m.p. 77–78° (52%) (14).

the spectra of **8** and **9** which do not have the appropriate number of carbon atoms in the alkyl group.

Experimental

Mass spectra were determined by Mr. D. Bain with an MS-12 mass spectrometer operating at 70 eV and an ion source temperature of 100°. The samples were introduced via the direct probe technique. Melting points and boiling points are uncorrected. Microanalyses were performed by Dr. F. B. Strauss, Microanalytical Laboratories, Oxford, England and Mr. R. M. Smith of the College of Pharmacy, University of Saskatchewan, Saskatoon. Gas–liquid chromatography was performed on a Pye Series 104 Gas Chromatograph equipped with a flame ionization detector. The glass column (5 ft × 0.25 in. o.d.) was packed with 4% SE-30 on acid washed and silanized 100/120 mesh Chromosorb W. The column temperature ranged from 110–250° and the nitrogen flow rate was 50 ml/min.

*General Procedure for the Preparation of Substituted 1-Phenyl-1-nonen-3-ones (Table 1, **1–6**)*

A mixture containing 2-octanone (0.60 mol), the appropriate aromatic aldehyde (0.50 mol), sodium hydroxide (0.25 mol), and water (300 ml) was heated under reflux with vigorous mechanical stirring for 24 h. After cooling to room temperature, the mixture was extracted with benzene, the organic extracts were washed with water and dried ($MgSO_4$). The benzene was evaporated *in vacuo* to give a crude product and unreacted aldehyde and 2-octanone were removed by distillation. The residue was purified by repeated distillation or recrystallization.

*1-Phenyl-1-penten-3-one (**8**)*

This compound was prepared from 2-butanone and benzaldehyde by the general method described previously. Four recrystallizations from petroleum ether (b.p. 40–60°) gave pure **8** (35%); m.p. 38–40°; lit. (15) m.p. 38–39°.

Anal. Calcd. for $C_{11}H_{12}O$: C, 82.46; H, 7.55. Found: C, 82.43; H, 7.41.

*1-(p-Chlorophenyl)-1-penten-3-one (**9**)*

The title compound was prepared (25%) by the general procedure described earlier (12 h reflux with mechanical stirring). Five recrystallizations from isopropanol gave the analytical sample, m.p. 77°.

Anal. Calcd. for $C_{11}H_{11}ClO$: C, 67.87; H, 5.70. Found: C, 67.95; H, 5.71.

*1-Phenyl-1,3-undecadien-5-one (**10**)*

A solution of sodium ethoxide (10% w/v, 10 ml) was added with vigorous mechanical agitation to a mixture of cinnamaldehyde (0.15 mol) and 2-octanone (0.15 mol) at 0°. The reaction mixture was stirred for 3 h, cooled to −10° for 48 h, and then water (100 ml) was added. The mixture was extracted with ether, washed with water, and dried ($MgSO_4$). Removal of the solvent *in vacuo* gave crude **10** as a yellow powder. Three recrystallizations from ether gave pure **10** (37%) as colorless crystals, m.p. 75–77°; lit. (16) m.p. 68°.

Anal. Calcd. for $C_{17}H_{22}O$: C, 84.25; H, 9.15. Found: C, 84.00; H, 9.12.

The authors wish to thank the National Research Council for a grant enabling the purchase of a A.E.I. MS-12 mass spectrometer to be made. One of the authors (W.G.T.) thanks the Medical Research Council for providing a studentship and financial support was also provided by Smith Kline and French Laboratories of Philadelphia, Pennsylvania. Our thanks are also extended to Mr. G. B. Baker and Miss J. L. McGillivray of the College of Pharmacy who prepared two of the compounds described in this work.

Can. J. Chem. Downloaded from www.nrcresearchpress.com by 210.87.254.40 on 09/05/12
For personal use only.

1. H. BUDZIKIEWICZ, C. DJERASSI, and D. H. WILLIAMS. Mass spectrometry of organic compounds. Holden-Day, San Francisco, 1967. Chapt. 3.
2. C. FENSELAU, W. G. DAUBEN, S. W. SHAFTER, and N. D. VIETMEYER. J. Am. Chem. Soc. **91**, 112 (1969).
3. A. J. BOWLES, E. F. H. BRITTAIN, and W. O. GEORGE. Org. Mass Spectrom. **2**, 809 (1969).
4. Y. M. SHEIKH, A. M. DUFFIELD, and C. DJERASSI. Org. Mass Spectrom. **4**, 273 (1970).
5. T. POSNER. Ber. **35**, 799 (1902).
6. T. POSNER. Ber. **37**, 502 (1904).
7. J. R. DIMMOCK, P. L. CARTER, and P. D. RALPH. J. Chem. Soc. B, 698 (1968).
8. J. R. DIMMOCK and W. G. TAYLOR. Details of the antineoplastic activity of these compounds against lymphoid leukaemia in mice and other pharmacological properties will be reported elsewhere.
9. U. CLAUSEN, H.-W. FEHLHABER, and K. KORTE. Tetrahedron, **22**, 3535 (1966).
10. J. RONAYNE, D. H. WILLIAMS, and J. H. BOWIE. J. Am. Chem. Soc. **88**, 4980 (1966).
11. J. K. MACLEOD, J. B. THOMSON, and C. DJERASSI. Tetrahedron, **23**, 2095 (1967).
12. A. M. DUFFIELD and O. BUCHARDT. Org. Mass Spectrom. **3**, 1043 (1970).
13. I. M. HEILBRON and F. IRVING. J. Chem. Soc. 931 (1929).
14. A. T. NIELSON and H. J. DUBIN. J. Org. Chem. **28**, 2120 (1963).
15. C. HARRIES and G. H. MÜLLER. Ber. **35**, 966 (1902).
16. Z. ZAFIRIADIS. Compt. rend. **230**, 452 (1950).

Can. J. Chem. Downloaded from www.nrcresearchpress.com by 210.87.254.40 on 09/05/12
For personal use only.

Isomeric Pyrimidone and Uracil Derivatives Obtained by Reaction of Barbiturates with Diazomethane[1]

G. A. NEVILLE AND H. W. AVDOVICH

Research Laboratories, Food and Drug Directorate, Department of National Health and Welfare, Ottawa, Canada

Received June 25, 1971

A re-examination of some recently reported studies by Ito *et al.* (1) of the action of diazomethane on barbituric acid, 1-methylbarbituric acid, and 5-ethyl- and 5-phenylbarbituric acids has resulted in the assignment of structures for some of the various possible positional isomers. These reactions were found to be more complex than previously indicated.

Les récentes études effectuées par Ito *et al.* (1) sur l'action du diazométhane sur l'acide barbiturique, l'acide méthyl-1 barbiturique, et sur les acides éthyl-5 et phényl-5 barbituriques, ont été réexaminées dans le but d'attribuer des structures à quelques uns des nombreux isomères de position possibles. Ces réactions semblent beaucoup plus complexes qu'on l'avait d'abord supposé.

Canadian Journal of Chemistry, **50**, 880 (1972)

Introduction

In a recent paper, Ito *et al.* (1) reported some results from the methylation of barbituric acid and its *N*-methyl, 5-alkyl, and 5,5-dialkyl derivatives with diazomethane. Unfortunately these workers encountered many of the same difficulties regarding structural assignment of the various possible isomeric pyrimidone and uracil derivatives formed on reaction of these barbiturates with diazomethane as we had experienced earlier with similar treatment of 1,5-dialkylbarbituric acids (2, 3). Although many new *O*-methyl and *N*-methyl derivatives of the tautomeric barbiturates are formed in these reactions, their positional isomerism is not easily elucidated from the usual p.m.r., i.r., and mass spectral data, and they are not easily or unambiguously obtained by alternative syntheses. It is the purpose of this communication to compare our findings with those of the Japanese workers and to reassess their structural conclusions on the basis of solvent and shift reagent studies of the various products by p.m.r. spectrometry.

In arriving at these structural assignments, use has been made of the relatively new paramagnetic shift reagent, tris-(dipivalomethanato)europium, $Eu(DPM)_3$, (4–6) and of the somewhat more common solvent effects in p.m.r. spectrometry. It appears, however, that this is the first example of the application of these techniques for structural elucidation of substituted pyrimidines. Various applications of the $Eu(DPM)_3$ shift reagent have been reviewed recently (7) together with an interpretation of the effect in terms of reversible complexation leading to pseudocontact shifts. In contrast, the magnitude and sign of proton resonance solvent shifts have been rationalized by means of reference plane rules (8–10) based on studies of various ketones and ethers. These rules have been generalized (11, 12): protons lying in front of the plane will tend to be deshielded in benzene (relative to an "inert" solvent) while those behind the plane will tend to be shielded in benzene. The shifts ($\Delta = \delta CCl_4 - \delta C_5H_5N$ p.p.m.) observed for pyridine are in general more negative than the corresponding benzene-induced shifts (13). The carbonyl plane "rule" is also applicable to pyridine-induced solvent shifts in some ketones (14), but the reference plane is displaced so that it passes through the α-carbons rather than the carbonyl carbon (13).

Some use has been made of the solvent shifts for methoxy-group resonances induced by trifluoroacetic acid (TFA) (15, 16) as an aid to structural elucidation. The downfield shift by TFA ($\Delta = \delta CCl_4 - \delta TFA$ p.p.m.) for methoxy-group resonances of several methoxybenzenes has been attributed to protonation of the methoxy-group (15) whereas with flavones protonation by TFA at both methoxy and carbonyl groups has been proposed (16).

[1]Presented at the 54th Annual Chemical Institute of Canada Conference, Halifax, Nova Scotia, June 1, 1971.

Can. J. Chem. Downloaded from www.nrcresearchpress.com by 210.87.254.42 on 09/05/12
For personal use only.

Can. J. Chem. Downloaded from www.nrcresearchpress.com by 210.87.254.42 on 09/05/12
For personal use only.

TABLE 1. Chemical shifts in p.p.m. downfield from TMS internal reference

Compound **1**	Solvent	H(C-5)	MeO (C-6)	N_1-Me	N_3-Me
a	TFA	5.63	4.08	—	—
b	TFA	5.70	4.13	3.50	—
*b**	$CDCl_3$	5.05	3.90	3.30	—
b	$\Delta_{TFA}^{CDCl_3}$	−0.65	−0.23	−0.20	—
c	$CDCl_3$	5.72	3.87	—	3.48
c	0.24 *M* $CDCl_3$ 0.031 *M* $Eu(DPM)_3$	−1.36	−0.21	—	−1.22
c	$\Delta_{TFA}^{CDCl_3}$	−0.62	−0.30	—	−0.38
d	$CDCl_3$	5.10	3.87	3.30	3.33
d	0.55 *M* $CDCl_3$ 0.041 *M* $Eu(DPM)_3$	−1.02	−0.58	−0.57	−0.70
d	CCl_4	4.93	3.87	3.18	3.27
d	C_6H_6	4.70	3.30	2.78	2.82
d	$\Delta_{C_6H_6}^{CCl_4}$	+0.23	+0.57	+0.40	+0.45
d	C_5H_5N	5.03	3.62	3.15	3.35
d	$\Delta_{C_5H_5N}^{CCl_4}$	−1.10	+0.25	+0.03	−0.08
d	TFA	5.93	4.18	3.58	3.60
d	$\Delta_{TFA}^{CCl_4}$	−1.00	−0.31	−0.40	−0.33

*Insoluble in benzene and too poorly soluble in $CDCl_3$ for use of $Eu(DPM)_3$.

TABLE 2. Chemical shifts in p.p.m. downfield from TMS internal reference for **1***e*

Solvent	H(C-5)	MeO (C-6)	$CH_2(N_1Et)$	$CH_2(N_3Et)$	$CH_3(N_1Et)$	$CH_3(N_3Et)$
$CDCl_3$	5.07	3.85	3.92	3.97	1.22	1.22
0.047 *M* $CDCl_3$ 0.011 *M* $Eu(DPM)_3$	−1.20	−0.05	−0.56	−1.55	−0.25	−0.73
CCl_4	4.93	3.87	3.85	3.88	1.15	1.20
C_6H_6	4.75	2.85	3.58	4.08	0.93	1.23
$\Delta_{C_6H_6}^{CCl_4}$	+0.18	+1.02	+0.27	−0.20	+0.22	−0.03
C_5H_5N	5.05	3.67	3.82	4.08	1.08	1.23
$\Delta_{C_5H_5N}^{CCl_4}$	−0.12	+0.20	+0.03	−0.20	+0.07	−0.03

Results

Methylation of Barbituric Acid and N-Alkyl Derivatives

When Ito *et al.* (1) treated a cold suspension of barbituric acid in ether with diazomethane for 10 min, they obtained as their major product (74%) a substance (m.p. 224–225° dec.) which they claimed to be 1-methyl-6-methoxyuracil (**1***b*) solely on the basis of p.m.r. spectral data in trifluoroacetic acid (TFA). We have also obtained this substance as the major derivative under similar conditions based on the similarity of chemical shift data in TFA; however, our material melts nearly 10° higher. Chemical shift data (Table 1) from solvent studies on both this compound and the isomeric *N*-methyl analog **1***c* indicate that **1***b* is the correct structure for this compound.

TABLE 3. Chemical shifts in p.p.m. downfield from TMS internal reference for **2**

Solvent	H(C-5)	OMe (C-2)	OMe (C-6)	N-Me
CCl_4	5.22	4.00	3.80	3.28
$CDCl_3$	5.43	4.03	3.83	3.37
$\Delta_{0.031\ M\ Eu(DPM)_3}^{0.20\ M\ CDCl_3}$	−1.40	−0.30	−0.15	−1.30
$\Delta_{C_6H_6}^{CCl_4}$	−0.32	+0.70	+0.82	−0.05
$\Delta_{TFA}^{CCl_4}$	−1.02	−0.35	−0.37	−0.43

In addition to the above compound, we obtained a second derivative (2%), not reported by the Japanese workers, which was shown to be 1,2-dihydro-2,6-dimethoxy-3-methyl-4-oxopyrimidine (**2**) by comparison of p.m.r. spectra (Table 3) with those of the same compound obtained by isomerization of *sym*-tri-

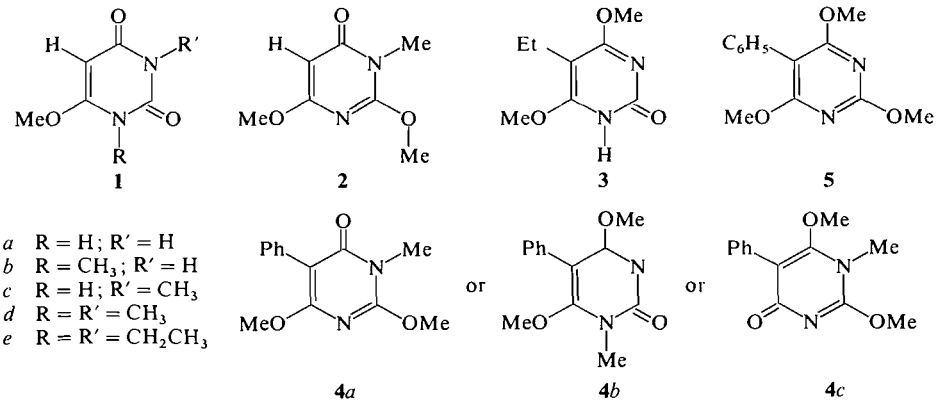

a R = H; R′ = H
b R = CH_3; R′ = H
c R = H; R′ = CH_3
d R = R′ = CH_3
e R = R′ = CH_2CH_3

1 **2** **3** **5** **4***a* **4***b* **4***c*

TABLE 4. Chemical shifts in p.p.m. downfield from TMS internal reference for **3***

Solvent	CH_3(Et)	CH_2(Et)	OMe (C-6)	OMe (C-4)	N-H
$CDCl_3$	1.05(t)	2.45(q)	3.95(a)	3.98(a)	10.0
TFA	1.15(t)	2.63(q)	4.25(b)	4.25(b)	—
$\Delta_{TFA}^{CDCl_3}$	−0.10	−0.18	−0.30	−0.27	
C_5H_5N	1.27(t)	2.75(q)	3.83(c)	3.85(c)	—
$\Delta_{C_5H_5N}^{CDCl_3}$	−0.22	−0.30	+0.12	+0.13	

*(a), $\Delta\delta = 0.04$; (b), $\Delta\delta = 0.01$; (c), $\Delta\delta = 0.02$; (t) = triplet, (q) = quartet.

methoxypyrimidine with methyl iodide. We also isolated a small quantity (10%) of 6-methoxyuracil (**1***a*) (m.p. 264–269° dec.) which was not found in this reaction by the Japanese workers. The same *O*-monomethyl compound was reported much earlier by Arndt (17) to be formed from barbituric acid with diazomethane.

Treatment of 1,3-dimethylbarbituric acid and 1,3-diethylbarbituric acid with excess diazomethane gives 1,3-dimethyl-6-methoxyuracil (**1***d*), first prepared by Biltz and Wittek (18), and 1,3-diethyl-6-methoxyuracil (**1***e*), a new derivative. Whereas the chemical shift data for 1,3-dimethyl-6-methoxyuracil (**1***d*) (Table 1) and 1,3-diethyl-6-methoxyuracil (**1***e*) (Table 2) confirm the expected structures, the relatively small differences in chemical shift between the protons of the *N*-alkyl substituents provide little assurance for the assignment of frequencies to the appropriate *N*-alkyl group.

In contrast to the Japanese workers who reported that treatment of 1-methylbarbituric acid with excess diazomethane over a 2 h period yields a mixture of 3-methyl-6-methoxyuracil (**1***c*)(77%), 1-methyl-6-methoxyuracil(**1***b*)(15%), and 1,3-dimethyl-6-methoxyuracil (**1***d*) (3%), we found that similar treatment of 1-methylbarbituric acid gives 1,3-dimethyl-6-methoxyuracil (**1***d*) as the major product. Again, the p.m.r. spectral evidence provided by Ito *et al.* (1) serves only to differentiate the two compounds **1***b* and *c*, but it remains inadequate as the sole basis of the assignment of structure to these positional isomers.

Methylation of 5-Ethyl- and 5-Phenylbarbituric Acid

The main product of the action of excess diazomethane on 5-ethylbarbituric acid for a 10 min period is 4,6-dimethoxy-5-ethylpyrimidone-2 (**3**) as previously reported (1). Our chemical shifts for **3** in TFA (Table 4) are identical with those reported by the Japanese workers; however, we were able to establish the non-equivalence of the two methoxy groups of **3** in TFA by scanning with the 100 Hz sweep width and confirmed the non-equivalence by observing slightly larger differences in the chemical shifts in $CDCl_3$ and pyridine solution.

On treating 5-phenylbarbituric acid overnight with excess diazomethane, Ito *et al.* (1) obtained a product (**4**) in low yield which they recognized

Can. J. Chem. Downloaded from www.nrcresearchpress.com by 210.87.254.42 on 09/05/12
For personal use only.

TABLE 5. Chemical shifts in p.p.m. downfield from TMS internal reference

Compound	Solvent	N_1-Me	OMe (C-2)	OMe (C-4)	Ar-H	OMe (C-6)
4*a*	CCl_4	3.35	3.85	4.00	7.30*	—
4*a*	C_6H_6	3.03	3.35	3.50	—	—
4*a*	$\Delta^{CCl_4}_{C_6H_6}$	+0.32	+0.50	+0.50		
4*a*	TFA	3.83	4.17	4.42	7.43*	—
4*a*	$\Delta^{CCl_4}_{TFA}$	−0.48	−0.32	−0.42	−0.13	
4*a*	$CDCl_3$	3.40	3.87	4.03	7.37*	—
4*a*	0.35 *M* $CDCl_3$	4.33	4.13	4.27	7.38*(3H)	—
	0.046 *M* $Eu(DPM)_3$				8.18*(2H)	—
5	$CDCl_3$	—	3.98	3.88	6.85	3.88

*Broad multiplet.

to be an *N,O,O*-trimethyl derivative. Although this compound was characterized by melting point, microanalysis, u.v., and p.m.r. spectra, these workers were not able to assign one of the three possible structures **4***a*, *b*, or *c* to the new derivative. In repeating this work, we also obtained **4** as the major product for which we have assigned the structure **4***a* on the basis of solvent and reagent shift studies (Table 5). In addition, we obtained 2,4,6-trimethoxy-5-phenylpyrimidine (**5**) as a minor product.

Discussion

Assignment of Structures

The compounds 1-methyl-6-methoxyuracil (**1***b*) and 3-methyl-6-methoxyuracil (**1***c*) were readily differentiated, and their structures were confirmed on the basis of solvent and shift reagent studies. In these compounds, the carbonyl oxygen at C-4 is expected from electronic considerations to be more favored for protonation than the ureido oxygen, and some evidence for protonation in such systems has been reported (19). From the chemical shift data (Table 1), it is seen that the largest downfield shifts in TFA relative to $CDCl_3$ ($\Delta^{CDCl_3}_{TFA}$) are given by the C-5 protons in each of **1***b* and *c* consistent with the above hypothesis. In addition, the methyl protons at N-3 of **1***c* show the next largest $\Delta^{CDCl_3}_{TFA}$ downfield shift appropriate to their proximity to a center inductively favored for development of positive charge. Because these properties also favor the C-4 oxygen as the donor for pseudocontact complexation (7) with $Eu(DPM)_3$, the marked deshielding of the C-5 and N-3 protons of **1***c* by $Eu(DPM)_3$, relative to their chemical shifts in $CDCl_3$, confirms the structure for 3-methyl-6-methoxyuracil (**1***c*).

The major product obtained by isomerization of *sym*-trimethoxypyrimidine with methyl iodide, which was also shown to be identical to a minor derivative resulting from methylation of barbituric acid, was deduced to have the structure 1,2-dihydro-2,6-dimethoxy-3-methyl-4-oxopyrimidine (**2**) from consideration of various solvent effects (Table 3) in addition to the shifts induced by $Eu(DPM)_3$. The relatively large and nearly equal upfield shifts for the C-2 and -6 methoxy protons of **2** in benzene relative to carbon tetrachloride ($\Delta^{CCl_4}_{C_6H_6}$) together with the smaller downfield shifts for the C-5 and N-methyl protons of **2** are compatible with the generalized reference plane rules for benzene solvent effects (11, 12). Additional support for the assignment of structure **2** to the major isomerized product is provided by the $\Delta^{CCl_4}_{TFA}$ downfield shifts (Table 3) which are largest for the C-5 and *N*-methyl protons consistent with the view that the C-4 oxygen is favored for protonation. On the same basis, complexation involving the C-4 oxygen with $Eu(DPM)_3$ would be expected to result in large downfield shifts for the C-5 and *N*-methyl protons of **2** as confirmed by the data in Table 3.

Only three possible positional isomers, **4***a*, *b*, or *c*, may be written for the major *O,O*-dimethyl-*N*-methyl derivative isolated from the reaction of 5-phenylbarbituric acid with diazomethane. The benzene solvent shifts relative to CCl_4 (Table 5) appear to favor **4***c* whereas the TFA solvent shifts tend to support structure **4***a* more than **4***b*. In contrast, the shifts observed with $Eu(DPM)_3$ demonstrate unequivocally

Can. J. Chem. Downloaded from www.nrcresearchpress.com by 210.87.254.42 on 09/05/12
For personal use only.

Can. J. Chem. Downloaded from www.nrcresearchpress.com by 210.87.254.42 on 09/05/12
For personal use only.

that the *N*-methyl and phenyl groups are adjacent to the carbonyl function.

It is also noteworthy that the multiplet character for the phenyl proton signal of **4***a* in $CDCl_3$ alone suggests coplanarity of the phenyl ring with the pyrimidine ring. Addition of $Eu(DPM)_3$ reagent causes the multiplet to appear as two new multiplets integrating for two and three protons, respectively. Since the two proton multiplet is at lowest field, this pattern appears to arise from the two adjacent ring protons that would be proximate to the carbonyl group in the coplanar model.

Frequency Assignment to N-Alkyl Protons and Non-equivalence of Methoxy Groups

Very small differences in chemical shift (p.p.m.) were observed between the two *N*-methyl frequencies of 1,3-dimethyl-6-methoxyuracil (**1***d*) in $CDCl_3$ (0.03), CCl_4 (0.09), C_6H_6 (0.04), C_5H_5N (0.20), and TFA (0.02) (Table 1). These small differences together with the small distinctions afforded by the values for $\Delta^{CCl_4}_{C_6H_6}$, $\Delta^{CCl_4}_{C_5H_5N}$, and $\Delta^{CCl_4}_{TFA}$ (Table 1) do not provide much assurance for the correct assignment of frequencies to the respective *N*-methyl groups of **1***d*. A similar situation was found to exist for 1,3-diethyl-6-methoxyuracil (**1***e*) (Table 2). In assigning these frequencies initially, the protons of the alkyl group at N_3 in both **1***d* and *e* were assumed to be in a more deshielding environment than those at N_1. These frequency assignments were then checked for consistency of their induced shifts by studying the effect of the $Eu(DPM)_3$ shift reagent on the N_3-alkyl and C-5 protons where the largest deshielding effects were expected for complexation at the C-4 carbonyl oxygen. The correctness of the initial frequency assignments and the assumption on which they were based are supported by the downfield shift of -0.70 p.p.m. for the N_3-methyl protons of 1,3-dimethyl-6-methoxyuracil (**1***d*) which is intermediate in magnitude between the downfield shifts for the C-5 and N_1-methyl protons of **1***d* (Table 1). An even more striking differentiation of the alkyl group frequencies is provided by $Eu(DPM)_3$ with 1,3-diethyl-6-methoxyuracil (**1***e*) where the N_3-methylene protons experience comparable deshielding (-1.55 p.p.m.) to the C-5 proton (-1.20 p.p.m.) in comparison to the N_1-methylene protons (-0.56 p.p.m.). The methyl protons of the N_3-ethyl substituent are similarly clearly distinguished from those of the N_1-ethyl group.

4,6-Dimethoxy-5-ethylpyrimidone-2 (**3**) is an almost symmetrically substituted molecule. Unfortunately the poor solubility of **3** in $CDCl_3$ precludes its study with the $Eu(DPM)_3$ shift reagent as a means of checking the assigned frequencies of the observed non-equivalent methoxy groups. In making the frequency assignments of Table 4, it was assumed that the C-4 methoxy group is in a more deshielded environment than the C-6 methoxy group because of the planar C=N—C=O moiety of the ring. The compound is also too insoluble in either carbon tetrachloride or benzene; thus, the limited chemical shift data are insufficient to settle this mute and interesting fine structural feature.

Experimental

Apparatus

The p.m.r. spectra were obtained with a Varian A-60A spectrometer from solutions (solvents indicated in Tables 1–5) usually 10–15% by weight in solute. No concentration effects were observed upon dilution, and chemical shifts, reported in p.p.m. downfield from tetramethylsilane (TMS) internal reference, are considered accurate to ± 0.02 p.p.m.

Melting point determinations were made either with a Thomas Unimelt capillary apparatus and reported uncorrected or with a precision melting apparatus (20) (prec.) containing Dow 550 fluid and utilizing Anschutz immersion thermometers.

Microanalyses were done by Bernhardt Mikroanalytisches Laboratorium, 5251 Elback uber Engelskirchen, Fritz-PreglStrasse 14–16, West-Germany.

Conditions of Methylation

Ethereal solutions of diazomethane were prepared from Diazald (Aldrich) according to the method of de Boer (21) and used immediately. In studying the methylations reported by the Japanese workers (1), we employed conditions judged to be similar to those indicated; namely, suspensions of reactants in anhydrous diethyl ether at ice-bath temperature were treated with excess cold ethereal diazomethane. We terminated reactions at the indicated time by adding a few drops of acetic acid.

Methylation of Barbituric Acid

Barbituric acid (1.00 g, B.D.H.) in diethyl ether (25 ml) was treated with excess ethereal diazomethane (75 ml) for 10 min.

6-Methoxyuracil (1a)

The solid phase (A) of the reaction mixture was separated from its supernatant liquid (B). On extraction with boiling absolute ethanol (C), phase A provided an insoluble fraction (0.11 g), m.p. 264–269° (dec.), whose structure was established from p.m.r. spectra (Table 1) to be 6-methoxyuracil (**1***a*). No improvement in the melting behavior of **1***a* was obtained following successive recrystallization from water,

Can. J. Chem. Downloaded from www.nrcresearchpress.com by 210.87.254.42 on 09/05/12
For personal use only.

and mass spectral analysis confirmed the expected molecular weight.

*1-Methyl-6-methoxyuracil (**1***b*)

On cooling, the hot supernatant liquid (C) yielded solid m.p. 210–245°. Subsequent recrystallizations from absolute ethanol raised the melting range to 235.5–239° (~50 mg). The p.m.r. spectral data (Table 1) indicated this material to be the same derivative (**1***b*) as reported by the Japanese workers (1) except for our higher melting range. The molecular weight was confirmed by mass spectrometry, and the structural assignment was verified by solvent and reagent shift studies as discussed above. The p.m.r. spectral examination of the mother liquor concentrate from phase C revealed a mixture of **1***a* and *b*.

*1,2-Dihydro-2,6-dimethoxy-3-methyl-4-oxopyrimidine (**2**)*

On rotary evaporation, the major supernatant liquid (B) provided an oil whose p.m.r. spectrum in TFA showed it to be rich in an *N*-methyl-dimethoxy derivative. By extracting an aqueous solution of this oil with carbon tetrachloride and treating the combined extracts with heptane and a little chloroform while employing ice-bath cooling, crystallization was induced. There was just sufficient material obtained for successive p.m.r. spectra in $CDCl_3$ and TFA (Table 3) which, on recovery, showed undepressed melting with admixed **2** obtained by isomerization of *sym*-trimethoxypyrimidine with methyl iodide.

Preparation of sym-Trimethoxypyrimidine

A methanolic solution (25 ml) of 2,4,6-trichloropyrimidine (5.0 g, 0.027 mol, Aldrich) was added in small portions to a freshly prepared solution of sodium methoxide (2.5 g, 0.108 mol, sodium/50 ml methanol). Vigorous exothermic reaction proceeded with precipitation of sodium chloride. The reaction mixture was allowed to cool to room temperature after which it was filtered. The filtrate was evaporated and the resulting residue was treated with chloroform to remove additional inorganic material. The oil obtained by stripping the chloroform crystallized on standing. Two recrystallizations from heptane provided crystals (0.9 g) melting 50–52°; lit. m.p. 53° (22). The p.m.r.: δ($CDCl_3$/TMS) 3.93, s, 6H(OCH_3 at C-4 and -6); 3.98, s, 3H(OCH_3 at C-2); 5.72, s, 1H(C-5).

Isomerization of sym-Trimethoxypyrimidine

sym-Trimethoxypyrimidine (0.75 g, 0.0044 mol, m.p. 50–52°) was dissolved in excess freshly distilled methyl iodide (20 ml), and the solution was heated under reflux for 30 h. The oil obtained after rotary evaporation showed evidence of being a three component mixture. On treatment with hot heptane, this mixture formed a small quantity of insoluble residue (X) while the remainder dissolved in the supernatant liquid (Y). Recrystallization of X from chloroform–petroleum ether gave the minor product of this isomerization identified from p.m.r. and mass spectra as 1,3-dimethyl-6-methoxyuracil (**1***d*) which we also found to be the major product in the 24 h methylation of barbituric acid with diazomethane.

On cooling, the supernatant liquid (Y) deposited a solid (m.p. 85–94°) whose p.m.r. spectra indicated the major compound to be a dimethoxy-monomethyl derivative. The mother liquor from this solid was found to contain mainly starting material and some of the minor product (**1***d*). The basis for assigning the structure 1,2-dihydro-2,6-dimethoxy-3-methyl-4-oxopyrimidine (**2**) to the major isomerization product is provided in the discussion.

Preparation of 1-Methylbarbituric Acid

Diethyl malonate (20 ml, 0.125 mol, n_D^{20} 1.4138, Aldrich) was condensed with methylurea (9.5 g, 0.130 mol, m.p. 82–90°, Aldrich) using freshly prepared sodium ethoxide (5.8 g, 0.252 mol of sodium/160 ml absolute ethanol). When a thick paste formed after the mixture had been heated under reflux for 3 h, the mixture was distilled to remove most of the ethanol. The cooled residue was treated with water (100 ml) then warmed to dissolve the cake. The solution was then acidified (7 ml concentrated H_2SO_4/100 ml H_2O). The solution was extracted with chloroform (4 × 30 ml) and evaporation of the combined extracts gave the crude solid (3.7 g, m.p. 98–115°). Recrystallization from ethanol gave crystals (2.1 g) melting 131.8–132.6° (prec.) lit. m.p. 132–133° (23). The p.m.r. δ($CDCl_3$/TMS): 3.30, s, 3H(N-CH_3); 3.65, s, 2H(C-5); 8.43, b, 1H(NH).

Methylation of 1-Methylbarbituric Acid

1-Methylbarbituric acid (0.5 g, m.p. 131.8–137.6°) in diethyl ether (25 ml) was treated with excess ethereal diazomethane (75 ml) over a 2 h period. The solid phase (A) of the reaction mixture was separated from the supernatant liquid (B). Solid A (70 mg) melted broadly and showed no improvement after recrystallization from ethanol. The p.m.r. spectra of the material in TFA indicated a complex mixture of several minor components.

*1,3-Dimethyl-6-methoxyuracil (**1***d*)*

Rotary evaporation of supernatant liquid (B) gave solid (430 mg, m.p. 120–145°) shown by p.m.r. spectra to be rich in 1,3-dimethyl-6-methoxyuracil (**1***d*). Subsequent recrystallization from chloroform–petroleum ether gave material (250 mg, m.p. 156–160°) which was confirmed by p.m.r. (Table 1) and mass spectra to be 1,3-dimethyl-6-methoxyuracil (**1***d*) and identical to that reported by Ito *et al.* (1) and by Biltz and Wittek (24).

Preparation of 5-Ethylbarbituric Acid

Diethyl ethylmalonate (20.0 g, 0.106 mol, n_D^{20} 1.4164, Aldrich) was condensed with urea (6.5 g, 0.108 mol) using freshly prepared sodium ethoxide (4.95 g, 0.219 mol of sodium/130 ml absolute ethanol). A thick paste formed during 4 h heating under reflux. The mixture was filtered while still warm, and the solid was dissolved in hot water (40 ml) and acidified to Congo red with concentrated hydrochloric acid. The instantly formed precipitate was recrystallized from boiling water to obtain solid (7.8 g) melting 193.0–194.0 (prec.); lit. m.p. 190° (25); 193–194° (26). The p.m.r. δ(TFA/TMS): 1.13, t, 3H(CH_3 of Et); 2.37, m, 2H(CH_2 of Et); 3.77, t, 1H(C-5); 9.95, b, 2H(NH); $J_{CH_2CH_3}$ = 7.0; J_{H_5,CH_2} = 3.4 Hz.

Methylation of 5-Ethylbarbituric Acid

5-Ethylbarbituric acid (1.00 g, m. 193–194°) in diethyl ether (25 ml) was treated with excess ethereal diazomethane (75 ml) during a ten minute interval. The reaction mixture was separated into a solid phase (M) and the supernatant liquid (N).

*4,6-Dimethoxy-5-ethylpyrimidone-2 (**3**)*

Pulverization of the solid phase (M) with chloroform left an insoluble fraction which was shown to be mainly

Can. J. Chem. Downloaded from www.nrcresearchpress.com by 210.87.254.42 on 09/05/12
For personal use only.

starting material. On evaporation, the chloroform extract gave solid (25 mg, m. 203–213°, dec.) whose p.m.r. spectra (Table 4) showed the compound to be 4,6-dimethoxy-5-ethylpyrimidone-2 (**3**) and identical to that reported by Ito *et al.* (1) except that non-equivalence of the two methoxy groups was observed in TFA, $CDCl_3$, and pyridine solution.

Exploratory investigation of the supernatant liquid (N) revealed a mixture of *N*-methylated derivatives present in very small quantity.

Preparation of 5-Phenylbarbituric Acid

Diethyl phenylmalonate (20.0 g, 0.0846 mol, n_D^{20} 1.4913, Aldrich) was condensed with urea (5.1 g, 0.090 mol) using freshly prepared sodium ethoxide (3.9 g, 0.170 mol of sodium/150 ml absolute ethanol). After 1½ h heating under reflux, a thick paste formed. The mixture was acidified while still warm to p*H* ~ 2 with 20% aqueous HCl (~ 100 ml). The remaining insoluble material was collected and found to melt at 252–257°. The p.m.r. δ(DMSO-d_6/TMS): 4.83, b, 1H(C-5); 7.37, s, 5H(C_6H_5); 11.3, b, 2H(NH). When the product could not be recrystallized from boiling water, ethanol, methanol, dioxane, glacial acetic acid, acetonitrile or ethyl acetate, a portion of the material was recrystallized from dimethylformamide to obtain a solid, m.p. 255–258°; lit. m.p. 264–266° (27).

Methylation of 5-Phenylbarbituric Acid

5-Phenylbarbituric acid (1.00 g, m.p. 252–257°) in diethyl ether (25 ml) was treated with excess ethereal diazomethane (75 ml) over a 24 h period.

3-Methyl-2,6-dimethoxy-5-phenylpyrimidone-4 (4a)

The reaction mixture was separated into a solid phase (A) (25 mg), which was shown to be starting material, and supernatant liquid (B). Evaporation of B gave a residue which when crystallized from chloroform – petroleum ether gave crystals (0.19 g, m.p. 148–154°) (C) and mother liquor (D). Further recrystallization of C from chloroform – petroleum ether gave solid melting 154–156.5° and having chemical shifts in TFA (Table 5) identical to those reported by Ito *et al.* (1) for their dimethoxy-*N*-methyl derivative (**4***a*, *b*, or *c*) of 5-phenylbarbituric acid. On the basis of solvent and shift-reagent p.m.r. studies, this compound was shown to have structure **4***a*.

Evaporation of mother liquor (D) gave solid (0.5 g) from which the minor product (50 mg), 2,4,6-trimethoxy-5-phenylpyrimidine (**5**) was separated from more of the major derivative, **4***a*, by successive crystallization from heptane.

Preparation of 1,3-Diethylbarbituric Acid

1,3-Diethylbarbituric acid was prepared following the procedure of Biltz and Wittek (24) by heating an acetic acid solution (20 ml) of *sym*-diethylurea (10.0 g, 0.0862 mol, Aldrich) and malonic acid (10.0 g, 0.0962 mol, Aldrich) under reflux on a water bath at 50–60° while acetic anhydride (20 ml, 0.212 mol) was added over a 40 min interval. Heating of the mixture was continued for an additional 6 h after which water (10 ml) was added, and the mixture was heated for ½ h at 70°.

The reaction mixture was distilled at reduced pressure to remove glacial acetic acid and acetic anhydride. The crude residue was dissolved in hot water (40 ml) and acidified with concentrated HCl (1 ml). On cooling in a refrigerator, the solution deposited crystals (1.6 g), m.p. 52.6–53.4° (prec.); lit. m.p. 52° (24). The p.m.r. δ($CDCl_3$/TMS): 1.22, t, 6H(CH_3 of NEt); 3.63, s, 2H(C-5); 3.93, q, 4H(CH_2 of NEt); $J_{CH_2CH_3}$ = 7.3 Hz.

Preparation of 1,3-Diethyl-6-methoxyuracil (1e)

1,3-Diethylbarbituric acid (0.50 g, 0.0027 mol, m.p. 52.6–53.4°) was dissolved in methanol (25 ml) at ice-bath temperature and treated with cold ethereal diazomethane (120 ml). Reaction was immediate and upon reaching completion with excess diazomethane, the mixture was evaporated to obtain an oil. Crystals (m.p. 56–63°) were obtained from a chloroform – petroleum ether solution of the oil during slow evaporation. Recrystallization of the solid from heptane gave crystals melting 68.2–69.6°; p.m.r. shifts (Table 2).

Anal. Calcd. for $C_9H_{14}N_2O_3$: C, 54.54; H, 7.11; N, 14.13. Found: C, 54.74, 54.74; H, 7.01, 6.94; N, 14.09, 13.92.

1. K. Ito, K. Nishiie, and M. Sekiya. J. Pharm. Jap. **90**, 188 (1970).
2. G. A. Neville. Anal. Chem. **42**, 347 (1970).
3. G. A. Neville. Can. J. Chem. In press.
4. C. C. Hinckley. J. Am. Chem. Soc. **91**, 5160 (1969).
5. J. K. M. Sanders and D. H. Williams. Chem. Commun. 422 (1970).
6. P. V. Demarco, T. K. Elzey, R. B. Lewis, and E. Wenkert. J. Am. Chem. Soc. **92**, 5734 (1970); J. Am. Chem. Soc. **92**, 5737 (1970).
7. J. K. M. Sanders and D. H. Williams. J. Am. Chem. Soc. **93**, 641 (1971).
8. J. D. Connolly and K. McCrindle. Chem. and Ind. 379 (1965).
9. D. H. Williams and N. S. Bhacca. Tetrahedron, **21**, 2021 (1965).
10. C. R. Narayanan and N. R. Bhadane. Tetrahedron Lett. 1557 (1968).
11. R. G. Wilson, D. E. A. Rivett, and D. H. Williams. Chem. and Ind. 109 (1969).
12. K. M. Baker and R. G. Wilson. J. Chem. Soc. B, 236 (1970).
13. J. Ronayne and D. H. Williams. *In* Annual review of NMR spectroscopy. Vol. 2. *Edited by* E. F. Mooney. Academic Press, London. 1969. p. 118.
14. D. H. Williams. Tetrahedron Lett. 2305 (1965).
15. R. G. Wilson and D. H. Williams. J. Chem. Soc. C, 2475 (1968).
16. R. G. Wilson and D. H. Williams. J. Chem. Soc. C, 2477 (1968).
17. F. Arndt. Chem. Abstr. **31**, 1006 (1937).
18. H. Biltz and H. Wittek. Ber. **54**, 1035 (1921).
19. D. Cook. Can. J. Chem. **44**, 335 (1966).
20. E. B. Hershberg. Ind. Eng. Chem. Anal. Ed. **8**, 312 (1936).
21. T. J. De Boer. Rec. Trav. Chim. **73**, 229 (1954).
22. E. Büttner. Ber. **36**, 2227 (1903).
23. T. Ukai, Y. Yamamoto, S. Kanetome. J. Pharm. Soc. Jap. **74**, 674 (1954).
24. H. Biltz and H. Wittek. Ber. **54**, 1035 (1921).
25. M. Conrad and M. Guthzeit. Ber. **15**, 2844 (1882).
26. E. H. Volwiler. J. Am. Chem. Soc. **47**, 2236 (1925).
27. H. J. Morsman. Helv. Chim. Acta, **18**, 1254 (1935).

Photolysis of Ammine and Alkylamine Chromium(III) Complexes in Water and Dimethylsulfoxide: Mechanistic Evidence from Luminescence and Medium Effects[1]

COOPER H. LANGFORD[2] AND LEIGH TIPPING

Department of Chemistry, Carleton University, Ottawa, Canada K1S 5B6

Received September 30, 1971

Photosolvolysis of $Cr(NH_3)_6^{3+}$, $Cr(NH_3)_5Cl^{2+}$, $Cr(CH_3NH_2)_5Cl^{2+}$, and $Cr(CH_3CH_2NH_2)_5Cl^{2+}$ in water and DMSO is described. Phosphorescence of $Cr(NH_3)_6^{3+}$ is completely quenched in base but loss of NH_3 is not. This implies that photosolvolysis arises in the quartet excited state and not the phosphorescent doublet. The increase in ammine quantum yield in DMSO as compared to water can be understood in terms of a tetragonal distortion model for the quartet which also accommodates phosphorescence activation energy data. Unfavorable solvation of Cl^- of $Cr(RNH_2)_5Cl^{2+}$ (R = H, CH_3, CH_3CH_2) after tetragonal distortion can also explain the reversal of solvent effect in these systems wherein quantum yields are lower in DMSO than in water for both release of RNH_2 and Cl^-.

On décrit ici la photosolvolyse de $Cr(NH_3)_6^{3+}$, $Cr(NH_3)_5Cl^{2+}$, $Cr(CH_3NH_2)_5Cl^{2+}$, et $Cr(CH_3CH_2NH_2)_5Cl^{2+}$ dans l'eau et le DMSO. La phosphorescence de $Cr(NH_3)_6^{3+}$ est complètement empêchée dans la base, mais la perte de NH_3 ne l'est pas. Cela implique que la photosolvolyse a son origine de l'état excité quadruplet et non pas du doublet phosphorescent. L'augmentation du rendement quantique d'amine dans le DMSO telle que comparée à l'eau peut être expliquée en termes de modèle à distorsion tétragonale pour le quadruplet, ce qui concorde bien avec les données d'énergie d'activation de la phosphorescence. Une solvatation défavorable de l'ion Cl^-, du $Cr(RNH_2)_5Cl^{2+}$ (R = H, CH_3, CH_3CH_2) après distorsion tétragonale peut aussi expliquer le renversement de l'effet de solvant dans ces systèmes où les rendements quantiques sont plus faibles dans le DMSO que dans l'eau et où dans les deux cas on a dégagement de RNH_2 et Cl^-.

Canadian Journal of Chemistry, **50**, 887 (1972)

Introduction

For some years now, there has been an active interest in photosubstitution reactions of Cr(III) complexes. (A comprehensive review considering in detail most of the observations noted briefly in this introduction will be found in ref. 1.) Quite a number of complexes of local O_h symmetry undergo remarkably comparable photosubstitution reactions under irradiation in their first quartet bands. Examples include $Cr(OH_2)_6^{3+}$ photoexchange with a quantum yield, ϕ, of ~ 0.1; $Cr(NCS)_6^{3-}$ with a photoaquation yield, ϕ, ~ 0.3; and $Cr(NH_3)_6^{3+}$ with $\phi \sim 0.4$. The approximate wavelength independence of such yields early led Schlafer's group and Plane's group to suggest that reaction was from the low lying ^2E state reached by intersystem crossing. This idea is satisfactory to account for reactions of O_h complexes, but Adamson has emphasized its inadequacy for mixed ligand complexes. In these systems, there is large selectivity with respect to which ligand is lost, and some evidence of wavelength dependence of ratios of yields for different reaction modes has been presented. Adamson emphasizes that, at the least, some reaction via the lowest quartet ($^4T_{2g}$ in O_h symmetry) is required to explain such results.

Chen and Porter (2) have recently observed that only 50% of the thiocyanate yielded from *trans* $Cr(NH_3)_2(NCS)_4^-$ can be quenched by the doublet quenching reagent $Cr(CN)_6^{3-}$. This observation provides essentially conclusive evidence for 50% of the thiocyanate loss occurring from the quartet prior to intersystem crossing. Moreover, Porter suggests that the quenched thiocyanate yield may originate from the thermal repopulation of the quartet. The solvent and temperature dependence of phosphorescence intensity from several Cr(III) complexes in solution has recently been reported from this laboratory (3). The results lend suggestive support to Porter's idea since they show that a principal pathway of doublet relaxation has an activation energy of 8 to 14 kcal mol^{-1} and is most plausibly assigned to quartet repopulation.

To complete our introduction, we note one more central fact about ammine complexes like $Cr(NH_3)_5Cl^{2+}$. The selectivity in photoaqua-

[1]We thank the National Research Council for generous financial support.

[2]To whom correspondence should be addressed.

Can. J. Chem. Downloaded from www.nrcresearchpress.com by 210.87.254.5 on 09/05/12
For personal use only.

Can. J. Chem. Downloaded from www.nrcresearchpress.com by 210.87.254.5 on 09/05/12
For personal use only.

tion is the reverse of selectivity in thermal aquation. In photosubstitution, ammine yields are much higher than chloride yields. This report considers the problems of photolysis $Cr(NH_3)_6^{3+}$, $Cr(NH_3)_5Cl^{2+}$, and $Cr(NH_2R)_5Cl^{2+}$ as they depend upon the change of solvent from H_2O to $(CH_3)_2SO$ (DMSO), a change leading to increase in phosphorescence intensity from $Cr(NH_3)_6^{3+}$, and as they depend upon changing pH from 3 to 12 which leads to quenching of $Cr(NH_3)_6^{3+}$ phosphorescence.

Experimental

Synthesis of Complexes

The preparation of chloropentakisalkylaminechromium(III) followed ref. 4. The purity of the compounds was confirmed by comparing spectra with those previously reported (5). The hexammine chromium(III) nitrate had previously been prepared. Its purity was confirmed spectrophotometrically (6).

Irradiation and Actinometry

The irradiation apparatus has been described (7). Chemical actinometry employed the reineckate system characterized by Wegner and Adamson (8). Total absorbance of light was achieved by irradiating 0.010 M complex solutions in 10 cm quartz spectrophotometer cells in which solutions were mixed by periodic shaking. All yields were corrected for thermal reaction carried out under identical conditions. Conditions were chosen to make thermal corrections very small.

Analytical Schemes

(i) ΔpH Method. Solutions of $Cr(NH_2R)_5Cl^{2+}$ and $Cr(NH_3)_6^{3+}$ were made up in 1.00×10^{-3} M $HClO_4$ with either $NaClO_4$ or $NaNO_3$ added to bring ionic strength to 0.50. Amine release and formation of aquo product were determined by using an Accumet model 210 pH meter and Riccieri and Schlafer's pH change calculation (9).

(ii) Spectrophotometric Analysis. $Cr(NH_3)_6^{3+}$ has extinction coefficients of 18 and 12 at 500 and 510 nm, $Cr(NH_3)_5OH^{2+}$ has an extinction coefficient of 43 at 510 nm, and $Cr(NH_3)_5OH_2^{3+}$ has an extinction coefficient of 32 at 500 nm. These differences were exploited using a Gilford 240 spectrophotometer to determine extent of reaction in solutions initially at p$H = 3$ and 12 after low conversion ($\leq 10\%$). Spectrophotometry was also applied to the reaction of $Cr(NH_3)_6^{3+}$ in DMSO. The extinction coefficient of $Cr(NH_3)_5DMSO^{3+}$, obtained by treating the chloride with $AgNO_3$, is 39 at 500 nm.

(iii) Amine titration in DMSO. Amine and alkylamine yields in DMSO were determined by titration of liberated base with 0.0100 M $HClO_4$. Reaction solutions were mixed with equal volumes of water and pH electrodes were preconditioned in DMSO–water mixtures.

(iv) Chloride titration. The small chloride yields were determined by potentiometric titration of Cl^- with 1.00×10^{-3} M $AgNO_3$ using a microburette, a Ag/AgCl electrode, a calomel electrode, and a Leeds and Northrup student potentiometer. There is no chloride blank in the system.

Phosphorescence Measurements

Phosphorescence spectra were recorded with an Aminco–Bowman spectrofluorimeter equipped with an R446S phototube from Aminco and 2 mm slits.

Results

In Table 1, quantum yields for the various reactions studied are collected with the exception of data on reactions of $Cr(NH_3)_6^{3+}$ as a function of pH which appear in Table 2. Table 3 records the pH dependence of intensity of 660 nm phosphorescence as a function of pH. Two comments are in order about Tables 2 and 3. First, pH dependence was examined only in solutions which could be maintained without buffers. This is because there was some evidence that buffer anions might be involved in quenching processes. Second, the reactions in base were examined at 0 °C to eliminate substantial thermal corrections. Figure 1 shows the emission spectra of $Cr(NH_3)_6^{3+}$ at p$H = 2$ and p$H = 12$.

Discussion

(1) Base Quenching and the Role of the Quartet

Hydroxide ion appears to quench the ^2E state of $Cr(NH_3)_6^{3+}$ effectively. At p$H = 12$, the emission is less than 5% of that observed at p$H = 3$. That is, perhaps, a reasonable result since we have failed to observe luminescence in solution from complexes of the type Cr-

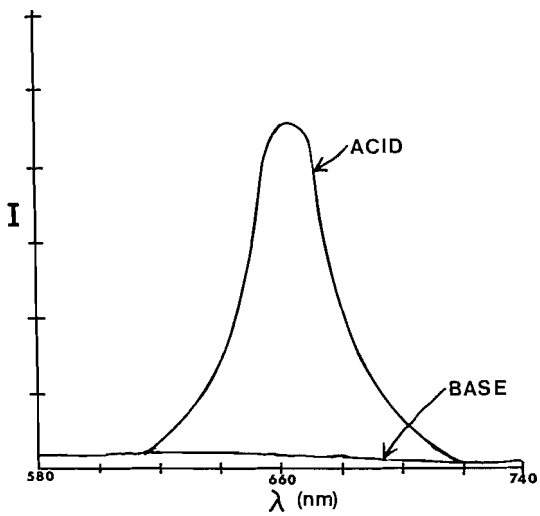

FIG. 1. Phosphorescence spectrum of $Cr(NH_3)_6^{3+}$ in acid (p$H = 2$) and base (p$H = 12$) under excitation at 465 nm. The blank superimposes on the result for basic solution.

Can. J. Chem. Downloaded from www.nrcresearchpress.com by 210.87.254.5 on 09/05/12
For personal use only.

TABLE 1. Quantum yields (ϕ) for release of RNH_2 and Cl^- at 25 °C

Complex	Medium	Analytical method*	Irradiation time (min)	ϕ_{RNH_2}	ϕCl^-
$Cr(NH_3)^{3+}$	$pH = 3$	pH	60	0.51†	
		S	60	0.4	
	DMSO	T	60	0.63	
		T	90	0.59	
		S	30	0.7	
		S	60	0.7	
		S	90	0.6	
$Cr(NH_3)_5Cl^{2+}$	$pH = 3$	pH	30	0.48	0.04‡
		pH	60	0.41	
	DMSO	T	30	0.30	
		T	45	0.28	
		T	180	—	<0.001
$Cr(CH_3NH_2)_5Cl^{2+}$	$pH = 3$	pH	30	0.44	
		pH	60	0.38	
	DMSO	T	90	0.18	
		T	90	0.20	
		T	180	—	<0.001
$Cr(CH_3CH_2NH_2)_5Cl^{2+}$	$pH = 3$	pH	60	0.40	
	DMSO	T	45	0.20	
		T	60	0.20	
		T	180	—	<0.001

*$pH = \Delta pH$ analysis, S = spectrophotometric analysis, T = titrimetric analysis.
†This yield is higher than that previously reported (see tabulations in ref. 1). But, we work at lower conversion and the agreement among analytical methods convinces us of, at least, the validity of the relative yields on which our discussion turns.
‡Quoted from the tabulations in ref. 1.

TABLE 2. Quantum yield for photolysis of 0.010 M $Cr(NH_3)_6^{3+}$ at 0 °C as a function of pH*

Initial pH	Irradiation time	ϕ_{NH_3}
3	150	0.2_8
4	60	0.2_5
11	60	0.2_3
12	180	0.2_3
13	60	0.1_7

*$\lambda_{irradiation} = 465$ nm (spectrophotometric analysis).

TABLE 3. Phosphorescence intensities as a function of pH at a $Cr(NH_3)_6^{3+}$ concentration of 0.010 M; $T = 22$ °C*

pH	Intensity (arbitrary units)
2.0	32
3.0	32
4.0	30
11.0	0.5
12.0	0.5
13.0	0.5
Blank (distilled H_2O)	0.5

*$\lambda_{excitation} = 465$ nm; $\lambda_{emission} = 660$ nm; slit width = 2 mm. The temperature dependence of this emission is characterized by an activation energy of 10.4 kcal mol^{-1} in H_2O. Corresponding studies in DMSO give an activation energy of 14 kcal mol^{-1} (3).

$(NH_3)_5X^{2+}$ (3) and a kinetically reasonable process for carrying the doublet through $Cr(NH_3)_5NH_2^{2+}$ in the presence of OH^- can be envisioned which does not require an unreasonable acidity constant. But, whatever the mechanism of hydroxide quenching, an argument parallel to Chen and Porter's (2) analysis of $Cr(NH_3)_2(NCS)_4^-$ leads to the conclusion that a *large part* of the ammine loss from $Cr(NH_3)_6^{3+}$ originates from the quartet prior to intersystem crossing because no more than one third appears to be subject to quenching. Since the main pathway of doublet relaxation in acid solution appears to be via thermal return to the quartet (3), it is probable that the part of the yield that is quenched also corresponds to reaction from the quartet when that state is reached by thermal repopulation.

Can. J. Chem. Downloaded from www.nrcresearchpress.com by 210.87.254.5 on 09/05/12
For personal use only.

(2) DMSO Effect on the Photolysis of $Cr(NH_3)_6^{3+}$

DMSO is observed to increase the ammine quantum yield from $Cr(NH_3)_6^{3+}$ and to increase the activation energy for phosphorescence decay. Base quenching and phosphorescence data require that we look at the properties of the quartet. To interpret the facts, we propose a specific speculative model for the behavior of a quartet excited state of $Cr(NH_3)_6^{3+}$ which we hope may prove useful in much of Cr(III) photochemistry. This model is based on Hammond's suggestion (10) that photoreaction results from internalization of electronic excitation and is best viewed as a problem in the theory of radiationless deactivation analogous to the problem of return of the excited state to the ground state. In particular, one feature of a "reactive" excited state should be its resemblance to the primary photoproduct so that its wavefunctions overlap those of the product to a degree competitive with the overlap with ground state wavefunctions.

The electronic configuration of a quartet octahedral Cr(III) complex is $t_{2g}^2 e_g$ in which a single σ^* orbital is occupied as in the ground state of a Cr(II), d^4, complex. The structure of Cr(II) complexes suggests that the vibrationally equilibrated Cr(III) complex should be subject to a strong tetragonal distortion. The doublet excited state with the configuration t_{2g}^3 has a potential surface very similar to the ground state as indicated by the correspondence between absorption and emission maxima (3) and a recent detailed analysis of the vibrational structure of phosphorescence (11). Figure 2 shows an *impression* (which can be only that in two dimensions) of the potential surfaces for the states ^2E and $^4T_{2g}$ as a function of a "tetragonal distortion parameter". Quartet surfaces with similar energy minima can cross the ^2E surface at higher energies as tetragonal distortion at the minimum increases. Such a model can explain higher activation energy for $^2E \rightarrow {}^4T$ thermal repopulation as a consequence of greater tetragonal distortion in the vibrationally equilibrated quartet. It also suggests why doublet relaxation occurs via the quartet; the ground state, ^4A, and the ^2E cross only at very high energies. Returning to reactivity, the less distorted quartet may be thought of as crossing the ground state at lower energy, and the more distorted quartet should cross the potential surface of a primary photo product related to O_h symmetry by a tetragonal distortion at lower energy. One (but only one) primary photo product would be a nearly square pyramidal nearly five coordinate intermediate that is suggestive of the commonly discussed transition state of thermal substitution.

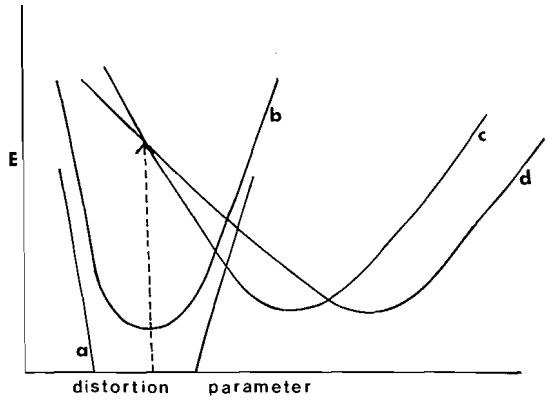

FIG. 2. An impression of the potential surfaces for the electronic states of $Cr(NH_3)_6^{3+}$ of interest in this study as a function of a "distortion parameter". The curves represent: (*a*) the $^4A_{2g}$ ground state; (*b*) the ^2E_g excited state; (*c*) the $^4T_{2g}$ excited state in aqueous solution; (*d*) the $^4T_{2g}$ excited state in DMSO solution.

(3) Effect of DMSO on the Photolysis of $Cr(NH_2R)_5Cl^{2+}$

The speculative model of the previous section can also accommodate the significant reversal of DMSO effect in the monochloro complexes. In this case, yields of RNH_2, and even more Cl^-, appear to be reduced by DMSO. If tetragonal distortion does occur along the axis including the *low field* Cl^- ligand, destabilization resulting from occupancy of a σ^* orbital will presumably be less, *and* destabilization due to occupancy of a π^* (t_{2g}) orbital (rendered antibonding by the Cl^- lone pairs) will also be minimized. But such a favored quartet requires projection of a Cl^- ligand into the solvent, and DMSO is known to be a poor solvent for Cl^- ion (12). So it is reasonable to assume that the H_2O and DMSO potential surfaces appear in reverse order from the way they are shown in Fig. 2. Distortion is smaller in DMSO. The profound reduction in Cl^- yield in DMSO means that relaxation of the distorted quartet to yield free Cl^- ion is quite unfavorable, but similarly, a less distorted quartet would be unfavorable as well to amine release.

We thank Dr. M. Parris for gifts of compounds and guidance in the synthesis of alkylamine complexes. Dr. Noel Kane-Maguire supplied phosphorescence data and valuable advice. Discussions with Dr. V. S. Sastri contributed significantly to formulation of the problem.

1. V. BALZANI and V. CARASSITTI. Photochemistry of coordination compounds. Academic Press, New York. 1970. Chap. 7.
2. S. CHEN and G. B. PORTER. Chem. Phys. Lett. **6**, 41 (1970).
3. N. A. P. KANE-MAGUIRE and C. H. LANGFORD. Chem. Commun. 895 (1971).
4. M. PARRIS and W. J. WALLACE. Can. J. Chem. **47**, 2257 (1969).
5. M. PARRIS. Private communication.
6. M. R. EDELSON and R. A. PLANE. Inorg. Chem. **2**, 231 (1964).
7. R. D. WILSON, V. S. SASTRI, and C. H. LANGFORD. Can. J. Chem. **49**, 679 (1971).
8. E. E. WEGNER and A. W. ADAMSON. J. Am. Chem. Soc. **88**, 314 (1966).
9. P. RICCIERI and H. L. SCHLAFER. Inorg. Chem. **9**, 727 (1970).
10. G. S. HAMMOND. Adv. in Photochem. **7**, 373 (1969).
11. T. V. LONG and D. J. B. PENROSE. J. Am. Chem. Soc. **93**, 632 (1971).
12. R. ALEXANDER and A. J. PARKER. J. Am. Chem. Soc. **89**, 5549 (1967).

Can. J. Chem. Downloaded from www.nrcresearchpress.com by 210.87.254.5 on 09/05/12
For personal use only.

Intermolecular Potentials from Differential Cross Sections: Ar + Ar

FERENC KALOS[1] AND ARTHUR E. GROSSER
Department of Chemistry, McGill University, Montreal, Quebec

Received September 23, 1971

The angular distribution of Ar + Ar scattering at $E = 9.16 \times 10^{-14}$ erg was measured out to the rainbow pattern (supernumerary rainbow and part of the rainbow peak) by the crossed molecular beam technique, with mass spectrometric detection. This distribution was compared to calculated differential cross sections. Total cross sections, and spectroscopic constants for Ar_2 were also calculated. The trial potentials were L.J.-12,6, L.J.-20,6, a modified Lennard–Jones potential (L.J.-14,12,8,6) and the Bobetic–Barker potential. The Bobetic–Barker potential is the one most consistent with cross section and spectroscopic experiments.

On a mesuré la distribution angulaire de la diffusion de Ar + Ar à $E = 9.16 \times 10^{-14}$ erg jusqu'au structure "arc-en-ciel" (l'arc-en-ciel supernuméraire et une partie du pic de l'arc-en-ciel) par la technique du faisceau moléculaire croisé, avec détection par spectrométrie de masse. On a comparé cette distribution aux sections efficaces différentielles. On a aussi calculé les sections efficaces totales et les constantes spectroscopiques pour Ar_2. Les potentiels d'essai étaient L.J.-12,6, L.J.-20,6, un potentiel de Lennard–Jones modifié (L.J.-14,12,8,6) et le potentiel de Bobetic–Barker. Le potentiel de Bobetic–Barker était celui qui se rapprochait le plus des expériences de la diffusion et des expériences spectroscopiques.

Canadian Journal of Chemistry, **50**, 892 (1972)

Introduction

The elucidation of the argon pair potential has recently received considerable attention: transport and virial data were analyzed by Dymond and Alder (1); Barker *et al.* (2–4) made use of the properties of the solid in addition to the virial data; the Ar_2 absorption spectrum in the vacuum ultraviolet was recently reported by Tanaka and Yoshino (5), and calculated vibrational energy levels for different potential functions have been compared with these data (6–7). Molecular beam measurements of the total scattering cross section at high energies (8–10) yielded the best available information on the interaction at short range, and such measurements at thermal energies (11) showed agreement with the calculated long-range force constant, C_6.

Measurements of the differential scattering cross section are potentially useful for the elucidation of the intermolecular potential in the region of the well. The first such measurements on Ar + Ar by Williams *et al.* (12) were confined to very small scattering angles, but since then, measurements extending into the region of rainbow scattering were reported by Cavallini *et al.* (13), who interpreted their data in terms of an assumed Lennard–Jones-12,6 potential. After a similar simple procedure of analysis, the measurements made in this laboratory (14) showed agreement with the results of Cavallini *et al.*[2] We have now elaborated a more refined scheme of analysis for our differential cross section measurements: properly velocity- and angle-averaged cross sections (*i.e.* theoretical angular distributions in the lab system) are calculated for various trial potentials and a matching of the measured angular distribution is attempted by trial and error. This procedure is more reliable than matching the locations only of the differential cross section extrema.

Experimental

The crossed molecular beam apparatus and the experimental technique have been described previously (14, 15). Briefly, a velocity selected primary beam ($v_0 = 518$ m/s) was crossed with a nozzle beam ($v_0 = 547$ m/s, speed ratio = 12.7). This arrangement resulted in a 17% FWHH spread in the relative velocity. The scattered species were detected by an ultrahigh vacuum mass spectrometer.

Calculations

Identical boson differential cross sections were evaluated for thirty trial potentials by the partial wave formula. The phase shifts η_l were obtained via the WKB approximation (for including symmetry oscillations, and fitted the data with a multiparameter potential.

[1]Present address: Department of Chemistry, Massachusetts Institute of Technology, Cambridge, Massachusetts 02139.

[2]Note added in proof: Parson, Siska, and Lee (23) have carefully measured the Ar + Ar differential cross section,

Can. J. Chem. Downloaded from www.nrcresearchpress.com by 210.87.254.5 on 09/05/12
For personal use only.

Can. J. Chem. Downloaded from www.nrcresearchpress.com by 210.87.254.5 on 09/05/12
For personal use only.

$0 \leqslant l \leqslant 200$), and via the Born approximation (for $202 \leqslant l \leqslant 500$) for the r^{-6} term of the potentials. The WKB phase shifts were evaluated using quadratures, and analytic integration from large r (where $V(r) \sim 0$); only every fourth phase ($\Delta l = 8$) was calculated, the others were obtained by interpolation of $\eta = \eta(l)$.[3]

The velocity and angle averaging of the computed cross sections, which was required for the comparison with the experiments was made the following way: the velocity distributions of the beams and the angular distribution of the wide (7.9° FWHH) secondary beam were each replaced by 3-point discrete distributions. As calculating cross sections for $3^3 = 27$ different energies did not appear necessary, this 27 point "overall" distribution was regrouped into 6 sets, mainly according to the value of the relative velocity. The beam velocities and crossing angle were averaged within each set, and then phase shifts were calculated for the collision energy of each set. The center-of-mass angles and Jacobians of transformation corresponding to certain laboratory angles (every $\frac{1}{4}°$) were then computed[4] (17) using the parameters (v_1, v_2, and crossing angle) of the set. The differential cross section was evaluated at these angles, transformed to the lab system, and these cross section contributions from the six sets were summed with proper weights. To account for the angular resolution of the detector and for the spread of the primary beam an angular averaging over a triangular distribution (0.75° FWHH) was made.

The mismatch between experiment and calculation was assumed to be given by χ^2. After subdividing the angular range into a number (4–8) of regions, χ^2 was evaluated for $I(\theta_L)$ *vs.* θ_L by

$$\chi^2 = \sum_{\text{regions}} \left\{ \frac{\left(\sum_{\substack{\text{points} \\ \text{in region}}} [I_{\text{expt}} - I_{\text{calc}}] \right)^2}{\sum_{\substack{\text{points} \\ \text{in region}}} I_{\text{calc}}} \right\}$$

Calculations of χ^2 for different numbers of regions reduced the uncertainty in its value.

[3]The phase shifts were compared with exact numerical calculations. The exact phase shift computer program (16) was kindly provided by Professor B. C. Eu.

[4]A correction was included for the use of a density detector.

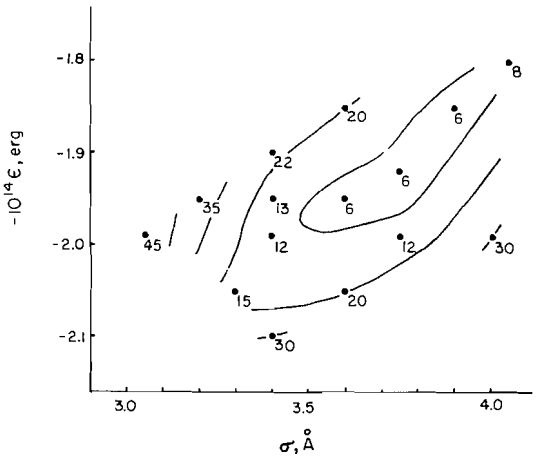

FIG. 1. Map of the fits by L.J.-12,6 potentials. The numbers mapped are 100 χ^2, and the contour lines represent equally good fits. The coordinate axes are the size parameter and well depth of the potential.

Total cross sections were also evaluated from the calculated phase shifts.

The spectroscopic constants have also become an important test of argon potentials since the Ar_2 spectra are now available (5). WKB eigenvalues and spectroscopic constants were also calculated for the trial potentials.

Results and Discussion

The trial potentials employed to fit the angular distribution were: the L.J.-12,6 and L.J.-20,6 potential functions, a modified Lennard–Jones potential, which will be discussed at a later point, and the Bobetic–Barker (3) multiparameter potential. Although it would be desirable to fit with a *flexible* multiparameter potential instead of the somewhat unrealistic L.J.-potential functions, the present experimental data would not be sufficient to establish the parameters of such a potential with any precision.

Lennard–Jones-n,6 Potentials

The results of fitting with L.J.-12,6 potentials are shown in Fig. 1; Table 1 lists the more successful potentials. A number of potential parameter combinations gave equally good fits and they are shown in Fig. 2. They illustrate that measurements of high angular and energy resolution and of high precision are required if a unique potential is to be deduced from differential cross section measurements alone. Table 1

TABLE 1.

(*a*) Lennard–Jones-12,6

Potential function No.	σ (Å)	$\varepsilon \times 10^{14}$ (erg)	χ^{2*}	Spectrum (cm^{-1}) ω_e	$\omega_e\chi_e$	$D_0°$	Total cross section† (Å^2)
25	3.75	1.92	0.06	22.18	1.51	84.32	497.1
11	3.60	1.95	0.06	23.10	1.61	85.23	446.0
24	3.90	1.85	0.06	21.04	1.41	81.47	538.7
28	4.05	1.80	0.08	20.09	1.32	79.54	585.9
2	3.40	1.99	0.12	24.95	1.88	86.37	378.4
9	3.75	1.99	0.12	22.68	1.62	87.61	509.8
20	3.40	1.95	0.13	24.64	1.87	84.51	369.0
27	3.30	2.05	0.15	26.00	1.99	88.7	357.1
22	3.60	2.05	0.20	23.83	1.63	89.92	466.7
				30.68 ± 0.37‡	2.56 ± 0.12‡	76.9‡	296.6§

(*b*) Other potentials

Potential function No.	σ (Å)	$\varepsilon \times 10^{14}$ (erg)	A‖	χ^{2*}	Spectrum (cm^{-1}) ω_e	$\omega_e\chi_e$	$D_0°$	Total cross section† (Å^2)
Bobetic–Barker								
1	3.4	1.94		0.12	26.8	2.17	82.81	284.3
14,12,8,6-modified L.J.								
10	3.40	2.03	1.26	0.29	28.69	2.47	87.08	299.2
33	3.15	2.05	0.36	0.31	28.79	2.50	87.41	278.8
34	3.35	2.10	1.14	0.34	28.78	2.35	90.14	298.9
43	3.50	1.95	1.64	0.36	27.76	2.42	83.69	301.8
31	3.60	2.00	2.27	0.38	27.48	2.24	86.37	320.0
30	3.35	1.95	0.97	0.41	27.89	2.45	83.23	288.5
L.J.-20,6								
42	3.40	1.95		0.69	29.97	2.91	80.40	293.7
					30.68 ± 0.37‡	2.56 ± 0.12‡	76.9‡	296.6§

*Fit to angular distribution at $E = 9.67 \times 10^{-14}$ erg.
†Calculated for $v = 760.75$ m/s.
‡Reference 5, experimental value.
§Reference 11, experimental value, corrected to $v = 760.75$ from 669 m/s using $v^{-2/5}$ velocity dependence.
‖Mixing coefficient.

also includes the total cross sections and spectroscopic constants. Bruch and McGee (6) have pointed out that agreement with experiment of ω_e and $\omega_e\chi_e$ should be more conclusive than the eigenvalues themselves.

As there is general agreement (1–3, 13, 18, 20) on the value of the size parameter, $\sigma = 3.4 \pm 0.05$ Å, it seems reasonable to apply this constraint to the L.J.-12,6 potentials, making potentials 2 and 20 the "best", with $\varepsilon = 2.00\,(\pm 0.07) \times 10^{-14}$ erg. This ε is in agreement with the differential cross section results of Cavallini *et al.* (13), but not with the transport data of Hogerworst (18), who found $\varepsilon(12,6) = 1.87 \times 10^{-14}$ erg, nor with the value deduced by Tanaka and Yoshino (5): $\varepsilon = 1.82 \times 10^{-14}$ erg. Searcy *et al.* (19) deduced even smaller well depths from the location of the first few quantum oscillations in the differential cross section, but we find many potentials yield similar interference patterns in the low angle region.

But even though the scattering data can be fitted fairly well by some L.J.-12,6 potentials, none of them yields the proper spectroscopic constants or total cross section. The L.J.-20,6 potential was much better in these latter respects, but did not fit the experimental angular distribution (Fig. 3).

Other Potentials

A modified Lennard–Jones, or 14,12,8,6 potential, as given by

$$[1] \qquad V(\rho) = 4\varepsilon_\infty(1 - A\rho^{-2})(\rho^{-12} - \rho^{-6})$$

where

$$[2] \qquad \rho \equiv r/\sigma$$

Can. J. Chem. Downloaded from www.nrcresearchpress.com by 210.87.254.5 on 09/05/12
For personal use only.

Can. J. Chem. Downloaded from www.nrcresearchpress.com by 210.87.254.5 on 09/05/12
For personal use only.

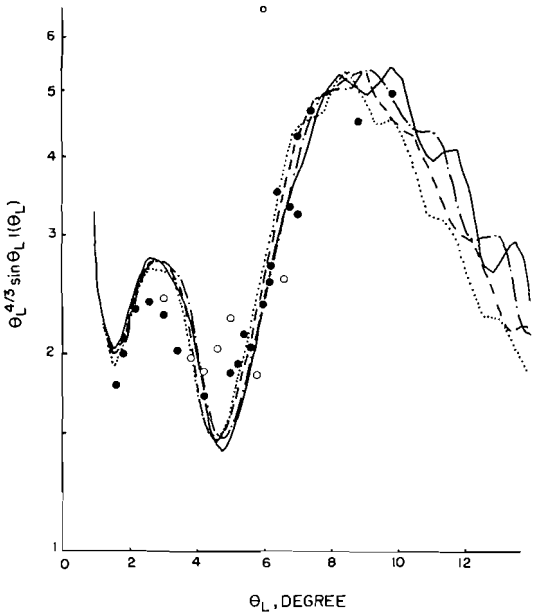

FIG. 2. The angular distribution of scattering in the laboratory system, weighted by $\theta_L^{4/3} \sin \theta_L$. The symbols indicate the statistical weights of the data points; ●: weight = 3, ○: weight = 1. The curves show calculated distributions for the following L.J.-12,6 potentials: -·- No. 25, — No. 11, --- No. 24, ··· No. 28. (The scale factor between the calculated curves and the experimental data was established by minimizing χ^2.)

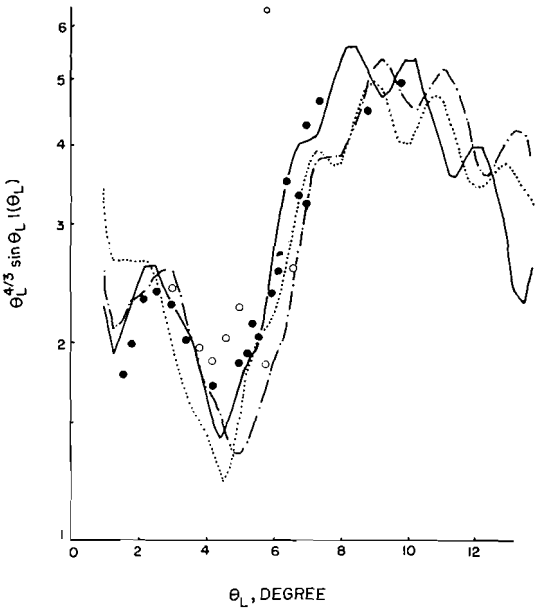

FIG. 3. The angular distribution of scattering in the laboratory system, weighted by $\theta_L^{4/3} \sin \theta_L$. The curves show calculated distributions for the following potentials: — No. 1, Bobetic–Barker; -·-·- No. 10, modified L.J.; ··· No. 42, L.J. – 20,6.

and

$$[3] \qquad \varepsilon_\infty \equiv C_6/4\sigma^6$$

has two adjustable parameters, σ, and the mixing coefficient, A. It employs the precisely known value (21, 22) of C_6 as an additional constraint. The purpose of this potential is to provide a two-parameter function which (by eq. 3) yields the correct long-range interaction. In fact, this potential closely resembles the Bobetic–Barker potential, as shown in Fig. 4. This potential family did not yield very good fits to the angular distribution, but was successful in reproducing $\omega_e\chi_e$.

The Bobetic–Barker potential[5] fits the experimental angular distribution very well (Fig. 3, Table 1*b*) and is much better than even the best L.J.-12,6 potentials in agreeing with the spectroscopic constants and total cross section.

In conclusion, while none of the potentials were able to reproduce the scattering, spectroscopic, and total cross section results, the Bobetic–Barker potential is most consistent with the data.

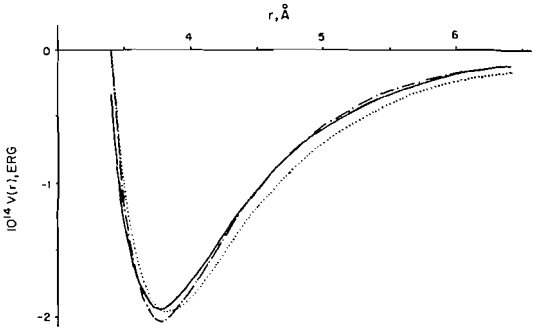

FIG. 4. Comparison of potential functions: — No. 1, Bobetic–Barker; -·-·- No. 10, modified L.J.; ··· No. 20, L.J. – 12,6.

Acknowledgment is made to the donors of the Petroleum Research Fund, administered by the American Chemical

[5]Given by the expression

$$V(r) = \varepsilon\left[e^{\alpha(1-R)} \sum_{i=0}^{i=5} A_i(R-1)^i - \sum_{i=0}^{i=2} C_{2i+6}/(\delta + R^{2i+6})\right]$$

where $R = r/r_m$ and the parameters are $E/k = 140.23$ °K, $r_m = 3.7630$ Å, $A_0 = 0.29214$, $A_1 = -4.41458$, $A_2 = -7.70182$, $A_3 = -31.9293$, $A_4 = -136.026$, $A_5 = -151.000$, $C_6 = 1.11976$, $C_8 = 0.171551$, $C_{10} = 0.013747$, $\alpha = 12.5$, and $\delta = 0.01$.

Society for partial support, along with National Research Council of Canada, Imperial Oil Co., and NATO, of this research. One of us (F.K.) thanks the Government of Quebec for a scholarship.

1. J. H. DYMOND and B. J. ALDER. J. Chem. Phys. **51**, 309 (1969).
2. J. A. BARKER and A. POMPE. Aust. J. Chem. **21**, 1683 (1968).
3. M. V. BOBETIC and J. A. BARKER. Phys. Rev. B **2**, 4169 (1970).
4. J. A. BARKER, M. L. KLEIN, and M. V. BOBETIC. Phys. Rev. B **2**, 4176 (1970).
5. Y. TANAKA and K. YOSHINO. J. Chem. Phys. **53**, 2012 (1970).
6. L. W. BRUCH and I. J. MCGEE. J. Chem. Phys. **53**, 4711 (1970).
7. C. T. CHEN and R. D. PRESENT. J. Chem. Phys. **54**, 3645 (1970).
8. A. B. KAMNEV and V. B. LEONAS. Dokl. Akad. Nauk SSSR **162**, 798 (1965); Sov. Phys. Dokl. **10**, 529 (1965).
9. I. AMDUR and E. A. MASON. J. Chem. Phys. **22**, 670 (1954).
10. S. O. COLGATE, J. E. JORDAN, I. AMDUR, and E. A. MASON. J. Chem. Phys. **51**, 968 (1969).
11. J. A. PHIPPS, G. D. MAGNUSON, and J. E. SCOTT, JR. Sixth Intern. Conf. on the Physics of Electronic and Atomic Collisions. (VI. ICPEAC, 1969). The MIT Press, Cambridge, Massachusetts. 1969. p. 188.
12. W. WILLIAMS, C. R. MUELLER, W. MCGUIRE, and B. SMITH. Phys. Rev. Lett. **22**, 121 (1969).
13. M. CAVALLINI, G. GALLINARO, L. MENEGHETTI, G. SCOLES, and U. VALBUSA. Chem. Phys. Lett. 7, 303 (1970).
14. F. KALOS. Ph.D. Thesis, McGill University, Montreal, Quebec. 1971.
15. F. KALOS and A. E. GROSSER. Chem. Phys. Lett. **6**, 537 (1970).
16. B. C. EU. J. Chem. Phys. **52**, 3021 (1970).
17. R. K. HELBING. J. Chem. Phys. **48**, 472 (1968); **50**, 4123 (1969).
18. W. HOGERWORST. Physica, **51**, 59 (1971); **51**, 77 (1971); **51**, 90 (1971).
19. J. SEARCY, K. WENDELL, C. R. MUELLER, and S. SHEEN. Chem. Phys. Lett. **8**, 123 (1971).
20. J. O. HIRSCHFELDER, C. F. CURTISS, and R. B. BIRD. Molecular theory of gases and liquids. John Wiley Co., New York. 1954.
21. A. DALGARNO. Adv. Chem. Phys. **12**, 143 (1967).
22. R. G. GORDON. J. Chem. Phys. **48**, 3929 (1968).
23. J. M. PARSON, P. E. SISKA, and Y. T. LEE. J. Chem. Phys. **56**, 1511 (1972).

Can. J. Chem. Downloaded from www.nrcresearchpress.com by 210.87.254.5 on 09/05/12
For personal use only.

The Master Equation for the Dissociation of a Dilute Diatomic Gas. VI. Solution of Coupled Sets of Master Equations

D. L. S. McELWAIN AND H. O. PRITCHARD

Centre for Research in Experimental Space Science, York University, Downsview, Ontario

Received October 18, 1971

Three coupled sets of master equations, representing the equilibration of $X_2 + Y_2 \rightleftarrows 2XY$ via atoms only, have been solved by the normal-mode technique; the set of 57 simultaneous differential equations describing the $H_2/D_2/2HD$ system was considered as a suitable trial model. It was found that at times (t) in excess of the longest vibrational relaxation time, even though some of the populations in the system appeared highly non-Boltzmann, all the phenomenological rate constants were well-behaved: they were either constant and obeyed the rate–quotient law, or they were dependent on t^2.

The paper concludes with a discussion of the information required before a full solution of the $X_2 + Y_2 \rightleftarrows 2XY$ reaction could be contemplated, and suggests methods by which an approximation to such a solution could be obtained.

Les trois ensembles couplés d'équations principales qui représentent l'équilibration de $X_2 + Y_2 \rightleftarrows 2XY$ à partir des atomes seuls, ont été résolus par la technique des modes normaux; l'ensemble des 57 équations différentielles simultanées qui décrit le système $H_2/D_2/2HD$ a été choisi comme modèle d'étude. On a constaté alors qu'aux temps (t) supérieurs au temps de relaxation vibrationnelle le plus long, toutes les constantes de vitesse phénoménologique avaient un bon comportement et cela, malgré un écart notable à la distribution de Boltzmann des populations du système dans certains cas. Ces vitesses étaient soit constantes et suivaient la loi en $1/k$ soit qu'elles dépendaient de t^2.

La note conclut par une discussion sur l'information exigée avant d'envisager la résolution complète de $X_2 + Y_2 \rightleftarrows 2XY$ et suggère des méthodes à partir desquelles une solution approchée peut être obtenue.

Canadian Journal of Chemistry, **50**, 897 (1972)

Introduction

Earlier papers in this series (I–5) have been concerned with the dissociation and recombination of a homonuclear diatomic gas at infinite dilution in a bath of *totally* inert atoms, and at such temperatures that rotational equilibration can be considered infinitely rapid.[1] In most of this work, the H_2 molecule has been used as a model, and having only 15 vibrational levels, can be represented by a set of 16 simultaneous differential equations; Part V addressed itself to the problem having a rather more dense energy-level spectrum, using D_2 as a model, and giving rise to a master equation of order 23. It is hoped that in future work, a more realistic description of the dissociation and recombination of a dilute homonuclear diatomic gas can be achieved by considering both rotational and vibrational interchanges; it should be mentioned in passing that for H_2, this will require the solution of almost 400 simultaneous differential equations and the assignment of some 70 000 translational–vibrational transition probabilities; for D_2 the problem is even more forbidding, with almost 700 simultaneous differential equations and some 200 000 translational–vibrational transition probabilities.

This paper addresses itself to a different problem, that of the solution of coupled sets of master equations. The need to solve coupled sets of master equations arises as soon as one tries to extend the very simple model with which we have worked so far in two very necessary directions: (*a*) The inclusion of bound states of MX in the dissociation–recombination scheme, *i.e.*

[1] $$X_2 + M \rightleftarrows X + X + M$$

[2] $$X_2 + M \rightleftarrows MX + X$$

[3] $$MX + M \rightleftarrows M + M + X$$

Here there are two coupled sets of equations, one representing reaction [1] as before and one representing reaction [3] (having one equation for each vibrational level of X_2 and MX, respectively), and they are coupled by two mechanisms, one through the atomic species which they share in common, and the other through the series of reaction [2]. In the face of a complete lack of any knowledge of the rates of reaction [2] as a function of the vibrational energy contents of both X_2 and MX, we felt that the exercise of solving these two coupled sets of

[1]Equations taken from papers in this series and used in the present paper are prefixed with the part numbers in Roman numerals.

Can. J. Chem. Downloaded from www.nrcresearchpress.com by 210.87.254.6 on 09/05/12
For personal use only.

Can. J. Chem. Downloaded from www.nrcresearchpress.com by 210.87.254.6 on 09/05/12
For personal use only.

equations would not advance our understanding significantly at the present time. We therefore turned our attention to

(*b*) The dissociation of a dilute heteronuclear diatomic gas, *i.e.*

[4] $$XY + M \rightleftarrows X + Y + M$$

[5] $$X + X + M \rightleftarrows X_2 + M$$

[6] $$Y + Y + M \rightleftarrows Y_2 + M$$

In this case, we have three sets of master equations, coupled via X and Y atoms. The complete description of the dissociation–recombination process for a heteronuclear diatomic molecule at experimentally attainable dilutions would also require the inclusion of reactions such as

[7] $$X + Y_2 \rightleftarrows XY + Y$$

[8] $$X_2 + Y \rightleftarrows XY + X$$

[9] $$X_2 + Y_2 \rightleftarrows 2XY$$

with a separate rate constant for each vibrational level of either reactants or products; and not to mention several permutations of reactions [2] and [3]. For the time being, reactions [7]–[9] must be omitted from the reaction scheme for two reasons. First, as in (*a*) above, we have no knowledge of the individual rate coefficients. Second, if we use the equilibration of $H_2 + D_2 \rightleftarrows 2HD$ as the simplest possible model for this type of reaction, we have to solve a set of 57 simultaneous differential equations, 15, 18, and 22 equations, respectively, representing the bound vibrational states of H_2, HD, and D_2, with one equation each for H and D atoms. Even excluding reactions [7], [8], and [9], we were unable to solve these 57 simultaneous equations by standard methods *e.g.* fifth-order Runge–Kutta, and it is clear therefore that the solution of the simple system of reactions [4], [5], and [6] at infinite dilution presents a problem which must be overcome before a complete solution to the heteronuclear diatomic dissociation reaction can even be contemplated; it is to this problem that we address ourselves in this paper.

Whilst it is not the aim of this work to try to describe the H_2/D_2 equilibration reaction, we prefer to maintain some contact with reality by performing our calculations within the experimental temperature range for the reaction. Shock-tube studies of the H_2/D_2 reaction have now been reported between 1000 and 3000 °K (6, 7), and we have performed our calculations for temperatures of 1500 and 2000 °K; the former is the lowest temperature at which our normal-mode procedure works well for H_2 and D_2 because of cancellation difficulties (3, 5) and the latter is the temperature to which most of our previous work relates. Following our previous philosophy (1–3, 8), it is assumed that translational and rotational equilibration occur instantaneously as the shock wave passes, and that reaction then proceeds to take place, starting with all the diatomic molecules in their $v = 0$ states. It is assumed that the translational–vibrational transition probabilities for H_2, HD, and D_2 have energy and temperature dependences given by eq. III(1) and that the energy-level spacings are those of Kolos and Wolniewicz (9, 10). The insensitivity of the overall behavior to imperfections in these assumptions is now well documented (2–4). Finally, it was assumed that at equilibrium there were 3.5×10^{16} molecules/cc each of $(H_2 + \frac{1}{2}H)$ and of $(D_2 + \frac{1}{2}D)$, the number of HD molecules being determined by the value of the appropriate equilibrium constant, which was calculated from the accepted energy-level scheme (10) by standard statistical mechanical methods. Thus, at 1500 and 2000 °K, respectively, there were 2.844×10^{17} and 2.780×10^{17} total (H + D) atoms (free and combined) per cc in the system, together with 3.5×10^{19} inert particles per cc. This choice of conditions facilitated comparison of the behavior of H_2 and D_2 in the mixed system with their separate behavior in earlier calculations (2, 3, 5) in which the total initial number of molecules was 3.5×10^{16} per cc in either case.

Normal-mode Factorization

Since the 57 simultaneous differential equations representing the system of reactions

[3*a*] $$HD + M \rightleftarrows H + D + M$$

[4*a*] $$H + H + M \rightleftarrows H_2 + M$$

[5*a*] $$D + D + M \rightleftarrows D_2 + M$$

in the translational–vibrational regime cannot be solved readily by conventional numerical methods, we follow our previous procedure (3) and recast them into normal modes. As far as possible, we will retain the same symbols as in that treatment, using unprimed symbols to describe the H_2 system, primed symbols for HD, and double-primed symbols for D_2. To recapitulate briefly, n_i represents the population of state $v = i$ of H_2 in molecules/cc. P_{ji} is the probability per collision of a transition from

Can. J. Chem. Downloaded from www.nrcresearchpress.com by 210.87.254.6 on 09/05/12
For personal use only.

state i to state j, and $\bar{P}_{ni}$ is the probability per collision of dissociation; $\tilde{n}_i$ represents the equilibrium population of state i at the temperature in question, and $\xi_i = n_i/\tilde{n}_i$. Thus, n_i' and n_i'' represent populations for HD and D_2, respectively, but to avoid as far as possible multiple superscripts, n_H ($=\frac{1}{2}[H]$) will be used for n_n and n_D ($=\frac{1}{2}[D]$) for n_n'' (there is no meaning to the quantity n_n'); also, a prime on a symbol implies that the subscripts carry primes. The numbers of bound vibrational levels are $n = 15$, $n' = 18$, and $n'' = 22$, and thus the 57 equations are

$$(1)\qquad \frac{dn_i}{dt} = [M]Z\left[\sum_{j=0}^{n-1}(P_{ij}n_j - P_{ji}n_i) + (\bar{P}_{in}n_H^2 - \bar{P}_{ni}n_i)\right] \qquad 0 \leqslant i \leqslant (n-1)$$

$$(2)\qquad \frac{dn_H}{dt} = [M]Z\left[\sum_{i=0}^{n-1}(\bar{P}_{ni}n_i - \bar{P}_{in}n_H^2) + \tfrac{1}{2}\sum_{i'=0}^{n'-1}(\bar{P}'_{ni}n_i' - \bar{P}'_{in}n_Hn_D)\right]$$

$$(3)\qquad \frac{dn_i'}{dt} = [M]Z\left[\sum_{j'=0}^{n'-1}(P'_{ij}n_j' - P'_{ji}n_i') + (\bar{P}'_{in}n_Hn_D - \bar{P}'_{ni}n_i')\right] \qquad 0 \leqslant i' \leqslant (n'-1)$$

$$(4)\qquad \frac{dn_D}{dt} = [M]Z\left[\sum_{i''=0}^{n''-1}(\bar{P}''_{ni}n_i'' - \bar{P}''_{in}n_D^2) + \tfrac{1}{2}\sum_{i'=0}^{n'-1}(\bar{P}'_{ni}n_i' - \bar{P}'_{in}n_Hn_D)\right]$$

$$(5)\qquad \frac{dn_i''}{dt} = [M]Z\left[\sum_{j''=0}^{n''-1}(P''_{ij}n_j'' - P''_{ji}n_i'') + (\bar{P}''_{in}n_D^2 - \bar{P}''_{ni}n_i'')\right] \qquad 0 \leqslant i'' \leqslant (n''-1)$$

The following detailed-balancing relationships hold:

$$(6)\qquad P_{ij}\tilde{n}_j = P_{ji}\tilde{n}_i \qquad \bar{P}_{in}\tilde{n}_H^2 = \bar{P}_{ni}\tilde{n}_i$$

$$(7)\qquad P'_{ij}\tilde{n}'_j = P'_{ji}\tilde{n}'_i \qquad \bar{P}'_{in}\tilde{n}_H\tilde{n}_D = \bar{P}'_{ni}\tilde{n}'_i$$

$$(8)\qquad P''_{ij}\tilde{n}''_j = P''_{ji}\tilde{n}''_i \qquad \bar{P}''_{in}\tilde{n}_D^2 = \bar{P}''_{ni}\tilde{n}''_i$$

These relationships are particularly important in establishing the required values for $\bar{P}_{in}$, $\bar{P}'_{in}$, and $\bar{P}''_{in}$. In terms of the reduced variable ξ_i, ξ_i', and ξ_i'', and writing $Q_{ij} = [M]ZP_{ij}$, etc., eqs. (1) to (5) become

$$(1a)\qquad \frac{d\xi_i}{dt} = \sum_{j=0}^{n-1}Q_{ji}(\xi_j - \xi_i) + \bar{Q}_{ni}(\xi_H^2 - \xi_i)$$

$$(2a)\qquad \frac{d\xi_H}{dt} = \tilde{n}_H\sum_{i=0}^{n-1}\bar{Q}_{in}(\xi_i - \xi_H^2) + \tfrac{1}{2}\tilde{n}_D\sum_{i'=0}^{n'-1}\bar{Q}'_{in}(\xi_i' - \xi_H\xi_D)$$

$$(3a)\qquad \frac{d\xi_i'}{dt} = \sum_{j'=0}^{n'-1}Q'_{ji}(\xi_j' - \xi_i') + \bar{Q}'_{ni}(\xi_H\xi_D - \xi_i')$$

$$(4a)\qquad \frac{d\xi_D}{dt} = \tilde{n}_D\sum_{i''=0}^{n''-1}\bar{Q}''_{in}(\xi_i'' - \xi_D^2) + \tfrac{1}{2}\tilde{n}_H\sum_{i'=0}^{n'-1}\bar{Q}'_{in}(\xi_i' - \xi_H\xi_D)$$

$$(5a)\qquad \frac{d\xi_i''}{dt} = \sum_{j''=0}^{n''-1}Q''_{ji}(\xi_j'' - \xi_i'') + \bar{Q}''_{ni}(\xi_D^2 - \xi_i'')$$

or, in more compact matrix notation

$$(9)\qquad \frac{d}{dt}\begin{pmatrix}\boldsymbol{\xi}\\ \xi_H\\ \boldsymbol{\xi}'\\ \xi_D\\ \boldsymbol{\xi}''\end{pmatrix} = \mathscr{A}\begin{pmatrix}\boldsymbol{\xi}\\ \xi_H\\ \boldsymbol{\xi}'\\ \xi_D\\ \boldsymbol{\xi}''\end{pmatrix} + \xi_H^2\begin{pmatrix}\bar{\boldsymbol{Q}}\\ \tilde{n}_Hw\\ \mathbf{0}\\ 0\\ \mathbf{0}\end{pmatrix} + \xi_H\xi_D\begin{pmatrix}\mathbf{0}\\ \frac{1}{2}\tilde{n}_Dw'\\ \bar{\boldsymbol{Q}}'\\ \frac{1}{2}\tilde{n}_Hw'\\ \mathbf{0}\end{pmatrix} + \xi_D^2\begin{pmatrix}\mathbf{0}\\ 0\\ \mathbf{0}\\ \tilde{n}_Dw''\\ \bar{\boldsymbol{Q}}''\end{pmatrix}$$

where

$$[\bar{Q}]_i = \bar{Q}_{ni}$$

and

$$w = -\sum_{i=0}^{n-1} \bar{Q}_{in}$$

likewise for primed and double-primed quantities. The matrix $\mathscr{A}$ has the form

$$\mathscr{A} = \begin{pmatrix} \mathbf{A} & \mathbf{0} & \mathbf{0} & \mathbf{0} & \mathbf{0} \\ \tilde{n}_H \boldsymbol{u}^T & 0 & \frac{1}{2}\tilde{n}_D(\boldsymbol{u}')^T & 0 & \mathbf{0} \\ \mathbf{0} & \mathbf{0} & \mathbf{A}' & \mathbf{0} & \mathbf{0} \\ \mathbf{0} & 0 & \frac{1}{2}\tilde{n}_H(\boldsymbol{u}')^T & 0 & \tilde{n}_D(\boldsymbol{u}'')^T \\ \mathbf{0} & \mathbf{0} & \mathbf{0} & \mathbf{0} & \mathbf{A}'' \end{pmatrix} \tag{10}$$

where

$$u_i = \bar{Q}_{in} = [\bar{Q}]_i \tilde{n}_i / \tilde{n}_H^2$$

and

$$A_{ij} = (1 - \delta_{ij})Q_{ji} - \delta_{ij}\left[\bar{Q}_{ni} + \sum_{k=0}^{n-1}(1 - \delta_{ki})Q_{ki}\right]$$

again, likewise for primed and double-primed quantities.

Now, following very closely our transformation of a single master equation to normal modes (3), we transform the composite vector $\boldsymbol{\xi}$ to a composite $\boldsymbol{\psi}$ by

$$\boldsymbol{\psi} = \mathbf{T}\boldsymbol{\xi} = \tilde{\mathbf{S}}\mathbf{E}\boldsymbol{\xi}$$

where

$$(E)_{ij} = \tilde{n}_i^{1/2}\delta_{ij}$$

and $\tilde{\mathbf{S}}\mathbf{E}\mathbf{A}\mathbf{E}^{-1}\mathbf{S} = \mathbf{D}$, a diagonal matrix; likewise $\mathbf{A}'$ and $\mathbf{A}''$. In detail

$$\begin{pmatrix} \boldsymbol{\psi} \\ \boldsymbol{\psi}_H \\ \boldsymbol{\psi}' \\ \boldsymbol{\psi}_D \\ \boldsymbol{\psi}'' \end{pmatrix} = \mathbf{T}\begin{pmatrix} \boldsymbol{\xi} \\ \boldsymbol{\xi}_H \\ \boldsymbol{\xi}' \\ \boldsymbol{\xi}_D \\ \boldsymbol{\xi}'' \end{pmatrix} \tag{11}$$

where

$$\mathbf{T} = \begin{pmatrix} \tilde{\mathbf{S}}\mathbf{E} & \mathbf{0} & \mathbf{0} & \mathbf{0} & \mathbf{0} \\ \mathbf{0} & \tilde{n}_H & \mathbf{0} & 0 & \mathbf{0} \\ \mathbf{0} & \mathbf{0} & \tilde{\mathbf{S}}'\mathbf{E}' & \mathbf{0} & \mathbf{0} \\ \mathbf{0} & 0 & \mathbf{0} & \tilde{n}_D & \mathbf{0} \\ \mathbf{0} & \mathbf{0} & \mathbf{0} & \mathbf{0} & \tilde{\mathbf{S}}''\mathbf{E}'' \end{pmatrix}$$

Thus eq. (9) becomes

Can. J. Chem. Downloaded from www.nrcresearchpress.com by 210.87.254.6 on 09/05/12
For personal use only.

$$(12)\quad \frac{\mathrm{d}}{\mathrm{d}t}\begin{pmatrix}\boldsymbol{\psi}\\ \psi_{\mathrm{H}}\\ \boldsymbol{\psi}'\\ \psi_{\mathrm{D}}\\ \boldsymbol{\psi}''\end{pmatrix}=\begin{pmatrix}\mathbf{D} & \mathbf{0} & \mathbf{0} & \mathbf{0} & \mathbf{0}\\ \tilde{n}_{\mathrm{H}}^2(\boldsymbol{\alpha})^{\mathrm{T}} & 0 & \frac{1}{2}\tilde{n}_{\mathrm{H}}\tilde{n}_{\mathrm{D}}(\boldsymbol{\alpha}')^{\mathrm{T}} & 0 & \mathbf{0}\\ \mathbf{0} & \mathbf{0} & \mathbf{D}' & \mathbf{0} & \mathbf{0}\\ \mathbf{0} & 0 & \frac{1}{2}\tilde{n}_{\mathrm{H}}\tilde{n}_{\mathrm{D}}(\boldsymbol{\alpha}')^{\mathrm{T}} & 0 & \tilde{n}_{\mathrm{D}}^2(\boldsymbol{\alpha}'')^{\mathrm{T}}\\ \mathbf{0} & \mathbf{0} & \mathbf{0} & \mathbf{0} & \mathbf{D}''\end{pmatrix}\begin{pmatrix}\boldsymbol{\psi}\\ \psi_{\mathrm{H}}\\ \boldsymbol{\psi}'\\ \psi_{\mathrm{D}}\\ \boldsymbol{\psi}''\end{pmatrix}$$

$$+\psi_{\mathrm{H}}^2\begin{pmatrix}\boldsymbol{\alpha}\\ w\\ \mathbf{0}\\ 0\\ \mathbf{0}\end{pmatrix}+\psi_{\mathrm{H}}\psi_{\mathrm{D}}\begin{pmatrix}\mathbf{0}\\ \frac{1}{2}w'\\ \boldsymbol{\alpha}'\\ \frac{1}{2}w'\\ \mathbf{0}\end{pmatrix}+\psi_{\mathrm{D}}^2\begin{pmatrix}\mathbf{0}\\ 0\\ \mathbf{0}\\ w''\\ \boldsymbol{\alpha}''\end{pmatrix}$$

where $\psi_{\mathrm{H}}=n_{\mathrm{H}}=\frac{1}{2}[\mathrm{H}]$ replaces what we previously (3) called ϕ; α_i, etc. $=(\boldsymbol{u}^{\mathrm{T}}\mathbf{E}^{-1}\mathbf{S})_i$, etc. for primed and double-primed indices. In expanded form (12) is

$$(13)\qquad \dot{\psi}_i(t)=d_i\psi_i(t)+\alpha_i n_{\mathrm{H}}^2(t)\qquad 0\leqslant i\leqslant(n-1)$$

$$(14)\qquad \dot{\psi}_i'(t)=d_i'\psi_i'(t)+\alpha_i' n_{\mathrm{H}}(t)n_{\mathrm{D}}(t)\qquad 0\leqslant i'\leqslant(n'-1)$$

$$(15)\qquad \dot{\psi}_i''(t)=d_i''\psi_i''(t)+\alpha_i'' n_{\mathrm{D}}^2(t)\qquad 0\leqslant i''\leqslant(n''-1)$$

$$(16)\qquad \dot{n}_{\mathrm{H}}(t)=\tilde{n}_{\mathrm{H}}^2\sum_{i=0}^{n-1}\alpha_i\psi_i(t)+wn_{\mathrm{H}}^2(t)+\tfrac{1}{2}\left[\tilde{n}_{\mathrm{H}}\tilde{n}_{\mathrm{D}}\sum_{i'=0}^{n'-1}\alpha_i'\psi_i'(t)+w'n_{\mathrm{H}}(t)n_{\mathrm{D}}(t)\right]$$

$$(17)\qquad \dot{n}_{\mathrm{D}}(t)=\tilde{n}_{\mathrm{D}}^2\sum_{i''=0}^{n''-1}\alpha_i''\psi_i''(t)+w''n_{\mathrm{D}}^2(t)+\tfrac{1}{2}\left[\tilde{n}_{\mathrm{H}}\tilde{n}_{\mathrm{D}}\sum_{i'=0}^{n'-1}\alpha_i'\psi_i'(t)+w'n_{\mathrm{H}}(t)n_{\mathrm{D}}(t)\right]$$

As was noted in eq. III(11), the integral form of eq. (13) is

$$(18)\qquad \psi_i(t)=\psi_i(0)\,\mathrm{e}^{d_it}+\alpha_i\int_0^t\mathrm{e}^{d_i(t-\tau)}\,n_{\mathrm{H}}^2(\tau)\,\mathrm{d}\tau$$

where, for $0\leqslant i\leqslant(n-2)$, the d_i are large in magnitude and negative; hence an asymptotic expansion can be made in powers of d_i^{-1}, retaining only one term, *i.e.*

$$(19)\qquad \psi_i(t)=\psi_i(0)\,\mathrm{e}^{d_it}+\alpha_i d_i^{-1}n_{\mathrm{H}}^2(0)\,\mathrm{e}^{d_it}-\alpha_i d_i^{-1}n_{\mathrm{H}}^2(t)\qquad 0\leqslant i\leqslant(n-2)$$

with similar results for $\psi_i'(t)$, $0\leqslant i'\leqslant(n'-2)$ and $\psi_i''(t)$, $0\leqslant i''\leqslant(n''-2)$. Thus only five differential equations remain

$$(13a)\qquad \dot{\psi}_{n-1}(t)=d_{n-1}\psi_{n-1}(t)+\alpha_{n-1}n_{\mathrm{H}}^2(t)$$

$$(14a)\qquad \dot{\psi}_{n-1}'(t)=d_{n-1}'\psi_{n-1}'(t)+\alpha_{n-1}'n_{\mathrm{H}}(t)n_{\mathrm{D}}(t)$$

$$(15a)\qquad \dot{\psi}_{n-1}''(t)=d_{n-1}''\psi_{n-1}''(t)+\alpha_{n-1}''n_{\mathrm{D}}^2(t)$$

$$(16a)\qquad \dot{n}_{\mathrm{H}}(t)=\tilde{n}_{\mathrm{H}}^2\alpha_{n-1}\psi_{n-1}(t)+\left[w-\tilde{n}_{\mathrm{H}}^2\sum_{j=0}^{n-2}\alpha_j^2d_j^{-1}\right]n_{\mathrm{H}}^2(t)+\tilde{n}_{\mathrm{H}}^2\sum_{j=0}^{n-2}\alpha_j[\psi_j(0)+\alpha_jd_j^{-1}n_{\mathrm{H}}^2(0)]\,\mathrm{e}^{d_jt}$$
$$+\tfrac{1}{2}\Bigg\{\tilde{n}_{\mathrm{H}}\tilde{n}_{\mathrm{D}}\alpha_{n-1}'\psi_{n-1}'(t)+\left[w'-\tilde{n}_{\mathrm{H}}\tilde{n}_{\mathrm{D}}\sum_{j'=0}^{n'-2}(\alpha_j')^2(d_j')^{-1}\right]n_{\mathrm{H}}(t)n_{\mathrm{D}}(t)$$
$$+\tilde{n}_{\mathrm{H}}\tilde{n}_{\mathrm{D}}\sum_{j'=0}^{n'-2}\alpha_j'[\psi_j'(0)+\alpha_j'(d_j')^{-1}n_{\mathrm{H}}(0)n_{\mathrm{D}}(0)]\,\mathrm{e}^{d_j't}\Bigg\}$$

Can. J. Chem. Downloaded from www.nrcresearchpress.com by 210.87.254.6 on 09/05/12
For personal use only.

$$(17a)\quad \dot{n}_D(t) = \tilde{n}_D^2\alpha''_{n-1}\psi''_{n-1}(t) + \left[w'' - \tilde{n}_D^2 \sum_{j''=0}^{n''-2} (\alpha''_j)^2 (d''_j)^{-1}\right] n_D^2(t)$$
$$+ \tilde{n}_D^2 \sum_{j''=0}^{n''-2} \alpha''_j \left[\psi''_j(0) + \alpha''_j (d''_j)^{-1} n_D^2(0)\right] e^{d''_j t}$$
$$+ \tfrac{1}{2}\left\{\tilde{n}_H\tilde{n}_D\alpha'_{n-1}\psi'_{n-1}(t) + \left[w' - \tilde{n}_H\tilde{n}_D \sum_{j'=0}^{n'-2} (\alpha'_j)^2 (d'_j)^{-1}\right] n_H(t) n_D(t)\right.$$
$$\left. + \tilde{n}_H\tilde{n}_D \sum_{j'=0}^{n'-2} \alpha'_j \left[\psi'_j(0) + \alpha'_j (d'_j)^{-1} n_H(0) n_D(0)\right] e^{d'_j t}\right\}$$

Equations (13*a*)–(17*a*) retain the symmetry characteristic of the reaction scheme.

Organization of the Calculation

The solution of the problem proceeds in the following way. First, the matrices **A**, **A**′, and **A**″ are constructed from the assumed translational–vibrational transition probabilities according to eq. (10), and each is diagonalized separately by methods described elsewhere (2, 11); for temperatures above 1500 °K, this is relatively straightforward if a wordlength of about 30 decimal places is available. The factorization into three separate calculations at this stage is due to the fact that the off-diagonal blocks in eq. (10) are all zero: they would only be non-zero if a collision with the third body were to bring about transmutations between H_2, HD, and D_2, *i.e.* only if the species H, D, H_2, HD, or D_2 were considered as third bodies in non-dilute systems; in such cases, sets of master equations would not only be coupled through the products H and D as they are here, but also through the third bodies, and the solution of such a complicated problem seems intractable in the present state of the art.

An initial distribution is then chosen, and for these calculations we always chose the reactants to be either $H_2 + D_2$, all in $v = 0$ and $v'' = 0$, or pure HD, all in $v' = 0$, together with the usual excess of inert gas M. These distributions are then transformed first to $\xi(0)$ etc. and then to $\psi(0)$ etc. using the eigenvectors **S**, **S**′, and **S**″ (eq. 11). Five differential equations (13*a*)–(17*a*) are then constructed and solved by a fifth-order Runge–Kutta procedure (12) using a step length chosen to be consistent with the desired accuracy; as explained previously (3) this has to be very short at the beginning but, as time progresses, can be made longer and longer as the large (and negative) d_i terms die out of the equations. Here, we used an empirical criterion for "desired accuracy": that the rate constants, as discussed below, were the same whether calculated from the eigenvalues d_{n-1}, d'_{n-1}, and d''_{n-1} by eqs. III(21) and III(22): from the instantaneous values of the upward and downward fluxes by equations II(6*b*) and II(11*b*), which are the differential forms of the rate expressions for dissociation and recombination respectively, or from the total amount of product formed in the given time via the appropriate integrated law; (*cf.* our earlier discussions of eq. II(7*b*) and of eqs. III(21) and III(22) which show that all three methods should agree once the time is sufficiently long that the induction period can be ignored). It is of interest to note that we had to use an order-of-magnitude shorter step length than calculations on H_2(3) or D_2(5) alone would have suggested in order to attain this consistency of the rate constants; perhaps this is in some way related to the fact that in all attempts to solve the original set of 57 equations by direct integration, the indications always were that a shorter step length was required, but we could never achieve it!

Having solved these five simultaneous differential equations (13*a*)–(17*a*) to the desired precision out to the particular time t, the ψ_i, ψ'_i, and ψ''_i are generated from the ψ_{n-1}, ψ'_{n-1}, ψ''_{n-1}, n_H and n_D by the $(n-1)$, $(n'-1)$, and $(n''-1)$ sets of algebraic equations (19), (19′), and (19″). The ψ_i are then transformed back to the ξ_i, and thence to the n_i, using the transformation $\mathbf{T}^{-1}\boldsymbol{\psi}$, since by eq. III(10)

$$\psi_i = \sum_{j=0}^{n-1} \tilde{S}_{ij}\tilde{n}_j^{1/2}\xi_j \qquad 0 \leqslant i \leqslant (n-1)$$

Can. J. Chem. Downloaded from www.nrcresearchpress.com by 210.87.254.6 on 09/05/12
For personal use only.

Can. J. Chem. Downloaded from www.nrcresearchpress.com by 210.87.254.6 on 09/05/12
For personal use only.

TABLE 1. *Typical population distributions in the dissociation of HD at 2000 °K; $t = 10^{-4}$ s*

Initial mixture
$[M] = 3.5 \times 10^{19}$ particles/cc
$[HD] = 1.39012 \times 10^{17}$ molecules/cc, all in the $v = 0$ state
Equilibrium distribution
$[H_2] = 3.47112 \times 10^{16}$ molecules/cc
$[HD] = 6.90119 \times 10^{16}$ molecules/cc
$[D_2] = 3.47336 \times 10^{16}$ molecules/cc
$[H] = 5.77560 \times 10^{14}$ atoms/cc
$[D] = 5.32804 \times 10^{14}$ atoms/cc

$\xi_i = n_i/\tilde{n}_i$	H_2	HD	D_2
ξ_0	2.188×10^{-12}	2.014	3.390×10^{-12}
ξ_1	2.217×10^{-12}	2.014	3.392×10^{-12}
ξ_2	2.531×10^{-12}	2.014	3.406×10^{-12}
ξ_3	5.357×10^{-12}	2.014	3.486×10^{-12}
ξ_4	2.724×10^{-11}	2.014	3.921×10^{-12}
ξ_5	1.728×10^{-10}	2.014	6.112×10^{-12}
ξ_6	1.001×10^{-9}	2.014	1.622×10^{-11}
ξ_7	4.989×10^{-9}	2.013	5.941×10^{-11}
ξ_8	2.106×10^{-8}	2.010	2.288×10^{-10}
ξ_9	7.430×10^{-8}	1.999	8.416×10^{-10}
ξ_{10}	2.156×10^{-7}	1.963	2.863×10^{-9}
ξ_{11}	5.034×10^{-7}	1.866	8.964×10^{-9}
ξ_{12}	9.119×10^{-7}	1.651	2.555×10^{-8}
ξ_{13}	1.235×10^{-6}	1.267	6.623×10^{-8}
ξ_{14}	1.368×10^{-6}	0.7647	1.544×10^{-7}
ξ_{15}	—	0.3728	3.217×10^{-7}
ξ_{16}	—	0.2036	5.906×10^{-7}
ξ_{17}	—	0.1657	9.390×10^{-7}
ξ_{18}	—	—	1.264×10^{-6}
ξ_{19}	—	—	1.464×10^{-6}
ξ_{20}	—	—	1.550×10^{-6}
ξ_{21}	—	—	1.571×10^{-6}
ξ_H	1.227×10^{-3}		
ξ_D	1.330×10^{-3}		

likewise for primed and double-primed quantities.

Using an IBM 360/50 machine, the three diagonalizations took altogether approximately 1 h of computer time for each temperature; thereafter, the integration was quite rapid (about 10^{-3} s of reaction time per min of computing). The time-consuming nature of the diagonalizations is to some extent a reflection of the unsuitable nature of our particular machine for these kinds of calculation; the word length is too short, and cumbersome four-length arithmetic has to be used; the same three matrices can be diagonalized with the required precision on a CDC 6600 machine in about 2 min.

Results

Tables 1 and 2 show sample population distributions for the time $t = 10^{-4}$ s for the dissociation of HD and for the reaction of H_2 with D_2, respectively. The data for H_2 and D_2 in Table 2 are indistinguishable from the distributions that H_2 and D_2 would have at the same time if they were dissociating *alone* under the same conditions. Qualitatively then, the description of each of the three dissociation processes is very similar to that which we have already described (2) but with one small difference. That is, that when a H_2 or a D_2 molecule dissociates into atoms, not only can the H or D atoms recombine back to the parent molecules, but they find another sink into which they can be trapped with a partner of the opposite kind. These product molecules appear to be

TABLE 2. *Typical population distributions in the reaction of H_2 with D_2 via reactions [3a], [4a], and [5a] at 2000 °K; $t = 10^{-4}$ s*

Initial mixture
$[M] = 3.5 \times 10^{19}$ particles/cc
$[H_2] = [D_2] = 6.95059 \times 10^{16}$ molecules/cc, all in the $v = 0$ state
Equilibrium distribution
$[H_2] = 3.47112 \times 10^{16}$ molecules/cc
$[HD] = 6.90119 \times 10^{16}$ molecules/cc
$[D_2] = 3.47336 \times 10^{16}$ molecules/cc
$[H] = 5.77560 \times 10^{14}$ atoms/cc
$[D] = 5.32804 \times 10^{14}$ atoms/cc

$\xi_i = n_i/\tilde{n}_i$	H_2	HD	D_2
ξ_0	2.002	2.680×10^{-12}	2.001
ξ_1	2.002	2.688×10^{-12}	2.001
ξ_2	2.002	2.762×10^{-12}	2.001
ξ_3	2.002	3.328×10^{-12}	2.001
ξ_4	2.002	7.139×10^{-12}	2.001
ξ_5	2.002	3.020×10^{-11}	2.001
ξ_6	2.001	1.538×10^{-10}	2.001
ξ_7	1.996	7.337×10^{-10}	2.001
ξ_8	1.974	3.202×10^{-9}	2.001
ξ_9	1.904	1.220×10^{-8}	2.000
ξ_{10}	1.716	4.016×10^{-8}	1.998
ξ_{11}	1.333	1.162×10^{-7}	1.991
ξ_{12}	0.7897	2.843×10^{-7}	1.972
ξ_{13}	0.3605	5.859×10^{-7}	1.926
ξ_{14}	0.1837	9.791×10^{-7}	1.826
ξ_{15}	—	1.286×10^{-6}	1.637
ξ_{16}	—	1.419×10^{-6}	1.333
ξ_{17}	—	1.449×10^{-6}	0.9385
ξ_{18}	—	—	0.5703
ξ_{19}	—	—	0.3448
ξ_{20}	—	—	0.2474
ξ_{21}	—	—	0.2228
ξ_H	1.051×10^{-3}		
ξ_D	1.502×10^{-3}		

TABLE 3. Rate constants for the dissociation* and recombination† of H_2, HD, and D_2 calculated by eqs. III(21) and III(22), or by eqs. II(6*b*) and II(11*b*)

T (°K)	k_d	k'_d	k''_d	k_r	k'_r	k''_r
1500	2.516×10^{-25}	2.787×10^{-25}	2.918×10^{-25}	1.544×10^{-34}	4.220×10^{-34}	2.559×10^{-34}
2000	1.248×10^{-21}	1.457×10^{-21}	1.645×10^{-21}	1.299×10^{-34}	3.268×10^{-34}	2.013×10^{-34}

*In cm^3 molecule^{-1} s^{-1}.
†In cm^6 molecule^{-2} s^{-1}.

formed with grossly non-Boltzmann population distributions amongst the vibrational levels.

Because there are apparently such distorted population distributions, at least in the product molecules, it is of interest to calculate the phenomenological rate constants for dissociation and recombination in the system. As standards for comparison, Table 3 presents the recombination and dissociation rate constants for H_2, HD, and D_2 calculated from the eigenvalues d_{n-1}, d'_{n-1}, and d''_{n-1} by equations III(21) and III(22). Note that k'_d lies between k_d and k''_d for reasons already explained (5). Note also that k'_r is roughly twice as big as the mean k_r and k''_r as required by the standard definitions due to the difference in symmetry number between homo- and hetero-nuclear diatomic molecules. The rate constants for these processes can be calculated from the population distributions and transition probabilities, as described before (2), the data in Table 1 yielding k'_d, k_r, and k''_r, and Table 2 k_d, k''_d, and k'_r. It turns out that all six rate constants are identical to those calculated from the eigenvalues, despite the fact that the population distributions of the newly formed product molecules look distorted. It is not surprising that the dissociation rate constants can be defined, since the population distributions of the reactants are so little affected by the alternative channel(s) open to the atoms, but perhaps it is surprising that the recombination rate constants are so well-behaved; however, inspection of the H_2 data in Table 1 reveals that the product-molecule distributions are similar to those obtaining in normal recombinations (2, 3, 13) apart from a rather large scaling factor. The effect of successively closer vibrational level spacings in H_2, HD, and D_2 also shows up in Tables 1 and 2: for the newly formed product molecules, there is both a better equilibration amongst the lower vibrational states, and a faster path for molecules down to the lower levels as the vibrational spacings come closer together (5).

One can define another kind of rate constant from the data in Tables 1 and 2, *viz.*

HD dissociation

$$(20)\quad R_{H_2} = k_f[M]\{[HD]^2 - K_m[H_2][D_2]\}$$

$$(20'')\quad R_{D_2} = k''_f[M]\{[HD]^2 - K_m[H_2][D_2]\}$$

$$(21')\quad -R_{HD} = k'_{dd}[M]\{[HD]^2 - K_m[H_2][D_2]\}$$

H_2/D_2 reaction

$$(20')\quad R_{HD} = k'_f[M]\{[H_2][D_2] - K_m^{-1}[HD]^2\}$$

$$(21)\quad -R_{H_2} = k_{dd}[M]\{[H_2][D_2] - K_m^{-1}[HD]^2\}$$

$$(21'')\quad -R_{D_2} = k''_{dd}[M]\{[H_2][D_2] - K_m^{-1}[HD]^2\}$$

with

$$(22)\quad K_m = \frac{[HD]^2}{[H_2][D_2]} = \frac{k_{dd}}{k_f} = \frac{k'_f}{k'_{dd}} = \frac{k''_{dd}}{k''_f}$$

The rate constants defined by eqs. (21), (21'), and (21'') are trivial, since the rate of disappearance of the diatomic in question is also related to the rate constant to be found in Table 3, *e.g.* at early times, neglecting the back reaction, we can write

$$(23)\quad k_{dd}[H_2][D_2] = k_d[H_2]$$

whence k_{dd} is simply $k_d/[D_2]$.

On the other hand, the rate constants for the formation of diatomics expressed in terms of the diatomics are not trivial, since they turn out to be time-dependent. The time dependency arises very simply, since using eq. (20') as an example, at early times before back reaction commences but long compared with the induction period, one can write (2)

$$\begin{aligned} R_{HD} &= k'_r[M][H][D] \\ &= k'_r[M]\{2k_d[M][H_2]t\}\{2k''_d[M][D_2]t\} \\ &= 4k'_rk_dk''_d[M]^3[H_2][D_2]t^2 \end{aligned}$$

whence

$$(24')\quad k'_f = 4k'_rk_dk''_d[M]^2t^2$$

Can. J. Chem. Downloaded from www.nrcresearchpress.com by 210.87.254.6 on 09/05/12
For personal use only.

Can. J. Chem. Downloaded from www.nrcresearchpress.com by 210.87.254.6 on 09/05/12
For personal use only.

The population distributions such as are shown in Tables 1 and 2, when cast in the form of eqs. (20), (20′), and (20″), all give t^2-dependent k_f rate constants conforming to eq. (24) etc., thus demonstrating the internal consistency of our population distributions and the accuracy of the integration. Had the rate expressions (20) and (21) excluded the term in [M] on the right hand side, eqs. (23) and (24) would have been appropriately different, but eq. (24) would still retain its dependence on t^2. In recent months, rate constants having a *first-power* t-dependence have been reported in two instances, in shock-tube studies of reactions in H_2/D_2 and HCl/D_2 systems (7, 14).

Towards a Complete Solution of the Heteronuclear Diatomic Dissociation Problem

The main purpose of the work described in this paper has been to show that although the 57 simultaneous differential equations representing the vibration–dissociation coupling of HD at infinite dilution cannot be solved by conventional integration, they can be solved by the normal-mode approach. It would seem therefore that the present type of solution represents a good starting point upon which to base an attempt at a complete solution of the problem, since it seems more than likely that even if rate coefficients were known for reactions [7], [8], and [9] with X = H and Y = D, direct numerical integration would fail as it did here. It is clearly a great simplification that the phenomenological rate constants are well-defined and well-behaved even though the population distributions are as far from Boltzmann as they appear to be in Tables 1 and 2. Thus, it seems that the first attempts at a complete solution should try to superimpose the atomic exchange reactions [7] and [8], and the molecular exchange reaction [9] on population distributions such as those presented in Tables 1 and 2. The effect of including such reactions will be to perturb the population distributions slightly, just as happens when vibration–vibration coupling is included into a simple vibration–dissociation coupling scheme; however, these changes in population are small (8) and would therefore not alter the overall rate appreciably. What will happen, however, is that the perturbation of the population distribution will be different for different concentrations of reactants, and so one will not find simple orders in the reactants, as we have explained previously (8): (*cf.* also ref. 15); we feel therefore that Kaufman's criticism (16) of Bauer's work on *this particular count* should be softened slightly. Thus, at the present stage of the art, given correct rate coefficients for the atomic and molecular exchange reactions between each pair of vibrational levels of reactant and product, one should easily predict the correct overall rate with moderate accuracy. One will not however be able to predict the order in reactants, nor the temperature coefficient of the rate; these must await the development of better integration techniques than those at present available.

As far as the special case of the H_2/D_2 system is concerned, there have been several discussions of the reaction (6, 7, 15, 17) and related ones (14, 18) using both normal Boltzmann and slightly perturbed distributions of reactants. Inspection of Tables 1 and 2, in the light of the results of ref. 8 discussed above, shows that no serious fallacy is introduced by assuming equilibrium population distributions, at least as far as the overall rate is concerned. Thus, with X = H and Y = D, reactions [7] and [8] are many orders of magnitude too slow to give the experimentally observed rates of equilibration of H_2 and D_2, as has been pointed out several times (6, 7, 15, 18). One is therefore left with the paradox that although most theoretical predictions put the activation energy barrier for the molecular exchange [9] very high indeed (19–22), that reaction would have to be very fast indeed to account for the observed rates (6, 15, 16, 23). In fact, if the observed Arrhenius temperature coefficients of around 40 kcal/mol can be assumed to be lower limits to the critical energy, any single molecular exchange process would need to have a P-factor of the order of 10^2 or more to account for the observed rates, which seems unlikely: there are however several such possible processes, and taken all together, they could collectively give rise to the observed rate if most of them had P-factors of the order of 10; this same factor of 10 arises in a somewhat different guise in other treatments (15). Thus, either the critical energy for the molecular exchange reaction is rather less than 40 kcal, although some theoretical predictions place it nearer 140 kcal, or there is some other exchange mechanism that has not yet been considered. The mechanism which is the subject of this paper is of course far too slow, as illustrated by the comparison of the extents of reaction shown in

Tables 1 and 2 with the experimental observation that complete equilibration is achieved in the order of 1 ms; however, this rate does have a t^2-dependence and accelerates rapidly as time progresses. Clearly the resolution of this paradox will require much detailed work along the lines suggested by Kaufman (16) and by Belford and Strehlow (23); however, an experimental search for an unsuspected source of atoms (24),[2] building up linearly with t, would seem to be well worthwhile in view of the recent discovery of a time-dependent rate (7), for whilst the model proposed by Kern and Nika does account for the observed form of the time dependence, it too fails to account satisfactorily for the high rate of the reaction. Also, the homogeneous ortho–para conversion of H_2 should have a similarly time-dependent rate law; the study of this reaction in a shock tube would present significant technical problems, but would be important not only for its own intrinsic interest, but also to throw more light on the isotopic exchange problem.

1. V. A. LoDato, D. L. S. McElwain, and H. O. Pritchard. J. Am. Chem. Soc. **91**, 7688 (1969).
2. D. L. S. McElwain and H. O. Pritchard. J. Am. Chem. Soc. **91**, 7693 (1969).

[2]Craig has calculated for us the rate of scrambling of H_2 and D_2 that would occur in the combustion of 20 p.p.m. O_2 in a 98:1:1 Ar:H_2:D_2 mixture and confirmed Schott's conclusion, quoted by Bauer and Ossa (6): thus, free O_2 which is present in these sorts of quantities (7) is certainly not responsible; it would seem that any other likely impurity atoms would have to be introduced into the shock-tube system during fabrication or cleaning processes (25).

3. D. L. S. McElwain and H. O. Pritchard. Thirteenth Symposium (International) on Combustion. The Combustion Institute, Pittsburgh, Pa. 1971. p. 37.
4. E. Kamaratos and H. O. Pritchard. Can. J. Chem. **49**, 2617 (1971).
5. D. L. S. McElwain and H. O. Pritchard. Can. J. Chem. **49**, 3915 (1971).
6. S. H. Bauer and E. Ossa. J. Chem. Phys. **45**, 434 (1966).
7. R. D. Kern and G. G. Nika. J. Phys. Chem. **75**, 1615 (1971); **75**, 2541 (1971).
8. D. L. S. McElwain and H. O. Pritchard. J. Am. Chem. Soc. **92**, 5027 (1970).
9. W. Kolos and L. Wolniewicz. J. Chem. Phys. **49**, 404 (1968).
10. R. J. LeRoy. J. Chem. Phys. **54**, 5433 (1971).
11. A. Wallis, D. L. S. McElwain, and H. O. Pritchard. Int. J. Quant. Chem. **3**, 711 (1969).
12. J. D. Lawson. SIAM J. Num. Anal. **3**, 593 (1966).
13. D. L. S. McElwain. Ph.D. Thesis, York University, Toronto, Ontario. 1970.
14. R. D. Kern and G. G. Nika. J. Phys. Chem. **75**, 171 (1971).
15. L. L. Poulsen. J. Chem. Phys. **53**, 1987 (1970).
16. F. Kaufman. Ann. Rev. Phys. Chem. **20**, 45 (1969).
17. K. Morokuma, L. Pedersen, and M. Karplus. J. Am. Chem. Soc. **89**, 5064 (1967).
18. P. Schechner, A. Burcat, and A. Lifshitz. J. Chem. Phys. **52**, 337 (1970).
19. H. Conroy and G. Malli. J. Chem. Phys. **50**, 5049 (1969).
20. R. N. Porter and L. M. Raff. J. Chem. Phys. **50**, 5216 (1969).
21. C. W. Wilson and W. A. Goddard. J. Chem. Phys. **51**, 716 (1969).
22. M. Rubinstein and I. Shavitt. J. Chem. Phys. **51**, 2104 (1969).
23. R. L. Belford and R. A. Strehlow. Ann. Rev. Phys. Chem. **20**, 237 (1969).
24. R. A. Craig. Unpublished results.
25. R. K. Boyd, G. Burns, T. R. Lawrence, and J. H. Lippiat. J. Chem. Phys. **49**, 3804 (1968).

Can. J. Chem. Downloaded from www.nrcresearchpress.com by 210.87.254.6 on 09/05/12
For personal use only.

n-Butylamine Adsorption onto Amorphous Silica

COLIN CLARK-MONKS[1] AND BRYAN ELLIS
Department of Glass Technology, University of Sheffield, Sheffield 10, Yorkshire, England

Received June 29, 1971

Gravimetric and infrared spectroscopic observations of *n*-butylamine adsorption onto silica have shown that strong adsorption is associated primarily with *isolated* surface hydroxyl groups and also with some *vicinal* surface groups. Adsorbed material can be totally removed from the surface by outgassing at elevated temperature (to 200 °C) without irreversible changes to the underlying surface. The interaction between adsorbed amine and ethylene oxide vapor has been investigated and a possible reaction mechanism is presented.

Les observations spectroscopiques infrarouge et de gravimétrie sur l'adsorption de la *n*-butylamine sur la silice ont montrées qu'une forte adsorption est essentiellement due à la présence de groupes hydroxyles isolés de surface et également à la présence de groupes vicinaux de surface. Les produits adsorbés peuvent être complètement éliminés de la surface par un dégazage à température élevée (200 °C) et ceci sans changement irréversible des surfaces sous-jacentes.

Canadian Journal of Chemistry, **50**, 907 (1972)

Introduction

The mechanism of amine adsorption onto siliceous surfaces has been the subject of several investigations (1,2–3,4) and it would appear that strong adsorption onto surfaces with low concentrations of surface hydroxyl groups is often associated with *isolated* hydroxyl units. *Isolated* hydroxyl groups are defined as groups which do not undergo interaction with other surface hydroxyl groups, being further than ~3 Å from their nearest neighbors. Other surface hydroxyl groups are close enough together to undergo mutual interactions and are usually classified as *vicinal* units. There has been some speculation on the precise nature of the adsorbed amine species, and the formation of a quaternary ammonium surface group has been postulated (2); however, this view is not confirmed by us.

In the present work, a detailed examination of *n*-butylamine adsorption onto a well-characterized silica surface has been carried out in order to ascertain the applicability of earlier suggested adsorption mechanisms, and the interaction of the adsorbed amine species with ethylene oxide vapor has been investigated. Both gravimetric and infrared spectroscopic observation of the adsorption behavior have been employed. The silica adsorbent used was amorphous, had a surface area of 356 ± 7 m^2/g, and a surface hydroxyl group concentration of 3.1 groups/100 Å^2 of which approximately 1.4 groups/100 Å^2 are considered to be *isolated* units. Characterization of the silica surface (17) has been previously reported (5).

[1]Present address: Technical Centre, Fiberglas Canada Ltd., P.O. Box 3005, Sarnia, Ontario.

Experimental

Adsorption was measured gravimetrically in a McBain–Bakr type of balance utilizing a fused silica spring. The balance system could be evacuated to a pressure of 10^{-6} Torr and was thermostatted in an air bath: the use of a furnace enabled adsorbent sample temperatures to be raised from ambient to 450 °C.

Infrared spectra were recorded using a cell which enabled direct observation of adsorption onto pressed silica discs. The cell was constructed from brass with removable potassium bromide windows which were polished before each experiment, and was similar to the design given by Kagel and Hersher (6). It was connected to a conventional vacuum rack. All spectra were corrected for background absorption due to vapor in the cell.

The amorphous silica used was a particulate pyrogenic material[2] and was thoroughly outgassed between 100 and 110 °C prior to experiment. Adsorbates used were *n*-butylamine (G.P.R.) and ethylene oxide (G.P.R.), and were thoroughly outgassed *in situ* before use.

Apparatus and experimental techniques are further detailed in ref. 5.

Results and Discussion

The adsorption isotherm measured gravimetrically at 23 °C was of the B.D.D.T (7) Type II, with a strong *irreversible* adsorption (8) being found on subsequent outgassing (Fig. 1). *Irreversibly* adsorbed material W_{irr}, was found

[2]Cab-O-Sil S17 (Cabot Carbon Ltd.).

Can. J. Chem. Downloaded from www.nrcresearchpress.com by 210.87.254.42 on 09/05/12
For personal use only.

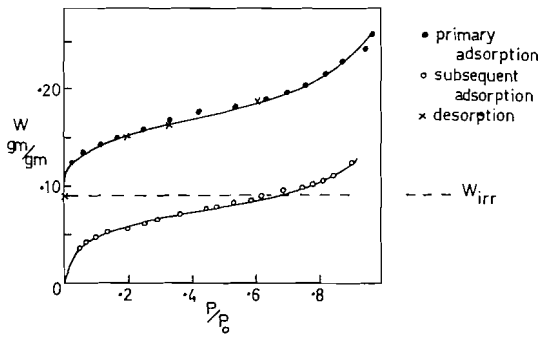

FIG. 1. Adsorption isotherms of *n*-butylamine onto the silica. $T = 23$ °C. ●, primary adsorption; ○, subsequent adsorption; X, desorption; --- W_{irr}.

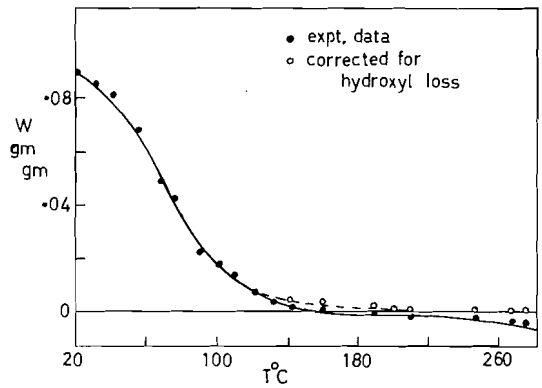

FIG. 2. Loss of *irreversibly* adsorbed *n*-butylamine with temperature (*in vacuo*).

to be 0.0893 g/g which is equivalent to 2.1 molecules/100 Å^2. Although *irreversible* adsorption may be associated with *isolated* surface hydroxyl groups as suggested elsewhere, in the present case adsorption must also be associated with other surface groups since the *isolated* site concentration is only approximately 1.4 groups/100 Å^2. Analysis of the secondary reversible adsorption isotherm using the B.E.T. equation (9) yields a "monolayer" capacity of $W_m = 0.466$ g/g which is equivalent to 1.1 molecules/100 Å^2, and it is interesting to note that $W_m + W_{irr} \simeq 3.2$ molecules/100 Å^2, which is similar to the total surface hydroxyl group concentration; therefore, adsorption in the first complete adsorbed layer may be in a 1-to-1 ratio with surface hydroxyl groups. Consideration of the adsorbate molecular shape and size (chain length >5 Å) shows that interaction with the surface must occur with the chain "end" to give such a result, and this is consistent with the conclusions advanced by Ross and Taylor (2). The latter authors also present isosteric heats of adsorption which show that there is a strong lateral interaction between adsorbed molecules containing amine groups. This indicates that there is some tendency to clustering around the primary adsorption sites.

An investigation of the outgassing characteristics of the silica plus *irreversibly* adsorbed material showed a gradual removal of material with increasing temperature (1 °C/min) until apparently total loss by 200 °C, Fig. 2. Correction of the total weight loss for surface hydroxyl group condensation (5) would agree with complete desorption of the amine which is later shown to be correct by infrared spectroscopy. Thus, there must be a strong but reversible surface interaction which may be consistent with the concept of an adsorbed quaternary ammonium species (2). This is not, however, confirmed by the present study. The adsorption residence time has been shown to depend critically on the energy of adsorption (10): thus, the present desorption results are readily interpreted qualitatively as showing that there is a distribution of site energies and that for some sites the adsorption energy must be high (>15 kcal/mol).

In order to properly clarify the nature of the interactions occurring, direct infrared spectroscopic observation of adsorption onto a pressed silica disc has been employed as previously described (5). The behavior on degassing at increased temperatures after adsorption of *n*-butylamine at room temperature is shown by the infrared spectra in Fig. 3. The silica has been thermally pretreated in air at 810 °C so that the available surface contained only *isolated* hydroxyl groups. Deuteration of this silica disc had previously shown that all the hydroxyl groups present were available to adsorbing vapors (5). Other spectra for adsorption onto a silica disc which had been thermally pretreated at 440 °C, and a disc which had not been thermally treated but which was pre-deuterated, are presented in Fig. 4. The spectra presented demonstrate that adsorption of *n*-butylamine is indeed primarily associated with the *isolated* surface hydroxyl sites because of the perturbation of the absorption band at 2.67 μ (3.63 μ, deuterated) which is assigned to those groups (4, 5, 11–13). Perturbation occurs with the appearance of a broad band around 3.5 μ superimposed on absorption bands

Can. J. Chem. Downloaded from www.nrcresearchpress.com by 210.87.254.42 on 09/05/12
For personal use only.

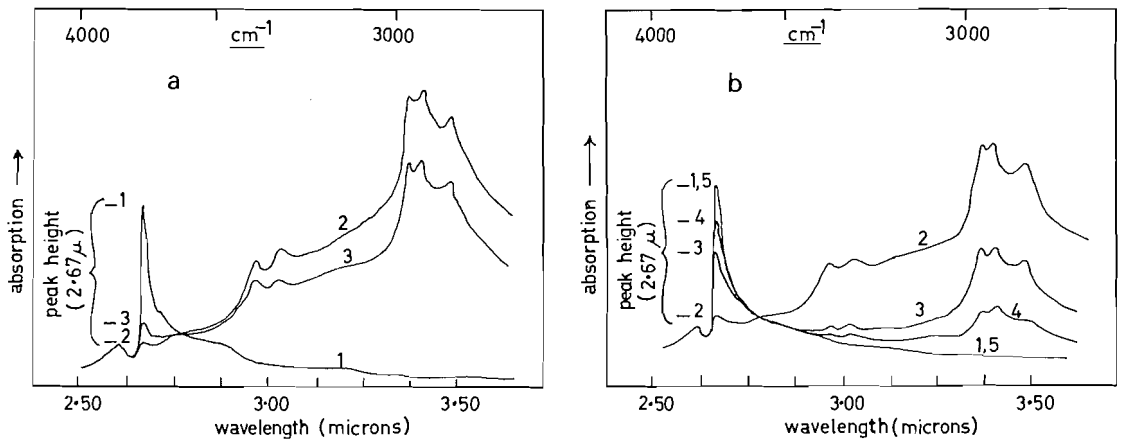

FIG. 3. (*a*) Adsorption of *n*-butylamine onto a pressed silica disc (pretreated at 810 °C). $T = 30$ °C. Trace *1*, initial spectrum of disc; trace *2*, with amine vapor at 12.0 τ; trace *3*, spectrum after outgassing (to 10^{-4} τ) following trace *2*. (*b*) *Irreversibly* adsorbed *n*-butylamine on pressed silica disc (pretreated at 810 °C), and its loss with increasing outgas temperature. Trace *1*, initial spectrum of disc; trace *2*, after exposure to amine vapor at 20 τ, followed by outgassing (10^{-4} τ) at 30 °C; trace *3*, subsequent outgas at 65 °C; trace *4*, subsequent outgas at 95 °C; trace *5*, subsequent outgas at 140 °C.

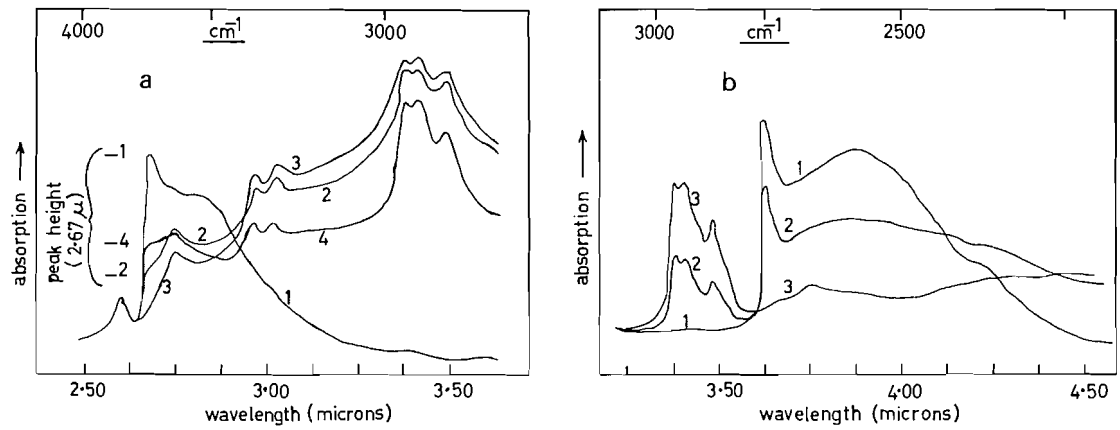

FIG. 4. (*a*) Adsorption of *n*-butylamine onto a pressed silica disc (pretreated at 440 °C), $T = 30$ °C. Trace *1*, initial spectrum of disc; trace *2*, with amine vapor at 3.5 τ; trace *3*, with amine vapor at 9.0 τ; trace *4*, outgassed (10^{-4} τ) after trace *3*. (*b*) Adsorption of *n*-butylamine onto a pressed silica disc (pre-deuterated), $T = 30$ °C. Trace *1*, initial spectrum of disc; trace *2*, with amine vapor at 0.5 τ; trace *3*, with amine vapor at 3.5 τ. Outgassing after trace *3* gave no spectral change.

at 2.95 to 3.05 μ (unperturbed N—H vibrations (14)) and at 3.45 μ (C—H vibrations) due to adsorbed *n*-butylamine. Similar effects have been previously recorded by Basila (1) for the adsorption of diethylamine onto silica. Evacuation at 30 °C following the adsorption of *n*-butylamine left a strongly adsorbed residue which, in the case of the thermally pretreated samples, remained with the perturbation of approximately all the *isolated* surface groups. In the case of the predeuterated sample (Fig. 4), adsorption and subsequent outgassing were suspected to have removed some of the deuterated hydroxyl groups by exchange with the reversibly adsorbed *n*-butylamine: the outgassed sample (with *irreversibly* adsorbed amine) was therefore re-deuterated by two exposures to saturated D_2O vapor for 2 min. The intensities of the absorption bands due to *irreversibly* adsorbed amine were not visibly affected by re-deuteration and the resulting spectrum was found to exhibit only a small proportion of residual *isolated* surface groups (peak height of the 3.63 μ absorption band $<10\%$ of the pre-

Can. J. Chem. Downloaded from www.nrcresearchpress.com by 210.87.254.42 on 09/05/12
For personal use only.

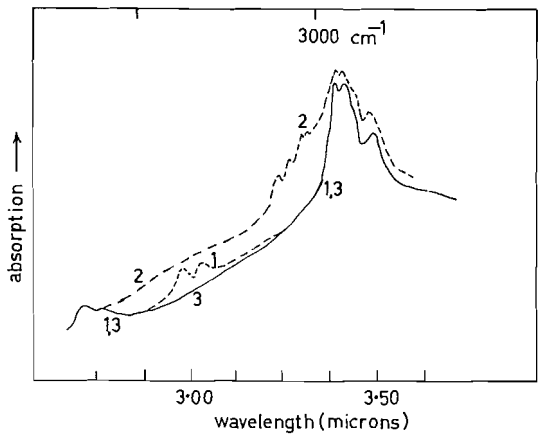

FIG. 5. Ethylene oxide adsorbing onto *irreversibly* adsorbed *n*-butylamine, $T = 30$ °C. Trace *1*, *irreversibly* adsorbed amine on silica disc; trace *2*, with ethylene oxide vapor present at 70 τ for 5 min; trace *3*, outgassed (10^{-4} τ) following trace *2*.

adsorption height). Re-deuteration also only has a small effect on the intensity of the absorption band near to 3.9 μ (which is assigned to *vicinal* surface groups (13), and the spectrum is only marginally different to the final trace presented in Fig. 4*b*. It is therefore concluded that although *irreversibly* adsorbed *n*-butylamine is primarily associated with *isolated* surface sites, some is also associated with *vicinal* surface sites (on the thermally untreated silica sample) which was concluded previously from consideration of the gravimetric data.

The observed outgassing behavior of the pretreated (810 °C) silica disc with *irreversibly* adsorbed *n*-butylamine, Fig. 3 shows that adsorbed species are completely removed by outgassing at 140 °C. Therefore, these observations demonstrate that no permanent and completely irreversible effects occur and that *irreversibly* adsorbed *n*-butylamine can be removed without affecting the surface structure, which supports the gravimetric evidence.

From the present infrared data, it appears unlikely that primary amines primarily adsorb as a quaternary ammonium species (2). Amine salts $(—NH_3)^+$ are reported to show an absorption band for N—H stretching vibration near to 3.2 μ (14), and whilst the spectra presented in Figs. 3 and 4 are not sufficiently well-defined to show beyond doubt that the amine salt is not formed it is clear that the unperturbed $—NH_2$ vibrations (14) (2.95 and 3.05 μ) are still present, which would not be the case if most of the amine had formed a quaternary ammonium species.

Confidence in the conclusion that the $—NH_2$ absorption bands are present in Figs. 3 and 4 is increased by the disappearance of these bands when ethylene oxide is adsorbed onto a silica with preadsorbed *n*-butylamine, Fig. 5. The adsorption of ethylene oxide onto this silica has been described previously (5) and it was shown that the adsorption at room temperature was completely reversible. The nature of the principal surface reaction between ethylene oxide and strongly adsorbed *n*-butylamine is not completely elucidated, but could possibly be formally represented as

[1]

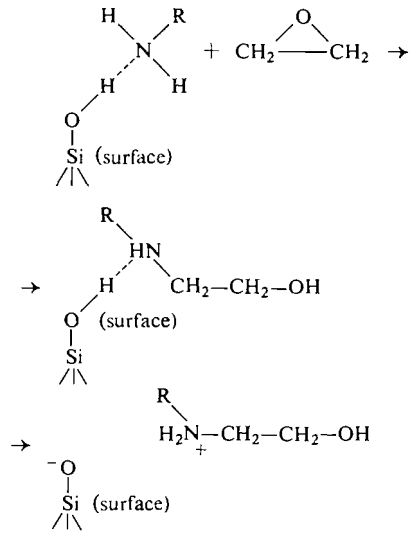

The formation of the quaternary ammonium species in this case may be allowed since a secondary amine is generally considered to be more basic than a primary amine (15). Such a reaction may satisfactorily explain the strong adhesion of epoxy resins cured with primary amines to siliceous surfaces (16) since ethylene oxide can be considered to be analogous to the resin end groups. However, the possibility of more than one surface reaction occurring should not be excluded and the real situation is probably highly complex.

These investigations therefore show that strong adsorption of *n*-butylamine onto silica surfaces occurs at room temperature onto primarily the *isolated* surface hydroxyl groups

Can. J. Chem. Downloaded from www.nrcresearchpress.com by 210.87.254.42 on 09/05/12
For personal use only.

but also involves other *vicinal* surface groups. The adsorbed species can be totally removed by outgassing at elevated temperatures without any permanent effects on the underlying surface structure. Previously suggested quaternary ammonium salt formation would now appear unlikely on the basis of the present infrared spectroscopic data.

Thanks are due to the Science Research Council for financial support, and to Cabot Carbon Ltd. for the donation of materials.

1. M. R. BASILA. J. Chem. Phys. **35**, 1151 (1961).
2. R. A. ROSS and A. H. TAYLOR. Proc. Brit. Ceram. Soc. **5**, 167 (1965).
3. W. HERTL and M. L. HAIR. J. Phys. Chem. **72**, 4676 (1968).
4. M. L. HAIR and W. HERTL. J. Phys. Chem. **73**, 4269 (1969).
5. (*a*) C. CLARK-MONKS. Ph.D. Thesis. The University of Sheffield. Sheffield, Yorkshire, England. 1970. (*b*) B. ELLIS, C. CLARK-MONKS, and K. ROWAN. Phys. Chem Glass. In press.
6. R. O. KAGEL and L. W. HERSHER. Appl. Spectrosc. **21**, 187 (1967).
7. S. BRUNAUER, L. S. DEMING, W. S. DEMING, and E. TELLER. J. Am. Chem. Soc. **62**, 1723 (1940).
8. C. CLARK-MONKS, B. ELLIS, and K. ROWAN. J. Coll. Int. Sci. **32**, 628 (1970).
9. S. BRUNAUER, P. H. EMMETT, and E. TELLER. J. Am. Chem. Soc. **60**, 309 (1938); S. BRUNAUER, L. E. COPELAND, and D. L. KANTRO. *In* The solid–gas interface, Vol. 1. *Edited by* E. A. Flood. Marcel-Dekker, New York. 1966. Chap. 3, p. 77.
10. J. H. DE BOER. The dynamical character of adsorption. Oxford University Press, 1953. p. 35.
11. F. W. HAMBLETON and J. A. HOCKEY. Trans. Faraday Soc. **62**, 1694 (1966).
12. J. B. PERI and A. L. HENSLEY. J. Phys. Chem. **72**, 2926 (1968).
13. F. H. HAMBLETON, J. A. HOCKEY, and J. TAYLOR. Trans. Faraday Soc. **62**, 795 (1966); **62**, 801 (1966).
14. L. SEGAL. J. Phys. Chem. **65**, 698 (1961).
15 J. MARCH. Advanced organic chemistry: reactions, mechanisms and structure. McGraw-Hill, 1968. p. 229.
16. J. A. GORBATKINA. Plate und Kautschuk, **13**, 145 (1966).
17. C. CLARK-MONKS and B. ELLIS. J. Coll. Int. Sci. To be published.

Can. J. Chem. Downloaded from www.nrcresearchpress.com by 210.87.254.42 on 09/05/12
For personal use only.

The Crystal and Molecular Structure of bis(triphenylphosphine)-(ethylene)platinum, $(PPh_3)_2PtC_2H_4$

P.-T. CHENG AND S. C. NYBURG

Lash Miller Chemical Laboratories, University of Toronto, Toronto 181, Ontario

Received September 1, 1971

The X-ray crystal structure analysis of the triphenyl–phosphine platinum ethylene complex $(PPh_3)_2PtC_2H_4$ is reported. The crystals belong to the monoclinic system $a = 16.46(3)$, $b = 10.85(2)$, $c = 17.85(3)$ Å, $\beta = 100.5(1)°$, space group $P2_1/a$, $Z = 4$ molecules per cell.

The ethylene C—C distance of 1.434(13) Å is in accord with that found when other transition elements form metallo-cyclopropanes. The structure has been refined by anisotropic full-matrix least-squares, the final R-factor being 0.043 for 4174 observed reflections.

On rapporte l'analyse par rayons-x de la structure cristalline du complexe triphénylphosphine éthylène platine, $(PPh_3)_2PtC_2H_4$. Les cristaux appartiennent au système monoclinique $a = 16.46(3)$, $b = 10.85(2)$, $c = 17.85(3)$ Å, $\beta = 10.05(1)°$, au groupe spatial $P2_1/a$, $Z = 4$ molécules par maille.

La distance C—C dans l'éthylène de 1.434(13) Å est concordante avec celle qu'on trouve quand d'autres éléments de transition forment des métallo-cyclopropanes. La structure a été raffinée par la méthode anisotropique matricielle des moindres carrés, le facteur R final étant de 0.043 pour les réflexions 4174 observées.

Canadian Journal of Chemistry, **50**, 912 (1972)

Introduction

The primary problem concerning the nature of the bonding of unsaturated molecules to transition metals is whether, when a carbon–carbon double bond is involved, the system should be described as a metallo-cyclopropane derivative or a π-adduct of the metal. The Dewar–Chatt–Duncanson (D–C–D) (1) representation of the bonding between ethylene and transition metals allows any reasonable oxidation state of the metal. In the case of platinum, the oxidation state could be between Pt(0) and Pt(II) depending upon the extent of back-donation.

Crystallographic data are accumulating on certain closely related complexes, *e.g.* $(PPh_3)_2PtC_2(CN)_4$ (2), $(PPh_3)_2PtC_2Cl_4$ (3), and $(PPh_3)_2NiC_2H_4$ (4). In order to make a critical appraisal of the D–C–D model and to learn the role played by the electron-withdrawing groups —CN and —Cl we have undertaken a three-dimensional X-ray analysis of the ethylene complex $(PPh_3)_2PtC_2H_4$, a brief report on which has already been published (5).

Experimental

The crystals of the ethylene adduct were supplied by Cook of this Department. They are colorless cuboids, stable under X-irradiation with major crystal forms {011}, {01$\bar{1}$}, and {100}. Unit cell dimensions were determined by measuring eleven 2θ, χ, and ϕ settings of strong ($h00$), ($0k0$), and ($00l$) reflections and refining by least squares. The crystal data are as follows:

$C_{38}H_{34}P_2Pt$ f.w. = 747

Monoclinic, $a = 16.46(3)$, $b = 10.85(2)$, $c = 17.85(3)$ Å, $\beta = 100.5(1)°$. $V = 3135$ Å^3, $\rho_0 = 1.56(1)$, $Z = 4$, $\rho_c = 1.58$ (25 °C; MoKα, $\lambda = 0.7107$ Å, $\mu = 47.7$ cm^{-1}).

Intensity data were collected by automated diffractometer using MoKα radiation in 2θ scan mode at 1° min^{-1} with $0 \leqslant \sin\theta \leqslant 0.4$. The scanning range at low 2θ was 1.6°. The crystal used was a small cube with *ca.* 0.3 mm edge and no absorption corrections were applied to the intensity data. The weighting scheme used was (6)

$$\sigma^2(F^2) = I/(LP)^2 + CF^4$$

where I is peak plus background intensity and C was taken as 0.02 to allow for instrumental instability. Of the 4678 independent reflections collected, 504 had $F^2 \leqslant \sigma(F^2)$ and were considered unobserved.

Determination of the Structure

From the Patterson function, the Pt atom coordinates were determined. (Space group $P2_1/a$ has four equivalent positions: (x, y, z), $(\bar{x}, \bar{y}, \bar{z})$, $(\frac{1}{2} + x, \frac{1}{2} - y, z)$, and $(\frac{1}{2} - x, \frac{1}{2} + y, \bar{z})$). Refinement was carried out using the full-matrix least-squares program XFLS (7). Atomic form factors used were those derived from Hartree–Fock wave functions (8), allowance being made for anomalous scattering. After three cycles of anisotropic refinement, the conventional R-factor converged smoothly to 0.047. In the last cycle, the largest shift was about 0.8σ and no abnormal thermal parameters were observed. At this stage the refinement of the non-hydrogen atomic positions was considered complete. The final positional and thermal

Can. J. Chem. Downloaded from www.nrcresearchpress.com by 210.87.254.105 on 09/05/12
For personal use only.

TABLE 1. Comparison of the structural data of $(PPh_3)_2PtC_2H_4$ and related complexes

Compound	Bond length (Å)			Bond angle (deg)		Dihedral angle (deg) (PMP)(CMC)	Reference
	C—C	M—C	M—P	C—M—C	P—M—P		
$(PPh_3)_2PtC_2H_4$	1.434(13)	2.106(8) 2.116(9)	2.265(2) 2.270(2)	39.7(4)	111.6(1)	1.6	This work
$(PPh_3)_2PtC_2(CN)_4$	1.49(5)	2.10(3) 2.12(3)	2.288(8) 2.291(9)	41.5(13)	101.4(3)	8.3	2
$(PPh_3)_2PtC_2Cl_4$	1.62(3)	2.02(3) 2.05(3)	2.278(8) 2.292(7)	47.1(10)	100.6(2)	12.3	3
$(PPh_3)_2NiC_2H_4$	1.43(1)	1.98(1) 2.00(1)	2.147(4) 2.157(4)	42.1(5)	110.5(2)	5.0	4

parameters and their estimated standard deviations are given in Tables 2 and 3.

All phenyl hydrogen atom positions were then calculated from a local program, using C...H = 1.07 Å. The hydrogen atoms were assigned the same thermal parameters as the carbon atoms to which they are bonded. Structure factor calculations, including contributions from these hydrogen atoms, lowered the *R*-factor to 0.043.

A difference Fourier synthesis at this stage gave no clearly defined ethylenic hydrogen atoms. The diffuse regions of electron density which were observed suggested that the hydrogen atoms were displaced somewhat away from the Pt atom to give a nonplanar ethylene molecule. It is impossible to be certain of this effect, however; if it were genuine it would resemble the displacements found for CN in $(PPh_3)_2PtC_2(CN)_4$ (2) and for Cl in $(PPh_3)_2PtC_2Cl_4$ (3).

The final bond distances and angles in the molecule are shown in Fig. 1 (*a*) and (*b*), the average standard deviations of the phenyl ring angles being 0.8°. Final F_o and F_c values have been placed in the Depository for Unpublished Data.[1]

Discussion

A diagram of the molecule viewed normal to the central coordination plane is given in Fig. 2. Important bond lengths of this and related complexes are given in Table 1.

The 1.434(13) Å C—C bond length is consistent with the length of 1.43 Å found in the

[1]Photocopy of the data is available from the Depository of Unpublished Data, National Science Library, National Research Council of Canada, Ottawa, Canada K1A 0S2.

TABLE 2. Fractional atomic coordinates $X10^5$ (e.s.d.'s in parentheses)

Atom	*x*	*y*	*z*
Pt	2885(2)	36135(3)	19725(2)
P(1)	11676(11)	41222(18)	30577(11)
P(2)	−6689(12)	51078(18)	16161(11)
C(001)	7191(58)	18741(78)	16770(53)
C(002)	28(59)	22327(76)	11370(47)
C(111)	12915(46)	29053(73)	37735(43)
C(112)	19781(54)	27735(94)	43350(49)
C(113)	20332(62)	18513(108)	48682(56)
C(114)	13997(75)	10213(94)	48305(52)
C(115)	6807(67)	11353(80)	42840(58)
C(116)	6365(57)	20676(71)	37412(45)
C(121)	9580(44)	54876(66)	36060(42)
C(122)	8224(46)	66005(71)	32314(46)
C(123)	5961(54)	76474(75)	35820(50)
C(124)	4732(60)	75741(87)	43315(58)
C(125)	5869(65)	64567(84)	47069(57)
C(126)	8342(54)	54215(87)	43620(47)
C(131)	22432(44)	43910(77)	29504(39)
C(132)	26438(55)	33556(93)	26935(52)
C(133)	34621(53)	35100(93)	25771(58)
C(134)	38582(51)	46133(109)	27291(56)
C(135)	34650(57)	56171(99)	29723(59)
C(136)	26526(50)	54898(80)	31071(49)
C(211)	−2237(46)	65702(65)	14109(40)
C(212)	5058(55)	65074(79)	11176(53)
C(213)	8576(64)	75923(99)	8936(58)
C(214)	4952(66)	87426(87)	9703(58)
C(215)	−2046(67)	87932(80)	12626(65)
C(216)	−5637(54)	77215(74)	14981(52)
C(221)	−13849(47)	54494(74)	22554(45)
C(222)	−21437(57)	60489(93)	20358(51)
C(223)	−26902(57)	62124(97)	25211(61)
C(224)	−24801(67)	57635(125)	32727(58)
C(225)	−17368(62)	52131(126)	34936(55)
C(226)	−11911(54)	50226(107)	29935(51)
C(231)	−14147(47)	48868(72)	7243(43)
C(232)	−19968(64)	39452(93)	6725(58)
C(233)	−25971(68)	38055(100)	231(66)
C(234)	−25952(60)	45449(105)	−5880(55)
C(235)	−19881(59)	54380(38)	−5657(51)
C(236)	−14132(51)	56092(78)	853(45)

Can. J. Chem. Downloaded from www.nrcresearchpress.com by 210.87.254.105 on 09/05/12
For personal use only.

TABLE 3. Thermal parameters $X10^5$ (e.s.d.'s in parentheses).
T.F. = $\exp -(h^2\beta_{11} + k^2\beta_{22} + l^2\beta_{33} + 2hk\beta_{12} + 2hl\beta_{13} + 2kl\beta_{23})$

Atom	β_{11}	β_{22}	β_{33}	β_{12}	β_{13}	β_{23}
Pt	242(1)	491(3)	223(1)	18(1)	1(1)	−1(1)
P(1)	236(7)	539(17)	235(7)	12(9)	15(5)	−4(9)
P(2)	266(8)	540(18)	243(7)	39(9)	6(6)	2(9)
C(001)	509(44)	544(72)	444(38)	240(48)	−64(33)	−217(45)
C(002)	573(46)	648(80)	308(31)	96(49)	−15(30)	−181(41)
C(111)	279(31)	687(79)	257(28)	53(41)	8(24)	−67(38)
C(112)	347(38)	1266(113)	302(32)	103(53)	−69(28)	66(50)
C(113)	445(45)	1346(123)	403(40)	169(64)	54(34)	388(59)
C(114)	790(64)	959(101)	266(33)	295(67)	147(37)	161(47)
C(115)	609(52)	610(85)	405(39)	66(51)	152(37)	53(45)
C(116)	559(45)	484(71)	270(29)	48(46)	117(29)	−50(37)
C(121)	244(29)	480(65)	271(27)	−91(35)	10(22)	−49(34)
C(122)	248(31)	637(77)	296(29)	−47(37)	5(24)	−1(37)
C(123)	412(38)	623(77)	360(33)	189(44)	75(28)	−53(41)
C(124)	458(44)	819(93)	482(41)	83(51)	112(34)	−150(50)
C(125)	537(48)	873(96)	384(37)	24(53)	199(35)	−147(48)
C(126)	394(38)	956(95)	262(29)	15(48)	70(27)	35(42)
C(131)	255(30)	911(89)	180(24)	21(41)	3(21)	51(37)
C(132)	334(36)	1242(111)	341(34)	151(51)	77(28)	−33(48)
C(133)	234(34)	1269(117)	442(40)	153(51)	28(29)	−19(52)
C(134)	233(33)	1556(136)	418(38)	7(57)	49(29)	167(59)
C(135)	347(40)	1216(114)	484(42)	−65(55)	128(33)	95(56)
C(136)	313(35)	889(89)	349(33)	−102(45)	50(27)	8(43)
C(211)	288(31)	558(69)	176(23)	72(36)	−44(21)	−84(31)
C(212)	348(37)	866(89)	355(34)	−64(45)	91(29)	10(43)
C(213)	542(48)	1130(112)	423(39)	−167(62)	115(35)	22(56)
C(214)	499(47)	885(102)	382(38)	−254(54)	0(34)	−26(47)
C(215)	510(49)	671(88)	526(45)	−79(50)	93(38)	−88(47)
C(216)	427(39)	507(74)	407(36)	10(44)	61(30)	−83(41)
C(221)	276(31)	750(79)	291(30)	45(40)	39(24)	4(38)
C(222)	399(42)	1199(107)	311(33)	180(53)	−61(29)	75(48)
C(223)	314(38)	1435(130)	461(42)	267(54)	90(33)	−78(56)
C(224)	526(51)	1821(157)	341(38)	128(76)	118(35)	−28(65)
C(225)	384(44)	2249(176)	317(36)	309(71)	75(32)	217(63)
C(226)	316(37)	1718(135)	278(32)	56(57)	−25(27)	−37(53)
C(231)	304(32)	638(75)	251(28)	−13(39)	5(23)	15(36)
C(232)	483(46)	981(103)	381(38)	−131(56)	−16(33)	70(51)
C(233)	473(51)	1503(141)	451(45)	−283(69)	−122(38)	−21(66)
C(234)	465(45)	1334(128)	319(37)	−133(60)	−190(32)	−70(56)
C(235)	447(43)	1036(97)	306(33)	−13(53)	−57(30)	14(46)
C(236)	367(36)	763(84)	265(29)	−66(43)	−24(26)	−27(40)

nickel analog (4). It is also compatible with the electron spectroscopic result (9) that there is a 0.8-electron transfer from Pt to C_2H_4. This $Pt \rightarrow C_2H_4$ back donation is sufficient to change the C=C bond to one with significant single bond character. Although this bond is shorter than the 1.49(5) Å found in $(PPh_3)_2PtC_2(CN)_4$ (2), the difference is not statistically significant; however, it is significantly shorter than the 1.62(3) Å found in $(PPh_3)_2PtC_2Cl_4$ (3). The shortest C—C bond of this type is found in Zeise's salt $KPtCl_3(C_2H_4).H_2O$, 1.37(3) Å (10), where however, the C—C vector is not in the coordination plane, but almost perpendicular to it (84°).

The Pt—C distances, 2.116(9) and 2.106(8) Å, are similar to those found in other platinum–olefin complexes, namely 2.10(3), 2.12(3) Å in $(PPh_3)_2PtC_2(CN)_4$, 2.02(3), 2.05(2) Å in $(PPh_3)_2$-PtC_2Cl_4. They are also compatible with the 1.98(1) and 2.00(1) Å found in $(PPh_3)_2NiC_2H_4$. Estimates of radii of transition elements atoms in their zero oxidation state do not seem to have been made. However the fact that the metallic

Can. J. Chem. Downloaded from www.nrcresearchpress.com by 210.87.254.105 on 09/05/12
For personal use only.

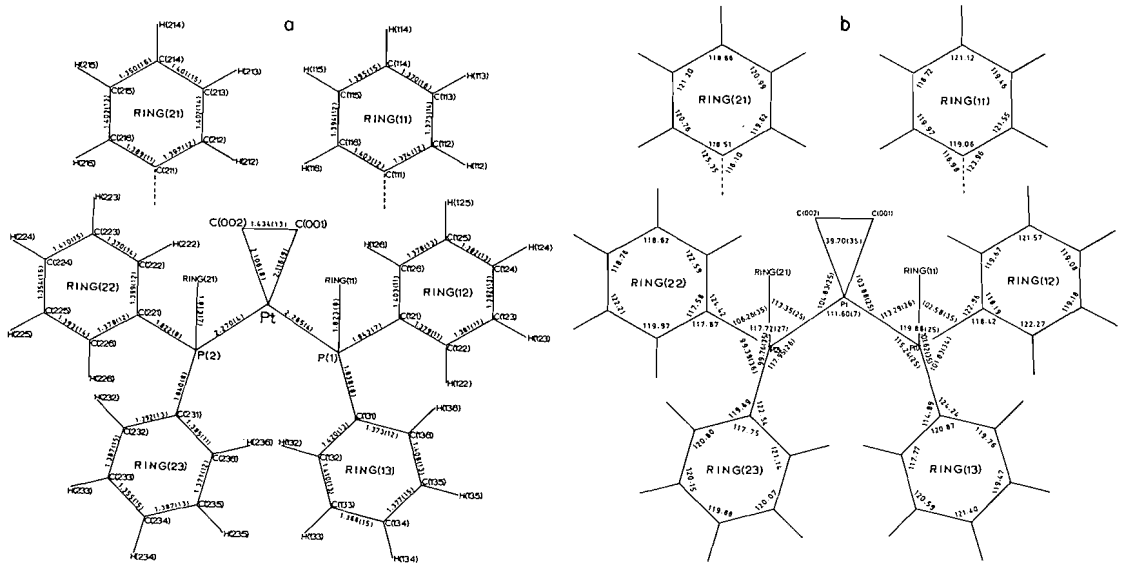

FIG. 1. (*a*) Bond lengths, (*b*) bond angles.

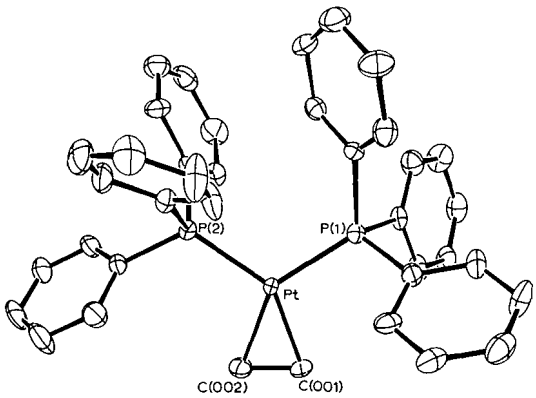

FIG. 2. Molecule of $(PPh_3)_2PtC_2H_4$ with 30% probability thermal ellipsoids.

radius of the Pt atom is estimated to be some 0.14 Å greater than the metallic radius of Ni is in accord with these results.

The Pt—P distances, 2.265(4) and 2.270(4) Å, are also compatible with, although shorter than, those found in the other complexes of known structure, namely 2.288(8), 2.291(9) Å in $(PPh_3)_2PtC_2(CN)_4$, 2.278(8), 2.292(7) Å in $(PPh_3)_2PtC_2Cl_4$; the shortenings are marginally significant.

The four atoms attached directly to the Pt atom are closely coplanar, the best least-squares plane, in real orthogonal coordinates, X along x and Z along z^* is $0.7158X + 0.4427Y - 0.5401Z = -0.2513$ with deviations of atoms (in Å) from this plane as follows: Pt, −0.0033; P(1), −0.0054; P(2), +0.0074; C(001), +0.0174; C(002), −0.0161. When the P—Pt—P and C—P—C parts are considered separately there is an interplanar angle of 1.6° between planes P—Pt—P and C—Pt—C, significantly smaller than that found in the related complexes, 8° in $(PPh_3)_2PtC_2(CN)_4$ and 12° in $(PPh_3)_2PtC_2Cl_4$. However, no close intramolecular or intermolecular contacts have been reported for any of the crystals of these complexes, so that observed non-coplanarities may be a feature of the isolated molecules. A modification of the Dewar–Chatt–Duncanson representation has been proposed (11) to rationalize these observations; it allows the metal-to-ligand back donation to involve both d_{xz} and $d_{x^2-y^2}$ (or d_{xy}) electrons. However, the involvement of the d_{xz} electrons in $(PPh_3)_2PtC_2H_4$ would be negligible since the central coordination plane is very close to planar.

We are grateful to Professor C. D. Cook and Mr. K. Y. Wan for helpful discussions. Thanks are due to National Research Council of Canada for generous financial support.

1. M. J. S. DEWAR. Bull. Soc. Chim. Fr. **18**, 79 (1951). J. CHATT and L. A. DUNCANSON. J. Chem. Soc. 2939 (1953).

Can. J. Chem. Downloaded from www.nrcresearchpress.com by 210.87.254.105 on 09/05/12
For personal use only.

2. G. BOMBIERI, E. FORSELLINI, C. PANATTONI, R. GRAZIANI, and G. BANDOLIS. J. Chem. Soc. A, 1314 (1970).
3. J. N. FRANCIS, A. MCADAM, and J. A. IBERS. J. Organomet. Chem. **29**, 131 (1971).
4. P.-T. CHENG, C. D. COOK, C. H. KOO, S. C. NYBURG, and M. T. SHIOMI. Acta Cryst. B **27**, 1904 (1971).
5. P.-T. CHENG, C. D. COOK, S. C. NYBURG, and K. Y. WAN. Inorg. Chem. **10**, 2210 (1971).
6. S. C. ABRAHAMS. Acta Cryst. **17**, 1327 (1964).
7. R. D. ELLISON. XFLS, An Extensively modified version of ORFLS. Report ORNL-TM-305, Oak Ridge National Laboratory. 1962. Unpublished.
8. D. T. CROMER and J. B. MANN. Acta Cryst. A **24**, 321 (1968).
9. C. D. COOK, K. Y. WAN, U. GELIUS, K. HAMRIN, G. JOHANSSON, E. OLSSON, H. SIEGBAHN, C. NORDLING, and K. SIEGBAHN. J. Am. Chem. Soc. **93**, 1904 (1971).
10. J. A. JARVIS, B. T. KILBOURN, and P. G. OWSTON. Acta Cryst. B **27**, 366 (1971).
11. F. R. HARTLEY. Chem. Rev. 799 (1969).

Can. J. Chem. Downloaded from www.nrcresearchpress.com by 210.87.254.105 on 09/05/12
For personal use only.

Quaternary Nitrogen Heterocycles. I. Equilibrium and Spectral Data for Pseudobase Formation by the *N*-Methyl Cations of Diazanaphthalenes

JOHN W. BUNTING AND WILLIAM G. MEATHREL
Department of Chemistry, University of Toronto, Toronto 181, Ontario

Received October 18, 1971

Equilibrium constants have been measured at 25° for the formation of pseudobases from the 2-methylphthalazinium, 1-methylquinoxalinium, 1-methyl-1,5-naphthyridinium, 6-methyl-1,6-naphthyridinium, 7-methyl-1,7-naphthyridinium, 1-methyl-1,8-naphthyridinium, 1-methyl-3-nitroquinolinium, and 2-methyl-4-nitroisoquinolinium cations. Ionization constants have also been obtained for ionization of some of these pseudobases to alkoxide anions. For each cation the site of hydroxide attack has been determined by comparison of the u.v. and p.m.r. spectra of the pseudobases, the corresponding methoxide adducts, and the lithium aluminum hydride reduction products. In all cases, except for the 1-methylquinoxalinium cation, only one major pseudobase species is present in solution, and ring-opening does not occur to any appreciable extent. The pseudobase of the 1-methylquinoxalinium cation exists in equilibrium with a considerable amount of its covalent hydrate from addition of water across the C_3—N_4 bond.

Les constantes d'équilibre ont été mesurées à 25° pour la formation de pseudobases à partir des cations méthyl-2 phthalazinium, méthyl-1 quinoxalinium, méthyl-1 naphthyridium-1,5, méthyl-6 naphthyridium-1,6, méthyl-7 naphthyridium-1,7, méthyl-1 naphthyridium-1,8, méthyl-1 nitro-3 quinolinium, et méthyl-2 nitro-4 isoquinolinium. Les constantes d'ionisation ont été aussi obtenues pour l'ionisation de quelques de ces pseudobases en anions alkoxyde. Pour chaque cation, le site d'attaque de l'hydroxyde a été déterminé par comparaison des spectres u.v., et r.m.p. des pseudobases, des composés d'addition méthoxyde correspondants et des produits de réduction par l'hydrure de lithium aluminium. Dans tous les cas, à l'exception du cation de la méthyl-1 quinoxalinium, il n'y a seulement qu'une espèce pseudobase majoritaire présente en solution, et l'ouverture du cycle ne se produit pas dans un pourcentage appréciable. La pseudobase du cation de la méthyl-1 quinoxalinium existe en équilibre avec un pourcentage important de son hydrate covalent résultant de l'addition de l'eau sur la liaison C_3—N_4.

Canadian Journal of Chemistry, **50**, 917 (1972)

Can. J. Chem. Downloaded from www.nrcresearchpress.com by 210.87.254.40 on 09/05/12
For personal use only.

Although pseudobase formation by quaternary nitrogen heterocycles in aqueous alkaline solutions is a generally accepted phenomenon (1, 2), there are few recent studies of this reaction in the aromatic nitrogen heterocycles. Beke (3) has reviewed studies of pseudobase formation in partially saturated nitrogen heterocycles (mainly naturally occurring 3,4-dihydroisoquinoline derivatives such as berberine and cotarnine), and has discussed the problem of ring–chain tautomerism which may occur in these systems between the pseudobase and a ring-opened amino-aldehyde. The evidence for pseudobase formation in quaternary hetero-aromatic systems rests mainly on the studies of Hantzsch (4), Decker (5), and Aston and Lasselle (6), although the structure of Hantzsch's often quoted (1, 2) "bimolecular ether", which is believed to be formed from the pseudobase of the 1-methylquinolinium cation, has recently been shown to be in error (7, 8).

There has been little attempt to correlate equilibria and kinetics of pseudobase formation with the structure of the quaternary ion. For the equilibrium (eq. 1) between the quaternary heterocyclic cation (Q^+) and the corresponding

[1] $$Q^+ + OH^- \rightleftharpoons QOH$$

pseudobase (QOH), we may define an equilibrium constant, K (eq. 2). Cooksey and Johnson (9), who have measured equilibrium constants for pseudobase formation by the *N*-cyano and *N*-methyl cations of some substituted quinolines and isoquinolines, have preferred to use the constant, K_{ROH}, (eq. 3) which is

[2] $$K = \frac{[QOH]}{[Q^+][OH^-]}$$

[3] $$K_{ROH} = \frac{[H^+][QOH]}{[Q^+]}$$

related to K through the ionic product of water, K_W, by $K = K_{ROH}.K_W$. The definition of K_{ROH} is similar in form to that of a classical Bronsted-acid ionization constant. It is convenient to express these equilibrium constants as pK_{ROH}

Can. J. Chem. Downloaded from www.nrcresearchpress.com by 210.87.254.40 on 09/05/12
For personal use only.

values, which are analogous to pK_a values for Bronsted acids, and which denote the pH at which the quaternary ion and pseudobase are present at equal concentrations. We shall use this formulation throughout the present paper. In sufficiently alkaline solutions the pseudobases may also lose a proton to form a pseudobase anion (QO^-) (an alkoxide ion) (9), and we shall denote the ionization constant for this process by K_{RO^-}.

For the 1-methylquinolinium and 2-methylisoquinolinium cations, appreciable pseudobase formation occurs only at pH values where subsequent irreversible reactions predominate (4, 5, 9), and consequently pK_{ROH} values for these cations cannot be measured directly. The presence of electron-withdrawing substituents makes the cations much more susceptible to nucleophilic attack by hydroxide ions, and reduces the pK_{ROH} values sufficiently that these values may be measured in pH regions where irreversible reactions are negligible (9). Apart from the studies by Johnson and coworkers, the only other pK_{ROH} values in the literature appear to be those for the *N*-methylacridinium cation (**1** $\rightleftharpoons$ **2**, $pK_{ROH} = 9.75$) (10), and the *N*-methylphenanthridinium (**3** (R = H) $\rightleftharpoons$ **4** (R = H), $pK_{ROH} = 10.4 \pm 0.2$) (11), and 5,6-dimethylphenanthridinium (**3** (R = Me) $\rightleftharpoons$ **4** (R = Me), $pK_{ROH} = 10.1 \pm 0.2$) (11) cations.

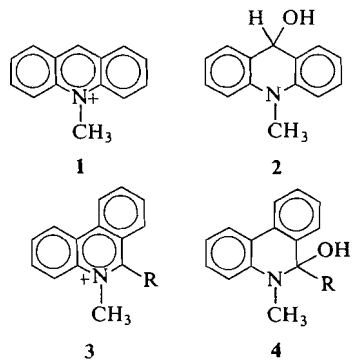

1 **2** **3** **4**

The lack of a comprehensive study of pseudobase formation by quaternary aromatic nitrogen heterocycles is rather surprising in view of the extensive investigations which have been made on the closely related covalent hydration of nitrogen heteroaromatic cations in aqueous acid (12–14). Numerous studies (15–18) have also been made on the formation of Meisenheimer complexes by the addition of nucleophiles to various electron-deficient aromatic molecules. The formation of these anionic covalent complexes is quite analogous to pseudobase formation, since both reactions involve nucleophilic attack on electron-deficient aromatic systems and result in loss of aromaticity because of the production of a saturated carbon atom in the ring.

As the initial step in a study to further the quantitative understanding of the influence of the structure of the heterocycle on pseudobase formation, we wish to report a study of the pseudobase formation by the *N*-methyl cations of phthalazine, quinoxaline, quinazoline, and the 1,*x*-naphthyridines ($x = 5$–8).[1] In addition to the measurement of pK_{ROH} and pK_{RO^-} (where accessible) values for each of these cations, we have determined the site of hydroxide attack by u.v. and p.m.r. spectral techniques.

Results

In each of phthalazine, quinoxaline, 1,5-naphthyridine, and 1,8-naphthyridine the two nitrogen atoms are equivalent and consequently the site of methylation in unequivocal. For 1,6- and 1,7-naphthyridine, in each of which the ring-nitrogen atoms are not equivalent, methylation with methyl iodide has been shown (21) to occur exclusively[2] on the isoquinoline-type nitrogen atom (*i.e.*, N-6 and -7 respectively). It has recently been shown (23) that methylation of quinazoline with methyl iodide produces a mixture of the 3-methyl- and 1-methylquinazolinium cations in the ratio of 5:1.

The u.v. spectra of each of the diazanaphthalene cations examined were pH dependent in aqueous solution. Typical spectra are shown in Figs. 1 (1-methyl-1,5-naphthyridinium iodide) and 2 (1-methylquinoxalinium iodide). The

[1]We have also confirmed that the 2-methylcinnolinium ion, which was believed by early workers to be the 1-methylcinnolinium ion (19, 20), does not form a pseudobase in aqueous alkali, but undergoes a demethylation reaction to give cinnoline as the major product (19).

[2]Jones and Wagstaff (22) have claimed the presence of 5–10% 1-methyl-1,6-naphthyridinium cation from the methylation of 1,6-naphthyridine. This claim is based on the observation of a small peak (δ 4.62 in DMSO-d_6) in the p.m.r. spectrum of their crude reaction product which they assign to the N-1 methyl protons of this cation. This peak was not present in our product.

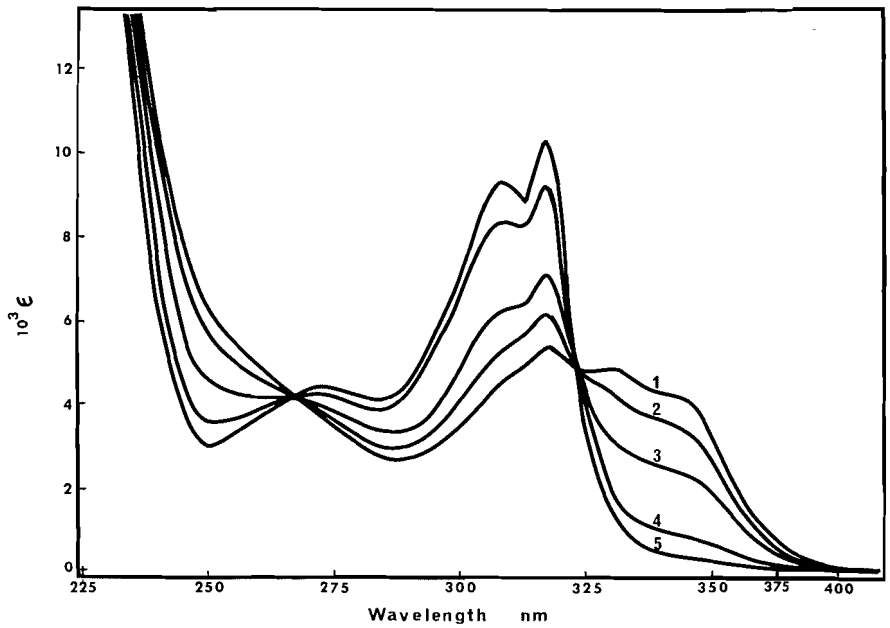

FIG. 1. The u.v. spectrum of 1-methyl-1,5-naphthyridinium iodide in water: 1, pH = 13.4; 2, pH = 13.0; 3, pH = 12.5; 4, pH = 12.0; 5, pH = 9.0.

presence of clean isosbestic points and the reversibility of the spectra upon re-acidification of alkaline solutions indicates that true equilibria, are being observed. The presence of two successive equilibria, as is apparent for the 1-methylquinoxalinium cation in Fig. 2, was also observed for the 2-methylphthalazinium cation, the 3-methylquinazolinium cation, and the 1-methyl-3-nitroquinolinium and 2-methyl-4-nitroisoquinolinium cations, but not for any other cation at less than pH 14. The u.v. spectral data for each species are collected in Table 1.

An equilibrium constant was calculated for each reaction for which an u.v. spectral change was observed. These constants are given, along with appropriate experimental data, in Table 2.

For the 1-methylquinolinium cation, pseudobase formation in aqueous solutions at pH < 15 is insufficient to allow spectroscopic observation. Above pH 15, u.v. spectral changes are apparent, but these are irreversible upon acidification. These changes seem to be due to the formation of 1-methyl-2-quinolone which has been isolated from more concentrated solutions of 1-methylquinolinium iodide in strong aqueous alkali. This product is presumably produced via the corresponding pseudobase which would be formed by hydroxide attack at C-2 of the heterocyclic cation. The data of Cooksey and Johnson (9) indicate that the difference in pK_{ROH} for five correspondingly substituted 1-methyl- and 1-cyano-quinolinium cations is $\Delta pK_{ROH} = 17.5 \pm 0.5$. If we use this ΔpK_{ROH} and the pK_{ROH} value (−1.05) for the unsubstituted 1-cyanoquinolinium cation (9), we may estimate the pK_{ROH} for pseudobase formation from the 1-methylquinolinium cation by hydroxide attack at C-2 to be $pK_{ROH} = 17.5 + (-1.05) = 16.5 \pm 0.5$. This value is consistent with the lack of observable reversible u.v. spectral changes at pH < 15, although it does not definitely establish that C-2 is preferred over C-4 as the site of hydroxide attack in the 1-methylquinolinium cation.

The 2-methylisoquinolinium cation has a pH-independent u.v. spectrum below pH 14. In more basic solutions, spectral changes do occur, but these changes are only partially reversible upon acidification. This suggests that an irreversible reaction is also occurring in addition to pseudobase formation, and 2-methyl-1-isoquinolone has been isolated from more concentrated solutions of this cation. The pK_{ROH} values are available (9) for only two pairs of corre-

Can. J. Chem. Downloaded from www.nrcresearchpress.com by 210.87.254.40 on 09/05/12
For personal use only.

Can. J. Chem. Downloaded from www.nrcresearchpress.com by 210.87.254.40 on 09/05/12
For personal use only.

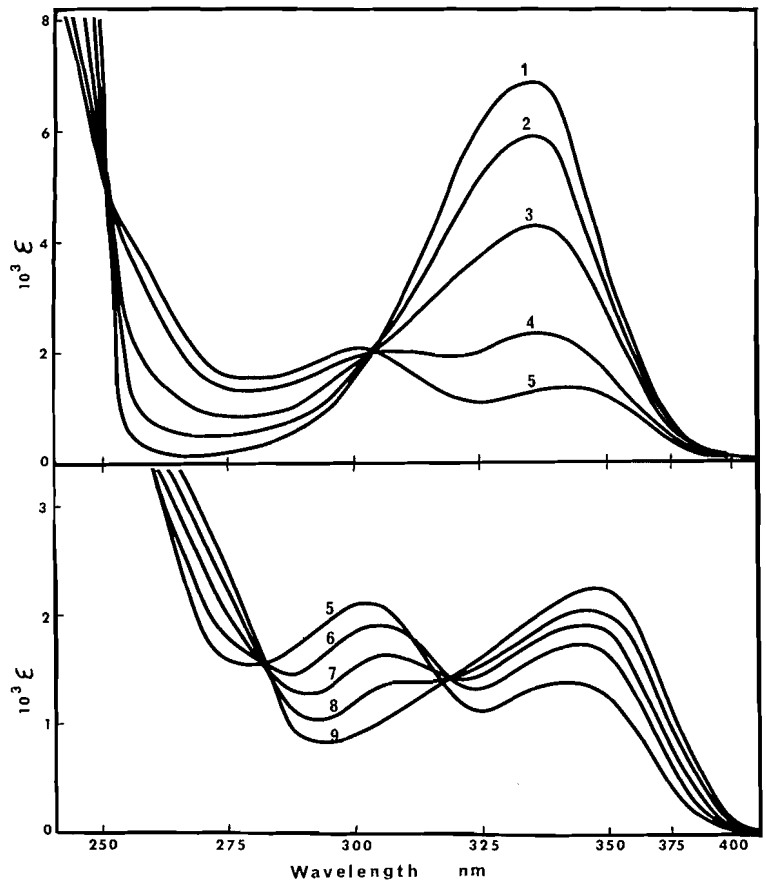

FIG. 2. The u.v. spectrum of 1-methylquinoxalinium iodide in water: 1, pH = 3.6; 2, pH = 7.9; 3, pH = 8.6; 4, pH = 9.2; 5, pH = 10.4; 6, pH = 11.9; 7, pH = 12.5; 8, pH = 13.0; 9, pH = 14.0.

spondingly substituted 2-methyl- and 2-cyano-isoquinolinium cations. The ΔpK_{ROH} values for 5-bromo and 4-bromo substitution are 17.3 and 17.2 respectively, although there is considerable experimental error in pK_{ROH} values of the 2-methylisoquinolinium cations used to calculate ΔpK_{ROH}. Using the $pK_{ROH}(-2.0)$ for the 2-cyanoisoquinolinium cation (24), we estimate $pK_{ROH} = 17.3 + (-2.0) = 15.3$ for the 2-methylisoquinolinium cation, which is consistent with the observed lack of spectral change for solutions of this cation at pH < 14.

The *N*-methyl-1,*x*-naphthyridinium cations have previously been oxidized (21, 25) with

[4]

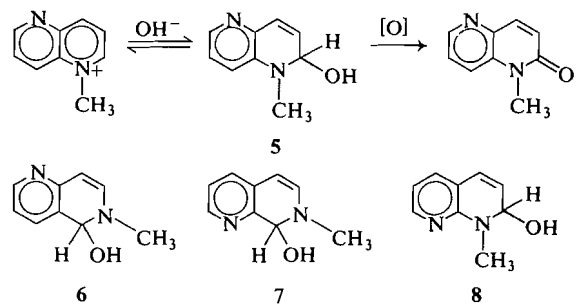

TABLE 1. The u.v. spectra of *N*-methyl heterocyclic cations in water

Cation	p*H*	λ_{max} (log ε)
1-Methylquinolinium	7	315(3.90)
2-Methylisoquinolinium	7	269(3.42), 276(3.43), 330(3.63)
1-Methylquinoxalinium	4	336(3.84)
	10.5	301(3.33), 340(3.13)
	14.5	347(3.41)
2-Methylphthalazinium	9	275(3.46), 317 (3.50)
	12	302(3.89)
	15	312(3.90)
1-Methyl-1,5-naphthyridinium	7	272(3.64), 307(3.97), 317(4.01)
	14	*272(3.98)*, 342(4.00)
6-Methyl-1,6-naphthyridinium	7	261(3.54), 271(3.41), 308(3.56), 318(3.55)
	14	340(3.86)
7-Methyl-1,7-naphthyridinium	7	268(3.70), 304(3.53), 316(3.49)
	14.2	320(3.96)
1-Methyl-1,8-naphthyridinium	7	303(4.02), 312(4.01)
	14	330(3.82)
1-Methyl-3-nitroquinolinium	3.4	318(3.83)
	8.7	313(3.40), 401(4.23)
	14	313(3.41), 410(4.16)
2-Methyl-4-nitroisoquinolinium	3	345(3.58)
	8	282(4.04), 402(4.10)
	14.5	285(3.78), 410(3.70)

alkaline potassium ferricyanide to keto products. These oxidations are believed to proceed via the pseudobase intermediates (**5**–**8**) (*e.g.* eq. (4)). To assume from these oxidation studies that **5**–**8** are the major pseudobase species present in alkaline solutions of these cations would be akin to the assumptions made by early workers in this field, and which resulted in much confusion about the nature of pseudobase equilibria (3). It is possible that any, or all, of **5**–**8** are only minor components of the total mixture of pseudobase species, but nevertheless, give rise to the kinetically controlled major oxidation products.

It is well known (26) that quinolinium derivatives are susceptible to nucleophilic attack at C-4 as well as at C-2, and the above oxidation studies cannot rule out the possibility that the pseudobases from the 1-methyl-1,5-naphthyridinium and 1-methyl-1,8-naphthyridinium cations may be mixtures of the pseudobases arising from hydroxide attack at C-4 and -2, with the latter pseudobase being much more readily oxidized than the former. In isoquinolinium derivatives, nucleophilic attack almost invariably occurs at C-1 (27). However, we feel that it is unreasonable to arbitrarily rule out **9** and **10** as species which are possibly present in appreciable amounts in the equilibrium pseudobase mixtures. The presence of the pseudobases in the ring-opened forms, *e.g.*, **11**, also cannot be ruled out by the isolation of the above oxidation products, since the ring-opened and ring-closed forms of each pseudobase will always be in equilibrium.

We have sought spectral evidence by which we might assign the structures of the major pseudobase species which are present in aqueous

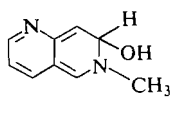

9

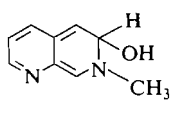

10

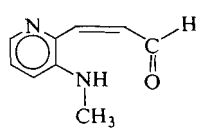

11

Can. J. Chem. Downloaded from www.nrcresearchpress.com by 210.87.254.40 on 09/05/12
For personal use only.

Can. J. Chem. Downloaded from www.nrcresearchpress.com by 210.87.254.40 on 09/05/12
For personal use only.

TABLE 2. Values of pK_{ROH} and pK_{RO^-} for some *N*-methyl heterocyclic cations at 25°

Cation	pK_{ROH}	K	pK_{RO^-}	λ (nm)*	pH Range†	n‡	Concentration (mM)*
1-Methylquinolinium	(16.5 ± 0.5)§	(3×10^{-3})					
2-Methylisoquinolinium	(~15.3)§	(~5×10^{-2})					
9-Methylacridinium	9.86 ± 0.06‖	1.4×10^{4}		341	9.2–10.4	8	0.076
2-Methylphthalazinium	11.04 ± 0.05	9.1×10^{2}		297	10.2–11.6	7	0.130
			13.0 ± 0.1	335	11.9–13.8	11	0.30
1-Methylquinoxalinium	8.62 ± 0.06¶	2.4×10^{5}		335	7.5–9.0	13	0.098
			12.62 ± 0.05¶	370	11.9–13.3	7	0.124
1-Methylquinazolinium	<7**	$>10^{7}$					
3-Methylquinazolinium	<7**	$>10^{7}$					
			12.47 ± 0.06	310	12.1–13.4	8	0.22
1-Methyl-3-nitroquinolinium	6.74 ± 0.06	1.8×10^{7}		402	6.2–7.9	10	0.040
			13.0 ± 0.1	450	12.1–13.3	6	0.065
2-Methyl-4-nitroisoquinolinium	5.03 ± 0.04††	9.3×10^{8}		402	4.6–5.4	8	0.060
			11.15 ± 0.04	‡‡			4.0
1-Methyl-1,5-naphthyridinium	12.67 ± 0.06	21		342	11.9–13.1	7	0.041
6-Methyl-1,6-naphthyridinium	12.33 ± 0.06	47		340	11.5–13.0	9	0.082
7-Methyl-1,7-naphthyridinium	13.1 ± 0.1	8.0		335	12.8–14.2	8	0.075
1-Methyl-1,8-naphthyridinium	12.44 ± 0.03	36		330	11.2–13.1	10	0.098

*Analytical wavelength and concentration.
†pH range over which pK_{ROH} or pK_{RO^-} was calculated.
‡Number of values included in average.
§Estimated as described in text.
‖Goldacre and Phillips report 9.75 (10).
¶Apparent pK_{ROH} and pK_{RO^-} values (see text).
**See text.
††Potentiometric titration gave 4.99 ± 0.03.
‡‡From potentiometric titration. Spectral change is too small for accurate spectrophotometric determination.

Can. J. Chem. Downloaded from www.nrcresearchpress.com by 210.87.254.40 on 09/05/12
For personal use only.

alkaline solutions of the heterocyclic cations included in the present study. It is not possible to obtain p.m.r. spectra of the pseudobases themselves in aqueous alkaline solution. Oils separate from these solutions at p.m.r. spectral concentrations. The main components of these oils are the oxidation products mentioned above, and are presumably formed by reactions similar to those which give rise to 1-methyl-2-quinolone in alkaline solutions of the 1-methylquinolinium cation. We have therefore measured u.v. and p.m.r. spectra for each cation in basic methanol solutions, and these spectral data are given in Table 3. It was hoped to identify the site(s) of methoxide attack from the p.m.r. spectrum of the reaction product, and then to compare the u.v. spectrum of each methoxide adduct with that of the corresponding pseudobase. Unlike the pseudobases, the methyl ethers can neither be easily oxidized to keto derivatives, nor can they undergo ring-opening reactions. Thus, a comparison of the u.v. spectra of corresponding methyl ethers and pseudobases will also be useful in determining whether appreciable amounts of ring-opened species, *e.g.* **11**, are present in equilibrium with the pseudobases.

Table 3 also contains spectral data for the dihydroheterocycles obtained by the reduction of each heterocyclic cation with 1 equiv of lithium aluminum hydride in ether. Reduction of both the 1-methylquinolinium and 2-methylisoquinolium cations with this reagent cannot be forced beyond the 1,2-dihydro stage (28). Use of a limited quantity of reducing agent ensured that the reduction of each of the *N*-methylnaphthyridinium cations occurred only in the much more reactive pyridinium ring. The p.m.r. spectrum of the reduction product of the 1-methylquinoxalinium cation confirms that this reduction cannot be stopped at the dihydro stage but proceeds to give 1-methyl-1,2,3,4-tetrahydroquinoxaline (29).

Discussion

1-Methylquinolinium Cation

Initially, upon dissolution of 1-methylquinolinium iodide in basic methanol-d_4(3 $M CD_3O^-$), the p.m.r. spectrum indicates a three proton singlet at δ 3.12 (N—CH_3), a five proton multiplet (δ 6.6–7.3), and a multiplet centered at δ 5.70 which integrates for slightly less than two

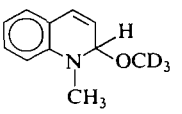

12

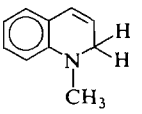

13

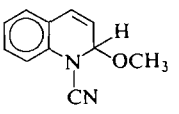

14

protons. The integration of this latter multiplet is time dependent, gradually decreasing relative to the other peaks, until eventually it becomes a time-insensitive one proton doublet centered at δ 5.66 ($J = 10$ Hz), with no concurrent change having occurred in the other peaks in the spectrum. We attribute this spectrum to 1,2-dihydro-2-trideuteromethoxy-1-methylquinoline (**12**) which is formed by attack of methoxide ion upon C-2 of the heterocyclic cation. This assignment is in good agreement with the spectrum of 1,2-dihydro-1-methylquinoline (**13**) which has been shown (30, 31) to be the reduction product of the 1-methylquinolinium cation by lithium aluminum hydride: ($CDCl_3$) δ 2.72, N—CH_3 (singlet, 3H); δ 3.99, H-2 (doublet of doublets, 2H, $J_{23} = 4$ and $J_{24} = 1.8$ Hz); 5.50–5.78, H-3 (multiplet, 1H, $J_{23} = 4$ and $J_{34} = 10$ Hz); 6.1–7.2, aromatic protons plus H-4 (multiplet, 5H). The coupling constants $J_{23} = 4$, $J_{24} = 1$, and $J_{34} = 10$ Hz, which are almost substituent independent, are typical of 1,2-dihydroquinolines and are sufficiently distinctive to differentiate the 1,2-dihydroquinolines from the corresponding 1,4-dihydroquinolines (31, 32). Thus, the spectrum of the methoxide adduct may be assigned as: δ 6.6–7.3, aromatic protons plus H-4; 5.66, H-3; 5.7, H-2, which exchanges with solvent deuterium in a base-catalyzed process. The C-3 and -4 protons have similar chemical shifts in **12** and **13**, while H-2 is approximately 1.7 p.p.m. (the solvents are different) further downfield in **12** than in **13** as expected from the substituent effect of the methoxyl group. The spectrum assigned to **12** is also in good agreement with that of 1-cyano-1,2-dihydro-2-methoxyquinoline (**14**) (32): (CCl_4) δ 6.02, H-2; 5.64, H-3; 6.78, H-4 ($J_{34} = 9.8$ Hz).

Further confirmation of the 1,2-dihydroquinoline structure for the methoxide adduct was provided by its u.v. spectrum. An absorption maximum in the vicinity of 340 nm is typical of the spectra of 1,2-dihydroquinolines (30, 33, 34), while 1,4-dihydroquinolines with no chromophoric substituents do not have absorption maxima above 300–310 nm (31, 32,

Can. J. Chem. Downloaded from www.nrcresearchpress.com by 210.87.254.40 on 09/05/12
For personal use only.

TABLE 3. The u.v. and p.m.r. spectra of some dihydro heterocycles

Compound	λ_{max} (nm)*	δ (p.p.m.)†								
		H-1	H-2	H-3	H-4	H-5	H-6	H-7	H-8	N-CH_3
1,2-Dihydro-2-methoxy-1-methylquinoline	265, 335	—	5.70	5.66	←———		6.6–7.3		———→	3.12
1,2-Dihydro-1-methylquinoline	345	—	3.99	5.64	←———		6.1–7.2		———→	2.72
1,2-Dihydro-1-methoxy-2-methylisoquinoline	277, 326, 334	6.10	—	6.60	5.66	←———		7.1–7.4	———→	3.22
1,2-Dihydro-2-methylisoquinoiine	328	4.12	—	6.00	5.24	←———		6.8–7.1	———→	2.69
1,2-Dihydro-2-methoxy-1-methylquinoxaline	‡	—	5.37	7.66	—	←———		6.9–7.5	———→	3.17§
2,3-Dimethoxy-1-methyl-1,2,3,4-tetrahydroquinoxaline	‡	—	4.62	4.62	—	←———		6.67	———→	3.23§
1-Methyl-1,2,3,4-tetrahydroquinoxaline	262, 313	—	←—3.2–3.6‖—→		—	←———		6.5–6.7	———→	2.87
1,2-Dihydro-1-methoxy-2-methylphthalazine	305	5.71	—	—	←———		7.3–7.6		———→	3.40
1,2-Dihydro-2-methylphthalazine	320	3.94	—	—	←———		7.0–7.8		———→	3.00
1,2-Dihydro-2-methoxy-1-methyl-1,5-naphthyridine	266, 345	—	5.60	6.12	7.03	—	7.89	←—7.24–7.29—→		3.17
1,2-Dihydro-1-methyl-1,5-naphthyridine	324, 335	—	4.14	5.95	6.50	—	7.79	←—6.7–7.0—→		2.72
5,6-Dihydro-5-methoxy-6-methyl-1,6-naphthyridine	337	—	8.37	7.16	7.71	6.02	—	6.86	5.61	3.22
5,6-Dihydro-6-methyl-1,6-naphthyridine	297, 333	—	8.22	←—6.7–7.1—→		4.30	—	6.31	5.22	2.78
7,8-Dihydro-8-methoxy-7-methyl-1,7-naphthyridine	316	—	8.32	←—7.2–7.6—→		5.46	6.64	—	5.90	3.24
7,8-Dihydro-7-methyl-1,7-naphthyridine	344	—	8.14	←—6.9–7.2—→		5.09	6.10	—	4.40	2.70
1,2-Dihydro-2-methoxy-1-methyl-1,8-naphthyridine	265, 330	—	5.77	5.90	¶	7.50	¶	8.10	—	3.27
1,2-Dihydro-1-methyl-1,8-naphthyridine	249, 315, 325	—	4.38	5.70	6.24	6.94	6.41	7.87	—	2.97

*Methoxy derivatives in methanol, others in chloroform.
†Methoxy derivatives in methanol-d_4, others in $CDCl_3$.
‡These compounds present as a mixture; u.v. spectrum: 304, 344.
§Assignments may be reversed.
‖Obscured by broad N—H signal.
¶δ 6.65–7.05 multiplet, H-4 and -6.

Can. J. Chem. Downloaded from www.nrcresearchpress.com by 210.87.254.40 on 09/05/12
For personal use only.

35). The spectrum of the methoxide adduct of the 1-methylquinolinium cation has a maximum at 335 nm, and is thus consistent with the presence of a 1,2-dihydroquinoline system.

Both the u.v. and p.m.r. spectral evidence are consistent with predominant methoxide attack at C-2 in the 1-methylquinolinium cation, and any product arising from C-4 attack can only be present to an extent less than 5%. It is also reasonable to assume, that in aqueous alkaline solutions, hydroxide ion would also preferentially attack this cation at C-2.

2-Methylisoquinolinium Cation

The p.m.r. spectrum of the 2-methylisoquinolinium cation in basic methanol-d_4 is readily assigned to 1,2-dihydro-1-trideuteromethoxy-2-methylisoquinoline (**15**): δ 7.1–7.4, aromatic protons (multiplet, 4H); 6.60, H-3 (doublet, 1H, $J_{34} = 7.5$ Hz); 5.66, H-4 (doublet, 1H, $J_{34} = 7.5$ Hz); 6.10, H-1 (singlet, 1H—but decreases with time due to exchange with solvent D); 3.22, *N*-CH_3 (singlet, 3H). The coupling constant, $J_{34} = 7.5$ Hz, is typical of 1,2-dihydroisoquinolines (32), and the methoxyl substituent effect on a singlet (2.0 p.p.m. relative to 1,2-dihydro-2-methylisoquinoline (Table 3)) is further evidence of methoxide attack at C-1. The u.v. spectra of the methoxide adduct (in methanol) and 1,2-dihydro-2-methylisoquinoline (in chloroform) are also quite similar, having long wavelength maxima at 334 and 328 nm, respectively. Thus, the spectral evidence is in accord with preponderant methoxide attack (and by implication, hydroxide attack) occurring at C-1 in the 2-methylisoquinolinium cation.

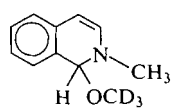

15

We have discussed the spectral data of these quinoline and isoquinoline derivatives in some detail, because we now wish to use these spectra as reference data for the assignment of structures to the pseudobases formed by hydroxide attack on the *N*-methyl cations of the diazanaphthalenes.

1-Methyl-1,5-naphthyridinium Cation

The u.v. spectrum of an alkaline solution of this cation has an absorption maximum at 342 nm, which is typical of 1,2-dihydroquinoline derivatives. The absorption maxima in the spectra of the methoxide adduct (345 nm) and lithium aluminum hydride reduction product (335 nm) are also indicative of 1,2-dihydroquinoline derivatives. These structural assignments are confirmed by p.m.r. spectral data. Thus, for the methoxide adduct, the protons in the dihydropyridine ring are assigned: δ 5.60, H-2 (doublet, 1H, $J_{23} = 4.5$ Hz); 6.12, H-3 (doublet of doublets, 1H, $J_{23} = 4.5$, $J_{34} = 10$ Hz); 7.03, H-4 (doublet, 1H, $J_{23} = 10$ Hz). These coupling constants are typical of 1,2-dihydroquinoline derivatives, and the methoxide adduct may be confidently assigned the structure **16**.

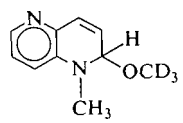

16

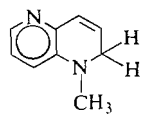

17

The chemical shift of H-2 is very similar to that for the same proton in the corresponding quinoline derivative **12**, while H-3 is further downfield due to the presence of N-5 and no longer overlaps with H-2. While H-4 is also presumably further downfield than in **12**, it is now clearly distinguishable from the aromatic protons H-6, -7, and -8 which have suffered even larger shifts as a result of the presence of N-5. The p.m.r. spectrum (Table 3) of the lithium aluminum hydride reduction product can likewise be confidently assigned to **17** by comparison with the spectrum of 1,2-dihydro-1-methylquinoline.

The similarity of the u.v. spectrum of the pseudobase to the spectra of **16** and **17**, which are definitely established as 1,2-dihydro-1,5-naphthyridines by their p.m.r. spectra, indicates that the predominant pseudobase species of the 1,5-naphthyridinium cation is **5**.

1-Methyl-1,8-naphthyridinium Cation

The u.v. spectra of this cation in aqueous alkali (p*H* 14) and basic methanol are very similar. Both spectra have absorption maxima at 330 nm and are completely reversible to the spectrum of the cation upon acidification. The p.m.r. spectrum of the methoxide adduct in basic methanol-d_4 may be assigned to **18** as follows: δ 3.27, *N*-CH_3 (s, 3H); 5.75–5.95, H-2 and -3 (m, 2H); 6.65–7.05, H-4 and -6 (m, 2H); 7.50, H-5 (doublet of doublets, 1H, $J_{56} = 7$,

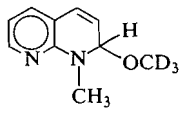

18

$J_{57} = 2$ Hz); 8.10, H-7 (doublet of doublets, 1H, $J_{67} = 5.5$, $J_{57} = 2$ Hz). The multiplet centered at δ 5.85 collapses on standing to a doublet ($J_{34} =$ 10 Hz) as a result of the exchange of H-2 for solvent deuterium (*cf.* 1-methylquinolinium cation). A similar spectral assignment (Table 3) is also consistent with the lithium aluminum hydride reduction product of the cation being 1,2-dihydro-1-methyl-1,8-naphthyridine.

Thus, the similarity of the u.v. spectra of the pseudobase from the 1-methyl-1,8-naphthyridinium cation and **18** indicate that **8** is the predominant pseudobase species present in aqueous alkaline solutions of this cation.

6-Methyl-1,6-naphthyridinium Cation

Aqueous alkaline solutions of this cation have an absorption maximum at 340 nm. In basic methanol this maximum is at 337 nm, while the spectrum of the lithium aluminum hydride reduction product has a maximum at 333 nm. These latter two maxima are at slightly longer wavelengths than in the corresponding isoquinoline derivatives, but the identity of these species as 1,2-dihydroisoquinoline derivatives is readily confirmed from their p.m.r. spectra (Table 3). In each case, the pair of doublets, with coupling constant 7.5 Hz for protons corresponding to H-3 and -4 of a 1,2-dihydroisoquinoline system is clearly visible. In the 1,6-naphthyridine series these protons (H-7 and -8) appear at δ 6.86 and 5.61 for the methoxide adduct and 6.31 and 5.22 for the reduction product, which are in close agreement with the chemical shifts for H-3 and -4 in the corresponding isoquinoline derivatives. In addition, the H-1 singlet of 1,2-dihydro-2-methylisoquinoline is 2.0 p.p.m. further upfield than in its 1-methoxy derivative, and a similar difference (1.7 p.p.m.) is observed for H-5 of the corresponding 5,6-dihydro-1,6-naphthyridine derivatives. Hence the structure of the methoxide adduct of the 6-methyl-1,6-naphthyridinium cation can confidently be assigned as **19**, and the similarity of the u.v. spectra of **19** and the pseudobase indicate that the predominant pseudobase species present in aqueous alkaline solutions of this cation is **6**.

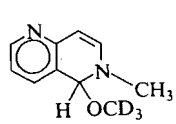

19

7-Methyl-1,7-naphthyridinium Cation

The p.m.r. spectra of this cation in basic methanol-d_4 and of its lithium aluminum hydride reduction product are readily assigned to 1,2-dihydroisoquinoline derivatives, *i.e.*, 7,8-dihydro-1,7-naphthyridines (Table 3). The u.v. spectra of the pseudobase (λ_{max} 320 nm) and the methoxide adduct (λ_{max} 316 nm) are very similar, and consequently the predominant pseudobase species present in alkaline solutions of this cation can be assigned structure **7** and so results from hydroxide attack at C-8.

2-Methylphthalazinium Cation

The reaction of this cation in aqueous alkaline solutions was first investigated by Gabriel and Muller in 1895 (36), and more recently by Smith and Otremba in 1962 (37). In both studies, the only products isolated were 1,2-dihydro-2-methylphthalazine (**20**) and 2-methyl-1-phthalazinone (**21**). It has been assumed (38) that these products arise from the disproportionation of an initially formed pseudobase **22**, although this species has not previously been confirmed as a component of the reaction mixture.

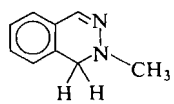

20

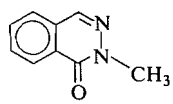

21

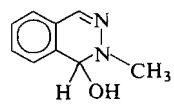

22

The p*H* dependence of the u.v. spectrum of this cation indicates the occurrence of two equilibria in alkaline solutions for which we have measured pK_a values of 11.04 and 13.0. We have confirmed that only **20** and **21** may be extracted from concentrated solutions of this cation in the region p*H* 10–13. However, chloroform extracts from very alkaline solutions (5 *N* KOH) contain a product with p.m.r. spectrum ($CDCl_3$): δ 3.38 (s, 3H), 5.75 (s, 1H), 7.23–7.57 (m, 5H). This spectrum is very similar to that of solutions of this cation in basic methanol-d_4 and which we assign to the methoxide adduct **23** as follows;

Can. J. Chem. Downloaded from www.nrcresearchpress.com by 210.87.254.40 on 09/05/12
For personal use only.

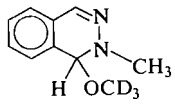

23

δ 3.40, N-CH_3 (s, 3H); 5.71, H-1 (s, 1H); 7.30–7.60, aromatic protons plus H-4 (m, 5H). Thus, the species extracted from strong alkali may be assigned the pseudobase structure **22**, and this assignment of structures **22** and **23** is also consistent with the spectrum of 1,2-dihydro-2-methylphthalazine (Table 3). The u.v. spectra of aqueous solutions of pH 12 and 15 are very similar (λ_{max} 302 and 312 nm, respectively), and so the observed equilibria may be assigned to pseudobase formation ($pK_{ROH} = 11.04$) and ionization of the pseudobase ($pK_{RO^-} = 13.0$).

Anion formation seems to stabilize the pseudobase with respect to disproportionation to **20** and **21**. The pseudobase also does not tend to disproportionate at an appreciable rate in chloroform solution.

1-Methylquinoxalinium Cation

The u.v. spectra of dilute aqueous alkaline solutions (pH 10.5) and basic methanolic solutions of this cation are very similar. Each spectrum has two absorption maxima; 301 and 340 nm (pH 10.5); 304 and 344 nm (CH_3O^-/CH_3OH). In more alkaline aqueous solutions (pH 14.5), the only maximum is at 347 nm. Two ionization constants (8.62 and 12.62) were obtained from the pH dependence of the u.v. spectrum.

Although aqueous solutions of the 1-methylquinoxalinium ion in dilute alkali (pH 9–12) are turbid at p.m.r. spectral concentrations, solution is complete in stronger alkali. The p.m.r. spectrum in 3 M NaOD in D_2O may be assigned to the anion **24** of the pseudobase from hydroxide attack at C-2: δ 3.05, N-CH_3 (s, 3H); 5.15, H-2 (d, 1H, $J = 3$ Hz); 6.7–7.3, aromatic protons (m, 4H); 7.67, H-3 (d, 1H, $J = 3$ Hz). This assignment of H-2 and -3 agrees well with the chemical shifts for the pyrazine ring protons in **25** (39): δ 5.20, 7.05 (doublets, $J = 3$ Hz).

The p.m.r. spectrum of the 1-methylquinoxalinium cation in basic methanol-d_4 is more complex than would be expected for 1,2-dihydro-2-trideuteromethoxy-1-methylquinoxaline: δ 3.17, 3.23 (singlets); 4.62 (s); 5.37 (d, $J =$ 3 Hz); 6.67 (s); 6.9–7.5 (m); 7.66 (d, $J = 3$ Hz).

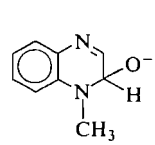

24

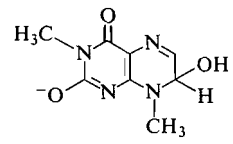

25

The doublets at δ 5.37 and 7.66 are of equal intensity and integrate for one quarter of the area of the multiplet, 6.9–7.5. The singlet at δ 6.67 is twice as intense as the singlet at 4.62. Integration of the peaks at δ 3.17 and 3.23 is difficult since they tend to overlap with one another and also with the signals from a small amount of solvent protiated methyl groups. Assignment of δ 7.66 to H-3, 5.37 to H-2, and 6.9–7.5 to the aromatic protons of **26**, would be consistent with the assignment made above for **24**. We suggest that the remaining peaks could then reasonably be assigned to the tetrahydroquinoxaline derivative (**27**), which would be formed by addition of a molecule of methanol across the C_3—N_4 bond of **26**. This assignment

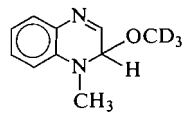

26

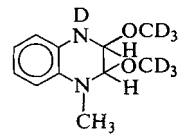

27

requires the chemical shifts of all the aromatic protons in **27** to be the same (δ 6.67), and also the chemical shifts of H-2 and -3 to be the same (δ 4.62) within the resolution obtained. As supporting evidence that the chemical shifts of the four aromatic protons in **27** should be similar, we note that the aromatic protons of o-phenylenediamine (in $CDCl_3$) give rise to only one signal (δ 6.68) and the signals from the aromatic protons of 1-methyl-1,2,3,4-tetrahydroquinoxaline occur as a very narrow multiplet centered at δ 6.60 ($CDCl_3$). The chemical shift (δ 4.62) for H-2 and -3 in **27** agrees well with the reported chemical shifts for the corresponding protons in **28** (δ 4.63) and **29** (δ 4.72, 4.83) (40).

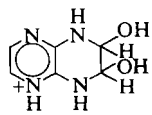

28

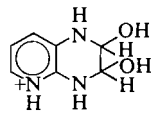

29

Can. J. Chem. Downloaded from www.nrcresearchpress.com by 210.87.254.40 on 09/05/12
For personal use only.

Can. J. Chem. Downloaded from www.nrcresearchpress.com by 210.87.254.40 on 09/05/12
For personal use only.

The tendency of quinoxaline derivatives to add two molecules of nucleophilic reagents to form tetrahydro derivatives is well known. Thus, quinoxaline itself readily adds two molecules of hydrogen cyanide or bisulfite ion across the 1,2- and 3,4- C=N bonds (41); 2,4-dihydroxypteridines add two equivalents of bisulfite ion in the pyrazine ring (42); and the cations of 1,4,5-triazanaphthalene, 1,4,5,8-tetra-azanaphthalene, and pteridine form covalent dihydrates by the addition of two molecules of water to the pyrazine ring (40, 43). We believe that this current observation of the addition of methoxide ion and methanol to the *N*-methylquinoxalinium cation represents the only case in which an appreciable amount of a dihydroquinoxaline monoadduct has been shown to be in equilibrium with the tetrahydroquinoxaline diadduct. The relative proportions of **26** and **27** in solution are independent of methoxide concentration from 0.01–3 *M*. From the integral ratios of (*i*) the aromatic proton peaks, and (*ii*) the H-2 proton peaks at several different base concentrations, we have estimated that the equilibrium mixture consists of 60% **26** and 40% **27**.

These observations on the reaction of the 1-methylquinoxalinium cation in basic methanol, raise the possibility that the pseudobase formed in aqueous alkali by hydroxide addition at C-2 may be sufficiently susceptible to addition of a molecule of water across the C_3—N_4 double bond, that appreciable amounts of the tetrahydroquinoxaline (**30**) may be present in dilute aqueous alkali (p*H* 9–12). As noted above, the quinoxaline pseudobase is insufficiently soluble in dilute aqueous alkali to allow a p.m.r. spectral investigation. However, the similarity of the u.v. spectra of the *N*-methylquinoxalinium cation in dilute aqueous alkali (λ_{max} 301, 340 nm) and basic methanol (λ_{max} 304, 344 nm) strongly suggests that **30** is present. Maxima in the vicinity of 300 nm are not typical of the spectra of 1,2-dihydroquinoline derivatives (30, 33, 34), but are typical of 1,2,3,4-tetrahydroquinoline derivatives (*e.g.*, 1,2,3,4-tetrahydroquinoline in ethanol, 299 nm (34); 1-methyl-1,2,3,4-tetrahydroquinoxaline in $CHCl_3$, 313 nm (Table 3)). We feel that the maxima at 304 and 344 nm in basic methanol solution should be assigned separately to **27** and **26**, respectively. This assignment then suggests that in dilute aqueous alkali the pseudobase **31** (λ_{max} 340 nm) is in equilibrium with a considerable amount of its covalent hydrate **30** (λ_{max} 301 nm). This conclusion is further supported by the fact that in strongly alkaline solutions, where we have shown by p.m.r. spectroscopy that only the anion **24** is present in any appreciable amount, the u.v. spectrum (Fig. 2) has only the absorption maximum (347 nm) typical of a 1,2-dihydroquinoline derivative. Thus the anion **24** is less susceptible to covalent hydration of the C_3—N_4 bond than the corresponding neutral molecule **31**.

30

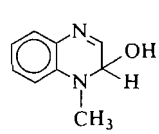

31

1- and 3-Methylquinazolinium Cations

The 3-methylquinazolinium cation is known to undergo hydroxide attack at C-4 to give the pseudobase **32** (44). More recently, we have shown that the 1-methylquinazolinium cation also undergoes hydroxide attack at C-4 to give the pseudobase **33** (23). The formation of both these pseudobases is complicated by their facile protonation to give the resonance-stabilized cations **34** and **35**. We have measured a pK_a value for protonation[3] of **32** of 7.77 ± 0.06 at 25° (Albert *et al.* (44) give 7.64 at 20°), and the free 1- and 3-methylquinazolinium ions are never present in aqueous solution to any appreciable extent. It is therefore not possible to measure pK_{ROH} values for these ions by any direct method, although they must each be less than 7.

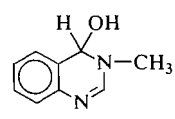

32

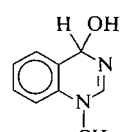

33

It would be useful to have estimates of pK_{ROH} values for these ions for comparison with the other diazanaphthalene cations in the present study, and to this end we have made use of the observation that the electronic effect of a pyridine-type ring nitrogen atom is very similar

[3]The pK_a for **33** is not known since it has never been obtained free of **32**. However, the basicities of **32** and **33** should be quite similar.

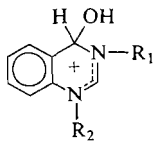

34 $R_1 = H$; $R_2 = CH_3$
35 $R_1 = CH_3$; $R_2 = H$

to that of a nitro group in the corresponding position of a homocyclic ring (45). Thus, we have measured the pK_{ROH} values for the 1-methyl-3-nitroquinolinium cation (6.74 ± 0.06) and for the 2-methyl-4-nitroisoquinolinium cation (5.03 ± 0.04) as models for the 1-methyl- and 3-methylquinazolinium cations, respectively.

The 1-methyl-3-nitroquinolinium cation has previously been shown (46) to undergo hydroxide attack at C-4 and so is directly comparable with the 1-methylquinazolinium cation, although the value of 6.94 should only be considered as an upper limit for pK_{ROH} for the latter species, since it is not possible to allow for steric effects from the presence of the nitro group ortho to C-4.

The 2-methyl-4-nitroisoquinolinium cation has not been previously studied, however, it is to be expected that it will be most susceptible to nucleophilic attack at C-1 (comparable to C-4 in the 3-methylquinazolinium cation) as are other isoquinolinium derivatives. The p.m.r. spectrum in strong alkali (3 *N* NaOD/D_2O) is consistent with the structure **36** for the pseudobase anion: δ 3.48, *N*-Me (s, 3H); 5.74, H-1 (s, 1H); 8.52, H-3 (s, 1H); 7.1–7.3, 8.33, aromatic protons (m, 4H). Although attack at C-3 cannot be definitely ruled out, we feel that it is unlikely that the nitro group will have sufficient influence to produce this abnormal mode of attack. This is substantiated by the fact that nucleophilic attack at C-2 between the nitro group and ring-nitrogen atom in the 1-methyl-3-nitroquinolinium ion is less important than at C-4 (46). Hence, the 2-methyl-4-nitroisoquinolinium cation should be an excellent model for the 3-methylquinazolinium cation, and since the nitro group is well removed from the site of hydroxide attack at C-1, the pK_{ROH} value for the 3-methylquinazolinium cation is probably quite close to 5.0.

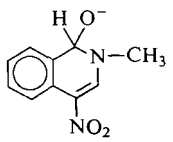

36

General Comparison of N-Methyl Diazanaphthalene Cations

Our spectral data establish that in all cases (except for the 1-methylquinoxalinium cation) there is only one major pseudobase species present in aqueous alkaline solutions of the cations that we have examined. Such studies will not, however, detect the presence of small amounts of other species (*e.g.*, from attack at C-4 in quinolinium ions or at C-3 in isoquinolinium ions). Much early work on the pseudobases was related to the possibility of their ring-opening to give amino-aldehydes (3). We have found no evidence for any significant amount of ring-opening of the pseudobases formed from the *N*-methyl cations of the diazanaphthalenes. In all cases, there is a close correspondence between the u.v. spectra of the pseudobases and the corresponding methoxy derivatives which cannot undergo ring-opening. The presence of any appreciable amount of the ring-opened species should be readily apparent since these species have quite distinctive u.v. spectra as a result of the increased conjugation in these molecules compared to the corresponding pseudobases; *e.g.*, **37**, λ_{max} 316 nm; **38**, λ_{max} 394 nm (39).

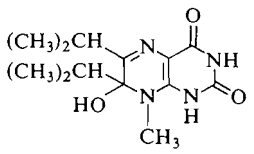

37

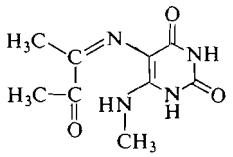

38

All of our data are consistent with the activation of heterocyclic cations to nucleophilic attack by the presence of a strongly electron-withdrawing azine nitrogen atom. The data of Table 2 indicate that there is little difference in the susceptibilities of the various *N*-methylnaphthyridinium cations to pseudobase formation. Thus the pK_{ROH} values for all the *N*-methyl-1,*x*-naphthyridinium cations lie in the range 12.4–13.1.

The presence of a further ring-nitrogen atom in the pyridine ring of a quinolinium or isoquinolinium cation usually causes a drastic increase in susceptibility to pseudobase formation

Can. J. Chem. Downloaded from www.nrcresearchpress.com by 210.87.254.40 on 09/05/12
For personal use only.

Can. J. Chem. Downloaded from www.nrcresearchpress.com by 210.87.254.40 on 09/05/12
For personal use only.

(*e.g.*, 1-methylquinoxalinium and 1- and 3-methylquinazolinium cations) although this effect may be attenuated to some extent (as in phthalazinium derivatives) if the electronic effect of the second nitrogen atom must be transmitted predominantly through the quaternary nitrogen to the site of nucleophilic attack.

The experimental pK_{ROH} value for the 1-methylquinoxalinium cation is not strictly comparable to the other values in Table 2 if a considerable amount of **30** is present as we have suggested. In this case, the measured value, pK^{app}_{ROH}, is defined by eq. 5, and the true pK_{ROH} for

$$[5] \qquad K^{app}_{ROH} = \frac{[H^+]([QOH] + [\mathbf{30}])}{[Q^+]} = K_{ROH}\left[1 + \frac{[30]}{[QOH]}\right]$$

the 1-methylquinoxalinium cation will be less than pK^{app}_{ROH} (8.62) by an amount equal to the value of log (1 + [**30**]/[QOH]). By assuming that the ratio of tetrahydro- to dihydroquinoxaline species in water will be similar to that found in methanol (2:3), we estimate a value of $pK_{ROH} \approx 8.4$ for the *N*-methylquinoxalinium cation. Similarly, for alkoxide ion formation from the pseudobase **31**, the measured value, $pK^{app}_{RO^-}$, is also a "mixed" constant, and is defined by eq. 6.

$$[6] \qquad K^{app}_{RO^-} = \frac{[H^+][QO^-]}{[QOH] + [\mathbf{30}]} = \frac{K_{RO^-}}{1 + \frac{[30]}{[QOH]}}$$

The presence of strongly electron-withdrawing substituents close to the hydroxyl group is necessary in order to increase the acidity of the pseudobases sufficiently to give pK_{RO^-} values less than 14 (Table 2). Anion formation by pseudobases of the *N*-methylnaphthyridinium cations is not appreciable in solutions of p*H* less than 14, which is in agreement with the data of Cooksey and Johnson (9) for anion formation by the pseudobases of the 1-methyl-5-nitroquinolinium cation ($pK_{RO^-} \sim 15$) and the 1-methyl-6,8-dinitroquinolinium cation ($pK_{RO^-} = 14.3$).

Experimental

Materials

Quinoline, isoquinoline, acridine, phthalazine, quinazoline, and quinoxaline were obtained commercially. 1,5-Naphthyridine (25), 1,6-naphthyridine (47), 1,8-naphthyridine (48), and 3-nitroquinoline (49) were synthesized as described in the literature. The synthesis of 4-nitroisoquinoline will be described separately.[4] 1,7-Naphthyridine was synthesized by a modification of the method of Baumgarten and Cook (50) for substituted 1,7-naphthyridines. 3-Nitro-4-picoline (4 gm) was converted to *N*-(3-amino-4-picolylidene)-*p*-toluidine (51). This crude product was dissolved in absolute ethanol (10 ml) and cooled in an ice bath. Aqueous potassium hydroxide (1 *N*; 1 ml) was added, and then cold acetaldehyde (2 ml) was added dropwise to the stirred iced solution. After refluxing for 2 h, the cooled solution was diluted with water (50 ml) and extracted with chloroform (3 × 50 ml). These combined extracts were extracted with hydrochloric acid (15%; 4 × 25 ml). These acid extracts were basified (KOH) and then re-extracted with chloroform. After drying over anhydrous magnesium sulfate and evaporation of the chloroform, 1,7-naphthyridine (147 mgm) was obtained by chromatographing the residue on a silica gel column with ethanol as eluent.

Methylations

The heterocyclic base was treated with excess methyl iodide, either neat or during reflux in a suitable solvent (acetone or ethanol). After removal of the solvent and excess methyl iodide, the solid residues were recrystallized to constant melting points which were in agreement with literature values. The only quaternary heterocyclic iodide that has not been previously reported is 2-methyl-4-nitroisoquinolinium iodide, m.p. 208–210°.

Anal. Calcd. for $C_{10}H_9IN_2O_2$: C 38.0; H 2.85; N 8.86. Found: C 38.0; H 3.07; N 8.68.

Reductions

The quaternary salt (100 mg) was suspended in anhydrous ether (30 ml) and lithium aluminum hydride (50 mg) was slowly added with stirring. After 5 min, the reaction mixture was poured into ice-water (50 ml). The aqueous layer was extracted with ether, and after drying over magnesium sulfate, the ether was removed on the rotary evaporator. The p.m.r. spectra of the oily products were recorded immediately, since these dihydronaphthyridines tend to decompose on standing in a similar manner to 1,2-dihydro-1-methylquinoline (30).

Methods

The p.m.r. spectra were obtained on a Varian T-60 spectrometer, using tetramethylsilane as an internal standard in $CDCl_3$ and CD_3OD solutions, and sodium 2,2-dimethyl-2-silapentane-5-sulfonate in D_2O. The u.v. spectra were recorded on a Unicam SP-800 spectrophotometer and absorption maxima were checked manually on a Beckman DU-2 instrument.

Spectrophotometric determinations of pK_{ROH} and pK_{RO^-} values were made as described by Albert and Serjeant (52) on a Beckman DU-2 spectrophotometer with cell compartment thermostatted at 25 ± 0.1°. In several cases, the optical density of the pure pseudobase species was not directly obtainable owing to subsequent reactions at high p*H* values, and so this value was obtained from the ordinate intercept of a plot of D *vs.* $a_{H^+}(D - D_c)$ where D_c is the optical density

[4] J. W. Bunting and W. G. Meathrel, Organic Preparations and Procedures International, submitted for publication.

of the pure heterocyclic cation and D is the optical density of a solution of the cation at hydrogen ion activity a_{H^+}. Specific experimental details for each compound are included in Table 2. Errors quoted are the greatest deviation from the average. Buffer solutions were those described by Perrin (53) (pH 2–10.6) and Bates (54) (pH 11–13). Solutions of pH greater than 13 were made up by dilution of standard potassium hydroxide solutions (55). All pH values below 13 were checked on a Corning Model 12 Research pH Meter. The potentiometric titration of 2-methyl-4-nitroisoquinolinium iodide was also performed according to Albert and Serjeant (56) using standard 0.05 M potassium hydroxide solution as titrant.

This research was supported by a grant from the National Research Council of Canada and a Province of Ontario Graduate Fellowship (W.G.M.).

1. A. Albert. Heterocyclic chemistry. Athlone Press, London, 1968. p.112.
2. M. H. Palmer. The structure and reactions of heterocyclic compounds. Edward Arnold Ltd., London, 1967. p.130.
3. D. Beke. Advan. Heterocycl. Chem. **1**, 167 (1963).
4. A. Hantzsch. Chem. Ber. **32**, 575 (1899); A. Hantzsch and M. Kalb. Chem. Ber. **32**, 3109 (1899).
5. H. Decker. J. prakt. Chem. **47**, 28 (1893); H. Decker and A. Kaufmann. J. prakt. Chem. **84**, 219 (1911).
6. J. G. Aston and P. A. Lasselle. J. Am. Chem. Soc. **56**, 426 (1934).
7. H. Vorsanger and J. J. Vorsanger. Bull. soc. chim. Fr. 589 (1970); H. Vorsanger, R. Ferrand, M. Mazza, and J. J. Vorsanger. Bull. soc. chim. Fr. 593 (1970).
8. W. G. Meathrel. M.Sc. Thesis. University of Toronto, Toronto, Ontario, 1970.
9. C. J. Cooksey and M. D. Johnson. J. Chem. Soc. B, 1191 (1968).
10. R. J. Goldacre and J. N. Phillips. J. Chem. Soc. 1724 (1949).
11. D. Magrath and J. N. Phillips. J. Chem. Soc. 1940 (1949).
12. A. Albert and W. L. F. Armarego. Advan. Heterocycl. Chem. **4**, 1 (1965).
13. D. D. Perrin. Advan. Heterocycl. Chem. **4**, 43 (1965).
14. A. Albert. Angew. Chem. Int. Ed. Engl. **6**, 919 (1967).
15. M. J. Strauss. Chem. Rev. **70**, 667 (1970).
16. M. R. Crampton. Advan. Phys. Org. Chem. **7**, 211 (1969).
17. P. Buck. Angew. Chem. Int. Ed. Engl. **8**, 120 (1969).
18. E. Buncel, A. R. Norris, and K. E. Russel. Quart. Rev. Chem. Soc. **22**, 123 (1968).
19. J. S. Morley and J. C. E. Simpson. J. Chem. Soc. 1354 (1949).
20. D. E. Ames and H. Z. Kucharska. J. Chem. Soc. 283 (1964).
21. W. W. Paudler and T. J. Kress. J. Heterocycl. Chem. **5**, 561 (1968).
22. R. A. Y. Jones and N. Wagstaff. J. Chem. Soc. D, 56 (1969).
23. J. W. Bunting and W. G. Meathrel. Can. J. Chem. **48**, 3449 (1970).
24. B. J. Huckings and M. D. Johnson. J. Chem. Soc. 5371 (1964).
25. H. Rapoport and A. D. Batcho. J. Org. Chem. **28**, 1753 (1963).
26. C. K. Ingold. Structure and mechanism in organic chemistry. Cornell Press, Ithaca, 1953. p. 577.
27. Reference 1. p. 114.
28. H. Schmid and P. Karrer. Helv. Chim. Acta, **32**, 960 (1949).
29. J. Druey and A. Hüni. Helv. Chim. Acta, **35**, 2301 (1952).
30. E. A. Braude, J. Hannah, and R. P. Linstead. J. Chem. Soc. 3249 (1960).
31. J. W. Bunting and W. G. Meathrel. Tetrahedron Lett. 133 (1971).
32. R. Bramley and M. D. Johnson. J. Chem. Soc. 1372 (1965).
33. K. Sutter-Kostic and P. Karrer. Helv. Chim. Acta, **39**, 677 (1956).
34. W. S. Johnson and B. G. Buell. J. Am. Chem. Soc. **74**, 4517 (1952).
35. N. J. Leonard and R. L. Foster. J. Am. Chem. Soc. **74**, 3671 (1952).
36. S. Gabriel and F. Müller. Chem. Ber. **28**, 1830 (1895).
37. R. F. Smith and E. D. Otremba. J. Org. Chem. **27**, 879 (1962).
38. R. C. Elderfield and S. L. Wythe. Heterocyclic compounds, Vol. 6. *Edited by* R. C. Elderfield. Wiley, New York, N.Y., 1957. p. 190.
39. W. Pfleiderer, J. W. Bunting, D. D. Perrin, and G. Nübel. Chem. Ber. **99**, 3503 (1966).
40. T. J. Batterham. J. Chem. Soc. C, 999 (1966).
41. F. W. Bergstrom and R. A. Ogg. J. Am. Chem. Soc. **53**, 245 (1931).
42. J. W. Bunting. Ph.D. Thesis. Australian National University, Canberra, 1967.
43. A. Albert, T. J. Batterham, and J. J. McCormack. J. Chem. Soc. B, 1105 (1966).
44. A. Albert, W. L. F. Armarego, and E. Spinner. J. Chem. Soc. 5267 (1961).
45. J. Clark and D. D. Perrin. Quart. Rev. Chem. Soc. **18**, 295 (1964).
46. T. Severin, D. Bätz, and H. Lerche. Chem. Ber. **101**, 2731 (1968).
47. T. J. Kress and W. W. Paudler. Chem. Commun. 3 (1967).
48. W. W. Paudler and T. J. Kress. J. Org. Chem. **32**, 832 (1967).
49. M. J. S. Dewar and P. M. Maitlis. J. Chem. Soc. 944 (1957).
50. H. E. Baumgarten and K. C. Cook. J. Org. Chem. **22**, 138 (1957).
51. H. E. Baumgarten and A. L. Kreiger. J. Am. Chem. Soc. **77**, 2438 (1955).
52. A. Albert and E. P. Serjeant. Ionization constants of acids and bases. Methuen, London, 1962. p. 69.
53. D. D. Perrin. Aust. J. Chem. **16**, 572 (1963).
54. R. G. Bates. Determination of pH. Wiley, New York, N.Y., 1964. p. 162.
55. H. S. Harned and M. A. Cook. J. Am. Chem. Soc. **59**, 496 (1937).
56. Reference 52. p. 43.

Can. J. Chem. Downloaded from www.nrcresearchpress.com by 210.87.254.40 on 09/05/12
For personal use only.

Substituent Effects in Dye-sensitized Photooxidation Reactions of Furans[1]

R. H. YOUNG, R. L. MARTIN, N. CHINH, C. MALLON, AND R. H. KAYSER

Department of Chemistry, Georgetown University, Washington, D.C. 20007

Received March 13, 1970[2]

The problems encountered in the normal method used to determine β values (rate of decay of singlet oxygen divided by the rate of its reaction with an organic compound) are discussed. The use of dilute solutions of organic acceptors for our measurements was found to give more reproducible values and simplified kinetics. These β values were used to obtain relative rate constants for a variety of substituted furans. Hammett plots were made to quantitate the substituent effects in order to explore the nature of singlet oxygen in the dye-sensitized photooxidation reactions of these furans. The calculated ρ values were compared with other photooxidation and Diels–Alder reactions. Hammett ρ values in a series of solvents were also calculated for the reaction of singlet oxygen with 2-arylfurans and increasing ρ values were correlated with decreasing solvent polarity.

On discute des problèmes rencontrés dans la méthode normale utilisée pour déterminer les valeurs de β (vitesse de désintégration de l'oxygène singulet divisée par la vitesse de sa réaction avec un composé organique). On trouve que l'utilisation de solutions diluées d'accepteurs organiques pour nos mesures donne des valeurs plus reproductibles et une cinétique simplifiée. On utilise les valeurs de β pour obtenir les constantes de vitesse relatives pour une variété de furannes substitués. On trace les graphes de Hammett pour concrétiser les effets de substituants afin d'explorer la nature de l'oxygène singulet dans les réactions de photooxydation sensibilisées au colorant de ces furannes. Les valeurs calculées de ρ sont comparées avec d'autres réactions d'oxydation et de Diels–Alder. On calcule aussi les valeurs de ρ de Hammett pour une série de solvants dans le cas de la réaction de l'oxygène singulet avec les 2-arylfurannes et on fait la corrélation entre des valeurs de ρ croissantes avec la polarité décroissante du solvant.

Canadian Journal of Chemistry, **50**, 932 (1972)

Introduction

There has been a recent revival of interest in the photooxidation of organic compounds. A number of recent reviews on photooxidation reactions aptly illustrate the large amount of recent work and current interest in this area (1). The postulated reactive intermediate in such photooxidations, singlet oxygen ($^1\Delta_g$), has been described as an electrophilic, discriminating species (2) which is "Diels–Alder-like" in its reactions (3). These reactions have also been described as being concerted in nature (1*b*, 4).

The involvement of singlet oxygen in type II dye-sensitized photooxidation reactions is well established (3, 5, 6). There is a variety of different reactions that would fall into this class of photooxidation reactions (1*b*). These include the photooxidation of alkenes with allylic hydrogens:

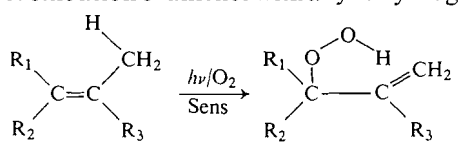

and the addition of singlet oxygen in a Diels–Alder manner to conjugated dienes:

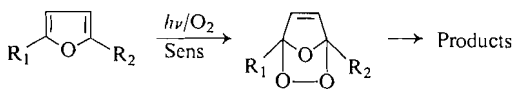

In some cases the initial photooxidation product is unstable and subsequent products are isolated.

Foote has studied the substituent effect for the photooxidation of substituted 2-aryl-3-methyl-2-butenes and obtained a Hammett ρ value of -0.93 (in methanol) when using σ constants (1*a*, 7). This low ρ value was said to indicate little polar character in the transition state of the reaction. However, even with this small substituent effect one might have expected the product ratio to vary with the substituent. In addition to a concerted mechanism, the substituent effect could be explained either by the formation of a partial charge-transfer complex as an initial

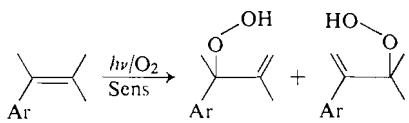

1 **2**

[1]Presented in part at the 52nd C.I.C. Conference, Montreal, Quebec, 1969.

[2]Revision received November 19, 1971.

Can. J. Chem. Downloaded from www.nrcresearchpress.com by 210.87.254.105 on 09/05/12
For personal use only.

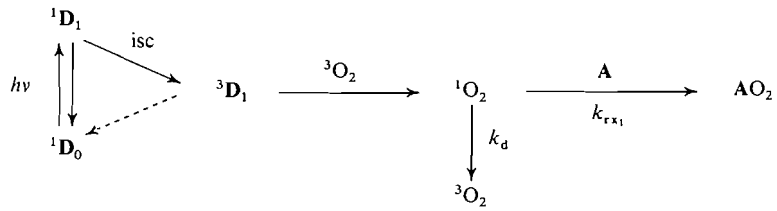

SCHEME 1

intermediate, or by the formation of a reactive intermediate as suggested by Kearns for such reactions (8). Substituent effects on subsequent reactions which would affect product ratios would be difficult to predict.

We have carried out a similar study of substituent effects for the photooxidation reaction of a series of substituted furans in order to compare these reactions with the results obtained by Foote and to typical Diels–Alder reactions.

Method

The most widely accepted mechanism (1) for photooxidation reactions is outlined in Scheme 1, where **A** is the organic acceptor; **D** is the sensitizer; isc is intersystem crossing; k_{rx_1} is the rate constant for the reaction; and k_d is the rate constant for the decay of singlet oxygen to ground state oxygen.

The velocity for the disappearance of A would then be given by:

$$-\frac{d[\mathbf{A}]}{dt} = K\frac{k_{rx_1}[\mathbf{A}]}{k_{rx_1}[\mathbf{A}] + k_d} = K\frac{[\mathbf{A}]}{[\mathbf{A}] + \beta}$$

where K is the rate of formation of singlet oxygen and $\beta = k_d/k_{rx_1}$.

Usually this β value is determined by plotting $1/\Phi_{-A}$ or $1/(-d[\mathbf{A}]/dt)$ *vs.* $1/[\mathbf{A}]$ when the values of β and [**A**] are comparable. However, the errors in this method are estimated to vary from $\pm 30\%$ up to $\pm 400\%$ (9). Competitive reactions used to determine relative β values were found to be more satisfactory and usually are acceptable when following product appearance (9). This latter method suffers from the limitations of g.l.p.c., the method most commonly used for analysis of these competitive reactions.

From the above equation it can be seen that at higher concentrations of **A** errors in the measurement of the velocity of the photooxidation reaction become magnified in the calculation of the β value for a particular reaction. We found some initial difficulties when using the standard method (a plot of $1/d[\mathbf{A}]/dt$) *vs.* $1/[\mathbf{A}]$) for the determination of β values. The errors in this method were such that small differences in the β values for some acceptors (2-arylfurans) could not be determined with any accuracy. It is only at low concentrations of acceptor ($[\mathbf{A}] \ll \beta$) that the maximum difference in the velocities of these reactions will be realized. At these lower concentrations of acceptors not only does one get maximum differences in velocity but the kinetics are simplified to pseudo first order. Then as the substituents of the furan are changed (all reaction conditions remaining constant) the relative β values (k_{rx_1} (rel.) $\equiv 1/\beta$ (rel.) for these reactions can be easily calculated from the slopes of first order plots. This method should enable even

$$-\frac{d\mathbf{A}}{dt} = K\frac{[\mathbf{A}]}{\beta}$$

$$\beta = \frac{k_d}{k_{rx_1}}$$

small differences in the rate constant (k_{rx_1}) to be meaningful. The method was used to obtain relative β values for a series of furans, principally the 2-arylfurans and is referred to as method A in this paper. Absolute β values were determined by relating these relative β values to that of 2,5-diphenylfuran which was determined by our alternate method (method B). Some preliminary results using method A for the 2-arylfurans were reported earlier (10).

For some furans method A was not applicable as it required the *change* in concentration of the furan acceptor to be followed at low concentrations (concentrations lower than the β value are necessary). For this and other reasons we have developed an alternative method (method B) for the direct determination of β values for

Can. J. Chem. Downloaded from www.nrcresearchpress.com by 210.87.254.105 on 09/05/12
For personal use only.

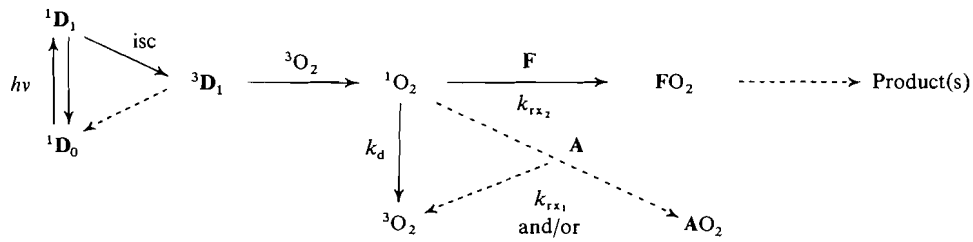

SCHEME 2

photooxidation reactions. This method is given in detail elsewhere (11).

Briefly the reaction scheme involved can be illustrated as Scheme 2, where **D** is a dye-sensitizer (Rose Bengal or methylene blue); **F** is a very reactive species (such as 1,3-diphenylisobenzofuran); and **A** is any compound which can quench the reaction between singlet oxygen and compound **F** either by reaction with the singlet oxygen (which occurs for all compounds in this paper) or by enhancing the intersystem crossing of singlet oxygen to ground state oxygen (unlikely to be important for the furans (12)). The technique involves working at very low concentrations of **F** and applying a Stern–Volmer quenching plot, the slope of which will be equivalent to k_{rx_1}/k_d or $1/\beta$. As shown elsewhere, this method gives quite acceptable results as compared to literature values (11).

These methods were applied to the determination of the β values for a large group of substituted furans and the results are recorded in Table 1. The versatility of these two methods is exemplified by their application to the reactions of singlet oxygen with a wide variety of furans.

Results and Discussion

The addition of singlet oxygen has been suggested to be mechanistically related to the Diels–Alder reaction (3). Little work has been done to confirm this suggestion. For this reason we have looked at some substituent and solvent effects on the dye-sensitized photooxidation reaction of a series of furans as examples of dienes. If singlet oxygen is a dienophile it is of interest to compare its reactivity to that of other dienophiles.

Hammett ρ plots were made for the reactions between singlet oxygen and a number of different substituted furans (eqs. 1–3).

The negative slope for the Hammett plots in all cases illustrates the electrophilic character of singlet oxygen. The low values obtained indicate only a small increase in polarity in the transition state of the reaction.

The ρ value for the reaction between singlet oxygen and the furans with substituents directly attached to the furan ring (including the phenyl-substituted furans) was calculated assuming that the σ values for the 2- and 3-substituents were equivalent to σ para and σ meta, respectively. There is a precedent for this assumption for

[1] 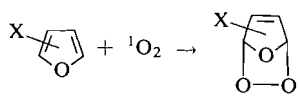 (methanol) $\rho = -2.48 \pm 0.21$

[2] 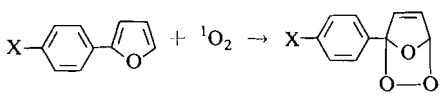 (methanol) $\rho = -0.836 \pm 0.085$[3]

[3] 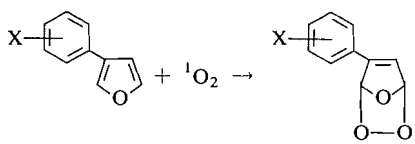 (methanol) $\rho = -0.699 \pm 0.051$

[3]This value differs only slightly from that previously reported (10). This is due to recently repeating this experiment using an improved, more automated technique.

Can. J. Chem. Downloaded from www.nrcresearchpress.com by 210.87.254.105 on 09/05/12
For personal use only.

Can. J. Chem. Downloaded from www.nrcresearchpress.com by 210.87.254.105 on 09/05/12
For personal use only.

TABLE 1. β-Values for the reaction of singlet oxygen with substituted furans (methanol solvent)

Compound	$\beta \times 10^3$ (M)*	Method used	Product reference
Furan	2.62	B	13
2-Methoxyfuran	0.39 0.41	B	—
Furfural alcohol	4.68 4.77	B	13
2-Acetylfuran	22.1 21.3	B	—
Furfural	79 81	B	13
2-Methylfuran	1.1		
2-Furoic acid	11.2 12.7	B	13
2,5-Dimethylfuran	0.28	B	14
2,5-Diphenylfuran	0.953†	B	15
3,4-Diphenylfuran	1.67	B	—
Furfuralamine	29.2 30.7	B	16
2-Phenylfuran	1.73 1.67	A	17
2-(*p*-Tolyl)furan	1.40 1.40	A	18
2-(*p*-Methoxyphenyl)furan	1.05 1.02	A	—
2-(*p*-Chlorophenyl)furan	2.71 3.03	A, B	18
3-Phenylfuran	2.86 2.82	B	19
3-(*p*-Tolyl)furan	2.42 2.35	B	—
3-(*p*-Methoxyphenyl)furan	2.04 1.83	B	—
3-(*p*-Bromophenyl)furan	4.36	B	—
3-(*p*-Fluorophenyl)furan	3.57 3.28	B	—
1,3-Diphenylisobenzofuran	0.073†	A	20

*Values determined by method B are for quenching of singlet oxygen, presumably by reaction with singlet oxygen.
†From ref. 11.

furans with substituents at the 2 and 3 positions of the furan molecule (21). However, our application deviates in that not only is there a para relationship between the substituent at the 2 position of the furan relative to the reactive site at the 5 position (assuming that —Ö— ≡ —C=C—) (21) but the reaction also involves bond formation at the site of the substituent. This is based on the assumption that there is a concerted addition of singlet oxygen to furan. (In a two-step addition reaction with a reaction at the 5 position, the rate determining step would involve a reasonable para type substituent interaction only.) It is possible that the inductive and resonance effects of the substituent at the 2 position on both the 2 and 5 positions would be important and linearly related. In addition, as the attacking dienophile (singlet oxygen) is small and most of the substituents are about the same size, variations in steric interactions should not be of major importance. For these reasons the assumption that σ para will represent the relative effect of the substituents on the electronic demands of the dienophile is probably a good one.

The three substituted furans involve a meta relation with C-5 and an ortho relation to C-2. For the attack of a dienophile on furan both σ meta and σ ortho should be considered for the 3-substituents. In our case only the 3-phenyl and the 3,4-diphenylfurans present this problem. The rate constants for these compounds correlate well with the other furans with the assumption that σ meta approximates the total inductive and resonance effects ($\sigma_p = -0.01$ and $\sigma_m = 0.06$). Again steric effects do not appear to be significant for these compounds.

Solvent Effects

In addition we have expanded this work to investigate the effect of other solvents on the photooxidation reaction of these furans. Previously solvent effects on the rate of reaction have been difficult to rationalize because the solvent can affect both the rate constant of reaction (k_{rx}) and the rate constant of decay (k_d) and hence the ratio of these two (β value) is ineffective for the study of solvent effects.

However, in the investigation of the changes in the calculated Hammett ρ value for reactions in various solvents we are looking at the effect of the solvent on relative rate constants of reaction only, and not the solvent effect on the rate constant of decay. Often there is a correlation between Hammett ρ values and the rate constant for reactions. The results from reactions in a series of solvents are given in Table 2.

[4] 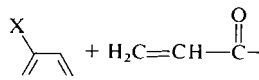 $\rho = -3.12$ (*vs.* σ^+) ref. 22

[5] 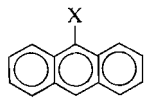 (chloroform) $\rho = -4.6$ ref. 23, our calculations *vs.* σ^+

[6] 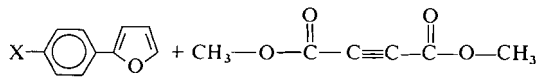 (ethanol) $\rho = -2.27$ ref. 24

[7] 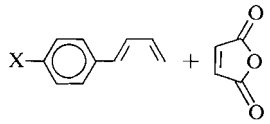 (dioxane) $\rho = -0.68$ ref. 25

[8] 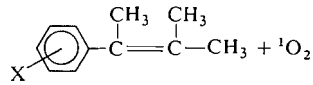 (methanol) $\rho = -0.93$ ref. 7

[9] 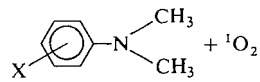 (methanol, quenching only) -1.7 ref. 26

TABLE 2. Hammett ρ values for the photooxidation of 2-arylfurans in different solvents

Solvent	ρ	$1/\varepsilon$	$1/\beta_{rel}$*
Dioxane	−2.13	0.453	—
n-Butanol	−1.03	0.0585	1.00
Methanol	−0.84	0.0308	2.02
Glycol	−0.45	0.0264	5.64
Water	−0.15	0.0127	3.27

*Determined for 2-(*p*-methoxyphenyl)furan.

It can be seen from Table 2 that there is a reasonable correlation between the Hammett ρ values and the polarity of the solvent. This is additional evidence for a *slightly* polar species being involved in the reaction of these furans with singlet oxygen.

In addition the effect of solvent on β values (for the 2-(*p*-methoxyphenyl)-furans) is largely due to its influence on the rate constant of reaction (k_{rx}). However, the β value in water is smaller than that for the less polar glycol solvent in contrast to expectations based on the Hammett ρ values. This may well indicate that the solvent is affecting the lifetime of singlet oxygen (k_d). This was later confirmed and is reported elsewhere (11). At the time of this observation this was the first evidence as to what role the solvent plays in photooxidation reactions (10).

The calculated Hammett ρ values for the photooxidation reactions of the furans can be related to a number of other reactions and interactions. Some of these are given in eqs. 4–9.

The Hammett ρ values calculated for the reaction between singlet oxygen and the directly substituted furans (1) ($\rho = -2.48$) can be compared to that calculated for reaction (4) ($\rho = -3.12$). Although the actual diene and reaction conditions vary it does appear that there may be a similarity in electrophylic character of the dienophiles. In comparison with the photooxidation of anthracene, (5), it is not surprising to see that this reaction yields a calculated Hammett ρ value ($\rho = -4.6$) which is higher than that obtained for the furans for two reasons:

(*1*) The less polar solvent should increase the calculated ρ value similar to the results reported in Table 2.

(*2*) The reactivity of anthracene with singlet oxygen is lower than furan with singlet oxygen and hence more susceptible to substituent effects.

The high ρ value does suggest the possibility for an unsymmetrical dipolar transition state during the cycloaddition reaction of singlet oxygen with anthracene.

Can. J. Chem. Downloaded from www.nrcresearchpress.com by 210.87.254.105 on 09/05/12
For personal use only.

Can. J. Chem. Downloaded from www.nrcresearchpress.com by 210.87.254.105 on 09/05/12
For personal use only.

In addition correlations between the photooxidation of the aryl-substituted furans and various other reactions, [6] and [7], can be made. It appears that singlet oxygen is less susceptible to the electronic effects of the substituents than is dimethyl acetylenedicarboxylate, but more susceptible than maleic anhydride.

The low Hammett ρ values calculated from the reactions of singlet oxygen with the 2- and 3-arylfurans (-0.836 and -0.699) compare favorably with that calculated by Foote from his photooxidation reactions of the 2-aryl-3-methyl-2-butenes in methanol (-0.93) (7). This illustrates the similarity of substituent effects on both classes of photooxidation reactions.

It is reasonable to expect a higher ρ value ($\rho = -2.46$) to be calculated for the reaction of singlet oxygen with the directly substituted furans than for the 2-aryl- and 3-arylfurans. The substituents in the latter cases are further removed from the reaction sites. In all cases the low Hammett ρ values indicate that the formation of a completely dipolar intermediate, **1**, is

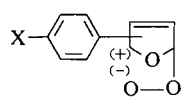

1

unlikely in methanol. In addition to the formation of a slightly polar transition state in a concerted cycloaddition mechanism, the negative slope of the Hammett plot could be due to the formation of a partial charge-transfer complex, **2**, with the π electrons as suggested by Koch (27) (Scheme 3).

The possibility that this could be real is enhanced when the Hammett ρ values from the photooxidation reactions are compared with that calculated from the quenching reactions of singlet oxygen by a number of substituted *N,N*-dimethylanalines. In the latter case we have recently found that the Hammett plots are a good probe of the mechanism of the quenching of singlet oxygen by amines (26) (Scheme 4).

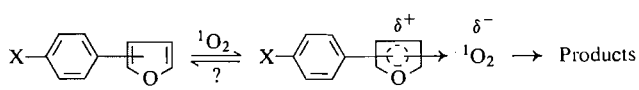

2

SCHEME 3

$$^1O_2 + NR_3 \underset{k_{-1}}{\overset{k_1}{\rightleftharpoons}} [^1O_2 \cdots\cdots NR_3]^{\delta^- \quad \delta^+} \xrightarrow{k_2} {}^3O_2 + NR_3$$

SCHEME 4

When singlet oxygen is quenched by the substituted *N,N*-dimethylanilines it was found that the Hammett ρ value was -1.7 (26). This value emphasizes the importance of the formation of the charge-transfer-like complex in the course of the quenching reaction. Clearly this must be kept in mind when considering photooxidation *reaction* mechanisms. It is conceivable that the substituent effect which is measured may result from the pre-equilibrium formation of a charge-transfer-like complex.

Conclusions

We have compared the photooxidation reactions of a number of furans to similar photooxidation reactions of alkenes, anthracenes, and to Diels–Alder reactions. We suggest that the mechanism of the reaction of singlet oxygen with the furans may be a concerted one-step addition to the diene and/or involve a pre-equilibrium complex. The lack of symmetry of some of the furans may cause some dissymmetry in the transition state, for example the 2-arylfurans. A correlation between the Hammett ρ values and the polarity of the solvent for a series of solvents confirms the expected solvent effect on the rate constant of reaction. Further evidence suggests that the solvent may also be affecting the rate constant for the decay of singlet oxygen. The solvent effect on the rate constant of reaction and on the rate constant of decay was later confirmed and is reported elsewhere (11).

Experimental

The kinetics studies were carried out using either an Aminco-SPF-125 spectrofluorometer or an Aminco filter fluorometer. The experimental procedure for the kinetic methods is given in detail in ref. 11.

The furans were obtained from a variety of sources. Furan and furfuryl alcohol were obtained from Aldrich and were redistilled prior to use. The 2-methoxyfuran and

2-acetylfuran were obtained from Aldrich and used as received. The furfural was obtained from Aldrich and was freshly distilled under vacuum (b.p. 54–55 °C/17 mm) prior to use.

2-Methylfuran was obtained from Eastman Chemicals and was redistilled. 2,5-Dimethylfuran was obtained from Research Organic/Inorganic Chemical Corporation and was redistilled. Furfural amine was obtained from Commercial Solvents Corporation and redistilled prior to use. The 2,5-diphenyl furan was obtained from Dr. A. Trozolo of Bell Laboratories and was used as received.

The 2-arylfurans were prepared by the method used by Ayres and Smith (24) and the 3-arylfurans prepared by a modification of the Wynberg method (19, 28).

The 3,4-diphenylfuran was prepared by the method according to Farnum and Burr (29) and by a Friedel–Crafts reaction of the 3,4-dibromotetrahydrofuran on benzene (19) followed by aromatization with sulfur.

The preparation of the 2- and 3-arylfurans and the products of their photooxidation reactions will be reported in detail in a later paper.

We would like to thank the Research Corporation and the donors of the Petroleum Research Fund, administered by the American Chemical Society (G-3021-A4) for partial support of this research. We would also like to acknowledge the American Instrument Company for the loan of a SPF-125 spectrophotofluorometer, and the National Science Foundation for support of C.M. (N.S.F. Undergraduate Research Participant, Summer 1969).

1. (*a*) C. S. FOOTE. Accts. Chem. Res. **1**, 104 (1968). (*b*) K. GOLLNICK. Advances in photochemistry. *Edited by* Noyes, Hammond, and Pitts. Interscience, 1969. p. 1. (*c*) Ann. N.Y. Acad. Sci. **171**, 1–103 (1970).
2. K. R. KOPECKY and H. J. REICH. Can. J. Chem. **43**, 2265 (1965).
3. E. MCKEOWN and W. A. WATERS. J. Chem. Soc. B, 1040 (1966).
4. (*a*) K. GOLLNICK. Oxidation of organic compounds. III. Adv. in Chem. 77. 1968. p. 78. (*b*) A. NICKON and J. F. BAGLI. J. Am. Chem. Soc. **83**, 1498 (1961).
5. C. S. FOOTE and S. WEXLER. J. Am. Chem. Soc. **86**, 3879, 3880 (1964).
6. E. J. COREY and W. C. TAYLOR. J. Am. Chem. Soc. **86**, 3881 (1964).
7. C. S. FOOTE and R. W. DENNY. J. Am. Chem. Soc. **93**, 5162 (1971).
8. A. W. FENICAL, D. R. KEARNS, and P. RADLICK. J. Am. Chem. Soc. **91**, 3396, 7771 (1969).
9. R. HIGGINS, C. S. FOOTE, and H. CHENG. Oxidation of organic compounds. III. Adv. in Chem. 77. 1968. p. 102.
10. R. H. YOUNG, N. CHINH, and C. MALLON. Ann. N.Y. Acad. Sci. **171**, 130 (1970).
11. R. H. YOUNG, K. WEHRLY, and R. L. MARTIN. J. Am. Chem. Soc. **93**, 5774 (1971).
12. G. A. HOLLINDEN and R. B. TIMMONS. J. Am. Chem. Soc. **92**, 4181 (1970).
13. G. O. SCHENCK. Ann. **584**, 156 (1953); E. KOCH and G. O. SCHENCK. Chem. Ber. **99**, 1984 (1966).
14. C. FOOTE and S. WEXLER. J. Am. Chem. Soc. **86**, 3879 (1964).
15. J. MARTEL. Compt. Rend. **244**, 626 (1957); C. DUFRAISSE, G. RIO, and A. RANJON. Compt. Rend. **264**, 516 (1967).
16. G. O. SCHENCK. Angew. Chem. **64**, 12 (1952).
17. R. H. YOUNG and N. CHINH. Unpublished research. Georgetown University; N. CHINH. Ph.D. Thesis. Georgetown University, 1970.
18. K. GOLLNICK and G. O. SCHENCK. Oxygen as a dienophile. 1,4-Cycloaddition reactions: the Diels–Alder reaction in heterocyclic syntheses. J. Hamer, Editor. Academic Press, New York, 1967. p. 288.
19. R. H. YOUNG and R. L. MARTIN. Unpublished research, Georgetown University, 1971.
20. C. DUFRAISSE and S. ECARY. Compt. Rend. **223**, 735 (1946).
21. Y. OTSUJI, Y. KODA, M. KULO, M. FURUKAWA, and E. IMATO. Nippon Kaguka Zasshi, **80**, 1297 (1959) (Chem. Abstr. 55–6476*g*).
22. T. INUKAI and T. KOJIMI. Chem. Commun. 1334 (1969).
23. E. J. BOWEN. Discuss. Faraday Soc. **14**, 143 (1953).
24. D. C. AYRES and J. R. SMITH. Chem. Commun. 886 (1967).
25. E. J. DEWITT, C. T. LESTER, and G. A. ROPP. J. Am. Chem. Soc. **78**, 2101 (1956).
26. R. H. YOUNG and R. KELLER. Submitted for publication.
27. E. KOCH. Tetrahedron, **24**, 6295 (1968).
28. H. WYNBERG. J. Am. Chem. Soc. **80**, 364 (1958).
29. D. G. FARNUM and M. BURR. J. Org. Chem. **28**, 1387 (1963).

Can. J. Chem. Downloaded from www.nrcresearchpress.com by 210.87.254.105 on 09/05/12
For personal use only.

Fully Fluorinated Alkoxides. Part VI. Derivatives of Hydroxyhexafluoroisobutyric Acid

J. T. PRICE, A. J. TOMLINSON, AND C. J. WILLIS[1]

Chemistry Department, University of Western Ontario, London 72, Ontario

Received October 5, 1971

Hydroxyhexafluoroisobutyric acid, $HOC(CF_3)_2COOH$, $H_2(HHIB)$, gives complexes with a variety of metals, acting as a chelating, dinegative ligand. Derivatives prepared include $[B(HHIB)_2]^-$, $[M(HHIB)_2]^{2-}$ (M = Ni, Cu, Co), $[M(HHIB)_3]^{3-}$ (M = Al, Cr, Mn, Fe), and mixed ligand complexes of Cu and Ni with HHIB and nitrogen- or phosphorus-containing ligands. In some cases, the HHIB anion appears to act as a tridentate ligand through carboxylate bridging. HHIB is close to water in the spectrochemical series.

L'acide hydroxyhexafluorobutyrique, $HOC(CF_3)_2COOH$, $H_2(HHIB)$, donne des complexes avec une variété de métaux, agissant comme ligand chélaté, dinégatif. Les dérivés préparés incluent $[B(HHIB)_2]^-$, $[M(HHIB)_2]^{2-}$ (où M = Ni, Cu, Co), $[M(HHIB)_3]^{3-}$ (M = Al, Cr, Mn, Fe) et des ligands mixtes du Cu et du Ni avec HHIB et des ligands contenant de l'azote et/ou du phosphore. Dans quelques cas, l'anion HHIB semble agir comme ligand tridenté au moyen de ponts carboxylates. HHIB se situe près de l'eau dans la série spectrochimique.

Canadian Journal of Chemistry, **50**, 939 (1972)

Can. J. Chem. Downloaded from www.nrcresearchpress.com by 210.87.254.105 on 09/05/12
For personal use only.

We have previously reported the use of perfluoropinacol, $HOC(CF_3)_2C(CF_3)_2OH$, (PFP) as a bidentate ligand forming stable, cyclic, derivatives of main group elements (1) and complexes with a variety of transition elements (2). In terms of the chelate ring structure, there is an obvious resemblance between these complexes and the familiar series of oxalato-complexes, although the acidity of PFP [$pK_a = 5.95$ (3)] is less than that of oxalic acid ($pK_a = 1.23$).

A third compound, structurally related to both of the above molecules, and having potential application as a chelating ligand, is hexafluoro-2-hydroxyisobutyric acid, $HOC(CF_3)_2COOH$, $H_2(HHIB)$.[2] This acid is readily made by hydrolysis of the cyanohydrin of hexafluoroacetone (4, 5) and has a pK_a of 2.1. Simple monobasic salts (*e.g.* with Cs^+ cation) are readily prepared, but the acid shows no evidence of a second dissociation in aqueous solution. This behavior is similar to that of PFP, and in both cases the stability of the singly ionized molecule may be attributed to intramolecular hydrogen bonding. However, it was expected that the presence of two trifluoromethyl groups in the HHIB molecule would increase the acidity of the hydroxylic proton so that, in complex ions, chelation would occur as the dinegative, bidentate ligand $^-OC(CF_3)_2COO^-$, (HHIB), rather than as a uninegative, bidentate species similar to the ion $HOC(CH_3)_2COO^-$, found with hydroxyisobutyric acid and other unfluorinated α-hydroxyacids (6).

Isolation of a range of stable complexes has confirmed that $H_2(HHIB)$ does behave in the expected manner. Complexes have been prepared of the types $[M(HHIB)_3]^{3-}$ ($M = Al^{3+}$, Cr^{3+}, Mn^{3+}, Fe^{3+}); $[M(HHIB)_2]^{2-}$ ($M = Co^{2+}$, Ni^{2+}, Cu^{2+}); $[M(HHIB)_2]^-$ (M = B), and mixed complexes including HHIB and other ligands. Although structures cannot be assigned with certainty in all cases, sufficient information is now available to give some idea of the properties of HHIB as a ligand. Compounds were prepared by interaction of $H_2(HHIB)$ with various metal ions, generally in methanolic solution, at suitable p*H*. The range prepared is shown in Table 1, and includes derivatives of all first-row transition elements from V to Cu. Electronic spectra are given in Table 2. Specific aspects of these compounds will now be discussed for the various elements.

Vanadium

As has been done with many other ligands, it was convenient to make the vanadyl complex $[VO(HHIB)_2]^{2-}$. This had a magnetic moment of 1.76 B.M., in the expected range; *cf.* $VO(acac)_2$ (acac = acetylacetone), $\mu_{eff} = 1.73$ B.M. (7). The electronic spectrum also re-

[1]To whom inquiries should be addressed.

[2]Throughout this paper, the acid is abbreviated to $H_2(HHIB)$ and the di-anion to HHIB.

Can. J. Chem. Downloaded from www.nrcresearchpress.com by 210.87.254.105 on 09/05/12
For personal use only.

TABLE 1. HHIB complexes

Compound	Formula	Carbon		Hydrogen		Fluorine		Other			Magnetic moment (B.M.)	Color
		Calcd.	Found	Calcd.	Found	Calcd.	Found	Calcd.		Found		
Cs(HHIB)	$CsC_4HF_6O_3$	14.0	14.2	0.3	0.6	33.1	33.1					white
$CsB(HHIB)_2$	$CsBC_8F_{12}O_6$	17.0	17.3	0.0	0.2	40.4	40.2					white
$K_3Al(HHIB)_3$	$K_3AlC_{12}F_{18}O_9$	18.6	18.2	0.0	0.3	44.2	44.6	Al,	3.5	3.8		white
$K_2VO(HHIB)_2(H_2O)$	$K_2VH_2F_{12}O_8$	16.5	16.8	0.4	0.5	39.0	38.7				1.76	purple
$Cs_3Cr(HHIB)_3(H_2O)$	$Cs_3CrC_{12}H_2F_{18}O_{10}$	13.1	13.1	0.2	0.2	31.1	30.7	Cr,	4.7	5.1	3.85	green
$Cs_3Mn(HHIB)_3$	$Cs_3MnC_{12}F_{18}O_9$	13.3	13.1	0.0	0.3	31.6	31.8	Mn,	5.1	5.0	4.97	black
$Cs_3Fe(HHIB)_3(H_2O)$	$Cs_3FeC_{12}H_2F_{18}O_{10}$	13.1	12.9	0.2	0.2	31.0	30.8	Fe,	5.1	4.7	5.84	pale yellow
$Cs_2Co(HHIB)_2(H_2O)_2$	$Cs_2CoC_8H_4F_{12}O_8$	12.2	11.7	0.5	0.3	29.2	29.0	Co,	7.6	8.0	3.88	purple–pink
$K_2Ni(HHIB)_2$	$K_2NiC_8F_{12}O_6$	17.3	16.8	0.0	0.2	40.9	40.4	Ni,	10.5	10.4	3.06	yellow–green
$K_2Cu(HHIB)_2$	$K_2CuC_8F_{12}O_6$	17.1	17.0	0.0	0.1	40.6	39.7	Cu,	11.3	11.3	1.85	blue
$en_2Ni(HHIB)_2$	$NiC_{12}H_{18}F_{12}N_4O_6$	23.9	23.5	3.0	3.1	37.9	37.7	Ni,	9.8	10.1	3.18	blue–violet
								N,	9.4	9.7		
$(Et_3P)_2Ni(HHIB)$	$NiC_{16}H_{30}F_6O_3P_2$	38.0	38.0	6.0	6.1	22.6	22.6	Ni,	11.6	11.7	dm	orange
								P,	12.2	12.2		
(diphos)Ni(HHIB)	$NiC_{30}H_{24}F_6O_3P_2$	54.1	54.5	3.6	3.7	17.1	17.6	Ni,	8.8	8.7	dm	yellow
								P,	9.3	9.3		
$K_2Ni(HHIB)(PFP)$	$K_2NiC_{10}F_{18}O_5$	17.8	18.0	0.0	0.2	50.4	49.8	Ni,	8.7	8.6	3.21	orange
$enCu(HHIB)_2$	$CuC_{10}H_{10}F_{12}N_2O_6$	22.0	21.9	1.9	2.1	41.8	41.5	Cu,	11.7	12.4	1.90	blue
								N,	5.2	5.7		
$en_2Cu(HHIB)_2$	$CuC_{12}H_{18}F_{12}N_4O_6$	23.8	24.3	3.0	3.1	37.7	38.0	Cu,	10.5	10.8	1.86	purple
								N,	9.3	9.5		
$(TMED)Cu(HHIB)_2$	$CuC_{14}H_{18}F_{12}N_2O_6$	27.9	28.0	3.0	3.1	37.9	38.2	Cu,	10.6	11.3	1.88	deep blue
								N,	4.7	4.9		
$(Me_3Si)_2HHIB$	$Si_2C_{10}H_{18}F_6O_3$	33.7	33.8	5.1	5.3							white

TABLE 2. Electronic spectra of HHIB complexes

Compound	Solvent*	Absorption frequencies, cm^{-1}
$K_2VO(HHIB)_2.H_2O$	d.r.	11 000–20 000(br) 23 800
	MeOH	13 700(10) 16 100(15) 18 500(16)
$Cs_2Cr(HHIB)_3.H_2O$	d.r.	14 700 20 800
	MeOH	16 800(51) 22 700(55)
	H_2O	16 700 22 800
$Cs_3Fe(HHIB)_3.H_2O$	d.r.	10 900 14 300 14 900 20 900
	MeOH	22 000(4)
$Cs_3Mn(HHIB)_3$	MeOH	22 000(br)
$Cs_2Co(HHIB)_2.2H_2O$	d.r.	10 500 16 900 17 900 20 000
	MeOH	11 800(4) 17 300(9) 19 200(9) 20 900(8)
$K_2Ni(HHIB)_2$	d.r.	13 600(sh) 13 800 21 000(sh) 24 400
	MeOH	8900(5) 14 300(6) 24 700(16)
$K_2Cu(HHIB)_2$	d.r.	15 400(br)
	MeOH	14 800(28)
$en_2Ni(HHIB)_2$	d.r.	11 200 18 200 28 200
	MeOH	10 500(9) 26 200(9) 27 500(13)
$(Et_3P)_2Ni(HHIB)$	d.r.	22 200
	MeOH	21 700(190)
(diphos)Ni(HHIB)	d.r.	25 000
	MeOH	23 500(200)
$K_2Ni(HHIB)(PFP)$	d.r.	8700 13 200 24 100
	MeOH	8700(3) 13 200(11) 24 700(2)
$enCu(HHIB)_2$	d.r.	15 400 18 200(sh)
	MeOH	15 700(25)
$en_2Cu(HHIB)_2$	d.r.	12 700 17 400
	MeOH	17 500(25)
$(TMED)Cu(HHIB)_2$	d.r.	15 600 18 800
	MeOH	15 800(27)

*d.r. = diffuse reflectance. Molar extinction coefficients in parentheses.

sembled that of similar vanadyl complexes, which have been extensively studied (7, 8). By analogy with the results of Ballhausen and Gray (7), the absorption bands at 13 700 and 16 000 cm^{-1} in the complex $[VO(HHIB)_2]^{2-}$ may be assigned to the $^2B_2 \rightarrow {}^2E(I)$ and $^2B_2 \rightarrow {}^2B_1$ transitions respectively. In the complex $VO(acac)_2$ they are found at 12 800 and 17 300 cm^{-1}. However, the same authors assign a band at 18 800 cm^{-1} in the spectrum of $[VO(tartrate)_2]^{2-}$ to the latter transition, so the assignments in $[VO(HHIB)_2]^{2-}$, where a band appears at 18 500 cm^{-1}, cannot be regarded as definite.

The complex crystallizes as a monohydrate, and the water molecule may possibly be coordinated to the vanadium atom *trans* to the oxygen atom. This would not affect the tetragonal symmetry of the ion, and would therefore have little effect on its properties. However, Jones has suggested (9) that only molecules with strong donor properties are capable of such coordination to five-coordinate vanadyl complexes.

Chromium

The geometry of the ion $[Cr(HHIB)_3]^{3-}$ cannot be exactly octahedral, as the ligand is unsymmetrical. However, the properties of the metal ion are consistent with its being regarded as at the center of an octahedral distribution of oxygen atoms. The visible spectrum shows bands at 16 800 and 22 700 cm^{-1} very similar to those observed in the hydrated $[Cr(H_2O)_6]^{3+}$ species at 17 400 and 24 700 cm^{-1} and assigned to the $^4A_{2g} \rightarrow {}^4T_{2g}(F)$ and $^4A_{2g} \rightarrow {}^4T_{1g}(F)$ transitions respectively (10). These figures lead to a

Can. J. Chem. Downloaded from www.nrcresearchpress.com by 210.87.254.105 on 09/05/12
For personal use only.

Can. J. Chem. Downloaded from www.nrcresearchpress.com by 210.87.254.105 on 09/05/12
For personal use only.

Dq value of 1700 cm^{-1} for HHIB, the same as that for water and very close to that of the oxalate ion (1740 cm^{-1}).

The analogous PFP complex of Cr^{3+} has not yet been prepared. The reason for this difference in behavior between HHIB and PFP is not obvious, but may be connected with a difference in the pK_a's of the two compounds.

Manganese

Here, as with chromium, a difference between PFP and HHIB was observed. The former gives the Mn(II) complex $[Mn(PFP)_2]^{2-}$ (2), whereas in the latter case oxidation by air occurs rapidly to give Mn(III) in the ion $[Mn(HHIB)_3]^{3-}$. Such ready oxidation has been noted previously in the formation of the complex $Mn(acac)_3$ (11). The validity of the formulation of the HHIB complex as an Mn(III) compound is shown by its magnetic moment of 4.95 B.M. [*cf.* $Mn(acac)_3$, 4.95 B.M. (12); $Mn(C_2O_4)_3^{3-}$, 4.81 B.M. (13)] and its visible spectrum, which shows a very broad absorption with a maximum at 21 800 cm^{-1} [*cf.* $Mn(H_2O)_6^{3+}$, $\nu = 22\,000$ cm^{-1} (14)].

Iron

The Fe(III) complex, $[Fe(HHIB)]_3^{3-}$, formed readily, as does the PFP complex. It had a magnetic moment of 5.84 B.M., similar to those of $[Fe(PFP)_3]^{3-}$ (6.0 B.M.), $Fe(acac)_3$ (5.95 B.M.) (15), and $[Fe(C_2O_4)_3]^{3-}$ (5.75 B.M.) (13). As is common with Fe(III) complexes, where there are no spin-allowed transitions, the electronic spectrum was very weak. Only one absorption was found in the solution spectrum ($\nu = 22\,000$ cm^{-1}), and meaningful assignments cannot be made.

Cobalt

The only cobalt complex isolated was the compound $Cs_2Co(HHIB)_2 \cdot 2H_2O$. This we presume to contain Co(II) in the six-coordinate ion $[Co(HHIB)_2(H_2O)_2]^{2-}$. However, its magnetic moment of 3.88 B.M. is unusually low, being equal to the spin-only value. Orbital contributions usually increase magnetic moments in Co(II) complexes above the spin-only value (16), typical values being in the range 4.5–5.1 B.M.

The visible spectrum of the complex is similar to that of the octahedral aquo complex, but shows some additional splitting which presumably results from departure from perfect octahedral symmetry.

Nickel

The Ni(II) complex, $[Ni(HHIB)_2]^{2-}$, differs considerably from the corresponding nickel complex of PFP in being green and paramagnetic ($\mu_{eff} = 3.06$) with visible spectra typical of octahedral Ni(II), whereas the PFP complex is purple, diamagnetic, and square planar. This difference we ascribe to additional coordination from the carboxylate oxygen in the ligand, making it effectively tridentate, a process common for oxalates but not possible in the PFP complex:

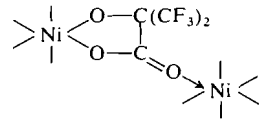

Such a structure would be broken down in solution, with solvent molecules replacing the bridging carboxylate groups around nickel, and, consistent with this, some differences are observed between the diffuse reflectance and methanol solution spectra.

Copper

The Cu(II) complex, $[Cu(HHIB)_2]^{2-}$, has a magnetic moment of 1.85 B.M. and is presumed to have a square planar arrangement of ligands, although the possibility of carboxylate bridging, similar to that suggested for nickel, cannot be entirely eliminated.

Mixed Ligand Complexes

The coordination of HHIB to Cu^{2+} or Ni^{2+} in the presence of nitrogen bases gives rise to a variety of mixed ligand complexes. Those isolated were of two stoichiometries; $en_2Ni(HHIB)_2$ and $en_2Cu(HHIB)_2$ (en = ethylenediamine), and $enCu(HHIB)_2$ and $(TMED)Cu(HHIB)_2$ (TMED = Tetramethylethylenediamine). The last two complexes showed several absorptions in their i.r. spectra in the region 2000–2700 cm^{-1}, characteristic of amine salts, while the remaining parts of their i.r. spectra were very similar to the salt $K_2[Cu(HHIB)_2]$ (Table 3). They may therefore be formulated as the amine salts $[H_2en]^{2+}[Cu(HHIB)_2]^{2-}$ and $[H_2TMED]^{2+}[Cu(HHIB)_2]^{2-}$.

In the other complexes, where there are two molecules of nitrogen base present for each

TABLE 3. Infrared spectra (cm^{-1}) as Nujol mulls

Compound	ν CO_2		ν C—O		ν C—C		δ CO_2
H_2(HHIB)	1760		995		825		665
Cs(HMIB)	1660	1375	1005	975	800		675
$CsB(HHIB)_2$	1770		1065	980	780		670
$K_3Al(HHIB)_3$	1710, 1685	1385	1030	975	845	760	675
$Cs_3Cr(HHIB)_3$	1655	1365	1020	975	835	755	665
$Cs_3Mn(HHIB)_3$	1650	1340	1032, 1015	975	825	810	665
$Cs_3Fe(HHIB)_3$	1655	1365	1020	975	825	755	670
$Cs_2Co(HHIB)(H_2O)_2$	1630	1375	1020	980	820		670
$K_2Ni(HHIB)_2$	1650	1400	1015	972	830	800	665
$K_2Cu(HHIB)_2$	1665	1380	1020	970	825	790	660

metal atom, absence of absorption in the 2000–2700 region rules out amine salts, while magnetic moment and visible spectra on the nickel complex suggest octahedral coordination. While a definite assignment of structure cannot be made, we suggest that one end of each HHIB ligand has been displaced to give the carboxylate complexes $HOC(CF_3)_2COOM(en)_2OOCC(CF_3)_2OH$ (M = Ni, Cu). No O—H absorption can be definitely assigned in the i.r. spectrum, but we have commented before on the difficulty of observing O—H frequencies in complexes of this type (17).

The two mixed ligand phosphine–HHIB complexes prepared were $(PEt_3)_2Ni(HHIB)$ and (diphos)Ni(HHIB) (diphos = 1,2-bisdiphenylphosphinoethane). Both were orange–yellow and diamagnetic, and are presumed to be square planar. They were conveniently made by the reaction of PEt_3 or diphos with the ion $[Ni(HHIB)_2]^{2-}$; only in the former case was the displacement of HHIB reversible.

The remaining mixed ligand complex characterized had a stoichiometry corresponding to K_2[(PFP)Ni(HHIB)]. Formulation as the double salt, $K_2Ni(PFP)_2.K_2Ni(HHIB)_2$, seems unlikely, as the magnetic moment of the compound (μ_{eff} = 3.21 B.M.) showed all nickel present to be paramagnetic and octahedral, whereas $K_2Ni(PFP)_2$ is diamagnetic. Its color, moreover, is orange, while $K_2Ni(PFP)_2$ is purple and $K_2Ni(HHIB)_2$ is yellow-green. Presumably some carboxylate bridging is present, bringing the coordination of the nickel up to six, but present evidence is not sufficient to determine the precise mode of attachment of the ligands.

Non-transition Element Complexes

The expected boron and aluminum complexes, $[B(HHIB)_2]^-$ and $[Al(HHIB)_3]^{3-}$ were readily prepared. Attempts to make a neutral tetrahedral complex, *e.g.* $Si(HHIB)_2$, were unsuccessful, but reaction of HHIB with hexamethyldisilazane gave the bis(trimethylsilyl) derivative $Me_3SiOC(CF_3)_2C(O)OSiMe_3$.

Infrared Spectra

Chelation of HHIB to metal ions would be expected to influence the frequency of the carboxylate stretching and bending modes, the alcoholic C—O stretch, and perhaps the C—C stretching mode. Frequencies associated with these vibrations are shown in Table 3. In addition, all complexes showed strong absorptions in the region 1150–1300 cm^{-1} associated with the CF_3 groups.

Considerable similarity is apparent between the spectra of all complexes. In particular, no significant difference is seen in the carboxylate frequencies in the nickel and copper complexes, where carboxylate bridging was postulated above on other evidence. Such coordination, if present, is presumably weak in nature.

It was not possible to make a definite assignment of frequencies associated with metal–oxygen bonds, since the region 450–600 cm^{-1}, where they might be expected, was complicated by the presence of C—F bending modes.

Isomerism in HHIB Complexes

Since the HHIB molecule is an unsymmetrical chelating agent, isomerism may be expected in the various complexes. Optical isomerism is possible for the tetrahedral species $[B(HHIB)_2]^-$,

Can. J. Chem. Downloaded from www.nrcresearchpress.com by 210.87.254.105 on 09/05/12
For personal use only.

TABLE 4. Preparation of complexes

Compound	HHIB/metal mole ratio	Solvent	Recrystallization from	Note*
$K_3Al(HHIB)_3$	3.3	EtOH	2-PrOH	
$K_2VO(HHIB)_2(H_2O)$	1.0	EtOH	2-PrOH	
$Cs_3Cr(HHIB)_3H_2O$	3.0	EtOH	2-PrOH	
$Cs_3Mn(HHIB)_3$	2.3	EtOH	EtOH	(*a*)
$Cs_3Fe(HHIB)_3(H_2O)$	3.3	EtOH	2-PrOH	
$Cs_2Co(HHIB)_2(H_2O)_2$	2.0	EtOH	2-PrOH	
$K_2Ni(HHIB)_2$	1.7	MeOH	EtOH	
$K_2Cu(HHIB)_2$	2.0	MeOH	EtOH	
$en_2Ni(HHIB)_2$	1.1	H_2O	EtOH	
$(Et_3P)_2Ni(HHIB)$	1.0	$MeOH/H_2O$	$EtOH/H_2O$	(*b*)
(diphos)Ni(HHIB)	1.0	$MeOH/H_2O$	$EtOH/H_2O$	(*c*)
$K_2Ni(HHIB)(PFP)$	1.0	MeOH	2-PrOH	(*d*)
$enCu(HHIB)_2$	1.0	H_2O	MeOH	
$en_2Cu(HHIB)_2$		EtOH	$EtOH/C_6H_{14}$	(*e*)
$(TMED)Cu(HHIB)_2$	1.0	H_2O	2-PrOH	(*f*)

*Notes: (*a*) Oxidation to Mn(III) was complete after stirring in air 30 min. (*b*) Carried out under nitrogen. (*c*) diphos added in MeOH/THF solution. (*d*) Ratio HHIB/PFP/Ni was 1:1:1. (*e*) Made by adding en to the preceding complex in EtOH. (*f*) KOH added to p*H* 6, then TMED added.

and geometric (*cis–trans*) isomerism for square planar ions $[M(HHIB)_2]^{2-}$, while the tris-chelated species $[M(HHIB)_3]^{3-}$ can show both geometric and optical isomerism.

In no case was any evidence found for the presence of more than one isomer, nor was it possible to decide which configuration was present. In the square planar complexes, a *trans*-configuration might be thought more likely on steric grounds, but no definite evidence is available. Crystallographic structure determinations are now in progress in an attempt to elucidate this point.

Conclusions

From the range of complexes prepared in this work, it appears that $H_2(HHIB)$ acts as a ligand in a manner resembling PFP or oxalic acid rather than its unfluorinated analogue. Although usually bidentate, there is some evidence for additional coordination through carboxylate bridging. Electronic spectra are generally similar to those of aquo complexes, placing HHIB close to water in the spectrochemical series.

Experimental

General

Volatile materials were manipulated on a conventional vacuum line. Infrared spectra were recorded on a Beckman IR-10 instrument and visible/u.v. spectra on Beckman DK-1 and Cary 14 instruments. Magnetic moments were determined at 25° by the Gouy method using $Hg[Co(CNS)_4]$ as standard. Microanalyses were performed by Alfred Bernhardt Laboratories. All analytical data are shown in Table 1.

Hydroxyhexafluoroisobutyric Acid

Hexafluoroacetone (50 g, 0.32 mol) was bubbled into a solution of potassium cyanide (17 g, 0.31 mol) in dried diethyl ether/tetrahydrofuran (400 ml, 5% THF v/v) at −30° over a 2 h period with stirring. Removal of solvent *in vacuo* gave the potassium salt of hexafluoroacetone cyanohydrin. Sulfuric acid (250 ml) was added and the resulting solution held at 180° for 48 h, during which time $H_2(HHIB)$ (38 g, 78%) distilled out. The product was recrystallized from benzene and had m.p. 81°.

Cs(HHIB)

$H_2(HHIB)$ (1.0 g, 4.7 mmol) was added to cesium hydroxide (0.7 g, 4.7 mmol) in water (10 ml). Cesium chloride (1.0 g) was added and the solution allowed to evaporate slowly. Crystals separating were recrystallized from 2-propanol to give the cesium salt of HHIB.

Complexes of HHIB

Most of the complexes were prepared by substantially the same route. The metal ion, usually as the sulfate, was mixed with a suitable quantity of $H_2(HHIB)$ in methanol or ethanol. The appropriate amount of base (CsOH, KOH, en, or phosphine) was then added and any precipitate (Cs_2SO_4, etc.) removed. The solution was then evaporated *in vacuo*, and the resulting complex recrystallized. Conditions for these preparations are listed in Table 4.

Cs[B(HHIB)$_2$]

Trimethyl borate (0.5 g, 5.0 mmol) was added to $H_2(HHIB)$ (2.1 g, 10 mmol) in methanol/benzene (15 ml) and the solution heated under reflux for 2 h. Removal of solvent left a gelatinous residue, which was added to aqueous cesium hydroxide (0.75 g, 5 mmol) containing cesium chloride (1 g). Crystals of $Cs[B(HHIB)_2]$ separated on evaporation and were recrystallized from 2-propanol.

Can. J. Chem. Downloaded from www.nrcresearchpress.com by 210.87.254.105 on 09/05/12
For personal use only.

Trimethylsilyl 2-Trimethylsiloxy-2-trifluoromethyl-3,3,3-trifluoropropionate

H_2(HHIB) (2.1 g, 10 mmol) and hexamethyldisilazane (4.8 g, 30 mmol) were heated to 80° for 4 h. Fractional distillation gave the trimethylsilyl-substituted product (b.p. 40°, 0.1 mm).

We thank the National Research Council of Canada for financial support in an operating grant and a scholarship (to J.T.P.).

1. M. ALLAN, A. F. JANZEN, and C. J. WILLIS. Can. J. Chem. **46**, 3671 (1968).
2. M. ALLAN and C. J. WILLIS. J. Am. Chem. Soc. **90**, 5343 (1968).
3. W. J. MIDDLETON and R. V. LINDSEY. J. Am. Chem. Soc. **86**, 4948 (1964).
4. I. L. KNUNYANTS *et al.* Khim. Nauka i Prom. **4**, 802 (1959).
5. R. FILLER and R. SHURE. J. Org. Chem. **32**, 1217 (1967).
6. C. K. PROUT *et al.* J. Chem. Soc. A, 2791 (1968).
7. C. J. BALLHAUSEN and H. B. GRAY. Inorg. Chem. **1**, 119 (1962).
8. S. M. HORNER, S. Y. TYREE, and D. L. VENEZKY. Inorg. Chem. **1**, 845 (1962).
9. M. M. JONES. J. Am. Chem. Soc. **76**, 5995 (1964).
10. T. M. DUNN. *In* Modern coordination chemistry. *Edited by* J. Lewis and R. G. Wilkins. Interscience, New York, N.Y., 1960. p. 289.
11. F. GACH. Monatsh. **21**, 98 (1900).
12. L. C. JACKSON. Proc. Roy. Soc. A, **140**, 695 (1933).
13. N. GOLDENBURG. Trans. Farad. Soc. **36**, 847 (1940).
14. H. HARTMANN and H. L. SCHLAFER. Z. Naturf. **6***a*, 754 (1951).
15. L. CAMBI and L. SZEGO. Ber. **64**, 2591 (1931).
16. B. N. FIGGIS and J. LEWIS. *In* Progress in inorganic chemistry. Vol. 6. *Edited by* F. A. Cotton. Interscience, New York, N.Y., 1964. p. 188.
17. C. MACDONALD, A. J. TOMLINSON, and C. J. WILLIS. Can. J. Chem. **49**, 2578 (1971).

Can. J. Chem. Downloaded from www.nrcresearchpress.com by 210.87.254.105 on 09/05/12
For personal use only.

Hydrolysis of Sulfamoyl Chlorides. II. Hydrogen Participation in the Hydrolysis of Diethyl and Methylethylsulfamoyl Chlorides[1]

E. C. F. Ko[2] AND R. E. ROBERTSON

Department of Chemistry, University of Calgary, Calgary, Alberta

Received October 19, 1971

Diethylsulfamoyl chloride (**2**) hydrolyzes eight times faster than dimethylsulfamoyl chloride (**1**). In **2** the secondary deuterium isotope effect was found to be about 2, hence hydrogen participation is important in the hydrolysis of this compound. The temperature coefficient of the enthalpy of activation ($\Delta C_p^{\ddagger}$) is exceptional (-39 cal mol^{-1} deg^{-1}) for a reaction presumably following an S_N1 mechanism. The kinetic solvent isotope effect was normal for such a mechanism. The corresponding value of $\Delta C_p^{\ddagger}$ for the hydrolysis of piperidylsulfamoyl chloride (**4**) was about the same as found for **2** while the value for the methylethyl isomer (**3**) was -66 cal deg^{-1} mol^{-1}, an intermediate value supporting an explanation based on solvent exclusion. Experiments in mixed solvents support the hypothesis that solvent reorganization is the major factor in determining the value of $\Delta C_p^{\ddagger}$ for **2** but not for **4**.

Le chlorure de diéthylsulfamoyle (**2**) hydrolyse huit fois plus vite que le chlorure de diméthylsulfamoyle (**1**). Dans **2**, l'effet isotopique secondaire du deutérium est trouvé à peu près égal à 2, par suite la participation de l'hydrogène est importante dans l'hydrolyse de ce composé. Le coefficient de température de l'enthalpie d'activation ($\Delta C_p^{\ddagger}$) est exceptionnel (-39 cal mol^{-1} deg^{-1}) pour une réaction suivant probablement un mécanisme S_N1. L'effet isotopique cinétique du solvant était normal pour un tel mécanisme. La valeur correspondante de $\Delta C_p^{\ddagger}$ pour l'hydrolyse du chlorure de pipéridylsulfamoyle (**4**) a été environ la même que celle trouvée pour **2** tandis que la valeur de l'isomère méthyléthyl (**3**) était de -66 cal deg^{-1} mol^{-1}, valeur intermédiaire étayant une explication fondée sur l'exclusion de solvant. Des expériences dans des solvants mélangés étayent l'hypothèse que la réorganisation du solvant est le facteur principal dans la détermination de la valeur de $\Delta C_p^{\ddagger}$ pour **2** mais non pas pour **4**.

Canadian Journal of Chemistry, **50**, 946 (1972)

The enthalpy of activation ($\Delta H^{\ddagger}$) for the hydrolysis of dimethylsulfamoyl chloride (**1**) (1) in water is characterized by a large negative temperature coefficient ($\Delta C_p^{\ddagger} = -76$ cal deg^{-1} mol^{-1}) a relatively small kinetic solvent isotope effect ($k_{H_2O}/k_{D_2O} = 1.30$) compared to the values found for other sulfonyl chlorides (2) and a small inverse γ-secondary deuterium isotope effect (1). Hall (3) has shown the rate of hydrolysis of **1** to be insensitive to weak or bulky nucleophilic reagents but accelerated by strong nucleophiles, a fact confirmed by Rogne (4). On the basis of these mechanistic indicators the conclusion that hydrolysis of **1** in water follows an S_N1 mechanism seems reasonable. However, we disagree with Hall as to the reason for the change over in mechanism in this particular case compared to the normal S_N2 mechanism found for the solvolysis of many other sulfonyl chlorides (5). We prefer to attribute the change in mechanism for the dimethylsulfamoyl chloride to effective steric hindrance to nucleophilic approach, rather than to enhanced electron release by the dimethylamino group. Thus the secondary γ-deuterium isotope effect found in the hydrolysis of dimethylsulfamoyl chloride was only about 1/6 value found for the ionization of dimethylamine (6). Moreover, in view of the small inverse secondary deuterium isotope effect found for the dimethyl compound, there seemed no obvious electron-release mechanism which could account for the large ($8\times$) acceleration in the rate of hydrolysis for the hydrolysis of diethylsulfamoyl chloride (**2**).

Thus the work reported here began with a search to identify the source of the accelerated rate of hydrolysis for the diethylsulfamoyl chloride and was subsequently extended to include the kinetics of the hydrolysis for methyl-ethyl (**3**) and piperidyl sulfamoyl chlorides (**4**).

Results and Discussion

The experimental procedures and calculations have been described previously (7). Details concerning the synthesis, characterization of the

[1]Presented in part at the Spring Conference, C.I.C., Halifax, Nova Scotia, 1971.

[2]Postdoctorate Fellow, 1970.

Can. J. Chem. Downloaded from www.nrcresearchpress.com by 210.87.254.42 on 09/05/12
For personal use only.

TABLE 1. Empirical constants for the three-parameter eq. 1 for the hydrolysis of sulfamoyl chlorides, RSO_2Cl

R	Solvent	A_1	$-A_2$	$-A_3$	n†
$(C_2H_5)_2N$	H_2O	64.59354	5925.375	18.70398	$28^{15}_{0.5}$
	H_2O–CH_3CN*	42.53552	4680.457	11.62047	32^{21}_{1}
$C_5H_{10}N$	H_2O	72.63695	6608.774	21.23280	30^{25}_{1}
	H_2O–CH_3CN*	60.73768	5809.054	17.63919	$29^{34}_{0.5}$
$C_2H_5NCH_3$	H_2O	97.68508	7641.611	29.91715	35^{25}_{0}

*0.95 mole fraction H_2O.
†$n^{T_2}_{T_1}$ = number of rate determinations; T_1, T_2 gives the temperature range over which rates were determined.

TABLE 2. Pseudo-thermodynamic quantities from the solvolysis of certain sulfamoyl chlorides, RSO_2Cl

R	Solvent	$\Delta H^{\ddagger}$ (cal mol^{-1})	$-\Delta S^{\ddagger}$ (cal mol^{-1} deg^{-1})	$-\Delta C_p^{\ddagger}$ (cal mol^{-1} deg^{-1})
$(C_2H_5)_2N$	H_2O	15 827±12	12.58±0.04	39±2
	H_2O–CH_3CN*	14 290±5	19.26±0.02	25±2
$C_5H_{10}N$	H_2O	17 505±5	9.26±0.02	44±1
	H_2O–CH_3CN*	15 907±5	16.11±0.02	37±1
$C_2H_5NCH_3$	H_2O	17 262±6	9.63±0.02	61±1
$(CH_3)_2N$†	H_2O	18 694±12	6.84±0.04	76±1
	H_2O–CH_3CN*	17 103±9	13.28±0.02	44±1

*0.95 mole fraction H_2O.
†Reference 1.

reactants, and solvents are given after this discussion.

Rate data determined by a conductance method are good to better than 1% for repetitive runs over a reasonable range of temperatures. These were fitted by the method of least squares to the empirical three constant equation

$$[1] \qquad \log k = A_1 + A_2/T + A_3 \log T$$

The corresponding constants for each compound are given in Table 1. These constants provide a convenient means of calculating rates for intermediate temperatures.

Granted the assumptions of the transition state hypothesis and the admissibility of attenuating the rate-temperature relationship, the empirical constants in Table 1 may be used to calculate the corresponding pseudothermodynamic parameters $\Delta H^{\ddagger}$, $\Delta S^{\ddagger}$, and $\Delta C_p^{\ddagger}$ (8). The values so calculated are given in Table 2. The errors in the rate determination for the hydrolysis of the *n*-propylsulfamoyl chloride are somewhat larger than normally acceptable for the determination of $\Delta C_p^{\ddagger}$ over the temperature range experimentally available, a fact we attribute to the low solubility of this compound. The rate constants for this compound ±1% are included in Table 4 for comparison.

TABLE 3. Relative hydrogen bonding tendencies for certain sulfamoyl chlorides

Compound	$\Delta\nu$ (cm^{-1})*
p-ClC_6H_4OH	0.0
$(CH_3)_2NSO_2Cl$	62.0
$(C_2H_5)_2NSO_2Cl$	65.0
CH_3SO_2Cl	65.0

*$\Delta\nu$(cm^{-1}) is the displacement of the complex band from that of the free *p*-chlorophenol (9).

According to the tests introduced by Kartha *et al.* for measuring the relative availability of unshared electrons for hydrogen bonding (9), these compounds show about the same tendency for hydrogen bonding as other sulfonyl chlorides (Table 3). Of course the conditions of the comparisons in Table 3 are quite different from those in our experiments, but if anything tend to accentuate hydrogen bonding.

The small inverse secondary deuterium isotope effect found for the hydrolysis of **1** appeared to

Can. J. Chem. Downloaded from www.nrcresearchpress.com by 210.87.254.42 on 09/05/12
For personal use only.

TABLE 4. First order rate constants and the relative rate for the hydrolysis of sulfamoyl chlorides RSO_2Cl at 15° in water and water/acetonitrile*

R	$10^3 k_{(H_2O)}$ (s^{-1})	Relative rate	$10^3 k_{(H_2O/CH_3CN)}$ (s^{-1})	Relative rate
$(C_2H_5)_2N$	10.61	8.3	5.140	6.4
$(nC_3H_7)_2N$	5.168	4.0	—	—
$C_2H_5NCH_3$	3.813	3.0	—	—
$C_5H_{10}N$	3.004	2.3	1.522	1.9
$(CH_3)_2N$†	1.275	1	0.8024	1

*0.95 mole fraction H_2O.
†Reference 1.

cancel the possibility that some electron release mechanism provided for the eight-fold increase in the rate of hydrolysis of **2** and a four-fold increase for **3** (Table 4). An examination of space-filling models showed that in these cases the sulfur group was effectively shielded from nucleophilic attack compared to *e.g.* methanesulfonyl chloride. In addition it was noted that the α-hydrogens were in a favorable configuration for hydrogen participation and could be activated by the adjoining methyl group. Hence the deuterated isomer $(CH_3CD_2)_2NSO_2Cl$ was synthesized and was shown to hydrolyze with a much reduced rate $k_H/k_D \simeq 2$, a value in the same range as found for the corresponding isotope effect from the hydrolysis of 3-methyl-2-butyl-bromide (10) and the corresponding mesylate in acetic acid (11), for *cis*-cyclopentyl-d_1 and *cis*-cyclohexyl-d_1 chlorides (12), *t*-butyl chloride (13), and the *cis*-4-*t*-butyl-cyclohexyl brosylate (14). All of these compounds on solvolysis show a relatively large secondary deuterium isotope effect $k_H/k_D \geqslant 2$. Shiner and Jewett attribute the large isotope effect in the case of the last example to the formation of a bridged non-classical carbonium ion (14) and the same description might well be applied to the examples given above. In the case of the diethylsulfamoyl-chloride, the ethyl groups block off nucleophilic attack on sulfur even more effectively than the methyl groups in **1** and the change in the secondary deuterium isotope effect from 0.95 to about 2 seems convincing evidence for hydrogen participation. In view of the favorable configuration noted above, such a conclusion was not too surprising, but for the same reason the value of $\Delta C_p^{\ddagger}$ (-39 cal mol^{-1} deg^{-1}) found for the hydrolysis of **2** was without precedent.

TABLE 5. First order rate constants in D_2O and k.s.i.e. for the hydrolysis of RSO_2Cl at 15°

R	$10^3 k_{D_2O}$ (s^{-1})	k.s.i.e.	Reference
$(C_2H_5)_2N$	8.239	1.29	This work
$C_5H_{10}N$	2.319	1.30	" "
$(CH_3)_2N$	—	1.33	1
C_6H_5	—	1.58	2
$(CH_3)_3CCl$	—	1.38 at 10°	15

The value of $\Delta C_p^{\ddagger}$ for the hydrolysis of the piperidyl compound, **4**, was about the same as found for **2** while the methyl-ethyl compound (**3**) had a value intermediate between that of **1** and **2**. The kinetic solvent isotope effect (k.s.i.e.) was about the same value as found for *t*-butyl chloride (15) (Table 5) and lower than found for the hydrolysis of other sulfonyl chlorides (2).

Previous to this work, in every example where a halide was expected to hydrolyze by the S_N1 mechanism, the enthalpy of activation was characterized by a large negative temperature coefficient in the order of -70 to -80 cal deg^{-1} mol^{-1} or possibly more negative (8). This was considered both normal, in view of repeated recurrence, and reasonable, since the transition state for this mechanism involved a greater degree of charge separation, hence a greater degree of solvent reorganization than characterized those solutes hydrolyzing by an S_N2 mechanism. Of course, solvent reorganization is but one of the possible causes of a temperature coefficient for $\Delta H^{\ddagger}$ though it is the one most easily identified. Impurities reacting at comparable rates to give ions (16), mixed kinetics (17), or partitioning of the type discussed by Alberg and Robinson (18) and by Scott and Robertson (19) are all possible sources

Can. J. Chem. Downloaded from www.nrcresearchpress.com by 210.87.254.42 on 09/05/12
For personal use only.

Can. J. Chem. Downloaded from www.nrcresearchpress.com by 210.87.254.42 on 09/05/12
For personal use only.

of non-zero $d\Delta H^{\ddagger}/dT$. In the present investigation careful analysis of starting material and of products gave no indication of impurities nor any reason to doubt that the reaction was analogous to the hydrolysis of the dimethylsulfamoyl chloride where the value of $\Delta C_p^{\ddagger}$ was found to be -76 cal deg^{-1} mol^{-1}.

Robertson and Sugamori (20) have shown in a detailed investigation of the hydrolysis of *t*-butyl chloride in acetonitrile–water mixtures that the addition of 5 mol % cosolvent changes the water value of $\Delta C_p^{\ddagger}$ of -80 cal deg^{-1} mol^{-1} to about -44 cal deg^{-1} mol^{-1}. There was no reason to suspect a change in mechanism for such a minor change in solvent, hence the large change in the value of $\Delta C_p^{\ddagger}$ was associated with a corresponding change in the solvent structure in the initial state and a corresponding reduction in solvent reorganization in the activation process. Applying the same test to **1** and **2** the value of $\Delta C_p^{\ddagger}$ for the dimethyl isomer was reduced from -76 ± 1 to -44 ± 1 cal deg^{-1} mol^{-1}, while the value for the diethyl isomer was reduced from -39 ± 2 to -25 ± 2 cal deg^{-1} mol^{-1}, approximately in the same proportion. Since we could find no evidence from rate measurements or from analytical sources to suggest that the value of $\Delta C_p^{\ddagger}$ for **2** was caused by molecular complexity or adventitiously, we concluded that the difference between the $\Delta C_p^{\ddagger}$ values for **1** and **2**, **3** and **4** for hydrolysis in water represented a real difference in the degree of solvent reorganization.

A straightforward rationalization of these results would be that the diethyl and piperidyl isomers offered sufficient steric hindrance to solvation that the effect of charge development at the transition state for these members was not sufficient to overcome water–water interaction, under the conditions of the experiments. The intermediate value of $\Delta C_p^{\ddagger}$ found for the methyl-ethyl isomer can be regarded as support for this explanation. While qualitatively acceptable, the difference seems too large: the value of -39 cal deg^{-1} mol^{-1} is more positive than for most halides (8). The possibility that **2** can react by mixed kinetics, *i.e.* with hydrogen participation and in the absence of this effect (11) is considered unlikely for two reasons. If direct solvent reaction is unlikely in the case for **1** for steric reasons, it will be even more unlikely in the case of **2**. An even better argument against a shift in the relative importance of k_s and k_Δ (11) is the constancy of k_H/k_D over the experimental temperature range, Table 6. An alternative suggestion which is advanced without further support is that the rate controlling step is the formation of the non-classical ion (14) and the transition state in this step comes at an early stage in charge development. But the fact that the same value of $\Delta C_p^{\ddagger}$ was found for the piperidyl isomer makes such a suggestion less likely than one based on solvent exclusion. Thus it appears that the hydrolysis of a halide in water by what would be considered an S_N1 mechanism need not necessarily be accompanied by a large degree of solvent reorganization and this implies a corresponding reduction in solvation of the transition state contrary to the classical requirement. However, in so far as we are aware a large negative value of $\Delta C_p^{\ddagger}$ (*e.g.* -80 cal deg^{-1} mol^{-1}) is still a general characteristic of an ionizing mechanism for halides in water. What is not left in doubt is that the temperature coefficient of $\Delta H^{\ddagger}$ ($\Delta C_p^{\ddagger}$) can give notice of differences in mechanism undetected by other indicators.

TABLE 6. Secondary deuterium isotope effect, k_H/k_D for the hydrolysis of $(CH_3CD_2)_2NSO_2Cl$ and its undeuterated analogue in water

Temperature (°C)	$10^3 k_H$ (s^{-1})*	$10^3 k_D$ (s^{-1})†	k_H/k_D
5.026	3.755	1.890	1.98
10.006	6.383	3.200	1.99
15.069	10.69	5.440	1.96

*Calculated from A_1, A_2, and A_3 in Table 1.
†Observed.

Finally we draw attention to the parallel correlation between the values of $\Delta H^{\ddagger}$ and $T\Delta S^{\ddagger}$ obtained for solvolysis of these compounds in water and in water containing 5 mol % acetonitrile (Fig. 1). In water it is surprising to note that the point corresponding to **4** lies closer to **1** than to **2**. Were the plot representative of solvent reorganization as judged by comparative values of $\Delta C_p^{\ddagger}$, **4** would be expected to lie closer to **2**. Against this apparent discrepancy we may cite a fact which points to some unspecified factor influencing the value of $\Delta C_p^{\ddagger}$ obtained for **4**. Whereas the value of $\Delta C_p^{\ddagger}$ for **2** was changed from -39 to -25 cal

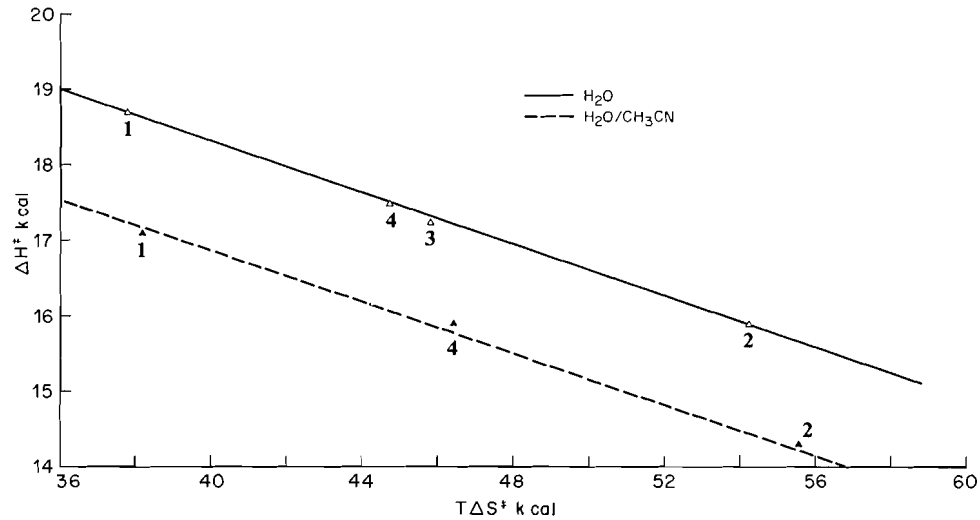

FIG. 1. Correlation of $\Delta H^{\ddagger}$ and $T\Delta S^{\ddagger}$ values for hydrolysis of a series of sulfamoyl chlorides.

TABLE 7. Physical properties of sulfamoyl chlorides RSO_2Cl boiling points and n.m.r. characteristics

R	b.p. (°C/mm Hg)	n.m.r. (proton integration ratio) τ
$(C_2H_5)_2N$	67–68/5	Triplet at 8.68 and quartet at 4.56 (3:2)
$(CH_3CD_2)_2N$	100–110 (oil-bath temperature)/5*	Singlet at 8.72; v.p.c. retention time = 3 min at column temperature 100°
$(nC_3H_7)_2N$	82/3	Triplet at 9.00, a distinctive quintet† at 8.27, and triplet at 6.74 (3:2:2)
$C_2H_5NCH_3$	58/2.5	Triplet at 8.70, singlet at 7.08, and quartet at 6.62 (3:3:2)
$C_5H_{10}N$	70/1	Two broad triplets at 6.70 and 8.25 (4:6)

*Distillation was in a micro tube with an inverted umbrella shaped formation at middle for collecting compound.

†The quintet observed is formed from the overlap of a quartet and a triplet.

deg^{-1} mol^{-1} on changing to the solvent mixture containing 5 mol % acetonitrile, the value for **4** was reduced by only 5 cal deg^{-1} mol^{-1}.

Experimental

Materials

Substituted sulfamoyl chlorides were prepared as previously outlined (1). The boiling points, comparable with those reported in the literature (21, 22) and the characteristics of n.m.r. spectra for these chlorides are summarized in Table 7.

The diethylsulfamoyl chloride -d_4 was checked by v.p.c. on Bendix 2500 analytical gas chromatograph using a 6 ft × $\frac{1}{4}$ in. glass column packed with 5% SE-30 on Chromosorb W. The retention times under the same conditions (3 min; column temperature = 100°) for deuterated and the undeuterated chlorides are comparable. Diethylamine-αd_4. DCl was prepared by the method reported by Werner (23). Acetaldehyde-αd_1 (Merck Sharp and Dohme, 1 g) was added to a solution of ammonium chloride-d_4 (Merck Sharp and Dohme) in D_2O (1 g, ND_4Cl in 4 ml D_2O). The solution was refluxed gently at first (~40 °C) and then at high temperature (not over 120°) overnight. The solution was then concentrated on a vacuum line to half of its volume and unreacted ND_4Cl was filtered off. The filtrate was then refluxed with fresh acetaldehyde-αd, (1 g) overnight. The solvent was evaporated to dryness on a vacuum line, and the residue was sublimed to collect diethylamine-αd_4 DCl (yield 0.9 g); no α-H by n.m.r.

Attempts made to synthesize di-isopropyl, diacetyl, phthalimidyl, and acetyl methyl sulfamoyl chlorides met with total failure. The first three reactions did not work, probably due to bulky amino groups. An attempt to synthesize acetyl methyl sulfamoyl chloride from acetamide and sulfuryl chloride gave a product b.p. 52°/3 mm Hg; n.m.r.: singlet at 6.53 τ. We are still trying to identify this product.

Methods for purification of solvents for measurement of rate and for product analysis were exactly similar to those outlined in the previous paper (1).

The authors are grateful for financial support from the National Research Council of Canada.

1. E. C. F. KO and R. E. ROBERTSON. J. Am. Chem. Soc. In press.
2. B. ROSSALL and R. E. ROBERTSON. Can. J. Chem. **49**, 1451 (1971).
3. H. K. HALL. J. Am. Chem. Soc. **78**, 1450 (1956).

Can. J. Chem. Downloaded from www.nrcresearchpress.com by 210.87.254.42 on 09/05/12
For personal use only.

4. O. ROGNE. J. Chem. Soc. B, 663 (1969).
5. R. E. ROBERTSON and B. ROSSALL. Can. J. Chem. **49**, 1441 (1971).
6. W. VAN DER LINDE and R. E. ROBERTSON. J. Am. Chem. Soc. **86**, 4505 (1964).
7. R. E. ROBERTSON and S. E. SUGAMORI. J. Am. Chem. Soc. **91**, 7254 (1969).
8. R. E. ROBERTSON. Progr. Phys. Org. Chem. **4**, 213 (1967).
9. V. B. KARTHA, R. N. JONES, and R. E. ROBERTSON. Pro. of Ind. Acad. of Sci. **18**, 216 (1963).
10. Y. INOMOTO, R. E. ROBERTSON, and G. SARKIS. Can. J. Chem. **47**, 4599 (1969).
11. S. WINSTEIN and J. TAKAHASHI. Tetrahedron **2**, 316 (1958).
12. H. S. GOLINKIN, D. M. PARBHOO, and R. E. ROBERTSON. Can. J. Chem. **48**, 1296 (1970).
13. L. HAKKA, A. QUEEN, and R. E. ROBERTSON. J. Am. Chem. Soc. **87**, 161 (1965).
14. V. J. SHINER and V. G. JEWETT. J. Am. Chem. Soc. **87**, 1382 (1965).
15. P. M. LAUGHTON and R. E. ROBERTSON. Can. J. Chem. **37**, 1491 (1959).
16. L. J. BRUBACKER, L. TREINDL, and R. E. ROBERTSON. J. Am. Chem. Soc. **90**, 4611 (1968).
17. A. QUEEN. Can. J. Chem. **45**, 1619 (1967).
18. W. J. ALBERY and B. H. ROBINSON. Trans. Faraday Soc. **85**, 980 (1969).
19. J. M. W. SCOTT and R. E. ROBERTSON. Can. J. Chem. **50**, 167 (1972).
20. R. E. ROBERTSON and S. E. SUGAMORI. In press.
21. W. W. BINKLEY and E. F. DEGERING. J. Am. Chem. Soc. **61**, 3250 (1939).
22. L. DENIVELLE. Bull. Soc. Chim. **3**, 2143 (1936).
23. E. A. WERNER. J. Chem. Soc. 844 (1917).

Can. J. Chem. Downloaded from www.nrcresearchpress.com by 210.87.254.42 on 09/05/12
For personal use only.

Can. J. Chem. Downloaded from www.nrcresearchpress.com by 210.87.254.40 on 09/05/12
For personal use only.

Acid-catalyzed Reactions of Cyclobutanones. II.[1] Generation of Acylium Ions from β,γ-Unsaturated Cyclobutanones

E. LEE-RUFF

Department of Chemistry, York University, Toronto, Ontario

Received October 5, 1971

Acid-catalyzed rearrangement of 3-methylene-2,2,4,4-tetramethylcyclobutanone (**1**) gave the γ-lactone of 2,2,3,4-tetramethyl-4-hydroxyvaleric acid. Reaction of 2,2,4,4-tetramethylcyclobutane-1,3-dione (**5**) with PPA gave diisopropylketone with evolution of carbon dioxide. Acylium ions are postulated as intermediates in both these reactions.

La transposition acido-catalysée du méthylène-3 tétraméthyl-2,2,4,4 cyclobutanone (**1**) conduit à la γ-lactone de l'acide tétraméthyl-2,2,3,4 hydroxy-4 valérique. La réaction de la tétraméthyl-2,2,4,4 cyclobutanedione-1,3 (**5**) avec le PPA conduit à la diisopropylcétone avec dégagement de dioxyde de carbone. Les ions acyliums sont postulés comme intermédiaires dans ces deux réactions.

Canadian Journal of Chemistry, **50**, 952 (1972)

The acid-catalyzed rearrangement of exocyclic α,β-unsaturated cyclobutanones has been shown to involve acylium ions as intermediates (1). The strain involved in having two sp^2 centers in an already strained cyclobutane ring (E_{strain} 26 kcal/mol) (2) would permit pathways of high activation energies in medium ring systems to operate in small rings. We wish to report some novel ring opening reactions of β,γ-unsaturated cyclobutanones in the presence of strong acid.

Rearrangement of 3-Methylene-2,2,4,4-tetramethylcyclobutanone (1) in Polyphosphoric Acid

Ketone **1** was prepared according to Hannon (3). Reaction of ketone **1** in polyphosphoric acid (PPA) (50/50 mixture of P_2O_5 and H_3PO_4) at 100° for 1 h resulted in a smooth conversion to the lactone **2** (see Scheme 1). Its structure was deduced from analytical and spectroscopic data as well as independent synthesis. Atmospheric hydrogenation of **1** resulted in an 80/20 mixture of the over-reduced alcohol **3** and the saturated ketone **4**. Jones oxidation of this mixture gave a quantitative yield of **4** which under Baeyer–Villiger oxidation conditions resulted in the exclusive formation of lactone **2**, identical in all respects with the sample obtained from the acid reaction of ketone **1**.

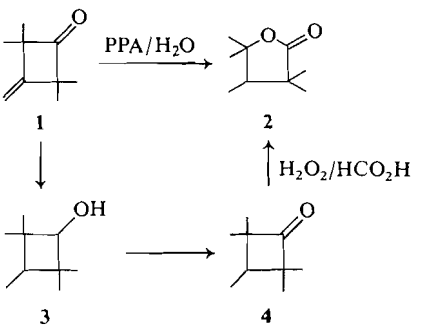

SCHEME 1

Reactions of 1,3-Cyclobutanediones in PPA

Commercial 2,2,4,4-tetramethylcyclobutane-1,3-dione (**5**) subjected to PPA at 100° for 1 h gave diisopropylketone (**6**) as the major product. Its structure was obtained from spectral data as well as comparison with an authentic sample.

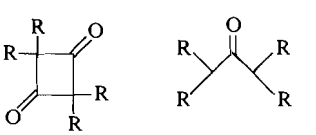

5 R = CH_3 **6** R = CH_3
5a R = C_6H_5 **6a** R = C_6H_5

[1]For paper I of this series see ref. 1.

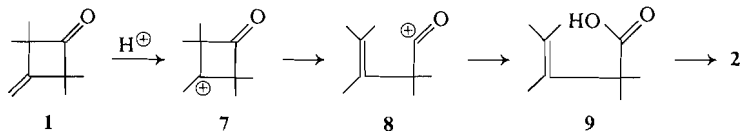

1 7 8 9

SCHEME 2

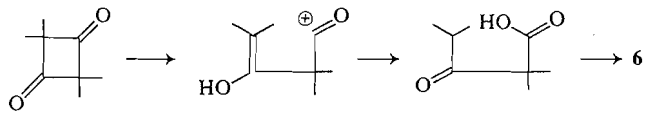

5 10 11

SCHEME 3

Evolution of carbon dioxide accompanied the acid reaction as evidenced by a positive test in passing the evolved gas through an aqueous solution of barium hydroxide under a stream of nitrogen. Under the same conditions 2,2,4,4-tetraphenylcyclobutane-1,3-dione (**5***a*) was inert.

Discussion

The formation of γ-lactone **2** from 3-methylene-2,2,4,4-tetramethylcyclobutanone (**1**) can be envisaged to proceed by Scheme 2. Although the carbonyl group in **1** would be preferentially protonated over the exo-methylene function, an equilibrium between the two species is established. Ring opening of **7** could compete over any other reaction pathway from the protonated ketone **1** to give acylium ion **8** which, upon reaction with water, gives rise to the β,γ-unsaturated carboxylic acid **9**. The cyclization of **9** to its lactone under the strong acid conditions is a common reaction.

A similar mechanism can be invoked for the formation of diisopropylketone from 2,2,4,4-tetramethylcyclobutane-1,3-dione (**5**). Protonation and ring opening could conceivably give rise to the acylium ion **10** (Scheme 3). Hydroxylation could result in the formation of 2,2,4-trimethyl-3-oxovaleric acid (**9**) which under these conditions could readily decarboxylate to diisopropylketone (**6**). The valeric acid derivative **9** was prepared from its methyl ester (4) which in turn is readily available from the alkali ring opening of 2,2,4,4-tetramethylcyclobutane-1,3-dione in methanol. Under the acid conditions it was shown that **9** gave a quantitative yield of ketone **6**.

Under completely anhydrous conditions 2,2,4,4-tetramethylcyclobutane-1,3-dione (**5**) has been reported to undergo an acid-catalyzed rearrangement to give lactone **12** (5) (eq. 1). In

[1] 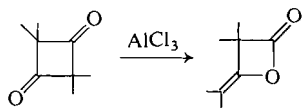

5 12

this case the acylium ion (aluminum chloride complex) cyclizes by intramolecular addition of enolate ion. The inertness of 2,2,4,4-tetraphenylcyclobutane-1,3-dione (***4a***) to acid-catalyzed ring opening lies in the inherent stability of the phenyl substituents. A similar kind of rearrangement would disrupt the aromaticity of one of the phenyl substituents.

Experimental

Melting points are uncorrected. The i.r. spectra were recorded with a Unicam SP 1000 instrument. The n.m.r. spectra were measured with a Varian A-60 and a Varian HA-100 instrument. Samples were dissolved in CCl_4 solution using tetramethylsilane as the internal standard. Vapor phase chromatography was performed on a Varian Aerograph 90-P instrument using 3% SE-30 on a Varaport 30 column at an operating temperature of 100°.

3-Methylene-2,2,4,4-tetramethylcyclobutanone (1)

This ketone was prepared by the method of Hannon in a private communication (3) which is described below.

Can. J. Chem. Downloaded from www.nrcresearchpress.com by 210.87.254.40 on 09/05/12
For personal use only.

Can. J. Chem. Downloaded from www.nrcresearchpress.com by 210.87.254.40 on 09/05/12
For personal use only.

The monophenylimine of 2,2,4,4-tetramethylcyclobutane-1,3-dione (2.0 g) (6) in 10 ml ether was added in one lot to a stirred suspension of triphenylphosphonium methyl iodide (4.2 g) and potassium *t*-butoxide (1.2 g) in sodium dried ether (50 ml) under an atmosphere of nitrogen. The canary-yellow colored mixture was stirred overnight, diluted with water, and extracted with ether. The ether layer was then dried over anhydrous magnesium sulfate and the ether was evaporated under vacuum. The solid residue was taken up in petroleum ether (b.p. 40–60°) and the solution cooled in ice. The triphenylphosphine oxide which precipitated (2.5 g) was removed by filtration and the filtrate extracted with a solution of 80% methanol: water (2 × 100 ml). This solution was back-extracted with petroleum ether and the combined petroleum ether lots washed with water and dried over magnesium sulfate. Removal of the petroleum ether left an oil which could be crystallized by scratching (1.8 g) m.p. 45–47°. The solid was purified by evaporative distillation (60°/3 mm) m.p. 47–48°.

The imine of 3-methylene-2,2,4,4-tetramethylcyclobutanone (0.9 g) was stirred and refluxed with 50% acetic acid (50 ml). A solid collected in the reflux condenser in a few minutes. This was washed back into the solution and refluxing continued for 1 h. After cooling, the excess acetic acid was destroyed by addition of solid sodium bicarbonate. The mixture was then extracted with ether and the ether layer was washed with water until neutral, dried over anhydrous magnesium sulfate, and evaporated to give an oil. The oil mixture was sublimed at room temperature at 25 mm pressure to give a crystalline material, m.p. 43–44° (lit. 42–43° (3)).

Reaction of 3-Methylene-2,2,4,4-tetramethylcyclobutanone (1) with PPA

A mixture of 500 mg of **1** and 1 g of PPA (1:1 mixture of P_2O_5 and H_3PO_4 aged for 24 h at 100°) was heated at 100° for 1 h in a flask equipped with a condenser. Water (5.0 ml) was added to the cooled mixture and 50 ml of ether was added for extraction. The ether layer was washed neutral with water, dried over anhydrous magnesium sulfate, and the ether evaporated to give an oil which crystallized after scratching. The crystalline mixture was purified by preparative v.p.c. to give a crystalline material (**2**) m.p. 55–56°; i.r.: 1775 cm^{-1} (C=O stretch); n.m.r.: 0.94 (3H, d, J = 7.5 Hz), 1.03 (3H, s), 1.01 (3H, s), 1.22 (3H, s), 1.33 (3H, s), 2.00 p.p.m. (1H, q, J = 7.5 Hz); *m/e* 156, (base peak 42 *m/e*).

Anal. Calcd. for $C_9H_{16}O_2$: C, 69.2; H, 10.3. Found: C, 69.0; H, 10.4.

Hydrogenation of 3-Methylene-2,2,4,4-tetramethylcyclobutanone (1)

Ketone **1** (500 mg) in 10 ml of ethyl acetate and 100 mg of PtO_2 was placed in an atmosphere of hydrogen overnight. The catalyst was filtered off and the ethyl acetate evaporated to give an oil which showed two peaks on v.p.c. in a ratio of 4:1. Both peaks were collected and had the following spectroscopic data. The major peak (**3**) was an oil, i.r.: 3420, 1120, 1065, 1015 (alcohol) cm^{-1}; *m/e*: 142. The minor peak (**4**) also was an oil, i.r.: 1786 cm^{-1} (C=O stretch, cyclobutanone); *m/e*: 140 (10 eV).

Jones Oxidation of the Hydrogenation Products of Ketone 1

The mixture (400 mg) obtained from the hydrogenation of ketone **1** was dissolved in 5.0 ml of acetone. To the cooled (0°) solution was added, dropwise, Jones reagent (7) until the yellow color persisted. Methanol was added dropwise until the yellow color disappeared. The solution was taken up in 50 ml ether, washed with water until neutral, dried over magnesium sulfate, and evaporated to give an oil **4** which had an identical i.r. spectrum with the minor component obtained from the hydrogenation of ketone **1**. The v.p.c. retention times were also identical.

Baeyer–Villiger Oxidation of Ketone 4

A mixture of 300 mg of ketone **4**, 1.0 ml of formic acid, and 0.5 ml of 30% H_2O_2 was stirred for 3 h. To this mixture was added 30 ml of ether. The ether extract was washed with 10% sodium bicarbonate solution and then 10% sodium sulfite solution, dried over anhydrous magnesium sulfate, and evaporated to give 270 mg of an oil which crystallized after scratching. This was further purified by preparative v.p.c. to give a crystalline product **2** m.p. 54–56°, which had identical i.r. and n.m.r. spectra with the material obtained from the acid reaction of ketone **1**, mixed m.p. 54–55°.

Reaction of 2,2,4,4-Tetramethylcyclobutane-1,3-dione (5) with PPA

A mixture of 1.0 g of **5** and 1.0 g of PPA was stirred at 100° for 1 h in a flask equipped with a condenser. Water (3.0 ml) was added to the cooled mixture. This was taken up in 50 ml of ether. The ether extract was washed with water until neutral, dried over anhydrous magnesium sulfate, and evaporated to give 800 mg of an oil which on v.p.c. showed two major peaks and one minor peak (<2% of mixture). The two major peaks were collected. The more polar one proved to be identical with 2,2,4,4-tetramethylcyclobutane-1,3-dione (**5**) by comparison of its i.r. spectrum and v.p.c. retention time. The less polar product showed i.r. and n.m.r. spectra identical with commercial sample of diisopropyl ketone. In a second run the gas evolved in the acid reaction was detected as CO_2 as evidenced by precipitation of $BaCO_3$ from an aqueous solution of barium hydroxide as the gas was passed through.

Reaction of 2,2,4,4-Tetraphenylcyclobutane-1,3-dione (4a) with PPA

The same procedure as for the PPA reaction with ketone **6** was repeated with 500 mg of ketone **6a**. After the usual work-up the starting material was recovered unchanged as shown by t.l.c., i.r., and n.m.r. spectra.

2,2,4-Trimethyl-3-oxovaleric Acid Methyl Ester

Dione **6** (2.0 g) in 10 ml of methanol containing 1.5 g of Na_2CO_3 and 5.0 ml of water was stirred at room temperature for 30 min. The mixture was taken up in 60 ml of ether, washed neutral with water, and evaporated to give 1.7 g of an oil, b.p. 92–93° (25 mm); i.r. 1720 (C=O, ketone), 1750 cm^{-1} (C=O stretch of ester); n.m.r.: 0.93 (6H, d, J = 7 Hz), 1.21 (6H, s), 2.71 (1H, q, J = 7 Hz), 3.55 p.p.m. (3H, s); *m/e*: 172.

2,2,4-Trimethyl-3-oxovaleric Acid (9)

A methanolic solution (5.0 ml) of 1.0 g of the methyl ester of **9** and 300 mg of sodium hydroxide was stirred at room temperature. Ether (25 ml) and water (5.0 ml) were added. The aqueous solution was separated and acidified with concentrated HCl solution. The acidified solution was re-extracted with 30 ml of ether. The ether layer was washed with water until neutral, dried over magnesium sulfate, and

evaporated to give 400 mg of an oil, b.p. 104° at 0.5 mm (lit. 105° at 0.5 mm (8)); i.r.: 3400–3100, 1720 cm^{-1} (carboxylic acid, broad peak): n.m.r.: 10.42 (1H, s, exchangeable with D_2O), 2.90 (1H, q, $J = 7$ Hz), 1.32 (6H, s), 1.03 p.p.m. (6H, d, $J = 7$ Hz).

*Reaction of 2,2,4-Trimethyl-3-oxovaleric Acid (**6**) with PPA*

The acid **6** (300 mg) was treated with PPA (0.5 g) using the identical procedure as described above for ketone **5**. Using the same work-up conditions 200 mg of an oil was obtained whose i.r. and n.m.r. spectra were identical with those of a commercial sample of diisopropyl ketone.

The author would like to thank the National Research Council of Canada for their financial support of this research.

1. E. Lee-Ruff, N. J. Turro, P. Amice, and J. M. Conia. Can. J. Chem. **47**, 2797 (1969).
2. C. T. Mortimer. Reaction heats and bond strengths. Pergamon Press, New York, N.Y. 1962. p. 45.
3. D. P. G. Hannon. J. Am. Chem. Soc. **90**, 4513 (1968).
4. R. Hasek, R. Clark, E. Elam, and J. C. Martin. J. Org. Chem. **27**, 60 (1962).
5. J. C. Martin. Belg. Pat. 617 253. Chem. Abstr. **59**, 451*f* (1963).
6. R. H. Hasek, E. V. Elam, and J. C. Martin. J. Org. Chem. **26**, 4340 (1961).
7. K. Bowden, I. H. Heilbron, E. R. H. Jones, and B. C. Weeden. J. Chem. Soc. **39** (1946).
8. B. Murin, W. Riedl, K. Risse, and M. Scheublin. Ber. **92**, 2033 (1959).

Erratum: Microwave Spectrum and Conformation of Tetrahydropyran

V. M. Rao and R. Kewley
Department of Chemistry, Queen's University, Kingston, Ontario

(Ref.: Can. J. Chem. **47**, 1289 (1969))

AND

Erratum: Microwave Spectrum of Morpholine

J. J. Sloan and R. Kewley
Department of Chemistry, Queen's University, Kingston, Ontario

(Ref.: Can. J. Chem. **47**, 3453 (1969))
Received November 29, 1971

Canadian Journal of Chemistry, **50**, 955 (1972)

When recalibrating the Stark cell during the determination of the dipole moment of 1,3-dioxane, an error was discovered in the earlier calibration, which had been used in the calculations of the dipole moments of tetrahydropyran (1) and morpholine (2). Correcting this calculation error and using the same experimental data (1, 2) the corrected values are:

	μ_a(D)	μ_c(D)	μ(D)
Tetrahydropyran	1.39(0.02)	0.74(0.02)	1.58(0.03)
Morpholine	1.53(0.01)	0.27(0.01)	1.55(0.02)

The μ values agree well with those measured in benzene solution of 1.55 (3) and 1.52 D(4), respectively.

Also in Table IX of the morpholine publication (2), the transition given as 2_{12}–3_{22} is actually 2_{21}—3_{22}.

1. V. M. Rao and R. Kewley. Can. J. Chem. **47**, 1289 (1969).
2. J. J. Sloan and R. Kewley. Can. J. Chem. **47**, 3453 (1969).
3. C. W. N. Cumper and A. I. Vogel. J. Chem. Soc. 3521 (1959).
4. M. Aroney and R. J. W. Lefèvre. J. Chem. Soc. 3002 (1958).

Can. J. Chem. Downloaded from www.nrcresearchpress.com by 210.87.254.40 on 09/05/12
For personal use only.

V.50
957-1986
1972

Canadian Journal of Chemistry

Published by THE NATIONAL RESEARCH COUNCIL OF CANADA

VOLUME 50 APRIL 1, 1972 NUMBER 7

Separation of Gas Mixtures by Accommodation Pumping

I. H. DOETSCH AND S. A. RYCE

Department of Chemistry, University of Victoria, Victoria, British Columbia

Received October 5, 1971

Enrichment of helium–argon gas mixtures by accommodation pumping in a 10-stage pump is described. With the warm half of the pump at room temperature, pumping ratios are reported for cold surfaces at 77, 195, and 273 °K.

L'enrichissement de mélanges gazeux hélium–argon, au moyen d'un pompage avec une pompe à 10-temps, est décrit. Avec une chaleur, moitié de celle de la pompe à la température de la pièce, les rapports de pompage sont rapportés pour des surfaces froides à 77, 195, et 273 °K.

Canadian Journal of Chemistry, **50**, 957 (1972)

Introduction

In recent studies Hobson (1–3) described a new development in vacuum pumping termed accommodation pumping, which is operative in the free-molecular and transition flow region. It is postulated by Hobson that the observed pumping action is a consequence of the difference in thermal accommodation between warm gas molecules impinging upon cold surfaces and cold molecules striking warm surfaces.

A typical pump, illustrated in Fig. 1, consists of volumes A and B connected by a U-tube made of Pyrex glass. The arm of the pump connected to B is smooth (untreated), whereas the tubulation adjoining A is "atomically rough" (leached in HCl). The pump contains helium or other gases at sufficiently low pressures such that the mean free path is greater than the internal diameter of the Pyrex U-tube. Typically for 8 mm i.d. of the tube, a suitable helium pressure is 10^{-4} Torr or less. With the assembly at a uniform temperature no pressure difference exists between volumes A and B, *i.e.*, $P_A = P_B$. However, when the U-tube is partially immersed in a cold bath at temperature T_1, a pumping action develops such that $P_A > P_B$. An atomistic interpretation of the phenomenon is that molecules arriving at a rough surface from both warm and cold regions are highly accommodated. On the smooth surfaces of the U-tube, however, collisions of warm molecules with cold surfaces are more likely to result in specular reflection than collisions of cold molecules with warm surfaces (1, 4). Thus in the temperature transition region in the smooth arm of the U-tube, molecules on the average maintain more readily

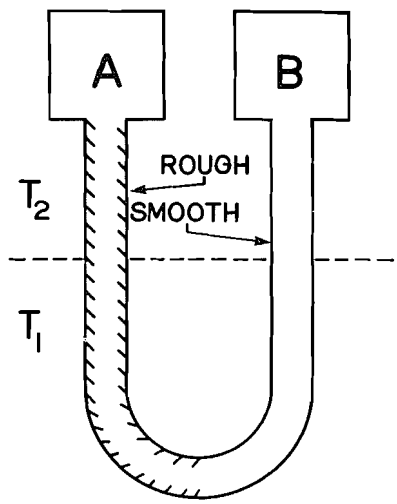

FIG. 1. Schematic of an accommodation pump. If $T_1 < T_2$, then $P_A > P_B$.

Can. J. Chem. Downloaded from www.nrcresearchpress.com by 210.87.254.40 on 09/05/12
For personal use only.

Can. J. Chem. Downloaded from www.nrcresearchpress.com by 210.87.254.40 on 09/05/12
For personal use only.

their velocity component in the direction leading to volume A. The net result of this action is an increase in the pressure ratio, P_A/P_B, over the value of unity for $T_2 = T_1$.

Following the notation of Hobson we have

$$[1] \qquad P_A/P_B = a^n$$

where a is the pressure- or pump-ratio for a single stage pump as described above, and n is the number of stages in series. Values of pump ratios for the inert gases in Pyrex systems were shown by Hobson to decrease with an increase in molecular weight. They ranged from 1.18 for helium to 1.05 for xenon. With a multistage pump ($n = 28$; $T_1 = 77$ °K; $T_2 = 295$ °K), pressure ratios for He of better than 20:1 were achieved. Hobson drew attention to the fact that accommodation pumps have no moving parts, require no working fluid, apparently have no low pressure limit and thus may have potential application as practical pumping devices.

It has occurred to us that the accommodation pumping principle may have applicability with some unique characteristics for the separation or enrichment of gas mixtures. For a binary mixture the ratio of the partial pressures of components 1 and 2 in volume A relative to that in volume B can be simply related to the individual pumping ratios. From eq. 1 we obtain

$$[2] \qquad (P_{1A}/P_{2A})/(P_{1B}/P_{2B}) = (a_1/a_2)^n$$

where the numerical subscript identifies the component.

If $a_1 = a_2$, no separation occurs. However, when $a_1 > a_2$, an enrichment in component 1 of the composition of volume A should accompany the net rise of pressure in A. Simultaneously volume B should be at a lower total pressure with an enrichment in component 2.

We report results of preliminary studies on the separation of mixtures of helium and argon by accommodation pumping. In qualitative agreement with eq. 2 significant enrichments were obtained.

Pumping ratios were obtained for helium and argon in single and ten-stage pumps at three values of T_1 ranging over about 200°. Pumping action was observed with a temperature difference ($T_2 - T_1$), of as little as 25°, with T_1 at 0 °C. An increase in the pumping efficiency of argon relative to helium was noted with an increase in the value of T_1.

Experimental

The apparatus consisted of a modified version of the system described by Hobson (1). Standard ultra-high vacuum procedures were employed to obtain background pressures of less than 10^{-9} Torr. Pressure measurements were performed with Veeco RG-75 ionization gauges generally operated at 1.0 mA emission current and thoroughly outgassed prior to measurement. Gauge pumping was observed in most cases but was considered to be of negligible influence on the determination of accommodation pumping ratios in the pressure range investigated. The relative sensitivities of the two gauges were obtained with the system at room temperature over the pressure ranges of interest. In all cases measurements were conducted at pressures requiring no correction for background gases.

Research grade helium and argon were employed in all experiments. The pump was immersed halfway in ice, Dry Ice–acetone, or liquid nitrogen, the top half always remaining at room temperature. The actual accommodation pumps consisted of 8 mm i.d. Pyrex (Corning No. 7740) tubing made into a single and a decade stage pump. The atomically rough surfaces (side A) were obtained by leaching in boiling 0.05 *N* HCl for about 100 h (1).

Pumping ratios were obtained individually with helium and argon at three values of T_1, *i.e.*, 77, 195, and 273 °K, both for the single and decade stage pumps.

Mixtures of helium and argon were tested in the decade pump only, for two values of T_1, 77 and 195 °K. Three sample flasks (A, B, and C) were initially attached to the accommodation pump. Flask A was connected to the roughened arm; B and C were attached to the smooth side of the pump. After introduction of the gas mixture into the system, sample flask C was severed from the apparatus by collapsing the connecting tubing with a torch to ascertain the initial composition of the gas mixture. Subsequently, the lower half of the decade pump was immersed in a cold bath to initiate pumping action. One of two procedural variations was followed after attainment of equilibrium. Either samples A and B were removed while the pump was cold or the cold pump was first fused at a raised section in the center loop and the system allowed to attain room temperature before subsequent sample removal. Since argon adsorbs appreciably at liquid nitrogen temperature, only the latter procedure permits the determination of the entire argon composition and allows the final composition of flasks A and B to be related to the initial composition in C.

Mass spectrometric analyses of the contents of the sample flasks were carried out with a Perkin–Elmer Hitachi RMU-7 instrument. Standard break-seal procedure through a common manifold was used to introduce the samples.

Results and Discussion

The general observations reported by Hobson (1) concerning the operation of accommodation pumps have been confirmed.

(a) Single Gas Analysis

Accommodation pumping ratios obtained in this work are shown in Table 1 for helium and argon at three values of T_1. No data have been

TABLE 1. Average values of pumping ratios in the pressure range 10^{-4} to 10^{-6} Torr; the mean deviation is given with the number of runs in parentheses; $T_2 = 298$ °K

Pump type	Gas	Average value of pumping ratio when T_1 = 77 °K	195 °K	273 °K
Single stage	Helium	1.215±0.004 (5)	1.065±0.003 (6)	1.012±0.002 (7)
Single stage	Argon	1.084±0.004 (7)	1.040±0.002 (7)	1.008±0.002 (6)
10-stage	Helium	3.00 ±0.05 (5)	1.42 ±0.01 (4)	1.068±0.003 (5)
10-stage	Argon	2.1 ±0.10 (4)	1.28 ±0.01 (5)	1.051±0.002 (5)

TABLE 2. Experimental values of a obtained from $P_A/P_B = a^n$

n	T_1 (°K)	a-value Helium Reference 1	Helium This work	Argon Reference 1	Argon This work
1	77	1.18	1.22	1.07	1.08
3	77	1.28	—	1.07	—
10	77	—	1.12	—	1.08
28	77	1.12	—	—	—
1	195	—	1.07	—	1.04
10	195	—	1.04	—	1.02
1	273	—	1.01	—	1.01
10	273	—	<1.01	—	<1.01

previously reported for values of T_1 at other than liquid nitrogen temperatures. It is of interest to note that a measurable pumping effect is observed with a temperature difference $(T_2 - T_1)$ as little as 25 °C for both gases.

A comparison of our multiple stage pumping ratios with those of Hobson (1) is not directly possible due to differences in the number of stages employed. However, if eq. 1 is assumed to be valid, the data can be evaluated in terms of the single stage pumping ratio, a, as shown in Table 2. It appears from these data, that eq. 1 is not, in fact, generally followed and that pumping efficiency probably decreases from some ideal value with an increase in the number of stages.

Hobson (1) has suggested that the pumping ratios of heavier gases might be improved relative to helium for larger values of T_2. Although we have not as yet tested this prediction, we have detected an increase in the pumping efficiency for argon relative to helium as the value of T_1 increases and possibly as the value of n decreases. These results are shown in Table 3. As in the case of Hobson's prediction for a change of T_2, the observed effect in changing T_1 can be interpreted as arising from a relative increase in specular reflections for argon as compared to helium at higher temperatures (5).

TABLE 3. Values of (a^n_{Ar}/a^n_{He})

n	a^n_{Ar}/a^n_{He} at 77 °K	195 °K	273 °K
1	0.89	0.97	~1.00
10	0.70	0.90	0.98

(b) Gas Mixtures

Binary mixtures of helium and argon were analyzed as previously described at total pressures between 10^{-4} and 10^{-2} Torr. This pressure region was chosen as a compromise to the opposing requirements of high precision in the gas analysis and maximum efficiency in accommodation pumping.

In those experiments at liquid nitrogen temperature in which the pump was severed while cold, the actual pumping effect for argon was partially masked by the subsequent desorption of argon from the warmed-up pump surfaces. The two severed halves of the system had nearly identical volumes so that any changes in the argon distribution between the final systems

Can. J. Chem. Downloaded from www.nrcresearchpress.com by 210.87.254.40 on 09/05/12
For personal use only.

TABLE 4. He/Ar Ratios for 10-stage pump

Trial	T_1 (°K)	A	B	C
1*	77	8.6 ±2.5	4.0 ±1.6	—
2†	77	0.33±0.03	0.13±0.02	0.21±0.02
3†	77	0.78±0.04	0.33±0.02	0.54±0.03
4*	195	0.90±0.03	0.81±0.04	0.80±0.03
5*	195	2.8 ±0.6	1.6 ±0.4	—

*Samples A and B removed with pump cold.
†Samples A and B removed with severed pump warm.

would be less likely to result from unequal cold surface-to-volume ratios. As an additional check, the same experiments were conducted at Dry Ice temperature and flasks A and B removed while the pump was cold.

Measurements are recorded in Table 4 as ratios of helium-to-argon uncorrected for the sensitivity of the mass spectrometer for the individual gases. Thus these data are not actual pressure ratios, and have no significance when compared within each column, since the partial and total pressures varied in each experiment. However, it is immediately apparent that the helium-to-argon ratio is greater in the rough arm of the pump than the smooth, as predicted. Sample C falls between the values for A and B (with the exception of the anomaly in trial 4).

The above results demonstrate the ability of accommodation pumps to partially separate gaseous mixtures. More detailed studies of the phenomenon are planned with a residual gas analyzer attached directly to the pump.

The authors gratefully acknowledge financial support of this work by the National Research Council of Canada. Discussions with Dr. J. P. Hobson were very helpful in furthering the project.

1. J. P. HOBSON. J. Vac. Sci. Technol. **7**, 351 (1970).
2. J. P. HOBSON. Bulletin of the Radio and Electrical Engineering Division, National Research Council of Canada, **20**, 2 (1970).
3. J. P. HOBSON. J. Vac. Sci. Technol. **8**, 290 (1971).
4. J. P. HOBSON. J. Vac. Sci. Technol. **6**, 257 (1969).
5. R. M. BARRER and D. NICHOLSON. Can. J. Chem. **43**, 896 (1965).

Can. J. Chem. Downloaded from www.nrcresearchpress.com by 210.87.254.40 on 09/05/12
For personal use only.

Nuclear Recoil Reactions in Organomanganese Compounds. VI. $IMn(CO)_5$ and $BrMn(CO)_5$

I. G. DE JONG AND D. R. WILES

Chemistry Department, Carleton University, Ottawa, Canada

Received July 19, 1971

Radiochemical reactions of ^{82}Br, ^{128}I, and ^{56}Mn have been studied in neutron-irradiated $BrMn(CO)_5$ and $IMn(CO)_5$. The parent compounds were found to contain 49 and 28% of the ^{82}Br and ^{128}I, but only 6 and 10% of the ^{56}Mn, respectively. The dimeric $[XMn(CO)_4]_2$ accounted for 28% of the ^{82}Br, but only about 2% of the ^{56}Mn. Some $^{56}Mn_2(CO)_{10}$ was also found. The radiochemical yields of several products were found to increase substantially on thermal treatment of the target material.

Reaction pathways are suggested which can account for the thermal effects, which involve halogen atom transfer and carbonyl transfer in the solid.

Des réactions radiochimiques de ^{82}Br, ^{128}I, et ^{56}Mn ont été étudiées dans l'irradiation neutronique de $BrMn(CO)_5$ et $IMn(CO)_5$. Les composés parents sont trouvés, contenant respectivement: 49 et 28% de ^{82}Br et ^{128}I, mais seulement 6 et 10% de ^{56}Mn. Le dimère $[XMn(CO)_4]_2$ rend compte pour sa part de 28% de ^{82}Br et seulement d'environ 2% de ^{56}Mn. Un peu de $^{56}Mn_2(CO)_{10}$ est aussi trouvé. Les rendements radiochimiques de plusieurs produits augmentent nettement avec le traitement thermique de matériaux cible.

Des voies de réactions sont suggérées pouvant rendre compte des effets thermiques, qui mettent en oeuvre le transfert atome d'halogène et le transfert carbonyle dans le solide.

Canadian Journal of Chemistry, **50**, 961 (1972)

Introduction

During the course of this study of the chemical behavior of ^{56}Mn atoms following their production by the $^{55}Mn(n,\gamma)$ reaction, we have observed several interesting aspects of the chemistry of isolated atoms and groups in manganese carbonyl compounds. Since the ligands involved have been entirely organic (—H, $—CH_3$, $—C_6H_5$, Cp), it appeared useful to extend our study to include some rather more electronegative ligands.

Recent evidence has led us to suspect (1, 2) that the $\cdot Mn(CO)_5$ radical is formed, or reformed, first and the other ligand is bonded later. Thus the (oversimplified) reaction series would be

$$[1] \quad Mn + CO + L \rightarrow Mn(CO)_5 + L \rightarrow LMn(CO)_5$$

and not

$$[2] \quad Mn + CO + L \rightarrow MnL + CO \rightarrow LMn(CO)_5$$

or

$$[3] \quad Mn + CO + L \rightarrow LMn(CO)_x + CO \rightarrow LMn(CO)_5$$

In particular, it is found for the compounds $LMn(CO)_5$, L = H (or D), CH_3, or C_6H_5, that the yield of radioactive $L^*Mn(CO)_5$ is qualitatively parallel to the readiness of the exchange of $L^*Mn(CO)_5$ with $IMn(CO)_5$ (the prefix asterisk indicates that the atom is radioactive). While no direct connection has been proven, it is highly suggestive of a stage such as $[L + Mn(CO)_5]$ being involved.

By changing the ligand L from the hydrocarbon ligands to a halogen, it seemed that if reaction 2 or 3 were the case, strong differences in the yields ought to result from the change in the ligand.

A further point regarding the choice of ligand is that both iodine and bromine themselves produce radioisotopes on neutron irradiation, so that the chemical behavior of two different elements could be studied in the same molecule. At the outset one can anticipate the exchange reactions of the ligands will be much more probable than those of the central atom. That is, the reaction

$$[4] \quad {}^*I + IMn(CO)_5 \rightarrow {}^*IMn(CO)_5 + I$$

is readily conceivable, while the reaction

$$[5] \quad {}^*Mn + IMn(CO)_5 \rightarrow I{}^*Mn(CO)_5 + Mn$$

seems to be less likely. The question then is whether this does make much of a difference to the yields of radioactive labelled products and if so, whether the effects can be isolated.

Experimental

The general nature of the experiments has been described earlier (3). The various compounds used were prepared as

Can. J. Chem. Downloaded from www.nrcresearchpress.com by 210.87.254.40 on 09/05/12
For personal use only.

Can. J. Chem. Downloaded from www.nrcresearchpress.com by 210.87.254.40 on 09/05/12
For personal use only.

TABLE 1. Radiochemical yields of ^{128}I, ^{82}Br, and ^{56}Mn in various chemical forms by neutron irradiation (at − 78 °C) of $IMn(CO)_5$ and $BrMn(CO)_5$[a]

Product	Yield (%) for target = $IMn(CO)_5$	Yield (%) for target = $BrMn(CO)_5$
$*XMn(CO)_5$	28.5	49
$X*Mn(CO)_5$	10.3	6.5
$[*XMn(CO)_4]_2$	—	28
$[X*Mn(CO)_4]_2$	1.7	2.0
$Mn_2(CO)_{10}$	3.0	1.9

[a]These data refer to samples given no thermal treatment following neutron irradiation. Chemical processing occurred at room temperature.

follows: (*i*), $IMn(CO)_5$, from $Mn_2(CO)_{10}$ and I_2 (4). (*ii*), $[IMn(CO)_4]_2$ by thermal decomposition of $IMn(CO)_5$ in cyclohexane under reflux (5). (*iii*), $BrMn(CO)_5$ from $Mn_2(CO)_{10}$ and Br_2 in cyclohexane at room temperature (6). (*iv*), $[BrMn(CO)_4]_2$ by thermal decomposition of $BrMn(CO)_5$ in refluxing hexane. (*v*), Purification was done by sublimation *in vacuo* and in the case of the pentacarbonyls also by silica gel chromatography. All synthetic work was performed in the dark, in nitrogen. Purity was checked using the infrared spectra taken on a Perkin–Elmer 237B.

Separation of the carrier species ($XMn(CO)_5$, $[XMn(CO)_4]_2$, and $Mn_2(CO)_{10}$) was effected using a combination of differential leaching and chromatography on silica gel and alumina columns. The dimeric species are markedly less soluble, so that the other compounds can be easily leached out into cold petroleum ether. Following this step, further purification is readily achieved by column chromatography. The remaining dimeric $[IMn(CO)_4]_2$ was chromatographed on silica gel using 5% $CHCl_3$ in petroleum ether. The dimeric $[BrMn(CO)_4]_2$ was not easily chromatographed, and was purified by fractional sublimation *in vacuo*, first at 55 °C to remove $BrMn(CO)_5$ and $Mn_2(CO)_{10}$ and then at 115 °C to sublime the $[BrMn(CO)_4]_2$.

Radioactivity measurements on the samples were made on the 847 keV γ of ^{56}Mn, the 445 keV γ of ^{128}I, and the 554 keV and 777 keV γ-rays of ^{82}Br. The statistical uncertainty in the data is estimated to be less than 5% of the reported value, except for $Mn_2(CO)_{10}$, which is 10%.

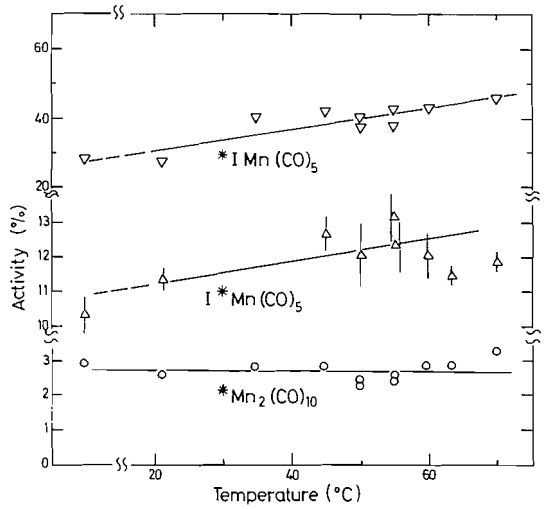

FIG. 1. Thermal annealing data for solid $IMn(CO)_5$ targets. Neutron irradiation at − 78 °C. Thermal treatment was for 6.0 min in all cases.

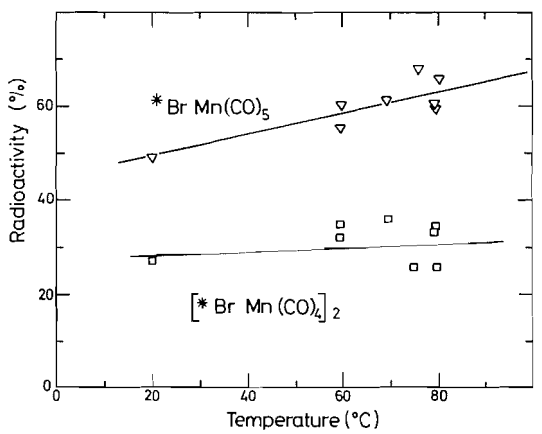

FIG. 2. Thermal annealing data for ^{82}Br containing products from solid $BrMn(CO)_5$ targets. Thermal treatment was for 6.0 min in all cases.

Results and Discussion

The results obtained from samples given no thermal treatment are given in Table 1, where the bromine data refer to 35.9 h ^{82}Br. Unfortunately we were unable to effect satisfactory separation quickly enough to get values for the 18-min ^{80}Br. For similar reasons some of the data for 25-min ^{128}I are less precise than those for the 2.58 h ^{56}Mn.

It is apparent from the data of Table 1 that in each case the yield of the radioactive halogen is greater than that of the radiomanganese in the same product compound. The yields in the dimeric compounds are considerably lower than those in the monomers, as perhaps might be expected, since the target matrix is that of the monomer.

The effect of thermal annealing on the radiochemical yields is shown in Fig. 1 for $IMn(CO)_5$ and in Figs. 2 and 3 for ^{82}Br and ^{56}Mn, respectively, in $BrMn(CO)_5$. From these figures it is evident that the various bromine- or iodine-containing products show largely parallel behavior with respect to the annealing temperature, and that different product compounds from the same target are not similar. We see

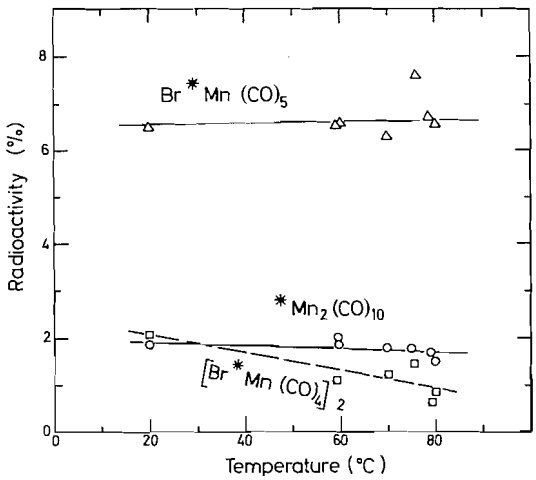

FIG. 3. Thermal annealing data for ^{56}Mn-containing products from solid $BrMn(CO)_5$ targets. Thermal treatment was for 6.0 min in all cases.

that (*a*) $*XMn(CO)_5$ shows a strong increase in yield; (*b*) $I*Mn(CO)_5$ has a much weaker increase while $Br*Mn(CO)_5$ remains unchanged; (*c*) $*Mn_2(CO)_{10}$ shows practically no effect; (*d*) $[*BrMn(CO)_4]_2$ seems to increase somewhat; (*e*) $[X*Mn(CO)_4]_2$ decreases.

Recent work by Groening and Harbottle (7) showing a distinctly stepwise increase of the retention in $Mo(CO)_6$ emphasizes that it is not safe to regard the *apparently linear* behavior shown in these figures as anything more precise than an *average trend.* To the extent that the straight lines may be valid representations of the data, the parameters of these lines are given in Table 2. Here again it is emphasized that the various product compounds have different thermal properties. This is evident in the values of α and of α/Y_{20}, which give the absolute and the relative temperature effects, respectively. In order to interpret the data, we make the *postulate* that, during the 6-min thermal treatment, only the one last ligand necessary to give a recoverable product is added by solid state reaction.

$*Mn_2CO_{10}$

The only exchange reactions which could reasonably give $*Mn_2CO_{10}$ are reactions of $*Mn(CO)_5$ with $XMn(CO)_5$ or with Mn_2CO_{10}.

$$\left.\begin{matrix}[6a]\ XMn(CO)_5 \\ [6b]\ Mn_2(CO)_{10}\end{matrix}\right\} + *Mn(CO)_5 \rightarrow *Mn_2(CO)_{10} + \begin{cases}\cdot X \\ \cdot Mn(CO)_5\end{cases}$$

TABLE 2. Parameters for the equation $Y_T = Y_{20} + \alpha\tau$, where Y_T is the radiochemical yield at temperature $T(°C) = 20 + \tau$

Target	Product	α	α/Y_{20}
$IMn(CO)_5$	$*IMn(CO)_5$	0.3	10×10^{-3}
	$I*Mn(CO)_5$	0.03	3×10^{-3}
	$[I*Mn(CO)_4]_2$	[a]	
	$Mn_2(CO)_{10}$	~0.000	~0
$BrMn(CO)_5$	$*BrMn(CO)_5$	0.24	5×10^{-3}
	$Br*Mn(CO)_5$	~0	~0
	$[*BrMn(CO)_4]_2$	0.04	1.5×10^{-3}
	$[Br*Mn(CO)_4]_2$	−0.02	-17×10^{-3}
	$Mn_2(CO)_{10}$	~0	~0

[a]This compound is distinctly non linear in its temperature dependence, and falls to about 0.6% in the vicinity of 60°.

These reactions have both been found earlier (1) not to occur in solution to a detectable extent during the short time of the experiment, and thus need not be considered further. As to solid state reactions, the data show that none occurs between 20 and 80 °C, since the yield of $*Mn_2(CO)_{10}$ is unchanged on heating. The same result was found on neutron irradiation of $Mn_2(CO)_{10}$. Since it has been shown (3) that reaction 6*b* does not occur at temperatures up to 60 °C, we feel it unlikely that reaction 6*a* plays a part. We conclude thus, that the observed $*Mn_2(CO)_{10}$ is formed by a very early epithermal (or prethermal) reaction.

$X*Mn(CO)_5$

For these species we must find a mechanism which distinguishes the different behaviors of the bromine and iodine compounds. The exchange reaction

$$[7]\quad *Mn(CO)_5 + XMn(CO)_5 \rightleftarrows X*Mn(CO)_5 + \cdot Mn(CO)_5$$

has been shown to occur rapidly for the iodine compound in petroleum ether solution, and presumably must also be rapid for X = Br. Thus, whether the species in the solid is $*Mn(CO)_5$ or $X*Mn(CO)_5$ could not be distinguished by the present data. Thus reaction 7, although possible, does not account for our data. The only other reaction consistent with the $I*Mn(CO)_5$ data is the transfer of a CO group in the solid compound

$$[8]\quad I*Mn(CO)_4 + IMn(CO)_5 \rightarrow I*Mn(CO)_5 + IMn(CO)_4$$

The existence of a $*Mn(CO)_4$ group in the solid state might also account for the data, through a reaction analogous to [8] followed then by

Can. J. Chem. Downloaded from www.nrcresearchpress.com by 210.87.254.40 on 09/05/12
For personal use only.

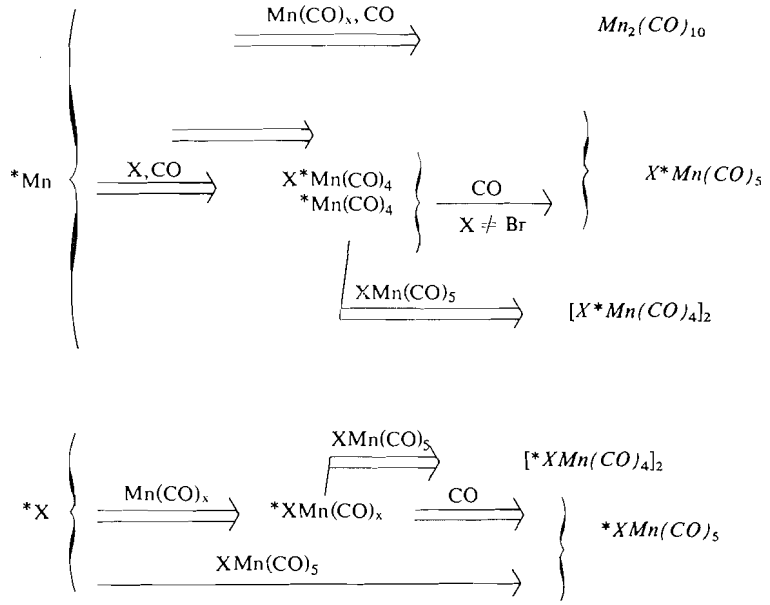

SCHEME 1. Schematic representation of possible reaction paths, both thermal and prethermal, to account for the observed radiochemical yields. ⇒ indicates a prethermal reaction, too fast to be observed, → indicates a reaction occurring during the annealing. Species in italics are the final observed *products*.

reaction 7. Participation of $*Mn(CO)_5$, as this last would suggest, is supported by the slight decrease in the yield of $I*Mn(CO)_5$ at $T \lesssim 60$, the temperature at which $\cdot Mn(CO)_5$ was found to decompose in crystalline $Mn_2(CO)_{10}$.

It seems, then, that the most likely route for formation of $I*Mn(CO)_5$ is through $I*Mn(CO)_4$ (or $*Mn(CO)_4$) formed epithermally and converted through reaction 8 (and reaction 7) to the final product. It is evident from the data for unannealed samples that a considerable amount of $X*Mn(CO)_5$ is formed prior to any heating, presumably by epithermal reactions.

In seeking an explanation for the absence of an annealing effect on $Br*Mn(CO)_5$ we can exclude differences in the lability of CO between the two compounds. While no direct information seems to be available on solid state exchanges, the indications from solution reactions (8) point to a greater CO lability in $BrMn(CO)_5$ than in $IMn(CO)_5$, while the data require quite the reverse. The remaining possibility is that the hypothetical starting compound for the annealing reaction 8, $BrMn(CO)_4$, is unstable even at room temperature so that either reaction 8 goes to completion very early or the $BrMn(CO)_4$ must decompose on being heated. The $Br*Mn(CO)_5$ which is found must then have been formed at a stage prior to the annealing.

*XMn(CO)$_5$

The bromine and iodine compounds behave in a qualitatively very similar manner in producing $*XMn(CO)_5$. One sees from Table 2 that the α values do not differ significantly, and that the values of α/Y_{20} are also similar. It is clear, then, that if reaction 8 is correctly applied to $X*Mn(CO)_5$, and the explanation regarding $Br*Mn(CO)_5$ is valid, this reaction path cannot be used to explain the data for $*XMn(CO)_5$.

The most reasonable reaction to be invoked is the exchange

$$[9] \qquad *X + XMn(CO)_5 \rightarrow *XMn(CO)_5 + X$$

which is able to account fully for the solid state reaction, in which the yields of both $*IMn(CO)_5$ and $*BrMn(CO)_5$ increase markedly during the annealing. It is apparent that if this same reaction were to occur rapidly in solution, then the final yield values would not be temperature dependent, since the two reactions would be indistinguishable. That reaction 9 evidently does not occur in solution may be due to rapid scavenging of the halogen atom, or to slowness

Can. J. Chem. Downloaded from www.nrcresearchpress.com by 210.87.254.40 on 09/05/12
For personal use only.

of the exchange in solution; we have not investigated these possibilities further.

$[*XMn(CO)_4]_2$ and $[X*Mn(CO)_4]_2$

Little can be said about these two compounds except to point out their occurrence as radioactive species. The fact that the radiochemical yield of $[Br*Mn(CO)_4]_2$ decreases during annealing while that of $[*BrMn(CO)_4]_2$ increases suggests the intervention of one or more intermediate species about which we have no further information. That the yield of the bromine-labelled dimer is an order of magnitude greater than that of the ^{56}Mn-labelled dimer points to different mechanisms of formation for the two. The fact that also the yields of the ^{82}Br- and ^{56}Mn-labelled monomers are in roughly the same ratio as of the dimer suggests that the developments may be parallel, following a different initial reaction. It seems reasonable to speculate that the precursor might be $XMn(CO)_x$ whose formation with *X is expected to be much more favorable than with *Mn. Following this, the reactions can be either CO transfer as in reaction 8 or dimerization.

Summary

In summary, it seems possible that the initial formation of $X*Mn(CO)_5$ and $*XMn(CO)_5$ may perhaps proceed through pathways similar to those in $RMn(CO)_5$. The effect of thermal treatment can only be explained through different reactions: addition of CO to $X*Mn(CO)_4$ to give $X*Mn(CO)_5$ and exchange of uncombined *X with the matrix to give $*XMn(CO)_5$.

We conclude that the formation of the observed radioactive products is consistent with the reactions shown schematically in Scheme 1.

We express our gratitude to the National Research Council of Canada for financial support, and to Atomic Energy of Canada, Limited, for providing neutron irradiation facilities.

1. I. G. DE JONG, S. C. SRINIVASAN, and D. R. WILES. J. Organometal. Chem. **26**, 119 (1971).
2. H. JAKUBINEK, S. C. SRINIVASAN, and D. R. WILES. Can. J. Chem. **49**, 2175 (1971).
3. I. G. DE JONG, S. C. SRINIVASAN, and D. R. WILES. Can. J. Chem. **47**, 1327 (1969).
4. E. O. BRIMM, M. A. LYNCH, and W. J. SESNY. J. Am. Chem. Soc. **76**, 3831 (1954).
5. E. W. ABEL and G. WILKINSON. J. Chem. Soc. 1501 (1959).
6. H. D. KAESZ, R. BAU, D. HENDRICKSON, and J. M. SMITH. J. Am. Chem. Soc. **89**, 2844 (1967).
7. H. R. GROENING and G. HARBOTTLE. Radiochim. Acta, **14**, 109 (1970).
8. A. WOJCICKI and F. BASOLO. J. Am. Chem. Soc. **83**, 525 (1961).

Can. J. Chem. Downloaded from www.nrcresearchpress.com by 210.87.254.40 on 09/05/12
For personal use only.

Determination of Conditions for the Suppression of $CH_3 + Sb(CH_3)_2 \rightarrow Sb(CH_3)_3$ and Evaluation of $D[(CH_3)_2Sb—CH_3]$

S. J. W. PRICE AND J. P. RICHARD

Chemistry Department, University of Windsor, Windsor 11, Ontario

Received October 25, 1971

The pyrolysis of trimethylantimony has been studied in a toluene carrier flow system over the temperature range 690–803 °K (total pressures 3.6–173.4 mm, contact times 1.0–13.5 s, decomposition 3.9–89.5%). The progress of the reaction was followed by measuring the amount of methane, ethane, and ethylbenzene formed. In 23 runs the undecomposed alkyl was also determined. The quantity found was in agreement with that expected from the product analysis if three methyl radicals are released for each molecule undergoing reaction. No heterogeneous reaction was detected.

Deuterium labeling led to the conclusion that regeneration of the parent alkyl occurred during the course of the decomposition. This regeneration reaction was effectively eliminated by working at toluene pressures above 150 mm. Least squares analysis of the results obtained under conditions where regeneration should not be important given

$$\log_{10} k/s^{-1} = 15.33 - (55\,900 \pm 1\,000)/2.3RT$$

The activation energy should be a good approximation to $D[(CH_3)_2Sb—CH_3]$.

Significant decomposition of $SbCH_3$ probably does not occur. It seems most likely that free Sb is formed via $2Sb(CH_3) \rightarrow Sb(CH_3)_2 + Sb$.

La pyrolyse du triméthylantimoine a été étudiée dans un système courant porteur de toluène sur la gamme de température de 690–803 °K (pressions totales 3.6–173.4 mm, temps de contact 1.0–13.5 s, décomposition 3.9–89.5%). La progression de la réaction est suivie en mesurant la quantité de méthane, d'éthane et d'éthylbenzène formée. Dans 23 essais, le produit alkylé non décomposé a été également déterminé. La quantité trouvée était en accord avec celle attendue à partir de l'analyse du produit dans le cas où les trois radicaux méthyle sont libérés pour chaque molécule qui subit des changements. Aucune réaction hétérogène n'a été détectée.

Le marquage au deutérium amène à la conclusion que la regénération du groupe alkyle d'origine se produit durant le temps de la décomposition. Cette réaction de regénération a été complètement éliminé en travaillant à des pressions de toluène supérieures à 150 mm. L'analyse des résultats par la méthode des moindres carrés dans des conditions où la regénération ne serait pas importante, a donné:

$$\log_{10} k/s^{-1} = 15.33 - (55\,900 \pm 1\,000)/2.3RT$$

L'énergie d'activation serait une bonne approximation à $D[(CH_3)_2Sb—CH_3]$.

Une décomposition notable de $SbCH_3$ ne se produit probablement pas.

Il semble beaucoup plus vraisemblable que l'antimoine libre se forme par la réaction $2Sb(CH_3) \rightarrow Sb(CH_3)_2 + Sb$.

Canadian Journal of Chemistry, **50**, 966 (1972)

Introduction

The pyrolysis of trimethylantimony has been previously studied in a toluene carrier flow system by Price and Trotman-Dickenson (1). The reaction was homogeneous but otherwise was not simple. The yields of methane and ethane fell far below the amount that would be expected if each alkyl molecule undergoing reaction released three methyl radicals. Furthermore, the overall rate constant, based on either volatile product analysis or antimony recovery from the reaction vessel, increased as the initial concentration of the alkyl decreased. At an initial concentration of 8×10^{-9} mol/cc they report

$$\log_{10} k/s^{-1} = 15.2 - 57\,000/2.3RT$$

based on metal recovery.

Previous work in this laboratory has shown that in similar studies ethylbenzene is always a significant product (2–5). The present work was undertaken to determine if inclusion of ethylbenzene in the product analysis would lead to a material balance or whether it would still be necessary to postulate formation of a polymer of the type $(SbCH_3)_n$. It was also hoped to

Can. J. Chem. Downloaded from www.nrcresearchpress.com by 210.87.254.42 on 09/05/12
For personal use only.

establish whether or not the fractional order behavior was due to regeneration of the parent alkyl and if so to try to find conditions such that the initial decomposition step could be isolated.

Experimental

Materials

(*a*) Dimethylmercury was taken from a stock prepared from mercuric chloride and methyl magnesium iodide (6–8). It had been stored under its own vapor pressure at room temperature. Vapor pressure measurements gave $\log_{10} P/\text{mm} = 7.61 - 1728/T$ (20 to 40 °C) in agreement with previous results (9, 10). The Raman spectrum was checked using a Spectra-Physics model 700 Raman Spectrometer equipped with a He–Ne gas laser. The following spectrum was obtained: 514(s), 1181(s), 2912(s), 2990(w) cm^{-1} in agreement with previously reported spectra (11, 12).

(*b*) Dimethylmercury-d_6 was prepared and stored in the same way (CD_3MgI used). Vapor pressure $\log_{10} P/\text{mm} = 6.97 - 1509/T$ (0 to 45 °C). Raman spectrum 472(s), 908(s), 2110(s), 2222(w) cm^{-1} in agreement with a previous study (11). An n.m.r. spectrum was taken using a Jeolco C60HL with TMS as external standard. No signals were obtained indicating that no significant amounts of undeuterated or partially deuterated alkyl were present.

(*c*) Trimethylantimony was prepared by heating antimony powder, dimethylmercury, and a trace of mercuric chloride in a sealed tube at 150 °C for at least 60 h (13). The product was separated by fractional distillation in an inert atmosphere. Vapor pressure $\log_{10} P/\text{mm} = 7.72 - 1696/T$ (8 to 40 °C) in agreement with reported values (1, 13–15). Raman spectrum: 188(s), 513(s), 1194(w), 1210(s), 2905(s), 2987(w) cm^{-1} in agreement with reported spectra (16). Nuclear magnetic resonance spectra (TMS as external reference): singlet at 1.3×10^{-6}.

(*d*) Trimethylantimony-d_9 was prepared ($Hg(CD_3)_2$ used) and purified in the same way as the undeuterated alkyl. Vapor pressure $\log_{10} P/\text{mm} = 7.61 - 1651/T$ (8 to 40 °C). Raman spectrum: 159 (s), 472 (s), 925(s), 942(w), 2112(s), 2239(w) cm^{-1}. As in the case of $Hg(CD_3)_2$, no n.m.r. signal was observed.

(*e*) Toluene from sulfonic acid (Eastman Organic X325) was used. Gas chromatographic analysis detected traces of xylenes and ethylbenzene. These were reduced to less than 40 p.p.m. by a fractional distillation in which a large tail fraction was discarded. The toluene was refluxed over sodium for 24 h and then degassed by bulb-to-bulb distillation.

Apparatus and Procedure

The experiments were carried out in a system similar to that used in previous work (17). The reaction vessel had a volume of 135 cc. To test for surface effects a vessel was packed with small quartz tubes. This vessel had a volume of 101 cc and a surface-to-volume ratio 20 times that of the unpacked vessel. Both vessels were treated with hot concentrated nitric acid before use. The residual acid was baked out under vacuum after the vessels were installed in the reaction system.

The gaseous products were analyzed using a Perkin–Elmer model 154 gas chromatograph equipped with a 1/4 in. × 6 ft silica gel column. The column was maintained at 80 °C, and a helium flow rate of 20 cm^3 per min was used.

The liquid products which condensed along with the toluene in an acetone – Dry Ice trap were analyzed using a Perkin–Elmer model 800 gas chromatograph equipped with a 150 ft × 0.02 in. i.d. Golay column coated with poly(propylene glycol). (Isothermal operation at 60 °C, flow rate 10 cm^3 per min.)

The mass spectrometric analyses were carried out using an AEI MS10 c2 mass spectrometer. Samples were handled in a conventional vacuum system and were admitted to the mass spectrometer through a porous leak. Gaseous products could be analyzed as obtained. In order to analyze the toluene solution collected in a trap at the outlet of the furnace for the extent of deuteration of the alkyls the solution was fractionally distilled and the first few drops used for mass spectral analysis. The yields were based on the most abundant isotopes of Sb and Hg, 121 and 202, respectively. Parent peaks were used with suitable correction for isotopic interferences (particularly from Hg199). As required analyses were carried out for $Sb(CH_3)_3$, $Sb(CH_3)_2CD_3$, $Sb(CD_3)_2CH_3$, $Sb(CD_3)_3$, $Hg(CH_3)_3$, $HgCH_3CD_3$, and $Hg(CD_3)_2$ at $m/e = 166$, 169, 172, 175, 232, 235, and 238, respectively.

Analysis of a grey deposit found at the outlet of the reaction zone for antimony was carried out by dissolving the deposit in hot concentrated HCl/Br_2. The resulting solution was treated with a saturated Na_2SO_3 solution to reduce the antimony and was then analyzed by titration with bromate (18).

Results and Discussion

The results obtained with $P > 150$ mm along with a few illustrative runs at 17 mm are given in Table 1. Pertinent features of these runs plus a large number of other runs at approximately 17, 30, 47, and 97 mm are given in Table 2 and Fig. 1. The results may be discussed in terms of the following mechanism:

$$[1] \quad Sb(CH_3)_3 \rightarrow Sb(CH_3)_2 + CH_3$$

$$[2] \quad Sb(CH_3)_2 \rightarrow SbCH_3 + CH_3$$

$$[3] \quad 2SbCH_3 \rightarrow Sb(CH_3)_2 + Sb$$

$$[4] \quad CH_3 + C_6H_5CH_3 \rightarrow C_6H_5CH_2 + CH_4$$

$$[5] \quad 2CH_3 \rightarrow C_2H_6$$

$$[6] \quad CH_3 + C_6H_5CH_2 \rightarrow C_6H_5CH_2CH_3$$

$$[7] \quad 2C_6H_5CH_2 \rightarrow (C_6H_5CH_2)_2$$

plus other minor processes characteristic of toluene carrier work (10). Very slight traces of ethylene were found in a few runs.

The runs at 17 mm in Table 1 were done under conditions similar to those used in the original toluene carrier study (1). In that study it was assumed that only negligible amounts of ethylbenzene were formed. This assumption was obviously incorrect.

Can. J. Chem. Downloaded from www.nrcresearchpress.com by 210.87.254.42 on 09/05/12
For personal use only.

TABLE 1. Experimental data for pyrolysis $Sb(CH_3)_3$

T^* (°K)	P (mm)	Initial $Sb(CH_3)_3$ (mol/cc × 10^9)	t_c (s)	$Sb(CH_3)_3$ used	CH_4	C_2H_6	Ethyl-benzene	k (s^{-1})
				(moles × 10^4)				
799.3 A	17.3	5.95	1.14	4.87	4.47	0.71	1.75	0.647
776.3 A	17.4	10.6	1.30	7.62	3.21	0.50	1.25	0.210
755.9	17.8	11.9	1.05	9.18	1.54	0.18	0.432	0.0835
766.7 P	171	19.0	8.61	4.02	9.43	0.13	0.98	0.251
766.7 P	172	19.1	8.66	4.00	9.62	0.11	0.91	0.260
753.7	161	4.64	5.67	1.99	2.82	0.01	0.22	0.132
753.8	161	13.1	6.42	3.30	5.35	0.05	0.58	0.147
752.6	157	18.7	3.90	5.83	6.00	0.08	0.75	0.128
753.1	157	28.7	4.07	8.58	8.94	0.12	1.18	0.127
746.4 P	173	31.1	8.98	5.25	7.47	0.10	0.77	0.085
743.1 P	168	45.3	9.46	4.35	5.39	0.09	0.59	0.068
736.4	173	24.6	11.39	5.24	5.71	0.05	0.41	0.044
736.4	173	30.0	11.45	5.31	6.33	0.07	0.53	0.050
735.7	151	86.1	6.97	15.01	10.52	0.27	1.43	0.047
724.0 P	172	49.7	9.36	6.43	4.25	0.04	0.33	0.030
715.8	170	43.9	12.36	4.32	2.55	0.03	0.23	0.020
715.3	169	55.7	12.66	5.34	2.92	0.03	0.27	0.018
714.4	170	50.1	11.65	6.96	3.52	0.05	0.26	0.018
713.7 P	160	41.9	9.52	3.99	1.37	0.02	0.10	0.014
705.9 P	159	94.3	9.94	5.75	1.72	0.02	0.10	0.012
705.2	168	79.8	13.23	4.88	1.68	0.03	0.16	0.011
690.3 P	171	38.3	9.94	4.67	0.50	0.00	0.05	0.0041
690.1	164	70.5	13.53	6.33	1.18	0.01	0.09	0.0052

*A, reaction vessel volume 156 cc; P, runs in packed vessel.

In the present work rate coefficients were calculated from the usual first order equation

$$k = \frac{2.303}{t_c} \log\left(\frac{1}{1-x}\right)$$

The fraction decomposed, x, may be calculated in two ways.

(*i*) From product analysis

$$x = \frac{\text{moles}(CH_4 + C_6H_5C_2H_5) + 2(\text{moles}\,C_2H_6)}{3(\text{moles}\,Sb(CH_3)_3\,\text{used})}$$

(*ii*) From alkyl recovery

$$x = \frac{g_{\text{alkyl used}} - g_{\text{alkyl recovered}}}{g_{\text{alkyl used}}}$$

The values of x calculated by these two methods for 23 runs are compared in Table 2. The basic agreement indicates that inclusion of reaction 6 in the mechanism resolves the discrepancy in the values of k_g and k_m reported in the original study (1). It is therefore not necessary to postulate the formation of a polymer of the type $(SbCH_3)_n$.

TABLE 2. Percent decomposition by product analysis and alkyl recovery

T (°K)	P (mm)	Decomposition %	
		Product analysis	Alkyl recovery*
801	32	77.7	80.6
800	6	64.8	63.7
800	24	49.9	48.6
799	21	55.0	55.7
799	17	52.3	56.9
789†	17	36.2	36.0
777‡	17	31.5	33.3
775	17	19.4	20.6
773	17	22.9	21.4
767	171	89.5	90.1
767	172	88.5	90.6
756	17	10.9	9.7
756	17	8.4	9.5
706	159	10.8	10.1

*From gas chromatographic analysis of the toluene collected at the outlet of the reaction vessel in a trap cooled by acetone – Dry Ice. Chromatographic conditions used were the same as those for ethylbenzene. Analyses were carried out immediately following a run and fresh standard solutions were used. The solutions have limited stability and care must be taken to avoid loss of alkyl by evaporation or rapid oxidation.

†Average of seven runs.

‡Average of four runs.

Can. J. Chem. Downloaded from www.nrcresearchpress.com by 210.87.254.42 on 09/05/12
For personal use only.

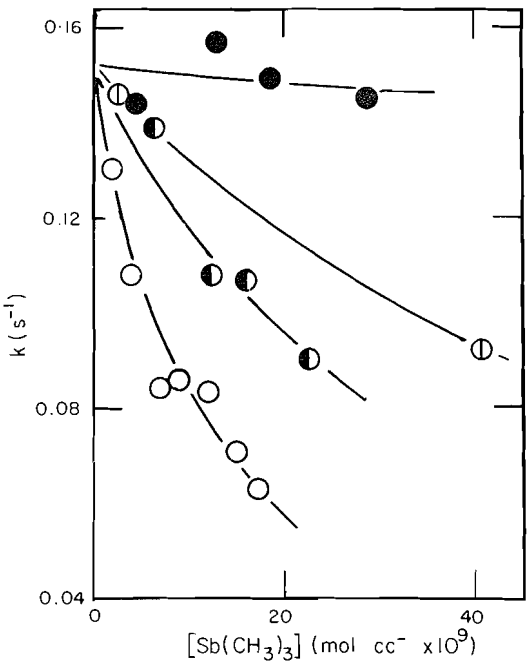

FIG. 1. Effect of alkyl concentration and toluene pressure on the first-order rate constant for the decomposition of $Sb(CH_3)_3$. The runs used were carried out between 753.0 and 755.9 °K. All points shown have been corrected to 755 °K. ○, 17 mm; ◐, 48 mm; ⦶, 97 mm; ●, 160 mm.

Even with a material balance a major problem still exists. The set of runs shown in Fig. 1 performed at 17 mm and 755 °K shows a dependence of k on the alkyl concentration similar to that determined by the previous workers (1). The dependence obviously diminishes as the toluene pressure is increased and in fact appears to be essentially negligible at 160 mm.

The observed concentration effect may be attributed to reaction −1 and possibly reaction 8. This may be seen by

$$[-1] \quad Sb(CH_3)_2 + CH_3 \rightarrow Sb(CH_3)_3$$

$$[8] \quad 2Sb(CH_3)_2 \rightarrow Sb(CH_3)_3 + SbCH_3$$

considering the results of a number of runs carried out using mixtures of either $Sb(CH_3)_3$ and $Sb(CD_3)_3$ or $Sb(CH_3)_3$ and $Hg(CD_3)_2$. These runs were carried out in total darkness as it was determined that methyl group exchange occurred at room temperature in the presence of light.

When $Sb(CH_3)_3$–$Sb(CD_3)_3$ mixtures were pyrolyzed at 17–20 mm toluene pressure extensive group exchange was observed as shown by the appearance of major peaks at $m/e = 169$ and 172 in the mass spectrum of the products. When $Sb(CH_3)_3$–$Hg(CD_3)_2$ mixtures were used (under the conditions used these two alkyls decompose at comparable rates) peaks appeared at 169, 172, and 175 with the major new peak being that at 169. As expected the lifetime of $HgCD_3$ was too short to allow time for formation of any measurable quantity of $HgCH_3CD_3$. It is therefore also highly unlikely that $HgCD_3$ will have time to react with $Sb(CH_3)_2$. The regeneration procedure in this mixture which leads to $Sb(CH_3)_2CD_3$ must then be $Sb(CH_3)_2 + CD_3 \rightarrow Sb(CH_3)_2CD_3$.

It was not possible to make quantitative comparisons between the $Sb(CH_3)_3$–$Sb(CD_3)_3$ and the $Sb(CH_3)_3$–$Hg(CD_3)_2$ systems. The extent of CD_3 group exchange in the latter system suggests that reaction −1 must be a major process in regeneration of alkyl in the $Sb(CH_3)_3$ pyrolysis. However, a significant contribution from reaction 8 cannot be ruled out.

When the toluene pressure was increased to 160 mm no mixing could be detected. This is in agreement with the essentially first order behavior shown at this pressure in Fig. 1 and with the results of the three runs at approximately 736 °K and 170 mm shown in Table 1.

The fact that the curves in Fig. 1 all extrapolate to approximately the same rate constant indicates that at least to a large extent the previously reported pressure dependence (1) was really just an observation of the decreasing extent of alkyl regeneration with increasing toluene pressure. In considering the magnitude of the effect of toluene concentration it should be remembered that in addition to reducing the CH_3 concentration by enhancing reaction 4, increasing the toluene pressure from 17 to 160 mm should increase k_2 by almost a factor of 3 (3). The toluene will also act as a third body in reaction 5 but this will be of less importance.

Basically then it is expected that the results obtained at 151–173 mm (Table 1) should have been obtained under conditions such that each $Sb(CH_3)_3$ undergoing reaction 1 releases three methyl radicals by a sequence of reactions in which the release of the first CH_3 is rate controlling and that under the conditions used no significant regeneration of alkyl will have occurred. The Arrhenius plot of results obtained

Can. J. Chem. Downloaded from www.nrcresearchpress.com by 210.87.254.42 on 09/05/12
For personal use only.

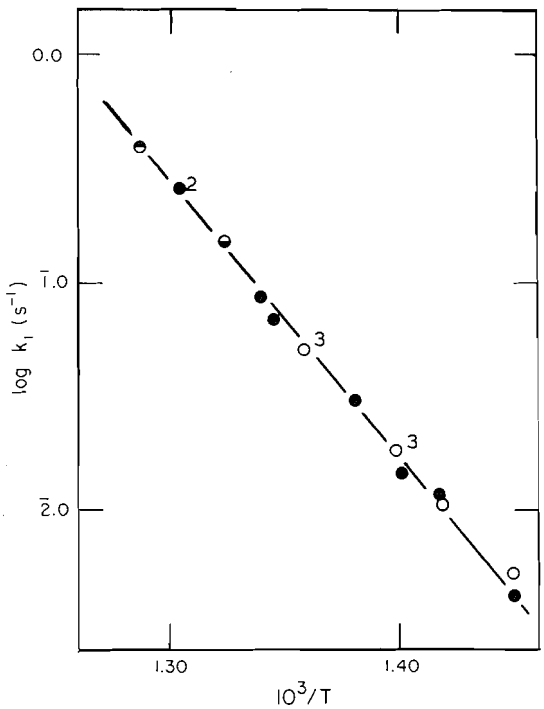

FIG. 2. Arrhenius plot of k_1 (toluene pressure >150 mm). ○, unpacked vessel; ●, packed vessel; ◒, zero concentration value from Fig. 1; ◓, zero concentration value at 776 °K obtained from extrapolation similar to that in Fig. 1 using results at 17, 29, and 48 mm with concentrations from 1.9–32 × 10^{-9} mol cc^{-1}.

under these conditions is shown in Fig. 2. The agreement between the experiments in the packed and unpacked vessel indicate that no detectable heterogeneous reaction is occurring Least squares analysis gives

$$\log_{10} k_1/s^{-1} = 15.33 - (55\,900 \pm 1\,000)/2.3RT$$

The observed activation energy should be a good approximation to $D[(CH_3)_2Sb—CH_3]$.

From ΔH^0_{f298} ($Sb(CH_3)_3$, g) = 1.4 kcal mol^{-1} (13), ΔH^0_{f298} (CH_3) = 33.2 kcal mol^{-1} (19) and ΔH^0_{f298} (Sb, g) = 62.7 kcal mol^{-1} (19) the sum

[3*a*] $$SbCH_3 \rightarrow Sb + CH_3$$

of the dissociation energies of reactions 1, 2, and 3*a* should be 160.9 kcal at 298 °K or approximately 158 kcal at 0 °K. Allowing a combined pressure dependence of E_2 and E_{3a} of 4 kcal then gives $E_2 + E_{3a} = 98$ kcal mol^{-1}.

At the temperatures and pressures used the A factor for reaction 2 should have a maximum value of about 10^{15}. If decomposition occurs via reactions 1, 2, and 3*a*, bearing in mind that three methyl radicals are obtained for each molecule undergoing reaction 1, then k_1 must be significantly smaller than k_2 and k_{3a}. Taking the rather conservative estimate that $2k_1 = k_2 = k_3$ leads to what should be considered a maximum value of $E_2 = 54$ kcal mol^{-1}. This then requires that $E_{3a} \geqslant 44$ kcal mol^{-1} and therefore the minimum value of A_3 would have to be $10^{12.1}$ s^{-1}, a value which is probably at least a factor of 10 too high (5).

The material balance indicated by the results in Table 2 rules out the formation of any major products other than CH_4, C_2H_6, $C_6H_5C_2H_5$, and Sb. However, further tests were made to see if any antimony containing compounds other than the parent alkyl could be detected. Negative results were obtained from both flame and electron capture gas chromatography. The only involatile products observed were dibenzyl and a grey deposit at the outlet of the furnace which on analysis showed 96.4% antimony. This deposit was built up over a number of runs and may have been subject to limited oxidation. However, the possibility that small amounts of $(SbCH_3)_n$ may have been present cannot be ruled out.

In conclusion it seems highly unlikely that reaction 3*a* occurs to any appreciable extent. The main steps in the decomposition of $Sb(CH_3)_3$ should be adequately represented by reactions 1, −1, 2, 3, and 8 with reactions −1 and 8 effectively suppressed at the temperatures and alkyl concentrations used in the present work when $P_{toluene} > \sim 150$ mm.

This work has been supported by a grant from the National Research Council of Canada.

1. S. J. W. PRICE and A. F. TROTMAN-DICKENSON. Trans. Faraday Soc. **54**, 1630 (1958).
2. S. J. W. PRICE and J. P. RICHARD. Can. J. Chem. **48**, 3209 (1970).
3. R. J. KOMINAR and S. J. PRICE. Can. J. Chem. **47**, 991 (1969).
4. R. J. KOMINAR, M. G. JACKO, and S. J. PRICE. Can. J. Chem. **45**, 575 (1967).
5. M. G. JACKO and S. J. W. PRICE. Can. J. Chem. **42**, 1198 (1964).
6. H. GILMAN and R. E. BROWN. J. Am. Chem. Soc. **51**, 928 (1929).
7. H. GILMAN and R. E. BROWN. J. Am. Chem. Soc. **52**, 3314 (1930).
8. C. S. MARVEL and V. L. GOULD. J. Am. Chem. Soc. **44**, 153 (1922).

Can. J. Chem. Downloaded from www.nrcresearchpress.com by 210.87.254.42 on 09/05/12
For personal use only.

9. S. J. W. PRICE and A. F. TROTMAN-DICKENSON. Trans. Faraday Soc. **53**, 939 (1957).
10. R. J. KOMINAR. Ph.D. Thesis, University of Windsor, Windsor, Ontario. 1968.
11. J. L. BRIBES and R. GAUFRES. J. Chim. Phys. **67**, 1168 (1970).
12. P. L. GOGGIN and L. A. WOODWARD. Trans. Faraday Soc. **56**, 1591 (1960).
13. L. H. LONG and J. F. SACKMAN. Trans. Faraday Soc. **51**, 1062 (1955).
14. E. J. ROSENBAUM and C. R. SANDBERG. J. Am. Chem. Soc. **62**, 1622 (1940).
15. C. H. BAMFORD, D. L. LEVI, and D. M. NEWITT. J. Chem. Soc. 468 (1946).
16. E. J. ROSENBAUM and T. A. ASHFORD. J. Chem. Phys. **7**, 554 (1939).
17. M. KRECH and S. J. PRICE. Can. J. Chem. **41**, 224 (1963).
18. N. H. FURMAM (*Editor*). Scott's Standard Methods of Chemical Analysis, 5th ed., Vol. 1. Van Nostrand. 1939.
19. Selected values of Chemical Thermodynamic properties, Natl. Bur. Std. U.S. Tech. Notes, No. 270-3. 1968.

Can. J. Chem. Downloaded from www.nrcresearchpress.com by 210.87.254.42 on 09/05/12
For personal use only.

The Kinetics of the Insertion Reaction of Tin(II) Chloride with a Mono-substituted Derivative of Cyclopentadienyliron Dicarbonyl Dimer

P. F. BARRETT AND W. J. JACOBS
Department of Chemistry, Trent University, Peterborough, Ontario

Received October 18, 1971

The kinetics of the thermal insertion reaction of $SnCl_2$ with the metal–metal bonded complex $(\pi\text{-}C_5H_5)_2Fe_2(CO)_3P(OC_6H_5)_3$ have been studied by following the change in the visible spectrum in THF over the temperature range 40.0 to 55.0 °C. The data are consistent with a two-stage mechanism involving the formation of an intermediate in which the iron–iron bond has been broken but the carbonyl bridges are left intact. From the activation enthalpy of 23.4 ± 0.5 kcal/mol for the formation of the intermediate it is concluded that the triphenyl phosphite has brought about a weakening of the iron–iron bond.

Les cinétiques de la réaction thermique d'insertion de $SnCl_2$ avec le complexe à liaison métal–métal $(\pi\text{-}C_5H_5)_2Fe_2(CO)_3P(OC_6H_5)_3$ ont été étudiés en suivant la variation dans le spectre visible, dans le THF sur un intervalle de température de 40.0 à 55.0 °C.

Les résultats sont compatibles avec un méchanisme en deux étapes comprenant la formation d'un intermédiaire dans lequel la liaison fer–fer a été cassé mais les ponts carbonyls sont gardés intact.

De l'enthalpie d'activation de 23.4 ± 0.5 kcal/mol pour la formation de l'intermédiaire on conclut que le triphényl phosphite occasionne l'affaiblissement de la liaison fer–fer.

Canadian Journal of Chemistry, **50**, 972 (1972)

Introduction

The kinetics of the insertion reaction of tin(II) halides into the metal–metal bond of $[\pi\text{-}C_5H_5Fe(CO)_2]_2$ has recently been reported and the data interpreted in a way to give an estimate of the iron–iron bond strength of 32 kcal/mol (1). Haines and du Preez (2, 3) have prepared a number of tertiary phosphine and phosphite mono-substituted derivatives of $[\pi\text{-}C_5H_5Fe(CO)_2]_2$. The triphenyl phosphite complex, $(\pi\text{-}C_5H_5)_2Fe_2(CO)_3P(OC_6H_5)_3$, was proposed to exist in solution as a mixture of *cis* and *trans* isomers containing two carbonyl bridges each but exchanging via a non-carbonyl bridged species analogous to the exchange proposed for the unsubstituted $[\pi\text{-}C_5H_5Fe(CO)_2]_2$ (4 and references therein). It was also found that tin(II) chloride reacted readily with the triphenyl phosphite derivative to produce $\pi\text{-}C_5H_5Fe(CO)_2Sn(Cl)_2Fe(CO)P(OC_6H_5)_3\pi\text{-}C_5H_5$ as the major product in which insertion of the tin(II) chloride has occurred (2).

We have begun in this laboratory a series of kinetic studies in an attempt to determine the effect of substituents on the strength of metal–metal bonds and in this paper report the kinetic investigation of the thermal insertion of $SnCl_2$ into the iron–iron bond of tricarbonyl(triphenylphosphite)di-π-cyclopentadienyldiiron, $(\pi\text{-}C_5H_5)_2Fe_2(CO)_3P(OC_6H_5)_3$.

Experimental and Results

Materials

Tricarbonyl(triphenylphosphite)di-π-cyclopentadienyldiiron, $(\pi\text{-}C_5H_5)_2Fe_2(CO)_3P(OC_6H_5)_3$, was prepared by the method of Haines and du Preez (3). Anhydrous tin(II) chloride and bromide were prepared as reported earlier (1). Tetrahydrofuran was purified by refluxing over sodium wire, and was freshly distilled and degassed by repeated freezing and thawing on a vacuum line before being used in the kinetic runs.

Reactions of Tin(II) Chloride with $(\pi\text{-}C_5H_5)_2Fe(CO)_3P(OC_6H_5)_3$

Haines and du Preez have pointed out that tin(II) chloride reacts readily with $(\pi\text{-}C_5H_5)_2Fe_2(CO)_3P(OC_6H_5)_3$ to produce the insertion product as well as other products including $[\pi\text{-}C_5H_5Fe(CO)_2]_2SnCl_2$ (2). We have confirmed these findings and have also shown two other possible reaction products to be $\pi\text{-}C_5H_5Fe(CO)_2SnCl_3$ and $\pi\text{-}C_5H_5Fe(CO)P(OC_6H_5)_3SnCl_3$. The former complex was identified from its properties quoted in the literature (5, 6). The ratio of the various products formed was highly sensitive to the degree of exposure of the reaction mixture to air. If only moderate care was taken to exclude air with nitrogen the products were almost exclusively a 50–50 mixture of the two —$SnCl_3$ species. With careful exclusion of air the product was mainly the insertion product with small amounts of $\pi\text{-}C_5H_5Fe(CO)P(OC_6H_5)_3SnCl_3$ and the unsubstituted insertion product $[\pi\text{-}C_5H_5Fe(CO)_2]_2SnCl_2$. Similar results were observed using $SnBr_2$.

To obtain the maximum yield of the insertion product, 50 ml of THF were refluxed under nitrogen for about 30 min to eliminate air. The degassed solvent was transferred to a second flask containing 0.5 g $(\pi\text{-}C_5H_5)_2Fe_2(CO)_3P(OC_6H_5)_3$ and 0.22 g $SnCl_2$ also under nitrogen. The resulting solution was refluxed for about 1 h, the solvent removed under reduced pressure, and the residue recrystallized from

Can. J. Chem. Downloaded from www.nrcresearchpress.com by 210.87.254.105 on 09/05/12
For personal use only.

Can. J. Chem. Downloaded from www.nrcresearchpress.com by 210.87.254.105 on 09/05/12
For personal use only.

dichloromethane and pentane. The first two products to come out of the solution were small amounts of π-$C_5H_5Fe(CO)P(OC_6H_5)_3SnCl_3$ and $[\pi$-$C_5H_5Fe(CO)_2]_2SnCl_2$ but the bulk of the product was the insertion product, π-$C_5H_5Fe(CO)_2Sn(Cl)_2Fe(CO)P(OC_6H_5)_3\pi$-$C_5H_5$. Some difficulties were encountered in isolating this species because of its high solubility and tendency to come out of solution as an oil.

π-$C_5H_5Fe(CO)P(OC_6H_5)_3SnCl_3$
Infrared in CH_2Cl_2: 1990 (s) cm^{-1}.
Anal. Calcd. for π-$C_5H_5Fe(CO)P(OC_6H_5)_3SnCl_3$: C, 42.13; H, 2.95; Cl, 15.54. Found: C, 42.80; H, 3.12; Cl, 15.55.

π-$C_5H_5Fe(CO)_2Sn(Cl)_2Fe(CO)P(OC_6H_5)_3\pi$-$C_5H_5$
Infrared in CH_2Cl_2: 2009 (s), 1963 (s) cm^{-1}.
Anal. Calcd. for π-$C_5H_5Fe(CO)_2Sn(Cl)_2Fe(CO)P(OC_6H_5)_3\pi$-$C_5H_5$: C, 45.09; H, 3.05; Cl, 8.59. Found: C, 44.55; H, 3.14; Cl, 10.42.

The microanalyses were performed by A. B. Gygli, Microanalysis Laboratory, Toronto, Ontario.

Kinetics

The thermal insertion of tin(II) chloride into the metal–metal bond of $(\pi$-$C_5H_5)_2Fe_2(CO)_3P(OC_6H_5)_3$ was studied by following the disappearance of the starting material at 560 nm using a Unicam SP800 spectrophotometer. There was some formation of the $-SnCl_3$ products initially, but then for at least 50% reaction, the insertion product was formed cleanly as indicated by the presence of an isosbestic point at 514 nm during this period. For each run 10 ml of a tin(II) chloride solution was made up in a glove bag in an atmosphere of nitrogen using degassed THF. This solution was then used to completely fill a 1 cm stoppered silica cell containing an amount of $(\pi$-$C_5H_5)_2Fe_2(CO)_3P(OC_6H_5)_3$ required to give an approximately 4×10^{-3} *M* solution. The cell containing the reaction solution was then quickly transferred to a thermostated cell holder in the spectrophotometer.

Pseudo first-order kinetics were observed in all cases with the tin(II) chloride in excess. Plots of log $(A_t - A_\infty)$, where A_t and A_∞ refer to the absorbances at 560 nm at times t and ∞, respectively, were linear during the time that the spectra passed through the isosbestic point at 514 nm, or about 50% reaction. A_∞ was calculated from a plot of the absorbance at 514 nm (the wavelength of the isosbestic) against the absorbance at 560 nm (the kinetic wavelength) for solutions containing different concentrations of pure π-$C_5H_5Fe(CO)_2Sn(Cl)_2Fe(CO)P(OC_6H_5)_3\pi$-$C_5H_5$ in 0.5 *M* $SnCl_2$ solutions in THF. From the absorbance at the isosbestic point in a given run the theoretical A_∞ could be determined from this graph.

The pseudo first-order rate constants, k_{obs} are plotted in Fig. 1 as a function of tin(II) chloride concentration. The line drawn through the experimental points is a theoretical one calculated on the basis of rate parameters derived by a least-squares treatment (7).

Discussion

Figure 1 shows the variation of the pseudo first-order rate constants k_{obs} with the concentration of tin(II) chloride for the thermal reaction of $(\pi$-$C_5H_5)_2Fe_2(CO)_3P(OC_6H_5)_3$ with excess

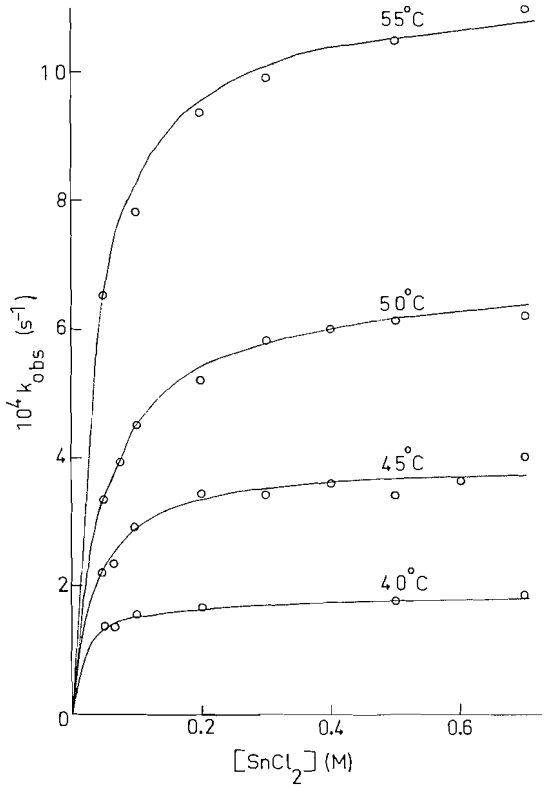

FIG. 1. Plot of the observed pseudo first-order rate constant *vs.* tin(II) chloride concentration for the thermal reaction $(\pi$-$C_5H_5)_2Fe(CO)_3P(OC_6H_5)_3 + SnCl_2 \rightarrow \pi$-$C_5H_5Fe(CO)_2Sn(Cl)_2Fe(CO)P(OC_6H_5)_3\pi$-$C_5H_5$ in THF. The curves drawn through the experimental points are theoretical lines calculated from the rate constants in Table 1.

$SnCl_2$ in THF at the temperatures indicated on the curves. As discussed previously for the insertion reaction of $SnBr_2$ with $[\pi$-$C_5H_5Fe(CO)_2]_2$ (1) the nature of this variation is consistent with the following two-stage mechanism:

$$A_2 \underset{k_{-1}}{\overset{k_1}{\rightleftharpoons}} A_2^* \xrightarrow[B]{k_2} ABA$$

where A_2 represents the metal–metal bonded iron complex $(\pi$-$C_5H_5)_2Fe_2(CO)_3P(OC_6H_5)_3$, A_2^* is a reactive intermediate, B is the tin(II) chloride, and ABA the insertion product. The rate equation for this reaction assuming the concentration of A_2^* to be small and invoking the steady state approximation for its concentration is

$$[1] \quad \frac{d[A_2]}{dt} = \frac{k_1 k_2 [B]/k_{-1}}{1 + k_2[B]/k_{-1}}[A_2] = k_{obs}[A_2]$$

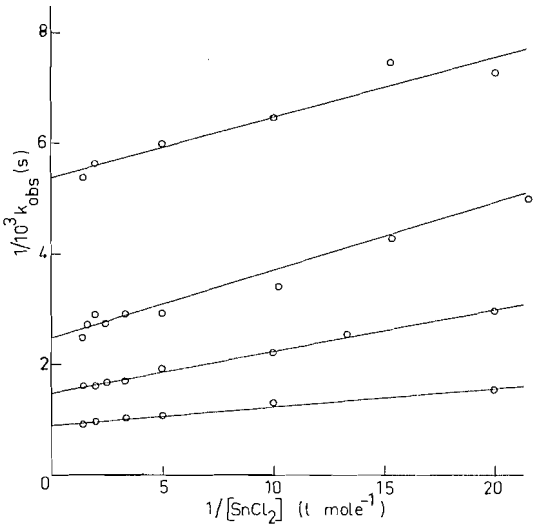

FIG. 2. Plot showing linear relationship between values of $1/k_{obs}$ and $1/[SnCl_2]$ taken from Fig. 1. The straight lines are least-squares plots and lead to the rate constants given in Table 1.

From eq. 1 the following expression can be obtained

$$[2] \qquad 1/k_{obs} = 1/k_1 + k_{-1}/k_1k_2[B]$$

and a plot of $1/k_{obs}$ against $1/[B]$ should yield a straight line with slope k_{-1}/k_1k_2 and intercept $1/k_1$. Figure 2 shows plots of this type for the reaction of $(\pi\text{-}C_5H_5)_2Fe_2(CO)_3P(OC_6H_5)_3$ with $SnCl_2$ and indicates that the data are in fact consistent with the proposed two-stage mechanism. The kinetic parameters together with their standard deviations are shown in Table 1 and were obtained from a least-squares treatment assuming equal uncertainties for all values of k_{obs}. The activation enthalpies and entropies and their standard deviations were obtained from a weighted least-squares treatment of the kinetic parameters (7).

Attempts were made to study the analogous insertion reaction using $SnBr_2$ instead of $SnCl_2$ but were not particularly successful. Although the reaction was very similar to that with $SnCl_2$, spectra of the reaction mixtures at various times drifted slowly but steadily from what should have been an isosbestic point. This suggested that some decomposition or side reactions were occurring but further attempts to remove oxygen from the system were not sufficient to eliminate the problem, and kinetic plots were gradual

TABLE 1. Kinetic parameters for the $SnCl_2$ thermal reaction*

Temperature (°C)	10^4k_1 (s^{-1})	$10^2k_{-1}/k_2$ (mol l^{-1})
40.0	1.86±0.06	2.1±0.3
45.0	3.95±0.12	3.9±0.3
50.0	6.71±0.08	5.0±0.2
55.0	11.2 ±0.3	3.7±0.3

*The uncertainties are standard deviations; $\Delta H_1^{\ddagger} = 23.4 \pm 0.5$; $\Delta H_{-1}^{\ddagger} - \Delta H_2^{\ddagger} = 5 \pm 2$ kcal mol^{-1}; $\Delta S_1^{\ddagger} = -0.6 \pm 1.6$; $\Delta S_{-1}^{\ddagger} - \Delta S_2^{\ddagger} = 9 \pm 5$ cal mol^{-1} deg^{-1}.

curves rather than straight lines. However, estimates of k_{obs} from the reactions indicated that the rate was independent of the concentration of $SnBr_2$ and that k_{obs} was approximately equal to the limiting value for k_1 obtained from the $SnCl_2$ reactions. This would suggest that k_2 was considerably greater for the $SnBr_2$ reaction than for the $SnCl_2$ reaction. This greater reactivity of $SnBr_2$ has also been observed in the insertion of tin(II) halides into the metal–metal bonds of $[PBu_3Co(CO)_3]_2$ (8), $[\pi\text{-}C_5H_5Fe(CO)_2]_2$ (1), and $[\pi\text{-}C_5H_5NiCO]_2$ (9). No evidence was obtained for a second order contribution to the rate as is observed in the reactions of $[PBu_3Co(CO)_3]_2$ and $[\pi\text{-}C_5H_5NiCO]_2$.

The activation parameters given in Table 1 are all concerned in total or in part with the formation or destruction of the reactive intermediate A_2^* and in order to say anything meaningful about these parameters it is necessary to postulate the possible nature of this intermediate. Since the original complex, $(\pi\text{-}C_5H_5)_2Fe_2(CO)_3P(OC_6H_5)_3$, exists mainly as a carbonyl bridged species in solution **1** (3), it would appear reasonable to suggest that the intermediate is also a carbonyl bridged species. Such intermediates have been postulated for the insertion reaction of $[\pi\text{-}C_5H_5Fe(CO)_2]_2$ (1) and $[PBu_3Co(CO)_3]_2$ (8) and also for ligand substitution reactions of $Mn_2(CO)_{10}$ (10), $Re_2(CO)_{10}$ (11), and their derivatives. There are two possible forms of such a reactive intermediate, **2** and **3**, but we cannot predict which would be formed on the basis of steric and electronic considerations.

The activation energy required to break both carbonyl bridges in $[\pi\text{-}C_5H_5Fe(CO)_2]_2$ has been estimated to be about 13 ± 2 kcal/mol (4). Because of the lowering of the carbonyl bridging as well as the terminal stretching frequencies in

Can. J. Chem. Downloaded from www.nrcresearchpress.com by 210.87.254.105 on 09/05/12
For personal use only.

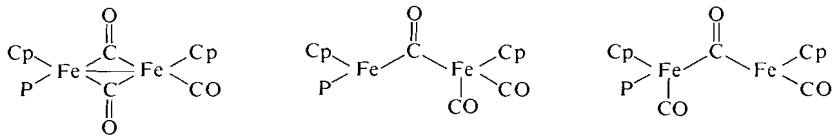

1 2 3

the phosphite substituted complex it has been suggested that the increased electron density on the metal due to the replacement of CO by phosphite is redistributed via π-bonding between the metal and the bridging carbonyl groups (3). For this reason it would appear that the carbonyl bridges are strengthened compared with the unsubstituted dimer and the energy required to break both bridges would be in excess of 13 kcal/mol. If the value of 23.4 kcal/mol for $\Delta H^{\ddagger}$ can be considered to be the energy required to break one carbonyl bridge plus one iron–iron bond, and if the energy required to rupture one carbonyl bridge is $\geqslant 7$ kcal/mol, an upper limit of about 16 kcal/mol can be placed on the energy to break the iron–iron bond. This value is only one half the value estimated at 32 kcal/mol for the iron–iron bond strength in the unsubstituted dimer $[\pi\text{-}C_5H_5Fe(CO)_2]_2$ (1).

On substitution of one CO by $P(OC_6H_5)_3$ the $\Delta S_1^{\ddagger}$ for the insertion reaction is reduced from $+45.5$ to -0.6 cal mol^{-1} deg^{-1}. This drastic change in $\Delta S_1^{\ddagger}$ seems unreasonable in view of the similarities proposed for the mechanisms and reactive intermediates in the two reactions. Although the open structure of the intermediates might accommodate more molecules of solvation than the reactants and give rise to a negative contribution to $\Delta S_1^{\ddagger}$, and although this contribution might be expected to be greater for the more polar $P(OC_6H_5)_3$ complex, these solvation effects could not account for such a large reduction in the $\Delta S_1^{\ddagger}$.

An alternative formulation for the reactive intermediate in the reaction of the $P(OC_6H_5)_3$ substituted complex is one in which only the iron–iron bond is ruptured and the two carbonyl bridges are left intact. This would seem reasonable if in fact the carbonyl bridges are strengthened by the presence of the $P(OC_6H_5)_3$ group as discussed above. The formation of an intermediate of this sort would be expected to involve a very small entropy change as is found experimentally. On the basis of this formulation of the intermediate the $\Delta H^{\ddagger}$ of 23.4 kcal/mol can be interpreted directly as the energy required to break the iron–iron bond, compared with 32 kcal/mol estimated in the unsubstituted dimer. Although the structure of the intermediate cannot be determined unequivocally, the latter proposal in which only the iron–iron bond is broken appears to agree better with the experimental data.

In the case of metal–metal bonds between transition metals in low oxidation states, ligands attached to the metals might be expected to play two opposing roles in their effect on the metal–metal bond strength. Substitution of carbon monoxide by poorer π-electron acceptor ligands would be expected to increase the electron density on the metal resulting in an expansion of the metal's filled non-bonding orbitals. This could result in increased repulsion between the metals due to interactions of these filled orbitals and lead to a weakening of the metal–metal bond. At the same time, however, the σ-bonding orbitals of the metal would also be expanded and the resulting increase in overlap would be expected to strengthen the metal–metal bond.

The former effect seems to predominate in the case of $[\pi\text{-}C_5H_5Mo(CO)_3]_2$. When this dimer is reacted with $P(OC_6H_5)_3$, the disubstituted dimer, $[\pi\text{-}C_5H_5Mo(CO)_2P(OC_6H_5)_3]_2$, is obtained. With the poorer π-bonding ligands $P(C_2H_5)_3$ and $P(n\text{-}C_4H_9)_3$, however, salt-like compounds of the type $[\pi\text{-}C_5H_5Mo(PX_3)_2(CO)_2][\pi\text{-}C_5H_5Mo(CO)_3]$ are formed (12). Thus the better π-bonding ligand $P(OC_6H_5)_3$ favors substitution while $P(C_2H_5)_3$ and $P(n\text{-}C_4H_9)_3$ apparently lead to repulsive interactions which result in the destruction of the metal–metal bond. On the basis of our study of the insertion reactions, the substitution of one carbonyl group in $[\pi\text{-}C_5H_5Fe(CO)_2]_2$ by $P(OC_6H_5)_3$ also appears to result in a reduction in the metal–metal bond strength. Substitution of second carbonyl group could lead to such a weakening of the metal–metal bond that the disubstituted complexes might not exist, and in

Can. J. Chem. Downloaded from www.nrcresearchpress.com by 210.87.254.105 on 09/05/12
For personal use only.

fact efforts to prepare these disubstituted complexes have not been successful (3).

The authors are indebted to the Department of University Affairs of the Province of Ontario and the National Research Council of Canada for financial support.

1. P. F. BARRETT and KENNETH K. W. SUN. Can. J. Chem. **48**, 3300 (1970).
2. R. J. HAINES and A. L. DU PREEZ. Chem. Commun. 1513 (1968).
3. R. J. HAINES and A. L. DU PREEZ. Inorg. Chem. **8**, 1459 (1969).
4. J. G. BULLITT, F. A. COTTON, and T. J. MARKS. J. Am. Chem. Soc. **92**, 2155 (1970).
5. F. BONATI and G. Wilkinson. J. Chem. Soc. 179 (1964).
6. M. J. MAYS and S. M. PEARSON. J. Chem. Soc. A, 136 (1969).
7. J. MANDEL. The statistical analysis of experimental data. Interscience Publ., New York. 1964. pp. 141–144 and pp. 272–278.
8. P. F. BARRETT and A. J. POË. J. Chem. Soc. A, 429 (1968).
9. P. F. BARRETT and R. R. CLANCY. Can. J. Chem. **49**, 2627 (1971).
10. L. I. B. HAINES, D. HOPGOOD, and A. J. POË. J. Chem. Soc. A, 421 (1968).
11. L. I. B. HAINES and A. J. POË. J. Chem. Soc. A, 2826 (1969).
12. R. J. HAINES, R. S. NYHOLM, and M. H. B. STIDDARD. J. Chem. Soc. A, 43 (1968).

Can. J. Chem. Downloaded from www.nrcresearchpress.com by 210.87.254.105 on 09/05/12
For personal use only.

Structure cristalline et moléculaire du thiocyanate mercurique

A. L. Beauchamp et D. Goutier
Département de Chimie, Université de Montréal, Montréal, Québec

Reçu le 17 septembre, 1971

$Hg(SCN)_2$ cristallise dans le système monoclinique, groupe spatial $C2/m$, $a = 10.878$ Å, $b = 4.042$ Å, $c = 6.435$ Å, $\beta = 95.28°$, $Z = 2$. La structure est résolue par la méthode de Patterson et l'affinement sur 217 réflexions observées indépendantes conduit à un facteur résiduel $R = 0.032$. Le mercure occupe les centres de symétrie de la maille et les atomes de soufre des groupes SCN, situés sur les plans de réflexion, assurent au mercure une coordination caractéristique linéaire. Le mercure interagit faiblement avec quatre atomes d'azote de molécules voisines, qui assurent l'environnement octaédrique au métal.

$Hg(SCN)_2$ crystals belong to the monoclinic space group $C2/m$ with $a = 10.878$ Å, $b = 4.042$ Å, $c = 6.435$ Å, $\beta = 95.28°$, and $Z = 2$. The structure was solved by the Patterson method and refined on 217 independent observed reflections to a R factor of 0.032. All the atoms are found on the planes of symmetry of the unit cell with mercury occupying centrosymmetric positions and forming collinear Hg—S bonds to two coplanar SCN groups. An octahedral environment is achieved through weak interaction of mercury with the nitrogen atoms on four neighboring molecules.

Canadian Journal of Chemistry, **50**, 977 (1972)

Introduction

Dans les composés qu'il forme avec l'ion thiocyanate SCN^-, le mercure bivalent se lie de préférence à l'atome de soufre. L'étude cristallographique de certains composés thiocyanatomercuriques semble indiquer une variation sensible de la longueur de la liaison Hg—S en fonction du nombre de coordination caractéristique (1) du mercure. Ainsi, on rapporte des liaisons Hg—S de 2.31 et 2.32 Å pour les molécules ClHgSCN et BrHgSCN, respectivement, où le mercure possède un nombre de coordination caractéristique de deux (2). Dans le sel complexe $K_2[Hg(SCN)_4]$, quatre atomes de soufre assurent au mercure une coordination caractéristique tétraédrique et on a observé des distances Hg—S de 2.54 Å (3). Enfin, dans le complexe *cis*-$Hg(SCN)_2$(1,10-Phénanthroline)$_2$, molécule monomère où le mercure est hexacoordonné, on observe des distances Hg—S voisines de 2.60 Å (4).

Bien que cette variation de la longueur de la liaison mercure–soufre semble significative, elle repose sur un nombre limité de données. En outre, dans certains cas, l'incertitude sur les distances interatomiques est mal connue. Il paraît donc souhaitable de recueillir des données additionnelles sur la longueur de la liaison Hg—S dans certains composés thiocyanatomercuriques. C'est dans ce but que nous avons déterminé la structure du thiocyanate mercurique.

Puff et Becker (5) ont mesuré la densité et les paramètres de maille de $Hg(SCN)_2$ et indiqué que les groupes spatiaux $C2$, Cm et $C2/m$ sont tous trois compatibles avec les absences systématiques notées. Cooney et Hall (6) ont conclu que les spectres de vibration de ce même composé favorisent le groupe centrosymétrique $C2/m$. Les résultats rapportés par ces auteurs sont largement confirmés par le présent travail.

Partie expérimentale

Formule = $Hg(SCN)_2$ Poids moléculaire = 316.75.

Maille monoclinique, groupe $C2/m$, $a = 10.878(8)$ Å, $b = 4.042(4)$ Å, $c = 6.435(6)$ Å, $\beta = 95.28(2)°$, $V = 281.7$ Å^3, $Z = 2$, $\rho_o = 3.71$ g cm^{-3} (5), $\rho_c = 3.734$ g cm^{-3}, $\mu = 282$ cm^{-1}, (20 °C, MoK$\bar{\alpha}$ 0.71069 Å, MoKβ 0.63225 Å).

L'évaporation lente d'une solution de $Hg(SCN)_2$ (Fisher Reagent) dans un mélange 1:1 eau–acétone a produit un dépôt de cristaux aciculaires b incolores. Une aiguille sectionnée de manière à obtenir un cristal de dimensions 0.062 mm × 0.090 mm × 0.029 mm a été utilisée tout au long de ce travail. Les diagrammes de Weissenberg et de précession ont permis de confirmer les paramètres de maille rapportés par Puff et Becker (5).

La détermination précise des paramètres de maille et les mesures d'intensité ont été effectuées sur un diffractomètre automatique Picker FACS-1. Les pics MoKβ de 8 réflexions distribuées sur l'ensemble de la sphère et comprises entre $18° \leqslant 2\theta \leqslant 27°$ ont d'abord été centrées dans l'ouverture du compteur par ajustement programmé des angles ω, χ, et 2θ de l'instrument. Ces valeurs d'angles ont ensuite permis d'affiner les paramètres cristallins par la méthode des moindres carrés décrite par Busing et Levy (7). Les déviations standard rapportées plus haut sont tirées des résultats du dernier cycle d'affinement.

Les intensités ont été mesurées avec la radiation MoKα

Can. J. Chem. Downloaded from www.nrcresearchpress.com by 210.87.254.6 on 09/05/12
For personal use only.

TABLEAU 1. Paramètres affinés selon le groupe $C2/m$ (déviation standard).
F.T. $= \exp\{-(\beta_{11}h^2 + \beta_{22}k^2 + \beta_{33}l^2 + 2\beta_{12}hk + 2\beta_{13}hl + 2\beta_{23}kl)\}$

	Equipoint (8)	x	y	z	β_{11}	β_{22}	β_{33}	β_{12}	β_{13}	β_{23}
Hg	*2a*	0*	0*	0*	0.0044(1)	0.0743(11)	0.0209(4)	0*	−0.0012(1)	0*
S	*4i*	0.1269(4)	0*	0.3222(7)	0.0076(4)	0.145(5)	0.023(1)	0*	0.0010(5)	0*
C	*4i*	0.2597(16)	0*	0.2261(22)	0.0075(17)	0.055(10)	0.014(3)	0*	−0.0020(19)	0*
N	*4i*	0.3580(16)	0*	0.1638(27)	0.0072(16)	0.121(16)	0.029(4)	0*	−0.0025(21)	0*

*Paramètres fixés par symétrie (10).

filtrée au zirconium, selon la technique du balayage $\theta/2\theta$ à raison de 1° (2θ) par min. Le balayage s'étendait sur un intervalle 2θ minimum de 1.60° centré sur le pic. A chacune des limites du balayage, le bruit de fond était compté durant 20 s. Les intensités des réflexions témoins 021, 401, et 003 ont été recueillies toutes les 30 mesures et n'ont manifesté aucune variation significative.

Les intensités intégrées des 743 réflexions (avec $h + k = 2n$) dans toute la sphère de 1.08 $Å^{-1}$ ($2\theta \leqslant 45°$) ont été mesurées. Quatre mesures ayant une intensité inférieure à 15% du bruit de fond ont été rejetées. Un facteur de transmission calculé selon l'équation des faces du cristal a servi à corriger chaque réflexion pour l'absorption. Après transformation des indices, ces données ont fourni 217 réflexions observées indépendantes (hkl, $hk\bar{l}$), qui ont été ensuite corrigées pour les effets de Lorentz et de polarisation.

Les calculs ont été effectués sur l'ordinateur CDC6400. Les versions modifiées des programmes suivants ont été utilisées: Ahmed et Huber, NRC-2 (traitement préliminaire des données); Ahmed et Singh, NRC-3 (correction pour l'absorption); Prewitt, SFLS5 (moindres carrés à matrice entière); Zalkin, FORDAP (cartes de Fourier et de Patterson); Johnson, ORTEP (traçage des figures).

Détermination de la structure

L'extinction systématique de toutes les réflexions dont $h + k \neq 2n$ conduit aux trois groupes spatiaux monocliniques $C2$, Cm, et $C2/m$. Dans les trois cas, les deux atomes de mercure doivent occuper une position spéciale d'ordre 2. On leur assigne arbitrairement les coordonnées (0,0,0) et $(\frac{1}{2},\frac{1}{2},0)$ respectivement, ce qui équivaut à déterminer l'origine de la maille cristalline.

Les atomes légers peuvent être localisés grâce à une synthèse tridimensionnelle de Patterson. La position relative des atomes de mercure permet de prévoir que les pics Hg—Hg se confondent avec l'origine et le centre de la face C de la maille de Patterson. Par ailleurs, à multiplicité égale, l'intensité des pics devrait varier dans l'ordre Hg—S > Hg—N > Hg—C > S—S. Sur la carte d'une portion représentative de la maille ($\frac{1}{4}$ de maille, $0 \leqslant u < \frac{1}{2}$, $0 \leqslant v < \frac{1}{2}$, $0 \leqslant w < 1$), on observe plusieurs pics de hauteurs diverses, qui se trouvent tous dans le plan $v = 0$. Les trois pics les plus intenses, situés respectivement à (0.13,0,0.32), (0.26,0,0.23) et (0.36,0,0.16), adoptent une disposition qui rappelle nettement le segment linéaire S—C—N. Leurs hauteurs relatives permettent de les identifier comme étant des pics Hg—S, Hg—C, et Hg—N de même multiplicité. Pour le groupe $C2/m$, on peut vérifier que les vecteurs interatomiques mercure–soufre (–azote ou –carbone) produisent 4 pics de multiplicité 4 par maille de Patterson, soit un seul par quart de maille. Par contre, pour les groupes $C2$ ou Cm, ces 4 pics se scindent en 8 pics de multiplicité 2 par maille, soit 2 pics par quart de maille. La présence d'une seule série de pics Hg—S, Hg—C, et Hg—N ne présentant pas de dissymétrie semble donc favoriser le groupe centrosymétrique $C2/m$. Néanmoins, la résolution limitée inhérente à la synthèse de Patterson ne permet pas d'exclure totalement de très légers écarts à la centrosymétrie, fait dont nous avons tenu compte lors de l'affinement.

Si le groupe est $C2/m$, le soufre, le carbone et l'azote occupent chacun une série de sites $4i$ $(x,0,z;\ \bar{x},0,\bar{z};\ \frac{1}{2}+x,\frac{1}{2},z;\ \frac{1}{2}-x,\frac{1}{2},\bar{z})$ (8). Dans chaque cas, x et z sont identiques aux valeurs de u et w lues sur la carte, puisque le mercure occupe l'origine de la maille cristalline. A l'aide des coordonnées ainsi déterminées, nous avons retrouvé sur la carte les pics peu intenses S—S, S—N, et S—C. La position de tous les atomes des deux molécules $Hg(SCN)_2$ se trouve ainsi déterminée.

Affinement

Les paramètres structuraux ont été affinés par moindres carrés à matrice entière. Les facteurs de diffusion f, ainsi que les facteurs de dispersion $\Delta f'$ et $\Delta f''$ du mercure et du soufre, proviennent de Cromer et Waber (9). Nous avons d'abord affiné la structure selon le groupe centrosymétrique $C2/m$, puis considéré les groupes $C2$ et Cm, afin de déterminer s'il existe des écarts significatifs à la centrosymétrie.

(*a*) Groupe $C2/m$. Nous avons affiné simultanément le facteur d'échelle, les coordonnées atomiques et les facteurs thermiques ajustables. Quatre cycles de moindres carrés avec des facteurs thermiques isotropes et des poids unitaires ont donné un facteur $R = \Sigma||F_o| - |F_c||/\Sigma|F_o|$ de 0.112. Dans les cycles suivants, nous avons utilisé des facteurs thermiques anisotropes et appliqué à chaque réflexion un poids w calculé selon l'équation $w = 1/(a + b|F_o| + c|F_o|^2)$, les constantes a, b, et c (3.64, −0.29, 0.007) étant ajustées de manière à assurer une distribution uniforme de l'écart pondéré moyen en fonction de $|F_o|$ et de $\sin\theta/\lambda$. Après cinq cycles, le facteur R s'établissait à 0.032, alors que le facteur $R_w = [\Sigma w(|F_o| - |F_c|)^2/\Sigma w|F_o|^2]^{1/2}$ était de 0.038. Les paramètres affinés sont réunis dans le Tableau 1. Une carte différence de Fourier calculée avec ces paramètres ne comportait que quelques pics significatifs (0.7–1.3 e/$Å^3$), tous situés à moins de 1.5 Å du mercure.[1]

(*b*) Groupe $C2$. Dans la maille de symétrie $C2$, le soufre,

[1]La liste des facteurs de structure est déposée en archives. On peut en obtenir une photocopie en s'adressant à la Bibliothèque Scientifique Nationale, Conseil National de Recherches du Canada, Ottawa, Canada K1A 0S2.

Can. J. Chem. Downloaded from www.nrcresearchpress.com by 210.87.254.6 on 09/05/12
For personal use only.

TABLEAU 2. Distances interatomiques et angles de liaison dans $Hg(SCN)_2$*

Liaisons	Distance (Å)	Liaisons	Angle (deg)
Hg—S(*a*)	2.381(6)	S(*b*)—Hg—S(*a*)	180 (sym.)
S(*a*)—C(*a*)	1.62 (2)	N(*a*+)—Hg—N(*b*−)	180 (sym.)
C(*a*)—N(*a*)	1.18 (3)	N(*a*−)—Hg—N(*b*+)	180 (sym.)
Hg—N(*a*+)	2.81 (1)	N(*a*−)—Hg—N(*b*−)	88.0 (4)
		N(*a*−)—Hg—N(*a*+)	92.0 (4)
		N(*a*−)—Hg—S(*a*)	88.2 (3)
		N(*b*−)—Hg—S(*a*)	91.8 (3)
		Hg—S(*a*)—C(*a*)	97.6 (5)
		S(*a*)—C(*a*)—N(*a*)	177.5 (13)
		Hg—N(*a*+)—C(*a*+)	132.7 (11)

*(*a*) $x,0,z$; (*b*) $\bar{x},0,\bar{z}$; (*a*+) $x-\frac{1}{2},\frac{1}{2},z$; (*a*−) $x-\frac{1}{2},-\frac{1}{2},z$; (*b*+) $\bar{x}+\frac{1}{2},\frac{1}{2},\bar{z}$; (*b*−) $\bar{x}+\frac{1}{2},-\frac{1}{2},\bar{z}$. Les déviations standard sur les distances tiennent compte des déviations standard sur les paramètres de maille.

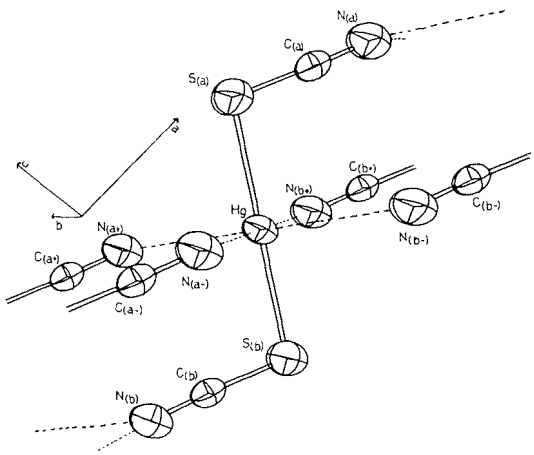

FIG. 1. Environnement du mercure dans le cristal de $Hg(SCN)_2$. Le mercure, situé sur le centre de symétrie à l'origine, et les groupes S(*a*)—C(*a*)—N(*a*) et S(*b*)—C(*b*)—N(*b*) centrosymétriquement équivalents, se trouvent sur le plan de symétrie $y = 0$ de la maille. Les autres atomes sont équivalents aux précédents par centrage de la face C et occupent les plans de symétrie à $y = \frac{1}{2}$ (*a*+ et *b*+) ou $y = -\frac{1}{2}$ (*a*− et *b*−). Les ellipsoïdes ont été tracées à partir des facteurs thermiques anisotropes et correspondent à un niveau de probabilité de 50%.

l'azote et le carbone occupent chacun une position générale *4c*. Au départ de l'affinement, nous avons utilisé les paramètres structuraux du Tableau 1. Dans ce groupe, les coordonnées *y* et les facteurs thermiques β_{12} et β_{23} des atomes légers sont également ajustables (10). Au point de convergence, l'écart entre les paramètres affinés et les valeurs correspondantes du Tableau 1 ne dépasse pas la somme de leurs déviations standard respectives. Les facteurs $R = 0.032$ et $R_w = 0.038$ sont identiques aux valeurs obtenues pour le groupe *C*2/*m*. Comme ces facteurs ne diminuent pas en passant du modèle *C*2/*m* (23 paramètres ajustables) au modèle *C*2 (32 paramètres ajustables), le groupe centrosymétrique *C*2/*m* est favorisé avec un degré de probabilité très élevé (11).

(*c*) Groupe *Cm*. Les atomes légers se trouvent nécessairement à proximité des plans de réflexion à $y = 0$ et $\frac{1}{2}$. Il n'est donc pas possible de les disposer sur des positions générales, puisque les distances entre des atomes situés à x,y,z et $x,\bar{y},z$ serait extrêmement courte. Le soufre, le carbone et l'azote constituent donc chacun deux paires non-équivalentes occupant des positions spéciales *2a*. Nous avons tenu compte de cette distribution des atomes sur les équipoints pour déterminer, à l'aide du Tableau 1, les coordonnées de départ.

L'affinement selon le groupe *Cm* ne converge pas. Au cours de cinq cycles successifs, les paramètres oscillent constamment autour de leurs valeurs initiales et le facteur *R* demeure au voisinage de 0.042. On observe une corrélation très élevée (coefficients de corrélation 0.80–0.95) entre les coordonnées *x* (ou *z*) d'atomes identiques supposés non-équivalents d'une part, entre ces mêmes coordonnées et les facteurs β_{ij} correspondants d'autre part. Ces résultats nous paraissent suffisants pour rejeter le groupe *Cm*.

En conclusion, l'affinement ne révèle pas d'écarts significatifs à la centrosymétrie. Nous admettons donc que la structure définie selon le groupe centrosymétrique *C*2/*m* est juste. Notons que Cooney et Hall ont tiré la même conclusion à la suite d'une étude des spectres de vibration de $Hg(SCN)_2$ (6).

Description de la structure et discussion

Les atomes se trouvent tous sur les plans de symétrie de la maille. L'atome de mercure et son environnement sont représentés à la Fig. 1.

Le Tableau 2 comporte un choix de distances interatomiques et les valeurs de certains angles. Les deux atomes de soufre S(*a*) et S(*b*) équivalents par centrosymétrie sont les seuls voisins immédiats du mercure et lui assurent une coordination caractéristique linéaire. L'angle Hg—S—C de 97.6(5)° est comparable à ceux qu'on observe généralement pour les groupes SCN coordonnés par le soufre (12). Les liaisons S—C (1.62(2) Å) et C—N (1.17(3) Å) possèdent les longueurs habituelles (13) et sont collinéaires

Can. J. Chem. Downloaded from www.nrcresearchpress.com by 210.87.254.6 on 09/05/12
For personal use only.

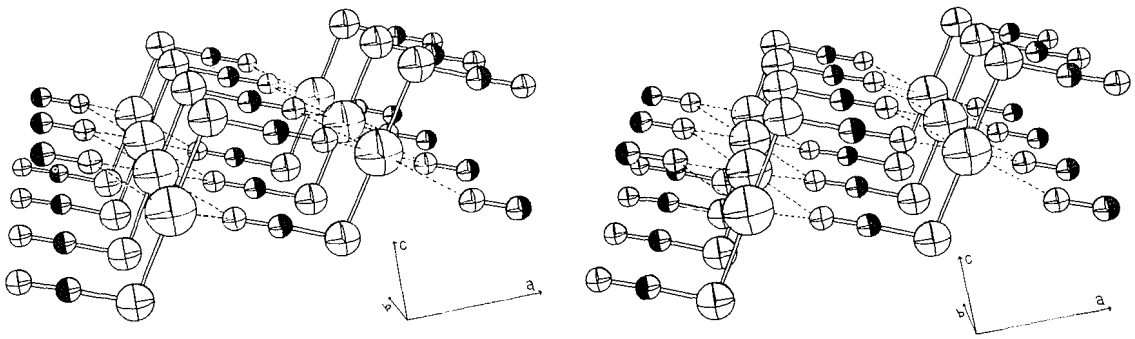

FIG. 2. Projection stéréoscopique d'une couche constituée de molécules $Hg(SCN)_2$ reliées entre elles. Les atomes sont représentés par des sphères et identifiés à la Fig. 3. Les traits pointillés indiquent les interactions intermoléculaires Hg—N. L'axe cristallographique *b* coincïde avec une rangée d'atomes de mercure.

aux erreurs expérimentales près (∠ S—C—N 177.5(13)°). La distance Hg—S de 2.381(6) Å est légèrement plus élevée que la somme des valeurs admises pour les rayons covalents du soufre (1.04 Å) et du mercure bicoordonné (1.30 Å) (1).

A l'état solide, plusieurs composés mercuriques bicovalents adoptent un empilement qui permet au métal d'interagir avec des atomes donneurs de molécules voisines. La Fig. 1 montre que le mercure est entouré de quatre atomes d'azote et possède ainsi un nombre de coordination *effectif* (1) de six. Les distances Hg—N (2.81(1) Å), toutes égales par symétrie, sont inférieures à la somme des rayons de van der Waals (3.1 Å) (1) et comparables aux distances Hg—N (2.74 Å) observées pour $Hg(CN)_2$ (14). Le mercure se trouve donc au centre d'un octaèdre constitué de quatre atomes d'azote et de deux atomes de soufre, ces derniers occupant des sommets opposés. Les angles S—Hg—N et N—Hg—N sont tous très voisins de 90 ou 180° selon le cas, de sorte que l'écart à la symétrie idéale D_{4h} est minime.

La Fig. 2 révèle la disposition relative de ces polyèdres dans le cristal. Des octaèdres voisins se partagent une arête N—N pour former une rangée infinie parallèle à l'axe *b*. Les rangées adjacentes sont décalées de *b*/2 l'une par rapport à l'autre, mais les segments S—Hg—S sont tous parallèles. Ces rangées se soudent l'une à l'autre par l'intermédiaire du carbone, qui relie chaque atome de soufre d'une rangée à un atome d'azote de la rangée voisine. Il en résulte des couches parallèles au plan *ab*, comme l'indique la Fig. 3. Entre ces couches, il n'existe apparemment que

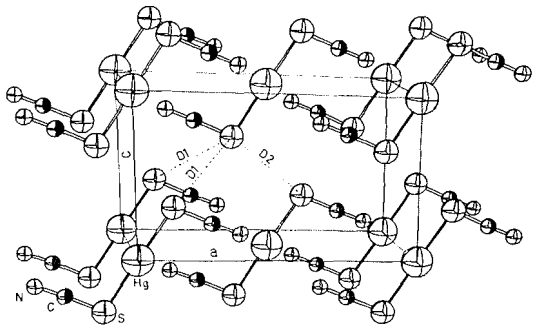

FIG. 3. Empilement des couches dans le cristal de $Hg(SCN)_2$. Les atomes sont représentés par des sphères. Entre atomes de couches différentes, seules les distances S—S ($D1 = 3.916(7)$ Å et $D2 = 3.747(7)$ Å) se rapprochent de la somme des rayons de van der Waals (3.6 Å).

des interactions faibles. Certains contacts S—S (3.75 et 3.92 Å) entre atomes de couches différentes sont les seuls qui se rapprochent de la somme des rayons de van der Waals (3.6 Å). Cette faible cohésion entre les couches est en accord avec la grande facilité de clivage des cristaux selon le plan *ab*.

La liaison Hg—S (2.381(5) Å) du thiocyanate mercurique est comparable à celles de CH_3-$SHgSCH_3$ (2.36(5) Å) (15) et du cinabre HgS (2.36(~5) Å) (16), mais sensiblement plus longue que celle de ClHgSCN (2.31(~2) Å) et BrHgSCN (2.32(~2) Å) (2). Ces composés ressemblent tous au thiocyanate, puisque le mercure *y* possède un nombre de coordination caractéristique de deux et complète sa coordinence effective par interaction avec des atomes voisins. Cependant, l'incertitude sur les longueurs de liaisons de certains composés et

Can. J. Chem. Downloaded from www.nrcresearchpress.com by 210.87.254.6 on 09/05/12
For personal use only.

relativement élevée. Il est donc prématuré de tirer des conclusions quant aux influences spécifiques de l'halogène ou du groupe rattaché au soufre. Une étude dans ce sens nécessiterait d'autres mesures plus précises de la longueur des liaisons Hg—S.

Nous tenons à remercier J. Hubert pour son intérêt et sa participation à la rédaction du présent manuscrit. Nous remercions également le Conseil National de Recherches du Canada pour une subvention de recherches.

1. D. GRDENIC. Quart. Rev. **19**, 303 (1965).
2. Z. V. ZVONKOVA et G. S. ZHDANOV. Zh. Fiz. Khim. **26**, 586 (1952).
3. Z. V. ZVONKOVA. Zh. Fiz. Khim. **26**, 1798 (1952).
4. A. L. BEAUCHAMP, B. SAPERAS et R. RIVEST. Can. J. Chem. **49**, 3579 (1971).
5. H. PUFF et H. BECKER. Acta Cryst. **18**, 299 (1965).
6. R. P. J. COONEY et J. R. HALL. Aust. J. Chem. **22**, 2117 (1969).
7. W. R. BUSING et H. A. LEVY. Acta Cryst. **22**, 457 (1967).
8. International tables for X-ray crystallography. Vol. I. Kynoch Press, Birmingham. 1969.
9. D. T. CROMER et J. T. WABER. Acta Cryst. **18**, 104 (1965). D. T. CROMER. Acta Cryst. **18**, 17 (1965).
10. W. J. A. M. PETERSE et J. H. PALM. Acta Cryst. **20**, 147 (1966).
11. W. C. HAMILTON. Acta Cryst. **18**, 502 (1965).
12. C. KUO-CHAN et M. A. PORAI-KOSHITS. Kristallografiya, **5**, 462 (1960).
13. A. FERRARI, A. BRAIBANTI, G. BIGLIARDI et A. M. LANFREDI. Acta Cryst. **18**, 367 (1965).
14. R. C. SECCOMBE et C. H. L. KENNARD. J. Organometal. Chem. **18**, 243 (1969).
15. D. C. BRADLEY et N. R. KUNCHUR. J. Chem. Phys. **40**, 2258 (1964).
16. K. L. AURIVILLIUS. Acta Chem. Scand. **4**, 1413 (1950).

Can. J. Chem. Downloaded from www.nrcresearchpress.com by 210.87.254.6 on 09/05/12
For personal use only.

Secondary Kinetic Isotope Effects in Bimolecular Nucleophilic Substitutions. V. The Role of the Solvent in the Reaction Between Methyl Iodide and Pyridine[1]

K. T. LEFFEK AND A. F. MATHESON[2]

Chemistry Department, Dalhousie University, Halifax, Nova Scotia

Received September 29, 1971

Secondary kinetic deuterium isotope effects are presented for the reaction of methyl-d_3 iodide and pyridine in four different solvents. Calculations on mass and moment of inertia change with deuteration in the initial state and an assumed tetrahedral transition state, together with internal rotational effects, are used to rationalize the inverse isotope effects. It is concluded from the variation of the isotopic rate ratio, that the transition state structure varies with solvent.

Les effets secondaires isotopiques cinétiques de deuterium sont présentés pour la réaction de l'iodure de méthyle d_3 et la pyridine dans quatre solvants différents. Les calculs de masses et de moments d'inertie qui varient avec la deutération dans l'état initial et un état de transition tétrahédrique supposé, conjointement avec les effets de rotation interne, sont utilisé pour rationaliser les effets isotopiques inverses. On conclut de la variation du rapport des vitesses isotopiques que la structure de l'état de transition varie avec le solvant.

Canadian Journal of Chemistry, **50**, 982 (1972)

Introduction

Several reports of secondary deuterium isotope effects in Menschutkin reactions between alkyl halides and sulfonates and tertiary amines have been made (1–5) and several different approaches have been used to rationalize the inverse isotope effects ($k_H/k_D < 1$) which have been usually observed. All of these have been at least partially successful despite the fact that the role of the solvent has always been assumed to introduce no rate change, an assumption which has some limited experimental basis (6–8). In this paper, secondary isotope effects measured in four different solvents are presented and an attempt is made to account for their magnitude, and at the same time use the rate ratios to draw some general conclusions about the role of the solvent in Menschutkin reactions.

The temperature dependence study of the isotope effect for the reaction of 2-picoline and methyl-d_3 iodide in solvent benzene reported in 1965 (1) gave values of $(\Delta H_D^{\ddagger} - \Delta H_H^{\ddagger})$ and $(\Delta S_D^{\ddagger} - \Delta S_H^{\ddagger})$ which were unusual at the time, in that the rate change was due almost entirely to a difference in the entropies of activation between the normal and deuterated compounds. When a correlation of the enthalpy and entropy contributions to the secondary deuterium isotope effect for 16 nucleophilic substitutions at saturated carbon was made (9), the result which presented the greatest anomaly was that for 2-picoline and methyl iodide.

It may be postulated that the anomalous behavior is due to the unusually non-specific role of the solvent. This is based partly on an analogy with the temperature dependence of the isotope effect of the thermal racemization of 9,10-dihydro-4,5-dimethyl-d_6-phenanthrene in both benzene and *n*-heptane measured by Mislow *et al.* (10). This result was not included in our correlation (9) because the reactions are not nucleophilic substitutions, but if the enthalpy and entropy contributions to the isotope effects for these reactions are plotted, they fall well below both lines, in a qualitatively similar manner to those for the 2-picoline–methyl iodide reaction in benzene. It would seem reasonable to assume that the specific role of the solvent in the racemization reactions would be minimal since the formation of the transition state involves no charge formation or destruction nor any electron redistribution. From the similar isotope effects, it may be inferred that a non-specific role toward the carbon seat of reaction is played by the solvent benzene in the Menschutkin reaction, although this may not be true for all solvents.

[1]Based on part of a thesis submitted by A. F. Matheson in partial fulfillment of the requirements for the degree of Doctor of Philosophy at Dalhousie University, 1969.

[2]Present address: Uniroyal Research Centre, Guelph, Ontario.

Can. J. Chem. Downloaded from www.nrcresearchpress.com by 210.87.254.6 on 09/05/12
For personal use only.

Can. J. Chem. Downloaded from www.nrcresearchpress.com by 210.87.254.6 on 09/05/12
For personal use only.

Origin of the Secondary Isotope Effect in Menschutkin Reactions

Leffek and MacLean (1) suggested that a substantial part of the isotope effect for the reaction of methyl-d_3 iodide and 2-picoline in benzene arose from an increase in the size of the barrier to rotation of the CH_3 and CD_3 groups on passage from the initial state to the transition state, which produced a positive $(\Delta S_D^{\ddagger} - \Delta S_H^{\ddagger})$ and also a positive $(\Delta H_D^{\ddagger} - \Delta H_H^{\ddagger})$ (which cancelled the negative zero-point energy contribution to the latter). At about the same time, Wolfsberg and Stern (11) developed a theoretical treatment which accounted for temperature independent isotope effects in terms of opposing changes in force constants during the activation process. Subsequently Brown and McDonald (4) interpreted secondary isotope effects in general, with particular reference to the reaction of substituted pyridines and methyl iodide, as a manifestation of the steric difference between normal and deuterated compounds. Kaplan and Thornton (5) also proposed a steric explanation for the inverse isotope effect, measured at a single temperature, for the reaction of *N,N*-dimethyl-d_6-aniline and methyl *p*-toluenesulfonate in nitrobenzene, and Leffek and Matheson (9) showed, by a temperature dependence study, that the rate change was predominantly an enthalpy of activation effect. However, the problem of the temperature independent effect (rate change due to entropy of activation effect only) has not been completely solved and we have carried out further calculations on model systems to reassess the contributions from the several sources.

Leffek and MacLean considered the mass and moment of inertia contributions to the isotope effect only qualitatively and assumed them to be small. We have now reconsidered some transition state models and found that if a tetrahedral transition state is assumed, *i.e.* identical to the final state, simply a mirror image of the initial state configuration, significant entropy of activation effects may result. The calculations were made following Wolfsberg and Stern (11) in a manner explained in the previous paper of this series (9). The initial state, CH_3Y, was assumed to have a C—Y bond length of 2.00 Å and the mass of Y was taken as 120.5 a.w.u. 109.5° was used for all the bond angles in the initial state and the transition state. Bond lengths for C—H and C—D were maintained at 1.07 Å (*i.e.* anharmonicity neglected) and atomic masses C = 12.0, H = 1.006, D = 2.012 were used. Table 1 shows some results of these calculations, from which it may be seen that, for this model system, closer approach of the nucleophile (X) gives a more positive value of $\Delta\Delta S_I^{\ddagger}$ and hence of $\Delta\Delta S_{MMI}^{\ddagger}$. Smaller changes in $\Delta\Delta S_{MMI}^{\ddagger}$ are produced by mass variation of X, since $\Delta\Delta S_I^{\ddagger}$ and $\Delta\Delta S_M^{\ddagger}$ vary in an opposing manner. The latter term is dominant, so that the reduction of the mass of X, compared to that of Y, yields a positive $\Delta\Delta S_{MMI}^{\ddagger}$.

TABLE 1. Calculated $\Delta\Delta S^{\ddagger}$ (cal mol^{-1} deg^{-1}) contributions from mass and moment of inertia changes for a nucleophilic substitution with a tetrahedral transition state

Transition state variables				
C—X[a] length (Å)	Mass of X[a] (a.w.u.)	$\Delta\Delta S_I^{\ddagger}$ [b]	$\Delta\Delta S_M^{\ddagger}$ [b]	$\Delta\Delta S_{MMI}^{\ddagger}$ [b]
1.0	120.5	+0.153	0.0	+0.153
2.0	120.5	0.0	0.0	0.0
3.0	120.5	−0.048	0.0	−0.048
2.0	60.25	−0.029	+0.051	+0.022
2.0	120.5	0.0	0.0	0.0
2.0	180.75	+0.013	−0.020	−0.007

[a] X is the attacking nucleophile.
[b] $\Delta\Delta S^{\ddagger} \equiv (\Delta S_D^{\ddagger} - \Delta S_H^{\ddagger})$.

In order to apply these general conclusions to the reaction of methyl iodide with 2-picoline, which is not a single atom nucleophile as used in the above calculation, only the nitrogen atom of the amine was considered, but it was assigned a mass of 93 a.w.u. This cut-off procedure has been discussed by Wolfsberg and Stern (11, 12) in their work with the force constant model. They have shown that this simplifying technique is a useful one in the qualitative understanding of the isotope effect. Making the assumption that the transition state is well advanced towards product, and that specific solvation is negligible, the formation of the transition state in the reaction of amine and methyl iodide will result in a bond contraction from 2.1 (C-1) to 1.47 Å (C—N), and a mass decrease from 127 (iodine) to 93 (2-picoline). Each of these factors will tend to reinforce the other to yield a positive $\Delta\Delta S_{MMI}^{\ddagger}$. It is difficult to give a reliable value for $\Delta\Delta S_{MMI}^{\ddagger}$ but +0.1 cal mol^{-1} deg^{-1} would be a reasonable estimate.

TABLE 2. Second-order rate constants and isotopic rate ratios for the reaction of methyl and methyl-d_3 iodide with pyridine at 50 °C

Solvent	CH_3I 10^4k_2(l mol^{-1} s^{-1}) (± standard error)	CD_3I 10^4k_2(l mol^{-1} s^{-1}) (± standard error)	k_H/k_D (± standard error)
Benzene	0.700[a]	0.761[a]	$0.91_9 \pm 0.002$[a]
Nitrobenzene	20.38 ± 0.17[b]	22.87 ± 0.08	$0.89_1 \pm 0.008$
2-Butanone	7.73 ± 0.07	9.03 ± 0.07	$0.85_7 \pm 0.010$
Ethanol	1.41 ± 0.01	$1.60 \pm 0.00_5$	$0.88_2 \pm 0.006$

[a]Reference 1.
[b]Literature values $10^4k_2 = 23.80$ (ref. 15), 21.30 (ref. 16) l mol^{-1} s^{-1}.

Thus, even though a tetrahedral product-like transition state may not be the most realistic, and there is evidence in the literature that in some solvents it is not (13), it is one possible way to account for part of the experimental value of +0.25 cal mol^{-1} deg^{-1} found for $\Delta\Delta S^{\ddagger}$ for this reaction (1).

The $\Delta\Delta H^{\ddagger}$ value is still best interpreted as a cancellation between a positive component from the changes in the barrier to internal rotation and a negative component from the zero-point energy source. Even with an assumed tetrahedral transition state there is evidence from Raman spectra (14, 15) that a small overall increase in the carbon–hydrogen vibrational frequencies will occur during the activation process.

The Dependence on Solvent of the Secondary Isotope Effect

The postulate that there is no specific involvement of the benzene solvent in reactions of methyl iodide and tertiary amines and that this is the reason why this particular reaction shows a poor correlation on the $\Delta\Delta H^{\ddagger}$ *vs.* $T\Delta\Delta S^{\ddagger}$ plot (9) leads to the conclusion that the secondary isotope effect should change when the solvent is changed to one having greater specific solvation with the transition state. This has been tested using several solvents, two dipolar aprotic solvents and one protic solvent, ethanol, in addition to the original benzene. The results are shown in Table 2. The rate constants for the reaction in benzene and nitrobenzene are in reasonable agreement with previous measurements (16, 17) and the 2-butanone and ethanol constants are of the same order of magnitude as earlier measurements in mixed solvents of acetone–water and ethanol–water (18). It may be noted, although it is not a novel observation, that the reaction rates do not follow the Hughes–Ingold theory of solvent effects (19) in that the reaction is not fastest in the most polar solvent, ethanol, nor do the rates correlate with the dielectric constants of the media. However, the rate is slowest in the least polar solvent, benzene, in agreement with the postulated minimal solvation stabilization of the transition state.

The isotopic rate ratios, also, do not correlate with solvent polarity, the bulk dielectric constant, nor with some of the empirical solvent parameters compiled by Reichardt (20). However, there is some indication of a parallel between the rate ratios and specific solvent–solute interactions. One measure of specific solvent–solute interactions has been advanced by Bellamy *et al.* (21) who measured the frequency shift for the stretching frequency of X—H dipoles between the vapor and dissolved species for a large number of solvents. Using the N—H bond of pyrrole as the X—H dipole the relative frequency shift $10^3\Delta\nu/\nu$, where $\Delta\nu$ is the X—H stretching frequency in the vapor minus that in the solvent, has a value of 20.4 for benzene, 22.9 for nitrobenzene, and 35 to 47 for ketones (39.6 for acetone). Limited though the data are, they do show that the greater the ability of the solvent to interact specifically with a dipole, the larger is the isotope effect. We suggest that as the specific solvent interaction increases as the solvent is changed, the transition state comes earlier on the reaction coordinate, *i.e.* is more like the usual trigonal-bipyramidal S_N2 transition state. Under these circumstances, increased crowding due to stiffening of the out-of-plane vibrational frequencies will render $\Delta\Delta H^{\ddagger}$ increasingly negative, yielding a larger inverse isotope effect.

Thus, the change in kinetic isotope effect with solvent may be interpreted in terms of the

Can. J. Chem. Downloaded from www.nrcresearchpress.com by 210.87.254.6 on 09/05/12
For personal use only.

TABLE 3. Reaction of methyl-d_3 iodide with pyridine in 2-butanone at 50.0 °C. Run 38

Initial concentration pyridine = 9.73×10^{-2} *M*
Initial concentration methyl-d_3 iodide = 2.011×10^{-2} *M*

Time (min)	Product concentration $\times 10^3$ (mol l^{-1})	$10^4 k_2$ (l mol^{-1} s^{-1})
0	0.871	—
6.98	1.568	9.147
10.27	1.872	9.035
12.41	2.067	8.988
14.45	2.250	8.947
16.83	2.467	8.958
18.81	2.644	9.070
21.29	2.870	8.994
24.02	3.115	9.025
25.87	3.281	9.049
28.38	3.504	9.084

Average $k_2 = 9.030 \times 10^{-4}$ (l mol^{-1} s^{-1})

amount of specific solvation of the transition state by the solvent, and the effect that this has upon the geometry of the transition state.

Experimental

Materials

The solvents nitrobenzene and 2-butanone were dried over calcium sulfate, fractionally distilled at atmospheric pressure, and the center cut of the distillates collected. Ethanol was dried by the method of Lund and Bjerrum and distilled.

Commercial methyl iodide and methyl-d_3 iodide were distilled immediately before use. Pyridine was dried first with potassium hydroxide pellets and then with calcium hydride. After fractional distillation the central cut was stored in an opaque container over calcium hydride and under nitrogen.

Kinetics

Each reactant, cooled to minimize volatilization, was weighed and quickly transferred to a 10 ml volumetric flask, dissolved in solvent and made up to the mark. Experiments were performed to determine the initial concentration of alkyl halide by titration, but the direct weighing technique gave more consistent and reliable results. The reaction mixture was prepared by mixing the appropriate volumes of the 10 ml stock solutions and injecting the mixture into a conductivity cell of 5 ml capacity (LKB-Producter AB Sweden). After temperature equilibration in a constant temperature oil-filled bath, conductivity measurements were taken at appropriate intervals of time and converted to concentrations by means of a previously determined calibration curve. The calibration curve had been set up using both methylpyridinium iodide and methyl-d_3 pyridinium iodide and the points for both compounds fell on a single smooth curve. Second-order rate constants were calculated from the integrated second-order equation.

A preliminary investigation for each reaction series was made to determine the optimum molar ratio of the reactants and the percent reaction range to yield consistent and reproducible rate constants. Identical conditions were then used for the deuterated analogue. The initial concentration of methyl iodide was always 2×10^{-2} *M* and the initial pyridine concentration was 0.1 *M* in nitrobenzene and 2-butanone and 0.2 *M* in ethanol. The reaction range, expressed as a percentage of initial methyl iodide consumed was 15–50% in nitrobenzene, 5–18% in 2-butanone, and 15–30% in ethanol. The second-order rate constants reported in Table 2 are the means of from two to four runs carried out for each reaction. A sample run is given in Table 3.

The authors are grateful for financial support by the National Research Council of Canada and for an NRCC studentship to A.F.M.

1. K. T. LEFFEK and J. W. MACLEAN. Can. J. Chem. **43**, 40 (1965).
2. J. J. ELLIOT and S. F. MASON. Chem. and Ind. 488 (1959).
3. E. S. LEWIS and W. J. FARRISEY. *Quoted in* E. S. Lewis. Tetrahedron, **5**, 142 (1959).
4. H. C. BROWN and G. J. MCDONALD. J. Am. Chem. Soc. **88**, 2514 (1966).
5. E. R. KAPLAN and E. R. THORNTON. J. Am. Chem. Soc. **89**, 6644 (1967).
6. G. J. FRISONE and E. R. THORNTON. J. Am. Chem. Soc. **90**, 1211 (1968).
7. H. STRECKER and H. ELIAS. Chem. Ber. **102**, 1270 (1969).
8. S. SELTZER and A. A. ZAVITSAS. Can. J. Chem. **45**, 2023 (1967).
9. K. T. LEFFEK and A. F. MATHESON. Can. J. Chem. **49**, 439 (1971).
10. K. MISLOW, R. GRAEVE, A. J. GORDON, and G. H. WAHL. J. Am. Chem. Soc. **86**, 1733 (1964).
11. M. WOLFSBERG and M. J. STERN. Pure and Appl. Chem. **8**, 225 (1964).
12. M. WOLFSBERG and M. J. STERN. J. Chem. Phys. **45**, 4105 (1966).
13. Y. C. MAC, W. A. MILLEN, A. J. PARKER, and D. W. WATTS. J. Chem. Soc. B, 525 (1967).
14. J. T. EDSALL. J. Chem. Phys. **5**, 225 (1937).
15. J. T. EDSALL and H. SCHEINBERG. J. Chem. Phys. **8**, 520 (1940).
16. H. W. THOMPSON and E. E. BLANDON. J. Chem. Soc. 1237 (1933).
17. H. C. BROWN and A. CAHN. J. Am. Chem. Soc. **77**, 1715 (1955).
18. R. A. FAIRCLOUGH and C. N. HINSHELWOOD. J. Chem. Soc. 538 (1937).
19. C. K. INGOLD. Structure and mechanism in organic chemistry. 2nd Ed. Cornell University Press, Ithaca, N.Y., 1969. p. 457.
20. C. REICHARDT. Angew. Chem. Int. Ed. **4**, 29 (1965).
21. J. BELLAMY, H. E. HALLAM, and R. L. WILLIAMS. Trans. Faraday Soc. **54**, 1120 (1958).

Can. J. Chem. Downloaded from www.nrcresearchpress.com by 210.87.254.6 on 09/05/12
For personal use only.

Secondary Kinetic Isotope Effects in Bimolecular Nucleophilic Substitutions. VI. Effect of α and β Deuteration of Alkyl Halides in their Menschutkin Reactions with Pyridine in Nitrobenzene[1]

K. T. LEFFEK AND A. F. MATHESON[2]

Chemistry Department, Dalhousie University, Halifax, Nova Scotia

Received September 29, 1971

A survey of kinetic, secondary deuterium isotope effects, for α, β, and γ deuterated alkyl halides reacting with pyridine in nitrobenzene solvent has been made. α-Deuterium effects have been measured for eight compounds, β-deuterium effects for four compounds, and one rate ratio for γ-deuteration is reported. The possible errors in the rate ratios for β-deuterated compounds, resulting from the elimination side reaction have been determined. The results are discussed in terms of transition state structure.

Une étude sur la cinétique des effets isotopiques secondaires du deutérium a été effectuée sur les halogénures d'alkyle α, β, et γ deutérés qui réagissent avec la pyridine dans le nitrobenzène. Les effets du deutérium en α ont été mesurés au moyen de huit composés, les effets du deutérium en β au moyen de quatre composés, et on rapporte un rapport de vitesse pour la deutération en γ. Les erreurs possibles dans les rapports de vitesse pour les composés β-deutérés, et qui résultent d'une réaction annexe d'élimination, ont été déterminées. Les résultats sont discutés en fonction de la structure de l'état de transition.

Canadian Journal of Chemistry, **50**, 986 (1972)

Introduction

Although many secondary deuterium isotope effects have been measured for nucleophilic substitutions at saturated carbon, systematic studies involving changes in the leaving group, the alkyl group, and the position of deuteration are not common. Robertson and co-workers (1–4) have provided the most complete set of data for solvolysis reactions in water of alkyl halides and sulfonates, and Brown and McDonald (5) have reported a series of measurements on various substituted deuterated pyridines reacting with alkyl iodides in nitrobenzene solvent. This paper presents a set of isotopic rate ratios for the reaction of a single nucleophile pyridine, with various deuterated alkyl compounds in the same solvent, nitrobenzene.

Results and Discussion

α-Deuterium Effects

In Table 1 the second-order rate constants and isotopic rate ratios are shown for α-deuterated alkyl iodides, bromides, and tosylate. The reactions were followed conductometrically for all but the methyl bromide reaction, for which the sealed tube technique was used with analysis for bromide ion by titration. All of the rate constants are at 50 °C, except for ethyl bromide, which was run at 35 °C.

The result of changing the leaving group from iodide, to bromide, to tosylate is to decrease the isotope effect, *i.e.* to bring the rate ratio closer to unity. This change is analogous to the behavior of methyl compounds solvolyzing in water (1) and if the rate ratios are plotted against $E_n - E_l$, where E_n is the Edward's nucleophilicity factor (6, 7) of the incoming nucleophile and E_l that of the leaving group, the three points yield a line parallel but not coincident with the one plotted by Seltzer and Zavitsas (8, 9). The order magnitude of the isotope effect (I > Br > OTs for inverse effects or OTs > Br > I for normal effects) has been explained (10, 11) for limiting solvolytic reactions proceeding via ion-pairs, in terms of the effect of the leaving group on the initial state. However, the non-solvolytic Menschutkin reaction is known to pass through an S_N2 transition state, and this transition state might be expected to yield a significant contribution to the isotope effect. In another non-solvolytic reaction, that of thiosulfate ion with methyl-d_3 iodide, bromide, and tosylate, the rate ratios contrast with the series above in

[1]Based on part of a thesis submitted by A. F. Matheson in partial fulfillment of the requirements for the Ph.D. degree at Dalhousie University, 1969. Presented in part at the 50th Annual Conference of the Chemical Institute of Canada, Toronto, Ontario, June 1967.

[2]Present address: Uniroyal Research Centre, Guelph, Ontario.

Can. J. Chem. Downloaded from www.nrcresearchpress.com by 210.87.254.40 on 09/05/12
For personal use only.

TABLE 1. Second-order rate constants and α-deuterium isotope effects for reactions of alkyl compounds with pyridine at 50.0 °C in nitrobenzene solvent

Alkyl compound	$10^6 k_H$(l mol^{-1} s^{-1}) (± standard error)	$10^6 k_D$(l mol^{-1} s^{-1}) (± standard error)	k_H/k_D (± standard error)	(k_H/k_D) per D
Methyl iodide*	2038 ± 17*	2287 ± 8*	$0.89_1 \pm 0.008$*	0.96_2
Methyl bromide	968 ± 3	1043 ± 3	$0.92_8 \pm 0.003$	0.97_5
Methyl tosylate	$715._3 \pm 4$	$727._8 \pm 7$	$0.98_2 \pm 0.01$	0.99_4
Ethyl iodide	$151._5 \pm 0.1$	$156._7 \pm 0.3$	$0.96_7 \pm 0.003$	0.98_3
Ethyl bromide†	$8.8_8 \pm 0.05$†	$9.1_8 \pm 0.03$†	$0.96_7 \pm 0.006$†	0.98_3
n-Propyl bromide	$13.2_6 \pm 0.15$	$13.8_1 \pm 0.15$	$0.96_0 \pm 0.015$	0.98_0
Isopropyl iodide‡	$9.44_4 \pm 0.011$‡	$9.40_5 \pm 0.01$‡	$1.00_4 \pm 0.002$‡	1.00_4
Isopropyl bromide	$0.95_2 \pm 0.009$	$0.99_3 \pm 0.011$	$0.95_8 \pm 0.014$	0.95_8

*Reference 17.
†Rate constants measured at 35.02 °C.
‡Rate constants measured at 49.92 °C.

giving values of 1.058, 1.031, and 1.12, respectively (9).

The ethyl-αd_2 iodide and bromide reactions give exactly the same rate ratio of 0.967 and isopropyl-αd_1 iodide gives a more normal ratio than the corresponding bromide. Thus the change in isotope effect between iodide and bromide leaving groups depends upon the alkyl radical and, therefore, is probably related to a large extent to the control of the transition state structure by the alkyl radical.

The trend towards a normal (> 1) rate ratio with α-methylation of the alkyl group for a constant leaving group is also observed in Table 1 and appears to be a general phenomenon (1, 2). This has been interpreted in zero-point energy terms, assuming that the $\Delta H^{\ddagger}$ isotope effect dominates that of $\Delta S^{\ddagger}$, which is true for several S_N2 reactions (12–14). The argument is that a tight S_N2 transition state, such as that for a methyl compound leads to an increase in the C—H bending frequencies during activation, which in turn leads to a faster rate for the deuterium compound than for the protium compound (15). A looser transition state resulting from charge delocalization within a carbon skeleton such as an isopropyl group, yields less increase (or in some cases a decrease) in the C—H (C—D) bending modes of vibration on going from the initial to the transition state and therefore a smaller inverse isotope effect. This implies that for isopropyl compounds, bond breaking is more important than bond making and that the entering and leaving groups are held, presumably by the steric effects of the methyl groups, at a greater distance from the α-C—H (or C—D) bond, which would, therefore, be relatively free in the transition state with respect to the bending vibrations. Thus the methyl halides have tighter transition states than ethyl or isopropyl halides and larger inverse isotope effects and, of the two halides, the larger iodide has the greater inhibition of the C—H and C—D bending vibrations in the transition state and hence the larger inverse isotope effect. For the methyl compounds, the more polarizable the leaving group, I > Br > OTs on the Edwards *E* scale (6, 7), the greater will be the degree of bond making in the transition state and hence the more crowded it will be, giving rise to a larger isotope effect.

The inverse isotope effect observed with isopropyl-αd_1 bromide may be due to the fact that a larger excess (eightfold) of nucleophile was used for this compound than for the others, which was necessitated by practical reasons. With such a large excess of pyridine the reaction tends to be a pyridinolysis, since the pyridine will tend to solvate the transition state preferentially, compared to nitrobenzene. This effective change to a solvent of more specific solvating power (16) will give a transition state for the reaction more reactant-like (17) and therefore more crowded with a larger isotope effect.

β-Deuterium Effects

Secondary β-deuterium isotope effects in S_N2 reactions present a problem in that some amount of E2 side reaction usually occurs concurrently and the elimination of a β-hydrogen (or deuterium) in the E2 reaction introduces a primary deuterium isotope effect of large magni-

Can. J. Chem. Downloaded from www.nrcresearchpress.com by 210.87.254.40 on 09/05/12
For personal use only.

TABLE 2. Product analyses and the percentage of elimination in the reactions of isopropyl halides with pyridine in nitrobenzene at 50 °C

Isopropyl halide	$10^3[HX]$* (mol l^{-1})	$10^3[X_2]$* (mol l^{-1})	$10^3[X^-]$* (mol l^{-1})	$\frac{100 \times E2}{E2 + S_N2}$ (%)†
Iodide	0.668	0.141	47.4_5	2.0
Bromide	0.707	—	94.8_2	0.7_4

*X ≡ Halogen

†Calculated from $\frac{100([HX] + 2[X_2])}{[X^-] + 2[X_2]}$

tude, typically a factor of 4 to 8 for the rate ratio (18, 19) although much larger values have been observed (20–22).

While the percentage of E2 to the total reaction is expected to be small for the quaternization reaction (23), it is apparent that even a small percentage could give rise to misleading, small, overall normal isotope effects. In order to determine the magnitude of this source of error a careful product analysis was carried out for the reactions of isopropyl iodide and bromide, for which the E2 side reaction is known to be larger than for the ethyl and *n*-propyl halides (24). The total product formed was obtained by potentiometric titration with aqueous silver nitrate and the elimination products were estimated by a non-aqueous acid–base titration following Brown and Cahn (25) plus, in the case of the iodide, a spectrophotometric determination of iodine which was presumed to have been formed by oxidation of some of the hydriodic acid (25). The analytical results are compiled in Table 2. As expected, the proportion of elimination is greater for the iodide than for the bromide (24). The value of 2% for the iodide may be compared with Brown and Cahn's approximate figure (25) of 3% for equal initial molar concentrations of methyl substituted pyridines and isopropyl iodide in the same solvent.

The possible error introduced into the secondary isotope effect by the elimination reaction may be estimated as follows:

$$S_N2 \text{ rate} = k_s[RX][C_5H_5N]$$

$$E2 \text{ rate} = k_E[RX][C_5H_5N]$$

$$\text{Observed rate} = k_{obs}[RX][C_5H_5N]$$

$$= (k_E + k_s)[RX][C_5H_5N]$$

$$[1] \qquad \left(\frac{k_H}{k_D}\right)_{obs} = \frac{k_E^H + k_s^H}{k_E^D + k_s^D}$$

If the secondary isotope effect, k_s^H/k_s^D, is assumed to be unity and the primary isotope effect k_E^H/k_E^D is written 'x', eq. 2 is obtained by dividing the numerator and denominator of eq. 1 by k_E^D.

$$[2] \qquad \left(\frac{k_H}{k_D}\right)_{obs} = \frac{x(k_s^H/k_E^H + 1)}{x.k_s^H/k_E^H + 1}$$

The numerical value of k_s^H/k_E^H for isopropyl iodide and bromide may be calculated from the figures in Table 2 as 49 and 133, respectively.

The observed rate ratio for isopropyl iodide, assuming no secondary isotope effect and a typical primary isotope effect ($x = 7$) would be $(k_H/k_D)_{obs} = 1.017$ and the largest possible ratio ($x = 700$) would be 1.020. For isopropyl bromide primary isotope effects of 7 and 700 would give rate ratios of 1.006 and 1.007. Therefore, for these small amounts of elimination the maximum error is about the same percentage as the elimination is of the total reaction.

Second-order rate constants for some β-deuterated alkyl halides and their isotopic rate ratios are shown in Table 3. In determining the isotope effects, the normal compound was always run simultaneously with the deuterated sample to eliminate errors such as temperature fluctuation and where the α and β effects were measured at widely separated time intervals, slight differences in k_H are noted. The corrected rate ratio was calculated assuming a primary isotope effect on the elimination reaction of 7. The elimination percentage was not investigated for the ethyl and *n*-propyl halides since it is expected to be very small indeed for these compounds (24).

Can. J. Chem. Downloaded from www.nrcresearchpress.com by 210.87.254.40 on 09/05/12
For personal use only.

TABLE 3. Second-order rate constants and isotopic rate ratios for the reaction of β-deuterated alkyl halides with pyridine at 50.0 °C in nitrobenzene solvent

	$10^6 k_H$(l mol^{-1} s^{-1}) (± standard error)	$10^6 k_D$(l mol^{-1} s^{-1}) (± standard error)	k_H/k_D (observed)	k_H/k_D* (corrected)	(k_H/k_D) per D (corrected)
Ethyl iodide	151.5±0.1	149.6±0.9	$1.01_3 \pm 0.006$	—	1.00_4
n-Propyl bromide	13.26±0.15	13.23±0.14	$1.00_2 \pm 0.015$	—	1.00_1
Isopropyl iodide	9.66±0.04	9.23±0.04	$1.04_7 \pm 0.006$	1.03_0	1.00_5
Isopropyl bromide	0.972±0.008	0.885±0.005	$1.09_9 \pm 0.011$	1.09_1	1.01_5

*Corrected assuming a primary isotope effect of 7 for the elimination reaction.

The results in Table 3 show that only in the isopropyl halides is the β-deuterium isotope effect significant, with the bromide giving a rate decrease with deuteration three times larger than the iodide. The direction and magnitude of the effects are not surprising in comparison to those observed in the water solvolysis reactions (4). Since the hydrolysis reactions give a temperature independent isotope effect for isopropyl compounds (26), it is not possible to specify the origin of the isotope effects in the pyridine reaction. However, that normal effects are observed does allow the conclusion that within the S_N2 mechanism there is a trend to a less crowded (or possibly a more S_N1-like) transition state for secondary compounds than for primary compounds, since this type of structure is required for normal isotope effects whether the explanation is made in terms of the hyperconjugative effects (27) or in terms of internal rotational contributions (26, 28).

The greater magnitude of the rate change for the bromide leaving group than for the iodide again indicates, as found for the α-effect that the iodide has a tighter, more crowded transition state. This trend is in agreement with the β-effect observed by Strecker and Elias (29) for the radiochloride exchange with isopropyl chloride ($k_H/k_D = 1.12$).

γ-Deuterium Effect

The relative rates of reaction were measured for *n*-propyl-γd_3 bromide and its normal analogue giving 13.32 and 13.26×10^{-6} l mol^{-1} s^{-1} respectively, possibly an inverse isotope effect of about $\frac{1}{2}$%, but the two rates are barely significantly different. This result is very similar to the γ-effect observed for *n*-propyl-γd_3 bromide reacting with thiosulfate ion (30) in 50% v/v ethanol–water $k_H/k_D = 0.990$ and very much smaller than the 8% inverse effect found for the same compound solvolyzing in water (3).

From these three results there appears to be an approximate correlation between the β and γ isotope effects with the β rate ratio becoming larger than unity as the γ rate ratio becomes less than unity. This suggests that both these effects depend on transition state geometry and is in accord with the earlier explanations (3), which postulated that the greater the β-hydrogen atom interaction with the central carbon atom p-orbital in the transition state (hyperconjugation), the greater would be the steric inhibition of the vibrations of the γ-hydrogens. The amount of hyperconjugation will be directly related to the degree of incipient positive charge on the central carbon atom in the transition state. Thus, for the three S_N2 reactions of *n*-propyl bromide, it may be concluded that the pyridine reaction has no such charge (or no S_N1 character or no ion-pair character), the thiosulfate ion reaction has a very small amount, and the hydrolysis a slightly larger amount.

Experimental

Materials

Nitrobenzene solvent was dried over anhydrous calcium sulfate and distilled at atmospheric pressure, boiling range 210.5–211 °C. Pyridine was dried with potassium hydroxide pellets and then with calcium hydride before fractional distillation. Material boiling between 115.2 and 115.7 °C was collected and stored in an opaque container over calcium hydride and under nitrogen.

Methyl bromide, previously cooled to −80° in an acetone–Dry Ice slurry was allowed to volatilize at 25–30°, passed through wash towers of concentrated sulfuric acid and glass wool, and collected and stored at −80°. All the other alkyl halides were dried over anhydrous calcium sulfate and fractionally distilled, after which they were stored in opaque containers in an atmosphere of nitrogen and over copper. Methyl tosylate was distilled under vacuum.

Can. J. Chem. Downloaded from www.nrcresearchpress.com by 210.87.254.40 on 09/05/12
For personal use only.

Can. J. Chem. Downloaded from www.nrcresearchpress.com by 210.87.254.40 on 09/05/12
For personal use only.

Commercial samples of methyl-d_3 bromide, ethyl-αd_2 iodide and bromide, *n*-propyl-αd_2 bromide, *n*-propyl-βd_2 bromide, isopropyl-βd_6 iodide and bromide, and *n*-propyl-γd_3 bromide were used without further purification. Commercial methyl-d_3 iodide was redistilled and stored in opaque sealed tubes. Methyl-d_3 tosylate, prepared by Jackson (9), was redistilled under vacuum. Ethyl-βd_3 iodide was prepared by reaction of ethyl-βd_3 tosylate (0.01 mol) with a slurry of dry potassium iodide (0.03 mol) in diethylene glycol (2 ml). The product was distilled from the reaction mixture at 45–50 °C under reduced pressure and collected in a liquid N_2 trap. After several redistillations the ethyl-βd_3 iodide was stored in an opaque sealed tube, under nitrogen, over copper. The yield was 59%. The absence of hydrogen on the β-carbon atom was confirmed by n.m.r. spectroscopy.

Isopropyl-αd_1 halides were prepared from isopropyl-αd_1 alcohol (Merck, Sharp & Dohme Ltd.) via the *p*-bromobenzenesulfonate (brosylate). The general method of Sekera and Marvel (31) was used to convert the alcohol to the brosylate, by reaction with *p*-bromobenzenesulfonyl chloride in anhydrous pyridine at −5 °C. A 57% yield of brosylate was obtained, melting at 31–32 °C. Isopropyl-αd_1 brosylate was converted to the iodide and bromide by reaction with the appropriate solid potassium halide, as described for ethyl-βd_3 iodide. Crude yields of about 60% were obtained and the halides were purified for kinetic work by g.l.c. using a very low column temperature. The deuteration of the compounds was confirmed by the n.m.r. spectra.

Analyses for Elimination Products

Ten sealed tubes each containing 4.402 ml of reaction mixture were prepared and allowed to react at 50° for about ten half-lives. For the isopropyl iodide reaction the substrate concentration was 0.0483 *M* and that of the pyridine 0.227 *M*, with a reaction time of 39 days. The corresponding figures for the isopropyl bromide reaction were 0.0973, 0.778 *M*, and 117 days. The total halide concentrations were determined by potentiometric titration against standard silver nitrate solution of approximately the same molarity as that of the pyridinium halide. Sharp end-points were obtained using wet acetone as solvent. Both reactions were found to be about 98% complete with respect to the isopropyl halide.

The hydrohalic acid concentrations were determined by potentiometric titration of the sample against potassium hydroxide in isopropanol solvent under an atmosphere of nitrogen. Blank titrations were run and the analyses corrected.

In the isopropyl iodide reaction a visible concentration of iodide was produced and this was estimated spectrophotometrically. A calibration curve of $\log_{10}$ (% transmittance), at a wavelength of 480 nm, *vs*, iodine concentration was set up by preparing solutions of iodine in a mixture of *N*-ethylpyridinium iodide and pyridine in nitrobenzene. This graph was linear. The ethyl product was used to stimulate the reaction mixture rather than the isopropyl compound because solutions of isopropylpyridinium iodide tend to redden on standing. Thus the iodine concentration recorded in Table 2 may have come from some decomposition of the substitution product as well as the elimination reaction, and the percentage elimination is, therefore, a maximum figure.

Kinetic Measurements

The runs were followed conductometrically in a manner very similar to that previously described (17), except for those involving methyl bromide. A calibration curve was constructed for each alkyl halide reaction and they were all very similar in form to that for trimethylphenylammonium tosylate in nitrobenzene (14). The conductivities were converted to concentrations and the second-order rate constants were calculated from the integrated second-order equation. The kinetics were followed to various reaction percentages up to 50% for most of the alkyl halides, but only up to 10% for the isopropyl compounds. The pyridine was always in excess, ranging from a factor of 2 to a factor of 8.

The methyl bromide runs were carried out using a sealed tube technique, similar to that described previously (28).

The authors are grateful for financial support by the National Research Council of Canada and for an NRCC Studentship to A.F.M.

1. J. A. Llewellyn, R. E. Robertson, and J. M. W. Scott. Can. J. Chem. **38**, 222 (1960).
2. K. T. Leffek, J. A. Llewellyn, and R. E. Robertson. Can. J. Chem. **38**, 1505 (1960).
3. K. T. Leffek, J. A. Llewellyn, and R. E. Robertson. J. Am. Chem. Soc. **82**, 6315 (1960).
4. K. T. Leffek, J. A. Llewellyn, and R. E. Robertson. Can. J. Chem. **38**, 2171 (1960).
5. H. C. Brown and G. J. McDonald. J. Am. Chem. Soc. **88**, 2514 (1966).
6. J. O. Edwards. J. Am. Chem. Soc. **76**, 1540 (1954).
7. J. O. Edwards. J. Am. Chem. Soc. **78**, 1819 (1956).
8. S. Seltzer and A. A. Zavitsas. Can. J. Chem. **45**, 2023 (1967).
9. G. E. Jackson and K. T. Leffek. Can. J. Chem. **47**, 1537 (1969).
10. V. J. Shiner, Jr., M. W. Rapp, E. A. Halevi, and M. Wolfsberg. J. Am. Chem. Soc. **90**, 7171 (1968).
11. V. J. Shiner, Jr. and W. Dowd. J. Am. Chem. Soc. **93**, 1029 (1971).
12. A. V. Willi and C. M. Won. J. Am. Chem. Soc. **90**, 5999 (1968).
13. A. V. Willi and C. M. Won. Can. J. Chem. **48**, 1452 (1970).
14. K. T. Leffek and A. F. Matheson. Can. J. Chem. **49**, 439 (1971).
15. L. Melander. Isotope effects on reaction rates. The Ronald Press Co., New York, N.Y. 1960. Chapt. 2.
16. J. Bellamy, H. E. Hallam, and R. L. Williams. Trans. Faraday Soc. **54**, 1120 (1958).
17. K. T. Leffek and A. F. Matheson. Can. J. Chem. This issue.
18. D. V. Banthorpe. Reaction mechanisms in organic chemistry. *Edited by* E. D. Hughes. Vol. II. Elimination reactions. Elsevier Publishing Co., New York, N.U., 1963. p. 18.
19. W. H. Saunders, Jr., D. G. Bushman, and A. F. Cockerill. J. Am. Chem. Soc. **90**, 1775 (1968).
20. E. S. Lewis and L. H. Funderburk. J. Am. Chem. Soc. **86**, 2531 (1964).
21. E. S. Lewis and L. H. Funderburk. J. Am. Chem. Soc. **89**, 2322 (1967).

22. R. P. BELL and D. M. GOODALL. Proc. R. Soc. (Lond.). *A***294**, 273 (1966).
23. Reference 18. p. 29.
24. J. HINE. Physical organic chemistry. *2nd Ed.* McGraw-Hill, New York, N.Y., 1962. p. 202.
25. H. C. BROWN and A. CAHN. J. Am. Chem. Soc. **77**, 1715 (1955).
26. K. T. LEFFEK, R. E. ROBERTSON, and S. E. SUGAMORI. Can. J. Chem. **39**, 1989 (1961).
27. Reference 15. p. 91.
28. K. T. LEFFEK and J. W. MACLEAN. Can. J. Chem. **43**, 40 (1965).
29. H. STRECKER and H. ELIAS. Chem. Ber. **102**, 1270 (1969).
30. K. T. LEFFEK. Can. J. Chem. **42**, 851 (1964).
31. V. C. SEKERA and C. S. MARVEL. J. Am. Chem. Soc. **55**, 345 (1933).

Can. J. Chem. Downloaded from www.nrcresearchpress.com by 210.87.254.40 on 09/05/12
For personal use only.

Kinetic Study of the Pyrolysis of Formaldehyde

C. J. CHEN AND D. J. MCKENNEY
Department of Chemistry, University of Windsor, Windsor, Ontario
Received August 17, 1971

Kinetics of the thermal decomposition of pure formaldehyde were studied over a temperature range of 466–516 °C and a pressure range of ~50–160 Torr. Arrhenius parameters and rate laws were determined for carbon monoxide, hydrogen and methanol as follows:

$$\frac{d[CO]}{dt} = [10^{11.8\pm0.4} \exp(-34\,400 \pm 1\,300/RT)][CH_2O]^{1.8}$$

$$\frac{d[H_2]}{dt} = [10^{8.7\pm1.0} \exp(-34\,000 \pm 3\,600/RT)][CH_2O]^{1.6}$$

$$\frac{d(CH_3OH)}{dt} = [10^{12.6\pm0.9} \exp(-36\,800 \pm 3\,600/RT)][CH_2O]^2$$

A mechanism is postulated which is qualitatively consistent with the experimental results but the activation energy for reaction 1

[1] $$2CH_2O \rightarrow CH_2OH + CHO \quad E = 37 \text{ kcal/mol}$$

is ~15 kcal/mol lower than predicted from recent thermochemical data, suggesting the possibility of a heterogeneous reaction.

Les cinétiques de la décomposition thermique du formaldéhyde pur sont étudiées dans un intervalle de température de 466–516 °C et un intervalle de pression de 50–160 Torr. Les paramètres d'Arrhénius et les lois de vitesse sont déterminés pour le monoxyde de carbone, l'hydrogène et le méthanol comme suit:

$$\frac{d[CO]}{dt} = [10^{11.8\pm0.4} \exp(-34\,400 \pm 1\,300/RT)][CH_2O]^{1.8}$$

$$\frac{d[H_2]}{dt} = [10^{8.7\pm1.0} \exp(-34\,000 \pm 3\,600/RT)][CH_2O]^{1.6}$$

$$\frac{d(CH_3OH)}{dt} = [10^{12.6\pm0.9} \exp(-36\,800 \pm 3\,600/RT)][CH_2O]^2$$

Un mécanisme est admis qui est qualitativement compatible avec les résultats expérimentaux mais l'énergie d'activation pour la réaction 1

[1] $$2CH_2O \rightarrow CH_2OH + CHO \quad E = 37 \text{ kcal/mol}$$

est ~15 kcal/mol plus faible que prévu à partir des récents résultats thermochimiques suggérant la possibilité d'une réaction hétérogène.

Canadian Journal of Chemistry, **50**, 992 (1972)

Introduction

In spite of the fact that formaldehyde is an important intermediate in many gas phase reactions (1–4) the detailed kinetics and mechanism of the pyrolysis is not completely established. Many photochemical investigations have been made (*e.g.* ref. 5) yet considerable doubt remains with regard to specific kinetic and thermochemical values related to CH_2O, CHO, CH_2OH, etc. (6).

The major process in the thermal decomposition is clearly a free radical chain reaction yielding CO and H_2 at temperatures above ~450 °C (7). Methanol is a relatively minor product which becomes increasingly important as the temperature is decreased (8). Klein *et al.* (7) proposed that methanol is produced by a homogeneous molecular reaction, whereas Calvert and Steacie (9) suggested a heterogeneous process. Gay *et al.* (10) detected CH_3O radicals mass spectrometrically at shock tube temperatures.

There are significant discrepancies in the measured activation energies. Fletcher (11) obtained 44.5 kcal/mol at 783–883 °K, while Gay *et al.* (10) calculated a value of 27.8 kcal/mol at 1535–2100 °K. Longfield and Walters (8) obtained 31 kcal/mol for methanol formation

Can. J. Chem. Downloaded from www.nrcresearchpress.com by 210.87.254.105 on 09/05/12
For personal use only.

Can. J. Chem. Downloaded from www.nrcresearchpress.com by 210.87.254.105 on 09/05/12
For personal use only.

at 666–731 °K. A simple Rice–Herzfield mechanism predicts an activation energy greater than 60 kcal/mol and does not account for CH_3OH formation.

The decomposition was shown to be second-order in the shock-tube work, approximately second-order at lower temperatures, and all mechanistic interpretations have been made on the assumption of straightforward second-order kinetics.

This work was undertaken with the intention of resolving some of the questions pertaining particularly to the low (< 700 °C) temperature results.

Experimental

Experiments were carried out in a conventional static vacuum system similar to that previously described (12). Formaldehyde was prepared by heating paraformaldehyde (Fisher "purified") under vacuum following an adaptation of Spence and Wild's (13) procedure. The storage vessel and connecting tubing were thoroughly dried and degassed using a yellow flame while pumping prior to the admission of formaldehyde. After six distillations, freshly prepared formaldehyde was stored at − 196 °C.

Carbon monoxide was analyzed by gas chromatography using a thermal conductivity detector and a 6 ft, 1/4 in. i.d. molecular sieve 5A column at 90 °C. Hydrogen yields were calculated by difference from pressure measurements of the non-condensible fraction. CH_2O was analyzed on a 6 ft, 1/4 in. Polypak column at 90 °C, using the thermal conductivity detector and also along with the CH_3OH determinations using a flame ionization detector and an ethofat (10% supported on Chromosorb T) column at 115 °C (14).

Pyrolyses were carried out over a temperature range of 466–516 °C (± 0.25 °C). No detectable temperature gradient over the length of reaction vessel was observed. The reactor was a 277 cc quartz cylinder, $S/V \simeq 1.3\ cm^{-1}$, and dead space < 2%.

"Conditioning" was accomplished by twice washing with hot (~ 80 °C) concentrated HNO_3, returning the vessel to the furnace and pumping for several hours. After a few runs the results became fully reproducible.

Between runs the reactor was evacuated to $< 10^{-4}$ Torr.

Results[1]

Virtually no polymerization took place in the storage vessel for periods of many weeks provided it remained condensed at − 196 °C. Slight polymerization occurred however, during the periodic warming of the trap when samples were taken for reaction. Analyses of the reactant gas by g.c. indicated < 0.01% H_2O and < 0.05% CH_3OH present as impurities. These could not be removed by as many as six distillations. A thin polymer film slowly accumulated (particularly) in the traps of the analytical system.[2]

In addition to CO, H_2, and CH_3OH, slight traces of two unidentified compounds (apparently secondary products) formed at rates of $< 10^{-11}$ mol/cc s were found among the products. Compounds looked for and *not* found were glyoxal, carbon dioxide, formic acid, dimethyl ether, and methane. Minor polymerization processes in the analytical system hindered precise analyses of small quantities of CH_3OH, yields of which were shown to be a function (exponential or higher order) of the length of time the products were held in the cold traps prior to g.c. analysis. For example the measured CH_3OH yield decreased by > 40% when the analysis was delayed by ~ 40 min. Since the amount of CH_2O was always many orders of magnitude larger, a relatively small loss by polymerization of the aldehyde was hardly noticeable but resulted in a major loss of CH_3OH. Similar decreases were observed for the secondary products. In addition, loss rates were not always reproducible. As a result a systematic study of secondary products was not attempted.

In the case of the CH_3OH, enough analyses were carried out to obtain a rate constant for a temperature of 418 °C. Otherwise estimates were made based on the difference between carbon monoxide and hydrogen yields. Consideration of the stoichiometric equations,

$$CH_2O \rightarrow CO + H_2$$
$$2CH_2O \rightarrow CH_3OH + CO$$

shows any excess of CO to be equal to the yield of CH_3OH.

Initial rates of carbon monoxide and hydrogen were calculated from slopes of yield–time plots. Figure 1 shows typical plots for carbon monoxide for five different initial pressures at 516 °C. Reaction times were generally varied from 6 to 120 s depending on the reaction rate. Decompositions were always < 5%. All plots showed good linearity, but extrapolated through a positive intercept (with the exception of CH_3OH

[1]Tables of analytical and kinetic data have been placed in the Depository of Unpublished Data, National Science Library, National Research Council, Ottawa, Canada K1A 0S2. Photocopies may be obtained upon request to the Depository.

[2]Polymerization is facilitated by adsorbed water and methanol (15).

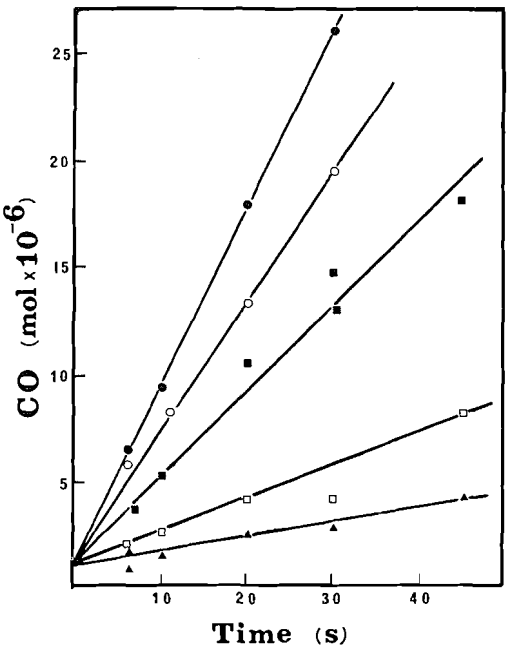

FIG. 1. Yield–time plot for carbon monoxide at 516.6 °C over five different initial formaldehyde pressures (Torr). ● 162.0; ○ 143.5; ■ 115.0; □ 71.0; ▲ 50.0.

which passed through the origin. Double logarithmic plots of initial rate *vs.* formaldehyde concentration had slopes of 1.8 ± 0.03 for carbon monoxide and 1.6 ± 0.04 for hydrogen. Similar plots for estimated methanol production showed an order of 2.0 ± 0.05. (Error limits indicate maximum uncertainty in slopes.) At higher pressures of formaldehyde the yields of carbon monoxide were approximately double those of hydrogen but the ratio decreased to about 1.3 at 50 mm pressure.

Arrhenius plots (Fig. 2) yielded the following rate constants for CO, H_2, and CH_3OH yields.

$$k_{CO} = 10^{11.8 \pm 0.4}\, e^{\frac{-34\,400 \pm 1\,300}{RT}}\ \text{cc}^{0.8}/\text{mol}^{0.8}\ \text{s}$$

$$k_{H_2} = 10^{8.7 \pm 1.0}\, e^{\frac{-34\,000 \pm 3\,600}{RT}}\ \text{cc}^{0.6}/\text{mol}^{0.6}\ \text{s}$$

$$k_{CH_3OH} = 10^{12.6 \pm 0.9}\, e^{\frac{-36\,800 \pm 3\,600}{RT}}\ \text{cc/mol s}$$

The uncertainty limits in these values are generous estimates of the maximum probable error. The hydrogen data were somewhat more scattered than in the carbon monoxide case as a result of the combined errors in the carbon monoxide analysis and manometer readings. The ratio CO/H_2 appears to increase with decreasing temperature if the data taken at 71 mm pressure of formaldehyde are neglected. If the trend is significant it implies that the activation energy for hydrogen production should be ~4 kcal greater than that for carbon monoxide production. Figure 2 also shows some results of previous research for comparison.

Discussion

There is no doubt that the pyrolysis of formaldehyde occurs predominantly by a chain mechanism (7) and for a compound as apparently simple as CH_2O the possible schemes would appear to be rather limited. Gay *et al.* (10) pyrolyzed formaldehyde over the temperature range of 1500 to 2100 °K in a shock tube, and considered a number of possible mechanisms. They were unable however, to establish conclusively which one was correct. Their detection of the methoxyl radical (CH_3O) mass spectrometrically points to the homogeneous formation of methanol since heterogeneous reactions were ruled out in their study. Many schemes were attempted in this work before deciding to discuss our data in terms of mechanism II of Gay *et al.* (10). At the lower temperatures involved in this work their scheme (below) had to be modified slightly (addition of reaction 3 and the third body required in reaction 6).

[1] $2CH_2O \rightarrow CH_2OH + CHO$

[2] $M + CH_2OH \rightarrow CH_2O + H + M$

[3] $CH_2OH + CH_2O \rightarrow CH_3OH + CHO$

[4] $M + CHO \rightarrow H + CO + M$

[5] $H + CH_2O \rightarrow H_2 + CHO$

[6] $M + 2CHO \rightarrow 2CO + H_2 + M$

Application of the steady state approximation leads to the following rate expressions, if at low temperature $k_3 > k_2$, $k_4 > k_2$, and the third body, M, corresponds to CH_2O.

$$[7]\quad \frac{-d[CH_2O]}{dt} = 3k_1[CH_2O]^2 + k_4\left(\frac{k_1}{k_6}\right)^{1/2}[CH_2O]^{3/2}$$

$$[8]\quad \frac{d[CO]}{dt} = 2k_1[CH_2O]^2 + k_4\left(\frac{k_1}{k_6}\right)^{1/2}[CH_2O]^{3/2}$$

Can. J. Chem. Downloaded from www.nrcresearchpress.com by 210.87.254.105 on 09/05/12
For personal use only.

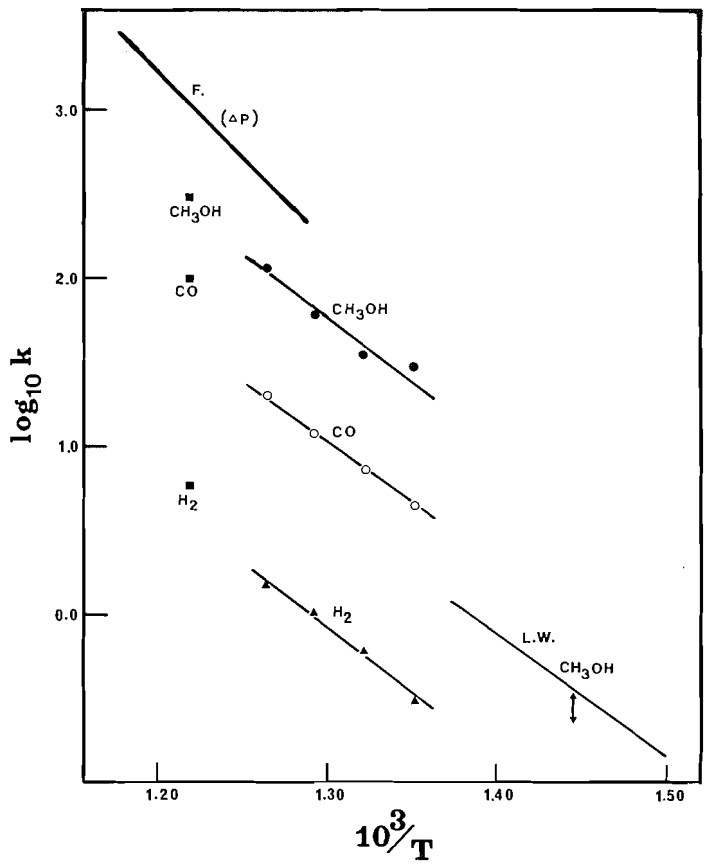

FIG. 2. Arrhenius plots for methanol, carbon monoxide, and hydrogen production. Results of some previous research are also shown. ● CH_3OH production (estimated); this work. ○ CO production; this work. ▲ H_2 production; this work. ↕ CH_3OH production (direct analyses); this work. ■ Calculated from Klein *et al.* (7) for products indicated. F from Fletcher (11); manometric data. L. W. from Longfield and Walters (8). CH_3OH analyses. Units: k_{CH_3OH} (cc/mol s); k_{CO} ($cc^{0.8}/mol^{0.8}$ s); k_{H_2} ($cc^{0.6}/mol^{0.6}$ s); k_{Δ_p} (cc/mol s).

$$[9]\quad \frac{d[H_2]}{dt} = k_1[CH_2O]^2 + k_4\left(\frac{k_1}{k_6}\right)^{1/2}[CH_2O]^{3/2}$$

$$[10]\quad \frac{d[CH_3OH]}{dt} = k_1[CH_2O]^2$$

Benson and O'Neal (16) recommended $k_4 = 10^{13.7}\exp(-19\ \text{kcal}/RT)$ and $k_2 = 10^{13.05}\exp(-29\ \text{kcal}/RT)$. k_3 can be estimated as $10^{11}\exp(-6\ \text{kcal}/RT)$ by comparison with similar abstraction reactions (17). At 500 °C, $k_3/k_2 \simeq 10^4$.

The rate of formation of carbon monoxide was 1.8 order with respect to formaldehyde, suggesting that both terms in eq. 8 are about equally important. In the hydrogen case the observed 1.6 order is in agreement with eq. 9 providing the second term dominates. Equations 8 and 9 are identical except for the factor of 2 appearing in eq. 8. This accounts for the higher order observed for CO. Reaction orders obtained in this work were supported by replotting Fletcher's (11) manometric data which led to 1.7 order dependence on formaldehyde pressure.

Rates of disappearance of CH_2O could not be determined precisely because measurements necessitated taking small differences of relatively large quantities, in addition to the occasional loss of small amounts in the analysis due to polymerization with the resultant uncertainties (±3%) being generally larger in magnitude than the rates to be measured. However, qualitative results showed approximate agreement with eq. 7.

The rate law for methanol production agreed with eq. 10.

Reactions 2, 4, and 6 were assumed to be in

Can. J. Chem. Downloaded from www.nrcresearchpress.com by 210.87.254.105 on 09/05/12
For personal use only.

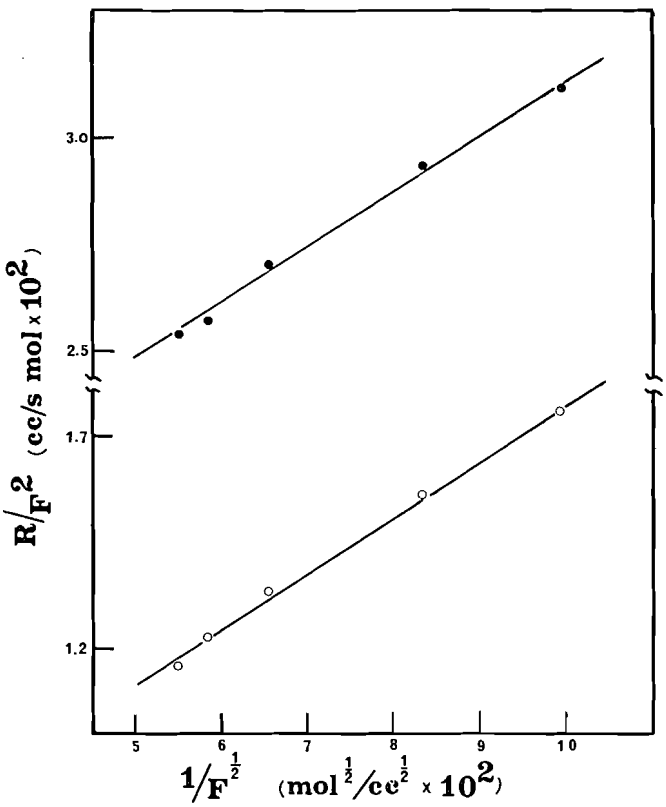

FIG. 3. Typical plots of initial rates divided by formaldehyde concentration squared *vs.* the reciprocal of the square root of formaldehyde concentration. Temperature 516.6 °C (eqs. 8 and 9). ● carbon monoxide data; ○ hydrogen data.

their pressure-dependent regions, an assumption justified by comparison with other three-, five-, and six-atom unimolecular processes (16) in roughly the same temperature and pressure range.

The derived rate laws were tested by appropriate plots of the experimental data. Typical plots of initial rate divided by formaldehyde concentration squared ($R(CO)/F^2$ and ($R(H_2)/F^2$) against $1/F^{1/2}$ at 516.6 °C are shown in Fig. 3. According to eqs. 8 and 9 the slopes and intercepts of such plots yield values of $k_4(k_1/k_6)$ and k_1. Subsequent Arrhenius plots produced eqs. 11–14. Equations 13 and 14 are

$$[11] \quad \log \{k_4(k_1/k_6)^{1/2}\}_{CO} = (8.4 \pm 0.3) - (32\,200 \pm 2\,200)/2.3RT$$

$$[12] \quad \log \{k_4(k_1/k_6)^{1/2}\}_{H_2} = (8.0 \pm 1.0) - (32\,600 \pm 1\,000)/2.3RT$$

$$[13] \quad \log (k_1)_{CO} = (12.2 \pm 0.6) - (37\,200 \pm 1\,200)/2.3RT$$

$$[14] \quad \log (k_1)_{H_2} = (11.4 \pm 0.3) - (36\,700 \pm 2\,750)/2.3RT$$

to be compared with that obtained from the experimental expression derived from estimated rates of methanol production (Fig. 2), eq. 15.

$$[15] \quad \log (k_1)_{CH_3OH} = (12.6 \pm 0.9) - (36\,800 \pm 3\,600)/2.3RT$$

(The subscripts on the left hand terms refer to CO, H_2, and CH_3OH plots.) Agreement is quite satisfactory in all cases.

While the above plots and derived parameters lend substantial support to the proposed mechanism, calculated thermochemical values show serious disagreement with these activation

Can. J. Chem. Downloaded from www.nrcresearchpress.com by 210.87.254.105 on 09/05/12
For personal use only.

Can. J. Chem. Downloaded from www.nrcresearchpress.com by 210.87.254.105 on 09/05/12
For personal use only.

energies. For example using more recent data from Fletcher and Pilcher (6), ΔH_f^0 (CH_2O) = -25.9 ± 0.11 kcal/mol, D(H—CHO) = 88.5 ± 0.9 kcal/mol, and from Fisher and Henderson (18), ΔH_f^0 (CH_2OH) = -8.4 ± 3.0 kcal/mol and calculating ΔH_f^0 (CHO) = 10.5 kcal/mol, ΔH^0 for reaction 1 is equal to 53.9 kcal/mol. At about 700 °K, $\Delta C_p T_0 \simeq 1.5$ kcal/mol and assuming $E_{-1} \simeq 0$, then $E_1 \simeq 52.4$ kcal/mol.

The value of the C—H bond dissociation energy in formaldehyde has been in dispute for many years (see for example (6, 19, 20) and references cited therein). Even using a "low" value (~ 80 kcal/mol) and a consistent set of enthalpies the result is still some 11 kcal/mol higher than the E_1 estimated from our experimental data.

The apparent low value for E_1 may imply a wall reaction in the initiation step, but the existing evidence on this point is inconclusive. Firstly, the existence of a positive intercept in the yield–time plots (Fig. 1) suggests possible participation of a rapid wall reaction in the very early stages of a "run" and since these intercepts were always effectively independent of initial pressure, the effect cannot be attributed to impurities. Secondly, heterogeneous reactions can be particularly troublesome when hydrogen production is relatively important (at least in paraffin pyrolyses) (21). Thirdly, decomposition rates are reported to be sensitive to the treatment and history of the reaction vessel (7). On the other hand, it has been shown (7, 8) that the reaction is more or less independent of the surface to volume ratio, hence a compensating termination step would be required. In addition, wall processes appear to be unlikely in view of the relatively close agreement between our low temperature data and those at shock wave temperatures (10).

Our data are reasonably consistent with the more recent pyrolysis studies (7, 10). For example, use of our rate constant for carbon monoxide formation (see Fig. 2), leads to calculated rates within approximately a factor of two of those observed by Klein *et al.* (7) at 547 °C.

The high temperature data of Gay *et al.* (10) are not shown in Fig. 2 but a long extrapolation of our results yields a rate constant (1500–2000 °K) ~ 20 times less than theirs. Fletcher's (11) early data based on a manometric study produced rate constants considerably higher than ours. The reason for the discrepancy is not clear. Fletcher did not elaborately dry his formaldehyde claiming that the reaction was unaffected by water vapor. He also observed higher rates using freshly prepared paraformaldehyde, possibly indicating the presence of traces of oxygen. Contamination of this sort could account for the higher rates.

Longfield and Walter's (8) data shown in Fig. 2 were based on four experiments over the temperature range of 393–458 °C and involved analyses of methanol. In this work 15 runs were carried out at 418 °C, leading to the result indicated by the double headed arrow (deviation) in Fig. 2. The agreement is apparently quite satisfactory. There are reasons, however, for doubting the accuracy of the rates based on methanol analyses. Losses were inevitable in all determinations due to polymerization and possibly secondary reactions. Our results indicate that these losses could be relatively large (order of magnitude). We therefore favor estimates based on the difference between CO and H_2 yields as more accurately representing initial rates of formation of methanol neglecting the small error due to possible termination products such as glyoxal.

According to the mechanism k_{CO} and k_{H_2} (observed) is given approximately by $k_4 (k_1/k_6)^{1/2}$. Using $E_4 \simeq 15$ (22), $E_6 \simeq 0$ and $E_1 \simeq 37$, then $E_{calc} \simeq 33.5$ as compared with $E_{exp} = 34$. The agreement may be fortuitous however, since E_1 was not independently determined. Use of Benson and O'Neal's (16) value, ($E_4 = 19$ kcal/mol) still leads to reasonable agreement. Using $E_1 \simeq 52$ (calculated above) yields $E_{calc} \simeq 41$ or 45, respectively.

The authors are grateful to the National Research Council of Canada for financial support.

1. D. J. McKENNEY and K. J. LAIDLER. Can. J. Chem. **41**, 1984 (1963).
2. R. KENWRIGHT, P. L. ROBINSON, and A. B. TRENWITH. J. Chem. Soc. 660 (1958).
3. N. N. SEMENOV. Photochemistry and reaction kinetics. *Edited by* P. G. Ashmore, F. S. Dainton, and T. M. Sugden. Cambridge University Press, 1967. p. 229.
4. J. H. KNOX. See ref. 3. p. 250.
5. S. GLICKER and L. J. STIEF. J. Chem. Phys. **54**, 2852 (1971).
6. R. A. FLETCHER and G. PILCHER. Trans. Faraday Soc. **66**, 794 (1970).
7. R. KLEIN, M. D. SCHEER, and L. J. SCHOEN. J. Am. Soc. **78**, 50 (1956).
8. J. E. LONGFIELD and W. D. WALTERS. J. Am. Chem. Soc. **77**, 6098 (1955).

9. J. G. CALVERT and E. W. R. STEACIE. J. Chem. Phys. **19**, 176 (1951).
10. I. D. GAY, G. P. GLASS, G. B. KISTIAKOWSKY, and H. NIKI. J. Chem. Phys. **43**, 4017 (1965).
11. C. J. M. FLETCHER. Proc. R. Soc. Ser. A. **141**, 41 (1933).
12. P. R. MCLEAN and D. J. MCKENNEY. Can. J. Chem. **48**, 1782 (1970).
13. R. SPENCE and W. WILD. J. Chem. Soc. 338 (1935).
14. K. J. BOMBAUGH and W. C. BULL. Anal. Chem. **34**, 1237 (1962).
15. R. SAUTEREY. Ann. Chim. **7**, 5 (1952).
16. S. W. BENSON and H. E. O'NEAL. Kinetic data on gas phase unimolecular reactions. NSRDS-NBS **21** (1970).
17. A. F. TROTMAN-DICKENSON and G. S. MILNE. Tables of bimolecular gas reactions. NSRDS-NBS **9** (1967).
18. I. P. FISHER and E. HENDERSON. Trans. Faraday Soc. **63**, 1343 (1967).
19. R. D. MCQUIGG and J. G. CALVERT. J. Am. Chem. Soc. **91**, 1590 (1969).
20. R. WALSH and S. W. BENSON. J. Am. Chem. Soc. **88**, 4570 (1966).
21. D. A. LEATHARD and J. H. PURNELL. Ann. Rev. Phys. Chem. *Edited by* H. Eyring. George Banta Co. Inc. **21**, 197 (1970).
22. J. G. CALVERT. J. Phys. Chem. **61**, 1206 (1957).

Can. J. Chem. Downloaded from www.nrcresearchpress.com by 210.87.254.105 on 09/05/12
For personal use only.

Organic Free Radical and Metal Complexes. 2,2-Diphenyl-1-picrylhydrazyl with Cu(I)

F. LEH[1] AND J. K. S. WAN

Department of Chemistry, Queen's University, Kingston, Ontario

Received August 16, 1971

Reactions of Cu(I)Cl, $Cu(II)Cl_2$, Cu(II) acetylacetonates, and Cu(II) *N*-methylsalicylalidiiminate with the stable free radical 2,2-diphenyl-1-picrylhydrazyl have been investigated. In all cases Cu(II) was reduced and the organic radical behaved as an electron donor-ligand to form complexes containing Cu(I). These novel free radical Cu(I) complexes were characterized by various spectroscopic methods, including e.s.r.

Les réactions des acétylacétonates de Cu(I)Cl, $Cu(II)Cl_2$, Cu(II) et du *N*-méthylsalicylalidiiminate de Cu(II) avec le radical libre stable diphényl-2,2 picryl-1 hydrazyl, ont été étudiés. Dans tous les cas Cu(II) a été réduit et le radical organique se conduit comme un ligand donneur d'électrons pour former des complexes contenant Cu(I). Ces nouveaux complexes radicaux libres Cu(I) ont été caractérisés par plusieurs méthodes spectroscopiques, dont la résonance du spin électronique.

Canadian Journal of Chemistry, **50**, 999 (1972)

Can. J. Chem. Downloaded from www.nrcresearchpress.com by 210.87.254.6 on 09/05/12
For personal use only.

Introduction

The stable free radical 2,2-diphenyl-1-picrylhydrazyl (DPPH) has been investigated extensively in solution and in the solid state by e.s.r. (1), n.m.r. (2), and optical absorption spectroscopy (3). Several diamagnetic monoalkali salts M^+ $DPPH^-$ have been prepared and characterized (4) and the reactions of DPPH with acidic centers in minerals have recently been investigated (5). Some preliminary observations on the reactions of Cu(II) acetylacetonates (6) and iron(II) (7) with DPPH have been reported. However, no details regarding the nature and products of the reactions have been published. In this paper we wish to report some evidence for the formation of Cu(I)DPPH complexes from the reactions of a variety of copper compounds with DPPH.

Experimental

Optical spectra were recorded with a Unicam SP 800 spectrophotometer and i.r. data were obtained from mull samples with a Perkin–Elmer 180 spectrometer with sodium chloride optics. Proton n.m.r. spectra were taken on a Bruker HX-60 high resolution instrument locked on tetramethylsilane as an internal standard. The e.s.r. spectra were obtained with a Varian V4502 spectrometer and spectral analysis was carried out by means of spectra simulation on an IBM 360/50 computer. Mass spectra were recorded on a JEOL high resolution mass spectrometer; the samples were introduced via the heated inlet at 100 °C and perfluorokerosene was used as mass standard.

[1]Postdoctoral Fellow, 1970–1972.

Satisfactory elementary analyses were performed by Schwarzkopf Microanalytical Laboratory. Molecular weights were determined by means of a Hewlett Packard vapor pressure osmometer with chloroform as solvent at 37.6 °C, using purified benzil as the standard.

Preparation of Mono(DPPH) Cu(I) Chloride

This complex was prepared by the following different methods.

(*a*) A solution of DPPH (0.39 g) in chloroform (20 ml) was added to a solution of Cu(II) chloride (0.34 g) in ethanol (10 ml). After 14 h the resulting solution was evaporated to half-volume and cooled in an ice-bath. The brown crystals were filtered off, washed with ether and ethanol, and dried (0.30 g, 61.4% yield), m.p. 174 °C (dec.).

Anal. Calcd. for DPPH–CuCl (mol. wt. 493): Cu, 12.8. Found (475 ± 25): Cu, 11.7.

(*b*) A mixture of DPPH–H (2,2-diphenyl-1-picrylhydrazine, 0.39 g) in chloroform (20 ml) and Cu(II) chloride (0.34 g) in ethanol (10 ml) was allowed to react for 14 h. The solvent was evaporated under vacuum and brown crystals were recovered and recrystallized (0.31 g, 63.3% yield), m.p. 177 °C (dec.).

Anal. Found for DPPH–CuCl (468 ± 25): Cu, 11.6.

(*c*) A brown solution resulted when excess Cu(I) chloride was suspended in an acetone solution of DPPH (0.39 g). The unreacted Cu(I) chloride was filtered off and the brown crystals were recrystallized from chloroform and ether, yield: 49.9%, m.p. 178 °C (dec.).

Anal. Found for DPPH–CuCl (475 ± 25): Cu, 11.8.

Preparation of Mono(DPPH) Cu(I) Acetylacetonate

Bis(acetylacetonate) Cu(II) (0.5 g) and DPPH (0.8 g) were dissolved in hot methanol (50 ml) and allowed to stand for 1 h at 60 °C. Evaporation of the solvent and recrystallization from chloroform–ether gave brown crystals (0.5 g, 50% yield), m.p. 145 °C (dec.).

Anal. Calcd. for DPPH–Cu(I) acetylacetonate (mol. wt. 556.6): C, 49.59; H, 3.41; Cu, 11.4. Found (535 ± 30): C, 50.6; H, 3.5; Cu, 10.8.

TABLE 1. Characteristic i.r. bands (cm^{-1}) of the DPPH–CuL complexes*

DPPH	DPPH–H	DPPH–CuCl	DPPH–Cu(acac)	DPPH–Cu(tfacac)	DPPH–Cu(salm)	Assignment
	3284 vw					N—H vib.
2961 vw	2954 vw	2971 vw				=C—H str.
		2946 vw				
1576 vs	1620 vs	1621 vs	1620 vs	1608 vs	1615 vs	NO_2 asym. str.
1599 vs	1595 vs	1591 vs				C=C(phenyl) vib.
			1593 vs	1592 vs		C=C(chelate) str.
			1535 vs	1528 vs		C=O str.
					1515 vs	C=N str.
756 s	759 s	765 s	754 ms	750 mw	720 m	NO_2 out of
716 s	724 s	726 s		737 m		plane deformation
699 s	693 s	694 s	693 ms	690 mw		C—NO_2 bending
			450 w	449 mw	458 m	Cu—O str.
					646 w	Cu—N str.

*w, weak; m, medium; s, strong; vs, very strong; (acac), acetylacetonate; (tfacac), trifluoroacetylacetonate; (salm), *N*-methyl salicylaldiiminate.

Preparation of Mono(DPPH) Cu(I) Trifluoroacetylacetonate

A solution of bis(trifluoroacetylacetonate) Cu(II) (0.74 g) in hot methanol was added to DPPH (0.80 g) in 50 ml methanol and the mixture was gently heated for 1 h. Evaporation of the solvent and recrystallization from chloroform–light petroleum ether gave brownish grey crystals (0.63 g, 40.9% yield), m.p. 148 °C (dec.).

Anal. Calcd. for DPPH–Cu(I) trifluoroacetylacetonate (mol. wt. 610.5): Cu, 10.4. Found (581 ± 30): Cu, 10.1.

Preparation of Mono(DPPH) Cu(I) N-Methyl Salicylaldiiminate

Bis(*N*-methyl salicylaldiiminato) Cu(II) (0.65 g) and DPPH (0.8 g) were dissolved in hot methanol (60 ml) and allowed to stand for 1 h at 60 °C. The solution began turning brown after several minutes; chromatography on silica gel and addition of diethyl ether yielded dark brown crystals (0.72 g, 50% yield), m.p. 151 °C (dec.).

Anal. Calcd. for DPPH–Cu(I) *N*-methyl salicylaldiiminate (mol. wt. 591.5): C, 52.74; H, 3.38; Cu, 10.7. Found (607 ± 30): C, 53.1; H, 3.5; Cu, 10.0.

Results and Discussions

Free radical complexes of the formulae DPPH–CuL (where L is one of the following: chloride ion, acetylacetone, trifluoroacetylacetone, *N*-methyl salicylaldiimine) have been synthesized by the reactions of Cu(I)Cl or $Cu(II)L_2$ with DPPH or DPPH–H in organic solvents. This type of complex containing the free radical ligand DPPH is novel and a report (8) on other metal complexes with organic radical ligands such as α,α′-bipyridyl and *O*-phenanthroline has only recently appeared. In the present study it is interesting to note that the DPPH–H is a stronger reducing agent than tertiary phosphines, since triphenylphosphine fails to reduce Cu(II) acetylacetonate to form the Cu(I) complex (9). In the reaction of DPPH–H, the primary reaction suggested by a referee could be:

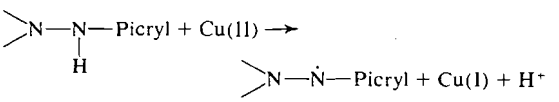

Using DPPH as the starting reagent in ethanol leads to the same product. This is probably due to the well known fact that DPPH is rather unstable in ethanol (10) and presumably reduces to give the DPPH–H.[2]

The i.r. absorption data of these DPPH–CuL complexes are given in Table 1. The assignments are based on the frequencies previously reported for Cu(II) acetylacetonates (11), Cu(II) bis-salicylaldehydeethylenediiminate (12), and those for the free radical DPPH. The C=O and C=N absorption bands are stronger in DPPH–CuL complexes than in their parent compounds and may be caused by the transmission of electron effects from the nitro substituents on the picryl ring moiety through the metal atom to the chelates of the complexes. For the assignments of the metal-oxygen stretching bands of acetylacetonate complexes, Nakamoto *et al.* (13) show the Cu(II)—O stretching mode occurring at 455 cm^{-1}. We tentatively assign the Cu(I)—O stretching at 450 and 448 cm^{-1} for DPPH–Cu(I) acetylacetonate and DPPH–Cu(I) trifluoroacetylacetonate, respectively. The two

[2]We are grateful to a referee who pointed out to us the possibility.

Can. J. Chem. Downloaded from www.nrcresearchpress.com by 210.87.254.6 on 09/05/12
For personal use only.

TABLE 2. The p.m.r. data for the DPPH–CuL complexes in deuterated acetone solvent at room temperature. Shifts are in Hz against internal standard TMS at 60 MHz

Compounds	Picryl ring	Phenyl ring	CH_3
2,2-Diphenyl-1-picrylhydrazine	534	434	—
DPPH	Not observed	434	—
DPPH–CuCl	538	435	—
DPPH–Cu(I) acetylacetonate	547	431	87.0
DPPH–Cu(I) trifluoroacetylacetonate	549	432	59.8
DPPH–Cu(I) *N*-methyl salicylaldiiminate	546	430	46.4

TABLE 3. The e.s.r. hyperfine coupling constants (G) of DPPH–CuL complexes in degassed dilute chloroform solutions at room temperature

Compound	A_{N_1} (Picryl N)	A_{N_2}	A_{N_2}/A_{N_1}
DPPH	9.90 ± 0.02	7.63 ± 0.02	0.77
DPPH–CuCl	9.80	7.70	0.79
DPPH–Cu(I) acetylacetonate	9.71	7.74	0.80
DPPH–Cu(I) trifluoroacetylacetonate	9.44	7.84	0.83
DPPH–Cu(I) *N*-methyl salicylaldiiminate	9.64	7.76	0.81

bands of the DPPH–Cu(I) *N*-methyl salicylaldiiminate at 458 and 646 cm^{-1} are assigned to the Cu—O and Cu—N vibrations, respectively.

Most organic radicals in dilute solutions have relatively long electron spin relaxation times resulting in very broad nuclear resonance signals. The proton resonance of the picryl ring of the free radical ligand DPPH can not be observed in solutions at various temperatures, but appears in the spectra of DPPH–CuL complexes by coordination. It seems likely that the use of coordination to study the n.m.r. of organic radicals will prove to be generally helpful in systems where the radicals have long relaxation times. The p.m.r. data for the DPPH–CuL complexes are presented in Table 2. The assignments for picryl ring, phenyl ring, and methyl protons are based on their intensities and previous observations of 2,2-diphenyl-1-picrylhydrazine (4, 14). In the spectrum of the uncomplexed DPPH, some small but definite spin density (1) on the picryl ring probably renders the picryl ring proton signals too broad for detection. When the DPPH is complexed to the Cu(I) ion via the picryl ring, the coordination could twist the picryl ring more out of the plane of the unpaired electron orbital, thus reducing the probability of spin delocalization and sharpening the picryl proton peaks for observation. For the observed small paramagnetic shift in these complexes, some remaining negative spin density is probably transferred directly from the picryl ring to the Cu(I) ion with the result that the absorption of the two picryl ring protons is displaced towards lower field. For the DPPH–Cu(I) acetylacetonates, the shift is slightly increased as the methyl group is replaced by an electron-withdrawing trifluoromethyl group.

The most characteristic physical property of these complexes DPPH–CuL is their paramagnetism due to the presence of an unpaired electron in the ligand DPPH; this has been studied by e.s.r. The spectra of polycrystalline samples of DPPH–CuL is found to consist of a single narrow symmetrical line centered at $g = 2.002$. In degassed dilute benzene solution, these complexes exhibit e.s.r. spectra of a major quintet with relative intensities approximately 1:2:3:2:1. The experimental spectra were analyzed in terms of two non-equivalent nitrogens (15, 16) with the larger nitrogen hyperfine coupling constant assigned to the picryl nitrogen, N_1 (15, 17). These coupling constants are reported in Table 3. In the case of DPPH–CuCl, further hyperfine structures arising from the interactions with the ring protons were also observed. It is seen from Table 3 that the ratio of A_{N_2}/A_{N_1} depends upon the nature of the chelates L. Walter (18) has rationalized substituent effects in terms of the relative impor-

Can. J. Chem. Downloaded from www.nrcresearchpress.com by 210.87.254.6 on 09/05/12
For personal use only.

TABLE 4. Optical absorption bands of the DPPH–CuL complexes

Compound	Solvent	λ_{max} (nm)	ε_{max} (l/mol cm)
DPPH	$CHCl_3$	530	11700
		332	15800
DPPH–CuCl	$CHCl_3$	319	19940
Cu(II) acetylacetonate	CH_3OH	659	50
		553	38
		301	26430
		254	18000
DPPH–Cu(I) acetylacetonate	CH_3OH	326	18900
		252	shoulder
Cu(II) trifluoroacetylacetonate	$CHCl_3$	680	34
		298	24000
DPPH–Cu(I) trifluoroacetylacetonate	$CHCl_3$	302	26170
Cu(II) *N*-methylsalicylaldiiminate	CH_3OH	635	99
		354	9804
		297	9400
		271	23180
		241	48040
DPPH–Cu(I) *N*-methylsalicylaldiiminate	CH_3OH	341	shoulder
		317	shoulder
		296	36830
		244	36560

tance of the following canonical forms in DPPH:

$$\underset{\mathbf{1}}{Ph_2N_{(2)}—\dot{N}_{(1)}—Picryl} \longleftrightarrow \underset{\mathbf{2}}{Ph_2^{+}\dot{N}_{(2)}—\dot{N}_{(1)}=Picryl^{-}}$$

Thus the electron-withdrawing nitro substituents in the picryl ring will stabilize form **2** relative to form **1**. Similarly, metal coordination with the picryl ring decreases the unpaired electron density on the picryl nitrogen and thus stabilizes the structure **2**.

The absence of the familiar characteristic Cu(II) e.s.r. signals in DPPH–CuL complexes is taken as evidence for Cu(I) formation. In addition, integration of the experimental e.s.r. signal intensities indicates approximately one unpaired electron per complex molecule.

The optical absorption band of the DPPH–CuL complexes together with those of their parent compounds are listed in Table 4. The distinct feature of the complexes spectra (Figs. 1 and 2) is the absence of both the absorptions at ~530 and ~670 nm which are present in the DPPH ligand and the parent Cu(II) compounds. The former absorption is due to the conjugated resonance structure of DPPH (3)

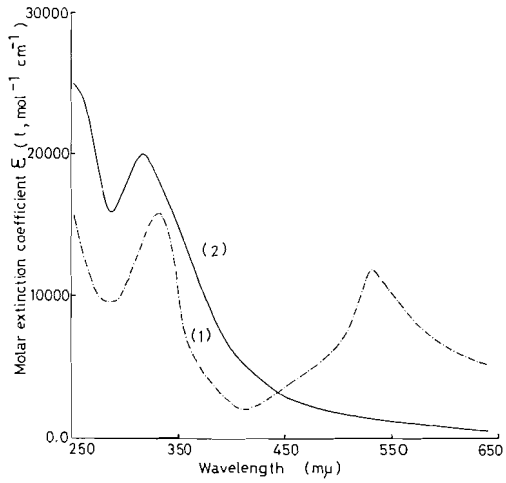

FIG. 1. Optical absorption spectra of: (*1*) DPPH and (*2*) DPPH–CuCl complex in chloroform.

while the latter has been assigned (19) to the P_π–d_π transition in the Cu(II) acetylacetonates. Cotton and co-workers (19) also suggested that the band at ~250 nm in the Cu(II) acetylacetonate spectra is a charge transfer band involving the promotion of a π-bonding electron

Can. J. Chem. Downloaded from www.nrcresearchpress.com by 210.87.254.6 on 09/05/12
For personal use only.

TABLE 5. Relative intensities of ions in the mass spectra of DPPH–CuL complexes at 75 eV and 100 °C

Ions	Relative intensity of ions from DPPH–CuL			
	L = Cl	Acetylacetonate	Trifluoroacetyl-acetonate	*N*-Methylsalicyl-aldiiminate
$[DPPH]^+$	36.5	47.1	40.2	10.3
$[DPPH-NO_2]^+$	4.4	9.6	8.3	3.8
$[DPPH-2NO_2]^+$	1.3	3.6	2.5	1.8
$[DPPH-3NO_2]^+$	13.0	15.9	11.3	5.5
$[(C_6H_5)_2N]^+$	100.0	100.0	100.0	100.0
$[C_6H_5N_2]^+$	2.4			
$[C_6H_5N_2]^+ + [CuOCCH]^+$		14.7	25.6	18.6
$[C_6H_5]^+$	58.8	27.9	28.1	48.0
$[CuC_6H_2 + 2NO_2]^+$	1.7	1.5	4.3	6.2
$[CuC_6H + 2NO_2]^+$	18.8	14.0	20.3	68.9
$[CuL]^+$	—	11.1	7.3	5.2
$[CuL-CH_3]^+$	—	4.0	1.2	2.4
$[CuL-CH_2CO]^+$	—	—	4.1	—
$[CuL-CF_3]^+$	—	—	3.5	—
$[CuL-2CH_3]^+$	—	2.3	—	—
$[CuL-NCH_3]^+$	—	—	—	15.5
$[CuL-NHCH_3]^+$	—	—	—	27.6
$[CuL-CH_2NCH_3]^+$	—	—	—	15.5
$[Cu]^+$	8.2	4.0	18.8	20.4
$[167]^+$	48.3	41.1	36.5	55.2

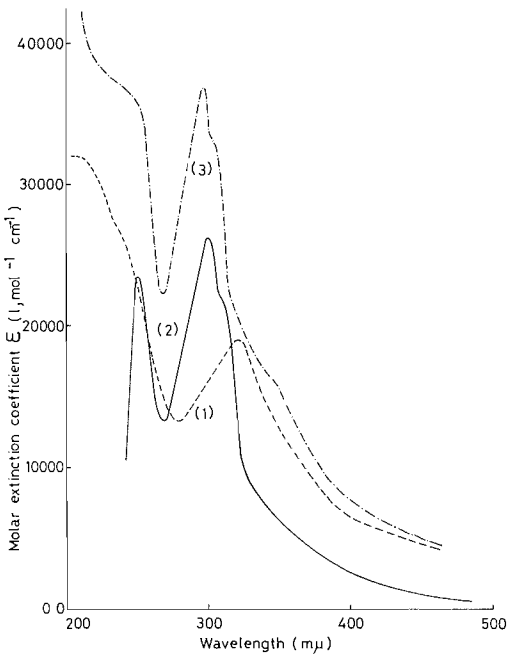

FIG. 2. Optical absorption spectra of: (*1*) DPPH–Cu(I) acetylacetonate in methanol, (*2*) DPPH–Cu(I) trifluoro-acetylacetonate in chloroform, and (*3*) DPPH–Cu(I) *N*-methyl salicylaldiiminate in methanol.

or a non-bonding electron of the oxygen to a metal orbital. However, in the DPPH–CuL complexes, bands in the 250 nm region are not resolved; the band at ~300 nm is probably due to an electronic transition in the diphenylamino moiety of the DPPH ligand (3) or a mixture of this with a π–π^* transition (19, 20) in the complexes.

Unlike the parent Cu(II) acetylacetonates, the DPPH–CuL complexes do not exhibit their parent peaks in their mass spectra, although they were expected to be thermally stable at temperatures well below their melting points. The relative intensities of all copper-containing ions and major ions from the ligand DPPH in the mass spectra of the complexes are given in Table 5. The abundant ions $[DPPH]^+$, $[CuC_6H(NO_2)_2]^+$, $[CuL]^+$ characterize the primary fragmentation of CuDPPH and CuL bonds in the complexes. The peaks at $m/e = 255$, 228, 170, 169, 168, 167, and 77 could be due to further fission of the $[DPPH]^+$ ion and indeed the base peak which appears in the mass spectra of all the complexes corresponds to the $[(C_6H_5)_2N]^+$ ion. For the DPPH–Cu(I) acetylacetonates, peaks at $m/e = 148$, 133, and 105 are consistent

Can. J. Chem. Downloaded from www.nrcresearchpress.com by 210.87.254.6 on 09/05/12
For personal use only.

with the fragmentation pattern of the $[CuL]^+$ ion (21).

Based upon the results presented, we conclude that we have synthesized some novel DPPH–CuL complexes and the complex formation is probably via the coordination of the Cu(I) ion with the picryl ring of the DPPH.

The authors are grateful to Professor K. E. Russell for many helpful discussions. This research is supported by the National Research Council of Canada and the Department of Public Health.

1. M. M. HEGYHATI. J. Chem. Phys. **50**, 3123 (1969) and references therein.
2. H. S. GUTOWSKY, H. KUSUMOTO, T. H. BROWN, and D. H. ANDERSON. J. Chem. Phys. **30**, 860 (1959); M. E. ANDERSON and G. E. PAKE. J. Chem. Phys. **33**, 1581 (1960).
3. A. T. BALABAN, P. T. FIANGOPOL, M. MARCULESCU, and J. BALLY. Tetrahedron, **13**, 258 (1961).
4. J. A. WEIL and G. A. JANUSONIS. J. Org. Chem. **27**, 1248 (1962).
5. D. H. SOLOMON and D. G. HAWTHORNE. J. Macromol. Sci. **A5**, 575 (1971).
6. K. UEHARA, M. TANAKA, and N. MURATA. Bull. Chem. Soc. Jap. **41**, 3034 (1968).
7. V. V. VOEVODSKII, R. I. ZUSMAN, and Y. N. MOLIN. Izv. Sib. Otd. Akad. Nauk. SSSR, Ser. Khim. Nauk. **3**, 127 (1968).
8. P. CLOPATH and A. V. ZELEWSKY. Chem. Commun. 47 (1971).
9. W. A. ANDERSON, A. J. CARTY, G. J. PALENIK, and G. SCHREIBER. Can. J. Chem. **49**, 746 (1971).
10. P. J. PROLL and L. H. SUTCLIFFE. Trans. Faraday Soc. **59**, 2090 (1963).
11. L. BELFORD, A. E. MARTELL, and M. CALVIN. J. Inorg. Nucl. Chem. **2**, 11 (1956).
12. K. UENO and A. E. MARTELL. J. Phys. Chem. **60**, 1270 (1956); K. NAKAMOTO. Infrared spectra of inorganic and coordination compounds. Interscience, New York, N.Y., 1963. p. 227.
13. K. NAKAMOTO, C. UDOVICH, and J. TAKEMOTO. J. Am. Chem. Soc. **92**, 3973 (1970).
14. J. HEIDBERG, J. A. WEIL, G. A. JANUSONIS, and J. K. ANDERSON. J. Chem. Phys. **41**, 1033 (1964).
15. M. M. CHEN, K. V. SANE, R. I. WALTER, and J. A. WEIL. J. Phys. Chem. **65**, 713 (1961).
16. A. R. FORRESTER, J. M. HAY, and R. H. THOMSON. Organic chemistry of stable free radicals, Academic Press, New York, N.Y., 1968. pp. 137–172.
17. R. W. HOLMBERG, R. LIVINGSTON, and W. T. SMITH. J. Chem. Phys. **33**, 541 (1960).
18. R. I. WALTER. J. Am. Chem. Soc. **88**, 1923 (1966).
19. J. P. FACKER, F. A. COTTON, and D. W. BARNUM. Inorg. Chem. **2**, 97 (1963).
20. B. R. JAMES, M. PARIS, and R. J. P. WILLIAMS. J. Chem. Soc. 4632 (1961).
21. C. REICHERT, G. M. BANCROFT, and J. B. WESTMORE. Can. J. Chem. **48**, 1362, 3213 (1970).

Can. J. Chem. Downloaded from www.nrcresearchpress.com by 210.87.254.6 on 09/05/12
For personal use only.

A Quantum Chemical Conformational Analysis of the Ethylenediamine Molecule

N. HADJILIADIS, A. DIOT, AND T. THEOPHANIDES
Department of Chemistry, University of Montreal, Montreal, Quebec

Received July 16, 1971

The conformational analysis of the ethylenediamine molecule has been studied by the LCAO-EHMO calculation method. The results indicate that the most stable conformation of the molecule is the *gauche* form, in which the angle N—C—C—N is *ca.* 63.0° measured from the *cis* form. This is in agreement with experimental data and can explain the fact that the ethylenediamine in its chelate complexes is always in the *gauche* form. In addition, the present results indicate that the *trans* form is the next most stable conformation of ethylenediamine in agreement with experimental results on bridging ethylenediamine metal complexes.

L'analyse conformationnelle de la molécule de l'éthylène diamine a été étudiée par la méthode de LCAO-EHMO. Le calcul indique que la conformation la plus stable est la forme *gauche*, avec un angle diédral N—C—C—N de 63.0°. Le résultat est en accord avec les résultats expérimentaux et explique la formation des complexes chélatés et pontés de cette molécule.

Canadian Journal of Chemistry, **50**, 1005 (1972)

Can. J. Chem. Downloaded from www.nrcresearchpress.com by 210.87.254.5 on 09/05/12
For personal use only.

Introduction

Several complexes of ethylenediamine with different metal ions have been prepared and studied. In these complexes the ethylenediamine molecule serves as a chelating agent, or gives the so-called bridged type complexes, where the two nitrogen atoms are bound with two metal ions. In all the chelated complexes of ethylenediamine the organic molecule has the *gauche* form. This has been proved in several cases by X-ray crystallography (1–3), while in the bridged complexes, the ethylenediamine is in the *trans* form (4–6), with a C_{2h} symmetry.

Although the complexes of ethylenediamine have been thoroughly studied, little is known about the conformation and stability of the conformers of the free ethylenediamine molecule. Infrared and Raman spectra of the liquid and solid ethylenediamine have been explained satisfactorily by assuming the *cis* conformer present as the major contributor of the spectra (7, 8).

A recent short communication (9) showed by gas electron diffraction studies that ethylenediamine is predominantly in the *gauche* form, with the dihedral angle N—C—C—N of 64.0 ± 5.0°, as measured from the *cis* position.

Results and Discussion

The present work reports the results of calculations on the ethylenediamine molecule using the extended Hückel theory, LCAO-EHMO method with the aid of the CDC-6400 computer and the program developed by Hoffmann and co-worker (10). In these calculations intermolecular interactions are not taken into account, *e.g.*, hydrogen bonding, aggregation, etc., and only one isolated molecule is considered. It is known that the above method gives excellent agreement with experimental conformational studies, (11–13) and predicts reliably the molecular structure.

Allen and Russel (13) have discussed at great length the reliability of this method. Blyholder and Coulson (12) recently concluded "that this method gives reasonably satisfactory results...".

The present result is another example confirming the usefulness of this essentially *naive and crude*[1] EHMO method, which appears to work so well in predicting preferred equilibrium conformations. Kier (11*a*), who made similar calculations, concludes that the EHMO method works well, because it includes in the input the precise 3-dimensional coordinates of the atoms.

We believe that the method will continue to work reasonably well as long as the simple sums of one-electron energies behave approximately as the true molecular energies, *i.e.*, the nuclear–nuclear repulsions and the electron–electron repulsions cancel out roughly (10*c*) or their difference varies slowly with distance.

In order of stability the *trans* conformer comes next to the *gauche* form. The small difference in energy between the 63° and 180° configurations

[1]We should like to express our appreciation to the referee who so forcefully pointed this out.

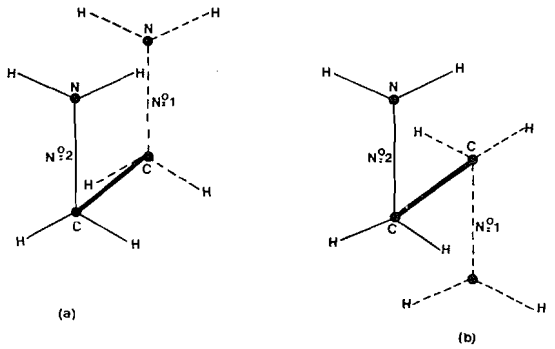

FIG. 1. Geometry of (*a*) *cis* and (*b*) *trans* ethylenediamine.

(Fig. 1) of the order of 0.05 eV (~1 kcal) suggests that the ethylenediamine molecule prefers the *gauche* conformation for normal chelates and the *trans* conformation for bridged complexes. The *cis* isomer is not favored energetically and this explains the non-existence of *cis*-chelated complexes.

The small difference of energy between the *gauche* and the *trans* conformers is also in perfect agreement with the gas electron diffraction study (9). The experimental radial distribution curves showed two peaks, one outstanding around 2.85 Å corresponding to the *gauche* conformation and one small peak around 3.8 Å indicating the presence of a small fraction of *trans* conformer (9).

Calculations

The MO's are obtained from eq. 1,

$$[1] \qquad \Phi_j = \sum_k \sum_r C_{jr_k}\chi_{r_k}$$

c_{jr_k} being the LCAO coefficients and χ_{r_k} being the normalized atomic orbitals of Slater's type. The overlap integrals, eq. 2,

$$[2] \qquad S_{r_k s_l} = \int \chi_{r_k}\chi_{s_l}\, d\tau$$

are calculated from Mulliken's formulas (14). The coulomb integrals for an orbital i ($\alpha_i = H_{ii}$) are taken as the appropriate valence state ionization potentials and the resonance integrals ($\beta_{ij} \equiv H_{ij}$) are computed from eq. 3,

$$[3] \qquad H_{ij} = 0.5\, K\,(H_{ij} + H_{jj})S_{ij}$$

where $K = 1.75$. The values of ionization potentials and of the Slater's coefficients were taken from the tables of Pilcher and Skinner (15, 16), correspondingly (Table 1).

TABLE 1. Values of ionization potentials and of Slater's coefficients

Valence shell	μ	H_{ii} (eV)
H (1s)	1.000	−13.6
C (2s)	1.625	−20.78
C (2p)	1.625	−11.31
N (2s)	1.950	−27.70
N (2p)	1.950	−14.78

TABLE 2. Values of angles and interatomic distances utilized

Bonds	Angle (deg)	Bond	Distance (Å)
HCH	109.27	CC	1.54
NCH	109.27	CC	1.47
HCC	109.27	CH	1.094
HNC	112.5	NH	1.011
NCC	109.8		

Accordingly, the secular determinant was set up and solved. The interatomic distances and the angles were taken from previous works (17–19, 3), in order to have the best representation of the molecule. The same values (Table 2) were also

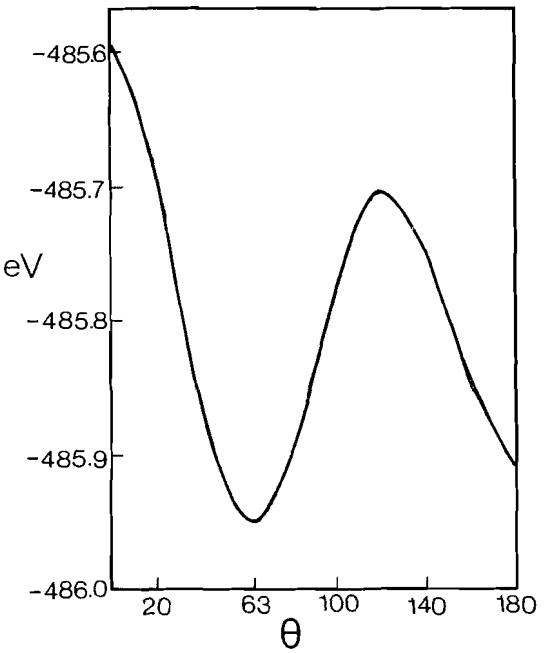

FIG. 2. Variation in energy going from the *cis* to the *trans* form. The abscissa represents the dihedral angles (θ) of each conformer with respect to the *cis* form.

Can. J. Chem. Downloaded from www.nrcresearchpress.com by 210.87.254.5 on 09/05/12
For personal use only.

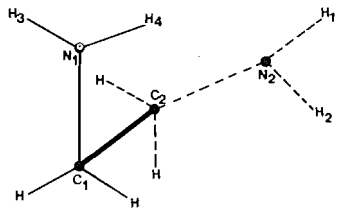

FIG. 3. The dihedral angle (θ) of the plane $C_1C_2N_2$ with respect to the *cis* form is approximately 63.0°. The H_1 is in the plane of $C_1C_2N_2$ and the H_2 to its right. The plane $C_1N_1H_4$ makes an angle of 57.0° with the $N_1C_1C_2$ plane, and the plane $C_1N_1H_3$, makes an angle of 63.0° with the plane $N_1C_1C_2$.

used in an infrared and Raman study with a normal coordinate analysis of the molecule (8).

In the first place, the calculations of the total electronic energy were performed on the *cis* form of the molecule, and the H—N—H angle was bisected by the N—C—C—N plane (Fig. 1*a*). Then the C—N bond No. 1 was rotated successively with a rotation interval of 20° until the *trans* form (180°) was obtained (Fig. 1*b*). In the vicinity of the minima, rotation intervals of 2° were also carried out to exactly determine the minimum of the potential.

The examination of the total electronic energy corresponding to these different geometries (Fig. 2) indicated that the most stable conformation of the molecule corresponded to a dihedral angle N—C—C—N of approximately 63.0°, with respect to the *cis* form.

The study of the rotation of the two NH_2 groups with respect to each other also indicated that the most stable conformation of the molecule is the *gauche* form as shown in Figs. 3 and 4.

This work was supported by the National Research Council of Canada. We would like to express our thanks to Professor S. Fliszar for the program utilized and for many discussions relating to the problems covered in this paper.

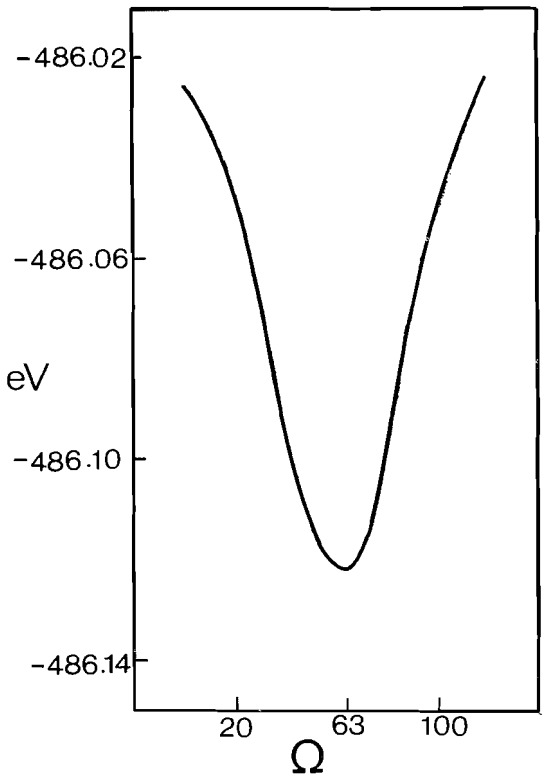

FIG. 4. Variation in energy by fixing the position of the $N_2H_1H_2$ group and rotating the $N_1H_3H_4$ group. The abscissa represents the dihedral angles (Ω) between the planes $C_1N_1H_3$ and $N_1C_1C_2$ (see Fig. 3).

1. L. N. SWINK and M. ATOJI. Acta Cryst. **13**, 639 (1960).
2. M. IWATA, K. NAKATZU, and Y. SAITO. Acta Cryst. **B25**, 2562 (1969).
3. F. DURANT, P. PIRET, and M. VAN MEERSSCHE. Acta Cryst. **23**, 780 (1967).
4. (*a*) P. C. KONG and T. THEOPHANIDES. Can. Spectrosc. **14**, 104 (1969). (*b*) T. THEOPHANIDES and P. C. KONG. Inorg. Chim. Acta, **5**, 485 (1971).
5. K. BRODERSON. Z. Anorg. U. Allgem. Chem. **298**, 142 (1959).
6. D. P. POWELL and A. SHEPPARD. J. Chem. Soc. 3089 (1959).
7. A. SABATINI and S. CALIFANO. Spectrochim. Acta, **16**, 677 (1960).
8. A. DIOT and T. THEOPHANIDES. Unpublished results.
9. A. YOKOZEKI and K. KUCHITSU. Bull. Chem. Soc. Jap. **43**, No. 8, 2644 (1970).
10. (*a*) R. HOFFMANN and W. N. LIPSCOMB. J. Chem. Phys. **36**, 2179, 3487 (1962). (*b*) R. HOFFMANN and W. N. LIPSCOMB. J. Chem. Phys. **37**, 2872 (1962). (*c*) R. HOFFMANN. J. Chem. Phys. **39**, 1397 (1963).
11. (*a*) L. B. KIER. Tetrahedron Lett. 1233 (1967). (*b*) J. RENARD and S. FLISZAR. J. Am. Chem. Soc. **92**, 2628 (1970).
12. G. BLYHOLDER and C. A. COULSON. Theor. Chim. Acta, **10**, 316 (1968).
13. L. C. ALLEN and J. D. RUSSEL. J. Chem. Phys. **46**, 1029 (1967).
14. R. S. MULLIKEN, C. A. RIEKE, D. ORLOFF, and H. ORLOFF. J. Chem. Phys. **17**, 1248 (1949).
15. G. PILCHER and H. A. SKINNER. J. Inorg. Nucl. Chem. **24**, 937 (1962).
16. R. S. MULLIKEN. J. Chem. Phys. **23**, 1833, 1841, 2338, 2343 (1955).
17. G. DELLEPIANE and G. ZERBI. J. Chem. Phys. **48**, 3573 (1968).
18. T. ASCHIDA and S. HIROKAWA. Bull. Chem. Soc. Jap. **36**, 704 (1963).
19. R. G. SNYDER and G. ZERBI. Spectrochim. Acta, **23A**, 391 (1967).

Can. J. Chem. Downloaded from www.nrcresearchpress.com by 210.87.254.5 on 09/05/12
For personal use only.

Reactions of 1,2,5-Triphenylphosphole and its Oxide, Sulfide, and Selenide with some Transition Metal Halides

D. BUDD, R. CHUCHMAN, D. G. HOLAH, A. N. HUGHES, AND B. C. HUI

Department of Chemistry, Lakehead University, Thunder Bay, Ontario

Received September 14, 1971

Reactions of 1,2,5-triphenylphosphole (TPP) and 1,2,5-triphenylphosphole oxide (TPPO), sulfide (TPPS), and selenide (TPPSe) with some transition metal halides have been studied in dry, oxygen-free organic solvents. The reactivity of these ligands is clearly a function of the oxidation states of the metal, with the order being M(II) < M(III) < M(IV) < M(V). For example the ligands do not react with the metal(II) halides (Mn, Fe, Ni), while rapid reactions occur with niobium(V) and tantalum(V). Iron(III) and copper(II) are both reduced by TPP. The complexes resulting from these studies are mostly simple adducts of the various metal halides, although other species such as phospholium salts $[TPPH^+][MCl_6^-]$ and oxytrichloride adducts, MOX_3.TPPO (M = Nb, Ta) are also described. In the phospholium salts, the phosphole ring is protonated at the phosphorus atom which is in direct contrast to pyrrole derivatives. The origin of the oxygen atom in the oxytrichloride complexes is discussed and compared with data on the analogous triphenylphosphine oxide systems, where cleavage of the P=O bond occurs.

Les réactions du triphényl-1,2,5 phosphole (TPP) et du triphényl-1,2,5 phosphole oxyde (TPPO), sulfure (TPPS), et séléniure (TPPSe) avec quelques halogénures de métaux de transition ont été étudiées dans des solvants organiques secs, en l'absence de tout oxygène. La réactivité de ces ligands est clairement fonction des états d'oxydation du métal, l'ordre étant M(II) < M(III) < M(IV) < M(V). Par exemple les ligands ne réagissent pas avec $M(II)X_2$ (Mn, Fe, Ni) tandis que des réactions rapides ont lieu avec le niobium (V), le tantale (V); le fer (III) et le cuivre (II) sont tous deux réduits par le TPP. Les complexes résultant de ces études sont pour la plupart des composés d'addition simple avec les divers halogénures métalliques bien que d'autres espèces telles que les sels de phospholium $[TPPH]^+[MCl_6]^-$ et des composés oxytrichlorés d'addition MOX_3. TPPO (M = Nb, Ta) sont aussi décrites. Dans les sels de phospholium, le cycle phosphole est protoné sur l'atome de phosphore ce qui est en contraste direct avec les dérivés du pyrrole. L'origine de l'atome d'oxygène dans les complexes oxytrichlorés est discutée et comparée avec les données des systèmes analogues de l'oxyde de triphénylphosphine où le clivage de la liaison P=O a lieu.

Canadian Journal of Chemistry, **50**, 1008 (1972)

Introduction

The coordinating properties of tertiary phosphines with transition metals have been extensively studied, but their fully unsaturated five-membered heterocyclic counterparts, the phospholes (*e.g.* **1**), which probably have considerable aromatic character (1), have not been investigated extensively as coordinating species.

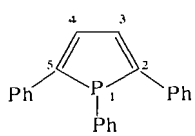

1

This is probably due to their relative inaccessibility until recently and also to their much lower basicity (1) which is evident in both their organic and inorganic reactions. This lower basicity of phospholes as well as other physical evidence, such as a low pyramidal inversion barrier (2), have been taken as evidence for the extensive delocalization of the phosphorus non-bonding electron pair into the phosphole ring (for a discussion of the aromatic character of the phosphole system, see ref. 3). If this is so, then presumably the phospholes will be weaker electron donors than the phosphines.

In one of the few studies of the phosphole system, it was found (4) that 1,2,3,4,5-pentaphenylphosphole reacts with $Fe(CO)_5$ to give P-bonded pentaphenylphosphole iron tetracarbonyl but that the reaction with $Fe_3(CO)_{12}$ gives pentaphenylphosphole iron tricarbonyl, in which bonding to the iron is through the diene π system of the heterocyclic ring. Similar reactions have been observed between 1,2,5-triphenylphosphole (**1**, TPP) and iron carbonyls (5) and P-bonded phosphole complexes have been obtained from carbonyls of chromium, molybdenum, tungsten, and nickel. Further-

Can. J. Chem. Downloaded from www.nrcresearchpress.com by 210.87.254.5 on 09/05/12
For personal use only.

Can. J. Chem. Downloaded from www.nrcresearchpress.com by 210.87.254.5 on 09/05/12
For personal use only.

more, the use of phosphole and phospholene cobalt carbonyl complexes as catalysts in hydroformylation reactions has also been reported (6). TPP also reacts with the chlorides of some 4d and 5d elements and adducts of Hg(II), Pd(II), Pt(II), and Rh(III) halides have been reported (7).

Phosphole oxide complexes have received brief mention (4, 5) in connection with their π-bonded $Fe(CO)_3$ complexes but otherwise have not been investigated as coordinating species. Similarly, phosphole sulfides and selenides have received little attention except by Braye *et al.* (4) who found that treatment of 1,2,3,4,5-pentaphenylphosphole sulfide with iron carbonyls results in complete cleavage of the P=S bond to give only the pentaphenylphosphole–$Fe(CO)_4$ complex. In short, most of the few reported reactions with phosphole derivatives have been with zero valent metal species.

Reactions of triphenylphosphine oxide, sulfide, and selenide with metal halides, particularly those of niobium(V) and tantalum(V) have been investigated by several groups (8–11). Thus, a direct comparison with the corresponding phosphole systems is possible and the influence of the heterocyclic ring and possible steric effects of the bulky phenyl groups may be ascertained. Examination of reactions of a wide range of transition metal halides in various oxidation states with the phosphole systems should also lead to information on the electronic structures of the ligands.

Results and Discussion

The fact that the phosphorus lone pair of electrons is not readily available for σ-bonding is immediately apparent by the fact that TPP does not react, under any of the conditions employed in this work, with the chlorides (anhydrous and hydrated) of silver(I), manganese(II), iron(II), cobalt(II), nickel(II), thorium(IV), and uranium(IV), although phosphine complexes of these metals, except for the last two (12), are well established (13).

However, with an approximately 1:1 ratio of TPP:$CuCl_2$ in methanol solution, a yellow crystalline diamagnetic solid of composition CuCl.TPP is obtained. A complex of the same stoichiometry can also be prepared as a white crystalline solid from the reactions between DBP[1] and copper(II). Also, reactions between freshly prepared copper(I) chloride and the phospholes **1** and **2** in methanol under reflux yield the same compounds (identical infrared spectra and X-ray powder diffraction patterns) as the complexes from the copper(II) reactions. It is well known that salts of copper(II) are readily reduced by tertiary phosphines and arsines (14) and this, together with the formation (15) of $CuCl.Ph_3P$ from Ph_3P and CuCl emphasizes the close resemblance between phospholes and Ph_3P in this system.

The reaction between iron(III) chloride and TPP in methylene chloride solution also results in reduction of the metal with the formation of iron(II) chloride and oxidation of the phosphole to the corresponding oxide TPPO. In the presence of an excess of iron(III) chloride, the complex $FeCl_3.2TPPO.0.5CH_2Cl_2$ is formed.

However, the chlorides and bromides of niobium(V) and tantalum(V) react readily with TPP producing 1:1 crystalline complexes (except for $NbBr_5$ which gives an oil). The iodides do not react, probably because the bonding energy is offset by greater steric interactions. The ready reaction of the phosphole in these cases is rather surprising in view of its much weaker basicity compared with tertiary phosphines (1), together with the fact that it reacts only slowly as a weak nucleophile with the strongly electrophilic dimethyl acetylenedicarboxylate (16), and shows no reaction with most of the above mentioned metal halides. With niobium(V) and tantalum(V) halides, the reaction begins immediately on addition of dry methylene chloride or benzene to a mixture of the reactants, and virtually quantitative yields of the 1:1 adducts are obtained when the mixtures are heated under reflux for 2 h. In this system, therefore, it appears that the energy barrier to reaction is substantially reduced and this is probably a function of the ability of these

[1]Work is currently being carried out in these laboratories on the donor properties of DBP, 9-phenyl-9-phosphafluorene **2**, a dibenzophosphole derivative.

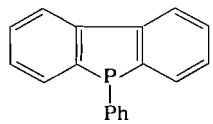

2

Can. J. Chem. Downloaded from www.nrcresearchpress.com by 210.87.254.5 on 09/05/12
For personal use only.

metal ions to accept electrons (note that niobium(V) and tantalum(V) readily accept electrons in the formation of 1:1 complexes with other poor donors, such as ethers and thioethers (17)).

The weakness of the metal phosphorus bond in these adducts is shown by their rapid hydrolysis on exposure to air and by the immediate displacement of the phosphole by coordinating solvents such as acetonitrile and (even) ether. On the other hand, ether does not displace Ph_3P from the $TaCl_5.Ph_3P$ complex nor is the latter as sensitive to hydrolysis by atmospheric moisture as is the phosphole adduct. However, the phosphole complexes are stable when stored under dry nitrogen and, indeed, $TaCl_5$.TPP sublimes unchanged at 155 °C under high vacuum (10^{-6} Torr).

When anhydrous HCl is bubbled through benzene solutions of $TaCl_5$.TPP and $NbCl_5$.TPP, crystalline products rapidly appear. The same products are also formed when the above benzene solutions are exposed to ethanol vapor in the glovebox atmosphere, or when trace amounts of ethanol, water, or hydrogen peroxide (30%) are added directly. (Note that there is no reaction when dry oxygen is bubbled through the solutions.) Chemical analyses of the products, together with the assignment of a sharp absorption band in the infrared spectrum at 2400 cm^{-1} to a P^+—H stretching frquency (18) suggest that the products should be formulated as phospholium salts $[TPPH^+][MCl_6^-]$ (M = Nb, Ta). Furthermore, when anhydrous DCl is passed into a benzene solution of $TaCl_5$.TPP (or when a trace of D_2O is added directly), the corresponding $[TPPD^+][TaCl_6^-]$ complex is produced showing the P—D stretching frequency at 1753 cm^{-1} (18) and having an X-ray powder pattern identical with that of $[TPPH^+][TaCl_6^-]$.

Methylene chloride appears to be the only solvent in which the phospholium salts show any real stability and even in this solvent, extensive decomposition occurs when the solutions are allowed to stand. However, molar conductivities measured rapidly in freshly prepared solutions (Table 1) are consistent with the complexes being formulated as 1:1 electrolytes. Thus the site of protonation in TPP (at least under conditions employed in this work) is the phosphorus atom. This is in contrast to pyrroles which protonate on the 2 or 3 positions of the ring (19) depending upon the substitution pattern. A further discussion of protonated phospholes is the subject of a separate communication (20). In reactions where ethanol was added directly to the $TaCl_5$.TPP solution, traces of an uncharacterized product containing metal, halide, ethoxy, and ligand were observed, indicating that the proton probably originates from the hydroxyl group of the ethanol.

TABLE 1. Molar conductivity data

Complex	Concentration (M)	Molar conductivity (ohm^{-1} cm^{-1} mol^{-1})
$[TPPH^+][TaCl_6^-]$	7.5×10^{-4}	6.6
$[Et_4N^+][I^-]$	1.85×10^{-3}	10.7
$[Et_4N^+][Cl^-]$	1.16×10^{-3}	8.25
β-$TaCl_5$.TPPO	5.5×10^{-3}	0.060
$Fe(S_2CN\ Et_2)_3$	1.07×10^{-3}	0.061

The orange crystalline $[TPPH^+][TaCl_6^-]$ complex is stable in air for several hours but is instantly hydrolyzed on addition of wet organic solvents. Attempts to replace $[TaCl_6^-]$ with other anions such as Cl^- and $[BPh_4]^-$ resulted in decomposition of the phospholium salt, probably indicating that a favorable lattice energy is required (and obtained) with the $[MCl_6^-]$ ions (M = Nb,Ta). The niobium complex appears to be much less stable, decomposes rapidly in air, and is generally much more difficult to isolate from the reactions described above than is the tantalum compound.

That this reaction is not restricted to TPP is apparent from the ease with which molecules such as $[Ph_3PH^+][TaCl_6^-]$ and $[DBPH^+][TaCl_6^-]$ are formed, although in these cases protonation at the phosphorus atom is not unexpected since both Ph_3P and DBP are considerably more basic than the phosphole. Other transition metal ions, such as $ZnCl_4^{2-}$, $FeCl_4^-$, UCl_6^{2-}, $PtCl_6^{2-}$, *etc.* do not appear to stabilize phospholium ions. For example the reaction of anhydrous $FeCl_3$ with TPP (2:1) and dry HCl in benzene, produces an extremely air-sensitive complex which shows in its infrared spectrum, a P—H stretching frequency at 2410 cm^{-1} and bands probably associated with the $FeCl_4^-$ anion at 335 and 390 cm^{-1} (21). This, together with chemical analyses, indicates that the complex could possibly be formulated as $[TPPH^+][FeCl_4^-].FeCl_3$ (*cf.* a double salt $[(pyH^+)$-

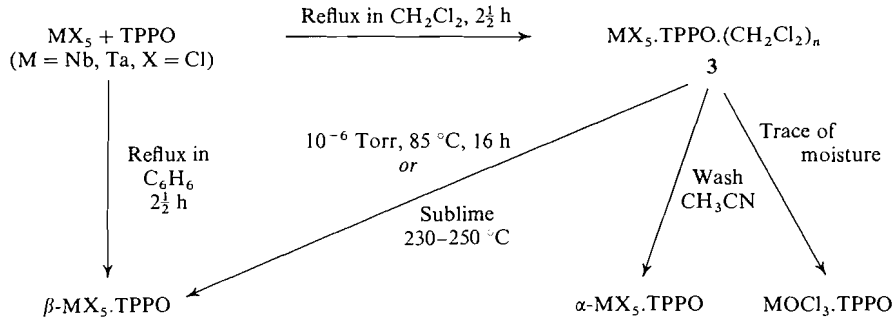

FIG. 1. Reactions of TPPO with niobium(V) and tantalum(V) halides.

$(FeCl_4^-)]_2.(pyH^+Cl^-)$ (py = pyridine) has been reported (22)). Similar reactions carried out with the $FeCl_3$:TPP ratio 1:1 result in the formation of a yellow hygroscopic solid which appears to be $[FeCl_2(TPP)_2^+][FeCl_4^-]$.

The donor properties of the phosphole system appear to be only marginally improved by incorporating an oxygen atom onto the phosphorus. Thus, no reaction was observed between 1,2,5-triphenylphosphole oxide (TPPO) and iron(II), nickel(II), and copper(II) chlorides after prolonged heating under reflux in methylene chloride or ethanol solution, while traces of a product were obtained from manganese(II). Cobalt(II) is the most reactive of the divalent 3d metals towards TPPO producing, in methylene chloride, a bright green solid, although all attempts to purify the complex (*e.g.* recrystallization, sublimation, and chromatography) resulted in decomposition. Bands in the visible (16 700 cm^{-1}) and near infrared (5900 cm^{-1}) regions in the reflectance spectrum of the crude compound strongly suggest the presence of tetrahedral cobalt(II) as is the case (23) with tertiary phosphine oxide complexes of cobalt(II) and therefore the complex is probably $CoCl_2.2TPPO$. A rapid reaction of TPPO also occurs with $FeCl_3$ producing $FeCl_3.2TPPO.0.5CH_2Cl_2$ and with thorium(IV) and uranium(IV) chlorides producing $MCl_4.2TPPO$ (M = Th,U) and $ThCl_4.3TPPO$. The halides $TaCl_5$ and $NbCl_5$ react immediately with TPPO to give 1:1 adducts in several crystalline forms, depending on the reaction conditions. These results are summarized in Fig. 1. Both α- and β-MX_5.TPPO can be converted back into the solvated adduct **3** by recrystallization from methylene chloride. Similar reactions occur with the pentabromides of both metals.

When the tantalum chloride adduct **3** (Fig. 1) is allowed to stand in a rubber-stoppered tube for several weeks, an orange colored precipitate of the oxytrichloride adduct $TaOCl_3.TPPO$ slowly forms. The origin of the oxygen atom in this species is of special interest in view of the oxygen abstraction from phosphine oxides by niobium(V). Thus, Fairbrother *et al.* (10) found that the reaction of $NbCl_5$ with an excess of Ph_3PO leads to the formation of $NbOCl_3.2Ph_3PO$ and probably Ph_3PCl_2, although the latter was not isolable. Other workers (8, 9, 11) report similar results although with $TaCl_5$, only the 1:1 complex, $TaCl_5.Ph_3PO$ was observed (8, 11). Fairbrother *et al.* (10) did obtain $TaOCl_3.2Ph_3PO$ but only by reacting $TaCl_5$ with $(Ph_3PO)_2.H_2O_2$, where the peroxide probably serves as the oxygen source. In view of the weaker P=O bond in the phosphole oxides (24) compared with Ph_3PO, it would appear likely that oxygen abstraction from this group should occur, particularly in reactions between $NbCl_5$ and TPPO.

However, no evidence for this was observed in reactions between either $TaCl_5$ or $NbCl_5$ with TPPO. Thus, when a benzene solution of $TaCl_5.TPPO$ is heated under reflux for up to 16 h with a 2 *M* excess of TPPO, no evidence (infrared, mass spectral) for cleavage of the P=O bond by formation of either a P-dichloride or the phosphole itself is observed. Indeed methylene chloride solutions of $TaCl_5.TPPO$ are stable indefinitely when kept in a ground-glass stoppered tube indicating clearly that in reactions producing $MOCl_3.TPPO$ complexes the oxygen atom comes from trace amounts of oxygen or water diffusing into the system and not from the P=O group. With the $NbCl_5.TPPO$ reaction, even a 1:3 molar ratio of reactants

Can. J. Chem. Downloaded from www.nrcresearchpress.com by 210.87.254.5 on 09/05/12
For personal use only.

TABLE 2. Some infrared stretching frequencies

Compound	ν(P=X) (X = O,S)	$\Delta\nu$(P=X)*	ν(M—Halide)
TPPO	1181	—	—
$CoCl_2$.2TPPO	1170	11 (40, 25)	315, 345
$FeCl_3$.2TPPO	1145	36 (70, 25)	375
$ThCl_4$.2TPPO	1062	119 (121, 26)	260
$ThCl_4$.3TPPO	1135	46 (122, 26)	260
	1100	81 (147, 26)	
UCl_4.2TPPO	1090	91 (124, 26)	270
	1063	118	
α-$TaCl_5$.TPPO	1064	117 (205, 9)	332
β-$TaCl_5$.TPPO	1064	117	336, 343
$TaBr_5$.TPPO.CH_2Cl_2	1053	128 (217, 9)	235
α-$NbCl_5$.TPPO	1058	128	355
β-$NbCl_5$.TPPO	1058	128	350, 365
$NbBr_5$.TPPO.CH_2Cl_2	1049	132	
$TaOCl_3$.TPPO†	1089	92 (50, 10)	338
TPPS	637	—	—
α-$TaCl_5$.TPPS	613/625‡	24/12‡ (48, 9)	342
β-$TaCl_5$.TPPS	613/625	24/12 (48, 9)	340
α-$NbCl_5$.TPPS	611/623	26/14 (53, 9)	365
β-$NbCl_5$.TPPS	611/623	26/14	355, 375

*Figures in parentheses are the shifts for similar Ph_3PO complexes together with the appropriate reference.
†Also shows a very strong absorption at 800 cm^{-1} due to the Ta=O group.
‡Impossible to unambiguously assign the P=S frequency and therefore either of the two figures may be correct.

produced only a trace (< 2%) of $NbOCl_3$.TPPO. This is not unreasonable in the light of the ready formation of NbX_5.TPPO (X = Cl,Br) from reactions between NbX_5 and TPPSe when oxygen is not rigorously excluded, *i.e.* oxygen pick-up in these cases appears to be at the phosphorus atom to form TPPO and *not* at the metal to form the Nb=O linkage. The reason for the difference in behavior between Ph_3PO and TPPO towards $NbCl_5$ is not clear.

Coordination of the ligand through the oxygen atom is confirmed in all the above mentioned complexes by shifts in the P=O stretching frequency on complexation (25). The shifts (Table 2) range from only 11 cm^{-1} for the crude cobalt(II) complex where interaction between the oxygen atom of the ligand and the metal is clearly extremely weak, to ~130 cm^{-1} for some of the niobium(V) and tantalum(V) species. In all cases, (except $TaOCl_3$.TPPO) the metal–oxygen bonds for the phosphole oxides are much weaker than for phosphine oxides. The complexes $ThCl_4$.3TPPO and UCl_4.2TPPO, along with several other complexes in the literature, show a splitting of the P=O band, the origin of which is not clearly understood (25–27). The remainder of the infrared spectrum of each compound is generally very similar to that of the free ligand except for the strong metal–halide absorptions in the 260–380 cm^{-1} region. The complexity of the spectra in the 300–500 cm^{-1} region rendered impossible the assignment of the M—O stretching frequency.

The phosphole sulfide (TPPS) and selenide (TPPSe) do not react with the divalent metals nor with thorium(IV) and uranium(IV). TPPS does, however, form a weak complex with $FeCl_3$, but on recrystallization of this, $FeCl_3$.2TPPO is formed. TPPS reacts with a slight excess (~10%) of $TaCl_5$ in benzene to give $TaCl_5$.TPPS.C_6H_6 from which the benzene is removed under high vacuum giving α-$TaCl_5$.TPPS. When the reaction is carried out in methylene chloride or benzene using strictly 1:1 ratios, a solvated adduct $TaCl_5$.TPPS.0.5CH_2Cl_2 of the β-phase is obtained. These observations are similar to those of Brown *et al.* (8) who noted that with $TaCl_5$ and $TaBr_5$, triphenylphosphine sulfide and the corresponding selenide give two different crystalline phases depending on the rate of crystallization. However, the reaction of $TaCl_5$ with TPPSe in both methylene chloride and benzene gives only a solvated β-phase (for which the X-ray powder pattern is identical with that

Can. J. Chem. Downloaded from www.nrcresearchpress.com by 210.87.254.5 on 09/05/12
For personal use only.

Can. J. Chem. Downloaded from www.nrcresearchpress.com by 210.87.254.5 on 09/05/12
For personal use only.

of β-$TaCl_5$.TPPS). With neither the sulfide nor the selenide was any abstraction by the metal of S or Se from the P=S or P=Se bonds observed, although both are substantially weaker than the P=O bond. Thus, the ligands TPPS and TPPSe are recovered intact on hydrolysis of the complexes, and high vacuum sublimation of $TaCl_5$.TPPS gives a mixture of the 1:1 adduct with some ligand. Similar observations have been recorded for substituted phosphine sulfides (8, 9, 11).

Tentative assignment of the P=S stretching frequencies are made in Table 2, and are in the general range expected for such molecules (18). Shifts of the P=S vibration on coordination of TPPS to niobium(V) and tantalum(V) are about 20 cm^{-1} (compared to 40–50 cm^{-1} in triphenylphosphine sulfide complexes). The P=Se shifts are extremely small, reflecting the weakness of the M—Se bond. The M—S, M—Se, and M—P frequencies, which would be expected to occur in the 200–400 cm^{-1} region have not been identified, largely because of the intense and very broad M–chlorine stretching frequencies which occur in this general region.

The very limited solubility of the niobium, tantalum, thorium, and uranium complexes precluded n.m.r. and molecular weight measurements. However, the fact that β-$TaCl_5$.TPPO is a non-electrolyte in methylene chloride (Table 1) is not inconsistent with the metal being 6-coordinate in this and similar molecules. The actinide complexes are too insoluble for conductivity studies, but the multiple P=O stretching frequencies in their infrared spectra could indicate the presence of non-equivalent ligands.

In summation, therefore, the donor properties of TPP, TPPO, TPPS, and TPPSe towards transition metals are extremely weak, especially with the lower valent metal salts. Their behavior towards Nb(V) and Ta(V) halides appears to follow rather closely the behavior of their triphenylphosphine analogues, although the greater basic strengths of the latter make them more powerful donors. Even with these strongly electron accepting metal halides, the weakness of the M—P bond in the phosphole complexes is evident and is consistent with the relative inaccessibility of the phosphorus lone pair brought about by delocalization into the ring, although steric effects may also be involved. Moreover, the heterocyclic ring clearly affects the electron density at the oxygen atom in the TPPO complexes where infrared data show the weaker TPPO—M link compared with the Ph_3PO—M bonds. A later publication will in fact concern TPPO complexes of rhodium where bonding to the metal occurs through the π system of the ligand (28).

Experimental

Niobium(V), tantalum(V), thorium(IV), and uranium(IV) halides were prepared by standard methods and purified by vacuum sublimation prior to use. The ligands TPP, TPPO, TPPS, and TPPSe were prepared as described by Campbell *et al.* (29). DBP was prepared by the method of Hoffmann (30) and its oxide by the reaction of H_2O_2 on the phosphole in methanol. Deuterated sulfuric acid (isotopic purity 99%) was obtained from Stohler Isotope Chemicals. Where necessary, reactions were carried out in a dry nitrogen-filled glove box (~100 p.p.m. oxygen). All solvents were degassed and stored over freshly activated molecular sieve (4A) under nitrogen. Methylene chloride and benzene were distilled from calcium hydride prior to degassing.

Physical Measurements

All physical measurements were carried out as previously described (31).

Analyses

Metal analyses (Nb, Ta, Th, U) were performed gravimetrically by hydrolysis of the complexes in an ethanol–aqueous ammonia solution followed by ignition of the precipitated hydroxide to the oxide. Chloride in the supernatant liquid was determined as silver chloride. Analytical data are recorded in Table 3. Where the ligand (TPPS) was not decomposed by the hydrolysis procedure, it was extracted into methylene chloride and determined spectrophotometrically (25 970 cm^{-1}, $\log \varepsilon$, 4.1 (29)). Organic microanalyses were carried out under the supervision of W. J. Buis at the Institute for Organic Chemistry, TNO, Utrecht, the Netherlands, and on a Perkin–Elmer 240 elemental analyzer in the Science Instrumentation Laboratory at this University.

Syntheses

1. CuCl.L (L = TPP, DBP)

A mixture of TPP (0.94 g) and $CuCl_2.2H_2O$ (0.59 g) in methanol (100 ml) was heated under reflux for 2 h, producing a yellow crystalline product (0.74 g, 90%, m.p., 251°).

The same product was also obtained by heating under reflux in methanol (150 ml) a mixture of TPP (0.44 g) and CuCl (0.12 g) for 4 h. The yellow filtrate, on evaporation, yielded a yellow crystalline solid which was recrystallized from benzene.

CuCl.DBP was prepared from either copper(II) or copper(I) following the procedures outlined above as a white crystalline solid, m.p. 254–256°.

2. Attempts to Prepare $[TPPH^+][FeCl_4^-]$

Freshly prepared anhydrous $FeCl_3$ and TPP in a ratio of 2:1 were suspended in purified benzene under a dry nitrogen atmosphere. Anhydrous HCl (dried with conc. H_2SO_4) was passed into the reaction mixture for ~1 h with stirring.

TABLE 3. Chemical analyses

Complex	Color	Found				Calculated			
		C	H	M	X	C	H	M	X
CuCl.TPP	yellow	64.1	4.1		8.8	64.24	4.17		8.62
CuCl.DBP	white	59.9	3.6		9.4	60.18	3.65		9.87
$[TPPH^+][FeCl_4^-].FeCl_3$?	orange-brown	40.2	3.3		34.8	39.20	2.69		36.9
$[FeCl_2(TPP)_2^+][FeCl_4^-]$?	yellow	52.4	3.7			55.68	3.61		
$FeCl_3.2TPPO.0.5CH_2Cl_2$	brown	62.0	4.0		12.8	62.10	4.07		12.37
$FeCl_3.2DBPO.CH_2Cl_2$	yellow	55.8	3.4		13.5	55.57	3.52		13.29
$ThCl_4.2TPPO$	orange-yellow	51.3	3.3	22.5	13.5	50.70	3.30	22.69	13.65
$ThCl_4.3TPPO$	orange	58.8	3.8	17.5	10.7	58.33	3.76	17.09	10.45
$UCl_4.2TPPO$	red	50.3	3.3	22.9	12.2	50.97	3.28	22.98	13.70
$TaCl_5.TPP$	dark brown	39.2	2.7	26.0	25.5	39.41	2.56	26.97	26.44
$[TPPH^+][TaCl_6^-]$	orange	36.9	2.5	25.7	29.6	37.37	2.57	25.58	30.09
$[DBPH^+][TaCl_6^-]$	white			27.0	31.7			27.62	32.49
$TaCl_5.TPPO.CH_2Cl_2$	bright red	36.0	2.6	23.4	22.6	35.81	2.48	23.45	22.98
α-$TaCl_5.TPPO$	bright red	38.9	2.6	26.9	25.6	38.49	2.50	26.35	25.83
β-$TaCl_5.TPPO$	bright red	38.7	2.7	26.3	25.3	38.49	2.50	26.35	25.83
$TaOCl_3.TPPO$	orange	41.7	2.9	27.3	17.3	41.83	2.71	28.64	16.84
β-$TaCl_5.TPPS.0.5C_6H_6$	red-brown	40.4	2.8	24.5	23.7	40.49	2.72	24.39	23.91
α-$TaCl_5.TPPS$	red-brown	49.0*		25.6	25.0	49.02*		25.75	25.24
α-$TaCl_5.TPPS.C_6H_6$	red-brown			23.4	22.3			23.17	22.71
β-$TaCl_5.TPPS$	red-brown	48.1*		25.8	24.5	49.02*		25.75	25.24
β-$TaCl_5.TPPSe.0.5C_6H_6$	red-brown	37.8	2.7	23.1	21.1	38.08	2.56	22.94	22.48
$[Ph_3PH^+][TaCl_6^-]$	white			27.0	31.2			27.53	32.39

*Ligand percentages, determined spectroscopically.

The mixture turned gummy and finally solidified, when the solid was separated and washed with benzene.

Similarly the reaction of TPP and anhydrous $FeCl_3$ in a ratio of 1:1 with HCl yielded a hygroscopic yellow solid which was recrystallized from chloroform.

3. $FeCl_3.2L$ (L = TPPO, TPPS, DBPO)

A mixture of TPPO (0.90 g) and $FeCl_3.6H_2O$ (0.37 g) was heated under reflux in methylene chloride (50 ml) for 4 h. The cooled reddish-brown solution was filtered and a brown crystalline solid separated as the solvent was removed (quantitative yield), m.p. 176–178°.

The other Fe(III) complexes were prepared similarly in methylene chloride solution, *n*-hexane being added to precipitate the compounds. Thus, $FeCl_3.2DBPO$ showed a m.p. of 168–170° while $FeCl_3.2TPPS$ decomposed on recrystallization.

4. $CoCl_2.2TPPO$

A mixture of TPPO and $CoCl_2.6H_2O$ (2:1 mole ratio) in methylene chloride was heated under reflux for 5 h. The reaction mixture was cooled and the excess of cobalt chloride was filtered off. The green filtrate was then evaporated to dryness and the residue recrystallized from 1:1 CH_2Cl_2/C_6H_6 solution as green needles (m.p. 257°). However, the product was contaminated with traces of unreacted ligand. Unsuccessful attempts were made to purify the complex by recrystallization, sublimation, and chromatography.

5. $MCl_4.2TPPO$ (M = Th,U), $ThCl_4.3TPPO$

These complexes were made by mixing the appropriate mole ratios of metal halide and TPPO in ethanol. The 1:2 complex formed immediately while the 1:3 complex formed after the mixture was heated under reflux for 12 h. The products which are air stable, were washed with ethanol and dried under high vacuum (10^{-6} Torr) for 12 h. $ThCl_4.3TPPO$ dissolves in methylene chloride from which $ThCl_4.2TPPO$ is precipitated on addition of pentane.

6. $TaCl_5.TPP$ ($NbCl_5.TPP$, $TaBr_5.TPP$)[2]

A mixture of $TaCl_5$ (0.65 g) and TPP (0.60 g) in methylene chloride/pentane (8:1) (9 ml) was heated under reflux for $2\frac{1}{2}$ h. The resulting dark-brown solution was centrifuged, stoppered, and cooled overnight, when dark-brown crystals (0.6–0.8 g, ~66%) were deposited. These were vacuum dried.

7. $[TPPH^+][TaCl_6^-]$ ($[TPPD^+][TaCl_6^-]$, $[TPPH^+][NbCl_6^-]$)

Anhydrous HCl (or DCl)[3] was bubbled through a benzene solution (8 ml) of $TaCl_5.TPP$ (0.5 g) producing immediately an orange solid. This was washed with benzene (3 × 6 ml), dried, and dissolved in methylene chloride. Addition of dry pentane immediately precipitated the orange product (~0.15 g) which was quickly centrifuged off and dried under vacuum. If the methylene chloride solution is allowed to stand for any length of time an unidentified yellow solid precipitates.

[2]The complexes shown in parentheses were isolated and identified by the fact that their X-ray powder patterns are identical with that of the compound for which the analyses are listed in Table 3.

[3]Made by heating dry sodium chloride (5 g) with degassed D_2SO_4 (0.5 ml).

Can. J. Chem. Downloaded from www.nrcresearchpress.com by 210.87.254.5 on 09/05/12
For personal use only.

Can. J. Chem. Downloaded from www.nrcresearchpress.com by 210.87.254.5 on 09/05/12
For personal use only.

8. $[Ph_3PH^+][TaCl_6^-]$, $[DBPH^+][TaCl_6^-]$

Treatment of a benzene solution (~5 ml) of $TaCl_5.Ph_3P$[4] and $TaCl_5$.DBP[4] (0.5–0.8 g) with anhydrous HCl resulted in the quantitative precipitation of white solids which were washed with benzene (2 × 5 ml), dried, and recrystallized from methylene chloride-pentane.

9. $TaCl_5.TPPO.CH_2Cl_2$ *(*$TaBr_5.TPPO.CH_2Cl_2$, $NbX_5.TPPO.CH_2Cl_2$, $X = Cl, Br$*)*

$TaCl_5$ (0.65 g) and TPPO (0.67 g) in methylene chloride (10 ml) were heated under reflux for 2 h. The resulting bright-red solid (~1 g, 80%) which was formed was dissolved in methylene chloride and recrystallized by slow evaporation of solvent to 1/3 volume. If the solid was precipitated by addition of pentane the solvent content varied between 0.5 and 1.5 mol.

10. α-$TaCl_5.TPPO$ *(*α-$NbCl_5.TPPO$*)*

When the solvated adduct (9) (0.5 g) was washed with acetonitrile (3 × 5 ml), it changed to a flocculent orange-red solid which was vacuum dried.

11. β-$TaCl_5.TPPO$ *(*β-$NbCl_5.TPPO$*)*

(*a*) The β phase was quantitatively obtained by heating (85 °C, 16 h) the adduct (9) under high vacuum (10^{-6} Torr). It also sublimed (together with some TPPO) when the adduct (9) was heated (230–250 °C) under high vacuum (10^{-6} Torr). (*b*) To a suspension of $TaCl_5$ (0.87 g) in benzene (10 ml), TPPO (0.82 g) was added and the mixture heated under reflux for $2\frac{1}{2}$ h. The red crystalline solid (~1.3 g, 80%) which separated was recrystallized from hot benzene.

12. $TaOCl_3TPPO$ *(*$NbOCl_3.TPPO$*)*

A methylene chloride solution (9 ml) of the adduct (9) (0.25 g) was set aside for 1 week in a rubber-stoppered tube. An orange solid (~30 mg) formed on the walls of the tube. This deposition was accelerated by direct exposure to the glove box atmosphere and frequent stirring. After two weeks, the solid (0.15 g, 70%) was removed, washed with methylene chloride (2 × 5 ml), and dried under vacuum.

13. $TaCl_5.TPPS.C_6H_6$ *(*$NbCl_5.TPPS.C_6H_6$*)*

A mixture of $TaCl_5$ (0.64 g) and TPPS (0.56 g) in benzene (5 ml) was heated under reflux for 2 h. The resulting deep-red solution was set aside for several hours during which large dark-red crystals (0.6 g, 50%) were deposited. More product was obtained by slow evaporation of the remaining solution.

14. α-$TaCl_5.TPPS$ *(*α-$NbCl_5.TPPS$*)*

The adduct (13) was pumped under high vacuum (10^{-6} Torr) at 85 °C for 6 h, yielding a red-brown solid.

15. β-$TaCl_5.TPPS$ *(*β-$NbCl_5.TPPS$*)*

A mixture of $TaCl_5$ (1.0 g) and TPPS (1.0 g) in methylene chloride or benzene (10 ml) was heated under reflux for $2\frac{1}{2}$ h. The crystalline solid (1.2 g, 60%) which was deposited on cooling was dried to a red-brown solid under high vacuum (10^{-6} Torr) at 85 °C for 14 h.

16. β-$TaCl_5.TPPSe$ *(*β-$NbCl_5.TPPSe$*)*

A mixture of $TaCl_5$ (1.1 g) and TPPSe (1.3 g) in benzene (10 ml) was heated under reflux for $2\frac{1}{2}$ h. The red-brown crystalline solid (1.5 g, 65%) which was formed was recrystallized from benzene solution and pumped under high vacuum (10^{-6} Torr) at 85° for 14 h.

In the corresponding $NbCl_5$ reaction, oxygen must be rigorously excluded to prevent the formation of $NbCl_5$.TPPO.

We thank the Senate Research Committee of Lakehead University and the National Research Council of Canada for generous financial support of this work.

1. L. D. Quin, J. G. Bryson, and C. G. Moreland. J. Am. Chem. Soc. **91**, 3308 (1969).
2. W. Egan, R. Tang, G. Zon, and K. Mislow. J. Am. Chem. Soc. **92**, 1442 (1970).
3. A. N. Hughes and C. Srivanavit. J. Heterocyclic Chem. **7**, 1 (1970).
4. E. H. Braye, W. Hübel, and I. Caplier. J. Am. Chem. Soc. **83**, 4406 (1961).
5. R. C. Cookson, G. W. A. Fowles, and D. K. Jenkins. J. Chem. Soc. 6406 (1965).
6. Shell Internationale Research Maatschappij N.V., Netherlands Patent Application, 6516164 (1966). Chem. Abstr. **66**, 28392r (1967).
7. R. A. Walton. J. Chem. Soc. A, 365 (1966).
8. D. Brown, J. F. Easey, and J. G. H. du Preez. J. Chem. Soc. A, 258 (1966).
9. D. Brown, J. Hill, and C. E. F. Rickard. J. Less-Common Metals, **20**, 57 (1970).
10. D. B. Copley, F. Fairbrother, and A. Thompson. J. Less-Common Metals, **8**, 256 (1965).
11. W. Van der Veer and F. Jellinek. Rec. Trav. Chim. **85**, 842 (1966).
12. D. Brown. Halides of the lanthanides and actinides, J. Wiley and Sons, Inc., London. 1968. p. 141.
13. G. Booth. Adv. Inorg. Radio Chem. **6**, 1 (1964).
14. R. S. Nyholm. J. Chem. Soc. 1257 (1952); K. Cohn and R. W. Parry. Inorg. Chem. **7**, 46 (1968).
15. F. Glocking and K. A. Hooton. J. Chem. Soc. 2658 (1962).
16. A. N. Hughes and S. Uaboonkul. Tetrahedron, **24**, 3437 (1968).
17. F. Fairbrother. The Chemistry of niobium and tantalum. Elsevier Publishing Company, Amsterdam. (1967).
18. D. E. C. Corbridge. Topics in Phosphorus Chemistry. **6**, 235 (1969).
19. Y. Chiang and E. B. Whipple. J. Am. Chem. Soc. **85**, 2763 (1963).
20. R. Chuchman, D. G. Holah, A. N. Hughes, and B. C. Hui. J. Heterocyclic Chem. **8**, 877 (1971).
21. K. Nakamoto. Infrared spectra of inorganic and coordination compounds. J. Wiley and Sons, Inc., New York. 1963. p. 106.

---

[4]To our knowledge, these compounds have not been prepared previously although the analogous niobium complex, $NbCl_5.Ph_3P$ has been reported (32) and was characterized on the basis of a chloride analysis of 22.10%. However, the theoretical percentage of chloride in $NbCl_5.Ph_3P$ is 33.35%. The tantalum complex was prepared by adding Ph_3P (0.75 g) to a suspension of $TaCl_5$ (0.96 g) in benzene (5 ml). The mixture was heated under reflux for $1\frac{1}{2}$ h, producing a bright yellow solution from which the yellow product was crystallized on addition of pentane.

Anal. Calcd. for $TaCl_5.Ph_3P$: Ta, 28.86; Cl, 28.28. Found: Ta, 28.7; Cl, 28.1.

$TaCl_5$.DBP was made in an analogous manner.

22. A. P. GINSBERG and M. B. ROBIN. Inorg. Chem **2**, 817 (1963).
23. O. A. SERRA and A. C. MASSABNI. Inorg. Nucl. Chem. Lett. **7**, 275 (1971), and references therein.
24. A. F. BEDFORD, D. M. HEINEKY, I. T. MILLAR, and C. T. MORTIMER. J. Chem. Soc. 2932 (1962).
25. F. A. COTTON, R. D. BARNES, and E. BANNISTER. J. Chem. Soc. 2199 (1960).
26. D. BROWN, J. HILL, and C. E. F. RICKARD. J. Chem. Soc. A, 497 (1970).
27. C. I. BRÄNDEN. Acta. Chem. Scand. **17**, 759 (1963) and references therein.
28. D. G. HOLAH, A. N. HUGHES, and B. C. HUI. To be published.
29. I. G. M. CAMPBELL, R. C. COOKSON, M. B. HOCKING, and A. N. HUGHES. J. Chem. Soc. 2184 (1965).
30. H. HOFFMANN. Chem. Ber. **95**, 2563 (1962).
31. P. R. HECKLEY, D. G. HOLAH, and D. BROWN. Can. J. Chem. **49**, 1151 (1971).
32. J. DESNOYERS and R. RIVEST. Can. J. Chem. **43**, 1879 (1965).

Can. J. Chem. Downloaded from www.nrcresearchpress.com by 210.87.254.5 on 09/05/12
For personal use only.

The Reactions of *N*,*N*′-Dimethylethylenediamine with Cyclic Phosphonitrilic Halides[1]

T. CHIVERS AND R. HEDGELAND

Department of Chemistry, The University of Calgary, Calgary 44, Alberta

Received October 25, 1971

The reactions of *N*,*N*′-dimethylethylenediamine with the cyclic phosphonitrilic halides $N_3P_3F_6$, $N_4P_4F_8$, $N_3P_3Cl_6$, and $N_4P_4Cl_8$ lead to spiro halogenophosphonitrilic imidazolidines of the type

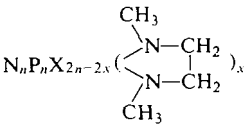

($n = 3, 4$; $x = 1, 2$; X = Cl, F) together with polymeric materials. Structure

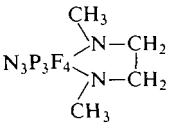

has also been prepared by fluorination of the corresponding chloride with KSO_2F and from $N_3P_3F_6$ and

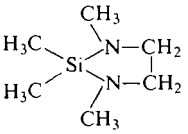

The ^1H and ^{19}F n.m.r., i.r., and mass spectra of the phosphonitrilic imidazolidines are discussed.

Les réactions entre la *N*,*N*′-diméthyléthylènediamine et les halogénures phosphonitriliques cycliques, $N_3P_3F_6$, $N_4P_4F_8$, $N_3P_3Cl_6$, et $N_4P_4Cl_8$, conduisent à des imidazolidines halogénophosphonitriliques spiro du type

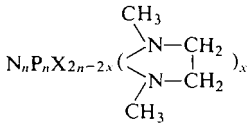

($n = 3, 4$; $x = 1, 2$; X = Cl, F), et à des produits polymériques. Le composé

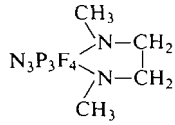

a également été préparé par fluoration des chlorures correspondant avec KSO_2F et à partir de $N_3P_3F_6$ et

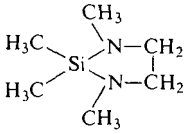

Les spectres r.m.n. (^1H et ^{19}F), de masse, et i.r. des imidazolidines phosphonitriliques sont discutés.

Canadian Journal of Chemistry, **50**, 1017 (1972)

[1]For a preliminary account see Chivers and Hedgeland (24).

Can. J. Chem. Downloaded from www.nrcresearchpress.com by 210.87.254.42 on 09/05/12
For personal use only.

Can. J. Chem. Downloaded from www.nrcresearchpress.com by 210.87.254.42 on 09/05/12
For personal use only.

Introduction

The reactions of cyclic phosphonitrilic chlorides (chlorocyclophosphazenes) with monofunctional amines have been investigated in considerable detail and different substitution pathways have been recognized (1). Geminally substituted spirocyclic derivatives of $N_3P_3Cl_6$ have been prepared from the difunctional amine, *o*-phenylenediamine (2). More recently the reactions of cyclic phosphonitrilic fluorides with amines, *e.g.* Me_2NH (3–5), $MeNH_2$ (4, 5), or Me_3SiNMe_2(3), have been shown to follow a non-geminal substitution pathway and, under appropriate conditions, good yields of the monoamino derivatives can be obtained. Deamination by hydrogen chloride or bromide provides an expeditious route to the corresponding monohalogeno or non-geminally substituted halogeno derivates of cyclic phosphonitrilic fluorides (3–7) which are otherwise difficult to purify (8, 9). In an attempt to extend this synthetic route to the preparation of *gem*-dihalogenophosphonitrilic fluorides we have investigated the reactions of *N,N'*-dimethylethylenediamine with the cyclic phosphonitrilic halides $N_nP_nX_{2n}$ ($n = 3, 4$; X = Cl, F). Geminal substitution occurs to give spiro halogenophosphonitrilic imidazolidines of the type

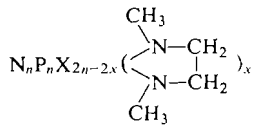

$(n = 3, x = 1, 2; n = 4, x = 1)$

Particularly in the case of $N_4P_4F_8$ oily, presumably polymeric, products were also formed. The reactions of the spiro compounds with hydrogen chloride or bromide gave adducts which could not be converted to the corresponding *gem*-dihalogenophosphonitrilic fluorides.

Experimental

General

The preparations of the phosphonitrilic imidazolines were carried out under an atmosphere of nitrogen, which was replaced by air in the work-up procedure. Hydrocarbon solvents were redistilled from calcium hydride before use. The following chemicals were obtained commercially and used without further purification: anhydrous diethyl ether (Mallinckrodt), hydrogen chloride, hydrogen bromide, dimethylamine (Matheson), *N,N'*-dimethylethylenediamine (Columbia Organic), dichlorodimethylsilane (Peninsular Chem Research), and potassium fluorosulfite (Ozark-Mahoning). $N_3P_3Cl_6$ and $N_4P_4Cl_8$ were purchased from Alfa Inorganics and recrystallized from petrol (30–60°) before use. $N_3P_3F_6$ and $N_4P_4F_8$ were prepared from the corresponding chlorides by the reaction with potassium fluorosulfite in paraffin oil at *ca.* 110° (10). 1,2,2,3-Tetramethyl-1,3-diaza-2-silacyclopentane was prepared by the method of Abel and Bush (11).

The following instruments were used for spectroscopic studies: ^1H n.m.r. spectra (Varian A60 and HA100), ^{19}F n.m.r. spectra (Varian HA100 operating at 94.1 MHz), i.r. spectra (Perkin–Elmer 337 and 621), mass spectra (Varian Atlas CH-5 operating at 70 eV and an accelerating voltage of 3 kV). The ^{19}F n.m.r. spectra were obtained for saturated solutions in benzene with CCl_3F as internal standard.

Carbon, hydrogen, and nitrogen analyses were carried out in this department by Mrs. S. Swaddle and Mr. R. Davidson, and by Organic Microanalyses, Montreal, Quebec who also performed the halogen analyses.

Preparation of gem-N,N'-Dimethylethylenediaminotetrafluorocyclotriphosphonitrile

(a) From N,N'-Dimethylethylenediamine

Hexafluorocyclotriphosphonitrile (27.0 g, 0.108 mol) in diethyl ether (250 ml) was cooled to −15° and *N,N'*-dimethylethylenediamine (19.1 g, 0.216 mol) in ether (100 ml) was added dropwise with continual stirring. After the addition was complete, the reaction mixture was allowed to come to room temperature and the insoluble *N,N'*-dimethylethylenediamine hydrofluoride was filtered off. Removal of solvent from the filtrate yielded white crystals of *gem*-N,N'-dimethylethylenediaminotetrafluorocyclotriphosphonitrile (13.6 g, 0.046 mol) which, after recrystallization from petroleum ether (30–60°), had m.p. 97°.

Anal. Calcd. for $C_4H_{10}F_4N_5P_3$: C, 16.2; H, 3.4; N, 23.6. Found: C, 16.1; H, 3.7; N, 23.9.

(b) From 1,2,2,3-Tetramethyl-1,3-diaza-2-silacyclopentane

Hexafluorocyclotriphosphonitrile (5.4 g, 0.024 mol) and 1,2,2,3-tetramethyl-1,3-diaza-2-silacyclopentane (3.5 g, 0.024 mol) were heated at 80° for 2 h in a sealed Carius tube under vacuum. Vacuum transfer gave difluorodimethylsilane (2.3 g, 0.024 mol) and a white solid which, after recrystallization from ether, was identified as *gem*-N,N'-dimethylethylenediaminotetrafluorocyclotriphosphonitrile (4.5 g, 0.015 mol) from its m.p. 93–95°, ^1H n.m.r. spectrum, and analysis.

Anal. Found: C, 16.4; H, 4.0; N, 22.9.

(c) From gem-N,N'-Dimethylethylenediaminotetrachlorocyclotriphosphonitrile

gem-N,N'-Dimethylethylenediaminotetrachlorocyclotriphosphonitrile (1.9 g, 0.005 mol) and an excess of potassium fluorosulfite (9.6 g) were heated to 105° for 4 h in paraffin oil (20 ml). White crystals were collected by sublimation (25°/0.01 mm) and identified as *gem-N,N'*-dimethylethylenediaminotetrafluorocyclotriphosphonitrile (0.25 g, 0.0007 mol) from the ^1H n.m.r. spectrum and m.p. 95°.

Preparation of gem-Bis(N,N'-dimethylethylenediamino)-difluorocyclotriphosphonitrile

In one preparation of *gem-N,N'*-dimethylethylenediaminotetrafluorophosphonitrile the insoluble white precipitate (mainly dimethylethylenediamine hydrofluoride) was heated under reflux with diethyl ether for 15 min. After filtration of the solution, white crystals began to precipitate which were identified as *gem*-bis(*N,N'*-dimethylethylene-

Can. J. Chem. Downloaded from www.nrcresearchpress.com by 210.87.254.42 on 09/05/12
For personal use only.

diamino)difluorocyclotriphosphonitrile (0.41 g, 0.0016 mol), m.p. 174°.

Anal. Calcd. for $C_8H_{10}F_2N_7P_3$: C, 27.8; H, 5.8; N, 28.4. Found: C, 27.2; H, 5.8; N, 27.8.

Preparation of gem-N,N'-Dimethylethylenediaminohexafluorocyclotetraphosphonitrile

Octafluorocyclotetraphosphonitrile (4.3 g, 0.013 mol) in toluene (150 ml) was cooled to − 78° and *N,N'*-dimethylethylenediamine (2.3 g, 0.026 mol) in toluene (50 ml) was added dropwise to the cooled solution with continual stirring. After the addition was complete, the solution was allowed to stir for a further 30 min at − 78°, and then the insoluble amine hydrofluoride was filtered off before the solution was allowed to come to room temperature. Solvent was removed rapidly on a rotary evaporator and finally on the vacuum line in a sublimation apparatus. The solid residue sublimed (25°/0.01 mm.) to give white crystals of *gem-N,N'*-dimethylethylenediaminohexafluorocyclotetraphosphonitrile (0.5 g, 0.0014 mol), m.p. 40° (dec.).

Anal. Calcd. for $C_4H_{10}F_6N_6P_4$: C, 12.6; H, 2.6; N, 22.1. Found: C, 12.8; H, 2.7; N, 22.2.

The residue from the sublimation, a brown oil containing some crystals, was chromatographed on a florisil column using petroleum ether (30–60°) as eluant to give impure *gem-N,N'*-dimethylethylenediaminohexafluorocyclotetraphosphonitrile.

Anal. Found: C, 13.2; H, 2.7; N, 20.4.

Preparation of gem-N,N'-Dimethylethylenediaminotetrachlorocyclotriphosphonitrile

Hexachlorocyclotriphosphonitrile (5.3 g, 0.015 mol) in ether (700 ml) was cooled to − 78°. *N,N'*-Dimethylethylenediamine (2.7 g, 0.031 mol) in ether (150 ml) was added dropwise over a period of 3 h to the cooled solution with continual stirring. The solution was allowed to reach room temperature overnight and then the insoluble amine hydrochloride was filtered off (1.9 g, 0.012 mol). Solvent was removed on the rotary evaporator, and the residue dissolved in hot hexane (150 ml). Insoluble material (0.13 g) was filtered off, and solvent was removed from the filtrate which deposited white crystals of *gem-N,N'*-dimethylethylenediaminotetrachlorocyclotriphosphonitrile (2.5 g, 0.007 mol), m.p. 114–116°.

Anal. Calcd. for $C_4H_{10}Cl_4N_5P_3$: C, 13.2; H, 2.8; N, 19.3; Cl, 39.1. Found: C, 13.1; H, 3.1; N, 19.2; Cl, 38.7.

Preparation of gem-Bis(N,N'-dimethylethylenediamino)-dichlorocyclotriphosphonitrile

Hexachlorocyclotriphosphonitrile (1.5 g, 0.0043 mol) and *N,N'*-dimethylethylenediamine (2.4 g, 0.028 mol) were heated at reflux in ether solution for 2 h. The insoluble amine hydrochloride (1.3 g, 0.0081 mol) was filtered off, and removal of solvent gave a white solid which, after recrystallization from toluene, was identified as *gem*-bis(*N,N'*-dimethylethylenediamino)dichlorocyclotriphosphonitrile (1.3 g, 0.0035 mol), m.p. 208° (dec.).

Anal. Calcd. for $C_8H_{20}Cl_2N_7P_3$: C, 25.4; H, 5.3; N, 25.6. Found: C, 24.7; H, 6.0; N, 24.4.

Preparation of gem-N,N'-Dimethylethylenediaminohexachlorocyclotetraphosphonitrile

Octachlorocyclotetraphosphonitrile (4.8 g, 0.010 mol) in ether (600 ml) was cooled to 0° and *N,N'*-dimethylethylenediamine (1.8 g, 0.020 mol) in ether (150 ml) was added dropwise during 3 h with continual stirring. The solution was allowed to come to room temperature overnight. The insoluble amine hydrochloride (1.5 g, 0.009 mol) was filtered off and solvent was removed to give a solid residue which was treated with boiling hexane. Insoluble material (0.28 g) was filtered off and removal of some solvent from the filtrate caused the precipitation of white crystals of *gem-N,N'*-dimethylethylenediaminohexachlorocyclotetraphosphonitrile (1.5 g, 0.003 mol), m.p. 91–92°.

Anal. Calcd. for $C_4H_{10}Cl_6N_6P_4$: C, 10.0; H, 2.1; N, 17.5; Cl, 44.7. Found: C, 9.6; H, 2.3; N, 17.2; Cl, 44.8.

Reaction of gem-N,N'-Dimethylethylenediaminotetrafluorocyclotriphosphonitrile with Anhydrous Hydrogen Chloride

gem-N,N'-Dimethylethylenediaminotetrafluorocyclotriphosphonitrile (0.87 g, 0.0029 mol) and an excess of anhydrous hydrogen chloride were heated in a sealed Carius tube under vacuum for 16 h at 130°. Vacuum transfer of the volatile products gave only unreacted hydrogen chloride. The white solid residue, which was stable at 160°, was tentatively identified as an adduct $N_3P_3F_4$ $(CH_3NCH_2CH_2NCH_3)_x$HCl ($x = 1$ or 2).

Anal. Calcd. for the mono-adduct: C, 14.5; H, 3.3; N, 21.1. Calcd. for the di-adduct: C, 13.0; H, 3.2; N, 18.9. Found: C, 13.9; H, 4.1; N, 20.0.

The i.r. spectrum (Nujol mull) 1280s, 1140w, 1115w, 1060s, 920s, 840sh, 810s, 727m, 670w, 505s cm^{-1}.

Discussion

The trimeric phosphonitrilic fluoride, $N_3P_3F_6$, reacts with either *N,N'*-dimethylethylenediamine in ether or, preferably, 1,2,2,3-tetramethyl-1,3-diaza-2-silacyclopentane in a sealed tube to

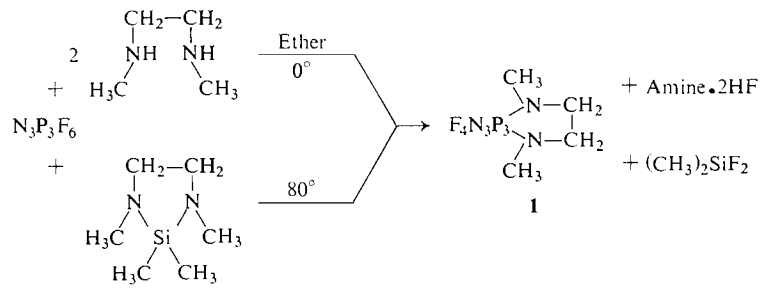

1

SCHEME 1

Can. J. Chem. Downloaded from www.nrcresearchpress.com by 210.87.254.42 on 09/05/12
For personal use only.

give *gem*-*N*,*N*′-dimethylethylenediaminotetrafluorocyclotriphosphonitrile (**1**) (see Scheme 1). Some of the disubstituted compound **2** was also isolated in the reaction with *N*,*N*′-dimethylethylenediamine.

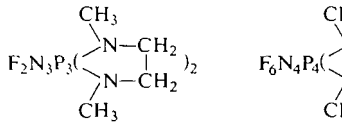

2

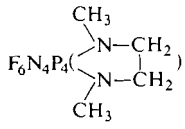

3

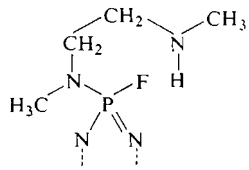

A

Similar reactions using the tetrameric fluoride, $N_4P_4F_8$, were mostly unsuccessful, yielding only a colorless oil which on standing turned brown, became more viscous, and after several days solidified. However, low yields of **3** were obtained from *N*,*N*′-dimethylethylenediamine using *dilute* solutions of the reactants in toluene at $-78°$ followed by a rapid work-up procedure. Apparently in the case of the tetramer the formation of a linear polymer is favored over the formation of the spiro derivative. Nucleophilic substitution by a difunctional amine will likely be a stepwise process, with the substitution of a fluorine by one of the amino groups as the first step. There are now two substitution processes that the monoamino derivative, **A**, can undergo. (*a*) The second amino group can substitute at the same phosphorus atom yielding a spiro derivative, or (*b*) the second amino group can substitute at a phosphorus atom on another phosphonitrilic molecule leading to the formation of linear polymers.[2] Consideration of cyclization kinetics shows that dilute solutions will favor the formation of the spiro derivative over the linear polymers as found experimentally.

It has previously been observed that other imidazolidines show a tendency to polymerize. For example, 1,2,2,3-tetramethyl-1,3-diaza-2-silacyclopentane polymerizes to a highly viscous liquid on standing, particularly in the presence of ammonium sulfate (11). The polymerization is reversible on heating. Similar behavior has been reported for the corresponding germanium imidazolidine, but attempts to prepare the tin analog gave a viscous liquid, apparently polymeric (12).

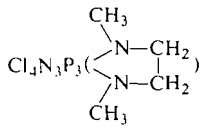

4

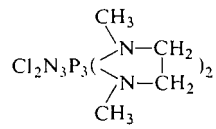

5

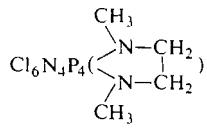

6

Both $N_3P_3Cl_6$ and $N_4P_4Cl_8$ react with *N*,*N*′-dimethylethylenediamine in a large volume of ether at $-10°$ to give good yields of the corresponding monosubstituted spiro compounds, **4** and **6**. The disubstituted derivative **5**, was obtained from $N_3P_3Cl_6$ and an excess of *N*,*N*′-dimethylethylenediamine under reflux in ether. More vigorous reaction conditions are apparently necessary to prepare the trisubstituted spiro compound.

Fluorination of the chloride **4** with potassium fluorosulfite in paraffin oil gave the corresponding fluoride **1**. Fluorination of the corresponding chlorides has also been used to prepare *cis*- and *trans*-1,3-$N_3P_3F_4(NMe_2)_2$ (6), $N_4P_4F_5(NMe_2)_3$, and $N_4P_4F_4(NMe_2)_4$ (from SbF_3) (7), and 1,2-$N_3P_3F_4(NH_2)_2$ (from CsF in acetonitrile) (13).

The reaction of an excess of anhydrous hydrogen chloride with **1** yielded an adduct tentatively identified as

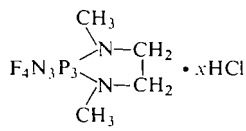

($x = 1$ or 2)

which was thermally very stable. An adduct is also formed initially in the reaction of $N_3P_3F_5NMe_2$ with hydrogen halides, but in this case heating effects decomposition (3–5).

$$N_3P_3F_5NMe_2.HX \xrightarrow[>70°]{HX} N_3P_3F_5X + Me_2NH.HX$$

(X = Cl, Br)

[2]Non-geminal substitution on the same phosphonitrilic molecule is considered to be unlikely for steric reasons.

Can. J. Chem. Downloaded from www.nrcresearchpress.com by 210.87.254.42 on 09/05/12
For personal use only.

The greater stability of the adduct in the case of the spiro compound may indicate a more basic exocyclic nitrogen than in $N_3P_3F_5NMe_2$. Some evidence to support this suggestion comes from measurements of the shifts in ν(C—D) of deuteriochloroform solutions of the compounds relative to ν(C—D) for pure deuteriochloroform. For $N_3P_3F_5NMe_2$, $\Delta\nu = 65\ cm^{-1}$ compared to $\Delta\nu = 77\ cm^{-1}$ for the spiro compound **1**. However, reservations have been expressed concerning this method of measuring base strengths (14).

The geminal structure of **1** (see Fig. 1) is indicated by its ^{19}F n.m.r. spectrum which shows only one doublet ($\delta = 68.4$ p.p.m., $J'_{PF} = 930$ Hz) corresponding to the $\equiv PF_2$ fluorines. The disubstituted compound **2** also shows a $\equiv PF_2$ doublet ($\delta = 65.5$ p.p.m., $J'_{PF} = 800$ Hz) and is thus assigned a geminal structure. The ^{19}F n.m.r. spectrum of **3** shows two doublets of relative intensity (2:1) ($\delta = 67.6$ p.p.m., $J'_{PF} = 840$ Hz; $\delta = 68.7$ p.p.m., $J'_{PF} = 835$ Hz) which have chemical shifts which are similar to those of *gem*-$N_4P_4F_6Cl_2$ (8) rather than those of non-geminal-$N_4P_4F_6(NMe_2)_2$ (3). The two doublets can therefore be assigned to nearest neighbor and antipodal $\equiv PF_2$ groups, respectively.

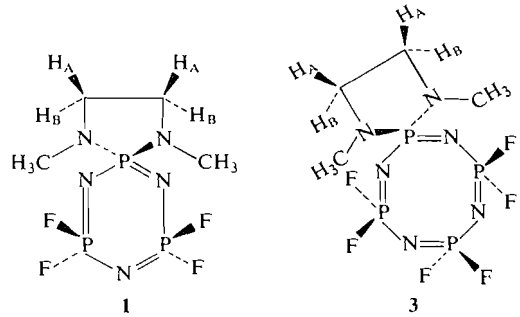

1 3

FIG. 1. Spiro fluorophosphonitrilic imidazolidines: *gem*-(*N*,*N*′-dimethylethylenediamino)tetrafluorocyclotriphosphonitrile (**1**) and *gem*-(*N*,*N*′-dimethylethylenediamino)-hexafluorocyclotetraphosphonitrile (**3**).

The ^1H n.m.r. spectra of the phosphonitrilic imidazolidines are shown in Figs. 2 and 3. The spectra of both **1** and **3** show two doublets of relative intensities 3:2, the doublet to low field is therefore assigned to the methylene protons and the doublet to high field to the *N*-methyl

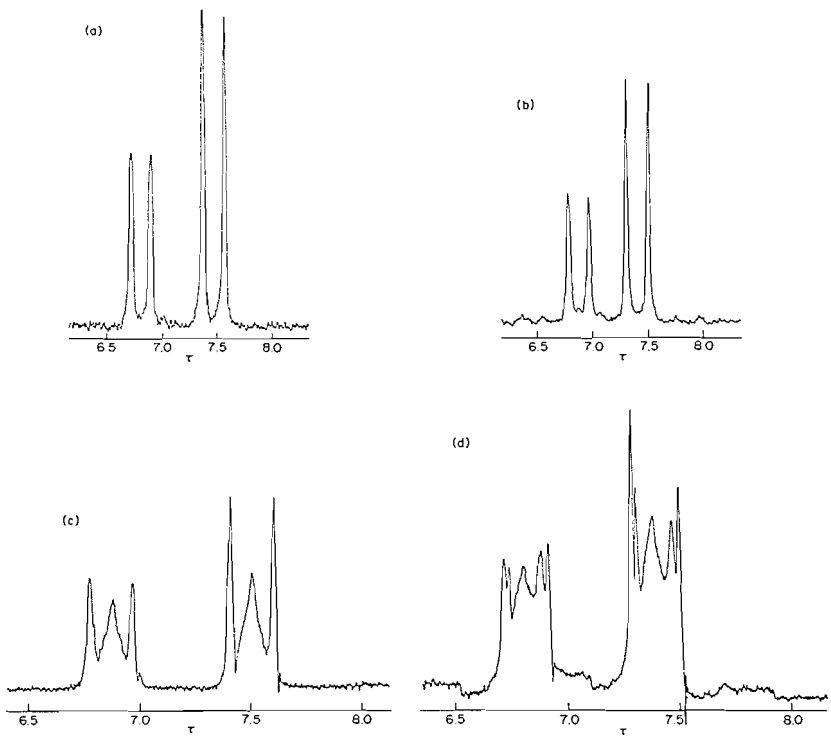

FIG. 2. The ^1H n.m.r. spectra of (*a*) *gem*-(*N*,*N*′-dimethylethylenediamino)tetrafluorocyclotriphosphonitrile (**1**); (*b*) *gem*-(*N*,*N*′-dimethylethylenediamino)hexafluorocyclotetraphosphonitrile (**3**); (*c*) *gem*-bis(*N*,*N*′-dimethylethylenediamino)-difluorocyclotriphosphonitrile (**2**); (*d*) *gem*-bis(*N*,*N*′-dimethylethylenediamino)dichlorocyclotriphosphonitrile (**5**).

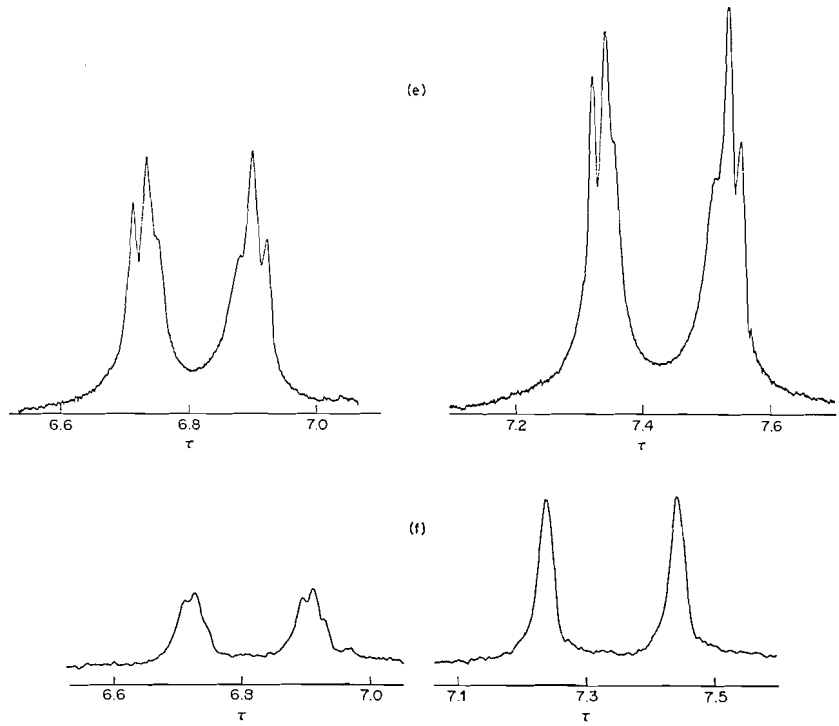

FIG. 3. The ^{1}H n.m.r. spectra of (*e*) *gem*-(*N*,*N*'-dimethylethylenediamino)tetrachlorocyclotriphosphonitrile (**4**); (*f*) *gem*-(*N*,*N*'-dimethylethylenediamino)hexachlorocyclotetraphosphonitrile (**6**).

protons. The separation of the doublets is independent of field strength and hence is assigned to ^{31}P–N–C–^{1}H coupling. These spectra confirm the geminal structures of **1** and **3** since a doublet of doublets is expected for non-geminal substitution *cf.* dimethylaminofluorophosphonitriles (3).

The apparent chemical equivalence of the methylene protons H_A and H_B in the ^{1}H n.m.r. spectra of the fluorophosphonitrilic imidazolidines **1** and **3** is perhaps unexpected and persists even at $-80°$. It should be noted however that unexpectedly simple ^{1}H n.m.r. spectra have previously been observed for the methylene protons in both phosphorus (15, 16) and boron (11) imidazolidines.

In the present examples a number of possible explanations can be given for this observation. Either (*a*) inversion, which is rapid with respect to *ca.* 0.01 s is occurring at the nitrogen atoms of the imidazolidine ring or, less likely (*b*) the imidazolidine ring is planar, or (*c*) protons H_A and H_B show accidental chemical shift equivalence. The sharp doublet observed for the *N*-methyl protons could arise if the *N*-methyl groups are (*a*) *cis*-oriented to the ring, or (*b*) coplanar with a planar ring (*i.e.* attached to trigonal nitrogen atoms), or (*c*) *trans* and inverting rapidly on the n.m.r. time scale. However, it excludes the possibility that the *N*-methyl groups are in a fixed *trans* position.

The ^{1}H n.m.r. spectra of the chlorides **4** and **6**, Fig. 3, are similar to those of the corresponding fluorides **1** and **3** except that splitting of the methylene proton doublets and of the *N*-methyl proton doublets (resolved for **4** only) into triplets is observed. This additional splitting (*ca.* 1 Hz) is probably due to long range coupling with the neighboring $\equiv PCl_2$ phosphorus atoms. Such interactions have previously been observed in the ^{1}H n.m.r. spectra of *cis*- and *trans*-1,3-$N_3P_3Cl_4(NMe_2)_2$ (6).

The ^{1}H n.m.r. spectra of the disubstituted compounds **2** and **5**, Fig. 2, are clearly not first-order and, in particular, a broad absorption is observed between the components of both the methylene proton doublet and the *N*-methyl proton doublet. This type of spectrum is

Can. J. Chem. Downloaded from www.nrcresearchpress.com by 210.87.254.42 on 09/05/12
For personal use only.

TABLE 1. ^{1}H n.m.r. data for some phosphorus imidazolidine derivatives

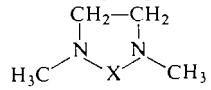

X*	N-CH_2			N-CH_3			Reference
	τ	J'_{PH}(Hz)	M†	τ	J'_{PH}(Hz)	M†	
P—C_6H_5	7.15	—	m	7.50	14.3	d	13
P—CH_3	6.95	—	m	7.45	14.7	d	13
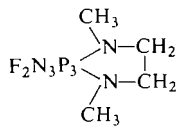	6.88	11.0	m	7.50	12.0	m	‡
$F_6N_4P_4$	6.87	11.5	d	7.42	12.0	d	‡
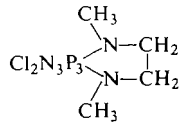	6.82	12.0	m	7.41	12.8	m	‡
$Cl_6N_4P_4$	6.82	11.1	m	7.34	12.2	d	‡
$Cl_4N_3P_3$	6.82	10.0	m	7.42	11.6	m	‡
$F_4N_3P_3$	6.81	10.8	d	7.45	10.7	d	‡
O=P—C_6H_5	6.7	—	d of d	7.47	10.0	d	14

*Measured as saturated solutions in CCl_4 *vs.* tetramethylsilane as internal standard.
†Multiplicity: s, singlet; d, doublet; m, multiplet.
‡This work.

characteristic of an $X_nAA'X'_n$ system (17) and has been observed for a large number of dialkylaminophosphonitrilic derivatives (3, 6, 18). The separation of the two outer components of these signals is $|J_{AX} + J_{AX'}|$. The spectrum of the chloride **5** shows further splitting of the outer components into doublets, presumably due to long range coupling with the unique $\equiv PCl_2$ phosphorus atom.

Table 1 shows the relevant ^{1}H n.m.r. parameters for a series of heterosubstituted imidazolidines. The chemical shifts for the methylene protons indicate the following order of electron withdrawal by phosphorus substituents, O=P—C_6H_5 > $N_3P_3X_4$ ~ $N_4P_4X_6$ > P—CH_3 > P—C_6H_5 (X = F, Cl).

The i.r. spectra of the phosphonitrilic imidazolidines are reported in Table 2. The actual symmetry of

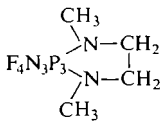

is at most C_{2V} (planar imidazolidine and phosphonitrilic rings) and is probably lower. The degeneracy of the ring vibration ν_{as}(PNP) and 1200–1300 cm^{-1} is therefore removed and peaks are observed at *ca.* 1250 cm^{-1} (**1**) and at 1240 and 1208 cm^{-1} (**2**). The decrease in ν_{as}(PNP) compared to $N_3P_3F_6$ (1290 cm^{-1}) (19) is consistent with weakening of the endocyclic π-bonding on replacement of fluorine by the less electronegative amino substituents, and is also observed for the tetrameric derivative (**3**)ν_{as}(PNP) 1385 cm^{-1} *cf.* ν_{as}(PNP) 1419 and 1438 cm^{-1} for $N_4P_4F_8$ (10). Other assignments can be made from a knowledge of the i.r. spectra of the phosphonitrilic fluorides (20) and chlorides (21) and their dialkylamino derivates (3). C—N antisym stretching 1160–1170 cm^{-1}; C_2NP sym. stretching 1030–1040 cm^{-1}; PF_2 asym. stretching 700–800 cm^{-1}; PCl_2 sym. and asym. stretching 500–600 cm^{-1}; and PF_2 deformation 480–500 cm^{-1}.

The partial mass spectra of the spiro compounds (**1**) and (**3**) and of $N_3P_3F_5NMe_2$, for

Can. J. Chem. Downloaded from www.nrcresearchpress.com by 210.87.254.42 on 09/05/12
For personal use only.

TABLE 2. The i.r. spectra of phosphonitrilic imidazolidines*

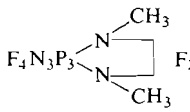	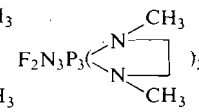	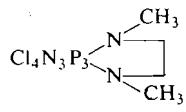	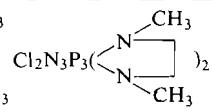	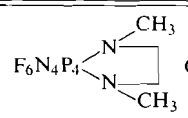	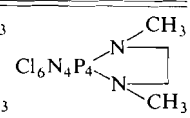
				1385 s	1325 s 1310 m
1280 sh 1245 sh 1230 vs	1240 s 1208 s	1250 s 1230 s	1225 s 1205 sh	1262 m 1250 sh 1212 m	
1160 s	1162 s 1115 sh	1180 vs 1140 sh	1160 s	1160 s 1120 sh	1160 m
1040 m	1030 s	1035 m	1030 s	1040 s	1040 m
932 m 905 vs	945 s 930 sh	948 m	940 s	980 s 960 sh 950 sh 935 vs 915 sh	985 w 945 m
803 s	892 m 868 m 852 m	880 w 865 m 845 m 805 m	860 m 810 m	865 w 820 m	885 m 825 w
747 vs	755 s 735 m	745 m	745 m	732 vs 702 vs	745 m 725 w
695 w	690 s	690 w 630 m	690 s		620 m
		585 sh 562 s 525 s	580 m 540 m		590 s 550 w 510 s
487 s 462 m	490 s 472 s	492 m	490 s	495 sh 488 vs 445 sh	488 sh 455 w

*Nujol mull.

comparison, were obtained. Noteworthy features include the fact that the parent ions exhibit the strongest peak in the spectra of the spiro compounds, (*m/e* 297, **1**; *m/e* 389, **3**) whereas the ion $N_3P_3F_5^+$ (*m/e* 230) is predominant in the spectrum of $N_3P_3F_5NMe_2$. The P + 1 peaks are larger than expected on the basis of natural isotopic abundances, especially for the spiro compounds. This may be due to the formation of a protonated ion PH^+, which suggests that the exocyclic nitrogen atom is more basic in the spiro compound than in $N_3P_3F_5NMe_2$ (*cf.* adduct formation with hydrogen halides). Strong peaks corresponding to fluorophosphonitrilic hydride ions *e.g.* $N_3P_3F_4H_2^+$ (*m/e* 213) were observed in the spectra of all three compounds. Halogenophosphonitrilic hydrides are not known although extensive attempts have been made to prepare them[3] (22, 23).

Financial support from the National Research Council of Canada is gratefully acknowledged.

1. R. A. SHAW. Rec. Chem. Progr. **28**, 243 (1967).
2. H. R. ALLCOCK and R. L. KUGEL. Inorg. Chem. **5**, 1016 (1966).
3. T. CHIVERS, R. T. OAKLEY, and N. L. PADDOCK. J. Chem. Soc. A, 2324 (1970). T. CHIVERS and N. L. PADDOCK Chem. Commun. 337 (1969).
4. O. GLEMSER, E. NIECKE, and H. W. ROESKY. Chem. Commun. 282 (1969).
5. O. GLEMSER, E. NIECKE, and H. THAMM. Z. Naturforsch. **25**b, 754 (1970).

[3]For example, the reaction between $N_4P_4F_7Br$ and tri-*n*-butyltin hydride gives tri-*n*-butyltin bromide in almost quantitative yield, but the major phosphonitrilic product is $N_4P_4F_8$ (T. Chivers and N. L. Paddock, unpublished data).

Can. J. Chem. Downloaded from www.nrcresearchpress.com by 210.87.254.42 on 09/05/12
For personal use only.

6. B. GREEN and D. B. SOWERBY. J. Chem. Soc. A, 987 (1970). B. GREEN and D. B. SOWERBY. Chem. Commun. 628 (1969).
7. B. GREEN and D. B. SOWERBY. Inorg. Nucl. Chem. Lett. **5**, 989 (1969).
8. J. EMSLEY and N. L. PADDOCK. J. Chem. Soc. A, 2590 (1968).
9. E. STEGER and D. KLEMM. J. Inorg. Nucl. Chem. **29**, 1812 (1967).
10. A. C. CHAPMAN, N. L. PADDOCK, D. H. PAINE, H. T. SEARLE, and D. R. SMITH. J. Chem. Soc. 3608 (1960).
11. E. W. ABEL and R. P. BUSH. J. Organometal. Chem. **3**, 245 (1965).
12. C. H. YODER and J. J. ZUCKERMAN. J. Am. Chem. Soc. **88**, 4831 (1966).
13. E. NIECKE, H. THAMM, and O. GLEMSER. Abstract C21, 6th International Symposium on Fluorine Chemistry, Durham, 1971.
14. E. W. RANDALL, C. H. YODER, and J. J. ZUCKERMAN. Inorg. Chem. **6**, 744 (1967).
15. M. K. DAS and J. J. ZUCKERMAN. Inorg. Chem. **10**, 1028 (1971).
16. C. H. YODER and J. J. ZUCKERMAN. J. Am. Chem. Soc. **88**, 2170 (1966).
17. R. K. HARRIS. Inorg. Chem. **5**, 701 (1966).
18. R. KEAT, S. K. RAY, and R. A. SHAW. J. Chem. Soc. 7193 (1965). R. KEAT and R. A. SHAW. J. Chem. Soc. A, 703 (1968).
19. J. EMSLEY. J. Chem. Soc. A, 109 (1970).
20. A. C. CHAPMAN and N. L. PADDOCK. J. Chem. Soc. 635 (1962).
21. L. W. DAASCH. J. Am. Chem. Soc. **76**, 3403 (1954).
22. C. H. KOLICH. Diss. Abstr. Int. **B31** (10), 5862 (1971).
23. B. V. LEVIN, Z. G. RUMYANTSEVA, and V. V. MIRONOVA. Izv. Akad. Nauk S.S.S.R., Neorg. Materialy, **3** (3), 586 (1967); Chem. Abstr., **67**, 49997*c* (1967).
24. T. CHIVERS and R. HEDGELAND. Inorg. Nucl. Chem. Lett. **7**, 767 (1971).

Can. J. Chem. Downloaded from www.nrcresearchpress.com by 210.87.254.42 on 09/05/12
For personal use only.

Chloroacetylation of 1-Azaphenothiazine

J. W. STEELE[1] AND W. K. ANDERSON[2]
Faculty of Pharmacy, University of Manitoba, Winnipeg, Manitoba R3T 2N2

AND

W. F. TRAGER
The School of Pharmacy, University of California, San Francisco Medical Center, San Francisco, California 94122

Received March 5, 1971[3]

The n.m.r. and mass spectral data are used to show that chloroacetylation of 1-azaphenothiazine gave 1-hydroxy-2-chloroacetyl-6-thia-10*b*-aza-2*a*-azoniaaceanthrylene hydroxide inner salt and not the expected 10-chloroacetyl-1-azaphenothiazine.

On utilise les données de r.m.n. et de spectrométrie de masse pour montrer que la chloro-acétylation de la 1-azaphénothiazine donne le sel interne suivant: l'hydroxyde de 1-hydroxy-2-chloro-acétyl-6-thia-10*b*-aza-2*a*-azoniaacéanthrylène et non pas le 10-chloroacétyl-1-azaphénothiazine auquel on s'attendait d'abord.

Canadian Journal of Chemistry, **50**, 1026 (1972)

Introduction

The synthesis of 10-chloroacetyl-1-azaphenothiazine was the initial key step in making one of several series of phenothiazine compounds (1) of potential therapeutic value. It is well known that phenothiazine can be chloroacetylated under a variety of conditions to yield 10-chloroacetylphenothiazine (2). However, treatment of 1-azaphenothiazine[4] in such standard reactions did not produce the desired 10-chloroacetyl-1-azaphenothiazine, nor indeed any identifiable product. A relatively pure product was eventually obtained in consistent yields by treating 1-azaphenothiazine (**1**) with chloroacetic anhydride and chloroacetic acid in dry dioxane and shown to be 1-hydroxy-2-chloroacetyl-6-thia-10*b*-aza-2*a*-azoniaaceanthrylene hydroxide inner salt (**2**).

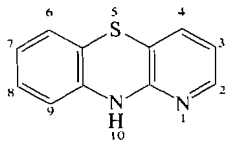

1

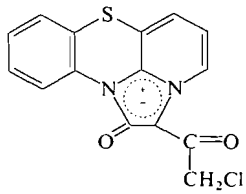

2

[1]Author to whom enquiries should be addressed, at the University of Manitoba.

[2]Present address: Department of Medicinal Chemistry, School of Pharmacy, State University of New York at Buffalo, Buffalo, N.Y. 14214.

[3]Revision received December 20, 1971.

[4]The 1-azaphenothiazine was prepared by direct thionation of 2-anilinopyridine in the presence of an iodine catalyst; see ref. 22.

Experimental

Melting points were determined on a Hoover Uni-melt apparatus and are uncorrected. The 60 MHz n.m.r. spectrum was determined on a Varian A-60 n.m.r. spectrometer and the 220 MHz spectra were determined on a Varian 220 MHz n.m.r. spectrometer, using tetramethylsilane as the internal standard. The mass spectra were determined on the AEI MS-902 high resolution mass spectrometer, modified to permit metastable scanning, at 70 eV and temperature of approximately 200° via the direct insertion probe. High resolution mass measurements were made at approximately 20 000 resolution (10% valley definition) using the electrical peak matching technique with perfluorotributylamine as standard. All measurements were within ±3 p.p.m. of the calculated values. The i.r. spectra were determined on a Beckman IR-8 instrument. Microanalyses were performed by either F. and E. Pascher, West Germany or Geller Laboratories, U.S.A.

Chloroacetylation of 1-Azaphenothiazine

A stirred mixture of 1-azaphenothiazine (50.0 g, 0.25 mol), chloroacetic anhydride (54.0 g, 0.32 mol), and chloroacetic acid (75.0 g, 0.79 mol) in 250 ml of dry dioxane was refluxed for 1 h. The hot mixture was poured into 1 l of hot water and the precipitate was collected and washed with warm 95% ethanol until the washings were colorless. The product (1-hydroxy-2-chloroacetyl-6-thia-10*b*-aza-2*a*-azoniaaceanthrylene hydroxide inner salt (**2**)) was obtained as a fluffy, yellow–green solid, (43.0 g) m.p. 275–277° (dec.); i.r. absorption (KBr) at 3150, 1672, 1613, 1486, 1439, 1389, 1362, 1333, 1282, 1253, 1188, 1140, 1092, 1029, 983, 843, 787, 766, 752, 730, 715, 653 cm^{-1}; *m/e* 318, 316 (M^+, $C_{15}H_9ClN_2O_2S$), 281, 267 ($C_{14}H_7N_2O_2S$), 253, 239, 225, 211, 200, 199 ($C_{11}H_7N_2S$), 184, 172, 168, 155, 140, 109, 108, 99, 98.

Anal. Calcd. for $C_{15}H_9ClN_2O_2S$: C, 56.87; H, 2.86; N, 8.85. Found: C, 56.99; H, 3.18; N, 8.60.

The chloroacetylation of 1-azaphenothiazine was attempted under basic conditions in a number of modifications. The best yield (40%) was obtained when a stirred mixture of 1-azaphenothiazine (1 mol), chloroacetyl chloride (2 mol), and excess potassium carbonate was refluxed for 3 h

Can. J. Chem. Downloaded from www.nrcresearchpress.com by 210.87.254.42 on 09/05/12
For personal use only.

Can. J. Chem. Downloaded from www.nrcresearchpress.com by 210.87.254.42 on 09/05/12
For personal use only.

in dioxane. The yield was unpredictable and the product was impure. After many recrystallizations from glacial acetic acid, the same fluffy, yellow–green solid, m.p. 275–277° (dec.), was obtained.

Hydrolysis of the Chloroacetylation Product

1-Hydroxy-2-chloroacetyl-6-thia-10*b*-aza-2*a*-azoniaaceanthrylene hydroxide inner salt was added to a mixture of concentrated hydrochloric acid (5 ml) and glacial acetic acid (15 ml) and refluxed for 15 min. The reaction mixture was made basic with sodium hydroxide solution and the resultant precipitate was collected. Recrystallization from 95% ethanol yielded 1-hydroxy-6-thia-10*b*-aza-2*a*-azoniaaceanthrylene hydroxide inner salt (**6**) as a buff colored solid, m.p. 198–199°. The average yield was approximately 50%.

Anal. Calcd. for $C_{13}H_8N_2OS$: C, 64.97; H, 3.35; N, 11.65. Found: C, 64.71; H, 3.62; N, 11.05.

Reaction of the Chloroacetylation Product with Piperidine

A stirred mixture of 1-hydroxy-2-chloroacetyl-6-thia-10*b*-aza-2*a*-azoniaaceanthrylene hydroxide inner salt (20.0 g, 0.07 mol), piperidine (18.8 g, 0.22 mol), and *N,N*-dimethylformamide (200 ml) was heated on a boiling water bath for 1 h. After cooling overnight in a refrigerator, the resultant precipitate was collected and washed with water. The filtrate and washings were poured into 1 l of water previously made alkaline (sodium carbonate) and the mixture filtered. The total solid collected was combined and recrystallized from isopropanol (charcoal) to yield fine yellow needle crystals, 18.0 g, m.p. 177–179° (dec.) (77%). This was shown to be 1-hydroxy-2-piperidinoacetyl-6-thia-10*b*-aza-2*a*-azoniaaceanthrylene hydroxide inner salt (**3**); n.m.r. in benzene-d_6 (220 MHz): δ 1.41 (m, 2H, γ protons of piperidine), 1.70 (m, 4H, β protons of piperidine), 2.84 (t, 4H, α protons of piperidine), 4.02 (s, 2H, methylene), 5.85 (m, 2H, H_2 and H_3), 6.40 (q, 1H, H_6), 6.51 (m, 1H, H_7), 6.71 (m, 1H, H_8), 9.23 (q, 1H, H_9), and 9.36 (q, 1H, H_4) p.p.m.; the signals at 5.85 and 9.36 p.p.m. form an ABX system (**5**), $J_{AB} = 8.0$, $J_{AX} = 7.0$, $J_{BX} = 0.8$ Hz; $H_A = 5.87$ and $H_B = 5.85$ p.p.m.; the signals at 6.40, 6.51, 6.71, and 9.23 p.p.m. represent four adjacent protons in an aromatic system (**4**), $J_{9,8} = 8.4$, $J_{9,7} = 1.3$, $J_{6,7} = 7.7$, $J_{6,8} = 1.7$, $J_{7,8} = 7.4$ Hz; *m/e* 365 (M^+, $C_{20}H_{19}N_3O_2S$), 282 ($M - C_5H_9N$), 267, 253, 240 ($C_{13}H_8N_2OS$; 282 – $CH_2{=}C{=}O$), 225, 211, 200 ($C_{11}H_8N_2S$), 199, 184, 172, 168, 166, 155, 140, 109, 108, 99, 98 ($C_6H_{12}N$).

Anal. Calcd. for $C_{20}H_{19}N_3O_2S$: C, 65.73; H, 5.24; N, 11.50. Found: C, 65.57; H, 5.54; N, 10.91.

The oxalate was prepared by mixing the amine (0.5 g) in warm, dry benzene (150 ml) with an equimolar concentration of anhydrous oxalic acid, also in dry benzene. The mixture was allowed to cool, when the salt precipitated as a yellow solid, m.p. 232.5–233° (dec.).

Anal. Calcd. for $C_{22}H_{21}N_3O_6S$: C, 58.00; H, 4.65. Found: C, 57.57; H, 4.95.

The methyl iodide derivative was prepared by mixing equimolar concentrations of amine and methyl iodide in dry benzene and allowing to stand overnight. The derivative was a yellow solid, m.p. 229.5–230° (dec.).

Results and Discussion

The chloroacetylation product would not form a hydrochloride salt, in sharp contrast to normal 10-substituted-1-azaphenothiazines which readily form quaternary salts at N-1 (3). Since the compound also lacked absorption characteristic of amine N—H stretch (3300–3500 cm^{-1})[5] or protonated ammonium $\overset{+}{N}$—H stretch (2300–2500 cm^{-1}), it was deduced that both the N-1 and the N-10 positions of the azaphenothiazine nucleus must be substituted and that there must be a cationic site.

In polar solvents, at temperatures of 100° or higher, the chloroacetylation product reacted with secondary amines to form a series of new compounds (4) in which the chlorine atom is replaced by the amine moiety, showing that the chlorine atom is covalently bonded and that the anionic site must be provided by an oxygen atom.

The mass spectrum confirmed the molecular formula as $C_{15}H_9ClN_2O_2S$ and showed a base peak at *m/e* 267 (loss of CH_2Cl) and ions at *m/e* 281 (loss of Cl) and 239 (loss of $COCH_2Cl$), proving that the chloroacetylation product contains a chloroacetyl residue.

The low solubility of the chloroacetylation product in all common organic solvents precluded determination of n.m.r. spectra. The piperidine condensation product (**3**) was soluble in deuteriochloroform and the 60 MHz spectrum showed signals attributable to the α, β, and γ protons of the piperidine ring, an isolated methylene unit, a complex five proton multiplet in the aromatic region (6.89 p.p.m.), a one proton multiplet at 9.04 p.p.m., and a one proton multiplet at 9.59 p.p.m.

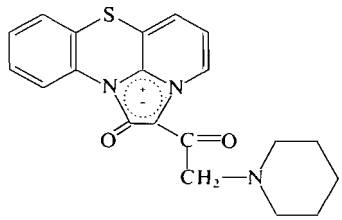

3

The 220 MHz spectrum in deuteriochloroform did not permit unambiguous assignments to be made for the lowfield protons but use of benzene-d_6 produced some dramatic solvent shifts and permitted interpretation of the resulting 220 MHz spectra. Analysis of these latter

[5]The i.r. spectrum of 1-azaphenothiazine in carbon disulfide exhibited absorption at 3390 cm^{-1}, attributed to the N—H stretching of the secondary amine function.

Can. J. Chem. Downloaded from www.nrcresearchpress.com by 210.87.254.42 on 09/05/12
For personal use only.

n.m.r. spectra showed that the piperidine derivative (1-hydroxy-2-piperidinoacetyl-6-thia-10*b*-aza-2*a*-azoniaaceanthrylene hydroxide inner salt) contained four adjacent protons in an aromatic system in which one (H_9 in structure **4**; quartet at 9.23 p.p.m.) is experiencing a strong deshielding effect. The remaining three lowfield protons are accounted for by an ABX system (5) with three adjacent protons in an aromatic ring, with one of the three again experiencing a strong deshielding effect (H_X in structure **5**; quartet at 9.36 p.p.m.).

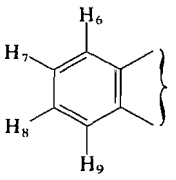

4

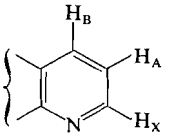

5

These data, together with mass spectral data from the piperidine derivative (6–10) (see Experimental) are consistent with the mesoionic structure **2** for the chloroacetylation product and structure **3** for the piperidine condensation product. Formation of structure **2** can be accounted for by initial chloroacetylation at N-10, followed by ring closure and proton abstraction to produce 1-hydroxy-6-thia-10*b*-aza-2*a*-azoniaaceanthrylene hydroxide inner salt (**6**). Further chloroacetylation of this with concomitant proton abstraction would yield structure **2**.

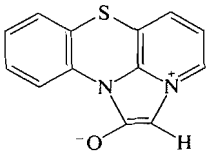

6

There are precedents for formation of cyclic structures such as is suggested here (11, 12). Proton abstraction to form structure **6** would presumably be driven by the formation of the aromatic mesoionic system. There is also ample precedent in the chemistry of mesoionic systems (13–15) for subsequent acylation of **6**. The final proton abstraction would again be driven by the formation of a stable aromatic system. The hydrolysis product (**6**) must be formed by reversal of the second acylation step.

None of the data presented thus far will allow differentiation between the postulated structure (**2**) given for the chloroacetylation product and the isomeric structure **7**. Mechanistically, one

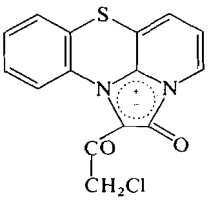

7

must decide whether N-1 or -10 of 1-azaphenothiazine is acylated in the first step. Jones and Katritzky (16) have studied potentially tautomeric pyridines and have found that 2-aminopyridine and 2-(methylamino)pyridine are acetylated exclusively (acetic anhydride/acetic acid) at the exocyclic nitrogen. Based on this information, preference is given to structure **2** as the chloroacetylation product of 1-azaphenothiazine. Supporting evidence for this selection has very recently been obtained in a study directed toward the chloroacetylation of aminosubstituted 2-aminopyridines (17).

The mesoionic 1,3-diazol-4-one system (**8**) is known (15, 18–21) but the chloroacetylation product (**2**) represents a new ring system (**9**) which is 6-thia-10*b*-aza-2*a*-azoniaaceanthrylene.

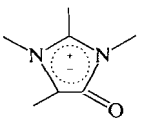

8

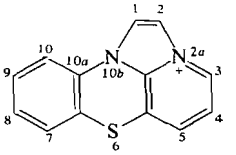

9

The chloroacetylation product is therefore 1-hydroxy-2-chloroacetyl-6-thia-10*b*-aza-2*a*-azoniaaceanthrylene hydroxide inner salt, the hydrolysis product (**6**) is 1-hydroxy-6-thia-10*b*-aza-2*a*-azoniaaceanthrylene hydroxide inner salt, and the piperidine derivative (**3**) is 1-hydroxy-2-piperidinoacetyl-6-thia-10*b*-aza-2*a*-azoniaaceanthrylene hydroxide inner salt.

The authors would like to thank Mr. Walter Kremers for technical assistance throughout the project, Mr. W. Garland of the School of Pharmacy, University of California, for the

mass spectral determinations and metastable scanning, and Dr. R. Reavill of the Division of Pure Chemistry, National Research Council of Canada, Ottawa, for assistance with some of the n.m.r. work.

W.K.A. gratefully acknowledges receipt of two Warner–Lambert Fellowships from Warner–Lambert (Canada) Ltd. and a grant from the Faculty of Graduate Studies, University of Manitoba. J.W.S. is also grateful for financial support from the National Research Council of Canada.

1. A. VON SCHLICHTEGROLL. Arzneimittelforsch. **8**, 489 (1958).
2. R. DAHLBOHM and T. EKSTRAND. Acta Chem. Scand. **5**, 102 (1951).
3. W. K. ANDERSON. The synthesis of substituted azaphenothiazine derivatives. M.Sc. Thesis. University of Manitoba, Winnipeg, Manitoba, May, 1965.
4. J. W. STEELE, W. K. ANDERSON, and W. F. TRAGER. In preparation.
5. J. A. POPLE, H. J. BERNSTEIN, and W. G. SCHNEIDER. High resolution nuclear magnetic resonance spectroscopy. McGraw–Hill, New York, N.Y. 1959. p. 132.
6. BUDZCKIEWICZ, C. DJERASSI, and D. H. WILLIAMS. Interpretation of mass spectra of organic compounds. Holden–Day Inc., San Francisco, California. 1964. p. 64.
7. M. BARBER and R. M. ELLIOTT. 12th Annual Conference On Mass Spectrometry and Allied Topics. Committee E 14, ASTM, Montreal, Quebec, 1964.
8. K. R. JENNINGS. J. Chem. Phys. **43**, 4176 (1965).
9. J. H. FUTTRELL, K. R. RYAN, and L. W. SIECK. J. Chem. Phys. **43**, 1832 (1965).
10. K. R. JENNINGS. Chem. Commun. 283 (1966).
11. A. E. TSCHITSCHIBABIN. Chem. Ber. **57**, 2092 (1924).
12. G. B. CHHEDA and R. H. HALL. J. Org. Chem. **34**, 3492 (1969).
13. W. D. BURROWS. J. Org. Chem. **31**, 3435 (1966).
14. G. V. BOYD and P. H. WRIGHT. Chem. Commun. 182 (1969).
15. A. LAWSON and D. H. MILES. J. Chem. Soc. 2865 (1959).
16. R. A. JONES and A. R. KATRITZKY. J. Chem. Soc. 1317 (1959).
17. W. K. ANDERSON and A. E. FRIEDMAN. Can. J. Chem. **49**, 668 (1971).
18. E. B. ROCHE and D. W. STANSLOSKI. J. Heterocycl. Chem. **7**, 139 (1970).
19. E. BESTHORN. Chem. Ber. **46**, 2761 (1913).
20. F. KROLLPFEIFFER and K. SCHNEIDER. Ann. **34**, 530 (1937).
21. W. L. MOSBY. The chemistry of heterocyclic systems with bridgehead nitrogen atoms, part one. Interscience Publishers, Inc., New York, N.Y. 1961. pp. 540–544.
22. W. A. SCHULER and H. KLEBE. Ann. **653**, 172 (1962).

Can. J. Chem. Downloaded from www.nrcresearchpress.com by 210.87.254.42 on 09/05/12
For personal use only.

Field and Resonance Components of Substituent Effects in Relation to the Hammett Equation

L. D. HANSEN[1] AND L. G. HEPLER

Department of Chemistry, University of Lethbridge, Lethbridge, Alberta

Received October 29, 1971

Following Swain and Lupton's analysis of substituent effects, we have taken $\Delta G^0 = a_e t_e + a_r t_r$ for a typical substituent effect reaction. In this equation a_e and a_r are substituent constants for electrostatic field and resonance effects while t_e and t_r are corresponding transmission coefficients. Both substituent constants and t_r are taken to be independent of solvent and temperature, while t_e is taken to depend on both solvent and temperature. General conclusions based on analysis of this model are the following. (*i*) A Hammett $\rho\sigma$ equation with constant σ values that are valid over a range of temperatures for a variety of reactions in several solvents can be obtained only when either the field or the resonance interaction is negligible compared with the other. (*ii*) A Hammett $\rho\sigma$ equation can be expected to hold for "similar" reaction series in a given solvent at one temperature even when both the field and resonance interactions are important. (*iii*) An isoequilibrium or isokinetic relationship can be expected only when the field interaction is dominant.

The general equations leading to these and other conclusions are presented so that one can later insert appropriate mathematical descriptions of detailed models and thereby obtain information about specific reactions.

En suivant l'analyse de Swain et Lupton sur les effets de substituants, nous avons pris $\Delta G^0 = a_e t_e + a_r t_r$ pour une réaction à effet de substituant typique. Dans cette équation a_e et a_r sont les constantes des substituants pour un champ électrostatique et pour des effets de résonance tandis que t_e et t_r sont les coefficients de transmission correspondants. Les constantes des substituants et t_r sont pris indépendamment du solvant et de la température et t_e dépend sur le solvant et la température. Les conclusions générales fondées sur l'analyse de ce modèle sont les suivantes. (*i*) Une équation de Hammett $\rho\sigma$ avec des valeurs constantes σ qui sont valables dans une gamme de températures pour une variété de réactions dans plusieurs solvants est obtenue seulement quand à la fois l'interaction de champ ou de résonance sont négligeables comparativement aux autres. (*ii*) On peut espérer une équation de Hammett $\rho\sigma$ pour des séries de réactions "similaires" dans un solvant donné à une température même lorsque les interactions de champ et de résonance sont importants. (*iii*) On peut attendre une relation d'isoéquilibre ou d'isocinétique seulement quand l'interaction de champ est prédominante.

Les équations générales amenant telles ou telles conclusions sont présentées autant que l'on peut insérer des descriptions mathématiques appropriées de modèles détaillées et par là obtenir une information sur les réactions spécifiques.

Canadian Journal of Chemistry, **50**, 1030 (1972)

Partly in response to the proliferation of sets of σ parameters designed to account for substituent effects on a huge variety of reactions, Swain and Lupton (1) have carried out a thorough statistical analysis that has led to a number of empirically useful and theoretically important conclusions.

The statistical analysis by Swain and Lupton (1) provided convincing evidence that all of the various sets of substituent constants in present or past use can be expressed as linear combinations of two terms, each of which may be regarded as representing one kind of interaction of substituent with reaction center. Although the validity of their statistical analysis is totally independent of the names assigned to these kinds of interactions and also independent of subsequent descriptions of these interactions, Swain and Lupton (1) have quite reasonably taken the two terms to represent field and resonance effects. Here it should be noted that they have carefully excluded from consideration those reactions in which steric effects could be significant.

In their efforts to separate field and steric effects, it was necessary for Swain and Lupton (1) to make (very reasonable) assumptions about certain substituents. In this connection they wrote the following: "...are convinced that the Hammett equation and other *free*-energy correlations work in spite of entropy variations, ..., and that such effects can be considered as sub-

[1]Permanent address: Department of Chemistry, University of New Mexico, Albuquerque, New Mexico, 87106.

Can. J. Chem. Downloaded from www.nrcresearchpress.com by 210.87.254.105 on 09/05/12
For personal use only.

Can. J. Chem. Downloaded from www.nrcresearchpress.com by 210.87.254.105 on 09/05/12
For personal use only.

components of the field effect". A recent thermodynamic analysis (2) of the Hammett equation has shown that entropy changes must be proportional to enthalpy changes if the $\rho\sigma$ relationship is to be exactly valid over a range of temperature. Good correlations of entropy and enthalpy changes with σ values have in fact been observed for several reaction series. On the other hand, as recognized by Swain and Lupton (1) and others (2), the Hammett equation does work (fairly well, not exactly) for many reaction series in which there are substantial variations from the enthalpy–entropy proportionality.

The ideas of the above discussion, combined with recognition that interpretation of entropy and enthalpy changes is often an important part of gaining some detailed understanding of substituent effects, have led us to include temperature and solvent as variables so that application of classical thermodynamics to an equation of the form suggested by Swain and Lupton (1) can lead to information about enthalpy and entropy changes in relation to substituent effects.

Before proceeding with our extension of the ideas of Swain and Lupton (1), it is worthwhile to write down one explicit chemical reaction equation to illustrate a substituent effect. Partly because effects of substituents on acidities as measured by acid ionization equilibrium constants are a common method of obtaining various σ values, and partly because of a later specific application of our theoretical equations to proton transfer reactions, we choose the following illustrative reaction equation:

[1] $$XPBH^{z}(S) + PB^{z-1}(S) = XPB^{z-1}(S) + PBH^{z}(S)$$

In this equation we have used (S) to emphasize that each solute species is in some solution and interacts with the solvent in ways that must be considered in relation to substituent effects. The letters X, P, and B represent the substituent, the "parent structure" (such as a benzene ring), and the basic site (such as $-COO^-$ or $-NH_2$), while z and $z-1$ represent integral charges. In all of our following discussion and development of theoretical equations we are concerned with quantities that refer to reaction series of type [1], with realization that analogous equations can be written to represent other reaction series.

In a few instances we have experimental results that refer directly to reactions of type [1]. More often, however, we have equilibrium constants for ionization of the parent acid (K_{PBH}) and the substituted acid (K_{XPBH}) that must be combined to give $K_1 = K_{XPBH}/K_{PBH}$ and thence $\Delta G_1^0 = \Delta G_{XPBH}^0 - \Delta G_{PBH}^0$. In similar fashion we can obtain ΔH_1^0 and ΔS_1^0 values from the experimental values for ionization of $XPBH^z$ and PBH^z. In all that follows we shall be concerned with thermodynamic quantities that refer to reactions of type [1], but note that similar equations can be written in terms of rate constants rather than equilibrium constants, and thus in terms of activation parameters such as $\Delta G^{\ddagger}$ and $\Delta H^{\ddagger}$.

Following Swain and Lupton (1), we consider substituent effects in terms of an appropriate combination of "field" and "resonance" components. For our present purposes, it is most convenient to use terminology similar to that of Swain and Lupton (1) with some of our own symbols.

We begin by taking the resonance contribution to the free energy (ΔG_r) of a reaction of type [1] to be given by a product of a substituent constant (a_r) times a transmission coefficient (t_r) so that we have

[2] $$\Delta G_r = a_r t_r$$

The substituent constant a_r depends only on the substituent while t_r depends on the parent skeleton P and on the ability of B to conjugate (resonance) with substituent X. We take both a_r and t_r to be independent of solvent, temperature, and pressure.

The field contribution to the free energy (ΔG_e), which can in principle be evaluated by way of classical electrostatic calculations, is similarly taken to be a product of substituent (a_e) and transmission (t_e) terms so that we have

[3] $$\Delta G_e = a_e t_e$$

Again, the substituent constant depends only on the substituent. The electrostatic field transmission coefficient depends on solvent, temperature, and pressure as well as on P and B.

The electrostatic models and derived equations of Kirkwood and Westheimer (3), Sarmousakis (4), and Tanford (5) provide considerable information about t_e, but for now we shall avoid any specific statements about the mathematical description of t_e while we develop the general consequences of eqs. 2 and 3.

Can. J. Chem. Downloaded from www.nrcresearchpress.com by 210.87.254.105 on 09/05/12
For personal use only.

We now combine eqs. 2 and 3 to obtain the total ΔG^0 for reactions of type [1] as

$$[4] \qquad \Delta G^0 = \Delta G_e + \Delta G_r = a_e t_e + a_r t_r$$

Here it should be emphasized that the form of eq. 4, as a sum of two terms is a direct consequence of the demonstration by Swain and Lupton (1) that a huge range of non-steric substituent effects can be described by appropriate linear combinations of two constants per substituent. Although we have followed Swain and Lupton (1) and others in assigning supposedly descriptive names to these terms, it must be understood that our conclusions (except where explicitly stated otherwise) are independent of our choice of names and mental pictures of the interactions that lead to these terms. However, we have gone beyond Swain and Lupton (1) in specifying that one of these terms is solvent, temperature, and pressure dependent.

Further combination of eq. 4 with the Hammett equation ($\log K_1 = \rho\sigma$) and $\Delta G^0 = -RT \ln K$ leads to

$$[5] \qquad a_e t_e + a_r t_r = -2.3RT\rho\sigma$$

This application of eq. 4 can apply accurately only when certain conditions are met, which we now explore.

In the special case where $a_e t_e = 0$ (or, more reasonably, $a_e t_e \ll a_r t_r$), we simplify eq. 5 to

$$[6] \qquad (t_r/T)(-a_r/2.3R) = \rho\sigma$$

Identification of (t_r/T) with ρ and $(-a_r/2.3R)$ with σ is consistent with our original definitions of a_r and t_r. This identification tells us that ρ should be a linear function of T^{-1}, as it is known to be (2).

Although there are some substituents that exert only a very small field effect ($a_e \simeq 0$), any extensive series of substituents will include some for which $a_e \neq 0$. Further, we have $t_e = 0$ only in the unattainable cases of infinite dielectric constant for solvent and infinite "internal dielectric constant" of reacting species or of infinite separation of substituent from reaction center. Thus neither a_e nor t_e can generally be zero, and we do not expect eq. 6 to be generally appropriate. It is still possible, however, that eq. 6 can be applicable as a good approximation to a reaction series involving highly conjugated species (so that resonance is important) in which the substituents are very far from the reaction center. For such reaction series, t_e could be so small and t_r so large that $a_e t_e \ll a_r t_r$.

Another special case is where $a_r t_r = 0$ (or $a_r t_r \ll a_e t_e$) so that eq. 5 becomes

$$[7] \qquad (t_e/T)(-a_e/2.3R) = \rho\sigma$$

Identification of (t_e/T) with ρ and of $(-a_e/2.3R)$ with σ is again consistent with our original definitions. Because t_e is clearly some function of the dielectric constant of the solvent, which depends on temperature, we must postpone comment on the temperature dependence of ρ in this case.

There are numerous substituents for which $a_r \simeq 0$, and numerous reaction series involving non-aromatic structures (represented by P in reaction 1) for which $t_r \simeq 0$. Thus we should expect to find that it is appropriate to interpret linear free energy relationships for many reaction series in terms of eq. 7.

The special cases that lead to eqs. 6 and 7 are so restrictive that we now turn to a more general justification for the widespread empirical successes of the Hammett equation. It is clear that any proportionality between the two additive terms on the left hand side of eq. 5 will suffice, but it is also clear that a_e and a_r are proportional to each other only for carefully selected substituents rather than for a wide range of substituents. We must therefore turn to detailed consideration of t_e and t_r.

The transmission coefficient t_r for resonance effects depends only on the particular reaction series under consideration (P and B in reaction 1) and is therefore a constant when only the substituent X is varied. Similarly, t_e is independent of X and is a constant when P, B, solvent, temperature, and pressure are held constant. Thus for a series of reactions (only X variable) at any specified temperature and pressure in a specified solvent, the ratio of these transmission coefficients is also a constant as indicated by

$$[8] \qquad t_r/t_e = b$$

The "constant" b is a function of solvent, temperature, and pressure because t_e is some function of the temperature and pressure dependent dielectric properties of the solvent.

Substitution of eq. 8 into eq. 5 now leads to

Can. J. Chem. Downloaded from www.nrcresearchpress.com by 210.87.254.105 on 09/05/12
For personal use only.

$$[9]\quad \left[\frac{t_e}{T}\right]\left[-\frac{a_e + a_r b}{2.3R}\right] = \left[\frac{t_r}{T}\right]\left[-\frac{(a_e/b) + a_r}{2.3R}\right] = \rho\sigma$$

We identify the t/T terms with ρ and the terms containing a_e, a_r, and b with σ and see that it is possible to obtain a linear free energy relationship of the form of the Hammett equation even when there are substantial contributions from both field and resonance effects. However, the presence of b in the terms we identify with σ has important consequences that we must consider carefully.

Since b is a function of temperature and solvent, we see that the original definition of σ as independent of temperature and solvent cannot be both generally and exactly true. That is, one may obtain a good $\rho\sigma$ correlation for a particular reaction in a given solvent at any one temperature, but at another temperature or with a different solvent, it will in general be necessary to use different values of σ (possibly only slightly different) as well as different values for ρ.

Equation 9 also shows that the Hammett equation with a single set of σ values cannot be generally applicable to different reactions series (P and B varied). This is because the value of the "constant" b depends on the particular reaction series (particular P and B) under consideration. However, the empirical successes of the Hammett equation suggest that the value of b is approximately constant (in a particular solvent at a specified temperature) as long as P and B are not changed too drastically, which can account for successful use of reaction independent σ values in these cases.

Now we summarize our conclusions based on eq. 9 as follows. (*i*) Only in the case of $b \simeq 0$ (field effects much larger than resonance effects) can we generally expect to find σ values that are independent of reaction, solvent, and temperature. When $b \simeq 0$, eq. 9 reduces to eq. 7. (*ii*) For "similar" reaction series b may be sufficiently close to a constant that σ values can appear to be independent of the particular reaction under consideration.

The presence of b (a function of temperature) in eq. 9 has consequences with respect to ΔH^0, ΔS^0, and ΔC_p^0 that are considered following application of some classical thermodynamic relationships to eq. 4.

We now differentiate eq. 4 with respect to temperature at constant pressure to obtain

$$[10]\quad \Delta S^0 = -a_e(\partial t_e/\partial T)_p$$

and combine eq. 10 with eq. 4 to obtain

$$[11]\quad \Delta H^0 = a_e t_e + a_r t_r - a_e T(\partial t_e/\partial T)_p$$

Now the ratio of ΔH^0 to ΔS^0 is

$$[12]\quad \frac{\Delta H^0}{\Delta S^0} = T - \frac{t_e}{(\partial t_e/\partial T)_p}\left[1 + \frac{a_r t_r}{a_e t_e}\right]$$

$$[12']\quad \frac{\Delta H^0}{\Delta S^0} = T - \frac{t_e}{(\partial t_e/\partial T)_p}\left[1 + \frac{a_r b}{a_e}\right]$$

Further differentiation of eq. 11 with respect to temperature leads to

$$[13]\quad \Delta C_p^0 = -a_e T(\partial^2 t_e/\partial T^2)_p$$

Thus the ratio of ΔS^0 to ΔC_p^0 is

$$[14]\quad \Delta S^0/\Delta C_p^0 = (\partial t_e/\partial T)_p/T(\partial^2 t_e/\partial T^2)_p$$

Differentiation of eq. 4 with respect to pressure at constant temperature leads to

$$[15]\quad \Delta V^0 = a_e(\partial t_e/\partial P)_T$$

and the ratio of ΔS^0 to ΔV^0 is

$$[16]\quad \Delta S^0/\Delta V^0 = -(\partial t_e/\partial T)_p/(\partial t_e/\partial P)_T = (\partial P/\partial T)_{t_e}$$

The linear relationship between ΔS^0 and ΔV^0 that is predicted by eq. 16 has been observed and discussed in another connection previously (6). Unfortunately, we have few experimental data that yield reliable ΔC_p^0 values and are therefore unable to make any definitive statement about the general applicability of eq. 14. We do, however, note that there is some empirical evidence from thermodynamic studies of the ionization of aqueous acids for a (roughly) linear relationship between ΔS^0 and ΔC_p^0 as required by eq. 14.

Accuracy of most experimental data is such that we are often limited to consideration of ΔH^0 and ΔS^0 (and maybe more especially $\Delta H^\ddagger$ and $\Delta S^\ddagger$) as temperature independent quantities. It then follows from $d\Delta H^0/dT = \Delta C_p^0$ and $d\Delta S^0/dT = \Delta C_p^0/T$ that we must often take $\Delta C_p^0 = 0$. From eq. 13 we have, therefore

$$[17]\quad (\partial^2 t_e/\partial T^2)_p = 0$$

Can. J. Chem. Downloaded from www.nrcresearchpress.com by 210.87.254.105 on 09/05/12
For personal use only.

and thence

[18] $t_e = C_1 + C_2T \qquad (\text{when } \Delta C_p^0 = 0)$

in which C_1 and C_2 are constants of integration. Now the ratio of transmission coefficients (eq. 18) becomes

[19] $b = t_r/(C_1 + C_2T) \qquad (\text{when } \Delta C_p^0 = 0)$

Substitution of eq. 18 in eq. 12 gives us

[20] $\Delta H^0/\Delta S^0 = -(C_1/C_2) - (a_r t_r/C_2 a_e)$

This eq. 20 shows that the ratio $\Delta H^0/\Delta S^0$ is a function of substituent, and that there should not be any general correlation of ΔH^0 with ΔS^0 for a reaction series that includes any wide range of substituents. This statement is entirely consistent with our earlier discussion of the consequences of the presence of b (a function of temperature) in the terms identified with σ in eq. 9. In the special case of negligible resonance contribution (*i.e.*, $t_r \simeq 0$), eq. 20 reduces to

[21] $\Delta H^0/\Delta S^0 = -(C_1/C_2) = \beta_i$

in which β_i is a constant for a particular reaction series in a specified solvent and is called the isoequilibrium (or isokinetic) temperature (2).

The treatment above shows that a simple isoequilibrium (or isokinetic) relationship can be generally expected only when temperature independent substituent effects (here called resonance effects that are described in terms of a_r and t_r) are very small compared to temperature dependent substituent effects (here called field effects that are described in terms of a_e and t_e). Thus we see that the requirements of an isoequilibrium (or isokinetic) relationship are more stringent than the requirements for a $\rho\sigma$ relationship for a reaction series in a specified solvent at a given temperature. This is a necessary requirement for any theory of substituent effects because there are numerous examples of reaction series for which there is a fairly good $\rho\sigma$ correlation while ΔH^0 and ΔS^0 vary in apparently erratic ways.

Possibly the most impressively extensive empirical support for an isoequilibrium relationship of the form of eq. 21 is provided by the linear relationship between ΔG^0 and ΔS^0 reported by Christensen, Izatt, and Hansen (7) for ionization of a large number of carboxylic acids. (Note that the isoequilibrium relationship $\Delta H^0/\Delta S^0 = \beta_i$ combined with $\Delta G^0 = \Delta H^0 - T\Delta S^0$ gives $\Delta G^0 = (\beta_i - T)\Delta S^0$, which is a linear relationship between ΔG^0 and ΔS^0.) It is consistent with a variety of evidence that field effects are more important than resonance effects for ionization of carboxylic acids, which in turn is consistent with our general equations and simplifications for the special case of resonance effects being small compared with field effects.

Now we turn to consideration of reaction series for which both ΔH^0 and ΔS^0 vary with temperature and for which we therefore have $\Delta C_p^0 \neq 0$. If we take ΔC_p^0 to be the same non-zero constant for each reaction in a particular series of reactions (only X variable), the solution of differential equation 13 leads to t_e being a function of a_e, which is contrary to the definitions of these quantities. Thus if $\Delta C_p^0 \neq 0$, it must be some function of substituent X and thence of a_e. Taking as the simplest case $\Delta C_p^0 = C_3 a_e$, the solution of differential equation 13 is

[22] $t_e = C_1 + C_2T - C_3T \ln T$

Substitution of eq. 22 in eq. 12 gives

[23] $$\frac{\Delta H^0}{\Delta S^0} = T - \frac{C_1 + C_2 - C_3T \ln T}{C_2 - C_3(1 + \ln T)} - \frac{a_r t_r}{a_e[C_2 - C_3(1 + \ln T)]}$$

Because eq. 23 is a function of substituent, we should not expect any general simple correlation between ΔH^0 and ΔS^0 values for any reaction series that includes a substantial range of substituents. Again, this statement is entirely consistent with our earlier discussion of eq. 9. In the special case where $t_r \simeq 0$, eq. 23 reduces to $\Delta H^0/\Delta S^0 = f(T)$ in which $f(T)$ is independent of substituent. Thus, for a reaction series in which field effects are dominant, we should expect to find a linear relationship between ΔH^0 and ΔS^0, with the slope depending on the temperature. Those who enjoy doing second order differential equations beyond the range of applicability of the model or accuracy of experimental data may express ΔC_p^0 as a function of temperature in eq. 13. Results that are obtained in this way are the same as above in that $\Delta H^0/\Delta S^0$ is in general a function of both temperature and substituent that reduces to a function of temperature when $t_r \simeq 0$.

Can. J. Chem. Downloaded from www.nrcresearchpress.com by 210.87.254.105 on 09/05/12
For personal use only.

In earlier discussions of eq. 7, which applies when resonance effects are negligible compared to field effects, we identified t_e/T with ρ and then postponed consideration of the temperature dependence of ρ. For the common case in which we are only justified in taking $\Delta C_p^0 = 0$, we have t_e expressed as a linear function of temperature in eq. 18, which leads to

$$[24] \qquad \rho = C_2 + (C_1/T)$$

It has previously been shown (2) that ρ is a similar function of temperature when the Hammett equation is valid over a range of temperature, and it has been shown in this paper that the Hammett equation with temperature and reaction independent σ can be generally valid only when field effects are dominant.

When $\Delta C_p^0 \neq 0$, we have obtained a more complicated expression for t_e as a function of temperature (eq. 22), which leads to

$$[25] \qquad \rho = (C_1/T) + C_2 - C_3 \ln T$$

Thus when $\Delta C_p^0 \neq 0$ we have ρ only approximately linear in T^{-1}, with the deviations from linearity of the form required by previous (2) classical thermodynamic analysis of the Hammett equation.

The thorough statistical analysis by Swain and Lupton (1) has clearly shown that there is no general empirical justification for consideration of more than two kinds of independent (non-steric) interactions leading to substituent effects. On this basis we are restricted to two additive terms in eq. 4. There are, however, a few reaction series involving ionization of aqueous acids for which we have unusually extensive and accurate data that can lead to empirical justification for a third additive term in eq. 4 and thence to extensions of many of the following equations. But at present we can only add a third term to eq. 4 by assuming a much more specific and detailed model for the interaction mechanisms of substituent with reaction center and for solutes with solvent than is appropriate in this paper. We shall return to this question in connection with subsequent investigations of the relationships between the general conclusions of this paper and earlier investigations of substituent effects (2–5).

We are grateful to Dr. Douglas Dolman for helpful discussions, to the National Institutes of Health for a U.S. Public Health Service Research Career Development Award (#5-K4-GM-42, 545-03) to L.D.H., and to the National Research Council of Canada, The Research Corporation, and the Petroleum Research Fund administered by the American Chemical Society for support of our experimental work that has led to the research reported here.

1. G. C. SWAIN and E. C. LUPTON, JR. J. Am. Chem. Soc. **90**, 4328 (1968).
2. L. G. HEPLER. Can. J. Chem. **49**, 2803 (1971).
3. J. G. KIRKWOOD and F. H. WESTHEIMER. J. Chem. Phys. **6**, 506 (1938); **6**, 513 (1938).
4. J. N. SARMOUSAKIS. J. Chem. Phys. **12**, 277 (1944).
5. C. TANFORD. J. Am. Chem. Soc. **79**, 5348 (1957).
6. L. G. HEPLER. J. Phys. Chem. **69**, 965 (1965).
7. J. J. CHRISTENSEN, R. M. IZATT, and L. D. HANSEN. J. Am. Chem. Soc. **89**, 213 (1967).

Nuclear Magnetic Resonance Studies of the Solution Chemistry of Metal Complexes. III. Acetylglycine Complexes of Cadmium, Zinc, and Lead[1]

DALLAS L. RABENSTEIN
Department of Chemistry, University of Alberta, Edmonton, Alberta

Received September 30, 1971

The aqueous solution chemistry of the cadmium, zinc, and lead complexes of acetylglycine has been investigated by proton magnetic resonance spectroscopy. These systems were investigated as models for the interaction of cadmium, zinc, and lead with the C-terminal end of peptides and proteins. The acid ionization constant of acetylglycine ($pK_a = 3.44$) and the formation constants of the cadmium ($\log K_{f1} = 1.23$), zinc ($\log K_{f1} = 0.86$), and lead ($\log K_{f1} = 1.38$, $\log K_{f2} = 1.20$) complexes at 25 °C were determined from chemical shift measurements ($K_{f1} = [ML^+]/[M^{2+}][L^-]$; $K_{f2} = [ML_2]/[ML^+][L^-]$). The rates of exchange of the peptide proton of acetylglycine in the free and complexed forms with solvent protons were measured from exchange-broadened n.m.r. spectra. The exchange rate of the peptide proton increases when the acetylglycine is complexed by these metals; in the case of the cadmium–acetylglycine complex the exchange rate is 53 times faster. The potential metal ion binding sites at the C-terminal end of peptides are discussed, and the possibility of chelation through an oxygen atom of the carboxylate group and an atom of the peptide linkage is considered.

La chimie des solutions aqueuses de complexes d'acétylglycine avec le cadmium, zinc, plomb a été étudiée pour la résonance magnétique nucléaire. Ces systèmes ont été choisis comme modèles pour l'étude de l'interaction du cadmium, zinc et plomb avec le carbone terminal des peptides et protéines. Les constantes d'ionisation acide de l'acétylglycine ($pK_a = 3.44$) et les constantes de formation des complexes avec le cadmium ($\log K_{f1} = 1.23$), zinc ($\log K_{f1} = 0.86$) et plomb ($\log K_{f1} = 1.38$, $\log K_{f2} = 1.20$) ont été déterminées à 25 °C par les mesures du déplacement chimique ($K_{f1} = [ML_2]/[M^{2+}][L^-]$; $K_{f2} = [ML_2]/[ML^+][L^-]$). Les vitesses d'échange avec le solvant du proton peptidique de l'acétylglycine, sous ses formes libre et complexée, ont été mesurées à partir de la bande large d'échange du spectre r.m.n. La constante de cet échange croît lorsque l'acétylglycine est complexé par ces métaux; dans le cas du complexe avec le cadmium, l'échange est 53 fois plus rapide. Les sites potentiels de liaison de l'ion métal avec le carbone terminal des peptides sont discutés, la possibilité de chélation avec un atome d'oxygène du groupe carboxylate et un atome de la liaison peptidique est considérée.

Canadian Journal of Chemistry, **50**, 1036 (1972)

Introduction

Structural studies of several metal-containing biological molecules have revealed that binding of a metal ion by a protein may involve functional groups separated by many amino acid residues along the chain (2). To a first approximation, the donor groups have been considered to act independently of one another with respect to the metal ion, except for steric interactions between them. Within this approximation, simple amino acids and peptides have been used as models for the study of metal–protein interactions (3).

We are presently investigating the interaction of metal ions with the potential coordination sites of peptides and proteins. In this paper, we wish to report the results of a proton magnetic resonance study of the interaction of a model compound for the C-terminal carboxylic acid group with the metal ions cadmium, zinc, and lead. Acetylglycine was chosen as the model compound because it has the peptide linkage characteristic of the C-terminal amino acid residue of a protein chain. In addition, there are no other coordination sites in acetylglycine known to form strong complexes with these metal ions. The complexation reactions have been quantitatively characterized from the dependence of the chemical shifts of the acetylglycine protons on solution conditions. The exchange kinetics of the peptide proton of both free and complexed acetylglycine have been determined by lineshape analysis of the collapse of spin–spin coupling to the peptide proton.

[1]For Part II, see ref. 1.

Experimental

Chemicals

Acetylglycine (Eastman Organic Chemicals) and reagent grade metal nitrate salts were used as received. Standardized solutions of the metal salts were prepared by the methods of Schwarzenbach (4).Tetramethylammonium (TMA) nitrate was prepared by titration of a 25% aqueous solution of

Can. J. Chem. Downloaded from www.nrcresearchpress.com by 210.87.254.6 on 09/05/12
For personal use only.

Can. J. Chem. Downloaded from www.nrcresearchpress.com by 210.87.254.6 on 09/05/12
For personal use only.

TMA hydroxide (Eastman Organic Chemicals) with HNO_3 to a neutral p*H*.

pH Measurements

All p*H* measurements were made at 25 °C with an Orion Model 701 p*H* meter equipped with a standard glass electrode and a fiber-tip, saturated calomel reference electrode. Saturated potassium acid tartrate and 0.01 *M* sodium tetraborate buffers, p*H* 3.56 and 9.18 at 25 °C, were used to standardize the p*H* meter.

Nuclear Magnetic Resonance Measurements

Nuclear magnetic resonance spectra were obtained on a Varian A-60D high-resolution spectrometer at a probe temperature of 25 ± 1 °C. Spectra were recorded at sweep rates of 0.1 Hz/s both for chemical shift measurements and line-shape measurements; sweep widths of 50 Hz were used. For line-shape measurements, each spectrum was recorded four or five times and the spectra were averaged.

Solutions used in the n.m.r. studies were prepared in distilled water from the appropriate amounts of crystalline acetylglycine and standardized metal nitrate solution. KNO_3 was added to the solution containing only acetylglycine to give an ionic strength comparable to that of the solutions containing the metal nitrates. HNO_3 or KOH was added to bring the solutions to the desired p*H* values. TMA nitrate was added to each solution at a concentration of approximately 0.01 *M* as a reference compound for chemical shift measurements, negative shifts representing resonances downfield from the central resonance of the TMA triplet. The central resonance of TMA is 3.17 p.p.m. downfield from the methyl resonance of sodium 3-(trimethylsilyl) 1-propane sulfonic acid (TMS*). At p*H* values greater than ~8, some hydrolysis of the peptide linkage occurred as indicated by drifting of p*H* to lower values. To minimize error due to changes in p*H*, n.m.r. spectra were obtained immediately after each sample was prepared. Successive scans showed little change in chemical shift or in line shape so that the change in p*H* while in the n.m.r. probe is considered to be small.

Results

Interpretation of the Nuclear Magnetic Resonance Spectra

The n.m.r. spectrum of the carbon-bonded protons of acetylglycine at p*H* 4.50 is shown in Fig. 1. The multiplet pattern for the methylene protons is a doublet of quartets resulting from spin–spin coupling to the peptide proton ($^3J_{HH} = 5.9$ Hz) and long-range coupling to the methyl protons ($^5J_{HH} = 0.3$ Hz). The spin states of the methyl protons which give rise to the quartet structure are given under the resonances for the methylene protons. These will be discussed with regard to the determination of the peptide proton exchange kinetics in a later section. Some structure appears in the resonance for the methyl protons, probably from coupling to both the peptide proton and the methylene protons. Due to the small coupling involved,

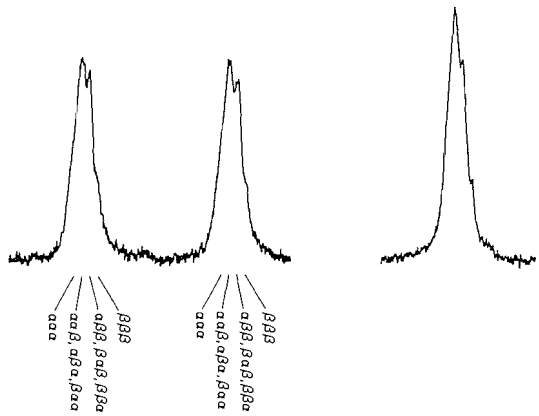

FIG. 1. 60 MHz proton n.m.r. spectrum of the carbon-bonded protons of acetylglycine at p*H* 4.50. The spin states of the methyl protons which give rise to the quartet structure are indicated below the resonances for the methylene protons.

however, it is not possible to determine the multiplicity of the methyl resonance. Similar long-range coupling through the same system of chemical bonds has been observed for *N*-methylacetamide (5).

Resonance patterns for the methylene protons at several p*H* values are shown in Fig. 2. The doublet of quartets collapses to a single quartet

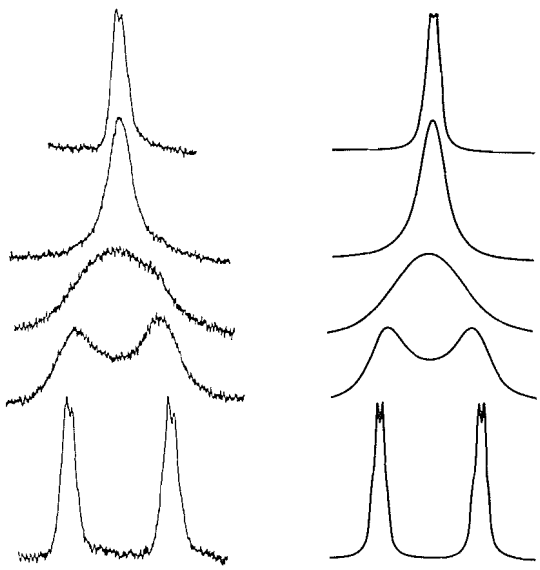

FIG. 2. Actual and computer-simulated 60 MHz proton n.m.r. spectra of the methylene group of acetylglycine at p*H* 4.50, 8.56, 8.93, 9.39, and 10.50, from bottom to top. Acetylglycine concentration 0.20 *M*. Temperature 25 °C.

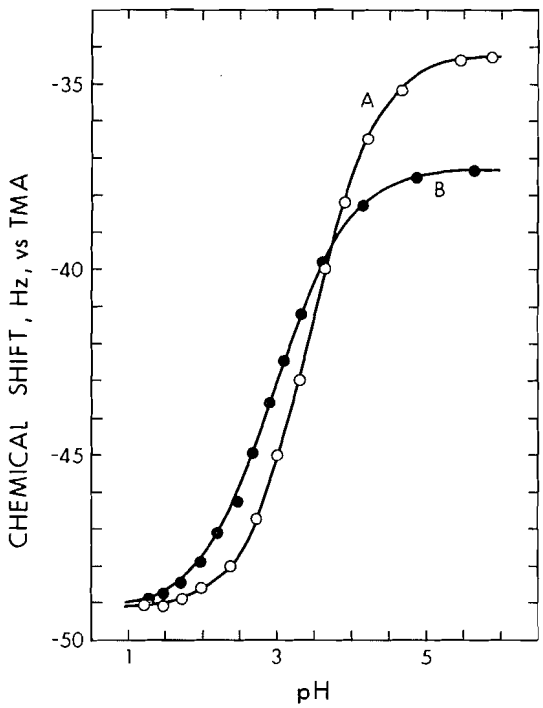

FIG. 3. p*H*-dependence of the chemical shift of the methylene protons of acetylglycine in (*A*) 0.20 *M* acetylglycine, 0.60 *M* KNO_3 and (*B*) 0.20 *M* acetylglycine, 0.20 *M* $Cd(NO_3)_2$. The smooth curves are the theoretical chemical shift behavior predicted with the acid ionization constant of acetylglycine and the formation constant of the cadmium–acetylglycine complex determined in this work. Temperature 25 °C.

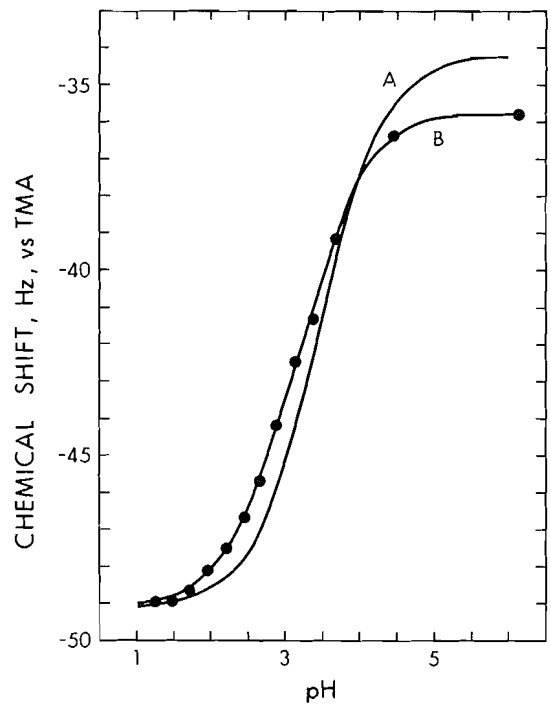

FIG. 4. p*H*-dependence of the chemical shift of the methylene protons of acetylglycine in (*A*) 0.20 *M* acetylglycine, 0.60 *M* KNO_3 and (*B*) 0.20 *M* acetylglycine, 0.20 *M* $Zn(NO_3)_2$. The smooth curves are the theoretical chemical shift behavior predicted with the acid ionization constant of acetylglycine and the formation constant of the zinc–acetylglycine complex determined in this work. Temperature 25 °C.

when the rate of exchange of the peptide proton with solvent protons is fast.

Chemical shifts of the resonances for the methyl and methylene protons are p*H*-dependent due to ionization of the carboxylic acid proton. The p*H*-dependence of the chemical shift of the methylene protons is shown by Curve *A* in Fig. 3. The chemical shift of the methyl protons changes from 66.5 to 67.9 Hz as the p*H* value is increased from 1.22 to 5.89.

Addition of an equimolar concentration of cadmium nitrate, zinc nitrate, or lead nitrate changes the p*H*-dependence of the chemical shifts of the methylene protons, as shown in Figs. 3, 4, and 5. In particular, the shift accompanying ionization of the carboxylic acid proton occurs over a lower p*H* range indicating displacement by the metal ion. At high p*H*, the chemical shift is different in the presence of the metal ions indicating different chemical shifts in the complexed and uncomplexed acetylglycine. With the metal containing solutions, the chemical shifts of the methyl protons leveled off at 67.5 Hz, independent of the metal ion.

The resonances for the methylene protons in the metal containing solutions also consist of a doublet of quartets, however, collapse to a single quartet begins at a lower p*H* when the metal ions are present. Because of precipitation, it was not possible to observe the ultimate collapse to a single quartet. The precipitates are probably metal hydroxides. The highest p*H* values that could be reached before precipitation for solutions containing 0.20 *M* metal nitrate and 0.20 *M* acetylglycine were 7.3, 6.2, and 5.6 for the cadmium, zinc, and lead systems.

Determination of the Acid Ionization Constant

The observed chemical shifts in the p*H* region where ionization of the carboxylic acid proton

Can. J. Chem. Downloaded from www.nrcresearchpress.com by 210.87.254.6 on 09/05/12
For personal use only.

Can. J. Chem. Downloaded from www.nrcresearchpress.com by 210.87.254.6 on 09/05/12
For personal use only.

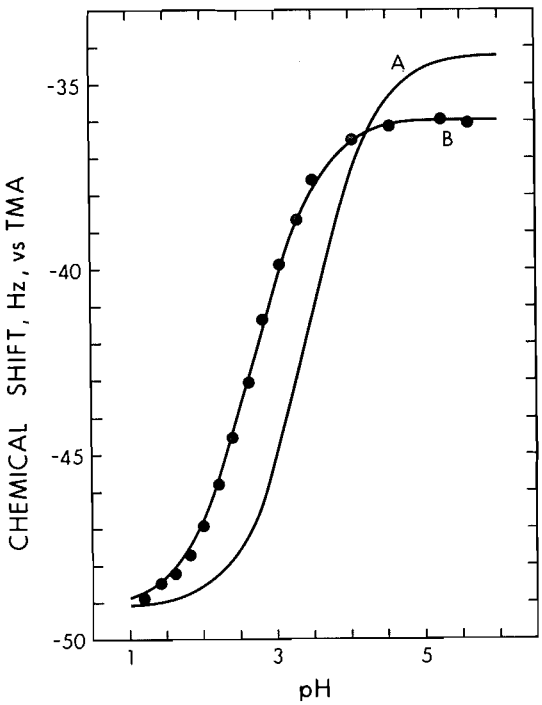

FIG. 5. p*H*-dependence of the chemical shift of the methylene protons of acetylglycine in (*A*) 0.20 *M* acetylglycine, 0.60 *M* KNO_3 and (*B*) 0.20 *M* acetylglycine, 0.20 *M* $Pb(NO_3)_2$. The smooth curves are the theoretical chemical shift behavior predicted with the acid ionization constant of acetylglycine and the formation constants of the lead–acetylglycine complexes determined in this work. Temperature 25 °C.

is occurring are the sums of the chemical shifts of the protonated and ionized forms, weighted according to the relative concentration of each species (6).

$$[1] \qquad \nu_{obsd} = P_{HL}\nu_{HL} + P_L\nu_L$$

where P is the fractional population of each species.

$$[2] \qquad 1 = P_{HL} + P_L$$

HL and L^- represent protonated and ionized acetylglycine, and ν the chemical shift of the acetylglycine in the species indicated. Ionization of the carboxylic acid proton is quantitatively expressed by the constant K_a, defined as

$$[3] \qquad K_a = \frac{[H^+][L^-]}{[HL]}$$

When $[HL] = [L^-]$, *i.e.* when $P_{HL} = P_L$, $K_a = [H^+]$. Equation 1 indicates that the K_a of acetylglycine equals the $[H^+]$ at which ν_{obsd} is midway between ν_{HL} and ν_L. A value for K_a of 3.64×10^{-4} was obtained in this way from the data in Fig. 3.

Determination of the Formation Constants

When some acetylglycine is complexed, the observed chemical shifts are a measure of the amount of complex formed from which the formation constants can be evaluated. The observed chemical shifts are the sums of the chemical shifts of the various protonated species, weighted according to the relative concentration of each species (7).

Acetylglycine complexes of varying stoichiometry presumably can form via a series of stepwise reactions. The formation constants for ML^+ and ML_2 are defined as follows

$$[4] \qquad K_{f1} = \frac{[ML^+]}{[M^{2+}][L^-]}$$

$$[5] \qquad K_{f2} = \frac{[ML_2]}{[ML^+][L^-]}$$

In this work, the solutions contained equimolar amounts of acetylglycine and metal nitrate. A consideration of the formation constants of the acetic acid complexes of these metal ions suggests that, for these solution conditions, ML^+ is the predominant acetylglycine complex. The observed chemical shift for this situation is given by eq. 6.

$$[6] \qquad \nu_{obsd} = P_{L_f}\nu_{L_f} + P_{ML}\nu_{ML}$$

where L_f is the uncomplexed ligand ($[L_f] = [L^-] + [HL]$) and ν_{L_f} is the chemical shift of acetylglycene at the particular p*H* in the absence of a complexing metal ion. Substitution of $1 - P_{ML}$ into eq. 6 for P_{L_f} and rearrangement leads to eq. 7.

$$[7] \qquad P_{ML} = \frac{\nu_{obsd} - \nu_{L_f}}{\nu_{ML} - \nu_{L_f}}$$

P_{ML} is related to the concentration of complex by eq. 8.

$$[8] \qquad [ML] = P_{ML}[L_t]$$

where $[L_t]$ is the total acetyl glycine concentration.

The chemical shift of acetylglycine in the complexed form is required for calculation of

Can. J. Chem. Downloaded from www.nrcresearchpress.com by 210.87.254.6 on 09/05/12
For personal use only.

the concentration of complex by this method. Equation 6 indicates that when ν_{obsd} equals ν_{L_f}, ν_{ML} equals ν_{obsd}. Thus ν_{ML} is equal to ν_{obsd} at the pH where the chemical shift *vs.* pH curve for acetylglycine crosses the chemical shift *vs.* pH curve for an acetylglycine solution containing the complexing metal ion.

Formation constants were calculated from the chemical shift data presented in Figs. 3, 4, and 5. The concentration of ML^+ was calculated for each data point using eqs. 7 and 8. The concentrations of uncomplexed metal and ligand were then obtained by difference. The concentration of uncomplexed ligand in the ionized form was calculated as $\alpha_1[L_f]$ where $\alpha_1 = K_a/(K_a + [H^+])$. Formation constants determined in this way were constant and independent of pH for the cadmium and zinc systems, and for the lead system at pH less than *ca.* 2.5. The values obtained are log $K_{f1} = 1.23$ with a standard deviation of 0.07 for cadmium, 0.86 with a standard deviation of 0.06 for zinc, and 1.38 with a standard deviation of 0.02 for lead at pH less than 2.5. Literature values are log $K_{f1} = 1.13$, 0.71, and 1.40 for cadmium, zinc, and lead, respectively, at an ionic strength of 0.4 and a temperature of 30 °C (8).

The dependence on pH in the lead system at pH greater than 2.5 indicates that, in this pH region, the lead system is not adequately described by considering only formation of PbL^+. Chemical shift data at pH greater than 2.5 were further evaluated to obtain K_{f2}. In this pH range, the observed chemical shift is given by eq. 9.

$$[9] \qquad \nu_{obsd} = P_{L_f}\nu_{L_f} + P_{PbL}\nu_{PbL} + P_{PbL_2}\nu_{PbL_2}$$

Assuming that the chemical shift of acetylglycine in PbL_2 equals its chemical shift in PbL^+, eq. 9 becomes

$$[10] \qquad \nu_{obsd} = P_{L_f}\nu_{L_f} + P_{L_c}\nu_{L_c}$$

where $P_{L_c} = P_{PbL} + P_{PbL_2}$. These relationships were used to calculate K_{f2} from the data in Fig. 5; a value of 16.0 with a standard deviation of 1.3 was obtained. No literature value is available for comparison with K_{f2}. To check the validity of the method used, the formation constants for the lead complexes of acetic acid, $Pb(OAc)^+$ and $Pb(OAc)_2$, were determined. As in the lead–acetylglycine system, the chemical shift of acetic acid in $Pb(OAc)_2$ was assumed to be the same as its chemical shift in $Pb(OAc)^+$. Formation constants obtained from chemical shift data are log $K_{f1} = 2.16$ and log $K_{f2} = 0.83$. Literature values for these formation constants are log $K_{f1} = 2.18$ and log $K_{f2} = 0.74$ (9).

Determination of the Rate of Peptide Proton Exchange

Collapse of the doublet of quartets to a single quartet as the pH is increased (Fig. 2) is due to an increase in the rate of exchange of the peptide proton with solvent protons. Two reactions considered to be possible exchange pathways in the pH region where collapse occurs are (5, 10–12)

$$[11] \qquad CH_3CONHCH_2CO_2^- + H_2O \overset{k_1}{\rightleftharpoons} CH_3CO\bar{N}CH_2CO_2^- + H_3O^+$$

$$[12] \qquad CH_3CONHCH_2CO_2^- + OH^- \overset{k_2}{\rightleftharpoons} CH_3CO\bar{N}CH_2CO_2^- + H_2O$$

The average lifetime, τ, of the peptide proton before transfer from acetylglycine is the kinetic parameter measured by n.m.r. Equation 13 is the rate equation for the above reactions in terms of this parameter.

$$[13] \qquad \frac{1}{\tau} = k_1 + k_2[OH^-]$$

The lifetime of the peptide proton was obtained from n.m.r. spectra in the pH range where collapse from a doublet of quartets to a single quartet takes place. Sheinblatt has previously reported the results of an n.m.r. study of the exchange kinetics of the peptide proton of acetylglycine (12). In his line-shape analysis of the collapsing spectra, the approximation apparently was made that the quartets are single lines. In the present work, exchange rates were determined from small amounts of collapse, especially in the presence of metal ions, which made it necessary to use a more rigorous line-shape treatment that included the quartet structure.

Collapse of the quartet structure by peptide proton exchange is due to exchange of the methylene protons between the eight environments giving the eight lines in the doublet of quartets. Spectra were simulated as a function of the lifetime of the peptide proton with Bloch phenomenological equations modified for trans-

Can. J. Chem. Downloaded from www.nrcresearchpress.com by 210.87.254.6 on 09/05/12
For personal use only.

TABLE 1. Kinetic data for exchange of the peptide proton of acetylglycine at 25 °C

p*H*	$1/\tau$, s^{-1}
7.82	4.7
8.34	5.7
8.56	13
8.80	20
8.93	28
9.11	38
9.27	70
9.39	91

fer of magnetization by eight-site exchange. This approach is valid for this system because the coupling is first-order (13). The treatment of McConnell and Meiboom was used to obtain modified Bloch equations for eight-site exchange (14, 15).

In simulating exchange-collapsed spectra, it was assumed that the spin states of the methyl protons (indicated in Fig. 1) do not change upon exchange of the peptide proton (13). Thus, exchange occurs only between those lines for which the spin states of the methyl protons are the same. The probabilities that the spin state of the peptide proton either will or will not change upon exchange are essentially equal. A line width of 0.32 Hz was used for each of the eight lines in the doublet of quartets in the absence of exchange. This value was obtained by comparing spectra calculated for different line widths with the experimental spectrum in Fig. 1.

The lifetime of the peptide proton at a particular p*H* value was obtained by comparing the partially collapsed spectrum with computer-simulated spectra. The most convenient parameters to measure from the simulated and observed spectra were line widths and valley-to-peak ratios. These parameters from simulated spectra were plotted *vs.* τ, and experimental τ values were obtained from experimental spectra using these plots.

The inverse of the lifetime of the peptide proton at several p*H* values in the region where collapse occurs is listed in Table 1. The experimental uncertainties in the τ values are from 10 to 15%. According to eq. 13, the intercept of a plot of $1/\tau$ *vs.* hydroxide concentration is k_1 and the slope is k_2. Treating the data with standard least-squares techniques (16), the intercept is essentially zero and the slope is $3.75 \times 10^6\ M^{-1}\ s^{-1}$ with a standard deviation of 0.18×10^6. The value obtained by Sheinblatt for k_2 is $2.7 \times 10^6\ M^{-1}\ s^{-1}$ (12). The theoretical spectra in Fig. 2 were computer-simulated for lifetimes calculated from the p*H* values indicated and the rate constant obtained in the present work.

When the solution contains acetylglycine and equimolar amounts of cadmium, zinc, or lead, collapse begins at significantly lower p*H* values than in the absence of complexing metal, indicating an acceleration of the rate of exchange upon complexation. The exchange kinetics of the complexed species can be obtained by modifying eq. 13 to include the complex. The resulting equation is

$$[14] \qquad \frac{1}{\tau} = k_2\beta_1[OH^-] + k_3\beta_2[OH^-]$$

where $\beta_1 = [\text{Acetylglycine}]_{\text{uncomplexed}}/[\text{Acetylglycine}]_{\text{total}}$ and $\beta_2 = [\text{Acetylglycine}]_{\text{complexed}}/[\text{Acetylglycine}]_{\text{total}}$. β_1 and β_2 were calculated at the p*H* of a particular data point using the formation constants determined above. k_3 was then determined using the k_2 reported above and the $1/\tau$ obtained by comparing experimental and computer-simulated spectra.

Measurement of k_3 was possible only for the cadmium complex; precipitation of presumably $Pb(OH)_2$ and $Zn(OH)_2$ prevented reaching p*H* values at which there was sufficient collapse for reliable measurement in the lead and zinc systems. However, some broadening of each of the quartets was observed at the highest p*H* values reached with the lead and zinc systems whereas in the absence of these metal ions no broadening was observed at similar p*H* values. Therefore, peptide proton exchange is faster also in the acetylglycine complexes of lead and zinc than in the uncomplexed form.

Data for the peptide proton exchange in the cadmium system are: $pH = 6.70$, $1/\tau = 5.0$; $pH = 6.84$, $1/\tau = 5.9$; $pH = 6.93$, $1/\tau = 6.7$; $pH = 7.09$, $1/\tau = 8.9$; $pH = 7.26$, $1/\tau = 13.3$. Evaluation of these data by eq. 14 yields a value of $2.0 \times 10^8\ M^{-1}\ s^{-1}$ with a standard deviation of 0.28×10^8 for the rate constant for exchange of the peptide proton in the cadmium–acetylglycine complex.

Can. J. Chem. Downloaded from www.nrcresearchpress.com by 210.87.254.6 on 09/05/12
For personal use only.

Discussion

The chemical shift data in Figs. 3, 4, and 5 indicate that acetylglycine is coordinated to cadmium, zinc, and lead. The carboxylate group is coordinated as evidenced by displacement of the ionization of the carboxylic acid proton to a lower p*H* region. The peptide linkage might also be coordinated to give a chelate structure; the peptide linkage is known to be a site of metal-binding in some simple dipeptides and tripeptides when coordination occurs at the N-terminal amino group (17). Binding of the peptide linkage has been proposed via the carbonyl oxygen, the protonated peptide nitrogen, and the deprotonated peptide nitrogen (17). Incomplete collapse of the multiplet structure from coupling to the peptide proton of acetylglycine indicates that in not more than a small fraction of the complexed species could the peptide proton be ionized. From previous work Co(II), Ni(II), Cu(II), and Pd(II) are the only divalent metals known to promote ionization of the peptide nitrogen with subsequent bonding at the deprotonated site (17–20). Therefore, any coordination of cadmium, zinc, or lead to the peptide linkage of acetylglycine in the p*H* regions studied in this work would be to the protonated peptide linkage.

Of the two potential coordination sites in the protonated peptide linkage, the carbonyl oxygen is considered the more basic site on the basis of n.m.r. studies of protonation of the amide linkage (5) and crystallographic (3, 21) and infrared (22, 23) studies of binding to the peptide linkage. Thus, when a metal ion is chelated at the N-terminal end of a peptide, as in the dipeptide and tripeptide complexes of several metal ions, chelation is through amino nitrogen atoms and carbonyl oxygen atoms (**1**).

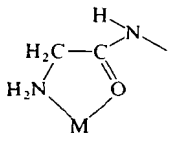

1

Chelation at the C-terminal end through an oxygen atom of the carboxylate group and the oxygen atom of the peptide linkage would lead to **2**. The seven-membered chelate ring in **2** is likely to be less stable than the five-membered ring in **1** (24), suggesting that the situation for chelation at the C-terminal end of peptides is not so ideal as at the N-terminal end.

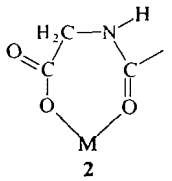

2

The formation constants for the acetylglycine complexes of cadmium, zinc, and lead also suggest that, if coordination does occur to the peptide linkage, it does not contribute significantly to the stability of the complex. The formation constants of complexes of these metals with a series of carboxylic acids, including acetylglycine, have been correlated with the basicity of the carboxylic acids, with no need for invoking chelation in the acetylglycine complexes (8).

Rabin and others have proposed that the peptide linkage exists as a resonance hybrid, primarily of the two forms

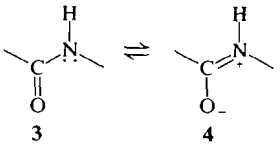

3 **4**

and that coordination at the oxygen, as in **1**, increases the importance of **4** (25). If so, coordination at the oxygen would tend to enhance the acidity of the peptide proton. In this work, it was found that coordination of acetylglycine to cadmium, zinc, and lead increases the rate of exchange of the peptide proton with solvent protons. In the cadmium complex, exchange is 53 times as fast as in uncomplexed acetylglycine. The increased lability may result from an inductive effect through the coordinated carboxylate group, or by interaction of the carbonyl oxygen of the peptide linkage with the metal. Interpretation of these results in terms of binding to the peptide linkage must await a better understanding of inductive effects on peptide proton exchange (11).

This research was supported in part by the National Research Council of Canada.

1. D. L. RABENSTEIN. Can. J. Chem. **49**, 3767 (1971).
2. L. J. BANASZAK, H. C. WATSON, and J. C. KENDREW. J. Mol. Biol. **12**, 130 (1965).
3. H. C. FREEMAN. Adv. Protein Chem. **22**, 255 (1967).
4. G. SCHWARZENBACH. Complexometric titrations. Interscience Publishers, New York. 1957.
5. A. BERGER, A. LOEWENSTEIN, and S. MEIBOOM. J. Am. Chem. Soc. **81**, 62 (1959).
6. E. GRUNWALD, A. LOEWENSTEIN, and S. MEIBOOM. J. Chem. Phys. **27**, 641 (1957).
7. D. L. RABENSTEIN and R. J. KULA. J. Am. Chem. Soc. **91**, 2492 (1969).
8. J. W. BUNTING and K. M. THONG. Can. J. Chem. **48**, 1654 (1970).
9. E. A. BURNS and D. N. HUME. J. Am. Chem. Soc. **78**, 3958 (1956).
10. M. SHEINBLATT. J. Am. Chem. Soc. **87**, 572 (1965).
11. M. SHEINBLATT. J. Am. Chem. Soc. **88**, 2123 (1966).
12. M. SHEINBLATT. J. Am. Chem. Soc. **92**, 2505 (1970).
13. E. GRUNWALD, A. LOEWENSTEIN, and S. MEIBOOM. J. Chem. Phys. **27**, 630 (1957).
14. H. M. MCCONNELL. J. Chem. Phys. **28**, 430 (1958).
15. S. MEIBOOM. J. Chem. Phys. **34**, 375 (1961).
16. J. MANDEL. The statistical analysis of experimental data. Interscience, New York. 1964.
17. P. J. MORRIS and R. B. MARTIN. Inorg. Chem. **10**, 964 (1971) and references cited therein.
18. R. B. MARTIN, M. CHAMBERLIN, and J. T. EDSALL. J. Am. Chem. Soc. **82**, 495 (1960).
19. E. W. WILSON, JR. and R. B. MARTIN. Inorg. Chem. **9**, 528 (1970).
20. H. DOBBIE and W. O. KERMACK. Biochem. J. **59**, 246 (1955); **59**, 257 (1955).
21. J. D. BELL, H. C. FREEMAN, A. M. WOOD, R. DRIVER, and W. R. WALKER. Chem. Commun. 1441 (1969).
22. N. C. LI and M. C. M. CHEN. J. Am. Chem. Soc. **80**, 5678 (1958).
23. N. C. LI, E. DOODY, and J. M. WHITE. J. Am. Chem. Soc. **79**, 5859 (1957).
24. A. E. MARTELL and M. CALVIN. Chemistry of the metal chelate compounds. Prentice-Hall, New York. 1952. p. 134.
25. B. R. RABIN. Trans. Faraday Soc. **57**, 785 (1961).

Can. J. Chem. Downloaded from www.nrcresearchpress.com by 210.87.254.6 on 09/05/12
For personal use only.

Photoreactions of Nitroso Compounds in Solution.[1] XX. Photoreduction, Photoelimination, and Photoaddition of Nitrosamines

Y. L. CHOW, M. P. LAU, R. A. PERRY, AND J. N. S. TAM

Department of Chemistry, Simon Fraser University, Burnaby 2, British Columbia

Received June 9, 1971

It has been established that alkylnitrosamines undergo photoreduction in methanol solutions in the presence of an acid to give the parent amine, formaldehyde, and *N*-aminoformamide. Where it is possible, an exchange reaction between the δ-hydrogen and the nitroso group is also observed during this photolysis. However, photoelimination also occurs in competition with photoreduction, the extent of which is dependent on the rates of the two photoprocesses. In aqueous solutions, *N*-nitrosamines predominantly undergo photoelimination. Those nitrosamines that undergo rapid photoelimination or photoreduction do not efficiently add to olefins photolytically. Conversely if photoaddition is retarded, a nitrosamine takes elimination or reduction pathways. Excitation of $n \rightarrow \pi^*$ or $\pi \rightarrow \pi^*$ transition band of *N*-nitrosamines gives virtually the same photoreaction patterns. Minor differences in the photoproducts are attributed to other secondary reactions.

Il a été établi que les alkylnitrosamines sont photoréduites dans des solutions de méthanol en présence d'un acide pour donner l'amine apparentée, du formaldéhyde et du *N*-aminoformamide. Lorsque c'est possible, on observe aussi une réaction d'échange entre l'hydrogène-δ et le groupe nitroso durant cette photolyse. Toutefois, la photoélimination arrive aussi en compétition avec la photoréduction, dont l'importance dépend des vitesses des deux procédés photolytiques. En solutions aqueuses, les *N*-nitrosamines subissent la photoélimination de façon prédominante. Ces nitrosamines qui subissent une photoréduction ou une photoélimination rapide ne s'additionnent pas photolytiquement aux oléfines de façon efficace. D'autre part, si la photoaddition est retardée, une nitrosamine entreprend un mécanisme d'élimination ou de réduction. L'excitation de la bande de transition $n \rightarrow \pi^*$ ou $\pi \rightarrow \pi^*$ des nitrosamines donne virtuellement les mêmes modèles de photoréaction. Des différences mineures dans les photoproduits sont attribuées à d'autres réactions secondaires.

Canadian Journal of Chemistry, **50**, 1044 (1972)

Previously we have demonstrated that an alkylnitrosamine is photolabile in the presence of an acid when irradiated in a Pyrex apparatus (>280 nm) (1, 2). Thus an aqueous solution of *N*-nitrosopiperidine (**1***a*) containing hydrochloric acid is photolytically decomposed to 2-piperidonoxime (**3***a*) and "isotripiperidein" (2). This process will be termed as photoelimination since various evidence indicates that the initial step of the reaction is the elimination of HNO to give alkylideneimine **2** (2–4). Examples of the photoinitiated addition of alkylnitrosamines to olefins (5–8), dienes (9), and acetylenes (10) have been described. This process, which also requires the presence of an acid, has been referred to as photoaddition. We have found that a nitrosamine also undergoes photolytically initiated reduction in the presence of an acid; the term photoreduction will be employed in describing this process. Further it has been observed that the pattern of these photodecompositions is virtually independent of the type of electronic excitation, *i.e.*, $n \rightarrow \pi^*$ or $\pi \rightarrow \pi^*$.

Through kinetic studies by flash excitation techniques we have recently demonstrated that the common reactive intermediate, aminium radical, is responsible for these photoreactions (1). In the light of this knowledge it is timely to discuss various photoprocesses and clarify the scope of these photoreactions.

Results

When a methanol solution of *N*-nitrosopiperidine (**1***a*) was photolyzed in the presence of hydrochloric acid, a large amount of piperidine (as its hydrochloride) was obtained and the expected photoelimination products were obtained in very low yields. This led us to re-examine carefully the photolysis both in methanol and in water solutions with respect to the different electronic excitations. Generally nonconjugated alkylnitrosamines show absorption maxima for the $n \rightarrow \pi^*$ transition band at ~340 nm and for the $\pi \rightarrow \pi^*$ transition at 230–240 nm with minima located at about the 300–320 nm region. For excitation of the $n \rightarrow \pi^*$ band, a filter solution of 2,7-dimethyl-3,6-diazacyclohepta-1,6-diene perchlorate was used to cut off the light energy below 340 nm.

[1]Part XIX of this series, see Chow *et al.* (21).

Can. J. Chem. Downloaded from www.nrcresearchpress.com by 210.87.254.40 on 09/05/12
For personal use only.

TABLE 1. Photolysis of *N*-nitrosopiperidine

Solvent	Type of irradiation	% yield			
		Piperidine HCl	Amidoxime **3***a*	Isotripiperidein	Other
H_2O	254 nm	24	—	19	—
H_2O	>340 nm	—	31	39	*
MeOH	254	42	2.2	—	†
MeOH	>340	57	3.5	—	‡

*2-Piperidone (1%) was also isolated.
†*N*-Piperidinoformamide (20%) and formaldehyde (as 2,4-DNPH) were isolated.
‡Formaldehyde (as 2,4-DNPH) and *N,N,N',N'*-bispentamethyleneurea were isolated.

For irradiation of the $\pi \rightarrow \pi^*$ band, a low pressure mercury resonance lamp (90% of energy output at 2537 Å) and a nickel sulfate solution were used so that the incident light energy in the 340–420 nm region was nil.

The results of the photolysis of *N*-nitrosopiperidine (**1***a*) under various conditions are summarized in Table 1 in which the percent yield of the products represents the percentage actually isolated. The photolysate after irradiation in methanol with the 254 nm light source was carefully analyzed and small amounts of 2-piperidonoxime (**3***a*) (2) and *N*-piperidinoformamide (**4***a*) were determined in addition to piperidine hydrochloride. From the methanol distillate, formaldehyde was isolated as its 2,4-DNPH derivative. The structure of formamide **4***a* was determined by direct comparison with an authentic sample prepared by a standard method (11), and by mass spectrometry in which the compound exhibited strong mass ions at 99 and 83 assignable to the fragments of M^+—CHO and M^+—NHCHO. It is pertinent to mention that the n.m.r. spectrum of formamide **4***a* (and other analogous compounds **4**) showed that the signal of the NH proton was coupled with the aldehyde proton ($J = 11$ Hz) indicating the former was not exchanging rapidly. However, in the photolysate obtained from the >340 nm irradiation, no trace of formamide **4***a* could be detected.

The photolysis of **1***a* was repeated in aqueous solutions with these two different light sources (Table 1). Careful analysis of the photolysate

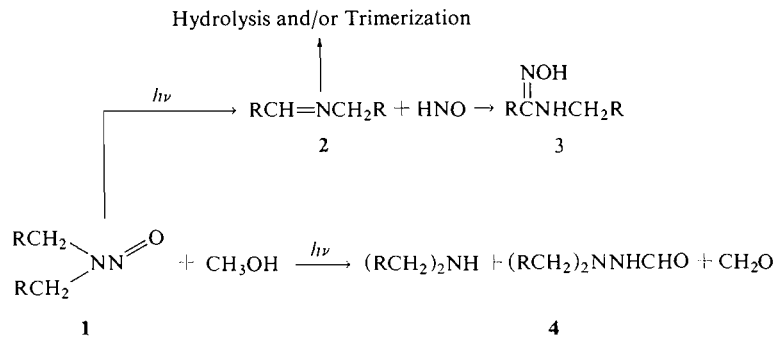

a R = $-CH_2CH_2CH_2-$
b R = C_4H_9
c R = C_6H_5

SCHEME 1

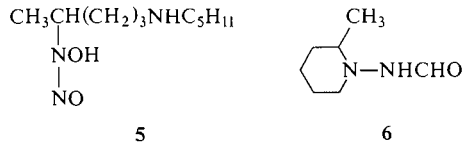

5 6

Can. J. Chem. Downloaded from www.nrcresearchpress.com by 210.87.254.40 on 09/05/12
For personal use only.

Can. J. Chem. Downloaded from www.nrcresearchpress.com by 210.87.254.40 on 09/05/12
For personal use only.

obtained from the >340 nm irradiation showed that oxime **3***a* (31%), "isotripiperidein" (39%) (2), and a trace amount of 2-piperidone had been formed; the last compound was assumed to be formed by hydrolysis of oxime **3***a*. These compounds were typical photoelimination products. Piperidine hydrochloride, if formed to a small extent, might have escaped detection. In contrast, irradiation with the 254 nm light source gave piperidine hydrochloride and "isotripiperidein" but no oxime **3***a*. The actual percent yields of these compounds were probably higher since recovery from aqueous solutions was generally not quantitative due to the compounds' high solubility in water. In each case, it was demonstrated that the photolysis did not take place in the absence of an acid.

Several nitrosamines were photolyzed in methanol in order to determine the photoreduction pattern. The pertinent cases will be discussed here. The complex photolysate from *N*-nitroso-di-*n*-pentylamine was analyzed to give valeraldehyde (35%), the parent amine (12%), *N*-di-*n*-pentylaminoformamide (**4***b*, 3%), 4-(*N*-nitrosohydroxylamino)-dipentylamine (**5**, 7%), and *N*-*n*-pentyl-pentanamidoxime (**3***b*, 1.5%); *n*-pentylamine was also isolated. Valeraldehyde was derived from the photoelimination product, imine **2***b*, through hydrolysis. The structures of both formamide **4***b* and amidoxime **3***b* were inferred after comparison of their spectral data with that of homologous compounds (2, 4) (see Experimental).

The molecular formula of nitrosohydroxylamine **5** was ascertained by high resolution mass spectrometry to be $C_{10}H_{23}N_3O_2$. The i.r. spectrum of this compound exhibited the major absorptions observed in the spectrum of 1-piperidino-2-(*N*-nitrosohydroxylamino)-3,3-dimethylbutane (8); this suggested the presence of a —N(NO)OH group. The location of the nitrosohydroxylamino group as shown in **5** was determined by n.m.r. decoupling experiments[2] by establishing that the methyl doublet (τ 8.59) was coupled with the methine proton (τ 5.7) with a coupling constant of 6.5 Hz. Nitrosohydroxylamine **5** and formamide **4***b* were, however, not detected when nitrosamine **1***b* was photolyzed with the >340 nm light source. The isolated photoproducts were amidoxime **3***b* (10%), valeraldehyde (>29%), and the parent amine (22%).

The photolysis of *N*-nitrosodibenzylamine in methanol solution with the 254 nm light source was gradually retarded as it proceeded due to an internal filter effect. It was assumed that the photoproducts were acting as internal filters to slow down the photoprocess. From the photolysate, *N*-benzylbenzamidoxime (**3***c*, 20%) (4), benzylamine (55%), and benzaldehyde (as its 2,4-DNPH) and its oxime were isolated; all these photoproducts were typical of photoelimination. Dibenzylamine was not isolated. In view of this result, the photolysis of *N*-nitroso-1,2,3,4-tetrahydroisoquinoline in methanol solution (7) was reinvestigated with the >340 nm light source. From the photolysate, 1-oximino-1,2,3,4-tetrahydroisoquinoline (7) was isolated in 87% yield and the parent amine only in 3% yield. The photoreduction was therefore very inefficient.

Photolysis of a methanol solution of *N*-nitroso-2-methyl-piperidine with the 254 nm light source gave a rather intractable crude product from which *N*-(2-methylpiperidino)formamide (**6**, >15%) was isolated. Under the same conditions, *N*-nitroso-*N*-methyl-cyclohexylamine (2) was photolyzed to give a 60% yield of *N*-methylcyclohexylamine. In addition, photodecomposition of *N*-nitroso-*N*-methylpentylamine *N*-nitroso-2-butylaminoethanol, and *N*-nitroso-2-(*t*-butylamino)ethanol were also investigated, but no radical departure from the above decomposition pattern was observed. The details of these photolyses are described in the thesis by one of us (12).

When a methanol solution of *N*-nitrosopiperidine and cyclohexene was irradiated with the 254 nm light source, 2-piperidinocyclohexanone (**7**, *ca.* 8%) and the corresponding oxime (**8**, 42%) (5) were isolated. Though the yield of the oxime estimated from the spectral data was about 60%, the isolation was hampered by the presence of a large amount of tarry product. The yields of both tar and the ketone were cut down to negligible amounts when the photoaddition was carried out with >340 nm irradiation. An excellent yield of oxime **8** was isolated readily from this photoaddition.

[2]The decoupling experiments have been carried out with a Varian HA-100 spectrometer through the kind assistance of Professor K. R. Kopecky to whom we are very grateful.

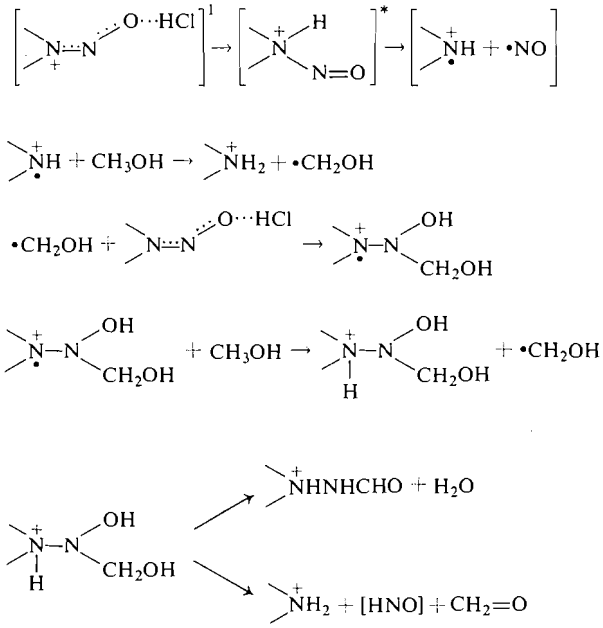

SCHEME 2

Discussion

From the kinetic studies by flash excitation, we have shown that a singlet excited nitrosamine–acid complex rapidly decays to the corresponding aminium radical. It is this aminium radical that undergoes elimination, reduction, and addition reactions (1). It has been noted that in photolyses of certain nitrosamines in methanol solution, instead of the expected reaction products, variable amounts of the parent amine have been isolated (2, 6, 7). Since nitrosamines have been shown to be stable in the absence of irradiation (2), the transformation to the parent amine is probably derived from a light-catalyzed process. That oxidation–reduction processes are involved in this transformation is readily shown by isolation of the formamides **4** and formaldehyde that are derived from oxidations of methanol. In an ethanol solution photolysis, acetaldehyde has been isolated (13) as the oxidation product, although the yields of both acetaldehyde and formaldehyde have not been quantitatively determined. The formyl group of the formamides **4** is apparently derived from oxidative coupling with methanol. In view of the known capacity of aminium radical to abstract hydrogen (14, 15) the following mechanism is suggested to account for the redox process. The ketyl radical $\cdot CH_2OH$ is proposed as a convenient carrier for the oxidation process and its formation is facilitated by the readily abstractable α-hydrogen.

The formation of hydroxylamine **5** in the photolysis of nitrosamine **1***b* can be regarded as an intramolecular oxidation process in which abstraction of the δ-hydrogen is favored by an entropy gain. This leads to the formation of the δ-nitroso compound which subsequently adds HNO to give **5** (8). The intramolecular exchange reaction between a hydrogen atom and a nitroso group has ample analogy in the Barton reaction (16) and nitrosamide photolysis (17, 18); the Hofmann–Löffler–Freytag reaction (15, 19) follows a similar reaction mechanism. An intermolecular hydrogen–nitroso group exchange reaction involving a labile allylic hydrogen has also been observed in the photolysis of **1***a* in the presence of Δ^9-octaline (20).

In the absence of hydrogen atom donating substrates, piperidinium radical preferentially undergoes photoelimination as shown in the photolysis of **1***a* in aqueous solutions. The proposed mechanism requires the elimination

Can. J. Chem. Downloaded from www.nrcresearchpress.com by 210.87.254.40 on 09/05/12
For personal use only.

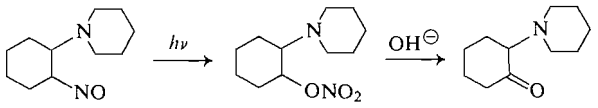

9 10 7

SCHEME 3

of an α-hydrogen atom from the aminium radical using nitric oxide as acceptor. The probability of elimination in an aminium radical is dependent upon the nature of the C—H bond to be broken and upon the steric factors around the C—H bond. Even in a methanol solution, the photoelimination takes place during photolysis of **1***b* since the rate of elimination is competitive with that of reduction (1). Since the elimination process is greatly facilitated by the involvement of a labile benzylic hydrogen in the photolysis of **1***c*, no photoreduction has been observed (3, 4). On the basis of a similar argument, the elimination process should dominate the photolysis of *N*-nitroso-1,2,3,4-tetrahydroisoquinoline; in this case, photoreduction has been observed to only a minute extent. It is pertinent to point out that in this case the photoelimination exclusively involves the benzylic hydrogen at the C-1 position.

On the other hand, it has been reported previously (5) that *N*-nitrosojervine and *N*-nitroso-*trans*-decahydroquinoline undergo photoreduction in methanol solutions faster than photoelimination, resulting in the exclusive formation of the parent amines. Photolyses of other nitrosamines indicate that the two rates are comparable and give both types of products (5). The structural features that facilitate photoreduction are however obscure at this stage. From the flash excitation studies of *N*-nitrosopiperidine it is shown that photoelimination is a unimolecular reaction while photoreduction is biomolecular (1). Since the latter rates are faster (1) than the former, for certain nitrosamines it is possible to adjust conditions so that one type of reaction takes place exclusively.

However, the formation of piperidinium chloride in the photolysis of **1***a* in an aqueous solution cannot be viewed as a photoreduction process, similar to that proposed in a methanol solution, since water is a poor hydrogen atom donating solvent. The photoelimination products, amidoxime **3***a* and "isotripiperidein", have been shown to be stable under the irradiation conditions with 254 nm light source.[3] Since the decay of the aminium radical is strictly first order and much slower than in methanol (1), an alternative mechanism for the formation of piperidinium chloride is required. It is envisaged that a photoinitiated hydrolysis of nitrosamine is responsible for this process; the details remain to be clarified.

An inspection of results shows that there are some superficial differences between $n \rightarrow \pi^*$ and $\pi \rightarrow \pi^*$ band photolysis. For example, in methanol it appears that formamide **4** is formed only in the irradiation with the 240 nm light source but not with the >340 nm source. In aqueous solution amidoxime **3***a* is not formed when $\pi \rightarrow \pi^*$ band of **1***a* is irradiated. Since these results are reproducible, it must be an intrinsic characteristic of the photoreaction. The causes effecting these discrepancies may be more than the wavelength effect of the light source. This difference may be ascribed to a secondary photoreaction in the irradiation with the 254 nm light source. Alternatively it may be due to a trivial difference in the vibrationally excited level of the intermediate in the respective cases.

Photoaddition of *N*-nitrosopiperidine to cyclohexene initiated by the 254 nm light source is as effective as that initiated by the >340 nm light source. However, in the former case a tarry by-product and cyclohexanone **7** are formed to a considerable extent apparently due to secondary photoreactions. Such secondary photoreactions are frequently observed phenomena; for example, photolysis of *N*-nitrosamides by $\pi-\pi^*$ band excitation generally causes a disproportionation of the *C*-nitroso compound intermediate (17, 18). It may be suggested that ketone **7** is formed via nitrate **10** from the nitroso intermediate **9** by analogy to the mechanism proposed in the photolysis of *N*-nitrosamides

[3]The protonated forms of **3***a* and isotripiperidein are not likely to serve as a source of hydrogen donor due to the polar effects of the aminium radical. We have not isolated other products that can be accounted for such secondary reaction.

Can. J. Chem. Downloaded from www.nrcresearchpress.com by 210.87.254.40 on 09/05/12
For personal use only.

Can. J. Chem. Downloaded from www.nrcresearchpress.com by 210.87.254.40 on 09/05/12
For personal use only.

(see Scheme 3) (17, 18). More complex reaction mixtures have been obtained in the photoaddition of **1***a* to cyclooctene and 3,3-dimethyl-1-butene with the 254 nm light source (12). Particularly in the latter case, the yield of the oxime corresponding to **8** is very low indicating the occurrence of extensive secondary photoreactions; the reasons for these secondary reactions have been discussed (8).

The success of photoaddition in methanol solutions under the present conditions is apparently dependent upon the competing rate of addition of aminium radical relative to the rates of reduction and elimination. The rate of addition of piperidinium radical (from **1***a*) to cyclohexene is about 5000 times faster than the reduction as has been shown by flash photolysis (1). It is readily understandable that the photoaddition predominates when cyclohexene is added to the irradiation mixture. Photoaddition of **1***a* to 3,3-dimethyl-1-butene is retarded by steric hindrance as has been previously discussed (8). In the latter photolysis, it is not surprising that the photoreduction product (**4***a*) has been isolated (8). On the other hand, *N*-nitroso-1,2,3,4-tetrahydroisoquinoline undergoes photoelimination so rapidly that no photoaddition to styrene can be observed (7). Styrene has been shown to be a far more reactive olefin than cyclohexene towards photoaddition since the rate determining step is an electrophilic attack of an aminium radical (6, 7).

Experimental

Unless specified otherwise, n.m.r. spectra were recorded with a Varian A 56/60 spectrometer in $CDCl_3$ using TMS as the internal standard, i.r. spectra in Nujol mulls or neat liquid with a Perkin–Elmer model 457 grating spectrophotometer, u.v. spectra with a Unicam SP 800 spectrophotometer, and mass spectra with an Hitachi RMU-6E instrument at 80 eV. Melting points were determined with a Fisher–Johns hot-stage and were uncorrected. Microanalyses were performed by Dr. A. Bernhardt, Elbach, West Germany.

General Procedure of Photolysis

Previously described photolysis procedures (2) were followed with two different light sources. For irradiation at $n \rightarrow \pi^*$ transition band (>350 nm) a Hanovia medium pressure mercury lamp was used in conjunction with a filter solution of 2,7-dimethyl-3,6-diazacyclohapta-1,6-diene perchlorate (0.1 g/1 l of water). The cold filter solution was circulated through the cold finger. This system permitted the irradiation at >350 nm.

For irradiation at $\pi \rightarrow \pi^*$ transition band of *N*-nitrosamines, a Nester Faust Model NFUV-300 low-pressure mercury resonance lamp (90% of the light output at 2537 Å) was employed; a saturated nickelous sulfate solution was used as a filter. The lamp was placed in a quartz cold finger through which the filter solution was circulated. This setup allowed us to excite the $\pi \rightarrow \pi^*$ transition band of nitrosamine (λ_{max} 230–240 nm) leaving the >340 nm region opaque.

The photolysis products were isolated in the usual way (2) and separated by column chromatography. The percentage yields of the products are summarized in Table 1. Authentic *N*-piperidino-formamide (**4***a*) was prepared by reacting *N*-aminopiperidine with formic acid and was recrystallized from petroleum ether to give white crystals: m.p. 76–78° (lit. m.p. 77–78°) (11); i.r. 3180, 3100, 1730, 1645, 657 cm^{-1}; n.m.r. τ 1.67 (d, $J = 10$ Hz, collapsed to singlet on D_2O exchange), 2.15 (NH), 7.27, and 8.4; *m/e* (%) 128 (M^+, 3), 99 (46), 83 (81), 55 (100) and 41 (35).

Anal. Calcd. for $C_6H_{12}N_2O$: C, 56.23; H, 9.44; N, 21.86. Found: C, 56.40; H, 9.43; N, 22.02.

Photolysis of N-Nitroso-2-methylpiperidine

A solution of *N*-nitroso-2-methylpiperidine (7.9 g) and concentrated hydrochloric acid (8.0 ml) in methanol (240 ml) was photolyzed with the 254 nm light source for 10 h. The photolysate was worked-up in the usual manner. The 2,4-DNPH of formaldehyde was isolated from the distillate. The parent amine was isolated as the hydrochloride from the residue of the photolysate. Chromatography of the basic extract gave *N*-(2-methyl-piperidino)formamide (**6**, 15%) as colorless crystals: m.p. 72–73°; i.r. 3200, 3080, 2725, 2670, 1694, 1660, 740, and 650 cm^{-1}; n.m.r. τ 8.92 (d, $J = 6$ Hz, 3H), 8.38 (6H), 6.91 (m, 1H), 2.31 (d, $J =$ 11 Hz, NH), 1.77 (d, $J = 11$ Hz, collapses to singlet on D_2O exchange); *m/e* (%) 143 (6), 142 (M^+, 4), 127 (27), 113 (45), 97 (100), 69 (52), 55 (70).

Anal. Calcd. for $C_7H_{14}N_2O$: C, 59.20; H, 9.85; N, 19.72. Found: C, 59.03; H, 9.71; N, 19.65.

Photolysis of N-Nitrosodibenzylamine (1c)

A solution of the nitrosamine (5.45 g) and concentrated hydrochloric acid (2.5 ml) in methanol (240 ml) was photolyzed with the 254 nm light source. The absorption at 340 nm decreased rapidly during the first hour but slowed to a static state after 2 h. The residue yielded benzylamine hydrochloride (1.69 g), after removal of a major portion of the methanol: m.p. 249–254°; n.m.r. (D_2O) τ 2.72 (5H), 6.03 (s, 2H). The mother liquor was analyzed in the usual manner. Upon chromatography the neutral extract gave benzaldehyde (910 mg), the nitrosamine (304 mg), and benzaldehyde oxime (211 mg). The basic extract was chromatographed to afford *N*-benzylbenzaldoxime (**3***c*, 1.02 g, 108–111°) (4) and benzylamine (80 mg).

Photolysis of N-Nitrosodipentylamine (1b)

A solution of the nitrosamine (4.36 g) and concentrated hydrochloric acid (5 ml) in methanol (240 ml) was photolyzed with the 254 nm light source for 3.5 h. After the usual working-up valeraldehyde (35%, as 2,4-DNPH, m.p. 103–105°), di-*n*-pentylamine (12%), and *n*-pentylamine were isolated. In addition, *N*-di-*n*-pentylaminoformamide (**4***b*) was isolated from the basic fraction as a colorless oil (3%); i.r. 3290, 3150, 1680, 1080, 1050, and 1005 cm^{-1}; n.m.r. τ 9.17 (t, 6H), 7.4 (5, 4H), and 1.85 (singlet after D_2O exchange); *m/e* (%) 200 (M^+ 7), 171 (10), 157 (1), 143 (94), 115 (56), 113 (28), 98 (99), 87 (41), 73 (100), and 43 (100).

Mol. Wt. Calcd. for $C_{11}H_{24}N_2O$: 200.1524. Found: 200.1526.

Similarly, *N*-pentylpentamidoxime (**3***b*) was also isolated as a colorless oil (1.5%): i.r. 3410, 3220, 1640, 942, 900, and 690 cm^{-1}; n.m.r. τ 9.08 (t, 6H), 7.82 (m, 2H), 6.9 (t, 2H); *m/e* (%) 186 (M^+ 22), 171 (8), 157 (15), 129 (22), 112 (42), 87 (97), and 30 (100).

Mol. Wt. Calcd. for $C_{10}H_{22}N_2O$: 186.1732. Found: 186.1728.

The basic aqueous solution was evaporated to dryness and the solid residue was extracted with methylene chloride to give a solid (395 mg). This solid was recrystallized from chloroform to afford colorless crystals of 4-(*N*-nitrosohydroxylamino)dipentylamine (**5**): m.p. 188–190°; i.r. 2680, 2480, 1600, 1395, 1230, 1200, 1145, 930, and 900 cm^{-1}; n.m.r. (D_2O) τ 5.7 (m, 1H), 7.01 (t, $J = 4$ Hz, 4H), 8.59 (d, $J =$ 6.5 Hz), and 9.05 (t, 3H); *m/e* (%) 217 (M^+ 3), 187 (7), 160 (22), 130 (100), 113 (15), 100 (100), and 98 (39).

Mol. Wt. Calcd. for $C_{10}H_{23}N_3O_2$: 217.1790. Found: 217.1785.

In a separate experiment, the nitrosamine (3.88 g) and concentrated hydrochloric acid (4 ml) in methanol (230 ml) were photolyzed with the >340 nm light source for 2 h. After the usual working-up valeraldehyde (as 2,4-DNPH, 1.6 g), *N*-pentylvaleroamidoxime (**3***b*, 375 mg, 10%), and di-*n*-pentylamine hydrochloride (22%) were isolated. In spite of a careful investigation, formamide **4***b* and *N*-hydroxylamine **5** were not obtained.

Photoaddition of N-Nitrosopiperidine to Cyclohexene

A solution of *N*-nitrosopiperidine (3.17 g), cyclohexene (2.72 g), and concentrated hydrochloric acid (3.5 ml) in methanol (240 ml) was photolyzed with the 254 nm light source for 1.5 h. The photolysate was analyzed in the usual manner (5, 6) to afford recovered nitrosamine (350 mg) in the neutral extract. A dark tarry material was in the basic extract and showed a medium absorption at 1710 cm^{-1}. The first crop of 2-piperidinocyclohexanone oxime (780 mg) was obtained by recrystallization of the crude resin. The mother liquor was chromatographed to afford 2-piperidinocyclohexanone (**7**, *ca.* 450 mg) and its corresponding oxime (**8**, 1.26 g). The fractions containing the ketone were collectively treated with hydroxylamine to give the oxime.

A solution of *N*-nitrosopiperidine (11 g), cyclohexene (9 g), and concentrated hydrochloric acid (15 ml) and methanol (450 ml) was photolyzed with the >350 nm light source. The usual analysis gave a basic extract which was crystallized to give oxime **8** (9.6 g); m.p. 102–105°. The residue (8 g) from the mother liquor was chromatographed on an alumina column to give oxime **8** (5.4 g) and a small amount of ketone **7**.

The authors are very grateful to the National Research Council of Canada and the President's Research Fund, Simon Fraser University, for financial support.

1. M. P. Lau, A. J. Cessna, Y. L. Chow, and R. W. Yip. J. Am. Chem. Soc. In press.
2. Y. L. Chow. Can. J. Chem. **45**, 53 (1967); Y. L. Chow. Tetrahedron Lett. 2333 (1964).
3. T. Axenrod and G. W. A. Milne. Tetrahedron, **24**, 5775 (1968).
4. E. M. Burgess and J. M. Lavanish. Tetrahedron Lett. 1221 (1964).
5. Y. L. Chow. Can. J. Chem. **43**, 2711 (1965).
6. Y. L. Chow, C. J. Colón, and S. C. Chen. J. Org. Chem. **32**, 2107 (1967).
7. Y. L. Chow and C. J. Colón. Can. J. Chem. **45**, 2559 (1967).
8. Y. L. Chow, S. C. Chen, and D. W. L. Chang. Can. J. Chem. **48**, 157 (1970).
9. Y. L. Chow, C. J. Colón, and D. W. L. Chang. Can. J. Chem. **48**, 1664 (1970).
10. Y. L. Chow and D. W. L. Chang. Chem. Commun. 64 (1971).
11. P. A. S. Smith and N. W. Kalenda. J. Org. Chem. **23**, 1599 (1958).
12. M. P. Lau. Ph.D. Thesis, Simon Fraser University, Burnaby, British Columbia, 1970.
13. S. C. Chen. Ph.D. Thesis, Simon Fraser University, Burnaby, British Columbia, 1970.
14. J. Spanswick and K. U. Ingold. Can. J. Chem. **48**, 546, 554 (1970).
15. M. E. Wolfe. Chem. Rev. **63**, 55 (1966).
16. M. Akhtar. Adv. Photochem. **2**, 263 (1963).
17. Y. L. Chow and J. N. S. Tam. J. Chem. Soc. C, 1138 (1970).
18. Y. L. Chow, J. N. S. Tam, and A. C. H. Lee. **47**, 2441 (1969).
19. R. S. Neale, N. L. Marcus, and R. G. Schepers. J. Am. Chem. Soc. **88**, 3051 (1966).
20. Y. L. Chow, S. C. Chen, K. S. Pillay, and R. A. Perry. Can. J. Chem. This issue.
21. Y. L. Chow, S. C. Chen, and D. W. L. Chang. Can. J. Chem. **49**, 3069 (1971).

Can. J. Chem. Downloaded from www.nrcresearchpress.com by 210.87.254.40 on 09/05/12
For personal use only.

Photoreactions of Nitroso Compounds in Solution.[1] XXI. Stereochemical Course of Photoaddition of Nitrosamines to some Cyclic Olefins and Conformational Isomers Generated by $A^{1,3}$-Interaction

Y. L. CHOW, S. C. CHEN, K. S. PILLAY, AND R. A. PERRY
Department of Chemistry, Simon Fraser University, Burnaby 2, British Columbia

Received June 9, 1971

The results of the photoadditions of *N*-nitrosopiperidine and *N*-nitrosodimethylamine to three substituted cyclohexenes are discussed in terms of an "electrophilic" free radical attack of the aminium radicals generated from the photolysis of the nitrosamines. The photoaddition to 4-*t*-butylcyclohexene gave all four possible oximes; the axial approach of the aminium radical was preferred over the equatorial approach. The photoadditions to 3-methylcyclohexene are highly stereoselective giving oxime pairs **1**–**2** and **4**–**5**. Both oximes in each pair have 2-amino and 6-methyl substituents in *trans*-relation; but locked in the alternative conformations through $A^{1,3}$ interaction of the oximino group. In this addition the aminium radical almost exclusively approaches the C-1 carbon of the most stable conformer from the axial side. The steric hindrance to all possible axial and equatorial approaches to conformers of olefins have been compared. Piperidinium radicals, however, abstract an allylic hydrogen from $\Delta^{9,10}$-octaline since the steric hindrance in the addition process is too great to overcome. The hydrogen abstraction process leads to an intermolecular hydrogen–nitroso group exchange reaction which is similar to that in the photolysis of nitrosamides. A pathway is suggested to account for the generation, *in situ*, of the heteroannular diene **28** from which oxime **17** could be derived by photoaddition in 1,4-mode.

On discute les résultats de photoadditions de *N*-nitrosopipéridine et de *N*-nitrosodiméthylamine à trois cyclohexènes substitués en termes d'une attaque par radical "électrophile" des radicaux aminium provenant de la photolyse des nitrosamines. La photoaddition au 4-*t*-butylcyclohexène a donné les quatre oximes possibles; l'approche axiale du radical aminium avait priorité sur l'approche équatoriale. Les photoadditions au 3-méthylcyclohexène sont très stéréosélectives, donnant les paires d'oxime **1**–**2** et **4**–**5**. Les deux oximes dans chaque paire ont les substituants 2-amino et 6-méthyle en relation *trans*; par contre ils sont figés dans des conformations alternatives par interaction $A^{1,3}$ du groupe oximino. Dans cette addition, le radical aminium approche presque exclusivement le carbone C-1 du conformère le plus stable par son côté axial. On a comparé l'empêchement stérique à toutes les approches axiales et équatoriales possibles sur des conformères d'oléfines. Toutefois, les radicaux pipéridinium enlèvent un hydrogène allylique au $\Delta^{9,10}$-octaline puisque l'empêchement stérique dans le procédé d'addition est trop important pour l'empêcher. Ce procédé d'abstraction d'un hydrogène nous amène à une réaction intermoléculaire d'échange de groupe hydrogène–nitroso, qui est semblable à celle qu'on rencontre dans la photolyse des nitrosamides. On suggère un mécanisme qui tient compte de la formation, *in situ*, du diène **28** hétéroannulaire à partir duquel l'oxime **17** pourrait être dérivé par photoaddition par un mode 1,4.

Canadian Journal of Chemistry, **50**, 1051 (1972)

Introduction

Photoaddition of a nitrosamine to a carbon–carbon double bond is an extraordinary reaction in that both acid-catalysis and photoenergy are required (2–4). The photoaddition occurs with a short chain process as suggested by the quantum yield of $2 \sim 3$. On the other hand, it is neither retarded by the presence of air (2) in the solution, nor in the presence of a quencher such as a diene (5). Recent work from this laboratory by the technique of flash excitation has established that the primary photoprocess is the decay of a singlet excited nitrosamine to aminium radical which initiates the addition to a double bond (6). Due to the cationic charge, an aminium radical is expected to be a very strong electrophilic species. The reactivity of the latter is, however, expected to be strongly under the influence of steric factors since even the smallest aminium radical, dimethylamino radical, is equivalent in size to isopropyl radical. In order to evaluate the steric factors controlling the stereochemical course of the photoadditions to olefins, photoaddition to 3-methyl- and 4-*t*-butylcyclohexenes and $\Delta^{9,10}$-octaline were studied.

Results

The conditions of the photoaddition have been described and discussed in our previous publications (2–4) and, in the present case, are also outlined in the Experimental. When a

[1]For paper XX of this series, see ref. 1.

Can. J. Chem. Downloaded from www.nrcresearchpress.com by 210.87.254.105 on 09/05/12
For personal use only.

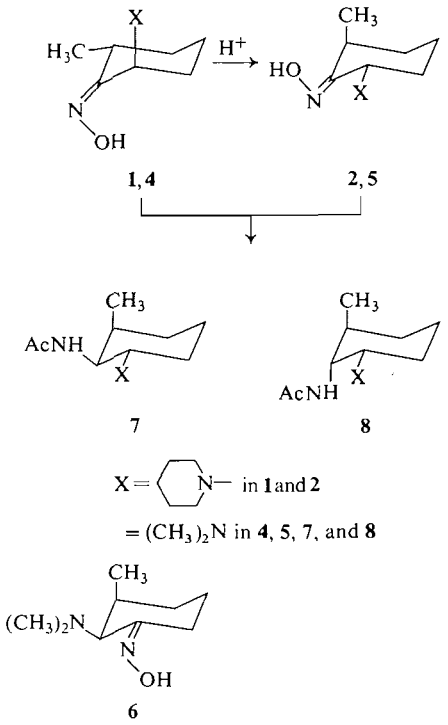

SCHEME 1

methanol solution containing equimolar quantities of *N*-nitrosopiperidine and 3-methylcyclohexene was irradiated in the presence of hydrochloric acid, two photoadducts, *syn,trans*-2-piperidino-6-methylcyclohexanone oxime[2] (**1**) and *anti,trans*-2-piperidino-6-methylcyclohexanone oxime (**2**), were obtained in 13 and 16% yield, respectively. In addition a small amount of *N*-piperidinoformamide (**3**) (1) was also isolated; but the amount of the neutral product was very small. In the presence of an excess of *N*-nitrosopiperidine and irradiation with a uranium glass filter, the yields of oximes **1** and **2** rose to 21 and 50%, respectively. Again no appreciable amount of the neutral product was obtained.

Both oxime **1** and **2** had the correct elemental analysis for the molecular formula of a 1:1 adduct, and exhibited characteristic i.r. absorption for the oxime group (7). The *anti*-oxime **2** dissolved readily in an aqueous solution of cupric sulfate (10%) to give a deep green solution indicating that chelation of the cupric ion had occurred[3] (8, 9). The blue color of cupric sulfate was, however, not affected when a methanol solution of the *syn*-oxime **1** was added. The presence of the *anti*-configuration in **2** and the *syn*-configuration in **1** were thus indicated.

The n.m.r. spectra provide information with regard to the configuration and conformation of the adducts and the relevant results are summarised in Table 1. The assignments of the lower field signals to C-2 and -6 protons are facilitated by the fact that the C-6 proton is coupled to the C—CH_3 group. The triplet ($J = 3.5$ Hz) at τ 6.18 in the spectrum of **1** is readily assigned to the C-2 equatorial proton while the C-6 proton is located at about τ 7.6 and partially hidden by the α-methylene signal of the piperidine ring. The chemical shift of the C-6 axial proton is comparable to that of the *anti*-α-axial proton of 4-*t*-butylcyclohexanone oxime (τ 7.95) (10) supporting the assignment of the axial orientation. The double doublet at τ 6.83 in the spectrum of **2** is assigned to the C-2 axial proton on the basis of the coupling constant. The broad multiplet at τ 6.35 ($w_{1/2} = 25$ Hz) is assigned to the equatorial proton at C-6 on the basis of the chemical shift value.[4] The orientations of the methyl group, equatorial in **1** and axial in **2**, are further supported by the observation that the coupling constant of the methyl group with the C-6 methine proton is larger for **2** (7 Hz) than for **1** (6.5 Hz); the coupling constant of an axial methyl proton with the vicinal methine proton in cyclohexane derivatives has been shown to be generally larger than that of the alternative conformation (11). Thus oximes **1** and **2** both possess piperidine and methyl groups oriented in a 1,3-*trans* relation and as the consequence of the $A^{1,3}$ interaction due to the oximino group (12, 13), the conformation of the ring is locked in the alternative orientations as shown. In agreement with this, oxime **1** was readily isomer-

[2]The *syn–anti* notation refers to the configuration of the oximino group and *cis–trans* notation is reserved for the configuration of the ring system. For the definition of *syn–anti* configuration, see ref. 2.

[3]So far, cupric sulfate tests of other *syn–anti* isomers have been successful, except in one bicyclic case. The *syn*-isomer of 2-*exo*-dimethylaminobicyclo[2,2,1]heptan-2-one oxime gave green coloration (unpublished results from this laboratory).

[4]The unpublished results from our laboratory show that the chemical shifts of the *syn*,equatorial proton at C-2 in various cyclohexanone oximes are as follows: 4-*t*-butylcyclohexanone oxime, τ 6.64; *cis*-3,5-dimethylcyclohexanone oxime, τ 6.68; 3-*t*-butylcyclohexanone oxime, τ 6.68.

Can. J. Chem. Downloaded from www.nrcresearchpress.com by 210.87.254.105 on 09/05/12
For personal use only.

TABLE 1. The n.m.r. data of the photoadducts to 3-methylcyclohexene*

	1	2	4	5
		Chemical shift (τ-value)		
OH	1.00(b)	1.54(b)	0.30(b)	1.06(b)
C-2	6.18(t)	6.83(dd)	6.23(t)	6.77(m)
N-CH_3	—	—	7.83(s)	7.60(s)
C-6	~7.6(m)	6.35(m)	7.25(m)	6.34(m)
C-CH_3	8.92(d)	8.87(d)	8.95(d)	8.86(d)
		Coupling constant (Hz)		
$J_{2,3e}$	~3.5	~4	3	4
$J_{2,3a}$	~3.5	~10	3	11
$J_{5e,6}$			2.5	~3
$J_{5a,6}$			10	~3
J_{6,CH_3}	6.5	7	6.5	7

*The spectra of oximes **4** and **5** were recorded with a Varian HA-100.

ized to **2** in the presence of hydrochloric acid; while the reverse isomerization did not take place. This is to be expected as piperidine ring is "bulkier" than methyl group.

The photoaddition of *N*-nitrosodimethylamine to 3-methylcyclohexene was run with a Rayonet photochemical reactor. The major photoadducts were *syn,trans*-2-dimethylamino-6-methylcyclohexanone oxime (**4**) and *anti,trans*-2-dimethylamino-6-methylcyclohexanone oxime (**5**) in 15 and 20% yield, respectively. A small amount (2%) of what appeared to be *anti,trans*-2-dimethylamino-3-methylcyclohexanone oxime (**6**) was also isolated. The proof of the structures and conformations of oximes **4** and **5** follows the same arguments as those used in the cases of **1** and **2**. In the present case the assignments of the protons and the configurations of the oximes were placed on a firmer basis by decoupling experiments; the relevant results and some examples of the decoupling are given in Table 1 and Figs. 1 and 2.

In both cases, the decoupling experiments (Figs. 1 and 2) related not only the signals of the C-6 proton and the *C*-methyl protons; but also located the signal due to the C-3 proton. The chemical shifts and the coupling patterns of the C-2 proton in **4** and **5** confirmed beyond any doubt their orientation as equatorial and axial, respectively. The narrow triplet, due to the C-6 proton in **5**, when decoupled from the *C*-methyl group, clearly indicates that the proton was equatorially oriented (Fig. 2*b*). The same decoupling operation in **4**, however, did not afford a clear coupling pattern. Judging from the width at half-height of the decoupled signal, an axial orientation of the C-6 proton was indicated.

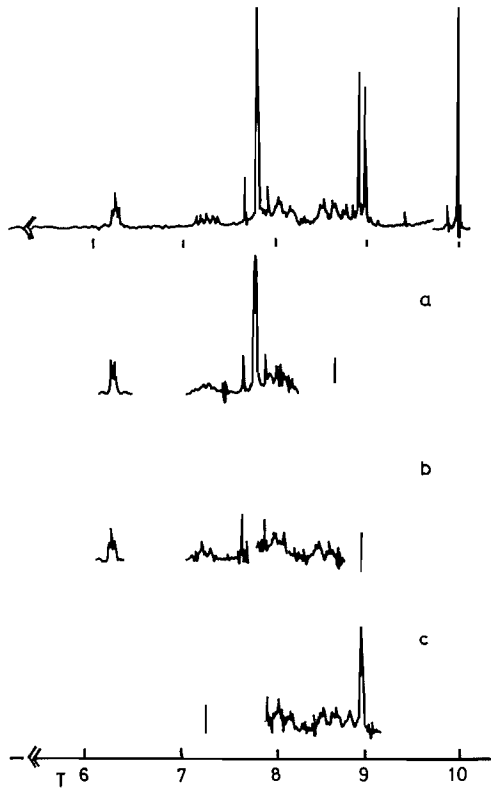

FIG. 1. The n.m.r. spectrum (100 MHz) of *syn,trans*-2-dimethylamine-6-methylcyclohexanone oxime (**4**) in pyridine: (*a*) irradiation at τ 8.78, (*b*) irradiation at τ 8.95, and (*c*) irradiation at τ 7.25.

The n.m.r. data shown in Table 1 and the decoupling results described above firmly placed

Can. J. Chem. Downloaded from www.nrcresearchpress.com by 210.87.254.105 on 09/05/12
For personal use only.

Can. J. Chem. Downloaded from www.nrcresearchpress.com by 210.87.254.105 on 09/05/12
For personal use only.

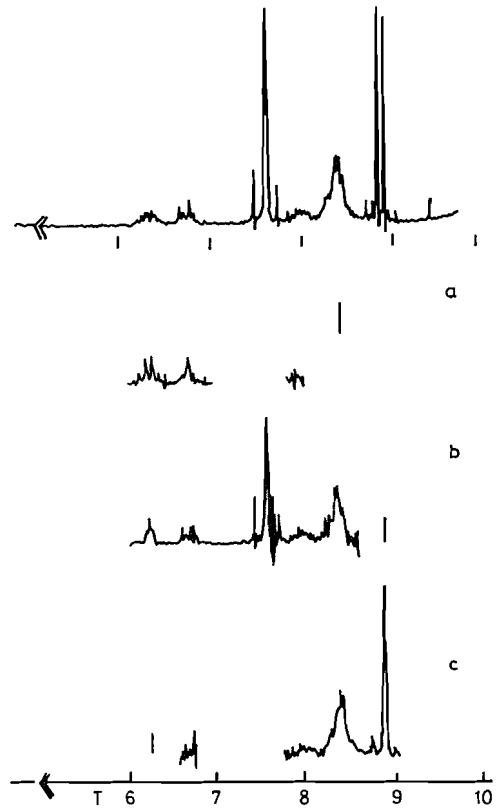

FIG. 2. The n.m.r. spectrum (100 MHz) of *anti,trans*-2-dimethylamino-6-methylcyclohexanone oxime (**5**) in pyridine: (*a*) irradiation at τ 8.35, (*b*) irradiation at τ 8.86, and (*c*) irradiation at τ 6.34.

the configuration and conformation of oximes **4** and **5** as shown. This is similar to the relation of oximes **1** and **2**; where they are forced to assume the alternative conformation though possessing the common *trans*-configuration at 2-amino-6-methyl groups. Further corroboration that oxime **5** possessed the *anti,trans*-configuration was given by the appearance of a deep green color on treatment with a copper sulfate solution.

The third isomer in the photoaddition of *N*-nitrosodimethylamine to 3-methylcyclohexene was obtained in a small quantity and was suggested to have the structure **6** on the basis of the following evidence. The *anti*-configuration of the oximino group was indicated according to the positive copper sulfate test (8, 9) exhibited by the compound.[3] The superimposed n.m.r. signal at τ 7.25 ~ 7.15 was integrated to be equivalent to two protons. One of these was clearly due to the C-6 equatorial proton as shown by a doublet ($J = 14$ Hz), each portion of which was further broadened. The remaining signals could be interpreted as a doublet with coupling constant of 2–3 Hz. The orientation of the equatorial 2-amino group and the axial 3-methyl group were suggested on the basis of the conformational energy of the substituents, which should have the *cis*-relation as indicated by the coupling constant of the methine protons. The structure **6** was also favored on consideration of the steric course of the approach of the reactant (*vide infra*).

In order to relate the configuration of oximes **1** and **2**, both compounds were reduced separately with lithium aluminum hydride followed by acetylation. From both operations the crude acetamide was shown to contain the same major and minor products; although the ratio from each preparation was slightly different. Both major and minor product acetamides showed i.r. absorption characteristic of the acetamido group, and an appropriate mass spectral pattern. The major product acetamide was shown to be 1-acetamido-2-*trans*-piperidino-6-*cis*-methylcyclohexane (**7**) and the minor one 1-acetamido-2-*cis*-piperidino-6-*trans*-methylcyclohexane (**8**).

The major product acetamide **7** exhibited n.m.r. signals at τ 3.35 and 6.30, the latter of which was sharpened to a double doublet ($J = 11$ and 4 Hz) when the former was removed by D_2O exchange. These results indicated that the τ 6.30 signal was due to the C-1 proton, oriented axially. The n.m.r. spectrum of the deuteriochloride of **7** exhibited the axial C-1 methine proton at τ 5.85 as a double doublet and the axial C-2 methine proton at τ 6.55 as a triplet each of which was further split to a doublet ($J = 11$ and 4.5 Hz). The orientations of the substitutions around the cyclohexane ring were such that both the 1-acetamido and 2-amino groups were equatorial and the 6-methyl was axial. The shifts of both the C-1 and -2 protons downfield as the consequences of the protonation of **7** were unusual. The minor acetamide **8** was obtained in impure state and showed a triplet n.m.r. signal at τ 5.98 ($J = 5.5$ Hz), indicating that the C-1 methine proton was equatorial. Although the signal due to the C-2 methine proton could not be observed clearly,

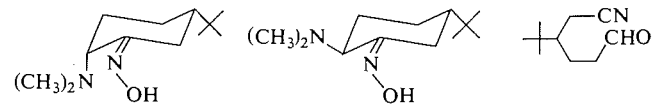

9 11 13

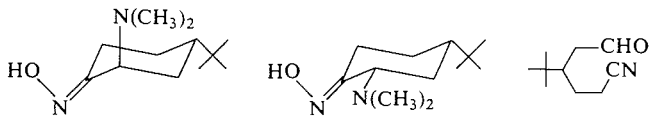

10 12 14

the configuration of **8** was provisionally assigned on the basis of the mechanism of the reduction.

The photoaddition of *N*-nitrosodimethylamine to 4-*t*-butylcyclohexene under the usual conditions afforded four isomeric oximes, *anti*, *cis*-2-dimethylamino-5-*t*-butylcyclohexanone oxime (**9**), *anti,trans*-2-dimethylamino-4-*t*-butylcyclohexanone oxime (**10**), *anti,trans*-2-dimethylamino-5-*t*-butylcyclohexanone oxime (**11**), and *anti-cis*-2-dimethylamino-4-*t*-butylcyclohexanone oxime (**12**), in that order of decreasing yield. The last two compounds were obtained in semi-pure state; each of which was contaminated by a small amount of the other. All four oximes **9**–**12** were shown to possess the *anti*-configuration as evidenced by positive cupric sulfate tests (8, 9). This was in agreement with the exclusive formation of the *anti*-oxime in the photoaddition to cyclohexene (2).

Oximes **9** and **11** were both transformed to 5-cyano-4-*t*-butyl-pentanal (**13**) through the Beckmann cleavage reaction (14–16). Pentanal **13** was characterized as 2,4-dinitrophenylhydrazone (2,4-DNPH, m.p. 127–128°). In the same manner, oxime **10** was cleaved to afford a different compound, 5-cyano-3-*t*-butylpentanal (2,4-DNPH, m.p. 125–126°). Due to the limited quantity available, oxime **12** was not cleaved in the same manner. While the i.r. and n.m.r. spectra of the two pentanals were distinctly different, it was not possible to establish the position of the *t*-butyl group unambiguously. This information enabled us to conclude that oximes **9** and **11** were the epimeric pair at the C-2 position having the same arrangement of the substituents around the cyclohexane ring. It is also clear that oxime **10** had a different arrangement of the substituents than oximes **9** and **11**. Oxime **10** was perhaps epimeric to oxime **12**.

The i.r. spectra of oxime **9** and **11** exhibit the C=N stretching band at 1650 and 1647 cm^{-1}, respectively, whereas the corresponding bands of **10** and **12** appear at 1670 and 1675 cm^{-1}, respectively, indicating their structural similarity (7). The mass spectra of oximes **9**–**10** determined under identical conditions are shown in Fig. 3 and unequivocally demonstrate that oximes **9** and **11** are one epimeric pair, while oximes **10** and **12** are the other. The significant feature of the mass spectra of oximes **9** and **11** is the most intense mass peak at *m/e* 84 which has been shown to correspond to the $C_5H_{10}N^+$ ion (**9***c*, 84.0812); but not to the $C_6H_{12}^+$ ion (84.0936) by exact mass determination (Found: 84.0811). A fragmentation scheme of oxime **9** or **11** to give **9***c* via **9***b* is proposed (see Scheme 2). This demands that the dimethylamino group must be related to the *t*-butyl group in a 1,4-orientation on the cyclohexane ring. The most intense mass peak at *m/e* 137 in the mass spectra of oxime **10** and **12** has been shown to correspond to the $C_9H_{15}N^+$ ion (**10***d*, 137.1204) by an exact mass determination (Found: 137.1178). This ion of *m/e* 137 is probably related to the ion of *m/e* 97 as proposed in Scheme 3. This scheme suggests that the *t*-butyl and the oximino groups are related in 1,4-fashion.

It is our aim now to ascertain the relative position of the *t*-butyl group in the respective pair of oximes. For this purpose, n.m.r. spectroscopy is shown to be the less ambiguous method.

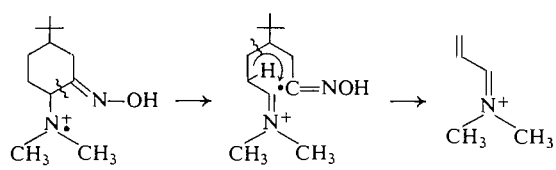

9*a* 9*b* 9*c* *m/e* 84

SCHEME 2

Can. J. Chem. Downloaded from www.nrcresearchpress.com by 210.87.254.105 on 09/05/12
For personal use only.

Can. J. Chem. Downloaded from www.nrcresearchpress.com by 210.87.254.105 on 09/05/12
For personal use only.

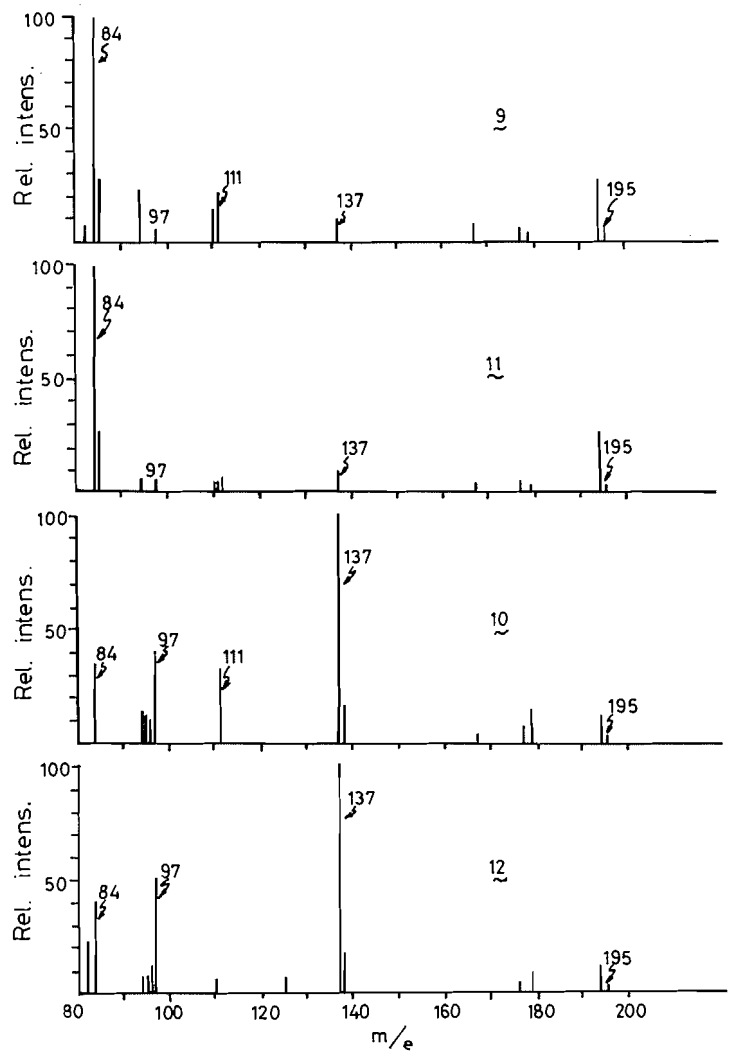

FIG. 3. Mass spectra (80 eV) of isomeric oximes **9**, **10**, **11**, and **12**.

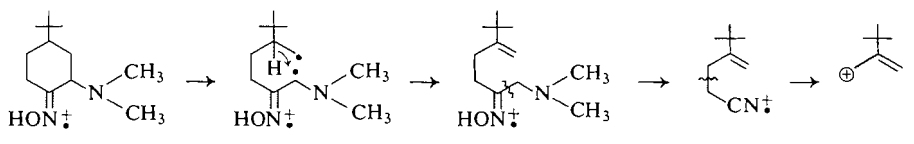

SCHEME 3

The n.m.r. results for these four oximes are summarized in Table 2 in which both the chemical shifts and coupling constants of oxime **9** have been confirmed by decoupling experiments. In all four n.m.r. spectra, the signals due to C-6 equatorial[4] and C–2 protons were readily identified in the range τ 6.25–6.45 and τ 7.25–6.79, respectively (Table 2). The C-2 proton in oxime **9** was equatorially oriented and that in oxime **11** axially, as shown by the coupling

TABLE 2. The n.m.r. data (100 MHz) of oximes **9**–**10** taken in pyridine solution

	9*	**10**	**11**†	**12**
		Chemical shift (τ-value)		
C-2	7.5(*t*)	7.16(t)	6.95(dd)	6.79(dd)
C-6e	6.25(d)	6.32(d)	6.42(d)‡	6.45(dt)
N-CH_3	7.82(s)	7.82(s)	7.47(s)	7.42(s)
C-CH_3	9.11(s)	9.20	9.15(s)	9.18(s)
		Coupling constant (Hz)		
$J_{2,3e}$	~3	3	5	4.5
$J_{2,3a}$	~3	3	10	10
$J_{5a,6a}$	12	—	11	
$J_{6a,6e}$	12.5	12	13	13

*The decoupling experiments also show that the chemical shifts of C-3 equatorial and C-6 axial are at τ 7.73 and 8.18, respectively.

†The decoupling experiments also show that the chemical shift of the C-6 axial proton is at τ 8.38.

‡The doublet is further broadened by small couplings.

patterns of the proton. The former is shown as a narrow triplet and the latter as a double doublet with a large and a small coupling constant. On the same grounds the C-2 proton of oxime **10** was assigned to the equatorial orientation and that of oxime **12** to the axial orientation. It was noted that in both pairs the chemical shifts of the axial protons (**11** and **12**) appeared at lower field than those of the equatorial protons (**9** and **10**). A similar reversal of the relative chemical shift positions for axial and equatorial protons was also found in α-bromocyclohexanones (17) and could be related to the conformation of the ring with respect to the anisotropic effects of the π-bond system.

The C-6 equatorial proton in all four oximes resonated in the expected range, in agreement with *syn*-α-equatorial protons of substituted cyclohexanone oximes with "frozen" conformations.[4] In all four oximes this proton signal was split to a doublet by the C-6 axial proton by a large geminal coupling constant. In oximes **9** and **11**, each signal was further broadened to the unresolved doublet by a small coupling (2–3 Hz) with C-5 (the carbon carrying the *t*-butyl group) axial proton. In the corresponding pair of oximes **10** and **12**, each signal of the doublet was weakly coupled (*ca.* 3 Hz) with the two C-5 protons as shown by the broad signal in **10** and the unresolved triplet in **12**. Furthermore, by the decoupling experiments, the C-6 axial proton in oximes **9** and **11** was shown to be a triplet and a double doublet, respectively, exhibiting large coupling constants (12 and 11 Hz, respectively) with the C-5 axial proton. This evidence allows us to place the *t*-butyl group at C-5 position for oximes **9** and **11** and at C-4 position for oximes **10** and **12**.

Photoaddition of *N*-nitrosopiperidine to Δ^9-octaline (**15**) was investigated under the standard photolysis conditions from which Δ^9-decalone-1 oxime (**16**, 30%) and 5-piperidino-Δ^9-decalone-1 oxime (**17**, 9%) were isolated. The isolation of these anomalous products was accompanied by a small yield of *N*-piperidinoformamide (3). For oxime **16**, the C=N stretching absorption at 1640 cm^{-1} and the u.v. absorption maximum at 237 nm indicated the presence of the con-

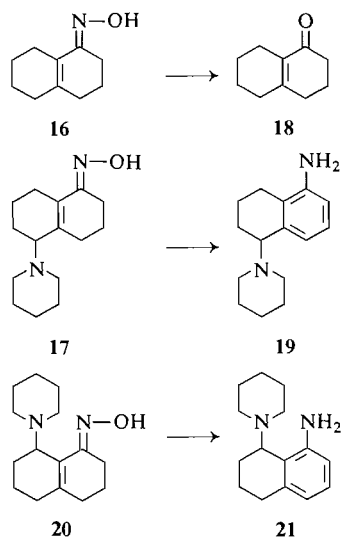

SCHEME 4

Can. J. Chem. Downloaded from www.nrcresearchpress.com by 210.87.254.105 on 09/05/12
For personal use only.

Can. J. Chem. Downloaded from www.nrcresearchpress.com by 210.87.254.105 on 09/05/12
For personal use only.

jugated enone oxime chromophor. Since the n.m.r. spectrum of oxime **16** did not show signal below τ 6, except the broad OH signal at τ 0.5, the tetra-substituted double bond was established. The identity of oxime **16** was established by the trans-oximation reaction with levulinic acid to give Δ^9-decalone, which was characterized by formation of its 2,4-DNPH. The melting points of oxime **16** and its derivatives are identical with those reported by Hückel and Blohm (18) and those by Campbell and Harris (19).[5] The configuration of oxime **16** must have the OH portion of the oximino group oriented *anti* to the olefinic bond since the alternative configuration would cause severe $A^{1,3}$ interaction (12, 13). The partially resolved triplet at τ 7.38 ($J = 6.5$ Hz) was assigned to two C-2 protons and the multiplet at τ 7.84 to the six allylic protons. The former assignment was justified in view of the similarity of the chemical shift to that of the α-*cis* protons of cyclohexanone oxime (τ 7.54). The magnetic equivalence of these C-2 protons also indicated that oxime **16** was flexible and rapidly interchanging among various conformations.

The basic oxime **17** contained a piperidine ring and the basic skeleton of oxime **16** as shown by i.r. (1633 cm^{-1}) and u.v. (237 nm) absorptions and the elemental analysis. The n.m.r. spectrum was not readily analyzable due to extensive overlapping of the signals (with the exception of the multiplet signal at τ 6.85 due to the tertiary allylic proton adjacent to the piperidino ring). Oxime **17** was transformed under the conditions of Semmler and Hofmann (20) to 1,2,3,4-tetrahydro-1-piperidino-5-aminonaphthalene (**19**), which exhibited appropriate mass peaks at *m/e* 230, 216, and 145 corresponding to the ions of M^+, $(M\text{-}NH_2)^+$ and $(M\text{-}C_5H_{10}N)^+$. The conclusion that the two amino groups were oriented in the 1,5-relation was supported by the comparable u.v. absorption curves of **19** and its dihydrochloride with those of 1-amino-5-di-(2′-chloroethylamino)-1,2-3,4-tetrahydronaphthalene and its dihydrochloride (21).[6] Structures **20** and **21**, the alternative possibilities to oxime **17** and aniline **19**, were not rigorously excluded. In view of the failure of the oxime and the aniline derivative to form Cu^{2+} or Ni^{2+} complexes (22), structures **20** and **21** could not be considered probable structures. From the mechanistic considerations (*vide infra*), no logical pathway could be formulated to arrive at structure **20**.

[5]The structure **16** was first suggested by Hückel and Blohm; but Campbell and Harris later erroneously reassigned the same compound to $\Delta^{8,9}$-decalone-1 oxime.

[6]The authors are grateful to the Director, Institute of Chemical-Pharmaceutical Research, Bucharest, Romania for the authentic samples.

Discussion

We have demonstrated that the primary photoprocess of a nitrosamine, in the presence of an acid, is the generation of the corresponding aminium radical from the singlet excited state of a nitrosamine–acid association complex (16). Further we have shown that piperidinium radical reacts with cyclohexene with a bimolecular rate constant of 2.4×10^7 M^{-1} s^{-1} (6). Although the aminium radical may be considered as an electrophilic species, it attacks a carbon–carbon double-bond by a purely free radical mechanism (see Scheme 5). However, it does not behave as an electrophilic reagent since a purely electrophilic attack would result in an electronic configuration of the nitrogen outer shell in excess of the limit imposed by the octet rule (see **22**). Further, a bridged aminium radical, such as **23**, cannot be rationally proposed as an intermediate on the same basis. The following discussion is based on free-radical addition of the aminium radical.

The investigation of the photoaddition to 4-*t*-butylcyclohexene, a conformationally "frozen" cyclohexene, affords an insight into the steric course of the initial attack of an aminium radical on the olefinic bond (Scheme 6). Although a more complex mixture of adducts has been obtained from the addition to this cyclohexene, the process is mechanistically less complicated since the olefinic bond is relatively free from a direct steric influence of the remote 4-*t*-butyl group. The isolation of all four possible oximes **9**–**12** indicates that the attack of the

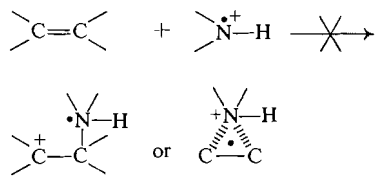

22 **23**

SCHEME 5

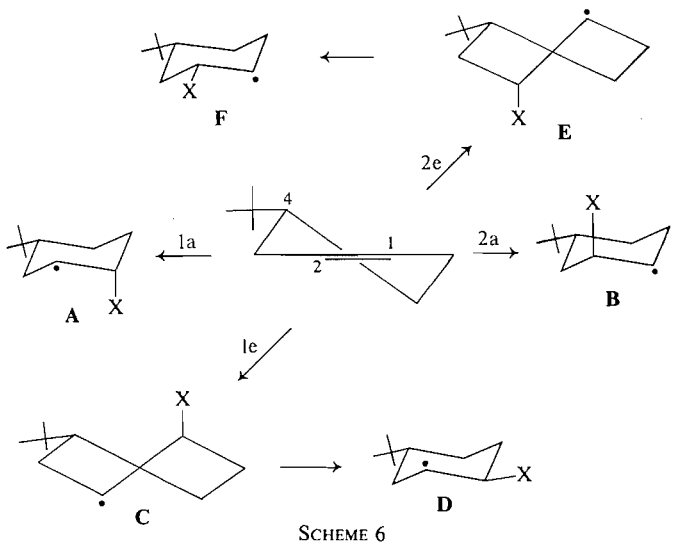

SCHEME 6

dimethylaminium radical is not stereospecific; but is stereoselective. Thus the aminium radical initiates the addition by preferentially attacking the C-1 position over the C-2 position. Between two available approaches to the respective carbon atom of the double-bond, it prefers to take the axial approach at both C-1 and -2 positions to give the intermediates **A** and **B**, respectively. The axial approach of the aminium radical at C-1 position (**A**) involves a nonbonded interaction from the C-5 axial hydrogen while that at C-2 (**B**) involves a similar interaction from the C-4 axial hydrogen. The latter is clearly more severe than the fomer due to compression from the 4-*t*-butyl group in **B**. The equatorial approaches[7] of the aminium radical at the C-1 and -2 positions led to the energetically unfavorable boat conformations **C** and **E**, respectively, that invert to chair conformations **D** and **F**. During the inversion of the boat conformation in **C** and **E**, the amino group would encounter eclipsing strain from the neighboring axial hydrogens. The total energies required in these two cases are apparently greater than those required in the axial approaches. It is not difficult to understand that the steric strain exerted by the C-3 axial hydrogen in **E** is more severe, owing to compression of the 4-*t*-butyl group. The same order of selectivity has been observed in the addition of methylthiyl radical to 4-*t*-butylcyclohexene (23). A similar steric effect has been shown in the light-induced addition of methane- and ethanethiol to *trans*-Δ^2-octaline to give a mixture in which the axial attack predominates over the equatorial one by a factor of *ca.* 10–1 (24). Since the "bulk" of the dimethylaminium radical is expected to be somewhat greater than that of the thiyl radicals, the lower selectivity observed in the present addition signifies that the aminium radical is more aggressive toward electrophilic attack, causing less stereochemical discrimination.

In the photoaddition to 3-methylcyclohexene (Scheme 7), the conformational equilibrium of the initial-state conformations has to be taken into account and the unknown steric strain imposed by the C-3 methyl group on various approaches of aminium radical has to be considered. It has been shown by a gas phase equilibrium (25), and supported by the recent theoretical calculation (26), that 3-methylcyclohexene exists mainly (85–90%) in the conformation with the methyl group at pseudoequatorial orientation. The conformer with the methyl group in pseudoaxial orientation, however, is also present in significant concentration. An attack of an aminium radical at the C-2 position in both conformations is considered to be severely restricted by compression of the C-3

[7]Strictly speaking, the mode of the attack leading to **C** and **E** is not precisely equatorial in conformational definition. If the attack and the inversion of the ring take place in a rapid succession, the net result and energetics can be approximated as an equatorial approach.

Can. J. Chem. Downloaded from www.nrcresearchpress.com by 210.87.254.105 on 09/05/12
For personal use only.

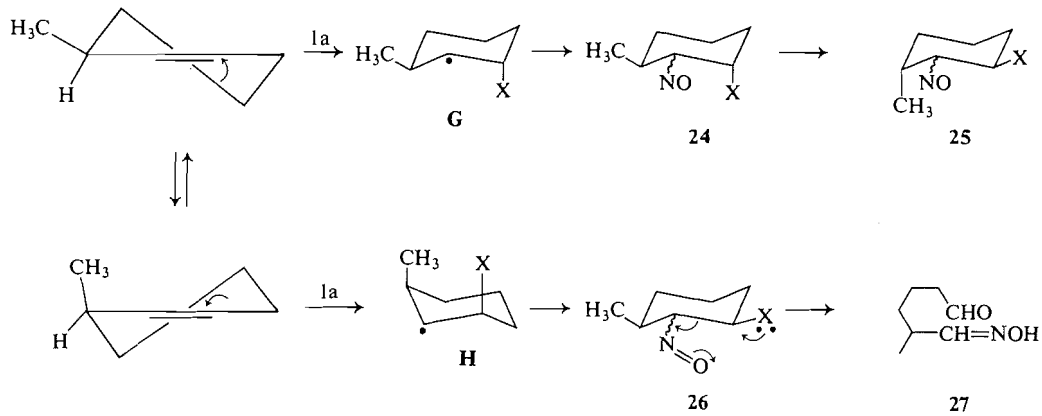

SCHEME 7

methyl group. The less hindered approaches at C-1 position in both conformations are visualized to follow the lowest energy pathways with axial approaches, for reasons similar to those stated in the previous case, leading to two possible intermediates with 1,3-*trans* (**G**) and 1,3-*cis* orientation (**H**). The latter intermediate appears less likely to form due to the 1,3-diaxial interaction between the amino and the methyl groups. The isolation of isomeric oximes (**1**–**2** and **4**–**5**) with two substituent groups (methyl and amino) solely in *trans*-orientation is in full accord with this argument. In both cases, the oxime pair is derived from tautomerization of the single *C*-nitroso compound in different conformations (**24** and **25**). The ratio in each pair is controlled by the rate of inversion, in competition with the rate of tautomerization. A small amount of the minor product **6** obtained in the photoaddition of *N*-nitrosodimethylamine apparently arises from an attack of dimethylaminium radical at the C-2 position. In accordance with the preferred axial approach of dimethylaminium radical, the *trans*-orientation of the substituents is assigned to **6**. Since piperidinium radical is "bulkier" than dimethylaminium radical, it is not surprising that the possible corresponding minor product in the photoaddition of *N*-nitrosopiperidine is not found.

The isomeric pairs of oximes (**1**–**2** and **4**–**5**) are interesting cases in which the 2-dimethylamino and 6-methyl groups, though in *trans*-relation in both cases, are locked in the alternative conformation by severe $A^{1,3}$ interactions generated by the oximino group (12, 13). The

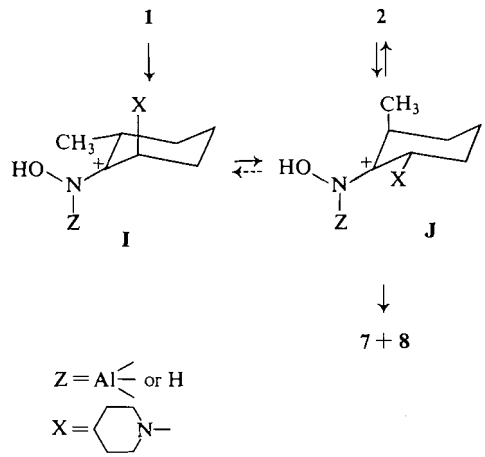

SCHEME 8

ready isomerization of oxime **1** to oxime **2** in an acidic solution is a good proof of the isomeric pair and apparently occurs through an intermediate such as the protonated species **I** (Scheme 8). The latter has been relieved of the $A^{1,3}$ interaction of the oximino group and rapidly inverts to more stable **J**; followed by deprotonation of **J** to give **2**. The result of the lithium aluminum hydride reduction of **1** and **2** can be explained on the same grounds. In both reductions the product-forming step, with hydride attack at the C-1 position, takes place from the common intermediate **J** to afford the observed configurational isomers **7** and **8**.

It is speculated that *C*-nitroso compound **26** (derived from **H**), though not a favored product, may also be formed in small quantity during photoaddition to 3-methylcyclohexene. The

Can. J. Chem. Downloaded from www.nrcresearchpress.com by 210.87.254.105 on 09/05/12
For personal use only.

Can. J. Chem. Downloaded from www.nrcresearchpress.com by 210.87.254.105 on 09/05/12
For personal use only.

tautomerization of **26** is certainly unlikely, since this process would entail a prior inversion to the 2,6-diaxial conformation of the substituents; the energy barrier of which appears to be too great to overcome (12). Among various other alternative decomposition routes, the cleavage pathway to **27** may be possible in analogy to the similar cleavage reaction observed previously (4). It is suspected that aldehyde **27** may have undergone various aldol condensations leading to a tarry material under the conditions of the experiment.

The photolysis of *N*-nitrosopiperidine in the presence of $\Delta^{9,10}$-octaline does not lead to the formation of a regular addition product. The failure of the addition can be traced to the 1,3-diaxial interactions due to the axial and pseudo-axial hydrogens. These hinder the approaches of piperidinium radical to the carbon–carbon double-bond. Since the addition pathway is sterically blocked, *N*-nitrosopiperidine undergoes an intermolecular hydrogen–nitroso group exchange reaction. The latter reaction is a process similar to Hofmann–Löffler–Freytag reaction (27), and is related to nitrosamide photolysis (28). Formation of oxime **16** must have taken place via hydrogen abstraction by the piperidinium radical to give **K**, which scavenges a nitroso group to afford the precursor to **16**. Such a hydrogen-abstraction process has been shown to take place between the piperidinium radical and methanol (1) although the rate is slower by 5000 times than its addition to cyclohexene according to flash excitation studies (6). This process also has been proposed as the initial step in Hofmann–Löffler–Freytag reaction (27). Indeed *N*-piperidinoformamide and *N*-dimethylaminoformamide, photoreaction products between the nitrosamines and methanol (1), have been isolated in these cases and also during other photoadditions. The present intermolecular hydrogen–nitroso group exchange reaction with an allylic hydrogen is so far the first instance observed in the photoreaction of nitrosamines.

The minor product of oxime **17** in this photoreaction can be derived from the photoaddition to a diene such as **28** in analogy to the established photoaddition pattern to dienes (5, 29). Since the olefin **15** used in this experiment has been shown, by v.p.c., to be completely free of diene **28**, this diene must be generated *in situ* during the photolysis. It is suggested that a hydrogen atom acceptor interacts with intermediate **K** to provide the heteroannular diene **28** (Scheme 9).

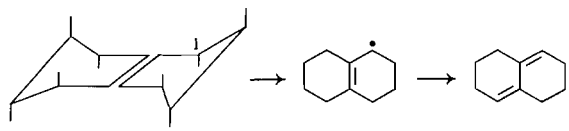

SCHEME 9

Experimental

Unless specified otherwise the i.r. spectra were recorded with a Perkin–Elmer 457 spectrometer in Nujol mulls or in liquid film, the mass spectra with an Hitatchi RMU-6E mass spectrometer (80 eV), and the n.m.r. spectra with a Varian A56/60 spectrometer in $CDCl_3$ solution using TMS as the internal standard. The decoupling experiments of n.m.r. spectroscopy were carried out with a Varian HA-100 spectrometer through the kind assistance of Professor K. R. Kopecky, The University of Alberta, Edmonton, Alberta. The melting points were measured with a Fisher–Johns hotstage and were corrected. The microanalyses were performed by Dr. A. Bernhardt, Elbach, West Germany.

Addition of N-Nitrosopiperidine to 3-Methylcyclohexene

(*a*) A methanol solution (320 ml) of *N*-nitrosopiperidine (4.75 g, 41.5 mmol), 3-methylcyclohexene (4.0 g, 41.5 mmol, Aldrich Chemical Co.), and concentrated hydrochloric acid (4.4 ml, 48 mmol) was irradiated with a 200 W Hanovia medium pressure mercury lamp (654A-36) for 2 h. The solvent was distilled off under reduced pressure, and the residue was treated with water (20 ml) and extracted with ether (30 ml × 3). The ether extract was dried ($MgSO_4$) and evaporated, leaving a light brown liquid (242 mg). Chromatography of this liquid on a silicic acid column (12 g) eluting with chloroform gave, after recrystallization from petroleum ether, *N*-piperidinoformamide (**3**), m.p. 70–72°, whose i.r. and n.m.r. were identical with those of an authentic sample (1).

The aqueous solution of the photolysate was then made basic with a saturated Na_2CO_3 solution. The white precipitate formed from the basic solution was filtered, dried in a desiccator to give crude crystals (4.03 g) which contained two compounds as indicated by t.l.c. analysis. One gram of this mixture was chromatographed on basic alumina (35 g). Elution with benzene (500 ml) gave *syn,trans*-2-piperidino-6-methylcyclohexanone oxime (**1**, 258 mg); m.p. 164–166° (dec.); i.r. 3350, 1670, 1135, 935, 740 cm^{-1}.

Anal. Calcd. for $C_{12}H_{22}N_2O$: C, 68.53; H, 10.54; N, 13.32. Found: C, 68.71; H, 10.43; N, 13.37.

Elution with 50% chloroform in benzene (100 ml) gave a mixture of **1** and isomer **2** (254 mg) in a ratio of *ca.* 1:10. Subsequent fractions from the same eluent (400 ml) contained *anti,trans*-2-piperidino-6-methylcyclohexanone oxime (**2**, 124 mg); m.p. 156–158° (dec.); i.r. 3250, 1670, 960, 880, and 800 cm^{-1}.

Anal. Calcd. for $C_{12}H_{22}N_2O$: C, 68.53; H, 10.54; N, 13.32. Found: C, 68.71; H, 10.43; N, 13.37.

The total yields of **1** and **2** were 13 and 16%, respectively. When a mixture of **1** and **2** was irradiated under the same

Can. J. Chem. Downloaded from www.nrcresearchpress.com by 210.87.254.105 on 09/05/12
For personal use only.

conditions of the photoaddition, the ratio of **1** to **2** was not changed.

(*b*) A methanol solution (200 ml) of 3-methylcyclohexene (2.0 g, 20.8 mmol), *N*-nitrosopiperidine (4.75 g, 41.5 mmol), and concentrated hydrochloric acid (4.4 ml, 52 mmol) was irradiated with a 200 W Hanovia lamp using a uranium glass filter. After complete disappearance of the nitrosamine absorption ($6\frac{1}{2}$ h), the photolysate was worked-up in the similar manner as described above. The acidic extract gave a mixture (220 mg) of recovered nitrosamine and amide **3** as indicated by i.r. spectroscopy and t.l.c. The yellowish basic extract was chromatographed to give oxime **1** (940 mg, 21.4%) and **2** (2.2 g, 50%).

Isomerization of syn,trans-2-Piperidino-6-methylcyclohexanone oxime (1)

A solution of oxime **1** (340 mg, 16 mmol) and hydrochloric acid (0.5 ml, 6 mmol) in methanol (40 ml) was stirred at 60° for 6 h. The resultant solution was worked-up in the usual manner to give a solid (320 mg) whose n.m.r. showed two pairs of doublets at τ 8.87 ($J = 7$ Hz) and 8.92 ($J = 6.5$ Hz), due to oximes **2** and **1** respectively, with an integration ratio of *ca.* 1:3. Silicic acid t.l.c. of this mixture eluted with 25% methanol in chloroform exhibited two spots at R_f 0.87 and 0.56, corresponding to oxime **1** and **2**, respectively. This mixture was chromatographed on a basic alumina column (10 g) to give pure oxime **2** (32 mg) together with recovered compound **1**.

Addition of N-Nitrosodimethylamine to 3-Methylcyclohexene

In a manner similar to the previous photolysis, a methanol solution (360 ml) of *N*-nitrosodimethylamine (3.08 g, 40.5 mmol), the olefin (4 g, 41.5 mmol) and concentrated hydrochloric acid (4 ml, 48 mmol) was irradiated using a single Rayonet RPR 3500 Å lamp. The photolysis was complete after 12 h. The methanol was removed under vacuum leaving a crude mixture which was treated with acetone to give a crystalline precipitate. The crystals were removed by filtration to give the hydrochloride of *anti,cis*-2-dimethylamino-3-methylcyclohexanone oxime (**6**) (400 mg). The hydrochloride was treated with saturated $NaHCO_3$ solution (20 ml) to give a suspension, which was filtered to give the free base (**6**, 159 mg, 2.3%). Recrystallization once from methanol and sublimation gave an analytical sample of **6**; m.p. 110–111.5°; i.r. 3230, 1655, 960, 925, and 885 cm^{-1}; n.m.r. τ 0.05 (s, 1H, D_2O exchangeable), 6.75–7.15 (m, 2H), 7.7 (m, superimposed, 1 H), 7.75 (s, 6H), 9.10 (d, $J = 7$ Hz, 3H).

Anal. Calcd. for $C_9H_{18}N_2O$: C, 63.49; H, 10.66; N, 16.45. Found: C, 63.44; H, 10.52; N, 16.28.

After removal of **6**, the filtrate was worked-up in the usual manner to give a basic fraction (3.2 g) which was chromatographed on a basic alumina column (100 g). A solid eluted with benzene was identified as *syn,trans*-2-dimethylamino-6-methylcyclohexenone oxime (**4**, 1.05 g, 15.2%), which was sublimed to give a pure compound; m.p. 121–122°; i.r. 3360, 2800, 1670, 995, 935 cm^{-1}.

Anal. Calcd. for $C_9H_{18}N_2O$: C, 63.49; H, 10.66; N, 16.45. Found: C, 64.61; H, 10.74; N, 17.07.

Further elution with 10% methanol in chloroform gave a solid, which was recrystallized from isopropanol to give *anti,trans*-2-dimethylamino-6-methylcyclohexanone oxime (**5**, 1.4 g, 20%); m.p. 105.5–107°; i.r. 3250, 3100, 1655, 1505, 960, and 900 cm^{-1}.

Anal. Calcd. for $C_9H_{18}N_2O$: C, 63.49; H, 10.66; N, 16.45. Found: C, 63.42; H, 10.96; N, 16.22.

Photoaddition of N-Nitrosodimethylamine to 4-t-Butylcyclohexene

4-*t*-Butylcyclohexene was prepared from an isomeric mixture of 4-*t*-butylcyclohexanols (Aldrich) according to the method of Sicher and co-workers (30).

Photoaddition of *N*-nitrosodimethylamine to 4-*t*-butylcyclohexene was carried out using a single Rayonet RPR 3500 Å lamp. A solution of the nitrosamine (2.22 g, 30 mmol), the olefin (4.15 g, 30 mmol), and concentrated hydrochloric acid (2.6 ml, 31 mmol) in methanol (300 ml) was photolyzed to completion (3 h). The photolysate was concentrated, neutralized ($NaHCO_3$ solution), and cooled to furnish a crystalline precipitate (500 mg). The crystals were removed by filtration, and shown by t.l.c. to contain exclusively one compound. Recrystallization twice from ethanol gave *anti,cis*-2-dimethylamino-5-*t*-butylcyclohexanone oxime (**9**); m.p. 200–201°; i.r. 3170, 3060, 1650, 1365, 962, 942, and 905 cm^{-1}.

Anal. Calcd. for $C_{12}H_{24}N_2O$: C, 67.88; H, 11.39; N, 13.19. Found: C, 67.86; H, 11.18; N, 13.16.

The aqueous filtrate was basified (Na_2CO_3) and extracted with CH_2Cl_2 (40 ml × 3), dried (Na_2SO_4), and evaporated to dryness. The gummy residue was chromatographed on a basic alumina column (100 g) in which 100 ml fractions were collected. Fractions 1–10 eluted with benzene gave a trace of a liquid which was not investigated. Fractions 11–14 eluted with $CHCl_3$ gave a mixture of two compounds. These fractions were combined for further purification. Fractions 15–18 gave exclusively one crystalline compound (283 mg). A small portion was sublimed to furnish pure *anti,trans*-2-dimethylamino-5-*t*-butylcyclohexanone oxime (**11**); m.p. 169–172°; i.r. 3160, 1647, 1367, 1040, 986, 932 cm^{-1}.

Fractions 19–22 from 5% methanol in $CHCl_3$ gave a resinous substance (336 mg) which on treatment with methanol afforded a crystalline solid (100 mg). Sublimation yielded pure *anti,cis*-2-dimethylamino-4-*t*-butylcyclohexanone oxime (**12**), m.p. 161–163°; i.r. 3200, 1675, 1367, 1060, 962, and 930 cm^{-1}. The last fraction eluted with 10% methanol in $CHCl_3$ gave a resin. Attempts to purify this substance were unsuccessful.

Fractions 11–14 obtained above were further chromatographed on a silicic acid column (50 g). The first fraction eluted with $CHCl_3$ (1 l) was *anti,trans*-2-dimethylamino-4-*t*-butylcyclohexanone oxime (**10**, 443 mg), recrystallized from ethyl acetate; m.p. 130–132°; i.r. 3200, 3100, 1670, 984, 960, 928, 918 cm^{-1}.

Anal. Calcd. for $C_{12}H_{24}N_2O$: C, 67.88; H, 11.39; N, 13.19. Found: C, 67.84; H, 11.17; N, 13.09.

Further elution with $CHCl_3$ (200 ml) gave a mixture of **9** and **10** (60 mg). Elution with 1% methanol in chloroform (700 ml) gave a single compound **9** (285 mg). The total yields of oximes **9**, **10**, **11**, and **12** were 13, 7.3, 4.5, and 1.6%, respectively.

Beckmann Cleavage of Oximes 9 and 11

A solution of oxime **9** (340 mg, 1.6 mmol) in a mixture of dioxane (30 ml) and water (5 ml) was placed in a 50 ml beaker, in which p*H* electrodes were immersed. The beaker was set in a water bath regulated at 45° on a magnetic stirrer. To the stirred solution, finely pulverized *p*-toluenesulfonylchloride (610 mg, 3.2 mmol) was added portionwise and subsequently neutralized with 2 *N* NaOH solution to

Can. J. Chem. Downloaded from www.nrcresearchpress.com by 210.87.254.105 on 09/05/12
For personal use only.

p*H* 7 after each addition so as not to bring the p*H* of the solution below 6. When all of the *p*-toluenesulfonylchloride had been introduced, the solution was allowed to cool to room temperature, then poured onto ice flakes (50 g). The ether extracts were dried (Na_2CO_3) and evaporated to give a liquid mixture (333 mg), which was purified on a silicic acid column (16 g). Elution with benzene gave *N,N*-dimethyltoluenesulfonamide (98 mg). The next fraction eluted from the same solvent gave a mixture (71 mg). Subsequent fractions gave a liquid, exhibiting a single spot on t.l.c. This liquid was tentatively assigned as 5-cyano-4-*t*-butylpentanal **13** (50 mg): i.r. 2880, 2715, 2250, 1725, and 1168 cm^{-1}; n.m.r. τ 0.34 (t, $J = 1$ Hz, 1H), 6.35 (m, 2H), 7.67 (m, 2H), 8.0 (m, 1H), 8.5 (m, 2H), and 9.02 (s, 9H). The 2,4-DNPH derivative of **13** was prepared in the usual manner to afford a yellow precipitate which was recrystallized from ethanol; m.p. 127–128° (dec.); n.m.r. τ −0.9 (s, 1H), 1.0 (d, $J = 2.5$ Hz, 1H), 1.75 (dd, $J = 2.5$ and 9.5 Hz, 1H), 2.45 (t, $J = 4.5$ Hz, 1H), 7.35–7.75 (m, 4H), 8.00 (m, 1H), 8.35–8.60 (m, 2H), 9.00 (s, 9H); *m/e* 345(14), 224(14), 206(23), 91(28), and 57(100).

A solution of oxime **11** (91 mg, 0.43 mmol) in a mixture of water (1 ml) and dioxane (10 ml) was similarly reacted as described above with *p*-toluenesulfonylchloride (82 mg, 0.86 mmol). The reaction mixture was worked-up to give 5-cyano-4-t-butylpentanal which was identical with that obtained from oxime **9**.

*Cleavage of Oxime **10***

In a similar fashion, oxime **10** (260 mg, 1.25 mmol) in dioxane (4.0 ml) and water (1.0 ml) was treated with *P*-toluenesulfonylchloride (466 mg, 2.5 mmol) giving a mixture of the sulfonamide and a ω-cyanoaldehyde; the latter was purified by chromatography to give 5-cyano-3-t-butylpentanal (**14**, 102 mg): i.r. 2885, 2720, 2260, 1725, 1095 cm^{-1}; n.m.r. τ −0.15 (t, $J = 1.5$ Hz, 1H), 7.40–7.80 (m, 4H), 8.10 (m, 2H), 8.60 (m, 1H), and 9.10 (s, 6H). The 2,4-DNPH derivative was prepared by the usual method to give the hydrazone of **14**: m.p. 125.5–126.5°; *m/e* 347(100), 224(16), 206, 152(52), and 83(74).

*Preparation of $\Delta^{9,10}$-Octalin (**15**)*

Crude $\Delta^{9,10}$-octalin was prepared according to Dauben and co-worker (31). Isomeric 2-decanol (Aldrich) (47.7 g, 310 mmol) was dehydrated with boric acid (19.5 g, 87 mmol) and isomerized with phosphorus pentoxide (12.3 g) to give a mixture of octalins, b.p. 190–196° (28.9 g, 69%). The crude product contained 73% of **15** as indicated by v.p.c. analysis. This mixture was fractionally distilled on a spinning band column to give 7.3 g (25%) of **15**, which showed single peak on v.p.c. (SE 30% column at 225°) analysis and whose n.m.r. spectrum exhibited two superimposed multiplets at τ 8.25 and 8.42 of 1 : 1 integration ratio. The i.r. showed three main absorptions at 2920, 1445, and 1161 cm^{-1}.

Addition of N-Nitrosopiperidine to $\Delta^{9,10}$-Octalin

A methanol solution (170 ml) of *N*-nitrosopiperidine (1.66 g, 14.5 mmol), $\Delta^{9,10}$-octalin (2.0 g, 14.7 mmol), and concentrated hydrochloric acid (1.4 ml, 17 mmol) was photolyzed in a Rayonet photoreactor using a 350 mμ lamp. After completion of the photolysis (3 h), the photolysate was concentrated, treated with water (10 ml), and extracted with ether (30 ml × 3). The ether solution was dried ($MgSO_4$) and evaporated to give a solid (760 mg, 30%). This solid was recrystallized from methanol and sublimed to give an analytical sample of Δ^9-decalone-1 oxime (16); m.p. 146–147° (lit. m.p. 147° (18)); i.r. 3300, 1640, 1025, and 960 cm^{-1}; n.m.r. τ −0.5 (s, 1H, D_2O exchangeable), 7.38 (t, $J = 6.5$ Hz, 2H), 7.84 (m, 6H); *m/e* 165(50), 148(100), 131(25), 119(25).

After work-up in the usual manner, the basic extracts gave a viscous liquid (895 mg), which was treated with methanol to give a crystalline precipitate. Recrystallization once from methanol yielded colorless needles of 5-piperidino-Δ^9-decalone oxime (**17**); m.p. 178–180°; i.r. 3230, 1633, 980, and 943 cm^{-1}; n.m.r. τ 0.3 (s, 1H, D_2O exchangeable), 6.85 (m, 1H), 7.30–7.90 (m, 10H), and 8.20–8.65 (m, 12H); *m/e* 248(18), 231(43), 148(51), 86(100).

Anal. Calcd. for $C_{15}H_{24}N_2O$: C, 72.54; H, 9.74; N, 11.28. Found: C, 72.74; H, 9.59; N, 11.13.

The mother liquor after removal of **17** was chromatographed on a silicic acid column (40 g). A solid (84 mg) eluted with $CHCl_3$ was identified as *N*-piperidinoformamide by direct comparisons with an authentic sample prepared from *N*-aminopiperidine and formic acid (1). The subsequent eluate from 5% methanol in $CHCl_3$ was found to be **17** (122 mg). The last fraction eluted with 10% methanol in $CHCl_3$ gave a gummy substance (50 mg), from which no pure compound could be isolated. Total yield of **17** was 402 mg (9%).

*Deoximation of **16***

Oxime **16** (100 mg, 0.6 mmol) was mixed with levulinic acid (2.7 ml) and 1.2 *N* hydrochloric acid (0.3 ml). The mixture was heated under reflux for 3 h. The resultant solution was then basified with saturated Na_2CO_3 solution, extracted with CH_2Cl_2 (30 ml × 3). The extracts were washed with water, dried (Na_2SO_4), and evaporated to give an impure substance (100 mg). The liquid ketone **18** (72 mg, 79%), i.r. 2930, 2865, 1660, 1632 cm^{-1}, was obtained by chromatography through a silicic acid column (35 g) eluting with $CHCl_3$. The 2,4-DNPH derivative of ketone **18** was obtained as a red solid and was recrystallized from ethanol to give crimson crystals; m.p. 265–266°, (lit. m.p. 264.5–265.5° (32)); i.r. 3330, 1620, 1585, 1330 cm^{-1}; *m/e* 331(21), 330(100), 119(21), 91(25).

*Aromatization of **17***

The oxime **17** (140 mg, 5.7 mmol) in acetic anhydride (0.2 ml) and acetic acid (1 ml) was placed in a two-necked pear-shaped flask equipped with a gas inlet and a condenser whose exit was attached to a calcium chloride tube. The mixture was saturated with anhydrous hydrogen chloride for 2 h at room temperature and then heated on a water bath for an additional 4 h. The resultant dark brown solution was evaporated to dryness under vacuum. The residue was treated with isopropanol to give 1,2,3,4-tetrahydro-1-piperidino-5-aminonaphthalene dihydrochloride (**19**, 92 mg, 61%) which was recrystallized from isopropanol m.p. 214–217° (dec.); i.r. 3410, 3315, 2525, 1625, 1600, 795, 720 cm^{-1}; n.m.r. (D_2O) τ 2.30–2.55 (m, 3H), 6.40–6.66 (m, 5H), 6.70 (t, $J = 6$ Hz, 2H); u.v. (MeOH) 210 and 250 nm.

The free base of **19** (53 mg) was obtained by dissolving the hydrochloride (80 mg) in saturated Na_2CO_3 solution and extracting with $CHCl_3$ (20 ml × 3). Sublimation of the crude product in a sealed tube gave a colorless liquid, 1,2,3,4-tetrahydro-1-piperidino-5-aminonaphthalene; i.r. 3460, 3370, 1640, 1575, 1325, 795 cm^{-1}; n.m.r. τ 1.90–2.40 (m, 2H), 2.63 (t, unresolved, $J = 6.5$ Hz, 1H), 6.70 (s, 2H,

D_2O exchangeable), 7.60 (m, 6H); u.v. (MeOH) 212 nm (ε 1.86×10^3), 235 (ε 11.5×10^2), 287 (ε 2.5×10^2); *m/e* 230(1), 146(12), 145(22), 130(100). The absorption spectra (in H_2O; 190–450 nm) of arylamine **19** were unaffected in the presence of Cu^{2+} or Ni^{2+} ion.

The u.v. absorption maxima of 1-amino-5-di(2-chloroethylamino-1,2,3,4-tetrahydro) naphthalene were at 209, 235, and 285 nm and its dihydrochloride at 208 and 235 nm.

Lithium Aluminum Hydride Reduction of Oxime **2** *and* **1**

To a suspension of LAH (164 mg, 3.2 mmol) in anhydrous tetrahydrofuran (THF, 10 ml), a solution of oxime **2** (300 mg, 1.4 mmol) in THF (10 ml) was added dropwise with stirring. The grey suspension was stirred for 1 h at room temperature and subsequently heated under reflux for 4 h. The resultant reaction mixture was decomposed with water, and magnesium sulfate was added to aid the coagulation of aluminum hydroxide. The solid was filtered and washed with THF. The THF solution was evaporated to give crude amines as colorless liquid (202 mg, 72%), i.r. 3400, 1590, 1165, and 110 cm^{-1}.

The crude amine mixture was acetylated with acetic anhydride and fused sodium acetate. After the usual work-up the crude acetamide exhibited two pairs of n.m.r. signals at 8.00 and 9.13 in one hand and τ 7.95 and 9.00 on the other: the ratio of the former pair to the latter pair was 3.5:1. The crude product was chromatographed on a silicic acid column to give two compounds. The less polar compound was contaminated by acetamide **7** and was the minor product 1-acetamido-2-*cis*-piperidino-6-*trans*-methylcyclohexane (**8**): i.r. 3300, 1645, and 1540 cm^{-1}; n.m.r. τ 5.98 (t, $J = 5.5$ after D_2O exchange), 7.95 (s, 3H), and 9.00 (d, $J = 7$ Hz). The major product (more polar) was sublimed to give 1-acetamido-2-*trans*-piperidino-6-*cis*-methylcyclohexane (**7**); m.p. 130–132°; i.r. 3250, 1635, 1555, and 1280 cm^{-1}; n.m.r. ($CDCl_3$) τ 3.35 (broad, 1H, D_2O exchangeable), 6.30 (m, $W_{1/2}$ *ca.* 20 Hz after D_2O exchange, 1H), 7.5 (m, 5H), 8.00 (s, 3H), and 9.13 (d, $J = 7$ Hz, 3H); n.m.r. (D_2O–DCl) τ 5.80 (dd, $J = 4$ Hz and 11 Hz), 6.65 (m, 5H); *m/e* 238(4), 179(13), 164(12), 124(100), and 84(31). The hydrochloride of **7** was recrystallized from 2-propanol; m.p. 254–256° (dec.); i.r. 3170, 2650, 1670, 1555, and 1290 cm^{-1}; n.m.r. ($CDCl_3$) τ 5.85 (dd, $J = 11$ and 4 Hz, 1H), 6.55 (dt, $J = 11$ and 4.5 Hz, 1H), 7.85 (s, 3H) and 8.79 (d, $J = 7$ Hz, 3H).

Oxime **1** (358 mg, 1.7 mmol) was reduced with LAH (196 mg, 5.2 mmol) and acetylated in the similar manner as described above. The crude acetamide showed similar n.m.r. spectra as that obtained above but the ratio of **7** to **8** was 5:1. On chromatograph of the mixture on alumina, acetamide **7** and the corresponding hydrochloride were obtained. The hydrochloride of **7** was readily soluble in chloroform and could be sublimed. The acetamide **8** was isolated in semi-pure state.

The authors are grateful to the National Research Council of Canada and to the President's Research Fund of Simon Fraser University for financial support.

1. Y. L. CHOW, M. P. LAU, R. A. PERRY, and J. N. S. TAM. Can. J. Chem. This issue.
2. Y. L. CHOW. Can. J. Chem. **43**, 2711 (1965).
3. Y. L. CHOW, C. J. COLÓN, and S. C. CHEN. J. Org. Chem. **32**, 2109 (1967).
4. Y. L. CHOW, S. C. CHEN, and D. W. L. CHANG. Can. J. Chem. **48**, 157 (1970).
5. Y. L. CHOW, C. J. COLÓN, H. H. QUON, and T. MOJELSKY. Can. J. Chem. This issue.
6. M. P. LAU, A. J. CESSNA, Y. L. CHOW, and R. W. YIP. J. Am. Chem. Soc. **93**, 3808 (1971).
7. Y. L. CHOW and C. J. COLÓN. J. Org. Chem. **33**, 2598 (1968).
8. H. P. FISCHER and C. A. GROB. Helv. Chim. Acta, **45**, 2528 (1962).
9. C. F. LINSTROEM and G. KOZLOWSKI. Z. Chem. **12**, 470 (1965).
10. W. F. TRAGER and A. C. HUITRIC. Tetrahedron Lett. 825 (1966).
11. A. SEGRE and J. I. MUSHER. J. Am. Chem. Soc. **89**, 706 (1967); E. L. ELIEL, M. H. GIANNI, and TH. H. WILLIAMS. Tetrahedron Lett. 741 (1962).
12. Y. L. CHOW, C. J. COLÓN, and J. N. S. TAM. Can. J. Chem. **46**, 2821 (1968).
13. F. JOHNSON. Chem. Rev. **68**, 375 (1968).
14. C. A. GROB and A. SIEBER. Helv. Chim. Acta, **50**, 2520, 2531 (1967) and the earlier references cited therein.
15. K. LUNKWITZ, W. PRITZKOW, and G. SCHMID. J. prak. chem. **37**, 319 (1968).
16. Y. L. CHOW. J. Am. Chem. Soc. **87**, 4642 (1965).
17. K. M. WELLMAN and F. G. BORDWELL. Tetrahedron Lett. 1703 (1963).
18. W. HÜCKEL and M. BLOHM. Ann. **502**, 114 (1933).
19. W. P. CAMPBELL and G. C. HARRIS. J. Am. Chem. Soc. **63**, 2721 (1941).
20. L. G. DONARUMA and W. Z. HELDT. Org. Reaction, **11**, 1 (1942).
21. F. KUIBAN, Z. DUNINITRESKU, and I. AMBRUSH. J. Gen. Chem. U.S.S.R. (Engl. Ed.) **34**, 1592 (1964).
22. A. ALBERT. Nature, **172**, 201 (1953); **177**, 433 (1956).
23. E. S. HUYSER and J. R. JEFFREY. Tetrahedron, **21**, 3083 (1965).
24. E. S. HUYSER, H. BENSON, and H. J. SINNIGE. J. Org. Chem. **32**, 622 (1967).
25. E. GIL-AV and J. SHABTAI. Chem. Ind. (London), 1630 (1959).
26. N. L. ALLINGER, J. A. HIRSCH, M. H. MILLER, and I. J. TYMIUSK. J. Am. Chem. Soc. **90**, 5773 (1968).
27. J. SPANSWICK and K. U. INGOLD. Can. J. Chem. **48**, 546, 554 (1970) and the references cited therein.
28. Y. L. CHOW, J. N. S. TAM, and A. C. H. LEE. Can. J. Chem. **47**, 2441 (1969); Y. L. CHOW and J. N. S. TAM. J. Chem. Soc. C, 1138 (1970).
29. Y. L. CHOW, C. J. COLÓN, and D. W. L. CHANG. Can. J. Chem. **48**, 1664 (1970).
30. J. SICHER, F. ŠIPOŠ, and M. TRICKY. Coll. Czech. Chem. Commun. **26**, 847 (1961).
31. W. G. DAUBEN, E. C. MARTIN, and G. J. FONKEN. J. Org. Chem. **23**, 1205 (1958).
32. A. K. HILL and R. T. CONLEY. J. Am. Chem. Soc. **82**, 645 (1960).

Can. J. Chem. Downloaded from www.nrcresearchpress.com by 210.87.254.105 on 09/05/12
For personal use only.

Photoreactions of Nitroso Compounds in Solution.[1] XXII. Stereochemical Consequences of the Photoaddition of *N*-Nitrosopiperidine to Conjugated Acyclic Dienes: a Nuclear Magnetic Resonance Study of Enone Oximes

Y. L. CHOW, C. J. COLÓN, H. H. QUON, AND T. MOJELSKY

Department of Chemistry, Simon Fraser University, Burnaby 2, British Columbia

Received June 9, 1971

In the presence of an acid, photoexcited *N*-nitrosopiperidine adds to conjugated acyclic 1,3-dienes to give the 1,4-adducts as the major product in addition to 1,2-adducts. In the photoaddition to 1,3-pentadienes the reverse 4,1-adduct and 4,3-adducts are also identified. These results suggest that a singlet photoexcited *N*-nitrosopiperidine–acid complex rapidly decays to piperidinium radical which irreversibly attacks the dienes as the first step, followed by either a short propagation step or a termination step to give *C*-nitroso compounds. The *C*-nitroso compounds are rapidly removed by irreversible tautomerization to the final oximes. The reactivity of the piperidinium radical toward conjugated double bonds decreases in the order of $RCH{=}CH_2$ > *cis*-RCH=CHR > *trans*-RCH=CHR. This mechanism is in accord with the following stereochemical results. Firstly, the newly-formed double bond in the 1,4-adduct (or the adduct of the reverse orientation) is exclusively *trans*-oriented. Secondly, the remaining double bonds in the 1,2-adducts maintain their original stereochemistry.

The stereochemistry of the photoadducts, enone oximes **1**–**11**, was determined by means of n.m.r. spectroscopy. From the correlation of the n.m.r. chemical shifts of these enone oximes it has been shown that (*i*) the α-olefinic proton generally resonates at a lower field than the β-olefinic proton (with one exception) and (*ii*) in changing from $CDCl_3$ to an aromatic solvent the α-olefinic proton and the α′-alkyl protons are deshielded by 0.3–0.05 p.p.m. while the β-olefinic proton is shifted only slightly either to a higher or a lower field. It is observed that the order of the chemical shifts of the olefinic protons and the aromatic solvent effects on the chemical shifts in these enone oximes are both opposite to those observed in enone systems.

En présence d'un acide, le *N*-nitrosopiperidine photoexcité réagit avec les 1,3-diènes acycliques conjugués pour donner lieu aux dérivés-1,4 comme produits principaux, de même qu'aux dérivés-1,2. Durant la photoaddition aux 1,3-pentadiènes, on a aussi observé la formation des dérivés-4,1 et 4,3. Ces résultats suggèrent qu'un complexe singulet photoexcité de *N*-nitrosopipéridine et d'acide se dissocie rapidement en radical pipéridinium qui attaque de façon irréversible les diènes d'abord, pour ensuite entreprendre une courte étape de propagation ou de terminaison pour donner les composés *C*-nitroso. Les composés *C*-nitroso sont rapidement éliminés par tautomérisation irréversible pour donner les oximes, qui sont les produits finaux. La réactivité du radical pipéridinium pour les doubles liaisons conjuguées se manifeste dans l'ordre décroissant suivant: $RCH{=}CH_2$ > *cis*-RCH=CHR > *trans*-RCH=CHR. Ce mécanisme est en accord avec les résultats stéréochimiques suivants. Premièrement, la double liaison nouvellement formée dans le dérivé-1,4 (ou le dérivé d'orientation opposée) est orienté exclusivement de manière *trans*. Deuxièmement, les autres doubles liaisons des dérivés-1,2 conservent leur stéréochimie originale.

On a déterminé par r.m.n., la stéréochimie des photodérivés oximes **1**–**11** énone. A partir de la corrélation des déplacements chimiques r.m.n. de ces oximes énone, on a pu démontrer que: (*i*) le proton α-oléfinique résonne généralement à champ plus faible que le proton β-oléfinique (à une exception près) et que (*ii*) si l'on passe du solvant $CDCl_3$ à un solvant aromatique, le proton α-oléfinique et les protons α-alkyl sont déblindés de 0.3–0.05 p.p.m. alors que le proton β-oléfinique est déplacé très légèrement soit à champ plus fort ou à champ plus faible. On observe que l'ordre des déplacements chimiques des protons oléfiniques et les effets de solvant aromatique sur les déplacements chimiques dans le cas de ces oximes énone sont tous deux opposés à ceux qu'on observe dans le cas des systèmes énone.

Canadian Journal of Chemistry, **50**, 1065 (1972)

Introduction

As mentioned in the previous paper (1) there are several features associated with the photoaddition of nitrosamine to an olefinic linkage. It is well-known that conjugated dienes are good electronic energy acceptors from excited states of carbonyl and other types of compounds (2–5). In view of this efficient quenching action it is generally regarded that other photochemical processes of an excited molecule with a diene, for example photocycloaddition of ketones, are unimportant (6). Nevertheless, we have observed an efficient photoaddition of *N*-nitrosopiperidine to butadiene as well as to some

[1]For paper XXI of this series, see ref. 1.

Can. J. Chem. Downloaded from www.nrcresearchpress.com by 210.87.254.42 on 09/05/12
For personal use only.

Can. J. Chem. Downloaded from www.nrcresearchpress.com by 210.87.254.42 on 09/05/12
For personal use only.

cyclic dienes (7). In this photoaddition, a number of questions arise regarding photoprocesses and addition processes (8). They are, for example, (*i*) the reactive species responsible for the addition, (*ii*) quenching of photoexcited states of *N*-nitrosopiperidine, if any, and the mechanism, (*iii*) the reactivity of the dienes, and finally (*iv*) the stereochemical course of the addition. In this report these questions are discussed in the light of the results obtained in photoadditions to a series of acyclic dienes.

The photoadditions of *N*-nitrosopiperidine to various acyclic dienes, *cis*- and *trans*-1,3-pentadienes and *cis,trans*- and *trans,trans*-2,4-hexadienes, were carried out with the same apparatus and under the same conditions as those used in the photoaddition to cyclic dienes reported in the previous publications (9, 10). The major product, the 1,4-adduct, was crystallized readily from the basic fraction of the crude product. The isolations of the minor products, the 1,2-adducts and the reverse adduct (4,1-adduct),[2] however, have to depend on careful column chromatography. The structures of the photoadducts were derived from the n.m.r., i.r., and mass spectral data; the n.m.r. spectroscopy was the most powerful tool in the present study. The discussion is based on the structure and stereochemistry displayed in **1**–**12**; the pertinent spectral data are given in the Experimental.

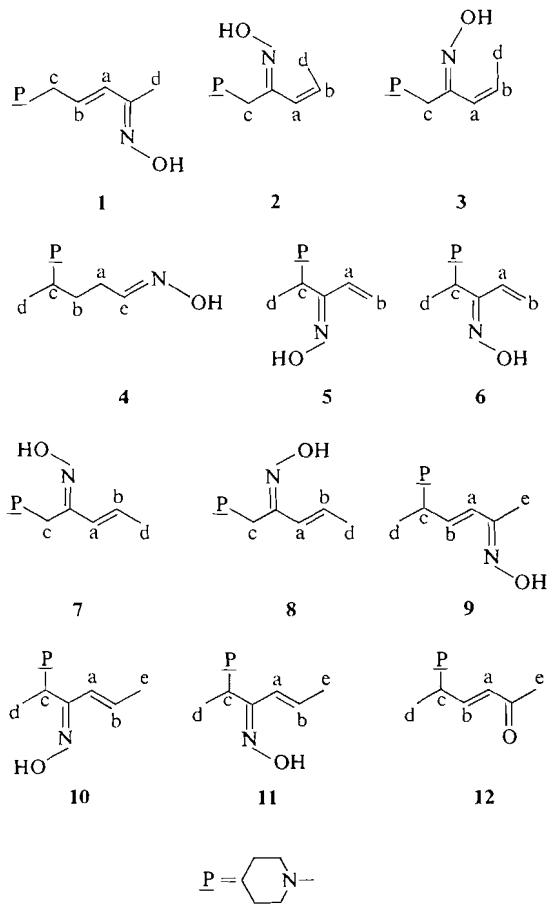

Photoaddition Products

The photoaddition to *cis*-1,3-pentadiene afforded the 1,4-adduct, *anti,trans*-5-piperidino-3-pentene-2-one oxime (**1**),[3] as the major product in addition to the 1,2-adducts, *syn,cis*-1-piperidino-3-penten-2-one oxime (**2**) and *anti, cis*-1-piperidino-3-penten-2-one oxime (**3**), all of which are isolated in pure form as demonstrated by t.l.c. Careful chromatography of the photolysate afforded, in addition, three compounds isolated in semi-pure state; they are the 4,1-adducts, *anti,trans*-4-piperidino-2-pentenal oxime (**4**), and 4,3-adducts, *syn*-**5** and *anti*-4-piperidino-1-penten-3-one oxime (**6**).

The photoaddition to *trans*-1,3-pentadiene gave the same 1,4-adducts, **1**, and the 4,1-adduct, **4**, as that obtained in the addition to *cis*-pentadiene though both in lesser yields. The 1,2-adducts, *syn,trans*-**7** and *anti,trans*-1-piperidino-3-pentene-2-one oxime (**8**), however, were isolated in higher percentage than their counterparts in the addition to *cis*-pentadiene. In addition, trace amounts of the reverse 4,3-adducts **5** and **6** were also detected by t.l.c. analysis.

The photoaddition to *cis,trans*-2,4-hexadiene gave the 1,4-adduct, *anti,trans*-5-piperidino-3-hexen-2-one oxime (**9**), and the 1,2-adducts, *syn,trans*-**10** and *anti,trans*-2-piperidino-4-hexen-3-one oxime (**11**). In addition a small amount of ketone derived, presumably, from the hydrolysis of **9**, *trans*-5-piperidino-3-hexen-2-one (**12**), was also isolated. The photoaddition to *trans,trans*-2,4-hexadiene gave the same 1,4- and 1,2-adducts but the latter adducts (**10** and **11**) were

[2]For convenience, the reverse addition products are referred to as 4,1-adducts or 4,3-adducts in this report.

[3]The *syn–anti* notation is used to express configuration of the oxime group and *trans–cis* notation for the configuration of the double bond. The definition of *syn–anti* configuration follows the convention adapted in our previous publication (ref. 7).

TABLE 1. Yields of nitrosopiperidine photoadditions to dienes

Diene	% of adducts			
	1,2-*syn*	1,2-*anti*	1,4-Adducts‡	4,1-Adducts§
Butadiene	10	16	57	—
cis-1,3-Pentadiene*	~3	8	72	12
trans-1,3-Pentadiene†	10	16	60	4
cis,trans-2,4-Hexadiene‖	3	7	85	—

*4,3-*syn*- and 4,3-*anti*-adducts were isolated in semipure state.
†4,3-*syn*- and 4,3-*anti*-adducts were detected in trace amount.
‡The 1,4-adduct to butadiene was mixture of *syn*- and *anti*-isomer. The 1,4-adducts to other dienes are *anti*-isomer.
§The 4,1-adduct was *anti*-isomer.
‖5-Piperidino-3-hexen-2-one was isolated in 2% yield.

obtained in only very small quantity (*ca.* 5% in total). For a comparison the percentage yields of these adducts are tabulated in Table 1.

The adducts exhibited typical i.r. absorptions for common linkages possessed by them (11), *i.e.*, the Bohlmann bands in the 2800–2600 cm^{-1} region, weak but distinct C=C and C=N stretching vibrations in the 1550–1690 cm^{-1} region and the multiple peaks of N—O stretching absorption near 900–1000 cm^{-1}. The stereochemistry of these adducts is readily interpreted from the n.m.r. spectra. Moreover, since we have also observed good correlation between chemical shifts and the nature of solvent, we will, therefore, discuss the n.m.r. results separately in the following section.

Nuclear Magnetic Resonance Data and the Structure

The n.m.r. study of the enone oximes obtained from photoaddition to cyclic dienes (7) has played an important role in clarifying the configuration and conformation of those adducts. The adducts derived from photoaddition to acyclic dienes exhibited well-defined signals in most cases and provided a good deal of information with regard to the structure and stereochemistry. Taking together the data available from our previous (7, 11) and present studies we have arrived at a few general rules that facilitate a decision on enone oxime structure.

First of all, *syn,anti*-isomerism of the oxime group is determined by the comparison of the chemical shifts of α- and/or α′-protons (with respect to the oxime group) in which the α-proton oriented at the same side of the OH group generally resonates at a lower field in comparison to that oriented at the opposite side. This relation holds true for other types of oximes, for an intramolecular comparison and for an intermolecular comparison where *syn–anti* pairs are available (7, 12, 13). Secondly, the *cis–trans* isomerism of the double bond is decided by well-known spin coupling constant correlations (14) in which coupling constants for *trans*-protons (11–17 Hz) are larger than that of *cis*-protons (6–12 Hz). Thirdly, the chemical shift of the α-olefinic proton of an enone oxime generally appears at a lower field than that of the β-olefinic proton (Table 2). Since the α- and β-olefinic protons could be accurately assigned on the basis of their coupling patterns with allylic protons where the spectra were well resolved, this relation could be obtained directly from Table 2 with the exception of **10**.

Where an isomeric pair exists, the *syn*- and *anti*-configurations are readily decided by the chemical shifts of the α- and α′-protons vicinal to the oximino group, for example **2–3**, **5–6**, **7–8**, and **10–11**. This correlation is also supported by some n.m.r. data on *syn* and *anti* enone oximes in the literature (12, 13). For the sole 1,4-adduct (**1** and **9**) obtained in the photoaddition, the *anti*-configuration was assigned on steric grounds (11); the *syn*-configuration would cause strong crowding of the OH group with the olefinic protons (either in *s-cis* or *s-trans* arrangement) due to coplanarity within the conjugated system (10). The *anti*-configuration of the 4,1-adduct **4** is indicated by the chemical shift of the aldoxime proton (H_e, τ 2.3) which is correlated better to the corresponding proton of *anti*-4-piperidino-2-butenal oxime (**14**, τ 2.28) than to that of the *syn*-isomer (**13**, τ 2.90) (7).

In deuteriochloroform solution these enone oximes generally show the appropriate proton signals for the assigned structures except that,

Can. J. Chem. Downloaded from www.nrcresearchpress.com by 210.87.254.42 on 09/05/12
For personal use only.

TABLE 2. The n.m.r. chemical shifts of the α-protons of the enone oximes

Compound†	Solvent‡	Chemical shift (τ-value)* H_a	H_b	Alkyl§
1	C	3.7 –3.95(3.82)		8.05
	P	3.38	3.93	7.87
2	C	4.10–4.40(4.25)		6.60
	P	3.69	4.20	6.41
3	C	3.85–4.3 (4.05)		6.85
	P	3.48	4.17	6.70
4	C	3.75–3.90(4.0)		2.30
	D	3.45	3.95	2.13
7	C	3.8 –4.2 (3.95)		6.65
	B	3.63	4.00	6.74
	P	3.6 –3.9 (3.78)		6.51
8	C	3.2 –3.8 (3.35)		6.87
	D	3.00	3.50	6.82
9	C	3.2 –4.0 (3.85)		8.01
	P	3.50	3.98	7.78
10	C	3.7 –4.1 (3.95)		6.57
	B	3.6 –4.0 (3.80)		6.38
	P	3.74	3.30	5.88
11	C	3.0 –3.7 (3.28)		6.67
	P	2.7 –3.2 (3.00)		6.48
12	C	3.94	3.18	7.71
	P	3.87	3.00	7.80
25	C	3.8 –4.2 (3.9)		6.96
	P	3.53	3.88	6.58
26	C	3.7 –4.2 (3.9)		5.95
	P	3.63	3.98	5.92

*Where the chemical shifts of H_a and H_b could not be located precisely, the range of signal is quoted and the center of gravity was given in the parentheses.

†Compound **25** is *anti*-4-piperidino-2-cyclohexenone oxime and compound **26** *syn*-2-piperidino-5-cyclohexenone oxime (see ref. 7).

‡C, deuteriochloroform; P, pyridine; D, hexadeuteriobenzene; B, benzene.

§The alkyl proton refers to the α-proton opposite to the olefinic proton or the aldehydic proton.

in most cases, the olefinic and the allylic protons are extensively coupled with second order interactions. The olefinic protons reveal themselves as narrow unresolved signals because the shift difference of α- and β-olefinic protons ($\Delta\nu$) is nearly equal to the coupling constant (J). The presence of virtual coupling in these cases is also indicated by the splitting pattern of the allylic protons (15). In pyridine or benzene solution the α-proton of the enone oximes is shifted downfield while the β-olefinic proton remains virtually unchanged. The separation of the olefinic proton signals caused by aromatic solvents apparently is sufficient to generate a first order coupling pattern (AMX_n) from which the estimated coupling constant of the olefinic protons is utilized to define the *cis–trans* configuration of the olefinic linkage.

The order of chemical shifts of α- and β-olefinic protons manifested by cyclic and acyclic enone oximes is just opposite to that of the corresponding protons of enones (16) and provides an interesting comparison. Taking the average chemical shifts for α- and β-olefinic protons of acyclic and six-membered enones as τ 4.00 and 3.10, respectively, (16, 17) it can be seen that in enone oximes, while the β-proton is more shielded by *ca.* 1 p.p.m., the α-proton emerges approximately in the same region with respect to the corresponding protons of enones (Table 2, comparisons in $CDCl_3$ solution). It is instructive to compare these data with those of ketone **12** in which α- and β-olefinic protons resonate at the expected chemical shifts for an enone. The apparent exception to the correlation is found in **11** which will be commented on later. The reversal of the order of the chemical shifts in enone oximes indicates that the contribution of the polar resonance form (16) in enone oximes is not as extensive as that involved in enones, or that the anisotropic effects of the oxime group are drastically different from those of the carbonyl group.

Aromatic solvent effects on chemical shifts of various protons in enone systems have been reported (17) and are explained by *s-cis* and *s-trans* conformation models. In the present case, on passing from $CDCl_3$ to pyridine solution, the β-olefinic proton is generally only slightly affected (either shielded or deshielded) but α-olefinic protons and α′-alkyl protons are deshielded by an average of 0.3 p.p.m. and 0.10–0.05 p.p.m., respectively. In every respect these trends are just the opposite to that observed in enones in which the β-olefinic proton and α′-alkyl protons are shielded and the α-olefinic proton is only slightly shielded or deshielded (17). This indicates the orientation of a collision complex between an enone oxime and an aromatic ring is markedly different from that involved in the enone itself.

The n.m.r. data on oximes **10** and **11** are found to be anomalous in several accounts with respect to the conclusion obtained so far. In oxime **10**, the chemical shift of the β-olefinic proton apparently resonates at a lower field than does that of

Can. J. Chem. Downloaded from www.nrcresearchpress.com by 210.87.254.42 on 09/05/12
For personal use only.

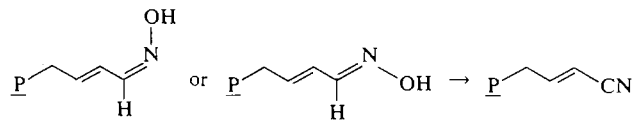

13 14 15

SCHEME 1

the α-olefinic proton, since the former is significantly coupled with the methyl group ($J = 6$ Hz) and the latter is only a slightly broadened doublet. Although the chemical shifts of the olefinic protons of oxime **11** cannot be located precisely due to a second order coupling, the same chemical shift pattern as that of **10** is suspected. A careful inspection of the data in Table 2 shows that on changing from $CDCl_3$ to pyridine solution, in oximes **10** and **11**, the β-olefinic proton is deshielded much more than the α-olefinic proton in contrast to other cases. The anisotropic effect of an oxime group and the related aromatic solvent effect are intimately connected to the molecular geometry. The observed anomalies of oximes **10** and **11** are attributed to a stereochemical variation of these two molecules from other enone oximes. A better understanding of these situations requires investigation of simpler model enone oxime systems and is being undertaken.

Stereochemical Course of the Photoaddition

As the structures of the product are firmly proved, the stereochemical course of photoaddition can be summarized as follows. First of all, the 1,4-addition to a conjugated diene (or reverse 4,1-addition) leads to the formation of the new *trans* double bond (such as **1**, **4**, and **9**). Secondly, the 1,2-addition to a diene retains the stereochemical integrity of the remaining 3,4-double bond (such as shown in **2**, **3**, **7**, **8**, **10**, and **11**). Thirdly, if a choice is available internally, a *cis*-double bond is attacked preferentially to a *trans*-double bond. Finally, the reverse addition (4,1-addition) is more prone to take place with *cis*-1,3-pentadiene than the *trans*-diene (**5** and **6**). These conclusions are confirmed by some quantitative experiments described below.

It has been demonstrated that photoaddition of *N*-nitrosopiperidine to butadiene gives a mixture of *syn*-**13** and *anti*-isomer **14**, of *trans*-4-piperidino-2-butenal oxime (7) as the major product. That oximes **13** and **14** are the *syn–anti* isomeric pair but not *cis–trans* isomers has been indicated by the n.m.r. data in the previous report and placed on a firmer basis now by facile Beckmann dehydration reaction. Decomposition of the tosylate of **14** or of a mixture of **13** and **14** gives quantitative yields of *trans*-4-piperidinocrotononitrile (**15**) (Scheme 1) as indicated by the clean n.m.r. spectra of the crude products (Fig. 1). A *cis–trans* mixture of 4-piperidinocrotononitrile was synthesized from a commercial crotononitrile (*cis–trans* mixture) by standard procedures. In order to find out if a trace amount of the *cis*-isomer corresponding to **13** (and/or **14**) is formed in the photoaddition to butadiene, a crude basic product was subjected to Beckmann dehydration to give a crude basic dehydration product. The n.m.r. spectrum of this latter basic product shows clean signals for **15** but no trace of the corresponding *cis*-isomer. In the photoadditions to *cis*- and *trans*-1,3-pentadienes, the n.m.r. spectra of each chromatographic fraction were carefully scrutinized but showed no signals expected for other 1,4-adducts.

In order to prove the second conclusion, advantage was taken that these 1,2-adducts undergo a facile Beckmann cleavage reaction aided by the lone pair electron of the piperidine ring as shown in **16** (Scheme 2) (18, 19). The cleavage of the tosylates **7**, **8**, **10**, or **11** under mild conditions gave only *trans*-crotononitrile as shown by v.p.c. analysis. Similarly, the tosylates of **2** and **3** gave only *cis*-crotononitrile.[4] Crude 1,2-adducts from the photoaddition to each diene were treated under the same conditions and the neutral ethereal extracts were examined by v.p.c. analysis. In the case of photoaddition to *cis*-1,3-pentadiene, the v.p.c. analysis of the ether extract indicated that only *cis*-crotononitrile (**18**) was obtained, that to *trans*-1,3-pentadiene only *trans*-crotononitrile, and that to

[4]A stronger base apparently isomerizes the crotononitriles since a treatment of the tosylate of **8** with 2 *N* sodium hydroxide solution gives *cis*- and *trans*-crotononitrile in the ratio of 20:80.

Can. J. Chem. Downloaded from www.nrcresearchpress.com by 210.87.254.42 on 09/05/12
For personal use only.

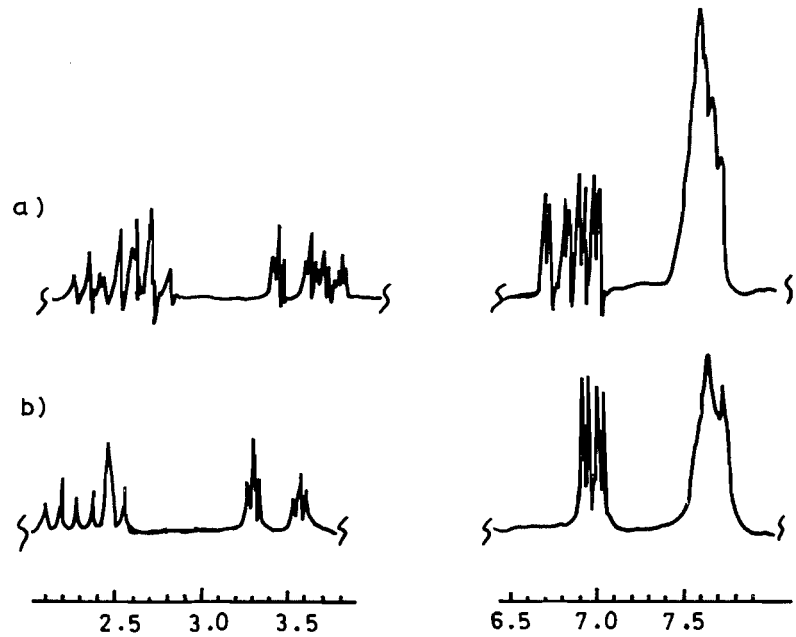

FIG. 1. The 60 MHz n.m.r. spectra of (*a*) the synthetic mixture of *cis* and *trans*-4-piperidino-crotononitrile and (*b*) the *trans*-isomer obtained from Beckmann cleavage reaction of a crude photolysate or a mixture of oximes **13** and **14**.

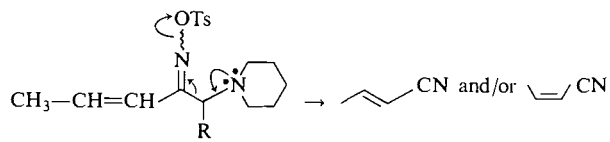

16 **17** **18**

R = H or CH_3

SCHEME 2

cis,*trans*-2,4-hexadiene, *trans*- and *cis*-crotononitrile were obtained in the ratio of 97:3. The last result also substantiates conclusion three and suggests that the *cis*-disubstituted double bond is more reactive than the *trans*-disubstituted bond. The fourth conclusion is related to the third one and explains the higher percentage yield of the reverse adducts in the photoaddition to *cis*-1,3-pentadiene than that to the *trans*-diene. The higher overall yields of the normal adducts (1,2- and 1,4-addition) in this case also indicates that the monosubstituted double bond is more reactive toward the aminium radical (*vide infra*) than the *cis*-disubstituted double bond which is, in turn, more reactive than the *trans*-disubstituted one.

In the presence of both *cis*,*trans*- and *trans*, *trans*-2,4-hexadienes in 1:1 ratio, however photoaddition to the dienes takes place indiscriminately; thus after the half-completion of the photoaddition, v.p.c. analysis of the residue indicated a 1:1 ratio of the two dienes. The same situation was also observed with a mixture of *cis*- and *trans*-1,3-pentadiene. The latter result is not unexpected since the monosubstituted double bond common to both pentadienes is more reactive than *cis*- and *trans*-disubstituted double bonds by a wide margin. The reactivities of *cis*,*trans*- and *trans*,*trans*-hexadienes toward the photoaddition are different but not significant enough to cause a discriminative attack on the double bonds.

Can. J. Chem. Downloaded from www.nrcresearchpress.com by 210.87.254.42 on 09/05/12
For personal use only.

TABLE 3. The quantum yields of the disappearance of *N*-nitrosopiperidine in methanolic HCl solutions*

Olefin	0.5 *N* HCl solution [Olefin] (mol/l)	Φ	0.06 *N* HCl solution [Olefin] (mol/l)	Φ
None	—	2.46	—	2.56
Cyclohexene	2.0×10^{-3}	2.74	2.6×10^{-3}	2.66
1,3-Pentadiene	2.0×10^{-3}	3.06	3.2×10^{-3}	3.02
trans,trans-2,4-Hexadiene	2.1×10^{-3}	3.05	2.4×10^{-3}	3.23
cis,trans-2,4-Hexadiene	2.3×10^{-3}	2.95	2.2×10^{-3}	3.31

*In both determinations the concentration of *N*-nitrosopiperidine is 2.05×10^{-3} mol/l. The solution was irradiated for 20 min during which about 25% of the nitrosamine disappeared. A commercial mixture of 1,3-pentadienes was used in which the ratio of *cis* to *trans* isomer was 40:60.

[1] 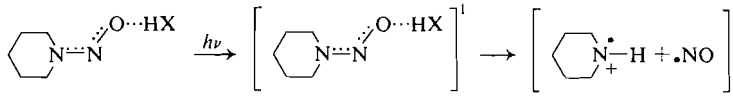

[2] 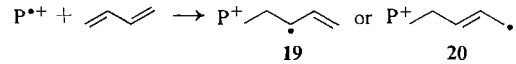

19 **20**

[3] 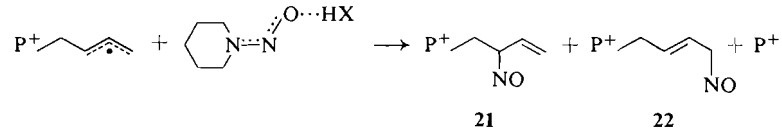

21 **22**

[4] 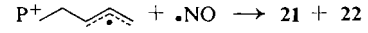

The conservation of the configuration of the disubstituted double bond in the 1,2-adducts resulting from these photoadditions indicates that the dienes are not isomerized during the irradiation. In theory various pathways for isomerization of the dienes are available and the possibility of the diene isomerization has to be checked independently. In particular, since the lowest triplet state energy of *N*-nitrosopiperidine (59 kcal/mol) (20) is nearly the same as those of the dienes (61 ~ 57 kcal/mol), isomerization of the dienes by triplet–triplet energy transfer is a good possibility. The recovered diene in each photoaddition was monitored with v.p.c. analysis and was found to contain no other diene than the starting one. The dienes are therefore not isomerized during the photoaddition.

Mechanism of Photoaddition

We have established that nitrosamine photoaddition is a stepwise process in which the aminium radical is the initial attacking species (20, 21). Further, it has been shown that the aminium radical is generated from the singlet excited state of a nitrosamine–acid association complex (20). The photoaddition mechanism therefore can be divided into two parts for the convenience of discussion, *i.e.*, the photoprocess that generates piperidinium radical, and the addition reaction initiated by the piperidinium radical.

The lack of isomerization of dienes, the high quantum yields of disappearance of nitrosamine (shown in Table 3), as well as the excellent yields of the adducts, suggest that virtually every collision of a diene with the piperidinium radical leads to the irreversible formation of the intermediate cation radical **19** or **20**. Although the piperidinium radical is an electrophilic species it must undergo free radical addition for the reason described previously (1, 21). It is significant that an abstraction of allylic protons, the typical reaction of the aminium radical as exemplified by the Hofmann–Löffler–Frytag

Can. J. Chem. Downloaded from www.nrcresearchpress.com by 210.87.254.42 on 09/05/12
For personal use only.

Can. J. Chem. Downloaded from www.nrcresearchpress.com by 210.87.254.42 on 09/05/12
For personal use only.

reaction (22), is not observed. It is concluded that an aminium radical is an extremely reactive species toward electrophilic addition, as may be expected from its cationic charge. An additional feature worthy of mentioning is that an aminium radical does not attack the remaining double bond of the hydrochloride of the adducts **1**–**12** owing to repulsion of the positive charges.

The addition products **21** and **22** are formed by two independent steps as shown in [3] and [4]. Step 3 is the propagation step corresponding to the short chain process as implied by the observed quantum yield of $3 \sim 4$. In view of the fact that the clean photoaddition occurs, this figure probably represents the chain length of the free radical processes. The termination step 4 enters into the picture quickly and may suggest that nitric oxide is located in the vicinity of the reaction site. The stereochemistry of the adducts is also decided by these two steps. The conservation of the remaining double bond in the 1,2-adduct indicates that steps 3 and 4 occur rapidly before the intermediate **19** (or **20**) has time to undergo rotation. The retention of the configuration of an allyl radical through rapid reaction of the radical has been demonstrated (25). If steps 3 and 4 are indeed rapid, an explanation is required for the failure to form *cis*-1,4-adduct along with the isolated *trans*-1,4-adducts (**13** and **14**) since under ordinary conditions 5% of the butadiene is in an *s-cis* conformation. It may be assumed that the activation energy required to form the *trans*-1,4-adduct is far smaller than that required for the *cis*-1,4-adduct. Steric controls over tautomerization of **21** and **22** to give the *syn*- and *anti*-oximes (**1**–**14**) has been discussed previously (11).

We have shown through kinetic studies by flash photolysis (20) that the piperidinium radical adds to cyclohexene faster than it abstracts hydrogen from methanol, by a factor of 5000. From a similar study, piperidinium radical is shown to add to 1,3-pentadienes with a bimolecular rate constant of $4.5 \times 10^7\ M^{-1}\ s^{-1}$; this is about 1.8 times faster than the rate constant of the addition to cyclohexene ($2.54 \times 10^7\ M^{-1}\ s^{-1}$). The rate constants explain explicitly why, during irradiation of a nitrosopiperidine–diene mixture in methanol solution, the photodecomposition of nitrosopiperidine (23) is not observed and affords the photoaddition product exclusively in a high yield. The same observation has been made previously in the photoaddition to unhindered olefins (such as 1-hexene and cyclohexene) (10, 24).

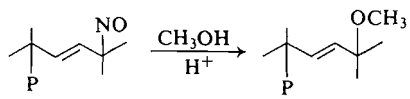

23 **24**

SCHEME 3

Investigation into the stereochemical course of an addition to a diene is often frustrated by reversible processes in [2], [3], and [4] and/or by an ionization of **21** and **22**. In the present case, fortunately, such processes are prevented since the *C*-nitroso compounds **21** and **22** are rapidly removed by tautomerization to the oximes, due to facile migration of the labile allylic proton (9). If *C*-nitroso compounds **21** and **22** are not removed rapidly, other side reactions involving **21** and **22** may set in as has been experienced in the low temperature photoaddition to cyclopentadiene (7). In particular, the photoaddition of nitrosopiperidine to 2,5-dimethyl-2,4-hexadiene under ordinary conditions appears to accumulate the adducts corresponding to **21** and **22** as witnessed by the deep blue color, which disappears on standing. Since the tautomeric pathway is not available for the 1,4-adduct corresponding to **22**, the labile nitroso group is presumably displaced by a methoxy group through an ionic pathway **23** → **24** (Scheme 3). The crude product, which could not be purified owing to its instability, exhibited strong n.m.r. signals for methoxy groups, thus supporting our hypothesis.

Generally speaking, though photoadditions to olefins are frequently encountered phenomena (26, 27), the direct addition of a photoexcited species to a diene is not a commonly observed process due to the fact that an electronically excited species preferentially transfers energy to the diene instead of physically attacking the diene (6). On the other hand, many examples of addition reactions of dienes by photosensitization are reported in the literature (27, 28). In the present case, it is not likely that the photoexcited nitrosopiperidine transfers its energy to a diene which initiates the addition process. This is further confirmed by the failure to sensitize the addition to 1,3-pentadienes using naphthalene as a sensitizer; an efficient

Can. J. Chem. Downloaded from www.nrcresearchpress.com by 210.87.254.42 on 09/05/12
For personal use only.

energy transfer from singlet excited state naphthalene to pentadienes has been demonstrated by Hammond and co-workers (3, 29).

The failure of singlet excited state nitrosopiperidine to isomerize dienes has further implications. First of all, the singlet energy transfer to dienes (30, 31) apparently does not take place. Secondly, the reverse process of the piperidinium radical attack [2], similar in concept to the Schenck mechanism (32, 33), does not occur significantly (*vide supra*). This is readily understandable since the reverse process entails the generation of a high energy species, the piperidinium radical. The first implication reflects the short singlet state lifetime of nitrosopiperidine, owing probably to a rapid decay to piperidinium radical. This is significant since even if the classical energy transfer fails to operate efficiently, quenching by an exciplex mechanism is possible at $0.5 \sim 0.3$ *M* concentration of a diene (3). In this regard it should be pointed out that nitrosoamine does form collision complexes with π-electron cloud of aromatic rings in the ground state (34) which should be a factor in favor of an exciplex formation. The total failure of an excited state nitrosamine to act as a sensitizer implies that the dissociation to an aminium radical is extremely facile.

Experimental

Unless specified otherwise the following experimental conditions prevail. The n.m.r. spectra were recorded with a Varian A56/60 spectrometer in $CDCl_3$ solution using TMS as the internal standard. Some n.m.r. spectra were taken with a Varian HA-100 spectrometer through kind assistance of Dr. K. R. Kopecky, the University of Alberta, Edmonton, Alberta. The coupling patterns of n.m.r. signals were presented as d for doublet, t for triplet, q for quartet, b for broad signals, and m for multiplet. A Perkin–Elmer RMU-6E mass spectrometer was used to record mass spectra with the chamber voltage at 80 eV. The i.r. spectra were recorded with a Perkin–Elmer 457 spectrophotometer in Nujol mull or liquid film. An Unicam SP-800 UV–Visible spectrophotometer was used to follow the progress of the reaction.

Material and General Photolysis Conditions

The commercial samples of *trans*-1,3-pentadiene (Aldrich Chemical Co.) and 2,4-hexadienes (Chemical Samples Co., Columbus, Ohio) were distilled and the purity checked by v.p.c. analysis. A pure *cis*-1,3-pentadiene (99%+) was prepared according to the procedure of Craig (35) from a mixture of *cis*- and *trans*-1,3-pentadienes.

In general the photoaddition was carried out according to the conditions described previously (9, 10) for the photoaddition to simple olefins. The t.l.c. was developed with chloroform containing a few percent of methanol and was used to monitor the purity of each fraction from column chromatography and to aid the identification of the *syn*- and *anti*-configuration of the oximes.

Photoaddition of N-Nitrosopiperidine to cis-1,3-Pentadiene

The nitrosamine (5.70 g, 0.05 mol), *cis*-1,3-pentadiene (4.0 g, 0.06 mol), and concentrated hydrochloric acid (5 ml, 0.06 mol) were dissolved in methanol (200 ml). This solution was irradiated with 450 W Hanovia lamp for 70 min. The solvent was removed under vacuum. The usual work-up gave a neutral ether extract which contained *N*-nitrosopiperidine (116 mg) as shown by i.r. and n.m.r. analysis. The basic fraction was extracted with $CHCl_3$ (50 ml × 3) to give a mixture of crystals and oil (9.7 g). To this mixture was added some ether and the mixture was cooled. Filtration of the mixture gave white crystals (3.73 g): m.p. 132–136°. These crystals were recrystallized from a mixture of benzene–Skellysolve B three times to afford *anti,trans*-5-piperidino-3-penten-2-one oxime (**1**); m.p. 141–142°; i.r. 3200, 1620, 1091, 1010–895 (multiple peaks), 763 cm^{-1}; n.m.r. τ 0.0 (b, OH), 3.82 (m, H_a and H_b), 6.92 (m with virtual coupling, H_c), 7.59 (m, 4H), 8.05 (s, H_d), 8.50 (m, 6H); n.m.r. (pyridine) τ 3.38 (dt H_a, $J = 16$ and 0.5 Hz), 3.93 (dt, H_b, $J = 16$ and 6 Hz), 6.96 (d, H_c, $J = 6$ Hz), 7.66 (m, 4H), 7.87 (s, H_d), 8.58 (m, 6H).

Anal. Calcd. for $C_{10}H_{18}N_2O$: C, 65.90; H, 9.95; N, 15.37. Found: C, 65.62; H, 9.85; N, 15.68.

The mother liquor was evaporated to dryness to give a mixture of crystals and oil (5.95 g). This mixture was chromatographed on silicic acid (60 g). The first six fractions eluted with 0–3% methanol in $CHCl_3$ (600 ml) gave fraction A as an oil (360 mg). Next six fractions eluted with 4% methanol in $CHCl_3$ gave fraction B (580 mg). With 8% methanol in $CHCl_3$ an oil (442 mg) was eluted as fraction D.

Fraction A showed one predominant spot at R_f 0.3 and two smaller spots at R_f 0.6 on the t.l.c. plate. The oil was rechromatographed on silicic acid (5 g) giving an oil (109 mg) as the first fraction eluted with $CHCl_3$. The n.m.r. spectrum showed this oil to be mostly *N*-nitrosopiperidine and another compound. This oil was then distilled (110°/0.1 mm Hg) to remove the more volatile nitrosamine giving a colorless resinous liquid (30 mg) of *syn*-4-piperidino-1-penten-3-one oxime (**5**); i.r. 3300, 1660, 1280, 1260, 1100, 995, 940 cm^{-1}; n.m.r. τ 3.74 (dd, H_a, $J = 17$ and 11 Hz), 4.65 (dd, H_b, $J = 17$ and 1 Hz), 4.8 (d, H_b, $J = 11$ Hz), 6.68 (q, H_c, $J = 7$ Hz), 8.72 (d, H_d, $J = 7$ Hz); mass spectrum *m/e* (relative intensity) 182 (6.2), 112 (88), 98 (90), 84 (100), 41 (92). The third fraction from this chromatograph gave an oil (27 mg) which showed single spot on a t.l.c. plate. This oil was distilled (100°/0.1 mm Hg) to afford a colorless oil identified as *syn,cis*-1-piperidino-3-penten-2-one oxime (**2**); i.r. 3300, 1640, 1110, 1000–900 cm^{-1} (multiple peaks); n.m.r. (pyridine) τ 3.69 (dq, H_a, $J = 12.5$ and 1 Hz), 4.2 (dq, H_b, $J = 12.5$ and 7 Hz), 6.41 (s, H_c), 7.54 (m, 4H), 7.91 (dd, H_d, $J = 7$ and 1 Hz); mass spectrum *m/e* (relative intensity) 182 (M^+, 3), 98 (100).

Fraction B consisted predominantly of a new compound as shown by t.l.c., and was rechromatographed on silicic acid (10 g). On eluting with 1% methanol in $CHCl_3$, an oil (230 mg, t.l.c. single spot) was obtained which was distilled in a small scale (90°/0.2 mm Hg) to give *anti,cis*-1-piperidino-3-penten-2-one oxime (**3**); i.r. 3350, 1643, 1459, 1370, 1300, 1270, 1110, 1008, 985, 940, 860, 760 cm^{-1}; n.m.r. τ 0.9 (b,

Can. J. Chem. Downloaded from www.nrcresearchpress.com by 210.87.254.42 on 09/05/12
For personal use only.

OH), 3.97 (d, H_a, $J = 12$ Hz), 4.21 (dq, H_b, $J = 12$ and 5.5 Hz), 6.85 (s, H_c), 7.61 (m, 4H), 8.23 (d, H_d, $J = 5.5$ Hz), 8.53 (m, 6H); n.m.r. (pyridine) τ 3.48 (dq, H_a, $J = 12$ and 1 Hz), 4.17 (dq, H_b, $J = 12$ and 7 Hz), 6.70 (s, H_c), 7.61 (m, 4H), 7.12 (dd, H_d, $J = 7$ Hz), 7.64 (m, 6H); mass spectrum at (20 eV) *m/e* (relative intensity) 182 (2), 164 (26), 98 (100).

Fraction C showed one predominant spot on t.l.c. analysis which corresponded to the 1,4-adduct **1**; n.m.r. τ 3.9 (m, 2H), 6.9 (m, 2H), 7.6 (m, 4H), 8.0 (s, 2H), 8.5 (m, 6H). In addition another minor spot could be detected in the t.l.c. plate which ran slightly ahead but superimposed on the spot of **1**. This spot contributed signals at τ 3.55 (dd, H_a, $J = 16$ and 7 Hz), 4.1 (m, H_b), 8.7 (d, $J = 6$ Hz) to the n.m.r. spectrum of the mixture. This minor compound is probably *anti*-4-piperidino-1-penten-3-one oxime (**6**).

Fraction D consisted of a mixture of **1** and another compounds as shown on the t.l.c. plate by an additional spot beside the spot of **1**. The n.m.r. of this mixture showed, in addition to the signals typical of **1**, signals at τ 2.3 (d, H_c, $J = 9$ Hz), 3.75 ~ 3.9 (m, superimposed with the olefinic proton signals of **1**), and 8.78 (d, H_d, $J = 7$ Hz). The ratio of the integration for the signals at τ 8.03 and τ 8.78 was 15:38, respectively, which indicated that this compound is about 70% of the total mixture. This fraction was recrystallized from 2-propanol to give a semi-pure compound of *anti,trans*-4-piperidino-2-pentenal oxime (**4**); n.m.r. (C_6D_6) τ 2.13 (d, H_c, $J = 9$ Hz), 3.45 (dd, H_a, $J = 16$ and 9 Hz), 3.95 (dd, H_b, $J = 16$ and 7 Hz), and 8.93 (d, H_d, $J = 7$ Hz). The percent yield of compound **4** was estimated by n.m.r. analysis to be 12%.

Photoaddition of N-Nitrosopiperidine to trans-1,3-Pentadiene

A solution of *N*-nitrosopiperidine (5.7 g, 0.05 mol), *trans*-1,3-pentadiene (3.74 g, 0.055 mol), and concentrated hydrochloric acid (5 ml) in methanol (200 ml) was photolyzed as previously described. The reaction was worked-up in the usual manner. The acidic ether extract gave a crude oil (36 mg) which was not investigated further. The basic extract was obtained by extracting with $CHCl_3$ (50 ml × 3) which, upon evaporation of the solvent, gave a resin (9.3 g). This resin was treated with ether to give crystals (3.6 g); superimposable i.r. and n.m.r. with those of **1**. The mother liquor was evaporated down to give a resin (5.29 g) which was chromatographed on silicic acid (60 g). The first compound eluted with $CHCl_3$ (100 ml) was a solid (670 mg) which showed a single spot by t.l.c. analysis and was recrystallized from cyclohexane to give *syn,trans*-1-piperidino-3-penten-2-one oxime (**7**); m.p. 96–97.5°; i.r. 3180, 1650, 1009, 1005–900 (multiple peaks) 863, 790 cm^{-1}; n.m.r. τ −0.9 (b, OH), 3.8 ~ 4.2 (m, H_a and H_b), 6.65 (s, H_c), 7.60 (m, 4H), 8.25, (d, H_d, $J = 5$ Hz), 8.54 (m, 6H); n.m.r. (benzene-d_6) τ 3.63 (d, H_a, $J = 16$ Hz), 4.0 (dq, H_b, $J = 16$ and 6 Hz), 6.74 (s, H_c), 8.38 (d, H_d, $J = 6$ Hz).

Anal. Calcd. for $C_{10}H_{18}N_2O$: C, 65.90; H, 9.95; N, 15.37. Found: C, 65.90; H, 9.73; N, 15.19.

The next fraction eluted with 2% methanol in $CHCl_3$ was an oil (1.4 g) which could be crystallized from petroleum ether to give white crystals (350 mg, t.l.c. single spot). They were sublimed (70°/0.2 mm Hg) to give *anti,trans*-1-piperidino-3-penten-2-one oxime **8**; m.p. 72–73.5°; i.r. 3250, 1640, 1113, 1118, 1000–940 (multiple peaks), 760 cm^{-1}; n.m.r. τ 0.9 (b, OH), 3.36 (m, H_a and H_b), 6.87 (s, H_c), 7.65 (m, 4H), 8.18 (d with virtual coupling, H_d, $J = 6$ Hz), 8.57 (m, 6H); n.m.r. (benzene-d_6) τ 3.0 (dq, H_a, $J = 16$ and 1 Hz), 3.5 (dq, H_b, $J = 16$ and 6 H), 6.82 (s, H_c), 8.42 (dq, H_d, $J = 6$ and 1 Hz). The mother liquors from the recrystallizations were combined to give a residue. This residue was slightly contaminated by **7** showing signals at τ 3.8 and 6.6. This residue was subjected to the amino group assisted Beckmann cleavage reaction (*vide infra*).

Continued elution with 2% methanol in $CHCl_3$ gave 1,4-adduct **1** (1.3 g); i.r. 3200, 1620, 1010–895 cm^{-1}; n.m.r. τ 3.82 (m, 2H), 6.92 (m, 2H), 7.59 (m, 4H), 8.05 (s, 3H), 8.50 (m, 6H). In the last fraction from this chromatography, 4,1-adduct **4** admixed with compound **1** was obtained as shown by the doublet at τ 2.34 and 8.78; the rest of the n.m.r. signals were superimposed with those of **1**.

Photoaddition of N-Nitrosopiperidine to cis,trans-2,4-Hexadiene

The photoaddition was carried out in the same manner as described above. The $CHCl_3$ extract (50 ml × 3) of the basic aqueous solution afforded a quantitative yield of crude adducts as a light yellow oil (10.0 g) which was chromatographed on silicic acid (60 g).

The first fraction A eluted with $CHCl_3$ was an oil (516 mg) and, on a t.l.c. plate, showed two predominant spots with R_f values of 0.42 and 0.29. Continued elution with $CHCl_3$ gave fraction B which was a mixture of two compounds showing spots on the R_f 0.16 and 0.08. The remaining fraction C (6.48 g) was eluted with 1 ~ 20% methanol in $CHCl_3$ to give predominantly the last compound showing R_f of 0.08 on t.l.c. analysis.

Fraction A was rechromatographed on silicic acid (15 g). Elution with $CHCl_3$ gave four consecutive fractions which showed a single spot on a t.l.c. plate. These fractions were combined (200 mg) and distilled to give a colorless oil (170 mg) of *syn,trans*-2-piperidino-4-hexen-3-one oxime (**10**); i.r. 3350, 1660, 1620, 1590, 1390, 1340, 1150, 1110, 990, 940 cm^{-1}; n.m.r. τ − 1.25 (b, OH), 3.7–4.1 (m, H_a and H_b), 6.57 (q, H_c, $J = 7$ Hz), 7.5 (m, 4H), 8.18 (d with virtual coupling, H_c, $J = 5$ Hz), 8.47 (m, 6H), 8.67 (d, H_d, $J = 7$ Hz); n.m.r. (pyridine) τ 3.3 (dq, H_b, $J = 16$ and 6 Hz), 3.74 (d, H_a, $J = 16$ Hz), 5.88 (q, H_c, $J = 7$ Hz), 8.23 (d, H_c, $J = 6$ Hz), 8.75 (d, H_d, $J = 7$ Hz); mass spectrum *m/e* (relative intensity) 196 (1), 111 (32), 84 (53), 41 (100). Continued elution with 1% methanol in $CHCl_3$ gave a fraction which on a t.l.c. plate showed a single spot. This oil was distilled on a small scale (100°/0.2 mm Hg) to give a colorless sample (40 mg) of *trans*-5-piperidino-3-hexen-2-one (**12**); i.r. 2950, 2800, 1678, 1630, 1450, 1360, 1258, 1110, 990 cm^{-1}; n.m.r. τ 3.18 (dd, H_b, $J = 17$ and 7 Hz), 3.94 (d, H_a, $J = 17$ Hz), 6.82 (quintet, H_c, $J = 7$ Hz), 7.5 (m, 4H), 7.71 (s, H_c), 8.46 (m, 6H), 8.76 (d, H_d, $J = 7$ Hz); mass spectrum (at 20 eV), *m/e* (relative intensity) 181 (4), 111 (46), 84 (100).

Fraction B was rechromatographed on silicic acid (15 g). Eluting with up to 1% methanol in $CHCl_3$ gave four fractions which were predominantly a new compound contaminated slightly by **11**. Continued elution with 2% methanol in $CHCl_3$ gave an oil (28 mg) which showed a single spot on a t.l.c. plate. This oil was distilled to afford an analytical sample of *anti,trans*-2-piperidino-4-hexen-3-one oxime (**11**); i.r. 3350, 2995, 1650, 1638, 1458, 1383, 1120, 963, 940 cm^{-1}; n.m.r. τ 0.9 (b, OH), 3.0 ~ 3.7 (m, H_a and H_b), 6.67 (q, H_c, $J = 7$ Hz), 7.50 (m, 4H), 8.12 (d with virtual coupling, H_c, $J = 6$ Hz), 8.50 (m, 6H), 8.73 (d, H_d, $J = 7$ Hz); mass spectrum *m/e* (relative intensity) 196 (1.8), 179 (5.4), 84 (8), 41 (100).

Can. J. Chem. Downloaded from www.nrcresearchpress.com by 210.87.254.42 on 09/05/12
For personal use only.

Anal. Calcd. for $C_{11}H_{20}N_2O$: C, 67.31; H, 10.27; N, 14.27. Found: C, 67.20; H, 10.26; N, 14.47.

One of the fractions from fraction C (single spot on t.l.c., 300 mg) was crystallized from petroleum ether: m.p. 83–85°. These crystals were recrystallized three times from petroleum ether and then sublimed (90°/0.2 mm Hg) to give white crystals of *anti,trans*-5-piperidino-3-hexen-2-one oxime (**9**); m.p. 88–89°; i.r. 3000, 1630, 1145, 1110, 1060, 980–900 (multiple peaks), 870, 840, 780, 675 cm^{-1}; n.m.r. τ −1.00 (b, OH), 3.2 ~ 4.0 (m, H_a and H_b), 6.95 (m, H_c), 7.52 (m, 4H), 8.01 (s, H_e), 8.52 (m, 6H), 8.78 (d, H_d, J = 6.5 Hz); n.m.r. (pyridine) τ 3.5 (d, H_a, J = 16 Hz), 3.98 (dd, J = 16 and 7 Hz), 7.78 (s, H_e), 6.92 (quintet, H_c, J = 7 Hz), 8.84 (d, H_d, J = 7 Hz).

Anal. Calcd. for $C_{11}H_{20}N_2O$; C, 67.31; 10.27; N, 14.27. Found: C, 67.25; H, 10.14; N, 14.40.

Beckmann Reaction of trans-4-Piperidino-2-butenal Oximes

A sample of the *anti,trans*-oxime **14** (m.p. 100–103°, 1.1 g) and *p*-toluenesulfonyl chloride (2.9 g) were added to cold triethylamine (50 ml). The mixture was stored in an ice box overnight and was flash evaporated under vacuum to remove triethylamine. The residue was stirred with aqueous sodium carbonate solution (10%) for 1 h and was extracted with ether (30 ml × 3). The ether solution was extracted with 2 *N* hydrochloric acid. The acid solution was basified and extracted with methylene chloride to give a crude basic product (1.02 g); i.r. 2790, 2820, 2240, 1640, 990, 960 cm^{-1}. The crude product was chromatographed on an alumina column (30 g) and eluted with benzene to give *trans*-4-piperidinocrotononitrile (**15**); i.r. 2800, 2780, 2220, 1638, 1345, 1150, 1120, 1035, 990, 960 cm^{-1}; n.m.r. τ 3.33 (dt, 1H, J = 16 and 5.5 Hz), 4.42 (dt, 1H, J = 16 and 1.8 Hz), 6.95 (dd, 2H, J = 5.5 and 1.8 Hz).

The picrate of **15** was recrystallized from a mixture of ethanol–benzene to give orange crystals; m.p. 155.5–156.5.

Anal. Calcd. for $C_{15}H_{17}N_5O_7$: C, 47.55; H, 4.52; N, 18.56. Found: C, 47.57; H, 4.63, N, 18.46.

A crude resin (1.59 g) obtained from the photoaddition of *N*-nitrosopiperidine to butadiene was, without further purification, dissolved in pyridine (30 ml). To this solution was added *p*-toluenesulfonyl chloride (3.0 g, 0.015 mol) as a finely ground powder. The solution was stirred at room temperature for 24 h. At this time, the pyridine was removed under vacuum leaving a dark black oil. This oil was treated with saturated K_2CO_3 solution and stirred for 1 h at room temperature. This solution was worked-up as shown above to afford a brown-black oil (860 mg). The oil was then distilled by bulb distillation at a vacuum of 0.2 mm Hg. The forerun collected distilled at a chamber temperature of 70–76° and the main distillate was collected at a temperature range of 76–88°. Both the forerun and the main fraction showed n.m.r. and i.r. spectra superimposable with that of *trans*-4-piperidinocrotononitrile (**15**).

Beckmann Reaction of cis-1-Piperidino-3-penten-2-one Oximes (2 and 3)

In a round bottom flask (50 ml) equipped with a condenser, pure oxime of **3** (244 mg, 0.0013 mol) was dissolved in pyridine (10 ml). The top of the condenser was closed with a stopper. To the solution was added *p*-toluenesulfonyl chloride (600 mg, 0.003 mol) and the resulting solution was stirred for 18 h. It was then treated with ether. The ether layer was washed with 2 *N* hydrochloric acid solution (30 ml × 3), and then with a saturated K_2CO_3 solution and lastly with water. The ether extract was then dried ($MgSO_4$) and filtered. The ether solution was distilled to a small volume (10 ml) in a distillation apparatus equipped with a Vigreux column (50 mm). This residual ether (10 ml) was examined by v.p.c. and n.m.r. The v.p.c. analysis (20 ft × 3/8 in., 30% SE–30, chromosorb, 100 ml of He/min, 120°) showed that no *trans*-crotononitrile was present. The n.m.r. showed signals at τ 3.5 (dq, 1H, J = 11 and 7 Hz), 4.66 (dq, 1H, J = 11 and 1.5 Hz), 8.0 (dd, 3H, J = 7 and 1.5 Hz).

The crude adduct obtained from the addition of *N*-nitrosopiperidine to *cis*-1,3-pentadiene was recrystallized to remove 1,4-adduct **1**. The mother liquor was evaporated to give a crude mixture. This crude material (1.73 g, 0.0095 mol) was dissolved in pyridine and cooled in an ice bath to 3° with constant stirring. To this solution was added finely powdered *p*-toluenesulfonyl chloride (3.8 g, 0.02 mol) and the resulting solution was stirred overnight. The temperature rose gradually to 22° after stirring for 18 h. The solution was diluted with ether (50 ml). The ether solution was worked-up as described above. The n.m.r. and v.p.c. analysis in the same manner (135 ml/min, 100°) showed only *cis*-crotononitrile.

Beckmann Reaction of trans-1-Piperidino-3-penten-2-one Oximes (7 and 8)

Pure oxime **8** (300 mg, 0.0016 mol) as finely ground crystals was dissolved in pyridine (15 ml). *p*-Toluenesulfonyl chloride (960 mg, 0.002 mol) was added and this solution was stirred for 16 h. The reaction was worked-up as previously described. A v.p.c. analysis (150 ml of He/min, 123°) and n.m.r. spectrum of the concentrated ether solution showed it to contain only *trans*-crotononitrile.

An analogous reaction was carried out in an aqueous 2% KOH solution. The recovered crotononitrile was analyzed to contain about 20% *cis* and 80% *trans* isomer by v.p.c. analysis (125 ml of He/min, 85°). The commercially available *cis*- and *trans*-crotononitrile mixture was stirred for 20 h in an aqueous 2% KOH solution. The *cis* to *trans* ratio was found to be unchanged.

The basic crude mixture obtained from a photoaddition *N*-nitrosopiperidine to *trans*-1,3-pentadiene was chromatographed on silicic acid (60 g). All the fractions that showed the presence of the minor components (other than **1**) by t.l.c. analysis were combined (2.124 g, 0.0118 mol). The oil was treated with *p*-toluenesulfonyl chloride (4.85 g, 0.025 mol) in pyridine (20 ml) for 16 h. The solution was then worked-up in the usual manner. The concentrated ether extract was examined by v.p.c. (120 ml of He/min, 126°) and n.m.r. and was shown to contain only *trans*-crotononitrile.

Beckmann Reaction of a Crude Mixture of trans-2-Piperidino-4-hexen-3-one Oximes (10 and 11)

The basic fraction obtained from the photoaddition of *N*-nitrosopiperidine to *cis,trans*-2,4-hexadiene was chromatographed and all the fractions that showed the presence of minor components (other than **9**) were combined to give a crude mixture (560 mg, 0.0029 mol). This crude mixture was treated with *p*-toluenesulfonyl chloride (1.3 g, 0.0065 mol) in pyridine (20 ml) for 22 h at room temperature and the solution was worked-up in the usual way. The ether extract was examined by v.p.c. analysis (30% SE–30 on chrom. W, 150 ml of He/min, 80°) and was shown to contain *cis*- and *trans*-crotononitrile in a ratio of 3:97 by mixed

Can. J. Chem. Downloaded from www.nrcresearchpress.com by 210.87.254.42 on 09/05/12
For personal use only.

injection. The retention times for the *trans*-crotononitrile was 8 min and for the *cis* isomer 9.5 min.

Attempts of Sensitized Isomerization of 1,3-Pentadienes

(*1*) *N*-Nitrosopiperidine (4.0 g, 0.035 mol) and a mixture of *cis*- and *trans*-1,3-pentadiene (40:60) in cyclohexane (360 ml) was irradiated for 18 h with a 200 *W* Hanovia lamp. At intervals the photolysis solution was analyzed by v.p.c. (20 ft × 3/8 in., 30% SE–30, chromosorb W, 86 ml of He/min, 85°). The 0 h sample showed the *trans:cis* ratio of 60:40; after 1 h irradiation 58.5:41.5; after 3 h, 59.5:40.5; after 18 h, 59.5:40.5. The retention time for *trans*-1,3-pentadiene was 16.5 min and for the *cis*-1,3-pentadiene 17.5 min under the conditions employed.

(*2*) *N*-Nitrosopiperidine (2.3 g, 0.02 mol) *cis*-1,3-pentadiene (2.2 g, 0.032 mol) and concentrated hydrochloric acid (2 ml, 0.024 mol) in methanol (1.4 l) were irradiated with a RPR 3500 Å lamp to about 80% completion (4 h). To this solution was added water (50 ml) followed by sodium bicarbonate (p*H* 7–8). The photolysate solution was partially distilled to collect 25 ml of distillate (b.p. 64–65°) while the receiver was cooled with an acetone–Dry Ice mixture. This distillate was examined by v.p.c. to show the peak for *cis*-1,3-pentadiene with a retention time 13.4 min. No peak having a retention time of *trans*-1,3-pentadiene (11.2 min) was present in the v.p.c. analysis.

(*3*) *N*-Nitrosopiperidine (3.42 g, 0.03 mol), *trans*-1,3-pentadiene (3.40 g, 0.05 mol), and concentrated hydrochloric acid (3 ml, 0.036 mol) in methanol (360 ml) was photolyzed for 5 h with a RPR 3500 Å lamp to completion. The remaining diene was examined by v.p.c. in the usual manner to show the peak of *trans*-1,3-pentadiene at 13 min but no peak at 14.2 min for *cis*-1,3-pentadiene.

Photolysis of N-Nitrosopiperidine in the Presence of cis- and trans-1,3-Pentadienes

A solution of *N*-nitrosopiperidine (2.3 g, 0.02 mol), concentrated hydrochloric acid (2 ml, 0.024 mol), and a (60:40) *cis* and *trans* mixture of 1,3-pentadiene (2.72 g, 0.04 mol) in methanol (380 ml) was irradiated for 5 h and was worked-up in the usual manner to afford the forerun (20 ml). The forerun was examined by v.p.c. (60 ml of He/min, 70°) to show that the *cis:trans* ratio of the 1,3-pentadiene was 60:40, having identical ratio as the 0 h sample. Under the conditions employed *trans*-1,3-pentadiene had a retention time of 19 min, the *cis* isomer 20.4 min.

Photolysis of N-Nitrosopiperidine in the Presence of cis,trans- and trans,trans-2,4-Hexadiene

A solution of *N*-nitrosopiperidine (2.51 g, 0.022 mol), concentrated hydrochloric acid (3 ml, 0.036 mol), *cis,trans*-2,4-hexadiene (1.64 g, 0.02 mol), and *trans,trans*-2,4-hexadiene (1.64 g, 0.02 mol) in methanol (200 ml) was irradiated as described above for 7 h. The photolysate was analyzed by v.p.c. (20 ft × 3/8 in., 30% SE–30, chromosorb W, 120 ml of He/min, 90°). This *cis,trans* isomer had a retention time of 16 min and the *trans,trans* isomer of 18.2 min. At 0 h the ratio of *cis,trans* to *trans,trans* isomer was 1:1 and at the end of photolysis the corresponding ratio was also 1:1.

Synthesis of 4-Piperidinocrotononitrile

A mixture of *N*-bromosuccinimide (17.8 g, 0.11 mol) and a *cis-trans* mixture of crotononitrile (10 g, 40:60 ratio) were refluxed in CCl_4 for 15 h. At this time, the succinimide had crystallized as top layer in the CCl_4 solution and was filtered. To the CCl_4 filtrate was then added piperidine (20 g, 0.24 mol). Upon standing at room temperature piperidine hydrobromide (15.5 g, 0.095 mol) precipitated and was filtered. The filtrate was then refluxed for 1 h. The CCl_4 was then removed under vacuum to give a brown oil which was dissolved in ether and the ether solution washed with water (50 ml × 3), dried ($MgSO_4$), and evaporated to give a crude oil (11.4 g): i.r. 2225, 1640, 1108. This oil was distilled to give a mixture of *trans*- and *cis*-4-piperidinocrotononitrile (76–82°/1.5 mm Hg); i.r. 2225, 1640, 1108 cm^{-1}; n.m.r. see Fig. 1.

Quantum Yield Determination for the Disappearance of N-Nitrosopiperidine

The quantum yield was determined by using a home-made merry-go-round apparatus (36) and in methanol solution containing a suitable concentration of unsaturated compounds at two hydrochloric acid concentrations (0.5 and 0.06 *N*). The solution was degassed by three cycles of freeze–pump–thaw processes. The light source was a PEK #202 high pressure mercury arc lamp and was filtered through a Corning CS-5-60 filter. In each run the duration or irradiation was 20 min. The decrease of *N*-nitrosopiperidine was monitored at the absorption peak at 350 nm. The chemical actinometry described by Hatchard and Parker (37) was used for the photon count which was determined to be $\sim 3 \times 10^{11}$ quanta/s/tube. The quantum yields listed in Table 3 were shown to be reproducible.

We thank the National Research Council of Canada and the President's Research Fund of Simon Fraser University for generous financial support of this work.

1. Y. L. Chow, S. C. Chen, K. S. Pillay, and R. A. Perry. Can. J. Chem. This issue.
2. P. J. Wagner and G. S. Hammond. Adv. Photochem. **5**, 21 (1968). S. L. Murov, R. S. Cole, and G. S. Hammond. J. Am. Chem. Soc. **90**, 2957 (1968); R. S. Cooke and G. S. Hammond. J. Am. Chem. Soc. **90**, 2958 (1968).
3. L. M. Stephenson, D. G. Whitten, G. F. Vesley, and G. S. Hammond. J. Am. Chem. Soc. **88**, 3665 (1966); L. M. Stephenson and G. S. Hammond. Pure Appl. Chem. **16**, 125 (1968).
4. T. R. Evans and P. A. Leermakers. J. Am. Chem. Soc. **91**, 5898 (1969).
5. N. J. Turro, J. C. Dalton, and D. S. Weiss. Org. Photochem. **2**, 1 (1969).
6. D. R. Arnold. Adv. Photochem. **6**, 301 (1968).
7. Y. L. Chow, C. J. Colón, and D. W. L. Chang. Can. J. Chem. **48**, 1664 (1970).
8. R. C. Fahey. Topics in Stereochem. **3**, 237 (1968).
9. Y. L. Chow, C. J. Colón, and S. C. Chen. J. Org. Chem. **32**, 2107 (1967).
10. Y. L. Chow, S. C. Chen, and D. W. L. Chang. Can. J. Chem. **48**, 157 (1970).
11. Y. L. Chow and C. J. Colón. J. Org. Chem. **33**, 2598 (1968).
12. W. F. Trager and A. C. Huitric. Tetrahedron Lett. 825 (1966).
13. R. H. Mazur. J. Org. Chem. **28**, 248 (1963); M. Dvolaitzky and A. S. Dreiding. Helv. Chim. Acta, **48**, 1988 (1965); W. L. Benson and A. E. Pohland. J. Org. Chem. **30**, 1129 (1965).

14. L. M. JACKMAN and S. STERNHELL. Application of nuclear magnetic resonance spectroscopy in organic chemistry. 2nd Ed. Pergamon Press, Oxford, 1969. Part 4.
15. Reference 14, part 2.
16. Reference 14, part 3.
17. C. J. TIMMONS. J. Chem. Soc. D, 576 (1965); J. V. HATTON and R. E. RICHARDS. Mol. Phys. **5**, 153 (1962).
18. Y. L. CHOW. J. Am. Chem. Soc. **87**, 4642 (1965).
19. C. A. GROB, H. P. FISCHER, H. LINK, and E. RENK. Helv. Chim. Acta, **46**, 1190 (1963); C. A. GROB and A. SIEBER. Helv. Chim. Acta, **50**, 2520, 2531 (1967).
20. M. P. LAU, A. J. CESSNA, Y. L. CHOW, and R. W. YIP. J. Am. Chem. Soc. **93**, 3808 (1971).
21. Y. L. CHOW, D. W. L. CHANG, and S. C. CHEN. Can. J. Chem. **49**, 3069 (1971).
22. M. E. WOLFE. Chem. Rev. **63**, 55 (1963).
23. Y. L. CHOW, M. P. LAU, R. A. PERRY, and J. N. S. TAM. Can. J. Chem. This issue.
24. Y. L. CHOW. Can. J. Chem. **43**, 2711 (1965).
25. C. WALLING and W. THALER. J. Am. Chem. Soc. **83**, 3877 (1961).
26. D. ELAD. Org. Photochem. **2**, 168 (1969).
27. O. L. CHAPMAN and G. LENZ. Org. Photochem. **1**, 283 (1967).
28. G. J. FONKEN. Org. Photochem. **1**, 107 (1967).
29. G. S. HAMMOND *et al.* J. Am. Chem. Soc. **86**, 3197 (1964).
30. G. S. HAMMOND and J. SALTIEL. J. Am. Chem. Soc. **85**, 2516 (1963).
31. W. G. HERKSTROETER and G. S. HAMMOND. J. Am. Chem. Soc. **88**, 4769 (1966).
32. N. C. YANG, J. L. COHEN, and A. SHAW. J. Am. Chem. Soc. **90**, 3264 (1968); N. C. YANG, K. R. NEUBERGER, and M. WRIGHTON. J. Am. Chem. Soc. **91**, 3658 (1969).
33. R. A. CALDWELL and S. P. JAMES. J. Am. Chem. Soc. **91**, 5184 (1969).
34. Y. L. CHOW and M. M. FESER. Chem. Commun. 239 (1967).
35. D. CRAIG. J. Am. Chem. Soc. **65**, 1006 (1943).
36. J. N. S. TAM. Ph.D. Thesis. Simon Fraser University, Burnaby, British Columbia, 1970.
37. C. G. HATCHARD and C. A. PARKER. Proc. Roy. Soc. (London), **A235**, 518 (1956).

Can. J. Chem. Downloaded from www.nrcresearchpress.com by 210.87.254.42 on 09/05/12
For personal use only.

The Stereochemistry of the Addition of Two Diazoalkanephosphonates to Norbornene and Norbornadiene; Photolysis of the Adducts. An Entry into the Dimethyl Tricyclo[2.1.1.$0^{2,4}$]octyl Phosphonate System

HENRY J. CALLOT[1] AND CLAUDE BENEZRA

Department of Chemistry, University of Ottawa, Ottawa, Canada K1N 6N5

Received July 15, 1971

Dimethyl phenyldiazomethyl- and methyldiazomethylphosphonates were treated with norbornene and norbornadiene and the configuration of the Δ^1-pyrazolines obtained (**3**–**8**) was deduced from n.m.r. by using the dihedral angular dependence relationship of vicinal $^{31}P,^1H$ couplings. The adducts were photolyzed under sensitized and non-sensitized conditions. The resulting cyclopropyl derivatives (**9**–**12** and **14**–**17**) were assigned configuration by using n.m.r. data. The results are discussed in terms of steric and electronic factors. The n.m.r. and mass spectral data are also discussed.

La réaction des phényldiazométhyl- et méthyldiazométhylphosphonates de diméthyle avec le norbornène et le norbornadiène a été étudiée et la configuration des Δ^1-pyrazolines obtenues (**3**–**8**) a été déduite par r.m.n. en utilisant la dépendance angulaire du couplage vicinal $^{31}P,^1H$. Les produits d'addition ont été photolysés dans des conditions sensibilisées et non sensibilisées. La configuration des dérivés cyclopropaniques formés (**9** à **12** et **14** à **17**) a été déterminée en utilisant les données de r.m.n. Les résultats sont discutés en termes de facteurs stériques et électroniques. Les données de r.m.n. et de masse sont également discutées.

Canadian Journal of Chemistry, **50**, 1078 (1972)

1,3-Dipolar cycloadditions are well documented by a large amount of studies, mostly stimulated by the important contribution of Huisgen and co-workers (1) in the field. Some controversy arose recently concerning the mechanism of the addition (2) but the "no-mechanism" concerted pathway originally proposed by Huisgen (3) seems to be generally accepted. The nature of the orientation (when either the dipole or the dipolarophile is unsymmetrical) is still obscure (3) and orbital symmetry considerations (4) do not permit predictions (5).

When the dipole contains a carbon bearing two different substituents, two stereoisomers can be obtained with a symmetrical olefin. This aspect of the stereochemistry of the cycloaddition has apparently received little attention although some examples of the formation of epimeric mixtures (6) and separation and determination of the configuration of epimers have been described recently (7). Strained olefins such as norbornene (**1**) and norbornadiene (**2**) are very reactive toward cycloadditions (1) and should provide an excellent model to study the "tertiary" aspects of the stereochemistry of the cycloadditions.[2] Our interest in phosphonates prompted us to study the cycloaddition of diazoalkanephosphonates $RC(N_2)P(O)(OCH_3)_2$ made readily available through the recent work of Regitz and co-workers (9, 10) and Marmor and Seyferth (11) to those strained olefins. Although the carbenoid-type behavior of those diazo compounds have been studied recently (generation of $R\ddot{C}P(O)(OCH_3)_2$ either by copper-catalyzed decomposition (11) or by photolysis), much less attention has been devoted to their potential as 1,3-dipolar reagents and the stereochemistry of the cycloaddition.

It was hoped to get some insight into the steric and electronic requirements of the cycloadditions and an entry into strained tricyclic systems containing the $P(O)(OCH_3)_2$ moiety through the decomposition of the intermediate Δ^1-pyrazolines expected. This work describes the reaction of dimethyl phenyldiazomethyl- ($R = C_6H_5$) and methyldiazomethyl ($R = CH_3$) phosphonates with norbornene and norbornadiene and the photolysis of the adducts.

[1]On leave of absence from C.N.R.S. (France). Present address: Institut de chimie, 1 Rue Blaise Pascal, Strasbourg, France.

[2]The "primary" aspects being the exclusive *cis* addition (1,3) (except for one case (8) recorded in the literature), the "secondary" aspects the exclusive *exo* addition to norbornene and norbornadiene systems (1), the "tertiary" aspects would be the formation of epimers (possible when the dipole bears two unlike substituents).

Can. J. Chem. Downloaded from www.nrcresearchpress.com by 210.87.254.105 on 09/05/12
For personal use only.

Can. J. Chem. Downloaded from www.nrcresearchpress.com by 210.87.254.105 on 09/05/12
For personal use only.

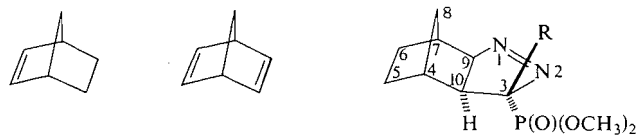

1 2 3 R = C_6H_5; 4 R = CH_3

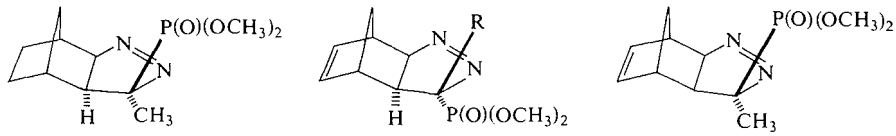

5 6 R = C_6H_5; 7 R = CH_3 8

Results

Cycloadditions

Cycloaddition of diazoalkanephosphonates $RC(N_2)P(O)(OCH_3)_2$ to norbornene **1** and norbornadiene **2** proceeds smoothly when a mixture containing the olefin, the diazo compound and methylene chloride is warmed at temperatures not exceeding 50 °C.

Interesting to note is the steric course of the addition: with norbornene, for instance, and dimethyl phenyldiazomethylphosphonate (R = Ph), only one pyrazoline, **3**, was formed. However when dimethyl methyldiazomethylphosphonate ($R = CH_3$) was treated with norbornene, two pyrazolines, **4** and **5** (ratio 4:1), epimeric at C-3 were obtained.

Assignment of the configuration of the pyrazolines follows from the examination of their 100 MHz n.m.r. spectra. *exo*-Junction of the pyrazoline ring to the bicyclo[2.2.1]heptyl moiety is shown by the absence of any H_9,H_7 or H_{10},H_4 couplings,[3] such absence of coupling being characteristic of an *endo* proton (12). Configuration at C-3 can be assigned from the different $^3J_{PH_{10}}$ couplings. In compounds **3** and **4** the 17.4 and 18.8 Hz couplings respectively are only compatible with a near-zero P,H dihedral angle (13), while the small 6.0 Hz P,H coupling in **5** can be ascribed to a near 120° dihedral angle.[4]

Similar results were obtained with norbornadiene: pyrazolines **6**–**8** were obtained and assigned stereochemistry based on the same considerations. Results for cycloadditions are summarized in Table 1.

Decomposition of the Pyrazolines

Thermal decomposition of Δ^1-pyrazolines generally results in the formation of olefins or cyclopropanes while photochemical decomposition leads mainly to cyclopropane derivatives (14, 15).

Photolyses of the above pyrazolines **3**–**8** were conducted in a Srinivasan–Griffith reactor. The pyrazolines were in benzene solutions and reacted in Vycor vessel.

Non-sensitized photodecomposition[5] of pyrazoline **3** was a clean reaction with complete stereoselectivity: only one compound, to which we assign structure **9** on the basis of the n.m.r.

[3]The numbering used for the pyrazolines **3**–**8** is based on the nomenclature of Chemical Abstracts (for example Chem.Abstr., subject index, **72**, 2338s, June 1970) for the 5,5,5-ring system of 4,7-methano-1*H*-indazole.

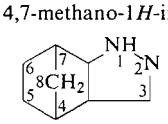

[4]One referee has questioned the validity of our assignments concerning the configurations of the pyrazoline, arguing that these were based on a given conformation of the pyrazoline ring. According to his comments, the large vicinal P,H_{10} coupling could also be ascribed a 180° P,H_{10} dihedral couple and the small P,H_{10} coupling to a 60°angle. When one builds Dreiding models of compound **3**–**8** it becomes clear that the pyrazoline ring is planar due to: (*1*) its attachment to the rigid bicyclo[2.2.1]heptyl moiety and (*2*) to the presence of the *N*=*N* bond. Only 120 and 0° dihedral vicinal angle arrangements between proton H-10 and groups at C-3 are thus possible.

[5]"Non-sensitized" photolyses were conducted at 3500 Å using a Pyrex filter while "sensitized" photolyses were performed at 2537 Å in the presence of benzophenone (see Experimental).

Can. J. Chem. Downloaded from www.nrcresearchpress.com by 210.87.254.105 on 09/05/12
For personal use only.

TABLE 1. Cycloadditions

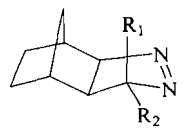

3, 4, and 5

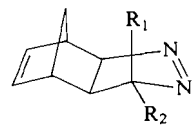

6, 7, and 8

Olefin	Diazoalkane phosphonate $RC(N)_2P(O)(OCH_3)_2$	Total yield* (%)	R_1	R_2		Pyrazolines† (%)	
Norbornene **1**	$R = C_6H_5$	92	C_6H_5	$P(O)(OCH_3)_2$	*anti*	(**3**)	100
			$P(O)(OCH_3)_2$	C_6H_5	*syn*		0
Norbornene **1**	$R = CH_3$	86‡	CH_3	$P(O)(OCH_3)_2$	*anti*	(**4**)	81
			$P(O)(OCH_3)_2$	CH_3	*syn*	(**5**)	19
Norbornadiene **2**	$R = C_6H_5$	90§	C_6H_5	$P(O)(OCH_3)_2$	*anti*	(**6**)	100
			$P(O)(OCH_3)_2$	C_6H_5	*syn*		0
Norbornadiene **2**	$R = CH_3$	84‡	CH_3	$P(O)(OCH_3)_2$	*anti*	(**7**)	78
			$P(O)(OCH_3)_2$	CH_3	*syn*	(**8**)	22

*Relative to the starting diazocompound.

†Relative yield of each epimeric pyrazoline: $\%anti + \%syn = 100$; the words *anti* and *syn* refer to the position of the dimethyl phosphono group relative to the C-8 bridge.

‡The *syn*/*anti* mixture was separated on column chromatography (weight of silica gel = 30 times weight of the mixture; eluent ether and ether–ethyl acetate mixtures).

§In another experiment on larger scale, the total yield was raised to 94 and 4% of the epimeric **6***a* pyrazoline (see theoretical part) was isolated along with 90% of the major isomer, **6**.

data, was formed. Sensitized photolysis of the pyrazoline[5] **3** resulted in complete loss of stereoselectivity: a 1:1 mixture of two epimers **9** and **10** was formed. Structures **9** and **10** were deduced from n.m.r. spectra: the large P,H_2 coupling (15.5 Hz) was assigned to compound **9** where the P,H_2 dihedral angle is near 0° (13) while the low 4.2 Hz P,H_2 coupling was consistent with structure **10**.

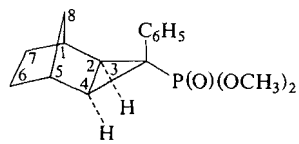

9

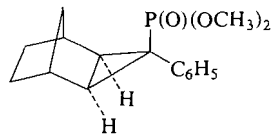

10

Thermal decomposition of pyrazoline **3** in boiling xylene for 40 h resulted in the formation of an intractable mixture in which n.m.r. showed the presence of ~35% of the cyclopropane **9** along with the unreacted pyrazoline **3** (*ca.* 25%) and unidentified products. Pyrolysis like photolysis led to the product with retention of configuration at C-3. No trace of the epimer **10** could be detected in the n.m.r. of the thermolytic mixture.

Although non-sensitized photolytic decomposition of the unsaturated analog, compound **6**, was less clean (the yield in cyclopropanes was lower, see Table 2) it was still highly stereoselective and only isomer **11** could be detected. The photolysis performed under sensitized conditions led to a mixture containing the cyclopropyl derivative **11**, its epimer at C-3, compound **12**, and isomeric unidentified compounds **13** in a 1.2:1:1.2 ratio.

Photolytic behavior of the methyl pyrazolines

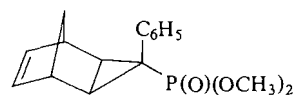

11

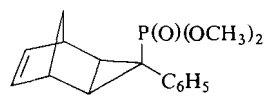

12

TABLE 2. Photolyses

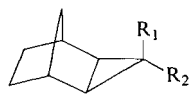

9, **10**, **14**, and **15**

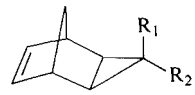

11, **12**, **16**, and **17**

Pyrazoline	Photolysis conditions	Total yield* (%)	R_1	R_2	Cyclopropanes† (%)		
3	Non-sensitized	96	C_6H_5	$P(O)(OCH_3)_2$	*anti*	(**9**)	100
			$P(O)(OCH_3)_2$	C_6H_5	*syn*	(**10**)	0
	Sensitized	94	C_6H_5	$P(O)(OCH_3)_2$	*anti*	(**9**)	50
			$P(O)(OCH_3)_2$	C_6H_5	*syn*	(**10**)	50
6	Non-sensitized	54	C_6H_5	$P(O)(OCH_3)_2$	*anti*	(**11**)	100
			$P(O)(OCH_3)_2$	C_6H_5	*syn*	(**12**)	0
	Sensitized	44	C_6H_5	$P(O)(OCH_3)_2$	*anti*	(**11**)	35
			$P(O)(OCH_3)_2$	C_6H_5	*syn*	(**12**)	65
4	Non-sensitized	96	CH_3	$P(O)(OCH_3)_2$	*anti*	(**14**)	100
			$P(O)(OCH_3)_2$	CH_3	*syn*	(**15**)	0
5	Non-sensitized	95	CH_3	$P(O)(OCH_3)_2$	*anti*	(**14**)	15–20
			$P(O)(OCH_3)_2$	CH_3	*syn*	(**15**)	80–85
7	Non-sensitized	75	CH_3	$P(O)(OCH_3)_2$	*anti*	(**16**)	100
			$P(O)(OCH_3)_2$	CH_3	*syn*	(**17**)	0
8	Non-sensitized	63	CH_3	$P(O)(OCH_3)_2$	*anti*	(**16**)	10–15
			$P(O)(OCH_3)_2$	CH_3	*syn*	(**17**)	85–90

*In % cyclopropane derivatives relative to the starting pyrazoline.
†Relative yield of each epimeric cyclopropane: % *anti* + % *syn* = 100; the words *anti* and *syn* refer to the position of the phosphorus relative to the C-8 bridge.

4 and **5** was of greater interest since epimers **4** and **5**, **7** and **8** were available. Photolyses were conducted under non-sensitized conditions.

Pyrazoline **4** led exclusively to the cyclopropane derivative **14** (96% yield). In turn, pyrazoline **5** with the dimethylphosphono group *syn* to the C-8 bridge led to a 1:4 mixture of cyclopropanes **14** and **15**. The corresponding

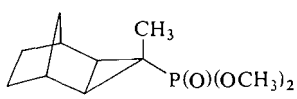

14

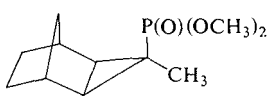

15

norbornadiene pyrazolines **7** and **8** gave comparable results. Configurations at C-3 in compounds **14** and **15** follow from a large (15.0 Hz in **14**) compared to a small (3.6 Hz in **15**) $^3J_{PH_2}$ coupling. In the norbornadiene series

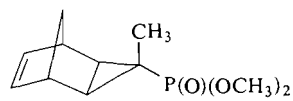

16

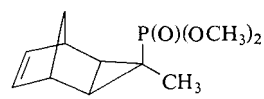

17

comparable results were obtained, and compounds **16** and **17** were isolated. Results for photolytic decomposition are summarized in Table 2.

Discussion

Steric Course of the Cycloaddition

On purely steric grounds, the results of the cycloaddition are unexpected. If one compares the Van der Walls radii of the phenyl group (half-thickness 1.7 Å) to that of the methyl group (2 Å) (16) the decreasing size order of the three substituents would be $P(O)(OMe)_2 >$

Can. J. Chem. Downloaded from www.nrcresearchpress.com by 210.87.254.105 on 09/05/12
For personal use only.

Can. J. Chem. Downloaded from www.nrcresearchpress.com by 210.87.254.105 on 09/05/12
For personal use only.

TABLE 3. The n.m.r. spectra of pyrazolines

	Chemical shifts (p.p.m.)								Couplings (Hz)					
Pyrazoline	P—O—CH_3	R—C_3	H_{10}	H_9	H_4	H_7	H_{5+6}	H_8	P—O—CH_3	P—C—CH_3	P,H_9	P,H_{10}	H_9,H_{10}	H_8,H_8
3 R = Ph	3.44 3.64	7.2–7.8	2.53	4.87	1.84	2.92	1.2–1.6	0.27 0.62	9.0	—	3.6	17.4	7.0	10.2
6 R = Ph	3.48 3.68	7.3–7.8	2.81	5.20	2.49	3.56	6.22	0.44 1.02	10.0	—	4.0	19.0	6.4	9.8
4 R = CH_3	3.74 3.80	1.66	2.20	4.77	2.06	2.91	1.1–1.7	0.51 1.04	10.4	17.6	4.2	18.8	7.1	11.0
5 R = CH_3	3.87 3.88	1.31	1.62	4.68	2.47	2.95	1.0–1.6	0.99	10.5	15.3	6.2	6.0	6.0	—
7 R = CH_3	3.72 3.80	1.67	2.32	5.06	2.64	3.50	6.18	0.64 1.37	10.2	17.2	4.0	18.4	6.5	9.2
8 R = CH_3	3.90	1.33	1.86	4.98	3.06	3.55	6.23	1.11 1.40	10.6	15.2	6.0	6.0	6.1	9.3

TABLE 4. The n.m.r. of cyclopropanes

	Chemical shifts (p.p.m.)						Couplings (Hz)			
Cyclopropane	P—O—CH_3	R—C_3 (R = Me or Ph)	H_{2+4}	H_{5+1}	H_{6+7}	H_8	P—O—CH_3	P—C—CH_3	P,H_{2+4}	H_8,H_8
9	3.57	7.23	1.69	2.41	1.3–1.5	0.27	10.4	—	15.5	—
10	3.42	7.1–7.4	1.53	2.69	1.0–1.6	0.93 2.07	10.8	—	4.2	12.2
11	3.56	7.28	1.94	2.95	6.53	0.51 0.67	10.4	—	14.8	10.2
12	3.52	7.2–7.6	1.78	3.32	6.56	1.28 2.25	10.8	—	4.0	10.8
14	3.70	1.32	1.28	2.46	1.2–1.6		10.4	15.0	15.0	
15	3.70	1.07	0.92	2.49	0.8–1.6		10.5	10.8	3.6	
16	3.69	1.52	1.51	2.96	6.57	1.01 1.46	10.2	15.5	15.0	10.0
17	3.74	1.17	1.20	3.05	6.46	1.11 2.10	10.5	11.2	3.5	10.6

Can. J. Chem. Downloaded from www.nrcresearchpress.com by 210.87.254.105 on 09/05/12
For personal use only.

phenyl > methyl.[6] One would have expected then more steric discrimination in the case of the methyl derivative (CH_3 being much less bulky than the phosphono moiety). The reverse is observed.

Electronic factors probably play an important role since the phenyl group stabilizes the diazo-compound relative to its methyl analog. Since the dimethyl methyldiazomethylphosphonate is more reactive, less discrimination is observed in this case and a mixture of pyrazolines **4** and **5** is obtained.[7]

Photolyses

Stereoselectivity of direct photolysis of pyrazolines compared to the absence of stereoselectivity in the photosensitized decomposition can be explained on the basis of different intermediate diradicals. Direct photolysis is believed to proceed through the intermediacy of a short-lived singlet species: time is therefore not sufficient to allow rotation about the C_{10}—C_3 bond and epimerization at C-3. In turn, photosensitized decomposition of pyrazolines occurs through a triplet (18), long lived enough to allow such bond rotation. Recent work confirms this general result concerning stereoselectivity (7).

In agreement with this is the finding that non-sensitized photodecomposition of pyrazolines **3**, **4**, **6**, and **7** was completely stereoselective while sensitized decomposition of pyrazolines **3** and **6** led to mixtures of cyclopropanes (see Table 2).

[6]No definite value for the size of the dimethylphosphono group is known; however, from X-ray data (17) it may be inferred that $P(O)(OMe)_2$ occupies as much space as a tert-butyl group although the length of the P—C bond (1.85 Å) compared to that of the C—C bond should make the dimethylphosphono group less bulky than $(CH_3)_3C$. Work to determine the *A* value for the phosphono group is in progress in this laboratory.

[7]In agreement with this hypothesis, is our recent finding that 4% of the epimeric pyrazoline **6***a* was isolated from the cycloaddition of $PhC(N_2)P(O)(OCH_3)_2$ to norbornadiene. Since norbornadiene is more reactive than norbornene (due to the presence of a second double bond), less discrimination is observed for the former.

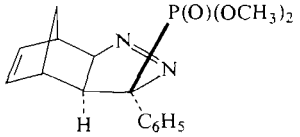

6*a*

There is a striking difference between the photolytic behavior of pyrazolines **4** and **7** on one hand and that of the epimeric pyrazolines **5** and **8** on the other hand. Complete stereoselectivity is found in the first case while in the second case, where the bulky dimethylphosphono group is *syn* to the C-8 bridge, there are 20% of the cyclopropanes **14** and **16** found with inversion of configuration at C-3. We propose as a possible explanation that the bulkiness of the dimethylphosphono group[6] results in such a steric compression in the intermediate **18** ($R = CH_3$) with the P *syn* to the C-8 bridge that even with a very short-lived singlet, rotation of C_3—C_{10} occurs, thus relieving some of the strain. Such a steric compression when the $P(O)(OCH_3)_2$ group is *syn* to the C-8 bridge is also reflected in the n.m.r. of the compounds (see below).

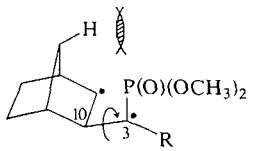

18

Nuclear Magnetic Resonance Spectra

The data on n.m.r. are summarized in Tables 3 and 4; some general features are worth comment.

In the pyrazolines, the chemical shift of the protons near C-3 strongly depends on the configuration at this center. This is very clear in the methyl series. For instance, the chemical shift of the methyl group in the *anti* compounds **4** and **7**[8] is 1.66 and 1.67 p.p.m. while in the *syn* derivatives **5** and **8** they are 1.31 and 1.33 respectively. There is also a large difference between the chemical shifts of H_{10} in the epimers: H_{10} resonates at higher field in the *syn* derivatives **5** and **8**.

Concerning the couplings, most of our assignments are based on the vicinal P,H_{10} couplings. For a near 120° dihedral angle, this coupling is equal to 6.0–6.2 Hz while a 0° angle results in a high 17.4–19.0 Hz coupling. These results are consistent with a Karplus-type variation of the vicinal P,H coupling (19). Another $^3J_{PH}$ coupling is of interest: the *P*—C—*CH*$_3$ coupling is sensi-

[8]The words *syn* and *anti* refer to the position of the phosphorus group relative to the C-8 bridge.

Can. J. Chem. Downloaded from www.nrcresearchpress.com by 210.87.254.105 on 09/05/12
For personal use only.

tive to the configuration at C-3. It is equal to 17.2 and 17.6 Hz in the *syn* compounds **4** and **7** while it drops to 15.2–15.3 in the *anti* derivatives **5** and **8**. It is probable that due to the bulkiness of the dimethylphosphono group some steric compression with the H_8 *syn* to the phosphono occurs, causing a deformation of the P—C—CH_3 angle. Such a compression is more severe in the cyclopropyl derivatives and is reflected by a larger drop in $^3J_{PCH_3}$ (see below).

Some long range P,H couplings can be noted: P,H_9 coupling varies from 3.6 to 6.2 Hz and is the largest when the phosphono group is *syn* to the C-8 bridge.

Almost the same features described above apply to the photo-products **9** to **17**. Interesting to note is the difference in the chemical shift of the H_8 protons depending on the C-3 configuration. In the phenyl derivatives (**9** to **12**) two general features can be described. A phenyl *syn* to the C-8 bridge results in shielding of the H_8 protons: (0.27 to 0.67 p.p.m.) while the effect of the dimethyl-phosphono group seems to be an enhancement of the chemical non-equivalence of the two hydrogens (about 1.0 p.p.m. $\Delta\delta$). The results are less clear-cut in the methyl series (**14** to **17**) but the same type of comment can be made.

Concerning the vicinal coupling, the dihedral dependence of $^3J_{PCH_3}$ allows the assignment of configuration of the cyclopropyl derivatives. As

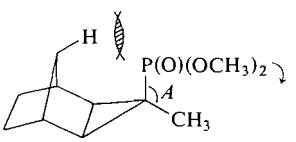

in the case of the pyrazolines, the *P*—C—*CH*$_3$ splitting strongly depends on the orientation of the bulky dimethylphosphono group. When this is *syn* to the C-8 bridge a substantial drop of this coupling occurs (from $\sim$ 15 to 11 Hz). This is unexpected since steric compression (between P and H_{8syn}) should cause the decrease of the P—C—C(H_3) bond angle *A* and result in the *increase* of the vicinal coupling (20). Other factors such as rehybridization of phosphorus in the *syn* derivatives could play a role.

Mass Spectra

Spectral data are summarized in Tables 5 and 7. Some salient features are worth comment.

Pyrazolines show no parent ion but instead an $M^+ - 28$ (loss of nitrogen) peak. In the norbornadiene series (compounds **6** and **7**) the major fragmentation is the retro-Diels–Alder path (loss of C_5H_6 after nitrogen has been eliminated) where the charge is carried by the moiety containing the phosphorus group. Loss of the elements of dimethyl phosphonate ($HP(O)(OCH_3)_2$($M^+ - 28$)-110 is an important process in both series as was shown for other phosphonates (21). In the unsaturated methyl derivatives **7** and **8**, it is interesting to note that the fragmentation pattern of those epimers seems to depend strongly on the configuration at C-3. When the $P(O)(OCH_3)_2$ group is *syn* to the C-8 bridge the retro-Diels–Alder process becomes minor and the prominent ion is the one corresponding to the loss of [$HP(O)(OCH_3)_2$]. The steric compression existing in the *syn* derivatives seems to be reflected also in the mass spectra.

Cyclopropyl derivatives exhibit spectra which are almost identical with those of the corresponding pyrazolines. It is possible that a common intermediate is involved, once nitrogen has been lost; the parent ion is more intense than the corresponding ($M^+ - 28$) peak of pyrazoline. In the saturated series (**9**, **10**, **14**, and **15**) one of the major fragmentation processes corresponds to the loss of 110 mass units ($C_2H_7O_3P$); note that in compounds **9** and **10** the base peak is the parent ion. In the unsaturated series (**11**, **12**, **16**, and **17**) two major fragmentation patterns are observed: the retro-Diels–Alder process (loss of C_5H_6) and the loss of 110 mass units. Here again the influence of the configuration at C-3 is determinant: when the phosphorus moiety is *syn* to the C-8 bridge (causing severe steric compression), the major process by far is the loss of the elements of dimethyl phosphonate.

Experimental

The i.r. spectra were recorded on a Beckman 20 i.r. Spectrometer either in chloroform solutions when the compound was a solid or as neat liquids. The n.m.r. spectra were run on a HA-100 Varian Spectrometer in deuterochloroform solutions, chemical shifts are given in δ p.p.m. values with TMS as internal reference. Mass spectra were recorded on a Hitachi–Perkin–Elmer RMU-6D Spectrometer at 70 eV. Analyses were performed in Organic Microanalyses laboratories (Dr. C. Daesslé) Montréal. Norbornene and norbornadiene were purchased from Aldrich company, and used without further purification. The silica gel used was purchased from Brinkman instru-

TABLE 5. Pyrazolines

Pyrazoline	m.p.(°C) (recryst. solvent, subl., or dist.)	Anal. Calcd. (Found) C	H	P	N	i.r. (cm^{-1})	Mass spectra *m/e* (%)	
3	116–117 (ether)	60.00 (60.18)	6.50 (6.56)	9.69 (9.52)	8.75 (8.89)	1595 (Phenyl) 1545 (N=N) 1240 (P=O)	292(86) 264(60) 213(50) 182(100) 155(58)	154(77) 153(50) 141(74) 115(65) 79(51)
6	84–85 (ether)	60.37 (60.12)	6.02 (5.86)	9.73 (9.51)	8.80 (8.91)	1600 (Phenyl) 1550 (N=N) 1225 (P=O)	290(30) 289(30) 224(100) 209(34) 181(32)	180(67) 179(67) 115(33) 85(60) 83(73)
4	38–39 (subl.)	51.16 (51.18)	7.36 (7.39)	12.02 (11.85)	10.85 (11.03)	1545 (N=N) 1250 (P=O)	230(62) 202(37) 121(26) 120(100) 110(39)	105(44) 93(40) 92(41) 91(48) 79(59)
5	oil (dist.)	51.16 (51.33)	7.36 (7.43)	12.03 (11.74)	10.85 (10.62)	1540 (N=N) 1255 (P=O)	230(42) 121(20) 120(100) 119(20) 110(34)	105(36) 93(26) 92(30) 91(37) 79(41)
7	65–66 (PE + subl.)	51.56 (51.30)	6.69 (6.71)	12.09 (11.89)	10.93 (10.81)	1540 (N=N) 1240 (P=O)	228(24) 227(34) 163(28) 162(100) 147(26)	119(33) 118(92) 117(86) 91(32) 79(27)
8	49–57 (subl.)	51.56 (51.18)	6.69 (6.57)	12.09 (12.31)	10.93 (11.20)	1540 (N=N) 1260 (P=O)	227(18) 162(25) 119(33) 118(100) 117(71) also: 228: 13%	110(29) 109(18) 91(33) 79(32) 77(19)

ments Canada: Merck silica gel 0.05–0.20 mm. Dimethyl phenyldiazomethylphosphonate: $C_6H_5C(N_2)P(O)(OCH_3)_2$ and dimethyl methyldiazomethylphosphonate $CH_3C(N_2)P(O)(OCH_3)_2$ were prepared according to Seyferth (11).

Cycloadditions

The general procedure was the following: mixtures of the diazo compound, the hydrocarbon (norbornene or norbornadiene) and methylene chloride were heated until complete disappearance of the yellow color of the diazo compound. The proportions used were as follows: (*1*) R = phenyl: *n* mmol of diazo, 10*n* mmol hydrocarbon, and *n* ml CH_2Cl_2, the mixtures were refluxed 3–4 days; (*2*) R = methyl: *n* mmol diazo, 60*n* mmol hydrocarbon, 4*n* ml CH_2Cl_2, about the 20 h reflux.

The adducts **3** and **6** were isolated by removal of the solvent and excess olefin by distillation. Compounds **4** and **5**, **7**, and **8** were separated by column chromatography. Yields are indicated in Table 1, physical constants and spectral data in Table 5.

Photolyses

Photolyses were conducted in a Srinivasan–Griffith reactor in benzene solutions using Vycor vessels, under nitrogen. There were two types of conditions: (*a*) "non-sensitized" photolyses were performed with a 3500 Å lamp using a Pyrex filter. (*b*) "sensitized" photolyses were performed with a 2537 Å lamp in the presence of benzophenone.

Experimental conditions are given in Table 6. Physical constants (m.p. and mass spectra) are given in Table 7. The duration of photolyses varied from 4 to 6 h, depending on the pyrazoline.

Anal. Calcd. for **9** and **10** (1:1 mixture): C, 65.60; H, 7.12; P, 10.36. Found: C, 65.74; H, 7.24; P, 10.10.

Anal. Calcd. for **16**: C, 57.89; H, 7.51; P, 13.57. Found: C, 58.14; H, 7.41; P, 13.32.

Compounds **11**, **12**, and **14** were correlated by hydrogenating the norbornadiene derivative into the norbornene derivative. Hydrogenations were carried out in a Parr hydrogenation apparatus for 2 h in methanol solutions in the presence of Pd/C at 2.7 atm. The yield was quantitative in each case and only one product was obtained.

Thus hydrogenation of compound **11** led to compound **9**, that of compound **12** to compound **10**, and finally compound **16** was transformed into compound **14**. Compounds **15**

Can. J. Chem. Downloaded from www.nrcresearchpress.com by 210.87.254.105 on 09/05/12
For personal use only.

TABLE 6. Photolyses conditions

Starting pyrazoline (g)	s./n.s.*	Benzene (ml)	Benzophenone (g)	Time (h)	Isolation conditions (after removal of the solvent)
3 (0.50)	n.s.	100	—	4	Isolation of the mixture (**9** + **10**) by recrystallization of the crude in cyclohexane. **9** and **10** were separated on column chromatography (silica gel; eluent ether).
3 (0.50)	s.	100	1.0	2	Isolation of the mixture (**9** + **10**) by column chromatography on silica gel (elution $CHCl_3$–AcOEt) separation of **9** and **10** as above (n.s.).
6 (0.95)	n.s.	100	—	5	Isolation of **11** and **12** by column chromatography on siligel (elution: $CHCl_3$–AcOEt).
6 (1.45)	s.	100	1.5	6	Same as above (eluent: ether).
4 (0.34)	n.s.	100	—	3.5	The crude was sublimated to give pure **14**.
5 (0.13)	n.s.	80	—	4	Sublimation – mixture **14** + **15** (estimated by n.m.r.).
7 (0.70)	n.s.	100	—	4	Chromatography on a silica gel column (eluent AcOEt) sublimation gave pure **16**.
8 (0.17)	n.s.	90	—	2.5	Same as above. A mixture of **16** + **17** is obtained.

*s., sensitized; n.s., non-sensitized conditions.

TABLE 7. Cyclopropane derivatives

Compound	m.p.(°C)	Mass spectra (%)		
9	107–109	293(18)	182(41)	128(18)
		292(100)	154(20)	115(25)
		237(19)	153(17)	
		213(26)	141(24)	
10	78–80	292(100)	181(26)	115(27)
		213(35)	167(25)	77(30)
		183(26)	154(34)	
		182(90)	141(33)	
11	55–60*	290(36)	180(57)	83(29)
		289(20)	179(45)	77(21)
		224(100)	178(23)	
		181(29)	165(20)	
12	oil*	290(43)	180(100)	115(24)
		289(21)	179(59)	77(18)
		224(50)	178(28)	
		181(59)	165(27)	
14	24–25	230(62)	110(30)	79(59)
		121(28)	105(38)	77(24)
		120(100)	93(29)	
		119(24)	91(40)	
15	oil*	M^+ 230(37)	93(54)	67(54)
		120(76)	91(75)	66(47)
		110(61)	79(100)	
		105(51)	77(50)	
16	55–57	228(30)	119(31)	79(35)
		227(32)	118(100)	77(27)
		163(23)	117(80)	
		162(100)	91(43)	
17	oil*	228(31)	119(42)	105(45)
		227(30)	118(100)	91(67)
		162(34)	117(82)	79(58)
		134(31)	110(40)	77(39)

*Contains a little of the other epimer.

and **17** were not pure enough to be analyzed but their mass spectra showed the same fragmentations (but with different peak intensity, see above) as the corresponding epimers (**14** and **16**), and the other spectral data were fully consistent with the proposed structures.

The authors wish to thank the National Research Council of Canada for financial support of this research (Grant No. A 5496) and the C.N.R.S. for a fellowship to one of us (H.J.C.).

1. R. HUISGEN. Angew. Chem. Int. Ed. **2**, 565 and 633 (1963); R. HUISGEN, R. GRASHEY, and J. SAUER. *In* The chemistry of alkenes. S. Patai, *ed.* Interscience, London, 1964. p. 739.
2. R. A. FIRESTONE. J. Org. Chem. **33**, 2285 (1968).
3. R. HUISGEN. J. Org. Chem. **33**, 2291 (1968).
4. R. B. WOODWARD and R. HOFFMANN. Conservation of orbital symmetry. Verlag Chemie GmbH, Weinheim, 1970.
5. G. W. COWELL and A. LEDWITH. Quart. Rev. 119 (1970).
6. H. PAUL, I. LANGE, and A. KAUSMANN. Chem. Ber. **98**, 1789 (1965).
7. P. B. CONDIT and R. G. BERGMANN. Chem. Commun. 4 (1971).
8. C. G. OVERBERGER, N. WEINSHENKER, and J. P. ANSELME. J. Am. Chem. Soc. **87**, 4119 (1965).
9. M. REGITZ, W. ANSCHUTZ, and A. LIEDHEGENER. Chem. Ber. **101**, 3734 (1968).
10. M. REGITZ. Angew. Chem. Int. Ed. **9**, 249 (1970) and references cited therein.
11. R. S. MARMOR and D. SEYFERTH. J. Org. Chem. **36**, 128 (1971) and references cited therein.
12. L. M. JACKMAN and S. STERNHELL. Application of NMR spectroscopy in organic chemistry. 2nd Ed. Pergamon Press, Oxford, 1969. p. 288–289.
13. C. BENEZRA. Tetrahedron Lett. 4471 (1969).

Can. J. Chem. Downloaded from www.nrcresearchpress.com by 210.87.254.105 on 09/05/12
For personal use only.

14. T. V. VAN AUKEN and K. L. RINEHART. J. Am. Chem. Soc. **84**, 3736 (1962); M. FRANCK-NEUMANN. Angew. Chem. **80**, 42 (1968); M. FRANCK-NEUMANN. Thèse Doctorat ès Sciences, Strasbourg, 1968 and references cited therein.
15. D. E. MCGREER and J. W. MCKINLEY. Can. J. Chem. **49**, 105 (1971) and references cited therein.
16. L. PAULING. The nature of the chemical bond. Cornell University Press, Ithaca, N.Y., 1945. p. 189.
17. G. SAMUEL and R. WEISS. Tetrahedron, **26**, 2995 (1970).
18. P. S. ENGEL and P. D. BARTLETT. J. Am. Chem. Soc. **92**, 5883 (1970) and earlier papers.
19. M. KARPLUS. J. Chem. Phys. **30**, 11 (1959).
20. Reference 12. p. 286.
21. H. J. CALLOT and C. BENEZRA. Org. Mass. Spectrom. **5**, 343 (1971).

Can. J. Chem. Downloaded from www.nrcresearchpress.com by 210.87.254.105 on 09/05/12
For personal use only.

Can. J. Chem. Downloaded from www.nrcresearchpress.com by 210.87.254.6 on 09/05/12
For personal use only.

NOTES

An Upper Bound to the Mole Fraction of Unbonded H_2O in Liquid Water at 25 °C

FABIO LENZI

Département de Génie Chimique, École Polytechnique, Université de Montréal, Montréal, Québec

Received October 19, 1971

Liquid water at 25 °C has been treated as a semi-ideal solution of relatively very volatile unbonded monomer dissolved in non-volatile hydrogen-bonded solvent. A mole fraction of less than 0.0016 has been found for unbonded water, in agreement with Stevenson's conclusion.

La notion que l'eau à l'état liquide à 25 °C peut être assimilée à une solution semi-idéale de monomère d'eau relativement très volatil dissout dans des fractions d'espèces liées (par liaisons d'hydrogène) et non-volatiles donne une limite supérieure de 0.0016 à la fraction molaire d'eau monomérique. Ceci est en accord avec les conclusions de Stevenson.

Canadian Journal of Chemistry, **50**, 1088 (1972)

Various estimates of the fraction of non-hydrogen-bonded (or less hydrogen-bonded species in two-state models not invoking monomeric water as such) species in liquid water have been listed (1–6). These range from values over 0.5 to 0.06 (4) to the very low values of monomer mole fraction contended by Stevenson (5). Levine and Perram (6) have calculated the mole fraction of monomeric water, x, between 273 and 373 °K according to different statistical-mechanical postulates. Their values of x at 273 °K lie between 0.054 and 0.0008.

It is assumed that monomeric or non-hydrogen-bonded water, if it could exist independently of other more hydrogen-bonded water species, would exert a vapor pressure p_0^* at least as large as that of liquid H_2S at the same temperature. At 25 °C the vapor pressure of H_2S is 15×10^3 Torr (7); whence the virtual or hypothetical vapor pressure of unbonded H_2O, p_0^*, would be at least 15×10^3 Torr and probably appreciably higher, since H_2O is lighter than H_2S, and liquid H_2S may itself be hydrogen-bonded to some extent.

Consider liquid water to be a semi-ideal solution[1] in the Dolezalek–Scatchard sense comprised of a relatively very volatile unbonded water fraction, x, dissolved in a relatively involatile hydrogen-bonded water solvent. Then at a given temperature the observed solution vapor pressure, p, mainly due to unbonded water, will be given by

$$p = p_0^* x$$

with p_0^* evaluated at the same temperature. Hence at 25 °C,

$$23.8 = (15 \times 10^3) x_{max}$$

where x_{max} is the maximum possible value of x since p_0^* is higher than the minimum 15×10^3 Torr assumed, and some of the observed 23.8 Torr may be due to H_2O molecules with some little hydrogen-bonding. Thus $x_{max} = 0.0016$.

This low figure for the fraction of completely unbonded H_2O molecules in liquid water at 25 °C supports Stevenson's conclusions (5) and some of Levine and Perram's models (6).

[1]Stokes and Robinson (8, 9) have successfully treated concentrated water–sucrose solutions semi-ideally; Crisci and Lenzi (10) have also interpreted kinetic data in aqueous H_2SO_4 and $HClO_4$ solutions up to 6 M in similar fashion.

1. M. FALK and T. A. FORD. Can. J. Chem. **44**, 1699 (1966).
2. B. E. CONWAY. Ann. Rev. Phys. Chem. **17**, 481 (1966).
3. D. EISENBERG and W. KAUZMANN. The structure and properties of water. Oxford University Press. Oxford, England. 1969. p. 258.
4. O. D. BONNER and G. B. WOOLSEY. J. Phys. Chem. **72**, 899 (1968).
5. D. P. STEVENSON. J. Phys. Chem. **69**, 2145 (1965).
6. S. LEVINE and J. W. PERRAM. Hydrogen-bonded solvent systems. Taylor & Francis Ltd. 1968. p. 115.
7. Handbook of Chemistry (Lange). 8th ed. Handbook Publishers Inc. 1952. p. 1473.
8. R. H. STOKES and R. A. ROBINSON. J. Phys. Chem. **70**, 2126 (1966).
9. R. H. STOKES and R. A. ROBINSON. J. Phys. Chem. **74**, 4453 (1970).
10. P. CRISCI and F. LENZI. Can. J. Chem. **49**, 2552 (1971).

Synthesis and Kinetic Behavior of Some *trans*-Diacidotetraamminerhodium(III) Complexes

A. J. POË[1] AND M. V. TWIGG

Lash Miller Chemical Laboratories, University of Toronto, Toronto 181, Ontario

Received June 10, 1971

A greatly improved preparation of *trans*-dichlorotetraamminerhodium(III) chloride has been devised that makes use of *trans*-hydridoaquotetraamminerhodium(III) as an intermediate. The new complexes *trans*-$[Rh(NH_3)_4Br_2]Br$ and *trans*-$[Rh(NH_3)_4I_2]I$ have also been prepared. The kinetics of some reactions of the dichlorocomplex have been studied over a range of temperatures, and the rate parameters are compared with those for the reactions of the analogous *bis*ethylenediamine complex.

La préparation du chlorure du *trans*-dichlorotétraamminerhodium(III) a été très nettement améliorée par l'utilisation du *trans*-hydridoaquotétraamminerhodium(III) comme intermédiaire. Deux nouveaux complexes, le *trans*-$[Rh(NH_3)_4Br_2]Br$ et le *trans*-$[Rh(NH_3)_4I_2]I$ ont également été préparés. Les cinétiques de quelques réactions avec les complexes dichloro ont été étudiées sur une échelle de température et les paramètres de vitesse ont été comparés avec ceux pour les réactions de complexes analogues du *bis*éthylènediamine.

Canadian Journal of Chemistry, **50**, 1089 (1972)

Can. J. Chem. Downloaded from www.nrcresearchpress.com by 210.87.254.6 on 09/05/12
For personal use only.

The *trans*-diacido*bis*ethylenediaminerhodium(III) complexes can be prepared from $RhCl_3(H_2O)_3$ in moderately good yields by fairly straightforward methods (1, 2) and their kinetic and thermodynamic behavior has received detailed study (3, 4). By contrast, similar methods lead to yields as low as 7% when applied to the tetraammine analogues and very little is known of their behavior (2, 3).

Convenient reactions, involving hydride catalysis (5), lead to the production of *trans*-$[RhL_4Cl_2]^+$ in high yields when L = pyridine or substituted pyridines ($pK_a = ca.\ 5$), but this method does not work when L is a more basic ligand such as ammonia ($pK_a = 9$) because unreactive "rhodium hydroxide" is precipitated. However, salts of $[Rh(NH_3)_5H]^{2+}$ have recently been isolated (6) and, while they are stable in ammoniacal solution, the strong *trans*- labilizing effect of the hydride ion is demonstrated by the existence of the equilibrium

$$[Rh(NH_3)_5H]^{2+} + H_2O \rightleftharpoons [Rh(NH_3)_4(OH_2)H]^{2+} + NH_3$$

In this note we describe the use of $[Rh(NH_3)_5H]^{2+}$ as an intermediate in the preparation, in high yield, of the *trans*-dichlorotetraamminerhodium(III) complex as the chloride or perchlorate salt. This complex is a convenient starting point for the preparation of a wide variety of new *trans*-tetraamminerhodium(III) complexes. We have used it to prepare the new bromo and iodo analogues, and have also studied the temperature dependence of the kinetics of some of its reactions in order to compare its behavior with the corresponding *bis*ethylenediamine complex.

[1]To whom all correspondence should be addressed.

Experimental

A solution of the hydridopentaamminerhodium(III) complex was prepared by treating a suspension of $[Rh(NH_3)_5Cl]Cl_2$ (Johnson Matthey and Co. Ltd.) (0.92 g) in aqueous ammonia (2.3 ml concentrated ammonia in 3.0 ml water) with zinc dust (0.8 g) for 3.5 min at 50°. After removal of the excess of zinc and a little precipitated rhodium metal by filtration through sintered glass, the very pale yellow solution of hydridopentaammine was chilled in ice and made slightly acid (pH 6–7) by cautious addition of concentrated hydrochloric acid. This solution was warmed at 35° for 1 min, when a small amount of a dark precipitate formed. After chilling in ice and adding potassium chloride (1 g), the solution was made strongly acid ($pH \leq 1$) with concentrated hydrochloric acid. Hydrogen peroxide (0.5 ml 30%) was quickly added and a small amount of a yellow precipitate formed. The mixture was transferred to a beaker and boiled for 30 min with dilute hydrochloric acid (30 ml, 5 *M*) and filtered. A golden yellow precipitate formed and was collected and washed with ice cold water on a filter, the product being dried over 'Drierite'. Yield 0.66 g (76%).

Anal. Calcd. for $[Rh(NH_3)_4Cl_2]Cl$: N, 20.2; Cl, 38.3. Found: N, 20.4; Cl, 38.2.[2]

Recrystallization from sodium perchlorate solution led to the corresponding perchlorate salt.

Anal. Calcd. for $[Rh(NH_3)_4Cl_2]ClO_4$: N, 16.4; Cl, 31.2. Found: N, 16.2; Cl, 31.0.

trans-Dibromotetraamminerhodium(III) Bromide

A solution of *trans*-$[Rh(NH_3)_4Cl_2]Cl$ (0.23 g) and sodium bromide (1 g) in water (50 ml) was boiled for 20 min. The

[2]Analyses by Alfred Bernhardt, 5251 Elbach über Engelskirchen, West Germany.

TABLE 1. Electronic absorption spectra of $[Rh(NH_3)_4X_2]^+$ and *trans*-$[Rh(en)_2X_2]^+$

	$[Rh(NH_3)_4X_2]X$		*trans*-$[Rh(en)_2X_2]ClO_4$	
X	λ (nm)	ε (cm^{-1} l mol^{-1})	λ (nm)	ε (cm^{-1} l mol^{-1})
Cl	415	74	407[a]	75[a]
	293	85	286[a]	125[a]
	209	3.2×10^4	—	—
	412[b]	66[b]	—	—
Br	441	111	425[a]	120[a]
	ca. 280(sh)	*ca.* 2.7×10^3	276[a]	3.0×10^3[a]
	236	2.7×10^4	231[a]	*ca.* 3.1×10^4[a]
I	471	288	462[c]	260[c]
	340	1.24×10^4	340[c]	1.43×10^4[c]
	271	2.45×10^4	269[c]	3.10×10^4[c]
	221	2.78×10^4	222[c]	2.00×10^4[c]

[a]Reference 13.
[b]Reference 1.
[c]Reference 14.

solution darkened from yellow to orange whereupon another portion of sodium bromide (1 g) was added and the solution boiled for a further 4 h. On standing, the cooled solution (20 ml) deposited orange crystals of *trans*-$[Rh(NH_3)_4Br_2]Br$ and this was filtered on a sinter, washed with a little ice cold water, and dried over 'Drierite'. Yield, 0.22 g (65%).

Anal. Calcd. for $[Rh(NH_3)_4Br_2]Br$: N, 13.6; Br, 58.4. Found: N, 13.7; Br, 58.2.

trans-Diiodotetraamminerhodium(III) Iodide

(*a*) The procedure used for preparing the dibromo complex was followed exactly but with sodium iodide replacing sodium bromide. A dark red precipitate formed after the first period of boiling and increased in amount during the longer period of boiling. It did not dissolve after boiling the diluted reaction mixture (300 ml for 30 min) and it was collected on a sinter, washed well with water, and air dried. Analysis showed it to be $Rh(NH_3)_3I_3$. Yield, 0.13 g (28.8%).

Anal. Calcd. for $Rh(NH_3)_3I_3$: N, 7.86; I, 71.2. Found: N, 8.02; I, 71.1.

The filtrate was concentrated to *ca.* 25 ml and the red-brown crystals of *trans*-$[Rh(NH_3)_4I_2]I$ filtered off, washed with a little ice cold water, and dried over 'Drierite'. Yield, 0.21 g (71.1%).

Anal. Calcd. for $[Rh(NH_3)_4I_2]I$: N, 10.2; I, 69.0. Found: N, 10.4; I, 68.8.

(*b*) A solution of *trans*-$[Rh(NH_3)_4Cl_2]Cl$ (0.046 g) and sodium iodide (0.4 g) in water (8 ml) was heated to 90° in a foil-wrapped test tube for 3.5 h. The crystals of $[Rh(NH_3)_4I_2]I$ that formed on cooling were filtered off, recrystallized from a dilute solution of sodium iodide, and finally washed with ice cold water and dried over 'Drierite'. Yield, 0.065 g (71%). All of the product was soluble in water and the electronic absorption spectrum was identical with the analyzed product formed in (*a*) above.

Electronic Absorption Spectra

Spectra were measured with Cary 16 and Perkin–Elmer 402 spectrophotometers and the main features are reported in Table 1, together with previously reported spectra for the analogous ethylenediamine complexes.

Kinetics of Reactions of trans-$[Rh(NH_3)_4Cl_2]^+$

The reactions with bromide and iodide were followed spectrophotometrically, by means of a Perkin–Elmer 402 spectrophotometer, at 270 and 344 nm, respectively, absorbance changes of *ca.* one unit being observed during the course of the reactions. When the reaction with bromide was followed by scanning the complete spectrum repeatedly, isosbestic points at 417 and 376 nm were observed. The ionic strength was controlled by the concentration of sodium bromide or iodide used.

Results are shown in Table 2 together with activation parameters calculated by a least squares procedure in which all rate constants, including those from ref. 3, were assumed to have the same % of uncertainty. The uncertainties quoted are standard deviations after appropriate allowance for the number of degrees of freedom so that 95% confidence limits can be obtained by doubling the standard deviations. Corresponding parameters for the reactions of the analogous ethylenediamine complex were similarly estimated by combining the results in refs. 3 and 7 (Table 2).

Discussion

The preparation of the dichlorotetraammine-rhodium(III) complex depends on the formation of *trans*-$[Rh(NH_3)_4(H_2O)H]^{2+}$ on careful warming of a neutral or very slightly acid solution of $[Rh(NH_3)_5H]^{2+}$. Simple addition of chloride to aqueous solutions of $[Rh(NH_3)_5H]^{2+}$ leads to some reduction to metallic rhodium (8) and we find that addition of chloride to the hydridoaquo complex leads to extensive reduction. However, if acid peroxide solution is added quickly to a fresh solution of hydridoaquo complex, reduction does not occur and good yields of the dichloro substitution product are obtained. It seems possible that the substitution

Can. J. Chem. Downloaded from www.nrcresearchpress.com by 210.87.254.6 on 09/05/12
For personal use only.

TABLE 2. Rate data for the reactions: *trans*-$[Rh\ A_4\ Cl_2]^+ \xrightarrow{X^-}$ *trans*-$[Rh\ A_4\ X_2]^+$

	A = NH_3				A_2 = en		
X	[NaX][a] (M)	Temperature (°C)	$10^5 k_{obs}$ (s^{-1})	X	[NaX][a] (M)	Temperature (°C)	$10^5 k_{obs}$ (s^{-1})
Br	0.1	92.5	28.9	I[c]	0.10	90.0	10.9
		88.1	18.8	OH^b	$pH = 8.9$	90	11.6
		84.3	14.0	I[c]	0.10	80.0	4.20
	0.05	82.6	11.4	OH^b	$pH = 9.9$	80	4.4
OH^b	$pH = 8.9$	80	8.5	OH	$pH = 9.9$	80	4.4
	$pH = 9.9$	80	8.9		$pH = 8.9$	80	4.2
	$pH = 12.7$	80	8.6	I[c]	0.10	75.0	2.50
Br	0.1	79.8	8.16			70.0	1.36
		74.7	5.00	OH^b	$pH = 8.9$	70	1.5
I	0.1	73.3	4.46				
Br	0.1	68.6	2.70				
$\Delta H^\ddagger = 24.11 \pm 0.39$ kcal mol^{-1}				$\Delta H^\ddagger = 24.81 \pm 0.56$ kcal mol^{-1}			
$\Delta S^\ddagger = -9.2 \pm 1.1$ cal mol^{-1} deg^{-1}				$\Delta S^\ddagger = -8.7 \pm 1.6$ cal mol^{-1} deg^{-1}			
$\sigma_k = \pm 3.3\%$				$\sigma_k = \pm 4.7\%$			

[a]Equal to ionic strength.
[b]Reference 3, ionic strength variable.
[c]Reference 7.

process occurs via reduction to an unstable $[Rh(NH_3)_4]^+$ intermediate which undergoes rapid *trans* oxidative addition by chlorine from the strongly oxidizing $HCl–H_2O_2$ mixture.

Reaction of the *trans*-dichloro complex with bromide presumably occurs via a simple aquation process, and this is confirmed by the kinetic behavior (*vide infra*). Reaction with iodide in the light produces the neutral complex $Rh(NH_3)_3I_3$ in addition to the *trans*-diiodo complex, but this does not occur in the dark. Reactions of diacido*bis*ethylenediaminerhodium(III) complexes are known to be light catalyzed (9) and it has recently been shown (10) that irradiation of $Rh(NH_3)_5I^{2+}$ produces aquated iodoamminerhodium(III) complexes. Normal laboratory light is evidently inducing similar photochemical replacement of ammonia in our systems.

The electronic spectra of aqueous solutions of the $[Rh(NH_3)_4X_2]^+$ complexes (X = Cl, Br, I) are very similar to those of the known *trans*-$[Rh(en)_2X_2]^+$ analogues, and this confirms our assignment of a *trans*-configuration to the tetraammine complexes. In each case the position of the lowest energy transition in the visible or near u.v. region of the spectrum indicates, as expected (11), that the rhodium in the ethylenediamine complexes experiences a slightly larger ligand field than that in the corresponding ammine complex.

As with its *bis*ethylenediamine analogue (1, 7) the rates of reaction of the *trans*-dichlorotetraammine complex are unaffected by the nature or concentration of the ligand which eventually replaces the coordinated chloride, or by the ionic strength to the extent that that was varied. No intermediate mixed complexes are seen, and there is no sign of any *trans* → *cis* isomerization.

The rate of aquation of the *trans*-$[Rh(NH_3)_4Cl_2]^+$ is about twice that of *trans*-$[Rh(en)_2Cl_2]^+$ at all the temperatures used. Similar behavior has been found for analogous cobalt(III) complexes where rates decrease with increasing numbers of chelate rings. This is consistent with smaller hydration energies of more highly chelated complexes, and a consequent smaller gain in hydration energies during the charge separation as the chloride leaves the complex. It is also consistent with the greater loss of ligand field stabilization energy expected for complexes containing more highly alkylated amines (12). However, $[Rh(NH_3)_5OH_2]^{3+}$ undergoes anation by chloride almost twice as slowly as does *trans*-$[Rh(en)_2(NH_3)OH_2]^{3+}$ under similar conditions (4). Since the effect of L.F.S.E. should be the

Can. J. Chem. Downloaded from www.nrcresearchpress.com by 210.87.254.6 on 09/05/12
For personal use only.

same for anation and aquation reactions this suggests that solvation is the more important factor, there being a *decrease* in solvation on forming the transition state in anation reactions. $\Delta H^{\ddagger}$ for *trans*-$[Rh(en)_2Cl_2]^+$ should, therefore, be higher than $\Delta H^{\ddagger}$ for *trans*-$[Rh(NH_3)_4Cl_2]^+$. The observed difference of 0.70 ± 0.69 kcal mol^{-1} allows this although the precision is unfortunately not sufficient to confirm it.

The authors are grateful to the National Research Council of Canada for partial support of this work.

1. S. A. JOHNSON and F. BASOLO. Inorg. Chem. **1**, 925 (1962).
2. S. A. ANDERSON and F. BASOLO. Inorg. Syn. **7**, 214 (1963).
3. S. A. JOHNSON, F. BASOLO, and R. G. PEARSON. J. Am. Chem. Soc. **85**, 1741(1963).
4. A. J. POË and K. SHAW. J. Chem. Soc. A, 393 (1970).
5. R. D. GILLARD, J. A. OSBORN, and G. WILKINSON. J. Chem. Soc. 1951 (1965).
6. K. THOMAS, J. A. OSBORN, A. R. POWELL, and G. WILKINSON. J. Chem. Soc. A, 1801 (1968).
7. H. L. BOTT, E. J. BOUNSALL, and A. J. POË. J. Chem. Soc. A, 1275 (1966).
8. K. THOMAS and G. WILKINSON. J. Chem. Soc. A, 356 (1970).
9. R. A. BAUER and F. BASOLO. J. Am. Chem. Soc. **90**, 2437 (1968).
10. T. KELLY and J. F. ENDICOTT. J. Am. Chem. Soc. **92**, 5733 (1970).
11. C. K. JØRGENSEN. Absorption spectra and chemical bonding in complexes. Pergamon Press, London. 1962. Chapt. 7.
12. F. BASOLO and R. G. PEARSON. Mechanisms of inorganic reactions. 2nd ed. John Wiley and Sons, Inc., New York. 1967. pp. 159–161.
13. H. L. BOTT and A. J. POË. J. Chem. Soc. 5931 (1965).
14. E. J. BOUNSALL and A. J. POË. J. Chem. Soc. A, 286 (1966).

Epimerization of Monosaccharides in Acetic Acid and Acetic Anhydride. Synthesis of D-Altrose

WALTER SOWA
Department of Organic Chemistry, Ontario Research Foundation, Sheridan Park, Ontario

Received November 25, 1971

Acetolysis of 1,2;5,6-di-*O*-isopropylidene-α-D-allofuranose occurred with inversion at C-2 in a medium composed of acetic acid, acetic anhydride, and sulfuric acid. D-Altrose was isolated in 45% yield by deacetylation and chromatographic separation of the mixture of products. Unsubstituted D-allose did not epimerize under the same reaction conditions.

L'acétolyse du 1,2;5,6-di-*O*-isopropylidène-α-D-allofuranose se produit avec une inversion en C-2 dans un milieu composé d'acide et d'anhydride acétiques et d'acide sulfurique. On isole le D-altrose avec un rendement de 45% par la désacétylation et la séparation chromatographique du mélange de produits. Le D-allose non-substitué ne s'est pas épimérisé dans les mêmes conditions de réaction.

Canadian Journal of Chemistry, **50**, 1092 (1972)

There are a number of routes to the altrose configuration of carbohydrates (1). The most practical preparation of D-altrose currently employed involves the reaction sequence methyl 4,6-*O*-benzylidene-α-D-glucopyranoside, methyl 4,6-*O*-benzylidene-2,3-di-*O*-*p*-tolysulfonyl-α-D-glucopyranoside, methyl 2,3-anhydro-4,6-*O*-benzylidene-α-D-allopyranoside, methyl 4,6-*O*-benzylidene-α-D-altropyranoside, α-D-altropyranose pentaacetate, β-D-altrose (2). The present report describes a simple procedure for the preparation of D-altrose on a small scale. It consists of acetolysis of 1,2;5,6-di-*O*-isopropylidene-α-D-allofuranose, deacetylation of the reaction mixture, and chromatographic separation of the products, D-allose and D-altrose. The isomerization bears some resemblance to the neolactose synthesis of Hudson and co-workers (*cf.* 1) in which the D-glucose moiety of lactose octaacetate is converted to D-altrose under the influence of aluminum trichloride and phosphorus pentachloride in chloroform. The synthesis from 1,2;5,6-di-*O*-isopropylidene-α-D-allofuranose is based on

Can. J. Chem. Downloaded from www.nrcresearchpress.com by 210.87.254.6 on 09/05/12
For personal use only.

same for anation and aquation reactions this suggests that solvation is the more important factor, there being a *decrease* in solvation on forming the transition state in anation reactions. $\Delta H^{\ddagger}$ for *trans*-$[Rh(en)_2Cl_2]^+$ should, therefore, be higher than $\Delta H^{\ddagger}$ for *trans*-$[Rh(NH_3)_4Cl_2]^+$. The observed difference of 0.70 ± 0.69 kcal mol^{-1} allows this although the precision is unfortunately not sufficient to confirm it.

The authors are grateful to the National Research Council of Canada for partial support of this work.

1. S. A. JOHNSON and F. BASOLO. Inorg. Chem. **1**, 925 (1962).
2. S. A. ANDERSON and F. BASOLO. Inorg. Syn. **7**, 214 (1963).
3. S. A. JOHNSON, F. BASOLO, and R. G. PEARSON. J. Am. Chem. Soc. **85**, 1741(1963).
4. A. J. POË and K. SHAW. J. Chem. Soc. A, 393 (1970).
5. R. D. GILLARD, J. A. OSBORN, and G. WILKINSON. J. Chem. Soc. 1951 (1965).
6. K. THOMAS, J. A. OSBORN, A. R. POWELL, and G. WILKINSON. J. Chem. Soc. A, 1801 (1968).
7. H. L. BOTT, E. J. BOUNSALL, and A. J. POË. J. Chem. Soc. A, 1275 (1966).
8. K. THOMAS and G. WILKINSON. J. Chem. Soc. A, 356 (1970).
9. R. A. BAUER and F. BASOLO. J. Am. Chem. Soc. **90**, 2437 (1968).
10. T. KELLY and J. F. ENDICOTT. J. Am. Chem. Soc. **92**, 5733 (1970).
11. C. K. JØRGENSEN. Absorption spectra and chemical bonding in complexes. Pergamon Press, London. 1962. Chapt. 7.
12. F. BASOLO and R. G. PEARSON. Mechanisms of inorganic reactions. 2nd ed. John Wiley and Sons, Inc., New York. 1967. pp. 159–161.
13. H. L. BOTT and A. J. POË. J. Chem. Soc. 5931 (1965).
14. E. J. BOUNSALL and A. J. POË. J. Chem. Soc. A, 286 (1966).

Epimerization of Monosaccharides in Acetic Acid and Acetic Anhydride. Synthesis of D-Altrose

WALTER SOWA

Department of Organic Chemistry, Ontario Research Foundation, Sheridan Park, Ontario

Received November 25, 1971

Acetolysis of 1,2;5,6-di-*O*-isopropylidene-α-D-allofuranose occurred with inversion at C-2 in a medium composed of acetic acid, acetic anhydride, and sulfuric acid. D-Altrose was isolated in 45% yield by deacetylation and chromatographic separation of the mixture of products. Unsubstituted D-allose did not epimerize under the same reaction conditions.

L'acétolyse du 1,2;5,6-di-*O*-isopropylidène-α-D-allofuranose se produit avec une inversion en C-2 dans un milieu composé d'acide et d'anhydride acétiques et d'acide sulfurique. On isole le D-altrose avec un rendement de 45% par la désacétylation et la séparation chromatographique du mélange de produits. Le D-allose non-substitué ne s'est pas épimérisé dans les mêmes conditions de réaction.

Canadian Journal of Chemistry, **50**, 1092 (1972)

There are a number of routes to the altrose configuration of carbohydrates (1). The most practical preparation of D-altrose currently employed involves the reaction sequence methyl 4,6-*O*-benzylidene-α-D-glucopyranoside, methyl 4,6-*O*-benzylidene-2,3-di-*O*-*p*-tolysulfonyl-α-D-glucopyranoside, methyl 2,3-anhydro-4,6-*O*-benzylidene-α-D-allopyranoside, methyl 4,6-*O*-benzylidene-α-D-altropyranoside, α-D-altropyranose pentaacetate, β-D-altrose (2). The present report describes a simple procedure for the preparation of D-altrose on a small scale. It consists of acetolysis of 1,2;5,6-di-*O*-isopropylidene-α-D-allofuranose, deacetylation of the reaction mixture, and chromatographic separation of the products, D-allose and D-altrose. The isomerization bears some resemblance to the neolactose synthesis of Hudson and co-workers (*cf.* 1) in which the D-glucose moiety of lactose octaacetate is converted to D-altrose under the influence of aluminum trichloride and phosphorus pentachloride in chloroform. The synthesis from 1,2;5,6-di-*O*-isopropylidene-α-D-allofuranose is based on

Can. J. Chem. Downloaded from www.nrcresearchpress.com by 210.87.254.105 on 09/05/12
For personal use only.

Can. J. Chem. Downloaded from www.nrcresearchpress.com by 210.87.254.105 on 09/05/12
For personal use only.

the observation that monosaccharides with a *cis*-configuration at C-2 and -3 generally form a mixture of C-2 epimers in an acetolysis medium containing a high concentration of acetic acid (*ca.* 90%) (3). This *cis* to *trans* conversion was first noted by Jerkeman with D-mannofuranose derivatives (4).

1,2;5,6-Di-*O*-isopropylidene-α-D-allofuranose is readily available by oxidation of 1,2;5,6-di-*O*-isopropylidene-α-D-glucofuranose with dimethyl sulfoxide–acetic anhydride (5) followed by borohydride reduction of the intermediate keto-sugar (6). The D-allose derivative was treated at room temperature with an approximately 9:1 mixture of acetic acid and acetic anhydride containing sulfuric acid. After the reaction had proceeded for 24 h, the mixture was worked-up, deacetylated with triethylamine, and chromatographed on paper to obtain D-altrose in 45% yield. The ratio of D-altrose to D-allose, as estimated by preparative paper chromatography, was 1.4 to 1. With a longer reaction time of 89 h, the results were virtually unchanged; the yield of D-altrose was 41% and the D-altrose to D-allose ratio was 1.3 to 1. The high conversion of 1,2;5,6-di-*O*-isopropylidene-α-D-allofuranose to D-altrose supports the suggestion that the acetolysis-inversion reaction occurs via the furanose form of a monosaccharide in which a *cis*-orientation of groups is capable of assuming a *trans*-orientation through acetoxonium ion intermediates (3, 4).

Previous work has demonstrated that some unsubstituted pyranose sugars are transformed into their C-2 epimers by the "epimerization" mixture. Thus D-mannose gave D-glucose and D-mannose in 0.3 to 1 ratio while D-ribose yielded a 0.85 to 1 mixture of D-arabinose and D-ribose (3). When D-allose was treated in the same manner, only a trace amount of D-altrose was detected by paper chromatography. It is possible that the lack of reactivity shown by free D-allose is due to acetylation of the sugar in the pyranose form before significant tautomerization to the furanose form can occur.

Experimental

General

Melting points were determined on a Fisher–Johns melting point apparatus and are uncorrected. Optical rotations were obtained with a Carl Zeiss photoelectric polarimeter Model 0.005° equipped with a sodium spectral light source. Chromatographic mobilities are quoted relative to D-glucose (R_G). Visualization reagents for paper chromatography were *p*-anisidine hydrochloride (7) and silver nitrate – sodium hydroxide (8).

Acetolysis of 1,2;5,6-Di-O-isopropylidene-α-D-allofuranose

1,2;5,6-Di-*O*-isopropylidene-α-D-allofuranose was prepared from 1,2;5,6-di-*O*-isopropylidene-α-D-glucofuranose by the dimethyl sulfoxide – acetic anhydride and borohydride route described previously (5) except that the intermediate 1,2;5,6-di-*O*-isopropylidene-α-D-*ribo*-3-hexulofuranose was crystallized as the hydrate (6, 9) to avoid chromatographic isolation of the product. Sulfuric acid (1.5 ml) was added to a stirred and cooled solution of the di-*O*-isopropylidene-D-allose (1.4 g) in acetic acid (30 ml) and acetic anhydride (4 ml). After 24 h at room temperature, the reaction mixture was poured into ice and water and the solution was extracted with chloroform. The chloroform extract was washed with saturated sodium bicarbonate solution and water, dried (Na_2SO_4), and evaporated to a syrup. This was deacetylated overnight in a mixture of methanol (20 ml), water (2.5 ml), and triethylamine (2.5 ml). The resulting mixture was evaporated to a syrup (0.945 g), one-half of which was separated on a sheet of Whatman 3MM paper (46 × 57 cm) in ethyl acetate – pyridine – water (8:2:1 v/v) to obtain D-allose (153 mg), $[\alpha]_D^{24}$ + 16.3° (*c* 4.6 in water), and D-altrose (216 mg), $[\alpha]_D^{24}$ +32.8° (*c* 3.5 in water). Reported specific rotations for D-allose and D-altrose are $[\alpha]_D^{20}$ +14° (*c* 1.3 in water) (10) and $[\alpha]_D^{20}$ +33° (*c* 4 in water) (2), respectively. The respective R_G values on Whatman No. 4 paper were 1.3 and 2.3. The D-altrose was characterized as its dibenzyl dithioacetal. The syrup (125 mg) was treated with trifluoroacetic acid (1.25 ml) and toluenethiol (0.125 ml) at room temperature for 5 h, the reaction mixture was evaporated to dryness, and the residue recrystallized from ethyl acetate and petroleum ether. The thioacetal had m.p. 119–120° and $[\alpha]_D^{24}$ + 39.8° (*c* 1.75 in pyridine). Literature values are m.p. 121–122° and $[\alpha]_D^{20}$ +39° (*c* 3 in pyridine) (2).

The recovered D-allose was characterized as the *p*-bromophenylhydrazone, m.p. 145–146°, reported value 145–147° (10). Another useful derivative of D-allose is the dibenzyl dithioacetal, prepared as above and crystallized from ethyl acetate. It has m.p. 108–109° and $[\alpha]_D^{24}$ −37.8° (*c* 0.4 in methanol).

Anal. Calcd. for $C_{20}H_{26}O_5S_2$: C, 58.51; H, 6.38; S, 15.63. Found: C, 58.44; H, 6.25; S, 15.41.

An acetolysis of 1,2;5,6-di-*O*-isopropylidene-α-D-allose was carried out for 89 h with other conditions unchanged. The dark-colored solution, after work-up, showed the presence of only D-allose and D-altrose by chromatographic examination. Preparative paper chromatography as before gave D-altrose in 41% yield and a 1.3 to 1 ratio of D-altrose to D-allose.

A sample of free D-allose (syrup, 500 mg) was treated with a mixture of acetic acid – acetic anhydride – sulfuric acid (15:2:0.75 v/v) for 24 h. After work-up of the reaction mixture in the usual manner, only a trace of D-altrose was detectable chromatographically.

The author is grateful to Mrs. Brigitte Licht for valuable technical assistance. The work was made possible by funds received from the Province of Ontario through the Department of Trade and Development.

1. N. K. RICHTMYER. Adv. Carbohydr. Chem. **1**, 37 (1945).
2. N. K. RICHTMYER. *In* Methods in carbohydrate chemistry. Vol. I. Academic Press, Inc., New York, N.Y. 1962. p. 107.
3. W. SOWA. Can. J. Chem. **49**, 3292 (1971).
4. P. JERKEMAN. Acta Chem. Scand. **17**, 2769 (1963).
5. W. SOWA and G. H. S. THOMAS. Can. J. Chem. **44**, 836 (1966).
6. O. THEANDER. Acta Chem. Scand. **18**, 2209 (1964).
7. L. HOUGH, J. K. N. JONES, and W. H. WADMAN. J. Chem. Soc. 1702 (1950).
8. W. E. TREVELYAN, D. P. PROCTER, and J. S. HARRISON. Nature, **166**, 444 (1950).
9. P. J. BEYNON, P. M. COLLINS, P. T. DOGANGES, and W. G. OVEREND. J. Chem. Soc. C, 1131 (1966).
10. F. L. HUMOLLER. *In* Methods in carbohydrate chemistry. Vol. I. Academic Press, Inc., New York, N.Y. 1962. p. 102.

Can. J. Chem. Downloaded from www.nrcresearchpress.com by 210.87.254.105 on 09/05/12
For personal use only.

Isothermal Compressibilities of Aqueous Solutions of Tetraalkylammonium Bromides

J. E. DESNOYERS AND P. R. PHILIP
Department of Chemistry, Université de Sherbrooke, Sherbrooke, Quebec

Received November 3, 1971

The standard isothermal apparent molal compressibilities, ϕ_K^0, of tetraalkylammonium bromides in water at 25° were calculated from known standard apparent molal adiabatic compressibilities, ϕ_{Ks}^0, expansitivites, ϕ_E^0, and heat capacities, ϕ_c^0. ϕ_K^0 is significantly different from ϕ_{Ks}^0 and depends mostly on the extrapolation procedure used to obtain ϕ_{Ks}^0 and on the precision of ϕ_E^0.

Les compressibilités isothermes apparentes molaires à l'état standard, ϕ_K^0, des bromures de tétraalkoylammonium dans l'eau à 25 °C ont été calculées à partir des valeurs apparentes molaires standards des compressibilités adiabatiques, ϕ_{Ks}^0, des expansitivités, ϕ_E^0, et des capacités calorifiques, ϕ_c^0. ϕ_K^0 diffère de façon appréciable de ϕ_{Ks}^0 et depend principalement de l'incertitude sur ϕ_E^0 et de la méthode d'extrapolation pour obtenir ϕ_{Ks}^0.

Canadian Journal of Chemistry, **50**, 1094 (1972)

The apparent molal volume ϕ_V of solutes is a useful function to characterize solute–solvent (1) and solute–solute interactions (2), especially with structured solvents like water. However, any interpretation of ϕ_V^0, the standard apparent molal volume at infinite dilution, must rely on some semi-empirical estimate of the intrinsic volume (1). In this respect, the study of the standard apparent molal expansitivities ϕ_E^0 or compressibilities ϕ_K^0 are most useful: if the ions are considered incompressible spheres, ϕ_E^0 and ϕ_K^0 depend only on ion–solvent interactions. For this reason, many recent studies (3–7) have been made on the compressibility of aqueous solutions.

It is not always easy to measure directly isothermal compressibilities β from which ϕ_K can be derived. Precise adiabatic compressibilities β_s are, on the other hand, easily accessible from sound velocity measurements (3), and they can be converted to isothermal compressibilities (in bars^{-1}) with the relation

$$[1] \qquad \delta = \beta - \beta_s = \frac{\alpha^2 T}{\sigma}$$

where α is the coefficient of thermal expansion (K^{-1}) and σ is the volumetric specific heat ($JK^{-1}\ cm^{-3}$). Unfortunately, α and σ are not always available as a function of concentration and the difference δ is often ignored in the interpretation of aqueous solutions. With alkali halides, δ is in fact small ($\sim 1\%$ of β), but this is not so with large organic salts like tetrabutylammonium bromide where Garnsey *et al.* (6) have shown that δ leads to differences between the isothermal and adiabatic apparent molal compressibilities, $\phi_K - \phi_{Ks}$, that are far from being negligible.

Precise heat capacity measurements of aqueous tetraalkylammonium bromides are now

1. N. K. RICHTMYER. Adv. Carbohydr. Chem. **1**, 37 (1945).
2. N. K. RICHTMYER. *In* Methods in carbohydrate chemistry. Vol. I. Academic Press, Inc., New York, N.Y. 1962. p. 107.
3. W. SOWA. Can. J. Chem. **49**, 3292 (1971).
4. P. JERKEMAN. Acta Chem. Scand. **17**, 2769 (1963).
5. W. SOWA and G. H. S. THOMAS. Can. J. Chem. **44**, 836 (1966).
6. O. THEANDER. Acta Chem. Scand. **18**, 2209 (1964).
7. L. HOUGH, J. K. N. JONES, and W. H. WADMAN. J. Chem. Soc. 1702 (1950).
8. W. E. TREVELYAN, D. P. PROCTER, and J. S. HARRISON. Nature, **166**, 444 (1950).
9. P. J. BEYNON, P. M. COLLINS, P. T. DOGANGES, and W. G. OVEREND. J. Chem. Soc. C, 1131 (1966).
10. F. L. HUMOLLER. *In* Methods in carbohydrate chemistry. Vol. I. Academic Press, Inc., New York, N.Y. 1962. p. 102.

Can. J. Chem. Downloaded from www.nrcresearchpress.com by 210.87.254.42 on 09/05/12
For personal use only.

Isothermal Compressibilities of Aqueous Solutions of Tetraalkylammonium Bromides

J. E. DESNOYERS AND P. R. PHILIP
Department of Chemistry, Université de Sherbrooke, Sherbrooke, Quebec

Received November 3, 1971

The standard isothermal apparent molal compressibilities, ϕ_K^0, of tetraalkylammonium bromides in water at 25° were calculated from known standard apparent molal adiabatic compressibilities, ϕ_{Ks}^0, expansitivites, ϕ_E^0, and heat capacities, ϕ_c^0. ϕ_K^0 is significantly different from ϕ_{Ks}^0 and depends mostly on the extrapolation procedure used to obtain ϕ_{Ks}^0 and on the precision of ϕ_E^0.

Les compressibilités isothermes apparentes molaires à l'état standard, ϕ_K^0, des bromures de tétraalkoylammonium dans l'eau à 25 °C ont été calculées à partir des valeurs apparentes molaires standards des compressibilités adiabatiques, ϕ_{Ks}^0, des expansitivités, ϕ_E^0, et des capacités calorifiques, ϕ_c^0. ϕ_K^0 diffère de façon appréciable de ϕ_{Ks}^0 et depend principalement de l'incertitude sur ϕ_E^0 et de la méthode d'extrapolation pour obtenir ϕ_{Ks}^0.

Canadian Journal of Chemistry, **50**, 1094 (1972)

The apparent molal volume ϕ_V of solutes is a useful function to characterize solute–solvent (1) and solute–solute interactions (2), especially with structured solvents like water. However, any interpretation of ϕ_V^0, the standard apparent molal volume at infinite dilution, must rely on some semi-empirical estimate of the intrinsic volume (1). In this respect, the study of the standard apparent molal expansitivities ϕ_E^0 or compressibilities ϕ_K^0 are most useful: if the ions are considered incompressible spheres, ϕ_E^0 and ϕ_K^0 depend only on ion–solvent interactions. For this reason, many recent studies (3–7) have been made on the compressibility of aqueous solutions.

It is not always easy to measure directly isothermal compressibilities β from which ϕ_K can be derived. Precise adiabatic compressibilities β_s are, on the other hand, easily accessible from sound velocity measurements (3), and they can be converted to isothermal compressibilities (in bars^{-1}) with the relation

$$[1] \qquad \delta = \beta - \beta_s = \frac{\alpha^2 T}{\sigma}$$

where α is the coefficient of thermal expansion (K^{-1}) and σ is the volumetric specific heat ($JK^{-1}\ cm^{-3}$). Unfortunately, α and σ are not always available as a function of concentration and the difference δ is often ignored in the interpretation of aqueous solutions. With alkali halides, δ is in fact small ($\sim 1\%$ of β), but this is not so with large organic salts like tetrabutylammonium bromide where Garnsey *et al.* (6) have shown that δ leads to differences between the isothermal and adiabatic apparent molal compressibilities, $\phi_K - \phi_{Ks}$, that are far from being negligible.

Precise heat capacity measurements of aqueous tetraalkylammonium bromides are now

TABLE 1. Standard apparent molal isothermal compressibilities of tetraalkylammonium bromides in water at 25 °C

Salt	ϕ_E^0 ($cm^3\ K^{-1}\ mol^{-1}$)	ϕ_c^0 ($JK^{-1}\ mol^{-1}$)	$\phi_{Ks}^0 \times 10^4$ ($cm^3\ bar^{-1}\ mol^{-1}$)	$\frac{2\delta_0}{\alpha_0}\phi_E^0 \times 10^4$	$\frac{\delta_0}{\sigma_0}\phi_c^0 \times 10^4$	$\phi_K^0 \times 10^4$ ($cm^3\ bar^{-1}\ mol^{-1}$)
Me_4NBr	0.111	109	−7.1	4.1	0.12	−3.1
Et_4NBr	0.132	388	−8.2	4.9	0.44	−3.7
n-Pr_4NBr	0.173	789	−11.8	6.4	0.89	−6.3
n-Bu_4NBr	0.255	1210	−23.3	9.5	1.37	−15.2
Ref.	9, 10	8	5			

available (8). Therefore, in view of the importance of these salts in the understanding of structural hydration effects, we have attempted to calculate the standard ϕ_K^0 from the available ϕ_{Ks}^0 (5, 6).

A simple relation between ϕ_K and ϕ_{Ks} can be derived if eq. 1 is combined with the basic apparent molal quantities (3)

$$[2] \qquad \phi_V = \frac{1000}{cd_0}(d_0 - d) + \frac{M}{d_0}$$

$$[3] \qquad \phi_E = \frac{1000}{c}(\alpha - \alpha_0) + \alpha_0\phi_V$$

$$[4] \qquad \phi_K = \frac{1000}{c}(\beta - \beta_0) + \beta_0\phi_V$$

$$[5] \qquad \phi_{Ks} = \frac{1000}{c}(\beta_s - \beta_{so}) + \beta_{so}\phi_V$$

$$[6] \qquad \phi_c = \frac{1000}{c}(\sigma - \sigma_0) + \sigma_0\phi_V$$

where c, d, and ϕ_c are the solution molarity, density, and apparent molal heat capacity respectively, and as usual the subscripts refer to the pure solvent. The difference $\phi_K - \phi_{Ks}$ is thus given by

$$[7] \qquad \phi_K - \phi_{Ks} = \frac{\delta}{\alpha}\left(1 + \frac{\alpha_0}{\alpha}\right)\phi_E - \frac{\delta_0}{\sigma}\phi_c + \left(\delta_0 - \frac{\delta\alpha_0}{\alpha}\right)\phi_V$$

At infinite dilution, eq. 7 reduces to

$$[8] \qquad \phi_K^0 - \phi_{Ks}^0 = \delta_0\left(\frac{2\phi_E^0}{\alpha_0} - \frac{\phi_c^0}{\sigma_0}\right)$$

This equation is equivalent to those of Harned and Owen (3), and of Garnsey *et al.* (6) (which has unfortunately been misprinted) but is much simpler in form.

The three parameters δ_0 (4.726×10^7 $bars^{-1}$), α_0 ($2.55 \times 10^{-4}\ K^{-1}$), and σ_0 ($4.1720 JK^{-1}\ cm^{-3}$) are known for pure water at 25 °C (4). The standard ϕ_c^0 are available for the tetraalkylammonium bromides (8) and are given in Table 1. The expansitivities ϕ_E^0 have been measured for the corresponding chlorides (9), but can be converted to the bromides, using the difference ϕ_E^0 (KBr) − ϕ_E^0 (KCl) = 0.032 $cm^3\ K^{-1}\ mol^{-1}$ derived from the data of Dunn (10), and these again are given in Table 1. It should be noted that the uncertainty on ϕ_E^0 is of the order of 10 to 20% with the tetraalkylammonium halides (9). Two sets of data exist for ϕ_{Ks}^0. Conway and Verrall (5) have plotted ϕ_{Ks} against $c^{1/2}$ and extrapolated to infinite dilution. This procedure implies that ϕ_{Ks} obeys Debye–Hückel's law which is true only at very low concentrations and may lead to some uncertainty in the extrapolated ϕ_{Ks}^0. On the other hand, Garnsey *et al.* (6) have estimated ϕ_{Ks}^0 directly from the variation of the sound velocity with concentration at low concentrations. This procedure in principle assumes that at low concentrations the solution is ideal and obeys Henry's law (no solute–solute interactions), which is certainly not the case in the concentration range studied. Even if they did use a correction term in $c^{3/2}$, this method of measuring ϕ_{Ks}^0 necessarily leads to an average value of ϕ_K at low concentrations. Since ϕ_{Ks}^0 is negative and $d\phi_{Ks}/dc^{1/2}$ is positive, the values of ϕ_{Ks}^0 of Garnsey *et al.* are all too positive; of course, this source of error is independent of the accuracy of the experimental data (not given), which may be superior to that of Conway and Verrall. In view of the better extrapolation procedure, the ϕ_{Ks}^0 of Conway and Verrall are taken as the most reliable and are given in Table 1.

As can be seen from Table 1, the main correction to ϕ_{Ks}^0 comes from the term in ϕ_E^0 and not in ϕ_c^0. Therefore, contrary to what is

Can. J. Chem. Downloaded from www.nrcresearchpress.com by 210.87.254.42 on 09/05/12
For personal use only.

usually believed, accurate expansitivities and approximate heat capacities are needed to convert ϕ_{Ks}^0 to ϕ_K^0. In the present case, the error on ϕ_c^0 is negligible but that on ϕ_K^0 appreciable (10 to 20%) and this leads to a corresponding uncertainty on ϕ_K^0.

The present calculations confirm the observation of Garnsey *et al.* (6) that ϕ_K^0 and ϕ_{Ks}^0 are significantly different and this difference should not be overlooked when discussing properties of organic molecules in aqueous solutions. There is no reason why reliable methods (dilatometers for example) could not be developed to measure accurate expansitivities. Expansitivities, compressibilities and heat capacities are closely related properties (all related to the second derivative of the chemical potential) and should, whenever possible, be studied together.

It is also obvious that better extrapolation procedures should be devised; the limiting Debye–Hückel slope A_K should be estimated, either in terms of ϕ_K or ϕ_{Ks}, so that the data could be fitted with an equation of the type

$$[9] \qquad \phi_K = \phi_K^0 + A_K c^{1/2} + B_K c$$

where B_K would be an adjustable parameter related to deviations of the Debye–Hückel theory, like in the case of apparent molal volumes (2) and heat capacities (8).

We are grateful to the Defence Research Board of Canada for financial assistance.

1. F. J. MILLERO. Structure and transport processes in water and aqueous solutions. *Edited by* R. A. Horne. Wiley-Interscience, New York, N.Y. 1971.
2. J. E. DESNOYERS, M. AREL, G. PERRON, and C. JOLICOEUR. J. Phys. Chem. **73**, 3346 (1969).
3. H. S. HARNED and B. B. OWEN. The physical chemistry of electrolyte solutions. Reinhold, 1958. Chapt. 8.
4. B. B. OWEN and P. L. KRONICK. J. Phys. Chem. **65**, 84 (1961).
5. B. E. CONWAY and R. E. VERRALL. J. Phys. Chem. **70**, 3952 (1966).
6. R. GARNSEY, R. J. BOE, R. MAHONEY, and T. A. LITOWITZ. J. Chem. Phys. **50**, 5222 (1969).
7. E. K. BAUMGARTNER and G. ATKINSON. J. Phys. Chem. **75**, 2336 (1971).
8. P. R. PHILIP and J. E. DESNOYERS. J. Solution Chem. Submitted.
9. F. J. MILLERO and W. DROST-HANSEN. J. Phys. Chem. **72**, 1758 (1968).
10. L. A. DUNN. Trans. Faraday Soc. **64**, 2951 (1968).

Electron Spin Resonance of γ-Irradiated Acetylacetone in Adamantane Matrix

W. H. WOLODARSKY AND J. K. S. WAN
Department of Chemistry, Queen's University, Kingston, Ontario

Received November 15, 1971

Electron spin resonance spectrum is observed when samples of solid adamantane doped with acetylacetone are γ-irradiated at room temperature. The spectrum is interpreted due to an enolized allylic radical $CH_3COCHC(OH)CH_2$.

On observe un spectre de résonance paramagnétique électronique lorsque des échantillons d'adamantane solide contenant de l'acétylacétone sont irradiés avec des rayons-γ à la température de la pièce. On interprète le spectre à cause de la présence d'un radical allylique énolisé: $CH_3COCHC(OH)\dot{C}H_2$.

Canadian Journal of Chemistry, **50**, 1096 (1972)

Introduction

At room temperature liquid acetylacetone is known to exist largely (about (80%) in the enolized form $CH_3COCHC(OH)CH_3$ (1). Such enolization would be expected to influence the reactivity of acetylacetone. Thus Rutbi (2) has suggested the primary radical processes in the γ-radiolysis of acetylacetone in both the keto and enol forms:

$$[1] \qquad CH_3COCH_2COCH_3 \rightsquigarrow CH_3\dot{C}O + \dot{C}H_2COCH_3$$

$$[2] \qquad CH_3COCHC(OH)CH_3 \rightsquigarrow \dot{C}H_3 + CH_3C(OH)CH\dot{C}O$$

$$[3] \qquad CH_3COCH_2COCH_3 \rightsquigarrow H + \dot{C}H_2COCH_2COCH_3$$

However, on secondary reactions involving

Can. J. Chem. Downloaded from www.nrcresearchpress.com by 210.87.254.42 on 09/05/12
For personal use only.

usually believed, accurate expansitivities and approximate heat capacities are needed to convert ϕ_{Ks}^0 to ϕ_K^0. In the present case, the error on ϕ_c^0 is negligible but that on ϕ_K^0 appreciable (10 to 20%) and this leads to a corresponding uncertainty on ϕ_K^0.

The present calculations confirm the observation of Garnsey *et al.* (6) that ϕ_K^0 and ϕ_{Ks}^0 are significantly different and this difference should not be overlooked when discussing properties of organic molecules in aqueous solutions. There is no reason why reliable methods (dilatometers for example) could not be developed to measure accurate expansitivities. Expansitivities, compressibilities and heat capacities are closely related properties (all related to the second derivative of the chemical potential) and should, whenever possible, be studied together.

It is also obvious that better extrapolation procedures should be devised; the limiting Debye–Hückel slope A_K should be estimated, either in terms of ϕ_K or ϕ_{Ks}, so that the data could be fitted with an equation of the type

$$[9] \qquad \phi_K = \phi_K^0 + A_K c^{1/2} + B_K c$$

where B_K would be an adjustable parameter related to deviations of the Debye–Hückel theory, like in the case of apparent molal volumes (2) and heat capacities (8).

We are grateful to the Defence Research Board of Canada for financial assistance.

1. F. J. MILLERO. Structure and transport processes in water and aqueous solutions. *Edited by* R. A. Horne. Wiley-Interscience, New York, N.Y. 1971.
2. J. E. DESNOYERS, M. AREL, G. PERRON, and C. JOLICOEUR. J. Phys. Chem. **73**, 3346 (1969).
3. H. S. HARNED and B. B. OWEN. The physical chemistry of electrolyte solutions. Reinhold, 1958. Chapt. 8.
4. B. B. OWEN and P. L. KRONICK. J. Phys. Chem. **65**, 84 (1961).
5. B. E. CONWAY and R. E. VERRALL. J. Phys. Chem. **70**, 3952 (1966).
6. R. GARNSEY, R. J. BOE, R. MAHONEY, and T. A. LITOWITZ. J. Chem. Phys. **50**, 5222 (1969).
7. E. K. BAUMGARTNER and G. ATKINSON. J. Phys. Chem. **75**, 2336 (1971).
8. P. R. PHILIP and J. E. DESNOYERS. J. Solution Chem. Submitted.
9. F. J. MILLERO and W. DROST-HANSEN. J. Phys. Chem. **72**, 1758 (1968).
10. L. A. DUNN. Trans. Faraday Soc. **64**, 2951 (1968).

Electron Spin Resonance of γ-Irradiated Acetylacetone in Adamantane Matrix

W. H. WOLODARSKY AND J. K. S. WAN
Department of Chemistry, Queen's University, Kingston, Ontario

Received November 15, 1971

Electron spin resonance spectrum is observed when samples of solid adamantane doped with acetylacetone are γ-irradiated at room temperature. The spectrum is interpreted due to an enolized allylic radical $CH_3COCHC(OH)CH_2$.

On observe un spectre de résonance paramagnétique électronique lorsque des échantillons d'adamantane solide contenant de l'acétylacétone sont irradiés avec des rayons-γ à la température de la pièce. On interprète le spectre à cause de la présence d'un radical allylique énolisé: $CH_3COCHC(OH)\dot{C}H_2$.

Canadian Journal of Chemistry, **50**, 1096 (1972)

Introduction

At room temperature liquid acetylacetone is known to exist largely (about (80%) in the enolized form $CH_3COCHC(OH)CH_3$ (1). Such enolization would be expected to influence the reactivity of acetylacetone. Thus Rutbi (2) has suggested the primary radical processes in the γ-radiolysis of acetylacetone in both the keto and enol forms:

$$[1] \qquad CH_3COCH_2COCH_3 \rightsquigarrow CH_3\dot{C}O + \dot{C}H_2COCH_3$$

$$[2] \qquad CH_3COCHC(OH)CH_3 \rightsquigarrow \dot{C}H_3 + CH_3C(OH)CH\dot{C}O$$

$$[3] \qquad CH_3COCH_2COCH_3 \rightsquigarrow H + \dot{C}H_2COCH_2COCH_3$$

However, on secondary reactions involving

Can. J. Chem. Downloaded from www.nrcresearchpress.com by 210.87.254.42 on 09/05/12
For personal use only.

radicals abstracting H atom from acetylacetonate, Rutbi considered only the abstraction from the methyl group of the substrate in the keto form. On the other hand, Cadogen *et al.* (3) have concluded that the abstraction reactions involving the keto and the enol forms of acetylacetone are quite different:

[4] $(CH_3)_3C\dot{O} + CH_3COCH_2COCH_3 \rightarrow CH_3CO\dot{C}HCOCH_3$

[5] $(CH_3)_3C\dot{O} + CH_3COCHC(OH)CH_3 \rightarrow CH_3COCHC(OH)\dot{C}H_2$ *or* $\dot{C}H_2COCHC(OH)CH_3$

The exact configurations of the enol radicals have not been elucidated.

The present investigation reports the e.s.r. evidence that when a H atom is removed from acetylacetone during the γ-radiolysis in an adamantane matrix, the predominant radical resulting is the enol radical with a specific configuration of $CH_3COCHC(OH)\dot{C}H_2$.

Experimental

Acetylacetone (PCR Inc.) and adamantane (Aldrich *puriss* grade) were used as supplied. Further purification proved to be unnecessary. Small quantities of acetylacetone were introduced into the adamantane matrix by recrystallization of the solid from acetylacetone. Samples were filtered, dried, and irradiated in air at room temperature in a 19 000 Ci source of ^{60}Co γ-rays. The dose rate was approximately 1 Mrad/h and the total dose was 0.1 to 0.2 Mrad. Electron spin resonance spectra were obtained with an X-band Varian V4502 spectrometer using 100 kc modulation and auxiliary equipment. Microwave power and modulation amplitude were adjusted to avoid saturation.

Results and Discussion

The general usefulness of using adamantane as the trapping matrix (cavity–molecule isolation) in radiolysis systems to improve the resolution of e.s.r. spectra has been amply demonstrated (see, for example, ref. 4).

A typical room temperature e.s.r. spectrum recorded when samples of the acetylacetone doped adamantane were γ-irradiated is given in Fig. 1. The g-value of this radical measured with reference to DPPH ($g = 2.0036$) was $2.0039 \pm .0001$. The hyperfine pattern of the spectrum leads to the conclusion that there are two "equivalent" protons of splitting 14.5 ± 0.2 G and one proton of splitting 9.5 ± 0.2 G.

There are several possibilities that may account for the observed e.s.r. spectrum, but the

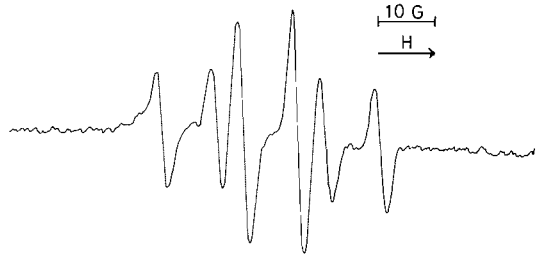

FIG. 1. The e.s.r. spectrum at room temperature from radicals trapped in an irradiated adamantane matrix containing acetylacetone.

radicals $\cdot CH_2COCH_3$ and $\cdot CH_2CHO$ could be immediately disregarded on the basis of their reported splitting constants and hyperfine pattern (5, 6). The possibility was thus narrowed to one of the three radicals, $CH_3CO\dot{C}HCOCH_3$ (I), $CH_3COCHC(OH)\dot{C}H_2$(II), and $CH_3C(OH)$-$CHCOCH_2$(III). Radical I with six "equivalent" methyl protons was considered unlikely to be responsible for the observed spectrum. Of radicals II and III, the former would be more stable with an allyl type structure (7). Also radical II would be expected to have a relatively large splitting of the methyne proton due to the π-electron delocalization through the allyl type structure. Recently, Hutterman *et al.* (8) have observed e.s.r. spectra of a similar allyl-type radical during the γ-radiolysis of single crystals of 5-methylcytosine:

[6]

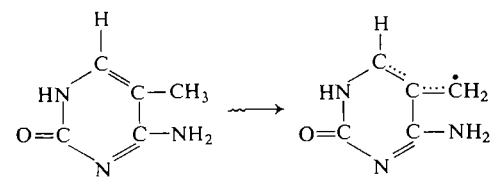

Their assignments of the two methylene protons ($a_H = 16.6$ G) and the methyne proton ($a_H = 7.7$ G) are consistent with an allyl-type radical as well as the radical II in the present system. Therefore, it is reasonable to assume that radical II is responsible for the observed e.s.r. spectrum.

The radical II was considered to be planar (9) and the small splitting of the hydroxy proton is not resolved experimentally. However, the reasons why the splitting from the methyl protons are not being observed can be better understood by considering other well-known

Can. J. Chem. Downloaded from www.nrcresearchpress.com by 210.87.254.42 on 09/05/12
For personal use only.

carbonyl-containing radicals such as the acetonyl $CH_3C\dot{O}CH_2$ (5) and the $HC\dot{O}CH_2$ (6) radical. With an allylic structure, radical II is expected to have appreciable spin density on the methyne carbon atom. Thus one can qualitatively consider radical II as a substituted acetonyl radical. Since the experimental hyperfine splitting for the methyl protons in the acetonyl radical is only 0.27 G (5), similar splittings in the radical II will be too small to be resolved in the present matrix study.

In conclusion, we interpreted the observed e.s.r. spectrum during the radiolysis of acetylacetone doped adamantane due to an enolized allyl radical $CH_3COCHC(OH)\dot{C}H_2$. The result suggests a specific and preferred site for the removal of a H atom from the predominant enol form of acetylacetone.

This research is supported by the National Research Council of Canada and the Department of Public Health.

1. K. H. MEYER and H. HOPFF. Ber. **54**, 579 (1921).
2. M. P. RUTBI. J. Chem. Phys. **60**, 1155 (1960).
3. J. I. CADOGEN, D. H. HEY, and T. T. SHARP. J. Chem. Soc. C, 1743 (1966).
4. D. E. WOOD and R. V. LLOYD. J. Chem. Phys. **53**, 3932 (1970); D. R. GEE and J. K. S. WAN. Can. J. Chem. **49**, 20 (1971); S. W. KANICK, R. E. LINDER, and A. C. LING. J. Chem. Soc. A. In press.
5. H. ZELDES, and R. LIVINGSTON. J. Chem. Phys. **45**, 1946 (1966).
6. A. L. BURLEY, R. O. C. NORMAN, and R. T. PRITCHETT. J. Chem. Soc. B, 849 (1966).
7. R. W. FESSENDEN and R. H. SCHULER. J. Chem. Phys. **39**, 2147 (1963).
8. J. HUTTERMAN, J. F. WARD, and L. S. MYERS, JR. Int. J. Radiat. Phys. Chem. **3**, 117 (1971).
9. K. MOROKUMA, H. KATO, T. YONEZAWA, and K. FUKUI. Bull. Chem. Soc. Jap. **38**, 1263 (1965).

A Total Synthesis of *dl*-Occidol

TSE-LOK HO
Department of Chemistry, University of Manitoba, Winnipeg, Manitoba

Received October 6, 1971

dl-Occidol has been synthesized from 3,6-dimethylphthalic anhydride.

On a synthétisé le *dl*-occidol à partir de l'anhydride 3,6-diméthyl-phtalique.

Canadian Journal of Chemistry, **50**, 1098 (1972)

The major sesquiterpene alcohol found in the essential oil of *Thuja occidentalis* L. is *d*-occidol. The structure depicted as in **1** (without stereochemical implication) was elucidated by Hirose and Nakatsuka (1), and the absolute configuration (*R*) of the chiral center at C-7 was established by correlation with *l*-santonin (2).

The biogenetically unusual features of occidol have aroused our interests in its synthetic endeavors. *dl*-Occidol has been previously synthesized by Hirose and Nakatsuka, starting from 5,8-dimethyl-1-tetralone in six steps (3). Unaware of the details of this work, the present author sometime ago also completed a shorter synthesis from the same intermediate (4).

In this publication, a totally different synthetic approach is disclosed. Examination of the sesquiterpene framework clearly indicates that occidol is symmetrical except for the single chiral center (C-7). This structural characteristic offers great advantages in synthetic design and facilitates execution thereof.

In this context, one may envisage that the substituted *o*-quinodimethane **A** is the ideal intermediate for our purpose. It is also anticipated that **A** would be adequately reactive toward olefins in participating a Diels–Alder type reaction. Specifically, an acrylic ester serving as the reaction partner fits perfectly well in elaborating the desired bicyclic skeleton.

3,6-Dimethylphthalic anhydride (5) was reduced to the diol **2***a* with lithium aluminum hydride. Treatment of this diol with phosphorus tribromide and pyridine gave the dibromide **2***b*.

Can. J. Chem. Downloaded from www.nrcresearchpress.com by 210.87.254.42 on 09/05/12
For personal use only.

carbonyl-containing radicals such as the acetonyl $CH_3C\dot{O}CH_2$ (5) and the $HC\dot{O}CH_2$ (6) radical. With an allylic structure, radical II is expected to have appreciable spin density on the methyne carbon atom. Thus one can qualitatively consider radical II as a substituted acetonyl radical. Since the experimental hyperfine splitting for the methyl protons in the acetonyl radical is only 0.27 G (5), similar splittings in the radical II will be too small to be resolved in the present matrix study.

In conclusion, we interpreted the observed e.s.r. spectrum during the radiolysis of acetylacetone doped adamantane due to an enolized allyl radical $CH_3COCHC(OH)\dot{C}H_2$. The result suggests a specific and preferred site for the removal of a H atom from the predominant enol form of acetylacetone.

This research is supported by the National Research Council of Canada and the Department of Public Health.

1. K. H. MEYER and H. HOPFF. Ber. **54**, 579 (1921).
2. M. P. RUTBI. J. Chem. Phys. **60**, 1155 (1960).
3. J. I. CADOGEN, D. H. HEY, and T. T. SHARP. J. Chem. Soc. C, 1743 (1966).
4. D. E. WOOD and R. V. LLOYD. J. Chem. Phys. **53**, 3932 (1970); D. R. GEE and J. K. S. WAN. Can. J. Chem. **49**, 20 (1971); S. W. KANICK, R. E. LINDER, and A. C. LING. J. Chem. Soc. A. In press.
5. H. ZELDES, and R. LIVINGSTON. J. Chem. Phys. **45**, 1946 (1966).
6. A. L. BURLEY, R. O. C. NORMAN, and R. T. PRITCHETT. J. Chem. Soc. B, 849 (1966).
7. R. W. FESSENDEN and R. H. SCHULER. J. Chem. Phys. **39**, 2147 (1963).
8. J. HUTTERMAN, J. F. WARD, and L. S. MYERS, JR. Int. J. Radiat. Phys. Chem. **3**, 117 (1971).
9. K. MOROKUMA, H. KATO, T. YONEZAWA, and K. FUKUI. Bull. Chem. Soc. Jap. **38**, 1263 (1965).

A Total Synthesis of *dl*-Occidol

TSE-LOK HO
Department of Chemistry, University of Manitoba, Winnipeg, Manitoba

Received October 6, 1971

dl-Occidol has been synthesized from 3,6-dimethylphthalic anhydride.

On a synthétisé le *dl*-occidol à partir de l'anhydride 3,6-diméthyl-phtalique.

Canadian Journal of Chemistry, **50**, 1098 (1972)

The major sesquiterpene alcohol found in the essential oil of *Thuja occidentalis* L. is *d*-occidol. The structure depicted as in **1** (without stereochemical implication) was elucidated by Hirose and Nakatsuka (1), and the absolute configuration (*R*) of the chiral center at C-7 was established by correlation with *l*-santonin (2).

The biogenetically unusual features of occidol have aroused our interests in its synthetic endeavors. *dl*-Occidol has been previously synthesized by Hirose and Nakatsuka, starting from 5,8-dimethyl-1-tetralone in six steps (3). Unaware of the details of this work, the present author sometime ago also completed a shorter synthesis from the same intermediate (4).

In this publication, a totally different synthetic approach is disclosed. Examination of the sesquiterpene framework clearly indicates that occidol is symmetrical except for the single chiral center (C-7). This structural characteristic offers great advantages in synthetic design and facilitates execution thereof.

In this context, one may envisage that the substituted *o*-quinodimethane **A** is the ideal intermediate for our purpose. It is also anticipated that **A** would be adequately reactive toward olefins in participating a Diels–Alder type reaction. Specifically, an acrylic ester serving as the reaction partner fits perfectly well in elaborating the desired bicyclic skeleton.

3,6-Dimethylphthalic anhydride (5) was reduced to the diol **2***a* with lithium aluminum hydride. Treatment of this diol with phosphorus tribromide and pyridine gave the dibromide **2***b*.

Can. J. Chem. Downloaded from www.nrcresearchpress.com by 210.87.254.5 on 09/05/12
For personal use only.

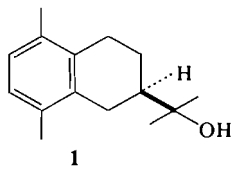

1

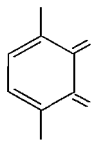

A

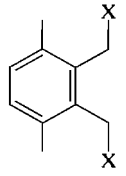

2

a X = OH
b X = Br

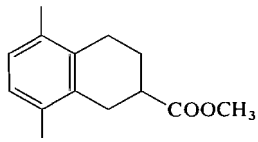

3

Generation of **A** from **2***b* was readily accomplished by reaction with activated zinc dust. In view of the expected reactivity of **A**, it was trapped *in situ* by methyl acrylate placed in the reaction vessel.

Alder and Fremery have reported cycloadditions between unsubstituted *o*-quinodimethane and a number of activated alkenes (6) to produce tetralin derivatives. The reaction may involve a [4 + 2] or an [8 + 2] process, both of which are thermally allowed on the basis of molecular orbital symmetry selection rules (7). A clear-cut case of [8 + 2] cycloaddition has appeared in the recent literature (8).

For the sake of convenience in isolating the ester **3**, the crude reaction mixture was saponified and the acidic material was re-esterified with diazomethane. Exposure of **3** to methyllithium in ether readily afforded *dl*-occidol. The synthetic compound is identical with natural *d*-occidol (kindly supplied by Dr. E. von Rudloff, Saskatoon) with respect to i.r., n.m.r., and t.l.c. properties.

Experimental

α^2,α^3-Dihydroxyprehnetene (2a)

To a stirred suspension of lithium aluminum hydride (1.80 g) in anhydrous ether (60 ml) was added a solution of 3,6-dimethylphthalic anhydride (2.50 g) in dry tetrahydrofuran (40 ml). It was heated under reflux for 18 h, cooled, and the excess hydride was cautiously destroyed by adding a saturated aqueous sodium sulfate solution. The granular suspension was filtered and the filter cake was leached with additional portions of tetrahydrofuran. Evaporation of the dried ($MgSO_4$) organic solution yielded the diol **2***a* (1.66 g, 70%); m.p. 62–64° (ether – petroleum ether); i.r. ($CHCl_3$) ν 3600, 3400 cm^{-1}; n.m.r. ($CDCl_3$) τ 7.60 (6H, s), 6.72 (2H, br.s), 5.20 (4H, s), 2.86 (2H, s).

Anal. Calcd. for $C_{10}H_{14}O_2$: C, 72.30; H, 8.43. Found: C, 72.53; H, 8.38.

α^2,α^3-Dibromoprehnetene (2b)

To a solution of the diol **2***a* (390 mg) and pyridine (0.4 ml) in ether (15 ml) was added dropwise 0.5 ml of phosphorus tribromide. After stirring at room temperature for 18 h, the reaction mixture was poured into ice water and extracted with ether. Removal of the solvent from the dried ($MgSO_4$) extracts gave the dibromide **2***b* as colorless crystals (540 mg, 79%); m.p. 97–98° (petroleum ether); i.r. ($CHCl_3$) no OH absorption; n.m.r. (CCl_4) τ 7.63 (6H, s), 5.36 (4H, s), 2.95 (2H, s).

Anal. Calcd. for $C_{10}H_{12}Br_2$: C, 41.10; H, 4.11. Found: C, 41.37; H, 4.28.

Methyl-ester 3

A stirred mixture of the dibromide **2***b* (200 mg), methyl acrylate (2.0 ml), and $CuSO_4$–activated zinc dust (2.0 g) in dimethoxyethane (40 ml) was refluxed for 15 h. It was concentrated *in vacuo*, and digested with benzene and water. The gummy substance obtained from the benzene layer was directly saponified with sodium hydroxide (1.0 g) in 50% aqueous methanol (30 ml) for 2 h at reflux. The hydrolysate was diluted with water (50 ml), washed with benzene, acidified, and extracted with chloroform (3 × 25 ml). The combined extracts were dried ($MgSO_4$), treated with ethereal diazomethane, and evaporated to dryness. Chromatography over neutral alumina (5 g) yielded the ester **3** (31 mg, 20%) on elution with benzene and benzene–ether mixture (9:1). This product was identical with a specimen prepared by another route (4), b.p. 125–130° (0.8 mm Hg); i.r. ($CHCl_3$) ν 1730 cm^{-1}; n.m.r. ($CDCl_3$) τ 7.79 (6H, s), 6.25 (3H, s), 3.05 (2H, s).

Anal. Calcd. for $C_{14}H_{18}O_2$: C, 77.06; H, 8.25. Found: C, 76.82; H, 8.38.

dl-Occidol (1)

A solution of ester **3** (1.1 g, 5.1 mmol) in ether (15 ml) was added slowly to methyllithium (20 ml, 1.2 *M* in ether) at room temperature and the reaction was allowed to proceed for 4.5 h before being poured into aqueous ammonium chloride. Extraction of the resulting mixture with ether (3 × 50 ml) and concentration *in vacuo* furnished a solid (1.1 g). Recrystallization of the product from petroleum ether yielded *dl*-occidol (668 mg, 60%); m.p. 99–100° (lit. (3) m.p. 101–102°); i.r. (CCl_4) ν 3620 cm^{-1}; n.m.r. (CCl_4) τ 8.78 (6H, s), 7.82 (6H, br,s), 3.13 (2H, s).

1. Y. Hirose and T. Nakatsuka. Bull. Agri. Chem. Soc. Japan, **23**, 143 (1959).
2. M. Nakazaki. Bull. Chem. Soc. Japan, **35**, 1387 (1962).
3. Y. Hirose and T. Nakatsuka. Bull. Agri. Chem. Soc. Japan, **23**, 253 (1959).
4. T.-L. Ho. Chem. Ind. 487 (1971).
5. M. S. Newman and B. T. Lord. J. Am. Chem. Soc. **66**, 733 (1944).
6. K. Alder and M. Fremery. Tetrahedron, **14**, 190 (1961).
7. R. B. Woodward and R. Hoffmann. Angew. Chem. Int. Ed. **8**, 781 (1969).
8. G. C. Farrant and R. Feldmann. Tetrahedron Lett. 4979 (1970).

Can. J. Chem. Downloaded from www.nrcresearchpress.com by 210.87.254.5 on 09/05/12
For personal use only.

Synthesis of 8,2′-Thioanhydroguanosine

K. K. OGILVIE, L. SLOTIN,[1] J. B. WESTMORE, AND D. LIN
Department of Chemistry, University of Manitoba, Winnipeg, Manitoba

Received November 15, 1971

The synthesis of 8,2′-thioanhydroguanosine is described. The anhydro ring is formed by displacement of bromine from position-8 and sulfonate from the 2′-position using sodium hydrogen sulfide.

On décrit la synthèse du 8,2′-thioanhydroguanosine. Le cycle anhydro est formé par le déplacement du brome de la position-8 et du sulfonate de la position-2′ en utilisant le sulfure acide de sodium.

Canadian Journal of Chemistry, **50**, 1100 (1972)

Can. J. Chem. Downloaded from www.nrcresearchpress.com by 210.87.254.40 on 09/05/12
For personal use only.

Introduction

Anhydronucleosides are important modifications of natural nucleosides. They are easily converted into either the natural ribo or sugar modified nucleosides (1, 2) and have also provided alternate synthetic routes to nucleotides (3–5). More recently a thioanhydropurine nucleoside has been used in studies of enzyme specificity (6).

While pyrimidine anhydronucleosides have received a great deal of attention (1), adenosine is the only purine nucleoside for which 8,2′- and 8,3′-anhydro derivatives have been extensively developed (2). Neither the *O* nor *S* 8,2′(8,3′)-anhydro derivatives of guanosine has been reported, although the 3′-methanesulfonate of 8,2′-*O*-anhydroguanosine has been described (7). We wish to report the synthesis of 8,2′-thioanhydroguanosine (**6**) which is readily converted to 2′-deoxyguanosine (7).

Results and Discussion

The synthesis of 8,2′-thioanhydroguanosine is outlined in Scheme 1. The 2-NH_2 group of 8-bromoguanosine (8) was protected with the dimethylaminomethylene group (9). The reaction between 8-bromoguanosine (**1**) and excess dimethylformamide dimethyl acetal gives 8-bromo-N^2-dimethylaminomethyleneguanosine (**2**) in 95% yield. Compound **2** was quantitatively converted to the 5′-monomethoxytrityl derivative **3**.

The essential step in the scheme is the introduction of a good leaving group on the 2′-position. Once this is achieved the 8,2′-thio bridge can be introduced in a single step (10).

The monomethoxytrityl group on the 5′-position screens the 3′-hydroxyl much more than it does the 2′-hydroxyl. As a result large sulfonating agents or triphenylmethyl chlorides react preferentially or exclusively at the 2′-position (10, 11).

For the above reasons we chose to react **3** with mesitylenesulfonyl chloride (MSCl). MSCl is a bulky sulfonating agent but one that does react with hydroxyl groups at a reasonable rate (12, 13). MSCl reacted with **3** in dry pyridine at room temperature for 2 days to produce **4***a* in 42% yield. Starting material **3** was also recovered (34%) from the reaction mixture. While others (10) using more basic conditions have detected small amounts of 3′-isomers from such reactions, we were unable to detect any **4***b*.[2] The structure of our product was confirmed as **4***a* by the subsequent steps which converted it into the 8,2′-thioanhydronucleoside **6** and 2′-deoxyguanosine (**7**).

Because we anticipated that N^2- and $O^{5'}$-protecting groups would be at least partially hydrolyzed during the step to form the anhydro-linkage, we decided to remove them completely before this step. The dimethylaminomethylene group was quantitatively removed from **4***a* using either a hydrazine hydrate solution (hydrazine hydrate : acetic acid : pyridine, 1 : 6 : 24) or ammonium hydroxide solution at room temperature. The monomethoxytrityl group was then removed using 80% acetic acid at room temperature for 3 h to produce 2′-mesitylenesulfonyl-8-bromoguanosine (**5**) in 77% overall yield from **4***a*.

To form the 8,2′-thioanhydro link, **5** was

[1]NRCC Scholarship Holder 1970–1971.

[2]Generally a 3′-substituted nucleoside moves more slowly than the 2′-isomer on silica gel t.l.c. (10, 14).

Can. J. Chem. Downloaded from www.nrcresearchpress.com by 210.87.254.40 on 09/05/12
For personal use only.

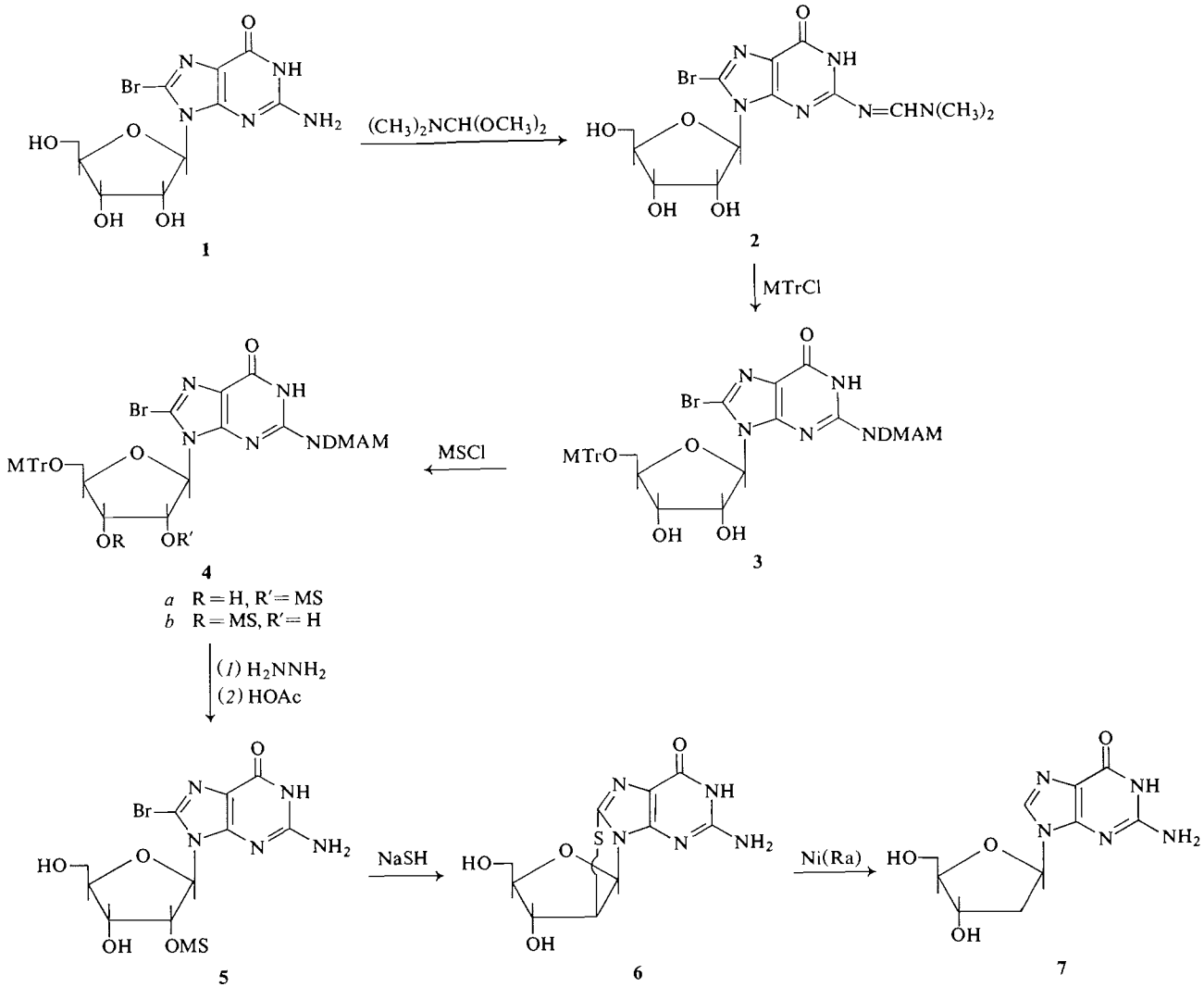

1 2 3 4 5 6 7

a R = H, R′ = MS
b R = MS, R′ = H

DMAM = Dimethylaminomethylene
MTrCl = Monomethoxytrityl chloride
MSCl = Mesitylenesulfonyl chloride

SCHEME 1

TABLE 1. Properties of guanosine derivatives

Compound	R_f (paper chromatography)		Ultraviolet spectra	
	Solvent A*	Solvent B*	Solvent	max, nm(ε)
Guanosine	0.28	0.53	Water	275(8400), 253(12700)
1	0.28	0.58	Water	262(15550), 269(14100)sh
2	0.29	0.64	Water	302(24400), 233(12600)
3	0.79	0.88	95% ethanol	309(24900), 284(17200)sh, 233(32800)
4a	0.88	0.92	95% ethanol	309(24800), 288(20300), 234(30000)
5	0.73	0.82	95% ethanol	275(12200)sh, 265.5(14100), 237(13100)
6	0.20	0.58	Water	283(13590), 268(16630)
7	0.32	0.62	Water	270(8600)sh, 253(12800)
3′-Deoxyguanosine	0.24	0.61	Water	270(8900)sh, 253(13100)

*Solvents described in General Methods (Experimental).

treated with sodium hydrogen sulfide in *N*,*N*-dimethylformamide. Using a six-fold excess of sodium mercaptan and a temperature of 70 °C for 20 h, a 16% yield of **6** was obtained. By increasing the temperature to 100 °C and using an 11-fold excess of sodium mercaptan the yield was increased to 40%.

Compound **6** was identified as 8,2′-thioanhydroguanosine (Table 1). Elemental analysis and the mass spectrum[3] of the tetrasilyl derivative (*m/e* 585) agreed with the assigned structure. Compound **6** was converted to 2′-deoxyguanosine (**7**) using Raney nickel. The synthetic 2′-deoxyguanosine was identical to authentic material (17) and is readily distinguished from 3′-deoxyguanosine (18, 19) by paper chromatography (Table 1).

Compound **7** was further characterized by acidic hydrolysis (20) to 2-deoxyribose which gave positive tests with Dische reagent (21) and cysteine – sulfuric acid reagent (22).

Experimental

General Methods

Descending paper chromatography was carried out on Whatman 3MM paper. The solvent systems employed were: solvent A, isopropyl alcohol – concentrated ammonium hydroxide – water (7:1:2); solvent B, ethanol–water (7:3). The solvents were prepared on a volume basis. Thin layer chromatography was carried out employing the ascending technique. All thin-layer chromatography was run on Eastman Chromagram Sheets 6060 (silica gel with fluorescent indicator) on strips 10 × 2 cm. Thick-layer chromatography was carried out on glass plates (20 × 20 cm) coated with a 2 mm thick layer of silica gel DSF-5 (Mondray Chemicals Ltd). Nucleosides and their derivatives were detected on paper chromatograms, thin and thick-layer sheets, using an u.v. source (Mineralite output 254 nm). Compounds containing *p*-monomethoxytrityl groups were detected on chromatography by spraying with 10% perchloric acid solution and drying them in a stream of warm air.

The i.r. spectra were obtained on a Perkin–Elmer 337 recording spectrophotometer using KBr disks for sample preparation. The u.v. spectra were obtained on a Cary Model 14 recording spectrophotometer. Mass spectra were obtained on a Hitachi RMU-6D instrument. Melting points were determined on a Fisher-Johns melting point apparatus and are reported uncorrected. Elemental analyses were performed by Galbraith Laboratories Inc., Knoxville, Tenn. Samples submitted to them were prepared by crystallization, lyophilization, or precipitation from tetrahydrofuran with hexane followed by heating in a drying apparatus over P_2O_5.

Reagent grade pyridine was distilled from *p*-toluenesulfonyl chloride, redistilled from calcium hydride, and stored over Linde Molecular Sieve. Reagent grade *N*,*N*-dimethylformamide (DMF) was dried by distillation from calcium hydride and stored over Linde Molecular Sieve. 8-Bromoguanosine (m.p. 191–194 °C) was prepared by the method of Shapiro and Agarwal (8).

*N^2-Dimethylaminomethylene-8-bromoguanosine(**2**)*

8-Bromoguanosine (3.63 g, 10 mmol) and *N*,*N*-dimethylformamide dimethyl acetal (5 ml, 50 mmol) were dissolved in DMF (50 ml) and stirred at room temperature for 12 h. The solvents were removed at reduced pressure and the residue was crystallized from water to yield 3.99 g (96%) of **2** (m.p. 216–218 °C, R_f 0.19 (THF)). Principal bands in the i.r. spectrum occurred at 5.85, 8.95, 11.95, and 12.85 μ.

Anal. Calcd. for $C_{13}H_{17}N_6O_5Br$: C, 37.42; H, 4.11; Br, 19.15. Found: C, 37.69; H, 4.20; Br, 19.08.

*5′-O-Monomethoxytrityl-N^2-dimethylaminomethylene-8-bromoguanosine (**3**)*

Compound **2** (3.78 g, 9.1 mmol) and monomethoxytrityl chloride (3.16 g, 10.2 mmol) were dissolved in pyridine (15 ml) and the solution was stirred at room temperature for 24 h. The solution was then poured into ice water with vigorous stirring. A precipitate formed which was collected by filtration, washed with water, and reprecipitated from

[3]A detailed mass spectral analysis of thioanhydropyrimidines will be reported shortly (15). See also Ikehara and co-workers (16).

Can. J. Chem. Downloaded from www.nrcresearchpress.com by 210.87.254.40 on 09/05/12
For personal use only.

Can. J. Chem. Downloaded from www.nrcresearchpress.com by 210.87.254.40 on 09/05/12
For personal use only.

tetrahydrofuran using hexane. The resulting white solid (m.p. 158° (dec.)) was collected by filtration (6.17 g, 99%) and identified as compound **3**. The thin-layer chromatographic properties of the material were: R_f 0.05 (ethyl acetate) and 0.41 (tetrahydrofuran). Principal bands in the i.r. spectrum occurred at 5.9, 8.55, and 14.3 μ.

Anal. Calcd. for $C_{33}H_{33}N_6O_6Br$: C, 57.48; H, 4.82; Br, 11.59. Found: C, 57.60; H, 4.95; Br, 11.84.

*5′-O-Monomethoxytrityl-2′-O-mesitylenesulfonyl-N^2-dimethylaminomethylene 8-bromoguanosine (**4a**)*

Compound **3** (1.0 g, 1.45 mmol) and mesitylenesulfonyl chloride (0.63 g, 2.9 mmol) were dissolved in pyridine (5 ml) and the solution was stirred at room temperature for 48 h. The solution was poured into ice water and the precipitate was collected by filtration and dissolved in chloroform (100 ml). The chloroform solution was dried over sodium sulfate, concentrated to a small volume, and applied to five thick-layer plates. These plates were developed twice in ether followed by one development in tetrahydrofuran. Three nucleoside bands were present at R_f 0.72, 0.48, and 0.20. The band at R_f 0.20 was eluted from the plates with ethanol and upon evaporation of the ethanol 55 mg of compound **2** were obtained. The band at R_f 0.48 was eluted with tetrahydrofuran and upon evaporation of the solvent 340 mg of compound **3** were obtained. The band at R_f 0.72 was also eluted with tetrahydrofuran and yielded 530 mg (42%) of compound **4a** (m.p. 148–150 °C). The thin-layer chromatographic properties of **4a** were: R_f 0.19 (ethyl acetate) and 0.68 (tetrahydrofuran). Principal bands in the i.r. spectrum occurred at 5.9, 8.48, 8.55, and 14.2 μ.

Anal. Calcd. for $C_{42}H_{43}N_6O_8Br$: C, 57.86; H, 4.97. Found: C, 58.50; H, 5.04.

5′-O-Monomethoxytrityl-2′-O-mesitylenesulfonyl-8-bromoguanosine

Method A. Compound **4a** (200 mg, 0.23 mmol) was dissolved in 3 ml of a solution containing 85% hydrazine hydrate – acetic acid – pyridine (1:6:24) and the solution was stirred at room temperature for 24 h. The solution was poured into ice water and the precipitate was collected by filtration to yield after drying 181 mg (96%) of 5′-*O*-monomethoxytrityl-2′-*O*-mesitylenesulfonyl-8-bromoguanosine (m.p. 162 °C (dec.)). Thin-layer chromatography showed R_f values of 0.18 (ethyl acetate) and 0.60 (tetrahydrofuran). Principal bands in the i.r. spectrum occurred at 5.85, 8.40, 8.50, and 14.2 μ.

Anal. Calcd. for $C_{39}H_{38}N_5O_8Br$: C, 57.35; H, 4.69; Br, 9.78. Found: C, 57.73; H, 4.62; Br, 11.11.

Method B. The dimethylaminomethylene group could be removed in 98% yield by stirring **4a** in concentrated ammonium hydroxide for 24 h.

*2′-O-Mesitylenesulfonyl-8-bromoguanosine (**5**)*

5′-*O*-Monomethoxytrityl-2′-*O*-mesitylenesulfonyl-8-bromoguanosine (500 mg, 0.61 mmol) was stirred in 80% acetic acid (10 ml) for 3 h at room temperature. The solvents were removed at reduced pressure and the residue was dissolved in tetrahydrofuran (3 ml) and applied to three thick-layer plates which were developed in tetrahydrofuran. A nucleoside band appeared at R_f 0.40 and was eluted with tetrahydrofuran. The product was collected by precipitation with hexane followed by filtration to yield 274 mg (80%) of **5** (m.p. 183° (dec.)). Principal bands in the i.r. spectrum occurred at 5.85, 8.40, and 8.50 μ.

Anal. Calcd. for $C_{19}H_{22}N_5O_7Br$: C, 41.92; H, 4.07; Br, 14.68. Found: C, 42.20; H, 4.27; Br, 14.59.

*8,2′-Thioanhydroguanosine (**6**)*

Method A. Compound **5** (50 mg, 0.093 mmol) and 0.2 ml of a 40% solution of NaSH (1.25 mmol) and water were added to DMF (3 ml) and the solution was heated at 100 °C for 18 h. The solution was cooled and applied to Whatman 3MM paper developed in solvent A. Two nucleoside bands appeared at R_f 0.73 and 0.19. The band at R_f 0.73 was eluted with water which was lyophilized to yield 24 mg of **5**. The band at R_f 0.19 was also eluted with water and the aqueous solution was lyophilized to yield 11 mg (39%) of **6** (m.p. 268 °C (dec.)). The mass spectrum of the tetrasilyl derivative showed a parent peak at *m/e* 585. Principal bands in the i.r. spectrum occurred at 5.9, 6.55, and 12.0 μ.

Anal. Calcd. for $C_{10}H_{11}N_5O_4S$: C, 40.40; H, 3.73; N, 23.56. Found: C, 40.34; H, 3.99; N, 23.05.

Method B. The above procedure was repeated using a six-fold excess of NaSH and a temperature of 70° for 18 h. The yield of **6** was 16%.

*2′-Deoxyguanosine (**7**)*

Compound **6** (10 mg, 0.034 mmol) was dissolved in water (1 ml) and the solution was heated at reflux with Raney nickel for 3 h. The product, 2′-deoxyguanosine (m.p. 215 °C (dec.)) was isolated by paper chromatography in solvent A and was identical in all respects to an authentic sample (17).

The product was hydrolyzed (20) to 2-deoxyribose which gave positive tests with Dische reagent (21) and cysteine – sulfuric acid reagent (22).

We wish to acknowledge financial support from the National Research Council of Canada.

1. J. J. Fox. Pure and Appl. Chem. **18**, 223 (1969).
2. M. Ikehara. Acts. Chem. Res. **2** 47 (1969).
3. M. Ikehara, S. Uesugi, M. Vasumoto. J. Am. Chem. Soc. **92**, 4735 (1970).
4. K. K. Ogilvie and D. Iwacha. Can. J. Chem. **48**, 862 (1970).
5. K. L. Nagpal and M. M. Dhar. Tetrahedron Lett. 47 (1968).
6. K. K. Ogilvie, L. Slotin, and P. Rheault. Biochem. Biophys. Res. Commun. **45**, 297 (1971).
7. M. Ikehara and K. Muneyama. J. Org. Chem., **32**, 3039 (1967).
8. R. Shapiro and S. C. Agarwal. Biochem. Biophys. Res. Commun. **24**, 401 (1966).
9. S. Zemlicka and A. Holy. Coll. Czech. Chem. Commun. **32**, 3159 (1967).
10. M. Ikehara and M. Kaneko. Tetrahedron, **26**, 4251 (1970).
11. N. C. Yung and J. J. Fox. J. Am. Chem. Soc. **83**, 3060 (1961).
12. R. Lohrmann and H. G. Khorana. J. Am. Chem. Soc. **88**, 829 (1966).
13. J. F. Bunnett and J. Y. Bassett, Jr. J. Am. Chem. Soc. **81**, 2104 (1959).

14. K. K. OGILVIE and D. IWACHA. Can. J. Chem. **47**, 495 (1969).
15. J. B. WESTMORE and K. K. OGILVIE. Unpublished results.
16. M. IKEDA, Y. Tamura, and M. Ikehara. J. Heterocycl. Chem. **7**, 1377 (1970).
17. Sigma Chemical Co.
18. K. K. OGILVIE and L. SLOTIN. Unpublished results.
19. L. GOODMAN. J. Org. Chem. **32**, 859 (1967).
20. M. IKEHARA and H. TADA. Chem. Pharm. Bull. (Tokyo), **15**, 94 (1967).
21. J. BUCHANAN. J. Chem. Soc. 3162 (1950).
22. J. BUCHANAN. Nature **164**, 443 (1949).

Can. J. Chem. Downloaded from www.nrcresearchpress.com by 210.87.254.40 on 09/05/12
For personal use only.

Can. J. Chem. Downloaded from www.nrcresearchpress.com by 210.87.254.42 on 09/05/12
For personal use only.

A Convenient Synthesis of Propargylic Esters and γ-Keto Esters. The Reaction of Trialkynylboranes with Ethyl Diazoacetate, and the Unidirectional Hydration of Propargylic Esters

JOHN HOOZ AND ROBERT B. LAYTON[1]

Department of Chemistry, University of Alberta, Edmonton, Alberta

Received January 7, 1972

Trialkynylboranes react with ethyl diazoacetate to provide propargylic esters. The process occurs under mild conditions (−20°) and in good yields. Propargylic esters undergo unidirectional mercuric ion-promoted hydration to afford good yields of γ-ketoesters.

Les trialcynylboranes réagissent avec le diazoacétate d'éthyle pour conduire aux esters propargyliques. La réaction se fait dans des conditions douces (−20°) et avec de bons rendements. Les esters propargyliques subissent une hydration unique, provoquée par les ions mercuriques, pour conduire aux esters γ-cétoniques avec de bons rendements.

Canadian Journal of Chemistry, **50**, 1105 (1972)

Although exploration of the synthetic applications of trialkylboranes is an area of active burgeoning development (1), the chemistry of their triacetylenic analogs, in marked contrast, has been almost completely unexplored. Studies directed toward elucidating the organochemical synthetic potential of these interesting derivatives have understandably been hampered by their intrinsic instability. Since they decompose above *ca.* −30°, trialkynylboranes[2] are usually synthesized as (stabilized) amine complexes (eq. 1).

$$[1]\quad 3RC{\equiv}CNa + BF_3\cdot Py \xrightarrow{\text{Pyridine}} (RC{\equiv}C)_3B\cdot Py$$

We have prepared solutions of triacetylenic boranes *in the absence of amine donors*, and utilized these reagents for a convenient mild synthesis of propargylic esters. The requisite organoborane is easily obtained by treating a lithium acetylide (from a terminal alkyne and *n*-butyllithium) with boron trifluoride etherate in tetrahydrofuran solvent[3] at −20° (eq. 2). Subsequent reaction with ethyl diazoacetate

$$[2]\quad 3RC{\equiv}CLi + BF_3\cdot OEt_2 \xrightarrow[-20^\circ]{\text{THF}} (RC{\equiv}C)_3B$$

provides good yields of the corresponding propargylic ester after hydrolysis (eq. 3). The

$$[3]\quad (RC{\equiv}C)_3B + N_2CHCOOC_2H_5 \xrightarrow[-N_2]{\text{THF, }-20^\circ} \xrightarrow{H_2O} RC{\equiv}CCH_2COOC_2H_5$$

reaction proceeds readily at −20°, and organoborane decomposition does not seriously interfere, as indicated by the results summarized[4] by eqs. 4–7.

$$[4]\quad (n\text{-}C_4H_9C{\equiv}C)_3B \xrightarrow[(88\%)]{100\%} n\text{-}C_4H_9C{\equiv}CCH_2COOC_2H_5$$

$$[5]\quad (C_6H_5C{\equiv}C)_3B \xrightarrow[(92\%)]{100\%} C_6H_5C{\equiv}CCH_2COOC_2H_5$$

$$[6]\quad (n\text{-}C_5H_{11}C{\equiv}C)_3B \xrightarrow[(87\%)]{97\%} n\text{-}C_5H_{11}C{\equiv}CCH_2COOC_2H_5$$

[1]Holder of a 1967 Science Scholarship.

[2]Evidence for their existence has been obtained at −60°, but attempts at isolation, under a variety of conditions, have led only to polymeric products (2). Reviews on unsaturated organoboron compounds are available (3, 4).

[3]In view of the fact that tris(phenylethynyl)borane forms a complex with tetrahydrofuran (5), the trialkynylboranes described herein may exist as THF complexes. No studies have been made of this matter, and these species are depicted as if uncomplexed merely for convenience and simplification.

[4]Numbers above and below the arrows represent g.l.p.c. and (unoptimized) isolated yields, respectively. The molar ratio of organoborane: diazoacetic ester varied from 1:1.3 to 1:2.

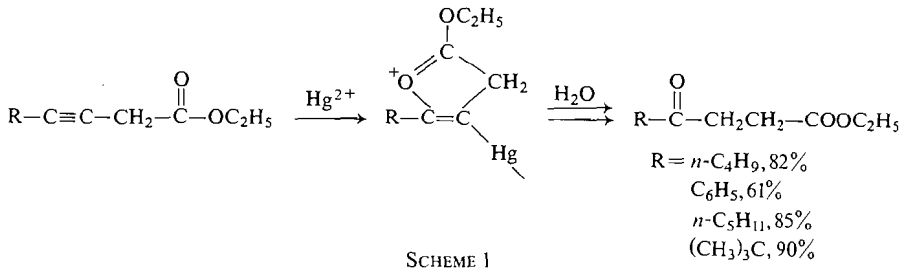

SCHEME 1

[7] $((CH_3)_3C—C\equiv C)_3B \xrightarrow[(63\%)]{83\%} (CH_3)_3C—C\equiv CCH_2COOC_2H_5$

Since propargylic esters are usually prepared by a multi-step sequence (6), this method offers a convenient, high-yield, abbreviated approach to these intermediates.

Moreover, mercuric ion-promoted hydration of β,γ-acetylenic esters occurs in a directionally-specific manner to produce γ-ketoesters. No β-ketoester formation could be detected. Although mechanistic studies have not as yet been undertaken, this regiospecific hydration may be

$$R—C\overset{Hg^{2+}}{\equiv}C—CH_2—COOC_2H_5$$

A

the ultimate outcome of an initial alkyne-Hg^{++} complex (**A**) leading to the more stable γ-carbonium ion as a consequence of the inductive (or field effect) exerted by carboethoxy.

Alternatively, regiospecificity may be the manifestation of carbonyl oxygen participation which results in formation of the more geometrically favorable five-membered ring.[5] Scheme 1 depicts this view, as well as isolated yields.

It is clear, however, that irrespective of which factor prevails, the present development provides a unique uncomplicated route to this class of compounds.[6]

However, in this propargylic ester synthesis, as in other organoborane-diazo reactions (9), only one organic moiety is utilized. In an attempt to circumvent this inherent difficulty, we briefly explored the reaction of dibutylheptynylborane[7] with ethyl diazoacetate in the hope of achieving selective migration of the alkynyl group. Surprisingly, the only ester product formed was ethyl hexanoate. This represents an interesting contrast to the behavior of the congeneric alanes, $R_2AlC\equiv CR$, which, in a variety of reactions, selectively transfer the ligand possessing the highest degree of *s*-character (11). We are continuing to explore the ramifications of these developments.

The experimental procedure is illustrated for the methylenecarbethoxylation of 1-heptyne, and the hydration of ethyl 3-nonynoate. To a solution of lithium 1-heptyne (from 1-heptyne (30 mmol) in 26 ml tetrahydrofuran and *n*-butyllithium[8] (30 mmol)) held at *ca.* $-20°$ was added, gradually, a solution of boron trifluoride etherate (40 mmol). The resulting solution was stirred an additional 0.5 h at *ca.* $-20°$, and a solution of ethyl diazoacetate (1.46 g, 12.8 mmol) was slowly added. After stirring for 1.5 h, water was added, the mixture stirred (*ca.* 20 min), then poured into ice water (200 ml). The aqueous phase was extracted with ether (three 30-ml portions) and the combined organic extract was dried (Na_2SO_4). The g.l.p.c. analysis indicated a 97% yield of ethyl 3-nonynoate. Solvent was removed *in vacuo* (rotary evaporator), and the crude residue was distilled to afford 1.44 g (87%) of ethyl 3-nonynoate, b.p. 90–91° (2.5 mm); n_D^{22} 1.4440; i.r. (liquid film) 1735 cm^{-1}; n.m.r. (τ, $CDCl_3$) 5.75 (2H, q, OCH_2CH_3), 6.70 (2H, t, $CH_2C{=}O$), 7.80 (2H, m, $CH_2CH_2C\equiv C$), 8.30–8.80 (6H, m, $(CH_2)_3$), 8.69 (3H, t, CH_3CH_2O), 9.09 (3H, t, $CH_3(CH_2)_3$); mass spectrum (70 eV) M^+ 182.

Anal. Calcd. for $C_{11}H_{18}O_2$: C, 72.49; H, 9.95. Found: C, 72.52; H, 9.76.

A mixture of ethyl 3-nonynoate (5.6 mmol),

[5]This possibility is analogous to proposals advanced to account for the unidirectional hydration of γ-ketoacetylenes (7).

[6]A variety of other approaches has been summarized (8).

[7]Prepared by reaction of dibutylboron bromide (10) with lithium 1-heptyne.

[8]A solution of *n*-butyllithium in hexane, obtained from Alfa Inorganics, Inc., was employed.

Can. J. Chem. Downloaded from www.nrcresearchpress.com by 210.87.254.42 on 09/05/12
For personal use only.

ethanol (50 ml), water (10 ml), concentrated sulfuric acid (3 drops), and mercuric sulfate (10 mg) was refluxed for 5 h. Solvent was removed *in vacuo* and the oily residue was dissolved in ether. The ethereal solution was washed with saturated sodium bicarbonate solution, dried (Na_2SO_4), and evaporated. Molecular distillation of the residue provided 1.00 g (85%) of ethyl 4-oxononanoate, n_D^{21} 1.4369; i.r. (liquid film) 1735, 1710 cm^{-1}; n.m.r. (τ, $CDCl_3$) 5.88 (2H, q, OCH_2CH_3), 7.41 (6H, m, $CH_2CO(CH_2)_2CO$), 8.65 (6H, m, $(CH_2)_3$), 8.75 (3H, t, CH_3CH_2O), 9.11 (3H, t, CH_3CH_2).

We thank the National Research Council of Canada for financial support of this work.

1. H. C. Brown. Accts. Chem. Res. **2**, 65 (1969).
2. E. C. Ashby and W. E. Foster. J. Org. Chem. **29**, 3225 (1964).
3. W. E. Davidsohn and M. C. Henry. Chem. Rev. **67**, 73 (1967).
4. A. V. Topchiev, A. A. Prokhorova, and M. V. Kurashev. Russ. Chem. Rev. **33**, 453 (1964).
5. U. Kruerke. Z. Naturforsch. **11***b*, 676 (1956).
6. M. S. Newman and J. H. Wotiz. J. Am. Chem. Soc. **71**, 1292 (1949).
7. G. Stork and R. Borch. J. Am. Chem. Soc. **86**, 935 (1964).
8. C. R. Noller. Chemistry of organic compounds. W. B. Saunders Company, Philadelphia, 1965.
9. J. Hooz, D. M. Gunn, and H. Kono. Can. J. Chem. **49**, 2371 (1971); J. Hooz and G. F. Morrison. Can. J. Chem. **48**, 868 (1970); J. Hooz and D. M. Gunn. Tetrahedron Lett. 3455 (1969); J. Hooz and D. M. Gunn. J. Am. Chem. Soc. **91**, 6195 (1969); J. Hooz and S. Linke. J. Am. Chem. Soc. **90**, 5936, 6891 (1968); J. Hooz and D. M. Gunn. Chem. Commun. 139 (1969).
10. J. R. Johnson, H. R. Snyder, and M. G. Van Campen, Jr. J. Am. Chem. Soc. **60**, 115 (1938).
11. J. Hooz and R. B. Layton. J. Am. Chem. Soc. **93**, 7320 (1971).

Can. J. Chem. Downloaded from www.nrcresearchpress.com by 210.87.254.42 on 09/05/12
For personal use only.

Can. J. Chem. Downloaded from www.nrcresearchpress.com by 210.87.254.42 on 09/05/12
For personal use only.

Canadian Journal of Chemistry

Published by THE NATIONAL RESEARCH COUNCIL OF CANADA

VOLUME 50 APRIL 15, 1972 NUMBER 8

Densities, Excess Volumes, Surface Tensions, Viscosities, and Dielectric Constants of the Systems: Methanol–Cyclohexane, Acetone–Methanol, Acetone–Cyclohexane, and Methanol–Cyclohexane–Acetone

A. N. CAMPBELL AND S. C. ANAND

Department of Chemistry, University of Manitoba, Winnipeg 19, Manitoba

Received October 7, 1971

The density, dielectric constant, change of volume on mixing, refractive index, surface tension, and viscosity of the methanol–cyclohexane system have been investigated experimentally at temperatures ranging from 25° to 50°. The same properties of the binary systems acetone–methanol and acetone–cyclohexane, as well as of the ternary system methanol–cyclohexane–acetone were determined experimentally at 25°. The critical region of the partially miscible system methanol–cyclohexane has been investigated by determining the above physical properties at temperatures above and below the critical solution temperature. A similar investigation of the ternary system has been made, isothermally at 25°, by investigating solutions lying in the neighborhood of the plait point.

The surface tension or a derived function of it, *viz.* the molecular surface energy, does not show a horizontal portion of the isotherm in the methanol–cyclohexane system, but the ternary system does show such a constant surface tension, probably fortuitously, all along the tangential line. The viscosity exhibits anomaly.

All the systems show azeotropic behavior. The methanol–cyclohexane and acetone–cyclohexane systems show marked deviations in molar polarization from linearity and this agrees with the thermodynamic data, which indicate larger than unity values for the activity coefficients of the components' behavior (1). The viscosity isotherms of all these systems give no indication of the formation of any stable compound.

On a étudié expérimentalement la densité, la constante diélectrique, le changement de volume au cours du mélange, l'indice de réfraction, la tension superficielle et la viscosité du système méthanol–cyclohexane à des températures allant de 25° à 50°. On a déterminé expérimentalement à 25° les mêmes propriétés des systèmes binaires: acétone–méthanol et acétone-cyclohexane, de même que celles des systèmes ternaires méthanol–cyclohexane–acétone. La région critique du système partiellement nuisible: méthanol–cyclohexane a été étudiée en déterminant les propriétés physiques citées plus haut, au-dessus et en bas de la température critique de la solution. Une enquête similaire sur les systèmes ternaires a aussi été faite, isothermiquement à 25°, en étudiant des solutions se trouvant au voisinage du point d'inflexion.

La tension superficielle ou une fonction dérivée, l'énergie moléculaire superficielle ne montre pas de partie horizontale de l'isotherme du système méthanol–cyclohexane, mais le système ternaire montre une tension superficielle constante, probablement fortuitement, le long de la ligne tangentielle. La viscosité est anormale.

Tous les systèmes ont un comportement azéotropique. Les systèmes méthanol–cyclohexane et acétone–cyclohexane démontrent des déviations marquées de polarisation molaire de la linéarité et ceci condorde avec les données thermodynamiques, qui indiquent des valeurs plus grandes de coefficients d'activité des composés (1). Les isothermes de viscosité de tous les systèmes ne donnent aucune indication sur la formation d'un composé stable.

Canadian Journal of Chemistry, **50**, 1109 (1972)

Introduction

The general purpose of a series of papers of which the present makes one is to investigate physical properties in the immediate neighborhood of the critical states, $L \rightleftarrows V$, and $L_1 \rightleftarrows L_2$. Homogeneity can be attained in both the above types by working at a temperature slightly above (or occasionally, slightly below) the critical temperature or the critical solution temperature, respectively. The region is of interest because the structure is colloidal or semi-colloidal, as is obvious from the scattering of light. Thermo-

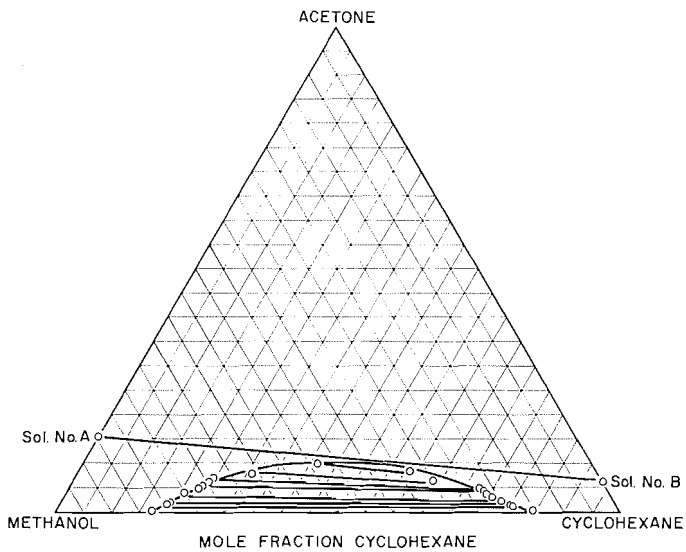

FIG. 1. Binodal curve data for the ternary system: methanol–cyclohexane–acetone at 25 °C.

dynamics requires that certain properties of consolute solutions be identical. The question arises of whether solutions of the same composition retain this identity slightly above the critical temperature. It has been suggested that this identity, *e.g.* of vapor pressure, is thermodynamically necessary for a range of temperature above the critical point, but this view now seems to be more or less abandoned. In fact, we have shown that for various systems, though identity is hard to prove, close similarity does persist above the critical temperature.

In the case of the equilibrium $L_1 \rightleftarrows L_2$, it is possible to study the physical properties isothermally by adding sufficient of a third component to render the system homogeneous. For this purpose we have invariably used acetone. In all the systems we have studied, a very little acetone was sufficient to produce homogeneity. Nevertheless, the two-component system has now become a three-component system and it becomes necessary to study not only the three-component system as such, but also the three binary systems of which it is composed. For obvious reasons, the partially miscible binary system merits attention, but so do the two binary systems involving acetone, since these may or may not be ideal. Only after this work has been completed is it possible to proceed to the investigation of the pseudo-binary system represented by solutions lying on the straight line tangential to the binodal curve (Fig. 1).

In a previous paper (1) we have dealt with the most important thermodynamic properties, *viz.* vapor pressure and heat of mixing. The properties now studied were taken more or less at random and in accordance with apparatus at our disposal. Some are rate processes and there is no *a priori* reason to suppose that any of them should be identical for different concentrations, even in the heterogeneous region. Thus, for example, it is not thermodynamically necessary that the surface tensions of two layers in equilibrium should be identical. It is, however, experimentally true in the majority of cases, that these physical properties change only slowly over the range of composition corresponding to the miscibility gap (at room temperature). Our numerical data for density, surface tension, viscosity, refractive indices, and dielectric constant, of the pure liquids, of the binary systems, and of the ternary system, are all to be found in the Depository of Unpublished Data, but for precise details of our experimental methods, reference should be made to ref. 3 and to previous publications (1, 2).[1]

[1]Complete set of tables is available from the Depository of Unpublished Data, National Science Library, National Research Council of Canada, Ottawa, Canada K1A 0S2.

Can. J. Chem. Downloaded from www.nrcresearchpress.com by 210.87.254.42 on 09/05/12
For personal use only.

Can. J. Chem. Downloaded from www.nrcresearchpress.com by 210.87.254.42 on 09/05/12
For personal use only.

Discussion of Results

Pure Liquids

Density and Surface Tension

For cyclohexane the average value of the temperature coefficient of density, dd/dt, is 0.0009 per deg, between 25° and 50°. For what it is worth, the parachor value is 240.61 ± 0.26, as against a calculated value (from atomic parachors) of 240.10. For methanol, the average value of the temperature coefficient of density, dd/dt is 0.00094 per deg, between 25° and 50°. The parachor value of methanol is 88.25 ± 0.18, as against a calculated value of 93.20 (or 92.0, depending on the values assigned to the atomic parachors). If any faith is to be placed in the parachor, the results indicate that cyclohexane is practically an inert solvent and methanol highly associated (4). The parachor value of methanol increases slightly with rising temperature, indicating a decrease in the degree of association with rising temperature.

Viscosity

Of numerous viscosity–temperature relations that we tested for cyclohexane, that of deGuzman (5) was found to be the best. The equation is

$$\eta = A.e^{E/RT}$$

where E is a positive constant, called the viscous heat. The average values of the constants A and E are 5.408×10^{-3} and 3024.5, respectively. The calculated viscosities obtained from this equation agree with the experimental values with an accuracy of 0.75%. DeGuzman's equation, however, fails entirely to apply to methanol: it is said that deGuzman's equation does not apply to polar liquids (6, 7).

An equation proposed by Bingham (8) was found the best for reproducing the experimental values for methanol:

$$T = A/\eta + C - B\eta$$

where η is the viscosity, T is the temperature in absolute degrees, and A, B, and C are constants. The average values of the constants A, B, and C are 31.414, 10.944, and 246.401, respectively. By means of this equation, the experimental values are reproduced with an accuracy of $\pm 0.50\%$,

Pelofsky (9) has related viscosity to surface tension (λ) by the following equation:

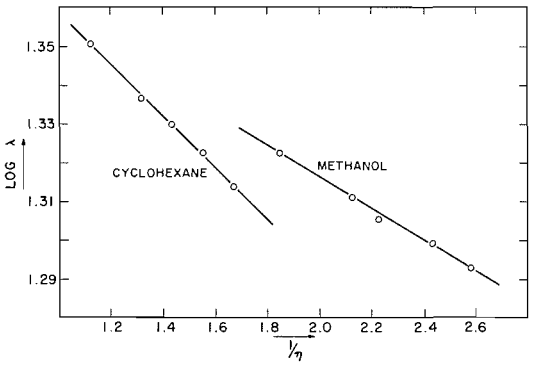

FIG. 2. Plot of logarithm of surface tension *vs.* reciprocal of viscosity for cyclohexane and methanol at different temperatures.

$$\lambda = A \exp B/\eta$$

where A and B are dimensionless constants. Plots of $\log \lambda$ *vs.* $1/\eta$ at 25°, 35°, 40°, and 50°, do indeed give straight lines, as the above equation requires, for cyclohexane and methanol (Fig. 2).

Binary and Ternary Systems

Excess Volumes

The excess volume is positive for all systems, except acetone–methanol, where it is slightly negative; in other words, for all systems except acetone–methanol there is an expansion on mixing the constituents. With acetone–methanol there is a very slight contraction. The expansion is greatest for the acetone–cyclohexane system. It is easy to explain the expansion as due to depolymerization of an associated liquid, but the slight contraction with acetone–methanol is not so easy to account for: contractions are usually associated with complex formation.

Viscosity and Dielectric Constant

There is neither maximum nor minimum on the viscosity isotherms of the binary systems, at 25°. According to Bamelis *et al.* (10) and Liler and Kosabovic (11), such viscosity isotherms are characteristic of those systems in which no addition compounds or compounds of low stability only are formed. The main factor, however, producing a viscosity isotherm of this shape is probably the disruption of the structure of polar liquids, such as methanol and acetone by the addition of cyclohexane.

The molar polarization, P' is defined by

$$P' = \frac{X_1M_1 + X_2M_2}{d_{\text{mixt}}} \cdot \frac{E-1}{E+2}$$

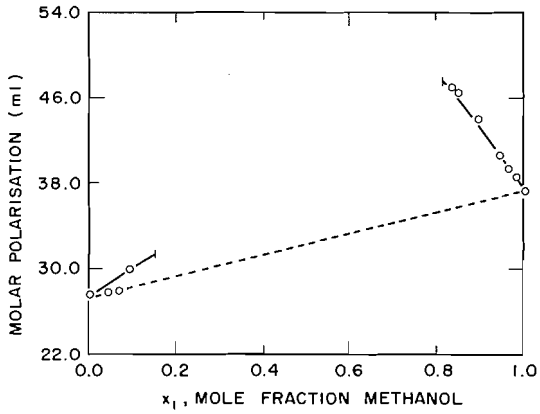

FIG. 3. Molar polarization of the methanol–cyclohexane system at 25 °C.

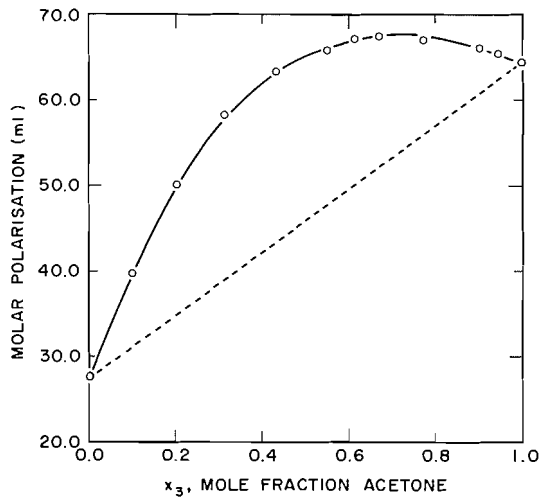

FIG. 4. Molar polarization of the acetone–cyclohexane system at 25 °C.

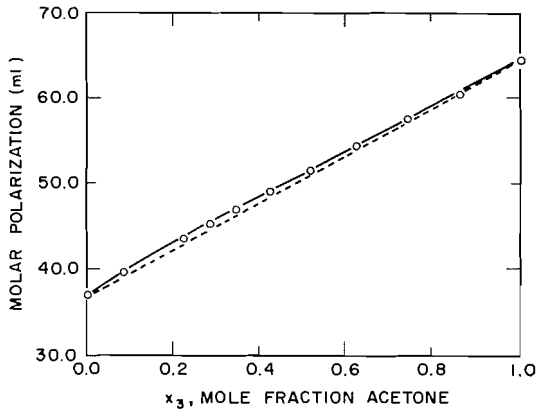

FIG. 5. Molar polarization of the acetone–methanol system at 25 °C.

where E is the dielectric constant and d the density of the mixture.

The distortion polarization is given by

$$P_d = \frac{n^2 - 1}{n^2 + 2} \cdot \frac{X_1 M_1 + X_2 M_2}{d_{mixt}}$$

where n is the refractive index.

Syrkin (12) proposed the following formula for orientation polarization,

$$P_i = \frac{P' - X_1 R_1 - X_2 R_2}{1 - \left(\frac{E-1}{E+2}\right)^2}$$

where P' is the molar polarization and R_1 and R_2 are the molar refractions of the pure components. The molar polarizations are represented graphically in Figs. 3, 4, and 5. All the graphs show positive deviation from linearity, that of methanol–cyclohexane being the greatest, followed by that of acetone–cyclohexane and again by that of acetone–methanol, where the deviation is very slight. This agrees with the observation of Campbell and Kartzmark (13, 14) that strong positive deviation from additivity in molar polarization is an indication of tendency towards formation of a miscibility gap. The statement of Campbell and Kartzmark received further support from the thermodynamic data as the activity coefficients of these systems show similar behavior (1).

When the Syrkin orientation polarization is plotted *vs.* mole fraction, a straight line is said to be obtained in the ideal case. Positive deviation indicates the existence of hydrogen bonding between the components. Negative deviation indicates dipole association, dipole-induced dipole interactions or there is a decrease in hydrogen bonding with dilution. The acetone–cyclohexane system shows negative deviation from additivity. The methanol–cyclohexane and acetone–methanol systems show both positive and negative deviations from additivity. The acetone–methanol system shows positive deviation at concentrations less than 0.52 mole fraction acetone and negative deviation at concentrations greater than 0.52. Thus, at higher concentrations of methanol some interaction may take place between methanol and acetone, while at higher concentrations of acetone, the methanol dissociates. As mentioned above, the

Can. J. Chem. Downloaded from www.nrcresearchpress.com by 210.87.254.42 on 09/05/12
For personal use only.

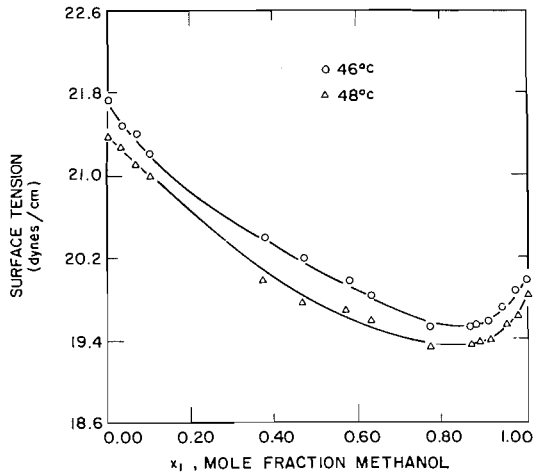

FIG. 6. Surface tension of the methanol–cyclohexane system near the critical solution temperature.

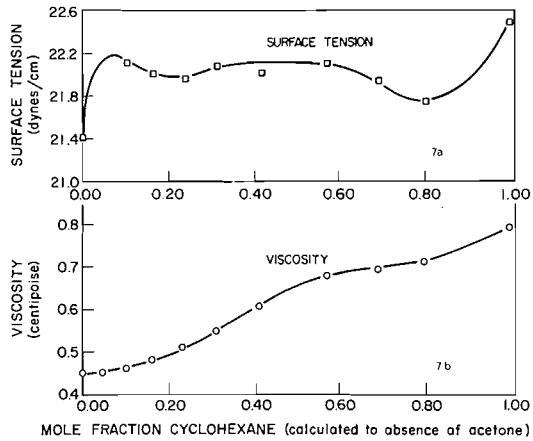

FIG. 7. Viscosities (*b*) and surface tensions (*a*) of such compositions of the ternary system: methanol–cyclohexane–acetone as lie on the tangential line AB (as shown in Fig. 1), and calculated to absence of acetone.

viscosity isotherm gives no indication of the formation of a stable addition compound.

Properties in the Neighborhood of the Critical Solution Temperature

Surface Tension for the Methanol–Cyclohexane System

The results are expressed graphically in Fig. 6 at two temperatures just above the critical solution temperature. For this system there is no temperature for which an isotherm has a range of constant surface tension, neither does thermodynamics require that this should be so. According to Hildebrand and Scott (15), systems showing large positive deviations from Raoult's law give rise to a minimum on the surface tension diagram. This is exemplified by the methanol–cyclohexane diagram which shows large positive deviations from Raoult's law, as well as partial miscibility. The molecular surface energy of cyclohexane is higher than that of methanol. This may indicate that the intermolecular forces between cyclohexane molecules are greater than those between methanol molecules.

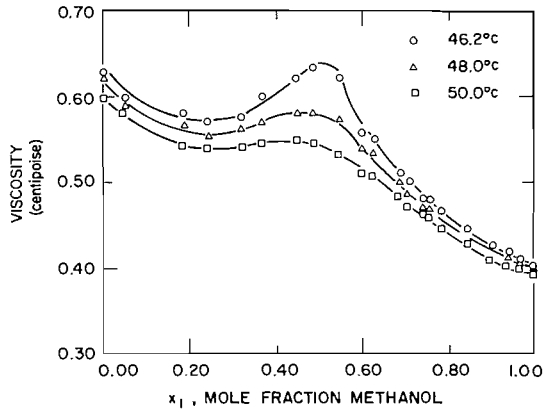

FIG. 8. Viscosity of the methanol–cyclohexane system near the critical solution temperature.

The isothermal (25°) data for such compositions of the ternary system: methanol–cyclohexane–acetone, as lie on the tangential line AB of Fig. 1, are plotted in Fig. 7*a*. The data are calculated to absence of acetone.

The graph indicates that over the critical range of composition and within the limits of experimental error, the surface tension may well be constant. This, however, may be accidental since the surface tensions of the parent solutions A and B differ but little.

Viscosity

As shown in Fig. 8 the anomalous increase in viscosity above the critical solution temperature extends over a considerable range of concentration, *viz.* 0.32 to 0.62 mole fraction methanol, in the methanol–cyclohexane system. This region agrees with the coexistence data of Campbell and Kartzmark (16). The magnitude of the anomalous increase in viscosity is of the order of 15 to 25%, near the critical solution temperature and critical composition. Various theories of viscosity near the critical solution temperature (17–20) explain this anomalous

Can. J. Chem. Downloaded from www.nrcresearchpress.com by 210.87.254.42 on 09/05/12
For personal use only.

increase in viscosity as due to the colloidal structure of the mixture near the critical solution temperature and this colloidal solution is idealized as a continuous medium, in which composition, density, and local viscosity all vary from point to point and are also time dependent.

Figure 7*b* shows the viscosity behavior of the ternary solutions in the neighborhood of the plait point. The viscosity varies more or less continuously with cyclohexane content, except that a small region of anomalous viscosity may be said to exist between 35 and 75 mol% cyclohexane.

The general conclusions of this part are: (*1*) the rule of Campbell and Kartzmark, *viz.* that systems showing strong positive deviation from additivity in molar polarization, exhibit partial miscibility, either at room temperature or some other temperature is confirmed. (*2*) In the pseudo-binary section of the ternary system, the surface tension is constant over the critical range, although there is no apparent reason for this. (*3*) The viscosity plot is, as always, anomalous over the critical range.

1. A. N. CAMPBELL and S. C. ANAND. Can. J. Chem. In press.
2. A. N. CAMPBELL, E. M. KARTZMARK, S. C. ANAND, Y. CHENG, H. P. DZIKOWSKI, and S. M. SKRYNYK. Can. J. Chem. **46**, 2399 (1968).
3. S. C. ANAND. Ph.D. Thesis. University of Manitoba, Winnipeg, Manitoba. 1970.
4. S. GLASSTONE. Text book of physical chemistry. MacMillan and Co., London. 1960.
5. J. DEGUZMAN. Anal. Fis. Quim. **9**, 353 (1913).
6. E. N. DAC. ANDRADE. Viscosity and plasticity. Heffer, Cambridge. 1947.
7. P. B. MACEDO and T. A. LITOVOTZ. J. Chem. Phys. **42**, 245 (1965).
8. E. C. BINGHAM. Fluidity and plasticity. 1st ed. McGraw-Hill, New York. 1922.
9. H. A. PELOVSKY. J. Chem. Eng. Data, **11** (3), 394 (1966).
10. P. BAMELIS, P. HUYSKENS, and E. MEEUSSEN. J. Chem. Phys. **62**, 158 (1965).
11. M. LILER and D. KOSABOVIC. Symposium of hydrogen bonding at Ljubljana, Pergamon Press, New York. 1959. p. 529.
12. Y. K. SYRKIN. Compt. rend. U.S.S.R. **35**, 43 (1942).
13. A. N. CAMPBELL and E. M. KARTZMARK. Can. J. Chem. **48**, 904 (1970).
14. A. N. CAMPBELL and E. M. KARTZMARK. Can. J. Chem. **47**, 619 (1969).
15. J. H. HILDEBRAND and R. L. SCOTT. Regular solutions. Prentice-Hall, New Jersey. 1962.
16. A. N. CAMPBELL and E. M. KARTZMARK. Can. J. Chem. **45**, 2433 (1967).
17. M. FIXMAN. J. Chem. Phys. **36**, 310 (1962).
18. M. FILMAN and W. BOTCH. J. Chem. Phys. **36**, 3100 (1962).
19. J. M. DEUTCH and H. ZIVANZIG. J. Chem. Phys. **46**, 1612 (1967).
20. K. KAWASAKI and M. TANAKA. Proc. Roy. Phys. Soc. **90**, 791 (1967).

Can. J. Chem. Downloaded from www.nrcresearchpress.com by 210.87.254.42 on 09/05/12
For personal use only.

Kinetics of the Mercury-Photosensitized Decomposition of Neopentane. Part I. The Overall Mechanism

E. FURIMSKY and K. J. LAIDLER

Department of Chemistry, University of Ottawa, Ottawa K1N 6N5, Canada

The mercury-photosensitized decomposition of neopentane was investigated from 230 to 335 °C, and at pressures from 3 to 280 Torr. The following were identified as primary products and their initial rates of formation measured over a range of conditions: H_2, CH_4, C_2H_6, i-C_4H_8, neohexane and dineopentyl. The results are explained in terms of a mechanism in which the primary step involves the split of neopentane (Nptn) into the neopentyl radical (Nptl) and H; Nptl then undergoes further reactions including a split into i-C_4H_8 + CH_3. Estimates are made of the free-radical concentrations at various temperatures and pressures. A simplified steady-state treatment is worked out and is shown to explain the pressure dependence of the rates of formation of the various primary products.

On a étudié la décomposition photosensibilisée au mercure du néopentane de 230 à 335 °C, à des pressions de 3 à 280 Torr. Les composés suivants ont été identifiés comme étant des produits primaires et leurs vitesses initiales de formation ont été mesurées dans un domaine de conditions: H_2, CH_4, C_2H_6, i-C_4H_8, néohexane, et dinéopentyl. On a expliqué les résultats en termes d'un mécanisme dans lequel l'étape primaire implique la dissociation du néopentane (Nptn) en radical néopentyl (Nptl) et H; Nptl réagit encore, notamment il se dissocie en i-C_4H_8 + CH_3. On a fait l'estimé des concentrations en radical libre à différentes températures et pressions. On a aussi développé un calcul d'état stationnaire et on a montré qu'il explique l'influence de la pression sur les vitesses de formation des différents produits primaires.

Canadian Journal of Chemistry, **50**, 1115 (1972)

Can. J. Chem. Downloaded from www.nrcresearchpress.com by 210.87.254.5 on 09/05/12
For personal use only.

Introduction

The method of photosensitization provides a valuable means of generating free radicals and of studying their subsequent reactions. Recent investigations in this laboratory have been concerned with the mercury-photosensitized decompositions of ethane (1), dimethyl ether (2–5), and propane (6, 7), the object being to obtain reliable kinetic parameters for the decompositions of the radicals produced, and to study the behavior over a range of pressures.

The present investigation is concerned with the mercury-photosensitized decomposition of neopentane. The present paper (Part I) is concerned with the experimental methods and results, and with an interpretation of the overall behavior as far as primary products are concerned. Conclusions about the kinetics of reactions of the neopentyl and methyl radicals, especially relative to pressure dependence, are described in the following paper (Part II). Part III is concerned with the kinetics and mechanisms of formation of the secondary products.

Several previous investigations have been concerned with the mercury-photosensitization of neopentane. In an early study Darwent and Steacie (8) established the main course of the reaction, but their measurements were necessarily made at fairly high conversions, so that there were complications due to secondary reactions. In addition, since their mercury saturator was at 20 °C, it is likely that the work was done under conditions of light inhomogeneity; the problems arising from this have been stressed by Loucks and Laidler (2). Their work indicated a very small quantum yield for H_2 production (*e.g.* 0.004 at 25 °C), and they concluded that an important initial step is the transfer of energy to a C_5H_{12} molecule. This, however, violates the spin-conservation rule (9), and is inconsistent with the most recent studies on the paraffins. It is now clear that an important factor leading to a low quantum yield in these experiments is the reaction of H atoms with *neo*-C_5H_{11} radicals, a process that is favored by the light inhomogeneity which leads to high concentrations of H and *neo*-C_5H_{11} at one side of the reaction vessel. Another possible reason for the apparent low quantum yield is the presence of olefin impurities in the *neo*-C_5H_{12}. A more recent investigation by Holroyd and Klein (10) indicated a much higher quantum yield than determined by Steacie and Darwent.

Norstrom, Strausz, and Gunning (11) have reinvestigated the quantum yield for the process, taking care to eliminate olefin impurities from the *neo*-C_5H_{12}. The values were much higher, and suggest that the true primary

Can. J. Chem. Downloaded from www.nrcresearchpress.com by 210.87.254.5 on 09/05/12
For personal use only.

quantum yield is unity, the main initial process thus being

$$Hg(^3P_1) + neo\text{-}C_5H_{12} \rightarrow neo\text{-}C_5H_{11} + H + Hg(^1S_0)$$

On the other hand, an investigation by Sato and Tsunashima (12) has led to a low quantum yield: however, an examination of their results suggests that there was considerable light inhomogeneity, and that there was confusion between primary and secondary products. Our own experiments confirm the conclusions of Gunning and co-workers (11) that the main initial step is the production of $neo\text{-}C_5H_{11} + H$.

Studies have also been made of the vacuum ultraviolet photolysis (13) and pyrolysis (14–17) of neopentane.

Experimental

Apparatus

The reaction was carried out in a static system. A cylindrical quartz reaction vessel was used; it had plane parallel windows at both sides, was about 9 cm in length and 5 cm in diameter, and its volume was 170 cc. It was wrapped in asbestos, and placed in a cylindrical copper collar 14 cm in length. This collar was well insulated and heated electrically, the heating being regulated by a thermo electric temperature controller activated by means of a thermocouple placed in the wall of the collar and reaching the middle of the reaction vessel. The temperature of the reaction vessel was measured at three positions by means of chromel–alumel thermocouples.

The lamp was a low-pressure lamp emitting the characteristic line spectrum of mercury vapor, with peak emission at 2537 Å. It was supported at 25 cm from the window of the reaction vessel and operated at room temperature; before each experiment it was warmed up for 20 min. The 1849 Å line was eliminated by use of a Corning filter C.S. No. 9–54.

The concentration of mercury in the reaction vessel was controlled by the temperature of a spiral trap in the head of the reaction vessel. The temperature of the trap was −15.3 °C.

Materials

The neopentane used was obtained from Phillips Petroleum Company with stated research grade purity of 99.92%; it was further purified, after thorough degassing by distillation from methylene chloride slush (−97 °C), to *n*-pentane slush (−132 °C). Only the middle fraction was used in the investigation. Gas chromatographic analysis of this sample showed no impurities in front of the neopentane peak; a very small peak (probably C_5) was observed on the tail of the neopentane peak; this peak changed very little after one hour's irradiation at 335 °C.

Dineopentyl(2,2,5,5-tetramethylhexane) and 2,2,4,4-tetramethylpentane were obtained from the American Petroleum Institute as API Standard Samples, and 2,2,3,3-tetramethylbutane was obtained from the Matheson-Coleman Co. These compounds were used for calibration without further purification. Neohexane (2,2-dimethylbutane) was obtained from the Aldrich Chemical Co. and was purified by distillation before being used for calibrations.

Procedure

Before each experiment the apparatus was evacuated to 10^{-5} Torr. Neopentane was saturated with mercury vapor by passing it over mercury at 0 °C and was then passed through a spiral trap containing mercury at −15.3 °C; it was then admitted to the reaction vessel. Special attention was paid to the mercury vapor pressure; at all times when the experiments were not being done the mercury saturator was kept at −196 °C (liquid N_2) in order to condense mercury remaining in the reaction vessel, and so to avoid an excess of mercury during the experiments.

The reaction was started by the removal of a shutter and was stopped by switching off the lamp. The reaction products and the remaining neopentane were trapped in a U-tube immersed in liquid N_2, and then underwent analysis.

Analysis

The reaction products were separated into three fractions: (*1*) non-condensables, (*2*) condensables at −196 °C (liquid N_2); (*3*) condensables at −97 °C (methylene chloride slush). In order to prevent loss of C_2 hydrocarbons, a solid N_2 trap (at −210 °C) was used in series with the liquid N_2 trap. Non-condensable products (H_2 and CH_4) were collected by Toepler pumping for 30 min. The type *2* condensables comprised C_2H_6, $i\text{-}C_4H_8$, and neohexane (primary products) and C_2H_4, C_3H_6, C_3H_8, and $i\text{-}C_4H_{10}$ (secondary products). Type *3* condensables comprised 2,2,5,5-tetramethylhexane (primary) and 2,2,3,3-tetramethylbutane and 2,2,4,4-tetramethylpentane (secondary products).

The volume of the non-condensables was first measured in the gas burette; they were then analyzed chromatographically using a 6 m column filled with 80–100 mesh Porapak Q at 0 °C. Fraction *2* was analyzed on an 8.5 column of 30% Squalane on 60–80 mesh Chromosorb P operating at 30 °C; this gave a very good separation of $i\text{-}C_4H_8$ and $i\text{-}C_4H_{10}$. Peak heights were found to be satisfactory except with *neo*-hexane, for which the area was measured. Fraction *3* was analyzed on a 0.5 m column of 30% Squalane on 60–80 mesh Chromosorb P; peak areas were measured because the accuracy of the yield measurements was limited when peak heights were measured. All columns used were 1/4 in. in diameter.

The gas chromatograph used was assembled from commercially available units. The detector used was of a thermistor type and was maintained at 30 °C. The detector was supplied from 6 batteries of 1.5 V (Mallory – M 900) connected in series. The output used was 8 V d.c. and the current through the filament of the detector was 200 mA. The signal from the detector was put through a 10 mV Leeds and Northrup Speedomax Type G recorder. A good baseline was obtained by installing Edwards pressure controllers in both the reference flow and the sensing flow. Greatest sensitivity is obtained when the carrier and the sample have widely differing conductivities; most products have low conductivities, and therefore helium, having a high conductivity, was used in all cases.

Reaction Conditions

A compromise had to be made between the temperature of the mercury saturator and the light homogeneity in the reaction vessel at a given reactant pressure. It was originally intended that the temperature of the saturator should be

Can. J. Chem. Downloaded from www.nrcresearchpress.com by 210.87.254.5 on 09/05/12
For personal use only.

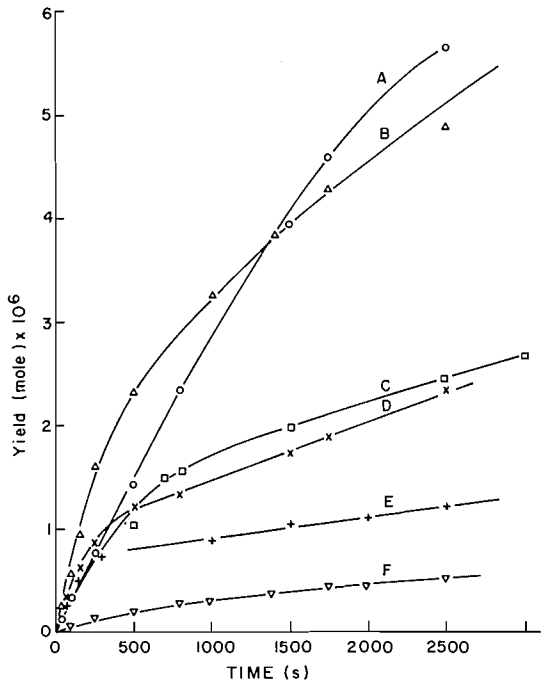

FIG. 1. Yield–time curves for primary products at a temperature of 286 °C and at pressure of 112 mm Hg. *A*, methane; *B*, *i*-C_4H_8; *C*, dineopentyl (at temperature of 256 °C); *D*, hydrogen; *E*, neohexane; *F*, ethane.

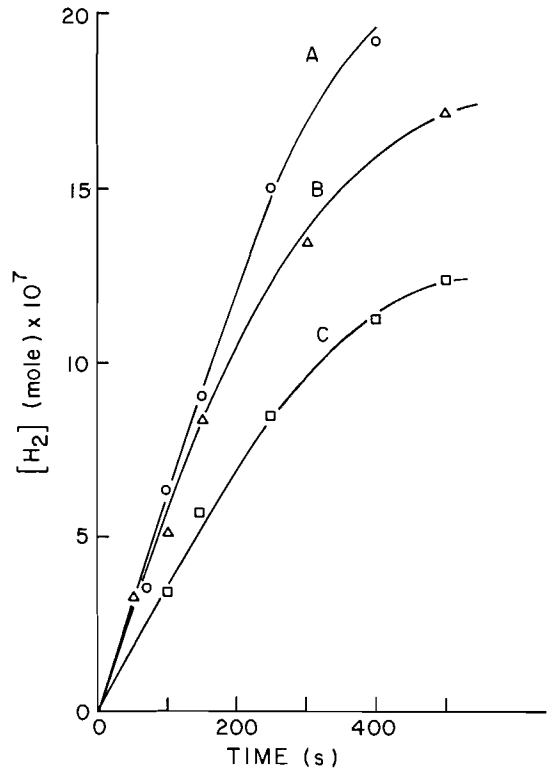

FIG. 2. Yield–time curves for production of hydrogen at 256 °C and at different pressures. *A*, 225; *B*, 110; and *C*, 27 mm Hg.

−32 °C, but the highest reactant pressure that could then be used was 108 mm. At 0 °C it was possible to use a reactant pressure of 530 Torr; however, the region of light inhomogeneity was approached. As a compromise the work was done at a saturator temperature of −15.3 °C, at which the vapor pressure of neopentane is 280 Torr.

Several runs were done to find the maximum temperature of the reaction system at which the rate became independent of pressure; this was found to be 310 °C. It was originally intended that this should be the highest temperature used in the study, but it was later found necessary to work up to 335 °C. At 230 °C, the lowest temperature employed, no measurable amount of ethane was formed; at 256 °C an accurate rate of ethane formation could be measured only at higher pressures. In order to obtain more complete information concerning the combination of CH_3 radicals, and to obtain some parameters for the H abstraction by CH_3 radicals, the experiments were also carried out at 335 °C. Unfortunately, at this temperature the region of constant rate of methane production was not reached.

The highest pressure used was 280 Torr, the vapor pressure of neopentane at the mercury saturator temperature (−15.3 °C). The accuracy of the analysis was limited in the low-pressure region. At 230 and 256 °C reliable rates could not be obtained below 16 and 10 Torr, respectively. At higher temperatures sufficient amounts of CH_4, C_2H_6, and *i*-C_4H_8 were produced at lower pressures, and accurate analyses could be made. Hydrogen also could not be analyzed satisfactorily at the lowest pressures.

Results and Interpretations

As primary products were analyzed: H_2, CH_4, C_2H_6, *i*-C_4H_8, neohexane (2,2-dimethylbutane), and dineopentyl (2,2,5,5-tetramethylhexane). The amounts of H_2, CH_4, *i*-C_4H_8, and neohexane were measured over the entire temperature range (230–335 °C). At 230 °C no measurable amounts of C_2H_6 were obtained. Dineopentyl was observed only at 230 and 256 °C, and at the lower temperature only an approximate rate of production could be obtained; at 286 °C it was detected only in small amounts at high conversions.

Figure 1 shows the yield–time curves at 286 °C for all primary products except dineopentyl, which was studied at 256 °C. The curves are linear only at very low conversions; the effect of secondary reactions on methane formation is evident at later stages.

Hydrogen Production

Typical yield–time curves for H_2 are shown in Fig. 2. The length of the linear region decreases

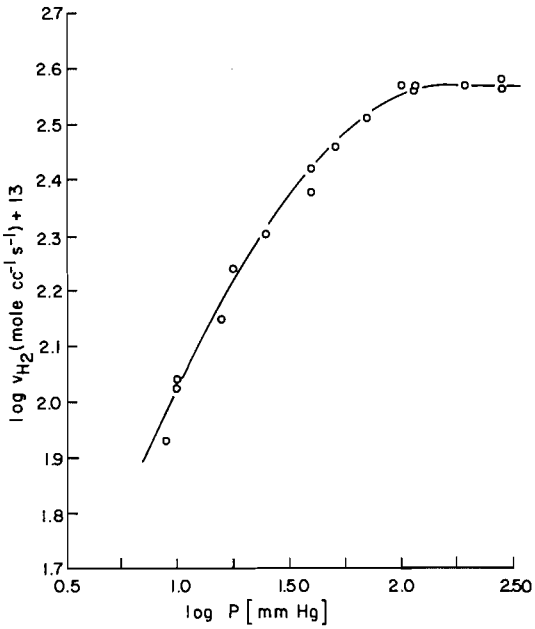

FIG. 3. Order plot for hydrogen production.

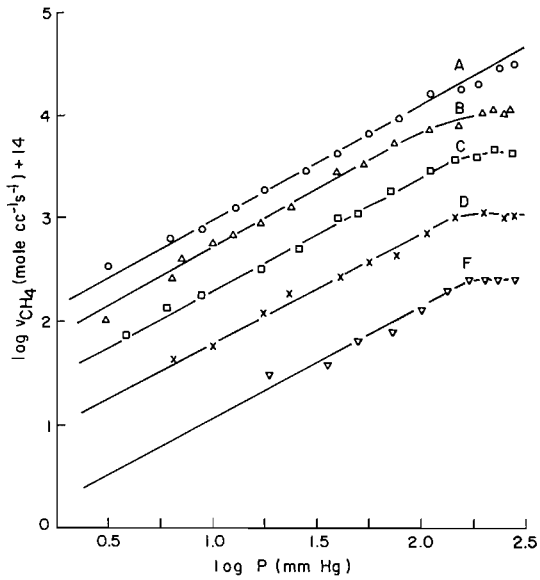

FIG. 4. Order plots for methane at different temperatures: *A*, 335; *B*, 310; *C*, 286; *D*, 256; and *E*, 230 °C.

with increase of temperature, owing to increase in i-C_4H_8 concentration with increase of temperature. Initial rates were obtained from the slopes in the linear region, and Fig. 3 shows a double logarithmic plot of the initial rate of H_2 production against the pressure; the order changes from 1.0 at low pressures to zero at higher pressures. Within the experimental error the rate of H_2 production shows no temperature dependence.

Methane Production

The methane yield–time curves were linear (*cf.* Fig. 1); secondary reactions are only important at very high conversions. Order plots of initial rates are shown in Fig. 4; the order varies from 1.0 at low pressures to zero at high pressures. An Arrhenius plot is shown in Fig. 5, for rates at 280 Torr; the activation energy is 28.8 kcal per mole.

Ethane Production

The ethane yield–time curves are initially linear and later show deviations from linearity. Order plots are shown in Fig. 6; the order changes from 1.0 at low pressures to zero at high pressures. An Arrhenius plot leads to an activation energy of 28.8 ± 0.5 kcal per mole.

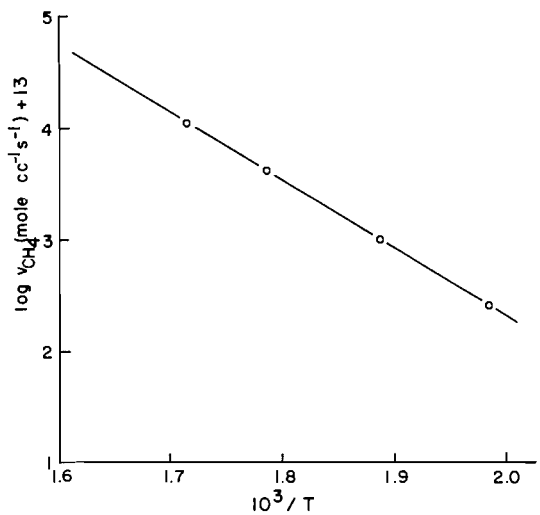

FIG. 5. Logarithm of the rate of methane production (at 280 mm Hg) against the reciprocal of the temperature.

Isobutene Production

The isobutene yield–time plots are also linear only at low conversions. The order plot (Fig. 7) leads to an order of 0.5 at low pressures and of zero at high pressures. The activation energy is 27.5 ± 0.5 kcal per mole.

Neohexane Production

The neohexane results were similar to those

Can. J. Chem. Downloaded from www.nrcresearchpress.com by 210.87.254.5 on 09/05/12
For personal use only.

Can. J. Chem. Downloaded from www.nrcresearchpress.com by 210.87.254.5 on 09/05/12
For personal use only.

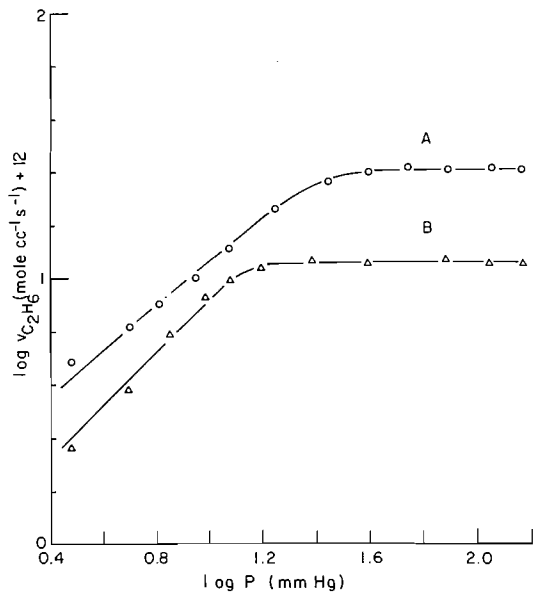

FIG. 6. Order plots for ethane: *A*, 335 and *B*, 310 °C.

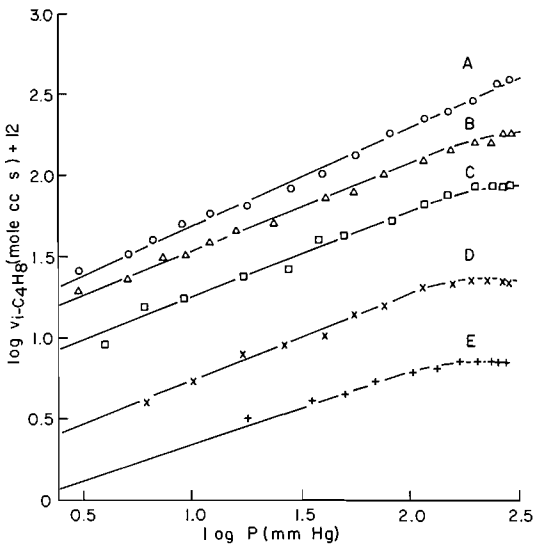

FIG. 7. Order plots of i-C_4H_8: *A*, 335; *B*, 310; *C*, 286; *D*, 256; and *E*, 230 °C.

for other primary products, but reliable rates could not be obtained at the low pressures. With increase of temperature the rate increased until 310 °C was reached, and then remained constant.

Dineopentyl Production

Because of the high boiling point of this product (140 °C) there are difficulties in measuring its yield; approximate rates could be measured only at 230 °C. Pressure was found to have little effect on the initial rates.

Secondary Products

Certain products, C_2H_4, C_3H_6, C_3H_8, i-C_4H_{10}, 2,2,3,3-tetramethylbutane, and 2,2,4,4-tetramethylpentane, were found to have an induction period, and are therefore formed in secondary reactions. The results for these products, and the nature of the secondary reactions, are considered in Part III.

Discussion

The results are consistent with the following reaction scheme, in which Nptn has been written for neopentane and Nptl for the *neo*-pentyl radical:

[1] $Hg + h\nu \rightarrow Hg^*$

[2] $Hg^* + Nptn \rightarrow Nptl + H + Hg$

[3] $Nptn + H \rightarrow Nptl + H_2$

[4] $Nptn + CH_3 \rightarrow Nptl + CH_4$

[5] $CH_3 + H \rightarrow CH_4$

[6] $Nptl \rightarrow i\text{-}C_4H_8 + CH_3$

[7] $Nptl + CH_3 \rightarrow C_6H_{14}$ (2,2′-dimethylbutane)

[8] $2CH_3 \rightarrow C_2H_6$

[9] $2Nptl \rightarrow C_{10}H_{22}$ (2,2,5,5-tetramethylhexane)

[10] $Nptl + H \rightarrow CH_3 + t\text{-}C_4H_9$

[11] $Nptl + H \rightarrow Nptn$

[12] $i\text{-}C_4H_8 + H \rightarrow C_4H_9$

It has been seen that the yield–time relations for all primary products except methane are linear only at low conversions; the deviations from linearity that are observed at later times are due to secondary reactions which have their origin in reaction 12. The secondary reactions are considered in Part III.

In the scheme proposed, H atoms are produced in the initial quenching reaction 2, which is believed to be the only source of H atoms. Most of the H atoms will undergo reaction 3, and reaction of H with Nptl (reactions 10 and 11) also probably occurs.

Nptl radicals are formed in the initial quenching reaction 2 and also in reactions 3 and 4; they can combine in reaction 9 to form dineopentyl and also combine with CH_3 to give neohexane (reaction 7). At higher temperatures (286 °C and higher) most of the Nptl

Can. J. Chem. Downloaded from www.nrcresearchpress.com by 210.87.254.5 on 09/05/12
For personal use only.

radicals decompose into i-C_4H_8 and CH_3 by reaction 6. At low pressures reaction 10 will predominate over 11, whereas 11 will be more important at higher pressures.

The main origin of CH_3 is reaction 6, but at lower pressures there will be some atomic cracking. With increase of temperature and pressure the removal of CH_3 by reaction 4 will become relatively more important with respect to 7 and 8.

Simplified Steady-State Treatment

Reactions 5 and 12 will not be included in the steady-state treatment. The steady-state equation for H then leads to

$$[13] \quad [H] = \frac{I_a\phi}{k_3[\text{Nptn}] + (k_{10} + k_{11})[\text{Nptl}]}$$

where I_a is the intensity of light and ϕ the quantum yield of H_2. The steady-state equation for CH_3, with reaction 8 omitted (since the yield of C_2H_6 is very low), leads to

$$[14] \quad [CH_3] = \frac{k_6[\text{Nptl}] + k_{10}[H][\text{Nptl}]}{k_4[\text{Nptn}] + k_7[\text{Nptl}]}$$

The sum of the steady-state equations for CH_3 and Nptl, with reaction 11 neglected, leads to

$$[15] \quad [\text{Nptl}] = \tfrac{1}{2}\left\{\left(\frac{k_7}{k_9}\right)^2 [CH_3]^2 + \frac{2I_a\phi}{k_9} + \frac{2k_3}{k_9}[H][\text{Nptn}]\right\}^{1/2} - \frac{k_7}{2k_9}[CH_3]$$

At higher temperatures dineopentyl was not detected, so that reaction 9 can be neglected; under these circumstances the Nptl concentration takes a simpler form:

$$[16] \quad [\text{Nptl}] = \frac{[\text{Nptn}](2k_3[H] + k_4[CH_3])}{k_6 + k_7[CH_3]}$$

Estimates of the steady-state concentrations of H, CH_3, and Nptl at different temperatures and pressures are given in Table 1. The concentrations of H atoms were obtained from

$$[17] \quad [H] = \frac{v_{H_2}}{k_3[\text{Nptn}]}$$

with k_3 calculated using $E_3 = 9.7$ kcal per mole and $A_3 = 10^{14}$ cc mol^{-1} s^{-1}. The concentrations of CH_3 were calculated from

$$[18] \quad [CH_3] = \frac{v_{CH_4}}{k_4[\text{Nptn}]}$$

using k_4 values obtained in the present study (*cf.* Part II). The Nptl concentrations were calculated using

$$[19] \quad [\text{Nptl}] = \frac{v_{i\text{-}C_4H_8}}{k_6}$$

using k_6 values obtained in the present work (*cf.* Part II).

The expressions for the rates as functions of the various reaction products are rather complicated; however, a simplified treatment, similar to that of Papic and Laidler (6), leads to a satisfactory interpretation of the behavior. Only a very brief account can be given; further details are to be found elsewhere (18). The arguments are based on the steady-state equations, and the estimated concentrations of free radicals (Table 1).

Hydrogen is formed mainly in reaction 3. Since the production of H atoms by reaction 2 is temperature independent, that of H_2 is expected to be also, in agreement with experiment. The reaction order for H_2 production varies from 1.0 at low pressures to zero at high pressures (Fig. 3). The steady-state rate of H_2 production is

$$[20] \quad v_{H_2} = v_3 = \frac{I_a\phi}{1 + \dfrac{(k_{10} + k_{11})[\text{Nptl}]}{k_3[\text{Nptn}]}}$$

At higher pressures v_{H_2} is thus $I_a\phi$, and is independent of [Nptn]. At low pressures v_{H_2} is proportional to $k_3[\text{Nptn}]/[\text{Nptl}]$. Reference to Table 1 shows that [Nptl] changes only slightly with pressure, so that the hydrogen production is approximately first order in Nptn.

At low pressures $v_{C_2H_6} = v_8$ predominates over $v_{CH_4} = v_4$. The ratio $v_{C_2H_6}/v_{CH_4}$ is equal to $k_8[CH_3]/k_4[\text{Nptn}]$, and use of the values in Table 1, and k_4 and k_8, shows that this ratio at about 10 Torr should be 1–2 depending on temperature, in agreement with experiment. The reaction order for CH_4 production varies from 1.0 at low pressures to zero at high pressures. The steady-state equation is

TABLE 1. The approximate concentrations (in mol/cc) of neopentane (Nptn) and of H atoms, CH_3 and neopentyl (Nptl) radicals

Pressure (mm Hg)	Temperature (°C)	[Nptn]	[CH_3]	[Nptl]	[H]
280	335	7.39×10^{-6}	11.2×10^{-13}	1.31×10^{-12}	1.29×10^{-16}
115	335	3.03×10^{-6}	12.9×10^{-13}	1.35×10^{-12}	2.7×10^{-16}
12	335	3.40×10^{-7}	10.3×10^{-13}	1.72×10^{-12}	—
280	310	7.70×10^{-6}	6.2×10^{-13}	2.22×10^{-12}	1.72×10^{-16}
115	310	3.14×10^{-6}	8.44×10^{-13}	1.85×10^{-12}	4.06×10^{-16}
9.5	310	2.61×10^{-7}	9.72×10^{-13}	2.22×10^{-12}	—
280	286	8.03×10^{-6}	3.22×10^{-13}	2.40×10^{-12}	1.10×10^{-16}
112	286	3.21×10^{-6}	4.91×10^{-13}	2.21×10^{-12}	2.14×10^{-16}
9.0	286	2.58×10^{-7}	4.86×10^{-13}	3.00×10^{-12}	6.80×10^{-16}
275	256	8.33×10^{-6}	1.47×10^{-13}	3.41×10^{-12}	3.48×10^{-16}
110	256	3.32×10^{-6}	2.39×10^{-13}	2.97×10^{-12}	8.41×10^{-16}
10	256	3.02×10^{-7}	2.21×10^{-13}	2.79×10^{-12}	27.60×10^{-16}
280	230	8.93×10^{-6}	6.10×10^{-14}	3.12×10^{-12}	5.46×10^{-16}
104	230	3.31×10^{-6}	7.40×10^{-14}	3.0×10^{-12}	14.5×10^{-16}
18	230	5.1×10^{-7}	5.8×10^{-14}	4.11×10^{-12}	45.0×10^{-16}

[21] $$v_{CH_4} = \frac{[\text{Nptl}](k_6 + k_{10}[\text{H}])}{1 + \dfrac{k_7[\text{Nptl}]}{k_4[\text{Nptn}]}}$$

At low pressures

[22] $$v_{CH_4} = \frac{k_4}{k_7}[\text{Nptn}](k_6 + k_{10}[\text{H}])$$

[H] varies much less than [Nptn] as the pressure changes from 10 to 110 Torr (Table 1), so that approximate first-order kinetics is expected. At high pressures reaction 10 is relatively unimportant and v_{CH_4} is now approximately k_6[Nptl]; since [Nptl] varies only slightly with pressure the kinetics are zero order.

Ethane production shows the same variation with pressure as methane production, and a similar explanation applies. Further aspects of the combination of methyl radicals are considered in Part II (following paper).

The order for i-C_4H_8 production is 0.5 at low pressures and zero at higher pressures (Fig. 7). The steady-state expression for the formation of this product is

[23] $$v_{i\text{-}C_4H_8} = v_6 = \frac{k_6}{2}\left\{\left(\frac{k_7}{k_9}\right)^2[\text{CH}_3]^2 + \frac{2I_a\phi}{k_9} + \frac{2k_3}{k_9}[\text{H}][\text{Nptn}]\right\}^{1/2} - \frac{k_6k_7[\text{CH}_3]}{2k_9}$$

At low pressures the predominant term is $2k_3$[H][Nptn]$/k_9$, and [H] is more or less independent of pressure; the dependence of $v_{i\text{-}C_4H_8}$ on [Nptn]$^{1/2}$ can therefore be understood on this basis. At higher pressures [H] becomes inversely proportional to [Nptn], and [CH_3] is fairly constant; the kinetics of formation of i-C_4H_8 is therefore zero order.

The work described in this and the following two papers was supported by a grant from the National Research Council of Canada.

1. L. F. LOUCKS and K. J. LAIDLER. Can. J. Chem. **45**, 2795 (1967).
2. L. F. LOUCKS and K. J. LAIDLER. Can. J. Chem. **45**, 2763 (1967).
3. L. F. LOUCKS and K. J. LAIDLER. Can. J. Chem. **45**, 2767 (1967).
4. L. F. LOUCKS. Can. J. Chem. **45**, 2775 (1967).
5. L. F. LOUCKS and K. J. LAIDLER. Can. J. Chem. **45**, 2785 (1967).
6. M. M. PAPIC and K. J. LAIDLER. Can. J. Chem. **49**, 535 (1971).
7. M. M. PAPIC and K. J. LAIDLER. Can. J. Chem. **49**, 549 (1971).
8. B. DE B. DARWENT and E. W. R. STEACIE. Can. J. Res. **B27**, 81 (1949).
9. K. J. LAIDLER. J. Chem. Phys. **15**, 712 (1947).
10. R. A. HOLROYD and G. W. KLEIN. J. Phys. Chem. **67**, 2273 (1963).
11. R. J. NORSTROM, O. P. STRAUSZ, and H. E. GUNNING. Can. J. Chem. **42**, 2140 (1964).

Can. J. Chem. Downloaded from www.nrcresearchpress.com by 210.87.254.5 on 09/05/12
For personal use only.

12. S. SATO and S. TSUNASHIMA. Bull. Chem. Soc. Jap. **37**, 563 (1964).
13. S. G. LIAS and D. AUSLOOS. J. Chem. Phys. **43**, 2748 (1965).
14. K. H. ANDERSON and S. W. BENSON. J. Chem. Phys. **43**, 3747 (1964).
15. J. ENGEL, A. COMBE, M. LETORT, and M. NICLAUSE. C.R. **244**, 453 (1957).
16. F. BARONNET, M. DZIERZYNSKI, G. M. COME, R. MARTIN, and M. NICLAUSE. Int. J. Chem. Kinetics, **3**, 197 (1971).
17. M. C. FLOWERS. Ann. Rep. Chem. Soc. A**66**, 166 (1969).
18. E. FURIMSKY. Ph.D. Thesis, University of Ottawa, Ottawa, Canada. 1971.

Can. J. Chem. Downloaded from www.nrcresearchpress.com by 210.87.254.5 on 09/05/12
For personal use only.

Kinetics of the Mercury-Photosensitized Decomposition of Neopentane. Part II. Reactions of the Methyl and Neopentyl Radicals

E. FURIMSKY AND K. J. LAIDLER

Department of Chemistry, University of Ottawa, Ottawa, K1N 6N5, Canada

Received September 2, 1971

The results of Part I are further analyzed with reference to certain of the elementary free-radical processes occurring. A fall-off in the methyl radical combination is observed at low pressures. Comparison of this process with the CH_3 + neopentane abstraction yields for the latter an activation energy of 11.5 kcal/mol and a frequency factor of 4.9×10^{11} cc mol^{-1} s^{-1}. The relative importance of CH_3 + neopentyl and neopentyl + neopentyl is compared. The decomposition of the neopentyl radical into i-C_4H_8 + CH_3 shows a fall-off at low pressures; the limiting activation energy at high pressures is 29.0 kcal/mol, while that at low pressure is 17.1 kcal/mol. The former value leads to 6.7 kcal/mol for the heat of formation of the neopentyl radical at 25 °C, to 21.3 kcal/mol for the heat of its dissociation into i-C_4H_8 + CH_3, and to 98.5 kcal/mol for the heat of dissociation of neopentane into neopentyl + H. Entropy values are also calculated in an approximate manner.

Les résultats de la partie I sont analysés plus en détails, en se référant à certains des procédés radicalaires élémentaires qui se produisent. On observe une chute brusque de la combinaison du radical méthyle à basses pressions. La comparaison de ce procédé avec l'abstraction de CH_3 + néopentane donne pour ce dernier une énergie d'activation de 11.5 kcal/mol et un facteur de fréquence de 4.9×10^{11} cc mol^{-1} s^{-1}. On compare l'importance relative de CH_3 + néopentyl et de néopentyl + néopentyl. La décomposition du radical néopentyl en i-C_4H_8 + CH_3 subit une brusque diminution à basses pressions; l'énergie d'activation limitante à hautes pressions est de 29.0 kcal/mol, tandis qu'à basses pressions elle est de 17.1 kcal/mol. La valeur précédente nous conduit à une chaleur de formation du radical néopentyl à 25 °C de 6.7 kcal/mol, une chaleur de dissociation en i-C_4H_8 + CH_3 de 21.3 kcal/mol et une chaleur de dissociation du néopentane en néopentyl + H de 98.5 kcal/mol. On calcule aussi approximativement les valeurs d'entropie.

Canadian Journal of Chemistry, **50**, 1123 (1972)

Can. J. Chem. Downloaded from www.nrcresearchpress.com by 210.87.254.6 on 09/05/12
For personal use only.

Introduction

The present paper is concerned with the detailed kinetics of certain reactions that occur in the mercury-photosensitized decomposition of neopentane, namely the combination and abstraction reaction of methyl radicals and the combination and decomposition reactions of the neopentyl radical.

Results and Discussion

Combination of Methyl Radicals

Several workers have studied the rate of the reaction[1]

$$CH_3 + CH_3 \xrightarrow{8} C_2H_6$$

under a variety of conditions; a matter of particular interest is the variation of the kinetics with pressure. Kistiakowsky and Roberts (1) and Dodd and Steacie (2) made a study of the photolysis of gaseous acetone at temperatures from 150 to 250 °C, and found the expected change of kinetics (from second to third order behavior) at pressures below 10 Torr. Toby and Weiss (3) studied the combination of CH_3 radicals in the photolysis of azomethane at pressures from 3 to 60 Torr, and in the temperature range of 25 to 180 °C. They observed a significant fall-off of the rate coefficient below 10 Torr. Loucks (4) examined the reaction from 200 to 300 °C and observed the beginning of fall-off at a pressure of 100 Torr.

Grotewold and co-workers (5, 6) photolyzed mixtures of azomethane and azoethane, and of azomethane and azopropane. They used the cross-combination of CH_3 radicals with higher radicals to characterize the effect of pressure, the assumption being that the combinations of CH_3 radicals with higher radicals will be pressure independent over the range of the experiments. Their conclusion was that the pressure fall-off at 15, 60, and 100 °C was at pressures about 100 times lower than would be expected from the previous studies.

The pressure dependence of the combination of CH_3 radicals as given by the present study is shown in Fig. 1. It is seen that a significant de-

[1]Reactions are numbered as in Part I (preceding paper).

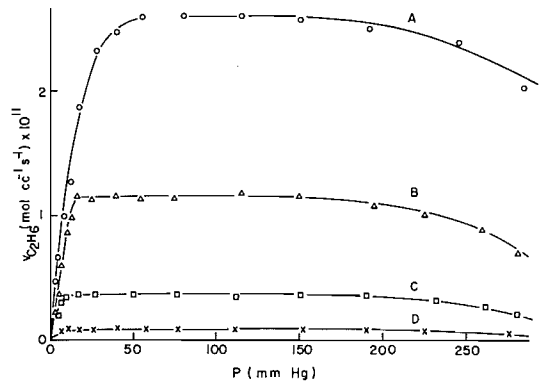

FIG. 1. Rates of ethane production plotted against pressure: *A*, 335; *B*, 310; *C*, 286; *D*, 256 °C.

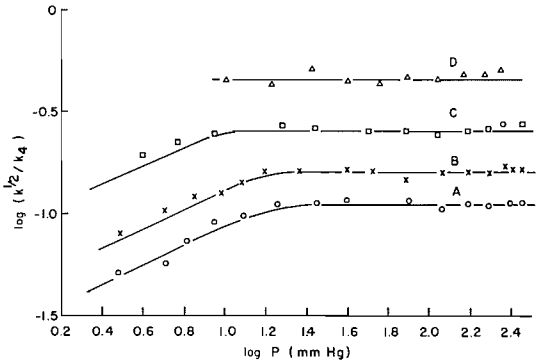

FIG. 2. log–log plots of $k_8^{1/2}/k_4$ against pressure: *A*, 335; *B*, 310; *C*, 286; *D*, 256 °C.

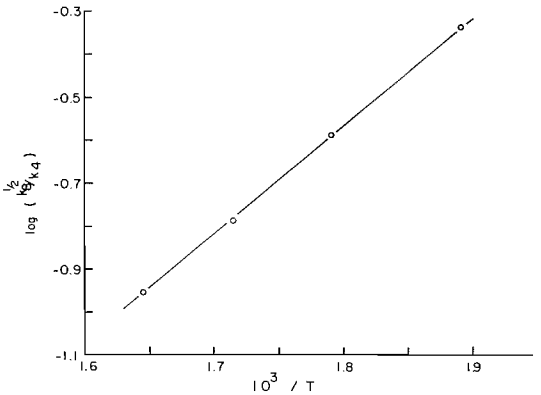

FIG. 3. Plot of logarithm of $k_8^{1/2}/k_4$ against reciprocal of temperature.

crease of the rate of C_2H_6 production occurs at 335 °C at pressures less than 35 Torr. At 310 °C the decrease is observed below about 15 Torr, and at 286 °C below 10 Torr. The conclusion can be drawn that an increase of temperature of about 25 °C results in about a twofold increase in the pressure at which the rate of ethane formation begins to decrease.

It is seen in Fig. 1 that the rate at first increases with increase in pressure and then reaches a constant value, after which there is a decrease in rate. Two explanations are possible:

(*1*) The combination reaction is suppressed by increase in pressure, which favors abstraction by CH_3 radicals.

(*2*) There is a second source of CH_3 radicals, such as the atom cracking reaction

$$H + Nptl \xrightarrow{10} CH_3 + t\text{-}C_4H_9$$

This will occur via an excited Nptn molecule, which is either quenched

$$Nptn^* + Nptn \rightarrow 2Nptn$$

or splits off CH_3

$$Nptn^* \rightarrow CH_3 + t\text{-}C_4H_9$$

The first explanation predominates at higher pressures, so that an increase in pressure suppresses this additional source of CH_3.

The present results can be analyzed by relating the combination reaction with the hydrogen abstraction reaction

$$CH_3 + Nptn \rightarrow Nptl + CH_4$$

which will show no pressure effect. The rates of abstraction and combination are

$$v_{CH_4} = v_4 = k_4[CH_3][Nptn]$$

$$v_{C_2H_6} = v_8 = k_8[CH_3]^2$$

whence

$$\frac{k_8^{1/2}}{k_4} = \frac{v_{C_2H_6}^{1/2}}{v_{CH_4}}[Nptn]$$

A double logarithmic plot of $k_8^{1/2}/k_4$, determined in this way, is shown in Fig. 2. The slope is seen to change from zero at high pressures to 0.5 at low pressures, indicating a change to third order as the pressure is lowered.

Figure 3 shows an Arrhenius plot of the $k_8^{1/2}/k_4$ values in the high pressure region. The effective activation energy is -11.5 kcal/mol, so that

$$E_8^{1/2} - E_4 = -11.5 \text{ kcal/mol}$$

If $E_8 = 0$, $E_4 = 11.5$ kcal/mol.

Can. J. Chem. Downloaded from www.nrcresearchpress.com by 210.87.254.6 on 09/05/12
For personal use only.

TABLE 1. Results for combination of neopentyl radicals

Temperature (°C)	Pressure (Torr)	Rate × 10^{12} (mol cc^{-1} s^{-1})				$\frac{v_6 + v_7}{2v_3 + v_4}$
		v_3	v_4	v_7	v_6	
230	36	27.5	0.37	4.5	4.12	0.155
230	104	37.5	1.20	4.5	5.88	0.139
230	240	38.1	2.47	4.5	6.93	0.141
256	27	20.1	1.37	11.5	8.73	0.480
256	110	35.0	6.60	11.5	21.2	0.430
256	225	36.5	10.70	11.5	22.4	0.410
286	50	28.6	10.80	26.6	43.9	1.030
286	112	33.1	26.40	26.6	61.3	1.010
286	230	35.7	41.20	26.6	80.3	0.96

A value of 10.4 kcal/mol has previously been tabulated as an average value for this reaction (7). Kerr and Timlin (8) compared this value with the activation energy for H abstraction by CH_3 radicals from $(CH_3)_4Si$, and they concluded that it is probably too low. Their own work gave 12.0 kcal/mol for E_4, in good agreement with the value obtained from Polanyi's theoretical equation $E = 0.49\ (D_{CH} - 74.3)$ with $D_{C-H} = 99$ kcal/mol. The value obtained in the present work supports the higher value preferred by these authors.

From the intercept in Fig. 3, and using $A_8 = 2.2 \times 10^{13}$ cc mol^{-1} s^{-1} (9), the frequency factor for the abstraction reaction is

$$A_4 = 4.9 \times 10^{11} \text{ cc mol}^{-1} \text{ s}^{-1}$$

Combination Reactions of Neopentyl Radicals

Neopentyl radicals combine mainly with methyl radicals

$$\text{Nptl} + \text{CH}_3 \xrightarrow{7} \text{C}_6\text{H}_{14}\ (2,2'\text{-dimethylbutane})$$

and with other neopentyl radicals,

$$2\text{Nptl} \xrightarrow{9} \text{C}_{10}\text{H}_{22}\ (2,2,5,5\text{-tetramethylhexane, dineopentyl})$$

Dineopentyl was found only at 230 and 256 °C (and at 286 °C in high conversion experiments), and only at 230 °C was it possible to obtain an approximate initial rate. However, some information about the amounts of Nptl radicals disappearing in reaction 9 can be obtained on the basis of the material balance. With the unimportant reactions 10 and 11 neglected,

$$2v_3 + v_4 = 2v_9 + v_6 + v_7$$

so that the ratio

$$\frac{2v_9 + v_6 + v_7}{2v_3 + v_4}$$

should be unity. The ratio

$$\frac{v_6 + v_7}{2v_3 + v_4} = \frac{v_{i\text{-}C_4H_8} + v_{C_6H_{14}}}{2v_{H_2} + v_{CH_4}}$$

will therefore express the fraction of Nptl radicals removed by reactions 6 and 7; the remainder will be removed by reaction 9. Results are given in Table 1. It is concluded that at 230 °C approximately 85% of the Nptl radicals are removed by reaction 9, and at 256 °C about 55%. At 286 °C the ratio is close to unity indicating that the combination reaction 9 is relatively unimportant.

Reactions 7 and 9 show a striking difference in temperature dependence. The rate of formation of neohexane increases with increase of temperature until 310 °C is reached, but there is a decrease at 335 °C; over the same range there is a decrease of dineopentyl production. Similar effects were found by Sato and Tsunashima (10). The observation can be explained on the basis of different thermal stabilities of dineopentyl and neohexane, the former being much less stable.

It is seen from Table 1 of Part I that the concentration of CH_3 increases strongly with increase of temperature, whereas that of Nptl slightly decreases. This effect favors the combination of CH_3 with Nptl with respect to combination of two Nptl radicals.

Decomposition of Neopentyl Radicals

Few previous studies have been concerned with the decomposition of the Nptl radical,

$$\text{Nptl} \xrightarrow{6} i\text{-}C_4H_8 + CH_3$$

Can. J. Chem. Downloaded from www.nrcresearchpress.com by 210.87.254.6 on 09/05/12
For personal use only.

TABLE 2. Results for the decomposition of neopentyl radicals

Temperature (°C)	Pressure (Torr)	Rate × 10^{12} (mol cc^{-1} s^{-1})				$\frac{v_6}{v_4 + v_7 + 2v_8}$
		v_4	v_8	v_7	v_6	
230	104	1.2	—	4.5	5.88	1.04
230	240	2.47	—	4.5	6.93	1.00
256	110	6.6	0.895	11.5	20.2	1.06
256	225	10.7	0.67	11.5	22.4	0.95
286	150	36.5	3.71	26.6	75.0	1.05
286	230	41.2	3.24	26.6	80.1	1.06
310	115	68.6	11.5	33.9	120.4	0.96
310	232	11.50	10.1	33.9	163.0	0.97
335	115	158.6	26.5	33.8	237.0	0.99
335	245	272.7	24.4	33.8	353.0	1.00

Anderson and Benson (11) investigated the process in a study of the pyrolysis of Nptn in the presence of HCl. For the rate constant at 742 °K they obtained $10^{3.3\pm0.3}$ with the following kinetic parameters:

$$\log A_6 = 13 \pm 1 \text{ s}^{-1} \qquad E_6 = 34 \pm 3.5 \text{ kcal/mol}$$

Sato and Tsunashima (10) studied the mercury-photosensitized decomposition of Nptn, and from the initial rates of i-C_4H_8 and CH_4 production they obtained $E_6 = 17.0 \pm 2$ kcal/mol. This value is much too low for a high-pressure value, and is to be compared with the low-pressure limiting value E_6^0 obtained in the present study.

It is expected that reaction 6 will be the only source of i-C_4H_8, and this can be checked through the material balance. The steady-state equation for CH_3 is

$$v_6 = v_4 + v_7 + 2v_8$$

so that the ratio

$$\frac{v_{i\text{-}C_4H_8}}{v_{CH_4} + v_{C_6H_{14}} + 2v_{C_2H_6}}$$

should be unity. This is confirmed by the values shown in Table 2.

The rate constant for reaction 6 can be obtained by considering the rates of reactions 4, 6, and 7, whence

$$\frac{v_4 v_6}{v_7} = \frac{k_4 k_6}{k_7}[\text{Nptn}]$$

Thus

$$\frac{k_4 k_6}{k_7} = \frac{v_{CH_4} v_{i\text{-}C_4H_8}}{v_{C_6H_{14}}[\text{Nptn}]}$$

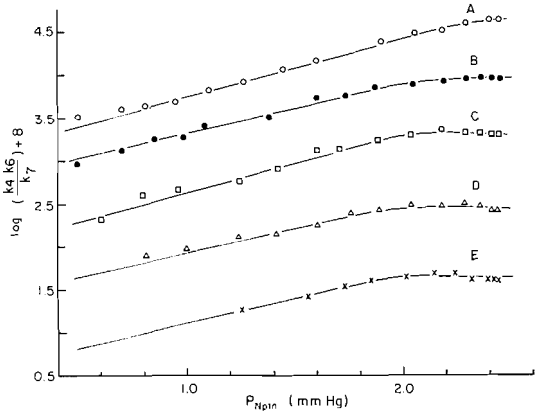

FIG. 4. A double logarithmic plot of k_4k_6/k_7 against the pressure of neopentane: *A*, 335; *B*, 310; *C*, 286; *D*, 256; and *E*, 230 °C.

A double-logarithmic plot of this function against [Nptn] is shown in Fig. 4. Reactions 4 and 7 are assumed to be pressure independent (*cf.* Rabinovitch and Setser (12) for evidence regarding the combination of CH_3 with larger radicals) so that the pressure dependence shown in Fig. 4 can be attributed to the behavior of reaction 6. Average values of k_6 at different temperatures and pressures are listed in Table 3; these values were calculated with $k_7 = 2.2 \times 10^{13}$ cc mol^{-1} s^{-1} and with the k_4 values obtained in the present study (*cf.* above).

Evaluation of the limiting high- and low-pressure rate constants was done by use of a plot of k^{-1} against $[\text{Nptn}]^{-1/2}$, as proposed by Schlag and Rabinovitch (13); such a plot is shown in Fig. 5 for a temperature of 310 °C. From the intercept the value of $k_7/k_4k_6^\infty$ is obtained, while from the slope of the linear part of the curve

Can. J. Chem. Downloaded from www.nrcresearchpress.com by 210.87.254.6 on 09/05/12
For personal use only.

Can. J. Chem. Downloaded from www.nrcresearchpress.com by 210.87.254.6 on 09/05/12
For personal use only.

TABLE 3. Rate constants for decomposition of neopentyl radicals at different temperatures and pressures

Pressure (Torr)	Rate constant, k_6, s^{-1}				
	230 °C	256 °C	286 °C	310 °C	335 °C
10	0.56	2.19	6.2	18.2	29.6
20	0.76	3.15	10.02	28.7	53.3
30	1.08	3.84	13.9	36.3	74.6
50	1.36	5.20	16.8	47.6	105.5
70	1.68	6.11	23.6	58.4	133.2
90	2.12	6.80	26.8	64.2	150.1
110	2.2	6.88	30.1	70.4	173.4
175	2.2	6.88	33.6	77.4	236.7
225	2.20	6.88	33.6	79.4	265.4
280	2.2	6.88	33.6	79.4	297.8

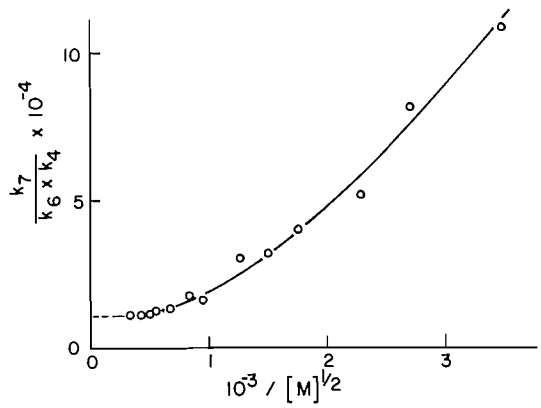

FIG. 5. A plot of k_7/k_4k_6 against $1/[\text{Nptn}]^{1/2}$ at 310 °C.

$k_7/k_4k_6^0$ is obtained. The Arrhenius plots lead to

$$E_6^\infty + E_4 - E_7 = 40.5 \text{ kcal/mol}$$

With $E_7 = 0$, and $E_4 = 11.5$ kcal/mol as obtained in the present study, it follows that the high-pressure activation energy E_6^∞ is 29.0 ± 0.5 kcal/mol. Use of $A_7 = 10^{13.34}$ cc mol^{-1} s^{-1} and $A_4 = 10^{11.7}$ cc mol^{-1} leads to a high-pressure preexponential factor A_6^∞ of 2.5×10^{13}. Thus

$$k_6^\infty = 2.5 \times 10^{13} \exp(-29.0/RT)\ s^{-1}$$

The entropy of activation $\Delta S_6^\ddagger$ is -0.5 cal deg^{-1} mol^{-1} (standard state 1 mol cc^{-1}).

A similar treatment for the limiting low-pressure rate constant leads to

$$k_6^0 = 5.8 \times 10^{10} \exp(-17.1/RT) \text{ cc mol}^{-1}\ s^{-1}$$

The activation energies for this radical decomposition are subject to an estimated error of ± 0.5 kcal/mol. The activation energy difference $E^\infty - E^0$ corresponds to about 12 effective degrees of freedom in the molecule; this is to be compared with a total of 42 degrees of freedom for the neopentyl radical.

Thermochemistry

Knowledge of E_6^∞ (29.0 kcal/mol) and of the activation energy E_{-6} for the reverse addition of CH_3 to i-C_4H_8 permits a calculation of the heat of formation of Nptl radicals. The activation energy for the addition of CH_3 to i-C_4H_8 has been given (14) as 6.9 kcal/mol; this includes addition to both terminal and non-terminal carbon atoms. We have taken, for non-terminal addition, a value of 8.3 kcal/mol, but this is admittedly a guess. These activation energies are related to ΔH_6 for the process

$$\text{Nptl} \rightarrow CH_3 + i\text{-}C_4H_8$$

by the expression

$$\Delta H_6(T) = E_6 - E_{-6} + \Delta nRT$$

where $\Delta n = 1$ in the present case. Enthalpy changes at other temperatures can be obtained from the relationship

$$\Delta H_6(T) = \Delta H_6(0\ ^\circ\text{K}) + \int_0^T \Delta C_p\, dT$$

There are difficulties with this procedure because of lack of heat capacities as a function of temperature. Another possibility is to use heat contents for Nptl, CH_3, and i-C_4H_8. Heat contents for Nptl are not available, but in the present work values for the analogous Nptn were used as giving a reliable estimate. Values of the integral obtained in this way are included in Table 4. The enthalpy change obtained from the experimental results is considered to refer to 550 °K, the middle of the temperature range employed. The heat contents at 550 °K for Nptn, CH_3, and i-C_4H_8 were obtained by extrapolation of the data of Rossini *et al.* (15).

The enthalpy change for the reaction at 0 °K is obtained from the expression

$$\Delta H_6\ (0\ ^\circ\text{K}) = E_6 - E_{-6} + RT - \int_0^T \Delta C_p\, dT$$

This leads to $\Delta H_6\ (0\ ^\circ\text{K}) = 19.0$ kcal/mol. From $\Delta H_6(T)$ it is then possible to calculate at various

TABLE 4. Thermodynamic quantities at different temperatures

T (°K)	$\Delta C_p dT$ (kcal/mol)	ΔH_6 (kcal/mol)	ΔH_f(Nptl) (kcal/mol)	D(Nptl—H) (kcal/mol)
0	0	19.0	14.7	97.6
298.2	2.3	21.3	6.7	98.5
550	2.8	21.8	2.2	98.9

temperatures the heat of formation of the Nptl radical, using the relationship

$$\Delta H_f(\text{Nptl}) = \Delta H_f(CH_3) + \Delta H_f(i\text{-}C_4H_8) - \Delta H_6$$

The resulting heats of formation of Nptl are listed in the fourth column of Table 4. In the literature (16) there is listed the heat of formation of Nptl only at 298.29; the value is exactly the same as that obtained in the present study.

The last column of Table 4 gives the enthalpy change for the process

$$\text{Nptn} \rightarrow \text{Nptl} + \text{H}$$

These values were calculated using the expression

$$D(\text{Nptl—H}) = \Delta H_f(\text{Nptl}) - \Delta H(\text{Nptn}) + \Delta H_f(\text{H})$$

A previous value of the C—H bond dissociation energy of Nptn at 298.2 °K is 100.0 kcal/mol (16), in good agreement with the present value.

The overall standard entropy change for the dissociation of Nptl into $CH_3 + i\text{-}C_4H_8$ is calculated from the present results to be

$$\Delta S_6 = 8.8 \text{ cal deg}^{-1} \text{ mol}^{-1}$$

for the standard state of 1 mol cc^{-1}, or 28.0 cal deg^{-1} mol^{-1} for the standard state of 1 atm. By use of this value and the entropies of CH_3 and $i\text{-}C_4H_8$ (15) the standard entropy of Nptl is calculated to be

$$S(\text{Nptl}) = 109.5 \text{ cal deg}^{-1} \text{ mol}^{-1} \text{ at } 550 \text{ °K}$$

(standard state 1 atm)

This is a very approximate value.

1. G. B. KISTIAKOWSKY and E. K. ROBERTS. J. Chem. Phys. **21**, 1637 (1953).
2. R. E. DODD and E. W. R. STEACIE. Proc. Roy. Soc. (London), A **223**, 283 (1954).
3. S. TOBY and B. H. WEISS. J. Phys. Chem. **68**, 2492 (1964).
4. L. F. LOUCKS. Can. J. Chem. **45**, 2775 (1967).
5. J. GROTEWOLD, E. A. LISSI, and M. G. NEUMANN. J. Chem. Soc. (A) 375 (1968).
6. F. CASAS, C. PREVITALI, J. GROTEWOLD, and E. A. LISSI. J. Chem. Soc. (A) **7**, 1001 (1970).
7. A. F. TROTMAN-DICKENSON and G. S. MILNE. Tables of bimolecular gas reactions, NSRDS-NBS9, 42 (1967).
8. J. A. KERR and D. TIMLIN. J. Chem. Soc. (A), 1241 (1969).
9. A. SHEPP. J. Chem. Phys. **24**, 939 (1956).
10. S. SATO and S. TSUNASHIMA. Bull. Chem. Soc. Jap. **37**, 543 (1964).
11. K. H. ANDERSON and S. W. BENSON. J. Chem. Phys. **43**, 3747 (1964).
12. B. S. RABINOVITCH and D. W. SETSER. Advan. Photochem. **3**, 1964.
13. E. W. SCHLAG and B. S. RABINOVITCH. J. Am. Chem. Soc. **82**, 5996 (1960).
14. R. J. CVETANOVIC and R. S. IRWIN. J. Chem. Phys. **46**, 1694 (1967).
15. F. D. ROSSINI *et al.* Selected values of physical and thermodynamic properties of hydrocarbons and related compounds. American Petroleum Institute Report, Carnegie Press, Pittsburg, 1953.
16. C. W. LARSON, E. A. HARDWIDGE, and B. S. RABINOVITCH. J. Chem. Phys. **50**, 2769 (1969).

Can. J. Chem. Downloaded from www.nrcresearchpress.com by 210.87.254.6 on 09/05/12
For personal use only.

Kinetics of the Mercury-Photosensitized Decomposition of Neopentane. Part III. The Secondary Reactions

E. FURIMSKY AND K. J. LAIDLER

Department of Chemistry, University of Ottawa, Ottawa, K1N 6N5, Canada

Received September 2, 1971

The following were identified as secondary products of the mercury-photosensitized decomposition of neopentane, and their maximal rates measured over a range of conditions: C_2H_4, C_3H_6, C_3H_8, i-C_4H_{10}, 2,2,3,3-tetramethylbutane, and 2,2,4,4-tetramethylpentane. A mechanism is proposed which explains the kinetics of formation of these products. It involves the reaction of H atom with i-C_4H_8 formed as a primary product; this leads to the formation of C_4H_9 which reacts further; one of its products is C_3H_6 which also reacts with H atoms.

On a identifié les produits secondaires suivants venant de la décomposition par photosensibilisation au mercure du néopentane, de même que leurs vitesses maximales mesurées dans un domaine de conditions: C_2H_4, C_3H_6, C_3H_8, i-C_4H_{10}, 2,2,3,3-tétraméthylbutane, et 2,2,4,4-tétraméthylpentane. On propose un mécanisme qui explique la cinétique de formation de ces produits. Il implique la réaction de l'atome de H avec i-C_4H_8 formé comme produit primaire; ceci amène à la formation de C_4H_9 qui réagit encore; un de ces produits est C_3H_6 qui réagit lui aussi avec les atomes de H.

Canadian Journal of Chemistry, **50**, 1129 (1972)

Introduction

The present investigation had necessarily to be carried out up to higher conversions than was the case with propane (1, 2), and as a result secondary products are observed; their yield–time curves show an induction period. The secondary products are i-C_4H_{10}, 2,2,3,3-tetramethylbutane (2,2,3,3-TMB), and 2,2,4,4-tetramethylpentane (2,2,4,4-TMP), and in smaller yields ethylene, propylene, and propane. Because of the relatively small number of primary products it was possible to analyse these secondary products and to obtain information about their origin. Table 1 summarizes the main results. The present paper is concerned with this problem.

Because of the very high quenching cross section of H_2 for $Hg(^3P_1)$ atoms (3) it is expected that H_2 formed in the early stages of the experiments will quench the mercury atoms with production of H atoms. These react with olefins (4–6), and there will therefore be reaction with i-C_4H_8, an important primary product, with the formation of a hot radical. Such hot radicals may decompose by C—C or C—H bond rupture, or may be deactivated by collision; they may then undergo their usual combination, disproportionation, and H-abstraction reactions.

In an early study on the photosensitized hydrogenation of i-C_4H_8 at 23 °C (7) the following products were observed: i-C_4H_{10} (52%), CH_4 (15%), 2,2,3,3-TMB (12%), neopentane (11.7%); C_2H_4, C_2H_6, C_3H_6, and C_3H_8 were observed as minor products. It was concluded that the sole products of the addition of H atom to i-C_4H_8 are t-C_4H_9 radicals, and that i-C_4H_9 radicals are either not formed at all or they

TABLE I. The yields of secondary products

Temperature (°C)	Pressure (Torr)	Time (s)	Concentration × 10^7 (mol)				
			C_2H_4	C_3H_6	C_3H_8	i-C_4H_{10}	2,2,3,3-TMB
310	40	1000	n.m.*	0.52	n.m.	4.4	n.m.
310	40	2000	0.12	0.76	0.23	11.3	3.4
310	40	3000	0.20	0.83	0.38	14.8	6.1
310	115	1000	n.m.	0.55	n.m.	4.9	n.m.
310	115	2000	0.11	0.80	0.20	12.1	3.2
310	115	2500	0.18	0.88	0.28	13.8	4.8

*n.m.—not measurable.

Can. J. Chem. Downloaded from www.nrcresearchpress.com by 210.87.254.42 on 09/05/12
For personal use only.

Can. J. Chem. Downloaded from www.nrcresearchpress.com by 210.87.254.42 on 09/05/12
For personal use only.

decompose or isomerize before reacting. At 300 °C a small amount of 2,4,4-trimethylpentene-1 was detected. A later study (8) of the reaction was concerned with the object of studying the disproportion–combination ratio for t-C_4H_9 radicals, a value of 2.2 ± 0.3 being obtained.

An extensive study on the addition of H atoms to olefins has recently been made by Falconer and Sunder (9). They investigated the relative rates of terminal and non-terminal addition of H atoms to i-C_4H_8 at room temperature, obtaining this from the amounts of products resulting from combination and disproportionation reactions of i-C_4H_9 radicals; at this temperature most of the i-C_4H_9 radicals were stabilized by collisions. The percentage of non-terminal addition was found to be 0.48, and the activation energy difference for non-terminal and terminal addition of H atoms to i-C_4H_8 was found to be 3.2 kcal/mol.

Results and Discussion

Mechanism

The secondary products obtained in the present investigation can be explained in terms of the following partial mechanism:

[1] $H + i\text{-}C_4H_8 \rightarrow t\text{-}C_4H_9^*$

[2] $H + i\text{-}C_4H_8 \rightarrow i\text{-}C_4H_9^*$

[3] $t\text{-}C_4H_9^* + M \rightarrow t\text{-}C_4H_9 + M$

[4] $i\text{-}C_4H_9^* + M \rightarrow i\text{-}C_4H_9 + M$

[5] $t\text{-}C_4H_9^* \rightarrow i\text{-}C_4H_8 + H$

[6] $t\text{-}C_4H_9^* \rightarrow C_3H_6 + CH_3$

[7] $i\text{-}C_4H_9^* \rightarrow i\text{-}C_4H_8 + H$

[8] $i\text{-}C_4H_9^* \rightarrow C_3H_6 + CH_3$

It is assumed that both t-$C_4H_9^*$ and i-$C_4H_9^*$ are produced by addition of H to i-C_4H_8. The former decomposes mainly by C—H bond rupture, into i-C_4H_8 and H (*i.e.* reaction 5 is more important than reaction 6), while i-$C_4H_9^*$ decomposes mainly by C—C rupture into $C_3H_6 + CH_3$ (reaction 8 is more important than reaction 7). The most recent evidence (10–13) is against isomerization of C_3 or C_4 alkyl radicals. It is expected that the decomposition of i-$C_4H_9^*$ will be much faster than that of t-$C_4H_9^*$, so that there is a much greater possibility for t-$C_4H_9^*$ to be stabilized as compared with i-$C_4H_9^*$; most of the i-$C_4H_9^*$ radicals will decompose before being stabilized by collision.

The following reactions, involving stabilized radicals, are also postulated to explain the observed products:

[9] $2t\text{-}C_4H_9 \rightarrow C_8H_{18}$(2,2,3,3-TMB)

[10] $2t\text{-}C_4H_9 \rightarrow i\text{-}C_4H_8 + i\text{-}C_4H_{10}$

[11] $t\text{-}C_4H_9 + \text{Nptn} \rightarrow i\text{-}C_4H_{10} + \text{Nptl}$

[12] $t\text{-}C_4H_9 + \text{Nptl} \rightarrow C_9H_{20}$(2,2,4,4-TMP)

[13] $t\text{-}C_4H_9 + CH_3 \rightarrow \text{Nptn}$

[14] $t\text{-}C_4H_9 + CH_3 \rightarrow CH_4 + i\text{-}C_4H_8$

There will also be some reaction of H with t-C_4H_9.

The propylene produced in reaction 8 will further react with H to give hot propyl radicals; according to Bradley *et al.* (14), more than 93% of this process leads to i-C_3H_7, which decomposes primarily into $C_3H_6 + H$. Addition of H to C_3H_6 leading to n-C_3H_7 is suggested by the fact that C_2H_4 is formed; this is not formed to an appreciable extent from i-C_3H_7. The following scheme of reactions must therefore be added:

[15] $H + C_3H_6 \rightarrow i\text{-}C_3H_7^*$

[16] $H + C_3H_6 \rightarrow n\text{-}C_3H_7^*$

[17] $i\text{-}C_3H_7^* \rightarrow C_3H_6 + H$

[18] $n\text{-}C_3H_7^* \rightarrow C_2H_4 + CH_3$

[19] $i\text{-}C_3H_7^* + M \rightarrow i\text{-}C_3H_7 + M$

[20] $n\text{-}C_3H_7^* + M \rightarrow n\text{-}C_3H_7 + M$

[21] $2C_3H_7 \rightarrow C_3H_6 + C_3H_8$

[22] $2C_3H_7 \rightarrow C_6H_{14}$

[23] $C_3H_7 + \text{Nptn} \rightarrow C_3H_8 + \text{Nptl}$

It is assumed, on the basis of previous evidence, that i-$C_3H_7^*$ does not isomerize to n-$C_3H_7^*$. The amount of ethylene produced accounted for about 10% of all C_2 and C_3 secondary products analyzed, so that there is substantial addition of H to C_3H_6 leading to the n-C_3H_7 radical.

It is possible to arrive at approximate information about the relative ratio of addition of H to i-C_4H_8 with the formation of i-$C_4H_9^*$ and t-$C_4H_9^*$ radicals. All of the C_2H_4, C_3H_6, and C_3H_8 have their origin in i-$C_4H_9^*$ radicals, and it is seen in Table 1 that those products account for about 3% of all the C_4H_9 radicals removed in secondary reactions at 310 °C. This result is approximate, however, since two opposing factors are also involved; (*1*) some of the C_3H_7 radicals are removed in combination reactions and (*2*) some of the t-C_4H_9 radicals are removed in reactions 13 and 14.

Can. J. Chem. Downloaded from www.nrcresearchpress.com by 210.87.254.42 on 09/05/12
For personal use only.

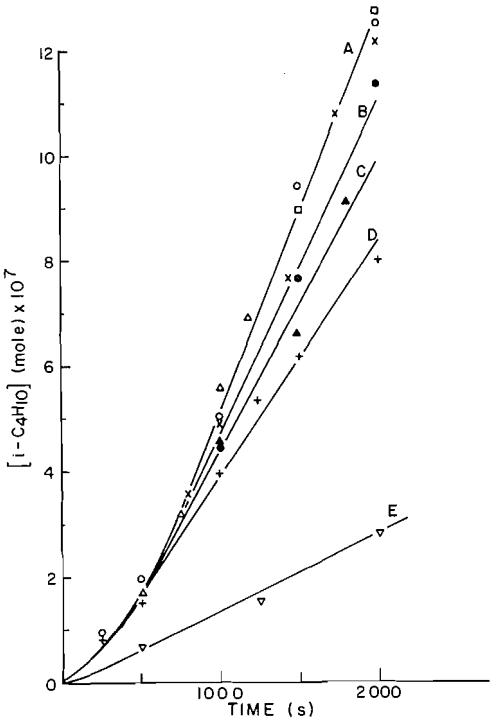

FIG. 1. Yield–time plot for isobutane production at 310 °C and at different pressures: *A*, higher than 54; *B*, 40; *C*, 24; *D*, 16; and *E*, 7 Torr.

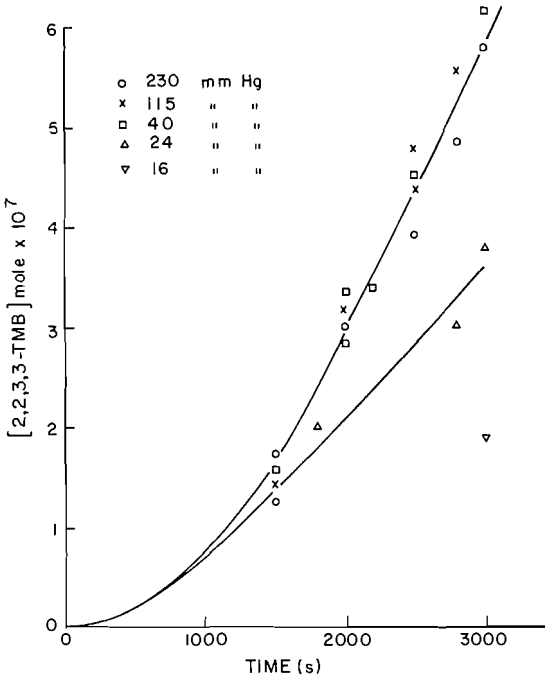

FIG. 2. Yield–time plot of 2,2,3,3-TMB production at different pressures and at 310 °C.

The present results were obtained at much higher temperature than that used by Falconer and Sunder (9). Because no products resulting from combination reactions of i-C_4H_9 radicals were detected, it is believed that in the present study the region of stabilization of i-C_4H_9 radicals was not reached and so most of the radicals decomposed. In view of the higher activation energy for non-terminal addition compared to terminal addition, as found by these authors, the increase of temperature will increase the percentage of non-terminal addition. On this basis one can explain the different results obtained in our investigation.

Production of Isobutane and 2,2,3,3-TMB

Typical yield–time plots for i-C_4H_{10} are shown in Fig. 1. Such plots show an induction period which decreases with increase in temperature. The maximal rates of i-C_4H_{10} production, obtained from the slopes in the linear region, are constant at pressures above 54 Torr at 310 °C. The pressure dependence at lower pressures is attributed to decrease of deactivation of the t-C_4H_9 radicals; an increasing fraction of the t-$C_4H_9^*$ radicals will decompose as the pressure is lowered. The activation energy is 3.6 ± 0.5 kcal/mol.

Typical yield–time plots for 2,2,3,3-TMB are shown in Fig. 2. The induction periods are longer than for i-C_4H_{10}, and increase with decrease of temperature. The activation energy is 2.8 ± 0.5 kcal/mol.

Both of these activation energies are comparable with those for the addition of H atoms to olefins.

The maximal rates for i-C_4H_{10} and 2,2,3,3-TMB production provide some information about the disproportion–combination ratio for t-C_4H_9 radicals:

$$\frac{k_d}{k_c} = \frac{v_{i\text{-}C_4H_{10}}}{v_{2,2,3,3\text{-TMB}}}$$

The ratios for different temperatures are summarized in Table 2. These values are subject to some error because of (*1*) the possibility of H abstraction by t-C_4H_9 radicals and (*2*) a limited accuracy in the analysis of 2,2,3,3-TMB. Listed values for k_d/k_c in the literature (15) vary from

Can. J. Chem. Downloaded from www.nrcresearchpress.com by 210.87.254.42 on 09/05/12
For personal use only.

TABLE 2. The maximal rates of i-C_4H_{10} and 2,2,3,3-TMB production, and the k_d/k_c ratio at different temperature

Temperature (°C)	Maximum rate (mol cc^{-1} s^{-1} × 10^{12})		k_d/k_c
	i-C_4H_{10}	2,2,3,3-TMB	
230	2.82	1.2	2.4
256	3.31	1.3	2.5
286	4.15	1.6	2.6
310	4.45	1.7	2.6

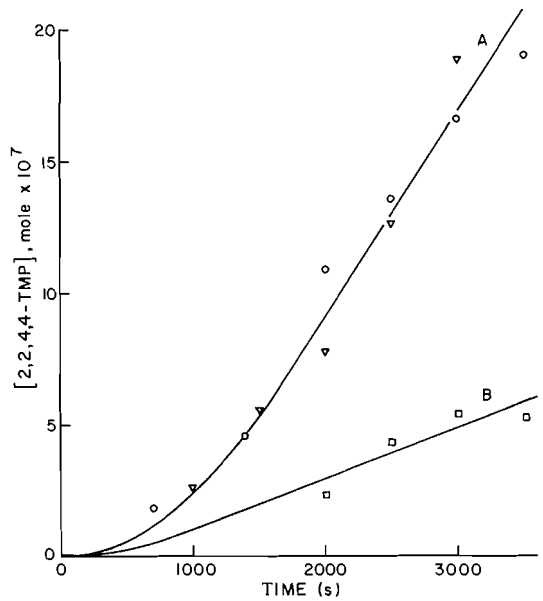

FIG. 3. Yield–time plot of 2,2,4,4-tetramethyl pentane production at different pressures and temperatures: *A*, 230 °C; ○, 54; ▽, 110; and *B*, 286 °C.

2 to 7.4; the present results support the lower values.

Production of 2,2,4,4-TMP

Typical yield–time curves for the production of 2,2,4,4-TMP are shown in Fig. 3. The yield decreases with temperature; little 2,2,4,4-TMP was found at 286 °C and none at 310 °C.

Production of Ethylene, Propylene, and Propane

Typical yield–time plots for these products are shown in Figs. 4, 5 and 6. The plot for C_3H_6 is S-shaped, owing to the fact that C_3H_6 is first formed in a secondary reaction and later is removed by addition of H atoms.

In high conversion experiments several very small peaks were observed for C_5 and C_6 hydrocarbons, but reliable analysis was not possible.

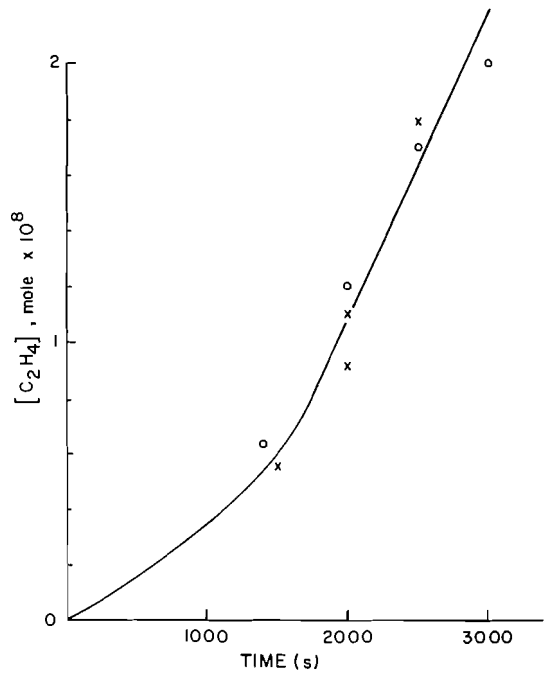

FIG. 4. Yield–time plot for ethylene production at 310 °C; ×, 115; ○, 40 Torr.

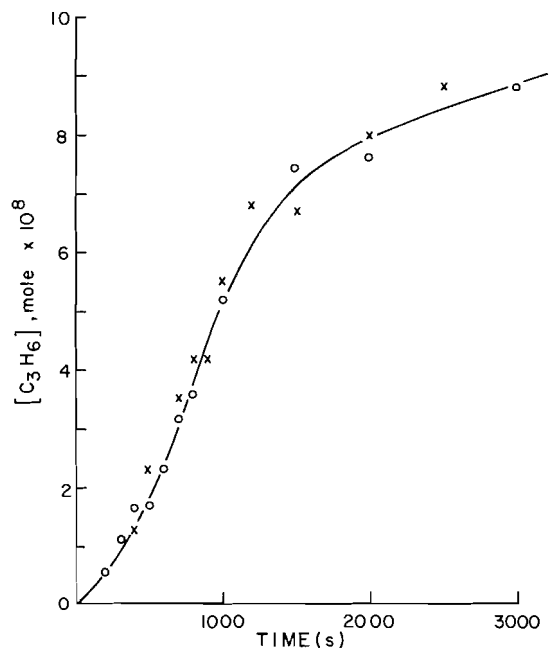

FIG. 5. Yield–time plot for propylene production at 310 °C, ×, 115 Torr; ○, 40 Torr.

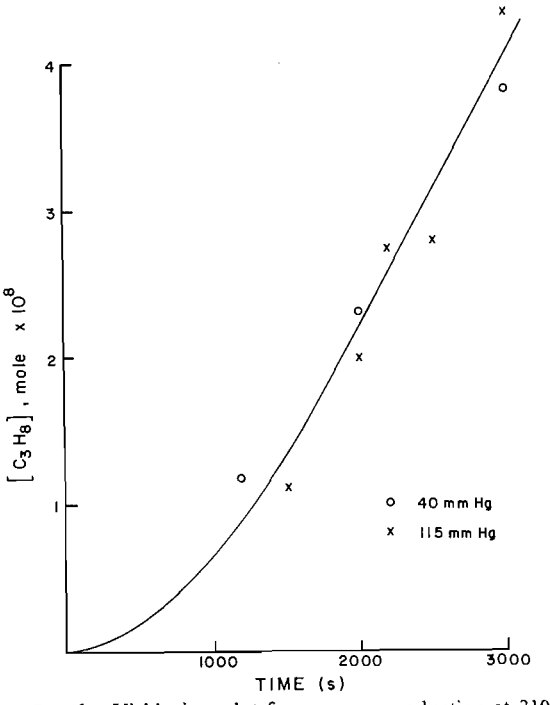

FIG. 6. Yield–time plot for propane production at 310 °C, ×, 115; ○, 40 Torr.

1. M. M. PAPIC and K. J. LAIDLER. Can. J. Chem. **49**, 535 (1971).
2. M. M. PAPIC and K. J. LAIDLER. Can. J. Chem. **49**, 549 (1971).
3. R. J. CVETANOVIC. Mercury photosensitized reactions, *In* Progr. Reaction Kinetics. Vol. 2. *Edited by* G. Porter. Pergamon Press, 1964.
4. R. J. CVETANOVIC, W. E. FALCONER, and K. R. JENNINGS. J. Chem. Phys. **33**, 1225 (1961).
5. K. R. JENNINGS and R. J. CVETANOVIC. J. Chem. Phys. **35**, 1235 (1961).
6. B. S. RABINOVITCH and R. W. DIESEN. J. Chem. Phys. **30**, 735 (1959).
7. W. J. MOORE and L. A. WALL. J. Chem. Phys. **17**, 1325 (1949).
8. P. J. BODDY and J. C. ROBB. Proc. Roy. Soc. A **249**, 233 (1959).
9. W. E. FALCONER and W. A. SUNDER. Int. J. Chem. Kinetics, **3**, 395 (1971).
10. J. A. KERR and A. C. LLOYD. Quart. Rev. **22**, 549 (1969).
11. W. M. JACKSON, J. R. NESBY, and B. DE B. DARWENT. J. Chem. Phys. **37**, 2256 (1962).
12. A. S. GORDON and J. R. NESBY. J. Chem. Phys. **33**, 1882 (1960).
13. M. C. LIN and K. J. LAIDLER. Can. J. Chem. **44**, 2927 (1966).
14. J. N. BRADLEY, H. W. MELVILLE, and J. C. ROBB. Proc. Roy. Soc. (London), A **236**, 339 (1956).
15. A. F. TROTMAN-DICKENSON and G. S. MILNE. Tables of bimolecular gas reactions, NSRDS-NBS9, **42**, 1967.

Can. J. Chem. Downloaded from www.nrcresearchpress.com by 210.87.254.42 on 09/05/12
For personal use only.

The Crystal Structure of Potassium Hydrogeniodate (V), $KIO_3.HIO_3$

G. KEMPER AND AAFJE VOS

Laboratorium voor Structuurchemie, Universiteit Groningen, Zernikelaan, Paddepoel, Groningen, The Netherlands

AND

H. M. RIETVELD

Reactor Centrum Nederland, Petten (N.H.), The Netherlands

Received August 9, 1971

The crystal structure of $KIO_3.HIO_3$ has been determined by three-dimensional single crystal X-ray diffraction and by neutron powder diffraction. The crystallographic data are $a = 7.025(2)$, $b = 8.206(2)$, $c = 21.839(5)$ Å, $\beta = 97.98(2)°$, space group $P2_1/c$, $Z = 8$ units $KIO_3.HIO_3$. The residual $R = [\Sigma|\Delta F|^2/\Sigma|F_0|^2]^{1/2}$ was 0.048 for 7516 independent X-ray reflections measured on a three-circle diffractometer with Zr-filtered Mo radiation. The results of the present study show good qualitative agreement with the structure recently determined by Chan and Einstein (7). The HIO_3 and IO_3^- groups are pyramidal, the I—O(H) bonds vary from 1.898 to 1.939(4) Å and the I—O bonds from 1.786 to 1.827(4) Å, these lengths are not corrected for the effects of thermal motion. Strong O—I . . . O interactions and electrostatic attractions between K^+ and $O^{\delta-}$ give slabs of thickness $\frac{1}{2}c \sin\beta \approx 10$ Å. The slabs are connected by hydrogen bonds of 2.710 and 2.694 Å.

On a déterminé la structure cristalline de $KIO_3.HIO_3$ par diffraction de rayons-X de cristaux uniques à trois dimensions et par diffraction de neutron de poudres. Les données cristallographiques sont $a = 7.025(2)$, $b = 8.206(2)$, $c = 21.839(5)$ Å, $\beta = 97.98(2)°$, le groupe spatial est $P2_1/c$, $Z = 8$ unités $KIO_3.HIO_3$. La valeur de $R = [\Sigma|\Delta F|^2/\Sigma|F_o|^2]^{1/2}$ résiduelle était de 0.048 pour 7516 réflexions de rayons-X indépendantes mesurées sur un diffractomètre tri-circulaire, au moyen d'une radiation de Mo filtrée par Zr. Les résultats de la présente étude sont en accord qualitatif avec la structure récemment déterminée par Chan et Einstein (7). Les groupes HIO_3 et IO_3^- sont pyramidaux, la longueur de lien I—O(H) varie de 1.898 à 1.939 Å et celle des liens I—O de 1.786 à 1.827 (4) Å, ces longueurs n'étant pas corrigées pour les effets de mouvement thermique. A cause des fortes interactions O—I . . . O et des attractions électrostatiques entre K^+ et $O^{\delta-}$, on obtient des plaques d'épaisseur $\frac{1}{2}c \sin\beta \approx 10$ Å. Les plaques sont reliées entre elles par des ponts hydrogènes de 2.710 et 2.694 Å.

Canadian Journal of Chemistry, **50**, 1134 (1972)

Introduction

The crystal structures of the oxygen acids and salts of iodine have aroused considerable interest because of the presence of short O—I...O distances indicative of strong O—I...O interactions.

For the iodates this strong interaction was observed first in $NaIO_3$ by MacGillavry and Panthaleon van Eck (1). In addition to the three oxygen atoms of the IO_3 group, each iodine atom in $NaIO_3$ is surrounded at short distances by three oxygen atoms of neighboring IO_3 groups in such a way that an irregular octahedron is formed. Similar surroundings of the iodine atoms occur in $Ce(IO_3)_4$ and in $LiIO_3$, giving rise in all cases to the formation of a three-dimensional network (2, 3).

In HIO_3 and in HI_3O_8 (in which HIO_3 and I_2O_5 groups can be distinguished) hydrogen bonds take part in the formation of the three-dimensional network (4–6) in addition to O—I...O interactions. In HI_3O_8 the iodine atom of the HIO_3 group is surrounded by seven oxygen atoms, whereas the remaining iodine atoms have six coordination (6).

To check the role of the hydrogen bonds in an acid iodate and to study the configuration of the different IO_3 groups, we have determined the crystal structure of $KIO_3.HIO_3$ by single crystal X-ray diffraction and by neutron powder diffraction. While our work was in progress an X-ray diffraction study of $KIO_3.HIO_3$ performed with fewer and less accurate reflection data, was published by Chan and Einstein (7). In the present paper our experimental work will be described and some additional information concerning the structure will be given.

Experimental

Crystal Data

$KIO_3.HIO_3$ f.w. = 390

Monoclinic, space group $P2_1/c$ with $a = 7.025(2)$, $b = 8.206(2)$, $c = 21.839(5)$ Å, $\beta = 97.98(2)°$, $V = 1246.7$ Å^3, $D_o = 4.0 \pm 0.5$ g/cm^3, $Z = 8$, $D_c = 4.16$ g/cm^3 (20 °C, $\lambda(CuK\alpha_1) = 1.54051$, $\lambda(CuK\alpha_2) = 1.54433$ Å).

The crystals were grown at room temperature by com-

plete evaporation of a solution of equimolar amounts of KIO_3 and HIO_3 in H_2O, the solution being placed over concentrated H_2SO_4 in a desiccator. The composition of the crystals was checked by chemical analysis. Form {001} is predominant and the crystals are slightly elongated along [010]. The cell dimensions were determined from zero layer line Weissenberg photographs calibrated with NaCl reflection spots. A least-squares program was used to calculate a, b, c, and β from the $\sin^2\theta/\lambda^2$ values of 64 reflections $0kl$ and 54 reflections $h0l$ with $45° < \theta < 80°$. The standard deviations estimated by the least-squares program are given in parentheses. The observed cell dimensions are not significantly different from the values reported by Chan and Einstein. The corresponding axial ratios and the angle β ($a:b:c = 0.856:1:2.661$, $\beta = 97.98°$) show reasonable agreement with the values given in Gmelin's Handbuch (8) for the monoclinic γ modification ($a:b:c = 0.857:1:2.590$, $\beta = 98.45$ after doubling the value given for c).

As reported by Chan and Einstein the systematic extinctions and the symmetry relations between the reflections indicate the space group to be $P2_1/c$. Initially we hesitated to adopt this space group as a large crystal of $KIO_3.HIO_3$ appeared to exhibit a strong piezoelectric effect (9). Later this effect was ascribed to a layer of KIO_3 which was shown to be present on the surface of the crystal by a zero layer line Weissenberg photograph of the crystal used for the piezoelectric test (10). The refinement of the structure described below shows that no difficulties are encountered in describing the structure in space group $P2_1/c$. It seems reasonable to assume that the strong second harmonic effect (11) reported at the end of ref. 7 is also caused by KIO_3 (or HIO_3) deposits.

X-Ray Diffraction Intensities

All intensities were obtained from a crystal with dimensions of 0.2, 0.25, and 0.1 mm along a, b, and c^*, respectively. The measurements were done on an automatic Nonius three-circle single crystal diffractometer with Zr-filtered Mo radiation, the b axis was mounted parallel to ϕ. The θ–2θ scan method was used with scan width $(0.7 + 0.5 \text{ tg } \theta)°$ and scan speed 1.2°/min. At each of the scan limits background measurements were done for half the scan time. All 10 827 independent reflections hkl with $\sin\theta/\lambda < 0.995$ Å^{-1} were considered. Due to the presence of a range selector integrated intensity and background measurements were carried out only for the 7516 reflections having a peak intensity above the level (just above zero) set by the range selector. Every 50 reflections one of the three chosen reference reflections was measured. The deviations of the intensities of these reflections from the respective average values appeared to be smaller than 5%. Corrections were made for the Lorentz and polarization effects, for the variations in the intensities of the reference reflections and for absorption ($\mu = 108$ cm^{-1}). The latter corrections were calculated according to the Busing and Levy (12) scheme; $6 \times 6 \times 6$ volume fragments and 6 bounding planes were considered.

Neutron Diffraction Data

In order to obtain additional information on the hydrogen positions, a neutron diffraction study was undertaken. Because no suitably large crystals for single crystal measurements were available, only powder samples were used. The high background scatter inevitable from powdered samples containing hydrogen was strongly reduced by deuterating the sample. This was done by dissolving I_2O_5 and KIO_3 in hot D_2O and crystallizing the $KIO_3.DIO_3$ by cooling.

The neutron diffraction data were collected on the powder diffractometer installed at the High Flux Reactor of the Reactor Centrum Nederland at Petten. The neutron wavelength was 2.5796(4) Å, obtained from the (111) plane of a copper crystal. As a second-order filter a piece of pyrolytic graphite with a thickness of 10 cm was employed (13). A Soller slit with a horizontal angular divergence of 30′ was placed between the reactor and the monochromator. A second slit of 10′ was placed in front of the BF_3 counter. The sample was contained in a cylindrical vanadium sample holder with a diameter of 2 cm. Powder diagrams from both the deuterated and undeuterated compound were obtained at room temperature and at liquid helium temperature.

Determination of the Structure

Determination of the Structure from the X-Ray Data

A rough model of the arrangement of the iodine atoms could be obtained from a three-dimensional Patterson synthesis. The positions of the K and O atoms were found by the heavy atom technique. The parameters of K, I, and O were refined on a TR4 computer with a least-squares program using the block diagonal approximation (14). All atoms (ions) were given anisotropic temperature factors and scattering factors corresponding with neutral atoms. The scattering factors were taken from Doyle and Turner (15), anomalous effects were not taken into account. All 7516 measured reflections were considered. In the final stages of the refinement the weighting scheme

$$w(hkl) = [\{w_c(hkl)\}^{-1} + p|F_o(hkl)|^2]^{-1}$$

was introduced in which $w_c(hkl)$ is the weight based on counting statistics, for the constant p the value 1.8×10^{-4} was chosen. Corrections for extinction were made according to Zachariasen (16). For the strongest reflection $12\bar{3}$ the extinction appeared to be as high as 26% in F. The residual $R = [\Sigma|\Delta F|^2/\Sigma|F_o|^2]^{1/2}$ and the weighted residual $R_w = [\Sigma w|\Delta F|^2/\Sigma w|F_o|^2]^{1/2}$ decreased to 0.048 and 0.043, respectively for the 7516 reflections used in the refinement. No systematic variations of $\langle w|\Delta F|^2\rangle$ with $|F|$ or with $\sin\theta/\lambda$ were observed. Typical deviations from the mean value found for the different groups are 15 and 25% for the former and latter case, respectively. A difference Fourier map showed no peaks greater than 2.0 e/Å^3 or lower than -1.8 e/Å^3 (standard deviation 0.5 e/Å^3).

The final coordinates and thermal parameters

TABLE 1. Final parameters*

(*a*) Final coordinates calculated by the least-squares programs, with standard deviations in parentheses

Atom	*x*	*y*	*z*
I(1)	0.16889(3)	0.10453(3)	0.65738(1)
I(2)	0.23147(3)	0.38738(3)	0.49976(1)
I(3)	0.66774(3)	0.36784(3)	0.65626(1)
I(4)	0.65247(3)	0.86048(3)	0.63591(1)
K(1)	0.24947(13)	0.87591(13)	0.50359(5)
K(2)	0.14460(14)	0.61345(12)	0.67125(5)
O(11)	0.0535(5)	0.2717(4)	0.6927(2)
O(12)	0.0155(5)	0.9355(4)	0.6699(2)
O(13)	0.0975(5)	0.1415(5)	0.5763(2)
O(21)	−0.0037(5)	0.3582(5)	0.4567(2)
O(22)	0.3206(5)	0.5460(4)	0.4534(2)
O(23)	0.3525(5)	0.2076(4)	0.4744(2)
O(31)	0.4144(4)	0.3927(4)	0.6357(2)
O(32)	0.6466(5)	0.2739(5)	0.7345(2)
O(33)	0.7436(5)	0.5655(4)	0.6852(2)
O(41)	0.4024(5)	0.8100(5)	0.6270(2)
O(42)	0.6652(5)	0.9005(4)	0.7239(2)
O(43)	0.6237(5)	0.0681(4)	0.6097(2)
H(1)†	0.552(4)	0.320(4)	0.754(1)
H(2)†	0.773(4)	0.842(4)	0.747(1)

*For numbering of atoms, see Fig. 2.
†Obtained by neutron powder diffraction.

(*b*) Thermal parameters (in 10^{-5} Å^2)*

Atom	U_{11}	U_{22}	U_{33}	$2U_{12}$	$2U_{23}$	$2U_{13}$
I(1)	1194(8)	1535(9)	1627(10)	−113(15)	−214(16)	227(14)
I(2)	1541(9)	1397(9)	1070(8)	90(15)	52(15)	378(14)
I(3)	1307(8)	1111(8)	1592(9)	−9(14)	−67(15)	287(14)
I(4)	1247(8)	1153(8)	1523(9)	14(14)	324(15)	630(13)
K(1)	1886(38)	2223(41)	1729(37)	−192(62)	435(65)	439(60)
K(2)	1891(38)	1708(37)	2728(46)	−331(61)	52(68)	133(67)
O(11)	2135(148)	1992(145)	2562(167)	180(229)	−1273(249)	817(248)
O(12)	1467(131)	2130(151)	3589(205)	−649(222)	1037(279)	556(257)
O(13)	2284(150)	3400(191)	1514(134)	−577(273)	−74(268)	−156(225)
O(21)	1657(132)	3380(189)	1947(147)	−208(256)	−142(274)	−692(218)
O(22)	2873(167)	2062(147)	1987(152)	−1001(251)	866(240)	1582(257)
O(23)	2381(150)	1794(137)	1934(144)	1003(225)	−258(224)	907(207)
O(31)	1089(111)	2555(153)	2347(151)	392(213)	−5(250)	−370(207)
O(32)	2598(167)	3129(183)	1893(152)	2065(277)	1450(268)	1200(255)
O(33)	2810(168)	1545(135)	2787(180)	−655(239)	−1203(249)	−649(274)
O(41)	1212(124)	3601(192)	2379(165)	−721(246)	337(289)	564(225)
O(42)	2066(137)	2295(146)	1409(123)	−16(228)	85(220)	616(210)
O(43)	3208(172)	1428(126)	1980(148)	860(236)	843(220)	959(257)

*The U_{ij} values are obtained from the formula $T(hkl) = \exp[-2\pi^2(h^2a^{*2}U_{11} + \ldots + 2hka^*b^*U_{12} + \ldots)]$.

are listed in Table 1. In Table 3 the observed and calculated structure factors (hydrogen atoms not included) are compared.[1] An analysis of the thermal parameters showed that these parameters can be described in terms of rigid body motions of independently vibrating IO_3 groups. Although not too much physical significance should be attached to this model because of the strong intermolecular interactions occur-

[1]Tabular data are available from the Depository of Unpublished Data, National Science Library, National Research Council of Canada, Ottawa, Canada K1A 0S2.

ring in the structure, libration corrections have been calculated for the I—O bonds. In Table 2*a* the corrected bond lengths are given in addition to the uncorrected values. The further discussion of the structure is based on the uncorrected coordinates given in Table 1.

Determination of the Hydrogen Positions

As the information content of a powder diagram is inherently low compared with single crystal measurements, it was decided to refine the hydrogen positions (and isotropic temperature factors) only and to keep the parameters of the other atoms fixed at the values determined by X-ray diffraction. The refinement was performed by the profile refinement method described by Rietveld (17). This method determines the estimates of the various parameters by finding a least-squares fit between the observed and calculated profile intensities y_i by minimizing the quantity $X_v^2 = \Sigma_i w_i[y_i(\text{obs}) - y_i(\text{calc})]^2/v$, where $y_i(\text{obs})$ and $y_i(\text{calc})$ are the observed and calculated values of the profile intensity measured at diffraction angle $2\theta_i$, w_i is the statistical weight, and v represents the number of degrees of freedom. The coherent scattering lengths used are: $b_H = -3.26 \times 10^{-13}$ cm, $b_D = 6.21 \times 10^{-13}$ cm, $b_K = 3.7 \times 10^{-13}$ cm, $b_I = 5.2 \times 10^{-13}$ cm, $b_O = 5.77 \times 10^{-13}$ cm. No significantly different hydrogen positions were found for the deuterated and undeuterated samples at room temperature and liquid helium temperature. The statistically most reliable results were obtained from the deuterated sample at room temperature. These have been given in Table 1*a* (for deuterium a B value of -0.5 (s.d. 1.2) Å^2 was obtained). The observed and calculated diffractometer profiles of $KIO_3.DIO_3$ are shown in Fig. 1.

During the refinement of the various samples it was found that the deuterated sample easily replaced its deuterium by hydrogen on contact with the atmosphere. The reversed exchange also took place, with the sample in a D_2O saturated atmosphere. No satisfactory explanation for this phenomenon has yet been found.

Structure Description and Discussion

The Three-dimensional Network

The structure reported and the description given in ref. 7 are essentially correct. The positions assumed by Chan and Einstein for the hydrogen atoms from the values obtained for I—O and O...O are confirmed by the present neutron diffraction study. Figure 2 is copied from ref. 7 except for the fact that in the present paper the atoms numbered in the figure correspond with those given in Table 1, moreover the hydrogen atoms have been added. Table 2, in which the atomic distances and valence angles are listed, are directly comparable with Table 2 of ref. 7.[2]

Some additional remarks can be made.

1. The surroundings of the K^+ ions are depicted in Fig. 3. For each of the K^+ ions all oxygen atoms have been projected unto the "best" plane through K^+ and five of its eight coordinating oxygen atoms. According to Chan and Einstein the coordination polyhedra can be best described as distorted square antiprisms. The squares around K(1) involve O(21)—O(22)—O(23)′—O(41) and O(13)—O(13)′—O(23)—O(43), respectively, for K(2) the squares are O(31)—O(42)—O(32)—O(41) and O(11)—O(33)—O(12)—O(21) (for the symmetry relations of these atoms to those in Fig. 2, see Table 2*b*).[3] Especially O(11) lies far from the idealized position.

2. From Fig. 2 it is seen that strong O—I...O interactions and electrostatic attractions between K^+ and $O^{\delta-}$ give slabs lying between $z = \frac{1}{4}$ and $z = \frac{3}{4}$ (and between $z = \frac{3}{4}$ and $z = 1\frac{1}{4}$ etc.) with a thickness of $\frac{1}{2}c \sin \beta \simeq 10$ Å. Successive slabs are connected by hydrogen bonds of 2.710 and 2.694 Å. The one independent O—I...O "bond" which crosses the plane $z = \frac{1}{4}$ (or $z = \frac{3}{4}$) is relatively weak, the relevant I...O distance [I(1)...O(33)] being the largest among those given in Table 2*b* and only 0.13 Å shorter than the accepted van der Waals distance of 3.55 Å (18). The layer-like structure explains the formation of crystals with form {001} predominant.

3. Comparison of the three I...O distances around the iodine atom I(1) of the $I(1)O_3^-$ group in $KIO_3.HIO_3$ (average value 3.16 Å) with the three I...O distances around the IO_3^- groups in $LiIO_3$ (average value 2.89 Å) shows that the I...O distances can vary appreciably,

[2] In ref. 7 the values of some of the interionic distances and angles are incorrect, errors occurring in the numbering of atoms and in the symmetry operations.

[3] We thank Dr. Einstein for sending us details of his description.

TABLE 2. Interatomic distances and angles

(*a*) I—O bond lengths*

Bond	Length (Å)	Average length (Å)
I(3)—O(31)	1.786 (1.792)	
I(3)—O(33)	1.795 (1.803)	1.792 (1.799)
I(4)—O(41)	1.789 (1.795)	
I(4)—O(43)	1.800 (1.806)	
I(2)—O(21)	1.800 (1.807)	
I(2)—O(22)	1.814 (1.820)	
I(2)—O(23)	1.827 (1.834)	1.810 (1.817)
I(1)—O(11)	1.819 (1.826)	
I(1)—O(12)	1.801 (1.806)	
I(1)—O(13)	1.799 (1.806)	
I(3)—O(32)	1.898 (1.904)	
I(4)—O(42)	1.939 (1.943)	1.919 (1.924)

*Values corrected for thermal libration in parentheses.

(*b*) I...O and K...O distances smaller than 3.5 Å

Bond	Distance (Å)	Symmetry*	Bond	Distance (Å)	Symmetry*
I(1)—O(31)	3.003	1*	I(3)—O(22)	2.509	2
O(41)	3.045	1*a*	O(43)	2.663	1
O(33)	3.423	3	O(11)	2.828	1*b*
I(2)—O(13)	2.861	1	I(4)—O(23)	2.468	2
O(21)	2.871	2*a*	O(12)	2.628	1*b*
O(31)	3.068	1	O(33)	2.690	1
O(22)	3.218	2			
K(1)—O(13)	2.797	2*a*	K(2)—O(11)	2.929	1
O(13)	2.980	1*c*	O(12)	2.793	1
O(21)	2.799	2*a*	O(21)	2.842	2*a*
O(22)	2.989	1	O(31)	2.808	1
O(23)	2.854	2	O(32)	2.700	3*a*
O(23)	2.910	1*c*	O(33)	2.902	1*d*
O(41)	2.812	1	O(41)	2.702	1
O(43)	2.783	2	O(42)	3.039	3

*(1), x,y,z; (1*a*), $x,y-1,z$; (1*b*), $x+1,y,z$; (1*c*), $x,y+1,z$; (1*d*), $x-1,y,z$; (2), $1-x,1-y,1-z$; (2*a*), $-x,1-y,1-z$; (3), $1-x,y-\frac{1}{2},\frac{3}{2}-z$; (3*a*), $1-x,y+\frac{1}{2},\frac{1}{2}-z$.

TABLE 2 *(Continued)*

(*c*) Angles (deg) around iodine atoms

	I(2)		I(1)		I(3)		I(4)	
I—O Contacts involved	Bonding O	Angle	Bonding O	Angle	Bonding O	Angle	Bonding O	Angle
Both I—O < 2.00 Å	O(21),O(22)	99.6	O(11),O(12)	101.8	O(31),O(32)	94.2	O(41),O(42)	93.2
	O(22),O(23)	101.5	O(12),O(13)	100.9	O(32),O(33)	96.1	O(42),O(43)	98.2
	O(23),O(21)	99.6	O(13),O(11)	102.2	O(33),O(31)	102.8	O(43),O(41)	96.8
2.40 Å < both I—O < 3.5 Å	O(21),O(22)	109.7	O(31),O(41)	104.6	O(22),O(43)	85.0	O(12),O(33)	86.0
	O(21),O(13)	94.4	O(41),O(33)	96.8	O(22),O(11)	101.0	O(23),O(12)	102.2
	O(13),O(22)	108.7	O(31),O(33)	101.8	O(11),O(43)	84.6	O(33),O(23)	99.0
	O(21),O(31)	81.2						
	O(22),O(31)	55.3						
	O(13),O(31)	64.7						
One I—O < 2.00 Å	O(21),O(22)	167.2	O(11),O(41)	167.5	O(31),O(11)	170.1	O(41),O(12)	169.9
2.40 Å < One I—O < 3.5 Å	O(22),O(13)	178.2	O(12),O(31)	178.3	O(32),O(22)	171.9	O(42),O(23)	176.2
	O(23),O(21)	172.7	O(13),O(33)	172.7	O(33),O(43)	169.2	O(43),O(33)	171.5
	O(21),O(13)	81.9	O(11),O(31)	76.8	O(31),O(22)	83.8	O(41),O(23)	87.8
	O(21),O(21)	75.9	O(11),O(33)	70.9	O(31),O(43)	87.2	O(41),O(33)	90.6
	O(22),O(22)	70.0	O(12),O(33)	78.6	O(32),O(11)	79.9	O(42),O(33)	77.3
	O(23),O(22)	76.0	O(12),O(41)	76.9	O(32),O(43)	87.1	O(42),O(12)	76.7
	O(23),O(13)	79.2	O(13),O(31)	78.4	O(33),O(22)	91.9	O(43),O(12)	86.0
	O(31),O(21)	137.6	O(13),O(41)	90.2	O(33),O(11)	85.8	O(43),O(23)	85.3
	O(31),O(22)	113.6						
	O(31),O(23)	98.9						
	O(22),O(21)	85.1						

TABLE 2 *(Concluded)*

(*d*) O...O distances smaller than 3 Å, and selected angles
(for hydrogen bonds see Table 2*e*)

Bond	Distance (Å)	Bonds	Angle (deg)
O(22)—O(31)	2.918	I(3)—O(32)—O(42)	108.4
O(23)—O(43)	2.933	I(4)—O(42)—O(32)	110.0
O(12)—O(42)	2.886	I(4)—O(42)—O(11)	121.9
O(33)—O(42)	2.950	I(1)—O(11)—O(42)	104.6
O(11)—O(42)	2.710*	O(32)—O(42)—O(11)	100.0
O(42)—O(32)	2.694*		

*Hydrogen bonds.

(*e*) The geometry of the hydrogen bonds

Bond	Distance (Å)	Bonds	Angle (deg)
O(32)—H(1)	0.92(4)	I(3)—O(32)—H(1)	114(3)
O(42)...H(1)	1.79(4)	I(4)—O(42)...H(1)	106(4)
O(32)...O(42)	2.694(6)	O(32)—H(1)...O(42)	167(4)
O(42)—H(2)	0.98(3)	I(4)—O(42)—H(2)	111(3)
O(11)...H(2)	1.76(3)	I(1)—O(11)...H(2)	105(2)
O(42)...O(11)	2.710(6)	O(42)—H(2)...O(11)	163(3)
		H(2)—O(42)...H(1)	108(3)

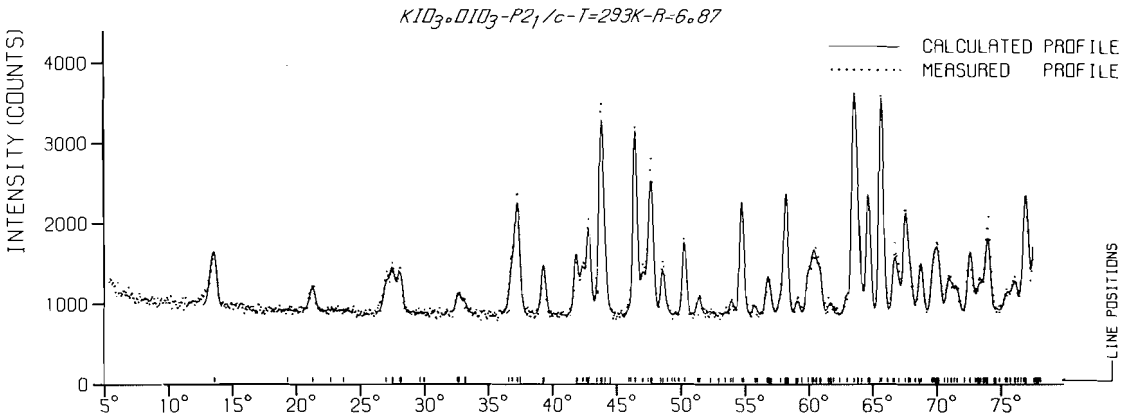

FIG. 1. Observed and calculated neutron diffraction profiles of $KIO_3.DIO_3$ at room temperature.

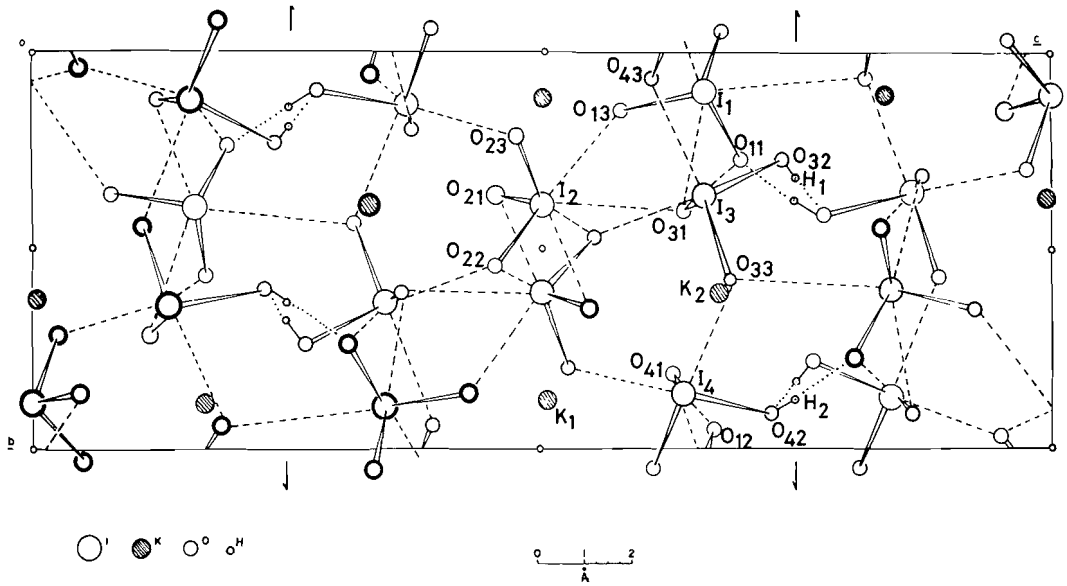

FIG. 2. Crystal structure of $KIO_3.HIO_3$ projected along the *a* axis. (Dotted lines indicate hydrogen bonds; dashed lines weak I...O interactions.)

even when the charge of the IO_3 group does not change. We think it possible that the I...O distances are influenced more by the packing in the crystal than by the charge of the IO_3 groups.

The Covalent I—O Bonds

As the present structure is more accurate than that described in ref. 7 a more detailed discussion of the I—O bonds can be given. The bond lengths and angles are listed in Table 2. The standard deviations calculated from the standard deviations in the coordinates (Table 1*a*) are 0.004 Å for the bond lengths and 0.2° for the angles.

Individual HIO_3 and IO_3^- groups can be described as $(HO)I^{2+}(O^-)_2$ and $I^{2+}(O^-)_3$, respectively, if no d orbitals are taken into account and as

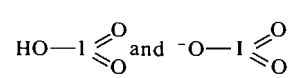

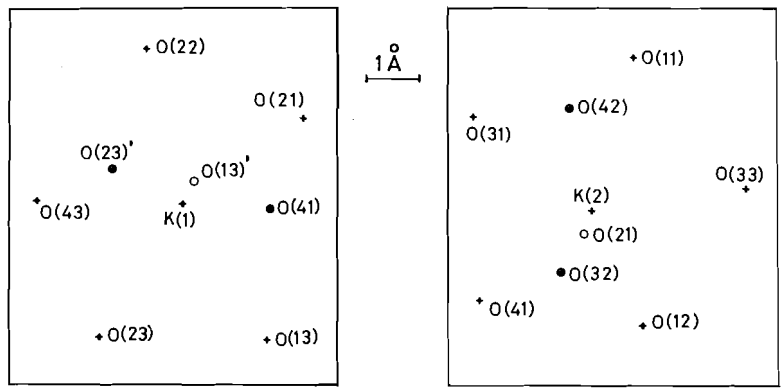

FIG. 3. Projection of K(1) and K(2) with their coordinating oxygen atoms on their respective "best" planes. Atoms within 0.4 Å from the "best" plane are marked +, those about 2.5 Å above or below the plane are marked ● or ○, respectively. O(13)′ = O(13;2*a*), O(23)′ = O(23;2), see Table 2*b*. The equations of the "best" planes are (*X*, *Y*, *Z* in Å along directions *a**, *b*, and *c*) $0.83742X - 0.11913Y + 0.53341Z = 6.07763$ (K_1) and $0.39309X - 0.08077Y + 0.91595Z = 13.90882$ (K_2).
The distances of the atoms to the respective planes of projection (in Å) are: K(1), 0.3; O(23), 0.1; O(43), −0.4; O(22), 0.4; O(21), −0.4; O(13), 0.0; O(23)′, 2.7; O(13)′, −2.5; O(41), 2.6; K(2), 0.2; O(41), −0.1; O(31), −0.2; O(11), 0.2; O(33), −0.3; O(12), 0.1; O(42), 2.5; O(21), −2.6; O(32), 2.6.

(plus appropriate resonance structures) with the use of d orbitals.[4] In view of this description three types of bonds with decreasing bond orders can be distinguished: (*a*) I—O in HIO_3, (*b*) I—O in IO_3^-, and (*c*) I—OH in HIO_3. The observed bond lengths in Table 2*a* show that in groups (*b*) and (*c*) the lengths of the bonds show significant variations. The bonds of type (*c*) are significantly longer than those of types (*a*) and (*b*). The difference between the latter two types, which is evidently small, is obscured by the observed variations. The small difference between bonds of type (*a*) and (*b*) will be due to the I—OH bond having partial double bond character (see below). We tentatively ascribe the observed variations of the I—O bond lengths in group (*b*) to the intermolecular interaction occurring in $KIO_3.HIO_3$, although we have not been able to detect a systematic correlation between the observed variations and the surroundings of the I—O bonds. The average value of I—O in IO_3^- (1.810 Å; group *b*) is in excellent agreement with the I—O bond lengths of 1.809 Å in $LiIO_3$(3).

The length of the I—OH bond I(3)—O(32) = 1.898 Å agrees with the value of 1.90 Å observed for the I—OH bonds in HIO_3 and in HI_3O_8(6). The bond I(4)—O(42) = 1.939 Å is significantly longer, probably due to the fact that O(42) acts both as a hydrogen donor and acceptor whereas O(32) acts as a hydrogen donor alone. The further interactions with the surroundings are approximately the same for the two I—OH bonds. The I—OH bonds can also be compared with the I—O—(I) bonds of the I_2O_5 groups in HI_3O_8 which are 1.96 ± 0.01 Å (6) and with those in I_2O_5 where lengths of 1.93 ± 0.02 Å have been observed (19). All these I—O bonds are shorter than the value 1.99 Å predicted by Schomaker–Stevenson's rule (20) and are thus likely to have a partial double bond character (for a further discussion see ref. 19).

[4]This description corresponds with the formal bond orders used by Chan and Einstein. Their description in terms of I^{5+} surrounded by O^{2-} is not reasonable.

We thank Dr. W. G. Perdok for the piezoelectric measurements. The calculations were done at the Computing Centre of the University of Groningen.

1. C. H. MACGILLAVRY and C. L. PANTHALEON VON ECK. Rec. Trav. Chim. Pays-Bas, **62**, 729 (1943).
2. D. T. CROMER and A. C. LARSON. Acta Cryst. **9**, 1015 (1956).
3. J. L. DE BOER, F. VAN BOLHUIS, R. OLTHOF-HAZEKAMP, and A. VOS. Acta Cryst. **21**, 841 (1966).
4. M. T. ROGERS and L. HELMHOLTZ. J. Am. Chem. Soc. **63**, 278 (1941).
5. B. S. GARRETT. ORNL-17. Oak Ridge National Laboratory, Tennessee. 1954.
6. Y. D. FEIKEMA and A. VOS. Acta Cryst. **20**, 769 (1966).
7. L. Y. Y. CHAN and F. W. B. EINSTEIN. Can. J. Chem. **49**, 468 (1971).
8. GMELIN. Handbuch der anorganischen Chemie. Jod **8**, 509 (1933).

9. G. KEMPER and A. VOS. Acta Cryst. **B26**, 302 (1970).
10. G. KEMPER and A. VOS. Acta Cryst. **B27**, 2286 (1971).
11. A. K. LEVINE. Lasers. Vol. 2. Marcel Dekker, Inc. 1968. p. 298.
12. W. R. BUSING and H. A. LEVY. Acta Cryst. **10**, 180 (1957).
13. B. O. LOOPSTRA. Nucl. Instr. Methods, **44**, 181 (1966).
14. D. W. J. CRUICKSHANK and D. E. PILLING. *In* Computing methods and the phase problem in X-ray crystal analysis. Pergamon Press. London. 1961.
15. P. A. DOYLE and P. S. TURNER. Acta Cryst. A**24**, 390 (1968).
16. W. H. ZACHARIASEN. Acta Cryst. A**24**, 212 (1968).
17. H. M. RIETVELD. J. Appl. Cryst. **2**, 65 (1969).
18. L. PAULING. The chemical bond. Cornell University Press. 1967. pp. 151–152.
19. K. SELTE and A. KJEKSHUS. Acta Chem. Scandinavica, **24**, 1912 (1970).
20. V. SCHOMAKER and D. P. STEVENSON. J. Am. Chem. Soc. **63**, 37 (1941).

Constantes de stabilité de cyano-complexes d'argent et produit de solubilité de AgCN

A. O. GÜBELI ET P. A. CÔTÉ

Département de Chimie, Université Laval, Québec, Québec

Reçu le 9 septembre 1971

On a appliqué la méthode des pentes à la détermination des constantes de formation cumulatives de $Ag(CN)_2^-$ et $Ag(OH)CN^-$ et à la mesure du produit de solubilité de AgCN, dans $NaClO_4$ 1 *M*, à 25 °C.

The slope method has been applied to the determination of the cumulative formation constants of $Ag(CN)_2^-$ and $Ag(OH)CN^-$ and to the measure of the solubility product of AgCN, in 1 *M* $NaClO_4$, at 25 °C.

Canadian Journal of Chemistry, **50**, 1144 (1972)

Can. J. Chem. Downloaded from www.nrcresearchpress.com by 210.87.254.40 on 09/05/12
For personal use only.

Introduction

La méthode des pentes, telle que proposée par Ste-Marie (1), était basée sur la basse solubilité des complexes, $[M]_{tot}$, comparée à la concentration totale de ligand (autre que OH^-) en solution, $[L]_{tot}$. Cette méthode a d'ailleurs été appliquée à l'étude de complexes de métaux en présence de NH_3 (2), H_2S (3), H_2Se (4), et H_2SeO_3 (5) entre autres.

Nous nous proposons de démontrer que, même si le rapport $[L]_{tot}/[M]_{tot}$ tend vers l'unité, la méthode des pentes peut s'appliquer à l'étude de solutions saturées de cyanure d'argent.

Traitement mathématique

Quand on précipite l'argent par un excès de cyanure, un ensemble d'équilibres simultanés s'établit en solution saturée,

$$H_2O \rightleftarrows H^+ + OH^-$$

$$HCN \rightleftarrows H^+ + CN^-$$

$$AgCN(s) \rightleftarrows Ag^+ + CN^-$$

et

$$Ag^+ + xOH^- + yCN^- \rightleftarrows Ag(OH)_x(CN)_y^{1-x-y}$$

dont les constantes respectives, K_e, k_1, K_{s0} et β_{xy}, sont représentées par les éqs. 1 à 4:

$$[1] \qquad K_e = a_H a_{OH}$$

$$[2] \qquad k_1 = \frac{a_H[CN^-]}{[HCN]}$$

$$[3] \qquad K_{s0} = [Ag^+][CN^-]$$

et

$$[4] \qquad \beta_{xy} = \frac{[Ag(OH)_x(CN)_y^{1-x-y}]}{[Ag^+]a_{OH}^x[CN^-]^y}$$

où a_H et a_{OH} représentent les activités de H^+ et OH^-, alors que [ ] indique la concentration de toute autre espèce.

Si nous posons que, dans une région du pH et pour un intervalle de concentration du ligand, un seul complexe mononucléaire[1] est prédominant en solution, on peut écrire

$$[5] \qquad [Ag]_{tot} = [Ag(OH)_x(CN)_y^{1-x-y}]$$

et

$$[6] \qquad [CN]_{tot} = [HCN] + [CN^-] + [CN]_{lié}$$

où

$$[7] \qquad [CN]_{lié} = y[Ag]_{tot}$$

A. Basse solubilité

Lorsque $[Ag(OH)_x(CN)_y^{1-x-y}]$ est très faible comparativement à la concentration totale du ligand en solution, il s'ensuit que

$$[8] \qquad [CN]_{tot} = [CN^-](F_cH)$$

où

$$[9] \qquad (F_cH) = ((a_H/k_1) + 1)$$

Substituant dans l'éq. 5, les éqs. 1, 3, 4, et 8, on obtient la relation

$$[10] \qquad [Ag]_{tot} = \beta_{xy}K_{s0}K_e^x[CN]_{tot}^{y-1}(F_cH)^{1-y}a_H^{-x}$$

dont les dérivées partielles sont les pentes caractéristiques de l'espèce métallique prédominante en solution

$$[11] \qquad \left(\frac{\partial pAg_{tot}}{\partial pH}\right)_{pCN_{tot}} = 1 - x - y$$

si $pH < pk_1 - 1$

[1]Limitation inhérente à la méthode de solubilité ((6), chapitre sur la solubilité).

Can. J. Chem. Downloaded from www.nrcresearchpress.com by 210.87.254.40 on 09/05/12
For personal use only.

[12] $$\left(\frac{\partial \mathrm{pAg_{tot}}}{\partial \mathrm{p}H}\right)_{\mathrm{pCN_{tot}}} = -x \qquad \text{si } \mathrm{p}H > \mathrm{p}k_1 + 1$$

et

[13] $$\left(\frac{\partial \mathrm{pAg_{tot}}}{\partial \mathrm{pCN_{tot}}}\right)_{\mathrm{p}H} = y - 1 \qquad \text{à tout p}H$$

Si on vérifie expérimentalement le comportement de Ag^+ en présence de cyanure d'argent, c'est-à-dire quand ($x = y = 0$) et pAg_{tot} est remplacé par pAg^+ dans les éqs. 11 à 13, on peut calculer le produit de solubilité de AgCN dans l'éq. 10, à condition que k_1 soit connu. La valeur de la constante de dissociation de HCN est, sur l'échelle de pH, le point où la pente de pAg^+ en fonction du pH passe de (+1) à (0). Il est, par la suite, possible d'identifier toute espèce prédominante par les pentes de la courbe de solubilité et d'en calculer la constante de formation cumulative, β_{xy}, dans l'éq. 10.

B. Haute solubilité

Si la concentration de $Ag(OH)_x(CN)_y^{1-x-y}$ est beaucoup plus élevée que la somme ($[HCN] + [CN^-]$), l'éq. 6 devient

[14] $$[CN]_{tot} = y[Ag]_{tot}$$

En y introduisant les éqs. 1 et 3 à 5, on tire

[15] $$[CN]_{tot} = y\beta_{xy}K_{s0}^{y}K_c^{x}[Ag^+]^{1-y}a_H^{-x}$$

dont les dérivées partielles sont caractéristiques de l'espèce prédominante en solution à tout pH, quand ($y > 1$):

[16] $$\left(\frac{\partial \mathrm{pAg}^+}{\partial \mathrm{p}H}\right)_{\mathrm{pCN_{tot}}} = x/(1-y)$$

et

[17] $$\left(\frac{\partial \mathrm{pAg}^+}{\partial \mathrm{pCN_{tot}}}\right)_{\mathrm{p}H} = 1/(1-y)$$

Dans un domaine de haute solubilité, on peut identifier une espèce prédominante, très stable, par les pentes des éqs. 16 et 17, si celle-ci contient plus d'un groupement cyanure lié au métal. Si un mono-cyano-complexe simple ou mixte devient prépondérant en solution, les pentes des éqs. 16 et 17 ne sont plus valables.

Puisque k_1 n'intervient pas dans l'éq. 15, on ne peut, dans une telle région, en déterminer la valeur de façon graphique.

Méthode expérimentale

Des réactifs de pureté garantie et de l'eau bidistillée ont servi à la préparation de toutes les solutions. Nous avons précipité le cyanure d'argent à partir de $AgClO_4$ et d'un excès de cyanure de sodium tel que AgCN(s) était toujours en équilibre avec la solution. La solution de $AgClO_4$ contenait un faible pourcentage de ^{110}Ag utilisé comme traceur radioactif. Le pH de chacune des solutions a été ajusté avec $HClO_4$ ou NaOH selon le cas et la molarité de $NaClO_4$ a été maintenue à l'unité. Les solutions saturées ont été agitées durant les premiers jours et laissées au repos pendant quatre semaines.

Une fois l'équilibre vérifié par échantillonnage périodique, nous avons procédé à la mesure de la solubilité totale de l'argent au moyen d'un compteur à scintillations de marque Philips et à la détermination de la concentration totale de cyanure par une méthode spectrophotométrique à l'aide du réactif *p*-phénylènediamine (7). Le pH a été mesuré au moyen d'un couple d'électrodes verre-calomel(sat.) reliées entre elles par un pont d'agar-agar. L'électrode de verre de marque Corning (No 476022), pouvant opérer entre pH = 0 et 14, a été étalonnée à l'aide de tampons Clark and Lubs et de solutions de HCl et NaOH. Ainsi, on a attribué à NaOH 0.1 et 1.0 M des pH de 12.88 et 13.83, étant donnés les $\gamma_\pm$ correspondants, 0.764 et 0.677 (8). On a apporté une correction due à la réponse de l'électrode aux ions Na^+ (toujours <0.04 unité de pH) (9). La concentration des ions Ag^+ a été obtenue en substituant à l'électrode de verre une électrode d'argent dans le couple décrit précédemment. Celle-ci a été étalonnée préalablement par rapport au produit de solubilité apparent de l'oxyde d'argent que nous avons déterminé radiométriquement dans $NaClO_4$ 1 M, à 25 °C. Cet étalonnage est basé sur l'équation de Nernst et sur l'identification par la méthode des pentes des espèces prédominantes Ag^+, AgOH et $Ag(OH)_2^-$ en équilibre avec Ag_2O(s). Le produit de solubilité apparent déterminé ($pK_{s0} = 7.82$) est en accord avec la valeur rapportée par Biedermann et Sillén (10).

Résultats

D'après la fig. 1, puisque la valeur de R ($R = pAg_{tot} - pCN_{tot}$) indique que le rapport $[CN]_{tot}/[Ag]_{tot}$ est grand pour p$H < 4$, on peut traiter les résultats de cette région (I) par l'hypothèse de basse solubilité. Cependant, pour $4 <$ p$H <$ 13, la solubilité totale de l'argent est comparable à celle du cyanure. Les résultats de ce domaine (II) correspondent à une région de haute solubilité. Puisque, pour p$H \geqslant 13$, R tend vers 0, cette partie de la courbe (III) est traitée séparément, car "y" tend vers l'unité.

Puisque la région de haute solubilité (II) cache la valeur de pk_1 (9.21, à dilution infinie et à 25 °C (11)), nous en avons effectué la détermination dans $NaClO_4$ 1 M, par titrage potentiométrique, selon une méthode analogue à celle d'Anderegg (12). Trois mesures pour des solutions de NaCN de concentrations variables nous ont donné comme valeur la plus probable de cette constante apparente, $pk_1 = 8.95$.

Les résultats des régions I et II ont pu être interprétés à l'aide de la méthode des moindres

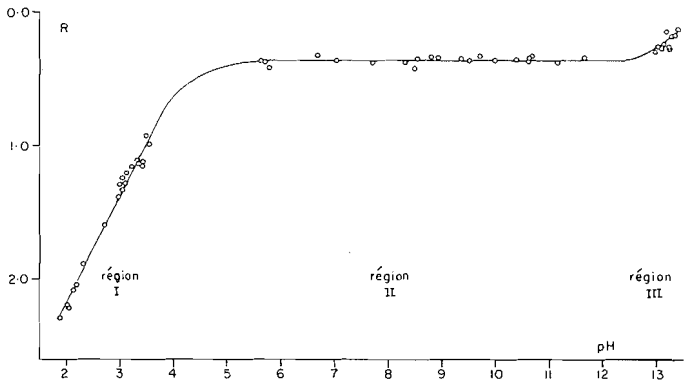

FIG. 1. Influence du pH sur R ($R = pAg_{tot} - pCN_{tot}$).

TABLEAU 1. Solubilité totale (pAg_{tot}) et cationique (pAg^+) de l'argent pour des valeurs variables de pCN_{tot}, $pH < 4$

pH	pCN_{tot}	pAg_{tot}	pAg^+
1.85	2.72	5.02	5.73
2.02	2.70	4.90	5.97
2.05	2.57	4.77	6.14
2.12	2.66	4.75	6.01
2.20	2.51	4.55	6.22
2.32	2.59	4.47	6.33
2.72	2.26	3.85	7.10
2.95	2.67	4.06	6.88
3.00	2.83	4.13	6.79
3.05	2.61	3.86	7.10
3.05	2.34	3.67	7.31
3.10	2.72	4.01	6.97
3.12	2.28	3.49	7.50
3.22	2.20	3.36	7.56
3.22	2.21	3.37	7.58
3.35	2.49	3.63	7.31
3.35	2.80	3.92	7.04
3.42	2.65	3.77	7.20
3.42	2.64	3.70	7.51
3.50	2.31	3.23	7.78
3.55	2.20	3.19	7.99

carrés appliquée à l'équation générale d'un plan, $Z = f(X,Y) = \alpha + \beta X + \gamma Y$. Ceci nous a permis d'évaluer des coefficients α, β, et γ qui ont orienté l'interprétation des données de solubilité totale et cationique.

Région I

Les résultats du tableau 1 permettent d'obtenir l'équation

$$[18] \quad pAg^+ = f(pH,pCN_{tot}) = 7.0 + 0.95pH - 1.1pCN_{tot}$$

qui confirme le comportement de Ag^+ selon les pentes des éqs. 11 et 13.

La valeur la plus probable du produit de solubilité apparent du cyanure d'argent peut être calculée d'après l'éq. 10

$$pK_{s0} = 15.54 \ (\sigma = \pm 0.06)$$

De plus, l'équation

$$[19] \quad pAg_{tot} = f(pH,pCN_{tot}) = 3.7 - 0.81pH + 1.0pCN_{tot}$$

montre la prédominance de $Ag(CN)_2^-$ en solution d'après les pentes des éqs. 11 et 13.

La valeur la plus probable de sa constante de formation cumulative apparente est

$$\log \beta_{02} = 20.14 \ (\sigma = \pm 0.05)$$

De ces constantes, on peut calculer

$$\log K_s = \log (\beta_{02} K_{s0}^2) = -10.94 = \log [Ag(CN)_2^-][Ag^+]$$

Région II

Les résultats groupés au tableau 2 permettent de confirmer que $[Ag]_{tot} = [Ag(CN)_2^-]$ d'après l'équation

$$[20] \quad pAg^+ = f(pH,pCN_{tot}) = 11 + 0.02pH - 1.1pCN_{tot}$$

car β et γ correspondent aux pentes des éqs. 16 et 17 quand $(x = 0)$ et $(y = 2)$. D'ailleurs, la valeur de α dans l'équation

$$[21] \quad pAg_{tot} = f(pH,pCN_{tot}) = 0.34 + 0.00pH + 1.0pCN_{tot}$$

Can. J. Chem. Downloaded from www.nrcresearchpress.com by 210.87.254.40 on 09/05/12
For personal use only.

Can. J. Chem. Downloaded from www.nrcresearchpress.com by 210.87.254.40 on 09/05/12
For personal use only.

TABLEAU 2. Solubilité totale (pAg_{tot}) et cationique (pAg^+) de l'argent pour des valeurs variables de pCN_{tot}, $4 < pH < 13$

pH	pCN_{tot}	pAg_{tot}	pAg^+
5.63	2.45	2.81	8.18
5.70	2.47	2.84	8.09
5.80	2.93	3.34	7.71
6.70	2.40	2.72	8.13
7.05	2.93	3.29	7.53
7.72	2.30	2.67	8.20
8.33	2.47	2.84	8.05
8.50	2.42	2.84	8.08
8.57	2.33	2.67	8.24
8.82	2.48	2.81	8.12
8.95	2.42	2.76	8.18
9.37	2.35	2.69	8.13
9.52	2.33	2.68	8.20
9.72	2.51	2.84	7.93
10.00	2.34	2.70	8.18
10.40	2.46	2.81	8.09
10.62	2.32	2.68	8.24
10.65	2.48	2.82	7.95
10.70	2.50	2.83	7.91
11.17	2.36	2.73	8.18
11.67	2.34	2.68	8.24

fournit une valeur approchée de ($\log y$), d'après l'éq. 14.

On vérifie de plus cette identification par le calcul de

$$\log K_s = -(pAg_{tot} + pAg^+)$$
$$= -10.89\ (\sigma = \pm 0.05)$$

Région III

Puisque, d'après le tableau 3, on observe que

$$1 < [CN]_{tot}/[Ag]_{tot} < 2$$

on peut écrire

[22] $$[Ag]^f_{tot} = [Ag]_{tot} - [Ag^+] - [Ag(CN)_2^-]$$
$$= [Ag(OH)_x(CN)^{-x}]$$

La constante K_s permet d'évaluer $[Ag]^f_{tot}$ et nous pouvons développer l'éq. 22

[23] $$[Ag]^f_{tot} = \beta_{x1} K_{s0} K_e^x a_H^{-x}$$

La dérivée totale, $(dpAg^f_{tot}/dpH)$, fournit la valeur numérique de x. Un tel graphique donne une pente de (-1) identifiant ainsi l'espèce $Ag(OH)CN^-$, dont nous avons calculé, à l'aide de $pK_e = 14.0$, la constante de formation cumulative apparente

$$\log \beta_{11} = 12.80\ (\sigma = \pm 0.08)$$

TABLEAU 3. Solubilité totale (pAg_{tot}), cationique (pAg^+) et différentielle (pAg^f_{tot}) de l'argent pour des valeurs variables de pCN_{tot}, $pH \geqslant 13$

pH	pCN_{tot}	pAg_{tot}	pAg^+	pAg^f_{tot}
13.00	2.49	2.79	8.06	3.74
13.05	2.65	2.90	7.92	3.69
13.10	2.76	3.02	7.80	3.65
13.15	2.80	3.04	7.74	3.67
13.20	3.10	3.24	7.38	3.57
13.25	2.59	2.85	7.92	3.46
13.27	2.66	2.93	7.84	3.51
13.30	2.96	3.14	7.50	3.45
13.35	2.99	3.16	7.35	3.38
13.40	3.05	3.18	7.30	3.37

Discussion

Le traitement mathématique proposé explique le comportement de l'argent en présence de cyanure, en milieu hétérogène. Les valeurs mesurées du produit de solubilité de AgCN et des constantes de formation cumulatives de $Ag(CN)_2^-$ et $Ag(OH)CN^-$ s'approchent de celles compilées par Sillén et Martell (13), si l'on tient compte des corrections à apporter à chacune d'elles pour les ramener à dilution infinie. Il est à noter que l'imprécision sur la mesure du pH en milieu très alcalin a pu affecter la valeur de β_{11}.

Dans l'intervalle de pH et de pCN_{tot} étudié, l'absence des espèces prédominantes $Ag(CN)_3^{2-}$ et $Ag(CN)_4^{3-}$ est en accord avec les résultats d'Ammar, Darwish et Rizk (14), et de Jones et Penneman (15) entre autres. En effet, puisque nous avons observé expérimentalement que

$$[CN^-] = \frac{K_{s0}}{[Ag^+]} \ll 1$$

il s'ensuit que, si AgCN(s) est en équilibre avec la solution,

$$\frac{[Ag(CN)_3^{2-}]}{[Ag(CN)_2^-]} = K_3[CN^-] \ll 1$$

et

$$\frac{[Ag(CN)_4^{3-}]}{[Ag(CN)_2^-]} = K_3 K_4 [CN^-]^2 \ll 1$$

où les valeurs de K_3 et K_4 ($\log K_3 = 0.70$ et $\log K_4 = -1.13$) sont tirées de la réf. 15.

Quant à l'espèce neutre, AgCN, sa solubilité, indépendante du pH et du pCN_{tot} en présence de AgCN(s), est reliée au produit de solubilité

par la relation

$$[AgCN] = \beta_{01} K_{s0} = K_{s1}$$

Etant donné la solubilité minimale observée (tableau 1), [AgCN] est nécessairement inférieure à 10^{-5}. Ceci est en accord avec la valeur estimée, $K_{s1} = 10^{-7}$, rapportée par Butler (16).

Nous tenons à remercier le Conseil National de Recherches du Canada pour son aide financière qui a permis la réalisation de ce travail et le Centreau de l'Université Laval pour l'instrumentation supplémentaire.

1. J. STE-MARIE. Thèse, Université Laval, Québec, Québec. 1966.
2. A. O. GÜBELI et J. STE-MARIE. Can. J. Chem. **46**, 1707 (1968); A. O. GÜBELI, J. HÉBERT, R. TAILLON, et P. A. CÔTÉ. Helv. Chim. Acta, **53**, 1229 (1970); **53**, 186 (1970).
3. A. O. GÜBELI et J. STE-MARIE. Can. J. Chem. **45**, 2101 (1967).
4. M. C. MEHRA et A. O. GÜBELI. Can. J. Chem. **48**, 3491 (1970); J. Less-Common Metals, **22**, 281 (1970).
5. M. C. MEHRA et A. O. GÜBELI. Radiochem. Radioanal. Lett. **2**, 61 (1969).
6. F. J. C. ROSSOTTI et H. ROSSOTTI. The determination of stability constants. McGraw-Hill Book Co. Inc. New York. 1961.
7. L. S. BARK et H. G. HIGSON. Talanta, **11**, 621 (1964).
8. L. MEITES. Handbook of analytical chemistry. McGraw-Hill Book Co. Inc. New York. 1963.
9. R. G. BATES. Determination of p*H*. John Wiley and Sons, Inc. New York. 1964.
10. G. BIEDERMANN et L. G. SILLÉN. Acta Chim. Scand. **14**, 717 (1960).
11. R. M. IZATT, J. J. CHRISTENSEN, R. T. PACK, et R. BENCH. Inorg. Chem. **1**, 828 (1962).
12. G. ANDEREGG. Helv. Chim. Acta, **40**, 1022 (1957).
13. L. G. SILLÉN et A. E. MARTELL. Stability constants. The Chemical Society. London. 1964. Spec. Publ. No. 17.
14. I. A. AMMAR, S. DARWISH, et K. RIZK. Electrochim. Acta, **12**, 647 (1967).
15. L. H. JONES et R. A. PENNEMAN. J. Chem. Phys. **22**, 965 (1954).
16. J. N. BUTLER. Ionic equilibrium. A mathematical approach. Addison-Wesley Publishing Co. Inc. Reading. 1964.

Can. J. Chem. Downloaded from www.nrcresearchpress.com by 210.87.254.40 on 09/05/12
For personal use only.

Microwave Spectrum, Dipole Moment, and Intramolecular Hydrogen Bond of 2-Methoxyethanol

PAUL BUCKLEY AND MIREILLE BROCHU

Département de Chimie et Centre de Recherches sur les Atomes et les Molécules, Université Laval, Québec

Received September 23, 1971

The minimum energy conformation of 2-methoxyethanol ($CH_3OCH_2CH_2OH$) has been determined from an analysis of its microwave spectrum. The rotational constants of the normal species are: $A = 12982.35$, $B = 2742.48$, and $C = 2468.10$ MHz; the dipole moment components are $\mu_a = 2.03$, $\mu_b = 1.15$, $\mu_c \simeq 0.25$, and $\mu = 2.36 \pm 0.03$ D. For the $CH_3OCH_2CH_2OD$ species: $A = 12385.71$, $B = 2724.74$, and $C = 2431.42$ MHz. The conformation consistent with this data is *gauche* about each of the C—C, C—O(H) and C—O(ether) bonds, having dihedral angles of $57 \pm 3°$, $45 \pm 5°$, and $8 \pm 3°$, respectively. This distorted conformation is one in which the hydroxyl hydrogen atom is approximately aligned with the nearest sp^3 lone pair electrons of the ether oxygen atom. Transitions in three excited torsional states have also been observed but no other rotational isomer was detected.

L'analyse du spectre de micro-ondes du méthoxy-2-ethanol ($CH_3OCH_2CH_2OH$) a permis d'en déterminer la conformation la plus stable. Les constantes rotationnelles de la molécule sont: $A = 12982.35$, $B = 2842.48$, et $C = 2468.10$ MHz; les composantes du moment dipolaire sont $\mu_a = 2.03$, $\mu_b = 1.15$, $\mu_c \simeq 0.25$, et $\mu = 2.36 \pm 0.03$ D. Pour l'espèce deutériée ($CH_3OCH_2CH_2OD$): $A = 12385.71$, $B = 2724.74$, et $C = 2431.42$ MHz. Ces données correspondent à une conformation *gauche* autour des liaisons C—C, C—O(H), et C—O(éther), les angles dièdres étant respectivement $57 \pm 3°$, $45 \pm 5°$, et $8 \pm 3°$. Dans cette conformation déformée, l'hydrogène hydroxylique est approximativement aligné avec l'un des doublets libres sp^3 de l'atome d'oxygène du groupement éther. Des transitions de trois états excités de torsion ont également été observées, mais aucun autre isomère rotationnel n'a été détecté.

Canadian Journal of Chemistry, **50**, 1149 (1972)

Can. J. Chem. Downloaded from www.nrcresearchpress.com by 210.87.254.40 on 09/05/12
For personal use only.

Introduction

The intramolecular hydrogen bond in 2-substituted ethanols is thought to be a weaker variety among hydrogen bonds, yet it appears to be the predominant factor determining the relative stability of molecular conformations. Extensive studies of the 2-substituted ethanols have shown that the minimum energy conformation is one in which an intramolecular hydrogen bond is favorable and that there are definite structural effects associated with its occurrence. Microwave spectroscopy has recently been used to determine the structure of four such molecules: fluoroethanol (1); chloro and bromoethanol (2) and aminoethanol (3). The OH···O interaction is an important example since the analogous OH···O intermolecular hydrogen bonds are among the strongest. The only intramolecular OH···O bond studied by microwave spectroscopy is glycolaldehyde (4) which presumably involves sp^2 hybridized lone pair electrons. 2-methoxyethanol, with sp^3 lone pairs on the ether oxygen atom and with four internal rotation axes, is an interesting case. Very little relevant structural data on this molecule exists. Infrared (5) and n.m.r. (6) spectra of 2-methoxyethanol in dilute solutions were interpreted in terms of a more stable *gauche* conformation about the C—C bond and a small population of a less stable *trans* isomer. The authors of the n.m.r. study suggested that the stability of the *gauche* isomer was not due to an intramolecular hydrogen bond since the acetyl derivative apparently also had a preferred *gauche* conformation.

Experimental

2-Methoxyethanol ($CH_3OCH_2CH_2OH$) was obtained from Anachemia Chemicals and used without further purification. The hydroxyl deuterated species ($CH_2OCH_2CH_2OD$) was prepared by esterifying the alcohol with boric acid and adding D_2O to the ester as required.

Microwave spectra were obtained at about -40 °C on a standard Stark modulation spectrometer, operating at 100 kHz, constructed in this laboratory. All frequency measurements were made with the oscillator phase locked to harmonics of voltage tunable 15 MHz crystal oscillators by means of a Microwave Systems MOS V stabilizer. The reference frequency was counted directly, markers being derived from the electronic counter. The frequencies are accurate to 50 kHz.

Results and Discussion

Ground State Spectra

The spectrum is characteristic of a prolate

TABLE 1. Assigned transitions of the ground state of $CH_3OCH_2CH_2OH$

Transition	ν_{obs}*	$\nu_{calc} - \nu_{obs}$	Transition	ν_{obs}	$\nu_{calc} - \nu_{obs}$
$1_{11} \leftarrow 0_{00}$	15450.45	0.00	$4_{22} \leftarrow 3_{21}$	20892.00	0.37
$1_{10} \leftarrow 1_{01}$	10514.18	0.06	$4_{13} \leftarrow 3_{12}$	21379.84	0.15
$2_{12} \leftarrow 1_{01}$	20386.72	−0.06	$4_{04} \leftarrow 3_{13}$	11209.99	0.32
$2_{12} \leftarrow 1_{11}$	10146.87	−0.08	$4_{13} \leftarrow 4_{04}$	11815.97	−0.09
$2_{02} \leftarrow 1_{01}$	10415.76	−0.04	$5_{15} \leftarrow 4_{14}$	25343.59	0.27
$2_{11} \leftarrow 1_{10}$	10695.45	0.09	$5_{05} \leftarrow 4_{04}$	25944.23	0.53
$2_{11} \leftarrow 2_{02}$	10794.00	0.06	$5_{24} \leftarrow 4_{23}$	26040.77	0.05
$3_{13} \leftarrow 2_{12}$	15216.88	−0.06	$5_{42} \leftarrow 4_{41}$	26066.36	−1.36
$3_{03} \leftarrow 2_{02}$	15609.97	0.03	$5_{41} \leftarrow 4_{40}$	26066.36	−1.35
$3_{22} \leftarrow 2_{21}$	15632.35	−0.60	$5_{33} \leftarrow 4_{32}$	26072.02	−1.10
$3_{21} \leftarrow 2_{20}$	15653.41	0.08	$5_{32} \leftarrow 4_{31}$	26072.43	−0.10
$3_{12} \leftarrow 2_{11}$	16039.91	0.08	$5_{23} \leftarrow 4_{22}$	26148.85	0.12
$3_{13} \leftarrow 2_{02}$	25187.76	−0.01	$5_{05} \leftarrow 4_{14}$	16871.41	0.76
$3_{12} \leftarrow 3_{03}$	11223.97	−0.03	$5_{14} \leftarrow 5_{05}$	12585.49	−0.03
$4_{14} \leftarrow 3_{13}$	20282.83	0.06	$6_{06} \leftarrow 5_{15}$	22602.30	1.45
$4_{04} \leftarrow 3_{03}$	20787.83	0.22	$6_{15} \leftarrow 6_{06}$	13551.13	0.11
$4_{23} \leftarrow 3_{22}$	20838.26	−0.16	$7_{16} \leftarrow 7_{07}$	14733.38	0.34
$4_{32} \leftarrow 3_{31}$	20853.82	−0.81	$8_{17} \leftarrow 8_{08}$	16152.70	1.11
$4_{31} \leftarrow 3_{30}$	20853.82	−0.40	$9_{18} \leftarrow 9_{09}$	17828.80	2.13

* ±0.05 MHz.

TABLE 2. Assigned transitions of the ground state of $CH_3OCH_2CH_2OD$

Transition	ν_{obs}*	$\nu_{calc} - \nu_{obs}$	Transition	ν_{obs}	$\nu_{calc} - \nu_{obs}$
$1_{11} \leftarrow 0_{00}$	14817.08	0.06	$3_{21} \leftarrow 2_{20}$	15494.89	−0.11
$1_{10} \leftarrow 1_{01}$	9954.31	−0.03	$3_{12} \leftarrow 2_{11}$	15904.26	−0.06
$2_{02} \leftarrow 1_{01}$	10305.69	0.06	$3_{12} \leftarrow 3_{03}$	10716.33	−0.03
$2_{11} \leftarrow 1_{10}$	10605.72	−0.07	$4_{13} \leftarrow 4_{04}$	11355.08	0.00
$2_{11} \leftarrow 2_{02}$	10254.21	0.03	$5_{14} \leftarrow 5_{05}$	12189.09	0.10
$3_{13} \leftarrow 2_{12}$	15024.53	−0.08	$6_{15} \leftarrow 6_{06}$	13240.12	0.45
$3_{03} \leftarrow 2_{02}$	15442.20	0.01	$7_{16} \leftarrow 7_{07}$	14531.96	0.97
$3_{22} \leftarrow 2_{21}$	15468.69	−0.20	$8_{17} \leftarrow 8_{08}$	16087.86	1.73

* ±0.05 MHz.

asymmetric rotor with transitions resulting from μ_a and μ_b components of the dipole moment. The μ_a R-, and μ_b Q-type transitions were readily identified by their characteristic patterns. Transitions were assigned by means of their resolvable Stark effect, line strengths, and by least-squares fitting of the frequencies. μ_b R-type transition frequencies were then predicted and measured. Some 38 lines of the ground state were measured in the range 8 to 26.5 GHz. Their frequencies are listed in Table 1 along with differences between the calculated and the observed values using the rotational constants listed in Table 4. Some of the higher J and K transitions show small deviations which are probably due to centrifugal distortion but an analysis was not performed. The rotational constants were derived from low J, K transitions showing negligible distortion effects. The constants were used to predict μ_c transition frequencies and a search was made, but no such transitions were found. The spectrum of the hydroxyl deuterated species is similar to that of the normal species and was assigned on the same basis. The observed transitions are listed in Table 2 and the rotational constants in Table 4. These constants and those of the normal species were used to determine the coordinates of the hydroxyl hydrogen atom in the principal inertial axis system; these are included in Table 4. The c coordinate turned out to be imaginary indicating that the hydrogen is near the a–b principal plane. Therefore a value close to zero is assumed for the c coordinate.

Can. J. Chem. Downloaded from www.nrcresearchpress.com by 210.87.254.40 on 09/05/12
For personal use only.

Can. J. Chem. Downloaded from www.nrcresearchpress.com by 210.87.254.40 on 09/05/12
For personal use only.

TABLE 3. Assigned transitions of the excited states of $CH_3OCH_2CH_2OH$

Transition	ν_{obs}*	$\nu_{calc} - \nu_{obs}$	Transition	ν_{obs}	$\nu_{calc} - \nu_{obs}$
		$v_{t1(CH_3)} = 1$			
$1_{11} \leftarrow 0_{00}$	15561.14	0.47	$3_{12} \leftarrow 3_{03}$	11342.80	0.05
	15561.79	−0.03		11343.03	0.02
$1_{10} \leftarrow 1_{01}$	10641.99	−0.06	$4_{13} \leftarrow 4_{04}$	11927.04	−0.05
				11927.61	−0.39
$2_{12} \leftarrow 1_{11}$	10110.83	−0.12	$5_{04} \leftarrow 4_{14}$	16634.73	0.45
$3_{13} \leftarrow 2_{12}$	15162.83	−0.02	$5_{14} \leftarrow 5_{05}$	12685.30	0.52
				12685.76	0.34
$3_{03} \leftarrow 2_{02}$	15551.76	0.15	$6_{15} \leftarrow 6_{06}$	13637.23	0.08
				13637.615	0.04
$3_{22} \leftarrow 2_{21}$	15573.10	−0.20	$7_{16} \leftarrow 7_{07}$	14801.10	0.80
$3_{21} \leftarrow 2_{20}$	15593.98	−0.08		14801.51	0.30
$3_{12} \leftarrow 2_{11}$	15976.40	0.04	$8_{17} \leftarrow 8_{08}$	16197.70	0.85
				16198.13	0.93
$9_{18} \leftarrow 9_{09}$	17846.25	1.71			
	17846.68	1.71			
		$v_{t2} = 1$			
$1_{11} \leftarrow 0_{00}$	15342.28	−0.05	$3_{21} \leftarrow 2_{20}$	15695.07	−0.07
$1_{10} \leftarrow 1_{01}$	10394.77	−0.01	$3_{12} \leftarrow 2_{11}$	16083.99	0.07
$2_{12} \leftarrow 1_{11}$	10171.84	−0.05	$4_{13} \leftarrow 4_{04}$	11708.57	−0.04
$2_{02} \leftarrow 1_{01}$	10442.80	0.02	$5_{05} \leftarrow 4_{14}$	17066.43	0.85
$2_{11} \leftarrow 1_{10}$	10725.03	0.04	$5_{14} \leftarrow 5_{05}$	12486.14	0.02
$2_{11} \leftarrow 2_{02}$	10676.80	0.21	$6_{15} \leftarrow 6_{06}$	13462.46	0.25
$3_{13} \leftarrow 2_{12}$	15254.30	−0.11	$7_{16} \leftarrow 7_{07}$	14658.49	0.63
$3_{03} \leftarrow 2_{02}$	15650.11	0.15	$8_{17} \leftarrow 8_{08}$	16094.34	2.35
$3_{22} \leftarrow 2_{21}$	15672.99	−0.36	$9_{18} \leftarrow 9_{09}$	17792.39	2.56
		$v_{t2} = 2$			
$2_{02} \leftarrow 1_{01}$	10471.91	0.08	$5_{05} \leftarrow 4_{14}$	17265.83	0.64
$3_{13} \leftarrow 2_{12}$	15293.43	0.60	$5_{14} \leftarrow 5_{05}$	12393.38	0.00
$3_{03} \leftarrow 2_{02}$	15693.55	0.02	$6_{15} \leftarrow 6_{06}$	13382.34	0.20
$3_{22} \leftarrow 2_{21}$	15716.97	−0.33	$7_{16} \leftarrow 7_{07}$	14594.60	0.64
$3_{21} \leftarrow 2_{20}$	15739.80	−0.09	$8_{17} \leftarrow 8_{08}$	16051.85	1.29
$3_{12} \leftarrow 2_{11}$	16132.02	0.02	$9_{18} \leftarrow 9_{09}$	17773.44	2.46
$4_{13} \leftarrow 4_{04}$	11606.32	−0.00			

*±0.05 MHz.

TABLE 4. Rotational constants* of $CH_3O(CH_2)_2OH$ and $CH_3O(CH_2)_2OD$ (in MHz)

Rotational constant	Value				
	$CH_3O(CH_2)_2OH$				$CH_3O(CH_2)_2OD$
	$v = 0$	$v_{t1}(CH_3) = 1$†	$v_{t2} = 1$	$v_{t2} = 2$	$v = 0$
A	12982.35	13101.80	12868.55	12757.95	12385.71
B	2742.48	2731.09	2750.43	2759.12	2724.74
C	2468.10	2459.87	2473.78	2479.76	2431.42
Principal inertia axis coordinates of the hydroxyl hydrogen atom:‡					
	$\lvert a_H \rvert = 1.095$		$\lvert b_H \rvert = 1.383$		$\lvert c_H \rvert = 0$§

*±0.05 MHz.
†Average of the two sets derived from doublet splittings.
‡±0.001 Å.
§The c coordinate is imaginary, this is an assumed value.

Can. J. Chem. Downloaded from www.nrcresearchpress.com by 210.87.254.40 on 09/05/12
For personal use only.

TABLE 5. Stark coefficients and dipole moment of 2-methoxyethanol*

Transition	M	$\Delta\nu/E^2 \times 10^4$ MHz (V/cm)$^{-2}$ Observed	Calculated
$4_{14} \leftarrow 3_{13}$	1	0.0309	0.0306
	2	0.156	0.153
$3_{12} \leftarrow 2_{11}$	1	−0.308	−0.311
	2	−1.221	−1.207
$3_{13} \leftarrow 2_{12}$	1	0.327	0.332
	2	1.343	1.334
$3_{12} \leftarrow 3_{03}$	3	0.593	0.607
	2	0.237	0.237
$2_{12} \leftarrow 1_{11}$	1	10.350	10.338

*$\mu_a = 2.03 \pm 0.02$; $\mu_b = 1.15 \pm 0.02$; $\mu_c \simeq 0.25$; $\mu = 2.36 \pm 0.03$ D.

Stark Effect and Dipole Moment

Stark effect measurements were performed on nine $\Delta M = 0$ transitions of five lines. The electric field was calibrated before and after measurements using the $2 \leftarrow 1$ transition of OCS with μ(OCS) taken as 0.71521 D (7). The second order Stark coefficients observed are listed in Table 5 along with the calculated values and the derived dipole moment components. The μ_a and μ_b dipole components are well determined from the measured lines but the μ_c component is not. Transitions more sensitive to this component were sought but no reasonably measurable lines were found. The measurements, however, restrict the value of μ_c to between 0 and 0.5 D, with a probable value not exceeding 0.25 D, since no μ_c transitions were observed. The total dipole moment determined is 2.36 ± 0.03 D, slightly higher than the two values, 2.0 (8) and 2.2 D (9), obtained from dielectric constant measurements in solution.

Spectra of Excited Torsional States

The ground state lines are accompanied by several weaker ones due to molecules in vibrationally excited states. These satellites exhibit the same Stark effects as the nearby ground state lines. This observation as well as the typical satellite pattern permitted the assignments listed in Table 3. Two series of lines have an intensity of about 0.5 with respect to the ground state. One series consists of doublets having an average spacing of 450 kHz for the perpendicular transitions and singlets for the parallel transitions. Each member of the doublet could be fit by rigid rotor theory; the average of the two close sets of constants is listed in Table 4. These lines are probably due to the first excited state of the CH_3 torsion about the CH_3—O bond and are labelled as v_{t1} (CH_3). Since the molecular structure is not well determined and the measured transitions are relatively insensitive, the barrier height was not calculated. The small splittings in the first torsional state imply that the barrier is greater than 2.5 kcal/mol, a value of the same order of magnitude as that observed for dimethyl ether (10) and methyl ethyl ether (11).

The other series is accompanied by a third having an intensity factor of approximately 0.3. In the absence of any low frequency infrared assignment it is difficult to positively identify the two states involved. The two remaining lowest frequency vibrations are the torsions about the C—C and C—O (ether) bonds. The relative intensities and the nearly linear changes in rotational constants suggest that the two series are due to the first and second excited states of one of these torsions. The states are labelled $v_{t2} = 1$ and $v_{t2} = 2$ in Table 4.

Conformation of 2-Methoxyethanol

The relatively simple rigid rotor spectrum observed indicates that one molecular conformation is predominant. This conformation can be identified and its three characteristic dihedral angles approximately determined from the

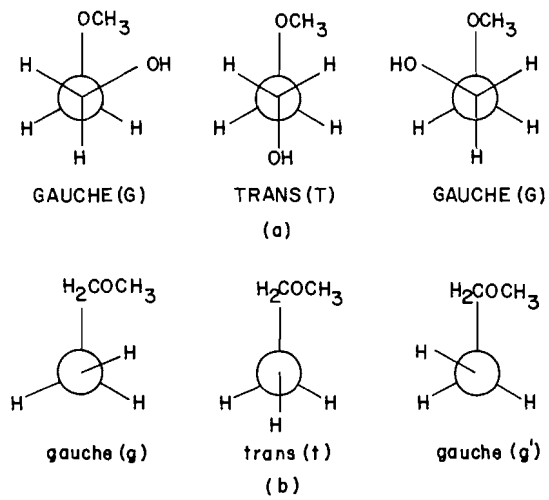

FIG. 1. Possible stable conformations of 2-methoxyethanol: (*a*) about the C—C axis; (*b*) about the C—O(H) axis.

TABLE 6. Comparison of observed and calculated parameters for various conformations

		Value			
		Calculated*			
			Gauche CC		
Parameter	Observed	*Trans* CC	*Gauche'* OH†	*Trans* OH†	*Gauche* OH†
A	12982.35	21754	13794	14333	13770
B	2742.48	2188	2606	2554	2634
C	2468.10	2031	2460	2414	2474
a_H	−1.095	−1.98	−1.90	−2.85	−1.43
b_H	1.385	0.46	1.02	0.37	1.14
c_H	~0	1.57	0.77	0.37	0.58
μ_a	2.03	1.7	1.1	0.15	2.05
μ_b	1.15	1.6	1.5	2.5	1.29
μ_c	~0.25	1.2	3.0	0.8	0.36

*Calculated assuming corresponding structural parameters of dimethyl ether and 2 haloethanols (see Table 7).
†COCC atoms coplanar, *gauche* dihedral angles set at 60°.

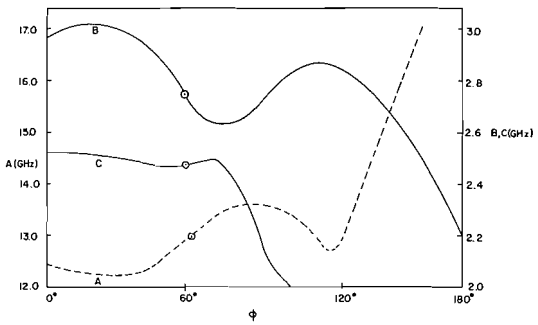

FIG. 2. Variation of rotational constants with OCC/CCO dihedral angle ($\phi = 0$ is *cis*). COH/OCC angle = 55°; COC/CCO angle = +12°. Circles are observed values.

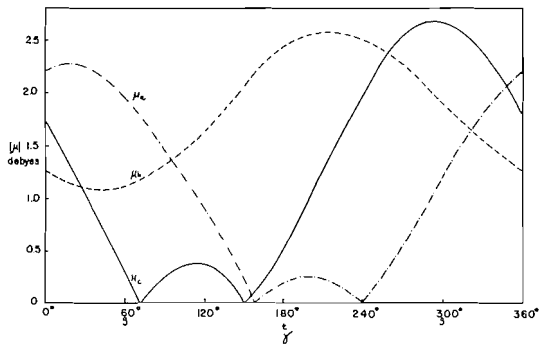

FIG. 3. Variation of dipole moment components with COH/OCC dihedral angle (γ). OCC/CCO angle = 60°, COC/CCO angle = +12°.

present data. Six possible stable conformations due to internal rotation about the C—C and C—O(H) bonds are shown in Fig. 1; not shown are those resulting from rotation of the methyl group as a whole about the C—O(ether) bond. Bond lengths and bond angles for the preliminary model were those determined from the extensive microwave spectra reported for dimethyl ether (10) and the 2-haloethanols (1, 2). With the methyl group fixed in its *trans* position making the COCC chain coplanar, the internal rotation angles about the C—C and C—O(H) bonds were varied and the nine parameters obtainable from the experimental data computed. The main results are summarized in Table 6 and in Figs. 2 and 3. Comparison of the observed and calculated parameters reveals that the minimum energy conformation must be *gauche–gauche* (*G–g*) about the C—C and C—O(H) bonds. In this minimum the hydroxyl hydrogen atom is directed toward the ether oxygen atom. The calculated principal axis coordinates of the hydrogen atom alone show this clearly. Although only relative values of calculated dipole moment components are significant, they do confirm this isomer since the others would give rise to quite different spectra than the one observed.

The initial model with *G–g* dihedral angles of 60° and a *trans* CH_3 group does not, however, reproduce the *A* and *B* rotational constants and the hydrogen coordinates sufficiently well; the differences are large enough to justify further refinement even though the problem is severely underdetermined. For instance, moving the CH_3 group out of the plane several degrees toward the OH group makes *A* and *B* simultaneously

Can. J. Chem. Downloaded from www.nrcresearchpress.com by 210.87.254.40 on 09/05/12
For personal use only.

Can. J. Chem. Downloaded from www.nrcresearchpress.com by 210.87.254.40 on 09/05/12
For personal use only.

TABLE 7. Structural parameters for the gauche–gauche–gauche conmation of 2-methoxyethanol

Structure	Bond	Distance (Å)	Bonds	Angle
Ether part*	C—H	1.09	COC	111°43′
	C—O	1.41	OCH_s	107°14′
			OCH_a	110°50′
			H_aCH_s	109°33′
			H_aCH_a	108°44′
			CCO	109°33′
Alcohol part†	C—H	1.09	COH	105°
	C—O	1.41	CCO	112°
	C—C	1.52	CCH	111°24′
	O—H	1.01	HCH	108°40′

Dihedral angle	Value (deg)	Parameter	Calculated range of observables‡
$C(H_3)OC/OCC$	8 ± 3	A	12880–13115 MHz
OCC/CCO	57 ± 3	B	2728–2794
CCO/COH	45 ± 5	C	2468–2483
		$\lvert a_H \rvert$	1.24–1.36 Å
		$\lvert b_H \rvert$	1.18–1.19
		$\lvert c_H \rvert$	0.10–0.20
		μ_a	2.07–2.30 D
		μ_b	1.08–1.29
		μ_c	0.36–0.52

*Assumed as in dimethyl ether (10).
†Assumed as in 2-haloethanols (1, 2).
‡Based on the assumed valence structure and the variation of the dihedral angles within the indicated limits.

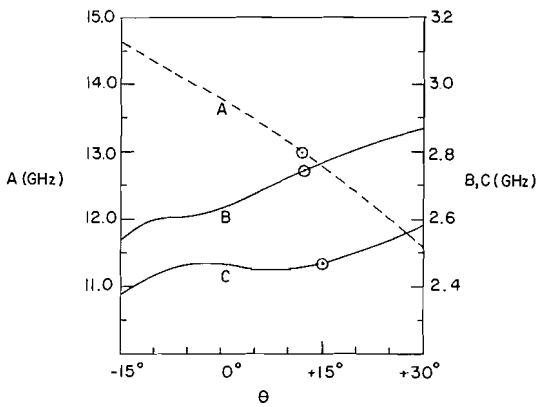

FIG. 4. Variation of rotational constants with COC/CCO dihedral angle (θ) $\theta = 0°$ COCC coplanar; $\theta = (+)$ CH_3 toward OH; $\theta = (-)$ CH_3 away from OH. Circles are observed values.

converge toward the experimental values (Fig. 4) but does not significantly affect the hydrogen coordinates. Decreasing the COH/CCO dihedral angle to about 45° has only a small effect on the rotational constants but brings the hydrogen c coordinate close to zero and improves the a and b coordinates. No combination of reasonable changes in the assumed valence structure alone, *e.g.*, varying the heavy atom lengths and angles or the OH lengths and COH angle, was found which could produce a similar convergence. A consistent fit to the nine parameters occurs for dihedral angles of $8 \pm 3°$, $45 \pm 5°$, and $57 \pm 3°$ about the C—O(ether), C—O(H), and C—C bonds, respectively (Table 7). The error limits quoted are somewhat arbitrary but probably exceed those resulting from changes in the valence structure; they apply for the assumed structure. Modifications of the valence structure and the dihedral angles simultaneously refer to an ultimate refinement which, of course, can only be determined by further isotopic substitution. Improvement of the hydrogen coordinates will depend mainly on the valence structure, particularly the OH length and the COH and CCO(H) angles. It seems clear that, whatever the final structure may be, the conformation responsible for the ground state spectrum is *gauche* about the three internal rotation axes, involving a rather closed COH/CCO dihedral angle and a methyl group oriented about 8° toward the hydroxyl group

Can. J. Chem. Downloaded from www.nrcresearchpress.com by 210.87.254.40 on 09/05/12
For personal use only.

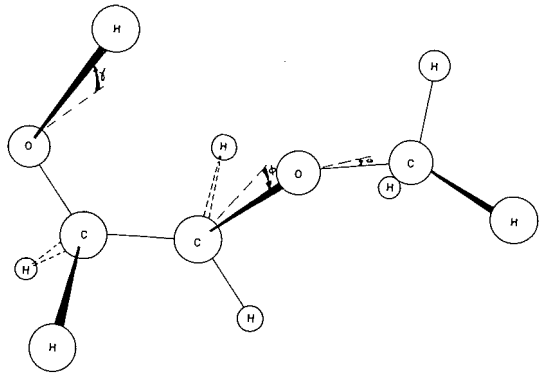

FIG. 5. Representation of the all-gauche conformation of 2-methoxyethanol. $\phi \simeq 57°$; $\gamma \simeq 45°$; $\theta \simeq 8°$.

(Fig. 5). The orientation of the methyl group about its axis is unknown but is presumably staggered with respect to the nearest methylene hydrogen atoms.

The vibrational satellites analyzed are due to molecules in the all-*gauche* conformation. Other weaker lines are present and while they have not been fully analyzed, they are probably due to other excited states of the same conformation. As mentioned previously the spectra of other molecular conformations would be quite different from that observed. Dipole moment calculations show that these would have been observable if an appreciable population existed; if another conformation was within 1 kcal/mol of the ground state.

The absence of any identifiable lines due to a *trans* (C—C) isomer is compatible with an enthalpy difference of 1.8 kcal/mol between the *gauche* and the *trans* isomers determined from infrared intensity measurements of dilute solutions (5). The infrared spectrum of the vapor obtained recently in this laboratory[1] shows only one band for each of the OH stretching and torsional vibrations at frequencies consistent with the all-*gauche* isomer (3635 and 360 cm^{-1}).

The Intramolecular Hydrogen Bond

The all-*gauche* conformation adopted by the molecule is one in which the hydroxyl hydrogen atom is approximately aligned with the nearest, tetrahedrally directed, sp^3 lone pair electrons of the ether oxygen atom. This alignment involves distortion of the usual staggered positions found in similar molecules. Despite the highly electronegative oxygen atoms, the dihedral angle about the C—C bond is the same or slightly smaller than in ethane, and is significantly smaller than in dichloroethane (70°) and the 2-haloethanols (63°). For this angle, however, the O···O nonbonded distance is approximately equal to the sum of the van der Waals radii, as observed in the 2-haloethanols. The hydroxyl hydrogen atom, some 15° away from the staggered minimum toward the unstable *cis* position eclipsing the C—C bond, is nearly as close as possible to the ether oxygen atom, the H···O distance being about 0.3 Å less than the sum of the van der Waals radii. In the haloethanols, the corresponding angle is 55°, making the OH and CX bonds parallel. It is difficult to predict the location of the methyl group about the C—O (ether) axis, but a *trans* methyl group would make all bonds staggered and the methyl and methylene hydrogens as far apart as possible. Small deviations from this geometry may not be significant in themselves, but it is significant that the methyl group is oriented out of the COCC plane *toward* the hydroxyl group: the immediate environment of the methyl group is the same on either side of that plane. In this position the lone pair orbital axis and the hydrogen atom are in the same plane. This would also occur for a COH/CCO dihedral angle of 60° if the CH_3 group was 30° out of the plane or, for a COH/CCO dihedral angle of 25–30° and a *trans* CH_3 group, but these are more distorted configurations. The other lone pair could become directed toward the hydrogen atom only if the methyl group turned 120° into an improbable, sterically unfavorable position.

The actual conformation is evidently a compromise between the intramolecular OH···O interaction and the opposing barrier forces. One can infer that in 2-methoxyethanol the compromise favors the intramolecular hydrogen bond and that the bond involves lone pair electrons. This is the same result as in 2-aminoethanol where the dihedral angles about the C—O (30°) and C—N (40°) bonds permit maximum interaction between the hydrogen atom and the nitrogen sp^3 lone pair electrons (3).

It is a pleasure to acknowledge the expert technical assistance of Marcel Rouillard, Jean-Paul Langlois, and Gaétan Genest during the construction of the microwave

[1]P. Buckley and G. W. Mines. To be published.

spectrometer, and Jean Weber's excellent computer programs. One of us (M.B.) wishes to thank the National Research Council of Canada for a post-graduate scholarship and we are grateful to NRCC and the Defense Research Board of Canada for operating grants.

1. K. S. BUCKTON and R. G. AZRAK. J. Chem. Phys. **52**, 5652 (1970).
2. R. G. AZRAK and E. B. WILSON, JR. J. Chem. Phys. **52**, 5299 (1970).
3. R. E. PENN and R. F. CURL, JR. J. Chem. Phys. **55**, 651 (1971).
4. K. M. MARSTOKK and H. M. MØLLENDAL. J. Mol. Structure, **5**, 205 (1970); **7**, 101 (1971).
5. P. J. KRUEGER and H. D. METTEE. J. Mol. Spectr. **18**, 131 (1965).
6. R. J. ABRAHAM and K. G. R. PACHLER. Molecular Physics, **7**, 165 (1964).
7. J. S. MUENTER. J. Chem. Phys. **48**, 4544 (1968).
8. W. H. BYERS. J. Chem. Phys. **7**, 175 (1939).
9. S. D. GOKHALE, N. L. PHALMKAR, and S. D. BHARVE. J. Univ. Bombay, **A11**, 56 (1943).
10. P. H. KASAI and R. J. MYERS. J. Chem. Phys. **30**, 1096 (1959).
11. D. R. HERSHBACH. Bibliography for hindered internal rotation and microwave spectroscopy. Lawrence Radiation Laboratory, Berkeley, California, UCRL-10404, 1963.

Can. J. Chem. Downloaded from www.nrcresearchpress.com by 210.87.254.40 on 09/05/12
For personal use only.

Etude par spectrométrie de vibration des composés d'addition formés entre le chlorure ou le bromure d'aluminium et le dimethylsulfoxyde

J. MEUNIER ET M. T. FOREL

Laboratoire de Spectrométrie de Vibration, associé au C.N.R.S., Université de Bordeaux I, 33-Talence, France

Reçu 9 novembre 1971

Les composés d'addition formés entre le chlorure ou le bromure d'aluminium et le diméthylsulfoxyde ou le diméthylsulfoxyde-d_6 ont été synthétisés. Deux composés solides différents $AlX_3.(dmso)_{1.5}$ et $AlX_3.(dmso)_6$ ont été isolés. L'analyse spectroscopique montre qu'ils sont ioniques et correspondent aux formules $[Al(dmso)_6]^{3+}.3AlX_4^-$ (I) ou $[Al(dmso)_6]^{3+}.3X^-$ (II). Une interpretation complète des spectres est effectuée. Les résultats concernant le cation $[Al(dmso)_6]^{3+}$ sont compatibles avec une symétrie D_{3d} pour les dérivés (I) et C_{2h} pour les dérivés (II). Ils montrent en outre une intéraction importante entre les ions X^- et les cations de la forme (II).

La constante de force de la liaison AlO a été déterminée; elle est proche de 1.8×10^5 dynes cm^{-1}.

Coordination compounds between $AlCl_3$ or $AlBr_3$ and $(CH_3)_2SO$ or $(CD_3)_2SO$ have been prepared. Two different solid compounds $(AlX_3).(dmso)_{1.5}$ and $AlX_3.(dmso)_6$ have been characterized. The vibration spectra show that they are ionic, $[Al(dmso)_6]^{3+}.3AlX_4^-$ (I) and $[Al(dmso)_6]^{3+}.3X^-$ (II). A complete assignment is proposed. Results are in good agreement with a D_{3d} symmetry for the cation of compound (I) and C_{2h} for the cation of compound (II). Strong interaction between the X^- ions and the methyl groups of the form (II) exist.

The (Al—O) bond force constant is close to 1.8×10^5 dynes cm^{-1}.

Canadian Journal of Chemistry, **50**, 1157 (1972)

Introduction

Les réactions de polymérisation du type Ziegler–Natta sont catalysées par des mélanges ternaires contenant un métal de transition, une base de Lewis et un dérivé de l'aluminium (*1*, 2).

Afin d'essayer de comprendre le rôle joué par les différents composants, nous avons étudié, grâce aux travaux déjà effectués au laboratoire, les composés d'addition susceptibles de se former entre les trihalogénures d'aluminium et le diméthylsulfoxyde (dmso).

Le composé d'addition $AlCl_3$.6dmso a été signalé par plusieurs auteurs (3 à 7) et certains ont suggéré l'existence du cation $[Al(dmso)_6]^{3+}$. Cet ion a d'ailleurs été mis en évidence par r.m.n. dans le complexe $Al(ClO_4)_3$.6dmso (8). Le dérivé $AlBr_3$.6dmso est également connu (7). Aucun spectre complet de ces composés n'a été publié et les travaux précédents ne citent que les fréquences des élongations ν(AlO) et ν(SO).

Conditions expérimentales

Les halogénures d'aluminium et le diméthylsulfoxyde proviennent de la maison Fluka A. G. Buchs. Le chlorure et le bromure d'aluminium sont sublimés sous vide, le dmso est distillé sur hydrure de calcium sous pression réduite. Le diméthylsulfoxyde deutérié (dmso-d_6) fabriqué par le C.E.A. est utilisé tel quel; son enrichissement isotopique est de 99.5%. L'éther éthylique est distillé sur sodium. Tous les produits sont manipulés sous atmosphère anhydre.

(a) Synthèse des composés d'addition

La méthode utilisée est celle décrite par Selbin et coll. (5): nous avons dissous dans l'éther éthylique une quantité connue d'halogénure d'aluminium puis ajouté un volume déterminé de dmso. Le précipité formé est recueilli sur un verre fritté et lavé à l'éther pour éliminer l'halogénure en excès. Différents solides ont été isolés en prenant des rapports $\rho = [dmso]/[AlX_3]$ compris entre 0.1 et 10.

(b) Spectres infrarouges et Raman

Les spectres d'absorption entre 4000 et 250 cm^{-1} sont enregistrés avec un appareil Perkin–Elmer 521. La région spectrale comprise entre 400 et 30 cm^{-1} est explorée à l'aide d'un spectromètre interférentiel R.I.I.C.

Les échantillons sont examinés en suspension dans le Nujol ou l'hexachlorobutadiène entre des faces de KRS 5 ou de polythène. Nous avons vérifié qu'elles ne sont pas dégradées au contact des produits.

Les spectres de diffusion sont obtenus à l'aide d'un spectromètre Coderg PH1 utilisant comme source un laser hélium–néon ($\lambda = 6328.17$ Å). En raison de la forte diffusion des poudres, certaines fréquences n'ont pu être déterminées.

Mise en évidence des différentes structures

Quand le rapport $\rho = [dmso]/[AlCl_3]$ augmente jusqu'à 1.5, les spectres infrarouges des précipités restent identiques. Ils correspondent à un composé bien défini de formule $AlCl_3.(dmso)_{1.5}$.

Pour des valeurs supérieures, de nouvelles bandes qui ne sont pas celles du dmso libre (9, 10) se juxtaposent aux précédentes. Ces absorptions augmentent en intensité avec ρ

Can. J. Chem. Downloaded from www.nrcresearchpress.com by 210.87.254.42 on 09/05/12
For personal use only.

Can. J. Chem. Downloaded from www.nrcresearchpress.com by 210.87.254.42 on 09/05/12
For personal use only.

TABLEAU 1. Spectres radiocristallographiques des poudres*

$Al(dmso)_6.3AlCl_4$		$Al(dmso)_6.3Cl$		$Sc(dmso)_6.3Br$†	
d	I_{rel}	d	I_{rel}	d	I_{rel}
9.4004	20	8.3702	30	8.6474	20
8.0364	20	7.0415	50	7.1176	40
5.8239	100	5.1989	10	5.3570	60
4.2668	20	4.7816	10	4.8079	60
4.1106	30	4.2520	60	4.3198	80
3.7983	20	4.1678	40	3.7590	10
3.6012	20	3.5090	100	3.5940	100
		3.3556	30	3.4564	40
		3.0093	10	3.0805	40
		2.9097	20	2.9700	60
		2.7809	10	2.8585	20

*d = distance réticulaire; intensité relative calculée en posant égale à 100 l'intensité de la bande la plus forte.
†Référence 11.

alors que les autres diminuent; elles subsistent seules quand $\rho = 6$. On est alors en présence d'un autre composé de formule $AlCl_3.(dmso)_6$.

Pour ρ supérieur à 6, les bandes du dmso libre apparaissent.

Les mêmes résultats sont obtenus avec le bromure d'aluminium.

Les stoechiométries des composés (I) $AlX_3.(dmso)_{1.5}$ et (II) $AlX_3.(dmso)_6$ avec X = Cl ou Br, ont été vérifiées pondéralement, par un dosage Charpentier–Vohlard de l'halogène et une microanalyse du carbone.

Pour les valeurs de ρ comprises entre 1.5 et 6 les précipités isolés correspondent à des mélanges des composés I et II dont les proportions sont définies par la réaction

$$AlX_3.(dmso)_{1.5} + 4.5\ dmso \rightarrow AlX_3.(dmso)_6$$

Nous avons effectué les spectres Debye–Scherrer des dérivés chlorés (formes I et II); ils ne sont pas identiques, ce qui confirme l'existence de deux structures différentes (tableau 1). Bien que le petit nombre de taches ne nous ait pas permis de déterminer le groupe d'espace, il semble que $AlCl_3.(dmso)_6$ soit isotype de $ScBr_3(dmso)_6$ (11) (tableau 1).

Les spectres infrarouges et Raman des composés de forme I présentent des bandes qui n'ont pas d'effet isotopique du deutérium et sont fortement déplacées par le changement d'halogène (figs. 1 et 2). Leurs fréquences correspondent à celles des ions AlX_4^- (12–14); les exclusions infrarouges–Raman sont celles du groupe de symétrie T_d (tableau 2).

La stœchiométrie et la présence des ions AlX_4^- suggèrent pour les composés de forme I la formule développée $[Al(dmso)_6]^{3+}.3AlX_4^-$.

La très grande similitude des spectres des dérivés de forme II, $AlCl_3(dmso)_6$ et $AlBr_3(dmso)_6$, montre qu'aucune bande ne peut être attribuée à une liaison Al—X (figs. 2 et 3); la même analogie est retrouvée pour les composés deutériés. En raison de la stœchiométrie, on doit être en présence de composés ioniques de formule $[Al(dmso)_6]^{3+}.3X^-$.

Des composés d'addition analogues, entre le chlorure de gallium et le diméthylsulfoxyde, ont été mis en évidence par Carty et Patel (15): $Ga(dmso)_6^{3+}.3GaCl_4^-$ et $Ga(dmso)_6^{3+}.3Cl^-$.

Discussion du spectre de vibration de l'ion $Al(dmso)_6^{3+}$

L'ion $Al(dmso)_6^{3+}$ possède au maximum la symétrie D_{3d} si l'on admet, comme le font tous les auteurs (3–7), que la liaison de coordination met en jeu l'atome d'oxygène. Nous avons dénombré dans cette hypothèse les vibrations d'un modèle $Al(OSC_2)_6$ (tableau 3). L'analyse des spectres repose sur l'examen de l'effet isotopique du deutérium et sur la comparaison avec le dmso libre (9) et le groupe AlO_6(16). Comme le changement d'halogène déplace les fréquences de 5 cm^{-1} au maximum, nous ne discuterons que les résultats relatifs aux dérivés bromés dont les spectres Raman sont les plus complets.

Dérivés $[Al(dmso)_6]^{3+}.3AlX_4^-$

(1) Vibrations du groupe AlO_6

Les fréquences de vibration du groupe AlO_6 ont été peu étudiées et les résultats de la littérature ne sont pas cohérents (16–19).

Entre 450 et 600 cm^{-1}, région où aucune fréquence de vibration du dmso n'est attendue, on observe pour le dérivé $[Al(dmso)_6]^{3+}.3AlBr_4^-$ deux bandes de diffusion à 492 et 461 cm^{-1} et une absorption à 539 cm^{-1} (Fig. 1); nous les attribuons aux mouvements ν(AlO). L'exclusion infrarouge–Raman suggère l'existence d'un centre de symétrie dans l'ion $Al(dmso)_6^{3+}$ et une symétrie locale O_h; elle est compatible avec le groupe D_{3d} si l'on admet que les niveaux A_{2u} et

Can. J. Chem. Downloaded from www.nrcresearchpress.com by 210.87.254.42 on 09/05/12
For personal use only.

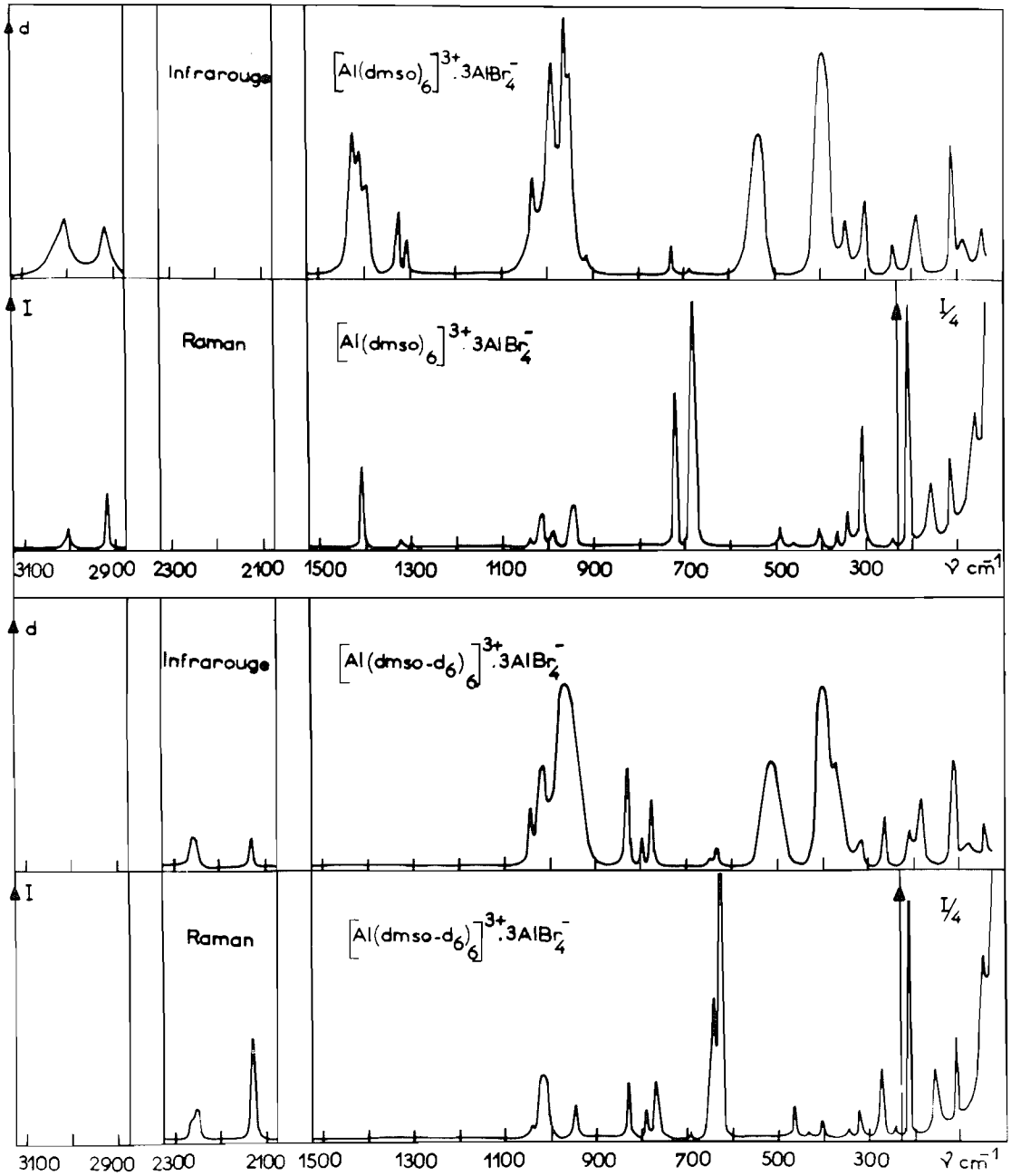

FIG. 1. Spectres infrarouges et Raman des composés bromés de forme I.

E_u ne sont pas séparés (tableau 3). La comparaison avec l'étude récente de l'ion $Al(H_2O)_6^{3+}$ (16) conduit à faire correspondre la raie Raman de plus haute fréquence à la vibration de symétrie A_{1g} (tableau 4). L'important effet isotopique du deutérium sur les élongations ν(AlO) montre qu'elles sont couplées avec les mouvements des ligandes.

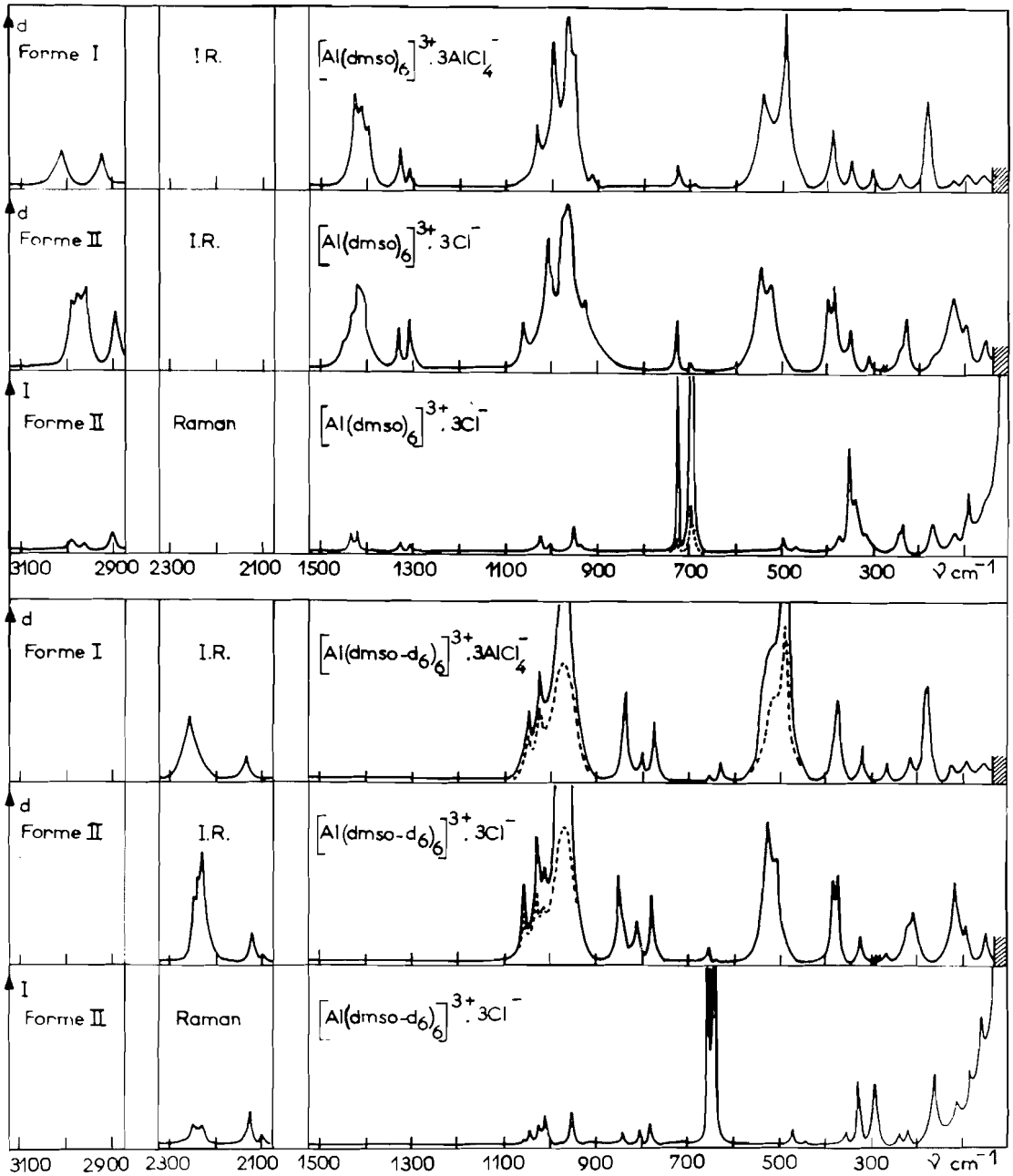

FIG. 2. Spectres infrarouges et Raman des composés chlorés.

Les déformations δ(OAlO) sont observées vers 300 cm^{-1} sur les spectres de l'hexahydrate d'aluminium (16); en raison de la masse du dmso elles sont attendues à des fréquences plus faibles dans l'ion $Al(dmso)_6^{3+}$. Nous les faisons correspondre à la raie à 161 cm^{-1} et à l'absorption à 188 cm^{-1}, car elles ne sont pas modifiées par la deutériation.

Tous les spectres présentent entre 210 et 250 cm^{-1} une bande qui n'a pas d'effet iso-

Can. J. Chem. Downloaded from www.nrcresearchpress.com by 210.87.254.42 on 09/05/12
For personal use only.

TABLEAU 2. Nombres d'ondes des vibrations fondamentales des ions AlX_4^-

$AlCl_3.(dmso)_{1.5}$		$AlCl_4^-$ (12)		$AlBr_3.(dmso)_{1.5}$		$AlBr_4^-$ (13, 14)		
Infrarouge	Raman	Infrarouge	Raman	Infrarouge	Raman	Infrarouge	Raman	Attributions
489	488	495	495	403	403	396	396	$\nu_a(AlX_4^-)\ F_2$
*	349	Inactive	349	*	210	Inactive	205	$\nu_s(AlX_4^-)\ A_1$
180	179	183	183	115	114	112	112	$\delta(AlX_4^-)\ F_2$
*	140	Inactive	145	*	*	Inactive	88	$\delta(AlX_4^-)\ E$

*Non observé.

topique en diffusion alors qu'elle s'abaisse de 31 cm^{-1} en infrarouge. En raison de cette différence de comportement, nous pensons qu'il ne s'agit pas du même mode de vibration et proposons d'attribuer la raie Raman à une déformation δ(OAlO) et la bande infrarouge à un mouvement du dmso.

(2) Vibrations des groupes dmso

Au-dessus de 600 cm^{-1}, les spectres de vibration du dmso libre et de l'ion $Al(dmso)_6^{3+}$ présentent le même nombre de bandes; les six dmso sont donc liée à l'aluminium de façon identique. Sauf dans la région 900–1100 cm^{-1} les fréquences infrarouges et Raman sont très voisines, ce qui indique un couplage très faible entre les groupes dmso.

Les fréquences des vibrations $\nu(CH_3)$, $\nu(CD_3)$, $\delta(CH_3)$, et ν(CSC) augmentent de 5 à 20 cm^{-1} par complexation.

Région 1100–750 cm^{-1}

Les nombres d'ondes infrarouges et Raman des mouvements $\delta(CD_3)$ et $r(CD_3)$ du dérivé $Al(dmso\text{-}d_6)_6.3AlBr_4$ coincident; ils sont en outre proches de ceux du dmso-d_6 libre; nous conservons la même attribution (tableau 4). L'absorption intense à 965 cm^{-1} provient alors de l'élongation ν(SO), la raie Raman correspondante est située à 948 cm^{-1}; il y a donc exclusion.

L'analyse des spectres de l'ion $Al(dmso)_6^{3+}$ montre que la vibration ν(SO) se retrouve à 945 cm^{-1} en Raman et à 960 cm^{-1} en infrarouge. Cet écart de fréquence indique un fort couplage entre les élongations des liaisons SO. La comparaison avec le dmso libre conduit à situer les balancements $r(CH_3)$ à 1031, 990, 950, et 909 cm^{-1}. La raie Raman à 1016 cm^{-1}, qui n'a pas d'homologue en absorption, provient peut-être d'un autre mode ν(SO). Dans ce cas la bande située à 1018 cm^{-1} dans le composé deutérié pourrait être due à la fois à ν(SO) et à un mouvement $\delta(CD_3)$, ce qui expliquerait sa forte intensité.

Ces résultats montrent que les six ligandes ont, autour de l'aluminium, une disposition centrosymétrique compatible avec la symétrie D_{3h} que nous avons proposée.

L'abaissement des fréquences ν(SO) par complexation et l'exclusion infrarouge–Raman confirment que la liaison de coordination s'effectue grâce à l'oxygène.

Région 750–200 cm^{-1}

Les bandes situées à 376, 321, et 266 cm^{-1} sur le spectre infrarouge de l'ion$[Al(dmso\text{-}d_6)_6]^{3+}$ se trouvent à des fréquences supérieures pour l'ion hydrogéné (tableau 4). Elles proviennent des mouvements de déformation δ(SO), γ(SO) et δ(CSC) attendus dans cette région spectrale.

Une seule de ces trois bandes a la même fréquence (321 cm^{-1}) en infrarouge et Raman. Nous l'attribuons à δ(CSC) car c'est le vibrateur qui peut le moins se coupler avec les mouvements de l'octaèdre.

Les déformations γ(SO) sont orthogonales aux élongations des liaisons AlO adjacentes, par contre, elles peuvent se coupler avec les mouvements δ(OAlO). Ces derniers étant situés vers 180 cm^{-1}, les vibrations de groupe γ(SO) sont déplacées vers les hautes fréquences: nous les faisons correspondre aux bandes infrarouges et Raman observées respectivement à 376 et 348 cm^{-1} (tableau 4).

L'absorption de plus basse fréquence, 266 cm^{-1}, est alors attribuée à δ(SO) abaissée par couplage avec ν(AlO); il lui correspond la raie Raman à 271 cm^{-1}.

Seule l'absorption à 212 cm^{-1} n'a pas été interprétée. Elle ne peut pas provenir d'une torsion des groupes CD_3 car le rapport iso-

Can. J. Chem. Downloaded from www.nrcresearchpress.com by 210.87.254.42 on 09/05/12
For personal use only.

Can. J. Chem. Downloaded from www.nrcresearchpress.com by 210.87.254.42 on 09/05/12
For personal use only.

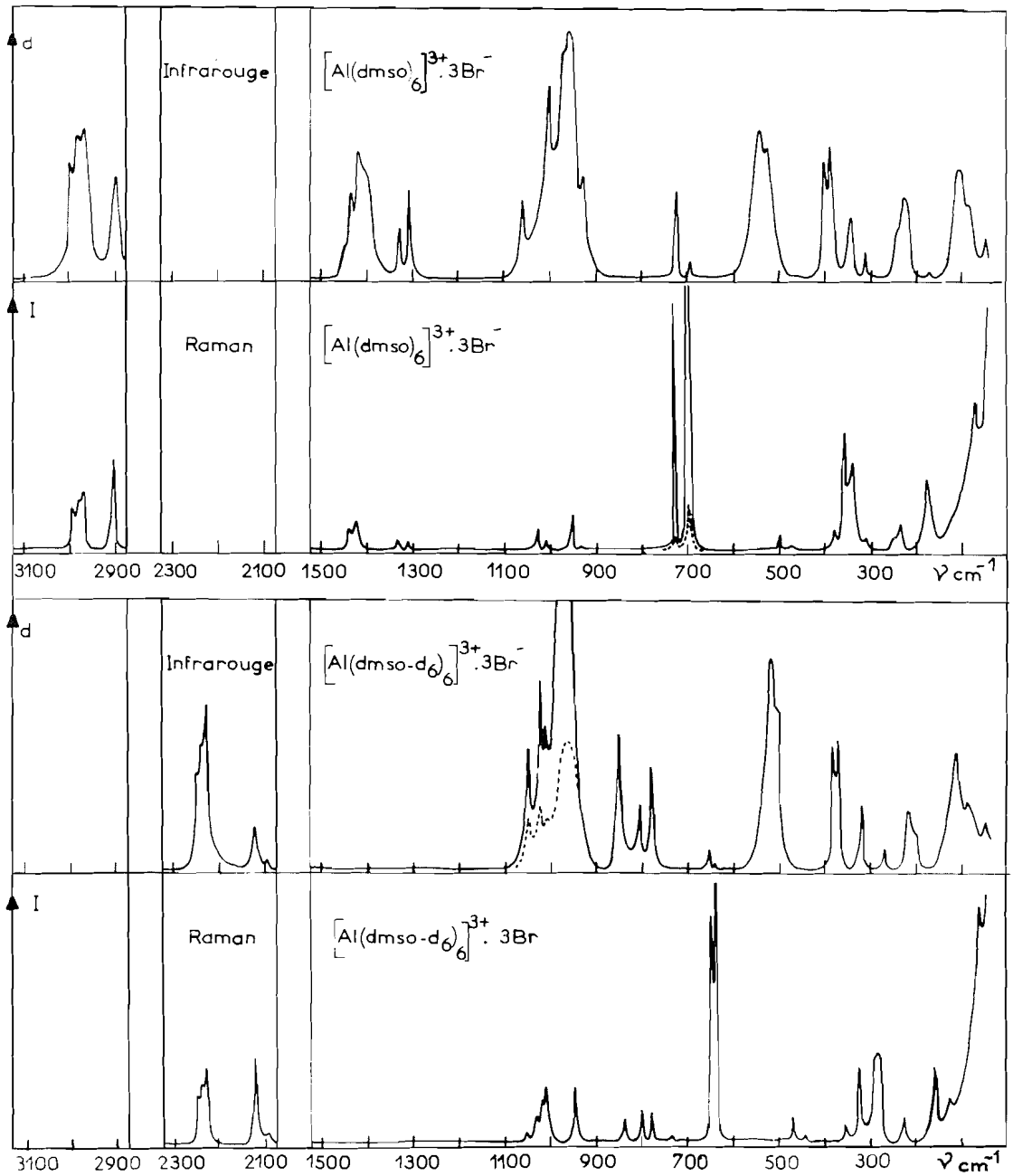

FIG. 3. Spectres infrarouges et Raman des composés bromés de forme II.

topique est trop faible ($\rho_{exp} = 1.14$ et $\rho_{th} \simeq 1.37$). Nous proposons de l'affecter à un mode mettant surtout en jeu δ(SO).

La formation de la liaison de coordination par l'intermédiaire de l'atome d'oxygène modifie donc l'ordre des fréquences δ(SO), γ(SO), et δ(CSC) par rapport à la molécule libre, contrairement à ce qui a été proposé par Berney et coll. (20) pour différents ions $[M(dmso)_6]^{n+}$.

TABLEAU 3. Dénombrement des vibrations d'un modèle $Al(OSC_2)_6$ de symétrie D_{3d}

	A_{1g}	A_{2g}	E_g	A_{1u}	A_{2u}	E_u
ν(SO)	1	0	1	0	1	1
ν_a(CSC)	0	1	1	1	0	1
ν_s(CSC)	1	0	1	0	1	1
ν(AlO)	1	0	1	0	1	1
δ(SO)	1	0	1	0	1	1
γ(SO)	0	1	1	1	0	1
δ(CSC)	1	0	1	0	1	1
δ(OAlO)	1	0	1	1	1	2
δ(AlOS)	1	0	1	0	1	1
t(S—O)	0	1	1	1	0	1
t(Al—O)	0	1	1	1	0	1
Activité	Raman	Inactive	Raman	Inactive	Infrarouge	Infrarouge

(3) Région inférieure à 200 cm^{-1}

L'absorption à 90 cm^{-1} qui est fortement abaissée par la deutériation doit provenir d'une déformation complexe de l'ion $[Al(dmso)_6]^{3+}$; le rapport isotopique est en effet très différent de ceux que l'on prévoit pour les vibrations de groupe non encore attribuées.

La fréquence de la bande située à 50 cm^{-1} est modifiée par la substitution du deutérium à l'hydrogène et du brome au chlore; nous la faisons correspondre à une vibration de réseau.

Dérivés $[Al(dmso)_6]^{3+}.3X^-$

Les bandes que nous venons d'attribuer aux vibrations de l'ion $[Al(dmso)_6]^{3+}$ des composés de forme I se retrouvent sur les spectres des composés de forme II; nous conserverons donc la même interprétation. Quelques modifications de fréquences et d'intensités sont cependant observées: nous allons les discuter.

(1) Vibrations des groupes méthyles

Les massifs attribués aux mouvements $\nu(CH_3)$ ou $\nu(CD_3)$ et $\delta(CH_3)$ présentent un plus grand nombre de maximums. Nous pensons que cette multiplicité provient de l'existence de groupes méthyles non identiques. En effet, ce phénomène est également observé pour les composés $[(CH_3)_2SO]_2PdX_2$ solides et dans ce cas les dilutions isotopiques montrent qu'il n'est pas dû à un effet de corrélation (21).

Les fréquences des élongations $\nu(CH_3)$ diminuent quand on passe de la forme I à la forme II alors que celles des déformations $\delta(CH_3)$ et des balancements $r(CH_3)$ augmentent (tableaux 4 et 5). Il en est de même pour les vibrations des groupes CD_3. Il y a donc intéraction spécifique entre les anions et les groupes méthyles. Celle-ci est d'autant plus forte que l'anion est plus petit, par contre Cl^- et Br^- ont des actions comparables. Ce résultat est en accord avec les travaux de Roche concernant l'influence des anions sur le méthyl de l'acétonitrile (22).

(2) Vibrations $\delta(SO)$ et $\gamma(SO)$

Les nombres d'ondes des mouvements δ(SO) augmentent et l'écart de fréquence entre les modes actifs en Raman et en infrarouge croît (tableau 5). La raie de diffusion vers 285 cm^{-1} du dérivé $[Al(dmso\text{-}d_6)_6]^{3+}.3Br^-$ est dédoublée mais ceci ne prove pas que le squelette $Al(OSC_2)_6$ ait une symétrie inférieure à D_{3d} puisque deux vibrations δ(SO) sont attendues en Raman pour ce groupe de symétrie (tableau 3). Les raies relevées vers 310 cm^{-1} sur les spectres des composés hydrogénés proviennent sans doute de vibrations de combinaison mettant en jeu les modes de réseau car le déplacement de fréquence par changement d'halogène est très supérieur à ceux relevés pour les autres mouvements de déformation de l'ion $[Al(dmso)_6]^{3+}$.

Les nombres d'onde des vibrations γ(SO) sont également augmentés; en outre, l'absorption infrarouge correspondante présente deux maximums séparés d'une douzaine de cm^{-1}. Un tel éclatement peut provenir d'un effet de corrélation dans le cristal, mais la simplicité du reste du spectre suggère qu'il s'agit plutôt de deux modes différents provenant d'une symétrie de site inférieure à D_{3d}: S_6 ou C_{2h} (tableau 3).

(3) Vibrations du groupe AlO_6

Les élongations ν(AlO) sont peu modifiées,

Can. J. Chem. Downloaded from www.nrcresearchpress.com by 210.87.254.42 on 09/05/12
For personal use only.

Can. J. Chem. Downloaded from www.nrcresearchpress.com by 210.87.254.42 on 09/05/12
For personal use only.

TABLEAU 4. Composés de forme I: nombres d'ondes des vibrations en cm^{-1}

$[Al(dmso)_6]^{3+}.3AlCl_4^-$		$[Al(dmso\text{-}d_6)_6]^{3+}.3AlCl_4^-$		$[Al(dmso)_6]^{3+}.3AlBr_4^-$		$[Al(dmso\text{-}d_6)_6]^{3+}.3AlBr_4^-$		
Infrarouge	Raman*	Infrarouge	Raman*	Infrarouge	Raman	Infrarouge	Raman	Attributions†
							2265 ép	
3009	3010	2258	‡	3005	3004	2253	2254	$\nu_a(CH_3)$, $\nu'_s(CH_3)$
2922	2923	2133	‡	2919	2918	2129	2129	$\nu_s(CH_3)$
1425				1423				
1412	1410	1045	‡	1410	1409	1044	1045	$\delta_a(CH_3)$, $\delta'_s(CH_3)$
1397				1395				
1326	‡	1022	‡	1324	1323	1017	1018	
1306				1304				$\delta_s(CH_3)$
					1041			
1033		834	‡	1031		832	831	$r_{//}(CH_3)$
	‡				1016			$\nu(SO)$ A_{1g}
992		798	‡	990	988	796	791	$r_\perp(CH_3)$
961		965		960		965		$\nu(SO)$ A_{2u}, E_u
	‡		‡		945		948	$\nu(SO)$ E_g
950		772	‡	950		771	770	$r_\perp(CH_3)$
910		‡	‡	909		‡	693	$r_{//}(CH_3)$
727	725	651	647	725	723	647	647	$\nu_a(CSC)$
689	687	636	634	687	685	635	633	$\nu_s(CSC)$
539		515		539		515		$\nu(AlO)$ A_{2u}, E_u
	‡		‡		492		464	$\nu(AlO)$ A_{1g}
	‡		‡		463		436	$\nu(AlO)$ E_g
489	488	488	‡	403	403	403	403	$\nu_a(AlX_4^-)$
389		374		392		376		γ (SO) E_u
	‡		‡		366		348	γ (SO) E_g
347	‡	320	‡	346	344	321	320	δ (CSC)
	312		‡		313		271	δ (SO) A_{1g}, E_g
304		267		302		266		δ (SO) A_{2u}
243		214		243		212		δ (SO) E_u
	‡		‡		243		243	δ (OAlO) E_g
	349		349		210		211	$\nu_s(AlX_4^-)$
189		189		189		188		δ (OAlO)
	162		‡		162		161	δ (OAlO) A_{1g}
180	179	180	‡	115	114	115	114	δ (AlX_4^-)
	140							δ (AlX_4^-)
120	122	121	‡	‡	‡			
90		83		90		~80		mouvements
					65		60	d'ensemble
55		53		46		45		vibration de réseau

*Spectres Raman pour lesquels seules les bandes les plus intenses ont pu être observées.
†Les types de symétrie sont ceux attendus si le cation $Al(dmso)_6^{3+}$ a la symétrie D_{3d}.
‡Non observée.

Can. J. Chem. Downloaded from www.nrcresearchpress.com by 210.87.254.42 on 09/05/12
For personal use only.

TABLEAU 5. Composés de forme II: nombres d'ondes des vibrations en cm^{-1}

$[Al(dmso)_6]^{3+}.3Cl^-$		$[Al(dmso\text{-}d_6)_6]^{3+}.3Cl^-$		$[Al(dmso)_6]^{3+}.3Br^-$		$[Al(dmso\text{-}d_6)_6]^{3+}.3Br^-$		
Infrarouge	Raman	Infrarouge	Raman	Infrarouge	Raman	Infrarouge	Raman	Attributions
2992	2987	2249	2250	2993	2995	2248	2248	$\nu_a(CH_3)$, $\nu'_s(CH_3)$
2983		2241	2243	2980	2980	2240	2240	
			2236					
2962	2965	2226	2228	2963	2970	2228	2232	
2898	2904	2120	2127	2896	2902	2119	2124	$\nu_s(CH_3)$
		2101	2101			2096	2096	
		2010	2009			2007	2005	
1455				1455				$\delta_a(CH_3)$, $\delta'_s(CH_3)$
1440	1436	1078		1435	1430	1078		
1423	1422	1054	1060	1421	1420	1051	1056	
1405			1044	1403			1038	
1331	1329	1027	1026	1330	1330	1024	1021	$\delta_s(CH_3)$
1308	1308	1012	1012	1307	1309	1012	1011	
1062		848	845	1061		848	841	$r_{//}(CH_3)$
	1026				1027			ν (SO)
1008	1006	809	806	1002	1005	805	801	$r_\perp(CH_3)$
974		780	784	972		778	780	$r_\perp(CH_3)$
965		970		963		970		ν(SO)
	950		953		950		950	ν(SO)
930	932	*	712	928	932	*	*	$r_{//}(CH_3)$
728	730	655	655	726	730	653	650	ν_a(CSC)
695	697	643	645	694	697	640	640	ν_s(CSC)
545		525		542		520		ν(AlO)
528		507		524		505		
	496		472		495		467	ν(AlO)
	470		440		468		440	ν(AlO)
402		385		402		386		γ(SO)
390		374		389		374		
	372		357		374		353	γ(SO)
350	352	321	327	346	350	319	323	δ (CSC)
	340		293		338		290	δ (SO)
							283	
310		273		310		271		δ (SO)
	317				308			
250		210		240		204		δ (SO)
230		225		225		220		δ (OAlO)
	254		240		248		230	δ (OAlO)
	233		223		232			
	170		164		170		160	δ (OAlO)
125	125	119	115	105		105	125	
100	95	94	90	90		87		
55		50	65	50	67	52	56	

*Non observée.

mais l'absorption centrée vers 530 cm^{-1} présente deux maximums séparés de 17 cm^{-1} environ, la largeur du massif à la demi-intensité restant du même ordre de grandeur.

Les déformations δ(OAlO) sont plus perturbées: la fréquence infrarouge est augmentée, la bande Raman vers 170 cm^{-1} présente un effet isotopique du deutérium de 8 cm^{-1} alors qu'elle ne varie pas dans les composés de forme I. Ceci suggère une modification des angles OAlO de l'ion $[Al(dmso)_6]^{3+}$.

Le doublet situé vers 230–250 cm^{-1} sur les spectres de diffusion peut correspondre à la raie à 243 cm^{-1} des dérivés de forme I. Dans ces conditions, trois mouvements δ(OAlO) sont actifs en Raman, ce qui est compatible avec une symétrie C_{2h}.

Evaluation de la constante de force de la liaison AlO

Nous avons effectué un calcul des modes normaux de vibration du squelette $Al(OSC_2)_6$ par la méthode de Wilson (23). Les paramètres géométriques sont égaux à ceux de l'ion $[Al(H_2O)_6]^{3+}$ (24) ou $[Fe(dmso)_4Cl_2]^+$ (25) pour les groupes AlO_6 et OSC_2 respectivement. L'angle AlOS a été posé égal à 120°. Les coordonnées de symétrie du groupe AlO_6 ont été écrites dans l'hypothèse d'une symétrie D_{3d}, par contre les six modèles C_2SO ont été considérés séparément.

Un champ de force approché a été obtenu en envisageant successivement les vibrations de AlO_6 et celles de C_2SO. Il conduit à une description assez satisfaisante des spectres de vibration et met en évidence les résultats suivants: (*1*) la constante de force des liaisons AlO est voisine de 1.8×10^5 dynes cm^{-1}, valeur proche de celles obtenus pour $(CH_3)_2OAlX_3$ (26). (*2*) les modes mettant surtout en jeu les coordonnées γ(SO) contiennent une forte participation de δ(OAlO); leurs fréquences sont supérieures à celles des mouvements δ(CSC) et δ(SO). (*3*) les six vibrations δ(CSC) sont calculées à la même fréquence. Pour les mouvements δ(SO), γ(SO), δ(OAlO), ν(AlO), et ν(SO) on attend par contre des éclatements assez importants entre les niveaux de symétries différentes.

Nous remercions Monsieur le Professeur Lascombe pour ses nombreux conseils, et Messieurs les Professeurs Gay et Maurin pour la détermination des spectres R.X.

Ce travail a bénéficié de l'aide matérielle de la S.N.P.A.

1. G. Wilke et coll. Angew. Chem. Internat. Ed. **5**, 151 (1966).
2. M. Uchino, Y. Chauvin, et G. Lefebvre. C.R. Acad. Sc. Paris, **265**, 103 (1967).
3. J. Reedijk, P. W. N. M. Van Leeuwen, et W. L. Groeneveld. Rec. Trav. Chim. Pays-Bas, **87**, 1073 (1968).
4. F. A. Cotton et R. Francis. J. Am. Chem. Soc. **82**, 2986 (1960).
5. J. Selbin, W. E. Bull, et L. H. Holmes. J. Inorg. Nucl. Chem. **16**, 219 (1961).
6. B. F. G. Johnson et R. A. Walton. Spectrochim. Acta, **22**, 1853 (1965).
7. C. G. Fuentes et S. J. Patel. J. Inorg. Nucl. Chem. **32**, 1575 (1970).
8. S. Thomas et W. L. Reynolds. J. Chem. Phys. **44**, 3148 (1966).
9. M. T. Forel et M. Tranquille. Spectrochim. Acta, **26A**, , 1023 (1970).
10. M. Tranquille, P. Labarbe, M. Fouassier, et M. T. Forel. J. Mol. Struct. **8**, 273 (1971).
11. F. Kütek, et F. Petrü. Czechoslovak Chem. Commun. **32**, 296 (1968).
12. D. E. H. Jones et J. L. Wood. Spectrochim. Acta, **23**, 2695 (1967).
13. K. Nakamoto. Infrared spectra of inorganic and coordination compounds. John Wiley and Sons, New York, 1963.
14. H. Siebert. Anwendungen der Schwingungespektroskopie in der anorganische chemie. Springer-Verlag, Berlin, 1966.
15. A. J. Carty, H. A. Patel, et P. M. Boorman. Can. J. Chem. **48**, 492 (1970).
16. A. I. Grigorev, V. A. Sipachev, et E. G. Pogodilova. Zh. Strukt. Chim. **11**, 458 (1970).
17. Y. Kermarrec. C.R. Acad. Sci. **258**, 836 (1964).
18. A. Silveira, M. A. Marques, et N. M. Marques. C.R. Acad. Sci. **252**, 3983 (1961).
19. V. Ananthanarayanan. J. Chem. Phys. **52**, 3844 (1970).
20. C. V. Berney et J. H. Weber. Inorg. Chem. **7**, 283 (1968).
21. M. Tranquille et M. T. Forel. Spectrochim. Acta. Sous presse.
22. J. P. Roche et P. V. Huong. J. Chim. Phys. **67**, 211 (1970).
23. E. B. Wilson, J. C. Decius, et P. C. Cross. Molecular vibration. McGraw-Hill Inc., New York, 1955.
24. D. R. Buchanan et P. M. Harris. Acta Cryst. **B24**, 954 (1968).
25. M. J. Bennett, F. A. Cotton, et D. L. Weaver. Acta Cryst. **23**, 581 (1967).
26. J. Derouault, M. Fouassier, et M. T. Forel. J. Mol. Struct. Sous presse.

Can. J. Chem. Downloaded from www.nrcresearchpress.com by 210.87.254.42 on 09/05/12
For personal use only.

Reactions of Chloramines with Ag(0) and Ag(I) States[1]

O. E. EDWARDS AND D. VOCELLE[2]

Biochemistry Laboratory, National Research Council of Canada, Ottawa, Canada K1A 0R6

AND

J. W. APSIMON[3]

Department of Chemistry, Carleton University, Ottawa, Canada K1S 5B6

Received June 15, 1971

Reactions of *N*-chloroazacyclooctane and *N*-chloroazacyclononane are described which give good yields of bicyclic amines. These are: (*a*) short chain homolytic reactions involving *neutral* nitrogen radicals initiated by ferrous ion or metallic silver; (*b*) apparent homogeneous reactions involving silver ion and bases; (*c*) reactions using silver oxide suspension which also require added bases.

Both rate and product composition for (*b*) and (*c*) are sensitive to oxygen indicating that they are homolytic processes, probably initiated by traces of silver metal. No evidence for involvement of discrete nitrenium ions was found. However, reaction of *N*-chloroisoquinuclidine with silver ions has the character of a heterolytic process, giving products completely distinct from those from its homolytic decomposition. The addition of *neutral* piperidino radicals to styrene is described.

On décrit les réactions du *N*-chloroazacycloactane et du *N*-chloroazacyclononane, qui donnent de bons rendements en amines bicycliques. Ce sont: (*a*) les réactions homolytiques de courtes chaînes impliquant des radicaux azote *neutres* initiés par l'ion ferreux ou l'argent métallique; (*b*) des réactions homogènes apparentes impliquant l'ion argent et des bases; (*c*) des réactions utilisant une suspension d'oxyde d'argent impliquant aussi l'addition de bases.

La vitesse et la composition du produit, dans les cas (*b*) et (*c*) sont sensibles à l'oxygène, indiquant que ce sont des procédés homolytiques, initiés probablement par des traces d'argent métalliques. On n'a pu prouver l'implication dans ces réactions des ions nitrénium. Toutefois, la réaction du *N*-chloroisoquinuclidine avec les ions argent possède le caractère d'un procédé hétérolytique, donnant des produits complètement distincts de ceux provenant de sa décomposition homolytique. L'addition de radicaux *neutres* pipéridino au styrène est aussi décrite.

Canadian Journal of Chemistry, **50**, 1167 (1972)

Substitution of nitrogen on saturated unactivated carbon has been achieved using protonated nitrogen radicals derived from chloramines (1) (Hofmann–Löffler–Freytag reaction), nitrogen radicals from chloramides (2*a*) and chlorolactams (2*b*), by chemically and photochemically generated alkoxycarbonyl nitrenes (3) and acyl nitrenes (4), and by nitrenium ions derived from oximes (5). Some time ago we reported transannular substitution of saturated carbon using electron-deficient nitrogen species derived from chloramines (6). We considered the reactive species to be nitrenium ions, $R_2N:^+$ as illustrated:

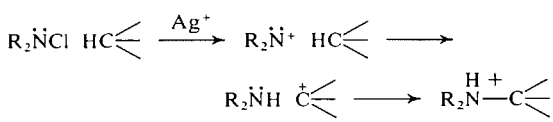

We now present evidence that the medium ring reactions are homolytic processes and that simple aliphatic nitrenium ions are not readily produced from chloramines by silver ions.

Attempted Generation of Nitrenium Ions

In our efforts to generate and observe reaction of nitrenium ions we studied medium ring amines. The efficient transannular hydride transfer to medium ring carbonium ions (7) encouraged us to expect similar reaction of any discrete or developing nitrenium ions. We first re-examined the early work of Fischer (8) on the deamination of 1,1-dialkylhydrazines. However, in agreement with his findings, the major reaction of *N*-aminoazacyclononane was frag-

[1]Issued as NRCC No. 12371. Presented in part at the Symposium on Reactive Intermediates, Laval University, Quebec City, September, 1964.

[2]NRCC Postdoctorate Fellow, 1964–1966. Present address: Université de Québec à Montréal, Montreal, Quebec.

[3]Guest worker, summer of 1964.

Can. J. Chem. Downloaded from www.nrcresearchpress.com by 210.87.254.42 on 09/05/12
For personal use only.

[1] 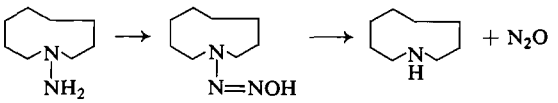

mentation to give N_2O and azacyclononane (eq. 1). A second alternative was hence attempted, the silver ion-promoted ionization of medium ring chloramines (eq. 2). The sub-

[2] $R_2NCl + Ag^+ \longrightarrow R_2N{:}^+ + AgCl$

strates chosen were *N*-chloroazacycloheptane (**1**), *N*-chloroazacyclooctane (**2**), *N*-chloroazacyclononane (**3**), and *N*-chloroazacyclodecane (**4**). In our early experiments (6) a rapid reaction

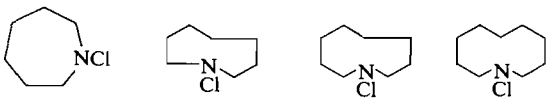

1 **2** **3** **4**

was observed for the eight- to ten-membered ring chloramines in several solvents, leading to bicyclic tertiary amines. However, in attempting to duplicate and extend these experiments it was discovered that medium ring chloramines and simple aliphatic chloramines that were *completely free of amine* were inert at room temperature to silver ions in aqueous dioxane, tetrahydrofuran, or acetonitrile. The other salient observations are:

(*1*) The addition of 0.1 to 0.2 *M* equiv of the corresponding amine to solutions of the silver perchlorate and the medium-ring chloramine initiated moderately rapid reaction in a nitrogen atmosphere. In aqueous dioxane (1 h[4]) the addition of the amine resulted in precipitation of silver oxide, but in aqueous acetonitrile (6 h[4]) the basic solution remained colorless[5] and only silver chloride precipitated.

(*2*) Fresh silver oxide, washed several times with water, induced rapid (*ca.* 2 h[4]) decomposition of medium ring chloramines under nitrogen. If the washing was much more thorough the initial reaction became very much slower, but was autocatalytic. Addition of 10 mol % of amine or ammonia or a trace of hydroxide ion eliminated the induction period. However, over 10 mol % of sodium hydroxide suppressed reaction.

(*3*) A large excess of silver ammonium ions gave moderately rapid decomposition of the chloramines but much metallic silver was produced by oxidation of products.

(*4*) The "homogeneous" reactions in aqueous acetonitrile were dramatically slowed if the nitrogen atmosphere was replaced by air. In addition negligible amounts of bicyclic amines were produced. The effect on the silver oxide-initiated reactions was less dramatic but qualitatively the same.

(*5*) In agreement with the observations of Gassman and Fox (10) *N*-chloroisoquinuclidine reacted slowly with silver nitrate in methanol at room temperature, but was rapidly decomposed at reflux temperature. It reacted very slowly (time for complete reaction greater than 45 h), with silver oxide at room temperature.

(*6*) *N*-Chloropiperidine was inert to a sample of silver oxide which rapidly reacted with *N*-chloroazacyclononane, and inert to the combination of silver perchlorate and 10 mol % of piperidine in 90% acetonitrile – 10% water.

The bicyclic product from *N*-chloroazacyclooctane was pyrrolizidine (**5**), and that from *N*-chloroazacyclononane was indolizidine (**6**). *N*-

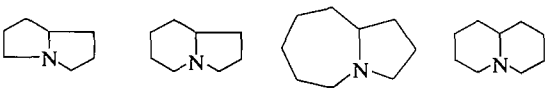

5 **6** **7** **8**

Chloroazacycloheptane gave negligible amounts of bicyclic products. It is interesting that *N*-chloroazacyclodecane gave 1-azabicyclo[5.3.0]-decane (**7**) as the major bicyclic product in reaction with Ag(I) although quinolizidine (**8**) was also produced. A summary of yields is presented in Table 1.

A second group of products from the silver ion or silver oxide reactions were aminoaldehydes. If the reaction products from *N*-chloroazacyclononane were directly converted to

[4]Mean time for complete reaction of *N*-chloroazacyclononane.

[5]Presumably both amine and acetonitrile (9) are acting as ligands, because hydroxide ion precipitates silver oxide from this solvent mixture.

Can. J. Chem. Downloaded from www.nrcresearchpress.com by 210.87.254.42 on 09/05/12
For personal use only.

TABLE 1.

Chloramine from	Atmosphere	Solvent*	Reagent	Added base† (mol %)	>NCl ‡ AgCl	Yield in % Bicyclic	Yield in % Parent	Runs	Time§ (h)
Azacyclononane	N_2	A	Ag	—	3	30	38	4	2
	"	"	$AgClO_4$	Non(10)	—	46	24	4	7
	"	"	"	$(CH_3)_3N$(10)	—	45	25	1	6
	Air	"	"	Non(10)	—	0	76	1	68
	N_2	"	"	Non(20)	—	31	17	3	3
	"	"	"	$(CH_3)_3N$(23)	—	29	10	1	8
	"	"	Ag_2O	—	—	48	<2	2	3
	Air	"	"	—	—	9	20	1	5
	N_2	D	Ag	—	2.5	45	38	1	5
	"	"	$AgClO_4$	Non(10)	—	68	0	1	1
	"	"	"	Non(20)	—	56	0	1	1
	"	"	Ag_2O	—	—	57	0	3	2
	"	"	"	NH_3(10)	—	55	0	1	2
	"	"	"	OH^-(5)	—	52	0	1	2
Azacyclooctane	N_2	A	Ag	—	>2	36	36	1	2
	Air	"	"	—	<2	19	28	1	6
	N_2	"	$AgClO_4$	Oct(10)	—	46	19	2	26
	Air	"	"	" "	—	0	50	1	96
	N_2	"	Ag_2O	—	—	72	0	1	4
	N_2	D	Ag	—	5	50	17	1	4
	"	"	$AgClO_4$	Oct(10)	—	78	0	1	4
	"	"	Ag_2O	—	—	72	0	2	7
Azacyclodecane	N_2	M‖	Ag	—	1	16	78¶	1	24
	"	A	"	—		11	32	1	20
	"	"	$AgClO_4$	Dec(10)	—	6	42	1	46
	"	D	Ag	—	3.4	6	24	1	20
	"	"	$AgClO_4$	Dec(10)	—	4	0	1	20

*A = 90% acetonitrile – 10% water (v/v). D = 80% dioxane – 20% water (v/v).
†Non = azacyclononane; Oct = azacyclooctane; Dec = azacyclodecane.
‡Ratio of chloramine consumed to silver chloride produced.
§Approximate time in hours for 100% reaction.
‖A mixture of 18 ml of dry acetonitrile and 2 ml of acetic anhydride was used as solvent.
¶Contains products from aldimines also.

hydrochlorides and isolated, the aldehyde group could be detected by a band at 1720 cm^{-1}. Alternatively if the products were acetylated, a neutral *N*-acetyl aldehyde (ν_{max} ($CHCl_3$) 1725 cm^{-1}) was obtained mixed with *N*-acetyl azacyclononane. However, when the free bases were isolated the aldehyde was converted to polymer.

A third type-product was the parent secondary amine. Only traces of azacyclononane were formed in reactions of *N*-chloroazacyclononane with silver oxide or in the silver ion – amine – chloramine reactions in aqueous dioxane, but up to 15% appeared in the products from "homogeneous" reaction in aqueous acetonitrile.

Since very little secondary base was formed, and the bicyclic products were readily separated from the amino aldehyde produced, the reaction using silver oxide provided convenient and mild routes to indolizidine and pyrrolizidine. We hope to extend the reactions to synthesis of natural products containing these ring systems.

As reported by Gassman and Fox (10) *N*-chloroisoquinuclidine gave a nearly quantitative yield of methoxy base **9** in the reaction with silver nitrate in methanol. However, the sluggish reaction of the chloramine with silver oxide only gave 6% of **9**. The major product was isoquinuclidine (**10**).

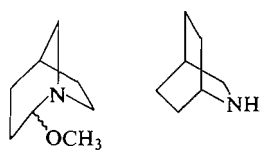

9 **10**

Can. J. Chem. Downloaded from www.nrcresearchpress.com by 210.87.254.42 on 09/05/12
For personal use only.

[3] 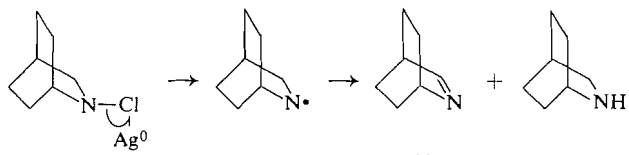

11

Metallic Silver-Initiated Reactions

As soon as it was recognized that amines were necessary to induce reaction between silver ions and chloramines, and the inevitable formation of silver oxide was noted in aqueous dioxane, we considered that metallic silver might play an important role in the reactions. Work in these laboratories had shown that fresh silver oxide rapidly oxidized some amines to carbinolamines (11, 12) while being reduced to metallic silver. Indeed small amounts of silver were detectable at the end of some of the present reactions. We hence examined the action of silver metal on medium ring and other chloramines.

The first attempts at inducing a silver catalyzed chloramine decomposition were made using a catalyst with a high specific surface developed for ethylene oxidation (13). Reaction was slow with this initiator or colloidal silver (14). However Tollens' silver (formaldehyde reduction of Tollens' solution) proved to be an effective and reproducible reagent when used in 2.5–3 *M* ratio. The amount of silver chloride produced was 20–40 mol %. The products from the medium ring chloramines were parent secondary amines, bicyclic amines, aldimines (appearing as polymer on work-up), and their hydrochlorides. Attack on solvent dioxane or tetrahydrofuran also took place. The reactions seem best formulated as homolytic processes giving *C*-chloro bases as primary products (see Discussion). However, no direct evidence for the formation of the *C*-chloro base in the silver catalyzed reaction was found. When the bases at the end of the reaction were converted to hydrochlorides, the resulting salt contained only a small excess of chlorine over that required for the hydrochlorides.

In order to further test the conception that homolytic initiation could lead to the above products, the chloramines were treated with fractional molar ratios of the one-electron reducing agents titanous and ferrous chlorides. Again short chain reactions resulted with the medium-ring chloramines (apparent chain length up to 10). The bicyclic bases were formed in comparable yields to those from the metallic silver-initiated reactions.

In marked contrast to the silver ion-promoted reaction (10) described above, *N*-chloroisoquinuclidine reacted with Tollens' silver in methanol to give a mixture of aldimine **11** and isoquinuclidine (eq. 3), but no trace of 2-methoxy-1-azabicyclo[3.2.1]octane (**9**). In the case of the reaction of both *N*-chloroisoquinuclidine and *N*-chloropiperidine with Tollens' silver, nearly 1 mol of silver chloride was produced, hence no chain reaction was involved (see Discussion).

We had earlier observed attack on tetrahydrofuran in the course of the reaction of silver ion with *N*-chloropiperidine (6), and had attributed this to hydride ion abstraction by nitrenium ions. However, since it now appears that nitrenium ions are not involved, the reaction was probably homolytic. We hence examined the decomposition of *N*-chloropiperidine in tetrahydrofuran brought about by metallic silver. As expected γ-hydroxybutyraldehyde was formed (see Scheme 2). Higher boiling neutral products with the spectroscopic characteristics of tetrahydrofuran dimer and polymer were also observed (Scheme 2).

In an attempt to produce further evidence for the homolytic character of the reactions, the reaction of *N*-chloropiperidine with silver was run in the presence of styrene. A moderate yield of a mixture of tertiary amines containing phenylethyl and piperidine units was obtained.

Discussion

The lowest energy reaction pathways for the N—Cl bond of chloramines are either homolytic fission, or heterolytic in the direction $N^- \cdots Cl^+$ in the presence of electron donors. However, heterolysis in the opposite sense can be forced in a E2 process such as the Ruschig reaction (15) (eq. 4). Another situation formally analogous to a retro-Prins reaction (16) in which chloride ion is liberated is illustrated as eq. 5. More unusual cases are the cyclization reported by

Can. J. Chem. Downloaded from www.nrcresearchpress.com by 210.87.254.42 on 09/05/12
For personal use only.

[4] 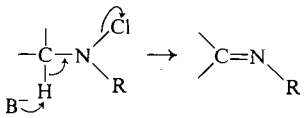

[5] 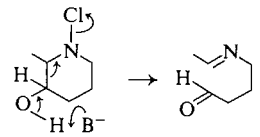

Adam and Schreiber (17) (eq. 6) and the rearrangement discovered by Benezra and Lusinchi (18) (eq. 7). The base in the latter two cases probably plays a secondary role following homolytic chlorination or thermal ionic rearrangement, respectively.

The present work demonstrates that the ionization of chloramine to nitrenium ions involves high activation energy, and in simple aliphatic cases silver ion pull on the halogen is not sufficient to effect this at room temperature. The work of Loeppky and Rotman (19) shows that the same is true of *N*-chloroketimines, silver assisted ionization only occurring synchronous with bond migration to nitrogen. Similarly most of the recent work of Gassman and coworkers, of Rautenstrauch, and of Horwell and Rees, can be accounted for without invoking discrete nitrenium ions. Their reactions can be considered as cases of σ-bond participation (10, 20) or π-electron participation (21, 22) in the ionization of the N—Cl bonds. The elevated temperature takes the place of silver ion pull in the pure solvolytic examples. The possible intrusion of homolytic reactions and acid catalyzed electrophilic chlorinations add uncertainty to mechanistic interpretation.

Our observations confirm that the reaction of *N*-chloroisoquinuclidine with silver nitrate in methanol is heterolytic in character since the products are strikingly distinct from those produced in the homolytic decomposition. The reaction probably involves σ-bond participation in the silver ion assisted ionization of the N—Cl bond.

The silver ion catalyzed rearrangements of azabicycloheptanes (23), the surprisingly rapid internal reaction of primary chloramines with olefinic double bonds discovered by Nagata and coworkers (24) and the silver ion catalyzed cycloaddition of unsaturated secondary chloramines described by Hobson and Riddell (25) present mechanistic problems that merit further study.

Much of the evidence suggested that our transannular reactions with Ag(I) species were push–pull heterolytic processes involving added base. This mechanism is illustrated for *N*-chloro-

[8] 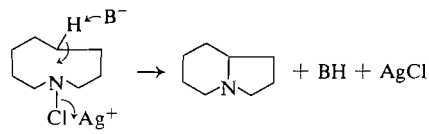

azacyclononane in eq. 8. The facts which appeared to support this were:

(*1*) Only traces of silver were formed when azacyclononane, indolizidine, or mixtures of these with aldimine (amino aldehyde) were left for 4 h under nitrogen in aqueous acetonitrile containing silver perchlorate. Hence the chance that a large amount of the product in the "homogeneous" reactions would arise in a silver-initiated homolytic process seemed small.

(*2*) The "homogeneous" reaction of the eight- and nine-membered ring chloramines with silver ion and base were much faster than those

[6] 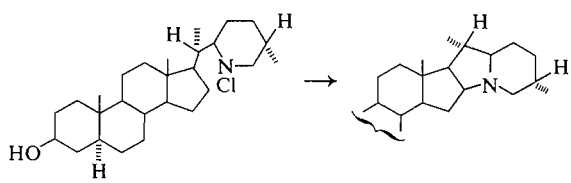

[7] 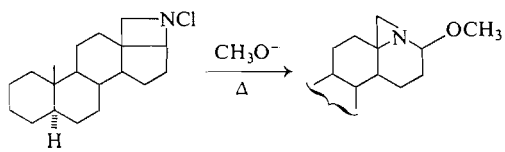

Can. J. Chem. Downloaded from www.nrcresearchpress.com by 210.87.254.42 on 09/05/12
For personal use only.

Can. J. Chem. Downloaded from www.nrcresearchpress.com by 210.87.254.42 on 09/05/12
For personal use only.

of *N*-chloroazacycloheptane and *N*-chloroazacyclodecane. *N*-Chloropiperidine was almost inert under these conditions. This is consistent with the unique possibility for the colinear arrangement Cl—N···C—H with close approach of the nitrogen and transannular carbon in the eight- and nine-membered rings.

(*3*) The complete or near absence of the parent secondary amine, which is the most characteristic homolytic product, in the reactions with silver oxide argues against a homolytic mechanism (yield of secondary amine in the metallic silver reactions up to 37%). The yield of bicyclic products in the silver oxide reactions was up to 20% greater than in the silver metal reactions (Table 1). In addition the probable heterolytic rearrangement of *N*-chloroisoquinuclidine described above encourages an interpretation of the medium ring reactions in heterolytic terms.

(*4*) The ratio of 1-azabicyclo[5,3,0]decane (**7**) to quinolizidine (**8**) from *N*-chloroazacyclodecane in the silver perchlorate promoted reactions (60:40) was reversed (40:60) in the homolytic reactions initiated by silver metal.

(*5*) Hydroxide ion or ammonia eliminated the induction period in the silver oxide initiated reactions. Neither seems likely to give metallic silver, hence a heterolytic process seemed likely, at least until products accumulated.

However, three observations are inconsistent with a heterolytic process.

(*a*) Radical trapping reactions showed that amine radicals were present in the "homogeneous" silver ion-initiated reactions in aqueous acetonitrile (26).

(*b*) The secondary amine produced (up to 15%) in these "homogeneous" reactions certainly arises by a homolytic process.

(*c*) The reaction of *N*-chloroazacyclooctane and *N*-chloroazacyclononane with silver perchlorate and parent amines in aqueous acetonitrile was almost stopped by the use of an air instead of a nitrogen atmosphere. In addition the yield of bicyclic products dropped sharply and very water-soluble products resulted.

As a consequence we are forced to conclude that the "homogeneous" reactions are homolytic chain reactions initiated by traces of silver, which are readily stopped by the good radical scavenger oxygen. The postulated reactions are outlined in Scheme 1.

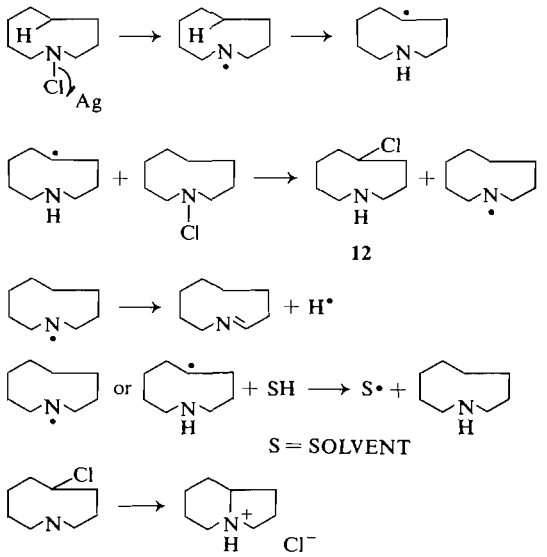

SCHEME 1

The aldimines produced could arise by hydrogen atom expulsion from the amine radical,[6] dismutation of the amine radicals, α-hydrogen abstraction from amines, or a Ruschig-type heterolytic process promoted by silver ion and base.

The generation of radicals using silver as a reducing agent has precedence in the preparation of triphenylmethyl radicals from triphenylmethyl chloride (27). Neutral alkylamino radicals have been generated previously by photolysis of amines (28) or decomposition (thermal, photochemical, or radical initiated) of tetrazenes (29) and chloramines (30). They have been shown to abstract hydrogen from carbon α to nitrogen (or eliminate a hydrogen atom from this carbon), producing dimers or imines (28). They are reported to have little tendency to add to carbon–carbon double bonds (29*b*) (see however, ref. 30).

Several cases of transannular hydrogen abstraction by carbon radicals are on record. Ourisson and coworkers discovered examples in the homolytic addition of carbon tetrachloride, etc. to longifolene and a medium ring analogue (31) and Traynham and Couvillon (32) described a similar reaction of cyclooctene (eq. 9). Hence there is good precedent for our postulated transannular radical reactions.

[6]Hydrogen has been identified as a reaction product (26).

[9] 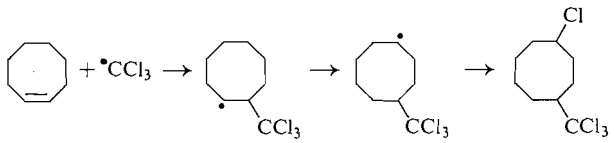

We conclude that the present work provides a new and convenient method of preparing *neutral* nitrogen radicals in solution and demonstrates their transannular attack on unactivated C—H bonds.

The dominant ring size for the reaction of *N*-chloroazacyclodecane with Ag(I) agrees with the favored six-membered cyclic transition state for hydrogen abstraction by oxygen radicals (33) and protonated nitrogen radicals (34) (see **13**).

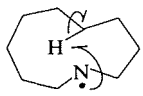

13

As indicated in point 3 above, the silver oxide initiated reactions (and the very comparable silver ion – chloramine – amine reactions in aqueous dioxane) are remarkable in that only very low yield of secondary amines are produced. This contrasts with the 17–38% of secondary amine in the Ag^0-initiated reactions in the same solvent. It was tempting to think that the absence of secondary amine ruled out a homolytic process, and that hence a special role of silver oxide surface (with adsorbed base) favored a heterolytic push–pull mechanism resembling eq. 8. Again however, the effect of air in slowing the reaction and the resulting sharp drop in yield of the bicyclic amines seems only consistent with a homolytic process. An explanation of the high efficiency of the transannular hydrogen atom abstraction in these cases could be that most of nitrogen radicals are formed on the silver oxide surface and adsorbed long enough that the carbon radicals are formed before the radicals have contact with other hydrogen sources. This also requires that the carbon radicals react very much more efficiently to abstract chlorine from chloramine molecules than to abstract hydrogen from solvent or other sources.

In the case of the isoquinuclidinyl radical, where no transannular hydrogen is accessible the dominant reaction is attack on the hydrogens α to the nitrogen of other radicals (dismutation) or elimination of a hydrogen atom. Attack on solvent methanol seems a less favored process. Since a full molar equivalent of silver chloride was formed, no chain reaction was involved. *N*-Chloropiperidine behaved similarly. However, the nitrogen radicals did attack solvent dioxane and tetrahydrofuran (see Scheme 2).

The reaction of *N*-chloropiperidine with silver in the presence of styrene in acetonitrile produced a roughly 38% yield of products arising from addition of the piperidine to styrene. Since the bases were tertiary (inert to hot acetic anhydride), the nitrogen radicals had added, rather than carbon radicals derived from them. This agrees with the work of Minisci and Galli (30), but not with the observations of Mackay and Waters (29*b*). Since 77% of the theoretical amount of silver chloride was formed, the intermediate benzyl radicals were inefficient abstractors of chlorine from *N*-chloropiperidine, and very few radical chains were initiated.

The minor importance of chain reactions in the homolytic decomposition of *N*-chloropiperidine and *N*-chloroisoquinuclidine is consistent with the statement of Minisci and coworkers (35) that neutral nitrogen radicals cannot sustain a chain reaction. Thus the chain reactions observed with the medium ring chloroamines are special cases and are probably a consequence of the transfer of the radical center to carbon (Scheme 1).

One surprising feature in the present work was the rapidity with which the *C*-chloro bases

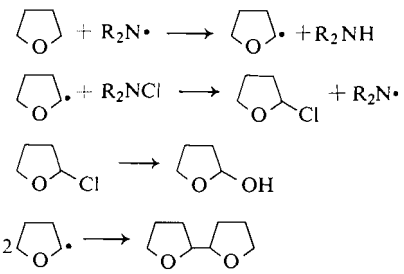

SCHEME 2

Can. J. Chem. Downloaded from www.nrcresearchpress.com by 210.87.254.42 on 09/05/12
For personal use only.

Can. J. Chem. Downloaded from www.nrcresearchpress.com by 210.87.254.42 on 09/05/12
For personal use only.

cyclized. However we subsequently found that even the *C*-chlorolactams corresponding to **12** cyclized spontaneously at room temperature (*2b*).

In an attempt to examine the possibility that initial radical formation might be followed by oxidation to nitrenium ions by silver ion (eq. 10), a methanol solution of *N*-chloroisoquinuclidine was treated at 5° with a mixture of Tollens'

$$[10] \qquad R_2NCl + Ag^0 \rightarrow R_2N\cdot + AgCl$$
$$R_2N\cdot + Ag^+ \rightarrow R_2N^+ + Ag^0$$

silver and silver perchlorate. The products were isoquinuclidine, methoxy base **9**, and imine **11**. This mixture could result from concurrent homolytic and ionic reactions, so we failed to demonstrate whether the radical oxidation takes place.

Summary

(*1*) Nitrenium ions *are not* generated from simple secondary chloramines in the presence of silver ions at room temperature.

(*2*) Secondary amino radicals can be generated from secondary chloramine by the action of silver metal. These efficiently abstract hydrogen from unactivated CH bonds. The transannular CH abstraction in medium rings leads to good yields of bicyclic amines. These reactions of *neutral* amine radicals may have synthetic utility where the strongly acid conditions of Hofmann–Löffler–Freytag reaction cannot be used.

(*3*) Neutral amine radicals add to styrene and induce polymerization.

Experimental

The i.r. spectra were obtained on a Perkin–Elmer model 257 grating spectrometer, and n.m.r. spectra on a Varian A-60A spectrometer. The g.l.c. was performed on the following columns: A, 6 ft × 1/4 in. SF-96 (fluorinated silicone) on fluoropak; B, 6 ft × 1/4 in. SE-30 (silicone gum rubber) on silanized Chromosorb W; C, 6 ft × 1/4 in. polyphenyl ether on Chromosorb W.

The yields of bicyclic products are minimum figures, since with the relatively small quantities used, losses were possible on isolation and distillation.

Chloramine determinations were done using 0.5 ml samples which were added to *ca.* 1 g of potassium iodide in 5 ml of methanol, 1 ml of water, and 1 ml of acetic acid. The iodine liberated was titrated with 0.1 *N* sodium thiosulfate.

Chloramine Preparation

In our earlier experiments either *N*-chlorosuccinimide or dichloramine-T in methylene chloride were used to convert the secondary amines to chloramines. However, the use of sodium hypochlorite proved much more convenient. The preparation is illustrated for azacyclononane.

A solution of 1 g of azacyclononane hydrochloride in 2 ml of water was added to 35 ml of a rapidly stirred cold 10–14% solution of sodium hypochlorite in water (strongly alkaline). The mixture was stirred for 1 h at room temperature, then extracted three times with 15 ml portions of pure pentane. The pentane layers were washed successively with water, very dilute sulfuric acid, water, then sodium carbonate solution. The dried solution (Na_2SO_4) was evaporated on a rotating evaporator under reduced pressure in a bath at 20 °C until the volume reached a few milliliters. The evaporation was then continued outside the bath until a thick oil remained. This was dissolved in the appropriate solvent and a 0.5 ml aliquot titrated iodimetrically (see general directions). The yield in all cases was over 90%.

Base Derivatives

The bases used were prepared by reduction of the corresponding lactams using lithium aluminum hydride in refluxing dioxane, followed by isolation as hydrochlorides.

Azacyclooctane hydrochloride, m.p. 178° (lit. m.p. 177° (36)); azacyclononane hydrochloride, m.p. 165° (lit. m.p. 164° (36)); azacyclodecane hydrochloride, laths from ethyl acetate, m.p. 119°, picrate, m.p. 193° (lit. m.p. 192° (37)); isoquinuclidine hydrochloride crystallized as thin plates from methanol – ethyl acetate, m.p. 302° dec. when immersed at 290° (lit. m.p. >300° (38)).

Pyrrolizidine picrate, m.p. 258–260°; mixed m.p. with an authentic sample (m.p. 256–258° (39)) was 258–260°.

Indolizidine picrate, m.p. 230°; mixed m.p. with an authentic sample (m.p. 230° (39)) was not depressed.

Azabicyclo[5.3.0]decane picrate, m.p. 212–216° was shown by g.l.c. of the base to contain *ca.* 15% of quinolizidine picrate. It gave a mixed m.p. of 210–214° with an authentic sample (m.p. 210–213° (40)) which was also shown by g.l.c. of the base to contain *ca.* 15% of quinolizidine picrate.

Tollens' Silver

Freshly washed silver oxide from 2 g of silver nitrate was suspended in 15 ml of water, and the minimum amount of concentrated ammonia added to effect solution. Aqueous formaldehyde was then added dropwise with stirring and cooling. The precipitated silver and mirror scraped from the walls was washed with water by decantation, then on a Hirsch funnel. It was kept moist, and used as soon as possible after preparation.

N-Chloroazacyclononane

The faintly yellow oil could be distilled over a short path using a bath at 65° under 8 mm pressure. It had λ_{max} 287 mμ, ε 390, and pK_a 1.2 in 95% ethanol. The protons α to the nitrogen resonated at δ 3.2 in deuterochloroform. It was stable in solution in pentane, aqueous acetonitrile, and aqueous dioxane in diffuse light. It was stable over a period of 7 h in a stirred mixture of 2 ml of dioxane and 11 mg of sodium hydroxide in 0.12 ml of water. It was also inert to a 3.5% solution (w/v) of azacyclononane in aqueous dioxane.

Solutions of the chloramine and silver perchlorate in aqueous acetonitrile or aqueous dioxane showed less than 10% drop in chloramine concentration in 20 h at room temperature in diffuse light.

Can. J. Chem. Downloaded from www.nrcresearchpress.com by 210.87.254.42 on 09/05/12
For personal use only.

N-Chloroazacyclooctane and N-Chloroazacyclodecane

These were obtained as nearly colorless oils from pentane solution. They were stable for at least 8 h in aqueous dioxane and aqueous acetonitrile, and in solutions of silver perchlorate in these solvents.

N-Chloropiperidine

The nearly colorless oil could be distilled over a short path at 45° under 10 mm pressure. It had ν_{max} 269 mμ, ε 380, and pK_a of 1.0 in 95% ethanol. The methylene groups α to the nitrogen gave a triplet with $J = 5.5$ Hz at δ 3.20 in deuterochloroform. It reacted to the extent of 9% in 19 h at room temperature in 80% dioxane – 20% water containing 4% (w/v) of silver perchlorate.

N-Chloroisoquinuclidine

This was recovered from pentane solution as a waxy white solid. An attempt to distill a sample over a short path at bath temperatures up to 80° under 8 mm pressure led to extensive decomposition. It gave n.m.r. signals in deuterochloroform at δ 3.12 (1H) and 3.50 (2H).

N-Nitrosoazacyclononane

Azacyclononane hydrochloride (2.34 g) in a mixture of water (20 ml) and concentrated hydrochloric acid (14 ml) was cooled to 0° and an aqueous solution of sodium nitrite at 0° (3.0 g in 10 ml) was added. The mixture was stirred for 1 h, ether extracted, and washed well with water. Drying and evaporation yielded *N*-nitrosoazacyclononane (2.5 g), b.p. 90–92°/10^{-3} mm; ν_{max} (film) 1630 cm^{-1} (—N=O).

Anal. Calcd. for $C_8H_{16}N_2O$: C, 61.51; H, 10.32; N, 17.93. Found: C, 61.21; H, 10.22; N, 17.51.

N-Aminoazacyclononane

N-Nitrosoazacyclononane (2.5 g) in dry ether (30 ml) was added to a vigorously stirred solution of lithium aluminum hydride (1 g) in ether (20 ml) and the mixture was stirred overnight at room temperature. Decomposition of the excess lithium aluminum hydride with saturated aqueous Rochelle salt, followed by ether extraction, drying, and evaporation yielded the substituted hydrazine (2.1 g), b.p. 75–80° (10^{-3} mm); ν_{max} 3300, 1600 cm^{-1} (—NH_2).

This compound could not be obtained completely pure for analysis but treatment of an ethyl acetate solution (50 mg in 5 ml) with methyl iodide gave an immediate precipitate of the corresponding methiodide (60 mg) which recrystallized as needles from methanol – ethyl acetate, m.p. 216–218°.

Anal. Calcd. for $C_{11}H_{25}N_2I$: N, 8.98; I, 40.70. Found: N, 8.63; I, 39.3.

Deamination of N-Aminoazacyclononane

N-Aminoazacyclononane (650 mg) was dissolved in 2 *N* HCl (20 ml) and cooled to 0°. Excess saturated aqueous sodium nitrite (*ca.* 1.2 g $NaNO_2$) was added and the mixture stirred at 0° for 1 h then ether was added. The ether layer after washing and drying was evaporated to yield an unstable neutral fraction (*ca.* 200 mg) which was not examined further.

The aqueous layer was basified (5% NaOH) and continuously extracted with ether overnight (caution! the base fraction is fairly soluble in water) which after careful removal of the ether at room temperature under vacuum yielded the basic fraction (270 mg). The g.l.c. (Perkin–Elmer model 154, Fluoropak QF 1 on Chromosorb 60–80) indicated over 95% of one component with retention time identical to azacyclononane. Treatment of the base fraction with HCl gas yielded the corresponding hydrochloride (m.p. and mixed m.p. 164°) and with methyl iodide in ethyl acetate the methiodide (m.p. and mixed m.p. 237–238°) was obtained.

The only other constituent of much longer retention time could not be obtained pure (preparative g.l.c. fractional crystallization of derivatives, column chromatography, t.l.c.) but was probably dimeric material (no N—H in i.r. or n.m.r., yet n.m.r. indicated an azacyclononane-type structure).

Reactions with Ag(I) Species

(A) N-Chloroazacyclononane

(1) With Silver Perchlorate and Azacyclononane in Dioxane–Water

A solution of 830 mg (5.13 mmol) of the chloramine and 90 mg (14 mol % relative to chloramine) of azacyclononane in 14.5 ml of 80% dioxane – 20% water (v/v) was prepared. The flask was flushed with nitrogen, then 1.5 g of silver perchlorate added with stirring. A light brown precipitate formed. The mixture was stirred under nitrogen in a water bath at 22 °C for 40 min, when no chloramine remained. The solution was acidified with hydrochloric acid (p*H* 3) and any remaining silver ion precipitated using aqueous sodium chloride solution. After filtration the solution was taken to dryness under reduced pressure. The base was liberated with sodium hydroxide, and extracted into ether. After removal of the ether it was distilled under 15 mm pressure (bath at 70°), yielding 504 mg of oil. This consisted of indolizidine and azacyclononane in the ratio 4.7:1 (g.l.c. on column B at 125 °C). The yield of indolizidine (correcting for samples removed for titration) was 68%.

A comparable run using 29 mol % of azacyclononane relative to chloramine gave a 56% yield of indolizidine.

(2) With Silver Perchlorate and Trimethylamine in Acetonitrile–Water

A mixture of 4.48 mmol of the chloramine, 0.42 mmol of trimethylamine, and 1.50 g (7.2 mmol) of silver perchlorate in 30 ml of 90% acetonitrile – 10% water gave an opalescent solution and a small white precipitate. The flask was flushed with nitrogen. Titration showed the following reaction rate: 1 h, 7%; 2 h, 28%; 3 h, 56%; 4 h, 83%; 5 h, 95%; 5.5 h, 97.5%. The remaining 27.5 ml was left overnight under nitrogen, then taken to p*H* 5 using dilute hydrochloric acid. The rest of the silver ion was precipitated using sodium chloride. The filtered solution was evaporated to *ca.* 1 ml under reduced pressure. Acetic anhydride (5 ml) and 1 g of anhydrous sodium acetate were added and the solution heated on the steam bath for 1 h. Methanol was then added and the solution refluxed for 0.5 h to destroy excess anhydride. The methanol and methyl acetate were removed under reduced pressure. The acetic acid was neutralized and the bases liberated using solutions of first sodium carbonate then sodium hydroxide. The crystalline mush was extracted thoroughly with ether (4 × 20 ml). Fifty milliliters of the ether was concentrated to 5 ml, then a saturated solution of picric acid in ether was added. The 401 mg of crystalline picrate was recrystallized from methanol, giving 316 mg, m.p. 230°, identical to indolizidine picrate. This corresponded to a 58% yield of indolizidine.

The remaining 30 ml of ether was extracted with dilute sulfuric acid, then water, dried, and concentrated. The 62 mg

Can. J. Chem. Downloaded from www.nrcresearchpress.com by 210.87.254.42 on 09/05/12
For personal use only.

of yellow amide showed i.r. bands in CH_2Cl_2 for amide (ν_{max} 1630 and 1670 cm^{-1}) and enol ester (ν_{max} 1780 cm^{-1}). Gentle hydrolysis using sodium carbonate in hot aqueous methanol converted the enol ester to amide aldehyde (ν_{max} ($CHCl_2$) 1722, 1665 cm^{-1}). The estimated amount of this was 10%. An attempt to obtain a crystalline derivative of the aldehyde(s) was unsuccessful.

(3) With Silver Perchlorate and Azacyclononane in Acetonitrile–Water

Fifty-three milligrams (0.42 mmol) of azacyclononane was added to a solution of 3.12 mmol of chloramine in 20 ml of 90% acetonitrile – 10% water (v/v). The p*H* of the solution was 10. After addition of 1.68 g (8.1 mmol) of silver perchlorate the p*H* dropped to 9. The reaction mixture was left under nitrogen at room temperature. The reaction was followed by iodimetric titration. The consumption of chloramine was: 35 min, 31%; 95 min, 63%; 4 h, 89%; 6 h, 96%. The reaction mixture (17.5 ml) was left overnight under nitrogen, then the base isolated as in run A1. The 240 mg of distilled base contained 62% indolizidine and 38% azacyclononane. The indolizidine yield based on chloramine used was 42%.

(4) With Silver Perchlorate and Indolizidine in Acetonitrile–Water

A parallel run to A3 but using indolizidine as base gave practically identical kinetics. The yield of indolizidine (isolated as picrate after removal of azacyclononane as *N*-acetyl derivative as in A2) was 40%.

(5) With Silver Ammonium Ions in Aqueous Acetonitrile

A solution of 335 mg (1.45 mmol) of silver oxide was prepared in 8 ml of acetonitrile and 4 ml of 28% aqueous ammonia. This was added to a solution of 2.0 mmol of the chloramine in 9.5 ml of 90% acetonitrile – 10% water (v/v). A dark precipitate formed at once. The rate of disappearance of chloramine was: 70 min, 40%; 130 min, 55%; 190 min, 64%. A solution of 340 mg of silver oxide in 2 ml of 28% ammonia was added. After a further 1 h the reaction was 90% complete. The solution (17.5 mol) was acidified with hydrochloric acid, filtered, and evaporated to small volume. The product contained approximately 10 mg of ether-soluble amide (ν_{max} (CH_2Cl_2) 1670 cm^{-1}). The base was recovered as in A1 (some tar produced) and distilled. It consisted of indolizidine (22% yield) and azacyclononane (22% yield). Hence, the bulk of the chloramine must have been converted to aminoaldehydes and/or amino acids. Metallic silver was present at the end of the reaction.

(6) With Silver Oxide in Aqueous Acetonitrile

A mixture of 1.14 g of moist well-washed freshly prepared silver oxide and 19.5 ml of a solution of 2.3 mmol of the chloramine in 90% acetonitrile – 10% water (v/v) was stirred under nitrogen at room temperature. The chloramine consumption was: 30 min, 32%; 1 h, 65%; 1.5 h, 87%; 2 h, 98%. The distilled base, recovered as in the above runs was pure indolizidine in 42% yield.

(7) With Silver Oxide in Aqueous Dioxane

An identical run to A6, using 80% dioxane – 20% water as solvent but identical silver oxide, showed a marked induction period. The rate was: 30 min, 7%; 1 h, 51%; 2 h, 86%; 3 h, 94%; 5 h, 100%. The distilled basic product had a composition 98.5% indolizidine and 1.5% azacyclononane. The indolizidine yield was 51%.

In another run which showed an even more pronounced induction period (5% reaction in 2 h; total time 8 h) the yield of indolizidine was 60%.

In a run with 21% reaction in 4 h, addition of 4 mol % of sodium hydroxide relative to chloramine, accelerated the reaction dramatically (complete in one more hour). A 52% yield of pure indolizidine was recovered.

In a run where presumably the silver oxide was not as thoroughly washed free of hydroxide ion, the reaction was complete in 1.5 h. The yield of pure indolizidine was 58%.

(8) With Silver Oxide and 10 Mol % Ammonia

A solution of 574 mg (4.5 mmol) of *N*-chloroazacyclononane in 25 ml of 80% dioxane – 20% water (v/v) was prepared. Silver oxide was prepared from 2.26 g (13 mmol) of silver nitrate then washed free of alkali. To 10 ml of the chloramine solution under nitrogen was added 40% of the silver oxide and the mixture stirred. The extent of reaction was: 1 h, 4%; 2 h, 58%; 3 h, 91.5%; 4 h, 100%. The recovered distilled base was pure indolizidine.

To the remaining 15 ml of chloramine solution was added 3.9 mg (0.23 mmol) of ammonia in water (0.14 ml) and the remaining silver oxide. The mixture was stirred under nitrogen. The rate of chloramine reaction was: 1 h, 66%; 2 h, 96%; 3 h, 100%. The product after distillation was pure indolizidine in a yield of 55% (picrate, m.p. 229–230° without recrystallization; mixed m.p. with authentic indolizidine picrate 230° dec.). The distillation residue, and the polymer produced on the isolation weighed 69 mg.

(B) N-Chloroazacyclooctane

(1) With Silver Oxide in 90% Acetonitrile – 10% Water (v/v)

To a solution of 2.98 mmol of the chloramine in 15 ml of solvent was added well-washed silver oxide from 2.44 g (14 mmol) of silver nitrate. The solution was stirred under nitrogen. The rate of chloramine reaction was: 1 h, 62%; 2 h, 93%; 3 h, 98%. After one extra hour the 18 ml of reaction mixture was acidified using hydrochloric acid, filtered, and the filtrate taken to a syrup under reduced pressure. The base was liberated using sodium hydroxide then extracted into ether. The recovered base was distilled, giving 213 mg (72% yield) of pyrrolizidine containing a trace of azacyclooctane.

(2) With Silver Oxide in Aqueous Dioxane

Well-washed silver oxide from 2.54 g (15 mmol) of silver nitrate was added to a solution of 3.1 mmol of the chloramine in 15 ml of 80% dioxane – 20% water, then the mixture stirred under nitrogen. The reaction was autocatalytic with the following percentage of chloramine reacted: 1 h, 18%; 2 h, 51%; 3 h, 78.5%; 5 h, 100%. The product, worked-up as in B1 gave a 66% yield of pyrrolizidine picrate, m.p. 258°.

(3) With Silver Perchlorate and Azacyclooctane in 90% Acetonitrile

A solution of 4.4×10^{-3} mol of *N*-chloroazacyclooctane and 9.5×10^{-4} mol of azacyclooctane was prepared in 40 ml of 90% acetonitrile – 10% water. This was split for parallel reactions in air and under nitrogen.

(*a*) Under nitrogen: The solution (25 ml) was stirred under nitrogen, then 1.58 g (7.6 mmol) of silver perchlorate added. The extent of reaction was 11% in 2 h, 72.5% in 9.5 h, and 98% in 21 h. The yield of pyrrolizidine was 50% and of azacyclooctane 13%. The silver chloride precipitate contained approximately 5 mg of silver metal.

Can. J. Chem. Downloaded from www.nrcresearchpress.com by 210.87.254.42 on 09/05/12
For personal use only.

(*b*) In air: Silver perchlorate (1.07 g, 5.16 mmol) was added to 15 ml of the solution, which was then stirred in air. The extent of reaction was 10% in 9.5 h, 35% in 21 h, and 84% in 68 h. The reaction was pushed to completion by addition of 20 mg of amine and stirring for a further 24 h. The product on work-up contained no pyrrolizidine, but gave azacyclooctane in 50% yield.

(C) N-Chloroazacycloheptane

(1) With Silver Perchlorate and Azacycloheptane in Aqueous Dioxane

Silver perchlorate (4.18 g, 20 mmol) was added to 30 ml of 80% dioxane – 20% water (v/v) containing 130 mg (1.3 mmol) of azacycloheptane and 11.46 mmol of *N*-chloroazacycloheptane. An autocatalytic reaction ensued. The rate of disappearance of chloramine was: 1 h, 10%; 2 h, 21%; 4 h, 58%; 6 h, 100%. The reaction mixture was worked-up as in run A2 giving an ether-insoluble tar, a small amount of oily tertiary amine picrate, and a 56% yield of *N*-acetylazacycloheptane.

(2) With Silver Oxide

Identical runs using the same silver oxide were made in two solvents. A solution of 5.9 mmol of chloramine in 25 ml of solvent, and silver oxide from 2.57 g (15 mmol) of silver nitrate was stirred under nitrogen at room temperature. The reaction in 90% acetonitrile – 10% water (36% in 5 h) was somewhat faster than that in 80% dioxane – 20% water (7% in 5 h) but was much slower than reactions of the larger-ring chloramines. The reaction in acetonitrile was complete after 22 h, but the one in dioxane was only 91% complete in that time. The base hydrochlorides were obtained as gums as in run 1. They were triturated with ether to remove neutral products. Chloroform solutions of the remaining hydrochlorides showed strong bands at 1655 cm^{-1} and weaker bands at 1722 cm^{-1} attributable to immonium ion and corresponding aldehyde, respectively. The bases were isolated using successively sodium carbonate and ether and sodium hydroxide and ether. A major product with much longer retention time than azacycloheptane (22 and 5 min respectively, column B at 110°) was present, presumably amino aldehyde. However, only *N*-acetylazacycloheptane was recovered after acetylation of the bases.

(D) N-Chloroazacyclodecane

(1) With Silver Oxide

The chloramine was inert to well-washed silver oxide in aqueous dioxane under nitrogen, but in one case striking autocatalysis was observed. The reaction was accelerated by addition of catalytic amounts of ammonia, trimethylamine, or azacyclodecane. In each case the main products isolated were a polymer (*ca.* 80% yield) and azacyclodecane (5–10% yield).

(2) With Silver Perchlorate and Azacyclodecane in Aqueous Dioxane

A solution of 3.78×10^{-3} mol of *N*-chloroazacyclodecane, 4.6×10^{-4} mol of azacyclodecane, and 1.28 g (6.2 mmol) of silver perchlorate in 20 ml of 80% aqueous dioxane was stirred under nitrogen. The extent of reaction was: 1 h, 25%; 3 h, 60%; 5 h, 73%. The remaining 17.5 ml of mixture was then stirred overnight to ensure complete reaction, acidified with hydrochloric acid, and the base recovered as in run A1. The ether and pentane-soluble base gave 208 mg of picrate. The g.l.c. (column B at 150°) showed it to contain an approximate 2% yield of each of 1-azabicyclo[5,3,0]decane and quinolizidine, and 11% of azacyclodecane (the amount added). The ether-insoluble polymeric base weighed 380 mg (83% yield). Thus the major product as in all other runs was aldimine. In a comparable run in air less than 10% of the chloramine reacted in 24 h.

Homolytic Medium Ring Reactions

(E) N-Chloroazacyclononane

(1) With Tollens' Silver in Aqueous Dioxane

A solution of 4.24 mmol of the chloramine (by iodimetry) in 20 ml of 80% dioxane – 20% water was prepared. Tollens' silver corresponding to 1.19 g (7 mmol) of silver nitrate was added to 15 ml of this solution and the mixture stirred under nitrogen. The amount of chloramine reacted was: 1 h, 71%; 2 h, 89%; 3 h, 93%. Fresh Tollens' silver was added, driving the reaction rapidly to completion. The solid was removed by filtration. By ammonia extraction and reprecipitation of the silver chloride, it was found to contain 156 mg of silver chloride. This represents approximately 40% of the chloramine reacted. The filtrate was titrated using dilute hydrochloric acid. The free base corresponded to 41% of the chloramine. When the base was liberated from the hydrochloride (NaOH) and extracted into ether some dark tar was formed. The composition of the ether-soluble base was 63% indolizidine and 37% azacyclononane by g.l.c. analysis on column B. The yield of indolizidine was 48%.

A sample of the total hydrochloride from the reaction contained 22.84% chlorine. Calculated for indolizidine hydrochloride, 21.8%.

(2) With Tollens' Silver in Aqueous Acetonitrile

A solution of 3.27 mmol of the chloramine in 25 ml of 84% acetonitrile – 16% water (v/v) was prepared. To 20 ml of this solution was added Tollens' silver from 0.72 g (4.25 mmol) of silver nitrate. The mixture was stirred under nitrogen. The chloramine reacted was: 1 h, 64%; 2 h, 75%. Tollens' silver from 0.39 g (2.3 mmol) of silver nitrate was added and stirring continued. After two more hours no chloramine remained. The silver chloride produced was 32% of theoretical and the free base present was 43% of theoretical. The liberated ether-soluble base (tar formed) contained 61% indolizidine and 39% azacyclononane. The yield of indolizidine was approximately 40%. The total base hydrochloride contained 23.25% halogen (calculated for indolizidine hydrochloride, 21.8%). Its i.r. spectrum contained no carbonyl or immonium ion bands.

In another run using 3.18 mmol of chloramine in 25 ml of 84% acetonitrile – 16% water, and silver from 1.42 g (8.35 mmol) of silver nitrate, the reaction was 97% complete in 1 h and complete in 2 h. The basic product was acetylated. The tertiary base gave a picrate, m.p. 230° dec., identical to indolizidine picrate. The *N*-acetyl derivative was mainly *N*-acetyl azacyclononane, but contained 4.25% chlorine. (Calculated for *N*-acetyl chloroazacyclononane, 17.42%.) The silver chloride produced corresponded to 33% of the reacted chloramine.

(3) With Ferrous Chloride in Aqueous Dioxane

Ferrous chloride tetrahydrate (66 mg, 0.33 mmol) was added to a solution of 530 mg (3.3 mmol) of the chloramine in 10 ml of 80% dioxane – 20% water (v/v). The mixture was stirred in the dark under nitrogen. Aliquots were removed at intervals, diluted with ether, the iron salts removed by a sodium carbonate wash, then the residual chloramine determined by iodimetry. The reaction was complete in 4 h.

Can. J. Chem. Downloaded from www.nrcresearchpress.com by 210.87.254.42 on 09/05/12
For personal use only.

The basic product was recovered as hydrochloride, then acetylated as in run A2. The tertiary base gave 561 mg of picrate, which after one recrystallization from methanol had m.p. 230–231° and proved identical to indolizidine picrate. The yield of indolizidine in this and other runs averaged near 50%.

(F) N-Chloroazacyclooctane

(1) With Tollens' Silver in Aqueous Dioxane

Tollens' silver from 2.05 g (12 mmol) of silver nitrate was added to 20 ml of a solution of *N*-chloroazacyclooctane (560 mg, 3.8×10^{-3} mol) in 80% dioxane – 20% water (v/v) under a nitrogen atmosphere. After 1 h, 80% of the chloramine had reacted; after 1.5 h, 96%, and 3.5 h, 97.5%. The 18 ml of mixture was filtered and the filtrate acidified to Congo red with hydrochloric acid. The solution was evaporated to a volume of a few milliliters on a rotating evaporator in a bath at 50°. The base was recovered by exhaustive extraction of the solution after basification with sodium carbonate, then sodium hydroxide. Some tar formed. The ether-soluble base was distilled (bath 70°, 15 mm), leaving a small residue. The distilled base (254 mg) was estimated by g.l.c. on column B to contain 195 mg of pyrrolizidine, the remainder being azacyclooctane. The yield of pyrrolizidine corrected for samples removed for titration was 50%.

The amount of silver chloride (99 mg) produced corresponded to a chain length of approximately five molecules of chloramine for each atom of silver converted.

(2) With Ferrous Chloride in Aqueous Dioxane

In two runs using 10 mol % of ferrous chloride tetrahydrate in 80% dioxane – 20% water, following the conditions in section E1, the reaction was complete in 4 h. Work-up as in E1 gave an average of 26% yield of picrate, m.p. 258–260°, undepressed with pyrrolizidine picrate.

(G) N-Chloroazacyclodecane

(1) With Ferrous Chloride in Aqueous Dioxane

The reaction was run as for *N*-chloroazacyclononane (see E3). The average yield of tertiary base estimated by removal of secondary base by acetylation was 39%. It gave a picrate, m.p. 220–221° after recrystallization from methanol. A mixture with authentic 1-azabicyclo[5.3.0]decane picrate (m.p. 210–221°) (40) melted at 210–221°. A g.l.c. examination of the base from these samples showed it to be a mixture of 86% 1-azabicyclo[5.3.0]decane and 14% quinolizidine. Similarly, g.l.c. of the base recovered from the total tertiary amine picrate showed it to contain approximately 45% of quinolizidine and 55% of azabicyclo[5.3.0]decane.

(2) With Silver in Acetonitrile and Acetic Anhydride

Tollens' silver from 3.0 g (17.6 mmol) of silver nitrate was added under nitrogen to a solution of 3.08×10^{-3} mol of *N*-chloroazacyclodecane in a mixture of 18 ml of dry acetonitrile and 2 ml of acetic anhydride. The extent of reaction was: 1 h, 35%; 3 h, 60%; 5.5 h, 75%; 21 h, 97%. The yield of tertiary base was 16% consisting of azabicyclo-[5.3.0]decane and quinolizidine in the ratio of 1 : 1.17.

N-Chloroisoquinuclidine Reactions

(a) With Silver Nitrate

A solution of 314 mg of the chloramine and 400 mg of silver nitrate powder was dissolved in 10 ml of reagent methanol. The solution was refluxed gently. After 1 h only 7% of the chloramine remained. Excess silver nitrate was then added, after which half an hour reflux completed the reaction. The excess silver ion was precipitated using sodium chloride solution, the solid removed by filtration, and the filtrate evaporated to near dryness under reduced pressure at 25 °C. Sodium hydroxide solution was added, and the base extracted into pure ether. The 224 mg of residue after evaporation of the ether gave only one peak (column A, 124°). Its n.m.r. spectrum contained a poorly defined one-hydrogen doublet centered at δ 3.80 and a methoxyl signal at δ 3.41, and was completely consistent with the product being the methoxy base **6**.

(b) With Silver Oxide

To a solution of 3.18×10^{-3} mol of chloramine in 15 ml of reagent methanol was added silver oxide (thoroughly washed with water, then methanol) from 0.5 g (2.9 mmol) of silver nitrate. The mixture was stirred under nitrogen. After reaction of 14% of the chloramine in the first hour the decomposition became very slow. After 21 h, 43% had reacted. Silver oxide from 1.55 g (9.1 mmol) of silver nitrate was added and the stirring continued. After a further 21 h, 78% had reacted. The basic solution was filtered and the filtrate taken to p*H* 3 with dilute hydrochloric acid in methanol. The solution was then taken to a volume of *ca.* 1 ml under reduced pressure and the residue extracted with pentane to remove any unchanged chloramine. After addition of 1 ml of saturated sodium carbonate solution followed by thorough extraction by ether, sodium hydroxide was added to the solution. It was again thoroughly extracted with ether. The combined ether solutions were distilled to give an oil. The g.l.c. on column B at 120° showed the volatile product to be almost pure isoquinuclidine, with only a few percent of the methoxy base **6**.

An experiment using 2.4×10^{-3} mol of chloramine and silver oxide from 423 mg (2.5 mmol) of silver nitrate in 15 ml of methanol was extremely slow at room temperature (18% in 20 h). However, refluxing for 3.5 h drove the reaction to completion. Again the volatile product was mainly isoquinuclidine with 14% of methoxy base **6**.

(c) With Metallic Silver

To a solution of 4.1 mmol of the chloramine in 19 ml of reagent methanol was added Tollens' silver from 1 g (5.9 mmol) of silver nitrate. The suspension was stirred under nitrogen. After 1 h, 72% of the chloramine had reacted; after 1.5 h, 87% reacted. Tollens' silver from 0.6 g of silver nitrate was added. After a further 4 h of stirring only 5% of the chloramine remained. The 17 ml of mixture was filtered and the basic solution (p*H* 10.7) titrated with 0.1 *N* hydrochloric acid (28 ml required, theory after subtracting the amounts removed by titration is 35 ml). The solution was taken to dryness under reduced pressure. The base was recovered by basifying with sodium carbonate (to avoid destroying the imine) extracting with ether, then basifying with sodium hydroxide and re-extracting with ether. The 360 mg of oil recovered from the ether showed two g.l.c. peaks corresponding to a new compound and isoquinuclidine in the approximate ratio of 1.75:1 (column A, 124°, 10 min, and 8 min, respectively). An ether solution of the mixture slowly deposited a white polymer, while a corresponding drop in intensity of the g.l.c. peak for the new compound occurred. Reduction of the mixture by sodium borohydride in methanol converted the new compound to isoquinuclidine (single g.l.c. peak).

In other runs the new compound was found to give an i.r. peak in ether at 1665 cm^{-1} and a —CH=N— signal at δ 9.7 in its n.m.r. spectrum. It was never obtained pure, but

Can. J. Chem. Downloaded from www.nrcresearchpress.com by 210.87.254.42 on 09/05/12
For personal use only.

this evidence is consistent with it being dehydroisoquinuclidine **7**. The silver chloride was extracted from the mixture with silver using ammonia. It was then reprecipitated and weighed. In each case it exceeded 94% of theoretical for one molar equivalent.

(d) With Metallic Silver and Silver Nitrate

The chloramine reacted very slowly with silver nitrate in methanol at 5 °C (5% in 2 h). Tollens' silver from 0.75 g of silver nitrate, and 716 mg of powdered silver nitrate were added to a solution of 550 mg of the chloramine in 15 ml of methanol at 5 °C. After 1 h, 41% of the chloramine had reacted. Tollens' silver from 0.75 g of silver nitrate was added and stirring continued. After one more hour at 5°, 59% had reacted. After a further 4 h at 15° the reaction was 91% complete. The reaction was allowed to run to completion overnight, then filtered. The solution was titrated using 0.1 *N* hydrochloric acid (13 ml required) to p*H* 4.5, then the silver ions in solution completely precipitated using sodium chloride. After filtration the solution was taken to dryness under reduced pressure. The liberated base showed the presence of imine (ν_{max} 1665 cm^{-1}; n.m.r. signal at δ 9.7; g.l.c. peak after 16.5 min, column C at 115°) methoxy base 6 (g.l.c. retention time 6.8 min, column C, 115°) and isoquinuclidine (g.l.c. retention time 4.5 min), in the ratio of 1:1.5:2.7. Sodium borohydride reduction of the mixture in methanol removed the 16.5 min g.l.c. peak.

N-Chloropiperidine

(1) With Tollens' Silver in Tetrahydrofuran

Tollens' silver from 2.1 g (12.3 mmol) of silver nitrate was added to a solution of 1.25 g (11.4 mmol) of the chloramine in 30 ml of 80% tetrahydrofuran – 20% water (v/v). The mixture was stirred under nitrogen at room temperature in diffuse light. The rate of chloramine reaction was: 50 min, 16%; 95 min, 41%; 7 h, 89%. The reaction was pushed to near completion by addition of more silver. After removal of the solid by filtration from the remaining 27 ml of the reaction mixture it was acidified using hydrochloric acid (7.8 mmol required, theoretical for no chain reaction, 10.5 mmol).

Forty percent of the solution was taken to near dryness under reduced pressure. The residue was extracted with ether, giving 14 mg of ether-soluble oil. This contained at least four components. Its n.m.r. spectrum (signal between δ 1.1 and 2.6 and broad signals centered at δ 3.4 and 3.9) resembled that expected for polymers of tetrahydrofuran. The base recovered from the salts was shown by g.l.c. on column B at 130° to be mainly piperidine with 6% of each of two amines with longer retention time.

To the remaining 60% of the solution was added 1 g of dinitrophenylhydrazine as its hydrochloride in methanol. After 1 h at room temperature the solution was evaporated to small volume under reduced pressure at 60°. The residue was distributed between dilute hydrochloric acid and chloroform. The chloroform-soluble fraction was a crystalline solid (150 mg). It was recrystallized twice from methanol–water, giving crystals with m.p. 115°.

Anal. Calcd. for $C_{10}H_{12}N_5O_4$: C, 44.78; H, 4.51; N, 20.89. Found: C, 44.69; H, 4.63; N, 21.11.

Its m.p. (lit. (41) m.p. 118°) and n.m.r. spectrum in $CDCl_3$ (δ 1.62, 2H singlet, absent when D_2O added; 1.8–2.9, 4H multiplets; 2H triplet centered at 3.88 with $J_1 = J_2 = 6$ Hz; 1H doublet centered at 9.2, $J = 2.5$ Hz) in addition to the aromatic hydrogens, were consistent with the compound being the 2,4-dinitrophenylhydrazone of γ-hydroxybutyraldehyde.

(2) With Tollens' Silver and Styrene in Acetonitrile

Freshly distilled acetonitrile and styrene (50°, 8 mm) were used. A solution was prepared of 1.25 g of the chloramine (10.4 mmol) and 1.0 g (9.6 mmol) of styrene in 19 ml of acetonitrile. This was flushed with nitrogen. While stirring under nitrogen, Tollens' silver from 1.13 g (6.6 mmol) of silver nitrate was added to the solution. After 0.5 h a second identical quantity of silver was added. The extent of chloramine reaction was: 2 h, 16%; 4 h, 23%. At this time, silver from 3 g (17.5 mmol) of silver oxide was added, and the stirring continued under nitrogen. In the total reaction time of 6 h, 45% had reacted; 9 h, 76%; 10.3 h, 87%.

The yellow solution was filtered and the precipitate washed with acetonitrile. Addition of 0.6 ml of glacial acetic acid reduced the p*H* to approximately 5. The solution was then evaporated to a volume of *ca.* 3 ml on a rotating evaporator in a bath at 45°. The residue was taken up in methylene chloride, extracted twice with 10 ml of 1 *N* sulfuric acid, then washed with sodium carbonate solution. The neutral product after heating under 0.5 mm pressure on the steam bath weighed 90 mg.

The base was recovered from the acid solution using methylene chloride as solvent. After removal of the methylene chloride the base was taken up in ether and the ether solution filtered from a small amount of solid. The ether yielded 675 mg of orange oil after warming to 40° under water pump vacuum. In an attempt to distill the oil in a chain of bulbs only a small quantity of crystalline solid came over at a bath temperature of 65° under 8 mm pressure. Under 0.5 mm at 80°, 54 mg of oil distilled, and a second fraction of 81 mg distilled at 115–120°. Some tar formed, and the ether-soluble part of the undistilled material weighed 391 mg. By comparison of the n.m.r. signals for aromatic hydrogens to the signals between σ 1.1 and 1.8 (isolated CH_2 groups) the ratio of piperidine groups to phenylethyl groups in the fractions was: 80°, 2.3:1; 120°, 2:1; and the residue, 1.3:1. All three fractions were inert to acetic anhydride at 90° (0.5 h) and the n.m.r. spectra of the recovered bases were unchanged. The chlorine content of the non-volatile base was 1.44%.

The amount of silver chloride produced in the reaction (1.03 g) was roughly 86% of 1 mol (compensated for incomplete reaction and aliquots removed).

We are grateful to M. G. Reinecke and N. J. Leonard for reference samples of bicyclic amines. We thank Mr. H. Seguin for analyses, Mrs. Joyce Lemke and Mr. M. Lesage for technical assistance, and Dr. G. Bernath for preparation of isoquinuclidine. We thank the Abbot Laboratories for financial support.

1. R. S. NEALE, M. R. WALSH, and N. L. MARCUS. J. Org. Chem. **30**, 3683 (1965).
2. (*a*) R. S. NEALE, N. L. MARCUS, and R. G. SCHEPERS. J. Am. Chem. Soc. **88**, 3051 (1966); M. OKAHARA, T. OHASHI, and S. KOMORI. Tetrahedron Lett. 1629 (1967). (*b*) O. E. EDWARDS, J. M. PATON, M. H. BENN, R. E. MITCHELL, C. WATANATADA, and K. N. VOHRA. Can. J. Chem. **49**, 1648 (1971).
3. W. LWOWSKI. *Editor*. Nitrenes. Interscience Publishers. New York. 1970. pp. 185–224.

4. I. BROWN and O. E. EDWARDS. Can. J. Chem. **45**, 2599 (1967); ref. 3, pp. 225–243.
5. Reference 3. pp. 405–419.
6. O. E. EDWARDS, D. VOCELLE, J. W. APSIMON, and F. HAQUE. J. Am. Chem. Soc. **87**, 678 (1965).
7. A. C. COPE, M. M. MARTIN, and M. A. MCKERVEY. Quart. Rev. **20**, 119 (1966).
8. E. FISCHER. Ann. **190**, 67 (1877). See also M. N. SHENG and A. R. DAY. J. Org. Chem. **28** 736 (1963).
9. S. E. MANAHAN and R. T. IWAMOTO. J. Electro. Anal. Chem. 213 (1967).
10. P. G. GASSMAN and B. L. FOX. J. Am. Chem. Soc. **89**, 338 (1967).
11. O. E. EDWARDS, F. H. CLARKE, and B. DOUGLAS. Can. J. Chem. **32**, 235 (1954).
12. O. E. EDWARDS, M. LOS, and L. MARION. Can. J. Chem. **37**, 1996 (1959).
13. A. CAMBRON and W. A. ALEXANDER. Can. J. Chem. **34**, 665 (1956).
14. T. I. TAYLOR and W. H. CONE. J. Am. Chem. Soc. **55**, 3512 (1933).
15. H. RUSCHIG, W. FIRTSCH, J. SCHMIDT-THOMÉ, and W. HAEDE. Chem. Ber. **88**, 883 (1955).
16. R. W. FRANCK and W. S. JOHNSON. Tetrahedron Lett. 545 (1963).
17. G. ADAM and K. SCHREIBER. Angew. Chem. **76**, 752 (1964).
18. C. BENEZRA and X. LUSINCHI. Can. J. Chem. **47**, 1547 (1969).
19. R. N. LOEPPKY and M. ROTMAN. J. Org. Chem. **32**, 4010 (1967).
20. P. G. GASSMAN and A. CARRASQUILLO. Chem. Commun. 495 (1969).
21. P. G. GASSMAN, F. HOYDA, and J. DYGOS. J. Am. Chem. Soc. **90**, 2716 (1968). V. RAUTENSTRAUCH. Chem. Commun. 1122 (1969). D. C. HORWELL and C. W. REES. Chem. Commun. 1428 (1969).
22. P. G. GASSMAN, G. CAMPBELL, and R. FREDERICK. J. Am. Chem. Soc. **90**, 7377 (1968).
23. P. G. GASSMAN and R. L. CRYBERG. J. Am. Chem. Soc. **91**, 2047 (1969).
24. W. NAGATA, S. HIRAI, K. KAWATA, and T. AOKI. J. Am. Chem. Soc. **89**, 5045 (1967).
25. J. D. HOBSON and W. D. RIDDELL. Chem. Commun. 1178, 1180 (1968).
26. O. E. EDWARDS and D. J. PASKOVITCH. Unpublished work.
27. H. LANKAMP, W. TH. NAUTA, and C. MACLEAN. Tetrahedron Lett. 249 (1968).
28. G. A. SWAN. J. Chem. Soc. 4822 (1965). C. H. BAMFORD. J. Chem. Soc. **12**, 17 (1939).
29. (*a*) R. E. JACOBSON, K. M. JOHNSTON, and G. H. WILLIAMS. Chem. and Ind. London, 157 (1967). (*b*) D. MACKAY and W. A. WATERS. J. Chem. Soc. (C), 813, (1966).
30. F. MINISCI and R. GALLI. Chimica e Industria (Milan). **45**, 1400 (1963).
31. D. HEMLINGER and G. OURISSON. Ann. **686**, 19 (1965); M. FISCH and G. OURISSON. Chem. Commun. 407 (1965).
32. J. G. TRAYNHAM and T. V. COUVILLON. J. Am. Chem. Soc. **89**, 3205 (1967).
33. D. H. R. BARTON, J. M. BEATON, L. E. GELLER, and M. M. PECHET. J. Am. Chem. Soc. **83**, 4076 (1961). J. KALVODA, K. HEUSLER, C. MERPTRE, P. WIELAND, G. ANNER, and A. WETTSTEIN. Gazzeta **93**, 140 (1963).
34. S. WAWZONEK and T. P. CULBERTSON. J. Am. Chem. Soc. **82**, 441 (1960).
35. T. MINISCI, R. GALLI, and G. POLLINA. Chemica e Industria (Milan), **47**, 736 (1965).
36. F. F. BLICKE and N. J. DOORENBOS. J. Am. Chem. Soc. **76**, 2317 (1954).
37. N. J. LEONARD, S. SWANN, and J. FIGUERAS. J. Am. Chem. Soc. **74**, 4620 (1952).
38. L. H. WERNER and S. RICCA. J. Am. Chem. Soc. **80**, 2733 (1958).
39. M. G. REINECKE and L. R. KRAY. J. Org. Chem. **29**, 1736 (1964).
40. N. J. LEONARD and W. C. WILDMAN. J. Am. Chem. Soc. **71**, 3089 (1949).
41. R. PAUL and S. TCHELITCHEFF. Bull. Soc. Chim. (France), 197 (1948).

Can. J. Chem. Downloaded from www.nrcresearchpress.com by 210.87.254.42 on 09/05/12
For personal use only.

The Formation of Alkenes by the Thermal Elimination Reaction of *N*-Methyl-4-Alkoxypyridinium Iodides. I. Scope of the Reaction

GEORGE H. SCHMID AND AARON W. WOLKOFF[1]

Department of Chemistry, University of Toronto, Toronto 181, Ontario

Received September 28, 1971

Twenty-one 4-alkoxypyridines and their corresponding *N*-methyl-4-alkoxypyridinium iodides have been prepared and the latter pyrolyzed at temperatures ranging from room temperature to 185° to give the olefins derived from the alkyl moiety in high yields.

On a préparé 21 alkoxypyridines-4 différents de même que les iodures correspondants *N*-méthyl-alkoxypyridinium-4; ces derniers produits ont été pyrolysés à des températures variant de la température de la pièce à 185°. Nous avons obtenu de cette façon les oléfines dérivées du groupe alkyl avec de bons rendements.

Canadian Journal of Chemistry, **50**, 1181 (1972)

Can. J. Chem. Downloaded from www.nrcresearchpress.com by 210.87.254.5 on 09/05/12
For personal use only.

In the course of an investigation of the solvolysis of a series of *N*-methyl-4-alkoxypyridinium iodides it proved impossible to prepare *N*-methyl-4-(Δ^2-cyclopentenoxy)pyridinium iodide and *N*-methyl-4-(1′-indanoxy)pyridinium iodide (1). Attempts to prepare these compounds by the treatment of neat 4-(Δ^2-cyclopentenoxy)-pyridine (**1**) and 4-(1′-indanoxy)pyridine (**2**) with methyl iodide led to the spontaneous formation of cyclopentadiene and indene respectively (Scheme 1). This elimination reaction is unusual since ethers are not generally prone to undergo this kind of elimination under these relatively mild conditions. The purpose of this paper is to report the generality of this thermal elimination reaction of *N*-methyl-4-alkoxypyridinium iodides.

Results and Discussion

The 4-alkoxypyridines used in this study were prepared by the reaction of an alkoxide with 4-chloropyridine (Scheme 2). The properties of the 4-alkoxypyridines, together with the yields and elemental analyses are given in Table 1. The

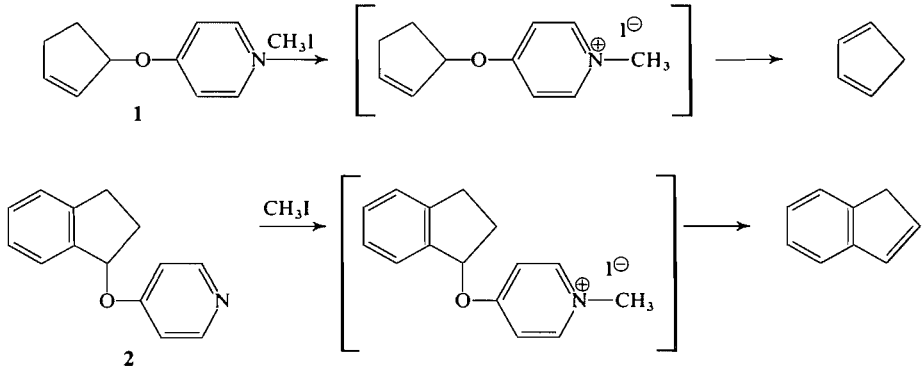

SCHEME 1

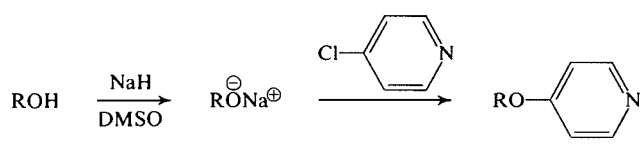

SCHEME 2

[1]Holder of NRCC Scholarship, 1967–1971.

Can. J. Chem. Downloaded from www.nrcresearchpress.com by 210.87.254.5 on 09/05/12
For personal use only.

TABLE 1. Properties of 4-Alkoxypyridines RO— 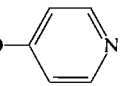

R–	% Yield	Boiling point °C (mm)	Elemental analysis[a] % Carbon Calcd.	% Carbon Found	% Hydrogen Calcd.	% Hydrogen Found	% Nitrogen Calcd.	% Nitrogen Found
Cyclopentyl	62	81 (0.075)[b]						
Cyclohexyl	67	88–92 (0.050)	74.54	74.44	8.53	8.73	7.90	8.08
Cycloheptyl	70	106 (0.075)	75.35	75.50	8.96	9.07	7.32	7.36
Cyclooctyl	36	114 (0.15)	76.06	75.99	9.33	9.66	6.82	6.80
trans-2-Methylcyclopentyl	61	75–90 (0.050)	74.51	74.41	8.53	8.40	7.90	8.01
2-Methylcyclopentyl (57.4% *cis*)	48	84–90 (0.050)						
trans-2-Methylcyclohexyl	46	102–104 (0.050)	75.35	75.68	8.96	9.03	7.32	7.44
2-Methylcyclohexyl (45.7% *cis*)	81	87 (0.020)						
2-Methylcyclohexyl (66.9% *cis*)	67	94–99 (0.050)						
Δ^2-Cyclohexenyl	51	103–104 (0.075)	Decomposed[c]					
2,2-Dimethylcyclohexyl	56	108–110 (0.10)	[d]					
Menthyl	56	113–125 (0.10)[e]	77.21	77.21	9.93	9.82	6.00	6.12
Neomenthyl	68	113–125 (0.090)[f]	77.21	77.25	9.93	10.06	6.00	5.92
n-Octyl	69	118–120 (0.20)	75.32	74.81	10.21	10.34	6.76	6.68
2-Octyl	70	99–100 (0.10)	75.32	75.39	10.21	10.29	6.76	6.92
1-Phenyl-1-propyl	88	101–105 (0.075)	78.84	78.96	7.09	7.19	6.57	6.64
1-*p*-Methoxyphenyl-1-propyl[g]	68	135–140 (0.125)[h]	74.05	74.01	7.04	6.97	5.76	5.85
1-*p*-Chlorophenyl-1-propyl	66	135–137 (0.95)	[d]					
1-*p*-Methylphenyl-1-propyl	60	133–142 (0.060)	79.26	79.45	7.54	7.55	6.16	6.25
1-Phenyl-2-propyl	24[i]	130 (0.020)	78.84	78.97	7.09	7.31	6.57	6.52
(–)-Isobornyl	44	115 (0.050)[e]	77.88	77.74	9.15	9.32	6.05	6.14
(+)-Bornyl	53	130–131 (0.075)	77.88	77.75	9.15	9.16	6.05	6.17

[a]Analytical samples were prepared by gas chromatography as described for the preparation of the cyclohexyl derivative (Experimental).
[b]Literature (1) b.p. 61–65° (0.075 mm).
[c]On attempting to prepare an analytical sample by gas chromatography (SE-30 column at 200°; flow rate of 200 ml He/min), the compound decomposed to give a product whose n.m.r. spectrum was consistent with that for 1,3-cyclohexadiene.
[d]Analyzed as methiodide derivative.
[e]Material partially solidified.
[f]Melting point 45–45.6°.
[g]An analytical sample was prepared by repeated recrystallization from pentane.
[h]Melting point 75.5–76.5°.
[i]Corrected for recovered starting alcohol; yields were not improved using the extraction procedure described in the Experimental.

Can. J. Chem. Downloaded from www.nrcresearchpress.com by 210.87.254.5 on 09/05/12
For personal use only.

preparation of 4-alkoxypyridines derived from tertiary alcohols (*e.g.* 1-methylcyclohexanol, *t*-amyl alcohol, and *t*-butyl alcohol) proved impossible undoubtedly due to the steric bulk of the alkyl groups. Attempts to separate *cis*- and *trans*-2-methylcyclohexanol by preparative g.l.c. failed, consequently, it was decided to use known *cis–trans* mixtures of the alcohol; one obtained commercially (45.1 + 1% *cis*) and another enriched in the *cis* isomer (66.9 ± 0.8% *cis*) by a spinning band distillation. Similarly pure *cis*-2-methylcyclopentanol could not be prepared in sufficient quantity to form the corresponding 4-alkoxypyridine. Again a *cis–trans* mixture was used whose composition was known.

The *N*-methyl-4-alkoxypyridinium iodides were prepared by the reaction of the 4-alkoxypyridines with methyl iodide, either neat or in ether. The properties of the *N*-methyl-4-alkoxypyridinium iodides, together with the yields and elemental analyses (where possible) are given in Table 2. In some cases where the methiodides were oils, yields were not determined and the elimination reaction was carried out directly on the oils.

The results of the elimination reactions are shown in Table 3. In most cases the product compositions are accurate within ±0.5%. In some cases where the component was present in small amounts (*ca.* 5%), the results are good to within ±1%.

Since pure *cis*-2-methylcyclohexanol could not be obtained, the result for the pyrolysis of *cis*-*N*-methyl-4-(2′-methylcyclohexoxy)pyridinium iodide was obtained by the extrapolation of the results from three *cis–trans* mixtures (including the pure *trans*-*N*-methyl-4-(2′-methylcyclohexoxy)pyridinium iodide). The result for the pyrolysis of *cis*-*N*-methyl-4-(2′-methylcyclopentoxy)pyridinium iodide was also obtained by extrapolation.

The decomposition temperatures given in Table 3 are the lowest temperatures at which the reactions could conveniently be studied. In some cases, methyl iodide was isolated along with the reaction products, making exact determination of the yields difficult. In all compounds studied the elimination did in fact take place, although for a few compounds, higher temperatures (>165°) were needed.

The elimination reaction occurs so that Saytzev orientation is observed; that is the more stable olefins are the major products. Geometrical orientation is heavily in favor of the *trans* olefin. A lack of stereospecificity is indicated by the fact that the *cis*- and *trans*-methiodides give similar (but not identical) product mixtures. Products arising from rearrangement can be seen in the case of the *n*-octyl and 2-methylcyclohexyl compounds. Compounds that are capable of forming stable carbonium ions (*e.g.* 1-*p*-methoxyphenyl-1-propanol and Δ^2-cyclohexenol) decompose spontaneously at room temperature to give the corresponding olefin.

The olefin products do not seem to have been formed under conditions of thermodynamic control. While an acid is generated, the experimental procedure involves distilling off the olefins as they are formed and consequently the olefins are in contact with the acid for only a short time. Furthermore, product composition of the pyrolysis carried out in dimethyl formamide as solvent is identical to that obtained by distilling off the olefin. In a solvent, equilibration of the olefins should be facilitated yet it is not observed. Therefore, it is concluded that isomerization of the products does not occur and since the reaction is irreversible, the products are the result of kinetic control.

Experimental

All m.p. and b.p. are uncorrected. Elemental analyses were carried out by A. B. Gygli of Toronto, Ontario.

Many of the alcohols used in this study were commercially available and were purified by distillation before use. Others were available as the corresponding ketones which were then reduced with lithium aluminum hydride to the required alcohol.

trans-2-Methylcyclohexanol, b.p. 87° (33 mm), was prepared in 38% yield by the hydroboration of 1-methylcyclohexene (3).

trans-2-Methylcyclopentanol, b.p. 144–148°, was prepared in 34% yield by the hydroboration of 1-methylcyclopentene (3).

2,2-Dimethylcyclohexanone, b.p. 49–50° (11 mm), was prepared in 42% yield by the method of Meinwald and Ouderkirk (4).

2,2-Dimethylcyclohexanol, b.p. 65° (11 mm) (lit. (5) b.p. 72° (13 mm)) was prepared in 75% yield by the lithium aluminum hydride reduction of 2,2-dimethylcyclohexanone.

(−)-Isoborneol was prepared in 50% yield according to the method of Toivonen (6), $[\alpha]_D^{22}$ −32.78° (94.7% optically pure). Gas chromatographic analysis showed the product to contain 5.8% borneol.

l-Menthone: Oxidation (7) of *l*-menthol by chromic acid, gave *l*-menthone, b.p. 85–92° (15 mm), $[\alpha]_D^{26}$ −28.4° (neat, 1 dm) (lit. (7) b.p. 66–67° (4 mm); $[\alpha]_D$ −29.9°) in 84% yield.

l-Menthol and d-Neomenthol: A mixture of these two alco-

Can. J. Chem. Downloaded from www.nrcresearchpress.com by 210.87.254.5 on 09/05/12
For personal use only.

TABLE 2. Properties of *N*-methyl-4-alkoxypyridinium iodides RO— 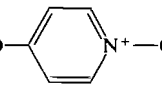 —CH_3I^-

R—	% Yield	Melting point °C	Elemental analysis[a] % Carbon Calcd.	% Carbon Found	% Hydrogen Calcd.	% Hydrogen Found	% Nitrogen Calcd.	% Nitrogen Found	% Iodine Calcd.	% Iodine Found
Cyclopentyl	88	112–114[b]								
Cyclohexyl	91	120	45.16	45.39	5.68	5.69	4.39	4.33	39.76	39.92
Cycloheptyl	91	114–115	46.86	46.98	6.05	6.17	4.20	4.24	38.08	38.16
Cyclooctyl	[c]	Oil								
trans-2-Methylcyclopentyl	57	100–101.5	45.16	44.51	5.68	5.92	4.39	4.43	39.76	39.60
2-Methylcyclopentyl (57.4% *cis*)	[c]	Oil								
trans-2-Methylcyclohexyl	87[d]	Oil	46.86	42.35	6.05	5.65	4.20	3.94	38.08	40.45
2-Methylcyclohexyl (45.7% *cis*)	[c]	Oil								
2-Methylcyclohexyl (66.9% *cis*)	[c]	Oil								
Δ^2-Cyclohexenyl[e]	138[f]	93–95								
2,2-Dimethylcyclohexyl	72	115–116	48.34	47.85	6.39	6.48	4.03	4.16	36.55	36.84
Menthyl	65	165.5–166.5	51.21	51.31	6.98	6.99	3.73	3.79		
Neomenthyl	77	162.5–163.5	51.21	51.41	6.98	6.90	3.73	3.71		
n-Octyl	69	88–89	48.15	48.10	6.93	6.91	4.01	3.93	36.34	36.51
2-Octyl	[c]	Oil								
1-Phenyl-1-propyl	97	Oil								
1-*p*-Methoxyphenyl-1-propyl	93[g]	94–95								
1-*p*-Chlorophenyl-1-propyl	90	124–125	46.12	46.19	4.64	4.56	3.59	3.64		
1-*p*-Methylphenyl-1-propyl	96[h]	138–140[i]								
1-Phenyl-2-propyl	[c]	Oil								
(−)-Isobornyl	90[j]	152–153.5	51.48	51.27	6.48	6.37	3.75	3.84	34.00	34.40
(+)-Bornyl	75	159–160	51.48	51.79	6.48	6.59	3.75	3.83		

[a]Analytical samples were prepared by recrystallization from acetone–ether as described in the Experimental; in some cases no analysis was done for iodine.
[b]Literature (1) m.p. 115.5–117°.
[c]Yield not determined; pyrolysis done directly on oil.
[d]An attempt was made to prepare an analytical sample by adding excess methyl iodide to a chromatographically pure sample of the pyridine ether followed by removal of the excess methyl iodide under vacuum (0.1 mm), but the analysis was not acceptable; no analysis was done on oils after this point.
[e]Decomposed at room temperature to give 1,3-cyclohexadiene.
[f]Probably contains some excess methyl iodide.
[g]Slowly decomposed at room temperature to give anethole.
[h]Sample turned yellow on standing; no analysis done.
[i]Decomposed at melting point.
[j]$[\alpha]_D^{23}$ −60.58° (*c* 18, EtOH).

Can. J. Chem. Downloaded from www.nrcresearchpress.com by 210.87.254.5 on 09/05/12
For personal use only.

TABLE 3. Products from pyrolysis of *N*-methyl-4-alkoxypyridinium iodides

R–	Decomposition temperature[a] (°C)	Product(s)[b]		% Yield[c]
Cyclopentyl	165	Cyclopentene		100
Cyclohexyl	165	Cyclohexene		90
Cycloheptyl	165	Cycloheptene		87
Cyclooctyl[d]	145–155	*cis*-cyclooctene[e]		76
trans-2-Methylcyclopentyl	145	1-Methylcyclopentene, 98.3%	3-Methylcyclopentene, <0.7%; [f] 1%	84
cis-2-Methylcyclopentyl[h]	145	1-Methylcyclopentene, 85.2%	3-Methylcyclopentene, 13.8%; [f] 1%	
trans-2-Methylcyclohexyl[d]	160–165	1-Methylcyclohexene, 86.2%	3-Methylcyclohexene, 8.7%; Methylene cyclohexane, 5.1%	>100[g]
cis-2-Methylcyclohexyl[h]	160–165	1-Methylcyclohexene, 95.1%	3-Methylcyclohexene, 4.9%; Methylene cyclohexane, <1%	
Δ^2-Cyclohexenyl[i]	25	1,3-cyclohexadiene		[j]
2,2-Dimethylcyclohexyl	190–200[k]	At least six products as seen gas chromatography[l]		>100[g]
Menthyl	170	Δ^2-Menthene, 11.1%	Δ^3-Menthene, 88.9%	>100[g]
Neomenthyl	160	Δ^2-Menthene, 4.8%[m]	Δ^3-Menthene, 95.2%[m]	>100[g]
1-Octyl	165[n]	Octene-1, 96.6%	*trans*-2-Octene, 3.4%	>100[g]
2-Octyl[d]	165	*trans*-2-Octene, 68.3%	*cis*-2-Octene, 23.9%; 1-Octene 7.8%	>100[g]
1-(*p*-Methoxyphenyl)-1-propyl	150[o]	*trans*-1-(*p*-Methoxyphenyl)-propene, >99.9%	*cis*-1-(*p*-Methoxyphenyl)-propane, <0.1%	[j]
1-Phenyl-1-propyl[a]	150[p]	*trans*-1-Phenylpropene, 98.0%	*cis*-1-Phenylpropene, 1.7%	67
1-(*p*-Chlorophenyl)-propyl	140	*trans*-1-(*p*-Chlorophenyl)-propene, 96.0%	*cis*-1-(*p*-Chlorophenyl)-propene, 4%	[j]
1-(*p*-Methylphenyl)-propyl	110	*trans*-1-(*p*-Methylphenyl)-propene, >99.5%	*cis*-1-(*p*-Methylphenyl)-propene, <0.5%	27
1-Phenyl-2-propyl[d]	150	*trans*-1-Phenylpropene, 91.7%	*cis*-1-Phenylpropene, 6.7%	100[g]
Isobornyl	150	Camphene, 99.1%[q]	Tricyclene, 0.9%[q]	60
Bornyl	185	Camphene, 87.9%[r]	Tricyclene, 2.1%[r]	28

[a]See text for explanation.
[b]Products were determined by gas chromatography and/or n.m.r. (unless otherwise stated); for experimental limits, see text.
[c]Reactions were studied over a period of 3 h (unless otherwise stated).
[d]Methiodide was an oil, so reaction done *in situ* and yields calculated on basis of weight of starting 4-alkoxypyridine.
[e]Product determined to be *cis* isomer by i.r. spectroscopy (2) (absorption at 11.2 and 13.3 μ; no absorption at 11.8 and 12.6 μ).
[f]1% unknown product; shown not to be methylenecyclopentane.
[g]Some methyl iodide produced, making yield over 100%; yields could not be determined exactly but were generally quite high (see text).
[h]Extrapolated graphically and normalized to 100%.
[i]Decomposed spontaneously on addition of methyl iodide.
[j]Yield not determined.
[k]When done at a lower temperature, relatively little product was obtained (37%).
[l]No further analysis attempted.
[m]Values corrected for 1.2% menthol in starting alcohol.
[n]Temperature accidently rose to 250° for 1/2 h.
[o]Decomposition complete after 10 min.
[p]Compound actually decomposed at a much lower temperature.
[q]Values corrected for 5.8% borneol in starting alcohol.
[r]Values corrected for 2.7% isoborneol in starting alcohol.

Can. J. Chem. Downloaded from www.nrcresearchpress.com by 210.87.254.5 on 09/05/12
For personal use only.

hols was prepared in 98% yield by aluminum isopropoxide reduction of *l*-menthone (8).

d-Neomenthol was isolated from the mixture of *l*-menthol and *d*-neomenthol by making use of the fact that *p*-nitrobenzoyl chloride reacts 16.3 times as fast with *l*-menthol as with *d*-neomenthol (9). In this way a 72% yield of *d*-neomenthol was prepared; b.p. 85° (10 mm) $[\alpha]_D^{16}$ 17.80° (homog: 1 dm). The specific rotation of the prepared neomenthol corresponds to a mixture of 98.8% *d*-neomenthol and 1.2% *l*-menthol.

1-p-Methylphenyl-1-propanol, b.p. 105° (12 mm) (lit. (10) b.p. 115–116° (13 mm)), was prepared by reaction of ethyl magnesium bromide with *p*-tolualdehyde.

Δ^2-*Cyclohexenol*, b.p. 61–64° (11 mm) (lit. (11) 164–166°), was prepared from cyclohexene according to the method of Alder and Flock (11).

4-Chloropyridine was prepared by neutralization of commercially available (Aldrich Chemical Co.) 4-chloropyridine hydrochloride. The hydrochloride salt (30 g; 0.20 mol) was dissolved in approximately 200 ml of water and cooled in an ice bath during dropwise addition of 120 ml of 10% sodium hydroxide. During the addition the solution turned dark brown. The solution was then extracted with three 200 ml portions of pentane. The combined pentane extracts were dried over anhydrous magnesium sulfate and filtered. After stripping off the solvent under vacuum (20 mm), the material was distilled at room temperature under high vacuum (0.050 mm) into a Dry Ice–acetone trap, to give 19.4 g (86% yield) of 4-chloropyridine. Care was taken not to warm the material since it dimerizes slowly at room temperature (and rapidly on heating) to a red water soluble solid which is thought to be *N*-(4′-pyridyl)-4-chloropyridinium chloride (12). The n.m.r. spectrum of 4-chloropyridine appears as a typical AA′XX′ with quartets centered at δ 7.3 and 8.6.

General Procedure for the Preparation of 4-Alkoxypyridines

A typical procedure is the preparation of 4-cyclohexoxypyridine.

In a dry 50 ml Erlenmeyer flask protected by a calcium chloride drying tube was placed 0.77 g (32.1 mmol) of sodium hydride which had been previously washed with dry hexane in a sintered glass filtering funnel to remove the mineral oil used as a dispersing agent. (In some cases, the sodium hydride dispersion was weighed directly into the reaction flask and stirred with about 25 ml of hexane and the hexane then removed by means of a pipette.) To this was added 10 ml dimethylsulfoxide (previously dried overnight over Linde Molecular Sieves, type 5A). The mixture was allowed to stir for one-half hour before 3.20 g (32.0 mmol) of cyclohexanol was added dropwise. (In those preparations where the alcohol was a solid, a concentrated solution of the alcohol in dimethylsulfoxide was employed.) Considerable foaming occurred and the solution turned dark brown. After the alcohol had been added, 3.63 g (32.0 mmol) of 4-chloropyridine was added and the solution allowed to stir overnight at room temperature. In later preparations a 15% excess of 4-chloropyridine was usually employed. The solution was filtered and the precipitate (sodium chloride) was washed with about 10 ml of hot benzene. The filtrate was concentrated on a rotary evaporator and then distilled under vacuum giving dimethylsulfoxide, b.p. 23° (0.050 mm) and 3.76 g (67% yield) of 4-cyclohexoxypyridine, b.p. 88–92° (0.050 mm). (It was found that an alternative work-up of extracting the product out of dimethylsulfoxide into pentane was equally satisfactory and did not significantly decrease the yields. For example, in the preparation of the 2-octyl derivative, the filtrate was divided into two parts, half being distilled directly and half worked-up using the extraction procedure, the yields were 70% and 64% respectively.)

Analytical samples of the 4-alkoxypyridines were prepared by gas chromatography on an SE-30 column (20 ft × 3/8 in. o.d.) at 200° using a flow rate of about 200 ml He/min.

General Procedure for the Preparation of N-Methyl-4-Alkoxypyridinium Iodides

All *N*-methyl-4-alkoxypyridinium iodides were prepared in essentially the same manner. In a typical procedure, 1.64 g (9.29 mmol) of 4-cyclohexoxypyridine was placed in a tightly stopped test tube. This was cooled in an ice bath while 2 ml (32.1 mmol) of methyl iodide was added. After allowing the solution to stand at 6° overnight, the excess methyl iodide was removed by means of a rotary evaporator. In this case, an oil resulted, but it was found that after keeping this oil under vacuum for a few hours, a red solid resulted. The solid was then recrystallized by dissolving it in acetone and adding ether until precipitation of the methiodide occurred. The solution was then filtered to give 2.70 g (91% yield) of *N*-methyl-4-cyclohexoxypyridinium iodide, m.p. 120°.

In some cases a solid was obtained immediately on removal of the excess methyl iodide or by allowing the oil to stand for a few days or by prolonged concentration on a rotary evaporation. For some compounds, crystallization was induced by dissolving the oil in acetone and adding ether just to the point of cloudiness. The solution was then allowed to stand overnight and then filtered to give crystals of the methiodide. Some of the methiodides failed to crystallize using these procedures and these were pyrolyzed directly without being fully characterized.

Product Studies

The pyrolysis reactions were done in the same general manner. In a typical procedure, 1.56 g (4.89 mmol) of *N*-methyl-4-cyclohexoxypyridinium iodide was placed in a 25 ml round bottom flask. To this was attached a short path distillation column. A tared test tube, fitted with a ground glass joint, was attached to the distillation column and cooled in a Dry Ice–acetone bath. The system was placed under vacuum (10 mm) and slowly heated by means of an oil bath. The solid melted at about 120° and at approximately 165°, the melt was observed to be boiling. Heating was continued until the boiling had ceased (about 3 h), leaving a red solid in the reaction flask. The product (cyclohexene in this case) was analyzed by gas chromatography and n.m.r. The yield of cyclohexene was 0.36 g (90%).

Those methiodides which gave pyrolysis products which were solids (isobornyl and bornyl derivatives) were pyrolyzed by means of a sublimation apparatus. The methiodide was placed in the bottom of the apparatus and heated while a vacuum was applied. The products were then trapped out on the walls of the cold finger.

Those methiodides which were oils were not actually isolated prior to elimination. A known weight of the 4-alkoxypyridine was placed in a flask and an excess of methyl iodide was added. After allowing the solution to stand over-

night, the excess methyl iodide was removed under vacuum and the resulting oil was then pyrolyzed directly. Yields were calculated on the basis of the weight of the starting 4-alkoxypyridine.

Continued financial support from the National Research Council of Canada is gratefully acknowledged.

1. A. BROWN. Ph.D. Thesis. University of Toronto, Toronto, Ontario, 1969.
2. A. C. COPE, R. A. PIKE, and C. F. SPENCER. J. Am. Chem. Soc. **75**, 3212, (1953).
3. H. C. BROWN and G. ZWEIFEL. J. Am. Chem. Soc. **83**, 2544, (1961).
4. J. MEINWALD and J. T. OUDERKIRK. J. Am. Chem. Soc. **82**, 480 (1960).
5. I. HEILBRON, *Ed.* Dictionary of organic compounds. Vol. 2. 4th Ed. Eyre and Spottiswoode Publishers Ltd., London. 1965. p. 1162.
6. H. TOIVONEN. Ann. Acad. Sc. Fennicae. Ser. A. II. No. **72**, (1956).
7. H. C. BROWN and C. P. GARG. J. Am. Chem. Soc. **83**, 2952 (1961).
8. D. S. NOYCE and D. B. DENNEY. J. Am. Chem. Soc. **72**, 5743 (1950).
9. W. J. GRUBB and J. READ. J. Soc. Chem. Ind. **53**, 52T, (1934).
10. R. YA. LEVINA. J. Gen. Chem. (USSR), **7**, 684, (1937).
11. K. ALDER and P. H. FLOCK. Ber. **89**, 1732, (1956).
12. J. P. WIBAUT and F. W. BROEKNAN. Rec. Trav. Chim. **58**, (1939).

Can. J. Chem. Downloaded from www.nrcresearchpress.com by 210.87.254.5 on 09/05/12
For personal use only.

The Formation of Alkenes by the Thermal Elimination Reaction of *N*-Methyl-4-alkoxypyridinium Iodides. II. An Investigation of the Mechanism

GEORGE H. SCHMID AND AARON W. WOLKOFF[1]

Department of Chemistry, University of Toronto, Toronto 181, Ontario

Received October 13, 1971

A comparison of the products from elimination reactions of a number of compounds containing various leaving groups with those containing the *N*-methyl oxypyridinium leaving group suggests that the elimination is not occurring by means of a simple E1 mechanism. Changing the anion of the salt from iodide to methylsulphate and tetrafluoroborate affects the product composition indicating that the anion is taking part in the reaction. The mechanism of this reaction appears to be on the E1-E2 borderline.

Une comparaison des produits de réactions d'élimination de certains composés contenant une variété de groupes labiles avec ceux contenant le groupe labile *N*-méthyl oxypyridinium suggère que l'élimination ne s'explique pas par un mécanisme simple de type E1. Lorsqu'on change l'anion du sel, soit le sulfate de méthyl ou le tétrafluoroborate à la place de l'iodure, la composition du produit est affectée, ce qui indique que l'anion prend part à la réaction. Le mécanisme de cette réaction semble être le résultat d'une contribution des deux mécanismes E1 et E2.

Canadian Journal of Chemistry, **50**, 1188 (1972)

Can. J. Chem. Downloaded from www.nrcresearchpress.com by 210.87.254.105 on 09/05/12
For personal use only.

We have found that *N*-methyl-4-alkoxypyridinium iodides decompose upon heating to give olefins and the hydroiodide of *N*-methyl-γ-pyridone (1). The olefins obtained from this reaction are not stereospecific and there is evidence that rearrangement occurs during the pyrolysis. These results suggest that the elimination is occurring by means of an E1 mechanism. A comparison of our results with elimination reactions carried out by other workers on 2-methylcyclohexyl and menthyl neomenthyl derivations (3–8) indicates that the mechanism is more complicated. In general, elimination reactions which are believed to occur by an E1 mechanism give almost identical product ratios from either the *cis* or *trans* starting material. Results obtained in this work for the pyrolysis of the oxypyridinium iodides show that the menthyl, neomenthyl, and 2-methylcyclohexyl derivatives give products which resemble those formed under E1 conditions. Still there are significant differences in the products from *cis* and *trans* isomers. The question arises as to whether or not the iodide ion does actually play a part in the reaction. Hence, additional product studies were attempted wherein modifications were made in the leaving group. Specifically, the counter-ion was changed from iodide to methylsulfate and tetrafluoroborate.

[1]Holder of NRCC Scholarship, 1967–1971.

The results for the pyrolysis of the *N*-methyl-4-(2′-octoxy)pyridinium salts are shown in Table 1. These results clearly show that the counter-ion affects the stereochemistry and regiospecificity of the products. The fact that the addition of 2,6-lutidine, a non-nucleophilic base, has little effect on the product ratios indicates that no isomerization of the initially formed olefins occurs.

These results can be compared with the dehydration of 2-octanol with phosphoric acid at 120–130° which gives *trans*/*cis* and 2-/1-olefin ratios of 1.06 and 4.71 respectively. These ratios are closer to those from the pyrolysis of the tetrafluoroborate salt than to those from the iodide salt. Since the dehydration proceeds by way of a carbonium ion, this indicates that the reaction of the tetrafluoroborate salt proceeds through a transition state resembling a carbonium ion (E1) while the iodide salt must react through a transition state that has some E2 character.

The results of the pyrolysis of optically active *N*-methyl-4-isobornoxypyridinium salts with varying counter ions are given in Table 2. All compounds upon pyrolysis gave 97–99% camphene and 1–3% tricyclene. Bornylene could not be detected as a product in any of the reactions. A significant drop in retention of optical activity of the camphene is observed on changing from the iodide and methyl sulfate salts to the

TABLE 1. Results of pyrolysis of *N*-methyl-4-(2′-octoxy)pyridinium salts

X^-	Decomposition temperature (°C)	1-Octene (%)	*cis*-2-Octene (%)	*trans*-2-Octene (%)	*trans*-/*cis*-2-Octenes	2-/1-Octenes	Yield (%)
I	165	7.8±0.2	23.9±0.1	68.3±0.3	2.85±0.03	11.82±0.36	[a]
CH_3SO_4	135–150	12.8±0.8	28.8±2.1	58.4±1.3	2.02±0.18	6.81±0.75	>100[b]
BF_4[c]	145	35.7±1.0	21.7±0.4	37.7±0.4	1.73±0.05	1.66±0.07	99
I[d]	110	4.3±0.8	25.1±0.9	70.6±0.8	2.81±0.14	22.30±5.52	[e]
I[d,f]	110	4.2±1.9	21.7±4.2	74.1±2.3	3.41±0.95	22.8[g]	[e]

[a]Some methyl iodide produced making yield greater than 100%.
[b]Some methylsulfate distilled over with products making yield greater than 100%.
[c]Reaction was accompanied by 4.9% of an unknown product (see Experimental).
[d]Pyrolysis carried out in dimethylformamide (0.0255 *M*).
[e]Yield not determined.
[f]In added 2,6-lutidine.
[g]Large experimental limits; due to uncertainty in % 1-octene.

TABLE 2. Elimination from *N*-methyl-4-isobornoxypyridinium salts

R^-	X^-	Decomposition temperature (°C)	Camphene[a] (%)	Tricyclene[a] (%)	Retention[b] of optical activity (%)	Yield (%)
Isobornyl[c]	I	150	99.1	0.9	63.2	60
Isobornyl	I[d]	110[e]	97.6	2.4	≈99	[f]
Isobornyl	CH_3SO_4	160	97.0	3.0	61.7	68
Isobornyl	BF_4	130	>99.5	<0.5	10.4	≈100

[a]Determined by gas chromatography; values are better than ±1% (average of least three determinations).
[b]Corrected for tricyclene.
[c]Values are corrected for 5.8% borneol in starting alcohol.
[d]0.1677 *M* solution of substrate in DMF (solution also contains 0.0539 *M* 2,6-lutidine).
[e]Allowed to react for 10 days.
[f]Yield not determined.

TABLE 3. Comparison of elimination reactions of *N*-methyl-4-isobornoxypyridinium salts and *N*-methyl-4-(2′-octoxy)pyridinium salts

Counter ion	Solvent	Isobornyl system: Retention of optical activity (%)	2-Octyl system: *trans*-/*cis*-2-Octenes	2-Octyl system: 2-/1-Octenes
I^-	DMF	≈99	2.81	22.30
I^-	—	63.2	2.85	11.82
$CH_3SO_4^-$	—	61.7	2.02	6.81
BF_4^-	—	10.4	1.73	1.66

tetrafluoroborate salt. As in the 2-octyl case, it is clear that the counter ion must be involved in some way.

The results of the reactions of the isobornyl and 2-octyl derivatives are strikingly similar. It seems that the percent retention of optical activity in the isobornyl system is related to that fraction of the reaction in which the counter-ion participates in removal of a proton. Similarly, in the 2-octyl case, the *trans*/*cis* olefin ratio, as well as the 2-/1-octene ratio, reflect that fraction of the reaction proceeding by a concerted pathway. A comparison of the results for the isobornyl and 2-octyl derivatives is shown in Table 3 and Fig. 1.

These results can be explained by means of the Theory of the Variable Transition State (9). According to this theory, in a series of bimolecular elimination reactions, as the base is made weaker the position of the transition state shifts towards the paenecarbonium extreme with a consequent decrease in the *trans*/*cis* and

Can. J. Chem. Downloaded from www.nrcresearchpress.com by 210.87.254.105 on 09/05/12
For personal use only.

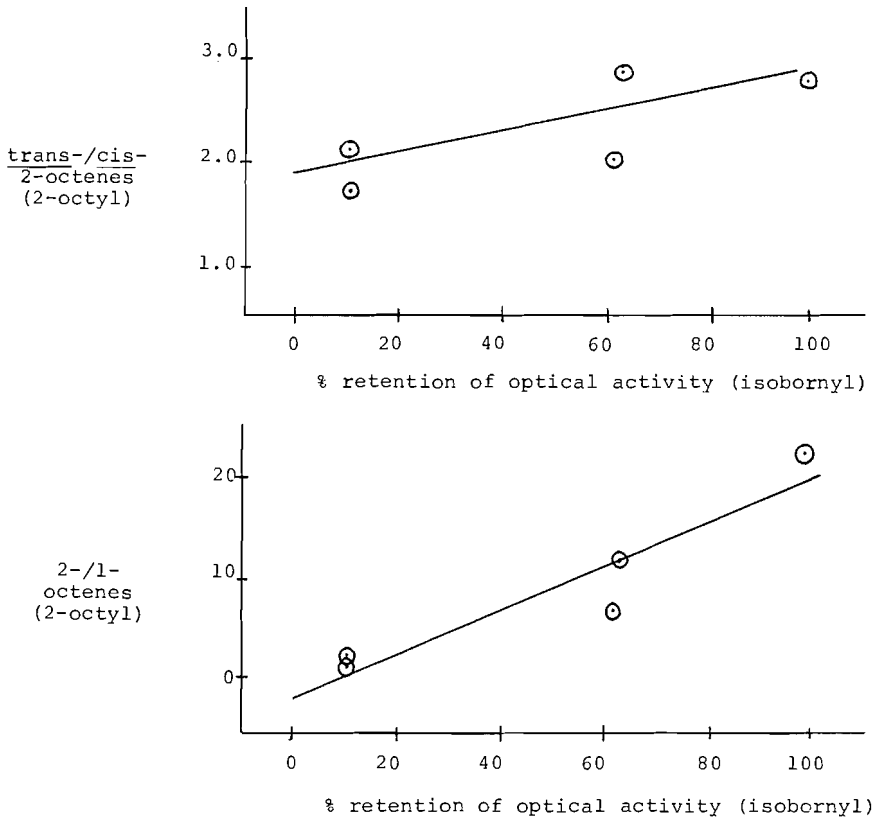

FIG. 1. Plot of the products of pyrolysis of *N*-methyl-4-(2′-octoxy)pyridinium iodide *vs.* the percent retention of optical activity of the products of pyrolysis of *N*-methyl-4-isobornoxypyridinium oxide.

2-/1-olefin ratios. This presumes, of course, that all the reactions are proceeding via transition states that are along the continuum between the paenecarbonium extreme and central regions.

In bimolecular elimination reactions there is a gap in the continuum between the E1 and the paenecarbonium extreme of the E2 mechanism. The reason for this is that there is a loss of entropy due to the inclusion of a base in the E2 transition state. The elimination of *N*-methyl-4-alkoxypyridinium iodides may represent reactions where this gap is bridged. In these reactions, the base is the counter-ion and is therefore present in the transition state for both the E1 and E2 component of the mechanism, leading to small entropy differences between the E1 and E2 transition states. Hence, one can visualize a continuum between E1 and E2 mechanisms for these reactions. Thus in the elimination reaction involving the tetrafluoroborate anion, which is a conjugate base of a very strong acid, little or no abstraction of a proton would be expected in the transition state and the mechanism would approach the E1 end of the continuum. With iodide as the anion the mechanism would approach the paenecarbonium extreme of the E2 mechanism. The results in Table 1, are in accord with this view. As the counter-ion becomes a weaker base, the ratio of 2-octenes/1-octene decreases to a value near that found in the acid-catalyzed dehydration of 2-octanol.

The results definitely indicate some participation of the counter-ion. In the 2-octyl and other acyclic systems as well as the monocyclic systems, the reaction probably proceeds via a concerted mechanism in which the transition state is very near to the E1 extreme. Because ionization of the C_2—O bond is facile in the isobornyl system the role of the iodide and

Can. J. Chem. Downloaded from www.nrcresearchpress.com by 210.87.254.105 on 09/05/12
For personal use only.

Can. J. Chem. Downloaded from www.nrcresearchpress.com by 210.87.254.105 on 09/05/12
For personal use only.

methylsulfate counter-ion is probably to aid in the loss of a proton from the initially formed carbonium ion.

Alternatively these results may be explained by a dual mechanism in which part of the reaction proceeds through an E1 transition state and in part through a transition state which is close to the paenecarbonium extreme of the E2 mechanism (10).

Experimental

All melting and boiling points are uncorrected. Elemental analyses were carried out by A. B. Gygli of Toronto, Ontario.

4-(−)-Isobornoxypyridine

The compound was prepared according to the procedure previously reported (1) in 44% yield, b.p. 115° (0.050 mm).

4-(2′-Octoxy)pyridine

The compound was prepared according to the procedure previously reported (1) in 70% yield, b.p. 99–100° (0.10 mm).

N-Methyl-4-(−)-isobornoxypyridinium Methylsulfate

To a solution of 1.2 g (5.19 mmol) of 4-(−)-isobornoxypyridine in about 15 ml of ether was added 1.5 ml (15.8 mmol) of dimethylsulfate. After about 2 min, a white precipitate formed. After allowing the mixture to stand overnight, it was filtered to give a white solid. Recrystallization of this solid from acetone gave 1.65 g (95% yield) of *N*-methyl-4-(−)-isobornoxypyridinium methylsulfate, m.p. 158–159°.

Anal. Calcd. For $C_{17}H_{27}SO_5N$: C, 57.12; H, 7.61; N, 3.92. Found: C, 57.23; H, 7.43; N, 4.06.

The n.m.r. δ ($CDCl_3$): multiplet at 0.8–2.3 (16H, methyl and ring protons); sharp singlet at 3.73 (3H, H—C—OSO_3^-); multiplet at 4.3–4.6 (methine α to oxypyridinium group) overlapping a singlet (*N*-methyl protons) at 4.37 (4H total); distorted doublet at 7.37 (2H, 3,5-pyridyl, $J = 7$ Hz); doublet at 8.90 (2H, 2,6-pyridyl, $J = 7$ Hz).

N-Methyl-4-(−)-isobornoxypyridinium Iodide

The compound was prepared according to the method previously reported (1) in 90% yield m.p. 152–153.5°.

N-Methyl-4-(−)-isobornoxypyridinium Tetrafluoroborate

To a solution of 1.00 g (2.68 mmol) of *N*-methyl-4-(−)-isobornoxypyridinium iodide in 15 ml of absolute ethanol, was added a solution containing 0.7 g of silver tetrafluoroborate in 23 ml of absolute ethanol until no further precipitation occurred (20 ml). The mixture was then filtered and the filtrate concentrated under vacuum to give white crystals. The material was recrystallized from water (to remove any excess silver tetrafluoroborate) to give 0.59 g (66% yield) of *N*-methyl-4-(−)-isobornoxypyridinium tetrafluoroborate, m.p. 127–129°. An analytical sample was prepared by a further recrystallization from water and then repeated recrystallizations from acetone–ether (as previously described (2), m.p. 132–132.5°.

Anal. Calcd. for $C_{16}H_{24}ONBF_4$: C, 57.58; H, 7.26; N, 4.20. Found: C, 57.68; H, 7.23; N, 4.29.

The n.m.r. δ ($CDCl_3$): multiplet at 0.7–2.0 (16H, methyl and cycloalkyl ring protons); multiplet at 4.1–4.6 (α-methine proton) overlapping a singlet (*N*-methyl) at 4.33 (4H total); doublet at 7.30 (2H, 3,5,-pyridyl, $J = 7.5$ Hz); doublet at 8.60 (2H, 2,6-pyridyl, $J = 7.5$ Hz). The i.r. λ_{max} ($CHCl_3$): 6.06, 6.60, 7.50, 9.54, (strong, BF_4) 10.77 μ.

Acid-catalyzed Dehydration of 2-Octanol

Treatment of 2-octanol with concentrated phosphoric acid at 120–130° gave a mixture consisting of 17.5% 1-octene, 40.0% *cis*-2-octene, and 42.5% *trans*-2-octene.

N-Methyl-4-(2′-octoxy)pyridinium Methylsulfate

To 1.0 g (4.83) of 4-(2′-octoxy)pyridine was added 1.5 ml (15.8 mmol) of dimethylsulfate. The mixture was allowed to stand for 48 h and then placed under vacuum overnight to remove any excess dimethylsulfate. The oily product was pyrolyzed directly at 135–150° to give 0.70 g (129% yield; contained some methylsulfate) of a mixture of olefins. Analysis by gas chromatography showed the mixture to contain 12.8 ± 0.8% 1-octene, 58.4 ± 1.3% *trans*-2-octene, and 28.8 ± 2.1% *cis*-2-octene.

N-Methyl-4-(2′-octoxy)pyridinium Iodide

The compound was prepared according to the method reported (1).

N-Methyl-4-(2′-octoxy)pyridinium Tetrafluoroborate

To a solution of 1.75 g (5.01 mmol) of *N*-methyl-4-(2′-octoxy)pyridinium iodide in 20 ml of absolute ethanol, was added a solution of 1.50 g (7.69 mmol) of silver tetrafluoroborate in 20 ml of ethanol until precipitation was complete. The mixture was filtered to remove the silver iodide, and the filtrate concentrated to give 1.45 g (91% yield) of an oil. The oil was pyrolyzed to give 0.55 g (99% overall yield) of a mixture of olefins. This mixture was analyzed by gas chromatography using a 13 ft × 1/4 in. o.d. column packed with dimethylsulfolane on Chromosorb G with a flow rate of 37 ml He/min at 35°. The mixture was found to be composed of 4.9% of an unknown compound, 35.7% 1-octene, 37.7% *trans*-2-octene, and 21.7% *cis*-2-octene.

Continued financial support from the National Research Council of Canada is gratefully acknowledged.

1. G. H. Schmid and A. W. Wolkoff. Can. J. Chem. This issue.
2. D. G. Botteron and G. P. Shulman. J. Org. Chem. **27**, 2007 (1962).
3. T. H. Brownlee and W. H. Saunders, Jr. Proc. Chem. Soc. 314 (1961).
4. E. D. Hughes, C. K. Ingold, and J. B. Rose. J. Chem. Soc. 3829 (1953).
5. W. Huckel, W. Tappe, and G. Legutke. Ann. **543**, 191 (1940).
6. E. D. Hughes and J. Wilby. J. Chem. Soc. 4094 (1960).
7. G. Baile, A. J. Parker, S. G. Smith, I. D. R. Stevens, and S. Winstein. J. Am. Chem. Soc. **92**, 115 (1970).
8. A. C. Cope and E. M. Acton. J. Am. Chem. Soc. **80**, 355 (1958).
9. J. F. Bunnett. Surv. Prog. Chem. **5**, 53 (1969).
10. J. F. Bunnett, G. T. Davis, and H. Tanida. J. Am. Chem. Soc. **84**, 1606 (1962).

Photoamidation of 3,4,6-Tri-*O*-acetyl-1,2-dideoxy-D-*arabino*-hex-1-enopyranose

ALEX ROSENTHAL AND A. ZANLUNGO

Department of Chemistry, The University of British Columbia, Vancouver, British Columbia

Received November 10, 1971

The acetone-initiated photochemical addition of formamide to 3,4,6-tri-*O*-acetyl-1,2-dideoxy-D-*arabino*-hex-1-enopyranose (**1**) afforded 3,4,6-tri-*O*-acetyl-2,6-anhydro-3-deoxy-D-*gluco*-heptonamide (**2**), 3,4,6-tri-*O*-acetyl-2,6-anhydro-3-deoxy-D-*manno*-heptonamide (**3**), and 3,4,6-tri-*O*-acetyl-1,5-anhydro-2-*C*-carbamoyl-1,2-dideoxy-D-*gluco*-hexitol (**4**) in a combined yield of about 75% (the ratio of yields of **2**, **3**, and **4** was approximately 2:2:3). In addition, trace quantities of the epimeric *manno* branched-chain adduct of **4**, and acetone adducts of **1** were formed. Lithium aluminum hydride reduction of **4** yielded a branched-chain aminopolyol, isolated as its *N*-acetyl derivative.

L'addition photochimique initiée par l'acétone de formamide au 3,4,6-tri-*O*-acétyl-1,2-didéoxy-D-*arabino*-hex-1-énopyranose (**1**) nous a conduit au 3,4,6-tri-*O*-acétyl-2,6-anhydro-3-déoxy-D-*gluco*-heptanomide (**2**), au 3,4,6-tri-*O*-acétyl-2,6-anhydro-3-déoxy-D-*manno*-heptonamide (**3**), et au 3,4,6-tri-*O*-acétyl-1,5-anhydro-2-*C*-carbamoyl-1,2-didéoxy-D-*gluco*-hexitol (**4**), dans un rendement global de 75% (le rapport des rendements de **2**, **3**, et **4** étant approximativement 2:2:3). De plus, des traces du dérivé épimérique branché *manno* de **4** et les dérivés acétone de **1** ont été formées. La réduction de **4** avec l'hydrure d'aluminium et de lithium a donné un aminopolyol branché, qu'on a isolé sous forme de dérivé *N*-acétyl.

Canadian Journal of Chemistry, **50**, 1192 (1972)

During work on the synthesis of homologues of puromycin we have investigated new routes for the preparation of amino sugars in which the amino-group is located in the branching residue. Branched-chain amino sugars have been synthesized by Overend and coworkers (1) by application of the nitromethane synthesis (2) to a methyl glycopyranosidulose. Similar application of the nitromethane synthesis to 1,2:5,6-di-*O*-isopropylidene-α-D-*ribo*-hexofuranos-3-ulose, followed by a deoxygenation reaction, enabled Albrecht and Moffatt (3) to prepare a a 3-deoxy-3-*C*-aminomethyl branched-chain amino sugar which was subsequently converted into a homologue of the aminonucleoside moiety of puromycin. Other workers (4, 5) have also synthesized branched-chain amino deoxy sugars by application of the nitromethane synthesis and the Wittig reaction to ketoses (6). In this paper we report a new route for the synthesis of deoxy branched-chain amino sugars, namely, by photochemical amidation of unsaturated carbohydrates. Although the photochemical amidation of olefins has been studied in considerable detail (6), the reaction has hitherto not been applied to the unsaturated carbohydrates. Of particular relevance to our investigation was the fact that Elad and Rokach (7) found that the reaction was stereospecific when applied to norbornene.

When an acetone solution of 3,4,6-tri-*O*-acetyl-1,2-dideoxy-D-*arabino*-hex-1-enopyranose (**1**) containing formamide and *t*-butyl alcohol was irradiated with u.v. light in a water-cooled apparatus (see Scheme 1) all of the starting material was consumed in 26 h, as

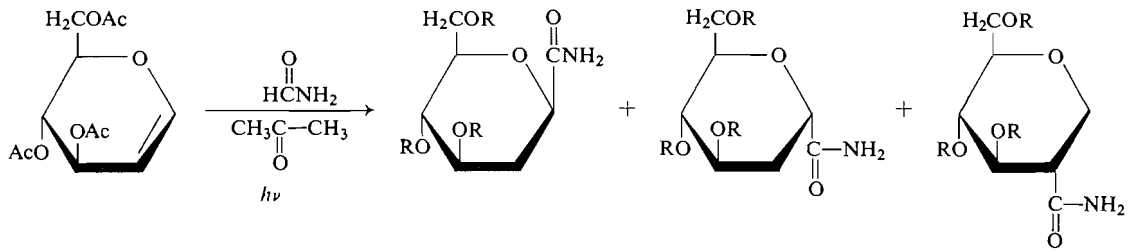

1

2 R = Ac
5 R = H

3 R = Ac
6 R = H

4 R = Ac
7 R = H

SCHEME 1

Can. J. Chem. Downloaded from www.nrcresearchpress.com by 210.87.254.5 on 09/05/12
For personal use only.

TABLE 1. Chromatography of photolysis products of 3,4,6-tri-*O*-acetyl-1,2-dideoxy-D-*arabino*-hex-1-enopyranose (**1**)

Developer	Volume (l)	Fraction	Weight (g)	Nature of material
6:4 Benzene – ethyl acetate	2.5	A	0.14	Mainly **1**
6:4 Benzene – ethyl acetate	1.2	B	0.17	Syrup
6:4:0.5 Benzene – ethyl acetate – ethanol	1.8	C	0.16	Syrup
6:4:0.5 Benzene – ethyl acetate – ethanol	0.5	D	1.38	**2** + **3** + ?
6:4:0.5 Benzene – ethyl acetate – ethanol	0.8	E	0.80	**2** + **3**
6:4:0.6 Benzene – ethyl acetate – ethanol	1.2	F	0.95	**2** + **3** + **4**
6:4:0.7 Benzene – ethyl acetate – ethanol	1.4	G	0.70	**3** + **4**
6:4:0.8 Benzene – ethyl acetate – ethanol	3.0	H	0.66	**4** + ?
6:4:1.2 Benzene – ethyl acetate – ethanol	2.0	I	0.19	Syrup

evidenced by monitoring the reaction mixture by t.l.c. As shown in Table 1 gradient column chromatography of the photolysis products on silica gel using benzene – ethyl acetate – ethanol as eluent afforded a partial separation of the three major carbamoyl components **2**, **3**, and **4** (combined yield about 75%) from the acetone adducts which were formed in trace quantities. The major components were clearly distinguishable and separable by t.l.c. However, a more efficacious procedure for separating large quantities of each component was by fraction crystallization. Thus crystallization of fractions E and F from ethyl acetate afforded pure crystalline 3,4,6-tri-*O*-acetyl-2,6-anhydro-3-deoxy-D-*gluco*-heptonamide (**2**). The acetylated *manno*-epimer (**3**) could only be obtained in pure crystalline form by first deacetylating an aliquot of fractions E and F followed by cellulose column chromatography of the deacetylated products using *n*-butanol–ethanol–water as developer. This procedure afforded the pure deacetylated *gluco* and *manno*-epimers, **5** and **6**. Acetylation of the manno epimer **6** with acetic anhydride and pyridine afforded, after silica gel chromatographic purification, crystalline 4,5,7-tri-*O*-acetyl-2,6-anhydro-3-deoxy-D-*manno*-heptonamide (**3**).

Although 3,4,6-tri-*O*-acetyl-1,5-anhydro-2-*C*-carbamoyl-1,2-dideoxy-D-*gluco*-hexitol (**4**) was clearly distinguishable from compounds **2** and **3** by t.l.c., attempts to prepare crystalline **4** by preparative t.l.c. were unsuccessful. On the other hand, when fractions F and G were deacetylated with methanolic sodium methoxide the deacetylated product readily afforded, on fractional crystallization from methanol, pure crystalline 2,5-anhydro-2-*C*-carbamoyl-1,2-dideoxy-D-*gluco*-hexitol (**7**) in 74% yield (based on fractions F and G only). The overall yield of **4** was approximately 30%. Acetylation of **7** in the usual way readily afforded crystalline 3,4,6-tri-*O*-acetyl-1,5-anhydro-2-*C*-carbamoyl-1,2-dideoxy-D-*gluco*-hexitol (**4**).

The principal remaining fraction H showed chromatographic evidence of the presence of **4**, and in addition, a fourth carbamoyl product in less than 5% yield. Attempts to isolate this fourth component in pure crystalline form were unsuccessful.

The complete structures of the photoamidation products **2**, **3**, and **4** and of the corresponding deacetylated products **5**, **6**, and **7** obtained from 3,4,6-tri-*O*-acetyl-1,2-dideoxy-D-*arabino*-hex-1-enopyranose (**1**) were readily deduced from their p.m.r. spectra. Carboxamidation at C-1 of **1** would give compounds **5** and **6** (after deacetylation), both possessing two C-3 methylene protons which would be expected to resonate at high field (about τ 8). On the other

Can. J. Chem. Downloaded from www.nrcresearchpress.com by 210.87.254.5 on 09/05/12
For personal use only.

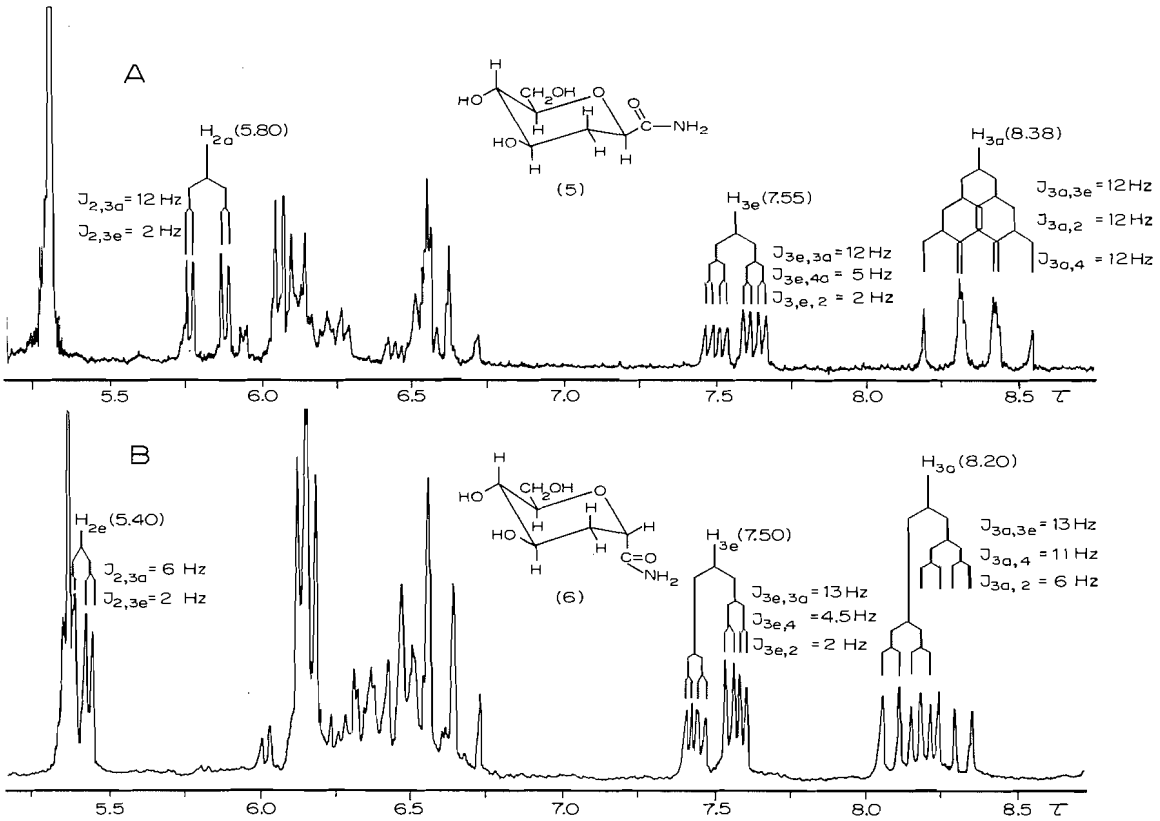

FIG. 1. Partial 100 MHz p.m.r. spectrum of (A), 2,6-anhydro-3-deoxy-D-*gluco*-heptonamide (**5**) and (B), 2,6-anhydro-3-deoxy-D-*manno*-heptonamide (**6**) in D_2O solution.

hand, were carboxamidation to occur at C-2 of the glycal, the resulting, branched-chain carbohydrate would have only one methine hydrogen atom, which would give rise to a high-field signal. It was possible to distinguish readily between the normal chain and branched-chain structures merely from a consideration of the resonance positions and relative intensities of the proton signals observed in the n.m.r. spectra (Figs. 1 and 2) of the unsubstituted compounds **5**, **6**, and **7**, or of their acetate derivatives **2**, **3**, and **4**. The spectra of **5** and **6**, measured in deuterium oxide solution, exhibited two octets at τ 7.5–8.4 equal to two hydrogens which clearly arise from the C-3 methylene protons. Hence both **5** and **6** are clearly normal-chain 2,6-anhydro-3-deoxy-heptonamides. The assignment of configuration at C-2 of both compounds was readily made from the multiplicities of the C-3 equatorial and axial hydrogen signals which occur at τ 7.5–8.2 or from the coupling constants of the C-2 hydrogen which resonates in the lowest-field region (τ 5.4–5.8). The p.m.r. spectrum of **5** (see Fig. 1A) clearly shows two quartets at τ 7.55 which were assigned to the C-3 equatorial hydrogen atom and an octet (two overlapping quartets) at τ 8.38 assigned to the C-3 axial hydrogen atom. On the basis of the observations of Lemieux and coworkers (8), the spin–spin coupling between the two C-3 methylene hydrogen atoms would be expected to be large, of the order of 12 Hz; additional coupling of each proton with neighboring protons on C-2 and -4 would also be large were a diaxial relationship to exist; otherwise it would be small. The observed splitting of H-3e into two quartets, showed indeed, the anticipated, large coupling (12 Hz) with the geminal H-3a. The orientation of the C-2 hydrogen was deduced from the width of the higher-field H-3a signal (36 Hz), this being practically equal to the sum of the three coupling constants ($J_{3a,3e}$,

Can. J. Chem. Downloaded from www.nrcresearchpress.com by 210.87.254.5 on 09/05/12
For personal use only.

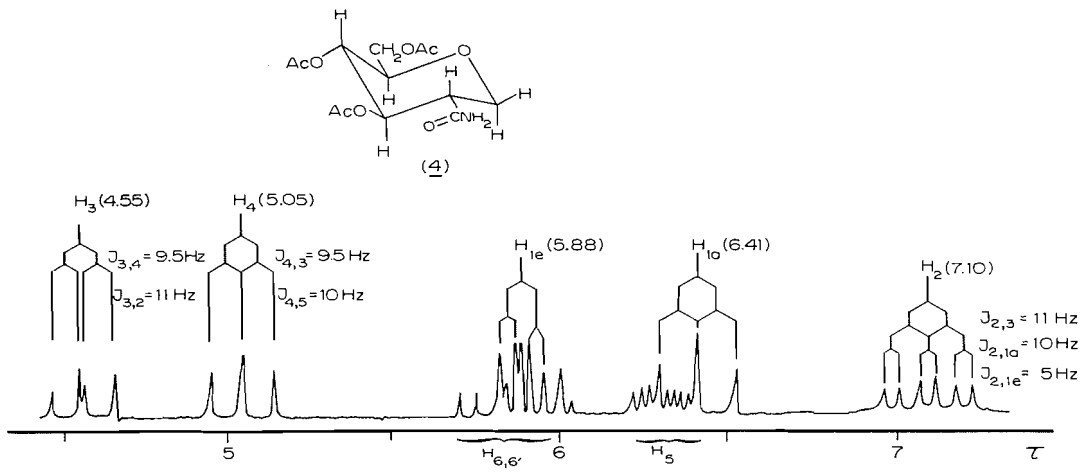

FIG. 2. Partial 100 MHz p.m.r. spectrum of 3,4,6-tri-*O*-acetyl-1,5-anhydro-2-*C*-carbamoyl-1,2-dideoxy-D-*gluco*-hexitol (**4**) in $(CD_3)_2$ C=O solution.

$J_{3a,2a}$, and $J_{3a,4a}$) with which the axial C-3 hydrogen atom was coupled to the equatorial C-3 hydrogen and to the two neighboring hydrogen atoms on C-2 and -4. Thus, as $J_{3a,3e}$ was 12 Hz, and $J_{3a,4a}$ must be about 12 Hz (H_{4a} is known to be axial), then $H_{3a,2a}$ must be 12 Hz; this large value could only be rationalized if H-2 and -3a are both axial. The two equatorial–axial interactions of H-3e with H-2 and -4 were assigned J values of 2 and 5 Hz respectively, to account for the observed octet of the lower-field group at τ 7.55. Corroboration of this assignment is readily seen by an analysis of the C-2 hydrogen signal at τ 5.80. Here one clearly sees two doublets having $J_{2a,3a} = 12$ and $J_{2a,3e} = 2$ Hz. The large J value can only arise if the C-2 hydrogen is in an axial orientation. In contrast, the *manno*-epimer **6** gave a spectrum (Fig. 2B) in which the C-2 hydrogen signal occurs at the expected lower field (τ 5.40) for an equatorial hydrogen and it also exhibits the lower J values of 6 and 2 Hz which would be expected to result from the coupling of the C-2 equatorial hydrogen to the C-3 axial and C-3 equatorial hydrogens. First order analysis of the p.m.r. spectra of the heptonamide acetate derivatives **2** and **3** in $CDCl_3$ solution gave the same structural assignments (see Experimental). In the spectrum of **2**, irradiation of the C-3 equatorial methylene hydrogen collapsed the C-2 axial hydrogen signals to a doublet, thus confirming the assignment of the low field pair of doublets to the C-2 hydrogen. Interestingly, the two epimeric 2,6-anhydro-3-deoxy-D-*gluco* (and D-*manno*) heptonamides **5** and **6**, respectively, exhibited p.m.r. spectra which were remarkably similar to the spectra of the two epimeric 2,6-anhydro-3-deoxy-D-*gluco* (and D-*manno*) heptitols obtained by hydroxymethylation (followed by deacetylation) of 3,4,6-tri-*O*-acetyl-1,2-dideoxy-D-*arabino*-hex-1-enopyranose (9). The complete structures of the latter compounds were rigorously proved by chemical means as well as by X-ray studies.

A similar first order analysis of the p.m.r. spectrum of the acetate of compound **4** in $CDCl_3$ solution (Fig. 2) readily showed that carboxamidation had occurred on C-2 of **1**. In this spectrum the lone high-field multiplet at τ 7.10 is equivalent to one hydrogen and therefore must be attributed to the C-2 methine hydrogen. Confirmation of this assignment and in addition, the orientation of the carboxamide group, was provided by double irradiation experiments (see Experimental). The magnitude of $J_{2,1a} = 10$ Hz, clearly indicates that H-2 must be axial and therefore compound **4** must be 3,4,6-tri-*O*-acetyl-1,5-anhydro-2-*C*-carbamoyl-1,2-dideoxy-D-*gluco*-hexitol. A parallel analysis of the p.m.r. parameters of the fourth acetylated carbamoyl carbohydrate (see Experimental) reveals a much narrower high-field multiplet positioned at τ 6.90–7.02 which must be due to the C-2 equatorial hydrogen. It is tentatively suggested, therefore, that the fourth carbamoyl carbo-

Can. J. Chem. Downloaded from www.nrcresearchpress.com by 210.87.254.5 on 09/05/12
For personal use only.

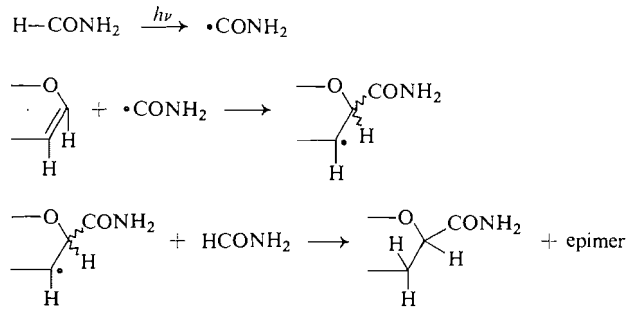

SCHEME 2

hydrate might be the expected epimeric *manno* C-2 branched-chain carbohydrate. Because this component occurred in very small amounts and could not be crystallized, no further definitive structural work was done.

Trace quantities of acetone adducts of **1** were also isolated from fraction B. Because these adducts could not be crystallized further work on them was abandoned.

Lithium aluminum hydride reduction of 3,4,6-tri-*O*-acetyl-1,5-anhydro-2-*C*-carbamoyl-1,2-dideoxy-D-*gluco*-hexitol (**4**) in tetrahydrofuran, followed by reacetylation of the product, yielded the branched-chain amino carbohydrate 2-*C*-acetamidomethyl-3,4,6-tri-*O*-acetyl-1,5-anhydro-1,2-dideoxy-D-*gluco*-hexitol.

The course of the reaction for the photochemical synthesis of 1:1 adducts of formamide and the unsaturated carbohydrate **1** may be illustrated by Scheme 2.

Although there was no stereospecificity in the addition of the carbamoyl free radical to C-1 of the glycal there was virtually exclusive stereospecificity in the attack of the same group on C-2 to afford the *gluco* branched-chain adduct **4** (equatorial product) and only a trace of the epimeric *manno* branched-chain adduct (axial product). In contrast to our findings it is interesting to note that Igarashi and Honma (10) found that in the free radical addition of thiolacetic acid to D-glucal triacetate the $CH_3\overset{O}{\overset{\|}{C}}—S\cdot$ free radical added exclusively to C-2 giving a preponderance of the axial product. It would therefore appear that no simplified explanation for the addition of carbamoyl free radicals to the unsaturated carbohydrate can be offered. Steric factors (7) undoubtedly play a role.

Experimental

Irradiations were made with a 450 W Hanovia medium pressure mercury vapor lamp with Corex filter under oxygen-free nitrogen. The reaction mixture was cooled internally with running water. Agitation of the reaction mixture was achieved with magnetic stirring. Purified nitrogen was bubbled for 2 h through the reaction mixture before irradiation. The progress of reactions and purity of products were checked by t.l.c. on silica gel G (benzene – ethyl acetate – ethanol, 5:5:1 v/v). Grace silica gel and Woelm neutral alumina were used for column chromatography. The i.r. spectra were recorded in Nujol with a Perkin–Elmer Model 337 spectrometer, and n.m.r. spectra were determined in deuteriochloroform solution with TMS as the internal standard using a Varian HA-100 spectrometer. The n.m.r. spectra of the deacetylated products were determined in deuterium oxide solution. Mass spectroscopy was obtained with a HMS-9 spectrometer. Optical rotations were measured at room temperature with a Perkin–Elmer automatic polarimeter Model 141. Chemical analyses were performed by Mr. P. Borda of the Microanalytical Laboratory, University of British Columbia.

*Photolysis of 3,4,6-Tri-O-acetyl-1,2-dideoxy-*D*-arabino-hex-1-enopyranose (**1**) in the Presence of Formamide and Acetone*

A mixture of 3,4,6-tri-*O*-acetyl-1,2-dideoxy-D-arabino-hex-1-enopyranose (**1**) (2.0 g), formamide (160 ml), *t*-butyl alcohol (30 ml), and acetone (10 ml) was irradiated for 30 min. A solution of (**1**) (2.20 g), *t*-butyl alcohol (10 ml), acetone (20 ml), and formamide (30 ml) was then added dropwise during 1 h and irradiation was continued for another 26 h (or until all starting material had disappeared as evidenced by t.l.c.). Alteration in the reaction conditions led to the formation of a more complex mixture of products. After the solution was concentrated to remove *t*-butyl alcohol and acetone by evaporation (30 mm pressure at 50°), the resulting solution was diluted with saturated aqueous sodium chloride solution (900 ml). The resulting solution was then extracted with dichloromethane (10 × 200 ml). The combined dichloromethane solution was washed with saturated aqueous sodium chloride solution (100 ml), dried over sodium sulfate, filtered, and concentrated under reduced pressure to yield a syrup (7.05 g). This syrup was applied to a silica gel column (520 g) and eluted by gradient elution chromatography using benzene – ethyl acetate – ethanol as developer as shown in Table 1.

Fraction A was mainly unreacted starting material **1**.

Can. J. Chem. Downloaded from www.nrcresearchpress.com by 210.87.254.5 on 09/05/12
For personal use only.

Can. J. Chem. Downloaded from www.nrcresearchpress.com by 210.87.254.5 on 09/05/12
For personal use only.

Fraction B was purified by preparative t.l.c. on silica gel G (benzene–ethanol, 97:3). The main zone, homogeneous by t.l.c., was twice distilled in high vacuum at 230° but could not be crystallized. Its i.r. in CCl_4 showed the absence of hydroxyl and ketone carbonyl group; m^+ 332; τ $(CD_3)_2CO$ 8.52 ($(CH_3)_2$), 8.05 (three acetyl groups).

Anal. Calcd. for $C_{15}H_{24}O_8$: C, 54.21; H, 7.28. Found: C, 53.95; H, 6.50.

Fraction C could not be purified by t.l.c.

Fraction D consisted of four compounds. High vacuum distillation of D at 200° removed non-carbohydrate material and left 0.46 g of a mixture of carboxamides **2** and **3**.

*3,4,6-Tri-O-acetyl-2,6-anhydro-3-deoxy-*D*-gluco-heptonamide (**2**) and 2,6-Anhydro-3-deoxy-*D*-gluco-heptonamide (**5**)*

Fractions E and F were crystallized from ethyl acetate to yield 0.23 g of **2**, m.p. 220°, $[\alpha]_D^{23}$ +31° (*c* 1.4, chloroform); i.r. (CCl_4), 3520 cm^{-1} (N—H); τ $CDCl_3$, 8.32 (two overlapping quartets, H-3a, $J_{3a,4}$ = 13.5, $J_{3a,2}$ = 13.5, $J_{3a,3e}$ = 13 Hz), 7.98, 7.96, 7.90 (acetyl), 7.36 (two quartets centered at 7.28 and 7.42 each peak separated by about 2.5 Hz, $J_{3e,3a}$ = 13 Hz), 6.32 (m, H-6), 5.96 (pair of doublets, H-2a, $J_{2a,3a}$ = 12.5, $J_{2a,3e}$ = 2.5 Hz doublets, H-2), 5.84 and 5.68 (m, 2H, H-7 and -7′), 5.05 (*t*, H-5), 4.88 (m, H-4, $J_{4a,3a}$ = 10, $J_{4a,5a}$ = 10 Hz), 4.22 and 3.55 (NH_2). Irradiation of H-3a and -3e collapsed H-2a to doublets; irradiation of H-2a affected H-3a and -3e.

Anal. of **2** Calcd. for $C_{13}H_{19}NO_8$: C, 49.21; H, 6.03; N, 4.41. Found: C, 49.21; H, 6.13; N, 4.36.

Compound **2** was deacetylated with 1 *M* methanolic sodium methoxide and the product deionized with IR-120 (H^+) resin in the usual way to yield, after crystallization from isopropyl alcohol, 2,6-anhydro-3-deoxy-D-glucoheptonamide (**5**), m.p. 194–196°; $[\alpha]_D^{22}$ +56° (*c* 2, water); c.d. $\Delta\varepsilon$ + 1.12 (λ_{max} 208 nm, water), $[\theta]_{208}^{30°}$ + 3636; $\Delta\varepsilon$ + 1.04 (λ_{max} 212 nm, methanol), $[\theta]_{212}^{30°}$ + 3432 (methanol); o.r.d. $[M]_{589}^{23}$ +98, $[M]_{220}^{23°}$ +858; i.r. (Nujol) 1670 (C=O), 1580 cm^{-1} (NH_2).

Anal. of **5** Calcd. for $C_7H_{13}NO_5$: C, 43.97; H, 6.83; N, 7.33. Found: C, 44.02; H, 7.09; N, 7.37.

Compound **5** was also obtained by deacetylating fractions E and F with sodium methoxide followed by cellulose column (60 cm × 3.2 cm) chromatography of the product (0.6 g) using *n*-butanol–ethanol–water (10:1:2) as developer. The fastest moving zone was compound **5**.

*2,6-Anhydro-3-deoxy-*D*-manno-heptonamide (**6**) and 4,5,7-Tri-O-acetyl-2,6-anhydro-3-deoxy-*D*-manno-heptonamide (**3**)*

The second zone (0.290 g, 9.3%) of the above cellulose chromatography was homogeneous by paper chromatography but could not be crystallized; $[\alpha]_D^{23}$ +39° (*c* 0.73, water), c.d. (water) $\Delta\varepsilon$ +0.614 $mol^{-1}cm^2$ (λ_{max} 228 nm), $[\theta]_{228}^{30}$ +2026; o.r.d. (water): $[M]_{589}^{23}$ +72; $[M]_{238}^{23}$ +730; $[M]_{211}^{23}$ −522; i.r. (Nujol) 1670 (C=O), 1585 cm^{-1} (NH_2).

Anal. of **6** Calcd. for $C_7H_{13}NO_5$: C, 43.97; H, 6.85; N, 7.33. Found: C, 43.55; H, 6.92; N, 6.87.

An aliquot of compound **6** (0.060 g) was acetylated with acetic anhydride and pyridine in the usual way. The syrupy acetate was purified by chromatography on silica gel column (10 cm × 1.3 cm) using benzene – ethyl acetate – ethanol (60:40:3) as developer. The main fraction was crystallized from ethyl acetate – *n*-hexane to yield 4,5,7-tri-*O*-acetyl-2,6-anhydro-3-deoxy-D-*manno*-heptonamide (**3**), m.p. 205–207°; $[\alpha]_D^{24}$ +16° (*c* 1, chloroform); i.r. (chloroform); 3520 and 3400 cm^{-1} (NH); τ $CDCl_3$ 7.97, 7.93 (acetyl), 7.95 (m, H-3a, $J_{3a,2}$ = 5.5 Hz), 7.50 (m, H-3e, $J_{3e,2}$ = 6, $J_{3e,3a}$ = 14, $J_{3e,4}$ = 5 Hz), 5.97 (m, H-6), 5.86 (m, H-7′), 5.61 (m, H-7), 5.55 (t, H-2, $J_{2,3e}$ = 5.5, $J_{2,3a}$ = 5.5 Hz), 5.12 (t, H-5, $J_{5,4}$ = 6.5, $J_{5,6}$ = 6.5 Hz), 4.88 (m, H-4, $J_{4,3a}$ = 8, $J_{4,5}$ = 8, $J_{4,3e}$ = 4.5 Hz). Irradiation at τ 4.88 changed H-3e signals into a pair of doublets, $J_{3a,3e}$ = 14, $J_{3e,2}$ = 5 Hz. Irradiation at 7.50 (H-3e) changed the H-4 signals into a pair of doublets.

Anal. of **3** Calcd. for $C_{13}H_{19}NO_8$: C, 49.21; H, 6.03; N, 4.41. Found: C, 48.77; H, 6.35; N, 4.70.

*1,5-Anhydro-2-C-carbamoyl-1,2-dideoxy-*D*-gluco-hexitol (**7**) and 3,4,6-tri-O-acetyl-1,5-anhydro-2-C-carbamoyl-1,2-dideoxy-*D*-gluco-hexitol (**4**)*

Attempts to prepare a pure crystalline sample of **4** by preparative t.l.c. of fractions F or G were unsuccessful. As a consequence fractions F and G (total 1.65 g) were combined and deacetylated in the usual way with methanolic sodium methoxide for 1 h. The resulting solution was deionized with Amberlite IR 120 (H^+) and the product **7** recrystallized several times from methanol (0.730 g), m.p. 214–215°, $[\alpha]_D^{22}$ +41° (*c* 2, water), c.d. $\Delta\varepsilon$ = 0.0563 $mol^{-1}cm^2$ (λ_{max} 225, water), $[\theta]_{225}^{30}$ − 186; $\Delta\varepsilon$ = +0.090 mol^{-1} cm^2 (λ_{max} 206, water), $[\theta]_{206}^{30}$ +297; o.r.d. $[M]_{310}^{23}$ +323, $[M]_{214}^{23}$ +648; i.r. (Nujol): 1660, amide I band; 1608 cm^{-1}, amide II band; τ D_2O 7.26 (H-2, two overlapping quartets, $J_{2,1e}$ = 5, $J_{2,1a}$ = 11, and $J_{2,3}$ = 11 Hz).

Anal. of **7** Calcd. for $C_7H_{13}NO_5$: C, 43.97; H, 6.85; N, 7.33. Found: C, 43.73; H, 6.74; N, 7.48.

Compound 7 (0.080 g) was acetylated with acetic anhydride and pyridine in the usual way to afford after crystallization from methanol – *n*-hexane 0.110 g (61%) of 3,4,6-tri-*O*-acetyl-1,5-anhydro-2-*C*-carbamoyl-1,2-dideoxy-D-*gluco*-hexitol (**4**), m.p. 126–127°, $[\alpha]_D^{21}$ +73° (*c* 2.5, chloroform), i.r. (CCl_4), 3520 and 3400 cm^{-1} (NH); τ ($(CD_3)_2$-C=O) 3.73 (NH_2), 7.90, 7.95, and 7.96 (acetyl), remaining peaks shown in Fig. 2. Irradiation at τ 4.55 changed the triplet at τ 5.05 to a doublet, $J_{4,5}$ = 10 Hz and changed the multiplet at τ 7.10 into a pair of doublets, $J_{2,1e}$ = 5 and $J_{2,1a}$ = 10 Hz. Irradiation at τ 7.10 collapsed the signals at τ 4.55 into a doublet, $J_{3,4}$ = 10 Hz and also affected the multiplets at τ 5.88 and 6.41.

Anal. of **4** Calcd. for $C_{13}H_{19}NO_8$: C, 49.21; H, 6.03; N, 4.41. Found: C, 49.22; H, 5.96; N, 4.27.

*3,4,6-Tri-O-acetyl-1,5-anhydro-2-C-carbamoyl-1,2-dideoxy-*D*-manno-hexitol*

Fraction H was fractionated by preparative t.l.c. to give **4** and a slightly contaminated syrupy product in low yield which is tentatively assigned to be 3,4,6-tri-*O*-acetyl-1,5-anhydro-2-*C*-carbamoyl-1,2-dideoxy-D-*manno*-hexitol on the basis of its n.m.r. spectrum, τ ($CDCl_3$) 6.90–7.02 (overlapping m, H-2), 6.23–6.5 (H-1a, H-5, two doublets at 6.25 and 6.40, H-1a, $J_{1a,2}$ = 3, $J_{1a,1e}$ = 13 Hz, H-5 signals overlapped H-1a signals), 5.6–6.0 (two doublets of H-1e overlapping H-6,6′ signals), 4.85 and 4.95 (H-3, two doublets, $J_{3,2}$ = 6, $J_{3,4}$ = 9 Hz), 4.6 (t, $J_{4,3}$ = 9, $J_{4,5}$ = 9 Hz), 3.5 and 4.2 (NH).

*2-C-Acetamidomethyl-3,4,6-tri-O-acetyl-1,5-anhydro-1,2-dideoxy-*D*-gluco-hexitol*

To a slurry of lithium aluminum hydride (0.160 g) in anhydrous tetrahydrofuran (10 ml) was added dropwise with magnetic stirring a solution of 3,4,6-tri-*O*-acetyl-1,5-anhydro-2-*C*-carbamoyl-1,2-dideoxy-D-*gluco*-hexitol (0.200

g) in 1.0 ml of tetrahydrofuran. After addition of 10 ml of tetrahydrofuran the reaction mixture was heated under reflux for 32 h. The reaction mixture was then cooled to 0° and excess lithium aluminum hydride was decomposed by dropwise addition of water. The solids were removed by filtration and washed with a 1:1 methanol–ethanol mixture (2 × 15 ml). The combined filtrates were evaporated under reduced pressure to yield a syrup which was then extracted with 20 ml of boiling methanol. The resulting filtrate was evaporated under reduced pressure to give 0.105 g of a syrup which gave a positive ninhydrin test. This syrup was acetylated with a 1:1 mixture of acetic anhydride and pyridine (1 ml) at room temperature for 24 h. After evaporation of the acetylating mixture under reduced pressure the product (0.154 g) was chromatographed on silica gel (13.5 × 1.3 cm) using 230 ml of 97:3 benzene–ethanol followed by 100 ml of 93:7 benzene–ethanol as eluent. The latter eluent on evaporation afforded a crystalline product which was recrystallized from ether and then ethyl acetate in benzene to give the title compound, yield 0.052 g (23%), m.p. 112–113°, $[\alpha]_D^{26}$ + 137° (*c* 2, chloroform), i.r. ($CHCl_3$) 3425 (NH), 1675 cm^{-1} (amide); τ $CDCl_3$, 8.04 ($CH_3\overset{O}{\overset{\|}{C}}-N$), 7.98, 7.95, and 7.94 (acetyl), 7.8–8 (m, overlapping acetyl peaks), 7.14 (m, 1H), 6.73 (t, H-1a, $J_{1a,2} = 12$, $J_{1a,1e} = 12$ Hz), 6.45 (m, 2H), 5.7–6.05 (overlapping peaks, 3H), 5.03 (m, H-3 and -4), 3.96 (NH). Irradiation at τ 8 altered the signals at τ 5.03.

Anal. Calcd. for $C_{15}H_{23}NO_7$: C, 52.20; H, 6.66; N, 4.06. Found: C, 52.31; H, 6.95; N, 4.12.

The support of the National Research Council of Canada is gratefully acknowledged.

1. S. W. Gunner, R. D. King, W. G. Overend, and N. R. Williams. J. Chem. Soc. C, 1954 (1970).
2. H. H. Baer. Adv. Carbohydr. Chem. **24**, 67 (1969).
3. H. P. Albrecht and J. G. Moffatt. Tetrahedron Lett. 1063 (1970).
4. G. J. Lourens. Tetrahedron Lett. 3733 (1969).
5. (*a*) A. Rosenthal and K. S. Ong. Tetrahedron Lett. 3981 (1969); (*b*) A. Rosenthal, K. S. Ong, and D. A. Baker. Carbohydr. Res. **13**, 113 (1970); (*c*) A. Rosenthal and K. S. Ong. Can. J. Chem. **48**, 3034 (1970); (*d*) A. Rosenthal, M. Sprinzl, and D. Baker. Tetrahedron Lett. 4233 (1970).
6. A. Rosenthal and D. Baker. Tetrahedron Lett. 397 (1969).
7. (*a*) D. Elad and J. Rokach. J. Org. Chem. **29**, 1855 (1964); (*b*) D. Elad and J. Rokach. J. Chem. Soc. 800 (1965); (*c*) D. Elad and J. Rokach. J. Org. Chem. **30**, 3361 (1965); (*d*) D. Elad and J. Rokach. J. Org. Chem. **31**, 4210 (1966).
8. R. U. Lemieux, R. K. Kullnig, H. J. Bernstein, and W. G. Schneider. J. Am. Chem. Soc. **80**, 6098 (1958).
9. (*a*) A. Rosenthal and H. J. Koch. Can. J. Chem. **43**, 1375 (1965); (*b*) A. Rosenthal. Advan. Carbohydr. Chem. **23**, 59 (1968).
10. K. Igarashi and T. Honma. J. Org. Chem. **35**, 606 (1970).

Can. J. Chem. Downloaded from www.nrcresearchpress.com by 210.87.254.5 on 09/05/12
For personal use only.

Etude de l'association du 2,6-di-ter-butylparacrésol avec la cyclohexanone

C. BOURDÉRON

Département de Chimie, Université de Montréal, Montréal, Québec

Reçu le 13 août 1971

Nous avons étudié, par spectroscopie i.r., jusqu'à la température de l'azote liquide l'association du 2,6-di-ter-butylparacrésol avec la cyclohexanone en solution. Dans un certain domaine de concentration nous avons pu mettre en évidence des complexes 1:1 et 1:2 (cyclohexanone–2,6-di-ter-butylparacrésol) et nous avons pu préciser la nature de ces complexes. Nous avons observé un phénomène d'induction de liaisons hydrogène par un solvant bromé.

The association between 2,6-di-tert-butylparacresol and cyclohexanone has been investigated in solutions down to liquid nitrogen temperature through the measurement of i.r. spectra. The presence of 1:1 and 1:2 complexes in a certain range of concentration was ascertained and the nature of these complexes was established. We observed solvent induced hydrogen bond formation in a bromine containing solvent.

Canadian Journal of Chemistry, **50**, 1199 (1972)

Can. J. Chem. Downloaded from www.nrcresearchpress.com by 210.87.254.105 on 09/05/12
For personal use only.

Introduction

L'emploi de basses températures est un avantage certain lorsqu'on étudie la liaison hydrogène et la mise au point dans ce laboratoire de verres résistant jusqu'à une température de -190 °C nous a permis d'envisager l'étude de complexes donneurs–accepteurs de proton jusqu'à cette température; la grande gamme de température utilisée nous permettant alors de calculer d'une manière précise les enthalpies de formation des divers complexes.

Les résultats obtenus par Asselin (1) montrent qu'à basse température des systèmes tels que: phénol–acétone, isopropanol–cyclohexanone dans des solvants neutres évoluent en fonction de la température. Dès -80 °C l'isopropanol se polymérise et l'accepteur de proton ne joue plus aucun rôle sur la polymérisation. Il faut donc choisir pour l'étude envisagée un alcool ou un phénol qui ne polymérise pratiquement pas même à basse température. Nous avons choisi le 2,6-di-ter-butylparacrésol (DTBPC).

Un certain nombre de résultats ont été publiés sur ce phénol et nous citerons les travaux de Wren et Lenthen (2) qui mesurant la constante d'association du système DTBPC–dioxanne pour deux températures (20 et 50 °C), trouvent dans les deux cas la même constante $K_c = 0.12$ et par un calcul d'erreur en déduisent que l'enthalpie de formation de la liaison hydrogène est inférieure à 1100 cal/mol. Ces auteurs étudient d'autres systèmes DTBPC – accepteurs de proton et ils montrent qu'il se forme souvent des complexes comportant plus de deux molécules ou des complexes bimoléculaires dans lesquels l'axe de la liaison O—H est soit dans le plan soit hors du plan du cycle benzènique.

Sakano *et al.* (3) montrent qu'il se forme préférentiellement des complexes de type 1:1 entre le 2,6-di-ter-butylphénol (molécule dont l'encombrement stérique du groupement OH est semblable à celui du DTBPC) et l'acétone, la *N,N*-diméthylacétamide et la pyridine.

Enfin, Ingold (4) dans une étude sur les 2,6-di-ter-butylphénols substitués en position 4 montre que l'axe du groupement OH est situé dans le plan du cycle benzènique.

Nous avons donc associé le DTBPC à différents accepteurs de proton dans différents solvants; suivant ces bases et ces solvants nous avons obtenu divers types de complexes. Le cas qui nous semble le plus intéressant est celui de l'association du DTBPC et de la cyclohexanone. Nous nous proposons d'étudier ce cas ici.

Partie expérimentale

Les solvants employés sont des mélanges dans des proportions 1:1 du CCl_3F (F11) et du méthylcyclopentane (MCP), du CCl_3F et du $C_2F_4Br_2$ (F114B2); tous ces composés ont été distillés sur anhydride phosphorique et conservés sur ce même produit.

Le 2,6-di-ter-butylparacrésol a été sublimé et la cyclohexanone distillée et conservée sur tamis moléculaire.

Les spectres ont été enregistrés sur un spectrophotomètre Perkin–Elmer, modèle 621.

Analyse des résultats spectraux

Lorsque l'on associe le DTBPC avec la cyclohexanone, on voit apparaître deux bandes

Can. J. Chem. Downloaded from www.nrcresearchpress.com by 210.87.254.105 on 09/05/12
For personal use only.

associées, l'une de haute fréquence: 3550 cm^{-1} environ, l'autre de basse fréquence: 3350 cm^{-1} environ. Ceci nous montre que plusieurs espèces associées coexistent, ou qu'un complexe comportant plusieurs molécules de DTBPC se forme. En utilisant comme solvant le mélange F11 + MCP, les deux bandes associées observées sont d'intensité croissante lorsque la température s'abaisse; d'autre part un effet de variation des concentrations nous montre que le rapport des intensités des deux bandes associées pour une température donnée varie avec les concentrations initiales, ce qui élimine l'hypothèse d'un seul complexe. Pour la même raison un équilibre du type suivant est à rejeter:

$$D + A \rightleftharpoons DA$$
$$D + A \rightleftharpoons (DA)'$$

équilibre, dans lequel DA et (DA)′ seraient des complexes qui se différentieraient par l'orientation respective de A et D. Nous pensons donc que les bandes observées indiquent la présence de plusieurs espèces associées: la bande de haute fréquence indique la présence d'un groupement O—H engagé dans une liaison hydrogène faible, celle de basse fréquence à un groupement O—H engagé dans une liaison hydrogène moyenne. Nous supposerons qu'il se forme deux types de complexes: des complexes cyclohexanone–DTBPC 1:1 et 1:2. Nous verrons à posteriori que cette supposition est confirmée.

L'équilibre envisagé se présentera sous la forme:

$$A + D \rightleftharpoons AD \qquad K_1 = c/a.d$$
$$AD + D \rightleftharpoons AD_2 \qquad K_2 = e/c.d$$

A, D, AD, et AD_2 représentent l'accepteur et le donneur de proton et les deux complexes formés; a, d, c, e les concentrations respectives à l'équilibre; a_0 et d_0 les concentrations initiales de l'accepteur et du donneur de proton.

Nous nous proposons de calculer les enthalpies de formation ΔH_1^0 et ΔH_2^0 des complexes AD et AD_2. Pour ce calcul il faut connaître les constantes K_1 et K_2 à plusieurs températures et ce serait facile si on pouvait connaître simultanément les concentrations a et d mais l'absorption des solvants empêche une telle détermination.

La calcul de d, concentration du DTBPC à l'équilibre se fera d'une manière classique; nous mesurerons le coefficient apparent d'extinction moléculaire ε_T de la bande OH libre nous en déduirons la concentration d à chaque température. Cependant si pour une petite gamme de température on peut considérer ε_T comme constant, dans la gamme que nous avons employée il n'en est pas de même. Avec différentes solutions de DTBPC de concentration connue, dans le mélange F11 + MCP nous avons établi la relation:

$$\varepsilon_T = 256 - 0.900\,(t - 25)$$

(Nous avons effectué les corrections dues à la concentration de volume.)

Un certain nombre de méthodes itératives existent pour calculer K_1 et K_2 (5, 6, 7) mais, en général, elles ne permettent pas de calculer ΔH_2^0.

Nous avons donc essayé d'adapter une méthode permettant le calcul des enthalpies de formation des différents complexes.

Des équilibres précédents on tire les relations:

$$d_0 = d + c + 2e$$
$$a_0 = a + c + e$$

ou:

$$d_0 - 2a_0 = d - 2a - c$$

en remplaçant c par $K_1.a.d$ on a

$$a = \frac{2a_0 + d - d_0}{2 + K_1 d}$$

$$K_2 = \frac{e}{c.d} = \frac{a_0 - a - K_1 da}{K_1 d^2 a}$$

Nous fixerons une valeur arbitraire de K_1 à 298 °K et de ΔH_1^0 puis par l'intégration de l'équation de Van't Hoff, nous déterminerons K_1 à diverses températures:

$$K_T = \exp\left[\log K_{(298\,^\circ K)} - \frac{\Delta H^0}{R}\cdot\left(\frac{1}{T} - \frac{1}{298}\right)\right]$$

Nous calculerons alors les K_2 correspondant et ΔH_2^0. Nous répéterons ces calculs pour une série de concentrations initiales a_0 et d_0 différentes. Il suffit ensuite de faire varier K_1 et ΔH_1^0 de façon à obtenir des valeurs pratiquement constantes de ΔH_2^0 et de K_2(298 °K) quelles que soient les concentrations initiales utilisées.

Les erreurs minimales sur ΔH_2^0 et K_2(298 °K) sont obtenues pour des valeurs légèrement différentes de K_1(298 °K) mais nous choisirons

TABLEAU 1. Calcul des constantes d'équilibre K_1 et K_2 et des concentrations des complexes AD et AD_2.* Concentration initiale en DTBPC: 0.065 M, en cyclohexanone: 0.0260 M; $-\Delta H_2^0$: 2.10 kcal/mol; coefficient de corrélation: 0.990

T (°C)	d_0	d	a_0	K_1	K_2	K_2 Moy	c	e
25	0.065	0.064	0.0260	0.6	3.5	1.9	0.001	0.000
−40	0.069	0.066	0.0278	1.0	4.6	5.4	0.001	0.000
−92	0.073	0.060	0.0294	2.1	30.2	21.6	0.003	0.004
−120	0.076	0.049	0.0304	3.9	67.5	67.1	0.003	0.011
−150	0.078	0.030	0.0315	10.1	460.3	400.4	0.002	0.023

*c et e sont calculées avec la constante K_2 Moy.

TABLEAU 2. Calcul des constantes d'équilibre K_1 et K_2 et des concentrations des complexes AD et AD_2. Concentration initiale en DTBPC: 0.096 M, en cyclohexanone: 0.055 M; $-\Delta H_2^0$: 2.21 kcal/mol; coefficient de corrélation: 0.998

T (°C)	d_0	d	a_0	K_1	K_2	K_2 Moy	c	e
25	0.096	0.092	0.055	0.6	2.0	1.9	0.003	0.000
−20	0.100	0.093	0.057	0.8	4.1	3.7	0.004	0.001
−40	0.102	0.092	0.058	1.0	5.6	5.4	0.005	0.002
−60	0.104	0.090	0.060	1.3	8.3	8.5	0.006	0.004
−75	0.106	0.086	0.061	1.6	12.4	12.7	0.006	0.007
−90	0.108	0.080	0.062	2.1	23.6	20.2	0.007	0.011
−105	0.110	0.067	0.063	2.8	37.0	34.9	0.007	0.018
−120	0.112	0.054	0.064	3.9	70.7	67.1	0.007	0.025
−135	0.114	0.040	0.065	6.0	140.9	148.8	0.006	0.034

TABLEAU 3. Calcul des constantes d'équilibre K_1 et K_2 et des concentrations des complexes AD et AD_2. Concentration initiale en DTBPC: 0.102 M, en cyclohexanone: 0.113 M; $-\Delta H_2^0$: 2.30 kcal/mol; coefficient de corrélation: 0.999

T (°C)	d_0	d	a_0	K_1	K_2	K_2 Moy	c	e
23	0.102	0.094	0.113	0.6	1.5	1.9	0.006	0.001
−75	0.113	0.079	0.125	1.6	9.7	12.7	0.011	0.011
−105	0.117	0.055	0.129	2.8	30.3	34.9	0.013	0.024
−120	0.119	0.043	0.132	3.9	49.1	67.1	0.011	0.032
−135	0.121	0.025	0.134	6.0	142.3	148.8	0.011	0.042
−150	0.123	0.013	0.137	10.1	385.1	400.4	0.010	0.050

comme valeur de K_1(298 °K) celle qui donne les meilleures valeurs de ΔH_2^0 et dans ce cas l'erreur maximum sur ΔH_2^0 sera de 5% (erreur déterminée à partir de la moyenne des différents ΔH_2^0). Nous verrons alors qu'il y a bon accord pour chaque série de mesures entre les constantes calculées à diverses températures et les constantes moyennes correspondantes déterminées à partir de toutes les séries.

Dans tous les cas on pourra alors vérifier que les coefficients de corrélation ont une valeur proche de 1, ce qui montre une bonne linéarité dans la courbe expérimentale $\log K_2 = f(1/RT)$.

Nous avons fait quatre séries de mesures à diverses concentrations en DTBPC et cyclohexanone.

Les calculs ont été effectués sur ordinateur. Après une série d'itérations nous avons obtenu pour ΔH_1^0, K_1(298 °K), ΔH_2^0 moy, K_2(298 °K) moy, les valeurs suivantes: K_1(298 °K) = 0.6, K_2(298 °K) = 1.9; $\Delta H_1^0 = -1.17$ kcal/mol, $\Delta H_2^0 = -2.21$ kcal/mol.

Dans les tableaux 1–4 nous donnons les résultats obtenus pour K_2, c, et e.

L'avantage de cette méthode est qu'elle n'exige pas que le nombre de mesures pour

Can. J. Chem. Downloaded from www.nrcresearchpress.com by 210.87.254.105 on 09/05/12
For personal use only.

Can. J. Chem. Downloaded from www.nrcresearchpress.com by 210.87.254.105 on 09/05/12
For personal use only.

TABLEAU 4. Calcul des constantes d'équilibre K_1 et K_2 et des concentrations des complexes AD et AD_2. Concentration initiale en DTBPC: 0.107 M, en cyclohexanone: 0.237 M; $-\Delta H_2^0$: 2.22 kcal/mol; coefficient de corrélation: 0.998

T (°C)	d_0	d	a_0	K_1	K_2	K_2 Moy	c	e
18	0.107	0.090	0.237	0.6	2.3	2.0	0.013	0.002
−60	0.116	0.070	0.257	1.3	8.4	8.5	0.021	0.012
−75	0.118	0.060	0.262	1.6	13.6	12.7	0.023	0.017
−90	0.120	0.070	0.266	2.0	21.1	20.2	0.023	0.023
−105	0.123	0.035	0.271	2.7	46.2	34.9	0.025	0.031
−120	0.125	0.025	0.276	3.9	74.6	67.1	0.023	0.038
−135	0.127	0.014	0.280	6.0	177.9	148.8	0.021	0.045
−150	0.129	0.007	0.286	10.1	398.7	400.4	0.017	0.052

chaque série soit le même; de plus les températures employées peuvent différer d'une série à l'autre.

On remarque que généralement l'erreur sur K_2 est grande à 25 °C, mais à cette température $d_0 - d$ est faible et l'erreur sur cette dernière quantité est grande.

Cependant on peut dire que les valeurs de K_2 coïncident pour les quatre séries de mesures et ceci confirme notre hypothèse sur les équilibres successifs avec formation de complexes 1:1 et 1:2.

L'examen des quatre tableaux nous montre en outre que bien qu'à la température ambiante la constante K_2 soit plus grande que la constante K_1, la concentration c est plus grande que la concentration e et que c passe ensuite par un maximum vers −100, −120 °C suivant les concentrations, tandis que e croît continuellement.

Discussion

Le complexe 1:2 peut se présenter sous deux formes, **1** et **2**.

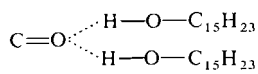

1

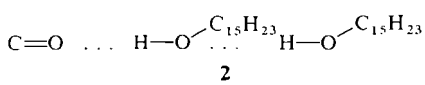

2

Lascombe (8) signale que pour un grand excès de donneur de proton par rapport à l'accepteur, on détecte des complexes de type **1**. Cependant Murrell (9) montre que les deux doublets libres de l'oxygène du groupement C=O sont différents, le premier est de caractère s très marqué et par conséquent très peu disponible pour former des liaisons hydrogène.

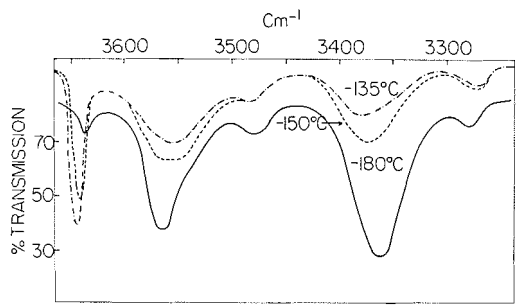

FIG. 1. Spectres du DTBPC (0.096 M) associé à la cyclohexanone (0.055 M) à différentes températures. Epaisseur de la cellule 0.1 mm; solvant F11 + MCP.

Ce dernier argument nous fait penser qu'en solution une structure de type **2** est plus probable.

L'examen de nos spectres (voir fig. 1) nous montre que nous voyons d'abord croître une bande à 3550 cm^{-1} environ et au fur et à mesure que la température diminue une deuxième bande apparaît à 3565 cm^{-1} environ et croît aussi régulièrement tandis qu'à un certain moment la bande située à 3550 cm^{-1} diminue d'intensité. Ce phénomène est d'autant plus visible que la concentration en cyclohexanone est faible et à condition que le complexe 1:2 se forme en quantité appréciable.

Ceci s'explique très bien lorsqu'on envisage une structure de type **2** et si nous faisons les attributions suivantes (fréquences obtenues à −190 °C):

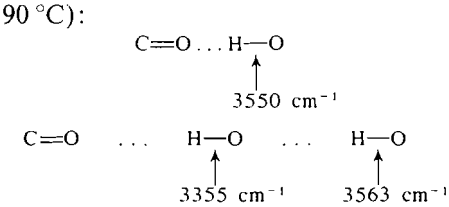

Nous avons vu par l'étude des constantes

Can. J. Chem. Downloaded from www.nrcresearchpress.com by 210.87.254.105 on 09/05/12
For personal use only.

d'équilibre que la concentration du complexe **1** doit croître jusqu'à -100 °C environ donc que l'intensité de la bande située à 3550 cm^{-1} doit croître elle aussi et ensuite que ce complexe est progressivement remplacé par le complexe 1:2 donc on doit voir la bande à 3550 cm^{-1} diminuer et elle doit être remplacée par la bande à 3565 cm^{-1}. Quant à la bande située à 3355 cm^{-1}, elle croît régulièrement.

Si on admet une relation croissante entre le déplacement de fréquence et l'énergie de formation d'un complexe, on s'aperçoit que le groupement C=O est meilleur accepteur que le complexe (C=O...H—O—$C_{15}H_{23}$), puisque la fréquence du groupement OH du complexe 1:1 est plus basse que celle du groupement OH terminal du complexe 1:2. Ce fait peut peut-être expliquer pourquoi il ne se forme qu'un complexe 1:2 (dans des gammes de concentration et de température importantes) car si on observait l'inverse on pourrait s'attendre à une polymérisation.

Il est à noter que notre attribution correspondant aux fréquences de vibration du groupement central OH du complexe 1:2 et du groupement OH du complexe 1:1 est semblable à celle que l'on ferait pour un dimère et un trimère d'alcool.

Il est difficile de mesurer la demi-largeur exacte des bandes associées du fait que la bande de haute fréquence est une bande double, cependant à -190 °C cette bande est presque simple et a une demi-largeur de 40 cm^{-1} tandis que la deuxième n'a qu'une demi-largeur de 45 cm^{-1} pour une fréquence de 3355 cm^{-1}. Ceci est assez surprenant car on s'attendrait à ce qu'une bande située aussi bas ait une demi-largeur beaucoup plus grande, cependant la fréquence de 3355 cm^{-1} ne correspond qu'à un seul vibrateur associé et non à un polymère. Cet exemple montre quand même que la relation $\Delta\nu_{\frac{1}{2}} = f(\Delta\nu)$ n'est pas générale. Ce fait est lié au degré de désordre qui existe dans le milieu. Il faut remarquer que dans ce cas de liaison hydrogène les groupements OH sont protégés de l'action du solvant par les groupements terbutyl et que ceci est une cause de l'amincissement des bandes OH associées.

Complexes de type 1:n

Le fait d'augmenter la concentration en cyclohexanone conduit graduellement suivant cette concentration à un nouveau phénomène et à un changement de l'équilibre envisagé (pour des concentrations en cyclohexanone de l'ordre de 0.6 *M* et en DTBPC de 0.1 *M*), l'application de notre méthode n'a donné aucun résultat (ce qui est normal du fait que nous avons un équilibre plus complexe). En effet pour des concentrations fortes en cyclohexanone nous voyons la bande associée à 3555 cm^{-1} baisser de fréquence continuellement lorsque la température diminue (il n'y a pas apparition de bande à 3563 cm^{-1} cependant elle peut être masquée par le massif à 3555 cm^{-1}), d'autre part la deuxième bande associée a une fréquence plus basse que précédemment 3320 cm^{-1}; les demi-largeurs pour ces bandes associées sont de 60 cm^{-1} pour la première et d'environ 100 cm^{-1} pour la deuxième (la mesure est assez imprécise du fait de l'absorption de 2ν C=O dans cette région). Pour une concentration initiale de 0.1 *M* en DTBPC et de 0.236 *M* en cyclohexanone on voit à -190 °C dans la région de 3300–3400 cm^{-1} deux bandes, l'une à 3350 cm^{-1}, l'autre à 3320 cm^{-1}, la deuxième devenant plus importante au fur et à mesure que l'on augmente la concentration en cyclohexanone; on passe donc progressivement d'un équilibre à un autre. Il est assez difficile de préciser la nature de ce troisième équilibre; cependant Gramstad et Van Binst (10) ont pu voir que l'on avait dans un certain domaine de concentration des complexes avec une molécule de phénol et deux d'accepteur de proton, ils ont même mesuré l'enthalpie de formation du complexe. Dans notre cas nous avons peut-être des complexes de même type ou des complexes de type 1:3, mais les spectres ne permettent pas de faire une attribution avec certitude.

Lorsqu'on reprend les spectres précédents en utilisant comme solvant le mélange 2F on s'aperçoit que lorsque la température diminue, il apparaît d'abord une bande associée dans la région de 3550 cm^{-1} et une autre dans la région de 3310 cm^{-1}, ensuite les bandes augmentent régulièrement en intensité et à une température voisine de -150 °C la première augmente beaucoup moins rapidement pour finalement diminuer d'intensité ou rester stationnaire suivant les concentrations, tandis que la deuxième devient très importante (fig. 2); dans ce cas la demi-largeur est de 92 cm^{-1} environ. Par comparaison avec les résultats précédents,

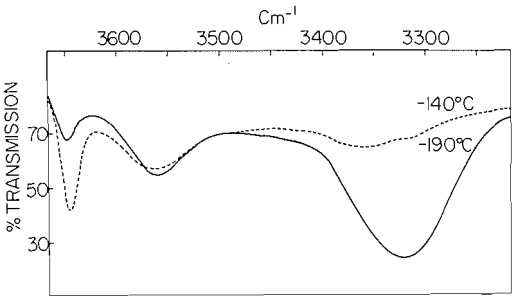

FIG. 2. Spectres du DTBPC (0.100 *M*) associé à la cyclohexanone (0.200 *M*) à deux températures. Epaisseur de la cellule 0.1 mm; solvant 2F.

il est probable que nous ayons obtenu un polymère et que ce polymère ait été induit par le $C_2F_4Br_2$; or dans ce composé seul les atomes de brome peuvent avoir été responsables d'une telle induction. Le mécanisme de l'interaction consiste probablement dans un transfert de charge de l'oxygène au brome.

Conclusion

L'étude du 2,6-di-ter-butylparacrésol nous a montré que ce composé ne forme pratiquement pas d'autoassociation même à la température de l'azote liquide, mais en présence d'accepteur de proton il forme des complexes de type 1:1 et 1:2. Ce résultat est un exemple d'induction de liaison hydrogène par le groupement C=O, cependant il nous est difficile de formuler des explications quant au mécanisme de cette induction. Dans un solvant contenant du brome ($C_2F_4Br_2$) nous avons même des complexes de type $1:n$, et nous avons un exemple d'induction de liaison hydrogène par le solvant.

Dans la gamme de température et de concentration ou le complexe 1:2 existe nous avons calculé son enthalpie de formation et proposé une structure pour ce complexe.

Je remercie tout particulièrement M. C. Sandorfy pour m'avoir aidé de ses conseils et pour avoir relu le manuscrit.

1. M. ASSELIN. Résultats non publiés.
2. J. J. WREN et P. M. LENTHEN. J. Chem. Soc. 2557 (1961).
3. T. K. SAKANO, S. L. ROCK, et R. M. HAMMAKER. Spectrochim. Acta, **25A**, 1195 (1969).
4. K. U. INGOLD. Can. J. Chem. **38**, 1092 (1960).
5. T. L. BROWN et M. KUBOTA. J. Am. Chem. Soc. **83**, 331 (1961).
6. K. B. WHETSEL et R. E. KAGARISE. Spectrochim. Acta, **18**, 315 (1962).
7. F. CRUEGE, P. PINEAU, et J. LASCOMBE. J. Chim. Phys. **64**, 1161 (1967).
8. J. LASCOMBE. Thèse de Doctorat, Bordeaux, 1960.
9. J. N. MURRELL. The theory of the electronic spectra of organic molecules. John Wiley Inc., Londres et New York, 1963.
10. T. GRAMSTAD et G. VAN BINST. Spectrochim. Acta, **22**, 1681 (1966).

Can. J. Chem. Downloaded from www.nrcresearchpress.com by 210.87.254.105 on 09/05/12
For personal use only.

Mechanism of Alcohol to Ester Rearrangement in Phosphorus Compounds[1]

A. F. JANZEN AND T. G. SMYRL
Department of Chemistry, University of Manitoba, Winnipeg, Manitoba

Received October 4, 1971

The kinetics of the base-catalyzed rearrangement of dialkyl 2-hydroxy-1,1,1,3,3,3-hexafluoroisopropylphosphonate, $(RO)_2P(O)C(OH)(CF_3)_2$ to 1,1,1,3,3,3-hexafluoroisopropyldialkyl phosphate, $(RO)_2P(O)OCH(CF_3)_2$, where R = methyl, ethyl, *n*-butyl, have been studied. Energies of activation and entropies of activation have been obtained and the base strength of the catalyst has been varied. A mechanism is proposed to account for the results.

Les cinétiques des transpositions baso-catalysées des dialkyl-2 hydroxy-1,1,1,3,3,3-hexafluoroisopropylphosphonates $(RO)_2P(O)C(OH)(CF_3)_2$ en 1,1,1,3,3,3-hexafluoroisopropyldialkyl phosphates, $(RO)_2P(O)OCH(CF_3)_2$ avec R = méthyle, éthyle, *n*-butyle, ont été étudiées. Les énergies d'activation et les entropies d'activation ont été obtenues et la force basique du catalyseur a été modifiée. Un mécanisme est proposé pour rendre compte des résultats.

Canadian Journal of Chemistry, **50**, 1205 (1972)

Introduction

Rearrangements involving isomeric alcohols and alkoxides are potentially useful in synthetic chemistry. Depending on the element M, a straightforward procedure may result in the preparation of one, but not the other, isomer.

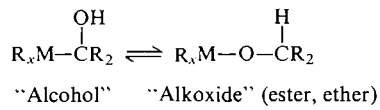

Considering only one example, namely the addition of metalloid–hydrogen bonds across carbonyl bonds, it is well known that B—H (1), Si—H (2), Ge—H, and Sn—H (3) bonds react with ketones to give alkoxides, whereas C—H, N—H, P—H, and As—H (4) bonds react with ketones to give alcohols.

Significant work has been carried out in the area of "alcohol–alkoxide" rearrangements. The Wittig rearrangement (M = C) involves the conversion of ether to alcohol in the presence of a strong base such as alkyllithium (5). The Brook rearrangement (M = Si) involves the conversion of alcohol to alkoxide in the presence of diethylamine (6, 7) whereas the reverse rearrangement, *i.e.* alkoxide to alcohol (M = Si) in the presence of *t*-butyllithium, has recently been reported by West and co-workers (8). Peddle and Ward have reported the alcohol to alkoxide rearrangement for M = Ge (9).

[1]Presented at the 54th Canadian Chemical Conference and Exhibition. Halifax, Nova Scotia, May 31–June 2, 1971.

A number of workers have reported base-catalyzed "alcohol–alkoxide" rearrangements involving phosphorus compounds (10) and a kinetic study, by the refractometric method, of phosphonate to phosphate rearrangement has been reported by Pudovik and co-workers (11).

In 1970 we reported the reaction of dialkyl phosphonates with hexafluoroacetone and found that in each case isomeric products were formed, the relative yield depending on the nature of

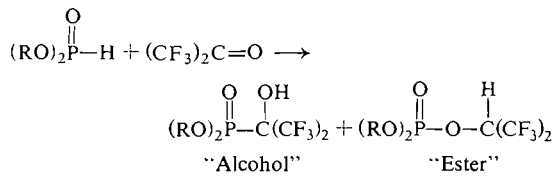

R (12). We further observed that rearrangement of alcohol to ester did not take place at room temperature in the absence of basic catalyst, *i.e.* under preparative conditions, and hence a rearrangement was not invoked to explain the relative yield of products.

To investigate this reaction further and determine under what conditions rearrangement does occur and what conditions give maximum yield of either alcohol or ester, a kinetic and mechanistic study was undertaken of the base-catalyzed rearrangement, in which R, base, and temperature were systematically varied.

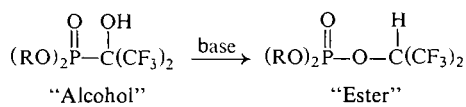

Can. J. Chem. Downloaded from www.nrcresearchpress.com by 210.87.254.40 on 09/05/12
For personal use only.

Can. J. Chem. Downloaded from www.nrcresearchpress.com by 210.87.254.40 on 09/05/12
For personal use only.

TABLE 1. Rates of rearrangement of $(CH_3O)_2P(O)C(OH)(CF_3)_2$ by pyridine in dichloromethane at 32.6 °C

Initial alcohol concentration (M)	Initial base concentration (M)	k_1' (s^{-1})	k_2 ($l\ mol^{-1}\ s^{-1}$)
0.99	1.71	5.18×10^{-4}	3.03×10^{-4}
0.49	1.71	5.15×10^{-4}	3.01×10^{-4}
0.99	2.57	7.92×10^{-4}	3.08×10^{-4}
0.49	2.57	7.82×10^{-4}	3.04×10^{-4}

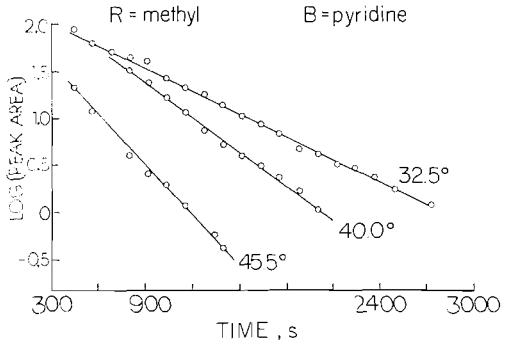

FIG. 1. Plot of log of peak area *vs.* time for rearrangement of $(CH_3O)_2P(O)C(OH)(CF_3)_2$ (0.99 M) with pyridine (2.57 M) in dichloromethane at various temperatures.

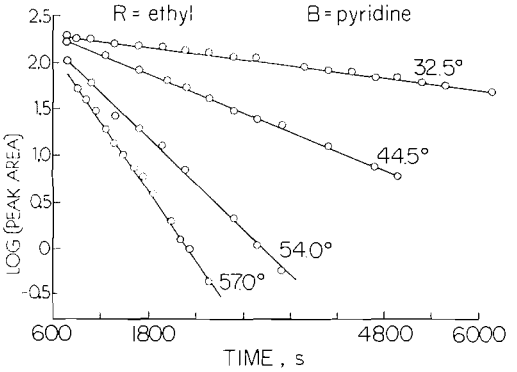

FIG. 2. Plot of log of peak area *vs.* time for rearrangement of $(C_2H_5O)_2P(O)C(OH)(CF_3)_2$ (1.22 M) with pyridine (2.57 M) in dichloromethane at various temperatures.

Kinetic Results

The chemical shifts of trifluoromethyl groups of alcohol and ester differ sufficiently (12) that ^{19}F n.m.r. techniques were suitable for measuring concentrations.

The base catalyst pyridine was added to the alcohol in dichloromethane as solvent and the disappearance of the alcohol doublet was followed as a function of time. Pseudo first order rate constants k_1' were obtained by plotting the logarithm of the peak area against time and the best value of the slope was calculated by the method of least squares. Dividing through by the base catalyst concentration, $k_1'/(\text{base}) = k_2$, gave a second order rate constant k_2 which is independent of initial concentration of alcohol and base, as shown in Table 1.

Alkyl substituents were varied and with the aid of a variable temperature probe on the n.m.r. instrument pseudo first order rate constants were determined at several temperatures for R = methyl (Fig. 1), R = ethyl (Fig. 2), and R = *n*-butyl (Fig. 3). The second order rate constant was obtained as described above and values of k_2 are given in Table 2.

It may be seen from Table 2 that rates of rearrangement decrease in the order R = methyl > ethyl > *n*-butyl, the second order rate constants being 8.03×10^{-4} (45.6°), 1.33×10^{-4} (44.6°), and 1.27×10^{-4} (51.4°) $l\ mol^{-1}\ s^{-1}$, respectively.

Plotting $\log k_2$ *vs.* $1/T$ gave linear plots from which the energy of activation was obtained. The entropy of activation and pre-exponential

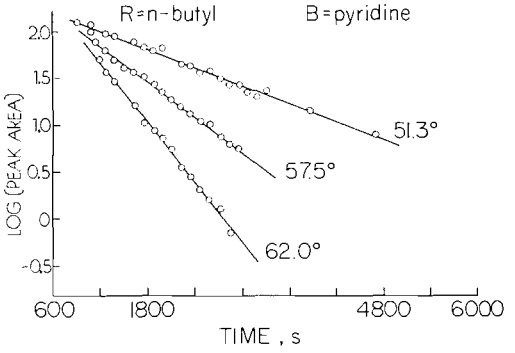

FIG. 3. Plot of log of peak area *vs.* time for the rearrangement of $(n\text{-}C_4H_9)_2P(O)C(OH)(CF_3)_2$ (1.18 M) with pyridine (2.57 M) in dichloromethane at various temperatures.

Can. J. Chem. Downloaded from www.nrcresearchpress.com by 210.87.254.40 on 09/05/12
For personal use only.

TABLE 2. Rates of rearrangement of $(RO)_2P(O)C(OH)(CF_3)_2$ by pyridine in dichloromethane

R	T (°C)	k_2 (1 mol^{-1} s^{-1})
CH_3	32.6	3.03×10^{-4}
	40.1	4.89×10^{-4}
	45.6	8.03×10^{-4}
C_2H_5	32.6	3.96×10^{-5}
	42.3	1.07×10^{-4}
	44.6	1.33×10^{-4}
	54.1	3.15×10^{-4}
	57.1	3.80×10^{-4}
n-C_4H_9	51.4	1.27×10^{-4}
	54.6	1.60×10^{-4}
	57.6	2.42×10^{-4}
	58.0	3.01×10^{-4}
	62.1	4.07×10^{-4}

TABLE 3. Energy of activation (E_a), entropy of activation ($\Delta S^{\ddagger}$), and logarithm of pre-exponent (log A) for $(RO)_2P(O)C(OH)(CF_3)_2$ rearrangement

R	E_a (k cal/mol)	$\Delta S^{\ddagger}$ (cal/mol degree)	log A
CH_3	14.6	−29.1	6.87
C_2H_5	19.8	−15.9	9.75
n-C_4H_9	24.5	−3.0	14.0

factor were calculated in the usual way (see experimental) and activation parameters are summarized in Table 3.

From the energies of activation it may be seen that the rate of rearrangement is favored in the order methyl > ethyl > *n*-butyl. On the other hand, the entropies of activation partly compensate for this trend since the negative entropies of activation are in the same order.

The effect of the basic catalyst on the rearrangement was also studied. Typical basic catalysts such as pyridine, dimethylsulfoxide, aniline, *N*-methylaniline, *N*,*N*-dimethylaniline, piperidine, and diethylamine, which differ widely in base strength[2] as measured by their pK_b, were added to the alcohol (R = methyl) in dichloromethane and the rearrangement studied at 33°. Rate constants k_1' and k_2 were obtained and, as shown in Table 4, the data indicate that, with the exception of *N*,*N*-dimethylaniline, the stronger the base the greater the rate of rearrangement.

[2]The base strength with respect to the alcohol in dichloromethane solution is not known and pK_b values are an approximation only.

TABLE 4. Effect of base catalyst (1.38 *M*) on rearrangement of $(CH_3O)_2P(O)C(OH)(CF_3)_2$ (1.10 *M*) in dichloromethane at 33 °C

Base	pK_b^*	k_2 (1 mol^{-1} s^{-1})
Dimethylsulfoxide	13	$\sim 7 \times 10^{-6}$
Aniline	9.37	1.11×10^{-4}
N-Methylaniline	9.15	1.47×10^{-4}
N,*N*-Dimethylaniline	8.85	1.02×10^{-4}
Pyridine	8.75	3.00×10^{-4}
Diethylamine	3.51	†
Piperidine	2.88	†

*Value for dimethylsulfoxide taken from Anal. Chem.; all others from "Handbook of chemistry and physics" (see ref. 17).
†Too fast for measurement by n.m.r. techniques.

Mechanism of Rearrangement

A reasonable mechanism for the alcohol to ester rearrangement must be consistent with second order kinetics and the observed activation parameters. If the mechanism was similar to that proposed by Brook, it would suggest that a common mechanism is possible for a variety of elements undergoing the "alcohol–alkoxide" rearrangement. Brook and co-workers (6) found that the base-catalyzed rearrangement of α-silylcarbinol (alcohol) to silyl ether (alkoxide) is first order in alcohol and first order in base and involves processes having low energies of activation but very high negative entropies of activation, and a cyclic three-membered transition state was postulated.

Pudovik and co-workers (11), who studied the thermal isomerization in the absence of solvent, of compounds **3**, **4**, and **5**, postulated a mechanism in which the oxygen atom of the hydroxyl group attacks the phosphorus atom, which then

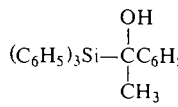

1

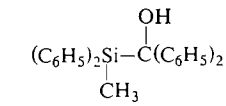

2

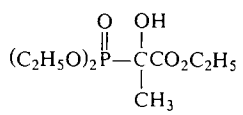

3

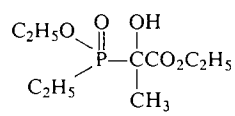

4

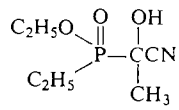

5

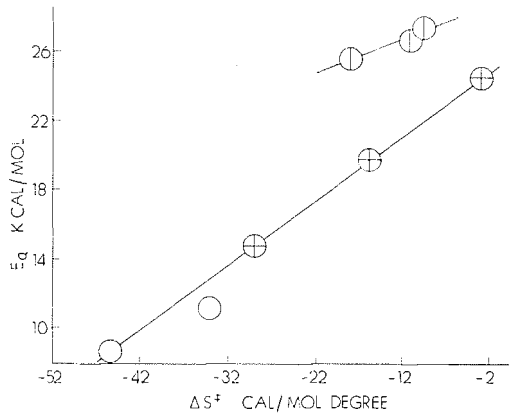

FIG. 4. Plot of E_a *vs.* $\Delta S^{\ddagger}$ for "alcohol to alkoxide" rearrangement: this work, ⊕; Brook *et al.* (6), ○; and Pudovik *et al.* (11), ⊙.

leads to cleavage of O—H and C—P bonds and formation of new C—O—P and C—H bonds.

To test for an isokinetic relationship, the energy of activation was plotted *vs.* the entropy of activation, as described by Leffler (13). As seen from Fig. 4, the results of this work and those of Brook for compounds **1** and **2** give an approximately linear plot, suggesting a common mechanism of rearrangement. On the other hand, the results of Pudovik for compounds **3**, **4**, and **5** are displaced towards higher energies of activation and more negative entropies of activation and since his results were obtained in the absence of solvent and catalyst it is not surprising that a different mechanism is implied by Fig. 4.

A reasonable mechanism that is consistent with the kinetics and activation parameters and, at the same time, is in agreement with the results obtained by Brook, is shown in eqs. 1–3.

Step 1 involves polarization of the hydroxyl oxygen, either through hydrogen bonding, which is expected to be particularly strong for pyridine and perfluoroalcohols (14), or through ionization to give the pyridinium ion. Hydrogen bonding in the starting compound involving phosphoryl oxygen and hydroxyl would probably be of smaller magnitude (15). Step 1 probably involves rapid proton exchange and the effect of increasing base strength of catalyst must be to shift the equilibrium to the right, in the direction of increased ionization.

Step 2 must then represent the rate determining step; in particular, it is postulated that the

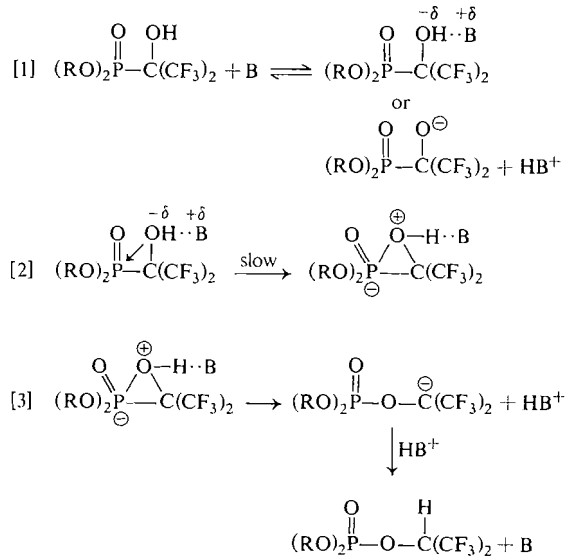

slow step is the intramolecular nucleophilic attack of the hydroxyl oxygen on the phosphorus atom, thereby implying that any substituent on the phosphorus atom which releases electron density to the phosphorus atom will increase the energy barrier to the transition state. Since the inductive (electron release) effect of alkyl groups is generally assumed to be in the order butyl > ethyl > methyl the argument is consistent with the trend found for the activation energies.

Step 3 involves collapse to final ester product, either through an intermediate carbanion followed by proton transfer, or directly via simultaneous cleavage of P—C bond and formation of C—H bond.

The negative entropies of activation are consistent with a constrained intermediate, namely a cyclic three-membered complex as postulated by Brook. For R = *n*-butyl the entropy of activation is only −3.0 e.u. and molecular models show that steric interactions are present between rotating *n*-butyl and trifluoromethyl groups. However, these steric interactions are not expected to differ greatly in the ground state and transition state and, in view of an isokinetic relationship, a cyclic three-membered transition state seems most reasonable.

It is interesting to speculate whether eqs. 2 and 3 could, under different conditions, represent equilibrium processes and permit the reverse rearrangement *i.e.* ester to alcohol. Undoubtedly a very strong base would be

Can. J. Chem. Downloaded from www.nrcresearchpress.com by 210.87.254.40 on 09/05/12
For personal use only.

Can. J. Chem. Downloaded from www.nrcresearchpress.com by 210.87.254.40 on 09/05/12
For personal use only.

required for carbanion formation, and we find that if *n*-butyllithium is added to ester (R = methyl) the characteristic ^{19}F n.m.r. doublet of the ester is replaced by a singlet, as required for the carbanion. Further n.m.r. examination showed that a P—C bond was not formed and we conclude that the reverse reaction did not go past the carbanion stage. What other factors, if any, could drive the equilibrium past the carbanion to the alcohol stage are not known at present, although the relative stabilities of P—C *vs.* P—O and $(RO)_2P(O)C(O^-)(CF_3)_2$ *vs.* $(RO)_2P(O)OC^-(CF_3)_2$ could be important (8).

Experimental

Conventional vacuum line techniques were used for handling volatile materials. Hexafluoroacetone, dialkyl phosphonates, and bases were purified by vacuum distillation or trap-to-trap distillation and their purity checked by i.r. and n.m.r. spectroscopy. Dichloromethane (B.D.H. Chemicals) was used without further purification. The n.m.r. spectra were obtained on a Varian A-56/60A spectrometer using 60 and 56.4 MHz for proton and fluorine, respectively.

Preparation of Dialkyl 2-Hydroxy-1,1,1,3,3,3-hexafluoroisopropylphosphonate, $(RO)_2P(O)C(OH)(CF_3)_2$, in High Yield

The procedure described previously (12) gave low yields for R = methyl and ethyl. Changing reaction conditions as described below substantially increased the yield.

Dimethyl phosphonate (2.40 g, 21.8 mmol) in dichloromethane (10.0 ml) was cooled to −196° and hexafluoroacetone (4.29 g, 25.8 mmol) was added. The reaction tube was sealed under vacuum and placed in a Dry Ice–acetone bath (−78°) which was allowed to evaporate and reach 25° over a period of 24 h. After this time the reaction tube was opened and excess hexafluoroacetone removed. The products were identified as dimethyl-2-hydroxy-1,1,1,3,3,3-hexafluoroisopropylphosphonate ("alcohol"), $(CH_3O)_2P(O)C(OH)(CF_3)_2$ (5.06 g, 84%), and 1,1,1,3,3,3-hexafluoroisopropyldimethyl phosphate ("ester"), $(CH_3O)_2P(O)OCH(CF_3)_2$ (0.96 g, 16%) on the basis of ^1H and ^{19}F n.m.r. and i.r. examination (12).

Diethyl phosphonate (3.01 g, 21.8 mmol) in dichloromethane (10.0 ml) and hexafluoroacetone (4.29 g, 25.8 mmol) were allowed to react as described above to give $(C_2H_5O)_2P(O)C(OH)(CF_3)_2$ (5.83 g, 88%) and $(C_2H_5O)_2P(O)OCH(CF_3)_2$ (0.80 g, 12%).

The compound $(C_4H_9O)_2P(O)C(OH)(CF_3)_2$ was prepared in yields of at least 90%, the remainder being $(C_4H_9O)_2P(O)OCH(CF_3)_2$, using the procedure outlined above or as described previously (12).

No rearrangement occurred when alcohols were kept at room temperature in the absence of basic catalyst. Furthermore, no rearrangement occurred when dialkyl phosphonates were added to the alcohols at room temperature.

One of the esters, namely $(CH_3O)_2P(O)OCH(CF_3)_2$, was found to be unstable in the presence of bases such as pyridine and diethylamine. After an induction period of approximately 30 min, the ester reacted with pyridine to give a new product containing the grouping $CH_3OPOCH(CF_3)_2$, as determined by ^1H and ^{19}F n.m.r. Approximately 50% of the ester had reacted after 24 h, and 66% after 48 h. Since this reaction was too slow to interfere with the kinetic results, it was not investigated further.

Kinetic Measurements

A Varian A-56/60A n.m.r. spectrometer, equipped with a variable temperature probe, was used to determine rate constants. The ^{19}F n.m.r. spectra showed well separated doublets due to trifluoromethyl groups of alcohol and isomeric ester (12).

In a typical kinetic run, a solution of alcohol in dichloromethane, in a standard n.m.r. tube, was allowed to reach thermal equilibrium in the sample probe of the n.m.r. spectrometer. The n.m.r. tube was then withdrawn and a measured amount of base added and the mixture shaken to ensure thorough mixing. The n.m.r. tube was re-inserted and the ^{19}F n.m.r. peaks due to alcohol and ester were recorded at regular intervals of time until at least 90% rearrangement had occurred. During the kinetic runs the integral heights of alcohol and ester were summed to check that sums remained constant *i.e.* to ensure that alcohol was converted only to ester.

Pseudo first order rate constants k_1' were obtained from a plot of the logarithm of alcohol peak area *vs.* the time and the best slope calculated by the method of least squares. Second order rate constants were obtained by dividing the pseudo first order rate constant by the concentration of base *i.e.* $k_2 = k_1'/(\text{base})$.

The Arrhenius energy of activation E_a was obtained by repeating the kinetic runs at several temperatures. An ethylene glycol temperature *vs.* chemical shift chart was used to calibrate the temperature of the n.m.r. probe, and the temperatures are accurate to ±1°. The temperature was checked before and after every run and if the temperature varied that particular run was discarded.

The entropy of activation was calculated from the equation

$$k = e\,\frac{kT}{h}\,e^{\Delta S^{\ddagger}/R}\,e^{-Ea/RT} \quad (16)$$

and A from

$$k = A\,e^{-Ea/RT} \quad \text{(ref. 16, p. 53)}$$

The rearrangement of $(CH_3O)_2P(O)C(OH)(CF_3)_2$ was studied at 33° in dichloromethane as a function of base strength of catalyst. Dimethylsulfoxide, aniline, *N*-methylaniline, *N*,*N*-dimethylaniline, pyridine, piperidine, and diethylamine were used and, in each case, k_1' and k_2 were determined and the results are shown in Table 4.

The financial assistance of the National Research Council of Canada is gratefully acknowledged.

1. G. W. PARSHALL. Inorg. Chem. **4**, 52 (1965).
2. A. F. JANZEN and C. J. WILLIS. Can. J. Chem. **43**, 3063 (1965); Inorg. Chem. **6**, 1900 (1967).
3. W. R. CULLEN and G. E. STYAN. Inorg. Chem. **4**, 1437 (1965).
4. C. G. KRESPAN and W. J. MIDDLETON. Fluorine chemistry review. Vol. 1. *Edited by* P. Tarrant. M. Dekker, New York, 1967.
5. G. WITTIG and L. LÖHMANN. Ann. **550**, 260 (1942); H. E. ZIMMERMAN. Molecular rearrangements. Part I. *Edited by* Paul de Mayo. Interscience, New York, N.Y., 1963. p. 372–377.
6. A. G. BROOK, G. E. LEGROW, and D. M. MACRAE. Can. J. Chem. **45**, 239 (1967).
7. G. J. D. PEDDLE and J. E. H. WARD. J. Organomet. Chem. **13**, 269 (1968).
8. R. WEST, R. LOWE, H. F. STEWART, and A. WRIGHT. J. Am. Chem. Soc. **93**, 282 (1971).
9. G. J. D. PEDDLE and J. E. H. WARD. J. Organomet. Chem. **14**, 131 (1968).
10. W. F. BARTHEL, B. H. ALEXANDER, P. A. GIANG, and S. A. HALL. J. Am. Chem. Soc. **77**, 2424 (1955); L. A. R. HALL, C. W. STEPHENS, and J. J. DRYSDALE. J. Am. Chem. Soc. **79**, 1768 (1957); I. S. BENGELSDORF. J. Org. Chem. **21**, 475 (1956); S. J. FITCH and K. MOEDRITZER. J. Am. Chem. Soc. **84**, 1876 (1962); V. S. ABRAMOV, N. I. D'YAKONOVA, and V. D. EFIMOVA. Zh. Obschei Khim. **39**, 1971 (1969).
11. A. N. PUDOVIK, I. V. GUR'YANOVA, L. V. BANDEROVA, and G. V. ROMANOV. J. Gen. Chem. USSR, **38**, 142 (1968).
12. A. F. JANZEN and R. POLLITT. Can. J. Chem. **48**, 1987 (1970).
13. J. E. LEFFLER. J. Org. Chem. **20**, 1202 (1955).
14. W. J. MIDDLETON and R. V. LINDSEY, JR. J. Am. Chem. Soc. **86**, 4948 (1964).
15. L. J. BELLAMY. Advances in infrared group frequencies. Methuen, London, 1968. p. 204.
16. K. J. LAIDLER. Chemical kinetics. 2nd ed. McGraw-Hill, New York, N.Y., 1965. p. 90.
17. C. A. STREULI. Anal. Chem. **30**, 997 (1958). Handbook of chemistry and physics. 51st ed. *Edited by* R. C. West. Chemical Rubber Co., Cleveland, 1970. p. D117.

Can. J. Chem. Downloaded from www.nrcresearchpress.com by 210.87.254.40 on 09/05/12
For personal use only.

Synthesis of Oligothymidylates on an Insoluble Polymer Support

K. K. OGILVIE AND K. KROEKER

Department of Chemistry, University of Manitoba, Winnipeg, Manitoba

Received August 26, 1971

The synthesis of a succinylated polystyrene polymer is described. The polymer is converted to the acid chloride form and condensed with thymidine derivatives. A number of methods for phosphorylation of polymer bound nucleosides were investigated and the synthesis of tetrathymidine triphosphate (TpTpTpT) is described.

On décrit la synthèse d'un polymère de styrène succinylé. Le polymère est transformé en chlorure d'acide et condensé avec les dérivés de thymidine. On a étudié plusieurs méthodes de phosphorylation des nucléosides attachés au polymère et on décrit la synthèse du dérivé triphosphaté de tétrathymidine (TpTpTpT).

Canadian Journal of Chemistry, **50**, 1211 (1972)

Can. J. Chem. Downloaded from www.nrcresearchpress.com by 210.87.254.42 on 09/05/12
For personal use only.

Introduction

The multistep synthesis of oligonucleotides on a polymer support offers a major advantage in that polymer-bound products may be easily separated from excess reagents and soluble by-products at each step. As a result a number of polymers have been investigated as supports for oligonucleotide synthesis. Hayatsu and Khorana (1) and Cramer *et al.* (2) have used soluble polystyrene polymers in which the reactive site was a triphenylmethyl chloride group. Melby and Strobach (3) have used a similar approach except that their polymer was insoluble in organic solvents. Letsinger *et al.* (4*a*) developed a crosslinked polystyrene "popcorn" polymer possessing a benzoyl functional group. Crosslinked polystyrene polymers have also been used by Kusama and Hayatsu (4*b*) and by Blackburn *et al.* (5). While nucleotides have been synthesized on all of these polymers yields are usually low. Further, conditions required to remove the nucleotide from the polymers also hydrolyze protecting groups from the nucleotide units.

We have investigated a succinylated polystyrene polymer as a support in nucleotide synthesis. Nucleosides would be bound to such a polymer via an acyl functional group which would be at a greater distance from the polymer backbone than in the "popcorn" polymer (4*a*). Since completion of our work Yip and Tsou (6) have reported use of an isotactic succinylated polystyrene polymer in ribooligonucleotide synthesis.

Results and Discussion

In any general useful synthesis, reagents should be readily available. For this reason we chose Biobeads S-X2, a commercially available (7) porous styrene–divinylbenzene copolymer and acylated it using succinic anhydride (Scheme 1).

When the acylation reaction was carried out at 60 °C using freshly sublimed aluminum chloride in nitrobenzene polymer **2** was obtained. Polymer **2** contained 0.39 mmol of succinyl group per gram of polymer. Polymer **2** was converted to the acid chloride form **3** on reaction with thionyl chloride in benzene with pyridine as catalyst. Polymer **3** reacted readily with thymidine or thymidine derivatives possessing a free 5′-hydroxyl but did not react with thymidine derivatives having only a free 3′-hydroxyl group. The thymidine content of polymer **4** was between 0.08 and 0.13 mmol of thymidine per gram of polymer. In all condensations a thymidine content of 0.11 mmol per gram of polymer was used.

Thymidine could not be removed from **4** using hydrazine solution.[1] Thymidine was easily removed from the polymer using 0.5 *N* NaOH in dioxane:water (1:1).

3′-*O*-Monomethoxytritylthymidine (T-MTr) reacted with **3** to produce **4***b* (R = monometh-

[1]This is in sharp contrast to the isotactic polymer of Yip and Tsou where the hydrazine solution did remove thymidine from the polymer. This must reflect a much greater degree of freedom for the side chain in the isotactic polymer as compared to the cross-linked polymer **4** (6).

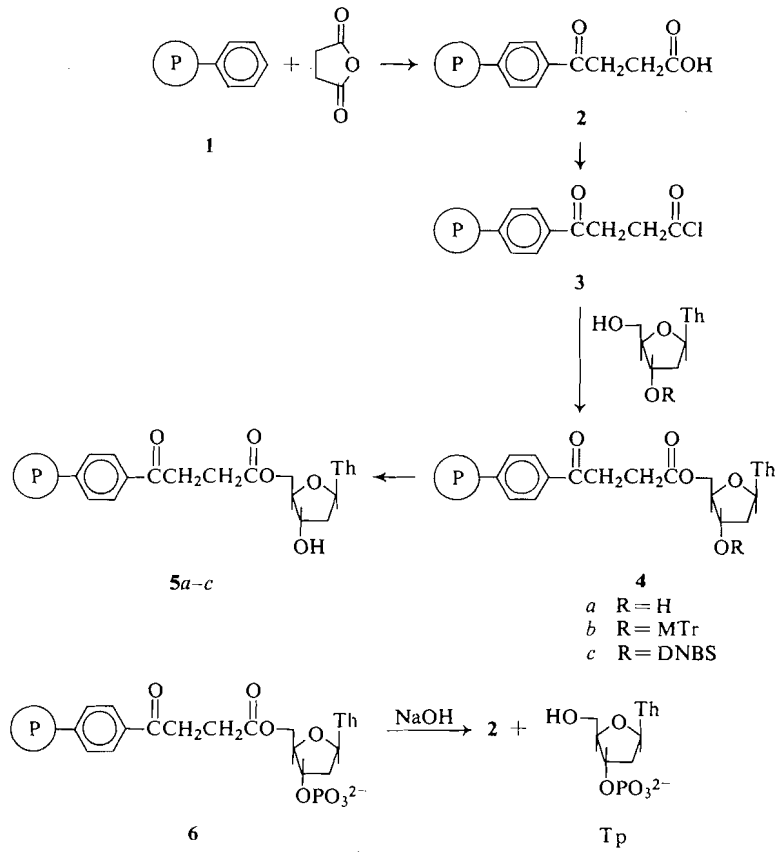

SCHEME 1

oxytrityl = MTr). Aqueous acetic acid, even at elevated temperatures, would not completely remove the methoxytrityl group from **4***b*. However, a 0.1% solution of trifluoroacetic acid in benzene completely removed the MTr group at room temperature.

3′-*O*-(2,4-Dinitrobenzenesulfenyl) thymidine also reacted readily with **3** to produce **4***c* (R = 2,4-dinitrobenzenesulfenyl = DNBS). The sulfenyl group was readily removed from **4***c* using thiophenol in pyridine.

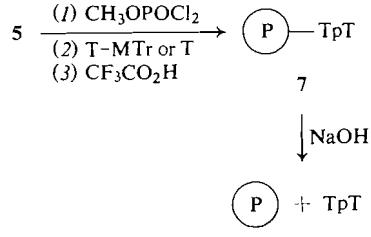

SCHEME 2

For investigation of phosphorylations on the polymer a polymer **5***b* containing 0.11 mmol of thymidine per gram of polymer was used. Using β-cyanoethyl phosphate with mesitylenesulfonyl chloride (MSCl) as condensing agent, 73% of the polymer bound thymidine was converted to thymidine-3′ phosphate (Tp). When dicyclohexylcarbodiimide was used in place of MSCl the yield of Tp was 65%. Methyl dichlorophosphate was the most convenient phosphorylating agent and gave a 75% conversion of thymidine to Tp.

Two different routes (Schemes 2 and 3) were used for the synthesis of nucleotide chains on the polymer (**5**). On the first approach (Scheme 2) polymer **5***b* was phosphorylated with methyl dichlorophosphate and the reactive intermediate was condensed directly with 3′-*O*-monomethoxytritylthymidine. After removal of the methoxytrityl group the nucleotidic material was cleaved from the polymer and a 38% yield of thymidylyl-(3′–5′)-thymidine (TpT) was ob-

Can. J. Chem. Downloaded from www.nrcresearchpress.com by 210.87.254.42 on 09/05/12
For personal use only.

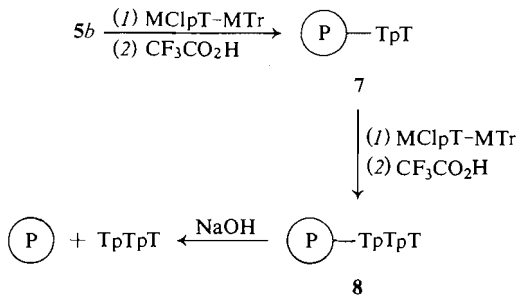

SCHEME 3

tained. The TpT so obtained was completely degraded by both snake venom and spleen enzymes.

This procedure was used with polymer **5***a*, condensing with unblocked thymidine at each step. The conversion of polymer bound thymidine to tetrathymidine triphosphate (TpTpTpT) was 4%.

The alternate route is outlined in Scheme **3**. Polymer **5***b* was condensed with methyl 3′-*O*-monomethoxytritylthymidine-5′ chlorophosphate (MeClpT–MTr) and the polymer was treated with trifluoroacetic acid to yield **7**. Analysis of a sample of **7** revealed a 34% conversion to TpT. Repeating the phosphorylation step with **7**, followed by acid and base hydrolysis gave thymidylyl-(3′–5′)-thymidylyl-(3′–5′)-thymidine (TpTpT) in 10% overall yield. The nucleotides produced by this route were completely degradable by snake venom and spleen enzymes.

These experiments show that the succinylated cross-linked polystyrene polymer can be conveniently used as a support for solid-phase synthesis of oligonucleotides containing entirely the natural 3′–5′ linkage. The yields for this polymer are slightly lower than for the isotactic polymer and this undoubtedly reflects increased steric hindrance at the reactive sites of the cross-linked polymer.

Experimental

General Methods

Paper chromatography was carried out by the descending technique on Whatman 3 mm paper. The solvent systems were: solvent A, 2-propanol – concentrated ammonium hydroxide – water (7:1:2); solvent B, 1-propanol – concentrated ammonium hydroxide – water (55:10:35). The solvents were prepared on a volume basis. Paper electrophoresis was performed using Whatman 3 mm paper in a Savant Flat Plate electrophoretic chamber with a Savant Flat Plate Model HV power supply operated at 2000 V for 1 h; the solution was buffered at p*H* 8.0 with 0.0033 *M* potassium dihydrogen phosphate and 0.063 *M* disodium hydrogen phosphate. Nucleosides and their derivatives were observed on paper strips by fluorescence in u.v. light (Mineralite).

The i.r. spectra were obtained with a Perkin–Elmer 337 recording spectrophotometer. All samples were prepared in KBr disks. The u.v. spectra were obtained on a Cary 14 recording spectrometer. The term OD unit refers to the extinction of the nucleotidic material in 1 ml of neutral solution in a quartz cell with a 1-cm light path.

Reagents and Chemicals

Reagent grade pyridine was distilled from *p*-toluenesulfonyl chloride, redistilled from calcium hydride, and stored over Linde Molecular Sieve. Pyridinium mono-β-cyanoethyl phosphate was prepared from the barium salt by passage over a column of Dowex 50WX8 resin (pyridinium form). The clear solution was first concentrated to a small volume and lyophilized to a gum. The gum was dissolved in pyridine and diluted to a known volume and stored in a sealed flask under refrigeration. Nucleotide products were characterized (chromatography and electrophoresis) by comparison to known compounds prepared by the "triester" method (8).

Enzyme Assays

The procedures used for snake venom and spleen phosphodiesterases have been described previously (8).

Methyl 3′-O-Monomethoxytritylthymidine-5′ Chlorophosphate (MClpT–MTr)

This compound was prepared by the method of Smrt and Catlin (9) as a stock solution in pyridine containing 0.11 mmol/ml of MClpT–MTr.

Succinylated Polystyrene (2)

(*a*) SX-2 resin (2 g), freshly sublimed aluminum chloride (2.13 g), and succinic anhydride (0.8 g, 8 mmol) were stirred in nitrobenzene (25 ml) at 60 °C for 1.5 h. The reaction mixture was poured into a beaker containing 25 ml of 6 *N* HCl and stirred for 10 min. The polymer was filtered, washed with water (3 × 25 ml), ethanol (3 × 25 ml), and benzene (3 × 25 ml), and then dried over phosphorus pentoxide. The acid content of the polymer was determined by adding excess standard sodium hydroxide solution (0.01 *M*) to a portion of the polymer and back titrating the excess NaOH with standard HCl (0.014 *M*) using phenolphthalein as indicator. The acid content of the polymer was found to be 0.39 mequiv/g. The i.r. spectrum (KBr disk) showed a broad strong absorption between 3600 and 2600 as well as between 1700 and 1600 cm^{-1}.

(*b*) The above procedure was repeated using reagent grade aluminum chloride directly. After 1.5 h the polymer had 0.10 mequiv of acid/g and at the end of 3 h contained 0.25 mequiv of acid/g.

Acid Chloride Polymer (Polymer 3)

Polymer **2** (100 mg) was added to a solution containing thionyl chloride (5 ml), pyridine (2.5 ml), and benzene (5 ml) and the mixture was heated at reflux for 5 h. The polymer (0.31 mequiv of chloride per gram of polymer by the indirect Volhardt method) was collected by filtration,

Can. J. Chem. Downloaded from www.nrcresearchpress.com by 210.87.254.42 on 09/05/12
For personal use only.

Can. J. Chem. Downloaded from www.nrcresearchpress.com by 210.87.254.42 on 09/05/12
For personal use only.

washed with dry benzene, and dried over phosphorus pentoxide. The i.r. spectrum (KBr disk) showed a strong acid chloride absorption at 1830 cm^{-1}.

Addition of Thymidine to Polymer 3

Polymer **3** (100 mg) and thymidine (100 mg, 0.4 mmol) were stirred in pyridine for 48 h at room temperature. The polymer was collected by filtration and washed with pyridine (25 ml), water (3 × 15 ml), and ethanol (3 × 15 ml) and then dried over phosphorus pentoxide. The i.r. spectrum (KBr disk) showed strong absorption between 1750 and 1660 cm^{-1}. The peak at 1830 cm^{-1} present in polymer **3** had disappeared.

Removal of Thymidine From Polymer 4a

(A) Sodium Hydroxide

Polymer **4***a* was treated with NaOH (0.5 N in dioxane: water, 1:1) for 48 h at room temperature. The reaction mixture was filtered and the filtrate neutralized with Dowex 50WX8 (pyridinium form). The filtrate was concentrated and applied to Whatman 3 mm paper which was then developed in solvent A. The nucleoside band (R_F^A 0.68) was eluted with water and the yield determined spectrophotometrically. The yield of thymidine bound to the polymer from several different preparations varied from 0.1 to 0.13 mmol/g of polymer.

(B) Hydrazine Hydrate Solution

Polymer **4***a* was treated with a solution containing hydrazine hydrate: acetic acid: pyridine (1:6:24) for periods up to 48 h. The solutions were separated from the polymer by filtration and applied to Whatman 3 mm paper for chromatography in solvent A. No thymidine was detected from any hydrazine hydrolysis.

Addition of 3′-Protected Thymidines to Polymer 3

In separate experiments 3′-*O*-monomethoxytrityl thymidine (10) and 3′-*O*-(2,4-dinitrobenzenesulfenyl)thymidine (11) were added to polymer **3** in the same manner as described above for thymidine. Analysis of the product polymers **4***b* and *c* by NaOH (method A above) showed the amount of nucleoside bound to the polymer varied from 0.08 to 0.13 mmol/g.

Removal of Protecting Groups From Polymer Bound Nucleosides

(A) Hydrolysis of the Monomethoxytrityl Group

Initially polymer **4***b* was treated with 80% acetic acid in water at room temperature for 24 h. Base hydrolysis (method A) showed that only partial hydrolysis of the monomethoxytrityl group had occurred. The same result was obtained with 80% acetic acid in a steam bath for 3 h. Finally a sample of polymer **4***b* was treated with trifluoroacetic acid (0.1% in chloroform) at room temperature for 6 h. Base hydrolysis (method A) of the polymer showed that the methoxytrityl group had been completely removed from the polymer-bound thymidine.

(B) Hydrolysis of the 2,4-Dinitrobenzenesulfenyl Group

Polymer **4***c* was stirred for 4 h with a pyridine solution containing two drops of thiophenol per ml of pyridine. The polymer was collected by filtration, washed with pyridine (25 ml), ethanol (3 × 15 ml), and water (3 × 15 ml). Base hydrolysis (method A) of the polymer yielded only thymidine, the 2,4-dinitrobenzenesulfenyl group had been completely removed.

Attempted Addition of 5′-Protected Thymidines to Polymer 3

When polymer **3** was treated with either 5′-*O*-monoethoxytritylthymidine (12) or 5′-*O*-(2,4-dinitrobenzenesulfenyl)thymidine (11) using the same conditions as described above for the 3′-protected derivatives, no esterification of the polymer occurred.

General Procedures for Phosphorylation of Nucleosides Bound to the Polymer

(I) Polymer **5***b* (100 mg containing 0.011 mmol of thymidine) and β-cyanoethyl phosphate (0.28 mmol, pyridinium form) were dried by evaporation of pyridine (4 × 1 ml). Mesitylenesulfonyl chloride (120 mg, 0.55 mmol) and pyridine (1.5 ml) were added and the mixture was stirred for 2 days at room temperature. Water (1.5 ml) was added and stirring continued for 24 h. The polymer was separated by filtration, washed with pyridine (25 ml), water (3 × 25 ml), and ethanol (3 × 25 ml), and dried over P_2O_5. A sample (50 mg) of the polymer was hydrolyzed with NaOH (method A) and the products thymidine (T) and thymidine-3′ phosphate (Tp) were separated by paper chromatography in solvent A. The bands were eluted with water to give 69 OD units of Tp (73%, R_F^A 0.09) at 267 nm and 25 OD units of T (R_F^A 0.67) at 267 nm.

(II) The above reaction was repeated except that dicyclohexylcarbodiimide (145 mg, 0.75 mmol) was used in place of mesitylenesulfonyl chloride and the reaction was stirred for 8 days. Analysis of the polymer gave 75 OD_{267} units of Tp (65%) and 40 OD_{267} units of T.

(III) Reaction I was repeated except that methyl dichlorophosphate was used in place of both β-cyanoethyl phosphate and mesitylenesulfonyl chloride. Analysis of the polymer (method A) after 24 h showed a 75% conversion to Tp. The yield was unaffected (71%) when the amount of methyl dichlorophosphate was doubled.

Synthesis of Thymidylyl-(3′–5′)-thymidine on the Polymer

Polymer **5***b* (100 mg containing 0.011 mmol of thymidine) was phosphorylated using method III. At the end of the condensation the polymer was washed thoroughly with dry pyridine (5 × 15 ml). A solution containing 3′-*O*-methoxytritylthymidine (26 ml, 0.05 mmol) in 1 ml of pyridine was added and the mixture was stirred for 4 days. The polymer was collected by filtration, washed with pyridine (3 × 15 ml) and chloroform (3 × 15 ml), and stirred for 6 h with 3 ml of trifluoroacetic acid (0.1% in chloroform). The polymer was collected by filtration, washed successively with chloroform (6 × 15 ml), ethanol (3 × 15 ml), and ether (3 × 15 ml), and a portion hydrolyzed by method A. Analysis of the products showed three products: thymidine (R_F^A 0.68, 29 OD_{267} units); thymidine-3′ phosphate (R_F^A 0.09, 30 OD_{267} units), and thymidylyl-(3′–5′)-thymidine (TpT, R_F^A 0.37, 71 OD_{267} units, 38%). The TpT so produced was completely degraded by both snake venom and spleen enzymes.

Synthesis of Thymidylylthymidylylthymidylylthymidine (TpTpTpT) on the Polymer

Polymer **5***a* (100 mg containing 0.011 mmol of thymidine) was phosphorylated as in method III and condensed with thymidine (0.05 mmol) as in the TpT preparation above. The polymer was washed with pyridine (25 ml), water (3 × 15 ml), ethanol (3 × 15 ml), and tetrahydrofuran (3 × 15 ml) and dried over P_2O_5. The phosphorylation, condensation, and washing steps were repeated twice more and the

TABLE 1. Products of TpTpTpT preparation on the polymer

Product	R_F^B	Identity	OD_{267} Units	% Yield
1	0.76	T	21	
2	0.64	TpT	18	10
3	0.53	TpTpT	10	3.8
4	0.47	TpTp	24	
5	0.43	Tp	34	
6	0.41	TpTpTpT	14	4
7	0.36	TpTpTp	15	

final polymer was hydrolyzed using method A. The products were identified by paper chromatography and electrophoresis by comparison with authentic material (8) and the results are shown in Table 1.

Synthesis of TpT using MClpT–MTr and Polymer 5b

Polymer **5***b* (50 mg, containing 5.5 μmol of thymidine) and 1 ml of the stock solution of MClpT–MTr were stirred together at room temperature for 4 days. The polymer was collected by filtration, washed with pyridine (25 ml), ethanol (3 × 15 ml), and chloroform (3 × 15 ml) and treated with trifluoroacetic acid 13 ml (0.1% in chloroform) for 6 h. The polymer was collected, washed successively with chloroform (6 × 15 ml), ethanol (6 × 15 ml), and tetrahydrofuran (3 × 15 ml), and dried over P_2O_5. Analysis of the product polymer by method A revealed a 38% yield of TpT relative to thymidine. The TpT was completely degraded by both snake venom and spleen enzymes.

Synthesis of Thymidylyl-(3–5′)-thymidylyl-(3′–5′)-thymidine using MClpT–MTr and Polymer 5b

Polymer **5***b* (50 mg, 5.5 μmol of thymidine) was treated exactly as above for the synthesis of TpT. However, after the trifluoroacetic acid treatment the polymer was dried and the condensation procedure using MClpT–MTr was repeated. Analysis of the polymer by method A showed a 10% yield of TpTpT based on the amount of thymidine originally bound to the polymer. The TpTpT so produced was completely degradable by both snake venom and spleen phosphodiesterases.

We wish to acknowledge financial support from the National Research Council of Canada.

1. H. HAYATSU and H. G. KHORANA. J. Am. Chem. Soc. **89**, 3880 (1967).
2. F. CRAMER, R. HELBIG, H. HETTLER, K. H. SCHEIT, and H. SELIGER. Angew. Chem. **78**, 640 (1966).
3. L. R. MELBY and D. R. STROBACH. J. Org. Chem. **34**, 421 (1969).
4. (*a*) R. L. LETSINGER, M. H. CARUTHERS, and D. M. JERINA. Biochem. **6**, 1379 (1967). (*b*) T. KUSAMA and H. HAYATSU. Chem. Pharm. Bull. **18**, 319 (1970).
5. C. M. BLACKBURN, M. J. BROWN, and M. R. HARRIS. J. Chem. Soc. (C), 2438 (1967).
6. K. F. YIP and K. C. TSOU. J. Am. Chem. Soc. **93**, 3272 (1971).
7. Bio-Rad Laboratories. Richmond, California.
8. R. L. LETSINGER and K. K. OGILVIE. J. Am. Chem. Soc. **91**, 3350 (1969).
9. J. SMRT and J. CATLIN. Tetrahedron Lett. 5081 (1970).
10. K. K. OGILVIE and R. L. LETSINGER. J. Org. Chem. **32**, 2365 (1967).
11. R. L. LETSINGER, J. FONTAINE, V. MAHADEVAN, D. A. SCHEXNAYDER, and R. E. LEONE. J. Org. Chem. **29**, 2615 (1964).
12. H. SCHALLER, G. WEIMANN, B. LERCH, and H. G. KHORANA. J. Am. Chem. Soc. **85**, 3821 (1963).

Can. J. Chem. Downloaded from www.nrcresearchpress.com by 210.87.254.42 on 09/05/12
For personal use only.

Reactions of Nitro Sugars. XXVI. Analysis and Separation of Stereoisomers by Nuclear Magnetic Resonance Spectroscopy and Column Chromatography of Benzylidene Derivatives[1]

HANS H. BAER AND WERNER RANK

Department of Chemistry, University of Ottawa, Ottawa, Canada K1N 6N5

Received November 18, 1971

Stereoisomeric methyl 4,6-*O*-benzylidene-3-deoxy-3-nitrohexopyranosides proved to be distinguishable by the chemical shifts of their benzylidene methine proton signals, and ratios of such isomers in mixtures could be estimated by signal integration. The method was applied to a reinvestigation of the epimeric distributions in which methyl 3-deoxy-3-nitro-α-D-hexopyranosides arise, firstly, in the nitromethane cyclization of 2-*O*-[(*S*)-formyl(methoxy)methyl]-(*R*)-glyceraldehyde and, secondly, in their base-catalyzed configurational equilibration via nitronates. Previous results were essentially confirmed as far as the preferred configurations are concerned but require some revision as to the relative abundance of less favored configurations. By preparative chromatography of benzylidene acetals and subsequent debenzylidenation, some nitrohexopyranosides of the α-D series were isolated for the first time in crystalline condition. Separation of isomers in the β-D series was improved by use of chromatography and by a new method involving differential reactivities of compounds toward alkali.

Les composés méthyl 4,6-*O*-benzylidène-3-déoxy-3-nitrohexopyranosides stéréoisomériques peuvent être différenciés par les déplacements chimiques des signaux du proton méthine benzylidène; de même on peut estimer les proportions de tels isomères dans les mélanges en intégrant le signal. La méthode a été appliquée à une nouvelle étude des distributions épimériques dans lesquelles les composés méthyl 3-déoxy-3-nitro-α-D-hexopyranosides apparaissent, premièrement dans la cyclisation du nitrométhane du 2-*O*-[(*S*)-formyl(méthoxy)méthyl]-(*R*)-glycéraldéhyde, et deuxièmement dans leur équilibre configurationnel catalysé par les bases, via les nitronates. Les résultats précédents ont été essentiellement confirmés en autant que les configurations les plus stables sont concernées, mais il doivent être revisés en ce qui a trait à l'abondance relative des configurations moins favorisées. Par chromatographie préparative des acétals de benzylidène et par la débenzylidénation subséquente, on a isolé quelques nitrohexopyranosides de la série α-D pour la première fois à l'état cristallin. On a amélioré la séparation des isomères dans la série β-D en utilisant la chromatographie et au moyen d'une nouvelle méthode impliquant les réactivités différentielles des composés envers les alcalins.

Canadian Journal of Chemistry, **50**, 1216 (1972)

Introduction

In synthetic work with nitro sugars, as indeed with carbohydrates in general, benzylidene acetals play a paramount role (1, 2). The most recent, extensive use of *O*-benzylidenated nitro sugars was made in syntheses of epoxynitro (3) and halonitro (4) glycosides. Prior publications had recorded the preparation of 4,6-*O*-benzylidene acetals derived from several, but not all, of the known methyl 3-deoxy-3-nitrohexopyranosides. The acetals were obtained, by standard procedures, mostly from pure glycosides and occasionally from non-crystallizable mixtures of stereoisomers (2). In conjunction with various synthetic projects we have now elaborated further the techniques of separating and characterizing nitro glycosides by way of benzylidenation. With n.m.r. spectroscopy as an analytical aid and column chromatography as a preparative tool, some nitro sugar derivatives were isolated for the first time, and the preparation of others was facilitated. Special benefit, however, accrued from benzylidenation when it was applied in studies on the stereochemistry of the sugar dialdehyde – nitromethane cyclization and the epimerization of glycoside nitronates.

Results

A convenient means of differentiating stereoisomeric methyl 4,6-*O*-benzylidene-3-deoxy-3-nitrohexopyranosides was found in the sharp n.m.r. singlet given by the methine proton of the benzylidene group. The chemical shifts of these signals proved indicative of sets of isomers (Table 1). Although in chloroform-*d* solution the shifts differed little in compounds having the *gluco* and *galacto* configurations, they permitted differentiation between these and *manno* and

[1]For Part XXV see ref. 10.

Can. J. Chem. Downloaded from www.nrcresearchpress.com by 210.87.254.105 on 09/05/12
For personal use only.

TABLE 1. Benzylidene methine and methoxyl proton n.m.r. signals (τ-scale)

Compound	Configuration	PhCH		OCH_3	
		in $CDCl_3$	in DMSO-d_6	in $CDCl_3$	in DMSO-d_6
2	α-D-*manno*	4.34	4.24	6.61	6.67
3	α-D-*talo*	4.42	4.32	6.60	6.66
4	α-D-*gluco*	4.48	4.34	6.55	6.63
5	α-D-*galacto*	4.50	4.40	6.56	
17	β-D-*gluco*	4.48	4.33	6.46	6.57
18	β-D-*galacto*	4.48	4.38	6.40	6.57
19	β-D-*manno*	4.32	4.26	6.44	6.58

talo isomers. In dimethylsulfoxide-d_6 solution, on the other hand, the *gluco* and *talo* derivatives had similar shifts but could be distinguished from the *manno* and *galacto* derivatives. The variations observed were distinctly larger than those recorded (5) for a number of non-nitro analogs. In fact, the signal separation in certain mixtures of isomers readily allowed quantitative determination of the component ratio by integration (Table 2, mixtures A–D). Thus, in three-component mixtures containing **2**, **3**, and **4** in varying proportions, the percentage of each compound could be measured with an accuracy of $\pm 4\%$ or better. On the other hand, the chemical shift of the methine proton was scarcely influenced by the anomeric configuration. However, anomers may be distinguished by their methoxyl proton resonances (Table 1) which tend to occur at higher field for axial groups than for equatorial ones (6).

Prompted by the feasibility of spectral identification and quantitative assay of certain benzylidene acetals, we decided to reinvestigate the configurational distributions in which stereoisomeric methyl 3-deoxy-3-nitro-α-D-hexopyranosides are formed (7, 8) in the nitromethane cyclization of 2-*O*-[(*S*)-formyl(methoxy)methyl]-(*R*)-glyceraldehyde (**1**, "D-hydroxymethyl-D′-methoxydiglycolaldehyde") and also those in which they exist after thermodynamically controlled epimerization (8). In the earlier work, the nitro glycosides had not been obtained in crystalline form; approximate estimates of product ratios in the amorphous mixtures could be gleaned from the amounts of amino sugars that were isolated, upon catalytic hydrogenation, partly by direct crystallization and partly by chromatographic procedures. Although the configurational preferences in these reactions had thereby been reasonably well established, no great accuracy could be claimed in a quantitative sense. A renewed study using improved techniques therefore appeared worthwhile.

A mixture of nitro glycosides was prepared, essentially as described (8), by the reaction of dialdehyde **1** with nitromethane followed by

TABLE 2. Analysis of acetal mixtures by n.m.r. spectroscopy

Mixture*	Composition		PhCH signals	
	Compounds	Ratio	τ-Values†	Intensity ratios
A	**2**, **3**, **4**	16.7:49.8:33.5	4.34 4.41 4.48	19.0:48.2:32.8
B	**2**, **3**, **4**	33.3:14.5:52.2	4.34 4.41 4.49	29.6:15.1:55.3
C	**19**, **3**, **4**	28.9:42.6:28.5	4.32 4.41 4.48	27.3:41.8:30.9
D	**19**, **3**, **17**	39.7:25.1:35.2	4.33 4.41 4.48	35.3:27.5:37.2
E	**2**, **3**, **4**, **5**		4.34 4.42 4.49‡	37.1:11.8:51.1‡
			(4.24 4.33§ 4.40)	42.0:49.2§:8.8
F	**2**, **3**, **4**, **5**		4.34 4.415 4.49‡	15.5:52.6:31.9‡

*A–D, standards made by mixing weighed amounts of crystalline compounds; E, mixture from nitromethane cyclization of **1** (see text); F, mixture from nitromethane cyclization followed by epimeric equilibration (see text).
†In $CDCl_3$ except for the set in parentheses, which refers to DMSO-d_6.
‡**4** + **5**.
§**3** + **4**.

Can. J. Chem. Downloaded from www.nrcresearchpress.com by 210.87.254.105 on 09/05/12
For personal use only.

Can. J. Chem. Downloaded from www.nrcresearchpress.com by 210.87.254.105 on 09/05/12
For personal use only.

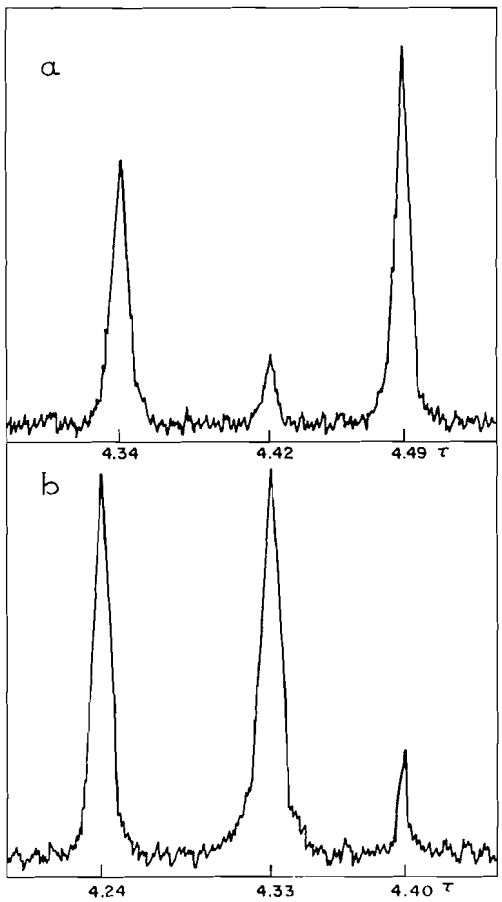

FIG. 1. Methine proton signals, in 100 MHz n.m.r. spectrum with 100 Hz sweep width, of nitromethane cyclization mixture from **1**, after benzylidenation; *a*, in $CDCl_3$; *b*, in DMSO-d_6.

deionization.[2] Exhaustive benzylidenation with benzaldehyde and zinc chloride gave a mixture of 4,6-acetals that showed methine proton signals assignable to the α-D-*manno* (**2**), α-D-*talo* (**3**), α-D-*gluco* (**4**), and α-D-*galacto* (**5**) isomers. In $CDCl_3$, there occurred three signals having an intensity ratio of 37:12:51, corresponding to **2**, **3**, and **4** + **5**. In DMSO-d_6, there occurred three signals with an intensity ratio 42:49:9, corresponding to **2**, **3** + **4**, and **5** (Fig. 1 and Table 2, mixture E). It is concluded from these data that the *manno* and *gluco* compounds, **2** and **4**, were present as main products in similar amounts (about 40% each), whereas the *talo* and *galacto* compounds, **3** and **5**, were minor products present to the extent of about 10% each. The acetal mixture was then chromatographed on silica gel, and substantial amounts of each isomer could be isolated in crystalline form. Complete separation was not achieved, but the proportions of isomers contained in mixed fractions were estimated spectroscopically, and summation of the yields indicated a ratio of 42:8:41:9 for **2**:**3**:**4**:**5**, in good agreement with the ratio found in the mixture prior to chromatography.

These results established in a more reliable, quantitative way what had been deduced earlier (8) from preparative separation of products on the amine stage, namely, that the *manno* and *gluco* configurations are favored in the nitromethane cyclization of **1** when kinetic control prevails. The results revealed, moreover, that the *talo* and *galacto* configurations are formed to a significant extent; the former had previously been observed to arise in an unspecified, small proportion and the latter had not been detected at all, under similar reaction conditions.[3]

We then proceeded to examine in the same way the isomer ratio that exists after the aforementioned nitro glycosides have been allowed to epimerize in aqueous, alkaline solution to the thermodynamic equilibrium of their nitronates. Equilibration and subsequent deionization of the nitronate mixture was performed as previously described (8), and the product was then benzylidenated. The acetal mixture in $CDCl_3$ solution showed three methine-proton peaks (τ 4.34, 4.415, and 4.49), and their intensity ratios were 15.5:52.5:32 in a 3-day epimerization experiment[4] (Fig. 2 and Table 2, mixture F). The first two signals corresponded to the α-D-

[2]The reaction time allowed for the nitromethane cyclization was 45 min whereas in the previous work (8) it was 25 min.

[3]It may be expected that minor changes in such conditions as reaction time (see footnote 2), temperature, or alkalinity of the medium could produce measurable variations in product ratios, owing to the interplay of kinetic and thermodynamic factors. In the nitromethane cyclization leading to analogous 6-deoxy glycosides, for instance, the *gluco* to *manno* ratio was about 1:1 after a reaction time of 25 min, but about 2:1 after 40 min; *talo* and *galacto* derivatives were minor products in either event (9). See also the discussion on this subject in ref. 10.

[4]In an independent experiment we found almost no difference in spectra from benzylidenations performed after nitronate epimerizations running for 3 and 5 days. This indicated that epimerization was essentially complete within 3 days.

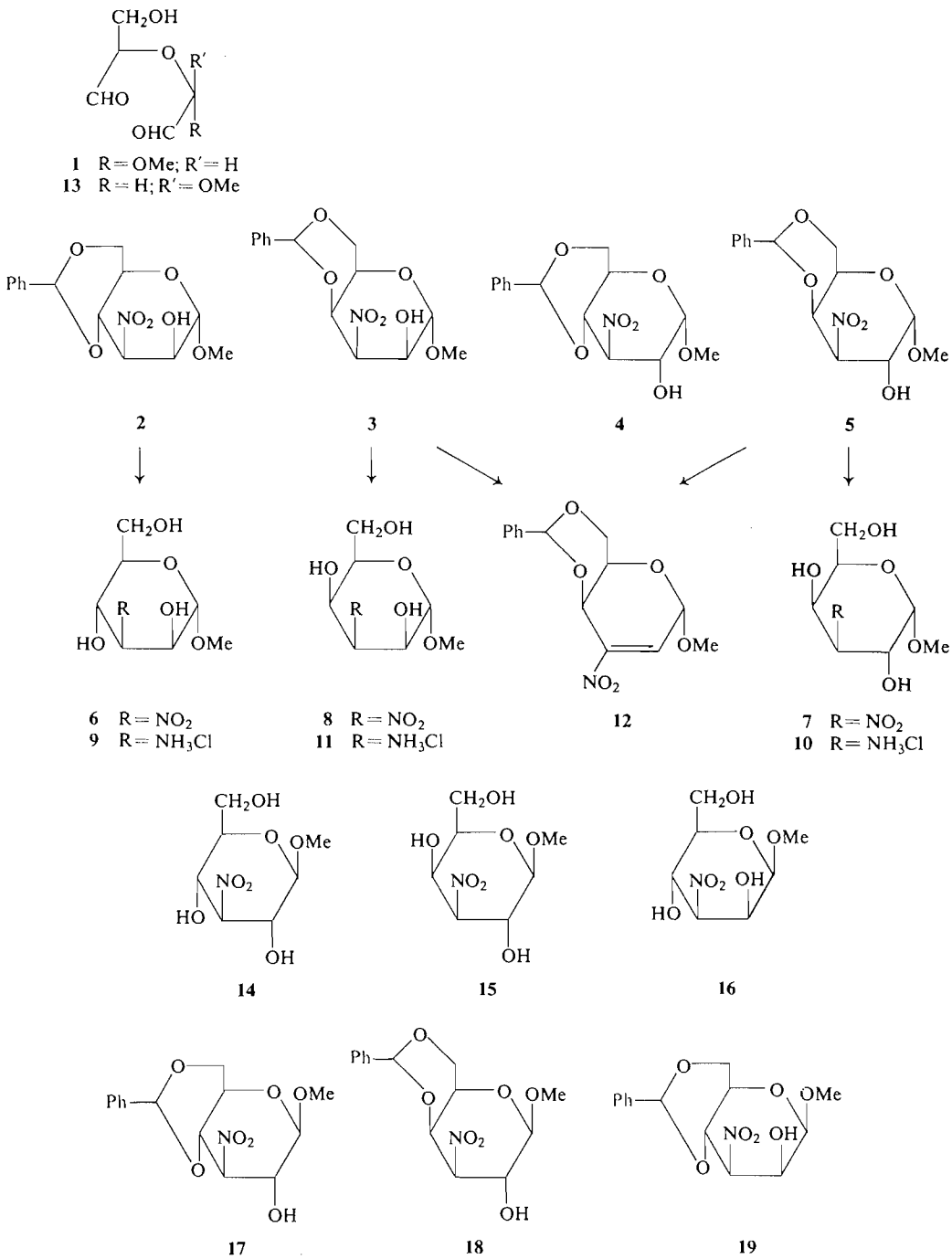

1 R = OMe; R′ = H
13 R = H; R′ = OMe

manno and α-D-*talo* isomers (**2** and **3**), respectively, and the third signal was due to the α-D-*gluco* (**4**) and α-D-*galacto* (**5**) isomers. Column chromatography confirmed this pattern, indicating the presence of **2**, **3**, **4**, and **5** in the ratio 15.5:51.5:20:13.

The direct evidence so obtained confirms the principal statement which was based on con-

Can. J. Chem. Downloaded from www.nrcresearchpress.com by 210.87.254.105 on 09/05/12
For personal use only.

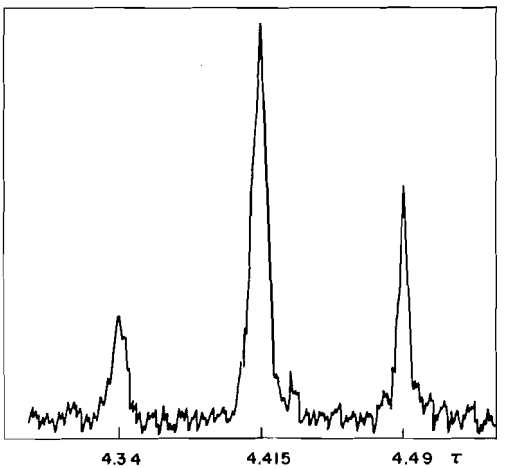

FIG. 2. Methine proton signals, in 100 MHz n.m.r. spectrum with 100 Hz sweep width, of nitromethane cyclization mixture from **1** after *epimerization* and subsequent benzylidenation; solvent, $CDCl_3$.

version into amine derivatives (8), namely that the nitro glycosides produced in the nitromethane cyclization of **1** epimerize, as nitronates, so as to generate chiefly the α-D-*talo* configuration at the expense of the α-D-*manno* and α-D-*gluco* configurations. Clearly, the nitronate of the α-D-*talo* compound is the thermodynamically most stable one. The experiments showed furthermore, that the amount of α-D-*galacto* isomer increases, if only slightly, during the epimerization. However, the relative stabilities of the nitronates of the α-D-*gluco* and α-D-*galacto* isomers have now been revealed to be in fact rather similar whereas, in the earlier work (8), the former had been underrated and the latter overestimated. The present results are for the most part in good harmony with those from a recent study (10) on analogous 6-deoxy glycosides in which, after nitronate equilibration, the *manno*:*talo*:*gluco*:*galacto* ratio was approximately 28:59:7:6.

In the course of the chromatographic separations just mentioned, methyl 4,6-*O*-benzylidene-3-deoxy-3-nitro-α-D-mannopyranoside (**2**) and its α-D-*galacto* isomer (**5**) were isolated for the first time. These acetals as well as the previously described (11) α-D-*talo* isomer (**3**) were debenzylidenated to furnish methyl 3-deoxy-3-nitro-α-D-mannopyranoside (**6**), -α-D-galactopyranoside (**7**), and -α-D-talopyranoside (**8**) as new, crystalline compounds. The structures of **6** and **8** were ascertained by catalytic hydrogenation giving the known, crystalline amino glycoside hydrochlorides **9** and **11**, respectively. Similarly, **7** afforded the corresponding amine hydrochloride (**10**) in crystalline form. In this case, however, further structural proof was needed since the amine had been obtained earlier (8) as a syrup of questionable purity only, and data of comparison were lacking. The α-D-*galacto* configuration was established by dehydration of the acetal **5** with hot acetic anhydride and sodium acetate, which produced known methyl 4,6-*O*-benzylidene-2,3-dideoxy-3-nitro-α-D-*threo*-hex-2-enopyranoside (**12**), *i.e.*, the same nitro olefin that was formed (11) by such dehydration from the α-D-*talo* isomer (**3**). The procedure for preparing **12** was improved in this connection.

Further preparative improvements to be recorded concern the separation of the three β-glycosides which are available (12, 13) by nitromethane cyclization of 2-*O*-[(*R*)-formyl-(methoxy)methyl]-(*R*)-glyceraldehyde (**13**, "D-hydroxymethyl-L′-methoxydiglycolaldehyde"), namely, methyl 3-deoxy-3-nitro-β-D-glucopyranoside (**14**), -β-D-galactopyranoside (**15**), and -β-D-mannopyranoside (**16**). Although preparation of **14** and **15** by direct crystallization is easy enough (14), it may be desirable to augment yields by working-up mother liquors that retain considerable quantities of material. Benzylidenation of such isomer mixtures from mother liquors has served (15) to separate components as their crystalline acetals (**17**–**19**), and in the Experimental we describe improved procedures involving fractional crystallization and column chromatography. Another method of separation was elaborated on the basis of the differential reactivities of **17**–**19** towards alkali; it represents a useful, preparative corollary to a recent communication on this subject (16). Thus, when a mixture of the three acetals (or a mixture of **18** and **19** alone) in chloroform solution was treated briefly with potassium hydroxide, the β-D-*manno* isomer **19** was quantitatively epimerized, and a mixture of **17** and **18** resulted. These two components then proved readily separable due to the fact that, under the conditions employed, the β-D-*galacto* isomer **18** forms a chloroform-insoluble, water-soluble nitronate whereas the β-D-*gluco* isomer **17** does not do so but remains soluble in chloroform and insoluble in water.

Can. J. Chem. Downloaded from www.nrcresearchpress.com by 210.87.254.105 on 09/05/12
For personal use only.

Can. J. Chem. Downloaded from www.nrcresearchpress.com by 210.87.254.105 on 09/05/12
For personal use only.

Experimental

The n.m.r. data were obtained from 100 MHz spectra taken on a Varian HA-100 instrument, using tetramethylsilane for the lock signal. For analysis of acetal mixtures, spectra were taken from approximately 10% solutions in chloroform-*d* or DMSO-d_6, at 100 Hz sweep width and 500 Hz sweep offset. The component ratios were determined by averaging three integrations of the methine proton signals and expressing each signal intensity in terms of percent of the sum of intensities. In standard mixtures, single integrations of a given signal deviated ± 1–2% from the average value, and the latter deviated ± 1–4% from the expected value.

The t.l.c. was performed on silica gel G (E. Merck AG) with carbon tetrachloride – ethyl acetate (7:3, v/v) as solvent unless specified otherwise. Ceric sulfate – sulfuric acid served as spray reagent. In column chromatography, silica gel refers to the 70-325 mesh ASTM product of E. Merck AG.

Separation of α-Glycosides

(a) Preparation of Nitro Glycoside and Acetal Mixtures

Preparation of the dialdehyde **1**, its cyclization with nitromethane in methanol solution containing sodium methoxide, and deionization of the product to give a mixture (E) of nitro glycosides was performed as previously described (8), with a minor modification.[2] The same applies to the preparation of the mixture (F) of epimerized nitro glycosides (8). Separation of crystalline methyl 3-deoxy-3-nitro-α-D-glucopyranoside by chromatography of mixture E on powdered cellulose has been recorded (15). Benzylidenation of mixtures E and F with benzaldehyde and zinc chloride had previously yielded the crystalline α-D-*gluco* (**4**) (15) and α-D-*talo* (**3**) (11) acetals, respectively. For the present studies, benzylidenated mixtures were prepared as previously described, but the syrups obtained were used for n.m.r. spectroscopy and column chromatography without prior removal of crystallizable components.

(b) Chromatography of Benzylidenated Mixture E

Crude, benzylidenated mixture E, obtained as a syrup (21.5 g) from **1** (0.068 mol, from 13.2 g of methyl α-D-glucopyranoside) was placed on a column (6.5 × 60 cm) containing 800 g of silica gel. Elution was performed with carbon tetrachloride – ethyl acetate mixtures of compositions (v/v) 7:3 (fractions 1–30), 1:1 (fractions 31–39), and 2:3 (fractions 40–80), the fractions being 75 ml in volume. All fractions were inspected by t.l.c., and the residues obtained after appropriate pooling and evaporation were examined by n.m.r. spectroscopy. Fractions 1–15 were free from carbohydrates but contained benzaldehyde (6.76 g). Fractions 16–21 yielded pure **2** (2.22 g). Fractions 22–30, 31–36, 37–39, 40–50, and 51 contained 4.49, 1.46, 0.43, 1.29, and 0.68 g of mixtures of **2**, **3**, and **4**. Fractions 52–63 and 75–80 were blank, and fractions 64–74 gave pure **5** (1.00 g). Thus the total, overall yield of nitro glycoside acetals was 11.57 g (54.7% of the theoretical based on starting methyl α-D-glucopyranoside). Individual yields, calculated by summation of pure fractions and spectroscopically-determined proportions of components in mixed fractions, were the following: **2**, 4.86 g (22.9%); **3**, 0.94 g (4.4%); **4**, 4.77 g (22.5%), and **5**, 1.00 g (4.7%).

When the column chromatography was performed with half the above glycoside load and with carbon tetrachloride – ethyl acetate mixture of constant composition (7:3), a somewhat better separation of the more mobile compounds, **2**, **4**, and **3** took place and parts of each were eluted as pure fractions, in that order, with mixed fractions occurring in between. However, the solvent was unsatisfactory for elution of slow-moving **5**.

(c) Chromatography of Benzylidenated Mixture E

A crude syrup (21.8 g) resulting from benzylidenation of a mixture (F) of epimerized nitro glycosides obtained from **1** was chromatographed. The technique detailed in section *b* was used except that the eluant composition was carbon tetrachloride–ethyl acetate in the ratios 4:3, 1:1, and 2:3 for fractions 1–24, 25–30, and 31–50, respectively. Fractions 1–10 contained benzaldehyde (5.6 g). Fractions 11–15 and 17–18 consisted of mixtures of **2** (1.20 g) and **4** (0.80 g), and of **4** (0.30 g) and **3** (0.55 g), respectively, the product ratios being determined from n.m.r. spectra. Fractions 16, 19–30, and 31–50 yielded virtually pure **4** (0.47 g), **3** (3.48 g), and **5** (1.03 g), respectively. Hence the total yield of nitro glycoside acetals was 7.83 g. Since the ratios of individual acetals were very similar before and after chromatography it appears that recovery was essentially complete. The weight deficit is attributed to benzaldehyde (5.6 g) and residual solvent in the starting syrup.

Characterization of α-D-Glycosides

Methyl 4,6-O-Benzylidene-3-deoxy-3-nitro-α-D-mannopyranoside (2)

Compound **2** as obtained from a chromatographic column was recrystallized for analysis from chloroform – petroleum ether; m.p. 138–139°, $[\alpha]_D$ +27.7° (*c*, 0.8 in $CHCl_3$).

Anal. Calcd. for $C_{14}H_{17}NO_7$ (311.3): C, 54.01; H, 5.51; N, 4.50. Found: C, 53.96; H, 5.56; N, 4.59.

Methyl 3-Deoxy-3-nitro-α-D-mannopyranoside (6)

The acetal **2** (300 mg) was debenzylidenated (17) by treatment with 3 ml of 90% trifluoroacetic acid at room temperature for 15 min. Completion of the reaction was ascertained by t.l.c. using ethyl acetate – petroleum ether (2:3). Water was added to the reaction mixture which was then evaporated. The residue was repeatedly evaporated with added water and ethanol, and the remaining syrup was dried *in vacuo* (206 mg, 96%; homogeneous on t.l.c.). Crystallization from tetrahydrofuran–ether furnished **6** (184 mg), m.p. 113–115°, $[\alpha]_D$ +44.5° (*c*, 0.9 in water).

Anal. Calcd. for $C_7H_{13}NO_7$ (223.2): C, 37.67; H, 5.87; N, 6.28. Found: C, 37.79; H, 5.93; N, 6.35.

A sample of **6** (100 mg) was dissolved in water (8 ml), 0.1 *N* HCl (5 ml), and platinum catalyst (from 50 mg of PtO_2) was added, and the mixture was hydrogenated overnight. Filtration and evaporation of the solution, followed by crystallization of the residue from 95% ethanol at 4° furnished 84 mg (81.5%) of methyl 3-amino-3-deoxy-α-D-mannopyranoside hydrochloride (**9**) in two batches, m.p. 234–236° (dec.) and 232–235° (dec.); $[\alpha]_D$ +57.5° (*c*, 0.3 in water). Reported: $[\alpha]_D$ +60° in water (7, 18), and decomposition at about 205° (7), 221–223° (8), 210–240° (18). Evidently the melting behavior is not very characteristic, it being probably influenced by traces of impurities and the mode of heating. A sample at hand from previous work in this laboratory melted with decomposition at 230–231° and caused no depression when admixed to new **9**. The i.r. spectra were identical.

Can. J. Chem. Downloaded from www.nrcresearchpress.com by 210.87.254.105 on 09/05/12
For personal use only.

Methyl 4,6-O-Benzylidene-3-deoxy-3-nitro-α-D-talopyranoside (3)

Compound **3** collected from the column showed m.p. 177–178°, $[\alpha]_D$ +66.8° (*c*, 1.1 in $CHCl_3$), and its i.r. spectrum was identical with that of an authentic sample. Reported (11): m.p. 175°, $[\alpha]_D$ +68° (in $CHCl_3$).

Methyl 3-Deoxy-3-nitro-α-D-talopyranoside (8)

The acetal **3** (200 mg) was debenzylidenated with trifluoroacetic acid as described for **2**, above. The reaction was complete after 20 min as indicated by t.l.c. with chloroform–acetone (7:3). The syrupy product (117 mg, 82%) was crystallized from chloroform to give **8** (93 mg), m.p. 86–87°; $[\alpha]_D$ +87.5° (*c*, 0.9 in water).

Anal. Calcd. for $C_7H_{13}NO_7$ (223.2): C, 37.67; H, 5.87; N, 6.28. Found: C, 37.46; H, 6.08; N, 6.12.

A sample of **8** (40 mg) was catalytically hydrogenated for 3 h in water (3 ml) and 0.1 *N* HCl (2 ml), in the presence of platinum catalyst (70 mg of PtO_2). Upon recrystallization of the product from 99% ethanol by slow addition of ethyl acetate, methyl 3-amino-3-deoxy-α-D-talopyranoside hydrochloride (**11**) was obtained in 99% yield; m.p. 187–188° (dec.), $[\alpha]_D$ +88.3° (*c*, 0.3 in water). Reported (8): m.p. 187–188 (dec.), $[\alpha]_D$ +90° (in water). Identity with an authentic sample was established by a mixture melting point (186–188° with dec.), comparison of i.r. spectra, and paper chromatography (8).

Methyl 4,6-O-Benzylidene-3-deoxy-3-nitro-α-D-glucopyranoside (4)

Compound **4** collected from a column showed m.p. 166–167°, $[\alpha]_D$ +86.5° (*c*, 0.7 in ethanol), and its i.r. spectrum was identical with that of an authentic sample. Reported (15): m.p. 167°, $[\alpha]_D$ +87.2° (in ethanol).

Methyl 4,6-O-Benzylidene-3-deoxy-3-nitro-α-D-galactopyranoside (5)

Compound **5** collected by column chromatography was recrystallized for analysis from ethyl acetate–petroleum ether; m.p. 166–167°, $[\alpha]_D$ +205° (*c*, 0.5 in $CHCl_3$).

Anal. Calcd. for $C_{14}H_{17}NO_7$ (311.3): C, 54.01; H, 5.51; N, 4.50. Found: C, 53.83; H, 5.51; N, 4.41.

Methyl 3-Deoxy-3-nitro-α-D-galactopyranoside (7)

The acetal **5** (94 mg) was debenzylidenated with trifluoroacetic acid as described for **2**, above. The reaction was complete after 30 min as shown by t.l.c. Crystallization of the syrupy product (67 mg) from chloroform afforded **7** (32 mg), m.p. 145–146°, $[\alpha]_D$ +209° (*c*, 0.4 in water). The remainder of **7** (35 mg) was recovered as a syrup.

Anal. Calcd. for $C_7H_{13}NO_7$ (223.2): C, 37.67; H, 5.87; N, 6.28. Found: C, 37.92; H, 6.02; N, 6.16.

Methyl 3-Amino-3-deoxy-α-D-galactopyranoside Hydrochloride (10)

Syrupy **7** (35 mg) in water (5 ml) and 0.1 *N* HCl (2 ml) was hydrogenated for 3 h in the presence of prereduced PtO_2 (50 mg). Evaporation of the filtrate followed by two coevaporations with ethanol gave crystalline **10** (34 mg) which upon recrystallization from ethanol melted with decomposition at 219–221° and had $[\alpha]_D$ +146.5° (*c*, 0.2 in water).

Anal. Calcd. for $C_7H_{16}ClNO_5$ (229.7): C, 36.61; H, 7.02; Cl, 15.44. Found: C, 36.76; H, 6.79; Cl, 15.71.

In agreement with the earlier observation on amorphous **10**, the mobility of the compound in paper chromatography (8) was lower than that of its isomers **9** and **11**.

Methyl 4,6-O-Benzylidene-2,3-dideoxy-3-nitro-α-D-threo-hex-2-enopyranoside (12)

A mixture of the acetal **5** (100 mg), anhydrous sodium acetate (200 mg), and acetic anhydride (2 ml) was heated on a steam bath for 30 min with continual swirling. The mixture was then poured into ice water (50 ml) which caused a white crystalline material to precipitate. The product, which was collected by filtration, washed well with cold water, and dried *in vacuo*, weighed 86 mg (91%) and melted at 175–177°. Recrystallization from ethyl acetate – petroleum ether raised the m.p. to 182–184°; reported (11), m.p. 185–186°. An i.r. spectrum was identical with that of **12** from the earlier work (11).

In like manner but with a reaction time of 15 min, **12** was obtained in 83% yield starting from the isomeric acetal **3**. Evidently, employment of steam-bath rather than reflux (11) temperature improved the yields in these dehydrations. Moreover, the procedure was more reliable than that formerly employed, which sometimes failed due to decomposition by overheating.

Separation of β-D-Glycoside Acetals

The preparation of dialdehyde **13** and its cyclization with nitromethane to give the nitro β-D-glycosides **14**, **15**, and **16** has been described (12–14*a*) as has the benzylidenation of these glycosides, individually as pure compounds and in mixtures recovered from mother liquors (14*b*, 15).

(a) Fractional Crystallization

Mother liquors that remained when upon nitromethane cyclization of **13** the bulk of crystallizable β-D-glucoside **14** had been collected (13) were evaporated, and the residue was benzylidenated. From the mixture of acetals so produced, the β-D-*galacto* isomer **18** can be obtained by fractional crystallization from ethanol in which it is the least soluble component. However, 6–8 recrystallizations are needed to achieve high purity. A more convenient procedure is to dissolve the mixture in a small amount of acetone and then to add chloroform, which causes precipitation of a material highly enriched in **18**. One subsequent recrystallization of the precipitate from ethanol usually is sufficient to give reasonably pure **18**, m.p. 229–231° (dec.). Reported (15): m.p. 230–231° (dec.). This procedure is probably the most convenient one for the preparation of larger quantities of **18**, as it renders unnecessary the use of isolated, crystalline **15** for benzylidenation.

The acetone–chloroform mother liquor from the above separation procedure is strongly enriched in the β-D-*manno* compound **19**, but purification of the latter by continued fractional crystallization could not be achieved. If pure **19** is desired without having to start with pure **16** and without resorting to chromatography, one may benzylidenate nitromethane cyclization mixtures from which the bulk of both **14** and **15** have been removed (13, 15). However, column chromatography proved advantageous for isolating **19**.

(b) Column Chromatography

The following example describes the separation of an acetal mixture containing mainly **18** and **19** (the latter preponderating) as well as a small proportion of **17**. The mixture (10 g) and a few grams of silica gel were intimately mixed by two coevaporations with acetone in a rotary evaporator, and the dry mass was then placed on a column (4.5 × 65 cm) containing 500 g of silica gel. Elution was performed with chloroform–acetone (7:3, v/v) at a rate of about 17 ml per

10 min. The eluate was inspected at intervals by t.l.c., and the fractions were suitably combined. The first 800 ml (approximately) of effluent was blank (it may be recycled). The following 300 ml contained β-D-*manno* derivative **19** which was obtained by evaporation and was recrystallized from ethanol to give a very pure product (5.23 g), m.p. 202°, $[\alpha]_D$ −112° (*c*, 1.2 in ethanol). Reported (15): m.p. 194–196° and 198–199°, $[\alpha]_D$ −107.5°. The next 60 ml of effluent yielded impure **19** (1.05 g, m.p. 189°) that contained some **17**. Continued elution with about 500 ml of solvent furnished the β-D-*galacto* derivative **18** (3.23 g) which emerged after a few blank fractions (or, in similar runs, with slight overlapping). Upon recrystallization from ethanol it showed m.p. 232°, $[\alpha]_D$ +25° (*c*, 1 in dimethylformamide). Reported (15): $[\alpha]_D$ +24.8°.

(c) Nitronate Formation

A mixture (1 g) containing mainly **18** and **19** along with a small proportion of **17** was dissolved in chloroform (40 ml), and an ethanolic, *N* potassium hydroxide solution (3.5 ml) was added. A voluminous precipitate occurred within 5 min, and t.l.c. of the reaction mixture, performed after 10 min with a neutralized sample, indicated absence of **19** and presence of both **17** and **18**. The reaction mixture was then shaken with 40 ml of water in which the precipitate dissolved. After phase separation the aqueous layer was extracted twice with chloroform which was combined with the organic phase. Excess acetone was then added to the aqueous phase and the solution was at once deionized with an acidic cation exchange resin. The filtrate was concentrated *in vacuo* to remove most of the acetone, whereby the β-D-*galacto* isomer **18** crystallized in chromatographically pure form (131 mg). The aforementioned chloroform phase was washed twice with water, dried over sodium sulfate, and evaporated to give chromatographically pure β-D-*gluco* isomer **17** (710 mg). The products were identified by their i.r. spectra and physical constants.

Support of this work by the National Research Council of Canada is gratefully acknowledged. Miss Ursula Eppenberger is thanked for her skilful technical assistance.

1. A. N. DE BELDER. Adv. Carbohydr. Chem. **20**, 219 (1965).
2. H. H. BAER. Adv. Carbohydr. Chem. Biochem. **24**, 67 (1969).
3. H. H. BAER and W. RANK. Can. J. Chem. **49**, 3192 (1971).
4. H. H. BAER and W. RANK. To be published.
5. N. BAGGETT, K. W. BUCK, A. B. FOSTER, and J. M. WEBBER. J. Chem. Soc. 3401 (1965).
6. S. A. BARKER, J. HOMER, M. C. KEITH, and L. F. THOMAS. J. Chem. Soc. 1538 (1963); R. U. LEMIEUX and B. FRASER-REID. Can. J. Chem. **42**, 532 (1964); H. H. BAER and G. V. RAO. Ann. **686**, 210 (1965).
7. H. H. BAER and H. O. L. FISCHER. J. Am. Chem. Soc. **82**, 3709 (1960).
8. H. H. BAER. J. Am. Chem. Soc. **84**, 83 (1962).
9. H. H. BAER and K. ČAPEK. Can. J. Chem. **47**, 99 (1969).
10. J. KOVÁŘ, K. ČAPEK, and H. H. BAER. Can. J. Chem. **49**, 3960 (1971).
11. H. H. BAER and F. KIENZLE. Can. J. Chem. **45**, 983 (1967).
12. H. H. BAER. Ber. **93**, 2865 (1960).
13. H. H. BAER and F. KIENZLE. Can. J. Chem. **41**, 1606 (1963).
14. H. H. BAER. *In* Methods in carbohydrate chemistry. Vol. VI. *Edited by* R. L. Whistler and J. N. BeMiller. Academic Press Inc., New York, N.Y. 1971. (*a*) [42]; (*b*) [53].
15. H. H. BAER, F. KIENZLE, and T. NEILSON. Can. J. Chem. **43**, 1829 (1965).
16. H. H. BAER and W. RANK. Can. J. Chem. **49**, 3197 (1971).
17. J. E. CHRISTENSEN and L. GOODMAN. Carbohydr. Res. **7**, 510 (1968).
18. A. C. RICHARDSON. J. Chem. Soc. 373 (1962).

Can. J. Chem. Downloaded from www.nrcresearchpress.com by 210.87.254.105 on 09/05/12
For personal use only.

The Effect of Heat on *cis*- and *trans*-Crotonic Acids: Alternatives to Direct *cis–trans* Isomerism[1]

M. B. HOCKING[2]

Research Department,[3] Dow Chemical of Canada Limited, Sarnia, Ontario

Received August 16, 1971

The thermal *cis–trans* equilibration of *cis*- and *trans*-crotonic acids (2-butenoic acids) has been examined at temperatures in the range 100–189°. The *trans* acid has been found to yield a mixture of at least five components, of which 9–11.6% was *cis*-crotonic acid, and 19.4–31.7% was a dimer of *trans*-crotonic acid. Heating *cis*-crotonic acid yielded similar final mixtures, but with an initial component of vinylacetic acid, not seen in the *trans* acid equilibrations. The rates of formation and identities of the components formed in these two sets of experiments, together with data for the thermal tautomerization of vinylacetic acid, are discussed with reference to suggested pathways for these transformations.

L'équilibration thermique *cis–trans* des acides crotoniques *cis* et *trans* (ou acides butène-2 oiques) a été examinée dans l'intervalle de température de 100–189°. L'acide *trans* donne alors un mélange d'au moins cinq composants parmi lesquels 9–11.6% d'acide crotonique *cis* et 19.4–31.7% d'acide crotonique *trans* à l'état de dimère. Le chauffage de l'acide *cis* donne des résultats finals semblables avec en plus un composant initial d'acide vinylacétique inconnu lors des équilibrations sur l'acide *trans*. Les vitesses de formation et les composants identiques formés dans ces deux séries d'expériences ainsi que les données sur la tautomérisation thermique de l'acide vinylacétique, sont discutés par rapport aux processus réactionnels suggérés pour ces transformations.

Canadian Journal of Chemistry, **50**, 1224 (1972)

Introduction

Morrell and Hanson (1), in their early study of the *cis*- and *trans*-crotonic acid equilibrium system, claimed that the equilibrium mixture at 172° consisted of 24% *cis*- and 76% *trans*. This was a sufficiently high proportion of *cis* to make separation of it from an equilibrium mixture produced by thermally isomerizing *trans* seem an attractive route to *cis*-crotonic acid. However, it was felt that temperatures below 172° were likely to be more propitious for *cis* isolation and Morrell and Hanson's data below this temperature were not obtained at equilibrium since their heating times were insufficient. Also their melting-point method of analysis, assuming a binary mixture, aroused a cautious treatment of the results since the possibility of another component being present was mentioned (1). Twenty-five years later, Skau and Saxton (2) confirmed the presence of a large proportion of a third component, a finding which reduced confidence in the values of Morrell and Hanson. Consequently, the equilibration of both *cis*- and *trans*-crotonic acids over a range of temperatures was re-examined with a view to using the results to prepare *cis*-crotonic acid from the *trans*, if the equilibrium was sufficiently favorable. The equilibration results and conclusions which can be drawn from these, are reported here.

[1]Contribution No. 150.

[2]Present Address: Department of Chemistry, University of Victoria, Victoria, B.C.

[3]Address for reprint requests.

Results

Equilibration of trans-Crotonic Acid

Heating *trans*-crotonic acid converted it to a mixture of at least five components (Scheme 1). Those predominating, *trans*- and *cis*-crotonic acids (**1**, **2**) and 3-hydroxybutyric acid *cis*- and *trans*-crotonates (**3***a*, *b*), have been isolated and identified with the aid of n.m.r. (3, 4). The more minor fifth component, the concentration of which was related to that of **3***a* and never rose above 7%, was more difficult to characterize. A combination of mass and proton spectroscopic methods together with quantitative bromination and hydrogenation established its identity as the trimer of crotonic acid, **4** (3). On long term heating at relatively high temperatures small amounts of a tetramer **5** were isolated, and there was evidence for the presence of higher oligomers (3).

The n.m.r. spectra of the pure components

Can. J. Chem. Downloaded from www.nrcresearchpress.com by 210.87.254.6 on 09/05/12
For personal use only.

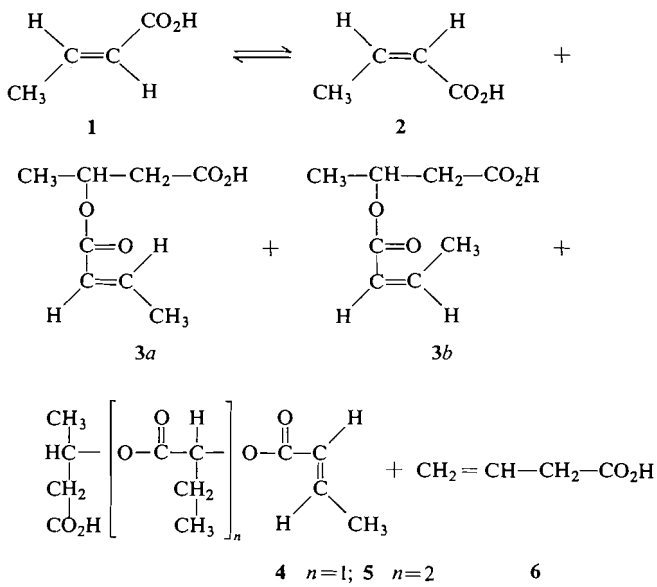

SCHEME 1. Products from crotonic acid on heating.

had been obtained (3, 4). Using these it was possible to determine the proportions of the components present in mixtures merely by integration of the composite n.m.r. spectrum. This was the method by which a series of equilibrations of small samples of *trans*-crotonic acid, each heated at temperatures ranging from 100–189°, was followed. The samples of *trans*-crotonic acid yielded mixtures which reached equilibrium after times ranging from about 8 h for the hottest to more than 250 h for the coolest runs.

The major component in all cases was *trans*-crotonic acid. In the runs in which there was reasonable certainty that equilibrium was reached in less than 250 h (Table 1) the molar concentrations of *trans*-crotonic acid ranged from a low of 51% to a high of 66%. Between 138 and 156° all the equilibrium percentage concentrations of *trans* were in the low or middle fifties (Table 2). However, the runs above 160° showed a 10% increase in the percentage of *trans* present at equilibrium, mostly at the expense of a dimer of crotonic acid, the next most abundant constituent.

The dimer of crotonic acid (3), the formation of which had been previously demonstrated (2), was the next most abundant component. Its concentration in the *trans* equilibrations ranged from around 30% at temperatures below 160° but dropped to around 20% at the higher temperatures (Fig. 1). This lower concentration at higher temperatures can probably be ascribed to an enhanced rate of cracking of the dimer back to crotonic acids (3).

The concentration of *cis*-crotonic acid in the equilibrium mixtures was found to be about 9% below 160° and to rise slightly to 11.5% above this temperature (Fig. 2); it never approached the 24% claimed earlier (1). This rise was proportionate to that of the *trans*-crotonic acid component above 160° and kept the *cis–trans* ratio within the narrow range of 0.16–0.18 (Table 2). For isolation of *cis*-crotonic acid (4), the lowest boiling component, this latter proportion was of importance since none of the dimer entered the distillation column.

Equilibrations of cis-Crotonic Acid

The thermal equilibrations of *cis*-crotonic acid, which were carried out after a quantity had been prepared (4) by successful use of the *trans*-crotonic acid equilibration, were expected to be fairly routine. Unexpectedly, a new component appeared in these, which was not seen in the *trans*-crotonic acid equilibrations. The additional compound was found by isolation and comparison of its physical properties with an authentic sample (5) to be vinylacetic acid (3-butenoic acid, **6**). The rate of change of the

Can. J. Chem. Downloaded from www.nrcresearchpress.com by 210.87.254.6 on 09/05/12
For personal use only.

TABLE 1. Changes in composition on heating pure *trans*-crotonic acid

Heating time (h)	Component acids in mixture* and run temperatures: % *cis*-Crotonic	% *trans*-Crotonic	Weight % dimer **3**	Weight % trimer **4**
		100° Run		
18	0	100	0	0
65	0	100	trace	0
		117° Run		
65	trace	87.7	10.3	2.0
137	3.7	69.2	22.6	4.5
233	3.8	55.5	33.9	6.8
		138° Run		
18	3.3	79.6	14.1	2.8
65	6.1	62.0	26.5	5.4
137	8.5	54.7	31.7	6.1
233	9.0	55.0	31.1	6.1
		147° Run		
18	5	70.9	20.0	4.1
65	8.3	59.0	27.2	5.5
137	8.9	56.9	28.5	5.7
233	8.3	50.5	34.3	6.9
		156.5° Run		
18	7.5	67.1	20.7	4.7
65	9.3	61.6	24.2	4.9
137	9.2	59.6	26.0	5.2
233	8.9	57.0	28.4	5.7
		179° Run		
18	11	65.1	19.9	4.0
65	10.5	65.5	20.0	4.0
137	11.5	64.5	20.0	4.0
233	11.6	63.9	20.2	4.4
		189° Run†		
4	9.0	72.3	15.6	3.1
8.5 (185°)	11.1	69.0	16.6	3.3
24 (182°)	11.6	66.1	18.6	3.7
48‡ (180°)	11.2	65.5	19.4	3.9

*Vinylacetic acid was never detected. It is estimated that 2% or greater would have been seen, if present.
†Extent of gradual cooling of bath indicated in time column.
‡Some resinification occurred obscuring n.m.r. resolution somewhat.

concentration of this compound is given in Table 3. In the first few hours of heating, its concentration rose to as high as 15% but subsequently fell to less than 1% of the total, both of these changes occurring more rapidly with higher temperatures.

The drop in vinylacetic acid concentration coincided with a significant rise in the proportion of *trans*-crotonic acid formed (Fig. 3, Table 3). Then very shortly after the simultaneous build-up of *trans*-crotonic acid and decline of vinylacetic acid, the dimer concentration began to rise very sharply (Table 3). In spite of an initial pronounced lag, the concentration of dimer

Can. J. Chem. Downloaded from www.nrcresearchpress.com by 210.87.254.6 on 09/05/12
For personal use only.

TABLE 2. Equilibrium compositions approached from both *cis*- and *trans*-crotonic acids

Temperature of equilibration (°C)	Equilibrium approached from: *cis*-Crotonic acid*			*trans*-Crotonic acid*			*cis*/*trans* from *trans* equilibria
	cis	*trans*	Dimer	*cis*	*trans*	Dimer	
100†	81.9	0	0	0	0	trace	
117‡	—	—	—	3.8	55.5	34.0	—
138	13.0‡	27.5‡	49.5‡§	9.0	55.0	31.0	0.16
147	—	—	—	8.3	50.5	34.5	0.16
156.5	9.0	50.5	34.2	8.9	57.0	28.5	0.16
179	—	—	—	11.6	64.0	20.0	0.18
189‖	—	—	—	11.6	65.5	19.5	0.18

*Reliability estimated to be about ±5% of value given. Two percent or less (approximate detection limit) vinylacetic acid might also have been present.
†Equilibrium not reached.
‡Probably not equilibrium values since 250 h heating time was insufficient at this temperature.
§Some resinification occurred, making good resolution impossible.
‖Temperature gradually dropped during run, see Table 1.

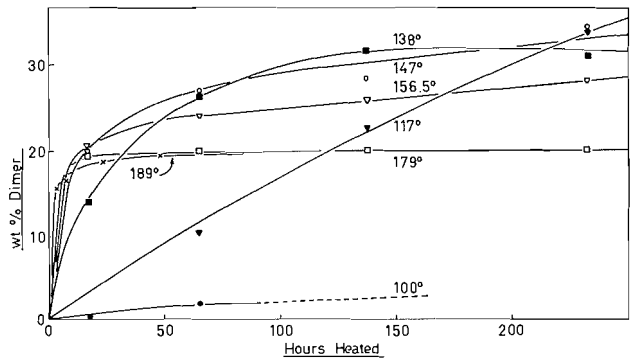

FIG. 1. Equilibration of *trans*-crotonic acid to dimer 3*a*. At 100°, ●; 117°, ▼; 138°, ■; 147°, ○; 156.5°, ∇; 179°, □; and 189°, ×.

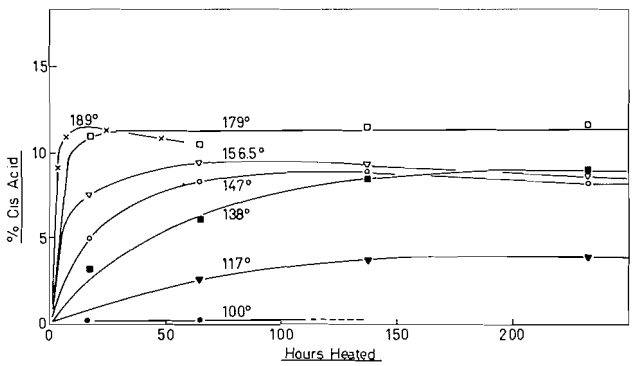

FIG. 2. Equilibration of *trans*-crotonic acid to *cis*. At 100°, ●; 117°, ▼; 138°, ■; 147°, ○; 156.5°, ∇; 179°, □; and 189°, ×.

during *cis*-crotonic acid equilibration reached the same levels as those obtained on equilibration of the *trans*, before the dimer concentration of the latter had reached equilibrium (*cf.* Tables 2 and 3).

cis-Crotonic acid was only slowly isomerized to the *trans* at 100° (Table 3). This made its isolation from the *trans* a practical proposition (4). At room temperature, over a period of 83 days, less than 1% of the *cis*-crotonic acid, if

Can. J. Chem. Downloaded from www.nrcresearchpress.com by 210.87.254.6 on 09/05/12
For personal use only.

TABLE 3. Changes in composition on heating 97% *cis*-crotonic acid

Heating time*	Component acids in mixture, and run temperatures				
	% Vinylacetic†	% *cis*-Crotonic	% *trans*-Crotonic	Weight % dimer **3**	Weight % trimer **4**
			25–27°		
0	3.3	96.7	0	0	0
83 days	2.8	96.4	0.8	0	0
			100°		
0	0	97.0	3.0	0	0
4.0	8.6	87.6	3.8	0	0
23.0	13.4	82.2	4.5	0	0
72.5	10.9	81.9	7.2	0	0
			138°		
0	0	97	3.0	0	0
0.5	14.5	82.1	3.4	0	0
1.5	14.8	80.5	4.7	0	0
4.0	12.3	78.8	8.9	0	0
7.5	13.7	73.8	12.5	0	0
23.0	14.5	57.5	28.0	0	0
31.0	9.3	53.8	36.9	trace	0
48.0	7.1	36.4	39.6	14.1	2.8
72.5	5.3	24.2	38.0	27.1	5.4
191.0‡	0	13.2	27.5	49.5	9.8
			156.5°		
0	0	97	3.0	0	0
4.5	10.2	66.2	23.6	0	0
8.0	14.6	50.5	32.7	2.2	0
24.0†	7.9	19.8	56.3	14.0	?
32.0	7.4	17.0	50.7	20.9	4.0
48.0	7.1	12.5	54.6	21.5	4.3
72.0	4.7	9.3	52.4	28.0	5.6
96.0	trace	8.7	53.3	31.7	6.3
168.0‡	0	11.8	52.2	30.0	6.0
264.0‡	0	13.6	50.4	29.9	6.1

*Time in hours, unless otherwise stated.
†Less than two percent vinylacetic acid might not have been detectable.
‡Poor n.m.r. resolution for these samples.

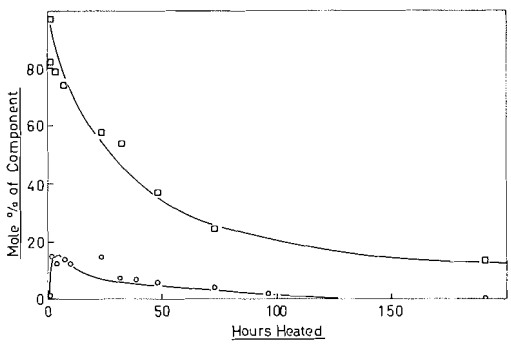

FIG. 3. Coincidence of vinylacetic acid losses to *cis*-crotonic acid losses at 138°. *cis*-Crotonic acid, □; vinylacetic acid, ○.

any, had isomerized to *trans* and no vinylacetic acid had formed. This indicated that it was much more stable than even recent literature reports would suggest (6).

Equilibration of trans-Crotonic Acid in the Presence of Catalysts

A few substances were tried, which might have had a catalytic effect on equilibrations. *trans*-Crotonic acid, with added alumina, *m*-benzenedisulphonic acid, or caustic, was heated at 138°, a temperature sufficient without catalysis to give easily observable and yet not too fast rates of formation of both *cis* acid and dimer. Alumina had a deleterious effect on the rates of formation

Can. J. Chem. Downloaded from www.nrcresearchpress.com by 210.87.254.6 on 09/05/12
For personal use only.

TABLE 4. Heating *trans*-crotonic acid at 138° in the presence of catalysts

Catalyst	Heating time (h)	Components of mixtures formed: % *cis*-Crotonic	% *trans*-Crotonic	% Dimer **3**	% Dimer **5**
Alumina	17	0	88.1	9.9	2.0
	114	5.3	56.7	31.7	6.3
m-Benzenedisulfonic acid	0.5	0	100	0	0
	2	0	94.9	5.1	0
	17	7.0	67.5	21.3	4.2
	114	8.2	55.8	30.0	6.0
Anhydrous sodium hydroxide	1.5	0	94.8	4.3	0.9
	4	0	83.4	13.9	2.7
	7.5	0	78.3	18.1	3.6
	23	3.5	60.2	31.3	5.0

of all three *trans* equilibration products (Table 4), perhaps because of a surface effect, and one equivalent of the strong organic acid accelerated quite markedly the appearance of all three. That the effects of alumina were not primarily the result of its basicity was evident on comparison of these with the results in the presence of caustic. The latter gave the most impressive acceleration of the appearance of dimer (as good as that obtained by heating at 189° without catalysis) but, at the same time, retarded the formation of *cis*-crotonic acid.

Ethyl *trans*-crotonate, with or without crotonic acid present, was found to be stable to geometrical or tautomeric isomerization at temperatures as high as 155° for periods of up to 16 h.

Discussion

The equilibrium concentrations and the approximate rates of geometrical isomerization on heating of either *cis*- or *trans*-crotonic acid at various temperatures was determined. These data indicated that a method of separation of *cis*-crotonic acid from a thermally equilibrated mixture obtained by heating the *trans* was practical. This has been demonstrated (4). In addition to this premeditated data utilization, methods for isolating the dimers **3***a* and *b* (3), and vinylacetic acid (5) have been devised and experimentally carried out. Here, the overall quite complicated crotonic acid equilibrium is discussed.

Direct double bond isomerism is unnecessary to explain the mechanism of formation of *cis* acid from the *trans* or vice versa since the results show alternative routes for either transformation. However, the equilibration runs show that the proportion of direct interconversion between **1** and **2** is not the predominant one at 100–140°, and is probably only as important as interconversions of **1** and **2** through **3** and **6**. Scheme 2 summarizes the overall qualitative picture demonstrated by these equilibrium studies.

Heating *trans*-crotonic acid can give rise to one or more of several products. At 100 and 117°, temperatures effecting relatively slow equilibration where an intermediate could be noticed, dimer **3***a* had formed to a considerable extent before any *cis*-crotonic acid had appeared. Hence, the formation of *cis* directly from the *trans* is improbable or at least very slow at these temperatures. However, for Scheme 2 to satisfy the principle of microscopic-reversibility (7, 8) there must be at least slow direct *cis* formation. The dimers and higher oligomers also arise

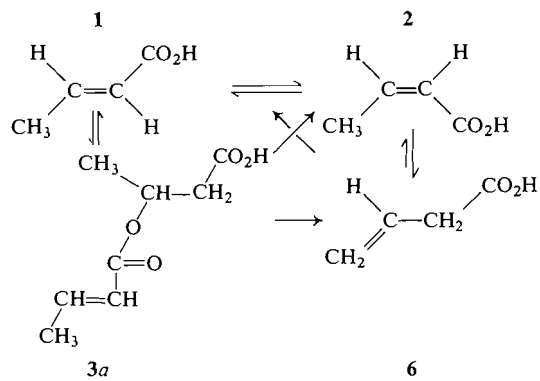

SCHEME 2. A representation of crotonic acid equilibria.

Can. J. Chem. Downloaded from www.nrcresearchpress.com by 210.87.254.6 on 09/05/12
For personal use only.

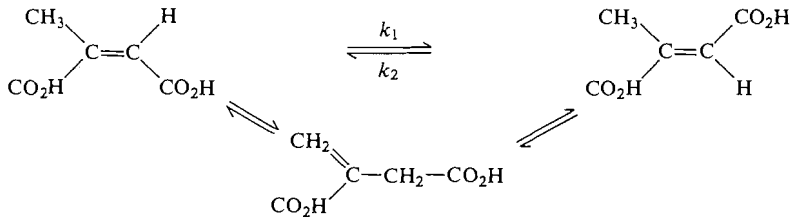

7 8 9

SCHEME 3. Citraconic (**7**), itaconic (**8**), mesaconic (**9**), acid equilibria.

TABLE 5. Rate of tautomerization of neat vinylacetic acid at 160°

	Proportions of components (%)		Net changes (%)	Changes in other* systems under same conditions (%)
	At start	After 5.5 h heating		
Vinylacetic acid	97.3	92.8	−4.5	0
cis-Crotonic acid	1.6	3.0	+1.4	−22.6
trans-Crotonic acid	1.1	4.2	+3.1	+17.9
Dimer **3**	0	0	0	+4.7

*See ref. 5.

primarily from *trans*-crotonic acid because this is the dominant component, and because *trans*-crotonic acid, having a less hindered carboxyl, could add more readily than *cis* to **1** or **2**. Some *cis*-crotonic acid does add to *trans* as evidenced by the appearance of **3***b* on long term heating (3).

cis-Crotonic acid in the room temperature stability test changed very little over a period of 80 days. The minute amount of *trans* formed was more at the expense of the vinylacetic component than of the *cis* (Table 3). In fact, if all the *trans* had arisen from vinylacetic acid with concomitant tautomerization of *cis* to vinylacetic acid, this would explain the observed concentration changes. Stepwise geometrical isomerization of this type is closely analogous to the citraconic, itaconic, mesaconic acid equilibrium (Scheme 3) investigated by Linstead and Mann (9). Their data can be mathematically fitted[4] to a system where k_1 and k_2 are 0.

At 160° in the crotonic acid system however, only 3.1% *trans* acid was formed from vinylacetic acid in the time taken for 20.6% to form from *cis*-crotonic acid (*cf.* Tables 3 and 5). Therefore, at this temperature most of the *trans* must have arisen directly from *cis*-crotonic acid.

[4]E. C. Clarke, Dow Chemical of Canada, Ltd., Sarnia, 1966. Personal communication.

The dimer **3***a* arises from *trans*-crotonic acid since it appeared almost immediately on heating *trans* acid whereas none appeared in the *cis*-crotonic acid equilibrations until well over 30% *trans* had formed (Tables 2, 3). The addition of *cis* to *trans* is the probable mode of formation of dimer **3***b*. No dimer appeared on short term heating of vinylacetic acid (Table 5). The dimers only continue to form an equilibrium concentration with *trans*-crotonic acid (Tables 2, 3). Cracking dimer **3** by heat (3) yields both of the crotonic acids and vinylacetic acid in about equilibrium proportions, as indicated in Scheme 2.

As for the various isomerization pathways open to vinylacetic acid, its neat tautomerization to crotonic acid confirms earlier work carried out in caustic (10). Vinylacetic acid was never seen in aliquots from *trans*-crotonic acid equilibrations; traces could have been present. The minute amounts found during dimer isolation procedures (3) probably arose either by tautomerization of the small amount of *cis* present or from the dimer via heat cracking. Vinylacetic acid obtained on the distillation of *trans*-crotonic acid (4) probably arose via the former route.

Large proportions of vinylacetic acid arose from the *cis*-crotonic acid on heating (Fig. 3)

Can. J. Chem. Downloaded from www.nrcresearchpress.com by 210.87.254.6 on 09/05/12
For personal use only.

Can. J. Chem. Downloaded from www.nrcresearchpress.com by 210.87.254.6 on 09/05/12
For personal use only.

and virtually none from the *trans*. That the *trans*-crotonic – vinylacetic acid equilibrium must be nearly completely on the side of the former has been demonstrated with initial crotonate salts in strong base (11, 12). However, that either isomer of crotonic acid should form more than a very small amount of vinylacetic acid was unexpected since it involved a double bond moving out of apparent resonance with a carbonyl group. For the *trans*, the apparent is true; hence the lack of a noticeable equilibrium proportion of vinylacetic acid (Table 1). But in α,β-unsaturated *cis*-acids generally, as has been pointed out by Newman (13), there is little carbonyl–olefin π-overlap due to mutual interaction of the *cis* groups twisting the carbonyl out of the plane of the olefinic double bond. Manipulation of a Stuart–Briegleb model of *cis*-crotonic acid confirmed Newman's general statement for this acid in particular and in addition demonstrated considerable steric strain. Therefore, the thermal tautomerization of *cis*-crotonic acid to vinylacetic acid can be explained on the basis of no significant loss of conjugative stabilization and relief of steric strain.

The stability to geometrical isomerization found for ethyl *trans*-crotonate can be attributed to a number of factors. It is unable to form a dimer analogous to **3**, and the olefinic double bond (14) has reduced permanent polarization and polarizability (14). Hence, even in the experiments where ester was heated in the presence of free acid no addition of the acid across ester double bonds and, consequently, no ester *cis–trans* isomerism occurred. Esterification of the ordinarily labile citraconic acid (**8**) has been found to stabilize it (15), but it has been found possible to isomerize and tautomerize esters of olefinic acids at somewhat higher temperatures (16) than used here. The high temperature data were interpreted as favoring a 1,5-prototropic shift as one pathway for interconversion of the *cis* esters (5).

The results support the suggestion that the interconversion of *cis*- and *trans*-crotonic acids is only partly direct; a significant proportion of the interconversion is via the intermediates **3** and **6**, especially at lower temperatures (100–140°). At higher temperatures and for certain of the catalytic experiments more transient intermediates might play a part in the equilibration. Isotopic labelling experiments may give more unequivocal answers.

Experimental

Boiling points are not corrected. The n.m.r. spectra were obtained at room temperature on deuteriochloroform solutions using a Varian A60 instrument and have been reported (3–6).

trans-Crotonic Acid Equilibrations

The thermostats used were as follows: 100°, boiling water; 117, 138, and 189°, stirred polyethylene glycol; 147, 156.5, and 179°, vapor phases of refluxing *sym*-tetrachloroethane, *n*-hexanol, and *o*-dichlorobenzene respectively. The heating media were frequently checked with the same calibrated thermometer and were constant to $\pm 0.5°$ over the periods used, except for the 189° polyethylene glycol bath. Mechanical difficulties caused the latter to cool to the indicated extent during the run. *trans*-Crotonic acid was freshly recrystallized (using decolorizing charcoal) from hexane just before the runs, and samples of about 4 g were placed in stoppered test tubes in each of the thermostats described above. The crotonic acid interface in each case was situated at least 2 in. below the level to which the test tubes were heated. Time for the start of heating at each temperature was staggered 5 min, the same order being observed for the withdrawal of aliquots of about 100 mg. With this aliquot put directly into a cold n.m.r. sample tube the equilibration was effectively quenched. Shortly after the aliquots were removed, deuteriochloroform (about 0.3 ml) and TMS were added to the tubes and, following analysis and integration of n.m.r. spectra, the concentrations were calculated (Table 2).

cis-Crotonic Acid Equilibrations

The equilibration of *cis*-crotonic acid was carried out in a strictly analogous way using 97% *cis* acid as the starting material (Table 3). Room temperature stability was determined on a 300 g sample in a nearly full amber bottle left on a bench top.

Catalyzed Equilibrations

The equilibrations by heat with catalysis of *trans*-crotonic acid were carried out in a way analogous to those without catalysis. Woelm basic alumina (1.2 g; activity 1) was kept well suspended in a melt of 4.2 g of the acid with a micro air-powered stirrer for a surface activity test. For the acid catalysis test a solution of *m*-benzenedisulfonic acid (0.1 g; 12 mol %) in 3.0 g of the *trans* acid was used. Anhydrous caustic (0.6 g; 21 mol %) was dissolved in a melt of 6.0 g of the *trans* acid to give the results in strongly basic media. Table 4 summarizes these results.

Equilibration of Vinylacetic Acid

A 5 g sample of neat vinylacetic acid was heated in a stoppered test tube and the changes in composition determined by n.m.r. (6). The results obtained are given in Table 5 and, for comparison, the changes noted in another system in which the initial presence of a large proportion of *cis*-crotonic acid gave ambiguous conclusions (*cis* → *trans vs. cis* → vinylacetic → *trans*, or mixed) is included.

Ester Equilibrations

A test-tube containing ethyl *trans*-crotonate (2.5 g) and

trans-crotonic acid (50 mg) was heated in a bath at 117° for 65 h and an aliquot was analyzed by n.m.r. No ethyl *cis*-crotonate had formed. One gram of the above solution was sealed into an n.m.r. tube and heated in a 138° bath for 120 h, and again, no *cis* ester formed. A further experiment at 155° using the *trans* ester alone sealed into an n.m.r. tube again showed no *cis* after 16 h heating.

Molar Composition Determination

Molar compositions of the equilibration components were determined from the integrated areas of the resonances of the largest proton groupings in each molecule. The integral for the saturated methylene resonance of vinylacetic acid at 179 and 186 Hz was multiplied by 3/2 to convert its integral to a molar proportion for a three proton resonance. The proportion of *cis*-crotonic acid present was clearly determined from the integral of its methyl resonance. The pair of doublets due to the olefinic methyl of dimer **3***a* inconveniently straddled those of the *trans* acid and likewise, the resonance of trimer **4** straddled the resonance doublet of the saturated methyl of **3**. However, both of these composite integrals were resolved using the ratios of these integrals to the integral of the relatively clear methylene doublet of **3**. The latter ratios were determined using both peak height and peak area ratios on two expanded and integrated spectra of different samples and were found to be consistent. These ratio approximations amounted to multiplying the integral of the methylene doublet of **3** by 3/2 to give the integral equivalent of a methyl of the dimer, which then was subtracted from both the dimer methyl *trans*-crotonic methyl composite integral and the dimer methyl-trimer methyl composite integral. The remainders were the *trans*-crotonic acid integral and the trimer integral respectively. For the dimer, which has twice the molecular weight of the other components, the integral for the methylene doublet was multiplied by three to give a six proton equivalence and this figure was used to calculate its molar proportions.

As a consequence of the approximations required to get meaningful data from the integrated spectra, the absolute values quoted should be treated with some caution though it is estimated that the error introduced should not be larger than $\pm 5\%$ of the value given.

Actual isolation of the components of the mixtures formed was relatively easy for some of them. For instance, *trans*-crotonic acid was recovered when required simply by dissolving the mixture with warming in a small amount of hexane and allowing to cool to room temperature. The isolation of *cis*-crotonic acid has been presented in detail (4), and vinylacetic acid, dimers, and higher oligomers were isolated by essentially distillation procedures (3, 5).

The assistance of H. D. Mak in obtaining most of the n.m.r. spectra is recorded with gratitude. The author thanks a referee for bringing the relevance of reference 16 to his attention.

1. R. S. MORRELL and E. K. HANSON. J. Chem. Soc. **85**, 1520 (1904).
2. E. L. SKAU and B. SAXTON. J. Am. Chem. Soc. **52**, 335 (1930).
3. M. B. HOCKING. Can. J. Chem. **47**, 822 (1969).
4. M. B. HOCKING. Synth. 482 (1971).
5. M. B. HOCKING. Can. J. Chem. **49**, 3889 (1971).
6. C. RAPPE. Acta. Chem. Scand. **17**, 2766 (1963) and references cited therein.
7. J. HINE. Physical organic chemistry. 2nd Edition. McGraw-Hill Book Company, Inc. New York. N.Y. 1962. p. 69.
8. R. A. ALBERTY and W. G. MILLER. J. Chem. Phys. **26**, 1231 (1957).
9. R. P. LINSTEAD and J. T. W. MANN. J. Chem. Soc. 726, (1931).
10. R. P. LINSTEAD and E. P. NOBLE. J. Chem. Soc. 614, (1934).
11. E. J. BOORMAN and R. P. LINSTEAD. J. Chem. Soc. 577, (1933).
12. D. J. G. IVES. J. Chem. Soc. 81, (1938).
13. M. S. NEWMAN. Steric effects in organic chemistry. John Wiley and Sons, Inc. New York. N.Y. 1956. p. 429.
14. Reference 7. p. 90.
15. E. H. KON and G. A. R. COULSON. J. Chem. Soc. 2568, (1932).
16. D. E. MCGREER and N. W. K. CHIU. Can. J. Chem. **46**, 2225 (1968).

Can. J. Chem. Downloaded from www.nrcresearchpress.com by 210.87.254.6 on 09/05/12
For personal use only.

Aromatic Halogenation with Titanium(IV) Chloride in Presence of Peroxytrifluoroacetic Acid

G. K. CHIP AND J. S. GROSSERT[1]

Department of Chemistry, Dalhousie University, Halifax, Nova Scotia

Received July 2, 1971

Titanium(IV) chloride in the presence of an oxidizing reagent such as peroxytrifluoroacetic acid is shown to chlorinate a variety of aromatic substrates. The substitution orientation patterns suggest that the reaction is an electrophilic substitution process, which possibly involves the intermediacy of hypochlorous acid. Chlorination fails to occur with ring systems bearing strongly deactivating substituents, but it proceeds very cleanly and in high yield with activated rings, *e.g.* phenol. The reaction conditions are mild and are adaptable for bromination or iodination as well as chlorination.

On montre que le chlorure de titanium(IV), en présence d'un agent oxydant tel l'acide péroxytrifluoroacétique, permet d'introduire un chlore sur plusieurs substrats aromatiques. Les modèles d'orientation de la substitution suggèrent que la réaction est un procédé de substitution électrophile, qui implique possiblement l'intermédiaire de l'acide hypochloreux. Il n'y a pas de substitution de chlore sur les noyaux portant des substituants fortement désactivants, mais elle se produit facilement, avec de bons rendements, dans le cas de noyaux activés, tel le phénol. Les conditions de réaction sont douces et peuvent être adaptées pour la bromuration et l'ioduration, aussi bien que pour la chloruration.

Canadian Journal of Chemistry, **50**, 1233 (1972)

Can. J. Chem. Downloaded from www.nrcresearchpress.com by 210.87.254.6 on 09/05/12
For personal use only.

Halogenation of aromatic rings is one of the more thoroughly investigated organic reactions, and it has been discussed in a wealth of chemical literature (1). Most reactions of this type fall into four general classes, *viz.* (*1*) reaction of electron-rich aromatic rings with molecular halogen; (*2*) reaction of less-activated rings with molecular halogen in the presence of a catalyst; (*3*) reaction of aromatic compounds with systems which furnish a positively charged halonium ion species (*e.g.* chlorine–silver acetate); and (*4*) direct halogenation of an aromatic molecule with halogen, apparently derived from reduction of a metal halide, but without the addition of any free halogen.

Of these four general approaches, the last-mentioned has been studied relatively little, although the use of iron(III) and antimony(V) chlorides as aromatic chlorinating agents has been known for over 100 years (2). Since that time, those metal halides which have received most attention include antimony(V), copper(II), iron(III), and vanadium(V) chlorides (3). It should be noted that metal halides may effect other transformations in addition to halogenation. Depending on the reaction conditions, nuclear coupling, side-chain attack in alkylbenzenes, disproportionation, and polymerization are known to occur (4, 5). In the nuclear chlorination of aromatic compounds with metal halides, various lines of evidence, including the predominant ortho/para orientation, point to an electrophilic substitution mechanism, although the actual attacking form of the metal halide is uncertain.

Titanium(IV) chloride by itself has never been reported to chlorinate aromatic compounds, but it has been used as a catalyst and as a solvent in the chlorination of aromatic rings by other metal halides (6). Previously, we reported that titanium(IV) chloride, in the presence of peroxytrifluoroacetic acid or *m*-chloroperbenzoic acid, will chlorinate aromatic compounds (7). In the present paper, we report further examples of aromatic chlorination with this system and present evidence for a proposed mechanism of the reaction.

Results and Discussion

In general, the chlorination reactions were performed in methylene chloride solvent at 0–20 °C with aromatic reactant–titanium(IV) chloride–peroxytrifluoroacetic acid in a 1:1:1 molar ratio. Aromatic substrates, which represent a range of different reactivities toward electrophiles, were chlorinated by this reaction; the results are presented in Table 1. The products

[1]To whom correspondence should be addressed.

TABLE 1. Chlorination of aromatic compounds with $TiCl_4$–CF_3CO_3H ([substrate]:[$TiCl_4$]:[CF_3CO_3H] = 1:1:1 for all experiments)

Substrate (mmol)	Reaction conditions: Time (h)	Reaction conditions: Temperature (°C)	Overall yield (%)	Isomer distribution
Benzene (3)	3	20	60	Chlorobenzene 100
Chlorobenzene (5)	9	20	40	*o*-Dichlorobenzene 40 *p*-Dichlorobenzene 60
Toluene (5)	3	20	90	*o*-Chlorotoluene 85 *p*-Chlorotoluene 15
Acetanilide (3)	4	20	76	*o*-Chloroacetanilide 27 *p*-Chloroacetanilide 48 2,4-Dichloroacetanilide 15 2,4,6-Trichlorophenol 10
p-Acetotoluidide (3)	10	20	86	2-Chloro-4-methylacetanilide 62 2,4,6-Trichloro-4-methylcyclohexa-2,5-dienone 15
p-Methoxyacetanilide (3)	6	20	85	3-Chloro-4-methoxyacetanilide 59 2,5-Dichloro-4-methoxyacetanilide 31 2,4,5-Trichloro-4-methoxycyclohexa-2,5-dienone 10
Mesitylene (3)	2	0	94	Trichloromesitylene 65 Mesitol 5 Unidentified products 30
p-Chloroacetanilide (2)	4	20	38	2,4-Dichloroacetanilide 100
Anisole (3)	3	20	94	*o*-Chloroanisole 52 *p*-Chloroanisole 28 2,4-Dichloroanisole 20
Phenol (5)	3	0	90	*o*-Chlorophenol 56 *p*-Chlorophenol 22 2,4-Dichlorophenol 22
Aniline (3)	4	20	64	*o*-Chloroaniline 34 *p*-Chloroaniline 23 2,4-Dichloroaniline 43
Biphenyl (3)	4	20	76	2-Chlorobiphenyl 68 4-Chlorobiphenyl 17
Benzoic acid (3)	28	64	—	Starting material
Nitrobenzene (3)	20	50	—	Starting material
Pyridine (3)	6	20	—	Starting material
Thiophene (3)	6	20	—	Starting material

were isolated and were identified by comparison with authentic materials or by their spectroscopic properties.

Benzene was converted to chlorobenzene with no detectable formation of dichlorobenzene. Toluene and chlorobenzene were monochlorinated also. Although there is considerable literature on chlorination of these two aromatics (8–10), it appears that the use of titanium(IV) chloride as a catalyst for chlorination with molecular chlorine has not been reported previously. In Table 2, we have included our results on this system, together with relevant literature data for other systems, in order to compare these with the reactions of the titanium(IV) chloride – peroxytrifluoroacetic acid reagent.

In the case of mesitylene, 94% was consumed and the products contained trichloromesitylene (65%) and mesitol (5%). Reaction of mesitylene with peroxytrifluoroacetic acid alone has been

Can. J. Chem. Downloaded from www.nrcresearchpress.com by 210.87.254.6 on 09/05/12
For personal use only.

Can. J. Chem. Downloaded from www.nrcresearchpress.com by 210.87.254.6 on 09/05/12
For personal use only.

TABLE 2. Chlorination reactions of toluene and chlorobenzene

Substrate	Catalyst	Chlorine source	Solvent	Reaction conditions: Time (h)	Reaction conditions: Temperature (°C)	Overall yield (%)	Isomer distribution (%): *o*	*m*	*p*	Reference
Toluene	$HClO_4$ / $AgClO_4$	$HOCl/H^+$	HOH	—	25.0	—	75	—	23	8
Toluene	$SbCl_5$	Cl_2	—	4.0	25–30	20*	72	2	26	9
Toluene	$FeCl_3$	Cl_2	—	2.3	25–30	5*	64	4	32	9
Toluene	—	$SbCl_5$	—	2.5	18–31	87	47	2	51	9
Toluene	$TiCl_4$	Cl_2§	CH_2Cl_2	3	25	95§	45	—	10†	‡
Toluene	$TiCl_4$	Cl_2‖	CH_2Cl_2	3	25	60‖	71	—	29	‡
Toluene	$TiCl_4$	$TiCl_4/CF_3CO_3H$	CH_2Cl_2	3	25	90‖	85	—	15	‡
Chlorobenzene	$HClO_4$	$ClClO_4$	CCl_4	1–8	25	—	36	—	62	10
Chlorobenzene	$FeCl_3$	Cl_2	—	3.5	40–55	35*	40	3	57	9
Chlorobenzene	—	$SbCl_5$	—	2.0	41–59	82	15	1	84	9
Chlorobenzene	$TiCl_4$	Cl_2§	CH_2Cl_2	9	25	90§	28	—	72	‡
Chlorobenzene	$TiCl_4$	Cl_2‖	CH_2Cl_2	3	25	37‖	30	—	70	‡
Chlorobenzene	$TiCl_4$	$TiCl_4/CF_3CO_3H$	CH_2Cl_2	9	25	40‖	40	—	60	‡

*Reaction not taken to completion.
†In addition, 45% 2,4-dichlorotoluene was obtained.
‡Present work.
§Excess of chlorine.
‖Molar ratio of reactants 1:1:1.

TABLE 3. Chlorination of aromatic compounds with $TiCl_4$–H_2O_2 at 20 °C

Substrate (mmol)	$TiCl_4$ (mmol)	H_2O_2 (90%) (mmol)	Reaction time (h)	Overall yield (%)	Isomer distribution			
					o	*p*	2,4-Dichloro	Residue
Acetanilide (3)	3	3	6	45	24	54	14	8*
Acetanilide (4)	3	6	6	52	29	56	9	6*
Acetanilide (1)	3	6	6	95	0	0	95	5*
Toluene (10)	10	10	7	40	75	25	0	0
Chlorobenzene (10)	10	10	9	21	40	60	0	0

*Shown to be 2,4,6-trichlorophenol.

reported to give mesitol in 45% yield, whereas this was increased to 88% by carrying out the same reaction in the presence of boron trifluoride (11). On the other hand, we have observed that aluminum(III) chloride–peroxytrifluoroacetic acid is a chlorinating system.[2] From these reactions it may be concluded that a Lewis acid will only enhance the reactivity of peroxytrifluoroacetic acid as a source of electrophilic hydroxyl if the Lewis acid itself will not become involved in a reaction to form a species less electrophilic than "HO^+".

Acetanilide gave a mixture of chloroacetanilides, in addition to 2,4,6-trichlorophenol.[3] With *p*-acetotoluidide, 2-chloro-4-methyl-acetanilide and 2,4,6-trichloro-4-methylcyclohexa-2,5-dienone were produced, the structure of this dienone being deduced from its spectral characteristics (see Experimental). On acetylation with acetic anhydride/*p*-toluenesulfonic acid, it rearranged to 3-methyl-2,4,6-trichlorophenyl acetate. This rearrangement rules out the possibility that the dienone might have been 3,4,5-trichloro-4-methylcyclohexa-2,5-dienone which, solely on spectral grounds, could not be unequivocally distinguished from the 2,4,6-trichloro-4-methyl isomer. Similarly, *p*-methoxyacetanilide gave 3-chloro-4-methoxyacetanilide, 2,5-dichloro-4-methoxyacetanilide and 2,4,5-trichloro-4-methoxycyclohexa-2,5-dienone, which proved to be much less stable than the similar dienone from *p*-acetotoluidide. The formation of 3-chloro- instead of 2-chloro-4-methoxyacetanilide is consistent with a dominance in substituent directive power of the methoxyl group over the *N*-acetylamino group (12).

Phenol was cleanly chlorinated with a mixture of titanium(IV) chloride and peroxytrifluoroacetic acid to give chlorophenols in 90% yield. No oxidation products of phenol, such as benzoquinone, could be detected; indeed, the reaction was remarkably smooth. Presumably, phenol first reacts with titanium(IV) chloride to form phenyl titanate (13) which is sufficiently nucleophilic to be chlorinated.

Aniline was chlorinated in 64% yield to *o*-chloroaniline (34%), *p*-chloroaniline (23%), and 2,4-dichloroaniline (43%). These products were identified by conversion to the corresponding chloroacetanilides which were analyzed by v.p.c. It is relevant to note that in this case too, no oxidation products could be detected, whereas the direct chlorination of most primary aromatic amines with free chlorine results in extensive oxidation (14).

Some aromatic compounds failed to undergo chlorination. Benzoic acid and nitrobenzene were too strongly deactivated to react, whereas pyridine and thiophene failed to react because of the nucleophilic heteroatoms which, on complexing with the titanium(IV) chloride, caused the ring to become highly deactivated toward electrophilic substitution (15).

Titanium(IV) chloride also chlorinates aromatic compounds in the presence of other peroxides. For example, acetanilide with titanium(IV) chloride–*m*-chloroperbenzoic acid in a 1:1:1 ratio gave a 56% yield of chloroacetanilides. Reaction with a mixture of titanium(IV) chloride and 90% hydrogen peroxide also gave chlorination products, although generally the yields were much lower than when using peroxytrifluoroacetic acid. Results for this system with three representative aromatic substrates are shown in Table 3.

Some conclusions concerning the mechanism of the chlorination reaction may be drawn at this point. The predominance of ortho/para

[2]G. K. Chip and J. S. Grossert. Unpublished data.

[3]We had previously reported (7) the absence of *o*-chloroacetanilide in this reaction. This was due to the inadequacy of t.l.c. separation techniques, and the presence of the ortho isomer has since been demonstrated unequivocally by the use of v.p.c.

Can. J. Chem. Downloaded from www.nrcresearchpress.com by 210.87.254.6 on 09/05/12
For personal use only.

TABLE 4. Chlorination of acetanilide with $TiCl_4$–CF_3CO_3H in the presence of added anions

Added anions (mmol)	Reaction conditions		Overall yield (%)	Products
	Time (h)	Temperature (°C)		
$(C_2H_5)_4N^+Cl^-$ (24)	8	20	97	2,4-Dichloroacetanilide
$(C_2H_5)_4N^+Br^-$ (24)	24	20	98	4-Bromoacetanilide
$(C_2H_5)_4N^+I^-$ (6)	18	40	80	4-Iodoacetanilide
$(C_2H_5)_4N^+F^-$ (9)	48	20	50	2-Chloroacetanilide (25%) 4-Chloroacetanilide (54%) 2,4-Dichloroacetanilide (21%)

substitution and the lack of attack on alkyl side chains point to a reaction which is electrophilic rather than radical in nature. The possibility that the active species is molecular chlorine was considered unlikely on the grounds of the product isomer distribution (*cf.* Table 2), and the fact that the decomposition of titanium(IV) chloride into titanium(II) chloride and chlorine is not known (16). Examination of the substitution pattern for all the substrates investigated pointed to an active species of relatively low specificity (and hence of relatively high reactivity), with a relatively small steric factor (17); we suggest that this is best accounted for by postulating hypochlorous acid, or a titanate ester thereof, as the active chlorinating species. The formation of hypochlorous acid by reaction between a peroxy acid and titanium(IV) chloride may be readily rationalized by eq. 1, and a corresponding reaction with hydrogen peroxide by eq. 2.

We have found two additional pieces of evidence to support eq. 1. Reaction of cyclohexene with titanium(IV) chloride–*m*-chloroperbenzoic acid gave 2-chlorocyclohexanol and *m*-chlorobenzoic acid as the only isolable products, eq. 3. No 2-chlorocyclohexyl *m*-chlorobenzoate or 1,2-dichlorocyclohexane could be isolated, which is in accord with the proposed mechanism.

Results from the addition of an excess of various halide anions to the reaction of acetanilide with titanium(IV) chloride–peroxytrifluoroacetic acid (3mmol of each) are given in Table 4. On addition of an excess of chloride ions, the appearance of a greenish-yellow color in the reaction flask indicated the liberation of chlorine gas. The sole product was 2,4-dichloroacetanilide, formed in 97% yield. With an excess of bromide ions, 4-bromoacetanilide was formed in 98% yield, whereas addition of iodide ions gave 4-iodoacetanilide in 80% yield. Addition of fluoride ions gave no fluorination, but only a mixture of chloroacetanilides. These results are as would be expected for a hypochlorite as the active species (18).

The formation of dienones during chlorination of acetanilides is a novel reaction, although their formation during halogenation of phenols is known (19). We have depicted in Scheme 1 our speculation on how the reaction may convert the amide function into a leaving group.

Titanium(IV) chloride is known to form complexes with acetanilide, although the structure of these is in doubt.[4] However, an adduct of the Vilsmeier–Haack type, analogous to the one proposed in Scheme 1, has been postulated (21)

[4]We have prepared a red titanium(IV) chloride–acetanilide complex, m.p. 160–164° (dec.), from methylene chloride solutions. This does not correspond to complexes reported in the literature (20) and we are investigating its structure.

[1] 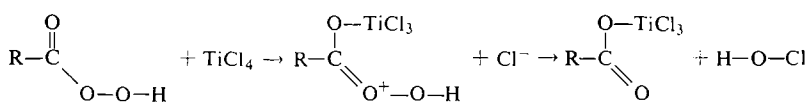

[2] 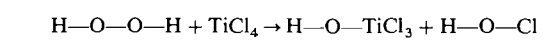

[3] 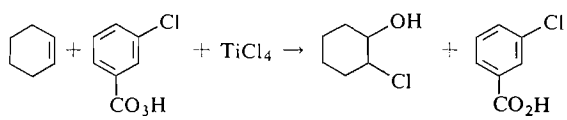

Can. J. Chem. Downloaded from www.nrcresearchpress.com by 210.87.254.6 on 09/05/12
For personal use only.

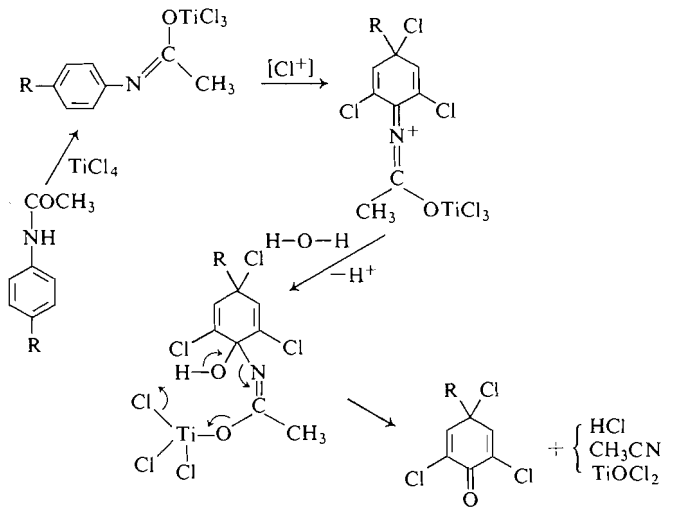

For R = —H or —CH_3; if R = —OCH_3, then chlorination pattern is changed

SCHEME 1

to decompose by expulsion of acetonitrile. As a result of this postulate, we examined the reaction mixture and did detect acetonitrile by v.p.c. and i.r. spectroscopy. On the basis of Scheme 1, mono- or dichlorinated dienones could have been expected but we have found no evidence of their presence.

We believe that this reaction offers a novel and versatile approach to the synthesis of halogenated aromatic compounds, and it may also have some potential for the synthesis of chlorohydrins. In particular, the reaction is easy to carry out, it occurs under mild, controlled conditions and it is applicable to chlorination of reactive molecules, such as aniline or phenol. We are exploring further its applicability to other systems.

Experimental

All melting points were recorded on a Fisher–Johns apparatus and are uncorrected. Infrared spectra were recorded (in $CHCl_3$) on a Perkin–Elmer Model 237B grating spectrophotometer. Ultraviolet spectra were obtained in 95% ethanol solutions on a Coleman–Hitachi Model 124 spectrophotometer. The n.m.r. spectra were determined in $CDCl_3$ on Varian Associates A-60 or T-60 spectrometers using tetramethylsilane as an internal standard. Mass spectra were taken on a C.E.C. Model 21-104 spectrometer operating at 70 eV. Vapor-phase chromatography was performed on a Hewlett–Packard Model 700 chromatograph, equipped with a flame ionization detector and a 6 ft × 1/8 in. stainless steel column (packed with a 15% DC-200/10% QF-1 mixture on 80–100 mesh acid-washed Chromosorb W) generally at 175°, with a nitrogen flow rate of 45 ml/min. Overall yields were calculated on the basis of consumption of starting aromatic substrate, and isomer ratios reflect the relative composition of the isolated product mixture.

Materials

Titanium tetrachloride (Matheson, Coleman & Bell) was refluxed over copper turnings for 4 h and then distilled, giving a colorless fraction, b.p. 136°. Methylene chloride was reagent grade (Fisher Scientific) and was dried over Linde molecular sieve 4A. Hydrogen peroxide (90%) was from the FMC Corporation, and chromatography was done using appropriate Merck products. Tetraethylammonium chloride was made by the method of Coppens *et al.* (22). All other materials were either reagent grade or were prepared by standard procedures.

Reaction of Acetanilide with Titanium(IV) Chloride and Peroxytrifluoroacetic Acid; General Procedure

An anhydrous solution of peroxytrifluoroacetic acid (11) was prepared by dissolving trifluoroacetic anhydride (0.63 ml, 3.2 mmol) in anhydrous methylene chloride (3 ml). After cooling to 0 °C, 90% hydrogen peroxide (0.09 ml, 3 mmol) was added while maintaining vigorous stirring until a homogeneous solution was obtained (15 min). The peracid solution was then added dropwise, during a 15 min period, to a cooled, well-stirred solution of acetanilide (405 mg, 3 mmol) and titanium(IV) chloride (0.33 ml, 3 mmol) in dry methylene chloride (15 ml), under N_2. After the addition of peracid was complete, the reaction mixture was stirred at room temperature for 4 h, during which time its color changed from dark orange to light yellow. The mixture was then hydrolyzed with cold water (50 ml). The product was extracted with methylene chloride, washed with water, 10% sodium bicarbonate, water again, and then dried over anhydrous sodium sulfate. The extract was concentrated and v.p.c. analysis showed that the product (formed in 76% overall yield) contained a mixture of *o*-chloro-

Can. J. Chem. Downloaded from www.nrcresearchpress.com by 210.87.254.6 on 09/05/12
For personal use only.

Can. J. Chem. Downloaded from www.nrcresearchpress.com by 210.87.254.6 on 09/05/12
For personal use only.

acetanilide (27%), *p*-chloroacetanilide (48%), 2,4-dichloroacetanilide (15%), and 2,4,6-trichlorophenol (10%). In some other experiments, the products were separated on preparative t.l.c. plates and the individual components were extracted and characterized by their melting points and spectroscopic properties.

Reactions of other aromatic substrates were carried out by a procedure identical with that described above. The reagent quantities, reaction conditions, yields, and isomeric distributions are presented in Table 1.

The aryl chlorides were identified by n.m.r. and v.p.c. techniques and in most cases by comparison of their physical properties with those of authentic samples.

Chlorination with Molecular Chlorine in the Presence of Titanium(IV) Chloride; General Procedure

A solution of chlorine (7 mmol) was prepared by bubbling molecular chlorine into methylene chloride (10 ml). This solution was then added to a mixture of acetanilide (7 mmol, 945 mg) and titanium(IV) chloride (7 mmol, 0.77 ml) in methylene chloride (20 ml). The reaction mixture was allowed to stir at room temperature for 5 h. After aqueous work-up, analysis of the organic fraction by v.p.c. indicated a mixture of ortho- and para-chloroacetanilide in the ratio 32:68 and in a 15% overall yield.

When a large excess of molecular chlorine was used in this reaction, only 2,4-dichloroacetanilide (in 96% yield) could be isolated. Similar reactions were carried out on toluene and on chlorobenzene. The results are reported in Table 2.

Reaction of Acetanilide with Titanium(IV) Chloride

The reaction of acetanilide and titanium(IV) chloride was repeated without the addition of peroxytrifluoroacetic acid. After aqueous work-up, the acetanilide recovery was essentially quantitative. No chloroacetanilides could be detected either by t.l.c. or v.p.c.

Reaction of p-Acetotoluidide with Titanium(IV) Chloride – Peroxytrifluoroacetic Acid

The same general procedure was followed. The crude reaction mixture (570 mg) was chromatographed on a column of neutral alumina, Brockman activity 1, 80–200 mesh. Elution with petroleum ether (b.p. 30–60°) gave a white solid (90 mg, 15%) which crystallized from petroleum ether (b.p. 30–60°), m.p. 89–90°. This was identified as 2,4,6-trichloro-4-methylcyclohexa-2,5-dienone from its spectral data: i.r. 1680, 1630 cm^{-1}, no NH or OH absorption; u.v. (95% EtOH) λ_{max} 251 nm (ε 8600), λ_{min} 288 nm; n.m.r. δ 1.98 (s, 3H), 7.21 p.p.m. (s, 2H); mass spectrum M^+ at 209.9399 a.m.u. (calculated for $C_7H_5OCl_3$, 209.9405 a.m.u.) with the isotopic ratio $M^+ + 2 : M^+ + 4 : M^+ + 6$ indicating three chlorine atoms. Further elution gave 2-chloro-4-methylacetanilide (340 mg, 62%, m.p. 117°, undepressed with an authentic sample) and 4-methylacetanilide (56 mg, 16%).

The cyclohexa-2,5-dienone was converted to its 2,4-dinitrophenylhydrazone by warming with an ethanolic solution of the hydrazine reagent. An orange solid precipitated immediately; water was added until the solution became cloudy, and the solid was extracted with chloroform, which was dried (Na_2SO_4). The solvent was evaporated and the residue was recrystallized from EtOH, giving orange-yellow plates, m.p. 160–161°, M^+ 390 a.m.u.

The dienone was converted to 3-methyl-2,4,6-trichlorophenyl acetate by refluxing with a mixture of acetic anhydride and *p*-toluenesulfonic acid for 20 h. The dark solution was poured into cold water and solid Na_2CO_3 added to neutralize excess acid. The product was extracted with chloroform, washed with water and dried (Na_2SO_4). Evaporation of the solvent gave a brown gum which was purified by column chromatography on silica gel. The product was recrystallized from petroleum ether (b.p. 30–60°) to give colorless prisms, m.p. 94–95°. The i.r. showed a band at 1760 cm^{-1} (ester C=O); n.m.r. showed a singlet at δ 2.3 (3H), a singlet at 2.08 (3H), and a singlet at 7.3 p.p.m. (1H).

Reaction of p-Methoxyacetanilide with Titanium(IV) Chloride – Peroxytrifluoroacetic Acid

The same general procedure was followed with *p*-methoxyacetanilide (495 mg, 3 mmol), titanium(IV) chloride (3 mmol), and peroxytrifluoroacetic acid (3 mmol). The crude reaction mixture (570 mg) was chromatographed on a column of neutral alumina, Brockman Activity 1, 80–200 mesh. Elution with petroleum ether (b.p. 30–60°)/benzene (3:1) gave a white solid (20 mg, 10%), m.p. 63–65°, identified as 2,4,5-trichloro-4-methoxycyclohexa-2,5-dienone by its spectral characteristics: i.r. 1665 and 1610 cm^{-1} (α,β-unsaturated C=O), no NH or OH adsorption; u.v. λ_{max} 235 nm (ε 8400); n.m.r. δ 3.84 (s, 3H, OCH_3), 6.83 (s, 1H), and 6.86 p.p.m. (s, 1H); mass spectrum M^+ 226 a.m.u. with the isotopic ratio indicating the presence of three chlorine atoms. This dienone was unstable and readily decomposed to a brown solid of undetermined composition, but which did appear to contain quinonoidal material.

Further elution gave 2,5-dichloro-4-methoxyacetanilide (153 mg, 31%) recrystallized from 95% ethanol, m.p. 194–195° (lit. (23) 189–190°), n.m.r. δ 2.20 (s, 3H, $-CH_3$), 3.87 (s, 3H, $-OCH_3$), 6.90 (s, 1H), 7.33 (broad s, 1H, NH, exchanged in D_2O), 8.17 p.p.m. (s, 1H); i.r. 3420 (NH), 1690 cm^{-1} (amide C=O), and 3-chloro-4-methoxyacetanilide (225 mg, 59%) recrystallized from ethanol, m.p. 92–93° (lit. (24) 94°).

Reactions with Titanium(IV) Chloride – Hydrogen Peroxide

The general procedure already outlined was followed, except that the appropriate amount of hydrogen peroxide (90%) was used in place of the peroxytrifluoroacetic acid. The two-phase system was stirred vigorously; the results are given in Table 3.

Reactions of Acetanilide with Titanium(IV) Chloride – Peroxytrifluoroacetic Acid in Presence of Added Anions

The same general procedure was followed, except that prior to the addition of the peroxytrifluoroacetic acid, a solution of tetraethylammonium chloride, bromide, or fluoride in methylene chloride was added. The results are presented in Table 4. Tetraethylammonium iodide was insoluble in methylene chloride and hence was added in methanol. At the end of this reaction, the solvent was evaporated, leaving a dark violet mass. This was thoroughly washed with cold water, leaving a violet solid which had m.p. 113° and smelled of iodine. The filtrate was extracted with benzene, and the extract was washed first with sodium thiosulfate, then with water, and dried (Na_2SO_4). Evaporation of the solvent gave *p*-iodoacetanilide, recrystallized from ethanol, m.p. 189–190° (lit. (25) 184°), The n.m.r. spectrum of this compound showed the characteristic AA′BB′ pattern

of a 1,4-disubstituted benzene and the mass spectrum showed the molecular ion at *m/e* 261 (C_8H_8NOI has mol. wt. 261).

Reaction of Cyclohexene with m-Chloroperbenzoic Acid–Titanium(IV) Chloride

Cyclohexene (246 mg, 3 mmol) was added to a stirred solution of *m*-chloroperbenzoic acid (517.5 mg, 3 mmol) and titanium(IV) chloride (0.33 ml, 3 mmol) in methylene chloride (20 ml) under N_2. The reaction was allowed to proceed at room temperature for 4 h. The mixture was hydrolyzed with water and the organic product was extracted with methylene chloride. The extract was washed with water and dried (Na_2SO_4). Evaporation of the solvent gave 493 mg of product which was washed with hot water to dissolve the *m*-chlorobenzoic acid. These washings were extracted with chloroform, which was dried and evaporated to give *m*-chlorobenzoic acid (212 mg, 45%), m.p. 155–156°, identical with an authentic sample.

The above product, having been washed with hot water, was extracted with methylene chloride, which was washed, dried and evaporated to give 2-chlorocyclohexanol (150 mg, 37%), the spectroscopic properties of which were identical to those of an authentic sample.

Identification of Acetonitrile

A reaction with acetanilide, as described in the general procedure, was repeated using 1,1,2,2-tetrachloroethane, b.p. 114°, as solvent. At the end of the reaction, the mixture was fractionated and the distillates were analyzed by v.p.c. and i.r. One fraction showed an absorption band in the i.r. spectrum at 2260 cm^{-1} and on the v.p.c. showed a peak corresponding to the retention time of authentic acetonitrile.

We thank the National Research Council of Canada and Dalhousie University for financial support, and Dr. W. D. Jamieson for the high-resolution mass spectrum.

1. For a general review of aromatic halogenation, see H. P. BRAENDLIN and E. T. MCBEE. *In* Friedel–Crafts and related reactions. Vol. III, Part 2. *Edited by* G. A. Olah. John Wiley and Sons, Inc., New York, 1964. Chapt. 46.
2. H. MÜLLER. J. Chem. Soc. **15**, 41 (1862).
3. P. KOVACIC. *In* Friedel–Crafts and related reactions. Vol. IV. *Edited by* G. A. Olah. John Wiley and Sons, Inc., New York, 1965. Chapt. 48.
4. P. KOVACIC and R. M. LANGE. J. Org. Chem. **28**, 968 (1963).
5. P. KOVACIC and A. K. SPARKS. J. Org. Chem. **28**, 972 (1963).
6. P. KOVACIC and C. WU. J. Org. Chem. **26**, 214 (1961).
7. J. S. GROSSERT and G. K. CHIP. Tetrahedron Lett. 2611 (1970).
8. P. B. D. DE LA MARE, J. T. HARVEY, M. HASSAN, and S. VARMA. J. Chem. Soc. 2756 (1958).
9. P. KOVACIC and A. K. SPARKS. J. Am. Chem. Soc. **82**, 5740 (1960).
10. R. O. C. NORMAN and G. K. RADDA. J. Chem. Soc. 3610 (1961).
11. H. HART, C. A. BUEHLER, and A. J. WARING. *In* Selective oxidation processes. Advances in chemistry series. No. 51. Am. Chem. Soc. Washington, D.C., 1965. Chapt. 1, and references therein.
12. P. B. D. DE LA MARE and J. H. RIDD. Aromatic substitution. Nitration and halogenation. Academic Press Inc., New York, 1959. Chapt. 10.
13. D. SCHWARTZ and W. CROSS. J. Chem. Engin. Data, **8**, 463 (1963); G. P. LUTSCHINSKY. Z. Anorg. Chem. **225**, 321 (1935).
14. H. P. CROCKER and R. WALSER. J. Chem. Soc. C, 1982 (1970); T. H. CHAS and L. P. CIPRIANI. J. Org. Chem. **26**, 1079 (1961).
15. Reference 12, Chapt. 15.
16. J. BARKSDALE. Titanium. Its occurrence, chemistry and technology. 2nd Ed. Ronald Press Co., New York, 1966. p. 99, 100.
17. R. O. C. NORMAN and R. TAYLOR. Electrophilic substitution in benzenoid compounds. Elsevier, Amsterdam, 1965. Chapts. 5, 11.
18. Reference 17, p. 126.
19. E. BERLINER. *In* Progress in physical organic chemistry. Vol. 2. *Edited by* S. G. Cohen, A. Streitwieser, Jr., and R. W. Taft. John Wiley and Sons, Inc., New York, 1964. p. 275; S. HUSAIN. Indian J. Chem. **6**, 81 (1968).
20. R. C. PAUL, B. R. SREENATHAN, and S. L. CHADHA. J. Inorg. Nucl. Chem. **28**, 1225 (1966); D. SCHWARTZ and R. HEYER. J. Inorg. Nucl. Chem. **29**, 1384 (1967).
21. J. L. MASSINGILL, JR., M. G. REINECKE, and J. E. HODGKINS. J. Org. Chem. **35**, 823 (1970).
22. G. D. COPPENS, D. N. KEVILL, and N. H. CROMWELL. J. Org. Chem. **27**, 3299 (1962).
23. M. GOI and K. KONISHI. J. Soc. Org. Synth. Chem. Japan, **12**, 189 (1954).
24. F. REVERDIN and F. ECKHARD. Ber. **32**, 2622 (1899).
25. F. D. CHATTAWAY and A. B. CONSTABLE. J. Chem. Soc. **105**, 124 (1914).

Can. J. Chem. Downloaded from www.nrcresearchpress.com by 210.87.254.6 on 09/05/12
For personal use only.

The Effect of Heat Treatment of Silica Gels on the Calorimetric Heats of Adsorption of Sulfur Dioxide up to One-twentieth Monolayer Coverage at 423 °K

R. W. GLASS AND R. A. ROSS

Department of Chemistry, Lakehead University, Thunder Bay, Ontario

Received November 15, 1971

Calorimetric heats of adsorption of sulfur dioxide have been determined at 423 °K for a series of silica gels heat-treated at 240, 550, 700, 800, and 900 °C. At the lowest surface coverage of 0.01 μmol m^{-2}, heats of 25 to 30 kcal mol^{-1} were observed. These values dropped rapidly with increasing coverage and approached "limiting" values of 6 to 7 and 12 kcal mol^{-1} for dehydroxylated and hydroxylated surfaces, respectively. To explain the results at lowest coverages an adsorbed complex involving multiple hydrogen bonds is proposed while at higher coverages it is suggested that single and dual site adsorbed species predominate for the dehydroxylated and hydroxylated surfaces, respectively. Sulfur dioxide adsorption isotherms on all gels at 423 °K obeyed the Langmuir equation.

Adsorbents were characterized by nitrogen adsorption–desorption isotherms at 77 °K and pore size distribution data were calculated from the desorption branch.

On a déterminé les chaleurs calorimétriques d'adsorption d'anhydride sulfureux à 423 °K pour une série de gels de silice traités à des chaleurs de 240, 550, 700, 800, et 900 °C. Lorsque la plus petite surface est couverte, soit 0.01 μmol m^{-2}, on observe des chaleurs de 25 à 30 kcal mol^{-1}. Ces valeurs diminuent rapidement lorsqu'on augmente la surface couverte et approchent des valeurs limites de 6 à 7 et 12 kcal mol^{-1} pour des surfaces respectivement, déhydroxylées et hydroxylées. Pour expliquer les résultats dans le cas d'une faible portion de surface couverte, on propose l'existence d'un complexe adsorbé qui implique des liaisons hydrogène multiples; pour une grande surface couverte, on suggère que des espèces adsorbées à site simple et double prédominent respectivement pour les surfaces déhydroxylées et hydroxylées. Les isothermes d'adsorption de l'anhydride sulfureux sur tous les gels à 423 °K obéissent à l'équation de Langmuir.

Les adsorbants sont caractérisés par des isothermes d'adsorption–désorption de l'azote à 77 °K et les données de distribution de la grandeur des pores sont calculées en se servant de la branche de désorption.

Canadian Journal of Chemistry, **50**, 1241 (1972)

Introduction

This investigation is an extension of the earlier studies of the adsorption of sulfur dioxide on various catalytic and porous solids (1, 2). Previously, results were described (1) for the adsorption of sulfur dioxide on silica gels in the temperature range 263 to 323 °K when both adsorption–desorption isotherms and isosteric heats for surface coverages above one-tenth of a monolayer were determined. These data showed that physisorption was the dominant process although some chemical interaction with surface hydroxy groups appeared to take place.

In the present work calorimetric heats of adsorption of sulfur dioxide for surface coverages below one-tenth of a monolayer have been determined at 423 °K for a series of silica gels heat-treated at temperatures between 240 and 900 °C. In addition, nitrogen adsorption–desorption isotherms for all gels have been measured at 77 °K and the pore size distributions calculated using the Cranston and Inkley method of analysis (3).

Experimental

Materials

Davison '923' grade silica gel with a particle size range 75–150 μ was used. Samples of this material were heat-treated in air at 240, 550, 700, 800, and 900 °C for 20 h. Immediately prior to making adsorption measurements all adsorbents were activated at 240 °C for 2 h, transferred to the appropriate apparatus, and then outgassed at 150 °C overnight at $<10^{-4}$ mm.

High-purity nitrogen (>99.99%; Canadian Liquid Air Ltd.) was used in the determination of the low-temperature nitrogen adsorption isotherms. Sulfur dioxide (Matheson Co.) was anhydrous quality and was drawn directly from the cylinder after line-flushing to a trap attached to the apparatus. It was then outgassed at 10^{-4} mm and vacuum distilled over trays of phosphorous pentoxide. Middle portions only were used and g.l.c. analyses show these to be >99.99% pure.

Apparatus

Heats of adsorption were determined calorimetrically in an apparatus similar to that described earlier (4), using the modified experimental technique for measurements above 273 °K (2).

Nitrogen adsorption–desorption isotherms at 77 °K were determined in an apparatus similar to that used by Joyner (5), and pore size distributions were calculated with the aid of an IBM 360/50 computer.

Hydroxyl group concentrations were determined (6) with

Can. J. Chem. Downloaded from www.nrcresearchpress.com by 210.87.254.42 on 09/05/12
For personal use only.

Can. J. Chem. Downloaded from www.nrcresearchpress.com by 210.87.254.42 on 09/05/12
For personal use only.

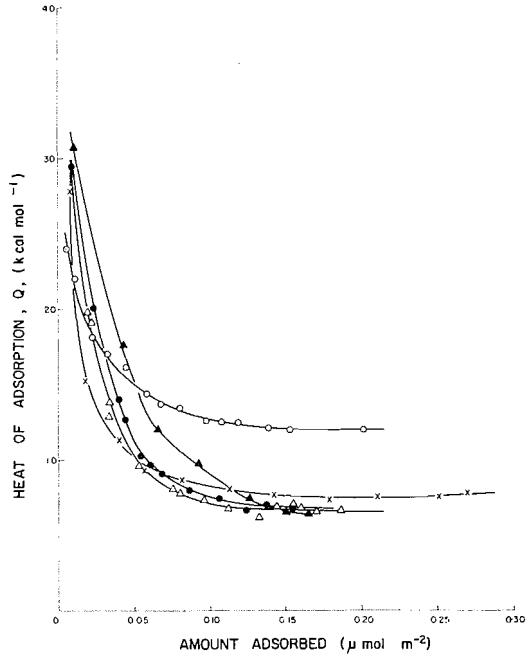

Fig. 1. Heat curves for the adsorption of sulfur dioxide at 423 °K on various heat-treated silica gels. Silica gel heat-treated at: 240 °C, ⊙; 550 °C, ×; 700 °C, ●; 800 °C, △; 900 °C, ▲.

a thermobalance (Stanton–Redcroft Model HT5A) at 1200 °C until a constant-weight value was recorded in a static air atmosphere.

Results

Heats of adsorption were determined for low surface coverages from 0.02 to 0.25 μmol m^{-2} on all five adsorbents at 423 °K. At this temperature, 0.70 μmol m^{-2} is approximately equivalent to one-tenth of a monolayer (2).

There was a tendency for the heats on all the adsorbents to level out at coverages above 0.12 μmol m^{-2}, following a relatively rapid fall between 0.02 and 0.06 μmol m^{-2}, Fig. 1.

Figure 2 shows the adsorption isotherms for sulfur dioxide at 423 °K. All are essentially linear while their slopes decrease with increase in the temperature of heat treatment of the specimens. Ultimately for gels heat-treated at 700, 800, and 900 °C the slopes are almost identical. Langmuir plots of these isotherm data are presented in Fig. 3.

Nitrogen Adsorption/Desorption Measurements

The nitrogen adsorption–desorption isotherms were very similar in shape while the amount of nitrogen adsorbed decreased with increase in temperature of heat treatment, as could be anticipated (7), Fig. 4. A large amount of nitrogen was adsorbed below $p/p_0 = 0.1$ followed by an almost linear adsorption path to $p/p_0 = 0.6$. Saturation was reached around $p/p_0 = 0.9$. The hysteresis loop extended between 0.4 and 0.7 p/p_0 in almost every case although the height of the hysteresis loop decreased with increasing temperature of heat treatment of the samples.

Pore size distributions calculated on a differential basis are shown in Fig. 5. The pore diam-

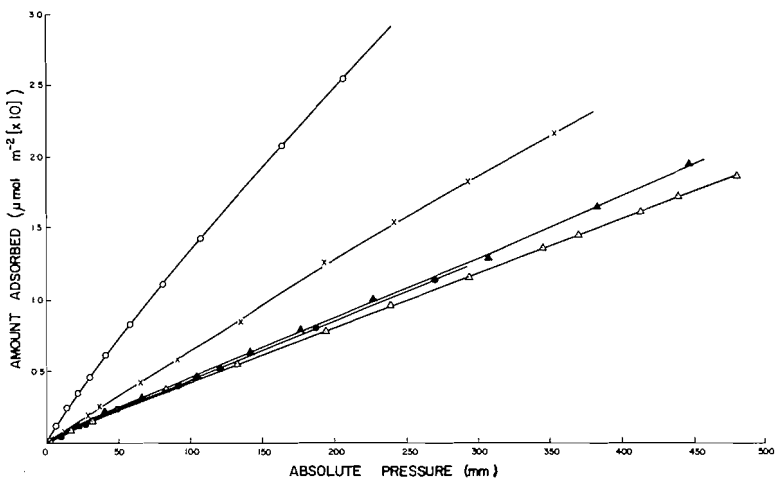

FIG. 2 Adsorption isotherms for sulfur dioxide at 423 °K on heat-treated silica gels. Silica gel heat-treated at: 240 °C, ⊙; 550 °C, ×; 700 °C, ●; 800 °C, △; 900 °C, ▲.

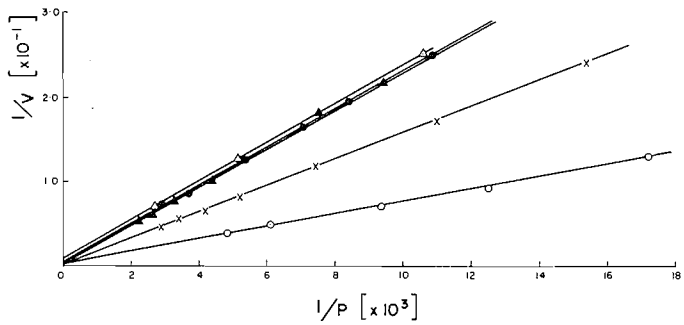

FIG. 3. Langmuir plots for the adsorption of sulfur dioxide at 423 °K on heat-treated silica gels. Silica gel heat-treated at: 240 °C, ⊙; 550 °C, ×; 700 °C, ●; 800 °C, △; 900 °C, ▲.

eter range was from below 20 to 55 Å for silica gels heat-treated at 240, 550, 700, and 800 °C. Maxima occur at about 15, 23, and 38 Å for all of these samples. For the sample heated at 900 °C, the pore diameter range increased to include diameters up to 85 Å, and when compared with the 550 °C sample there were 40% fewer pores of diameter 23 Å and a considerable increase in the numbers of pores <20 Å diameter. Similar results were recorded earlier (7) although the maximum at about 15 Å was not observed.

Table 1 summarizes the data obtained for surface areas (B.E.T. plots), hydroxyl group concentrations and the "limiting heats" of adsorption for sulfur dioxide on each of the heat-treated samples.

Discussion

The high heats of adsorption for sulfur dioxide of 25 to 30 kcal mol^{-1} occur at surface coverages of less than one-hundredth of a monolayer with all samples. These values are too high to be explained by a purely physical adsorption process (8). Earlier it was proposed (2) that in the absence of surface dehydration, adsorption heats of 25 kcal mol^{-1} for sulfur dioxide on silica gel could be explained by the formation of a total of four hydrogen bonds between the oxygen atoms in the sulfur dioxide molecule and adjacent hydroxyl groups on a hydroxylated gel surface. For the interactions at lowest coverages on the heat-treated gels a similar adsorbed complex may occur. While there is infrared evidence (9) that after heat treatment at 800 °C, only isolated hydroxyl groups remain on silica gel surfaces, it is stressed that the bonding arrangement is proposed for extremely low surface hydroxyl group concentrations outside the scope of detection by present infrared techniques. At coverages greater than one-fiftieth of a monolayer, the heats, 6 to 7 kcal mol^{-1}, are more in agreement with infrared studies (9)

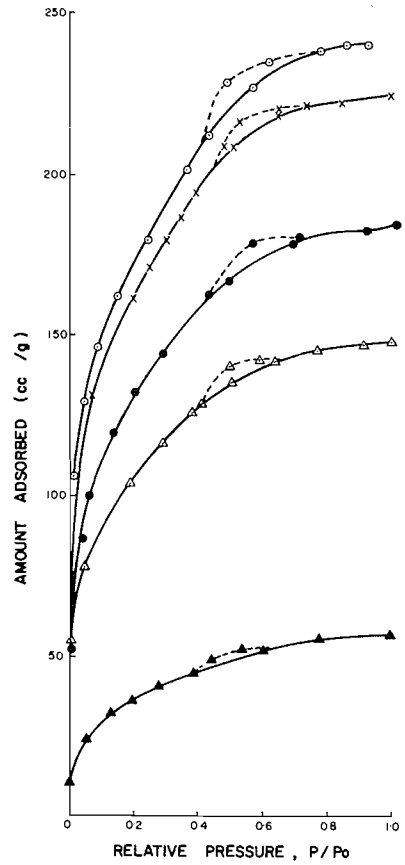

FIG. 4. Nitrogen adsorption–desorption isotherms at 77 °K on heat-treated silica gels. Silica gel heat-treated at: 240 °C, ⊙; 550 °C, ×; 700 °C, ●; 800 °C, △; 900 °C, ▲.

Can. J. Chem. Downloaded from www.nrcresearchpress.com by 210.87.254.42 on 09/05/12
For personal use only.

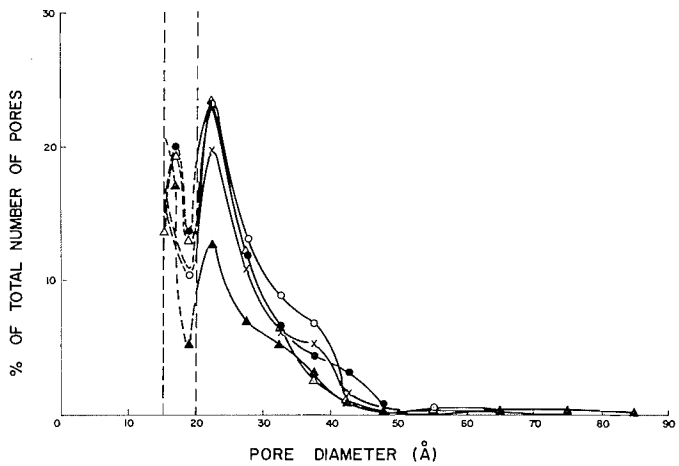

FIG. 5. Differential pore size distributions of heat-treated silica gels based on desorption leg of nitrogen isotherm. Pore size distribution data based on applications of the Kelvin equation are not valid for pores of less than 15 to 20 Å diameter when nitrogen is used as adsorbate (ref. 16, p. 58). Silica gel heat-treated at: 240 °C, ⊙; 550 °C, ×; 700 °C, ●; 800 °C, △; 900 °C, ▲.

TABLE 1. Surface areas, hydroxyl group concentrations, and "limiting"* heats of adsorption of sulfur dioxide for heat-treated silica gels

Temperature of heat treatment (°C)	Surface area ($m^2\ g^{-1}$)	Hydroxyl group concentration ($\mu mol\ m^{-2}$)	'Limiting' heat of adsorption (kcal mol^{-1})
240	630	7.2	12.0
550	580	2.4	7.5
700	490	1.3	6.6
800	385	1.2	6.6
900	135	1.1	6.5

*The "limiting" heat of adsorption is defined here, for practical convenience, as that value which appears constant over at least the final 30% of the total range of surface coverage measured.

since the formation of a single hydrogen bond of this nature involves between 3 and 6 kcal mol^{-1} of energy (10).

The hydroxyl group concentrations, Table 1, are similar for the samples heat-treated at 700, 800, and 900 °C. Although it has been suggested (11) that the gravimetric method of determining surface hydroxyl group concentrations does not take into account the possibility of bulk water desorption, Uytterhoeven (12) has shown that the total hydroxyl group content of silica xerogels is located at the surface as soon as the material is annealed at a temperature of 600 °C or higher. Thus, the concentrations quoted here give an excellent indication of surface hydroxyl group concentrations. Further, since the surface hydroxyl group concentration for the silica gel heat-treated at 700 °C is very similar to that determined for the samples heat-treated at 800 and 900 °C, it is reasonable to conclude that the chemical structures of the surfaces of these silica gels do not differ much and hence similar sulfur dioxide heat curves would be expected, Fig. 1.

The "limiting" values of the heats at coverages $> 0.2\ \mu mol\ m^{-2}$ may be explained by the adsorption of sulfur dioxide on a largely uniform surface. Previously (1) in studies of the adsorption of sulfur dioxide at 263 °K, boiling point, isosteric heat values of 7 to 7.5 kcal mol^{-1} were observed at around $\theta = 0.8$ for a 240 °C gel. This value was close to that of the heat of liquefaction of sulfur dioxide under these conditions and a physical adsorption process could be envisaged for that region of surface coverage up

Can. J. Chem. Downloaded from www.nrcresearchpress.com by 210.87.254.42 on 09/05/12
For personal use only.

Can. J. Chem. Downloaded from www.nrcresearchpress.com by 210.87.254.42 on 09/05/12
For personal use only.

to completion of the monolayer. However, at 473 °K the heat of liquefaction (13) is 1.7 kcal mol^{-1} at a pressure of 68.67 atm and clearly a liquefaction mechanism cannot be used to explain the present results.

The heat curve obtained for the 900 °C gel does not fall as rapidly as those for the 700 and 800 °C samples. At a given coverage the heat of adsorption is 1–2 kcal greater up to a coverage of 0.12 μmol m^{-2} and although the surface hydroxyl group concentrations of the gels are very similar, the pore structure of the 900 °C gel is different from the other two (Fig. 5). More than 25% of the pores have diameters less than 20 Å while the gels heat-treated at 700 and 800 °C have few, if any, pores of these dimensions. This phenomenon is most probably related to the onset of bulk sintering (14) and loss of pore volume above 800 °C which is close to the Tammann temperature for this material (0.5 T_m). The additional 1–2 kcal mol^{-1} of adsorption heat has been detected previously and may be explained by restricted adsorption in pores of diameters approaching molecular dimensions (15).

The 'limiting' heats of 7.5 and 12.0 kcal mol^{-1} for the 550 and 240 °C samples respectively, are in accord with their higher hydroxyl group concentrations and hence with the increased possibility that hydroxyl groups would be more favorably spaced to accommodate more than one OH···O type of linkage with adsorbed sulfur dioxide molecules. Confirmation of this possibility is evident from Fig. 2 which shows that the amount of sulfur dioxide adsorbed depends significantly on the hydroxyl group concentration.

The shapes of the sulfur dioxide isotherms are typical (ref. 16, p. 80) of those which obey the Langmuir equation for low pressures or small adsorptions, especially when capillary condensation or multilayer adsorption phenomena may be excluded (see, for example ref. 16, p. 80). These exclusions are appropriate to the present studies for isotherms determined at 7° below the critical temperature of sulfur dioxide and only up to a maximum coverage of less than 5% of a monolayer. Further, (*i*) the isotherms are linear above surface coverages of 0.08 μmol m^{-2} coincident with the point at which the adsorption heats begin to level out (Fig. 1) and (*ii*) the slopes of the Langmuir plots are proportional to the heats of adsorption (ref. 16, p. 80) (Fig. 3). When all of these factors are combined there results very strong evidence in favor of the Langmuir model of adsorption which allows the additional conclusion that the free energy of adsorption does not vary with the surface coverage (ref. 16, p. 80) above 0.08 μmol m^{-2}.

1. W. J. Jones and R. A. Ross. J. Chem. Soc. A, 1021 (1967).
2. R. W. Glass and R. A. Ross. Can. J. Chem. **49**, 2832 (1971).
3. R. W. Cranston and F. A. Inkley. Adv. Catal. **9**, 143 (1957).
4. E. Robinson and R. A. Ross. J. Chem. Soc. A, 2521 (1969).
5. L. G. Joyner. Scientific and industrial glass blowing and laboratory techniques. *Edited by* W. E. Barr, and V. J. Anhorn, Pittsburgh, Instruments Publishing Company. 1949.
6. A. V. Kiselev. *In* Colston Papers. Vol. 10, Butterworths, London. 1958.
7. A. H. Taylor and R. A. Ross. J. Chem. Eng. Data, **14** (3), 347 (1969).
8. S. J. Gregg. Surface chemistry of solids. Chapman and Hall, London. 1961.
9. M. L. Hair. Infrared spectroscopy in surface chemistry. Edward Arnold, London. 1967.
10. A. V. Kiselev and V. I. Lygin. Infrared spectra of adsorbed species. *Edited by* L. H. Little, Academic Press, New York. 1966.
11. B. G. Linsen. Physical and chemical aspects of adsorbents and catalysts. Academic Press, London. 1970.
12. J. Uytterhoeven, E. Hellinckx, and J. Fripiat. Silic. Ind. **28**, 241 (1963).
13. D. Bienstock, L. W. Brunn, E. M. Murphy, and H. E. Benson. Bureau of Mines Information Circular, 7836 (1958).
14. N. Henry and R. A. Ross. J. Chem. Soc. 4265 (1962).
15. J. H. de Boer. The dynamical character of adsorption. University Press, Oxford. 1968.
16. S. Brunauer. The solid–gas interface. Vol. 1. *Edited by* E. A. Flood, Marcel Dekker Inc., New York. 1967.

Hindered Rotation in Styryl Anions[1]

S. BROWNSTEIN AND D. J. WORSFOLD

Division of Chemistry, National Research Council of Canada, Ottawa, Canada K1A 0R9

Received November 26, 1971

Magnetically non-equivalent meta-protons, and occasionally ortho-protons, were observed on the benzene ring in styryl anions. With some cations and solvents it was possible to follow the coalescence of the peaks with increasing temperature and obtain Arrhenius activation energies for rotation of the phenyl group.

On observe des protons-méta magnétiquement non-équivalents et occasionnellement des protons-ortho sur le noyau benzénique dans les anions styryl. Il a été possible, avec quelques cations et solvants, de suivre la coalescence des pics avec l'augmentation de la température et d'obtenir les énergies d'activation d'Arrhénius pour la rotation du groupe phényle.

Canadian Journal of Chemistry, **50**, 1246 (1972)

Can. J. Chem. Downloaded from www.nrcresearchpress.com by 210.87.254.40 on 09/05/12
For personal use only.

Introduction

The planar character of benzylic anions has been demonstrated in some of the organometallic compounds formed from styrene and α-methylstyrene by reason of their proton resonance spectra (1, 2). For example when α-methylstyrene is reacted with potassium in tetrahydrofuran solution, it forms a dimer anion, 2,5-diphenyl-2,5-dipotassiohexane (3). The planar character about the benzylic carbon atoms of this molecule is evidenced by the doubling of the n.m.r. absorptions of both the ortho- and meta-protons, and by the sharpness of the single methylene signal. 2,5-Dideutero-2,5-diphenylhexane by comparison no longer has a single peak for the methylene protons, but a quartet, and exists also in two isomeric forms.

Similarly the adducts of *t*-butyllithium with one molecule of either styrene or α-methylstyrene show resonances in two places for both ortho and meta protons at suitable temperatures. In the case of the styryl compound this is below room temperature.

The spectrum of the potassium dimer compound appears to be independent of temperature up to 75 °C. Above this temperature side reactions start to become significant. Both the lithium compounds have spectra which are temperature and solvent dependent. The phenyl group appears to rotate at speeds fast on the n.m.r. time scale at 0° for the styryl compound and 50° for the α-methylstyryl compound. In the former it is the meta-protons which show the greater separation at low temperature, the ortho for the latter. From comparison of exchange broadened spectra of these protons with computer generated curves (5), it is possible to obtain rates of rotation and the Arrhenius activation energy for the rotation process.

Experimental

All preparations were made in an all glass vacuum apparatus, using sublimed tertiary butyllithium, and styrene and α-methylstyrene purified as before (6).

2,5-Diphenyl-2,5-dipotassiohexane (**1**) was prepared in tetrahydrofuran-d_8 by shaking a 5% solution of α-methylstyrene with excess sodium–potassium alloy for 2 days at room temperature. The solution was filtered under vacuum into the n.m.r. sample tube.

2-Lithio-2-phenyl-4,4-dimethylpentane (**2**) was prepared in benzene by reacting equimolar amounts of *t*-butyllithium-d_9 with α-methylstyrene. The product precipitated and was filtered and dissolved in tetrahydrofuran-d_8.

1-Lithio-1-phenyl-3,3-dimethylbutane (**3**) was prepared by adding a solution of styrene in benzene containing 10% tetrahydrofuran to a benzene solution of an equimolar amount of *t*-butyllithium. Tetrahydrofuran was then added to give a 50% tetrahydrofuran–benzene solvent mixture.

All spectra were obtained on a "Varian Associates HA-100" spectrometer. Proton spin decoupling was performed with audio side band modulation in the usual manner. Temperature calibration was done as previously described (5). The data were fitted by least square techniques and the errors quoted are standard deviations.

Results

The generalized formula for the phenyl portion of these compounds is

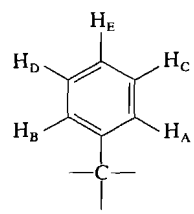

[1]NRCC No. 12389.

TABLE 1. Resonance and exchange parameters

Compound	1	2	3
δA^a	4.855	5.18	6.050
δB	5.430	5.56	6.050
δC	5.937	6.06	6.434
δD	6.040	6.13	6.576
δE	4.235	4.45	5.385
$J_{A-B}{}^b$	2.6		
J_{A-C}	8.1	8	8.2
J_{A-D}	0.5		
J_{A-E}	0.9		1.0
J_{B-C}	0.5		
J_{B-D}	8.3	8	8.3
J_{B-E}	0.9		1.0
J_{C-D}	1.6		~2
J_{C-E}	6.0	6	6.5
J_{D-E}	6.0	6	6.5
E^c	Too large to measure	14±1	11.9±0.8
Charge on ring	0.89	0.80	0.61

[a]In p.p.m. to low field of tetramethylsilane.
[b]In Hz.
[c]The Arrhenius activation energy in kcal/mol.

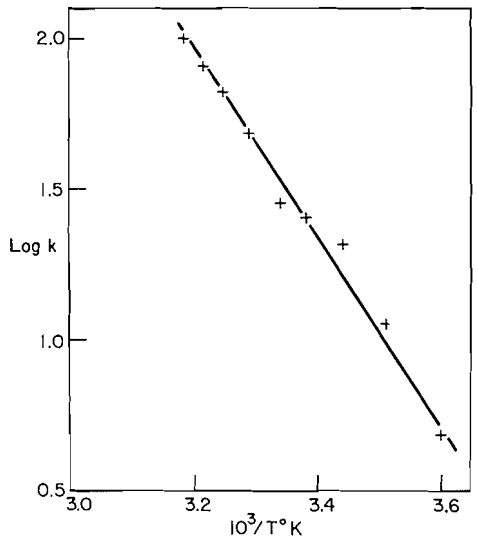

FIG. 1. The rate constants for phenyl rotation in 3 as a function of the temperature; k is in s^{-1}.

The chemical shifts and coupling constants of the aromatic protons in these three compounds are given in Table 1. The assignments were confirmed with the simplified spectra obtained by selective decoupling in double resonance experiments and by comparison of the experimental spectra with theoretical spectra calculated for the appropriate parameters. The chemical shifts of the meta protons of **3** are sensitive to the relative amounts of tetrahydrofuran and benzene. Since **3** has a greater thermal stability the lower the concentration of tetrahydrofuran in solution, a solvent composition was chosen with a minimum of tetrahydrofuran consistent with an adequate separation of the meta-proton signals and a sufficiently low freezing point. The chemical shift and spin coupling constants are consistent with, but of higher precision than, those previously reported (1, 2).

Also given in Table 1 are Arrhenius activation energies for the phenyl rotation in compounds **2** and **3**, derived from the rate constants obtained from spectra taken over a range of temperatures. These results for compound **3** are plotted in Fig. 1 and the spectra shown in Fig. 2. The calculation of the rate constants for rotation about the phenyl–carbon bond are straightforward for compound **2** where each of the well-separated ortho-protons gives a doublet due to spin coupling with the adjacent meta-proton. The meta-proton region of compound **3** is considerably more complex but can be simplified to a four line pattern, in the absence of rotation, by spin decoupling the para-proton. Because of the symmetry of the benzene ring this double irradiation will not affect the transfer of magnetization for the meta-protons.

The hindrance to rotation of the phenyl ring has been ascribed to the delocalization of the charge of the anion away from the α carbon atom, adjacent to the metal atom, to the ring. To delocalize the charge the α carbon atom has to adapt an sp^2 configuration, with the remaining electrons in the residual p orbital which projects above and below the plane of the other carbon bonds (7). The greatest overlap with the π electrons will occur when the phenyl ring and the substituents on the α carbon atom are coplanar. The activation energy for rotation about this bond is then a measure of the electron overlap.

The degree of delocalization of the charge can be measured by estimating the charge on the ring carbons. This is done by comparing the upfield shift of their p.m.r. absorption with the corresponding position in the neutral parent compound. The calculated total charge on the five ring carbons attached to protons is also given in Table 1. Two factors probably affect the degree of delocalization. Firstly, the change from a potassium to lithium as counterion probably concentrates the charge on the α

Can. J. Chem. Downloaded from www.nrcresearchpress.com by 210.87.254.40 on 09/05/12
For personal use only.

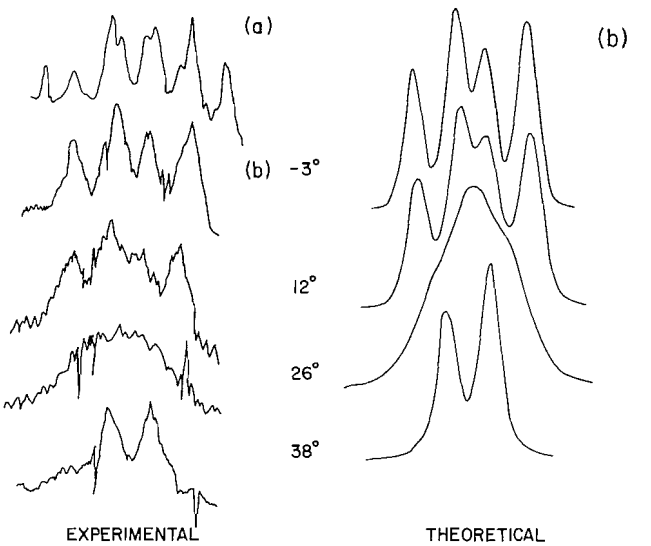

FIG. 2. Experimental and theoretical spectra of the meta-protons of **3**. (*a*) Without decoupling of the para-proton; (*b*) with decoupling of the para-proton.

carbon atom. This is because both are probably contact ion pairs (8) and the carbon lithium interionic distance is smaller. Also on changing from a styryl to an α-methylstyryl compound, the additional methyl substituent on the α carbon appears to increase the charge on the ring.

The compound with the highest delocalization of the charge did not show evidence for rotation, on the n.m.r. time scale, at temperatures below that where decomposition becomes rapid, probably because of high activation energy. The activation energies of the other two compounds are in order of the ring charge, and in general there appears to be a correlation between the degree of delocalization and the activation energy.

Similar barriers to rotation have been found for phenylallyl alkali metal salts (9). The hindrance to rotation occurs in both the allyl group and the bond linking it to the phenyl ring. The activation energy for the latter process was 13.9 kcal/mol when the counterion was lithium and the solvent tetrahydrofuran. This increases somewhat when the counterion is sodium or potassium. In the lithium compound the charge on the ring appears to be near 0.5 e, somewhat lower than the styryl compounds, although the activation energy is high. However, the more extensive conjugation of the phenylallyl system could contribute to the rotation barrier.

1. S. BYWATER and D. J. WORSFOLD. J. Organomet. Chem. **33**, 273 (1971).
2. K. TAKAHASHI, M. TAKAKI, and R. ASAMI. J. Phys. Chem. **75**, 1062 (1971).
3. C. L. LEE, J. SMID, and M. SZWARC. J. Phys. Chem. **66**, 904 (1962).
4. D. R. WEYENBURG. J. Org. Chem. **30**, 3237 (1965).
5. S. BROWNSTEIN, E. C. HORSWILL, and K. U. INGOLD. Can. J. Chem. **49**, 1350 (1971).
6. D. J. WORSFOLD. J. Polym. Sci. Part A, **5**, 2783 (1967).
7. R. WAACK, M. A. DORAN, E. B. BAKER, and G. A. OLAH. J. Am. Chem. Soc. **88**, 1272 (1966).
8. F. S. DAINTON, G. A. HARPELL, and K. J. IVIN. Eur. Polym. J. **5**, 395 (1969).
9. V. R. SANDEL, S. V. MCKINLEY, and H. H. FREEDMAN. J. Am. Chem. Soc. **90**, 495 (1968).

Can. J. Chem. Downloaded from www.nrcresearchpress.com by 210.87.254.40 on 09/05/12
For personal use only.

Metal–Ammonia Reduction. Part I. The Reduction of α,ω-Diarylalkanes and Triphenylmethanes

D. N. BUTLER AND R. MILBURN

Department of Chemistry, York University, Toronto, Ontario

Received June 4, 1971[1]

The Birch reductions of 15 α,ω-diarylalkanes, **1***a*, *b*, *c* ($n = 1$–5) and of triphenylmethane (**3***a*) and tris-(*p*-methoxyphenyl)methane (**3***b*) are described. In every case reduction proceeds independently in each ring to furnish the products, namely, α,ω-bis(2′,5′-dihydroaryl)alkanes, **2***a*, *b*, *c* ($n = 1$–5), and tris(2′,5′-dihydroaryl)methanes, **4***a*, *b*.

Acid hydrolysis of the enol ethers **2***b*, *c* ($n = 1$–5) and **4***b* affords the corresponding ketones **6** ($n = 1$–5), **7** ($n = 1$–5), and **8**.

On décrit les réductions de Birch de quinze α,ω-diarylalcanes, **1***a*, *b*, *c* ($n = 1$–5), du triphénylméthane (**3***a*) et du tris(*p*-méthoxyphényl)méthane (**3***b*). Dans chaque cas, la réduction agit indépendamment dans chaque noyau pour conduire aux produits, soient les α,ω-bis(2′,5′-dihydroaryl)alcanes, **2***a*, *b*, *c* ($n = 1$–5), et les tris(2′,5′-dihydroaryl)méthanes, **4***a*, *b*.

L'hydrolyse acide des éthers d'énol **2***b*, *c* ($n = 1$–5) et **4***b* nous amène aux cétones correspondantes **6** ($n = 1$–5), **7** ($n = 1$–5), et **8**.

Canadian Journal of Chemistry, **50**, 1249 (1972)

Relatively few unconjugated diarylalkanes have been subjected to the Birch reduction conditions. Those that have been reported (1*a*–*g*) mostly involve steroid or related systems. Only one triphenylmethane, *viz.* tris(*m*-methoxyphenyl)methane has been reduced (1*g*).

This paper describes the reduction of the α,ω-diphenylalkanes of the type **1** ($n = 1$–5) and the characterization of the products **2** ($n = 1$–5).

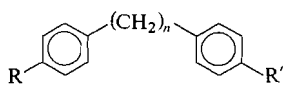

1

a R = R′ = H
b R = H; R′ = OCH_3
c R = R′ = OCH_3
($n = 1$–5)

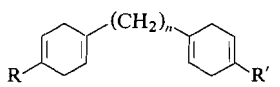

2

a R = R′ = H
b R = H; R′ = OCH_3
c R = R′ = OCH_3
($n = 1$–5)

The analogous chemistry arising from the reduction of triphenylmethane (**3***a*) and tris-(*p*-methoxyphenyl)methane (**3***b*) to the respective products **4***a* and *b* is also described.

[1]Revision received December 7, 1971.

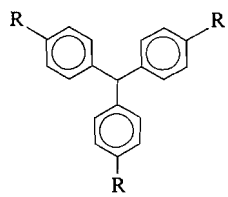

3

a R = H
b R = OCH_3

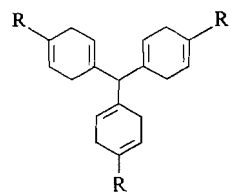

4

a R = H
b R = OCH_3

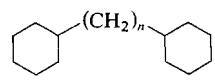

5

($n = 1$–5)

The 15 starting materials, **1**, were either known or synthesized by standard methods (see Experimental). The reductions using lithium, *t*-butyl alcohol, tetrahydrofuran, and liquid ammonia at −33° were carried out at much higher dilutions than usually described to keep diarylalkanes in solution (1*a*). The product yields were all better than 90% of theory. The reduction products were characterized by elemental and spectroscopic analysis, and by some chemical reactions described below, and all corresponded to the expected α,ω-bis(2′,5′-dihydroaryl)alkanes **2** ($n = 1$–5).

Compounds **2***a* ($n = 1$–5) were catalytically hydrogenated and all absorbed approximately 4 mol of hydrogen giving rise to the correspond-

Can. J. Chem. Downloaded from www.nrcresearchpress.com by 210.87.254.5 on 09/05/12
For personal use only.

Can. J. Chem. Downloaded from www.nrcresearchpress.com by 210.87.254.5 on 09/05/12
For personal use only.

ing α,ω-dicyclohexylalkanes **5** ($n = 1$–5). These liquids **5** ($n = 1$–5) showed characteristic absorptions for saturated C—H bonds in i.r. and p.m.r. spectra, and in all cases produced the predicted intense parent ion in the mass spectra. The reduction products **2***a* ($n = 1$–5) were all easily oxidized back to their aromatic precursors by the action of 2,3-dichloro-5,6-dicyanobenzoquinone.

Gas liquid chromatographic analysis of the reduction products of compounds **1***a* ($n = 1$–5) revealed them all to be mixtures of two components. In each case, the major component (90–95%) was shown by collection and mass spectrometry to be the expected tetraolefin **2***a* ($n = 1$–5) whilst the minor component (5–10%) appeared to be an over-reduced product having a molecular weight two mass units greater than that of the major product. Cyclohexenes (and even cyclohexanes) have been mentioned (2) as minor products of the Birch reduction of benzenes and are proposed to arise via either a base-catalyzed conjugation/re-reduction pathway, or initial 1,2-hydrogen addition competing with the usual 1,4-addition.

Entirely similar chemistry was encountered in the reduction of triphenylmethane to the hexahydro-compound **4***a*. In this case the proportion of over-reduced product increased to nearly 25% of the total reduction material. Again, hydrogenation and oxidation proceeded as expected to afford tricyclohexylmethane and triphenylmethane respectively, as indicated by spectroscopic examination. The structure of the over-reduced product (*m/e* 252) was not further investigated.

There was no problem with over-reduction of the ten methoxyl-carrying α,ω-diarylalkanes **1***b*, *c* or with tris(*p*-methoxyphenyl)methane, **3***b*. All these reduction products **2***b*, *c* and **4***b* were essentially pure directly from the reaction. However, upon vacuum distillation of the reduction products **2***b*, *c* ($n = 1$–5), it was evident by the appearance of vicinally coupled vinyl protons in the p.m.r. spectra that partial conjugation of the two double bonds in the methoxyl-containing ring or rings was occurring. Thermal conjugation of 2,5-dihydroanisoles has been reported and utilized in obtaining Diels–Alder adducts from these systems (3). No attempt was made to distil **4***b*.

Following the Birch method (4), small quantities of the ten enol ethers **2***b*, *c* ($n = 1$–5) and **4***b* were warmed in tetrahydrofuran with 2 *N* sulfuric acid to produce the ketones **6** ($n = 1$–5), the diketones **7** ($n = 1$–5), and the triketone, **8**.

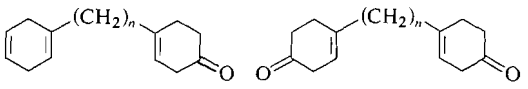

6 ($n = 1$–5)

7 ($n = 1$–5)

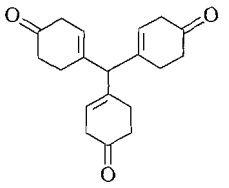

8

In all cases by this treatment, it was observed that the enol ether C=C stretching frequency near 1700 cm^{-1} was replaced by a C=O stretch near 1725 cm^{-1} in the i.r. spectra and the characteristic enol ether vinyl C—H absorption near δ 4.47 p.p.m. in the p.m.r. spectra disappeared along with the methoxyl group absorptions near δ 3.45 p.p.m. Although insufficient quantities of the ketones **6** ($n = 1$–5), **7** ($n = 1$–5), and **8** were available for an evaluation of their melting points or boiling points, these compounds all showed spectral characteristics in their i.r. and p.m.r. spectra consistent with their formulations. They all (except for compound **8**) showed the expected parent ions in their respective mass spectra. For the triketone **8**, the P-28 (loss of CO) at *m/e* 270 was observed as the highest peak. All the ketones were characterized as their 2,4-dinitrophenylhydrazones.

From the preceding results it seems likely that the Birch reduction of compounds containing two or more unconjugated benzenoid rings will take place via the predictable stepwise reduction of the individual rings to furnish the bis- or poly-dihydroaromatic compounds as the major product.

Experimental

All melting points and boiling points are uncorrected. The i.r. spectra were determined on a Unicam SP1000 spectrophotometer as Nujol mulls or in carbon tetrachloride solution. The p.m.r. spectra were recorded on a Varian A-60 instrument in carbon tetrachloride using tetramethylsilane

Can. J. Chem. Downloaded from www.nrcresearchpress.com by 210.87.254.5 on 09/05/12
For personal use only.

(TMS) as the internal standard. The g.l.c. separations were made on a Varian Aerograph Series 1700 instrument using a 6 ft × 0.25 in. column packed with 3% Silicone Rubber gum, SE 30 on 100/120 mesh Varaport #30 support. Mass spectra were taken at 70 eV using a Hitachi–Perkin–Elmer RMU-6E instrument. Microanalyses were obtained from A. B. Gygli, Toronto, Ontario.

α,ω-Diarylalkanes, 1a, b, c, and Triphenylmethanes, 3a, b

Compounds **1***a* ($n = 1$), **1***a* ($n = 2$), and **3***a* were purchased from Eastman Chemical Company. The following diarylalkanes are listed with their appropriate reference. **1***a* ($n = 3$) (5), **1***a* ($n = 4$) (6), **1***a* ($n = 5$) (7), **1***b* ($n = 1$) (8), **1***b* ($n = 2$) (9), **1***b* ($n = 3$) (10), **1***c* ($n = 1$) (11), **1***c* ($n = 2$) (12), **1***c* ($n = 3$) (13), **1***c* ($n = 4$) (14), **1***c* ($n = 5$) (15), **3***b* (16).

p-(4-Phenylbutyl)anisole, 1b (n = 4)

A mixture of *p*-(4-phenylbutyryl)anisole (17) (50 g), triethylene glycol (150 ml), and 90% hydrazine hydrate (60 g) was heated under reflux for 15 min. Potassium hydroxide pellets (50 g) were then added and the mixture heated for 30 min at 195–200°, during which time the water that formed was distilled off. The mixture was then diluted with water (600 ml) and extracted with ether (3 × 200 ml). This ether extract was dried (anhydrous Na_2SO_4), filtered, and evaporated. Vacuum distillation of the resulting oil afforded the product **1***b* ($n = 4$) (32 g), b.p. 136–138° (0.06 mm), m.p. 31–33°.

Anal. Calcd. for $C_{17}H_{20}O$: C, 84.96; H, 8.39. Found: C, 85.29; H, 8.53.

p-(5-Phenylpentyl)anisole, 1b (n = 5)

1-*p*-Methoxyphenyl-5-phenylpent-1-en-3-one was prepared from benzylacetone (18) and anisaldehyde according to the method of Pond and Shoffstall (19). This material was first catalytically hydrogenated then the ketone function reduced as for **1***b* ($n = 4$). The product **1***b* ($n = 5$) was a colorless liquid, b.p. 138–140° (0.03 mm).

Anal. Calcd. for $C_{18}H_{22}O$: C, 84.99; H, 8.72. Found: C, 85.19; H, 8.53.

General Metal–Alcohol–Ammonia Reduction Procedure

The reductions were conducted in a three-necked 1 l flask, equipped with an ammonia inlet tube, a Dry Ice/acetone cooled Dewar condenser, and a dropping funnel. Liquid ammonia was transferred directly from the cylinder to the flask and the inlet tube replaced with a stopper. Then the aromatic substance (0.01 mol) was added, followed by excess *t*-butyl alcohol (5 ml) and sufficient tetrahydrofuran to affect solution. The lithium metal (0.1 g atom) was added in small pieces until the reaction was seen to slow down; then the remainder of the lithium was added. The blue reaction mixture was allowed to stand for 2 h and then quenched by the addition of solid ammonium chloride to discharge the blue color. Most of the ammonia was allowed to evaporate; then water and petroleum ether (30–60°) was added. The organic phase was separated, washed with water, dried over anhydrous magnesium sulfate, and then evaporated to give the reduction products in essentially quantitative yield. These products were either vacuum distilled or recrystallized from ethanol or ethanol–water mixtures. In the cases of the enol ether products **2***b*, *c* and **4***b* distillation brought about partial conjugation of the double bonds in the methoxyl-carrying ring or rings as indicated in the p.m.r. spectra of the distillates.

The analytical, physical, and spectroscopic data for all the reduction products have been placed in the Depository of Unpublished Data.[2] Compound **2***b* ($n = 5$) represents a typical example. 1-(2′-5′-Dihydrophenyl)-3-(2″,5″-dihydro-4″-methoxyphenyl)propane, **2***b* ($n = 5$), m.p. 66–68°; i.r. (CCl_4) 1654, 1670, 1702 cm^{-1}; p.m.r. (CCl_4) δ 5.60 (2H, m), 5.30 (2H, m), 4.47 (1H, m), 3.44 (3H, s), 2.61 (8H, m), 1.91 (4H, m), 1.34 (6H, m) p.p.m.; mass spectrum parent ion *m/e* 258, calcd. 258.

Anal. Calcd. for $C_{18}H_{26}O$: C, 83.67; H, 10.14. Found: C, 83.72; H, 9.94.

General Hydrolysis Procedure for the Enol Ethers, 2b, c and 4b

The enol ethers, **2***b*, *c* ($n = 1$–5) and **4***b* (approximately 100 mg) were each warmed on a water bath for 10 min with tetrahydrofuran (5 ml) and 2 *N* H_2SO_4 (2 ml). The reaction mixtures were then diluted with water and extracted with ether. The ether layers were dried over anhydrous Na_2SO_4, filtered, and evaporated giving crude ketones **6** ($n = 1$–5), **7** ($n = 1$–5), and **8**. The i.r., p.m.r., and mass spectra were taken in each case and all were consistent with the assigned structures. No evidence for acid-catalyzed conjugation to α,β-cyclohexenones of the β,γ-cyclohexenone moieties was found in the p.m.r. spectra.

The 2,4-dinitrophenylhydrazones were prepared in the usual way (20). These yellow compounds showed no evidence of conjugation of the incyclic double bond as indicated by the p.m.r. spectra. Their analytical and physical data have been placed in the Depository of Unpublished Data.[2]

Hydrogenations

The hydrocarbons, **2***a* ($n = 1$–5) and **4***a*, were individually reduced in ethyl acetate using 10% palladium-on-charcoal catalyst. When hydrogen uptake ceased, the catalyst was filtered off and the solvent evaporated to leave the product.

Oxidations

The hydrocarbons, **2***a* ($n = 1$–5) and **4***a*, were individually shaken in benzene with excess 2,3-dichloro-5,6-dicyanobenzoquinone for 2 h. The mixture was filtered and the filtrate passed through a short column of alumina (Woelm-activity grade 1). The clear eluate was evaporated and the product shown to be identical to the respective starting materials **1***a* ($n = 1$–5) and **3***a* by direct comparison.

The authors wish to thank the National Research Council of Canada and the Department of University Affairs of the Province of Ontario for their financial assistance.

1. (*a*) A. J. Birch and S. M. Mukherji. J. Chem. Soc. 2531 (1949). (*b*) H. H. Inhoffen, D. Kampe, C. Cordes, K. Muller, and W. Milkowski. Ann. **674**, 36 (1964). (*c*) A. J. Birch and H. Smith. J. Chem. Soc. 1882 (1951). (*d*) A. J. Birch and H. Smith. J. Chem. Soc. 4909 (1956). (*e*) J. Reiner and W. Jenny. Helv. Chim. Acta, **52**, 1624 (1969). (*f*) J. L. Marshall and T. K. Folsom. Tetrahedron Lett. 753 (1971). (*g*) V. S. Gaind and S. M. Mukherji. Curr. Sci. (India), **25**, 336 (1956).

[2]Copies of the material in the depository may be obtained from: Depository of Unpublished Data, National Science Library, National Research Council of Canada, Ottawa, Canada K1A 0S2.

2. A. P. KRAPCHO and A. A. BOTHNER-BY. J. Am. Chem. Soc. **81**, 3658 (1959).
3. I. ALFARO, W. ASHTON, L. D. MCMANUS, R. C. NEWSTEAD, K. L. RABONE, N. A. J. ROGERS, and W. KERNICK. Tetrahedron, **26**, 201 (1970).
4. A. J. BIRCH. J. Chem. Soc. 593 (1946).
5. H. WEIDLICH. Chem. Ber. **74**, 1209 (1941).
6. J. S. SALKIND and B. FUNDYLER. Chem. Ber. **69**, 128 (1936).
7. N. L. ALLINGER and D. J. CRAM. J. Am. Chem. Soc. **76**, 2362 (1954).
8. E. PRATT, R. F. PRESTON, and J. D. DRAPER. J. Am. Chem. Soc. **72**, 285 (1951).
9. NG. PH. BUU-HOI, NG. HOAN, and NG. D. XUONG. Rec. Trav. Chim. **71**, 1367 (1950).
10. R. ROGER, P. DEMERSEMAN, J. P. LECHARTIER, and A. CHEUTIN. J. Org. Chem. **27**, 3808 (1962).
11. L. CONOVER and D. TARBELL. J. Am. Chem. Soc. **72**, 3586 (1950).
12. E. M. RICHARDSON and E. E. REID. J. Am. Chem. Soc. **62**, 413 (1940).
13. P. PFEIFFER and P. A. NEGREANU. Chem. Ber. **50**, 1476 (1917).
14. D. C. AYRES and R. C. DENNEY. J. Chem. Soc. 4506 (1961).
15. W. BORSCHE. Chem. Ber. **52**, 2078 (1919).
16. H. BURTON and G. W. H. CHEESEMAN. J. Chem. Soc. 832 (1953).
17. NG. PH. BUU-HOI, NG. HOAN, and NG. D. XUONG. J. Chem. Soc. 3499 (1951).
18. J. KERN, R. SHRINER, and R. ADAMS. J. Am. Chem. Soc. **47**, 1157 (1925).
19. I. J. POND and A. S. SHOFFSTALL. J. Am. Chem. Soc. **22**, 666 (1900).
20. G. D. JOHNSON. J. Am. Chem. Soc. **73**, 5888 (1951).

Can. J. Chem. Downloaded from www.nrcresearchpress.com by 210.87.254.5 on 09/05/12
For personal use only.

Use of $Eu(fod)_3$ Shift Reagent and Solvent Effects in Structural Elucidation of Novel Isomeric Pyrimidones and Model Methoxylated Pyrimidines[1]

GEORGE A. NEVILLE

Research Laboratories, Food and Drug Directorate, Department of National Health and Welfare, Ottawa, Canada

Received July 29, 1971

1-Ethyl-1,6-dihydro-2,4-dimethoxy-5-methyl-6-oxopyrimidine (**1***a*) and 1,5-diethyl-1,6-dihydro-2,4-dimethoxy-6-oxopyrimidine (**2***a*) are shown to be the correct positional isomers, respectively, for the major *O,O*-dimethyl derivatives isolated from the reaction products of 1-ethyl-5-methylbarbituric acid (**1**) and the new 1,5-diethylbarbituric acid (**2**) with excess diazomethane. In addition to the above compounds, the behavior of 2,4-dimethoxypyrimidine (**3**), 4,6-dimethoxypyrimidine (**4**), 2,4,6-trimethoxypyrimidine (**5**), and 6-chloro-2,4-dimethoxypyrimidine (**6**) were studied by p.m.r. spectrometry in various solvents. The relatively new shift reagent, $Eu(fod)_3$ was used in these studies because of its affinity for weak electron donors such as ethers.

On montre que le 1-éthyl-1,6-dihydro-2,4-diméthoxy-5-méthyl-6-oxopyrimidine (**1***a*) et le 1,5-diéthyl-1,6-dihydro-2,4-diméthoxy-6-oxo-pyrimidine (**2***a*) sont les isomères de position corrects, respectivement pour les dérivés principaux *O,O*-diméthyl isolés des produits de réaction de l'acide 1-éthyl-5-méthylbarbiturique (**1**) et du nouvel acide 1,5-diéthylbarbiturique (**2**) avec le diazométhane. En plus des composés précédents, le comportement du 2,4-diméthoxypyrimidine (**3**), du 4,6-diméthoxypyrimidine (**4**), du 2,4,6-triméthoxypyrimidine (**5**), et du 6-chloro-2,4-diméthoxypyrimidine (**6**) a été étudié par spectrométrie r.m.p. dans différents solvants. On a utilisé le relativement nouvel agent de déplacement $Eu(fod)_3$ dans ces études à cause de son affinité pour les donneurs faibles d'électrons tels que les éthers.

Canadian Journal of Chemistry, **50**, 1253 (1972)

Introduction

In an earlier paper (1), where it was shown that *N*-methylation of 5,5-disubstituted barbiturates is predominant with the methylating agent diazomethane, reference was made to the formation of various products with *O*-methyl proton signals from 1,5-dialkylbarbituric acids by the action of excess diazomethane. Although no difficulty was experienced in recognizing the nature of the substituents of these products by p.m.r. spectrometry, the correct positional isomerism could not be established from the usual p.m.r., i.r., and mass spectral data. In addition, the various isomers are not easily and unambiguously obtained by alternative synthesis. It is the purpose of this communication to establish that **1***a* and **2***a* are the correct structures for the crystalline *O,O*-dimethyl derivatives isolated from 1-ethyl-5-methylbarbituric acid (**1**) and 1,5-diethylbarbituric acid (**2**), respectively, by the action of diazomethane. In arriving at these structural assignments, use has been made of the recently reported tris-1,1,1,2,2,3,3-heptafluoro-7,7-dimethyl-4,6-octanedione)-europium(III), $Eu(fod)_3$, as a paramagnetic shift reagent (2) and of solvent effects in p.m.r. spectrometry. The $Eu(fod)_3$ shift reagent appears to be superior to the more common and somewhat older shift reagent, tris-(dipivalomethanato)europium, $Eu(DPM)_3$, recently reviewed by Sanders and Williams (3), because it is more soluble than $Eu(DPM)_3$ in non-alcoholic solvents and has complexing properties such that it will affect weak electron donors such as ethers and esters. For comparison, four model pyrimidines of known structure, 2,4-dimethoxypyrimidine (**3**), 4,6-dimethoxypyrimidine (**4**), 2,4,6-trimethoxypyrimidine (**5**), and 6-chloro-2,4-dimethoxypyrimidine (**6**), were subjected to similar solvent and shift reagent studies. An earlier example of the application of these techniques for structural elucidation of isomeric pyrimidone and uracil derivatives has been reported from these laboratories (4).

[1]Presented in part at the 54th C.I.C. Conference, Halifax, N.S., June 1, 1971.

Results and Discussion

Structural Elucidation of the Pyrimidones

Excluding *O,N*-dimethyl derivatives which are minor products of the action of excess diazomethane in 1-ethyl-5-methylbarbituric acid (**1**) and 1,5-diethylbarbituric acid (**2**), only one of the structures **1***a*, *b*, *c* and **2***a*, *b*, *c*, respectively

Can. J. Chem. Downloaded from www.nrcresearchpress.com by 210.87.254.6 on 09/05/12
For personal use only.

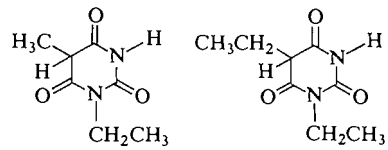

1 2

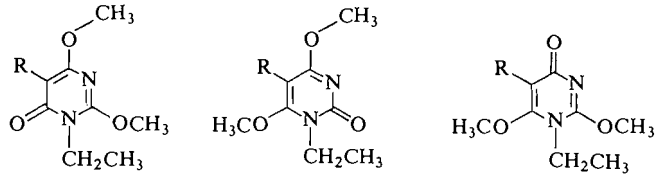

1*a* R = CH_3 1*b* R = CH_3 1*c* R = CH_3
2*a* R = CH_2CH_3 2*b* R = CH_2CH_3 2*c* R = CH_2CH_3

TABLE 1. The p.m.r. solvent shift data (δ in p.p.m. downfield from internal TMS)
1-Ethyl-1,6-dihydro-2,4-dimethoxy-5-methyl-6-oxopyrimidine (1*a*)

Solvent	O—Me (C-2)	O—Me (C-4)	CH_2(Et) (N-1)	CH_3 (C-5)	CH_3(Et) (N-1)
CCl_4	3.97 (s)	3.85 (s)	3.93 (q)	1.77 (s)	1.18 (t)
$\Delta^{CCl_4}_{C_6H_6}$	+0.40	+0.48	+0.08	−0.43	+0.13
$\Delta^{CCl_4}_{C_5H_5N}$	+0.15	+0.05	−0.05	−0.32	+0.03
$\Delta^{CCl_4}_{TFA}$	−0.37	−0.38	−0.47	−0.40	−0.25

1,5-Diethyl-1,6-dihydro-2,4-dimethoxy-6-oxopyrimidine (2*a*)

Solvent	O—Me (C-2)	O—Me (C-4)	CH_2(Et) (N-1)	CH_2(Et) (C-5)	CH_3(Et) (N-1)	CH_3(Et) (C-5)
CCl_4	3.98 (s)	3.85 (s)	3.92 (q)	2.30 (q)	1.18 (t)	0.97 (t)
$\Delta^{CCl_4}_{C_6H_6}$	+0.40	+0.47	+0.08	−0.47	−0.12	−0.08
$\Delta^{CCl_4}_{C_5H_5N}$	+0.17*	+0.03*	−0.07	−0.37	−0.02	−0.17
$\Delta^{CCl_4}_{TFA}$	−0.37	−0.40	−0.48	−0.38	−0.27	−0.20

*In pyridine, these peaks resolved by 0.01 p.p.m. (s) singlet, (q) quartet, (t) triplet.

can be assigned to the major *O,O*-dimethyl product from each of **1** and **2**.

Using the solvent shift data of Table 1, one can deduce the most likely structure for the positional *O,O*-dimethyl isomer formed from each of **1** and **2**. For ketones and ethers, the magnitude and sign of the proton resonance solvent shifts have been rationalized by means of reference plane rules (5–7). These rules have been generalized (8, 9): protons lying in front of the plane will tend to be deshielded in benzene (relative to an "inert" solvent) while those behind the plane will tend to be shielded in benzene. The shifts ($\Delta = \delta CCl_4 - \delta C_5H_5N$ p.p.m.) observed for pyridine are in general more negative than the corresponding benzene-induced shifts (10). The carbonyl plane "rule" is also applicable to pyridine-induced solvent shifts in some ketones (11), but the reference plane is displaced so that it passes through the α-carbons rather than the carbonyl carbon (10). By these rules one finds that the benzene shifts ($\Delta = \delta CCl_4 - \delta C_6H_6$ p.p.m.) support structures **1***a* and **2***a* best, and similarly, the pyridine shifts support structures **1***a* and **2***a* best.

Some use has been made of the solvent shifts for methoxy-group resonances induced by trifluoroacetic acid (TFA) (12, 13) as an aid to structural elucidation. The downfield shift by

Can. J. Chem. Downloaded from www.nrcresearchpress.com by 210.87.254.6 on 09/05/12
For personal use only.

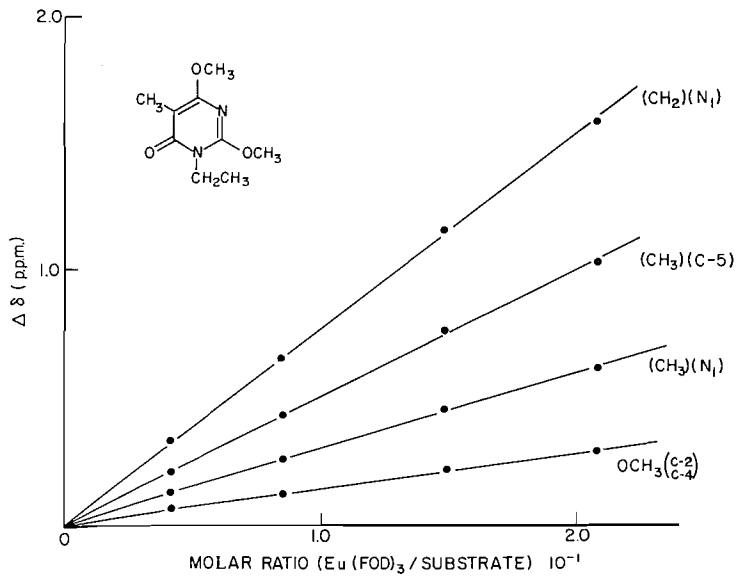

FIG. 1. Normalized Eu(fod)$_3$ induced p.m.r. shifts for 1-ethyl-1,6-dihydro-2,4-dimethoxy-5-methyl-6-oxopyrimidine (**1***a*) in $CDCl_3$ solution.

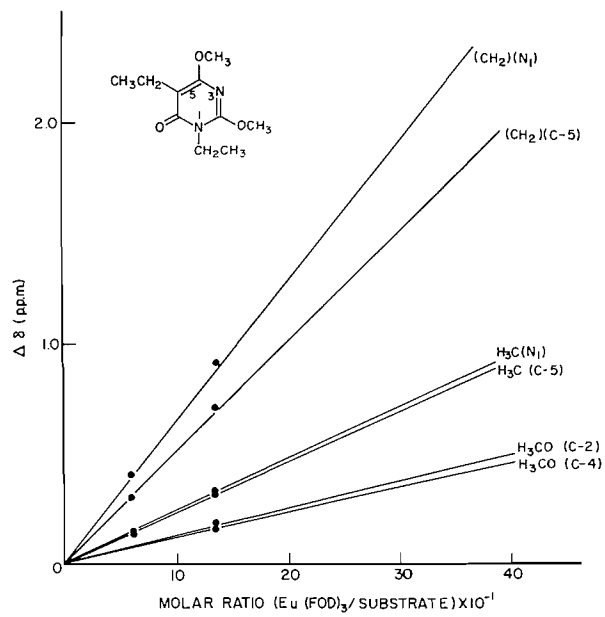

FIG. 2. Normalized Eu(fod)$_3$ induced p.m.r. shifts for 1,5-diethyl-1,6-dihydro-2,4-dimethoxy-6-oxopyrimidine (**2***a*) in $CDCl_3$ solution.

TFA ($\Delta = \delta CCl_4 - \delta TFA$ p.p.m.) for methoxy-group resonances of several methoxybenzenes has been attributed to protonation of the methoxy group (12) whereas with flavones protonation by TFA at both methoxy and carbonyl groups has been proposed (13). The TFA solvent shift data of Table 1 support structures **1***a* and **2***a* best assuming protonation at the carbonyl oxygen only.

The structural assignments for **1***a* and **2***a*, based on solvent studies, were confirmed from chemical shift behavior (Figs. 1 and 2) observed

Can. J. Chem. Downloaded from www.nrcresearchpress.com by 210.87.254.6 on 09/05/12
For personal use only.

Can. J. Chem. Downloaded from www.nrcresearchpress.com by 210.87.254.6 on 09/05/12
For personal use only.

TABLE 2. Variation of deshielding gradients with functionality

Compound	Functional group	Gradient (p.p.m./mol $Eu(fod)_3$ per mol substrate)	Solvent
1*a*	CH_2 (N-1)	7.5	$CDCl_3$
	CH_3 (C-5)	4.9	
	CH_3 (N-1)	3.0	
	OCH_3 (C-2,3)	1.4	
2*a*	CH_2 (N-1)	6.3	$CDCl_3$
	CH_2 (C-5)	5.1	
	CH_3 (N-1)	2.3	
	CH_3 (C-5)	2.3	
	OCH_3 (C-2)	1.2	
	OCH_3 (C-4)	1.1	
3	OCH_3 (C-2)	7.8	$CDCl_3$
	OCH_3 (C-4)	4.4	
	H (C-5)	3.7	
	H (C-6)	1.5	
4	H (C-5)	5.7	$CDCl_3$
	OCH_3 (C-2,4,6)	4.3	
5	H (C-5)	6.0	CCl_4
	OCH_3 (C-4,6)	4.8	
	OCH_3 (C-2)	4.5	
6	OCH_3 (C-2)	6.3	$CDCl_3$
	OCH_3 (C-4)	3.9	
	H (C-5)	3.7	

with $Eu(fod)_3$, shift reagent. In selecting **1***a* as the correct structure, it was noted that both methoxy resonances are nearly equally affected by the shift reagent and have the same deshielding gradients of 1.4 p.p.m. (Table 2). Although structure **1***b* is best suited by symmetry for this deshielding, assuming complexation at the carbonyl oxygen by the shift reagent, the asymmetrical location of one ring nitrogen would not be expected to alter the chemical shifts greatly. In contrast, the similarly strong deshielding of both the CH_2(Et) protons at N-1 and of the C-5 methyl protons (gradients of 7.5 and 4.9 p.p.m., respectively) by the shift reagent can only be accounted for on the basis of structure **1***a*. Confirmation of structure **2***a* was likewise based on the similarity of deshielding of the methoxy resonances (gradients of 1.1 and 1.2 p.p.m., Table 2) and on the similar but larger deshielding of the CH_2(Et) and CH_3(Et) protons at N-1 and C-5 (gradients of 6.3, 2.3 and 5.1, 2.3 p.p.m., respectively). It is concluded, therefore, that the major products formed by the action of diazomethane on **1** and **2** are 1-ethyl-1,6-dihydro-2,4-dimethoxy-5-methyl-6-oxopyrimidine (**1***a*) and 1,5-diethyl-1,6-dihydro-2,4-dimethoxy-6-oxopyrimidine (**2***a*), respectively.

Solvent and Eu(fod)$_3$ Shift Studies with Some Methoxylated Pyrimidines

The assignment of chemical shifts to methoxylated and methylated pyrimidine rings has been difficult due to very small or negligible differences in these values among structurally similar derivatives. Nishiwaki (14) has reported that the methoxy signal of 2,4-dimethoxy-6-methylpyrimidine appears as a singlet in carbon tetrachloride (3.83 p.p.m.) or in acetic acid (4.00 p.p.m.) while two distinct bands (4.33 and 4.27 p.p.m.) were seen for this pyrimidine in trifluoroacetic acid. The signal at lower field was assumed to be the C-2 methoxy because this signal is likely to be affected more extensively by protonation of the nitrogen atom. Ma and Warnhoff (15) have reported that methoxyl groups show a negligible shift (+0.03 to −0.11 p.p.m.) on changing from deuterochloroform to perdeuteroacetic acid and only a small (−0.08 to −0.37 p.p.m.) further downfield shift in trifluoroacetic acid.

In considering the assignment of the correct structure *a*, *b*, or *c* to compounds **1** and **2**, the known compounds 2,4-dimethoxypyrimidine (**3**), 4,6-dimethoxypyrimidine (**4**), 2,4,6-trimethoxypyrimidine (**5**), and 6-chloro-2,4-dimethoxypyrimidine (**6**) were studied for solvent effects in the hope that frequency assignments made with this series of compounds would aid in the structural elucidation of **1** and **2**. These frequency data (Table 3), however, do not prove helpful by analogy in selecting the correct structure for **1** and **2**. The aromatic solvent shifts indicate that competitive complexation is occurring at different sites with the simpler substrates (**3**–**6**) to produce the range of values observed. Competitive complexation undoubtedly contributes to the character of the solvent shifts recorded for **1** and **2** even though these two compounds possess a carbonyl function which usually exerts a stronger polarizing influence in such solvent effects.

The relative solvent shifts for **3**, **4**, **5**, and **6** in trifluoroacetic acid ($\Delta_{TFA}^{CCl_4}$) (Table 3) show the largest downfield shift for the C-5 proton with

TABLE 3. The p.m.r. solvent shift data (δ in p.p.m. downfield from internal TMS) for some methoxylated pyrimidines

Solvent	C-5	C-6	OMe C-2	OMe C-4	OMe C-6	H(C-2)	J^*H_5,H_6(Hz)
2,4-Dimethoxypyrimidine (**3**)							
$CDCl_3$	6.37(d)†	8.18(d)	4.00	3.97	—		5.6
CCl_4	6.27(d)	8.10(d)	3.92	3.92	—		5.8
$\Delta^{CCl_4}_{C_6H_6}$	+0.24	+0.22	+0.17	+0.32			5.8 (C_6H_6)
$\Delta^{CCl_4}_{C_5H_5N}$	−0.11	−0.13	0.00	+0.09			5.7 (C_5H_5N)
$\Delta^{CCl_4}_{TFA}$	−0.56	−0.12	−0.46	−0.41			7.0 (TFA)
4,6-Dimethoxypyrimidine (**4**)							J^*H_2,H_5(Hz)
$CDCl_3$	6.03(d)	—	—	3.95	3.95	8.45 (d)	0.8
CCl_4	5.93(d)	—	—	3.90‡	3.90‡	8.33 (d)	0.7
$\Delta^{CCl_4}_{C_6H_6}$	−0.12	—	—	+0.23	+0.23	−0.15	0.8 (C_6H_6)
$\Delta^{CCl_4}_{C_5H_5N}$	−0.24	—	—	+0.02	+0.02	—	0.9 (C_5H_5N)
$\Delta^{CCl_4}_{TFA}$	−0.69	—	—	−0.38	−0.38	−0.45	0.6 (TFA)
2,4,6-Trimethoxypyrimidine (**5**)							
$CDCl_3$	5.72	—	3.98	3.93	3.93		
CCl_4	5.58	—	3.90	3.88	3.88		
$\Delta^{CCl_4}_{C_6H_6}$	−0.22	—	+0.22	+0.25	+0.25		
$\Delta^{CCl_4}_{C_5H_5N}$	−0.29	—	0.00	+0.03	+0.03		
$\Delta^{CCl_4}_{TFA}$	−0.57	—	−0.42	−0.34	−0.34		
6-Chloro-2,4-dimethoxypyrimidine (**6**)							
$CDCl_3$	6.40	—	4.02	3.97	—		
CCl_4	6.32	—	3.95‡	3.95‡	—		
$\Delta^{CCl_4}_{C_6H_6}$	+0.17	—	+0.33	+0.45	—		
$\Delta^{CCl_4}_{TFA}$	−0.60	—	−0.47	−0.42	—		

*Measured on the 100 Hz sweep width.
†d, Doublet.
‡No resolution on the 100 Hz sweep width.

smaller deshielding for the C-2 proton (*e.g.* **4**) or for the methoxyl protons at C-2 (*e.g.* **3**, **5**, **6**). These shifts are in accord with some delocalization of charge through a protonated nitrogen atom; however, the larger downfield shift for the C-5 proton is opposite to what Nishiwaki found for TFA solutions of 4-hydroxy-6-methylpyrimidine and 5-bromo-4-hydroxy-6-methylpyrimidine (14) where the C-2 proton moves downfield more than 1 p.p.m. in TFA relative to chloroform. Similarly, the results of these studies of the effect of TFA on the simpler substrates (**3**–**6**) are of little help in selecting the correct structures for **1** and **2** where protonation of the carbonyl oxygen appears to be more favored than a ring nitrogen.

In studying the effect of Eu(fod)$_3$ on 2,4-dimethoxypyrimidine (**3**), one is surprised to find that it is the C-2 methoxy protons which show the largest deshielding gradient (7.8 p.p.m.) Table 2 and Fig. 3. It would appear that complexation[2] of Eu(fod)$_3$ involves the C-2 methoxy oxygen rather than the C-4 methoxy oxygen atom which might have been expected to have the higher electron density. Reversal of the methoxy assignments shows appreciable non-linearity in graphical representation of the C-4 methoxy proton shifts. It is also interesting to note from Fig. 3 that the deshielding gradient (3.7 p.p.m.) for the C-5 proton of 2,4-di-

[2]A referee has noted that complexation may involve a nitrogen of the pyrimidine ring instead of the oxygen of an *O*-methyl group because of the fact that pyridine is tightly complexed with lanthanide reagents while anisole is not. While this may be the case for some pyrimidine derivatives, complexation does not appear to involve the N-1 site, more favored than N-3 as a Lewis base, of 2,4-dimethoxypyrimidine because H (C-6) shows the smallest deshielding gradient (Fig. 3) of all protons of this molecule.

Can. J. Chem. Downloaded from www.nrcresearchpress.com by 210.87.254.6 on 09/05/12
For personal use only.

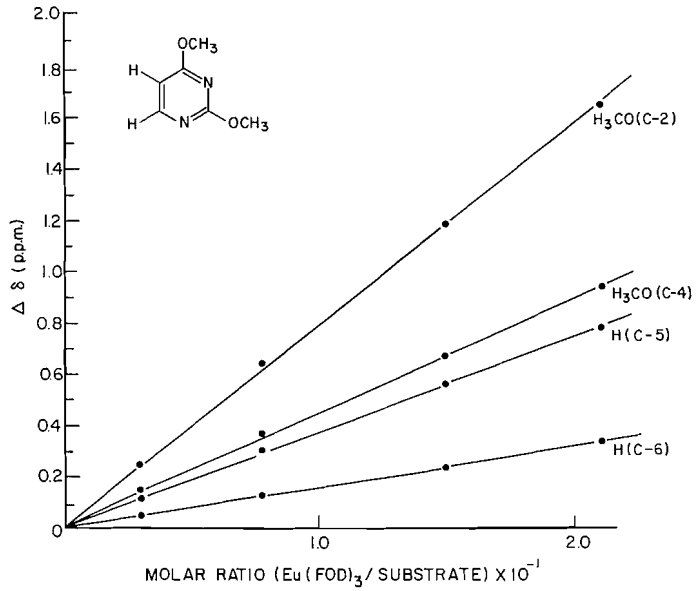

FIG. 3. Normalized $Eu(fod)_3$ induced p.m.r. shifts for 2,4-dimethoxypyrimidine in $CDCl_3$ solution.

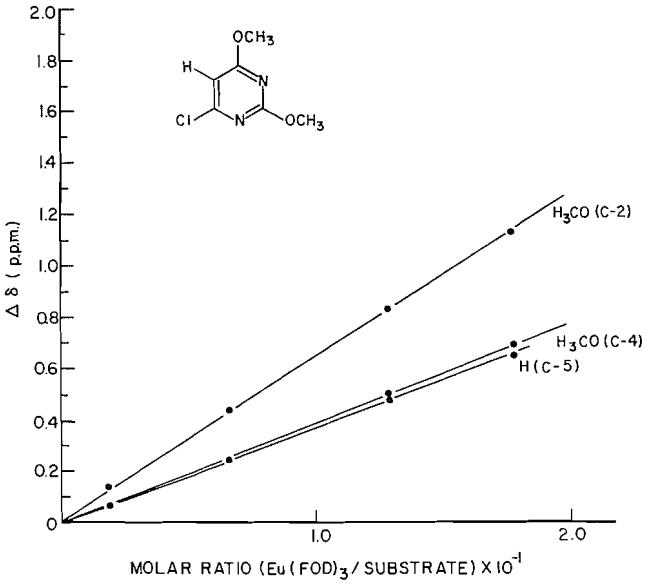

FIG. 4. Normalized $Eu(fod)_3$ induced p.m.r. shifts for 6-chloro-2,4-dimethoxypyrimidine in $CDCl_3$ solution.

methoxypyrimidine is significantly greater than that for the C-6 proton which is more proximate to the site of complexation. This reversal in deshielding effect with distance may be due to a dominant ring inductive effect influencing the para-proton more than the meta-proton, or it may arise in this instance by the influence of the angular dependence term $(3 \cos^2 X_i - 1)$ of the McConnell equation (16) applicable to pseudo-contact complexation. Recent mathematical considerations of the geometry in regions of angular dependence for simple model compounds showing an anomalous upfield shift with Eu shift reagents have shown that the

Can. J. Chem. Downloaded from www.nrcresearchpress.com by 210.87.254.6 on 09/05/12
For personal use only.

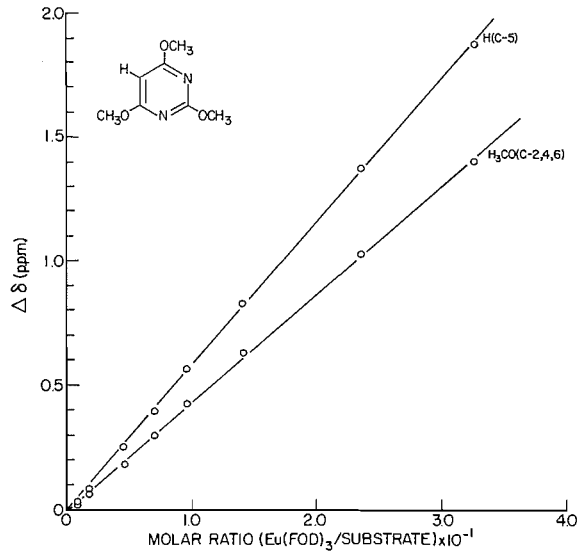

FIG. 5. Normalized Eu(fod)$_3$ induced p.m.r. shifts for 2,4,6-trimethoxypyrimidine in $CDCl_3$ solution.

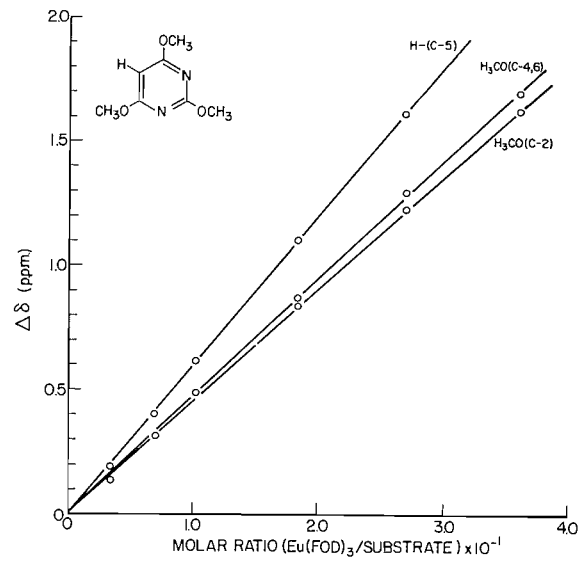

FIG. 6. Normalized Eu(fod)$_3$ induced p.m.r. shifts for 2,4,6-trimethoxypyrimidine in CCl_4 solution.

angular term can override the distance term and result in anomalously small (but not necessarily with reversed sign) deshielding effects (17).

Support for the assignments and complexation model for 2,4-dimethoxypyrimidine was obtained from similar studies of the effect of Eu(fod)$_3$ on 6-chloro-2,4-dimethoxypyrimidine (**6**) (Fig. 4) where the presence of the chloro substituent was not found to alter the electronic character of the pyrimidine ring sufficiently to alter the mode of complexation. The C-2 methoxyl protons of **6** show the largest deshielding gradient (6.4 p.p.m.) (Fig. 4) whose somewhat smaller value than 7.8 p.p.m. for the C-2 methoxyl protons of 2,4-dimethoxypyrimidine cannot be attributed entirely to the electron withdrawing effect of the chloro substituent of **6** because the C-5 proton of both **3** and **6** shows the same gradient of 3.7 p.p.m. (Table 2).

In contrast to the above examples, no dif-

Can. J. Chem. Downloaded from www.nrcresearchpress.com by 210.87.254.6 on 09/05/12
For personal use only.

Can. J. Chem. Downloaded from www.nrcresearchpress.com by 210.87.254.6 on 09/05/12
For personal use only.

ferentiation is made between the 2 and 4 (or 6) methoxyl protons of 2,4,6-trimethoxypyrimidine (**5**) by $Eu(fod)_3$ in $CDCl_3$ solution (Fig. 5). In addition the C-5 proton of **5** shows a larger deshielding gradient (5.7 p.p.m.) (Table 2) than the methoxyl protons (4.3 p.p.m.) which suggests that a different complexation geometry may be involved with this molecule. In carbon tetrachloride solution Fig. 6, $Eu(fod)_3$ does permit one methoxyl group of *sym*-trimethoxypyrimidine (**5**) to be distinguished from the other two, but this distinction is only possible at higher molar concentrations of $Eu(fod)_3$ shift reagent, i.e. $>0.1\ M$ $Eu(fod)_3$/substrate. In this instance because the peak integrating for three protons consistently occurred upfield from the peak integrating for six protons, the former was assigned to the C-2 methoxyl group and complexation was assumed to involve either the C-4 or -6 methoxyl oxygen atom consistent with the large gradient (6.0 p.p.m.) for the C-5 proton of *sym*-trimethoxypyrimidine in CCl_4 solution.

It is apparent from these studies of the effect of various solvents and of the shift reagent, $Eu(fod)_3$, in model pyrimidines (**3**–**6**) for the novel methoxylated pyrimidones **1** and **2** that very subtle effects are involved which make the choice of model compounds difficult. From these studies, it appears that the structural evidence presented for the pyrimidones **1***a* and **2***a* is best considered on its own merits and internal consistency.

Experimental

Proton Magnetic Resonance Studies

The p.m.r. shifts were measured with a Varian A-60A spectrometer with a probe temperature of 40°. The shifts are believed accurate to ± 0.02 p.p.m.

The $Eu(fod)_3$ shift reagent was obtained from Merck Sharp and Dohme Canada Limited, P.O. Box 898, Pointe Claire–Dorval 700, Quebec.

Syntheses

The conditions for barbiturate synthesis and various physicochemical properties of 1-ethyl-5-methylbarbituric acid (**1**) have been described (18).

*1,5-Diethylbarbituric Acid (**2**)*

Diethyl ethylmalonate (20.0 g, 0.107 mol, n_d^{20} 1.4164, Aldrich) was condensed with ethylurea (9.5 g, 0.110 mol, m.p. 92–94 °C, Aldrich) during 3 h heating under reflux in absolute ethanol (150 ml) containing dissolved sodium (5.0 g, 0.221 mol). The reaction mixture was diluted with water (200 ml), acidified with concentrated hydrochloric acid to Congo red, and left to crystallize overnight in a refrigerator. The crude dry solid (9.2 g, 50%) was recrystallized twice from boiling heptane containing sufficient benzene to maintain miscibility of the oily solute to obtain the analytical sample, m.p. 89.2–91.5° (precision m.p., ref. 19).

Anal. Calcd. for $C_8H_{12}N_2O_3$: C, 52.17; 6.57; N, 15.21. Found: C, 51.96, 52.03; H, 6.45, 6.43; N, 15.37, 15.42.

The p.m.r. spectrum: δ in $CDCl_3$ relative to TMS internal reference: 0.97 (t), CH_3 (C—Et); 1.20 (t), CH_3(N—Et); 2.18 (m) CH_2 (C—Et); 3.45 (t), CH (C-5); 3.93 (q), CH_2(N—Et); 9.32 (broad), NH.

*1-Ethyl-1,6-dihydro-2,4-dimethoxy-5-methyl-6-oxopyrimidine (**1***a*)*

Treatment of a methanolic solution of 1-ethyl-5-methylbarbituric acid (**1**) (m.p. 146.8–147.5 °C) with excess ethereal diazomethane (20) at 0–5 °C and subsequent evaporation gave an oil which crystallized on standing. The crude solid (m.p. 71–80 °C, 15% yield) was recrystallized twice from heptane to obtain an analytical sample of **1***a*, m.p. 80.5–82.2°(corr.) (19).

Anal. Calcd. for $C_9H_{14}N_2O_3$: C, 54.54; H, 7.11; N, 14.13. Found: C, 54.99, 55.29; H, 7.23, 7.30; N, 14.53, 14.51.

*1,5-Diethyl-1,6-dihydro-2,4-dimethoxy-6-oxopyrimidine (**2***a*)*

Similar treatment and handling of a methanolic solution of 1,5-diethylbarbituric acid (**2**) (m.p. 89.2–91.5 °C) gave a crude solid (m.p. 76–81 °C, 28% yield). Two recrystallizations from heptane gave the analytical sample of **2***a* (m.p. 85.6–87.2 °C (corr.) (19).

Anal. Calcd. for $C_{10}H_{16}N_2O_3$: C, 56.59; H, 7.60; N, 13.20. Found: C, 56.32, 56.33; H, 7.54, 7.45; N, 13.25, 13.30.

The p.m.r. spectrometry indicated the mother liquor fractions from both reactions using diazomethane to be complex mixtures of *O*,*N*-dimethyl and *O*,*O*-dimethyl positional isomers.

Methoxylated Pyrimidines

2,4-Dimethoxypyrimidine (**3**) and 6-chloro-2,4-dimethoxypyrimidine (**6**) were used as received from the Aldrich Chemical Co.

*4,6-Dimethoxypyrimidine (**4**)*

A methanolic solution (25 ml) of 4,6-dichloropyrimidine (10.0 g, 0.067 mol, Aldrich) was added in small portions to a freshly prepared methanolic solution of sodium methoxide (4.50 g, 0.20 mol Na/75 ml methanol). The exothermic reaction was allowed to proceed just below the boiling point of the mixture. The reaction mixture was allowed to cool to room temperature before the sodium chloride by-product was removed by filtration. The filtrate was stripped of methanol, and the resulting oil was distilled at reduced pressure to obtain liquid b.p. 36–40°/0.2 mm; lit. b.p. 85°/16 mm (21). The product was verified by p.m.r. spectral analysis (Table 3).

*2,4,6-Trimethoxypyrimidine (**5**)*

A methanolic solution (25 ml) of 2,4,6-trichloropyrimidine (5.0 g, 0.027 mol, Aldrich) was added in small portions to a freshly prepared methanolic solution of sodium methoxide (2.55 g, 0.108 mol Na/50 ml methanol). The reaction proceeded with bubbling and the evolution of heat. The

mixture was allowed to cool to room temperature before the precipitated sodium chloride was removed by filtration. The filtrate was reduced to an oil by rotary evaporation. The oil crystallized on standing. Three recrystallizations of the solid from heptane gave crystals (0.9 g) m.p. 50–52°; lit. m.p. 53° (22). The product was verified by p.m.r. spectral analysis (Table 3).

The author is grateful to Mr. H. W. Avdovich of these laboratories for preparative work and p.m.r. spectra.

1. G. A. NEVILLE. Anal. Chem. **42**, 347 (1970).
2. R. E. RONDEAU and R. E. SIEVERS. J. Am. Chem. Soc. **93**, 1525 (1971).
3. J. K. M. SANDERS and D. H. WILLIAMS. J. Am. Chem. Soc. **93**, 641 (1971).
4. G. A. NEVILLE and H. W. AVDOVICH. Can. J. Chem. **50**, 880 (1972).
5. J. D. CONNOLLY and R. MCCRINDLE. Chem. and Ind. 379 (1965).
6. D. H. WILLIAMS and N. S. BHACCA. Tetrahedron, **21**, 2021 (1965).
7. C. R. NARAYANAN and N. R. BHADANE. Tetrahedron Lett. 1557 (1968).
8. R. G. WILSON, D. E. A. RIVETT, and D. H. WILLIAMS. Chem. and Ind. 109 (1969).
9. K. M. BAKER and R. G. WILSON. J. Chem. Soc. B, 236 (1970).
10. J. RONAYNE and D. H. WILLIAMS. *In* Annual review of NMR spectroscopy. Vol. 4. *Edited by* E. F. Mooney. Academic Press, London, 1969. p. 118.
11. D. H. WILLIAMS. Tetrahedron Lett. 2305 (1965).
12. R. G. WILSON and D. H. WILLIAMS. J. Chem. Soc. C, 2475 (1968).
13. R. G. WILSON and D. H. WILLIAMS. J. Chem. Soc. C, 2477 (1968).
14. T. NISHIWAKI. Tetrahedron, **23**, 2657 (1967).
15. J. MA and E. WARNHOFF. Can. J. Chem. **43**, 1849 (1965).
16. H. M. MCCONNELL and R. E. ROBERTSON. J. Chem. Phys. **29**, 1361 (1958).
17. J. P-K. TONG and C. H. LANGFORD. Private communication.
18. G. A. NEVILLE, H. W. AVDOVICH, and A. W. BY. Can. J. Chem. **48**, 2274 (1970).
19. E. B. HERSHBERG. Ind. Eng. Chem. Anal. Ed. **8**, 312 (1936).
20. T. J. DEBOER. Rec. Trav. Chim. **73**, 229 (1954).
21. D. J. BROWN and J. S. HARPER. J. Chem. Soc. 1298 (1961).
22. E. BÜTTNER. Ber. Dtsch. chem. Ges. **36**, 2227 (1903).

Can. J. Chem. Downloaded from www.nrcresearchpress.com by 210.87.254.6 on 09/05/12
For personal use only.

A Proton Nuclear Magnetic Resonance Study of the Exchange Reactions of Acetonitrile – Boron Trihalide Adducts with Excess Acetonitrile[1,2]

J. FOGELMAN AND J. M. MILLER[3]

Department of Chemistry, Brock University, St. Catharines, Ontario

Received July 21, 1971

Proton n.m.r. studies of the mechanism for exchange of excess acetonitrile with $CH_3CN{\cdot}BX_3$ (X = F, Cl, Br) adducts show that the rates and activation energy for dissociation are influenced by solvent effects when mixed solvents such as $C_6H_5NO_2/CH_2Cl_2$ or CD_3NO_2/CH_2Cl_2 are used. On extrapolation to inert solvent conditions, first order activation energies are obtained which are in close agreement with previously measured dissociation energies of acetonitrile adducts in solution. The relative rates of dissociation are $CH_3CN{\cdot}BF_3 > CH_3CN{\cdot}BCl_3 > CH_3CN{\cdot}BBr_3$; in agreement with previous experimental evidence that the strength of the donor–acceptor band varies as $CH_3CN{\cdot}BBr_3 > CH_3CN{\cdot}BCl_3 > CH_3CN{\cdot}BF_3$.

Des études par r.m.n. de protons concernant le mécanisme d'échange d'un excès d'acétonitrile avec des dérivés $CH_3CN{\cdot}BX_3$ (X = F, Cl, Br) montrent que les vitesses et l'énergie d'activation de la dissociation sont influencées par les effets de solvants quand des solvants mixtes, tels $C_6H_5NO_2/CH_2Cl_2$ ou CD_3NO_2/CH_2Cl_2 sont utilisés. On obtient, par extrapolation aux conditions de solvant inerte, les énergies d'activation de premier ordre; celles-ci concordent très bien avec les énergies de dissociation de dérivés d'acétonitrile en solution mesurées précédemment. Les vitesses de dissociation relatives sont, dans l'ordre $CH_3CN{\cdot}BF_3 > CH_3CN{\cdot}BCl_3 > CH_3CN{\cdot}BBr_3$; ces résultats sont en accord avec les faits expérimentaux précédents qui montraient que la force de la bande donneur–accepteur varie dans l'ordre $CH_3CN{\cdot}BBr_3 > CH_3CN{\cdot}BCl_3 > CH_3CN{\cdot}BF_3$.

Canadian Journal of Chemistry, **50**, 1262 (1972)

Can. J. Chem. Downloaded from www.nrcresearchpress.com by 210.87.254.6 on 09/05/12
For personal use only.

Introduction

It has previously been reported (1) that the downfield chemical shift of acetonitrile–boron trihalide adducts increase in the same order as the acceptor power of the boron trihalides, and also that the exchange with excess acetonitrile proceeded rapidly at room temperature. We now report an n.m.r. kinetic study of the exchange process

$$CH_3CN{\cdot}BX_3 + CH_3CN^* \rightleftarrows CH_3CN + CH_3CN^*{\cdot}BX_3 \qquad (X = F, Cl, Br)$$

De Roos and Oliver (2) have shown that for a first order, dissociation dependent, exchange of the type

$$AB \underset{}{\overset{k_1}{\rightleftharpoons}} A + B \qquad \text{(slow)}$$

$$A + B^* \underset{}{\overset{k_2}{\rightleftharpoons}} AB^* \qquad \text{(fast)}$$

the inverse mean lifetime of adduct species AB, *i.e.* $1/\tau_{AB}$, obtainable from the n.m.r. line widths, is independent of the concentration of either the adduct AB or free base B, *i.e.* $1/\tau_{AB} = k_1$. Similarly, the inverse mean lifetime of the free base has the following concentration dependence, $1/\tau_B = k_1[AB]/[B]$.

For the second order reaction

$$AB + B^* \underset{k_2}{\overset{k_1}{\rightleftharpoons}} B + AB^*$$

the concentration dependence of the mean lifetimes are $1/\tau_{AB} = k_1[B]$ and $1/\tau_B = k_1[AB]$. Thus, from changes in n.m.r. line widths with concentration the order of reaction may be obtained. Such n.m.r. studies have been reviewed recently for organometallic systems (3–5).

Cowley and Mills (6) have shown that for the exchange reaction of $(CH_3)_3N{\cdot}B(CH_3)_3$ with excess acid or base, the rate determining step is dissociation of the adduct. Henold *et al.* (7) have argued that steric hindrance is the explanation for first order rather than second order exchange in Cowley and Mills' work. An additional factor which makes second order displacements at boron less favorable is the increase in activation energy from repulsive terms between groups bonded to boron when the small boron atom must go through a five coordinate transition state. In this work we report on

[1]Presented in part at the 52nd Chemical Institute of Canada Conference, Montreal, Quebec, June, 1969.

[2]Abstracted in part from the Brock University M.Sc. Thesis of J. F. (1969).

[3]Address all correspondence to this author.

TABLE 1. Concentration dependence of the lifetimes and rate of exchange for $CH_3CN \cdot BBr_3 + CH_3CN$

Temperature (°C)	[AB]* ($M \times 10^2$)	[B]† ($M \times 10^2$)	$1/\tau_{AB}$ (s^{-1})	$1/\tau_B$ (s^{-1})	$\frac{1}{\tau_B}\frac{[B]}{[AB]}$ (s^{-1})
−1.4	5.45	5.59	2.89	1.73	1.77
	3.14	4.91	2.89	1.45	2.27
	4.70	14.1	2.89	0.74	2.22
	1.42	12.9	2.73	—‡	—
	1.57	21.3	2.36	—‡	—
+5.5	5.45	5.59	3.74	2.10	2.15
	3.14	4.91	4.05	1.89	2.95
	4.70	14.1	4.27	1.24	3.72
	1.42	12.9	4.81	—‡	—
	1.57	21.3	3.96	—‡	—
+9.3	5.45	5.59	5.53	5.40	5.54
	3.14	4.91	6.50	3.17	4.95
	4.70	14.1	5.47	1.73	5.19
+20.7	5.45	5.59	12.2	12.4	12.7
	3.14	4.91	10.2	9.6	15.0
	4.70	14.1	14.1	4.3	12.9

*AB is $CH_3CN \cdot BBr_3$.
†B is CH_3CN.
‡Acetonitrile peak shows only slight exchange broadening.

exchange of acetonitrile with $CH_3CN \cdot BX_3$, where the acetonitrile is certainly much less sterically hindered and serves as a test of Henold's argument.

Experimental

$CH_3CN \cdot BX_3$ adducts were prepared from acetonitrile (dried over molecular sieve followed by vacuum distillation), and freshly distilled boron trihalides as previously described (1). The BF_3 adduct was washed with dry benzene prior to vacuum sublimation (25 °C) while the BCl_3 and BBr_3 adducts were sublimed directly at 85 and 150°, respectively. All manipulations of the adducts were carried out in a nitrogen filled dry box. The n.m.r. samples were prepared using weighed samples of adduct in capped n.m.r. tubes, the solvent and excess acetonitrile being added by syringe in the dry box. Samples were stored at −78 °C prior to use.

The ^1H n.m.r. spectra were recorded on a Varian A-60 equipped with a V-6040 variable temperature unit modified to function over a temperature range of +200 to −150 °C. Temperatures were calibrated using a Varian methanol sample and the corrected calibration curves of Van Geet (8). Spectra were calibrated by audio side bands from a HP4204A decade oscillator monitored by an El Dorado 224 frequency counter.

The A-60 was also equipped with a C-1024 time averaging computer which was used for some measurements on the more dilute samples. Other accessories included a V-6058A homonuclear decoupler and an NMR Specialties HD-60 heteronuclear decoupler operating at 19.25 MHz for ^{11}B decoupling. No coupling to ^{11}B was observed.

Line widths were measured at half height and were approximately corrected for natural line widths by subtracting the width of the TMS reference line, since under the low temperature conditions of our experiments the TMS and pure acetonitrile line widths were approximately the same (0.45 ± 0.05 Hz). The TMS simultaneously provided a monitor of spectrometer resolution. We were unable to measure the line width of the adducts in the absence of exchange so our correction for natural line width is only an approximation. It is probably quite reasonable by analogy with $Me_3N \cdot BX_3$ adducts which we observe to have line widths similar to trimethylamine itself (0.50 and 0.47 Hz, respectively), under conditions of no exchange.

Straight line fits of the kinetic data were computed using a least squares program.

Results and Discussion

(I) Acetonitrile–Boron Tribromide System

This system exhibited the slowest exchange rate of the three described, and could be studied under slow exchange conditions at temperatures not far from ambient (−5 to 25 °C). However, nitrobenzene or nitrobenzene–dichloromethane mixtures had to be used as solvents since the already limited solubility of $CH_3CN \cdot BBr_3$ in dichloromethane decreased rapidly on reducing temperature. Studies were carried out at several temperatures with varied concentration of adduct and free base. Typical results are shown in Table 1.

It can be seen that these data show the

Can. J. Chem. Downloaded from www.nrcresearchpress.com by 210.87.254.6 on 09/05/12
For personal use only.

TABLE 2. Activation energies and entropies and rate constants for $CH_3CN \cdot BBr_3 + CH_3CN$ in nitrobenzene–dichloromethane solution

$[C_6H_5NO_2]$ (M in CH_2Cl_2)	E_A (kcal/mol)	$\Delta S^{\ddagger}$ (e.u.)	k_1 at 6.5 °C (s^{-1})
9.74	11.9±1.0	−14.5	4.65
9.54	11.9±1.0	−14.2	4.80
5.96	14.4±1.0	−5.3	7.09
4.13	15.8±1.0	−1.8	10.4
2.99	16.9±1.0	+7.9	15.2

behavior expected for a first order dissociation controlled reaction, namely; (*a*) $1/\tau_{AB}$ is independent of concentration, *i.e.* $1/\tau_{AB} = k_1$; and (*b*) $1/\tau_B$ is concentration dependent, but when multiplied by the ratio of free base to adduct concentrations is constant within experimental error and approximately equal to $1/\tau_{AB}$.

The activation energy for this dissociation process in neat nitrobenzene was determined from a plot of ln $1/\tau$ *vs.* $1/T$ °K. These activation energies were 11.6 ± 0.4 and 12.1 ± 0.4 kcal/mol as determined from the adduct and free base peaks, respectively. These values are low when compared to 19.1 kcal/mol for the dissociation energy of $CH_3CN \cdot BBr_3$ measured by Blackborow and Lockhart (9). A solvent effect was suspected so activation energies and entropies of activation were determined at various concentrations of nitrobenzene in dichloromethane as shown in Table 2.

Since the reaction of nitrobenzene with the boron trihalides is a well known reaction (10), second order interactions with nitrobenzene are possible, namely

$$PhNO_2 + CH_3CN \cdot BX_3 \rightleftarrows CH_3CN + PhNO_2 \cdot BX_3$$

Such a reaction could also affect the concentrations of base and adduct used in the calculations. However, we found that, within experimental error, the ratios of adduct to free base as measured by electronic or planimeter integration of the n.m.r. spectra were the same as the ratios originally added to the n.m.r. tubes, so the free acetonitrile–adduct equilibrium is not seriously disturbed.

Participation of a competitive reaction with the solvent could still greatly affect the n.m.r. line widths. The fact that $1/\tau_{AB}$ is constant with changes in adduct or acetonitrile concentration would still be consistent with a pseudo first order reaction for constant nitrobenzene concentration. Participation of a third species in the exchange is also indicated by the fact that $[B]/\tau_B[AB]$, although constant, is not exactly equal to $1/\tau_{AB}$.

The low activation energy and negative entropy at higher nitrobenzene concentrations is consistent with increasing participation of nitrobenzene in the exchange reactions. If the activation energy is plotted against nitrobenzene concentration, and extrapolated to zero nitrobenzene concentration, *i.e.* pure dichloromethane solvent, the extrapolated activation energy is 18.5 ± 1.0 kcal/mol, in good agreement with the measured dissociation energy in solution, 19.1 kcal/mol (9).

Thus, in the absence of nitrobenzene, dissociation of $CH_3CN \cdot BBr_3$ would be the rate determining step for exchange with excess acetonitrile. A S_N1 mechanism has been reported by Blackborow and Lockhart for the reaction of aromatic amines with $CH_3CN \cdot BBr_3$ adduct (11), although they also report a mechanistic crossover with the BCl_3 adduct reacting via a S_N2 mechanism.

The effect of nitrobenzene concentration on the observed rate constants indicates that in addition to the probable second order attack of nitrobenzene on the acetonitrile adduct, further complicating processes are involved which will be discussed later.

(II) Acetonitrile–Boron Trichloride System

Exchange of excess acetonitrile with the adduct $CH_3CN \cdot BCl_3$ was more rapid than for the corresponding BBr_3 adduct, and thus lower temperatures (−35 to −55 °C) were required for observation of the ^1H n.m.r. spectra of both free base and adduct under conditions of slow exchange. Lower temperatures necessitated using the mixed solvent system, nitrobenzene–dichloromethane. The mechanism of exchange was again elucidated from a study of adduct and free base line widths on varying concentrations of both adduct and free base as shown in Table 3.

For BCl_3 as was the case for the BBr_3 adduct $1/\tau_{AB} = k_1 = [B]/\tau_B[AB]$. Unlike the reaction of aromatic amines with acetonitrile adducts (9) for which there is a crossover from S_N1 to S_N2 mechanism on changing from the bromide to the chloride adduct, we find that both

Can. J. Chem. Downloaded from www.nrcresearchpress.com by 210.87.254.6 on 09/05/12
For personal use only.

TABLE 3. Concentration dependence of the lifetimes and rate of exchange for $CH_3CN \cdot BCl_3 + CH_3CN$

Temperature (°C)	[AB]* ($M \times 10^2$)	[B]† ($M \times 10^2$)	$1/\tau_{AB}$ (s^{-1})	$1/\tau_B$ (s^{-1})	$\frac{1}{\tau_B}\frac{[B]}{[AB]}$ (s^{-1})
−34	4.10	13.8	11.2	2.95	9.93
	4.63	10.5	11.8	4.65	10.59
	6.04	7.29	10.7	7.76	9.36
	5.85	4.79	9.58	14.0	11.45
	6.78	3.53	13.7	24.7	12.84
−39	4.10	13.8	7.45	1.26	4.24
	4.63	10.5	6.50	2.36	5.35
	6.04	7.29	6.69	4.37	5.27
	5.85	4.79	6.72	5.03	4.11
	6.78	3.53	6.44	16.56	8.61
−43	4.10	13.8	3.93	0.53	1.79
	4.63	10.5	3.52	1.38	3.13
	6.04	7.29	3.49	2.83	3.41
	5.85	4.79	3.99	5.25	4.29
	6.78	3.53	3.90	6.38	3.32

*AB is $CH_3CN \cdot BCl_3$.
†B is CH_3CN.

TABLE 4. Evaluation of activation energy for the exchange of $CH_3CN \cdot BCl_3 + CH_3CN$*

Temperature (°C)	$1/T \times 10^3$ ($°K^{-1}$)	$1/\tau_{AB}$ (s^{-1})	$1/\tau_B$ (s^{-1})
Run I			
−35.7	4.211	9.11	7.73
−38.8	4.266	8.23	7.13
−41.2	4.310	5.15	5.09
−42.8	4.340	4.81	4.08
−45.5	4.393	2.89	2.07
−47.7	4.436	—	1.70
Run II			
−51.3	4.507	1.60	0.85
−47.5	4.431	2.14	1.45
−44.8	4.378	2.83	1.98
−42.7	4.338	3.49	3.20
−40.1	4.290	5.37	3.52
−38.9	4.268	6.57	4.08
−35.8	4.212	8.95	7.07
−34.2	4.184	11.4	7.60

*Solvent = $C_6H_5NO_2/CH_2Cl_2$ = 1/1.19.

adducts exchange with excess acetonitrile via a dissociative mechanism.

A plot of ln k_1 *vs.* $1/T$ based on typical data in Table 4 led to activation energies of 12.5 ± 0.6 and 12.8 ± 0.6 kcal/mol from the adduct and free base line widths, respectively. These values are again below the 18.1 kcal/mol measured

TABLE 5. Activation energies and entropies and rate constants for $CH_3CN \cdot BCl_3 + CH_3CN$ in nitrobenzene–dichloromethane solution

$[C_6H_5NO_2]$ (M in CH_2Cl_2)	E_A (kcal/mol)	$\Delta S^{\ddagger}$ (e.u.)	k_1 at −42 °C (s^{-1})
6.63	10.7±0.4	−17.1	3.86
6.30	10.9±2.0	—	—
5.74	11.9±1.8	—	—
5.48	11.7±0.2	—	—
5.35	11.9±0.9	−8.9	5.12
4.76	12.7±0.7	+6.9	6.25
4.45	12.8±0.3	—	6.50
2.96	14.6±1.3	—	—

dissociation energy of $CH_3CN \cdot BCl_3$ (9), and as was the case for the BBr_3 adduct the effect of solvent concentration on activation energy was examined (Table 5).

These results show the same trend as for the BBr_3 adduct, an increase in rate, entropy of activation and energy of activation on decreasing the nitrobenzene concentration. On extrapolation to pure dichloromethane an activation energy of 17.7 ± 1.0 kcal/mol is obtained, in good agreement with the 18.1 kcal/mol dissociation energy for $CH_3CN \cdot BCl_3$ calculated by Blackborow and Lockhart (9). This is further confirmation of a dissociative mechanism, complicated in the mixed solvent system by pseudo

Can. J. Chem. Downloaded from www.nrcresearchpress.com by 210.87.254.6 on 09/05/12
For personal use only.

Can. J. Chem. Downloaded from www.nrcresearchpress.com by 210.87.254.6 on 09/05/12
For personal use only.

first order reaction with nitrobenzene, and other complications.

Deuteronitromethane was also used as a solvent system for a study of $CH_3CN \cdot BCl_3 + CH_3CN$. Slow exchange conditions were observed at higher temperatures (-35 to -17 °C) than required for the nitrobenzene–dichloromethane mixed solvent system. The results were not as accurate as those discussed above, but all indications were that a similar exchange mechanism was operative in CD_3NO_2 as well.

(III) Acetonitrile–Boron Trifluoride System

$CH_3CN \cdot BF_3$ had the highest solubility of the three adducts studied, but being the most weakly bonded it was not surprising to find that it exchanged most rapidly. It proved impossible to cool this system below the coalescence point (≈ -100 °C) without precipitation of the adduct. A mixed solvent system, CD_3NO_2/CH_2Cl_2 was found to have a low enough freezing point, while maintaining its ability to dissolve the adduct, to permit studies down to about -95 °C, still in the region for fast exchange.

Activation energies were calculated based on the exchange broadening of the single peak observed, typical data being given in Table 6 for a system where adduct and free base concentration were the same.

Again the activation energies were lower than the 12.5 kcal/mol calculated for dissociation of $CH_3CN \cdot BF_3$ in solution (12), so the measurements were performed over a series of solvent concentrations (Table 7).

These values, if extrapolated to pure CH_2Cl_2 solvent correspond to an activation energy of 11.2 ± 0.6 kcal/mol; similar to the value for the dissociation energy of $CH_3CN \cdot BF_3$ in solution. By analogy, therefore, to the trichloride and tribromide adducts, for which the extrapolated activation energy corresponded to the dissociation energy, and which were independently shown by concentration studies to exchange with acetonitrile via a first order dissociative mechanism, we conclude that the $CH_3CN \cdot BF_3$ adduct also exchanges via a dissociative mechanism.

(IV) Other Considerations

As the nitrobenzene concentration was decreased, the rate of exchange increased (Table 8).

TABLE 6. Evaluation of activation energy for the exchange of $CH_3CN \cdot BF_3 + CH_3CN$*

Temperature (°C)	$1/T \times 10^3$ ($°K^{-1}$)	Line width (Hz)
−80.2	5.20	4.82
−83.0	5.26	6.12
−86.0	5.34	7.64
−89.2	5.44	10.4
−92.0	5.52	13.2
−95.0	5.61	14.1

*Solvent = CD_3NO_2/CH_2Cl_2; 8.09 *M* in CD_3NO_2.

TABLE 7. Variation of activation energy with solvent composition for the exchange of $CH_3CN \cdot BF_3 + CH_3CN$

$[CD_3NO_2]$ (*M* in CH_2Cl_2)	E_A (kcal/mol)
4.45	8.16±0.3
5.93	8.17±0.5
6.72	7.40±0.5
8.09	6.30±0.1

TABLE 8. Solvent dependence of exchange rates

(*a*) $CH_3CN \cdot BCl_3$

$PhNO_2$ (*M*)	$1(\tau_{CH_3CN \cdot BCl_3}$ (Hz)		
	−37.1	−42.2	−46.3 (°C)
6.63	6.57	3.86	2.42
5.35	9.17	5.12	2.77
4.76	12.72	6.25	3.42

(*b*) $CH_3CN \cdot BBr_3$

$PhNO_2$ (*M*)	$1/\tau_{CH_3CN \cdot BBr_3}$ (Hz)	
	6.5	0(°C)
9.74	4.65	2.83
9.54	4.80	2.71
4.49	7.09	4.57
4.26	10.4	6.49
2.75	15.2	10.1

For the two competing reactions, [1] and [2],

[1] $CH_3CN \cdot BX_3 \rightarrow CH_3CN + BX_3$

[2] $PhNO_2 + CH_3CN \cdot BX_3 \rightarrow CH_3CN + PhNO_2 \cdot BX_3$

we expect in the first case the adduct peak width $1/\tau_{AB} = k$, and in the second, $1/\tau_{AB} = k[PhNO_2]$, the exact opposite to that shown by the data in Table 8. This slower rate of exchange, and

Can. J. Chem. Downloaded from www.nrcresearchpress.com by 210.87.254.6 on 09/05/12
For personal use only.

perhaps part of the negative entropy of activation at high nitrobenzene concentrations might be explained by a solvent cage effect such as that described by Rutenberg *et al.* (13), which can also result in a lower apparent activation energy. A solvent cage effect which would prevent rapid diffusion of the free acid and base after dissociation could be a partial explanation for both the slower reaction rate and negative entropy of activation (indicative of some ordering process) at higher concentrations of nitrobenzene. At low nitrobenzene concentration the positive entropy of activation observed is consistent with the dissociative process.

Solvent viscosity does not appear to be seriously involved since there is no apparent broadening of the TMS reference line with increasing nitrobenzene concentration.

The observed effect of solvent on activation energies may alternatively be approached from an electrostatic point of view. If the donor–acceptor bond is considered as a dipole $\overset{\delta^- \delta^+}{B—N}$ with Coulombic attraction involved, then the energy to separate the charges will be inversely proportional to the dielectric constant of the medium. Higher concentrations of nitrobenzene (dielectric constant = 34; compared to $CH_2Cl_2 = 9$) will increase the dielectric constant of the medium and lower the energy for charge separation, in agreement with the observations reported above.

Schmulback and Ahmed (14) in a conductometric study of the boron trihalides in acetonitrile solution have shown that BBr_3 and BCl_3 exhibit weak electrolytic behavior and that BX_4^- is present in their solutions. Therefore, the possibility of ionic species being involved in the exchange had to be considered. Reactions of type [3] and [4] may be postulated, or alternately, [5] and [6]. However, for all reactions of this type, the n.m.r. line width for the adduct peak, $1/\tau_{AB}$, would be expected to be concentration dependent, in particular, dependent upon adduct concentration. Since it has been shown above that $1/\tau_{AB}$ is independent of concentration we can, therefore, eliminate ionic species as serious participants in the exchange. In addition, an ionic mechanism would promote more rapid reaction in solutions of higher dielectric constant, the exact opposite to that observed. The ^{19}F n.m.r. spectra of the $CH_3CN \cdot BF_3$ system did not show any BF_4^- present.

[3] $$2CH_3CN \cdot BX_3 \overset{k_1}{\rightleftharpoons} \underset{\text{ion pair}}{[(CH_3CN)_2BX_2^+, BX_4^-]} \overset{k_2\ (\text{slow})}{\rightleftharpoons} (CH_3CN)_2BX_2^+ + BX_4^-$$

[4] $$CH_3CN^* + (CH_3CN)_2BX_2^+ \overset{\text{fast}}{\rightleftharpoons} (CH_3CN)(CH_3CN^*)BX_2^+ + CH_3CN$$

[5] $$(CH_3CN)_2BX_2^+ \overset{k_3\ (\text{slow})}{\rightleftharpoons} CH_3CN + CH_3CNBX_2^+$$

[6] $$CH_3CNBX_2^+ + CH_3CN^* \overset{k_4\ (\text{fast})}{\rightleftharpoons} (CH_3CN)(CH_3CN^*)BX_2^+$$

TABLE 9. Comparison of activation energies with heats of dissociation in solution

Adduct	E_A (kcal/mol)	ΔH_{Dissn} (kcal/mol)	Reference
$CH_3CN \cdot BF_3$	11.2±0.6	12.5	12
$CH_3CN \cdot BCl_3$	17.7±1.0	18.1	9
$CH_3CN \cdot BBr_3$	18.5±1.0	19.1	9

In conclusion we can say that the exchange of excess acetonitrile with acetonitrile–boron trihalide adducts proceeds in absence of solvent complications, via a first order dissociative mechanism

$$CH_3CN \cdot BX_3 \overset{\text{slow}}{\rightleftharpoons} CH_3CN + BX_3$$

$$CH_3CN^* + BX_3 \overset{\text{fast}}{\rightleftharpoons} CH_3CN^* \cdot BX_3$$

The rate of dissociation of these adducts is in the order $BF_3 > BCl_3 > BBr_3$ and the extrapolated activation energies for exchange parallel the dissociation energy of the adducts in solution (see Table 9), in agreement with the accepted order of Lewis acidity, $BBr_3 > BCl_3 > BF_3$.

This work also shows that, unlike the gallium adducts, (5) for which first or second order exchange mechanisms may be explained on steric grounds, this is not the case for boron, since the sterically unhindered acetonitrile exchanges via a first order mechanism.

We thank the National Research Council of Canada and the Ontario Department of University Affairs for financial support, and Dr. J. S. Hartman for helpful discussions.

1. J. M. MILLER and M. ONYSZCHUK. Can. J. Chem. **44**, 899 (1966).
2. J. B. DEROOS and J. P. OLIVER. Inorg. Chem. **4**, 1741 (1965).
3. T. L. BROWN. Accts. Chem. Res. **1**, 23 (1968).

4. A. H. COWLEY and J. L. MILLS. J. Am. Chem. Soc. **91**, 2911 (1969).
5. N. S. HAM and T. MOLE. Progr. Nucl. Mag. Res. **4**, 91 (1969).
6. J. P. OLIVER. Adv. Organometal. Chem. **8**, 167 (1970).
7. K. L. HENOLD, J. B. DEROOS, and J. P. OLIVER. Inorg. Chem. **8**, 2035 (1969).
8. A. L. VAN GEET. Anal. Chem. **40**, 2227 (1968).
9. J. R. BLACKBOROW and J. C. LOCKHART. J. Chem. Soc. A, 3015 (1968).
10. H. C. BROWN. J. Chem. Soc. 1248 (1956).
11. J. R. BLACKBOROW and J. C. LOCKHART. Chem. Commun. 726 (1968).
12. Private communication from M. ONYSZCHUK, McGill University, Montreal, Quebec; calculated for BF_3 in condensed phase.
13. A. C. RUTENBERG, A. A. PALKO, and J. S. DRURY. J. Phys. Chem. **68**, 976 (1964).
14. C. D. SCHMULBACK and I. Y. AHMED. Inorg. Chem. **2**, 508 (1963).

Can. J. Chem. Downloaded from www.nrcresearchpress.com by 210.87.254.6 on 09/05/12
For personal use only.

Five-coordinate Tertiary Phosphine and Arsine Adducts of Copper(hexafluoroacetylacetonate)$_2$

R. A. ZELONKA AND M. C. BAIRD

Department of Chemistry, Queen's University, Kingston, Ontario

Received September 14, 1971

1:1 adducts of copper(hexafluoroacetylacetonate)$_2$ with a number of phosphorous and arsenic ligands have been prepared and characterized by their electronic, infrared, n.m.r. (^{1}H and ^{19}F), and e.s.r. spectra.

Des produits d'addition 1:1 entre l'hexafluoroacétylacétonate de cuivre(II) et un certain nombre de ligands phosphoreux et arséniques, ont été préparés et caractérisés au moyen des spectres électroniques, infrarouges, r.m.n. (^{1}H et ^{19}F), et r.s.e.

Canadian Journal of Chemistry, **50**, 1269 (1972)

Can. J. Chem. Downloaded from www.nrcresearchpress.com by 210.87.254.40 on 09/05/12
For personal use only.

Introduction

The coordination chemistry of copper with tertiary phosphines and arsines has been extensively studied (1, 2) and complexes of these ligands with copper(I) are well known. Copper(II) salts, however, are readily reduced by tertiary phosphines and arsines, and to our knowledge, no copper(II) complexes of phosphines or arsines have been satisfactorily characterized. We have recently reported that the powerful Lewis acid copper(II) hexafluoroacetylacetonate, Cu(hfac)$_2$, forms 1:1 adducts with di-*t*-butyl nitroxide (3) and we now describe reactions of Cu(hfac)$_2$ with tertiary phosphines and related compounds to form five-coordinate 1:1 adducts of the general formula Cu(hfac)$_2$·L. A preliminary report of this work has appeared (4).

Experimental

Anhydrous Cu(hfac)$_2$ was prepared by the method of Bertrand and Kaplan (5) and dried *in vacuo* over sulfuric acid at room temperature. The tertiary phosphines used were purchased from Maybridge Chemical Company, while the compounds $OPPh_3$ (6), $SPPh_3$ (7), $OAsPh_3$ (8), and $SAsPh_3$ (9) were prepared as described in the literature.

Cu(hfac)$_2$·L, L = PPh_3, $PMePh_2$, PMe_2Ph, PEt_3, PBu_3, $AsPh_3$

The complexes were prepared by mixing equimolar amounts of Cu(hfac)$_2$ and the ligand in deaerated, anhydrous cyclohexane under nitrogen. In all cases, the blue Cu(hfac)$_2$ solutions turned deep green. The solvent and any unreacted starting materials (Cu(hfac)$_2$ and the liquid phosphines are volatile) were removed under vacuo at room temperature, leaving a dark green oil of the 1:1 adduct. In the case of PPh_3 and $AsPh_3$, the oil slowly crystallized; the other adducts are liquids at room temperature. The compounds obtained are somewhat unstable, both in the solid state and in solution and could not be purified by recrystallization, sublimation, or distillation. Analytical data are shown in Table 1. The low molecular weight of the arsine adduct suggests that it is largely dissociated in solution.

Cu(hfac)$_2$·L, L = $OPPh_3$, $SPPh_3$, $OAsPh_3$, $SAsPh_3$

The above procedure gave pale green, crystalline 1:1 adducts in all cases except $SPPh_3$, whose adduct was very unstable. Analytical data are shown in Table 1.

Cu(hfac)·2L, L = PPh_3, $AsPh_3$

Addition of PPh_3 to a methanolic solution of Cu(hfac)$_2$ (molar ratio 2.5:1) at room temperature resulted in rapid color changes from light green to dark green to yellow. On concentration of the solution, yellow crystals of the product precipitated in virtually quantitative yield. The same compound was also prepared by heating a 2.5:1 mixture of PPh_3 and Cu(hfac)$_2$ at 90 °C. An extremely malodorous mixture of gases was evolved; n.m.r. and mass spectroscopy showed that the mixture was predominantly hexafluoroacetylacetone, although some unidentified higher weight fluorocarbons were also present.

The orange arsine derivative was obtained in 40% yield by fusing the reactants at 70 °C for 1 h.

Both compounds were recrystallized from methanol. Analytical data are shown in Table 1.

Physical Measurements

Infrared spectra were obtained on Beckman IR-10 and Perkin–Elmer 180 infrared spectrometers, mass spectra on a Jeolco JMS-OISC high resolution mass spectrometer, optical spectra on a Unicam SP820 spectrophotometer, e.s.r. spectra on a Varian V450Z spectrometer with auxiliary equipment, and n.m.r. spectra on a Bruker HX60 spectrometer with internal TMS and hexafluorobenzene lock for proton and fluorine spectra, respectively. Melting points were determined using a Gallenkamp melting point apparatus and are corrected. Molecular weights were determined in deaerated chloroform using a Hewlett–Packard 302B vapor pressure osmometer operating at 37 °C.

Air-sensitive samples were prepared and run under nitrogen as much as possible. Exposure to air, when necessary was kept to a minimum.

Magnetic susceptibilities of the compounds in chloroform solutions were determined by the method of Evans (10). The magnetic moments listed in Table 1 were calculated

TABLE 1. Analytical data

Compound	Melting point (°C)	Analysis						μ_{eff} (B.M.)
		Calculated			Found			
		C(%)	H(%)	Molecular weight	C(%)	H(%)	Molecular weight	
$Cu(hfac)_2 \cdot PPh_3$	65–66.5	45.45	2.32	740	45.57	2.52	740	1.65
$Cu(hfac)_2 \cdot AsPh_3$	66–68	42.90	2.19	784	43.43	2.52	478	1.67
$Cu(hfac)_2 \cdot PMePh_2$	—	40.75	2.23	678	40.47	2.37	698	1.63
$Cu(hfac)_2 \cdot PMe_2Ph$	—	35.11	2.13	616	35.40	2.53	632	1.70
$Cu(hfac)_2 \cdot PEt_3$	—	32.26	2.88	596	32.22	2.82	588	1.74
$Cu(hfac)_2 \cdot PBu_3$	—	38.86	4.30	680	38.48	4.29	683	1.76
$Cu(hfac)_2 \cdot OPPh_3$	98–99	44.49	2.27	754	44.28	2.25	756	1.89
$Cu(hfac)_2 \cdot OAsPh_3$	115–116	42.04	2.14	800	41.85	2.23	752	1.83
$Cu(hfac)_2 \cdot SAsPh_3$	94–95	41.22	2.10	816	41.96	2.24	543	1.80
$Cu(hfac) \cdot 2PPh_3$	153–154	61.93	3.93	795	61.22	3.89	790	Diamagnetic
$Cu(hfac) \cdot 2AsPh_3$	129–130	55.77	3.54	883	55.91	3.45	727	Diamagnetic

using the equation

$$\mu_{eff} = 2.84[(\chi'_M - N\alpha)T]^{1/2}$$

where χ'_M is the molar susceptibility corrected for the diamagnetic susceptibility of the ligands and $N\alpha$ is the temperature-independent paramagnetism of copper(II).

Results and Discussion

Anhydrous $Cu(hfac)_2$ reacts rapidly with tertiary phosphines to form the deep green 1:1 adducts $Cu(hfac)_2 \cdot PR_3$. Although the compounds cannot be purified using standard techniques, the analytical data in Table 1, especially the molecular weights, and the physical properties of the reaction products are completely consistent with their formulation as 1:1 adducts rather than mixtures of reactants. Their structures are presumably square pyramidal, as are similar systems (11). There was no color change and apparently no reaction, on adding tertiary phosphines to solutions of Cu(acetylacetonate)$_2$. This is in accord with the fact that $Cu(hfac)_2$ is a much better Lewis acid than the non-fluorinated derivative (12).

The presence of copper(II) rather than copper(I) is indicated by the magnetic moments, which are close to the expected spin-only value for one unpaired electron. Some of the magnetic moments are somewhat lower than normal; it is possible that partial reduction of the copper occurred in these cases, especially since the compounds decompose slowly in air, even in the solid state. The $OPPh_3$ and $OAsPh_3$ adducts were prepared for purposes of comparison; the former has been incorrectly reported (13) as being an oil. The phosphine and arsine complexes are definitely different from the corresponding oxide complexes, showing that oxidation of the ligands had not occurred, and that the new compounds do contain copper–phosphorous and copper–arsenic bonds.

The infrared spectra of the copper(II) adducts were essentially superpositions of the spectra of $Cu(hfac)_2$ and the phosphines in the region 4000 cm^{-1} to 300 cm^{-1}, the ligand bands shifting at most only a few cm^{-1}.

Nakamoto *et al.* (14) have assigned a weak band at 415 cm^{-1} in the spectrum of $Cu(hfac)_2$ to a Cu—O stretching mode. We find that this band (which appears at 418 cm^{-1} in the spectra of our samples) has an apparent counterpart in the spectrum of hexafluoroacetylacetone, a weak band appearing at 430 cm^{-1}. A new, strong band does appear, however, in the spectrum of $Cu(hfac)_2$ at 279 cm^{-1}, beyond the region scanned by Nakamoto *et al.* Although the latter band seems rather low for a copper–oxygen stretch, we question the previous assignment.

On forming the monoadduct of triphenylphosphine, medium intensity bands at 358 and 323 cm^{-1} in the spectrum of $Cu(hfac)_2$ shift to 353 and 314 cm^{-1}, and strong bands at 279 and 204 cm^{-1} are replaced by a series of bands at 258, 230, 213, and 182 cm^{-1}. Assignments of these bands are difficult at present but may

Can. J. Chem. Downloaded from www.nrcresearchpress.com by 210.87.254.40 on 09/05/12
For personal use only.

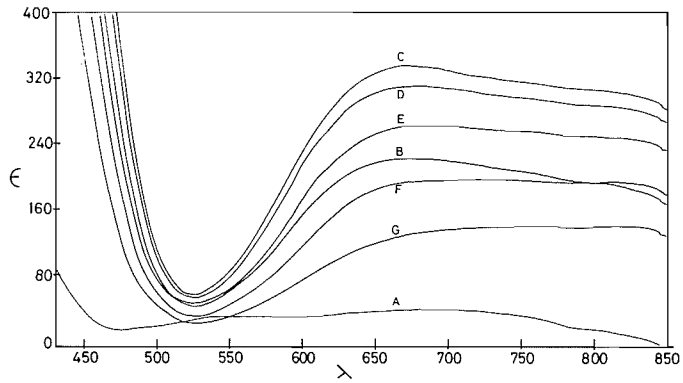

FIG. 1. Visible spectra of cyclohexane solutions of $Cu(hfac)_2$ (5×10^{-3} *M*) in the presence of triphenylphosphine. Phosphine:copper ratios: *A*, 0.0; *B*, 0.50; *C*, 1.0; *D*, 2.0; *E*, 5.0; *F*, 10; *G*, 20.

involve copper–phosphorous and/or copper–oxygen stretching modes.

The optical spectra of solutions of $Cu(hfac)_2$ in the presence of varying concentrations of triphenyl phosphine are shown in Figs. 1 and 2. The predominant changes are large increases in the intensities of the band envelopes in the regions 370–450 and 550–850 mμ as the phosphine:copper ratio increases to approximately unity. The increase in intensity of the low energy (d–d transition) band envelope is indicative of adduct formation, and similar observations have been reported for the 1:1 adducts of $Cu(hfac)_2$ with nitrogen (15, 16) and oxygen (3, 12, 17)

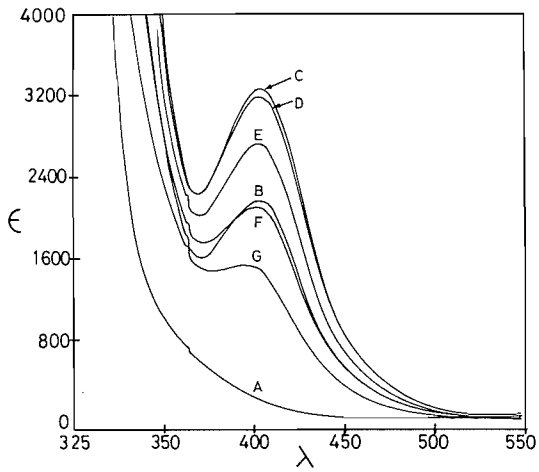

FIG. 2. Ultraviolet–visible spectra of cyclohexane solutions of $Cu(hfac)_2$ (5×10^{-4} *M*) in the presence of triphenylphosphine. Phosphine:copper ratios: *A*, 0.0; *B*, 0.50; *C*, 1.0; *D*, 2.0; *E*, 5.0; *F*, 10; *G*, 20.

TABLE 2. Optical spectra of the copper complexes

Compound	Wavelength* (mμ)	ε (l/mol cm)
$Cu(hfac)_2 \cdot PPh_3$	674	292
	410	1920
$Cu(hfac)_2 \cdot AsPh_3$	680	53
$Cu(hfac)_2 \cdot PMePh_2$	676	172
	391	1740
$Cu(hfac)_2 \cdot PMe_2Ph$	720	140
	380 (sh)	1430
$Cu(hfac)_2 \cdot PEt_3$	746	75
$Cu(hfac)_2 \cdot PBu_3$	740	156
$Cu(hfac)_2 \cdot OPPh_3$	740	52
$Cu(hfac)_2 \cdot OAsPh_3$	812	70
$Cu(hfac)_2 \cdot SAsPh_3$	740	82
$Cu(hfac) \cdot 2PPh_3$	364 (sh)	1160
$Cu(hfac) \cdot 2AsPh_3$	360 (sh)	973

*sh = shoulder.

donors. Funck and Ortolano (18) have recently reported the color changes on adding a series of aryl phosphines to solutions of $Cu(hfac)_2$, although no complexes were isolated and thus no explanation for the spectral changes could be given.

Wavelengths and approximate molar extinction coefficients for the 1:1 adducts studied are listed in Table 2. Since formation of the five-coordinate complexes necessarily causes loss of the inversion center of the molecule, thus relaxing the parity selection rule forbidding d–d transitions, it is reasonable to expect that the increases in the extinction coefficients of the d–d bands are related to the degree of the perturbation of the copper(II) electronic system on formation of the adducts. On this basis, the relative strengths of the interactions would

Can. J. Chem. Downloaded from www.nrcresearchpress.com by 210.87.254.40 on 09/05/12
For personal use only.

Can. J. Chem. Downloaded from www.nrcresearchpress.com by 210.87.254.40 on 09/05/12
For personal use only.

appear to be $PPh_3 > PMePh_2 > PBu_3 > PMe_2Ph > PEt_3$. The extinction coefficient of the arsine derivative is probably low because of partial dissociation. There is no correlation of the band intensities with the basicities of these ligands in polar solvents (19, 20).

As is shown in Figs. 1 and 2, the addition of more than one equivalent of triphenylphosphine to a cyclohexane solution of $Cu(hfac)_2$ results in a decrease in the intensity of the absorption bands in the region 600 to 850 mμ. The decrease in color could be caused by a redox reaction yielding the yellow $Cu(hfac)\cdot 2PPh_3$ (as occurs in methanol) or by the formation of a 2:1 adduct, as has been observed for some nitrogen donors (16). The latter suggestion seems more likely, as the decrease in intensity is not observed in the more polar chloroform, in which a redox reaction might be favored. The reduction in the extinction coefficient can be rationalized in terms of formation of a *trans* 2:1 adduct, since the molecule would become centrosymmetric and the parity selection rule forbidding d–d transitions would apply.

The mass spectra of $Cu(hfac)_2\cdot PPh_3$, $Cu(hfac)_2\cdot PEt_3$, and $Cu(hfac)_2\cdot AsPh_3$ at 70 eV did not show the molecular ion lines, although lines attributable to PPh_3^+, PEt_3^+, and $AsPh_3^+$ were observed. In contrast to the relative intensities of the lines in the mass spectrum of $Cu(hfac)_2$ (21, 22), the lines assigned to the ions $[Cu(hfac)_2]^+$, $[Cu(hfac)_2 - CF_3]^+$, $[Cu(hfac)_2 - 2CF_3]^+$, and $[Cu(hfac)_2 - 4CF_3]^+$ were more intense than the lines corresponding to the ions CF_3^+, $hfac - CF_3^+$, and $hfac^+$. Similar results were reported for the $Cu(hfac)_2$ adduct of di-*t*-butylnitroxide (3). It seems likely that the energy of the ionizing electrons was largely dissipated in breaking the copper–phosphorous or –arsenic bond, leaving the rest of the molecule relatively intact.

The major lines in the mass spectrum of $Cu(hfac)\cdot 2PPh_3$ were attributable to the ions $[Cu(hfac)\cdot PPh_3]^+$, $[CuPPh_3]^+$, and PPh_3^+.

The n.m.r. spectra of the copper(II) complexes were in all cases broadened because of the paramagnetism. In those cases where spectra were obtained, the proton chemical shifts were usually in the "normal" regions for chemically similar diamagnetic compounds or were shifted only slightly. The chemical shifts and linewidths are listed in Table 3. The proton linewidths of the phosphine complexes provide further evidence for their formulation as complexes of copper(II), since the linewidths are much greater than those of the diamagnetic copper(I) complexes, and are even significantly greater than the linewidths of the copper(II) complexes of $OPPh_3$, $OAsPh_3$, and $SAsPh_3$, the correct formulation of which is not in doubt. If the phosphine complexes somehow did not have phosphorous bonded to copper(II), the n.m.r. linewidths should be much smaller.

The ^{19}F resonance of $Cu(hfac)_2$ in chloroform is too broad to observe because of the short fluorine spin–lattice relaxation time induced by the unpaired electron. We have previously shown (3) that spin exchange between $Cu(hfac)_2$ and the stable free radical, di-*t*-butylnitroxide, can cause sufficient electron spin relaxation that the ^{19}F spectrum can be observed. It is now seen that coordination of a tertiary phosphine to $Cu(hfac)_2$ can also shorten the fluorine relaxation time, possibly by delocalization of spin density from the copper(II) into the phosphine ligand via d_π–d_π bonding between copper and phosphorous. Thus the spin density on the fluorine atoms, and hence the linewidth, would be decreased. It is perhaps significant that the order of increasing ^{19}F isotropic shifts from the diamagnetic positions ($PPh_3 < PMePh_2 < PBu_3 < PMe_2Ph < PEt_3$) parallels the order of increasing fluorine resonance linewidths (the $AsPh_3$ derivative is omitted from consideration because of dissociation). The $OPPh_3$, $OAsPh_3$, and $SAsPh_3$ derivatives exhibited no ^{19}F spectra, presumably because the resonances were too broad to be observed.

On the basis of ^{19}F resonance positions and linewidths, the interactions of $Cu(hfac)_2$ is strongest with PPh_3 decreasing along the series. The greatest degree of electronic interaction is expected to remove the largest proportion of electron density from the ^{19}F nuclei, leading to a resonance position exhibiting the smallest isotropic shift relative to the diamagnetic position. This series of relative $Cu(hfac)_2$–phosphine interactions parallels the apparent trend established on the basis of the magnitude of the extinction coefficients of the complexes.

Furthermore, the proton resonances of the neutral ligands of the PEt_3, $OPPh_3$, $OAsPh_3$, and $SAsPh_3$ complexes are relatively narrow, suggesting less delocalization of spin density

TABLE 3. Nuclear magnetic resonance data

Compound		Chemical shift*	Linewidth (p.p.m.) $\Delta\nu_{1/2}$
$Cu(hfac)_2 \cdot PPh_3$	Ph	−7.7	3.3
	Ring	−3.4	2.0
	F	−85.3	5.0
$Cu(hfac)_2 \cdot AsPh_3$	Ph	−8.5, −6.6	2.6
	Ring	−1.2	0.6
	F	†	—
$Cu(hfac)_2 \cdot PMePh_2$	Ph	−7.4	10.0
	Ring	†	—
	Me	−3.1	6.7
	F	−87	35
$Cu(hfac)_2 \cdot PMe_2Ph$	Ph	−7.4	2.4
	Ring	0.0	0.8
	Me	−1.3	3.0
	F	−115	61
$Cu(hfac)_2 \cdot PEt_3$	Ring	†	—
	CH_2	−4.3	5.7
	Me	−1.8	2.3
	F	†	—
$Cu(hfac)_2 \cdot PBu_3$	Ring	0.0	0.3
	Butyl	−0.9, −1.6	2.0
	F	−91	40
$Cu(hfac)_2 \cdot OPPh_3$	Ph	−7.7	0.47
	Ring	−2.4	0.70
	F	†	—
$Cu(hfac)_2 \cdot OAsPh_3$	Ph	−7.3, −7.6, −8.3	1.6
	Ring	−4.0	0.6
	F	†	—
$Cu(hfac)_2 \cdot SAsPh_3$	Ph	−7.3, −7.5, −8.0	1.3
	Ring	−0.12	0.5
	F	†	—
$Cu(hfac) \cdot 2PPh_3$	Ph	−7.28	0.09
	Ring	−5.58	0.08
	F	−84.85	0.31
$Cu(hfac) \cdot 2AsPh_3$	Ph	−7.27	0.10
	Ring	−5.72	0.12
	F	−85.12	0.20

*Protons, p.p.m. downfield from TMS; fluorine, p.p.m. downfield from C_6F_6.
†Not observed.

into these ligands. Calculations suggest (23) that dipolar shifts of the ^{19}F resonances should be negligible in these systems, and thus the isotropic shifts may be expected to be proportional to the spin densities on the fluorine atoms.

The most conclusive evidence for copper–phosphorous bonding was obtained from the e.s.r. spectra of the complexes. The e.s.r. spectrum of $Cu(hfac)_2$ in chloroform solution (g 2.14, $a_{Cu} \sim 71$ G) at room temperature is shown in Fig. 3. The lower field lines are broadened because the tumbling rate does not average out the anisotropies. The spectrum of $Cu(hfac)_2 \cdot PMe_2Ph$ is shown in Fig. 4. The four-line spectrum of copper(II) ($I = 3/2$) is split into eight lines by coupling with the phosphorous ($I = 1/2$). The e.s.r. data for the five phosphine complexes are listed in Table 4. The spectra are all similar, although the overlap of the quartets of the triphenylphosphine adduct is such that a sextet (intensities 1:1:2:2:1:1) is observed. Because of dissociation of the

Can. J. Chem. Downloaded from www.nrcresearchpress.com by 210.87.254.40 on 09/05/12
For personal use only.

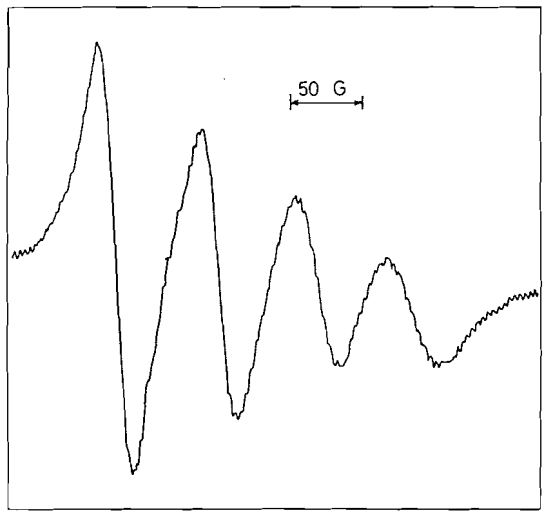

FIG. 3. Electron spin resonance spectra of $Cu(hfac)_2$ in chloroform at 300 °K.

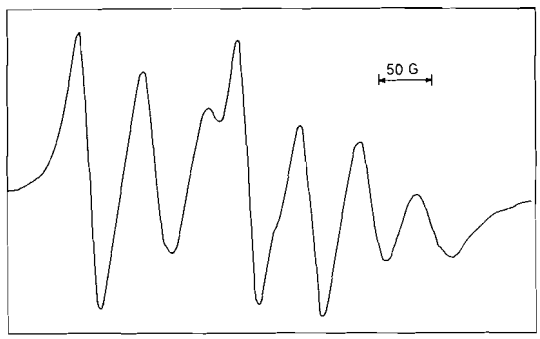

FIG. 4. Electron spin resonance spectrum of $Cu(hfac)_2 \cdot PMe_2Ph$ in chloroform at 300 °K.

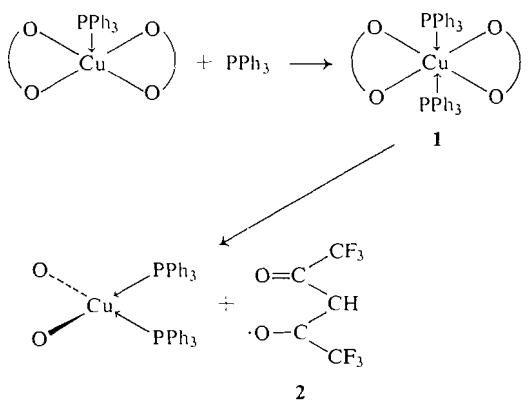

FIG. 5. Suggested mechanism for the reduction of $Cu(hfac)_2 \cdot PPh_3$ to $Cu(hfac) \cdot 2PPh_3$.

TABLE 4. Electron spin resonance data

Compound	g	a_{Cu} (G)	a_p (G)
$Cu(hfac)_2 \cdot PPh_3$	2.13	59	132
$Cu(hfac)_2 \cdot PMePh_2$	2.13	62	140
$Cu(hfac)_2 \cdot PMe_2Ph$	2.14	60	146
$Cu(hfac)_2 \cdot PBu_3$	2.13	58	139
$Cu(hfac)_2 \cdot PEt_3$	2.13	59	137

complex, the spectrum of the triphenylarsine adduct is essentially that of $Cu(hfac)_2$.

The possibility that the observed spectrum is only that of a small amount of a copper(II) impurity can be rejected because the magnetic moments (Table 1) clearly show that the oxidation state of the copper is +2 rather than +1. In addition, the intensities of the lines in the e.s.r. spectra of the phosphine complexes are comparable with the intensities of the lines in the spectrum of $Cu(hfac)_2$, while the g values are quite different.

There have been several recent reports of observations of phosphorous superhyperfine interactions in the e.s.r. spectra of transition metal complexes. Kramolowsky and Schmidt (24) and Cullen and co-workers (25) have studied the e.s.r. spectra of the series of compounds $Fe(NO)_2LX$ (L = tertiary phosphine; X = Cl, Br), observing values of a_p in the region 31–78 G. Henrici-Olivé and Olivé (26), on the other hand, observed phosphorous splittings of 25–36 G for a series of vanadium(IV)–tertiary phosphine complexes. Thus the degree of spin density delocalization from metal-to-phosphorous is somewhat greater in the copper than in the iron and vanadium systems.

Although, as expected, the copper hyperfine splitting is reduced on going from $Cu(hfac)_2$ to the phosphine adducts, there is no correlation between either of these quantities and the isotropic shifts/linewidths of the ^{19}F n.m.r. resonances. Clearly the mechanism of delocalization of spin density from the copper(II) into the ligands is very complicated, and results in the placing of spin density on fluorine, phosphorous, and the organic groups of the coordinated tertiary phosphines.

The mechanism of the reduction of the copper(II) by excess triphenyl phosphine probably involves coordination of a second phosphine to give the unstable, octahedral complex $Cu(hfac)_2 \cdot 2PPh_3$ (Fig. 5, 1). This step could be

Can. J. Chem. Downloaded from www.nrcresearchpress.com by 210.87.254.40 on 09/05/12
For personal use only.

followed by homolytic cleavage of a copper–oxygen σ-bond to form $Cu(hfac)\cdot 2PPh_3$ and the radical **2**. The latter could then abstract a hydrogen atom from, say, a solvent molecule to form hexafluoroacetylacetone. This type of reaction has been suggested by Carty and co-workers (27) as an efficient procedure for the preparation of copper(I) complexes such as $Cu(hfac)\cdot 2PPh_3$.

We thank the International Nickel Company of Canada for a scholarship to R.A.Z. and the National Research Council of Canada for financial assistance. We are also indebted to Dr. J. K. S. Wan for assistance in running the e.s.r. spectra.

1. G. BOOTH. *In* Advances in inorganic chemistry and radiochemistry. Vol. 6. *Edited by* H. J. Emeleus and A. G. Sharpe. Academic Press, New York. 1964. p. 47.
2. W. E. HATFIELD and R. WHYMAN. *In* Transition metal chemistry. Vol. 5. *Edited by* R. L. Carlin. Marcel Dekker, New York. 1969. p. 138.
3. R. A. ZELONKA and M. C. BAIRD. Chem. Commun. 1448 (1970); J. Am. Chem. Soc. **93**, 6066 (1971).
4. R. A. ZELONKA and M. C. BAIRD. Chem. Commun. 780 (1971).
5. J. A. BERTRAND and R. I. KAPLAN. Inorg. Chem. **5**, 489 (1966).
6. C. SRETTAS and A. R. ISBELL. J. Org. Chem. **27**, 2573 (1962).
7. V. MIGIDICHIAN. Organic synthesis. Vol. 1. Reinhold Publishing Corp., New York. 1957.
8. A. W. JOHNSON. J. Org. Chem. **25**, 183 (1960).
9. W. T. REICHLE. Inorg. Chem. **1**, 650 (1962).
10. D. F. EVANS. J. Chem. Soc. 2003 (1959).
11. D. P. GRADDON. Coord. Chem. Rev. **4**, 1 (1969).
12. W. PARTENHEIMER and R. S. DRAGO. Inorg. Chem. **9**, 47 (1970).
13. N. C. LI, S. M. WANG, and W. R. WALKER. J. Inorg. Nucl. Chem. **27**, 2263 (1965).
14. K. NAKAMOTO, Y. MORIMOTO, and A. E. MARTELL. J. Phys. Chem. **66**, 346 (1962).
15. L. L. FUNCK and T. R. ORTOLANO. Inorg. Chem. **7**, 567 (1968).
16. W. R. WALKER and N. C. LI. J. Inorg. Nucl. Chem. **27**, 2255 (1965).
17. C. H. KE and N. C. LI. J. Inorg. Nucl. Chem. **28**, 2255 (1966).
18. L. L. FUNCK and T. R. ORTOLANO. J. Inorg. Nucl. Chem. **33**, 1205 (1971).
19. K. ISSLEIB and H. BRUCHLOS. Z. Anorg. Allg. Chem. **316**, 1 (1962).
20. B. I. STEPANOV, A. I. BOKANOV, and B. A. KOROLEV. Teor. Eksp. Khim. **4**, 354 (1968); Chem. Abstr. **69**, 63 217 (1968).
21. S. SASAKI, Y. ITAGAKI, T. KUROKAWA, K. NAKANISHI, and A. KASAHARA. Bull. Chem. Soc. Jap. **40**, 76 (1967).
22. C. REICHERT, J. B. WESTMORE, and H. D. GESSER. Chem. Commun. 782 (1967).
23. R. A. ZELONKA and M. C. BAIRD. Unpublished results.
24. R. KRAMOLOWSKY and J. SCHMIDT. Z. Naturforsch. **256**, 1487 (1970).
25. J. P. CROW, W. R. CULLEN, F. G. HERRING, J. R. SAMS, and R. L. TAPPING. Inorg. Chem. **10**, 1616 (1971).
26. G. HENRICI-OLIVÉ and S. OLIVÉ. Angew. Chem. Int. ed. **9**, 957 (1970).
27. W. A. ANDERSON, A. J. CARTY, G. J. PALENIK, and G. SCHREIBER. Can. J. Chem. **49**, 761 (1971).

Can. J. Chem. Downloaded from www.nrcresearchpress.com by 210.87.254.40 on 09/05/12
For personal use only.

The Structures of the Trihydroxyflavans from the Acid-catalyzed Rearrangement and Dimerization of 3-Carene-2,5-dione[1]

I. W. J. Still and D. J. Snodin[2]

Lash Miller Chemical Laboratories, Department of Chemistry, University of Toronto, Toronto 181, Ontario

Received October 15, 1971

The structures of the trimethyl ethers of three of the four mechanistically probable trihydroxyflavans derived by acid-catalyzed rearrangement and dimerization of 3-carene-2,5-dione have been assigned on spectroscopic grounds and by analogy with earlier results obtained under conditions which precluded dimerization. Confirmation of these assignments has been obtained by the unambiguous synthesis of two of the isomeric trimethyl ethers from simple aromatic precursors.

Les structures des triméthyl éthers de trois parmi les quatre trihydroxyflavanes possibles quant au mécanisme, et qui dérivent d'une transposition acido-catalysée et d'une dimérisation du carène-3 dione-2,5, ont été attribuées en se fondant sur des données spectroscopiques et par analogie avec des résultats précédents obtenus dans des conditions qui excluent toute dimérisation. La confirmation de ces attributions a été obtenue par une synthèse non ambigüe de deux des triméthyl éthers isomères, à partir de progéniteurs aromatiques simples.

Canadian Journal of Chemistry, **50**, 1276 (1972)

Can. J. Chem. Downloaded from www.nrcresearchpress.com by 210.87.254.40 on 09/05/12
For personal use only.

As part of our investigation of the chemistry of the bicyclo[4.1.0]heptane derivative, 3-carene-2,5-dione (**1**) (1–3) we examined the effect of concentrated hydrochloric acid at room temperature. After a very brief interval a pale brown solid precipitated in 77% yield from the initially clear yellow solution. The same product was obtained on similar treatment of **1** with concentrated sulfuric acid, albeit in lower yield. The nature of this solid product, actually a mixture of isomers, is the subject of the present study.

Preliminary i.r. examination of the solid product revealed intense hydrogen-bonded hydroxyl absorption in the range 3600–3100 and a moderately strong band at 1600 cm^{-1} indicative of aromatic character. A bathochromic shift in the u.v. absorption maximum from 295 to 312 nm on addition of potassium hydroxide to a methanolic solution, and the ready solubility in aqueous alkali provided further indications of the presence of a phenolic group or groups in the product, although ferric chloride tests were consistently negative. The mass spectrum of the product showed an apparent molecular weight of 328, with major fragment ions occurring at *m/e* 165 and 164. The n.m.r. spectrum showed two main sets of broad resonances, in the aromatic region at δ 6.5–8.0 and in the region 0.9–3.2 p.p.m. From the complexity of the spectra in general and from the difficulty in obtaining analytical samples of reproducible melting point, we concluded that we were probably dealing with a mixture of at least two components. Furthermore, because of solubility problems we felt that conversion of the dimeric rearrangement product to a more tractable derivative would be rewarding.

Various attempts at esterification of the product were unsuccessful but methylation with excess methyl sulfate under mild conditions produced a viscous yellow oil which contained only traces of unreacted hydroxyl. A preliminary analysis of this oil by t.l.c. indicated that there were at least three major components present. The mass spectrum of the mixture revealed an apparent molecular weight of 370, indicating the presence of three hydroxyl groups in the original product, all presumably phenolic in nature from the ease of methylation. Column chromatography of the methylated product, using a large ratio of adsorbent (Grade I alumina) to substrate, led to the elution in ether–hexane of four isomeric products, referred to subsequently in the order of elution as methylated dimers **A**–**D**. Relative yields of **A**–**D** and details of the n.m.r. and mass spectra appear in Table 1.

The n.m.r. spectra of **A**, **C**, and **D** confirmed in each case the presence of three methoxyl

[1]Presented in part at the Annual Conference of the Chemical Institute of Canada, Halifax, Nova Scotia, May 31–June 2, 1971.

[2]Postdoctoral Fellow, 1969–1970.

TABLE 1. Spectral data for methylated dimers **A**, **C**, and **D**

Dimer	n.m.r. (δ) in CCl_4				Mass spectra (relative intensity)†	
	Aromatic	OCH_3	CH_2	CH_3		
A (15%)	6.83 (1H, s)	3.77	2.82 (1H, d)	2.12	370	(27)
(*p, p*-)*	6.75 (1H, s)	3.68	1.88 (1H, d)	2.07	192	(100)
	6.55 (1H, s)	3.51	($J = -14$ Hz)	1.58	179	(31)
	6.48 (1H, s)			1.21	178	(23)
				0.66		
B (8%)‡						
(*p, m*-)*						
C (41%)	6.81 (1H, d)	3.72	2.72 (1H, d)	2.20	370	(49)
(*m, p*-)*	6.74 (1H, s)	3.64	1.96 (1H, d)	2.11	192	(100)
	6.50 (1H, s)	3.48	($J = -14$ Hz)	1.63	191	(24)
	6.45 (1H, d)			1.23	179	(73)
	($J = 3$ Hz)			0.69	178	(79)
					177	(24)
D (36%)	6.61 (1H, d)	3.76	2.69 (1H, d)	2.30	192	(42)
(*m, m*-)*	6.55–6.40 (3H, m)	3.65	1.98 (1H, d)	2.23	179	(35)
	($J = 3$ Hz)	3.51	($J = -14$ Hz)	1.66	178	(100)
				1.25	—	—
				0.70	(370, 9%)	

*These designations refer to the disposition of the hydrogens in the benzo- and phenyl rings, respectively, of the flavan system.
†Only relative intensities > 20% are indicated.
‡This is an estimated yield, based on n.m.r. spectra of **B** contaminated with varying amounts of **A** and **C**.

groups and five methyl groups, three of which are attached to sp^3 carbon atoms. Assuming from the original mass spectral evidence that a mixture of dimers ($C_{20}H_{24}O_4$) had been formed, then the fourth oxygen present in addition to the three hydroxyl groups must be accounted for by an ether functionality. At this point, the results of related experiments which we had conducted on the rearrangement of **1** in acetic anhydride–sulfuric acid mixtures (1) led us to the conclusion that the products obtained in the present investigation might well be trihydroxyflavans produced by the acid-catalyzed dimerization of the *o*-isopropenylphenols, **4** and **5**, arising from acid-catalyzed ring opening of the cyclopropane ring in **1**. The facility of flavan formation in such cases had been demonstrated earlier by Baker and his collaborators (4). The selectivity of the acid-catalyzed opening of the cyclopropane ring in **1**, apparent in our earlier study (1), is not so evident from the distribution of both "symmetrical" (**A** and **D**) and "mixed" (**B** and **C**) products in Table 1. This may be regarded as supporting evidence for our contention that the reaction leading to the formation of the phenolic diacetates described in ref. 1 is actually initiated by acetylium ions rather than by protons, giving rise to the observed selectivity by virtue of the much greater difficulty of electrophilic attack by a bulky ion at the sterically crowded C-2 carbonyl group site. The mechanism proposed for the formation of the trihydroxyflavans in the present reaction appears in Scheme 1. Further evidence in support of our gross structural assignment arises from the presence of major fragment ions in the mass spectra of **A**, **C**, and **D** at *m/e* 192 and 178. This

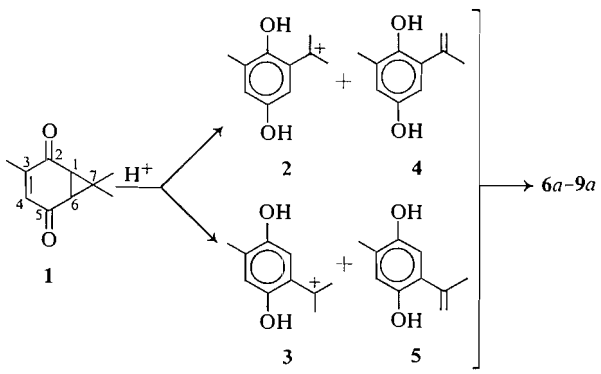

SCHEME 1

Can. J. Chem. Downloaded from www.nrcresearchpress.com by 210.87.254.40 on 09/05/12
For personal use only.

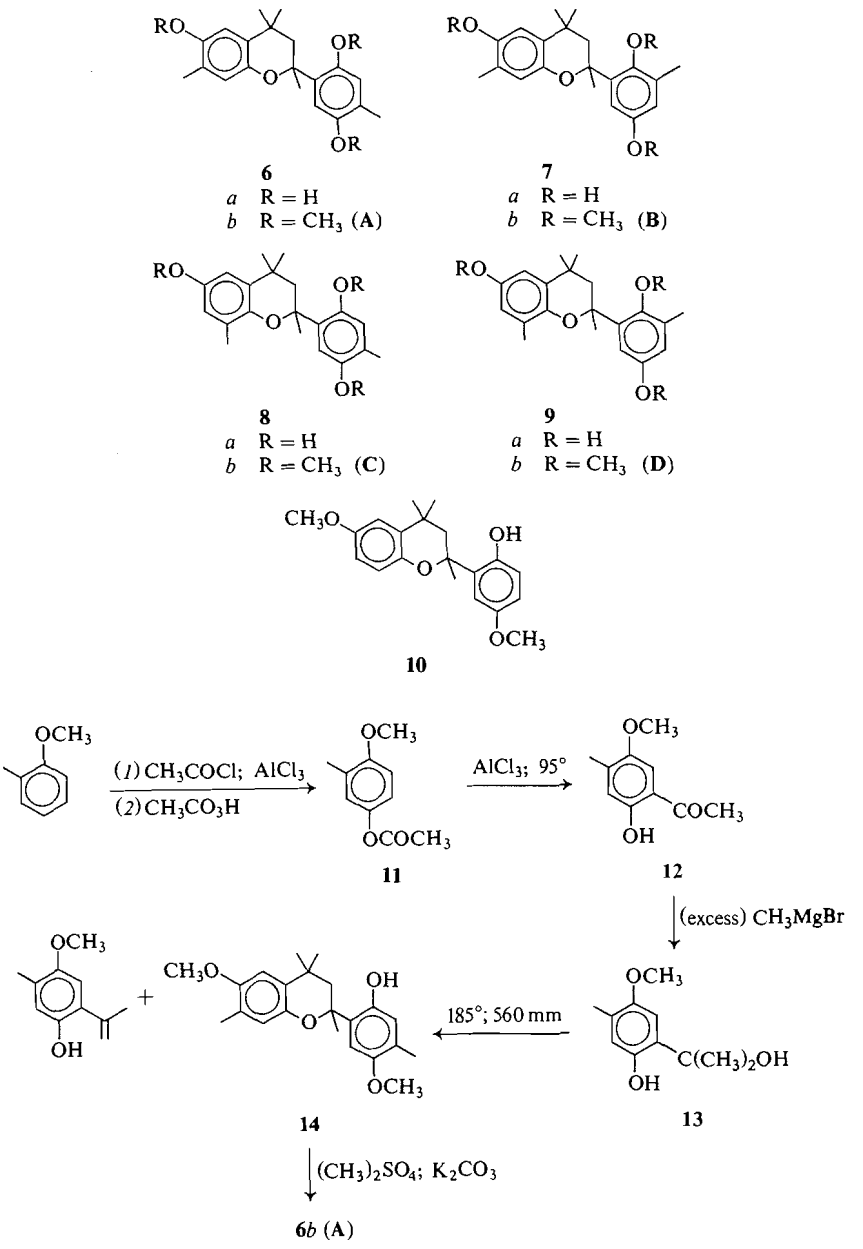

SCHEME 2

is indicative of a *retro*-Diels–Alder type of disintegration, observed previously (5–7) as being characteristic of flavan derivatives.

The individual assignments of structures **6***b*–**9***b* to the methylated products **A**–**D** respectively, and hence of structures **6***a*–**9***a* to the original phenolic products, were made largely on the basis of the n.m.r. spectra and in particular from an inspection of the aromatic region. The spectrum of methylated dimer **A** revealed four singlets of equal intensity between δ 6.48 and 6.83 p.p.m. and thus the *p*,*p*-relationship of the hydrogens in each aromatic ring, as represented in structure **6** was assigned. On the

Can. J. Chem. Downloaded from www.nrcresearchpress.com by 210.87.254.40 on 09/05/12
For personal use only.

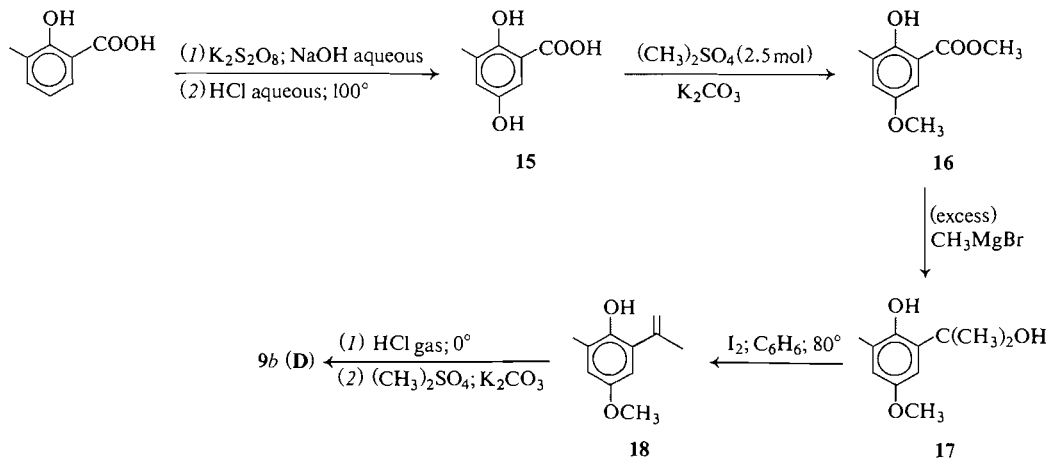

SCHEME 3

other hand, the dimer **D** was assigned structure **9** because its spectrum possessed the most complex aromatic region, δ 6.40–6.55 (m, 3H) and 6.61 (1H, d, $J = 3$ Hz), in accord with expectation for the *m*-orientation of the hydrogens in both aromatic rings. The structural assignments for both **A** and **D** have been confirmed by unambiguous syntheses (see Schemes 2 and 3).

The remaining dimers **B** and **C** resulting from "mixed" coupling of the carbonium ion precursors **2** and **3** with the isopropenylphenols **4** and **5** were more difficult to differentiate. Methylated dimer **C** was assigned structure **8** on the following grounds. Mechanistic analogy to the result obtained in the acetic anhydride – sulfuric acid system (1) and the observed preponderance of **D** over **A** (see Table 1) suggests that formation of carbonium ion **2** would be preferred and thus one might reasonably expect that the *m,p*-mixed dimer would be formed in greater amount than the *p*-, *m*-mixed dimer. The methylated dimer **B** could never be obtained free of contamination with **A** and **C**, and thus analytical, n.m.r., and mass spectral data are not reported for this isomer. The general similarity of its i.r., u.v., and n.m.r. spectra, to those of **A**, **C**, and **D**, however, as well as very similar elution properties lead us very tentatively to assign the remaining mechanistically probable structure **7** to this isomer. One remaining feature of interest in the n.m.r. spectra of **A**, **C**, and **D** is the relatively large chemical shift difference (0.71–0.94 p.p.m.) observed for the two methylene protons in the heterocyclic rings of the flavans. Bowman *et al.* (8) have observed a similar difference (0.70 p.p.m.) and an identical coupling constant ($J = -14$ Hz) for the two methylene protons in the closely related structure **10**.

The synthetic routes to the methylated dimers **A** and **D** from *o*-methylanisole and 2-hydroxy-3-methylbenzoic acid (*o*-cresotic acid), respectively, are illustrated in Schemes 2 and 3, and were generally straightforward, with satisfactory yields being obtained in all steps. In Scheme 2, dehydration of **13** proceeded almost quantitatively, producing a mixture of the monomeric and dimeric dehydration products in a ratio of 1:4. In Scheme 3, the crucial hydroxylation step to produce the dihydroxybenzoic acid derivative **15** with the desired substitution pattern proceeded in 43% yield (9). The iodine-catalyzed dehydration of the tertiary alcohol **17** produced the monomeric *o*-isopropenylphenol **18** almost quantitatively and strong acid catalysis was required to produce dimerization. The presumed intermediate monohydroxy-dimethoxyflavan was not isolated and the synthesis of **9***b* was completed by methylation. The synthetic routes provide additional, indirect support for the mechanistic scheme already described in Scheme 1, in that an *o*-isopropenylphenol derivative is a presumed intermediate in each case.

Experimental

General

The i.r. spectra (cm^{-1}) in CCl_4 solution or as otherwise specified were recorded on a Perkin–Elmer 337 grating spectrophotometer and the u.v. spectra (in methanol) on a

Can. J. Chem. Downloaded from www.nrcresearchpress.com by 210.87.254.40 on 09/05/12
For personal use only.

Can. J. Chem. Downloaded from www.nrcresearchpress.com by 210.87.254.40 on 09/05/12
For personal use only.

Unicam SP 800 recording instrument. The n.m.r. spectra (δ) were obtained on Varian A-60 and HA-100 instruments in the solvents specified, using tetramethylsilane as the internal standard. Mass spectra were recorded on a Bell and Howell 21-490 spectrometer and the elemental analyses were performed by A. B. Gygli, 329 St. George Street, Toronto and by the Scandinavian Microanalytical Laboratory, Herlev, Denmark. Column chromatography was performed using silica gel (Davison Chemical, Grade 923, 100–200 mesh) or neutral alumina (Fisher Grade I, 80–200 mesh) and Fisher A.C.S. grade solvents. All melting points and boiling points are uncorrected.

*3-Carene-2,5-dione (**1**)*

This compound was synthesized and purified by a previously published procedure (10).

*Reaction of **1** with Concentrated HCl*

3-Carene-2,5-dione (2.0 g) was finely powdered and added rapidly to concentrated HCl (50 ml) with stirring at 25 °C. After 2–3 min a pale brown precipitate appeared and the acid solution was poured into iced water (100 ml). The precipitate was filtered off, washed thoroughly with ice-cold water, 5% sodium hydrogen carbonate solution, and finally again with ice-cold water before drying in a vacuum desiccator for 2 days. The crude product (1.55 g, 77%) was recrystallized from a variety of mixed solvents such as ether–hexane, methylene chloride–petroleum ether (30–60°) but no purified sample with a range of melting of less than 5° could be obtained. (The melting points varied from 160–190° depending on the solvent system used.)

The mass spectrum of this product showed an apparent molecular ion at *m/e* 328, while the n.m.r. spectrum (acetone-d_6) looked exceedingly complex. The i.r. spectrum showed a broad OH band at 3600–3100 and prominent peaks at 1600 and 1485 indicative of aromatic character. The u.v. spectrum showed a prominent maximum at 295 nm (ε, 7000).

Methylation of Mixture of Dimers

The product (1.05 g) obtained as described above was methylated under standard conditions with an excess of methyl sulfate in acetone in the presence of anhydrous potassium carbonate. Examination of the i.r. spectrum of the viscous yellow oil (1.13 g) so obtained revealed almost no residual OH absorption bands. Chromatography of the crude methylation product on alumina (850 g) and examination of the fractions by following changes in the intensity of the 295 nm band in the u.v. led to the isolation of four main fractions designated **A**, **B**, **C**, and **D** in the order of their elution. The product **A** began to elute with 12% ether–hexane and the last traces of **D** were eluted with ether. The four isomers accounted for essentially all of the substrate chromatographed. The i.r. spectra of **A**–**D** showed general similarities with no hydroxyl or carbonyl absorption and peaks characteristic of —OCH_3 at 2830, as well as the aromatic bands at 1600 and 1490. The details of the n.m.r. and mass spectra of **A**, **C**, and **D**, as well as the relative yields of the methylated dimers, appear in Table 1.

Methylated dimer **A**, **6***b* was recrystallized from methanol, m.p. 115–116°.

Anal. Calcd. for $C_{23}H_{30}O_4$: C, 74.56, H; 8.16. Found: C, 74.72, H; 8.09.

Methylated dimer **C**, **8***b* was recrystallized from 60% aqueous ethyl alcohol, m.p. 96.5–97.5°.

Anal. Calcd. for $C_{23}H_{30}O_4$: C, 74.56; H, 8.16. Found: C, 74.71; H, 8.13.

Methylated dimer **D**, **9***b* was recrystallized from 50% aqueous ethyl alcohol, m.p. 94–94.5°.

Anal. Calcd. for $C_{23}H_{30}O_4$: C, 74.56; H, 8.16. Found: C, 74.82; H, 7.96.

*4-Methoxy-3-methylphenyl Acetate (**11**)*

4-Methoxy-3-methylacetophenone (11) was converted to 4-methoxy-3-methylphenyl acetate by the procedure of Bowman *et al.*, (8). The product was obtained as a pale yellow oil (19.2 g, 51%), b.p. 136–138°/20 mm; i.r. 2835, 1770, 1503, 1210; n.m.r. ($CHCl_3$-d_1) 2.24 (3H, s), 2.29 (3H, s), 3.80 (3H, s), and 6.85 (3H, m) p.p.m. The mass spectrum showed the expected molecular ion at *m/e* 180 (17) and major fragment ions at *m/e* 138 (100) and 123 (68).

Anal. Calcd. for $C_{10}H_{12}O_3$: C, 66.65; H, 6.71. Found: C, 66.42; H, 6.73.

*2-Hydroxy-5-methoxy-4-methylacetophenone (**12**)*

Fries rearrangement of **11** (18.4 g) was carried out by adding aluminum chloride (15 g) to the ice-cold acetate. A vigorous reaction occurred as the flask warmed up to room temperature. The reaction mixture was then stirred at 90° for 16 h before cooling and adding 2 *N* HCl (80 ml). The resulting yellow solid was extracted with ether and the combined extracts in turn extracted thoroughly with cold 2 *N* NaOH solution. The alkaline solution was strongly acidified with concentrated HCl and the product steam-distilled (a total of 1100 ml was collected). Extraction of the phenol with ether gave, on evaporation of the dried extract, a yellow solid (7.8 g). Recrystallization from aqueous ethyl alcohol afforded **12** as small yellow needles (5.9 g, 38%), m.p. 108–109°. (Some unreacted starting material was recovered from the neutral fraction in the original ethereal extract.) The i.r. 2850, 2830, 1650, 1630 (sh), 1585, 1495; n.m.r. ($CHCl_3$-d_1) 2.22 (3H, s), 2.57 (3H, s), 3.82 (3H, s), 6.78 (1H, s), and 6.99 (1H, s); u.v. λ_{max} 230 (ε, 16 100), 265 (ε, 9900), 352 nm (ε, 5100). The mass spectrum showed the expected molecular ion at *m/e* 180 (63) and further peaks at 165 (100), 147 (11), and 137 (10).

Anal. Calcd. for $C_{10}H_{12}O_3$: C, 66.65; H, 6.71. Found: C, 66.64; H, 6.70.

*2-(2-Hydroxy-5-methoxy-4-methylphenyl)-2-propanol (**13**)*

The substituted acetophenone, **12** (2.83 g, 0.016 mol) in ether (15 ml) was added to a refluxing ethereal solution of methylmagnesium bromide, prepared from magnesium (1.13 g, 0.047 g-atom) and excess methyl bromide. After refluxing the reaction mixture for 1 h under N_2, saturated ammonium chloride solution (10 ml) was added dropwise until a clear supernatant ethereal layer was obtained. Separation and drying of the ethereal layer gave on evaporation a white solid. Recrystallization from petroleum ether (b.p. 60–70°) with the aid of charcoal gave the expected tertiary alcohol (2.53 g, 82%); m.p. 70–71°; i.r. 3640, 3420, 2815, 1495; n.m.r. ($CHCl_3$-d_1) 1.63 (6H, s), 2.14 (3H, s), 3.74 (3H, s), 5.13 (1H, s), 6.57 (1H, s), 6.67 (1H, s). (The phenolic proton was not detected.) The mass spectrum showed a molecular ion at *m/e* 196 (20) and major fragment ions at 178 (100) and 163 (76).

Can. J. Chem. Downloaded from www.nrcresearchpress.com by 210.87.254.40 on 09/05/12
For personal use only.

Anal. Calcd. for $C_{11}H_{16}O_3$: C, 67.32; H, 8.22. Found: C, 67.12; H, 8.11.

Dehydration of ***13****: Formation of 2-(2-Hydroxy-5-methoxy-4-methylphenyl)-6-methoxy-2,4,4,7-tetramethylchroman (****14****)*

The tertiary alcohol **13** (2.75 g) was heated at 185°/580 mm for 1 h and a product (0.37 g, 18%), b.p. 174–176°/11 mm, was collected. This was shown to be the expected *o*-isopropenylphenol derivative (see Scheme 2) arising from simple dehydration; i.r. 3530, 2830, 1620, 1500, and 911; n.m.r. ($CHCl_3$-d_1) 2.11 (3H, s), 2.17 (3H, s), 3.76 (3H, s), 5.13 (1H, bs), 5.31 (1H, bs), 5.52 (1H, bs), 6.60 (1H, s), and 6.70 (1H, s).

The glassy residue in the distilling flask was extracted with hot benzene and the solvent evaporated. Trituration with petrol afforded white crystals of **14**, (2.06 g, 81%) which were recrystallized from petroleum ether (b.p. 60–70°, m.p. 106–107°; i.r. 3420, 2830, 1500; n.m.r. ($CHCl_3$-d_1) 1.13, 1.39, 1.70, 2.12, 2.18, 3.70, 3.77 (each 3H, s) 2.0 (1H, d), and 2.67 (1H, d)($J = -14$ Hz), 6.69 (4H, m), and 7.56 (1H, s). The mass spectrum showed the expected molecular ion at *m/e* 356 (42) and major fragment ions at *m/e* 180 (13), 179 (96), 178 (100), and 163 (16).

Anal. Calcd. for $C_{22}H_{28}O_4$: C, 74.13; H, 7.92. Found: C, 74.15; H, 7.89.

*2-(2,5-Dimethoxy-4-methylphenyl)-6-methoxy-2,4,4,7-tetramethylchroman (****6b****)*

Methylation of **14** (0.95 g) using methyl sulfate and anhydrous potassium carbonate in acetone under standard conditions afforded the expected methyl ether, ***6b*** (0.87 g, 88%), m.p. 114–115° on recrystallization from aqueous ethyl alcohol, undepressed on admixture with a pure sample of methylated dimer, **A**. The i.r., n.m.r., and mass spectra of the synthetic sample were identical with those of dimer **A**.

*2,5-Dihydroxy-3-methylbenzoic Acid (****15****)*

A solution of 2-hydroxy-3-methylbenzoic acid (Eastman Kodak) (10 g, 0.067 mol) in 10% NaOH solution (125 ml), was cooled to 10° and a saturated aqueous solution of potassium perdisulfate ($K_2S_2O_8$) (18 g in 350 ml, 0.067 mol) was added with stirring, over a period of 5 h. During this period, the temperature was never allowed to rise above 15°. The reaction was then stirred overnight at 25° before acidifying first with solid CO_2 and then to p*H* 4 with 2 *N* HCl. Extraction with ether and washing the ethereal extract (water, saturated brine) afforded on drying ($MgSO_4$) and evaporation some unreacted starting material (4.6 g); i.r. (Nujol) 3250–2300, 1670, 1605; m.p. 166–167°, undepressed on admixture with 2-hydroxy-3-methylbenzoic acid.

The p*H* of the residual aqueous solution was readjusted to about p*H* 8 with (solid) $NaHCO_3$, and the solution evaporated to dryness at 60°, under vacuum. The brown solid residue was extracted thoroughly on the steam bath with three portions of 90% aqueous ethyl alcohol (500 ml in total) according to the modified procedure of Baker and Brown (9). The residue (6.5 g) obtained on evaporation was then hydrolyzed on the steam bath with 2 *N* HCl for 1 h, in the presence of a layer of ether. Removal of the ethereal layer, washing (brine), and drying ($MgSO_4$) gave the crude dihydroxybenzoic acid derivative (3.9 g) which afforded the expected product (2.65 g, 43%) on recrystallization from 20% aqueous ethyl alcohol; m.p. 222–223° (dec.) (lit (12) m.p. 215° (dec.)); i.r. (Nujol) 3290–2400, 1660, 1605; n.m.r. (DMSO-d_6) 2.18 (3H, s), 6.97 (1H, d, $J = 3.2$ Hz), and 7.14 (1H, d, $J = 3.2$ Hz) p.p.m. (The acidic protons were unobservable.) The mass spectrum showed the expected molecular ion at *m/e* 168 (46) and major fragment ions at 150 (100) and 121 (74).

Anal. Calcd. for $C_8H_8O_4$: C, 57.14; H, 4.80. Found: C, 56.76; H, 4.86.

*Methyl 2-Hydroxy-5-methoxy-3-methylbenzoate (****16****)*

Esterification of the acid **15** was accompanied by concomitant methylation of the unhindered phenolic group when carried out by treating **15** (2.37 g, 14.5 mmol) with methyl sulfate (4.5 g, 36 mmol) and anhydrous potassium carbonate (5.0 g) in anhydrous acetone (20 ml). After refluxing for 2 h and stirring at room temperature overnight, the product was isolated as a semi-solid material (3.5 g). Chromatography on silica gel (80 g) and elution with 10% ether–benzene led to the recovery of pure **16** (1.71 g, 62%), m.p. 78–79° on recrystallization from petroleum ether (b.p. 60–70°); i.r. 3200, 2835, 1685, 1615; n.m.r. (CCl_4) 2.22 (3H, s), 3.68 (3H, s), 3.89 (3H, s), 6.83 and 6.97 (each 1H, d, $J = 3.2$ Hz), 10.44 (1H, s) p.p.m. The mass spectrum showed the expected molecular ion at *m/e* 196 (41), with major fragment ions at 164 (100), 136 (23), and 121 (14).

Anal. Calcd. for $C_{10}H_{12}O_4$: C, 61.21; H, 6.17. Found: C, 61.54; H, 6.44.

*2-(2-Hydroxy-5-methoxy-3-methylphenyl)-2-propanol (****17****)*

The ester **16** (1.5 g, 7.5 mmol) in ether (35 ml) was added to a refluxing solution of methylmagnesium bromide, prepared from magnesium (0.65 g, 0.0265 g-atom) and excess methyl bromide in ether (15 ml) over 0.75 h and the reaction mixture refluxed for a further 2 h. Addition of saturated ammonium chloride solution (15 ml), extraction with ether, and evaporation afforded a pale brown solid (1.46 g) which gave a white solid (0.99 g, 66%) on recrystallization from petroleum ether (b.p. 60–70°), m.p. 99–100°; i.r. (Nujol) 3415, 3165, 2850, and 1605; n.m.r. ($CHCl_3$-d_1) 1.60 (6H, s), 2.21 (3H, s), 3.70 (3H, s), 4.73 (1H, s), 6.52 and 6.66 (each 1H, d, $J = 3.0$ Hz) p.p.m. The mass spectrum showed the expected molecular ion at *m/e* 196 (23), and major fragment ions at *m/e* 179 (21), 178 (100), 163 (37), 135 (11), 131 (31), and 119 (14).

Anal. Calcd. for $C_{11}H_{16}O_3$: C, 67.32; H, 8.22. Found: C, 67.08; H, 8.02.

*2-(2-Hydroxy-5-methoxy-3-methylphenyl)propene (****18****)*

The tertiary alcohol **17** (490 mg) was refluxed for 5 h in anhydrous benzene (10 ml) containing iodine (5 mg). The cooled reaction mixture was washed successively with 5% sodium hydrogen sulfite solution, water, and saturated brine. Drying ($MgSO_4$) and evaporation afforded a mobile colorless oil (412 mg, 93%). The i.r. spectrum (liquid film) showed peaks at 3520, 2835, 1605, and 910, and the n.m.r. spectrum (CCl_4) 2.05, 2.18, 3.66 (each 3H, s), 5.08 (1H, bs), 5.16 (1H, s), 5.31 (1H, bs), 6.36 (1H, d, $J = 3.2$ Hz), and 6.50 (1H, d, $J = 3.2$ Hz) p.p.m. were in accord with expectation for the simple dehydration product **18**.

*2-(2,5-Dimethoxy-3-methylphenyl)-6-methoxy-2,4,4,8-tetramethylchroman (****9b****)*

Anhydrous hydrogen chloride was bubbled through the

o-isopropenylphenol derivative **18** (380 mg) for 15 min at $-10°$ (*cf.* Baker *et al.* (4)) and the reaction mixture allowed to warm to 25° (1 h). Excess iced water (100 ml) was added and the product extracted with ether. Washing the ethereal extracts (water, $NaHCO_3$ solution, water, and saturated brine), drying ($MgSO_4$), and evaporation afforded a very viscous pale yellow gum (355 mg) which did not crystallize on standing or cooling. Further purification was not attempted and the viscous oil was dissolved in anhydrous acetone (10 ml) containing methyl sulfate (200 mg) and anhydrous potassium carbonate (250 mg). After refluxing the mixture for 2 h and stirring overnight at 25°, the methylation product was isolated as a yellow gum (375 mg). Chromatography on silica gel (80 g) gave, on elution with 7% ether in benzene, a fraction (179 mg) which partly crystallized on standing. Isolation of the solid product (65 mg), m.p. 93–95°, was achieved by adding ice-cold pentane and thorough washing with the same solvent. The melting point of the product on admixture with pure methylated dimer "**D**" was undepressed (91–94°), and the identity of the two materials was further confirmed by comparison of the i.r., n.m.r., and mass spectra.

We thank the National Research Council of Canada for generous support of this work. Preliminary experiments by Mr. R. W. Mulligan and Mr. G. W. Nathan are gratefully acknowledged.

1. I. W. J. Still and G. W. Nathan. Can. J. Chem. **48**, 1013 (1970).
2. I. W. J. Still, C. J. Macdonald, and Y.-N. Oh. Can. J. Chem. **48**, 1526 (1970).
3. I. W. J. Still and D. T. Wang. Can. J. Chem. **46**, 1583 (1968).
4. W. Baker, D. F. Downing, A. E. Hewitt-Symonds, and J. F. W. McOmie. J. Chem. Soc. 3796 (1952), and references therein.
5. A. Pelter, P. Stainton, and M. Barber. J. Heterocycl. Chem. **2**, 262 (1965).
6. K. Heyns and H.-F. Grutzmacher. Ann. **675**, 134 (1964).
7. R. G. Cooke and J. G. Down. Tetrahedron Lett. 1037 (1970).
8. D. F. Bowman, F. R. Hewgill, and B. R. Kennedy. J. Chem. Soc. (C) 2274 (1966).
9. W. Baker and N. C. Brown. J. Chem. Soc. 2303 (1948).
10. G. L. Buchanan, R. A. Raphael, and I. W. J. Still. J. Chem. Soc. 4372 (1963).
11. G. Stadnikoff and A. Baryschewa. Ber. **61**, 1996 (1928).
12. Chemische Fabrik Schering. Deut. Rep. Pat. 81 297 (1895).

Can. J. Chem. Downloaded from www.nrcresearchpress.com by 210.87.254.40 on 09/05/12
For personal use only.

Oligoribonucleotide Synthesis. IV.[1] Approach to Block Synthesis

EVA S. WERSTIUK AND THOMAS NEILSON

Department of Biochemistry, McMaster University, Hamilton, Ontario

Received August 3, 1971

A convenient block synthesis for oligoribonucleotides of predetermined sequence is developed. Preparation and deblocking of protected tetranucleotide, Ph_3COCH_2CO.O-U(Thp)p(Cl_3Et)A^{bz}(Thp)p(Cl_3Et)U(Thp)p-(Cl_3Et)A^{bz}(Thp)-OH (**8**) to give UpApUpA is described. Phosphorylation of HO-U(Thp)-OH derivative (**1**; R = Ph_3COCH_2CO) and subsequent coupling with HO-A^{bz}(Thp)-OH (**4**) gave protected UpA (**5**). Specific removal of triphenylmethoxyacetyl group from **5** is accomplished by dilute methanolic ammonia. 5′-Hydroxyl group of resulting UpA derivative (**7**) is condensed with the 3′-phosphate derivative of **5** to give **8** in good overall yield.

Ease of mild alkaline cleavage, convenient ceric sulfate spray detection and enhancement of solubility, make the triphenylmethoxyacetyl group an excellent choice for 5′-protection of nucleoside derivatives.

Une synthèse commode des oligoribonucléotides de séquence déterminée est développée. La préparation et la déprotection du tétranucléotide (**8**), Ph_3COCH_2CO.O-U(Thp)p(Cl_3Et)A^{bz}(Thp)p(Cl_3Et)UThp)p-(Cl_3Et)A^{bz}(Thp)-OH en UpApUpA est décrite. La phosphorylation du dérivé (**1**) de HO-U(Thp)-OH (où R = Ph_3COCH_2CO) et le couplage ultérieur avec **4** = HO-A^{bz}(Thp)-OH donnant **5** = UpA protégé. L'enlèvement spécifique du groupe triphénylméthoxyacétyle sur **5** est effectué par une solution diluée d'ammoniac dans le méthanol. Le groupe hydroxyl-5′ du dérivé UpA **7** qui en résulte, est condensé sur le groupe phosphate au 3′ de **5** pour donner **8** avec un bon rendement global.

La facilité du clivage alcalin dans des conditions douces, la détection commode par pulvérisation de sulfate cérique et l'accroissement de la solubilité font du groupe triphénylméthoxyacétyle un réactif de choix pour la protection en 5′ de dérivés nucléosides.

Canadian Journal of Chemistry, **50**, 1283 (1972)

Synthesis of "tailor-made" oligoribonucleotides of defined length and sequence to function as model transfer RNAs in various site recognition studies, is an attractive proposition (1). Already some oligoribonucleotide fragments from enzymic digestions on native molecules have shown similar but reduced activities relative to their precursors (2, 3). To determine the exact points of interaction within these fragments, series of oligoribonucleotides with single base changes should be prepared and their binding assayed.

Chemical synthesis of oligoribonucleotides is still in the developmental stage, the literature (1, 4–7) only offers the preparation of trinucleotides. Deoxyoligoribonucleotide synthesis on the other hand, is more advanced because use is made of fragment coupling methods in which short sequences prepared by a stepwise method are linked together to give sequences of greater length. One example of a block synthesis being applied to the preparation of oligoribonucleotide has been reported (8). However, the conditions necessary for coupling protected trinucleotides, caused extensive cleavage to the starting material. Perhaps triisopropylbenzenesulfonyl chloride (TPS) activation of the phosphodiester linkages of these protected trinucleotides promoted undesirable coupling at the diphosphate centers producing unstable phosphotriester intermediates (attachment of three ribofuranosyl residues to one phosphate) which break down on work-up giving mixtures of many different species containing phosphodiester linkages.

Elimination of these undesirable side-reactions should be possible using protected trinucleotides which contain phosphotriester linkages, the "third" ester substituent being the easily removable β,β,β-trichloroethyl. Only the phosphate destined to become the new internucleotidic link should be allowed to be secondary. TPS activation in pyridine should be inert towards phosphotriester centers and reaction restricted to the terminal diphosphate sites ensuring linear sequences and excluding branched species. In a previous communication, a stepwise synthesis for short oligoribonucleotides using phosphotriester intermediates was described (1). However, in order to couple these

[1]For part III, see ref. 1.

Can. J. Chem. Downloaded from www.nrcresearchpress.com by 210.87.254.6 on 09/05/12
For personal use only.

Can. J. Chem. Downloaded from www.nrcresearchpress.com by 210.87.254.6 on 09/05/12
For personal use only.

short sequences, the 5′-trityl group must be removed specifically so that a new internucleotide link can be created at that 5′-position. Unfortunately, acid hydrolysis necessary for cleavage also deblocks the tetrahydropyranyl groups which protect the hydroxyls at the 2′-positions. A new protecting group to substitute for the terminal 5′-trityl group was sought bearing in mind that its removal conditions must be neutral, but not catalytic, or mildly alkaline.

A 2,4-dinitrobenzenesulfenyl group appeared to be a reasonable choice, its removal being effected by hydrogen sulfide in pyridine. 5′-(2,4-Dinitrobenzenesulfenyl)-2′-*O*-tetrahydropyranyluridine (**1**; R = 2,4-dinitrobenzenesulfenyl) was prepared from 2′-*O*-tetrahydropyranyluridine (**1**; R = H) (9) using a literature method (10). However, on phosphorylation with *β*,*β*,*β*-trichloroethyl phosphate and TPS in pyridine (11), the dinitrobenzenesulfenyl group was found to be too sensitive and this approach had to be abandoned.

Various substituted acetates were next considered. Sensitivity to alkaline cleavage increases in the series: acetate, methoxyacetate, and phenoxyacetate, the last two being removed by dilute methanolic ammonia in 1–2 h (12). Since ammonolysis of benzamido groups on the heterocyclic bases required 1–2 days under the same conditions, specific de-*O*-acylation should be possible at position 5′. 5′-*O*-Methoxyacetyl-2′-*O*-tetrahydropyranyluridine (**1**; R = $MeOCH_2CO$—) was prepared from 2′-*O*-tetrahydropyranyluridine (**1**; R = H) (9). Phosphorylation with *β*,*β*,*β*-trichloroethyl phosphate and TPS (11) was successful but on work-up, the pyridinium salt (**2**; R = $MeOCH_2CO$—) could not be extracted with methylene chloride. Apparently, the molecule is not as lipophilic as the corresponding 5′-trityl analogue (1). Since no other simple isolation procedure was available, this approach also was set aside. To make the 5′-grouping more lipophilic, the corresponding 5′-*O*-phenoxyacetate derivative (**1**; R = $PhOCH_2CO$—) was prepared from 2′-*O*-tetrahydropyranyluridine (**1**; R = H) (9) in 79% yield. Phosphorylation (11) to give pyridinium salt (**2**; R = $PhOCH_2CO$—) was successful and isolation presented no problems. Coupling with a further mole of 2′-*O*-tetrahydropyranyluridine (**1**; R = H) gave protected UpU (**3**; R = $PhOCH_2CO$—) in 44% yield. Steric interference between the neighboring 2′-*O*-tetrahydropyra-

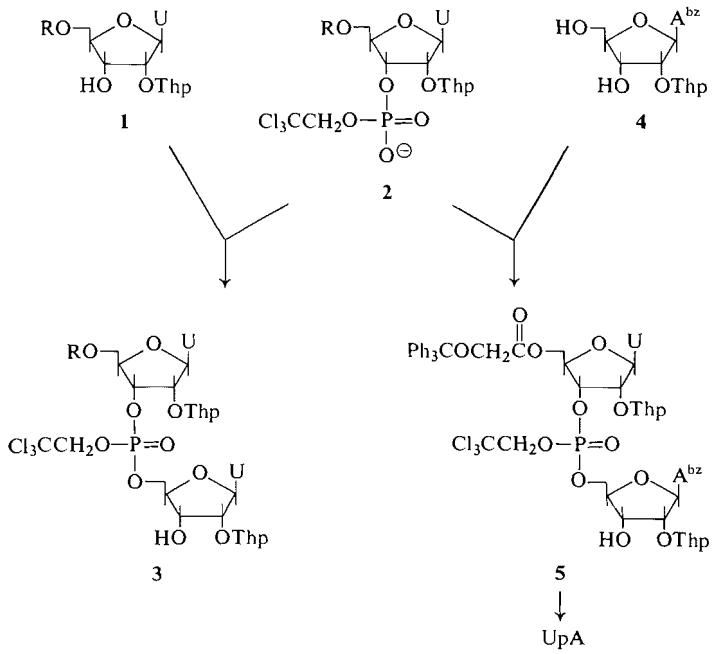

SCHEME 1

Can. J. Chem. Downloaded from www.nrcresearchpress.com by 210.87.254.6 on 09/05/12
For personal use only.

nyl group and the bulky TPS complex, together with the secondary nature of the 3′-hydroxyl group, ensures specific 5′-condensation (1). Removal of the phenoxyacetyl group was accomplished using 0.1 *N* ammonia in methanol for 1 h to give 2′-*O*-tetrahydropyranyluridylyl (3′-β,β,β-trichloroethyl-5′) 2′-*O*-tetrahydropyranyluridine (**4**; R = H) quantitatively. Thus, the 5′-position could be deblocked specifically leaving the rest of the protection intact.

Stepwise synthesis using groups other than trityls at the 5′-position had one inherent disadvantage in that detection of the product during its formation in the actual reaction or during column purification, was unsatisfactory. Compounds containing various trityl groups exhibit distinctive yellow–orange color on development with a ceric sulfate spray (1), whereas, those containing phenoxyacetyl groups give the ubiquitous brown coloration. Combination of trityl and phenoxyacetyl groups led directly to the "evolution" of a triphenylmethoxyacetyl group, compounds containing which, should be detectable by ceric sulfate spray, possess the necessary lipophilicity for extraction as a pyridinium salt, and be deblocked with dilute methanolic ammonia. Since cleavage of the trityloxyacetyl to the corresponding hydroxyacetyl would not be necessary and in fact, would be undesirable, the stable triphenylmethyl derivative was chosen.

Standard tritylation on methyl glycolate was carried out. Deesterification of the product gave sodium triphenylmethoxyacetate which on neutralization yielded the parent acid in good overall yield. The sodium salt was used in further reactions, the parent acid being required for characterization.

2′-*O*-Tetrahydropyranyl-5′-triphenylmethoxyacetyluridine (**1**; R = Ph_3COCH_2CO—) was prepared from 2′-*O*-tetrahydropyranyluridine (**1**; R = H) (9) in good yield. Phosphorylation using pyridinium β,β,β-trichloroethylphosphate and TPS (11) to give 3′-phosphate derivative (**2**; R = Ph_3COCH_2CO—) was successful and isolation was routine. Coupling with 1 mol of N^6-benzoyl-2′-*O*-tetrahydropyranyladenosine (**4**) (13) gave the protected dinucleotide, 2′-*O*-tetrahydropyranyl-5′-*O*-triphenylmethoxyacetyluridylyl (3′-β,β,β-trichloroethyl-5′)N^6-benzoyl-2′-*O*-tetrahydropyranyladenosine (**5**)[2] in *ca.* 90% yield over the two steps. Again reaction would be expected to occur specifically at position 5′ of **4**.

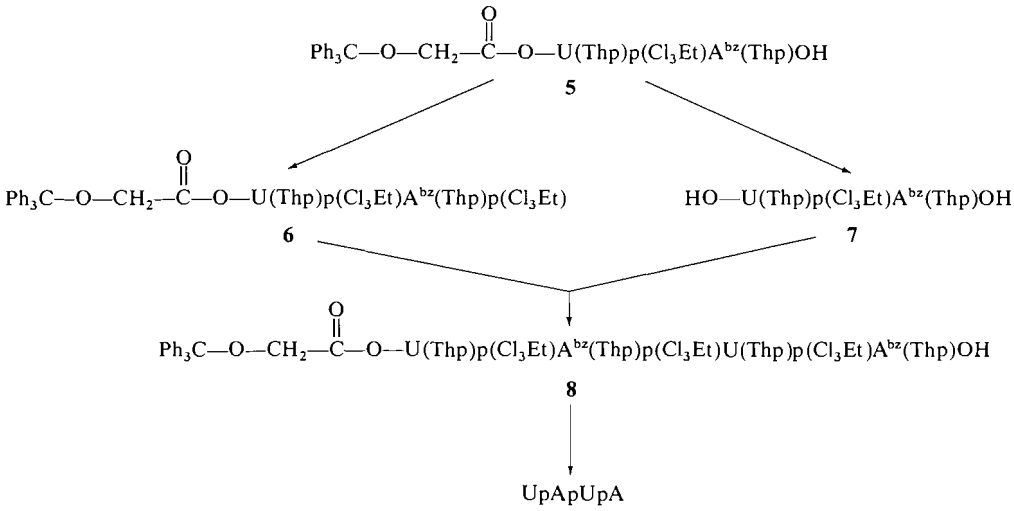

SCHEME 2

[2]To condense the huge structural formulae necessary to describe protected oligoribonucleotides shown in the flow sheet, a shorthand method suggested by the IUPAC-IUB commission on Biochemical Nomenclature is adopted (14).

For example, 2′-*O*-tetrahydropyranyl-5′-triphenylmethoxyacetyluridylyl (3′-β,β,β-trichloroethyl-5′)N^6-benzoyl-2′-*O*-tetrahydropyranyladenosine can be written as Ph_3COCH_2CO.O-U(Thp)p(Cl_3Et)A^{bz}(Thp)OH.

TABLE 1. The p.m.r. comparison of diastereoisomers of 7

Protons	Chemical shifts (δ in p.p.m.) High R_F isomer	Low R_F isomer	Signal J in Hz
2 of A	8.72	8.80	1H-s
8 of A	8.67	8.75	1H-s
o-PhCO and 6 of U	8.00	8.00	3H-m
m- and *p*-PhCO	7.60	7.60	3H-m
1′ of A	6.25	6.20	1H-d (both 6)
1′ of U	6.05	6.00	1H-d (both 8)
C-methylene of Thp	1.50	1.58	12H-broad m

Inspection of the t.l.c. of **5** showed two spots (R_F 0.70 and 0.62) in unequal amounts. An enriched sample of the major component (lower R_F) was isolated (45%) using careful column chromatography, p.m.r. data being obtained only for this component. Existence of isomerization around the tertiary phosphate of **5** could result in a pair of diastereoisomers,[3] the inequality in amounts resulting from the steric restrictions towards the reacting species in the second step of internucleotidic link formation. Complete removal of protection (1) on isomeric mixture **5** gave a single molecular species. Since deblocking will ultimately remove any chirality at phosphotriester centers, further transformations were carried out on the unseparated mixture.

Removal of the trityloxyacetyl group from **5** (both components) was smoothly accomplished in dilute methanolic ammonia to give protected dinucleotide **7** which on t.l.c. was shown to consist of an unequal mixture. Column chromatography on silica gel gave a major component (R_F 0.52) and a minor component (R_F 0.60) in the ratio of 2:1 and in a total yield of 93%. The p.m.r. spectra of these two isomers are summarized in Table 1. Each set of data indicated the correct structure for **7**. The subtle differences in chemical shifts could be explained by the occurrence of a diastereoisomeric pair. Prolonged methanolic ammonia treatment on unresolved **7** only gave debenzoylated materials; no interconversion was detected, the ratio of 2:1 remaining constant. Although the two components of **7** could be isolated, the unseparated mixture was used in further condensations.

Convenient specific removal of the triphenylmethoxyacetyl group from dinucleotide derivative (**5**) to give dinucleotide derivative (**7**) possessing free hydroxyl groups at both its 3′ and 5′ positions, meant that a block synthesis for oligoribonucleotides could now be undertaken. Dinucleotide derivative **5** was phosphorylated using the pyridinium salt of β,β,β-trichloroethylphosphate and TPS in pyridine to give pyridinium salt of 3′-phosphate derivative **6** which was successfully isolated by methylene chloride extraction. Immediate coupling of **6** with 1 mol of **7** gave the protected tetranucleotide **8** in 93% yield over two steps. As mentioned previously, the 5′-hydroxyl of a nucleoside derivative will participate preferentially in the second step of internucleotidic link formation, consequently the 5′-hydroxyl group of dinucleotide derivative **7** might be expected to react likewise to give specific 3′–5′ phosphotriester linkages. The t.l.c. of material **8** gave an extended oval spot as would be anticipated from a mixture of eight components (three chiral centers). The p.m.r. spectrum was too complicated for interpretation. Complete deblocking of **8** using the three step procedure described previously (1) gave the free tetranucleoside triphosphate, UpApUpA, as a single species in 95% yield.

Pancreatic ribonuclease treatment of UpApUpA gave ApUp as well as Up and A in the correct ratio. Combined pancreatic ribonuclease and alkaline phosphatase treatment of UpApUpA gave ApU as well as U and A in the correct ratio. Snake venom diesterase treatment on ApU gave A and pU in the correct ratio. Snake venom diesterase treatment of UpApUpA gave U, pA, and pU in the correct ratio. Complete digestions in each case confirmed the fidelity of the 3′–5′-diphosphate linkages (<1%,

[3]Existence of diastereoisomeric pairs of phosphotriesters has been reported independently (15).

Can. J. Chem. Downloaded from www.nrcresearchpress.com by 210.87.254.6 on 09/05/12
For personal use only.

TABLE 2. The R_{Up}'s of free oligoribonucleotides and nucleotide markers

Compound	Paper chromatography (Whatman No. 1) solvent A	Thin-layer chromatography (cellulose)*		
		Solvent A	Solvent B	Solvent C
UpApUpA	0.36	0.57	0.18	0.57
UpA	1.50	2.35	0.68	1.03
ApU	1.30	1.65	0.86	1.54
ApUp	0.74	0.40	0.14	0.43
U	2.15	5.2	2.50	5.5
A	1.92	3.5	3.25	7.3
pA	0.72	0.74	1.42	1.42
pU	0.93	0.64	0.78	0.72
Up	1.00	1.00	1.00	1.00

*Solvents: A, EtOH – 1 *M* NH_4OAc, p*H* 7.5 (7:3, v/v); B, 1-BuOH – glacial HOAc – H_2O (5:3:2, v/v); C, 2-PrOH – concentrated NH_4OH – H_2O (7:1:2, v/v).

2′–5′ linkage). Thus enzymic digestion confirmed the synthesis of tetranucleoside triphosphate (UpApUpA) and characterized ApU which contained the internucleotidic link formed between the two original UpA fragments (Table 2).

Extension to general block synthesis of oligoribonucleotides of predetermined sequence and length is now underway.

Experimental

The p.m.r. spectra were recorded on a Varian T60 or Varian HA-100 spectrometer in 10–15% (w/v) DMSO-d_6 – D_2O solutions, and line positions are reported in p.p.m. from the reference (TMS).

Silica gel (Baker Analyzed Reagent) was used for column chromatography; and Analtech prescored silica gel plates were employed for t.l.c. The plates were usually developed in 5 or 10% methanol in methylene chloride mixtures. The t.l.c. detection was carried out using a ceric sulfate spray (1 g $H_4Ce(SO_4)_4$ in 10% aqueous sulfuric acid solution) and followed by heating the plates at 300–400 °C. Compounds containing a trityl group develop as yellow spots, while others appear as brown colorations.

Paper chromatography was performed using the descending technique on Whatman No. 1 or 3 MM paper. Analtech pre-coated cellulose plates (Avicel F) were used for t.l.c. of deblocked nucleotides. The solvent system employed for p.c. and t.l.c. on cellulose was ethanol – 1 *M* ammonium acetate, p*H* 7.5 (7:3, v/v). A short wave u.v. lamp was used for detection.

It was essential that moisture be excluded from all coupling reactions. After evaporation *in vacuo* of the pyridine solution, normal pressure was restored with dry nitrogen and *not* atmospheric air. All such evaporations were carried out in the temperature range 30–40 °C.

Emulsion, frequently obtained during methylene chloride extractions of aqueous pyridine solutions, was broken by the addition of a few milliliters of saturated sodium chloride solution.

*5′-O-Phenoxyacetyl-2′-O-tetrahydropyranyluridine (**1**; R = $PhOCH_2CO$)*

Lower R_F diastereoisomer of 2′-*O*-tetrahydropyranyluridine (**1**; R = H) (9) (110 mg) was added to an anhydrous pyridine solution (5 ml) of phenoxyacetic acid (51 mg) and TPS (101 mg). Reaction proceeded overnight at room temperature and was followed by t.l.c. (R_F 0.25 → 0.55 in 5% CH_3OH–CH_2Cl_2). On the disappearance of starting material, ice (10 g) was added and the mixture extracted with methylene chloride (3 × 25 ml). The combined extracts were washed with water (2 × 25 ml) and evaporated *in vacuo* to an oil, the last traces of pyridine being removed by co-distillation with toluene (2 × 10 ml). The major component was purified using silica gel chromatography with methanol – methylene chloride as solvent to give a solid foam (122 mg, 79%). The p.m.r. data indicated monoesterification, signals (δ TMS) at 7.67 (1H-doublet, $J \simeq$ 8 Hz; 6 proton of U); 7.2 (5H-multiplet; phenyl protons); 5.93 (1H-doublet, $J \simeq 5$ Hz; 1′-anomeric proton); 5.63 (1H-doublet, $J \simeq 8$ Hz; 5 proton of U); 4.80 (2H-singlet; OCH_2CO); 4.70 (1H-singlet; Thp acetal proton); 4.1 (7H-broad multiplet; sugar protons and O—CH_2 of Thp); 1.57 p.p.m. (6H-broad multiplet; C—CH_2's of Thp). Non-reactivity towards trityl chloride confirmed 5′-substitution.

*5′-O-Phenoxyacetyl-2′-O-tetrahydropyranyluridine-3′-β,β,β-trichloroethylphosphate (**2**; R = $PhOCH_2CO$)*

Bis-cyclohexylamine salt (133 mg, 1.25 equiv) of mono-β,β,β-trichloroethylphosphate (11) was dissolved in anhydrous pyridine (10 ml) (warming was necessary) and converted to its corresponding pyridinium salt by repetitive evaporation *in vacuo* and solution in pyridine (4 × 10 ml).

Triisopropylbenzenesulfonyl chloride (TPS) (181 mg, 2.5 equiv) was added to the pyridinium salt in pyridine (10 ml). Thirty minutes later, 5′-*O*-phenoxyacetyl-2′-*O*-tetrahydropyranyluridine (122 mg, 1 equiv; R_F 0.55 in 5% CH_3OH–CH_2Cl_2) was added as a pyridine solution (5 ml). The reaction mixture was sealed under nitrogen and left at room temperature for 1–2 days in the dark. The t.l.c. indicated the phosphorylation was complete (R_F 0.55 → 0.05 in 5% CH_3OH–CH_2Cl_2). Ice (2 g) was added and the quenched reaction left for 30 min, poured into ice-water

Can. J. Chem. Downloaded from www.nrcresearchpress.com by 210.87.254.6 on 09/05/12
For personal use only.

Can. J. Chem. Downloaded from www.nrcresearchpress.com by 210.87.254.6 on 09/05/12
For personal use only.

(20 ml), and then extracted with methylene chloride (4 × 20 ml). The combined organic extracts were washed with distilled water (2 × 20 ml). Methylene chloride was removed by evaporation *in vacuo* and replaced by anhydrous pyridine (10 ml). This pyridine solution containing the pyridinium salt (**2**; R = $PhOCH_2CO$) of the desired nucleotide derivative was used immediately to form blocked dinucleotide derivatives.

*5′-O-Phenoxyacetyl-2′-O-tetrahydropyranyluridylyl(3′-β,β,β-trichloroethyl-5′)2′-O-tetrahydropyranyluridine (**3**; R = $PhOCH_2CO$)*

TPS (91 mg, 1.25 equiv) was added to the pyridine solution of blocked uridylate derivative (**2**; R = $PhOCH_2CO$) prepared in the previous experiment and activation was allowed to proceed for 30 min at room temperature. The lower R_F diastereoisomer of 2′-*O*-tetrahydropyranyluridine (**1**; R = H) (9) (90 mg, 1.1 equiv) dissolved in anhydrous pyridine (5 ml) was added and the sealed reaction mixture was left at room temperature for 1–2 days in the dark. The t.l.c. indicated coupling was complete (R_F 0.05 → 0.50 in 5% CH_3OH–CH_2Cl_2). Ice (2 g) was added and after 30 min the aqueous pyridine solution was poured into ice-water (20 ml) and extracted with methylene chloride (4 × 20 ml) and evaporated *in vacuo* to an oily residue, the last traces of pyridine being removed by co-distillation with toluene (2 × 10 ml). The residue was dissolved in methylene chloride (50 ml) and subjected to column chromatography on silica gel. Elution with 2% CH_3OH–CH_2Cl_2 gave the appropriate fractions which were pooled and evaporated *in vacuo* to give the blocked dinucleotide (**3**; R = $PhOCH_2$-CO) (110 mg, 44%) as a solid foam. The p.m.r. spectrum showed signals (δ TMS) at 7.43 (2H-superimposed doublets, both $J \simeq 8$ Hz; 6 protons of Us); 6.9 (5H-multiplet; phenyl protons); 5.80 (2H-superimposed doublets, $J \simeq 6$ and 7 Hz; 1′-anomeric protons); 5.48 (2H-superimposed doublets, both $J \simeq 8$ Hz; 5 protons of Us); 4.71 (2H-singlet; OCH_2-CO); 4.60 (2H-superimposed singlets; Thp acetal protons); 4.1 (16H-broad multiplet; sugar protons, O—CH_2 of Thps and O—CH_2 of Cl_3CCH_2O); 1.57 p.p.m. (12H-broad multiplet; C—CH_2's of Thps).

*2′-O-Tetrahydropyranyluridylyl(3′-β,β,β-trichloroethyl-5′)2′-O-tetrahydropyranyluridine (**3**; R = H)*

5′-*O*-Phenoxyacetyl-2′-*O*-tetrahydropyranyluridylyl(3′-β,β,β-trichloroethyl-5′)2′-*O*-tetrahydropyranyluridine (**3**; R = $PhOCH_2CO$) (40 mg) was dissolved in 0.1 *N* methanolic ammonia (5 ml). Reaction was followed by t.l.c. in 10% CH_3OH–CH_2Cl_2 (R_F 0.65 → 0.43) and was complete in 30 min. Evaporation *in vacuo* gave a residue which was extracted with anhydrous ether (6 × 5 ml) to leave a solid foam (22 mg, 81%). The p.m.r. spectrum showed signals (δ TMS) at 7.30 (2H-superimposed doublets, $J \simeq 8$ Hz; 6 protons of Us); 6.00 (2H-superimposed doublets, both $J \simeq 6$ Hz; 1′ anomeric protons); 5.63 (2H-superimposed doublets, both $J \simeq 8$ Hz; 5 protons of Us); 1.53 p.p.m. (12H-broad multiplet C—CH_2's of Thps); no $PhOCH_2CO$ signals.

Methyl Triphenylmethoxyacetate

A mixture of methyl glycolate (5.0 g, 0.055 mol), triphenylchloromethane (18.0 g, 0.065 mol) in anhydrous pyridine (50 ml) was set aside at room temperature in the dark. After 2 days ice (20 g) was added, and stirring continued for a further hour. The reaction mixture was then poured into ice-water (200 ml) and repeatedly extracted with methylene chloride (3 × 50 ml). Combined organic extracts were washed and evaporated to dryness *in vacuo*. Last traces of pyridine were removed by co-distillation with toluene (3 × 30 ml) to give a solid residue (16.2 g) which was used in the next reaction. A pure sample of the methyl ester was obtained by chromatography on silica gel in 20–30% methylene chloride – hexane mixtures. The p.m.r. spectrum of methyl triphenylmethoxyacetate showed signals (δ TMS) at 7.28 (15H-multiplet; trityl aromatic protons); 3.75 (2H-singlet; —OCH_2CO protons); and 3.58 p.p.m. (3H-singlet; OCH_3 protons).

Sodium Triphenylmethoxyacetate

To a suspension of crude methyl triphenylmethoxyacetate (16.2 g) in ethanol (75 ml), 4 *N* sodium hydroxide solution (75 ml) was added, and the reaction mixture stirred at room temperature. After 16 h t.l.c. indicated *ca.* 90% hydrolysis of the ester (R_F 0.95 → 0.0–0.20 in 10% CH_3OH–CH_2Cl_2). The reaction mixture was then poured into ice-water (100 ml) and repeatedly extracted with methylene chloride (4 × 50 ml). Combined organic extracts were evaporated *in vacuo*, and residue (20.0 g) triturated with benzene (2 × 30 ml), then hexane (6 × 30 ml) to give sodium salt of triphenylmethoxyacetic acid (15.10 g, 84% yield over two steps) which was used directly for reactions involving nucleosides described below.

Acid (1.67 g) m.p. 101–103° was obtained by neutralizing a methylene chloride solution of the sodium salt (1.84 g in 40 ml) with Dowex 50W (pyridinium form) and crystallization from petroleum ether (30–60°). The p.m.r. spectrum of triphenylmethoxyacetic acid showed signals (δ TMS) at 8.5 (1H-broad singlet; —COOH proton); 7.35 (15H-multiplet; trityl aromatic protons); and 3.60 p.p.m. (2H-singlet; —OCH_2CO protons).

Anal. Calcd. for $C_{21}H_{18}O_3$ (mol. wt. 318.35): C, 79.22; H, 5.70. Found: C, 79.31; H, 5.60.

The mass spectrum of triphenylmethoxyacetic acid (recorded at 200°) showed a strong M^+ peak at 318 *m/e*; and further peaks at 259 (M-59, corresponding to fragment Ph_3C—O—; and loss of —CH_2—COOH), 243 (M-75, corresponding to fragment Ph_3C—, and loss of —O—CH_2—COOH).

*2′-O-Tetrahydropyranyl-5′-O-triphenylmethoxyacetyluridine (**1**; R = Ph_3COCH_2CO)*

Sodium triphenylmethoxyacetate (2.72 g, 0.008 mol) was evaporated *in vacuo* from anhydrous pyridine (2 × 30 ml) and finally its volume reduced to *ca.* 20 ml. The solution was sealed under nitrogen, TPS (1.34 g, 0.0044 mol) added, and the reaction mixture allowed to stand at room temperature for 2 h. The low R_F diastereoisomer of 2′-*O*-tetrahydropyranyluridine (**1**; R = H) (9) (1.31 g, 0.004 mol; R_F 0.40 in 10% CH_3OH–CH_2Cl_2) was evaporated from anhydrous pyridine (2 × 30 ml) and finally its volume reduced to *ca.* 10 ml. This solution was then added to the triphenylmethoxyacetic acid–TPS complex (prepared above) and the reaction mixture set aside at room temperature for 1–2 days in the dark. A further portion of TPS (0.33 g, 0.0011 mol) was added after 1 day to ensure complete esterification. After 2 days t.l.c. indicated *ca.* 90% conversion into a product of R_F 0.80 in 10% CH_3OH–CH_2Cl_2. Ice (20 g) was then added to the mixture, and

Can. J. Chem. Downloaded from www.nrcresearchpress.com by 210.87.254.6 on 09/05/12
For personal use only.

stirring continued for a further hour. The reaction mixture was then poured into ice-water (100 ml) and repeatedly extracted with methylene chloride (6 × 30 ml). The combined organic extracts were washed, and evaporated to dryness *in vacuo*. The yellow glass obtained was purified by chromatography on silica gel (40 g) in methylene chloride. Elution with methylene chloride (400 ml) removed some impurity (R_F 0.78). Elution with 0.5% methanol – methylene chloride mixture yielded some impure product (0.336 g). Pure 2′-*O*-tetrahydropyranyl-5′-*O*-triphenylmethoxyacetyluridine (1.32 g, 53%) (R_F 0.82 in 10% CH_3OH–CH_2Cl_2) was obtained by elution with 1.0–1.5% methanol – methylene chloride mixtures (400 + 400 ml). The p.m.r. spectrum showed signals (δ TMS) at 7.38 (16H-multiplet; trityl aromatic protons and 6-proton of U); 5.90 (1H-doublet; $J \simeq 6$ Hz; 1′-anomeric proton); 5.50 (1H-doublet; $J \simeq 8$ Hz; 5-proton of U); 4.75 (1H-singlet; Thp acetal proton); 3.80 (2H-singlet; OCH_2CO); 1.58 p.p.m. (6H-broad multiplet; C—CH_2 of Thp).

Anal. Calcd. for $C_{35}H_{36}N_2O_9$ (mol. wt. 628.658): C, 66.87; H, 5.77; N, 4.46. Found: C, 67.15; H, 5.89; N, 4.21.

The mass spectrum of 2′-*O*-tetrahydropyranyl-5′-*O*-triphenylmethoxyacetyluridine (recorded at 370°) showed *no* M^+ peak, but peaks at 385 *m/e* (M-243, loss of Ph_3C—); 355 (M-273, loss of Ph_3C—O—); 326 (M-302; loss of Ph_3C—O—CH_2—CO—); 243 (M-385; loss of —O—CH_2—CO—O—U(Thp)—OH); 241 (M-387; loss of Ph_3C—O—CH_2—CO—, and Thp); 215 (M-413; loss of Ph_3C—O—CH_2—CO—, and uracil base); 112 (M-514; loss of Ph_3C—O—CH_2—CO—, Thp and ribose).

2′-*O*-Tetrahydropyranyl-5′-*O*-triphenylmethoxyacetyluridine (**1**; R = Ph_3COCH_2CO) (145 mg, R_F 0.82 in 10% CH_3OH–CH_2Cl_2) was suspended in dilute methanolic ammonia (5 ml, prepared by tenfold dilution of saturated (at 0°) methanolic ammonia with methanol) and stirred at room temperature. After 1 h t.l.c. indicated complete regeneration of starting material (**1**; R = H) (R_F 0.43 in 10% CH_3OH–CH_2Cl_2).

2′-O-Tetrahydropyranyl-5′-O-triphenylmethoxyacetyluridine-3′-β,β,β-trichloroethyl Phosphate (2; R = Ph_3COCH_2CO)

Bis-cyclohexylamine salt (2.25 g, 0.005 mol; 2 equiv) of mono-β,β,β-trichloroethyl phosphate (**11**) was dissolved in anhydrous pyridine (50 ml) with warming, and converted to its pyridinium salt by repetitive evaporation *in vacuo* and solution in pyridine (5 × 50 ml). The TPS (3.02 g, 0.01 mol; 4 equiv) was then added to the pyridinium salt in pyridine (50 ml). After 1 h a pyridine solution of 2′-*O*-tetrahydropyranyl-5′-*O*-triphenylmethoxyacetyluridine (**1**; R = Ph_3COCH_2CO) (1.5 g, 0.0025 mol; 1 equiv; R_F 0.82 in 10% CH_3OH–CH_2Cl_2) was added to the yellow solution and the reaction mixture sealed under nitrogen and set aside at room temperature in the dark. After 1–2 days t.l.c. indicated complete conversion into a product of R_F 0.0–0.24 in 10% CH_3OH–CH_2Cl_2. Ice (20 g) was added and the quenched reaction left for 30 min, poured into ice-water (250 ml), and repeatedly extracted with methylene chloride (4 × 50 ml). The combined organic extracts were washed with distilled water (4 × 50 ml). Methylene chloride was removed by evaporation *in vacuo* and replaced by anhydrous pyridine (50 ml). This pyridine solution, containing the pyridinium salt of (**2**; R = Ph_3COCH_2CO) was used immediately to form blocked dinucleotide phosphate derivatives.

2′-O-Tetrahydropyranyl-5′-O-triphenylmethoxyacetyluridylyl(3′-β,β,β-trichloroethyl-5′)N⁶-benzoyl-2′-O-tetrahydropyranyladenosine (5)

TPS (0.80 g, 0.0027 mol; 1.1 equiv) was added to the blocked uridylate derivative (**2**; R = Ph_3COCH_2CO) and activation allowed to proceed for 30 min at room temperature in the dark. The low R_F diastereoisomer of N^6-benzoyl-2′-*O*-tetrahydropyranyladenosine (**4**) (1.70 g, 0.0037 mol; 1.5 equiv; R_F 0.48 in 10% CH_3OH–CH_2Cl_2) dissolved in anhydrous pyridine (30 ml) was added and the reaction mixture sealed under nitrogen, and set aside at room temperature for 2–3 days in the dark. On the second day a further portion of TPS (0.36 g, 0.55 equiv) was added to ensure complete coupling. After 3 days t.l.c. indicated *ca.* 90% conversion into a product of R_F 0.62–0.70 in 10% CH_3OH–CH_2Cl_2. Ice (20 g) was then added to the mixture, and stirring continued for further 30 min. The reaction mixture was then poured into ice-water (200 ml) and repeatedly extracted with methylene chloride (5 × 50 ml). The combined organic extracts were washed with water (5 × 30 ml) and evaporated *in vacuo*. The last traces of pyridine were removed by co-distillation with toluene (3 × 30 ml). Methylene chloride (30 ml) was then added to the residue, and the precipitated tri-isopropylbenzenesulfonic acid was filtered off. The filtrate was purified by chromatography on silica gel (120 g) in methylene chloride. Elution with 2.5–3.0% methanol – methylene chloride mixtures (1 + 1 l) yielded a *ca.* 4:1 mixture of **5** and **4** (3.2 g, R_F 0.62–0.70; and 0.45 in 10% CH_3OH–CH_2Cl_2). This mixture could *not* be purified further by chromatography, so it was treated with an excess of *p*-anisylchlorodiphenylmethane (0.45 g, 1.5 mmol, *ca.* 1.1 equiv, based on a 4:1 mixture of **5** and **4**) in anhydrous pyridine (30 ml). The reaction mixture was set aside at room temperature in the dark. After 16 h t.l.c. indicated *complete* conversion of **4** into N^6-benzoyl-5′-*O*-*p*-methoxytrityl-2′-*O*-tetrahydropyranyladenosine (R_F 0.84 in 10% CH_3OH–CH_2Cl_2). Ice (20 g) was then added, and stirring continued for further 30 min. The reaction mixture was then poured into ice-water (250 ml), and repeatedly extracted with methylene chloride (5 × 50 ml). The combined organic extracts were washed with water (5 × 50 ml), and evaporated *in vacuo* to give a yellow glass. This mixture was separated by chromatography on silica gel (50 g) in methylene chloride. Washing the column with methylene chloride (200 ml); 0.5–1% methanol – methylene chloride mixtures (200 + 200 ml) removed the trityl alcohol. Elution with 2.0% methanol – methylene chloride mixture (800 ml) yielded the 5′-*O*-*p*-methoxytrityl ether of **4** (0.8 g, R_F 0.83 in 10% CH_3OH–CH_2Cl_2). Continued elution with 2.5% methanol – methylene chloride mixture (800 ml) yielded a mixture of the isomers of **5** (0.262 g, R_F 0.80 and 0.72 in 10% CH_3OH–CH_2Cl_2) of an enriched sample of the lower R_F isomer **5** (1.44 g; 45% yield) was obtained by eluting the column with 3.0% methanol – methylene chloride mixture (400 ml). Further 0.25 g of an impure sample of **5** was isolated on elution with 4% methanol – methylene chloride mixture (400 ml).

The p.m.r. spectrum of the lower R_F isomer showed signals (δ TMS) at 8.65 and 8.60 (2H-singlets: 2- and 8-protons of A) 8.20 (2H-multiplet; *o*-benzoate protons); 7.42 (19H-multiplet; trityl aromatic protons, 6-proton of U; and other benzoate protons); 6.38 (1H-doublet; $J \simeq 4$ Hz; 1′-anomeric proton of A); 6.02 (1H-doublet; $J \simeq 6$ Hz;

Can. J. Chem. Downloaded from www.nrcresearchpress.com by 210.87.254.6 on 09/05/12
For personal use only.

1′-anomeric proton of U); 5.65 (1H-doublet; $J \simeq 8$ Hz; 5-proton of U); 3.95 (2H-singlet; OCH_2CO); 1.78 p.p.m. (6H-broad multiplet; C-methylenes of Thp).

Uridylyl(3′–5′)adenosine (UpA)

A solution of 2′-*O*-tetrahydropyranyl-5′-*O*-triphenylmethoxyacetyluridylyl(3′-β,β,β-trichloroethyl-5′)N^6-benzoyl-2′-*O*-tetrahydropyranyladenosine (**5**) (15 mg, R_F 0.62–0.70 in 10% CH_3OH–CH_2Cl_2) in *N*,*N*-dimethylformamide (1.0 ml) was stirred at 50° with Cu–Zn couple (*ca.* 20 mg). After 1 day t.l.c. indicated complete conversion of starting material into a product of R_F origin in 10% CH_3OH–CH_2Cl_2. Half saturated methanolic ammonia (1 ml) was then added, and the reaction mixture stirred at room temperature for 2 days. *N*-Ammonia solution (1 ml) was added, and the Cu–Zn couple filtered off, and washed well with dilute ammonia. The combined filtrate and washings were carefully concentrated *in vacuo* and the solution p*H* brought to 8–10. Dowex 50 W (NH_4^+ form; *ca.* 1 g) was added, and the mixture stirred at room temperature for 15 min. The resin was filtered off and washed well with water. The combined filtrate and washings were concentrated *in vacuo* to *ca.* 20 ml. The p*H* of the solution was then adjusted to 2.0 with 0.1 *N* hydrochloric acid solution, and the reaction mixture stirred at room temperature. After 2 days t.l.c. on cellulose plates indicated that the hydrolysis was complete (R_F 0.76 → 0.32) UpA (144 o.d.$_{260}$ 93%, R_{Up} 1.50) was isolated and purified using preparative paper chromatography.

2′-O-Tetrahydropyranyluridylyl(3′-β,β,β-trichloroethyl-5′)N^6-benzoyl-2′-O-tetrahydropyranyladenosine (7)

2′-*O*-Tetrahydropyranyl-5′-*O*-triphenylmethoxyacetyluridylyl(3′-β,β,β-trichloroethyl-5′)N^6-benzoyl-2′-*O*-tetrahydropyranyladenosine (**5**) (0.516 g; 0.004 mol; R_F 0.62–0.70 in 10% CH_3OH–CH_2Cl_2) was suspended in dilute methanolic ammonia (50 ml, prepared by tenfold dilution of a saturated (at 0°) methanolic ammonia with methanol) and stirred at room temperature. After 1 h t.l.c. indicated complete conversion into *two* products of R_F 0.60 and 0.52 in 10% CH_3OH–CH_2Cl_2 in a ratio of *ca.* 1:2. The reaction mixture was then evaporated *in vacuo*, and the mixture separated by chromatography on silica gel (15 g) in methylene chloride. Washing the column with methylene chloride (200 ml) and 0.5–1.0% methanol–methylene chloride mixtures (200 + 200 ml) removed the triphenylmethoxyacetamide. Elution with 2.5% methanol–methylene chloride mixture (400 ml) yielded the pure high R_F isomer (R_F 0.60; 0.073 g). Continued elution with 3.0–4.0% methanol–methylene chloride mixtures (400 + 200 ml) gave a mixture (R_F 0.60 + 0.52; 0.131 g). Finally, pure low R_F isomer was obtained (R_F 0.52, 0.166 g) on elution with 5% methanol–methylene chloride mixture (400 ml) (total yield: 0.370 g, 93%). For the p.m.r. spectra: see Table 1.

2′-O-Tetrahydropyranyl-5′-O-triphenylmethoxyacetyluridylyl(3′-β,β,β-trichloroethyl-5′)N^6-benzoyl-2′-O-tetrahydropyranyladenosine-3′-β,β,β-trichloroethyl Phosphate (6)

Bis-cyclohexylamine salt (0.180 g, 0.0004 mol, 2 equiv) of mono-β,β,β-trichloroethyl phosphate was converted into its pyridinium salt as described previously. TPS (0.240 g, 0.0008 mol; 4 equiv) was then added to the pyridinium salt. After 1 h a pyridine solution of **5** (0.260 g, 0.0002 mol; 1 equiv; R_F 0.62–0.70 in 10% CH_3OH–CH_2Cl_2) was added to the yellow solution, and the reaction mixture sealed under nitrogen and set aside at room temperature in the dark. After 2 days t.l.c. indicated complete conversion of starting material into a product of R_F 0.0–0.30 in 10% CH_3OH–CH_2Cl_2. Ice (5 g) was then added followed 30 min later by a similar methylene chloride extraction as described for (**2**; R = Ph_3COCH_2CO). Blocked UpAp **6** was obtained as its pyridinium salt in pyridine and was used immediately in the next step.

2′-O-Tetrahydropyranyl-5′-O-triphenylmethoxyacetyluridylyl(3′-β,β,β-trichloroethyl-5′)N^6-benzoyl-2′-O-tetrahydropyranyladenylyl(3′-β,β,β-trichloroethyl-5′)-2′-O-tetrahydropyranyluridylyl(3′-β,β,β-trichloroethyl-5′)N^6-benzoyl-2′-O-tetrahydropyranyladenosine (8)

TPS (66 mg, 0.22 mmol; 1.1 equiv) was added to the pyridine solution of blocked UpAp **6** pyridinium salt prepared above. After 1 h a mixture of isomers of 2′-*O*-tetrahydropyranyluridylyl(3′-β,β,β-trichloroethyl-5′)N^6-benzoyl-2′-*O*-tetrahydropyranyladenosine (**7**) (300 mg, 0.30 mmol; 1.5 equiv; R_F 0.60 + 0.52 in 10% CH_3OH–CH_2Cl_2) was added, and the reaction mixture sealed under nitrogen, and set aside at room temperature for 2–4 days in the dark. After 2 days a further portion of TPS (66 mg, 0.22 mmol; 1.1 equiv) was added to ensure complete coupling. After 4 days t.l.c. indicated *ca.* 90% conversion into a product of R_F 0.80–0.88 in 10% CH_3OH–CH_2Cl_2. After a similar work-up described for **5** the product was purified by chromatography on silica gel (20 g) and alumina (5.0 g) in methylene chloride.

Elution with 1% methanol–methylene chloride mixture (200 ml) yielded an impurity (62 mg, R_F 0.94 in 10% CH_3OH–CH_2Cl_2). Elution with 2.0–2.5% methanol–methylene chloride mixtures (200 + 200 ml) gave the faster R_F isomer (32 mg, $R_F \simeq 0.6$ in 10% CH_3OH–CH_2Cl_2). Continued elution with 3.0% methanol–methylene chloride mixture (400 ml) yielded a mixture of the isomers (0.308 g, $R_F \simeq 0.60 + \simeq 0.55$ in 10% CH_3OH–CH_2Cl_2). Finally, the lower R_F isomers (0.316 g, $R_F \simeq 0.55$ in 10% CH_3OH–CH_2Cl_2) were obtained, contaminated with some unreacted starting material **7**. The last impure fraction (0.316 g) was re-chromatographed on silica gel (10 g) and alumina (5.0 g) in methylene chloride. Enriched lower R_F isomers of **8** were obtained (0.133 g, $R_F \simeq 0.55$ in 10% CH_3OH–CH_2Cl_2) on eluting the column with 3.0–3.5% methanol–methylene chloride mixtures (400 + 400 ml). A mixture, containing **8** + **7** (0.092 g, R_F 0.55–0.37 in 10% CH_3OH–CH_2Cl_2) was finally eluted with 4.0–5.0% methanol–methylene chloride mixtures (400 + 200 ml). (Combined yield of enriched isomers of **8**: 0.032 + 0.308 + 0.133 g; 93%.) Since no single isomer could be isolated, no p.m.r. spectrum was recorded.

Uridylyl(3′–5′)adenylyl(3′–5′)uridylyl(3′–5′)adenosine (UpApUpA)

A solution of 2′-*O*-tetrahydropyranyl-5′-*O*-triphenylmethoxyacetyluridylyl(3′-β,β,β-trichloroethyl-5′)N^6-benzoyl-2′-*O*-tetrahydropyranyladenylyl(3′-β,β,β-trichloroethyl-5′)-2′-*O*-tetrahydropyranyluridylyl(3′-β,β,β-trichloroethyl-5′)-N^6-benzoyl-2′-*O*-tetrahydropyranyladenosine (**8**) (15 mg, R_F 0.60–0.55 in 10% CH_3OH–CH_2Cl_2) in *N*,*N*-dimethylformamide (1.0 ml) was stirred at 50° with Cu–Zn couple (*ca.* 20 mg). After 1 day t.l.c. indicated complete conversion of starting material into a product of R_F: origin in 10% CH_3OH–CH_2Cl_2. Half-saturated methanolic ammonia

Can. J. Chem. Downloaded from www.nrcresearchpress.com by 210.87.254.6 on 09/05/12
For personal use only.

(1 ml) was then added, and the reaction mixture stirred at room temperature for 2 days. *N*-Ammonia solution (1 ml) was added, and Cu–Zn couple filtered off and washed well with dilute ammonia. Combined filtrate and washings were carefully concentrated *in vacuo* and the solution p*H* brought to 8–10. Dowex 50 W (NH_4^+ form; *ca* 1 g) was added, and the mixture stirred at room temperature for 15 min. The resin was filtered off and washed well with water. The combined filtrate and washings were concentrated *in vacuo* to *ca.* 20 ml. The p*H* of the solution was then adjusted to 2.0 with 0.1 *N* hydrochloric acid solution, and the reaction mixture stirred at room temperature. After 2 days t.l.c. on cellulose indicated that the hydrolysis was complete. (R_F 0.80 → 0.07) UpApUpA (260 o.d.$_{260}$, 95%; R_{Up} 0.36) was isolated and purified using preparative paper chromatography.

Enzymatic Analysis of UpApUpA

Pancreatic RNase Digestions

A solution of the ammonium salt of UpApUpA (10 o.d.) in 0.2 ml of Tris buffer (0.1 *M*; p*H* 8.0) was digested completely at 37° with 100 λ of Pancreatic Ribonuclease (Calbiochem., Grade A, 1 mg/ml) for 16 h. Paper chromatographic analysis showed the expected products (Up + ApUp + A) of R_{Up} 1.04, 0.74, 1.92 respectively, in the correct ratio. The t.l.c. analysis also showed the expected products (Up + ApUp + A) of R_{Up} 0.93, 0.40, 3.50 respectively in correct ratio.

To the above incubation mixture further 100 λ of Bacterial alkaline phosphatase (Worthington, 0.5 mg/ml) was added. Paper chromatographic analysis showed the expected products (U + ApU + A) of R_{Up} 2.15, 1.30, 1.92 respectively, in the correct ratio. The t.l.c. analysis also showed the expected products (U + ApU + A) of R_{Up} 5.2, 1.65, 3.55 respectively in correct ratio.

Snake Venom Diesterase Digestions

A solution of the ammonium salt of UpApUpA (10 o.d.) in 0.2 ml of Tris buffer (0.1 *M*; p*H* 8.0) was digested completely at 37° with 100 λ of Snake Venom Diesterase (Worthington, 1 mg/ml) for 16 h. Paper chromatographic analysis showed the expected products (U + 2pA + pU) of R_{Up} 2.10, 0.72, 0.93 respectively in correct ratio. The t.l.c. analysis also showed the expected products (U + 2pA + pU) of R_{Up} 5.2, 0.74, 0.64 respectively, in correct ratio.

A solution of the ammonium salt of ApU (18 o.d.) isolated by preparative paper chromatography from PRNase–Alk phosphatase digestion (40 o.d. scale), in 0.2 ml Tris buffer (0.1 *M*; p*H* 8.0) was digested completely at 37° with 100 λ of Snake Venom Diesterase for 16 h. Paper chromatographic analysis showed the expected products (A + pU) of R_{Up} 1.94, 0.92 respectively, in the correct ratio. The t.l.c. analysis also showed the expected products (A + pU) of R_{Up} 3.55, 0.65 respectively, in the correct ratio.

Financial assistance from the Medical Research Council of Canada is gratefully acknowledged.

1. T. Neilson and E. S. Werstiuk. Can. J. Chem. **49**, 3004 (1971).
2. B. F. C. Clark, S. K. Dube, and K. A. Marcker. Nature, **219**, 484 (1968).
3. N. Imura, G. B. Weiss, and R. W. Chambers. Nature, **222**, 1147 (1969).
4. R. Lohrman, D. Söll, H. Hayatsu, E. Ohtsuka, and H. G. Khorana. J. Am. Chem. Soc. **88**, 819 (1966).
5. A. Holy and J. Smrt. Coll. Czech. Chem. Commun. **31**, 3800 (1966).
6. B. E. Griffin and C. B. Reese. Tetrahedron, **25**, 4057 (1969).
7. E. Ohtsuka, K. Murao, M. Ubasawa, and M. Ikehara. J. Am. Chem. Soc. **92**, 3441 (1970).
8. E. Ohtsuka, M. Ubasawa, and M. Ikehara. J. Am. Chem. Soc. **93**, 2296 (1971).
9. B. E. Griffin, M. Jarman, and C. B. Reese. Tetrahedron, **24**, 639 (1968).
10. G. W. Grams and R. L. Letsinger. J. Org. Chem. **33**, 2589 (1968).
11. F. Eckstein. Chem. Ber. **100**, 2228 (1967).
12. C. B. Reese and J. C. M. Stewart. Tetrahedron Lett. 4273 (1968).
13. T. Neilson and E. S. Werstiuk. Can. J. Chem. **49**, 493 (1971).
14. IUPAC-IUB Commission on Biochemical Nomenclature. Biochem. **9**, 4022 (1970).
15. P. O. P. Ts'O and co-authors. J. Am. Chem. Soc. **93**, 6657 (1971).

Can. J. Chem. Downloaded from www.nrcresearchpress.com by 210.87.254.6 on 09/05/12
For personal use only.

Selective Reduction of Carbohydrate Nitroolefins[1,2]

HANS H. BAER AND WERNER RANK

Department of Chemistry, University of Ottawa, Ottawa, Canada K1N 6N5

Received November 18, 1971

Reduction of the four stereoisomeric methyl 4,6-*O*-benzylidene-2,3-dideoxy-3-nitro-hex-2-enopyranosides (**1**–**4**) with sodium borohydride gave in 80–90% yield the corresponding saturated nitro glycosides that possess an equatorial nitro group (**5**–**8**). Reduction of **1**–**4** with zinc and acetic acid gave in similar yields the corresponding 2,3-dideoxy-3-oximino glycosides (**9**–**12**). Two of the latter were deoximated to 2,3-dideoxy-3-oxo sugar derivatives.

La réduction des quatre méthyl 4,6-*O*-benzylidène-2,3-didéoxy-3-nitro-hex-2-énopyranosides (**1**–**4**) stéréoisomères par le borohydrure de sodium conduit avec un rendement de 80–90% aux nitro glycosides saturés correspondants qui possèdent un groupe nitro en position équatoriale (**5**–**8**). La réduction de **1**–**4** par le zinc dans l'acide acétique conduit avec un rendement similaire aux 2,3-didéoxy-3-oximino glycosides correspondants (**9**–**12**). Parmi ces derniers, deux ont été soumis à une désoximation pour conduire aux sucres 2,3-didéoxy-3-oxo.

Canadian Journal of Chemistry, **50**, 1292 (1972)

In early work on nitro sugars, which has been comprehensively reviewed by Sowden (1), conversion of polyhydroxy-α-nitroalkenes into saturated nitro alditols was achieved by palladium-catalyzed hydrogenation in ethanolic solution. Use of ethyl acetate as the solvent has been said (1) to diminish the selectivity of this hydrogenation. Nevertheless, in our own previous work, which dealt with glycosides containing an endocyclic α-nitroalkene grouping, facile and selective hydrogenation of the olefinic bond by palladium on charcoal in an ethyl acetate medium has been observed in certain cases. Thus, the methyl 4,6-*O*-benzylidene-2,3-dideoxy-3-nitrohex-2-enopyranosides with β-D-*erythro* (**1**) and β-D-*threo* (**2**) configuration gave high yields of the saturated methyl 4,6-*O*-benzylidene-2,3-dideoxy-3-nitro-β-D-*arabino*- and β-D-*lyxo*-hexopyranosides, **5** and **6**, respectively (2, 3). In the corresponding α-anomers, on the other hand, the same procedure was not selective. Thus, the α-D-*erythro* (**3**) and α-D-*threo* (**4**) olefins afforded saturated nitro glycosides (**7** and **8**) in lesser yields, and these were accompanied by substantial proportions (49 and 30%) of oximes, namely the methyl 4,6-*O*-benzylidene-2,3-dideoxy-3-oximino-α-D-*erythro*- and α-D-*threo*-hexopyranosides, **11** and **12**, respectively (4). An explanation for the differential behavior of α- and β-glycosides in these catalytic hydrogenations has been given (4).

We now describe selective chemical reductions by which the four nitroolefins (**1**–**4**) have afforded in 80–90% yields either the saturated nitro compounds (**5**–**8**) or the oximes (**9**–**12**), regardless of configuration. Sodium borohydride in ethanol, first applied to nitroalkenes including one from the carbohydrate series by Shechter and coworkers (5), smoothly gave **5**–**8**. There was no evidence for formation of the corresponding 3-epimers (with axial nitro group) or other reduction products.[3]

Reduction with zinc and acetic acid, a method known to convert nitroalkenes into oximes (7, 8), was then applied to **1**–**4**, and oximino glycosides were produced exclusively. In addition to the known α-glycosides **11** and **12**, their β-anomers **9** and **10** were thus obtained for the first time. Acetylation of **9** and **10** gave the corre-

[1]Part XXVII in a series on reactions of nitro sugars. For Part XXVI see ref. 15.

[2]Presented before the Joint Conference of the Chemical Institute of Canada and the American Chemical Society, Toronto, Ontario, May 25, 1970.

[3]Szarek and coworkers (6) have reported that borohydride reduction of benzyl 2-*O*-benzyl-3,4-dideoxy-4-nitro-α-D-*glycero*-pent-3-enopyranoside produces an axial nitro group, the product having the β-L-*threo* configuration. Furthermore, they have reduced in the same way carbohydrate derivatives containing an exocyclic α-nitroalkene group.

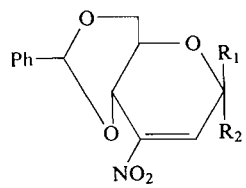

1 $R^1 = OMe; R^2 = H$
3 $R^1 = H; R^2 = OMe$

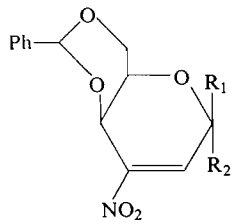

2 $R^1 = OMe; R^2 = H$
4 $R^1 = H; R^2 = OMe$

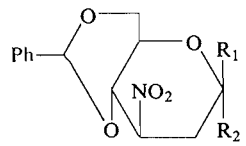

5 $R^1 = OMe; R^2 = H$
7 $R^1 = H; R^2 = OMe$

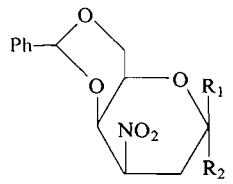

6 $R^1 = OMe; R^2 = H$
8 $R^1 = H; R^2 = OMe$

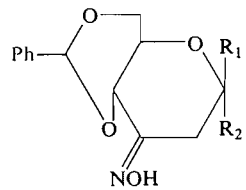

9 $R^1 = OMe; R^2 = H$
11 $R^1 = H; R^2 = OMe$

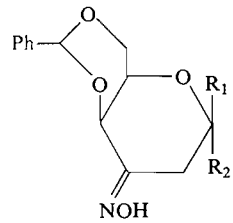

10 $R^1 = OMe; R^2 = H$
12 $R^1 = H; R^2 = OMe$

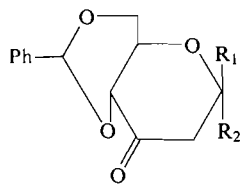

15 $R^1 = H; R^2 = OMe$
16 $R^1 = OMe; R^2 = H$

sponding acetoximino derivatives **13** and **14**. The i.r. and n.m.r. spectral data confirmed the structures (see Experimental).

The facile availability of oximino from nitro sugars may provide an attractive avenue to oxo sugars as an alternative to oxidative procedures. Lemieux and coworkers (9) have successfully deoximated 2-oximino glycosides by use of levulinic acid (10). To test this method in the present series it was applied to **11**, giving known methyl 4,6-*O*-benzylidene-2-deoxy-α-D-*erythro*-hexopyranosid-3-ulose (**15**) (11, 12) in 77% yield. Similar deoximation of **9** quantitatively produced the β-anomer (**16**) of **15**.

Experimental

The methyl 4,6-*O*-benzylidene-2,3-dideoxy-3-nitro-hex-2-enopyranosides **1** (2, 13), **2** (13, 14), **3** (4), and **4** (4, 15) were prepared as described in the literature. Special reference is made to improved procedures for preparation of some of the nitro glycoside precursors required (15). Reactions were monitored by t.l.c. on silica gel G plates with mixtures of ethyl acetate and petroleum ether (b.p. 30–60°) as irrigating solvent. The i.r. spectra were taken from Nujol mulls. The n.m.r. data were obtained from 100 MHz spectra taken with a TMS lock signal. Specific rotations were measured in an automatic polarimeter at room temperature and in sample concentrations of 0.5–1.2%.

Reductions with Sodium Borohydride

A solution of sodium borohydride (50 mg) in ethanol (5 ml) was mixed with the solution of a given nitroolefin (100 mg) in ethanol (10 ml), and the reaction mixture was magnetically stirred at room temperature. Reaction times were 3 h for **1**, 2 h for **2**, and **1** h for **3** and **4**. Sodium ion was then removed by cation exchange, the resin was washed well with ethanol, and the combined filtrate and washing solvent was evaporated to dryness. Several portions of methanol were then evaporated from the residue which was finally recrystallized from ethyl acetate–petroleum ether (b.p. 30–60°) to give the pure saturated nitro glycoside. The following results were obtained.

Methyl 4,6-O-Benzylidene-2,3-dideoxy-3-nitro-β-D-arabino-hexopyranoside (5) from 1

Yield, 87%; m.p. 149–150°; $[\alpha]_D$ −96.1° (in chloroform). Reported (2): m.p. 148–149°, $[\alpha]_D$ −95.5°.

Methyl 4,6-O-Benzylidene-2,3-dideoxy-3-nitro-β-D-lyxo-hexopyranoside (6) from 2

Yield, 89%; m.p. 177–179°; $[\alpha]_D$ +21.7° (in dimethylformamide). Reported (3): m.p. 176°; $[\alpha]_D$ +15.2°.

Methyl 4,6-O-Benzylidene-2,3-dideoxy-3-nitro-α-D-arabino-hexopyranoside (7) from 3

Yield, 91%; m.p. 108–110°; $[\alpha]_D$ +67.0° (in chloroform). Reported (4): m.p. 112°; $[\alpha]_D$ +67°.

Methyl 4,6-O-Benzylidene-2,3-dideoxy-3-nitro-α-D-lyxo-hexopyranoside (8) from 4

Yield, 81%; m.p. 108–109°; $[\alpha]_D$ +155.5° (in dimethylformamide). Reported (4): m.p. 108°.

Reductions with Zinc and Acetic Acid

To the solution of a given nitroolefin (293 mg, 1 mmol) in ether (30 ml) was added zinc dust (600 mg) and 4 *N* acetic acid (1.5 ml). The mixture was heated under reflux for 1 h, filtered, and evaporated to give a residue from which several portions of added methanol were evaporated. Finally, recrystallization of the residue from ethyl acetate–petroleum ether furnished the pure oximino glycoside.

Methyl 4,6-O-Benzylidene-2,3-dideoxy-3-oximino-β-D-erythro-hexopyranoside (9) from 1

Yield, 87%; m.p. 233°; $[\alpha]_D$ −16.4° (*c*, 0.8 in chloroform); ν_{max} 3360 (broad; OH) and 1660 cm^{-1} (weak; C=N), no NO_2 band. The n.m.r. data: in $CDCl_3$ containing a small

Can. J. Chem. Downloaded from www.nrcresearchpress.com by 210.87.254.6 on 09/05/12
For personal use only.

Can. J. Chem. Downloaded from www.nrcresearchpress.com by 210.87.254.6 on 09/05/12
For personal use only.

amount of DMSO-d_6 a 1-proton singlet (=N—OH) that disappeared on adding D_2O occurred at -0.5 τ. Other data refer to DMSO-d_6 solution: τ 2.57 (5-proton narrow multiplet, C_6H_5); 4.28 (1-proton singlet, PhCH); 5.33 (1-proton quartet, H-1, $J_{1,2a} = 8$, $J_{1,2e} = 3$ Hz); 5.60 (1-proton doublet, H-4, $J_{4,5} = 9.5$ Hz); 5.70 (1-proton quartet, H-6e, $J_{6a,6e} = 10$, $J_{5,6e} = 4.5$ Hz); 6.17 (1-proton triplet, H-6a, $J_{6a,6e} = J_{5,6a} = 10$ Hz); 6.45 (1-proton sextet of H-5, partly obscured by overlapping signals due to OCH_3 and H-2e in the 6.6–6.7 τ region); 7.90 (1-proton quartet, H-2a, $J_{2a,2e} = 15$, $J_{1,2a} = 8$ Hz). Compare also the published 60 MHz spectrum (4) of the α-anomer **11**.

Anal. Calcd. for $C_{14}H_{17}NO_5$ (279.3): C, 60.21; H, 6.14; N, 5.02. Found: C, 60.40; H, 6.19; N, 5.07.

*Methyl 4,6-O-Benzylidene-2,3-dideoxy-3-oximino-β-*D*-threo-hexopyranoside (**10**) from **2***

Yield, 81%; m.p. 215–216°; $[\alpha]_D$ −61.5° (in chloroform); ν_{max} 3370 (broad, OH) and 1650 cm^{-1} (very weak, C=N), no NO_2 band. The n.m.r. data: in $CDCl_3$ solution containing a small amount of DMSO-d_6 a 1-proton singlet occurred at τ −0.7 (=NOH); it disappeared on addition of D_2O. Spectrum in DMSO-d_6: τ 2.64 (5-proton narrow multiplet, C_6H_5); 4.32 (1-proton singlet, PhCH); 6.60 (OCH_3 signal). The ring proton signals were poorly resolved.

Anal. Calcd. for $C_{14}H_{17}NO_5$ (279.3): C, 60.21; H, 6.14; N, 5.02. Found: C, 60.12; H, 6.09; N, 4.92.

*Methyl 4,6-O-Benzylidene-2,3-dideoxy-3-oximino-α-*D*-erythro-hexopyranoside (**11**) from **3***

Yield, 88%; m.p. 197–199°; $[\alpha]_D$ +171° (in chloroform). Reported (4): m.p. 203° (dec.), $[\alpha]_D$ +172°.

*Methyl 4,6-O-Benzylidene-2,3-dideoxy-3-oximino-α-*D*-threo-hexopyranoside (**12**) from **4***

Yield, 86%; m.p. 220–221°, $[\alpha]_D$ +248° (in chloroform). Reported: m.p. 219–220° dec. (4, 16), $[\alpha]_D$ +257° (16).

*Methyl 3-Acetoximino-4,6-benzylidene-2,3-dideoxy-β-*D*-erythro-hexopyranoside (**13**)*

Oxime **9** (100 mg) was acetylated overnight at room temperature with acetic anhydride (1 ml) and pyridine (2 ml). The reaction mixture was poured into ice water, which produced a white solid precipitate that was washed with cold water, dried, and recrystallized from ethanol. The acetate **13** (107 mg, 93%) melted at 216° and showed $[\alpha]_D$ −15.6° (in chloroform), ν_{max} 1770 cm^{-1}. The n.m.r. data (in $CDCl_3$): τ 2.55 (multiplet of C_6H_5); 4.36 (1-proton singlet, PhCH); 5.32 (quartet, H-1, $J_{1,2a} = 8$, $J_{1,2e} = 3$ Hz); region about 5.5 and 6.0–6.4 (partly overlapping signals corresponding to 4 protons, H-4, 5, 6, 6′); 6.48 (OCH_3 singlet); 6.51 (quartet partially overlapped by OCH_3 signal, H-2e, $J_{1,2e} = 3$, $J_{2a,2e} = 16$ Hz); 7.60 (quartet, H-2a, $J_{1,2a} = 8$, $J_{2a,2e} = 16$ Hz), 7.81 (3-proton singlet, $OCOCH_3$).

Anal. Calcd. for $C_{16}H_{19}NO_6$ (321.3): C, 59.80; H, 5.92; N, 4.36. Found: C, 59.72; H, 5.99; N, 4.21.

*Methyl 3-Acetoximino-4,6-O-benzylidene-2,3-dideoxy-β-*D*-threo-hexopyranoside (**14**)*

Acetylation of oxime **10**, performed exactly as that of **9**, gave **14** in a yield of 78%; m.p. 163–164°, $[\alpha]_D$ +83.8° (in chloroform), ν_{max} in Nujol, 1770 cm^{-1}. The n.m.r. data (in $CDCl_3$): substituent resonances at τ 2.6 (5-proton multiplet, C_6H_5), 4.38 (1-proton singlet, PhCH), 6.46 (singlet, OCH_3), 7.85 (singlet, $OCOCH_3$). There were poorly resolved signals integrating for 4 protons in the τ 5.3–5.9 region and 2 protons in the τ 6.5–6.7 region. A 1-proton quartet was centered at τ 7.47 (H-2a, $J_{1,2a} = 10$, $J_{2a,2e} = 15$ Hz).

Anal. Calcd. for $C_{16}H_{19}NO_6$ (321.3): C, 59.80; H, 5.92; N, 4.36. Found: C, 59.78; H, 6.08; N, 4.37.

*Methyl 4,6-O-Benzylidene-2-deoxy-α-*D*-erythro-hexopyranosid-3-ulose (**15**)*

To a solution of oxime **11** (200 mg) in ethanol (10 ml) was added levulinic acid (4 ml) and 0.1 *N* hydrochloric acid (1 ml). The mixture was allowed to stand at room temperature for 4 h after which it was diluted with water (25 ml) and concentrated *in vacuo* to remove ethanol. The remaining, largely aqueous, solution was extracted with chloroform (3 × 20 ml) which was then washed with *M* sodium bicarbonate solution (2 × 10 ml) and twice with water (2 × 10 ml). Evaporation of the dried (Na_2SO_4) chloroform solution gave crystalline **15** which was recrystallized from 2-propanol. The yield was 142 mg (77%); m.p. 176–177°, $[\alpha]_D$ +155° (in ethyl acetate). Reported: m.p. 177–178° (11), 174–176° (12), $[\alpha]_D$ +159° (11).

*Methyl 4,6-O-Benzylidene-2-deoxy-β-*D*-erythro-hexopyranosid-3-ulose (**16**)*

The oxime **9** was treated with levulinic acid exactly as described above for **11**. Compound **16** crystallized from the reaction mixture in 99% yield. It melted at 193–195°, and at 194–195° after recrystallization from 2-propanol; $[\alpha]_D$ −51.5° (in chloroform); ν_{max} 1725 cm^{-1} (C=O). The n.m.r. data (in $CDCl_3$): τ 2.56 (multiplet, C_6H_5), 4.41 (singlet, PhCH), 5.22 (quartet, H-1, $J_{1,2e} = 4$, $J_{1,2a} = 8$ Hz), 5.52 (quartet, H-6e, $J_{5,6e} = 4.5$, $J_{6a,6e} = 10$ Hz), 5.65 (doublet, H-4, $J_{4,5} = 11$ Hz), 6.08 (triplet, H-6a, $J_{5,6a} = J_{6a,6e} = 10$ Hz), 6.3–6.5 (multiplet, H-5), 6.46 (singlet, OCH_3), 7.25 (two overlapping quartets, H-2a and -2e).

Anal. Calcd. for $C_{14}H_{16}O_5$ (264.3): C, 63.62; H, 6.10. Found: C, 63.46; H, 6.30.

This work was supported by the National Research Council of Canada.

1. J. C. Sowden. Adv. Carbohydr. Chem. **6**, 291 (1951).
2. H. H. Baer and T. Neilson. Can. J. Chem. **43**, 840 (1965).
3. H. H. Baer and F. Kienzle. Can. J. Chem. **43**, 3074 (1965).
4. H. H. Baer and F. Kienzle. Can. J. Chem. **45**, 983 (1967).
5. H. Shechter, D. E. Ley, and E. B. Roberson, Jr. J. Am. Chem. Soc. **78**, 4984 (1956). See also A. I. Meyers and J. C. Sircar. J. Org. Chem. **32**, 4134 (1967).
6. W. A. Szarek, D. G. Lance, and R. L. Beach. Carbohydr. Res. **13**, 75 (1970).
7. D. V. Nightingale and J. R. Jones. J. Am. Chem. Soc. **66**, 352 (1944).
8. V. V. Perekalin. Unsaturated nitro compounds. Goskhimizdat. Leningrad, 1961. Translated by L. Mandel. Israel Program for Scientific Translations Ltd. Jerusalem, 1964.
9. R. U. Lemieux, R. Suemitsu, and S. W. Gunner. Can. J. Chem. **46**, 1040 (1968).
10. C. H. DePuy and B. W. Ponder. J. Am. Chem. Soc. **81**, 4629 (1959).
11. B. Flaherty, W. G. Overend, and N. R. Williams. J. Chem. Soc. 398 (1966).

12. A. ROSENTHAL and P. CATSOULACOS. Can. J. Chem. **46**, 2868 (1968).
13. H. H. BAER. *In* Methods in carbohydrate chemistry. Vol. VI. *Edited by* R. L. Whistler and J. N. BeMiller. Academic Press, Inc. New York, N.Y. 1971.
14. H. H. BAER, F. KIENZLE, and T. NEILSON. Can. J. Chem. **43**, 1829 (1965).
15. H. H. BAER and W. RANK. Can. J. Chem. This issue.
16. P. J. BEYNON, P. M. COLLINS, and W. G. OVEREND. Proc. Chem. Soc. 342 (1964).

Can. J. Chem. Downloaded from www.nrcresearchpress.com by 210.87.254.6 on 09/05/12
For personal use only.

Can. J. Chem. Downloaded from www.nrcresearchpress.com by 210.87.254.5 on 09/05/12
For personal use only.

Canadian Journal of Chemistry

Published by THE NATIONAL RESEARCH COUNCIL OF CANADA

VOLUME 50 MAY 1, 1972 NUMBER 9

Studies on the Decomposition of Tetra-alkylammonium Salts in Solution. V. Rates and Activation Parameters of Salts Containing Substituted-benzyl or Other Active Groups

E. C. F. KO AND K. T. LEFFEK

Department of Chemistry, Dalhousie University, Halifax, Nova Scotia

Received July 22, 1971

First order rate constants and activation parameters are reported for the decomposition in chloroform and acetone solvents of a series of 4-substituted-benzylphenyldimethylammonium bromides and iodides and also of a series of tetra-alkylammonium bromides which contain no benzyl group. The results are discussed in terms of general mechanism of these reactions, which are unimolecular "ionic internal" nucleophilic substitutions.

On rapporte les constantes de vitesse du premier ordre et les paramètres d'activation pour la décomposition dans le chloroforme et l'acétone d'une série de bromures et d'iodures de benzylphényldiméthylammonium substitués en position-4 et d'une série de bromures de tétra-alkylammonium ne contenant aucun groupe benzyle. Les résultats sont discutés à la lumière des mécanismes généraux dans ces réactions qui sont des substitutions nucléophiles unimoléculaires "ionique interne".

Canadian Journal of Chemistry, **50**, 1297 (1972)

Introduction

The evidence from earlier studies (1–4) shows that tetra-alkylammonium iodides, which contain a benzyl group, decompose in chloroform solution by a unimolecular reaction of the ammonium ion, probably associated in the form of a triple ion. These decompositions are clean and invariably yield benzyl iodide and a tertiary amine. Structural variations on that portion of the substrate which is transformed to the tertiary amine can be explained, qualitatively, in terms of electronic effects of the substituents (2). Reasonably linear plots for the Hammett ($\rho - \sigma$) correlation, for $\Delta H^{\ddagger}$ *vs.* $\Delta S^{\ddagger}$, and for $\Delta G^{\ddagger}$ *vs.* $\Delta S^{\ddagger}$ exist for these compounds, which confirm the direction of movement of electrons during the activation process and the fact that all the decompositions follow the same basic mechanism. Secondary deuterium isotope effects (benzyl-1,1-d_2) on the rate of decomposition of one salt indicated that the benzyl carbon atom had considerable carbonium ion character in the transition state (4).

Hammett correlations for the decomposition of benzylphenyldimethylammonium iodides and bromides, containing para-substituted benzyl groups, were reported (3) and this paper, which concludes the series on this reaction, describes the effect of this structural change on the activation parameters for the same compounds and for seven other tetra-alkylammonium salts containing various active groups other than benzyl.

Results and Discussion

The first order rate constants for the decomposition reactions were obtained by the application of the Guggenheim method to the integrated first order rate equation (5). However, straight line plots were obtained, only when the measured conductance was used rather than the stoichiometric concentration of the salt. Since the salts are known to exist in chloroform solution mainly as ion-pairs (6), this means that the velocity of reaction is proportional to the concentration of single ammonium ion or triple ions (1). The rate constants, collated in Table 1, therefore, are calculated with respect to the concentration of the ammonium ion (or triple ion). All the values quoted are the means of at

TABLE 1. Specific first order rate constants for the decomposition of tetra-alkylammonium salts in solution

Compound	Concentration (10^2 M)	$10^5 k_1$ (s^{-1}) 20°	25°	30°	35°	40°	45°	50°	55°	60°
(I) Chloroform solvent										
(*a*) $4\text{-}XC_6H_4CH_2\cdot C_6H_5\cdot(CH_3)_2N^+Br^-$										
4-CH_3O	1.8 –3.1	—	—	—	30.0	53.0	100	183	353	
4-CH_3	3.0 –4.5	—	—	—	—	12.5	23.6	43.3	82.0	144
4-H	4.6 –9.1	—	—	—	—	6.1	12.3	22.8	44.0	85.8
4-Br	3.9 –4.5	—	—	—	—	5.56	11.3	21.8	42.2	77.6
4-NO_2	1.0*	—	—	—	—	7.82	15.7	26.4	55.0	92.0
(*b*) $4\text{-}XC_6H_4CH_2\cdot C_6H_5\cdot(CH_3)_2N^+I^-$										
4-CH_3O	1.8 –4.9	—	43.7	75.3	142	247	441	—	—	—
4-CH_3	2.6 –4.7	—	—	17.0	32.0	60.4	116	222	—	—
4-H†	5.0	—	5.53	11.6	23.8	47.7	93.2	—	—	—
4-Br	3.3 –4.3	—	—	8.0	16.3	32.5	60.7	124	—	—
4-NO_2	0.5*	—	—	15.0	29.3	59.4	122	264	—	—
(*c*) $R\cdot C_6H_5\cdot(CH_3)_2N^+Br^-$										
$CH_2{=}CH{-}CH_2$	3.71–3.88	—	—	—	—	1.11	2.18	4.32	8.43	16.5
$CH_3CH{=}CH{-}CH_2$	3.84–4.93	—	—	—	—	7.00	12.2	22.2	40.6	73.2
$C_6H_5CH{=}CH{-}CH_2$	3.74–4.07	—	—	—	15.2	26.1	46.3	86.0	153	—
$C_6H_5(CH_3)CH{-}$	3.86–4.26	6.63	14.5	31.4	65.8	137	—	—	—	—
$C_6H_5COCH_2$	3.85–4.20	—	—	—	—	1.04	2.09	3.69	7.39	13.6
$(CH_3)_2CH$	2.33–4.55	—	—	—	—	—	—	0.367	0.672	1.33
C_2H_5‡	2.97–3.18	—	—	—	—	—	—	0.212	0.395	0.725
(II) Acetone solvent										
(*a*) $4\text{-}XC_6H_4CH_2\cdot C_6H_5\cdot(CH_3)_2N^+Br^-$										
4-CH_3O	0.5*	—	—	—	15.0	29.0	48.5	100	167	—
4-CH_3	1.4*	—	—	—	—	9.60	18.5	36.7	65.2	—
4-H	1.2*	—	—	—	2.96	6.86	14.0	27.3	48.8	—
4-Br	0.2*	—	—	—	—	8.00	16.6	30.4	59.6	—
4-NO_2	0.3*	—	—	—	7.15	13.7	27.7	51.3	96.3	—
(*b*) $4\text{-}XC_6H_4CH_2\cdot C_6H_5\cdot(CH_3)_2N^+I^-$										
4-CH_3O	1.2 –3.6	—	18.7	35.7	63.3	114	187	—	—	—
4-CH_3	2.2 –3.2	—	—	—	16.9	29.1	53.8	94.0	—	—
4-H	1.3*	—	—	—	8.64	15.9	30.5	55.0	100	—
4-Br	2.3 –3.5	—	—	7.15	13.5	25.1	45.7	79.3	—	—
4-NO_2	0.5*	—	—	—	15.7	32.9	60.5	116	204	—
(*c*) $R\cdot C_6H_5\cdot(CH_3)_2N^+Br^-$										
$CH_2{=}CH{-}CH_2$	1.05–1.14	—	—	—	0.634	1.20	2.49	4.50	9.38	—
$CH_3CH{=}CH{-}CH_2$	1.7*	—	—	—	2.4	4.40	7.96	15.1	28.1	—
$C_6H_5CH{=}CH{-}CH_2$	1.0*	—	—	—	7.15	13.3	27.7	50.8	87.8	—
$C_6H_5(CH_3)CH$	0.45*	—	—	—	11.4	25.7	47.1	95.1	183	—

*Saturated solutions at room temperature; the quoted figures are approximate.
†Reference 1.
‡Complex reaction (see text).

least two determinations and some runs were performed for a number of the salts at various concentrations within the stated ranges. No variation of rate constant with concentration was observed. Activation parameters were calculated from the rate constants in Table 1 and are shown in Table 2.

Ethyldimethylphenylammonium bromide decomposed in chloroform to give a mixture of dimethylaniline and ethylmethylaniline and the corresponding ethyl and methyl bromides, and the reported rate constants for this salt were calculated from the total rate. All the other salts decomposed cleanly, each giving only two pro-

Can. J. Chem. Downloaded from www.nrcresearchpress.com by 210.87.254.5 on 09/05/12
For personal use only.

Can. J. Chem. Downloaded from www.nrcresearchpress.com by 210.87.254.5 on 09/05/12
For personal use only.

TABLE 2. Activation parameters for the decomposition of tetra-alkylammonium salts in solution

	Compound	$CHCl_3$ solvent $\Delta H^{\ddagger}$ (kcal mol^{-1})*	$CHCl_3$ solvent $\Delta S^{\ddagger}$ (cal mol^{-1} deg^{-1})*	$CHCl_3$ solvent $\Delta G^{\ddagger}$ (kcal mol^{-1})§	$(CH_3)_2CO$ solvent $\Delta H^{\ddagger}$ (kcal mol^{-1})*	$(CH_3)_2CO$ solvent $\Delta S^{\ddagger}$ (cal mol^{-1} deg^{-1})*	$(CH_3)_2CO$ solvent $\Delta G^{\ddagger}$ (kcal mol^{-1})§
(*a*)	$4\text{-}XC_6H_4CH_2\cdot C_6H_5\cdot(CH_3)_2N^+Br^-$						
	4-CH_3O	24.7±0.4	5.5±1.1	23.0	24.4±0.5	3.0±1.4	23.4
	4-CH_3	25.5±0.1	4.8±0.4	24.0	26.3±0.3	7.0±0.8	24.1
	4-H	26.3±0.4	6.1±1.1	24.4	26.8±0.2	7.5±0.7	24.3
	4-Br	27.5±0.2	9.9±0.5	24.4	27.0±0.3	9.1±1.0	24.2
	4-NO_2	25.6±0.5	4.4±1.6	24.2	26.6±0.3	8.9±0.8	23.8
(*b*)	$4\text{-}XC_6H_4CH_2\cdot C_6H_5\cdot(CH_3)_2N^+I^-$						
	4-CH_3O	21.9±0.1	−0.5±0.8	22.1	21.7±0.3	−2.8±0.9	22.6
	4-CH_3	25.2±0.1	7.4±0.6	22.9	22.8±0.3	−1.9±0.6	23.4
	4-H†	24.0±0.2	4.6±0.3	22.6	24.5±0.2	2.1±0.7	23.8
	4-Br	26.5±0.1	10.1±0.8	23.3	23.5±0.1	0.0±0.4	23.5
	4-NO_2	27.9±0.4	15.8±1.3	23.0	25.7±0.3	7.5±0.9	23.4
(*c*)	Salts with no benzyl group $R\cdot C_6H_5\cdot(CH_3)_2N^+Br^-$						
	$CH_2{=}CHCH_2$—	27.9±0.4	7.9±1.1	25.4	27.0±0.6	5.1±1.8	25.4
	$CH_3CH{=}CHCH_2$—	24.4±0.5	0.4±1.5	24.3	24.7±0.5	0.3±1.6	24.6
	$C_6H_5CH{=}CHCH_2$—	22.9±0.7	−1.7±2.2	23.4	25.6±0.6	5.4±1.8	23.9
	$C_6H_5(CH_3)CH$—	27.7±0.2	16.7±0.5	22.5	27.6±0.6	12.9±1.7	23.6
	$C_6H_5COCH_2$—	26.5±0.5	3.4±1.5	25.4	—	—	—
	$(CH_3)_2CH$—	28.1±0.7	3.4±2.2	27.0	—	—	—
	CH_3CH_2—‡	26.3±0.1	−3.1±0.2	27.3	—	—	—

*Figures after ± signs are standard deviations.
†Reference 1.
‡Complex reaction (see text).
§Calculated at 40 °C.

Can. J. Chem. Downloaded from www.nrcresearchpress.com by 210.87.254.5 on 09/05/12
For personal use only.

ducts, the dimethylaniline and the corresponding alkyl halide.

Rate Constants and Anion Identity

For a simple S_N1-type reaction the rate constant should be independent, not only of the concentration of the nucleophile, but also of its identity. In this case, the anion of the salt is the nucleophile and it may be calculated from Table 1 that the iodides react 5 to 8 times faster in chloroform and 2 to 4 times faster in acetone, than the bromides. This phenomenon is not novel, since it was reported by Hughes, Ingold, and coworkers in their study of S_N1 and E1 reactions in sulfur dioxide solvent (7–11) and was also observed by the same workers for certain reactions of triphenylmethyl chloride in benzene solvent (12, 13). From the evidence available, it is postulated that the phenomenon should appear when unimolecular reactions take place in solvents of low dielectric constant. Hughes, Ingold, and coworkers found that, in nitromethane, dielectric constant about 40, the effect was absent (14, 15). Consistent with this, the present work illustrates that the effect is greater in chloroform, dielectric constant 4.6, than in acetone, dielectric constant 20.7.

The long range electrostatic forces which must be present in solutions of ions or ion-pairs in solvents of low polarity were seen as the source of the deviation from typical S_N1 behavior by Ingold (13), although the details of the explanation were conceived in slightly different terms at different times; first in terms of an intermediate mechanism (9), then as a ubiquitous presence of the nucleophile in the reacting system (12, 13) and then again in terms of intermediate mechanisms (16). The present results seem to fit better the concept of the ubiquitous presence of the nucleophile in the form of ammonium ion-pairs.

On this basis, the least complicated picture of the reaction mechanism is a decomposition of a triple ion containing the anion nucleophile. With most of the substrate present as ion-pairs, the triple-ion concentration will be equal to the stoichiometric concentration of salt, times the degree of ionization of the ion-pairs, and a decomposition involving only a triple-ion will give a reaction order of one-half in the stoichiometric concentration of salt or an order of unity with respect to the conductivity of the solution. We call this a unimolecular reaction because there is one entity, *i.e.* one triple-ion, present in the transition state. Thus, the halide atom in the alkyl halide product comes from within the triple-ion which contains the decomposing ammonium ion. If it came from another ion-pair or another triple-ion a different kinetic order would be observed, and such a reaction would be S_N2. Although our observed mechanism is unimolecular and therefore properly written S_N1, it is not a simple S_N1 reaction and for this reason we have called it an "ionic internal nucleophilic substitution". This terminology is an extension of the unimolecular S_Ni mechanism as found *e.g.* in reactions of alkyl chlorosulfites (17).

With the halide ion present in the triple ion in the transition state, it is possible to explain the rate difference between bromide and iodide as a catalytic effect or in terms of a more specific covalent bonding between the halide and the carbon seat of reaction. To estimate the relative importance of these sources of rate differences the secondary kinetic isotope effects were studied for α-deuterated benzyl compounds (4) and were found to be much larger than the literature values for non-solvolytic S_N2 reactions and almost as large as the values found for typical limiting S_N1 reactions. Thus, the benzyl compound decomposition involves a carbonium ion, but this carbonium ion may, in fact, always be an ion-pair (4) since the halide ion is present in the transition state.

For the compounds shown in section *c* of Table 1, in which there is no benzyl group, the rate of reaction is seen to correlate approximately with the ease with which the reacting alkyl group can accommodate positive charge on the central carbon. Even when the reacting group is a saturated alkyl radical such as isopropyl or ethyl, the reaction goes very slowly and in the case of ethylphenyldimethylammonium ion some methyl cleavage was also observed. All these reactions show the same kinetics. In these circumstances it is reasonable to postulate a similar mechanism for all the reactions. This can be accomplished by postulating some covalent bonding between the halide ion and the methyl carbon in the transition state, which does not alter the S_N1 designation of the reaction. However, such covalent bonding cannot be completely dominating because the methyl and ethyl groups cleave more slowly than the isopropyl

TABLE 3. Purification of some tetra-alkylammonium salts

Alkyl(R)phenyl-dimethyl ammonium bromide	Medium of recrystallization (by volume)	Melting point (°C)
$CH_2{=}CHCH_2$	Ethanol/acetone(1:10)	134–135
$CH_3CH{=}CHCH_2$	Ethanol/acetone(1:25)	143–144
$C_6H_5CH{=}CHCH_2$	Ethanol/acetone(1:20)	129–130
$C_6H_5CH(CH_3)$	Ethanol/ether*	125–126
$C_6H_5COCH_2$	Ethanol	126–127
$(CH_3)_2CH$	Ethanol/ether(1:10)	205–207
C_2H_5	Ethanol/ether(1:10)	197–198

*The salt is very unstable on heating. The purification was done by dissolving in a minimum amount of ethanol and precipitating with dried ether. This was repeated three times.

group, that is, the alkyl groups are still in the classical order for alkyl halides reacting by a simple S_N1 mechanism rather than the S_N2 relative rate order.

Thus, the general mechanism of the triple-ion decomposition is via a transition state which contains a central carbon atom carrying some positive charge with some covalent bonding to the halide. For benzylic compounds the positive charge is large and covalent bonding quite small, whereas for saturated alkyl group cleavage these two factors must be more evenly balanced.

Activation Parameters

Within the substituted benzyl series of compounds some overall trends may be seen in the activation parameters given in Table 2. Electron releasing para-substituents are associated with smaller enthalpies of activation, a result which is expected if the reaction involves some build-up of positive charge on the benzylic carbon atom in the transition state since this would be stabilized by electron release from this substituent. The entropies of activation are, in general, compensating, with less than $1\frac{1}{2}$ kcal mol^{-1} spread in the free energy of activation. The positive $\Delta S^{\ddagger}$ values are expected for any reaction in which one molecule gives rise to two molecules of product, but the values in Table 2 are rather small and some even negative. Undoubtedly, there is a contribution to $\Delta S^{\ddagger}$ from changes in the solvation shell during reaction but it is not possible to determine the relative sizes of the contributions from the measured $\Delta S^{\ddagger}$ values of the present data.

The activation parameters for the substrate molecules containing no benzyl group in section *c* of Table 2 show much more variation and this probably reflects the differing amounts of carbonium-ion-pair character in the transition states of the different reacting groups.

Experimental

Materials

The preparation and properties of the para-substituted benzylphenyldimethylammonium salts have already been described (3). The other ammonium bromides were prepared similarly, from redistilled dimethylaniline and the corresponding alkyl bromide, purified from commercial materials. The reactions of dimethylaniline with isopropyl bromide and ethyl bromide are extremely slow. The former bromide was heated, without solvent, with the amine at about 120 °C for 125 h and gave a 9% yield and the latter at 50° for 18 h for a 10% yield. The other bromides gave quantitative yields. The methods of purification of these salts are summarized in Table 3.

Kinetics

The rate measurements were carried out as previously described (1).

Product Analyses

The reaction mixtures, after about 10 half-lives, were analyzed by v.p.c. using two columns, a silicon gum rubber SE30 and a 30% Carbowax. The first column separated the anilines and some high boiling alkyl bromides effectively at a column temperature of about 180°, and the latter was used to separate the low boiling alkyl bromides at a column temperature about 140°. The peaks were identified by comparing the retention times with those of authentic samples under identical conditions. All the reactions gave only two products except ethylphenyldimethylammonium bromide (see Results and Discussion).

The authors are grateful for financial support by the National Research Council of Canada.

1. K. T. LEFFEK and F. H-C TSAO. Can. J. Chem. **46**, 1215 (1968).

Can. J. Chem. Downloaded from www.nrcresearchpress.com by 210.87.254.5 on 09/05/12
For personal use only.

2. J. T. BURNS and K. T. LEFFEK. Can. J. Chem. **47**, 3725 (1969).
3. E. C. F. KO and K. T. LEFFEK. Can. J. Chem. **48**, 1865 (1970).
4. E. C. F. KO and K. T. LEFFEK. Can. J. Chem. **49**, 129 (1971).
5. E. A. GUGGENHEIM. Phil. Mag. **2**, 538 (1926).
6. J. M. STEWART and K. E. WEALE. J. Chem. Soc. 2849 (1965).
7. L. C. BATEMAN, E. D. HUGHES, and C. K. INGOLD. J. Chem. Soc. 1011 (1940).
8. L. C. BATEMAN, E. D. HUGHES, and C. K. INGOLD. J. Chem. Soc. 1017 (1940).
9. M. L. BIRD, E. D. HUGHES, and C. K. INGOLD. J. Chem. Soc. 634 (1954).
10. C. A. BUNTON, C. H. GREENSTREET, E. D. HUGHES, and C. K. INGOLD. J. Chem. Soc. 642 (1954).
11. C. A. BUNTON, C. H. GREENSTREET, E. D. HUGHES, and C. K. INGOLD. J. Chem. Soc. 647 (1954).
12. E. D. HUGHES, C. K. INGOLD, S. F. MOK, S. PATAI, and Y. POCKER. J. Chem. Soc. 1265 (1957).
13. C. K. INGOLD. Proc. Chem. Soc. 279 (1957).
14. E. GELLES, E. D. HUGHES, and C. K. INGOLD. J. Chem. Soc. 2918 (1954).
15. P. B. D. DE LA MARE, E. D. HUGHES, C. K. INGOLD, and Y. POCKER. J. Chem. Soc. 2930 (1954).
16. C. K. INGOLD. Structure and mechanism in organic chemistry. 2nd Ed. Cornell University Press. New York. N.Y. 1969. p. 507.
17. Reference 16. p. 537.

Can. J. Chem. Downloaded from www.nrcresearchpress.com by 210.87.254.5 on 09/05/12
For personal use only.

The Effect of Pressure on the Rate of Acetolysis of a Charge-transfer Complex

R. K. WILLIAMS, J. J. LOVEDAY, AND A. K. COLTER
Department of Chemistry, University of Guelph, Guelph, Ontario

Received December 1, 1971

Rates of acetolysis of the π acceptor 2,4,7-trinitro-9-fluorenyl *p*-toluenesulfonate, with and without added 9-methylanthracene donor, have been measured at 1, 680, and 1362 atm at 55.2 °C. The volume of activation for acetolysis of uncomplexed ester was -27 cm^3 mol^{-1} while that for acetolysis of the 1:1 complex was -33 cm^3 mol^{-1}, relative to uncomplexed reactants. The mechanistic significance of these results is discussed.

On a mesuré les vitesses d'acétolyse de l'accepteur π 2,4,7-trinitro-9-fluorenyl *p*-toluènesulfonate, avec ou sans donneur 9-méthylanthracène à 1, 680, et 1362 atm, à 55.2 °C. Le volume d'activation pour l'acétolyse de l'ester non-complexé était de -27 cm^3 mol^{-1} tandis que celui de l'acétolyse du complexe 1:1 était de -33 cm^3 mol^{-1}, comparativement aux réactifs non-complexés. On discute de la signification mécanistique des résultats.

Canadian Journal of Chemistry, **50**, 1303 (1972)

Can. J. Chem. Downloaded from www.nrcresearchpress.com by 210.87.254.40 on 09/05/12
For personal use only.

Introduction

Acetolysis of the π acceptor 2,4,7-trinitro-9-fluorenyl *p*-toluenesulfonate (**1**) is strongly accelerated by a variety of π donors (1). The kinetics of acetolysis in the presence of added donor are consistent with a mechanism involving substrate (ROTs) and donor (D) in equilibrium with 1:1 complex (ROTs·D), with concurrent acetolysis of uncomplexed and complexed substrate (Scheme 1). The greater reactivity of the 1:1 complex (rate constant k_c) is assumed to arise through electron supply from donor to acceptor in an electronically-deficient transition state.

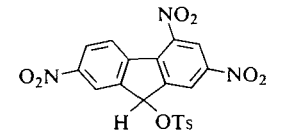

1

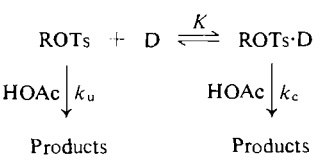

SCHEME 1

The influence of pressure on the catalyzed reaction is of particular interest for several reasons. First, the spectroscopic properties of typical π donor–π acceptor complexes are sensitive to pressure, both in solution (2, 3) and in the solid state (4, 5). An increase in pressure is almost invariably accompanied by a bathochromic shift in the charge-transfer absorption maximum and an increase in the intensity of the charge-transfer band. Since the catalytic effectiveness of aromatic donors in acetolysis of **1** also increases with an increase in the wavelength of the charge-transfer maximum (1) the chemical properties of charge-transfer complexes might be expected to be unusually pressure sensitive. The influence of pressure on k_c is of interest with regard to the structure of the complexed transition state, particularly with relation to the charge delocalization in the complex. Volumes of complex formation for a series of π donor and π acceptors in methylcyclohexane and methylene chloride were found by Ewald (3) to range between -2 and -12 cm^3 mol^{-1}.

The present study seeks to estimate the influence of pressure on the uncatalyzed acetolysis of **1** and on the acetolysis catalyzed by 9-methylanthracene donor. A previous investigation (6) has established that 9-methylanthracene is a very effective catalyst, with $K = 6.4$ l mol^{-1} and $k_c/k_u = 4.6 \times 10^2$ at 70°.

Experimental

Materials

9-Methylanthracene (Aldrich) was purified by crystallization from ethanol to m.p. 78–79°. 2,4,7-Trinitro-9-fluorenyl *p*-toluenesulfonate, m.p. 202–204°, was prepared as previously described (7). Anhydrous acetic acid was prepared by refluxing a 0.02 *M* solution of freshly fractionated acetic anhydride in reagent grade glacial acetic acid for 24 h, followed by fractionation to remove excess acetic anhydride.

Can. J. Chem. Downloaded from www.nrcresearchpress.com by 210.87.254.40 on 09/05/12
For personal use only.

Standard 0.002 *M* sodium acetate in glacial acetic acid was prepared as previously described.

Kinetic Measurements

The kinetic procedures have been described previously (8). First order behavior was observed at all donor concentrations studied and rate constants were obtained by least squares analysis of a plot of residual ester concentration *vs.* time. The pressure vessel and technique for its use were essentially as described by Koskikallio and Whalley (9). The reaction vessel was a 100 ml glass syringe lubricated with silicone grease and placed inside a standard $4\frac{3}{4}$ in. o.d. pressure vessel supplied by the American Instrument Co., Silver Spring, Maryland. The syringe was connected by an 18 gauge steel hypodermic needle to a micro control valve supplied by the High Pressure Equipment Co., Erie, Pennsylvania. Samples of 10 ml volume were extracted at intervals of time without releasing the pressure. White mineral oil was used as pressurizing fluid. The silicone grease used to lubricate the syringe was found to provide an effective barrier between the oil and the reaction solution.

Treatment of Data

The assumed mechanism leads to eq. 1 relating the observed rate constant, k_{obs}, and the stoichiometric donor concentration, $[D]_0$ (8). A plot of $(k_{obs} - k_u)^{-1}$ *vs.* $[D]_0^{-1}$

$$[1] \qquad \frac{1}{k_{obs} - k_u} = \frac{1}{k_c - k_u} + \frac{1}{K(k_c - k_u)[D]_0}$$

leads to a straight line of intercept $(k_c - k_u)^{-1}$ and slope $K(k_c - k_u)^{-1}$ from which both k_c and K can be obtained, provided that values of k_{obs} can be measured to an accuracy of $\pm 1\%$ or better. In the present work we were unable to obtain data of sufficient accuracy to determine the pressure dependence of k_c and K separately. However, $K(k_c - k_u)$, the reciprocal of the slope of the plot according to eq. 1, could be determined to about $\pm 4\%$. Since $k_c \gg k_u$ for 9-methylanthracene, $K(k_c - k_u) \approx k_c K$. The values listed in Table 2 were obtained by a simple least squares analysis of the data according to eq. 1 treating k_{obs} from each rate run as an individual point.

Calculation of the volumes of activation corresponding to the rate constants k_u and $k_c K$ was based on eq. 2 (10). Plots of log k_u and log $(k_c K)$ *vs.* pressure were linear within

$$[2] \qquad \left(\frac{\partial \ln k}{\partial P}\right)_T = -\frac{\Delta V^{\ddagger}}{RT}$$

the experimental error up to 1362 atm (Fig. 2), and values of $\Delta V^{\ddagger}$ were obtained from the least squares slopes of these plots.

Results

The observed first order rate constants obtained in this study are listed in Table 1. Figure 1 shows plots of $(k_{obs} - k_u)^{-1}$ *vs.* $[D]_0^{-1}$ for 1, 680, and 1362 atm. Values of $(k_c - k_u)K$ derived from the slopes of the plots in Fig. 1 are listed in Table 2. Figure 2 shows plots of log (k_p/k_o) *vs.* pressure for the rate constants k_u and $k_c K$, where (k_p/k_o) is the ratio of the rate constant

TABLE 1. Summary of kinetic results*

[9-Methylanthracene] (M)†	$10^6 k_{obs}$ ± average deviation (s^{-1})	No. of runs averaged
	Pressure = 1 atm	
0	0.149	1
0.0479	24.5±0.5	3
0.0575	28.9±1.6	3
0.0718	31.8±0.8	3
0.0957	38.1±1.9	4
0.150	55.6±3.0	3
0.200	57.9±2.4	2
	Pressure = 680 atm	
0	0.304	1
0.0330	42.1±0.5	3
0.0479	57.0±3.0	4
0.0575	64.1±0.3	3
0.0718	73.7±3.5	3
0.0957	93.1±1.2	3
0.125	112.8±8.9	3
	Pressure = 1362 atm	
0	0.598	1
0.0330	83.4±1.4	3
0.0479	100.0±0.8	3
0.0575	118.1±3.2	3
0.0718	133.5±3.5	3
0.0957	158.5±3.6	4

*Ester concentration = 0.002 *M*, temperature = 55.2 °C.
†At 25.0 °C.

TABLE 2. Results of analysis of kinetic data

Pressure (atm)	$10^4 K(k_c - k_u)$* (l mol^{-1} s^{-1})
1.0	6.72±0.30
680.0	15.4 ±0.5
1362.0	34.6 ±1.3

*Listed with standard deviations from least squares analysis according to eq. 1. Taken as equal to $k_c K$ within the experimental error.

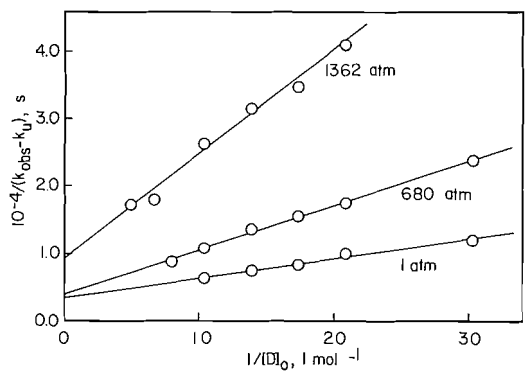

FIG. 1. Plot of $1/(k_{obs} - k_u)$ *vs.* $1/[D]_0$.

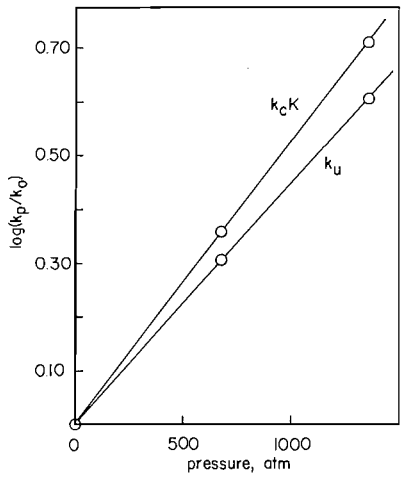

Fig. 2. Plot of log (k_p/k_o) *vs.* pressure.

TABLE 3. Volumes of activation*

$\Delta V^{\ddagger}$ corresponding to	
k_u	k_cK
-27.2 ± 0.8 cm^3 mol^{-1}	-32.6 ± 1.6 cm^3 mol^{-1}

*Listed with standard deviations from least squares analysis (Experimental).

at a given pressure to its value at atmospheric pressure. Table 3 lists values of the volumes of activation, $\Delta V^{\ddagger}$, corresponding to the rate constants k_u and k_cK.

Discussion

The value of $\Delta V^{\ddagger}$ for acetolysis of uncomplexed ester, -27 cm^3 mol^{-1}, is of little diagnostic value with regard to the structure of the uncomplexed transition state. First, there are no published results on *p*-toluenesulfonate acetolyses with which we can compare our results. Secondly, $\Delta V^{\ddagger}$ is likely to be rather insensitive to the extent of solvent nucleophilic participation in the transition state (11). However, a considerable amount of other evidence (12), including the catalysis by aromatic donors, points to a transition state having considerable carbonium ion character and the present results are not inconsistent with this picture.

The significance of the two volumes of activation measured in the present work can be seen by reference to Scheme 2 which is an

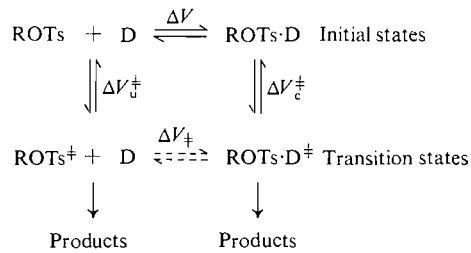

SCHEME 2

expansion of the mechanism outlined in Scheme 1 to include equilibrium between initial and transition states (13). The quantity k_cK is simply the rate constant for acetolysis via the 1:1 complex based on uncomplexed reactants. The volume of activation based on k_cK is equal to $\Delta V + \Delta V_c^{\ddagger}$, or $\Delta V_u^{\ddagger} + \Delta V_{\ddagger}$ in Scheme 2. The difference between the two volumes of activation measured in the present work (5 cm^3 mol^{-1}) can therefore be viewed as the volume of the uncomplexed transition state plus donor minus the volume of the complexed transition state, *i.e.*, $-\Delta V_{\ddagger}$. On this basis, $\Delta V_{\ddagger}$ (-5 cm^3 mol^{-1}) is within the range of values observed by Ewald (3) (above) for formation of a variety of π complexes.

Considering: (*a*) the usual magnitude of the variation of the charge-transfer absorption frequency with pressure (2, 3) and, (*b*) the magnitude of the variation of k_c and k_cK with the frequency of the charge-transfer maximum for different donors (1), one might have expected a much larger variation of k_cK with pressure. Such a variation in the chemical properties of the complex with pressure would show up as a negative contribution to $\Delta V^{\ddagger}$ for acetolysis via the 1:1 complex. Using data reported in the literature (1, 3) we have calculated that this contribution could be as large as -10 cm^3 mol^{-1}. Why no such dramatic effect was observed in the present work we cannot yet say. Possibly it may be obscured by the effects of extensive charge delocalization in the complexed transition state. The measured value of $\Delta V_{\ddagger}$ (-5 cm^3 mol^{-1}) is consistent with a contribution of, say, -8 to -10 cm^3 mol^{-1} due to complexation, which is within the range found by Ewald (3), and a contribution of $+3$ to $+5$ cm^3 mol^{-1} due to charge delocalization, which is within the range estimated by le Noble and co-workers (14) for several solvolysis

Can. J. Chem. Downloaded from www.nrcresearchpress.com by 210.87.254.40 on 09/05/12
For personal use only.

reactions involving neighboring σ bond participation.

This research was supported in part by grants from the University of Guelph Research Advisory Board and the National Research Council of Canada.

1. A. K. COLTER and S. H. HUI. J. Org. Chem. **33**, 1937 (1968), and earlier papers in this series.
2. J. R. GOTT and W. G. MAISCH. J. Chem. Phys. **39**, 2229 (1963).
3. A. H. EWALD. Trans. Faraday Soc. **64**, 733 (1968).
4. D. R. STEPHENS and H. G. DRICKAMER. J. Chem. Phys. **30**, 1518 (1959).
5. A. H. KADHIM and H. W. OFFEN. J. Chem. Phys. **48**, 749 (1968), and earlier papers in this series.
6. A. L. MCKENNA, III. Ph.D. Thesis, Carnegie-Mellon University, Pittsburgh, Pennsylvania, January, 1970.
7. A. K. COLTER and S. S. WANG. J. Org. Chem. **27**, 1517 (1962).
8. A. K. COLTER, S. S. WANG, G. H. MEGERLE, and P. S. OSSIP. J. Am. Chem. Soc. **86**, 3106 (1964).
9. J. KOSKIKALLIO and E. WHALLEY. Trans. Faraday Soc. **55**, 809 (1959).
10. M. G. EVANS and M. POLANYI. Trans. Faraday Soc. **31**, 875 (1935).
11. W. J. LE NOBLE. *In* Progress in physical organic chemistry. Vol. 5. *Edited by* A. Streitwieser, Jr. and R. W. Taft. Interscience Publishers, New York, N.Y. 1967. p. 307.
12. A. K. COLTER and M. R. J. DACK. *In* Molecular complexes. Vol. 1. *Edited by* R. Foster. London. In press.
13. J. L. KURZ. J. Am. Chem. Soc. **85**, 987 (1963).
14. W. J. LE NOBLE, B. L. YATES, and A. W. SCAPLEHORN. J. Am. Chem. Soc. **89**, 3751 (1967).

Can. J. Chem. Downloaded from www.nrcresearchpress.com by 210.87.254.40 on 09/05/12
For personal use only.

Studies on Metal Carboxylates. Part II.[1] Cobalt(II) and Nickel(II) Complexes of Certain Pyridine Carboxylic Acids and Pyridine-3-Sulfonic Acid: Magnetic and Spectral Studies

A. ANAGNOSTOPOULOS[2]

Department of Chemistry, University of Reading, Reading, Berkshire, U.K.

R. W. MATTHEWS[3]

Department of Chemistry, University of Western Ontario, London, Ontario

AND

R. A. WALTON[4]

Department of Chemistry, Purdue University, Lafayette, Indiana 47907

Received October 6, 1971

Several pyridine carboxylate complexes of cobalt(II) and nickel(II) have been prepared and their spectral and magnetic properties and X-ray powder patterns used to establish their stereochemistry. The cobalt(II) complex of pyridine-3-carboxylic acid $Co[3\text{-}py(CO_2)]_2 \cdot 4H_2O$, whose crystal structure we have previously reported, was used as a model for a consideration of the structural details of these complexes. Like the latter cobalt(II) derivative, the nickel(II) complex of pyridine-3-carboxylic acid and the cobalt(II) and nickel(II) complexes of pyridine-4-carboxylic acid and pyridine-3-sulfonic acid, isolated as their tetrahydrates, are formulated as non-classical zwitterions. Comparisons are made with the related pyridine carboxylate complexes of silver(II).

On a préparé plusieurs complexes carboxylate de pyridine de cobalt(II) et de nickel(II) et on a utilisé leurs propriétés spectrales et magnétiques et leurs spectres de poudres par rayons-X pour établir leur stéréochimie. Le complexe de cobalt(II) de l'acide pyridine-carboxylique-3 $Co[3\text{-}py(CO_2)]_2 \cdot 4H_2O$, dont la structure cristalline a été rapportée précédemment, a été utilisé comme modèle dans l'étude des détails structuraux de ces complexes. Comme le dérivé du cobalt(II) précédent, le complexe de nickel(II) de l'acide pyridine-3 carboxylique et les complexes de cobalt(II) et de nickel(II) l'acide pyridine-4 carboxylique et de l'acide pyridine-3 sulfonique, isolés sous forme de tétrahydrates, sont formulés comme étant des zwitterions non-classiques. On compare ensuite ces complexes à ceux de l'argent(II), soient les complexes pyridine carboxylate.

Canadian Journal of Chemistry, **50**, 1307 (1972)

Introduction

In our studies of pyridine carboxylates of silver(II) (2–6), we have investigated the structural features of certain of these species in order to provide a basis for the interpretation of their spectral and magnetic properties, and to better understand their chemical reactivity, in particular their role as oxidizing agents. Unlike pyridine-2-carboxylic acid (picolinic acid), the pyridine-3- and -4-carboxylic acids (nicotinic and isonicotinic acids, respectively) cannot act as chelating ligands, although they can conceivably bridge metal atoms in several ways (structures **1**, **2**, or **3**), or act as monodentate

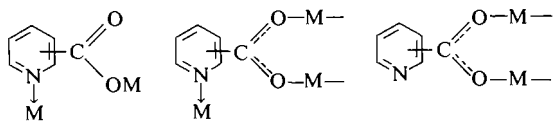

1 **2** **3**

donors. We have previously noted (2) that the temperature range magnetic properties of $Ag[3\text{-}py(CO_2)]_2$, which is not isomorphous with $Cu[3\text{-}py(CO_2)]_2$, could be interpreted in terms of the presence of a pronounced antiferromagnetic interaction, although we have as yet no information on the structural details of this polymeric complex. Accordingly, we decided to investigate the cobalt(II) and nickel(II) complexes of several pyridine carboxylic acids in which $-CO_2H$ groups were present in the 3- and 4- positions. We chose these particular systems since (*i*), the complexes

[1]Part I, ref. 1.

[2]Present address: Department of Chemistry, University of Patras, Patrae, Greece.

[3]Present address: University Chemical Laboratory, Lensfield Road, Cambridge CB2 1EW, U.K.

[4]To whom correspondence should be addressed.

Can. J. Chem. Downloaded from www.nrcresearchpress.com by 210.87.254.5 on 09/05/12
For personal use only.

Can. J. Chem. Downloaded from www.nrcresearchpress.com by 210.87.254.5 on 09/05/12
For personal use only.

can generally be isolated in the pure state in nicely crystalline form and should be suitable for single-crystal X-ray studies, and (*ii*), from a study of their magnetic and spectral properties we should be able to establish the gross stereochemistry of the metal atoms fairly readily, and thereby deduce the nature of the pyridine carboxylate coordination. The results of this investigation are now reported.

Experimental Section

The pyridine carboxylic acids were all commercially available (Aldrich, B.D.H., Koch-Light, or Mersey Chemicals Ltd.) and were used without further purification. Pyridine-3-sulfonic acid (Aldrich) was recrystallized twice from water before use. Henceforth, the acids and their anions are abbreviated *N*-py(X) where $X = CO_2^-$, CO_2H, SO_3^-, or SO_3H and *N* denotes the position of X in the pyridine ring, py.

Preparation of the Complexes

Complexes $ML_2 \cdot 4H_2O$ where M = Co or Ni and L = 3-py(CO_2), 4-py(CO_2), or 3-py(SO_3). The ligand (2.2 mol) was dissolved in dilute, aqueous sodium hydroxide and the p*H* of the solution adjusted to *ca.* 6 with dilute nitric acid. The solution was filtered, warmed to *ca.* 60° and added to a warm solution of the metal(II) nitrate hexahydrate (1.0 mol) in a small volume of water. The product precipitated immediately from solution. After the solution had cooled to room temperature, the product was collected, washed with water, ethanol, and ether, and dried *in vacuo* over calcium chloride.

Complexes $M[2,3\text{-}py(CO_2)(CO_2H)]_2 \cdot 2H_2O$ where M = Co or Ni. Pyridine-2,3-dicarboxylic acid (2.2 mol) was dissolved in dilute aqueous sodium hydroxide and the solution adjusted to p*H* 4–5 using dilute nitric acid. The solution was filtered, warmed to *ca.* 60° and added to a warm solution of the metal(II) nitrate hexahydrate (1.0 mol) in a small volume of water. After allowing the solution to stand at 0–5° for a few hours, the complex precipitated and was filtered off, washed with water, ethanol, and ether, and dried *in vacuo* over calcium chloride. The same product was also obtained when a metal to ligand ratio of 1.1:1.0 was used.

Complexes $Co[2,5\text{-}py(CO_2)_2] \cdot 4H_2O$ *and* $Ni[2,5\text{-}py(CO_2)_2] \cdot 5H_2O$. Pyridine-2,5-dicarboxylic acid monohydrate (1.0 mol) was dissolved in dilute aqueous potassium carbonate solution. The solution was brought to p*H ca.* 6 with dilute nitric acid, boiled for a few minutes to expel CO_2, filtered, and added to a warm solution of the metal(II) nitrate hexahydrate (1.1 mol) in a small volume of water. On cooling to room temperature, the product precipitated from solution. After collection the product was washed with water, ethanol, and ether, and dried *in vacuo* over calcium chloride.

Complex $Ni[2,5\text{-}py(CO_2)(CO_2H)]_2 \cdot 3H_2O$. Pyridine-2,5-dicarboxylic acid monohydrate (2.2 mol) was dissolved in a large volume of boiling water. After filtering the hot solution, it was further boiled while a solution of nickel(II) nitrate hexahydrate (1.0 mol) in a small volume of water was added dropwise. The product precipitated immediately and was collected by filtering the hot reaction mixture through a heated Buchner funnel. The product was washed with boiling water, ethanol, and ether, and dried *in vacuo* over calcium chloride.

Attempts to prepare the cobalt analog of this complex by a similar procedure yielded products which analyzed closely for $Co[2,5\text{-}py(CO_2)(CO_2H)]_2 \cdot 1\frac{1}{2}\ H_2O$.

Anal. Calcd. for $C_{14}H_{11}N_2O_{9.5}Co$: C, 40.2; H, 2.7; N, 6.7. Found: C, 39.7; H, 2.6; N, 6.7.

Analyses

Cobalt. The complexes were destroyed by boiling with a 1:1 mixture of concentrated sulfuric and perchloric acids. After dilution the solution was buffered, treated with R-nitroso salt and the cobalt determined spectrophotometrically.

Nickel. The complex was dissolved in concentrated hydrochloric acid and the solution made alkaline with concentrated ammonia solution (28%). The nickel was determined gravimetrically as the dimethylglyoxime complex.

Carbon, Hydrogen, and Nitrogen. These elements were determined in the microanalytical laboratory at the University of Reading and by A. Bernhardt, Germany.

Colors, elemental and thermogravimetric analyses for the complexes are shown in Table 1.

Physical Measurements

Since the complexes were found to be insoluble in polar and non-polar solvents, visible–u.v. spectra were determined by the diffuse reflectance technique on Unicam SP 700 and Cary 14 spectrophotometers. Infrared spectra were recorded as Nujol and hexachlorobutadiene mulls on Perkin–Elmer PE 457 and Beckman IR 10 spectrophotometers. Magnetic susceptibility measurements were made on a Newport Instruments variable temperature Gouy balance system. Mercury tetrathiocyanatocobaltate(II) was used as calibrant and diamagnetic corrections were estimated from Pascal's constants.

Thermogravimetric analyses were made using a Stanton thermogravimetric balance. The X-ray powder patterns were determined on a Philips X-ray diffractometer (PW 1051) using filtered Cu–$K_{\alpha 1}$ radiation ($\lambda = 1.5405$ Å).

Results and Discussion

A series of complexes of cobalt(II) and nickel(II) with pyridine carboxylic acids containing acid groups in the 3-, 4-, 2,3-, and 2,5-positions has been prepared, together with related complexes of pyridine-3-sulfonic acid. Complexes with metal to ligand ratios of 1:2 were obtained for mono-acidic ligands and pyridine-2,3-dicarboxylic acid, while ratios of 1:2 and 1:1 were obtained using pyridine-2,5-dicarboxylic acid. The presence of water of hydration in all the complexes was confirmed by the observation of ν(O—H) bands in the i.r. spectra, and by thermogravimetric analyses (Table 1).

Can. J. Chem. Downloaded from www.nrcresearchpress.com by 210.87.254.5 on 09/05/12
For personal use only.

TABLE 1. Elemental and thermogravimetric analyses for the complexes

Compound	Color	Analysis (%) Found Metal	C	H	N	Calcd. Metal	C	H	N	Total decomposition T* (°C)	Weight loss (%) Found	Calcd.	Removal of water T† (°C)	Weight loss (%) Found	Calcd.
$Co[3\text{-}py(CO_2)]_2\cdot 4H_2O$	Pink	15.8	38.4	4.4	7.5	15.7	38.4	4.3	7.5	480	78.9	78.6‡	No stepwise loss of water		
$Ni[3\text{-}py(CO_2)]_2\cdot 4H_2O$	Pale blue	15.6	38.6	4.5	7.6	15.7	38.4	4.3	7.5	750	79.7	80.1§	No stepwise loss of water		
$Co[4\text{-}py(CO_2)]_2\cdot 4H_2O$	Pale orange	15.6	38.3	4.3	7.5	15.7	38.4	4.3	7.5	470	78.2	78.6‡	120–220	19.6	19.2
$Ni[4\text{-}py(CO_2)]_2\cdot 4H_2O$	Blue-green	15.6	38.4	4.5	7.6	15.7	38.4	4.3	7.5	600	79.6	80.1§	120–230	19.9	19.2
$Co[3\text{-}py(SO_3)]_2\cdot 4H_2O$	Orange	13.2	26.3	3.8	6.3	13.1	26.9	3.6	6.3	650	74.6	||	100–300	16.3	16.1
$Ni[3\text{-}py(SO_3)]_2\cdot 4H_2O$	Pale blue	12.9	25.6	3.6	6.3	13.1	26.9	3.6	6.3	650	80.0	||	80–320	16.4	16.1
$Co[2,3\text{-}py(CO_2)(CO_2H)]_2\cdot 2H_2O$	Orange	14.0	40.1	3.1	6.7	13.8	39.4	2.8	6.6	500	81.0	81.2‡	200–320	30.4	29.0¶
$Ni[2,3\text{-}py(CO_2)(CO_2H)]_2\cdot 2H_2O$	Pale blue	13.2	39.7	2.9	6.7	13.8	39.4	2.8	6.6	500	82.3	82.5§	200–350	29.9	29.1¶
$Co[2,5\text{-}py(CO_2)_2]\cdot 4H_2O$	Orange	19.9	28.4	3.7	4.9	19.9	28.4	3.6	4.7	470	72.0	72.9‡	40–220	25.1	24.3
$Ni[2,5\text{-}py(CO_2)_2]\cdot 5H_2O$	Pale blue	19.0	26.3	4.5	4.5	18.7	26.8	4.2	4.5	640	76.0	76.2§	80–260	28.1	28.7
$Ni[2,5\text{-}py(CO_2)(CO_2H)]_2\cdot 3H_2O$	Pale blue	12.9	38.3	3.0	6.4	13.2	37.8	3.2	6.3	500	83.1	83.2§	60–250	12.7	12.2

*Temperature at which decomposition was complete.
†Temperature range for first stepwise weight loss.
‡Assuming Co_3O_4 residue.
§Assuming NiO residue.
||Stoichiometry of residue unknown.
¶Assuming loss of $2H_2O + 2CO_2$.

Can. J. Chem. Downloaded from www.nrcresearchpress.com by 210.87.254.5 on 09/05/12
For personal use only.

TABLE 2. X-Ray diffraction powder patterns for $M[3\text{-py}(CO_2)]_2\cdot 4H_2O$, M = Co, Ni

$Co[3\text{-py}(CO_2)]_2\cdot 4H_2O$		$Ni[3\text{-py}(CO_2)]_2\cdot 4H_2O$	
Relative intensity	d (Å)	Relative intensity	d (Å)
25	7.56	20	7.49
100	6.60	95	6.56
13	6.31	11	6.24
75	6.09	100	6.06
13	5.37	16	5.34
50	4.27	42	4.24
31	4.24	20	4.19
63	3.99	53	3.95
25	3.91	24	3.88
13	3.59	9	3.56
63	3.47	93	3.45
31	3.36	29	3.33
6	3.30	4	3.27
13	3.14	11	3.13
19	3.06	22	3.05
31	3.03	35	3.02
13	2.81	9	2.80
19	2.71	16	2.68
31	2.67	28	2.66
13	2.61	7	2.58
13	2.58	7	2.56
19	2.50	15	2.48
19	2.48	11	2.47
6	2.36	5	2.37
37	2.19	29	2.17

TABLE 3. X-ray diffraction powder patterns for $M[4\text{-py}(CO_2)]_2\cdot 4H_2O$, M = Co, Ni

$Co[4\text{-py}(CO_2)]_2\cdot 4H_2O$		$Ni[4\text{-py}(CO_2)]_2\cdot 4H_2O$		
Relative intensity	d (Å)	Relative intensity	d (Å)	
10	8.76	18	8.63	
6	6.19	13	6.15	
100	5.56	100	5.50	
10	4.56	9	4.51	
3	4.42	4	4.37	
2	4.17	—	—	
3	4.10	4	4.04	
4	3.60	4	3.60	
19	3.40	33	3.39	
3	3.28	—	—	
9	3.22	11	3.19	broad
8	3.14			
5	3.09	7	3.08	
3	2.98	4	2.94	
3	2.89	4	2.89	
2	2.76	4	2.76	
4	2.70	7	2.70	
9	2.28	11	2.25	

The X-ray powder data (Tables 2–5) for the complexes $M[3\text{-py-}(CO_2)]_2\cdot 4H_2O$, $M[4\text{-py-}(CO_2)]_2\cdot 4H_2O$, $M[3\text{-py}(SO_3)]_2\cdot 4H_2O$ and $M[2,3\text{-py}(CO_2)(CO_2H)]_2\cdot 2H_2O$ (M = Co, Ni) shows that each cobalt complex is isomorphous with its nickel analog and a consideration of the d values and intensities suggests that the complexes are isostructural. The 1:1 complexes of cobalt and nickel with pyridine-2,5-dicarboxylic acid are not isomorphous (Table 6).

As a basis for considering the magnetic and spectral properties of these complexes, we had previously (7) established the structure of crystalline $Co[3\text{-py}(CO_2)]_2\cdot 4H_2O$ from a 3-dimensional single crystal X-ray analysis which revealed a slightly distorted octahedral environment around cobalt, comprising a planar array of aqueous oxygens and two axial nitrogens (structure **4**). This species can clearly be formu-

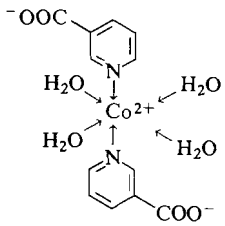

4

lated as a non-classical zwitterion. The magnetic and electronic spectral properties (Tables 7 and 8) of this complex are as expected typical of a pseudo-octahedral environment (8, 9) and since these properties are similar to those of the cobalt(II) complexes of pyridine-4-carboxylic acid and pyridine-3-sulfonic acid, it is reasonable to conclude that octahedral coordination around the cobalt atom prevails throughout the series. Likewise, the nickel complexes have similar magnetic and electronic spectral properties and these are characteristic (8, 9) of approximate octahedral coordination around the metal ion. The isomorphism of the related cobalt and nickel complexes confirms this conclusion, and so we can envisage similar structures to **4** for $M[4\text{-py}(CO_2)]_2\cdot 4H_2O$ and $M[3\text{-py}(SO_3)]_2\cdot 4H_2O$. Previous work by Sacconi (10) and Kleinstein and Webb (11) is of relevance to these conclusions. In these two earlier studies, room temperature magnetic moments were

Can. J. Chem. Downloaded from www.nrcresearchpress.com by 210.87.254.5 on 09/05/12
For personal use only.

TABLE 4. X-Ray diffraction powder patterns for $M[3\text{-py}(SO_3)]_2\cdot 4H_2O$, M = Co, Ni

$Co[3\text{-py}(SO_3)]_2\cdot 4H_2O$		$Ni[3\text{-py}(SO_3)]_2\cdot 4H_2O$	
Relative intensity	d (Å)	Relative intensity	d (Å)
22	7.17	24	7.20
100	6.49	100	6.44
29	6.11	23	6.07
4	5.13	4	5.10
4	4.90 broad	5	4.91
—	—	4	4.82
40	4.40	31	4.37
32	4.33	27	4.35
47	4.10	41	4.08
19	3.80	11	3.79
31	3.77	35	3.72
4	3.58	4	3.58
7	3.50	4	3.46
22	3.32	19	3.31
25	3.24	20	3.22
25	3.19	28	3.18
6	3.03	7	3.02
6	2.96	4	2.09
8	2.58	7	2.58
4	2.46	7	2.44
4	2.41	—	—
8	2.19	5	2.18
4	2.13	4	2.14

recorded for $M[3\text{-py}(CO_2)]_2\cdot 4H_2O$ (M = Co, Ni) and $Ni[4\text{-py}(CO_2)]_2\cdot 4H_2O$ which are in reasonable agreement with our more complete data. However, Kleinstein and Webb (11) concluded from a study of these three complexes, together with the anhydrous salts and several nitrogen base adducts of the type $M[X\text{-py}(CO_2)]_2\cdot nL$, where $n = 4$ for $L = NH_3$ and $n = 2$ for L = pyridine and β- or γ-picoline, that "small differences in the electronic spectra and magnetic moments of the cobalt(II) and nickel(II) complexes produced by the introduction of water or base indicate little change in the structure of the complexes." This clearly is not the case since we have demonstrated that the tetrahydrates are mononuclear species in which the $-COO^-$ groups are not coordinated. On the other hand, dehydration of these derivatives must be accompanied by gross structural changes, with the $-COO^-$ groups now becoming incorporated in the first coordination sphere with the resulting formation of polymeric species. However, it seems possible that a MO_4N_2 (M = Co, Ni) structural unit is preserved since the electronic absorption spectra of the anhydrous complexes (11) are still indicative of a pseudo-octahedral stereochem-

TABLE 5. X-Ray diffraction powder patterns for $M[2,3\text{-py}(CO_2)(CO_2H)]_2\cdot 2H_2O$, M = Co, Ni

$Co[2,3\text{-py}(CO_2)(CO_2H)]_2\cdot 2H_2O$		$Ni[2,3\text{-py}(CO_2)(CO_2H)]_2\cdot 2H_2O$	
Relative intensity	d (Å)	Relative intensity	d (Å)
13	6.61	15	6.61
100	6.31	100	6.30
9	6.03	10	6.00
17	5.72	—	—
14	5.19	24	5.19
11	5.08	10	5.07
10	4.81	—	—
9	4.33	5	4.33
9	4.23	—	—
7	4.04	10	4.02
39	3.83	34	3.82
14	3.64	12	3.64
16	3.52	—	—
9	3.48	10	3.47
4	3.30	—	—
86	3.14	70	3.14
13	3.08	7	3.01
13	2.92	15	2.92
6	2.65	—	—
6	2.61	7	2.59

TABLE 6. X-Ray diffraction powder patterns for cobalt(II) and nickel(II) complexes of pyridine-2,5-dicarboxylic acid

$Co[2,5\text{-}py(CO_2)_2]\cdot 4H_2O$		$Ni[2,5\text{-}py(CO_2)_2]\cdot 5H_2O$		$Ni[2,5\text{-}py(CO_2)(CO_2H)]_2\cdot 3H_2O$	
Relative intensity	d (Å)	Relative intensity	d (Å)	Relative intensity	d (Å)
10	12.28	59	10.72	100	12.36
22	9.41	100	7.80	28	6.11
33	8.47	6	6.46	21	5.87
100	6.58	76	6.09	7	5.19
54	6.05	30	5.61	9	4.96
8	5.83	13	5.34	7	4.67
24	5.57	31	5.16	14	4.06
6	5.19	17	5.00	7	3.38
14	4.93	61	4.52	5	3.26
25	4.75	26	4.29	14	3.13
25	4.44	41	4.25	5	3.05
13	4.23	13	4.17	5	2.90
14	3.99	57	3.88	4	2.55
11	3.79	11	3.83	4	2.44
16	3.47	41	3.72	4	2.27
6	3.38	11	3.41		
27	3.29	28	3.34		
51	3.09	15	3.27		
10	3.03	9	3.18		
13	2.85	70	3.11		
11	2.68	24	3.06		
21	2.64	7	2.91		
14	2.52	9	2.83		
11	2.47	24	2.79		
8	2.35	7	2.76		
8	2.22	7	2.70		
13	2.15	17	2.67		
13	2.00	17	2.64		
		9	2.57		
		11	2.49		
		15	2.29		

TABLE 7. Summary of magnetic properties of cobalt(II) and nickel(II) complexes*

Complex	μ_{eff} at 303 °K	μ_{eff} at 79 °K	θ (°K)†
$Co[3\text{-}py(CO_2)]_2\cdot 4H_2O$	4.80	4.14	+24
$Co[4\text{-}py(CO_2)]_2\cdot 4H_2O$	4.78	4.15	+24
$Co[3\text{-}py(SO_3)]_2\cdot 4H_2O$	4.78‡	—	—
$Co[2,3\text{-}py(CO_2)(CO_2H)]_2\cdot 2H_2O$	4.84	4.31	+18
$Co[2,5\text{-}py(CO_2)_2]\cdot 4H_2O$	4.70	4.19	+19
$Ni[3\text{-}py(CO_2)]_2\cdot 4H_2O$	3.11	2.85	+10
$Ni[4\text{-}py(CO_2)]_2\cdot 4H_2O$	3.16	2.91	+11
$Ni[3\text{-}py(SO_3)]_2\cdot 4H_2O$	3.24‡	—	—
$Ni[2,3\text{-}py(CO_2)(CO_2H)]_2\cdot 2H_2O$	3.15	2.89	+8
$Ni[2,5\text{-}py(CO_2)_2]\cdot 5H_2O$	3.02‡	—	—
$Ni[2,5\text{-}py(CO_2)(CO_2H)]_2\cdot 3H_2O$	3.22	2.93	+9

*Temperature range magnetic susceptibility studies were carried out at eleven temperatures between 303 and 79 °K. Full details of the magnetic data are available on request to R.A.W.

†The constants θ were determined from plots of $1/X'm$ *vs.* temperature, assuming Curie–Weiss law behavior.

‡Magnetic susceptibility measurements for these complexes were recorded at room temperature only (294 °K).

Can. J. Chem. Downloaded from www.nrcresearchpress.com by 210.87.254.5 on 09/05/12
For personal use only.

TABLE 8.
(*a*) Diffuse reflectance spectra of cobalt(II) complexes*

Cobalt(II) complexes	Absorption maxima ($\times 10^{-3}$ cm^{-1}) and assignments†		
	$^4T_{1g} \rightarrow {}^4T_{2g}$ (ν_1)	$^4T_{1g} \rightarrow {}^4T_{1g}$(P) ($\nu_3$)	Charge-transfer
Co[3-py(CO_2)]$_2$·4H_2O	8.2	19.4	37.3
Co[4-py(CO_2)]$_2$·4H_2O	8.9	20.3; 21.3	31.6sh; 36.2
Co[3-py(SO_3)]$_2$·4H_2O	8.4	20.0	37.2
Co[2,3-py(CO_2)(CO_2H)]$_2$·2H_2O	8.7	18.9sh; 20.4	29.2; 36.4
Co[2,5-py(CO_2)$_2$]·4H_2O	8.8	20.2	30.4; 37.6

(*b*) Diffuse reflectance spectra of nickel(II) complexes

Nickel(II) complexes	$^3A_{2g} \rightarrow {}^3T_{2g}$ (ν_1)	$^3A_{2g} \rightarrow {}^3T_{1g}$(F) ($\nu_2$)	$^3A_{2g} \rightarrow {}^3T_{1g}$(P) ($\nu_3$)	Charge-transfer
Ni[3-py(CO_2)]$_2$·4H_2O	9.5	15.5	25.8	37.0
Ni[4-py(CO_2)]$_2$·4H_2O	9.8	15.9	26.4sh	31.5sh; 36.2
Ni[3-py(SO_3)]$_2$·4H_2O	9.7	15.7	26.2	37.4
Ni[2,3-py(CO_2)(CO_2H)]$_2$·2H_2O	9.5sh; 11.0	16.5	29.9sh	35.6
Ni[2,5-py(CO_2)$_2$]·5H_2O	9.5	15.6	26.9sh	31.6sh; 37.3
Ni[2,5-py(CO_2)(CO_2H)]$_2$·3H_2O	9.5	16.4	29.0sh	35.0sh; 37.0

*MgO used as reference.
†See ref. 9.

istry. We suggest that the adducts M[X-py-(CO_2)]$_2$·2L (11), may represent an intermediate structural situation, with coordination from the nitrogen atoms of the pyridine carboxylic acid and the nitrogen base L, and an oxygen atom of the —COO^- group (structure **5**).

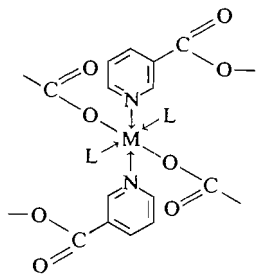

5

The isomorphous pair of complexes derived from pyridine-2,3-dicarboxylic acid, M[2,3-py-(CO_2)(CO_2H)]$_2$·2H_2O are seen to have magnetic and spectral properties characteristic of pseudo-octahedral species (Tables 7 and 8). These are also reminiscent of the related properties of the corresponding complexes of pyrazine-2,3-dicarboxylic acid, M[2,3-pyz-(CO_2)(CO_2H)]·2H_2O (12). These complexes must contain a MO_4N_2 moiety, and we believe that they have a structure in which the two water molecules are coordinated (structure **6**)[5] rather

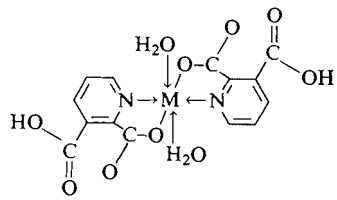

6

than the alternative in which the primary coordination sphere is completed by weak "interactions" with the —COOH groups in the 3 positions of *adjacent* M[2,3-py(CO_2)(CO_2H)]$_2$ molecules. This latter possibility is realized in the related silver(II) complex Ag[2,3-py(CO_2)-(CO_2H)]$_2$·2H_2O, in which the stereochemistry about silver approaches square-planar (5, 6). Support for this conclusion comes from our observation that this silver(II) derivative is not

[5]A related stereochemistry has been found for the nickel(II) and zinc(II) complexes of pyridine-2-carboxylic acid, M[2-py(CO_2)]$_2$·4H_2O (13, 14); the remaining two water molecules per formula unit are hydrogen-bonded within the lattice.

Can. J. Chem. Downloaded from www.nrcresearchpress.com by 210.87.254.5 on 09/05/12
For personal use only.

isomorphous with the cobalt(II) and nickel(II) complexes considered here.

The final group of complexes which we have investigated are those derived from pyridine-2,5-dicarboxylic acid. Although 1:1 complexes $Co[2,5\text{-}py(CO_2)_2]\cdot 4H_2O$ and $Ni[2,5\text{-}py(CO_2)_2]\cdot 5H_2O$ are not isomorphous, it seems probable that they also possess pseudo-octahedral structures, with some water molecules involved in the first coordination sphere while the remainder are incorporated into the lattice via a complex hydrogen-bonding network. While we have isolated the 1:2 complex $Ni[2,5\text{-}py(CO_2)(CO_2H)]_2\cdot 3H_2O$, a species whose thermal properties have been reported previously (15), we did not isolate the previously reported $Co[2,5\text{-}py(CO_2)(CO_2H)]_2\cdot 4H_2O$ (15). Rather we found that the product from this latter system analyzed as a lower hydrate. However, its infrared spectrum was virtually identical to that of the above nickel(II) complex and its powder pattern, while more complex than that for $Ni[2,5\text{-}py(CO_2)(CO_2H)]_2\cdot 3H_2O$, showed all but two weak lines characteristic of the latter system. The extra lines observed in the powder pattern of the cobalt(II) complex are not due to the presence of $Co[2,5\text{-}py(CO_2)_2]\cdot 4H_2O$ or the free acid. Accordingly, this product may be a mixture of $Co[2,5\text{-}py(CO_2)(CO_2H)]_2\cdot 3H_2O$ and an unidentified impurity.

Infrared mull spectra (4000–600 cm^{-1}) have been recorded for all the complexes described in this investigation. At the present time, we feel that detailed analyses of these spectra are not justified, particularly with regard to any deductions as to the nature of the carboxylate groups. One of the main reasons for this is that the hydrated complexes of these different pyridine carboxylic acids have lattices which are stabilized by different degrees of hydrogen-bonding, in which interactions between $-COO^-$, $-COOH$ and H_2O are clearly extremely important. Consequently, modifications of the $\nu(C{-}O)$ vibrations can arise from strong hydrogen-bonding effects. An inspection of the spectra of these complexes clearly shows that as expected the isomorphous pairs of complexes have virtually identical spectra.[6]

One of us (R.W.M.) gratefully acknowledges financial support from the University of Western Ontario; A.A. thanks the Greek Ministry of Co-ordination for financial support, and R.A.W. acknowledges the award of a grant from the Camille and Henry Dreyfus Foundation.

1. H. Gaw, W. R. Robinson, and R. A. Walton. Inorg. Nucl. Chem. Lett. **7**, 695 (1971).
2. G. W. A. Fowles, R. W. Matthews, and R. A. Walton. J. Chem. Soc. A, 1108 (1968).
3. M. G. B. Drew, G. W. A. Fowles, R. W. Matthews, and R. A. Walton. J. Am. Chem. Soc. **91**, 7769 (1969).
4. M. G. B. Drew, R. W. Matthews, and R. A. Walton. J. Chem. Soc. A, 1405 (1970).
5. M. G. B. Drew, R. W. Matthews, and R. A. Walton. Inorg. Nucl. Chem. Lett. **6**, 277 (1970).
6. M. G. B. Drew, R. W. Matthews, and R. A. Walton. J. Chem. Soc. A, 2959 (1971).
7. A. Anagnostopoulos, M. G. B. Drew, and R. A. Walton. Chem. Commun. 1241 (1969).
8. B. N. Figgis and J. Lewis. Prog. Inorg. Chem. **6**, 37 (1964), and references therein.
9. C. J. Ballhausen. Introduction to Ligand Field Theory, McGraw-Hill, 1962, pp. 256, 261.
10. L. Sacconi. Ann. Chim. **40**, 386 (1950).
11. A. Kleinstein and G. A. Webb. J. Inorg. Nucl. Chem. **33**, 405 (1970).
12. R. W. Matthews and R. A. Walton. Inorg. Chem. **10**, 1433 (1971).
13. H. Loiseleur, G. Thomas, B. Chevrier, and D. Grandjean. Chem. Commun. 182 (1967).
14. P. Lumme, G. Lundgren, and W. Mark. Acta Chem. Scand. **23**, 3011 (1969).
15. G. Dascenzo and W. W. Wendlandt. Gazz. Chim. Ital. **100**, 371 (1970).

[6]Full details of these spectra are available on request to R.A.W.

Can. J. Chem. Downloaded from www.nrcresearchpress.com by 210.87.254.5 on 09/05/12
For personal use only.

The Crystal and Molecular Structure of Tetrameric Phosphonitrilic Isothiocyanate

J. BRIAN FAUGHT

Department of Chemistry, Dalhousie University, Halifax, Nova Scotia

Received November 4, 1971

The crystal structure of tetrameric phosphonitrilic isothiocyanate, $N_4P_4(NCS)_8$, has been determined by three-dimensional X-ray studies from data collected on a Picker FACS-1 automated diffractometer. The compound crystallizes in the triclinic space group $P\bar{1}$ with $a = 8.098(8)$, $b = 8.018(7)$, $c = 9.937(10)$ Å, $\alpha = 104.08(7)$, $\beta = 99.42(7)$, $\gamma = 95.42(7)°$, and one molecule per unit cell. The structure was solved from 1766 independent non-zero reflections and refined to a conventional R factor of 0.063. Nitrogen atoms of two isothiocyanate groups are bonded to each phosphorus atom of the eight-membered phosphorus–nitrogen ring. The ring has a chair configuration. The average dimensions of the structure are $P—N_{ring} = 1.543 \pm 0.017$, $P—N_{isothiocyanate} = 1.644 \pm 0.011$, $N—C = 1.168 \pm 0.008$, $C—S = 1.535 \pm 0.009$ Å, $P\hat{N}_{ring}P = 140.2 \pm 1.8°$, $N_{ring}\hat{P}N_{ring} = 120.2 \pm 1.3°$, $N_{iso}\hat{P}N_{iso} = 100.1 \pm 1.0°$, $P\hat{N}C = 151.1 \pm 9.0°$, and $N\hat{C}S = 176.6 \pm 1.1°$.

La structure cristalline du tétramère de l'isothiocyanate phosphonitrilique, $N_4P_4(NCS)_8$, a été déterminée par diffraction de rayons-X à partir de données tridimensionnelles obtenues sur un diffractomètre automatique Picker FACS-1.

La maille trichinique de ce composé est monomoléculaire de dimensions: $a = 8.098(8)$, $b = 8.018(7)$, $c = 9.937(10)$ Å, $\alpha = 104.08(7)$, $\beta = 99.42(7)$ et $\gamma = 95.42(7)°$, et appartient au groupe spatial $P\bar{1}$.

La structure a été déterminée à partir de 1766 reflexions uniques observées et affinée jusqu'à une valeur de 0.063 du facteur d'accord R.

A chaque atome de phosphore du cycle à 8 atomes N_4P_4 sont liée deux groupes isothiocyanate par l'intermédiaire de leur atome d'azote. Le cycle a la configuration chaise. Les dimensions moyennes de la structure sont: P—N(cycle) = 1.543(17), P—N(isothiocyanate) = 1.644(11), N—C = 1.168(8), C—S = 1.535(9) Å, ∠PN(cycle)P = 140.2(18)°, ∠N(cycle)PN(cycle) = 120.2(13)°, ∠N(iso)PN(iso) = 100.1(10)°, ∠PNC = 151.1(90)° et ∠NCS = 176.6(11)°.

Canadian Journal of Chemistry, **50**, 1315 (1972)

Introduction

The crystal structures of a number of tetrameric phosphonitrilic halides have been reported, including the fluoride (1) and two forms of the chloride (2, 3). Other tetrameric phosphonitrilic compounds which have eight similar substituents have been studied and these include the $[NP(CH_3)_2]_4$ (4), $[NP(NMe_2)_2]_4$ (5), and $[NP(OCH_3)_2]_4$ (6). This paper reports the X-ray analysis of tetrameric phosphonitrilic isothiocyanate and is the first tetrameric phosphonitrilic pseudohalide studied so far.

Experimental

Crystal Structure Analysis

Tetrameric phosphonitrilic isothiocyanate was prepared according to the method of Audrieth and co-workers (7, 8). Crystals suitable for structural analysis were prepared from a solution of tetrameric phosphonitrilic isothiocyanate in *n*-heptane at room temperature. Crystal data are as follows:

$N_4P_4(NCS)_8$ f.w. = 644.5

Triclinic, $a = 8.098(8)$, $b = 8.018(7)$, $c = 9.937(10)$ Å, $\alpha = 104.08(7)°$, $\beta = 99.42(7)°$, $\gamma = 95.42(7)°$, $V = 611.2$ Å^3, $\rho_{obs} = 1.70 \pm 0.01$ g cc^{-1}, $Z = 1$, $\rho_{calc} = 1.751$ g cc^{-1} (22 °C, MoK_α, $\lambda = 0.7107$ Å).

The unit cell dimensions and their estimated standard deviations were obtained from a least-squares refinement of 12 independent reflections. The possible space groups are $P1$ or $P\bar{1}$.

Intensity data were collected on a Picker FACS-1 automated four-circle diffractometer. The a axis of the crystal (0.044 × 0.056 × 0.028 cm) was mounted parallel to the ϕ axis of the diffractometer. The take-off angle was 2°; β-filtered MoK_α radiation was used. All reflections were measured with a scintillation counter and attenuators were inserted when necessary.

The four octants, hkl, $hk\bar{l}$, $h\bar{k}l$, $h\bar{k}\bar{l}$ were explored in the 2θ range 4–50° using the moving-crystal, moving-counter technique with a 2θ scan rate of 1°/min. The $5\bar{4}0$ reflection was monitored after every 20 measurements, and the maximum variation of the intensity was ±1.5% of the average intensity of the reflection. The linear absorption coefficient for MoK_α radiation $\mu = 9.67$ cm^{-1}. No absorption or extinction corrections were applied.

The results of the E-statistics are given in Table 1. These results suggest that the crystal is centric and therefore, the space group is $P\bar{1}$ (no. 2) (9).

The structure was determined by the application of symbolic addition procedures (10). The programs of Hall and Ahmed were used (11). The sulfur and 2 phosphorus atoms were found readily in the E-map, and with this skeleton, the 6 N and 4 C atoms were located. A structure factor calculation based on these 16 atoms, with the thermal parameter for all atoms except S set to 4.0 Å^2, B for S = 5.0 Å^2, led to an R

Can. J. Chem. Downloaded from www.nrcresearchpress.com by 210.87.254.105 on 09/05/12
For personal use only.

TABLE 1. *E*-Statistics for $N_4P_4(NCS)_8$

Parameter	Value		
		Theoretical	
	Observed	Centric	Acentric
Mean $\|E\|$	0.817	0.798	0.886
Mean $\|E\|^2$	1.015	1.000	1.000
Mean $\|E^2 - 1\|$	0.945	0.968	0.736
$\%\|E\| > 3$	0.33	0.30	0.01
$\%\|E\| > 2$	3.96	5.00	1.80
$\%\|E\| > 1$	33.80	32.00	37.00

factor of 0.412 where

$$R = \frac{\Sigma \| F_o | - | F_c \|}{\Sigma | F_o |}$$

The refinement was carried out using a modification of the Busing, Martin, and Levy program ORFLS (12). All observed reflections were assigned unit weights and the quantity minimized was $\Sigma w \| F_o | - | F_c \|^2$. After full matrix least squares refinement of the positional and isotropic thermal parameters, R was reduced to 0.166 and R_2 was 0.162 where

$$R_2 = \left[\frac{\Sigma w (|F_o| - |F_c|)^2}{\Sigma w (F_o)^2} \right]^{1/2}$$

The thermal motion of the atoms was then treated anisotropically. Because of the limitation on the number of parameters that could be refined at one time, the refinement was carried out in sections, each section included the 4 ring atoms and 2 complete isothiocyanate groups. After 12 such cycles of anisotropic refinement, R was reduced to 0.063 and $R_2 = 0.083$. In the final cycles of refinement, the largest ratio of shift to standard deviation was found to be 0.07. Unobserved reflections were not included in the least squares refinements, but the structure factors of all the unobserved reflections were calculated and no inconsistencies were found. A final difference map was calculated, and for the most part, the highest peaks associated with this map were 0.3 e $Å^{-3}$. However, two peaks of intensity 0.6 e $Å^{-3}$ were observed, and each of these was in the region of a phosphorus and two isothiocyanate nitrogen atoms. The refinement was deemed to be complete at this point.

The scattering curves for neutral P, N, C, and S atoms were taken from the compilation of Hanson *et al.* (13). No corrections for $\Delta f'$ and $\Delta f''$ were made for P and S because they are quite small, 0.1 and 0.2 for both P and S (14).

Results and Discussion

A drawing of the molecule of tetrameric phosphonitrilic isothiocyanate viewed perpendicular to the *a*–*b* plane is shown in Fig. 1. The atom notation is indicated in this drawing. The centrosymmetric phosphorus atoms are also labelled.

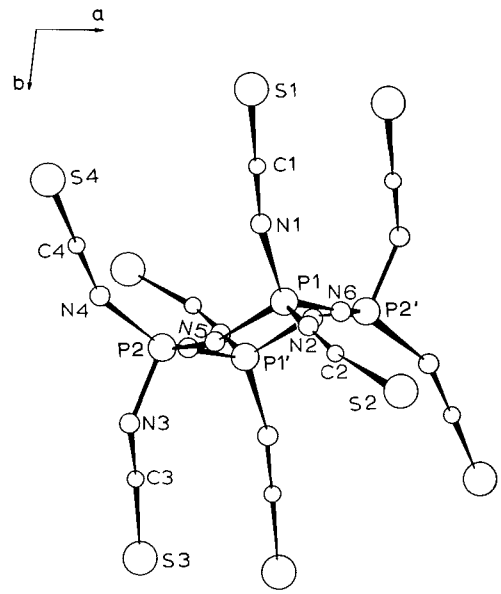

FIG. 1. A view of the molecule $N_4P_4(NCS)_8$ perpendicular to the *a*–*b* plane.

Table 2 contains the list of final fractional coordinates of the atoms and their anisotropic thermal parameters. The final observed and calculated structure factors based on these positional and thermal parameters may be obtained from the Depository of Unpublished Data.[1] Table 3 is a list of the calculated bond lengths and angles with standard deviations.

There are four independent P—N bond lengths in the ring and these vary from 1.523 to 1.565 Å and a root-mean-square (r.m.s.) deviation of 0.017 Å; the standard deviation calculated from least squares for an individual bond length is 0.008 Å. Ansell and Bullen (6) suggest that there is a correlation between the P—N bond length in a tetrameric phosphonitrilic ring and the electronegativity of the exocyclic atom bonded to the phosphorus atom. This does not hold true for this case, and it is evident that the electronegativity of the nitrogen atom is not a good approximation of the electronegativity of the isothiocyanate group. However, the electronegativity suggested by Huheey (15) for the isothiocyanate group, 4.2 on the Pauling scale, also does not fit this correlation well.

[1]Tabular data are available from the Depository of Unpublished Data, National Science Library, National Research Council of Canada, Ottawa, Canada, K1A 0S6.

Can. J. Chem. Downloaded from www.nrcresearchpress.com by 210.87.254.105 on 09/05/12
For personal use only.

Can. J. Chem. Downloaded from www.nrcresearchpress.com by 210.87.254.105 on 09/05/12
For personal use only.

TABLE 2. Positional and thermal parameters* for $N_4P_4(NCS)_8$

Atom	x	y	z	U_{11}†	U_{22}	U_{33}	U_{12}	U_{13}	U_{23}
P(1)	0.5362(3)	0.9345(2)	0.2987(2)	454(11)	399(10)	387(10)	45(8)	188(9)	102(8)
P(2)	0.2627(2)	1.0616(2)	0.4285(2)	379(10)	382(10)	471(11)	103(8)	134(9)	120(8)
S(1)	0.4032(5)	0.3824(3)	0.1480(3)	1506(31)	437(14)	869(20)	55(16)	108(20)	70(13)
S(2)	0.8538(4)	1.1469(5)	0.0697(4)	903(22)	1151(25)	1101(25)	10(19)	566(19)	520(20)
S(3)	0.2492(5)	1.6001(3)	0.5231(3)	1264(26)	417(13)	920(21)	112(14)	117(18)	135(13)
S(4)	−0.0784(4)	0.6293(4)	0.1731(3)	916(22)	793(19)	870(21)	−187(14)	73(17)	−106(13)
N(1)	0.4611(12)	0.7312(10)	0.2246(10)	1280(82)	416(46)	973(68)	−102(47)	253(59)	0(43)
N(2)	0.6049(10)	0.9915(11)	0.1661(7)	687(49)	1041(62)	536(44)	158(44)	301(39)	394(44)
N(3)	0.1931(10)	1.2484(9)	0.4285(9)	746(52)	400(41)	892(57)	219(36)	98(43)	189(38)
N(4)	0.0857(9)	0.9293(9)	0.3558(8)	472(41)	549(43)	778(52)	−9(34)	118(37)	54(39)
N(5)	0.3902(9)	1.0390(9)	0.3278(7)	594(43)	709(46)	599(43)	267(36)	332(35)	271(36)
N(6)	0.6887(9)	0.9549(11)	0.4167(7)	550(43)	987(58)	492(41)	183(40)	115(34)	304(40)
C(1)	0.4389(11)	0.5812(11)	0.1922(8)	645(54)	513(50)	434(44)	55(40)	69(39)	84(37)
C(2)	0.7166(11)	1.0616(11)	0.1293(8)	561(49)	663(52)	437(44)	124(40)	246(39)	207(39)
C(3)	0.2229(10)	1.3997(11)	0.4715(9)	551(50)	509(50)	554(49)	147(39)	42(39)	191(40)
C(4)	0.0188(10)	0.7981(11)	0.2762(9)	455(45)	541(49)	551(49)	61(38)	122(38)	148(41)

*The form of the expression is $\exp[-2\pi^2(a^{*2}h^2U_{11} + \ldots + 2a^*b^*hkU_{12} + \ldots)]$.
†$U_{ij} \times 10^4$.

TABLE 3. Interatomic distances and angles (e.s.d.'s in parentheses)

Atoms	Distance (Å)	Atoms	Angle (deg)
P(1)—N(1)	1.628(9)	N(1)—P(1)—N(2)	100.8(4)
P(1)—N(2)	1.655(8)	N(1)—P(1)—N(5)	109.6(4)
P(2)—N(3)	1.649(7)	N(1)—P(1)—N(6)	111.8(4)
P(2)—N(4)	1.644(8)	N(2)—P(1)—N(5)	105.8(4)
P(1)—N(5)	1.538(7)	N(2)—P(1)—N(6)	107.6(4)
P(1)—N(6)	1.523(8)	N(5)—P(1)—N(6)	119.3(4)
P(2)—N(5)	1.544(7)	N(3)—P(2)—N(4)	99.3(4)
P(2)—N(6′)	1.565(8)	N(3)—P(2)—N(5)	106.8(4)
N(1)—C(1)	1.156(12)	N(3)—P(2)—N(6′)	110.4(4)
N(2)—C(2)	1.175(12)	N(4)—P(2)—N(5)	110.5(4)
N(3)—C(3)	1.171(11)	N(4)—P(2)—N(6′)	106.5(4)
N(4)—C(4)	1.171(11)	N(5)—P(2)—N(6′)	121.1(4)
C(1)—S(1)	1.532(9)	P(1)—N(1)—C(1)	164.6(6)
C(2)—S(2)	1.523(9)	P(1)—N(2)—C(2)	146.5(7)
C(3)—S(3)	1.546(9)	P(2)—N(3)—C(3)	145.7(6)
C(4)—S(4)	1.537(10)	P(2)—N(4)—C(4)	147.7(8)
		P(1)—N(5)—P(2)	138.9(2)
		P(1)—N(6)—P(2′)	141.5(6)
		S(1)—C(1)—N(1)	178.1(8)
		S(2)—C(2)—N(2)	175.5(5)
		S(3)—C(3)—N(3)	175.9(4)
		S(4)—C(4)—N(4)	176.8(5)

There are no significant differences on bond angles of a given type and the mean values for the ring are $P\hat{N}P = 140.2 \pm 1.8°$, $N\hat{P}N = 120.2 \pm 1.3°$, and $X\hat{P}X = 100.1 \pm 1.0°$, where X is the exocyclic N atom. These values are compared with other tetrameric phosphonitrilic derivatives in Table 4. Several features stand out from this comparison. The angle at N in the ring is larger than all except that of the fluoride. In partially substituted derivatives only the fluoride derivatives have angles larger than 140°. The other feature is the $X\hat{P}X$ angle, which is comparable to the angle in the fluoride derivative. These angles along with the short P—N bond length seem to indicate that there is a greater inductive effect from the isothiocyanate group than all other substituents except for the fluoride substituent.

The isothiocyanate groups have the following mean values: P—N = 1.644 ± 0.011 Å, N—C = 1.168 ± 0.008 Å, C—S = 1.535 ± 0.009 Å, $P\hat{N}C$ 151.1 ± 9.0°, $N\hat{C}S = 176.6 \pm 1.1°$. The P—N bond length is considerably shorter than the presumed single bond length of 1.77 Å found in the $NaPO_3NH_3$ species (16). The C—S bond length is shorter than that of any other reported isothiocyanate (17). This amounts to more than double bond character. The N—C length indicates a bond order of three.

There is no simple valence bond canonical structure to explain the bond lengths in this isothiocyanate structure, but this is not uncommon (see for example ref. 17). The best simple representation can be made in the following structure:

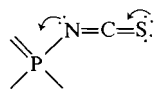

TABLE 4. Comparison of various features of the rings of tetrameric phosphonitrilic derivatives

Compound	Bond distance (Å)		Bond angle (deg)			Reference
	P—N	P—X*	PNP	NPN	XPX*	
$N_4P_4F_8$	1.51	1.51	147	123	100	1
K—$N_4P_4Cl_8$	1.57	2.00	131	121	103	2
T—$N_4P_4Cl_8$	1.56	1.99	134, 138	121	103	3
$N_4P_4(CH_3)_8$	1.60	1.81	132	120	104	4
$N_4P_4(N(CH_3)_2)_8$	1.58	1.68	133	120	104	5
$N_4P_4(OCH_3)_8$	1.57	1.58	132	121	106	6
$N_4P_4(NCS)_8$	1.54	1.64	140	120	100	This work

*X is the exocyclic group bonded to the P atom.

TABLE 5. Dihedral angles of ring bonds for chair configuration tetrameric phosphonitrilic compounds*

Compound	Dihedral angle (deg)			
	P(1)—N(6)	P(1)—N(5)	P(2)—N(5)	P(2′)—N(6)
$N_4P_4Cl_8$ (T form)	76	59	45	20
$N_4P_4Ph_4Cl_4$	76	62	42	24
$N_4P_4Ph_4(NHCH_3)_4$	95	73	53	21
$N_4P_4(NCS)_8$	57	59	33	26

*Data taken from ref. 20 except for $N_4P_4(NCS)_8$.

Delocalization of the nitrogen lone pair would not only result in a shorter P—$N_{(exo)}$ bond length but also a PN̂C angle greater than 120°. The PN̂C angle is interesting from another aspect. Of the 4 independent angles, three are quite close to 146° while the fourth is 164.5°. This difference is significant, but was also noticed in the structure of trimeric phosphonitrilic isothiocyanate (18). Hazell (19) has suggested that there is a relationship between the MN̂C angle and the N—C and C—S bond lengths. N—C distances generally decrease and C—S distances generally increase with increasing MN̂C angle. M is the atom to which the NĈS group is bonded. In this case, the N—C bond length corresponding to the largest PN̂C angle is 0.02 Å shorter than the average of the other three N—C bond lengths, with a least-squares estimated standard deviation of 0.01 Å on these bond lengths. However, that particular C—S bond length shows no corresponding increase.

Since the molecule occupies a center of symmetry, the ring has the chair configuration. The nitrogen atoms are 0.35 and 0.30 Å out of a plane described by the 2 crystallographically independent phosphorus atoms and the center of symmetry. The equation of this plane is

$$-0.3064\,X' - 0.9459\,Y' - 0.1066\,Z' + 7.5922 = 0$$

where X', Y', and Z' are an orthogonal set of axes, X' along a, Y' in the ab plane, and Z' along c^*. If the phosphonitrilic ring were to exhibit perfect $2/m$ symmetry, the dihedral angles of the bonds P(1)—N(6) would be equal to that of P(1)—N(5) and that of P(2)—N(5) equal to P(2′)—N(6). The dihedral angles of other chair forms of tetrameric phosphonitrilic derivatives are listed in Table 5. The numbering of the atoms has been changed to compare with the present work. Tetrameric phosphonitrilic isothiocyanate has a ring very close to $2/m$ symmetry. The mirror plane is that plane passing through atoms P(1) and P(1′) while the diad axis passes through P(2) and P(2′).

A molecular packing diagram projected on the a–b plane is shown in Fig. 2. The crystal packing appears to be dominated by the isothiocyanate groups, which participate in all of

Can. J. Chem. Downloaded from www.nrcresearchpress.com by 210.87.254.105 on 09/05/12
For personal use only.

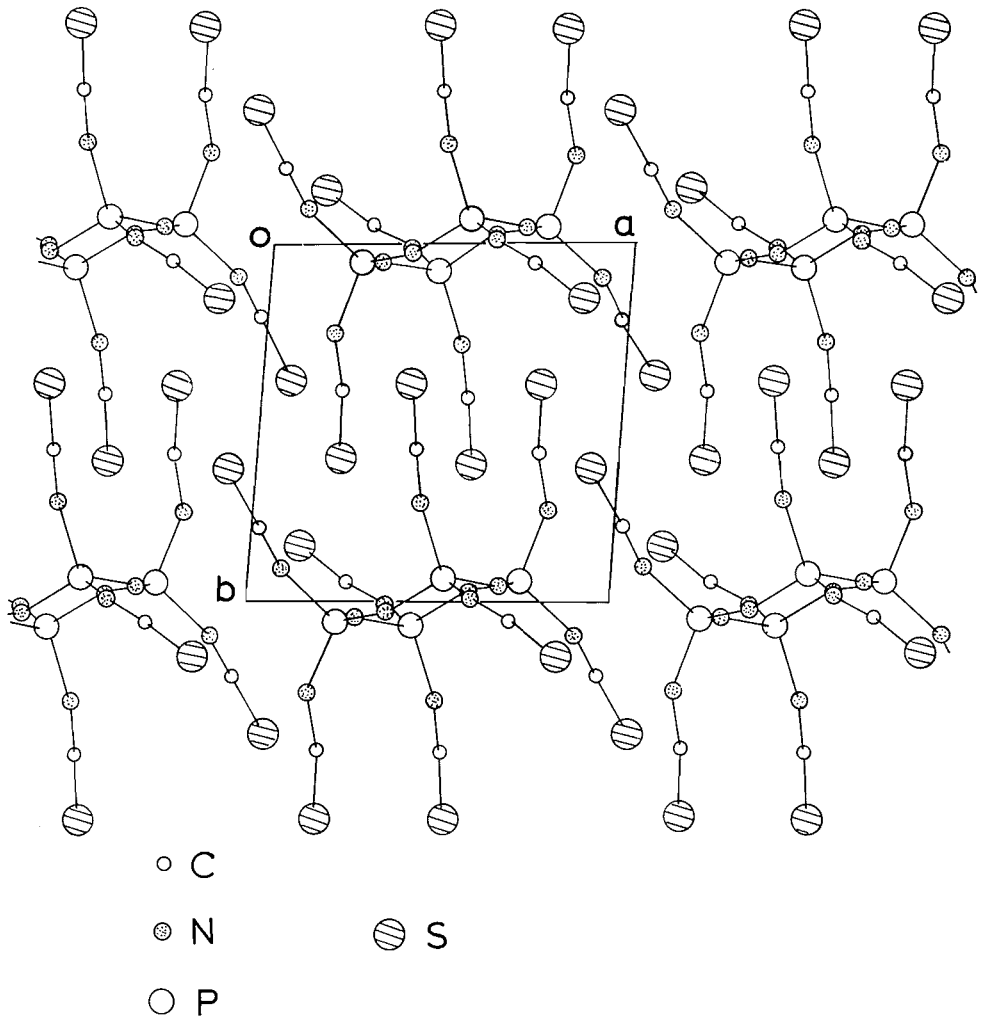

FIG. 2. Packing diagram of tetrameric phosphonitrilic isothiocyanate.

the closest intermolecular contacts. Most of the short intermolecular contacts are between two isothiocyanate groups. The shortest S...S distance is 3.91 Å, while the shortest S...N, N...N, N...C, C...C, and C...S distances are 3.63, 3.38, 3.42, 3.72, and 3.60 Å, respectively. None of these distances are smaller than the sum of the van der Waals radii of the two atoms.

The author wishes to thank Professor Harry Lynton of the University of New Brunswick for the use of the automated diffractometer. He also wishes to thank Mr. Peter S. White for help with computer problems and the National Research Council of Canada for financial support.

All computations were done on the IBM 360/50 and the CDC 6400 of the Dalhousie University Computer Centre.

1. H. McD. McGeachin and F. R. Tromans. J. Chem. Soc. 4777 (1961).
2. R. Hazekamp, T. Migchelsen, and A. Vos. Acta Cryst. **15**, 539 (1962).
3. A. J. Wagner and A. Vos. Acta Cryst. B**24**, 707 (1968).
4. M. W. Dougill. J. Chem. Soc. 5471 (1961).
5. G. J. Bullen. J. Chem. Soc. 3193 (1962).
6. G. B. Ansell and G. J. Bullen. J. Chem. Soc. A, 2498 (1971).
7. R. J. A. Otto and L. F. Audrieth. J. Am. Chem. Soc. **80**, 5894 (1958).
8. G. Tesi, R. J. A. Otto, F. G. Sherif, and L. F. Audrieth. J. Am. Chem. Soc. **82**, 528 (1960).

Can. J. Chem. Downloaded from www.nrcresearchpress.com by 210.87.254.105 on 09/05/12
For personal use only.

9. International tables for X-ray crystallography. Vol. 1. The Kynoch Press, Birmingham, England. 1969. p. 75.
10. J. KARLE and I. L. KARLE. Acta Cryst. **21**, 849 (1966).
11. F. R. AHMED, S. R. HALL, M. E. PIPPY, and C. P. HUBER. NRC-crystallographic programs for the IBM/360 system. National Research Council of Canada, Ottawa, 1970.
12. W. R. BUSING, K. O. MARTIN, and H. A. LEVY. ORFLS, a Fortran crystallographic least-squares program. U.S. Atomic Energy Commission Report ORNL-TM-305. Oak Ridge National Laboratory, Oak Ridge, Tennessee. 1962.
13. H. P. HANSON, F. HERMAN, J. D. LEA, and S. SKILMAN. Acta Cryst. **17**, 1040 (1964).
14. D. H. TEMPLETON. *In* International tables for X-ray crystallography. Vol. III. The Kynoch Press, Birmingham, England. 1968. pp. 213–216.
15. J. E. HUHEEY. J. Phys. Chem. **70**, 2086 (1966).
16. D. W. J. CRUICKSHANK. Acta Cryst. **17**, 671 (1964).
17. Y. M. CHOW. Inorg. Chem. **9**, 794 (1970).
18. J. B. FAUGHT, T. MOELLER, and I. C. PAUL. Inorg. Chem. **9**, 1656 (1970).
19. A. C. HAZELL. J. Chem. Soc. 5745 (1963).
20. G. J. BULLEN, P. R. MALLINSON, and A. H. BURR. Chem. Commun. 691 (1969),

Can. J. Chem. Downloaded from www.nrcresearchpress.com by 210.87.254.105 on 09/05/12
For personal use only.

Desorption of Hydrogen from Palladium and Palladium–Silver Alloys followed by Differential Scanning Calorimetry

D. ARTMAN AND TED B. FLANAGAN

Chemistry Department, University of Vermont, Burlington, Vermont

Received October 18, 1971

Differential scanning calorimetric curves have been obtained corresponding to the desorption of hydrogen from palladium and palladium–silver alloys. There was no evidence for the existence of an exotherm, following the endothermic desorption of hydrogen, which has been previously found and attributed to the relaxation of a metastable, expanded hydrogen-free palladium lattice. Heats of desorption have been evaluated from the areas of the endotherms and these are reasonable in the light of values obtained by other techniques. Comparisons of scanning curves for palladized and unpalladized hydrogen-containing silver–palladium alloys demonstrate that solid-state diffusion cannot be the slow step for the former but may be for the latter.

Nous avons obtenu des courbes de balayage calorimétrique différentiel correspondant à la désorption de l'hydrogène du palladium et des alliages palladium–argent. Nous n'avons pas remarqué l'existence d'un exotherme à la suite de la désorption endothermique de l'hydrogène, tel que trouvé auparavant et attribué à la relaxation d'un réseau du palladium métastable, étendu et exempt d'hydrogène. Nous avons évalué les chaleurs de désorption à partir des surfaces des endothermes et ces valeurs sont raisonnables à la lumière des valeurs obtenues par d'autres techniques. La comparaison entre les courbes de balayage pour des alliages argent–palladium contenant de l'hydrogène, palladiés et non-palladiés, démontre que la diffusion à l'état solide ne peut pas être l'étape lente pour la première, mais peut l'être pour la deuxième.

Canadian Journal of Chemistry, **50**, 1321 (1972)

Palladium and its alloys with high palladium contents have the ability to absorb large amounts of hydrogen (1). If their surfaces are not especially activated by, *e.g.*, palladium black, this hydrogen will remain within the sample in a metastable state, *i.e.*, under conditions where $\mu_H^{metal} > \mu_H^{gas}$. When they are heated, hydrogen is evolved. This suggests that thermoanalytic techniques may be readily applicable to hydrogen-containing samples of palladium and its alloys. No one has, to our knowledge, applied these techniques to hydrogen-containing palladium, save Michel and Michel (2) who followed the loss of hydrogen from a palladium specimen in nitrogen using differential thermal analysis (DTA). The DTA curve obtained by Michel for Pd/H_2 in the β-phase exhibits an endothermic peak with a maximum at 175 °C corresponding to the desorption of hydrogen (2). Subsequently an exothermic peak, which was even larger than the endothermic one, appeared with a maximum at *ca.* 280 °C. This latter peak was attributed to the relaxation of the extended hydrogen-free lattice to its normal lattice spacing. Michel and co-workers (3) have presented ancillary evidence that hydrogen may be removed from palladium without an accompanying relaxation of the lattice. To a limited extent, Gibb *et al.* (4) have supported their finding, *i.e.*, the magnetic susceptibility can remain low despite the fact that a considerable fraction of hydrogen may be removed from a hydrogen-containing palladium sample in the β-phase. Other workers (5) have not supported Michel's suggestion. It is of interest to repeat these early thermoanalytic investigations on samples of high purity in order to reexamine the possibility of the occurrence of the metastable lattice.

An additional motive was to determine if a thermoanalytical approach could provide accurate thermochemical data on these important systems. Considerable thermodynamic data are available for the hydrogen/palladium and the silver/palladium/hydrogen systems (1). Most data are derived from pressure–temperature equilibrium data rather than from calorimetric measurements. Calorimetric measurements on palladium/hydrogen have been limited (1) and there are none available for the interaction of hydrogen with palladium alloys.

The most extensive calorimetric investigation of the palladium/hydrogen system is that of Nace and Aston (6). They found an average value for ΔH of -40.19 kJ/mol H_2 for absorption into the α/β two-phase region (25 °C) which is consistent with the results of earlier workers who found an average of -38 kJ/mol (1). For hydrogen concentrations exceeding

Can. J. Chem. Downloaded from www.nrcresearchpress.com by 210.87.254.105 on 09/05/12
For personal use only.

Can. J. Chem. Downloaded from www.nrcresearchpress.com by 210.87.254.105 on 09/05/12
For personal use only.

those corresponding to the two-phase region, H-to-Pd, atomic ratio, = 0.58 (25 °C), calorimetric data are unavailable. It is known that at 1 atm hydrogen pressure absorption ceases at H-to-Pd = 0.69 (1) (25 °C). To attain values of H-to-Pd greater than this, either high pressures of gaseous hydrogen are required (7) or the maintenance of a non-equilibrium concentration of hydrogen atoms such as produced by gaseous discharges or heated tungsten filaments (8). It is of interest to explore the feasibility of thermoanalytic techniques for the determination of enthalpies of desorption at values of $n > 0.69$ because direct calorimetric approaches at these concentrations are fraught with potential experimental difficulties.

Experimental

Palladium and silver–palladium wires (99.99% purity, 0.027 cm diam) were charged with hydrogen employing the technique of spontaneous absorption from solution (9) to H-to-metal values of 0.65 and 0.45, respectively. This method was employed in order to avoid non-homogeneous charging often associated with electrolytic introduction of hydrogen. Contents in excess of H/Pd = 0.65 were obtained by gas phase reaction of hydrogen atoms and palladium (8). Contents were determined by weighing the specimen before and after degassing and also by measurement of the hydrogen evolved following heating of a segment of the sample *in vacuo*.

The samples were cut into many small pieces (~1–6 mg) and then the course of desorption was followed by differential scanning calorimetry (Dupont). The heating rate was generally 15 °C min^{-1} and the purge rate, ~100 cc min^{-1}.

In order to prepare samples with catalytically active surfaces, they were charged electrolytically with hydrogen and then submerged into a palladium chloride solution. Palladium was spontaneously deposited upon the surface of the metal creating a very active surface for the $H_2 \leftrightarrow 2H^*$ reaction (10). The samples were then kept in distilled water until they were transferred to the DSC cell in a wet condition where they were purged with helium in order to remove the water at room temperature before being heated.

The major difficulty in obtaining meaningful results was the accuracy of the calibration. The samples were placed directly onto the sample platforms and were short enough so that their entire lengths were in contact with the sensing element. Calibration based upon the transition In(s) → In(l), where the Indium was placed in an aluminum pan, did not lead to accurate data. The geometry and size of the calibration sample must approximate the hydrogen-containing sample as closely as possible. Measurements of the heat capacity of aluminum wire (diam 0.08 cm, wt ≅ 3–4 mg, ~3 mm long) provided relatively successful calibration. Aluminum wire was chosen over palladium itself because of its considerably larger heat capacity, *i.e.*, 0.949 J g^{-1} deg^{-1} (Al) and 0.250 J g^{-1} deg^{-1} (Pd).

Results and Discussion

A typical differential scanning calorimetric run is shown in Fig. 1 for an unactivated sample of composition $PdH_{0.65}$. Runs were performed in either nitrogen (as Michel and Michel (2)) or in helium in order to avoid reaction of the absorbed hydrogen with oxygen. It can be seen that there is no evidence of an exothermic process following the endothermic desorption of hydrogen (2). Such an exothermic peak was never noted in the numerous runs carried out in this research. For $PdH_{0.65}$, hydrogen commences to be evolved at *ca.* 150 °C and the maximum occurs at approximately 265 °C.

Heats of Desorption

Further support for the finding that the lattice relaxes after desorption of hydrogen can be

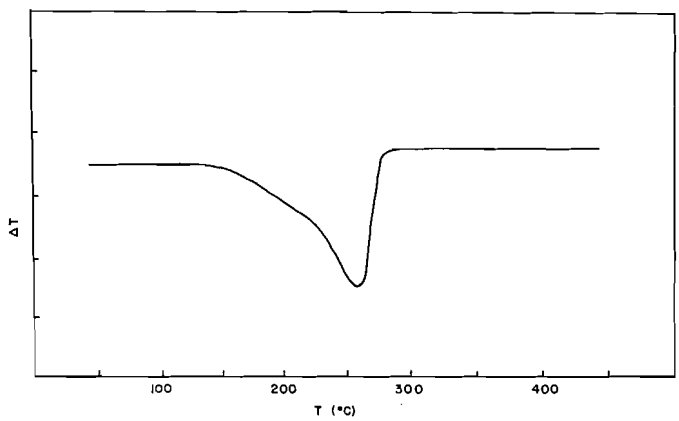

FIG. 1. Typical DSC run for unactivated $PdH_{0.65}$ in the presence of helium.

Can. J. Chem. Downloaded from www.nrcresearchpress.com by 210.87.254.105 on 09/05/12
For personal use only.

TABLE 1. Integral heats of desorption of hydrogen from Palladium and Ag(20%)/Pd

Sample type (unpalladized)	Endotherm$_{max}$ (°C)	ΔH (kJ/mol H_2)
$PdH_{0.65}$	265 ± 10	37.8
$PdH_{0.81}$	245	36.6
$PdH_{0.92}$	205	27.2
$Ag(20\%)PdH_{0.45}$	235	38.3

gained from a quantitative evaluation of the endothermic peaks. The value of ΔH_{des} can be determined for the process

$$[1] \qquad \frac{2}{x} PdH_x \rightarrow \frac{2}{x} Pd + H_2$$

Results are given in Table 1 for values of ΔH_{des} corresponding to reaction 1 (integral heats of desorption).

The composition $PdH_{0.65}$ (Table 1) exceeds that of the β-phase boundary (25 °C) only slightly (1), and, therefore, a natural comparison is that between the observed heat of desorption of $PdH_{0.65}$ (reaction 1) and the often determined value corresponding to the $\beta \rightarrow \alpha$ transformation. The error introduced into this comparison by the larger partial molar heat of desorption which obtains for the $PdH_{0.65}$ sample in the range H-to-Pd > 0.58 is only 1% and a comparable error arises from the fact that the desorption product is not α-phase palladium/hydrogen but pure palladium. These errors, however, are well within the present experimental precision. The value reported for the integral heat of desorption per mole of H_2 for $PdH_{0.65}$ (Table 1) is the average of ten determinations with two different DSC cells. The average values found for the two different cells with separate calibration determinations were within 1.2 kJ/mol H_2 of each other.

Values in the literature reported for the $\beta \rightarrow \alpha$ transition are greater than those for the $\alpha \rightarrow \beta$ transition because of the presence of hysteresis (1). Calorimetric values have not been determined for the desorption of hydrogen from β-phase palladium. Wicke and Nernst (11) report 39.9 kJ/mol H_2 for the heat of desorption from −30 to 50 °C. Lewis (1) has collected all available data for the two-phase pressures and, surprisingly, a single Arrhenius straight line can be drawn through these extensive data (−30 to 290 °C) with a value for $\Delta H_{\beta \rightarrow \alpha}$ of 40.9 kJ/mol H_2. The value reported here is within experimental error of these previously reported values. The convenience of this technique makes it quite useful, *e.g.*, it requires only small samples (1–6 mg) and is very rapid.

Wicke and Nernst (11) give an expression for the partial molar heat of desorption of hydrogen from the β-phase of Pd/H_2, *i.e.*, $\Delta \bar{H} = 96.7 - 90.0 \times (H/Pd)$ kJ/mol H_2. This expression can be integrated between values of H-to-Pd of 0.58 and 0.81 and, together with the two-phase heat, an integral heat of desorption of 37.7 kJ/mol H_2 can be calculated to compare with the value shown in Table 1; a similar treatment applied to $PdH_{0.92}$ gives 36.1 kJ/mol H_2. The results for the $PdH_{0.81}$ alloy are not unreasonable, but the calculated heat for the largest hydrogen content alloy is in poor agreement with the experiment (Table 1). It is quite possible that the analytical expression for $\Delta \bar{H}$ (11) is not suitable for H-to-Pd values greater than 0.81. It can be shown from Table 1 that the partial desorption of hydrogen from $PdH_{0.92}$ to $PdH_{0.81}$ is exothermic, yet a distinguishable exothermic peak is not observed when $PdH_{0.92}$ is heated; therefore, there is no tendency for the "exothermic" hydrogen to be desorbed before the rest of the hydrogen.

The differential heat of solution of hydrogen at small hydrogen contents is greater in Ag(20%)/Pd than in pure palladium (12) so that the reported value (Table 1) supports this trend. Further quantitative calorimetric data are needed for the desorption of hydrogen from palladium alloys.

Kinetics of Desorption

Figure 2 shows the differential calorimetric scanning curve for a palladized and a bright, *i.e.*, unpalladized, sample of hydrogen-containing Ag(20%)/Pd. It is of interest to note that the endothermic peak which appears at about 235 °C for the bright sample has shifted to about 80 °C for the palladized sample. This demonstrates that solid state diffusion cannot be the rate-limiting step for desorption from the bright sample; such a slow step may be obtained for the palladized sample. (A comparison of the desorption rates was made with silver/palladium alloys rather than pure palladium in order to avoid complications due to the presence of the two phases.) It is known that a coating of palladium

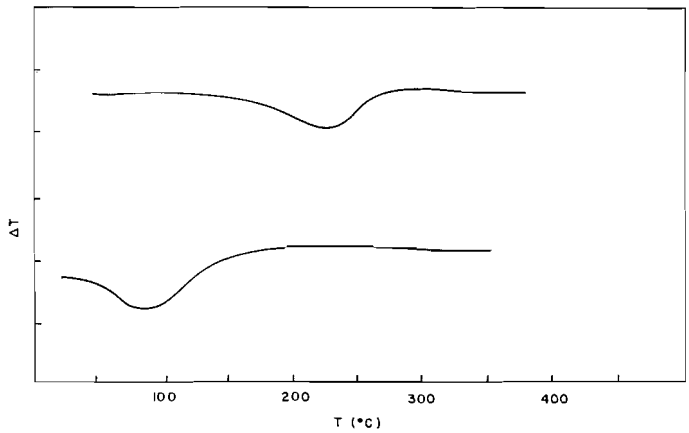

FIG. 2. DSC plots for hydrogen containing Ag(20%)Pd specimens. Upper curve is of a bright sample and lower is of a palladized specimen.

black can sufficiently activate the surface of palladium so that surface steps are not rate-controlling for permeation experiments (13). Palladized samples of hydrogen-containing Ag(35%)/Pd and Ag(45%)/Pd were also subjected to scanning runs. The endothermic peaks for these samples occurred at 140 and 160 °C, respectively. Züchner (14) has recently measured the diffusion coefficients in this system and noted that the diffusion coefficients decline with silver content so that it would be expected for the endothermic peaks to shift to progressively higher temperatures as observed here.

Numerical evaluation of the diffusion coefficients using approximate solutions of the cylindrical diffusion problem with the assumption that the surface concentration during desorption is zero, lead to values of D which are too small. It is quite likely that the assumed boundary condition, $c_{H_2} = 0$ at the surface, is invalid under the experimental conditions. This general approach for the determination of diffusion parameters deserves further attention because of its great convenience.

1. F. A. LEWIS. The palladium/hydrogen system. Academic Press, London, 1967.
2. A. MICHEL and M. MICHEL. Compt. rend. **221**, 551 (1945).
3. A. MICHEL and M. GALLISOT. Compt. rend. **208**, 434 (1939).
4. T. R. P. GIBB, J. MACMILLAN, and R. J. ROY. J. Phys. Chem. **70**, 3024 (1966).
5. J. C. BARTON, F. A. LEWIS, and I. WOODWARD. Trans. Faraday Soc. **59**, 434 (1963).
6. D. M. NACE and J. G. ASTON. J. Am. Chem. Soc. **79**, 3619 (1957).
7. B. BARANOWSKI and R. WISNIEWSKI. Phys. Stat. Sol. **35**, 593 (1969).
8. W. A. OATES and T. B. FLANAGAN. Nature, **231**, 19 (1971).
9. T. B. FLANAGAN and F. A. LEWIS. Trans. Faraday Soc. **55**, 1400 (1959).
10. E. WICKE. Private communication.
11. E. WICKE and G. H. NERNST. Ber. Bunsenges. phys. Chem. **68**, 224 (1964).
12. H. BRODOWSKY and E. POESCHEL. Zeit. phys. Chem. N.F. **44**, 143 (1965).
13. E. WICKE and G. HOLLECK. Zeit. phys. Chem. N.F. **46**, 125 (1965).
14. H. ZÜCHNER. Zeit. Naturforsch. **25a**, 1490 (1970).

Can. J. Chem. Downloaded from www.nrcresearchpress.com by 210.87.254.105 on 09/05/12
For personal use only.

Complexes de platine avec des dérivés acétyléniques $Pt(R_1R_2C(OH)—C\equiv C—C(OH)R_1R_2)_2$

FERNANDE D. ROCHON[1] ET T. THEOPHANIDES

Département de chimie, Université de Montréal, Montréal, Québec

Reçu le 12 août 1971

Les complexes $Pt(ac)_2$ où $ac = R_1R_2C(OH)—C\equiv C—C(OH)R_1R_2$ ont été étudiés. Les composés sont mononucléaires, non ioniques et diamagnétiques. Les résultats expérimentaux semblent indiquer que les ligands ne sont pas réarrangés dans le complexe. L'ordre de la liaison C≡C a été partiellement réduit et il y a probablement une distorsion assez importante de la molécule acétylénique. Une structure où les deux ligands acétyléniques sont liés par des ponts hydrogène est proposée.

La réaction des complexes $Pt(ac)_2$ avec la triphénylphosphine a été étudiée. On a la réaction suivante:

$$Pt(ac)_2 + 2PPh_3 \rightarrow Pt(PPh_3)_2(ac) + ac$$

Complexes of the type $Pt(ac)_2$ where $ac = R_1R_2C(OH)—C\equiv C—C(OH)R_1R_2$ have been studied. The compounds are mononuclear, non ionic, and diamagnetic. The experimental results seem to indicate that the ligands are not rearranged in the complex. The order of the triple bond has been partially reduced and there is an important distortion of the acetylenic molecule. A structure with the two ligands hydrogen bonded is proposed.

The complexes $Pt(ac)_2$ react with triphenylphosphine according to the following equation:

$$Pt(ac)_2 + 2PPh_3 \rightarrow Pt(PPh_3)_2(ac) + ac$$

Canadian Journal of Chemistry, **50**, 1325 (1972)

Dans un article précédent (1), nous avons rapporté la synthèse d'une nouvelle série de complexes de platine avec des dérivés acétyléniques de formule générale $Pt(ac)_2$. Six composés dans la série ont été préparés où $ac = R_1R_2C(OH)—C\equiv C—C(OH)R_1R_2$.

Résultats

Les complexes $Pt(ac)_2$ sont formés comme produits secondaires de la réaction suivante:

$$K_2PtCl_4 + ac \rightarrow K[Pt(ac)Cl_3] + KCl$$

L'analyse élémentaire indique la composition $Pt(ac)_2$ (1). Les composés sont non-ioniques, diamagnétiques et monomères (tableau 1).

Spectres de masse

Le spectre de masse de tous les complexes $Pt(ac)_2$ montrent des pics moléculaires correspondant aux trois isotopes du platine 194, 195, et 196. Ce phénomène est très intéressant puisque les ligands ac n'ont pas montré de pics moléculaires. Le fragment le plus élevé dans le spectre de masse des ligands correspond à la masse $M^+ - 17$ (perte probable d'un groupement hydroxyle). L'intensité relative de ce pic ($M^+ - 17$) est faible, environ 1%. Par contre, tous les complexes $Pt(ac)_2$ possèdent des pics moléculaires. L'intensité relative du pic M^+ varie de 1 à 16%. La stabilité du ligand dans la chambre d'ionisation semble donc plus grande lorsqu'il est coordiné au métal. La première partie du spectre de masse des complexes (fragments ne contenant pas de platine) ressemble beaucoup au spectre de masse du ligand correspondant.

TABLEAU 1. Poids moléculaire

Complexe*	Poids moléculaire Théor.	Sp. de masse (^{195}Pt)	Solution dans l'acétone†
$Pt(ac^1)_2$	535.54	535	562
$Pt(ac^2)_2$	591.69	591	615
$Pt(ac^3)_2$	591.69	591	608
$Pt(ac^4)_2$	703.89	703	673
$Pt(ac^5)_2$	703.89	703	730
$Pt(ac^6)_2$	639.72	639	600

*$ac^1 = (CH_3)(C_2H_5)C(OH)—C\equiv C—C(OH)(CH_3)(C_2H_5)$;
$ac^2 = (C_2H_5)_2C(OH)—C\equiv C—C(OH)(C_2H_5)_2$;
$ac^3 = (CH_3)(C_3H_7)C(OH)—C\equiv C—C(OH)(C_3H_7)(CH_3)$;
$ac^4 = (CH_3)(C_5H_{11})C(OH)—C\equiv C—C(OH)(C_5H_{11})(CH_3)$;
$ac^5 = (C_2H_5)(C_4H_9)C(OH)—C\equiv C—C(OH)(C_4H_9)(C_2H_5)$;
$ac^6 =$ 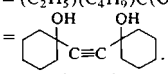 .

†Les complexes étant peu solubles dans l'acétone, ces résultats sont approximatifs.

Résonance magnétique nucléaire

Les spectres de résonance magnétique nucléaire du complexe $Pt(ac^1)_2$ et du ligand cor-

[1]Adresse actuelle: Université du Québec à Montréal, Montréal, Québec.

TABLEAU 2. Spectre de résonance magnétique nucléaire

τ (p.p.m.)				
ac^1				
CCl_4	DMSO-d_6	$Pt(ac^1)_2$ DMSO-d_6	Intensité relative	Attribution
9.01	9.08	9.10	3 (triplet)	CH_3 (de C_2H_5)
8.60	8.68	8.63	3 (singulet)	CH_3
8.42	8.45	8.34	2 (quadruplet)	CH_2
5.88 (conc. 0.30 m/l)	5.06 (conc. 0.15 m/l)	5.29 (conc. 0.037 m/l)	1 (singulet)	OH

respondant ($ac^1 = (CH_3)(C_2H_5)C(OH)—C\equiv C—C(OH)(CH_3)(C_2H_5)$) ont été mesurés dans le diméthylsulfoxyde-d_6 à la température ambiante entre 0 et 30 p.p.m. (τ). Les résultats ont été notés sur le tableau 2. Les spectres n'ont pas été mesurés dans l'acétone-d_6 puisque les complexes ne sont pas suffisamment solubles. Les spectres du diol ac^1 et du complexe $Pt(ac^1)_2$ sont semblables. Les mêmes intensités relatives ont été notées, indiquant la présence de deux groupements hydroxyles par ligand dans le complexe tout comme dans le diol même. On peut donc conclure que l'environnement des groupements hydroxyles du diol et du complexe n'est pas très différent.

Le spectre de résonance magnétique nucléaire des autres composés de la série n'a pas été mesuré, puisque leur solubilité est insuffisante, ou il y a décomposition du complexe en solution. Les complexes en solution se décomposent sous l'effet de la chaleur.

Spectres électroniques

Le spectre électronique des complexes $Pt(ac)_2$, mesuré dans l'acétonitrile, a montré la présence de trois transitions, à 46 700 ($\varepsilon \sim 7\,500$), à 39 200 ($\varepsilon \sim 1\,500$), et à 35 200 cm^{-1} ($\varepsilon \sim 1\,500$) (tableau 3) (DDI).[2]

Les trois transitions observées ont été attribuées à des transferts de charge à cause des grands coefficients d'extinction moléculaire et de l'énergie relativement grande des transitions. En se basant sur les travaux de Denning, Hartley, et Venanzi (3) et sur le fait que dans les complexes de Pt(0) la liaison π semble très importante, on peut attribuer ces transitions à des transferts d'électrons d'une orbitale d du métal à une orbitale π^* (antiliante) du ligand, donc $M \rightarrow L$, $d \rightarrow \pi^*$.

L'absence de transition d–d dans le spectre électronique semble indiquer la configuration électronique d^{10} pour le platine. Par conséquent, les complexes $Pt(ac)_2$ sont probablement des complexes de Pt(0).

Spectres infrarouges

Le spectre infrarouge des ligands ac et des complexes $Pt(ac)_2$ (fig. 1) a été mesuré de 4000 à 200 cm^{-1}. Le tableau 4 montre la position d'absorption des vibrateurs O—H et C≡C.

Les complexes sont complètement insolubles dans les solvants neutres, excepté $Pt(ac^5)_2$ qui est légèrement soluble dans le tétrachlorure de carbone. Trois bandes d'absorption ont été notées, à 3600, 3530 et 3335 cm^{-1} (fig. 2). Il semble donc y avoir une liaison hydrogène intramoléculaire et une liaison hydrogène intermoléculaire.

Une absorption très intense située entre 1880 et 1904 cm^{-1} a été attribuée à la vibration C≡C. Il y a probablement une distorsion assez importante de la molécule acétylénique et la vibration devient active et très forte dans l'infrarouge. Dans la molécule libre, la triple liaison est observée dans le Raman autour de 2230 cm^{-1} (18). La fréquence du vibrateur C≡C est abaissée à cause de l'interaction entre le platine et la triple liaison. La possibilité que cette absorption soit causée par une vibration Pt—H a été écartée, puisque la deutération n'a pas altéré cette absorption (tableau 4). Le vibrateur Pt—H absorbe généralement autour de 2100 cm^{-1} (2, 4). Donc les complexes ne sont pas des hydrures. Les complexes $Pt(ac)_2$ absorbent à une valeur intermédiaire entre les

[2]Dépôt des données inédites. Les photocopies des tableaux 3, 5, et 6 peuvent être obtenues, sur demande adressée aux archives des documents non publiés, à la Bibliothèque scientifique nationale, au Conseil national de recherches du Canada à Ottawa, Canada K1A 0S2.

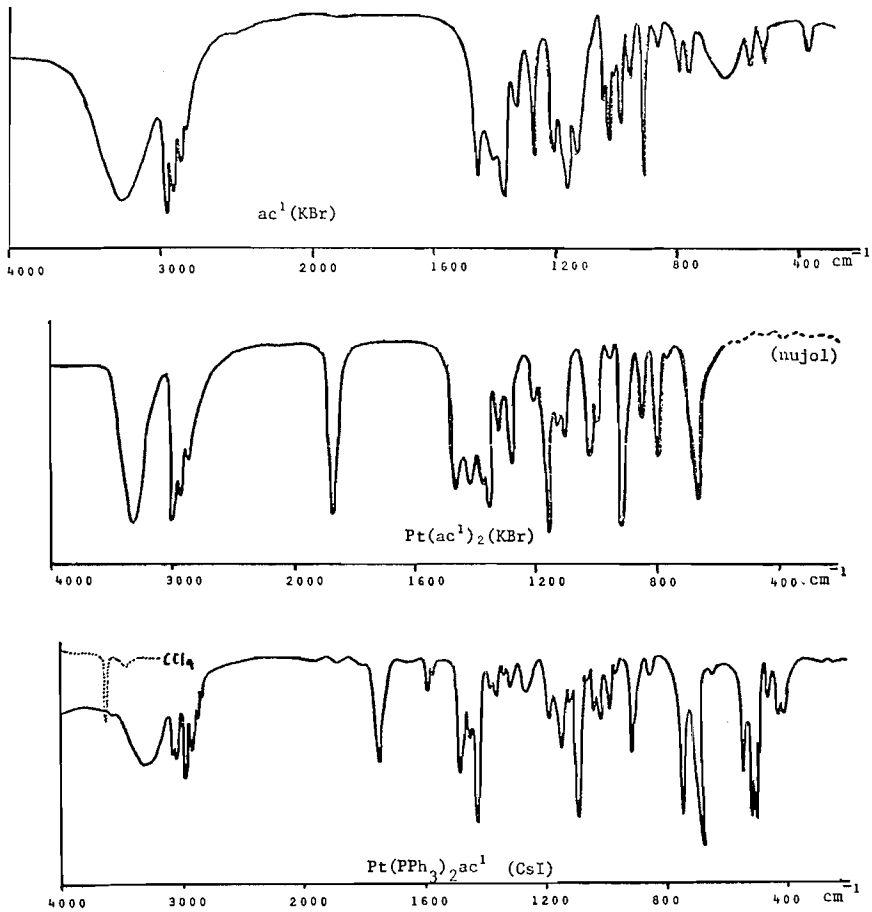

FIG. 1. Spectres infrarouges du ligand ac^1 et des complexes $Pt(ac^1)_2$ et $Pt(PPH_3)_2(ac^1)$.

TABLEAU 4. Spectres infrarouges

Composé	ν_{O-H} (cm^{-1}) Solide	ν_{O-H} (cm^{-1}) CCl_4	$\nu_{C\equiv C}$ (cm^{-1}) solide
ac^1	3280	3610	
$Pt(ac^1)_2$	3290	insoluble	1890
$Pt(ac^1)_2$ deutéré	2450 (ν_{O-D})	insoluble	1891
ac^2	3260	3610	
$Pt(ac^2)_2$	3380	insoluble	1904
ac^3	3260	3610	
$Pt(ac^3)_2$	3300	insoluble	1885
ac^4	3300	3610	2230 R†
$Pt(ac^4)_2$	3260	insoluble	1880
ac^5	3295	3610	
$Pt(ac^5)_2$	3365	3600, 3530*	1889
ac^6	3360	3610	
$Pt(ac^6)_2$	3220	insoluble	1880

*Voir texte.
†R: Raman (18), $(CH_3)_2C(OH)C\equiv C(OH)(CH_3)_2$ montre 2 raies à 2224 et 2248 cm^{-1}.

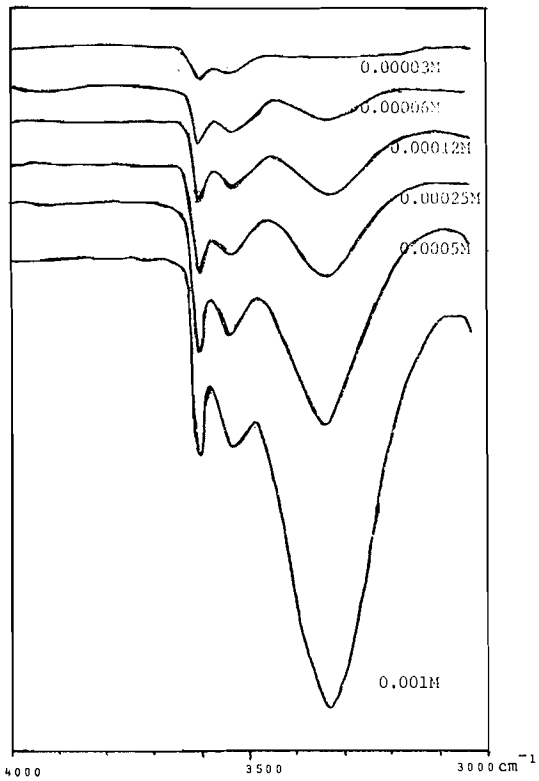

FIG. 2. Spectre infrarouge de $Pt(ac^5)_2$ dans CCl_4.

complexes de platine II (ex. $K[Pt(ac)Cl_3]$ $\nu_{C\equiv C} = 2000\ cm^{-1}$) et les complexes de platine(0) de type $[Pt(PPh_3)_2(ac)]$ ($\nu_{C\equiv C} \simeq 1750\ cm^{-1}$). Plusieurs complexes possédant une absorption similaire ont été décrits dans le passé (2, 4–9). Chatt a signalé l'existence possible de toute une série de complexes de platine variant entre les deux sortes de liaisons ($\nu_{C\equiv C} = 2000$ et $1750\ cm^{-1}$). Collman et Kang (10), en se basant sur leurs résultats de complexes de rhodium et d'iridium avec des composés acétyléniques, ont noté le même phénomène et ont conclu que les deux sortes de liaison correspondaient à des descriptions extrêmes d'une transformation graduelle.

Les spectres infrarouges ($700–200\ cm^{-1}$) des ligands et des complexes ont été mesurés dans le Nujol. Les bandes observées ont été notées dans le tableau 5 (DDI).[2]

Réaction avec la triphénylphosphine

Lorsqu'on ajoute très lentement une solution de triphénylphosphine dans l'hexane à une suspension du complexe $Pt(ac)_2$ dans l'hexane, la réaction suivante a lieu:

$$Pt(ac)_2 + 2PPh_3 \rightarrow Pt(PPh_3)_2(ac) + ac$$

$Pt(PPh_3)_2(ac)$ où (ac) est un dérivé acétylénique a été préparé selon la méthode décrite par Chatt et ses collaborateurs (11) ainsi que par Allen et Cook (12) et comparé au produit final de la réaction de $Pt(ac)_2$ avec PPh_3. L'analyse élémentaire, le point de fusion, le poids moléculaire, la susceptibilité magnétique et le spectre infrarouge des deux composés obtenus par les deux méthodes se sont révélés identiques.

Les complexes $Pt(PPh_3)_2(ac)$ sont diamagnétiques. Les poids moléculaires mesurés dans l'acétone varient de 425 à 465. Ces complexes semblent se décomposer en solution pour donner l'espèce monocoordinée $Pt(PPh_3)$, probablement solvatée. Ugo, Cariati, et La Monica (13) ont observé pour le complexe $Pt(PPh_3)_2$ (*P.M.* théorique = 719) un poids moléculaire de 464 dans le benzène et de 395 dans l'acétone.

Le tableau 6 (DDI)[2] montre la position d'absorption des vibrateurs O—H et C≡C à l'état solide dans l'infrarouge des complexes $Pt(PPh_3)_2(ac)$. L'ordre de la liaison C—C a été réduit puisque le vibrateur absorbe à environ $1750\ cm^{-1}$.

Les spectres de masse des complexes $Pt(PPh_3)_2(ac)$ n'ont pas montré de pics moléculaires ni de fragments contenant du platine. Les fragments sont surtout ceux du glycol acétylénique (ac) correspondant. Il y a probablement la décomposition suivante du complexe $Pt(PPh_3)_2(ac)$

$$Pt(PPh_3)_2(ac) \rightarrow Pt(PPh_3)_2 + (ac)$$

Le glycol acétylénique étant beaucoup plus volatil que le complexe $Pt(PPh_3)_2$, les fragments observés sur le spectre de masse sont surtout ceux du glycol acétylénique.

Discussion

La réaction du $Pt(ac)_2$ avec la triphénylphosphine est particulièrement intéressante pour prouver que le ligand acétylénique est intact dans le complexe. Les deux ligands sont probablement liés au platine par la triple liaison puisqu'ils sont facilement enlevés. Ils sont vraisemblablement liés au platine d'une façon

identique puisqu'une seule vibration C≡C est observée dans le spectre infrarouge.

En se basant sur nos résultats, nous proposons la structure suivante (fig. 3).

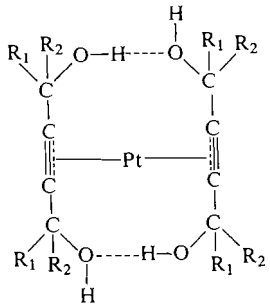

FIG. 3. Structure proposée pour les complexes $Pt(ac)_2$.

Cette structure semble concorder avec tous nos résultats expérimentaux. Les deux triples liaisons ne sont probablement pas parallèles, à l'extrême elles pourraient être perpendiculaires. Il y a une distorsion, probablement cis, assez importante des ligands acétyléniques. Jusqu'à maintenant, toutes les structures déterminées par diffraction des rayons X ont montré des distorsions cis de la molécule acétylénique, vers le côté opposé au platine. Le nombre de coordination du platine est deux et l'hybridation probable dp, puisque dans le complexe $Pt(PPh_3)_2(PhC{\equiv}CPh)$ les orbitales s ne prennent pas part à l'hybridation (14). Il y a des ponts hydrogène entre les groupements hydroxyles des deux ligands acétyléniques.

La stabilité très grande de ces complexes à l'état solide, semble indiquer l'existence d'un excès de charge négative sur le métal zérovalent. Plusieurs auteurs (15, 16) croient que les liens π sont plus forts dans les coordinations linéaires et trigonales que dans les coordinations tétraédriques. Il semble qu'avec une configuration d^{10}, la charge négative sur le métal est plus facilement dispersée sur le ligand (liaison π) lorsque le nombre de coordination est petit. La liaison π (rétro-donation) est donc très importante. Cette interaction est facilitée par la présence sur l'alcyne de groupements électronégatifs (deux groupements hydroxyles) qui diminuent l'énergie des orbitales π^* (antiliantes) du ligand acétylénique permettant un lien π très fort. La donation d'électrons du métal à l'orbitale π^* (antiliante) du ligand est donc un facteur électronique très important dans ce genre de composés.

Partie expérimentale

Les points de fusion ont été déterminés avec un appareil Fisher–Johns et ne sont pas corrigés.

Un appareil Hitachi Perkin–Elmer 115 a été utilisé pour déterminer les poids moléculaires. Les complexes $Pt(ac)_2$ et $Pt(PPh_3)_2(ac)$ ont été analysés dans l'acétone (Fisher A-20) à une température de 37.8 °C. Le benzil (*P.M.* = 210.22) a été utilisé comme standard pour préparer la courbe de calibration.

Les spectres électroniques ont été mesurés avec un spectrophotomètre Cary 14.

Un appareil Perkin–Elmer 621 a été utilisé pour mesurer les spectres infrarouges entre 4000 et 200 cm^{-1}. Le spectromètre était fréquemment vérifié avec un échantillon de polystyrène. Les ajustements standards de l'appareil ont été utilisés. Les spectres des échantillons solides ont été mesurés par la méthode de dispersion dans des pastilles de bromure de potassium ou d'iodure de césium. Des cellules de chlorure de sodium, de bromure de potassium, de KRS-5 et de quartz (région 3500 cm^{-1}) de différentes épaisseurs ont été utilisées pour mesurer les spectres de composés en solution. Un appareil pour sécher l'atmosphère a été utilisé pour les spectres dans l'infrarouge lointain. Un spectrophotomètre Perkin–Elmer 457 a également été utilisé à l'occasion.

Les mesures de conductivité ont été faites avec un conductomètre Radiometer de type CDM 2d et une cellule conductométrique Radiometer de type CDC 104.

La susceptibilité magnétique des complexes a été mesurée à la température ambiante par la méthode de Faraday avec un appareil ALPHA muni d'un électroaimant modèle No 9506. La distance entre les pointes des pôles est de $1\frac{1}{2}$ pouce. Un régulateur de courant ALPHA type 110 a été utilisé ainsi qu'une électrobalance Cahn Rg et un enregistreur Varian G 1000. La contribution diamagnétique du panier en quartz a été soustraite. $HgCo(SCN)_4$ a été utilisé comme standard pour calibrer l'appareil.

Les quatre appareils suivants ont été utilisés pour les spectres de résonance magnétique nucléaire: Varian A 60, Jeol C 60 H, Jeol 100 Mc 4 H et Perkin–Elmer R 12.

Les spectres de masse ont été mesurés avec un appareil Hitachi Perkin–Elmer R.M.U.-6D. L'énergie du faisceau d'électrons ionisants était de 70 eV, la température de la chambre à ionisation étant maintenue à 250 °C.

Préparation des ligands

Diméthyl-3,6 octyne-4 diol-3,6 (ac^1) a été obtenu de Air Reduction Chemical and Carbide Company et recristallisé dans le tétrachlorure de carbone p.f. 49°.

Spectre r.m.n. (CCl_4) (τ (p.p.m.), intensité relative, attribution): 9.01, 3 triplet, CH_3 (de C_2H_5); 8.60, 3 singulet, CH_3; 8.42, 2 quadruplet (?), CH_2; 5.88, 1 singulet, OH.

Diéthyl-3,6 octyne-4 diol-3,6 (ac^2) a été préparé d'après la méthode décrite par Theophanides (17). Le glycol a été recristallisé dans l'hexane p.f. 76°.

Spectre r.m.n. (CCl_4) (τ (p.p.m.), intensité relative, attribution): 9.00, 6 triplet, CH_3; 8.46, 4 multiplet, CH_2, 7.85, 1 singulet, OH).

Diméthyl-4,7 décyne-5 diol-4,7 (ac^3) a été préparé par la même méthode que celle décrite dans la référence (17) en substituant la pentanone-3 par la pentanone-2. Le glycol a été recristallisé dans l'hexane-*n* p.f. 62–63°.

Spectre r.m.n. (CCl_4) (τ (p.p.m.), intensité relative, attribution): 9.05, 3 multiplet, CH_3 (de C_3H_7); 8.61, 3 singulet, CH_3; 8.45, 4 multiplet, CH_2; 7.37, 1 singulet, OH.

Diméthyl-6,9 tétradécyne-7 diol-6,9 (ac^4) a été préparé par la même méthode (17) en utilisant l'heptanone-2. Le ligand a été recristallisé dans l'hexane-*n* p.f. 84–85°.

Spectre r.m.n. (CCl_4) (τ (p.p.m.), intensité relative, attribution): 9.1, 8.6, 14 multiplet, CH_3 (de C_5H_{11}), CH_3 et CH_2; 7.21, 1 singulet, OH.

Diéthyl-5,8 dodécyne-6 diol-5,8 (ac^5) a également été préparé par la même méthode (17). L'heptanone-3 a été utilisé. Le glycol a été recristallisé dans l'hexane-*n* p.f. 71°.

Spectre r.m.n. (CCl_4) (τ (p.p.m.), intensité relative, attribution): 9.0, 6 multiplet, CH_3; 8.5, 8 multiplet, CH_2; 7.3, 1 singulet, OH.

Di(hydroxy-1 cyclohexyl)-1,2 acétylène (ac^6) a été préparé par la même méthode (17). La cyclohexanone a été utilisée. Le glycol acétylénique a été recristallisé dans l'hexane-*n* p.f. 105–106°.

Spectre r.m.n. (CCl_4) (τ (p.p.m.), intensité relative, attribution): 8.40, 10 multiplet, CH_2; 6.60, 1 singulet, OH.

Préparation des complexes $Pt(ac)_2$

0.002 *m* de K_2PtCl_4 est dissous dans 25 ml de solvant. Le solvant est une solution de 40% d'éthanol dans l'eau. La solution de K_2PtCl_4 est filtrée pour enlever les particules insolubles et on ajoute 0.005 *m* de ligand (ac) à la solution. Le mélange est ensuite chauffé sur un bain-marie pendant cinq minutes et laissé au repos pendant au moins 12 h. Un précipité brun se forme lentement. Le précipité est alors filtré et lavé avec de l'hexane-*n*. On obtient alors un produit beige ou brun pâle que l'on cristallise deux fois dans l'acétone. Un produit blanc, cristallisé en forme d'aiguille est finalement obtenu. Les rendements sont bas, de 5 à 18% et varient avec le ligand.

L'analyse élémentaire des complexes $Pt(ac)_2$ a déjà été publiée (1). $Pt(ac^1)_2$: p.f. 164–173° (déc.); $Pt(ac^2)_2$: p.f. 186–192° (déc.); $Pt(ac^3)_2$: p.f. 145°; $Pt(ac^4)_2$: p.f. 148°; $Pt(ac^5)_2$: p.f. 145°; $Pt(ac^6)_2$: p.f. 190–197° (déc.).

Préparation des complexes $Pt(PPh_3)_2(ac)$

(a) Ces complexes ont été préparés selon les méthodes décrites dans la littérature par Chatt et ses collaborateurs (11) et par Allen et Cook (12) afin de comparer ces complexes avec ceux que nous avons isolés comme produits de la réaction des complexes $Pt(ac)_2$ avec la triphénylphosphine.

(b) Ces complexes peuvent également être préparés selon la réaction suivante:

$$Pt(ac)_2 + 2PPh_3 \xrightarrow{\text{hexane-}n} Pt(PPh_3)_2(ac) + ac$$

0.00005 *m* de $Pt(ac)_2$ sont ajoutés à 10 ml d'hexane-*n*. Le mélange est agité avec un agitateur magnétique. 0.0001 *m* de triphénylphosphine est dissous dans 15 ml d'hexane-*n*. Cette dernière solution est ajoutée goutte à goutte très lentement à la suspension contenant le complexe $Pt(ac)_2$. L'addition doit durer environ 8 h et l'agitation doit être continuelle. La réaction est quantitative. Des rendements de 80% sont obtenus. Les complexes ne sont pas recristallisés puisqu'ils se décomposent facilement en solution.

$Pt(PPh_3)_2(ac^1)$ p.f. 125–132° (déc.), $\chi g(c.g.s.) = -0.3 \times 10^{-6}$ et *P.M.* (acétone) = 445 (théoriquement = 889).

Anal. calc.: C, 62.14; H, 5.90; P, 6.97. Trouvé: C, 61.93; H, 5.43; P, 6.74.

$Pt(PPh_3)_2(ac^5)$ p.f. 108–114° (déc.), $\chi g(c.g.s.) = -0.4 \times 10^{-6}$ et *P.M.* (acétone) = 438 (théoriquement = 973).

Anal. calc.: C, 64.18; H, 6.22; P, 6.37. Trouvé: C, 64.24; H, 6.10; P, 6.23.

$Pt(PPh_3)_2(ac^6)$ p.f. 105–135° (déc.), $\chi g(c.g.s.) = -0.4 \times 10^{-6}$ et *P.M.* (acétone) = 435 (théoriquement = 941).

Anal. calc.: C, 63.82; H, 5.57; P, 6.59. Trouvé: C, 63.18; H, 5.49; P, 6.61.

Notre vive appréciation va au Conseil National de Recherches du Canada et à l'Imperial Oil Co. Ltée pour l'aide financière accordée.

1. F. D. ROCHON et T. THEOPHANIDES. Can. J. Chem. **46**, 2973 (1968).
2. D. M. ROUNDHILL et H. B. JONASSEN. Chem. Commun. 1233 (1968).
3. R. G. DENNING, F. R. HARTLEY, et L. M. VENANZI. J. Chem. Soc. 1322 (1967).
4. J. H. NELSON, H. B. JONASSEN, et D. M. ROUNDHILL. Inorg. Chem. **8**, 2591 (1969).
5. J. L. BOSTON, S. O. GRIM, et G. WILKINSON. J. Chem. Soc. 3468 (1963).
6. J. CHATT, G. A. ROWE, et A. A. WILLIAMS. Proc. Chem. Soc. 208 (1957).
7. E. O. GREAVES, C. J. L. LOCK, et P. M. MAITLIS. Can. J. Chem. **46**, 3879 (1968).
8. T. L. GILCHRIST, J. F. GRAVELING, et C. W. REES. Chem. Commun. 821 (1968).
9. J. CHATT. Chimica inorganica. Accad. Nazl. Lincei, Roma, 113 (1961).
10. J. P. COLLMAN et J. W. KANG. J. Am. Chem. Soc. **89**, 844 (1967).
11. J. CHATT, R. G. GUY, L. A. DUNCANSON, et D. T. THOMPSON. J. Chem. Soc. 5170 (1963).
12. A. D. ALLEN et C. D. COOK. Can. J. Chem. **42**, 1063 (1964); Can. J. Chem. **41**, 1235 (1963).
13. R. UGO, F. CARIATI, et G. LA MONICA. Chem. Commun. 868 (1966).
14. J. H. NELSON, K. S. WHEELOCK, L. C. CUSACHS, et H. B. JONASSEN. Chem. Commun. 1019 (1969).
15. R. UGO. Coord. Chem. Rev. **3**, 319 (1968).
16. L. MALATESTA, R. UGO, et S. CENINI. Adv. Chem. Ser. **62**, 318 (1966).
17. T. THEOPHANIDES. Mémoire de M.A. Université de Toronto, Toronto, Ontario, 1961.
18. FORREST F. CLEVELAND, et M. J. MURRAY. J. Am. Chem. Soc. **62**, 3186 (1940).

Fluorescence and Phosphorescence of 2,3-Pentanedione

A. W. JACKSON AND A. J. YARWOOD
Department of Chemistry, McMaster University, Hamilton, Ontario
Received August 9, 1971

The fluorescence and phosphorescence yields on photolysis of 2,3-pentanedione were investigated at various temperatures. The processes involved in the formation and removal of both the singlet and triplet states are considered. The data agree qualitatively and quantitatively with the results of an earlier study of the lifetime of the triplet state. It is shown that delayed fluorescence is not observed in the pentanedione system. A mechanism is proposed that can correlate the temperature variation of both the lifetime and quantum yield data.

On a étudié les rendements de fluorescence et de phosphorescence durant la photolyse du 2,3-pentanedione à différentes températures. On examine les procédés impliqués dans la formation et la disposition des états singulet et triplet. Les résultats que nous obtenons sont en accord qualitatif et quantitatif avec ceux provenant d'une étude précédente sur le temps de demi-vie de l'état triplet. On montre que la fluorescence retardée n'est pas observée dans le système pentanedione. On propose un mécanisme qui peut expliquer la variation de température du temps de demi-vie et des résultats de rendement quantique.

Canadian Journal of Chemistry, **50**, 1331 (1972)

Can. J. Chem. Downloaded from www.nrcresearchpress.com by 210.87.254.105 on 09/05/12
For personal use only.

The electronically excited singlet and triplet states of diketones are of low energy. As a result, diketones, particularly biacetyl, have often been used as acceptors in studies of both singlet and triplet energy transfer (1–3). The features required of an acceptor in sensitization studies have been considered by Noyes and Unger (3), and in many respects 2,3-pentanedione fulfils the criteria. An earlier study investigated the radiationless processes involving the triplet state in the photochemistry of 2,3-pentanedione through measurement of the phosphorescence lifetime (4). This investigation considers the photochemical processes involving both the singlet and triplet states of 2,3-pentanedione. The temperature dependence of the fluorescence and phosphorescence yields is studied and the data correlated with the phosphorescence lifetime data.

Experimental

The 2,3-pentanedione was purified in the manner described earlier (4). The equipment used in the emission measurements with wavelength resolution was also described (4). However, in this research the luminescence spectra were corrected for the quantum efficiency of the photomultiplier and the bandwidth and transmission factor of the monochromator. A standard lamp (Electro Optics Associates, Type 101) was used to calibrate the monochromator–photomultiplier arrangement. The quantum yields were determined using quinine sulfate ($\phi = 0.55$) as a standard (5, 6) and the incident light intensities were determined using potassium ferrioxalate actinometry (7).

Measurements were also made of the relative yields of fluorescence and phosphorescence. The excitation source for these studies was a 60 W medium pressure mercury lamp operated from a Gates Omnirange power supply. The light was focussed to produce parallel light which passed through a filter holder. Interference filters supplied by Baird Atomic were used to isolate wavelengths of 313, 365, 405, and 436 nm. A portion of the light passed by the filter was reflected by a quartz plate onto a photocell (GE Type 935). The signal was displayed on a recorder and measured the intensity of the light entering the system. The majority of the light was transmitted by the plate, passed through a cell and was focussed onto a second photocell, and the output measured on an electrometer (Keithley 610C). The cell and thermostatically controlled box were described earlier (4).

Light emitted by the sample through the side window of the cell passed down a tube mounted to reduce the scattered light and restrict the portion of the cell viewed. The emission at 460 and 527 nm was isolated using interference filters (Baird Atomic, bandwidth at half peak transmittance about 10 nm) and measured using a photomultiplier (EMI 6256 cooled to −80 °C) and an electrometer (Keithley 610C).

The relative yield of emission, Q_λ, at 460 or 527 nm was determined in the experiments and is defined by

$$Q_\lambda = \frac{l_\lambda - l_\lambda^0}{g(l_{trans}^0 - l_{trans})}$$

where $(l_\lambda - l_\lambda^0)$ is the difference between the emission readings with and without sample in the cell. $(l_{trans}^0 - l_{trans})$ is the difference between the transmitted photocell readings without and with sample in the cell. For a particular exciting wavelength the electrometer readings were corrected to some arbitrary value of the incident light intensity.

The quantity g is a geometric factor that takes into account that the actual incident light causing emission in the region viewed by the photomultiplier varies as the amount of light absorbed varies. In this case, $g = [\sinh(\varepsilon c\delta/2)]/[\sinh \varepsilon cl/2]$ where α is the natural extinction coefficient, c is the concentration in mol l^{-1}, $\delta = 10$ mm, is the length viewed by the photomultiplier, and $l = 100$ mm, is the length of the cell.

The value of Q was also corrected (8) for reflection effects in the cell. A further correction was necessary for the emission data at 460 nm. This is due to reabsorption of the

Can. J. Chem. Downloaded from www.nrcresearchpress.com by 210.87.254.105 on 09/05/12
For personal use only.

fluorescence by the sample before its detection by the photomultiplier. The illuminated section of the cell in these experiments had a width $2a$ and the distance between the outer edge of the illuminated area and the cell window was also a (where $a = 13$ mm). The "inner filter" correction factor assumed that the light emitted by a region of thickness dx a distance x from the cell wall that reached the cell wall was $I_x = Ae^{-\alpha cx}.dx$. The total light that reached the wall as a result of illumination in the region between a and $3a$ from the wall was thus $I_{total} = A[e^{-\alpha ca} - e^{-3\alpha ca}]/\alpha c$. In the absence of the "inner filter" effect the light intensity would be $2a$A so the correction factor was $2a\alpha c/[e^{-\alpha ca} - e^{-3\alpha ca}]$. Now $\alpha = 2.303\varepsilon$ where ε is the decadic extinction coefficient and the correction factor was calculated using $\varepsilon = 4.0$ for 460 nm excitation.

In some experiments the narrow band interference filters were not used to select the wavelength viewed by the photomultiplier. Instead, a glass filter (CS 3-72) covered the photomultiplier and restricted the emitted light so that only wavelengths greater than 470 nm were recorded by the photomultiplier (type 1P28 in these experiments). The total emission was recorded, then oxygen added, and the fluorescence intensity recorded. The phosphorescence intensity was taken as the difference between the total and the fluorescence intensities.

Results

The absorption spectrum of 2,3-pentanedione in the gas phase is shown in Fig. 1. The spectrum consists of two systems. The system at shorter wavelengths extends from less than 220 nm to greater than 320 nm with a maximum at 253 nm ($\varepsilon = 31.5\ M^{-1}\ cm^{-1}$). The only structure observed is a shoulder at 280 nm. The longer wavelength system extends from less than 340 nm to greater than 465 nm. Some structure is observed in the system and no absorption is detected at wavelengths longer than 480 nm.

The luminescence spectrum of 2,3-pentanedione was determined by irradiating a sample (15 Torr) in the vapor phase at 24 °C. The emission extends from less than 430 nm to greater than 610 nm. The corrected total emission spectrum is shown in Fig. 2, and the emission profile was identical for excitation at 365, 405, and 436 nm. The emission at longer wavelengths, associated with a long lived species from earlier phosphoroscope experiments, disappeared on addition of 20 Torr of oxygen. The profiles of the emission after addition of oxygen were identical at the three excitation wavelengths used. The corrected spectrum observed in presence of oxygen is also shown in Fig. 2 (note that the figure indicates only the emission profiles and that curve B is not to the same scale as curve A).

The absolute quantum yields of emission were determined with respect to quinine sulfate as a standard and the results are shown in Table 1. A further check of the quantum yield of emission was made using the relative yield apparatus.

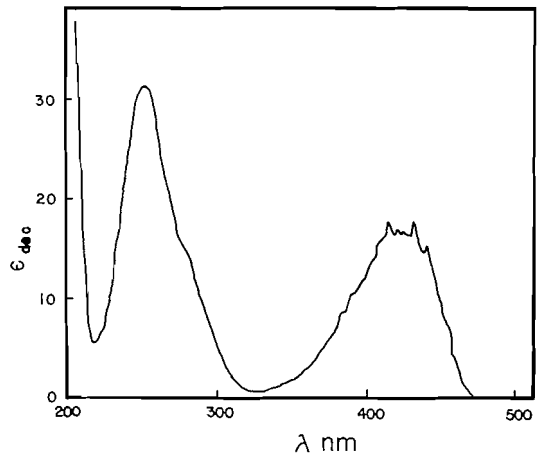

FIG. 1. Absorption spectrum of 2,3-pentanedione in gas phase at 24 °C.

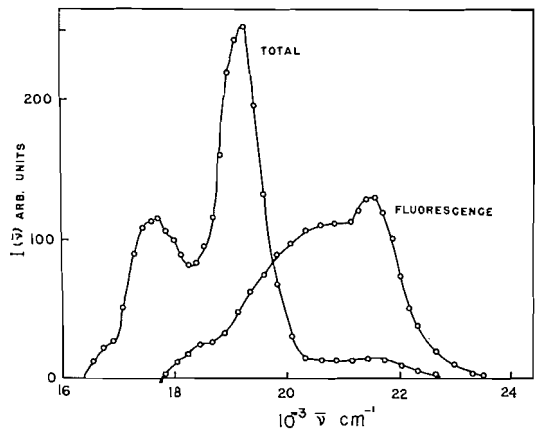

FIG. 2. Corrected emission spectra of 2,3-pentanedione excited at 405 nm. *A*, total emission. *B*, emission in presence of 20 Torr oxygen, not to the same scale as *A*.

TABLE 1. Quantum yields of emission of 2,3-pentanedione (15 Torr) at 23 °C excited at various wavelengths

λ_{ex} (nm)	ϕ_f	ϕ_p
436	0.0011	0.019
405	0.0011	0.019
365	0.00063	0.010

Can. J. Chem. Downloaded from www.nrcresearchpress.com by 210.87.254.105 on 09/05/12
For personal use only.

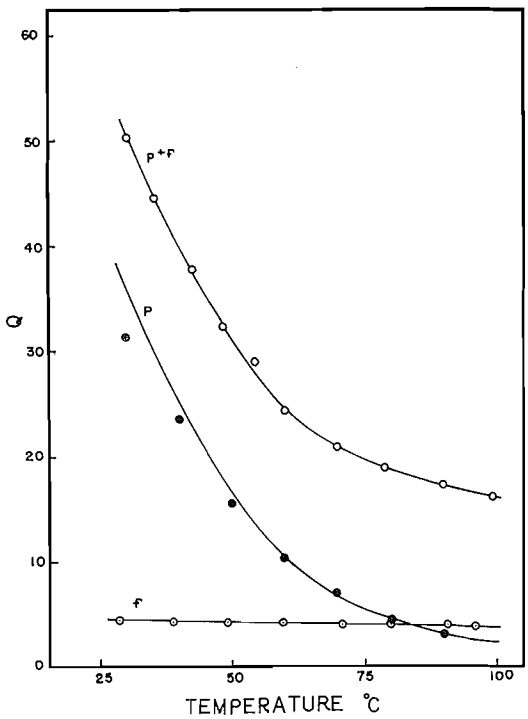

FIG. 3. Variation of total emission, fluorescence and phosphorescence yields with temperature. Pentanedione concentration = 2.2×10^{-4} M. $\lambda_{ex} = 436$ nm. (The total emission (p + f) curve is displaced 10 units vertically.)

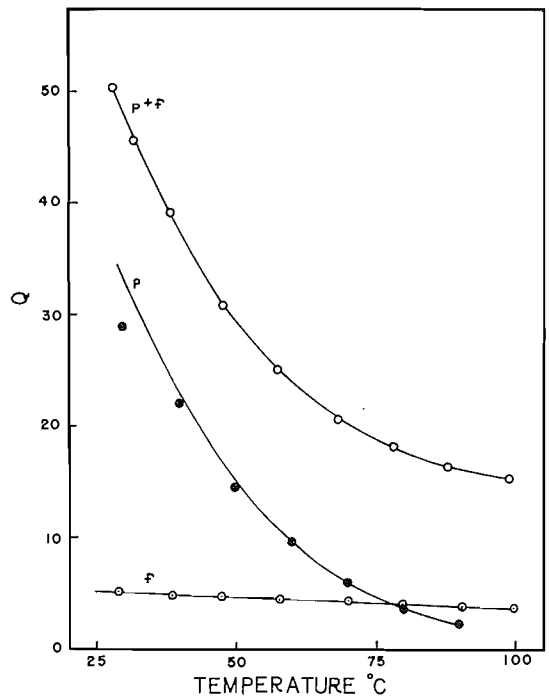

FIG. 4. Variation of total emission, fluorescence and phosphorescence yields with temperature. Pentanedione concentration = 1.2×10^{-3} M. $\lambda_{ex} = 436$ nm. (The total emission curve is displaced vertically by 10 units.)

The emission spectra of 2,3-pentanedione and butanedione are very similar and butanedione (biacetyl) was used as a relative standard ($\phi = 0.18$ (9)). The quantum yield of total emission of 2,3-pentanedione at 14 Torr at 30 °C was found to be 0.022. Initial experiments were conducted using the oxygen quenching technique to monitor the fluorescence. Since the emission filter passed only wavelengths longer than 470 nm, where absorption by the diketone is negligible, the "inner filter" correction was not applied. In these studies, a more extensive temperature range was investigated and various excitation wavelengths were used. The results for a low concentration of pentanedione (2.2×10^{-4} M) excited at 436 nm, are shown in Fig. 3, while the results of excitation at 365 nm are shown in Fig. 4 for 1.2×10^{-3} M pentanedione. Figures 5 and 6 show the data for 6.1×10^{-3} M pentanedione excited at 436 and 365 nm, respectively.

Other relative yield experiments involved excitation at 436 nm and used the filter technique to discriminate between the fluorescence and the phosphorescence. The values of Q_f and Q_p were measured at various pentanedione pressures at 50.0, 70.0, and 90.0 °C. There was no significant variation in Q_f over the concentration range studied. The variation in Q_p is presented in Fig. 7 in the form Q_p^0/Q_p vs. concentration at various temperatures. Q_p^0 is the phosphorescence yield at zero pressure for 436 nm excitation.

In one sequence of experiments, the fluorescence yield of pentanedione (1.4×10^{-3} M) at 40.0 °C was measured as an inert gas (perfluoroethane) was added. No change in Q_f was detected for 436 nm excitation up to a perfluoroethane concentration of 5×10^{-2} M.

Discussion

The visible and ultraviolet absorption spectrum of 2,3-pentanedione in the vapor phase is shown in Fig. 1 and shows clearly the absorptions expected for a diketone in the 260 and 420 nm regions. The long wavelength absorption

Can. J. Chem. Downloaded from www.nrcresearchpress.com by 210.87.254.105 on 09/05/12
For personal use only.

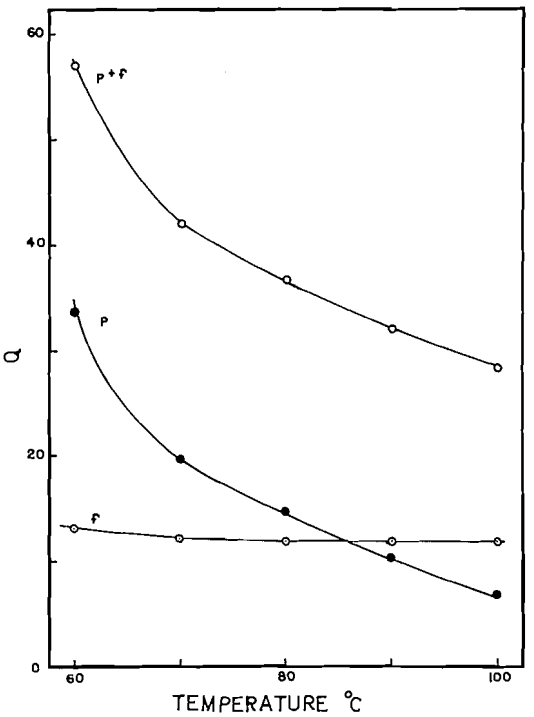

FIG. 5. Variation of total emission, fluorescence and phosphorescence yields with temperature. Pentanedione concentration = 6.1×10^{-3} M. $\lambda_{ex} = 436$ nm. (The total emission curve is displaced vertically by 10 units.)

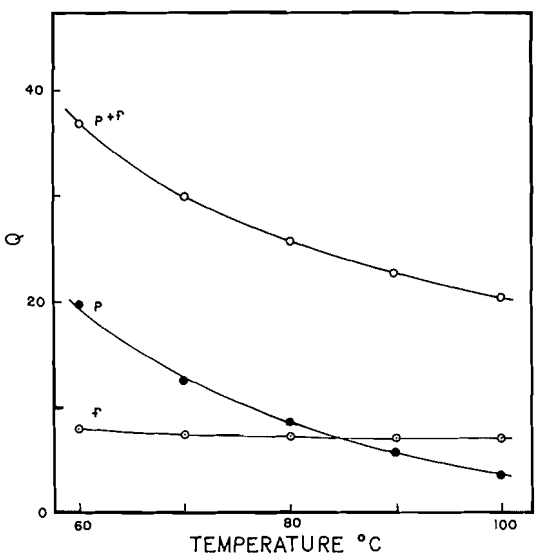

FIG. 6. Variation of total emission, fluorescence and phosphorescence yields with temperature. Pentanedione concentration = 6.1×10^{-3} M. $\lambda_{ex} = 365$ nm. (The total emission curve is displaced by 10 units vertically.)

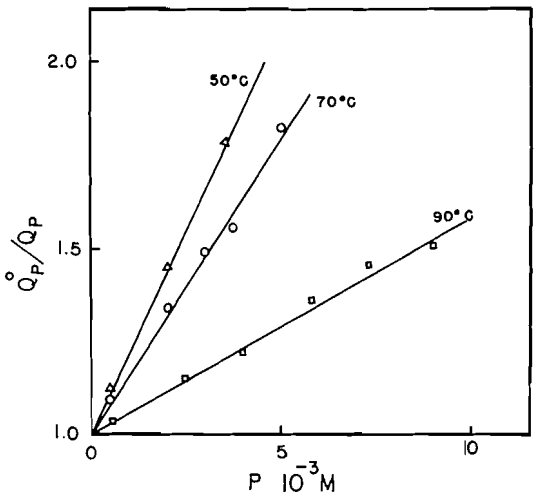

FIG. 7. Variation of Q_p^0/Q_p with pentanedione concentration. $\lambda_{ex} = 436$ nm.

of 2,3-pentanedione shows considerable structure and this transition can be classified as $n\pi^*$ by analogy with biacetyl and glyoxal (10, 11). In the short wavelength region, pentanedione in the gas phase has a structureless absorption with a maximum at 255 nm ($\varepsilon \simeq 30\ M^{-1}\ cm^{-1}$) which can be compared with those of biacetyl at 270 nm ($\varepsilon \simeq 12\ M^{-1}\ cm^{-1}$) (8) and chlorobiacetyl at 265 nm ($\varepsilon \simeq 240\ M^{-1}\ cm^{-1}$) (12). The short wavelength absorption of diketones is often considered as the second $n\pi^*$ transition. However, on the basis of solvent effects on the absorption spectra and calculations of the position and intensity of the absorption band this assignment can be questioned (24).

From the absorption spectrum, the natural radiative lifetime of the excited state can be estimated. Although, there are several formulae (13) available, the simple expression $\tau_0^{-1} = 2.88 \times 10^{-9} \nu^{-2} \int \varepsilon\, d\bar{\nu}$ was used to obtain τ_0 as 8.1×10^{-6} s. Although the formula is valid only for atomic absorption with resonance fluorescence, it is useful in comparing the natural radiative lifetime of the $^1n\pi^*$ state with that of biacetyl, 8.5×10^{-6} s (14). This confirms that the long wavelength excitation in 2,3-pentanedione is similar to that of biacetyl.

The corrected luminescence spectrum of 2,3-pentanedione, Fig. 2, shows that excitation in the $n\pi^*$ band leads to emission in the blue and green regions of the spectrum. The stronger

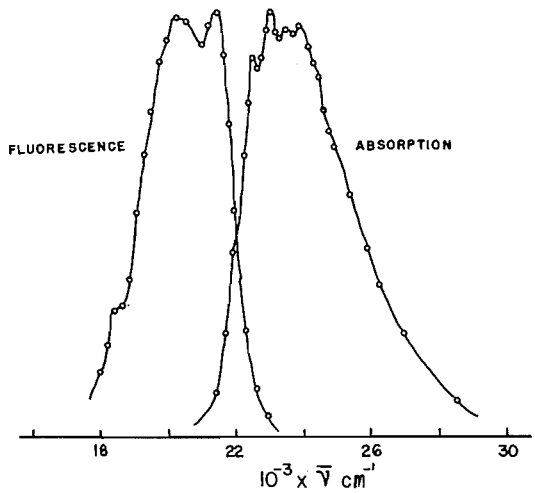

FIG. 8. Relationship between fluorescence and absorption spectrum.

green emission has already been shown to be associated with a long lived species (4) and is the phosphorescence. Figure 2 shows that the green emission is quenched by a low pressure of oxygen and the remaining blue emission is fluorescence.

The absorption and fluorescence spectra can be used to estimate the energy of the 0–0 transition. Figure 8 shows the approximate "mirror image" relationship between the fluorescence and absorption spectra and a value of 63.2 kcal is obtained for the singlet 0–0 transition in pentanedione. Since the onset of the fluorescence and phosphorescence spectra leads to a S_1–T_1 splitting of 9.2 kcal then the T_1–S_0 0–0 energy is 54.0 kcal. This value can be compared with the 54.7 kcal obtained by Hammond and co-workers (15) for 2,3-pentanedione in a 3-methyl pentane matrix at 77 °K. It is also very similar to the energy, 55 to 57 kcal, of the triplet state of biacetyl (16).

The fluorescence and phosphorescence yields are collected in Table 1. For excitation at 405 nm, the phosphorescence is about seventeen times greater than the fluorescence at 23 °C. Thus, the total emission spectrum in Fig. 2 is essentially the phosphorescence spectrum with a small contribution from the fluorescence at about 21 500 cm^{-1}.

A comparison between the triplet lifetime and luminescence yield data can be made from the relative yield data collected using the oxygen quenching technique. The results for excitation at various wavelengths and concentrations are shown in Figs. 3–6. There are two features common to the data. The fluorescence yield varies only slightly with the temperature and the phosphorescence yield varies significantly with the temperature.

The variation in the fluorescence yield is not large, about 10% between 30 and 100 °C. Since the quantum yield of fluorescence is small, then the quantum yield of fluorescence directly measures the ratio of the fluorescence emission and radiationless process rate constants for excitation at long wavelengths. It is likely that the reduction in Q_f with temperature is due to a small increase in the radiationless rate constant from the singlet state.

In contrast to the slight variation in the fluorescence yields with temperature, the phosphorescence variation is dramatic. As the singlet state is the precursor of the triplet state, the contrast in behavior could be due to the destruction of some intermediate between the emitting levels of the singlet and triplet states or to the processes removing the triplet. The phosphorescence lifetime study (4) has already shown that the processes removing the triplet state are strongly temperature dependent so the following mechanism can be considered for the long wavelength photolysis.

[1] $P + h\nu \rightarrow {}^1P^0$

[2] ${}^1P^0 \rightarrow P + h\nu_f$

[3] ${}^1P^0 \rightarrow {}^3P^h$

[4] ${}^3P^h + P \rightarrow {}^3P^0 + P$

[5] ${}^3P^0 \rightarrow P + h\nu_p$

[6] ${}^3P^0 \rightarrow$ radiationless removal

[7] ${}^3P^0 + P \rightarrow$ removal

When k_2 is small compared to k_3 the quantum yield of phosphorescence, ϕ_p, is given by

$$[8] \qquad \phi_p = \frac{k_5}{k_5 + k_6 + k_7(\mathrm{P})} = \tau_p k_5$$

where τ_p is the phosphorescence lifetime. Thus, if the mechanism is correct and k_5 does not vary with the temperature, then the variation of ϕ_p should be described by the variation of τ_p. This is tested in Figs. 3–6 where the continuous curve representing the variation of the phosphorescence yield with temperature is obtained as the

Can. J. Chem. Downloaded from www.nrcresearchpress.com by 210.87.254.105 on 09/05/12
For personal use only.

Can. J. Chem. Downloaded from www.nrcresearchpress.com by 210.87.254.105 on 09/05/12
For personal use only.

difference between the curves for the total emission yield and the fluorescence yield. The open circles on the total emission and fluorescence curves represent experimental data. The filled circles close to the phosphorescence curve in Figs. 3–6 represent the variation of the phosphorescence lifetime (4) with temperature for a particular pentanedione concentration. The lifetime data are plotted using $Q_p = \text{constant} \times \tau_p$ and the value of the constant was chosen by substitution at a temperature in the middle of the temperature range (a quantitative comparison of the phosphorescence yield and lifetime data is considered later).

The correlation of the lifetime and yield data is good and the mechanism described above is adequate to describe the behavior on long wavelength excitation. The temperature variation due to decomposition of intermediate levels between the vibrationally equilibrated singlet and triplet levels cannot be detected at these concentrations even for 365 nm excitation.

The variation of the fluorescence yield of pentanedione with temperature is similar to that of biacetyl. Groh (17) reports that a reduction of about 30% is observed for the fluorescence yield at 200 °C compared with 30 °C. The variation of the phosphorescence yield with temperature was studied by Coward and Noyes (18) and has been re-investigated by Noyes *et al.* (19). They showed that at low temperature the decomposition of the triplet state occurred by triplet–triplet annihilation and that at high temperature by thermal decomposition. Any thermal decomposition of the triplet state of pentanedione would have to compete with the rapid unimolecular reaction proposed for that triplet state and thermally induced decomposition was not detected.

As discussed above, excitation of pentanedione at 436 nm forms the singlet state with an energy about 3 kcal above the 0–0 level. The quantum yield of formation of vibrationally equilibrated singlet level is effectively unity at this wavelength since spontaneous dissociation is unlikely. This assumption is confirmed by the fact that the fluorescence quantum yield is independent of the pressure of pentanedione for 436 nm excitation at 50.0, 70.0, and 90.0 °C. Again, the data also indicate that there is no bimolecular quenching process involving the excited singlet state that can be detected in the 0–0.01 M concentration range (only processes with rate constants greater than $3 \times 10^9\ M^{-1}\ s^{-1}$ can be detected).

The behavior of pentanedione with respect to the self-quenching of the fluorescence cannot be compared directly to that of biacetyl since the variation of the fluorescence yield of biacetyl excited at 436 nm has not been studied at a variety of temperatures and pressures. However, the photochemical decomposition of biacetyl has been studied under these conditions and the behavior can also be described without including a bimolecular quenching process of the vibrationally equilibrated singlet with the ground state species (20).

A more detailed investigation of the dependence of the phosphorescence yield on pentanedione concentration was undertaken using the relative yield apparatus with interference filters for the selection of the fluorescence and phosphorescence. The results are shown in Fig. 7 in a simple Stern–Volmer plot. This indicates that the self-quenching reaction of the triplet state involves a bimolecular reaction of the vibrationally equilibrated triplet molecule with the molecule of pentanedione in its ground state. This is just the conclusion reached in the phosphorescence lifetime study (4). The phosphorescence yield data can be discussed in terms of eq. 8 which can be rearranged to

$$[9] \qquad \frac{\phi_p^0}{\phi_p} = 1 + k_7\tau_0(\mathrm{P})$$

where τ_0 and ϕ_p^0 are the phosphorescence lifetime and quantum yield extrapolated to zero pentanedione pressure. The variation of τ_0 with temperature is already known (4) and, in conjunction with the values of the slopes in Fig. 7, k_7 can be evaluated from the phosphorescence yield data, on the basis of the above mechanism. The results are shown in Table 2. The agreement is good and supports the mechanism presented above.

The possibility of E-type delayed fluorescence in the pentanedione photolysis was also investigated. The phenomenon has been observed in many systems and is associated with the thermal excitation of the triplet state to the singlet state. It has been detected in molecules characterized

TABLE 2. Comparison of rate constants for self-quenching of triplet state from τ_p and Q_p data

Temperature (°C)	k_7 from τ_p (M^{-1} s^{-1})	k_7 from Q_p (M^{-1} s^{-1})
50.0	5.3×10^5	7.5×10^5
70.0	1.5×10^6	2.5×10^6
90.0	2.5×10^6	2.0×10^6

by a small triplet–singlet energy gap, *e.g.* benzil in solution (21) and biacetyl in the gas phase (22).

The mechanism of the reactivation can be considered as

[10] $$^3P + M \rightarrow {}^3P^v + M$$

[11] $$^3P^v + M \rightarrow {}^3P + M$$

[12] $$^3P^v \rightarrow {}^1P$$

It can be shown from a detailed consideration of the differential equations that describe the mechanism (23) for the pentanedione system that reactivation from the triplet would not affect the lifetime of the triplet. This arises because the major process removing the singlet state is a rapid intersystem crossing to reform the triplet. Thus, triplet lifetime studies could not show the presence of a reactivation process, *i.e.* delayed fluorescence, in the system. The fluorescence yield from pentanedione was measured as a function of the concentration of an added inert gas, perfluoroethane. It was found that the fluorescent yield was constant for pentanedione (concentration of 1.4×10^{-3} M) at 40 °C excited at 436 nm as the perfluoroethane concentration varied up to about 5×10^{-2} M. Delayed fluorescence cannot be detected under those conditions in the pentanedione system. The difference between the pentanedione and biacetyl (22) systems in this regard may be due to the shorter lifetime of the triplet pentanedione, so that more rapid processes are in competition with reactivation in this case.

We thank the National Research Council of Canada for financial support.

1. H. ISHIKAWA and W. A. NOYES, JR. J. Chem. Phys. **37**, 583 (1962).
2. P. G. BOWERS and G. B. PORTER. J. Phys. Chem. **68**, 2982 (1964).
3. W. A. NOYES, JR. and I. UNGER. Advan. Photochem. **4**, 49 (1966).
4. A. W. JACKSON and A. J. YARWOOD. Can. J. Chem. **49**, 987 (1971).
5. W. H. MELHUISH. J. Opt. Soc. Amer. **54**, 183 (1964).
6. J. N. DEMAS and G. A. CROSBY. J. Phys. Chem. **75**, 991 (1971).
7. C. A. PARKER. Photoluminescence of solutions. Elsevier, New York, 1968.
8. J. G. CALVERT and J. N. PITTS, JR. Photochemistry. Wiley, New York, 1966.
9. A. GANDINI and K. O. KUTSCHKE. Proc. Roy. Soc. A, **306**, 511 (1968).
10. H. M. MCMURRY. J. Chem. Phys. **9**, 241 (1942).
11. A. D. WALSH. Trans. Faraday Soc. **42**, 66 (1946).
12. A. W. JACKSON and A. J. YARWOOD. Unpublished work.
13. J. B. BIRKS and I. H. MUNRO. Progress in reaction kinetics. Vol. 4. Pergamon, New York, 1967.
14. G. M. ALMY and S. ANDERSON. J. Chem. Phys. **8**, 805 (1943).
15. W. G. HERKSTROETER, A. A. LAMOLA, and G. S. HAMMOND. J. Am. Chem. Soc. **86**, 4537 (1964).
16. J. W. SIDMAN and D. S. MCCLURE. J. Am. Chem. Soc. **77**, 6461 (1955).
17. H. J. GROH. J. Chem. Phys. **21**, 674 (1955).
18. N. A. COWARD and W. A. NOYES, JR. J. Chem. Phys. **22**, 1207 (1954).
19. W. A. NOYES, JR., M. A. MULAC, and M. S. MATHESON. J. Chem. Phys. **36**, 880 (1962).
20. G. F. SHEATS and W. A. NOYES, JR. J. Am. Chem. Soc. **77**, 1421, 4532 (1955).
21. C. A. PARKER and T. A. JOYCE. Chem. Commun. 1421 (1968).
22. S. H. NG. Doctoral Dissertation. University of New Brunswick, Fredericton, New Brunswick. 1970.
23. A. W. JACKSON. Doctoral Dissertation. McMaster University, Hamilton, Ontario. 1971.
24. G. W. KING and G. KIDD. Private communication.

Can. J. Chem. Downloaded from www.nrcresearchpress.com by 210.87.254.105 on 09/05/12
For personal use only.

Emission and Deactivation of the Excited States of 2,3-Pentanedione

A. W. JACKSON AND A. J. YARWOOD
Department of Chemistry, McMaster University, Hamilton, Ontario
Received August 9, 1971

Vibrationally excited singlet and triplet states of 2,3-pentanedione are formed by photolysis at 365 nm. The processes removing these excited states in the gas phase are studied by measuring the fluorescence and phosphorescence yields. Fluorescence can occur from the vibrationally excited, as well as the vibrationally equilibrated, singlet state. The fluorescence and phosphorescence data are considered in terms of mechanisms which involve either weak or strong collisions. Although the data cannot distinguish between the alternatives, there are two significant conclusions. The fluorescence data require that emission occur from at least two levels in the singlet manifold. To explain the phosphorescence data, the highest emitting singlet level must not lead to a vibrationally equilibrated triplet state.

Les états excités vibrationnels singulet et triplet du 2,3-pentanedione sont formés par photolyse à 365 nm. On étudie les procédés qui enlèvent ces états excités en phase gazeuse en mesurant les rendements de fluorescence et de phosphorescence. La fluorescence peut provenir de l'état singulet vibrationnel excité aussi bien qu'équilibré. On considère les résultats de phosphorescence et de fluorescence en termes de mécanismes qui impliquent des collisions fortes ou faibles. Quoique les résultats ne permettent pas de distinguer les cas intermédiaires, on arrive à deux conclusions significatives. Les résultats de fluorescence impliquent que l'émission se fait à partir d'au moins deux niveaux à l'état singulet. Pour expliquer les résultats de phosphorescence, le niveau singulet émetteur le plus élevé ne doit pas conduire à un état vibrationnel triplet équilibré.

Canadian Journal of Chemistry, **50**, 1338 (1972)

Introduction

The deactivation of vibrational energy is a topic that is central to the problem of describing the photochemical behavior of molecules excited at short wavelength in the gas phase. The deactivation is particularly clearly shown in the photochemistry of the iodine molecule (1, 2). The resonance fluorescence spectrum observed at very low iodine pressure changes on the addition of an inert gas. The spectrum includes new emission lines, due to the iodine molecules in new vibrational and rotational levels formed by collisional deactivation. The early research on iodine has been consolidated in an extensive series of recent papers, *e.g.* ref. 3.

The photochemistry of polyatomic molecules, particularly carbonyl compounds, has also contributed to an understanding of the deactivation of vibrational energy. The first paper (4) on the photochemistry of hexafluoroacetone included a consideration of vibrational excitation, and the photochemistry of hexafluoroacetone has been a fruitful field of endeavor (5, 6). Much of the discussion has concerned the problem of whether deactivation is by a single strong collision, or by a weak collision mechanism in which vibrational energy is removed in a cascade process (7–11). The problem has also been considered in the photochemistry of chloropentafluoroacetone (12) and biacetyl (13–15).

This paper is concerned with the emission and deactivation of the excited states of 2,3-pentanedione. The results are consistent with fluorescence from the vibrationally excited singlet state, and the problem of vibrational deactivation is investigated through measurement of the fluorescence and phosphorescence yields.

Experimental and Results

The details of the experimental procedure were given earlier (16). The quantum yields of fluorescence (ϕ_f) and phosphorescence (ϕ_p) of 2,3-pentanedione (15 Torr) excited at 436 and 405 nm were reported (16) as 0.0011 and 0.019, respectively; whereas, on excitation at 365 nm ϕ_f was 0.00063 and ϕ_p was 0.010.

The effect of adding a high pressure of an inert gas on the emission yields of pentanedione was investigated. At all excitation wavelengths the emission profiles were unchanged in the presence of 1000 Torr of sulfur hexafluoride. Also, for excitation wavelengths of 436 and 405 nm, the absolute yields are unaffected by the addition of inert gas. However, at 365 nm excitation, the values of the fluorescence and phosphorescence yields increased to 0.0012 and 0.020, *i.e.* to essentially those found when 405 and 436 nm excitation was used.

The enhancement of the emission in the presence of added

Can. J. Chem. Downloaded from www.nrcresearchpress.com by 210.87.254.40 on 09/05/12
For personal use only.

Can. J. Chem. Downloaded from www.nrcresearchpress.com by 210.87.254.40 on 09/05/12
For personal use only.

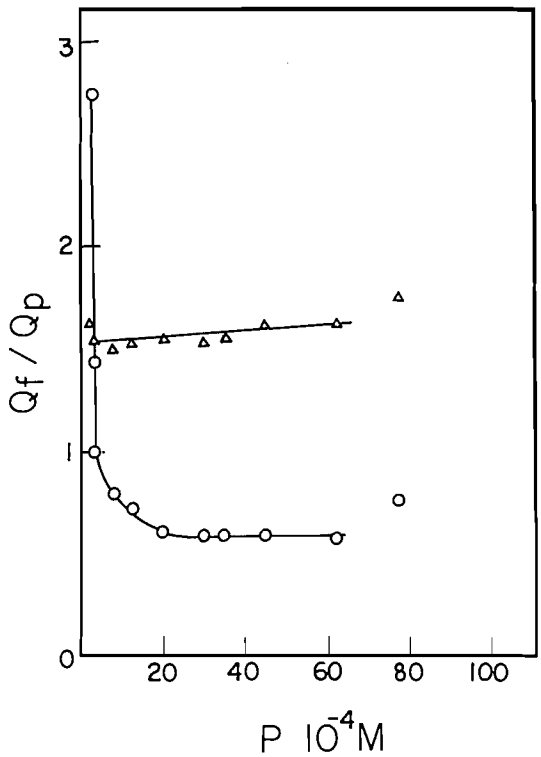

FIG. 1. Ratio of fluorescence to phosphorescence yields as a function of pentanedione concentration at 70 °C. ○, $\lambda_{ex} = 365$ nm. △, $\lambda_{ex} = 405$ nm. The data for $\lambda_{ex} = 405$ nm are displaced one unit vertically.

gas for excitation at 365 nm was further investigated through measurements of the relative fluorescence and phosphorescence yields. In one study the phosphorescence yields were determined from the difference between the total emission yield and the fluorescence yield (which was taken as the emission yield in the presence of oxygen). The ratios of the relative fluorescence and phosphorescence yields at 70 °C as a function of the pentanedione concentration are shown in Fig. 1 for excitation at 405 and 365 nm.

A more detailed investigation of the luminescence behavior at low pressures was carried out using narrow band interference filters to select the fluorescence and phosphorescence. Figure 2 shows the individual fluorescence and phosphorescence yields of pentanedione at 90 °C for 365 nm excitation. The value $Q_{f\infty}$ corresponds to the value of Q_f when 1000 Torr of methyl chloride were added to the sample at a concentration of 1.0×10^{-2} M.

The behavior on 365 nm excitation was also investigated at a lower temperature, 30.0 °C. Due to the low vapor pressure of 2,3-pentanedione at this temperature, the experiment was carried out at a fixed pressure of pentanedione, and various pressures of sulfur hexafluoride were added. The results are shown in Fig. 3, where Q_e, the yield of total emission, *vs.* sulfur hexafluoride pressure is plotted.

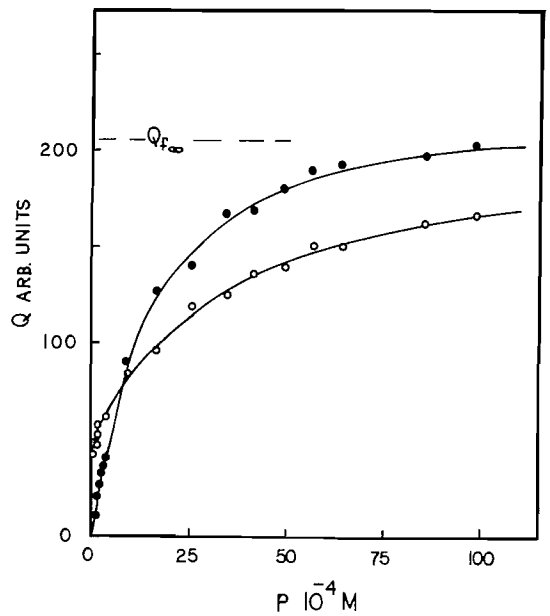

FIG. 2. Variation of fluorescence and phosphorescence yields as a function of pentanedione at 90 °C. ○, fluorescence yield. ●, phosphorescence yield.

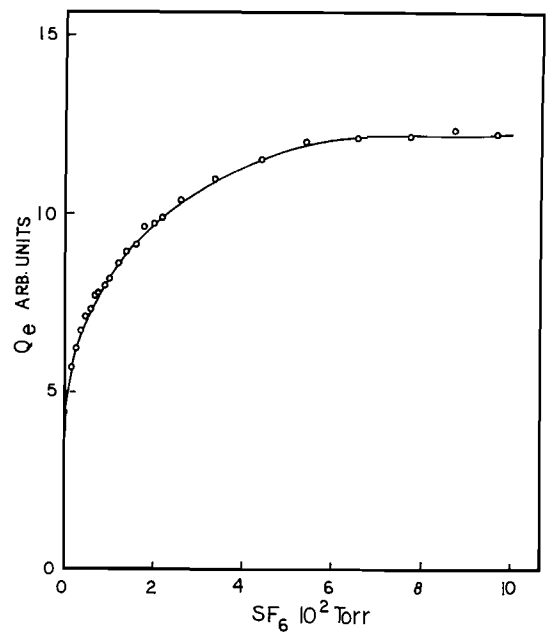

FIG. 3. Variation of total emission yield of pentanedione with pressure of sulfur hexafluoride at 30 °C. Pentanedione pressure = 10.7 Torr, $\lambda_{ex} = 365$ nm.

Can. J. Chem. Downloaded from www.nrcresearchpress.com by 210.87.254.40 on 09/05/12
For personal use only.

Discussion

There is a distinct difference between the luminescence behavior observed on excitation at 405 nm and at 365 nm, since $\phi_f = 0.00063$ for $\lambda_{ex} = 365$ nm compared with $\phi_f = 0.0011$ for $\lambda_{ex} = 405$ nm. The phosphorescence yield is also lower for the shorter wavelength excitation at low pressures. The pressure of the system also has a large influence, since the addition of 1000 Torr of sulfur hexafluoride to 15 Torr of pentanedione changes the emission yields observed on excitation at 365 nm to the values observed on excitation at 405 nm. The differences are shown very clearly in the data taken using the relative yield apparatus. At high concentrations, the ratio of fluorescence to phosphorescence yields (oxygen quenching technique) is approximately the same for 365 and 405 nm excitation at 70 °C, Fig. 1. However, at low concentrations there is a dramatic increase in the ratio for 365 nm excitation which is not detected for 405 nm excitation.

This feature of the system was further investigated using narrow band interference filters to isolate the fluorescence and phosphorescence wavelengths. The results for pentanedione at 90 °C are shown in Fig. 2. Again the excitation wavelength is 365 nm, but in Fig. 2 the individual values of Q_f and Q_p are presented. This shows that as the concentration is decreased, it is the phosphorescence yield that decreases rapidly to zero whereas the fluorescence is finite. Thus, the ratio $Q_f : Q_p$ in Fig. 1 increases at low concentration for 365 nm excitation because the phosphorescence yield has decreased rather than the fluorescent yield increased. This indicates the formation of the emitting level of the triplet depends upon a collisional process.

Another interesting point concerning the data of Fig. 2 is the enhancement of the fluorescence (and phosphorescence) as the concentration increases. Similar fluorescence enhancement has been observed in biacetyl (14, 15), hexafluoroacetone (10), and chloropentafluoroacetone (12) and has been interpreted in terms of a model involving competition between radiation and radiationless processes in the excited singlet state.

The variation of the fluorescence yield with concentration in the low concentration region cannot be reasonably extrapolated to the origin (although this does not show very clearly in Fig. 2). This is a particularly noteworthy aspect of the system and suggests that pentanedione excited at short wavelength at low concentration can emit from vibrationally excited levels of the excited singlet state. Consequently, the mechanisms to be discussed all involve emission from vibrationally excited singlet states.

The following scheme represents an initial kinetic model that considers vibrational deactivation in the singlet state and can account for emission from vibrationally excited singlet levels and collisional dependence of the phosphorescence. The fluorescence behavior is considered first.

Scheme A

[1] $S_0 + h\nu \rightarrow S_1^v$

[2] $S_1^v \rightarrow S_0 + h\nu_f$

[3] $S_1^v \rightarrow$ removal

[4] $S_1^v + M \rightarrow S_1^0 + M$

[5] $S_1^0 \rightarrow S_0 + h\nu_f$

[6] $S_1^0 \rightarrow T_1^v$

Absorption of light [1] can populate a vibrationally excited singlet state S_1^v that can fluoresce $h\nu_f$ [2], be removed in a radiationless process [3], or be vibrationally deactivated in a single collision by a species M [4] to form S_1^0. The vibrationally equilibrated excited singlet level S_1^0 can fluoresce [5] or can intersystem cross [6] to form a vibrationally excited triplet state T_1^v.

Application of the steady state approximation to this system gives for the quantum yield of fluorescence ϕ_f,

$$[7] \quad \phi_f = \frac{k_2}{k_2 + k_3 + k_4(M)} + \frac{k_4 k_5(M)}{(k_5 + k_6)(k_2 + k_3 + k_4(M))}$$

If it is assumed that $k_2 = k_5$, and that $k_2 \ll k_3$ and $k_5 \ll k_6$ (since the fluorescence yield is small) then

$$[8] \quad \phi_f = \frac{k_2}{k_3 + k_4(M)} \left\{ 1 + \frac{k_4(M)}{k_6} \right\}$$

This expression may be rearranged in several ways to yield a functional dependence that can be tested using the data. One method is to recognize the limits of the fluorescence quantum yield

Can. J. Chem. Downloaded from www.nrcresearchpress.com by 210.87.254.40 on 09/05/12
For personal use only.

at high and low concentrations, ϕ_{f_∞} and ϕ_{f_0}.

$$\text{As (M)} \rightarrow 0, \qquad \phi_f \rightarrow \phi_f^0 = k_2/k_3$$

$$\text{As (M)} \rightarrow \infty, \qquad \phi_f \rightarrow \phi_f^\infty = k_2/k_6$$

Inserting these limits gives

$$[9] \qquad \phi_f - \phi_f^0 = \frac{k_2 k_4(\text{M})(k_3 - k_6)}{k_3 k_6(k_3 + k_4(\text{M}))}$$

$$[10] \qquad \phi_f^\infty - \phi_f = \frac{k_2(k_3 - k_6)}{k_6(k_3 + k_4(\text{M}))}$$

which gives the dimensionless equation

$$[11] \qquad \frac{\phi_f - \phi_f^0}{\phi_f^\infty - \phi_f} = \frac{k_4}{k_3}(\text{M}) = \frac{Q_f - Q_f^0}{Q_f^\infty - Q_f}$$

Equation 11 is tested in Fig. 4 using the fluorescence data of Fig. 2. The value of Q_f^0 was obtained by extrapolating the experimental curve of Fig. 2 to zero concentration and the value of Q_f^∞ was taken as the relative fluorescence yield when about 1000 Torr of methyl chloride were added to the pentanedione. It can be seen from Fig. 4 that the dependence is well described by a straight line passing through the origin. The fit is particularly good since the dimensionless quantity $(Q_f - Q_f^0)/(Q_f^\infty - Q_f)$ contains three experimentally determined quantities and accumulates the experimental errors.

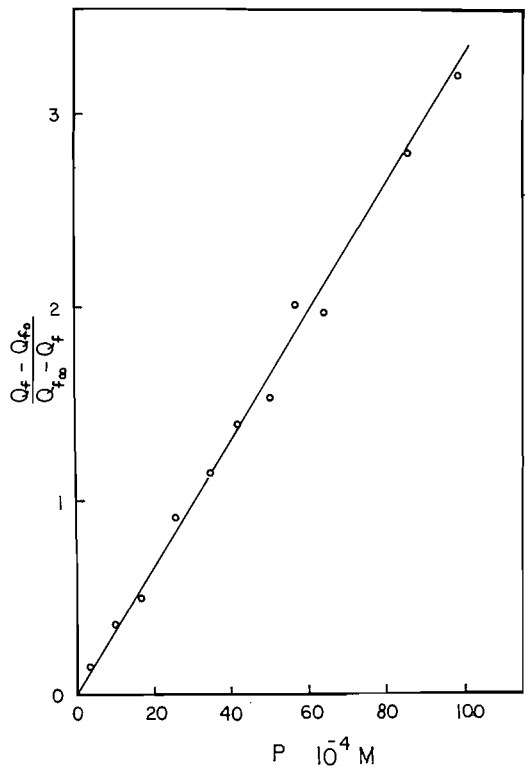

FIG. 4. Dependence of the dimensionless fluorescence function on pentanedione concentration at 90 °C, $\lambda_{ex} = 365$ nm.

The conclusion from this test is that a model in which there are two emitting levels in the singlet manifold that are connected through a strong collision is consistent with the fluorescence data. Although a model in which there is only one emitting singlet level would also predict a linear relation for Fig. 4 it is not consistent with the finite intercept for ϕ_f in Fig. 2. The rate constant k_3 can be estimated from $Q_f^\infty/Q_f^0 = k_3/k_6 = 4.4$. The rate constant k_6 can be estimated as about 2×10^8 s^{-1} (from the natural radiative lifetime and the fluorescence yield) and if it is assumed that the rate constant does not change with temperature then $k_3 \simeq 8.8 \times 10^8$ s^{-1}. The slope of the line in Fig. 4 is given by k_4/k_3 ($= 330 \pm 20\ M^{-1}$) and so $k_4 \simeq 2.9 \times 10^{11}\ M^{-1}$ s^{-1}. This value can be compared with the collision frequency (about $2 \times 10^{11}\ M^{-1}$ s^{-1}) and indicates that within the context of this mechanism every collision successfully deactivates the vibrationally excited singlet species.

Fluorescence is a useful tool in studying collisional deactivation in the gas phase and much work (8, 9, 12) has been carried out to distinguish between strong and weak collisional deactivation mechanisms. Accordingly, a mechanism was constructed for pentanedione involving more than two excited singlet levels to discover how the fluorescence behavior would be modified. This weak collision mechanism is:

Scheme B

$$[12] \qquad S_0^0 + h\nu \xrightarrow{\text{labs}} S_1^v$$

$$[13] \qquad S_1^v \longrightarrow \text{removal}$$

$$[14] \qquad S_1^v \longrightarrow S_0^n + h\nu_f$$

$$[15] \qquad S_1^v + \text{M} \longrightarrow S_1^{v'} + \text{M}$$

$$[16] \qquad S_1^{v'} \longrightarrow \text{removal}$$

$$[17] \qquad S_1^{v'} \longrightarrow S_0^n + h\nu_f$$

$$[18] \qquad S_1^{v'} + \text{M} \longrightarrow S_1^0 + \text{M}$$

$$[19] \qquad S_1^0 \longrightarrow S_0^n + h\nu_f$$

$$[20] \qquad S_1^0 \longrightarrow T_1^v$$

Can. J. Chem. Downloaded from www.nrcresearchpress.com by 210.87.254.40 on 09/05/12
For personal use only.

This mechanism involves an extra vibrationally excited singlet level $S_1^{v'}$ and the removal steps are radiationless processes. This situation is more complicated than Scheme A but can be treated if simplifying assumptions are made. These assumptions are: (*a*) the spontaneous emission rate constants are the same from the three levels, *i.e.* $k_{14} = k_{17} = k_{19}$; and that in each case the radiative rate constant is small compared to the radiationless rate constants; (*b*) the vibrational quenching efficiency is independent of the level in singlet manifold, *i.e.* $k_{15} = k_{18}$; and, (*c*) the intersystem crossing rate constant is the same from the intermediate level as from the thermally equilibrated level, *i.e.* $k_{16} = k_{20}$.

Under these conditions $\phi_f^0 = k_{14}/k_{13}$, $\phi_f^\infty = k_{14}/k_{20}$, and $(Q_f - Q_f^0)/(Q_f^\infty - Q_f) = k_{15}(M)/k_{13}$; which is the same form as Scheme A. Scheme B, with the same assumptions, is indistinguishable from Scheme A since the $S_1^{v'}$ level has the same processes controlling its fate as the S_1^0 level.

Changes in the mechanism can cause only small changes in fluorescence behavior. This is emphasized by considering Scheme C, which is a modification of Scheme B in which k_{16} is now set equal to k_{13} rather than k_{20}. Under these circumstances, retaining assumptions *a* and *b* above,

$$[21] \quad \phi_f = \frac{k_{14}}{k_{13} + k_{15}(M)} + \frac{k_{14}k_{15}(M)}{(k_{13} + k_{15}(M))^2} + \frac{k_{14}k_{15}^2(M)^2}{k_{20}(k_{13} + k_{15}(M))^2}$$

and this can be rearranged to

$$[22] \quad \frac{1}{\phi_f - \phi_f^0} = \frac{k_{20}k_{13}(k_{13} + k_{15}(M))^2}{k_{15}^2 k_{14}(k_{13} - k_{20})(M)^2}$$

The prediction of this mechanism is tested using eq. 22 in Fig. 5, where $(M)/(Q_f - Q_f^0)^{1/2}$ *vs.* (M) is plotted. A straight line dependence is indeed found and shows that Scheme C is also in accord with the experimental data. Thus, the data do not distinguish between the three models presented above.

An important feature of the above mechanisms is the suggestion that vibrationally excited levels of the excited singlet diketone can fluoresce. This might be expected to cause a shift in the profile of fluorescence as a function of wavelength at low concentrations. No change in the profile was detected in this research, but experiments could only be carried out at pressures greater than 15 Torr. Experiments with more sensitive equipment and much lower pressures would be useful.

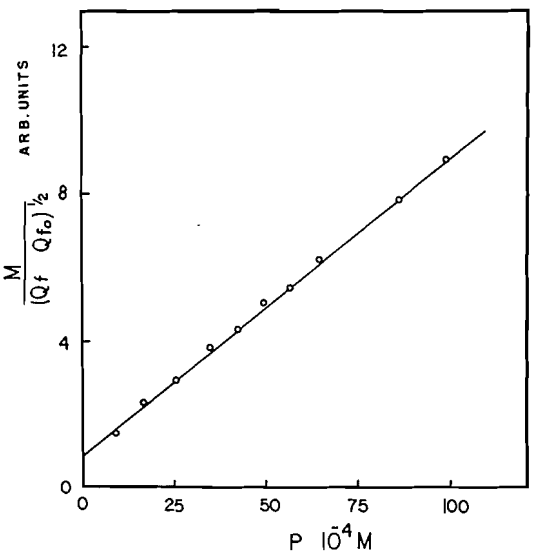

FIG. 5. Test of fluorescence Scheme C at 90 °C, $\lambda_{ex} = 365$ nm.

The phosphorescence behavior expected on the basis of Scheme A can now be considered. If it is assumed that only those molecules which intersystem cross from the S_1^0 level of the singlet manifold give triplet molecules capable of phosphorescence, then the quantum yield of T_1^v is

$$[23] \quad \phi_{T_1}^v = \frac{k_4(M)}{k_2 + k_3 + k_4(M)} \times \frac{k_6}{k_5 + k_6}$$

Since $k_5 \ll k_6$ and $k_2 \ll k_3$ then $\phi_{T_1}^v = k_4(M)/(k_3 + k_4(M))$. Further, if vibrational deactivation occurs without loss of population in the triplet manifold then the quantum yield of triplet in the emitting level is also given by $\phi_{T_1}^0 = k_4(M)/(k_3 + k_4(M))$. The processes removing the triplet state in its vibrationally equilibrated level have been considered earlier (17), and the quantum yield of phosphorescence ϕ_p is given by

$$[24] \quad \phi_p = k_p \tau_p k_4(M)/(k_3 + k_4(M))$$

where k_p is the rate constant for phosphorescence emission and τ_p the phosphorescence lifetime.

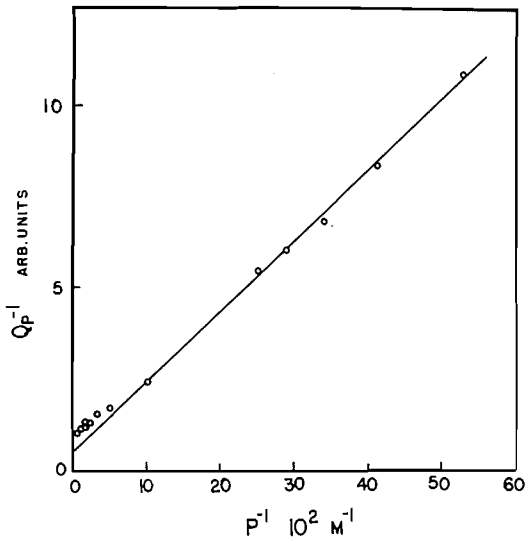

FIG. 6. Variation of the reciprocal of the phosphorescence yield with the reciprocal of the pentanedione concentration at 90 °C, $\lambda_{ex} = 365$ nm.

Equation 24 can be rearranged to

$$[25] \qquad \frac{1}{\phi_p} = \frac{1}{k_p\tau_p}\left\{\frac{k_3}{k_4} \times \frac{1}{(M)} + 1\right\}$$

If one neglects the variation of τ_p with pentanedione concentration, then this predicts that Q_p^{-1} *vs.* $(M)^{-1}$ should be linear. This is tested in Fig. 6, where the data are derived from Fig. 2. The dependence is linear at low concentrations but deviates at high concentrations; the high deviation can be reconciled with self-quenching of the triplet state (17). From the slope of Fig. 6, the ratio k_4/k_3 can be calculated as 250 M^{-1}. This value is sensitive to the extrapolated intercept of Fig. 6 and uses a value of $k_p\tau_0 = 2 \times 10^{-3}$ at 90 °C. It can be compared directly with the value of 330 M^{-1} determined in the fluorescence study. Considering the error involved in determining the intercept of Fig. 6, the agreement between the rate constant ratios determined from the fluorescence and phosphorescence data is very good. This emphasizes the internally consistent nature of Scheme A.

The phosphorescence model assumes that only those triplet molecules which originate from the vibrationally equilibrated level of the singlet state successfully reach the emitting equilibrated level of the triplet state. This implies that the radiationless process [3] does not yield triplet molecules capable of deactivation to the equilibrated level of the triplet. Process [3] could involve decomposition through the singlet manifold or intersystem crossing to a dissociative triplet state. At 90 °C, a rate constant for decomposition of the triplet of greater than 5×10^9 s^{-1} would effectively prevent deactivation to emitting levels of the triplet.

It is interesting to note the approximations necessary in Schemes B and C to provide agreement with the phosphorescence behavior. In both cases, if the S_1^v level is the only level incapable of yielding vibrationally quenchable triplets then the same functional dependence is found as for Scheme A.

Even though a choice cannot be made between the three alternatives, there are two important common features: (*a*) to explain the fluorescence data at least two levels in the singlet manifold must emit; (*b*) to explain the phosphorescence data the highest emitting singlet level must not be capable of giving thermally equilibrated triplet states.

The results of the enhancement experiments at 30.0 °C with sulfur hexafluoride can now be considered. Since the phosphorescence is about seventeen times the intensity of the fluorescence at 30.0 °C, the total emission yield plotted in Fig. 3 is effectively the phosphorescence yield. The deactivation phenomena in a mixture of gases can be discussed within the framework of a strong collision mechanism in the manner recommended by Caro, Grotewold, and Lissi (14). In the following Scheme, M is sulfur hexafluoride and P is the pentanedione.

Scheme A'

[26] $S_0^0 + h\nu \rightarrow S_1^v$

[27] $S_1^v \rightarrow$ radiationless removal

[28] $S_1^v + M \rightarrow S_1^0 + M$

[29] $S_1^v + P \rightarrow S_1^0 + P$

[30] $S_1^0 \rightarrow T_1^0$

[31] $T_1 \rightarrow S_0 + h\nu_p$

[32] $T_1 \rightarrow$ radiationless removal

If $Y = \phi_p^0/\phi_p$ where ϕ_p^0 and ϕ_p are the phosphorescence quantum yields in the absence and presence of M, and if $F = Y/(1 - Y)$, then the steady state approximation in Scheme A' leads to

$$[33] \qquad F = \frac{1}{(M)}\frac{k_{29}(P)^2}{k_{28}} + \frac{k_{29}^2(P)^2}{k_{27}k_{28}} + \frac{k_{29}(P)}{k_{27}}$$

Can. J. Chem. Downloaded from www.nrcresearchpress.com by 210.87.254.40 on 09/05/12
For personal use only.

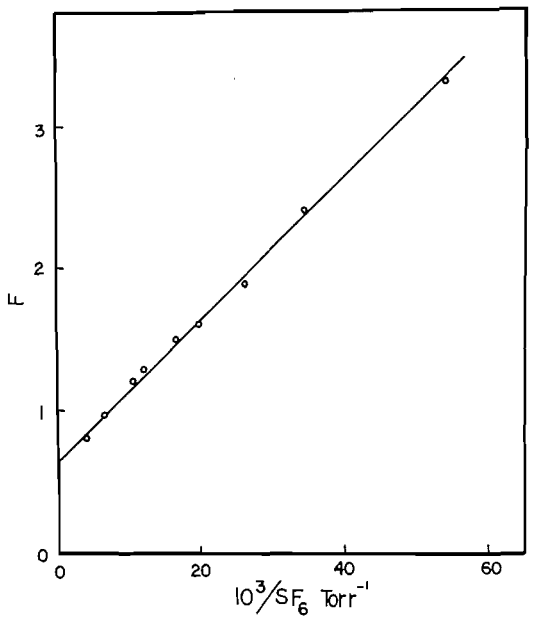

FIG. 7. Variation of F with the reciprocal of the sulfur hexafluoride pressure at 30 °C, $\lambda_{ex} = 365$ nm.

For a particular pentanedione concentration this predicts a linear relation between F and $1/(M)$. Figure 7 shows a plot of F *vs.* the reciprocal of the sulfur hexafluoride pressure for the data of Fig. 3. From the slope and intercept of Fig. 7, the ratios $k_{29}/k_{27} = 1.04 \times 10^3\ M^{-1}$ and $k_{29}/k_{28} = 2.94$ at 30.0 °C can be derived. The sulfur hexafluoride molecule is about one-third as efficient as the pentanedione molecule in deactivating the excited singlet state and this result is in agreement with the data obtained on the deactivation of the excited singlet state of biacetyl (15).

The value of $k_{29}/k_{27} = 1.04 \times 10^3\ M^{-1}$ at 30.0 °C derived from the sulfur hexafluoride experiments can be compared with the value of the similar rate constant ratio (k_4/k_3) derived from the pure pentanedione experiments at 90.0 °C (330 and 250 M^{-1} from the fluorescence and phosphorescence experiments, respectively). The smaller value of the ratio at the higher temperature suggests that process [3] involving radiationless removal has increased at the higher temperature, since the rate constant k_4 is not likely to change greatly.

The research on pentanedione can be compared with that on biacetyl. Phosphorescence behavior of biacetyl on excitation at 365 nm has been reported by several workers (13–15), and was also described by a strong collision mechanism. There is a very recent preliminary study (18) of interference effects on the helium quenching of fluorescence of biacetyl (at 0.05 Torr) on excitation at 405 nm, but excitation at shorter wavelengths was not considered in detail.

In summary, the fluorescence behavior of pentanedione with varying pressure during 365 nm photolysis is consistent with emission from vibrationally excited levels of the singlet state. Examination of the variation with pressure does not distinguish between a strong and weak collision mechanism for deactivation in the singlet manifold. An internally consistent model for the phosphorescence data is proposed in which the highest emitting singlet level is not capable of forming vibrationally equilibrated triplet states.

We thank the National Research Council of Canada for financial support.

1. R. W. WOOD. Phil. Mag. **12**, 499 (1906).
2. C. ARNOT and C. A. MCDOWELL. Can. J. Chem. **36**, 114 (1958).
3. R. L. BROWN and W. KLEMPERER. J. Chem. Phys. **41**, 3072 (1964); J. I. STEINFELD and W. KLEMPERER. J. Chem. Phys. **42**, 3475 (1965).
4. P. B. AYSCOUGH and E. W. R. STEACIE. Proc. Roy. Soc. A, **234**, 476 (1956).
5. H. OKABE and E. W. R. STEACIE. Can. J. Chem. **36**, 137 (1956).
6. G. GIACOMETTI, H. OKABE, and E. W. R. STEACIE. Proc. Roy. Soc. A, **250**, 287 (1959).
7. G. B. PORTER and B. T. CONELLY. J. Chem. Phys. **33**, 81 (1960).
8. A. N. STRACHAN, R. K. BOYD, and K. O. KUTSCHKE. Can. J. Chem. **42**, 1345 (1964).
9. P. G. BOWERS and G. B. PORTER. J. Phys. Chem. **70**, 1622 (1960).
10. A. GANDINI, D. A. WHYTOCK, and K. O. KUTSCHKE. Proc. Roy. Soc. A, **306**, 541 (1968).
11. A. M. HALPERN and W. R. WARE. J. Chem. Phys. **53**, 1969 (1970).
12. H. S. SAMANT and A. J. YARWOOD. Can. J. Chem. **48**, 2611 (1970).
13. H. ISHIKAWA. Doctoral Dissertation. University of Rochester, Rochester, N.Y. 1962.
14. E. CARO, J. GROTEWOLD, and E. A. LISSI. Chem. Commun. 318 (1969).
15. E. AUBIN, J. GROTEWOLD, and E. A. LISSI. J. Chem. Soc. A, 516 (1971).
16. A. W. JACKSON and A. J. YARWOOD. Can. J. Chem. This issue.
17. A. W. JACKSON and A. J. YARWOOD. Can. J. Chem. **49**, 987 (1971).
18. A. NITZAN, J. JORTNER, J. KOMMANDEUR, and E. DRENT. Chem. Phys. Lett. **9**, 273 (1971).

Can. J. Chem. Downloaded from www.nrcresearchpress.com by 210.87.254.40 on 09/05/12
For personal use only.

Theory of Enthalpy of Mixing in Reactive Charge Asymmetrical Molten Salt Systems. Part II. Ternary Solutions

S. N. FLENGAS AND J. M. SKEAFF[1]

Department of Metallurgy and Materials Science, University of Toronto, Toronto 181, Ontario

Received October 14, 1971

The enthalpies of mixing for a reacting charge asymmetrical ternary molten salt system have been calculated on the basis of an extension of a previously developed model for binary systems. The enthalpy of mixing is considered to consist of a reaction term and a mixing term; the former results from the formation of the tetrahedrally coordinated complex species MCl_4^{2-} and the latter from the mixing of the products of reaction according to quasichemical theory modified to account for charge asymmetry.

The ternary model enables the prediction of the integral enthalpies from a knowledge of the interaction parameters determined for the two charge asymmetrical binary systems. The calculations are compared with experimentally measured integral enthalpies of mixing in the ternary system $MnCl_2$–NaCl–CsCl, and shown to give accurate predictions of the behaviour of the system.

On a calculé les enthalpies de mélange d'un système ternaire de sel fondu à charge réactive assymétrique sur la base d'une extension d'un modèle développé auparavant pour les systèmes binaires. On considère que l'enthalpie de mélange consiste en un terme de réaction et un terme de mélange; le premier terme résulte de la formation d'espèces complexes tétraédriquement coordinées MCl_4^{2-} et le dernier du mélange de produits de réaction selon la théorie quasi-chimique, modifiée pour tenir compte de l'assymétrie de charge.

Le modèle ternaire rend possible la prédiction des enthalpies intégrales, connaissant les paramètres d'interaction déterminés pour les deux systèmes binaires à charge assymétrique. On compare les calculs avec les enthalpies intégrales de mélange, mesurées expérimentalement, dans le système ternaire $MnCl_2$–NaCl–CsCl et on montre qu'ils prédisent de façon précise le comportement du système.

Canadian Journal of Chemistry, **50**, 1345 (1972)

Introduction

In a previous publication (1) from this laboratory the enthalpies of mixing of the charge asymmetrical molten salt systems of the type MCl_2–ACl (where M represented Mn, Fe, Co, Ni, Mg, and Cd, and A represented Li, Na, K, Rb, and Cs) measured elsewhere (2–4) were interpreted on the basis of a quasichemical model in which the mixing process was separated into a reaction and a mixing step. The heat evolved during the reaction step was attributed to the formation of a tetrahedrally coordinated complex MCl_4^{2-}, and that associated with the mixing step was calculated by the application of a regular solution treatment which accounted for charge asymmetry in the liquid. For the latter calculation the coordination number of the solution was taken to be proportional to the concentration average coordination number of the cationic species present.

The adjustable parameters predicted by this treatment were shown to be physically meaningful as they related to the structural properties of the melts.

As indicated previously, the presence of tetrahedrally coordinated complex species in mixtures of mono- and divalent melts is supported by cryoscopic (5*a*) and spectrophotometric evidence (5*b*). According to Papatheodorou and Kleppa (2–4), the exothermic heats of mixing observed in these systems could be attributed to the formation of the MCl_4^{2-} complex species and to dispersion effects. The treatment is semi-qualitative and the various adjustable parameters are assigned arbitrary values.

Pelton and Thompson (6) calculated the concentration dependence of the heats and entropies of mixing in the $MgCl_2$–ACl type binary systems for about 60% of the composition range using a dissociating complex ion model based on the $MgCl_4^{2-}$ species. The model does not account for charge asymmetry or vibrational contributions to the entropies of mixing and also makes the questionable assumption that *pure* $MgCl_2$ consists of "free" Mg^{2+} and complex MCl_4^{2-} species related by a dissociation constant.

Also, recently Østwold (7) developed a model

[1]Present address: Metallurgisk Institutt Norges Tekniske Høgskole, Trondheim, Norway.

Can. J. Chem. Downloaded from www.nrcresearchpress.com by 210.87.254.5 on 09/05/12
For personal use only.

Can. J. Chem. Downloaded from www.nrcresearchpress.com by 210.87.254.5 on 09/05/12
For personal use only.

which is quite similar to that proposed by Pelton and Thompson (6) with the main difference that, although charge asymmetry is accounted for in the calculation of the enthalpy of the solution, it is ignored in the calculation of the entropy.

Experimental data and theoretical interpretations are almost totally lacking for ternary charge asymmetrical fused salt systems. In the present investigation the previously proposed quasichemical model developed for charge asymmetrical binary fused salt systems is extended to ternary systems. The method is applied to the enthalpies of mixing of the system $MnCl_2$–NaCl–CsCl as determined in a previous investigation (8) in this laboratory. The isothermal heats of mixing were measured by means of a high temperature isoperibol solution calorimeter which is also described elsewhere (8). The ternary model enables the prediction of the integral enthalpies of mixing in the ternary system from the knowledge of the interaction parameters of the two binary systems $MnCl_2$–NaCl and $MnCl_2$–CsCl.

Complexes in Fused Salts

The concept of complexes in fused salts is based upon the following postulates (1):

(*1*) The fused salt is a continuous and highly charged medium, and as a result interlocking anionic and cationic quasi-lattices exist to preserve local electrical neutrality.

(*2*) A non-ionic solvent capable of separating ionic species such as water is not present.

(*3*) The difference between a complexed and a non-complexed state, involving a cation M^{2+} and an anion X^-, is simply defined by a characteristic average "shorter" bond distance M—X for the complexed state as compared to the M—X bond distance for the non-complexed state.

(*4*) Complexed ionic species must still belong to their respective quasi-lattices and not disrupt the continuity of the phase. Hence the ligands X in a complex MX_n interact with the surrounding A^+ cations in the sequence

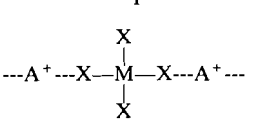

whereby an anion X is always a cation "bridging" species.

(*5*) Under such restrictions, the complex represents a coordinated configuration of the type MX_n which may be treated as a statistical entity.

(*6*) The formation of a complex is initiated by the presence of foreign cations A^+ which compete poorly with the central cations M^{2+} for the same ligands X^-. Accordingly, the charge density of the cation A^+ is related to its capability of promoting or preventing the formation of complexes.

(*7*) The coordination number of a given monovalent cation is taken to be one-half of that of a divalent cation, with respect to a monovalent anion ligand. The coordination number of a solution containing both mono- and divalent cations is taken to be the ion-fraction average of that of the two cations.

Composition Representation Within a Ternary System

The composition of a ternary system is usually represented by points within an equilateral triangle in which the points of 100% of each component are situated at the corners.

Any composition point P is found by drawing through P, lines parallel to each of the three sides. The complement of the perpendicular distance from each corner to the respective line through P gives the amount of the particular component. If the composition variable is the mole fraction, then the values thereby ascertained must satisfy the relationship

$$[1] \qquad x_1 + x_2 + x_3 = 1$$

where 1, 2, and 3 are the components of the ternary.

A tie-line from 1 to the 2, 3 binary represents compositions for which

$$[2] \qquad t' = \frac{x_3}{x_2} = \text{constant}$$

but since t' goes to infinity as x_2 goes to zero, it is more convenient to define

$$[3] \qquad t = \frac{x_3}{x_2 + x_3}$$

which is seen to be always finite and to lie between 0 and 1.

When x_1 is constant then $1 - (x_2 + x_3)$ is also constant and the parameter, y, is defined as

Can. J. Chem. Downloaded from www.nrcresearchpress.com by 210.87.254.5 on 09/05/12
For personal use only.

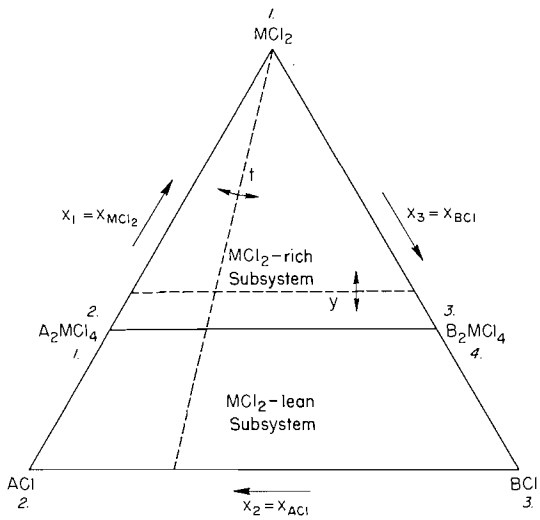

FIG. 1. Division of the ternary system MCl_2–ACl–BCl into two subsystems.

$$y = x_2 + x_3 = 1 - x_1 \quad [4]$$

$t = 0$ in the *1–2* binary, and $t = 1$ in the *1–3* binary; for pure component *1*, $y = 0$ and $y = 1$ for all values of t in the *2–3* binary.

Calculation of the Enthalpies of Mixing in Reactive Charge Asymmetrical Ternary Fused Salt Systems

The concentration dependence of the enthalpy of mixing in reactive charge asymmetrical ternary fused salt systems will be derived on the basis of the complex ion model (1).

The thermodynamic properties of a ternary system of the type MCl_2–ACl–BCl, where M represents a divalent cation and A and B represent two different monovalent metal cations, may be predicted by postulating that the behavior of the ternary system is a function of the constituent binaries. As an extension of the approach to binary systems, the ternary is divided into two composition ranges at $y = 2/3$: a MCl_2-rich three component subsystem, MCl_2–A_2MCl_4–B_2MCl_4 and a four component subsystem A_2MCl_4–ACl–BCl–B_2MCl_4, as shown in Fig. 1.

For both regions the total enthalpy of mixing in the ternary, ΔH_{tot}, is considered to consist in a reaction term ΔH_R, and a mixing term, ΔH_{mix}, *i.e.* $\Delta H_{M,T} = \Delta H_R + \Delta H_M$. In a solution of composition (y,t), the actual mole fractions of the three component reactants are

$$x_{MCl_2} = x_M = 1 - y$$
$$x_{ACl} = (1 - t)y \quad [5]$$
$$x_{BCl} = ty$$

The complex forming reactions are

$$2ACl + MCl_2 \rightarrow A_2MCl_4 \quad [6]$$
$$2BCl + MCl_2 \rightarrow B_2MnCl_4$$

The Subsystem MCl_2–A_2MCl_4–B_2MCl_4

For convenience, the subscripts *1*, *2*, and *3* will refer to the components as they appear in the heading of this section.

The reaction term is comprised of the two following heat effects: (*i*)

$$y(1-t)ACl + \tfrac{1}{2}y(1-t)MCl_2 \rightarrow \tfrac{1}{2}y(1-t)A_2MCl_4 \quad [7]$$

for which the enthalpy is

$$\Delta H_{12} = \tfrac{1}{2}y(1-t)b_{R_{12}} \quad [8]$$

and (*ii*)

$$yt BCl + \tfrac{1}{2}yt MCl_2 \rightarrow \tfrac{1}{2}yt B_2MCl_4 \quad [9]$$

for which the enthalpy is

$$\Delta H_{13} = \tfrac{1}{2}yt b_{R_{13}} \quad [10]$$

where $b_{R_{12}}$ and $b_{R_{13}}$ are the reaction parameters of the binary systems MCl_2–ACl and MCl_2–BCl, respectively. The total "reaction heat" is thus

$$\Delta H_R = \tfrac{1}{2}y[(1-t)b_{R_{12}} + tb_{R_{13}}] \quad [11]$$

After the stoichiometric reaction has taken place, the solution consists of

$$n_1 = (2 - 3y) \text{ moles of unreacted } MCl_2$$
$$n_2 = y(1-t) \text{ moles of } A_2MCl_4 \quad [12]$$
$$n_3 = yt \text{ moles of } B_2MCl_4$$

The mixing reaction to be considered is thus

$$n_1MCl_2 + n_2A_2MCl_4 + n_3B_2MCl_4 \rightarrow [(MCl_2)_{n_1}(A_2MCl_4)_{n_2}(B_2MCl_4)_{n_3}] \quad [13]$$

for which the energy of mixing is

$$\Delta E^{int}_{mix} = E_{soln} - n_1E^0_{MCl_2} - n_2E^0_{A_2MCl_4} - n_3E^0_{B_2MCl_4} \quad [14]$$

In this region, the ionic fractions N are

$$N_{M^{2+}} = \frac{n_1}{\Sigma n_+}, \qquad N_{A^+} = \frac{2n_2}{\Sigma n_+}$$

$$[15] \qquad N_{B^+} = \frac{2n_3}{\Sigma n_+}, \qquad N_{Cl^-} = \frac{2n_1}{\Sigma n_-}$$

$$N_{MCl_4^{2-}} = \frac{n_2 + n_3}{\Sigma n_-} = N_{Cl^*}$$

where $\Sigma n_+ = (n_1 + 2n_2 + 2n_3)$ and $\Sigma n_- = (2n_1 + n_2 + n_3)$. The symbol Cl* refers to chloride bonded within a complex.

The significant interactions in this ternary for the pure components and for the solution are considered to be those involving nearest neighbors only. The coordination number of A^+ or B^+ will be $Z_1/2$ and that of M^{2+} will be Z_1. Thus the average coordination number will be

$$[16] \qquad \bar{Z} = Z_1 N_{M^{2+}} + \tfrac{1}{2} Z_1 N_{A^+} + \tfrac{1}{2} Z_1 N_{B^+}$$

and substitution of the concentration terms for the ionic fraction yields

$$[17] \qquad \bar{Z} = \frac{n_1 + n_2 + n_3}{n_1 + 2n_2 + 2n_3} Z_1$$

The total number of bonds in solution will thus be $(n_1 + n_2 + n_3)NZ_1/2$ which N is now Avogadro's number.

The pure liquid components are characterized by the interactions M–Cl, A–Cl*, and B–Cl*. In addition to these the solution contains the interactions A–Cl, B–Cl, and MCl*.

From eq. 14, following the method which is applicable to regular solutions extended to ternary systems, the expression for the integral internal energy of mixing is given as

$$[18] \quad \Delta E_M = \tfrac{1}{2} NZ_1[(n_1 + n_2 + n_3)(N_{M^{2+}}.N_{Cl^-}\varepsilon_{MCl} + N_{M^{2+}}.N_{Cl^*}\varepsilon_{M-Cl^*} + N_{A^+}.N_{Cl^-}\varepsilon_{A-Cl} + N_{A^+}.N_{Cl^*}\varepsilon_{A-Cl^*} + N_{B^+}.N_{Cl^-}\varepsilon_{B-Cl} + N_{B^+}.N_{Cl^*}\varepsilon_{B-Cl^*}) - (n_1\varepsilon_{M-Cl} + n_2\varepsilon_{A-Cl^*} + n_3\varepsilon_{B-Cl^*})]$$

where nearest neighbor bond energies of the same kind are taken to have the same value in the solution as in the corresponding pure material. With the introduction of the expressions for the ionic fractions, factoring, rearranging and assuming that $P\,dV_{mix} = 0$, we obtain the following expression for the integral enthalpy of mixing

$$[19] \quad \Delta H_{mix} = \frac{NZ_1}{2\Sigma n_+ . \Sigma n_-}\{[n_1^2 n_2(4\varepsilon_{A-Cl} + \varepsilon_{M-Cl^*} - 3\varepsilon_{M-Cl} - 2\varepsilon_{A-Cl^*}) + 2n_1 n_2^2(2\varepsilon_{A-Cl} + \tfrac{1}{2}\varepsilon_{M-Cl^*} - \varepsilon_{M-Cl} - \tfrac{3}{2}\varepsilon_{A-Cl^*}) + n_1^2 n_3(4\varepsilon_{B-Cl} + \varepsilon_{M-Cl^*} - 3\varepsilon_{M-Cl} - 2\varepsilon_{B-Cl^*}) + 2n_1 n_3^2(2\varepsilon_{B-Cl} + \tfrac{1}{2}\varepsilon_{M-Cl^*} - \varepsilon_{M-Cl} - \tfrac{3}{2}\varepsilon_{B-Cl^*}) + n_1 n_2 n_3(2\varepsilon_{M-Cl^*} - 4\varepsilon_{M-Cl} + 4\varepsilon_{A-Cl} - 3\varepsilon_{A-Cl^*} + 4\varepsilon_{B-Cl} - 3\varepsilon_{B-Cl^*})]\}$$

The interaction energies in parentheses may be rearranged to take the form of simple functions of the interaction parameters previously determined for the binary systems MCl_2–ACl and MCl_2–BCl for the MCl_2-rich regions. For example, for the MCl_2–ACl binary these were

$$[20] \qquad \begin{aligned} b_1' &= \tfrac{1}{2} NZ_1(2\varepsilon_{ACl} + 0.5\varepsilon_{MCl^*} - 2\varepsilon_{MCl} - 0.5\varepsilon_{ACl^*}) \\ b_2' &= \tfrac{1}{2} NZ_1(2\varepsilon_{ACl} + 0.5\varepsilon_{MCl^*} - \varepsilon_{MCl} - 1.5\varepsilon_{ACl^*}) \end{aligned}$$

where N is the Avogadro number. The parameters for the MCl_2–BCl system are obtained by substituting all the A's in eq. 20 with B's.

From eqs. 11, 19, and 20 the final expression for the total enthalpy of mixing in terms of the y and t concentration parameters is

$$[21] \quad \Delta H_{mix}^{int} = \frac{y(2-3y)(1-t)}{8(1-y)}\left[\frac{2-3y}{4(2-y)}(b_1')_{1,2} + (b_2')_{1,2}\right] + \frac{(2-3y)yt}{8(1-y)}\left[\frac{2-3y}{4(2-y)}(b_1')_{1,3} + (b_2')_{1,3}\right] + \frac{y}{2}[(1-t)(b_R)_{1,2} + t(b_R)_{1,3}]$$

which is valid for $2/3 > y > 0$ and $0 < t < 1$. It is thus possible to predict the properties of the ternary system from a consideration of the parameters determined for two of the constituent binaries.

Can. J. Chem. Downloaded from www.nrcresearchpress.com by 210.87.254.5 on 09/05/12
For personal use only.

Can. J. Chem. Downloaded from www.nrcresearchpress.com by 210.87.254.5 on 09/05/12
For personal use only.

The Subsystem A_2MCl_4–ACl–BCl–B_2MCl_4

In the composition range defined by $1 > y > 2/3$ and $1 > t > 0$, the solution consists of n_1 g-mol of A_2MCl_4, n_2 g-mol of ACl, n_3 g-mol of BCl, and n_4 g-mol of B_2MCl_4, and contains the ionic species A^+, B^+, Cl^-, and MCl_4^{2-}. The complex configuration MCl_4^{2-} results from the reaction between MCl_2 and the stoichiometrically required Cl^- anions provided by the ACl and BCl components.

The solution may be considered as being formed from a binary mixture containing ACl and A_2MCl_4 or BCl and B_2MCl_4 to which either BCl or ACl are added, respectively. In the first case, for example, addition of BCl to a ACl–A_2MCl_4 mixture shall affect the thermodynamic stability of the already existing complex configurations and in this case increase their strength to an extent proportional to the concentration average of the two ligand donors. With respect to the bond energy within a complex, a solution containing the nominal A_2MCl_2, and B_2MCl_4 components should be characterized at each ACl/BCl ratio by a single value for the energy of the M–Cl* type interaction.

The reaction part of the enthalpy of mixing is therefore calculated as the concentration average of the contributions of the two complex species A_2MCl_4 and B_2MCl_4.

Although the system A_2MCl_4, ACl, BCl, and B_2MCl_4 appears to be a reciprocal salt mixture which ordinarily would be treated from the point of view of stable pairs determined by an exchange reaction between ACl and B_2MCl_4 or BCl and A_2MCl_4, the concentration dependent thermodynamic stability of the MCl_4 complex configuration enables the treatment of the system in terms of the four nominal components. Hence, exchange reactions of the type

$$2ACl + B_2MCl_4 \rightarrow A_2MCl_4 + 2BCl$$

should not be taken into account.

Considering a solution consisting of X_1 g-mol of MCl_2, X_2 g-mol of ACl, and X_3 g-mol of BCl, the nominal quaternary composition is calculated on the assumption that the gram-moles of A_2MCl_4 and B_2MCl_4 present are proportional to the ratio of ACl/BCl.

From a mass balance based on eq. 6, the quaternary composition is defined as

$$\begin{aligned} n_1 &= X_1(1-t) && \text{g-mol } A_2MCl_4 \\ n_2 &= X_2 - 2X_1(1-t) && \text{g-mol ACl} \\ n_3 &= X_3 - 2X_1 t && \text{g-mol BCl} \\ n_4 &= X_1 t && \text{g-mol } B_2MCl_4 \end{aligned} \quad [22]$$

The reaction part of the enthalpy of mixing is therefore given as

$$\Delta H_R = (1-y)[(1-t)(b_R)_{1,2} + t(b_R)_{1,3}] \quad [23]$$

where $(b_R)_{1,2}$ and $(b_R)_{1,3}$ refer to the reaction parameters in the ACl–MCl_2 and BCl–MCl_2 binary systems.

The mixing part of the total enthalpy of mixing may be calculated by extending the previous treatment to the quaternary concentration range.

For this purpose, only next nearest neighbor type interactions with respect to an alkali cation shall be considered as being significant. Thus, the pure liquid components are characterized by the interactions Cl*ACl*, ClACl, ClBCl, Cl*BCl*. In addition to these the solution contains the interactions Cl*ACl and Cl*BCl.

The number of bonds for the common coordination number Z_1 of the A^+ and B^+ cations is given as $\frac{1}{2}NZ_1(2n_1 + n_2 + n_3 + 2n_4)$. Accordingly, the concentration dependence of the enthalpy of mixing is calculated as:

$$\begin{aligned} \Delta H_M = \tfrac{1}{2}NZ_1\{&[(2n_1 + n_2 + n_3 + 2n_4)[(N^2_{Cl^*}.N_{A^+}\varepsilon_{Cl^*ACl^*}) + (N^2_{Cl^-}.N_{A^+}\varepsilon_{ClACl}) + (N^2_{Cl^-}.N_{B^+}\varepsilon_{ClBCl}) \\ &+ (N^2_{Cl^*}.N_{B^+}\varepsilon_{Cl^*BCl^*}) + (2N_{Cl^*}.N_{A^+}.N_{Cl^-}\varepsilon_{Cl^*ACl}) + (2N_{Cl^*}.N_{B^+}.N_{Cl^-}\varepsilon_{Cl^*BCl})] \\ &- 2n_1\varepsilon_{Cl^*ACl^*} - n_2\varepsilon_{ClACl} - n_3\varepsilon_{ClBCl} - 2n_4\varepsilon_{Cl^*BCl^*}]\} \end{aligned} \quad [24]$$

where

$$N_{Cl^-} = \frac{n_2 + n_3}{\Sigma n_-}, \qquad N_{MCl_4^{2-}} = N_{Cl^*} = \frac{n_1 + n_4}{\Sigma n_-}$$

$$N_{A^+} = \frac{2n_1 + n_2}{\Sigma n_+}, \qquad N_{B^+} = \frac{n_3 + 2n_4}{\Sigma n_+}$$

and

$$\Sigma n_- = n_1 + n_2 + n_3 + n_4, \qquad \Sigma n_+ = 2n_1 + n_2 + n_3 + 2n_4$$

With the introduction of the expressions for the ionic fractions eq. 24 may be rearranged as

$$[25]\quad \Delta H_M = \tfrac{1}{2}NZ_1\Big[\frac{(n_1+n_4)^2}{\Sigma n_-^2}[n_2(\varepsilon_{Cl^*ACl^*} - \varepsilon_{ClACl}) + n_3(\varepsilon_{Cl^*BCl^*} - \varepsilon_{ClBCl})]$$
$$+ \frac{2(n_2+n_3)^2}{\Sigma n_-^2}[n_4(\varepsilon_{ClBCl} - \varepsilon_{Cl^*BCl^*}) + n_1(\varepsilon_{ClACl} - \varepsilon_{Cl^*ACl^*})]$$
$$+ \frac{2(n_1+n_4)(n_2+n_3)}{\Sigma n_-^2}[2n_1(\varepsilon_{ClACl^*} - \varepsilon_{Cl^*ACl^*}) + n_2(\varepsilon_{Cl^*ACl} - \varepsilon_{ClACl})]$$
$$+ n_3(\varepsilon_{Cl^*BCl} - \varepsilon_{ClBCl}) + 2n_4(\varepsilon_{Cl^*BCl} - \varepsilon_{Cl^*BCl^*})\Big]$$

The interaction energies in parentheses may be expressed as simple functions of the interaction parameters previously determined for the binary systems MCl_2–ACl and MCl_2–BCl for the MCl_2-lean regions. For example, for the MCl_2–ACl binary these were (1)

$$[26]\quad b_1 = \tfrac{1}{2}NZ_1(\varepsilon_{Cl^*ACl^*} + \varepsilon_{ClACl} - 2\varepsilon_{Cl^*ACl})$$
$$b_2 = \tfrac{1}{2}NZ_1(4\varepsilon_{ClACl^*} - 3\varepsilon_{Cl^*ACl^*} - \varepsilon_{ClACl})$$

Replacement of A's with B's yields the corresponding parameters in the MCl_2–BCl binary system. Factoring of eq. 25, rearranging in terms of the interaction parameters, and introducing the y and t composition variables, we obtain the following expression for the mixing part of the total enthalpy

$$[27]\quad \Delta H_M = \frac{(1-y)^2(2-3y)}{(2y-1)^2}[(1-t)(2b_1+b_2)_{1,2} + t(2b_1+b_2)_{1,3}]$$
$$+ \frac{2(3y-2)^2(1-y)}{(2y-1)^2}[(1-t)(2b_1+b_2)_{1,2} + t(2b_1+b_2)_{1,3}]$$
$$- \frac{(1-y)(3y-2)^2}{(2y-1)^2}[(1-t)(3b_1+b_2)_{1,2} + t(3b_1+b_2)_{1,3}]$$
$$+ \frac{2(1-y)^2(3y-2)}{(2y-1)^2}[(1-t)(b_1+b_2)_{1,2} + 2t(b_1+b_2)_{1,3}]$$

The total enthalpy of mixing is calculated by adding eqs. 27 and 23. The partial molar enthalpies of mixing are readily obtained by partial differentiation of the corresponding equations for the total enthalpies of mixing.

Application of the Treatment to the Ternary System $MnCl_2$–NaCl–CsCl

The enthalpies of mixing in the binary systems, $MnCl_2$–NaCl and $MnCl_2$–CsCl, and in the ternary system $MnCl_2$–NaCl–CsCl were determined calorimetrically at 820 °C and are reported in a previous publication (8). The interaction parameters b_1, b_2, b_1', b_2', and $(b_R)_{1,2}$, $(b_R)_{1,3}$ for the two binary systems $MnCl_2$–NaCl and $MnCl_2$–CsCl are given in Table 1.

The contributions to the total enthalpy of mixing over the entire composition range from reaction and mixing effects have been calculated from eq. 21 for the MCl_2-rich region and eqs. 23 and 27 for the MCl_2-lean region using the data in Table 1 and are given in Table 2.

Can. J. Chem. Downloaded from www.nrcresearchpress.com by 210.87.254.5 on 09/05/12
For personal use only.

TABLE 1. Interaction parameters

	Parameter value (cal/mol)				
		$MnCl_2$-rich		$MnCl_2$-lean	
Binary system	b_R	b'_1	b'_2	b_1	b_2
$MnCl_2$–NaCl (1–2)	−4 500	−7 435	−2 300	−127	−1 100
$MnCl_2$–CsCl (1–3)	−13 200	−23 240	−8 000	+840	−2 600

*For a binary system of the type MCl_2–ACl, in the composition range $1.0 > X_{MCl_2} > 1/3$ it has been shown (1) that

$$\Delta H_M = 0.5X_{ACl}.b_R + \frac{(X_{MCl_2} - 0.5X_{ACl}).0.5X_{ACl}}{(2X_{MCl_2} - 0.5X_{ACl})}\left[\frac{X_{MCl_2} - 0.5X_{ACl}}{X_{MCl_2} + 0.5X_{ACl}}b'_1 + b'_2\right]$$

In the composition range $1/3 > X_{MCl_2} > 0$

$$\Delta H_M = X_{MCl_2}.b_R + \frac{(X_{ACl} - 2X_{MCl_2})X_{MCl_2}}{X_{ACl} - X_{MCl_2}}\left[\frac{X_{ACl} - 2X_{MCl_2}}{X_{ACl} - X_{MCl_2}}b_1 + b_2\right]$$

where, $b_R = 3\Delta H_M$ at $X_{MCl_2} = 1/3$.

TABLE 2. Contributions to the total enthalpy (cal/mol) of mixing from reaction and mixing effects calculated from theory

	$t = 0.25$			$t = 0.50$			$t = 0.75$		
Y	ΔH_R	ΔH_M	$\Delta H_{M,T}$	ΔH_R	ΔH_M	$\Delta H_{M,T}$	ΔH_R	ΔH_M	$\Delta H_{M,T}$
0	0	0	0	0	0	0	0	0	0
0.15	−500	−474	−974	−663	−644	−1307	−827	−812	−1639
0.30	−1000	−733	−1733	−1325	−997	−2322	−1654	−1257	−2911
0.45	−1500	−711	−2211	−1988	−970	−2958	−2481	−1224	−3705
0.60	−2000	−324	−2324	−2650	−445	−3095	−3308	−559	−3867
0.67	−2225	0	−2225	−2950	0	−2950	−3680	0	−3680
0.75	−1668	−282	−1950	−2213	−382	−2595	−2760	−487	−3247
0.85	−1001	−235	−1236	−1328	−309	−1637	−1655	−391	−2046

It is seen that the mixing effects are significant and cannot be ignored, particularly in the $MnCl_2$-rich regions where the mixing contributions are comparable to the reaction enthalpy. Mixing contributions to the total enthalpy of mixing are also significant in the $MnCl_2$-lean region and amount to about 20% of the total heat.

The calculated total enthalpies of mixing over the entire concentration range are compared with the experimental values in Fig. 2.

Solid lines in this figure are calculated while the points are experimental. It is seen that the agreement is within ±100 cal, which is within the stated uncertainty of the experimental data (8), with the exception of two points at about $y = 0.4$ which appear to deviate more than this amount. It should be noted that the b-values used for the calculations are those determined in this laboratory (8). The enthalpies of mixing of the $MnCl_2$–NaCl and $MnCl_2$–CsCl system measured by Papatheodorou and Kleppa (2) are more negative by about 18% from the former and if used in the present model calculations would predict more negative total enthalpies of mixing. The foregoing binary systems have also been investigated in this laboratory by the e.m.f. method (9) and the electrochemically obtained enthalpies of mixing are close to the calorimetric results (8).

The application of the proposed quasichemical model to the NaCl–CsCl–$MnCl_2$ ternary

Can. J. Chem. Downloaded from www.nrcresearchpress.com by 210.87.254.5 on 09/05/12
For personal use only.

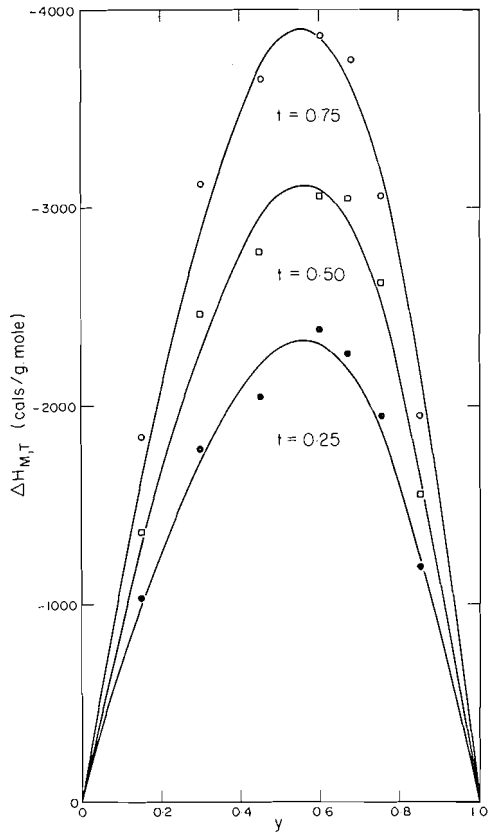

FIG. 2. Total enthalpy of mixing in the ternary system $MnCl_2$–NaCl–CsCl. Solid lines are calculated from theory, points are experimental (8).

system constitutes a severe test of the theory. As indicated the maximum integral enthalpies of mixing in the two constituent binary systems NaCl–$MnCl_2$ and CsCl–$MnCl_2$ occur at about 33 mol% $MnCl_2$, which is the stoichiometric composition for the formation of a tetrahedrally coordinated complex species. In addition, these heats have been found (8) to have the widely different values of 1600 and 4600 cal/g-mol, respectively, and available quasichemical models based on ideality and simple additivity are not expected to be valid.

1. S. N. FLENGAS and A. S. KUCHARSKI. Can. J. Chem. In press.
2. G. N. PAPATHEODOROU and O. J. KLEPPA. J. Inorg. Nucl. Chem. **33**, 1249 (1971).
3. G. N. PAPATHEODOROU and O. J. KLEPPA. J. Inorg. Nucl. Chem. **32**, 889 (1970).
4. F. G. MCCARTY and O. J. KLEPPA. J. Phys. Chem. **70**, 1249 (1966).
5. (*a*) H. FLOOD and S. URNES. Zeit. fur Electrochem. **59**, 834 (1955). (*b*) D. M. GRUEN and R. L. MCBETH. Pure Appl. Chem. **6**, 23 (1963).
6. A. D. PELTON and W. T. THOMPSON. Can. J. Chem. **48**, 1585 (1970).
7. T. ØSTVOLD. EMF measurements for the determination of partial Gibbs energies and entropies of mixing of the alkali chlorides in liquid mixtures with $MnCl_2$. Dept. of Chem. NLHT – The University of Trondheim, Norway.
8. J. M. SKEAFF. Ph.D. Thesis. University of Toronto, Toronto, Ontario. 1971.
9. A. S. KUCHARSKI and S. N. FLENGAS. To be published.

Can. J. Chem. Downloaded from www.nrcresearchpress.com by 210.87.254.5 on 09/05/12
For personal use only.

The Hydrolysis of *t*-Butyl Chloride in Aquo-Organic Mixtures: Heat Capacity of Activation and Solvent Structure[1]

R. E. ROBERTSON[2] AND S. E. SUGAMORI

Division of Chemistry, National Research Council of Canada, Halifax, Nova Scotia and Department of Chemistry, The University of Calgary, Calgary 44, Alberta

Received October 19, 1971

The temperature dependence of the rate of solvolysis of *t*-butyl chloride in mixtures of tetrahydrofuran and of acetonitrile in water have been determined. In the high-water range both minor co-solvents lead to a reduction in the value of $\Delta H^{\ddagger}$ similar to that found previously where alcohol was the co-solvent. However, a remarkable difference in the values of $\Delta C_p^{\ddagger}$ across the same concentration range reflected a difference in the effect of these two co-solvents on the structural properties of the several solvent media. Where tetrahydrofuran or alcohols are the minor co-solvent, $\Delta C_p^{\ddagger}$ becomes much more negative until that concentration is reached where the quasi-aqueous structure collapses. Where acetonitrile is the minor co-solvent $\Delta C_p^{\ddagger}$ becomes more positive relative to the value found for hydrolysis in water until a value of about -40 cal deg^{-1} mol^{-1} is reached. The implication of these findings concerning the nature of solvation of weakly polar solutes in such mixtures is discussed.

On a déterminé l'influence de la température sur la solvolyse du chlorure de *t*-butyl dans des mélanges de tétrahydrofuranne et d'acétonitrile dans l'eau. Dans le domaine de haute concentration en eau, les deux co-solvants mineurs mènent à une réduction de la valeur de $\Delta H^{\ddagger}$ semblable à celle qu'on a trouvé précédemment, où l'alcool était le co-solvant. Toutefois, une différence remarquable dans les valeurs de $\Delta C_p^{\ddagger}$ dans le même domaine de concentration reflète une différence de l'effet de ces deux co-solvants sur les propriétés structurales des différents milieux de solvants. Lorsque la tétrahydrofuranne ou les alcools sont le co-solvant mineur, $\Delta C_p^{\ddagger}$ devient beaucoup plus négatif jusqu'à ce qu'on atteigne la concentration où la structure quasi-aqueuse s'effondre. Lorsque l'acétonitrile est le co-solvant mineur, $\Delta C_p^{\ddagger}$ devient plus positif comparativement à la valeur qu'on trouve pour l'hydrolyse dans l'eau, jusqu'à ce qu'on atteigne une valeur d'environ -40 cal deg^{-1} mol^{-1}. On discute de l'implication de ces résultats relativement à la nature de la solvatation des solutés faiblement polaires dans de tels mélanges.

Canadian Journal of Chemistry, **50**, 1353 (1972)

For some time we have been exploring the changes in the temperature coefficient of $\Delta H^{\ddagger}$ ($\Delta C_p^{\ddagger}$) as an indicator of the degree of reorganization of water structure associated with ionogenic reactions in water (1). Recently we have shown that remarkable changes occur in $\Delta C_p^{\ddagger}$ (as well as in $\Delta H^{\ddagger}$ and $\Delta S^{\ddagger}$ (2)) when this coefficient was determined for the same compound, *t*-butyl chloride, solvolyzing in a series of alcohol–water mixtures. The changes $\Delta H^{\ddagger}$ and $\Delta S^{\ddagger}$ in this study were similar to those reported previously (3). Arnett and co-workers have shown (4–6) that the changes in $\Delta H^{\ddagger}$ obtained from the hydrolysis of *t*-butyl chloride across a series of alcohol–water mixtures in the high-water range are closely equivalent to the corresponding changes in $\Delta \bar{H}_s$ characterizing the transfer of the solute from its pure liquid state to aqueous solution. The effect for non-electrolytes was much larger than for those electrolytes which could be regarded as models for the transition state in the above reaction. From this they concluded that the decrease in $\Delta H^{\ddagger}$ noted above was the consequence of an increase in $\Delta \bar{H}_s$ of the initial state. The corresponding $\Delta C_p^{\ddagger}$ values (2) support this hypothesis and further clarify the effect of temperature on the reorganization of solvents in such systems.

In this paper we determine $\Delta C_p^{\ddagger}$ for the solvolysis of *t*-butyl chloride in a series of tetrahydrofuran mixtures where the structure of the mixture appears to be enhanced over that in water and in acetonitrile–water mixtures where there is evidence of a break-down of water structure over the same concentration range. Attempts to obtain reproducible results in urea–water mixtures based on the assumption that urea would act as a structure-breaker (7) failed to yield data of sufficient accuracy for our purpose. Similar attempts with ethylene glycol as the minor co-solvent were unsuccessful.

[1]NRCC No. 12359.

[2]To whom correspondence should be addressed (at Calgary).

Can. J. Chem. Downloaded from www.nrcresearchpress.com by 210.87.254.40 on 09/05/12
For personal use only.

TABLE 1. Empirical constants for equation: $\log_{10} k = A/T + B \log_{10} T \times C$ for tetrahydrofuran/water mixtures

Mole fraction H_2O	Experimental density 25 °C	$-A$	$-B$	C
1.0		10340.7211	40.7885	134.0848
0.95	0.9892	11246.8012	53.5655	168.0508
0.90	0.9805	5530.7180	9.4917	38.9226
0.80	0.9604	6483.9122	13.0764	49.8148

TABLE 2. Empirical constants for equation: $\log_{10} k = A/T + B \log_{10} T + C$ for acetonitrile/water mixtures

Mole fraction H_2O	Experimental density 25 °C	$-A$	$-B$	C
1.0		10340.7211	40.7885	134.0848
0.95	0.9797	8552.7410	30.4969	102.2833
0.90	0.9613	6987.8153	19.1637	68.5529
0.80	0.9254	7086.0932	18.6517	66.7686

Experimental

For all the rate determinations, A.R. *t*-butyl chloride was purified by distillation and passage through Al_2O_3 for absorption, and was shown to be kinetically pure. The stock sample was shielded from light and placed in a desiccator which was opened only for removal of samples.

Solvolyzing Media

Distilled H_2O was passed through an ion exchange column (Rexyn R208-1-300-H-OH) and used without further purification.

Acetonitrile was of spectroscopic grade and used without further purification. Tetrahydrofuran was purified by distillation from sodium carbonate. The adherence of rate data to strict first-order behavior was taken as evidence that no deleterious impurity was present.

All concentrations used throughout this investigation were mixed by volume and then checked by density measurements. Densities of the mixtures were done prior to and at the end of each series. Enough of each solvent mixture was made to complete the series of studies. Incremental amounts were siphoned from a stock bottle provided with a double vapor trap. Value of densities, volume ratios, and mole fractions are given in Tables 1 and 2.

Kinetic Studies

Rates of reaction were determined by a conductance method using Queen-type stirred conductance cells. Temperatures were controlled by a Tronac system (Tronac, Provo, Utah) and measured by means of a platinum resistance thermometer.

Rate data were collected by means of our Auto-Ram (2) save for the highest rates, where the system used previously for the study of hydrolysis of *t*-butyl chloride in water was adopted.

The suitable initial concentration range for kinetic studies on the halide was determined, as in previous studies, by trial and error. At the concentration range $< 10^{-3}$ *M* the *t*-butyl chloride was assumed to exist in true solution; *i.e.* in a condition which led to reproducible, strictly first-order-rate behavior with small random experimental error. Any appreciable increase above that range led to non-linear behavior attributed to incipient micelle formation. When this was observed the initial concentration was reduced by a safe margin. The consistency of results was taken as sufficient justification for this technique, in the absence of some independent method of detection of supersaturation. It is suspected that micelle formation can take place in binary systems at low concentrations more readily than in water even though one component of the binary is a much better solvent for the halide than water. This tendency toward phase separation at low concentrations was more notable where acetonitrile was the co-solvent than for the alcohols (2) or in the presence of tetrahydrofuran, as the minor co-solvent.

Results and Discussion

The rate data[3] for the solvolysis of *t*-butyl chloride over a range of temperatures were fitted to the usual three constant equation $\log k = A/T + B \log T + C$ by the method of least squares. The values so obtained for the indicated concentrations of solvent mixtures are given in Tables 1 and 2. The pseudo-thermodynamic quantities, $\Delta H^{\ddagger}$, $\Delta S^{\ddagger}$, and $\Delta C_p^{\ddagger}$ derived from these empirical terms by accepting transition state assumptions and the approximation that $d\Delta C_p^{\ddagger}/dT = 0$, are given in Tables 3 and 4. Calculated rates at 10 °C are included for convenience, though these will not be discussed.

[3]Values of individual rates are available from the Depository of Unpublished Data, National Science Library, National Research Council of Canada, Ottawa, Canada K1A 0S2.

Can. J. Chem. Downloaded from www.nrcresearchpress.com by 210.87.254.40 on 09/05/12
For personal use only.

TABLE 3. Pseudo-thermodynamic parameters for the hydrolysis of *t*-butyl chloride in a series of tetrahydrofuran–water mixtures

Solvent V/V	Mole fraction H_2O	$-\Delta C^{\ddagger}$ (cal mol^{-1} deg^{-1})	$\Delta H^{\ddagger}$ (cal mol^{-1})	$\Delta S^{\ddagger}$ (cal mol^{-1} deg^{-1})	k_1 ($s^{-1} \times 10^{-5}$)
80.8:19.2	0.95	108±6	20759±30	1.1±0.1	93.3
66.6:33.4	0.90	21±3	19404±48	−7.7±0.2	13.0
47.0:53.0	0.80	28±5	21748±132	−5.2±0.4	0.705

TABLE 4. Pseudo-thermodynamic parameters for the hydrolysis of *t*-butyl chloride in a series of acetonitrile–water mixtures

Solvent V/V	Mole fraction H_2O	$\Delta C_p^{\ddagger}$ (cal mol^{-1} deg^{-1})	$\Delta H^{\ddagger}$ (cal mol^{-1})	$\Delta S^{\ddagger}$ (cal deg^{-1} mol^{-1})	k_1 ($s^{-1} \times 10^{-5}$)
Water	1.0	−83±4.5	23830	14.4	
86.5:13.5	0.95	−63±4	21412±11	4.8 ±0.04	194.7
75.6:24.4	0.90	−40±4	20628±17	0.16±0.06	77.5
58.0:42.0	0.80	−39±2	21366±34	−1.2 ±0.1	10.1

It is assumed that under the experimental conditions, *t*-butyl chloride reacts according to the classical S_N1 mechanism (8) as amplified by Winstein and co-workers (9, 10) and generalized by Sneen and Larsen (11). We assume that the solute is first activated to an intermediate indistinguishable from the intimate-ion-pair, stabilized in part by external interaction with the solvent and in part by hyperconjugation (12, 13). It does not seem that this latter stabilizing effect alters significantly over the solvent range investigated here (14, 15), hence we assume that charge development at the transition state is relatively constant across the series of solvent mixtures.

The pattern of change in $\Delta H^{\ddagger}$ and $\Delta S^{\ddagger}$ values found here across a series of solvent mixtures of tetrahydrofuran–water and acetonitrile–water mixtures are similar to the pattern found for the hydrolysis of *t*-butyl chloride in alcohol–water mixtures (Fig. 1) (2) and about the same as reported earlier by Winstein and Fainberg (3). The latter authors analyzed the factors determining $\Delta H^{\ddagger}$ in a Haber-type cycle but for lack of the necessary initial state data were forced to treat their extensive kinetic data and derived values of $\Delta H^{\ddagger}$ and $\Delta S^{\ddagger}$ by an empirical classification of little, if any, predictive value. This lack of supplementary calorimetric data was met in part by Arnett and co-workers (4) who, as we have noted above, provided a neat hypothesis to explain the

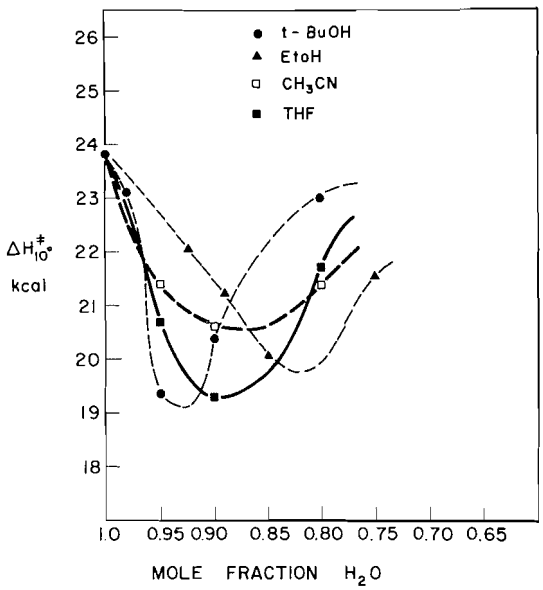

FIG. 1. A correlation of changes in $\Delta H^{\ddagger}$ with changes in the concentration of the organic co-solvent.

changes in $\Delta H^{\ddagger}$ and $\Delta S^{\ddagger}$ reported by Winstein and Fainberg (3). In an extensive survey of enthalpy changes for the solution of a wide range of neutral and charged species in aqueous binaries where the mole fraction of the organo-co-solvent was small ($x_2 = 0.2$ mole fraction or less) changes in $\Delta \bar{H}_s$ for neutral molecules were found to bear a striking relationship to corre-

Can. J. Chem. Downloaded from www.nrcresearchpress.com by 210.87.254.40 on 09/05/12
For personal use only.

Can. J. Chem. Downloaded from www.nrcresearchpress.com by 210.87.254.40 on 09/05/12
For personal use only.

sponding changes in $\Delta H^{\ddagger}$ over the same range of solvent composition.

The changes in $\Delta \bar{H}_s$ were found to be very much less for the solution of tetramethylammonium chloride and trimethylsulfonium chloride than for non-electrolytes in the same series of alcohol–water mixtures. If these salts were accepted as approximate models for the transition state in the hydrolysis of *t*-butyl chloride, the reasonable deduction followed that the reduction in the values in $\Delta H^{\ddagger}$ on the addition of small increments of alcohol to water (Fig. 1) were the consequence of compensating changes in the solvation of the initial state. Specifically Arnett and co-workers claimed that the addition of small increments of alcohol to water produce an increase in structuredness, a view supported by many others (4, 16–18). In the terminology of Nemethy and Scheraga (19) the presence of the non-electrolyte caused a shift in the water–water equilibrium toward a greater degree of hydrogen bonding. This extended quasi-aqueous structure is sensitive to changes in temperature (2, 20) and pressure (21). It is the former characteristic which is of interest here.

The capacity of water to maintain a quasi-aqueous structure presumably through an extension of co-operative hydrogen bonding in the presence of increasing concentrations of weakly polar alkyl groups is distinctly limited, a limit depending in an obvious way on the size of the alkyl groups (2, 20, 22). Any addition of co-solvent beyond that limit leads to a rapid change in the properties of the solvent consistent with a "break-down" in solvent structure. In such cases it is concluded that the hydrogen-bonding maintaining extended co-operative structure is weaker than the thermal agitation tending to disorganize structure.

Solvent Structure in Alcohol–Water Mixtures

It will be recognized that the above observations and deductions are simply an extension of the observations published more than 25 years ago by Frank and Evans (16) in which they introduced the idea that non-electrolytes when dissolved in water caused a shift toward greater structuredness rather than occupying interstitial sites in an ice-like lattice (23). In that paper Frank and Evans made passing reference to what has become known as the "iceberg hypothesis". This graphic term provided an instant if imprecise description of the effect of weakly polar solutes on water structure — sufficiently true to be useful, sufficiently imprecise by implication to be misleading (24). Recently, a common misinterpretation of this hypothesis has been criticized by Grunwald and Ralph (25, 26). Apparently, these authors would de-emphasize the possible structural effect of weakly polar solutes on adjacent water structure and attempt to account for the unique characteristics of such aqueous solutions in terms of London dispersion forces. No one is likely to deny that such forces are present and contribute to the overall effect. We find it equally unlikely that this interpretation will provide an adequate explanation for the extrema observed in the thermodynamic quantities reported by Arnett (4) and Ben-Naim (17) who favor the structural hypothesis. In particular we take exception to likening the iceberg hypothesis to a "suit of armour" for which Grunwald and Ralph would substitute a "form-fitting sweater". The latter light-hearted suggestion is reminiscent of the surface-tension hypothesis of Langmuir while the former is a graphic figure based on the idea that the presence of the weakly polar solute "strengthens" (4) the water structure, an idea which may follow naturally enough from the analogy but which is inconsistent with our kinetic results (2). Thus while we agree with Grunwald and Ralph that the iceberg hypothesis is misleading, we disagree with the alternative they propose. In particular the substitution of solute–solvent interaction (London forces) as the dominant factor does not provide for sudden changes in properties of organo-aqueous mixtures in the high water range (A).[4] We assume, as a working hypothesis, that the changes in such properties as heat of mixing, partial molal volume, velocity of ultrasound (20) are less a function of solvent–solute interaction than of altered solvent–solvent interaction. This assumption is important for it determines the interpretation we attach to the changes in the values of $\Delta C_p^{\ddagger}$ found for ionogenic reactions across a series of such solvent mixtures in range A. Equally important

[4]In range A, some degree of three-dimensional quasi-aqueous structure is maintained. On the addition of sufficient co-solvent (range B) this extended structure can no longer be maintained.

Can. J. Chem. Downloaded from www.nrcresearchpress.com by 210.87.254.40 on 09/05/12
For personal use only.

is the observation that non-electrolytes have somewhat larger effects than small ions on the properties of the solvent mixture (4–6). Since solvolytic reactions such as the solvolysis of *t*-butyl chloride involve the transformation of a non-electrolyte to a charged transition state, we assume that the changes in $\Delta C_p^{\ddagger}$ in range A for a series of solvent mixtures reflect mainly changes in the initial state solvation of the reactant. Thus the central idea we have used for the interpretation of the large negative values of $\Delta C_p^{\ddagger}$ found in these reactions in mixed solvents is the same as that for the corresponding values for solvolysis in water (2), *i.e.* the value of this coefficient is mainly determined by the effect of temperature on that component of $\Delta H^{\ddagger}$ required to reorganize the solvent shell adjacent to the reactant from dominant water–water interaction to ion–water interaction. We note (Fig. 1) that the $\Delta H^{\ddagger}$ values obtained from the solvolysis of *t*-butyl chloride in a series of alcohol–water mixtures (range A) decrease as the alcohol concentrations increase. Whatever the detailed description of the solvation shell, each added increment of alcohol appears to move the initial state solvation shell closer to that of the transition state. Proceeding on the assumption that the values of $\Delta C_p^{\ddagger}$ found for solvolysis in such mixtures are dependent on $d\Delta H^{\ddagger}/dT$ and that $d\Delta \bar{H}_s/dT$ is small by comparison, then we note that in range A (Fig. 2) the incremental addition of alcohol has the effect of making $\Delta C_p^{\ddagger}$ more negative, *i.e.*, the quasi-aqueous structure becomes more sensitive to a change in temperature relative to water. Hence we conclude that as the concentration of co-solvent is increased the initial state solvation shell in equilibrium with aqueous mixture becomes *extended* and *weakened*. The ability of the system to maintain a quasi-aqueous structure (*i.e.*, a three-dimensional hydrogen-bonded network or some combination of clusters (27) or cages (28)) is limited, and beyond a critical concentration the quasi-aqueous structure is replaced by a solvent with quite different characteristics as judged by previously noted criteria (20). Here $\Delta C_p^{\ddagger}$ for the above reaction has a value in the range -30 – -40 cal deg^{-1} mol^{-1} and is relatively insensitive to solvent composition (29). From the above we conclude that our $\Delta C_p^{\ddagger}$ values for the solvolysis of *t*-butyl chloride in alcohol–water mixtures serve to underline the weakness in those hypotheses which claim that the addition of a non-electrolyte "strengthens" the adjacent water structure.[5]

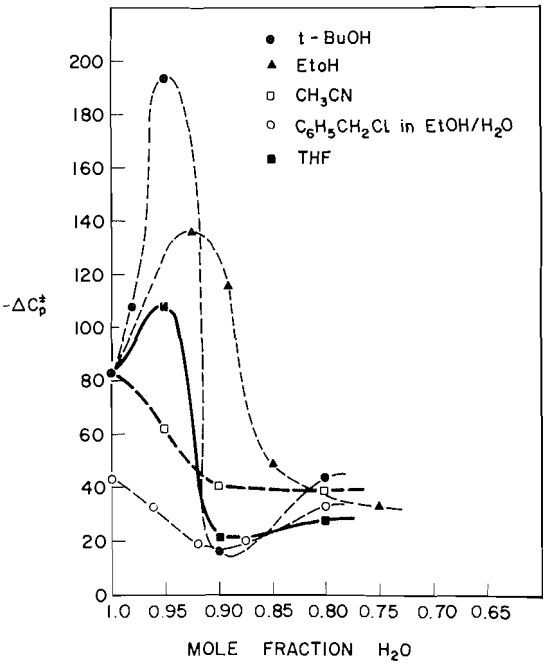

FIG. 2. A correlation of the changes in $\Delta C_p^{\ddagger}$ with changes in the concentration of the organic co-solvent.

Solvolysis in Tetrahydrofuran–Water Mixtures

The trend in values of $\Delta H^{\ddagger}$, $\Delta S^{\ddagger}$, and $\Delta C_p^{\ddagger}$ found for the solvolysis of *t*-butyl chloride in a range of tetrahydrofuran–water mixtures are similar to the corresponding values in alcohol–water mixtures over the same concentration range. This suggests that the major effect of this co-solvent on water structure (30, 31) is similar to that of the alcohols in agreement with Arnett's generalization with respect to the effect of non-electrolytes on water structure (4).

Tetrahydrofuran is a solvent of low ionizing power (32), hence the major effect of THF on the rate will be a consequence of the modifying effect on water structure. Since $\Delta H^{\ddagger}$ is observed to decrease and $\Delta C_p^{\ddagger}$ becomes more negative

[5]In the case of ethanol being added to water, the implication seems to be that some ethanol strengthens the adjacent water structure; further successive increments strengthen it more until presumably the structure is so strong that it falls apart under the influence of thermal fluctuation. This progression lacks logic. It also underlines the implied fallacy in the iceberg analogy, as frequently interpreted.

Can. J. Chem. Downloaded from www.nrcresearchpress.com by 210.87.254.40 on 09/05/12
For personal use only.

through the high water range (A) and the change in both terms is assumed to be related to the structural stability of the initial state solvation shell which is disrupted in the activation process, we are led to the same conclusion as reached with respect to results of solvolytic studies in alcohol–water mixtures: that the co-solvent over the initial range modifies and weakens the quasi-aqueous structure toward reorganization (but see ref. 33). As before, we assume that charge development at the transition state does not alter appreciably over the concentration range (14, 15) and that $d\bar{H}_s/dT \gg dH^{\ddagger}/dT$. Beyond a critical concentration of tetrahydrofuran ($x_2 = 0$–0.05 m) the quasi-aqueous structure undergoes a major collapse, and the value $\Delta C_p^{\ddagger}$ becomes more positive (-30 to -40 cal deg^{-1} mol^{-1}), *i.e.* the system becomes much less sensitive to a change in temperature. Values of $\Delta C_p^{\ddagger}$ in this range (B) are too large to arise from the temperature dependence of the dielectric constant of the bulk-solvent (34) and at the moment are not explained. It seems likely, however, that the assumption $d\bar{H}_s/dT \gg dH^{\ddagger}/dT$ is no longer valid.

Solvolysis in Acetonitrile–Water Mixtures

The effect of acetonitrile on water structure is quite different from that of alcohol or of THF as co-solvents in range A. Thus Blandamer and co-workers (35, 36) found no minimum in the plot of excess partial molal volume *vs.* x_2 for water rich acetonitrile mixtures (in contrast to that found for *t*-butanol–water mixtures). They conclude from a comparison of the enthalpy of mixing and from i.r. spectra that in contrast to the effect of *t*-butanol as a co-solvent, acetonitrile appears to compete successfully with water–water interaction. Such intercomponent interaction leads to endothermic mixing (37) due to the breakdown of water-structure in contrast to the exothermic effect in the *t*-butanol–water binary, and to a lowering of the temperature of maximum density of water (38) in contrast to the effect of alcohol (20). The competition between water–water interaction and water–acetonitrile interaction shifts in favor of the former with decreasing temperature; phase separation occurring at -1 °C. We have found that *t*-butyl chloride or cyclohexyl bromide enhance this tendency giving rise to a separation of two ternary phases at low concentrations. As a result no method was found which permitted a characterization of saturation solubility of these solutes over a series of H_2O–MeCN mixtures as was done for cyclohexyl bromide in *t*-butanol–H_2O mixtures (2). This characteristic imposed the practical limitation that the initial concentration of *t*-butyl chloride in kinetic studies be reduced well below 10^{-3} M in order to ensure uncomplicated kinetics.

That $\Delta H^{\ddagger}$ decreased initially in the three systems (Fig. 1) was taken as prima facie evidence that the initial addition of each co-solvent in some manner weakened the initial state solvation shell. The very different trend in $\Delta C_p^{\ddagger}$ is evidence that this structure modification is different for co-solvents such as alcohols and tetrahydrofuran and for acetonitrile. In the former mixtures, the solvent structure is extended and weakened and thus rendered more sensitive to changes in temperature ($-\Delta C_p^{\ddagger}$ is increased), in the latter the acetonitrile appears to act as a structure breaker. This characteristic will be reflected in the initial state solvation of the *t*-butyl chloride and hence in the temperature dependence of that part of the enthalpy of activation required for solvent reorganization. Rather simply, since the acetonitrile appears to act like small ions and partially melt the water structure (4, 16) less structure remains to be influenced by a change in temperature. Qualitatively, at least, this argument accommodates the opposed differences in the apparent values of $\Delta C_p^{\ddagger}$ in these systems, *i.e.* for the cases where the co-solvent extends and so weakens the initial solvent shell and for the case where the co-solvent is a structure breaker. Both types of structure modification would be expected to show a reduction in the structural component of $\Delta H^{\ddagger}$ with increasing concentration of the co-solvent in range A. The modifying word "apparent" might well be prefixed to $\Delta H^{\ddagger}$ as well as $\Delta C_p^{\ddagger}$. Of necessity the quantities $\Delta H^{\ddagger}$, $\Delta S^{\ddagger}$, and $\Delta C_p^{\ddagger}$ are derived from rates determined over a range of temperatures. Since the solvent is sensitive to a change of temperature, the purist might claim that data from different systems are being compared (39). This argument becomes bothersome only if one insists on absolute values. In the present study the apparent temperature coefficient of $\Delta H^{\ddagger}$ ($\Delta C_p^{\ddagger}$) provides a useful insight into the different effects of certain co-solvents on water structure and so requires no further justification.

Can. J. Chem. Downloaded from www.nrcresearchpress.com by 210.87.254.40 on 09/05/12
For personal use only.

Solvent Structure $\Delta H^{\ddagger}$ *and* $\Delta S^{\ddagger}$

Granted the above deductions are consistent with our data we are left with an apparent anomaly. Thus, many authors have concluded (40, 41) that D_2O has more structure than H_2O at comparable temperatures. Certainly it would seem that the higher freezing point, the higher temperature of maximum density, the higher viscosity and the lower the conductance values, the lower rate of self diffusion are physical indicators which are consistent with such a conclusion.[6] Similarly, it is the conclusion of many authors beginning with the classical paper of Frank and Evans (16) that the presence of a weakly polar solute in water leads to an enhancement of structure. Whether that enhancement takes the form of enhanced fluttering cluster formation or of incipient clathrate formation or of some combination involving the occupancy of interstitial sites are questions of detail. Since the initial state solvent shell about a reactant in such a solvent mixture must necessarily be in equilibrium with that mixture, the initial state solvent shell will reflect the co-operative nature of that mixture. The important fact is the claim that the structure is enhanced and/or strengthened.

We have shown that if *t*-butyl chloride is hydrolyzed in H_2O and in D_2O, the $\Delta H^{\ddagger}$ for the reaction is higher in the latter and we have attributed this increase in $\Delta H^{\ddagger}$ to the greater degree of structure which must be reorganized (42) in the activation process. In this and in our previous paper (2) we note that on the addition of alcohol or THF to water, $\Delta H^{\ddagger}$ for the solvolysis of *t*-butyl chloride decreases in range A and the results obtained by Arnett and co-workers show that this decrease probably arises from a change in the nature of the initial state solvation shell. That a nominal increase in structure in D_2O over H_2O and in alcohol–water or THF–water mixtures over water alone as reaction media for the solvolysis of *t*-butyl chloride can be responsible for both an increase and a decrease in $\Delta H^{\ddagger}$ seems improbable unless the word "structure" refers to different types of co-operative interaction. We note further that in the D_2O/H_2O comparison the difference in k_{obs} is determined by the difference reduced by a compensating change in $\Delta S^{\ddagger}$, while in the mixed solvents the decrease in $\Delta H^{\ddagger}$ was more than cancelled by an opposing change in $\Delta S^{\ddagger}$ and the decrease in k_{obs} was far larger. This is hardly surprising in view of the much greater change in solvent. That a structure-maker such as THF and a structure-breaker such as acetonitrile when co-solvents in water should lead to a similar though by no means equal decrease in $\Delta H^{\ddagger}$ is less anomalous when the quite different trends in the accompanying values of $\Delta C_p^{\ddagger}$ are taken into consideration. While the latter factor may have important contributions from sources other than the solvent structure (see above) it is interesting to note that the difference in conductance between K^+ and Cs^+ in ethanol–water mixtures ($x_2 = 0.08$) is twice as great as it is in water, suggesting that the more highly "structured" solvent mixture discriminates better or is more sensitive to the structure-breaking power of ions than water (20). Our results suggest that the addition of alcohol or THF to water both extends and weakens the structure toward reorganization by a charged transition state relative to water. Such structural interpretations if valid are inseparable from the accompanying changes in entropy, and here the picture is not at all clear. The idea that there is more structure in D_2O than in H_2O and hence requires a greater input of energy in the activation process is borne out by the relative value of $d_l\Delta H^{\ddagger}$ and $d_l\Delta S^{\ddagger}$, where the difference in $\Delta H^{\ddagger}$ is dominant (42). In the organo–solvent mixtures $\Delta H^{\ddagger}$ has lower values but the rate is controlled by an opposed shift in $\Delta S^{\ddagger}$ relative to the value in water. It could be argued that in the solvent mixture, the gain in entropy is reduced but this is hardly consistent with the idea advanced to account for the more negative values of $-\Delta C_p^{\ddagger}$ or the idea of a more extended co-operative initial state solvent shell. This lack of consistency between the values of $\Delta C_p^{\ddagger}$ and $\Delta S^{\ddagger}$ has been noted previously (43) but has not been resolved.

[6]Holtzer and Emerson have recently questioned this conclusion and have noted that just the opposite conclusion might be drawn from a consideration of dielectric constant differences (24).

1. R. E. ROBERTSON. Progr. Phys. Org. Chem. Vol. 4, 213 (1967).
2. R. E. ROBERTSON and S. E. SUGAMORI. J. Am. Chem. Soc. **91**, 7254 (1969).
3. S. WINSTEIN and A. H. FAINBERG. J. Am. Chem. Soc. **79**, 5937 (1957).
4. E. M. ARNETT, W. G. BENTRUDE, J. J. BURKE, and P. MCDUGGLEBY. J. Am. Chem. Soc. **87**, 1541 (1965).

5. E. M. ARNETT, W. G. BENTRUDE, and P. MCDUGGLEBY. J. Am. Chem. Soc. **87**, 2048 (1965).
6. E. M. ARNETT, P. MCDUGGLEBY, and J. J. BURKE. J. Am. Chem. Soc. **85**, 1350 (1963).
7. H. S. FRANK and F. FRANKS. J. Chem. Phys. 4746 (1967).
8. C. K. INGOLD. Structure and mechanism in organic chemistry. Cornell University Press, Ithaca, New York. 1953. Chap. 7.
9. S. WINSTEIN, E. CLIPPINGER, A. H. FAINBERG, and G. C. ROBINSON. J. Am. Chem. Soc. **76**, 2597 (1954); Chem. Ind. 664 (1954).
10. S. WINSTEIN, B. APPEL, R. BAKER, and A. DIAZ. Chem. Soc. Special Publication No. 19, 109 (1965).
11. R. A. SNEEN and J. W. LARSEN. J. Am. Chem. Soc. **91**, 362 (1969).
12. V. J. SHINER, JR., B. L. MURR, and G. HEINEMAN. J. Am. Chem. Soc. **85**, 2413 (1963).
13. V. J. SHINER, JR. Tetrahedron, **5**, 243 (1959).
14. G. FRISONE and E. R. THORNTON. J. Am. Chem. Soc. **90**, 1211 (1968).
15. L. HAKKA, A. QUEEN, and R. E. ROBERTSON. J. Am. Chem. Soc. **87**, 161 (1965).
16. H. S. FRANK and M. EVANS. J. Chem. Phys. **13**, 507 (1945).
17. A. BEN-NAIM. J. Phys. Chem. **69**, 1922 (1965).
18. G. L. BERTRAND, F. L. MILLERO, C. WU, and L. G. HEPLER. J. Phys. Chem. **70**, 699 (1966).
19. G. NEMETHY and H. A. SCHERAGA. J. Chem. Phys. **36**, 3382 (1962).
20. F. FRANKS and D. J. G. IVES. Quart. Rev. **20**, 1 (1966).
21. S. J. DICKSON and J. B. HYNE. Can. J. Chem. **49**, 2394 (1971).
22. E. M. ARNETT, W. B. KOVER, and J. V. CARTER. J. Am. Chem. **91**, 4028 (1969).
23. D. D. ELEY. Trans. Faraday Soc. **35**, 1281 (1939).
24. A. HOLTZER and M. E. EMERSON. J. Phys. Chem. **73**, 26 (1969).
25. E. GRUNWALD and E. RALPH. J. Am. Chem. Soc. **89**, 4405 (1967).
26. E. GRUNWALD, R. L. LIPNICK, and E. RALPH. J. Am. Chem. Soc. **91**, 4333 (1969).
27. H. S. FRANK and W. Y. WEN. Discuss. Faraday Soc. **24**, 133 (1957).
28. W. F. CLAUSEN and M. F. POLGLASE. J. Am. Chem. Soc. **74**, 4817 (1952).
29. G. KOHNSTAM. The transition state. Special Pub. 16, 179, Chem. Soc. London, 1962.
30. M. J. STACKELBERG and B. METHUEN. Z. Electrochem. **62**, 130 (1958).
31. S. R. GOUGH and D. W. DAVIDSON. Can. J. Chem. **49**, 2691 (1971).
32. S. G. SMITH, A. H. FAINBERG, and S. WINSTEIN. J. Am. Chem. Soc. **83**, 618 (1961).
33. A. BEN-NAIM and G. MORAN. Trans. Faraday Soc. **61**, 821 (1965).
34. D. D. ELEY and W. F. K. JONES. Trans. Faraday Soc. **35**, 1313 (1939).
35. D. A. ARMITAGE, M. J. BLANDAMER, M. J. FOSTER, N. J. HIDDEN, K. W. MORCOM, M. C. R. SYMONDS, and M. J. WOOTEN. Trans. Faraday Soc. **64**, 1193 (1968).
36. M. J. BLANDAMER, D. E. CLARKE, T. A. CLAXTON, M. F. FOX, N. J. HIDDEN, J. OAKES, M. C. R. SYMONDS, and M. J. WOOTEN. Chem. Commun. 273 (1967).
37. J. B. HYNE and M. ESTEP. Private communication.
38. B. G. WADA and S. UMEDA. Bull. Chem. Soc. Jap. **35**, 1797 (1962).
39. D. J. G. IVES and P. D. MARSDEN. J. Chem. Soc. 649 (1965).
40. J. L. KAVANAU. Water and solute–water interaction. Holden-Day Inc. San Francisco. 1964.
41. G. NEMETHY and H. A. SCHERAGA. J. Chem. Phys. **41**, 680 (1964).
42. L. TREINDL, R. E. ROBERTSON, and S. E. SUGAMORI. Can. J. Chem. **47**, 3397 (1969).
43. R. E. ROBERTSON, B. ROSSALL, S. E. SUGAMORI, and L. TREINDL. Can. J. Chem. **47**, 4199 (1969).

Can. J. Chem. Downloaded from www.nrcresearchpress.com by 210.87.254.40 on 09/05/12
For personal use only.

^{13}C Nuclear Magnetic Resonance Studies. XX. ^{13}C Shieldings of Several Allyl Alcohols. Geometric Dependence of ^{13}C Shieldings[1]

H. BROUWER[2] AND J. B. STOTHERS

Department of Chemistry, University of Western Ontario, London, Ontario

Received October 25, 1971

The ^{13}C spectra of 21 methyl- and halo-substituted 2-propenols have been determined. The shielding data are discussed with particular emphasis on their dependence on the orientation of the 3-halo substituents. Linear regression analyses of the results gave sets of additive parameters which correlate the shieldings with reasonable precision ($\leqslant 1$ p.p.m.). A similar set of parameters has been generated from the published data for acyclic alkenes: these parameter sets are intercompared. The results of complete analysis of the proton spectra of most of the alcohols are also presented.

On a déterminé le spectre au ^{13}C de 21 dérivés méthylés et halogénés du 2-propenol. On discute des données de blindage en insistant particulièrement sur leur effet dans l'orientation des substituants halogénes en position-3. Les analyses de régression linéaire des résultats ont donné des ensembles de paramètres additifs qui nous fournissent les blindages avec une précision raisonnable ($\leqslant 1$ p.p.m.). Un ensemble similaire de paramètres a été tiré des données publiées pour les alcènes acycliques: on compare ces paramètres avec ceux qu'on a obtenus. On présente aussi les résultats de l'analyse complète des spectres de protons de la plupart des alcools.

Canadian Journal of Chemistry, **50**, 1361 (1972)

Can. J. Chem. Downloaded from www.nrcresearchpress.com by 210.87.254.40 on 09/05/12
For personal use only.

Introduction

In an earlier part of this series, ^{13}C n.m.r. spectra of several unsaturated aliphatic systems were discussed and the results of an examination of α,β-unsaturated carboxylic acids and esters compared with earlier data (1). These results clearly showed that olefinic ^{13}C shieldings exhibit a marked dependence on the orientation of substituents bonded to the olefinic carbons. Furthermore, these shieldings were correlated by a linear expression entirely analogous to that employed for acyclic saturated hydrocarbons (2),

$$[1] \qquad \delta_C^i = K + \sum_j A_j n_{ij}$$

where δ_C^i, the shielding of the ith olefinic carbon, is given by a summation of specific substituent parameters, A_j; n_{ij}, is the number of such substitutions and K, a constant, corresponds to the shielding in the parent system. Similar correlations, initially proposed by Savitsky and Namikawa (3) and by Grant and Paul for saturated hydrocarbons (2), and methylcyclohexanes (4), have proved to be valuable in the analysis of more complex systems; a good example is the steroid study by Reich *et al.* (5).

In the paper presenting the first results of a systematic study of the ^{13}C spectra of alkenes, Retcofsky and Friedel (6) noted the general trends exhibited by olefinic shieldings upon alkyl substitution but, for practical reasons, these authors did not investigate the shieldings of carbons bonded to the olefinic nuclei. In our previous report, we noted that the carboxyl carbon shieldings of acrylic acids and esters are essentially independent of substituent orientation whereas olefinic methyl carbons exhibit a marked geometrical dependence. As an extension of our study of stereochemical effects on ^{13}C shieldings, we have determined the ^{13}C spectra of a series of substituted allyl alcohols to examine the variation of these shieldings as a function of substitution and substituent geometry. Additive correlations have been found for the olefinic and carbinyl carbon shieldings which may be compared with similar data which have been generated from the published results for acyclic alkenes. In this paper these correlations are discussed and compared with the results for saturated systems. In addition, the proton parameters for most of the allyl alcohols are presented.

Experimental

Materials

All of the alcohols employed in this study are known compounds and were obtained as commercial samples or prepared by published procedures. In all cases, their physical properties agreed well with literature values and the proton

[1]Part XVIII, ref. 24. Part XIX, ref. 25.

[2]Holder of NRCC Scholarships, 1966–1970.

Can. J. Chem. Downloaded from www.nrcresearchpress.com by 210.87.254.40 on 09/05/12
For personal use only.

TABLE 1. Proton parameters of some substituted 2-propen-1-ols, RC(X)=C(Y)CH_2OH*
(δ_H, p.p.m. from TMS; J in Hz)

(a) Shieldings

R	X	Y	Carbinyl Z	Carbinyl E	Vinyl C-2 Z	Vinyl C-2 E	Vinyl C-3 Z	Vinyl C-3 E	Methyl Z	Methyl E
H	H	H	4.046		5.916		5.064(*E*) 5.209(*Z*)			
CH_3	H	H	4.07	3.92	†	†	†	†	1.62	1.67
CH_3	CH_3	H	3.97		5.31				1.65(*Z*) 1.72(*E*)	
H	H	CH_3	3.922				4.899(*Z*) 4.763(*E*)		1.712	
CH_3	H	CH_3	3.85				5.39		1.60 1.60	
H	Cl	H	4.279	4.064	5.922	6.016	6.075	6.200		
CH_3	Cl	H	4.169	4.036	5.628	5.757			2.121	2.108
H	Cl	CH_3	4.223	3.983			5.805	6.044	1.830	1.783
H	Br	H	4.228	4.025	6.285	6.298	6.221	6.323		
CH_3	Br	H	4.134	4.011	5.835	6.015			2.315	2.291
H	I	H	4.146	4.002	6.439	6.630	6.306	6.350		
CH_3	I	H	4.074	3.992	5.722	6.325			2.539	2.459

(b) Coupling constants

R	X	Y	J_{vic} J_{12} Z	J_{12} E	J_{23} Z	J_{23} E	Long-range $J_{HC=CCH_2}$ Z	$J_{HC=CCH_2}$ E	$J_{HC=CCH_3}$ Z	$J_{HC=CCH_3}$ E	$J_{H_2CC=CCH_3}$ Z	$J_{H_2CC=CCH_3}$ E	Other
H	H	H	5.04		10.45 17.21		−1.52 (*trans*) −1.81 (*cis*)						1.73(J_{gem})
H	H	CH_3					−1.10 (*trans*) −1.60 (*cis*)		−0.92 (*trans*) −1.48 (*cis*)				1.96(J_{gem}) 0.54($J_{H_2CCCH_3}$)
CH_3	CH_3	H	6.80						−1.3 (*trans*) −1.3 (*cis*)				
H	Cl	H	6.00	5.93	7.22	13.32	−1.72	−1.62					
CH_3	Cl	H	6.16	7.40					−1.30	−1.25	1.32	0.77	
H	Cl	CH_3					−1.10	−1.43	−1.60	−1.50			0.2(*Z*)$J_{H_2CCCH_3}$ 0.5(*E*)
H	Br	H	5.71	5.76	7.24	13.59	−1.60	−1.68					
CH_3	Br	H	5.87	7.25					−1.37	−1.38	1.37	0.80	
H	I	H	5.60	5.40	7.69	14.45	−1.67	−1.66					
CH_3	I	H	5.76	6.95					−1.57	−1.55	1.37	0.82	

*Relative orientation of substituents indicated by convention of Blackwood *et al.* (7); *Z*-isomers have highest priority groups on the same side of the double bond.
†Not analyzed.

Can. J. Chem. Downloaded from www.nrcresearchpress.com by 210.87.254.40 on 09/05/12
For personal use only.

spectra were recorded to insure that the samples employed for ^{13}C spectra were of high purity.

Spectra

For detailed analysis, proton spectra were recorded on a Varian HA-100 spectrometer using 5 mol % solutions in CCl_4. The spectra were analyzed using the LAOCOON III program and the parameters obtained were employed to calculate 60 MHz spectra. As a check on the analysis, the latter were compared with spectra obtained on a Varian HA-60 instrument; for these comparisons, calculated spectra were plotted using the n.m.r. Plot II program, kindly supplied by Dr. S. Castellano. Confirmation of the geometry of several of the examples was obtained by nuclear Overhauser enhancement measurements on samples of the alcohols or the methyl esters from which the alcohols were prepared.

The ^{13}C spectra were determined for 25% (v/v) solutions in *p*-dioxane using a frequency-swept, field-locked spectrometer operating at 15.1 MHz; the proton-decoupled solvent signal served as the lock signal. This instrument was controlled with a Varian 620i computer. In most cases, ^{13}C spectra were obtained from ten, 50-s scans over 250 Hz; the sweep unit was a Wave-Tek III VCO. Proton decoupling was accomplished with a "home-built" decoupler utilizing a Frequency Electronics 60 MHz VCO whose output was amplified to provide up to 6 W of r.f. power at the probe. Frequency modulation with a HP 3722A noise generator provided noise modulation of the decoupler output. A Varian V4336 probe[3] which permitted the use of 12 mm spinning samples was employed. In this instrument, the sample temperature was *ca.* 40°.

The ^{13}C shieldings (δ_C) are given relative to TMS by conversion of the raw data, measured from dioxane, using the value 67.4 p.p.m. for the shielding of dioxane.

Results

The results of analysis of the proton spectra using the LAOCOON III program are listed in Table 1. In general, individual shieldings were initially estimated from first-order analysis and the coupling constants from the observed spacings; these parameters were used to generate a theoretical spectrum and the transitions matched with those observed as the input for iterative convergence on a best fit. As an example the 100 MHz spectra of allyl alcohol, observed and calculated, are illustrated in Fig. 1. It is interesting that the r.m.s. error for fitting all lines is 0.06 if all coupling constants except the geminal ones are assumed to be positive whereas the r.m.s. error is 0.04 if the allylic couplings are negative. Thus the latter assignment is preferred and is in agreement with the earlier results for methyl allyl ether and allyl chloride (8).

The ^{13}C shielding data are collected in Table 2. Assignments for the methyl and carbinyl carbon signals were straightforward since the former appear at higher field, δ_C 12–33, while the latter absorb near 60 p.p.m. For the compounds in which each olefinic carbon is bonded to a single proton the specific carbon signals were identified by the differences in the one-bond coupling constants observed in spectra obtained without proton-decoupling. The J_{CH} values for olefinic carbons bearing polar groups are larger than those exhibited by carbons bonded to sp^3-carbons (9). Confirmation of these assignments was provided by the results for the methyl substituted homologs since the shielding changes produced by replacement of an olefinic hydrogen with a methyl group are well known (1, 6), *i.e.*, the substituted carbon is deshielded while its neighbor is shielded.

Discussion

(a) General Trends

Although significant proton chemical shift differences are found between geometrical isomers, the largest difference is only *ca.* 0.2 p.p.m. In general, the methyl protons are slightly shielded in the *E*-3-halobut-2-en-1-ols and the carbinyl protons are deshielded by up to 0.2 p.p.m. in the *Z*-isomers, both relative to the values for the corresponding analogs. Similarly the carbinyl protons are deshielded and the α-olefinic proton shielded in the *Z*-3-substituted-2-propen-1-ols relative to the *E*-isomers. The somewhat larger vicinal coupling constants for the carbinyl protons in the substituted alcohols compared to the value for the parent compound indicate that the rotamer population is affected by the 3-substituents. The microwave spectrum of allyl alcohol itself (10) indicates that the preferred rotamer is the *gauche* form **1** for which the vicinal coupling will be the average of a *trans* ($\phi = 180°$) and a *gauche* ($\phi = 60°$) interaction or *ca.* $(11.5 + 2.8)/2 = 7.2$ Hz assuming that the vicinal coupling constants for specific dihedral angles are approximately the same as those found for 3-methoxypropene (11). Since J_{vic} for rotamer **2** having an eclipsed hydroxyl is expected to be *ca.* 2.8 Hz, the observed value of 5.04 Hz for allyl alcohol indicates that **1** and **2** are present in approximately equal amounts. It is interesting that the introduction of a *cis*-3-methyl group, as in 3-methyl-2-buten-1-ol, serves to increase J_{vic} substantially, a trend consistent

[3]We wish to thank Varian Associates, Palo Alto, California, for the loan of this probe for these studies.

Can. J. Chem. Downloaded from www.nrcresearchpress.com by 210.87.254.40 on 09/05/12
For personal use only.

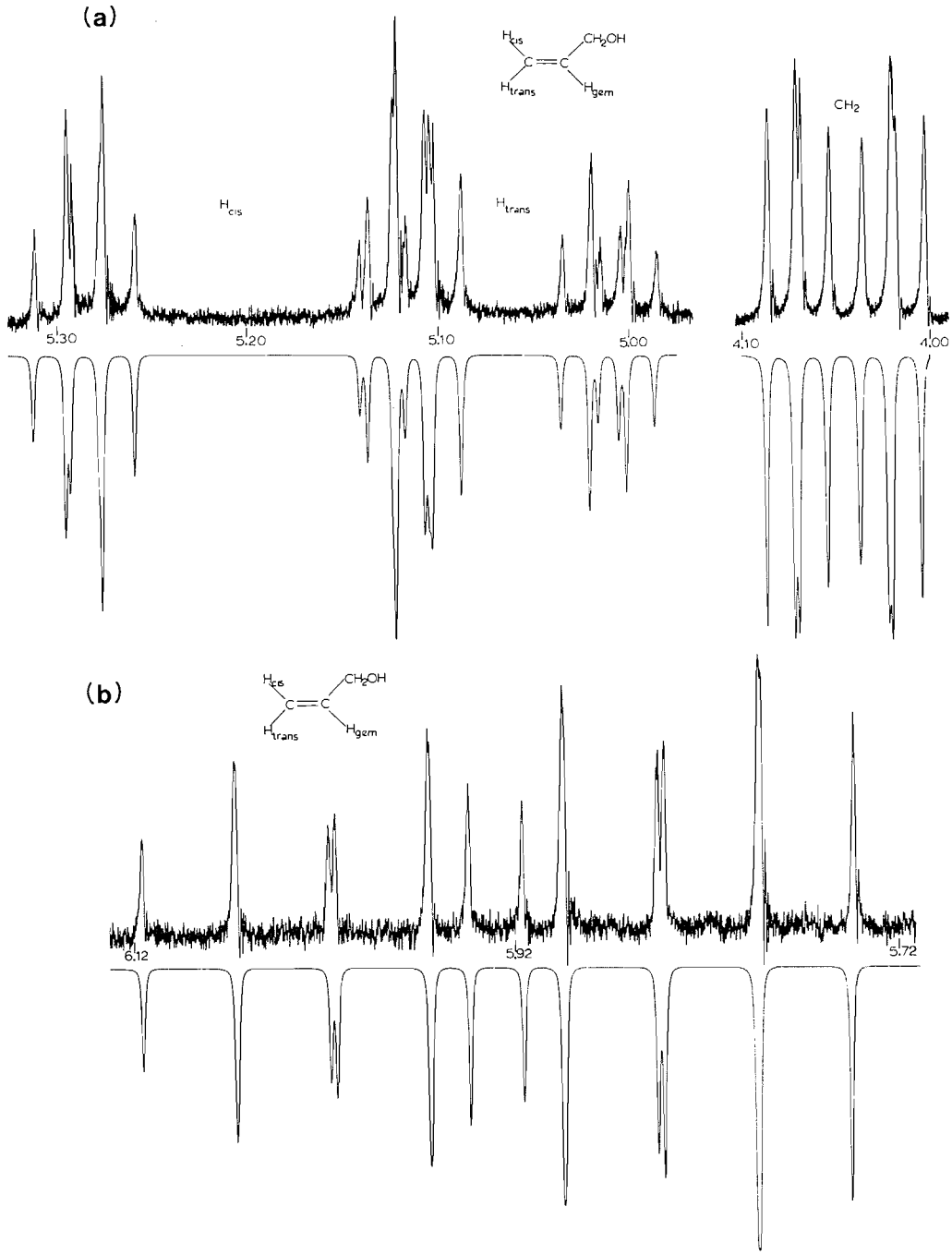

FIG. 1. Theoretical and experimental 100 MHz proton spectra of allyl alcohol (*a*) higher field region, (*b*) absorption for H_{gem}.

TABLE 2. ^{13}C Shieldings in some substituted allyl alcohols, RC(X)=C(R′)CH_2OH* (δ_C, p.p.m. from TMS)

			C-1		C-2		C-3		CH_3	
R	X	R′	*Z*	*E*	*Z*	*E*	*Z*	*E*	*Z*	*E*
H	H	H	63.3		139.1		113.7			
CH_3	H	H	57.9	62.9	131.4	132.1	125.3	126.0	12.7	17.3
H	H	CH_3	66.2		146.2		108.7		18.9	
CH_3	CH_3	H	58.8		125.7		133.7		17.6	
									25.4	
CH_3	H	CH_3	60.5	68.1	136.5	136.7	120.8	118.8	12.8	12.9
									21.9	12.9
H	Cl	H	58.1	60.9	132.9	134.2	118.3	119.3		
CH_3	Cl	H	60.1	56.6	127.0	128.3	130.7	132.5	25.6	20.7
H	Cl	CH_3	60.6	65.5	139.4	139.5	111.8	113.9	23.2	17.5
H	Br	H	60.7	62.5	135.9	138.4	107.5	106.8		
CH_3	Br	H	62.2	59.2	130.1	132.8	122.2	122.6	28.4	23.3
H	I	H	65.7	64.7	142.0	146.8	81.2	76.8		
CH_3	I	H	67.0	59.7	136.3	141.7	99.7	96.9	33.3	28.0

*Relative orientation of substituents indicated by the convention of Blackwood *et al.* (7); *Z*-isomers have highest priority groups on the same side of double bond.

with an appreciable increase in the concentration of forms corresponding to **1** in the rotamer equilibrium. Furthermore, the *E*-isomer for each of the 3-halobutenols exhibits the larger J_{vic} by 1.2–1.4 Hz. Although it is difficult to estimate the effect of the 3-halo substituents on the magnitude of this coupling constant, the differences for J_{vic} between *Z*- and *E*-isomers in the 3-halopropenols are very much smaller (0.05–0.2 Hz) possibly indicating little change in the preferred conformation of the hydroxymethyl group in these alcohols.

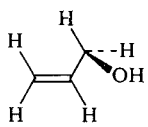

1

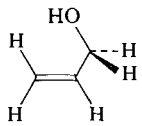

2

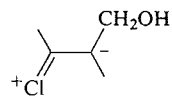

3

Although no regular trend is observed for the allylic proton–proton couplings as a function of geometry the homoallylic interactions ($J_{HCC=CCH}$) are consistently larger for a *transoid* disposition of carbons α to the double bond, 1.35 *vs.* 0.77 Hz. Perhaps this difference would be helpful for stereochemical assignments in related systems but both isomers would be required.

Perhaps the most striking trend exhibited by the ^{13}C shielding data (Table 2) is the upfield shift found for methyl and carbinyl carbons if eclipsed, *i.e.*, in a *cis*-orientation, with respect to another methyl group compared to the shieldings in the corresponding *trans*-isomers. For example, the methyl carbons are equivalent (δ_C 12.9) in *E*-2-methyl-2-buten-1-ol but differ by 9.1 p.p.m. in the *Z*-isomer. In the latter case, the signal at δ_C 21.9 may be assigned to the 2-methyl carbon and the 12.8 p.p.m. peak to the terminal methyl. A similar shielding difference (7.6 p.p.m.) is observed for the carbinyl carbons in these two isomers with that in the former at higher field. The terminal methyls in 3-methyl-2-buten-1-ol also differ appreciably (7.8 p.p.m.). By comparison with the remaining methyl carbon shieldings a consistent pattern emerges such that the more shielded carbon is eclipsed with either a methyl or carbinyl carbon. It is interesting that the carbinyl carbons are much less sensitive to the configuration of the 3-halogens. The differences ($\delta_C^E - \delta_C^Z$) between the *Z*- and *E*-3-halo-2-propen-1-ols are 2.8 (Cl), 1.8 (Br), and −1.0 p.p.m. (I), but, in the corresponding 3-halo-2-buten-1-ols, the *E*-isomers consistently exhibit the more shielded carbinyl carbons (*i.e.*, in those isomers in which the carbinyl and terminal methyl carbons are eclipsed). As noted above the methyl carbons in the latter series are shielded by *ca.* 5 p.p.m. relative to the *Z*-isomers.

(b) Regression Analyses

To test for the existence of an additive rela-

Can. J. Chem. Downloaded from www.nrcresearchpress.com by 210.87.254.40 on 09/05/12
For personal use only.

TABLE 3. Substituent parameters governing carbinyl ^{13}C shieldings in substituted allyl alcohols (in p.p.m.)*

Parameter	A_j	No. of examples
α-Me	3.9±0.4	5
β-Me	1.8±0.4	12
β-Cl	−0.6±0.4	6
β-Br	1.3±0.6	4
β-I	2.6±0.6	4
cis-Me	−6.3±0.5	6
cis-Cl	−3.7±0.5	3
cis-Br	−2.6±0.7	2
cis-I	1.0±0.7	2
Constant, K	61.8	
Standard error	±0.7	

*Positive values denote downfield shifts.

tionship for substituent effects on the carbinyl carbon shieldings the results were analyzed using a linear regression program to furnish the parameters, A_j, listed in Table 3. Using these parameters and expression [1] the shieldings of the ith carbinyl carbon in this series of alcohols can be estimated with an overall precision of ±0.7 p.p.m. The constant term K is expected to be close to the value for allyl alcohol itself although, in fact, it differs from the latter by 1.5 p.p.m. It may be noted that two parameters are required for each *cis*-substituent which, as a first approximation, may perhaps be regarded as a subdivision into polar and steric components. If this view is valid, it is apparent that the largest steric effect is that exerted by a *cis*-β-methyl group.

With the exception of the iodo derivatives, the shieldings of the olefinic carbons in these alcohols are much less sensitive to substituent geometry than those of the sp^3-hybridized carbons. Although the C-2 nuclei show a general tendency to absorb at somewhat higher fields in the *Z*-isomers, the C-3 shieldings follow no consistent pattern. In general, the differences between *Z*- and *E*-isomers are <2 p.p.m. for both centers. In the iodo derivatives, however, the *Z*-C-2 nuclei are shielded by *ca.* 5 p.p.m. relative to their *E*-counterparts while the C-3 nuclei show the opposite behavior. While it is clear that iodine exerts pronounced effects on the shieldings of its neighboring carbons, a rationalization of the trends cannot yet be offered. This problem has been discussed in some detail for other olefinic systems (12, 13) but a satisfactory explanation was not presented.

Since the trends observed for the methyl-substituted systems appeared to be similar to those previously reported for the simpler alkenes it seemed reasonable to examine the available data by linear regression analysis to test for a possible additive correlation. In their initial report on olefinic shieldings in alkenes, Retcofsky and Friedel (6) noted the consistent effects of alkyl substitution on these shieldings but did not attempt a detailed analysis of their somewhat limited data. Because of the appearance of additional data (13–16) and the finding that saturated hydrocarbon shieldings may be correlated through expression [1], we have analyzed the alkene data to obtain the parameters listed in the second column of Table 4; these are analogous to those found for the alkanes by Grant and Paul (2). More parameters are required for the alkenes since the effect of an alkyl substituent is transmitted to the olefinic carbons by two pathways (*a*) entirely through σ-bonds or (*b*) through the π-bond. The two factors for each position relative to the olefinic carbons are distinguished by the superscripts, σ and π, respectively. As in the alkanes (2), the shieldings of branched systems relative to those for linear alkenes show that branching attenuates the substituent effects such that additional parameters are required to correlate the data. Substitution on the double bond is accounted for by the *gem* parameters while the effects of branching at the α-, β-, or γ-sp^3-carbons are the *mult* factors. Finally, a factor for the *cis*-disposition of alkyl groups is required to achieve a reasonable correlation. It may be noted that the constant term K of 122.1 p.p.m. is remarkably close to the observed value (16) for ethylene (δ_C 122.8). Even though the majority of the data employed in this analysis was obtained by rapid-passage techniques for which the precision is *ca.* ±0.3 p.p.m. at best, the standard error of 0.9 p.p.m. for the correlation indicates that the parameters should be helpful for estimations in related systems. As a comparison of the effect of a hydroxymethyl group with that of a methyl substituent on the olefinic shieldings, the data for the methyl-substituted allyl alcohols were included in a second analysis to obtain the results listed in the final column of Table 4. Clearly the alkyl effects

Can. J. Chem. Downloaded from www.nrcresearchpress.com by 210.87.254.40 on 09/05/12
For personal use only.

TABLE 4. Substituent parameters for alkenes and methyl substituted allyl alcohols (in p.p.m.)*

Parameter†	Acyclic alkenes A_j	Acyclic alkenes No. of examples	Alkenes and 2-propen-1-ols A_j	Alkenes and 2-propen-1-ols No. of examples
α	+11.0±0.4	76	+11.3±0.4	85
β^{π}	−7.1±0.4	76	−7.1±0.4	85
β^{σ}	+6.0±0.3	52	+6.0±0.3	52
γ^{π}	−1.9±0.3	52	−1.8±0.3	52
γ^{σ}	−1.0±0.3	30	−1.0±0.3	30
δ^{π}	+1.1±0.3	32	+1.2±0.3	32
δ^{σ}	+0.7±0.4	16	+0.8±0.4	16
ε	+0.2±0.3	26	+0.2±0.3	26
cis-alkyl	−1.2±0.3	37	−1.2±0.3	45
gem^{α}	−4.9±0.5	13	−5.0±0.5	17
gem^{β}	+1.2±0.5	13	+1.4±0.5	17
$mult^{\sigma}$	+1.3±0.6	5	−1.1±0.6	5
$mult^{\pi}$	−0.7±0.6	5	−0.6±0.6	5
α-CH_2OH			+17.4±0.5	7
β^{π}-CH_2OH			−6.7±0.5	7
Constant, K	122.1		121.9	
Standard error	±0.9		±0.9	

*Positive values indicate downfield shifts.
†Superscript indicates mode of transmission to carbon of interest (see text).

TABLE 5. Substituent parameters for 3-halo-2-propen-1-ols (in p.p.m.)*

Substituent	A_j C-2	A_j C-3	No. of examples
CH_2OH	+25.2±1.2	0.0	21
CH_3	8.4±0.9	+11.8±0.9	17
Cl	−6.5±1.2	+5.4±1.2	6
Br	−2.0±1.2	−5.8±1.2	4
I	+6.2±1.2	−33.1±1.2	4
cis-Cl	−0.7±1.0	−1.0±1.0	4
cis-Br	−2.7±1.1	+0.8±1.3	2
cis-I	−4.8±1.1	+3.7±1.1	2
gem(Me, X)	+4.1±1.1	+2.5±1.1	6
Constant, K	114.0		
Standard error	±1.1		

*A positive value indicates a downfield shift.

are similar in the alcohols since the precision of the individual factors as well as that overall is comparable. It is interesting that the β^{π}-effect of the CH_2OH group (−6.7 ±0.5 p.p.m.) is essentially the same as that of the CH_3 group (−7.1 ±0.4 p.p.m.). Thus, except for its enhanced α-effect, the hydroxymethyl group is comparable to a methyl function.

A regression analysis of the olefinic data for the 3-halo-2-propenols was also carried out with the results listed in Table 5. The constant term, 114.0 p.p.m., compares well with the observed value for the β-carbon in allyl alcohol, 113.7 p.p.m. As a result of the choice of a reference point for the analysis, the β^{π}-factor for the CH_2OH group is given as 0.0 p.p.m. but if the value of this factor from the previous analysis is employed (−6.7 p.p.m.) the constant term becomes 120.7 p.p.m. which is in fair agreement with the ethylene shielding. On the latter basis the α-effect of the CH_2OH group is 18.5 p.p.m. compared with the value of 17.4 p.p.m. found

Can. J. Chem. Downloaded from www.nrcresearchpress.com by 210.87.254.40 on 09/05/12
For personal use only.

Can. J. Chem. Downloaded from www.nrcresearchpress.com by 210.87.254.40 on 09/05/12
For personal use only.

from the preceding analysis. In view of the relatively small number of compounds, the overall standard error of ± 1.1 p.p.m. seems remarkably small, and indicates that an additive relation indeed exists.

(c) Origins of the Trends

Although the existence of additive relations for ^{13}C shieldings has been recognized for several years (17) various attempts to place these on a firm theoretical basis have not been particularly successful; a general review and discussion of the various approaches employed is available (18). For linear saturated hydrocarbons Grant and Paul (2) found that the ^{13}C shieldings can be correlated with five parameters representing the effects of replacing a hydrogen atom by a methyl group at the α, β, γ, δ, and ε position with respect to the carbon of interest. For acyclic systems in general, additional parameters are required to account for the attenuation of these five parameters caused by branching along the main chain. The results of the analysis described in the preceding section are discussed in terms of the alkane parameters in the following.

Only one of the factors for the carbinyl shieldings (Table 3) is operative entirely through σ-bonds, the "α-Me" parameter. Since this factor corresponds to the β-effect of alkyl carbons in alkanes it is expected to be positive, *i.e.*, deshielding, but its magnitude is less than half that found for the saturated hydrocarbons (2). A similar attenuation of the effect is apparent from the data for several acyclic alcohols (19) but the effect in the allyl alcohols is even smaller. Clearly, the hydroxyl group strongly attenuates the "β-effect" of alkyl carbons but it is difficult to comment on the trend because the origin of the β-effect is not yet understood.

The remaining factors in Table 3 are analogous to the γ-effects in alkanes and are of special interest because these appear to arise, at least in part, from steric perturbations between closely-lying atoms. In fact, a simple model has been proposed to account for the observed trends in terms of steric polarization arising from nonbonded interactions between neighboring hydrogens (20). Several examples are available to support this idea, on a qualitative basis, since it is generally found that carbons in sterically hindered environments tend to absorb at higher fields than the corresponding nuclei in electronically similar positions but without close neighbors. For example, in methylcyclohexanes axial methyl groups appear at consistently higher fields than their equatorial counterparts (4). In saturated acyclic systems it seems reasonable to assume that the γ-effect arises primarily from interactions in *gauche* rotamers. By virtue of the double bond in the allyl alcohols, however, the 3-substituents are constrained to either eclipsed or *trans* orientations relative to the carbinyl carbon and, as a first approximation, the effects of the substituents may be subdivided into "polar" and "steric" components; in this manner the "*cis*-X" factors may be taken as the "steric" components for each substituent and the "β-X" factors represent the "polar" component. Implicit in this interpretation and the regression analysis is the assumption that the latter factor is independent of configuration. On this basis, it is apparent that, in general, 3-substituents tend to deshield the γ-carbon. Chlorine is the exception to this trend since the β-Cl effect is -0.6 p.p.m., possibly as a result of some contribution of resonance forms such as **3** which would increase the electron density at C-2. Presumably, delocalization of this sort is less likely with the larger halogens such that their inductive effects dominate the electron distribution along the carbon chain. Although it is apparent that *cis*-3-substituents tend to shield the carbinyl carbon relative to the effects of the *trans*-groups, it is difficult to offer even a semi-quantitative assessment of the trend. It is of interest, however, to examine the internuclear separation between the *cis*-groupings. To this end, the coordinates of the *cis*-isomers were computed, using the COORD program of Baird and Dewar (21), to compare the data for different possible rotamers. For example, the interatomic distances between X and the eclipsed H in **4** were obtained as listed in the first column of

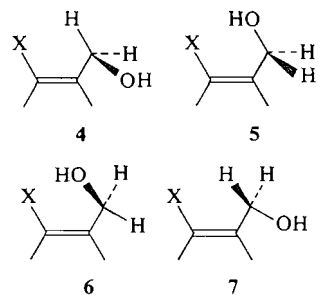

4 **5** **6** **7**

TABLE 6. Interatomic separations of nearest neighbors in *cis*-allyl alcohol rotamers,[a] $XCH{=}CHCH_2OH$ (in Å)

	Rotamer				$(\Sigma r^*)^b$	
	4	5	6			
X	X···H	X···O	X···H	X···O	X···H	X···O
H	2.266	2.241	2.701	2.801	2.40	2.60
Cl	2.331	2.215	2.857	2.910	3.00	3.20
Br	2.378	2.239	2.922	2.963	3.15	3.35
I	2.447	2.283	3.009	3.035	3.35	3.55

[a]Assuming normal bond angles and the following bond distances: C—H, 1.095; =C—H, 1.085; C—O, 1.43; =C—C, 1.51; C=C, 1.335; =C—Cl, 1.719; =C—Br, 1.890; =C—I, 2.092 Å.
[b]Sum of the van der Waals radii.

Table 6. Although only **1** and **2** were considered in the earlier analysis of rotamer distribution in allyl alcohol, the interatomic distances between nearest neighbors in the corresponding rotamers for the series of allyl alcohols, **4** and **5**, are much smaller than the sum of the van der Waals radii for each pair of neighboring atoms indicating that severe repulsive interactions would occur. The separation between nearest neighbors is markedly increased, however, by rotation to **6** as shown by the data in Table 6. Furthermore, the J_{vic} values for the carbinyl protons in **6** are expected to be similar to those in **1**. As noted above the configuration of the 3-halogen atoms has little effect on the observed J_{vic} couplings but, since each is larger than J_{vic} in allyl alcohol itself, it seems unlikely that **7** is a major contributor. For the crotyl alcohols, the proton data indicate that the carbinyl group is oriented as in **4** (or **6**) but with $X = CH_3$ the interatomic separation of nearest neighbors is less than the sum of the van der Waals radii for all orientations of the methyl group, having a maximum

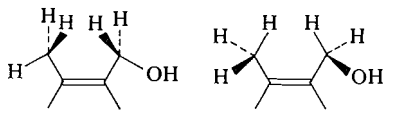

8 **9**

value of 2.317 Å for **8** and a minimum (1.423 Å) in **9**. Clearly the carbinyl group will experience appreciable nonbonded interactions in each. Of the various "*cis*-X" factors in Table 3 that for the methyl group is largest which may be a consequence of the differences in polarizability of the substituents as well as differences in the rotameric equilibria. Because the interatomic distances listed in Table 6 were computed for normal bond lengths and angles, the individual values are less meaningful than the general trend since a slight increase in, for example, the $C_1—C_2—C_3$ angle would increase the separation between nearest neighbors. Evidence for some splaying of this angle in *Z*-2-butene has been presented (22). In addition, the interatomic separation would be affected by a small rotation of the carbinyl group about the $C_1—C_2$ bond. These possibilities coupled with the lack of hard information on the rotamer populations limit one to a purely qualitative assessment of the trends. It would appear, however, that rotamers such as **6** may be important in the alcohols having elipsed methyl and carbinyl groups.

Turning to the olefinic shielding parameters (Table 4) it is immediately apparent that the factors for σ-bonded networks are qualitatively analogous to those found from the saturated hydrocarbon data although the α-effect is somewhat larger and the β-factors smaller. The most striking difference between the two sets of parameters is the *shielding* β-effect through a π-bond. While hyperconjugation may be suggested as a possible cause of the effect, its magnitude (-7.1 p.p.m.) is remarkably large. In fact, it is comparable, in absolute value, to the β-effect in saturated systems ($+9.4$ p.p.m.) which, as noted above, remains unexplained. A similar reversal of the β-effect is found for Cl and Br which in 1-haloalkanes tend to deshield β-carbons by *ca.* 10 p.p.m. (23) whereas their β^{π}-effects are shielding (Table 5). The parameters in Table 5 may be compared with a similar set generated for α,β-unsaturated carboxylic acids and esters (1) to assess the effect of conjugation on the sensitivity of the olefinic shield-

Can. J. Chem. Downloaded from www.nrcresearchpress.com by 210.87.254.40 on 09/05/12
For personal use only.

Can. J. Chem. Downloaded from www.nrcresearchpress.com by 210.87.254.40 on 09/05/12
For personal use only.

ings to polar substituents. In general, the "polar" components as represented by the entries for Cl, Br, and I in Table 5 are more negative than the corresponding values for the conjugated carboxyl derivatives, whereas the "*cis*-X" factors are more positive for the allyl alcohols.

In summary, it would appear that the additive parameters generated from the currently available data will be useful for estimating ^{13}C shieldings in closely-related systems although a detailed theoretical interpretation of the trends is not yet available.

We wish to thank the National Research Council of Canada for operating funds to support this project and Varian Associates, Palo Alto, California for the loan of the probe employed in this study.

1. H. BROUWER and J. B. STOTHERS. Can. J. Chem. **50**, 601 (1972).
2. D. M. GRANT and E. G. PAUL. J. Am. Chem. Soc. **86**, 2984 (1964).
3. G. B. SAVITSKY and K. NAMIKAWA. J. Phys. Chem. **67**, 2430 (1963); **68**, 1956 (1964).
4. D. K. DALLING and D. M. GRANT. J. Am. Chem. Soc. **89**, 6612 (1967).
5. H. J. REICH, M. JAUTELAT, M. T. MESSE, F. J. WEIGERT, and J. D. ROBERTS. J. Am. Chem. Soc. **91**, 7445 (1969).
6. R. A. FRIEDEL and H. L. RETCOFSKY. J. Am. Chem. Soc. **85**, 1300 (1963).
7. J. E. BLACKWOOD, C. L. GLADYS, A. E. PETRARCA, W. H. POWELL, and J. E. RUSH. J. Chem. Soc. D, 30 (1968).
8. A. A. BOTHNER-BY, S. CASTELLANO, S. J. EBERSOLE, and H. GUNTHER. J. Am. Chem. Soc. **88**, 2466 (1966).
9. W. MCFARLANE. Quart. Rev. **23**, 187 (1969).
10. A. N. MURTY and R. F. CURL. J. Chem. Phys. **46**, 4176 (1967).
11. A. A. BOTHNER-BY, S. CASTELLANO, and H. GUNTHER. J. Am. Chem. Soc. **87**, 2439 (1965) and references cited therein.
12. G. B. SAVITSKY and K. NAMIKAWA. J. Phys. Chem. **67**, 2754 (1963).
13. G. E. MACIEL, P. D. ELLIS, J. J. NATTERSTAD, and G. B. SAVITSKY. J. Mag. Res. **1**, 589 (1969).
14. E. LIPPMAA, S. RANG, O. EISEN, and T. PEHK. Eesti NSV Tead. Akad. Toim keem-geol. **16**, 351 (1967).
15. S. RANG, E. LIPPMAA, T. PEHK, and O. EISEN. Eesti NSV Tead. Akad. Toim keem-geol. **17**, 294 (1968).
16. S. W. COLLINS and D. M. GRANT. Unpublished observations.
17. P. C. LAUTERBUR. J. Am. Chem. Soc. **83**, 1838, 1846 (1961).
18. J. B. STOTHERS. Carbon-13 NMR Spectroscopy. Academic Press. New York, N.Y. 1972.
19. J. D. ROBERTS, F. J. WEIGERT, J. I. KROSCHWITZ, and H. J. REICH. J. Am. Chem. Soc. **92**, 1338 (1970).
20. D. M. GRANT and B. V. CHENEY. J. Am. Chem. Soc. **89**, 5315 (1967).
21. Quantum Chemistry Exchange Program. Indiana University No., Bloomington, Ind. 1360.
22. A. ALMENNINGEN, I. M. ANFINSEN, and A. HALLAND. Acta Chem. Scand. **24**, 43 (1970).
23. T. D. BROWN. Ph.D. thesis. University of Utah, 1966.
24. J. B. STOTHERS, I. S. Y. WANG, D. OUCHI, and E. W. WARNHOFF. J. Am. Chem. Soc. **93**, 6702 (1971).
25. M. H. CHISHOLM, H. C. CLARK, L. E. MANZER, and J. B. STOTHERS. Chem. Commun. 1627 (1971).

Rearrangement Studies with ^{14}C. XXXVI. Solvolysis of 1-^{14}C-2-Phenylethyl Tosylate in Aqueous Acetic Acid with or without Added Sodium Azide

C. C. LEE, D. UNGER, AND SHARON VASSIE

Department of Chemistry and Chemical Engineering, University of Saskatchewan, Saskatoon, Saskatchewan

Received September 3, 1971

Solvolyses of 1-^{14}C-2-phenylethyl tosylate (**1**-OTs-1-^{14}C) were carried out in HOAc and H_2O solvent systems with or without added NaN_3. In the absence of added azide ion, the products obtained from a given solvent mixture of HOAc–H_2O, **1**-OAc-^{14}C, and **1**-OH-^{14}C, showed essentially the same extent of rearrangement of the ^{14}C-label from C-1 to -2. In the presence of added azide ion, the rearrangement in the **1**-N_3-^{14}C was less than that found in the **1**-OAc-^{14}C or **1**-OH-^{14}C. The results are interpreted in terms of concurrent direct displacement to give product and product formation from the ethylenephenonium ion.

Les solvolyses du ^{14}C-1 phényl-2 éthyl tosylate (OTs-**1**-^{14}C-1) ont été menées dans des systèmes AcOH–H_2O, avec ou sans addition de NaN_3. En l'absence de l'ion azoture, les produits obtenus à partir d'un mélange donné AcOH–H_2O, c'est-à-dire -OAc-**1** ^{14}C et OH-**1** ^{14}C, montrent essentiellement le même pourcentage de réarrangement du ^{14}C marqué du C-1 au -2. En présence de N_3^-, le réarrangement de N_3-**1** ^{14}C est inférieur à celui trouvé pour OAc-**1** ^{14}C ou OH-**1** ^{14}C. Les résultats sont interprétés par une compétition entre un déplacement direct conduisant au produit et la formation de ce dernier par l'intermédiaire de l'ion éthylène phénonium.

Canadian Journal of Chemistry, **50**, 1371 (1972)

The acetolysis of 1-^{14}C-2-phenylethyl tosylate (**1**-OTs-1-^{14}C) has been extensively investigated (1 and references given therein) and the results have generally been attributed to two competing processes, namely, a direct displacement (solvent assisted or k_s pathway) and reaction via the ethylenephenonium ion (**2**) (anchimerically assisted or k_Δ pathway) (1–3). On the other hand, the work of Sneen and Larsen (4, 5) suggested the possibility that such solvolyses could proceed solely through an ion-pair mechanism. Very recently however, Schleyer and coworkers (6, 7) have utilized the azide ion as a probe for the k_s process and have interpreted their results as in support of the concurrent mechanism. In the present work, solvolyses of **1**-OTs-1-^{14}C in H_2O–HOAc with or without added NaN_3 were carried out, and the isotope position rearrangements in the different products, **1**-OAc-^{14}C, **1**-OH-^{14}C, and **1**-N_3-^{14}C, were ascertained in an attempt to obtain data that might be pertinent in differentiating between the concurrent k_s and k_Δ processes and the single ion-pair mechanism. Moreover, since in all previous solvolytic studies with **1**-OTs-1-^{14}C, only a single product from a given reaction has been analyzed for isotopic scrambling, it is of interest to determine the extents of scrambling in the different products obtained from a solvolysis under conditions that could give rise to more than one product.

The solvolyses of **1**-OTs-1-^{14}C in water and acetic acid solvent systems were carried out by heating under reflux 0.05 mol of the substrate per 100 ml of solvent for 24 h. The products were analyzed and separated by v.p.c. and then oxidized to benzoic acid whose ^{14}C-activity gave the extent of isotope position rearrangement from C-1 to -2. The results are summarized in Table 1. In the case of the solvolysis in pure water, because of the low solubility of the **1**-OTs-1-^{14}C, the reaction mixture was not homogeneous. The unreacted tosylate was recovered and degraded by conversion to **1**-Br-^{14}C followed by oxidation to PhCOOH. It was found that in both runs in water, the recovered tosylate showed only 0.4% rearrangement of the ^{14}C-label from C-1 to -2. Since it is known that ion-pair return is suppressed in a highly ionizing solvent (8), the small amount of rearrangement observed in the recovered tosylate would suggest that ion-pair return in this solvent was not extensive, although the possibility that solvolysis of **1**-OTs-1-^{14}C in H_2O may not involve the symmetrical ethylenephenonium tosylate ion-pair could not be excluded.

The data in Table 1 indicate that when aqueous acetic acid was used as solvent, the resulting **1**-OH-^{14}C and **1**-OAc-^{14}C showed essentially the same amount of isotope position rearrangement. Moreover, the yields of **1**-OH and **1**-OAc were almost directly related to the

Can. J. Chem. Downloaded from www.nrcresearchpress.com by 210.87.254.6 on 09/05/12
For personal use only.

TABLE 1. Data from solvolyses of 1-^{14}C-2-phenylethyl tosylate (**1**-OTs-1-^{14}C) in water and acetic acid solvent systems

Solvent (H_2O:HOAc)*	Product yield (%)†		Specific activity (c.p.m./mmol)				Rearrangement to C-2 (%)	
	1-OH	**1**-OAc	**1**-OH‡	PhCOOH	**1**-OAc§	PhCOOH	**1**-OH	**1**-OAc
100:0¶	39.2		259 000	42 200			16.3	
100:0¶	31.8		450 500	74 600			16.6	
80:20	70.0	21.5	498 200	88 100	63 300	11 300	17.7	17.8
80:20	68.3	24.0	457 100	82 200	74 400	13 100	18.0	17.7
50:50	47.3	52.5	85 900	16 200	160 800	173 200	18.9	18.5
50:50	45.7	55.9	82 200	14 800	29 800	32 300	18.0	18.6
20:80	16.6	81.0	71 800	16 800	143 300	33 300	23.4	23.2
20:80	16.5	81.0	222 400	50 300	769 800	174 300	22.6	22.6
0:100		83.5			518 200	163 500		31.6
0:100		89.2			441 700	137 300		31.1

*By volume.
†Obtained by v.p.c. analysis.
‡Assayed as the α-naphthylurethane.
§Hydrolyzed to **1**-OH and then assayed as the α-naphthylurethane.
¶The **1**-OTs-1-^{14}C was not completely dissolved in these runs.

relative amounts of H_2O and HOAc in the solvent mixture. These findings thus failed to provide evidence for a difference in k_s contributions by the two components of the solvent mixture. A possible explanation of the identical amounts of rearrangement in the two products might be that the products arose from a single intermediate, such as an ion-pair (4, 5). Alternatively, the nucleophilic characters of H_2O and HOAc might not be sufficiently different to cause any observable difference in the k_s contributions, or the ion-pair might be insensitive to the nucleophilic differences between H_2O and HOAc. Since the azide ion is a strong nucleophile and since it has been used as a mechanistic probe for the k_s process (6, 7), the work was extended to include the solvolyses of **1**-OTs-1-^{14}C in HOAc or 50:50 (by volume) H_2O–HOAc in the presence of added NaN_3. The results, recorded in Table 2, showed that the rearrangement of the ^{14}C-label to C-2 was indeed lower in the **1**-N_3-^{14}C than in the **1**-OAc-^{14}C or **1**-OH-^{14}C, in accord with the anticipation of a greater k_s contribution in the formation of **1**-N_3-^{14}C. However, the variations in the extents of rearrangement, shown in both Tables 1 and 2, require further interpretations.

Utilizing the concurrent mechanism (1, 6, 7), when two or more products are formed in a given solvolysis of **1**-OTs-1-^{14}C, the isotope position rearrangement in each product is the composite result of product formation from the phenonium ion **2** and from the direct displacement involving rearranged starting material that resulted from ion-pair returns. As an illustration, Scheme 1 shows the possible processes involved in the acetolysis of **1**-OTs-1-^{14}C in the presence of added azide ion. Analogous to Scheme 1, if the two nucleophiles were HOAc and H_2O, and if the pseudo-first order rates for the k_s processes in the reaction with HOAc and with H_2O, k_A and k_W, were not significantly different, for a solvolysis in a given H_2O–HOAc mixture, there would be no significant difference in the extents of rearrangement of the label in the two products, **1**-OH-^{14}C and **1**-OAc-^{14}C, as was observed (Table 1). It may also be noted from Table 1 that the amount of rearrangement in the products increases with increasing proportions of HOAc in the solvent. This could be attributable to a greater tendency for ion-pair return when the solvent contains more HOAc. It has been pointed out earlier that for solvolysis of **1**-OTs-1-^{14}C in H_2O the recovered starting material was only 0.4% rearranged. On the other hand, Coke and coworkers (1) have found extensive ion-pair returns in the solvolysis of **1**-OTs-1-^{14}C in unbuffered HOAc; for example, after a reaction time of 22 h at 115°, the recovered tosylate was 26.1% rearranged. The greater extent of ion-pair return would result in a greater overall rearrangement since the k_s process would give rise to more rearranged product besides the rearrangement arising from the Fk_Δ process.

For the solvolyses in the presence of added azide ion, the k_s process involving azide ion, or $k_N[N_3^-]$, apparently could compete with $f_N k_\Delta$

Can. J. Chem. Downloaded from www.nrcresearchpress.com by 210.87.254.6 on 09/05/12
For personal use only.

Can. J. Chem. Downloaded from www.nrcresearchpress.com by 210.87.254.6 on 09/05/12
For personal use only.

TABLE 2. Data from solvolyses of 1-^{14}C-2-phenylethyl tosylate (**1**-OTs-1-^{14}C) in HOAc or 50:50 (by volume) H_2O–HOAc with added NaN_3*

	Product yield (%)†			Specific activity (c.p.m./mmol)						Rearrangement to C-2 (%)		
Solvent	**1**-OH	**1**-OAc	**1**-N_3	**1**-OH‡	PhCOOH	**1**-OAc§	PhCOOH	**1**-N_3¶	PhCOOH	**1**-OH	**1**-OAc	**1**-N_3
HOAc		96.4	4.1			303 200	24 600	20 700	1170		8.1	5.7
HOAc		93.7	4.2			286 900	22 900	21 000	1240		8.0	5.9
H_2O–HOAc	39.5	38.3	21.4	123 500	13 000	140 900	13 600	92 100	1840	10.5	9.7	2.0
H_2O–HOAc	35.8	36.3	26.7	106 300	11 300	155 500	14 700	132 100	2540	10.6	9.5	1.9

*The reaction mixture was 0.5 *M* in **1**-OTs-1-^{14}C and 0.7 *M* in NaN_3; the reaction was effected by heating under reflux for 24 h.
†Obtained by isotope dilution calculations.
‡Assayed as the α-naphthylurethane.
§Hydrolyzed to **1**-OH and then assayed as the α-naphthylurethane.
¶Reduced to **1**-NH_2 and then assayed as *N*-phenethyl-*N'*-phenylurea.

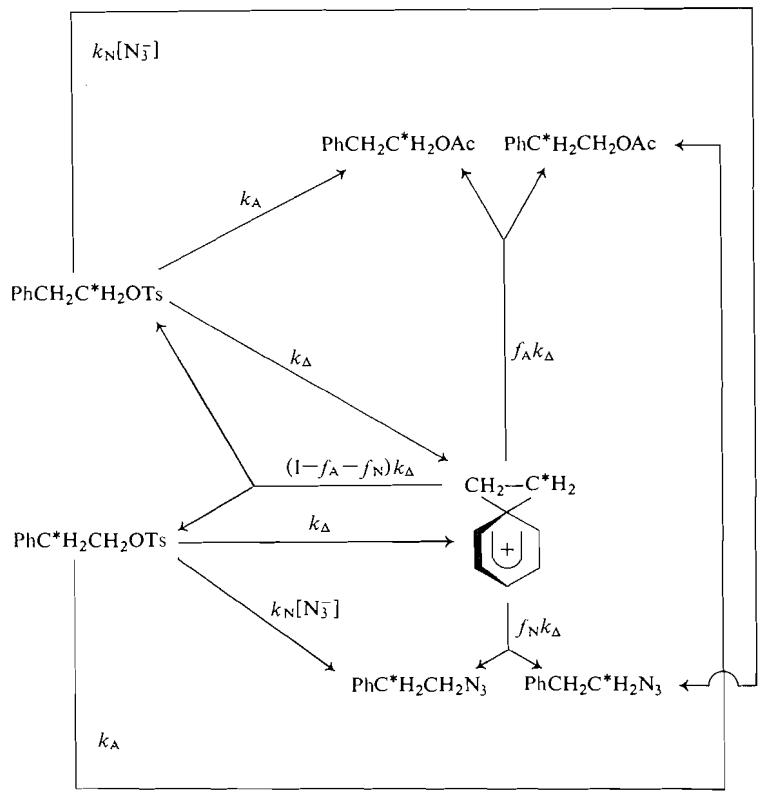

SCHEME 1

more effectively than did k_A in competing with f_Ak_Δ (or k_W in competing with f_Wk_Δ), thus resulting in lesser amounts of isotopic scrambling in the 1-N_3-^{14}C than in the 1-OAc-^{14}C or 1-OH-^{14}C (Table 2). It is seen from Table 2 that for the reaction in HOAc with added azide ion, only about 4% of 1-N_3-^{14}C was formed as product, but this product showed nearly 6% rearrangement of the label from C-1 to -2. On the other hand, solvolysis in 50:50 H_2O–HOAc gave more than 20% 1-N_3-^{14}C as product, which, however, showed only about 2% rearrangement of the isotopic label. The greater yield of 1-N_3-^{14}C in H_2O–HOAc could be the result of a greater availability of the azide ion for displacement reactions, possibly because NaN_3 might be more readily ionized in H_2O–HOAc than in HOAc. The greater amount of rearrangement in the 1-N_3-^{14}C obtained from the solvolysis in HOAc is likely due to more ion-pair returns in HOAc than in H_2O–HOAc; thus the formation of 1-N_3-^{14}C would involve reactions with more extensively rearranged 1-OTs-^{14}C in HOAc than in H_2O–HOAc.

Finally, a comparison of the data in Tables 1 and 2 shows that the presence of added azide ion has the effect of decreasing the extent of rearrangement in the products, 1-OAc-^{14}C and 1-OH-^{14}C. Such differences in the amounts of rearrangement are not unexpected since the overall observed rearrangement should be highly dependent on reaction conditions (1). A factor that might have played an important part in decreasing the rearrangement could be that in the presence of added NaN_3, the reaction rate would likely be enhanced (6, 7), and there would be lesser opportunity for the occurrence of many cycles of ion-pair formation and ion-pair return, thus resulting in a lower amount of rearrangement in the reaction product. Thus all the results obtained in the present work could be explained by, and hence lend further support to, the occurrence of competing k_s and k_Δ processes, involving direct displacement to give product as well

Can. J. Chem. Downloaded from www.nrcresearchpress.com by 210.87.254.6 on 09/05/12
For personal use only.

as product formation from the phenonium ion, as illustrated in Scheme 1.

Experimental

Solvolyses

The solvolyses were carried out by heating under reflux for 24 h 0.5 *M* solutions of **1**-OTs-1-^{14}C in the appropriate solvent (HOAc or H_2O–HOAc). In the experiments with H_2O as solvent, 0.05 mol of **1**-OTs-1-^{14}C in 100 ml of H_2O was heated, but a homogeneous solution was not obtained and much of the tosylate remained as a molten oil during the period of reflux. When the solvolysis was effected in the presence of added NaN_3, the concentration of NaN_3 was 0.7 *M*. In some preliminary work, 0.5 *M* NaN_3 was utilized, but the higher concentration of 0.7 *M* was chosen in order to raise somewhat the yields of **1**-N_3-^{14}C. The following is a typical experiment carried out with added NaN_3.

A solution of 3.452 g (0.0125 mol) of **1**-OTs-1-^{14}C (9) and 1.134 g (0.0175 mol) of NaN_3 in 25 ml of 50:50 (by volume) H_2O–HOAc was heated under reflux for 24 h. Appropriate amounts of ordinary **1**-N_3 (10), **1**-OAc, and **1**-OH were added as carriers. The mixture was then subjected to vacuum distillation (about 20 mm) to remove most of the solvent. Ice-water was then added, followed by neutralization with 5% NaOH solution. The resulting material was continuously extracted for 24 h with ether. The extract was dried over $MgSO_4$, the ether removed, and the products were recovered by preparative v.p.c., using a Pye Automatic Preparative Chromatograph with a 10-ft, 3/8-in. copper column packed with 20% silicone DC 710 on 60/80 mesh Chromosorb W. Knowing the weights of the carriers and the appropriate specific activities, the yields of the three products were obtained by isotope dilution calculations.

In the solvolyses without added NaN_3, instead of isotopic dilution, the yields were determined by v.p.c. analyses using 1-phenylethanol as an internal standard, a preliminary injection of the product mixture from each solvolysis having shown that 1-phenylethanol was not present as a product. An aerograph 200 Chromatograph with flame ionization detector fitted with a 25-ft, 1/8-in. copper column packed with 20% silicone DC 710 on 60/80 mesh Chromosorb W was utilized for the analyses.

Degradations

Samples of the v.p.c. purified **1**-OH-^{14}C, **1**-OAc-^{14}C, and **1**-N_3-^{14}C, diluted further with carriers if necessary, were converted to appropriate solid derivatives for radioactivity assays. **1**-OH-^{14}C was treated with α-naphthyl isocyanate to give the α-naphthylurethane, m.p. 117–118° (lit. (11), m.p. 119°). The **1**-OAc-^{14}C was hydrolyzed by heating with 10% NaOH to give **1**-OH-^{14}C which was, in turn, converted to the α-naphthylurethane. The **1**-N_3-^{14}C was reduced with $LiAlH_4$ to give **1**-NH_2-^{14}C (12) which was converted, by treatment with phenyl isocyanate, to *N*-phenethyl-*N'*-phenylurea, m.p. 153–154° (lit. (13) m.p. 153.5–154.5°).

The remaining portions of the **1**-OH-^{14}C, **1**-OAc-^{14}C, and **1**-N_3-^{14}C, after the derivative preparations, were oxidized directly with alkaline $KMnO_4$ (9) to give benzoic acid, whose radioactivity measured the ^{14}C content at the C-2 position of these products.

The **1**-OTs-^{14}C recovered from the solvolysis in H_2O was converted to **1**-Br-^{14}C by treatment with LiBr in dry acetone (14). The **1**-Br-^{14}C so obtained was also oxidized to benzoic acid (9) in order to ascertain the extent of rearrangement.

The authors wish to express sincere appreciation to Professor P. v. R. Schleyer for valuable comments and for suggesting the use of NaN_3 in this study. The financial assistance given by the National Research Council of Canada is gratefully acknowledged.

1. J. L. Coke, F. E. McFarlane, M. C. Mourning, and M. G. Jones. J. Am. Chem. Soc. **91**, 1154 (1969).
2. P. v. R. Schleyer and C. J. Lancelot. J. Am. Chem. Soc. **91**, 4297 (1969).
3. J. M. Harris, F. L. Schadt, P. v. R. Schleyer, and C. J. Lancelot. J. Am. Chem. Soc. **91**, 7508 (1969).
4. R. A. Sneen and J. W. Larsen. J. Am. Chem. Soc. **91**, 362 (1969).
5. R. A. Sneen and J. W. Larsen. J. Am. Chem. Soc. **91**, 6031 (1969).
6. D. J. Raber, J. M. Harris, R. E. Hall, and P. v. R. Schleyer. J. Am. Chem. Soc. **93**, 4821 (1971).
7. D. J. Raber, J. M. Harris, and P. v. R. Schleyer. J. Am. Chem. Soc. **93**, 4829 (1971).
8. W. G. Young, S. Winstein, and H. L. Goering. J. Am. Chem. Soc. **73**, 1958 (1951).
9. C. C. Lee, G. P. Slater, and J. W. T. Spinks. Can. J. Chem. **35**, 1417 (1957).
10. P. A. S. Smith and B. B. Brown. J. Am. Chem. Soc. **73**, 2435 (1951).
11. M. Frankel and S. Patai. Tables for identification of organic compounds. 2nd ed. The Chemical Rubber Co., Cleveland, 1964. p. 44.
12. J. H. Boyer. J. Am. Chem. Soc. **73**, 5865 (1951).
13. W. H. Carothers and G. A. Jones. J. Am. Chem. Soc. **47**, 3051 (1925).
14. D. P. Thornbill and C. C. Lee. Can. J. Chem. **41**, 2482 (1963).

Can. J. Chem. Downloaded from www.nrcresearchpress.com by 210.87.254.6 on 09/05/12
For personal use only.

Sur la reduction par les hydrures complexes de benzyl-3 camphres

JEAN-CLAUDE RICHER ET ARMAND ROSSI[1]

Département de Chimie, Université de Montréal, B.P. 6128, Montréal, Québec

Reçu le 22 mars 1971[2]

La synthèse de benzyl-3 camphres et les résultats obtenus lors de leur réduction par les hydrures complexes sont rapportés; les divers benzyl-3 bornéols qui en dérivent, ont été isolés et caractérisés.

Benzyl-3 camphors have been prepared and the stereochemistry of their reduction by complex hydrides is reported; the corresponding benzyl-3 borneols have also been prepared and characterized.

Canadian Journal of Chemistry, **50**, 1376 (1972)

Can. J. Chem. Downloaded from www.nrcresearchpress.com by 210.87.254.6 on 09/05/12
For personal use only.

Introduction

Dans le cadre de nos travaux (1, 2) sur les facteurs influençant les quantités relatives d'addition 1:2 *vs.* 1:4, lors de la réduction par les hydrures complexes, de méthylène-3 camphres (**1**), nous avons été amenés à préparer les benzyl-3 camphres **2** et **3**. La stéréochimie de leur réduction a été examinée. La structure et la configuration des produits obtenus ont été établies. Les résultats de cette étude font l'objet de la présente communication.

Partie expérimentale

Les points de fusion sont déterminés sur un "Hot Stage Apparatus" de la compagnie Reichert (Autriche) à l'aide d'un thermomètre calibré. Les indices de rotation sont mesurés à l'aide d'un polarimètre modèle 80 de la compagnie O. C. Rudolph; le benzène est utilisé comme solvant et une moyenne de cinq lectures est effectuée pour chaque mesure. Les spectres i.r. sont pris sur un spectromètre modèle IR-8 de la compagnie Beckman; les spectres des alcools et des cétones sont pris en solution dans le CCl_4. Les spectres u.v. sont mesurés dans l'éthanol à 95% à l'aide d'un appareil Spectronic 505 de la compagnie Bausch et Lomb. Les spectres de masse sont déterminés sur un spectromètre de masse Hitachi, modèle RMU 60, à 70 eV; ces spectres sont rapportés sous forme de schémas dans la thèse de doctorat de M. Armand Rossi. Les spectres r.m.n. sont pris sur des spectromètres Jeol modèle C-60H et 4H-100; à moins d'indications contraires le solvant utilisé est $CDCl_3$ et les déplacements chimiques se réfèrent au TMS utilisé d'une façon interne. Les spectres des produits des différentes séries se ressemblent beaucoup et afin d'éviter de fastidieuses répétitions nous n'avons résumé dans le tableau 1 que les caractéristiques spectrales des dérivés contenant le groupe *p*-méthylphényle. Les analyses par c.p.g. sont effectuées sur un appareil F et M 700 de la compagnie Hewlett Packard. Les colonnes utilisées sont: (A) carbowax 20M 5%, hyprose 2.5%, KOH 2.5% sur chromosorb W 60/80, longueur 16 pd, diamètre 1/8 p; (B) LAC 728 10% sur Diatoport S 80/100, longueur 8 pd, diamètre 1/8 p. Les temps de rétention en minutes de chacun des produits et les conditions expérimentales permettant de faire une analyse complète de tous les produits de chaque série sont résumés dans le tableau 2. Les c.p.g. préparatives sont effectuées sur un appareil Varian du type 90 P. La colonne utilisée de 12 pd de longueur et 1/4 p de diamètre est remplie de chromosorb W 30/60 portant 15% de carbowax 20M, 5% d'hyprose et 5% de KOH.

Benzylidène-3 camphres (1)

Suivant le protocole expérimental suggéré par Haller (3), 5 g de sodium en fil sont ajoutés à une solution de 30 g de camphre dans 300 ml de benzène anhydre; le tout est porté à reflux, sous agitation, pendant 18 h. Après refroidissement de la solution, le sodium n'ayant pas réagi est retiré avec une spatule; 30 g de benzaldéhyde approprié, fraîchement distillé, sont alors ajoutés. Après 4 h d'agitation à la température ambiante, le mélange est versé dans 500 ml d'eau. La solution est extraite au benzène, les fractions benzéniques lavées à l'eau, séchées sur du sulfate de sodium anhydre et évaporées. La recristallisation des benzylidène-3 camphres (**1**) dans l'éthanol absolu conduit aux dérivés désirés avec des rendements variant entre 50 et 70%; leurs caractéristiques physiques et spectrales sont résumées dans le tableau 3.

Benzyl-3 camphres (2 et 3)

D'une manière générale, 3 g de cétone insaturée **1** sont hydrogénés sous pression normale, à la température ambiante, en présence de palladium sur charbon (5%) dans 80 ml d'éthanol absolu. Après avoir éliminé le catalyseur par filtration, l'évaporation du solvant conduit à des mélanges contenant environ 80% de cétone *exo* **2**; ce pourcentage est déterminé en intégrant en r.m.n. le signal du méthyle 8 de l'isomère *exo* par rapport à l'ensemble des méthyles 8, 9 et 10. La chromatographie de 2 g de mélange sur 250 g de gel de silice en utilisant le benzène comme éluant permet d'obtenir la cétone **2***a* à l'état pur; par ailleurs la recristallisation des autres mélanges permet d'isoler les cétones **2***b*, *c*, et *d* à l'état pur; les constantes physiques et les caractéristiques spectrales de ces dérivés sont rapportées dans le tableau 3.

L'équilibration des mélanges d'hydrogénation (ou des

[1]Les résultats rapportés dans cette communication sont extraits en partie de la thèse soumise par M. Armand Rossi en vue de l'obtention du grade de Ph.D., Faculté des Sciences, Université de Montréal, janvier 1971.

[2]Revision reçue le 14 décembre 1971.

Can. J. Chem. Downloaded from www.nrcresearchpress.com by 210.87.254.6 on 09/05/12
For personal use only.

TABLEAU 1. Caractéristiques en r.m.n. du *p*-méthylbenzylidène-3 camphre et de ses produits de réduction*

	CH_3 (10)	CH_3 (9)	CH_3 (8)	CH_3 aromatique	H-2	H-3 CH(A)H(B) benzylique	H_v	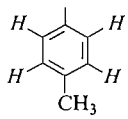 CH_3	*J* (Hz)
1*b*	1.00	1.03	0.81	2.30	—	— — —	7.27s	7.22, 7.43s, d	
2*b**	0.95	0.63	0.77	2.15	—	2.03 2.43 3.40	—	7.00s	H_AH_3 3.0 H_BH_3 10.0 H_AH_B 13.6
3*b*†	0.92	0.65	0.58	2.13	—	massif 2.0–3.5	—	6.97s	—
5*b*	0.99	0.87	0.96	2.35	3.94d	— — —	6.60dd	7.20s	H_2H_v 1.6 H_2H_4 0.6(?)
6*b*	0.96	0.92	0.82	2.35	4.29t	— — —	6.50dd	7.17s	H_2H_v 1.6 H_2H_{6x} 1.6
7*b*	0.93	0.80	1.24	2.32	3.77d	2.07 2.78 3.03	—	7.11s	H_3H_B 7.0 H_2H_3 8.0 H_3H_A 8.0 H_AH_B 14.1
8*b*	0.87	0.83	1.04	2.20	3.22d	massif 2.2–3.3	—	7.10s	H_2H_3 3.6
9*b*	0.83	0.88	0.88	2.36	3.96dd	massif 2.1–3.0	—	7.10s	H_2H_3 9.2 H_2H_{6x} 1.5
10*b*	0.85	0.85	1.05	2.31	3.87dd	massif 2.7–3.0	—	7.10s	H_2H_3 5.1 H_2H_{6x} 1.8

*s, Singulet; d, doublet; dd, doublet dédoublé; t, triplet; H_v, proton vinylique; H_x, proton *exo*.
†Solvant C_6D_6.

TABLEAU 2. Temps de rétention (min) en c.p.g. des différents produits préparés

Conditions	Produit de la série	**1**	**2** et **3**	**5**	**6**	**8**	**10**	**7**	**9**
A-1*	*a*	19	12	25	27	16		21	
A-2	*b*	25	16	31	34	21		25	
A-3	*c*	33	16	39	42	22		30	
A-4	*d*	20	15	32	35	23		29	
B-1†	*a*	—	28	50	58	32	35	38	41
B-2	*b*	—	21	décomposé		24	26	29	32
B-3	*c*	—	23	décomposé		26	29	34	38
B-4	*d*	—	26	42	48	30	33	35	38

*Les conditions A se réfèrent aux résultats obtenus avec la colonne A en maintenant l'injecteur à 230 °C, le détecteur à 250 °C et un débit d'azote de 85 ml/min; la température de la colonne étant (1) de 185 °C; (2) de 180 °C; (4) 175 °C, et (3) la température de la colonne est augmentée de 1 °C/min jusqu'à 210 °C en partant de 180 °C.
†Les conditions B se réfèrent aux résultats obtenus avec la colonne B en maintenant l'injecteur à 220 °C, le détecteur à 240 °C et un débit d'azote de 65 ml/min; la température de la colonne étant (1) de 180 °C; (2) de 190 °C; (3) de 210 °C et (4) de 180 °C.

cétones **2** pures) est effectuée en chauffant à 80 °C une solution contenant 2 g de méthylate de sodium et 2 g de cétone à équilibrer dans 80 ml de méthanol pendant 24 h. L'extraction des produits à la manière habituelle conduit avec des rendements pratiquement quantitatifs à des mélanges renfermant 7% de cétone *exo* **2** et 93% de cétone *endo* **3**. La chromatographie sur colonne de gel de silice permet d'isoler les cétones **3***a* et *d* pures par r.m.n.; il suffit de recristalliser les mélanges d'équilibration dans l'éther de pétrole pour obtenir les cétones **3***b* et *c* à l'état pur; les constantes physiques et les caractéristiques spectrales de ces dérivés sont résumées dans le tableau 3.

*p-Méthylbenzyl-3 endo camphre-3d (**4**)*

A 300 mg de *p*-méthylbenzyl-3 *exo* camphre (**2***b*) en solution dans 5 ml de méthanol-*O-d* sont ajoutés 300 mg de méthylate de sodium. Après agitation pendant 24 h à 80 °C, le mélange est hydrolysé avec 5 ml de D_2O. Le tout est extrait à la manière habituelle; après recristallisation dans l'éther de pétrole, le dérivé **4** est obtenu. Son point de fusion est

Can. J. Chem. Downloaded from www.nrcresearchpress.com by 210.87.254.6 on 09/05/12
For personal use only.

TABLEAU 3. Constantes physiques et caractéristiques spectrales des composés préparés

Produits	p.f. (°C)	$[\alpha]_D^{24}$	concentration (g/100 ml)	i.r. (ν cm^{-1}) C=O	C=C	C—O	OH non lié	OH lié	u.v. λ_{max}(nm) (ε)	p.f. (°C) *p*-nitrobenzoates	Spectre de masse M^+
1*a*	97[a,b]	+412[c,d]	1.350	1730	1640	—	—	—	291(18 800), 222(7750)	—	240
b	98.5–99.5[e]	+429[f]	1.615	1727	1642	—	—	—	301(20 500), 226(7300)	—	254
c	124–126[g]	+441[h]	1.680	1725	1640	—	—	—	317(20 500), 230(7600)	—	270
d	104–105	+369	4.035	1730	1650	—	—	—	286(17 400), 221(6800)	—	258
2*a*	huile	+18.5	5.975	1740	1606	—	—	—	—	—	242
b	73–75	+20.9	1.245	1740	1613	—	—	—	—	—	256
c	51–53	+28.0	1.462	1739	1612	—	—	—	—	—	272
d	53–54	+17.9	2.425	1740	1616	—	—	—	—	—	260
3*a*	huile	+86.2[i]	4.870	1739	1612	—	—	—	—	—	242
b	48–50	+77.4	1.770	1738	1612	—	—	—	—	—	256
c	70–71[j]	+76.5[i]	1.424	1737	1612	—	—	—	—	—	272
d	huile	+71.5	1.725	1740	1614	—	—	—	—	—	260
5*a*	93–94[k]	+333[k]	1.177	—	—	1065	3640	3480	255(15 450)	169–171	242
b	105–106	+335	0.740	—	—	1065	3625	3470	255(18 500)	158–160	256
c	75–77	+338	1.830	—	1608	1064	3640	3480	261(17 700)	123–125	272
d	107–108	+328	1.600	—	1612	1067	3635	3490	252(13 500)	138	260
6*a*	69–70[l]	+355[l]	1.375	—	—	1059	3690	3420	256(18 400)	98–99	242
b	huile	+346	0.800	—	—	1057	3630	3400	260(18 600)	73–75	256
c	105	+356	1.515	—	1609	1060	3620	3450	264(20 000)	129	272
d	60–61	+343	1.070	—	1607	1057	3620	3400	256(13 300)	60–61	260
7*a*	huile	+28.3	1.840	—	1605	1045	3650	3500	—	96–97	244
b	huile	+28.2	1.133	—	—	1045	3610	3510	—	103–105	258
c	89	+30.8	1.850	—	1610	1040	3660	3550	—	80–82	274
d	huile	+30.8	2.365	—	1610	1045	3660	3520	—	132	262

Continué

Can. J. Chem. Downloaded from www.nrcresearchpress.com by 210.87.254.6 on 09/05/12
For personal use only.

TABLEAU 3. (*Conclu*)

Produits	p.f. (°C)	$[\alpha]_D^{24}$	concentration (g/100 ml)	i.r. (ν cm^{-1}) C=O	C=C	C—O	OH non lié	OH lié	u.v. λ_{max} (nm) (ε)	p.f. (°C) *p*-nitrobenzoates	Spectre de masse M+
8*a*	huile	+10.8	1.330	—	—	1067	3630	3490	—	108–109	244
b	64–65	+10.6	1.125	—	—	1068	3645	3490	—	120–121	258
c	51–52	+5.9	1.415	—	—	1069	3660	3500	—	109–110	274
d	45–46	+14.6	1.845	—	1615	1070	3640	3490	—	92–93	262
9*a*	47–48	+28.2	2.195	—	1612	1055	3640	3515	—	79–81	244
b	huile	+27.8	1.598	—	1611	1055	3640	3505	—	92–93	258
c	46–47	+19.4	2.598	—	1610	1052	3640	3505	—	82–85	274
d	39–40	+15.4	1.618	—	1613	1055	3647	3500	—	84–85	262
10*a*	huile	+49.4	1.800	—	1610	1050	3635	3490	—	92–93	244
b	69–71	+30.5	1.180	—	1610	1050	3640	3500	—	102–103	258
c	40–41	+38.4	1.170	—	1611	1045	3635	3490	—	100–102	274
d	46–47	+40.8	1.320	—	1611	1050	3640	3480	—	93–94	262

[a]Littérature (3), 95–96 °C.
[b]Littérature (5), 98–98.5 °C.
[c]Littérature (6), +418°.
[d]Littérature (7), +406°.
[e]Littérature (8), 98 °C.
[f]Littérature (9), +458°.
[g]Littérature (10), 125 °C.
[h]Littérature (7), +456°.
[i]Littérature (11), p.f., 51–52 °C et $[\alpha]_D$ +97°.
[j]Littérature (10), p.f., 71 °C et $[\alpha]_D$ +85°.
[k]Littérature (6 et 4), p.f., 92–93.5 °C et $[\alpha]_D$ +368°.
[l]Littérature (6), p.f., 68–69 °C et $[\alpha]_D$ +338°.

TABLEAU 4. Réduction des *p*-méthylbenzyl-3 camphres (**2***b* et **3***b*) par les hydrures complexes

Agent réducteur	Réduction de **2***b*				Réduction de **3***b*			
	8*b*	**10***b*	**7***b*	**9***b*	**8***b*	**10***b*	**7***b*	**9***b*
$LiAlH_4/Et_2O$*	1.9	2.0	96.1	—	67.2	—	3.6	29.2
$LiAl(OtBu)_3H/THF$†	2.8	1.4	95.8	—	62.6	—	3.9	33.5
LDPA/Pyridine‡	6.4	4.1	65.5	24.0	18.6	—	4.5	76.9
$NaBH_4$/*iso*-PrOH§	33.3	4.6	30.6	31.5	44.2	3.0	14.6	38.2
$NaBH_4$/diglyme‖	11.4	6.0	70.8	11.8	43.2	0.8	11.6	44.4
$NaBH_4$/diglyme/2% H_2O¶	1.6	4.5	92.7	1.2	48.1	—	3.8	48.1

*Voir réf. 12; réaction effectuée au reflux de l'éther et complète après 4 h.
†Voir réf. 13; réaction effectuée à 70 °C et complète après 6 h.
‡Voir réf. 14; réaction effectuée à 35 °C, après 72 h, environ 15% de la cétone n'a pas réagi.
§Voir réf. 15; réaction effectuée à 70 °C et complète après 48 h.
‖Voir réf. 16; réaction effectuée à 70 °C, après 48 h environ 70% de la cétone n'a pas réagi.
¶Voir réf. 16; réaction effectuée à 70 °C, complète après 48 h.

identique à celui du dérivé **3***b*. La spectrométrie de masse révèle que le produit est monodeutéré à 87%. Les signaux dus au $-CH_2$ benzylique apparaissent, dans le spectre r.m.n., sous la forme de deux doublets ($J = 14.4$ Hz) à 2.37 et 3.30 p.p.m.

*Benzylidène-3 isobornéols (**5**) et bornéols (**6**)*

D'une manière générale, ces dérivés sont obtenus de la façon suivante: dans un ballon de 100 ml surmonté d'une colonne Vigreux, contenant 2.5 g de cétone **1** dans 60 ml d'alcool isopropylique, sont ajoutés 12 g d'isopropylate d'aluminium. Le mélange est porté à un léger reflux de façon à ce que l'acétone formée puisse distiller au fur et à mesure de sa formation. Lorsqu'il ne se forme plus d'acétone (1 à 4 jours), le mélange réactionnel est jeté dans 300 ml d'une solution de soude à 5%. Les produits sont alors extraits avec des rendements pratiquement quantitatifs. La chromatographie sur gel de silice en utilisant le benzène comme éluant permet d'isoler les alcools insaturés **5** et **6** à l'état pur. Les constantes physiques et les caractéristiques spectrales de ces alcools sont résumées dans le tableau 3.

*Benzyl-3 bornéols (**7**, **8**, **9** et **10**)*

*Benzyl-3 exo isobornéols (**7**)*

Ces alcools sont obtenus par le procédé suivant: 1.5 g de cétone **2** en solution dans 20 ml d'éther anhydre sont ajoutés à une suspension de 1 g de $LiAlH_4$ dans 30 ml d'éther anhydre. Après un reflux de 4 h, l'excès d'hydrure est détruit en ajoutant 50 ml d'une solution de soude à 5%. Les produits extraits à la manière habituelle renferment environ 96% des alcools désirés **7** et 4% de l'épimère **8**. La chromatographie sur gel de silice permet d'isoler les dérivés **7***a*, *b*, et *d* à l'état pur; il suffit de recristalliser dans l'éther de pétrole les produits bruts de la réaction pour récupérer l'acool **7***c* chromatographiquement pur. Les constantes physiques et les caractéristiques spectrales de ces alcools sont résumées dans le tableau 3.

*Benzyl-3 endo isobornéols (**8**) et bornéols (**9**)*

La réduction des benzyl-3 *endo* camphres (**3**) par $LiAlH_4$ suivant le mode opératoire donné précédemment conduit à des mélanges réactionnels contenant environ 67% des alcools **8**, 29% des alcools **9**, et 4% des alcools **7**. La chromatographie de ces mélanges sur colonne de gel de silice, en utilisant le benzène comme éluant, permet d'isoler les alcools **8***a*, **8***d*, **9***a*, et **9***d* à l'état pur. Les alcools **8***b*, **8***c*, **9***b*, et **9***c* à l'état pur sont obtenus par c.p.g. préparative. Les constantes physiques et les caractéristiques spectrales des alcools **8** et **9** sont résumées dans le tableau 3.

*Benzyl-3 exo bornéols (**10**)*

L'hydrogénation de 600 mg de benzylidène-3 bornéols (**6**) (ou isobornéols **5**) à pression normale, à la température ambiante et en présence de palladium à 5% sur charbon dans 40 ml d'éthanol absolu conduit à des mélanges contenant 54% de benzyl-3 *exo* bornéols (**10**) et 46% de benzyl-3 *endo* bornéols (**9**) (ou 85% de benzyl-3 *exo* isobornéols **7** et 15% de benzyl-3 *endo* isobornéols **8**).

La c.p.g. préparative permet de séparer quantitativement les deux isomères et d'isoler les bornéols **10** à l'état pur. Les constantes physiques et les caractéristiques spectrales de ces alcools **10** sont rapportées dans le tableau 3.

*Stéréochimie de la réduction des p-méthylbenzyl-3 exo (**2***b*) et endo (**3***b*) camphres par les hydrures complexes*

Considérations générales. Les techniques opératoires utilisées pour ces réductions ont fait l'objet de nombreuses descriptions. Le tableau 4 résume les résultats obtenus. Les références appropriées à ces techniques y sont rapportées.

Réduction par une solution de L.D.P.A. dans la pyridine

La solution de tétrakis-(*N*-déhydropyridil) aluminate de lithium (L.D.P.A.) est préparée d'après la méthode décrite par Lansbury et Peterson (14) (1 g de $LiAlH_4$/100 ml de pyridine). Dans un flacon fermé hermétiquement par un bouchon de caoutchouc et renfermant 128 mg de cétone à réduire en solution dans 5 ml de pyridine sont introduits, à l'aide d'une seringue, 20 ml de la solution de L.D.P.A. (environ 5 mmol). Le mélange est maintenu à 35 °C pendant 72 h. L'hydrolyse est effectuée avec une solution d'acide chlorhydrique très diluée (2%). L'extraction à l'éther est effectuée à la manière habituelle (rendement 80–90%). Les mélanges réactionnels sont examinés par c.p.g.

Discussion des résultats

Configurations des produits obtenus

Les spectres r.m.n. des benzylidène-3 camphres (**1**) ne présentent qu'un seul signal (7.28–7.10 p.p.m.) correspondant à un proton vinylique. Celui-ci apparaît à des champs relativement

Can. J. Chem. Downloaded from www.nrcresearchpress.com by 210.87.254.6 on 09/05/12
For personal use only.

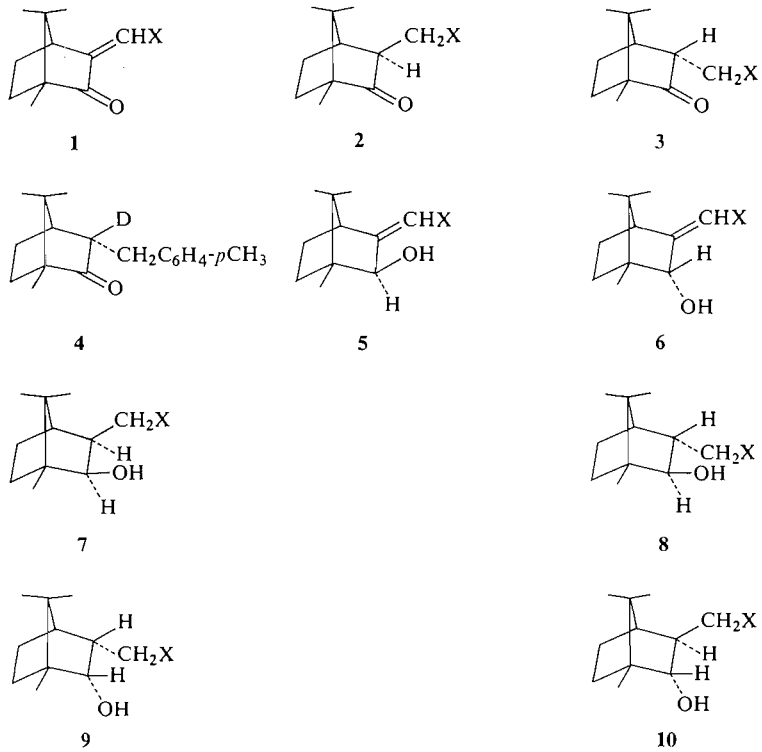

a X = C_6H_5— *c* X = *p*-$CH_3OC_6H_4$—
b X = *p*-$CH_3C_6H_4$— *d* X = *m*-FC_6H_4—

faibles, dû au déblindage par le groupement carbonyle, confirmant ainsi, en accord avec les travaux de Sotiropoulos (17), la configuration *trans* de ces dérivés.

Il est admis généralement (18) que dans la série du camphre, les composés *endo* sont plus stables que les composés *exo*. Les configurations des benzyl-3 *exo* (**2**) et *endo* (**3**) camphres ont donc été attribuées en se basant sur les résultats obtenus lors de leur mise à l'équilibre en milieu alcalin (*exo*/*endo* = 7/93). En r.m.n., la constante de couplage nulle entre les protons H-3 et -4 confirme l'attribution faite aux dérivés *exo* **2**, en accord avec les valeurs déjà rapportées (19) pour des systèmes comportant un proton *endo* en position 3. Les spectres des cétones *endo* **3** sont plus complexes à analyser, la constante de couplage entre H-3 et -4 n'est plus égale à zéro et il n'est pas exclu que le proton en position 3 soit également couplé avec celui en position 5-*exo* dans un système en W(20). De l'étude des spectres r.m.n. des cétones *exo* **2** et *endo* **3**, il ressort également que les chaînes benzyliques existent dans des conformations privilégiées. En effet, le proton en position 3 et les deux protons benzyliques des benzyl-3 *exo* camphres (**2**) apparaissent sous la forme d'un système ABX qui a été analysé et pour lequel $\delta_A = 2.43$, $\delta_B = 2.03$, et $\delta_X = 3.40$ p.p.m. avec $J_{AB} = 10.0$, $J_{AX} = 13.6$, et $J_{BX} = 3.0$ Hz. Les déplacements chimiques très différents pour les protons H_A et H_X et les constantes de couplage observées seraient compatibles avec l'existence de conformations privilégiées **A** *ou* **B**.

Pour des dérivés de la benzyl-2 hydrindanone, présentant des spectres r.m.n. comparables à ceux de nos produits, Imbach *et al.* propose (21)

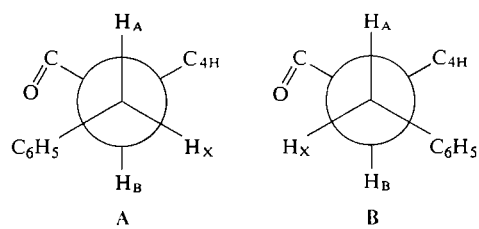

A B

Can. J. Chem. Downloaded from www.nrcresearchpress.com by 210.87.254.6 on 09/05/12
For personal use only.

TABLEAU 5. Constantes de couplage entre H-2 et -3 pour quelques bornanols-2 substitués en position 3

Stéréochimie	OH-2 Benzyl-3	OH-2 Amino-3	OH-2 OH-3‡	Valeurs théoriques‡
-2 *exo* -3 *exo*	8.0	7.8*	7.7	8.2
-2 *exo* -3 *endo*	3.6	3.4*	2.3	2.4
-2 *endo* -3 *endo*	9.2	9.0*	9.0	8.2
-2 *endo* -3 *exo*	5.1	3.6†	2.2	2.4

*Voir réf. 27.
†Voir réf. 28.
‡Voir réf. 29.

la conformation **A**. En considérant le fait que le proton H_X apparaît à un champ plus bas que H_A, nous sommes portés à croire, à la suite de l'interprétation de Mathieson (22) qu'il est plus approprié de suggérer que les benzyl-3 *exo* camphres (**2**) existent sous la conformation **B**. Les protons benzyliques du *p*-méthylbenzyl-3 *endo* camphre-3*d* (**4**) apparaissent respectivement à 2.37 (H_A) et 3.30 p.p.m. (H_B) avec $J_{AB} = 14.4$ Hz; nous pouvons donc considérer que les cétones **3** et **4** existent préférentiellement sous la conformation **C**. Il faut noter que dans chacune de ces confor-

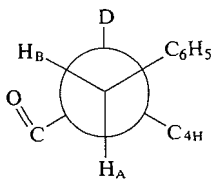

C

mations, considérées comme préférentielles sur la base de la r.m.n., le groupe phényle se trouve toujours dans la position la moins encombrée stériquement, c'est-à-dire entre H-3 (ou D) et C_4H.

Les configurations des benzylidène-3 isobornéols (**5**) et bornéols (**6**) découlent de leur mode de préparation (23), si on considère que dans des conditions de formations équilibrantes les bornéols **6** sont obtenus de façon prépondérante. La stéréochimie de ces composés est confirmée par l'étude en r.m.n. de la position et du type de couplage des protons carbinoliques (C*H*OH). Flautt et Erman (24) ont constaté que le signal dû à un tel proton est localisé à des champs plus forts pour les isomères *exo* (proton *endo*). Les benzylidène-3 isobornéols (**5**) (proton *endo*) et bornéols (**6**) (proton *exo*) donnent respectivement pour le proton en position 2 un signal à 3.95 et 4.31 p.p.m. Les couplages auxquels sont soumis de tels protons caractérisent également l'environnement stéréochimique dans lequel ils se trouvent. Les protons *endo* (H_{2n}) des benzylidènes-3 isobornéols (**5**) sont couplés uniquement avec le proton vinylique (H_v) ($J_{H_{2n}H_v} = 1.6$ Hz) et se présentent sous la forme de doublets, alors que pour les benzylidène-3 bornéols (**6**) les mêmes protons en position *exo* (H_{2x}) sont de plus couplés possiblement à longue distance (couplage en W) (25) avec le proton en position 6 *exo* ($J_{H_{2x}H_v} = 1.6$, $J_{H_{2x}H_{6x}} = 1.6$ Hz) et apparaissent sous forme de triplets assez mal définis.

Enfin, bien que les configurations relatives des quatre benzyl-3 bornéols (**7**–**10**) découlent directement de leur mode de formation, c'est essentiellement la comparaison, en r.m.n., des constantes de couplage entre les protons H-2 et -3 et les valeurs données par Karplus (26) pour les dérivés de l'éthane qui permet d'attribuer une configuration aux diastéréoisomères de bornanes substitués. Les constantes de couplage entre les protons H-2 et -3 de quelques bornéols substitués en position 3 sont résumés dans le tableau 5. Il est intéressant de noter que cette constante de couplage augmente d'une façon plus ou moins prononcée avec l'encombrement du substituant en position 3: —OH, —NH_2, et —$CH_2C_6H_5$. L'introduction du groupe hydroxyle en position 2 *exo* ou benzyle en position 3 *exo*, pour les dérivés étudiés, peut être la cause de certaines distorsions dans la molécule, faisant varier ainsi les valeurs des angles dièdres, par rapport à celles observées dans un bornane non substitué et expliquer les écarts observés pour les constantes de couplage entre les protons H-2 et -3 et les valeurs théoriques attendues (29). Conformément aux remarques faites précédemment pour les benzylidène-3 bornéols (**5** et **6**) le signal relatif au proton 2 *endo* apparaît à des

Can. J. Chem. Downloaded from www.nrcresearchpress.com by 210.87.254.6 on 09/05/12
For personal use only.

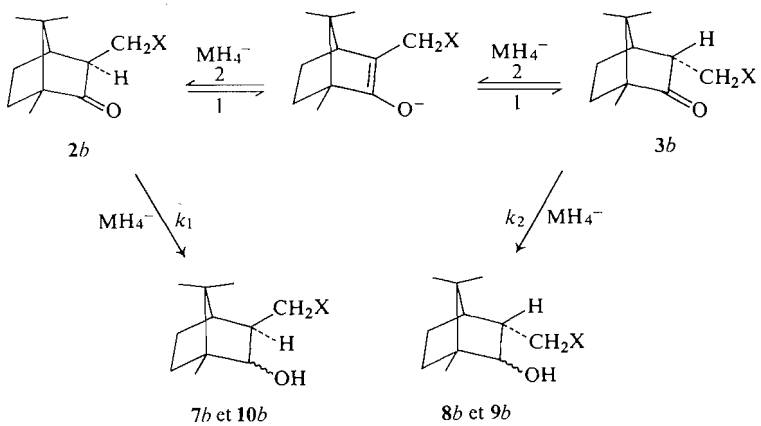

SCHÉMA 1

champs plus forts que celui correspondant au proton 2 *exo*; de plus, des couplages à longue distance entre les protons H(-2 *exo*) et H(-6 *exo*) de l'ordre de 1.5 Hz sont observés pour les dérivés **9** et **10**.

Stéréochimie de la réduction des p-méthylbenzyl-3 camphres (2b et 3b)

Un premier aspect des données rapportées dans le tableau 4 mérite des commentaires. La réduction des cétones **2***b* et **3***b* par le L.D.P.A. ou par $NaBH_4$ conduit à des quantités appréciables de produits provenant d'une réduction de la cétone épimère de celle mise en réaction. Ces résultats sont à rapprocher de ceux d'Erman et Flautt (30) qui observent, au cours de la réduction par $NaBH_4$ dans le méthanol des *p*-anisyl-2 *endo* et *exo* épicamphres, uniquement la formation de *p*-anisyl-2 *endo* épiisobornéol. Cette tendance à l'épimérisation, observée au cours de ces réductions ne semble pas générale pour toutes les cétones bicycliques substituées en α du groupe carbonyle puisqu'elle n'est pas observée lors de la réduction des méthyl-3 norbornanones (31). Les résultats obtenus au cours du présent travail s'accommodent bien avec le schéma 1 qui tient compte des faits suivants: (*a*) le pourcentage relatif des alcools isomères **7***b* *vs.* **10***b* formés au cours des réductions des deux cétones **2***b* et **3***b* reste le même; (*b*) la même remarque est valable pour le pourcentage relatif des alcools isomères **8***b* *vs.* **9***b*; (*c*) la proportion importante d'isomérisation (17.6%) obtenue pour la réduction par $NaBH_4$ dans le propanol-2 du *p*-méthylbenzyl-3 *endo* camphre (**3***b*) comparée au résultat de la mise à l'équilibre des deux cétones isomères **2***b* et **3***b* (*exo*/*endo* = 7/93 suggère que la réduction de l'isomère **2***b*, pour lequel le groupe carbonyle reste facilement accessible par la face *endo* de la molécule complètement dégagée, se fait plus rapidement que celle du dérivé **3***b*, déplaçant l'équilibre entre les deux cétones vers la formation du dérivé *exo* **2***b*.

D'une façon plus générale, la stéréochimie de la réduction de cétones cycliques a fait l'objet de nombreux travaux et est maintenant essentiellement rationalisée en fonction d'une théorie complètement stérique (32) ou de la variante proposée par Cherest et Felkin (33) faisant intervenir des effets de torsions. Appliqués aux dérivés du camphre, ces concepts permettent de prévoir que les réductions conduiront de façon prépondérante aux alcools *exo* (23, 31, 34–37). L'examen des résultats rapportés dans le tableau 6 permet de réaliser que l'introduction du groupe *p*-méthylbenzyle *exo* en position 3 de la cétone **2***b* ne fait qu'augmenter la stéréospécificité de la réaction comparée aux résultats obtenus lors de la réduction du camphre et de l'apocamphre. En accord avec ces théories, l'introduction d'un groupe *p*-méthylbenzyle-3-*endo* dans la cétone **3***b* ralentit l'attaque de l'hydrure s'approchant par la face *endo* du carbonyle en position 2. Le pourcentage de réduction par la face *exo* se trouve

Can. J. Chem. Downloaded from www.nrcresearchpress.com by 210.87.254.6 on 09/05/12
For personal use only.

TABLEAU 6. Réduction de quelques cétones bicycliques*

Cétone réduite	$LiAlH_4$ éther	$LiAlHO(t\text{-}Bu)_3$ THF	$NaBH_4$/ *iso*-PrOH	$NaBH_4$/ diglyme	$NaBH_4$/ diglyme 2% H_2O	LDPA/ pyridine
Camphre	92†	93†	86‡	—	—	62.5§
Apocamphre	90‖	—	78.4¶	—	—	—
2*b*	98**	98.7**	87**	92**	95**	92**
3*b*	69.7††	65.1††	52††	49††	50††	19.5††

*Les résultats rapportés dans ce tableau expriment le pourcentage normalisé d'alcool *exo* au cours des réductions indiquées.
†Valeurs tirées de la réf. 34.
‡Valeur tirée de la réf. 37.
§Valeur trouvée au cours du présent travail.
‖Valeur tirée de la réf. 36.
¶Valeur tirée de la réf. 35.
Valeurs tirées du tableau 4; elles expriment des pourcentages normalisés d'alcools **7*b* par rapport à **10***b*.
††Valeurs tirées du tableau 4; elles expriment des pourcentages normalisés d'alcools **8***b* par rapport à **9***b*.

ainsi considérablement augmenté, ce qui explique la proportion croissante d'alcool *endo*.

Enfin, les résultats obtenus lors des réductions par le L.D.P.A. ont retenu notre attention. En effet, Lansbury (14) rapporte qu'après avoir laissé le camphre en contact avec une solution de L.D.P.A. pendant 5 jours, 98% de cétone n'ayant pas réagi sont récupérés. La même réaction reprise dans des conditions identiques à celles décrites par ces auteurs nous conduit avec un rendement de 90% à un mélange formé de 62.5% d'isobornéol et 37.5% de bornéol. Cette différence de réactivité reste inexpliquée. Alors qu'il est probable que la présence du groupe *p*-méthylbenzyle en position 3 favorise l'action du L.D.P.A. sur les cétones 2 et 3 conformément aux résultats obtenus pour la réduction de benzophénones dans des conditions identiques (14). Les pourcentages élevés de bornéols (37.5%) et de *p*-méthylbenzyle-3-*endo* bornéol (**9***b*, environ 80%) obtenus respectivement pour les réductions du camphre et du *p*-méthylbenzyle-3-*endo* camphre (**3***b*) s'expliquent si nous admettons à la suite de Lansbury et MacLeay (38) que le L.D.P.A. est moins soumis à l'encombrement stérique des réactifs que les autres hydrures; son comportement serait intermédiaire entre celui de $NaBH_4$ et du produit d'addition du butyllithium sur la pyridine (39).

Les auteurs remercient vivement le Conseil National de Recherches du Canada, le Ministère de l'Education du Québec, et le Conseil des Arts du Canada pour l'aide financière apportée sous forme d'octroi et de bourses.

1. J. C. RICHER et Y. PÉPIN. Can. J. Chem. **48**, 1226 (1970).
2. J. C. RICHER et C. LAMARRE. Can. J. Chem. **45**, 1581 (1967).
3. A. HALLER. C. R. Acad. Sc. Paris, **113**, 22 (1891).
4. A. HALLER. C. R. Acad. Sc. Paris, **112**, 1270 (1891).
5. P. SCHENONE, G. MINARDI, et G. BIGNARDI. Il Farm. Ed. Sc. **23**, 983 (1968).
6. J. KOSSANYI, B. FURTH, et J. P. MORIZUR. Tetrahedron, **26**, 395 (1970).
7. A. HALLER et R. LUCAS. C. R. Acad. Sc. Paris, **180**, 1803 (1925).
8. A. HALLER et BAUER. C.R. Acad. Sc. Paris, **148**, 1490 (1909).
9. A. HALLER. C.R. Acad. Sc. Paris, **154**, 742 (1912).
10. A. HALLER et P. T. MULLER. C.R. Acad. Sc. Paris, **128**, 1370 (1899).
11. A. HALLER. C.R. Acad. Sc. Paris, **112**, 1490 (1891).
12. D. S. NOYCE et L. J. DOLBY. J. Org. Chem. **26**, 3619 (1961).
13. H. C. BROWN et R. F. MCFARLIN. J. Am. Chem. Soc. **78**, 252 (1956).
14. P. T. LANSBURY et J. O. PETERSON. J. Am. Chem. Soc. **85**, 2236 (1963).
15. D. M. S. WHEELER et J. W. HUFFMAN. Experientia, **16**, 516 (1960).
16. W. R. JACKSON et A. ZURGIYAH. J. Chem. Soc. 5280 (1965).
17. J. SOTIROPOULOS. Thèse Doctorat, Faculté des Sciences de Toulouse, France.
18. C. F. WILCOX JR., M. SEXTON, et M. F. WILCOX. J. Org. Chem. **28**, 1079 (1963).
19. J. PARELLO, C. BERTRAND, et P. BEDOS. Bull. Soc. Chim. France, 5034 (1968).
20. A. RASSAT, C. W. JEFFORD, J. M. LEHN, et B. WAEGELL. Tetrahedron Lett. 233 (1964).
21. J. L. IMBACH, G. MAURY, et N. H. CROMWELL. Bull. Soc. Chim. France, 3389 (1969).
22. D. W. MATHIESON. Nuclear magnetic resonance for organic chemists. Academic Press, 1967, p. 32.
23. H. KRIEGER, K. MANNINEN, et J. PAASIVIRTA. Suomen Kem. **B39**, 8, 1966.
24. T. J. FLAUTT et W. F. ERMAN. J. Am. Chem. Soc. **85**, 3212 (1963).
25. J. C. DAVIS et T. VAN AUKEN. J. Am. Chem. Soc. **87**, 3900 (1965).
26. M. KARPLUS. J. Chem. Phys. **30**, 11 (1959).
27. A. H. BECKETT, N. T. LAN, et G. R. MCDONOUGH. Tetrahedron, **25**, 5693 (1969).

Can. J. Chem. Downloaded from www.nrcresearchpress.com by 210.87.254.6 on 09/05/12
For personal use only.

28. S. THOREN. Acta Chem. Scand. **24**, 1851 (1970).
29. F. A. L. ANET. Can. J. Chem. **39**, 789 (1961).
30. W. F. ERMAN et T. J. FLAUTT. J. Org. Chem. **27**, 1526 (1962).
31. H. KRIEGER et K. MANNINEN. Suomen Kem. **38B**, 175 (1965).
32. J. C. RICHER. J. Org. Chem. **30**, 324 (1965).
33. M. CHEREST et H. FELKIN. Tetrahedron Lett. 2205 (1968).
34. R. HOWE, E. C. FRIEDRICH, et J. WINSTEIN. J. Am. Chem. Soc. **87**, 379 (1965).
35. S. BECKMAN et R. MEZGER. Chem. Ber. **89**, 2738 (1956).
36. H. C. BROWN et J. MUZZIO. J. Am. Chem. Soc. **88**, 2811 (1966).
37. H. C. BROWN et H. R. DECK. J. Am. Chem. Soc. **87**, 5620 (1965).
38. P. T. LANSBURY et R. E. MACLEAY. J. Am. Chem. Soc. **87**, 831 (1965).
39. R. A. ABRAMOVITCH, W. C. MARSH, et J. G. SAHA. Can. J. Chem. **43**, 2631 (1965).

Can. J. Chem. Downloaded from www.nrcresearchpress.com by 210.87.254.6 on 09/05/12
For personal use only.

Nuclear Magnetic Resonance Studies of some Trimethyl Tin Carbamates

A. E. LEMIRE AND J. C. THOMPSON[1]

Lash Miller Chemical Laboratories, University of Toronto, Toronto 181, Ontario

Received November 24, 1971

The low temperature n.m.r. spectra of some trimethylstannyl esters of *N,N*-dimethylcarbamic acid, *N,N*-dimethyldithiocarbamic acid, and *N,N*-dimethylmonothiocarbamic acid have been examined. Activation parameters for hindered rotation about the C—N bond in the trimethylstannyl ester of *N,N*-dimethylmonothiocarbamic acid have been determined to be: in hexane solution, $E_a = 17.0 \pm 0.5$ kcal/mol, $\Delta H^{\ddagger}_{298.2} = 16.4 \pm 0.5$ kcal/mol, $\Delta G^{\ddagger}_{298.2} = 16.4 \pm 0.4$ kcal/mol, $\Delta S^{\ddagger}_{298.2} = 0.2 \pm 2.0$ e.u.; in chloroform solution, $E_a = 19.9 \pm 0.5$ kcal/mol, $\Delta H^{\ddagger}_{298.2} = 19.3 \pm 0.5$ kcal/mol, $\Delta G^{\ddagger}_{298.2} = 16.6 \pm 0.4$ kcal/mol, $\Delta S^{\ddagger}_{298.2} = 9.1 \pm 2.0$ e.u.

Nous avons examiné les spectres r.m.n. à basse température de quelques esters triméthylstannyl des acides *N,N*-diméthylcarbamique, *N,N*-diméthyldithiocarbamique et *N,N*-diméthylmonothiocarbamique. Nous avons déterminé les paramètres d'activation pour la rotation gênée autour du lien C—N dans l'ester triméthylstannyl de l'acide diméthylmonothiocarbamique: (en solution dans l'hexane) $E_a = 17.0 \pm 0.5$ kcal/mol, $\Delta H^{\ddagger}_{298.2} = 16.4 \pm 0.5$ kcal/mol, $\Delta G^{\ddagger}_{298.2} = 16.4 \pm 0.4$ kcal/mol, $\Delta S^{\ddagger}_{298.2} = 0.2 \pm 2.0$ e.u.; (en solution dans le chloroforme) $E_a = 19.9 \pm 0.5$ kcal/mol, $\Delta H^{\ddagger}_{298.2} = 19.3 \pm 0.5$ kcal/mol, $\Delta G^{\ddagger}_{298.2} = 16.6 \pm 0.4$ kcal/mol, $\Delta S^{\ddagger}_{298.2} = 9.1 \pm 2.0$ e.u.

Canadian Journal of Chemistry, **50**, 1386 (1972)

Introduction

The question of hindered rotation about C—N bonds has long aroused interest, and increasingly, dynamic n.m.r. studies have been made on amide and amide-like systems. While some of the early data appear to be unreliable, the use of total line shape techniques has led to an increasing body of information that will allow systematic comparisons (1) of barriers to rotation both in amides (2–4) and thioamides (4, 5).

Less information is available, however, on carbamate and thiocarbamate systems (1, 6–9). Such systems, while analogous to amides and thioamides, are potentially even more interesting. If one represents them as compounds of the general formula RR′NC(X)YR″, then one sees that one may study the effects of X, Y, R, R′, and R″ functional groups upon the barrier to rotation about the C—N bond.

This paper is one in a series of systematic studies (8, 9) of carbamate and thiocarbamate esters of the group IV elements. By such studies, one may, hopefully, discover not only the effect on hindered rotation of various substituents, but also make comparisons of bonding modes used by different members of the group IV series.

[1]To whom correspondence should be addressed.

Experimental

(a) Methods

The techniques for obtaining and analyzing n.m.r. spectra have been described previously (8). Temperatures were measured using the methanol and ethylene glycol standards supplied by Varian Associates and employing the equations reported by Van Geet (10, 11). Temperatures are believed to be accurate to ± 0.3 °K when using the glycol method and ± 0.8 °K when using methanol. The solutions were sealed in n.m.r. tubes under vacuum. Values of T_2^* were obtained from the low temperature line width of the *N*-methyl protons and modified by a correction factor obtained from the $-SnMe_3$ or $CHCl_3$ peak, in order to take into account temperature and homogeneity changes. All n.m.r. spectra were obtained from a Varian A56/60D n.m.r. spectrometer.

(b) Preparation of Compounds

The preparations of all compounds used in this study are given in refs. 12–14.

Results

(a) $Me_2NC(O)SSnMe_3$

The *S*-trimethylstannyl ester of *N,N*-dimethylmonothiocarbamic acid was studied in *n*-hexane and chloroform solutions.

In a 10 mol% solution in hexane, the *N*-methyl protons give rise to two resonances with a low temperature equilibrium separation of 13.4 c.p.s. It is interesting to note that, while the collapse seems to be symmetrical over most of the region of exchange, at low temperatures the low field *N*-methyl resonance is slightly broader

Can. J. Chem. Downloaded from www.nrcresearchpress.com by 210.87.254.40 on 09/05/12
For personal use only.

TABLE 1. Some representative peak widths at low temperatures

Compound	Solvent	Temperature (°K)	*N*-methyl resonances (c.p.s.)		$SnMe_3$ resonance (c.p.s.)
			Low field	High field	
$Me_2NC(O)SSnMe_3$	*n*-Hexane	254.3	0.77	0.58	0.68
		276.7	1.17	0.92	0.65
		290.3	1.39	1.33	0.63
	$CHCl_3$	254.3	0.57	0.55	0.98
		276.7	0.79	0.81	1.19
		290.3	1.11	1.14	1.16
$Me_2NC(S)SSnMe_3$	*n*-Hexane	227.7	0.68		0.63
$Me_2NC(O)OSnMe_3$	CCl_4	248.2	0.90		0.70

TABLE 2. Activation parameters of some carbamate and thiocarbamate esters

Compound	Solvent	E_a (kcal/mol)	$\Delta H^{\ddagger}_{298.2}$ (kcal/mol)	$\Delta G^{\ddagger}_{298.2}$ (kcal/mol)	$\Delta S^{\ddagger}_{298.2}$ (e.u.)	Reference
$Me_2NC(O)SSnMe_3$	*n*-Hexane	17.0±0.5	16.4±0.5	16.4±0.4	0.2±2	This work
	$CHCl_3$	19.9±0.5	19.3±0.5	16.6±0.4	9.1±2	This work
$Me_2NC(S)SSnMe_3$	*n*-Hexane		No splitting observed			This work
	$CHCl_3$		No splitting observed			This work
$Me_2NC(O)OSnMe_3$	*n*-Hexane		No splitting observed			This work
	$CHCl_3$		No splitting observed			This work
$Me_2NC(O)SMe$	*n*-Hexane		No splitting observed			8
	$CHCl_3$	16.6±1.0	16.2±1.0	14.5±0.5	5.1±4	This work

than the high field *N*-methyl resonance. Some representative peak widths are given in Table 1. The two peaks collapse to a singlet at 315 °K.

In a 10 mol% solution in chloroform, the *N*-methyl resonances have a low temperature equilibrium separation of 12.7 c.p.s.; they again collapse to a singlet at 315 °K.

In this case, the line widths of the two *N*-methyl peaks are essentially the same at low temperatures as shown in Table 1.

The low field *N*-methyl also shows the greatest shift in benzene and hence, as in amides, is assigned to be the methyl group *trans* to the carbonyl (1).

The peak separation in the absence of exchange showed only a small temperature dependence, increasing slightly with decreasing temperature in the case of hexane solutions and decreasing slightly with decreasing temperature in the chloroform solutions. This effect was taken into account in the calculations by varying $\delta\omega_\infty$ for best fit.

Arrhenius plots yielded the activation parameters in Table 2.

A study of this compound has also been recently made using *o*-dichlorobenzene as a solvent (15).

(b) $Me_2NC(S)SSnMe_3$

This compound exhibits a singlet for the *N*-methyl protons at room temperature both in *n*-hexane and in chloroform solutions.

No splitting of the *N*-methyl signal was noted at temperatures as low as 221.1 °K for a 12 mol% solution in $CHCl_3$ or as low as 227.7 °K for an 8 mol% solution in *n*-hexane.

(c) $Me_2NC(O)OSnMe_3$

The trimethylstannyl ester of *N*,*N*-dimethylcarbamic acid also exhibits a singlet for the *N*-methyl protons at room temperature in chloroform, *n*-hexane, and carbon tetrachloride solutions.

In a 17 mol% solution in chloroform, no splitting of the *N*-methyl signal was observed at temperatures down to 221.1 °K. No splitting was observed at 248.2 °K for a dilute solution in carbon tetrachloride or at 279.3 °K for a dilute solution in *n*-hexane.

Can. J. Chem. Downloaded from www.nrcresearchpress.com by 210.87.254.40 on 09/05/12
For personal use only.

Can. J. Chem. Downloaded from www.nrcresearchpress.com by 210.87.254.40 on 09/05/12
For personal use only.

Discussion

The activation parameters obtained in this study are summarized in Table 2.

Of the three esters, the trimethylstannyl ester of *N*,*N*-dimethyldithiocarbamic acid is the one which has been most extensively studied in the past.

Infrared spectra were not conclusive in determining whether the structure was a non-cyclic monomer or a monomer containing a cyclic SnSCS ring in which the tin atom is 5-coordinated (13, 14).

Sheldrick *et al.* (16, 17) carried out a crystal structure determination and found that in the solid there is indeed some distortion of the tetrahedral coordination of the tin.

The lack of any splitting of the *N*-methyl resonance at low temperatures found in our study supports a symmetric structure in which tin is 5-coordinated in solution. A very similar situation was found with the trimethylsilyl ester (9).

The trimethylstannyl ester of *N*,*N*-dimethylcarbamic acid has also been studied both by Lappert and co-workers (13) and Dalton and Jones (14). From the i.r. data, both sets of workers conclude that the compound has a polymeric structure. Our n.m.r. data are consistent with this hypothesis since in a polymeric structure the two *N*-methyl environments would be identical. However, a cyclic monomer is also consistent with the n.m.r. data.

The structure of the *S*-trimethylstannyl ester of *N*,*N*-dimethylmonothiocarbamic acid is still ambiguous. While the n.m.r. data show that hindered rotation does occur about the C—N bond, it cannot distinguish between the two possible structures **1***a* or **1***b*, since in each case the two *N*-methyl positions are non-equivalent.

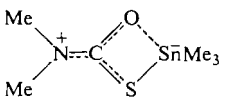

1*a*

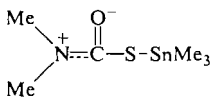

1*b*

In view, however, of the tendency of tin to 5-coordination (16–18), the first structure is, at least, quite possible.

Our previous studies of analogous methyl and trimethylsilyl esters allow some comparisons to be made (8, 9).

First, the free energy of activation, $\Delta G^{\ddagger}_{298.2}$, is lower in $Me_2NC(O)SSnMe_3$ than in either $Me_2NC(S)OMe$ and $Me_2NC(S)OSiMe_3$.

This is in keeping with the general pattern observed by several workers of the barriers to rotation in amides being lower than in thioamides (3, 4, 6, 8, 9).

The barrier is also higher than in the almost exactly analogous methyl ester, $Me_2NC(O)SMe$. Again, this is to be expected, since the lower barrier in $Me_2NC(O)SMe$ relative to amides has been explained (6) in terms of a resonance contribution of the type:

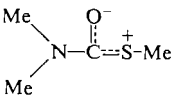

1*c*

In the case of structure **1***b*, this resonance contribution may be reduced by donation of electrons on sulfur into empty tin orbitals; it has however been suggested that tin d orbitals are too diffuse to take part in (p–d)π bonding (19).

Alternatively, formation of a 5-membered ring would also tend to increase the barrier relative to $Me_2NC(O)SMe$, as electron withdrawal from the oxygen into tin acceptor orbitals on forming the ring system should tend to further facilitate the donation of the lone pair on nitrogen into the $N^+{=}C{=}O^-$ system. The bonding in the ring, in this case, might involve either tin d orbitals or a 3-center bond formed from an sp^3 orbital of tin as postulated in compounds such as $(C_6H_5)_3Sn(Ox)$ (19).

The possibility of dimeric and other polymeric species of the trimethylstannyl ester of *N*,*N*-dimethylmonothiocarbamic acid at low temperatures is, of course, not precluded. Indeed formation of dimeric species may be the explanation for the different widths of the *N*-methyl peaks at low temperatures.

If the formation of dimers did occur at low temperatures, then the environment of the

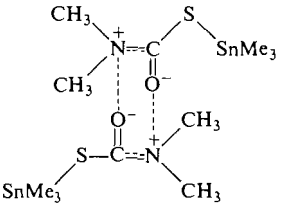

Can. J. Chem. Downloaded from www.nrcresearchpress.com by 210.87.254.40 on 09/05/12
For personal use only.

N-methyl group *cis* to the carbonyl would probably be slightly different in the dimer than in the monomer, and formation and destruction of dimeric species would hence lead to some broadening of its peak.

On the other hand, the difference in environment for the *trans* *N*-methyl group would probably not be substantially different between the monomer and dimer and hence this peak would not be as broadened.

In the more polar solvent chloroform, in which one would expect the molecule to be better solvated and dimerization not so likely to occur, there is indeed no substantial inequality of the line widths at low temperatures.[2]

It should be noted that in some cases other workers have observed unequal line widths for the *N*-methyl peaks in amides. For example, Neuman *et al.* noted this in a study of *N*,*N*-dimethylacetamide (3).

In this latter case, however, the workers attributed the asymmetric *N*-methyl line shapes to the unequal coupling with the *N*-methyl protons of the hydrogens of the other methyl group.

While this explanation seems quite reasonable for the situation in *N*,*N*-dimethylacetamide, the effect noted in the trimethylstannyl ester of *N*,*N*-dimethylmonothiocarbamic acid is unlikely to be due to spin–spin coupling, since the protons of the ester grouping are seven bonds removed from the *N*-methyl protons.

A similar broadening has been reported in the compound $(CH_3)_2ClSn[SSeCN(CH_3)_2]$ (20) and attributed to a coupling of the CH_3 protons *trans* to the selenium atom with the ^{77}Se isotope (natural abundance 7.58%). However, in view of our results, it appears this interpretation is incorrect.

Finally let us consider the results in chloroform solutions: solvation could occur by the formation of a hydrogen bond between the hydrogen on chloroform and the unshared electron pairs either on the carbonyl oxygen or on the ester sulfur.

In either case, this would be expected to raise the barrier to rotation: in the first case, by increasing the polarity of the $\bar{N}$=–C=–$\bar{O}$ system, and in the second case, by reducing the contribution of the resonance form **1***c*. And, indeed, the barrier to rotation in both $Me_2NC(O)SSnMe_3$ and $Me_2NC(O)SMe$ appears to be higher in chloroform solution than in hexane solution.

We thank the National Research Council of Canada for financial support, and the Ontario Department of University Affairs and the University of Toronto for fellowship support to A.E.L.

1. W. E. STEWART and T. H. SIDDALL, III. Chem. Rev. **70**, 517 (1970).
2. M. RABINOVITZ and A. PINES. J. Am. Chem. Soc. **91**, 1585 (1969).
3. R. C. NEUMAN, JR. and V. JONAS. J. Am. Chem. Soc. **90**, 1970 (1968).
4. R. C. NEUMAN, JR., D. N. ROARK, and V. JONAS. J. Am. Chem. Soc. **89**, 3412 (1967).
5. T. H. SIDDALL, III, W. E. STEWART, and F. D. KNIGHT. J. Phys. Chem. **74**, 3580 (1970).
6. T. M. VALEGA. J. Org. Chem. **31**, 1150 (1966).
7. C. E. HOLLOWAY and M. H. GITLITZ. Can. J. Chem. **45**, 2659 (1967).
8. A. E. LEMIRE and J. C. THOMPSON. Can. J. Chem. **48**, 824 (1970).
9. A. E. LEMIRE and J. C. THOMPSON. J. Am. Chem. Soc. **93**, 1163 (1971).
10. A. L. VAN GEET. Anal. Chem. **40**, 2227 (1968).
11. A. L. VAN GEET. Anal. Chem. **42**, 679 (1970).
12. H. TILLES. J. Am. Chem. Soc. **81**, 714 (1959).
13. T. A. GEORGE, K. JONES, and M. F. LAPPERT. J. Chem. Soc. 2157 (1965).
14. R. F. DALTON and K. JONES. J. Chem. Soc. A, 590 (1970).
15. C. Y. YODER, A. KOMORIYA, J. E. KOCHANOWSKI, and F. H. SUYDAM. J. Am. Chem. Soc. **93**, 6515 (1971).
16. G. M. SHELDRICK and W. S. SHELDRICK. J. Chem. Soc. A, 490 (1970).
17. G. M. SHELDRICK, W. S. SHELDRICK, R. F. DALTON, and K. JONES. J. Chem. Soc. A, 493 (1970).
18. W. P. NEUMANN. The organic chemistry of tin. Interscience Publishers, 1970, p. 17.
19. ROKURO OKAWARA and MASANORI WADA. Advances in organometallic chemistry. Vol. 5. Academic Press, 1967, p. 137.
20. TAKASHI KAMITANI and TOSHIO TANAKA. Inorg. Nucl. Chem. Lett. **6**, 91 (1970).

[2]A referee has suggested that the unequal line widths might be due to unequal quadrupole coupling with the low temperature structure in hexane solution.

Electron Spin Resonance Studies of Thiocarbonyl Anion Radicals

LEON J. AARONS[1] AND F. C. ADAM
Department of Chemistry, University of Calgary, Calgary, Alberta
Received October 25, 1971

The temperature dependence of the e.s.r. spectra of a series of sodium reduced thiones is reported. The thioketyls thiobenzophenone, *p,p'*-dimethoxythiobenzophenone, xanthene-9-thione, thioxanthene-9-thione, and their ketone analogues have been studied. Several show temperature-dependent sodium hyperfine structure near room temperature, but dissociate at lower temperatures to give spectra of thioketyl anions with no sodium coupling and markedly different *g*-values. Ring proton hyperfine splittings are found to be independent of the ion pairing process and independent of temperature. Models of ion pairing are discussed. Comparison is made to uhf–scf–mo calculations.

La variation des spectres r.p.e. en fonction de la température est décrite pour une série de thiones réduites par le sodium. Les thiocétyles (thiobenzophénone, diméthoxy-*p,p'*-thiobenzophénone, xanthène thione-9, thioxanthène thione-9) ainsi que leurs analogues cétoniques ont été étudiés. Pour plusieurs d'entre eux, la structure hyperfine du sodium montre une dépendance avec la température dans une zone voisine de la température ambiante, qui se dissocie aux températures plus basses en donnant les spectres des anions thiocétyles sans couplage avec le sodium et avec des valeurs *g* très différentes. On a trouvé que les multiplicités hyperfines pour les protons du cycle sont indépendantes de la température et du processus d'appariement ionique selon des modèles qui sont discutés. Une comparaison est faite avec les calculs uhf, scf et mo.

Canadian Journal of Chemistry, **50**, 1390 (1972)

Introduction

Although extensive research has been performed on aromatic ketyls (1) little work has been done on the analogous thioketyls, although the preparation and e.s.r. spectra of a few such compounds have been reported (2). The present investigation was undertaken to study the temperature dependence of the hyperfine couplings of this type of molecule and to improve, if possible, the understanding of the formation of ketyl ion pairs.

Since the early studies of Adam and Weissman (3) on the benzophenone ketyl, and of Atherton and Weissman on the sodium naphthalenide system (4), there has been considerable interest in the properties of ion pairs. Although the exact nature of these species is still not fully understood, aromatic ketyl ion pairs have proved to be particularly useful in such studies due to their greater stability and their tendency to form contact ion pairs, presumably because of the localization of negative charge in the carbonyl function. Aromatic hydrocarbons do not generally have such highly localized charge centers and as a result do not show as great a tendency to form tight ion pairs. For instance ketyls exhibit alkali metal couplings in the ethereal solvent dimethoxyethane (DME) while most hydrocarbon anions do not (5). The ketyl solutions in DME require additions of up to 40 volume per cent of a polar solvent such as dimethylformamide before the e.p.r. spectrum of the metal-free anion is obtained (6).

The alkali metal splitting of ketyl ion pairs usually decreases as the temperature is lowered (7). Several mechanisms have been suggested to explain this behavior of which the following two are the most frequently cited (1*c*).

Firstly McClelland (8) has calculated the most stable position of the alkali metal ion to be in the vicinity of the carbonyl group using as a perturbation the electrostatic interaction between the ions. It was proposed (9) that, in fact, the alkali metal ion lies in the nodal plane of the π-electrons at low temperatures but spends a proportionately greater time out of this nodal plane and in regions of higher π-electron spin density as the temperature is raised. This notion is similar in kind to that proposed by Atherton and Weissman for sodium naphthalenide (4), a concept which was later improved upon and put on a more theoretical basis by Aono and Oohashi (10).

The latter authors considered the temperature-dependent metal splittings to arise from configurational mixing between the ionic ground state, characterized by $\psi(Ar^-, Na^+)$, with an

[1]Present address: Department of Chemistry, University of Manchester, Manchester, England.

Can. J. Chem. Downloaded from www.nrcresearchpress.com by 210.87.254.105 on 09/05/12
For personal use only.

Can. J. Chem. Downloaded from www.nrcresearchpress.com by 210.87.254.105 on 09/05/12
For personal use only.

excited charge transfer state ψ(Ar, Na). The amount of mixing was dependent upon the amplitude of the oscillations of the sodium nucleus about a low energy configuration which was characterized by small metal couplings.

While no formal bonding occurs between the aryl anion and the metal cation in the description of Aono, the treatment can be extended to the ketyl system if it is assumed that the sodium nucleus undergoes torsional oscillations about the carbonyl bond. In analogy to the temperature dependence observed in the β-proton coupling constants of simple aliphatic radicals (11), it may be presumed that the coupling is given by an expression of the sort (12)

$$a_M = \rho_c(B_0 + B_2 \cos^2 \theta)$$

wherein ρ_c is the spin density at the π carbon atom while θ is the dihedral angle between this π orbital and the O—M bond as viewed down the C—O axis. In this manner, temperature variations in the hydroxyl splitting of biacetyl semidione radical could be explained as resulting from restricted torsional oscillations whose amplitude increases with temperature. This in turn determines the mean values of $\cos^2\theta$ and hence the magnitude of the coupling constant (13). For the particular case of the hydroxyl proton, the coupling decreases with increasing temperature. This was accounted for by a large negative value of $B_0(-9$ Oe), which included contributions from spin density delocalized onto the oxygen atom.

The rather more ionic nature of the metal to oxygen bond and the consequent lability of the metal ion compared to that of the proton prompted Hirota (7*a*, 14) to propose a second model to explain the temperature dependence of metal hyperfine coupling in ketyls. This model involves rapid equilibration between structurally different ion pairs which owe their difference mostly to the degree of solvation of the metal ion. This particular approach is supported by evidence from conductivity experiments (15) which show that both ion pairs and solvent separated ion pairs exist in solution, and that the relative amounts vary with temperature. The e.p.r. spectra suggest that the metal–ketone systems exhibit two main types of ion pairs which are termed "tight ion pairs", with large alkali metal splittings, and "loose ion pairs" or "solvent separated ion pairs" which have small or zero metal couplings. The temperature dependence of the thermodynamic equilibrium between the two ketyl forms accounts for the variation of the alkali–metal coupling with temperature. Although more than one type of ion pair has been observed in the spectra of hydrocarbon radical ions (16) only contact ion pairs have been detected in ketyl spectra in ethereal solvents. More recently Hirota and coworkers (7*b*) have suggested that there are in fact two kinds of tight ion pairs, with different metal coupling constants, which arise according to whether the cation is found primarily in a low-energy, low (negative) spin density configuration in the plane of the molecule, or in a second out-of-plane position characterized by large (positive) spin densities. As a result, the temperature dependence does not involve the solvent separated forms but only tight ion pairs. Specific solvation of the cation at the in-plane sites may then force the cation to a predominantly out-of-plane position giving rise to an increase in the metal coupling with polarity using mixed solvents. The carbonyl C^{13} and *g*-value shifts which accompany the changes in metal coupling can be predicted by a McClelland-type calculation which considers only the coulombic perturbation of the cationic charge upon the energy levels of the anions (7*c*) although the metal splittings themselves are not given by this procedure.

In this paper we present the experimental results of an e.p.r. study from which a comparison between a variety of sodium ketyls and the analogous sodium thioketyls can be made. The spectra are obtained using pure ethereal solvents. This avoids the complications arising from specific solvation effects in mixed solvents which are alluded to above. Uhf–scf calculations have also been carried out for the same compounds. Neither the experimental evidence nor the computations give results which are entirely consistent with the models described above.

Experimental

Table 1 gives the parent ketones which were studied, and notes the commercial sources from which they were obtained. The thioketones there listed were prepared from their oxygen analogues by heating the molten ketone with neat P_2S_5, or by refluxing a toluene solution of the ketone in the presence of excess P_2S_5 (17). Also included in Table 1 are the uncorrected melting points. Thiobenzophenone is not recorded because of its extreme sensitivity to air and mois-

TABLE 1. Carbonyls and thiocarbonyls

Compound	Symbol	Source	Melting point (°C)
Benzophenone	B	Eastman Chemicals	—
Thiobenzophenone	BS	P_2S_5, neat	*(19)
Xanthone	X	Fluke "purum"	—
Xanthene-9-thione	XS	P_2S_5/toluene	153–154 (20)
Thioxanthone	TX	K & K Labs., Inc.	—
Thioxanthene-9-thione	TXS	P_2S_5/toluene	167 (20)
p,p'-Dimethoxybenzophenone	DMB	K & K Labs., Inc.	—
p,p'-Dimethoxythiobenzophenone	DMBS	P_2S_5/toluene	113–115 (20)

*No melting point recorded as the compound decomposed on contact with air.

TABLE 2. Representative metal and ring proton coupling constants for the oxy-and thioketyl ions and ion pairs studied

System (ref.)	Coupling constants (Oe)*					g-value	T (°C)
	a_1	a_2	a_3	a_4	a_M		
B–Na (21)	2.60	0.88	3.45	0.88	1.16	2.0037	23
BS–Na	2.41	0.94	2.85	0.94	3.62	2.0068	23
	2.41	0.93	2.85	0.93	—	2.0079	−56
X–Na	3.88	0.88	3.88	<0.20	0.98	2.0036	22
XS–Na	3.42	0.77	3.42	0.39	3.43	2.0057	22
	3.42	0.78	3.42	0.39	—	2.0063	−50
TX–Na	3.50	0.98	3.50	0.37	1.00	2.0039	22
TXS–Na	2.97	0.90	2.97	0.64	3.33	2.0066	23
	2.94	0.86	2.83	0.50	—	2.0073	−68
DMB–Ca (21)	2.86	0.97	0.29†	0.97	—	2.0037	23
DMBS–Na (22)	2.58	0.98	0.28†	0.98	3.85	2.0058	23
DMBS–Na (22)	‡					2.0063	−42

*All metal-ketyl combinations observed in DME.
†Methoxyl proton splittings.
‡Poorly resolved.

ture, either of which rapidly convert it back to benzophenone. This particular thioketone was purified by vacuum sublimation and could also be satisfactorily stored under vacuum. Preparations of the compounds so obtained showed no carbonyl stretch in the i.r. spectrum and no trace of the benzophenone ketyl e.s.r. spectrum could be detected when a sample was slightly reduced in DME over a sodium mirror. The purification method was therefore deemed satisfactory for the present study.

The homodyne X-band spectrometer used for the e.s.r. studies is a unit built up from precision components following a design by Buckmaster and Dering (18). It uses a Currie, McLaughlan and Len MOS-1 phase-lock unit for klystron stabilization. This is fed by an A.F.C. circuit which operates at 6 KHz, using a small amount of the reflected carrier signal from the cavity to effect the stabilization. Field modulation was at a nominal 10 KHz. Signal was detected by a balanced pair of L-4164 Philco backward diodes and amplified using a Princeton Applied Research HR-8 lock-in amplifier. Field markers were obtained using a Harvey Wells F-10 gaussometer unit monitored by a Hewlett–Packard 5168-L frequency counter. Klystron frequencies were determined using a combination of the Hewlett–Packard counter to determine the base frequency of the crystal of the MOS-1 (nominally 15 MHz) which controls the klystron, and a Hewlett–Packard wavemeter which gives sufficient resolution (±5 MHz) to determine the particular harmonic of the crystal to which the klystron was locked. Several preliminary studies were carried out using a Varian 4502 spectrometer at the University of Sydney, Sydney, N.S.W., Australia.

The ethereal solvents used were distilled from lithium aluminum hydride and stored over sodium potassium alloy under vacuum. All samples were prepared using standard high vacuum techniques. Low temperature spectra were obtained by passing a stream of cold dry nitrogen gas past the sample in a quartz dewar insert set in the cavity.

Results

(A) Experimental

The hyperfine coupling constants and *g*-values of the radicals studied are given in Table 2. The

Can. J. Chem. Downloaded from www.nrcresearchpress.com by 210.87.254.105 on 09/05/12
For personal use only.

numbering scheme used is as follows:

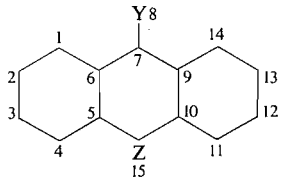

For benzophenone (B) and thiobenzophenone (BS), Z represents two non-bonded hydrogen atoms while Y = O and S respectively. Xanthone (X) and xanthene-9-thione (XS) have Z = O with Y = O and S respectively; finally thioxanthone (TX) and thioxanthene-9-thione (TXS) have Z = S with Y = O and S respectively. In most cases the coupling constants quoted in Table 2 were checked by comparison of the experimental spectrum with a computor stimulated spectrum based on the measured coupling constants and line widths, assuming Lorentzian line shapes. The spectra were plotted on a Calcomb 565 Digital Incremental Plotter. Representative samples of the spectra with their simulations are shown in Figs. 1–3. The assignments of the coupling constants given in Table 2 were made in the case of the thioketyls by comparison to their oxygen analogues, and from the results of uhf-scf-mo calculations to be described later. The assignments given also conform to those obtained by Sevilla and Vincow (23) for xanthyl radicals deuterated in either the 2 or 3 positions.

As can be seen from the results in Table 2, the spectra of the thioketyls are qualitatively quite similar to the corresponding oxyketyls. The decrease in proton hyperfine splittings at most

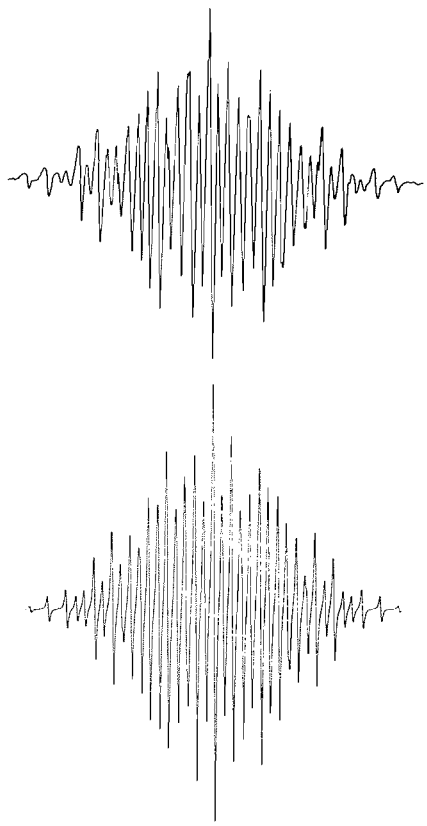

FIG. 1. Proton hyperfine spectrum of the thiobenzophenone–sodium ketyl at −56 °C in dimethoxyethane (upper) and (lower) a computor simulated spectrum. These spectra contain no sodium ($I = 3/2$) splittings.

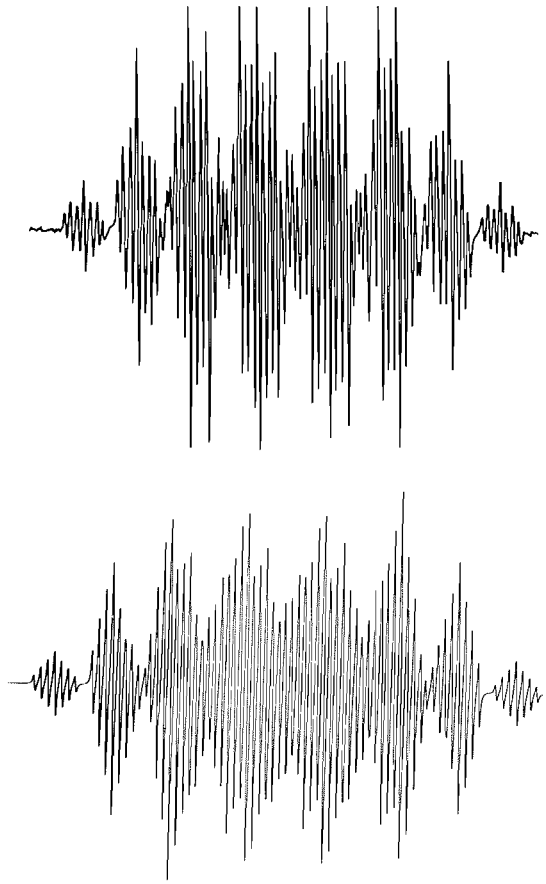

FIG. 2. Hyperfine spectrum of the xanthione–sodium ketyl in dimethoxyethane at 22 °C (upper) and (lower) a computor simulated comparison spectrum. These spectra show a temperature-dependent sodium hyperfine splitting.

Can. J. Chem. Downloaded from www.nrcresearchpress.com by 210.87.254.105 on 09/05/12
For personal use only.

Can. J. Chem. Downloaded from www.nrcresearchpress.com by 210.87.254.105 on 09/05/12
For personal use only.

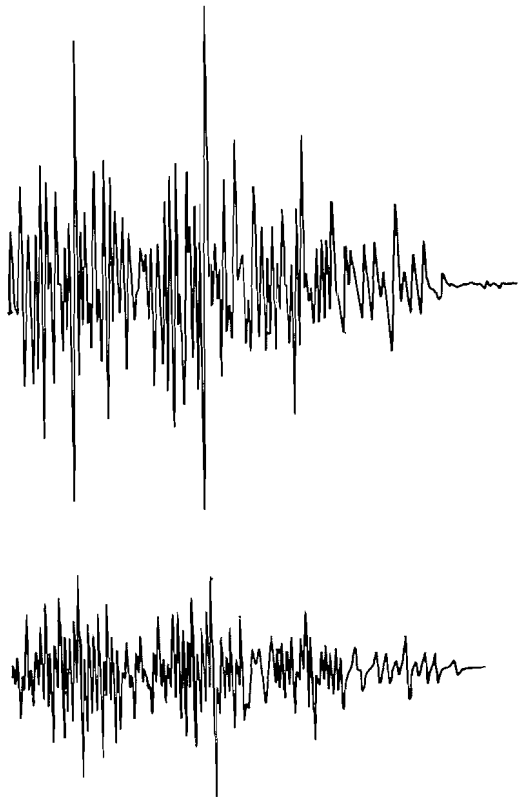

FIG. 3. The highfield half of the hyperfine spectrum of thioxanthione–sodium ketyl in tetrahydrofuran at 22 °C (upper) and a computor simulated comparison spectrum. This hyperfine spectrum does not show marked temperature variation.

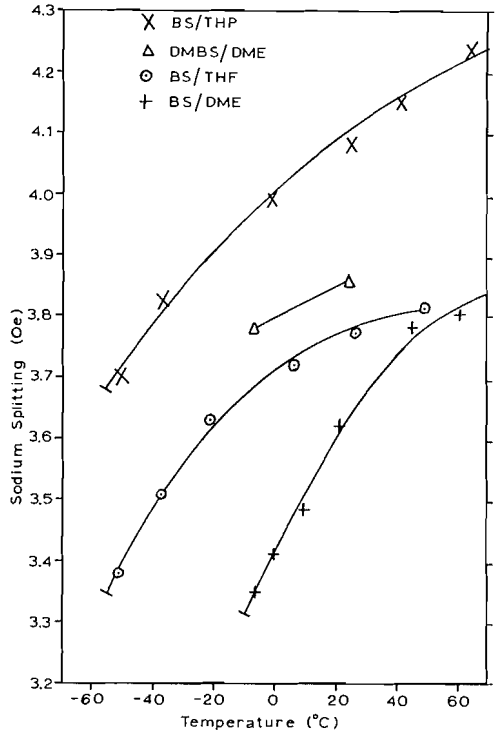

FIG. 4. Plot of sodium nuclear hyperfine coupling constant a_{Na} as a function of temperature for the thiobenzophenone ketyl in various ether solvents.

ring positions indicates that greater spin density accumulates in the thiocarbonyl moiety than is found in the corresponding carbonyl function. This is evident in all pairs of ketyls of thioketyls studied. The ring proton splittings of the xanthene derivatives were in general larger than the corresponding hyperfine couplings of the unbridged compounds. This can probably be attributed to the nonplanarity of the latter compounds which results from the strong steric repulsion between the ortho protons at positions 5 and 10 (24) whereas the xanthene derivatives are constrained to be planar. As the phenyl groups are twisted out of the plane of the central carbonyl group, the resonance integral for the extracyclic 5–7 and 7–9 bonds decreases with the result that the spin density is withdrawn from the rings and augments that already present in the carbonyl or thiocarbonyl groups (24).

No differences in the ortho proton couplings at sites, 1, 5, 10, and 14 were observed in the spectra of the unbridged thioketyl anions of BS and DMBS. The splittings of the meta sites at 2, 6, 12, and 13 were also found to be equal. Some differences might have been expected on the basis of the mo spin density calculations and because of the observations of Takeshita and Hirota (6) who found only pairwise equivalence between the ortho sites in benzophenone anions at low temperatures. The inherently greater line widths (0.1–0.3 Oe) of these compounds and the more complex hyperfine spectrum of the DMBS anion do not encourage a more detailed study into this effect.

The thioketyls exhibited relatively larger sodium coupling constants of about 4 Oe compared to the 1 Oe splittings (25) commonly obtained for the oxyketyls and in general they show a similar temperature dependence, in that this splitting decreases as the temperature is lowered. Plots of this effect are given in Figs. 4 and 5 for some of the compounds and solvents

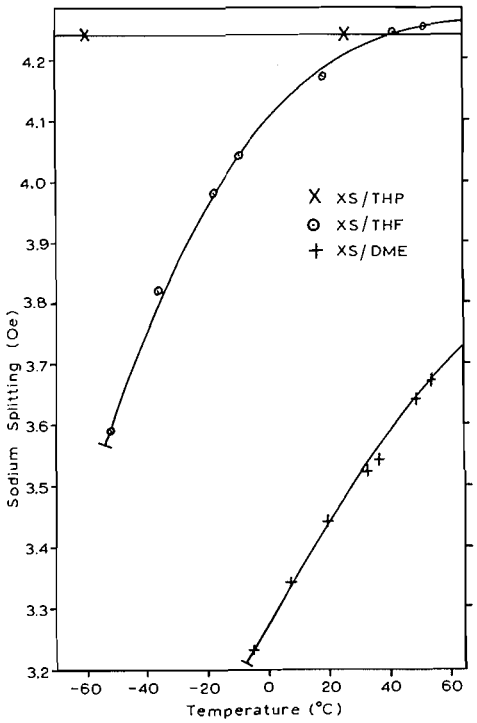

FIG. 5. Plot of the sodium hyperfine coupling constant a_{Na} as a function of temperature for the xanthione ketyl in different ether solvents.

studied. As can be seen the alkali metal splittings show a considerable solvent sensitivity for any particular ketyl. The variation in the coupling constant decreases at higher temperatures and is in fact essentially constant for both Na–TXS and Na–XS in tetrahydropyran (THP).

While the thioketyls do show analogous temperature dependence to the oxygen compounds, they do differ in one extremely important aspect. This behavior is typified by Na–BS in DME which shows a well resolved spectrum in the region +50 to −10 °C with the temperature dependent sodium splittings noted in Fig. 4. Within the accuracy of our measurements the *g*-value (2.0068) and the proton hyperfine splittings are independent of temperature in this range. Below −10 °C a complex and unsymmetrical spectrum was observed to evolve, which appears to be a superposition of the above spectrum upon a second spectrum which accounts for the entire absorption below −40 °C. The low temperature spectrum itself has no metal splitting and a different *g*-value (2.0079). No marked change in the proton coupling constants from the high temperature form is observed. Both the proton splittings and the *g*-value appear unchanged as the temperature is lowered to the gel point of the solvent near −80 °C. The suggestion may be made that the ion pairs observed at elevated temperatures can be considered to be more or less completely dissociated at the lower temperatures. This occurs with a jump, rather than a gradual shift, in the *g*-value, and a loss of, rather than a gradual decrease in the alkali metal splitting. At the same time essentially no change in the ring proton hyperfine splittings is observed. The temperature at which the dissociation occurs is indicated in Figs. 4 and 5 by the termination of the curves.

That the low temperature form is the free ion, and not an isomer of the ion pair in which the sodium ion shifted to a different position of low spin density in the ion pair, is shown by the following experiment. We have taken a preparation of BSNa in DME and added tetra-*n*-butyl ammonium perchlorate. At room temperature a spectrum is obtained with no sodium splittings, proton couplings of 2.43 (4H), 2.82 (2H), and 0.94 Oe (4H) and a *g*-value of 2.0072. These should be compared to the values obtained for the low temperature form for the BS anion in Table 2. Clearly the "free ion" is obtained in this case not because of solvent action, but because the size of the cation precludes the close association required for the formation of the tight ion pair.

A final observation concerning the metal splittings in the thioketyl ion pairs can be seen from Figs. 2 and 3 in that the hyperfine lines corresponding to $M_{Na} = \pm 3/2$ and $M_{Na} = \pm 1/2$ have the same peak-to-peak heights. Thus no selective broadening (1*b*) occurs in these systems to indicate that the sodium ion oscillates rapidly between a bound and an unbound state. If such an oscillation occurs, it must proceed at a frequency much lower than the alkali hyperfine line widths or less than $\sim 10^5$ s^{-1}.

The larger *g*-values of the thioketyls as compared to the oxyketyls result from the heavy atom effect (26) which can mostly be ascribed to the sulfur atom since it has a spin-orbit coupling parameter $\xi_S = -382$ cm^{-1} compared to that of oxygen, $\xi_O = -152$ cm^{-1}, and of carbon, $\xi_C = -28$ cm^{-1}. Shifts of the *g*-value away from

Can. J. Chem. Downloaded from www.nrcresearchpress.com by 210.87.254.105 on 09/05/12
For personal use only.

TABLE 3. Calculated and observed spin densities for free ions of the free ketyl ions and the thioketone analogues. XR and XSR are the ether and thioether neutral radical species which correspond to the ion pair

	Position								
Compound	1	2*	3	4*	5	6	7	8	15
B	0.073	−0.036	0.123	−0.052	0.097	0.058	0.189	0.342	—
Obs	0.096	0.033	0.128	0.033	0.096	—	—	—	—
BS	0.061	−0.037	0.095	−0.045	0.074	0.014	0.042	0.649	—
Obs	0.089	0.035	0.106	0.035	0.089	—	—	—	—
X	0.123	−0.065	0.150	−0.044	0.076	0.000	0.169	0.336	0.021
Obs	0.144	0.034	0.144	0.007	—	—	—	—	—
XR	0.144	−0.080	0.124	−0.080	0.135	−0.115	0.632	0.076	0.035
XS	0.083	−0.046	0.099	0.027	0.047	0.003	0.008	0.665	0.011
Obs	0.127	0.030	0.127	0.014	—	—	—	—	—
XSR	0.120	−0.067	0.104	−0.064	0.110	−0.090	0.472	0.281	0.026
TX	0.134	−0.071	0.155	−0.035	0.064	−0.005	0.157	0.325	0.033
Obs	0.132	0.036	0.132	0.013	—	—	—	—	—
TXS	0.090	−0.050	0.101	−0.021	0.039	−0.001	0.006	0.663	0.015
Obs†	0.108	0.034	0.113	0.023	—	—	—	—	—

*Signs of observed spin densities not determined from e.p.r. spectra.
†Spin densities at 1 and 3 assigned on basis of calculated values.

the free electron value $g_e = 2.0023$ can accordingly be related linearly to the spin density on the sulfur atom (*2b*). For those ketyls which dissociate at lower temperatures, the *g*-values are consistently larger than for the ion pairs observed at higher temperatures. This is the expected result since the unpaired electron is completely delocalized onto the sulfur atom of the free ion, while in the covalent limit for the ion pair, the sulfur atom would behave more like a thioether linkage with most of the spin density on the adjacent carbon atom at position 7. There are, however, alternative explanations of this *g*-value jump (*vide infra*), and every reason to believe that the covalently bound ion pair is not a good approximation. However, the relative insensitivity of the *g*-values to changes in solvent, temperature and counterion does support the contention that the low temperature form is in fact the free ion. The relatively small *g*-shifts observed for the ion paired species in different solvents and at various temperatures contrast markedly with the strong dependence exhibited by the metal coupling constants to both these factors. Whatever is happening to cause this variation does not apparently result from appreciable changes in the spin density at the sulfur atom.

(B) Calculations

Spin densities were calculated using the Pariser, Parr, and Pople (PPP) technique, a method which is described thoroughly elsewhere (27, 28). The bridged compounds were regarded as planar (23) while benzophenone and thiobenzophenone anions were assumed to be non-planar with each phenyl ring counter-rotated from the planar configuration by 30° to the carbonyl (thiocarbonyl) group. This was the angle calculated (29) to give the lowest total energy considering both the π-electron delocalization energy and the steric repulsion energies which vary as the rings are rotated (30). The parameters used will be described in more detail in ref. 29. The additional values required in the present calculations are those involving the ether and thioether linkages at position 15. In the notation of ref. 29, the ionization potentials I_O and I_S are taken as -33.9 (39) and -20.0 eV (40) respectively, while the repulsion integrals γ_O and γ_S are 20.0 (41) and 10.84 eV (40) respectively. The resonance integrals β are calculated using Mulliken's approximation (42) with β_{co} ($r = 1.37$ Å) $= -2.16$ eV and β_{cs} ($r = 1.71$ Å) $= -1.6$ eV. (40) The calculated spin densities appear in Table 3 along with the experimental spin densities (ρ_i) for the free ions. The latter were obtained from the measured proton hyperfine coupling constants (a_i) using McConnell's relationship (31)

$$\rho_i = a_i/Q_H$$

with Q_H taken to be -27.0 Oe.

Calculations were also carried out for the

Can. J. Chem. Downloaded from www.nrcresearchpress.com by 210.87.254.105 on 09/05/12
For personal use only.

Can. J. Chem. Downloaded from www.nrcresearchpress.com by 210.87.254.105 on 09/05/12
For personal use only.

covalently bonded analogues of the ion pairs for X and XS. These are symbolized by XR and XSR in Table 3, and are the compounds which would result if the metal atom were replaced by a non-polar group such as an alkyl group. The atomic parameters used for position 8 in these calculations are the same as those used at position 15 in the free ion computations. The effect of the alkyl group upon the π-bonding was not considered in the ether and thioether analogues. As can be seen, the spin densities at the ring positions do not change very much as a result of this substitution, but the spin density in the central group shifts sharply from the heteroatom in the free ion to the carbon atom at 7 in the "ion pair". This agrees with the experimental observation that the g-value of the free ion is significantly greater than that of the ion pair, if the presumption could be made that the S—M bond has considerable covalent character. While it would have been desirable to carry out the calculations taking the effect of the sodium atom more directly into account, such computations cannot be readily accommodated within the framework of the PPP approximation.

Discussion

While little attempt has been made to vary the atomic parameters of the mo calculations in order to obtain the best fit with the proton hyperfine spectra, it can be seen that in general the agreement with experiment is quite reasonable. The computations reflect the parallel behavior of the oxy and thio compounds with regard to planarity and to the insertion of different bridging elements. Also reproduced is the reduction in spin density observed for the ring positions of the thioketyls as compared to their oxygen analogues. As has been seen, the greatest change in spin densities, comparing the free ion to the covalently bound species XR and XSR, occurs at the central positions 7 and 8 while the changes within the ring are fairly modest, as experimentally observed. XR and XSR represent one extreme case for the association process and it would be expected that when the metal–ketyl bond has a rather more ionic nature, the real situation would lie somewhere between this limit and that given by X or XS free anions. It appears that the jump in g-value that occurs upon dissociation may therefore result from a redistribution of only that spin density found within the thiocarbonyl group, while the spin distribution in more remote parts of the molecule remains nearly the same. In any case it is apparent that the sodium ion is closely associated with the heteroatom in the ion pairs of both the oxy and thioketyl systems. Regardless of their detailed structure, it is clear that the rate of dissociation of these ion pairs to yield the free ions must occur slowly on the time scale of the present measurements; if this were not so the spectra of two distinct species could not be observed in the same solution, and one would expect instead a gradual change in both the averaged g-value and the mean metal splitting between the two extremes representing the bound and unbound ketyl anions. If the sodium ion exchange rate were not extremely rapid then one would expect broadening of the $M_{Na} = \pm 3/2$ lines relative to the $M_{Na} = \pm 1/2$ lines as well. Because of these observations it does not appear as if the original Hirota model can be used to explain the situation represented by the thioketyls. While the variation in sodium couplings may well result from rapid exchange between structurally different contact ion pairs such as proposed in his later models, the process cannot involve the low temperature species observed here.

The plots of a_{Na} *vs.* temperature as seen in Figs. 4 and 5 have the general appearance expected for restricted torsional oscillators with low energy barriers to rotation (32). According to this scheme, both TXS and XS in THP would be regarded as "free rotors" since the metal hyperfine coupling is both large and constant with respect to temperature changes. The g-value shifts are also fairly large in these compounds which indicates that the expression given in the introduction should be modified to take explicit account of the spin density on the sulfur atom. The computations for XSR also suggest that this is an appropriate step since the spin density at position 8 is by no means a negligible quantity. The general features of the situation can be expressed in the relationship

$$a_M = \rho_C(\theta)(B_0 + B_2 \cos^2 \theta) + \rho_S(\theta)B_3$$

in which θ retains its earlier meaning and the angular dependencies of ρ_C and ρ_S result from the fact that these values depend upon the C—S π overlap; as the torsional amplitude increases, ρ_S will decrease and probably ρ_C will increase. This oscillation accounts for the temperature dependence of the metal couplings, but since

Can. J. Chem. Downloaded from www.nrcresearchpress.com by 210.87.254.105 on 09/05/12
For personal use only.

ρ_C does not contribute to the g-value shift, it also predicts that the g-value should change with temperature. This is not observed. Nor is it very apparent why the ketyls TXS and XS should behave so differently in three such similar solvents, behaving as free rotors in THP but as restricted rotors in DME. It seems reasonably clear that at least part of the resistance to free rotation about the C—S axis arises from the π character of this bond, yet the computed bond orders are not reduced materially between XS (0.5113) and XSR (0.4408) and in either case represent a much higher barrier to rotation than would be expected for a "free rotor". While a significant reduction in bond order occurs between X (0.6199) and XR (0.2693) it is felt that the more polar nature of the O—M bond would favor the higher value so that the situation is similar for the oxyketyl ion pairs as well. For these reasons it appears as if the torsional oscillator model does not adequately account for the experimental observations.

The effect of solvent in the dissociation process itself follows the qualitative trends outlined by Aten *et al.* (33) in that the energy of solvation increases with increasing dielectric constant and decreasing radii of the ions. In accordance with the negative temperature coefficient of the dielectric constant for the solvents studied here, solvation of the metal ions becomes stronger as the temperature is lowered, and results in the ultimate dissociation. DME has the highest dielectric constant and also the highest dissociation temperatures, while THP has the lowest dielectric constant and does not in fact induce the dissociation of TXS or XS above the freezing point. It appears that there is a strong competition between the solvent and the anion to complete the solvation sheath of the metal ion. This factor may account for some of the observations which have been made for the ion pairs, in that the effect of the solvent probably does not end with the process of association but continues to affect the polarity of the bond which joins the metal to the ketyl ion. Since the g-values suggest there is considerable spin density on the sulfur atom even in the ion pair, it can be presumed that the S—M bond lies in the π-nodal plane of the thiocarbonyl group. The usual description of π-σ interactions in systems of this sort suggests the Q values depend only on the covalent (non-polar) part of the σ bonding description and smaller couplings due to spin polarization effects are expected as the ionic character (polarity) of this bond increases. The couplings also depend on the spin density of the heteroatom, as do the g-values. The temperature dependence of the metal hyperfine couplings in the ion pair could then result from changes in the dielectric behavior of the medium which are reflected in the polarity of the S—Na bond and hence the Q value, while the spin density (and hence g-values) in the π-system remain largely unchanged. Such changes as are observed would be in the direction of the free ion as the dielectric constant of the solvent increases but would not include such specific solvation effects as are observed in mixed solvents (*7b*). The eventual dissociation process must be considered as distinct from these effects although obviously not unrelated. Thus XSK with the more polar S—K bond has a g-value of 2.0058 compared to the value of 2.0057 for XSNa in DME at room temperature. In the three solvents, the TSXNa ion pair has g-values of 2.0064, 2.0065, and 2.0066 in THP, THF, and DME respectively while the sodium couplings are 4.11, 3.85, and 3.33 Oe, in the same order. Similar results obtain for XSNa.

The free ions also show a slight shift with the different solvents but in the reverse direction. This we attribute to solvation effects involving the unshared electron pairs (n-electrons) on the sulfur atom. Since the g-value shifts arise from terms of the sort (34, 35)

$$\Delta g_{xx} = -\frac{2\xi_S \rho_S \langle \sigma | l_x | \pi \rangle \langle \pi | l_x | \sigma \rangle}{\Delta E_{\sigma \to \pi}}$$

and because the resonance denominator is smallest for $n \to \pi$ transitions, the largest contribution will come from molecular excitations involving the non-bonding electrons of the sulfur atom. As is also well known, the $n \to \pi$ transitions are characteristically blue shift bands (36) so that $\Delta E_{n \to \pi}$ increases with the polarity of the solvent. It is for this reason our g-values are much higher for BS in DME (2.0079) than those obtained by Heller in ethanol–water mixtures (2.0054) (*2b*), where the n-electrons are specifically solvated by the protonic solvents. The analogous situation is observed for the radicals RS· in aqueous systems ($g = 2.0105$) (37) compared to similar "dry" radicals in hydrocarbon

Can. J. Chem. Downloaded from www.nrcresearchpress.com by 210.87.254.105 on 09/05/12
For personal use only.

glasses which yield mean g-values of about 2.0250 (38). The ionic association process of interest in the present case is different only in kind from the solvation effects recorded above. In fact if one considers the sulfur atoms to be unhybridized in the free ketyl ions in non-polar solvents but to be sp^2 hybrids in the ion pair, one would expect a reduction in the g-shift of about 33% for constant spin density in the $3p_z\pi$ orbital. This presumes the electron pair binding the metal ion does not contribute to the g-value shift at all. Considering the polarity of the S—M bond, this is probably an over-statement of the fact. The actual shifts decrease by only 20% between the free ion and the ion pairs of the thioketyls, and it is not certain whether the observed jump is due to this effect or whether a shift in the spin density away from the sulfur atom has also occurred. Since the latter will be accompanied by an increase in the C^{13} coupling constant of the carbonyl atom, studies are presently under way to investigate further the dissociation phenomenon using isotopically substituted thioketyls.

Finally it should be noted that the model used by Aono and Oohashi can be readily applied to the present study. The magnitude of the sodium couplings requires a spin density of only about 0.01 in the sodium orbitals. Solvation of the metal ion would decrease its electron affinity and hence decrease this spin density, to give the observed temperature dependence. Solvation of the anion produces the opposite effect. The model does not require any particular bonding structure to be ascribed to the ion pair, except to say that the metal ion resides primarily in regions of low potential energy. The only conceptual difficulty which appears to arise is that concerning the actual dissociation process. If this results when the ketyl anion is replaced by a solvent molecule in the ion envelope of the cation, then the model differs little from the one suggested above. Since furthermore this model includes the perturbing effect of the cation on the anionic energy levels, it contains the essential features of the calculation carried out by Takeshita and Hirota (7*c*) and may well be the best approach to take for future computations based on this system.

The technical assistance of Mr. Glenn Smith and financial support of the Defence Research Board of Canada and the Isaac Walton Killam Foundation are gratefully acknowledged.

1. (*a*) P. B. Ayscough and R. Wilson. Proc. Chem. Soc. 229 (1962). (*b*) P. H. Rieger and G. K. Fraenkel. J. Chem. Phys. **37**, 2811 (1962). (*c*) N. Hirota. *In* Radical ions. *Edited by* E. T. Kaiser and L. Keven. Interscience, New York, (1968).
2. (*a*) E. G. Janzen and C. M. Dubose, Jr. J. Chem. Phys. **70**, 3372 (1966). (*b*) H. C. Heller. J. Am. Chem. Soc. **89**, 4288 (1967).
3. F. C. Adam and S. I. Weissman. J. Am. Chem. Soc. **80**, 1518 (1958).
4. N. M. Atherton and S. I. Weissman. J. Am. Chem. Soc. **83**, 1330 (1961).
5. A. H. Reddoch. J. Chem. Phys. **43**, 225 (1965).
6. T. Takeshita and N. Hirota. J. Chem. Phys. **51**, 2146 (1969).
7. (*a*) N. Hirota. J. Am. Chem. Soc. **89**, 32 (1967). (*b*) K. S. Chen, S. W. Mao, K. Nakamura, and N. Hirota. J. Am. Chem. Soc. **93**, 6004 (1971). (*c*) T. Takeshita and N. Hirota. J. Am. Chem. Soc. **93**, 6421 (1971).
8. B. J. McClelland. Trans. Faraday Soc. **57**, 1458 (1961).
9. G. W. Canters and E. deBoer. Mol. Phys. **13**, 395 (1967).
10. S. Aono and K. Oohashi. Prog. Theor. Phys. (Kyoto), **30**, 162 (1963); **32**, 1 (1964).
11. R. W. Fessenden. J. Chem. Phys. **61**, 1570 (1964).
12. A. Horsfield, J. R. Morton, and D. H. Whiffen. Mol. Phys. **4**, 425 (1961).
13. P. B. Ayscough and R. E. D. McClung. Mol. Phys. **20**, 35 (1971).
14. N. Hirota and R. Kreilick. J. Am. Chem. Soc. **88**, 614 (1966).
15. T. E. Hogen-Esch and J. Smid. J. Am. Chem. Soc. **88**, 307, 318 (1966).
16. N. Hirota. J. Phys. Chem. **71**, 127 (1967).
17. Beilstein. **17**^{2}, 382.
18. H. A. Buckmaster and J. C. Dering. J. Sci. Inst. **43**, 554 (1966).
19. R. W. Bost and B. O. Cosby. J. Am. Chem. Soc. **57**, 1404 (1935).
20. A. Schonberg, O. Schutz, and S. Nickel. Ber. **16B**, 1375 (1928).
21. C. R. Kepford. Ph.D. Thesis. The University of Calgary, Calgary, Alberta, 1968.
22. R. Wickson. Unpublished report. The University of Calgary, Calgary, Alberta, 1969.
23. M. D. Sevilla and G. Vincow. J. Phys. Chem. **72**, 3635 (1968).
24. H. R. Falle and F. C. Adam. Can. J. Chem. **44**, 1387, 1397 (1966).
25. N. Hirota and S. I. Weissman. J. Am. Chem. Soc. **86**, 2537, 2538 (1964).
26. D. S. McClure. J. Chem. Phys. **20**, 682 (1952); **17**, 905 (1949).
27. R. Pariser and R. G. Parr. J. Chem. Phys. **21**, 466, 767 (1953).
28. A. Bristock and J. A. Pople. Trans. Faraday Soc. **50**, 901 (1954).
29. F. C. Adam and L. J. Aarons. Can. J. Chem. This issue.

30. W. G. LAIDLAW and R. B. FLEWWELLING. Can. J. Chem. **48**, 2158 (1970).
31. H. M. MCCONNELL. J. Chem. Phys. **24**, 632 (1956).
32. P. B. AYSCOUGH, M. C. BRICE, and R. E. D. MCCLUNG. Mol. Phys. **20**, 41 (1971).
33. A. C. ATEN, J. DIELEMAN, and G. J. HOITINK. Disc. Faraday Soc. **29**, 182 (1960).
34. H. M. MCCONNELL and R. E. ROBERTSON. J. Phys. Chem. **61**, 1018 (1957).
35. A. CARRINGTON and A. D. MCLACKLAN. *In* Introduction to magnetic resonance. Harper Row, 1967.
36. H. M. MCCONNELL. J. Chem. Phys. **20**, 700 (1952).
37. C. NICOLAU and H. DERTINGER. Rad. Res. **42**, 62 (1970).
38. J. SKELTON and F. C. ADAM. Can. J. Chem. **49**, 3536 (1971).
39. M. J. S. DEWAR and T. MORITA. J. Am. Chem. Soc. **91**, 796 (1969).
40. J. FABIAN, A. MEHLHORN, and R. ZAHRADNIK. J. Phys. Chem. **72**, 3975 (1968).
41. F. P. BILLINGSLEY and J. E. BLOOR. Theoret. Chem. Acta, **11**, 325 (1968).
42. R. S. MULLIKEN. J. Chem. Phys. **46**, 675 (1949).

Can. J. Chem. Downloaded from www.nrcresearchpress.com by 210.87.254.105 on 09/05/12
For personal use only.

Kinetics and Mechanism for the Hydrolysis of Chlorothionoformate and Chlorodithioformate Esters in Water and Aqueous Acetone

D. M. McKINNON AND A. QUEEN

Parker Chemistry Laboratory, University of Manitoba, Winnipeg, Manitoba

Received October 1, 1971

The effects of structural changes on the rates of hydrolysis of a series of chlorothionoformate esters and the analogous chlorodithioformate esters have been studied. For both classes of compound, the reactivity is enhanced by increased electron donation by the hydrocarbon group. These results, the activation parameters for the hydrolyses of the methyl compounds, and the solvent isotope effect are shown to be consistent with the operation of the S_N1 mechanism.

Les effets de modifications structurales sur les vitesses d'hydrolyse d'une série d'esters chlorothionoformates et d'esters chlorodithioformates analogues, ont été étudiés. Pour les deux classes de composés, la réactivité est accrue si l'on augmente le pouvoir donneur d'électrons du groupe hydrocarbure. Ces résultats concernant les paramètres d'activation pour les hydrolyses des composés méthylés et l'effet isotopique du solvant, sont consistants avec l'intervention d'un mécanisme S_N1.

Canadian Journal of Chemistry, **50**, 1401 (1972)

Introduction

Previous studies (1–3) have established that chloroformate esters (**1**; X = Y = O) and chlorothiolformate esters (**1**; X = S, Y = O) hydrolyze much more slowly than other acid chlorides, a feature that is most reasonably attributed to initial state conjugation, **2**. This effect is enhanced by structural changes that increase electron donation by the hydrocarbon group (R) (3, 4) and is diminished in compounds where the hetero-atom (X) has only a limited tendency to use its unshared electrons for π-bond formation. Thus, chloroformates are much less reactive than their thio analogues (3).

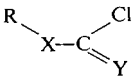

1

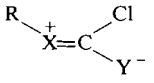

2

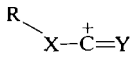

3

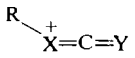

4

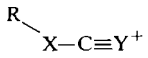

5

Whereas chloroformates hydrolyze by the addition–elimination mechanism 1 (2), chlorothiolformates and dimethylcarbamyl chloride react unimolecularly with water (mechanism 2) (3). These differences have been explained in the following terms.

(*i*) It is first of all assumed that, irrespective of the mechanism of hydrolysis, the nucleophile is supplied by the solvation shell surrounding the molecule. Hence for a given compound, the operative mechanism is determined by the differences in the transition state energies.

(*ii*) In the series of compounds (**1**; Y = O; X = O, S, NR), the inductive effect of the hetero atom (X) opposes its mesomeric effect, when this can operate. This latter tendency would act to stabilize a forming acylium ion (**4**; Y = O) but would be much reduced in the bimolecular formation of a tetrahedral intermediate (**6**; Y = O).

(*iii*) For the chloroformates, the inductive and mesomeric effects almost cancel so that the

[1] 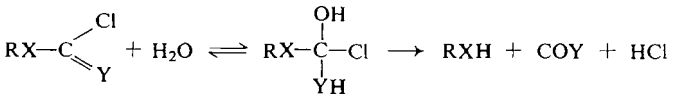

6

[2] 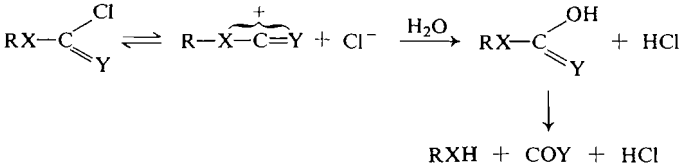

Can. J. Chem. Downloaded from www.nrcresearchpress.com by 210.87.254.6 on 09/05/12
For personal use only.

TABLE 1. Rate constants for the hydrolysis of chloroformate and thiochloroformate esters in water and aqueous acetone

Compound	Solvent	Temperature (°C)	k ($\times 10^4$ s^{-1}) C_6H_5	CH_3	C_2H_5	i-C_3H_7	Reference
RO—(CO)—Cl	Water	4.62	20.55	0.6738	0.4110	1.015	2
RS—(CO)—Cl	Water	4.62	1.060	4.733	26.69	116.9	3
RO—(CS)—Cl	Water	4.96	0.3740	1.732	25.36		This work
RS—(CS)—Cl	70% aqueous acetone	4.94	0.2477	1.264	7.955	42.17	This work
RO—(CS)—Cl	70% aqueous acetone	20.23		0.09924		15.81	This work

TABLE 2. The effects of temperature on the rates of hydrolysis of methyl chlorothionoformate in water and methyl chlorodithioformate in 70% aqueous acetone

Compound	Solvent	Temperature (°C)	($k \times 10^4$ s^{-1})	Mean temperature (°C)	$\Delta H^{\ddagger}$ (cal/mol)	$\Delta S^{\ddagger}$ (cal/mol deg)
CH_3O—(CS)—Cl	Water	4.438	1.628 ± 0.004	14.6	24767	13.5
		14.960	8.805 ± 0.008			
		24.396	35.34 ± 0.08			
CH_3S—(CS)—Cl	70% aqueous acetone	4.937	1.271 ± 0.004	12.6	20180	−3.7
		12.619	3.524 ± 0.004			
		20.230	8.992 ± 0.006			

S_N1 mechanism is not particularly favored, whereas mechanism 1 is promoted by the electron-withdrawing properties of the hetero atom (X = O).

(*iv*) For the other compounds, the inductive effects of nitrogen and sulfur are much smaller than for oxygen but the corresponding mesomeric effects are either particularly large (X = NR) or still appreciable (X = S) so that significant stabilization of the corresponding acylium ions is possible. However, it has been pointed out (3) that, in the case of the chlorothiolformate esters, the degree of cancellation of the two effects may be such that the observed unimolecular hydrolysis of these compounds reflects the favorable entropy terms for this mechanism rather than significantly reduced activation energies.

In these earlier studies it was not possible to determine the degree to which the carbonyl oxygen influenced reactivity and mechanism. However, its effect is unlikely to be negligible. For example, mesomerism should delocalize the charge in acylium ions (**5**; Y = O). As a logical extension of this work we have measured the rates of hydrolysis of the analogous chlorothionoformates (**1**; X = O, Y = S) and chlorodithioformates (**1**; X = Y = S). No previous kinetic studies of these compounds have been reported.

Results

First order rate constants for the hydrolyses of the chlorothionoformate esters in water at 5 °C are listed in Table 1 where they are compared with values for the corresponding reactions of chloroformates and chlorothiolformates, calculated from previous data (2, 3). The hydrolysis of isopropyl chlorothionoformate in water was too fast to be measured but its reactivity towards 70% aqueous acetone at 20 °C is compared with that of the methyl compound. The alkyl chlorodithioformates were not readily dissolved in water and also reacted too rapidly for convenient kinetic studies. However, they hydrolyze at convenient rates in 70% aqueous acetone and data for 5 °C are given in Table 1.

Table 2 gives rate constants for the hydrolyses of methyl chlorothionoformate and methyl chlorodithioformate at different temperatures in water and 70% aqueous acetone, respectively. Enthalpies and entropies of activation are

Can. J. Chem. Downloaded from www.nrcresearchpress.com by 210.87.254.6 on 09/05/12
For personal use only.

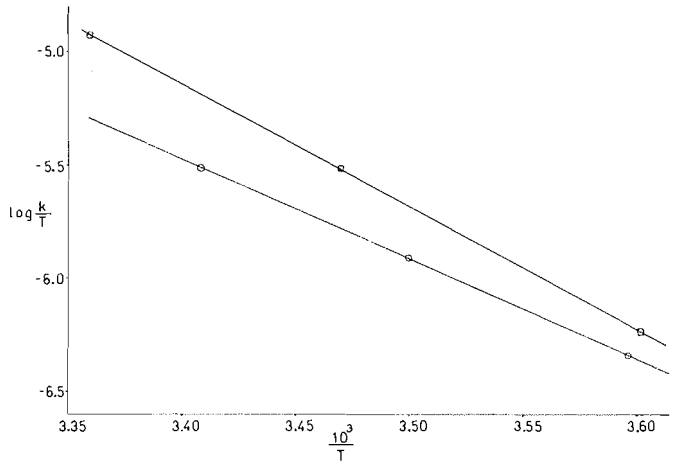

FIG. 1. Plots of $\log k/T$ *vs.* $1/T$ for the hydrolysis of methyl chlorothionoformate in water ⊡ and the hydrolysis of methyl chlorodithioformate in 70% aqueous acetone ⊙.

assumed to be constant over the experimental temperature ranges and evaluated from plots of $\log kT^{-1}$ against T^{-1} (Fig. 1). Close examination of these plots shows that they are slightly curved, consistent with decreases of the standard heat capacities of the systems during the activation processes, as previously reported for many solvolytic reactions (5, 6). At this time we have not attempted to measure heat capacities of activation for any of the reactions now studied. However, because of the indicated variations in the activation parameters, the values in Table 2 are assumed to refer to the averages of the experimental temperatures.

The chlorothionoformates hydrolyze rapidly to yield hydrochloric acid, carbonyl sulfide, and the corresponding alcohol. In agreement with this conclusion, the rate of hydrolysis of the methyl compound at 15.2 °C ($k = 8.82 \times 10^{-4}$ s^{-1}), determined by following the rate of collapse of the absorption peak at 247 mμ (Fig. 2) is in good agreement with the value calculated from the conductometric rate constants given in Table 2.

Methyl trithiocarbonate was the only organic material formed when methyl chlorodithioformate (2 ml) was reacted with 70% aqueous acetone (100 ml) at 20 °C. When a similar experiment was carried out with refluxing solvent, methanethiol and methyl trithiocarbonate were formed. These results indicate that the initial products of hydrolysis of methyl chlorodithioformate are hydrochloric acid, carbonyl sulfide, and methanethiol. This latter product reacts rapidly with methyl chlorodithioformate as it is added to the reaction mixture. However, it seems unlikely that trithiocarbonate esters would be formed in significant amounts when the substrates are in the low concentrations (*ca.* 10^{-4} *M*) used in the kinetic experiments. In agreement with this conclusion, the rate of hydrolysis of methyl chlorodithioformate in 70% aqueous acetone at 15.2 °C ($k = 4.89 \times 10^{-4}$ s^{-1}), determined by following the rate of change of optical density at 325 mμ (Fig. 3), is in good agreement with the value calculated from the data in Table 2. This result shows that methyl trithiocarbonate, which absorbs strongly at this wave-

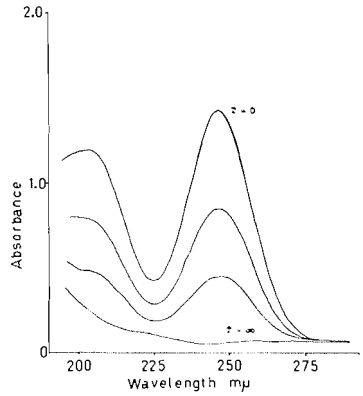

FIG. 2. Changes in the u.v. absorption spectrum of methyl chlorothionoformate in water with time.

Can. J. Chem. Downloaded from www.nrcresearchpress.com by 210.87.254.6 on 09/05/12
For personal use only.

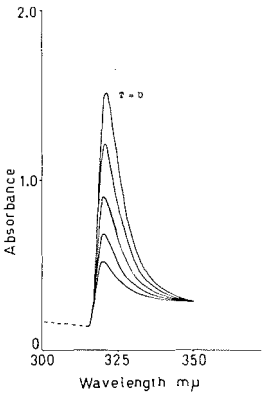

FIG. 3. Changes in the u.v. absorption spectrum of methyl chlorodithioformate in 70% aqueous acetone with time.

length, ($\varepsilon = 5700$ l mol^{-1} cm^{-1}), is not formed at low concentrations of the substrate.

Discussion

The relatively low reactivities of the compounds listed in Table 1, when compared to that of acetyl chloride (7), show that initial state conjugation is important for all of them. The smaller mesomeric effect of sulfur than oxygen is consistent with the reactivity relationships:

$$CH_3O—(CO)—Cl < CH_3S—(CO)—Cl$$
$$CH_3O—(CS)—Cl < CH_3S—(CS)—Cl$$

However, the different order of reactivity for the phenyl compounds

$$C_6H_5O—(CO)—Cl \gg C_6H_5S—(CO)—Cl$$
$$C_6H_5O—(CS)—Cl < C_6H_5S—(CS)—Cl$$

indicates that the same mechanistic differences that apply to chloroformates (**1**; X = Y = O) and chlorothiolformates (**1**; X = S, Y = O) cannot apply to chlorothionoformates (**1**; X = O, Y = S) and chlorodithioformates (**1**; X = Y = S). In fact, the differences in the rate sequences between the four classes of compounds show that those containing sulfur must react by different mechanisms to the chloroformates, which follow mechanism 1. By analogy with the chlorothiolformate esters, the increase of reactivity of the chlorothionoformates and chlorodithioformates with increasing electron donation by the group (R) indicates that these compounds also hydrolyze by S_N1 mechanisms 2. In the case of methyl chlorodithioformate, alternative processes involving alkyl–sulfur bond fission have been excluded by identification of methanethiol and methyl trithiocarbonate as products of hydrolysis (see above). Moreover, v.p.c. did not indicate the presence of methanol in the reaction mixture.

It is necessary, however, to consider the possibility that the present reactions may involve conversion of the thiono compounds to the corresponding carbonyl compounds. Presumably, the reaction would involve the formation of tetrahedral intermediates (**7**; X = O or S) as in mechanism 3. In the case of the chlorothionoformates, the initial products would be chloroformates (**8**; X = O) which would hydrolyze bimolecularly (steps *6*, *7*, and *8*). Two experimental facts argue against this possibility. These are that excellent first order rate constants were obtained over at least three half lives and that the reactivities of the chloroformates are much too low to account for the observed rates, if the phenyl compounds are excluded from consideration. Moreover, it is difficult to see why this pathway should be characterized by the observed differences of reactivity. In the case of the chlorodithioformates, the intermediates (**8**; X = S) would be chlorothiolformates which do hydrolyze unimolecularly. However, once again the high reactivities of the dithio compounds and the excellent first order rate constants are not in accord with mechanism 3, steps *1–5* and *9–12*. Unimolecular hydrolysis of the present compounds is therefore indicated.

In accord with these mechanistic assignments, the enthalpies of activation for the hydrolyses of the methyl compounds (Table 2) are much greater than those reported (2) for bimolecular hydrolysis of chloroformates. The positive entropy of activation for the hydrolysis of methyl chlorothionoformate in water is similar to the value reported for the corresponding reactions of *t*-butyl chloride (5, 8) and methyl chlorothiolformate (3), as is the solvent deuterium isotope effect, $k(D_2O)/k(H_2O) = 0.78$ at 4.96 °C. The entropy of activation for the hydrolysis of methyl chlorodithioformate in 70% aqueous acetone is comparable to values reported by Kohnstam (6) for S_N1 solvolyses in this solvent, if due allowance is made for temperature differences. The entropy terms for S_N2 reactions are much more negative.

Can. J. Chem. Downloaded from www.nrcresearchpress.com by 210.87.254.6 on 09/05/12
For personal use only.

[3]

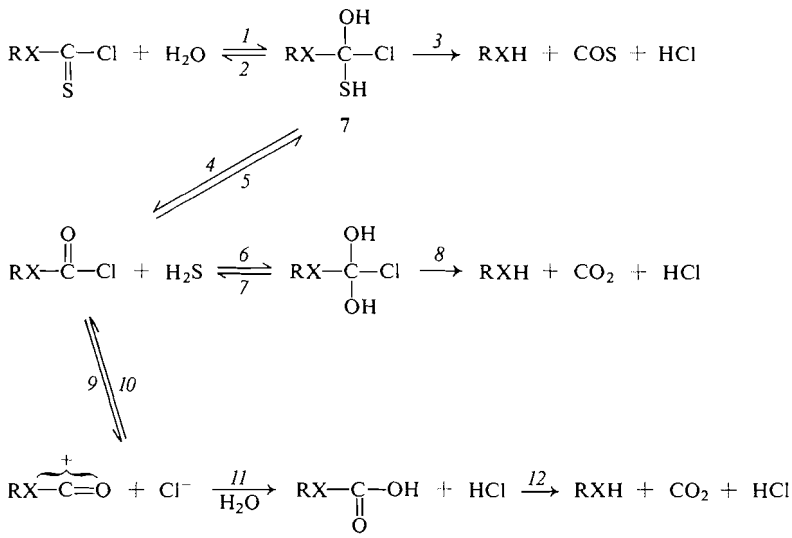

TABLE 3. Boiling points of thionochloroformate and dithiochloroformate esters*

R	X	Y	Yield (%)	Present work: Boiling point (°C)	Present work: Pressure (mm)	Literature: Boiling point (°C)	Literature: Pressure (mm)	Reference
CH_3	O	S	51	105–107		105–107		15
C_2H_5	O	S	38	136				16
i-C_3H_7	O	S†	35	35	4			This work
C_6H_5	O	S	48	93		92.5		17
CH_3	S	S	64	157–158		156–159		18
C_2H_5	S	S	65	64	8	63	6	18
i-C_3H_7	S	S‡	47	40	10			This work
C_6H_5	S	S	54	135		135		19

*General formula R—X—(CY)—Cl.
†Anal. Calcd. for C_4H_7ClOS: C, 34.9; H, 5.1; Cl, 25.7; S, 23.1. Found: C, 34.8; H, 5.2; Cl, 25.5; S, 22.8.
‡Anal. Calcd. for $C_4H_7ClS_2$: C, 31.1; H, 4.5; Cl, 23.0; S, 41.5. Found: C, 31.2; H, 4.4; Cl, 23.1; S, 41.3.

These results clearly show that replacement of either of the oxygen atoms of a chloroformate by sulfur is sufficient to cause a change from bimolecular hydrolysis (mechanism 1) to unimolecular hydrolysis (mechanism 2). Hence, the combined effects of two strongly electron-withdrawing groups (*e.g.*, the oxygen atoms of the chloroformates) are necessary to dictate bimolecular hydrolysis. It follows that all unsubstituted acyl chlorides should react unimolecularly with water, a conclusion that is supported by data for acetyl halides (7, 9). Trifluoroacetyl chloride should hydrolyze bimolecularly and trifluorothioacetyl chloride unimolecularly, but data to test these conclusions are not available. However, although benzoyl chloride seems to solvolyze by a bimolecular process (10), it has been suggested (11) that thiobenzoyl chlorides may react unimolecularly with methanol.

Experimental

Materials

The chlorothionoformate and chlorodithioformate esters were prepared by established methods (see Table 3) from thiophosgene and the corresponding alcohols and thiols, respectively. The compounds were purified by fractional distillation and shown to contain at least 99.4% of hydrolyzable chlorine.

Water was triply distilled from weakly alkaline potassium permanganate. Analar grade acetone was first distilled from alkaline permanganate and then from hydroquinone using a long fractionating column. 70% aqueous acetone was

Can. J. Chem. Downloaded from www.nrcresearchpress.com by 210.87.254.6 on 09/05/12
For personal use only.

prepared by mixing acetone (70 volumes) and water (30 volumes).

Measurement of Rates

The conductance methods used in these studies have been previously described (2, 12) as have the methods of calculating the rate constants. For the reactions in aqueous acetone, the resistance readings were converted to concentrations by means of large scale calibration curves. These curves were derived from measurements made using the completely reacted solutions of the various substrates, successive dilutions of these solutions being made so as to cover the complete ranges of conductance observed in the kinetic experiments.

Products of Hydrolysis

Methyl chlorothionoformate (4 ml) was shaken for 15 h with water (100 ml) and a sample (20 μl) of the solution examined by means of v.p.c. using a Poropak column. Methanol was identified as a component of the solution.

Methyl chlorodithioformate (2 ml) was added dropwise to 70% aqueous acetone (100 ml) in a flask fitted with a stirrer and a cold trap immersed in an acetone–Dry Ice bath. After 6 h there was no volatile material in the trap. The reaction mixture was evaporated to about a quarter of the original volume under reduced pressure and then extracted with methylene chloride (10 ml). After drying the extract and distilling off the solvent the yellow product was distilled at atmospheric pressure, b.p. 222 °C. The n.m.r. spectrum in deuterochloroform showed a single peak at 7.25 τ while the mass spectrum gave major peaks for masses 138 and 91, a smaller one at mass 76, and minor peaks at masses 47, 45, and 18. These results indicated that the product was methyl trithiocarbonate which is reported to boil at 225 °C (13). A sample of this compound was prepared by reacting methyl chlorodithioformate with methanethiol and shown to have identical properties to the above sample.

A similar experiment was carried out using refluxing 70% aqueous acetone. Methyl trithiocarbonate was again identified as a product but in this case the cold trap contained a volatile substance as well as a large amount of acetone. The volatile contents of the trap were reacted with a solution of 2,4-dinitrofluorobenzene in ethanol as previously described (3) to yield a yellow solid. Part of this solid was soluble in hot ethanol and the solution, on standing, yielded crystals of 2,4-dinitrophenyl methyl sulfide, m.p. and mixed m.p. with an authentic sample 126 °C (lit. 127 °C (14)). The insoluble fraction has not yet been identified.

The authors gratefully acknowledge the award of grants by the National Research Council of Canada. They also thank Miss Julia Queen for her careful measurements of the rates in the mixed solvents.

1. E. W. CRUNDEN and R. F. HUDSON. J. Chem. Soc. 3748 (1961).
2. A. QUEEN. Can. J. Chem. **45**, 1619 (1967).
3. A. QUEEN, T. A. NOUR, M. N. PADDON-ROW, and K. PRESTON. Can. J. Chem. **48**, 522 (1970).
4. R. LEIMU. Ber. **70**, 1040 (1937).
5. R. E. ROBERTSON. Prog. Phys. Org. Chem. **4**, 213 (1967).
6. G. KOHNSTAM. Adv. Phys. Org. Chem. **5**, 121 (1967).
7. R. F. HUDSON and G. E. MOSS. J. Chem. Soc. 5157 (1962).
8. P. M. LAUGHTON and R. E. ROBERTSON. Can. J. Chem. **34**, 1714 (1956). W. J. ALBERY and B. H. ROBINSON. Trans. Faraday Soc. **65**, 1623 (1969).
9. C. A. BUNTON and J. H. FENDLER. J. Org. Chem. **31**, 2307 (1966).
10. B. BENSLEY and G. KOHNSTAM. J. Chem. Soc. 4747 (1957).
11. S. SCHEITHAUER and R. MAYER. Ber. **98**, 838 (1965).
12. R. L. HEPPOLETTE and R. E. ROBERTSON. J. Am. Chem. Soc. **83**, 1834 (1961).
13. M. DELEPINE and P. SCHVING. Bull. Soc. Chim. Fr. **7**, 895 (1910).
14. R. W. BOST, J. O. TURNER, and R. D. NORTON. J. Am. Chem. Soc. **54**, 1985 (1932).
15. D. MARTIN and W. MUCKE. Ber. **98**, 2059 (1965).
16. W. AUTENREITH and H. HEFNER. Ber. **58**, 2151 (1925).
17. G. HILDETAG and R. PHILIPPSON. Monatsber. Dtsch. Akad. Wiss. Berlin. **6**, 585 (1964).
18. H. G. GODT and R. E. WANN. J. Org. Chem. **26**, 9047 (1961).
19. H. RIVIER. Bull. Soc. Chim. Fr. **1**, 737 (1907).

Can. J. Chem. Downloaded from www.nrcresearchpress.com by 210.87.254.6 on 09/05/12
For personal use only.

Steroids and Steroidases. XIV.[1] Studies on the Reactions of 2-Lithio-1,3-dithianes with Steroids Possessing Spiroepoxide Functions at C-3[2]

J. Bryan Jones and Roger Grayshan

Department of Chemistry, University of Toronto, Toronto 181, Ontario

Received December 2, 1971

The scope of the reactions of lithio-dithianes with spiro-epoxides for various stereospecific functionalizations of alicyclic systems has been illustrated by their application to spiro-3α- and -3β-oxiranes of the 5α-cholestane and 5α-androstane series.

La portée des réactions entre les lithio-dithianes et les époxydes spiranniques pour fonctionnaliser de façon stéréospécifique les systèmes cycliques a été illustrée par des applications sur les oxirannes-3α et 3β spiranniques dans les séries 5α-cholestane et 5α-androstane.

Canadian Journal of Chemistry, **50**, 1407 (1972)

Can. J. Chem. Downloaded from www.nrcresearchpress.com by 210.87.254.5 on 09/05/12
For personal use only.

The reactions of a 2-lithio-1,3-dithiane anion with appropriate 1,2 epoxides have been demonstrated to provide a versatile, convenient, and flexible method for the stereospecific introduction of substituents into the steroid nucleus (1*a*, *c*). The facility with which such reactions occurred encouraged us to explore the scope of lithio-dithiane-epoxide reactions further and the investigations have now been successfully extended to spiro-epoxides.

The ease with which spiro-epoxides would undergo reaction with dithiane anions, and establishment of the stereochemical integrity of the reactions, were evaluated on the readily available spiro-3α- and -3β-oxiranyl-5α-cholestanes **1** and **4**. The synthetic sequences followed are outlined in Scheme 1.

Treatment of 5α-cholestan-3-one with dimethylsulfonium methylide according to the literature procedure (2) gave a 95% yield of a mixture of **1** and **5** in the ratio 3:2. Although pure samples of **1** and **5** had not been obtained by this method in the previous work (2), it was found that separation of the two epimers could be effected by careful preparative layer chromatography (p.l.c.). The supply of the 3α-oxide **1** was augmented by its preparation in 80% yield from the 5α-cholestan-3-one-dimethylsulfoxonium methylide reaction (2) and in view of the more ready availability of the latter oxide, the initial experiments were carried out on the sequence of reactions involving compounds **1**–**4**.

When the 3α-epoxide **1** was kept with 2-lithio-1,3-dithiane in tetrahydrofuran at 0° for 2 days, the spiro-epoxide ring opened smoothly to give

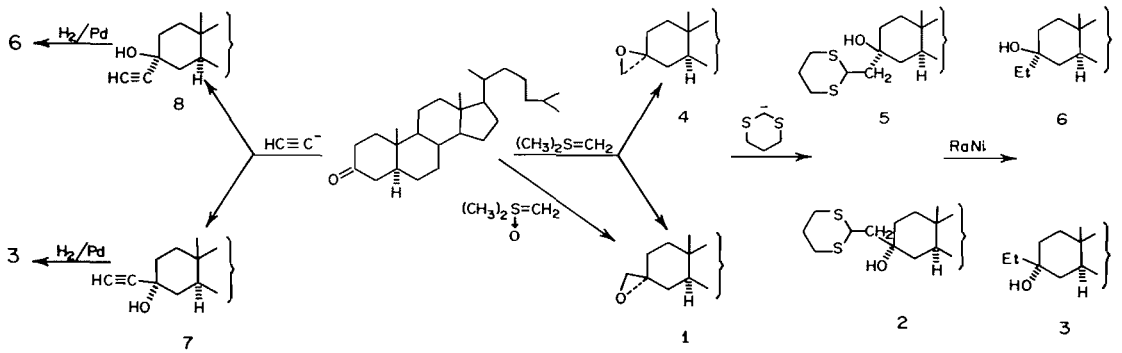

SCHEME 1

[1]For part XIII see ref. 1*a*.

[2]A communication on some of this work has been published (1*b*).

Can. J. Chem. Downloaded from www.nrcresearchpress.com by 210.87.254.5 on 09/05/12
For personal use only.

the hydroxydithianyl compound **2** in 85% yield. Although from the mode of formation of **2**, little doubt existed with regard to the stereochemistry at C-3, Raney nickel desulfurization of **2** to the hydroxyethyl derivative **3** (92% yield) was carried out in order to provide a convenient reference compound for which unambiguous assignment of the C-3 geometry could be made. That the C-3 configuration of **3** was as designated was confirmed by its preparation by catalytic hydrogenation of 3β-ethynyl-3α-hydroxy-5α-cholestane (**7**), the stereochemistry of which had been established previously (3).[3]

The corresponding reactions in the 3β-epoxide series proceeded with equal facility and treatment of **4** with 2-lithio-1,3-dithiane as described above yielded **5** in 86% yield. The C-3 configuration of the latter compound was again confirmed by its desulfurization (in 88% yield) to the corresponding hydroxyethyl derivative **6** which was shown to be identical with an authentic sample of 3α-ethyl-3β-hydroxy-5α-cholestane prepared by catalytic hydrogenation of the ethynyl compound **8** of known geometry (3).

The above results confirmed our expectations with regard to the facility of spiro-epoxide-dithiane reactions and their potential for stereospecific exocyclic functionalization of the steroid nucleus. Although all of our studies in this area had up to this time involved conversion of the dithianyl substituents into alkyl groups, several other types of transformations of these versatile intermediates have been well documented (5). Accordingly, attention was turned towards the application of the spiro-epoxide reactions for the introduction of functional groups other than alkyl. The compounds considered first were the βγ- and αβ-unsaturated ketoandrostanes **9** and **10** which were of interest to us as a potential substrate and inhibitor respectively of the Δ^5-3-ketoisomerase of *P. testosteroni*. Furthermore, it was desired to evaluate the biological activities of androstanes possessing C-3 functions of the 2′-oxopropyl type. The reactions carried out are outlined in Scheme 2. A mixture of spiro-3α-(**11**) and spiro-3β-oxiranyl-5α-androstan-17β-ol (**12**) in the proportions of 1:2 was obtained in 90% yield by reaction of 17β-hydroxy-5α-

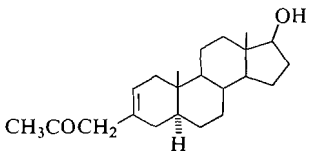

9

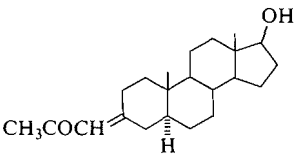

10

androstan-3-one with dimethylsulfonium methylide. The stereochemistry and spectral characteristics of **11** and **12** had been established previously (2) and corroboration of the assigned C-3 geometries was provided by a comparison of the spectral data of **11** and **12** with those determined for the analogous oxiranes of the cholestane series **1** and **4**. The proportions of each of **11** and **12** present were estimated from the areas of the characteristic epoxide CH_2 n.m.r. peaks at δ 2.61 and 2.57 p.p.m. respectively. The individual oxiranes could not be purified by any of the usual chromatographic methods and the subsequent dithiane reactions were therefore carried out on the mixture of the two epoxides.[4] Treatment of the epoxide mixture with 2-lithio-2-methyl-1,3-dithiane in tetrahydrofuran at 0° for 2 days yielded 68% of the corresponding dithianyl addition products **13** and **14**. The n.m.r. spectra of each isomer were quite distinctive, with the main differences being reflected in the positions of the C-19 methyl and dithianyl methyl peaks. For the 3α-hydroxy derivative **13**, these protons resonated at δ 0.75 and 1.77 p.p.m. respectively, while for the 3β-epimer **14**, they appeared at δ 0.85 and 1.80 p.p.m. Correlation of the n.m.r. spectra of **13** and **14** with the correct C-3 configuration was made using the C-19 methyl resonance of the corresponding cholestane analogues **2** and **5**, which occur at δ 0.74 and 0.83 p.p.m. respec-

[3]A 3-ethyl-3-hydroxy-5α-cholestane has been reported previously (4). A comparison of the physical data for this compound with those of the current work shows that this material has the same C-3 configuration as **3**.

[4]Repeated fractional recrystallization of the epoxide mixture has been reported (2) to give low yields of each of the pure epimers. However, in view of the quantities of material required to complete the proposed synthetic schemes, and the ease with which the subsequently obtained dithianyl acetates **15** and **16** could be separated, it was decided to bypass the epoxide separation procedure.

Can. J. Chem. Downloaded from www.nrcresearchpress.com by 210.87.254.5 on 09/05/12
For personal use only.

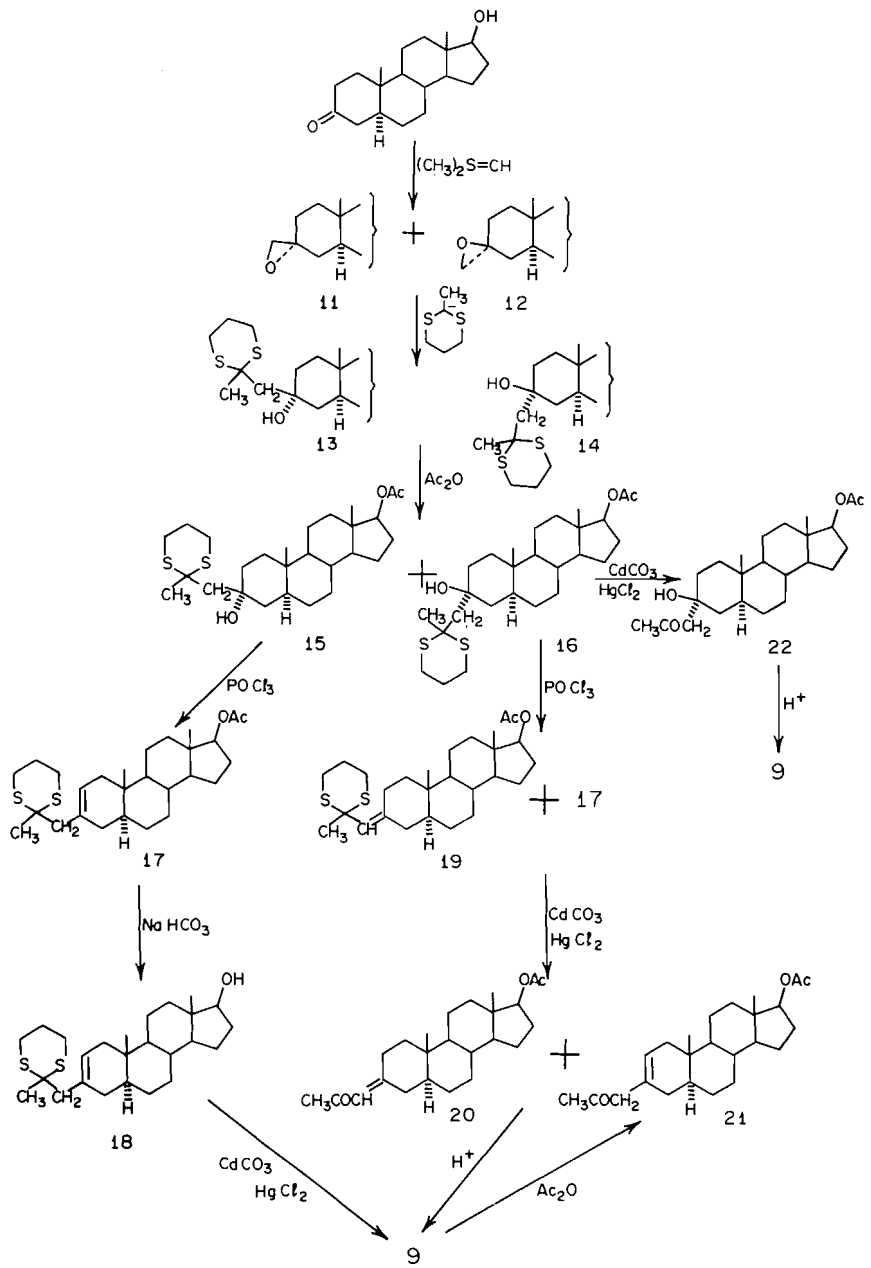

SCHEME 2

tively, for reference. The C-19 chemical shift differences for both pairs of epimers, **2** and **5**, and **13** and **14**, reflect C-19 deshielding by the C-3β hydroxyl groups which does not occur in the 3α-hydroxy compounds.

Since no further experiments could reasonably be carried out unless pure C-3 hydroxydithiane compounds could be obtained, the mixture of **13** and **14** was converted into the corresponding 17β-acetates **15** and **16** with acetic anhydride. Fortunately, the two acetates exhibited small differences in their chromatographic behavior

Can. J. Chem. Downloaded from www.nrcresearchpress.com by 210.87.254.5 on 09/05/12
For personal use only.

and following several fractional p.l.c. separations pure samples of each epimer were obtained.[5] The C-3 configurations of the hydroxydithianyl 17β-acetates were again assigned using the chemical shifts of the C-19 n.m.r. peaks as a basis for the correlation. For the 3α-hydroxyacetate **15**, the C-19 proton resonance occurred at δ 0.76 and for the 3β-hydroxy analogue **16** at δ 0.85 p.p.m.

It was anticipated that of the two desired en-ones **9** and **10**, the non-conjugated $\beta\gamma$-unsaturated isomer **9** would be thermodynamically the less stable,[6] and consequently it was decided to attempt its preparation first by introduction of the Δ^2-double bond prior to ketonization of the dithianyl function. Accordingly, elimination of the axial 3α-hydroxyl groups of **15** was effected with phosphoryl chloride in pyridine to give the Δ^2-compound **17** in 83% yield. The predominant formation of the Δ^2-isomer **17** (C-2 H at δ 5.45 p.p.m.) was expected on thermodynamic grounds. However, some of the less stable Δ^3-isomer was formed as evidenced by the C-4 olefin resonance at 0.28 p.p.m. higher field (6) than that of the C-2 vinyl peak of **17**. No still higher field n.m.r. peak ascribable to an exocyclic olefinic proton was observed. The small amounts of the Δ^3-compound formed during the preparation of **17** did not pose any separation problem since they were readily isomerized to the desired Δ^2-isomer by a trace of acid. Hydrolysis of the 17β-acetate of **17** under conditions which did not affect the dithianyl group was accomplished with sodium bicarbonate in methanol and the 17β-hydroxy product **18** was obtained in quantitative yield. Subsequent ketonization of the dithianyl function with the aqueous cadmium carbonate/mercuric chloride reagent (5) proceeded smoothly to give 49% of 3-(2′-ketopropyl)-5α-androst-2-en-17β-ol (**9**). That the product was the desired $\beta\gamma$-nonconjugated isomer was confirmed by the spectral data.

To our surprise, treatment of **9** with acid or base under a variety of conditions did not effect the expected isomerization to the conjugated isomer **10**. This was the first indication that for **9** and **10** the normal order of the thermodynamic stability of $\beta\gamma$- and $\alpha\beta$-unsaturated ketones was reversed. In order to obtain the desired compounds possessing an exocyclic C-3 double bond, phosphoryl chloride mediated dehydration of the 3β-hydroxydithiane **16** was carried out and the mixture of exocyclic olefinic **19** and Δ^2-dithianyl **17** products expected (7) was formed in 79% yield. However, the desired isomer **19** (identified by the C-19 methyl n.m.r. peak at δ 0.78) was the minor component. Disappointingly, separation of **17** and **19** could not be achieved even by repeated fractional p.l.c. and the mixture was therefore converted directly into the corresponding ketones **21** and **20** by hydrolysis under neutral conditions with aqueous cadmium carbonate/mercuric chloride. The $\beta\gamma$-unsaturated ketoacetate **21** was readily separated by p.l.c. and showed characteristic n.m.r. peaks at δ 0.80 (C-19 CH_3), 5.48 (C-2 H), and 2.99 p.p.m. (C-3 CH_2). This compound was also obtained in 89% yield by acetylation of **9** with acetic anhydride.

The presence in the mixture of the conjugated ketone **20** was established by the positions of the n.m.r. resonances of the C-19 methyl (δ 0.92) and COCH= (δ 5.99 p.p.m.) protons. Unfortunately, a pure sample of the conjugated ketone **20** could not be obtained owing to the facility with which it isomerized to **21** even under the mildest p.l.c. conditions. The attempts to prepare the $\alpha\beta$-unsaturated ketones **20** and **10** were therefore discontinued and the remaining mixture of **20** and **21** was converted directly to the $\beta\gamma$-unsaturated ketone **9** with aqueous methanolic hydrochloric acid.

The ketone **9** was also obtained smoothly *via* treatment of the dithianylacetate **16** with cadmium carbonate/mercuric chloride to give the hydroxy ketone **22** (62%). The subsequent acid-catalyzed hydrolysis and concomitant dehydration of **22** proceeded in 93% yield. Following the delineation of the reactions outlined in Scheme 2, it was found that quantities of **9** could be conveniently accumulated by direct ketonization of the mixture of the 17β-alcohols **11** and **12** (or their 17β-acetates **13** and **14**) obtained from the initial dithian-epoxide reaction.

With the ketone **9** being thermodynamically more preferred than its conjugated isomer **10**, our initial aim of studying its enzymic isomerization could obviously not be realized. It is unusual

[5]Small amounts of the two 3,17-diacetates were also present in the acetylated mixture. However, these were easily separated from the desired 17β-monoacetates **15** and **16** during the p.l.c. purification procedure.

[6]As discussed later, the converse was found to be true.

Can. J. Chem. Downloaded from www.nrcresearchpress.com by 210.87.254.5 on 09/05/12
For personal use only.

for a non-conjugated ketone to be the more stable and it is therefore of interest to consider some of the factors which would affect the relative stabilities of **9** and **10**. Spectral analyses of acid- or base-equilibrated mixtures of **9** and **10** indicated that the conjugated isomer is present to the extent of 1–2%. Thus the $\beta\gamma$-unsaturated compound **9** is favored by at least 2–3 kcal/mol (8). The marked propensity in 5α-steroids for a double bond to occupy the Δ^2-position in preference to C-3-exocyclic (9) would be a major component in the overall free energy balance favoring **9**. However, that this factor is not of overriding importance is demonstrated by the fact that for steroids analogous to **9** and **10**, but with $\alpha\beta$-unsaturated aldehyde (4, 10, 11), acid (4, 10), ester, and nitrile (12, 13) functions at C-3, the conjugated isomers are favored in each case. Such apparent contradictions are not restricted to the steroids. For example, similar reversals of isomer stabilities are observed with unsaturated keto- and carboxy-derivatives of cyclohexane (14, 15) and in view of the conflicting data currently available it is evident that a satisfactory rationalization for the relative stability of $\beta\gamma$-unsaturated ketones such as **9** must await further studies.

Experimental

Details of analytical methods, instrumentation, criteria of purity etc. used were as described previously (1). All p.l.c. separations were effected on silica gel G. Final drying of tetrahydrofuran was accomplished by distillation from lithium aluminum hydride. The i.r. and n.m.r. spectra were recorded on CCl_4 and $CDCl_3$ solutions respectively.

Spiro-3α-oxiranyl-5α-cholestane (1) and Spiro-3β-oxiranyl-5α-cholestane (4)

A 95% yield of a mixture of the spiro-oxiranylcholestanes **1** and **4** in the ratio 3:2 (by n.m.r.) was obtained by reaction of 5α-cholestan-3-one with dimethylsulfonium methylide in tetrahydrofuran according to the procedure of Cook *et al.* (2). The epoxides were separated by p.l.c. using benzene–hexane (1:1) as developing solvent. Final recrystallizations from methanol yielded the 3α-epoxide **1**, m.p. 127–128° (lit. (16) m.p. 129–130°) and the 3β-epoxide **4**, m.p. 172–173° (lit. (16) m.p. 175–176°).

3β-(2′-(1,3-Dithianyl))methyl-5α-cholestan-3α-ol (2)

To a solution of 2-lithio-1,3-dithiane (1 g, 8.1 mmol) prepared by the slow addition of *n*-butyl lithium (4.7 ml of a 1.6 *M* hexane solution, 8.1 mmol) to 1,3-dithiane (0.9 g, 8.1 mmol) in freshly dried tetrahydrofuran (21 ml) at −20° under dry nitrogen (5) was added spiro-3α-oxiranyl-5α-cholestane (**1**, 1.08 g, 2.7 mmol) in dry tetrahydrofuran (7 ml), also at −20°. After keeping for 2 days at 0° the mixture was poured into water (500 ml) and extracted with ether (4 × 50 ml). The combined ether extracts were washed with water (2 × 25 ml) and then dried ($MgSO_4$) and evaporated. The residual gum was purified by p.l.c. using ether–benzene (1:50) as developing solvent followed by recrystallization from ether–methanol to give the 3β-dithianyl-methyl-5α-cholestan-3α-ol **2** (1.2 g) m.p. 190°; i.r. 1278 and 914 cm^{-1} (dithianyl); n.m.r. δ 0.64 (C-18 CH_3), 0.74 (C-19 CH_3), 1.90 (2H, d, J = 7 Hz, C-3 CH_2), and 4.29 p.p.m. (1 H, t, J = 7 Hz, HCS_2).

Anal. Calcd. for $C_{32}H_{56}OS_2$: C, 73.8; H, 10.8; S, 12.3. Found: C, 73.9; H, 10.8; S, 12.3.

3β-Ethyl-5α-cholestan-3α-ol (3)

The above 3β-dithianyl-3α-ol **2** (0.15 g, 0.29 mmol) in ethanol (30 ml) was refluxed with freshly prepared Raney nickel (1.5 g) for 4 h. The filtered ethanolic solution was then evaporated to give 3β-ethyl-5α-cholestan-3α-ol (**3**, 0.11 g) which after recrystallization from ether–methanol was identical with an authentic sample, m.p. and mixed m.p. 109–110°.

The authentic sample was prepared in quantitative yield from 3β-ethynyl-5α-cholestan-3α-ol (**7**) m.p. 104–105° (obtained according to the procedure of Giraud *et al.* (3)) by hydrogenation in ethanol over 10% Pd–C; n.m.r. δ 0.66 (C-18 CH_3) and 0.74 p.p.m. (C-19 CH_3).

Anal. Calcd. for $C_{29}H_{52}O$: C, 83.4; H, 12.6. Found: C, 83.5; H, 12.7.

3α-(2′-(1,3-Dithianyl))methyl-5α-cholestan-3β-ol (5)

2-Lithio-1,3-dithiane (0.9 g, 7.1 mmol) in freshly dried tetrahydrofuran (18 ml) at −20° was reacted with spiro-3β-oxiranyl-5α-cholestane (**4**, 0.99 g, 2.5 mmol) in dry tetrahydrofuran (7 ml) as described above for the 3α-hydroxy isomer **2**. The p.l.c. purification with ether–benzene (1:20) as developing solvent gave the 3α-dithianylmethyl-5α-cholestan-3β-ol **5** (1.09 g), m.p. 132°, after recrystallization from ether–methanol; i.r. 1278 and 914 cm^{-1} (dithianyl); n.m.r. δ 0.64 (C-18 CH_3), 0.83 (C-19 CH_3), 2.14 (2H, d, J = 6.5 Hz, C-3 CH_2), and 4.19 p.p.m. (1H, t, J = 6.5 Hz, HCS_2).

Anal. Calcd. for $C_{32}H_{56}OS_2$: C, 73.8; H, 10.8; S, 12.3. Found: C, 73.9; H, 11.1; S, 12.1.

3α-Ethyl-5α-cholestan-3β-ol (6)

The 3α-dithianyl-3β-hydroxycholestane **5** described above (0.21 g, 0.4 mmol) in ethanol (40 ml) was heated under reflux for 4 h with freshly prepared Raney nickel (2 g). Filtration of the mixture followed by evaporation yielded 3α-ethyl-5α-cholestan-3β-ol (**6**, 0.51 g). The material obtained was identical, m.p. and mixed m.p. 138–138.5°, n.m.r. δ 0.66 (C-18 CH_3) and 0.83 p.p.m. (C-19 CH_3), with a sample prepared (quantitative yield) by hydrogenation in ethanol over 10% Pd–C of 3α-ethynyl-5α-cholestan-3β-ol (**8**) m.p. 165–167° (3).

Anal. Calcd. for $C_{29}H_{52}O$: C, 83.4; H, 12.6. Found: C, 83.3; H, 12.6.

The Reactions of 2-Lithio-2-methyl-1,3-dithiane with Spiro-3α-oxiranyl-5α-androstan-17β-ol (11) and Spiro-3β-oxiranyl-5α-androstan-17β-ol (12)

5α-Androstan-17β-ol-3-one and dimethylsulfonium methylide were reacted as described by Cook *et al.* (2) to give, after p.l.c. purification, a 90% yield of a mixture of the spiro-epoxides **11**, n.m.r. δ 0.75 (C-18 CH_3), 0.87 (C-19 CH_3), and 2.62 p.p.m. (2H, broad s, C-3 CH_2), and **12**, n.m.r.

Can. J. Chem. Downloaded from www.nrcresearchpress.com by 210.87.254.5 on 09/05/12
For personal use only.

δ 0.75 (C-18 CH_3), 0.88 (C-19 CH_3), and 2.57 p.p.m. (2H, broad s, C-3 CH_2) in the ratio 1:2.

To a solution of 2-lithio-2-methyl-1,3-dithiane (8.25 g, 60 mmol), prepared by the slow addition of *n*-butyl lithium (3.78 g, 60 mmol, 36.75 ml of a 1.6 *M* in hexane solution) to 2-methyl-1,3-dithiane (7.95 g, 60 mmol) in freshly dried tetrahydrofuran (150 ml) at $-20°$ under nitrogen (5), was added the above mixture of spiro-epoxides **11** and **12** (4.3 g, 14 mmol) dissolved in dry tetrahydrofuran (37 ml) at $-20°$. The mixture was kept for 2 days at 0° and was then worked-up as described previously for the analogous cholestane compounds **2** and **5**. The p.l.c. purification of the gum obtained yielded 4.2 g of an inseparable mixture of the 3α-hydroxydithiane **13**, n.m.r. δ 0.73 (C-18 CH_3), 0.75 (C-19 CH_3), and 1.77 p.p.m. (CH_3CS_2), and the 3β-hydroxy-dithiane **14**, n.m.r. δ 0.73 (C-18 CH_3), 0.85 (C-19 CH_3), and 1.80 p.p.m. (CH_3CS_2).

The above mixture of **13** and **14** (4.2 g) was refluxed with acetic anhydride (20 ml) for 20 min and the cooled reaction mixture was then evaporated. Fractional p.l.c. of the residue (4.8 g) using ethylacetate–hexane (1:4) developments yielded samples of the two 17β-acetates. The 17β-acetoxy-3β-(2′-oxopropyl)-5α-androstan-3α-ol 1,3-propylenethioketal (**15**) was recrystallized from methanol to give 0.46 g of material m.p. 184°; i.r. 908 cm^{-1} (dithianyl); n.m.r. δ 0.76 (C-18 CH_3), 0.78 (C-19 CH_3), 1.78 (3 H, s, CH_3CS_2), 2.03 (3 H, s, 17β-OAc), 2.18 (2 H, s, C-3 CH_2), and 4.59 p.p.m. (1 H, t, $J = 7.5$ Hz, C-17α H).

Anal. Calcd. for $C_{27}H_{44}O_3S_2$: C, 67.5; H, 9.2; S, 13.4. Found: C, 67.5; H, 9.4; S, 13.4.

The 17β-acetoxy-3α-(2′-oxopropyl)-5α-androstan-3β-ol 1,3-propylenethioketal (**16**) fraction was recrystallized from methanol to give 0.8 g of pure material, m.p. 136–137°, i.r. 906 cm^{-1} (dithianyl); n.m.r. δ 0.79 (C-18 CH_3), 0.85 (C-19 CH_3), 1.81 (3H, s, CH_3CS_2), 2.04 (3H, s, 17β-OAc), 2.30 (2H, s, C-3 CH_2), and 4.59 p.p.m. (1H, t, $J = 7.5$ Hz, C-17α H).

Anal. Calcd. for $C_{27}H_{44}O_3S_2$: C, 67.5; H, 9.2; S, 13.4. Found: C, 67.8; H, 9.4; S, 13.5.

*17β-Acetoxy-3-(2′-oxopropyl)-5α-androst-2-ene 1.3-propylenethioketal (**17**)*

Phosphoryl chloride (7 ml) was added dropwise with vigorous stirring at 0° to the dithianyl acetate **15** (0.35 g, 0.73 mmol) in dry pyridine (70 ml). The mixture was stirred overnight at 20° and was then poured into ice-water and extracted with ether (3 × 50 ml). The ether extracts were washed *rapidly* with ice-cold 0.1 *N* aqueous hydrochloric acid (50 ml) and were then dried ($MgSO_4$) and evaporated. The residual solid was purified by p.l.c. using ether–benzene (1:1) as developing solvent followed by recrystallization from ether–methanol to give the 17β-acetoxy-Δ^2-dithiane **17** (0.28 g) m.p. 164–165°; i.r. 908 cm^{-1} (dithianyl); n.m.r. δ 0.77 (C-18 CH_3), 0.79 (C-19 CH_3), 1.67 (3H, s, CH_3CS_2), 2.03 (3H, s, C-17β OAc), 2.58 (2H, s, C-3 CH_2), 4.60 (1H, t, $J = 7$ Hz, C-17α H), and 5.45 p.p.m. (1H, m, C-2 H).

Anal. Calcd. for $C_{27}H_{42}O_2S_2$: C, 70.1; H, 9.2; S, 13.9. Found: C, 70.1; H, 9.2; S, 14.0.

*17β-Hydroxy-3-(2′-oxopropyl)-5α-androst-2-ene 1.3-propylenethioketal (**18**)*

The 17β-acetate **17** (0.22 g) in methanol (40 ml) containing saturated aqueous sodium bicarbonate (2 ml) was refluxed for 12 h and then poured into water (200 ml). Extraction with chloroform (3 × 50 ml) followed by evaporation of the dried ($MgSO_4$) chloroform solution yielded the 17β-hydroxy-Δ^2-dithiane **18** (0.18 g) m.p. 158–159°, i.r. 3460, and 908 cm^{-1} (dithianyl); n.m.r. δ 0.75 (6H, s, C-18 and C-19 CH_3), 1.67 (3H, s, CH_3CS_2), 2.58 (2H, s, C-3 CH_2), 3.65 (1H, t, $J = 7$ Hz, C-17α H), and 5.45 (1H, m, C-2 H).

*Preparation and Attempted Isolation of 17β-Acetoxy-3-(2′-oxopropylidene)-5α-androstane (**20**)*

Phosphoryl chloride (25 ml) was added dropwise with vigorous stirring at 0° to the 3β-hydroxydithianyl acetate **16** (1.1 g, 2.3 mmol) in dry pyridine (250 ml). The mixture was stirred for a further 12 h at 20° and was then worked-up as described above for **17**. The product (0.84 g) was not resolvable by p.l.c. but was shown by n.m.r. analysis to be a mixture of the Δ^2-dithiane **17** isolated previously and 17β-acetoxy-3-(2′-oxopropylidene)-5α-androstane 1,3-propylidenethioketal (**19**), n.m.r. δ 0.78 (C-18 CH_3), 0.88 (C-19 CH_3), 1.83 (3H, s, CH_3CS_2), 2.03 (3H, s, C-17β OAc), and 5.33 p.p.m. (1H, s, COCH=).

The above mixture of **17** and **19** (0.8 g) in acetone–water (80 ml, 20:1) was stirred with mercuric chloride (0.8 g) and cadmium carbonate (0.8 g) at 20° for 1 day and was then filtered and evaporated (5). The residue was extracted with chloroform (100 ml) and the chloroform solution dried ($MgSO_4$) and evaporated. Fractional p.l.c. of the residue (0.56 g) with ether–benzene (1:15) as the developing solvent yielded only the Δ^2-ketone **21** (characterized as described later) in a pure form. The desired exocyclic olefin **20** present in the fractions isomerized progressively during the p.l.c. procedure and isolation of a pure sample by this approach was precluded by its instability.

*17β-Acetoxy-3α-(2′-oxopropyl)-5α-androstan-3β-ol (**22**)*

A solution of the 3β-hydroxydithianylacetate **16** (0.3 g, 0.63 mmol) in acetone–water (30 ml, 20:1) was treated with mercuric chloride (0.3 g) and cadmium carbonate (0.3 g) by the general ketonization procedure detailed in the attempted preparation of **20**. P.l.c. purification with ether–benzene (2:3) as developing solvent, followed by recrystallization from ether–methanol gave 17β-acetoxy-3α-(2′-oxopropyl)-5α-androstan-3β-ol (**22**, 0.15 g), m.p. 164–165°; i.r. 3534 and 1718 cm^{-1} (broad).

Anal. Calcd. for $C_{24}H_{38}O_4$: C, 73.8; H, 9.7. Found: C, 73.9; H, 9.8.

*17β-Hydroxy-3-(2′-oxopropyl)-5α-androst-2-ene (**9**)*

*(a) From the Pure Dithiane **18***

The dithiane **18** (0.18 g, 0.43 mmol) was dissolved in acetone–water (20 ml, 20:1) and the dithianyl function hydrolyzed in the presence of mercuric chloride (0.2 g) and cadmium carbonate (0.2 g) by the general procedure described for compound **20**. P.l.c. of the crude product with ether–benzene (1:4) as the developing solvent and recrystallization from cold ether afforded 17β-hydroxy-3-(2′-oxopropyl)-5α-androst-2-ene (**9**, 70 mg), m.p. 110–111°; i.r. 1708 cm^{-1}; n.m.r. 0.77 (6H, s, C-18 and C-19 CH_3), 2.13 (3H, s, CH_3CO), 3.01 (2H, s, C-3 CH_2), 3.64 (1H, t, $J = 8$ Hz, C-17α H), and 5.48 p.p.m. (1H, m, C-2 H).

Anal. Calcd. for $C_{22}H_{34}O_2$ (mol. wt. 330.2559): C, 80.0; H, 10.4. Found (330.2553 (mass spectrum)): C, 80.1; H, 10.3.

(b) From Mixtures of ***13*** *and* ***14****, and* ***15*** *and* ***16***

In a typical experiment, a mixture of the 17β-acetates **15** and **16** (2 g) was dissolved in acetone–water (200 ml, 20:1) and treated with mercuric chloride (2 g) and cadmium carbonate (2 g) in the usual way. The gum (1.5 g) obtained was then refluxed for 1 day in methanol (150 ml) containing 10% aqueous hydrochloric acid (10 ml). Purification of the product as in section *a* yielded 1.4 g of **9**, m.p. 110–111°.

When the 17β-hydroxy compounds **13** and **14** were used, the final acid-catalyzed hydrolysis step was omitted.

(c) From a Mixture of ***20*** *and* ***21***

The mixture of the unsaturated ketones **20** and **21** (0.1 g) obtained from **19**, dissolved in methanol (20 ml) containing 0.1 *N* aqueous hydrochloric acid (1 ml), was heated under reflux for 12 h. The usual work-up and purification afforded **9** (80 mg), m.p. 108–110°.

(d) From ***22***

Hydrolysis of the 17β-acetate **22** (0.14 g) as described for section *c* above yielded 0.11 g of **9**, m.p. 110–111°.

Equilibration of **9** by treatment with methanolic hydrochloric acid or methanolic sodium hydroxide did not result in the formation of a detectable amount of the $\alpha\beta$-unsaturated isomer **10**.

*17β-Acetoxy-3-(2′-oxopropyl)-5α-androst-2-ene (****21****)*

The 17β-ol **9** (0.1 g) and acetic anhydride (5 ml) were refluxed for 20 min. The mixture was then evaporated and purified by p.l.c. (developing solvent ether–benzene (1:12)) followed by recrystallization from ether–methanol to give **21** (98 mg), m.p. 123–124°; i.r. 1718 cm^{-1} (broad); n.m.r. δ 0.76 (C-18 CH_3), 0.80 (C-19 CH_3), 2.03 (3H, s, C-17β-OAc), 2.13 (3H, s, CH_3CO), 2.99 (2H, s, C-3 CH_2) and 5.48 p.p.m. (C-2 H).

We express our thanks to the National Research Council of Canada and to the University of Toronto School of Graduate Studies for the award (to R.G.) of a Postdoctoral Fellowship.

1. (*a*) J. B. Jones and R. Grayshan. Can. J. Chem. **50**, 810 (1972); (*b*) Chem. Commun. 741 (1970); (*c*) Chem. Commun. 141 (1970).
2. C. E. Cook, R. C. Corley, and M. E. Wall. J. Org. Chem. **33**, 2789 (1968).
3. A. M. Giraud, A. Rassat, P. Witz, and G. Ourisson. Bull. Soc. Chim. Fr. **31**, 3240 (1964).
4. N. A. Milas and C. P. Priesing. J. Am. Chem. Soc. **80**, 2189 (1958).
5. E. J. Corey and D. Seebach. Angew. Chem. Int. Ed. **4**, 1075 (1965); D. Seebach. Synth. 17 (1969).
6. G. M. L. Cragg, C. W. Davey, D. N. Hall, G. D. Meakins, E. E. Richards, and T. L. Whateley. J. Chem. Soc. C, 1266 (1966).
7. D. N. Kirk and P. M. Shaw. J. Chem. Soc. C, 182 (1970).
8. E. L. Eliel, N. L. Allinger, S. J. Angyal, and G. A. Morrison. Conformational analysis. Interscience, New York, 1965, p. 11.
9. R. C. Cookson, D. P. G. Hamon, and R. E. Parker. J. Chem. Soc. 5014 (1962).
10. N. A. Milas. U.S. Pat. 2 997 486.
11. W. Nagata and Y. Hayase. Ger. Pat. 1 911 768.
12. G. Drefahl, K. Ponsold, and H. Schick. Chem. Ber. **97**, 2011 (1966).
13. A. K. Bose and R. T. Dahill. J. Org. Chem. **30**, 505 (1965).
14. J. K. Groves and N. Jones. Tetrahedron Lett. 1161 (1970).
15. H. Gerlach. Helv. Chim. Acta, **49**, 1291 (1966).
16. B. N. Blackett, J. M. Coxon, M. P. Hartshorn, and C. N. Muir. Tetrahedron, **25**, 1479 (1969).

Can. J. Chem. Downloaded from www.nrcresearchpress.com by 210.87.254.5 on 09/05/12
For personal use only.

Steroids and Steroidases. XV.[1] Investigations of Some 2-Lithio-1,3-dithiane Reactions Directed Towards the Introduction of Corticoid and Related Functions at C-17 of the Steroid Nucleus[2]

J. Bryan Jones and Roger Grayshan

Department of Chemistry, University of Toronto, Toronto 181, Ontario

Received December 2, 1971

The potential of 2-lithio-1,3-dithiane reactions for the introduction of corticoid and related C-17 functions into the steroid nucleus has been explored. Although attempts to effect the direct addition of the dithiane reagents to C-17 ketones met with limited success, reactions of C-17 spiroepoxides were found to provide a convenient entry into routes to homocorticoid compounds.

La possibilité d'introduire le système corticoide et les fonctions apparentées sur le carbone C-17 du noyau stéroide a été explorée avec les réactions du lithio-2 dithiane-1,3. Bien que les essais d'addition directe entre les réactifs dithiane et les cétones C-17 soient d'un succès limité, on a constaté que les réactions avec les spiroépoxydes C-17 fournissent une voie convenable permettant l'accès aux composés homocorticoides.

Canadian Journal of Chemistry, **50**, 1414 (1972)

As a result of previous studies (1) evaluating the potential of 2-lithio-1,3-dithiane reactions for effecting stereospecific introductions of various functional groups into the steroid nucleus, we became interested in the possible utilization of dithiane reagents for the elaboration of C-17 functions of the corticoid types. Corey and his co-workers had demonstrated that their additions to carbonyl groups were often facile (2) and reaction of an appropriately substituted dithiane with a steroidal C-17 ketone therefore presented itself as an attractive initial step to the desired 17-hydroxy-20-oxo function outlined in Scheme 1. From the literature (3, and references therein) regarding the stereochemistry of addition of nucleophiles to steroid-17-ones, the hydroxydithianyl intermediate **2** was expected to be a mixture of the two C-17 epimers with the 17β-hydroxy compound predominating. However, it was hoped that the proportion of the 17α-hydroxy epimer present would be sufficient to make the route a viable one for the preparation of steroids possessing the general C-17 corticoid pattern represented in partial structure **3**.

The hydroxymethyldithiane, **1**, R = CH_2OH required for the introduction of the characteristic 17,21-dihydroxy-20-oxo corticoid function via the projected reactions of Scheme 1 was not a

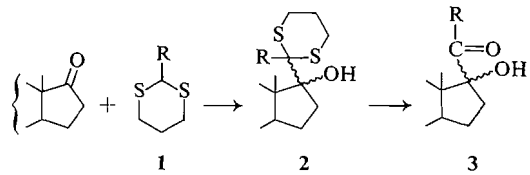

1 **2** **3**

Scheme I

known compound and the validity of the approach was evaluated initially using the readily available 2-methyl analogue **1**, R = CH_3. The potential cortexolone precursor androst-4-ene-3,17-dione, with its Δ^4-3-keto moiety protected as the Δ^5-ethylene ketal, was selected for the initial experiments. The ethylene ketal **4** was reacted with 2-methyl-1,3-dithiane anion and the 17β-hydroxy-17α-dithianyl derivative **5** was obtained in 59% yield (see Scheme 2). Disappointingly, t.l.c. and spectral analyses (*e.g.* only one C-18 CH_3 n.m.r. peak at δ 0.99 p.p.m.) did not indicate that any significant amount of the epimer with the desired 17α-hydroxy configuration was formed during the addition reaction. The hydroxydithiane **5** was unstable and at room temperature decomposed with discoloration to give a mixture of much more polar (by t.l.c.) compounds. Accordingly, the dithiane **5** was subjected to the neutral mercuric chloride – cadmium carbonate in aqueous acetone deketalization conditions (2) immediately following its p.l.c. purification. However, in spite of repeated hydrolysis attempts, none of

[1]For Part XIV see reference 1*a*.

[2]A summary of part of this work was included in a preliminary communication (1*b*).

Can. J. Chem. Downloaded from www.nrcresearchpress.com by 210.87.254.105 on 09/05/12
For personal use only.

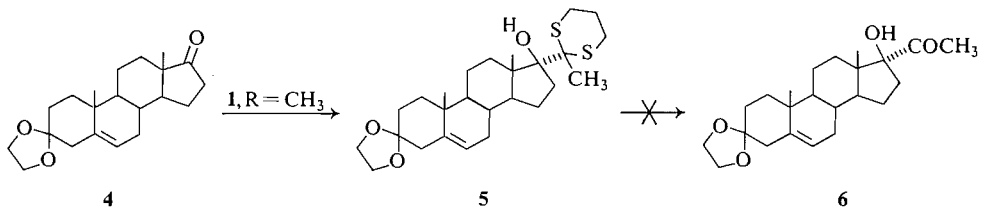

4 5 6

SCHEME 2

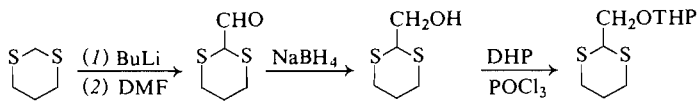

7 1, R = CH_2OH 8

SCHEME 3

the 17-hydroxy-20-ketone **6** could be detected in the multiple component reaction mixture. This was not entirely unexpected in view of the predilection of α-ketols to undergo further reactions (4). In order to prevent such complications, protection of the 17-hydroxyl group of **5** as the acetate was considered, but our endeavors to effect 17-acetylation of **5** under a variety of conditions resulted only in the formation of complex reaction mixtures. An alternative attempt to preclude α-ketol and subsequent decompositions by dehydration of **5** with thionyl chloride to the corresponding Δ^{16}-dithiane, for which re-introduction of a hydroxyl function into the required 17α-orientation following the dithiane hydrolysis step was an attractive possibility, was equally unrewarding.

Subsequently, the synthesis of 2-hydroxymethyl-1,3-dithiane (**1**, R = CH_2OH) was achieved as outlined in Scheme 3. A formyl group was introduced at C-2 of 1,3-dithiane by reaction of its anion with dimethylformamide and the unstable 2-formyl-1,3-dithiane (**7**) obtained was reduced directly with sodium borohydride to give the hydroxymethyl compound **1**, R = CH_2OH in 82% yield. Its n.m.r. spectrum in DMSO-d_6-D_2O was a complex one in which the eight-line AB_2 pattern of the C-2 H and hydroxymethylene protons was superimposed on the C-4 and -6 methylene multiplets centered at δ 2.85 p.p.m. Spin decoupling of the C-2 and $CH_2O(D)$ protons resulted in their collapse to singlets at δ 4.07 and 3.68 p.p.m. respectively. Surprisingly, **1**, R = CH_2OH was recovered unchanged when treated with toluene-*p*-sulfonic acid in benzene under conditions effecting dehydration of its substituted analogues (2).[3]

The dithianyl anion of 2-hydroxymethyl-1,3-dithiane required for effecting the C-17 carbonyl addition reaction of Schemes 1 and 2 could not be formed owing to the insolubility of the lithium alkoxide salt formed when **1**, R = CH_2OH was treated with *n*-butyllithium in tetrahydrofuran. Consequently, the hydroxyl group was protected as the tetrahydropyranyl ether with the product **8** being obtained in 83% yield (after p.l.c. purification). On mixing with *n*-butyllithium in tetrahydrofuran in the usual way, the tetrahydropyranyl derivative **8** appeared to form the desired anion. Unfortunately, it proved to be unstable in the basic reaction medium (*cf.* footnote 3 and ref. 5) and could not be trapped even using the standard (2) alkylation with methyl iodide assay. In view of the difficulties encountered with respect to formation of the desired dithianyl anions, and the problems associated with the generation of α-ketol functions from intermediates such as **5**, work on the Scheme 1 approach to cortico-steroids was discontinued.

Attention was then focussed on related routes to homocorticoid derivatives based on dithiane-spiro-epoxide reactions as outlined in Scheme 4. That reactions of dithiane anions with steroidal

[3]This attempt to prepare 2-methylene-1,3-dithiane was prompted by the report of its instability when formed under basic conditions (5).

Can. J. Chem. Downloaded from www.nrcresearchpress.com by 210.87.254.105 on 09/05/12
For personal use only.

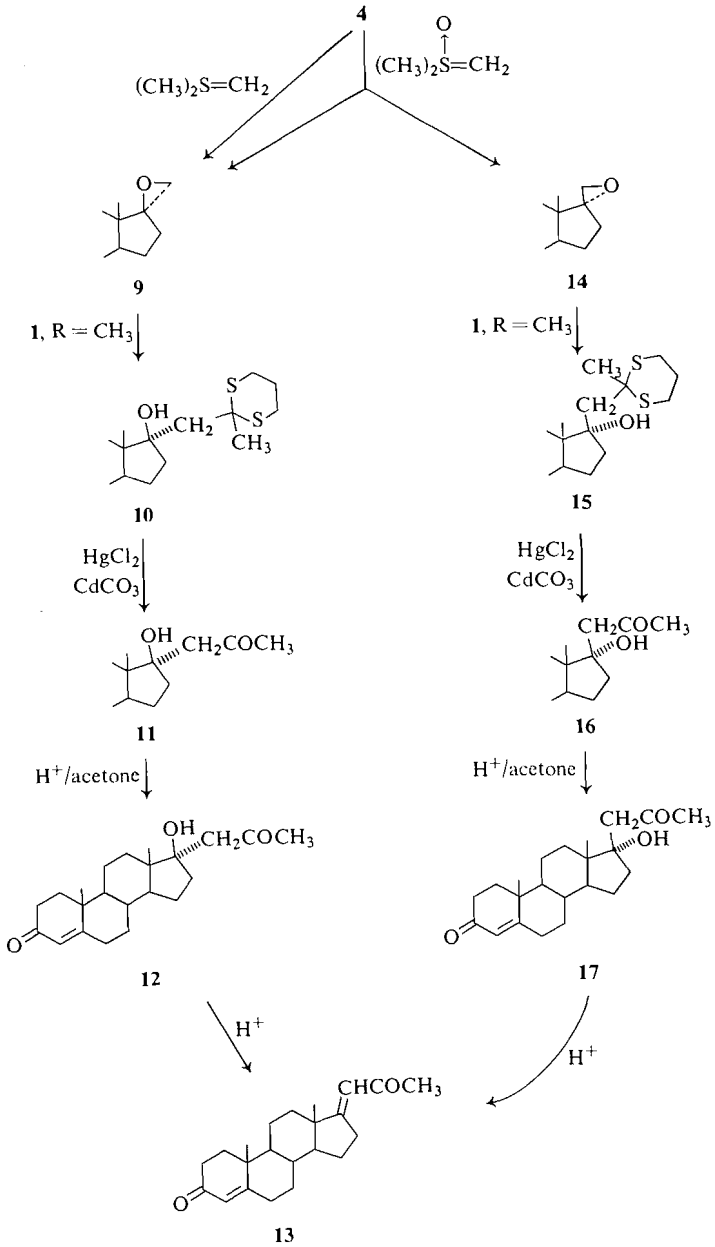

SCHEME 4

C-3 spiro-epoxides occurred smoothly and stereospecifically had been established previously (1*a*) and the corresponding reactions with C-17 spiro-oxiranes have now been shown to be equally facile. As shown in Scheme 4 the feasibility of the reactions contemplated was again explored with the readily available 2-methyl dithiane **1**, R = CH_3. The C-17 epoxides were prepared by reaction of the Δ^5-3-ethyleneketal **4** with dimethylsulfoxonium methylide (6), which gave a 96% yield of an inseparable mixture of the two epimers **9** and **14**, or with sulfonium methylide (6) which yielded the 17β-oxirane **9** exclusively in 97% yield (3). Since of

Can. J. Chem. Downloaded from www.nrcresearchpress.com by 210.87.254.105 on 09/05/12
For personal use only.

Can. J. Chem. Downloaded from www.nrcresearchpress.com by 210.87.254.105 on 09/05/12
For personal use only.

the two epoxides only the latter oxirane **9** was available in a pure form it was used in the initial experiments.

Opening of the epoxide ring of **9** with 2-methyl-1,3-dithianyl anion proceeded smoothly to give the 17β-hydroxydithiane **10** in 69% yield. In contrast to our experience with compound **5**, no difficulties were encountered during the mercuric chloride–cadmium carbonate mediated hydrolysis of the dithianyl group of **10** and the 17β-hydroxyketone **11** was obtained in 94% yield. Removal of the C-3 ethyleneketal function was effected with toluene-*p*-sulfonic acid in acetone to give 17α-acetonyltestosterone **12** (78%). When the acidic reaction conditions were applied for a more prolonged period, dehydration of **12** occurred to give 68% of the $\Delta^{17,20}$-homoprogesterone **13**.

The 17-hydroxy-21-oxo-compound **12** obtained by the above route has a C-17 configuration opposite to that present in naturally occurring cortico-steroids. Accordingly, in order to obtain the corresponding "homocorticoid" compound of the epimeric 17α-hydroxy series, the reactions were repeated using the 17α-oxirane **14**. As mentioned above, the mixture of C-17 epoxides containing **14** obtained by reaction of **4** with dimethylsulfoxonium methylide could not be resolved. The mixture was calculated to contain **9** and **14** in the ratio of ~2:1 by measurement of the relative intensities of the C-18 CH_3 peaks at δ 0.90 and 0.84 p.p.m. respectively and, after p.l.c. purification, it was used directly in the subsequent experiments. On reaction with the anion of **1**, R = CH_3, the corresponding hydroxydithianes **10** and **15** were obtained and p.l.c. separation afforded pure samples of each in 68 and 62% yields respectively from their parent epoxides. The sample of the 17β-hydroxy epimer **10** was identical with the material obtained previously from the pure oxirane **9**. The C-17 epimeric relationship of **10** and **15** was most readily illustrated by the chemical shift differences of the C-18 CH_3 peaks in the n.m.r. spectra (0.87 and 0.69 p.p.m. respectively). Neutral hydrolysis of **15** under the conditions applied to the corresponding 17β-epimer **10** gave 58% of the 17α-hydroxy-21-ketone **16** possessing the desired C-17 homocorticoid configuration and substitution pattern. Subsequent ketonization of the 3-ethyleneketal function of **16** to generate the 17α-hydroxyhomoprogesterone **17**, was again readily effected by acid-catalyzed exchange with acetone. However, owing to the ease with which the 17α-hydroxyl group of **17** underwent acid-catalyzed elimination during the work-up procedure, a significant proportion of the dehydrated product **13** was also formed. This situation contrasts with that in the corresponding 17β-series where the rate of ketonization of **10** was much greater than that of the subsequent elimination reaction.[4]

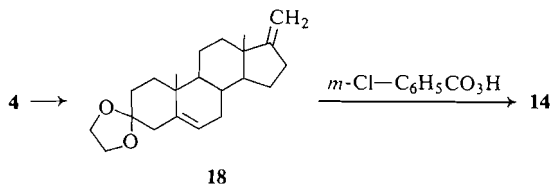

18

SCHEME 5

The samples of $\Delta^{17,20}$-homoprogesterone **13** obtained from both the 17α- and 17β-routes proved identical in all respects and all the t.l.c. and spectral data indicated that only one of the two $\Delta^{17,20}$-geometrical isomers was present. Assuming that the dehydrations of both **12** and **17** involve a *trans*-antiparallel elimination mechanism, examinations of molecular models suggest that an E configuration (7) 17,20-olefinic bond should be formed preferentially.

Subsequently, a more satisfactory route to the starting 17α-oxirane **14** was developed as outlined in Scheme 5. The C-17 ketone **4** was converted into the 17-methylene compound **18** in 77% yield using the normal Wittig procedure. On treatment of **18** with *m*-chloroperoxybenzoic acid in chloroform the main product was the desired 17α-oxirane **14** with the epimeric epoxide **9** present to a very minor extent. Use of peroxyacetic acid as the epoxidizing reagent afforded a mixture containing both C-17 and C-5,6 epoxides.

With relatively pure 17α-spiroepoxide **14** available, an extension of the reactions of Scheme 4 to the preparation of a "true homocorticoid", such as the C-22-hydroxy derivative of **17**, using the dithianes **1**, R = CH_2OH or **8** was attempted. However, presumably for the reasons discussed earlier in connection with C-17 carbonyl addition, none of the products

[4]The compounds of the 17α-hydroxy series were generally found to be less stable than their 17β-counterparts.

Can. J. Chem. Downloaded from www.nrcresearchpress.com by 210.87.254.105 on 09/05/12
For personal use only.

resulting from opening of the epoxide ring in the desired manner could be detected in any of the numerous experiments carried out. A parallel investigation using the 17β-oxirane **9** was equally discouraging.

From the above and previous (1) results it is now apparent that although reactions involving dithiane anions provide a valuable addition to the methods available for the stereospecific introduction of biologically interesting and other functions into the steroid framework, the method is not as generally applicable as had been hoped.

Experimental

If not included below, all general procedures, purification and analytical methods, criteria of purity, spectral analyses, etc. were carried out as detailed previously (1*a*,*c*, 3). Silica gel G was used for all p.l.c. separations.

17α-Acetyl-3,3-ethylenedioxyandrost-5-en-17β-ol 1,3-Propylenethioketal (5)

To a solution of 2-lithio-2-methyl-1,3-dithiane (2.3 g, 16.7 mmol), prepared from *n*-butyllithium (1.05 g, 16.7 mmol, 10.25 ml of a 1.6 *N* hexane solution) and 2-methyl-1,3-dithiane (**1**, R = CH_3, 2.21 g, 16.7 mmol) in freshly dried tetrahydrofuran (50 ml) at −20° under nitrogen (2), was added 3,3-ethylenedioxyandrost-5-en-17-one (**4**, 1.2 g, 3.63 mmol, prepared as described previously (3, 8)) in dry −20° tetrahydrofuran (17 ml). After keeping for 2 days at 0° the reaction mixture was worked-up in the usual (1*a*,*c*) way. The p.l.c. purification using ether–benzene (1:9) development yielded unchanged **4** (0.36 g) and the 17β-hydroxydithiane **5** (0.99 g) as an unstable foamy powder; i.r. ($CHCl_3$) 3497 and 909 cm^{-1} (dithianyl); n.m.r. ($CDCl_3$) δ 0.99 (C-18 CH_3), 1.03 (C-19 CH_3), 2.03 (3H, s, CH_3CS_2), 3.96 (4H, s, OCH_2CH_2O), and 5.29 p.p.m. (1H, m, C-5 H).

Anal. Calcd. for $C_{26}H_{40}O_3S_2$: C, 67.2; H, 8.7; S, 13.8. Found: C, 67.2; H, 8.8; S, 13.8.

2-Hydroxymethyl-1,3-dithiane (1, R = CH_2OH) and its Tetrahydropyranyl Ether (8)

Dimethylformamide (1.28 g, 16.6 mmol) was added quickly with stirring to a −20° solution of 2-lithio-1,3-dithiane (1 g, 8.3 mmol) prepared in a nitrogen atmosphere as described above in dry tetrahydrofuran (20 ml). A white solid precipitated almost immediately and the mixture was then poured into water (100 ml) and acidified with 1 *N* aqueous hydrochloric acid (20 ml). The clear aqueous solution was then extracted with chloroform (3 × 50 ml) and the combined extracts were washed with water until neutral and then dried ($MgSO_4$). Evaporation of the chloroform solution gave 2-formyl-1,3-dithiane as an oily liquid which was immediately redissolved in methanol (100 ml) containing 1 ml of water. Sodium borohydride (0.95 g, 25 mmol) was added and the solution kept at 20° until frothing ceased (30 min). The reaction solution was concentrated, diluted with water (100 ml), and extracted with chloroform (3 × 50 ml). The dried ($MgSO_4$) chloroform extracts were evaporated and the oily product purified by p.l.c. with ether–benzene (1:2) development. 2-Hydroxymethyl-1,3-dithiane (**1**, R = CH_2OH) was obtained as a gum (700 mg), i.r. ($CHCl_3$) 3400 (broad) and 907 cm^{-1} (dithianyl); n.m.r. (d_6-DMSO, and with D_2O added), δ 1.9 (2H, distorted t, J = 8 Hz, C-5 CH_2), 2.85 (6H, t, J = 5 Hz, C-4 and -6 CH_2), 3.6–4.2 (3H, AB_2 m, collapsing to two singlets at 3.68 (line 7) and 4.07 (line 3) on spin decoupling, C-2 H and CH_2O(D)).

Mol. Wt. Calcd. for $C_5H_{10}OS_2$: 150.0173. Found (mass spectrum): 150.0177.

Treatment of the above hydroxymethyldithiane (**1**, R = CH_2OH, 1.34 g, 8.7 mmol) and purified dihydropyran (1.46 g, 17.4 mmol) in purified chloroform (10 ml) at 0° with purified phosphoryl chloride (0.02 ml), followed by p.l.c. (ether–benzene (2:3) development) purification yielded the tetrahydropyranylether **8** (1.76 g) as a gum.

Mol. Wt. Calcd. for $C_{10}H_{18}O_2S_2$: 234.0748. Found (mass spectrum): 234.0748.

3,3-Ethylenedioxy-17β-hydroxy-7α-(2′-oxopropyl)androst-5-ene 1,3-Propylenethioketal (10)

3,3-Ethylenedioxy-spiro-17β-oxiranylandrost-5-ene (**9**) was prepared according to the literature procedure (3).

To a solution of 2-lithio-2-methyl-1,3-dithiane (4.13 g, 30 mmol) under nitrogen in −20° freshly dried tetrahydrofuran (80 ml) was added the spiro-17β-epoxide **9** (1.72 g, 5 mmol) in freshly dried −20° tetrahydrofuran. The reaction mixture was then kept for 2 days at 0° and worked-up in the usual (1*a*,*c*) way. The p.l.c. purification with ether–benzene (1:9) development, followed by recrystallization from ether, gave the 17β-hydroxy dithianyl compound **10** (1.62 g) m.p. 164–165°; i.r. (CCl_4) 3448 and 907 cm^{-1} (dithianyl); n.m.r. ($CDCl_3$) δ 0.87 (C-18 CH_3), 1.04 (C-19 CH_3), and 1.87 p.p.m. (3H, s, CH_3CS_2).

Anal. Calcd. for $C_{27}H_{42}O_3S_2$: C, 67.7; H, 8.8; S, 13.4. Found: C, 67.7; H, 8.6; S, 13.5.

3,3-Ethylenedioxy-17β-hydroxy-17α-(2′-oxopropyl)androst-5-ene (11)

The 17β-hydroxydithiane (**10**, 0.6 g, 1.26 mmol) was dissolved in acetone (60 ml) containing water (2.5 ml) at 20°. Mercuric chloride (0.6 g) and cadmium carbonate (0.6 g) were then added and the mixture was stirred for 24 h (2). A further 0.2 g each of mercuric chloride and cadmium carbonate were then added and stirring continued for another 5 h. The reaction mixture was then filtered and evaporated and purified by p.l.c. (ether–benzene (3:7) development) to give 3,3-ethylenedioxy-17β-hydroxy-17α-(2′-oxopropyl)-androst-5-ene (**11**, 460 mg) m.p. 192–195°; i.r. (CCl_4) 3521 and 1705 cm^{-1}; n.m.r. ($CDCl_3$) δ 0.90 (C-18 CH_3), 1.05 (C-19 CH_3), and 2.21 p.p.m. (3H, s, CH_3CO).

17β-Hydroxy-17α-(2′-oxopropyl)androst-4-en-3-one (12)

The 17β-hydroxy-2′-oxopropyl ketal **11** (460 mg) in acetone (80 ml) containing toluene-*p*-sulfonic acid (10 mg) was stirred at 20° until the t.l.c. monitoring process indicated that C-3 ketonization was almost complete (4 h). The mixture was then poured into water (200 ml) and extracted with ether (3 × 25 ml). The usual (1*a*,*c*) work-up procedure followed by p.l.c. purification (with ether–benzene (7:3) as developing solvent) and recrystallization from ether afforded 17β-hydroxy-17α-(2′-oxopropyl)androst-4-en-3-one (**12**, 320 mg) m.p. 133–134°; i.r. ($CHCl_3$) 3480 and 1701 cm^{-1};

Can. J. Chem. Downloaded from www.nrcresearchpress.com by 210.87.254.105 on 09/05/12
For personal use only.

n.m.r. ($CDCl_3$) δ 0.90 (C-18 CH_3), 1.20 (C-19 CH_3), and 2.20 p.p.m. (3H, s, CH_3CO).

Anal. Calcd. for $C_{22}H_{32}O_3$: C, 76.7; H, 9.4. Found: C, 76.9; H, 9.5.

*17-(2′-Oxopropyl)androsta-4,17(20)-diene-3,21-dione (**13**)*

Prolonged (36 h) treatment of 17β-hydroxy-17α-(2′-oxopropyl)androst-4-en-3-one (**12**, 25 mg) with acidic acetone as described above effected dehydration smoothly to give the diene-dione **13**. Purification by p.l.c. (ether–benzene (3:2) development) followed by recrystallization from ether gave 16 mg of the product m.p. 177–178°; i.r. ($CHCl_3$) 1672, 1661, and 1613 cm^{-1}; n.m.r. ($CDCl_3$) δ 0.88 (C-18 CH_3), 1.21 (C-19 CH_3), 2.20 (3H, s, CH_3CO), 5.75 (1H, broad s, C-14 H), and 5.95 p.p.m. (1H, t, $J = 2.5$ Hz, C-20 H).

Anal. Calcd. for $C_{22}H_{30}O_2$: C, 80.9: H, 9.3. Found: C, 80.8; H, 9.2.

*Preparation of a Mixture of the Spiro-17β- and 17α-Oxiranyl Epimers **9** and **14** by Reaction of 3,3-Ethylenedioxyandrost-5-en-17-one (**4**) with Dimethylsulfoxonium Methylide*

A 53.8% suspension of sodium hydride in mineral oil (1.2 g, 30 mmol) was washed with petroleum ether (b.p. 40–60°) by decantation in a nitrogen atmosphere. Trimethylsulfoxonium iodide (7.2 g, 32.7 mmol) was then added and dimethylsulfoxide (20 ml) was allowed to drip slowly into the reaction flask. After the evolution of hydrogen had ceased (20–30 min) 3,3-ethylenedioxyandrost-5-en-17-one (**4**, 3 g, 9.1 mmol) obtained by the standard literature procedure (3, 8) dissolved in *hot* dimethylsulfoxide (75 ml) was added without delay (3, 6, 9). The mixture was stirred for 4 h at 20°, and was then heated at 55° for 3 h during which time the reaction solution became clear. Water (300 ml) was added and the mixture extracted with ether (4 × 75 ml). The ether extracts were washed with water (2 × 50 ml), dried ($MgSO_4$), and evaporated. The product (3 g) was purified by column chromatography on alumina. The mixture obtained contained the 17β- and 17α-epoxides **9** and **14** in the ratio ~2:1 (estimated by n.m.r.) and could not be resolved into its individual component epoxides by p.l.c. or by fractional recrystallization (*cf.* 9, 10). The t.l.c. and n.m.r. characteristics of each epoxide were identical with those observed above for **9** (3) and below for **14**.

*3,3-Ethylenedioxy-17α-hydroxy-17β-(2′-oxopropyl)androst-5-ene 1,3-Propylenethioketal (**15**)*

The above mixture of spiro-17β-(**9**) and spiro-17α-(**14**) oxiranes (3 g, 8.7 mmol) in dry −20° tetrahydrofuran (25 ml) was added to 2-lithio-2-methyl-1,3-dithiane (5.5 g, 40 mmol) prepared in freshly dried tetrahydrofuran (100 ml) at −20° under nitrogen. The mixture was then allowed to stand at 0° for 2 days. The normal work-up procedure (1*a*,*c*) gave 2.6 g of an unstable mixture of the hydroxydithianes **10** and **15** in the ratio of ~2:1 (by n.m.r.). Several fractional p.l.c. purifications with ether–benzene (1:14) developments gave pure samples of the 17β-hydroxy epimer **10** (0.41 g, identical with the material obtained above) and 3,3-ethylenedioxy-17α-hydroxy-17β-(2′-oxopropyl)androst-5-ene 1,3-propylenethioketal (**15**, 0.25 g) as an unstable glassy foam, i.r. ($CHCl_3$) 3410 and 907 cm^{-1} (dithianyl); n.m.r. ($CDCl_3$) δ 0.69 (C-18 CH_3), 1.05 (C-19 CH_3), and 1.78 p.p.m. (3H, s, CH_3CS_2).

Anal. Calcd. for $C_{27}H_{42}O_3S_2$: C, 67.7; H, 8.8; S, 13.4. Found: C, 67.6; H, 8.9; S, 13.3.

*3,3-Ethylenedioxy-17α-hydroxy-17β-(2′-oxopropyl)androst-5-ene (**16**)*

The 17α-hydroxydithiane **15** (0.23 g), 0.48 mmol) was dissolved in acetone (20 ml) containing water (1 ml) and mercuric chloride (0.23 g) and cadmium carbonate (0.23 g) were then added (2). The mixture was stirred at 20° for 8 h after which time t.l.c. analysis indicated that complete reaction had taken place. The filtered reaction solution was evaporated and the residue redissolved in chloroform (50 ml), dried ($MgSO_4$), and evaporated. The p.l.c. purification, with ether–benzene 1:1 developing solvent, and recrystallization from ether yielded the 17α-hydroxy-17β-(2′-oxopropyl) compound **16** (0.11 g) m.p. 163–166°; i.r. (CCl_4) 3535 and 1706 cm^{-1}; n.m.r. ($CDCl_3$) δ 0.69 (C-18 CH_3), 1.04 (C-19 CH_3), and 2.20 p.p.m. (3H, s, CH_3CO).

Anal. Calcd. for $C_{24}H_{36}O_4$: C, 74.2; H, 9.3. Found: C, 74.4; H, 9.5.

*17α-Hydroxy-17β-(2′-oxopropyl)androst-4-en-3-one (**17**)*

A solution of 3,3-ethylenedioxy-17α-hydroxy-17β-(2′-oxopropyl)androst-5-ene (**16**, 100 mg, 0.26 mmol) in acetone (20 ml) containing toluene-*p*-sulfonic acid (10 mg) was stirred at 20° until t.l.c. analysis indicated C-3 ketonization to be complete (2 h). The solvent was then removed by evaporation (during which process some elimination of the C-17α-OH occurred) and the residue was purified by p.l.c. with ether–benzene (1:1) as the developing solvent. Recrystallization of the two main fractions from ether gave the $\Delta^{17(20)}$ elimination product **13** (30 mg), identical in all respects with the sample obtained previously, and 17α-hydroxy-17β-(2′-oxopropyl)androst-4-en-3-one (**17**, 30 mg) m.p. 125–127°; i.r. ($CHCl_3$) 3520, 1704, 1664, and 1616 cm^{-1}; n.m.r. ($CDCl_3$) δ 0.72 (C-18 CH_3), 1.20, (C-19 CH_3), 2.20 (3H, s, CH_3CO), and 5.63 p.p.m. (1H, s, C-4 H).

Anal. Calcd. for $C_{22}H_{32}O_3$: C, 76.7; H, 9.4. Found: C, 76.8; H, 9.4.

*3,3-Ethylenedioxy-17-methylene-androst-5-ene (**18**)*

3,3-Ethylenedioxyandrost-5-en-3-one (**4**, 7 g, 21.3 mmol) in dry benzene (140 ml) was added dropwise with stirring at 20° to triphenylphosphonium methylide (prepared from methyltriphenylphosphonium bromide (25.2 g, 70 mmol) and potassium *t*-butoxide (14 g, 125 mmol)) in dry dimethyl sulfoxide (125 ml) by the usual Wittig procedure (11). The mixture was kept at 20° until t.l.c. indicated the reaction to be complete (~24 h) and was then poured into water (500 ml) and extracted quickly with ether (4 × 50 ml). The ether solution was washed with water (2 × 50 ml), then dried immediately with $MgSO_4$ and evaporated. The residue was column chromatographed on Florisil (benzene elution) to give 3.2 g of the 17-methylene-3-ketal **18**. A fraction containing its hydrolysis product, 17-methyleneandrost-4-en-3-one, was reketalized with ethylene glycol and toluene-*p*-sulfonic acid in benzene, and p.l.c. purification afforded a further 1.2 g of **18**. Unchanged starting material **4** (1.1 g) was also recovered. Recrystallization from ether–methanol effected final purification of 3,3-ethylenedioxy-17-methyleneandrost-5-ene (**18**) m.p. 157–158°; n.m.r. ($CDCl_3$) δ 0.82 (C-18 CH_3), 1.07 (C-19 CH_3), 4.0 (4H, s, OCH_2CH_2O), 4.69 (2H, s, $=CH_2$), and 5.4 p.p.m. (1H, s, C-4 H).

Anal. Calcd. for $C_{22}H_{32}O_2$: C, 80.4; H, 9.8. Found: C, 80.4; H, 10.0.

*3,3-Ethylenedioxy-spiro-17α-oxiranylandrost-5-ene (**14**)*

m-Chloroperoxybenzoic acid (0.94 g, 5.5 mmol) in pure chloroform (10 ml) was added dropwise with stirring during 10 min to the 17-methyleneketal **18** (1.5 g, 4.6 mmol) in pure chloroform (25 ml) at 0°. After stirring for a further 30 min at 0°, chloroform (100 ml) was added and the solution was washed with 5% aqueous sodium bicarbonate (50 ml) and then with water (50 ml). The chloroform solution was dried immediately ($MgSO_4$) and evaporated. The p.l.c. purification (silica gel G, ether–benzene (1:6) development) gave unchanged starting material (0.4 g) and an oxirane fraction (1.4 g) which was shown by n.m.r. to be predominantly the 17α-epimer **14**. Recrystallization from ether–methanol provided a sample m.p. 163–167°, n.m.r. ($CDCl_3$) δ 0.83 (C-18 CH_3), 1.04 (C-19 CH_3), 2.75 (2H, C-20 CH_2),[5] 4.03 (4H, s, OCH_2CH_2O) and 5.23 p.p.m. (1H, broad s, C-5 H).

This work was carried out during the tenure of a University of Toronto School of Graduate Studies Postdoctoral Fellowship (awarded to R.G.) and was supported by the National Research Council of Canada.

[5]This peak was a broadened singlet in which some signs of the splitting pattern of an AA′ quartet could be detected. *cf.* refs. (3, 12).

1. (*a*) J. B. Jones and R. Grayshan. Can. J. Chem. This issue. (*b*) Chem. Commun. 741 (1970); (*c*) Can. J. Chem. **50**, 810 (1972).
2. E. J. Corey and D. Seebach. Angew. Chem. Int. Ed. **4**, 1075, 1077 (1965); D. Seebach. Synth. 17 (1969).
3. J. B. Jones and J. D. Leman. Can. J. Chem., **49**, 2420 (1971).
4. *e.g.* R. Dolique. *In* Traité de chimie organique. *Edited by* V. Grignard. Masson et Cie., Paris. **8**, 93 (1947).
5. R. M. Carlson and P. M. Helquist. Tetrahedron Lett. 173 (1969).
6. E. J. Corey and M. Chaykovsky. J. Am. Chem. Soc. **84**, 3782 (1962); **87**, 1353 (1965).
7. J. E. Blackwood, C. L. Gladys, K. L. Loening, A. E. Petraca, and J. E. Rush. J. Am. Chem. Soc. **90**, 509 (1968).
8. H. J. Dauben, B. Loken, and H. J. Ringold. J. Am. Chem. Soc. **76**, 1359 (1954).
9. C. E. Cook, R. C. Corley, and M. E. Wall. J. Org. Chem. **33**, 2789 (1968).
10. D. Bertin and L. Nedelec. Bull. Soc. Chim. Fr. **31**, 2140 (1964).
11. A. Maercker. *In* Organic reactions. *Edited by* A. C. Cope. J. Wiley and Sons, New York, N.Y. **14**, 270 (1965).
12. D. N. Kirk and M. A. Wilson. J. Chem. Soc. C, 414 (1971).

Can. J. Chem. Downloaded from www.nrcresearchpress.com by 210.87.254.105 on 09/05/12
For personal use only.

Can. J. Chem. Downloaded from www.nrcresearchpress.com by 210.87.254.42 on 09/05/12
For personal use only.

The Preparation of 1,2-Dimethylarsinohexafluorocyclopentene, 1,2-Dimethylarsinooctafluorocyclohexene, and Related Mixed Ligands

L. S. CHIA AND W. R. CULLEN

Chemistry Department, University of British Columbia, Vancouver 8, British Columbia

Received December 15, 1971

Dimethylarsine reacts with the compounds $FC{=}CF(CF_2)_{n/2}$ to give the ligands

$$(CH_3)_2AsC{=}C\,As(CH_3)_2(CF_2)_{n/2},$$

$f_n$fars ($n = 4, 6, 8$). The reaction of diphenylphosphine with $(CH_3)_2AsC{=}CF(CF_2)_{n/2}$ results in the mixed ligands

$$(CH_3)_2AsC{=}CP(C_6H_5)_2(CF_2)_{n/2},$$

f_nAsP ($n = 4, 6, 8$).

La diméthylarsine réagit avec les composés $FC{=}CF(CF_2)_{n/2}$ pour donner les ligands

$$(CH_3)_2AsC{=}C\,As(CH_3)_2(CF_2)_{n/2},$$

$f_n$fars ($n = 4, 6, 8$). La réaction de la diphénylphosphine avec $(CH_3)_2AsC{=}CF(CF_2)_{n/2}$ conduit à un mélange de ligands

$$(CH_3)_2AsC{=}CP(C_6H_5)_2(CF_2)_{n/2},$$

f_nAsP ($n = 4, 6, 8$).

Canadian Journal of Chemistry, **50**, 1421 (1972)

Reaction of the ditertiary arsine ligand $f_4$fars,

$$(CH_3)_2AsC{=}CAs(CH_3)_2CF_2CF_2,$$

with metal carbonyl compounds has provided a number of novel compounds. The related ditertiary phosphines $f_n$fos which are prepared by treating the perfluorocycloolefin with diphenylphosphine have also been described (1,

[1] $$2(C_6H_5)_2PH + FC{=}\!\!=\!\!=CF \rightarrow (C_6H_5)_2PC{=}\!\!=\!\!=CP(C_6H_5)_2 + 2HF \quad (n = 4, 6, 8)$$

and references therein). In this note we wish to describe an improved synthesis of $f_4$fars and its elaboration to the isolation of $f_6$fars and $f_8$fars. We also describe the preparation of the mixed ligands f_4AsP and f_8AsP

$$(CH_3)_2AsC{=}CP(C_6H_5)_2(CF_2)_{n/2}$$

($n = 4, 8$) and an improved synthesis of f_6AsP.

Experimental

All reactions were carried out in sealed tubes. Volatile reactants were manipulated in a conventional vacuum system. The preparation of f_4AsP is given as an example. This is also listed in Table 1 together with the conditions used to isolate the other ligands. The analytical data for new compounds are given in Table 2.

Preparation of 1-Diphenylphosphino-2-dimethylarsinotetrafluorocyclobutene (f_4AsP)

1-Dimethylarsinopentafluorocyclobutene was obtained by treating perfluorocyclobutene with dimethylarsine (2). The arsinocyclobutene (35.5 g, 0.143 mol) and diphenylphosphine (26.0 g, 0.140 mol) were sealed under vacuum in a thick-walled Pyrex tube. After shaking for 2 days at 20° the tube was opened. The solid product was dissolved in acetone and the residue was filtered off. The acetone was then removed *in vacuo* and the resulting residue (an orange oil) was dissolved in the minimum amount of methylene chloride and chromatographed on a Florisil column. A 1:1 diethyl ether–petroleum ether mixture eluted a pale yellow band. After removal of the solvent, pale yellow crystals were obtained which were purified by rechromatography and recrystallization from diethyl ether–petroleum ether to give colorless crystals of f_4AsP (43.0 g, 74%); m.p. 39°.

TABLE 1. Reaction conditions for the preparation of new ligands

Reactants	Conditions		Product	Yield (%)
	T(°C)	Time (days)		
c-C_4F_6, $(CH_3)_2AsH$	80	2	$f_4$fars*	55
c-C_5F_8, $(CH_3)_2AsH$	100	6	$f_6$fars*	61
c-C_6F_{10}, $(CH_3)_2AsH$	150	8	$f_8$fars†	59
$(CH_3)_2AsC{=}CFCF_2CF_2$, $(C_6H_5)_2PH$	20	2	f_4AsP†	74
$(CH_3)_2AsC{=}CF(CF_2)_2CF_2$, $(C_6H_5)_2PH$	20	13	f_6AsP†	60
$(CH_3)_2AsC{=}CF(CF_2)_3CF_2$,*‡ $(C_6H_5)_2PH$	20	50	f_8AsP†§	20

*Purified by distillation.
†Purified by chromatography on Florisil and crystallization.
‡Prepared in 48% yield from c-C_6F_{10} and $(CH_3)_2AsH$ by heating at 150° for 7 days.
§A pale yellow solid, m.p. ~70°, which is difficult to purify. Satisfactory microanalytical data were not obtained for this product.

TABLE 2. Analytical data for new compounds*

Compound	m.p. (°C) [b.p. (°C mm Hg)]	Found (%)			Calculated (%)		
		C	H	F	C	H	F
$(CH_3)_2AsC{=}CAs(CH_3)_2(CF_2)_2CF_2$	[84 (0.1)]	28.0	3.10	29.6	28.1	3.16	29.7
$(CH_3)_2AsC{=}CAs(CH_3)_2(CF_2)_3CF_2$	51	27.5	2.78	34.7	27.7	2.79	35.0
$(CH_3)_2AsC{=}CF(CF_2)_3CF_2$	[30 (0.1)]	27.7	1.88	49.0	27.6	1.74	49.1
$(CH_3)_2AsC{=}CP(C_6H_5)_2CF_2CF_2$	39	51.7	3.92	18.0	52.1	3.90	18.4

*All compounds are colorless.

Results and Discussion

Previous syntheses of $f_4$fars involved the reaction of dimethylarsine with 1-dimethylarsino-2-chlorotetrafluorocyclobutene (3). This two-step process was undesirable and since the $f_n$fos ligands were best prepared from the perfluorocycloolefins (eq. 1) the corresponding reactions using dimethylarsine were investigated. This has resulted in a convenient single step synthesis of $f_4$fars and the two new ditertiary arsines $f_6$fars and $f_8$fars. Unlike the reaction of

$$[2]\quad 2(CH_3)_2AsH + FC{=}^{\ulcorner(CF_2)_{n/2}\urcorner}{=}CF \rightarrow (CH_3)_2AsC{=}^{\ulcorner(CF_2)_{n/2}\urcorner}{=}CAs(CH_3)_2 + 2HF \qquad n = 4, 6, 8$$

eq. 1, where only disubstitution occurs, the reaction of eq. 2, can be stopped if required at the monosubstitution stage. This has previously been demonstrated when $n = 4$ and 6 (2) and in the present investigation the monosubstituted compound with $n = 8$ has been isolated. The products of eq. 3 react further with diphenylphosphine to afford the mixed ligands f_nAsP.

$$[3]\quad (CH_3)_2AsH + FC{=}^{\ulcorner(CF_2)_{n/2}\urcorner}{=}CF \rightarrow (CH_3)_2AsC{=}^{\ulcorner(CF_2)_{n/2}\urcorner}{=}CF + HF \qquad n = 4, 6, 8$$

$$[4]\quad (CH_3)_2AsC{=}^{\ulcorner(CF_2)_{n/2}\urcorner}{=}CF + (C_6H_5)_2PH \rightarrow (CH_3)_2AsC{=}^{\ulcorner(CF_2)_{n/2}\urcorner}{=}CP(C_6H_5)_2 + HF \qquad n = 4, 6, 8$$

The synthesis of f_6AsP ($n = 6$) has been described (1) but it has now been found that if the reaction of eq. 4 is carried out at 20° rather than 45°, with a corresponding increase in the reaction time, the yield is considerably increased. Two other mixed ligands f_4AsP and f_8AsP can be obtained by the same method although f_8AsP has been characterized only by its spectroscopic properties.

In general, all these reactions involving perfluorocycloolefins require more forcing conditions as the ring size is increased which is probably a consequence of ring strain (4).

The n.m.r. spectra of all the new compounds

Can. J. Chem. Downloaded from www.nrcresearchpress.com by 210.87.254.42 on 09/05/12
For personal use only.

TABLE 3. The n.m.r. data for new compounds*

Compound	^{19}F	^{1}H
f_4AsP	106.6(2), 107.2(2)	1.34(6), 7.50(10)
f_6AsP	104.8(2), 105.2(2), 131.7(2)	1.30(6), 7.46(10)
f_6fars	103.8(4), 130.3(2)	1.33
f_8AsP	101.9(2), 102.5(2), 133.0(2), 134.0(2)	1.30(6), 7.35(10)
f_8fars	102.0(4), 133.4(4)	1.38
$(CH_3)_2AsC{=}CF(CF_2)_3CF_2$	110.4(1), 102.6(2), 117.0(2), 133.8(2), 134.7(2)	1.37

*Obtained using Varian HA100 and T60 spectrometers. Chemical shifts are reported in p.p.m. downfield from TMS and upfield from $CFCl_3$. All resonances are multiplets except the upfield ^1H resonances. The numbers in parentheses are relative areas.

TABLE 4. The i.r. spectra of new compounds*

f_4AsP	3128w, 3058m, 3032m, 2988w, 2902m, 2804vw, 1975vw, 1952w, 1880w, 1809w, 1660vw, 1587w, 1573w, 1484m, 1438s, 1420m, 1384w, 1350m, 1308vs, 1262m, 1227vs, 1186w, 1150vs, 1105vs, 1073m, 1032m, 1005m, 972vw, 918w, 900m, 864m, 831s, 802m, 744vs, 712m, 696vs, 675m, 622vw, 585w, 576w, 558w, 535m, 498m, 478m
f_6fars	2982w, 2911m, 2812w, 2511vw, 1940vw, 1820vw, 1552m, 1422s, 1331vs, 1276s, 1258s, 1239vs, 1226vs, 1189vs, 1131vvs, 1093vs, 993vs, 910w, 899m, 865m, 847m, 829m, 790m, 580m, 567m, 531w, 468w
f_6AsP	3129vw, 3066m, 3048m, 3007w, 2994w, 2910m, 2847w, 2810w, 1970vw, 1950w, 1887vw, 1810w, 1755vw, 1655vw, 1616w, 1588w, 1573w, 1540m, 1485m, 1437s, 1423m, 1417m, 1331vs, 1307m, 1277s, 1262s, 1241vs, 1228vs, 1203w, 1187vs, 1135vs, 1093vs, 1075m, 1032m, 1001vs, 902m, 867m, 846m, 822w, 803m, 775w, 748s, 731m, 698s, 578w, 565w, 554w, 518w, 496w, 468w, 430w
f_8fars	2982w, 2914m, 2810vw, 2479vw, 1569m, 1424s, 1418s, 1343vs, 1312m, 1259m, 1208vs, 1188vs, 1175vs, 1159vs, 1102vs, 1035vs, 975vs, 898s, 866s, 846m, 817w, 725w, 642m, 619w, 576w, 565w, 524w, 502w, 415w
f_8AsP	3132vw, 3066m, 3050m, 3008w, 2998w, 2941w, 2913m, 2847w, 1966vw, 1948w, 1884w, 1806w, 1772vw, 1750vw, 1591w, 1567w, 1485m, 1439s, 1420m, 1343vs, 1325s, 1272s, 1261s, 1209vs, 1194vs, 1175vs, 1164vs, 1114vs, 1104vs, 1074w, 1035vs, 1008m, 972vs, 942w, 901m, 865m, 847w, 833w, 787w, 747vs, 739vs, 719m, 698vs, 643w, 622w, 580w, 570w, 550w, 520w, 495m, 482m, 470w
$(CH_3)_2AsC{=}CF(CF_2)_3CF_2$	2929vw, 2915w, 2820vw, 2816vw, 1664s, 1425m, 1357w, 1340s, 1296vs, 1288m, 1266m, 1253m, 1231vs, 1205vs, 1169vs, 1135vs, 1113vs, 1067m, 1031vs, 964vs, 910m, 870m, 855m, 809w, 775vw, 697w, 670m, 631m, 622m, 581m, 571w, 555m, 508m, 432w, 415w

*Spectra were run using a Perkin–Elmer 457 instrument. Samples were run as liquid films or KBr disks except in the region 1350–600 cm^{-1} where CS_2 solutions were used.

(Table 3) were as expected. In all cases the complex ^{19}F resonance associated with CF_2 groups adjacent to $(CH_3)_2As$ or $(C_6H_5)_2P$ moieties are in the region 102–107 p.p.m. More remote CF_2 groups absorb considerably upfield (> 130 p.p.m.). The vinylic fluorine atom in 1-dimethylarsinononafluorocyclohexene absorbs at 110.4 p.p.m.

The i.r. spectra of the compounds are listed in Table 4. It has been pointed out before (3) that ν(C=C) of the symmetrical ligands f_4fars and f_nfos is not strong as is now found for f_6fars and

Can. J. Chem. Downloaded from www.nrcresearchpress.com by 210.87.254.42 on 09/05/12
For personal use only.

$f_8$fars, and the mixed ligands f_nAsP. Indeed, because of this, it is difficult to assign this band with any certainty. In the monosubstituted series $(CH_3)_2AsC{=}CF(CF_2)_{n/2}$ the strong ν(C=C) changes very little with ring size, it being 1662, 1661, and 1664 cm^{-1} for $n = 4$, 6, and 8 respectively. In the C—F stretching region, the pattern and position of absorption for the di-substituted compounds ($f_n$fars, f_nAsP, $f_n$fos) with a given ring size is very similar. The ν(C—F) are $1308 \pm 4, \sim 1227, 1154 \pm 5, 1106 \pm 6$ cm^{-1} for $n = 4$; $\sim 1331, 1236 \pm 3, 1187 \pm 3, 1136 \pm 5, 1092 \pm 2, 1000 \pm 7$ cm^{-1} for $n = 6$; and $1344 \pm 1, 1213 \pm 5, 1193 \pm 5, 1177 \pm 2, 1162 \pm 4, 1109 \pm 7, 1038 \pm 3, 980 \pm 8$ cm^{-1} for $n = 8$.

All the derivatives which possess a $(CH_3)_2As$ group show a doublet in the region 565–585 cm^{-1} which is associated with As—CH_3 stretching vibrations and which is fairly insensitive to the nature of the other substituents on the arsenic(III) atom. The values for other compounds not listed in Table 4 are 568, 581, $f_4$fars; 565, 580, $(CH_3)_2AsC{=}CF(CF_2)_2CF_2$; 562, 584 cm^{-1} $(CH_3)_2AsC{=}CFCF_2CF_2$.

The financial assistance of the National Research Council of Canada is gratefully acknowledged.

1. J. P. Crow and W. R. Cullen. Inorg. Chem. **10**, 2165 (1971).
2. W. R. Cullen, P. S. Dhaliwal, and G. E. Styan. J. Organometal. Chem. **6**, 364 (1966).
3. W. R. Cullen. Fluorine Chem. Rev. **3**, 73 (1969).
4. R. F. Stockel, F. Megson, and M. T. Beachem. J. Org. Chem. **33**, 4395 (1968).

Synthesis of 6-*O*-(4-*O*-Methyl-β-D-glucopyranosyl)-D-galactose

J. M. Berry and G. G. S. Dutton
Chemistry Department, University of British Columbia, Vancouver 8, British Columbia

Received December 13, 1971

6-*O*-(4-*O*-Methyl-β-D-glucopyranosyl)-D-galactose has been synthesized by a Koenigs–Knorr reaction. The disaccharide is most readily characterized in the form of the crystalline glycosyl alditol peracetate.

Le 6-*O*-(4-*O*-methyl-β-D-glucopyranosyl)-D-galactose a été synthétisé selon la methode de Koenigs–Knorr. Le disaccharide est plus facilement identifié sous forme du glycosyl alditol peracétate.

Canadian Journal of Chemistry, **50**, 1424 (1972)

In studying the structure of acidic polysaccharides it is often more convenient to carry out fragmentation after the uronic acid function has been reduced, a transformation which is readily achieved with diborane (1) or complex hydrides (2, 3). Similarly, an aldobiouronic acid may more readily be characterized as the derived neutral disaccharide (*e.g.* 4, 5). The aldobiouronic acid 6-*O*-(4-*O*-methyl-β-D-glucopyranosyluronic acid)-D-galactose is found in many plant gums (6–8) and it is thus of interest to prepare 6-*O*-(4-*O*-methyl-β-D-glucopyranosyl)-D-galactose. This note reports the synthesis and characterization of this disaccharide and of the related disaccharide alditol.

4-*O*-Methyl-D-glucose was prepared by Hakomori methylation (9) of 2,3:5,6-di-*O*-isopropylidene-D-glucose dimethyl acetal which was obtained via the diethyl thioacetal and purified through the crystalline *p*-nitrobenzoate (10). This sugar was identified as the osazone (10, 11) and the β-D-tetraacetate (12), both crystalline.

2,3,6-Tri-*O*-acetyl-4-*O*-methyl-α-D-glucopyranosyl bromide was condensed with 1,2:3,4-di-*O*-isopropylidene-α-D-galactopyranose (13) in chloroform using freshly prepared silver oxide (14). The reaction product was deacetylated with sodium methoxide to give 6-*O*-(4-*O*-methyl-β-D-glucopyranosyl)-1,2:3,4-di-*O*-isopropylidene-D-galactopyranose as a crystalline material in 62% yield. Preliminary experiments showed that the ketal groups could be removed with minimal hydrolysis of the glycosidic linkage by 0.05 *N* sulfuric acid on a steam bath for 40 min. Hydrolysis in this way gave 6-*O*-(4-*O*-methyl-β-D-glucopyranosyl)-D-galactose as a

Can. J. Chem. Downloaded from www.nrcresearchpress.com by 210.87.254.42 on 09/05/12
For personal use only.

$f_8$fars, and the mixed ligands f_nAsP. Indeed, because of this, it is difficult to assign this band with any certainty. In the monosubstituted series $(CH_3)_2AsC{=}CF(CF_2)_{n/2}$ the strong ν(C=C) changes very little with ring size, it being 1662, 1661, and 1664 cm^{-1} for $n = 4$, 6, and 8 respectively. In the C—F stretching region, the pattern and position of absorption for the di-substituted compounds ($f_n$fars, f_nAsP, $f_n$fos) with a given ring size is very similar. The ν(C—F) are $1308 \pm 4, \sim 1227, 1154 \pm 5, 1106 \pm 6$ cm^{-1} for $n = 4$; $\sim 1331, 1236 \pm 3, 1187 \pm 3, 1136 \pm 5, 1092 \pm 2, 1000 \pm 7$ cm^{-1} for $n = 6$; and $1344 \pm 1, 1213 \pm 5, 1193 \pm 5, 1177 \pm 2, 1162 \pm 4, 1109 \pm 7, 1038 \pm 3, 980 \pm 8$ cm^{-1} for $n = 8$.

All the derivatives which possess a $(CH_3)_2As$ group show a doublet in the region 565–585 cm^{-1} which is associated with As—CH_3 stretching vibrations and which is fairly insensitive to the nature of the other substituents on the arsenic(III) atom. The values for other compounds not listed in Table 4 are 568, 581, $f_4$fars; 565, 580, $(CH_3)_2AsC{=}CF(CF_2)_2CF_2$; 562, 584 cm^{-1} $(CH_3)_2AsC{=}CFCF_2CF_2$.

The financial assistance of the National Research Council of Canada is gratefully acknowledged.

1. J. P. Crow and W. R. Cullen. Inorg. Chem. **10**, 2165 (1971).
2. W. R. Cullen, P. S. Dhaliwal, and G. E. Styan. J. Organometal. Chem. **6**, 364 (1966).
3. W. R. Cullen. Fluorine Chem. Rev. **3**, 73 (1969).
4. R. F. Stockel, F. Megson, and M. T. Beachem. J. Org. Chem. **33**, 4395 (1968).

Synthesis of 6-*O*-(4-*O*-Methyl-β-D-glucopyranosyl)-D-galactose

J. M. Berry and G. G. S. Dutton
Chemistry Department, University of British Columbia, Vancouver 8, British Columbia

Received December 13, 1971

6-*O*-(4-*O*-Methyl-β-D-glucopyranosyl)-D-galactose has been synthesized by a Koenigs–Knorr reaction. The disaccharide is most readily characterized in the form of the crystalline glycosyl alditol peracetate.

Le 6-*O*-(4-*O*-methyl-β-D-glucopyranosyl)-D-galactose a été synthétisé selon la methode de Koenigs–Knorr. Le disaccharide est plus facilement identifié sous forme du glycosyl alditol peracétate.

Canadian Journal of Chemistry, **50**, 1424 (1972)

In studying the structure of acidic polysaccharides it is often more convenient to carry out fragmentation after the uronic acid function has been reduced, a transformation which is readily achieved with diborane (1) or complex hydrides (2, 3). Similarly, an aldobiouronic acid may more readily be characterized as the derived neutral disaccharide (*e.g.* 4, 5). The aldobiouronic acid 6-*O*-(4-*O*-methyl-β-D-glucopyranosyluronic acid)-D-galactose is found in many plant gums (6–8) and it is thus of interest to prepare 6-*O*-(4-*O*-methyl-β-D-glucopyranosyl)-D-galactose. This note reports the synthesis and characterization of this disaccharide and of the related disaccharide alditol.

4-*O*-Methyl-D-glucose was prepared by Hakomori methylation (9) of 2,3:5,6-di-*O*-isopropylidene-D-glucose dimethyl acetal which was obtained via the diethyl thioacetal and purified through the crystalline *p*-nitrobenzoate (10). This sugar was identified as the osazone (10, 11) and the β-D-tetraacetate (12), both crystalline.

2,3,6-Tri-*O*-acetyl-4-*O*-methyl-α-D-glucopyranosyl bromide was condensed with 1,2:3,4-di-*O*-isopropylidene-α-D-galactopyranose (13) in chloroform using freshly prepared silver oxide (14). The reaction product was deacetylated with sodium methoxide to give 6-*O*-(4-*O*-methyl-β-D-glucopyranosyl)-1,2:3,4-di-*O*-isopropylidene-D-galactopyranose as a crystalline material in 62% yield. Preliminary experiments showed that the ketal groups could be removed with minimal hydrolysis of the glycosidic linkage by 0.05 *N* sulfuric acid on a steam bath for 40 min. Hydrolysis in this way gave 6-*O*-(4-*O*-methyl-β-D-glucopyranosyl)-D-galactose as a

Can. J. Chem. Downloaded from www.nrcresearchpress.com by 210.87.254.42 on 09/05/12
For personal use only.

Can. J. Chem. Downloaded from www.nrcresearchpress.com by 210.87.254.42 on 09/05/12
For personal use only.

syrup in 90% yield. Examination by paper chromatography showed a very small amount (<5%) of monosaccharide and pure disaccharide was obtained as a syrup by passage through Dowex 50W X2 (Li^+) (15). The disaccharide had $[\alpha]_D \sim 0°$ in water consistent with the assignment of a β-D-linkage. According to Hudson's rules (16) the calculated values for $[\alpha]_D$ are approximately +93 and −6° for α-D- and β-D-(1→6) links.

The disaccharide consumed 4.9–5.0 mol of periodate and successive borohydride reduction and total hydrolysis gave ethylene glycol and 2-*O*-methyl-D-erythritol identified by g.l.c. of their trimethylsilyl derivatives (17). Methylation (Hakomori) of the disaccharide followed by methanolysis and g.l.c. indicated the presence of 2,3,4,6-tetra-*O*-methyl-D-glucose together with 2,3,4- and 2,3,5-tri-*O*-methyl-D-galactose (18). It is of interest to note that the Hakomori method of methylation, like the Kuhn reagents (19), gives a high proportion of the furanose isomer. The peak areas for the 2,3,4- and 2,3,5-isomers were in the approximate ratio of 3:2. No satisfactory crystalline derivatives were obtained from the disaccharide which was most conveniently characterized as the glycosyl alditol acetate, m.p. 104–106°. The n.m.r. spectrum of the free glycosyl alditol in deuterium oxide showed $J_{1,2}$ 7.5 Hz (τ 5.3) consistent with a β-D-linkage (20).

Experimental

Thin-layer chromatography was carried out using solvent systems A and B on silica gel. Plates were developed by spraying with 50% aqueous sulfuric acid and heating to about 150° for 3–5 min. Paper chromatograms using solvent systems C and D were developed using silver nitrate in acetone for reducing sugars (21) and sodium periodate – benzidine for non-reducing compounds (22). Solvent A, ethyl ether – toluene (2:1); B, butanone–water azeotrope; C, ethyl acetate – pyridine–water (4:1:1); D, ethyl acetate – acetic acid–formic acid – water (18:3:1:4). Gas–liquid chromatography was carried out on a F and M 720 instrument using columns: (*a*) 8 ft × 1/4 in. 20% SF 96 on 80–100 mesh Diatoport S, (*b*) 4 ft × 1/4 in. 5% butanediol succinate on 80–100 mesh Diatoport S, and (*c*) 2 ft × 1/4 in. 20% SE 30 (F and M Division, Hewlett–Packard, Arondale, Pennsylvania). The n.m.r. spectra were recorded on a Varian HA-100 instrument using tetramethylsilane as internal standard except as noted. Optical rotations were measured at 23 ± 1° on a Rudolph polarimeter model 219 and later on a Perkin-Elmer model 141 polarimeter. Melting points are uncorrected. Solvents were removed *in vacuo* at a bath temperature not exceeding 40°.

4-O-Methyl-D-glucose

2,3:5,6-Di-*O*-isopropylidene-D-glucose dimethyl acetal (10 g) (10) was dissolved in dry methyl sulfoxide (100 ml), a solution of methyl sulfinyl anion (0.6 *M*, 120 ml) was added and the solution left 45 min at room temperature (23). Excess methyl iodide was then added while keeping the temperature below 25°. Thin-layer chromatography in solvent A showed the reaction to be complete in 30 min. Petroleum ether (65–110°, 400 ml) and water (200 ml) were added and the water layer extracted with petroleum ether (8 × 100 ml). The combined solvent extracts were washed, dried, and concentrated to give a syrup (9.6 g) which was heated for 4 h at 60° with sulfuric acid (0.05 *N*, 100 ml). Neutralization ($BaCO_3$) and concentration gave crude 4-*O*-methyl-D-glucose (5.7 g), [α] +49° (*c*, 2 in water). A pure sample obtained by sodium methoxide deacetylation of the tetraacetate had [α] +60.0° (*c*, 2.8 in water), lit. (11) $[\alpha]_D$ +61.1° (*c*, 2 in water); $R_{glucose}$ 2.65 (solvent C). Phenylosazone m.p. 158–160°, (lit. (10, 11) m.p. 158–160°).

Crude 4-*O*-methyl-D-glucose (4.5 g) was acetylated with acetic anhydride (32 ml) and anhydrous sodium acetate (2.25 g) to give the tetraacetate, (3.58 g), m.p. 98–100°. 1,2,3,6-Tetra-*O*-acetyl-4-*O*-methyl-β-D-glucopyranose (**1**) was recrystallized from cyclohexane and had m.p. 102–103°, $[\alpha]_D$ −8.1° (*c*, 2.3 in chloroform), (lit. (12) m.p. 98–99°, $[\alpha]_D$ −7° (*c*, 2 in chloroform)), the n.m.r. data ($CDCl_3$) $J_{1,2}$ 8.0 Hz (τ 4.40) (24).

Anal. Calcd. for $C_{15}H_{22}O_{10}$: C, 49.70; H, 6.12. Found: C, 49.62; H, 6.05.

2,3,6-Tri-O-acetyl-4-O-methyl-α-D-glucopyranosyl Bromide (**2**)

Tetraacetate (**1**) (1.6 g) was dissolved in cold hydrogen bromide in glacial acetic acid (32%, 28 ml) and the solution allowed to stand at room temperature for 45 min. Chloroform (50 ml) was added and the solution was shaken with water (50 ml). The aqueous layer was extracted with chloroform (3 × 25 ml) and the combined extracts were washed with saturated sodium hydrogen carbonate (2 × 50 ml) and cold water (2 × 25 ml). Evaporation of the dried chloroform gave (2) as a syrup (1.8 g), [α] +190° (*c*, 4.2 in chloroform).

6-O-(4-O-Methyl-β-D-glucopyranosyl)-1,2:3,4-di-O-isopropylidene-D-galactopyranose (3)

1,2:3,4-Di-*O*-isopropylidene-D-galactopyranose (**4**) (600 mg, 2.5 mmol, distilled syrup), freshly prepared silver oxide (2.0 g), and Drierite (2.0 g, finely powdered, preheated to 200° *in vacuo*) were stirred for 1 h in absolute chloroform (15 ml) at room temperature. A solution of the bromide **2** (1.5 g, 3.7 mmol) in absolute chloroform (8 ml) was then added over 2 h with continuous stirring. Thin-layer chromatography (solvent A) showed R_f values as follows: **2**, 0.54; product, 0.44; **4**, 0.33; and a compound, assumed to be a degradation product of **2**, at 0.28. Thin-layer chromatography further showed that the reaction was complete 30 min after the final addition. The mixture was filtered, the solid was washed with chloroform, and the filtrate and washings evaporated to a syrup which was reacted directly with sodium methoxide (0.1 *N*, 30 ml). After 30 min sodium ion was removed with Amberlite IR 120 resin and the methanol evaporated to give a solid product, m.p. 168–170° (680 mg, 62%). Recrystallization from ethanol (4 ml/g)

gave pure **3** m.p. 174–175°, $[\alpha]_D$ −60.5° (*c*, 0.8 in methanol), R_f (t.l.c., solvent B) 0.50.

Anal. Calcd. for $C_{19}H_{32}O_{11}$: C, 51.88; H, 7.35; OMe, 6.93. Found: C, 52.25; H, 7.39; OMe, 7.11.

*6-O-(4-O-Methyl-*D*-glucopyranosyl)-*D*-galactose*

Compound **3** (600 mg) was heated on a steam bath for 40 min in sulfuric acid (0.05 *N*, 30 ml). Passage through Duolite A-4 resin and concentration gave the disaccharide as a syrup (486 mg), $[\alpha]_D$ +4° (*c*, 1 in water); $R_{glucose}$ 0.34 (solvent C); 0.26 (solvent D) on paper chromatography. These conditions of hydrolysis were chosen when 0.5 *N* sulfuric acid and Amberlite IR-120 resin were found to give glycosidic cleavage and 0.01 *N* sulfuric acid required heating for 90 min. Removal of isopropylidene groups was followed by t.l.c. in solvent B and paper chromatography (solvents C and D) was used to check on glycosidic cleavage. Purification of 100 mg of disaccharide on Dowex 50W X2 (Li^+) gave a recovery of 94 mg, $[\alpha]_D$ ~0° (*c*, 1 in water). Solid products were obtained by reaction with phenylhydrazine, aniline (m.p. 145–147°) and *p*-nitrobenzoyl chloride (m.p. 153–156°) none of which gave satisfactory analyses.

The g.l.c. of the per(trimethylsilyl) disaccharide (column c at 260°) gave one peak (~15%) at 7.3 min and two unresolved peaks at 10.7 min (per(trimethylsilyl)sucrose 5.5 min).

Anal. Calcd. for $C_{13}H_{24}O_{11}$: C, 43.82; H, 6.74. Found (after drying over P_2O_5 at 68° for 3 days): C, 43.63; H, 7.09.

Reaction of the pure disaccharide (10.40, 10.50 mg) in duplicate oxidations with sodium metaperiodate (0.015 *M*, 20 ml) at room temperature in the dark showed a rapid uptake of 4 mol with the consumption of periodate becoming constant (4.9, 5.0 mol) in 18 h (25). Iodate and excess periodate were removed by addition of barium acetate and sodium borohydride was added. The polyalcohol, obtained by deionization, distillation with methanol and concentration, was hydrolyzed (1.0 *N* H_2SO_4, 5 ml, 100°, 4h) and the neutralized ($BaCO_3$) hydrolyzate converted to trimethylsilyl derivatives. Injection in hexane, onto column *a* programmed from 120 to 195° at 2°/min, gave peaks identical to authentic standards of the per(trimethylsilyl) derivatives of ethylene glycol (5.3 min) and 2-*O*-methyl-D-erythritol (27.2 min) (4, 26).

Pure disaccharide (28 mg) in dry methyl sulfoxide (2.0 ml) was methylated using methyl sulfinyl anion (1.5 *M*, 1.0 ml) and methyl iodide (6.0 ml). Methanolysis and examination of the methyl glycosides on column *b* programmed from 130 to 190° at 2°/min showed peaks corresponding to methyl 2,3,4,6-tetra-*O*-methyl-D-glucosides (5.1, 7.7 min), methyl 2,3,5-tri-*O*-methyl-D-galactofuranosides (15.9 min), and methyl 2,3,4-tri-*O*-methyl-D-galactopyranosides (21.3 min).

*6-O-(4-O-Methyl-β-*D*-glucopyranosyl)-*D*-galactitol (5)*
*[1-O-(4-O-Methyl-β-*D*-glucopyranosyl)-*L*-galactitol]*

Disaccharide (180 mg) was reduced with sodium borohydride (360 mg) in water (18 ml) for 4 h. Passage through cation exchange resin, concentration and distillation with methanol gave **5** ($R_{glucose}$ 0.34, solvent C; 0.33 solvent D) which was acetylated with acetic anhydride (10 ml) and anhydrous sodium acetate (500 mg). The peracetate of **5** was obtained as a syrup which crystallized on seeding with crystals obtained by g.l.c. Crude yield 346 mg, m.p. 95–100°. Two recrystallizations from ethanol (20 ml/g) gave 6-*O*-(4-*O*-methyl-β-D-glucopyranosyl)-D-galactitol octaacetate m.p. 104–106°, $[\alpha]_D$ −31.3° (*c*, 2.2 in chloroform), R_f 0.35 solvent A). Retention time on column *c* at 275° 8.0 min (sucrose octaacetate 5.1 min). The n.m.r. spectrum of the acetate in $CDCl_3$ did not show clearly the signal for the anomeric proton but the free alditol **5** in D_2O showed $J_{1,2}$ 7.5 Hz (τ 5.53, Me_4Si external) (20).

Anal. Calcd. for $C_{29}H_{42}O_{19}$: C, 50.12; H, 6.10. Found: C, 50.09; H, 6.07.

The authors wish to acknowledge financial support from the National Research Council of Canada and the interest of Dr. P. E. Reid.

1. F. Smith and A. M. Stephen. Tetrahedron Lett. **7**, 17 (1960).
2. D. A. Rees and J. W. B. Samuel. Chem. Ind. (London), 2008 (1965).
3. G. G. S. Dutton and S. Kabir. Anal. Lett. **4**, 95 (1971).
4. G. O. Aspinall and R. M. Fairweather. Carbohydr. Res. **1**, 83 (1965).
5. G. O. Aspinall, J. J. Carlyle, and R. Young. Carbohydr. Res. **7**, 421 (1968).
6. G. O. Aspinall. Adv. Carbohydr. Chem. **24**, 333 (1969).
7. R. W. Bailey. Oligosaccharides. Pergamon Press, London, 1965.
8. F. Smith and R. Montgomery. Chemistry of plant gums and mucilages. Reinhold, New York, 1959.
9. S. Hakomori. J. Biochem. (Tokyo), **55**, 205 (1964)
10. B. D. Kohn and P. Kohn. J. Org. Chem. **28**, 1037 (1963).
11. E. J. Bourne and S. Peat. Adv. Carbohydr. Chem. **5**, 145 (1950).
12. K. K. De and T. E. Timell. Carbohydr. Res. **4**, 72 (1967).
13. A. L. Raymond and E. F. Schroeder. J. Am. Chem. Soc. **70**, 2785 (1948).
14. B. Helferich and W. Klein. Justus Liebigs Ann. Chem. **450**, 219 (1926).
15. J. K. N. Jones, R. A. Wall, and A. O. Pittet. Can. J. Chem. **38**, 2285 (1960).
16. C. S. Hudson. Collected papers. Academic Press, New York, 1946, p. 660.
17. C. C. Sweeley, R. Bentley, M. Makita, and W. W. Wells. J. Am. Chem. Soc. **85**, 2497 (1963).
18. C. T. Bishop. Adv. Carbohydr. Chem. **19**, 95 (1964).
19. H. G. Walker, M. Gee, and R. M. McCready. J. Org. Chem. **27**, 2100 (1962).
20. J. N. C. Whyte. Anal. Biochem. **42**, 476 (1971).
21. W. E. Trevelyan, D. P. Procter, and J. S. Harrison. Methods Carbohydr. Chem. **1**, 21 (1962).
22. H. T. Gordon, W. Thornburg, and L. N. Werun. Anal. Chem. **28**, 849 (1956).
23. P. A. Sandford and H. E. Conrad. Biochem. **5**, 1508 (1966).
24. R. U. Lemieux, R. K. Kullnig, H. J. Bernstein, and W. E. Schneider. J. Am. Chem. Soc. **80**, 6098 (1958).
25. G. O. Aspinall and R. J. Ferrier. Chem. Ind. (London), 1216 (1957).
26. S. Karácsonyi and M. Kubacková. Coll. Czech. Chem. Commun. **34**, 2002 (1969).

Can. J. Chem. Downloaded from www.nrcresearchpress.com by 210.87.254.42 on 09/05/12
For personal use only.

Conformational Studies of the Benzophenone and Thiobenzophenone Radical Anions

F. C. ADAM AND LEON J. AARONS[1]

Department of Chemistry. University of Calgary. Calgary. Alberta

Received October 25, 1971

A conformational energy map is calculated for the anions of benzophenone and thiobenzophenone, using a Bartell repulsion potential. A low energy configuration is obtained in which the phenyl rings are counterrotated by 30° from the planar form. The energy barrier to concerted rotation is also calculated and found to be in reasonable agreement with the findings of Takeshita and Hirota for the oxyketyl. Spin density distributions are also given.

Un diagramme d'énergie conformationnelle a été calculé pour les anions de la benzophénone et du thiobenzophénone en se servant d'un potentiel de répulsion de Bartell. On obtient une configuration de faible énergie dans laquelle les noyaux phényl effectuent une contre-rotation de 30° relativement à la forme planaire. On calcule aussi la barrière énergétique à la rotation concertée et notre résultat est en accord avec les découvertes de Takeshita et Hirota sur l'oxycétyl. On donne aussi les distributions de densité de spin.

Canadian Journal of Chemistry, **50**, 1427 (1972)

Recent electron spin resonance (e.s.r.) studies by Takeshita and Hirota (1) have shown that at low temperatures the benzophenone radical anion has two sets of non-equivalent ortho protons. These result from the fact that at low temperatures the frequency of rotation of the phenyl rings is low compared to the frequency difference between the hyperfine couplings at the two sites. Adam and Falle (2) have suggested that the phenyl rings in radicals of the diaryl methyl type undergo a concerted rotation; this motion must occur with a minimum loss of delocalization energy but because of the steric repulsion energy between the ortho groups the system goes through a configuration in which only one ring is coplanar with the carbonyl group. The frequency of this rotation increases at higher temperatures until it is much greater than the difference in hyperfine couplings in which case identical couplings are observed from all ortho sites. Because of an interest in the structure of the benzophenone and thiobenzophenone anion radicals and their ion pairs (3), we have undertaken a theoretical study of the conformation of these systems.

The method used is similar to that used by Laidlaw and Flewwelling (4) and involves the minimization of the total energy (E_T) defined by:

$$E_T = E_\pi + E_S$$

[1]Present address: Department of Chemistry, University of Manchester, Manchester, England.

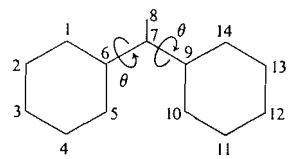

FIG. 1. Geometry of systems studied.

where E_π is the total π-electron energy and E_S is the steric repulsion energy.

E_π was calculated using the Pariser–Parr–Pople (PPP) (5) technique. The numbering system and geometry of the system is shown in Fig. 1. All C—C bonds of the aromatic rings were taken as 1.40 Å and extracyclic C—C bonds (6—7 and 7—9) as 1.48 Å. The C—O and C—S bonds (7—8) were taken as 1.23 and 1.71 Å, respectively (6). The C—H bonds were taken as 1.08 Å. The parameters used in the calculation are listed in Table 1.

E_S was calculated using the formulae of Bartell (10) which are given by eqs. 1, 2, and 3 for C—C, C—H, and H—H nonbonded repulsions respectively with V in eV and r in Å. The total repulsion energy was obtained by summing over all pairs of interacting atoms.

$$[1] \qquad V_{CC}(r) = 12\,800r^{-12} - 1.41 \times 10^3 r^{-6}$$

$$[2] \qquad V_{CH}(r) = [-5.42 + 1.94 \times 10^3 \times \exp(-r/0.490)]r^{-6}$$

$$[3] \qquad V_{HH}(r) = -2.14r^{-6} + 2.86 \times 10^2 \times \exp(-r/0.245)$$

Can. J. Chem. Downloaded from www.nrcresearchpress.com by 210.87.254.42 on 09/05/12
For personal use only.

TABLE 1. Values of parameters used in conformational calculations for the free benzophenone and thiobenzophenone anion radicals

Integral*	Value (eV)	Reference	Integral†	Value (eV)	Reference
I_c	−11.22	5*a*	β_{cc}	−2.39	5*a*
I_O	−17.1	7	β_{ce}‡§	$-2.10\cos\theta$	5*a*
I_s	−18.0		β_{co}§	−2.69	8
γ_c	16.53	5*a*	β_{cs}	−2.39	9
γ_O‖	14.97	7			
γ_s‖	17.93	7			

*I_X, ionization potential of atom X; γ_X, electron repulsion integral for atom X.
†β_{xy}, resonance integral between atoms x and y.
‡For extracyclic 6—7 and 7—9 bonds.
§Calculated by Mulliken's approximation.
‖Calculated using Paoloni's formula $\gamma_\mu = 3.29\ Z_\mu$.

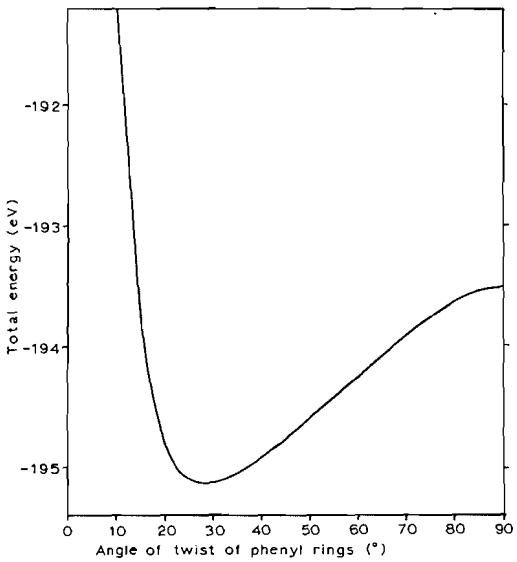

FIG. 2. Conformational energy map for benzophenone anion. The map for thiobenzophenone anion radical can be superimposed on this one shown except the minimum value occurs at an energy of −194.7 eV and the 90° value is −193.2 eV.

TABLE 2. Calculated and observed spin densities for the free benzophenone and thiobenzophenone anion radicals

Position	Planar	$\theta = 30°$	Observed*
	Benzophenone		
1, 14	0.0777	0.0734	0.096
2, 13	−0.0379	−0.0362	0.033
3, 12	0.1297	0.1239	0.128
4, 11	−0.0560	−0.0519	0.033
5, 10	0.1047	0.0966	0.096
7	0.1642	0.1887	
8	0.3490	0.3417	
	Thiobenzophenone		
1, 14	0.0592	0.0611	0.089
2, 13	−0.0359	−0.0374	0.035
3, 12	0.0975	0.0952	0.106
4, 11	−0.0476	0.0446	0.035
5, 10	0.0798	0.0735	0.089
7	0.0204	0.0422	
8	0.6540	0.6487	

*Spectra taken by sodium reduction in 1,2-dimethoxyethane (3) at reduced temperature (−50 °C). Experimental spin densities were calculated using McConnell's relation (14), $a_i = Q\rho_i$ where Q is a parameter taken as −27.0 Oe.

The conformations in which each ring has been rotated through equal and opposite angles (θ) were considered to be the low energy configurations as suggested by Adam and Falle (2). The formulae failed to give reasonable results around $\theta = 0°$ but these regions are obviously energetically unfavorable due to ortho proton–proton repulsion so these values were ignored. The conformational energy maps for benzophenone and thiobenzophenone are shown in Fig. 2. Both curves suggested minima in E_T at about 30°.

The results of our calculation suggest that both the benzophenone and thiobenzophenone radical anions are non-planar. The decrease in steric repulsion, which results mainly from the interaction between the ortho groups 5 and 10, compensates for the loss in π delocalization energy. The angle of rotation in the benzophenone radical anions is slightly reduced from that of benzophenone in the crystal (11) (33°) and that calculated by Hoffman and Swenson (12) (38°) for the ground state of benzophenone This is in accord with a suggestion of Rieger and

Can. J. Chem. Downloaded from www.nrcresearchpress.com by 210.87.254.42 on 09/05/12
For personal use only.

Fraenkel (13) who noticed that the calculated bond order between the carbonyl carbon atom and the phenyl rings increased from 0.323 in neutral benzophenone to 0.428 in the anion.

The barrier to concerted rotation was calculated as the energy difference between the above conformation with $\theta = 30°$, and that in which one ring is perpendicular to, and the other is coplanar with, the carbonyl group. The result is 0.34 eV, ($\sim$7.5 kcal mol^{-1}), about twice as large as the barrier to rotation of the phenyl rings found experimentally by Takeshita and Hirota (1) *i.e.* about 5 kcal mol^{-1} for the benzophenone radical anion. A value of 0.39 eV was found for thiobenzophenone. Finally the results of the spin density calculations for the benzophenone and thiobenzophenone anions in the planar ($\theta = 0°$) and non-planar ($\theta = 30°$) conformations are given in Table 2. It is evident from the table that the calculated ring proton spin densities are relatively insensitive to twist of the phenyl rings. Hence the comparison of calculated and observed hyperfine splitting constants could prove misleading if used as a basis for configurational studies concerning these compounds. The use of conformational energy maps would appear to be a more satisfactory technique.

1. T. Takeshita and N. Hirota. J. Chem. Phys. **51**, 2146 (1969).
2. F. C. Adam and H. R. Falle. Can. J. Chem. **44**, 1387, 1397 (1966).
3. F. C. Adam and L. J. Aarons. Can. J. Chem. This issue.
4. W. G. Laidlaw and R. B. Flewwelling. Can. J. Chem. **48**, 2158 (1970).
5. (*a*) R. Pariser and R. G. Parr. J. Chem. Phys., **21**, 466, 767 (1953); (*b*) A. Bristock and J. A. Pople. Trans. Faraday Soc. **50**, 901 (1954).
6. Chem. Soc. Spec. Publ. **11**, 1958.
7. R. D. Brown and M. L. Heffernan. Trans. Faraday Soc. **54**, 757 (1958).
8. R. S. Mulliken. J. Chim. Phys. **46**, 675 (1949).
9. H. C. Longuet-Higgins. Trans. Faraday Soc. **41**, 173 (1949).
10. L. S. Bartell. J. Chem. Phys. **32**, 827 (1960).
11. E. B. Fleischer, N. Sung, and S. Hawkinson. J. Phys. Chem. **72**, 4311 (1968).
12. R. Hoffmann and J. R. Swenson. J. Phys. Chem. **74**, 415 (1970).
13. P. H. Rieger and G. K. Fraenkel. J. Chem. Phys. **37**, 2811 (1962).
14. H. M. McConnell. J. Chem. Phys. **24**, 764 (1956).

Quenching of Fluorescence of Chloropentafluoroacetone by Saturated Hydrocarbons

A. J. Yarwood

Department of Chemistry, McMaster University, Hamilton, Ontario

Received August 9, 1971

Saturated hydrocarbons can quench the electronically excited singlet state of a simple ketone in the gas phase. Measurements on the quenching of the fluorescence yield of chloropentafluoroacetone at 23 °C show that different saturated hydrocarbons can deactivate the excited singlet state with varying efficiencies. The quenching rate constants are reported and possible relationships considered.

Les hydrocarbones saturés peuvent réprimer l'état singulet électroniquement excité d'une cétone simple en phase gazeuse. Des mesures de répression du rendement de la fluorescence du chloropentafluoroacétone à 23 °C montrent que certains hydrocarbones saturés peuvent désactiver l'état excité singulet avec une efficacité variable. On rapporte les constantes de vitesse de répression et on considère les relations possibles.

Canadian Journal of Chemistry, **50**, 1429 (1972)

Introduction

The quenching of electronically excited states by saturated hydrocarbons has played an important part in the growing understanding of the interaction of excited states and quenching molecules. One of the first quantitative studies in the area of photosensitized reactions was by Bates (1), who investigated the quenching of the

Can. J. Chem. Downloaded from www.nrcresearchpress.com by 210.87.254.42 on 09/05/12
For personal use only.

Fraenkel (13) who noticed that the calculated bond order between the carbonyl carbon atom and the phenyl rings increased from 0.323 in neutral benzophenone to 0.428 in the anion.

The barrier to concerted rotation was calculated as the energy difference between the above conformation with $\theta = 30°$, and that in which one ring is perpendicular to, and the other is coplanar with, the carbonyl group. The result is 0.34 eV, ($\sim$7.5 kcal mol^{-1}), about twice as large as the barrier to rotation of the phenyl rings found experimentally by Takeshita and Hirota (1) *i.e.* about 5 kcal mol^{-1} for the benzophenone radical anion. A value of 0.39 eV was found for thiobenzophenone. Finally the results of the spin density calculations for the benzophenone and thiobenzophenone anions in the planar ($\theta = 0°$) and non-planar ($\theta = 30°$) conformations are given in Table 2. It is evident from the table that the calculated ring proton spin densities are relatively insensitive to twist of the phenyl rings. Hence the comparison of calculated and observed hyperfine splitting constants could prove misleading if used as a basis for configurational studies concerning these compounds. The use of conformational energy maps would appear to be a more satisfactory technique.

1. T. Takeshita and N. Hirota. J. Chem. Phys. **51**, 2146 (1969).
2. F. C. Adam and H. R. Falle. Can. J. Chem. **44**, 1387, 1397 (1966).
3. F. C. Adam and L. J. Aarons. Can. J. Chem. This issue.
4. W. G. Laidlaw and R. B. Flewwelling. Can. J. Chem. **48**, 2158 (1970).
5. (*a*) R. Pariser and R. G. Parr. J. Chem. Phys., **21**, 466, 767 (1953); (*b*) A. Bristock and J. A. Pople. Trans. Faraday Soc. **50**, 901 (1954).
6. Chem. Soc. Spec. Publ. **11**, 1958.
7. R. D. Brown and M. L. Heffernan. Trans. Faraday Soc. **54**, 757 (1958).
8. R. S. Mulliken. J. Chim. Phys. **46**, 675 (1949).
9. H. C. Longuet-Higgins. Trans. Faraday Soc. **41**, 173 (1949).
10. L. S. Bartell. J. Chem. Phys. **32**, 827 (1960).
11. E. B. Fleischer, N. Sung, and S. Hawkinson. J. Phys. Chem. **72**, 4311 (1968).
12. R. Hoffmann and J. R. Swenson. J. Phys. Chem. **74**, 415 (1970).
13. P. H. Rieger and G. K. Fraenkel. J. Chem. Phys. **37**, 2811 (1962).
14. H. M. McConnell. J. Chem. Phys. **24**, 764 (1956).

Quenching of Fluorescence of Chloropentafluoroacetone by Saturated Hydrocarbons

A. J. Yarwood

Department of Chemistry, McMaster University, Hamilton, Ontario

Received August 9, 1971

Saturated hydrocarbons can quench the electronically excited singlet state of a simple ketone in the gas phase. Measurements on the quenching of the fluorescence yield of chloropentafluoroacetone at 23 °C show that different saturated hydrocarbons can deactivate the excited singlet state with varying efficiencies. The quenching rate constants are reported and possible relationships considered.

Les hydrocarbones saturés peuvent réprimer l'état singulet électroniquement excité d'une cétone simple en phase gazeuse. Des mesures de répression du rendement de la fluorescence du chloropentafluoroacétone à 23 °C montrent que certains hydrocarbones saturés peuvent désactiver l'état excité singulet avec une efficacité variable. On rapporte les constantes de vitesse de répression et on considère les relations possibles.

Canadian Journal of Chemistry, **50**, 1429 (1972)

Introduction

The quenching of electronically excited states by saturated hydrocarbons has played an important part in the growing understanding of the interaction of excited states and quenching molecules. One of the first quantitative studies in the area of photosensitized reactions was by Bates (1), who investigated the quenching of the

Can. J. Chem. Downloaded from www.nrcresearchpress.com by 210.87.254.5 on 09/05/12
For personal use only.

Can. J. Chem. Downloaded from www.nrcresearchpress.com by 210.87.254.5 on 09/05/12
For personal use only.

$^3P_1$ state of mercury by saturated hydrocarbons. More recent research has shown that the processes involved in the triplet mercury quenching are quite complex (2–7).

The triplet states of not only atoms, but also molecules, can be deactivated by collisions with saturated hydrocarbons. Thus, the photoreduction of aromatic ketones in solution is a well documented reaction (8) and the photoreduction of the triplet state of acetone in *n*-hexane has been reported (9). The first example of a photoreduction in the gas phase was reported by Whittemore and Swarc (10). They found that hexafluorobiacetyl was reduced on photolysis in the vapor and in solution in presence of saturated hydrocarbons. A chemical effect of isobutane was proposed by Kutschke and coworkers (11, 12,) to explain the observed quenching in the photolysis of hexafluoroacetone. Direct measurements (13) of the effect of isobutane on the phosphorescence lifetime of hexafluoroacetone in the gas phase showed clearly that there was an interaction ($k_Q = 1.2 \times 10^8\ M^{-1}\ s^{-1}$) between the isobutane and the triplet state of hexafluoroacetone.

Although the interaction of the triplet state of atoms and molecules with saturated hydrocarbons is now well-illustrated, there is little research reported on the interaction of electronically excited singlet states with saturated hydrocarbons. This paper reports the quenching of the electronically excited singlet state of chloropentafluoroacetone by saturated hydrocarbons in the gas phase.

Experimental

Chloropentafluoroacetone was supplied by Allied Chemical Co. and was purified as described earlier (14). The following hydrocarbons were C.P. grade chemicals supplied by Matheson Co. (all were used after distillation at suitable low temperatures in which large head and tail fractions were discarded): ethane, propane, *n*-butane, 2-methylpropane, and 2,3-dimethylpropane. Philips Research grade 2-methylpropane was also studied. The 2-methylbutane (Philips Pure grade), *n*-pentane (Matheson, Coleman and Bell, spectroquality), and germane (a gift of Dr. T. Birchall) were also used after distillation at low temperature. The cyclopentane and 2,3-dimethylbutane (Chemical Samples Co.) were both greater than 99.9% pure and were used after being deaerated.

The fluorescence equipment used in this study has been described earlier (15). In this investigation similar techniques were used; however, in all cases the ketone and hydrocarbon were mixed using an efficient all-glass pump that was driven magnetically.

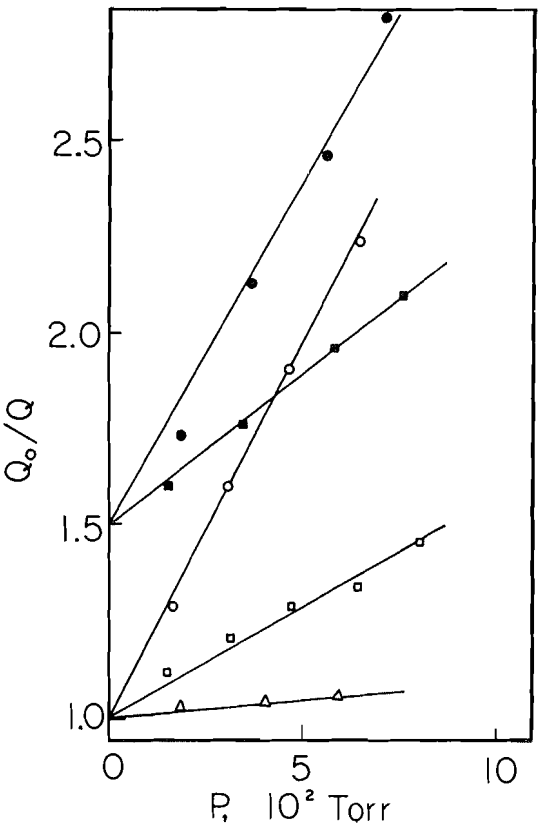

FIG. 1. Quenching of fluorescence of chloropentafluoroacetone. ○, 2-methylpropane; □, 2,2-dimethylpropane; △, ethane; ●, *n*-butane; ■, propane. N.B. The *n*-butane and propane data are displaced vertically in 0.5 units.

Results

The fluorescence of chloropentafluoroacetone (temperature, 23 °C and pressure, 200 ± 5 Torr) was excited at 313 nm and the quenching efficiencies of the hydrocarbons were deduced from the decreased fluorescence intensities when the hydrocarbons were present. Figure 1 shows the results for *n*-butane, propane, 2-methylpropane (Research grade sample), 2,2-dimethylpropane, and ethane. There are good linear relations between Q_0/Q and the pressure of the quencher. Q is the relative fluorescence yield in the presence of the quencher and Q_0 the relative fluorescence yield for the pure ketone. Figure 2 shows the Stern–Volmer plots for 2,3-dimethylbutane and *n*-pentane. Figure 3 includes the data for cyclopentane, germane, and 2-methyl-

Can. J. Chem. Downloaded from www.nrcresearchpress.com by 210.87.254.5 on 09/05/12
For personal use only.

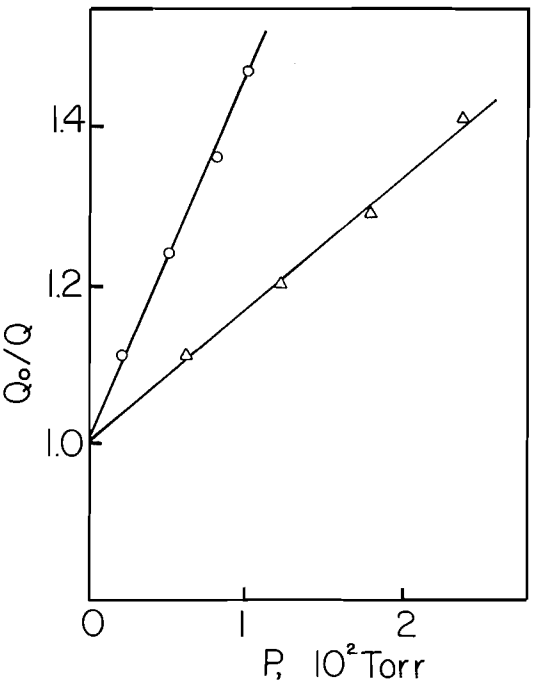

FIG. 2. Quenching of fluorescence of chloropentafluoroacetone. ○, 2,3-dimethylbutane; △, *n*-pentane.

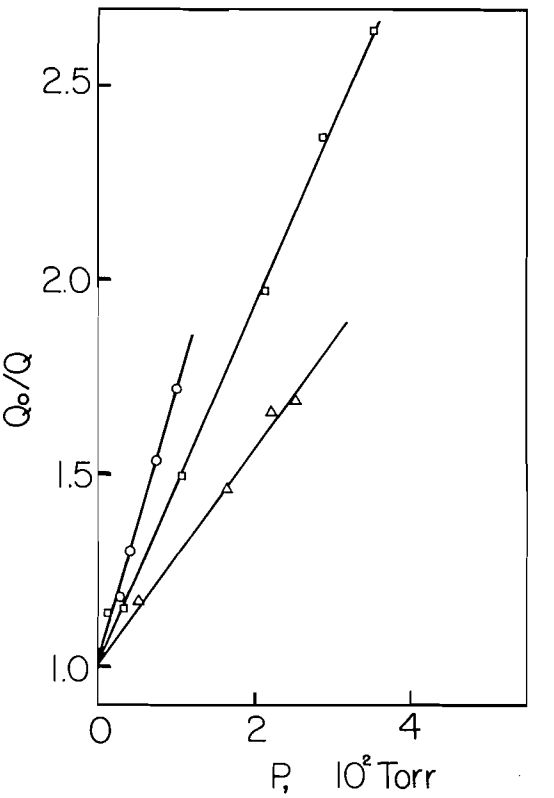

FIG. 3. Quenching of fluorescence of chloropentafluoroacetone. ○, cyclopentane; □, germane; △, 2-methylbutane.

butane. In each case good linear behavior is observed.

Discussion

Only fluorescence is observed when chloropentafluoroacetone is excited in the n,π^* band in the gas phase (14). On excitation at 313 nm, it was found that the relative fluorescence yield Q_0 was independent of the ketone pressure when the pressure was larger than about 150 Torr. Thus, deactivation of the initially populated vibrationally excited singlet levels is expected to be complete at a pressure of 200 Torr. The quenching efficiencies reported are for ketone molecules in low vibrational levels of the electronically excited singlet state.

The plots of Q_0/Q *vs.* pressure of quencher shown in Figs. 1–3 are linear, so the kinetics of the quenching can be explained in terms of a simple bimolecular quenching reaction (rate constant k_Q). The slopes of the lines in the figures are related to $k_Q\tau$ where τ is the actual lifetime of the ketone singlet state in the absence of quencher. τ has been measured (14) as 3.5×10^{-8} s and the quenching rate constants for the hydrocarbons are shown in Table 1.

TABLE 1. Rate constants for quenching of singlet chloropentafluoroacetone

Quencher	$k_Q(M^{-1}\ s^{-1})$
Ethane	5.0×10^7
Propane	4.1×10^8
n-Butane	9.4×10^8
2-Methylpropane	1.0×10^9
n-Pentane	9.0×10^8
2-Methylbutane	1.5×10^9
2,2-Dimethylpropane	3.0×10^8
Cyclopentane	3.7×10^9
2,3-Dimethylbutane	2.5×10^9
Germane	2.5×10^9

Since the saturated hydrocarbons could contain small amounts of olefins as impurities, care was taken in the purification procedure. The first experiments were, in fact, done using a sample of C.P. grade 2-methylpropane supplied

Can. J. Chem. Downloaded from www.nrcresearchpress.com by 210.87.254.5 on 09/05/12
For personal use only.

by Matheson. The results of that experiment are not shown in figures since the quenching rate constant obtained was essentially the same as for the research grade sample studied later, Fig. 1. It is believed that the rate constants shown in Table 1 represent intrinsic quenching by the saturated hydrocarbons. The quenching behavior of saturated hydrocarbons on the excited singlet state of a simple ketone was discovered independently by Kutschke (17) in a study of the fluorescence of hexafluoroacetone.

Recently the quenching by unsaturated hydrocarbons of the singlet state of chloropentafluoroacetone was reported (15) and an intriguing relationship between the rate constants was noted. For olefins that do not contain electron-withdrawing groups, it was found that there was a linear relation between the logarithm of the quenching rate constant and the ionization potential of the quenching molecule. The possibility of a similar relationship in the quenching by saturated hydrocarbons was considered. For many of the molecules, the data were consistent with the notion that a quencher with a high ionization (*e.g.* ethane, $5 \times 10^7\ M^{-1}\ s^{-1}$, 11.5 eV) had a lower quenching rate constant than a quencher with a low ionization potential (*e.g.* 2-methylbutane, $1.5 \times 10^9\ M^{-1}\ s^{-1}$, 10.3 eV). However, the correlation could not encompass all the data since the results for cyclopentane and 2,2-dimethylpropane deviated significantly. The quenching rate constant for 2,2-dimethylpropane is $3.0 \times 10^8\ M^{-1}\ s^{-1}$ and it has an ionization potential of 10.4 eV (16), whereas cyclopentane, with an ionization potential of 10.5 eV, has a quenching rate constant of $3.7 \times 10^9\ M^{-1}\ s^{-1}$. The quenching rate constant observed for 2,2-dimethylpropane is much smaller than might have been anticipated on the basis of a relation with the ionization potential.

When the individual values are considered some interesting aspects of the quenching are noticed. The values of the rate constants for the sequence ethane, propane, 2-methylpropane, 2,2-dimethylpropane suggest that the interaction of the excited singlet state ketone molecule is with the carbon–hydrogen bond. The rate constant for quenching by molecules with tertiary C—H bonds is larger than that for molecules with secondary bonds and this in turn is greater than that for molecules with primary C—H bonds. This suggestion is supported by the data on the substituted butanes. The rate constants increase along the series *n*-butane, 2-methylbutane and 2,3-dimethylbutane; also, the rate constant for 2-methylbutane is larger than that for 2-methylpropane.

The rate constant increases along the series ethane ($5 \times 10^7\ M^{-1}\ s^{-1}$), propane ($4.1 \times 10^8\ M^{-1}\ s^{-1}$) and *n*-butane ($9.4 \times 10^8\ M^{-1}\ s^{-1}$), but the value is smaller for *n*-pentane ($9.0 \times 10^8\ M^{-1}\ s^{-1}$) than for *n*-butane. Therefore, the quenching rate constant cannot be considered as a simple additive function of the number of methylene groups in quenching molecules. It should also be noted that the rate constant of cyclopentane quenching is more than twice that for quenching by *n*-pentane; germane is a surprisingly efficient quenching molecule.

In summary, saturated hydrocarbons can quench the electronically excited singlet state of chloropentafluoroacetone. The rate constants are consistent with the view that the interaction is with the carbon–hydrogen bond. The sequence of quenching ability of carbon–hydrogen bonds is tertiary > secondary > primary.

I thank the National Research Council of Canada for financial support and Dr. K. O. Kutschke for communicating his results prior to publication.

1. J. R. Bates. J. Am. Chem. Soc. **52**, 3825 (1930); **54**, 569 (1932).
2. B. de B. Darwent. J. Chem. Phys. **18**, 1532 (1950).
3. R. J. Cvetanovic. J. Chem. Phys. **23**, 1208 (1955).
4. Y. Rousseau and H. E. Gunning. Can. J. Chem. **41**, 465 (1963).
5. S. Penzes, A. J. Yarwood, O. P. Strausz, and H. E. Gunning. J. Chem. Phys. **43**, 4524 (1965).
6. K. Yang. J. Am. Chem. Soc. **87**, 5294 (1965).
7. J. M. Campbell, S. Penzes, H. S. Sandu, and O. P. Strausz. Int. J. Chem. Kin. **3**, 175 (1971).
8. J. G. Calvert and J. N. Pitts, Jr. Photochemistry. Wiley, New York, 1966, p. 533.
9. P. J. Wagner. J. Am. Chem. Soc. **88**, 5672 (1966).
10. I. M. Whittemore and M. Swarc. J. Phys. Chem. **67**, 2492 (1963).
11. A. N. Strachan, R. K. Boyd, and K. O. Kutschke. Can. J. Chem. **42**, 1345 (1964).
12. S. N. Khanna and K. O. Kutschke. Can. J. Chem. **44**, 1465 (1966).
13. A. Gandini and K. O. Kutschke. Can. J. Chem. **44**, 1720 (1966).
14. H. S. Samant and A. J. Yarwood. Can. J. Chem. **48**, 2611 (1970).
15. H. S. Samant and A. J. Yarwood. Can. J. Chem. **49**, 2053 (1971).
16. D. W. Turner. Adv. Phys. Org. Chem. **4**, 31 (1966).
17. K. O. Kutschke. Private communication.

The Cotton Effects of Conjugated Homoannular Dienes. I. The Non-generality of the Rule of Moscowitz[1]

J. LESSARD[2]
Division of Chemistry, National Research Council of Canada, Ottawa, Canada
AND
L. RUEST AND CH. R. ENGEL[3]
Department of Chemistry, Laval University, Quebec, Quebec

Received July 9, 1971

The non-generality of the diene rule of Moscowitz, relating the helicity of a non-planar conjugated homoannular diene to the sign of its Cotton effect, is discussed. We report the preparation of 3β-bromoacetoxy-16α-ethyl-16²-cyano-16²,21-cyclo-5α-pregna-17,21-diene, the X-ray crystallographic analysis of which confirms, as reported by Ahmed and Pollard, the stereochemistry which we previously assigned to the parent alcohol and acetate. We also report the synthesis of the methyl ketonic analogues of these dienonitriles and show that their sodium borohydride reduction product still has a Cotton effect in contradiction to the diene rule. The implications of these and other experiments are discussed.

On discute la non-généralité de la règle diénique de Moscowitz qui met en relation l'hélicité de dienes homoannulaires conjugués non planaires au signe de leurs effets Cotton. Nous rapportons la préparation du bromoacétoxy-3β éthyl-16α cyano-16² cyclo-16²,21 (5α)pregnadiène-17,21 dont l'analyse cristallographique aux rayons X, rapportée dans une publication parallèle par Ahmed et Pollard, confirme la stéréochimie que nous avons attribuée précédemment aux dérivés 3β-hydroxy et 3β-acétoxy et qui est en opposition avec la règle de Moscowitz. Nous décrivons la synthèse des analogues méthylcétoniques de ces diénonitriles et montrons que la réduction du groupe cétonique ne résulte pas dans une inversion du signe de l'effet Cotton. Nous discutons, ensemble avec d'autres données, les implications de ces expériences.

Canadian Journal of Chemistry, **50**, 1433 (1972)

In previous publications in our series on cyanoethylations and Michael additions, we have shown that the cyanoethylation of certain α,β-unsaturated aldehydes and ketones may take place in the γ-position, with cyclization, leading to allylic cyclohexenols, substituted in the α′-position by a nitrile group, and to derivatives of such products, such as conjugated dienonitriles arising by dehydration of the alcohols (1, 3–7). The experiments had been carried out with a steroid aldehyde (4, 5), an aldehyde of the D-homo steroid series (6), an aldehyde derived from decalin (1, 7), and a steroid ketone (3) (*cf.* partial formula **i**). On the basis of chemical and physical evidence, in particular of n.m.r. analyses, we assigned to the main reaction products of the steroidal carbonyl compounds (with a five-membered D-ring) a β-hydrogen-configuration at the new ring junction, position 16 (*cf.* partial structures **ii** and **iii**) (3, 5, 8). These assignments were, however, in opposition to the diene rule of Moscowitz (9) which relates the sign of the Cotton effect of a non-planar homoannular diene to its helicity (*cf.* 1, 4–8). Since our findings seemed to represent the first exceptions to this rule which has rendered important services in stereochemical structure determinations, it appeared opportune to confirm our conclusions by a crystallographic X-ray analysis.

We therefore prepared the bromoacetate **1***b*

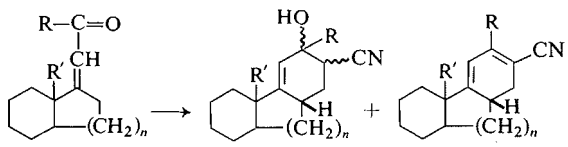

i **ii** **iii**

$n = 1, 2$
R = H; CH_3
R′ = H; CH_3

[1]This communication represents paper VII in the series on Cyanoethylations and Michael Additions, and paper XXXVI in the series on Steroids and Related Products; for paper VI of the first series see ref. 1, for paper XXXV of the second series, ref. 2.

[2]Present address: Department of Chemistry, University of Sherbrooke, Sherbrooke, Quebec.

[3]To whom correspondence should be addressed.

Can. J. Chem. Downloaded from www.nrcresearchpress.com by 210.87.254.105 on 09/05/12
For personal use only.

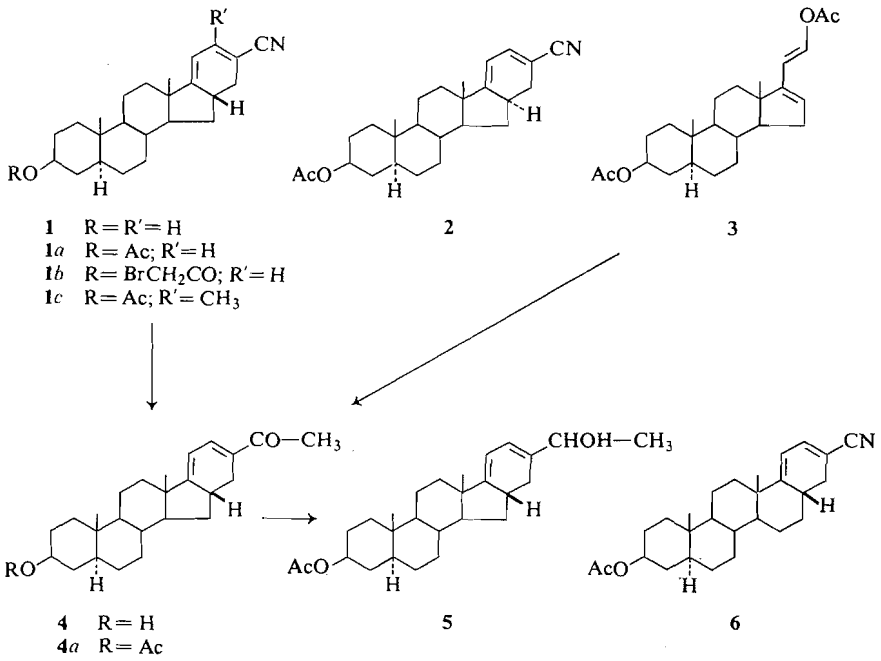

1 R = R' = H
1*a* R = Ac; R' = H
1*b* R = $BrCH_2CO$; R' = H
1*c* R = Ac; R' = CH_3

2 **3**

4 R = H
4*a* R = Ac

5 **6**

of 16α-ethyl-16²-cyano-16²,21-cyclo-5α-pregna-17,21-dien-3β-ol (**1**), as described in the Experimental. The product which, just as the free alcohol **1** and the acetate **1***a*, exhibits a negative Cotton effect, in opposition to Moscowitz' rule, was subjected by Ahmed and Pollard of the National Research Council of Canada to a crystallographic X-ray analysis which confirmed fully our stereochemical assignments and thus the non-generality of the diene rule. Ahmed and Pollard report their results in a parallel publication (10).

We demonstrated the limitations of the diene rule not only by the "exceptional" Cotton effects of the dienonitriles **1**, **1***a*, and **1***b*, the methyl ketonic analogue **1***c* of dienonitrile **1***a*, and the 16-epimer **2** of dienonitrile **1***a*, but also by those of the conjugated dienones **4** and **4***a*, which we had prepared by a Diels–Alder addition of acrylonitrile to the enol acetate **3** (8) and now also by the reaction of dienonitrile **1***a* with methyllithium (see Experimental).

One could have envisioned that the "exceptional" Cotton effects of these homoannular dienes be related to their conjugation with a nitrile function or a carbonyl function. We therefore reduced dienone **4***a* with sodium borohydride; the resulting product (*cf.* **5**), still showed an "abnormal", negative, Cotton effect which makes such a hypothesis improbable. A referee has kindly drawn to our attention that the sign of the Cotton effect of a steroidal 5α-hydroxy 6α-acetoxy 7,14-diene is opposite to that of the 5,6-unsubstituted product and that conclusions drawn from the Cotton effect of an allylic conjugated dienol are, therefore, subject to caution. We may also refer in this respect to a very recent article by Beecham *et al.* (11), in which the determining influence of allylic oxygen on the Cotton effects of non-planar dienes is demonstrated. However, in these examples, the allylic oxygen is attached directly to a ring and has a fixed geometry, a situation which does not prevail in the case of "aliphatic" allylic alcohols of type **5**. Furthermore, as already reported (6), dienonitrile **6** of the D-homo steroid series, to which, on the grounds of chemical and n.m.r. evidence, we assign a 17β-hydrogen configuration, shows a "normal", positive, Cotton effect, in agreement with Moscowitz' rule, in spite of the conjugation of the diene system with a nitrile group, so that the "anomaly" of the other Cotton effects observed by us can definitely not be rationalized solely on the grounds of the conjugation of the diene system with a nitrile or keto group or, for that matter, on the grounds

Can. J. Chem. Downloaded from www.nrcresearchpress.com by 210.87.254.105 on 09/05/12
For personal use only.

TABLE 1. Optical data of the dienonitriles **1***a*, **1***b*, **1***c*, **2**, and **6**, of the dienone **4** and the dienol **5**

Compound	Helicity of diene	Long-wavelength extremum				Agreement with diene rule
		o.r.d.		c.d.*		
1*a*	Right-handed	$[\Phi]_{321}$(dioxane)	−16200†	$\Delta\varepsilon_{297}$(EtOH)	−9.8	−
1*b*	Right-handed	$[\Phi]_{314}$(MeOH)	−31650‡[a]	$\Delta\varepsilon_{297}$(EtOH)	−12.1	−
				$\Delta\varepsilon_{295}$(cyclohexane)	−10.4§	−
1*c*	Right-handed	$[\Phi]_{314}$(MeOH)	−19600‡[b]	$\Delta\varepsilon_{295}$(EtOH)	−11.8	−
2	Left-handed	$[\Phi]_{322}$(dioxane)	+19400†	$\Delta\varepsilon_{303}$(EtOH)	+‖	−
6	Right-handed	$[\Phi]_{320}$(MeOH)	+9374‡[c]	$\Delta\varepsilon_{304}$(EtOH)	+6.2	+
4	Right-handed			$\Delta\varepsilon_{317}$(dioxane)	−7.02‡[d]	−
5	Right-handed	$[\Phi]_{290}$(dioxane)	−6446‡[a]			−

*If not otherwise stated, recorded by Prof. G. Wagnière and Mr. R. Geiger, on a Jouan 185 spectrograph.
†Recorded by Prof. P. Crabbé on a Jasco ORD/UV spectropolarimeter.
‡*cf.* (*a*) Experimental; (*b*) ref. 3; (*c*) ref. 6; (*d*) ref. 8.
§Recorded by Prof. A. Burgstahler on a Cary 60 spectropolarimeter with 6001 c.d. attachment.
‖Not sufficient quantities of material were available for a quantitative evaluation.

of allylic substitution with an aliphatic hydroxy group.

The pertinent optical data of the homoannular dienes discussed in this publication are summarized in Table 1[4] and related to the helicities of the diene systems and to the signs of the Cotton effects expected on the grounds of the diene rule of Moscowitz. We are greatly indebted to Prof. G. Wagnière and Mr. R. Geiger, University of Zurich, Switzerland, for the c.d. measurements, and to Prof. P. Crabbé, Syntex S.A., Mexico, for the o.r.d. curves of dienes **1***a* and **2**, and we also thank sincerely Prof. A. Burgstahler, University of Kansas, Lawrence, Kansas, for having kindly supplied us with the c.d. measurement of dienonitrile **1***b* in another solvent. As already indicated, it is apparent that the D-homo dienonitrile is the only product of this series whose Cotton effect is in agreement with the diene rule of Moscowitz, although one may note that the magnitude of this Cotton effect is lower than that of the Cotton effects of the other dienonitriles under discussion. The relatively low value of the negative o.r.d. extremum of the allylic dienol **5** (which is, actually, a mixture of epimeric alcohols) could point to a potentiating effect of a nitrile group in conjugation with the diene system, if one compares it with the extrema of the dienonitriles of the steroid series with a non-expanded D-ring. However, the consideration of both the sign and the magnitude of the Cotton effect of dienonitrile **6** of the D-homo series clearly indicates how cautious one has to be in attempting to establish such correlations. It seems that at this stage the only reasonably safe conclusion which may be drawn from our results is the assumption that the sign of the long-wavelength Cotton effect of complex homoannular dienes appears to depend to an appreciable extent on the environment of the optically active chromophore. This would become plausible if one accepts the recent suggestion of Burgstahler and Barkhurst (12) that the optical activity of nonplanar dienes were not due primarily to the inherent chirality of the diene system but to asymmetric perturbations of the double bond components. However, it must be pointed out that our results are also in opposition to the "axial allylic diene rule", proposed by Burgstahler and Barkhurst, which rationalizes the observed effects on the grounds of "asymmetric perturbations of the chromophore . . . through excited-state interactions with their allylic axial or pseudo-axial bonds".

On the other hand, our tentative suggestion (1, 3) that the apparently anomalous optical properties of our steroid dienes may be related to the fact that in these compounds one of the double bonds of the diene system is attached to a rigid five-membered ring, must be abandoned, or must at least be regarded as an over-simplification. Indeed, in a recent communication[5] (13),

[4]Copies of the original spectra are available from the Depository of Unpublished Data, National Science Library, National Research Council of Canada, Ottawa, Canada K1A 0S2.

[5]We sincerely thank Prof. P. Crabbé for sending us the manuscript prior to publication.

Can. J. Chem. Downloaded from www.nrcresearchpress.com by 210.87.254.105 on 09/05/12
For personal use only.

Can. J. Chem. Downloaded from www.nrcresearchpress.com by 210.87.254.105 on 09/05/12
For personal use only.

Crabbé and Guzmán describe a homoannular diene (B-nor-androsta-2,4-dien-3β-ol), one of the double bonds of which is attached to a rigid five-membered ring and which, in spite of that fact, exhibits a "normal" Cotton effect. Its relatively low magnitude could possibly confirm an influence of the size of the ring to which the diene system is attached but, evidently, other structural features also influence the optical activity of the chromophore.[6] Hence, a more detailed study becomes necessary for the explanation of the particular optical behavior of our pentacyclic steroid dienes. Work in this direction has been initiated in our laboratory.

Experimental[7]

3β-Bromoacetoxy-16α-ethyl-16^2-cyano-16^2,21-cyclo-5α-pregna-17,21-diene (1b)

To a solution of 200 mg of 3β-hydroxy-16α-ethyl-16^2-cyano-16^2,21-cyclo-5α-pregna-17,21-diene (**1**) (5), m.p. 199–200°, in 4 ml of absolute benzene and 0.06 ml of pyridine, 0.048 ml of bromoacetyl bromide was added and the mixture was left at room temperature for 15 h. The precipitate was filtered and washed with absolute benzene, the washings were combined with the filtrate which was then taken to dryness *in vacuo*. The crystalline residue was dried by repeated evaporation with benzene and recrystallized from ether–hexane to give 230 mg (86%) of the bromoacetate **1***b*, m.p. 187–189°. For analysis, a sample was recrystallized twice from ether–hexane; m.p. 191–191.5°; $[\alpha]_D^{25}$ −255.5° (*c*, 1.00 in $CHCl_3$); o.r.d. (*c*, 0.0012 in CH_3OH, 50 mm cell): $[\alpha]_{450}$ −500, $[\alpha]_{400}$ −1080, $[\alpha]_{350}$ −3000, $[\alpha]_{322}$ −6325, $[\alpha]_{314}$ −6670 (min), $[\alpha]_{308}$ −5670, $[\alpha]_{288}$ 0, $[\alpha]_{270}$ +4590, $[\alpha]_{258}$ +5340 (max), $[\alpha]_{244}$ +4840, $[\alpha]_{230}$ +4170° (negative Cotton effect); λ_{max} (EtOH) 296 nm (ε 11 130); ν_{max} (KBr) 3050 (vinylic hydrogens), 2180 (conjugated nitrile), 1740 (acetate), 1658 and 1572 (conjugated double bonds), 1285 (acetate), 1112, 1002, 988, 855, 840, and 680 cm^{-1}; n.m.r.: δ ($CDCl_3$) 1.84 (s) (18- and 19-CH_3), 2.35 (m) (16^1-CH_2), 2.70 (m) (16β-H), 3.78 (s) ($BrCH_2CO$), 4.80 (m) (3α-H), 5.60 (d of d, J = 5.0 and 2.5 Hz) (20-H), and 6.72 (d of d, J = 5.0 and 2.0 Hz) (21-H) (A/B system).

Anal. Calcd. for $C_{26}H_{34}O_2NBr$: C, 66.16; H, 7.26; N, 2.97; Br, 16.93. Found: C, 66.34; H, 7.22; N, 3.03; Br, 16.99.

[6]Crabbé and Guzmán indeed point out significant changes in the magnitude of Cotton effects upon changes of certain substituents (13).

[7]The melting points were taken in evacuated capillaries and the temperatures were corrected. The microanalyses were performed by the microanalytical laboratory of Drs. F. and E. Pascher, Bonn, Germany, to whom we are much obliged. For chromatography non-alkaline aluminum oxide Woelm, activity III, and Davison's silica gel no. 923 were used. The i.r. spectra were recorded on a Beckman model IR-4 spectrophotometer, the u.v. spectra on a Beckman model DK-1A spectrophotometer, the rotatory dispersion curves on a Jasco ORD/UV-5 instrument, and the n.m.r. spectra on a Varian A-60 spectrometer, in deuteriochloroform, tetramethylsilane serving as internal standard.

3β-Acetoxy-16α-ethyl-16^2-acetyl-16^2,21-cyclo-5α-pregna-17,21-diene (4a)

To a solution of 132 mg of 3β-acetoxy-16α-ethyl-16^2-cyano-16^2,21-cyclo-5α-pregna-17,21-diene (**1***a*) (4, 5) in 10 ml of absolute ether, 3.5 ml of a 0.5 *N* ethereal methyllithium solution was added in the course of 4 h. The progress of the reaction was followed by t.l.c. analysis. The formation of the methyl ketones **4** and **4***a* seemed to come to an end when a proportion of 1:2 of the ketones and the starting material was attained. The reaction mixture was poured into ice water and the precipitate was extracted with ether. The ethereal layer was washed with water and dried over sodium sulfate. The solvent was evaporated and the amorphous residue (125 mg) subjected to preparative t.l.c. on silica gel, using a benzene–ether (4:1) system. Two principal fractions were separated. The first one afforded 26 mg of *16α-ethyl-16^2-acetyl-16^2,21-cyclo-5α-pregna-17,21-dien-3β-ol (4)*, m.p. 180–185°, ν_{max} ($CHCl_3$) 3610 and 3450 (hydroxyl), 3010 (vinylic hydrogens), 1662, 1645, and 1575 ($\alpha,\beta,\gamma,\delta$-unsaturated ketone), 1040 cm^{-1} (hydroxyl). The product was acetylated in the usual fashion in 1 ml of pyridine with 0.5 ml of acetic anhydride. The crude reaction product (28 mg), m.p. 162–172°, representing *3β-acetoxy-16α-ethyl-16^2-acetyl-16^2,21-cyclo-5α-pregna-17,21-diene (4a)* was purified by preparative t.l.c. on silica gel, with the system benzene–ether (95:5), to give 18.5 mg of the pure methyl ketone **4***a*, m.p. 182–184°, not depressed upon admixture of a sample prepared from enol acetate **3** (8); $[\alpha]_D$ −204, $[\alpha]_{578}$ −214, $[\alpha]_{546}$ −251, $[\alpha]_{436}$ −609, $[\alpha]_{365}$ −3590° (*c*, 0.1 in dioxane); λ_{max} (EtOH) 318 nm (ε 12 700); ν_{max} ($CHCl_3$) 3005 (vinylic hydrogens), 1748 (acetate), 1662, 1647, and 1575 ($\alpha,\beta,\gamma,\delta$-unsaturated ketone), 1264 and 1248 (acetate), 1026 cm^{-1} (acetate and alcohol); n.m.r.: δ($CDCl_3$) 6.97 (d of d, J = 5.5 and 2.5 Hz) (21-H), 5.67 (d of d, J = 5.5 and 2.0 Hz) (H-20), 4.70 (m) (3α-H), 3.2-2.6 (complex absorption, three protons: 16β-H, 16$^1\alpha$-H, and 16$^1\beta$-H), 2.28 (methyl ketone), 2.02 (acetate), 0.87 (19- and 18-CH_3).

The second main fraction consisted of 33 mg of dienonitrile **1**, m.p. 194–197°, whose i.r. and n.m.r. spectra were identical with those of an authentic sample (5). Acetylation under the usual conditions in 1 ml of pyridine with 0.5 ml of acetic anhydride gave 33 mg of crude *acetoxy dienonitrile 1a* which, upon purification by t.l.c., gave 30 mg of pure product, m.p. 170–172°, ξ_{max} (EtOH) 299 nm (ε 10 100), identified by the determination of a mixture melting point and by the comparison of its infrared spectrum with that of an authentic product (**5**).

Reduction of 3β-Acetoxy-16α-ethyl-16^2-acetyl-16^2,21-cyclo-5α-pregna-17,21-diene (4a)

To a solution of 15 mg of the acetyl diene **4***a* in 3 ml of absolute alcohol containing traces of pyridine (to avoid acidity), 5.5 mg of sodium borohydride was added portionwise, within 2 h. After that period, the reaction mixture did not contain any starting material, as evidenced by thin-layer analysis. The product was poured into ice water and acidified at 0° with 0.1 *N* hydrochloric acid to p*H* 4, the precipitate was extracted at 0° with ether, the ethereal layer was washed with iced sodium bicarbonate solution and with ice water, and was dried over sodium sulfate. Removal of the solvent *in vacuo*, at a bath temperature not exceeding 35°, gave 16 mg of crude, crystalline *3β-acetoxy-16α-ethyl-16^2-(1ξ-hydroxyethyl)-16^2,21-cyclo-5α-pregna-17,21-diene (5)*. Recrystallization from ether–hexane gave a purified product, m.p. 168–172°, showing only minor impurities, by t.l.c. analysis.

A further purification was not possible since the product is extremely labile; λ_{max} (EtOH) 268 nm (ε 7100); ν_{max} ($CHCl_3$) 3600 and 3440 (hydroxyl), 1728 (acetate), 1665 and 1612 (weak bands of the conjugated diene), 1260 (acetate), 1030 cm^{-1} (acetate and alcohol); n.m.r.: δ ($CDCl_3$) 5.90 (21-H), 5.48 (20-H), 4.73 (m) (3α-H), 2.58 (H on OH-substituted carbon), 2.05 (acetate), 1.32 (d, $J = 6.5$ Hz) (CH_3 of side chain), 1.28 (d, $J = 6.5$ Hz) (CH_3 of side chain[8], 0.88 and 0.87 (19- and 18-CH_3); o.r.d. (*c*, 0.013 in dioxane[9]): $[\alpha]_{450}$ −220, $[\alpha]_{325}$ −827, $[\alpha]_{310}$ −1120, $[\alpha]_{300}$ −1430, $[\alpha]_{290}$ −1570 (min), $[\alpha]_{275}$ −675, $[\alpha]_{265}$ 0, $[\alpha]_{255}$ +375 (max), $[\alpha]_{245}$ 0 (negative Cotton effect). The allylic alcohol was too labile to be subjected to an elemental analysis. An attempt to reoxidize it with Jones' reagent (14) resulted primarily in decomposition but a very small quantity of the unsaturated ketone (**4***a*) seemed to have been formed, according to thin-layer analysis.

We sincerely thank Prof. G. Wagnière and Mr. R. Geiger, Zurich, Prof. P. Crabbé, Mexico, and Prof. A. W. Burgstahler, Lawrence, Kansas, for c.d. and o.r.d. measurements and for allowing us to include some details of these measurements in this paper. We are also very grateful to Professors Burgstahler and Crabbé for communicating to us various results prior to publication, as well as for stimulating discussions. Our appreciation is expressed to Mrs. J. Capitaine for her valuable collaboration in some of the experiments, and to Mr. D. Capitaine and Mrs. G. Pelletier for devoted technical assistance. The support of this project by the National Research Council of Canada is gratefully acknowledged.

[8]We rationalize the appearance of two peaks by the assumption that the reduction leads to two epimeric alcohols.

[9]Freshly treated with aluminum oxide, activity I, and twice redistilled.

1. CH. R. ENGEL. Chimia, **25**, 169 (1971).
2. CH. R. ENGEL, R. C. RASTOGI, and M. N. ROY CHOWDHURY. Steroids, **19**, 1 (1972).
3. CH. R. ENGEL, V. S. SALVI, and L. RUEST. Can. J. Chem. **48**, 3425 (1970).
4. CH. R. ENGEL and J. LESSARD. J. Am. Chem. Soc. **85**, 638 (1963).
5. CH. R. ENGEL and J. LESSARD. Can. J. Chem. **48**, 2819 (1970).
6. CH. R. ENGEL and L. RUEST. Can. J. Chem. **48**, 3136 (1970).
7. *Cf.* also: CH. R. ENGEL, J. LESSARD, L. RUEST, and S. BORY. Abstracts of communications. 5th International symposium on the chemistry of natural products. London, 1968, pp. 358–359.
8. S. BORY and CH. R. ENGEL. Bull. Soc. Chim. Fr., 3043 (1970).
9. A. MOSCOWITZ, E. CHARNEY, U. WEISS, and H. ZIFFER. J. Am. Chem. Soc. **83**, 4661 (1961).
10. D. R. POLLARD and F. R. AHMED. Acta Cryst. B**27**, 1976 (1971).
11. A. F. BEECHAM, A. MCL. MATHIESON, S. R. JOHNS, J. A. LAMBERTON, A. A. SIOUMIS, T. J. BATTERHAM, and I. G. YOUNG. Tetrahedron **27**, 3725 (1971).
12. A. W. BURGSTAHLER and R. C. BARKHURST. J. Amer. Chem. Soc. **92**, 7601 (1970).
13. P. CRABBÉ and A. GUZMÁN. Chem. & Ind., 851 (1971).
14. K. BOWDEN, J. M. HEILBRON, E. R. H. JONES, and B. C. L. WEEDON. J. Chem. Soc. 39 (1946); A. BOWERS, T. G. HALSALL, E. R. H. JONES, and A. J. LEMIN. J. Chem. Soc. 2548 (1953).

Search for the N–N_2 Exchange Reaction

RICHARD K. LYON

Corporate Research Laboratories, Esso Research and Engineering Company, Linden, New Jersey 07036

Received August 5, 1971

Since N_3 is a stable molecule, one might expect the N–N_2 exchange reaction to occur readily; however, if the reaction exists, its rate constant is $\leq 8 \times 10^6$ cc/mol s at 1000 °C. An explanation in terms of spin conservation is discussed.

Etant donné que N_3 est une molécule stable, on pourrait prévoir que la réaction d'échange N–N_2 apparaisse aisément; cependant, si la réaction existe, sa constante de vitesse est $\leq 8 \times 10^6$ cc/mol s à 1000 °C. Une explication en termes de conservation de spin est discutée.

Canadian Journal of Chemistry, **50**, 1437 (1972)

The exchange reaction $^{18}O + {}^{32}O_2 \rightarrow {}^{16}O + {}^{34}O_2$ has been demonstrated to be a facile process, occurring with an activation energy of only 1.1 ± 0.4 kcal/mol (1). The generally accepted mechanism is $^{18}O + {}^{32}O_2 \rightarrow {}^{50}O_3^* \rightarrow {}^{16}O + {}^{34}O_2$ where O_3^* is an ozone molecule with enough internal energy to decompose. One might expect that this mechanism would be general, *i.e.*, if ABC is a stable triatomic molecule, and if the reaction A + BC → AB + C is not endothermic, then the reaction should be rapid, occurring with little or no activation energy. Consistent with this expectation, the activation energies for the reactions ^{18}O, $^{18}O + C^{16}O \rightarrow$

Can. J. Chem. Downloaded from www.nrcresearchpress.com by 210.87.254.105 on 09/05/12
For personal use only.

A further purification was not possible since the product is extremely labile; λ_{max} (EtOH) 268 nm (ε 7100); ν_{max} ($CHCl_3$) 3600 and 3440 (hydroxyl), 1728 (acetate), 1665 and 1612 (weak bands of the conjugated diene), 1260 (acetate), 1030 cm^{-1} (acetate and alcohol); n.m.r.: δ ($CDCl_3$) 5.90 (21-H), 5.48 (20-H), 4.73 (m) (3α-H), 2.58 (H on OH-substituted carbon), 2.05 (acetate), 1.32 (d, $J = 6.5$ Hz) (CH_3 of side chain), 1.28 (d, $J = 6.5$ Hz) (CH_3 of side chain[8], 0.88 and 0.87 (19- and 18-CH_3); o.r.d. (*c*, 0.013 in dioxane[9]): $[\alpha]_{450}$ −220, $[\alpha]_{325}$ −827, $[\alpha]_{310}$ −1120, $[\alpha]_{300}$ −1430, $[\alpha]_{290}$ −1570 (min), $[\alpha]_{275}$ −675, $[\alpha]_{265}$ 0, $[\alpha]_{255}$ +375 (max), $[\alpha]_{245}$ 0 (negative Cotton effect). The allylic alcohol was too labile to be subjected to an elemental analysis. An attempt to reoxidize it with Jones' reagent (14) resulted primarily in decomposition but a very small quantity of the unsaturated ketone (**4***a*) seemed to have been formed, according to thin-layer analysis.

We sincerely thank Prof. G. Wagnière and Mr. R. Geiger, Zurich, Prof. P. Crabbé, Mexico, and Prof. A. W. Burgstahler, Lawrence, Kansas, for c.d. and o.r.d. measurements and for allowing us to include some details of these measurements in this paper. We are also very grateful to Professors Burgstahler and Crabbé for communicating to us various results prior to publication, as well as for stimulating discussions. Our appreciation is expressed to Mrs. J. Capitaine for her valuable collaboration in some of the experiments, and to Mr. D. Capitaine and Mrs. G. Pelletier for devoted technical assistance. The support of this project by the National Research Council of Canada is gratefully acknowledged.

[8]We rationalize the appearance of two peaks by the assumption that the reduction leads to two epimeric alcohols.

[9]Freshly treated with aluminum oxide, activity I, and twice redistilled.

1. CH. R. ENGEL. Chimia, **25**, 169 (1971).
2. CH. R. ENGEL, R. C. RASTOGI, and M. N. ROY CHOWDHURY. Steroids, **19**, 1 (1972).
3. CH. R. ENGEL, V. S. SALVI, and L. RUEST. Can. J. Chem. **48**, 3425 (1970).
4. CH. R. ENGEL and J. LESSARD. J. Am. Chem. Soc. **85**, 638 (1963).
5. CH. R. ENGEL and J. LESSARD. Can. J. Chem. **48**, 2819 (1970).
6. CH. R. ENGEL and L. RUEST. Can. J. Chem. **48**, 3136 (1970).
7. *Cf.* also: CH. R. ENGEL, J. LESSARD, L. RUEST, and S. BORY. Abstracts of communications. 5th International symposium on the chemistry of natural products. London, 1968, pp. 358–359.
8. S. BORY and CH. R. ENGEL. Bull. Soc. Chim. Fr., 3043 (1970).
9. A. MOSCOWITZ, E. CHARNEY, U. WEISS, and H. ZIFFER. J. Am. Chem. Soc. **83**, 4661 (1961).
10. D. R. POLLARD and F. R. AHMED. Acta Cryst. B**27**, 1976 (1971).
11. A. F. BEECHAM, A. MCL. MATHIESON, S. R. JOHNS, J. A. LAMBERTON, A. A. SIOUMIS, T. J. BATTERHAM, and I. G. YOUNG. Tetrahedron **27**, 3725 (1971).
12. A. W. BURGSTAHLER and R. C. BARKHURST. J. Amer. Chem. Soc. **92**, 7601 (1970).
13. P. CRABBÉ and A. GUZMÁN. Chem. & Ind., 851 (1971).
14. K. BOWDEN, J. M. HEILBRON, E. R. H. JONES, and B. C. L. WEEDON. J. Chem. Soc. 39 (1946); A. BOWERS, T. G. HALSALL, E. R. H. JONES, and A. J. LEMIN. J. Chem. Soc. 2548 (1953).

Search for the $N-N_2$ Exchange Reaction

RICHARD K. LYON

Corporate Research Laboratories, Esso Research and Engineering Company, Linden, New Jersey 07036

Received August 5, 1971

Since N_3 is a stable molecule, one might expect the $N-N_2$ exchange reaction to occur readily; however, if the reaction exists, its rate constant is $\leq 8 \times 10^6$ cc/mol s at 1000 °C. An explanation in terms of spin conservation is discussed.

Etant donné que N_3 est une molécule stable, on pourrait prévoir que la réaction d'échange $N-N_2$ apparaisse aisément; cependant, si la réaction existe, sa constante de vitesse est $\leq 8 \times 10^6$ cc/mol s à 1000 °C. Une explication en termes de conservation de spin est discutée.

Canadian Journal of Chemistry, **50**, 1437 (1972)

The exchange reaction $^{18}O + {}^{32}O_2 \rightarrow {}^{16}O + {}^{34}O_2$ has been demonstrated to be a facile process, occurring with an activation energy of only 1.1 ± 0.4 kcal/mol (1). The generally accepted mechanism is $^{18}O + {}^{32}O_2 \rightarrow {}^{50}O_3^* \rightarrow {}^{16}O + {}^{34}O_2$ where O_3^* is an ozone molecule with enough internal energy to decompose. One might expect that this mechanism would be general, *i.e.*, if ABC is a stable triatomic molecule, and if the reaction $A + BC \rightarrow AB + C$ is not endothermic, then the reaction should be rapid, occurring with little or no activation energy. Consistent with this expectation, the activation energies for the reactions ^{18}O, $^{18}O + C^{16}O \rightarrow$

Can. J. Chem. Downloaded from www.nrcresearchpress.com by 210.87.254.42 on 09/05/12
For personal use only.

Can. J. Chem. Downloaded from www.nrcresearchpress.com by 210.87.254.42 on 09/05/12
For personal use only.

$C^{18}O + {}^{16}O, N + NO \rightarrow N_2 + O$, and $O + CN \rightarrow CO + N$ have been reported to be 6.9 (1), 0.2 (2), and 2.4 kcal/mol (3), respectively. To the author's knowledge there is only one reported exception to this expectation. Back and Mui (4), in an attempt to observe the reactions $^{15}N + {}^{28}N_2 \rightarrow {}^{29}N_2 + {}^{14}N$ and $^{14}N + {}^{30}N_2 \rightarrow {}^{29}N_2 + {}^{15}N$, injected $^{30}N_2$ into a stream of active nitrogen flowing through a hot tube. No formation of $^{29}N_2$ was observed and the authors estimate an upper limit for the exchange reaction rate constant, k_E, of 4×10^8 cc/mol s at 1000 °C. As pointed out by Benson (5), the great majority of reported A factors for metathesis reactions involving atoms may be represented as $10^{14 \pm 0.5}$ cc/mol s and values less than 10^{13} cc/mol s are theoretically implausible. Hence, the data of Back and Mui imply that the nitrogen atom molecule exchange reaction has an activation energy greater than 25 kcal. Back and Mui very tentatively suggested this might mean that N_3 is an unstable, highly repulsive structure, but subsequently Douglas and Jones (6) proved that N_3 is a stable molecule.

The author decided to investigate the nitrogen atom molecule exchange reaction by a different and more sensitive method. This method is the measurement as a function of temperature of the formation of $^{29}N_2$ during the ^{60}Co gamma irradiation of $^{28}N_2$–$^{30}N_2$ mixtures. Let $G^0_{^{29}N_2}$ be the yield per 100 eV absorbed of $^{29}N_2$ measured at room temperature. Dawes and Back (7) have demonstrated that chain reaction does not occur at room temperature. If at some higher temperature isotopic mixing occurs via a nitrogen atom chain reaction, it can be readily shown that

$$[1] \quad G_{^{29}N_2} - G^0_{^{29}N_2})/G^0_{^{29}N_2} = 2\alpha(1-\alpha)k_E \times [N_2]\tau_N G_N / G^0_{^{29}N_2}$$

where α is the mole fraction of $^{28}N_2$ in the $^{28}N_2$–$^{30}N_2$ mixture (0.671 in the present experiments), $[N_2] = [^{28}N_2] + [^{30}N_2]$, τ_N is the nitrogen atom lifetime and G_N is the yield per 100 eV absorbed of nitrogen atoms. In the above expression, isotope effects are neglected. $G^0_{^{29}N_2}$ depends on α and is $2\alpha(1-\alpha)G_{EX}$ where G_{EX} is the total exchange yield. G_N and G_{EX} have been determined by Dawes and Back (7) and are 8.84 and 7.30. If τ_N may be estimated from literature data, the right side of eq. 1 contains no unknown quantities except k_E. Hence measurement of the formation of $^{29}N_2$, over a temperature range in which chain reaction begins, provides a measurement of k_E.

The experimental procedures used were those which are standard in radiation chemistry. Samples were placed in a small furnace which had provisions for holding ^{60}Co plates in reproducible positions. One hundred hours was a typical irradiation time. The only crucial point relates to the purity of the $^{28}N_2$–$^{30}N_2$ mixtures used. Sample preparation was done on a high vacuum system on which all essential parts were made of quartz and were baked out at 600 °C and 10^{-6} Torr. Lif-O-gen Research grade $^{28}N_2$ and $^{30}N_2$ from Isomet were treated with well-degassed copper at 600 °C for 22 h. The mixture was then transferred by condensation with liquid He into a manifold of 18 quartz capsules, 1.0 cm i.d. and 9 cm long. The capsules were provided with sealoff constrictions. The quartz in the vicinity of the constrictions had been degassed by heating under vacuum with a torch to slightly less than the softening point of quartz. Sealoff was done by rapid application of a small hydrogen oxygen flame. Blank experiments showed that isotopic mixing did not occur during sealoff of the capsules. The sample capsules were then placed inside larger quartz capsules, and the latter were evacuated and sealed off. This double-walled construction prevents atmospheric oxygen from diffusing into the sample (8).

The experimental results are readily summarized (Table 1). Thermal blank experiments up to 1094 °C showed no significant production of $^{29}N_2$ due to either four center gas phase reactions or heterogeneous processes. The change of the $^{29}N_2$ to $^{30}N_2$ ratio per hour of irradiation time is $(1.10 \pm 0.13) \times 10^{-4}$ at room temperature and $(1.10 \pm 0.04) \times 10^{-4}$ at 900–1000 °C. Hence, $(G_{^{29}N_2} - G^0_{^{29}N_2})/G^0_{^{29}N_2}$ is 0 ± 0.2 at 1000 and 900 °C. The mass spectra done for $^{28}N_2$–$^{29}N_2$–$^{30}N_2$ analysis showed no impurities. High sensitivity mass spectral analysis, done after irradiation at 1000 °C with a CEC 21-104 mass spectrometer, showed traces of argon and carbon dioxide to be present. If oxygen was present, it was below the threshold of detectability, estimated to be less than 10^{-4} times the mass 30 peak, or 33 p.p.m. based on total nitrogen.

Again the N–N_2 exchange reaction has escaped detection, and only an upper limit for k_E can be calculated. Using literature data a

TABLE 1. Summary of experimental results

Conditions	$[^{29}N_2]/[^{30}N_2]$	$\Delta([^{29}N_2]/[^{30}N_2])/\Delta t$*
Starting mixture A ($\alpha = 0.887$)	0.0747 ± 0.0002	
Mixture A, 24 h at 924 °C, no radiation	0.0730	
Mixture A, 140 h at 924 °C, no radiation	0.0754	
Mixture A, 94 h at 1000 °C, no radiation	0.0758	
Mixture A, 138.5 h at 1000 °C, no radiation	0.0726	
Mixture A, 95 h at 1093 °C, no radiation	0.0762	
Average, heated samples of Mixture A	0.0746 ± 0.0014	
Starting mixture B ($\alpha = 0.671$)	0.0274 ± 0.010	
Mixture B, 72 h at 1000 °C, no radiation	0.0266	
Mixture B, 192.5 h at 1094 °C, no radiation	0.0265	
Mixture B, irradiated 168 h at room temperature	0.0481	1.23×10^{-4}
Mixture B, irradiated 285.2 h at room temperature	0.0554	0.98×10^{-4}
Mixture B, irradiated 91.1 h at 900 °C	0.0380	1.16×10^{-4}
Mixture B, irradiated 69.1 h at 1000 °C	0.0348	1.07×10^{-4}
Mixture B, irradiated, 163.2 h at 1000 °C	0.0450	1.08×10^{-4}

*Δt is irradiation time in h.

lower limit for τ_N may be calculated. The only important nitrogen atom removal processes are recombination and reaction with catalytic impurities. Impurities which are consumed by reaction with nitrogen atoms need not be considered, since they will be exhausted shortly after the start of irradiation. Due to the low dose rate (2×10^{13} eV/cc s) used in these experiments, recombination occurs chiefly by diffusion to the walls. D_{N,N_2} is reported to be 0.37 cm^2/s at 300 °K and 760 Torr (9). This implies $D_{N,N_2} = 2.5$ cm^2/s at the 1273 °K and 960 Torr. Using the solution given by Carslaw and Jaeger (10) for the analogues heat conduction problem, one may calculate that the average time for the nitrogen atoms to diffuse to the wall is 0.0122 s. Hence the average lifetime of nitrogen atoms with respect to wall recombination is $\tau_{WR} \geqslant 0.0122$ s. O_2 is the only impurity both likely to be present and known to have a high rate constant for catalytic nitrogen atom removal. The reaction sequence is $N + O_2 \rightarrow NO + O$ and $N + NO \rightarrow N_2 + O$, followed by wall recombination of the oxygen atoms. Wilson (11) has determined k_{N+O_2} to be $1.4 \times 10^{13} \exp(-7900/RT)$ cc/mol s. Hence at 1000 °C and $O_2 \leqslant 33$ p.p.m. the lifetime of nitrogen atoms towards scavenging by oxygen, τ_{O_2}, is $(2k_{N,O_2}[O_2])^{-1}$, *i.e.*, $\geqslant 0.0020$ s. The effective lifetime, τ_N, is $(\tau_{WR}^{-1} + \tau_{O_2}^{-1})^{-1}$ and $\tau_N \geqslant 0.0017$ s.

On this basis, one calculates $k_E \leqslant 8 \times 10^6$ cc/mol s at 1000 °C. If the A factor for the exchange reaction is greater than 10^{13} cc/mol s (the minimum theoretically acceptable value), the activation energy must be greater than 36 kcal. From this example, it would appear that the existence of a bonding intermediate is not a sufficient condition for the occurrence of a facile exchange reaction.

It might be argued that the principal of spin conservation must also be considered, *i.e.*, that facile reaction is to be expected if and only if the triatomic intermediate possesses an energetically accessible electronic state which correlates with reactants and products. The suggestion that a reaction which is overall spin-allowed may be slow because access to the transition state is spin forbidden is not new. It has been previously proposed to explain the slowness of the ion molecules $O^+(^4S) + N_2(^1\Sigma) \rightarrow NO^+(^1\Sigma) + N(^4S)$, which may occur via the $N_2O^+(^1\Sigma)$ ground state only by a slow spin-forbidden step (ref. 12 and references cited therein). The $N-N_2$ exchange reaction is isoelectronic with and involves the same states as this ion–molecule reaction, so the same explanation appears applicable. If one accepts that the rate determining step in the $N-N_2$ exchange is the spin-forbidden step $N(^4S) + N_2(^1\Sigma) \rightarrow N_3^*(^1\Sigma)$, then it may reasonably be compared with another spin-forbidden reaction $O(^3P) + N_2(^1\Sigma) \rightarrow N_2O^*(^1\Sigma)$. The rate constant of the latter reaction may be calculated from the observed rate constant for N_2O unimolecular decomposition in the high pressure limit (13) and the equilibrium constant. One obtains $k_{O+N_2} = 3 \times 10^9$

Can. J. Chem. Downloaded from www.nrcresearchpress.com by 210.87.254.42 on 09/05/12
For personal use only.

exp $(-18500/RT)$ cc/mol s which at 1000 °C is 2×10^6 cc/mol s. This value appears quite compatible with the upper limit for k_{N+N_2} observed in these experiments.

1. S. JAFFE and F. S. KLEIN. Trans. Faraday Soc. **62**, 3135 (1966).
2. M. A. A. CLYNE and B. A. THRUSH. Nature, **189**, 56 (1961).
3. J. C. BODEN and B. A. THRUSH. Proc. Roy. Soc. A**305**, 93 (1968).
4. R. A. BACK and J. Y. P. MUI. J. Phys. Chem. **66**, 1362 (1962).
5. S. W. BENSON. Thermochemical kinetics, Wiley and Sons, New York. 1968. p. 99.
6. A. E. DOUGLAS and W. J. JONES. Can. J. Phys. **43**, 2216 (1965).
7. D. H. DAWES and R. A. BACK. J. Phys. Chem. **69**, 2385 (1965).
8. F. J. NORTON. Nature, **191**, 701 (1961).
9. R. A. YOUNG. J. Chem. Phys. **34**, 1295 (1961).
10. H. S. CARSLAW and J. C. JAEGER. Conduction of heat in solids. Oxford University Press, Oxford, England. 1959. p. 191.
11. W. E. WILSON. J. Chem. Phys. **46**, 2017 (1967).
12. A. L. SCHMELTEKOPF, E. E. FERGUSON, and F. C. FEHSENFELD. J. Chem. Phys. **48**, 2966 (1968).
13. H. A. OLSCHEWSKI, J. TROE, and H. G. WAGNER. Ber. Bunsenges. Phys. Chem. **70**, 450 (1966).

Can. J. Chem. Downloaded from www.nrcresearchpress.com by 210.87.254.42 on 09/05/12
For personal use only.

Non-Steady-State Kinetics for a Double-Intermediate Enzyme Mechanism: The Case of High Enzyme Concentrations

NASRAT H. HIJAZI AND KEITH J. LAIDLER

Department of Chemistry, University of Ottawa, Ottawa, Canada K1N 6N5

Received December 14, 1971

An equation has been derived for the non-steady-state kinetics arising from the mechanism

$$E + A \underset{k_{-1}}{\overset{k_1}{\rightleftharpoons}} EA \xrightarrow[X]{k_2} EA' \xrightarrow{k_3} E + Y$$

in which the concentration of enzyme E is greatly in excess of that of the substrate A; EA and EA′ are two intermediates and X and Y the products. Solutions for the rate of formation of the first product X were given by Kasserra and Laidler. The present work is concerned with the rate of formation of Y. A general equation is derived for the rate of production of Y, and it is shown that under certain simplifying conditions, easily realized in practice, the rate law reduces to $y = a_0(1 - e^{-k_3 t})$; study of the rate of formation of Y therefore leads to a determination of k_3.

Une équation a été obtenue pour les cinétiques en état stationnaire non constant provenant du mécanisme suivant:

$$E + A \underset{k_{-1}}{\overset{k_1}{\rightleftharpoons}} EA \xrightarrow[X]{k_2} EA' \xrightarrow{k_3} E + Y$$

La concentration en enzyme est en large excès par rapport à celle du substrat A; EA et EA′ représentent deux intermédiaires et X et Y deux produits. Les solutions concernant la vitesse de formation du premier produit X ont été données par Kasserra et Laidler. Le présent travail concerne la vitesse de formation de Y. Une équation générale a été obtenue pour la vitesse de formation de Y et il est montré que sous des conditions simplifiées, aisément réalisables en pratique, la loi de vitesse se réduit à $y = a_0(1 - e^{-k_3 t})$; l'étude de la vitesse de formation de Y conduit alors à une détermination de k_3.

Canadian Journal of Chemistry, **50**, 1440 (1972)

A considerable number of enzyme systems follow a mechanism of the type

$$E + A \rightleftharpoons EA \xrightarrow[X]{} EA' \longrightarrow E + Y$$

Here the enzyme E and substrate A form an addition complex which splits off a product X to form a second intermediate EA′ (*e.g.* an acyl enzyme); this gives the enzyme and a second product Y, usually by a solvolytic reaction. Steady-state studies do not yield a satisfactory separation of rate constants, but this can be

exp $(-18500/RT)$ cc/mol s which at 1000 °C is 2×10^6 cc/mol s. This value appears quite compatible with the upper limit for k_{N+N_2} observed in these experiments.

1. S. JAFFE and F. S. KLEIN. Trans. Faraday Soc. **62**, 3135 (1966).
2. M. A. A. CLYNE and B. A. THRUSH. Nature, **189**, 56 (1961).
3. J. C. BODEN and B. A. THRUSH. Proc. Roy. Soc. A**305**, 93 (1968).
4. R. A. BACK and J. Y. P. MUI. J. Phys. Chem. **66**, 1362 (1962).
5. S. W. BENSON. Thermochemical kinetics, Wiley and Sons, New York. 1968. p. 99.
6. A. E. DOUGLAS and W. J. JONES. Can. J. Phys. **43**, 2216 (1965).
7. D. H. DAWES and R. A. BACK. J. Phys. Chem. **69**, 2385 (1965).
8. F. J. NORTON. Nature, **191**, 701 (1961).
9. R. A. YOUNG. J. Chem. Phys. **34**, 1295 (1961).
10. H. S. CARSLAW and J. C. JAEGER. Conduction of heat in solids. Oxford University Press, Oxford, England. 1959. p. 191.
11. W. E. WILSON. J. Chem. Phys. **46**, 2017 (1967).
12. A. L. SCHMELTEKOPF, E. E. FERGUSON, and F. C. FEHSENFELD. J. Chem. Phys. **48**, 2966 (1968).
13. H. A. OLSCHEWSKI, J. TROE, and H. G. WAGNER. Ber. Bunsenges. Phys. Chem. **70**, 450 (1966).

Can. J. Chem. Downloaded from www.nrcresearchpress.com by 210.87.254.6 on 09/05/12
For personal use only.

Non-Steady-State Kinetics for a Double-Intermediate Enzyme Mechanism: The Case of High Enzyme Concentrations

NASRAT H. HIJAZI AND KEITH J. LAIDLER

Department of Chemistry, University of Ottawa, Ottawa, Canada K1N 6N5

Received December 14, 1971

An equation has been derived for the non-steady-state kinetics arising from the mechanism

$$E + A \underset{k_{-1}}{\overset{k_1}{\rightleftharpoons}} EA \xrightarrow[X]{k_2} EA' \xrightarrow{k_3} E + Y$$

in which the concentration of enzyme E is greatly in excess of that of the substrate A; EA and EA′ are two intermediates and X and Y the products. Solutions for the rate of formation of the first product X were given by Kasserra and Laidler. The present work is concerned with the rate of formation of Y. A general equation is derived for the rate of production of Y, and it is shown that under certain simplifying conditions, easily realized in practice, the rate law reduces to $y = a_0(1 - e^{-k_3 t})$; study of the rate of formation of Y therefore leads to a determination of k_3.

Une équation a été obtenue pour les cinétiques en état stationnaire non constant provenant du mécanisme suivant:

$$E + A \underset{k_{-1}}{\overset{k_1}{\rightleftharpoons}} EA \xrightarrow[X]{k_2} EA' \xrightarrow{k_3} E + Y$$

La concentration en enzyme est en large excès par rapport à celle du substrat A; EA et EA′ représentent deux intermédiaires et X et Y deux produits. Les solutions concernant la vitesse de formation du premier produit X ont été données par Kasserra et Laidler. Le présent travail concerne la vitesse de formation de Y. Une équation générale a été obtenue pour la vitesse de formation de Y et il est montré que sous des conditions simplifiées, aisément réalisables en pratique, la loi de vitesse se réduit à $y = a_0(1 - e^{-k_3 t})$; l'étude de la vitesse de formation de Y conduit alors à une détermination de k_3.

Canadian Journal of Chemistry, **50**, 1440 (1972)

A considerable number of enzyme systems follow a mechanism of the type

$$E + A \rightleftharpoons EA \xrightarrow[X]{} EA' \longrightarrow E + Y$$

Here the enzyme E and substrate A form an addition complex which splits off a product X to form a second intermediate EA′ (*e.g.* an acyl enzyme); this gives the enzyme and a second product Y, usually by a solvolytic reaction. Steady-state studies do not yield a satisfactory separation of rate constants, but this can be

Can. J. Chem. Downloaded from www.nrcresearchpress.com by 210.87.254.6 on 09/05/12
For personal use only.

achieved by studies under non-steady-state conditions.

Usually such investigations, using high-speed kinetic techniques, have been carried out under the usual enzyme-kinetic conditions, with the substrate present in great excess of the enzyme. There is then a transient non-steady-state phase prior to the establishment of the steady state, and an analysis of the results in this region in principle leads to some of the rate constants. Solutions of the equations under these conditions have been given by Ouellet and Laidler (1) and by Ouellet and Stewart (2). The equations are, however, rather complex and only become sufficiently simple for application to experimental results if certain conditions are satisfied. One of these is that the substrate is in sufficiently great excess to saturate the enzyme. However, it is sometimes impossible to achieve this.

Non-steady-state studies with the enzyme present in great excess of the substrate offer some advantages in this connection, the resulting kinetic equations being simpler and more directly applicable to the experimental results. Kasserra and Laidler (3) have obtained equations for the kinetics of formation of the first product X under these conditions. They found that there was no establishment of a steady state, the concentration of X rising steadily to a limiting value equal to the initial concentration of A. Under certain conditions, which are easily realized in practice, the rise is an exponential one with a rate constant of k_2. Kasserra and Laidler applied their equations to a trypsin-catalyzed reaction and obtained k_2.

The solution for the formation of Y presents some difficulties which have been overcome in the present work.

Theoretical

The reaction scheme is

$$\begin{array}{ccccccc} \mathrm{E} + \mathrm{A} & \underset{k_{-1}}{\overset{k_1}{\rightleftharpoons}} & \mathrm{EA} & \xrightarrow{k_2} & \mathrm{EA'} & \xrightarrow{k_3} & \mathrm{E} + \mathrm{Y} \\ & & & \searrow \mathrm{X} & & & \\ e_0 \quad a_0 - m - n - y & & m & x & n & & e_0 \quad y \end{array}$$

The concentrations of the various species are indicated in small letters. Since E is in great excess the amounts of enzyme tied up in EA and EA′ are insignificant. The differential rate equations are

[1] $\dot{m} = k_1 e_0 (a_0 - m - n - y) - (k_{-1} + k_2)m$

[2] $\dot{n} = k_2 m - k_3 n$

[3] $\dot{x} = k_2 m$

[4] $\dot{y} = k_3 n$

Kasserra and Laidler eliminated n between eqs. 1 and 2 and obtained a differential equation for which a solution was possible. The equation for m was

[5] $$m = M(\mathrm{e}^{-Ft} - \mathrm{e}^{-Gt})$$

where

[6] $$F = \tfrac{1}{2}(P - \sqrt{P^2 - 4Q})$$

[7] $$G = \tfrac{1}{2}(P + \sqrt{P^2 - 4Q})$$

[8] $$M = \frac{k_1 e_0 a_0}{G - F}$$

[9] $$P = k_1 e_0 + k_{-1} + k_2$$

[10] $$Q = k_1 k_2 e_0$$

Equations 3 and 5 lead readily to the following equation for x:

[11] $$x = \frac{k_2 M}{F}(1 - \mathrm{e}^{-Ft}) - \frac{k_2 M}{G}(1 - \mathrm{e}^{-Gt})$$

A comparable procedure in which m is eliminated between eqs. 1 and 2 unfortunately leads to a differential equation in $\ddot{n}$, $\dot{n}$, n and n^2 which cannot be solved. An alternative procedure has therefore been used; the equation for m has been inserted into eq. 2 and the resulting equation solved. Insertion of eq. 5 into eq. 2 gives

[12] $$\dot{n} = k_2 M\,(\mathrm{e}^{-Ft} - \mathrm{e}^{-Gt}) - k_3 n$$

which has to be solved subject to the boundary condition $t = 0$, $n = 0$, $\dot{n} = 0$. The solution is obtained by finding an integrating factor ρ such that

[13] $$\rho\dot{n} + \rho k_3 n = \frac{\mathrm{d}(\rho n)}{\mathrm{d}t} = n\dot{\rho} + \rho\dot{n}$$

Comparison of coefficients leads to $\dot{\rho} = \rho k_3$ where

[14] $$\rho = \mathrm{e}^{k_3 t}$$

Then

[15] $$\frac{\mathrm{d}(\rho n)}{\mathrm{d}t} = \rho k_2 M\,(\mathrm{e}^{-Ft} - \mathrm{e}^{-Gt})$$

Can. J. Chem. Downloaded from www.nrcresearchpress.com by 210.87.254.6 on 09/05/12
For personal use only.

or

$$[16] \quad ne^{k_3 t} = \int_0^t e^{k_3 t}\, k_2 M\, (e^{-Ft} - e^{-Gt})\, dt$$

Integration then leads to

$$[17] \quad n = \left(\frac{k_2 M}{k_3 - F}\right) e^{-Ft} - \left(\frac{k_2 M}{k_3 - G}\right) e^{-Gt} - k_2 M \left(\frac{1}{k_3 - F} - \frac{1}{k_3 - G}\right) e^{-k_3 t}$$

Substitution of this into eq. 4 and integration subject to the boundary condition $t = 0$, $n = 0$, $y = 0$ gives

$$[18] \quad y = \frac{k_2 k_3 M}{F(k_3 - F)} (1 - e^{-Ft}) - \frac{k_2 k_3 M}{G(k_3 - G)} (1 - e^{-Gt}) - k_2 M \left(\frac{1}{k_3 - F} - \frac{1}{k_3 - G}\right)(1 - e^{-k_3 t})$$

This is the general equation for the time course of production of the second product Y.

When $t \to \infty$ it is possible to show, by expressing F, G, and M in terms of eqs. 6–8, that y reaches a limiting value of a_0; *i.e.* all of the substrate is eventually converted into product. There is no steady state, y rising in a complex exponential fashion until it becomes a_0.

An Approximate Solution

Under many conditions the Y production may be satisfactorily approximated by an expression involving only a single exponential term $e^{-k_3 t}$. In general $P^2 \gg Q$ and $G \gg F$, in which case, by a single expansion, it can be shown that

$$[19] \quad F \approx \frac{Q}{P}$$

$$[20] \quad G \approx P$$

If in addition

$$[21] \quad F \gg k_3$$

eq. 18 will be dominated by the final term and reduces, with the above inequalities, to

$$[22] \quad y = a_0 (1 - e^{-k_3 t})$$

The inequality 21 requires that

$$[23] \quad \frac{k_1 k_2 e_0}{k_1 e_0 + k_{-1} + k_2} \gg k_3$$

which requires that k_2 is sufficiently large in comparison with k_3, and is not too large in comparison with $k_1 e_0$. The analysis of experimental results in terms of the simplified eq. 22 obviously must be done in conjunction with other non-steady-state studies in which the relative magnitude of $k_1 e_0$ and k_2 can be established.

1. L. Ouellet and K. J. Laidler. Can. J. Chem. **34**, 146 (1956).
2. L. Ouellet and J. A. Stewart. Can. J. Chem. **37**, 737 (1959).
3. H. P. Kasserra and K. J. Laidler. Can. J. Chem. **48**, 1793 (1970).

Erratum: Vibrational Spectra of SiH_4 and SiD_4–SiH_4 Mixtures in the Condensed States

R. P. Fournier and R. Savoie
Centre de recherches sur les atomes et les molecules et Département de chimie, Université Laval, Québec
AND
Nguyen Dinh The, R. Belzile, and A. Cabana
Departement de chimie, Université de Sherbrooke, Sherbrooke, Québec

Received February 29, 1972
(Ref.: Can. J. Chem. **50**, 35 (1972))
Canadian Journal of Chemistry, **50**, 1442 (1972)

The date of receipt of the article was incorrectly given. It should read August 13, 1971.

Can. J. Chem. Downloaded from www.nrcresearchpress.com by 210.87.254.6 on 09/05/12
For personal use only.

Canadian Journal of Chemistry

Published by THE NATIONAL RESEARCH COUNCIL OF CANADA

VOLUME 50 MAY 15, 1972 NUMBER 10

Primary Processes in the Vacuum Ultraviolet Photolysis of Ethyl Fluoride at 147 nm[1]

S. C. CHAN,[2] Y. INEL,[3] AND E. TSCHUIKOW-ROUX

Department of Chemistry, University of Calgary, Calgary 44, Alberta

Received January 13, 1972

The photolysis of C_2H_5F at 147 nm was studied at room temperature. The principal products include C_2H_3F, C_2H_2, C_2H_4, CH_4, and C_2H_6. The principal primary photochemical reactions involve the molecular elimination of HF and H_2, and, to a lesser extent, C—F and C—C bond fission. The effect of reactant and added inert gas pressure on the product yields has been investigated and it was found that the stabilization/decomposition ratio, C_2H_4/C_2H_2, displays opposite pressure dependence with ethyl fluoride and argon. This result is interpreted in terms of the higher energy transfer efficiency of the C_2H_5F molecule.

La photolyse à 147 nm de C_2H_5F a été étudiée à la température de la pièce. Les produits principaux incluent C_2H_3F, C_2H_2, C_2H_6, CH_4, et C_2H_6. Les principales réactions photochimiques primaires impliquent l'élimination moléculaire de HF et de H_2, et, à un degré moindre, la rupture des liaisons C—F et C—C. L'effet des corps réagissants et de l'addition de gaz inertes sur les rendements en produits a été étudié et il a été trouvé que le rapport stabilisation/décomposition, C_2H_4/C_2H_2, joue dans le sens inverse d'une dépendance de la pression avec le fluorure d'éthyle et l'argon. Ce résultat est interprété en termes d'une efficacité de transfert d'énergie plus élevée pour la molécule de C_2H_5F.

Canadian Journal of Chemistry, **50**, 1443 (1972)

Introduction

The unimolecular decomposition of C_2H_5F has been the subject of investigation by several workers. In the shock tube pyrolysis of C_2H_5F (1), the primary reaction was found to be molecular elimination of HF. The same mechanism was also observed in the case of excited C_2H_5F formed by chemical activation (2), while in the mercury photosensitized decomposition (3) H atom elimination appeared to be predominant. In the vacuum-ultraviolet photolysis at 147 nm the amount of energy available is very large (194 kcal) leading to a high level of excitation of the initially energized C_2H_5F molecules, and hence several reaction paths could be possible. A preliminary study of this system at 25 °C was carried out in order to identify the primary photochemical reactions.

Experimental

The experimental method was the same as described previously (4). A standard liquid oxygen cooled xenon resonance lamp was used as the light source. The lamp was equipped with a LiF window and was operated from a microwave power generator (Raytheon, Model PGM-10). The emission spectrum of the lamp which was scanned from 110 to 190 nm, showed the prominent resonance line at 147 nm and a minor contribution (~1%) at 129.6 nm. A Watson gas circulation pump was incorporated as part of the reaction vessel to prevent secondary photolysis. Analysis of products was performed by gas chromatography at 50 °C (Varian Aerograph, Model 1700) using a flame ionization detector. A 10 foot Porapak N column (80–100 mesh) was used and the flow rate of the He carrier gas was 30 ml/min. The reactant which was obtained from Peninsular Chemresearch Inc. was purified by pumping it at ethanol slush bath temperature (−117 °C) to remove low boiling impurities. Chromatographic analysis showed a residual impurity of less than 0.1% isobutane. Matheson nitric oxide and

[1]Work supported by the National Research Council of Canada.

[2]Post Doctorate Fellow, 1971–1972.

[3]Post Doctorate Fellow, 1970–1971. Present address: Department of Chemistry, Bosphorus University, Bebek, P.K. 2, Istanbul, Turkey.

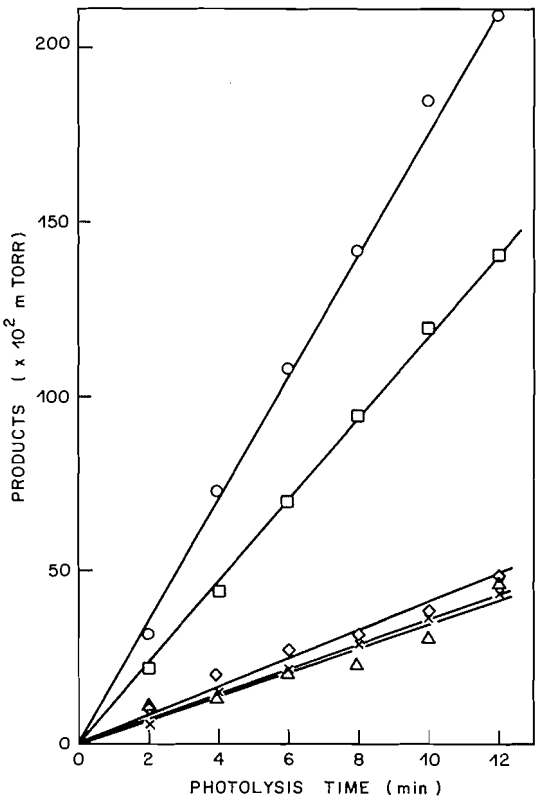

FIG. 1. Variation of the yield with photolysis time in the decomposition of C_2H_5F (12 Torr) at 25 °C. ○, C_2H_3F; □, C_2H_2; ◇, C_2H_4; ×, CH_4; and △, C_2H_6.

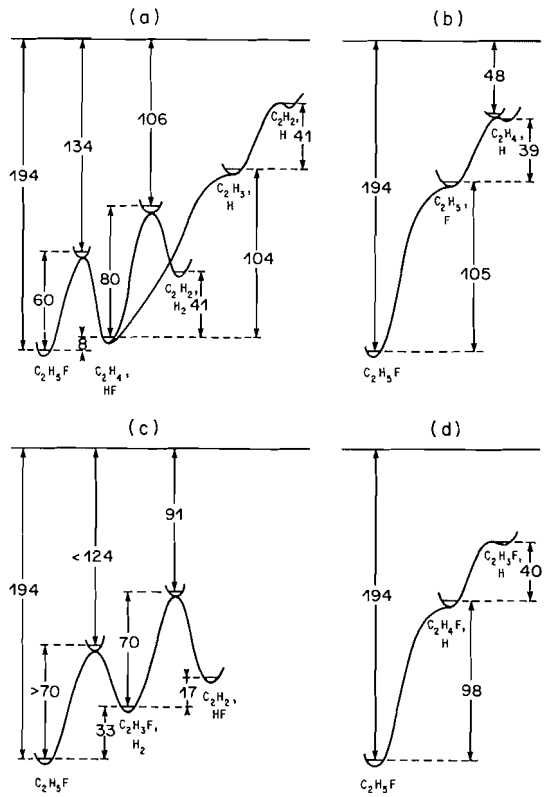

FIG. 2. Schematic energy diagrams in the photochemical decomposition of C_2H_5F at 147 nm. (*a*) HF elimination; (*b*) C—F bond fission; (*c*) H_2 elimination; and (*d*) C—H bond fission. Energy is in kcal/mol. ΔH^0 of various reactions are based on ΔH_f^0 given in ref. 9. Activation energies are discussed in text.

argon of 98.5 and 99.995% stated purity, respectively, were used without further purification.

Results and Discussion

The principal reaction products are C_2H_3F, C_2H_2, C_2H_4, CH_4, and C_2H_6. No attempt was made to identify other minor products with retention times longer than that of the reactant. Preliminary experiments have demonstrated that at short photolysis time and low conversion (< 1%) the yield of products is linear with respect to the irradiation time (Fig. 1). No deviation from linearity was observed up to at least 12 min, which indicates that within this time scale, secondary photolysis of the reaction products is not important. All subsequent diagnostic experiments had irradiation times of either 10 or 15 min.

The presence of C_2H_4 and C_2H_3F as products points to the possibilities of the following primary reactions:

[1] $C_2H_5F \xrightarrow{h\nu} C_2H_5F\dagger$

[2] $C_2H_5F\dagger \longrightarrow C_2H_4^* + HF$

[3] $\longrightarrow C_2H_5\cdot^* + F$

[4] $\longrightarrow C_2H_3F^* + H_2$

[5] $\longrightarrow C_2H_4F\cdot^* + H$

The thermochemical data of these and some subsequent reactions are given in Fig. 2. Although reactions 2 to 5 are all endothermic, they are energetically allowed since the energy in the excited C_2H_5F is 194 kcal. The radicals produced in reactions 3 and 4 could split H atoms to give ethylene and vinyl fluoride

[6] $C_2H_5\cdot^* \rightarrow C_2H_4 + H$

[7] $C_2H_4F\cdot^* \rightarrow C_2H_3F + H$

The ethylene and vinyl fluoride molecules produced in reactions 2 and 4 respectively are

Can. J. Chem. Downloaded from www.nrcresearchpress.com by 210.87.254.6 on 09/05/12
For personal use only.

TABLE 1. Photolysis of C_2H_5F at 147 nm

Run	$P_{C_2H_5F}$ (Torr)	P_{Ar} (Torr)	P_{NO} (Torr)	Photolysis time (min)	Peak area*			C_2H_4/C_2H_2†
					C_2H_4	C_2H_3F	C_2H_2	
1	4	186	0	15	22	234	232	0.152
2	4	125	0	15	27	288	282	0.154
3	4	0	0	15	58	316	432	0.21
4	4	0	1.12	15	32	328	364	0.141
5	4	0	1.23	15	35	316	376	0.149
6	4	0	7.2	15	34	266	324	0.168
7	4	0	24	15	32	214	274	0.187
8	4	298	7.7	15	22	182	175	0.194
9	4	322	0	10	10	129	120	0.133
10	4	214	0	10	16	166	158	0.162
11	39	0	0	10	76	408	320	0.38
12	24	0	0	10	56	312	280	0.32
13	14.4	0	0	10	56	306	270	0.31
14	8.3	0	0	10	29	153	160	0.29
15	2.0	0	0	10	26	123	178	0.23

*Relative sensitivities of C_2H_4, C_2H_3F, and C_2H_2 are 1.60, 1.51, and 1.00, respectively.
†Ratio of the absolute yield of C_2H_4 to C_2H_2.

"hot" and could undergo further decomposition to give acetylene. In contrast, those molecules that are produced by radical decomposition, reactions 6 and 7, do not have sufficient energy to split further (see Fig. 2).

[8] $$C_2H_4^* \rightarrow C_2H_2 + H_2$$

[9] $$\rightarrow C_2H_3 + H$$

[10] $$C_2H_3F^* \rightarrow C_2H_2 + HF$$

[11] $$\rightarrow C_2H_3 + F$$

[12] $$C_2H_3 \rightarrow C_2H_2 + H$$

The activation energy of reaction 2 has been shown to be 60 kcal (1) and that of reaction 4 could not be less than 70 kcal (5), hence the excess energy in the excited C_2H_5F molecules with respect to these two reactions is 134 kcal and less than 124 kcal, respectively (Fig. 2). From an energetic point of view, these two reaction channels should be competitive, with the former slightly favored. The product distribution shows that whereas the yield of C_2H_3F and C_2H_2 is comparable the yield of C_2H_4 is much less, and hence a necessary conclusion is that the precursor of C_2H_2 is mainly the excited C_2H_4.

When ~30% of NO was added to the reactant (Runs 4 and 5), the yield of C_2H_4 and C_2H_2 decreased, which suggests that the radical reactions 6 and 12 are partly responsible for their formation. On the other hand, the results also indicate that these reactions play only a minor role: in the case of acetylene, the radical mechanism accounts for less than one-sixth of its yield; while in the case of ethylene, the yield is decreased by one-half, but it should be emphasized that most of the ethylene (~90%) initially formed by molecular elimination decomposes into acetylene (Table 1). The yield of C_2H_3F is unaffected by the presence of NO which implies that the radical reactions 5 and 7 are not important in its production. This then suggests that C_2H_3F is indeed produced by the molecular elimination reaction 4. If so, it is somewhat surprising to find that these excited vinyl fluoride molecules do not further decompose into C_2H_2 and HF since the permissible maximum excess energy is 91 kcal with respect to HF elimination (Fig. 2*c*). Photolysis of C_2H_3F at 147 nm has, however, demonstrated that at low pressure HF elimination may be insignificant (4).

Some experiments were carried out with excess nitric oxide; however, the additional NO would probably only act as an inert additive and favor the stabilization of C_2H_4 with respect to its decomposition into C_2H_2. In addition, it was also observed that the presence of an inert additive, such as Ar, reduces the absolute yield of all products. This could be explained by the stabilization of the initially energized C_2H_5F molecules.

Further, a most interesting observation is the variation of the ratio C_2H_4/C_2H_2 with total pressure. Since C_2H_4 is the precursor of C_2H_2,

Can. J. Chem. Downloaded from www.nrcresearchpress.com by 210.87.254.6 on 09/05/12
For personal use only.

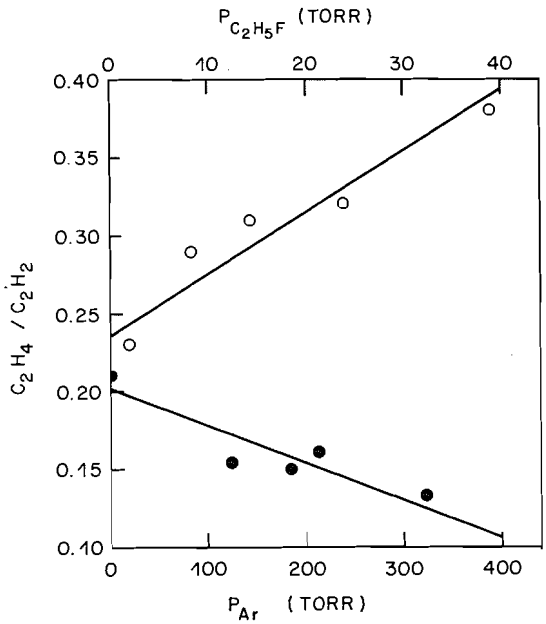

FIG. 3. Variation of the ratio C_2H_4/C_2H_2 with C_2H_5F (open circles) and Ar pressure (filled circles).

this ratio reflects the competition between stabilization and decomposition. In the pure C_2H_5F system, the ratio increases with pressure, whereas in the C_2H_5F–Ar system with a constant amount of C_2H_5F, the ratio decreases with increasing Ar pressure (Fig. 3). It is proposed that the difference in the deactivating efficiency between C_2H_5F and Ar is instrumental in these observed opposite pressure effects. Part of the C_2H_4 molecules are produced by the decomposition of $C_2H_5\cdot$ (reaction 6) and they are stable towards further decomposition. Inert added gas in the system could stabilize the radicals and thus have a diminishing effect on the ratio C_2H_4/C_2H_2. It has been shown that the energy transfer efficiency of a molecule in general increases with its molecular complexity (6); it is thus expected that C_2H_5F is much more efficient than argon. For example, it has been shown (5) in the case of highly excited vinyl fluoride that CF_4 is about ten times more efficient than He in deactivating the "hot" molecule. Ethylene produced by HF elimination from C_2H_5F may have as much as 186 kcal of energy; the activation energy for its decomposition into C_2H_2 is 80 kcal (7), hence its possible excess energy is 106 kcal (Fig. 2*a*). Ethyl radicals produced by F elimination (reaction 3) may have 89 kcal of energy. The endothermicity for decomposition into C_2H_4 and H is 39 kcal, and the activation energy of the reverse reaction is ~2 kcal (8), hence the activation energy of the forward reaction is 41 kcal and thus $C_2H_5\cdot$ has a maximum excess energy of 48 kcal with respect to its decomposition, Fig. 2*b*. Therefore, the excess energy of C_2H_5 radical is much less than that of C_2H_4. While this does not necessarily mean that its rate of decomposition is also slower, our results as discussed below seem to indicate that it is the case. Ethyl fluoride being a polyatomic molecule is expected to be very efficient in removing energy from both the excited C_2H_4 and $C_2H_5\cdot$; however, the formation of the radical (reaction 3) and its subsequent decomposition to ethylene (reaction 6) is only a minor reaction as compared to the initial production of ethylene (reaction 2) by a molecular reaction, hence the stabilization of C_2H_4 is dominant and the ratio C_2H_4/C_2H_2 increases with the pressure of C_2H_5F. On the other hand, argon being a monatomic gas is not an efficient deactivator. Its stabilizing effect would be negligible in the decomposition of C_2H_4, but a small effect may be expected in the case of $C_2H_5\cdot$ decomposition in that fewer deactivating collisions would be required to render the radical "undecomposable". This could explain the observed decrease in the ratio C_2H_4/C_2H_2 with increasing argon pressure. One could speculate that at sufficiently high argon pressure, this trend will be reversed. In order to study the variation of C_2H_4/C_2H_2 with pressure as a simple stabilization–decomposition competition, one has to remove the radical reaction. Indeed, in the C_2H_5F–NO–Ar system, we observed that the ratio C_2H_4/C_2H_2 does increase with Ar pressure (Runs 6 and 8).

In the above discussion and also in Fig. 2, we have assumed that all the excess energy resides in the larger species produced in a reaction. This is in general not true, but the error thus introduced will not invalidate the argument put forward.

Our results also indicate that C—C bond fission may occur in the primary photochemical act as shown indirectly by the presence of CH_4 and C_2H_6 in the product mixture. There is some evidence that CH_4 is produced by a molecular mechanism.

Can. J. Chem. Downloaded from www.nrcresearchpress.com by 210.87.254.6 on 09/05/12
For personal use only.

1. P. CADMAN, M. DAY, and A. F. TROTMAN-DICKENSON. J. Chem. Soc. A, 2498 (1970).
2. G. O. PRITCHARD and R. L. THOMMARSON. J. Phys. Chem. **71**, 1674 (1967).
3. P. M. SCOTT and K. R. JENNINGS. J. Phys. Chem. **73**, 1513 (1969).
4. A. W. KIRK and E. TSCHUIKOW-ROUX. J. Chem. Phys. **53**, 1924 (1970).
5. E. TSCHUIKOW-ROUX and S. KODAMA. J. Chem. Phys. **50**, 5297 (1969).
6. S. C. CHAN, B. S. RABINOVITCH, J. T. BRYANT, L. D. SPICER, T. FUJIMOTO, Y. N. LIN, and S. P. PAVLOU. J. Phys. Chem. **74**, 3160 (1970).
7. A. W. KIRK and E. TSCHUIKOW-ROUX. J. Chem. Phys. **51**, 2247 (1969).
8. R. D. PENZHORN and B. DE B. DARWENT. J. Chem. Phys. **55**, 1508 (1971).
9. NSRDS-NBS 26. Ionization potentials, appearance potentials and heats of formation of gaseous positive ions. U.S. Department of Commerce. 1969.

Can. J. Chem. Downloaded from www.nrcresearchpress.com by 210.87.254.6 on 09/05/12
For personal use only.

Silver Plated Bimolecular Lipid Membranes

A. PETKAU AND W. S. CHELACK

Medical Biophysics Branch, Whiteshell Nuclear Research Establishment, Atomic Energy of Canada Limited, Pinawa, Manitoba

Received November 3, 1971

The electrochemical reduction of silver ions at the surface of a model phospholipid membrane proceeds without the application of an electric field. The silver deposition is dependent on I^- and I_2. The charge transfer complexes formed by iodine with phospholipids and cholesterol are the most probable donors for the electron transfer reaction. Cholesterol membranes do not show the silver deposition unless an external electrical field is applied. An account for the difference is given on the basis of dissimilar ion distribution profiles within phospholipid and cholesterol membranes.

La réduction électrochimique des ions argents à la surface d'une membrane de phospholipide se fait sans l'application d'un champ électrique. La décomposition de l'argent ne dépend que de I^- et de I_2. Les complexes de transfert de charge, formés par l'iode avec les phospholipides et le cholestérol, sont probablement les donneurs lors de la réaction de transfert électronique. Les membranes de cholestérol ne provoquent pas de décomposition d'argent à moins qu'un champ électrique ne soit appliqué. Ces différences sont rationalisées sur la base d'une distribution ionique différente à l'intérieur des membranes de phospholipide et de cholestérol.

Canadian Journal of Chemistry, **50**, 1448 (1972)

Introduction

The existence of electrochemical reactions at membrane surfaces has been suggested as a basis for understanding the membrane potential and some aspects of ion transport (1). The model proposes that the electron transfer reaction is accelerated by an electric field applied across the double layer of a membrane/water interface. Recently, the electrochemical formation of metallic films of silver, platinum, and mercury at the surface of a membrane prepared from a solution of oxidized cholesterol has been described (2). The development of the metallic film was only seen following the application of a 50 mV potential in a direction which moved negative charge carriers from the iodide side to the metal ion side of the membrane. In terms of relating this phenomenon to the foregoing model it is of interest to determine whether the externally applied field is essential. It is conceivable that the existence of dissimilar electrochemical processes at the two intrafaces of a membrane might generate potential gradients within it that facilitated the deposition of the metal film at one intraface. In this report the results of attempts to silver plate cholesterol and phospholipid membranes in the absence of an applied electric field are described. It was found that cholesterol membranes did not develop any visible metallic film while phospholipid membranes did.

Experimental Procedure

Membrane Material

The composition of the phospholipid material has been described previously (3). In our experience the formation of a durable membrane lasting up to 21 days requires that cerebrosides, phosphatidylethanolamine, phosphatidyl inositol, and phosphatidyl serine are present in the solution from which the membrane is made. It therefore seems likely that these phospholipid components were present in the membrane as well.

Fatty acid analysis of the membrane material by gas chromatography indicated that about half of them contained one or more unsaturated carbon–carbon bonds.

Cholesterol (Reagent grade, Fisher) chromatographed as a single spot and was used without further purification.

Membrane Formation

The phospholipid material was dissolved in a minimal quantity of the apolar solvent, *n*-tetradecane, and then applied by the brush technique (4) to a 3 mm diameter aperture in a Teflon septum separating the two 4 ml aqueous compartments of a lucite cell. The lucite cell was symmetrically shaped about the Teflon septum and attached to the stage of a horizontally mounted microscope by means of a ball bearing. Microscopic observation of either side of the membrane under obliquely incident light was possible by rotating the cell back and forth through an angle of 180°. Once a membrane was formed in distilled water at 37 °C and had thinned to a bilayer, the plating solutions of reagent grade $AgNO_3$ (20 μM), KI (20 μM), and I_2 (2 μM), in that order, were added to the water. The $AgNO_3$ and KI, I_2 solutions were added to opposite sides of the membrane. Both sides of the membrane were then observed for the appearance of silver.

Results

Within 3–5 min after the addition of iodine a

Can. J. Chem. Downloaded from www.nrcresearchpress.com by 210.87.254.5 on 09/05/12
For personal use only.

fine granular deposit became visible on the Ag^+ ion side of the membrane. In 15 min the granules became more coarse and had the reflectance, lustre, and metallic appearance of silver. The plated membrane ruptured within 30 min unless the initial amount of $AgNO_3$, added to one compartment, was reduced to 2 μM. In this case the membrane would last at least 7 h but the density of the sparkling granules was diminished giving the affected side of the membrane a speckled appearance. The opposite side of the membrane, exposed to KI and I_2, remained black as before.

The plating process was carried out in darkness as well, to determine if the microscope illuminating light might have had any noticeable effect. No change in the time of occurrence or in the appearance of the granules was observed. Illumination of the membrane was therefore not essential to the development of the silver deposit, suggesting that it was not due to a photochemical effect.

The metallic nature of the silver deposit was investigated by an indirect method. Color transparencies of the deposit were taken and compared both by transmission and incident light microscopy with similar transparencies obtained by photographing under the same light films (10–1000 Å in thickness) of Ag, AgI, and $AgNO_3$ deposited on pieces of darkened B & W film. It was found that the color transparencies of the Ag, AgI, and $AgNO_3$ films could be readily distinguished from one another and that those obtained of the Ag film corresponded with the color transparencies of the silver deposit seen on the black phospholipid membrane. Additional evidence for the metallic nature of the silver deposit was obtained by confirming earlier work (2) that the deposit did not reduce the conductivity of the membrane. By comparing the similarity in appearance of the two sets of transparencies it could be estimated that the thickness of the silver deposit on the membrane was somewhere between 10–100 Å.

The nature of the silver deposition reaction was investigated by measuring the amount of time (plating time) required to reduce a given quantity of Ag^+, as determined by visual inspection of the deposit, when the concentration of the reactants was varied one at a time. In Fig. 1 the dependence of the plating time on the concentration of iodide (I^-), keeping $[Ag^+] =$ 2 μM and $[I_2] = 0.02$ μM, is shown on a log–log plot. A first-order reaction is suggested by the linear relationship. Since the amount of Ag^+ reduced is an infinitesimal amount of the total number of Ag^+ ions initially present in the one 4 ml compartment the result shown in Fig. 1 does not distinguish between a homogeneous and heterogeneous reaction involving I^-. A similar linear relationship was obtained between the plating time and the I_2 concentration keeping $[Ag^+] = 2$ μM and $[I^-] = 20$ μM.

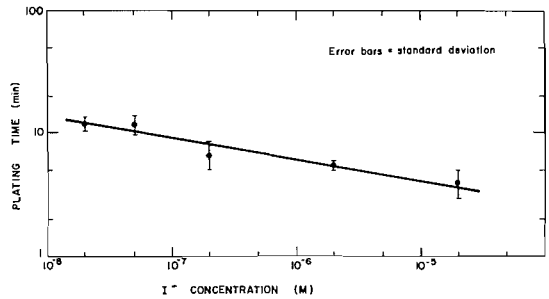

FIG. 1. Plating time vs. I^- concentration in the aqueous phase. $[Ag^+] = 2$ μM; $[I_2] = 0.02$ μM. Temperature = 37 °C.

The addition of I_2 to the aqueous phase containing the iodide ions was necessary since no plating was apparent without it. The effect of I_2 in promoting the silver plating might be attributable to the greatly increased permeability of the membrane to iodide due to the formation of polyiodides (I_3^-, I_5^-, etc.). Because of their larger size and lower surface charge density the polyiodides partition into the low dielectric region of the membrane phase more readily than iodide (5). The polyiodides, particularly I_3^-, may therefore be the source of electrons for the reduction of Ag^+. Alternatively, the formation of donor–acceptor complexes of I_2 with a lipid membrane (17) may increase the electrical conductivity of the membrane sufficiently to allow the silver reduction to occur at a measurable rate. Furthermore, the deposit of metallic silver on the membrane may then be interpreted as support for the electronic nature of the donor–acceptor charge transfer reactions (18).

In Fig. 2 the dependence of the plating time on the concentration of Ag^+, keeping $[I^-] = 20$ μM and $[I_2] = 2$ μM, is shown as a semi-log plot. The linear relationship with negative slope does not suggest a first-order reaction involving Ag^+ but is consistent with the fact that the total

Can. J. Chem. Downloaded from www.nrcresearchpress.com by 210.87.254.5 on 09/05/12
For personal use only.

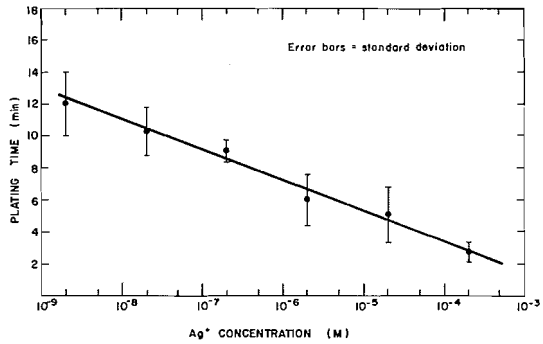

FIG. 2. Plating time vs. Ag^+ concentration in the aqueous phase. $[I^-] = 20\ \mu M$; $[I_2] = 2\ \mu M$. Temperature = 37 °C.

number of Ag^+ ions sorbed to the membrane at equilibrium will depend on the Ag^+ concentration in the aqueous phase as well as on the time required for an equilibrium distribution to be achieved.

With $[AgNO_3] = 2\ \mu M$ in one compartment and $[KI] = 2\ \mu M$, $[I_2] = 0.02\ \mu M$ in the other, the phospholipid membrane developed within a few seconds a self electromotive force of 132 mV as measured with a pair of closely matched platinum electrodes and a high impedance electrometer voltmeter. The aqueous phase containing the Ag^+ was positive. Increasing the resultant electric field by the application in the same direction of transmembrane potentials between 0–300 mV did not alter the plating time appreciably. The limitation may be due to space charge effects within the membrane. On the other hand reversal in polarity of the applied potential (10–100 mV) increased the plating time exponentially. At −100 mV no evidence of a deposit on the Ag^+ side of the membrane was seen.

Cholesterol membranes generated a self electromotive force of 82 mV (Ag^+ solution positive) when separating aqueous solutions of $AgNO_3$ (2 μM) from KI (2 μM) and I_2 (0.02 μM). The magnitude of the transmembrane potential is substantially less than the 132 mV measured for phospholipid membranes. In the absence of any relative change in electrical conductivity of the two kinds of membranes in the presence of I^- and I_2 (5, 6) this difference is likely due to dissimilar ion distributions within the membranes and will be discussed later. Attempts to silver plate membranes formed from a solution of chromatographically pure

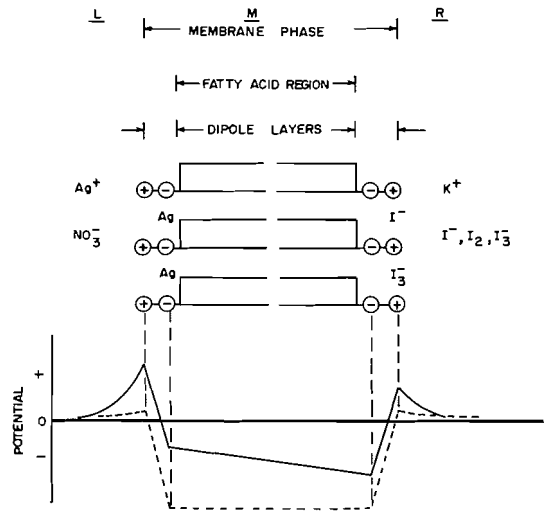

FIG. 3. A schematic illustration of silver plating on the left hand side L of an idealized black, bimolecular, phospholipid membrane M of area 0.06 cm^2. Following the addition of $AgNO_3$ (20 μM) and KI (20 μM), I_2 (2 μM) to aqueous phases L and R, respectively, the initial potential profile, represented for the case of distilled water by the broken line in the bottom of the diagram, is changed in a manner qualitatively illustrated by the solid line. Electron transfer to sorbed Ag^+ in intraface L from charge transfer complexes bound within the membrane is facilitated by the resultant electric fields. The silver deposit is visible within 5 min under low power microscopy (35×) of membrane surface L while surface R remains black.

cholesterol in *n*-tetradecane failed unless an external electric field was applied. A potential of 50 mV (Ag^+ solution positive) resulted in silver plating in 5–6 min.

Discussion

A basis for the difference in applied electric field requirements for silver plating to occur on phospholipid and cholesterol membranes may be sought in their structures. A number of components of the phospholipid material, from which the membranes were made, contain hydrophilic groups with a permanent dipole at near neutral p*H*. While the orientation of the hydrophilic groups with respect to the membrane is not firmly established the available evidence favors a distribution of orientations (7–9) rather than the perpendicular (10, 11) or coplanar (12, 13) alone. Sorption of counterions may realign a major proportion of the polar groups in the fully extended perpendicular direction (14) as shown schematically in Fig. 3.

Can. J. Chem. Downloaded from www.nrcresearchpress.com by 210.87.254.5 on 09/05/12
For personal use only.

Can. J. Chem. Downloaded from www.nrcresearchpress.com by 210.87.254.5 on 09/05/12
For personal use only.

The derivative force of the intrafacial potential existing in the region of the fixed dipoles then redistributes the counterions. Calculations have shown that the density of cations is maximal in the plane of fixed negative charge while the population of anions is highest in the plane of fixed positive charge. Furthermore, the concentration of counterions may be much higher in the polar layers than in the nearby aqueous phase (14). The redistribution alters the intrafacial potential profile somewhat in a manner shown by the solid line in the bottom diagram of Fig. 3. The magnitude of the change in the maximum and minimum potentials within the dipole layer from their values in distilled water, given by the broken line, depends on the densities of the counterions within the layer which, in turn, may be related to the affinity of the membrane to them (15). The ionic species in R, particularly I_3^-, permeate the membrane phase more readily than those in L; therefore the maximum and minimum potentials in the dipole layer of intraface R will be less than their respective values in intraface L. The solid line joining the two potential minima may then indicate in a general way the potential gradient across the low dielectric, fatty acid region. This potential may bias electron transfer from donors within the membrane to the sorbed Ag^+ ions. The strong positive potential ($4\,kT/e$ or more where the symbols have their usual meaning (14)) in the plane of fixed positive charge of intraface L is perhaps of more importance in facilitating electron entry at the anodic sites, that is, at the sorbed Ag^+ ions.

The development of the potential of 132 mV prior to any evidence of silver plating of the phospholipid membrane may then have an electrochemical component. This suggests an explanation for the failure of cholesterol membranes to silver plate in the absence of an applied potential. Cholesterol membranes lack the dipole layers within the membrane phase, the intrafacial potentials associated with them, and consequently the capacity to generate the increased ion density and intrafacial electric field similar to that of the bimolecular phospholipid membrane. An external potential must therefore be applied to satisfy the silver plating requirement of an increased Ag^+ ion density at the cholesterol membrane–water interface and/or a suitable electric field to promote electron transfer (16).

The electron transfer reaction of the plating process may be represented by the following redox couples:

$$2I^- \rightarrow I_2 + 2e^-$$
$$Ag \leftarrow Ag^+ + e^-$$

The reducing and oxidizing components are initially sorbed to opposite sides of the phospholipid membrane. However, the polyiodide ions (I_{2n+1}^-) are readily formed in the presence of iodine and they have a strong affinity for phospholipid membranes (6). The possibility that the plating process is simply the result of I_{2n+1}^- diffusion through the membrane is unlikely for the following reasons. The photographic results and the conductivity measurements indicate that the silver deposit is metallic and not a precipitate of AgI or $AgNO_3$. The lack of any measurable flux of ^{131}I through a lipid membrane in the presence of KI and under conditions where ^{131}I-labelled I_{2n+1}^- ions or I_2 diffused along favorable electrical and/or chemical gradients (6) suggests further that the polyiodide ions within the membrane are bound. This is consistent with spectrophotometric evidence for iodine complexes both with phospholipids and cholesterol (17). The bound complexes may, however, undergo relaxations (19) and transfer charge in a manner that is formally equivalent to diffusion of I_{2n+1}^- through the membrane. The electronic nature of the charge transfer is consistent with the mechanism of conductivity of a phospholipid membrane in an iodide–iodine system (19) and accounts for the silver deposition as well.

The skillful technical assistance of Mrs. M. C. Shierman is much appreciated. The helpful comments of Drs. J. O'M. Bockris and L. J. Mandel on the manuscript are acknowledged.

1. J. O'M. Bockris. Nature, **224**, 775 (1969).
2. H. C. Pant and B. Rosenberg. Chem. Phys. Lipids, **6**, 39 (1971).
3. A. Petkau and W. S. Chelack. Biochim. Biophys. Acta, **135**, 812 (1967).
4. P. Mueller, D. O. Rudin, H. T. Tien, and W. C. Wescott. Circulation, **26**, 1167 (1962).
5. A. Finkelstein and A. J. Cass. J. Gen. Physiol. **52**, No. 1, Part 2, 145 (1968).
6. M. K. Jain, A. Strickholm, F. P. White, and E. H. Cordes. Nature, **227**, 705 (1970).
7. V. A. Parsegian. J. Theor. Biol. **15**, 70 (1967).
8. V. A. Parsegian. Science, **156**, 939 (1967).

9. L. J. LIBERTINI, A. S. WAGGONER, P. C. POST, and O. H. GRIFFITH. P.N.A.S. **64**, 13 (1969).
10. H. T. TIEN. J. Theor. Biol. **16**, 97 (1967).
11. D. O. SHAH and J. H. SCHULMAN. J. Lipid Res. **8**, 227 (1967).
12. T. HANAI, D. A. HAYDON, and J. TAYLOR. J. Theor. Biol. **9**, 278 (1965).
13. B. A. PETHICA. *In* H. S. Rooke, Surface Activity and the Microbial Cell, S.C.I. Monograph No. 19 London, 1965, p. 85.
14. C. J. GILLESPIE. Biochim. Biophys. Acta, **203**, 47 (1970).
15. A. PETKAU and W. S. CHELACK. Biochim. Biophys. Acta, **203**, 34 (1970).
16. YE. A. LIBERMAN, V. P. TOPALY, L. M. TSOFINA, and A. M. SHKROB. Biofizika, **14**, 56 (1969).
17. B. BHOWMIK, G. L. JENDRASIAK, and B. ROSENBERG. Nature, **215**, 843 (1967).
18. B. ROSENBERG and B. B. BHOWMIK. Chem. Phys. Lipids, **3**, 109 (1969).
19. L. I. BOGUSLAVSKY, F. I. BOGOLEPOVA, and A. V. LEBEDEV. Chem. Phys. Lipids, **6**, 296 (1971).

Can. J. Chem. Downloaded from www.nrcresearchpress.com by 210.87.254.5 on 09/05/12
For personal use only.

Infrared and Raman Spectra of Single Crystals of Anhydrous Strontium Formate

N. R. McQUAKER[1] AND K. B. HARVEY[2]

Department of Chemistry, University of British Columbia, Vancouver 8, British Columbia

Received August 20, 1971

The infrared absorption of single crystals of anhydrous strontium formate has been measured in the region 4000 to 500 cm^{-1}. The internal fundamentals of two sets of crystallographically non-equivalent types of formate ions are identified. Frequencies of external fundamentals are tentatively inferred from absorption bands appearing in the second order spectrum. Measurement of laser excited Raman spectra in the region 700–10 cm^{-1} has yielded assignments for all of the expected translational modes. None of the librational modes were observed.

L'absorption infrarouge de monocristaux de formiate de sodium anhydre a été mesurée dans la région allant de 4000 à 500 cm^{-1}. Les vibrations fondamentales internes de deux séries d'ions formates de types de cristallographie non équivalents sont identifiées. Les fréquences de vibrations fondamentales externes sont déduites expérimentalement des bandes d'absorption apparaissant dans le spectre du second ordre. La mesure dans la région 700–10 cm^{-1} du spectre Raman obtenu par excitation au laser a permis d'attribuer tous les modes de translation attendus; aucun mode librationnel n'a été observé.

Canadian Journal of Chemistry, **50**, 1453 (1972)

Introduction

The mid-infrared absorption spectrum of polycrystalline $Sr(HCO_2)_2$ has been reported by previous workers (1–3). Evidently no single crystal absorption studies have been reported. The X-ray crystal studies of $Sr(HCO_2)_2$ (4, 5) indicate an orthorhombic structure (D_2^4-$P2_12_12_1$) with four molecules per unit cell. Under the D_2^4 space group all atoms must lie on general positions of multiplicity four. Thus, there are two sets of crystallographically independent formate ions. The vibrational spectrum of the internal fundamentals should be sensitive to the presence of the two types of formate ions and indeed the expected frequency doubling has been observed (1–3). However, the assignments are incomplete and it was hoped that by using single crystals and polarized radiation that more complete assignments could be made. This has been possible and in addition frequencies of external fundamentals are inferred from absorption bands appearing in the second order spectrum. In order to check for the presence of these external fundamentals we have measured the laser excited Raman spectra in the region 700–10 cm^{-1}. Assignments are made for all of the expected translations. The librations, however, did not appear with observable intensity.

The mid-infrared spectra of polycrystalline $Sr(HCO_2)_2$ and $Sr(DCO_2)_2$ have also been recorded.

Experimental

The $Sr(HCO_2)_2$ was obtained from Baker and Adamson Ltd. and the $Sr(DCO_2)_2$ was obtained from Merke, Sharp, and Dohme Ltd. Both compounds were of reagent grade. The single crystals of $Sr(HCO_2)_2$ were grown by controlled evaporation of a saturated solution held at 85 °C. After three to four weeks of growth a typical crystal (of sphenoidal habit) had dimensions of 25 × 15 × 10 mm. The principal face of these crystals was the (010) face elongated in the *c* direction.

In the polycrystalline studies the samples were prepared as thin films. These films were mechanically deposited on potassium bromide supports. The technique used has been described elsewhere (6). The thin single crystal slices were prepared using a refinement of the technique described by Charlton and Harvey (7). A polarizing microscope was used to determine the relative orientation of the crystal axes and to confirm the quality of the crystal. In all cases the crystals were clear and exhibited sharp extinction. Observation of the interference figures also allowed us to confirm that the crystals were ground to within 2° of the perpendicular of the axis of observation. The thicknesses of the crystals were measured on a Zeiss Light-section microscope and were found to be approximately 25 μ.

The infrared spectra were recorded in the region 4000–500 cm^{-1} using a Perkin–Elmer 421 spectrometer. All spectra were recorded against a dry air background purged of CO_2. The spectrometer was calibrated against known spectra (8) and the error of measurement is estimated to be less than ± 2 cm^{-1}.

The laser excited Raman spectra of the single crystals were recorded using a Spex (model 1400) spectrophotometer which was equipped with a cooled ITT photolube detector (FW-130) and a Spectra Physics 165 Argon laser. A right angle scattering geometry was used and the exciting wave-

[1]Present address: Department of Electrical Engineering, University of Waterloo, Waterloo, Ontario.

[2]Dr. K. B. Harvey passed away September 27, 1970.

Can. J. Chem. Downloaded from www.nrcresearchpress.com by 210.87.254.42 on 09/05/12
For personal use only.

TABLE 1. Correlation table for the internal fundamentals*

Vibration	Free ion symmetry (C_{2v})		Site group symmetry (C_1)		Factor group symmetry (D_2)
ν_1,ν_2,ν_3	a_1	→	a	→	a,b_1,b_2,b_3
ν_4,ν_5	b_1	→	a	→	a,b_1,b_2,b_3
ν_6	b_2	→	a	→	a,b_1,b_2,b_3

*This table is repeated twice: once for formate ions I and once for formate ions II.

length used was the 5145 Å line at a power of around 500 mW. The instrument was calibrated with a neon discharge lamp and the uncertainty in the measured frequencies is estimated to be less than ± 2 cm^{-1}.

Results and Discussion

Internal Lattice Vibrations

Under the D_2 factor group the irreducible representation for the internal fundamentals may be summarized as

$$\Gamma(\text{internal}) = 12a + 12b_1 + 12b_2 + 12b_3$$

These 48 internal normal vibrations may be considered to arise from the 6 normal vibrations of the HCO_2^- ion through the presence of the two sets of four crystallographically independent formate ions in the unit cell. The correlation table for the factor group (correlation field) splitting of the HCO_2^- ion appears in Table 1.

Reference to Table 1 shows that under D_2 each free ion mode is split into four crystal vibrations of symmetries a, b_1, b_2, and b_3. The b_1, b_2, and b_3 components of the free ion mode appear in the infrared single crystal spectra when the incident radiation is polarized along the $z(c)$, $y(b)$, and $x(a)$ axes, respectively. The resulting $b_1/b_2/b_3$ splittings are a direct measure of the correlation field splitting. However, in practice it is usually found that correlation field effects do not give significant splittings (see for example, ref. 9). Accordingly, we may make the assignments according to the following scheme: ν_1 through ν_6 for the first set of four crystallographically independent HCO_2^- ions and ν_1' through ν_6' for the second set. We will subsequently refer to formate ions of the first and second sets as formate ions of types I and II.

Even though we do not expect significant $b_1/b_2/b_3$ frequency shifts to be associated with a particular free ion mode we can expect significant $b_1/b_2/b_3$ intensity changes. This is because in the single crystal the orientations of the oscillating dipoles which give rise to the internal fundamentals are fixed relative to the incident polarized radiation. The orientation of the various dipoles will depend upon the location of the hydrogen, oxygen and carbon atoms of formate ions I and II. The positions of the hydrogen atoms are not known. However, the positions of the oxygen and carbon atoms fix C—O bond lengths of 1.24 Å in all cases (4, 5) and if we assume effective C_{2v} site symmetries for formate ions I and II we can compute the various dipole orientations relative to the crystal axes. In the limit of the oriented gas model (see for example, ref. 10) the relative infrared absorption intensities along the x, y, and z axes are given by the appropriate values of the squares of the dipole direction cosines. In Table 2 the relative intensities along the x, y, and z axes are given for the C_{2v} vibrations, ν_i and ν_i', associated with formate ions I and II. The magnitude of the ν_i/ν_i' splittings will largely be a reflection of differences in the C_{2v} geometry of ions of types I and II. The parameters that can show variation without destroying the assumed C_{2v} geometries are the C—H bond lengths and the O—C—O bond angles. It is known that formate ions of type I have an O—C—O bond angle of 130° and that those of type II have a corresponding bond angle of 129° (4, 5). Since the positions of the hydrogen

TABLE 2. Relative absorption intensities along the crystal axes*

Vibration	C_{2v} symmetry	Relative intensities $\|\|x$	$\|\|y$	$\|\|z$
ν_1,ν_2,ν_3	a_1	0.0659	0.0908	0.8431
ν_4,ν_5	b_1	0.5320	0.4673	0.0007
ν_6	b_2	0.4039	0.4398	0.1563
ν_1',ν_2',ν_3'	a_1	0.7510	0.0001	0.2490
ν_4',ν_5'	b_1	0.1777	0.2754	0.5469
ν_6'	b_2	0.0711	0.7237	0.2053

*The ν_i and ν_i' refer to formate ions I and II, respectively.

Can. J. Chem. Downloaded from www.nrcresearchpress.com by 210.87.254.42 on 09/05/12
For personal use only.

TABLE 3. Infrared frequencies of polycrystalline strontium formate*

Assignment	Frequency (cm^{-1})				
	$Sr(HCO_2)_2$				$Sr(DCO_2)_2$, this work
	Ref. 1	Ref. 2	Ref. 3	This work	
$\nu_3(\delta OCO)a_1$	763	763	763	*763*	*755*
	780	781	781	*779.5*	772
	784	785	786	*783.5*	*776*
$\nu_6(\rho CH)b_2$	1082	1085	1087	*1084*	*919*
	1350		1351	1349	
$\nu_2(\nu CO)a_1$	1360			*1359.5*	*1340*
		1362	1364	*1362.5*	
	1369	1374	1374	1368	
$\nu_5(\omega CH)b_1$	1381	1397	1399	*1393.5*	*1013*
	1387.5	1401	1404	*1399*	*1039*
$\nu_4(\nu CO)b_1$	1580	1572	1572	*1570*	*1562*
		1590		*1593*	*1593*
		1653		1651	1650
	2720			2720	
	2775			2775	
$\nu_1(\nu CH)a_1$	2872	2849	2874	*2872*	*2160*
					2183
	2925			2925	

*Frequencies in italics are those of internal fundamentals.

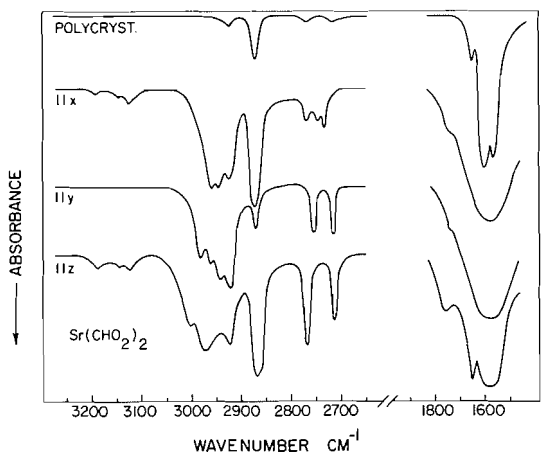

FIG. 1. Infrared spectra in the region 3300–1500 cm^{-1} of polycrystalline $Sr(HCO_2)_2$ and single crystal slices of $Sr(HCO_2)_2$ polarized along the x, y, and z axes. The thickness of the crystal slices is 25 ± 3 μ.

atoms are not known any difference in the C—H bond lengths cannot be compared.

There is only one $Sr(HCO_2)_2$ internal fundamental which does not show a ν_i/ν_i' splitting (or frequency doubling) and this is $\nu_1/\nu_1'(a_1)$. In both the polycrystalline and single crystal spectra (Fig. 1) a single ν_1/ν_1' absorption at 2872 cm^{-1} (Tables 3 and 4) is observed. If equal ν_1 and ν_1' oscillator strengths are assumed the strong ν_1/ν_1' intensities observed along the x and z axes and the weak intensity observed along the y axis can be compared with a predicted $x/y/z$ intensity ratio of 0.8/0.1/1.1. As already suggested the remaining two internal fundamentals possessing a_1 symmetry under C_{2v} show frequency doubling. In the polycrystalline spectrum of $Sr(HCO_2)_2$ there are four absorptions in the vicinity of $\nu_2/\nu_2'(a_1)$ (Fig. 2). These appear at 1349, 1359.5, 1362.5, and 1368 cm^{-1}. In the single crystal spectra very intense absorptions appear at 1360 cm^{-1} along both the x and z axes and a less intense absorption appears at 1363 cm^{-1} along the y axis. Since Table 2 indicates that ν_2' will have essentially zero intensity along the y axis the 1363 cm^{-1} absorption must be assigned as ν_2. The 1360 cm^{-1} absorption can then be assigned as ν_2'. The 1349 and 1368 cm^{-1} absorptions appearing in the polycrystalline spectrum are evidently obscured by the intense ν_2/ν_2' absorptions appearing in the single crystal spectra. These two apparently anomalous absorptions

Can. J. Chem. Downloaded from www.nrcresearchpress.com by 210.87.254.42 on 09/05/12
For personal use only.

TABLE 4. Infrared frequencies of single crystals of strontium formate*

	Frequency (cm^{-1})†			
	Observed			
Assignments	$\|\|x$	$\|\|y$	$\|\|z$	Calculated
	748 vvw		748 vvw	
	756 vvw		756 m	
ν_3	763 m	763 m	763 vs	
	766 w		766 s	
	775 m			
			779.5 m	
ν_3'	783.5 vs		783.5 s	
		786 m	787 w	
ν_6	1070 vvw	1070 vvw	1070 vvw	
ν_6'	1084 vw	1084 vs	1084 w	
ν_2'	1360 vvs		1360 vvs	
ν_2		1363 vvs		
		1374 ms		
		1383 ms		
ν_5	1393 vs	1393 vs		
ν_5'	1399 s	1399 s	1399 s	
ν_4/ν_4'	1580 vvs	1580 vvs	1580 vvs	
$\nu_4/\nu_4' + 70$			1650 vs	
$\nu_4/\nu_4' + 155$	1735 w	1735 w		
$\nu_4/\nu_4' + 180$			1760 mw	
$\nu_2/\nu_2' + \nu_3$			2130 vvw	2124
$\nu_2/\nu_2' + \nu_3'$	2152 vvw			2145
$\nu_3/\nu_3' + \nu_5/\nu_5'$	2165 vvw	2165 vvw	2165 vvw	2174
$\nu_3/\nu_3' + \nu_4/\nu_4'$	2349 vvw	2349 vvw	2349 vvw	2359
$\nu_2/\nu_2' + \nu_6$	2434 vvw	2434 vvw	2434 vvw	2431
$\nu_2/\nu_2' + \nu_6'$	2448 vvw	2448 vvw	2448 vvw	2445
$2(\nu_2/\nu_2')$		2721 w	2721 m	2722
$\nu_2/\nu_2' + \nu_5$	2745 w			2754
$\nu_2/\nu_2' + \nu_5'$	2753 vw			2760
$2\nu_5$		2760 w		2786
$2\nu_5'$	2775 vw		2775 ms	2798
ν_1/ν_1'	2872 vs	2872 w	2872 vs	
$\nu_2/\nu_2' + \nu_4$	2925 ms	2925 s	2925 ms	2931
$\nu_2/\nu_2' + \nu_4'$	2944 ms	2944 ms		2954
$\nu_4 + \nu_5$	2965 ms	2965 ms		2963
$\nu_4 + \nu_5'$			2975 ms	2969
$\nu_4' + \nu_5$		2988 m		2986
$\nu_4' + \nu_5'$			2998 m	2992
	3125 vvw		3125 vvw	
$2\nu_4$	3143 vvw		3143 vvw	3140
$2\nu_4'$	3190 vvw		3190 vvw	3186
$\nu_1/\nu_1' + \nu_3$	3631 vvw		3631 vvw	3635
$\nu_1/\nu_1' + \nu_3'$	3648 vvw		3648 vvw	3656

*The calculated second order frequencies use $\nu_i/\nu_i' = (\nu_i + \nu_i')/2$. $\nu_4/\nu_4' = 1580\ cm^{-1}$ has components at 1570 and 1593 cm^{-1} (see Table 3). The calculated second order frequencies use $\nu_4 = 1570\ cm^{-1}$ and $\nu_4' = 1593\ cm^{-1}$.

†v = very, s = strong, m = medium, w = weak.

may be associated with the lines observed at 1374 and 1383 cm^{-1} in the single crystal spectra. Their assignment is discussed later. The final internal vibration of a_1 symmetry is $\nu_3/\nu_3'(a_1)$. It is found that in the polycrystalline spectrum there are three absorptions in the vicinity of ν_3/ν_3'. These appear at 763, 779.5, and 783.5 cm^{-1}. Of these only the 763 cm^{-1} line appears along the y axis. Since ν_3' will have essentially zero intensity along the y axis the assignment

Can. J. Chem. Downloaded from www.nrcresearchpress.com by 210.87.254.42 on 09/05/12
For personal use only.

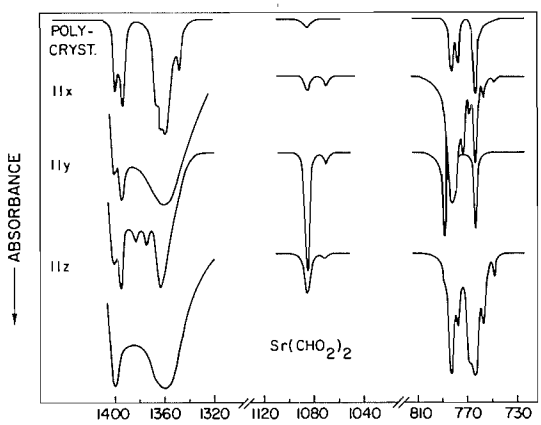

FIG. 2. Infrared spectra in the region 1500–700 cm^{-1} of polycrystalline $Sr(HCO_2)_2$ and single crystal slices of $Sr(HCO_2)_2$ polarized along the x, y, and z axes. The thickness of the crystal slices is 25 ± 3 μ.

suggested for the 763 cm^{-1} line is ν_3. The observed ν_3 intensity ratios of medium/medium/very strong along the $x/y/z$ axes are in agreement with the predicted ratio of 0.07/0.09/0.84. The 783.5 cm^{-1} absorption has an intensity ratio along the x/z axes of very strong/strong. This ratio is consistent with the predicted ν_3' ratio of 0.75/0.25. We may note that ν_3/ν_3' may be considered as an O—C—O bending vibration and that the frequency shift $\nu_3' - \nu_3 = 20.5$ cm^{-1} is compatible with the one degree decrease in the O—C—O bond angle as we go from formate ion I to formate ion II. Evidently the apparently anomalous line observed at 779.5 cm^{-1} in the polycrystalline spectrum must be considered along with the additional lines appearing in the single crystal spectra at 748, 756, 766, 775, and 786 cm^{-1}. The assignment of these lines is discussed in the following section.

Under C_{2v} there are two internal vibrations of b_1 symmetry. These are ν_4/ν_4' and ν_5/ν_5'. In the polycrystalline spectrum ν_4/ν_4' frequencies appear at 1570 and 1593 cm^{-1}. In the single crystal spectra the resolution of this doublet is completely obscured by very intense absorptions which appear along all three crystal axes. The ν_5/ν_5' frequencies at 1393 and 1399 cm^{-1} appear in the polycrystalline spectrum as a well resolved doublet. The predicted intensity of ν_5 along the z axis is essentially zero. Thus the absorption appearing along the z axis at 1399 cm^{-1} is assigned as ν_5'. As expected both ν_5 and ν_5' appear with considerable intensity along both the x and y axes.

The one remaining C_{2v} internal vibration is $\nu_6/\nu_6'(b_2)$. Only one component is observed in the polycrystalline spectrum. It appears at 1084 cm^{-1}. The observed single crystal intensities of the 1084 cm^{-1} absorption along the $x/y/z$ axes are very weak/very strong/weak. These may be compared with the corresponding predicted ν_6' intensities of 0.07/0.72/0.21. In the single crystal spectra ν_6 appears only very weakly at 1070 cm^{-1} along all three crystal axes. Comparison of intensities shows that the ν_6' intensity is much greater than the ν_6 intensity. Evidently the different C_{2v} geometries of formate ions I and II result in markedly different oscillator strengths in the case of ν_6 and ν_6'.

The foregoing results have shown that the assumption of effective C_{2v} site symmetries for formate ions I and II predicts relative intensities for the internal vibrations which are consistent with experimental observation. Thus, we may conclude that the assumption of effective C_{2v} site symmetries is a reasonably good one. Using this assumption we have been able to distinguish between the assignments ν_i and ν_i'. These assignments are summarized in Tables 3 and 4. Table 3 also includes the previously unreported frequencies of the internal fundamentals of $Sr(DCO_2)_2$. It is seen that the ν_i/ν_i' frequency doubling where $i = 2$, 3, and 4 is of comparable magnitude in both $Sr(HCO_2)_2$ and $Sr(DCO_2)_2$. This, however, is not the case for ν_1/ν_1' and ν_5/ν_5'. These frequencies are dependent on the motions of the hydrogen and deuterium atoms and the much greater ν_1/ν_1' and ν_5/ν_5' frequency doubling in $Sr(DCO_2)_2$ suggests a non-equivalence associated with the deuterium atoms of formate ions I and II which is not present in the case of $Sr(HCO_2)_2$.

Combinations and Overtones

We may associate the $Sr(HCO_2)_2$ absorptions appearing at 748, 756, 766, 775, 779.5, and 786 cm^{-1} in the single crystal spectra with the 772 cm^{-1} absorption appearing in the polycrystalline spectrum of $Sr(DCO_2)_2$. The close correspondence between the $Sr(HCO_2)_2$ wavenumbers and the $Sr(DCO_2)_2$ wavenumber suggests that hydrogen atom motion does not play a significant role in determining these second

Can. J. Chem. Downloaded from www.nrcresearchpress.com by 210.87.254.42 on 09/05/12
For personal use only.

Can. J. Chem. Downloaded from www.nrcresearchpress.com by 210.87.254.42 on 09/05/12
For personal use only.

order frequencies. Tentative assignments are to overtones and combinations involving librational motions about the C—H and C—D axes. The assumption of these assignments places frequencies for the librational motion of the oxygen atoms in the region 374–398 cm^{-1}. We may note that the unusually strong intensity of some of these second order absorptions may be due to Fermi resonance with ν_3 and ν_3'.

The intensities of the $Sr(HCO_2)_2$ bands at 1349, 1368, 1374, and 1383 cm^{-1} are also likely enhanced by Fermi resonance; *i.e.*, ν_2/ν_2' and ν_5/ν_5' lie nearby. It is possible that these apparently anomalous lines are due to overtones and combinations involving librational motions perpendicular to the C—H axes. The frequencies of these librational motions will be strongly dependent on the motion of the hydrogen atoms. This would explain the absence of these second order absorptions in the vicinity of ν_2/ν_2' in the $Sr(DCO_2)_2$ spectrum. The assumption of the assignments mentioned placed frequencies for librational motions involving motion of the hydrogen atom in the region 674–691 cm^{-1}. Although this region of the spectrum was studied the expected first order absorptions did not appear. This is analogous to the case for both the NH_4^+ ions (9, 11) and BH_4^- ions (6, 12) where the expected librational frequencies appear only in the second and third order spectra.

There are three bands appearing on the high wavenumber side of ν_4/ν_4' which may be assigned as ν_4/ν_4' in combination with translations. If we place ν_4/ν_4' at 1580 cm^{-1} the inferred translational frequencies are placed at 70, 155, and 180 cm^{-1}. Absorption bands assigned as ν_4 in combination with translations are also observed in the single crystal spectra of $Na(HCO_2)$(7). In this case the inferred translational frequencies are placed at 57, 107, and 138 cm^{-1}.

All the remaining bands appearing in the second order spectrum may be tentatively assigned to either combinations or overtones of internal fundamentals (see Table 4). The observed ($k = 0$) frequencies of the internal fundamentals may be used to predict the frequencies of combinations and overtones in the zero wavevector limit. Thus, discrepancies between observed and calculated second order frequencies may be due to the combination of phonons of non zero (but equal and opposite) wavevector (13) as well as to anharmonicity and Fermi resonance effects. The enhanced intensities of the combination and overtone bands in the region 2700–3025 cm^{-1} are likely due to Fermi resonance with ν_1/ν_1' which lies at 2872 cm^{-1}.

A summary of the second order wavenumbers appears in Table 4.

External Lattice Vibrations

The external lattice vibrations include those of optical translatory (o.t.), optical libratory (o.l.), and acoustical translatory (a.t.) origin. The respective irreducible representations are

$$\Gamma(\text{o.t.}) = 9a + 8b_1 + 8b_2 + 8b_3$$

$$\Gamma(\text{o.l.}) = 6a + 6b_1 + 6b_2 + 6b_3$$

$$\Gamma(\text{a.t.}) = b_1 + b_2 + b_3$$

Optical crystal modes of all four symmetry species are Raman active. The Raman tensor elements and their corresponding symmetry species are: α_{xx}, α_{yy}, and α_{zz} for a; α_{xy} for b_1; α_{zx} for b_2, and α_{yz} for b_3. As previously indicated, crystal modes of b_1, b_2, and b_3 symmetries are infrared active and are polarized along the $z(c)$, $y(b)$, and $x(a)$ crystal axes, respectively. We may note that the infrared active vibrations may be split due to the accompanying long range electrostatic forces. For example, $b_1 \rightarrow b_1(\text{TO}) + b_1(\text{LO})$ where TO and LO respectively refer to transverse optical and longitudinal optical phonons. The TO/LO phonons are expected to appear in the Raman spectrum when the direction of phonon propagation is perpendicular/parallel to the phonon polarization. Since $Sr(HCO_2)_2$ is anisotropic the magnitude of the frequency difference for a particular TO/LO splitting will depend upon the direction of phonon propagation with respect to the appropriate crystal axis.

In the present work attempts to observe the LO modes were unsuccessful. Apparently the signs of the electro-optic coupling coefficients are such that destructive interference occurs (13). This has also been found to be the case for the ammonium halides (9, 14).

Reference to Fig. 3 shows the spectra for the α_{zz}, α_{xz}, α_{xy}, and α_{zy} polarizations. The notation used to label the spectra is the same as that introduced by Damen, Porto, and Tell (15). For example, the spectrum labelled $y(zz)x$ corre-

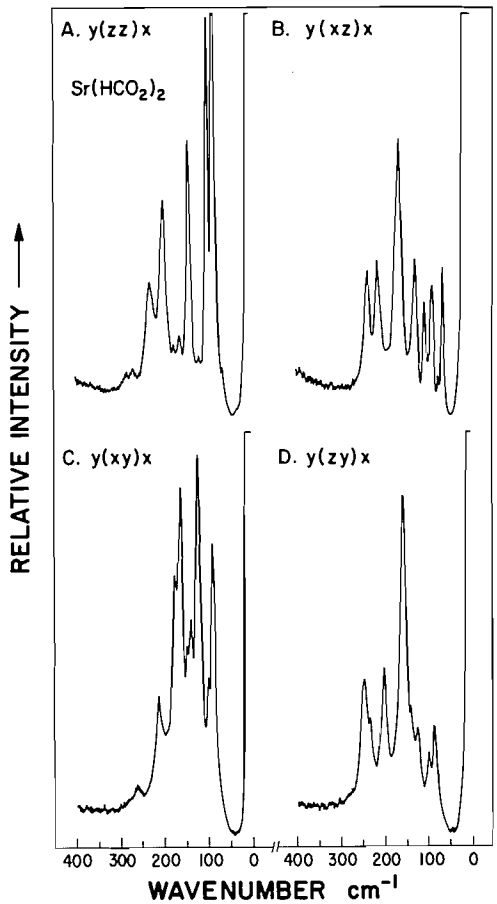

FIG. 3. Raman spectra in the region 0–400 cm^{-1} of a single crystal of $Sr(HCO_2)_2$: (*A*), α_{zz} component showing *a* vibrations; (*B*), α_{xz} component showing b_2 vibrations; (*C*), α_{xy} component showing b_1 vibrations; (*D*), α_{zy} component showing b_3 vibrations.

sponds to a right angle scattering geometry with the incident radiation propagating in the *y* direction (polarized in the *z* direction) and the scattered radiation propagating in the *x* direction (polarized in the *z* direction). The polarizability tensor α_{zz} determines this spectrum.

It was found that crystal modes arising from librations of the HCO_2^- ions did not appear with observable intensity. This also compares with the case of the ammonium halides where the expected librational modes appear very weakly, if at all (9, 16). However, it is seen from Table 5 that all 33 of the crystal modes arising from translations of the HCO_2^- and Sr^+ ions have been accounted for. Since $Sr(HCO_2)_2$ has

TABLE 5. Translational frequencies (cm^{-1}) of anhydrous strontium formate*

a symmetry	b_1 symmetry	b_2 symmetry	b_3 symmetry
228 w	212 w	233 w	247 mw
198 m	175 ms	212 mw	233 w
174 vw	160 vvs	161 s	201 mw
161 vw	147 m	125 mw	156 vs
138 s	137 m	104 w	140 w
117 vvw	121 vvs	87 mw	124 w
95 vvs	98 mw	72 vvw	98 vw
82 vvs	87 s	62 mw	87 w
64 vvw			

*v = very, w = weak, m = medium, s = strong.

4 Sr^+ ions and 8 HCO_2^- ions per unit cell the accidental degeneracies and near degeneracies observed can be expected. The observation of translational frequencies in the region 60–250 cm^{-1} is consistent with the continuous infrared absorption observed in the region ν_4/ν_4' to $\nu_4/\nu_4' + 250\ cm^{-1}$ where the ν_4/ν_4' frequency is taken as 1580 cm^{-1}. If we assume the combination of $k = 0$ phonons for the three absorption maxima of origin ν_4/ν_4' + translation appearing in the ν_4/ν_4' to $\nu_4/\nu_4' + 250\ cm^{-1}$ region then $k = 0$ translations are predicted at 70, 155, and 180 cm^{-1}. These frequencies compare with the Raman frequencies observed at 72, 156, and 175 cm^{-1}.

Three scatterings in addition to the translations assigned in Table 5 appear. These are observed at 263 cm^{-1} (*xy* polarization) and 269 and 282 cm^{-1} (*zz* polarization). It is likely that these scatterings are due to multiphonon processes involving the combination of two translations. Since the $k = 0$ selection rules are relaxed either optical or acoustical phonons of equal and opposite wavevector may contribute to the intensity of the scatterings at 263, 269, and 282 cm^{-1}.

Thanks are due to Professors A. Anderson and B. H. Torrie of University of Waterloo for the use of their Raman facility. The financial assistance of the National Research Council of Canada and of the University of British Columbia is gratefully acknowledged.

1. K. B. HARVEY, B. A. MORROW, and H. F. SHURVELL. Can. J. Chem. **41**, 1181 (1963).
2. C. J. H. SCHUTTE and K. BUIJS. Spectrochim. Acta, **20**, 187 (1964).

Can. J. Chem. Downloaded from www.nrcresearchpress.com by 210.87.254.42 on 09/05/12
For personal use only.

3. J. D. DONALDSON, J. F. KNIFTON, and S. D. ROSS. Spectrochim. Acta, **20**, 847 (1964).
4. I. NITTA and Y. SAITO. X-Rays, **5**, 89 (1949).
5. T. SUGAWARA, M. KAKUDO, Y. SAITO, and I. NITTA. X-Rays, **6**, 85 (1949).
6. K. B. HARVEY and N. R. MCQUAKER. Can. J. Chem. **49**, 3272 (1971).
7. T. L. CHARLTON and K. B. HARVEY. Can. J. Chem. **44**, 2717 (1966).
8. IUPAC Tables of Wavenumbers for the Calibration of Infrared Spectrophotometers. Butterworth, Washington, D.C., 1961.
9. K. B. HARVEY and N. R. MCQUAKER. J. Chem. Phys. **55**, 4390 (1971).
10. A. BREE and R. ZWARICH. Spectrochim. Acta, **27A**, 599 (1971).
11. N. E. SCHUMAKER and C. W. GARLAND. J. Chem. Phys. **53**, 392 (1970).
12. K. B. HARVEY and N. R. MCQUAKER. Can. J. Chem. **49**, 3282 (1971).
13. R. LOUDON. Adv. Phys. **13**, 423 (1964).
14. C. H. PERRY and R. P. LOWNDES. J. Chem. Phys. **51**, 3648 (1969).
15. T. C. DAMEN, S. P. S. PORTO, and B. TELL. Phys. Rev. **142**, 570 (1966).
16. J. R. DURIG and D. J. ANTION. J. Chem. Phys. **51**, 3639 (1969).

Can. J. Chem. Downloaded from www.nrcresearchpress.com by 210.87.254.42 on 09/05/12
For personal use only.

The Effect of Aromatic Tertiary Amines on the Copper(II) Catalyzed Decarboxylation of 3-Oxo-Glutaric Acid

K. N. LEONG AND M. W. LISTER

Department of Chemistry, University of Toronto, Toronto 181, Ontario

Received November 24, 1971

The kinetics of the copper(II) catalyzed decarboxylation of 3-oxo-glutaric acid have been investigated in unbuffered solutions at 25 °C and 0.60 *M* ionic strength, both in the presence of aromatic tertiary amines, and with hydrated copper ions alone. The amines used were 2,2′-bipyridyl and 1,10-phenanthroline. Equilibrium constants for the formation of the various copper complexes were determined with a copper ion selective electrode, particularly for the species CuAB, where A is the 3-oxo-glutarate ion, and B is an aromatic amine. The kinetic behavior was then interpreted as arising from the simultaneous decarboxylation of all the species present containing a 3-oxo-glutarate ligand. The resulting rate constants indicated that some kinetic effect was transmitted through the copper from the base to the 3-oxo-glutarate, but the effect was relatively small, and the bulk of the catalytic effect caused by the base arose from changes in equilibrium concentrations.

Les cinétiques de la décarboxylation de l'acide oxo-3 glutarique, catalysé par le cuivre(II), ont été étudiées dans des solutions non tamponées à 25 °C et à une force ionique de 0.60 *M*; ceci à la fois en présence d'amines aromatiques tertiaires et avec des ions hydratés du cuivre uniquement. Les amines utilisées sont la bipyridyle-2,2′ et la phénanthroline-1,10. Les constantes d'équilibre pour la formation des divers complexes du cuivre ont été déterminées au moyen d'une électrode sélectives en cuivre, spécialement dans le cas d'espèces CuAB, où A est l'ion oxo-3 glutarate et B une amine aromatique. Le comportement cinétique a alors été interprété en fonction d'une décarboxylation simultanée de toutes les espèces présentes contenant le ligand oxo-3 glutarate. Les constantes de vitesse qui en résultent, indiquent qu'un certain effet cinétique est transmis de la base vers l'oxo-3 glutarate par l'intermédiaire du cuivre; cet effet demeure cependant petit et l'importance de l'effet catalytique provoqué par la base provient de modifications dans les concentrations à l'équilibre.

Canadian Journal of Chemistry, **50**, 1461 (1972)

Can. J. Chem. Downloaded from www.nrcresearchpress.com by 210.87.254.105 on 09/05/12
For personal use only.

Introduction

The decarboxylation of β-keto dicarboxylic acids is catalyzed by transition metal ions (1), and the reaction has been shown to occur through the spontaneous decomposition of the 1:1 complex of formula MA^-, where M^{2+} is a divalent metal ion, and A^{2-} is the dianion of the keto acid. The catalytic effect of the metal ion may be appreciably enhanced when the 1:1 complexes of the metal ion are added instead of simply the hydrated metal ion (2–7). Presumably the decarboxylation now proceeds through a new reactive species, and it is shown in the present work that reasonably consistent rate constants are obtained, if it is assumed that this species is the 1:1:1 tertiary complex MAB, where B is the amine. Since aliphatic amines and phosphines are relatively ineffective in promoting decomposition, it is presumed that the delocalized π-systems of the aromatic amine are involved. The overall catalytic rate constant, k_{cat}, is defined by

$$d[CO_2]/dt = k_{H_2A}[H_2A] + k_{HA^-}[HA^-] + k_{A^{2-}}[A^{2-}] + k_{cat}T_M[A^{2-}]$$

where T_M is the total metal ion concentration, and k_{H_2A}, k_{HA} and $k_{A^{2-}}$ are the first-order rate constants of the unionized acid, the monoanion, and the dianion, respectively. If the mechanism of the metal ion catalysis is made up of two parts.

$$M^{2+} + A^{2-} \overset{K_{MA}}{\rightleftharpoons} MA \xrightarrow{k_{MA}} CO_2 + \text{product}$$

and

$$MB^2 + A^{2-} \overset{K_{MAB}}{\rightleftharpoons} MAB \xrightarrow{k_{MAB}} CO_2 + \text{product}$$

then k_{cat} is evidently a function of both the equilibrium constants K_{MA} and K_{MAB}, and the rate constants k_{MA} and k_{MAB}. Thus the enhanced catalytic effect caused by the amine may result from either changes in equilibrium constants, or in rate constants, or in both. These two effects can be separated by means of kinetic measurements alone (5), provided enough data are available, but in the present work it was felt that more accuracy would be achieved by measuring the equilibrium constants separately, and using them to interpret the kinetic data. The equilibrium measurements were made by means of a copper(II) ion sensitive electrode. This paper reports equilibrium and kinetic measure-

ments on the decomposition of 3-oxo-glutaric acid in the presence of 2,2′-bipyridyl and 1,10-phenanthroline.

Experimental

Chemicals

3-Oxo-glutaric acid, prepared essentially as described by Ingold and Nickolls (8), was recrystallized from ethyl acetate and stored over silica gel in an evacuated desiccator. The melting point was 134–135 °C, and the apparent molecular weight, determined by titration against sodium hydroxide was 146.3 (calculated for $C_5H_6O_5$ is 146.1). The purity of the acid was also determined from the amount of carbon dioxide released on complete decarboxylation, and this agreed to within 0.2% with the calculated amount.

All other chemicals were of reagent grade. 2,2′-bipyridyl and 1,10-phenanthroline were obtained from the Fisher Scientific Company, and were recrystallized from water. The melting points were then 70.3 and 101.5 °C, respectively. Copper(II) nitrate and sodium nitrate (used to control ionic strength) were "Baker Analysed" reagents, and were recrystallized from water. The stock solutions of copper(II) nitrate were analyzed by EDTA titration.

Potentiometric Measurements

Equilibria were investigated by potentiometric measurements on a Beckman research p*H* meter. All measurements were on solutions at 25.00 ± 0.01 °C, and at a constant ionic strength of 0.60 *M*, adjusted by sodium nitrate. Equilibrium constants for copper complex formation were determined by means of a copper(II) ion selective electrode (model 94-29, Orion Research Inc.). The electrode was calibrated by means of copper(II) nitrate solutions varying from 1.00×10^{-4} to 2.00×10^{-2} *M*, containing also 0.60 *M* sodium nitrate. A plot of electrode potential against log $[Cu^{2+}]$ gave a very good straight line, with a slope of 29.60 mV. This calibration allowed the measured voltages to be interpreted as copper(II) concentrations, and from these concentration equilibrium constants were calculated.

The hydrogen ion concentrations were obtained by means of a glass electrode, with a calomel reference electrode, using the Beckman research p*H* meter. The meter was standardized with 0.05 *M* potassium hydrogen phthalate at 25.0 °C. It was then calibrated in terms of hydrogen ion concentration by measurements on dilute nitric acid in 0.6 *M* sodium nitrate. It was found that the p*H* reading and $-\log [H^+]$ differed by a constant factor. Consequently, meter readings could be converted to hydrogen ion concentrations.

Kinetic Measurements

These were carried out manometrically in a constant volume apparatus. The manometer was regularly calibrated by the carbon dioxide liberated from known amounts of sodium bicarbonate plus acid. In each kinetic run a weighed amount of 3-oxo-glutaric acid, usually 17 to 18 mg, was suspended above 10 ml of a solution containing the other reagents. The 3-oxo-glutaric acid was in a container which could be released by a magnetically operated plunger. The solution was frozen, and the apparatus was evacuated and sealed. The solution and manometer were then completely immersed in a thermostat at 25 °C. The 3-oxo-glutaric acid was introduced by withdrawing the plunger, and the reaction was followed by measurements of pressure.

Results

Stability Constants of Copper(II) 3-Oxo-glutarate Complex

Known volumes of stock solutions of 3-oxo-glutaric acid, sodium hydroxide, sodium nitrate, and copper(II) nitrate (this was added last) were pipetted into a double-walled beaker maintained at 25.0 °C. The copper ion selective electrode and the reference electrode were placed in the solution, and the voltage readings were noted at 1 min intervals for 10 min. In general the potential was unchanged over this period, but small drifts (less than 0.05 mV per min) occurred in some cases. The potential used in calculation was then the value extrapolated to the time of mixing. Glass electrode measurements were more difficult as the p*H* drifted at the rate of about 0.01 p*H* units per min, owing to the decarboxylation reaction. The p*H* values used were those extrapolated to the time of mixing. The p*H* was always well below 4, to avoid enolization of the CuA complex which had been shown to occur at higher p*H* (9). It will be seen below that there is no drift in the calculated equilibrium constants with p*H*, so presumably the assumption, made in the calculations, that negligible enolization occurs, is justified. The results are given in Table 1. The equilibrium constant, K_{CuA}, defined as $[CuA]/[Cu^{2+}][A^{2-}]$, was calculated on the assumption that only H_2A, HA^-, A^{2-}, Cu^{2+}, CuA, H^+, and NO_3^- were present (apart from sodium nitrate). The ionization constants of 3-oxo-glutaric acid were taken to be 9.70×10^{-4} and 1.52×10^{-4} (9).

In Table 1, T_s is the total concentration of 3-oxo-glutaric acid, T_M is the total copper, and [NaOH] is the net concentration of added sodium hydroxide, after allowing for its reaction with nitric acid contained in the stock copper nitrate solution; it would, of course, also react with the 3-oxo-glutaric acid. The mean value of K_{CuA} is 150 M^{-1}, with a root-mean-square deviation of 4. This may be compared with the value of 114 M^{-1} (root-mean-square deviation of 40) obtained earlier from concentration cell measurements (9).

Can. J. Chem. Downloaded from www.nrcresearchpress.com by 210.87.254.105 on 09/05/12
For personal use only.

Can. J. Chem. Downloaded from www.nrcresearchpress.com by 210.87.254.105 on 09/05/12
For personal use only.

TABLE 1. Stability constant of copper(II) 3-oxo-glutarate complex at 25.0 °C, ionic strength 0.60

Run	10^3[NaOH] (M)	10^3T_s (M)	10^3T_M (M)	10^3[Cu^{2+}] (M)	10^4[H^+] (M)	K_{CuA} (M^{-1})
1	27.33	18.26	8.00	4.03	1.61	155
2	24.43	19.66	8.00	4.74	2.99	150
3	17.10	12.45	6.00	3.87	2.08	142
4	17.12	11.44	4.00	2.32	1.39	152
5	18.64	15.62	6.00	3.84	3.15	156
6	24.46	20.40	4.00	2.19	2.82	150
7	11.16	10.72	3.37	2.56	3.83	145
8	17.21	17.36	3.34	2.24	4.30	153
9	17.19	17.93	4.56	3.19	4.79	148

TABLE 2. Stability constant of the ternary copper(II), 2,2′-bipyridyl, 3-oxo-glutarate complex at 25 °C

Run	10^3[NaOH] (M)	10^3T_s (M)	10^3T_M (M)	10^3T_B (M)	10^5[Cu^{2+}] (M)	10^4[H^+] (M)	K_{CuAB} (M^{-1})
1	31.70	22.69	9.60	9.63	9.90	2.50	366
2	31.24	23.20	6.00	6.06	4.69	2.30	328
3	29.79	23.79	7.20	7.27	6.50	3.13	378
4	30.12	23.15	4.80	4.84	3.90	2.41	314
5	17.56	11.17	4.00	4.01	5.83	1.23	351
6	27.84	18.57	8.00	8.04	7.31	1.85	399
7	27.86	20.12	6.00	6.06	4.47	2.20	411

TABLE 3. Stability constant of the ternary copper(II), 1,10-phenanthroline, 3-oxo-glutarate complex at 25 °C

Run	10^3[NaOH] (M)	10^3T_s (M)	10^3T_M (M)	10^3T_B (M)	10^5[Cu^{2+}] (M)	10^4[H^+] (M)	K_{CuAB} (M^{-1})
1	30.44	21.78	6.00	6.00	8.81	1.98	254
2	31.41	22.48	7.20	7.20	9.82	2.16	327
3	36.72	26.23	8.40	8.40	10.70	2.17	299
4	37.21	26.62	4.80	4.80	5.92	1.80	220
5	32.05	26.67	6.00	6.00	9.60	3.11	259
6	33.34	27.76	7.20	7.20	10.86	3.34	314
7	36.72	25.16	6.40	6.40	8.27	1.63	203

Stability Constants of Copper(II) Ternary Complexes

The equilibrium constants, K_{CuAB}, defined by $K_{CuAB} = [CuAB]/[CuB^{2+}][A^{2-}]$, where B is 2,2′-bipyridyl or 1,10-phenanthroline, were also determined by the copper ion selective electrode. The techniques were the same as before, except that the stock copper nitrate solution had had an equimolar amount of one of the amines added to it. The results are given in Tables 2 and 3. As before, the pH was adjusted by sodium hydroxide, and the concentrations given are those in excess of the nitric acid contained in the stock copper solution. In calculations of K_{CuAB}, the solutions were considered to contain the following species: H_2A, HA^-, A^{2-}, Cu^{2+}, CuA, CuB^{2+}, CuB_2^{2+}, CuAB, H^+, Na^+ and NO_3^-. Sodium nitrate was used to adjust the ionic strength to 0.60, as before. Since only one new constant, K_{CuAB}, is being determined, a value can be found from each mixture, by means of the usual mass balance and equilibrium equations; these values are given in Tables 2 and 3. The calculations also require values for the acid ionization constants of the BH^+ species, and stability constants for

TABLE 4. Rate of copper(II) catalyzed decarboxylation of 3-oxo-glutaric acid

Run	10^3[NaOH] (M)	10^3T_s (M)	10^3T_M (M)	10^4[H$^+$] (M)	10^4k_{obs} (s^{-1})	10^3k_{CuA} (s^{-1})
1	14.15	12.53	10.80	3.69	4.50	1.95
2	16.33	12.49	10.80	2.53	5.78	2.10
3	18.18	12.66	6.00	2.44	2.70	2.00
4	17.74	12.59	10.80	1.98	5.80	1.92
5	17.90	12.53	9.00	1.79	5.23	1.92
6	18.07	12.59	7.20	1.68	4.57	1.95
7	18.27	12.46	5.00	1.44	3.70	1.95
8	18.37	12.53	4.00	1.40	2.78	1.83
9	18.46	12.46	3.00	1.29	2.38	1.97
10	19.79	12.59	10.80	1.22	6.62	1.90

the formation of CuB^{2+} and CuB_2^{2+}. The values used were for 2,2′-bipyridyl: $K_{BH^+} = 3.30 \times 10^{-5}$ (10), $K_{CuB} = 1.26 \times 10^8$, and $\beta_{CuB_2} = 2.98 \times 10^{13}$ (11); and for 1,10-phenanthroline, $K_{BH^+} = 1.10 \times 10^{-5}$ (12), $K_{CuB} = 1.12 \times 10^9$, and $\beta_{CuB_2} = 5.62 \times 10^{15}$ (11).

The average values of K_{CuAB}, with their root-mean-square deviations, are: B = 2,2′-bipyridyl, $K_{CuAB} = 364$ (r.m.s. = 33); B = 1,10-phenanthroline, $K_{CuAB} = 268$ (r.m.s. = 44).

Kinetic Measurements

Mixtures containing copper(II) nitrate, 3-oxo-glutaric acid, and aromatic amine were made up, adjusted to a pH between 3 and 4, and their rates of carbon dioxide evolution were measured, as described above. The rate was always found to be first order in total 3-oxo-glutaric acid, and the apparent rate constant, k_{obs}, defined by

$$d[CO_2]/dt = k_{obs}T_s$$

was calculated for each run. It is known that H_2A, HA^-, A^{2-} and CuA all decarboxylate, and hence contribute to k_{obs}; and in the calculations below we have assumed that the CuAB species also contribute. The product of the reaction, 3-oxo-butanoic acid itself decarboxylates, but experiments have shown (9, 13) that its rate of decarboxylation is much slower, and is not catalyzed by copper (14). Consequently this possible second stage was ignored. With these assumptions, k_{obs} is related to the various rate constants by the equation

$$k_{obs}.T_s = k_{H_2A}[H_2A] + k_{HA^-}[HA^-] + k_{A^{2-}}[A^{2-}] + k_{CuA}[CuA]$$

where k_{H_2A}, etc. are the first-order rate constants for the decomposition of the corresponding species. When an aromatic base was present, an additional term k_{CuAB}[CuAB] was included in the equation. The values of k_{H_2A}, k_{HA^-}, $K_{A^{2-}}$ were known from earlier work (9), and at 25 °C and an ionic strength of 0.60 were taken to be: $k_{H_2A} = 2.08 \times 10^{-5}$, $k_{HA^-} = 4.83 \times 10^{-5}$, and $k_{A^{2-}} = 0.17 \times 10^{-5}$ s^{-1}. Table 4 gives the results of some further measurements on the rate of the copper-catalyzed reaction, as before at 25 °C and an ionic strength of 0.60. The mean value of k_{CuA} is 1.95×10^{-3} s^{-1} with a root-mean-square deviation of 0.07×10^{-3}. This is lower than the value reported earlier (9), but much of the difference arises from the revised value of the equilibrium constant K_{CuA}. It can be seen from Table 4 that k_{CuA} did not change with pH over the range investigated.

Results with amines also present are given in Tables 5 and 6. The reactions were followed to 65 to 70% completion, and gave good first-order plots over this range. The equilibrium concentrations of all species were calculated, and hence k_{CuAB}. It might have been expected that, owing to the various competing reactions and equilibria, a first-order plot would not be closely followed, but in fact it was. This can be explained, at least in part, by supposing that the 3-oxo-butanoic acid also formed complexes with the copper ions and with CuB^{2+} ions to much the same extent as 3-oxo-glutaric acid, and that the bulk of the reaction arose from the catalyzed part. As before, experiments were at 25 °C and an ionic strength of 0.60. Although there is some scatter of the values of k_{CuAB}, they seem to be constant enough to support the view that a species of formula CuAB is responsible for changes in the rate on adding the aromatic

Can. J. Chem. Downloaded from www.nrcresearchpress.com by 210.87.254.105 on 09/05/12
For personal use only.

TABLE 5. Effect of 2,2′-bipyridyl on copper catalyzed decarboxylation of 3-oxo-glutaric acid

Run	10^3[NaOH] (M)	10^3T_S (M)	10^3T_M (M)	10^3T_B (M)	10^4[H^+] (M)	10^4k_{obs} (s^{-1})	10^3k_{CuAB} (s^{-1})
1	15.83	12.39	6.36	6.10	3.15	6.18	2.53
2	16.45	12.44	5.47	5.32	2.68	5.92	2.58
3	18.69	12.59	9.60	9.63	2.34	9.98	2.68
4	19.40	12.46	11.20	11.23	2.11	11.02	2.57
5	19.18	12.46	8.00	8.02	1.81	9.23	2.67
6	19.68	12.59	6.40	6.42	1.50	8.18	2.72
7	20.48	12.46	7.68	7.70	1.26	9.58	2.65
8	19.57	12.46	3.61	3.62	1.18	5.25	2.73
9	20.17	12.59	4.80	4.81	1.17	6.43	2.62
10	19.88	12.70	1.99	2.02	1.05	3.13	2.77

TABLE 6. Effect of 1,10′-phenanthroline on copper catalyzed decarboxylation of 3-oxo-glutaric acid

Run	10^3[NaOH] (M)	10^3T_S (M)	10^3T_M (M)	10^3T_B (M)	10^4[H^+] (M)	10^4k_{obs} (s^{-1})	10^3k_{CuAB} (s^{-1})
1	15.14	12.46	6.02	6.00	3.30	3.32	1.62
2	15.63	12.39	5.47	5.48	2.89	3.58	1.82
3	18.16	12.53	11.52	11.52	2.56	6.30	1.72
4	18.76	12.59	12.97	12.97	2.46	6.73	1.67
5	18.94	12.49	9.60	9.60	1.95	5.98	1.72
6	19.72	12.59	7.68	7.68	1.51	5.23	1.66
7	20.71	12.56	10.80	10.81	1.38	6.98	1.68
8	19.19	12.53	3.18	3.18	1.25	2.77	1.77
9	19.86	12.53	3.61	3.59	1.09	2.92	1.62
10	20.50	12.46	5.76	5.76	1.02	4.67	1.73

amine. It can be seen that there is no drift with pH over the range used. The average values of k_{CuAB} and root-mean-square deviations are: B = 2,2′-bipyridyl, $k_{CuAB} = 2.65 \times 10^{-3}$ s^{-1} (r.m.s. = 0.07); B = 1,10-phenanthroline, $k_{CuAB} = 1.70 \times 10^{-3}$ s^{-1} (r.m.s. = 0.06).

Discussion

The results of the present work, and some other relevant data, are summarized in Table 7, where the logarithms of various equilibrium or rate constants are given. The equilibrium constants are all for reactions of the type $X + Y \rightleftharpoons XY$, and the columns are accordingly headed X or Y, and $K = [XY]/[X][Y]$. Where CuB^{2+} is mentioned, B is the same base as appears in the first column.

Some comments may first be made on the equilibrium constants. As is commonly found, the stronger amine base also binds more strongly to Cu^{2+}, but A^{2-}, though of comparable strength as a base, attaches much less strongly to Cu^{2+}. The constants for the attachment of A^{2-} to CuB^{2+} are not very different from that for A^{2-} to Cu^{2+} (hydrated). The stronger amine base gives the weaker combination of A^{2-} to CuB^{2+}, possibly because the stronger base has transferred somewhat more negative charge to the copper ion, and so has weakened its attraction to the negatively charged A^{2-}. If the reaction $A^{2-} + Cu^{2+} \rightarrow CuA$ is considered as one of this series, with water molecules acting as the base already bound to copper, then the equilibrium constant and the basicity of water do not fit this trend: A^{2-} attaches much less strongly to Cu^{2+}aq than might be expected from the basicity of water. This difference is presumably due to the possibility of back-bonding from the copper to the empty orbitals in the π electron systems of the aromatic amines, which would make the copper atom to be relatively more positively charged. However, the effect, at least as estimated from the equilibrium constants, is apparently not very large.

It was noted above that a second molecule

Can. J. Chem. Downloaded from www.nrcresearchpress.com by 210.87.254.105 on 09/05/12
For personal use only.

TABLE 7.
(*a*) Logarithms of equilibrium constants*

X	Y	log *K*	X	Y	log *K*
Bipy	H^+	4.48	Bipy	CuB^{2+}	5.50
Phen	H^+	4.96	Phen	CuB^{2+}	6.70
A^{2-}	H^+	3.82			
Bipy	Cu^{2+}	8.10	Bipy	CuA	8.49
Phen	Cu^{2+}	9.05	Phen	CuA	9.30
A^{2-}	Cu^{2+}	2.18			
CuB^{2+}	A^{2-}	2.56			
CuB^{2+}	A^{2-}	2.43			
Cu^{2+}	A^{2-}	2.18			

*Bipy = 2,2′-bipyridyl; phen = 1,10-phenanthroline.

(*b*) Rate constants

Species	log *k*
A^{2-}	−5.77
CuA	−2.71
CuA bipy	−2.58
CuA phen	−2.77

of base, in CuB_2^{2+}, is attached appreciably less strongly than the first. This must also be true of the 3-oxo-glutarate ion, since the values of K_{CuA}, obtained above on the assumption that no CuA_2^{2-} was present, were fairly constant. The presence of considerable quantities of CuA_2^{2-} would lead to variations in the values of K_{CuA} obtained from different runs. It was in fact found that if the values of K_{CuA} are plotted against $[A^{2-}]$, and a line is drawn through the points by least-mean-squares, this line has a positive slope corresponding to β_{CuA_2} (defined as $[CuA_2^{2-}]/[Cu^{2+}][A^{2-}]^2$) equal to 1300 M^{-2}. The scatter of points is so large that this value is not very reliable, but it is true to say that the constant could not be much larger without the presence of CuA_2^{2-} being obvious from the measurements. If this value of β_{CuA_2} is correct, only about 0.5 to 2.5% of the total copper would be present as CuA_2^{2-} in our runs measuring K_{CuA}, while 25 to 50% is present as CuA, and somewhat lower percentages would hold for the kinetic runs. The matter is raised here because it is evident that CuAB is relatively stable compared with CuA_2^{2-} and CuB_2^{2+}. The equilibrium constant of

$$CuA_2^{2-} + CuB_2^{2+} \rightleftharpoons 2\,CuAB$$

is equal to $K_{CuAB}^2 K_{CuB}^2/\beta_{CuA_2}\beta_{CuB_2}$; and if β_{CuA_2} is taken as 1300 M^{-2}, then this reaction has an equilibrium constant of 40 000 if B = 2,2′-bipyridyl, and 12 000 if B = 1,10-phenanthroline. The CuAB species is more strongly favored for the weaker base. If A and B were attached at random to the copper, the equilibrium constant would be 4, and even allowing for the uncertainty in β_{CuA_2} there can be no doubt that the actual equilibrium constant is considerably larger. Other examples of this selective effect are, of course, known, for instance in the stability of the rather similar catecholiato-2,2′-bipyridyl copper(II) complex (15).

The rate constants collected in Table 7 also show effects from the ligand B, but not to a great extent; and indeed one of the main conclusions to be drawn from this work is that, at least for the present system, large changes in reactivity are not induced in the 3-oxo-glutaric acid by effects transmitted through the copper. It is, of course, true that we are comparing the effect of CuB^{2+} with a hydrated copper, possibly $Cu(H_2O)_2^{2+}$ attached to A^{2-}, but both 2,2-bipyridyl and 1,10-phenanthroline induce considerably larger ligand field splitting than does water; see, for instance, ref. 16. The ligand field splitting is almost the same for these two bases, while their effect on the rate of reaction is in a different direction. The gross catalytic

Can. J. Chem. Downloaded from www.nrcresearchpress.com by 210.87.254.105 on 09/05/12
For personal use only.

effect, that is the actual acceleration of the reaction, is proportional to K_{CuAB}, k_{CuAB}, and this product is 0.96 for 2,2′-bipyridyl, 0.48 for 1,10-phenanthroline, as compared with 0.34 for hydrated copper ions. These numbers show that the accelerating effect of the base largely arises from changes in the equilibrium concentrations in the solution. At present it does not seem possible to suggest detailed reasons for the small changes observed in the rate constants.

We wish to thank the National Research Council of Canada for financial assistance, and one of us (K.N.L.) is also grateful to the Ontario Department of University Affairs for the award of an Ontario Graduate fellowship.

1. R. W. HAY. Rev. Pure Appl. Chem. **13**, 157 (1963).
2. J. V. RUND and R. A. PLANE. J. Am. Chem. Soc. **86**, 367 (1964).
3. R. W. HAY and K. N. LEONG. Chem. Commun. 800 (1967); J. Chem. Soc. (A), 3639 (1971).
4. P. R. BONTCHEV and V. MICHAYLOVA. J. Inorg. Nucl. Chem. **29**, 2945 (1967).
5. J. V. RUND and K. G. CLAUS. J. Am. Chem. Soc. **89**, 2256 (1967).
6. J. V. RUND and K. G. CLAUS. Inorg. Chem. **7**, 860 (1968); **8**, 59 (1969).
7. J. V. RUND and K. G. CLAUS. J. Catal. **15**, 304 (1969).
8. C. K. INGOLD and L. C. NICKOLLS. J. Chem. Soc. **121**, 1642 (1922).
9. D. W. LARSON and M. W. LISTER. Can. J. Chem. **46**, 823 (1968).
10. W. A. E. MCBRYDE. Can. J. Chem. **45**, 2093 (1967).
11. H. IRVING and D. H. MELLOR. J. Chem. Soc. 5222 (1962).
12. H. IRVING and D. H. MELLOR. J. Chem. Soc. 3457 (1955).
13. R. W. HAY and M. A. BOND. Aust. J. Chem. **20**, 1823 (1967).
14. A. KORNBERG, S. OCHOA, and A. H. MEHLER. J. Biol. Chem. **174**, 159 (1948).
15. R. GRIESSER and H. SIGEL. Inorg. Chem. **9**, 1238 (1970).
16. B. N. FIGGIS. Introduction to ligand fields. Interscience Publishers, New York. 1966. p. 244.

Can. J. Chem. Downloaded from www.nrcresearchpress.com by 210.87.254.105 on 09/05/12
For personal use only.

Magnetic Susceptibilities of $^2T_2$ Ions. Part 1

ALAN D. WESTLAND

Department of Chemistry, University of Ottawa, Ottawa, Canada, K1N 6N5

Received November 4, 1971

An expression for the magnetic susceptibility of octahedral d^1 complexes is derived exactly in terms of an orbital reduction factor k taking into account the presence of the formal ^2E excited state. Sample calculations show that the improved expression gives results for susceptibility which are lower at times by several percent from those given by previous expressions. The results given by Figgis using Kotani's method are adequately precise when the spin–orbit coupling constant is no larger than $\sim 0.1\ Dq$.

Une expression pour la susceptibilité magnétique des complexes octaédraux d^1 est dérivée exactement en termes de facteur k de réduction d'orbitale qui tient compte de la présence de l'état excité défini ^2E. Des exemples de calculs montrent que l'expression améliorée donnent des résultats pour la susceptibilité qui sont plus bas dans certains cas de plusieurs pourcents par rapport à ceux donnés par les expressions précédentes. Les résultats donnés par Figgis utilisant la méthode de Kotani sont d'une précision convenable lorsque la constante de couplage spin–orbite n'est pas plus grande que $\sim 0.1\ Dq$.

Canadian Journal of Chemistry, **50**, 1468 (1972)

Introduction

The magnetic behavior of T-state ions shows large departures from spin-only character. The effective magnetic moment of octahedral d^1 and d^4 ions shows particularly strong temperature dependence with decreasing temperature, approaching zero at $T = 0$ in some instances, *e.g.* in ReF_6 (1). Kotani (2) and Liehr (3) have provided the theoretical background for an understanding of such behavior. However, the expressions given by these authors for the magnetic susceptibility of d^1 ions contain assumptions which have a considerable effect upon the results of calculations. Gerloch (4) has treated fully the similar case of d^9 ions in a tetrahedral field and included axial distortion in his calculations. His basis set of wavefunctions were not diagonalized with respect to spin–orbit coupling and this fact combined with the complications due to distortion made it impossible to write down an explicit expression for the susceptibility. We report here an exact expression for the susceptibility of $^2T_2$ ions and show thereby the extent to which the Kotani and Liehr expressions are in error. As Gerloch has treated d^9 ions already (4), we shall concentrate here on the d^1 case.

The $^2T_{2g}$ state gives under the influence of spin–orbit coupling a ground state quartet, $\Gamma_8(T_{2g})$ and a doublet, $\Gamma_7(T_{2g})$. There is a further quartet, $\Gamma_8(E_g)$, lying at still higher energy. The eigenfunctions corresponding to these states can be called $\Psi_8(t_{2g})^{a,b,c,d}$, $\Psi_7(t_{2g})^{a,b}$, and $\Psi_8(e_g)^{a,b,c,d}$, where the superscripts designate individual spinors. Using zero-order functions the matrix elements for the magnetic operator

$$\langle \Psi_8(t_{2g}) | l_z + 2s_z | \Psi_8(t_{2g}) \rangle$$

are zero so there is no paramagnetic contribution from the ground state through the first-order Zeeman terms. There is a second-order Zeeman contribution because the non-diagonal matrix elements

$$\langle \Psi_8(t_{2g}) | l_z + 2s_z | \Psi_7(t_{2g}) \rangle$$

are non-zero. To this temperature independent contribution to the susceptibility, Kotani added the first-order terms arising from thermal excitation to the $\Gamma_7(T_{2g})$ state. This is relevant when the energy difference between the $\Gamma_7(T_{2g})$ and $\Gamma_8(T_{2g})$ states is not large with respect to kT. This energy difference is $3\zeta/2$ where ζ is the spin–orbit coupling constant (3).

Liehr argued that when $\zeta \gg kT$, *i.e.* for heavy elements, the excitation to the $\Gamma_7(T_{2g})$ state is unimportant, but mixing of the $\Psi_8(e_g)$ wavefunctions into the $\Gamma_8(T_{2g})$ functions becomes quite important. Such intermixing makes the ground state diagonal matrix elements non-zero and a temperature dependent contribution to the susceptibility is produced. The susceptibility of heavy d^1 ions always shows some temperature dependence.

While Kotani neglected the intermixing of

Can. J. Chem. Downloaded from www.nrcresearchpress.com by 210.87.254.40 on 09/05/12
For personal use only.

Can. J. Chem. Downloaded from www.nrcresearchpress.com by 210.87.254.40 on 09/05/12
For personal use only.

wavefunctions, Liehr allowed the wavefunctions to mix and applied the resulting corrections to the diagonal matrix elements. The resulting expressions of Kotani and Liehr are useful in calculations dealing with first row and third row elements, respectively. It seemed doubtful that either expression would give accurately the magnetic susceptibility of certain second row ions such as $NbCl_6^{2-}$. We have now corrected the off-diagonal matrix elements to take account of orbital mixing and this has resulted in a decrease in calculated susceptibilities which amounted to several percent in some cases.

Theory

Wavefunctions

First order corrected strong field wavefunctions took the form

$$\Psi_8^s(t_{2g}) = \sin\eta\Gamma_8^s(t_{2g}) - \cos\eta\Gamma_8^s(e_g)$$

where

$$s = a, b, c, d$$

and

$$\tan 2\eta = -\frac{\sqrt{6}\zeta}{\zeta/2 + 10Dg}$$

and $\Gamma_8^s(t_{2g})$ as well as $\Gamma_7^s(t_{2g})$ and $\Gamma_8^s(e_g)$ are zero-order d orbitals transforming correctly under the double group O' (5). Hereinafter we use

$$\Psi_7^s(t_{2g}) = \Gamma_7^s(t_{2g})$$

Matrix Elements

The wavefunctions are diagonal under spin–orbit coupling. The energy matrix is thus

$$\begin{array}{cc} \Gamma_8(T_{2g}) & \Gamma_7(T_{2g}) \\ \left|\begin{array}{cc} -\frac{\zeta}{2} - \sqrt{\frac{3}{2}}\,\zeta\cot\eta & 0 \\ 0 & \zeta \end{array}\right| & \end{array}$$

The general matrix element under the magnetic operator is

$$\langle\Psi_n^s(t_{2g})|kl_z + 2s_z|\Psi_m^s(t_{2g})\rangle\beta H$$

Here k is the orbital reduction factor (6). It may be noted that Figgis revised Kotani's work by incorporating k into the magnetic operator (7). The use of a single k parameter to account for the reduction of all matrix elements is not entirely satisfactory (8), but little else can be done at this time. Liehr implicitly set k equal to unity. The energy matrix becomes

$$\begin{array}{cccccc} \Psi_8^a(t_{2g}) & \Psi_7^a(t_{2g}) & \Psi_8^b(t_{2g}) & \Psi_7^b(t_{2g}) & \Psi_8^c(t_{2g}) & \Psi_8^d(t_{2g}) \\ \left|\begin{array}{cccccc} a_{11} & a_{12} & & & & \\ & a_{22} & & & & \\ & & a_{33} & a_{34} & & \\ & & & a_{44} & & \\ & & & & a_{55} & \\ & & & & & a_{66} \end{array}\right| & & & & & \end{array}$$

where

$$a_{11} = \left[\frac{k-1}{3}\sin^2\eta + \frac{8k}{6}\sin\eta\cos\eta - \cos^2\eta\right]\beta H$$

$$a_{12} = \left\{\frac{\sqrt{2}}{3}\sin\eta\left[k + 1 + \sin\eta - \frac{2k}{3}\cos\eta\right]\right\}\beta H$$

$$a_{22} = \frac{2k+1}{3}\beta H$$

$$a_{33} = -a_{11}$$

$$a_{34} = a_{12}$$

$$a_{44} = -a_{22}$$

$$a_{55} = [(1-k)\sin^2\eta - \cos^2\eta]\beta H$$

$$a_{66} = -a_{55}$$

The magnetic susceptibility may be obtained from the standard formula (9) using the above listed independent matrix elements. We therefore have

$$[1]\quad \chi_M = N(2e^{\zeta/kT} + e^{-\zeta/kT})^{-1}\left\{\left[\frac{(a_{11}/H)^2 + (a_{55}/H)^2}{kT} + \frac{4}{3\zeta}(a_{12}/H)^2\right]e^{\zeta/2kT} + \left[\frac{(a_{22}/H)^2}{kT} - \frac{4}{3\zeta}(a_{12}/H)^2\right]e^{-\zeta/kT}\right\}$$

If ζ is large relative to kT, the quantity $e^{-\zeta/kT}$ becomes negligible and the susceptibility is given by

$$[2]\quad \chi_M = N\left[\frac{(a_{11}/H)^2 + (a_{55}/H)^2}{kT} + \frac{2}{3\zeta}(a_{12}/H)^2\right]$$

When $k = 1.0$ this differs from Liehr's expression only in the term a_{12} being more accurate but, as is shown below, this is an important difference. Following Liehr, we may make the

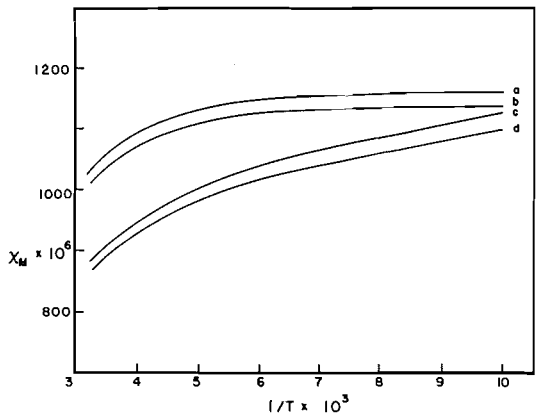

FIG. 1. Calculated mole susceptibility in e.s.u. for $\zeta = 300\ cm^{-1}$, $Dq = 2500\ cm^{-1}$. (*a*) Kotani equation, $k = 1.0$. (*b*) Equation 1, $k = 1.0$. (*c*) Kotani equation, $k = 0.7$. (*d*) equation 1, $k = 0.7$.

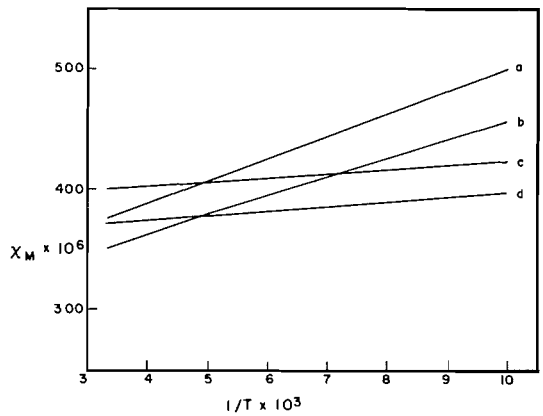

FIG. 2. Calculated mole susceptibility in e.s.u. for $\zeta = 900\ cm^{-1}$, $Dq = 2500\ cm^{-1}$. (*a*) Kotani equation, $k = 0.7$. (*b*) Equation 1, $k = 0.7$. (*c*) Liehr equation, $k = 1.0$. (*d*) Equation 1, $k = 1.0$.

expression easier to handle by writing it as

$$[3]\quad \chi_M = \frac{N\beta^2}{3kT}[1/4(1+\cos 2\eta)(19 - 13\cos 2\eta - 4\sqrt{6}\sin 2\eta)] + \frac{2N}{3\zeta}(a_{12}/H)^2$$

It is most probable that k will differ from unity in any specific instance so that expression 3 probably has little general applicability. Programs for these various expressions were written in Fortran and the results compared with those from previous methods of calculation.

Results and Discussion of Sample Calculations

Good agreement is expected between eq. 1 and the Kotani–Figgis calculations when the spin–orbit coupling is small relative to Dq. Figure 1 shows a comparison of results for a rather extreme case of $\zeta = 300\ cm^{-1}$ and $Dq = 2500\ cm^{-1}$. The agreement is good enough for dealing with typical experimental data in which errors of $\pm 1\%$ are to be expected. The difference between the calculations should get larger with increasing ζ. Figure 2 shows an example of this for $\zeta = 900\ cm^{-1}$ and $k = 0.7$. Here the difference is $\sim 9\%$ at 100 °K. For this choice of parameters (but with $k = 1.0$ of course) the Liehr expression also gives differing results. The magnetic susceptibility of MoX_6^- would therefore be given accurately only by the more detailed calculation.

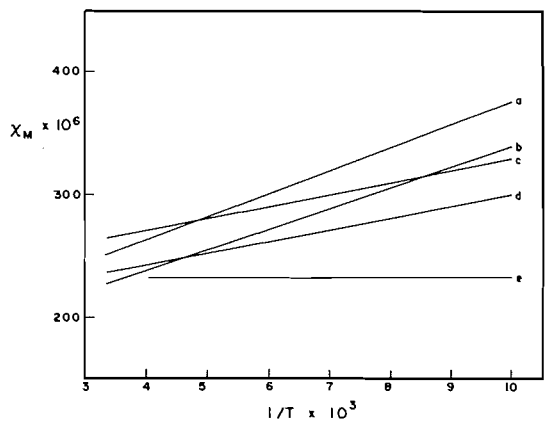

FIG. 3. Calculated mole susceptibility in e.s.u. for $\zeta = 1500\ cm^{-1}$, $Dq = 2500\ cm^{-1}$. (*a*) Kotani equation, $k = 0.7$. (*b*) Equation 1, $k = 0.7$. (*c*) Liehr equation, $k = 1.0$. (*d*) Equation 1, $k = 1.0$. (*e*) Kotani equation, $k = 1.0$.

We originally expected good results from the Liehr expression when ζ was several times kT in magnitude. For $\zeta = 1500\ cm^{-1}$ and $Dq = 2500\ cm^{-1}$, we see from Fig. 3 that considerable discrepancy persists. This originates in the temperature independent term owing to the fact that Liehr did not include mixing of the $\Gamma_8(T_{2g})$ and $\Gamma_8(E_g)$ states in the second-order Zeeman effect. The second-order term is more important in general than the temperature dependent part.

The Kotani–Figgis calculation is correct near the room temperature but there is virtually no temperature dependent contribution when $k = 1.0$. The error is consequently very large at low

Can. J. Chem. Downloaded from www.nrcresearchpress.com by 210.87.254.40 on 09/05/12
For personal use only.

temperatures. When k is small, the Kotani–Figgis procedure gives a fairly good estimate of the temperature dependent term but the temperature independent part is not correct.

It may be concluded that the detailed calculation is called for over almost the whole range of possible values of the spin–orbit coupling parameter. However, it is found that there is virtually exact agreement between the results of eq. 2 and those of eq. 1 for most choices of ζ and Dq. Equation 2, which can be used without the aid of a computer, is thus to be preferred in most cases. Calculations with eq. 2 are accurate to about 0.1% when $\zeta = 4kT$, to 0.5% when $\zeta = 3kT$, and are high by 3.6% when $\zeta = 2kT$.

Susceptibilities which are linear in $1/T$ are accurately given by eq. 2 but as promotion of electrons to the $\Gamma_7(T_{2g})$ state becomes appreciable with increasing temperature, the true susceptibility begins to fall short of that given by the linear relationship.

Some general statements can be made about axial distortions. If the octahedron is subjected to an elongation along a three-fold or four-fold axis, there is very little effect on the susceptibility at low temperatures. At high temperatures there will be a slight drop in susceptibility as indicated by Figgis' data (7). Compression along an axis has a large effect, especially at low temperatures where the susceptibility tends to be increased. The error involved in neglect of orbital mixing decreases with increasing distortion, so that for highly distorted complexes, Figgis' results are probably quite accurate. Large distortions are to be expected only with substituted octahedra, MX_3Y_3, etc.

1. W. MOFFITT, G. L. GOODMAN, M. FRED, and B. WEINSTOCK. Mol. Phys. **2**, 109 (1959).
2. M. KOTANI. J. Phys. Soc. Jap. **4**, 293 (1949).
3. A. D. LIEHR. J. Phys. Chem. **64**, 43 (1960).
4. M. GERLOCH. J. Chem. Soc. (A), 2023 (1968).
5. C. J. BALLHAUSEN. Introduction to ligand field theory. McGraw-Hill, New York. 1962. p. 117.
6. K. W. H. STEVENS. Proc. Roy. Soc. A**219**, 542 (1953).
7. B. N. FIGGIS. Trans. Faraday Soc. **57**, 198 (1961).
8. M. GERLOCH and J. R. MILLER. Prog. Inorg. Chem. **10**, 1 (1968).
9. J. H. VAN VLECK. The theory of electric and magnetic susceptibilities. Oxford. 1932. p. 235.

Can. J. Chem. Downloaded from www.nrcresearchpress.com by 210.87.254.40 on 09/05/12
For personal use only.

Etude spectroscopique des dérivés du peroxyde d'hydrogène. V. Les percarbonates $KHCO_4$ et $K_2C_2O_6$ [1]

PAUL A. GIGUÈRE ET DENIS LEMAIRE

Centre de Recherches sur les Atomes et les Molécules, Université Laval, Québec 10, Québec

Reçu le 15 décembre 1971

Les deux percarbonates $KHCO_4$ et $K_2C_2O_6$ ont été préparés à l'état pur en vue d'étudier leurs spectres infrarouges et Raman. Le permonocarbonate est assez instable et fortement hygroscopique. L'anion HCO_4^- forme des ponts d'hydrogène très forts, quoique un peu moins que ceux du bicarbonate HCO_3^-. Quant à l'anion $C_2O_6^{2-}$, il semble plan et centrosymétrique d'après le petit nombre de bandes en infrarouge et en Raman. Dans ces deux ions la vibration de valence O—O a une fréquence assez voisine de celle de H_2O_2, dû sans doute au couplage avec des vibrations voisines. Pour fin de comparaison on a étudié de la même façon le peroxyhydrate $K_2CO_3.3H_2O_2$.

The two percarbonates $KHCO_4$ and $K_2C_2O_6$ were prepared by chemical or electrolytic methods in order to measure their infrared and Raman spectra. The permonocarbonate is unstable and very hygroscopic. The HCO_4^- anion forms quite strong intermolecular hydrogen bonds, although somewhat less so than the bicarbonate anion. As for the $C_2O_6^{2-}$ anion, the rather small number of its infrared and Raman bands suggests a planar and centrosymmetric configuration. In both percarbonates the O—O vibration shows nearly the same frequency as in H_2O_2, presumably due to coupling with neighboring vibrations. For comparison purposes the peroxyhydrate $K_2CO_3.3H_2O_2$ was studied likewise.

Canadian Journal of Chemistry, **50**, 1472 (1972)

Introduction

Les percarbonates alcalins, qui entrent dans la composition de plusieurs détersifs domestiques, sont connus depuis très longtemps. En fait les premières descriptions de préparations par électrolyse remontent à la fin du siècle dernier (1, 2). Cependant, ils ont été l'objet de sérieuses controverses quant à leur nature et à leur composition. La difficulté venait d'abord de leur caractère instable et hygroscopique qui les rend difficiles à isoler à l'état pur. De plus, on les a longtemps confondus avec les peroxyhydrates des carbonates ou bicarbonates alcalins qui, eux aussi, dégagent de l'oxygène actif par hydrolyse. Le test dit de Riesenfeld-Liebhafsky (3), qui a servi pendant longtemps à distinguer entre les persels et les peroxyhydrates, n'a en fait de valeur absolue que lorsqu'il est positif (4, 5). Aujourd'hui, grâce aux méthodes physiques comme la spectroscopie, on peut distinguer entre les vrais percarbonates et les carbonates peroxyhydratés.

Les premiers, qui sont le résultat d'une réaction chimique, sont de deux sortes; soit les permonocarbonates, de formule $MHCO_4$, et les perdicarbonates, $M_2C_2O_6$. (Les composés de formule M_2CO_4 rapportés dans la littérature (4) ne semblent pas réels.) Par contre, les peroxyhydrates s'obtiennent pas simple cristallisation d'un carbonate à partir d'une solution aqueuse de peroxyde d'hydrogène. Ils sont difficiles à caractériser comme entités définies.

On ne possède aucune donnée sur la structure de ces composés. La seule étude par diffraction des rayons X de $K_2C_2O_6$ a été faite par la méthode des poudres pour fins analytiques (6). Elle n'a pas permis d'établir la symétrie ni les dimensions de la maille fondamentale. Le spectre infrarouge, étudié par les mêmes auteurs, a été interprété selon une formule entièrement covalente, ce qui ne saurait convenir. Les carbonates de sodium et de potassium peroxyhydratés ont déjà été étudiés par spectroscopie infrarouge et par analyse thermique différentielle (7).

Méthodes expérimentales

Nous avons suivi la méthode décrite par Firsova et ses collaborateurs (8) qui consiste à ajouter lentement du peroxyde d'hydrogène assez concentré à une solution refroidie à -20 °C, de KOH à 50% dans l'eau, de façon à atteindre un rapport KOH/H_2O_2 de 1. On y fait ensuite passer un courant de gaz carbonique pendant une heure environ. Le précité blanc ainsi obtenu est filtré à froid sur un entonnoir à disque de verre fritté, puis lavé avec de l'alcool absolu et de l'éther anhydre, préalablement re-

[1]Présenté au 18ième Symposium de Spectroscopie du Canada à Toronto, octobre 1971.

Can. J. Chem. Downloaded from www.nrcresearchpress.com by 210.87.254.5 on 09/05/12
For personal use only.

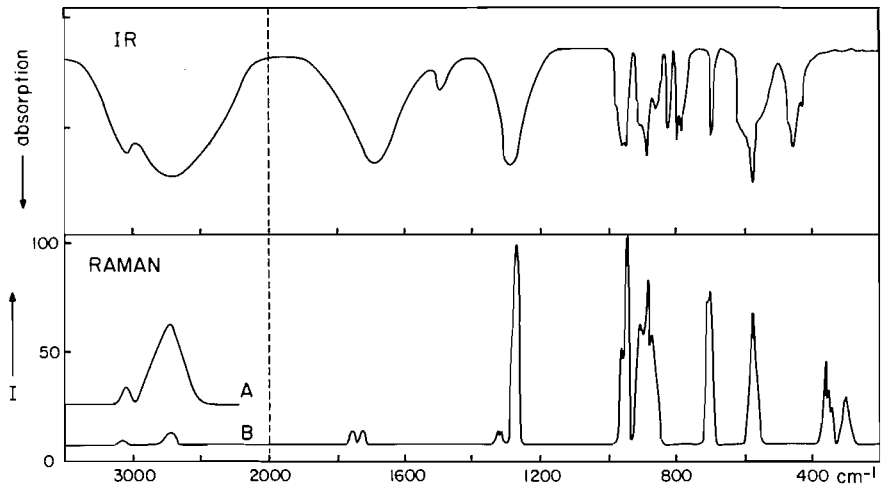

FIG. 1. Spectres de vibration de $KHCO_4$ à la température de l'azote liquide.

froidis, et finalement séché dans un courant d'air très sec. Parce que $KHCO_4$ perd lentement de son oxygène actif, même à température ambiante, nos spectres ont toujours été pris avec des échantillons frais. Pour plus de certitude nous avons analysé le produit utilisé, d'abord par acidimétrie, après décomposition du peroxyde avec MnO_2, puis par émission atomique pour doser le potassium. Les résultats concordaient avec la formule à 0.5% près.

Les échantillons de $K_2C_2O_6$ ont été préparés par électrolyse selon la technique décrite par Firsova (9). Le produit final était un solide pulvérulent, blanc, légèrement teinté de bleu tel que noté par les auteurs russes. Quoique beaucoup plus stable que $KHCO_4$, le perdicarbonate $K_2C_2O_6$ est hygroscopique et s'hydrolyse facilement en bicarbonate avec perte d'oxygène. Enfin le peroxyhydrate de formule hypothétique $K_2CO_3.3H_2O_2$ a été obtenu tel que décrit précédemment (4, 10).

Pour les spectres infrarouges les échantillons furent préparés par dispersion, sous l'atmosphère rigoureusement sèche, des poudres finement broyées dans du Nujol, du Fluorolube ou de l'hexachloro-1,3 butadiène, selon les régions à étudier. On étalait la suspension entre deux disques de NaCl ou de CsI, sauf dans le cas de $KHCO_4$ qui attaquait ces matériaux. Il a fallu alors employer des disques neufs de AgCl. Notons que la technique de la pastille de KBr, utilisée par les auteurs russes (6) avec $K_2C_2O_6$, donne des spectres de qualité inférieure. A en juger par la diminution d'intensité des bandes du percarbonate, ce dernier doit réagir lentement avec le bromure. Avec $KHCO_4$ la réaction était beaucoup plus rapide. Kyrki (11) a rapporté un phénomène semblable, quoique moins prononcé, avec le persulfate $KHSO_5$.

Pour l'infrarouge lointain la dispersion de $K_2C_2O_6$ dans le Nujol était pressée entre des disques de silicum. Enfin pour l'étude de l'effet Raman, la poudre tassée dans un capillaire de Pyrex était éclairée à incidence normale par le faisceau laser. Le percarbonate $K_2C_2O_6$ a pu être ainsi étudié à température ambiante, mais avec $KHCO_4$ et le peroxyhydrate il a fallu refroidir les échantillons avec de l'azote liquide pour empêcher la décomposition par le faisceau laser à argon ionisé (Coherent Radiation, modèle 52). Les spectromètres étaient les mêmes que précédemment (12).

Discussion des résultats

Le percarbonate $KHCO_4$

Les bandes infrarouges et Raman (Fig. 1) ont été attribuées (Tableau 1) dans l'hypothèse d'une configuration plane de l'anion HCO_4^-. Celle-ci en effet nous semble plus probable (du moins pour le squelette) étant donné que la résonance entre les trois structures canoniques doit conférer un certain caractère π à la liaison C—O_2H. De toute façon les spectres ne sauraient nous renseigner là-dessus puisque même selon la symétrie C_s toutes les vibrations doivent être actives tant en infrarouge qu'en Raman.

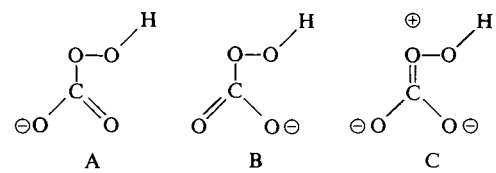

Ainsi les douze vibrations fondamentales se répartissent en neuf de classe a′ (dans le plan) et trois a″ (hors du plan). Pour fin de comparaison nous donnons également les fréquences en infrarouge de l'anion HCO_3^- (13). A noter que les bandes les plus fortes de ce dernier à 1960/1943 et 1017 cm^{-1} sont absentes de nos spectres des deux percarbonates. C'est là la meilleure preuve de la pureté chimique de

Can. J. Chem. Downloaded from www.nrcresearchpress.com by 210.87.254.5 on 09/05/12
For personal use only.

TABLEAU 1. Fréquences (en cm^{-1}) des principales bandes de $KHCO_4$

Raman	Infrarouge	Attributions	$NaHCO_3$ (13)
	3030	Combinaison	3060m
			2910m
2730	2700	Valence O—H $\nu_1(a')$	2560/2410F
			1960/1943F
—	1680	Valence C=O asym. $\nu_2(a')$	1698m
			1661/1618F
	1492	Déformation OOH $\nu_3(a')$	1458/1405FF
1273	1286	Valence C=O sym. $\nu_4(a')$	1300FF
961/942	955/945	" C—O $\nu_5(a')$	1052/1038m
	910	Torsion OH $\nu_{10}(a'')$	1017F
906			
884	882	Valence O—O $\nu_6(a')$	—
869			
	853/825	Déformation CO_2 $\nu_7(a')$	837F
	795/782		
701	692	" CO_3 $\nu_{11}(a')$	703/693FF
577	605/575	" OCO_2 $\nu_8(a')$	650m
	450	" COO $\nu_9(a')$	
	417		
360		Torsion C—O(?) $\nu_{12}(a')$	
300			

nos échantillons, puisque les percarbonates se décomposent ou s'hydrolysent en bicarbonates (4, 8).

La fréquence de ν_{O-H} est ici relativement basse, quoique moins basse que dans les bicarbonates (13–16). Ces derniers forment des liaisons hydrogène particulièrement fortes, avec des distances O—H...O de 2.61 Å. D'après les relations empiriques usuelles on peut évaluer ces distances à 2.64 Å dans HCO_4^-, et les distances O—H, à environ 1.04 Å; ce qui correspond à une énergie de l'ordre de 7 kcal mol^{-1}. On peut donc en conclure que ces liaisons hydrogène sont du type inter-, et non pas intramoléculaire. En effet, dans ce dernier cas elles seraient beaucoup plus faibles (distance H...O d'à peu près 1.9 Å) et non linéaires.

Les vibrations du squelette ont été attribuées sans tenir compte des effets de couplage possible. Les vibrations de valence C=O ont des fréquences légèrement inférieures, et celle de la liaison C—O, de beaucoup inférieure aux vibrations correspondantes dans l'anion HCO_3^-. On a une situation analogue dans H_2SO_5 par rapport à H_2SO_4 (11, 12). Quant à la vibration de valence O—O, on retrouve ici pratiquement la même fréquence que dans la molécule H_2O_2 (3), tout comme dans l'acide de Caro et ses sels. Notons en passant que cette vibration O—O se traduit par un triplet en Raman. (Le pic à 906 cm^{-1} semble trop aigu pour le mode de torsion OH.) C'est une indication que la maille cristalline contient plus de deux anions, avec vibrations en phase et hors de phase. La même explication vaut pour la multiplicité des composantes de la bande de déformation ν_7 en infrarouge.

Le percarbonate $K_2C_2O_6$

A priori deux configurations sont possibles pour l'anion $C_2O_6^{2-}$ selon que les deux groupes CO_3 reliés par le pont peroxyde sont dans le même plan ou non. La première semble plus probable; d'abord par analogie avec l'anion persulfate $S_2O_8^{2-}$ (17), et ensuite d'après les indications de nos spectres (Fig. 2). En effet, le nombre de bandes y est assez restreint. Il est vrai qu'elles coïncident parfois en infrarouge et en Raman, mais ceci est inévitable vu la multiplicité de certains modes. Selon une structure plane et centrosymétrique (C_{2h}) les dix-huit fondamentales de l'anion $C_2O_6^{2-}$ se subdivisent en quatre classes (Tableau 2).

Nos attributions ne tiennent pas compte des effets de couplage particulièrement importants dans la région de 700 à 900 cm^{-1}. C'est sans doute à ce phénomène qu'il faut attribuer la fréquence remarquablement élevée de la vibration de valence O—O. Intuitivement on s'attendrait à une fréquence sensiblement inférieure

Can. J. Chem. Downloaded from www.nrcresearchpress.com by 210.87.254.5 on 09/05/12
For personal use only.

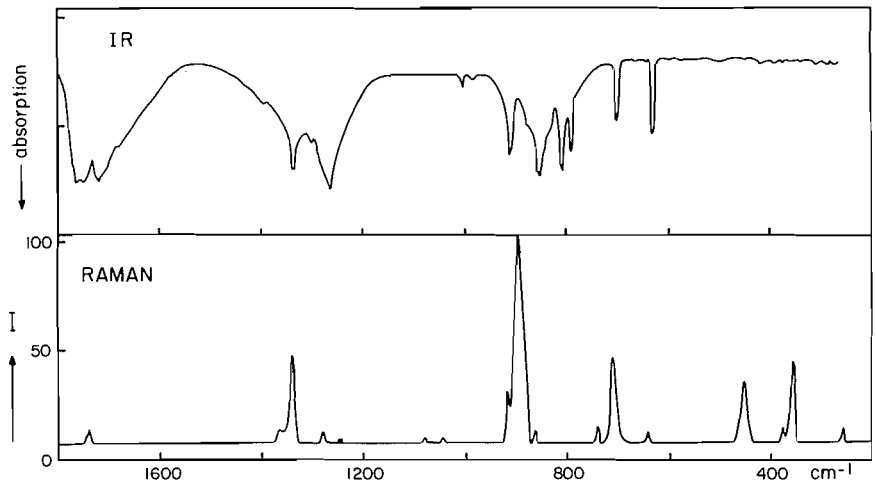

FIG. 2. Spectres de vibration à température ambiante d'un échantillon de $K_2C_2O_6$ préparé par électrolyse de K_2CO_3.

d'après l'effet de masse. Ainsi dans le cas quelque peu analogue de l'anion $S_2O_8^{2-}$ la vibration O—O se situe vers 830 cm^{-1} (18). Mais alors que dans ce dernier la vibration la plus proche est à 1090 cm^{-1}, dans $C_2O_6^{2-}$ au contraire les vibrations C—O sont beaucoup plus rapprochées. Les modes de torsion autour des liaisons C—O et O—O peuvent être identifiés d'après leur symétrie. Ainsi la plus basse fréquence Raman à 353 cm^{-1} doit appartenir au mode symétrique ν_9. La fréquence infrarouge la plus rapprochée est à 282 cm^{-1}. L'écart considérable s'explique par le couplage interne assez faible. Les forces de rappel sont surtout d'origine externe dans ce cas-ci.

De façon générale nos spectres infrarouges concordent assez bien avec ceux des auteurs soviétiques (6), sauf que leurs fréquences sont

TABLEAU 2. Spectres de vibration de $K_2C_2O_6$ (fréquences en cm^{-1})

Raman	Infrarouge: Ce travail	Infrarouge: Référence 6	Attributions
1742			ν_1 (a_g) Val. C=O
	1750/1715	1750/1720	ν_{13}(b_u) "
1337/1275			ν_2 (a_g) "
	1337/1265	1356/1290	ν_{14}(b_u) "
913			ν_3 (a_g) " C—O
	910	920	ν_{15}(b_u) "
893			ν_4 (a_g) " O—O
861			ν_5 (a_g) Def. CO_2
	865/855	878	ν_{16}(b_u) "
	810	820	ν_{17}(b_u) " OCO_2
	793		ν_8 (a_u) " CO_3
731			ν_6 (a_g) " OCO_2
710	702		ν_{11}(b_g) " CO_3
	630	637	ν_{18}(b_u) " OOC
450			ν_7 (a_g) " OOC
	282		ν_9 (a_u) Torsion C—O
353			ν_{12}(b_g) " O—O
	140		Réseau
	110		"
	88		"
	64		"

Can. J. Chem. Downloaded from www.nrcresearchpress.com by 210.87.254.5 on 09/05/12
For personal use only.

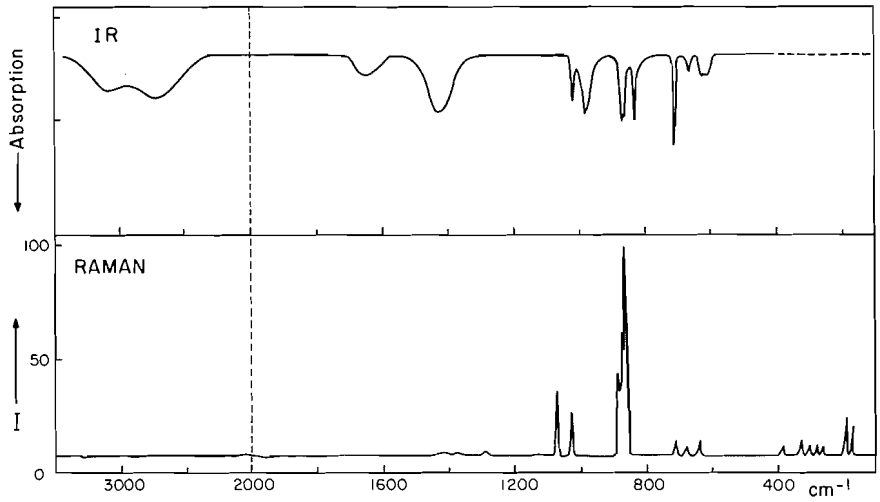

FIG. 3. Spectres d'un échantillon de peroxyhydrate censé de composition $K_2CO_3.3H_2O_2$, enregistrés à −180 °C.

toutes décalées de quelque 10 cm^{-1} par rapport aux nôtres. En outre ils n'ont pu résoudre toutes les composantes des bandes entre 800 et 1000 cm^{-1}. Aussi, en l'absence de données Raman, ont-ils attribué à la vibration O—O leur forte bande à 878 cm^{-1}. Par ailleurs leur interprétation selon une structure entièrement covalente les conduit à représenter l'atome de carbone avec une seule liaison double et deux liaisons simples, soit

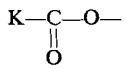

Une telle structure est évidemment inacceptable d'après la théorie de la liaison chimique. Il ne fait aucun doute que les percarbonates alcalins sont de nature ionique.

Les peroxyhydrates

Les carbonates alcalins peroxydratés sont trop instables pour être isolés à l'état pur. On a prouvé par l'analyse thermique différentielle (7) qu'ils contiennent toujours plus ou moins d'eau, d'où les diverses formules qu'on trouve dans la littérature. La situation se complique encore du fait que les carbonates mêmes, qui sont assez hygroscopiques, montrent des différences considérables dans leurs spectres lors de l'hydratation (19). Il n'est donc pas surprenant que les spectres des peroxyhydrates varient beaucoup d'un échantillon à l'autre, et même avec le temps pour un échantillon donné.

La Fig. 3 a été reconstituée d'après les spectres d'échantillons censés de composition $K_2CO_3.3H_2O_2$. Cependant la bande à 1650 cm^{-1} atteste bien la présence d'eau (de cristallisation ou de décomposition). Les fréquences principales correspondent bien à celles déjà trouvées (7) mais notre interprétation diffère dans certains cas. Ainsi des deux bandes de valence O—H à 3300 et 2700 cm^{-1}, nous attribuons la seconde aux liaisons hydrogène avec les anions carbonate, vraisemblablement plus fortes que les autres, entre H_2O_2 et H_2O. Les fondamentales de l'anion CO_3^{2-} sont diversement affectées dans les peroxyhydrates. Ainsi le mode de valence antisymétrique, qui donne un doublet dans le carbonate anhydre et son hydrate, ne produit ici qu'une seule bande large vers 1420 cm^{-1} en infrarouge. Par contre le mode symétrique, absent en infrarouge dans le carbonate anhydre, donne une bande fine à 1060 cm^{-1} dans l'hydrate et à 1013 cm^{-1} dans le peroxyhydrate. En Raman on trouve un doublet à 1071/1026 cm^{-1}. La bande assez large à 980 cm^{-1} en infrarouge seulement a été attribuée (7) à la rotation gênée ou libration des molécules d'eau. Nous croyons qu'elle appartient plutôt aux molécules de peroxyde vu l'analogie avec la bande à 940 cm^{-1} dans $KF.H_2O_2$ (20). La vibration de valence O—O du peroxyde d'hydrogène est difficile à identifier car elle coïncide exactement avec la déformation dans le plan de CO_3^{2-}. Cette dernière est probablement seule à l'origine du doublet à 865–830

Can. J. Chem. Downloaded from www.nrcresearchpress.com by 210.87.254.5 on 09/05/12
For personal use only.

cm^{-1} en infrarouge car la bande O—O des peroxydes symétriques n'y est jamais très intense. En Raman, au contraire, la vibration ν_2 du carbonate est souvent absente ou très faible, même dans le cas des hydrates. Le pic intense à 865 cm^{-1} avec pics secondaires à 870 et 876 cm^{-1} serait donc dû surtout à ν_{O-O}. Enfin une étude spectroscopique plus poussée de ces composés mal définis ne semble pas justifiable pour le moment vu l'intérêt plutôt académique de la question.

Ce travail a été exécuté avec l'aide financière du Conseil National de Recherches du Canada. Les auteurs remercient le professeur O. Gübeli pour les analyses par émission atomique et le docteur J. L. Arnau pour l'enregistrement des spectres Raman.

1. E. J. Constam et A. von Hansen. Z. Elektrochem. 3, 137 (1896).
2. A. H. Lymn. J. Soc. Chem. Ind. **16**, 406 (1897).
3. W. C. Schumb, C. N. Satterfield, et R. I. Wentworth. Hydrogen peroxide. Reinhold, New York, 1955, p. 460.
4. J. R. Partington et A. H. Fathallah. J. Chem. Soc. 1934 (1950).
5. P. A. Giguère et A. W. Olmos. Can. J. Chem. **34**, 689 (1956).
6. G. S. Karetnikov et M. F. Sorokina. Zh. Fiz. Khim. **39(2)**, 364 (1965). [Russ. J. Phys. Chem. **39(2)**, 187 (1965)].
7. C. Rocchiccioli. C. R. **261**, 361 (1965).
8. T. P. Firsova, A. N. Molodkina, T. G. Morozova, et I. V. Aksenova. Zh. Neorg. Khim. **9(5)**, 1066 (1964); [Russ. J. Inorg. Chem. **9(5)**, 583 (1964)].
9. A. Kh. Mel'nikov, T. P. Firsova, et A. N. Molodkina. Zh. Neorg. Khim. **7(6)**, 1237 (1962); [Russ. J. Inorg. Chem. **7(6)** 637 (1962)].
10. M. G. Celis et J. R. Massaguer. An. R. Soc. Esp. Fis. Quim. **51***B*, 693 (1955).
11. J. R. Kyrki. Suomen Kemistilehti, B**38**, 51 (1965).
12. J. L. Arnau et P. A. Giguère. Can. J. Chem. **48**, 3903 (1970).
13. A. Novak, P. Saumagne, et L. D. C. Bok. J. Chim. phys. **60**, 1385 (1963).
14. K. Nakamoto, Y. A. Sarma, et H. Ogoshi. J. Chem. Phys. **43**, 1177 (1965).
15. D. L. Bernitt, K. O. Hartman, et I. C. Hisatsune. J. Chem. Phys. **42**, 3553 (1965).
16. L. Couture-Mathieu. J. Phys. Rad. **11**, 541 (1950) et **15**, 531 (1954).
17. W. H. Zachariasen et R. C. L. Mooney. Z. Krist. **88**, 63 (1934).
18. A. Simon et H. Richter. Z. anorg. allgem. Chem. **315**, 196 (1962).
19. C. J. H. Schutte et K. Buijs. Spectrochim. Acta, **17**, 921 (1961).
20. Hélène Roy et P. A. Giguère. Rev. Chim. Min. **7**, 1053 (1970).

Can. J. Chem. Downloaded from www.nrcresearchpress.com by 210.87.254.5 on 09/05/12
For personal use only.

The Constituents of *Nauclea diderrichii*. Part II. Isolation and Classification of Constituents; Simple β-Carboline and Pyridine Alkaloids[1]

STEWART MCLEAN AND D. G. MURRAY

Department of Chemistry, University of Toronto, Toronto 181, Ontario

Received October 25, 1971

The bark of *Nauclea diderrichii* (Rubiaceae) has afforded a considerable number of constituents, mainly alkaloids. For convenience these have been placed in four categories: (*1*) simple β-carbolines, (*2*) simple pyridines, (*3*) indole-pyridines, and (*4*) miscellaneous substances. Isolation procedures and the elucidation of the structures of constituents in categories (*1*) and (*2*) are described in this paper. Spectroscopic evidence supported by synthesis has been used to assign structures **1**, **2**, **3**, and **4** to the four simple β-carbolines and structures **5**, **6**, **7**, and **8** to the four simple pyridines isolated.

L'écorce du *Nauclea diderrichii* (Rubiaceae) a donné un nombre considérable de produits constitués surtout d'alcaloides. Dans un but pratique, ceux-ci ont été classés en quatre catégories: (*1*) les β-carbolines simples, (*2*) les pyridines simples, (*3*) les indoles-pyridines, et (*4*) les substances diverses. Les moyens de purification ainsi que la détermination des structures des substances appartenant à la catégorie (*1*) et (*2*) sont décrits dans cet article. Des preuves spectroscopiques et des synthèses ont permis d'attribuer les structures **1**, **2**, **3**, et **4** aux quatre β-carbolines simples et les structures **5**, **6**, **7**, et **8** aux quatre pyridines simples isolées.

Canadian Journal of Chemistry, **50**, 1478 (1972)

We recently described in a preliminary communication (1*a*) the isolation of a number of alkaloids from the bark of a West African tree, *Nauclea diderrichii* (*Sarcocephalus diderrichii*). We were able to demonstrate the co-occurrence of indole alkaloids, presumed to be derived from tryptamine or tryptophan, and pyridine alkaloids that are probably of monoterpenoid origin, and evidence was presented that some of the alkaloids isolated, referred to as indole-pyridines, contained structural units derived from both of these classes and were of considerable structural novelty. In the present discussion attention will be focussed on the simpler alkaloids to which structures have been confidently assigned; experience with these alkaloids has helped us to discern in the more complex alkaloids (1*b*) structural features which appear to reveal a pattern, probably related to the biogenetic origins of these secondary plant metabolites (1*c*), which can then be applied to generate or test suggestions regarding the structures of some of the more complex alkaloids.

Isolation and Classification of Constituents

Although the genus *Nauclea* L. (*Sarcocephalus* Afzel. ex R. Br.) of the family Rubiaceae is widely distributed in tropical areas (2), contains species with reputations in native medicine (3), and is botanically closely related (4) to species from which constituents of considerable chemical interest have been isolated, it appears to have attracted remarkably little phytochemical interest (3).

We have investigated the bark of *N. diderrichii*, obtained from Nigeria, and isolated a considerable number of constituents, principally alkaloids, of chemical interest. Isolation procedures used were based on those commonly used for the extraction of alkaloids: typically, the dried, ground bark was extracted repeatedly with cold methanol, the extract was concentrated under reduced pressure, the components were partitioned between dilute hydrochloric acid and chloroform, and the basic fraction was recovered from the acidic solution after it had been treated with ammonia. The crude "total bases" isolated corresponded to between 0.01 and 0.075% of the dried bark. It should be noted that included in the "total bases" were components which were later found to be non-basic and that the use of ammonia as a standard practice in the extraction and the subsequent chromatography led to questions which will be discussed subsequently (1*b*). The t.l.c. showed that the "total bases" comprised an extremely complex mixture of components, and repeated preparative t.l.c. was required to effect their separation. In some cases it was possible to purify the compounds isolated

[1]Our preliminary communication (1*a*) is considered to be Part I of this series. This account is taken from the Ph.D. thesis of D. G. Murray, University of Toronto, 1971.

Can. J. Chem. Downloaded from www.nrcresearchpress.com by 210.87.254.5 on 09/05/12
For personal use only.

Can. J. Chem. Downloaded from www.nrcresearchpress.com by 210.87.254.5 on 09/05/12
For personal use only.

to a satisfactory level of homogeneity, but in others the very small amount of material available precluded further purification, and material that would, under better circumstances, have been considered of unsatisfactory homogeneity was studied.

In no case, however, was sufficient material available for investigation of its structure by standard methods requiring combustion analysis and rational degradation. Instead, it was necessary in every case to carry out first a careful mass spectrometric examination of the component to determine its molecular formula and to obtain any available structural information from its fragmentation pattern; other spectroscopic methods were then used, to the extent that the amount of material and its solubility allowed, in order to derive as much additional structural information as possible. On the basis of the information thus obtained, a structure was proposed as a working hypothesis with a degree of confidence that varied from case to case. It was then necessary to turn either to direct comparison with authentic material in the few cases where the compound appeared to have been described previously, or to an unambiguous synthesis of the compound when no previous account of a substance of the proposed structure could be found.

At the present time it has not been possible to carry the elucidation of structure to a satisfactory conclusion in every case, but sufficient progress has been made to allow us to see the development of a pattern in the structures that is of considerable interest and significance in the chemistry of secondary plant metabolites, and this has induced us to report our present results even in those cases where the evidence allows only a part structure to be proposed or a structural hypothesis to be advanced tentatively. It is convenient at this stage to divide the materials isolated into four categories: (*1*) simple β-carbolines, (*2*) simple pyridines, (*3*) indole-pyridines (N_3 alkaloids which appear to contain a tryptamine-derived unit and an independent pyridine unit), and (*4*) miscellaneous substances.

(1) Simple β-Carbolines

The four products (**1**, **2**, **3**, **4**) isolated that are in this category are conveniently described first since they were easily related to compounds of known structure. The identity of harman (**1**), a widely distributed and well-known alkaloid, was confirmed by comparison with authentic material. 3-Carbomethoxyharman (**2**) does not appear to have been obtained previously as a natural product, but a glycoside of the free acid has been found (5) and the ester has been synthesized from tryptophan (6); synthetic material we obtained by the same procedure (6) served to confirm the identity of natural **2**. 1-Carbomethoxynorharman (**3**) has previously been described as a natural product (7); it has also been synthesized from harman (8) and this synthesis was used to establish the identity of our natural material. 1-Carboxamidonorharman (**4**) seems not to have been described previously; its identity was established by comparison with an authentic sample derived from synthetic **3**.

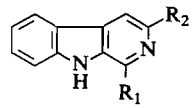

1 $R_1 = Me$; $R_2 = H$
2 $R_1 = Me$; $R_2 = CO_2Me$
3 $R_1 = CO_2Me$; $R_2 = H$
4 $R_1 = CONH_2$; $R_2 = H$

It is recognized that **4** may be an artifact derived from **3** or a related compound during the isolation process, which involved the use of ammonia at two stages. Attempts to prepare **3** and **4** via the corresponding acid chloride were abandoned in favor of Fischer esterification of the carboxylic acid and ammonolysis of the ester when it was found that the treatment of the hydrochloride of the carboxylic acid with refluxing thionyl chloride led to a considerable amount of chlorination of the β-carboline; the corresponding chlorination of a pyridine ring is known to occur (9), but under somewhat more vigorous conditions than we used.

A few features of the mass spectra of these β-carbolines (10) deserve comment since they have some diagnostic value. The base peak at M − 58 (5) in the spectrum of **2** does not correspond to an ion in the normal fragmentation pattern of an ester of an aromatic acid (11) (for which peaks are also present), and is best accounted for on the basis of a process such as:

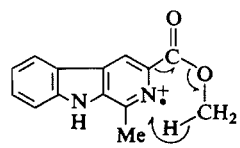

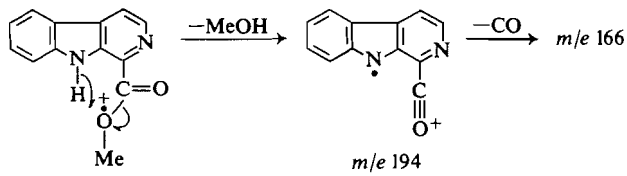

SCHEME 1

Accurate mass measurements and metastable ion evidence support this proposal. A corresponding fragmentation would be expected for **3** and the M − 58 peak is, indeed, prominent; however, the base peak is at M − 60 and apparently arises from a process involving the indole nitrogen (see Scheme 1). A significant peak is visible at *m/e* 194, and accurate mass measurements and metastable ion evidence are in accord with the sequence shown. Fragmentation of **4** apparently follows closely related pathways leading to peaks corresponding to M − CONH, M − NH_3 and M − $CONH_3$; accurate mass measurements and metastable ion evidence again provided support for the proposal, and replacement with deuterium of the hydrogen atoms bonded to nitrogen produced the anticipated spectral shifts.

(2) Simple Pyridines

Four alkaloids (**5**, **6**, **7**, **8**) in this class were isolated, and their structures were assigned on the basis of their spectroscopic properties and confirmed by synthesis. Despite the structural simplicity of the compounds, only two of them (**6** and **8**) could be found in the literature, and these appear in a patent (12) without description of their physical characteristics or origin.

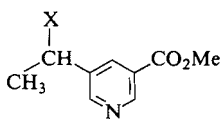

5 X = OMe
6 X = OH
7 X = NH_2

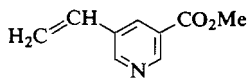

8

In each case the molecular formula was determined from the mass spectrum; the parent ion of **7** was not observed but its formula was determined by accurate mass measurement of fragment ions (M − 1 and M − 15). The spectrum of each of the alkaloids (**5**, **6**, **7**) with a saturated side-chain showed significant M − 1 and M − 15 peaks, the latter providing the base peak, which are attributed to fragmentation with loss of the methine hydrogen or methyl group of the side-chain. The normal aromatic ester fragmentation (11) is less clearly visible in these spectra, but in the spectrum of **8** it represents the dominant pathway and intense M − 31 and M − 59 peaks are observed.

The i.r. spectrum of each alkaloid showed a peak at 5.80 μ (with a shoulder at 5.82 μ), and the n.m.r. spectrum showed a methyl singlet near τ 6, indicative of the carbomethoxy function assigned to the alkaloid. The i.r. and n.m.r. spectra also provided the evidence that led to the recognition of the structure of the side-chain characteristic of each alkaloid, and the appearance, in the region of the n.m.r. spectrum associated with the protons of a pyridine ring, of an AMX pattern with $J_{AM} \simeq 0$ and $J_{AX} \simeq J_{MX} \simeq 2$ Hz allowed the substitution pattern of the ring to be assigned with confidence. It was observed that the appearance of the AMX pattern in the n.m.r. was markedly affected by the condition of the sample, and the presence of a trace of acid caused loss of the fine structure, with the signals at lower field being most strongly affected; the amount of peak broadening exhibited varied considerably and unpredictably, so that in some cases it was almost negligible, while in others it was sufficient to cause the signals to be submerged in the background noise. This was of considerable practical importance both here and in later cases, since spectroscopic samples that appeared pure in other respects were frequently clearly contaminated with slight traces of acid and it became our standard practice to remove the broadening by shaking the solution of the sample in chloroform-*d* with an aqueous base. The situation is also of considerable intrinsic interest since a detailed explanation of it encounters difficulties. It appears to have been observed previously (13) but was attributed to other causes, and several studies of the spectra of pyridinium salts and the influence of acidic solvents on the spectra of pyridines have been

Can. J. Chem. Downloaded from www.nrcresearchpress.com by 210.87.254.5 on 09/05/12
For personal use only.

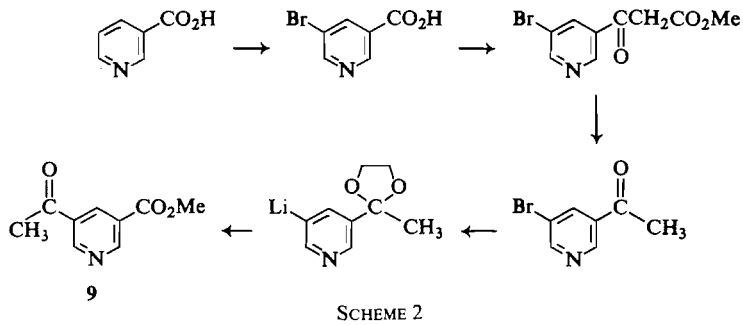

SCHEME 2

reported (14) but without reference to the effect of traces of acid in a solvent such as chloroform-*d*.

The structures **5**, **6**, **7**, and **8** were finally established by comparisons of natural and synthetic materials. The synthetic route (Scheme 2), which proved unexpectedly troublesome, required the preparation of the key intermediate 3-acetyl-5-carbomethoxypyridine (**9**). An obvious route to the intermediate can be drawn from 3,5-pyridinedicarboxylic acid and requires a Claisen condensation of methyl acetate at one carbomethoxy group of the diester, but this gave unsatisfactory results, even though it appears to have worked well for the ethyl ester (15); the utilization of sodium methylsulfinylmethide (16) did not prove a successful variant. The reaction of dimethylcadmium with the acid chloride of 5-carbomethoxy-3-pyridinecarboxylic acid, for which we developed a satisfactory synthesis similar to one described recently by Wenkert *et al.* (17), led to some of the required product, but the yield was unsatisfactory, and the product ketone was contaminated with substantial amounts of the carbinol resulting from further reaction of the ketone with dimethylcadmium. The most successful route to **9** started with nicotinic acid which was converted through the hydrochloride of its acid chloride to 5-bromonicotinic acid; this, after esterification, was converted to the corresponding methyl ketone by Claisen condensation (18); the ketone was then protected as the ethylene ketal, the pyridyllithium compound was formed, and this was converted to **9** by carbonation and esterification.

Sodium borohydride reduced **9** to **6**, structurally identical with the natural material. The synthetic alcohol **6** was converted by methanolysis of its mesylate to the methyl ether **5**, structurally identical with the natural alkaloid. The dehydration of **6** to **8** was successfully accomplished by treatment with phosphorus pentoxide (19) or *p*-toluenesulfonic acid and this provided material suitable for establishing the structure of the alkaloid; it can be noted, however, that yields in this reaction were variable and that polymerization of **6** was a serious side reaction in the toluenesulfonic acid procedure. Reduction by zinc and acetic acid of the oxime of **9** formed **7**, structurally identical with the natural alkaloid.

The natural materials (**5**–**8**) were obtained in small quantities as oils and, with the exception of one sample of **5**, resisted attempts to crystallize them. These materials, **8** excepted, showed optical activity but because of the small amount of material available, specific rotations could not be determined with precision and confidence and it could not be established whether partial racemization of some of the samples had occurred in the case of **6** or whether variations arose from differences in the purity of the samples and instrumental difficulties. The synthetic samples were, of course, racemic and with the exception of **7**, were obtained crystalline.

Experimental

Melting points were determined on a calibrated Thomas–Kofler micro hot stage unless otherwise specified. Unless otherwise indicated, chloroform solutions were used to obtain i.r. spectra and the wavelengths of significant absorptions are reported in μ. Methanol solutions were used to obtain u.v. spectra and the wavelengths of maximum absorption (λ_{max}) are reported in mμ followed by the extinction coefficient (ε) in parentheses. Chloroform-*d* solutions with tetramethylsilane as an internal standard were used to obtain n.m.r. spectra and chemical shifts are reported on the τ scale followed in parentheses with an indication of the multiplicity of the signal and the number of protons associated with it; an indication is given for those n.m.r. spectra which were obtained after the chloroform-*d* solution had been shaken with base, usually 10% potassium carbonate in deuterium oxide. Spectrometers used were a

Can. J. Chem. Downloaded from www.nrcresearchpress.com by 210.87.254.5 on 09/05/12
For personal use only.

Can. J. Chem. Downloaded from www.nrcresearchpress.com by 210.87.254.5 on 09/05/12
For personal use only.

Perkin–Elmer 237B for i.r. spectra, a Bausch and Lomb Spectronic 505, a Perkin–Elmer 350, or a Unicam SP.800A for u.v. spectra, and a Varian A-60, A-56/60D, T-60, or HA-100 for n.m.r. spectra (values at 100 MHz are reported unless otherwise indicated). Routine mass spectra were determined at 70 eV on a CEC 21-490 or an AEI MS-902 spectrometer and the *m/e* values of significant ions are reported followed in parentheses with a figure showing the height of the peak relative to that of the base peak (100%); accurate mass measurements were made on the AEI MS-902 spectrometer. Optical rotations were determined with a Bendix–Ericsson ETL-NPL Automatic Polarimeter Type 143A. Analytical t.l.c. procedures used pre-coated Merck silica gel F254 plates, aluminum oxide F254 type T plates, cellulose F plates, or Baker-flex aluminum oxide 1B-F sheets. Preparative t.l.c. was carried out with hand-coated plates (0.5 or 1.0 mm) prepared from Merck silica gel G or aluminum oxide G type E with 3% of an electronic phosphor (excited at 254 mμ) present, or with pre-coated Merck silica gel F254 or aluminum oxide F254 type T plates which contained an electronic phosphor. Chromatograms were examined by irradiation at 254 mμ, and also by exposure of the plates to iodine in some cases.

The *N. diderrichii* bark was obtained through the good offices of Professor D. M. James, Department of Pharmacology, University of Ibadan, Nigeria. The present work was carried out on six shipments of bark, received over a period of several years and apparently collected from trees of various ages.

Standard Isolation and Extraction Procedures

Coarsely ground dry bark was covered with methanol and allowed to soak for 24 h, the methanol was drained off, and the procedure was repeated with fresh methanol.[2] The extract obtained was filtered and concentrated under reduced pressure to about 5% of its original volume, and the material obtained from four successive extractions was pooled. The concentrate was acidified with 5% hydrochloric acid and extracted twice with chloroform. The aqueous phase was basified with 10% ammonia and extracted three times with chloroform (about one third of the volume of the aqueous solution each time). This chloroform extract was washed with water, concentrated under reduced pressure to about 5% of its original volume, and thoroughly extracted with 5% hydrochloric acid. The acidic extract was then basified with 5% ammonia and thoroughly extracted with chloroform. The final chloroform extract, after it had been washed with water and concentrated under reduced pressure provided the "total bases" as a brown syrup (about 0.05% of the starting bark).

The "total bases" were subjected to a primary separation by preparative t.l.c. using silica gel plates and elution with 84:14:1 methylene chloride – methanol–ammonia (concentrated). This separation afforded about 12 fractions, each of which was examined by analytical t.l.c. to determine the best conditions for further separation. The secondary separation was carried out by preparative t.l.c. on silica gel or alumina plates and elution by various combinations of the following solvents: hexane, benzene, ether, ethyl acetate, acetone, methanol, methylene chloride, and chloroform. Systems of particular value were 5:2:3 benzene–acetone–methanol for the more polar fractions, 7:2:1 methylene chloride–acetone–methanol for intermediate cases, and 6:4 hexane–acetone for less polar fractions. Each fraction obtained was subjected to further separations by preparative t.l.c. in the manner just described until each component was obtained in as homogeneous a condition as seemed possible.

In runs which avoided ammonia, it was replaced by 10% aqueous sodium carbonate during the extraction and by triethylamine during the separation by t.l.c.

Simple β-Carbolines

Harman (1)

Harman was obtained as a white solid, m.p. 205–229°,[3] which was identical with authentic harman, m.p. 238°; the t.l.c. behavior (four systems) and the i.r., n.m.r., and mass spectra of the two samples were compared to establish their identity.

3-Carbomethoxyharman (2)

Compound **2** was obtained, after recrystallization from methanol, as a white solid, m.p. 249–253° (dec.). Spectroscopic characteristics: i.r. 2.90 (sharp), 3.07 (broad), 5.82; n.m.r. (60 MHz) 0.95 (broad; 1), 1.16 (s; 1), 1.77 (d, $J = 8$ Hz; 1), 2.2–2.9 (complex; 3), 5.98 (s; 3), 7.18 (s; 3); mass spectrum 241 (7), 240 (29), 209 (4), 183 (16), 182 (100), 181 (35), 180 (4), 179 (8), 155 (4), 154 (13), 153 (5), 128 (5), 127 (8), 105 (17), 91 (6), 90.5 (4), 77 (14), 76 (5), 63 (4), 51 (4); metastable 138.1 (calcd. for 240 → 182: 138.0); mass measurements calcd. (found): $C_{14}H_{12}N_2O_2$, 240.08988 (240.0898); $C_{13}H_9N_2O$, 209.07149 (209.0711); $C_{12}H_{10}N_2$, 182.08440 (182.0845); $C_{12}H_9N_2$, 181.07657 (181.0764). An authentic sample of 3-carbomethoxyharman was synthesized (6) and obtained as fine needles, m.p. 250–253° (lit. (6, 5) 245°, 252–253°) and shown to be spectroscopically identical with the natural material isolated and to have the same t.l.c. behavior.

1-Carbomethoxynorharman (3)

Compound **3** was obtained as white crystals, m.p. 162–167°, by sublimation of the crude base and recrystallization of the sublimate from acetone–hexane. Spectroscopic characteristics: i.r. 2.91 (sharp), 5.77 (weak), 5.89 (strong); mass spectrum 227 (10), 226 (63), 194 (15), 169 (11), 168 (84), 167 (25), 166 (100), 165 (8), 140 (19), 139 (18), 114 (12), 113 (8), 88 (5), 84 (5), 83.5 (5), 83 (6), 63 (5); metastables 142.1 (calcd. for 194 → 166: 142.0), 124.8 (calcd. for 226 → 168: 124.8); mass measurements calcd. (found): $C_{12}H_6N_2O$, 194.04801 (194.0476); $C_{11}H_8N_2$, 168.06875 (168.0684); $C_{11}H_6N_2$, 166.05310 (166.0531). An authentic sample of 1-carbomethoxynorharman was synthesized by condensation of harman with benzaldehyde followed by oxidation with potassium permanganate in aqueous pyridine and Fischer esterification of the free acid produced; procedures used followed those in the literature (8) with minor modifications. The crystalline product, m.p. 160–166° (lit. (8) 165–166°, 168°) was spectroscopically identical with the natural material isolated and had the same t.l.c. behavior; n.m.r. 0.13 (broad; 1), 1.49 (d, $J = 5$ Hz; 1), 1.95 (d, $J = 7$ Hz, with further splitting; 1), 2.02 (d, $J = 5$ Hz; 1), 2.2–2.8 (complex; 3), 5.93 (s; 3).

[2]A referee has commented that this procedure may lead to the production of methylesters as artifacts.

[3]As with many of the components obtained in this way, insufficient material was available to allow its purification to a sharp melting point by repeated recrystallization.

Can. J. Chem. Downloaded from www.nrcresearchpress.com by 210.87.254.5 on 09/05/12
For personal use only.

1-Carboxamidonorharman (4)

Compound **4** was isolated as a crystalline solid which was sublimed and then recrystallized from methylene chloride; it was obtained as white needles, m.p. 224–226° (sealed tube). Spectroscopic characteristics: i.r. 2.84, 2.91 (sharp), 2.95 (sharp), 5.97; u.v. 214 (36 000), 240 (shoulder, 17 400), 244 (18 200), 250 (shoulder, 17 000), 270 (17 800), 298 (10 000), 366 (5900); mass spectrum 212 (16), 211 (100), 194 (27), 168 (21), 167 (21), 166 (96), 165 (9), 141 (5), 140 (19), 139 (19), 114 (14), 113 (8), 105.5 (7), 88 (6), 63 (6), 57 (6), 55 (6), 44 (8), 41 (6); metastables 178.2 (calcd. for 211 → 194: 178.4), 142.1 (calcd. for 194 → 166: 142.0); mass measurements calcd. (found): $C_{12}H_9N_3O$, 211.07456 (211.0747); $C_{12}H_6N_2O$, 194.04801 (194.0475); $C_{11}H_8N_2$, 168.06875 (168.0684); $C_{11}H_6N_2$, 166.05310 (166.0532). An authentic sample of 1-carboxamidonorharman was synthesized by dissolving the corresponding methyl ester, **3**, in methylene chloride and stirring the solution for a prolonged period (2–3 weeks) at room temperature with concentrated aqueous ammonia. This afforded material, m.p. 227–229° (sealed tube) identical in spectra and t.l.c. behavior with the natural material; n.m.r. 1.58 (d, $J = 5.5$ Hz; 1), 1.84 (d, $J = 7.5$ Hz, with further splitting; 1), 1.89 (d, $J = 5.5$ Hz; 1), 2.2–2.9 (complex; 3).

Simple Pyridines

Members of this group were obtained as oils (**5** subsequently crystallized) and their structures were deduced from their spectroscopic characteristics. Authentic (racemic) samples of these compounds were synthesized and identities were established by comparison of the t.l.c. behavior (at least four systems) and the i.r., n.m.r., and mass spectra of the natural and synthetic materials.

3-Acetyl-5-carbomethoxypyridine (9)

3-Acetyl-5-bromopyridine was prepared from nicotinic acid essentially by the method of Bachman and Micucci (18) and converted to its ethylene ketal (95% yield) by treatment of a refluxing solution of the ketone in benzene with excess ethylene glycol and a catalytic amount of *p*-toluenesulfonic acid in a Dean–Stark apparatus for 1 day. The product, after sublimation and recrystallization from methylene chloride, formed thick, colorless plates, m.p. 77–78°.

Anal. Calcd. for $C_9H_{10}NO_2Br$: C, 44.29; H, 4.13; N, 5.74; Br, 32.74. Found: C, 44.10; H, 4.27; N, 5.59; Br, 33.22.

A solution of the ketal (11.5 g; 47 mmol) in 60 ml of dry tetrahydrofuran was slowly added to a solution of *n*-butyllithium (about 220 mmol) in 90 ml of hexane diluted with 100 ml of tetrahydrofuran and maintained in a bath at −40° under dry nitrogen. The temperature was allowed to rise to −15° over 15 min, and the reaction mixture was poured on to 500 g of freshly crushed Dry Ice which was kept agitated during this period and for a further 5 min. The brown residue which remained after the solvent and excess Dry Ice had evaporated was partitioned between chloroform and 10% aqueous ammonia. The aqueous phase was acidified with concentrated hydrochloric acid, washed with chloroform, neutralized with concentrated ammonia, and evaporated to dryness, the last traces of moisture being removed under vacuum (≃1 mm). The residue was ground to a powder and treated for 24 h with 700 ml of refluxing methanol containing 3% of hydrogen chloride. The reaction mixture was cooled to about 35°, and about 600 ml of the solvent was removed under reduced pressure with no increase in temperature; 800 ml of 5% hydrochloric acid was then added to the solution at room temperature and the acidic solution was allowed to remain for 30 min (to hydrolyze the dimethyl ketal formed during the esterification). The solution was then cooled, made basic with concentrated ammonia, and thoroughly extracted with chloroform. The extract afforded a brown solid (3.3 g; about 39% yield) which was taken up in 400 ml of boiling hexane, a small amount of insoluble residue was removed, and the solution was evaporated to dryness. The product, **9**, was recrystallized from water and obtained as white needles, m.p. 90–92°.

Anal. Calcd. for $C_9H_9NO_3$: C, 60.33; H, 5.06; N, 7.82. Found: C, 60.08; H, 5.35; N, 7.99.

The i.r. 5.79, 5.91; n.m.r. (60 MHz) 0.55 (d, $J = 2$ Hz; 1), 0.62 (d, $J = 2$ Hz; 1), 1.15 (3 peaks, 2 Hz spacings; 1), 5.97 (s; 3), 7.30 (s; 3); mass spectrum 180 (5), 179 (42), 165 (10), 164 (100), 148 (18), 137 (10), 136 (33), 120 (10), 104 (18), 78 (13), 50 (12), 43 (34).

3-Carbomethoxy-5-chlorocarbonylpyridine

This pyridine was prepared by the partial hydrolysis of methyl dinicotinate and treatment of the acid formed with thionyl chloride. A solution of potassium hydroxide (1.2 g; 22 mmol) in 20 ml of methanol containing 2 ml of water was added dropwise over 10 min to a stirred solution of dimethyl 3,5-pyridinedicarboxylate (4.00 g; 20.5 mmol) in 60 ml of methanol, and the solution was stirred at room temperature for 3 days. Solvent was removed under reduced pressure and the white residue was partitioned between water and methylene chloride (600 mg of starting material was recovered from the organic phase). The aqueous solution was evaporated to dryness under reduced pressure, and the white residue was ground to a coarse powder and refluxed in a dry atmosphere for 6 h in 150 ml of benzene containing 30 ml of thionyl chloride. Removal of the solvent and unchanged thionyl chloride under reduced pressure left a white residue and trituration of this with a solvent (dry benzene or ethanol-free chloroform) afforded a solution of the required acid chloride that was used in subsequent reactions. Evaporation of the solvent (benzene) left a solid residue (3.0 g) from which a crystalline sample of the acid chloride was obtained, m.p. 74–79° (lit. (17) 78°) after recrystallization from hexane; i.r. (methylene chloride) 5.66, 5.78; n.m.r. (60 MHz) 0.48 (d, $J = 2$ Hz; 1), 0.51 (d, $J = 2$ Hz; 1), 1.00 (3 peaks, 2 Hz spacings; 1), 5.97 (s, 3).

Treatment of a solution of the acid chloride in benzene with excess dimethylcadmium converted it to the ketone **9**, but yields were unsatisfactory and substantial amounts of the corresponding carbinol were also obtained.

3-Carbomethoxy-5-(1'-hydroxyethyl)pyridine (6)

A solution of sodium borohydride (102 mg; 2.7 mmol) in 10 ml of methanol was added with stirring over a period of 3 min to a solution of the ketone **9** (800 mg; 4.5 mmol) in 35 ml of methanol cooled to 5°. The reaction mixture was stirred at 5° for 5 min and at room temperature for 30 min, and 200 ml of 5% hydrochloric acid was added. After 30 min the solution was basified with ammonia and extracted with methylene chloride. The extract afforded a residue (692 mg; about 86% yield) which, when recrystallized from acetone, yielded the alcohol **6** as stout, colorless crystals, m.p. 53–56° (*p*-nitrobenzoate, m.p. 139–142°).

Can. J. Chem. Downloaded from www.nrcresearchpress.com by 210.87.254.5 on 09/05/12
For personal use only.

Anal. Calcd. for $C_9H_{11}NO_3$: C, 59.66; H, 6.12; N, 7.73. Found: C, 59.81; H, 6.11; N, 7.77.

The i.r. 2.78 (sharp), 2.97 (broad), 5.80, 5.82 (shoulder); u.v. 216 (7600), 267 (2450), 274 (shoulder); n.m.r. 0.91 (d, $J = 2$ Hz; 1), 1.21 (d, $J = 2$ Hz; 1), 1.61 (3 peaks, 2 Hz spacings; 1), 4.93 (q, $J = 7$ Hz; 1), 6.03 (s; 3), 6.17 (broad; 1), 8.46 (d, $J = 7$ Hz; 3); mass spectrum 181 (22), 180 (6), 167 (10), 166 (100), 164 (10), 150 (16), 138 (47), 134 (22), 106 (20), 104 (18), 78 (18), 77 (13), 59 (10), 51 (15), 50 (10), 43 (18).

This material was identical by the criteria listed above with the natural material; samples of natural **6** from two different lots of plant material showed $[\alpha]_D^{26}$ +23° (*c* 2.5, MeOH) and $[\alpha]_D^{25}$ +14° (*c* 2.2, MeOH).

3-Carbomethoxy-5-(1'-methoxyethyl)pyridine (5)

The synthetic alcohol **6** (1.67 g; 9.2 mmol) was converted to its mesylate by treatment for 3 days at −12 to −15° with 2.4 ml of methanesulfonyl chloride (31.6 mmol) in 40 ml of dry pyridine. The mesylate, which was obtained as a gummy solid (2.36 g), was refluxed in 25 ml of anhydrous methanol for 2 h. The reaction mixture was concentrated to an oil, treated with 150 ml of 5% aqueous potassium carbonate, and extracted with methylene chloride. The extract afforded a product (1.53 g) which was the desired ether **5** contaminated with about 15% of the starting alcohol **6**. By preparative t.l.c. (silica gel, 92:8 methylene chloride–methanol) the ether **5** (981 mg, 55% conversion) was obtained substantially pure; after sublimation and recrystallization from hexane it formed white needles, m.p. 43–46°. An analytical sample was obtained by resublimation of this product.

Anal. Calcd. for $C_{10}H_{13}NO_3$: C, 61.52; H, 6.71; N, 7.18. Found: C, 61.47; H, 6.78; N, 7.19.

The i.r. 5.80, 5.82 (shoulder); u.v. 216 (8300), 266 (2600), 273 (shoulder); n.m.r. (60 MHz) 0.77 (d, $J = 2$ Hz; 1), 1.19 (d, $J = 2$ Hz; 1), 1.65 (3 peaks, 2 Hz spacings; 1), 5.53 (q, $J = 7$ Hz; 1), 6.00 (s; 3), 6.70 (s; 3), 8.51 (d, $J = 7$ Hz; 3); mass spectrum 195 (4), 194 (5), 181 (12), 180 (100), 174 (3), 164 (17), 138 (6), 134 (5), 104 (10), 87 (8), 78 (6), 77 (8), 59 (12), 43 (19).

This product was identical by the criteria listed above with the natural material; natural **5** was obtained as an oil, $[\alpha]_D^{26}$ +50° (c 5.0, MeOH). A sample of natural **5** crystallized on prolonged standing at −15°, and sublimation and recrystallization of this from hexane afforded white needles, m.p. 47–48°.

3-Carbomethoxy-5-vinylpyridine (8)

A mixture of the synthetic alcohol **6** (817 mg; 4.5 mmol), phosphorus pentoxide (6.4 g; 45 mmol), and *m*-dinitrobenzene (590 mg) in 200 ml of xylene was stirred and refluxed for 1.75 h with exclusion of moisture. The reaction mixture was cooled in an ice bath and the supernatant liquor was separated by decantation from the gummy residue that remained. Both the liquid phase and the residue were thoroughly extracted with 10% hydrochloric acid to which ice had been added. The combined acid extracts were washed with benzene, cooled, basified with concentrated ammonia, and extracted with methylene chloride. The extract was concentrated to a syrup which was subjected to separation by t.l.c. (silica gel, 95:5 methylene chloride–methanol). The dehydrated product (110 mg; 15% yield; variable) was obtained as a syrup which was recrystallized from chilled hexane. (A procedure using *p*-toluenesulfonic acid in place of phosphorus pentoxide also provided **8** but it was contaminated with a polymer that appeared to result from transesterification of **6**.) The product (**8**) was obtained as sticky needles which melted over the range 50–75°. Spectroscopic characteristics: i.r. 5.80, 5.82 (shoulder), 6.13; u.v. 215 (15 500, end absorption), 241 (7400), 283 (1800); n.m.r. (60 MHz) 0.89 (d, $J = 2$ Hz; 1), 1.21 (d, $J = 2$ Hz; 1), 1.66 (3 peaks, 2 Hz spacings; 1), 3.23 (dd, J values 18, 11 Hz; 1), 4.07 (d, $J = 18$ Hz; 1), 4.53 (d, $J = 11$ Hz; 1), 6.03 (s; 3); mass spectrum 164 (14), 163 (100), 162 (3), 133 (11), 132 (98), 131 (11), 104 (63), 77 (27), 51 (29); mass measurement calcd. (found): $C_9H_9NO_2$, 163.06333 (163.0634).

This product was identical by the criteria listed above with the natural material **8**, which was obtained as an oil.

3-Carbomethoxy-5-(1'-aminoethyl)pyridine (7)

The ketone **9** (1.00 g; 5.6 mmol) was converted to its oxime by adding a solution of hydroxylamine hydrochloride (1.56 g; 22.4 mmol) and sodium carbonate (1.21 g; 11.4 mmol) in 6 ml of water to a solution of the ketone in 10 ml of methanol and heating the mixture on a steam bath for 1 h. Dilution with water and extraction with methylene chloride afforded the oxime (53% yield) which was recrystallized from methanol and obtained as white needles, m.p. 169–171°.

Anal. Calcd. for $C_9H_{10}N_2O_3$: C, 55.66; H, 5.19; N, 14.43. Found: C, 55.79; H, 5.29; N, 14.49.

The i.r. 2.80 (sharp), 3.04 (broad), 5.79, 6.14 (weak); n.m.r. (60 MHz) 0.76 (d, $J = 2$ Hz; 1), 0.83 (d, $J = 2$ Hz; 1), 1.42 (3 peaks, 2 Hz spacings; 1), 6.00 (s; 3), 7.68 (s; 3); mass spectrum 195 (11), 194 (100), 178 (60), 163 (84), 162 (13), 147 (10), 136 (11), 135 (20), 122 (24), 120 (11), 119 (10), 104 (14), 78 (11), 50 (12), 42 (18).

Zinc powder (13 g; 200 mmol) was added over a period of 2.25 h to a stirred solution of the oxime (576 mg; 3.0 mmol) in 50 ml of glacial acetic acid containing 6 ml of water. After the mixture had been filtered and the residue washed with 100 ml of dilute acetic acid, the filtrate and washings were diluted with 400 ml of water, made basic with concentrated ammonia, and thoroughly extracted with methylene chloride. The amine **7** (491 mg; 75% yield) was obtained from the extract as a syrup with the following spectroscopic characteristics: i.r. 3.01 (broad), 5.82, 5.80 (shoulder); u.v. 217 (10 700), 268 (2950); n.m.r. (60 MHz) 0.99 (d, $J = 2$ Hz; 1), 1.21 (d, $J = 2$ Hz; 1), 1.66 (3 peaks, 2 Hz spacings; 1), 5.72 (q, $J = 7$ Hz; 1), 6.03 (s; 3), 7.83 (broad; 2), 8.56 (d, $J = 7$ Hz; 3); mass spectrum 180 (2), 179 (6), 166 (22), 165 (100), 149 (7), 138 (10), 107 (7), 106 (7), 105 (8), 104 (6), 78 (8), 77 (5), 44 (25); mass measurements calcd. (found): $C_9H_{11}N_2O_2$, 179.08205 (179.0828); $C_8H_9N_2O_2$, 165.06640 (165.0663); $C_8H_9N_2O$, 149.07149 (149.0718); $C_7H_8NO_2$, 138.05550 (138.0556).

The *p*-nitrobenzoyl derivative was obtained as white needles, m.p. 154–157° (phase change 100–110°).

Anal. Calcd. for $C_{16}H_{15}N_3O_5$: C, 58.35; H, 4.59; N, 12.76. Found: C, 58.64; H, 4.80; N, 12.75.

Synthetic and natural **7** were identical by the criteria listed above; the natural material was an oil which was optically active, $[\alpha]_D^{25}$ +27° (c 0.34, MeOH), but this value may contain a substantial error because of the small amount of sample available.

This work was supported by a grant from the National Research Council of Canada; scholarships (to D.G.M.)

from the same source and from the Province of Ontario are also gratefully acknowledged. We thank Professor D. M. James and Dr. S. O. A. Bamgbose for plant collections and for their interest in this work.

1. (*a*) S. McLEAN and D. G. MURRAY. Can. J. Chem. **48**, 867 (1970). (*b*) D. G. MURRAY, A. SZAKOLCAI, and S. McLEAN. Can. J. Chem. This issue. (*c*) S. McLEAN and D. G. MURRAY. Can. J. Chem. This issue.
2. J. C. WILLIS. A dictionary of the flowering plants and ferns. 7th ed. *Revised by* H. K. Airy Shaw. Cambridge University Press, London, 1966.
3. J. CAIMENT-LEBLOND. Thesis (Pharmacien). University of Paris, France, 1957; F. E. KING and L. JURD. J. Chem. Soc. 1192 (1953); L. J. WEBB. An Australian phytochemical survey; II. Alkaloids in Queensland flowering plants. Bulletin No. 268. Commonwealth Scientific and Industrial Research Organization. Melbourne, Australia. 1952. p 74; L. A. SILVA, L. N. PRISTA, and A. C. ALVES. Garcia Orta. **11**, 89 (1963); Chem. Abstr. **62**, 9458*a* (1965); E. FUJITA, T. FUJITA, and T. SUZUKI. Chem. Pharm. Bull. (Tokyo), **15**, 1682 (1967).
4. B. VERDCOURT. Bull. Jard. Bot. Etat. Brux. **28**, 209 (1958).
5. L. D. ANTONACCIO and H. BUDZIKIEWICZ. Monatsh. Chem. **93**, 962 (1962).
6. H. R. SNYDER, C. H. HANSCH, L. KATZ, S. M. PARMERTER, and E. C. SPAETH. J. Am. Chem. Soc. **70**, 219 (1948).
7. H. ACHENBACH and K. BIEMANN. J. Am. Chem. Soc. **87**, 4177 (1965); V. DEULOFEU. *In* Ethnopharmacologic search for psychoactive drugs. D. H. Efron, editor. Publ. No. 1645, United States Department of Health, Education, and Welfare. 1967, p. 398.
8. H. R. SNYDER, H. G. WALKER, and F. X. WERBER. J. Am. Chem. Soc. **71**, 527 (1949); C. KUMP, J. SEIBL, and H. SCHMID. Helv. Chim. Acta, **46**, 498 (1963).
9. H. MEYER and R. GRAF. Chem. Ber. **61**, 2202 (1928); R. GRAF, E. LEDERER-PONZER, V. KOPETZ, R. PURKERT, and P. LASZLO. J. Prakt. Chem. (2) **138**, 244 (1933).
10. R. T. COUTTS, R. A. LOCOCK, and G. W. A. SLYWKA. Org. Mass Spectrom. **3**, 879 (1970).
11. H. BUDZIKIEWICZ, C. DJERASSI, and D. H. WILLIAMS. Mass spectrometry of organic compounds. Holden-Day Inc., San Francisco, California, 1967.
12. F. E. CISLAK. U.S. Pat. 2 938 037 (1960); Chem. Abstr. **55**, 1664*d* (1961).
13. J. PALECEK, L. PTACKOVA, and J. KUTHAN. Collect. Czech. Chem. Commun. **34**, 427 (1969).
14. I. C. SMITH and W. G. SCHNEIDER. Can. J. Chem. **39**, 1158 (1961); V. M. S. GIL and J. N. MURRELL. Trans. Faraday Soc. **60**, 248 (1964); G. KOTOWYCZ, T. SCHAEFER, and E. BOCK. Can. J. Chem. **42**, 2541 (1964); J. B. MERRY and J. H. GOLDSTEIN. J. Am. Chem. Soc. **88**, 5560 (1966).
15. R. LUKES and P. VACULIK. Chem. Listy, **51**, 1510 (1957); Chem. Abstr. **52**, 1163*c* (1958).
16. E. J. COREY and M. CHAYKOVSKY. J. Am. Chem. Soc. **86**, 1639 (1964).
17. E. WENKERT, K. G. DAVE, I. DAINIS, and G. D. REYNOLDS. Aust. J. Chem. **23**, 73 (1970).
18. G. B. BACKMAN and D. D. MICUCCI. J. Am. Chem. Soc. **70**, 2381 (1948).
19. H. A. IDDLES, E. H. LANG, and D. C. GREGG. J. Am. Chem. Soc. **59**, 1945 (1937).

Can. J. Chem. Downloaded from www.nrcresearchpress.com by 210.87.254.5 on 09/05/12
For personal use only.

The Constituents of *Nauclea diderrichii*. Part III. Indole-Pyridine Alkaloids

D. G. MURRAY, A. SZAKOLCAI, AND STEWART MCLEAN
Department of Chemistry, University of Toronto, Toronto 181, Ontario

Received October 25, 1971

Six alkaloids isolated from the bark of *Nauclea diderrichii* have been shown to have structures that contain both indole and pyridine units. Because of the small amounts available of each constituent, investigation of structure has been confined mainly to the application of spectroscopic techniques; these have shown that all of these alkaloids belong to the novel indole-pyridine class, and have led us to propose structures or part structures with varying degrees of confidence for each of the alkaloids. Structure **1** was deduced for naucledine, $C_{18}H_{15}N_3O_2$, and confirmed by synthesis. Its spectroscopic characteristics indicate that naucleder ine, $C_{19}H_{19}N_3O_2$, has structure **3**, but this has not yet been confirmed by synthesis. Evidence is presented that nauclechine, $C_{21}H_{21}N_3O_3$, has part structures **6** and **7**, and it is suggested that these can be incorporated in structure **8**. A working hypothesis for the structure of nauclexine, $C_{18}H_{17}N_3O_2$, is represented by **9**. Two alkaloids, ND-363C, $C_{21}H_{21}N_3O_3$, and ND-305B, $C_{19}H_{19}N_3O$, are closely related, the latter being formally derived from the former by removal of a carbomethoxy group; each appears to exist as an equilibratible pair of isomers containing an indolic (substituted β-carboline) and a pyridine part linked together in a manner which may incorporate a spiro carbinolamine ether (as in **12**) that can form ring-opened or solvated derivatives in some solvents.

Il a été montré que six alcaloides isolés à partir de l'écorce de *Nauclea diderrichii* ont des structures comprenant à la fois des unités indole et pyridine. Par suite des petites quantités disponibles, la détermination de structure s'est faite essentiellement par des techniques spectroscopiques; celles-ci ont montré que tous ces alcaloides appartiennent à la nouvelle classe indole-pyridine. Cela nous a conduit à proposer des structures ou des parties de structure, dépendant du degré de confiance pour chacun des alcaloides. La structure **1**, proposée pour la naucl édine, $C_{18}H_{15}N_3O_2$, a été confirmée par synthèse. Les propriétés spectroscopiques de la naucl édérine, $C_{19}H_{19}N_3O_2$, nous font proposer la structure **3**, mais cela n'a pas encore été confirmé par synthèse. Des preuves sont présentées d'après lesquelles la naucléchine, $C_{21}H_{21}N_3O_3$, aurait en partie les structures **6** et **7**, et il est suggéré que celles-ci peuvent être incorporées dans la structure **8**. Une hypothèse de travail pour la structure de la naucléxine, $C_{18}H_{17}N_3O_2$, est représentée par **9**. Deux alcaloides, ND-363C, $C_{21}H_{21}N_3O_3$, et ND-305B, $C_{19}H_{19}N_3O$, sont étroitement apparentés; le dernier dérivant du premier par abstraction du groupe carbométhoxy; chacun semble exister sous forme d'une paire d'isomères équilibrable, contenant une partie indolique (β-carboline substituée) et une partie pyridinique, liées entre eux d'une façon qui pourrait faire intervenir un spiro carbinolamine éther (comme dans **12**) qui peut donner des produits d'ouverture de cycle ou des produits solvatés dans certains solvants.

Canadian Journal of Chemistry, **50**, 1486 (1972)

We have recently described the isolation from the bark of *Nauclea diderrichii* of a considerable number of constituents which we have placed for convenience in four categories (1, 2). The alkaloids of the first two categories, β-carbolines and pyridines, have already been described in detail (2) and we turn now to the third category, a novel group of alkaloids which we have called the indole-pyridines. Six alkaloids have been placed in this category, and although the complete structure of only one of them has been established with complete confidence at this time, their structural novelty leads us to report the evidence which allows us to place them in this category and to assign to each a provisional structure or part structure. Since the appearance of our preliminary communication (1), the isolation from another member of the Rubiaceae of two other alkaloids of this class has been reported (3).

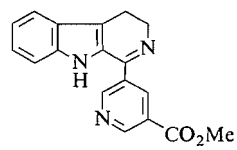

1

The first alkaloid, which we shall call naucledine, has been assigned structure **1**. It was isolated as crystals which melted over the range 84–90°; the wide range may result from the thermal instability of the compound, a dihydro-β-carboline. The formula, $C_{18}H_{15}N_3O_2$, was derived from its mass spectrum, which showed

Can. J. Chem. Downloaded from www.nrcresearchpress.com by 210.87.254.40 on 09/05/12
For personal use only.

Can. J. Chem. Downloaded from www.nrcresearchpress.com by 210.87.254.40 on 09/05/12
For personal use only.

a strong parent ion and, apart from a strong M − 1 peak, fragment ions of low relative intensity. The complex u.v. spectrum included a prominent peak at 328 mμ which showed a marked bathochromic and hyperchromic change in the presence of acid; this appearance and behavior is very similar to that described for the spectra of 1-aryl-3,4-dihydro-β-carbolines (4). The i.r. spectrum showed the sharp peak at 2.90 μ characteristic of an unassociated indolic NH group and carbonyl absorption near 5.80 μ which resembled that ascribed to the methyl ester functions of the pyridine alkaloids described previously (2). The characteristic signals of the aromatic protons of an indole appeared in the n.m.r. spectrum between τ 2.2 and 3.0 and the signals associated with a 3,5-disubstituted pyridine (2) appear at τ 0.81, 0.85, and 1.33; treatment of the sample with NaOD in D_2O was required to remove broadening of the pyridyl protons, and this also removed the indolic NH signal. The *O*-methyl signal was at τ 6.04, and the remaining four protons produced a symmetrical pattern of two-proton multiplets ("triplets") at τ 5.90 and 7.00 which resembled the pattern produced by the corresponding methylene groups of oxogambirtannine (5).

The structure of naucledine, **1**, was deduced from the results outlined here, and confirmed by synthesis of **1** from the acid chloride of 5-carbomethoxy-3-pyridinecarboxylic acid, available from the synthetic work we have already described in connection with the pyridine alkaloids (2). The synthesis was effected by the reaction of the acid chloride with tryptamine and the cyclization of the amide so formed to **1**, identical with natural naucledine, under Bischler–Napieralski conditions. As a preliminary to this synthesis we carried out the corresponding reactions starting with the model compounds 3- and 4-pyridinecarboxylic acid in order to discover conditions suitable for each step; this exploration was all the more necessary in the light of a report (6) that the Bischler–Napieralski cyclization failed with the amide derived from tryptamine and 3-pyridinecarboxylic acid. Our initial efforts confirmed that the cyclization failed under the conditions described (6), but we found that cyclization of the amides was successful in refluxing phosphorus oxychloride, albeit with extremely low conversion in the case of the isomer derived from 4-pyridinecarboxylic acid, and these conditions were then used in the synthesis of naucledine. In each case these Bischler–Napieralski conditions led to the formation of a by-product which appeared to be the aromatized β-carboline.

The second alkaloid in this category, which we shall refer to as naucledérine, has the formula $C_{19}H_{19}N_3O_2$ and is crystalline, but, once again, our samples melted over a considerable range, 102–124°, and showed signs of resolidifying and remelting at a higher temperature. The u.v. spectrum with a maximum at 276 mμ (ε, 9550) and a shoulder at 290 mμ could be accounted for as the summation of separate indole and pyridine chromophores (in contrast to the case of naucledine), and the i.r. spectrum showed N—H absorption, including a sharp 2.90 μ peak, and the 5.80 μ absorption characteristic of the ester group of the pyridine alkaloids described previously (2). The n.m.r. spectrum showed the patterns characteristic of aromatic protons of an indole and of a 3,5-disubstituted pyridine, and a three-proton singlet at τ 6.14 indicated that a methyl ester was present; one of the aliphatic protons formed an apparent triplet with 4 Hz spacings at τ 5.73 and the remainder were responsible for a complex pattern near τ 6.8. Peaks, which were removed when the sample was treated with D_2O, appeared at τ 1.61 and 7.55 and were attributed to the NH protons of an indole and an aliphatic secondary amine, respectively; support for the latter assignment was obtained when naucledérine formed an amide on acylation.

If it is assumed that naucledérine is derived from tryptamine without modification of the $—CH_2CH_2N<$ unit, three structures (**2**, **3**, **4**) must be considered for the alkaloid on the basis of the evidence presented so far. The mass spectrum provided evidence that structure **2** is a very unlikely possibility since it contained no significant peak at *m/e* 171, which corresponds to the most abundant fragment ion in the spectrum of 1-alkyltetrahydro-β-carbolines (7). Instead, the base peak was at *m/e* 279 ($M - C_2H_4N$ by accurate mass measurement), and the molecular ion peak was next in intensity, followed by a strong peak corresponding to $M - CH_3N$. Fragmentations of **3**

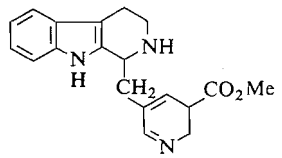

2

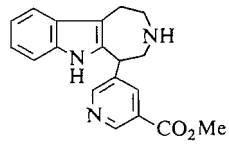

3

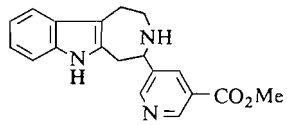

4

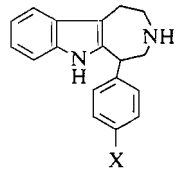

5

leading to the observed ions can be postulated, but it is more difficult to provide a rational explanation for the loss of C_2H_4N as the principal fragmentation of a molecule of formula **4**. Compounds of formula **5** have been described recently (8) and we are extremely grateful to Dr. K. Freter for generous samples of **5** (X = H and X = Cl). These show a marked similarity to naucleferine in their spectroscopic characteristics, particularly significant being the mass spectral fragmentation pattern which corresponded closely to that of naucleferine, especially with respect to the most intense peaks. The n.m.r. spectrum of **5** (X = Cl) also resembled that of naucleferine in showing the signal for one proton as an apparent triplet with 4.5 Hz spacings at τ 5.79, a multiplet near τ 6.8 attributed to the aliphatic protons, and the signal for the NH proton of the seven-membered ring at τ 7.63. The evidence presented here leads us to propose with a considerable degree of confidence that naucleferine has structure **3**, and we are currently attempting to establish this with complete certainty by a total synthesis.

The third alkaloid of this class, given the name nauclechine, m.p. 108–114°, has the formula $C_{21}H_{21}N_3O_3$. As with naucleferine, its u.v. spectrum is compatible with the presence in the molecule of separate indole and pyridine chromophores, and its i.r. spectrum shows strong absorption in the 2.8–3.1 μ region with a sharp peak, appropriate for an indolic NH, at 2.91 μ, and a carbonyl peak at a wavelength, 5.83 μ, very slightly longer than that observed previously in the spectra of the esters of 3-pyridinecarboxylic acids (2). A three-proton singlet at τ 5.94 in the n.m.r. spectrum supported the proposal that we again had the methyl ester of a pyridinecarboxylic acid, and the signals for the aromatic protons and the exchangeable NH proton of an indole were also present; when the sample was treated with D_2O, in addition to the loss of the indole NH signal at τ 1.28, a peak was lost from the envelope near τ 6.2, and this peak is attributed to the OH proton of an alcohol. The n.m.r. spectrum also provided evidence that the molecule contained a pyridine unit, but, in this case the signals observed were one-proton singlets at τ 0.98 and 1.42, and are assigned to the protons at positions 2 and 6 of a 3,4,5-trisubstituted pyridine. The part of the spectrum associated with aliphatic protons is complex, but a one-proton doublet, $J = 6.5$ Hz (slightly broadened by further weak coupling) at τ 5.08 is well separated on the low field side, and is attributed to a proton on a carbon atom carrying an OH group and attached to a pyridine ring; double irradiation showed that this proton was coupled to a proton at τ 6.49, which appeared to have an additional coupling, $J = 12.5$ Hz, to a third proton at τ 7.19; two slightly broadened peaks at the edge of the aliphatic envelope can be accounted for as the low field component (a doublet at τ 5.80, $J = 15.0$ Hz) of a second, independent three-spin system in which the proton at lowest field is coupled strongly ($J = 15.0$ Hz) to a proton at τ 6.54 and weakly ($J < 1$ Hz) to a proton at τ 6.22, and the latter two protons are themselves coupled with $J = 9.0$ Hz. In the mass spectrum the molecular ion at *m/e* 363 provides the base peak, an intense M − 1 peak is present, and strong peaks are observed at *m/e* 184, 183, 170, 169, and 156, a pattern that is characteristic of the tetrahydro-β-carbolines, such as yohimbine, in which positions 1 and 2 are further annelated; the spectrum in these regions bears, in fact, a strong resemblance to that of ajmalicine, and accurate mass measurement of the ions listed shows, furthermore, that they have the same formulae as those appearing in the fragmentation of ajmalicine (9). In addition, the spectrum has peaks at *m/e* 332 (M − OCH_3) and 346 (M − OH), and these fragmentations, verified by accurate mass measurements, are characteristic of the methyl ester of an aromatic carboxylic acid and a benzylic-type alcohol, respectively (10).

The evidence presented here is entirely in accord with the presence of both of the part

Can. J. Chem. Downloaded from www.nrcresearchpress.com by 210.87.254.40 on 09/05/12
For personal use only.

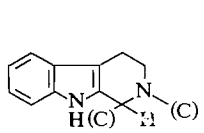

6

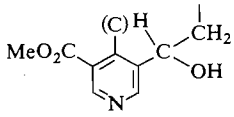

7

structures **6** and **7** in nauclechine. In particular, the mass spectral evidence for **6**, with no further substitution of the tetrahydro-β-carboline, is compelling; the n.m.r. evidence requires a 3,4,5-trisubstituted pyridine as in **7** and the n.m.r., i.r., and mass spectra all indicate the types of substituents illustrated, but they do not show unequivocally that the groups are in the order shown. The order appears probable when comparison is made with the simple pyridine alkaloids described previously, and when **6** and **7** are combined in **8**, a credible explanation can be given of all of the available data. In addition to the features already dis-

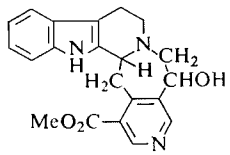

8

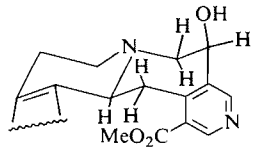

8*a*

cussed with respect to the individual part structures, the protons on the seven-membered ring incorporated in **8** would be expected to give rise in the n.m.r. spectrum to two separate three-spin systems, and the analysis outlined above shows that the spectrum does satisfy this requirement. A reasonable stereochemical arrangement (**8***a*) of the molecule can be suggested in explanation of the coupling constants observed: in each three-spin system the methylene protons have a strong mutual coupling, but only one proton in each pair has the appropriate angular relationship with the vicinal proton to couple appreciably with it; the chemical shift assignments are reasonable, with the proton on the carbon bearing the OH group being at lowest field (τ 5.08) in one set, but in the other three-spin set, the low field resonance (τ 5.80) must be assigned to the quasi-equatorial methylene proton, and its unusually low value must be associated with the location of the proton in the plane of the pyridine ring and adjacent to the carbomethoxy group. The presence of a Bohlmann band (11) in the i.r. spectrum is in accord with the suggested stereochemistry.

In summary, we propose that the structure of nauclechine is constituted of the components **6** and **7**; **8** represents a combination of these part structures that is entirely in accord with the available data, but the evidence falls short of establishing unequivocally that nauclechine has this structure.

The fourth alkaloid, which we shall refer to as nauclexine, was isolated as a small amount of crystalline substance, $C_{18}H_{17}N_3O_2$, m.p. 229–232°, from only one lot of bark. Its u.v. spectrum, which clearly distinguishes it from the other alkaloids we have obtained, indicates that it is a 2-acylindole, but its intense absorption at 300 mμ, which is unaffected by the addition of either acid or base, is at a wavelength 10–15 mμ shorter than that of typical 2-acylindole alkaloids (12). Its i.r. spectrum shows a very strong peak at 6.13 μ at the upper end of the range associated with the carbonyl group of 2-acylindole alkaloids and about 0.05 μ above a typical value (12); the i.r. spectrum also shows a sharp peak at 2.91 μ, indicative of an indolic NH, superimposed on a broader peak centered at about 3.05 μ. Because of the poor solubility of nauclexine in chloroform-*d*, its n.m.r. spectrum was obtained under special conditions (see Experimental). In the aromatic region of the spectrum, evidence of an indole was present, but the broadening of the lower field peaks associated with protons on a pyridine ring did not allow a confident assignment of the substitution pattern on the pyridine ring to be made. The only other useful deduction that can be drawn from the spectrum is that a multiplet at τ 4.89 has the characteristics expected for the signal of a proton on a carbon attached to a pyridine ring and carrying an OH group. There is, therefore, presumptive evidence that nauclexine contains a disubstituted pyridine ring and a 2-acylindole unit. If the molecule retains the $—CH_2CH_2N<$ unit of a tryptamine precursor, only one carbon atom remains unassigned and this must be placed between the nitrogen and the CHOH unit since the alkaloid does not appear to be a carbinolamine.

If all of these deductions were firmly grounded, and the usual 3,5-disubstitution pattern of the pyridine ring could be established, structure

Can. J. Chem. Downloaded from www.nrcresearchpress.com by 210.87.254.40 on 09/05/12
For personal use only.

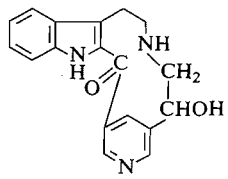

9

9 would represent nauclexine; unfortunately the quality of the data does not permit us to go further than suggesting this interesting structure as a working hypothesis. The unusual 11-membered ring, produced by a meta-bridging of the pyridine ring, has the virtue of providing an explanation for the failure of the amine and ketone to form a transannular carbinolamine bridge since such a bridge would produce a very highly strained system; however, a severe constraint of this sort is not obligatory since the position of the equilibrium between the amino ketone and carbinolamine forms can depend on more subtle stereochemical features than this (13). The mass spectrum of nauclexine is compatible with structure **9**. It is characterized by the presence of an extremely intense peak at *m/e* 199 ($C_{12}H_{11}N_2O$ by accurate mass measurement), much stronger than any other peak in the spectrum, which can be assigned to an ion resulting from loss of the pyridine by fragmentation at the picolyl position and, accompanied by a hydrogen transfer, cleavage between the carbonyl group and the pyridine ring. Peaks corresponding to those in picraphylline and burnamicine (14) were observed at *m/e* 129, 130, 143, and 144; significant peaks were also observed at *m/e* 157, 169, 170, 171, and 184. The absence of a peak corresponding to M − OH was unexpected, but it may be noted that all of the peaks corresponding to ions, including the parent ion, of higher mass than the base peak were of low intensity.

The next alkaloid, which we shall refer to by its laboratory designation ND-363C (the number indicating the assigned molecular weight), was isolated as a viscous syrup which, on the basis of its t.l.c. behavior, appeared to be homogeneous. The formula $C_{21}H_{21}N_3O_3$ was assigned to it by accurate mass measurement of the parent ion in the mass spectrum, and evidence was seen in the i.r. spectrum that we once again had a molecule which was both an indole (2.90 μ) and a carbomethoxypyridine (5.80 μ). The u.v. spectrum was extremely distinctive: ND-363C, in methanol containing added alkali, produced a spectrum with absorption of moderate intensity between 250 and 300 mμ that was very similar to that of the alkaloids containing separate indole and pyridine chromophores, while a solution in methanol containing added acid produced a dramatically different spectrum, characterized by intense absorption at 364 mμ, and the spectrum of a solution in methanol alone showed both sets of peaks with intensities between the limits in acid and alkali. The n.m.r. spectrum of ND-363C is extremely complex, but a considerable simplification in its interpretation can be achieved if it is postulated that it arises from two closely related species present in equal concentrations so that each set of peaks is doubled (but sometimes coincident). In the low field region of the spectrum, four doublets, at τ 0.85, 0.99, 1.17, and 1.50, and two triplets, at τ 1.68 and 2.20, can be assigned to overlapping patterns resulting from two 3,5-disubstituted pyridines; complex absorption between τ 2.5 and 3.0 has an integrated area on this basis corresponding to the aromatic protons of two indole moieties; multiplets at τ 4.70 and 5.08 each of which has the appearance of an X part of an AMX system, can each be assigned to one proton and singlets at τ 6.09 and 6.34 are associated with two different methyl esters; signals that correspond to protons exchangeable with D_2O are present at τ 0.99 and 8.22 but it is difficult to be confident about the number of protons related to them, the low field peak being reasonably assigned on the present basis to the superimposition of the NH signals of two indole units but the high field peak being considerably more intense (it could correspond to as many as three protons on each of the two molecular species); the remaining signals fall between τ 6 and 7.5 and are complex and poorly resolved.

The doubling of the n.m.r. spectrum could arise if ND-363C were a dimeric or pseudodimeric molecule (15), but we have no evidence that the molecular weight is higher than the assigned value, and at present we prefer to explain our results by proposing that ND-363C exists as two isomers that can be readily equilibrated and are, therefore, inseparable by t.l.c. The u.v. spectra of ND-363C are compatible with the presence in the molecule of the car-

Can. J. Chem. Downloaded from www.nrcresearchpress.com by 210.87.254.40 on 09/05/12
For personal use only.

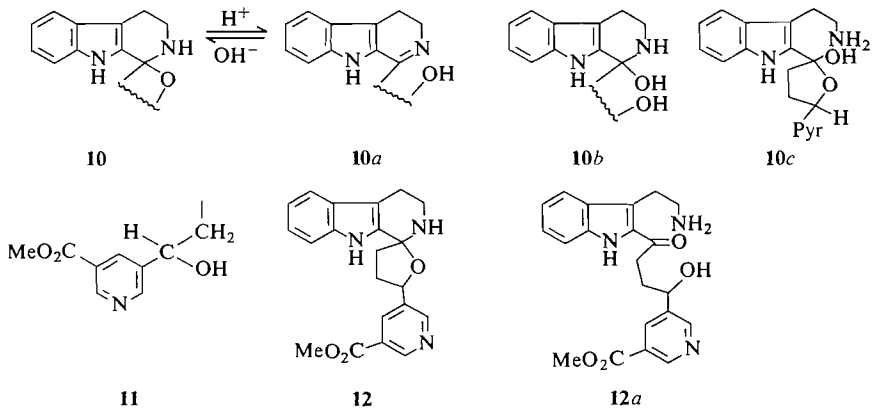

10 **10*a*** **10*b*** **10*c***

11 **12** **12*a***

binolamine ether of part structure **10** which can equilibrate with the open form **10*a***; in addition, the i.r. and n.m.r. evidence points to the presence of two units of part structure **11**, the multiplets at τ 4.70 and 5.08 being taken as evidence for the presence of a hydrogen on a carbon bearing an oxygen, a methylene group and a pyridine ring. If **10** and **11** are now combined in **12**, it can be seen that ND-363C could well exist in chloroform solution as the two diastereoisomers of **12**, epimeric at the spiro junction, equilibratible through **10*a***, of comparable free energy, and therefore present in approximately equal concentrations. Evidence contrary to this hypothesis is seen in the u.v. spectrum of ND-363C in neutral methanol where it is assumed that a considerable amount of the form **10*a*** is present and it is necessary to argue that the discrepancy arises because of the different solvents used to obtain the u.v. and n.m.r. spectra. It is more difficult to find a satisfactory explanation for the presence at τ 8.22 in the n.m.r. spectrum of strong peak that is removed by treatment of the sample with deuterium oxide. It is tempting to suggest that the equilibrium mixture contains a further component that is a hydrated species such as **10*b*** or *c*, and it can be seen that all of these structures can be derived, at least formally, by cyclizations of the open keto form, **12*a***, of the molecule through condensations of the carbonyl group with the hydroxy or amino functions or both; it should be noted, however, that only those derivatives which are chiral at both carbon centers bearing an oxygen function can exist as diastereoisomeric pairs and that the n.m.r. evidence can be satisfied only if all of the protons on oxygen or nitrogen have effectively the same chemical shift, but interconversion of diastereoisomers is not rapid enough to produce time-averaged signals in the rest of the molecule. The mass spectrum provides no evidence that the isolated sample is hydrated, and, although it is possible that a complex equilibrium between different forms, each of which predominates under different conditions, may supply the complete explanation, further work, when we have isolated sufficient alkaloid, will be required to establish this.

The mass spectrum of ND-363C provided evidence that the molecular formula is $C_{21}H_{21}N_3O_3$ and that no ions of higher mass, corresponding to a dimeric alkaloid and its fragment ions or a hydrated species, could be found; the appearance of peaks at *m/e* 130, 156, and 169 and the absence of an appreciable M − 1 peak supported the postulate that the structure was based on a tetrahydro-β-carboline which lacked a hydrogen at C-1 (9), and the presence of a peak corresponding to M − OCH_3 was in accord with the presence of the methyl ester of a pyridinecarboxylic acid (10). However, two peaks in the spectrum present problems on first examination; the base peak at *m/e* 348, which corresponds to M − CH_3 and the prominent peak at *m/e* 198. The loss of a methyl radical is a rare but not unprecedented fragmentation process (16) if the molecule does not have a preformed methyl group but we know of no case in which such a fragmentation produces the base peak. The n.m.r. spectrum of ND-363C provided no evidence for the presence of a methyl group, other than that of the ester function which would not be expected to frag-

Can. J. Chem. Downloaded from www.nrcresearchpress.com by 210.87.254.40 on 09/05/12
For personal use only.

ment by loss of a methyl radical (10). We have sought to reconcile these conflicting pieces of evidence by utilizing a distinctive feature of **12**. An important site of cleavage of the molecular ion of **12** can be expected to be the spiro center, and two ions formed by rupture at *a* or *b* are of particular significance, the former leading, after transfer of a hydrogen, to ion **A** which can be expected to form a stable fragment

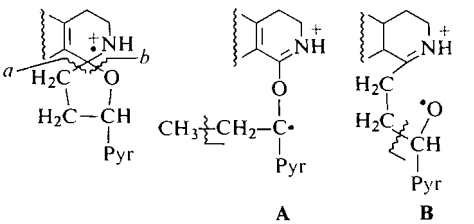

A **B**

ion by loss of a methyl radical; rupture at *b* would lead to ion **B** which would then lose the pyridyl portion of the molecule along with the CHO unit as an uncharged fragment and leave an ion of *m/e* 198.

A further alkaloid, designated ND-305B, appears to be very closely related to ND-363C, and, indeed, all of the observable properties of ND-305B can be accounted for on the basis that its structure is the same as that of ND-363C with the carbomethoxy group removed. It has the formula $C_{19}H_{19}N_3O$, its i.r. spectrum lacks the carbonyl absorption but retains the NH absorption, and its u.v. spectrum resembles that of ND-363C both in appearance and in behavior in acid or base. The n.m.r. spectrum of ND-305B shows a very close correspondence to that of ND-363C except that the methoxyl signals are now absent and the protons of the pyridine ring lead to a complex multiplet in the low field region of the spectrum. As with ND-363C, the problem regarding the presence of a high field signal, now at τ 8.21 due to protons exchangeable with D_2O also remains, as does the question of the origin of peaks at $M - CH_3$ and *m/e* 198 in the mass spectrum of ND-305B; the latter data do, however, demonstrate that the methyl radical is not lost from a carbomethoxy group (in ND-363C such a process was conceivable but highly improbable), and that the *m/e* 198 peak arises from the portion of the molecule that does not contain the pyridine ring. In short, the above discussion of the nature of ND-363C applies equally well to ND-305B, except that the carbomethoxy group is absent in the latter, and the results obtained for ND-305B buttress to some extent the conclusions based on ND-363C alone. The alkaloids, apparently equilibratible pairs of isomers, contain an indole (substituted β-carboline) part and a pyridine part which are linked together in a manner that has not yet been fully explained, but probably involves a function such as a carbinolamine ether that allows equilibration through a reversible cyclization.

In summary, the evidence presented allows us to place the six alkaloids in the novel class we have called the indole-pyridines; the complete structure of naucledine has been deduced and confirmed by synthesis, while for the other alkaloids additional features of their structures have been described and structural proposals have been advanced with varying degrees of confidence. However, there still remains the question of whether or not these are truly natural products, or whether they are artifacts produced in isolation procedures which used ammonia (2). It is known that some so-called pyridine alkaloids arise in this way (17). In our studies we have attempted to rule out this possibility by carrying out an isolation and separation of the alkaloids by a procedure that rigorously avoided the use of ammonia (2). Unfortunately, the only base isolated and identified on that occasion was a simple pyridine (compound **6** in ref. 2); while this result shows that the pyridine nucleus did not necessarily arise by the incorporation of ammonia used in the isolation procedure, the absence of the more interesting and more complex indole-pyridines described above is cause for concern. However, if these substances were artifacts, they would nevertheless have been the transformation products of natural precursors which were, themselves, structurally related indole alkaloids, and these were not isolated either under these conditions. We have noted previously (2) that the yields of individual alkaloids from different batches of bark were extremely variable and we consequently consider that the status of the indole-pyridines as natural products is still not proven; their interest as chemical entities remains, regardless of their origin.

Can. J. Chem. Downloaded from www.nrcresearchpress.com by 210.87.254.40 on 09/05/12
For personal use only.

Can. J. Chem. Downloaded from www.nrcresearchpress.com by 210.87.254.40 on 09/05/12
For personal use only.

Experimental

A description of routine instrumentation, spectroscopic conditions, extraction procedures, etc. has already been given (2).

Naucledérine

Naucledine was separated in t.l.c. systems of relatively low polarity. It was recrystallized from methanol and obtained as pale yellow needles, melting over the range 84–90°. Spectroscopic characteristics: i.r. 2.90 (sharp), 3.07 (broad), 5.79, 5.82 (shoulder); u.v. 220 (26 000, end absorption), 232 (shoulder), 248 (shoulder), 267 (shoulder), 328 (8900); 352 (shoulder); in MeOH–HCl 220 (18 000; end absorption), 252 (9800), 269 (shoulder), 306 (13 000); n.m.r. (solution treated with 6% NaOD in D_2O) 0.81 (d, $J = 2$ Hz; 1), 0.85 (d, $J = 2$ Hz; 1), 1.33 (3 peaks, 2 Hz spacings; 1) (prior to treatment of the sample with NaOD, these three signals gave unresolved single peaks and an additional one-proton peak appeared at 1.05), 2.2–3.0 (complex; 4), 5.90 and 7.00 (each 3 peaks, 8 Hz spacings; each 2), 6.04 (s; 3); mass spectrum 306 (20), 305 (100), 304 (85), 303 (15), 290 (3), 277 (5), 276 (4), 247 (7), 246 (8), 245 (12), 244 (11), 219 (9), 218 (18), 217 (14), 216 (6), 191 (5), 190 (7), 143 (12), 140 (6), 123 (6), 122.5 (8), 115 (8), 109 (6), 95.5 (7); metastable 303.7 (calcd. for 305 → 304: 303.1); mass measurements calcd. (found): $C_{18}H_{15}N_3O_2$, 305.11643 (305.1181); $C_{17}H_{13}N_2O_2$, 277.09770 (277.0966); $C_{16}H_{11}N_3$, 245.09530 (245.0950); $C_{15}H_{10}N_2$, 218.08440 (218.0835); $C_{10}H_9N$, 143.07350 (143.0743).

Naucledérine

Naucledérine was obtained from fairly polar t.l.c. systems. It was obtained as a syrup which was soluble in methanol and this solution deposited crystals which were then almost insoluble in methanol. The crystals melted over a wide range, typically 102–124°, partially resolidified on further heating and remelted at higher temperatures, typically in the range 172–183°. Two different samples of the crystals had $[\alpha]_D^{26}$ −13° (c 0.8, $CHCl_3$) and $[\alpha]_D^{25}$ 0° (c 3.3, $CHCl_3$). Spectroscopic characteristics: i.r. 2.90 (sharp), 3.03 (broad), 5.80, 5.82 (shoulder); u.v. 224 (40 700), 276 (9550), 290 (shoulder); n.m.r. (solution treated with K_2CO_3/D_2O) 1.03 (d, $J = 2$ Hz; 1), 1.48 (d, $J = 2$ Hz; 1), 1.88 (3 peaks, 2 Hz spacings; 1) (prior to treatment of the sample with K_2CO_3/D_2O, these three signals gave unresolved single peaks and an additional one-proton peak appeared at 1.61), 2.4–3.0 (complex; 4), 5.73 (3 peaks, 4 Hz separations; 1), 6.14 (s; 3), 6.5–7.0 (complex; 6), (2.45 (broad; 1; present only prior to treatment of sample with D_2O)); mass spectrum (a peak at 335 of variable intensity was probably produced by a contaminant), 322 (13), 321 (59), 293 (9), 292 (44), 291 (17), 280 (20), 279 (100), 277 (14), 266 (3), 247 (6), 233 (7), 219 (12), 218 (8), 204 (7), 191 (4), 167 (6), 165 (5), 156 (4), 130 (7), 57 (7), 43 (10), 42 (12); metastables 290.2 (calcd. for 292 → 291: 290.0), 265.8 (calcd. for 321 → 292: 265.7), 262.9 (calcd. for 292 → 277: 262.4), 242.5 (calcd. for 321 → 279: 242.5); mass measurements calcd. (found): $C_{19}H_{19}N_3O_2$, 321.14773 (321.1468); $C_{18}H_{16}N_2O_2$, 292.12118 (292.1210); $C_{17}H_{15}N_2O_2$, 279.11335 (279.1124); $C_{17}H_{13}N_2O_2$, 277.09770 (277.0977); $C_{16}H_{14}N_2O_2$, 266.10553 (266.1051); $C_{15}H_{11}N_2$, 219.09222 (219.0914); $C_{10}H_{13}N_3O$, 191.10586 (191.1057); $C_8H_{13}N_3O$, 167.10586 (167.1056). *p*-Bromobenzoyl chloride in pyridine reacted with the alkaloid to form a crystalline derivative, m.p. 207–210°; i.r. 2.90 (sharp), 3.06 (broad), 5.80, 5.83 (shoulder), 6.15; mass measurements calcd. (found): $C_{26}H_{22}N_3O_3{}^{81}Br$, 505.08254 (505.0828); $C_{26}H_{22}N_3O_3{}^{79}Br$, 503.08451 (503.0835); $C_{19}H_{16}N_2O_2$ (fragment ion) 304.12118 (304.1212).

The model 5-phenylhexahydroazepinoindole **5** (X = H) kindly provided by Dr. K. Freter (Pharma-Research Canada, Ltd.) provided the following mass spectrum: 263 (10), 262 (47), 234 (5), 233 (27), 232 (16), 230 (4), 221 (18), 220 (100), 219 (7), 218 (15), 217 (16), 204 (5), 115 (5), 108.5 (4), 43 (4), 42 (5); metastables 216.5 (calcd. for 220 → 218: 216.1), 208.1 (calcd. for 233 → 220: 207.7), 207.1 (calcd. for 262 → 233: 207.2), 203.8 (calcd. for 233 → 218: 204.0), 184.8 (calcd. for 262 → 220: 184.7); mass measurements calcd. (found): $C_{18}H_{18}N_2$, 262.14700 (262.1471); $C_{17}H_{15}N$, 233.12045 (233.1194); $C_{16}H_{14}N$, 220.11262 (220.1132). The corresponding chloro derivative **5** (X = Cl) showed: 289 (19), 297 (12), 296 (58), 294 (5), 269 (11), 268 (12), 267 (32), 266 (18), 257 (6), 256 (33), 255 (20), 254 (100), 252 (7), 232 (25), 231 (10), 230 (10), 219 (13), 218 (32), 217 (35), 216 (6), 204 (6), 148 (7), 130 (11), 115 (7), 108.5 (5), 102 (5), 43 (11), 42 (14).

Nauclechine

Nauclechine was obtained from t.l.c. systems of intermediate polarity. It was recrystallized from chilled methanol and isolated as white crystals, m.p. 108–114°. Spectroscopic characteristics: i.r. 2.91 (sharp), 3.00 (broad), 3.60 (Bohlmann band (11)), 5.83; u.v. 224 (40 700), 272 (10 050), 288 (shoulder); n.m.r. (solution treated with K_2CO_3/D_2O) 0.98 (s; 1), 1.42 (s; 1) (prior to treatment of the sample with K_2CO_3/D_2O these two peaks were broadened and an additional one-proton peak appeared at 1.28), 2.4–3.0 (complex; 4), 5.08 (2 peaks, 6.5 Hz spacing; collapsed to singlet by irradiation at 6.49; 1), 5.80 (2 peaks, 15.0 Hz spacing; 1), 5.94 (s; 3), 6–7.5 (complex; 8; included in this was a set of peaks centered at 6.49 indicating one proton with J values 12.5 and 6.5 Hz, the latter coupling being removed by irradiation at 5.08; the signals overlapped a set of peaks indicating one proton with J values 15.0 and 9.0 Hz; pairs of peaks with spacings of 9.0 and 12.5 Hz respectively appeared at 6.22 and 7.19; an additional broad signal at ≃6.2 was present only prior to treatment of the sample with D_2O); mass spectrum 364 (23), 363 (100), 362 (87), 361 (5), 348 (5), 347 (6), 346 (22), 332 (10), 303 (5), 185 (10), 184 (48), 183 (43), 182 (7), 171 (13), 170 (39), 169 (55), 168 (10), 167 (6), 157 (9), 156 (32), 155 (10), 154 (11), 144 (16), 143 (16), 142 (6), 130 (11), 129 (9), 128 (8), 127 (5), 117 (5), 116 (5), 115 (10), 86 (6), 84 (9), 77 (7), 65 (5), 57 (5), 51 (5), 49 (12), 43 (8), 42 (9), 41 (5); metastable 361.6 (calcd. for 363 → 362: 361.0); 15 eV spectrum 363 (100), 362 (29), 184 (6), 183 (6), 170 (6); mass measurements calcd. (found): $C_{21}H_{21}N_3O_3$, 363.15829 (363.1575); $C_{21}H_{20}N_3O_2$, 346.15555 (346.1551); $C_{20}H_{18}N_3O_2$, 332.13990 (332.1398), $C_{12}H_{12}N_2$, 184.10005 (184.1006); $C_{12}H_{11}N_2$, 183.09222 (183.0923), $C_{11}H_9N_2$, 169.0760 (169.07657), $C_{11}H_{10}N$, 156.0815 (156.08132).

Nauclexine

Nauclexine was obtained from t.l.c. systems of intermediate polarity. It was recrystallized from a mixture

Can. J. Chem. Downloaded from www.nrcresearchpress.com by 210.87.254.40 on 09/05/12
For personal use only.

of methylene chloride and methanol and isolated as off-white needles, m.p. 229–232°, which appeared to be weakly laevorotatory in methanol but an accurate value for the specific rotation could not be measured because of the very small amount of material available. Spectroscopic characteristics: i.r. 2.91 (sharp), 3.05 (broad), 6.13 (v. strong); u.v. 226 (17 800), 235 (14 800), 300 (15 850); n.m.r. (dilute solution in 98:2 $CDCl_3$–CD_3OD; 150 scans CAT; peak areas obtained only very approximately) 0.21 (broad; 1), 2.0–3.0 (complex; ?), 4.89 (m; 1), 6.0–7.1 (complex; 6); (dilute solution in 1:1 $CDCl_3$–CD_3OD; 150 scans CAT) additional (one-proton ?) peaks appear at 0.97, 1.36, and 1.53; the 4.89 multiplet appears to have 4 peaks with 5.0, 2.5, and 5.0 Hz spacings, and at 7.03 there is an apparent two-proton triplet, $J = 7.0$ Hz; mass spectrum 307 (9), 200 (20), 199 (100), 184 (2), 171 (5), 170 (5), 169 (8), 157 (4), 144 (10), 143 (8), 130 (6), 129 (9), 128 (5), 115 (6), 102 (4), metastables 168.7 (calcd. for 171 → 170: 169.0), 147.0 (calcd. for 199 → 171: 146.9), 145.2 (calcd. for 199 → 170: 145.2), 129.0 (calcd. for 307 → 199: 129.0), 121.3 (calcd. for 171 → 144: 121.3); 15 eV spectrum 307 (100), 199 (40); mass measurements calcd. (found): $C_{18}H_{17}N_3O_2$, 307.13208 (307.1336); $C_{12}H_{11}N_2O$, 199.08714 (199.0869); $C_{11}H_9N_2$, 169.07657 (169.0764); $C_{10}H_{10}N$, 144.08132 (144.0816); C_9H_7, 115.05478 (115.0546).

Alkaloid ND-363C

This alkaloid was separated by moderately polar t.l.c. systems and was obtained as a syrup which appeared homogeneous in five t.l.c. systems. Spectroscopic characteristics: i.r. 2.90 (sharp), 3.04 (broad), 5.80, 5.82 (shoulder); u.v. 223 (31 500), 252 (6900), 271 (7100), 291 (4800), 360 (6500); in MeOH–HCl 223 (16 200, end absorption), 250 (11 200), 266 (shoulder), 364 (18 600); in MeOH–KOH 223 (38 900), 274 (8700), 281 (shoulder), 290 (shoulder); n.m.r. (solution treated with K_2CO_3/D_2O; the number of protons assigned to each signal is based on the assumption that two $C_{21}H_{21}N_3O_3$ units are present) 0.85 (d, $J = 2$ Hz; 1), 0.99 (d, $J = 2$ Hz; 1), 1.17 (d, $J = 2$ Hz; 1), 1.50 (d, $J = 2$ Hz; 1); 1.68 (3 peaks, 2 Hz spacings; 1), 2.20 (3 peaks; 2 Hz spacings; 1), (prior to treatment of the sample with K_2CO_3/D_2O, these six signals appeared as unresolved peaks and the 0.99 signal corresponded to a total of 3 protons), 2.4–3.0 (complex; 8), 4.70 (4 peaks, spacings 6, 3, and 6 Hz; 1), 5.08 (4 peaks, spacings 6, 1, and 6 Hz; 1), 6.09 (s; 3), 6.34 (s; 3), 6.4–7.5 (complex; ≃16), 8.22 (s; ≃6; present only prior to treatment of the sample with D_2O); mass spectrum 364 (6), 363 (18), 349 (24), 348 (100), 332 (2), 316 (4), 199 (7), 198 (25), 197 (6), 172 (9), 170 (7), 169 (12), 165 (5), 164 (13), 157 (6), 156 (6), 155 (9), 154 (7), 144 (10), 143 (6), 134 (5), 130 (11), 129 (9), 128 (5), 115 (6), 104 (5), 77 (7); metastables 334.0 (calcd. for 363 → 348: 333.6), 287.0 (calcd. for 348 → 316: 286.9); 13 eV spectrum 363 (100), 348 (39), 198 (91); mass measurements calcd. (found): $C_{21}H_{21}N_3O_3$, 363.15829 (363.1578); $C_{20}H_{18}N_3O_3$, 348.13482 (348.1345); $C_{20}H_{18}N_3O_2$, 332.13990 (332.1401); $C_{19}H_{14}N_3O_2$, 316.10860 (316.1089).

Alkaloid ND-305B

This alkaloid was separated by more polar t.l.c. systems and was obtained as a syrup that appeared by t.l.c. to be homogeneous. Spectroscopic characteristics: i.r. 2.90 (sharp), 3.10 (broad); u.v. 224 (30 900), 250 (shoulder), 262 (shoulder), 284 (7800), 292 (7250), 310 (shoulder), 360 (5400); in MeOH–HCl 224 (16 200, end absorption), 251 (13 800), 365 (17 400); in MeOH–KOH 215 (47 900, end absorption), 223 (shoulder), 269 (10 250), 283 (9800), 291 (shoulder); n.m.r. (solution treated with K_2CO_3/D_2O; the number of protons assigned to each signal is based on the assumption that two $C_{19}H_{19}N_3O$ units are present) 1.3–1.5 (complex; ≃6; prior to treatment of the sample with D_2O the peak at 1.32 was higher), 2.2 (two peaks, 7 Hz spacing and fine splitting; 1), 2.47 (m; ≃1), 2.5–3.0 (complex; ≃8), 4.71 (4 peaks, spacings 6, 3, and 6 Hz; 1), 5.08 (4 peaks, spacings 6, 1, and 6 Hz; 1), 6.1–7.6 (complex; ≃18), 8.21 (s; ≃6; present only prior to treatment of the sample with D_2O); mass spectrum 305 (16), 291 (23), 290 (100), 199 (13), 198 (20), 183 (9), 182 (10), 156 (7), 155 (9), 154 (8), 144 (10), 143 (7), 130 (12), 129 (10), 128 (7), 115 (7), 106 (19), 78 (12), 77 (10); metastable 275.9 (calcd. for 305 → 290: 275.7); mass measurements calcd. (found): $C_{19}H_{19}N_3O$, 305.15281 (305.1531); $C_{18}H_{16}N_3O$, 290.12934 (290.1299).

Synthesis of 1-(3'-Pyridyl)-3,4-dihydro-β-carboline (Model Compound)

N-Nicotinoyl-β-(3-indolyl)ethylamine (125 mg; 0.47 mmol) prepared from tryptamine and the hydrochloride of nicotinoyl chloride (6), was suspended in phosphorus oxychloride (13.4 g; 87 mmol) and the mixture was refluxed for 2 h. Phosphorus oxychloride was removed on a rotary evaporator, the brown oily residue was dissolved in dilute acetic acid and, after filtration, the solution was made basic with ammonia and extracted with chloroform. The extract afforded a brown oil which was purified by preparative t.l.c. on silica gel with elution by 99:1 acetone–methanol. The product was obtained as an oil (34 mg; 28% yield) which could not be crystallized. Spectroscopic characteristics: i.r. 2.89, 6.18, 6.29, 6.37, 6.54; u.v. 213 (end absorption), 230 (shoulder), 244 (shoulder), 328 (9500); n.m.r. (solution treated with $NaOD/D_2O$) −0.85 (s; 1; observed only prior to treatment with D_2O), 1.03 (d, $J = 2$ Hz; 1); 1.68 (dd, J values 6, 2 Hz; 1), 1.96 (dt, J values 8, 2 Hz; 1), 2.42 (m; 1), 2.80 (complex; 4), 6.99 (3 peaks, 8 Hz spacings; 2), 7.06 (3 peaks, 8 Hz spacings; 2).

Synthesis of Naucledine (1)

3-Carbomethoxy-5-chlorocarbonylpyridine (2.4 g; 12 mmol) in 120 ml of carefully dried ethanol-free chloroform (2) was added to tryptamine (2.4 g; 15 mmol) dissolved in 60 ml of dry ethanol-free chloroform and 90 ml of dry pyridine, and refluxed for 2.5 h. Precipitated salts were removed by filtration and the filtrate was evaporated to dryness in a rotary evaporator. The residue was treated with 200 ml of 5% ammonia and extracted with four 100 ml portions of chloroform. The extract afforded a white residue (2.5 g) from which the tryptamide (1.0 g; 50% yield) was obtained as crystals, m.p. 168.5–169.5°, by recrystallization from methanol.

Anal. Calcd. for $C_{18}H_{17}N_3O_3$: C, 66.86; H, 5.30; N, 13.00. Found: C, 67.12; H, 5.33; N, 12.96.

Spectroscopic characteristics; i.r. (Nujol) 2.98 (sharp), 3.01 (broad), 5.85, 6.02, 6.24, 6.45; u.v. 222 (end absorption), 273 (10 100), 290 (8300); n.m.r. (DMSO-d_6) −0.90 (s; 1), 0.65 (d, $J = 2$ Hz; 1), 0.73 (d, $J = 2$ Hz; 1), 0.88 (t, $J = 5$ Hz; 1), 1.22 (3 peaks, 2 Hz spacings; 1), 2.2–3.1 (complex;

5), 6.08 (s; 3), 6.36 (m; 2), 6.96 (3 peaks, 7 Hz spacings; 2); mass spectrum 323 (10), 164 (6), 144 (18), 143 (100), 131 (13), 130 (82), 103 (10), 44 (22), 43 (51).

Treatment of the tryptamide (1.0 g; 3.1 mmol) with phosphorus oxychloride (100 g) in the manner described above for the model compound yielded a crude product (0.61 g) from which naucledine (52% yield) could be obtained by preparative t.l.c. on silica gel with elution by 99:1 acetone–methanol. The synthetic material, m.p. 84–90° (dec.) did not depress the melting point of natural naucledine and the two materials were identical in t.l.c. and spectroscopic characteristics.

Anal. Calcd. for $C_{18}H_{15}N_3O_2$: C, 70.80; H, 4.95; N, 13.76. Found: C, 70.66; H, 5.00; N, 13.50.

This work was supported by a grant from the National Research Council of Canada; scholarships (to D.G.M.) from the same source and from the Province of Ontario are also gratefully acknowledged. This acount is taken from the Ph.D. thesis of D.G.M., University of Toronto, 1971, and the M.Sc. thesis of A.S., University of Toronto, 1970.

1. S. McLean and D. G. Murray. Can. J. Chem. **48**, 867 (1970).
2. S. McLean and D. G. Murray. Can. J. Chem. This issue.
3. J.-L. Pousset, A. Bouquet, A. Cave, A. Cave, and R.-R. Pars. C.R. Acad. Sci. Paris Ser. C, **272**, 665 (1971).
4. Y. Kanaoka, E. Sato, and Y. Ban. Chem. Pharm. Bull. **15**, 101 (1967).
5. L. Merlini, R. Mondelli, G. Nasini, and M. Hesse. Tetrahedron, **23**, 3129 (1967).
6. L. Marion, R. H. F. Manske, and M. Kulka. Can. J. Res. **24B**, 224 (1946).
7. R. T. Coutts, R. A. Locock, and G. W. A. Slywka. Org. Mass Spectrom. **3**, 879 (1970).
8. K. Freter. Justus Liebigs Ann. Chem. **721**, 101 (1969).
9. H. Budzikiewicz, C. Djerassi, and D. H. Williams. Structure elucidation of natural products by mass spectrometry. Vol. 1. Holden-Day, Inc., San Francisco, California, 1964. Chapt. 9.
10. H. Budzikiewicz, C. Djerassi, and D. H. Williams. Mass spectrometry of organic compounds. Holden-Day, Inc., San Francisco, California, 1967.
11. F. Bohlmann. Angew. Chem. **69**, 641 (1957). J. Skolik, P. J. Krueger, and M. Wiewiorowski. Tetrahedron, **24**, 5439 (1968).
12. J. A. Weisbach and B. Douglas. Chem. Ind. (London), 623 (1965); 233 (1966).
13. M. Gorman and J. Sweeny. Tetrahedron Lett. 3105 (1964). W. I. Taylor. *In* The alkaloids. Vol. XI. *Edited by* R. H. F. Manske. Academic Press, Inc., New York, N. Y., 1968. Chapt. 2.
14. M. F. Bartlett and W. I. Taylor. J. Am. Chem. Soc. **85**, 1203 (1963). J. Levy, G. Ledouble, J. LeMen, and M.-M. Janot. Bull. Soc. Chim. Fr. 1917 (1964).
15. G. A. Cordell, G. F. Smith, and G. N. Smith. Chem. Commun. 191 (1970). G. Buchi, R. E. Manning, and S. A. Monti. J. Am. Chem. Soc. **85**, 1893 (1963).
16. E. Lund, H. Budzikiewicz, J. M. Wilson, and C. Djerassi. J. Am. Chem. Soc. **85**, 1528 (1963). B. Willhalm, A. F. Thomas, and F. Gautschi. Tetrahedron, **20**, 1185 (1964).
17. W. A. Ayer and T. E. Habgood. *In* The alkaloids. Vol. XI. *Edited by* R. H. F. Manske. Academic Press, Inc., New York, N.Y., 1968. Chapt. 12. H. Budzikiewicz, C. Horstmann, K. Pufahl, and K. Schreiber. Chem. Ber. **100**, 2798 (1967). N. L. Marekov and S. S. Popov. Tetrahedron, **24**, 1323 (1968). N. K. Hart, S. R. Johns, and J. A. Lamberton. Aust. J. Chem. **22**, 1283 (1969).

Can. J. Chem. Downloaded from www.nrcresearchpress.com by 210.87.254.40 on 09/05/12
For personal use only.

The Constituents of *Nauclea diderrichii*. Part IV. Miscellaneous Substances; Biogenetic Considerations

STEWART MCLEAN AND D. G. MURRAY
Department of Chemistry, University of Toronto, Toronto 181, Ontario

Received October 25, 1971

Basic substances isolated from the bark of *Nauclea diderrichii* and not placed in one of the three earlier alkaloidal categories include an alkaloid, $C_{21}H_{26}N_2O_4$, designated ND-370, and an amorphous material that appears to be an alkaloidal glycoside. Also isolated were the non-basic substances benzamide and antiarol (3,4,5-trimethoxyphenol), and two monoterpenoids given the names naucleol and naucledal; the spectroscopic characteristics of naucleol, $C_9H_{14}O_3$, can be accounted for by structure **1***a*, and those of naucledal, $C_{10}H_{12}O_4$, by structure **2***a*, but the data do not establish the structures unequivocally. The structural relationships between the various constituents isolated from this plant and their possible biogenetic implications are discussed.

Les substances basiques isolées à partir de l'écorce de *Nauclea diderrichii*, et qui n'appartiennent pas à l'une des trois premières catégories d'alcaloides, incluent un alcaloide, $C_{21}H_{26}N_2O_4$, désigné par ND-370, et un produit amorphe qui semble être un glycoside du type alcaloide. Il a également été isolé les substances non basiques, benzamide et antiarol (triméthoxy-3,4,5 phénol), et deux monoterpénoides auxquels il a été donné les noms de naucléol et nauclédal. Les caractéristiques spectroscopiques du naucléol, $C_9H_{14}O_3$, peuvent être rationalisées par la structure **1***a*, et celles du nauclédal, $C_{10}H_{12}O_4$, par la structure **2***a*; les données ne permettent cependant pas d'établir les structures d'une façon certaine. Les relations de structure entre les différents produits isolés à partir de cette plante et leurs incidences biogénétiques possibles sont discutées.

Canadian Journal of Chemistry, **50**, 1496 (1972)

In our study of the bark of *Nauclea diderrichii* we divided the constituents extracted into four categories (1, 2); we have discussed already the alkaloids of the first three categories (2, 3) and we turn now to the fourth category, miscellaneous substances, which includes alkaloids that do not fit in an earlier category and non-basic compounds. With the completion of an account of the four categories of constituents, a review of their structural characteristics reveals relationships of probable biogenetic significance, and the pattern that becomes apparent then provides some reinforcement for the structural assignments that have been made, in some cases very tentatively, on spectroscopic grounds (3).

(a) Alkaloids

Two alkaloids of undetermined structure are presently placed in this category. The first, m.p. 209–211°, designated ND-370, has the formula $C_{21}H_{26}N_2O_4$, isomeric with a number of tryptamine–monoterpene alkaloids, but does not appear to be identical with any alkaloid described previously. The second alkaloid is an amorphous substance of high molecular weight, which we believe is an alkaloidal glycoside, but we have not yet succeeded in obtaining the aglycone.

(b) Non-basic Compounds

Although the original plant extract was subjected to a sequence of acid–base partitions (2), several fractions ultimately separated by t.l.c. proved to be non-basic, a situation that is not without precedent (4). Two compounds of established structure are benzamide and antiarol; the isolation of benzamide from a plant has only rarely been described (4*a*, 5) and it may well be an artifact of our isolation procedure, which used ammonia at two stages; antiarol, 3,4,5-trimethoxyphenol, is also of fairly rare occurrence (6).

Two compounds appear to be monoterpenoids that have not been described previously. The first, which we shall call naucleol, is a colorless oil of formula $C_9H_{14}O_3$, based on accurate mass measurement of the parent ion in its mass spectrum. The i.r. spectrum provided evidence that the molecule contained an alcohol function, a δ-lactone and a trisubstituted ethylene grouping. The n.m.r. spectrum showed a one-proton quartet at τ 4.38, $J = 7$ Hz, that was slightly broadened and a three-proton doublet at τ 8.30, $J = 7$ Hz, and double irradiation confirmed that the protons responsible for these multiplets were mutually coupled; this provides evidence that the trisubstituted ethylene contained $CH_3CH{=}C<$.

Can. J. Chem. Downloaded from www.nrcresearchpress.com by 210.87.254.40 on 09/05/12
For personal use only.

Can. J. Chem. Downloaded from www.nrcresearchpress.com by 210.87.254.40 on 09/05/12
For personal use only.

A set of four peaks (broadened only very slightly by further coupling) at τ 5.33 was shown by comparison of the 100 MHz and 60 MHz spectra to be an AB quartet with $J = 13$ Hz; the chemical shift of the multiplet and the absence of vicinal coupling, taken with the evidence that a δ-lactone is present, lead us to conclude that the quartet arises from the methylene group shown explicitly in part structure **1**.

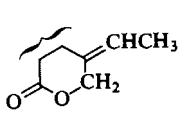

1

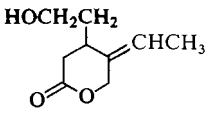

1*a*

A signal at τ 7.0, removed on treatment of the sample with D_2O, and a two-proton triplet at τ 6.32, $J = 6$ Hz, which was shown by double irradiation to be coupled to a two-proton multiplet at about τ 8.3 (overlapping the methyl doublet) provide evidence that the remainder of the molecule consists of a hydroxyethyl side chain, which clearly must be placed α or β to the carbonyl group. The three protons so far unaccounted for give rise to two sets of signals in the n.m.r. spectrum that can be interpreted as forming an ABX pattern (with some further couplings present), as would be expected for either placement of the hydroxyethyl side chain; a set of eight sharp peaks centered at τ 7.35 can be recognized as the AB part of the pattern ($J_{AB} = 16$ Hz) and this has no appreciable coupling involving protons outside of the ABX set, while the X proton appears to give a broad unresolved multiplet at about τ 6.9. It is difficult to use the chemical shift evidence to place the hydroxyethyl side chain, but the couplings just described, which indicate that the AB protons have a geminal relationship and that neither is involved in allylic coupling, lead us to favor placement at the β-carbon, as shown in **1***a*. At the present moment no strong evidence can be brought to bear on the question of the stereochemistry of the ethylidene side chain.

The mass spectrum of naucleol can be rationalized on the basis of structure **1***a*, but does not provide *a priori* evidence for this structure. The spectrum is complex and included in it are peaks corresponding to $M - CH_3$, $M - H_2O$, $M - (H_2O + C_2H_4)$ and the base peak at *m/e* 81 ($C_6H_9^+$).

A small amount of the second monoterpenoid, designated naucledal, was obtained as a colorless syrup from one lot of plant material. Since the substance seemed to be rather unstable, particularly in the presence of base, it proved to be impossible to obtain it homogeneous, and the presence of persistent impurities made an interpretation of the spectroscopic data more than usually difficult since a judgment had to be made about which peaks were associated with the principal component and which were produced by impurities. Nevertheless, some features of the molecule appear to be well established and of sufficient interest to warrant their description.

The formula was shown by accurate mass measurement of the parent ion in the mass spectrum to be $C_{10}H_{12}O_4$. The u.v. spectrum showed an absorption maximum at 246 mμ ($\varepsilon \simeq 6600$) with a shoulder at 285 mμ, but considerable doubt about the value of the extinction coefficients remains because of the inhomogeneity of the sample. The i.r. spectrum showed a weak band at 3.66 μ, strong and broad absorption at 5.80–5.89 μ, and a sharp intense peak at 6.21 μ; it was concluded that absorption in the OH-stretching region was due to the presence of an impurity. These spectroscopic characteristics are consistent with the presence in the molecule of an aldehyde group and an iridoid system, $RO_2C—C{=}C—O$ (7). The n.m.r. spectrum provides confirmation for the presence in the molecule of an aldehyde group since there is a one-proton doublet at τ 0.04, $J = 2.5$ Hz; double irradiation showed that the proton responsible for this is coupled to a proton which gives rise to a doublet of doublets at τ 7.58 with J values of 10 and 2.5 Hz. The 10 Hz coupling of the latter appears to be with a proton which gives rise to a multiplet which is part of a complex pattern near τ 5.63; irradiation at τ 5.63 also caused the collapse of a three-proton doublet, $J = 6$ Hz, at τ 8.53. A further significant signal is an apparent doublet at τ 2.22, $J = 2$ Hz, associated with one proton. If the evidence for the presence of both an aldehyde and an iridoid system can be accepted, the part structure **2** is compatible with the n.m.r. chemical shifts of all of the protons shown explicitly and, with the reservation that the coupling constant between H_b and H_d appears to be about zero, the J values ($J_{ab} = 10$; $J_{bc} = 2.5$; $J_{de} = 2$ Hz) are reasonable for this structure (8). Completion of the

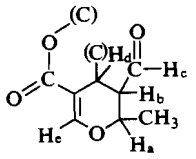

2

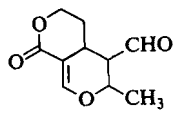

2*a*

structure to afford **2***a* provides a reasonable working hypothesis for naucledal. The mass spectrum is again complex and relatively uninformative with regard to structure: there is an appreciable molecular ion and, among others, significant peaks for $M - CH_3$, $M - H_2O$, and $M - CHO$.

Biogenetic Considerations

The co-occurrence of simple β-carbolines, simple pyridines, and the alkaloids we have called indole–pyridines raises questions of considerable interest regarding their biosynthesis, and the isolation of monoterpenoids and a constituent that appears to be a tryptamine–monoterpene indole alkaloid makes the metabolic situation even more intriguing. Although detailed biogenetic speculation can not be justified, a few comments on the structural relationships observed and their possible significance appear appropriate.

It is generally accepted that alkaloidal β-carbolines are derived from tryptophan, and the recent intense interest in the biosynthesis of the *Corynanthe–Strychnos, Aspidosperma,* and *Iboga* groups of alkaloids has led to the recognition that these alkaloids are formed from a tryptamine unit and a monoterpenoid unit, and the description of many of the details of the intricate network of metabolic pathways involved has now been placed on a firm experimental foundation (9). The so-called pyridine alkaloids (10) fall into two classes: those that are of monoterpenoid origin and those that are not.

Naucleol and naucledal are clearly monoterpenoid and the relationship between the structures advanced for them (**1***a* and **2***a*, respectively) and intermediates on the pathway leading from mevalonate through geraniol, loganin, and secologanin (9) can readily be seen (Scheme 1). Routes to **1***a* from loganin or one of its congeners require the removal of a one-carbon unit, the opening of the cyclopentane ring and adjustment of the oxidation level; a route from secologanin to 2*a* can readily be suggested, and, in this connection, the structural relationship between **2***a* and the alkaloid gentioflavine, which has been shown to be of mevalonate origin (11), is noteworthy.

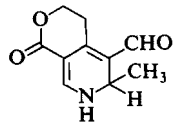

Gentioflavine

The simple pyridine alkaloids we have isolated (2) are 3,5-disubstituted, a pattern that appears to be without precedent in known pyridine alkaloids; routes to 3,4,5-tri-substituted pyridine alkaloids from monoterpenoid precursors through, for example, secologanin can readily be seen, and in the present cases it is probable that the substituent has been lost from position 4 at some stage. The simple β-carbolines (2) appear to be derived from tryptamine or tryptophan and a second component of uncertain origin, while the alkaloids we have isolated and called indole-pyridines (3) appear to be derived from tryptamine and a pyridine unit related to the simple pyridine alkaloids present in the plant. The pyridine unit is generally 3,5-disubstituted, the same pattern as that found in the simple pyridines; an exception to this generalization, nauclechine (3), with a 3,4,5-trisubstituted pyridine unit, provides support for the supposition that the pyridine units in the other alkaloids have lost the substituent originally present at position 4. With building blocks of 3,5-disubstituted (as in **3**) and 3,4,5-trisubstituted (as in **4**) pyridines available,

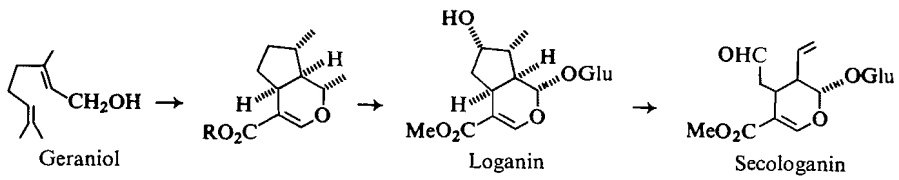

Geraniol Loganin Secologanin

SCHEME 1

Can. J. Chem. Downloaded from www.nrcresearchpress.com by 210.87.254.40 on 09/05/12
For personal use only.

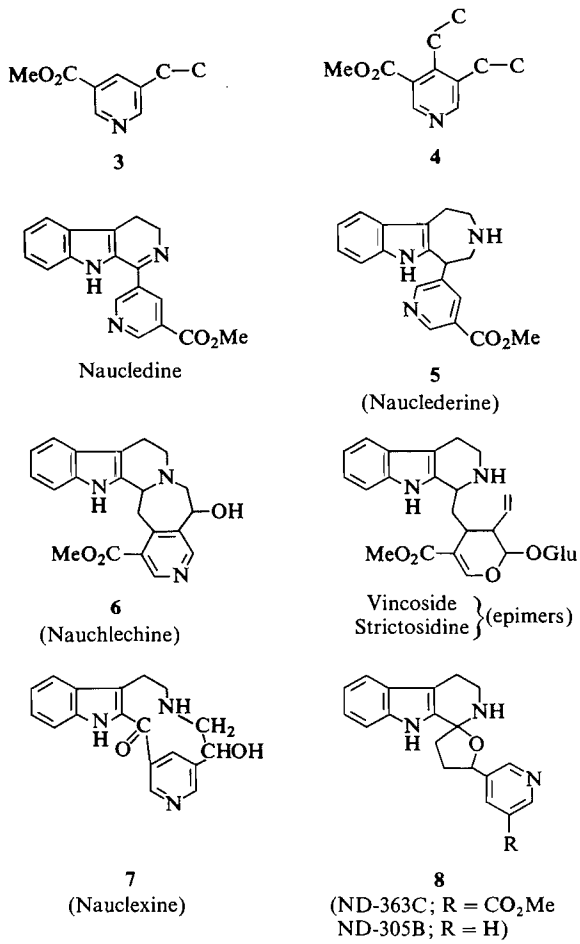

routes to all of the structures proposed for the indole–pyridine alkaloids (3) can be suggested.

In the case of naucledine, the structure of which has been established, one carbon of the two-carbon side chain of the precursor **3** has been lost, while in naucledine the complete two-carbon unit is retained and, in the structure (**5**) preferred for the alkaloid, it is incorporated in a tetrahydroazepine ring. It is attractive to speculate that both alkaloids were derived from a precursor (**3**) in which an oxidized two-carbon side chain condensed with tryptamine and then lost a one-carbon unit by, for example, decarboxylation to form naucledine or underwent ring expansion to lead on to naucledine. Nauclechine provides the example of an alkaloid derived from a precursor of form **4**, and the structure (**6**) suggested for it fits nicely into the pattern; furthermore, it is instructive to examine this structure in conjunction with the structures of alkaloids which incorporate a secologanin unit with little modification, such as vincoside and strictosidine (12) and some of the alkaloids of *Adina cordifolia* (13). Nauclexine is constructed from a tryptamine unit and a disubstituted pyridine unit but considerable uncertainty remains regarding the details of its structure; however, structure **7**, which has been very tentatively suggested for it, fits the present pattern. The related alkaloids ND-363C and ND-305B can also be considered to be derived from a unit such as **3**, decarbomethoxylated in the case of ND-305B, and a tryptamine unit; it is clear, however, that a further two-carbon unit must be incorporated and, even if structures based on **8** can be established for these alkaloids,

Can. J. Chem. Downloaded from www.nrcresearchpress.com by 210.87.254.40 on 09/05/12
For personal use only.

Can. J. Chem. Downloaded from www.nrcresearchpress.com by 210.87.254.40 on 09/05/12
For personal use only.

the order in which the necessary linkages are made is uncertain.

However, it is also possible to suggest that the indole–pyridine alkaloids could arise by a process that first unites the tryptamine and monoterpenoid components (and the isolation of ND-370 indicates that this path is open in any case) and the latter is subsequently transformed into a pyridine. This question can be usefully pursued only when it has been established that these materials are genuine natural products (3); however, the substances we have isolated, regardless of their origin, provide a valid problem in structural chemistry, and the fact that structural relationships between the more complex alkaloids and possible simpler precursors can be recognized and chemically reasonable routes for the elaboration of larger molecules can be proposed, provides some support for the tentative assignments made to some of the indole–pyridine alkaloids.

Experimental

Details of standard instrumentation, spectroscopic and chromatographic conditions, and isolation procedures have already been given (2).

ND-370

This alkaloid was isolated as a solid which, on recrystallization from methanol, formed white needles, m.p. 203–209° (phase change 77–84°); sublimed material, m.p. 209–211°. Spectroscopic characteristics: i.r. 2.90 (sharp), 3.03 (broad); u.v. 221 (18 200), 248 (4600), 268 (3500), 290 (shoulder), 363 (7250); in MeOH–HCl 221 (8500; end absorption), 246 (7600), 364 (15 500); in MeOH–KOH 223 (25 700), 274 (5900), 281 (6000), 290 (4700); n.m.r. 1.62 (s; 1; removed by D_2O), 2.4–3.0 (complex; 4), 5.08 (d, $J = 3.5$ Hz; 1), 5.18 (dd, J values 10 and 2.5 Hz; 1), 5.46 (d, $J = 6.5$ Hz, with further splitting; 1), 6.07 (d, $J = 10.5$ Hz; 1), 6.46 (s; 3), 6.55 (s; 3), 6.7–8.7 (complex; $\simeq 11$); mass spectrum 370 (5), 369 (2.5), 339 (4.5), 310 (5), 278 (2), 269 (2), 268 (3), 254 (2.5), 253 (20), 252 (100), 251 (3.5), 225 (3), 223 (4), 212 (2), 211 (3), 209 (2), 199 (3), 198 (5), 186 (3), 184 (2), 170 (3), 169 (2.5), 168 (2), 167 (2), 158 (2), 157 (4), 156 (2.5), 155 (2.5), 154 (2), 143 (3), 134.5 (3), 130 (3), 129 (6), 128 (2), 115 (2), 94 (4), 85 (3), 84 (2), 67 (2); metastables 260.2 (calcd. for 370 → 310: 259.8), 249.3 (calcd. for 310 → 278: 249.2), 204.9 (calcd. for 310 → 252: 204.9), 197.4 (calcd. for 252 → 223: 197.3); mass measurements calcd. (found): $C_{21}H_{26}N_2O_4$, 370.18926 (370.1884); $C_{20}H_{23}N_2O_3$, 339.17087 (339.1709); $C_{19}H_{22}N_2O_2$, 310.16813 (310.1681); $C_{18}H_{18}N_2O$, 278.14191 (278.1413); $C_{16}H_{17}N_2O_2$, 269.12900 (269.1283); $C_{16}H_{16}N_2O$, 252.12626 (252.1265).

Naucleol

Naucleol was obtained as syrup which could not be freed of small amounts of contaminants. Spectroscopic characteristics: i.r. 2.77 (sharp), 2.90 (broad), 5.74, 5.97 (v. weak); (liquid film) 2.93 (broad), 5.78, 5.97 (shoulder), 12.09; n.m.r. 4.38 (q, $J = 7$ Hz, with further splitting $\simeq 1$ Hz; 1; collapsed to broadened singlet by irradiation at 8.30), 5.33 (4 slightly broadened peaks, spacings 13, 12, and 13 Hz; at 60 MHz spacings are 13, 5, and 13 Hz; 2), 6.32 (t, $J = 6$ Hz, collapsed by irradiation at 8.30; 2), 6.7–7.1 (complex; 2; treatment with D_2O reduces area at $\simeq 7.0$), 7.35 (AB part of ABX system, $J_{AB} = 16$ Hz, $J_{AX} \simeq 6$ Hz, $J_{BX} \simeq 6.5$ Hz), 8.30 (d, $J = 7$ Hz, superimposed on broader multiplet; total 5; irradiation at 4.38 collapsed the doublet, and irradiation at 6.32 caused partial collapse of the multiplet); mass spectrum 171 (7), 170 (30), 169 (2), 155 (19), 153 (7), 152 (18), 142 (10), 141 (62), 140 (6), 139 (6), 137 (9), 127 (20), 126 (33), 125 (44), 124 (29), 123 (13), 111 (73), 110 (23), 109 (34), 108 (12), 107 (20), 99 (31), 98 (32), 97 (43), 96 (22), 95 (60), 93 (32), 91 (19), 83 (32), 82 (31), 81 (100), 80 (23), 79 (60), 77 (26), 71 (30), 69 (51), 67 (75), 55 (71), 54 (22), 53 (48), 43 (57), 42 (25), 41 (98), 39 (62), 31 (36); metastables 135.9 (calcd. for 170 → 152: 135.9), 121.1 (calcd. for 155 → 137: 121.1), 117.0 (calcd. for 170 → 141: 117.0), 101.2 (calcd. for 152 → 124: 101.2), 93.5 (calcd. for 170 → 126: 93.4), 78.1 (calcd. for 152 → 109: 78.2), 77.1 (calcd. for 81 → 79: 77.0), 72.5 (calcd. for 170 → 111: 72.5); mass measurements calcd. (found): $C_9H_{14}O_3$, 170.09430 (170.0935); $C_8H_{11}O_3$, 155.07082 (155.0710); $C_9H_{12}O_2$, 152.08373 (152.0837); $C_8H_{13}O_2$, 141.09156 (141.0914); $C_7H_9O_3$, 141.05517 (141.0552); $C_7H_{10}O_2$, 126.06808 (126.0678); $C_7H_9O_2$, 125.06026 (125.0600); $C_8H_{12}O$, 124.08882 (124.0888); $C_7H_8O_2$, 124.05243 (124.0524); $C_7H_{11}O$, 111.08099 (111.0810); C_7H_{11}, 95.08608 (95.0862); C_6H_7O, 95.04969 (95.0494).

Naucledal

Naucledal was isolated as a small amount of colorless syrup that could not be obtained free of impurities. Spectroscopic characteristics: i.r. 2.8 (impurity ?), 3.66 (weak), 5.80–5.89 (broad and strong), 6.21 (sharp and strong); u.v. 246 ($\simeq 6600$), 285 ($\simeq 1300$; shoulder); n.m.r. (60 MHz), 0.04 (d, $J = 2.5$ Hz; 1; collapsed by irradiation at 7.58), 2.22 (d, $J = 2$ Hz slightly broadened; 1), 3.2 (broad; impurity ?), 5.0–8.8 complex spectrum in which can be seen at 7.58 (dd, J values 10, 2.5 Hz; 2.5 Hz coupling removed by irradiation near 0.04 and multiplet partially collapsed by irradiation at 5.63; 1) and at 8.53 (d, $J = 6$ Hz; collapsed by irradiation at 5.63; 3); mass spectrum 197 (6), 196 (35), 181 (32), 178 (29), 170 (10), 169 (8), 168 (8), 167 (38), 165 (12), 153 (10), 152 (20), 151 (10), 150 (12), 149 (12), 141 (18), 140 (10), 139 (30), 137 (10), 135 (10), 127 (17), 126 (11), 125 (20), 124 (12), 123 (14), 122 (12), 121 (22), 111 (21), 109 (23), 108 (15), 105 (11), 98 (24), 97 (31), 95 (37), 93 (22), 91 (26), 81 (50), 79 (41), 77 (28), 69 (55), 67 (44), 55 (45), 53 (49), 43 (56), 41 (100), 39 (89); metastables 167.0 (calcd. for 196 → 181: 167.2), 161.7 (calcd. for 196 → 178: 161.7), 142.1 (calcd. for 196 → 167: 142.3), 105.2 (calcd. for 139 → 121: 105.3), 89.1 (calcd. for 167 → 122: 89.1), 78.1 (calcd. for 111 → 93: 77.9), 77.1 (calcd. for 81 → 79: 77.1); mass measurements calcd. (found): $C_{10}H_{12}O_4$, 196.07356 (196.0732); $C_9H_9O_4$, 181.05009 (181.0501); $C_{10}H_{10}O_3$, 178.06300 (178.0628); $C_9H_{11}O_3$, 167.07082 (167.0708); $C_8H_{11}O_2$, 139.07591 (139.0755).

Benzamide and antiarol (3,4,5-trimethoxyphenol) were isolated and identified by comparison with authentic samples; the reference sample of antiarol (6, 14) was kindly furnished by Professor Carl Djerassi.

This work was supported by a grant from the National Research Council of Canada; scholarships (to D.G.M.) from the same source and from the Province of Ontario are also gratefully acknowledged. This account is taken from the Ph.D. Thesis of D.G.M., University of Toronto, 1971.

1. S. McLEAN and D. G. MURRAY. Can. J. Chem. **48**, 867 (1970).
2. S. McLEAN and D. G. MURRAY. Can. J. Chem. This issue.
3. D. G. MURRAY, A. SZAKOLCAI and S. McLEAN. Can. J. Chem. This issue.
4. (*a*) N. K. HART, S. R. JOHNS, and J. A. LAMBERTON. Aust. J. Chem. **22**, 1283 (1969). (*b*) S. R. JOHNS and J. A. LAMBERTON. Aust. J. Chem. **22**, 1315 (1969).
5. G. J. PERSINOS, M. W. QUIMBY, A. R. MOTT, N. R. FARNSWORTH, D. H. ABRAHAM, H. H. S. FONG, and R. N. BLOMSTER. Planta Med. **15**, 361 (1967).
6. W. KARRER. Konstitution und Vorkommen der organischen Pflanzenstoffe. Birkhäuser Verlag, Basel, 1958. p. 97.
7. L. H. BRIGGS, B. F. CAIN, P. W. LE QUESNE, and J. N. SCHOOLERY. Tetrahedron Lett. 69 (1963). F. E. BADER. Helv. Chim. Acta, **36**, 215 (1953). H. INOUYE, S. UEDA, and Y. NAKAMURA. Tetrahedron Lett. 5229 (1966). F. KORTE, K.-H. BUCHEL, and L. SCHIEFER. Chem. Ber. **91**, 759 (1958).
8. H. INOUYE, T. YOSHIDA, Y. NAKAMURA, and S. TOBITA. Tetrahedron Lett. 4429 (1968). B. GILBERT, J. A. BRISSOLESE, N. FINCH, W. I. TAYLOR, J. M. WILSON, and C. DJERASSI. J. Am. Chem. Soc. **85**, 1523 (1963). E. WENKERT, B. WICKBERG, and C. LEIGHT. Tetrahedron Lett. 822 (1961).
9. A. I. SCOTT. Acc. Chem. Res. **3**, 151 (1970) provides a recent review.
10. W. A. AYER and T. E. HABGOOD. The alkaloids. Vol. XI. *Edited by* R. H. F. Manske. Academic Press, Inc., New York, N.Y., 1968. Chapt. 12.
11. N. MAREKOV and S. POPOV. Izv. Otd. Khim. Nauki, Bulg. Akad. Nauk. **2**, 575 (1970); Chem. Abstr. **73**, 15051*y* (1970).
12. K. T. D. DE SILVA, G. N. SMITH, and K. E. H. WARREN. Chem. Commun. 905 (1971).
13. R. T. BROWN and L. R. ROW. Chem. Commun. 453 (1967). R. T. BROWN, K. V. J. RAO, P. V. S. RAO, and L. R. ROW. Chem. Commun. 350 (1968). L. MERLINI and G. NASINI. Gazz. Chim. Ital. **98**, 974 (1968).
14. P. CRABBE, P. R. LEEMING, and C. DJERASSI. J. Am. Chem. Soc. **80**, 5258 (1958).

Can. J. Chem. Downloaded from www.nrcresearchpress.com by 210.87.254.40 on 09/05/12
For personal use only.

The Influence of the 2-Alkoxy Group and of C-5 Substituents on the Direction of Reductive Cleavage of 2-Alkoxytetrahydrofurans by AlH_2Cl in Ether Solution[1]

P. C. Loewen, Miss L. P. Makhubu, and R. K. Brown

Department of Chemistry, University of Alberta, Edmonton, Alberta

Received November 29, 1971

The AlH_2Cl hydrogenolysis of ether solutions of 2-alkoxytetrahydrofurans in which the alkoxy group is either CH_3O, C_2H_5O, *i*-C_3H_7O, or *t*-C_4H_9O, gives only those products resulting from ring C—O bond cleavage. However, substituents at C-5 of 2-methoxytetrahydrofuran exert a strong effect on the ratio of ring to *exo* C—O bond cleavage. Thus, alkyl (electron donor) groups at C-5 promote an increase in the amount of *exo* cleavage, the proportion increasing from 62.5 to 100% as the C-5 alkyl group is changed from CH_3 to *t*-C_4H_9. In contrast, electron withdrawing substituents, CH_3OCH_2— and C_6H_5, at C-5 favor ring cleavage to the extent of 93 and 84% respectively.

The results are interpreted in terms of the influence that these substituents exert through their electronic properties on the relative ease of attainment of the transition state leading to either ring C—O or *exo* C—O bond cleavage. However, evidence is provided to show that the bulk steric effect of these substituents also controls, though to a minor extent, the proportion of ring to *exo* cleavage.

Les hydrogénolyses par AlH_2Cl de solutions éthérées de tétrahydrofurannes alcoolates-2, où le group alcoolate est soit CH_3O, C_2H_5O, *i*-C_3H_7O, ou *t*-C_4H_9O, conduisent uniquement aux produits résultant de la rupture de la liaison C—O du cycle. Cependant, les substituants sur C-5 dans le méthoxy-2 tétrahydrofuranne, exercent un effet important sur le rapport: rupture de la liaison C—O du cycle sur rupture de la liaison C—O exocyclique. C'est ainsi que des groupes alkyles (donneurs d'électrons) sur C-5 favorisent le pourcentage de clivage exocyclique; les pourcentages augmentant de 62.5 à 100% si le groupe alkyle passe de CH_3 à *t*-C_4H_9. Au contraire, des substituants en C-5 attracteurs d'électrons, CH_3OCH_2— et C_6H_5, favorisent la rupture du cycle jusqu'à des proportions de 93 et 84% respectivement.

Les résultats sont interprétés en fonction de l'influence qu'exercent ces substituants, par leurs propriétés électroniques, sur la facilité relative de formation de l'état de transition conduisant ultérieurement à la rupture de la liaison C—O soit du cycle soit exocyclique. Cependant, des preuves ont été apportées afin de montrer que l'encombrement stérique de ces substituants contrôle également, bien qu'à un degré moindre, les proportions de clivage cyclique et exocyclique.

Canadian Journal of Chemistry, **50**, 1502 (1972)

Introduction

It has been shown (1) that the proportion of ring C—O bond cleavage to side chain C—O bond cleavage of 2-alkoxytetrahydropyrans (Scheme 1, **1**, $n = 2$) resulting from the hydrogenolysis by a 1:1 mixture of $AlCl_3$ and $LiAlH_4$ in ether depends upon the nature of the alkyl group of the 2-alkoxy substituent and also upon the nature of the C-6 substituent. The percent ring cleavage increased in the order 30, 60, 60, 82, 87 when the alkyl group of the 2-alkoxytetrahydropyran was CH_3, C_2H_5, *n*-C_4H_9, *i*-C_3H_9, and *t*-C_4H_9 respectively (**1**, $R' = H$ in each case). This was attributed to the relative electron donor ability of the alkyl group of the 2-alkoxy moiety to facilitate attainment of the transition state leading to the intermediate oxocarbonium ion involved in ring cleavage compared to the ease of obtaining the alternate intermediate oxocarbonium ion involved in the departure of the 2-alkoxy group with simultaneous ring retention (Scheme 1, routes *a* and *b* respectively, $n = 2$, $R' = H$, R = alkyl). Attainment of the transition state leading to the oxocarbonium ion was considered to be the slow and rate determining step, while hydride addition to this ion was fast and nonreversible. A similar explanation, involving the C-6 substituent was advanced to explain the 6, 60, and 80% proportion of ring cleavage found in the $LiAlH_4$–$AlCl_3$ hydrogenolysis respectively of the *cis–trans* mixture of 6-methyl-2-methoxy-

[1]In part from the thesis of P. C. Loewen submitted to the Faculty of Graduate Studies, University of Alberta as part of the requirements for the Ph.D. degree, 1969, and the thesis of Miss L. P. Makhubu submitted to the Faculty of Graduate Studies, University of Alberta as part of the requirements for the M.Sc. degree, 1967.

Can. J. Chem. Downloaded from www.nrcresearchpress.com by 210.87.254.42 on 09/05/12
For personal use only.

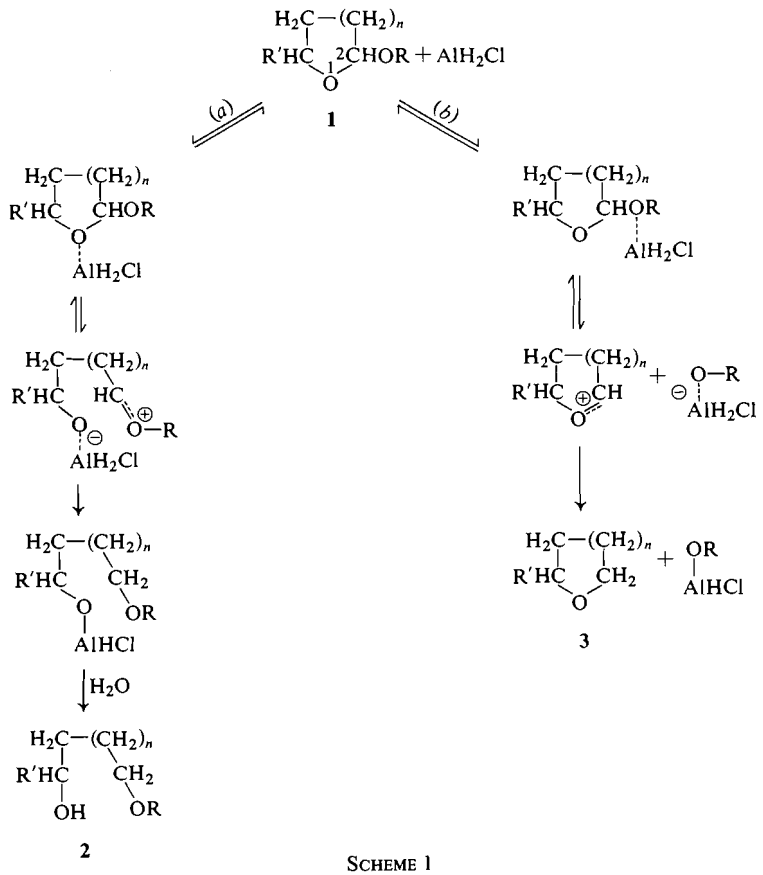

SCHEME 1

tetrahydropyran, and the separate *cis* and *trans* isomers of 2-methoxy-6-methoxymethyltetrahydropyran (1).

The present paper describes the results of the extension of this study to the hydrogenolysis by 1:1 $LiAlH_4$–$AlCl_3$ (*i.e.* AlH_2Cl (2, 3)) of 2-alkoxytetrahydrofurans and of some 5-substituted 2-methoxytetrahydrofurans (Scheme 1, **1**, $n = 1$).

Results and Discussion

Preparation of 2-Alkoxytetrahydrofurans and 5-Substituted 2-Alkoxytetrahydrofurans

The unsubstituted 2-alkoxytetrahydrofurans were prepared by the reaction of the appropriate alcohol with α-formyl-γ-butyrolactone (previously obtained from the base-catalyzed reaction of γ-butyrolactone (**4**, R′ = H) with ethyl formate), followed by alkaline hydrolysis and subsequent decarboxylation of the product (Scheme 2), a procedure based on that of Korte *et al.* (4, 5). For R′ = H, the yield of the ester **6** decreased in the order 90, 41, 29, ~0% when R was CH_3, C_2H_5, *i*-C_3H_7, and *t*-C_4H_9 respectively, a result thought to be due to the relatively greater steric interference of R as its bulk increased. Decarboxylation of the 2-alkoxy-3-carboxytetrahydrofuran in the conversion of **6** to **7** was accompanied by the dihydrofuran **8**. However, by the acid-catalyzed reaction of the mixture of **7** and **8** with the alcohol ROH, **7** could be obtained quite readily, free of **8**.

The same procedure shown in Scheme 2 was used to convert the γ-substituted γ-butyrolactones **4** (R′ = CH_3, *i*-C_3H_7, *t*-C_4H_9) to the corresponding 2-methoxy-5-substituted tetrahydrofurans. Apart from the commercially available γ-valerolactone (**4**, R′ = CH_3), the required γ-alkyl-γ-butyrolactones were made satisfactorily by the reaction of the appropriate

Can. J. Chem. Downloaded from www.nrcresearchpress.com by 210.87.254.42 on 09/05/12
For personal use only.

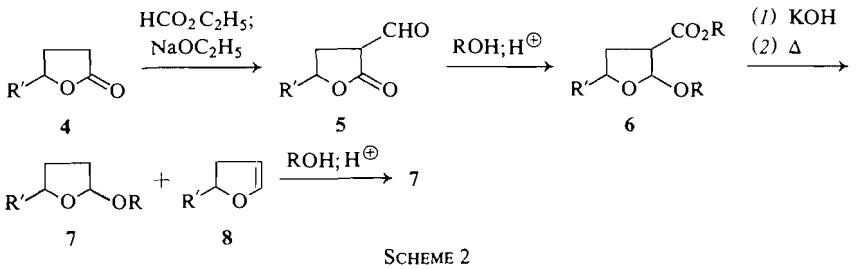

SCHEME 2

methyl ketones **9** ($R' = i\text{-}C_3H_7$ or $t\text{-}C_4H_9$) with dimethylamine and titanium tetrachloride (Scheme 3), a method which produces the terminal enamine **10** (6), which was then condensed with ethyl bromoacetate to provide the γ-ketoester **11** (7). The ester **11** could then be reduced and the product subsequently cyclized to the γ-substituted γ-butyrolactone **4** (Scheme 3). This method was unsuccessful for the preparation of γ-phenyl-γ-butyrolactone from acetophenone, since the conversion of **11** ($R' = C_6H_5$) to **4** ($R' = C_6H_5$) with sodium borohydride (Scheme 3) was quite unsatisfactory. However, **4** ($R' = C_6H_5$) could be obtained in satisfactory yield from the base-catalyzed reaction of styrene oxide with diethyl malonate, and the product hydrolyzed and decarboxylated.

We were unable to prepare γ-methoxymethyl-γ-butyrolactone (**4**, $R' = CH_3OCH_2$) to take advantage of its conversion to **7** ($R' = CH_3OCH_2$, $R = CH_3$) by the route shown in Scheme 2. However, 2-methoxy-5-methoxymethyltetrahydrofuran was made satisfactorily by the reaction of a peroxy acid with the methyl ether of 2-hydroxymethyl-2,3-dihydro-3*H*-pyran (**12**, $R = CH_3$) to produce the diol **13** (8) which in turn was oxidized with metaperiodic acid (Scheme 4). To avoid extensive decomposition, the product **14** was not isolated or purified, but instead subjected directly to acid-catalyzed reaction with methanol to produce the acetal **15** ($R = CH_3$).

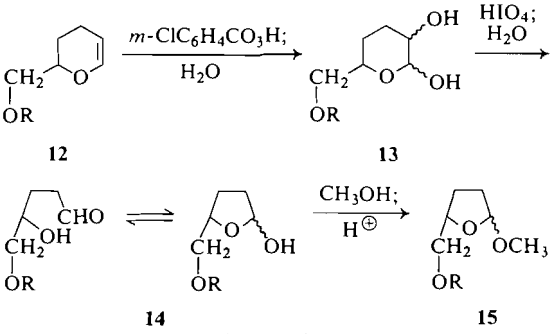

SCHEME 4

Hydrogenolyses

(a) Of 2-Alkoxytetrahydrofurans

Only two products were obtained from the hydrogenolysis of each of the 2-alkoxytetrahydrofurans (*cf.* routes *a* and *b* in Scheme 1, $n = 1$). These usually were easily identified by comparison of the g.l.c. retention times with those of authentic samples. In all cases of doubt, the products were isolated by preparative g.l.c. and then identified by comparison of their p.m.r. and i.r. spectra and physical constants with those of authentic compounds. In those

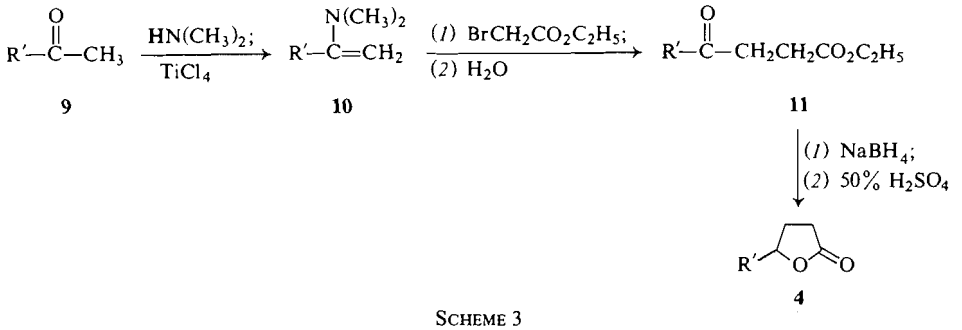

SCHEME 3

Can. J. Chem. Downloaded from www.nrcresearchpress.com by 210.87.254.42 on 09/05/12
For personal use only.

TABLE 1. Room temperature hydrogenolysis of unsubstituted and 5-substituted 2-alkoxytetrahydrofurans by AlH_2Cl in ether

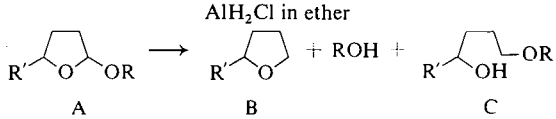

A B C

Experiment	Compound A R′	Compound A R	Reduction* time (h)	Extent of reduction (%)	Total recovery (%)	Reduction products as % of product B	Reduction products as % of product C
1	H	CH_3	2.25	100	86†	0	100
2	H	C_2H_5	2.25	100	82†	0	100
3	H	i-C_3H_7	2.25	100	80†	0	100
4	H	t-C_4H_9	2.25	100	86†	0	100
5‡	CH_3OCH_2	CH_3	2.0	100	85	6.5	93.5
6‡	CH_3	CH_3	2.0	100	80	62.5	37.5
7‡	i-C_3H_7	CH_3	2.0	100	90	86	14
8‡	t-C_4H_9	CH_3	2.0	62	80	~100	trace
			8.0	100	95	~100	trace
9‡	C_6H_5	CH_3	2.0	85	92	15.7	84.3
			48.	100	90	15.5	84.5
10‡	CH_3	i-C_3H_7	3.0	100	80	6.8	93.2

*This time generally was more than enough for complete reaction. Most were complete in a fraction of the time indicated and in these cases no starting material remained. All products were stable to the reaction conditions.

†Recovery was based on the actual % yield of product C obtained by distillation and does not include B or CH_3OH since the latter could not be estimated by g.l.c.

‡*cis–trans* mixtures of A were reduced in each case. The p.m.r. spectra indicated that the two isomers were present in the ratio from 1:1 to 2:3.

cases wherein authentic compounds were not available or reported, the isolated products were characterized in the usual way. All hydrogenolysis products were stable under the reaction conditions. Product ratios were determined by g.l.c. peak areas, uncorrected for detector response since usually the observed areas corresponded well within 5% of the expected area, and only a few deviated at the most by 10%. In all cases there was no doubt as to the preferred direction of reductive cleavage. The results of the hydrogenolysis reactions are shown in Table 1 in which structure A represents the substituted or unsubstituted 2-alkoxytetrahydrofuran while structures B and C represent the products from *exo* cleavage and ring (*endo*) cleavage respectively.

Experiments 1–4 in Table 1 show that when R′ = H in A, only ring cleavage occurs, regardless of whether R is CH_3, C_2H_5, i-C_3H_7, or t-C_4H_9. This is in sharp contrast to the findings for the hydrogenolysis of the analogous 2-alkoxytetrahydropyrans where both ring and *exo* cleavage products were formed, with the latter decreasing in relative amount as the alkyl group changed from CH_3 to t-C_4H_9. It is clear that exclusive ring cleavage occurs regardless of the inductive or steric effect of the alkyl substituent R. Since it has been shown that there is a stronger association of Lewis acids with tetrahydrofuran than with the analogous acyclic ether (9–11), it is possible that this factor submerges any inductive or steric influence of the alkyl group R and hence the Lewis acid AlH_2Cl associates exclusively or nearly so with the ring oxygen, the first step in the reductive cleavage of the C—O bond of acetals. It is to be expected that the stronger association of the Lewis acid with the ring oxygen would produce a greater extent of C—O bond breaking in the transition state, resulting in the strong preference for ring cleavage (route *a*, Scheme 1, $n = 1$, R′ = H). That a polar effect of the alkyl group is still operative, although it is unable to manifest itself in terms of the direction of reductive cleavage, is clearly shown by the competitive reaction of a 1:1 mixture of 2-ethoxy- and 2-t-butoxytetrahydrofuran with a limited amount of AlH_2Cl, sufficient to hydrogenolyze only one-half of the total acetal. It was found again that only ring cleavage products were obtained, but the ratio of the 2-t-butoxy- to 2-ethoxytetrahydrofuran reduced was 78:22, thus showing that the t-butyl group is more

Can. J. Chem. Downloaded from www.nrcresearchpress.com by 210.87.254.42 on 09/05/12
For personal use only.

TABLE 2. Room temperature hydrogenolysis of ether solution of 2-benzyloxytetrahydrofuran by AlH_3, AlH_2Cl, $AlHCl_2$, and $AlHCl_2 + AlCl_3$*

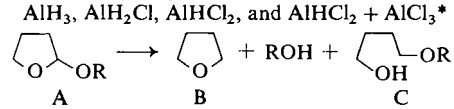

A B C

($R = C_6H_5CH_2^-$)

Experiment no.	Reagent	Extent of reduction (%)	Total material recovery (%)	% reduction product as B	% reduction product as C
1	AlH_3	67.5	84	20.5	79.5
2	AlH_2Cl	100	95	48.5	51.5
3	$AlHCl_2$	100	90	90.5	9.5
4	$AlHCl_2:AlCl_3$ (4:1)	100	91	91.3	8.7

*All reactions were allowed to proceed for 2 h.

effective in facilitating attainment of the transition state leading to oxocarbonium ion formation.

Eliel *et al.* (12) have reported the hydrogenolysis of four 2-alkoxytetrahydrofurans by a mixture of $AlCl_3$ and $LiAlH_4$ and found that generally both *exo* and *endo* cleavage occurred. The percentage of *exo* and *endo* cleavage products actually obtained by them in each case where the alkyl group was *t*-butyl, cyclohexyl, *n*-hexyl, and benzyl were, respectively, a trace and 58, 15 and 63, 40 and 27, 83 and 4. They concluded from this that the steric effect of the C-2 alkoxy group was more important than was the basicity of the ring oxygen in directing the course of reductive cleavage. The discrepancy between our results and those reported (12) might be due to the fact that we employed as reducing system a 1:1 mixture of $AlCl_3$ and $LiAlH_4$ which provides AlH_2Cl (2, 3) whereas Eliel *et al.* (12) used a 4:1 mixture of $AlCl_3$ and $LiAlH_4$, which provides a 1:4 mixture of $AlCl_3$ and $AlHCl_2$ (2, 3). This view is supported by the data in Table 2 which show the results of the hydrogenolysis of 2-benzyloxytetrahydrofuran by the series of reagents AlH_3, AlH_2Cl, $AlHCl_2$, and the 4:1 mixture of $AlHCl_2$ with $AlCl_3$ (Eliel's reagent). The latter two hydrogenolyzing reagents provide the *exo* and *endo* cleavage products, B and C, in the proportion 90.5:9.5 and 91.3:8.7 respectively, nearly the same as the proportion of 83:4 reported (12). However, reduction by AlH_2Cl provides the same products in the proportion *exo*:*endo* = 48.5:51.5. The failure to obtain exclusive ring cleavage with AlH_2Cl as was found for the alkoxytetrahydrofurans may be due to the electron withdrawing character of the phenyl group which would then cause the benzyloxy moiety to destabilize the transition state leading to ring cleavage, thus overcoming to some extent the overwhelming tendency of the Lewis acid to coordinate with the ring oxygen which is followed by ring cleavage. AlH_3 also provides the *exo* and *endo* cleavage products, but in the proportion 20.5:79.5. It is clear from the data in Table 2 that those hydrogenolyzing agents which are the strongest Lewis acids provide the greatest proportion of *exo* cleavage.

(b) Of 5-Substituted 2-Alkoxytetrahydrofurans

Hydrogenolysis of the 5-alkyl-2-methoxytetrahydrofurans, as *cis–trans* mixtures, provides both *exo* and *endo* cleavage products B and C. As the C-5 alkyl group R′ is changed from CH_3 to i-C_3H_7 to t-C_4H_9, the percent *exo* cleavage is respectively 62.5, 86, and ~100% (experiments 6–8, Table 1). It is clear that in these three cases, the greater "basicity" of the ring oxygen is counteracted by other forces. Two factors, either separately or in concert, could account for these results. The first is due to the electron donor property of the C-5 alkyl group (R′) competing progressively more effectively in lowering the energy required to attain the transition state leading to the formation of the oxocarbonium ion involved in ring retention, than does the *exo* oxygen's alkyl group in attaining the alternate oxocarbonium ion (*i.e.* route *b* is preferred over route *a* in Scheme 1). The second factor is due to the steric effect of the C-5 alkyl substituent, added to that of the C-2 methoxy group, decreasing the ease of associa-

Can. J. Chem. Downloaded from www.nrcresearchpress.com by 210.87.254.42 on 09/05/12
For personal use only.

Can. J. Chem. Downloaded from www.nrcresearchpress.com by 210.87.254.42 on 09/05/12
For personal use only.

tion of the Lewis acid with the ring oxygen, thus causing preference for route *b* (Scheme 1). It is to be noted that such a steric effect has been advanced to account for the lower "basicity" of 2-methyltetrahydrofuran and of 2,5-dimethyltetrahydrofuran compared to that of tetrahydrofuran itself (10, 11).

In an attempt to determine the relative effectiveness of the polar and steric influences, substituents were incorporated in structure **1** at C-5, which provided the bulk required, but were electron withdrawing in character. If the steric effect is predominant, hydrogenolysis of these C-5 substituted 2-methoxytetrahydrofurans should provide primarily B, the product from *exo* cleavage (route *b*, Scheme 1). On the other hand, if the polar effect is of predominant importance, then the ring cleavage product C should be preferred (route *a*, Scheme 1). In this connection it is known that the phenyl group has an effective bulk slightly greater than that of the isopropyl group, as shown by their respective A values of 2.1–3.0[2] and 1.8–2.5 kcal/mol determined in the cyclohexane system (13). Experiments 5 and 9 (Table 1) show that hydrogenolysis of 2-methoxy-5-methoxymethyltetrahydrofuran and of 2-methoxy-5-phenyltetrahydrofuran (both as *cis–trans* mixtures) provide the ring cleavage products in the proportion of 93.5 and 84.5% respectively. This appears to show that it is the electronic rather than the steric effect which is of major importance in determining the direction of reductive cleavage. However, the ability of oxygen ethers and of the phenyl group to associate with Lewis acids such as $AlCl_3$, and thus quite likely with AlH_2Cl, might cause the C-5 substituents, $R' = CH_3OCH_2$ and C_6H_5, to assist in keeping the AlH_2Cl in the vicinity of the ring oxygen, rather than with the C-2 oxygen atom, and in this way favor ring cleavage.

A further attempt to determine the relative effectiveness of polar and steric influences was made by hydrogenolyzing 5-methyl-2-isopropoxytetrahydrofuran. In this compound the polar effects on the acetal unit of the isopropyl group and of the portion of the structure at C-5

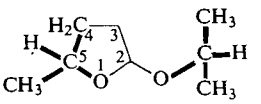

D

should be similar since the latter moiety approximates the isopropyl group in its electron donor ability. This feature is shown in structure D in which the comparable sections are emphasized. In this case only the bulk of the substituents and the relative "basicity" of the two oxygen atoms should control the direction of reductive cleavage. Experiment 10, Table 1, shows that ring cleavage occurs to the extent of 93.2%. This clearly demonstrates the importance of the greater "basicity" of the ring oxygen. If steric effects were predominant in controlling the direction of cleavage, one would expect that 5-methyl-2-isopropoxytetrahydrofuran (experiment 10) would suffer *exo* cleavage *at least* to the same extent as did 5-methyl-2-methoxytetrahydrofuran (experiment 6). This is clearly not the case, and fortifies our view that electronic factors as well as the "basicity" of the ring oxygen play dominant roles in the direction of reductive cleavage of 2-alkoxytetrahydrofurans. However, the fact that 2-isopropoxytetrahydrofuran undergoes *only* ring cleavage (experiment 3) while 5-methyl-2-isopropoxytetrahydrofuran provides, upon hydrogenolyses, as much as 6.8% of the *exo* cleavage product, B, might be interpreted as evidence that some steric effect is exerted by the C-5 substituent. Hence the steric effect of the C-5 substituent could provide at least some of the reason why hydrogenolysis of 5-alkyl-2-methoxytetrahydrofuran produces an increasing proportion of *exo* cleavage product B (62.5 → 86 → 100%) as the C-5 group is changed from CH_3 to i-C_3H_7 to t-C_4H_9.

All of the 5-substituted 2-alkoxytetrahydrofurans were mixtures of the *cis* and *trans* isomers, a fact readily determined by the two sets of quartets in the p.m.r. spectrum of each compound due to the anomeric proton. The signal areas showed that the proportion of isomers ranged from 1:1 to 3:2, but we were unable to determine which of the 3:2 mixture was *cis* or *trans*. Although it has been shown that the signals for the α protons of *trans*-2,5-dimethyltetrahydropyran appear at lower field than do those of the *cis* isomer (14, 15), the signals for the α protons of several other *cis*-

[2]Recent calculations involving phenylcyclohexane (35) show that the energy difference could be as high as 3.6 kcal/mol between the axial phenyl group in the preferred "perpendicular" orientation and the equatorial phenyl group in the preferred "parallel" orientation.

Can. J. Chem. Downloaded from www.nrcresearchpress.com by 210.87.254.42 on 09/05/12
For personal use only.

trans-2,5-disubstituted tetrahydrofurans appeared either at nearly the same position in the spectrum or in some cases the *trans* α proton signals occurred at slightly higher field than did those of the *cis* isomer. Accordingly, the p.m.r. spectrum was of no assistance in identifying the *cis* or *trans* isomer. All our attempts to separate the isomers by g.l.c. failed, in spite of the variety of columns employed. Our interest in identifying the *cis* or *trans* isomer lay in the possibility that one isomer might prefer to undergo *exo* cleavage, while the other would prefer *endo* cleavage. This might well have been the situation for 5-methyl-2-methoxytetrahydrofuran since the ratio of *exo*:*endo* cleavage is 62.5:37.5 while the isomer ratio is 3:2. However, since all the other 5-substituted 2-alkoxytetrahydrofurans employed in this work hydrogenolyzed either *exo* or *endo* to the extent of at least 80% while their proportion of *cis–trans* isomers ranged from 1:1 to 3:2, it is unlikely that the relative amount of *cis* and *trans* isomers is an important factor in determining the direction of hydrogenolysis. This view is supported by the results obtained from the treatment of the *cis–trans* mixtures of each of the three compounds 5-methyl-, 5-isopropyl-, and 5-*t*-butyl-2-methoxytetrahydrofuran with an amount of AlH_2Cl insufficient to hydrogenolyze all of the acetal. In all three cases the proportion of *cis–trans* isomers in the remaining unreacted material was the same as that in the starting material, and also the proportion of *exo* to *endo* cleavage was the same as that found when complete hydrogenolysis occurred.

Experimental

All boiling points and melting points are uncorrected.

Gas liquid chromatographic analyses were made with an F and M model 700 instrument equipped with 12 ft × 1/8 in. columns packed with either (*a*) Carbowax 20 M, 20% on Gas-Chrom P (60–80 mesh), (*b*) Apiezon T or Apiezon L, 10% on Chromosorb W (60–80 mesh), or (*c*) butanediol succinate, 20% on Chromosorb W (60–80 mesh). Helium was the carrier gas at a flow rate of ~40 ml/min. For preparative g.l.c., an Aerograph Autoprep, Model A-700 (Wilkens Instrument and Research Co.) was used. The columns employed were (*a*) 12 ft × 1/4 in. packed with Carbowax 20 M, 20% on Gas Chrom P (60–80 mesh), (*b*) 12 ft × 1/4 in., packed with butanediol succinate, 20% on Chromosorb W (60–80 mesh), (*c*) 6 ft × 1/4 in., packed with Apiezon T, 10% on Chromosorb W (30–60 mesh), and (*d*) 12 ft × 1/4 in., packed with 10% Carbowax 20 M and 10% silicone rubber on Chromosorb W (30–60 mesh). Helium was the carrier gas. The type of column and its temperature was dependent on the boiling point of the compounds. For most analyses on the F and M, Model 700, the temperature was linearly programmed to achieve better resolution, with a temperature increase of 15 °C/min starting from 50 °C. The terminal temperature depended upon column stability.

Quantitative analyses by g.l.c. were made by measuring the signal areas directly, uncorrected for detector response since observed and correct areas differed by less than 5% in most cases, though in a few this difference was as much as 10%.

The i.r. spectra were recorded with a Perkin–Elmer Model 337 instrument.

The p.m.r. spectra, all referred to tetramethylsilane, were recorded with a Varian Associates A-60 instrument operated by Mr. R. Swindlehurst and assistants, and an HR-100 spectrometer operated by Mr. G. Bigham. The p.m.r. spectra of all new compounds described below agreed completely with the structures proposed.

Elemental analyses were carried out by Mrs. D. Mahlow of this Department. These agreed well with the expected values.

Solvents were removed by rotary evaporator under reduced pressure unless otherwise stated.

Preparation of 2-Alkoxytetrahydrofurans (see Table 3)

The 2-alkoxy-3-carboalkoxytetrahydrofurans (compounds **1–4** in Table 3) were prepared by the published procedure (4). These were saponified (4) and decarboxylated at 100–120° to provide compounds **5–7**. Compounds **8** and **9** were prepared by literature directions (12).

Preparation of 5-Substituted 2-Alkoxytetrahydrofurans

cis-trans-5-Methyl-2-methoxytetrahydrofuran

3-Carbomethoxy-5-methyl-2-methoxytetrahydrofuran (5), b.p. 97° at 20 mm, η_D^{26} 1.4310; lit. b.p. 84° at 9 mm (5), was saponified (4) to the acid, yield 92%. The oil was decarboxylated at 100–110° to *cis-trans*-5-methyl-2-methoxytetrahydrofuran; yield 42%, b.p. 108–109° at 695 mm; η_D^{30} 1.4127, η_D^{22} 1.4080.

cis-trans-5-Isopropyl-2-methoxytetrahydrofuran

The reaction of 5.7 g (0.05 mol) of 2-dimethylamino-3-methyl-1-butene (6) with 8.35 g (0.05 mol) of ethyl bromoacetate following general directions (7) provided 2.3 g (32%) of *methyl β-isobutyrylpropionate*, b.p. 86–87° at 8 mm; η_D^{22} 1.4270.

A cold (0°) solution of methyl β-isobutyrylpropionate (2.0 g, 0.013 mol) in 20 ml of dry methanol was vigorously stirred while sodium borohydride (0.25 g, 0.0064 mol) was added in small portions. The mixture was then stirred overnight at room temperature. Excess methanol was then removed and 4 ml of aqueous sulfuric acid (1:1) was added to the stirred residue. The ether extracts (3 × 30 ml) were dried ($MgSO_4$), and freed from solvent. Distillation gave 1.5 g (93%) of γ-isopropyl-γ-butyrolactone, b.p. 56° at 0.5 mm; η_D^{20} 1.4416; lit. b.p. 98° at 15 mm; η_D^{25} 1.4410 (18).

The lactone (3.6 g, 0.15 mol) was condensed with ethyl formate according to general directions (4) to provide 16 g (81%) of *3-carbomethoxy-5-isopropyl-2-methoxytetrahydrofuran*, b.p. 70° at 1 mm; η_D^{24} 1.4392. This ester (6 g, 0.03 mol) was saponified (4) to give 4.1 g (74%) of the crude viscous

TABLE 3. Physical constants of several 2-alkoxytetrahydrofurans

No.	Compound R	Compound R′	b.p.°/mm Hg	η_D/°C	Literature b.p.°/mm Hg	Literature η_D/°C	Reference
1	CH_3	CO_2CH_3	94/5	1.4357/25	81/13	—	4
2	C_2H_5	$CO_2C_2H_5$	110/19	1.4318/25	—	—	
3	i-C_3H_7	CO_2-i-C_3H_7	108–110/15 (crude)		—	—	
4*	t-C_4H_9	CO_2-t-C_4H_9					
5	CH_3	H	101–102/699	1.4104/24	105–107/	1.4132/14	16
6	C_2H_5	H	110–112/699	1.4105/26	125/	1.4148/20	17
7	i-C_3H_7	H	117–119/699	1.4109/24	132/	1.4147/20	17
8	t-C_4H_9	H	126–127/699	1.4171/25	34–40/10	1.4186/20	12
9	$C_6H_5CH_2$	H	114/7	1.5120/24	102/4		12

*Isolation gave only 3-carbo-t-butoxy-4,5-dihydrofuran, m.p. 45–46°.

liquid *3-carboxy-5-isopropyl-2-methoxytetrahydrofuran.* This crude acid, in 20 ml of quinoline containing a trace of cupric sulfate, was heated at 200–210° under nitrogen. The product, collected in a Dry Ice–acetone cooled flask, contained *5-isopropyl-2-methoxytetrahydrofuran* contaminated with *2-isopropyl-2,3-dihydrofuran.* Treatment of this mixture for 6 h at room temperature with 5 ml of methanol containing a trace of *p*-toluenesulfonic acid, followed by addition of sodium carbonate (2 g), filtration, and distillation, gave *cis-trans-5-isopropyl-2-methoxytetrahydrofuran* (28% from the γ-isopropyl-γ-butyrolactone), b.p. 80° at 95 mm; η_D^{25} 1.4172. The g.l.c. analysis on butanediol succinate column showed two overlapping peaks in the area ratio of ~3:2.

cis-trans-5-t-Butyl-2-methoxytetrahydrofuran

Pinacolone (19) obtained from pinacol hydrate (20), was converted to the enamine 2-dimethylamino-3,3-dimethyl-1-butene (6), yield, 63%, b.p. 105° at 690 mm; η_D^{22} 1.4308; lit. b.p. 57° at 71 mm; η_D^{25} 1.4293 (6).

From the enamine (45 g) and ethyl bromoacetate there was obtained 16 g (38%) of *methyl β-pivalylpropionate* following the directions used for the reaction of methyl α-bromopropionate with enamines (7); b.p. 80° at 4 mm; η_D^{22} 1.4303.

Sodium borohydride reduction of methyl β-pivalylpropionate, followed by acid-catalyzed cyclization of the product as described above for the conversion of methyl β-isobutyrylpropionate to γ-isopropyl-γ-butyrolactone, gave γ-*t*-butyl-γ-butyrolactone; yield, 98% from the ketoester, b.p. 74° at 2 mm; η_D^{22} 1.4453.

Reaction of this lactone with ethyl formate (4) gave a 63% yield of crude *5-t-butyl-3-carbomethoxy-2-methoxytetrahydrofuran* containing 3–4% of unreacted lactone which could not be removed by usual fractional distillation; b.p. of crude, 95% at 3 mm; η_D^{25} 1.4380. The crude ester was saponified (4) and the impure free acid decarboxylated in quinoline as above to provide *cis-trans-5-t-butyl-2-methoxytetrahydrofuran*; yield from the lactone, 10%; b.p. 97° at 110 mm; η_D^{23} 1.4257. The g.l.c. on butanediol succinate showed two separate peaks in the area ratio 55:45.

cis-trans-2-Methoxy-5-phenyltetrahydrofuran

γ-Phenyl-γ-butyrolactone was prepared by the reaction of styrene oxide (21) with diethyl malonate as described (22) but with sodium hydride in 1,2-dimethoxyethane under nitrogen as the condensing system; yield, 54%; b.p. 123° at 0.8 mm; η_D^{23} 1.5392; lit. b.p. 130° at 1.5 mm (22); $\eta_D^{15.4}$ 1.5418 (23).

Reaction of this lactone with ethyl formate (4) gave *3-carbomethoxy-2-methoxy-5-phenyltetrahydrofuran*; yield, 78%; b.p. 125° at 0.5 mm; η_D^{22} 1.5124.

Saponification (4) gave the free acid which was decarboxylated (4) to *cis-trans-2-methoxy-5-phenyltetrahydrofuran* (54% from the lactone); b.p. 85° at 0.8 mm; η_D^{24} 1.5130. The g.l.c. on an Apiezon T column showed a single broad peak for the *cis–trans* mixture.

cis-trans-2-Methoxy-5-methoxymethyltetrahydrofuran

Methylation (25) of 2-hydroxymethyl-3,4-dihydro-2*H*-pyran (24) gave a 70% yield of *2-methoxymethyl-3,4-dihydro-2H-pyran*; b.p. 58–60° at 30 mm; η_D^{24} 1.4458; lit. b.p. 60° at 20 mm; $\eta_D^{17.5}$ 1.4508 (26).

To a solution of 80% *m*-chloroperoxybenzoic acid (55 g, 0.2 mol) in 400 ml of wet ether at 0°, was added dropwise 2-methoxymethyl-3,4-dihydro-2*H*-pyran (26 g, 0.2 mol). The mixture was warmed to room temperature, stirred for 24 h, then freed from ether. A chloroform solution of the residue, separated from the sparingly soluble *m*-chlorobenzoic acid, was washed with aqueous sodium bicarbonate till neutral. The bicarbonate washings in turn were washed with chloroform. The combined chloroform extracts were dried ($MgSO_4$), separated from the solid and freed from solvent to give 30 g (99%) of crude *2,3-dihydroxy-6-methoxymethyltetrahydropyran.* The crude diol (16 g, 0.1 mol) was added dropwise to a solution of periodic acid (22.5 g, 0.1 mol) in 200 ml of a 1:1 mixture of dioxane and water. The resulting mixture was stirred for 12 h, then neutralized with solid sodium bicarbonate. The slightly alkaline solution was extracted continuously for 24 h with chloroform and the extracts dried with $MgSO_4$ containing some sodium thiosulfate to remove iodine. The filtered solution was freed from solvent to give 11.5 g (88.5%) of the crude hemiacetal *cis-trans-2-hydroxy-5-methoxymethyltetrahydrofuran.* This was dissolved in 100 ml of dry methanol containing a few drops of concentrated hydrochloric acid and left at room temperature for 6 h. This was then stirred for 15 min with excess solid sodium bicarbonate. Removal of the solid, and separation of solvent by fractional distillation gave a residue

Can. J. Chem. Downloaded from www.nrcresearchpress.com by 210.87.254.42 on 09/05/12
For personal use only.

Can. J. Chem. Downloaded from www.nrcresearchpress.com by 210.87.254.42 on 09/05/12
For personal use only.

which was distilled to provide *cis-trans-2-methoxy-5-methoxymethyltetrahydrofuran*; yield, 7.1 g (55%); b.p. 65° at 50 mm; η_D^{25} 1.4242.

cis-trans-2-Isopropoxy-5-methyltetrahydrofuran

A solution of 6.8 g (0.05 mol) of 2-methoxy-5-methyltetrahydrofuran in 20 ml of isopropyl alcohol containing a trace of *p*-toluenesulfonic acid was heated in an apparatus arranged for downward distillation while nitrogen was bubbled through the solution. A mixture of methanol and isopropyl alcohol distilled between 60–80°. Distillation was continued till only isopropyl alcohol came over (80°). The cooled residue was stirred with solid sodium bicarbonate, filtered, and fractionally distilled to give 4.3 g (60%) of the furan; b.p. 136–139° at 700 mm; η_D^{25} 1.4112.

The g.l.c. on butanediol succinate showed one broad symmetrical peak.

Preparation of Authentic Hydrogenolysis Products

The 4-Alkoxy-1-butanols from Ring Cleavage of 2-Alkoxytetrahydrofurans

The following compounds were prepared by the general procedure (12) starting with 4-chloro-1-butanol and 3,4-dihydropyran and then using the appropriate alcohol.

4-Methoxy-1-butanol, b.p. 60° at 19 mm; η_D^{26} 1.4194; lit. b.p. 59–63° at 7 mm; η_D^{25} 1.4189 (27).

4-Ethoxy-1-butanol, b.p. 78° at 18 mm; η_D^{26} 1.4201; lit. b.p. 83–84° at 16 mm; η_D^{20} 1.4229 (28).

4-Isopropoxy-1-butanol, b.p. 87° at 15 mm; η_D^{24} 1.4237.

4-t-Butoxy-1-butanol was obtained in 86% yield from AlH_2Cl hydrogenolysis of 2-*t*-butoxytetrahydrofuran (see below for general method); b.p. 95–96° at 17 mm; η_D^{25} 1.4253; lit. b.p. 72–74° at 10 mm; η_D^{18} 1.4301 (12).

Compounds Expected from Ring Cleavage of 5-Substituted-2-alkoxytetrahydrofurans

5-Methoxy-2-pentanol

This compound was obtained as the chief product from the AlH_2Cl hydrogenolysis of 2-methoxy-5-methyltetrahydrofuran by the general procedure described later in this paper; yield, 50%; b.p. 65° at 20 mm; η_D^{25} 1.4220.

6-Methoxy-2-methyl-3-hexanol

A solution of 11 g (0.085 mol) of γ-isopropyl-γ-butyrolactone (see above for preparation of *cis-trans*-5-isopropyl-2-methoxytetrahydrofuran) in 10 ml of dry ether was added dropwise to a solution of lithium aluminum hydride (2.0 g, 0.053 mol) in 100 ml of ether kept at 5° in an ice bath. After the addition, the mixture was stirred for 2 h at room temperature and then an aqueous 15% solution of potassium hydroxide was added till no further lithium aluminate precipitated. The solid was separated and the filtrate freed from ether. The residue was distilled to give *5-methyl-1,4-hexanediol* as a colorless liquid (7.6 g, 69%); b.p. 80° at 0.1 mm; η_D^{19} 1.4553.

To a vigorously stirred solution of this diol (2.5 g, 0.019 mol) and methyl iodide (5.4 g, 0.038 mol) in 50 ml of dry 1,2-dimethoxyethane (DME) was added 0.76 g (0.019 mol) of sodium hydride (obtained from 60% sodium hydride in paraffin washed with pentane and dried under nitrogen) in small portions. The resulting mixture was stirred at room temperature for 2 h, then freed from DME. An ether solution of the residue was filtered and the filtrate dried ($MgSO_4$) and subsequently freed from solid and from ether. The residue when distilled gave *6-methoxy-2-methyl-3-hexanol* as a colorless liquid, b.p. 58° at 1 mm; η_D^{20} 1.4343.

The g.l.c. analysis showed only one symmetrical peak with retention time identical to that of the high boiling product obtained from the hydrogenolysis of 5-isopropyl-2-methoxytetrahydrofuran.

6-Methoxy-2,2-dimethyl-3-hexanol

A solution of lithium aluminum hydride (2.4 g, 0.063 mol) in 100 ml of dry ether was cooled in ice to 5° and added dropwise to a solution of 10 g (0.058 mol) of methyl β-pivalylpropionate (see above for preparation of *cis-trans*-5-*t*-butyl-2-methoxytetrahydrofuran) in 20 ml of ether. The reaction mixture was then treated as described for the analogous reduction of γ-isopropyl-γ-butyrolactone with the hydride; yield of *5,5-dimethyl-1,4-hexanediol*, 8.1 g (81%); b.p. 82–84° at 0.1 mm; η_D^{24} 1.4565.

Monomethylation of this diol followed the same procedure described above for the monomethylation of 5-methyl-1,4-hexanediol, to provide *6-methoxy-2,2-dimethyl-3-hexanol* in 61% yield; b.p. 82–83° at 6 mm; η_D^{24} 1.4350.

The g.l.c. showed a single symmetrical peak with retention time identical to that of the trace amount of high boiling product obtained from the hydrogenolysis of 5-*t*-butyl-2-methoxytetrahydrofuran.

4-Methoxy-1-phenyl-1-butanol

The reaction (29) of diethyl malonate with 1-bromo-2-methoxyethane, but using sodium hydride in dry DME under nitrogen, gave 36 g (45%) of *diethyl (2-methoxyethyl)-malonate*; b.p. 111° at 6 mm; η_D^{22} 1.4238; lit. b.p. 110° at 6 mm (29). Hydrolysis (29) gave 4-methoxybutyric acid (82%); b.p. 93° at 4 mm; η_D^{25} 1.4226; lit. b.p. 105° at 7 mm; η_D^{20} 1.4251 (29). Acid-catalyzed reaction of the acid with methanol gave *methyl 4-methoxybutyrate* (45%), b.p. 100° at 100 mm; η_D^{24} 1.4058.

Lithium metal (0.32 g, 0.04 mol) was added to vigorously stirred dry ether (100 ml) which had been flushed with dry nitrogen. To this stirred suspension was added dropwise, 3.14 g (0.02 mol) of bromobenzene. After all the metal had been consumed, the solution under nitrogen was stirred at room temperature for 2 h, and then 1.2 g (0.01 mol) of 4-methoxybutyric acid in 50 ml of ether was added slowly. The solution was stirred overnight at room temperature. Water (10 ml) was then slowly added to the stirred mixture. The ether layer was separated and dried ($MgSO_4$). Removal of the solid and then the solvent gave crude *4-methoxy-1-phenyl-1-butanone*. To this ketone (0.9 g, 0.051 mol), dissolved in 30 ml of dry tetrahydrofuran cooled to −10° in a Dry Ice–acetone bath, was added 1.0 g (0.026 mol) of sodium borohydride. After the addition, the solution was stirred overnight at room temperature and then carefully neutralized with 50% aqueous sulfuric acid using a drop of phenolphthalein as indicator. The excess tetrahydrofuran was removed and the residue dissolved in ether. The solid was separated by filtration and the filtrate freed from ether. Distillation of the residue gave 0.8 g (89%) of *4-methoxy-1-phenyl-1-butanol*; b.p. 94–95° at 0.1 mm; η_D^{23} 1.5150.

The g.l.c. on a column containing Apiezon T showed a single symmetrical peak with retention time identical to that of the high boiling product from the hydrogenolysis of 2-methoxy-5-phenyltetrahydrofuran.

5-Isopropoxy-2-pentanol

This was obtained as the chief product from AlH_2Cl

Can. J. Chem. Downloaded from www.nrcresearchpress.com by 210.87.254.42 on 09/05/12
For personal use only.

hydrogenolysis of 2-isopropoxy-5-methyltetrahydrofuran according to the procedure described later in this paper. The alcohol was isolated from the mixture of products by preparative g.l.c. on a butanediol succinate column. The microboiling point was 65–66° at 8 mm; η_D^{24} 1.4225.

Compounds Expected from exo Cleavage; the 2-Alkyltetrahydrofurans and 2-Phenyltetrahydrofuran

Tetrahydrofuran and *2-methyltetrahydrofuran*, from Eastman Kodak Co.

2-Isopropyltetrahydrofuran

The following extensive modification of the general procedure (30) for conversion of a 1,4-diol to the tetrahydrofuran was employed. *p*-Toluenesulfonylchloride (9.8 g, 0.052 mol) in a minimum amount of 2,6-lutidine was added dropwise to a hot (100°) stirred solution of 6.8 g (0.052 mol) of 5-methyl-1,4-hexanediol (prepared above) in 25 ml of 2,6-lutidine. The solution was then stirred for 1 h at 100°, and subsequently distilled. The material boiling at 120–130° was redistilled through a 3-in. Vigreux column; b.p. 114° at 700 mm; g.l.c. showed it to contain 2,6-lutidine (10%). Preparative g.l.c. on a butanediol succinate column at 150° gave pure *2-isopropyltetrahydrofuran*, η_D^{19} 1.4217. The g.l.c. showed one symmetrical peak with retention time identical to that for the low boiling product obtained from the hydrogenolysis of 5-isopropyl-2-methoxytetrahydrofuran.

2-t-Butyltetrahydrofuran

The compound, 5,5-dimethyl-1,4-hexanediol (prepared above) was cyclized to *t-butyltetrahydrofuran* by the modified method used to make 2-isopropyltetrahydrofuran. 2,4,6-Collidine was used in place of 2,6-lutidine and the solution obtained after the period of heating at 100° was stirred into ether. The residue, after removal of solid and solvent, distilled at 125° at 695 mm. The collidine impurity was removed by preparative g.l.c. on a Carbowax column at 150°; η_D^{22} 1.4248.

2-Phenyltetrahydrofuran

$LiAlH_4$ reduction of methyl β-benzoylpropionate (prepared above) by the method used above to reduce methyl β-pivalylpropionate gave *1-phenyl-1,4-butanediol* (84%); b.p. 129–130° at 0.3 mm; η_D^{23} 1.5409. The liquid solidified on standing, m.p. 65–66°.

The diol was cyclized to *2-phenyltetrahydrofuran* by the method used to prepare 2-*t*-butyltetrahydrofuran above but 2,6-lutidine was the base employed. The product boiled at 80° at 3 mm but contained some lutidine. Preparative g.l.c. on an Apiezon T column gave pure material; η_D^{23} 1.5283; lit. b.p. 107 at 15 mm; η_D^{20} 1.5299 (31).

2-Methoxymethyltetrahydrofuran

Reaction of furfuryl alcohol with methyl iodide and sodium hydride (25) gave *2-methoxymethylfuran* (40%); b.p. 80° at 120 mm; η_D^{23} 1.4521; lit. b.p. 134–135° at 762 mm; η_D^{20} 1.4573 (32).

The 2-methoxymethylfuran (5.6 g, 0.05 mol), hydrogenated at 60 p.s.i. and room temperature with rhodium on alumina (33), gave 3.85 g (69%) of 2-methoxytetrahydrofuran; b.p. 90° at 135 mm; η_D^{23} 1.4248; lit. b.p. 140–144° at 715 mm (34).

The g.l.c. showed one symmetrical peak of retention time identical to that of the minor product obtained from hydrogenolysis of 2-methoxy-5-methoxymethyltetrahydrofuran.

General Procedure for the Hydrogenolysis of 2-Alkoxytetrahydrofurans

To a solution of lithium aluminum hydride (0.30 g, 0.0079 mol) in 30 ml of dry ether, cooled to 5° in an ice bath, was added dropwise an ether solution of aluminum chloride, previously prepared by the addition of 1.05 g (0.0079 mol) of the aluminum chloride in small portions to 30 ml of dry ether kept at 5°. The resulting "mixed hydride" (AlH_2Cl (2, 3)) solution was stirred at room temperature for 15 min and then a solution of the 2-alkoxytetrahydrofuran (0.0156 mol) in ether (30 ml) was added dropwise. The resulting mixture was stirred at room temperature for the appropriate time (usually 2 h), whereupon an aqueous 15% solution of potassium hydroxide was slowly dropped in until no further reaction occurred. The colorless precipitate of lithium aluminate was separated by filtration and washed with ether. The combined washings and filtrate were freed from solvent by fractional distillation. The residue (recovery 80–95%) was analyzed by g.l.c. and the products identified by comparison of their retention times with those of authentic substances. In cases of doubt regarding identity the products were isolated by preparative g.l.c. and their i.r. and p.m.r. spectra were compared with those of authentic substances.

The authors thank the National Research Council of Canada for financial support for a part of this work.

One of us (P. C. Loewen) thanks the National Research Council of Canada for the award of a Bursary, and the Isaac Killam Memorial Fund of the University of Alberta for the award of a Fellowship.

1. U. E. Diner and R. K. Brown. Can. J. Chem. **45**, 2547 (1967).
2. E. C. Ashby and J. Prather. J. Am. Chem. Soc. **88**, 729 (1966).
3. U. E. Diner, H. A. Davis, and R. K. Brown. Can. J. Chem. **45**, 207 (1967).
4. F. Korte and H. Machleidt. Chem. Ber. **88**, 1685 (1955).
5. F. Korte, K-H Büchel, D. Scharf, and A. Zschocke. Chem. Ber. **92**, 884 (1959).
6. W. A. White and H. Weingarten. J. Org. Chem. **32**, 213 (1967).
7. G. Stork, A. Brizzolara, H. Landesman, J. Szmuszkovicz, and R. Terrell. J. Am. Chem. Soc. **85**, 207, (1963).
8. S. A. Barker, J. S. Brimacombe, A. B. Foster, D. H. Whiffen, and G. Zweifel. Tetrahedron, **7**, 10 (1959).
9. H. C. Brown and R. M. Adams. J. Am. Chem. Soc. **64**, 2557 (1942).
10. E. M. Arnett and C. Y. Wu. J. Am. Chem. Soc. **84**, 1684 (1962).
11. F. J. Cioffi and S. T. Zenchelsky. J. Phys. Chem. **67**, 357 (1963).
12. E. L. Eliel, B. E. Nowak, R. A. Daignault, and V. G. Badding. J. Org. Chem. **30**, 2441 (1965).
13. E. L. Eliel, N. L. Allinger, S. J. Angyal, and G. A. Morrison. Conformational analysis. Interscience Publishers Inc., New York, 1966. p. 44.
14. M. L. Michailovic, R. I. Manuzic, L. Zigic-Manuzic, T. Bosnjak, and Z. Cekovic. Tetrahedron, **23**, 215 (1967).

15. D. GAGNAIRE and P. MONZEGLIO. Bull. Soc. Chim. Fr. 474 (1965).
16. R. PAUL and S. TCHELITCHEFF. Bull. Soc. Chim. Fr. 197 (1948).
17. S.-O. LAWESSON and C. BERGLUND. Arkiv. für Kemi, **17**, 475 (1961).
18. R. P. LINSTEAD and H. N. RYDON. J. Chem. Soc. 580 (1933).
19. G. A. HILL and E. W. FLOSDORF. Org. Synth. Coll. Vol. I, 451 (1941).
20. R. ADAMS and E. W. ADAMS. Org. Synth. Coll. Vol. I, 448 (1941).
21. C. GOLUMBIC and D. L. COTTLE. J. Am. Chem. Soc. **61**, 996 (1939).
22. R. R. RUSSELL and G. A. VANDERWERF. J. Am. Chem. Soc. **69**, 11 (1947).
23. I. HEILBRON and H. M. BUNBURY. Dictionary of organic compounds. Vol. II. Eyre and Spottiswoode, London, 1953.
24. F. SWEET and R. K. BROWN. Can. J. Chem. **46**, 2289 (1968).
25. U. E. DINER, F. SWEET, and R. K. BROWN. Can. J. Chem. **44**, 1591 (1966).
26. R. PAUL and S. TCHELITCHEFF. Bull. Soc. Chim. Fr. 808 (1952).
27. W. F. GRESHAM. U.S. Pat. 2 504 407 (1950). Chem. Abstr. **44**, 5902 (1950).
28. C. CRISAN. Ann. Chim. **13**, 436 (1956).
29. M. H. PALOMAA and A. KENETTI. Chem. Ber. **64**, 797 (1931).
30. D. D. REYNOLDS and W. O. KENYON. J. Am. Chem. Soc. **72**, 1593 (1950).
31. W. B. RENFROW, D. OAKES, C. LAUER, and J. A. WALTER. J. Org. Chem. **26**, 935 (1961).
32. W. R. KIRNER. J. Am. Chem. Soc. **50**, 1958 (1928).
33. J. H. STOCKER. J. Org. Chem. **27**, 2288 (1962).
34. W. R. KIRNER. J. Am. Chem. Soc. **52**, 3251 (1930).
35. N. L. ALLINGER and M. T. TRIBBLE. Tetrahedron Lett. 3259 (1971).

Can. J. Chem. Downloaded from www.nrcresearchpress.com by 210.87.254.42 on 09/05/12
For personal use only.

Acidity Function Behavior in Aqueous-organic Solvents. I. The H_0, H_0''', and H_A Functions in 70% DMSO–H_2O

KEITH YATES AND GRAEME WELCH[1]

Department of Chemistry, University of Toronto, Toronto 5, Ontario

Received November 9, 1971

The H_0, H_0''', and (in part) the H_A acidity functions have been determined in 70% DMSO–water for the sulfuric acid concentration range 0–85%. In sharp contrast to purely aqueous acid systems the H_0 (primary aniline) and H_0''' (tertiary aniline) scales in DMSO–water are closely parallel over a wide range of acidity. This provides clear experimental demonstration that linearity of log (ionization ratio) *vs.* acidity function with unit slope is not a sufficient condition that a base is obeying a given acidity function. When the three acidity functions in DMSO–water are shifted to a purely aqueous standard state, their order is completely reversed from that observed in aqueous acids. These differences in behavior are discussed in terms of cation solvation by DMSO molecules only.

Les fonctions d'acidité H_0, H_0''', et (en partie) H_A, ont été déterminées dans un mélange à 70% DMSO–eau pour des concentrations en acide sulfurique allant de 0 à 85%. A l'encontre des systèmes acides purement aqueux, les échelles H_0 (aniline primaire) et H_0''' (aniline tertiaire) sont, dans le DMSO–eau, étroitement parallèles sur une vaste échelle d'acidité. Ceci constitue une bonne preuve expérimentale d'après laquelle la linéarité du log (rapport d'ionisation) par rapport à la fonction d'acidité avec une pente unitaire ne constitue pas une condition suffisante pour affirmer qu'une base obéit à une fonction d'acidité donnée. Lorsque les trois fonctions d'acidité dans le DMSO–eau sont déplacées vers un état standard purement aqueux, leur ordre est complètement inversé par rapport à celui observé en milieu acide aqueux. Ces différences de comportements sont rationalisées en termes d'une solvatation cationique par les seules molécules de DMSO.

Canadian Journal of Chemistry, **50**, 1513 (1972)

Introduction

In the 14 years following the Paul and Long (1) review of the Hammett acidity function H_0 (2), confidence in the generality and utility of this concept has been seriously undermined. Recent work in this field has concentrated on the construction of a variety of acidity scales[2] based on structurally different classes of organic base, or has been essentially empirical in its approach. Examples of the latter are the determination of pK_a values based on H_0 at half-protonation (3), the ϕ-parameter treatment of Bunnett and Olsen (4), the *m*-value approach of Yates and McClelland (5) and more recently the $\Delta H - \Delta G$ correlations studied by Arnett and co-workers (6). Although these methods may give reasonable estimates of the relative basicities of a series of organic compounds (4), or may prove useful in rate-acidity correlations (4, 5), there is considerable uncertainty associated with the relationship between the pK_a values obtained and the defined standard state (usually dilute aqueous solution). Apart from the intrinsic desirability of trying to place all weak bases on a common quantitative scale, the very large number of organic reactions which involve proton transfers between weakly basic sites require a much more complete knowledge of acidity function behavior.

Although attempts have been made to explain the differences between various acidity functions in terms of the hydration requirements of the indicator species involved (9–11), these have not been quantitatively successful, and it appears that neither the increasing number of aqueous acidity functions nor empirical correlation methods are likely to provide a better fundamental understanding of the problem.

The greater proportion of acidity function work has concentrated on strong mineral acid – water solvent systems, and there is much less information available concerning the comparable behavior of acidity functions in non-aqueous or partly aqueous solutions. A more extensive knowledge of their behavior in these systems might be expected to lead to interesting comparisons and possibly a better insight into the acidity function problem. Although a few attempts have been made in this direction (12, 13), most acidity scales in other than purely

[1]Present address: Department of Chemistry, McGill University, Montreal, Quebec.

[2]Two recent reviews (7, 8) give comprehensive accounts of these acidity functions and their measurement.

Can. J. Chem. Downloaded from www.nrcresearchpress.com by 210.87.254.40 on 09/05/12
For personal use only.

TABLE 1. The pK_a values of primary anilines (25 °C)

No.	Indicator	pK_a*	Mean deviation†	r‡
1	3-Nitroaniline‖	0.78	0.02	—
2	2,4-Dichloroaniline‖	0.02	0.09	—
3	3-Methyl-4-nitroaniline‖	−0.59	0.03	0.999
4	4-Nitroaniline	−1.09	0.06	0.997
5	3,5-Dinitroaniline	−1.63	0.07	0.997
6	2-Nitroaniline	−2.22	0.08	0.998
7	4-Chloro-2-nitroaniline	−2.94	0.14	0.990
8	2,5-Dichloro-4-nitroaniline§	(−3.57)	(0.24)	0.987
9	2-Chloro-6-nitroaniline	−4.77	0.06	0.994
10	2,6-Dichloro-4-nitroaniline	−5.52	0.03	0.991
11	2,4-Dinitroaniline	−6.29	0.11	0.987
12	2,6-Dinitroaniline	−7.32	0.04	0.998
13	4-Chloro-2,6-dinitroaniline	−7.98	0.01	0.997
14	2-Bromo-4,6-dinitroaniline	−8.68	0.02	0.993
15	3-Methyl-2,4,6-trinitroaniline	−10.33	0.05	0.997

*Referred to a standard state of 70% (w/w) DMSO–H_2O.
†Mean deviation of $\Delta \log I$ values.
‡Correlation coefficient.
§This indicator was not used to construct H_0.
‖Not previously used as H_0 indicator.

aqueous-mineral acid solutions have been constructed with more practical aims such as application to specific kinetic problems. In this and succeeding papers in the series, work will be described concerning an investigation into the comparative behavior of structurally different bases in a predominantly non-aqueous solvent system, sulfuric acid in DMSO–water. It was hoped that by studying not only the acidity functions themselves, but also solvent effects on pK_a values and activity coefficients, a better insight would be obtained into the reasons for the divergent behavior observed in purely aqueous-acid systems, which has been termed by Arnett and Mach (14) "acidity function failure". In this paper the comparative behavior of the H_0, H_0''', and in part, the H_A functions in 70% DMSO–water are considered, and contrasted with available data in purely aqueous acid systems.

Experimental

Solvents

Dimethyl sulfoxide (Fisher Reagent grade) was purified by a modification[3] of the fractional distillation method of Schläfer and Schaffernicht (15). The purity was checked by freezing point determination, only samples with f.p. above 18.54 °C being accepted. The physical properties of the DMSO were in good agreement with those tabulated by Butler (16), Martin *et al.* (17), and Agamie (18). Sulfuric acid solutions were prepared by diluting ice cold solutions of aqueous sulfuric acid with a cooled solution of DMSO–H_2O of the appropriate concentration to yield a final composition containing H_2SO_4 in 70% (w/w) DMSO–H_2O. The H_2SO_4 concentration was checked by potentiometric titration with standardized aqueous alkali. The acids were stored in glass bottles fitted with ground glass stoppers. Specimen acids were checked periodically but showed no change of titre with time. Acids more than 3 months old, however, developed a strong odor and showed evidence of weak absorption in the 300–260 nm regions of the u.v. spectrum. These acids were discarded.

Indicators

The indicators used to construct the H_0 and H_0''' acidity scales are listed in Tables 1 and 2.

Indicators 4, 6–15 (Table 1) and 3–14 (Table 2) form series used previously to construct H_0 (19) and H_0''' (20) scales in this laboratory. Indicators 1, 2, and 5 (Table 1) and 1 (Table 2) were commercially available compounds, which were recrystallized or sublimed to constant m.p., Table 1: 1, 112° (lit. (21) 112°); 2, 62° (lit. (21) 63°) 5, 162° (lit. (22) 163°); Table 2: 1, 63° (lit. (22) 63°).

N,N-Dimethyl-3-methyl-4-nitroaniline and 3-methyl-4-nitroaniline were prepared by nitration of *N,N*-dimethyl-*m*-toluidine, and *m*-toluidine respectively, using standard methods. Nitration of *N,N*-dimethyl-*m*-toluidine gave only the desired product which was purified by recrystallization from aqueous ethanol, m.p. 84° (lit. (22) 84°). Nitration of *m*-toluidine gave a mixture of 3-methyl-6-nitroaniline and 3-methyl-4-nitroaniline which were separated on an alumina column using benzene as eluant. 3-Methyl-4-nitroaniline had m.p. 133° (lit. (22) 134°).

2-Pyrrolecarboxamide and 4-methoxybenzamide were samples prepared previously to construct the H_A acidity scale (11).

The preparation of indicator solutions and the spectro-

[3]Details of this method are given in the Ph.D. Thesis of G. Welch, University of Toronto, Toronto, Ontario, 1969.

Can. J. Chem. Downloaded from www.nrcresearchpress.com by 210.87.254.40 on 09/05/12
For personal use only.

TABLE 2. The pK_a values of tertiary anilines (25 °C)

No.	Indicator	pK_a*	Mean deviation†	r‡
1	*N*,*N*-Dimethyl-3-nitroaniline§	−0.16	0.02	—
2	*N*,*N*-Dimethyl-3-methyl-4-nitroaniline§	−1.22	0.10	0.987
3	*N*,*N*-Dimethyl-4-nitroaniline	−1.96	0.09	0.995
4	*N*,*N*-Diethyl-2,4-dinitroaniline	−2.43	0.11	0.992
5	*N*(2,4-Dinitrophenyl)-piperidine	−2.73	0.03	0.992
6	*N*,*N*-Dimethyl-2,6-dinitro-4-methylaniline	−4.23	0.16	0.997
7	*N*,*N*-Dimethyl-2,4-dinitro-1-naphthylamine	−4.86	0.08	0.999
8	*N*,*N*-Dimethyl-2,6-dinitro-4-chloroaniline	−5.13	0.13	0.989
9	*N*-Methyl-4-nitrodiphenylamine	−5.68	0.15	0.981
10	*N*-Methyl-4-nitro-4′-bromo-diphenylamine	−6.37	0.05	0.992
11	*N*,*N*-Diethyl-2,4,6-trinitroaniline	−7.10	0.13	0.996
12	*N*,*N*-Dimethyl-2,4,6-trinitroaniline	−7.85	0.03	0.999
13	*N*-Methyl-4-bromo-2′,4′-dinitro-diphenylamine	−8.83	0.02	0.989
14	*N*-Methyl-*x*,4-dibromo-2′,4′-dinitrodiphenylamine	−10.00	0.12	0.993

*Referred to a standard state of 70% (w/w) DMSO–H_2O.
†Mean deviation of Δ log *I* values.
‡Correlation coefficient.
§Not previously used as H_0′′ indicator.

photometric measurements were carried out (at least in duplicate) by standard methods.

Treatment of Data

(*i*) Absorbance values at each acid concentration were interpolated from the recorder trace at a number of wavelengths (usually 5 to 7) symmetrically disposed about λ_{max}. (*ii*) The absorbance values at λ_{max} were plotted against concentration to give the usual sigmoid curves from which the best values of A_B and A_{BH^+} (18) were interpolated. The acid concentrations from which these values were chosen were then used to define A_B and A_{BH^+} at other wavelengths. (*iii*) The log *I* (*I* = ionization ratio = $[BH^+]/[B]$) values were calculated for each wavelength at a given acid concentration and the mean and standard deviation of log *I* calculated. It was hoped that *i* and *ii* would minimize any medium effect on *A*, A_B, and A_{BH^+} (which were in any case usually small in this solvent system) and that *iii* would reduce random experimental error to a minimum and give an indication of its magnitude. The values of λ_{max}, log *I*, σ (log *I*), and absorbance (at λ_{max}) are shown in Table 3.

Experimental Error in log I Values

Kresge and Chen (23) have shown that the error function for log *I* of aniline indicators is approximately symmetrical about log $I = 0$ and has a shallow minimum over the range log $I = \pm 1.5$. This treatment assumes that the spectrophotometer error is independent of the absorbance, but for the Bausch and Lomb 505 used in this work the error was found to be an approximately linear function of this quantity. Introduction of this variable into the error function results in a considerable asymmetry (minimum error at log $I = \pm 0.4$) and this was confirmed by comparison of the calculated error function with the experimental σ (log *I*) values. On this basis the overlap procedure for the log *I* – concentration curves was carried out where possible over the range −1.0 to +1.5.

Results and Discussion

Choice of Solvent System

The particular choice of 70% DMSO–H_2O as solvent system for the acid was based on two main considerations. Firstly, it is of sufficiently high dielectric constant that normal dissociation equilibria will be uncomplicated by ionic association phenomena. Secondly, it is sufficiently different from purely aqueous acid systems that other than trivial changes might be observed. The system pure DMSO–H_2SO_4[4] also seems satisfactory to meet the above requirements but was rejected for practical reasons, particularly because the high solubility of organic indicators in DMSO would preclude facile determination of activity coefficients by solubility measurements.

[4]Since the start of this work an H_0 acidity function has been reported for pure DMSO–H_2SO_4 (24).

Can. J. Chem. Downloaded from www.nrcresearchpress.com by 210.87.254.40 on 09/05/12
For personal use only.

Can. J. Chem. Downloaded from www.nrcresearchpress.com by 210.87.254.40 on 09/05/12
For personal use only.

Despite the fact that a three-component system (H_2SO_4–DMSO–H_2O) is intrinsically less desirable, the particular solvent composition 70% (w/w) DMSO–H_2O has a number of attractive features. The dielectric constant (61.7) (25) is sufficiently high to prevent significant ion-pairing phenomena, and more important, it has been shown that in this mole fraction region (*ca.* 2:1; H_2O:DMSO) the solvent properties are least like those of either of the pure solvents (26–28). Although DMSO, like water, is a highly associated solvent (29), the degree of disorganization with respect to the pure liquids in the solvent structure of the binary system is at a maximum (28, 30, 31) near the composition chosen. It was hoped that replacement of the solvent by added H_2SO_4 would thus result in a much less drastic alteration of the solvent characteristics than would be the case either with pure DMSO or pure water as solvent. This expectation is supported by the small variations in activity coefficient for neutral aniline bases in this particular solvent mixture (32).

Results

The H_0 and H_0''' acidity scales were constructed in 70% (w/w) DMSO–H_2O by standard methods using the established sequence of primary aniline indicators (Table 1) listed by Jorgenson and Hartter (33) and tertiary aniline indicators (Table 2) listed by Arnett and Mach (10). In addition, the lower acidity of this solvent system required the use of five more strongly basic indicators which are indicated in Tables 1 and 2.

The log I values for each set of indicators showed very satisfactory parallelism when plotted against % H_2SO_4 (w/w) in the conventional manner, except indicator 8 (2,5-dichloro-4-nitroaniline). This indicator was therefore omitted from the overlap calculation of H_0.[5] The parallelism of the remaining indicator slopes, within the measurable protonation range, demonstrates that each set conforms to the necessary condition of the Hammett activity coefficient postulate, despite the radical change in solvent composition. Thus construction of acidity scales is a no less valid procedure in this system than in purely aqueous mineral acid solutions.

[5]Details of the calculations and indicator curves are available elsewhere (34).

The pK_a values for the "anchor" indicators, 3-nitroaniline and *N*,*N* dimethyl-3-nitroaniline, were obtained from the least squares intercepts of plots of log $C_B C_{H^+}/C_{BH^+}$ *vs.* C_{H^+}. The values obtained were 0.78 and 0.16 respectively. The probable error in these values is ± 0.02 log units and the value for 3-nitroaniline is in excellent agreement with that interpolated from the results of Wolford (35) (0.80). No previous values for the tertiary aniline could be found, but the low value is in qualitative agreement with the pK_a values obtained for other tertiary anilines in DMSO–H_2O (36).

The pK_a values for the less basic indicators were obtained from the usual overlap technique (19, 33). The log I values were overlapped in the protonation region from log $I = -1.0$ to $+1.5$, the asymmetry arising from the analysis of the standard deviations of the individual log I values (see Experimental). The only significant exceptions to this were indicators 9 (-1.33 at 40%) and 15 (-1.27 at 72%) and indicator 7 (-1.22 at 34%) where the extended log I range was necessary to achieve a reasonable degree of overlap. These values are still within the normal accepted range, and the average degree of uncertainty in the Δ log I values (~ 0.05 log unit) is within the usual range of uncertainty for measurements of this type. The H_0 and H_0''' were calculated from the pK_a values and log I values interpolated from the regression lines, using the equation

$$H_0 = pK_a - \log I$$

The H_0 and H_0''' values derived from each indicator were averaged and are shown in Tables 3 and 4 along with the mean deviation of each point. The two functions are plotted in Fig. 1 and it can be seen that smooth curves may be drawn through the experimental points. At low concentrations (less than 5% H_2SO_4) the two functions converge satisfactorily to define the beginning of a pH scale for this solvent system.

It was originally hoped that the H_A (amide) acidity function (11) could also be constructed in this solvent system. However, the end absorption of the DMSO in the solvent limited spectrophotometric measurements to only two indicators, 2-pyrrolecarboxamide and 4-methoxybenzamide.

TABLE 3. The H_0 values for H_2SO_4–DMSO–H_2O solutions at 25 °C

Concentration (%)	H_0	Mean deviation	Indicator	Concentration (%)	H_0	Mean deviation	Indicator
1.00	0.86	0.03	1, 2	46.00	−4.18	0.02	7, 9
2.00	0.53	0.07	1, 2	48.00	−4.48	0.04	7, 9
4.00	0.06	0.09	1, 2, 3, 4	50.00	−4.85	0.01	9, 10
6.00	−0.25	0.05	1, 2, 3, 4	52.00	−5.18	0.01	9, 10
8.00	−0.45	0.04	1, 2, 3, 4	54.00	−5.44	0.08	9, 10, 11
10.00	−0.60	0.05	1, 2, 3, 4	56.00	−5.77	0.05	9, 10, 11
12.00	−0.75	0.04	2, 3, 4, 5	58.00	−6.12	0.03	9, 10, 11
14.00	−0.92	0.03	2, 3, 4, 5	60.00	−6.41	0.01	10, 11, 12
16.00	−1.08	0.03	2, 3, 4, 5	62.00	−6.81	0.05	10, 11, 12
18.00	−1.25	0.03	2, 3, 4, 5	64.00	−7.26	0.08	10, 11, 12, 13
20.00	−1.38	0.08	2, 3, 4, 5, 6	66.00	−7.66	0.02	11, 12, 13, 14
22.00	−1.53	0.07	3, 4, 5, 6	68.00	−8.10	0.01	12, 13, 14
24.00	−1.71	0.05	3, 4, 5, 6	70.00	−8.52	0.02	12, 13, 14
26.00	−1.89	0.05	3, 4, 5, 6	72.00	−8.99	0.05	13, 14, 15
28.00	−2.03	0.02	3, 4, 5, 6	74.00	−7.39	0.02	13, 14, 15
30.00	−2.15	0.06	4, 5, 6, 7	76.00	−9.81	0.03	14, 15
32.00	−2.35	0.07	4, 5, 6, 7	78.00	−10.21	0.07	14, 15
34.00	−2.55	0.06	4, 5, 6, 7	80.00	−10.40	—	15
36.00	−2.80	0.03	5, 6, 7	82.00	−10.84	—	15
38.00	−3.02	0.05	5, 6, 7	84.00	−11.22	—	15
40.00	−3.23	0.08	5, 6, 7	86.00	−11.57	—	15
42.00	−3.54	0.06	6, 7, 9	88.00	−11.93	—	15
44.00	−3.80	0.10	6, 7, 9	90.00	−12.29	—	15

TABLE 4. The H_0'' values for H_2SO_4–DMSO–H_2O solutions at 25 °C

Concentration (%)	H_0	Mean deviation	Indicator	Concentration (%)	H_0	Mean deviation	Indicator
2.00	0.57	—	1	44.00	−4.80	0.11	6, 7, 8, 9
4.00	0.13	—	1	46.00	−5.12	0.07	6, 7, 8, 9
6.00	−0.16	—	1	48.00	−5.41	0.06	7, 8, 9, 10
8.00	−0.34	0.07	1, 2	50.00	−5.75	0.05	7, 8, 9, 10
10.00	−0.53	0.05	1, 2	52.00	−6.09	0.07	7, 8, 9, 10
12.00	−0.80	0.05	1, 2, 3	54.00	−6.36	0.12	8, 9, 10, 11
14.00	−1.02	0.05	1, 2, 3	56.00	−6.64	0.03	8, 9, 10, 11
16.00	−1.27	0.07	1, 2, 3	58.00	−7.00	0.07	9, 10, 11, 12
18.00	−1.45	0.08	1, 2, 3	60.00	−7.43	0.05	10, 11, 12
20.00	−1.77	0.09	2, 3, 4	62.00	−7.88	0.09	10, 11, 12, 13
22.00	−1.89	0.08	2, 3, 4, 5	64.00	−8.40	0.03	11, 12, 13
24.00	−2.13	0.08	2, 3, 4, 5	66.00	−8.93	0.07	12, 13, 14
26.00	−2.37	0.08	2, 3, 4, 5	68.00	−9.35	0.03	12, 13, 14
28.00	−2.56	0.01	3, 4, 5	70.00	−9.75	0.03	13, 14
30.00	−2.80	0.02	3, 4, 5	72.00	−10.14	0.09	13, 14
32.00	−3.02	0.04	3, 4, 5	74.00	−10.39	—	14
34.00	−3.20	0.10	3, 4, 5, 6	76.00	−10.72	—	14
36.00	−3.47	0.08	3, 4, 5, 6	78.00	−11.05	—	14
38.00	−3.84	0.06	4, 5, 6, 7	80.00	−11.39	—	14
40.00	−4.15	0.09	5, 6, 7	82.00	−11.72	—	14
42.00	−4.38	0.17	5, 6, 7, 8	84.00	−12.05	—	14

Discussion

Although the relationship between the H_0 and H_0'' functions in 70% DMSO–H_2O is qualitatively similar to that observed in aqueous acid systems (10), there are two very significant differences. Firstly, at low acid concentrations, H_0 is the more negative function, as shown in Fig. 2. This result is opposite to that observed

Can. J. Chem. Downloaded from www.nrcresearchpress.com by 210.87.254.40 on 09/05/12
For personal use only.

Can. J. Chem. Downloaded from www.nrcresearchpress.com by 210.87.254.40 on 09/05/12
For personal use only.

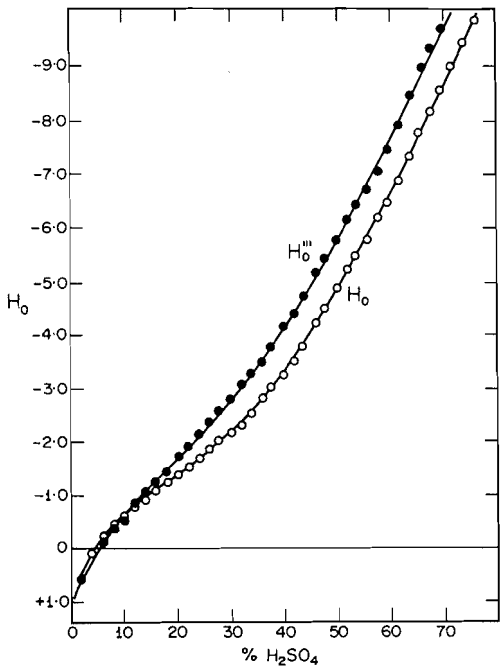

FIG. 1. Curves of the H_0 and H_0''' acidity functions in 70% DMSO–H_2O as a function of acid concentration.

for strong mineral acid – water systems, but is similar to the behavior observed by Arnett in *p*-toluenesulfonic acid.[6] Secondly, for most of the acid concentration range, the two acidity functions are essentially parallel as shown in Fig. 1, unlike in aqueous systems where the two functions continually diverge. Again, Arnett and Mach have reported similar (14) behavior for H_0 and H_0''' in aqueous *p*-toluenesulfonic acid, but in this system only a limited range of acidity could be studied.

The rapid divergence of H_0 and H_0''' in purely aqueous acids (which exceeds experimental error even in 4% H_2SO_4) indicates that the solvation requirements of anilinium ions are extremely sensitive to structure, in aqueous solutions. In the DMSO–H_2O system, although the very strong hydrogen-bonding capabilities of DMSO might have been expected to maintain, or increase the difference between anilinium and *N*,*N*-dimethylanilinium ion solvation, it apparently does not. This suggests that perhaps only one DMSO molecule can be really effective in stabilizing both types of ion, through formation of one strong hydrogen-bond. Arnett and Mach (14) have suggested that the analogous behavior observed in *p*-toluenesulfonic acid might be due to a strong salting in effect on the neutral base. This does not readily explain the crossing of the two functions, and in DMSO–H_2O both ions and neutral bases are strongly salted in. Activity coefficient measurements (32) show that both primary and tertiary anilines are salted in to almost the same extent, and that the difference in protonation behavior arises mainly from the activity coefficient behavior of the ionic species.

Acidity Function "Failure"

The most important difference between the aqueous and 70% DMSO–H_2O acidity scales is the near parallelism of H_0 and H_0''' in the latter solvent, as shown in Fig. 1. The difference in acidity function behavior between the two solvent systems is plotted in Fig. 3 in the manner suggested by Arnett and Mach (14), as a measure of acidity function "failure". It is evident that such "failure" occurs in both systems, but that it is less serious in DMSO–H_2O, particularly at high acid concentrations. It is interesting that in both systems, the point where acidity function differences start to level off corresponds to the region where the basic solvent molecules are fully protonated. In DMSO–H_2O this occurs at lower acid concentrations because of the higher molecular weight of DMSO; since this is approximately 100 times more basic than water (37), the proportion of hydronium ions in any solution should be low. It is interesting that in the regions where acidity function levelling occurs in DMSO–H_2O there are still free (unprotonated) water molecules available. That levelling still occurs suggests that these molecules are primarily involved in solvating protonated DMSO,[7] perhaps in a 2:1 structure as shown

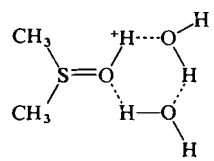

[6]Although the difference shown in Fig. 2 is small, it is outside the limits of experimental error and the ultimate convergence of H_0 and H_0''' at the lowest concentrations shows that it does not arise from an error in one of the "anchor" pK_a values.

[7]It has been generally assumed that protonation of DMSO occurs on oxygen. However, Olah *et al.* have recently reported evidence in favor of protonation on sulfur in superacid solutions (38).

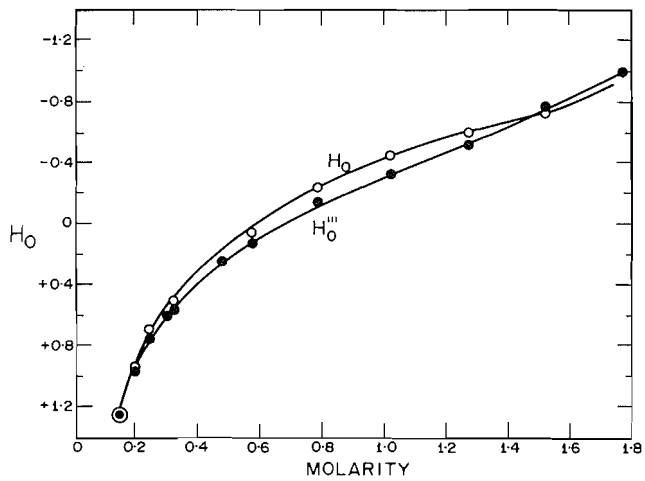

FIG. 2. Curves of the H_0 and H_0''' acidity functions in 70% DMSO–H_2O at low acid concentration.

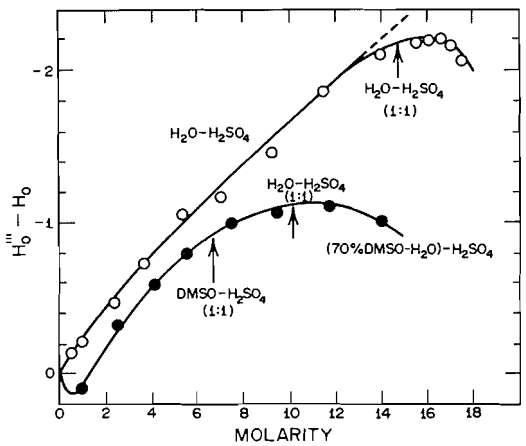

FIG. 3. Plots of $H_0''' - H_0$ as a measure of "acidity function failure" in aqueous H_2SO_4 and in (70% DMSO–H_2O)–H_2SO_4.

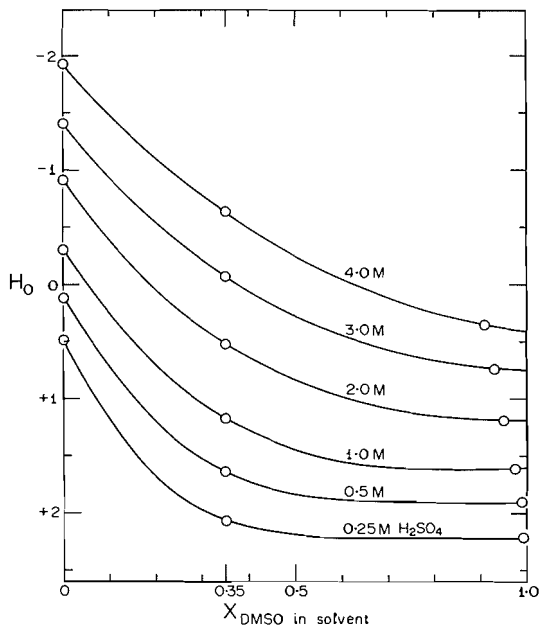

FIG. 4. Dependence of H_0 on solvent composition in the DMSO–H_2O system as a function of acid concentration.

The possibility that H_2O is significantly protonated in these systems can be discounted from a consideration of the effect of solvent composition on acidity in DMSO–H_2O systems. Using the limited data available (24) values of the H_0 function at different acid concentrations are plotted against mole fraction of water in Fig. 4. It is evident that although 70% DMSO–H_2O contains twice as many water molecules as DMSO molecules, the overall behavior of this system resembles that of pure DMSO–acid solutions much more closely than that of purely aqueous acids.

Two important points arise from the above discussion. Firstly, over an extensive range of acidity the DMSO–H_2O system has the potential of exhibiting ideal acidity function behavior with respect to primary and tertiary anilines, and possibly other types of base. For example, if the standard state were to be shifted from the pure solvent to the concentrated acid region, the two scales H_0 and H_0''' could be made to be almost superimposable over a range of about 7 H_0 units. It may be that other DMSO–H_2O compositions could be used to define a general

Can. J. Chem. Downloaded from www.nrcresearchpress.com by 210.87.254.40 on 09/05/12
For personal use only.

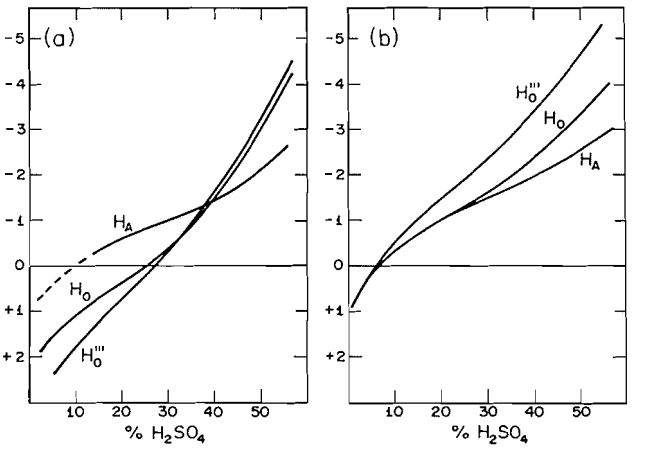

FIG. 5. Comparison of the H_0, H_0''', and H_A acidity scales in (*a*) 70% DMSO–H_2O and (*b*) H_2O, both referred to dilute aqueous solution as standard state.

acidity scale, applicable for the direct quantitative comparison of weak organic bases of a variety of different structural types. If this were possible it would be very valuable in restoring the utility of the acidity function approach to both equilibria and kinetics.

Secondly, the extensive parallelism of the two scales provides an excellent illustration that a log (indicator-ratio) – H_0 slope of unity is not a *sufficient* condition that the Hammett activity coefficient postulate be satisfied (*i.e.* $\log f_B f_{AH^+}/f_{BH^+} f_A = 0$). Either of the scales in DMSO–H_2O would give unit slope for both primary and tertiary anilines of a wide range of basicity, but if the incorrect scale were chosen, the pK_a values obtained would be in error by at least one log unit with respect to the defined standard state.

Amide Bases in DMSO–H_2O

It is unfortunate that practical difficulties have prevented the construction of an H_A scale in the solvent system. Even if the problems concerning the spectrophotometric measurements were overcome the weakly acidic nature of the solvent combined with the generally weak basicity of amides would make the determination of the pK_a for a suitable "anchor" indicator very difficult. The method of establishing the H_A function in aqueous acids (11) could not be used in DMSO–H_2O either, since the log I curves for 2-pyrrolecarboxamide and 2-nitroaniline are not only not parallel, but actually intersect in the measureable log I region.

However, the amides investigated appear to be stronger bases in DMSO–H_2O than might have been expected. The log I curves are shifted to lower concentrations with respect to 2-nitroaniline than is the case in aqueous acids. The reason for this is not clear, but it may reflect a greater sensitivity of the amide conjugate acid molecules to solvation by DMSO, compared with anilinium ions.

Acidity Functions in DMSO–H_2O Referred to the Aqueous Standard State

In order to avoid ambiguities in interpretation, the discussion so far has dealt with acidity functions based on a standard state of 70% DMSO–H_2O. The more usual procedure is to refer non-aqueous acidity scales to a standard state of ideal dilute aqueous solution. The validity of this procedure is sometimes questionable and the acidity scale thus defined may not be independent of the nature of the initial "anchor" indicator (12). In the present case the procedure appears to be justified by the parallel indicator plots obtained (also see later) and has been carried out by anchoring the scales to the aqueous pK_a of the initial indicator (H_0, 3-nitroaniline, pK_a = 2.5 (39); H_0''' *N,N*-dimethyl 3-nitroaniline, pK_a = 2.63 (40); H_A, 2-pyrrolecarboxamide, pK_a = 1.23) (11). The graphs of the three functions (referred to the aqueous standard state) in the two solvent systems (H_2O and DMSO–H_2O) are shown in Fig. 5.

The replacement of some of the water molecules in the solvent by DMSO clearly produces a dramatic change in the relationship between

Can. J. Chem. Downloaded from www.nrcresearchpress.com by 210.87.254.40 on 09/05/12
For personal use only.

Can. J. Chem. Downloaded from www.nrcresearchpress.com by 210.87.254.40 on 09/05/12
For personal use only.

the different acidity functions; in fact at moderate H_2SO_4 concentrations the relative order of the three scales has been completely reversed from the situation in aqueous systems. Also despite the DMSO–H_2O medium being considerably less acidic than a purely aqueous medium the weakly basic amides are protonated nearly 1000 times more readily than the strongly basic tertiary anilines, relative to their behavior in aqueous solutions.

The considerable differentiation between the acidity scales in this solvent raises a number of questions about the interpretation of divergent behavior in aqueous mineral acids. Following the work of Taft (9) these differences have been frequently interpreted in terms of the numbers of possible hydrogen bonding sites available. In order to explain the apparent hydration changes occurring during protonation of amides in aqueous solutions, multiple hydrogen bonded structures have been postulated (11).

Apart from the neglect of activity coefficient terms, this type of interpretation must now be considered of dubious value since it assumes that the interaction energy is of comparable magnitude for each of the different hydrogen bonds possible. In the DMSO–H_2O system similar multiple hydrogen bonded structures are not possible, because DMSO cannot act as a proton donor. As a result only three DMSO molecules at most may be used to stabilize the amidonium ion, the same number as may be formally ascribed to the anilinium ion.

In this case solvation must be of a completely different nature, involving either weak S...H—O hydrogen bonds, or dipolar interactions of the type suggested to explain the properties of pure DMSO (29). Despite the similarity in the number of specific hydrogen bond sites for DMSO in amides and primary amines, the relative behavior of H_A and H_0 is very different; also despite the difference in these sites between primary and tertiary amines the H_0 and H_0''' functions are much more similar. This suggests that solvent stabilization of cations of weak organic bases must involve highly specific interactions which cannot be suitably represented by simple parametric functions of the bulk solvent activity.

In Fig. 5*a* the three acidity functions do not converge to a single line in dilute solution. This is the expected result since the acidity value measures the relative protonating ability of the solvent with respect to an infinitely dilute solution of acid in water. There is no reason for this difference to be the same for different structural bases. However, when the scales are plotted on a suitable concentration scale, such as mole fraction H_2SO_4, then $H_0(H_2O)$, and H_0(DMSO–H_2O) converge at high concentrations. This is a necessary and valid confirmation that both acidity scales are thermodynamically consistent, since the protonating ability of 100% H_2SO_4 toward a given type of base, with respect to the aqueous standard state, should be identical irrespective of the solvent through which it is approached.

The choice of water as a standard state is purely arbitrary, and the acidity functions shown in Fig. 5 owe their relative positions to the *difference* in the specific interactions in pure water and pure DMSO–H_2O. The question of the choice of standard states, the pK_a values obtained in DMSO–H_2O and the relationship of these factors to acidity function behavior will be considered in a later paper in this series.

The continued financial assistance of the National Research Council of Canada is gratefully acknowledged. We are also grateful to the Government of the Province of Ontario for awards of Ontario Graduate Fellowships to one of us (G.J.W.) and to Prof. E. M. Arnett for the gift of eleven tertiary aniline indicators.

1. M. A. PAUL and F. A. LONG. Chem. Rev. **57**, 1, (1957).
2. L. P. HAMMETT and A. J. DEYRUP. J. Am. Chem. Soc. **54**, 2721 (1932).
3. G. C. LEVY, J. D. CARGIOLO, and W. RACELA. J. Am. Chem. Soc. **92**, 6838 (1970).
4. J. F. BUNNETT and F. P. OLSEN. Can. J. Chem. **44**, 1899 (1966).
5. K. YATES and R. A. MCCLELLAND. J. Am. Chem. Soc. **89**, 2680 (1967).
6. E. M. ARNETT, R. P. QUIRK, and J. J. BURKE. J. Am. Chem. Soc. **92**, 1260 (1970); E. M. ARNETT, P. QUIRK, and J. W. LARSEN. J. Am. Chem. Soc. **92**, 3977 (1970).
7. C. H. ROCHESTER. Acidity functions. Academic Press New York. N.Y., 1970. Chapt. 1.
8. R. H. BOYD. *In* Solute–solvent interactions. *Edited by* J. F. Coetzee and C. D. Ritchie. Marcel Dekker, New York, N. Y. 1969. Chapt. 3.
9. R. W. TAFT, JR. J. Am. Chem. Soc. **82**, 2965 (1962).
10. E. M. ARNETT and G. W. MACH. J. Am. Chem. Soc. **86**, 2671 (1964).
11. K. YATES, J. STEVENS, and A. R. KATRITZKY. Can. J. Chem. **42**, 1957 (1964).
12. N. F. HALL and W. F. SPENGEMAN. J. Am. Chem. Soc. **62**, 2487 (1940).
13. B. NAHLOVSKY and V. CHVALOVSKY. Coll. Czech. Chem. Commun. **33**, 3122 (1968).

14. E. M. ARNETT and G. W. MACH. J. Am. Chem. Soc. **88**, 177 (1966).
15. H. L. SCHLÄFER and W. SCHAFFERNICHT. Angew. Chem. **72**, 618 (1960).
16. J. N. BUTLER. J. Electroanal. Chem. and Interface Electrochem. **14**, 89 (1967).
17. D. MARTIN, A. WEISE, and H. J. NICLAS. Angew. Chem. Int. Ed. **6**, 318 (1967).
18. C. AGAMIE. Bull. Soc. Chim. Fr, 1021 (1965).
19. K. YATES and H. WAI. J. Am. Chem. Soc. **86**, 5408 (1964).
20. H. WAI. Ph.D. Thesis. University of Toronto, Toronto, Ontario, 1968. p.14.
21. Handbook of chemistry and physics. 44th Ed. Chemical Rubber Publishing Co., 1963.
22. Dictionary of organic compounds. 4th Ed. Eyre and Spottiswood, London, 1965.
23. A. J. KRESGE and H. T. CHEN. Anal. Chem. **41**, 74, (1969).
24. A. G. COOK and G. W. MASON. J. Inorg. Nucl. Chem. **28**, 2579 (1966).
25. Y. DOUCET, F. CALMER-PERAULT, and M. T. DURAND. C. R. Acad. Sc. Paris, **260**, 1878 (1965).
26. J. M. C. COWIE and P. M. POPOROWSKI. Can. J. Chem. **39**, 2240 (1961).
27. J. KENTAMAA and J. J. LINDBERG. Soumen Kemistil. **33B**, 32, 98, 104 (1960).
28. G. J. SAFFORD, P. C. SCAEFFER, P. S. LUNG, G. F. DOEBBLER, G. W. BRADY, and E. F. X. LYDEN. J. Chem. Phys. **50**, 2140 (1969).
29. H. L. CLEVER and E. F. WESTHEIMER. J. Phys. Chem. **74**, 1309 (1970).
30. K. H. JONG and J. B. HYNE. Can. J. Chem. **48**, 2423 (1970).
31. A. J. PARKER. Quart. Rev. **16**, 163 (1962).
32. K. YATES and G. WELCH. Unpublished results (part II of this series).
33. M. J. JORGENSON and D. R. HARTTER. J. Am. Chem. Soc. **85**, 876 (1963).
34. G. J. WELCH. Ph.D. Thesis. University of Toronto, Toronto, Ontario, 1969.
35. R. K. WOLFORD. J. Phys. Chem. **68**, 3392 (1964).
36. K. YATES and G. WELCH. Can. J. Chem. **50**, 474 (1972).
37. I. M. KOLTHOFF, M. K. CHANTOONI, and S. BHOWMIK. J. Am. Chem. Soc. **90**, 23 (1968).
38. G. A. OLAH, A. T. KU, and J. A. OLAH. J. Org. Chem. **35**, 3904 (1970).
39. D. D. PERRIN. Dissociation constants of bases in aqueous solution. Butterworths, London. 1965.
40. M. M. FICKLING, A. FISCHER, B. R. MANN, J. PACKER, and J. VAUGHAN. J. Am. Chem. Soc. **81**, 4226 (1959).

Can. J. Chem. Downloaded from www.nrcresearchpress.com by 210.87.254.40 on 09/05/12
For personal use only.

The Electron Paramagnetic Resonance Spectrum of the Phenalane Anion[1]

D. H. PASKOVICH[2] AND A. H. REDDOCH

Division of Chemistry, National Research Council of Canada, Ottawa K1A 0R6, Canada

Received November 18, 1971

The phenalane anion has been prepared by the reaction of alkali metals in ether solutions of both phenalane and phenalene. The electron paramagnetic resonance spectra of both the radical and of its ion pairs with sodium and with lithium in THF are reported. At room temperature there is an alternating linewidth involving the β protons caused by conformational interconversion of the axial and equatorial positions. At -80 °C the γ protons are not equivalent and the corresponding coupling constants are resolved.

L'anion phénalane a été préparé par l'actione des métaux alcalins sur des solutions éthérées de phénalane et de phénalène. Les spectres r.p.e. du radical ainsi que ceux des paires d'ions formées entre celui-ci et le sodium ou le lithium dans le THF, sont rapportés. A la température de la pièce, il se produit une alternation de largeur de raie impliquant les protons en β et provoquée par une interconversion conformationnelle des positions axiales et équatoriales. A -80 °C les protons en γ ne sont pas équivalents et les constantes correspondantes de couplage peuvent être résolues.

Canadian Journal of Chemistry, **50**, 1523 (1972)

Introduction

In the course of a study of the chemistry and e.p.r. spectra of aromatic hydrocarbon radicals (1, 2) a new species, the phenalane anion, has been prepared. This is an alkyl substituted naphthalene and the coupling constants of its e.p.r. spectrum are consistent with those of a number of other such species including 1,8-dimethylnaphthalene (3, 4), trihydropyrenyl (1), and acenaphthene (5). The dynamic aspects of this radical as reflected in the alternating linewidth of the β protons are consistent with those of the related species trihydropyrenyl (1) and the hexahydropyrene anion (6, 7). In these three cases the conformational changes become slow enough at low temperatures to show the inequivalence of the axial and equatorial β protons. A similar splitting could occur for the γ protons since they are geometrically inequivalent in these conformations, although a lower temperature may be required since the smaller difference is more readily averaged. This splitting has not in fact been reported for trihydropyrenyl but it is reported here for the phenalane anion. A recent reinterpretation (8) of the hexahydropyrene anion spectrum shows that such a splitting occurs there also, although it is unresolved.

Experimental

The phenalane anion was prepared from phenalane by treating the hydrocarbon with sodium or lithium in either 1,2-dimethoxyethane (DME) or tetrahydrofuran (THF). The solvents were purified by distillation from $LiAlH_4$ and were stored *in vacuo* over benzophenone ketyl. The radical was prepared by reacting an ether solution of the hydrocarbon with a sodium mirror in a pyrex U-tube using high-vacuum technique. When lithium was used, freshly cut pieces of metal were added to the tube just before evacuation.

Sodium phenalanide in THF formed an ion pair. In DME it gave a poorly resolved e.p.r. spectrum at room temperature which was probably that of the ion pair. At -80 °C in DME the spectrum was that of the free ion. Lithium phenalanide formed an ion pair in THF at 26 °C which dissociated on dilution or cooling. In DME it appeared to be dissociated at 26 °C and below.

The same radical anion was also produced from phenalene by a multistep reduction in either THF or DME. In view of the drying technique described above for the ethers, water is not likely to be the source of the protons for the reduction of the phenalene. However, instances are known where the ether is a proton source when intensive alkali reduction is attempted (9–11).

Phenalene in solution gives a well-resolved spectrum of the neutral phenalenyl radical which presumably is formed by the decomposition of a peroxy intermediate arising from the reaction of the hydrocarbon with traces of atmospheric oxygen (12). When an ethereal solution of phenalene is reacted with an alkali metal the phenalenyl e.p.r. spectrum rapidly disappears as this species is reduced to a diamagnetic monoanion. Further reduction produces a dianion which abstracts a proton from the ether solvent. This partially reduced species then undergoes further stepwise reduction until the phenalanide ion is produced.

[1]NRCC No. 12448.

[2]National Research Council of Canada Visiting Scientist 1967–1968. Present address: Air Pollution Control Division, Environment Canada, Tunney's Pasture, Ottawa K1A 0H3, Canada.

Can. J. Chem. Downloaded from www.nrcresearchpress.com by 210.87.254.40 on 09/05/12
For personal use only.

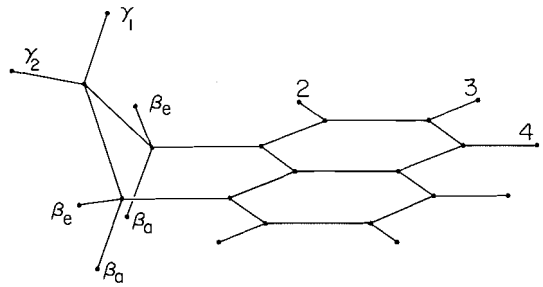

FIG. 1. Structure of phenalane anion and nomenclature used.

The spectra were studied with a Varian E3 spectrometer together with a Varian variable temperature accessory.

Discussion

The proton coupling constants for the phenalane anion (Fig. 1) at room temperature (Fig. 2) are reported in Table 1 together with corresponding values for some other substituted naphthalene anions. For these latter species only the values of the coupling constants relevant to the discussion are included and the various proton sites have been arbitrarily numbered and lettered to correspond with the designations used here for the analogous sites in the phenalane anion. Within the limited precision of the present measurements, about 0.02 G, the coupling constants did not change significantly with temperature, solvent or ion pair formation, except for the splitting of the β and γ protons at low temperature. At $-80\,^{\circ}C$ (Fig. 3) the γ protons of the phenalanide radical, which have a coupling constant of 0.43 G at room temperature, show values of 0.53 and 0.36 G, while the individual coupling constants of the axial and equatorial β protons are 8.62 and 2.24 G respectively. Since $a\ (25\,^{\circ}C) = 0.43$ is almost exactly the average of 0.53 and 0.36 it is clear that the latter two coupling constants have the same sign. Similarly since $a_{\beta} + a_{\beta'} = 10.75$ is almost exactly the sum of 8.62 and 2.24 these two constants must also have a common sign although not necessarily that of the γ protons. The aromatic protons at $-80\,^{\circ}C$ have coupling constants of 4.49, 1.90, and 1.55 G. In the ion pair with Na in the THF at 26 °C the Na coupling constant is 0.92 G. The corresponding Li coupling in THF at 26 °C is 0.18 G.

The assignments of the proton coupling constants of the phenalane anion are made by analogy with the other species cited in the table. The assignments for most of these other species, except acenaphthene (5), are essentially theoretical and have not been proven by deuteration. The resulting picture for phenalane seems quite reasonable but the 2 and 3 positions must be regarded as tentative in the absence of deuteration experiments.

The reduction of symmetry caused by the aliphatic substituents on the naphthalene, as measured by the difference $a_2 - a_3$ is greater in phenalanide than in dimethylnaphthalenide but less so than in acenaphthenide. The coupling constants a_4 also suggest this reduction in that they decrease monotonically but not linearly as $a_3 - a_2$ increases. The sum $a_2 + a_3$, although fairly constant for each of the substituted molecules, is less than in naphthalenide (13), while the lowest values occur in hexahydropyrenide, pyracenide (14), and diplieadanide (15) where there are two bridges which may be regarded as four alkyl substituents. This result probably reflects a spin density reduction in the aromatic part of the radical by the alkyl groups in a manner similar to that discussed by Fischer (16) for methyl substituents in alkyl radicals, although in the latter case the effect is larger. As Fischer points out, such effects may become more complex in charged species such as those considered here. Moreover, in these polyatomic aromatics it is really the total spin density in the π system rather than that on individual carbons which should be considered to avoid the effects of spin redistribution within that system caused by the substituents. Other details of the coupling constants of the aromatic protons seem reasonable. A very detailed treatment of the spin densities of alkyl substituted naphthalenes has been given by Moss *et al.* (17). In view of the difficulties they encountered, this topic will not be pursued further here.

The e.p.r. spectra of several radicals with —$(CH_2)_3$— bridges have now been reported including trihydropyrenyl (1), both the cation and the anion of hexahydropyrene (6, 7) and the present example of the phenalane anion. As can be seen in Table 2 the ratio of the coupling constants of the axial and equatorial β protons is near 4 in each case. This value reflects the

Can. J. Chem. Downloaded from www.nrcresearchpress.com by 210.87.254.40 on 09/05/12
For personal use only.

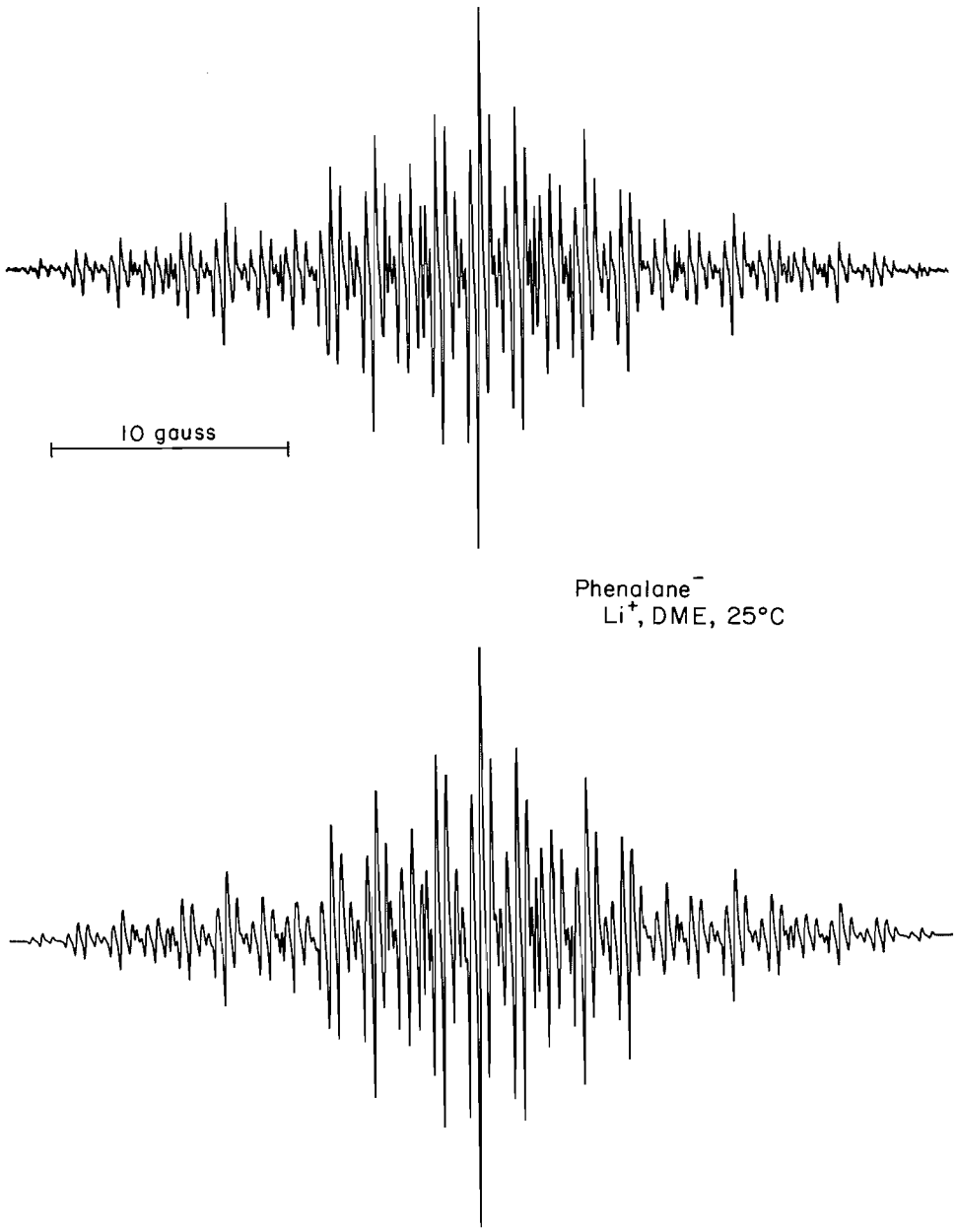

FIG. 2. The e.p.r. spectrum of phenalane anion at room temperature. The upper is experimental, the lower simulated using coupling constants (gauss): $a_2 = 1.52$, $a_3 = 1.89$, $a_4 = 4.44$, $a_a + a_e = 10.75$, $a_\gamma = 0.43$, and width = 0.07. The alternating linewidth limit in which the β protons give a 1:4:1 triplet is assumed.

common geometry of these species as the following discussion will show.

The coupling constants of β protons in aliphatic radicals may be described by the equation suggested by Heller and McConnell (18),

$$a = (B_0 + B_2 \cos^2 \theta)\rho \quad [1]$$

where θ is the angle between the projections of

Can. J. Chem. Downloaded from www.nrcresearchpress.com by 210.87.254.40 on 09/05/12
For personal use only.

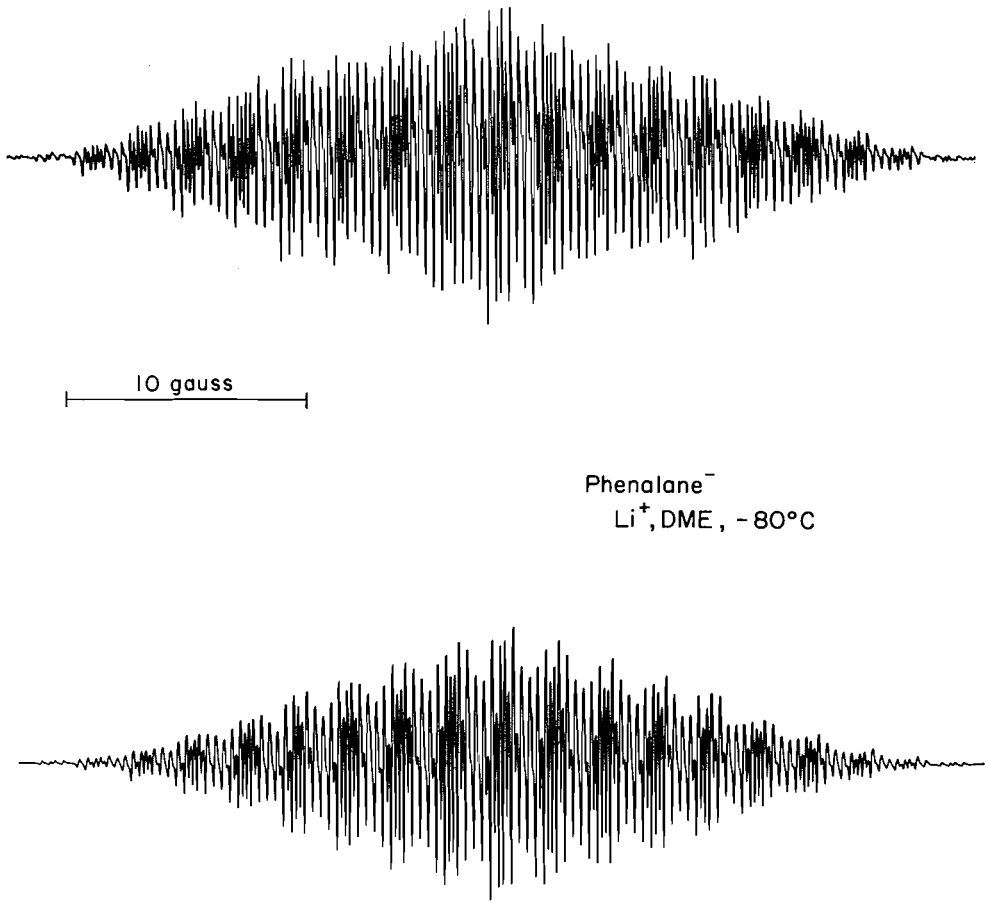

FIG. 3. The e.p.r. spectrum of phenalane anion at −80 °C. The upper is experimental, the lower simulated using coupling constants (gauss): $a_2 = 1.55$, $a_3 = 1.90$, $a_4 = 4.49$, $a_a = 8.62$, $a_e = 2.24$, $a_{\gamma 1} = 0.53$, $a_{\gamma 2} = 0.36$, and width = 0.07.

the CH bond and the axis of the p orbital on a plane perpendicular to the C—C bond. Whiffen (19) has proposed that $B_0 = 3.6$ and $B_2 = 51$ G. If it is assumed that the axial and equatorial angles differ by 120°, *i.e.*

$$\theta_e = \theta_a + 120° \quad [2]$$

then eq. 1, applied to the two coupling constants, yields the following equations:

$$a_a = (B_0 + B_2 \cos^2 \theta_a)\rho \quad [3a]$$

$$a_e = [B_0 + B_2 \cos^2 (\theta_a + 120°)]\rho \quad [3b]$$

By dividing eq. 3*a* by eq. 3*b*, ρ is eliminated.

$$a_a/a_e = (\cos^2 \theta_a + B_0/B_2)/[\cos^2 (\theta_a + 120°) + B_0/B_2] \quad [4]$$

This can be solved for θ_a and, from eq. 3*a*, ρ can be obtained.

The results for each of the species are shown in Table 2. For comparison, the axial angle calculated geometrically assuming tetrahedral and trigonal bond angles with aliphatic and aromatic bond lengths of 1.541 and 1.395 Å is −3.4°, *i.e.* the axial C—H bonds point slightly toward each other. This implies a slight strain of about 3° at the γ carbon, which however, may be distributed around the ring.

The agreement between the angles calculated from the coupling constants and those calculated geometrically is remarkable. In the case of the trihydropyrenyl the calculated spin density 0.219 is also very good, the value from McConnell's relation being 6.3/28 = 0.225 and

Can. J. Chem. Downloaded from www.nrcresearchpress.com by 210.87.254.40 on 09/05/12
For personal use only.

TABLE 1. Proton coupling constants in gauss of alkyl substituted naphthalene anions

Anion	$a_a + a_c$	a_γ	a_2	a_3	a_4	$a_2 + a_3$	Reference
Phenalane	10.75	0.43	1.52	1.89	4.44	3.41	This work
1,8-Dimethylnaphthalene			1.60	1.78	4.64	3.38	3
Hexahydropyrene	9.87	0.41	1.68	1.68		3.36	7
Acenaphthene			1.04	2.42	4.17	3.46	5
Pyracene			1.58	1.58		3.16	14
Naphthalene			1.78	1.78	4.92	3.56	13
Diplieadane	7.70		1.57	1.57		3.14	15

TABLE 2. Coupling constants in gauss and derived angles and spin densities

Radical	Coupling constants			a_a/a_c	θ_a	ρ	Reference
	a_a	a_c	a_γ				
Phenalane$^-$	8.62	2.24	0.43	3.84	−2.9	0.157	This work
H_3 pyrenyl	11.97	2.99	0.45	4.00	−3.7	0.219	1
H_6 pyrene$^-$	8.03	2.02	0.41	3.98	−3.6	0.147	7
H_6 pyrene$^+$	14.70	3.64	0.36	4.03	−3.9	0.269	7
(2 conformers)	14.63	3.90		3.75	−2.4	0.267	
Diplieadane$^-$	6.28	1.35	0.22	4.65	−43.8		15
(2 conformers)	6.16	1.57		3.93	−45.6		

the McLachlan value being 0.218 (20). The spin densities derived for the other species are not very good as can be seen by comparing the values for the hexahydropyrene anion and cation. The reason for this is that Whiffen's coefficients were selected for systems with the spin in a nonbonding orbital and hence will not apply to ion radicals with hyperconjugation. However since $B_0 \ll B_2$ the calculated angles are not very dependent on B_2. Thus if B_0 is taken as 0, eq. 4 is independent of B_2 and the resulting angles are in the range $-0.1°$ to $1.0°$, which are still reasonable. Moreover if the ratio B_0/B_2 were not strongly dependent on the charge of the radicals, as may be approximately true, then the above values would again yield good angles but poor spin densities for the ions.

In addition to the solution $\theta_a = -3.7°$ for eq. 4 when $a_a/a_c = 4$, there is another solution $\theta_a \simeq -45°$. This, curiously, applies to the diplieadane anion (15) where the coupling constant ratio is also approximately 4. The solutions for the two conformers are given in Table 2. These are also in very good agreement with the angle expected geometrically of 42.5°. The geometric value could be in error by about 1° because of a small amount of strain which can be seen in the geometric model and which will probably be distributed over the various bond angles. Claridge *et al.* (15) did not get quite such good agreement because they neglected B_0 in eq. 4. This is not as good an approximation for diplieadane where the $\cos^2$ terms are small, as it is in the other ions.

The γ protons are not geometrically equivalent in the static conformations and their coupling constants should be different. This has been seen by ENDOR experiments in a somewhat different radical, di-*t*-butylcyclohexylphenoxy, by Adams and Atherton (21). In a reinterpretation of the hexahydropyrene anion spectrum Claridge and Peake (8) have deduced from the line shape that at low temperatures the proton coupling constants are 0.50 and 0.36 G. These values are very similar to those reported here for the phenalane anion, where the splitting has been resolved.

An attempt was made to apply the spin polarization theory of Barfield (22) to the radicals in Table 2. Since this model was applied to a localized spin on a single aliphatic chain it was adapted for the present purposes by taking $a_\gamma = B'(c_1^2 + c_8^2)$ where B' is Barfield's a_γ as given by his eq. 32 and c_1 and c_8 are Hüchel coefficients for the lowest antibonding orbital of naphthalene. (An alternative form $B'(c_1 + c_8)^2$ does

Can. J. Chem. Downloaded from www.nrcresearchpress.com by 210.87.254.40 on 09/05/12
For personal use only.

not apply here, giving $a_\gamma = 0$ since $c_1 = -c_8$ by symmetry.) The result is $a_{\gamma 1} = 0.17$ and $a_{\gamma 2} = -0.06$ G. These magnitudes and opposite signs, which are obtained for any reasonable geometry, do not agree with the experimental results. This failure may result, as Barfield suspected (22), from long range couplings. It should be noted however that these γ protons cannot have direct overlap or hyperconjugative interaction with the unpaired electron for reasons of symmetry. Such interactions are possible with some of the other spin polarized π electrons, however.

The Na coupling constant with phenalane is only slightly smaller than that with naphthalene in THF (13), 1.04 G, or with acenaphthene in THF (23), 1.08 G. Similarly the Li coupling with phenalane is the same as that with naphthalene in THF (13), 0.18 G. Since the alkali ion splittings should be rather sensitive to the structure of the ion pair (24) these results suggest that the position of the cation in THF is not much affected by the addition of the aliphatic substituents to the naphthalene skeleton.

We are grateful to Drs. R. F. Adams and N. M. Atherton for showing us a preprint of their work on conformational effects prior to publication. We are also indebted to Drs. R. F. C. Claridge and B. M. Peake for sending us a manuscript, part of which was devoted to the phenalanide radical. Where our papers overlap, the agreement is quite satisfying.

1. F. Gerson, E. Heilbronner, A. H. Reddoch, D. H. Paskovich, and N. C. Das. Helv. Chim. Acta, **50**, 813 (1967).
2. A. H. Reddoch and D. H. Paskovich. Chem. Phys. Lett. **3**, 351 (1969).
3. C. de Waard and J. C. M. Henning. Phys. Lett. **4**, 31 (1963).
4. F. Gerson, B. Weidmann, and E. Heilbronner. Helv. Chim. Acta, **47**, 1951 (1964).
5. J. P. Colpa and E. de Boer. Mol. Phys. **7**, 333 (1964).
6. E. de Boer and A. P. Praat. Mol. Phys. **8**, 291 (1964).
7. M. Iwaizumi and T. Isobe. Bull. Chem. Soc. Jap. **38**, 1547 (1965),
8. R. F. C. Claridge and B. M. Peake. Mol. Phys. **18**, 137 (1970).
9. W. G. Schneider. *In* Nuclear magnetic resonance in chemistry. *Edited by* B. Pesce. Academic Press, New York. 1965. p. 63.
10. M. I. Terekhova, L. N. Kurkovskaya, E. S. Petrov, N. N. Shapet'ko, and A. I. Shatenshtein. Zhur. Org. Khim. **6**, 2359 (1970).
11. K. K. Brandes and R. J. Gerdes. Z. Naturforsch. **25***b*, 176 (1970).
12. P. B. Sogo, M. Nagasaki, and M. Calvin. J. Chem. Phys. **26**, 1343 (1957).
13. C. L. Dodson and A. H. Reddoch. J. Chem. Phys. **48**, 3226 (1968).
14. E. de Boer and E. L. Mackor. Proc. Chem. Soc. 23 (1963).
15. R. F. C. Claridge, D. R. A. Leonard, and B. M. Peake. Mol. Phys. **19**, 737 (1970).
16. H. Fischer. Z. Naturforsch. **20***a*, 428 (1965).
17. R. E. Moss, N. A. Ashford, R. G. Lawler, and G. K. Fraenkel. J. Chem. Phys. **51**, 1765 (1969).
18. C. H. Heller and H. M. McConnell. J. Chem. Phys. **32**, 1535 (1960).
19. D. H. Whiffen. *In* La structure hyperfine magnétique des atomes et des molécules. *Edited by* R. Lefebvre and C. Moser. Centre National de la Recherche Scientifique, Paris. 1967. p. 169.
20. A. D. McLachlan. Mol. Phys. **3**, 233 (1960).
21. R. F. Adams and N. M. Atherton. Mol. Phys. **17**, 673 (1969).
22. M. Barfield. J. Phys. Chem. **74**, 621 (1970).
23. A. M. Hermann, A. Rembaum, and W. R. Carper. J. Phys. Chem. **71**, 2661 (1967).
24. I. B. Goldberg and J. R. Bolton. J. Phys. Chem. **74**, 1965 (1970).

Can. J. Chem. Downloaded from www.nrcresearchpress.com by 210.87.254.40 on 09/05/12
For personal use only.

Complex Fluorides with Perovskite Structure: Thermal Analyses, Calorimetry, and Infrared Spectra

K. C. PATIL AND E. A. SECCO

Chemistry Department, St. Francis Xavier University, Antigonish, Nova Scotia

Received August 13, 1971

Thermal decomposition and infrared spectral results are reported for complex fluorides of the type NH_4MF_3 where M = Cd, Zn, Cu, Ni, Co, Mn.

On rapporte les résultats relatifs aux décompositions thermiques et aux spectres infrarouges de complexes fluorés du type NH_4MF_3 avec M = Cd, Zn, Cu, Ni, Co, Mn.

Canadian Journal of Chemistry, **50**, 1529 (1972)

Can. J. Chem. Downloaded from www.nrcresearchpress.com by 210.87.254.5 on 09/05/12
For personal use only.

Introduction

Complex fluorides of the type AMF_3, where A = alkali metal and M = bivalent transition metal, with a perovskite structure have attracted some interest (1). X-Ray diffraction, magnetic and i.r. studies have been reported (2–6). Nagakawa *et al.* (7) and more recently, Lane *et al.* (8) have carried out normal coordinate analysis of the vibrational spectrum of this compound type in the region 700–200 cm^{-1} and have assigned all the observed i.r. absorption frequencies.

The purpose of this paper is to complement the work by Roscoe and Haendler (9) and report the mode of decomposition, heat of decomposition, and infrared spectral data for NH_4MF_3, where M = Cd, Zn, Cu, Ni, Co, Mn.

Experimental

All the compounds studied here were prepared by following accepted procedures (2, 4). These compounds were identified by their X-ray diffraction patterns (10) recorded on a Norelco diffractometer unit using CuK_α radiation or MoK_α radiation as previously described (11).

Thermal analyses and calorimetry were done with the instrumentation and platinum ware described earlier (12–14).

The i.r. spectra of the compounds were recorded on a Perkin–Elmer Model 180 spectrophotometer using the standard pellet technique with KBr as the matrix material or as Nujol mulls with CsI windows.

Results and Discussion

The results of thermogravimetry and differential thermal analyses, along with heat of decomposition data, are tabulated in Table 1. The observed weight losses from TG and the single endotherm observed in DTA heating curves show all the compounds to decompose in one step to yield the simple metal fluoride as the residue, *viz.*,

$$[1] \qquad NH_4MF_{3(s)} \rightarrow MF_{2(s)} + NH_4F_{(g)}$$

The metal fluoride was confirmed by its characteristic X-ray diffraction pattern.

The last column listing the ΔH of decomposition shows a quasi-constant value of 34 ± 1 kcal/mol for most compounds, suggesting the

TABLE 1. Thermal analysis of NH_4MF_3 compounds

Compound	Thermogravimetry temperature range (°C)*	% of total weight lost		Differential thermal analysis, peak temperature (°C)*	ΔH† (cal/mol)
		Observed	Calculated		
NH_4MnF_3	200–300	28.48	28.47	310	38.5 ±0.5
NH_4CoF_3	230–300	27.10	27.63	290	30.4 ±0.5
NH_4NiF_3	200–300	26.70	27.60	290	34.98±0.50
NH_4CuF_3	200–270	26.08	26.82	250	34.2 ±0.2
NH_4ZnF_3	200–290	26.49	26.42	250	33.87±0.25
NH_4CdF_3	150–230	20.00	19.73	205	33.30±0.20

*One-step process and single endotherm.
†All determinations were done in duplicate; ΔH values accompanied by average deviations.

TABLE 2. Infrared absorption band frequencies of NH_4MF_3 compounds*

	Frequency (cm^{-1})						
	NH_4 species					MF_6 species	
Compound	ν_3	$\nu_2 + \nu_4$	$2\nu_4$	$\nu_4 + \nu_6$	ν_4	ν_1	ν_2
NH_4MnF_3	3250(s)	3100(m)	2865(sh)	—	1430(s)	390(s)	250(m)
NH_4CoF_3	3280(s)	3110(m)	2860(sh)	—	1425(s)	420(s)	250(m)
NH_4NiF_3	3280(s)	3110(m)	2860(sh)	—	1430(s)	425(s)	255(m)
NH_4CuF_3	3240(s)	3110(m)	2890(sh)	—	1430(s)	485(s)	270(m)
NH_4ZnF_3	3290(s)	3120(m)	2880(sh)	—	1425(s)	420(s)	275(m)
NH_4CdF_3	3200(s)	3080(m)	2880(sh)	1800(w)	1440(s)	400(s)	—

*s = strong; m = medium; w = weak; sh = shoulder.

nature of bonding between the MF_2 and NH_4F units to be strikingly similar in these compounds.

The i.r. absorption frequencies with their assignments in the 4000–180 cm^{-1} region are presented in Table 2; the assignments are made on the model reported for AMF_3 compounds (4, 7, 8). Our spectral data display a high degree of internal consistency for the various assignments; these data are also in agreement with the existing literature values.

The slight variation in the observed lattice frequencies, 390–425 cm^{-1}, is attributed to the nature of the metal. On the other hand, the higher lattice frequency in the case of NH_4CuF_3 is assumed to originate from a distorted perovskite structure (2). The observation of the 1800 cm^{-1} in NH_4CdF_3 is believed to arise from the combination $(\nu_4 + \nu_6)$ and its presence is rationalized in terms of increased H-bonding.

Grateful acknowledgment is made to the National Research Council of Canada and the University Council for Research for financial support of this research program.

1. P. D. PEACOCK. Prog. Inorg. Chem. **2**, 193 (1960).
2. R. L. MARTIN, R. S. NYHOLM, and N. C. STEPHENSON. Chem. Ind. 83 (1956).
3. H. M. HAENDLER, F. A. JOHNSON, and D. S. CROCKET. J. Am. Chem. Soc. **80**, 2662 (1958).
4. D. S. CROCKET and H. M. HAENDLER. J. Am. Chem. Soc. **82**, 4158 (1960).
5. D. S. CROCKET and R. A. GROSSMAN. Inorg. Chem. **3**, 644 (1964).
6. R. D. PEACOCK and D. W. A. SHARP. J. Chem. Soc. 2762 (1959).
7. J. NAGAKAWA, A. TSUCHIDA, and T. SHIMANOUCHI. J. Chem. Phys. **47**, 982 (1967).
8. A. P. LANE, D. W. SHARP, J. M. BARRACLOUGH, D. H. BROWN, and D. A. PATERSON. J. Chem. Soc. (A) **1**, 94 (1971).
9. S. L. ROSCOE and H. M. HAENDLER. Inorg. Chem. Acta, **1**, 73 (1967).
10. Am. Soc. Test. Materials File Index.
11. E. A. SECCO. Can. J. Chem. **42**, 2143 (1964).
12. O. K. SRIVASTAVA and E. A. SECCO. Can. J. Chem. **45**, 579 (1967).
13. P. RAMAMURTHY and E. A. SECCO. Can. J. Chem. **47**, 2185 (1969).
14. P. RAMAMURTHY and E. A. SECCO. Can. J. Chem. **46**, 3605 (1968).

Can. J. Chem. Downloaded from www.nrcresearchpress.com by 210.87.254.5 on 09/05/12
For personal use only.

Photolysis of Di-*tert*-butyl Peroxide at High Pressure

C. K. YIP AND H. O. PRITCHARD

Centre for Research in Experimental Space Science, York University, Downsview, Ontario

Received November 15, 1971

Di-*tert*-butyl peroxide has been photolyzed at 2537 Å in the gaseous phase in the presence of up to 47 amagats (2.10 mol/l) of propane and of cyclopropane. It was confirmed that no acetone is formed in the limit of infinite hydrocarbon concentration and therefore that the primary *chemical* act leading to the eventual formation of acetone is the formation of two *tert*-butoxy radicals from the excited peroxide molecule; in addition, some crude information was obtained concerning relative rates of photochemical *vs.* deactivation processes. It was also found that at these densities the *tert*-butoxy radical formed in the photolysis of di-*tert*-butyl peroxide did not appear to differ in chemical reactivity from the *tert*-butoxy radical formed in the thermal decomposition of di-*tert*-butyl peroxide.

Le peroxyde de di-*tert*-butyle a été photolysé en phase gazeuse à 2537 Å en présence d'une quantité allant jusqu'à 47 "amagats" (2.10 mol/l) de propane et de cyclopropane. On a confirmé l'absence de toute formation d'acétone dans la limite d'une concentration infinie en hydrocarbure et de là, que la première attaque chimique conduisant à la formation éventuelle d'acétone est la formation de deux radicaux tertio-butoxyles à partir de la molécule de peroxyde excitée; de plus, on a obtenu quelques informations brutes concernant le rapport des vitesses relatives du processus photochimique et du processus de désactivation. On a également trouvé que pour ces concentrations, le radical tertio-butoxyle issu de la photolyse du peroxyde de ditertio-butyle ne semble pas avoir une réactivité chimique différente du même radical issu du même peroxyde formé lors de la décomposition thermique.

Canadian Journal of Chemistry, **50**, 1531 (1972)

Can. J. Chem. Downloaded from www.nrcresearchpress.com by 210.87.254.42 on 09/05/12
For personal use only.

We have shown recently, from a study of the thermal decomposition of di-*tert*-butyl peroxide in the presence of high pressures of propane, that the primary process in the thermal decomposition of the peroxide is the formation of two *tert*-butoxy radicals (1). The reader should not be misled by the use of the word pressure into thinking that these experiments are concerned with the theory of unimolecular reactions, nor with the transition state theory: pressure, in the sense used here, is synonymous with density or concentration, but the use of the word pressure more clearly conveys the nature of the experimental techniques; the purpose is simply to establish a relationship between the rates of formation of reaction products and the *concentration* of the reactant substrate, and hence by extrapolation to infinite concentration of the substrate, to make inferences concerning the primary act in the initiating reaction. In this paper, we describe an attempt to extend our earlier work on the thermal decomposition of di-*tert*-butyl peroxide to the parallel photochemical decomposition.

Experimental Details

The preparation and purification of all the materials, the ferrioxalate actinometry, and the methods of analysis used in this work have all been documented adequately in earlier papers (1–4).

The photolysis cell was constructed (5) from stainless steel: it consisted of two parts, the body which had a bore of 0.375 in., and a lid to which the window was attached; the two parts were bolted together and the assembled vessel had an internal volume of 12 cc. Since the cell was filled by conventional vacuum techniques, it was necessary for the window seal to operate under both high pressures and a vacuum. The window itself was a 1 in. diameter, 0.375 in. thick, polished quartz plate. The basis of the high-pressure seal was simply the abutment of the polished quartz plate onto the polished stainless-steel surface of the lid of the vessel, together with a very thin smear of lubricant. Using silicone grease, for example, the vessel was tested up to 50 amagats of CO_2 at room temperature, but for higher temperature work with hydrocarbons, we used a thin film of Dow Corning silicone adhesive; this proved to be highly satisfactory, and although it can be removed with acetic acid, we have not so far found it necessary to dismantle the seal. For vacuum work, it was necessary to support the window from the inside against atmospheric pressure: this was done with a stainless-steel spring of suitable strength. There were two O-ring seals in the system, one between the body of the vessel and the lid, and the other at a union to the filling tube: in our early experiments, we sealed these with conventional neoprene O-rings, but their absorptive capacity for hydrocarbons, and particularly for acetone, was far too great and gave rise to irreproducible results: lead O-rings on the other hand were perfectly satisfactory.

The cell was filled on a vacuum line using liquid nitrogen to trap the materials into the bottom of the vessel: it was then isolated (with a needle valve close to the filling-tube union) and transferred to a temperature-controlled oil bath, where

Can. J. Chem. Downloaded from www.nrcresearchpress.com by 210.87.254.42 on 09/05/12
For personal use only.

it was illuminated for the required time from a low-pressure mercury lamp placed directly above the vessel; it was then reattached to the vacuum system for the analysis of the reaction products, as described previously (1–3). Care was taken to ensure the lamp operated under similar conditions in each experiment, and that its position was the same in relation to the cell, but no attempt was made to monitor the light intensity. However, the internal consistency of the results of experiments carried out in random order confirms an acceptable consistency of light intensity throughout this series of experiments; in fact, however, constancy of the light intensity is unimportant in respect of the principal aims of this work, as described in (*b*) and (*c*) below.

The extinction coefficient of gaseous di-*tert*-butyl peroxide is quite low (6.14 l mol^{-1} cm^{-1} at 2537 Å and 1.31 mol^{-1} cm^{-1} at 3130 Å) (6) and it was necessary with our particular lamp to irradiate the cell for from 1–3 h (depending on pressure) in order to achieve 1% decomposition: initial amounts of peroxide of about 9.8×10^{-5} mol were found to be sufficient to achieve a reliable analysis. The principal output of the lamp was at 2537 Å, with weaker lines near 2968 and 3022 Å and so on into the visible. Interposing a 1 mm Pyrex plate between the lamp and the reaction vessel reduced the photolysis yields below our level of detection, and since only the radiation at 2537 Å was removed by the glass, it can be safely assumed that we are concerned with a photochemical process initiated almost exclusively by radiation with a wavelength of 2537 Å. We hope that in future experiments of this kind, it will be possible to study an interesting molecule with a higher extinction coefficient, in which case proper wavelength selection by monochromator would be possible.

The rate of the homogeneous thermal decomposition ceases to be significant below 90 °C (2), but there appears to be a small heterogeneous reaction at lower temperatures, and we were forced to operate at 70 °C in order to reduce the dark-reaction corrections to less than 10% of the smallest product in all cases.

Results and Discussion

(a) Variation of Overall Quantum Yield with Hydrocarbon Concentration

The simplest possible photochemical reaction scheme that one can write is

[1] $$P + h\nu \rightarrow P^*$$

[2] $$P^* + M \rightarrow P + M$$

[2′] $$P^* + P \rightarrow P + P$$

[3] $$P^* \rightarrow P + h\nu,\ h\nu'$$

[4] $$P^* \rightarrow 2t\text{-BuO}$$

where P represents the peroxide molecule, and M represents a substrate molecule. In this crude treatment, step 3 will be ignored since the small amounts, if any, of fluorescence and phosphorescence which could occur would be impossible to distinguish kinetically with the other uncertainties which are present. Thus a steady-state

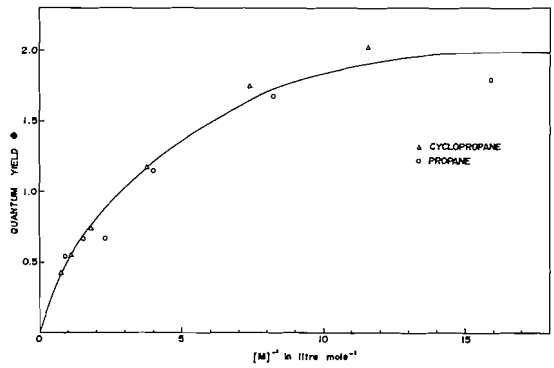

FIG. 1. Overall quantum yield for the photolysis of di-*tert*-butyl peroxide in the presence of propane and cyclopropane (M) at 70 °C.

treatment suggests that the quantum yield of *tert*-butoxy radicals, measured from the sum of the rates of formation of acetone and *tert*-butanol will have two limiting forms, *viz*:

$$\text{As } [M] \rightarrow \infty \qquad \Phi \rightarrow \frac{2k_4}{k_2[M]}$$

$$\text{As } [M] \rightarrow 0 \qquad \Phi \rightarrow \frac{2k_4}{k_2'[P] + k_4} \rightarrow 2 \quad (\text{as } [P] \rightarrow 0)$$

Thus, one would expect the quantum yield to fall from $\Phi = 2$ as the concentration of M is increased, and eventually tend to zero at high [M], hyperbolically. It is well known (6–8) that the low pressure quantum yield is about 2, and our own rough measurements support this observation. The variation of overall quantum yield with substrate concentration is shown in Fig. 1 in the form of a plot of Φ against $[M]^{-1}$; propane and cyclopropane are more or less indistinguishable from each other in their behavior. One would have perhaps expected the plot to become linear before concentrations of 1 mol/l (22.4 amagats) were reached, and this may indicate that the denominator in the high pressure expression for the quantum yield is wrong by an additive constant, possibly owing to the omission of processes like reaction 3. Nevertheless, it would appear that for both hydrocarbons $2k_4/k_2$ is of the order of 0.5 mol l^{-1}: the upper limit of k_2 will be of the order of the collision number *i.e.* 4.4×10^{11} mol^{-1} l s^{-1}; thus k_4 has an upper limit of about 1×10^{11} s^{-1}, but more precise information on k_2 will be

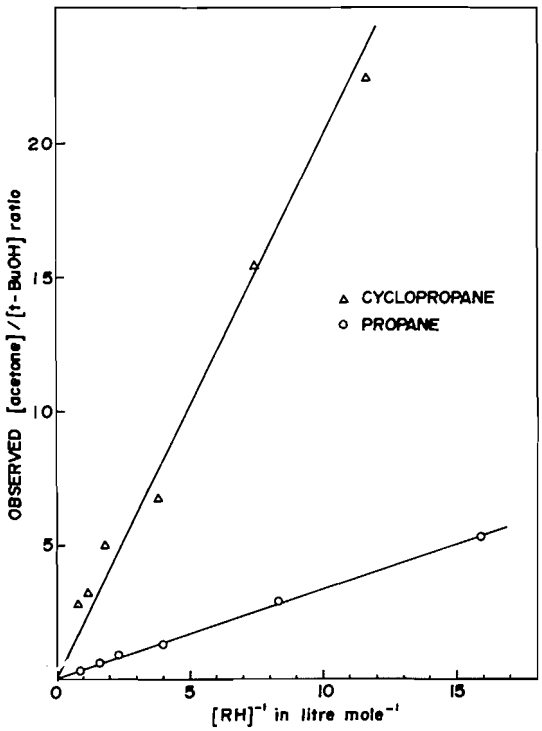

FIG. 2. Variation of [acetone]/[*t*-BuOH] ratio as a function of hydrocarbon concentration at 70 °C; propane: $k_5/k_6 = 0.34$ mol l^{-1}; cyclopropane: $k_5/k_6 = 2.0$ mol l^{-1}.

required before a more realistic value for the lifetime of P* can be given.

(b) Variation of the Ratio of Acetone to tert-Butanol Formation with Hydrocarbon Concentration

The question then arises as to whether step 4 represents the only "chemical" step by which the excited peroxide molecule P* decomposes with the eventual formation of either *tert*-butanol or (acetone plus ethane), or whether there are any concerted processes which form acetone directly. Evidence from liquid phase photolyses would suggest that there is no direct formation of acetone (9) since at quite a low temperature with reactive substrates, no acetone was found. However, these observations are qualitative in nature, and do not reveal the quantitative complementary yield feature described below.

Following our earlier analysis of the problem in the case of the thermal decomposition of di-*tert*-butyl peroxide (1), we plot in Fig. 2 the ratio of the rate of formation of acetone to that of *tert*-butanol against the reciprocal of the hydrocarbon concentration $[RH]^{-1}$, where RH is either propane or cyclopropane. At high RH concentrations, the reaction scheme suggested by McMillan and Wijnen (10) should reduce to

[4] $\quad P^* \rightarrow 2t\text{-BuO}$

[5] $\quad t\text{-BuO} \rightarrow CH_3COCH_3 + CH_3$

[6] $\quad t\text{-BuO} + RH \rightarrow t\text{-BuOH} + \text{etc.}$

whence such plots should be straight lines passing through the origin with slopes of k_5/k_6. For both hydrocarbons, the observed acetone/*tert*-butanol ratios do fall on acceptable straight lines passing through the origin. This shows unambiguously that, as in the thermal reaction (1), the *tert*-butoxy radical is the sole precursor of acetone, and that therefore the dominant primary chemical act is the formation of two *tert*-butoxy radicals; of course, there may also be other minor primary photochemical processes, such as the one which is said to give oxygen and butyl radicals (11).

(c) Relative Reactivities of tert-Butoxy Radicals Formed Thermally and Photochemically

The results of the preceding sections, together with our earlier results on the thermal decomposition (1) demonstrate that in both cases, the sequence of reactions 4–6 represents satisfactorily, at high hydrocarbon concentration, the evolution of the reaction once the critical state has been passed. Whilst the critical state is not necessarily the P* in reaction 4, but could be some precursor of P*, it is clear that the critical states are different in the two cases. In the thermal case, at the high-pressure limit, it is simply a molecule containing more than the critical energy $\varepsilon^*(\varepsilon^* \approx 38$ kcal/mol) within its internal degrees of freedom. In the photochemical case, the molecule P* could have up to 112 kcal/mol of internal energy, distributed between electronic, vibrational, and rotational excitation, and the actual amount, and its distribution will depend very much upon the history of the molecule since the spectroscopic absorption took place. McMillan (8) has suggested that in the 100 Torr total-pressure range, the photolysis of di-*tert*-butyl peroxide yields excited *tert*-butoxy radicals whose rate constant for abstraction from isobutane (k_6) is normal, but whose rate constant for dissociation (k_5) is enhanced, and

Can. J. Chem. Downloaded from www.nrcresearchpress.com by 210.87.254.42 on 09/05/12
For personal use only.

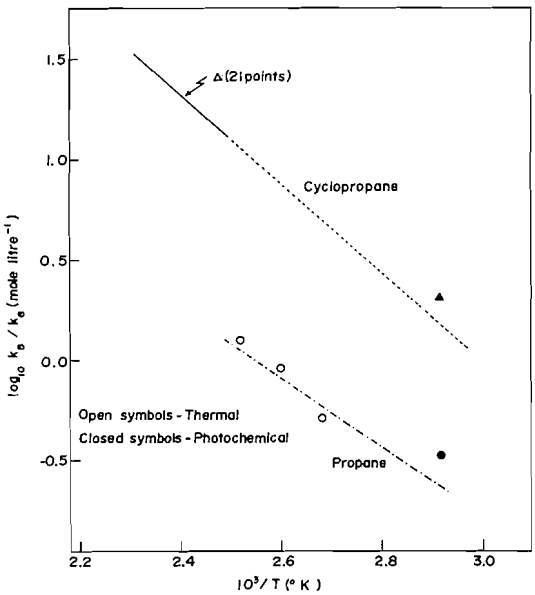

FIG. 3. Comparison of k_5/k_6 for thermally and photochemically produced *tert*-butoxy radicals.

that this excitation can be collisionally quenched. The fact that the data in Fig. 2 fall on acceptable straight lines implies that in all our experiments the collision rate is sufficiently high that all our *tert*-butoxy radicals are thermalized. Figure 3 shows an attempt to corroborate this conclusion in that it compares our earlier thermal data for propane and cyclopropane (the latter all taken at densities above 1 mol l^{-1} of hydrocarbon) with the present photochemical data (taken at densities in the range 0.05 to 1 mol l^{-1}). It can be seen that the value of k_5/k_6 for cyclopropane obtained in the photochemical experiments at 70 °C lies very close to the extrapolation of our higher-temperature thermal data (3); likewise for propane, somewhat less convincingly, since the original thermal data (1) are somewhat scattered. Thus our conclusion would be that in this pressure range we cannot distinguish between the reactivities of *tert*-butoxy radicals formed from di-*tert*-butyl peroxide either thermally, or photochemically by 2537 Å radiation.

Finally, we note that there is a high-pressure thermal value for k_5/k_6 with isobutane at one temperature (3) which lies very close indeed to the Arrhenius extrapolation of the low-pressure photolysis data of McMillan (12): however, interpretation of the latter results appears to be complicated by the hot-radical effects noted above (8) allowance for which spoils the agreement; it is also possible to deduce crude data for k_5/k_6 from experiments using *tert*-butyl hypochlorite as a photolytic source at about 200 Torr (13), but these results do not extrapolate well either towards the high-pressure high-temperature thermal result. However, unimolecular fall-off effects can be discounted as a source of these discrepancies since it is known (14, 15) that $P_{1/2}$ for reaction 5 is about 80 Torr near 500 °K: all the low pressure photolysis experiments were performed near 300 °K (12, 13), and since it is generally expected (16) that the fall-off moves to lower pressures at lower temperature, one would not expect the rate in the 100–200 Torr region to be more than about 20% below its high-pressure limit; this leaves the data on k_5/k_6 for RH = isobutane in a relatively unsatisfactory state.

1. C. K. YIP and H. O. PRITCHARD. Can. J. Chem. **47**, 4708 (1969).
2. D. H. SHAW and H. O. PRITCHARD. Can. J. Chem. **46**, 2721 (1968).
3. C. K. YIP and H. O. PRITCHARD. Can. J. Chem. **49**, 2990 (1971).
4. B. K. DUNNING, D. H. SHAW, and H. O. PRITCHARD. J. Phys. Chem. **75**, 580 (1971).
5. C. K. YIP. Ph.D. Thesis, York University, Downsview, Ontario. 1972.
6. D. H. VOLMAN and W. M. GRAVEN. J. Am. Chem. Soc. **75**, 3111 (1953).
7. L. M. DORFMAN and Z. W. SALSBURG. J. Am. Chem. Soc. **73**, 255 (1951).
8. G. R. MCMILLAN. J. Am. Chem. Soc. **84**, 2514 (1962).
9. H. B. HENBEST, J. A. W. RIED, and C. J. M. STIRLING. J. Chem. Soc. 5239 (1961); 1220 (1964).
10. G. R. MCMILLAN and M. H. J. WIJNEN. Can. J. Chem. **36**, 1227 (1958).
11. H. M. FREY. Proc. Chem. Soc. 385 (1959).
12. G. R. MCMILLAN. J. Am. Chem. Soc. **82**, 2422 (1960).
13. J. L. BROKENSHIRE, A. NECHVATAL, and J. M. TEDDER. Trans. Faraday Soc. **66**, 2029 (1970).
14. M. F. R. MULCAHY and D. J. WILLIAMS. Aust. J. Chem. **17**, 1291 (1964).
15. P. CADMAN, A. F. TROTMAN-DICKENSON, and A. J. WHITE. J. Chem. Soc. (A), 2296 (1971).
16. A. F. TROTMAN-DICKENSON. Gas kinetics. Butterworths, London. 1955. p. 62.

Can. J. Chem. Downloaded from www.nrcresearchpress.com by 210.87.254.42 on 09/05/12
For personal use only.

Spectroscopie de masse des *gem*-diesters cycliques. Fragment anhydride

KRZYSZTOF JANKOWSKI, JEAN COUTURIER, ET JEAN-YVES DAIGLE
Département de Chimie, Université de Moncton, Moncton, Nouveau-Brunswick

Reçu le 16 mars 1971[1]

La spectroscopie de masse des quatre *gem*-diesters sur les cycles à trois, quatre, cinq, et six est apportée. L'analyse des spectres est présentée par les schémas 1–5 et tableaux. Les ions métastables permettent d'identifier le fragment anhydride.

Mass spectra of four *gem*-diesters on three-, four-, five-, and six-member rings are analyzed. The fragmentation patterns of the investigated compounds supported by metastable ions are illustrated by Schemes 1–5 and Tables. A new fragment anhydride is proposed.

Canadian Journal of Chemistry, **50**, 1535 (1972)

Can. J. Chem. Downloaded from www.nrcresearchpress.com by 210.87.254.5 on 09/05/12
For personal use only.

Les spectres de masse de quelques *gem*-diesters ont été l'objet de quelques publications (1, 2). Dans cet article nous analysons les spectres de masse des quatre *gem*-diesters: le cyclopropanedicarboxylate-1,1 d'éthyle (**1**), cyclobutanedicarboxylate-1,1 d'éthyle (**2**), cyclopentanedicarboxylate-1,1 d'éthyle (**3**), et cyclohexanedicarboxylate-1,1 d'éthyle (**4**).

Malgré la ressemblance des structures des quatre produits, le comportement de l'ester sur le cycle à trois est bien différent de celui sur le cycle à quatre, et seulement pour les esters sur les cycles à cinq et à six peut-on observer certaines analogies. Les quatre diesters représentent des systèmes à deux centres ionisables: groupement carbonyle ou oxygène du groupement éthoxy.

Les pics moléculaires sont de très faible intensité, ne dépassant pas 4%, et on n'observe pas de pic $M^{\oplus} - 1$. Les pics parents pour les produits **3** et **4** sont des fragments hydrocarboniques C_nH_{2n-1} provenant de la rupture des cycles correspondants:

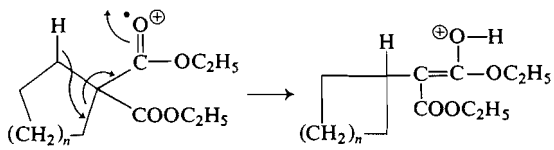

$n = 1$ ou 2 — *m/e* 55 ou 69 (100%)

Le même fragment est peu intense pour la rupture des cycles à trois et à quatre (les produits **1** et **2**). La fragmentation du dérivé deutérié d_4 du composé **4**, le produit **5**, ayant les deutériums introduits dans les positions 2′ et 6′, donne le pic parent à 72, et confirme cette voie de la fragmentation.

Le pic parent pour le produit **1** (*m/e* 141) correspond à la rupture classique (3) d'une des liaisons CO—OEt, avec la formation d'un ion $R—CO^{\oplus}$ (une perte de $29—OC_2H_5$). Cette fragmentation devient peu importante pour les produits **2**–**4** suivant l'ordre croissant du cycle.

Le diester **2** donne le pic parent à *m/e* 29 correspondant à la rupture du type:

$$R—CO—\dot{O}^{\oplus}—C_2H_5 \rightarrow C_2H_5^{\oplus} + R—CO—O^{\bullet}$$

Ce mode de fragmentation classique des esters (3) est assez important pour les autres esters (35–75%).

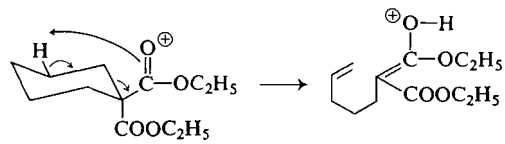

Les ruptures classiques des esters prévoient également la formation des pics correspondant à la fragmentation "H" selon Biemann (3, 4). Nous mentionnons également cette possibilité, certains pics importants résultent de cette fragmentation, surtout pour les cycles à cinq et à six. Surtout pour le produit **5** observe-t-on le fragment hydrocarbonique correspondant au transfert d'hydrogène en β de la substitution (intensité = 60%).

Quant aux clivages α (tableau 1) plusieurs pics sont identifiés, correspondant aux fragmentations du type $R—COOR_1 \rightarrow R_1^{\oplus}$, $R—C{\equiv}O^{\oplus}$, $OR_1^{\oplus}$, $R—COO^{\oplus}$. On n'observe pas de fragment du type $R—COOR_1^{\oplus} - 18$, correspondant à une perte d'eau, normalement présent dans les

[1]Revision reçu le 1 février 1972.

TABLEAU 1. Clivages α I (%)

	$R—COOC_2H_5^{\oplus}$	$C_2H_5^{\oplus}$ —RCOO	$R—C\equiv O^{\oplus}$ —OC_2H_5	$OC_2H_5^{\oplus}$ —R—CO	$R—COO^{\oplus}$ —C_2H_5	$R^{\oplus}$ —$COOC_2H_5$	$R—H^{\oplus}$ —$COOC_2H_4$	$R—OC_2H_5^{\oplus}$ (ou RCOOH)* —CO (ou C_2H_5)	$COOC_2H_5^{\oplus}$	$CH_2=CHO^{\oplus}$	$R—COOC_2H_5^{\oplus}-27$
1		73.2	100	22.0	0.8	63.6	20.4	26.7	3.0	20.1	24.4
2		100.0	18.1	15.4	1.0	14.5	7.4	—	5.4	40.7	2.7
3		35.6	0.7	3.5	1.0	1.7	2.5	—	6.1	5.7	2.0
4		36.5	0.7	2.1	0.7	0.8	—	—	12.7	14.0	2.1

*Le spectre de masse (h) prouve une perte de CO.

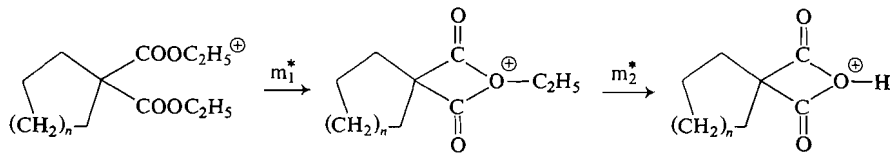

SCHÉMA 1

TABLEAU 2. Ions métastables $a \xrightarrow{m_1^*} b \xrightarrow{m_2^*} c$

	n	a	m_1^* calc.	m_1^* observé	b	m_2^* calc.	m_2^* observé	c
2	0	200	120.1	120.7	155	104.0	104.5	127
3	1	214	133.4	133.8	169	117.6	118.2	141
4	2	228	146.9	147.4	183	131.3	131.6	155

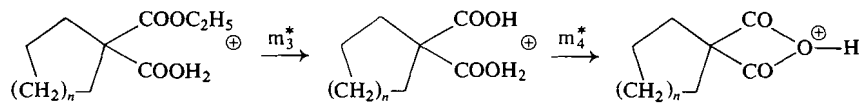

SCHÉMA 2

TABLEAU 3. Ions métastables $d \xrightarrow{m_3^*} e \xrightarrow{m_4^*} c$

	n	d	m_3^* calc.	m_3^* observé	e	m_4^* calc.	m_4^* observé	c
3	1	187	135.2	135.7	159	125.0	125.6	141
4	2	201	148.9	149.4	173	138.9	139.6	155

spectres des esters (3). Nous avons également observé le fragment $M^{\oplus} - 27$, qui a déjà été mentionné par d'autres auteurs (2), et qui a été identifié comme résultant d'une perte de C_2H_3 (ions métastables, voir également le schéma 2 et tableau 3).

Nous avons également identifié quelques fragmentations non classiques. D'abord, des fragments anhydrides *b* et *c* sont supportés par toute une série d'ions métastables (schéma 1 et tableau 2) pour les produits **2**–**4**. Les ions métastables pour le produit **1** ne sont pas observés. Toutefois, d'autres fragments possédant la même masse que *b* peuvent être suggérés.

Les fragments *c* peuvent aussi être obtenus comme le résultat des clivages représentés par schéma 2 (tableau 3). Cette fragmentation n'a pas été retracée pour le produit **1** et **2**. Biemann et collaborateurs en discutant le cas d'octoile mentionnent une structure semblable (4, 5).

Can. J. Chem. Downloaded from www.nrcresearchpress.com by 210.87.254.5 on 09/05/12
For personal use only.

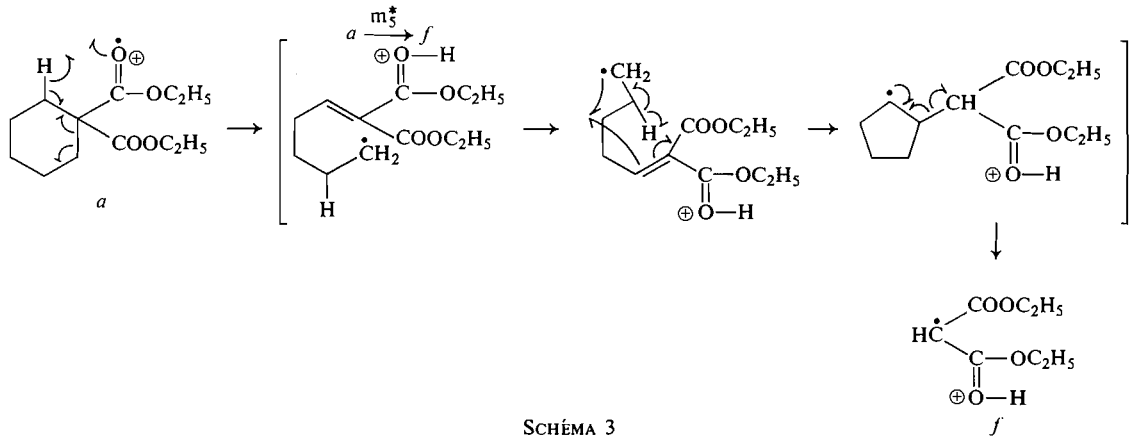

SCHÉMA 3

TABLEAU 4. Ions métastables $a \xrightarrow{m_5^*} f$

		m_5^*		
	a	calc.	observé	*f*
3	214	119.6	119.9	160
4	228	112.3	112.7	160
5	232	111.7	111.9	161

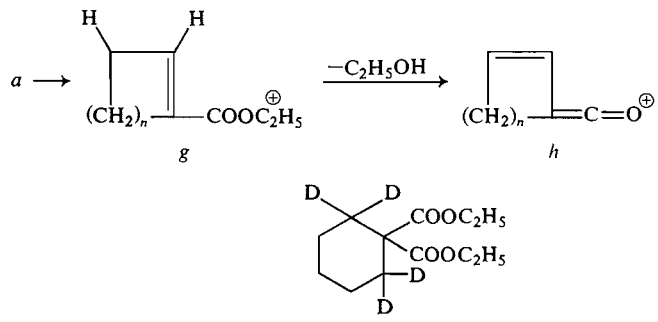

SCHÉMA 4

Une autre fragmentation, mentionnée par la littérature (1) a été trouvée par des ions métastables et l'étude du spectre du produit deutérié. En effet, les produits **3**, **4**, et **5** donnent le clivage malonique selon le schéma 3 (tableau 4).

Finalement, le produit deutérié **5** a été utilisé pour retracer la fragmentation cétènique selon le schéma 4 (tableau 5). Cette fragmentation a été observée pour tous les produits et confirmée par les ions métastables. Le fragment *g* pour le cycle à six peut également donner le clivage rétro-Diels–Alder (schéma 5). Cette fragmentation est supportée par l'ion métastable comme dans le schéma 5. Des fragmentations pareilles ont déjà été observées (1, 2).

Partie expérimentale

Les spectres de masse ont été enregistrés sur un appareil Hitachi RMU-6D et Picker-AEI-MS 30 (250°, 70eV). Les spectres ne sont pas corrigés sur l'abondance isotopique naturelle. Les composés **1**–**3** sont des produits commerciaux (Fluka, pureté minimum de 99%), le produit **4** a été obtenu

Can. J. Chem. Downloaded from www.nrcresearchpress.com by 210.87.254.5 on 09/05/12
For personal use only.

TABLEAU 5. Ions métastables $g \xrightarrow{m_6^*} h$

	n	g	m_6^* calc.	m_6^* observé	h	m* (%) m apparenté
1	0	112 (51.0)	38.9	39.5	66 (7.0)	5.8
2	1	126 (4.2)	50.8	51.4	80 (7.8)	5.0
3	2	140 (3.2)	63.1	63.5	94 (3.3)	6.1
4	3	154 (4.7)	75.7	75.8	108 (3.0)	13.3
5(d_4)	3	157 (4.2)	78.5	78.9	111 (2.7)	14.7

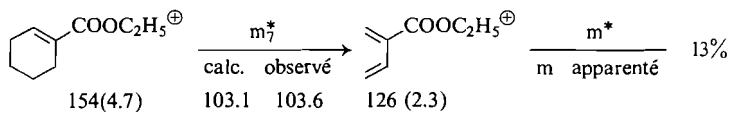

154(4.7) 103.1 103.6 126 (2.3)

SCHÈMA 5

par l'action du dibromo-1,5 pentane sur le malonate d'éthyle (6). Le produit **5**, pureté isotopique d_4 65% minimum, a été obtenu selon la procédure modifiée de Julia (7).

Les auteurs remercient le Conseil National de Recherches du Canada pour l'aide apportée à ce travail sous forme d'octroi de recherche (A 5976). Nous remercions également Dr. Y. Rousseau de l'Université de Montréal pour la réalisation de deux spectres et le Conseil de Recherches de l'Université de Moncton pour la subvention de recherche.

1. K. JANKOWSKI et A. ZAMOJSKI. Ann. Soc. Chim. Pol. **43**, 967 (1969); K. JANKOWSKI, A. ZAMOJSKI, A. KONOWAL, et J. JURCZAK. Ann. Soc. Chim. Pol. **43**, 1459 (1969).
2. J. H. BOWIE, D. H. WILLIAMS, S.-D. LAWESSON, et G. SCHROLL. J. Org. Chem. **31**, 1792 (1966); D. A. BAK et K. CONROW. J. Org. Chem. **31**, 3608 (1966).
3. H. BUDZIKIEWICZ, C. DJERASSI, et D. WILLIAMS. Interpretation of mass spectra of organic compounds. Holden–Day Inc., San Francisco, 1965. p. 11.
4. K. BIEMANN. Mass spectrometry. Application to organic chemistry. McGraw-Hill, New York, N.Y. 1965. pp. 119, 197.
5. F. W. MCLAFFERTY et S. GÖHLKE. Anal. Chem. **31**, 2076 (1959). E. M. EMERY. Anal. Chem. **32**, 1495 (1960).
6. G. BERGSON et A. BIEZAIS. Arkiv. Kem. **22**, 475 (1964).
7. M. JULIA et M. MAUMY. Bull. Soc. Chim. France, 434 (1966). R. SRINIVASAN et C. E. CREMER. J. Am. Chem. Soc. **87**, 1647 (1965).

Can. J. Chem. Downloaded from www.nrcresearchpress.com by 210.87.254.5 on 09/05/12
For personal use only.

Spectroscopie de masse des *gem*-diesters épimères

KRZYSZTOF JANKOWSKI, JEAN COUTURIER, ET ROBERT TOWER
Département de Chimie, Université de Moncton, Moncton, Nouveau-Brunswick

Reçu le 12 août 1971

Nous présentons l'analyse des spectres de masse de trois *gem*-diesters dihydropyranniques substitués en position 2. Nous avons identifié, entre autre, la fragmentation rétro-Diels–Alder, absente pour les autres produits dans cette famille. La fragmentation majoritaire a été l'aromatisation du cycle dihydropyrannique.

The analysis of mass spectra of three 2-substituted dihydropyran *gem*-diesters is presented. The retro-Diels–Alder fragmentation, absent in the other members of the group, was identified. The major fragmentation was the aromatization of the dihydropyran ring.

Canadian Journal of Chemistry, **50**, 1539 (1972)

Can. J. Chem. Downloaded from www.nrcresearchpress.com by 210.87.254.5 on 09/05/12
For personal use only.

Nous avons récemment apporté quelques précisions sur la fragmentation des *gem*-diesters sur les dihydropyrannes ou les composés carbocycliques (1–3). Présentement, nous analysons les spectres de masse de trois produits: méthyl-2 dihydro-5,6-α-pyranne-dicarboxylate-6,6 d'éthyle (**1**), le diméthyl-2β,5β-dihydro-5,6-α-pyranne-dicarboxylate-6,6 d'éthyle (**2**), et le diméthyl-2β,5α-dihydro-5,6-α-pyranne-dicarboxylate-6,6 d'éthyle (**3**). Les épimères **2** et **3** doivent normalement donner le même spectre (4). En effet, nous avons observé les mêmes fragments, mais l'intensité des fragments enregistrés plusieurs fois dans les mêmes conditions est différente pour les épimères **2** et **3**. Il est à souligner que les différences dans l'intensité des ions des deux épimères sont normalement beaucoup plus petites.

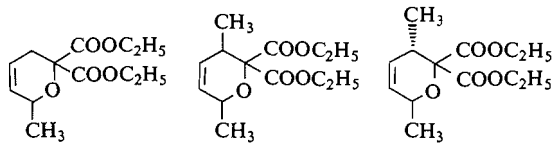

1 **2** **3**

Les ions moléculaires des trois produits sont très peu intenses et correspondent à une ionisation de l'oxygène du cycle. L'ionisation de l'oxygène du carbonyle n'a pas été retracée.

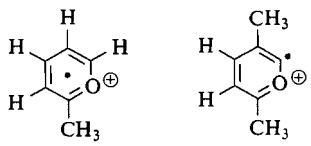

$P^{\oplus}$ (**1**) $P^{\oplus}$ (**2**)

Le processus majoritaire de la fragmentation est celui de l'aromatisation du cycle.

Un ion de base pour le produit **1** ($m/e = 95$) possède une structure aromatique. Le produit **2** donne un ion de base du même genre que le précédant ($m/e = 108$).

Le produit épimère **3** a donné un ion 100% à $m/e = 167$, ce qui correspond en plus à une perte d'un des deux groupements méthyles (en position 2 ou 5). Les ions possibles peuvent donc être $P_1^{\oplus}$ (**3**) ou $P_2^{\oplus}$ (**3**).

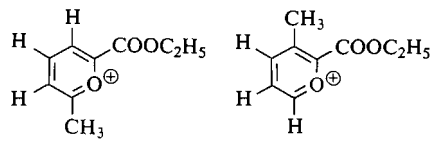

$P_1^{\oplus}$ (**3**) $P_2^{\oplus}$ (**3**)

Nous avons choisi une structure $P_2^{\oplus}$ (**3**) comme étant plus probable à l'issu de l'argumentation suivante:

(*a*) La fragmentation doit se faire d'abord dans une position 5, *p.ex.* la conjugaison avec le carbonyle (voir schéma 1).

(*b*) Une perte d'un hydrogène en position 5 dans l'étape de la formation d'un ion 100% va donner un radical plus stable qu'une perte de CH_3 dans la même position. Un ion $m/e = 182$ est donc très intense.

(*c*) A partir d'un $m/e = 182$ il n'y a pratiquement pas de perte d'hydrogène en position 5 (intensité $m/e = 181$ inférieure à 3%), mais le fragment correspondant à une perte de 15 unités donne un ion 100%.

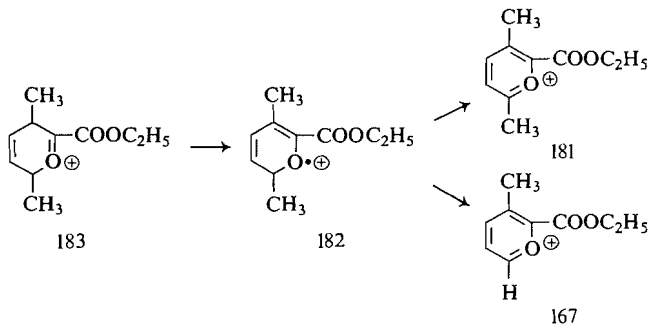

183 182 181 167

SCHÉMA 1

(*d*) Finalement, le produit **1** démontre également un ion intense à $m/e = 154$ (voir schéma 2) obtenu à partir d'un ion $m/e = 169$ en l'absence

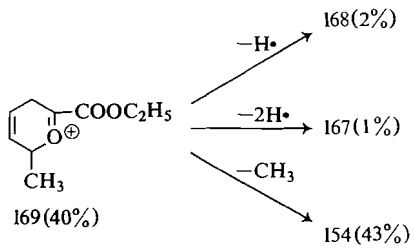

SCHÉMA 2

du fragment $m/e = 167$, ce qui prouve indirectement notre proposition. Le fragment analogue ($m/e = 167$) pour le produit **2** est également fort ($\sim 60\%$). Ceci semble prouver une dépendance de la facilité de départ du méthyl-5 et sa position dans l'espace. Les principaux fragments observés s'expliquent par schéma 3.

La majorité des fragmentations présentées dans le schéma 3 sont identiques avec celles déjà mentionnées par nous-mêmes (1–3). La structure *a*, possèdant le même poids moléculaire que la structure *b*, a été choisie en se servant de la méthode de détermination de masse exacte (exact mass measurement).

En effet, nous avons trouvé pour le produit **2** la composition $C_7H_7O_3$ (masse calculée: 139.0392, observée: 139.0407), au lieu de $C_8H_{11}O_2$ (masse calculée: 139.0759).

Dans une région inférieure à $m/e = 90$, on retrouve les fragments bien connus pour les

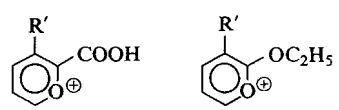

a $C_7H_7O_3$ (139) *b* $C_8H_{11}O_2$ (139)

clivages aromatiques des groupements ester et des fragments du type des ions cyclopropylydiums. Les plus intenses sont $m/e = 66$, 54, et 42 pour les produits **2** et **3**, ainsi que 67 et 43 pour le produit **1** (voir schéma 4). Pour le produit **2**, la fragmentation $a \rightarrow b$ est supportée par un ion métastable à 44.5 (calculée, 44.2). Cependant, les fragments du type *b* peuvent être obtenus par la voie compétitive plutôt que par la voie consécutive.

Contrairement aux cas déjà examinés, le clivage malonique (1, 3) n'a pas été retracé. On n'observe également pas de fragments $M^{\oplus} - 43$, ce qu'élimine une possibilité de l'ionisation du carbonyle. Vraisemblablement, la substitution d'une position 2 du cycle empêche cette rupture. On ne remarque pas l'ion anhydride (3).

Outre les processus de la fragmentation déjà décrits, nous avons confirmé par les ions métastables quelques fragmentations importantes (tableau 1).

L'identification de la fragmentation rétro-Diels–Alder, suggérée pour les autres produits dans cette série (1), constitue une particularité de ces spectres. Nous avons constaté que la substitution d'une position 2 du cycle dihydropyrannique est absolument importante pour observer cette dernière fragmentation. La substitution des positions 3 et 4 par un alkyle ou d'une position 2 par un radical alkoxy ne fait pas apparaître cette fragmentation (5–6).

Les dérivés pyranniques se caractérisent par des clivages menant à la formation de fragments diéniques (7, 8).

On dénote l'absence du fragment correspondant à une partie diénophile déjà observé (1). Ceci démontre l'importance de la substitution dans la position 2 pour ce genre de clivages.

Can. J. Chem. Downloaded from www.nrcresearchpress.com by 210.87.254.5 on 09/05/12
For personal use only.

Can. J. Chem. Downloaded from www.nrcresearchpress.com by 210.87.254.5 on 09/05/12
For personal use only.

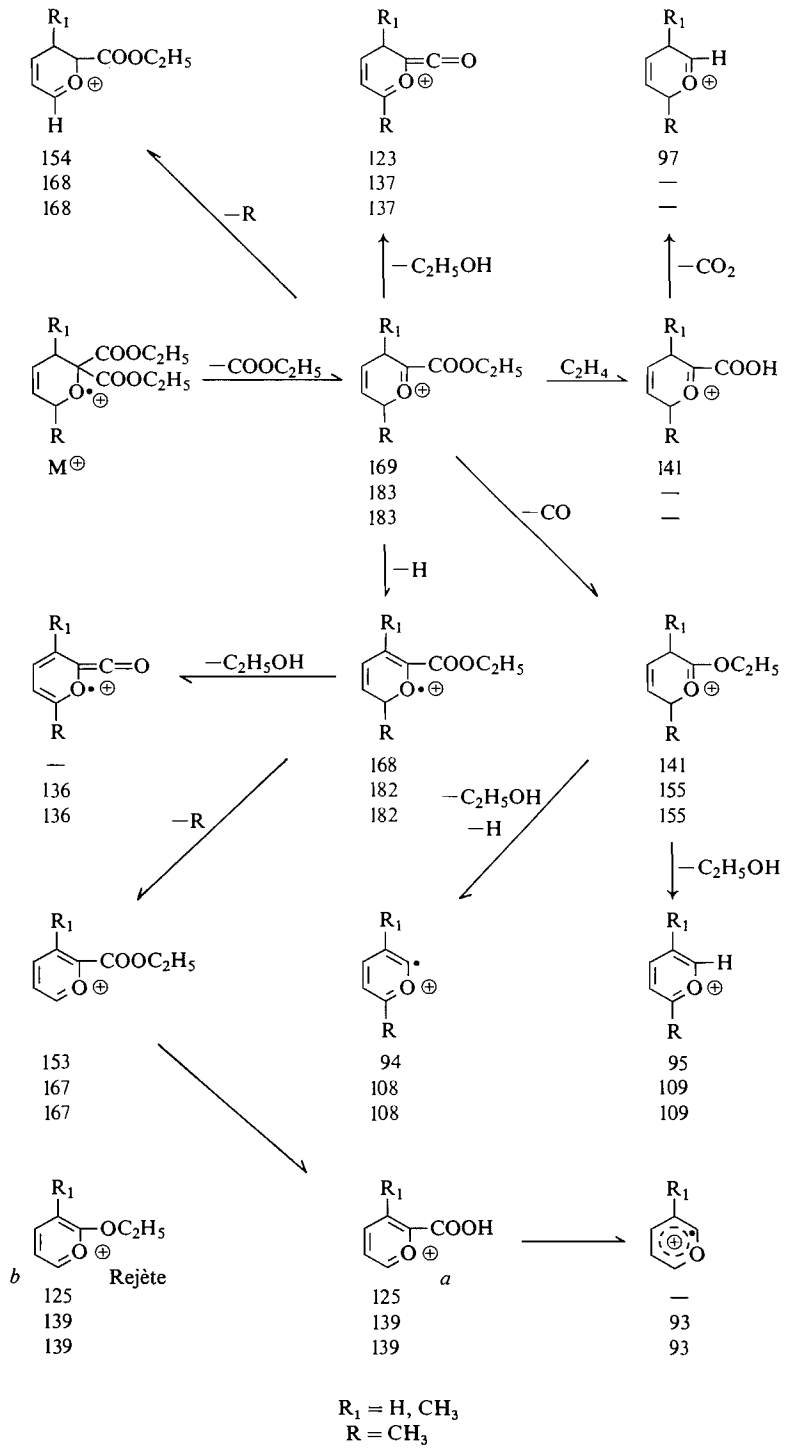

SCHÉMA 3

Can. J. Chem. Downloaded from www.nrcresearchpress.com by 210.87.254.5 on 09/05/12
For personal use only.

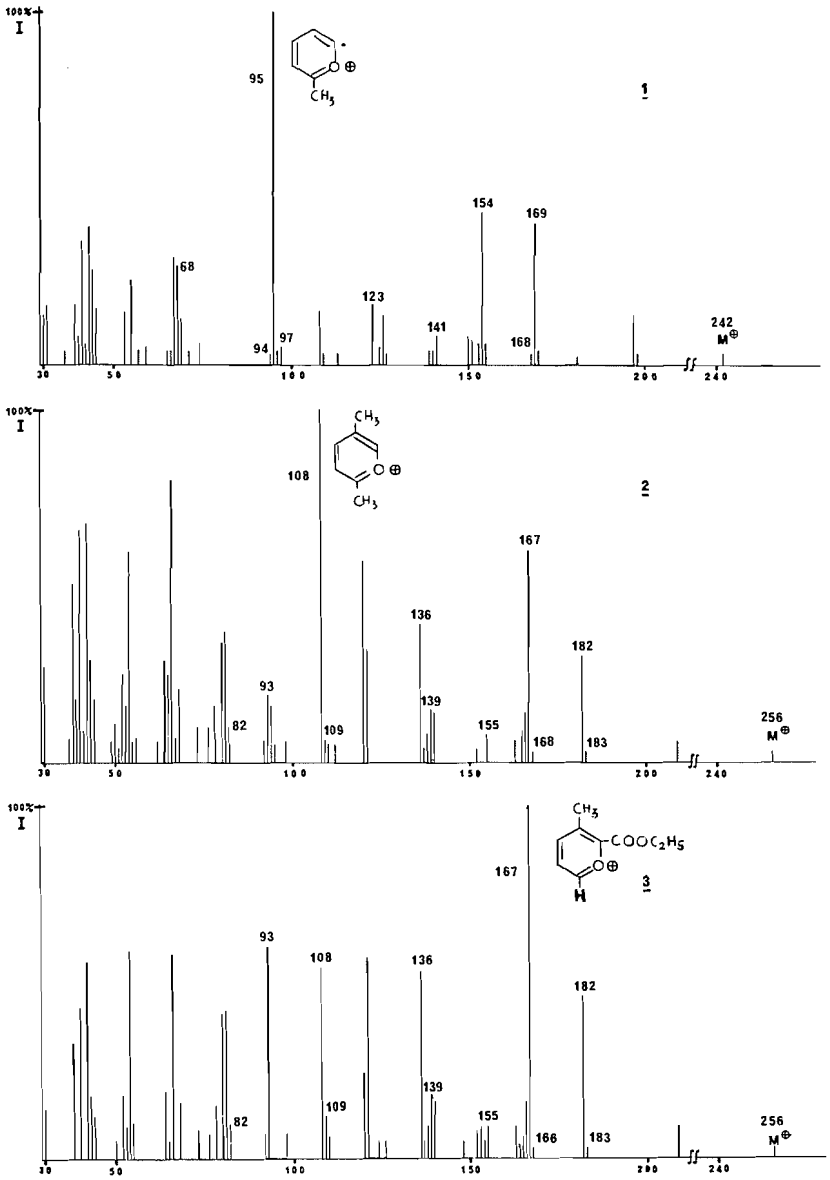

FIG. 1. Spectre de masse des produits **1–3**.

2, 3 $C_5H_6^{\oplus\bullet} \xrightarrow{-12} C_4H_6^{\oplus\bullet} \xrightarrow{-12} C_3H_6^{\oplus}$

1 $C_5H_7^{\oplus\bullet} \longrightarrow C_3H_7^{\oplus}$

SCHÉMA 4

L'augmentation de la température d'enregistrement du spectre augmente l'intensité des fragments correspondant à la fragmentation rétro-Diels–Alder. Cependant, même si le fragment diénophile ($m/e = 174$) apparaît, ceci peut s'expliquer par un clivage thermique (9).

Partie expérimentale

Les spectres de masse ont été réalisés sur des appareils Varian MAT 111, et AEI MS-30 (250°, 70 eV). Seuls les pics d'intensité relative $\geqslant 4\%$ sont mentionnés, exception faite des ions moléculaires (Fig. 1). Les spectres ont été

TABLEAU 1. Ions métastables

N°	*a*	*b*	$a \xrightarrow{m_1^*} b$ Calculé	Observé	Type de la fragmentation (R_1 = H ou CH_3; R = CH_3)
1	169	123	89.5	89.6	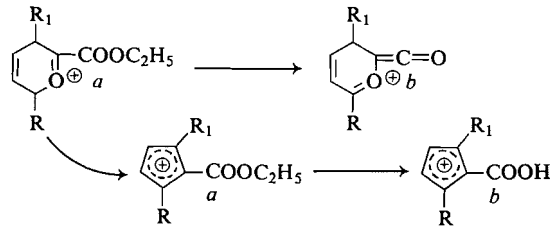
2	183	137	102.6	103.1	
3	183	137	102.6	103.3	
1	151	123	100.2	100.6	
2	165	137	113.7	114.2	
3	165	137	113.7	114.2	
2	137	93	63.1	63.5	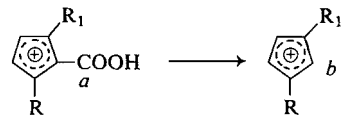
3	137	93	63.1	63.5	
1	169	141	117.6	117.8	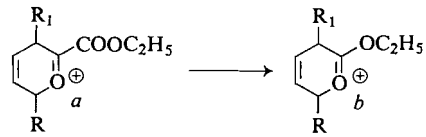
2	183	155	131.3	131.8	
3	183	155	131.3	131.6	
1	242	68	19.1	19.6	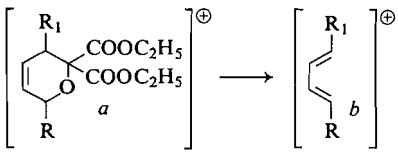
2	256	82	26.3	26.6	
3	256	82	26.3	26.8	

corrigés sur l'abondance isotopique naturelle. Les ions métastables ont été détectés par la méthode d'observation des spectres. Une tolérance de 0.1–0.4 unités de masse sur la valeur observée pour les spectromètres semicirculaires doit être suggérée (10). Les composés **1–3** ont été synthétisés par nous-mêmes (11–12).

Les auteurs remercient le Conseil National de Recherches du Canada pour l'aide apportée à ce travail sous forme d'octroi de recherche (A 5976) et le Conseil de Recherches de l'Université de Moncton pour la subvention de recherche. Nous remercions le Dr. Y. Rousseau, Université de Montréal et la compagnie Varian Associates of Canada Ltd., pour la réalisation de trois de nos spectres. Nous tenons à remercier pour ses discussions le Dr A. Zamojski, Institut de Chimie Organique, PAN.

1. K. JANKOWSKI et A. ZAMOJSKI. Ann. Soc. Chim. Polonorum, **43**, 967 (1969).
2. K. JANKOWSKI, A. ZAMOJSKI, A. KONOWAL, et J. JURCZAK. Ann. Soc. Chim. Polonorum, **43**, 1459 (1969).
3. K. JANKOWSKI, J. COUTURIER, et J.-Y. DAIGLE. Can. J. Chem. Cette issue.
4. K. BIEMANN. Mass spectrometry. Organic chemical application. McGraw-Hill, Inc., New York, N.Y. 1962. p. 145–9.
5. J. JURCZAK, A. KONOWAL, et A. ZAMOJSKI. Ann. Soc. Chim. Polonorum. **44**, 67 (1970).
6. J. JURCZAK, A. KONOWAL, E. BARANOWSKA, et A. ZAMOJSKI. Ann. Soc. Chim. Polonorum, **44**, 143 (1970).
7. D. C. DEJONGH et K. BIEMANN. J. Am. Chem. Soc. **85**, 2289 (1963).
8. N. K. KOCHETKOV, N. S. WULFSON, O. S. CHIZHOV, et B. M. ZOLOTAREV. Tetrahedron, **19**, 2209 (1963).
9. W. J. GENSLER, J. E. STOUFFER, et R. G. MCINNIS. J. Org. Chem. **32**, 200 (1967).
10. Voir la réf. 4. p. 155.
11. K. JANKOWSKI et J. COUTURIER. Can. J. Chem. En préparation.
12. O. ACHMATOWICZ et A. ZAMOJSKI. Ann. Soc. Chim. Polonorum, **35**, 799, 1251 (1961).

Can. J. Chem. Downloaded from www.nrcresearchpress.com by 210.87.254.5 on 09/05/12
For personal use only.

An Unusual Oppenauer Oxidation of (±) Ophiocarpine

V. ŠMULA AND R. H. F. MANSKE
Department of Chemistry, University of Waterloo, Waterloo, Ontario

AND

R. RODRIGO
Waterloo Lutheran University, Waterloo, Ontario

Received November 23, 1971

The Oppenauer oxidation of (±) ophiocarpine has been carried out to yield 3-(2′-vinyl-3′,4′-methylenedioxy) phenyl-4-hydroxyisoquinoline (**2**). Photolysis of this compound gave 3,4-dimethoxy-11,12-methylenedioxy-8,9-dihydro[1]benzoxepino(2,3-*c*) isoquinoline (**7**), whereas photolysis of the methyl ether of **2** produced *N*-norchelerythrine.

La réaction d'oxydation d'Oppenauer sur la (±) ophiocarpine conduit au 3-(2′-vinyl-3′,4′-méthylènedioxy) phényl-4-hydroxyisoquinoléine (**2**). La photolyse de ce composé conduit au 3,4-diméthoxy-11,12-méthylènedioxy-8,9-dihydro[1]benzoxepino(2,3-*c*) isoquinoléine (**7**), alors que la photolyse de l'éther méthylé de **2** conduit au *N*-norchelerythrine.

Canadian Journal of Chemistry, **50**, 1544 (1972)

The modified (1) Oppenauer oxidation of a secondary alcohol function has been previously used with some success in the alkaloid field (2). We have applied this reaction to the oxidation of (±) ophiocarpine (**1**).

The benzylic secondary alcohol group in ophiocarpine might be expected to suffer oxidation under the conditions of the reaction and the resulting 13-ketotetrahydroberberine would almost certainly undergo further transformations in the presence of the strong base used. Such compounds have not been isolated, presumably because of their facile dehydrogenation to 13-hydroxyprotoberberinium salts. Hence our interest in this reaction.

The oxidation carried out under Woodward's (1) conditions using dioxan as the solvent gave in *ca.* 60% yield 3-(2′-vinyl-3′,4′-methylenedioxy) phenyl-4-hydroxy-7,8-dimethoxyisoquinoline (**2**). The structure of **2** was evident from its p.m.r. spectrum which showed the characteristic pattern for the ABX system of the styrene unit with the coupling constants and chemical shifts of expected magnitude. The spectrum also contained a singlet integrating for one proton at δ 9.08 which could be assigned to the H-1 of the isoquinoline system (3). The resonances of the remaining protons were unexceptional. This structure was supported by the i.r. spectrum, (ν_{-OH} 3540 cm^{-1}) and by elemental analysis.

Several mechanisms may be written to rationalize the formation of this interesting product. By analogy with Woodward's original proposal (1) for the oxidation of the secondary alcohol group, it is possible to visualize a similar oxidation at the tertiary nitrogen atom which could be followed by a Hofmann elimination to yield **2** (Scheme 1).

In order to test this hypothesis the reaction was repeated with (±) canadine (**3**) and with berberinium chloride (**4**). In both cases the

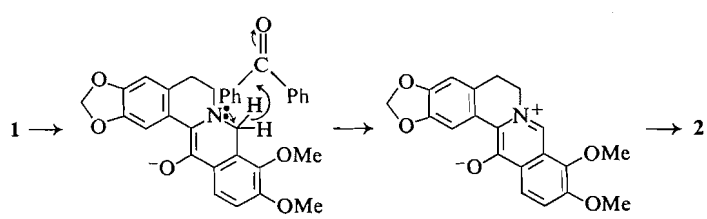

SCHEME 1

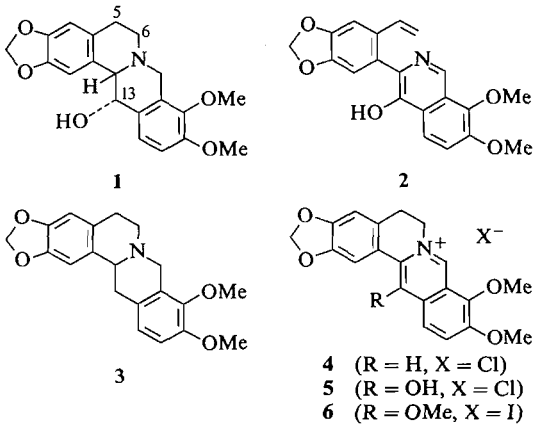

starting material was recovered and no elimination products were obtained. The reaction was successful however, with 13-hydroxyberberinium chloride (**5**) and 13-methoxyberberinium iodide (**6**) (4). The product **2** was obtained in *ca.* 60% yield in the former case and *ca.* 20% yield in the latter.

It is therefore evident that the reaction does not take place via a simple Hofmann degradation and that the presence of an oxygen function at C-13 is indispensable for proton abstraction at C-5 and cleavage of the C_6—N bond. Two different mechanisms which recognize this fact are illustrated in Scheme 2. In the first instance proton transfer directly across ring B (in the boat conformation) from C-5 to -14 is postulated. Alternatively, the results may be rationalized by proposing a 1,3 proton transfer which is followed by a concerted rearrangement–elimination step. Minor variations of either mechanism could account for all the results stated above. There is however no easy way of deciding between them.

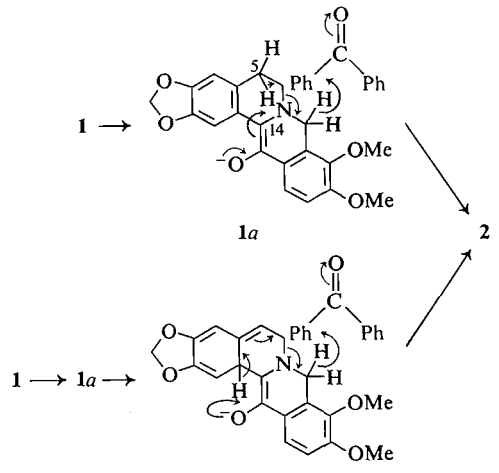

SCHEME 2

It has been recently shown (5) that *N*-methyl-1,2-dihydroisoquinolines similar to **2** are smoothly converted through an electrocyclic process to benzophenanthridine derivatives upon photolysis under suitable conditions. The photolysis of **2** was therefore attempted using a 3500 Å lamp and Pyrex filter under nitrogen in benzene solution.

This gave, *inter alia* the oxepine **7** readily recognized by the absence of the vinyl signals and presence of an A_2X_2 system consisting of two triplets centered at 4.8 and 2.83 δ (J_{AX} = 6.0 Hz). This structure was confirmed by the i.r. spectrum of **7** which was lacking in hydroxyl absorption. The oxepine **7** appears to be the first example of a new tetracyclic system.

In order to block such a photo-addition reaction compound **2** was methylated with diazomethane to the *O*-methyl ether **8** which showed the presence of the extra methoxyl group at 3.62 δ in its p.m.r. spectrum, an upfield shift of > 0.4 p.p.m. from the other two methoxyl groups at 4.06 and 4.14 δ. This shift is easily accounted for by the anisotropic effect of the benzene ring at position 3 of the isoquinoline system, in a non-coplanar conformation.

Photolysis of **8** under the same conditions as before led directly to *N*-norchelerythrine **9**. By analogy with the earlier work (5) the conversion may be regarded as an electrocyclic process followed by spontaneous elimination of methanol and concomitant aromatization (Scheme 3). The n.m.r. spectrum of **9** was fully compatible with its structure while the m.p. and the u.v. spectrum were identical with that of *N*-norchelerythrine already published (6).

This reaction therefore completes a three step conversion of a protoberberine to a fully aromatic benzophenanthridine. It may have some practical advantages over the earlier method (5) in that no dehydrogenation steps are required subsequent to the photolysis.

Experimental

Melting points were determined using a Fisher Meltemp unit and are uncorrected. The p.m.r. spectra were recorded using the frequency sweep mode of a Varian HA-100 spec-

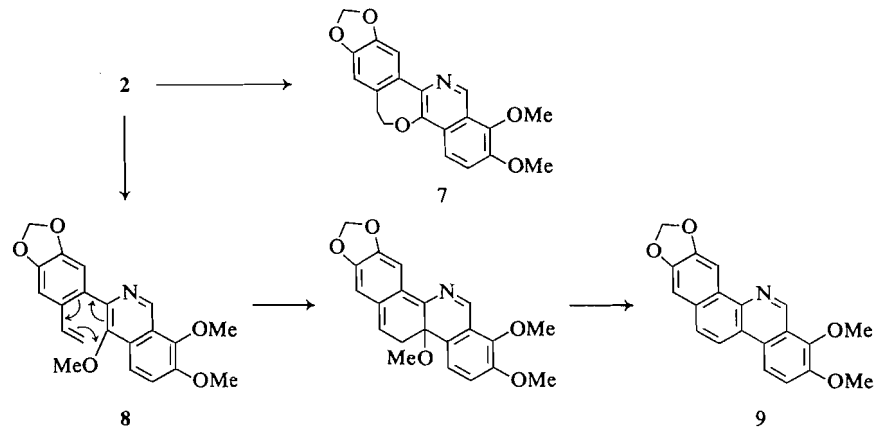

SCHEME 3

trometer. Samples were dissolved in $CDCl_3$, unless otherwise specified, using added TMS as the internal locking signal. Chemical shifts were measured relative to TMS. A Beckman I.R. 10 spectrometer was used to record the i.r. spectra and a Coleman–Hitachi EPS-3T spectrophotometer was used for the u.v. spectra.

3-(2'-Vinyl-3',4'-methylenedioxy)phenyl-4-hydroxy-7,8-dimethoxy Isoquinoline (2)

(*a*) Ophiocarpine (57 mg) in dry dioxan (3.5 ml) was refluxed under nitrogen with potassium *t*-butoxide (80 mg) and benzophenone (150 mg) for 20 h. The solvent was removed under reduced pressure and the residue extracted with 2% hydrochloric acid. The acid extract was washed with ether, basified with ammonia, extracted with chloroform, dried ($MgSO_4$) and evaporated to dryness. The residue was crystallized from methanol (33 mg) m.p. 191–192°.

The u.v. spectrum: λ_{max}^{EtOH} 235, 270(sh), 302, and 355 nm; log ε_{max} 4.56, 4.29, 4.12, and 3.61 respectively. The i.r. spectrum: $\nu_{max}^{CHCl_3}$ 3540 cm^{-1}. The n.m.r. spectrum (δ): 4.02 (3H, s) and 4.05 (3H, s), 6.00 (2H, s), 6.88 (1H, s), 7.17 (1H, s), 9.15 (1H, s), 5.11 (1H, d, d) 5.61 (1H, d, d) 6.44 (1H, q) ($J_{AB} = 18$ and $J_{AX} = 11$ Hz); 7.47 (1H, d) 7.95 (1H, d) ($J_{AB} = 9$ Hz).

Anal. Calcd. for $C_{20}H_{17}NO_5$: C, 68.37; H, 4.88; N, 3.99. Found: C, 68.31; H, 5.14; N, 4.26.

(*b*) 13-Hydroxyberberinium chloride (**5**, 52 mg) in dry dioxan (10 ml) was refluxed under nitrogen with potassium *t*-butoxide (79 mg) and benzophenone (140 mg) for 42 h. The solvent was evaporated under reduced pressure and the residue extracted with 2% hydrochloric acid. The acid extract was washed with ether, basified with ammonia, extracted with chloroform, dried ($MgSO_4$), and evaporated. The residue was purified by t.l.c. (silica gel chloroform – 5% acetone) and crystallized from methanol (26 mg). It was identical in all its properties with **2**.

(*c*) 13-Methoxyberberinium iodide (**6**, 116 mg) in dry dioxan (12 ml) was refluxed under nitrogen with benzophenone (500 mg) and potassium *t*-butoxide (230 mg) for 36 h. The subsequent isolation and purification was carried out as before (17 mg.).

Reactions *b* and *c* were also successful without benzophenone. (±) Canadine (**3**) and berberinium chloride (**4**) were recovered unchanged after reactions by the above procedure.

Methylation of 2

Compound **2** (372 mg) was dissolved in methylene chloride (30 ml) and treated with excess ethereal diazomethane at room temperature for 24 h. The solvents and excess diazomethane were allowed to evaporate and the residue purified by chromatography on a silica gel column in benzene–acetone (9:1). The product **8**, was a thick oily semi-solid (310 mg) homogeneous on t.l.c. The n.m.r. spectrum; virtually identical with **2** but for an extra singlet (3H) at 3.62 δ.

3,4-Dimethoxy-11,12-methylenedioxy-8,9-dihydro[1]-benzoxepino[2,3-c] Isoquinoline (7)

Compound **2** (75 mg) was dissolved in dry benzene (100 ml) and irradiated in a Rayonet reactor at 3500 Å under nitrogen for 2 h. The solvent was evaporated and the residue purified by preparative t.l.c. (silica gel, benzene–acetone, 9:1) and crystallized from ethanol (25 mg) m.p. 145–147°. The u.v. spectrum: λ_{max}^{EtOH} 233, 264, 320, and 363 nm; log ε_{max} 4.59, 4.33, 4.34, and 3.82 respectively. The n.m.r. spectrum (δ): 2.83 (2H, t) and 4.80 (2H, t) ($J_{AX} = 6$ Hz), 4.01 (3H, s) 4.06 (3H, s), 5.98 (2H, s), 6.75 (1H, s), 7.47 (1H, s), 9.13 (1H, s), 7.45 (1H, d), and 7.95 (1H, d) ($J_{AB} = 9.0$ Hz).

Anal. Calcd. for $C_{20}H_{17}NO_5$: C, 68.37; H, 4.88; N, 3.99. Found: C, 68.50; H, 5.06; N, 3.99.

N-Norchelerythrine (9)

Compound **8** (100 mg) in dry benzene (50 ml) was irradiated in a Rayonet reactor at 3500 Å under nitrogen for 4 h. The mixture was worked-up as before to yield the product which was crystallized from ethanol (52 mg), m.p. 215° (lit. 212–214°). The u.v. spectrum was identical with that already published (6). The n.m.r. spectrum (δ): 4.10 (3H, s), 4.17 (3H, s), 6.16 (2H, s), 7.24 (1H, s), 8.75 (1H, s), 9.78 (1H, s) 7.58 (1H, d), and 8.36 (2H, d) ($J_{AB} = 9.2$ Hz) and 7.86 (1H, d) ($J_{A'B'} = 9.0$ Hz).

We wish to thank Dr. D. B. MacLean, McMaster University, Hamilton, Ontario for the 100 MHz n.m.r. spectrum of

2. Support from the National Research Council of Canada is gratefully acknowledged.

1. R. B. WOODWARD, N. L. WENDLER, and F. V. BRUTSCHY. J. Am. Chem. Soc. **67**, 1425 (1945).
2. E. W. WARNHOFF and P. REYNOLDS-WARNHOFF. J. Org. Chem. **28**, 1431 (1963), and references therein.
3. A. TAURINS and R. K. C. HSIA. Can. J. Chem. **49**, 4054 (1971).
4. T. TAKEMOTO and Y. KONDO. Yakugaku Zasshi. **82**, 1413 (1962): Chem. Abstr. **59**, 689c (1963).
5. M. ONDA, K. YONEZAWA, and K. ABE. Chem. Pharm. Bull (Tokyo), **19**, 31 (1971).
6. A. S. BAILEY and C. R. WORTHING. J. Chem. Soc. 4534 (1956).

cis-5-Cyclooctene-1,2-dione and its Ethylene Ketals[1]

PETER YATES, E. G. LEWARS, AND P. H. MCCABE
Lash Miller Chemical Laboratories, University of Toronto, Toronto 5, Ontario

Received December 21, 1971

Oxidation of *cis-cis*-1,5-cyclooctadiene with hydrogen peroxide gives *cis*-5-cyclooctene-*trans*-1,2-diol (**3**) which is converted to *cis*-5-cyclooctene-1,2-dione (**6**) on treatment with dimethyl sulfoxide and acetic anhydride. Bromination of **6** is accompanied by transannular bonding to give a dibromo keto ether **9***a* or *b*. Ketalization of **6** with ethylene glycol gives a monoketal **11** and two diketals **12** and **13** with 1,3-dioxolane and 1,4-dioxane rings, respectively. Bromination of **12** with bromine or pyridinium perbromide is accompanied by transannular bonding and fission of one of the 1,3-dioxolane rings to give a dibromo monoketal ether **15***a* (or *b*). Bromination of **12** with *N*-bromosuccinimide followed by dehydrobromination gives a cyclooctadiene-1,2-dione diketal **20***a* (or *b*).

L'oxydation par l'eau oxygénée du cyclooctadiène-1,5 *cis-cis* donne le *cis*-cyclooctène-5 diol-1,2 *trans* (**3**) qui est converti en *cis*-cyclooctène-5 dione-1,2 (**6**) par traitement avec le diméthylsulfoxyde et l'anhydride acétique. La bromation de **6** est suivie de la formation d'une liaison transannulaire pour conduire au dibromocétoéther **9***a* ou *b*. La cétalisation de **6** avec l'éthylèneglycol donne un monocétal **11** et deux dicétals **12** et **13** avec respectivement des cycles dioxolane-1,3 et dioxane-1,4. La bromation de **12** par le brome ou par le perbromure de pyridinium est suivie de la formation d'une liaison transannulaire et de la scission d'un des cycles dioxolane-1,3 pour donner un dibromo monocétaléther **15***a* (ou *b*). La bromation de **12** par le *N*-bromosuccinimide suivie d'une déhydrobromation, conduit au cyclooctadiène dione-1,2 dicétal **20***a* (ou *b*).

Canadian Journal of Chemistry, **50**, 1548 (1972)

Can. J. Chem. Downloaded from www.nrcresearchpress.com by 210.87.254.6 on 09/05/12
For personal use only.

In an earlier paper in this series (2) we discussed the interest underlying the chemistry of 1,2-cyclooctatetraenoquinone (**1**) and its 1,4 isomer as a result of their potential aromaticity. We described a synthesis of dibenzo[*a*,*e*]cyclooctene-5,6-diene (**2**), the dibenzo analogue of **1**, and demonstrated that its eight-membered ring is not aromatic. It was pointed out that the latter observation could not be taken as implying the absence of aromaticity in the parent monocyclic compound **1**, since the benzenoid rings of **2** might damp the aromaticity of the eight-membered ring (3). We report now on some synthetic approaches to **1**, which, although not crowned with success, have provided results of interest in the area of eight-membered ring chemistry.

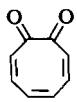

1

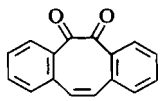

2

Oxidation of *cis-cis*-1,5-cyclooctadiene with hydrogen peroxide and formic acid followed by basic hydrolysis gave *cis*-5-cyclooctene-*trans*-1,2-diol (**3**) as a colorless oil in 55% yield. The stereochemistry is assigned as *trans* on the basis of analogy with analogous hydroxylation reactions (4). The preparation of this diol by hydrolysis of the corresponding epoxide has been reported previously in the patent literature (5) and in a review (6). The diol afforded an oily diacetate (**4**) and a crystalline dibrosylate (**5**); the spectra of **3**–**5** were in full accord with these structural assignments (see Experimental).

Oxidation of **3** with dimethyl sulfoxide and acetic anhydride (7) gave *cis*-5-cyclooctene-1,2-dione (**6**) as a very pale yellow crystalline solid in 30–50% yield.[2] Its i.r. spectrum showed bands at 5.80 and 5.85 μ, which can be attributed to the antisymmetrical and symmetrical coupled stretching vibrations of the two carbonyl groups (9). The relatively small separation of these bands indicates that the coupling is weak. This is in accord with the existence of **6** in the conformation **7** in which the non-bonding interactions of the hydrogen atoms and the dipole–dipole interaction of the carbonyl groups are minimized. The intercarbonyl angle in this conformation is *ca.* 120°, which would account

[1]Cyclooctatetraenoquinones. III. For paper II in this series, see ref. 1*a*. A preliminary account of part of this work has appeared (1*b*).

[2]The dione **6** was also obtained, in low yield, when 1,2-dibromo-*cis*-5-cyclooctene (8) was heated with collidine and dimethyl sulfoxide.

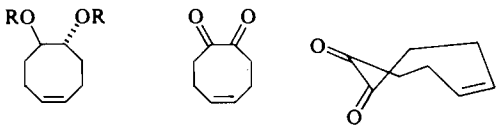

3 R = H
4 R = $COCH_3$
5 R = $SO_2C_6H_4Br$-*p*

6 7

for the fact that the carbonyl-stretching vibrations are only weakly coupled (10). The u.v. spectrum of **6** has maxima at 281 (ε 35), 289 (sh, ε 31), and 347 mμ (ε 17). This contrasts with many α-diketones which are bright yellow due to maxima in their electronic spectra at >360 mμ. However, it is well established (11) that this long wavelength maximum is shifted to shorter wavelength when the intercarbonyl angle is in the range 90–140°. In particular the spectrum may be compared with that of 3,3,8,8-tetramethylcyclooctane-1,2-dione: *ca.* 287 (ε 35), 296 (ε 43), and 343 mμ (ε 21) (12). This diketone is considered to exist in a crown conformation in which the intercarbonyl angle is 110–140°. The close similarity of its spectrum to that of **6** shows that no special effect due to non-bonded interaction of the ethylenic and carbonyl systems of the latter can be adduced from its electronic spectrum.

Treatment of **6** with *o*-phenylenediamine in boiling acetic acid gave the quinoxaline **8**. Treatment with bromine in carbon tetrachloride gave a dibromo compound. The i.r. spectrum of this product showed that bromination had been accompanied by transannular bonding to give a keto ether with structure **9***a* or *b*. A band at 5.76 μ is attributable to the carbonyl-stretching vibration shifted to lower wavelength than normal because of dipole–dipole interaction

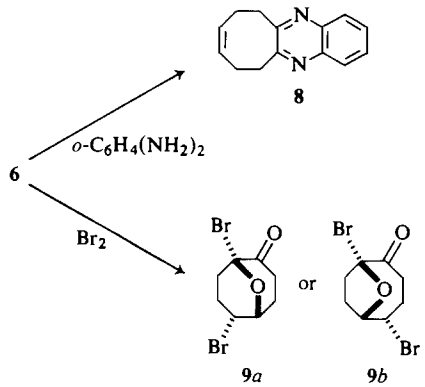

with the adjacent carbon–bromine bond, and strong bands between 9 and 10.5 μ, absent in the spectrum of **6**, are attributable to the ether linkage. The p.m.r. spectrum of the bromination product is also in accord with this formulation, showing two one-proton multiplets at δ 4.1–4.6 and 4.6–5.0. The formation of **9***a* (or *b*) is considered to occur via the bromonium ion **10** (Scheme 1). The stereochemistry depicted in **9***a* (and *b*) is assigned on the basis of Scheme 1. Attempted bromination of **6** with *N*-bromosuccinimide gave intractable tarry mixtures.

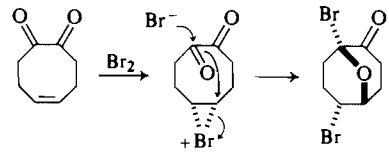

6 10 9*a*

SCHEME 1

Treatment of **6** with ethylene glycol and *p*-toluenesulfonic acid in boiling dichloromethane in a Soxhlet apparatus with calcium hydride or molecular sieves in the thimble gave a mixture of three products, **11**–**13**. The product distribution (determined by v.p.c.) as a function of time is shown in Table 1. Thus, the diketal **12** could be obtained in good yield by crystallization of the product mixture after the reaction had been allowed to proceed for 2 weeks, while the diketal **13** could be isolated, albeit in low yield, by crystallization of the product mixture after 2–3 days at reflux. The monoketal **11** was best obtained by treatment of **6** with acetone ethylene ketal and boron trifluoride etherate for 5 h at 25°; the major product was **11**, which was

TABLE 1. Product distribution in the ketalization of 6*

	Yield (%)†			
Time (h)	**6**	**11**	**12**	**13**
15	47	17	12	24
37	27	18	27	28
101	—	29	57	14
188	—	21	75	4
310	—	5	92	3

*A solution of **6** (2.00 g), ethylene glycol (2.00 g), and *p*-toluenesulfonic acid (0.10 g) was boiled under reflux in a flask fitted with a Soxhlet extractor holding Type 4A molecular sieves. Several further additions of ethylene glycol (totaling 5.00 g) and *p*-toluenesulfonic acid (totaling 0.30 g) were made.

†Determined by v.p.c. analysis (3% SE-30 on Chromosorb P, 200°).

Can. J. Chem. Downloaded from www.nrcresearchpress.com by 210.87.254.6 on 09/05/12
For personal use only.

TABLE 2. Spectra of the ketals **11**, **12**, and **13**

	11	**12**	**13**
$\lambda_{max}^{CCl_4}$ (μ)	5.80, 8.39, 9.19, 10.52	8.51, 9.20, 9.30, 9.56, 9.72, 10.48	9.10
δ^{CDCl_3}	1.5–1.8 (m, 2 H), 2.0–2.4 (m, 2 H), 2.4–2.7 (m, 4 H), 3.8–4.1 (m, 4 H), 5.5–5.8 (m, 2 H)	1.6–1.9 (m, 4 H), 2.0–2.4 (m, 4 H), 3.7–4.0 (m, 8 H), 5.4–5.8 (m, 2 H)	2.0–2.65 (m, 8 H), 3.5–4.3 (m, 8 H), 5.45–5.7 (m, 2 H)
m/e (relative abundance, %)*	182(5), 154(18), 125(16), 86(100), 67(11)	226(2), 154(10), 125(20), 86(100), 67(13)	226(0.1), 180(15), 170(31), 136(37), 108(28), 94(18), 86(53), 81(35), 80(100), 68(26), 67(54)

*Molecular ion peak and peaks with relative abundance > 10%.

accompanied by **12** and unconsumed **6**. The spectra of the ketals are given in Table 2.

The structures of the diketals **12** and **13** were assigned on the basis of deketalization studies. Treatment of **13** in acetone with boron trifluoride etherate or concentrated hydrochloric acid at room temperature gave the diketone **6**,

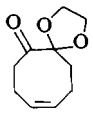

11

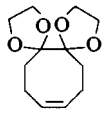

12

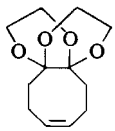

13

while treatment of **12** gave the monoketal **11**, which was stable under these conditions. Reaction of **12** in ether with 6 *N* hydrochloric acid rapidly gave **11**, which was slowly converted to **6**. These observations, which are summarized in Scheme 2, show that **13** is converted to **6** without forming **11**, while **12** is converted to **6** via **11**, in accord with the structural assignments.

Corroboratory evidence for these assignments is provided by the mass spectra of the diketals and their relationship to the mass

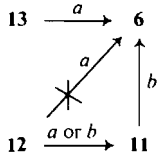

a $BF_3 \cdot Et_2O$ or 12 *N* HCl aqueous in acetone
b 6 *N* HCl aqueous in ether

SCHEME 2

spectrum of the monoketal. It is clear that there is a close relationship of the spectrum of **11** with that of **12**, but not of **13**. The salient features of the spectra of **11** and **12** can be interpreted in terms of Scheme 3, which involves processes that have been postulated previously to account for the mass spectra of related compounds (13, 14). The spectrum of **13** is considerably more complex than that of **12**; it can be interpreted in terms of earlier postulates (14), but detailed discussion is deferred in the absence of accurate

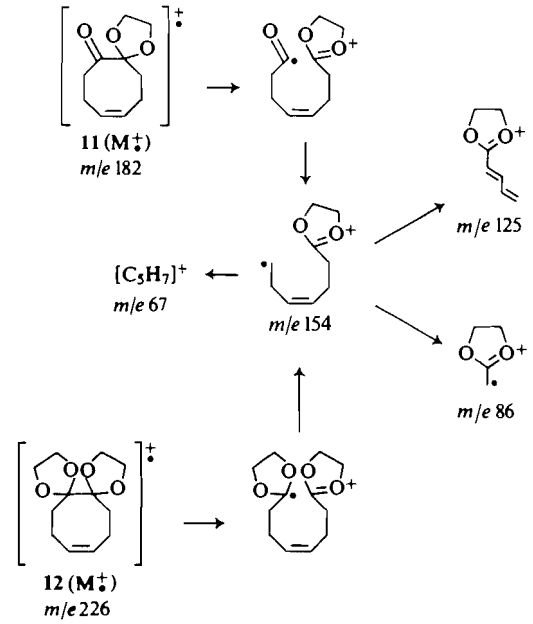

SCHEME 3

Can. J. Chem. Downloaded from www.nrcresearchpress.com by 210.87.254.6 on 09/05/12
For personal use only.

Can. J. Chem. Downloaded from www.nrcresearchpress.com by 210.87.254.6 on 09/05/12
For personal use only.

mass measurements. Attention may be drawn, however, to the strong peak at *m/e* 86, which most probably has the same origin as the peaks at *m/e* 86 in the spectra of **11** and **12**. This may at first sight be considered to be anomalous; however, Fuchs (14*a*) has observed related fragmentations of 1,4,5,8-tetraoxadecalins upon electron impact to ions considered to be dioxolane derivatives.

The relationship among the p.m.r. spectra of **11**–**13** also corroborates these structural assignments. The multiplets due to the protons of the $-OCH_2CH_2O-$ groups in the spectra of **11** and **12** are considerably narrower than the corresponding multiplet in the spectrum of **13**, which appears as a well-defined AA′BB′ system. This difference is attributable to the greater rigidity of the dioxane rings in **13** relative to the dioxolane rings in **12** (14*a*). It is also noteworthy that the $-OCH_2CH_2O-$ multiplet in **12** is centered at slightly lower field than that in **13** in correspondence with observations on related pairs of isomers (14*a*).

It can be seen from Table 1 that while **13** is formed more rapidly than **12**, the latter is highly favored thermodynamically. The greater stability of **12** is attributable both to entropy (*vide supra*) and enthalpy factors. The latter stem from the more severe non-bonded interactions in **13**, which must perforce have the dioxane rings *cis* fused. The same stability relationship appears to hold for the two diketals of 1,2-cyclohexanedione, although in this case insufficient data are available for rigorous structural assignment (15). The stability relationship is reversed in the case of the diketals of acenaphthenequinone; this relationship has been interpreted in terms of the relative stabilities of diprotonated intermediates (14*b*). However, we consider that it reflects the greater thermodynamic stability of the dioxane type diketal relative to the dioxolane type diketal in this case, due to the absence of non-bonded interactions of the dioxane ring hydrogen atoms with the hydrogen atoms of the diketone residue, thus making the interactions in the dioxolane rings systems paramount in determining the stability relationship.

A brief study was also made of the *thio*-ketalization of **6**. Treatment with 1,2-ethanedithiol and boron trifluoride in ether at room temperature gave the monothioketal **14**; however, prolonged reaction with these reagents at room temperature or at reflux failed to produce a dithioketal. The monothioketal **14** was resistant to hydrolysis with mercuric chloride and cadmium carbonate in aqueous acetone (*cf.* (16)), and was not further investigated.

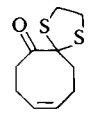

14

Bromination of diketal **12** with bromine or pyridinium perbromide gave a dibromo compound whose p.m.r. spectrum indicated that it was not the product derived by simple addition of bromine to the double bond of **12**. The nature of the product was revealed when it was found that treatment with potassium *t*-butoxide in ether gave a monodehydrobromination product whose spectra indicated the presence of a vinyl ether group,$-OCH=CH_2$. The presence of this group was confirmed by the fact that hydrolysis of the dehydrobromination product with boiling acidic methanol gave acetaldehyde, identified as its 2,4-dinitrophenylhydrazone. On the basis of these observations the dibromo compound is formulated as **15***a* or *b* and its dehydrobromination product as **16***a* or *b*. The other product formed in the hydrolysis of **16**, which could also be obtained by hydrolysis of **15**, was not fully characterized, but its spectra were consistent with its formulation as **17***a* or *b*.

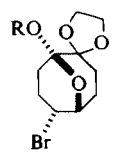

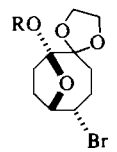

15*a* R = CH_2CH_2Br **15***b* R = CH_2CH_2Br
16*a* R = $CH=CH_2$ **16***b* R = $CH=CH_2$

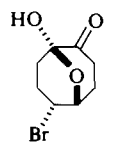

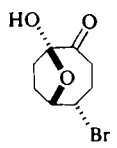

17*a* **17***b*

The formation of **15***a* from **12** is envisaged to occur via the bromonium ion **18** as in Scheme 4 (a closely related scheme would lead to **15***b*). The stereochemistry shown in **15**–**17** is assigned on the basis of Scheme 4.

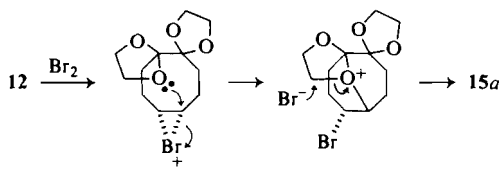

18

SCHEME 4

Bromination of the diketal **12** on a small scale with *N*-bromosuccinimide or 1,3-dibromo-5,5-dimethylhydantoin gave a monobromo compound that is formulated as **19***a* or *b* on the basis of its p.m.r. spectrum and its conversion to a conjugated diene on dehydrobromination (*vide infra*). Unfortunately, the reaction was capricious and the yield of **19** was very variable. Large scale reactions gave low yields of **19**, which was accompanied by two dibromination products.

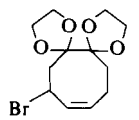

19*a*

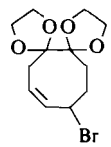

19*b*

One of these was found to be identical with the dibromo compound **15** obtained from the reaction of **12** with bromine or pyridinium perbromide. The other had similar spectra and is considered to be the other member of the **15***a*, **15***b* pair.

Dehydrobromination of **19** with potassium *t*-butoxide in dimethyl sulfoxide gave a product $C_{12}H_{16}O_4$ that is assigned structure **20***a* or *b*[3] on the basis of the following data. Its i.r. spectrum showed a weak-to-medium intensity band at 6.14 μ, similar to that in 1,3-cyclooctadiene. Its u.v. spectrum showed the presence of a *cisoid* conjugated diene system: $\lambda_{max}^{C_6H_{14}}$ 230 mμ (ε 4300) (*cf.* 1,3-cyclooctadiene: $\lambda_{max}^{C_6H_{14}}$ 227 mμ (ε 5500)). Its p.m.r. spectrum had signals at δ 2.1–2.7 (m, 4 H), 3.8–4.05 (m, 8 H), 5.65–6.0 (m, 4 H). On hydrogenation over palladium/charcoal it gave the diketal **21** of 1,2-cyclooctanedione, which was also obtained by hydrogenation of **12**, and whose structure was established by its preparation from 1,2-cyclooctanedione and ethylene glycol in the presence of *p*-toluenesulfonic acid.[4]

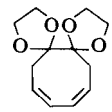

20*a*

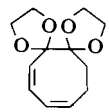

20*b*

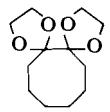

21

Experimental

Melting points were determined in capillary tubes with a Thomas-Hoover "Uni-Melt" apparatus. Melting and boiling points are uncorrected. The i.r. spectra were recorded in carbon tetrachloride, unless otherwise specified, n.m.r. spectra were recorded in deuteriochloroform, unless otherwise specified. The t.l.c. was carried out on silica gel with development with dichloromethane. Solutions in organic solvents were dried with anhydrous magnesium sulfate. "Aqueous work-up" signifies that the reaction solution was poured into about three times its volume of water, the mixture was extracted three times with dichloromethane, and the dichloromethane solution was washed three times with water, dried, and evaporated.

cis-5-Cyclooctene-trans-1,2-diol (3)

In a 1-l round-bottomed flask equipped with a magnetic stirring bar, a dropping funnel, and a thermometer, was placed *cis-cis*-1,5-cyclooctadiene (57 ml, 50 g, 0.46 mol). The flask was immersed in an ice bath, and stirring was commenced. A mixture of hydrogen peroxide (33%; 50 ml, 55 g, 0.50 mol) and 99% formic acid (310 ml) was added at a rate such as to keep the temperature of the reaction mixture at 40–45°; this required 30 min. When almost all of the hydrogen peroxide and formic acid had been added, the remaining portion was added at a rate such as to allow the temperature of the reaction mixture to reach 55°, when the mixture became homogeneous. The mixture was stirred for 5 min without cooling, during which the temperature showed no tendency to rise, and then heated at 65° for 2 h, at the end of which period peracid was shown to be absent (negative starch–iodide reaction). Formic acid and water (270 ml) were removed at the rotary evaporator. The residue was stirred and cooled in an ice-bath while a solution of sodium hydroxide (28 g, 0.7 mol) in water (120 ml) was cautiously added. The mixture was heated on the steam bath for 2 h. Concentrated hydrochloric acid was added to make the reaction mixture neutral. The mixture was heated on the steam bath, and the water was removed by flash distillation at the water aspirator. The residue was distilled to give **3** as a clear, colorless, virtually odorless, mobile oil (26 g, 39%), b.p. 99–100° (0.45 mm) (lit. (5) 153–155° (16 mm)); λ_{max} (liquid film) 3.01 μ; $\delta(CCl_4)$ 1.2–2.8 (m, 8 H), 3.4–3.7 (m, 2 H), 4.30 (broad s, 2 H), 5.58 (t, $J = 4$ Hz, 2 H).

Anal. Calcd. for $C_8H_{14}O_2$: C, 67.57; H, 9.93. Found: C, 67.65; H, 9.87.

When **3** was prepared on a 1 *M* scale, it was found con-

[3]It is not excluded that the diene is a mixture of **20***a* and *b*. Preliminary experiments indicated that this product could be brominated with *N*-bromosuccinimide to give a monobromo derivative; however, this route to the corresponding triene was not pursued because of the difficulties encountered in the preparation of **19**.

[4]Compound **21** was the major product formed on diketalization of 1,2-cyclooctanedione; its p.m.r. spectrum is in accord with the assignment to it of a structure analogous to **12** rather than **13** (*vide supra*). It is not excluded that a diketal analogous to **13** is also formed.

Can. J. Chem. Downloaded from www.nrcresearchpress.com by 210.87.254.6 on 09/05/12
For personal use only.

Can. J. Chem. Downloaded from www.nrcresearchpress.com by 210.87.254.6 on 09/05/12
For personal use only.

venient to extract the alkaline reaction mixture with chloroform; the chloroform extracts were dried and evaporated, and the residue was distilled to give **3** in 55% yield.

cis-5-Cyclooctene-trans-1,2-diol Diacetate (4)

In a 10-ml Erlenmeyer flask were placed the diol **3** (1.05 g, 7.4 mmol), acetic anhydride (6 ml), and concentrated sulfuric acid (1 drop). The flask was stoppered and the mixture was left at 23° for 13 h. The reaction mixture was poured into water (30 ml) and allowed to stand at 23° for 5 h with occasional swirling. The reaction mixture now consisted of a pale yellow oil beneath an aqueous layer; it was left at 2° for 6 days, but crystallization of the oil did not occur. The aqueous layer was extracted with dichloromethane, and the extract was washed with water, dried, and evaporated to give a pale yellow liquid, which was combined with the oil from the original reaction mixture to give the crude diacetate **4** (1.3 g, 77%). Vapor phase chromatography (10% NPGS on Chromosorb P, 10 ft × 0.25 in. copper column, 200°) indicated the presence of *ca.* 90% of one component; this was collected to give the diacetate **4** as a colorless liquid; λ_{max} 5.74, 7.30, 8.15 μ; $\delta(CCl_4)$ 1.4–2.8 (m, 14 H, including s, δ 1.93), 5.02 (t, $J = 4$ Hz, 2 H), 5.67 (t, $J = 5$ Hz, 2 H).

Anal. Calcd. for $C_{12}H_{18}O_4$: C, 63.70; H, 8.02. Found: C, 63.64; H, 7.94.

cis-5-Cyclooctene-trans-1,2-diol Bis-p-bromobenzenesulfonate (5)

The diol **3** (0.50 g, 3.5 mmol) in pyridine (5 ml) was stirred at 0°, and powdered *p*-bromobenzenesulfonyl chloide (1.80 g, 7.0 mmol) was added during 1 min. The colorless solution was maintained at 10° for 12 h. The reaction mixture was poured into 5% hydrochloric acid (70 ml), and the resulting suspension was extracted with ether (4 × 30 ml). The combined ethereal extracts were washed once with water, once with saturated aqueous sodium bicarbonate, and once with brine. The organic layer was dried, and most of the ether was removed on the rotary evaporator to give the dibrosylate **5** as colorless needles (636 mg, 30%), m.p. 126–127° (dec.); δ 1.7–2.6 (m, 8 H), 4.75–5.0 (m, 2 H), 5.5–5.7 (m, 2 H), 7.4–7.8 (m, 8 H).

Anal. Calcd. for $C_{20}H_{20}Br_2O_6S_2$: C, 41.39; H, 3.47; Br, 27.54; S, 11.05. Found: C, 41.65; H, 3.35; Br, 27.66; S, 11.05.

cis-5-Cyclooctene-1,2-dione (6)

The diol **3** (41 g), dimethyl sulfoxide (Fisher Certified, dried with Linde type 4A molecular sieves; 400 ml), and acetic anhydride (200 ml) were allowed to stand at 23° for 24 h in a stoppered flask. The light yellow–green reaction mixture was poured into 1 *N* hydrochloric acid (1200 ml) with cooling with a water bath at room temperature, and the mixture was stirred for 40 min while being maintained at room temperature. The mixture was extracted with dichloromethane (3 × 200 ml), and the dichloromethane extracts were washed twice with water and once with dilute aqueous sodium bicarbonate. The organic layer was dried and evaporated to give a yellow–green liquid, which was distilled to give the enedione **6** as a light yellow–green liquid (17 g; 43%), b.p. 60–72° (*ca.* 0.3 mm). This was redistilled to give 14 g (35%) of **6**, b.p. 45–56° (0.25 mm). Crystallization was effected by dissolving the liquid in pentane and leaving the solution at −20° for a few hours. This gave **6** as a pale yellow–green solid (12.5 g, 31%), m.p. 31–35°; recrystallization gave virtually colorless prisms, m.p. 35–36°; λ_{max} 5.80, 5.85 μ; λ_{max} (C_6H_{14}) 281 (ε 35), 290 (sh, ε 31), 346 (ε 17) mμ (end absorption; ε 370 at 220 mμ); $\delta(CCl_4)$ 2.1–2.8 (m, 8 H), 5.6–6.0 (m, 2 H); *m/e* 138.

Anal. Calcd. for $C_8H_{10}O_2$: C, 69.54; H, 7.30. Found: C, 69.25; H, 7.31.

Reaction of 1,2-Dibromo-cis-5-cyclooctene with Dimethyl Sulfoxide and Collidine. Formation of 6

1,2-Dibromo-*cis*-5-cyclooctene was prepared by treating *cis-cis*-1,5-cyclooctadiene with bromine as described by Willstätter and Veraguth (8). The product was a colorless, very air-sensitive liquid, b.p. 104–105° (2 mm) (lit. (8) b.p. 142–143° (14 mm)); $\delta(CCl_4)$ 1.5–3.1 (m, 8 H), 4.4–4.9 (m, 2 H), 5.5–5.9 (m, 2 H).

1,2-Dibromo-*cis*-5-cyclooctene (415 mg, 1.55 mmol), collidine (2 ml), and dimethyl sulfoxide (5 ml) (17) were heated at 125° under nitrogen for 24 h. The very dark mixture was poured into an equal volume of water and the mixture was extracted with dichloromethane. The dichloromethane extracts were washed successively with dilute hydrochloric acid, aqueous sodium bicarbonate, and water. The organic layer was dried and evaporated to give a mobile orange liquid (88 mg); λ_{max} 5.75, 5.81, 5.86, 6.01 μ. Vapor phase chromatography (10% NPGS on Chromosorb P, 10 ft × 0.25 in. copper column, temperature programmed from 150–220° at 5.9°/min) showed more than nine major peaks. The component with retention time identical with that of **6** was collected and shown to be **6** by i.r. spectral comparison.

Reaction of 6 with o-Phenylenediamine. Formation of 8

The enedione **6** (1.00 g, 7.25 mmol), *o*-phenylenediamine (0.784 g, 7.24 mmol), and acetic acid (18 ml) were heated on the steam bath for 1 h. Water (*ca.* 60 ml) was added to the hot solution until it was slightly cloudy, and the solution was allowed to cool. The solution deposited **8** as almost colorless needles (1.33 g, 87.5%), m.p. 118–119°; δ 2.45–2.9 (m, 4 H), 3.1–3.5 (m, 4 H), 5.45 (m, 2 H), 7.4–8.1 (m, 4 H).

Anal. Calcd. for $C_{14}H_{14}N_2$: C, 79.96; H, 6.71; N, 13.32. Found: C, 80.12; H, 6.69; N, 13.31.

Reaction of 6 with Bromine. Formation of 9a or b

Bromine (236 mg, 1.47 mmol) in carbon tetrachloride (1 ml) was added to the enedione (200 mg, 1.45 mmol) in carbon tetrachloride (1 ml) at −30°. The solution was allowed to warm to room temperature, during the course of which the orange color of the bromine faded. The solution was evaporated at 30° to give a viscous, light amber oil (430 mg). This was subjected to preparative t.l.c.; from the main band there was obtained the dibromide **9***a* or *b* (173 mg, 40%), m.p. 70–72°. Recrystallization from ether gave colorless prisms, m.p. 77–77.5°; λ_{max} 5.76, 9.25, 9.75, 10.36 μ; $\delta(CCl_4)$ 1.7–3.1 (m, 8 H), 4.1–4.6 (m, 1 H), 4.6–5.0 (m, 1 H); *m/e* 296, 298, 300.

Anal. Calcd. for $C_8H_{10}Br_2O_2$: C, 32.24; H, 3.38; Br, 53.63. Found: C, 32.43; H, 3.45; Br, 54.01.

Ketalization of 6.[5] *Formation of 11, 12, and 13*[6] *and their Reconversion to 6*

(a) Monoketal 11

The enedione **6** (2.00 g, 14.5 mmol) was dissolved in

[5]See, also, Table 1.

[6]See Table 2 for spectra of compounds **11**, **12**, and **13**.

Can. J. Chem. Downloaded from www.nrcresearchpress.com by 210.87.254.6 on 09/05/12
For personal use only.

acetone ethylene ketal (18) (7.5 g, 72.5 mmol) in benzene (10 ml), and boron trifluoride etherate (0.5 ml) was added. The mixture was allowed to stand at 25° for 5 h, when v.p.c. (3% SE-30 on Chromosorb P, 10 ft × 0.25 in. copper column, 200°) indicated it to consist of the enedione **6**, the monoketal **11**, and the diketal **12**, in the ratio 14:65:21. The reaction mixture was poured into aqueous 5% sodium bicarbonate, and the mixture was extracted twice with dichloromethane. The extracts were shaken once with brine, dried, and evaporated to give a yellow oil (2.35 g). Recrystallization from dichloromethane–hexane gave sticky, off-white platelets which were sublimed at 60° (0.01 mm) to give the monoketal **11** as a snow white solid (689 mg, 26%), m.p. 58–62°. Resublimation gave short needles, m.p. 63.5–64.5°.

Anal. Calcd. for $C_{10}H_{14}O_3$: C, 65.91; H, 7.74. Found: C, 65.79; H, 7.61.

The monoketal **11** was unaffected by treatment with acetone containing catalytic amounts of boron trifluoride etherate or hydrochloric acid, but could be converted to the enedione **6** by treatment with aqueous acid (*vide infra*).

(b) Diketal ***12***

In a 500-ml, two-necked, round-bottomed flask fitted with a glass stopper and a Soxhlet extractor holding calcium hydride were placed the enedione **6** (19.48 g, 0.141 mol), ethylene glycol (53.59 g, 0.86 mol), *p*-toluenesulfonic acid (1.0 g), and dichloromethane (300 ml). The mixture was heated at reflux, and the reaction was monitored by withdrawing aliquots and quickly replacing the stopper; the aliquots were subjected without work-up to v.p.c. analysis (3% SE-30 on Chromosorb P, 10 ft × 0.25 in. copper column, 200°). After 12 days, more *p*-toluenesulfonic acid (1.0 g) was added, and after 14 days, a further 1-g portion was added. After 16 days the product mixture consisted of the monoketal **11**, diketal **12**, and diketal **13** in the ratio 7:91:2. The mixture was concentrated to 80 ml by distillation. The concentrate was shaken once with saturated aqueous sodium bicarbonate (80 ml) and once with water (80 ml) and the organic layer was dried. The resulting amber solution was passed through a column of basic alumina (Woelm, activity 1; 35 g, 6.5 × 3 cm) to give an almost colorless solution that was evaporated to give 27.8 g (87%) of diketal **12** (92% purity (v.p.c.)) as a pale yellow oil which soon crystallized. Recrystallization from hexane gave 24.4 g (76%) of **12**, m.p. 67.5–68°.

Anal. Calcd. for $C_{12}H_{18}O_4$: C, 63.70; H, 8.02; O, 28.29. Found: C, 64.03; H, 7.94; O, 28.59.

The diketal **12** could be readily converted to the monoketal **11** as follows. The diketal (50 mg), 4 *N* hydrochloric acid (6 ml) and ether (7 ml) were stirred at 23°. The reaction was monitored by withdrawing aliquots of the upper, ethereal layer, running these through a little magnesium sulfate, washing the drying agent with a dry ether, evaporating the combined, dried, ethereal solutions and recording the i.r. spectrum. After 2.5 h, the upper, ethereal layer was removed, and the aqueous layer was extracted once with ether. The combined ethereal solutions were shaken once with water and once with brine, and the organic layer was dried and evaporated to give a colorless oil (37 mg, 92%), the i.r. spectrum of which was identical with that of monoketal **11**. The oil was recrystallized from hexane to give rosettes of colorless elongated prisms (32 mg, 79%), m.p. 63–64°; mixed m.p. with monoketal **11** (m.p. 64–65°), 64–64.5°. The diketal **12** was also readily converted to **11** with acetone containing a little hydrochloric acid or boron trifluoride etherate, as shown by v.p.c. analyses; under these conditions **11** was not converted to the enedione **6** after several days.

The diketal **12** (40 mg), 6 *N* hydrochloric acid (5 ml), and ether (2.5 ml) were stirred at 23°. The reaction was monitored by withdrawing aliquots of the ethereal layer and subjecting them without work-up to v.p.c. analysis (3% SE-30 on Chromosorb P, 10 ft × 0.25 in. copper column, 200°). After 40 min the reaction mixture consisted of the enedione **6** and the monoketal **11** in the ratio 1:99; none of the diketal **12** was detected. After 63 h the ratio of **6** to **11** was 60:40. After 9 days the mixture contained only about 1% of **11**. The ethereal layer was extracted twice with dichloromethane, and the combined dichloromethane and ethereal solutions were washed once with water, dried, and evaporated to give **6** (20 mg, 83%) as a colorless oil which soon crystallized. The i.r. spectrum of this oil was very similar to that of pure **6**. Molecular distillation at 60°/10 mm gave a colorless oil shown to be **6** by i.r. and n.m.r. spectral comparison and by t.l.c. and v.p.c. analysis.

(c) Diketal ***13***

In a 100-ml, two-necked, round-bottomed flask fitted with a glass stopper and a Soxhlet extractor holding Linde type 4A molecular sieves, were placed the enedione **6** (1.00 g, 7.25 mmol), ethylene glycol (1.02 g, 16.4 mmol), *p*-toluenesulfonic acid (50 mg), and dichloromethane (70 ml). The mixture was heated at reflux, and the reaction was monitored by withdrawing a few drops of the solution and quickly replacing the stopper; the aliquot was evaporated and its i.r. spectrum was compared with that of a zero-time aliquot. After 71 h, the decrease in intensity of the carbonyl-stretching band appeared to have ceased. More ethylene glycol (0.5 g) and *p*-toluenesulfonic acid (50 mg) were added, and heating was continued. After 117 h, the carbonyl band was very weak. The nearly colorless solution was shaken with 70 ml of saturated aqueous sodium bicarbonate, and the organic layer was washed twice with water, dried, and evaporated to give a mushy, light yellow solid (1.27 g); λ_{max} 5.80 (vw), 8.5, 9.1, 9.2, 9.3 μ. Recrystallization from hexane gave diketal **13** as colorless platelets (211 mg, 13%), m.p. 118–121°. Further recrystallization gave **13**, m.p. 121–122°.

Anal. Calcd. for $C_{12}H_{18}O_4$: C, 63.70, H, 8.02. Found: C, 63.55; H, 7.92.

When the diketal **13** (3 mg) was dissolved in acetone (0.5 ml) and concentrated hydrochloric acid (1 drop) was added, t.l.c. indicated that comparable amounts of **13** and the enedione **6** were present after 5 h. Another drop of hydrochloric acid was added after 24 h. After 43 h at 23°, t.l.c. showed essentially only one spot, corresponding to **6**. The solution was evaporated to give an oil the i.r. spectrum of which was virtually identical with that of **6**. Treatment of **13** with acetone containing a catalytic quantity of boron trifluoride etherate also effected conversion to **6**.

Thioketalization of ***6****. Formation of* ***14***

A solution of **6** (103 mg, 0.75 mmol) in anhydrous ether (20 ml) was treated with 1,2-ethanedithiol (0.70 ml, 8.2 mmol) and boron trifluoride etherate (4 ml). After the mixture had stood at room temperature for 44 h it was diluted with ether and washed with dilute aqueous sodium hydroxide and water. The ethereal solution was dried and

Can. J. Chem. Downloaded from www.nrcresearchpress.com by 210.87.254.6 on 09/05/12
For personal use only.

evaporated to give **14** as a pale yellow viscous oil (140 mg, 88%). Trituration with hexane–dichloromethane in a Dry Ice bath gave a solid, which was crystallized from hexane–ether to give colorless needles, m.p. 48–49°; λ_{max} 5.88 μ; δ 2.0–3.0 (m, 8 H), 3.23 (s, 4 H), 5.65 (m, 2 H); *m/e* 214.

Anal. Calcd. for $C_{10}H_{14}OS_2$: C, 56.03; H, 6.58; S, 29.92. Found: C, 56.00; H, 6.34; S, 29.96.

Extension of the reaction time to 116 h at room temperature or 70 h at reflux did not lead to further reaction of the monothioketal.

Bromination of ***12*** *with Pyridinium Perbromide or Bromine. Formation of* ***15***

In a 10-ml Erlenmeyer flask were placed the diketal **12** (200 mg, 0.885 mmol), pyridinium perbromide ("pyridinium hydrobromide perbromide") (283.5 mol), and hexane (6 ml). The flask was stoppered and the mixture was stirred at 23° for 70 min, during the course of which the red color of the perbromide faded. When the contents of the flask had become almost colorless, starch–iodide paper showed the absence of perbromide. The mixture was filtered and the pyridinium bromide (146 mg, 104%) was washed well with hexane. The combined hexane solutions were concentrated and warmed to dissolve the solid that separated. On standing the solution deposited **15** as colorless needles (266 mg, 94%), m.p. 76–77.5°; λ_{max} 9.48 μ; δ 1.7–2.6 (m, 8 H), 3.3–3.6 (m, 2 H), 3.6–4.4 (m, 7 H), 4.4–4.8 (m, 1 H); *m/e* 384, 386, 388.

Anal. Calcd. for $C_{12}H_{18}Br_2O_4$: C, 37.33; H, 4.70; Br, 41.40. Found: C, 37.14; H, 4.84; Br, 41.60.

When **12** was treated with bromine in carbon tetrachloride, evaporation of the solution gave an oil, whose i.r. spectrum was virtually identical with that of **15**.

Dehydrobromination of ***15****. Formation of* ***16***

In a 50-ml Erlenmeyer flask were placed **15** (386 mg, 1.00 mmol), potassium *t*-butoxide (229 mg, 2.04 mmol), and ether (20 ml). The flask was stoppered and the mixture was stirred at 23° for 30 min, when t.l.c. indicated that no starting material was present. The mixture was washed with water (20 ml) and with brine (50 ml), dried, and evaporated to give **16** (297 mg, 98%) as a colorless oil which soon crystallized. Recrystallization from hexane gave colorless needles (182 mg, 61%), m.p. 81–82°; λ_{max} 6.13 (m), 9.36 (sh), 9.44 μ; δ 1.6–2.8 (m, 8 H), 3.7–4.2 (m, 6 H), 4.41 (d, $J = 14$ Hz, 1 H), 4.6–4.9 (m, 1 H), 6.64 (dd, $J = 6.5$, 14 Hz, 1 H); *m/e* 304, 306.

Anal. Calcd. for $C_{12}H_{17}BrO_4$: C, 47.23; H, 5.62; Br, 26.19. Found: C, 47.13; H, 5.56; Br, 26.37.

Hydrolysis of ***15****. Formation of* ***17***

Compound **15** (300 mg), methanol (10 ml), and 5 *N* hydrochloric acid (5 ml) were heated at reflux. The reaction was monitored by withdrawing aliquots, evaporating them, evacuating at < 1 mm to remove water, and recording the i.r. spectra and thin layer chromatograms of the residues. After 48 h, 3 ml of concentrated hydrochloric acid was added. After 5 days, t.l.c. showed mainly one spot, of lower mobility than **15**. Aqueous work-up gave **17** as a colorless oil (137 mg, 75%). Crystallization from dichloromethane–hexane gave colorless prisms, m.p. 91–100°; on recrystallization the melting point varied erratically, although it was always in the range 80–100°. The compound showed one spot on t.l.c. Sublimation at 90° (0.01 mm) gave a colorless solid, m.p. 75–81°; λ_{max} 2.95 (m), 5.83 μ; δ 1.7–3.0 (m, 8 H), 4.0–5.0 (m, *ca.* 3 H); *m/e* 234, 236.

Hydrolysis of ***16****. Formation of Acetaldehyde and* ***17***

In a 50-ml two-necked flask fitted with a nitrogen inlet tube and a condenser were placed **16** (315 mg, 1.03 mmol), methanol (10 ml), and 5 *N* hydrochloric acid (5 ml). The mixture was heated at reflux for 2.5 h while a slow stream of nitrogen was passed through the flask and the condenser into two testtubes, each holding a solution of 2,4-dinitrophenylhydrazine (200 mg, 1.0 mmol) in methanol (8 ml) containing concentrated sulfuric acid (20 drops). Yellow needles were deposited in the first, but not the second, of these tubes. After 1.5 h the tubes were interchanged, but no solid was deposited in the tube that held the clear dinitrophenylhydrazine solution after a further 1 h; however, t.l.c. showed that acetaldehyde 2,4-dinitrophenylhydrazone was present in solution. The yellow needles (93 mg), m.p. 147–149°, were collected by filtration. Recrystallization from methanol gave yellow needles, m.p. 166.5–168°, identified as acetaldehyde 2,4-dinitrophenylhydrazone by mixed m.p. 167–168° with an authentic sample (m.p. 167–168°), and by i.r. spectral and t.l.c. comparison. Further acetaldehyde 2,4-dinitrophenylhydrazone (132 mg; total yield of crude product, 97%) could be isolated by aqueous work-up of the filtrate from the tube containing the crystalline product and the clear solution from the other tube.

Aqueous work-up of the reaction mixture from the hydrolysis of **16** gave **17** as a turbid oil (236 mg, 98%). Crystallization from dichloromethane–hexane gave colorless prisms, m.p. 83–95°; the m.p. varied erratically on further crystallization, but remained in the range 80–95°. This compound was identical with that obtained above by hydrolysis of the dibromide **15**.

Bromination of ***12*** *with N-Bromosuccinimide or 1,3-Dibromo-5,5-dimethylhydantoin. Formation of* ***19***

The diketal **12** (505 mg, 2.23 mmol), *N*-bromosuccinimide (829 mg, 4.65 mmol), azobisisobutyronitrile (26 mg), and carbon tetrachloride (25 ml) were heated at reflux under a drying tube for 1 h. The mixture was allowed to cool and the opalescent solution was filtered through a plug of glass wool. The filtrate was evaporated, and the residue was freed of β-bromopropionyl isocyanate (19) at 23° (0.1 mm). The resulting colorless oil was swirled with carbon tetrachloride, and the cloudy solution was passed through a short column of basic alumina (Woelm activity, grade 1; 5 g, 10 × 0.7 cm). The eluate was evaporated to give the bromo compound **19** as a colorless oil (501 mg, 74%) that partially crystallized on standing. Recrystallization from hexane gave colorless prisms, m.p. 102–103°; δ 1.45–3.0 (m, 6 H), 3.8–4.3 (m, 8 H), 4.8–5.55 (m, 1 H), 5.6–6.0 (m, 2 H); *m/e* 304, 306.

Anal. Calcd. for $C_{12}H_{17}BrO_4$: C, 47.23; H, 5.62; Br, 26.19. Found: C, 47.14; H, 5.52; Br, 26.24.

Similar treatment of **12** with 1,3-dibromo-5,5-dimethylhydantoin and azobisisobutyronitrile in hexane also gave **19**. With this reagent, as with *N*-bromosuccinimide, the yields of **19** were very variable, and were considerably reduced when the scale of the reaction was increased. Chromatography of a crude reaction product mixture that was shown by p.m.r. spectroscopy to contain a low proportion of **19** was carried out on basic alumina (Woelm activity, grade 1) in carbon tetrachloride. Elution with this solvent followed

by 10–50% dichloromethane in carbon tetrachloride gave in addition to **19**, the dibromo compound, **15***a* (or *b*), obtained from the reaction of **12** with pyridinium perbromide, and another dibromo compound, **15***b* (or *a*), which was obtained as colorless broad needles, m.p. 80–81°, after crystallization from hexane; δ 1.7–2.6 (m, 8 H), 3.3–3.6 (m, 2 H), 3.8–4.5 (m, 8 H).

Anal. Calcd. for $C_{12}H_{18}Br_2O_4$: C, 37.33; H, 4.70; Br, 41.40. Found: C, 37.48; H, 4.62; Br, 41.30.

Dehydrobromination of ***19****. Formation of* ***20***

A 50-ml, two-necked flask fitted with a septum cap and a nitrogen inlet tube connected to a mercury bubbler was flame-dried at 20 mm, and the hot flask was filled with nitrogen by admitting nitrogen and evacuating three times. In the flask were quickly placed a magnetic stirring bar and potassium *t*-butoxide (355 mg, 3.18 mmol). The flask was again evacuated and filled with nitrogen twice. Dimethyl sulfoxide (Fisher Certified, dried with molecular sieves; 10 ml) was injected through the septum cap and the mixture was stirred to dissolve the potassium *t*-butoxide, and then the bromo compound **19** (674 mg, 2.21 mmol) in dimethyl sulfoxide (10 ml) was injected. The reaction mixture was stirred under nitrogen at 23° for 12 h. Aqueous work-up gave the crude diene **20** as a yellow oil (390 mg, 79%). This was chromatographed on a column of basic alumina (Woelm activity, grade 1; 9.5 × 1.0 cm). Elution with benzene gave **20** as a colorless, mobile liquid (238 mg, 48%). The crude diene could also be purified by molecular distillation at 80° (0.01 mm). This gave a colorless mobile liquid; λ_{max} 6.14 μ (w); λ_{max} (C_6H_{14}) 230 mμ (ε 4300); δ (CCl_4) 2.1–2.7 (4 H), 3.8–4.05 (m, 8 H), 5.65–6.0 (m, 4 H); *m/e* 224.

Anal. Calcd. for $C_{12}H_{16}O_4$: C, 64.27; H, 7.19. Found: C, 64.23; H, 7.48.

When **19** was subjected to v.p.c. (10% SE-30 on Chromosorb P, 10 ft × 0.25 in. copper column, 200°) it decomposed, giving rise to four peaks. The material corresponding to the peak of shortest retention time (28%) was collected. It was shown to be **20** by i.r. spectral, v.p.c., and t.l.c. comparison.

1,2-Cyclooctanedione Diketal ***21***

The diketal **12** (207 mg) in ethyl acetate (3 ml) was hydrogenated over 10% palladium/charcoal at room temperature and atmospheric pressure. After 2.5 h 1 *M* equiv of hydrogen had been taken up and there was no further uptake. Filtration and evaporation of the solution followed by evacuation at 0.01 mm for 5 min gave **21** (169 mg, 81%) as a colorless oil; λ_{max} 8.46, 9.22, 9.54, 10.52 μ; δ 1.4–2.0 (m, 12 H), 3.7–4.0 (m, 8 H).

Anal. Calcd. for $C_{12}H_{20}O_4$: C, 63.13; H, 8.83. Found: C, 63.28; H, 8.90.

Hydrogenation of the diketal **20** under the same conditions gave a colorless oil (87%) with an i.r. spectrum very similar to that of the product from **12**, but with an additional weak band at 5.74 μ. Preparative v.p.c. (10% SE-30 on Chromosorb P, 200°) gave a product that was shown to be **21** by i.r. and p.m.r. spectral comparison and by mixed v.p.c. and t.l.c. analysis.

Treatment of 1,2-cyclooctanedione with ethylene glycol and *p*-toluenesulfonic acid in dichloromethane as for the ketalization of **6** to **12** gave a product mixture that was shown by v.p.c. analysis to consist largely of one component. Isolation of this by preparative v.p.c. (10% SE-30 on Chromosorb P, 200°) gave a colorless oil that was shown to be **21** as before.

We thank the National Research Council of Canada for generous support of this work. One of us (E.G.L.) gratefully acknowledges the awards of an Alcan Jamaica Independent Overseas Scholarship, a Shell Canada Fellowship, a Special Open University of Toronto Fellowship, and an NRCC Scholarship.

1. (*a*) P. YATES and E. G. LEWARS. Can. J. Chem. **48**, 796 (1970); (*b*) P. YATES and E. G. LEWARS. Chem. Commun. 1537 (1971).
2. P. YATES, E. G. LEWARS, and P. H. MCCABE. Can. J. Chem. **48**, 788 (1970).
3. M. STILES and A. J. LIBBEY, JR. J. Org. Chem. **22**, 1243 (1957).
4. D. SWERN. Org. React. **7**, 378 (1953).
5. P. LAFONT and H. MENAND. Fr. Pat. 1 294 313 (1962); Chem. Abstr. **57**, 16437 (1962).
6. A. C. COPE, M. M. MARTIN, and M. A. MCKERVEY. Quart. Rev. **20**, 119 (1966).
7. J. D. ALBRIGHT and L. GOLDMAN. J. Am. Chem. Soc. **89**, 2416 (1967).
8. R. WILLSTÄTTER and H. VERAGUTH. Ber. **38**, 1975 (1905).
9. W. G. DAUBEN and W. W. EPSTEIN. J. Org. Chem. **24**, 1595 (1959).
10. W. H. T. DAVISON. J. Chem. Soc. 2456 (1951).
11. N. J. LEONARD, A. J. KRESGE, and M. ŌKI. J. Am. Chem. Soc. **77**, 5078 (1955).
12. N. J. LEONARD and P. M. MADER. J. Am. Chem. Soc. **72**, 5388 (1950).
13. H. BUDZIKIEWICZ, C. DJERASSI, and D. H. WILLIAMS. Mass spectrometry of organic compounds. Holden-Day, San Francisco. 1967. p. 266.
14. (*a*) B. FUCHS. Tetrahedron Lett. 1747 (1970); (*b*) A. I. COHEN, I. T. HARPER, and S. D. LEVINE. Chem. Commun. 1610 (1970).
15. R. H. JAEGER and H. SMITH. J. Chem. Soc. 160 (1955).
16. N. PAPPAS and H. R. NACE. J. Am. Chem. Soc. **81**, 4556 (1959).
17. D. N. JONES and M. A. SAEED. J. Chem. Soc. 4657 (1963).
18. H. J. DAUBEN, JR., B. LÖKEN, and H. J. RINGOLD. J. Am. Chem. Soc. **76**, 1359 (1954).
19. H. W. JOHNSON, JR. and D. E. BUBLITZ. J. Am. Chem. Soc. **79**, 753 (1957); J. C. MARTIN and P. D. BARTLETT. J. Am. Chem. Soc. **79**, 2533 (1957).

Can. J. Chem. Downloaded from www.nrcresearchpress.com by 210.87.254.6 on 09/05/12
For personal use only.

Primary Yields and Mechanisms in the Radiolysis of N_2O from High Intensity Electron Pulse Irradiations of N_2O–O_2 Mixtures[1]

C. WILLIS,[2] A. W. BOYD, AND P. E. BINDNER

Physical Chemistry Branch, Chalk River Nuclear Laboratories, Atomic Energy of Canada Limited, Chalk River, Ontario

Received November 15, 1971

The yields of N_2, O_2, NO, and O_3 have been measured from the Febetron radiolysis of N_2O–O_2 mixtures with and without SF_6. A mechanism consistent with the yields from 0–100% O_2 and with known ionic abundances and reaction rate data has been derived. The major features of this mechanism are both dissociative neutralization of N_2O^+ and excitation of N_2O to give $N_2(X^1\Sigma)$ and $O(^1D)$ and smaller amounts of $N_2(B^3\Pi)$ and $O(^3P)$. The large yields of NO and N_2 observed are mainly due to reaction of $O(^1D)$ with N_2O to give both N_2 and O_2 and NO.

Les rendements en N_2, O_2 et NO et O_3 ont été mesurés à partir de la radiolyse Febetron des mélanges de N_2O–O_2 avec et sans SF_6. Un mécanisme tenant compte des rendements de 0 à 100% en O_2, des abondances ioniques connues et des données cinétiques de la réaction, a été déduit. Les caractéristiques majeures de ce schéma sont à la fois une neutralisation dissociative de N_2O^+ et une excitation de N_2O pour donner $N_2(X^1\Sigma)$ et $O(^1D)$ ainsi que des quantités plus faibles en $N_2(B^3\Pi)$ et $O(^3P)$. Les rendements élevés en NO et N_2 obtenus sont dus essentiellement à la réaction de $O(^1D)$ avec N_2O qui conduit à N_2, O_2 et NO.

Canadian Journal of Chemistry, **50**, 1557 (1972)

Introduction

The radiolytic behavior of nitrous oxide has been extensively investigated (1–11) but the identities and yields of the primary species and the mechanisms leading to the stable products are still uncertain. Nitrous oxide dissociates to give nitrogen atoms, oxygen atoms, nitrogen molecules, and nitric oxide molecules in various energy states but because of their high reactivity with N_2O most of these species are not easily scavenged.

A second more general problem is that of determining which ionic reactions occur. In gas phase radiolysis at conventional low dose rates (10^{16}–10^{20} eV g^{-1} s^{-1}) a variety of ion–molecule reactions often occur before charge neutralization so that the primary ionic species cannot easily be related to product yields. The ionic behavior of nitrous oxide is further complicated by dissociative electron attachment.

We have previously shown (11, 12) that at the very high dose rates (10^{26}–10^{28} eV g^{-1} s^{-1}) from Febetron pulses the reduction in ion-lifetime with respect to neutralization eliminates many ion–molecule reactions and allows identification of the neutralization products of the primary ions. In this work the reduction at high dose rates in the stable product yields on the addition of SF_6 is assumed to be due to the suppression of dissociative neutralization of the primary positive ions. This has been shown to be the most probable behavior of SF_6 in a number of gaseous systems. We have determined the reduction in the product yields of N_2O on the addition of SF_6 at high dose rates (11, 13). These results combined with the mass spectrum of N_2O (from conventional mass spectrometry) and ion–molecule reaction rate data do give some information as to the products of the neutralization reactions but not enough to obtain the yields of the primary species.

The approach taken in the present work was to measure the ozone yield in N_2O–O_2 mixtures with and without SF_6. Although this is very complicated in continuous irradiation it can be done easily for single Febetron pulses. This allows us to distinguish $O(^1S)$, $O(^1D)$ and $O(^3P)$ oxygen atoms. It is known that both singlet states react rapidly with N_2O whereas the triplet ground state does not.

These data, taken in conjunction with the extensive work of Young, Black, and Slanger (14–19) on the photochemistry of N_2O and on the behavior of the various species formed, have allowed us to present a fairly complete mechanism for the radiolytic behavior of N_2O and N_2O–O_2 mixtures and also to add to our understanding of the radiolytic behavior of O_2.

[1]AECL No. 4175.

[2]Present address: Chemistry Department, University of the West Indies, Kingston, Jamaica.

Can. J. Chem. Downloaded from www.nrcresearchpress.com by 210.87.254.5 on 09/05/12
For personal use only.

Can. J. Chem. Downloaded from www.nrcresearchpress.com by 210.87.254.5 on 09/05/12
For personal use only.

Experimental

Irradiations

The irradiation source used, a Febetron 705,[3] has been described previously (20, 21). For the determination of nitrogen, oxygen, and nitrite yields the samples were irradiated in quartz cells (22). The ozone yields were determined using a stainless steel optical cell with internal mirrors and a conventional optical detection system (23). The quartz cells had volumes of 80 ml and the average dose in these was 10^{20} eV g^{-1}. The volume of the optical cell was 1 l and the average dose 10^{19} eV g^{-1}.

Dosimetry

The dose in the quartz cells was determined by irradiations of pure N_2O at 1 atm pressure taking $G(N_2) = 12.4 \pm 0.3$. This value has previously been determined absolutely for the conditions of the experiments by adiabatic calorimetry (24, 25). The dose in the optical system was determined by irradiations of pure oxygen between 200 and 600 Torr taking $G(O_3) = 12.8 \pm 0.6$ (26–29).

Analyses

N_2, O_2

These were determined for pure N_2O using a McLeod gauge and a calibrated CEC 610 mass spectrometer. In the N_2O–O_2 mixtures, nitrogen was determined by gas chromatography using a 15C Loenco gas chromatograph with a Linde 5X molecular sieve column and thermal conductivity detection.

NO, NO_2

The NO formed in both N_2O and N_2O–O_2 was converted to NO_2 before analysis by freezing in liquid N_2. The NO_2 was measured using the method of Shinn (30). Our use of this method has been previously described (31).

O_3

The ozone from N_2O–O_2 mixtures was determined optically at 254 nm (32). The concentration of ozone in the optical cell was measured at three different times after the pulse: at ~10 ms, this gave the ozone yields, $G(O_3)_0$, prior to any appreciable reaction with NO; at ~10 s, this gave the ozone yield, $G(O_3)_i$, after all the NO in the system had reacted; and at ~30 min, this gave the ozone yield, $G(O_3)_f$, after the reaction with NO_2 was complete but before any appreciable thermal decomposition of O_3.

[1] $$NO + O_3 \rightarrow NO_2 + O_2$$
$$k_1 = 1.25 \times 10^{-14} \text{ cm}^3 \text{ molecule}^{-1} \text{ s}^{-1} \quad (33)$$

[2] $$NO_2 + O_3 \rightarrow NO_3 + O_2$$
$$k_2 = 7 \times 10^{-17} \text{ cm}^3 \text{ molecule}^{-1} \text{ s}^{-1} \quad (33)$$

Materials

The N_2O, O_2, and SF_6 were all Matheson C.P. grade. For the N_2, O_2, and nitrite determinations the N_2O and SF_6 were freed of permanent gases by several freeze–pump–thaw cycles. No difference in O_3 yields was observed using both purified N_2O and SF_6 and these gases taken directly from the tank. The reagents used in the nitrite determination were aqueous solutions of Fisher (Reagent grade) *N*-naphthylethylenediamine dihydrochloride 0.1%, Eastman Organic Chemicals (C.P.) sulfanilamide 0.2%, and Anachemia (Reagent Grade) HCl 5 *N* solution.

[3]Manufactured by Field Emission Corporation, McMinnville, Oregon, U.S.A.

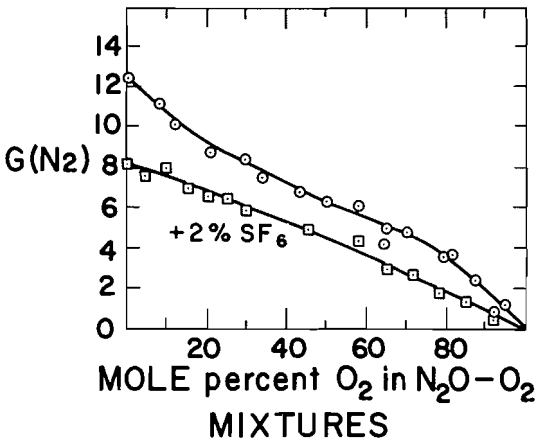

FIG. 1. Nitrogen yields from the Febetron radiolysis of N_2O–O_2 mixtures at 2×10^{27} eV g^{-1} s^{-1}, 700 Torr, and 25 °C.

Results

N_2 Yields

The nitrogen yield from pure N_2O is $G(N_2) = 12.4$ and this is reduced to $G(N_2) = 8.1$ on the addition of SF_6. The nitrogen yields in N_2O–O_2 mixtures are shown in Fig. 1.

O_2 Yield

The residual yield of O_2 in pure N_2O is $G(O_2)_r = 2.1 \pm 0.2$ as determined by mass spectrometry and gas chromatography. This oxygen yield is measured after all nitric oxide has reacted to give nitrogen dioxide.

[3] $$2NO + O_2 \rightarrow 2NO_2$$

[3*a*] $$NO + O \rightarrow NO_2$$

This oxygen yield, taken in conjunction with the nitrogen yield, by mass balance for the three product system N_2, O_2, NO_2 gives $G(NO_2)_r = 5.5$.

$$G(NO_2)_r = \tfrac{2}{3}(G(N_2) - 2G(O_2)_r)$$

Assuming all the nitrogen dioxide originates via reaction 3 or 3*a*, the initial oxygen yield formed in the radiolysis can be calculated by mass balance to be $G(O_2)_i = 4.8$.

$$G(O_2)_i = \tfrac{1}{2}(G(N_2) - \tfrac{1}{2}G(NO))$$

where
$$G(NO) = G(NO_2)_r = 5.5$$

In the presence of SF_6 the measured yield of O_2 is $G(O_2)_r \approx 1.0$ and hence for the three product system N_2, O_2, NO the initial yields are $G(O_2)_i \approx 3$, $G(NO) \approx 4$.

Can. J. Chem. Downloaded from www.nrcresearchpress.com by 210.87.254.5 on 09/05/12
For personal use only.

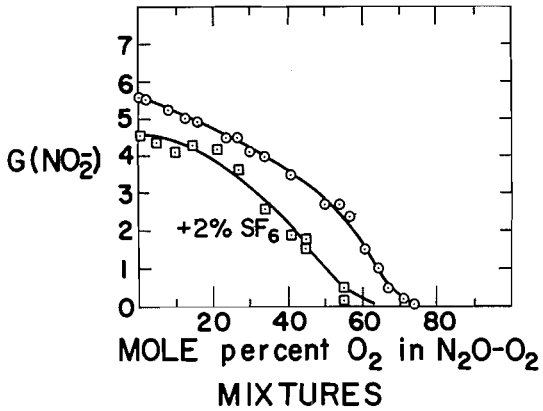

FIG. 2. Nitrite yields from the Febetron radiolysis of N_2O–O_2 mixtures at 2×10^{27} eV g^{-1} s^{-1}, 700 Torr, and 25 °C.

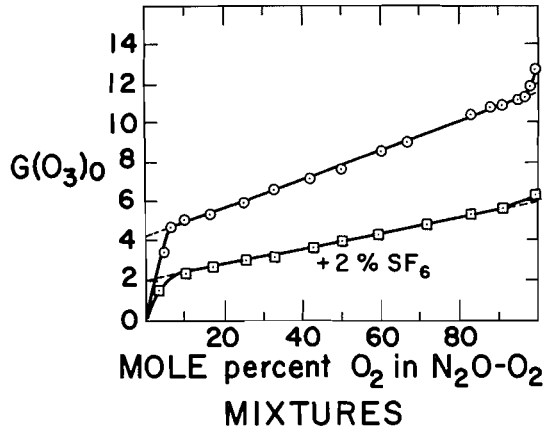

FIG. 4. Initial ozone yields in the Febetron radiolysis of N_2O–O_2 mixtures at 2×10^{26} eV g^{-1} s^{-1}, 700 Torr, and 25 °C.

NO Yields

Assuming no NO_2 is formed initially, the yield of NO from pure N_2O from the analysis of nitrite ion is $G(NO) = 5.6$ in good agreement with that derived from the residual O_2 yield. In N_2O–SF_6 this yield is reduced to $G(NO) = 4.6$ in fair agreement with the O_2 measurements.

In the N_2O–O_2 mixtures we tried to determine the NO yield from both nitrite measurements and the difference in O_3 yields ($G(NO) = G(O_3)_0 - G(O_3)_i$). The results are shown in Figs. 2 and 3. As can be seen the two sets of values do not agree. In the presence of O_3 the NO_2 formed in reaction 1 will react as in reaction 2.

[2] $$NO_2 + O_3 \rightarrow NO_3 + O_2$$

The lower yields obtained by the nitrite method can then be explained by the disappearance of NO_3 in reaction 4

[4] $$NO_3 + NO_2 \rightarrow N_2O_5$$

In the presence of SF_6 neither method appears to be reliable. Again, assuming no NO_2 is formed initially the yields of NO from the O_3 difference measurements $G(NO) \approx 1$ are much lower than those obtained from nitrite measurements and this implies that SF_6 interferes with the analytical method using O_3 yield differences.

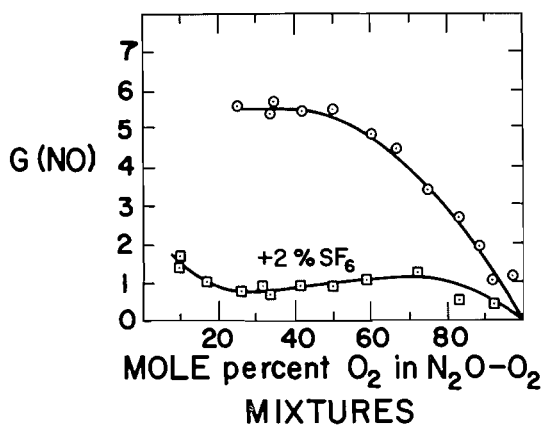

FIG. 3. Nitric oxide yields from the difference in O_3 yields from the Febetron radiolysis of N_2O–O_2 mixtures at 2×10^{26} eV g^{-1} s^{-1}, 700 Torr, and 25 °C.

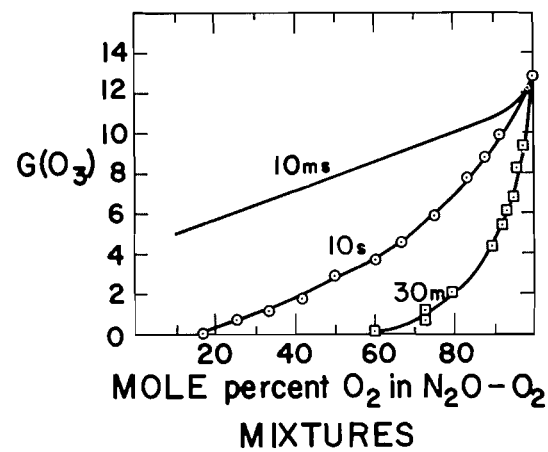

FIG. 5. Ozone yields in the Febetron radiolysis of N_2O–O_2 mixtures at 2×10^{26} eV g^{-1} s^{-1}, 700 Torr, and 25 °C at different times after the pulse.

Can. J. Chem. Downloaded from www.nrcresearchpress.com by 210.87.254.5 on 09/05/12
For personal use only.

TABLE 1. Stable product yields in the radiolysis of N_2O and N_2O–SF_6

Parameter	Value		
	Pure N_2O	$N_2O + SF_6$	ΔG
Dose rate = 10^{26}–10^{27} eV g^{-1} s^{-1}			
$G(N_2)$	12.4±0.3	8.1	4.3
$G(O_2)$	4.8	2.9	1.9
$G(NO)$	5.6	4.6	1.0
$G(-N_2O)$	15.2	10.4	4.8
$G(O_3)_0$ (extrapolated)	4.3	1.9	2.4
Dose rate = 10^{16} eV g^{-1} s^{-1}			
$G(N_2)$	10.0	8.1	1.9
$G(O_2)$	3.8	3.2	0.6
$G(NO)$	5.1	3.3	1.8
$G(-N_2O)$	12.5	9.7	2.8

The ozone yields determined from measurement of the ozone concentration at 10 ms after the electron pulse, $G(O_3)_0$, are shown in Fig. 4. As can be seen, the intercepts with the yield axis for pure N_2O extrapolated from intermediate concentrations of O_2 are 4.3 G units in the absence and 1.9 G units in the presence of SF_6.

Figure 5 gives the ozone yields at the three times described above. Using kinetic photometry the decrease in the ozone concentration as a function of time due to reaction with NO_2 was measured in the range 10–1000 s. The order of the disappearance reaction was greater than 1 and the half-life was ~200 s. The rate appeared to be inversely proportional to pressure over the range 300–1000 Torr.

Discussion

The discussion of the results will be in two parts, pure N_2O and N_2O–O_2 mixtures.

Pure N_2O

Our high dose rate yields of stable products from pure N_2O are given in Table 1 along with the yields obtained at low dose rates by Takao and Shida (8). Their values for pure N_2O are in good agreement with those of Jones and Sworski (5). Also included in this table are the values of $G(O_3)_0$ extrapolated from intermediate concentrations of oxygen to pure N_2O. As will become evident from the following discussion, this extrapolated ozone yield is considered to be a direct measure of the yield of oxygen atoms in a ^3P state.

To use the values from Table 1 to determine the yields of primary species and the mechanisms in N_2O radiolysis it is necessary to consider the possible ionic and neutral species. Reactions of ionic species and neutral species relevant to both pure N_2O and N_2O–O_2 mixtures are listed in Tables 2 and 3. These will be discussed in detail in the following sections.

Ionic Processes

The energy required to form an ion pair in nitrous oxide is 32.9 eV (34) and hence $G(e^-) = 3.05$. Taking this value in conjunction with mass spectrometrically measured abundances (35), the yields of the primary positive ions are as follows:

[5] $N_2O \rightarrow N_2O^+ + e$ $\quad G = 1.90$

[6] $N_2O \rightarrow NO^+ + N + e$ $\quad G = 0.59$

[7] $N_2O \rightarrow N^+ + NO + e$ $\quad G = 0.25$

[8] $N_2O \rightarrow N_2^+ + O + e$ $\quad G = 0.21$

[9] $N_2O \rightarrow O^+ + N_2 + e$ $\quad G = 0.10$

The low ionization potential of nitric oxide ($I.P.$ $(NO^+) = 9.25$ eV (36)) precludes any charge transfer from this ion to N_2O ($I.P.$ $(N_2O^+) = 12.88$ eV (36)) and we must assume NO^+ ions survive to be neutralized by a negative ion. N^+ ions, formed in reaction 7, will react with N_2O to give NO^+ and N_2, as in reaction 10

[10] $N^+ + N_2O \rightarrow NO^+ + N_2$

N_2^+ ions can react with N_2O in two ways, reactions 11 and 12

[11] $N_2^+ + N_2O \rightarrow NO^+ + N_2 + N$

[12] $N_2^+ + N_2O \rightarrow N_2O^+ + N_2$

O^+ ions can also react in two ways, reactions 13 and 14

[13] $O^+ + N_2O \rightarrow N_2O^+ + O$

[14] $O^+ + N_2O \rightarrow N_2 + O_2^+$

but because of the low yield of O^+ and the low value of k_{14} reaction 14 will be neglected.

These are the only ion–molecule reactions expected to occur in the single pulse, high dose rate radiolysis of pure N_2O. As we have discussed previously (11) the rate constant for the attachment of the electron to N_2O is far too low for this reaction to compete with neutralization even at atmospheric pressure for Febetron dose rates. Similarly any ionic reactions with

TABLE 2. Ionic reactions relevant to N_2O and N_2O–O_2 mixtures

Reaction	Rate constant (cm^3 molecule^{-1} s^{-1})	Reference
$N^+ + N_2O \rightarrow NO^+ + N_2$	5.5×10^{-10}	43
$N_2^+ + N_2O \rightarrow NO^+ + N_2 + N$	4×10^{-10}	43
$N_2^+ + N_2O \rightarrow N_2O^+ + N_2$	5×10^{-10}	44
$O^+ + N_2O \rightarrow N_2O^+ + O$	4×10^{-10}	43
$O^+ + N_2O \rightarrow N_2 + O_2^+$	2×10^{-11}	43
$N_2^+ + O_2 \rightarrow N_2 + O_2^+$	1×10^{-10}	45–49
$N_2^+ + O_2 \rightarrow NO^+ + NO$	$<5 \times 10^{-14}$	46, 50
$N_2^+ + NO \rightarrow N_2 + NO^+$	5×10^{-10}	46, 51
$N^+ + O_2 \rightarrow NO^+ + O$	5×10^{-10}	47, 51
$N^+ + O_2 \rightarrow N + O_2^+$	4.5×10^{-10}	45, 51
$O_2^+ + NO \rightarrow NO^+ + O_2$	7.2×10^{-10}	51
$O^+ + O_2 \rightarrow O_2^+ + O$	2×10^{-11}	45, 52, 53
$N^+ + NO \rightarrow NO^+ + N$	8×10^{-10}	51
$O^+ + NO \rightarrow NO^+ + O$	$\leqslant 2.5 \times 10^{-11}$	51
$O_2^- + O_3 \rightarrow O_3^- + O_2$	3×10^{-10}	54
$O_2^- + NO \rightarrow NO_2^- + O$	$<1 \times 10^{-12}$	55
$O_2^- + N_2O \rightarrow O_3^- + N_2$	$\sim 10^{-11}$	56
$O_2^- + NO_2 \rightarrow NO_2^- + O_2$	2×10^{-10}	57
$O_3^- + NO \rightarrow NO_3^- + O$	1×10^{-11}	54
$O_3^- + NO \rightarrow NO_2^- + O_2$	$<1 \times 10^{-11}$	56
$NO_2^- + O_3 \rightarrow NO_3^- + O_2$	1.8×10^{-11}	58
$O_3^- + NO_2 \rightarrow NO_2^- + O_3$	7×10^{-10}	57
$NO_3^- + NO \rightarrow NO_2^- + NO_2$	$<1 \times 10^{-11}$	59
$NO_2^- + NO_2 \rightarrow NO_3^- + NO$	$\sim 4 \times 10^{-12}$	59
$O_4^- + NO \rightarrow NO_3^- + O_2$	2.5×10^{-10}	59
$N_2O^- + O_2 \rightarrow O_3^- + N_2$	fast	60
$O^- + O \rightarrow O_2 + e$	1.9×10^{-10}	54
$O^- + N \rightarrow NO + e$	2.2×10^{-10}	54
$O^- + O_3 \rightarrow O_3^- + O$	7×10^{-10}	54

products including those suggested by Gorden and Ausloos (4) can be neglected at these dose rates. Thus before neutralization the yields of species from reactions 5–14 should be those given in Table 4.

Consider, now, how the yields of the ionic and neutral species in Table 4 can be related to the product yields in Table 1. The addition of SF_6 will be assumed to suppress dissociative neutralization.

The two positive ions, resulting from primary ionic processes, are NO^+ and N_2O^+. The neutralization of NO^+ by a free electron is certainly dissociative and may give both $N(^2D)$ and $N(^4S)$ nitrogen atoms (37). Considering the energy level diagram of Gilmore (38), the most probable neutralization reactions are

[15] $NO^+ + e \rightarrow N(^2D) + O(^3P)$

[16] $NO^+ + e \rightarrow N(^4S) + O(^1D)$

The $N(^2D)$ atoms will then react with N_2O via reaction 17 and the $O(^1D)$ atoms via reactions 18 and 19.

[17] $N(^2D) + N_2O \rightarrow N_2 + NO$

[18] $O(^1D) + N_2O \rightarrow N_2 + O_2$

[19] $O(^1D) + N_2O \rightarrow 2NO$

The products of the neutralization of N_2O^+ by a free electron are not known nor is a detailed energy level diagram of N_2O available. Possible neutralization reactions are

[20] $N_2O^+ + e \rightarrow N_2(X^1\Sigma) + O(^1D)$ (or $O(^1S)$)

[21] $N_2O^+ + e \rightarrow N_2(B^3\Pi) + O(^3P)$

[22] $N_2O^+ + e \rightarrow N(^2D) + NO(X^2\Pi)$

[23] $N_2O^+ + e \rightarrow N_2(A^3\Sigma) + O(^3P)$

[24] $N_2O^+ + e \rightarrow N(^4S) + NO$

Since $N(^4S)$ will react very rapidly with NO to form $N_2(X^1\Sigma)$ and $O(^3P)$, via reaction 25

[25] $N(^4S) + NO \rightarrow N_2(X^1\Sigma) + O(^3P)$

Can. J. Chem. Downloaded from www.nrcresearchpress.com by 210.87.254.5 on 09/05/12
For personal use only.

TABLE 3. Atom, radical and excited state reactions

Species	Reactant	Products	Rate constant* (cm^3 $molecule^{-1}$ s^{-1})	Reference
$O(^3P)$	$O(^3P) + M$	$O_2 + M$	2×10^{-33}	61
	$N(^4S) + M$	$NO + M$	1×10^{-32}	61, 62
	N_2O		Very slow	63
	$NO + M$	$NO_2 + M$	9×10^{-32}	64, 65
	$O_2 + M$	$O_3 + M$	2.8×10^{-34}	66, 67
			8.9×10^{-34}	68
	N_2		Very slow	33
	O_3	$2O_2$	1×10^{-14}	69
$O(^1D)$	N_2O	$N_2 + O_2$	9×10^{-11}	19, 70
	N_2O	$2NO$	9×10^{-11}	19, 70
	N_2O	$N + NO_2$	$<5 \times 10^{-13}$	19, 70
	N_2O	$O(^3P) + N_2O$	Very slow	19, 70
	NO	$O(^3P) + NO$	1.5×10^{-10}	19
	O_2	$O(^3P) + O_2$	4×10^{-11}	19, 71, 72
	N_2	$O(^3P) + N_2$	5×10^{-11}	72, 73, 75
	O_3	$2O_2$	3×10^{-10}	73
$O(^1S)$	N_2O	$N_2 + O_2$	1.6×10^{-11}	15, 17, 74
	N_2O	$2NO$	1.6×10^{-11}	15, 17, 74
	NO	$O(^1D) + NO$	5.5×10^{-10}	15, 17
	O_2	$O(^1D) + O_2$	5×10^{-13}	15, 17
	N_2	$O(^1D) + N_2$	$<10^{-16}$	15, 17
$N(^4S)$	$N(^4S) + M$	$N_2 + M$	4×10^{-33}	61, 62, 75, 76
	N_2O		Very slow	77
	NO	$N_2 + O(^3P)$	2×10^{-11}	78
	O_2	$NO + O(^3P)$	$1.2 \times 10^{-11} \exp\left(\frac{-3225}{T}\right)$	69, 79–82
	O_3	$NO + O_2$	3.7×10^{-13}	78
$N(^2D)$	N_2O	$N_2 + NO$	3×10^{-12}	15, 18
	NO	$N_2 + O(^3P)$	1.8×10^{-10}	15, 18
	O_2	$NO + O(^3P)$	6.5×10^{-12}	18
	N_2	$N(^4S) + N_2$	$<6 \times 10^{-15}$	18
$N_2(A^3\Sigma)$	N_2O	$2N_2(X^1\Sigma) + O$	Very slow	74, 83
	N_2O	Quenching	6.4×10^{-12}	16
	NO	Quenching	7×10^{-11}	16
	O_2	Quenching	3.8×10^{-12}	16
	N_2	Quenching	$<7 \times 10^{-15}$	16
$N_2(B^3\Pi)$	N_2O	$2N_2(X^1\Sigma) + O(^1S)$ ($N_2 + N + NO$?)	1.6×10^{-10}	16
	N_2O	Quenching	1.6×10^{-10}	16
	NO	Quenching	2.4×10^{-10}	16
	O_2	Quenching	1.1×10^{-10}	16
	N_2	Quenching	2.7×10^{-11}	16

*For 3 body reactions (where M is a reactant), the rate constant units are cm^6 $molecule^{-2}$ s^{-1}.

and since in pure N_2O the only fate of $N_2(A^3\Sigma)$ is deactivation to $N_2(X^1\Sigma)$, reaction 24 is indistinguishable from reaction 23. The neutral species formed in reactions 20–22 and 24 will react as in reactions 17–19 and 26 and 27.

[26] $N_2(A^3\Sigma) + N_2O \rightarrow N_2(X^1\Sigma) + N_2O$

[27] $N_2(B^3\Pi) + N_2O \rightarrow 2N_2(X^1\Sigma) + O(^3P)$

Assuming SF_6 suppresses dissociative neutralization,

[28] $e + SF_6 \rightarrow SF_6^-$

[29] $NO^+ + SF_6^- \rightarrow NO\,(+ SF_6)$

[30] $N_2O^+ + SF_6^- \rightarrow N_2O\,(+ SF_6)$

we can use the difference in yields to determine

Can. J. Chem. Downloaded from www.nrcresearchpress.com by 210.87.254.5 on 09/05/12
For personal use only.

TABLE 4. Ionic and neutral species yields from primary ionic processes (reactions 5–13)

Yield								
e	N_2O^+	NO^+	N_2	NO	O	N	$(-N_2O)$	Reaction
1.9	1.9						1.9	[5]
0.59		0.59				0.59	0.59	[6]
0.25				0.25			0.25	[7]
0.21					0.21		0.21	[8]
0.10			0.10				0.10	[9]
		0.25	0.25				0.25	[10]
		0.09	0.09			0.09	0.09	[11]
	0.12		0.12				0.12	[12]
	0.10				0.10		0.10	[13]
3.05	2.12	0.93	0.56	0.25	0.31	0.68	3.61	Total

TABLE 5. Neutralization reactions in pure N_2O

	Reaction	Yield
[15]	$NO^+ + e \rightarrow N(^2D) + O(^3P)$	a
[16]	$NO^+ + e \rightarrow N(^4S) + O(^1D)$	b
[20]	$N_2O^+ + e \rightarrow N_2(X^1\Sigma) + O(^1D)$	c
[21]	$N_2O^+ + e \rightarrow N_2(B^3\Pi) + O(^3P)$	d
[22]	$N_2O^+ + e \rightarrow N(^2D) + NO$	e
[23]	$N_2O^+ + e \rightarrow N_2(A^3\Sigma) + O(^3P)$	f
[17]	$N(^2D) + N_2O \rightarrow N_2 + NO$	$a + e$
[18]	$O(^1D) + N_2O \rightarrow N_2 + O_2$	$\frac{1}{2}(b + c)$
[19]	$O(^1D) + N_2O \rightarrow 2NO$	$\frac{1}{2}(b + c)$
[27]	$N_2(B^3\Pi) + N_2O \rightarrow 2N_2(X^1\Sigma) + O(^3P)$	d
[26]	$N_2(A^3\Sigma) + N_2O \rightarrow N_2(X^1\Sigma) + N_2O$	f
[29]	$NO^+ + SF_6^- \rightarrow NO\ (+ SF_6)$	
[30]	$N_2O^+ + SF_6^- \rightarrow N_2O\ (+ SF_6)$	

the extent of the various reactions. Table 5 shows a listing of the processes associated with neutralization. From this we can derive the following relationships[4]

$$\Delta G(N_2) = 4.3 = a + \frac{3b}{2} + \frac{3c}{2} + 2d + e + f$$

$$\Delta G(NO) = 1.0 + 0.93 = a + c + 2e$$

$$\Delta G(O(^3P)) = 2.4 = a + b + 2d + f$$

$$\Delta G(N_2O^+) = 2.12 = c + d + e + f$$

$$\Delta G(NO^+) = 0.93 = a + b$$

The equivalent equation for $\Delta G(O_2)$ is not a further equation as it can be considered to have been derived by mass balance. Thus we have 6 unknown parameters and only 5 equations and a unique solution is not possible. The relationships which can be uniquely derived are as follows: from neutralization

$$G(N_2(A^3\Sigma)) = f = 0.37$$

$$G(N_2(B^3\Pi)) = d = 0.55$$

$$G(O(^1D)) = (b + c) = 1.40$$

$$G(N(^2D)) = (a + e) = 0.73$$

and

$$c + e = 1.20$$

As will be shown below, very little $N(^2D)$ is formed from N_2O by direct excitation (less than 1%). If we assume that very little is formed by neutralization reactions, *i.e.* $e \approx 0$, then we can obtain a complete solution giving

$$a = 0.73$$

$$b = 0.20$$

$$c = 1.20$$

Neutral Processes

The measured product yields from N_2O–SF_6 mixtures are

$$G(N_2) = 8.1$$

$$G(O_2) = 2.9$$

$$G(NO) = 4.6$$

and

$$G(O^3P) = 1.8$$

The contributions from ionic processes other than neutralization are (see Table 4)

$$G(N_2) = 0.56$$

$$G(NO) = 0.25$$

$$G(O\ \text{atoms}) = 0.31$$

$$G(N\ \text{atoms}) = 0.68$$

[4]Reaction 25 adds $\frac{1}{2}b$ to $\Delta G(N_2)$, eliminates b from $\Delta G(NO)$ and adds b to $\Delta GO(^3P)$.

Can. J. Chem. Downloaded from www.nrcresearchpress.com by 210.87.254.5 on 09/05/12
For personal use only.

Can. J. Chem. Downloaded from www.nrcresearchpress.com by 210.87.254.5 on 09/05/12
For personal use only.

If we assume both N atoms and O atoms are in their ground states, ^4S and ^3P, respectively, then all $N(^4S)$ will react with NO, as in reaction 25. The net contributions from neutral dissociation will be

$$G(N_2)_n = 8.1 - 1.24 = 6.86$$

$$G(NO)_n = 4.6 + 0.68 - 0.25 - 0.93 = 4.10$$

$$G(O_2)_n = 2.9 - 0.5 = 2.40 - \tfrac{1}{2}G(O^3P) = 2.00$$

$$G(O(^3P))_n = 1.8 - 0.99 = 0.81$$

where the -0.93 contribution to $G(NO)_n$ comes from reaction 29.

Using a similar argument to that used when discussing neutralization reactions for N_2O^+, possible distinguishable dissociations are

[31] $N_2O \rightsquigarrow N_2(X^1\Sigma) + O(^1D)$ (or ^1S)

[32] $N_2O \rightsquigarrow N_2(A^3\Sigma) + O^3(P)$

[33] $N_2O \rightsquigarrow N_2(B^3\Pi) + O^3(P)$

[34] $N_2O \rightsquigarrow N(^2D) + NO$

Taking the yields of these reactions to be g, h, i, and j, respectively and using the reaction data of the species involved the following relationships can be derived

$$G(N_2)_n = 6.86 = \tfrac{3}{2}g + h + 2i + j$$

$$G(NO)_n = 4.10 = 2j + g$$

$$G(O_2)_n = 2.00 = \tfrac{1}{2}g$$

$$G(O(^3P))_n = 0.81 = h + 2i$$

Again, solving these equations simultaneously, we do not get a complete solution. We get

$$g = 4.00, \quad (h + i) = 0.81, \quad \text{and} \quad j = 0.05$$

This implies that, only 1% of the neutral dissociative excitation process yields $N(^2D)$ + NO ($j = 0.05$). Thus, as stated the parallel dissociation occurring in neutralization would not be expected to be very large and will be neglected giving a unique solution to simultaneous equations for neutralization.

The same argument cannot be used to resolve h and i for the neutral dissociative processes. Formation of $N_2(B^3\Pi)$ followed by subsequent reaction with N_2O cannot be distinguished from direct formation of $N_2(A^3\Sigma)$ followed by simple quenching. To that extent, differentiation becomes somewhat academic and we shall arbitrarily assume that no $N_2(B^3\Pi)$ is formed *i.e.* $i = 0$.

TABLE 6. Overall mechanism for N_2O radiolysis

Reaction		G
$N_2O \rightsquigarrow N_2O^+ + e$		1.90
$NO^+ + N + e$		0.59
$N^+ + NO + e$		0.25
$N_2^+ + O + e$		0.21
$O^+ + N_2 + e$		0.10
	Total	3.05
$N_2O \rightsquigarrow N_2(X^1\Sigma) + O(^1D)$		4.00
$N_2(A^3\Sigma) + O(^3P)$		0.81
$N(^2D) + NO(X^2\Pi)$		0.05
	Total	4.86

The primary yields for pure N_2O are given in Table 6. These species react as in Table 5 to give the observed stable product yields.

N_2O–O_2 Mixtures

The value of W for O_2 is 30.6 eV/ion pair (39) and from mass spectrometric results (see refs. 37–43 in ref. 27) the yields of reactions 35 and 36 are

[35] $O_2 \rightsquigarrow O_2^+ + e$ $\quad G = 3.17$

[36] $O_2 \rightsquigarrow O^+ + O + e$ $\quad G = 0.1$

The total yield of O atoms from direct excitation in O_2 is 6.2 (27). Small amounts of N_2O added to oxygen decrease the measured ozone yield by about 1.0 G unit. Since the ionization potential of N_2O is greater than that of O_2 this decrease cannot be due to charge exchange. But, as the data listed in Table 3 show $O(^1S)$ reacts about 100 times faster with N_2O than with O_2. This decrease can therefore be taken as a measure of the $O(^1S)$ yield in pure oxygen radiolysis. The equivalent results in O_2–SF_6 mixtures give a decrease in yield with N_2O of ~ 0.3 G units. Thus, it would seem that there is a neutralization yield of $O(^1S)$ from oxygen of $G(O(^1S))_{ionic} = 0.7$.

If we assume that both direct excitation and neutralization yield one singlet state oxygen atom and one triplet state oxygen atom, then the yields from oxygen would be

Neutralization

[37] $O_2^+ + (O_2^-) \rightarrow O_2 + O^1D + O^3P$
$G = 2.57 \quad 2.57$

[38] $O_2^+ + (O_2^-) \rightarrow O_2 + O^1S + O^3P$
$G = 0.7 \quad 0.7$

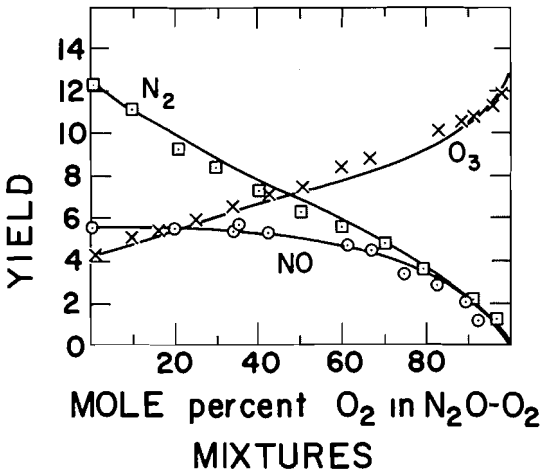

FIG. 6. Comparison of experimental and calculated yields in the Febetron radiolysis of N_2O–O_2 mixtures. —, Calculated values; □, $G(N_2)$ experimental value; ○, G(NO) experimental value; ×, $G(O_3)$ experimental value.

Excitation

[39] $O_2 \rightsquigarrow O^1D + O^3P$
$G = 2.75 \quad 2.75$

[40] $O_2 \rightsquigarrow O^1S + O^3P$
$G = 0.3 \quad 0.3$

A ratio of 9:1 for reactions 37 and 38 has been obtained by Zipf (40) by direct observation of $O(^1D)$ and $O(^1S)$ in an afterglow in O_2–rare gas mixtures. In pure oxygen the fate of both $O(^1D)$ and $O(^1S)$ will be deactivation to $O(^3P)$ ultimately leading to ozone (at high dose rates). However, in O_2–N_2O mixtures the $O(^1D)$ and $O(^1S)$ will react in accordance with the data given in Table 3.

We now have the yields of the primary species in both pure N_2O and pure O_2. Combining these yields with the rate constants for the reactions of these species given in Tables 2 and 3 and the mole fractions of N_2O and O_2 will give values for the final products in the N_2O–O_2 mixtures. Since practically all of the primary species react only with N_2O or O_2 the product yields can be estimated by simple arithmetic. However, calculation by computer is much less tedious, easier, and more accurate. The programs developed by Schmidt (41, 42) have proved to be very useful for this type of calculation. The input to this program consisted of the primary species yields in the mixtures obtained from the values in Table 6 and reactions 37–40 and the weight fractions of N_2O and O_2, the reactions and rate constants in Table 3 and the molar concentrations of N_2O and O_2.

As noted in Table 2 the rate of charge transfer from N_2O^+ to O_2 is not known. If we assume that there is no charge exchange or if we assume that charge exchange is very rapid (*i.e.* with a rate constant of 5×10^{-10} cm^3 molecule^{-1} s^{-1}) then a reasonably good fit of the calculated yields to the experimental yields is obtained. This fit can be improved by assuming a rate constant for charge exchange from N_2O^+ to O_2 of 1.2×10^{-11} cm^3 molecule^{-1} s^{-1}. The calculated yields using this value for k are compared with the experimental results in Fig. 6.

Conclusions

The mechanism for the Febetron radiolysis of N_2O presented in this paper gives good agreement with the experimental yields when used as the basis for calculating yields in N_2O–O_2 mixtures.

This agreement and the simple relationship between excitation processes and the resultant product yields shows that the major excitation reaction in N_2O is formation of $N_2(X^1\Sigma)$ and $O(^1D)$. As discussed, the other excitation reactions may give, in addition to $O(^3P)$, $N_2(A^3\Sigma)$, or $N_2(B^3\Pi)$ and we cannot distinguish between formation of these two excited states of N_2.

Because of the formation of NO^+ as well as N_2O^+ the contributions of the possible neutralizations are more difficult to determine. We have had to neglect the formation of $N(^2D)$ and NO in N_2O^+ neutralization to obtain values for the other neutralization reactions of N_2O^+ and those of NO^+.

Further work is needed to justify this neglect and to determine the yields of $N_2(A^3\Sigma)$ and $N_2(B^3\Pi)$ in excitation.

The product yields in the N_2O–O_2 mixtures in addition to testing the mechanism for N_2O provide values for the yields of $O(^1S)$, $O(^1D)$, and $O(^3P)$ in the neutralization of O_2^+ and the excitation of O_2.

Since the ionic reactions occurring in N_2O at low dose rates are not known it is difficult to determine the consistency of our mechanism with low dose rate product yields. As shown in

Can. J. Chem. Downloaded from www.nrcresearchpress.com by 210.87.254.5 on 09/05/12
For personal use only.

Table 1 the yields at the two dose rates in the presence of SF_6 are similar but this similarity may be in part fortuitous. It is reasonable, however, to assume that the yields from dissociative excitation are dose-rate independent.

The same considerations apply to the yields in the nitrous oxide–hydrocarbon mixtures of Takao *et al.* (9). Their qualitative conclusions concerning formation of both excited and ground state O atoms are in agreement with our mechanism. But because the ionic contributions are not known no quantitative comparison can be made.

1. B. P. Burtt and J. F. Kircher. Rad. Res. **9**, 1 (1958).
2. R. W. Hummel and J. A. Hearne. Nature, **188**, 734 (1960).
3. G. R. A. Johnson. J. Inorg. Nuc. Chem. **24**, 461 (1962).
4. R. Gorden and P. Ausloos. J. Res. Natl. Bus. Std. **69A**, 79 (1965).
5. F. T. Jones and T. J. Sworski. J. Phys. Chem. **70**, 1546 (1966).
6. J. T. Sears. J. Phys. Chem. **73**, 1143 (1969).
7. R. W. Hummel. Chem. Commun. 995 (1969).
8. S. Takao and S. Shida. Bull. Chem. Soc. Jap. **43**, 2766 (1970).
9. S. Takao, V. Hatano, and S. Shida. Bull. Chem. Soc. Jap. **44**, 873 (1971); J. Phys. Chem. **75**, 3178 (1971).
10. A. W. Boyd, C. Willis, and O. A. Miller. Can. J. Chem. **47**, 351 (1969).
11. C. Willis, A. W. Boyd, and D. A. Armstrong. Can. J. Chem. **47**, 3783 (1969).
12. C. Willis and A. W. Boyd. Proceedings of the IV International Congress of Radiation Research, Evian, France, 1970. In press.
13. A. W. Boyd, D. A. Armstrong, C. Willis, and O. A. Miller. Rad. Res. **40**, 255 (1969).
14. R. A. Young, G. Black, and T. G. Slanger. J. Chem. Phys. **48**, 2067 (1968).
15. R. A. Young, G. Black, and T. G. Slanger. J. Chem. Phys. **49**, 4769 (1968).
16. R. A. Young, G. Black, and T. G. Slanger. J. Chem. Phys. **50**, 303 (1969).
17. R. A. Young, G. Black, and T. G. Slanger. J. Chem. Phys. **50**, 309 (1969).
18. G. Black, T. G. Slanger, G. A. St. John, and R. A. Young. J. Chem. Phys. **51**, 116 (1969).
19. R. A. Young, G. Black, and T. G. Slanger. J. Chem. Phys. **49**, 4758 (1969).
20. C. Willis, O. A. Miller, A. E. Rothwell, and A. W. Boyd. Rad. Res. **35**, 428 (1968).
21. C. Willis, A. W. Boyd, A. E. Rothwell, and O. A. Miller. Int. J. Radiat. Phys. Chem. **1**, 373 (1969).
22. C. Willis, A. W. Boyd, and O. A. Miller. Can. J. Chem. **47**, 3007 (1969).
23. W. A. Seddon, C. Willis, M. J. Young, and E. B. Selkirk. Atomic Energy of Canada Limited Report AECL-3853 (1971).
24. C. Willis, O. A. Miller, A. E. Rothwell, and A. W. Boyd. Adv. Chem. **81**, 539 (1968).
25. C. Willis, A. W. Boyd, and O. A. Miller. Rad. Res. **46**, 428 (1971).
26. A. W. Boyd, C. Willis, R. Cyr, and D. A. Armstrong. Can. J. Chem. **47**, 4715 (1969).
27. C. Willis, A. W. Boyd, M. J. Young, and D. A. Armstrong. Can. J. Chem. **48**, 1505 (1970).
28. J. A. Ghormley, C. J. Hochanadel, and J. W. Boyle. J. Chem. Phys. **50**, 419 (1969).
29. G. M. Meaburn, D. Perner, J. LeCalve, and M. Bourene. J. Phys. Chem. **72**, 3920 (1968).
30. M. B. Shinn. Ind. Eng. Chem. Anal. Ed. **13**, 33 (1941).
31. C. Willis, A. W. Boyd, and M. J. Young. Can. J. Chem. **48**, 1515 (1970).
32. W. B. DeMore and O. Raper. J. Phys. Chem. **68**, 4212 (1964).
33. F. E. Niles. J. Chem. Phys. **52**, 408 (1970).
34. G. G. Meisels. J. Chem. Phys. **41**, 51 (1964).
35. A. Cornu and R. Massot. Compilation of mass spectral data. Heyden and Sons, London, 1966.
36. J. L. Franklin, J. G. Dillard, H. M. Rosenstock, J. T. Herron, K. Draxl, and F. H. Field. NSRDS-NBS-26 (1969).
37. D. F. Strobel. J. Geophys. Res. **76**, 2441 (1971).
38. F. R. Gilmore. J. Quant. Spectrosc. Radiat. Transfer **5**, 369 (1965).
39. R. Cooper and R. A. Mooring. Austr. J. Chem. **21**, 2417 (1968).
40. E. C. Zipf. Bull. Am. Phys. Soc. **15**, 418 (1970).
41. K. H. Schmidt. USAEC Research and Development Report ANL-7199 (1966).
42. K. H. Schmidt. USAEC Research and Development Report ANL-7693 (1970).
43. G. A. W. Derwish, A. Galli, A. Giardini-Guidoni, and G. G. Volpi. J. Chem. Phys. **40**, 3450 (1964).
44. E. W. McDaniel, V. Cermak, A. Dalgarno, E. E. Ferguson, and L. Friedman. Ion–molecule reactions. Wiley Interscience, New York. 1970. p. 326.
45. P. Warneck. Planet. Space Sci. **15**, 1349 (1967).
46. P. Warneck. J. Geophys. Res. **72**, 1651 (1967).
47. W. L. Fite, J. A. Rutherford, W. R. Snow, and V. A. J. Van Lint. Disc. Farad. Soc. **33**, 264 (1962).
48. D. E. Golden, J. Sinnott, R. N. Varney. Phys. Rev. Lett. **20**, 239 (1968).
49. R. F. Stebbings, B. R. Turner, and J. A. Rutherford. J. Geophys. Res. **71**, 771 (1966).
50. A. Galli, A. Giardini-Guidoni, and G. G. Volpi. J. Chem. Phys. **39**, 518 (1963).
51. P. D. Goldan, A. L. Schmeltekopf, F. C. Fehsenfeld, H. I. Schiff, and E. E. Ferguson. J. Chem. Phys. **44**, 4095 (1966).
52. M. J. Copsey, D. Smith, and J. Sayers. Planet. Space Sci. **14**, 1047 (1966).
53. F. C. Fehsenfeld, P. D. Goldan, A. L. Schmeltekopf, and E. E. Ferguson. Planet. Space. Sci. **13**, 579 (1965).
54. F. C. Fehsenfeld, A. L. Schmeltekopf, H. I. Schiff, and E. E. Ferguson. Planet. Space Sci. **15**, 373 (1967).
55. E. E. Ferguson, F. C. Fehsenfeld, and A. L. Schmeltekopf. Adv. Chem. **80**, 83 (1969).
56. E. W. McDaniel, V. Cermak, A. Dalgarno, E. E. Ferguson, and L. Friedman. Ion–molecule reactions. Wiley Interscience, New York. 1970. p. 334.
57. J. A. Rutherford and B. R. Turner. J. Geophys. Res. **72**, 3795 (1967).

Can. J. Chem. Downloaded from www.nrcresearchpress.com by 210.87.254.5 on 09/05/12
For personal use only.

58. F. C. FEHSENFELD and E. E. FERGUSON. Planet. Space Sci. **16**, 701 (1968).
59. F. C. FEHSENFELD, E. E. FERGUSON, and D. K. BOHME. Planet. Space Sci. **17**, 1759 (1969).
60. E. E. FERGUSON. Can. J. Chem. **47**, 1185 (1969).
61. I. M. CAMPBELL and B. A. THRUSH. Proc. Roy. Soc. (London) Series A, **296**, 201 (1967).
62. C. B. KRETSCHMER and H. L. PETERSEN. J. Chem. Phys. **39**, 1772 (1964).
63. F. KAUFMAN. Prog. React. Kinet. **1**, 1 (1961).
64. A. A. WESTENBERG and N. DE HAAS. J. Chem. Phys. **40**, 308, 7 (1964).
65. F. S. KLEIN and G. T. HERRON. J. Chem. Phys. **41**, 1285 (1964).
66. M. C. SAUER. J. Chem. Phys. **71**, 3311 (1967).
67. M. C. SAUER and L. M. DORFMAN. J. Am. Chem. Soc. **87**, 3801 (1965).
68. M. F. R. MALCAHY and D. J. WILLIAMS. Trans. Farad. Soc. **64**, 59 (1968).
69. H. I. SCHIFF. Can. J. Chem. **47**, 1903 (1969).
70. P. M. SCOTT, K. F. PRESTON, R. J. ANDERSON, and L. M. QUICK. Can. J. Chem. **49**, 1808 (1971).
71. W. B. DEMORE. J. Chem. Phys. **52**, 4309 (1970).
72. G. PARASKEVAPOULOUS, K. F. PRESTON, and R. J. CVETANOVIC. J. Chem. Phys. **54**, 3907 (1971).
73. D. R. SNELLING and E. J. BAIR. J. Chem. Phys. **47**, 228 (1967).
74. J. Y. YANG and F. M. SERVIDIO. J. Chem. Phys. **47**, 4817 (1967).
75. K. M. EVENSON and D. S. BIRCH. J. Chem. Phys. **45**, 2450 (1966).
76. M. A. A. CLYNE and J. H. STEDMAN. J. Chem. Phys. **71**, 3071 (1967).
77. F. KAUFMAN and J. R. KELSO. J. Chem. Phys. **28**, 510 (1958).
78. L. F. PHILLIPS and H. I. SCHIFF. J. Chem. Phys. **36**, 1509 (1962).
79. F. KAUFMAN. DASA Reaction Rate Handbook 14-1 (1967).
80. A. S. VLASTARAS and C. A. WINKLER. Can. J. Chem. **54**, 2837 (1967).
81. W. E. WILSON. J. Chem. Phys. **46**, 2017 (1967).
82. G. B. KISTIAKOWSKY and G. G. VOLPI. J. Chem. Phys. **35**, 237 (1961).
83. G. B. KISTIAKOWSKY and G. G. VOLPI. J. Chem. Phys. **27**, 1141 (1957).

Can. J. Chem. Downloaded from www.nrcresearchpress.com by 210.87.254.5 on 09/05/12
For personal use only.

The Acid-catalyzed Isomerization of the Adducts of Azodiacyls with Cyclopentadiene and 1,3-Cyclohexadiene

MISS C. Y-J. CHUNG, DONALD MACKAY, AND T. D. SAUER

Department of Chemistry, University of Waterloo, Waterloo, Ontario

Received December 2, 1971

The isomerization of the Diels–Alder adducts of azodiacyls with cyclopentadiene and 1,3-cyclohexadiene is powerfully catalyzed by strong protic acids and by Lewis acids. In adducts from *p*-substituted azodibenzoyls with cyclopentadiene the catalytic effect increases with electron release by the substituent.

L'isomérisation des produits d'addition de la réaction de Diels–Alder entre les azodiacyles et le cyclopentadiène et le cyclohexadiène-1,3 est très fortement catalysée par des acides protiques forts et par les acides de Lewis. Dans les produits d'addition entre les azodibenzoyles *p*-substitués et le cyclopentadiène, l'effet catalytique augmente avec l'effet donneur d'électrons du substituant.

Canadian Journal of Chemistry, **50**, 1568 (1972)

Can. J. Chem. Downloaded from www.nrcresearchpress.com by 210.87.254.42 on 09/05/12
For personal use only.

A number of reactions which proceed by [3,3] sigmatropic pathways are known to be catalyzed by Lewis acids (1–3) or by protic acids (2, 4–8). Many of these isomerizations involve allyl substituents in the Claisen (1), the dienol-benzene (6), or the dienone-phenol (7, 8) rearrangements. The catalyzed reactions are not all necessarily concerted (5).

Recently we have shown that the adducts **2** of azodiacyls **1** and cyclopentadiene undergo a [3,3] sigmatropic rearrangement to the racemic ($R_1 = R_2$) or isomeric ($R_1 \neq R_2$) *cis* bicyclic 1,3,4-oxadiazines **3** and **4** (9, 10). We now wish to report that this isomerization also is exceedingly sensitive to acid catalysis and to show how this catalysis can be utilized in studies of these and related isomerizations.

Qualitatively the effect could be simply demonstrated by adding traces of strong acids, *e.g.* hydrogen chloride or trifluoroacetic acid (TFA) to solutions of **2***a* in a wide range of solvents and evaporating the solutions to give the pure oxadiazine. In an inadvertent proof of the catalysis an attempt to purify a slightly colored sample of the very labile adduct **2***b* (10) in a pentane solution containing commercial activated charcoal led to the recovery of pure **3***b*;[1] the charcoal was found to give a p*H* of 2 to an aqueous suspension.

On a more quantitative basis (Table 1) the half-life of **2***a* which was 11 h in heptane at 62° was reduced to 1.3 s by the inclusion of 1.3×10^{-1} *M* TFA (1% v/v) or to 1.3 min by 1.3×10^{-2} *M* hydrogen chloride. Similarly 1.3×10^{-1} *M* TFA reduced the half-life of **2***b* in heptane at 52° from 22 min to 2.0 s. The isomerizations, which were all cleanly first order in adduct, were followed by u.v. spectrophotometry of dilute solutions (*ca.* 10^{-4} *M*), the slow thermal ones by the repeated scan technique (9), and the fast acid-catalyzed ones by following the development of the C=N chromophore of **3***a* at 290 nm and of **3***b* at 250 nm.

On a preparative scale the isomerization of **2***a* could be achieved under a wide range of conditions, at room temperature or by heating, in solutions containing TFA in excess or in amounts as little as 0.1 equiv. Typically a 2% solution of **2***a* in benzene could be isomerized

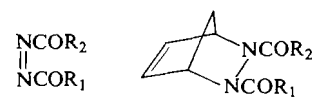

1 **2**

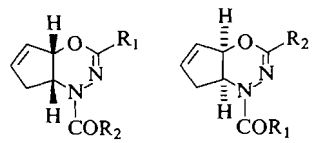

3 **4**

a $R_1 = R_2 = Ph$
b $R_1 = R_2 = CMe_3$
c $R_1 = R_2 = p\text{-}MeOC_6H_4$
d $R_1 = R_2 = p\text{-}O_2NC_6H_4$
e $R_1 = p\text{-}O_2NC_6H_4$; $R_2 = p\text{-}MeOC_6H_4$

[1]For racemic oxadiazines the simple notation for one enantiomer will be used.

Can. J. Chem. Downloaded from www.nrcresearchpress.com by 210.87.254.42 on 09/05/12
For personal use only.

TABLE I. Uncatalyzed and acid-catalyzed isomerization of adducts of azodiacyls in heptane

Adduct	Temperature (°C)	Acid concentration (M)	Half-life (s)
2*a*	62	—	3.9×10^4
		1.3×10^{-1}*	1.3
		1.3×10^{-2}†	78
		2.8‡	5.4×10^3
2*b*	52	—	1.3×10^3
		1.3×10^{-1}*	2.0
7	62	—	1.6×10^9§
		1.3×10^{-1}*	5.1×10^4

*TFA.
†Hydrogen chloride.
‡Acetic acid.
§Estimated by comparison of catalyzed isomerization rates of 7 and **2***a*, see text.

by refluxing for 3 min with 0.1 equiv of TFA. In all cases evaporation of the solutions gave crystalline product containing a small amount of TFA derived material (weak i.r. absorption at 1780 cm^{-1}) but washing with dilute ammonia removed this to give the oxadiazine in high yield (>90%) and purity.

The conversion of **2***a* into **3***a* is in fact quantitative, all solution spectra of **2***a* in the presence of TFA eventually becoming superimposable on those of pure **3***a* with the same amount of TFA added. The changes in the spectra of **3***a* induced by TFA are very minor suggesting that protonation of **3***a* is negligible. Thus the u.v. absorption band of the PhC=N chromophore in heptane was unreduced in intensity by the addition of 1.3×10^{-1} M TFA and showed a hypsochromic shift of only 6 nm. Though complete protonation transfer to pyridine, quinoline, and other heterocyclic bases by TFA in hexane has been detected by u.v. spectroscopy (11), it is likely that with the much less basic heterocycle **3***a* only proton association can occur in saturated hydrocarbon solvents. The observed band shift in heptane may be due to this.

The generality of the catalysis was explored for other protic acids and for Lewis acids. The isomerization of **2***a* was followed by n.m.r. spectroscopy in the presence of *p*-toluenesulfonic acid (0.2 equiv), boron trifluoride etherate (0.2 equiv), and tin (IV) chloride (1.0 equiv). In each case the reaction was markedly accelerated and was essentially quantitative on work-up of the solutions. Acetic acid was, however, rather ineffective; a 17% (v/v, 2.8 M) solution of it in heptane at 62° isomerized **2***a* only seven times faster than the isomerization in pure heptane.

Aqueous hydrochloric acid also catalyzed the isomerization but first order kinetics were not observed on u.v. analysis, the oxadiazine being slowly hydrolyzed. Thus solutions of **2***a* and **3***a* in excess of 0.1 M aqueous ethanolic hydrochloric acid for 1 day at room temperature gave identical end products containing at least four components (t.l.c.) and showing strong absorption in the OH/NH region of the i.r. spectrum. The instability of the dihydro derivative of **3***a* to aqueous acid has already been discussed (9).

The nature of the complex between the acid and the substrate in the transition state in hydrocarbon solvents must be speculative. The site of complexation is probably the same as that of protonation in solvents where proton transfer is possible. In simple amides the evidence is now conclusive that protonation occurs on oxygen (12), but no comparable studies have been carried out on hydrazides.

If, by analogy with amides, complexation in hydrocarbon solvents occurs at oxygen, then for a concerted reaction the representation **5** might reasonably describe the geometry leading to the transition state for the product **3**; in **5** the electrophilic oxygen initiates attack by the olefinic π electrons. A similar picture pertains to complexation at nitrogen, the likelihood of this alternative depending on the pyramidal (sp^3) as opposed to the planar (sp^2) character of the N—C=O system, since if the former is dominant complexation, like protonation, would relieve repulsion between lone electron pairs.[2] The involvement of an open protonated structure, *e.g.* **6**, in a non-concerted pathway cannot be discounted. In the absence of species

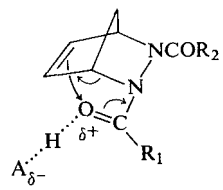

5

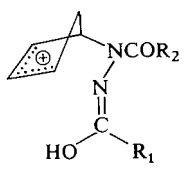

6

[2]As a referee has suggested, even if the *N*-complexed (or protonated) species is less stable than its *O*-counterpart it might nevertheless provide the preferred isomerization path; the two species would of course be in rapid equilibrium.

TABLE 2. Effect of *p*-substituent on the ratio of TFA (1.3×10^{-3} *M*)-catalyzed to uncatalyzed isomerization in benzene at 70.0°

Adduct **2**	*p*-Substituent	Uncatalyzed half-life (min)	Catalyzed half-life (min)	Rate enhancement
d	NO_2	32.4	20.0	1.6
a	H	145	1.38	105
c	MeO	95	0.17	560

capable of diverting it, the ring closure of **6** might be highly stereospecific and lead to the observed high yields of *cis* oxadiazines.

There are two predictable consequences of the invocation of **5**, or its *N*-complexed counterpart. The first is that in the case of two different symmetrical adducts under the same conditions that with the more basic amide group should be more susceptible to catalytic rate enhancement relative to the uncatalyzed (thermal) reaction. This is vividly borne out by the isomerization rates of **2***a*, *c*, and *d* in benzene at 70° (Table 2) in which the ratio of catalyzed (1.3×10^{-3} *M* TFA) to uncatalyzed rates increases with electron release from the aryl group.

The second consequence is that in the transformation of an unsymmetrical adduct ($R_1 \neq R_2$) to the mixture of isomeric oxadiazines, the isomer distribution for the thermal reaction must alter for the catalyzed reaction in the direction of the isomer derived through the transition state complexed at the more basic amide group. This is well illustrated utilizing again the substituent effects of the nitro and methoxy groups. In the absence of acid the yield from **2***e* of oxadiazine **4***e* was $40 \pm 5\%$ (10) but with 1.3×10^{-1} *M* TFA it was $85 \pm 5\%$, showing the predicted increase in participation of the anisamide group. A practical method is thus suggested of improving the yields of those oxadiazines which are minor products in the thermal isomerization of unsymmetrical adducts.

As part of a general study of the effect of the nature of the bridge on the stability of adducts of azodiacyls and cyclic 1,3-dienes we synthesized the [2.2.2]diazabicyclo derivatives **7**, m.p. 157–158°, and **8**, m.p. 126.5–127.5°, from cyclohexadiene in yields of 60 and 28% respectively. These adducts, unlike their cyclopentadiene counterparts, were completely stable at temperatures up to 150°. At 200° isomerization was complete in 1.5 h for **7** and 45 min for **8** (cf. likewise the greater stability of **2***a* than *b* (10)). The products **9**, m.p. 164.5–165.5°, and **10**, m.p. 66–67°, were identified as oxadiazines by their spectroscopic properties, in particular by the C=N chromophore in the u.v. spectrum at 294 nm for **9** and at 240 nm for **10**, and by the diagnostic (9, 10) splitting pattern of the *cis* tertiary hydrogens in the n.m.r. spectrum.[3]

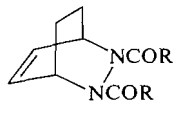

7 R = Ph
8 R = CMe_3

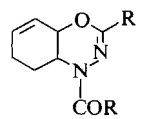

9 R = Ph
10 R = CMe_3

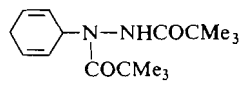

11

Rate values in solution could not therefore be obtained for **7** and **8** using the u.v. analytical technique described for the cyclopentadiene adducts, which isomerized readily in solution <90°. In view of the powerful catalytic effect of acids discussed above it seemed reasonable that isomerization rates for **7** and **8** might be brought within a range suitable for determination by u.v. spectrophotometry.

Refluxing of **7** in benzene containing 1.3×10^{-1} *M* TFA for 20 h indeed gave an 88% yield of **9**, along with small amounts of NH/OH containing material (i.r. spectrum), presumably arising by a solvolytic process. When the acid-catalyzed (1.3×10^{-1} *M*) reaction was followed

[3]The properties of the dihydro derivative of **9**, and of its precursor **7** and its dihydro derivative, were the same as those described (13, 14) for samples obtained by independent synthesis.

Can. J. Chem. Downloaded from www.nrcresearchpress.com by 210.87.254.42 on 09/05/12
For personal use only.

Can. J. Chem. Downloaded from www.nrcresearchpress.com by 210.87.254.42 on 09/05/12
For personal use only.

by repeated scan u.v. spectrophotometry at 62° in heptane the first order rate plot gave, as expected, a straight line fit only for the early stages. From the initial slope a rate constant of isomerization of 1.35×10^{-5} s^{-1} was obtained, corresponding to a half-life of 14.3 h. This value is greater than that for the adduct **2***a* by a factor of 3.9×10^4, representing a $\Delta\Delta G^{\ddagger}$ of 7.0 kcal mol^{-1} between the two adducts.

If the isomerizations for the [2.2.1] and the [2.2.2] ring systems are mechanistically analogous in both the catalyzed and the uncatalyzed case, so that the only energy differences in the $\Delta G^{\ddagger}$ terms arise from the differences in the bridge size, then the $\Delta\Delta G^{\ddagger}$ value is also applicable to the uncatalyzed reaction. On this basis the uncatalyzed rate constant for **7** in heptane at 62° has an estimated value of 4.4×10^{-10} s^{-1}, corresponding to a half-life of about 50 years.

Solvolytic pathways appeared to predominate when the isomerization of **8** was attempted in the presence of TFA in refluxing heptane. No **10** could be detected among the several products though it was in fact shown to be stable to the reaction conditions. Boron trifluoride etherate was more successful. A 1.6×10^{-3} *M* solution of it in heptane caused a 50% conversion of **8** to **10** after reflux for 15 min. Longer reflux times or higher catalyst concentrations led to the accumulation of by-products.

The synthesis of both cyclohexadiene adducts **7** and **8** was accompanied by the formation of much NH containing material which in the case of the azodibenzoyl reaction was not examined further. The azodipivaloyl reaction gave, as well as **8**, its dihydro derivative dipivaloylhydrazine, isolated in 40% yield from the total reaction product by water extraction (and probably arising by oxidation of cyclohexadiene to benzene), as well as a second 1:1 product of the azo compound and the diene. The latter was separated from **8** in 14% yield by silica gel chromatography, and was shown to be the product **11** of the "ene reaction" of the azo compound with the diene; this pathway is known to be the main one in the reaction of the diene with diethyl azodicarboxylate (15). The identity of **11** follows from the symmetrical pattern of the four vinyl protons and the presence of one N—H exchangeable with D_2O in its n.m.r. spectrum, and from the appearance only of end absorption in its u.v. spectrum.

Experimental

The following spectrometers were used: for i.r., a Beckman IR 10; for u.v., a Coleman EPS-3T Hitachi with a cell compartment heated by a constant temperature circulating pump; for n.m.r., a Varian T60 or HA100.

Microanalyses were done by The Baron Consulting Co., P.O. Box 663, Orange, Conn., U.S.A.

Solvents were purified and dried by conventional means. Anhydrous magnesium sulfate was used as drying agents for solutions in organic solvents. Melting points are uncorrected.

Compounds 1–4

All the azo compounds **1**, the adducts **2**, and their isomers **3** and **4** have been described or referred to earlier (10).

2,3-Dibenzoyl-2,3-diazabicyclo[2.2.2]oct-5-ene (7)

A solution of azodibenzoyl (1.19 g, 5 mmol) and 1,3-cyclohexadiene (Aldrich Chemical Co., 1.2 g, 15 mmol) in carbon tetrachloride (20 ml) was kept in the dark at room temperature for 20 h. Removal of some crystalline material (NH absorption in its i.r. spectrum) and concentration of the faintly orange filtrate gave slightly impure **7** (60%). Three crystallizations from ethanol and drying at 80° for 20 h gave prisms, m.p. 157–158° (lit. (14) m.p. 151–152°); $\nu(CCl_4)$ 1697, 1659 cm^{-1} (C=O); λ_{max} (EtOH) 220 (ε 14 500), 255 nm (ε 7850); $\tau(CDCl_3)$ 2.2–2.8 (10 phenyl H), 3.5 (2 vinyl H, broad), 4.6 and 5.2 (2 *tert* H, both broad[4]), 7.7 (2 methylene H, broad), 8.5, 8.7 p.p.m. (2 methylene H, doublet).

Hydrogenation of **7** was carried out in ethanol using di-imide generated by reaction of hydrazine with hydrogen peroxide. A solution of **7** (0.318 g, 1 mmol) in ethanol (15 ml) containing 95% hydrazine (1.2 ml) was brought to about 50° and 50% hydrogen peroxide (1.2 ml) in ethanol (6 ml) was added dropwise with vigorous stirring at a rate so as to maintain the temperature below the boiling point. The solution was finally stirred for 1/2 h and evaporated and the residue twice crystallized from aqueous ethanol giving 2,3-dibenzoyl-2,3-diazabicyclo[2.2.2]octane (80%) as needles, m.p. 174–176° (lit. (14) m.p. 171.5–172.5°); ν(Nujol) 1668 and 1632 cm^{-1} (C=O); λ_{max} (EtOH) (ε 15 700), 250 nm (ε 7580); $\tau(CDCl_3)$ 2.2–2.9 (10 phenyl H), 5.1 and 5.9 (2 *tert* H, both broad), 7.4–8.7 p.p.m. (8 methylene H).

cis-1-Benzoyl-4a,7,8,8a-tetrahydro-3-phenyl-1H-4,1,2-benzoxadiazine (9)

The adduct **7** was kept at 200° in a sealed evacuated tube for 1.5 h. The slightly colored melt crystallized on cooling and had an i.r. spectrum identical with that of analytical oxadiazine obtained as needles, m.p. 164.5–165.5°, from ethanol; $\nu(CCl_4)$ 1660 and 1650 (C=O, C=N, not necessarily respectively) 1091 cm^{-1} (C—O—C); λ_{max} (EtOH) 294 nm (ε 16 900); $\tau(CDCl_3$, 100 MHz) 2.1–2.9 (10 phenyl H), 3.7–4.1 (2 vinyl H, overlapping with complex splitting), 5.13 (C_{8a}—H, two triplets, $J_{8a,4a} = J_{8a,8A} = 3.6$ Hz, $J_{8a,8B} = 12$ Hz), 5.42 (H_{4a}, triplet containing $J = 3.6$ and another comparable splitting), 7.6 (C-7 methylene H_2, complex), 7.9, 8.3 p.p.m. (C-8 methylene AB system, $J_{AB} = 12$ Hz).

[4]They coalesce at higher temperatures. A fuller account of the properties and stability of 2,3-diazabicyclo[2.2.*n*] adducts from azodibenzoyl will be discussed in a forthcoming publication.

Can. J. Chem. Downloaded from www.nrcresearchpress.com by 210.87.254.42 on 09/05/12
For personal use only.

Anal. Calcd. for $C_{20}H_{18}N_2O_2$: C, 75.45; H, 5.70; N, 8.80. Found: C, 75.16; H, 5.66; N, 8.34.

Hydrogenation with di-imide, as described for 7, gave *cis*-1-benzoyl-4*a*,5,6,7,8,8*a*-hexahydro-3-phenyl-1*H*-4,1,2-benzoxadiazine (82%), m.p. 162.5–163.5° (lit. (13) m.p. 163–164°) on crystallization from ethanol; $\nu(CCl_4)$ 1636, 1625 (C=O, C=N), 1094 cm^{-1} (C—O—C); λ_{max} (EtOH) 220 (ε 16 500), 291 nm (ε 15 800); $\tau(CDCl_3)$ 2.0–2.8 (10 phenyl H), 5.15 and 5.50 (2 *tert* H, both complex), 7.5–8.6 p.p.m. (8 methylene H).

*2,3-Dipivaloyl-2,3-diazabicyclo[2.2.2]oct-5-ene (**8**)*

A solution of azodipivaloyl (7.6 g, 38 mmol) and 1,3-cyclohexadiene (6.0 g, 75 mmol) in carbon tetrachloride (75 ml) was refluxed in the dark under nitrogen for 3 days. The red–brown solution was evaporated and the residual gum was triturated with hexane to give an off-white solid (9.0 g) containing three major and one minor product (t.l.c. on silica gel). Extraction of the solid with water gave from the extracts 1,2-dipivaloylhydrazine (3.0 g, 40%), which was purified by sublimation and identified by m.p. and mixed m.p., and by its i.r. and n.m.r. spectrum.

The water insoluble fraction was chromatographed in portions on silica gel using as eluant a mixture of ether: benzene: petroleum ether: ethyl acetate in the proportions 1:2:10:10. The first and main fraction was the *adduct* **8** (3.0 g total, 28%) which was crystallized from aqueous acetone as long needles, m.p. 126.5–127.5°; $\nu(CCl_4)$ 1712, 1642 cm^{-1} (C=O); u.v. end absorption only (EtOH or *iso*-octane); $\tau(CDCl_3)$ 3.57 (2 vinyl H, triplet, $J = 4.0$ Hz), 4.97 (2 *tert* H, broad singlet), 7.67–8.17 (4 methylene H, complex), 8.73 p.p.m. (18 *tert*-butyl H, singlet).

Anal. Calcd. for $C_{16}H_{26}N_2O_2$: C, 69.03; H, 9.41; N, 10.06. Found: C, 69.27; H, 9.64; N, 10.06.

Further elution gave the "ene" product *1,2-dipivaloyl-1-(2,5-cyclohexadienyl)hydrazine* (**11**) (1.50 g total, 14%), an analytical sample of which was prepared by recrystallization from aqueous acetone and then vacuum sublimation as fine prisms, m.p. 159–160°; $\nu(CCl_4)$ 3405 (NH, broad), 1715, 1657 cm^{-1} (C=O); u.v. end absorption only (EtOH); $\tau(CDCl_3$, 100 MHz) 2.99 (1 NH, broad singlet, exchangeable with NaOD), 3.97 (C_2—H and C_6—H, broad unsymmetrical doublet, $J = 10$ Hz, A_2 portion of A_2B_2), 4.19 (C_1—H, center portion only visible, but chemically shifted downfield from $C_{2,6}$—H as a broad multiplet in benzene-d_6), 4.37 (C_3—H and C_5—H, B_2 portion), 7.33 (C-4 methylene H_2, complex, at least 10 lines), 8.76, 8.80 p.p.m. (9 *tert* butyl H each, sharp singlets).

Anal. Found: C, 68.98; H, 9.33; N, 10.51.

*cis-1-Pivaloyl-4a,7,8,8a-tetrahydro-3-tert-butyl-1H-4,1,2-benzoxadiazine (**10**)*

The adduct **8** was heated in a sealed evacuated tube at 200° for 45 min. The *oxadiazine* **10** crystallized on cooling and had m.p. 64.5–66° directly. Recrystallization from aqueous acetone raised this to 66–67°; $\nu(CCl_4)$ 1650 cm^{-1} (C=O, C=N); λ_{max} (EtOH) 240 nm (ε 12 000); $\tau(CDCl_3$, 100 MHz) 3.97 (C_5—H, two triplets, $J_{5,6} = 9.5$, $J_{5,4a} = 3.3$ Hz), 4.12 (C_6—H, complex), 5.44 (C_{8a}—H, two triplets, $J_{8a,4a} = J_{8a,8A} = 3.6$, $J_{8a,8B} = 12$ Hz), 5.73 (C_{4a}—H, broadened triplet containing $J = 3.3$ and 3.6 Hz), 7.7 (C-7 methylene H_2, complex), 8.3 (C-8 methylene H_2, complex), 8.64 and 8.80 p.p.m. (9 *tert* butyl H each, sharp singlets).

Anal. Calcd. for $C_{16}H_{26}N_2O_2$: C, 69.03; H, 9.41; N, 10.06. Found: C, 69.11; H, 9.25; N, 9.98.

*TFA-Catalyzed Isomerization of **2a** to **3a** on a Preparative Scale*

TFA (4.9 μl, 0.1 equiv) was added to a refluxing solution of **2***a* (200 mg, 0.66 mmol) in benzene and the refluxing was maintained for 3 min. The solution was evaporated, the residue was triturated with two drops of methanol to induce crystallization, dilute aqueous ammonia was added, and the precipitate (180 mg, 90%) was collected. Its i.r. spectrum was superimposable on that of analytically pure **3***a*.

*Effect of Aqueous Acid on **2a** and **3a***

Solutions of the adduct **2***a* or its isomer **3***a* (152 mg, 0.5 mmol) in 77% aqueous ethanol containing 0.10 *M* hydrochloric acid reacted completely in about 1 day at room temperature. Evaporation gave gummy solid residues which were identical in all respects, having superimposable i.r. and u.v. spectra and containing four components (t.l.c.).

The effect of the same solvent medium on a very dilute solution (*ca.* 10^{-4} *M*) of adduct was monitored at 35° by following the increase in absorbance at 290 nm (see below for details of kinetic experiments), which reached a maximum after 55 min and then began to fall. An estimate of the initial slope of a first order rate plot gave a half-life of 20 min.

*Isomerization of **2a** by Other Catalysts*

In the following the isomerization of the adduct **2***a* was followed by n.m.r. spectroscopy (probe temperature 35°).

(a) p-Toluenesulfonic acid: 19 mg (0.2 equiv) was added to a solution of the adduct (152 mg, 0.5 mmol) in dimethylsulfoxide-d_6 (1 ml). Reaction was complete in about 8 h.

(b) Boron trifluoride etherate: 14.2 mg (0.2 equiv) in chloroform-*d* (0.25 ml) was added to a solution of the adduct (152 mg, 0.5 mmol) in chloroform-*d* (0.25 ml). Reaction was complete before the spectrum could be run.

(c) Tin(IV) chloride: 26 mg (1 equiv) in methylene chloride (0.5 ml) was added to a solution of the adduct (76 mg, 0.25 mmol) in methylene chloride (0.5 ml). The reaction was monitored in the region of absorption of the CH_2 group and was complete in about 4 min. Lesser amounts of catalyst caused incomplete isomerization.

In the work-up for reactions *a* and *b* the solutions from the n.m.r. tube were evaporated to dryness in a stream of nitrogen and dilute aqueous ammonia was added. The oxadiazine crystallized and was filtered off. The i.r. spectrum was identical with that of analytically pure material.

In reaction *c*, dilute aqueous ammonia was added and the methylene chloride extracts were dried and evaporated. The residue was slightly gummy and had a weak absorption in the NH region of its i.r. spectrum, but one crystallization from aqueous methanol gave pure oxadiazine.

*TFA-Catalyzed Isomerization of **2e** to **3e** and **4e***

A solution of **2***e* (0.2 g, 0.69 mmol) in benzene (50 ml) containing TFA (1.3×10^{-1} *M*) was refluxed for 2 min and then evaporated. Integration of the methoxy signals in the n.m.r. spectrum at 100 MHz (10) showed the presence of 85 ± 5% of **4***e*, before and after work-up with dilute aqueous ammonia.

*TFA-Catalyzed Isomerization of **7** to **9***

A solution of 7 (80 mg, 0.25 mmol) in benzene (30 ml)

Can. J. Chem. Downloaded from www.nrcresearchpress.com by 210.87.254.42 on 09/05/12
For personal use only.

containing TFA (1%, 1.3×10^{-1} *M*) was refluxed for 20 h and then evaporated to dryness in a stream of nitrogen. An excess of dilute aqueous ammonia was added and the crystalline residue (70 mg, 88%) filtered off. Its spectrum was the same as that of pure **9**, and it had m.p. and mixed m.p. 163.5–164.5° after crystallization from aqueous ethanol. The balance of the reaction product was found in the ammoniacal filtrate by evaporation to dryness and extraction of the residue with methylene chloride which gave a gummy solid with i.r. absorption in the OH/NH and C=O regions.

Attempted Isomerization of **8** *to* **10** *with Acid Catalysts*

(a) Trifluoroacetic Acid

A sample of **8** was refluxed in heptane containing 1.3×10^{-1} *M* TFA for 15 min and evaporated. The residue was taken up in carbon tetrachloride and extracted with aqueous ammonia. The organic layer was dried and shown by t.l.c. on silica gel to contain at least four products, none of which was **8** or **10**.

Control experiment: A sample of **10** was recovered essentially pure when refluxed as above for 20 min.

(b) Boron Trifluoride Etherate

The adduct (0.318 g, 1.14 mmol) was refluxed for 15 min in heptane (45 ml) containing 1.6×10^{-3} *M* boron trifluoride etherate and the clear solution was evaporated under reduced pressure. The n.m.r. analysis of the residue in carbon tetrachloride showed it to be an equimolar mixture of **8** and **10**; silica gel t.l.c. showed a trace of a third substance. Column chromatography on silica gel using ether:benzene:petroleum ether:ethyl acetate in the proportions 1:2:20:20 as eluant gave the oxadiazine (163 mg, 51%) as the first material eluted, identified by n.m.r. and i.r. spectroscopy.

Refluxing with a more concentrated (1.8×10^{-2} *M*) solution of TFA for 30 min caused complete reaction of **8**, but the oxadiazine was then contaminated with two N—H containing products.

Kinetic Determinations by Ultraviolet Spectrophotometry

Dilute solutions in the range 10^{-4}–10^{-5} *M* were used in 10 mm quartz cells (Hellma Canada Ltd.) with Teflon stoppers. These gave an excellent fit, allowing no evaporation losses over periods of several days, even within 10° of the solvent boiling point.

The purely thermal reactions in heptane and the reaction in heptane containing acetic acid were carried out by the repeated scan technique used in earlier work (9). The thermal reactions in benzene were followed by measuring the increase in absorbance with time at a suitable fixed wavelength, 325 nm for **2***a*, 335 nm for **2***c*, and 340 nm for **2***d*.

All the TFA-catalyzed reactions on the compounds **2***a–d* were also followed at a fixed wavelength using an external recorder (Beckman Ten-Inch Linear) running at a suitable high speed. An average of at least three runs was used in each case. The solutions in the cell were all brought to the required temperature and the TFA introduced using a 10 or 50 μl syringe as appropriate. For reactions whose half-lives were greater than a few seconds the cell was stoppered, shaken manually, and immediately returned to the compartment. For the very fast reactions the cell compartment lid was replaced by a styrofoam cover fitted with an electrical contact and a hole directly above the sample cell. Through this and through one of two holes in the Teflon stopper of the cell passed a stainless steel stirrer; the other hole permitted passage of the syringe needle. Immediately after injection of the TFA the solution was stirred with two strokes of the stirrer which was then held above the light path while the absorbance change was being recorded.

In the hydrogen chloride-catalyzed reaction the heptane was saturated with the gas and the solution standardized by titration. The required amount was then introduced with the microsyringe.

All the reactions, catalyzed or uncatalyzed, gave excellent first order kinetics throughout.

The isomerization of **7** in heptane at 62° in the presence of 1.3×10^{-1} *M* TFA was also followed by the repeated scan technique. The curves passed through an isobestic point at 263 nm for the first 5 h but then drifted away from this point. A pure sample of the oxadiazine **9** was used to obtain a value for A_∞, the final absorbance which would have been observed in a quantitative isomerization. The initial slope of the plot of $\ln (A_\infty - A_t)$ against t gave the rate constant for the isomerization.

We wish to thank the National Research Council of Canada for financial assistance.

1. P. Fahrni, A. Habich, and H. Schmid. Helv. Chim. Acta, **43**, 448 (1960).
2. P. Yates and P. Eaton. Tetrahedron, **12**, 13 (1961).
3. R. C. Cookson, J. Hudec, and R. O. Williams. J. Chem. Soc. C, 1382 (1967).
4. L. S. Besford, R. C. Cookson, and J. Cooper. J. Chem. Soc. C, 1385 (1967).
5. R. C. Cookson and D. C. Warrell. J. Chem. Soc. C, 1391 (1967).
6. H.-J. Hansen, B. Sutter, and H. Schmid. Helv. Chim. Acta, **51**, 828 (1968), and references therein.
7. B. Miller. *In* Mechanisms of molecular migrations. *Edited by* B. S. Thyagarajan. Vol. 1. Interscience Publishers, New York, N.Y., 1968. p. 247.
8. B. Miller. J. Am. Chem. Soc. **91**, 2170 (1969); **92**, 6246 (1970).
9. D. Mackay, J. A. Campbell, and C. P. R. Jennison. Can. J. Chem. **48**, 81 (1970).
10. J. A. Campbell, D. Mackay, and T. D. Sauer. Can. J. Chem. **50**, 371 (1972).
11. G. Coppens, C. Gillet, J. Nasielski, and E. Vander Donckt. Spectrochim. Acta, **18**, 1441 (1962).
12. G. A. Olah, A. M. White, and D. H. O'Brien. Chem. Rev. **70**, 561 (1970).
13. T. Taguchi, J. Ishibashi, T. Matsuo, and M. Kajima. J. Org. Chem. **29**, 1097 (1964).
14. R. Askani. Chem. Ber. **98**, 2551 (1965).
15. B. Franzus. J. Org. Chem. **28**, 2954 (1963).

Sulfonation and Isomerization of some Halogenobenzenesulfonic Acids[1]

H. CERFONTAIN, MRS. A. KOEBERG-TELDER, AND W. A. ZWART VOORSPUY

Laboratory for Organic Chemistry, Nwe Achtergracht 129, University of Amsterdam, Amsterdam, The Netherlands

Received January 10, 1972

The behavior of the isomeric halogenobenzenesulfonic acids (halogen = F, Cl, and Br) in sulfuric acid was studied. In 115% H_2SO_4 at 25° only sulfonation takes place. Both the ortho- and para-isomers yield the 1-halogenobenzene-2,4-disulfonic acid, whereas the meta-isomers yield a mixture of mainly 3,4- and 3,5- with some 2,5-disulfonic acid.

In 98.1% H_2SO_4 at 150–170°, both sulfonation and isomerization occur. The ortho-isomers are sulfonated to the 2,4-disulfonic acid and isomerized to the para-isomer in competing reactions. The para-isomers are sulfonated to the 2,4-disulfonic acids much more slowly than the ortho-isomers. The least reactive are the meta-isomers which in competing reactions are sulfonated to a mixture of mainly 2,5- and 3,5- disulfonic acids, and isomerized to the para-isomers which eventually yield the 2,4-disulfonic acids.

It is suggested that the formation of the 3,4-disulfonic acids from the meta-isomers in 115% H_2SO_4 proceeds by an intramolecular rearrangement of the initially formed arenepyrosulfonic acids.

Le comportement des acides halogénobenzènesulfoniques isomères (halogène = F, Cl, Br) dans l'acide sulfurique a été étudié. A 25° dans l'acide sulfurique à 115%, seule la sulfonation a lieu. Les isomères ortho et para donnent tous deux l'acide halogéno-1 benzène disulfonique-2,4 tandis que les isomères méta conduisent à un mélange constitué principalement des acides disulfoniques-3,4 et -3,5 et un peu de -2,4.

Dans l'acide sulfurique à 98.1% à 150–170°, la sulfonation et l'isomérisation ont lieu toutes les deux. Les isomères ortho sont sulfonés en acide disulfonique-2,4 et isomérisés en para dans des réactions compétitives. Les isomères para donnent les acides disulfoniques-2,4 beaucoup plus lentement que pour les analogues ortho. Les moins réactifs sont les isomères méta qui, dans des réactions compétitives, sont sulfonés en un mélange d'acides disulfoniques-2,5 et -3,5 surtout et isomérisés en para pour donner éventuellement les acides disulfoniques-2,4.

On pense que la formation des acides disulfoniques-3,4 à partir des isomères méta dans H_2SO_4 115%, se fait selon un réarrangement intramoléculaire des acides arènepyrosulfoniques initialement formés.

Canadian Journal of Chemistry, **50**, 1574 (1972)

In connection with a study on the sulfonation of the halogenobenzenes (1, 2), an investigation was made of the sulfonation and isomerization of the fluoro-, chloro-, and bromobenzenesulfonic acids in sulfuric acid.[2] In 115% H_2SO_4 at 25°, only sulfonation occurs, whereas in 98.1% H_2SO_4 at 150–170° both sulfonation and isomerization occur. In 98.1% H_2SO_4 the halogenobenzenesulfonic acids are present in the un-ionized form ($ArSO_3H$) (4). In 115% H_2SO_4 they will be present mainly in the protonated form ($ArSO_3H_2^+$) and possibly partly in the pyrosulfonic acid form (ArS_2O_7H) (5, 6). The actual species undergoing sulfonation in fuming sulfuric acid is, however, the unionized sulfonic acid (5, 7).

Results and Discussion

Nuclear Magnetic Resonance Spectra

Information concerning the products formed with the halogenobenzenesulfonic acids in 98.1 and 115% H_2SO_4 was obtained from an analysis of the n.m.r. spectra. In order to make a comparison possible, the 115% H_2SO_4 mixtures were diluted to 98% H_2SO_4.

The assignments of the n.m.r. spectra of the three sets of reference compounds, *m*-, *p*-, and 2,4-disulfonic acid in 98.1% H_2SO_4 as solvent, are given in Table 1. The n.m.r. spectra of the sulfonation mixtures of the *m*-halogenobenzenesulfonic acids in 115% H_2SO_4 after dilution are given in Fig. 1. The formation of 2,3-disulfonic acid is considered highly improbable. In assigning the various absorptions we therefore took into account the possible presence of the three other disulfonic acid isomers. The results are listed in Table 1. The agreement between the assigned chemical shifts and those calculated on the basis of the principle of the additivity of substituent shifts is in general satisfactory.

Sulfonation in 115% H_2SO_4 at 25°

The n.m.r. spectra obtained on leaving both the *o*- and the *p*-halogenobenzenesulfonic acids in 115% H_2SO_4 at 25° for 7 days are identical

[1]Aromatic sulfonation, part 35. Preceding paper, ref. 27.

[2]The iodobenzenesulfonic acids behave differently. They suffer from deiodation in the Jacobsen reaction (2, 3).

Can. J. Chem. Downloaded from www.nrcresearchpress.com by 210.87.254.5 on 09/05/12
For personal use only.

Can. J. Chem. Downloaded from www.nrcresearchpress.com by 210.87.254.5 on 09/05/12
For personal use only.

TABLE 1. The n.m.r. data of halogenobenzenedisulfonic acids (5 wt. %) in 98% H_2SO_4

Halogen	Positions of sulfo groups	Chemical shift (p.p.m.)*†					$J_{n,m}$ (Hz)							
		H_2	H_3	H_4	H_5	H_6	1,2	1,3	1,5	1,6	2,3	2,6	3,5	5,6
Br	3-SO_3H	8.30(8.27)		8.12(8.05)	7.72(7.73)	8.12(8.12)								
	4-SO_3H	8.00(8.00‡)	8.00(8.00)											
	2,4-$(SO_3H)_2$		8.80(8.44)		8.32(8.29)	8.32(8.17)								
	3,4-$(SO_3H)_2$§	(8.44)			(8.17)	(8.29)								
	3,5-$(SO_3H)_2$§	8.64(8.56)		8.64(8.49)										
	2,5-$(SO_3H)_2$		(8.17)	(8.22)		(8.44)								
Cl	3-SO_3H	8.18(8.12)		8.00(8.00)	7.81(7.79)	7.97(7.97)						1.8		
	4-SO_3H	7.80(7.85)	8.11(8.06)								9.0			
	2,4-$(SO_3H)_2$		8.80(8.50)		8.42(8.35)	8.11(8.02)							1.8	8.8
	3,4-$(SO_3H)_2$§	8.48(8.29)			8.47(8.23)	8.12(8.14)						1.9		8.5
	3,5-$(SO_3H)_2$§	8.48(8.41)		8.60(8.44)										
	2,5-$(SO_3H)_2$		(8.23)	(8.17)		(8.29)								
F	3-SO_3H	‖(7.78)		‖(7.87)	‖(7.80)	‖(7.63)								
	4-SO_3H	7.53(7.51)	8.20(8.07)				8.9	4.8			8.9			
	2,4-$(SO_3H)_2$		8.7 (8.51)		8.5 (8.36)	7.83(7.68)		5.9		9.0			2.1	9.0
	3,4-$(SO_3H)_2$§	8.25(7.95)			8.57(8.24)	7.85(7.80)	8.1		4.9	8.1		2.2		9.0
	3,5-$(SO_3H)_2$§	8.25(8.07)		8.6 (8.51)										
	2,5-$(SO_3H)_2$		(8.24)	(8.04)		(7.95)								

*The data between brackets were calculated on the basis of the additivity principle of substituent effects, using the shift data for the halogens as given by Hayamizu and Yamamoto for C_6H_5Br and C_6H_5Cl (8) and by Suhr for C_6H_5F (9), and for the sulfonic acid substituent as determined recently by Ris for 85% H_2SO_4 (10) ($\Delta\delta_o = 0.44$, $\Delta\delta_m = 0.17$ and $\Delta\delta_p = 0.29$ p.p.m.).

†Chemical shifts are relative to external TMS in CCl_4 (50 vol. %).

‡The calculated chemical shifts are relative to the chemical shift of *p*-bromobenzenesulfonic acid, which was made the same as the shift of the experimentally observed singlet absorption.

§Assigned spectra.

‖Observed multiplet inbetween $\delta = 7.6$ and 8.1 p.p.m.

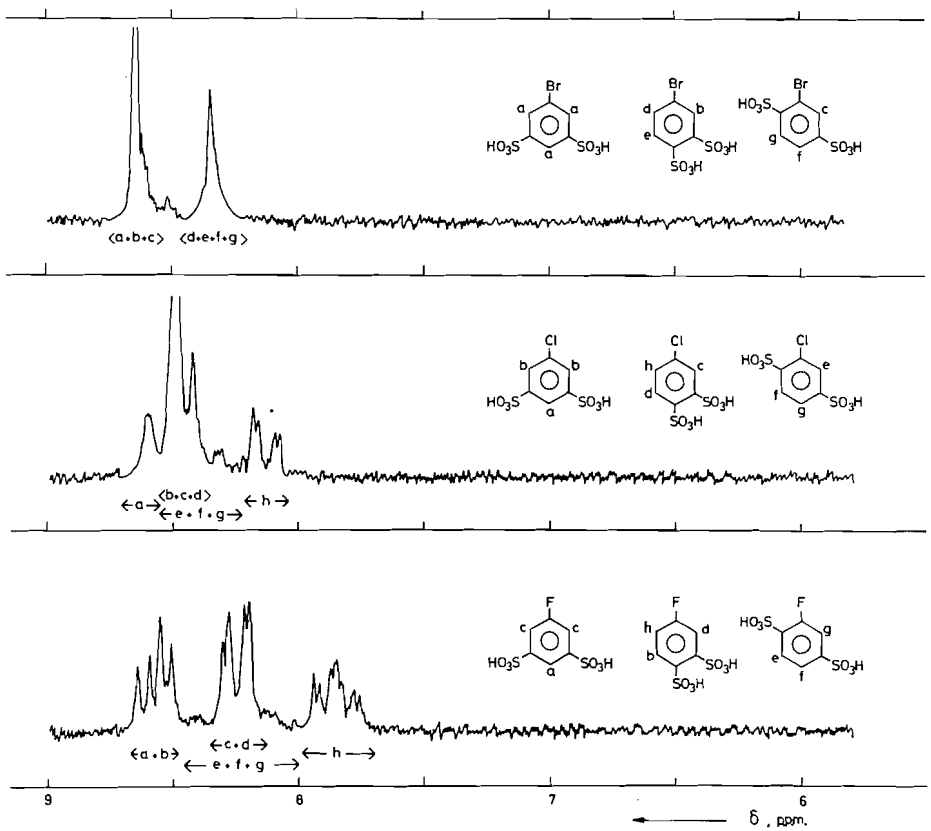

FIG. 1. The n.m.r. spectra with assignments of the sulfonation mixtures of *m*-$XC_6H_4SO_3H$ in 115% H_2SO_4 at 25°, after dilution to 98% H_2SO_4.

with those of the pure 2,4-disulfonic acid, indicating that this compound is the exclusive product.

The disulfonic acid isomer distribution in the sulfonation of the *m*-halogenobenzenesulfonic acids in 115% H_2SO_4 was determined by a three-component analysis of the n.m.r. spectra depicted in Fig. 1, each in terms of the three possible disulfonic acids. The results are given in Table 2 together with those for other meta-substituted benzenesulfonic acids. As is evident from the data for *m*-chlorobenzenesulfonic acid, the isomer distribution is kinetically controlled. Moreover Olivier has shown that the principal product under apparently thermodynamically controlled conditions is the chlorobenzene-3,5-disulfonic acid (13). The data of Table 2 illustrate that sulfonation ortho, meta, and para to the sulfonic acid group can be effected. The ratio of 3,4- to 3,5-disulfonic acid follows the order F > Cl > Me > *t*-Bu > H = 0. This order parallels the ability of the conjugative electron release of these substituents to the para-position. It therefore seems to emphasize the requirement of mesomeric electron release by the substituent at position 1 in order to effect sulfonation at position 4.

The degree of sulfonation at position 4 of the 3-halogenobenzenesulfonic acids is very much greater for the reaction in 115 than for that in 98% H_2SO_4 (*cf.* Tables 2 and 5). This may be explained in terms of a specific additional route for the introduction of a sulfo group ortho to the sulfonic substituent in the case of sulfonation in fuming sulfuric acid. In 115% H_2SO_4 the sulfonic acid substrate will be present mainly as the pyrosulfonic acid (6), and possibly in part as ArS_3O_9H.[3] Intramolecular rearrangement of the

[3]The presence of the entity $H_2S_3O_{10}$ in fuming sulfuric acid > 108% H_2SO_4 seems to be firmly established (14–17).

Can. J. Chem. Downloaded from www.nrcresearchpress.com by 210.87.254.5 on 09/05/12
For personal use only.

TABLE 2. Sulfonation of meta-substituted benzenesulfonic acids in 115% H_2SO_4 at 25°

Substituent	Reaction time (days)	Isomer distribution of disulfonic acid products (%) 2,5-	3,4-	3,5-	Reference
F	7	11±4	75±4	14±2	
Cl	7	11±4	46±3	43±3	
	14	10±4	50±3	40±3	
Br	7			46±5	
Me*		35±1	14±1	51±1	11
t-Bu*		0	16±1	84±1	10
H†		5.4±1.0	≤0.5	94.6±1.0	11, 12

*In 104% H_2SO_4.
†The sulfonation of benzenesulfonic acid in 101–109% H_2SO_4 at 25° yields 2.8% *p*- and 97.2% *m*-disulfonic acid (12).

pyrosulfonic acid can then lead to the formation of the σ-complex **1** with eventual formation of the 3,4-disulfonic acid (reaction 1).[4] The assigned sulfonating entity in the normal sulfonation of arenesulfonic acids in highly concentrated fuming sulfuric acid is $H_2S_4O_{13}$ (7). Sulfonation of the *m*-halogenobenzene-

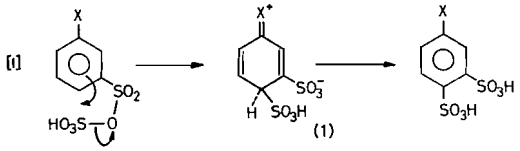

(pyro)sulfonic acids at position 4 by this bulky reagent seems on the other hand less probable for steric reasons.

Reaction in 98.1% H_2SO_4 at High Temperatures

The reactions of the halogenobenzenesulfonic acids occurring in 98.1% H_2SO_4 at 150° at low substrate concentration (0.7 mmol/l) were followed by means of u.v. absorption measurements. All reactions were found to be of the first order in the substrate.

With the *o*- and *p*-isomers as substrate, the composition of the reaction mixtures was analyzed by a three-component u.v. analysis using the *o*-, *p*-, and 2,4-disulfonic acid as reference compounds (19, 20). With the *o*-halogenobenzenesulfonic acids as substrate, the para-isomer and the 2,4-disulfonic acid are formed in a constant ratio. Apparently the two products are formed in competing reactions. On starting with the para-halogenobenzenesulfonic acids a very much slower reaction with formation of 2,4-disulfonic acid is observed. Typical experiments are given in Table 3. The kinetic results can be described in terms of reactions 2–4. The rate

TABLE 3. Reaction of *o*- and *p*-fluorobenzenesulfonic acid in 98.1% H_2SO_4 at 150°

Substrate	Reaction time (ks)	Fluorobenzenesulfonic acids, mmol/kg ortho-	para-	2,4-di-	para 2,4-di-
ortho	0.060	0.29	0.005	0.006	0.8
	0.60	0.17	0.06	0.09	0.7
	0.90	0.12	0.08	0.11	0.7
para	0.075	—	0.40	—	
	9.0	—	0.34	0.07	
	25.5	—	0.26	0.17	
	86.4	—	0.10	0.32	

TABLE 4. Isomerization and sulfonation rate constants (ks^{-1}) for the halogenobenzenesulfonic acids in 98.1% H_2SO_4 at 150°

Halogen	${}_ik_{o,p}$	${}_sk_o$	${}_sk_p$	k_m
fluoro	0.39	0.50	0.016	0.0074
chloro	0.37	0.34	0.0075	
bromo	0.40	0.45	0.0067	0.0013

[4]It may well be that the oxygen atom inbetween the two sulfur atoms of the pyrosulfonic acid has to be protonated first, or complexed by sulfur trioxide first, in order to allow the intramolecular ring sulfonation. In this connection the observation of the necessity of an additional molecule of sulfur trioxide in the aromatic sulfonylation by an arene-pyrosulfonic acid (18) seems of related interest.

Can. J. Chem. Downloaded from www.nrcresearchpress.com by 210.87.254.5 on 09/05/12
For personal use only.

Can. J. Chem. Downloaded from www.nrcresearchpress.com by 210.87.254.5 on 09/05/12
For personal use only.

TABLE 5. Reaction of *m*-halogenobenzenesulfonic acids (5 wt. %) in 98.1% H_2SO_4 at 170°; reaction mixture composition

Time (h)	Br (%)						Cl (%)						F (%)				
	m	*p*	*m* + *p*	2,4	(2,5 + 3,4)	3,5	*m*	*p*	2,4	2,5	3,4	(2,5 + 3,5)	*m*	*p*	2,4	2,5	(3,4 + 3,5)
4			97	0	—*	2.6*											
20.5													50	8	22†	20†	—†
24			64	24	—*	12*			20			14					
72			34	46	—*	20*			46			20	13	8	61†	18†	—†
144			21	52	—*	27*			58			23	3	6	74†	17†	—†
306			18	46	—*	36*	0	13	48	⩽7	0	39	⩽0.5	6	74	16	4
546	0	10		47	10	33	0	13	45	⩽7	0	43	0	7	72	14	7

*Data calculated on the assumption of the absence of the 2,5- and 3,4-disulfonic acid. This assumption does not affect the content of the 2,4-isomer, but only that of the 3,5-isomer. The assumption seems fair, as the total yield of the 2,5- + 3,4-isomers for the 546 h experiment amounts to only 10%.

†Data calculated on the assumption of the absence of the 3,4- and 3,5-disulfonic acid.

[2] $\text{ortho} \xrightarrow{{}_ik_{o,p}} \text{para}$

[3] $\text{ortho} \xrightarrow{{}_sk_o} \text{2,4-di}$

[4] $\text{para} \xrightarrow{{}_sk_p} \text{2,4-di}$

constants are listed in Table 4. The small variations in the isomerization rate constant ${}_ik_{o,p}$ and the sulfonation rate constant ${}_sk_p$ indicate the close balance between the mesomeric, inductive, and steric effects of the halogens. The constancy of ${}_sk_o$ indicates the balance between the mesomeric and the inductive effect (2).

The isomerization of arenesulfonic acids can be described as an intermolecular process, *i.e.* it proceeds via protiodesulfonation and subsequent sulfonation (21, 22). The amount of ortho- and meta-substitution in the sulfonation of the halogenobenzenes is only very small (1, 2). Therefore, in first approximation, the reported isomerization rate constants ${}_ik_{o,p}$ are equal to the desulfonation rate constants.

The reaction of a given *m*-halogenobenzenesulfonic acid (5 wt. %) in 98.1% H_2SO_4 at 170° was followed in time by recording the n.m.r. spectra of the withdrawn samples after cooling to ~32°. The compositions of the reaction mixtures, calculated by multicomponent analysis of the n.m.r. spectra, are given in Table 5. The *m*-halogenobenzenesulfonic acids in 98.1% H_2SO_4 at 170° undergo both sulfonation with formation of 2,5-, 3,5-, and possibly some 3,4-disulfonic acid, and isomerization with formation of the para-isomer, which is then sulfonated to yield the 2,4-disulfonic acid. At very high reaction times, when the starting compound is almost completely converted, the relative amount of the 3,5-disulfonic acid still increases and does so at the expense of the 2,4-isomer. The isomerization of chlorobenzene-2,4-disulfonic acid into the 3,5-isomer has been reported before as occurring in concentrated aqueous sulfuric acid at 300° (23). These isomerizations may proceed via the sequence 2,4-$(SO_3H)_2 \rightarrow$ 4-$SO_3H \rightarrow$ 3-$SO_3H \rightarrow$ 3,5-$(SO_3H)_2$, or via the sequence 2,4-$(SO_3H)_2 \rightarrow$ 2,5-$(SO_3H)_2 \rightarrow$ 3,5-$(SO_3H)_2$.

The ratio of isomerization to sulfonation of the *m*-halogenobenzenesulfonic acids was estimated from the low conversion ratio (4- + 2,4-)/(2,5- + 3,4- + 3,5-) to be 2.3 ± 0.5, 3.1 ± 0.6, and 4.0 ± 0.7 for the bromo-, chloro-, and fluoro-compound respectively.

The interconversion of the *m*- and *p*-chlorobenzenesulfonic acids in concentrated sulfuric acid at 185–220° was studied by Spryskov and Kachurin (24, 25), who reported equilibrium constants (24).

Experimental

The synthesis of the halogenobenzenesulfonates and the 2,4-disulfonates has been described previously (1, 2).

The u.v. absorption measurements were made with a Cary 14 recording spectrophotometer. The rate constants for the disappearance of a given halogenobenzenesulfonic acid in 98.1% H_2SO_4 were obtained from the u.v. spectra of the samples taken after appropriate reaction times, *viz.* from the slope of either log $|E_t - E_\infty|$ for a chosen wavelength or log |substrate| against reaction time. The former method was employed with the meta-isomers. The latter method was used with the ortho- and para-isomers; for these substrates the composition of the reaction mixtures was analyzed by a three-component, three-wavelengths u.v. analysis using *o*-, *p*-, and 2,4-disulfonic acid as reference compounds (19, 20).

The n.m.r. spectra were recorded with an A60 or HA100 Varian spectrometer using TMS in CCl_4 as an external standard. The substrate concentrations of the potassium or sodium halogenobenzenesulfonates for the reactions in 98.1% H_2SO_4 at 170° and in 115% H_2SO_4 at 25° were 5 and 10 wt. % respectively. The 115% H_2SO_4 mixtures were quenched with dilute sulfuric acid to yield 5 wt. % solutions in 98% H_2SO_4 as well; the n.m.r. spectra were recorded from these 98% H_2SO_4 solutions.

The composition of the reaction mixtures of the *m*-halogenobenzenesulfonic acids was determined by multicomponent n.m.r. analysis with the assignments of Table 1, using a method similar to that described extensively in connection with the analysis of the isomeric anthracenesulfonic acids (26).

The authors are greatly indebted to Dr. C. W. F. Kort for advice and to Miss M. Boomgaard for assistance.

1. C. W. F. KORT and H. CERFONTAIN. Rec. Trav. Chim. **86**, 865 (1967).
2. C. W. F. KORT and H. CERFONTAIN. Rec. Trav. Chim. **88**, 860 (1969).
3. H. CERFONTAIN. Mechanistic aspects in aromatic sulfonation and desulfonation. Interscience, New York, 1968. p. 221–226.
4. B. W. SCHNITGER and H. CERFONTAIN. Rec. Trav. Chim. **91**, 199 (1972).
5. H. CERFONTAIN. Rec. Trav. Chim. **80**, 296 (1961).
6. E. A. ROBINSON and V. SILBERBERG. Can. J. Chem. **44**, 1437 (1966).
7. C. W. F. KORT and H. CERFONTAIN. Rec. Trav. Chim. **88**, 1298 (1969).
8. K. HAYAMIZU and O. YAMAMOTO. J. Mol. Spectrosc. **28**, 89 (1968).

Can. J. Chem. Downloaded from www.nrcresearchpress.com by 210.87.254.5 on 09/05/12
For personal use only.

9. H. SUHR. Anwendungen der kernmagnetischen resonanz in der organischen chemie. Springer-Verlag, Berlin, 1965, p. 170.
10. C. RIS. Forthcoming Thesis. University of Amsterdam.
11. A. KOEBERG-TELDER and H. CERFONTAIN. Unpublished results.
12. A. J. PRINSEN, A. KOEBERG-TELDER, and H. CERFONTAIN. Tetrahedron, **26**, 1953 (1970).
13. S. C. J. OLIVIER. Rec. Trav. Chim. **37**, 307 (1918).
14. P. A. GIGUERE and R. SAVOIE. Can. J. Chem. **38**, 2467 (1960).
15. R. J. GILLESPIE and E. A. ROBINSON. Can. J. Chem. **40**, 658 (1962).
16. G. E. WALRAVEN. J. Chem. Phys. **40**, 2326 (1964).
17. K. STOPPERKA. Z. Anorg. Allgem. Chem. **345**, 264 (1966).
18. J. K. BOSSCHER and H. CERFONTAIN. Tetrahedron, **24**, 6543 (1968).
19. J. M. ARENDS, H. CERFONTAIN, I. S. HERSCHBERG, A. J. PRINSEN, and A. C. M. WANDERS. Anal. Chem. **36**, 1802 (1964).
20. H. CERFONTAIN. Rec. Trav. Chim. **84**, 551 (1965).
21. Reference 3, p. 206.
22. A. KOEBERG-TELDER, A. J. PRINSEN, and H. CERFONTAIN. J. Chem. Soc. B, 1004 (1969).
23. S. C. J. OLIVIER. Rec. Trav. Chim. **38**, 351, 356 (1919).
24. O. I. KACHURIN and A. A. SPRYSKOV. Izv. Vysshykh Ucheb. Zavedenii, Khim. i Khim. Tekhnol. 52 (1958); Through Chem. Abstr. **53**, 11285 (1959).
25. A. A. SPRYSKOV and O. I. KACHURIN. J. Gen. Chem. USSR. **28**, 2250 (1958).
26. A. KOEBERG-TELDER and H. CERFONTAIN. Rec. Trav. Chim. **91**, 22 (1972).
27. Z. R. H. NIENHUIS, W. J. SPILLANE, and H. CERFONTAIN. Can. J. Chem. This issue.

Can. J. Chem. Downloaded from www.nrcresearchpress.com by 210.87.254.5 on 09/05/12
For personal use only.

The Electrochemical Reduction of Compounds with the —N=C—C=N— Group. III *as*-Triazines

JEAN PINSON, JEAN-PIERRE M'PACKO, AND NICOLE VINOT

Laboratoire de Chimie Organique Structurale, Université de Paris VI, 8 Rue Cuvier, Paris V, France

AND

JOSEPH ARMAND AND PHILIPPE BASSINET

Laboratoire de Chimie IV, Université de Paris VI, 8 Rue Cuvier, Paris V, France

Received November 19, 1971

The electrochemical reduction of *as*-triazines 3-one or -thione leads to a 1,4-dihydro derivative which rearranges into a 4,5-dihydro compound which is further reducible to an imidazolone or a tetrahydro *as*-triazine 3-one. In the case of simple *as*-triazine the 1,4-dihydro compound rearranges either to a 1,2- or to a 4,5-dihydro compound. This last derivative can be reduced to an imidazole or a tetrahydro *as*-triazine. The mechanisms are discussed.

La réduction électrochimique des *as*-triazine ones-3 ou thiones-3 conduit à un dérivé dihydro-1,4 qui se transpose en un dérivé dihydro-4,5 lui-même réductible en imidazolone ou en tétrahydro *as*-triazine one-3. Dans le cas des *as*-triazines simples, le dérivé dihydro-1,4 se réarrange en dihydro-1,2 ou 4,5 *as*-triazine. Ce dernier composé peut être réduit en imidazole ou en tétrahydro *as*-triazine. Les mécanismes sont discutés.

Canadian Journal of Chemistry, **50**, 1581 (1972)

Introduction

It has already been shown that the —N=C—C=N— group is electrochemically reduced at a mercury electrode according to eq. 1. The reaction is valid whether this group

[1] —N=C—C=N— + $2e^-$ + $2H^+$ ⇌ —HN—C=C—NH—

is included in an aromatic ring (quinoxalines (1)), in a non-aromatic ring (dihydro-5,6 pyrazines (2)), or in an open-chain compound (α-diimines (3)), and even if the substituents on the two carbons are different. It seemed interesting to study the electrochemical reduction of compounds with the same —N=C—C=N— group, but with different substituents on the two nitrogen atoms; this is the case of *as*-triazines. We have studied both *as*-triazine 3-one (or -thione) and simple *as*-triazines.

Results and Discussion

1. as-Triazines 3-One (or Thione)

We will first describe the polarography and the controlled potential reduction in hydro-organic medium of 5,6-diphenyl *as*-triazine 3-one (**1**), 5,6-diphenyl 2-methyl *as*-triazine 3-one (**2**), and 5,6-diphenyl *as*-triazine 3-thione (**3**). The polarography and the controlled potential electrolysis of the corresponding 4,5-dihydro compounds will then be described.

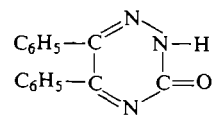

1

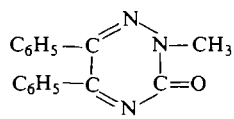

2

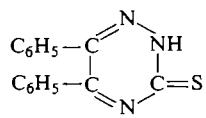

3

1.1 Reduction of as-Triazines 3-One (or-Thione)

1.1.1. Polarography and behavior in hydro organic medium

The stability of **1**, **2**, and **3** has been examined by u.v. spectroscopy in water–acetonitrile media at different p*H*. Compounds **1** and **2** are stable between p*H* 1 and 12, while **3** is only stable at p*H* > 7. The 5,6-diphenyl 2-methyl *as*-triazine 3-thione decomposes rapidly over the whole p*H* range.

Can. J. Chem. Downloaded from www.nrcresearchpress.com by 210.87.254.105 on 09/05/12
For personal use only.

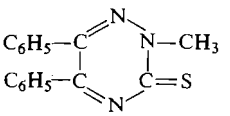

Compound **1** shows over the whole pH range studied ($c = 2.10^{-3}$ M, 20% CH_3CN) a single two-electron wave (3), the half-wave potential of which varies linearly with the pH as $E_{1/2} = -0.13 - 0.080$ pH (Fig. 1). In the case of **2** a single two-electron wave is observed in acidic medium, the $E_{1/2}$ of which varies linearly with the pH. At pH higher than 5 the wave height decreases while the height of a second wave, at more negative potential, increases. The $E_{1/2}$ of the second wave does not vary with the pH. This can be interpreted by supposing that the first wave corresponds to the reduction of protonated species and the second wave to the reduction of neutral species.

The sum of the heights of the first and the second wave remains constant and above pH 6 only the second wave is present.

The polarograms of **3** are strongly perturbed by adsorption phenomena. The half-wave potentials are given in Table 1.

1.1.2. Electrolyses in dilute solutions

We will describe the typical case of **1** at pH 1 (50% CH_3CN). The polarograms drawn in the course of electrolyses of dilute solutions under an argon atmosphere show that an anodic wave appears, the half-wave potential of which is close to that of the cathodic wave of **1**, followed by a cathodic wave at more negative potentials. (Fig. 2).

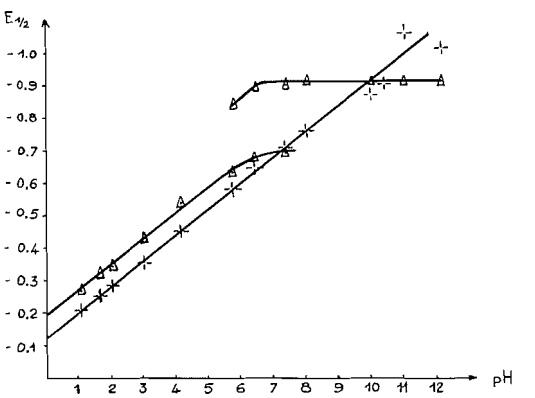

FIG. 1. The pH dependence of half-wave potentials $E_{\frac{1}{2}}$ (V/SCE) of **1** (-⊹-) and **2** (△).

TABLE 1. Half-wave potentials (V/SCE)

pH	1	3	5	7	9	11
1	−0.21	−0.37	−0.53	−0.69	−0.85	−1.01
2	−0.26	−0.44	−0.60	−0.69 −0.90	−0.92	−0.92
3				−0.6	−0.8	−1.0

As the electrolysis proceeds the height of the anodic wave increases until it reaches about a quarter of the height of the cathodic wave of **1** and then decreases.

At the end of the electrolysis (consumption of 2 F/mol) only a cathodic wave, the height of which is close to that of **1**, remains. If the electrolyse is interrupted before the second cathodic wave appears and if the flow of argon is stopped, the anodic wave decreases rapidly and the wave of **1** reappears at its original height.

At pH 6.30 (50% methanol) an anodic wave, the height of which remains constant, appears while a white compound precipitates; but no cathodic wave can be seen. At pH 11 (50%

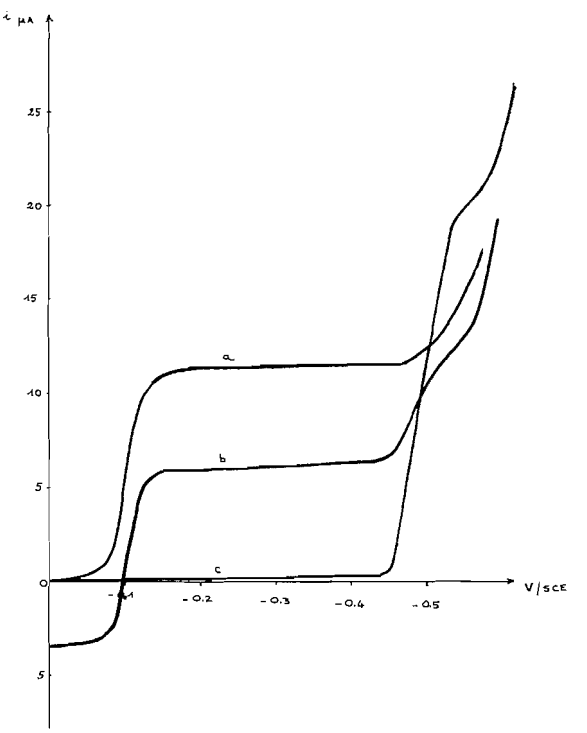

FIG. 2. Polarograms registered during the electrolysis of **1** (pH 1, CH_3CN 50%, c 2×10^{-3} M); a, beginning; b, $c_1 = 10^{-3}$ M; c, end.

Can. J. Chem. Downloaded from www.nrcresearchpress.com by 210.87.254.105 on 09/05/12
For personal use only.

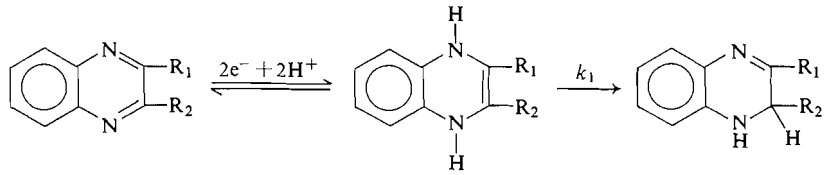

SCHEME 1

TABLE 2. Half-wave potentials (V/SCE)

	pH	1.0*	6.30†	7.90†	11.0†
1	$E_{\frac{1}{2}c}$	−0.21	−0.50		−0.92
	$E_{\frac{1}{2}a}$	−0.17	−0.47		
2	$E_{\frac{1}{2}c}$	−0.25	−0.57; −0.88		−0.81
	$E_{\frac{1}{2}a}$	−0.21	−0.51		
3	$E_{\frac{1}{2}c}$			−0.71	−1.00
	$E_{\frac{1}{2}a}$			−0.57	

*20% CH_3CN.
†50% CH_3CN.

methanol) for **1** and **2** no anodic or cathodic wave appears; for **3** a cathodic wave is observed at potentials close to that of the background discharge. However, cyclic voltametry carried out on a hanging mercury drop shows that in basic medium the primary reduction compound of **1**, **2**, and **3** presents an anodic peak (*i.e.* for **1** pH 10.1, CH_3OH 50%, $v = 0.2\ V\ s^{-1}$, $E_c = -1.00$, $E_a = -0.66$ V, $i_a = 0.7\ i_c$).

Table 2 gives the half-wave potentials of **1**, **2**, and **3** ($E_{1/2c}$) and of the anodic waves of the primary reduction compounds ($E_{1/2a}$).

A similar phenomenon has already been observed in the electrochemical reduction of quinoxalines (1); it has been shown that the anodic wave corresponds to a 1,4-dihydro derivative of type —NH—C=C—NH— which rearranges into a derivative of type —N=C—CH—NH— which is reducible at the dropping mercury electrode at more negative potentials than the starting quinoxaline (Scheme 1). It will be shown that reaction Scheme 2 is proved by preparative electrolyses. This is in good agreement with the fact that the following compound shows an anodic wave and reoxidizes rapidly in the air as has been shown by Kwee and Lund (4).

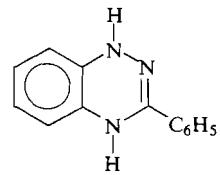

It must be noticed that as in the case of quinoxalines the rearrangement rate (which varies with the solvent, the pH, and the buffer composition) is under control of a general acidobasic catalysis.

Thus the electrochemical reduction in dilute solution of compounds **1**, **2**, and **3** yields a very oxidizable compound which shows an anodic wave and rearranges more or less rapidly, according to the pH, into a derivative evidencing a cathodic wave.[1]

1.1.3. Preparative electrolyses

Preparative electrolyses are carried out at 25° on a mercury pool, under argon. A saturated calomel electrode was used.

5,6-Diphenyl as-triazine 3-one (1). In acidic medium (pH 1, $E = -0.35$ V), a white compound precipitates in the course of the electrolysis. This compound is identified, by com-

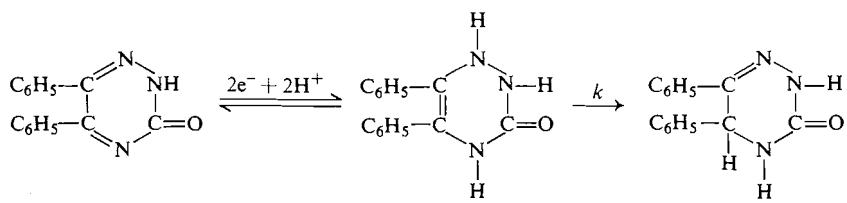

SCHEME 2

[1]The electrochemical reduction of *as*-triazines into 1,4-dihydro compounds is electrochemically irreversible ($E_{\frac{1}{2}c} \neq E_{\frac{1}{2}a}$).

Can. J. Chem. Downloaded from www.nrcresearchpress.com by 210.87.254.105 on 09/05/12
For personal use only.

Can. J. Chem. Downloaded from www.nrcresearchpress.com by 210.87.254.105 on 09/05/12
For personal use only.

parison with an authentic sample (5), as the 4,5-dihydro 5,6-diphenyl *as*-triazine 3-one (**4**). In neutral medium (p*H* 6, $E = -0.95$ V) an easily reoxidizable white compound precipitates in the course of the electrolysis. It is the 1,4-dihydro 5,6-diphenyl *as*-triazine 3-one, as shown by its spectroscopic properties. In solution this compound shows the same anodic wave as that observed in the electrolysis of **1** in dilute solution. In basic medium (p*H* 11, $E = -1.10$ V) the same product as in acidic medium is obtained.

5,6-Diphenyl 2-methyl as-triazine 3-one (2). In acidic medium (p*H* 1, $E = -0.35$ V) an easily reoxidizable white compound precipitates in the course of the electrolysis. It is identified by its spectroscopic properties as the 1,4-dihydro 5,6-diphenyl 2-methyl *as*-triazine 3-one. It shows the same anodic wave as that observed in the course of the electrolysis of **2** in dilute solution. In basic medium (p*H* 11, $E = -1.05$ V) a white compound precipitates which is identified by comparison with an authentic sample (5) as the 4,5-dihydro 5,6-diphenyl 2-methyl *as*-triazine 3-one (**5**). This same compound can also be obtained in acidic medium, by leaving the solution under argon several hours after the end of the electrolysis.

5,6-Diphenyl as-triazine 3-thione (3). In neutral medium (p*H* 7.5, $E = -0.90$ V) a yellow compound precipitates in the course of the electrolysis. This easily oxidizable compound which shows in solution the same anodic wave as that observed in the electrolysis of **3** in dilute solutions is the 1,4-dihydro 5,6-diphenyl *as*-triazine 3-thione. In basic medium (p*H* 11, $E = -1.10$ V) the 4,5-dihydro 5,6-diphenyl *as*-triazine 3-thione (**6**) precipitates in the course of the electrolysis.

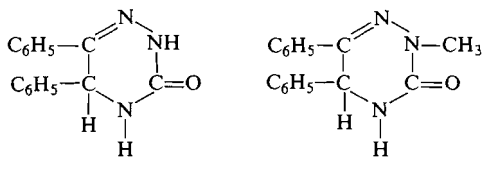

4 **5**

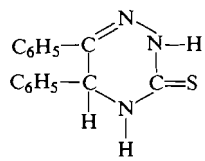

6

TABLE 3. Half-wave potentials (V/SCE)

p*H*	1.30	3.05	5.50	10.30
4	−0.97	−1.15	−1.33	
5	−1.00	−1.14	−1.33	
6			−1.60	−1.90

In conclusion, the preparative electrolysis supports Scheme 2. The primary reduction compound is a 1,4-dihydro triazine which presents an anodic wave at the dropping mercury electrode and is easily oxidizable. This 1,4-dihydro triazine rearranges into a 4,5-dihydro triazine with a rate depending on the medium.

1.2. 4,5-Dihydro as-Triazines 3-One (or Thione)

1.2.1. Polarography of the 4,5-dihydro derivatives

These compounds are reducible in certain p*H* ranges only and then show a single wave the height of which varies with the p*H*. The half-wave potentials are given in Table 3 ($c = 2.10^{-3}$ *M*, 40% CH_3CN).

1.2.2. Electrolysis of 4,5-dihydro derivatives

4,5-Dihydro 5,6-diphenyl as-triazine 3-one (4). In the course of the electrolysis of **4**, in acidic medium (p*H* 0.93, $E = -1.00$ V), a white compound precipitates which is identified by comparison with an authentic sample (5) as the 4,5-diphenyl imidazole 2-one (**7**). By making the filtrate alkaline (p*H* 11) a second compound precipitates: the *trans*-1,4,5,6-tetrahydro 5,6-diphenyl *as*-triazine 3-one (**8***b*) (5). In neutral medium, only the *cis*-1,4,5,6-tetrahydro 5,6-diphenyl *as*-triazine 3-one (**8***a*) is obtained.

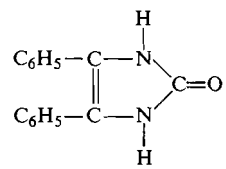

7

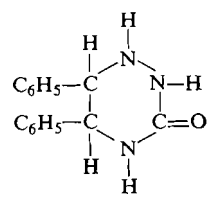

8

a cis
b trans

4,5-Dihydro 5,6-diphenyl 2-methyl as-triazine 3-one (5). The reduction in acidic medium gives the 4,5-diphenyl 1-methyl imidazole 2-one **9**.

4,5-Dihydro 5,6-diphenyl as-triazine 3-thione

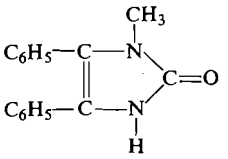

9

(6). In the course of the reduction of **6** in basic medium (p*H* 10.67, $E = -2.00$ V) the *cis*-1,4,5,6-tetrahydro 5,6-diphenyl *as*-triazine 3-thione **10** precipitates. Thus, the reduction of 4,5-dihydro compounds leads to two different kinds of

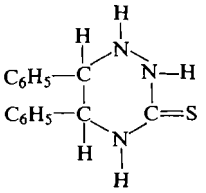

10

compounds: the 1,4,5,6-tetrahydro triazines and the 2-imidazolones. It has been shown that under the conditions of the electrolysis, the imidazolone does not come from the corresponding tetrahydrotriazine. No imidazolone can be detected in a solution of the tetrahydrotriazine which has been allowed to stand for a time equivalent to the length of an electrolysis. The reaction scheme can be rationalized as shown in Scheme 3.

Scheme 3 is in good agreement with the reduction of phenylhydrazones in acidic medium (6) and with the scheme proposed by Kwee and Lund (4) for benzotriazines. The cleavage of the N_1—N_2 bond needs a preliminary protonation of the N_2 nitrogen, a quaternary ammonium then being a good leaving group. In the case of **5** only the imidazolone is obtained in acidic medium, this can be explained by the higher basicity of the N_2 nitrogen which carries a methyl group.

2. as-Triazines

We will describe the case of 5,6-diphenyl *as*-triazine (**11**) and 3,5,6-triphenyl *as*-triazine (**12**).

2.1. Behavior in Hydroorganic Medium and Polarography

Compounds **11** and **12** are stable in hydroorganic medium over the whole p*H* range.

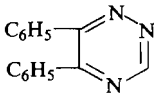

11

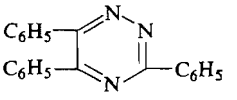

12

Compound **11** ($c = 10^{-3}$ *M*, 40% CH_3OH) shows two two-electron waves up to p*H* 7; at higher p*H* only the first wave remains; its half-wave potential (V/SCE) varies linearly with the p*H* as $E_{1/2} = -0.14 - 0.066$ p*H*. Compound **12** ($c = 10^{-4}$ *M*, 40% MeOH) behaves similarly; the second wave exists only up to p*H* 8. The half-wave potential of the first wave varies linearly with the p*H* as: $E_{1/2} = -0.23 - 0.062$ p*H*. The half-wave potentials are presented in Table 4.

2.2. Electrolysis in Dilute Solutions

An electrolysis of **11** under argon at a potential corresponding to the first plateau ($c = 2.10^{-3}$ *M*, p*H* 3.65, 50% CH_3OH, $E = -0.60$ V) gives

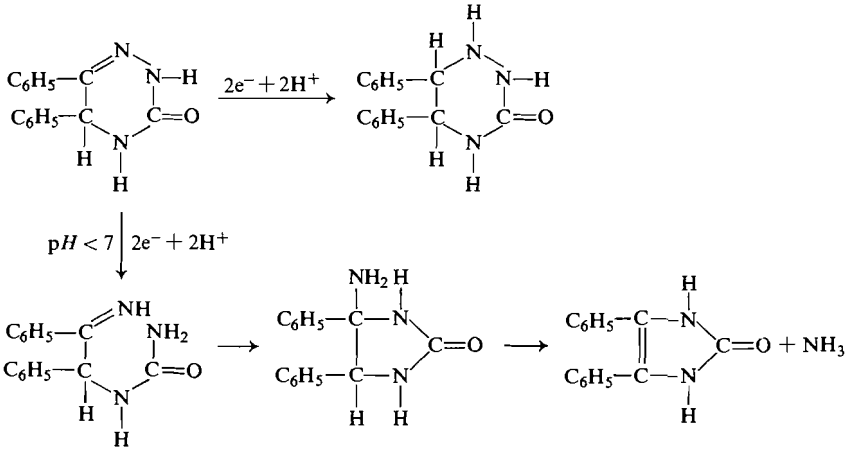

SCHEME 3

Can. J. Chem. Downloaded from www.nrcresearchpress.com by 210.87.254.105 on 09/05/12
For personal use only.

TABLE 4. Half-wave potentials (V/SCE)

pH	1	3	5	7	9	11	
11	−0.21	−0.34	−0.47	−0.60	−0.74	−0.87	1st wave
	−0.88	−0.97	−1.15	−1.36			2nd wave
12	−0.29	−0.41	−0.54	−0.66	−0.79	−0.91	1st wave
	−0.77	−0.88	−1.05	−1.42			2nd wave

a compound which shows an anodic wave at a potential slightly more positive than the cathodic wave of the starting compound. The height of the anodic wave never exceeds about a tenth of the height of the cathodic wave of **11**. At the end of the electrolysis, after consumption of about 2 F/mol, only a cathodic wave, the half-wave potential of which is slightly different from that of the second wave of **11**, remains. The same phenomenon is observed at p*H* 6.20 ($E = -0.80$ V), while at p*H* 12.83 ($E = -1.20$ V) no anodic wave appears. Cyclic voltametry carried out on a hanging mercury drop shows that in alkaline medium the primary reduction compound also shows an anodic peak (p*H* 12.96, CH_3OH 50%, $v = 0.2$ V s^{-1}, $E_c = -1.00$, $E_a = -0.72$ V, $i_a = 0.9\, i_c$). The same behavior is observed for **12**. Table 5 gives the half-wave potentials of **11** and **12** ($E_{1/2c}$) and of the anodic waves of the primary reduction compounds ($E_{1/2a}$).

The similarity of the results obtained in the electrolysis in dilute solutions of **11** and **12** with those of compounds **1**, **2**, and **3** indicates that a 1,4-dihydro derivative is obtained as the primary reduction compound. This 1,4-dihydro compound then undergoes a rearrangement.

2.3. Preparative Electrolysis

*3,5,6-Triphenyl as-Triazine (**12**)*

Reduction on the first plateau. In the course of an electrolysis at p*H* 3.60 ($E = -0.70$ V) a white compound precipitates which is identified as the 1,2-dihydro 3,5,6-triphenyl *as*-triazine **13**. By extracting the filtrate with ether a second compound, the 4,5-dihydro 3,5,6-triphenyl *as*-triazine **14**, is obtained. A reduction at p*H* 13.5 ($E = -1.30$ V) leads only to the 4,5-dihydro 3,5,6-triphenyl *as*-triazine **14**. The spectroscopic properties of **14** do not allow a definite choice between a 4,5-dihydro structure and a 5,6-dihydro structure. However the analogy of polarographic behavior between **14** and **4**, **5**, and **6** points to a 4,5-dihydro compound. Besides, the 5,6-dihydro derivative would probably be irreducible at the dropping mercury electrode.

Reduction on the second plateau. By adding water to the electrolysis solution (p*H* 3.60, $E = -1.30$ V, 4 F/mol) the 2,4,5-triphenyl imidazole **15** is obtained and by neutralizing the filtrate with sodium bicarbonate the *cis*-1,4,5,6-tetrahydro 3,5,6-triphenyl *as*-triazine **16** precipitates. The reduction at p*H* 6.20 ($E = -1.40$ V) only leads to the 2,4,5-triphenyl imidazole **15**. The 5,6-diphenyl *as*-triazine **11** gives similar results.

2.4. Reduction of 4,5-Dihydro Compounds

The 1,2-dihydro derivatives are not reducible at the dropping mercury electrode, but the 4,5-dihydro *as*-triazine shows a two-electron wave ($E_{1/2}$ given in Table 6).

A preparative electrolysis of **14** at p*H* 3.60 ($E = -1.20$ V) yields the *cis*-1,4,5,6-tetrahydro 3,5,6-triphenyl *as*-triazine **16**.

2.5. Reduction Mechanism

The different steps of the electrochemical reduction of **12** are given in Scheme 4. The primary reduction compound for **11** and **12** is the 1,4-dihydro derivative characterized by its

TABLE 5. Half-wave potentials (V/SCE) (50% CH_3OH)

	pH	3.6	6.0	13.0
11	$E_{\frac{1}{2}c}$	−0.38	−0.53	−1.00
	$E_{\frac{1}{2}a}$	−0.34	−0.51	—
12	$E_{\frac{1}{2}c}$	−0.45	−0.60	−1.04
	$E_{\frac{1}{2}a}$	−0.40	−0.57	—

TABLE 6. Half-wave potentials (V/SCE) (50% CH_3OH)

pH	3.60	6.00	13.00
4,5-Dihydro 5,6-Diphenyl *as*-Triazine	−0.95	−1.32	−1.40
4,5-Dihydro 3,5,6-Triphenyl Triazine **14**	−0.97	−1.06	−1.45

Can. J. Chem. Downloaded from www.nrcresearchpress.com by 210.87.254.105 on 09/05/12
For personal use only.

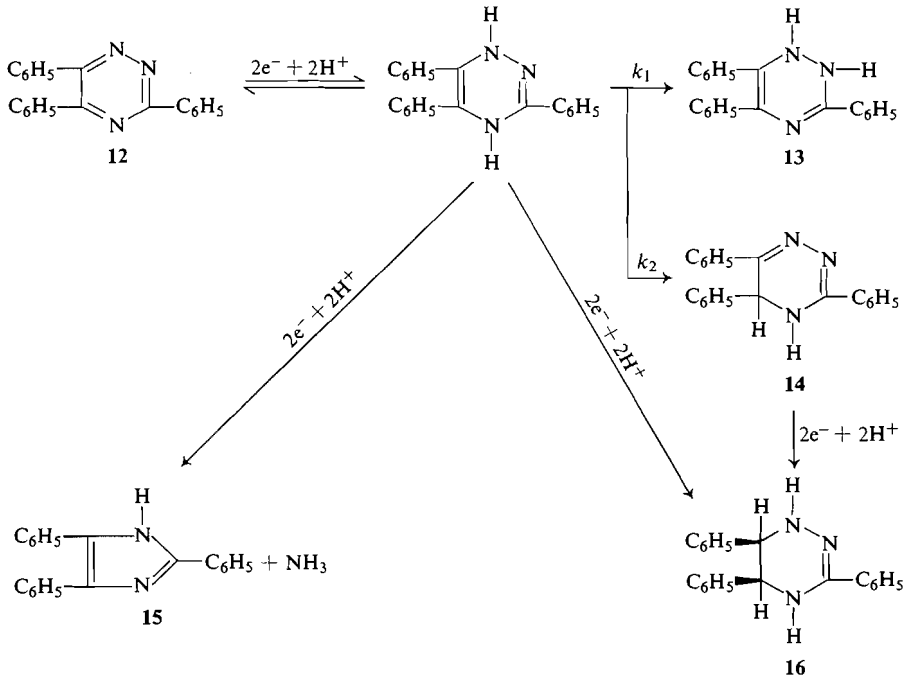

SCHEME 4

anodic wave, but it rearranges too quickly to be isolated. The 1,2- and 4,5-dihydro derivatives are obtained through two competitive reactions; it has been shown that under the conditions of the electrolysis these two compounds do not transform into each other; in the solution and during the time of the electrolysis the 1,2-dihydro compound does not give the 4,5-dihydro compound; in the same way the 4,5-dihydro compound does not give the 1,2-dihydro compound. The relative amount of these two compounds is strongly dependent on the p*H*. The 1,4-dihydro *as*-triazine shows two polarographic waves: an anodic wave (corresponding to the reoxidation into the starting compound) and a cathodic wave (the second wave observed on the polarograms of *as*-triazine). The reduction of the 1,4-dihydro *as*-triazine leads either to an imidazole or to a 1,4,5,6-tetrahydro triazine; here also the relative amount of the two compounds depends strongly on the p*H*. Scheme 5 could explain the formation of the imidazole. At last the 4,5-dihydro *as*-triazine is itself reducible, it corresponds to the cathodic wave observed at the end of the electrolysis of **11** and **12** in dilute solutions, and leads to a 1,4,5,6-tetrahydro *as*-triazine.

3. Remarks on the Stereochemistry of 1,4,5,6-tetrahydro as-Triazines

The n.m.r. spectra of **8**, **10**, and **16**, after addition of D_2O, show that either one or the other of the two possible isomers is obtained. The molecular models show that the ring takes a half chair conformation as cyclohexene and the two phenyl groups can be either *cis* or *trans* to each other. The coupling constants are: $J_{H_5-H_6} = 4.0$ for **10**, 8.2 for **8***b*, 4.0 for **8***a*, and 4.0 Hz for

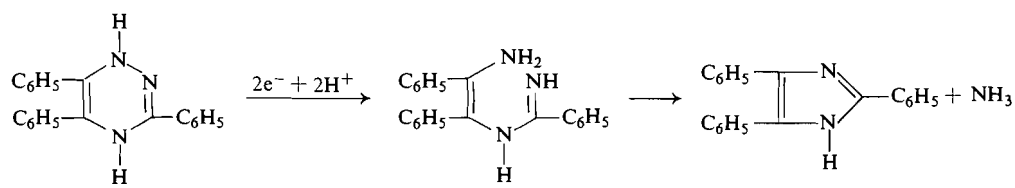

SCHEME 5

Can. J. Chem. Downloaded from www.nrcresearchpress.com by 210.87.254.105 on 09/05/12
For personal use only.

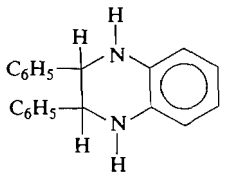
(Ref.7)

$J_{H_2-H_3}$ = 2.6–2.7 Hz (*cis*)
$J_{H_2-H_3}$ = 7.0–8.2 Hz (*trans*)

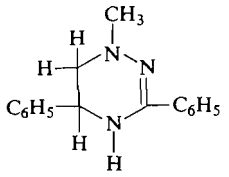
(Ref.8)

$J_{H_5-H_6}$ = 7.40 Hz (*trans*)

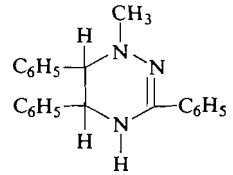
(Ref.8)

$J_{H_5-H_6}$ = 6.68 Hz (*trans*)

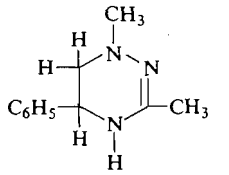
(Ref.8)

$J_{H_5-H_6}$ = 7.35 Hz (*trans*)

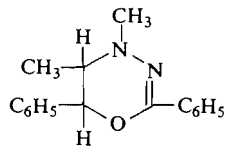
(Ref.9)

$J_{H_5-H_6}$ = 2.90 Hz (*cis*)
$J_{H_5-H_6}$ = 7.45 Hz (*trans*)

CHART 1

16. Chart 1 shows the values found in the literature. Therefore **8***b* is a *trans* derivative. The 5 and 6 protons are *trans* axial–axial with a dihedral angle of about 180°, and the two phenyl groups are in equatorial position. On the contrary **8***a*, **10**, and **16** are certainly *cis*-tetrahydro triazines. The coupling constant of 4.0 Hz obtained for **8***a*, **10**, and **16** is somewhat greater than the coupling constants given above. This may be due to a deformation of the ring which decreases the dihedral angle $C_5H—C_6H$ and thus increases the J_{H_5}–J_{H_6} coupling constant.

Thus, these results are different from that obtained in the electrochemical reduction of quinoxalines. These last compounds always yield *cis*-tetrahydro quinoxalines (1). These differences can be explained in the following way: the dihydroquinoxalines, **4** (in neutral medium), **6**, and **14** would be adsorbed when the last proton is fixed. On the contrary, the stereochemically determining step in the reduction of **4** in acidic medium, that is the fixation of the last proton, would take place in the bulk of the solution. The most stable isomer where the two phenyl groups are equatorial would then be obtained.

Conclusion

(*1*) Although the two substituents on the nitrogen atoms of the studied compounds are very different, the observed primary reduction mechanism is similar to that of the compounds with the —N=C—C=N— group previously studied (eq. 1).

(*2*) The electrochemical reduction of *as*-triazines allows selective preparation of some compounds which cannot be obtained by chemical reduction (5,10,11,16): the 1,4-dihydro *as*-triazines 3-one (or -thione), the 4,5-dihydro *as*-triazines, and the 1,4,5,6-tetrahydro *as*-triazines or *as*-triazinones. These last compounds are obtained stereoselectively.

Experimental

The apparatus and techniques used have been described previously (1). The cathodic compartment of the electrolytic cell is a glass cylinder of 85 mm diameter and the anodic compartment which fits in the cathodic compartment is a glass cylinder of 50 mm diameter closed at its lower end by a fine fritted glass. The organic cosolvents used in the elec-

Can. J. Chem. Downloaded from www.nrcresearchpress.com by 210.87.254.105 on 09/05/12
For personal use only.

Can. J. Chem. Downloaded from www.nrcresearchpress.com by 210.87.254.105 on 09/05/12
For personal use only.

trolyses are either methanol or acetonitrile (for solubility reasons). It has been checked that the nature of the cosolvent does not change the results of the electrolyses. All the compounds gave correct elemental analysis.

1. Controlled Potential Electrolysis of as-Triazines 3-One (or -Thione)

1.1 Reduction of 5,6-Diphenyl as-Triazine 3-One (1)

Compound **1** is prepared according to Biltz and Stellbaum (12) by condensation of semicarbazide hydrochloride with benzile in boiling acetic acid. Yellow crystals, m.p. 224°, are obtained.

Reduction of 1 in acidic medium

A solution is prepared from 100 cm^3 CH_3CN, 40 cm^3 1 *N* H_2SO_4, 60 cm^3 of water. Three grams of **1** are dissolved in 150 cm^3 of this solution (p*H* 0.97). In the course of the electrolysis ($E = -0.35$ V, 2.0 F/mol) a white compound precipitates, m.p. 176°, 2 g (yield 67%) identified as **4** (4,5-dihydro 5,6-diphenyl *as*-triazine 3-one) by comparison (i.r., n.m.r.) with an authentic sample.

Reduction at pH 6.3

A solution (200 cm^3) is prepared from 100 cm^3 CH_3OH, 40 cm^3 1 *N* NaOH, 3.6 g of succinic acid, and water. Compound **1** (0.5 g) is dissolved in 150 cm^3 of this solution, the rest of it being used as anolyte. In the course of the electrolysis ($E = -0.95$ V, 2.0 F/mol) a white compound precipitates, recovered under nitrogen in a glove box. The product is identified as the 1,4-dihydro 5,6-diphenyl *as*-triazine 3-one (370 mg, yield 75%, m.p. 150°). The n.m.r. spectrum (DMSO-d_6): NH 1 proton(s) δ 6.30, 1 proton(s) 8.05, and 1 proton(s) 8.26 p.p.m. which can be displaced by D_2O; C_6H_5 10 protons(m) 7.00–7.60 p.p.m. The i.r. spectrum (KBr pellet) ν_{NH} 3280 (m), 3200 cm^{-1} (m), $\nu_{C=O}$ 1680 cm^{-1} (s). The product reoxidizes rapidly in the air.

1.2 Reduction of 5,6-Diphenyl 2-Methyl as-Triazine 3-One

Compound **2** is prepared according to Biltz and Stellbaum (12).

Reduction in acidic medium

Compound **2** (0.5 g) is dissolved in 150 cm^3 of a solution prepared from 100 cm^3 CH_3CN, 40 cm^3 1 *N* H_2SO_4, and 60 cm^3 H_2O. In the course of the electrolysis (p*H* 0.97; $E = -0.35$ V, 2.0 F/mol) a white compound precipitates, recovered under nitrogen in a glove box (350 mg, yield 70%, m.p. 153° (alcohol)). This compound is easily oxidized in the air. The n.m.r. spectrum (DMSO-d_6) N—CH_3 3 protons(s) δ 2.91, N_1—H 1 proton(s) 6.60, N_4H 1 proton(s) 8.46 p.p.m., both NH protons are displaced by addition of D_2O; C_6H_5 10 protons(m) 7.0–7.5 p.p.m. The i.r. spectrum (KBr pellet) ν_{NH} 3.200 (m), $\nu_{C=O}$ 1670 cm^{-1} (s). This allows assignment of the 1,4-dihydro 2-methyl *as*-triazine 3-one formula to this compound (in particular, there is no C—H protons in the n.m.r. spectrum).

Reduction in basic medium pH 11

A solution is prepared from 100 cm^3 CH_3OH, 1.7 g CO_3HNa, 4 cm^3 1 *N* NaOH, and 100 cm^3 of water. Compound **2** (0.5 g) is dissolved in 150 cm^3 of this solution. A white precipitate appears in the course of the electrolysis ($E = -1.05$ V, 2.1 F/mol); 350 mg, yield 70%, m.p. 195° (alcohol); n.m.r. spectrum (DMSO-d_6): N—CH_3 3 protons(s) δ 3.31, C_5—H 1 proton(d) 5.78, N_4H 1 proton(d) 8.13 p.p.m. $J_{C_5H-N_4H} = 4.0$ Hz; the addition of D_2O transforms the doublet of C_5H in a singlet and N_4H is displaced. The i.r. spectrum (KBr pellet) ν_{NH} 3200, $\nu_{C=O}$ 1680 cm^{-1}. This compound is identical (t.l.c., i.r., m.p., n.m.r.) to the compound obtained by hydrogenation of **2** in the presence of Raney nickel (5) and to that obtained by electrolysis of **2** in acidic medium when the solution is kept under argon several hours after the end of the electrolysis. Thus this compound is the 5,6-diphenyl 2-methyl 4,5-dihydro *as*-triazine 3-one **5**.

1.3. Reduction of 5,6-Diphenyl as-Triazine 3-Thione (3)

Compound **3** is prepared according to Klosa (13)

Reduction in neutral medium

A solution is prepared from 120 cm^3 CH_3OH, 50 cm^3 1 *N* NaOH, 30 cm^3 H_2O, and 3.9 g citric acid. Compound **3** (0.5 g) is dissolved in 150 cm^3 of this solution. In the course of the electrolysis (p*H* 7.42, $E = -0.90$ V, 1.8 F/mol) a yellow compound precipitates which is recovered in a glove box under nitrogen (350 mg, yield 70%), m.p. 210° (alcohol). The n.m.r. spectrum (DMSO-d_6): N_1H 1 proton(s) δ 6.5, N_4H 1 proton(s) 9.5, both NH are displaced by addition of D_2O, C_6H_5 10 protons(m) 7.0–7.6 p.p.m. The i.r. spectrum (KBr pellet) ν_{NH} 3150, $\nu_{N-C=S}$ 1530 (s), $\nu_{C=S}$ 1220 cm^{-1}. In solution this compound is easily oxidized by air to **3**. Thus, this compound is the 1,4-dihydro 5,6-diphenyl *as*-triazine 3-thione **6**.

Reduction in basic medium

A solution is prepared from 100 cm^3 CH_3OH, 100 cm^3 of water, 1.7 g CO_3HNa and 4 cm^3 1 *N* NaOH. Compound **3** (0.5 g) is dissolved in 150 cm^3 of this solution (p*H* 10.64). In the course of the electrolysis ($E = -1.00$ V, 1.9 F/mol) a white compound precipitates (350 mg, yield 70%) F = 222° (alcohol). The n.m.r. spectrum (DMSO-d_6): C_5H 1 proton (d) δ 5.71, N_4H 1 proton (d) 9.70, $J_{C_5H-N_4H} = 4.0$ Hz, N_2H 1 proton(s) 11.50 C_6H_5 10 protons(m) 7.0–8.0 p.p.m. The addition of D_2O displaces the peaks at 11.50 and 9.70 p.p.m. and transforms into a singlet the doublet at 5.71 p.p.m. The i.r. spectrum (KBr pellet) ν_{NH} 3150 and 3350 (m), $\nu_{N-C=S}$ 1550 (s) and $\nu_{C=S}$ 1180 cm^{-1} (s). The compound thus obtained is identical (n.m.r., i.r., t.l.c., and m.p.) to the compound obtained by hydrogenation of **3** by Raney nickel (11), this ascertains the structure of this compound: 4,5-dihydro 5,6-diphenyl *as*-triazine 3-thione (**6**).

2. Controlled Potential Electrolysis of 4,5-Dihydro as-Triazines

2.1 4,5-Dihydro 5,6-Diphenyl as-Triazine 3-One (4)

Reduction in acidic medium

A solution is prepared from 100 cm^3 CH_3CN, 60 cm^3 H_2O, and 40 cm^3 *N* H_2SO_4; 1.5 g of **4** are dissolved in 150 cm^3 of this solution. In the course of the electrolysis ($E = -1.00$ V, p*H* 0.93) white crystals precipitate (700 mg, yield 50%), m.p. 318° (alcohol) n.m.r. spectrum (DMSO-d_6): 2 NH 2 protons(s) δ 10.51 which are displaced by addition of D_2O, C_6H_5 10 protons (s) 7.33 p.p.m. The i.r. spectrum (KBr pellet) ν_{NH} 3200 (s), $\nu_{C=O}$ 1690 cm^{-1} (s). This compound is identical (n.m.r., t.l.c.) to the 4,5-diphenyl imidazole 2-one (5). When the filtrate is concentrated and made slowly alkaline to p*H* 11, a second white compound precipitates: the *trans*-1,4,5,6-tetrahydro 5,6-diphenyl *as*-triazine 3-one **8***b* (700 mg, yield 45%), m.p. 220° (alcohol). The n.m.r. spectrum (DMSO-d_6 + D_2O) C_5H or C_6H 1 proton (d) δ 3.83, C_6H or C_5H 1 proton (d) 4.70 ($J_{H_5-H_6} = 8.2$ Hz),

Can. J. Chem. Downloaded from www.nrcresearchpress.com by 210.87.254.105 on 09/05/12
For personal use only.

C_6H_5 10 protons (m), 7.1–7.4 p.p.m. The i.r. spectrum (KBr pellet) ν_{NH} 3400 (m) and 3200 (s), $\nu_{C=O}$ 1655 cm^{-1} (s).

Reduction in neutral medium

A solution is prepared from 125 cm^3 CH_3CN, 50 cm^3 1 *N* NaOH, 3.9 g citric acid, and 75 cm^3 H_2O; 0.5 g of **4** is dissolved in 200 cm^3 of this solution. The compound which precipitates during the electrolysis (p*H* 5.98, $E = -1.50$ V) is the *cis*-1,4,5,6-tetrahydro 5,6-diphenyl *as*-triazine 3-one **8***a* (150 mg, yield 30%), m.p. 240° (alcohol). The n.m.r. spectrum (DMSO-d_6 + D_2O): C_5H or C_6H 1 proton (d) δ 4.50, C_6H or C_5H 1 proton (d) 4.93 ($J_{H_5-H_6}$ = 4.0 Hz), C_6H_5 10 protons (m) 6.8–7.3 p.p.m. The i.r. spectrum (KBr pellet): ν_{NH} 3200 (m) $\nu_{C=O}$ 1670 cm^{-1} (s).

2.2 4,5-Dihydro 5,6-Diphenyl 2-Methyl as-Triazine 3-One

Reduction in acidic medium

A solution is prepared from 100 cm^3 CH_3CN, 40 cm^3 1 *N* H_2SO_4, 60 cm^3 H_2O; 300 mg of **5** are dissolved in 150 cm^3 of this solution. In the course of the electrolysis (p*H* 0.93 $E = -1.00$ V, 2 F/mol) the 4,5-diphenyl 3-methyl imidazole 2-one precipitates (150 mg, yield 50%), m.p. 228° (alcohol). The n.m.r. spectrum (DMSO-d_6): N—CH_3, 3 protons (s) δ 2.95, N—H 1 proton(s) 10.71 displaced by addition of D_2O, C_6H_5 10 protons (m) 7.18 and 7.45 p.p.m. The i.r. spectrum (KBr pellet) ν_{NH} 3100 (s), $\nu_{C=O}$ 1730 cm^{-1} (s).

*2.3. 4,5-Dihydro 5,6-Diphenyl as-Triazine 3-Thione (**6**)*

Reduction in basic medium

A solution is prepared from 100 cm^3 CH_3OH, 100 cm^3 H_2O, 4 cm^3 1 *N* NaOH, and 1.7 g CO_3HNA; 0.5 g of **6** is dissolved in 150 cm^3 of this solution (p*H* 10.67). In the course of the electrolysis ($E = -2.00$ V) the *cis*-1,4,5,6-tetrahydro 5,6-diphenyl *as*-triazine 3-thione **10** precipitates (300 mg, yield 60%), m.p. 215° (alcohol). The n.m.r. spectrum (DMSO-d_6): C_5H and C_6H 2 protons (m) δ 4.20 and 4.90, N_1H 1 proton (d) 5.36 (J_{NH-CH} = 11 Hz), N_4H 1 proton (d) 8.73 ($J_{N_4H-C_5H}$ = 4.0 Hz), N_2H 1 proton(s) 9.56 p.p.m. By addition of D_2O the spectrum becomes more simple, the N—H are displaced, the C_5H and C_6H appear as doublets δ = 4.44 and 4.83 p.p.m., $J_{C_5H-C_6H}$ = 4.0 Hz. The i.r. spectrum (KBr pellet), ν_{NH} 3150 (s), $\nu_{N-C=S}$ 1560 (s), $\nu_{C=S}$ 1220 cm^{-1} (s).

3. Controlled Potential Electrolysis of as-Triazines

*3.1. 5,6-Diphenyl as-Triazine (**11**)*

Compound **11** is prepared according to ref. 14.

*3.2. 3,5,6-Triphenyl as-Triazine (**12**)*

Compound **12** is prepared according to Metze (15).

Electrolysis on the First Plateau

A solution is prepared from 5.3 g of citric acid, 15 cm^3 1 *N* NaOH, 110 cm^3 H_2O, 125 cm^3 CH_3CN, and 2 g $NaClO_4$. Compound **12** (700 mg) is dissolved in 200 cm^3 of this solution (p*H* 3.60). The temperature of the solution is maintained at about 10°. In the course of the electrolysis ($E = -0.70$ V) a white compound precipitates, m.p. 264.5° (washed with alcohol and ether) 163 mg (yield 23%). This compound is the 1,2-dihydro 3,5,6-triphenyl *as*-triazine **13**. The n.m.r. spectrum (DMSO-d_6): C_6H_5 (m) δ 7.40 p.p.m., no C—H proton appears on this spectrum. The i.r. spectrum (KBr pellet): ν_{NH} 3180 (m) and 3380 cm^{-1}. Water (200 cm^3) is added to the filtrate which is extracted with ether. A white compound is thus obtained, m.p. 249.5° (alcohol) 440 mg (yield 63%). This compound is the 4,5-dihydro 3,5,6-triphenyl *as*-triazine **14**. The n.m.r. spectrum (DMSO-d_6): C_5H 1 proton(s) δ 5.93, C_6H_5 15 protons (m) 7.2–8.2 p.p.m. The i.r. spectrum (KBr pellet) ν_{NH} 3260 cm^{-1} (m). Compound **14** is also obtained alone (98 mg) by reduction of **12** (124 mg) in basic medium (0.1 *N* NaOH, 50% CH_3CN, p*H* 13.47, $E = -1.30$ V) (yield 80%).

Electrolysis on the Second Plateau

Compound **12** (700 mg) is dissolved in the same solution as above (p*H* 3.60). At the end of the electrolysis ($E = -1.30$ V, 4.1 F/mol) 200 cm^3 of water are added and 300 mg (yield 80%) of a white compound m.p. 282° are filtered. This compound is identified (n.m.r., i.r., t.l.c.) by comparison with an authentic sample (16) as the 2,4,5-triphenyl imidazole **15**. The filtrate is neutralized with sodium bicarbonate and a second product precipitates (145 mg, yield 20%): the *cis*-1,4,5,6-tetrahydro 3,5,6-triphenyl *as*-triazine **16**. The n.m.r. spectrum (DMSO-d_6 + D_2O): C_5H or C_6H 1 proton (d) δ 4.31, C_6H or C_5H 1 proton (d) 4.81 ($J_{H_5-H_6}$ = 4.0 Hz), C_6H_5 15 protons (m) 6.7–8.0 p.p.m.

A reduction of **12** at p*H* 6.20 (700 mg of **12** in 200 cm^3 of a solution of 5.3 g citric acid, 6 ml 1 *N* NaOH, 125 cm^3 H_2O, and 125 cm^3 CH_3CN; $E = -1.40$ V, 4.2 F/mol) gives only the 2,4,5-triphenylimidazole **15** (yield 55%).

*3.2. Electrolysis of the 4,5-Dihydro 3,5,6-Triphenyl as-Triazine (**14**)*

The electrolysis of 300 mg of **14** at p*H* 3.60 (same solution as above) ($E = -1.20$ V, 2.2 F/mol) gives, after neutralization of the solution with sodium bicarbonate, 135 mg (yield 45%) of *cis*-1,4,5,6-tetrahydro 3,5,6-triphenyl *as*-triazine **16**.

1. J. Pinson and J. Armand. Coll. Czech. Chem. Commun. **36**, 585 (1971).
2. J. Pinson and J. Armand. Bull. Soc. Chim. Fr. 1764 (1971).
3. B. Fleet. J. Electroanal. Chem. **25**, 289 (1970).
4. S. Kwee and H. Lund. Acta Chem. Scand. **23**, 2711 (1969).
5. M. Polonovski, M. Pesson, et P. Rajzman. Bull. Soc. Chim. Fr. 1166 (1955).
6. H. Lund. Acta Chem. Scand. **13**, 249 (1959).
7. R. Aguilera, J. C. Duplan, and C. Nofre. Bull. Soc. Chim. Fr. 4491 (1968).
8. D. L. Trepanier, E. R. Wagner, J. Harris, and A. D. Rudzik. J. Med. Chem. **9**, 881 (1966).
9. D. L. Trepanier and V. Sprancmanis. J. Org. Chem. **29**, 2151 (1964).
10. N. Vinot and J. P. M'Packo. Comptes Rend. **270**, 1042 (1970).
11. J. P. M'Packo and N. Vinot. Comptes Rend. **271**, 1021 (1970).
12. H. Biltz and C. Stellbaum. Ann. Chem. **339**, 243 (1905).
13. J. Klosa. Archiv. Pharm. **288**, 465 (1955).
14. P. V. Laasko, R. Robinson, and H. P. Vandrewala. Tetrahedron, **1**, 103 (1957).
15. R. Metze. Chem. Ber. **87**, 1540 (1954).
16. R. Metze and G. Scherowsky. Chem. Ber. **92**, 2481 (1959).

Can. J. Chem. Downloaded from www.nrcresearchpress.com by 210.87.254.40 on 09/05/12
For personal use only.

Kinetics of Sulfonation of Phenylmethanesulfonic Acid[1]

MRS. Z. R. H. NIENHUIS, W. J. SPILLANE,[2] AND H. CERFONTAIN

Laboratory for Organic Chemistry, Nwe Achtergracht 129, University of Amsterdam, Amsterdam, The Netherlands

Received January 10, 1972

The kinetics of the sulfonation of phenylmethanesulfonic acid in 96.32–99.96% H_2SO_4 has been studied and partial rate factors for the $—CH_2SO_3H$ substituent are reported.

Les cinétiques de la sulfonation de l'acide phénylméthanesulfonique dans H_2SO_4 96.32–99.96% ont été étudiées et les facteurs partiels de vitesse pour le substituant $—CH_2SO_3H$ sont rapportés.

Canadian Journal of Chemistry, **50**, 1591 (1972)

With a view to elucidating the mechanism of sulfonation of phenylmethanesulfonic acid (α-toluenesulfonic acid) and comparing its reactivity with that of benzene (1) and of deactivated aromatic substrates, *e.g.* halogenobenzenes (2, 3) and polyfluorobenzenes (4), we have studied the homogeneous sulfonation of phenylmethanesulfonic acid in sulfuric acid ranging in concentration from 96.32 to 99.96%. The pseudo first order rate constants are given in Table 1.

In the sulfuric acid range of this study, phenylmethanesulfonic acid is present mainly in the unionized form.[3]

The relative reactivities of *p*-difluorobenzene, phenylmethanesulfonic acid, bromobenzene (3), and benzene (1) in 96.3% sulfuric acid at 25° are approximately 1:110:31 600:690 000 respectively.[4] Thus the reactivity of phenylmethanesulfonic acid lies somewhat closer to *p*-difluorobenzene than to bromobenzene.

For sulfonation in 99.7 ± 0.1% sulfuric acid the composition of the resulting disulfonic acid mixture was determined by n.m.r. to be 4 ± 1%, *o*-; 48 ± 10%, *m*-; and 48 ± 10% *p*-sulfophenylmethanesulfonic acid. For sulfonation in sulfuric acid decreasing in concentration from 99.8 to 96.5% H_2SO_4 during the sulfonation, the isomer distribution is the same within experimental error.

TABLE 1. Pseudo first order rate constant for the sulfonation of phenylmethanesulfonic acid at 25.0°

H_2SO_4 (wt. %)	${}_{ps}k_1 \times 10^4$ (s^{-1})
99.960 ± 0.002	155
99.915 ± 0.005	44.3
99.82 ± 0.02	9.7
99.63 ± 0.01	3.13
99.29 ± 0.02	1.18
98.75 ± 0.02	0.617
98.40 ± 0.05	0.385
,, ,,	1.82 (38.3°)
,, ,,	8.0 (50.4°)
96.32 ± 0.05	0.091

The correlation of the pseudo first order overall rate constant for sulfonation with the activity of $H_2S_2O_7$ [5] at the various sulfuric acid concentrations is similar for phenylmethanesulfonic acid and *p*-difluorobenzene (Fig. 1). Because of the similarity in isomer distribution at low and high sulfuric acid concentration this correlation does apply to the ortho-, meta-, and para-substitution of phenylmethanesulfonic acid. The present kinetic results may therefore be explained in terms of the mechanism proposed previously for *p*-difluorobenzene (4).

[1]Aromatic sulfonation, part 34. Preceding paper, see ref. 14.

[2]Present address: University College, Galway, Eire.

[3]Arenesulfonic acids (5, 6) and methanesulfonic acid (6) behave as weak bases in sulfuric acid more concentrated than 100% H_2SO_4, whereas they behave as weak acids in sulfuric acid less concentrated than 95% H_2SO_4 (half-deprotonation takes place at 82–84% H_2SO_4) (7, 8).

[4]${}_{ps}k_1$ for *p*-difluorobenzene in 96.3% sulfuric acid at 25° was obtained by extrapolation from the data of (4) to be 8.5×10^{-8} s^{-1}.

[5]The activities of $H_2S_2O_7$ were taken from refs. 4 and 9.

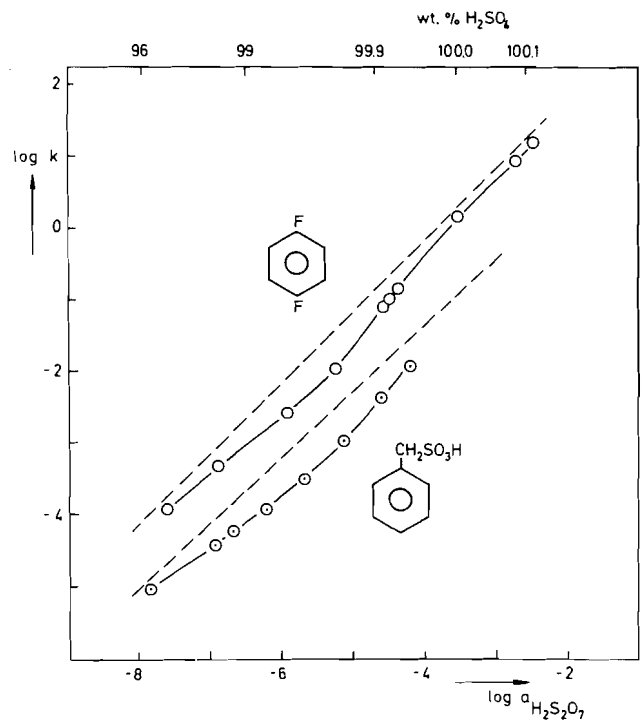

FIG. 1. Correlation of pseudo first order rate constant for sulfonation with the activity of $H_2S_2O_7$.

The temperature dependence of the overall rate of reaction was determined in 98.4% sulfuric acid, and corresponds with $E_a = 24.7$ kcal/mol. Since the sulfonation of phenylmethanesulfonic acid leads mainly to para- and meta-substitution which, by absence of steric hindrance will exhibit similar frequency factors, the activation energy value applies to both meta- and para-substitution. The present value of 24.7 kcal/mol is about 6 kcal/mol greater than observed for the sulfonation of benzene in 91–96% sulfuric acid (1).

The partial rate factors of phenylmethanesulfonic acid for sulfonation in 96.3% sulfuric acid at 25° were calculated from its reactivity relative to benzene (0.000160:1) and the sulfonation isomer distribution to be $f_o = (0.19 \pm 0.05) \times 10^{-4}$, $f_m = (23 \pm 5) \times 10^{-4}$, and $f_p = (46 \pm 10) \times 10^{-4}$. The substituent effect of the $-CH_2SO_3H$ group will be discussed and compared with the effects of the $-SO_3H$ and the $-CH_2C(CH_3)_3$ substituents in a forthcoming publication.

Whereas reaction of phenylmethanesulfonic acid in concentrated *aqueous* sulfuric acid leads to clean sulfonation, reaction with *fuming* sulfuric acid, *i.e.* >100% H_2SO_4, instead leads to decomposition with evolution of sulfur dioxide (smell).

Experimental

General

The u.v. measurements were made with a Zeiss PMQ2 spectrophotometer fitted with a thermostatically controlled cell holder. The n.m.r. spectra were recorded with a HA 100 Varian n.m.r. spectrometer equipped with a Time Averaging Computer, using TMS in CCl_4 (50 vol %) as external standard.

The potassium salt of phenylmethanesulfonic acid was prepared as described by Johnson and Ambler (10) by the action of potassium sulfite on benzyl chloride.

Anal. Calcd. for $C_7H_7O_3SK$: C, 39.98; H, 3.36; S, 15.25; K, 18.59. Found: C, 40.00; H, 3.48; S, 15.42; K, 18.60.

Rate Measurements

Rates were measured by following the u.v. extinction at an appropriate wavelength (*e.g.* 276 nm) with time. Pseudo first order rate constants were determined from plots of either log $|E_t - E_\infty|$ *vs.* time (1) or log $|E_{t+\Delta t} - E_t|$ *vs.* time (11). The latter method (the Guggenheim method) was used in most runs because some drift in the value of E_∞ was noticed. All rate runs were followed to at least 88% conversion and each run was repeated at least once. The rate constants obtained are accurate to within 5% with

Can. J. Chem. Downloaded from www.nrcresearchpress.com by 210.87.254.40 on 09/05/12
For personal use only.

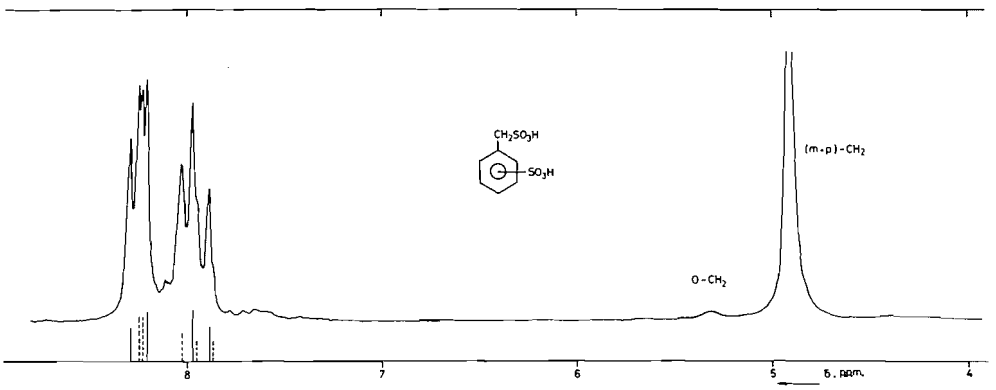

FIG. 2. Typical multiple scan (194 ×) n.m.r. spectrum of the sulfonation mixture of phenylmethanesulfonic acid in 96.5% H_2SO_4.

the exception of the rate constant obtained in 99.96% sulfuric acid which is accurate to within 10% (four determinations).

Isomer Distribution

Two samples of known amounts of substrate and 99.8% sulfuric acid (32 mg + 5.3 g and 101 mg + 1.7 g respectively) were placed in glass-stoppered flasks, and the mixtures were maintained at 25.0° for at least 2 days after which time the monosulfonation was complete. The final sulfuric acid concentration had then decreased to 99.5 and 96.5% H_2SO_4 respectively. The n.m.r. spectra of the sulfuric acid reaction mixtures exhibited two methylene singlets at δ 4.90 and 5.32 p.p.m. respectively and two slightly overlapping complex multiplets centered at δ 7.95 and 8.25 p.p.m. respectively for the aromatic hydrogens (Fig. 2). The ratio of the areas of the methylene to aromatic hydrogens was 0.50 ± 0.02. After the spectra had been compared with those of the three toluenesulfonic acids (12, 13) and with that of phenylmethanesulfonic acid (measured in 95% sulfuric acid), the singlet absorption at δ 5.32 p.p.m. was assigned to the benzylic hydrogens of *o*-sulfophenylmethanesulfonic acid and the singlet absorption at δ 4.90 p.p.m. to those of the *p*- and *m*-isomer. The ratio of *o*- *vs.* the sum of the *m*- and *p*-isomer was determined by measuring the ratio of the areas of the two benzylic hydrogen absorption peaks. The low field aromatic absorption comprises the absorption of the 2- and 4-hydrogens of 3- and of the 3- and 5-hydrogens of 4-sulfophenylmethanesulfonic acid, the high field absorption those of the other aromatic hydrogens. The AA′BB′ absorption pattern of the *p*-isomer is indicated schematically in Fig. 2. by full lines, the main absorption peaks of the *m*-isomer are indicated by dotted lines; these patterns are similar to those of *p*- and *m*-toluenesulfonic acid respectively (13). The ratio of the *p*- and *m*-isomer was estimated from the aromatic hydrogen pattern to be 1.0 ± 0.2.

The authors acknowledge gratefully the assistance of Mrs. A. Koeberg-Telder.

1. A. W. KAANDORP, H. CERFONTAIN, and F. L. J. SIXMA. Rec. Trav. Chim. **81**, 969 (1962).
2. C. W. F. KORT and H. CERFONTAIN. Rec. Trav. Chim. **86**, 865 (1967).
3. C. W. F. KORT and H. CERFONTAIN. Rec. Trav. Chim. **88**, 860 (1969).
4. C. W. F. KORT and H. CERFONTAIN. Rec. Trav. Chim. **88**, 1298 (1969).
5. R. J. GILLESPIE. Rev. Pure Appl. Chem. (Australia), **9**, 1 (1959).
6. S. K. HALL and E. A. ROBINSON. Can. J. Chem. **42**, 1113 (1964).
7. H. CERFONTAIN and B. W. SCHNITGER. Rec. Trav. Chim. **91**, 199 (1972).
8. A. KOEBERG-TELDER, C. VAN LENTEN, and H. CERFONTAIN. Unpublished results.
9. C. W. F. KORT and H. CERFONTAIN. Rec. Trav. Chim. **87**, 24 (1968).
10. T. B. JOHNSON and J. A. AMBLER. J. Am. Chem. Soc. **36**, 372 (1914).
11. M. AHMAD and J. HAMER. J. Chem. Educ. **41**, 249 (1964).
12. H. DE VRIES and H. CERFONTAIN. Rec. Trav. Chim. **86**, 873 (1967).
13. C. RIS. Forthcoming thesis. University of Amsterdam, Amsterdam, The Netherlands.
14. C. RIS and H. CERFONTAIN. Rec. Trav. Chim. **91**, 583 (1972).

Can. J. Chem. Downloaded from www.nrcresearchpress.com by 210.87.254.40 on 09/05/12
For personal use only.

Hindered Rotation in Carbamates: A Kinetic Anomaly

P. T. INGLEFIELD AND S. KAPLAN

Jeppson Laboratory, Chemistry Department, Clark University, Worcester, Massachusetts 01610

Received September 10, 1971

The energy barriers to hindered rotation in two carbamate structures have been measured by total line-shape analysis of the high resolution n.m.r. spectrum. Conclusions are presented concerning the influence of solvent on the nature of the transition state in such processes and the existence of frequency factors outside the normal expected range for a unimolecular transformation.

Les barrières d'énergie pour la rotation empêchée dans deux carbamates ont été mesurées au moyen d'une analyse complète raie-forme du spectre r.m.n. à haute résolution. Des conclusions sont présentées en ce qui concerne l'influence du solvant sur la nature de l'état de transition dans de tels processus et sur l'existence de facteurs de fréquence à l'extérieur du domaine normal attendu pour une transformation unimoléculaire.

Canadian Journal of Chemistry, **50**, 1594 (1972)

Can. J. Chem. Downloaded from www.nrcresearchpress.com by 210.87.254.42 on 09/05/12
For personal use only.

Introduction

There has been considerable controversy in recent years concerning the energetics of the barrier to hindered rotation about the C—N bond in simple amide structures as determined by n.m.r. methods(1). It has become abundantly clear that in order to obtain reliable kinetic information a total line-shape analysis must be made of the steady state n.m.r. spectrum or a similar complete analysis made of the transient response of the nuclear spin system to a sequence of radio-frequency pulses (2, 3). The systematic errors inherent in these methods have been discussed at length (1–5) and it is concluded that in the high resolution method any instrumental line broadening will introduce a systematic error which will tend to increase the value obtained for the rate constant in the slow exchange region ($k < \delta$) and decrease its value in the fast exchange region ($k > \delta$). This is the most common type of error present in such studies and gives rise naturally to a low value for the Arrhenius activation energy, a low frequency factor, and consequently a large negative entropy of activation. This is readily apparent in a comparison between more recent determinations and those of an earlier vintage (3).

The above conclusions often lead the experimenter to suspect measured barriers which exhibit large negative entropies of activation for a unimolecular process. It should be pointed out, however, that although the frequency factors for most unimolecular reactions lie in the expected theoretical range of 10^{12} to 10^{14} s^{-1} (corresponding to $\Delta S^{\ddagger} \approx 0$), values are obtained outside this range if an entropy increase or decrease accompanies the formation of the transition state (6). In the case of a simple amide in solution in a polar solvent the possibility of differential solvation between the ground state and the transition state exists and caution should be used in disregarding reproducible negative entropies of activation when they may well be an indication of preferential solvation in the transition state. We will present some measurements made in this laboratory on systems which we believe fall into this category. We will comment on these measurements and those recently reported by Lemire and Thompson (7), on similar systems, with which we are in substantial agreement. We also report some conclusions concerning the nature of the transition state for the hindered rotation process in the amide structure when solvation is an important consideration.

Experimental

N:*N*-Dimethylmethylcarbamate and *N*:*N*-dimethylmethylthiocarbamate were prepared by reacting *N*:*N*-dimethylcarbamoyl and thiocarbamoyl chloride with methanol in pyridine solvent in a pressure capped bottle heated on a steam bath for 3 h. The resultant mixture was washed and extracted with ether and the compounds purified using a Hewlett Packard 776 Preparative Gas Chromatograph. Each sample was thoroughly degassed and sealed *in vacuo* in a 5 mm o.d. n.m.r. tube.

The n.m.r. measurements were made on a JEOLCO JNM-C-6OH spectrometer operating in the internal lock mode. The instrument is equipped with a variable temperature controller JES-VT-2 and the temperature monitored by means of a thermocouple placed near the sample and calibrated by

TABLE 1. Activation parameters

Compound	Solvent	E_a (kcal/mol)	$\Delta G^{\ddagger}$ (kcal/mol)	$\Delta S^{\ddagger}$ (e.u.)	References
$Me_2NC(O)OMe$	Neat	Unobserved*	—	—	This work
					7
	10% in $CDCl_3$	14.3 ± 1.0	15.2	-5 ± 3	This work
$Me_2NC(S)OMe$	Neat	13.6 ± 0.6	18.0	-15 ± 4	This work
	Neat	14.5 ± 0.4	17.4	-11.7	7
	10% in $CDCl_3$	13.9 ± 0.3	17.7	-13 ± 2	This work
	1.5% in C_6H_{12}	14.2 ± 0.5	17.1	-11.7	7

*No non-equivalence observed for the NMe_2 resonance.

the method of Van Geet (8). The volumes used in the calibration and the samples were identical and the flow of heating air was kept constant thus minimizing any error due to temperature gradients within the sample. The sample temperatures are estimated to be accurate to $\pm 0.4°$.

The line-shape analysis of the high resolution p.m.r. spectra was accomplished by computer fitting as described previously (3). The value of the linewidth in the absence of exchange ($1/T_2^*$) was monitored at each temperature using the signal from a trace amount of $CHCl_3$ in the samples. The linewidth of $CHCl_3$ was identical to N—CH_3 at low temperatures indicating that inhomogeneity effects outweigh any quadrupolar broadening; it remained approximately constant at about 0.5 Hz. Both k (the rate constant) and $\delta\omega$ (the chemical shift between the methyl groups) were varied in order to obtain the best fit. $\delta\omega$ exhibited a small increase with temperature but did not vary appreciably over the temperature range studied. The errors quoted represent a 90% confidence interval in the least squares deviation calculations. An error propagation calculation assuming a rate constant precision of 2%, based on the criticalness of the computer fits, yields errors of approximately the same magnitude.

Results and Discussion

The results are given in Table 1 for *N*:*N*-dimethylmethylcarbamate and *N*:*N*-dimethylmethylthiocarbamate together with those of Lemire and Thompson (7). The results clearly demonstrate reproducible negative values of $\Delta S^{\ddagger}$ for the hindered rotation process. In the $Me_2NC(O)OMe$ case we observed no splitting of the —NMe_2 peak at low temperatures in the neat liquid in agreement with previous workers and in the 10 mol % solution in $CDCl_3$ a chemical shift of 1.8 Hz at 60 MHz was apparent at -23 °C, indicating considerable solvent interaction. Because of the small shift the precision on the activation parameters in this molecule is low. In the $Me_2NC(S)OMe$ molecule the chemical shift is much larger: $\delta = 11.9$ Hz in the neat liquid and $\delta = 15.0$ Hz in the 10 mol % solution in $CDCl_3$; again indicative of considerable solvation with the polar solvent. The activation parameters for this molecule are in good agreement with those obtained by Lemire and Thompson.

It is well known that the ground state structure in these molecules is planar or nearly planar due to the delocalization of the lone pair of electrons on nitrogen (**I** in Fig. 1) giving rise to the partial double bond character of the N—C bond. On rotation about the N—C bond breakdown of the conjugation between the N lone-pair π electrons and the carbonyl π-system would be expected with a corresponding change in hybridization at the N atom. The resulting trigonal pyramid configuration at the N atom leads to two possible transition states (**II** and **III** in Fig. 1). Support for the existence of these configurations has been recently reported from the results of a molecular orbital calculation in the CNDO/2 approximation (9) for possible configurations of the transition state for the hindered rotation in formamide. The CNDO study also confirms that $\mu_{II} > \mu_I > \mu_{III}$ and excellent agreement is obtained with the experimental dipole moment in the ground state configuration (**I**). The predicted energy difference between **II** and **III** is small and **II** could easily be the favored structure in a polar media due to mutual dipole–dipole interactions. Since $\mu_{II} > \mu_I$ preferential solvation in the transition state could easily account for the negative values obtained for

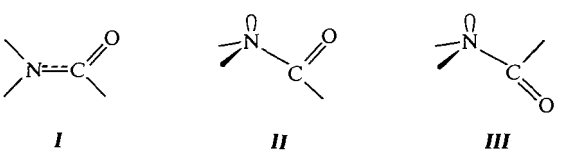

I *II* *III*

FIGURE 1

Can. J. Chem. Downloaded from www.nrcresearchpress.com by 210.87.254.42 on 09/05/12
For personal use only.

$\Delta S^{\ddagger}$. In the neat liquids the results are more difficult to rationalize unless a larger mutual dipole–dipole interaction leads to a decrease in entropy in transition state **II**. The large negative entropy of activation obtained for the cyclohexane solution of $Me_2NC(S)OMe$ by Lemire and Thompson is not in agreement with this explanation. However, we feel that the agreement between both laboratories in the results in polar media is the overriding consideration. The lower energy barriers obtained for these carbamates in comparison to many other amides (1, 3) is felt to be due to a slight decrease in C—N bond order caused by the inductive effect of the electronegative OCH_3 group.

In conclusion, we can say that considerable caution must be used in evaluating data on hindered rotations in amides since in view of our conclusions the possibility of having a negative $\Delta S^{\ddagger}$ for the process is not unreal. It is unfortunate that the precision of the frequency factor (or $\Delta S^{\ddagger}$) determination is so low in the n.m.r. method otherwise it would be possible to obtain detailed information on the exact nature of the transition state from a variable solvent study.

The authors wish to thank Dr. K. N. Shaw of the University of Waterloo, Waterloo, Ontario, for helpful discussion. Financial support was provided by a Biomedical Sciences Support Grant to Clark University by N.I.H.

1. W. H. Siddall, III and T. H. Stewart. Chem. Rev. **70**, 517 (1970).
2. A. Allerhand, H. S. Gutowsky, J. Jonas, and R. A. Meinzer. J. Am. Chem. Soc. **44**, 3185 (1966).
3. P. T. Inglefield, E. Krakower, L. W. Reeves, and R. Stewart. Mol. Phys. **15**, 65 (1968).
4. T. Drakenberg and S. Forsen. J. Phys. Chem. **74**, 1 (1970).
5. T. Drakenberg, K. V. Dahlquist, and S. Forsen. Acta Chem. Scand. **24**, 694 (1970).
6. S. Benson. The foundations of chemical kinetics. McGraw-Hill. 1960. p. 264.
7. A. E. Lemire and J. C. Thompson. Can. J. Chem. **48**, 824 (1970).
8. A. L. Van Geet. Anal. Chem. **40**, 2227 (1968).
9. K. N. Shaw and L. W. Reeves. Chem. Phys. Lett. **10**, 89 (1971).

Can. J. Chem. Downloaded from www.nrcresearchpress.com by 210.87.254.42 on 09/05/12
For personal use only.

Zeise's Salt, $K[Pt(C_2H_4)Cl_3]$, Anhydrous and Monohydrate and the Platinum–Olefin Interaction

J. Hubert, P. C. Kong, F. D. Rochon, and T. Theophanides
Department of Chemistry, University of Montreal, Montreal, Quebec

Received December 14, 1971

Zeise's salt, anhydrous and monohydrate, has been prepared by a new method similar to the original method used by Zeise. The infrared and laser Raman spectra of the anhydrous Zeise's salt together with the infrared spectra of the deutero and bromo analogs, are reported and discussed. The vibrational spectra are interpreted in terms of a cyclopropane-like ring structure, obtained by the insertion of the platinum atom into the double bond.

Le sel de Zeise, $K[Pt(L)X_3]$ ($L = C_2H_4$, $X = Cl$), a été préparé par une nouvelle méthode. Les spectres infrarouges et Raman laser du sel de Zeise anhydre à l'état solide sont discutés. Les spectres infrarouges des analogues, pour lesquels $L = C_2D_4$, $X = Cl$ et $L = C_2H_4$, $X = Br$, sont également rapportés. Les absorptions dues à l'interaction platine-double liaison ont été interprétés en fonction d'un modèle cyclique de type cyclopropane, $(CH_2)_2PtX_3$.

Canadian Journal of Chemistry, **50**, 1596 (1972)

Introduction

The platinum–ethylene bonding in Zeise's salt and the metal insertion into the double bond exhibits unusual features.

There have been conflicting reports concerning the platinum–olefin vibrations in the i.r. spectrum of Zeise's salt (1, 2) and similar platinum–olefin complexes (3, 4). The i.r. spec-

$\Delta S^{\ddagger}$. In the neat liquids the results are more difficult to rationalize unless a larger mutual dipole–dipole interaction leads to a decrease in entropy in transition state **II**. The large negative entropy of activation obtained for the cyclohexane solution of $Me_2NC(S)OMe$ by Lemire and Thompson is not in agreement with this explanation. However, we feel that the agreement between both laboratories in the results in polar media is the overriding consideration. The lower energy barriers obtained for these carbamates in comparison to many other amides (1, 3) is felt to be due to a slight decrease in C—N bond order caused by the inductive effect of the electronegative OCH_3 group.

In conclusion, we can say that considerable caution must be used in evaluating data on hindered rotations in amides since in view of our conclusions the possibility of having a negative $\Delta S^{\ddagger}$ for the process is not unreal. It is unfortunate that the precision of the frequency factor (or $\Delta S^{\ddagger}$) determination is so low in the n.m.r. method otherwise it would be possible to obtain detailed information on the exact nature of the transition state from a variable solvent study.

The authors wish to thank Dr. K. N. Shaw of the University of Waterloo, Waterloo, Ontario, for helpful discussion. Financial support was provided by a Biomedical Sciences Support Grant to Clark University by N.I.H.

1. W. H. Siddall, III and T. H. Stewart. Chem. Rev. **70**, 517 (1970).
2. A. Allerhand, H. S. Gutowsky, J. Jonas, and R. A. Meinzer. J. Am. Chem. Soc. **44**, 3185 (1966).
3. P. T. Inglefield, E. Krakower, L. W. Reeves, and R. Stewart. Mol. Phys. **15**, 65 (1968).
4. T. Drakenberg and S. Forsen. J. Phys. Chem. **74**, 1 (1970).
5. T. Drakenberg, K. V. Dahlquist, and S. Forsen. Acta Chem. Scand. **24**, 694 (1970).
6. S. Benson. The foundations of chemical kinetics. McGraw-Hill. 1960. p. 264.
7. A. E. Lemire and J. C. Thompson. Can. J. Chem. **48**, 824 (1970).
8. A. L. Van Geet. Anal. Chem. **40**, 2227 (1968).
9. K. N. Shaw and L. W. Reeves. Chem. Phys. Lett. **10**, 89 (1971).

Can. J. Chem. Downloaded from www.nrcresearchpress.com by 210.87.254.42 on 09/05/12
For personal use only.

Zeise's Salt, $K[Pt(C_2H_4)Cl_3]$, Anhydrous and Monohydrate and the Platinum–Olefin Interaction

J. Hubert, P. C. Kong, F. D. Rochon, and T. Theophanides
Department of Chemistry, University of Montreal, Montreal, Quebec

Received December 14, 1971

Zeise's salt, anhydrous and monohydrate, has been prepared by a new method similar to the original method used by Zeise. The infrared and laser Raman spectra of the anhydrous Zeise's salt together with the infrared spectra of the deutero and bromo analogs, are reported and discussed. The vibrational spectra are interpreted in terms of a cyclopropane-like ring structure, obtained by the insertion of the platinum atom into the double bond.

Le sel de Zeise, $K[Pt(L)X_3]$ ($L = C_2H_4$, $X = Cl$), a été préparé par une nouvelle méthode. Les spectres infrarouges et Raman laser du sel de Zeise anhydre à l'état solide sont discutés. Les spectres infrarouges des analogues, pour lesquels $L = C_2D_4$, $X = Cl$ et $L = C_2H_4$, $X = Br$, sont également rapportés. Les absorptions dues à l'interaction platine-double liaison ont été interprétés en fonction d'un modèle cyclique de type cyclopropane, $(CH_2)_2PtX_3$.

Canadian Journal of Chemistry, **50**, 1596 (1972)

Introduction

The platinum–ethylene bonding in Zeise's salt and the metal insertion into the double bond exhibits unusual features.

There have been conflicting reports concerning the platinum–olefin vibrations in the i.r. spectrum of Zeise's salt (1, 2) and similar platinum–olefin complexes (3, 4). The i.r. spec-

Can. J. Chem. Downloaded from www.nrcresearchpress.com by 210.87.254.42 on 09/05/12
For personal use only.

trum of Zeise's salt has been investigated by many investigators (1–5). The platinum–olefin vibrations have been assigned in Zeise's monohydrate salt, but the presence of water of crystallization in the molecule obscured the 500 cm^{-1} region and resulted in a controversy over the Pt–olefin band assignments (2, 5).

The early work of Babuskin *et al.* (5*c*), which was the first attempt to interpret all the bands of the molecule, showed that the ethylene double bond, on complexation, becomes single and that the Pt—C bond strength was quite similar to a normal covalent bond. The recent vibrational studies of Hiraishi (2*b*), as well as the earlier work of Pradilla-Sorzano and Fackler (2*a*), are in agreement with the conclusions of the Russian workers.

Powell and Sheppard (5*b*) studied the n.m.r. spectra of a number of olefin complexes including Zeise's salt and came to the conclusion that the C—C bond is a weakly perturbed double bond and that the olefinic molecule is firmly bound to the platinum. This conclusion seems to be contradictory.

Earlier, Chatt and Duncanson (10), from a few features of the i.r. spectra of Zeise's salt, namely, a weak absorption in the region 1500–1525 cm^{-1}, concluded that this very weak band was due to the C=C double bond absorption lowered on complexation by 100–140 cm^{-1}. This interpretation implies a weakly perturbed double bond. However, the molecular model they proposed, based on Dewar's model of σ- and π-bonding, indicates a strong interaction of the metal with the double bond in agreement with the high stability of their complexes. This also is a contradictory conclusion.

Zeise's salt, anhydrous and monohydrate, has been prepared by a new method similar to the original method used by Zeise.

Results

Preparation of Zeise's Salt by a New Method

The slow reduction of ethanol by an acetylenic glycol (ac = $(C_4H_9)(C_2H_5)(OH)C—C\equiv C—C(OH)(C_2H_5)(C_4H_9)$ or $(CH_3)_3C—C\equiv C—C(C_2H_5)_3$) gave as main product Zeise's salt (yield: 50–60%). The acetylenic glycol is used as a reducing agent to transform ethanol into ethylene *in situ*. Potassium tetrachloroplatinate (II) reacts with ethanol in the presence of the acetylenic glycol as follows:

$$K_2PtCl_4 + C_2H_5OH + ac \xrightarrow{H_2O} K[Pt(C_2H_4)Cl_3] + KCl + ac.H_2O$$

The complex is recrystallized from acetone–ether or water–HCl solutions.

In the above reaction, the water seems to attack the triple bond and hydration with polymerization of the acetylenic glycol takes place. The acetylenic ligand could not be recovered after the reaction and a brown oil was always formed. The presence of the acetylenic glycol and of ethanol are essential for the preparation, since it was impossible to isolate the Zeise's salt without one of them. The reaction is similar to the method used by Zeise to prepare $K[Pt(C_2H_4)Cl_3].H_2O$

$$PtCl_2 + KCl + C_2H_5OH \xrightarrow{\Delta} K[Pt(C_2H_4)Cl].H_2O$$

Discussion

The i.r. and laser Raman spectra of the anhydrous Zeise's salt, the i.r. spectra of the deutero and the bromo analogs are reported in Table 1. Survey i.r. spectra of the anhydrous salts, $K[Pt(C_2H_4)Cl_3]$, $K[Pt(C_2D_4)Cl_3]$, and $K[Pt(C_2H_4)Br_3]$ and the hydrated salt $K[Pt(C_2H_4)Cl_3].H_2O$ are shown in Figs. 1 and 2. Laser Raman spectra are shown in Fig. 3.

The spectrum of the monohydrate salt is identical to that reported by Nakamoto and Grogan (1).

From the spectra, it is evident that the band at 490 cm^{-1} cannot be assigned to water of crystallization, since the band is present in the spectra of the hydrated salt, in the anhydrous salt and also in the bromo analog. It cannot be assigned to a combination band, since both complexes $K[Pt(C_2H_4)Cl_3]$ and $[Pt(C_2H_4)Cl_2]_2$ show an absorption band around 490 cm^{-1} and their far i.r. spectra are very different from each other. Similarly, this band is observed in the spectra of the complexes $[(Pt(C_2H_4)Cl_2)_2en]$, $[(Pt(C_2D_4)Cl_2)_2en]$, $[(Pt(C_2H_4)Br_2)_2en]$, and of $[(Pt(C_2H_4)ClBr)_2en]$ (6).

Both bands at 490 and 400 cm^{-1} are due to Pt—C stretchings. The assignment was carried out according to Hiraishi (2*b*). The bands at 400 cm^{-1} (ν_5) and at 490 cm^{-1} (ν_{12}) are respectively assigned to the symmetric and the anti-

TABLE 1. Observed frequencies for the Zeise's salt and its analogs*

Assignment (ref. 8*b*)	$K[PtCl_3(C_2H_4)].H_2O$ (solid)	$K[PtCl_3(C_2H_4)]$ Infrared (solid)	$K[PtCl_3(C_2H_4)]$ Raman (solid)	$K[PtCl_3(C_2D_4)]$ infrared (solid)	$K[PtBr_3(C_2H_4)]$ infrared (solid)
ν_{21}		3100 w	3070(5)		
ν_{15}	3080 w	3080 vs		2330 b,w	3080 w
ν_1				2210 vw	
ν_9	3005 w	3005 vw		2180 vw	
$\nu_4 + \nu_{11}$	2025 m	2025 w		1580 w	2037 w
ν_2	1520 w	1510 vw		966 m	
ν_{10}	1425 vs	1420 vs		1060 vs	1420 vs
ν_3	1250 m	1250 w	1253(50)		1245 w
ν_{16}	1180 b,w	1180 w		1005 vw	1180 b,w
ν_{11}	1025 vs	1032 vs		830 sh	1020 sh
	1010 sh	1025 vs		816 s	1016 vs
ν_4	960 vw	970 vw		730 vw	960 vw
ν_{23}	840 w	840 w			836 w
ν_{17}	730 m	730 m		534 m	723 s
	720 sh	725 sh			710 sh
ν_{12}	480 b,m	490 s	489(40)	450 m	484 m
ν_5	390 m	400 s	395(50)	384 m	393 m
ν_6	336 vs	336 vs	335(100)	336 vs	241 s
ν_{18}	330 sh	328 sh		326 sh	225 sh
ν_7	300 m	302 s	299(20)	302 s	
ν_{13}			212(80)		
ν_{14}			180(50)		

*The intensities of the Raman lines are relative to the strongest line (100). w = weak, m = medium, s = strong, sh = shoulder, b = broad.

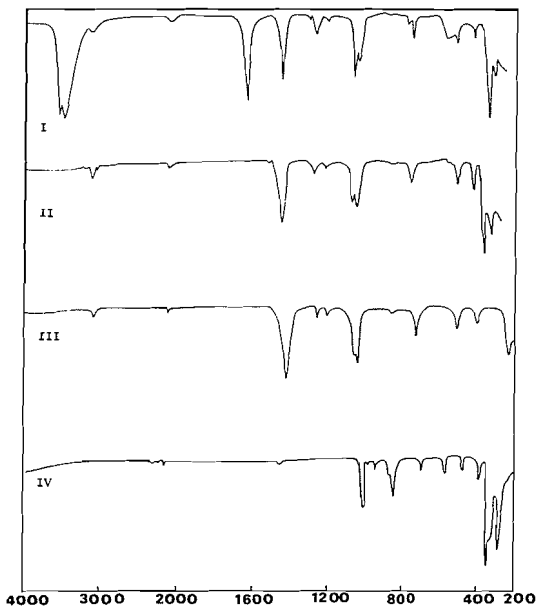

FIG. 1. Survey spectra of (*I*), $K[Pt(C_2H_4)Cl_3].H_2O$; (*II*), $K[Pt(C_2H_4)Cl_3]$; (*III*), $K[Pt(C_2H_4)Br_3]$; (*IV*), $K[Pt(C_2D_4)Cl_3]$.

symmetric Pt—C stretching vibrations. These bands are shifted on deuteration to 384 and 450 cm^{-1} and are found at 393 and 484 cm^{-1} for the bromo analog. The Raman band at 1253 cm^{-1} is assigned to C—C (ν_3) stretching (2*b*) from polarization data and the band at 299 cm^{-1} has been assigned to the Pt—Cl (*trans*) symmetric stretching. The 212 cm^{-1} band can be tentatively assigned to the PtC_2 rocking (2*b*) and the 180 cm^{-1} band to the Cl—Pt—Cl in-plane deformation (3*b*).

The recent X-ray study on the Zeise's salt monohydrate showed that the two types of platinum–chlorine bond (*i.e. cis* and *trans*) lengths are within one e.s.d. Therefore the difference in length cannot unambiguously be attributed to the *trans*-influence, since the surroundings of the chlorine atoms are different (7). An older neutron diffraction study (9) indicates that the four hydrogen atoms of the ethylene lie in a plane. The two carbon atoms are 0.18 Å above this plane toward the platinum atom. Thus the hydrogen atoms bend back significantly (9) and this should be consistent

Can. J. Chem. Downloaded from www.nrcresearchpress.com by 210.87.254.42 on 09/05/12
For personal use only.

Can. J. Chem. Downloaded from www.nrcresearchpress.com by 210.87.254.42 on 09/05/12
For personal use only.

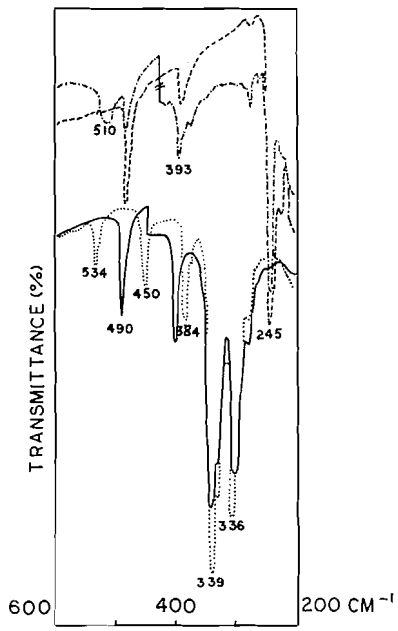

FIG. 2. Infrared spectra of Zeise's salt anhydrate (—); its deutero analog (...), the bromo analog monohydrate (-.-.-.), and the bromo analog anhydrate (---), in the region 600–200 cm^{-1} in Nujol mulls and between CsI plates.

with a strongly perturbed C—C bond. However, the authors (9) reported a C—C length of 1.354 (15) Å compared to 1.37 (3) Å obtained by X-ray diffraction (7). These distances are fairly short, but the uncertainties on the bond lengths are relatively great and the values should be interpreted with great care.

The two platinum–carbon bond distances are not significantly different (2.121 (19) and 2.134 (19) Å). These values are not too far from a platinum–carbon σ-type bond (2.076) (15) Å (8).

A ring structure with two Pt—C— σ-type bonds and one C—C single bond with some double bond character as in the case of cyclopropane or ethylene oxide is considered for $(CH_2)_2Pt$ to interpret the vibrational spectra (2*a*, 5*c*). This model can be obtained by insertion of the platinum atom into the double bond of the olefin:

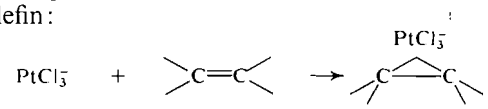

$PtCl_3^-$ seems to be similar in its chemical properties to CH_2 in cyclopropane, indicating that

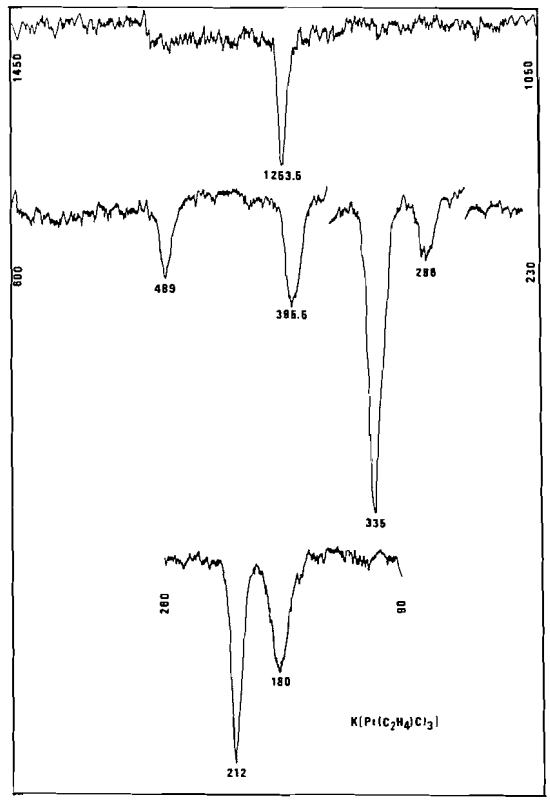

FIG. 3. Laser Raman spectra of the Zeise's salt anhydrate.

$PtCl_3^-$ has an electron affinity comparable to that of the group X in the series of molecules $X(CH_2)_2$, where X = CH_2, O, S, HN, *i.e.*, the molecules cyclopropane, ethylene oxide, ethylene sulfide, and ethylene amide. The angle $C\hat{X}C$ is decreasing as the atom X increases in size, cyclopropane (67°), ethylene oxide (60°), ethylene sulfide (48°), and Zeise's salt (39°) seems to fall well in the trend.

Experimental

The i.r. spectra between 4000 and 200 cm^{-1} were obtained with a Perkin–Elmer 621 i.r. spectrophotometer. Nujol or C_4Cl_6 mulls and KBr or CsI techniques were employed to record the spectra. Calibration of the frequencies was made with a polystyrene film and water vapor. Raman spectra were obtained with a Jarell Ash Raman spectrophotometer using He–Ne laser excitation at 6328 Å. The samples were examined as crystalline powders.

$K[Pt(C_2H_4)Cl_3].H_2O$ was prepared according to the method described by Chatt and Duncanson (10). The anhydrous salt $K[Pt(C_2H_4)Cl_3]$ was obtained by recrystallization

in 4 *N* hydrochloric acid. The water and HCl were evaporated in a desiccator under reduced pressure.

The salt was also prepared by the following method: potassium tetrachloroplatinite (0.002 *M*) was dissolved in 15 ml of water and the solution was filtered. A solution of 10 ml of 5,8-diethyl-6,6-dodecyne-5,8 diol or 2,2-dimethyl-5,5-diethyl-3-heptyne (0.005 *M*) in ethanol was added to the above solution. The mixture was stirred for a few minutes and left for a week. It was then filtered and the filtrate evaporated to dryness. The residue was washed with anhydrous ether and dissolved in 20 ml acetone. This was filtered and evaporated to dryness. Finally Zeise's salt was recrystallized slowly in a refrigerator in a mixture of acetone–anhydrous ether. Yield, 60%.

$K[Pt(C_2D_4)Cl_3]$ was prepared using ethylene-d_4 gas in D_2O and following the method described in ref. 10.

$K[Pt(C_2H_4)Br_3].H_2O$ was prepared by the above method (10) using a water solution of K_2PtBr_4. The red colored complex is extracted with acetone and recrystallized from acetone–ether. The i.r. spectrum of the complex was identical to the reported spectrum (2*a*).

$K[Pt(C_2H_4)Br_3]$ anhydrous was obtained by recrystallization in tetrahydrofuran or in 4 *N* hydrobromic acid and following the procedure as for $K[Pt(C_2H_4)Cl_3]$.

We wish to thank Johnson, Matthey and Mallory Ltd., for the loan of platinum chloroplatinite and the National Research Council of Canada for financial assistance. Many thanks also to Dr. I. S. Butler, McGill University for the use of the Jarell Ash Raman spectrophotometer.

1. M. J. GROGAN and K. NAKAMOTO. J. Am. Chem. Soc. **88**, 5454 (1966).
2. (*a*) J. PRADILLA-SORZANO and J. P. FACKLER, JR. J. Mol. Spectrosc. **22**, 80 (1967). (*b*) JIRO HIRAISHI. Spectrochim. Acta, 25A, 749 (1969).
3. (*a*) T. THEOPHANIDES. Inorg. Chim. Acta, **3**, 391 (1970). (*b*) T. THEOPHANIDES. Unpublished results.
4. G. T. BEHNKE and K. NAKAMOTO. Inorg. Chem. **7**, 2030 (1968).
5. (*a*) H. B. JONASSEN and J. E. FIELD. J. Am. Chem. Soc. **79**, 1275 (1957). (*b*) D. B. POWELL and N. SHEPPARD. Spectrochim. Acta, **13**, 69 (1958). (*c*) A. A. BABUSKIN, L. A. GRIBOV, and A. D. GEL'MAN. Russ. J. Inorg. Chem. **4**, 695 (1959).
6. P. C. KONG and T. THEOPHANIDES. Can. Spectrosc. 104 (1969).
7. J. A. J. JAVIS, B. T. KILBOURN, and P. G. OWSTON. Acta Cryst. B**27**, 366 (1971).
8. R. MASON, G. B. ROBERTSON, and P. O. WHIMP. J. Chem. Soc. A 535 (1970).
9. W. C. HAMILTON and K. KLANDERNAN. Acta Cryst. A**25**, S172 (1969).
10. J. CHATT and L. A. DUNCANSON. J. Chem. Soc. 2939 (1953).

Conductivity and Viscosity of the Tetrabutylammonium Bromide – Carbon Tetrachloride System

K. F. DENNING AND JAMES A. PLAMBECK

Department of Chemistry, University of Alberta, Edmonton, Alberta

Received July 20, 1971[1]

Conductivity and viscosity measurements have been made on tetra-*n*-butylammonium bromide–carbon tetrachloride solutions for the mole ratio range 1:40 to 1:2 at temperatures from 25 to 40 °C. At any individual concentration, both conductivity and viscosity follow an Arrhenius type temperature dependence. Viscosity increases exponentially with tetrabutylammonium bromide concentration while conductivity has a maximum at approximately 1:5 mole ratio $R_4NBr-CCl_4$.

Des mesures de conductivité et de viscosité ont été effectuées sur des solutions constituées d'un mélange de bromure de tétra-*n*-butylammonium-tétrachlorure de carbone; les rapports molaires utilisés varient de 1:40 à 1:2 pour des températures allant de 25 à 40 °C. Pour chaque concentration individuelle, la conductivité ainsi que la viscosité dépendent de la température par une relation du type d'Arrhénius. La viscosité augmente d'une façon exponentielle avec la concentration en bromure de tétrabutylammonium, alors que la conductivité passe par un maximum pour un rapport molaire de 1:5 $R_4NBr-CCl_4$.

Canadian Journal of Chemistry, **50**, 1600 (1972)

Solutions containing low concentrations of ionic salts, and fused ionic salts, have long been used as electrolytic media, and their conductivities and viscosities are well known. Mixtures which have "solute" and "solvent" present in comparable amounts are less well characterized. Such mixtures can be prepared from tetrabutylammonium halides and carbon tetrachloride (1). We have used such mixtures in

[1]Revision received February 1, 1972.

Can. J. Chem. Downloaded from www.nrcresearchpress.com by 210.87.254.42 on 09/05/12
For personal use only.

in 4 *N* hydrochloric acid. The water and HCl were evaporated in a desiccator under reduced pressure.

The salt was also prepared by the following method: potassium tetrachloroplatinite (0.002 *M*) was dissolved in 15 ml of water and the solution was filtered. A solution of 10 ml of 5,8-diethyl-6,6-dodecyne-5,8 diol or 2,2-dimethyl-5,5-diethyl-3-heptyne (0.005 *M*) in ethanol was added to the above solution. The mixture was stirred for a few minutes and left for a week. It was then filtered and the filtrate evaporated to dryness. The residue was washed with anhydrous ether and dissolved in 20 ml acetone. This was filtered and evaporated to dryness. Finally Zeise's salt was recrystallized slowly in a refrigerator in a mixture of acetone–anhydrous ether. Yield, 60%.

$K[Pt(C_2D_4)Cl_3]$ was prepared using ethylene-d_4 gas in D_2O and following the method described in ref. 10.

$K[Pt(C_2H_4)Br_3].H_2O$ was prepared by the above method (10) using a water solution of K_2PtBr_4. The red colored complex is extracted with acetone and recrystallized from acetone–ether. The i.r. spectrum of the complex was identical to the reported spectrum (2*a*).

$K[Pt(C_2H_4)Br_3]$ anhydrous was obtained by recrystallization in tetrahydrofuran or in 4 *N* hydrobromic acid and following the procedure as for $K[Pt(C_2H_4)Cl_3]$.

We wish to thank Johnson, Matthey and Mallory Ltd., for the loan of platinum chloroplatinite and the National Research Council of Canada for financial assistance. Many thanks also to Dr. I. S. Butler, McGill University for the use of the Jarell Ash Raman spectrophotometer.

1. M. J. GROGAN and K. NAKAMOTO. J. Am. Chem. Soc. **88**, 5454 (1966).
2. (*a*) J. PRADILLA-SORZANO and J. P. FACKLER, JR. J. Mol. Spectrosc. **22**, 80 (1967). (*b*) JIRO HIRAISHI. Spectrochim. Acta, 25A, 749 (1969).
3. (*a*) T. THEOPHANIDES. Inorg. Chim. Acta, **3**, 391 (1970). (*b*) T. THEOPHANIDES. Unpublished results.
4. G. T. BEHNKE and K. NAKAMOTO. Inorg. Chem. **7**, 2030 (1968).
5. (*a*) H. B. JONASSEN and J. E. FIELD. J. Am. Chem. Soc. **79**, 1275 (1957). (*b*) D. B. POWELL and N. SHEPPARD. Spectrochim. Acta, **13**, 69 (1958). (*c*) A. A. BABUSKIN, L. A. GRIBOV, and A. D. GEL'MAN. Russ. J. Inorg. Chem. **4**, 695 (1959).
6. P. C. KONG and T. THEOPHANIDES. Can. Spectrosc. 104 (1969).
7. J. A. J. JAVIS, B. T. KILBOURN, and P. G. OWSTON. Acta Cryst. B**27**, 366 (1971).
8. R. MASON, G. B. ROBERTSON, and P. O. WHIMP. J. Chem. Soc. A 535 (1970).
9. W. C. HAMILTON and K. KLANDERNAN. Acta Cryst. A**25**, S172 (1969).
10. J. CHATT and L. A. DUNCANSON. J. Chem. Soc. 2939 (1953).

Conductivity and Viscosity of the Tetrabutylammonium Bromide – Carbon Tetrachloride System

K. F. DENNING AND JAMES A. PLAMBECK

Department of Chemistry, University of Alberta, Edmonton, Alberta

Received July 20, 1971[1]

Conductivity and viscosity measurements have been made on tetra-*n*-butylammonium bromide–carbon tetrachloride solutions for the mole ratio range 1:40 to 1:2 at temperatures from 25 to 40 °C. At any individual concentration, both conductivity and viscosity follow an Arrhenius type temperature dependence. Viscosity increases exponentially with tetrabutylammonium bromide concentration while conductivity has a maximum at approximately 1:5 mole ratio $R_4NBr–CCl_4$.

Des mesures de conductivité et de viscosité ont été effectuées sur des solutions constituées d'un mélange de bromure de tétra-*n*-butylammonium-tétrachlorure de carbone; les rapports molaires utilisés varient de 1:40 à 1:2 pour des températures allant de 25 à 40 °C. Pour chaque concentration individuelle, la conductivité ainsi que la viscosité dépendent de la température par une relation du type d'Arrhénius. La viscosité augmente d'une façon exponentielle avec la concentration en bromure de tétrabutylammonium, alors que la conductivité passe par un maximum pour un rapport molaire de 1:5 $R_4NBr–CCl_4$.

Canadian Journal of Chemistry, **50**, 1600 (1972)

Solutions containing low concentrations of ionic salts, and fused ionic salts, have long been used as electrolytic media, and their conductivities and viscosities are well known. Mixtures which have "solute" and "solvent" present in comparable amounts are less well characterized. Such mixtures can be prepared from tetrabutylammonium halides and carbon tetrachloride (1). We have used such mixtures in

[1]Revision received February 1, 1972.

Can. J. Chem. Downloaded from www.nrcresearchpress.com by 210.87.254.6 on 09/05/12
For personal use only.

Can. J. Chem. Downloaded from www.nrcresearchpress.com by 210.87.254.6 on 09/05/12
For personal use only.

studying interesting electrochemical reactions, as will be reported elsewhere, and in this paper report the viscosity, conductivity, and density of the tetrabutylammonium bromide–carbon tetrachloride system. The concentrations considered correspond to a mole ratio range of 1:40 tetrabutylammonium bromide:carbon tetrachloride, where the solution was free-flowing, to 1:2 where the solution was extremely viscous. In this range the terms solute and solvent do not have any meaningful connotations and it is probably better to consider such mixtures as quasi-molten salts.

The literature of the dilute solutions dates back to the classic work of Walden (2) and Fuoss and Krauss (3). The latter measured the conductivity of tetraalkylammonium salts in benzene (dielectric constant 2.28 at 20 °C; that of carbon tetrachloride is very similar, 2.24) and, at concentrations far lower than those used in the present work, *i.e.* less than 0.2 *M*, observed a minimum in the equivalent conductivity *vs.* concentration curve. This was interpreted on the basis of ion association equilibria. Lind and Sageman (4) worked from the other end of the concentration scale. These authors measured the conductivities of fused tetraalkylammonium salts to which up to 0.06 mole fraction of nonelectrolytes had been added. They held that the observed increase in specific conductivity on these additions was due to the reduction in total friction on a given ion as the number of its ionic neighbors decreased. In the present study it was found that mole fractions of tetrabutylammonium bromide as high as those used by Lind and Sageman could be obtained only at high enough temperatures that decomposition of the halide became rapid. When cooled these highly viscous liquids became glassy solids. The highest concentration obtainable for a liquid at 30 °C was slightly over a 1:2 mole ratio of tetrabutylammonium bromide:carbon tetrachloride. The bromide salt was chosen as being the best compromise between high solubility and ease of solution preparation. The behavior of the other tetrabutylammonium halides is similar, insofar as our few studies have indicated, and that of some other tetraalkylammonium halides with smaller alkyl groups is somewhat similar although the solubilities in carbon tetrachloride are usually much lower.

Experimental

Chemicals

The tetra-*n*-butylammonium bromide (No. 7377, Eastman Organic Chemicals Ltd.) was dried under vacuum (5) or purified by dissolution in carbon tetrachloride and removal of solvent, followed by recrystallization from ethyl acetate and drying. The m.p. of material from either treatment was 117–119 °C, and no difference in conductivity due to treatment was observable. The carbon tetrachloride (Mallinckrodt Analytical Reagent) was used as supplied; use of redistilled material produced no observable change in solution conductivities.

Apparatus

Conductivities were measured at 1 kHz using a General Radio Company 1650-A Impedance Bridge. The Pyrex cell used platinized platinum electrodes 1 cm × 1 cm approximately 1 cm apart; the cell constant was determined with aqueous KCl before and after the series of determinations and found to be 0.717 cm. Viscosities were measured with a calibrated Cannon-type viscometer. Densities were obtained from the weight of an accurately measured volume of liquid and used to calculate the volume mole fractions given in Table 1.[2] All experiments were carried out in a water bath (Gebruder Haake, Type NBE) thermostated to ±0.05 °C and the temperature range for all data was 25 to 40 °C.

Procedure

Sets of measurements for both conductivity and viscosity were made with increasing and decreasing temperatures; no differences were noted, indicating no decomposition at 40 °C over the few minutes required for measurement. Decomposition was observed at higher temperatures. Six to ten temperatures were used in each set. These data, a summary at 30 °C, and the least-squares results for the Arrhenius form discussed below have been placed in the Depository of Unpublished Data. Least-squares calculations were carried out with the aid of the IBM 360/67 computer at the University of Alberta. Copies of the programs used are obtainable from the authors.

Results and Discussion

The viscosity at 30 °C increases exponentially with concentration over the range accessible in these experiments (Fig. 1). The analogous plot for specific conductivity, Fig. 2, is quite different, showing first an increase and then a decrease. The maximum appears in the region of approximately 1:5 mole ratio of tetrabutylammonium bromide to carbon tetrachloride.

The temperature dependence of conductivity (Λ) and viscosity (ν) at any individual concentration follows the expected Arrhenius form, *i.e.* $\Lambda = Ae^{-B/T}$ and $\nu = A'e^{B'/T}$, very well. The relationship between exponential terms and

[2]Tabular data are available from the Depository of Unpublished Data, National Science Library, National Research Council of Canada, Ottawa, Canada K1A 0S2.

Can. J. Chem. Downloaded from www.nrcresearchpress.com by 210.87.254.6 on 09/05/12
For personal use only.

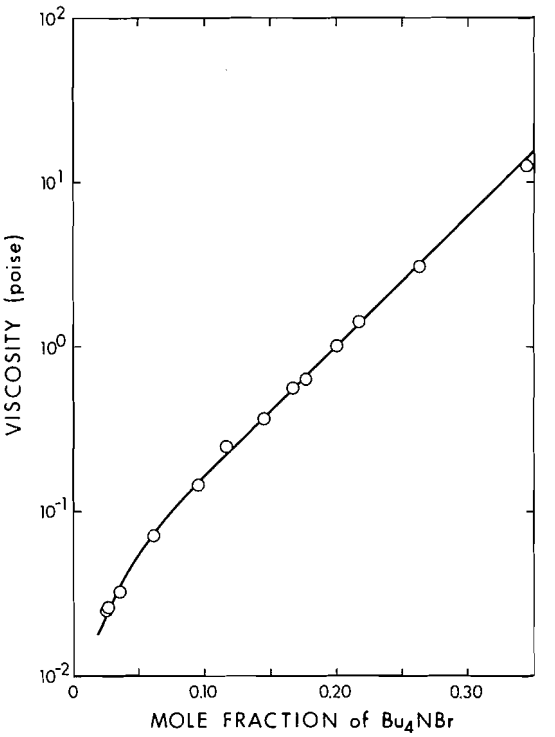

FIG. 1. Viscosity as a function of mole fraction of Bu_4NBr.

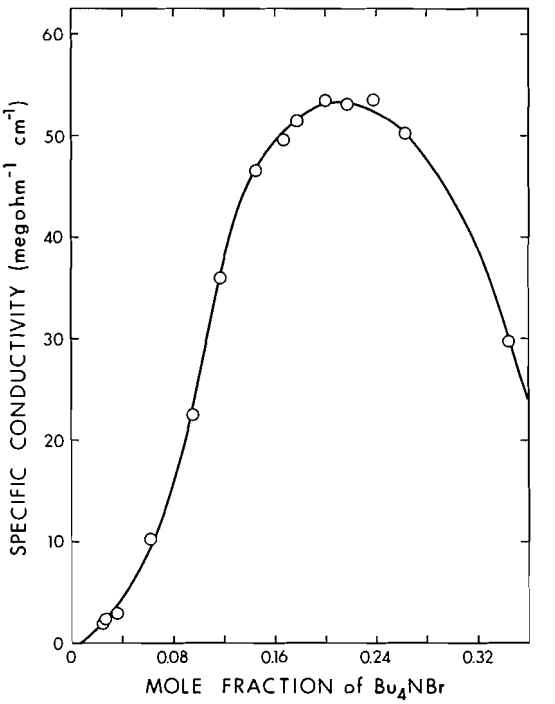

FIG. 2. Specific conductivity as a function of mole fraction of Bu_4NBr.

concentration is shown in Fig. 3, where the *B, B′* parameters are expressed as free energies of activation. The free energies of activation in the "dilute solutions" of the salt in carbon tetrachloride obtained from these conductivity measurements are in excellent agreement with the value of 1.96 kcal/mol calculated for the *pure fused tetrabutylammonium bromide* from the conductivity data of Lind *et al.* (5). It is not surprising that the free energy of activation from the viscosity data does not agree as the mechanisms for the two processes are different (6). In both cases the free energy of activation increases rapidly as the mole fraction of salt increases beyond 0.2, indicating that mass transport becomes much more difficult; on the basis of the data of Lind *et al.*, this should be followed by a subsequent decrease in the free energy of activation. Such a peaking behavior has previously been observed by Bloom (7) in ionic salt–ionic salt binary melts and by Boston, Grantham and Yosim (8) in $AlCl_3$–KCl mixtures, where it is ascribed to compound formation at the peak composition.

The formation of one or more complexes between the salt and carbon tetrachloride would be in general agreement with the observed change in conductivity with concentration shown in Fig. 2, although the rapid increase in viscosity with concentration alone should bring about some decrease in conductivity. The two are related, although not simply, since their product cannot be expected to be a constant in this concentration range. A complex at mole ratio 1:4.8 (and others at 1:1 and 2:1) was found by McDaniel and Deiters (9) through isothermal vapor pressure measurements on the tetrabutylammonium chloride–carbon tetrachloride system, and similar complexes are expected here.

The molar conductivity of these solutions in the peak region is approximately 0.03 cm^2 ohm^{-1} mol^{-1} at 25 °C, which is intermediate between that of highly conducting media, such as aqueous tetrabutylammonium bromide whose molar conductivity is 97.6 cm^2 ohm^{-1} mol^{-1} (10), and the virtually nonconducting carbon tetrachloride. It appears to be significantly greater than the molar conductivity of pure

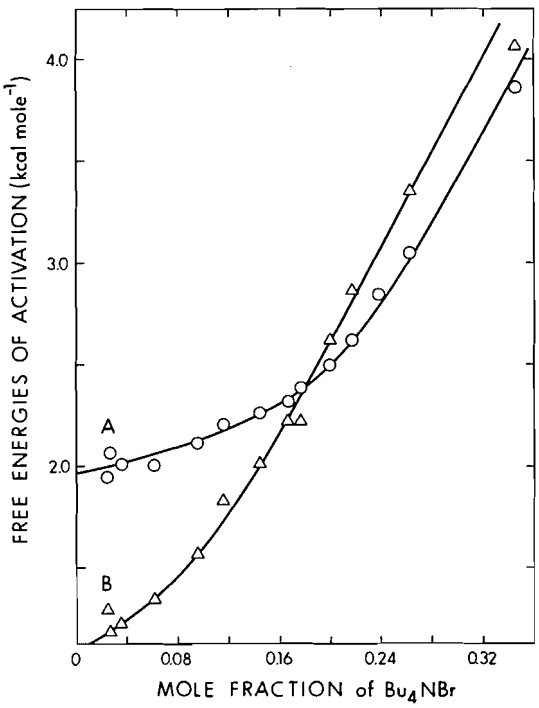

FIG. 3. Free energies of activation as a function of mole fraction of Bu_4NBr; Curve *A*, conductivity data; curve *B*, viscosity data.

fused tetrabutylammonium bromide, which we calculate as 0.012 cm^2 ohm^{-1} mol^{-1} by extrapolation of the data of Lind *et al.* (5) to 25 °C, but the extrapolation is well beyond the temperature range in which these authors' measurements were made.

The concentration–conductivity of the 1:5 mole ratio mixture permits cell resistances as low as 10 000 ohms at room temperature in reasonably practical electrolysis cells, and this mixture was therefore selected for further investigation.

The authors wish to thank the National Research Council of Canada for financial support.

1. R. D. GREEN, J. S. MARTIN, W. B. CASSIE, and J. B. HYNE. Can. J. Chem. **47**, 1639 (1969). R. D. GREEN. Ph.D. Thesis, University of Alberta, Edmonton, Alberta. (1968).
2. P. WALDEN. Z. Phys. Chem. **147**, 1 (1930).
3. R. M. FUOSS and C. A. KRAUSS. J. Am. Chem. Soc. **55**, 3614 (1933).
4. J. E. LIND, JR. and D. R. SAGEMAN. J. Phys. Chem. **74**, 3269 (1970).
5. J. E. LIND, JR., H. A. A. ABDEL-REHIM, and S. W. RUDICH. J. Phys. Chem. **70**, 3610 (1966).
6. YU. K. DELMARSKII and B. F. MARKOV. Electrochemistry of fused salts. *Translated by* A. Peiperl. *Edited by* R. E. Wood. Sigma Press, Washington, D.C., 1961, p. 21.
7. H. BLOOM. Chemistry of molten salts. Benjamin, New York, 1967. p. 91.
8. C. R. BOSTON, L. F. GRANTHAM, and S. J. YOSIM. J. Electrochem. Soc. **117**, 28 (1970).
9. D. H. MCDANIEL and SR. R. M. DEITERS. J. Am. Chem. Soc. **88**, 2607 (1966).
10. R. A. ROBINSON and R. H. STOKES. Electrolyte solutions. 2nd. ed. Butterworths, London, 1959. p. 463.

Can. J. Chem. Downloaded from www.nrcresearchpress.com by 210.87.254.6 on 09/05/12
For personal use only.

Equilibrium Dissociation Pressures of $NbBr_5$ over $NbBr_4$

A. D. WESTLAND AND D. LAL
Department of Chemistry, University of Ottawa, Ottawa, Canada, K1N 6N5

Received December 9, 1971

Equilibrium pressures of the dissociation of niobium tetrabromide into pentabromide and tribromide:

$$(5-x)NbBr_4(s) \rightleftharpoons NbBr_x(s) + (4-x)NbBr_5(g)$$

where x lies in the range 2.67 to 3.03 have been measured over the temperature range 275–365 °C. The dissociation pressures were determined by measuring the dew points of $NbBr_5$ vapor in a closed system containing $NbBr_4$ and $NbBr_x$. The equilibrium decomposition pressure of $NbBr_4$ at a given temperature was found to be much lower than that of $NbCl_4$, thereby indicating that $NbBr_4$ is significantly more stable than $NbCl_4$.

Les pressions d'équilibre pour la dissociation du tétrabromure de niobium en pentabromure et tribromure:

$$(5-x)NbBr_4(s) \rightleftharpoons NbBr_x(s) + (4-x)NbBr_5(g)$$

où x appartient au domaine allant de 2.67 à 3.03, ont été mesurées sur l'échelle de température 275–365 °C. Les pressions de dissociation ont été déterminées par la mesure du point de rosée de la vapeur de $NbBr_5$ dans un récipient fermé, contenant $NbBr_4$ et $NbBr_x$. La pression d'équilibre à la décomposition de $NbBr_4$, pour une température donnée, est beaucoup plus basse que celle de $NbCl_4$; ceci indiquant que $NbBr_4$ est plus stable que $NbCl_4$.

Canadian Journal of Chemistry, **50**, 1604 (1972)

Introduction

There is a lack of thermochemical data for compounds of less familiar elements such as niobium and tantalum. For example, there is considerable disagreement in the literature regarding the melting point of $NbBr_5$. Whether this variation is due to impurities in the various samples or other experimental errors is not clear.

The tetrahalides of niobium undergo thermal disproportionation (1, 2) to the corresponding pentahalide and a lower halide at elevated temperatures according to the equation:

$$(5-x)NbBr_4(s) \rightleftharpoons NbBr_x(s) + (4-x)NbBr_5(g)$$

where x may vary between the limits 2.67 and 3.03 (2). Thus a knowledge of equilibrium pressures of NbX_5 is desirable for work with these compounds at elevated temperatures. In the preparation of NbX_4, it is necessary to maintain a high pressure of NbX_5 by having an excess of NbX_5 present as a liquid. Moreover, knowledge of the decomposition pressures of NbX_5 is extremely important in the difficult separation of the pure metals niobium and tantalum.

Schäfer, Bayer, and Lehmann (3) have measured the decomposition pressures of $NbCl_5$ over $NbCl_4 + NbCl_x$ by a dew point method. We have used their technique to measure the equilibrium dissociation pressures of $NbBr_5$ over $NbBr_4$ and $NbBr_x$. The dew point method permits the determination of pressure of the major component in a gaseous mixture of $NbBr_5$, $NbBr_4$, and $NbOBr_3$.

Experimental

The design of the apparatus and the experimental procedure employed have been described in detail by Schäfer *et al.* (3).

Apparatus

The apparatus was a Pyrex glass vessel, 20 mm in diameter and about 100 mm long, which contained the sample to be studied. A cold finger, for observing the $NbBr_5$ condensate, extended about 20–25 mm into the upper part of the vessel. The cold finger contained a constant boiling liquid, a heater, and a thermocouple. The temperature of the liquid in the cold finger was adjusted by means of a manostat which controlled the pressure over the liquid. A vapor mantle surrounded the upper part of the reaction vessel and its temperature was kept well above the dew point temperature so that condensate only appeared on the cold finger and not on the inner surface of the reaction vessel.

Measurement

The sample was transferred to the reaction vessel in a rigorously dry nitrogen atmosphere. The temperature of the solid sample was adjusted by an aluminum block, the temperature of which was measured close to the solid sample and kept constant to ± 0.2 °C. The temperature of the vapor mantle was kept about 20° higher than the dew point temperature.

Can. J. Chem. Downloaded from www.nrcresearchpress.com by 210.87.254.42 on 09/05/12
For personal use only.

Can. J. Chem. Downloaded from www.nrcresearchpress.com by 210.87.254.42 on 09/05/12
For personal use only.

To effect a measurement, the temperature in the cold finger was lowered from a point about 20° above the dew point until the condensate appeared on the upper part of the cold finger. A slight raising of the temperature caused the condensate to disappear.

Initially the dew point was approached from above by lowering the temperature in steps of 5°, followed by 2° steps, and finally in steps of 0.5°. This was repeated several times to get consistent readings.

The observation of the condensate at the cold finger was done with the aid of adequate lighting and a magnifying lens. Much care was taken to distinguish between liquid and crystalline condensate. A crystalline condensate of $NbBr_5$ was red-orange and its whisker-like growth on the cold finger was easily recognized. Appearance of liquid condensate, which was very deep orange, was somewhat more difficult to observe.

At high furnace temperatures, fine needles of $NbBr_4$ deposited on the cold finger but this deposition caused little interference in the observation of the dew point. Moreover, it was an easy matter to sublime the $NbBr_4$ crystals back to the bottom part of the reaction vessel by placing the vessel in a temperature gradient.

The unavoidable presence of $NbOBr_3$, in small amounts, caused problems in the initial stages of the measurements. Its appearance on the cold finger was similar to that of $NbBr_5$ crystals. However, with little experience it was possible to differentiate between the shiny orange-red crystals of $NbBr_5$ and the dull yellow-brown crystals of $NbOBr_3$. It should be mentioned that $NbOBr_3$ may dissolve in liquid $NbBr_5$. Schäfer and Pietruck (4) have shown that in the case of the chloride, the solubility was rather small and it did not markedly affect the saturation pressure of $NbCl_5$. We expect that the bromide system is similar in this respect.

The static method employed here for measuring the vapor pressure is superior to the dynamic method because the former method allows the equilibrium to be established over a period of time while the dynamic method requires the equilibrium to be established instantaneously. Schäfer and Dohmann (5) have shown that in the case of $NbCl_4$ decomposition, equilibrium is established only slowly. We would expect that the bromide system would show essentially the same behavior. To ensure that the equilibrium was established, we proceeded in the following way: The aluminum furnace was heated to a predetermined temperature. Readings were carried on for several days and the dew point remained unchanged. Then the temperature of the furnace was altered by ±3° and the dew point redetermined. A corresponding change of a few degrees in dew point was observed. Return to the original furnace temperature gave the original dew point. The changes in the vapor pressures with respect to temperature were too great to be accounted for by temporary Boyles' Law expansion. Therefore the changes in pressure are attributable to shifts in the equilibrium and the pressures are reproducible with respect to furnace temperature.

Results and Discussion

The dew point measurements are given in the curves of Fig. 1. The results of two different samples show excellent agreement. In Fig. 1 the two segments of the plot corresponding to solid and liquid condensed phases intersect at the melting point of $NbBr_5$. Table 1 gives melting points obtained by various workers.

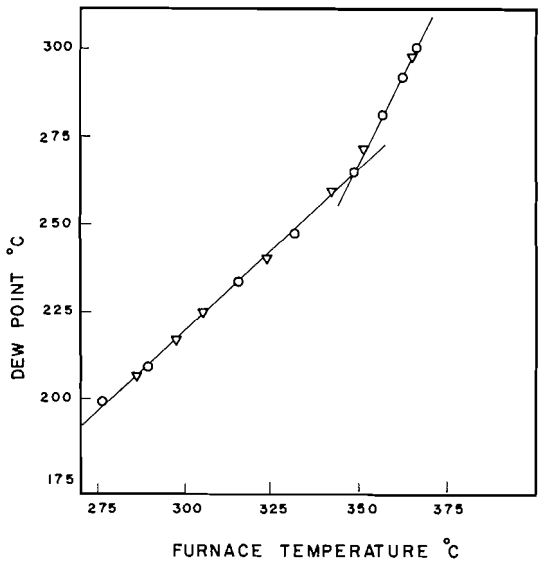

FIG. 1. The variation of dew point with furnace temperature: ○, sample No. 1; △, sample No. 2.

TABLE 1. Melting point data for $NbBr_5$

Melting point (°C)	Reference
254	6
255	7
267.5	8
265.2	9
264.5	This work

To utilize the dew point data, saturation pressures of $NbBr_5$ were needed. Two previous investigations of the vapor pressures of $NbBr_5$ have been reported. Alexander and Fairbrother (8) employed a static method using a Bourdon type gauge. We evaluated their data for temperatures above 239° by the method of least squares and obtained the following equations for the temperature dependence of vapor pressure:

$$\log_{10} p = 13.17 \pm 0.15 - (6.17 \pm 0.01)\frac{10^3}{T} \qquad (239\text{–}269\ ^\circ\text{C})$$

$$\log_{10} p = 9.30 \pm 0.06 - (4.08 \pm 0.01)\frac{10^3}{T} \qquad (270\text{–}360\ ^\circ\text{C})$$

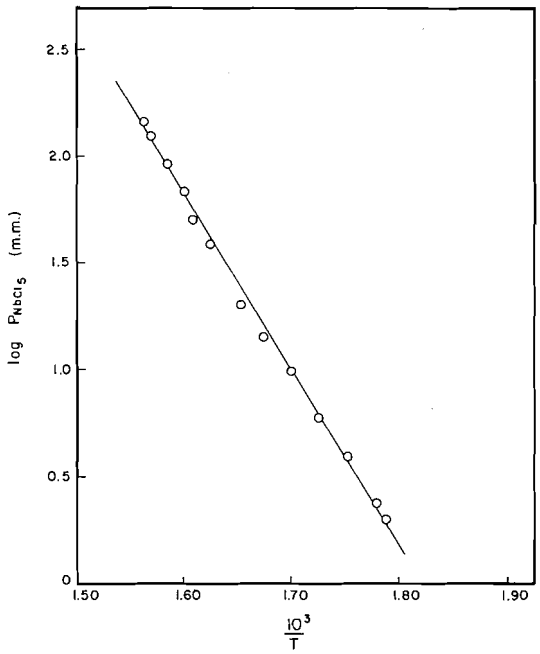

FIG. 2. Equilibrium decomposition pressures of $NbBr_5$ over $NbBr_4$.

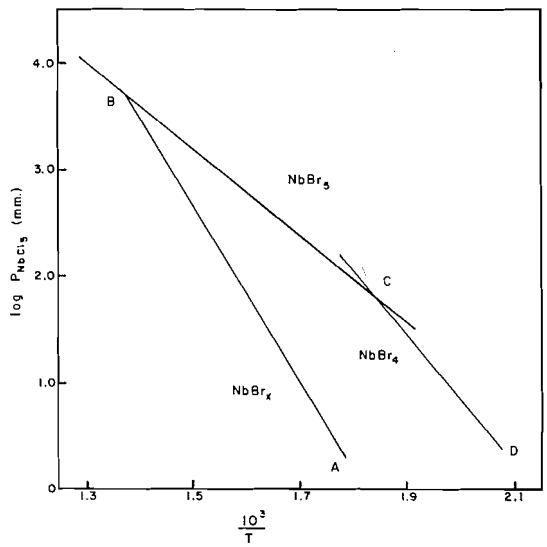

FIG. 3. Existence regions of various niobium bromide phases.

Berdonosov *et al.* (6) employed a radioactive tracer technique to a static method to obtain their data. They give the following equations for the dependence of vapor pressure on temperature

$$\log_{10} p = 12.52 \pm 0.33 - (5.782 \pm 0.158)\frac{10^3}{T}$$

(205–252 °C)

$$\log_{10} p = 9.784 \pm 0.260 - (4.347 \pm 0.147)\frac{10^3}{T}$$

(252–350 °C)

There is reasonably good agreement between the two sets of results only for the higher temperatures. Berdonosov *et al.* certainly show many more experimental points at low temperatures. However, our melting point value (Table 1) differs considerably from that given by Berdonosov *et al.* but agrees well with that of Alexander and Fairbrother. For this reason and also because Alexander and Fairbrother used direct pressure measurements, we have chosen to use their data.

Decomposition Pressures of $NbBr_4$

Saturation pressures of $NbBr_5$ at the dew point correspond to the decomposition pressures of $NbBr_4$. The decomposition pressures are given in Fig. 2. The following equation for the temperature dependence of decomposition pressures was obtained by the method of least squares

$$\log_{10} p\text{NbBr}_5 \text{ (over NbBr}_x \text{ and NbBr}_4) =$$

$$15.02 \pm 0.38 - (8.25 \pm 0.03)\frac{10^3}{T}$$

The straight line in Fig. 2 was obtained by the use of the above equation.

Figure 3 shows the existence region of solid $NbBr_4$. Line AB is the dissociation pressure curve obtained in this work. Below this line $NbBr_x$ and $NbBr_5$ vapor do not react to form $NbBr_4$. The line BCD is the vapor pressure curve for solid and liquid $NbBr_5$. Thus the tetrabromide phase is stable only within the conditions bounded by the figure ABCD. The maximum temperature region at which solid $NbBr_4$ can exist is found from Fig. 3 to be approximately 454°. It is assumed in the diagram that $NbBr_4$ is insoluble in liquid $NbBr_5$. One would expect as in the chloride system (10) that $NbBr_4$ is soluble in liquid $NbBr_5$. This would cause some reduction in the vapor pressure of

Can. J. Chem. Downloaded from www.nrcresearchpress.com by 210.87.254.42 on 09/05/12
For personal use only.

liquid $NbBr_5$ and the line BC would be depressed. Consequently, the quadruple point would also be somewhat lower than the point indicated. That this is not too serious an error is seen from the melting point data for $NbBr_5$ in Table 1, which indicates that the solubility of $NbBr_4$ in liquid $NbBr_5$ is not substantial.

A comparison of the $NbBr_4$ and the $NbCl_4$ decompositions indicates that the bromide is much the more stable compound. At 300° we obtained a pressure of 4.3 Torr for the $NbBr_5$ pressure while Schäfer *et al.* (3) obtained 230 Torr for the pressure over $NbCl_4$ at 300°.

The coefficient of the temperature dependent term in the equation for $\log p$ leads to a value of 37.8 kcal for the heat of the decomposition reaction producing 1 mole of $NbBr_5$ vapor. This corresponds to the decomposition of $(5-x)/(4-x)$ moles of $NbBr_4$. The composition of the lower bromide should lie close to the upper limit of its homogeneity range, *i.e.* x should be about 3.03 (2). However, as x may vary somewhat with temperature, its value is uncertain and the reaction is not well defined. The above value for the heat of reaction should be understood accordingly.

This work was supported by a grant from the National Research Council of Canada.

1. R. E. McCarley and B. A. Torp. Inorg. Chem. **2**, 540 (1963).
2. H. Schäfer, C. Göser, and L. Bayer. Z. anorg. allgem. Chem. **265**, 258 (1951).
3. H. Schäfer, L. Bayer, and H. Lehmann. Z. anorg. allgem. Chem. **268**, 268 (1952).
4. H. Schäfer and C. Pietruck. Z. anorg. allgem. Chem. **267**, 174, 180 (1951).
5. H. Schäfer and K. Dohmann. Z. anorg. allgem. Chem. **300**, 1 (1959).
6. S. S. Berdonosov, A. V. Lapitskii, and E. K. Bakov. Russ. J. Inorg. Chem. **10**, 173 (1965).
7. L. A. Nisel'son and T. D. Sokolova. Russ. J. Inorg. Chem. **9**, 1117 (1964).
8. K. M. Alexander and F. Fairbrother. J. Chem. Soc. S223 (1949).
9. G. Brauer (*Editor*). Handbook of preparative inorganic chemistry. Vol. 2, 2nd ed. Academic Press, 1965. p. 1313.
10. H. Schäfer and C. Pietruck. Z. anorg. allgem. Chem. **266**, 151 (1951).

A Convenient Synthesis of Monobromogermane

J. W. Anderson, G. K. Barker, J. E. Drake[1] and R. T. Hemmings
Department of Chemistry, University of Windsor, Windsor, Ontario

Received December 23, 1971

Monobromogermane, GeH_3Br, is conveniently prepared by the reaction of boron tribromide with germane.

Le monobromogermane, GeH_3Br, est aisément préparé par action du tribromure de bore sur le germane.

Canadian Journal of Chemistry, **50**, 1607 (1972)

The most common starting materials for studies of germyl compounds are the monohalogenogermanes, GeH_3X (X = F, Cl, Br, I). We wish to report a preparative method for monobromogermane which we believe has some advantages over the previously reported methods.

Monobromogermane was first prepared from germane and hydrogen bromide with an aluminum bromide catalyst (1) but the yields are as low as 10% (2). A particular disadvantage of this method is that the product tends to undergo decomposition possibly because of trace amounts of aluminum bromide carried over from the reaction vessel. A second method involves repeatedly passing germane over heated silver bromide (3) giving yields of 30%. A frequently used method is the reaction of bromine and germane (4). Although yields as high as 91% have been claimed for this reaction, it requires a large number of additions and separations and even with care the optimum yields are

[1]To whom correspondence should be addressed. No reprints will be available.

Can. J. Chem. Downloaded from www.nrcresearchpress.com by 210.87.254.42 on 09/05/12
For personal use only.

liquid $NbBr_5$ and the line BC would be depressed. Consequently, the quadruple point would also be somewhat lower than the point indicated. That this is not too serious an error is seen from the melting point data for $NbBr_5$ in Table 1, which indicates that the solubility of $NbBr_4$ in liquid $NbBr_5$ is not substantial.

A comparison of the $NbBr_4$ and the $NbCl_4$ decompositions indicates that the bromide is much the more stable compound. At 300° we obtained a pressure of 4.3 Torr for the $NbBr_5$ pressure while Schäfer *et al.* (3) obtained 230 Torr for the pressure over $NbCl_4$ at 300°.

The coefficient of the temperature dependent term in the equation for $\log p$ leads to a value of 37.8 kcal for the heat of the decomposition reaction producing 1 mole of $NbBr_5$ vapor. This corresponds to the decomposition of $(5-x)/(4-x)$ moles of $NbBr_4$. The composition of the lower bromide should lie close to the upper limit of its homogeneity range, *i.e.* x should be about 3.03 (2). However, as x may vary somewhat with temperature, its value is uncertain and the reaction is not well defined. The above value for the heat of reaction should be understood accordingly.

This work was supported by a grant from the National Research Council of Canada.

1. R. E. McCarley and B. A. Torp. Inorg. Chem. **2**, 540 (1963).
2. H. Schäfer, C. Göser, and L. Bayer. Z. anorg. allgem. Chem. **265**, 258 (1951).
3. H. Schäfer, L. Bayer, and H. Lehmann. Z. anorg. allgem. Chem. **268**, 268 (1952).
4. H. Schäfer and C. Pietruck. Z. anorg. allgem. Chem. **267**, 174, 180 (1951).
5. H. Schäfer and K. Dohmann. Z. anorg. allgem. Chem. **300**, 1 (1959).
6. S. S. Berdonosov, A. V. Lapitskii, and E. K. Bakov. Russ. J. Inorg. Chem. **10**, 173 (1965).
7. L. A. Nisel'son and T. D. Sokolova. Russ. J. Inorg. Chem. **9**, 1117 (1964).
8. K. M. Alexander and F. Fairbrother. J. Chem. Soc. S223 (1949).
9. G. Brauer (*Editor*). Handbook of preparative inorganic chemistry. Vol. 2, 2nd ed. Academic Press, 1965. p. 1313.
10. H. Schäfer and C. Pietruck. Z. anorg. allgem. Chem. **266**, 151 (1951).

A Convenient Synthesis of Monobromogermane

J. W. Anderson, G. K. Barker, J. E. Drake[1] and R. T. Hemmings
Department of Chemistry, University of Windsor, Windsor, Ontario

Received December 23, 1971

Monobromogermane, GeH_3Br, is conveniently prepared by the reaction of boron tribromide with germane.

Le monobromogermane, GeH_3Br, est aisément préparé par action du tribromure de bore sur le germane.

Canadian Journal of Chemistry, **50**, 1607 (1972)

The most common starting materials for studies of germyl compounds are the monohalogenogermanes, GeH_3X (X = F, Cl, Br, I). We wish to report a preparative method for monobromogermane which we believe has some advantages over the previously reported methods.

Monobromogermane was first prepared from germane and hydrogen bromide with an aluminum bromide catalyst (1) but the yields are as low as 10% (2). A particular disadvantage of this method is that the product tends to undergo decomposition possibly because of trace amounts of aluminum bromide carried over from the reaction vessel. A second method involves repeatedly passing germane over heated silver bromide (3) giving yields of 30%. A frequently used method is the reaction of bromine and germane (4). Although yields as high as 91% have been claimed for this reaction, it requires a large number of additions and separations and even with care the optimum yields are

[1]To whom correspondence should be addressed. No reprints will be available.

Can. J. Chem. Downloaded from www.nrcresearchpress.com by 210.87.254.40 on 09/05/12
For personal use only.

seldom attained. Monobromogermane may also be prepared from germane and thionyl bromide in high yields (5) but there are difficulties involved in purifying and handling thionyl bromide.

We have found that monobromogermane is conveniently prepared from germane and boron tribromide according to reaction 1 in yields of over 70%.

$$[1] \qquad 6GeH_4 + 2BBr_3 \rightleftharpoons 6GeH_3Br + B_2H_6$$

After the two reactants are mixed and left at $-78°$ for 1–2 h, the pure GeH_3Br can be readily separated from the reactants or other products. Adherence to experimental conditions such as the starting ratio of reactants provides consistently high yields.

Experimental

The reactions were carried out on a conventional Pyrex–glass vacuum line. The typical reaction vessel (a flask with cold-finger for condensing in reactants and a ball-joint for connection to the vacuum line) had a capacity of *ca.* 250 ml. Germane (Mathieson) and boron tribromide (Alfa) were obtained commercially. They were degassed at -196 and $-78°$, respectively, and their purity checked by their i.r. spectra (6, 7) which were recorded on a Beckman IR 12 spectrometer. Boron tribromide (1.1 mmol) and germane (3.9 mmol) were condensed at $-196°$ into the reaction vessel.

The $-196°$ bath was replaced with a $-78°$ bath (Dry Ice–acetone) and the mixture left for 1–2 h. The volatile products were then distilled from the reaction vessel leaving traces of an unidentified yellow solid, and passed through a series of U-traps surrounded by baths at $-45°$ (fraction *A*), $-95°$ (fraction *B*), and $-196°$ (fraction *C*). The contents of the $-95°$ trap (fraction *B*) were again passed through traps at -63, -95, and $-196°$ when the $-95°$ fraction was pure monobromogermane (2.9 mmol). It was initially identified by its vapor pressure and i.r. spectrum (1, 4) and its purity further checked by its ^1H n.m.r. spectrum (8).

The unreacted germane could be recovered from fraction *C* which consisted of diborane and germane which were identified spectroscopically (9, 6). The mixture was condensed into a large excess of triethylamine and the products volatile at $-78°$ were distilled off. Further passage through a trap at $-126°$ gave germane (0.6 mmol) in a trap at $-196°$. The fraction *A* was shown spectroscopically (8, 10) to be small quantities of dibromogermane.

We wish to thank the National Research Council of Canada for financial support.

1. L. M. Dennis and P. R. Judy. J. Am. Chem. Soc. **51**, 2321 (1929).
2. T. N. Srivastava, J. E. Griffiths, and M. Onyszchuk. Can. J. Chem. **40**, 739 (1962).
3. K. M. Mackay, P. Robinson, E. J. Spanier, and A. G. MacDiarmid. J. Inorg. Nucl. Chem. **28**, 1377 (1966).
4. J. E. Griffiths, T. N. Srivastava, and M. Onyszchuk. Can. J. Chem. **40**, 579 (1962).
5. R. T. Hemmings. Unpublished work.
6. W. B. Steward and H. H. Nielsen. Phys. Rev. **48**, 861 (1935).
7. T. Wentink and V. H. Tiesu. J. Chem. Phys. **28**, 826 (1958).
8. E. A. V. Ebsworth, S. G. Frankiss, and A. G. Robiette. J. Mol. Spectrosc. **12**, 299 (1964).
9. R. C. Lord and E. Nielsen. J. Chem. Phys. **19**, 1 (1951).
10. T. N. Srivastava, J. E. Griffiths, and M. Onyszchuk. Can. J. Chem. **41**, 2101 (1963).

Can. J. Chem. Downloaded from www.nrcresearchpress.com by 210.87.254.40 on 09/05/12
For personal use only.

Formation Constants of Copper(II) and Zinc(II) with *N*-salicylideneanthranilic Acid in 50–50 Water–dioxane

R. K. MEHTA AND R. K. GUPTA
Department of Chemistry, University of Jodhpur, Jodhpur, India

Received June 29, 1971

Protonation constants of *N*-salicylideneanthranilic acid and formation constants of its Cu(II) and Zn(II) complexes have been studied potentiometrically in 50% dioxane (vol/vol) solutions ($\mu = 0.1$ sodium perchlorate) at 30 ± 0.2 °C. The color changes observed during titrations have been related to the formation of different complex species in solution. The formation constants are in fair agreement with the Irving and Williams rule.

On a étudié au moyen de méthodes potentiométriques les constantes de protonation de l'acide *N*-salicylidène anthranilique et les constantes de formation de ses complexes avec Cu(II) et Zn(II), dans des solutions (vol/vol) 50% dans le dioxanne ($\mu = 0.1$ perchlorate de sodium), à 30 ± 0.2 °C. Les changements de couleur observés pendant les titrages ont été associés à la formation des différents complexes dans la solution. Les constantes de formation sont en accord avec la règle de Irving et Williams.

Canadian Journal of Chemistry, **50**, 1609 (1972)

Introduction

N-salicylideneanthranilic acid (H_2SA) reacts with different metal ions to form colored compounds in aqueous solution. Although the magnetic data of some of its solid complexes including those of Cu(II) and Zn(II) have been reported, no work appears to have been done potentiometrically for the step-wise formation of these complexes in solution (1, 2). It was, therefore, considered interesting to investigate these complexes adopting the Calvin–Bjerrum p*H*-titration technique as used by Irving and Rossotti (3–5). The step-wise proton–ligand stability constants of the ligand and the metal–ligand stability constants of the metal complexes have been determined in 50% dioxane at 30 ± 0.2 °C as the ligand and its complexes are insoluble in water.

Experimental

Apparatus

A precision p*H*-meter (Type: OP-205 No. 837) with a wide range glass-calomel electrode assembly was calibrated at two p*H* values (4.0 and 7.0) with suitable buffers. An inert atmosphere of nitrogen was maintained in the potentiometric cell through the solution.

Stock Solutions

Aqueous solutions of the metal ions were prepared from $CuSO_4$ and $Zn(NO_3)_2$ (BDH-AnalaR) and standardized by usual procedures (6). Sodium perchlorate (BDH-AnalaR) solution in double distilled water was prepared (1.0 *M*) and estimated by the standard method (7). Standard carbonate free sodium hydroxide (E. Merck) was prepared and its solution in 50% dioxane was used as a titrant (5). Dioxane was refluxed with sodium for 24 h and freshly distilled before use. The H_2SA was prepared (2) spectroscopically pure, the required quantity was dissolved in dioxane and the solution standardized potentiometrically (7).

Calvin–Bjerrum pH-titration Technique (3–5)

Four mixtures (as shown in Fig. 1) were prepared, titrated with progressive addition of an alkali solution (*ca.* 0.1 *M*), and the titration curves were plotted (Fig. 1). The protonation constants of H_2SA were calculated from the titration curves I and II.

Results and Discussion

Proton–Ligand System

H_2SA is a weak acid due to the presence of a phenolic and a carboxylic group in its molecule. Its formation curve (Fig. 2) extends up to $\bar{n}_A = 2.0$ which indicates the formation of the species HSA^- and SA^{2-} in solution. H_2SA dissociates in two steps. The values of log K_1^H and log K_2^H were found by (*i*) interpolation at half $\bar{n}_A$ values and (*ii*) interpolation at various $\bar{n}_A$ values, as shown in Table 1 (8).

A change of color from colorless to orange takes place at p*H* 7.2, which corresponds to the $\bar{n}_A$ value of approximately 1.0. But at $\bar{n}_A \approx 1.0$, the species HSA^- is the predominant species. Since there is no marked change in the color of the species HSA^- and SA^{2-}, it appears that the species H_2SA (in 50% dioxane) is colorless, changing to orange species SA^{2-} at $\bar{n}_A > 1.0$.

Metal–Ligand System

Copper(II)–H_2SA System

The formation curve (Fig. 3) for this system

Can. J. Chem. Downloaded from www.nrcresearchpress.com by 210.87.254.6 on 09/05/12
For personal use only.

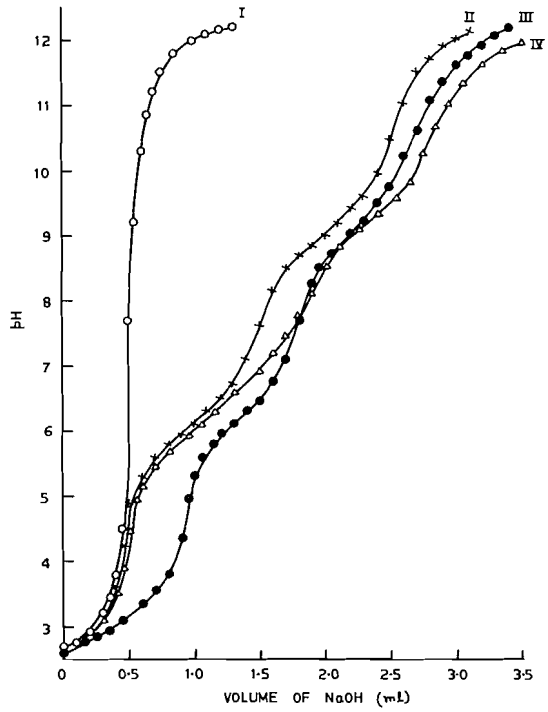

FIG. 1. Titration curves of Cu(II) and Zn(II)–H_2SA complexes: curve *I*, 5.0 ml 0.01 *M* $HClO_4$ + 2.0 ml 1 *M* $NaClO_4$ + 3.0 ml water + 10.0 ml dioxane; curve *II*, 10.0 ml 0.01 *M* H_2SA + 5.0 ml 0.01 *M* $HClO_4$ + 2.0 ml 1 *M* $NaClO_4$ + 3.0 ml water; curve *III*, 10.0 ml 0.01 *M* H_2SA + 5.0 ml 0.01 *M* $HClO_4$ + 2.0 ml 1 *M* $NaClO_4$ + 2.0 ml 0.01 *M* $CuSO_4$ + 1.0 ml water; curve *IV*, 10.0 ml 0.0 *M* H_2SA + 5.0 ml 0.01 *M* $HClO_4$ + 2.0 ml 1 *M* $NaClO_4$ + 2.0 ml 0.01 *M* $Zn(NO_3)_2$ + 1.0 ml water.

TABLE 1. Protonation constants of H_2SA at 30 ± 0.2 °C

Method	$\log K_1^H$	$\log K_2^H$	$\log \beta_2^{H*}$
(*i*) Interpolation at half $\bar{n}_A$ values	9.05	6.09	15.14
(*ii*) Interpolation at various $\bar{n}_A$ values	9.07	6.09	15.16
Mean	9.06	6.09	15.15

*Equals $\log K_1^H \log K_2^H$.

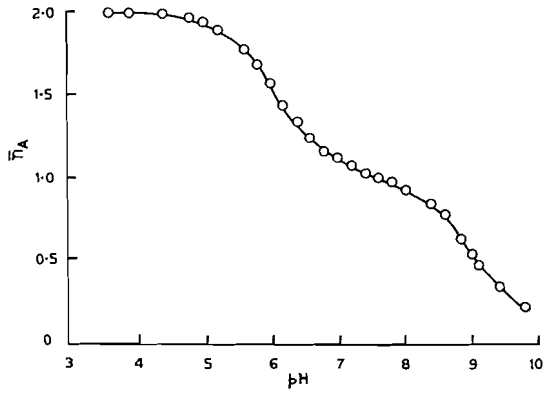

FIG. 2. Formation curve of proton–ligand system of H_2SA.

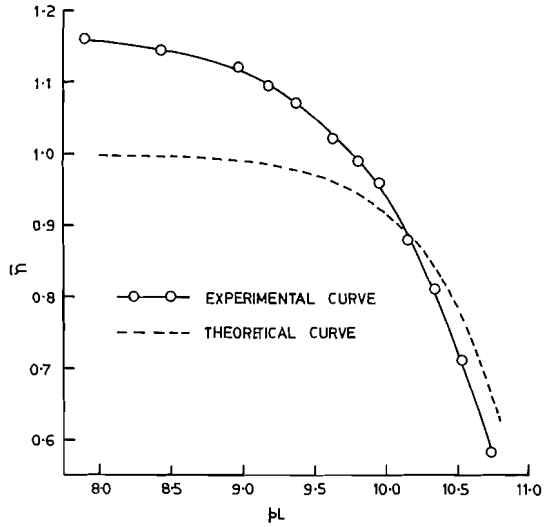

FIG. 3. Formation curve of Cu(II)-H_2SA system.

is incomplete at both ends and it is not symmetrical about its midpoint. Therefore, its formation constant, $\log K_1 = 11.05$, was calculated by interpolation at various $\bar{n}$ method. In Fig. 3 the deviation between the experimental (curve *A*) and theoretical (curve *B*) curves is observed only beyond $\bar{n} \approx 0.9$. From the nature of the experimental curve it appears that at $\bar{n} \approx 1.1$ the complex starts hydrolyzing with the result that 1:2 species does not exist.

In this system the formation of different species in solution is evident from the color change observed during the titration. A yellowish-green color appears in the p*H* range of 3.2–4.6. The p*H* 4.0 corresponds to $\bar{n} \simeq 1$ from which it may be concluded that the 1:1 species is yellowish-green in color.

Zinc(II)–H_2SA System

In this system the formation curve *A* (Fig. 4) attains maxima at $\bar{n} \approx 1.9$ which indicates that 1:1 and 1:2 complexes are formed. The values of $\log K_1$ and $\log K_2$ as obtained by Bjerrum's

Can. J. Chem. Downloaded from www.nrcresearchpress.com by 210.87.254.6 on 09/05/12
For personal use only.

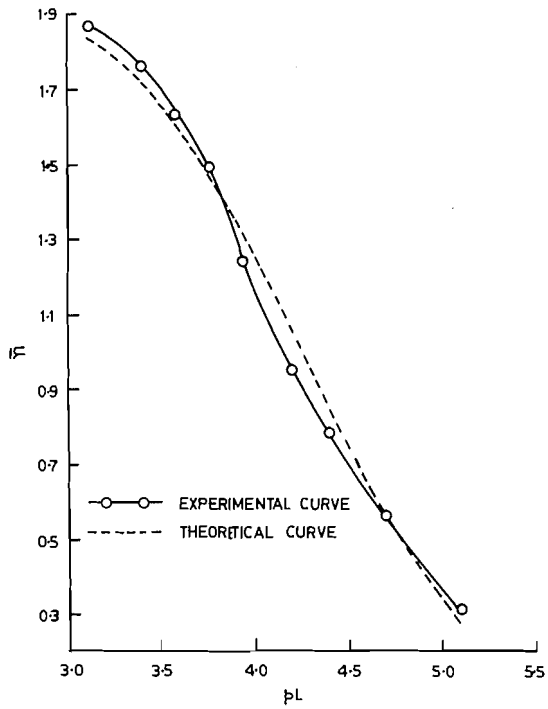

FIG. 4. Formation curve of Zn(II)–H_2SA system.

TABLE 2. Formation constants of zinc(II)–H_2SA Complex at 30 + 0.2 °C

Method	log K_1	log K_2	log β_2*
(*i*) Interpolation at half $\bar{n}$ values	4.69	3.84	8.53
(*ii*) Successive approximations	4.65	3.89	8.54
(*iii*) Correction term	4.62	3.80	8.42
Mean	4.65	3.84	8.49

*Equals log K_1K_2.

half $\bar{n}$ values method (3) were refined by interpolation at half $\bar{n}$ values method, correction term method and the method of "successive approximations" (8) as shown in Table 2. The theoretical formation curve *B* (Fig. 4) was thus derived by using log $K_1 = 4.65$ and log $K_2 = 3.84$. A perusal of the experimental and theoretical curves indicates negligible deviation.

In this system a lemon-yellow color appears in the p*H* range of 6.0–7.2. The p*H* 6.8 corresponds to $\bar{n} > 0.5$ and it may be concluded that the 1:1 species formed is lemon-yellow in color. The color becomes deep yellow in the p*H* range of 7.4–8.4 indicating the formation of 1:2 species. The p*H* 7.9 corresponds to $\bar{n} \approx 1.5$. Beyond p*H* 8.7, the complex starts decomposing which results in the hydrolysis of the metal ion.

The formation constants of Cu(II) and Zn(II) complexes with H_2SA are in fair agreement with the Irving and Williams rule (9).

1. R. K. MEHTA, S. P. RAO, and R. C. KAPOOR. Ind. J. Chem. 7, 933 (1969).
2. R. H. HOLM, G. W. EVERETT, JR., and A. CHAKRAVORTY. Progress in inorganic chemistry. Vol. VII. Interscience Publishers Inc., New York, 1966, pp. 83–214.
3. J. BJERRUM. Metal ammine formation in aqueous solution. Haase, Copenhagen, 1941.
4. M. CALVIN and K. W. WILSON. J. Am. Chem. Soc. **67**, 2003 (1945).
5. H. IRVING and H. S. ROSSOTTI. J. Chem. Soc. 2904 (1954).
6. A. I. VOGEL. A Textbook of quantitative inorganic analysis. 3rd ed. Longmans, London, 1961, pp. 241, 497, 533, 910.
7. G. BIEDERMANN. Arkiv Kemi. **9**, 277 (1956).
8. H. IRVING and H. S. ROSSOTTI. J. Chem. Soc. 3397 (1953).
9. H. IRVING and R. J. P. WILLIAMS. J. Chem. Soc. 3192 (1953).

Can. J. Chem. Downloaded from www.nrcresearchpress.com by 210.87.254.6 on 09/05/12
For personal use only.

Can. J. Chem. Downloaded from www.nrcresearchpress.com by 210.87.254.40 on 09/05/12
For personal use only.

Canadian Journal of Chemistry

Published by THE NATIONAL RESEARCH COUNCIL OF CANADA

VOLUME 50 JUNE 1, 1972 NUMBER 11

The Wetting Properties of Aqueous Solutions of Valeric Acid on Solid Surfaces

A. B. PONTER

Department of Chemical Engineering, University of New Brunswick, Fredericton, New Brunswick

AND

A. P. BOYES

Department of Chemical Engineering, University of Birmingham, England

Received October 1, 1971

Contact angles are reported for aqueous solutions of valeric acid on copper, stainless steel and polytetrafluoroethylene surfaces in equilibrium with their own vapors at atmospheric pressure and 25 °C. It is demonstrated that the dependency on concentration for the polytetrafluoroethylene surface is in accord with theory.

Les angles de contact sont rapportés pour des solutions aqueuses d'acide valérique sur des surfaces en cuivre, en acier inoxydable et en polytétrafluoroéthylène, en équilibre avec leurs propres vapeurs sous pression atmosphérique et à 25 °C. Il a été démontré que la dépendance par rapport à la concentration pour une surface en polytétrafluoroéthylène est en accord avec la théorie.

Canadian Journal of Chemistry, **50**, 1613 (1972)

Introduction

The spreading coefficient, the wetting energy and the surface tension of a liquid spreading on a plane solid surface are related by the expression

$$[1] \qquad S_c = W_e - \gamma_{LV}$$

where S_c is the spreading coefficient, W_e is the wetting energy, and γ, interfacial free energy with subscript LV referring to liquid–vapor, SL to solid–liquid, and SV to solid–vapor, interfaces. The wetting energy may be expressed in terms of the surface energies at the solid–vapor and solid–liquid interface by the expression

$$[2] \qquad W_e = \gamma_{SV} - \gamma_{SL}$$

In the presence of a surfactant, the spreading coefficient increases partly by the lowering of the surface tension of the liquid and partly by an increase in the wetting energy, the wetting energy being increased by adsorption of the surfactant at the solid–liquid interface causing a decrease in γ_{SL} by an amount which is maximum when the solid–vapor interfacial free energy is unaffected by the surfactant. Such changes can be regarded as an interfacial surface pressure and may be used in conjunction with the Gibbs' equation to derive the excess of concentration at the solid–liquid interface which is equal to $RT\,\mathrm{d}\,\pi_{SL}/\mathrm{d}\,(\ln c)$, where π is surface pressure, R is gas constant, and T is temperature. Fowkes and Harkins (1) measured contact angles of aqueous solutions on paraffin wax and other low energy surfaces as a function of surfactant concentration. Assuming that adsorption at the solid–air interface was negligible, they used Young's equation to calculate the spreading pressure of the surfactant at the solid–liquid interface. Thus

$$[3] \qquad \gamma_{SL^o} - \gamma_{SL} = \gamma_{LV} \cos\theta - \gamma_{LV^o} \cos\theta$$

where the superscript zero refers to the system without surfactant and θ is the contact angle. They were then able to calculate adsorption by the use of Gibbs' equation. It was found that

adsorption at the paraffin–solution interface was very similar to that at the solution–air interface, surface excess and spreading pressures had approximately the same magnitude, and surface equations of state were similar at each interface.

Adsorption from solution at the solid–liquid interface is usually measured either by the depletion of the solute concentration, by using adsorbing molecules which have been rendered radioactive, by the effect on friction measurements or the effect on contact angles (Alexander (2)). Smolders (3) used contact angles to study adsorption at the mercury–solution interface, and Asahara and Goto (4), to observe the adsorption of surfactants at the paraffin wax–solution interface. Ruch and Bartell (5), Schulman and Leja (6), and Ténèbre (7) used various forms of the Young equation coupled with the Gibbs' equation to derive the adsorption from contact angle measurements. However, adsorption at the solid–vapor interface in their systems made it impossible to resolve adsorption at the solid–liquid interface. Padday (8) measured the spreading coefficient of solutions of sodium lauryl sulfate and Aerosol OT on a wax surface. The surface tensions of the spreading solutions were measured, then used to derive the wetting energy. From a plot of the wetting energy *vs.* the logarithm of the concentration of the surfactant he was able to derive the saturation adsorption. In the systems chosen the solid–vapor interfacial free energy was not in fact affected by surfactants, the whole change of wetting energy being derived from changes in γ_{LV}. Bernett and Zisman (9, 10) studied the wettability of low energy surfaces by aqueous solutions of non-fluorinated and fluorinated surfactants.

Using Fowkes and Harkins' original observations that adsorption is similar at the solid–liquid and liquid–air interface, then at constant T and P

$$[4] \qquad \frac{d\gamma_{SL}}{dc} = \frac{d\gamma_{SV}}{dc}$$

where c is the concentration of surfactant or

$$[5] \qquad \frac{d\gamma_{SL}}{d\gamma_{LV}} = 1$$

Differentiating Young's equation with respect to γ_{LV} gives

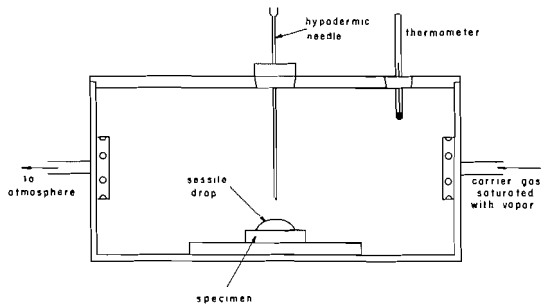

FIG. 1. Diagram of apparatus employed for contact angle measurement at equilibrium conditions at atmospheric pressure and 25 °C.

$$[6] \qquad \frac{d\cos\theta}{d\gamma_{LV}} = \frac{\dfrac{d\gamma_{SV}}{d\gamma_{LV}} - \dfrac{d\gamma_{SL}}{d\gamma_{LV}}}{\gamma_{LV}} - \frac{\cos\theta}{\gamma_{LV}}$$

Using eq. 4 and the assumption that $d\gamma_{SV}/d\gamma_{LV} = 0$

$$[7] \qquad \frac{d\cos\theta}{d\gamma_{LV}} = -\frac{1}{\gamma_{LV}}(1 + \cos\theta)$$

Integrating eq. 6 between the limits γ_c and γ_{LV} gives

$$[8] \qquad \cos\theta = \frac{(2\gamma_c - \gamma_{LV})}{\gamma_{LV}}$$

where γ_c is the critical surface tension. The experimental data of Bernett and Zisman (9) for the wettability of polyethylene by aqueous solutions of non-fluorinated surfactants showed good agreement with eq. 8; so their results are consistent with those of Fowkes and Harkins that adsorption is similar at the solid–liquid and liquid–air interfaces and that adsorption at the solid–air interface is negligible.

Experimental

For this investigation contact angles of a series of aqueous valeric acid solutions ranging from $6.68 \times 10^{-4} - 1 \times 10^{-1}$ M were measured on polytetrafluoroethylene ($R_A = 0.44$ μin.), stainless steel ($R_A = 1.02$ μin.), and copper ($R_A = 1.01$ μin.) surfaces in the apparatus shown in Fig. 1 (R_A is center-line average of surface roughness). Contact angles were measured using a travelling microscope fitted with a goniometer eyepiece and were reproducible to $\pm 1°$. The solid samples were prepared as outlined in Figs. 2 and 3 and the surface roughness measured, as the center-line average, on a Talysurf meter. The water used in the experiments was triply distilled, each stage incorporated a surface overflow device which continuously removed contaminants. Using a Du Noüy ring

Can. J. Chem. Downloaded from www.nrcresearchpress.com by 210.87.254.40 on 09/05/12
For personal use only.

Can. J. Chem. Downloaded from www.nrcresearchpress.com by 210.87.254.40 on 09/05/12
For personal use only.

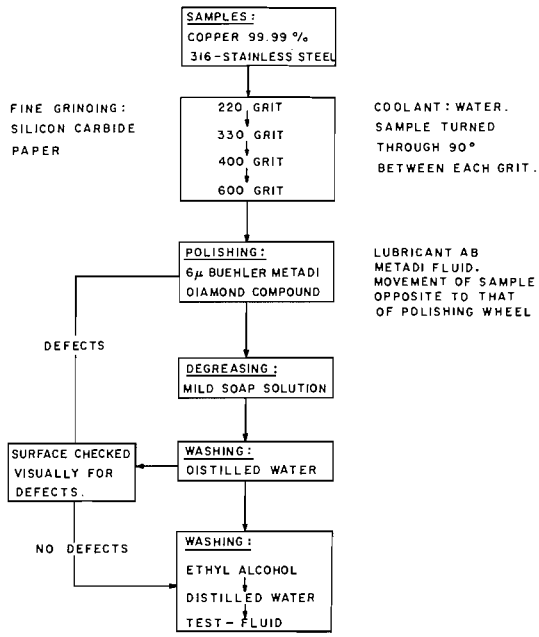

FIG. 2. Preparation procedure for copper and stainless steel specimens.

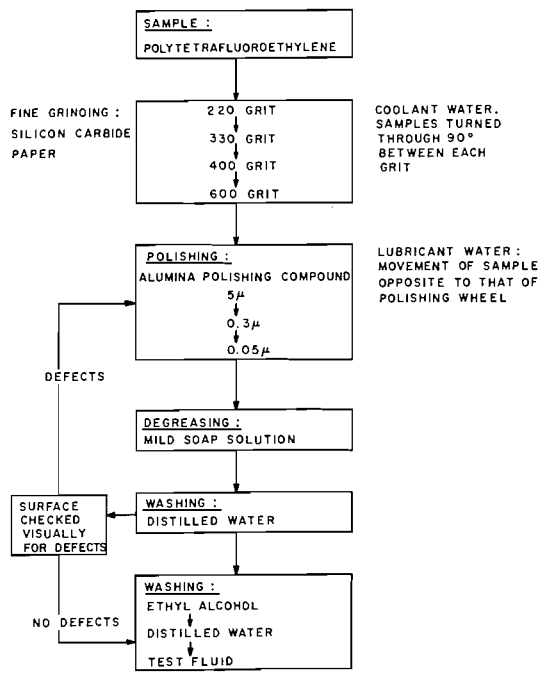

FIG. 3. Preparation procedure for polytetrafluoroethylene specimens.

TABLE 1. Contact angles of valeric acid – water system on a polytetrafluoroethylene surface ($R_A = 0.44$ μin.) at atmospheric pressure and room temperature

Composition (M)	Contact angle (deg)
6.68×10^{-4}	108
1.13×10^{-3}	108
1.63×10^{-3}	108
3.52×10^{-3}	108
4.98×10^{-3}	108
1.00×10^{-2}	108
5.00×10^{-2}	103
1.00×10^{-1}	92
Pure valeric acid	26

TABLE 2. Contact angles of valeric acid – water system on a stainless steel surface ($R_A = 1.02$ μin.) at atmospheric pressure and room temperature as a function of time

Time (min)	Contact angle (deg) for concentration of valeric acid		
	4.98×10^{-3} M	0.1 M	Pure valeric acid
1	68	63	0
5	68	63	0
10	68	63	0
20	68		
30	68		
40	68		

balance the final product was shown to have a surface tension of 72.8 dyn/cm at 20 °C which is in excellent agreement with reported values.

Before each run the solid specimen was prepared as mentioned and left to soak in the test solution before use. The sample was then introduced into the observation box and tested to be horizontal using an optical method. Argon gas, 99.999% purity, was passed through four contacting cells, which were partially filled with solution of the same composition as the test solution, and then through the observation cell before finally being passed to a vent. After approximately 30 min a sample of the test solution was placed onto the solid surface by means of a syringe fitted with a hypodermic needle, care being taken to ensure that the drop was formed slowly until the equilibrium drop height had been achieved and that withdrawal of the needle did not disturb the drop. Contact angles were measured as a function of time using a travelling microscope fitted with a goniometer eyepiece. The reported values are an average of five readings and were reproducible to $\pm$ 1°. The results are presented in Tables 1–3.

TABLE 3. Contact angles (deg) of valeric acid – water system on a copper surface ($R_A = 1.01$ μin.) at atmospheric pressure and room temperature as a function of time

	Contact angle (deg) when composition of valeric acid (molar) =								
Time (min)	6.68×10^{-4}	1.13×10^{-3}	1.63×10^{-3}	3.52×10^{-3}	4.98×10^{-3}	0.01	0.05	0.1	Pure valeric acid
1	88	86	87	89	87	82	71	68	0
5	88	86	87	89	87	82	71	68	
10	88	86	87	89	87	82	71	68	
20	87	85	85	88	85	81	71		
30	87	85	85	88	85	81	71		
40	87	85	85	88	85	81	71		

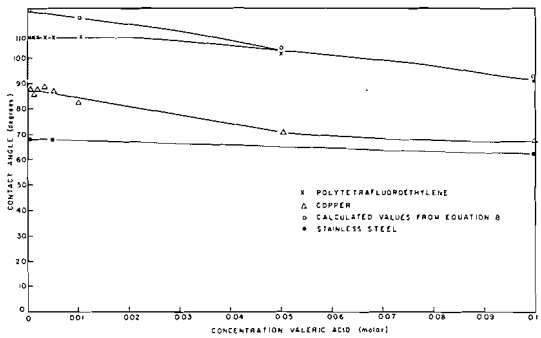

FIG. 4. Contact angles of aqueous valeric acid solutions on solid surfaces.

Discussion

It is evident from Fig. 4 that the contact angle remains constant up to a concentration of 1×10^{-2} M and then decreases with increasing valeric acid concentration. A comparison of results for contact angles obtained in these experiments, using the polytetrafluoroethylene surface ($\gamma_c = 18.5$ dyn/cm) with those predicted using eq. 8 are presented in Fig. 4. The polytetrafluoroethylene surface is chosen since eq. 8 is derived on the assumption that $d\gamma_{SV}/d\gamma_{LV} = 0$. The theory will not be expected to hold for the metal surface where adsorption at the solid–vapor interface will occur. Both results are in very good agreement except for concentrations below 0.05 M. A similar deviation in behavior is exhibited with the surface tension data of Meissner and Michaels (11) who showed for values below 0.1 M that the experimental and calculated values of surface tension of valeric acid solutions diverge in a similar manner. The effect of the valeric acid concentration on the surface tension is not great over the range 0–0.01 M (Meissner and Michaels (11)) since valeric acid is only a weak surfactant and thus no change in contact angle would be expected. No variation of contact angle with time occurs. However, with the copper and stainless steel results, the values of the contact angles varied slightly with time; this probably being partly due to adsorption of the valeric acid at the solid–vapor interface.

1. F. M. FOWKES and W. D. HARKINS. J. Am. Chem. Soc. **62**, 3377 (1940).
2. A. E. ALEXANDER. Proc. III Int. Congr. Surf. Act. Köln **2**, 60 (1960).
3. C. A. SMOLDERS. Rec. Trav. Chim. **80**, 650 (1961).
4. T. ASAHARA and K. GOTO. J. Chem. Soc. Japan Ind. Chem. Sect. **58**, 864 (1955).
5. R. J. RUCH and L. S. BARTELL. J. Phys. Chem. **64**, 513 (1960).
6. J. H. SCHULMAN and J. LEJA. Kolloid, Z. **136**, 77 (1954).
7. L. TÉNÈBRE. Mem. Serv. Chim. Etat (Paris), **40**, 77 (1955).
8. J. F. PADDAY. Chem. Phys. Appl. Surf. Act. Substr. Proc. 4th Int. Congr. **2**, 299 (1964).
9. M. K. BERNETT and W. A. ZISMAN. J. Phys. Chem. **63**, 1241 (1959).
10. M. K. BERNETT and W. A. ZISMAN. J. Phys. Chem. **63**, 1911 (1959).
11. H. P. MEISSNER and A. S. MICHAELS. Ind. Eng. Chem. **41**, 2782 (1949).

Can. J. Chem. Downloaded from www.nrcresearchpress.com by 210.87.254.40 on 09/05/12
For personal use only.

Effect of Electric Field Strength on the Free Ion Yields in the X-Radiolysis of Liquids: Influence of Molecular Structure and Temperature[1]

J.-P. DODELET, P. G. FUOCHI,[2] AND G. R. FREEMAN

Chemistry Department, University of Alberta, Edmonton 7, Alberta

Received November 22, 1971

The relative increase in the free ion yield with increasing field strength E, expressed as G_{fi}^{E}/G_{fi}^{0}, is smaller when the following quantities are larger: (*1*) dielectric constant, (*2*) temperature, and (*3*) separation distance between the geminate ion–electron pairs. The field dependence $(dG_{fi}^{E}/dE)/G_{fi}^{0}$ equals $9.7/\varepsilon T^2$ cm/V at low E, but at higher fields it is affected by the above three factors and by E itself. Results obtained from the liquids propane (123–233 °K), 2-methylpropane (isobutane, 148–294 °K), 2,2-dimethylpropane (neopentane, 295 °K), argon (87 °K), oxygen (87 °K) and argon–oxygen solutions (87 °K) are presented and analyzed according to a theoretical model. Several types of ion–electron separation (y) distribution functions are tested. Within the framework of the model a power function $F(>y) = y_{min}\, y^{-x}$ with $x < 4$ provides a good interpretation of the results when $G_{fi}^{0} < 0.2$; a Gaussian distribution function provides the best interpretation of the field effects when $G_{fi}^{0} > 0.2$. Either the y distribution has a Gaussian core with a more gently sloping tail, or distributions are more Gaussian-like in liquids in which the electron ranges are greater. The electron range in pure argon ($b = 1300$ Å) is much smaller than had been expected and is only 2.6 times greater than that in liquid methane ($b = 500$ Å at 120 °K). Phonon emission by 10–0.01 eV electrons in liquid argon may be relatively efficient and might involve transient states of the type Ar_2^*.

L'accroissement relatif du rendement en ion libre avec le champ E, exprimé par G_{fi}^{E}/G_{fi}^{0}, est plus faible lorsque les grandeurs suivantes croissent: (*1*) la constante diélectrique, (*2*) la température, (*3*) la distance séparant les paires ion–électron géminées. La variation du champ $(dG_{fi}^{E}/dE)/G_{fi}^{0}$ est égale à $9.7/\varepsilon T^2$ cm/V pour E faible mais aux champs plus élevés elle est affectée par les trois facteurs cités ci-dessous et par E lui-même. Les résultats obtenus à partir des liquides propane (123–233 °K) méthyl-2 propane (isobutane, 148–294 °K) diméthyl-2,2 propane (néopentane, 295 °K), argon (87 °K), oxygène (87 °K), et argon–oxygène en mélange (87 °K), sont présentés et analysés selon un modèle théorique. Différents types de fonctions de distribution pour la séparation ion–électron sont essayés. Dans le cadre du modèle une fonction puissance $F(>y) = y_{min}\, y^{-x}$ avec $x < 4$ fournit une bonne interprétation des résultats pour $G_{fi}^{0} < 0.2$; une fonction de distribution gaussienne donne la meilleure interprétation des effets du champ pour $G_{fi}^{0} > 0.2$. La distribution y a soit une allure de type gaussien au centre finissant par une légère inclinaison soit une allure réellement gaussienne pour les liquides dans lesquels la distance parcouru par les électrons est plus grande. Le parcours de l'électron dans l'argon pur ($b = 1300$ Å) est beaucoup plus petit que celui attendu; il est seulement 2.6 fois plus grand que dans le méthane liquide ($b = 500$ Å à 120 °K). L'émission de phonons par les électrons de 10–0.01 eV dans l'argon liquide peut être relativement efficace et pourrait impliquer des états de transition du type Ar_2^*.

Canadian Journal of Chemistry, **50**, 1617 (1972)

Introduction

The free ion yield in an irradiated liquid increases with increasing applied electric field strength at field strengths greater than about 1 kV/cm (1–12). Jaffé (2) developed a theory to explain the effect of applied field strength on the escape of ions from the columnar tracks of high L.E.T. radiations such as α particles. He also noted that the experimentally observed field effects in β and γ (low L.E.T.) irradiated liquids were similar in form but smaller in magnitude to that for α irradiation (2, 3). However, the assumptions involved in the columnar ionization model were most questionable for low L.E.T. irradiations (2).

More recently (7) it seemed preferable to interpret electric field effects in γ irradiated liquids in terms of a model developed by Onsager (13) for high pressure gases irradiated by low L.E.T. radiations. Onsager assumed that ions and electrons were generated in isolated pairs and that the laws of Brownian motion apply to both types of charge. The Onsager model has been applied successfully to a limited number of systems such as *n*-hexane (7, 9, 11).

[1]Financial assistance was received from the National Research Council of Canada.

[2]Permanent address: Consiglio Nazionale delle Ricerche, Laboratorio di Fotochimica e Radiazioni d'Alta Energia, 40126 Bologna, Italy.

Can. J. Chem. Downloaded from www.nrcresearchpress.com by 210.87.254.5 on 09/05/12
For personal use only.

Can. J. Chem. Downloaded from www.nrcresearchpress.com by 210.87.254.5 on 09/05/12
For personal use only.

However, the discovery of the influence of molecular structure on the free ion yields in liquid hydrocarbons (10, 14, 15) makes it necessary to examine the Onsager model in liquid hydrocarbons with different molecular structures.

The free ion yield at low field strengths increases with increasing sphericity of the hydrocarbon molecule (15). A series of molecules with increasing sphericity is propane <2-methylpropane (isobutane) <2,2-dimethylpropane (neopentane). The free ion yields have been measured as functions of applied field strength in these liquids at different temperatures and the Onsager model has been applied to the data. The results are reported in this article.

Application of the model to the X-radiolysis of liquid argon, oxygen, and argon–oxygen solutions is also included.

Experimental

Materials

Phillips research grade propane, 2-methylpropane, and 2,2-dimethylpropane were purified by the method outlined earlier (15).

Matheson ultrahigh-purity argon was further purified as previously described (16), but using a more convenient quartz U-trap in which 150 g of activated coconut charcoal had been heated to 500 °C and evacuated to $<10^{-4}$ Torr over a period of two weeks.

Equipment and Technique

(a) Conductance Cell

The conductance cell was similar to that described earlier (16) except that a Kovar seal around the collector lead gave better electrostatic shielding against moving charges in the refrigerant baths and reduced the noise in the signals. The electrode spacing in a typical cell was $L = 0.49$ cm and the effective area of the collecting electrode was $A = 1.14\ \text{cm}^2$. The cell constant (L/A, cm^{-1}) was measured conductiometrically, using standard KCl solutions.

The refrigerants were liquid argon for 87 °K, isopentane slush for 123 °K, *n*-pentane slush for 148 °K, methanol slush for 183 °K and chlorobenzene slush for 233 °K.

(b) Sample Preparation

The conductance cells were filled by vacuum techniques. The argon–oxygen solutions were prepared by distilling pure oxygen into the cell containing part of the argon, followed by the rest of the argon. The solution was then distilled into a side-reservoir and back into the cell to hasten the mixing of the components. The amount of oxygen added was measured by a *PVT* technique, using a Pyrex spiral gauge connected to a mercury differential manometer.

(c) Measurement of the Free Ion Yield

The charge clearing method (14, 16, 17) was used with minor modification. A van de Graaff accelerator delivered 1 μs pulses of 1.7 MeV X-rays (absorbed dose/pulse = 2–5 $\times 10^{10}$ eV/cm^3). The current after a radiation pulse or blank (no pulse from the van de Graaff) was monitored with a Tektronix 549B oscilloscope containing a type 1A7 plug-in.

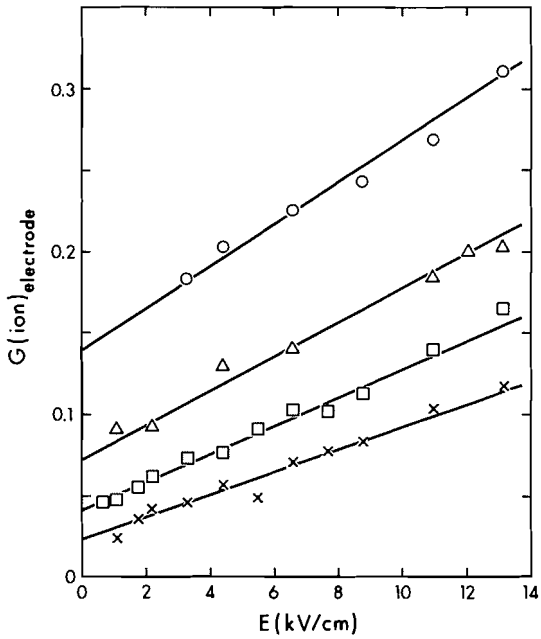

FIG. 1. Yield of ions collected at each electrode as a function of applied field strength in propane. Temperature: ○, 233; △, 183; □, 148; ×, 123 °K. The curves through the points were calculated using the *y* distribution function YP with $x = 2.5$ at all temperatures (see text).

For each measurement, sixteen alternate signals and blanks were fed into a low drift, high sensitivity integrator and averaged with a Fabritek 1062. The integration time for each signal and blank was 3 s. The averaged signals and blanks were then subtracted with the 1062. Sensitivities as high as 0.1 pC/cm were obtained.

Dosimetry

The dose in each pulse was monitored by measuring the charge collected on the gold target. The monitor was calibrated by thermoluminescent dosimetry, using doses of 10^{12}–10^{13} eV/cm^3 in the thermoluminescent crystals. The LiF crystals of the Harshaw model 2000 Thermoluminescent Analyser were calibrated against the Fricke dosimeter, using a ^{60}Co source. Conversion of dosimetry from one medium to another was done on the basis of their relative electron densities.

Physical Properties of the Liquids

The densities (18, 19), dielectric constants (19, 20), dipole moments (20), and viscosities (18, 21) of the liquids were obtained by extrapolation or calculation from data in the references indicated.

Results

Propane

The *G* value of ions collected at each electrode increased linearly with increasing field strength up to 13 kV/cm (Fig. 1). The yield extrapolated to zero-field strength may be taken as the free

TABLE 1. Free ion yields and rates of increase with increasing field strength in liquid hydrocarbons

T (K)	G_{fi}^{0}*	$10^6 \frac{dG^*}{dE}$ (ion cm/100 eVV)	$10^4 \frac{dG}{dE}/G_{fi}^{0*}$ (cm/V)	$\left(\frac{9.69}{\varepsilon T^2}\right)10^4$ (cm/V)	ε	G_{fi}‖	G_{tot}
C_3H_8							
123	0.023†	7.1‡	3.1	3.11	2.05	0.026	4.1¶
148	0.040†	9.0‡	2.3	2.23	1.98	0.043	
183	0.075†	10.0‡	1.3	1.52	1.90	0.076	
233	0.143†	12.2‡	0.9	1.00	1.79	0.12	
$(CH_3)_3CH$							
148	0.11±0.02	21∓2	1.9	2.13	2.07	0.12	4.2¶
183	0.13±0.01	18∓1	1.4	1.99	1.99	0.14	
233	0.21±0.01	24∓4	1.1	0.96	1.87	0.22	
294	0.31±0.01	19∓2	0.6	0.64	1.75	0.31	
$(CH_3)_4C$							
294	1.10±0.05	7∓2§	0.6	0.62	1.80	1.0	4.3**

*Empirical.
†±0.005.
‡∓0.8. At a given temperature, taking a higher value of G_{fi}^{0} results in a lower value of dG/dE.
§Initial slope.
‖Measured by applying a 2–8 kV/cm electric field 1–6 μs after the end of the radiation pulse. Values taken from ref. 22.
¶Averages of gas phase values reported by refs. 36–38.
**Assumed.

ion yield in the absence of an applied field, G_{fi}^{0}. Measurements were made at four temperatures ranging from 123 to 233 °K. Both G_{fi}^{0} and the field dependence dG/dE increased with increasing temperature (Fig. 1). However, the relative rate of increase of G_{fi}^{0} was greater than that of dG/dE (Table 1).

A sample at 183 °K was studied up to 26 kV/cm to permit a more thorough test of the theoretical model. The points in Fig. 2 represent the averages of two experiments. The average precision of the measurements was ±3%. The ion yield increased linearly with field strength up to 26 kV/cm, within experimental error.

2-Methylpropane

The yield of ions collected at the electrodes in 2-methylpropane also increased linearly with field strength up to 13 kV/cm, within experimental error (Fig. 3). Although G_{fi}^{0} increased with increasing temperature the field dependence dG/dE was essentially independent of temperature between 148 and 294 °K (Table 1).

2,2-Dimethylpropane

The ion yield was measured at 294 °K at field strengths up to 24 kV/cm. The yield increased less than linearly with increasing field strength (Fig. 4), in agreement with an earlier report (12). It is difficult to estimate the initial slope of a curve, but from a plot with an expanded E axis it was estimated that $dG/dE = (7 \pm 2)10^{-6}$ ion cm/100 eV V, with $G_{fi}^{0} = 1.10 \pm 0.05$.

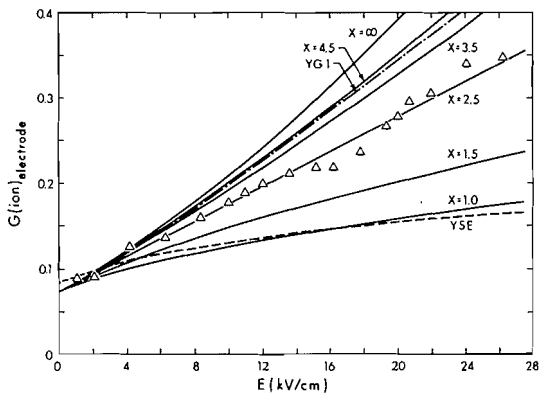

FIG. 2. Yield of ions collected in propane at 183 °K as a function of applied field strength. △, experimental. The curves were calculated with the following y distribution functions: —, YP with the x value indicated; -·-·-·, YG1; ---, YSE.

Theory

The model was developed by Onsager (13) to explain the effect of an applied electric field on the amount of "initial recombination" of ion–electron pairs that were generated in high pressure gases by β and γ radiations. It has been

Can. J. Chem. Downloaded from www.nrcresearchpress.com by 210.87.254.5 on 09/05/12
For personal use only.

Can. J. Chem. Downloaded from www.nrcresearchpress.com by 210.87.254.5 on 09/05/12
For personal use only.

extended to interpret the effect of an applied electric field on the yield of free ions in γ irradiated liquids (7). According to this model, the probability $\phi(y)^E$ that a thermalized electron–ion pair of initial separation distance y will escape geminate neutralization in the presence of an applied field E can be represented by an infinite series (7):

$$[1]\quad \phi(y)^E = e^{-r/y}\,[1 + \beta r + 0.375\beta^2 r^2 - 0.750\beta^2 ry + 0.0695\beta^3 r^3 - 0.417\beta^3 r^2 y + 0.417\beta^3 ry^2 + 0.0076\beta^4 r^4 - 0.091\beta^4 ry^3 + 0.274\beta^4 r^2 y^2 - 0.183\beta^4 ry^3 + \ldots\ldots]$$

where $\beta = \xi E/600\,kT$, $r = \xi^2/\varepsilon kT$, $\xi = 4.803 \times 10^{-10}$ e.s.u., E is expressed in V/cm, k is Boltzmann's constant, T is the absolute temperature, and ε is the dielectric constant of the medium.

The free ion yield in the presence of an applied field is then

$$[2]\quad G_{fi}^E = G_{tot}\int_0^\infty F(y)\,e^{-r/y}\,[1 + \beta r + 0.375\beta^2 r^2 - 0.750\beta^2 ry + \ldots]\,dy$$

where $F(y)dy$ is the fraction of thermalized electron–ion pairs with initial separation distances between y and $y + dy$, and G_{tot} is the total number of ion–electron pairs generated per 100 eV absorbed by the fluid.

By inserting the values of the appropriate constants one sees that $\beta r = 9.69E/\varepsilon T^2$. Similarly, the ratio of the free ion yield in the presence of an applied field E to that at zero applied field strength is

$$[3]\quad G_{fi}^E/G_{fi}^0 = \frac{\displaystyle\int_0^\infty F(y)\,e^{-r/y}\left[1 + \frac{9.690E}{\varepsilon T^2} + \frac{35.21E^2}{\varepsilon^2 T^4} - \frac{4.214\times 10^4 E^2}{\varepsilon T^3}\,y + \ldots\right]dy}{\displaystyle\int_0^\infty F(y)\,e^{-r/y}\,dy}$$

$$= 1 + \frac{9.690E}{\varepsilon T^2} + \frac{35.21E^2}{\varepsilon^2 T^4} - \frac{4.214\times 10^4 E^2}{\varepsilon T^3}\,\frac{\displaystyle\int_0^\infty F(y)\,e^{-r/y}\,y\,dy}{\displaystyle\int_0^\infty F(y)\,e^{-r/y}\,dy} + \ldots.$$

The initial slope of a plot of G_{fi}^E/G_{fi}^0 against E should equal $9.69/\varepsilon T^2$. This is equivalent to the ratio of the initial slope to the intercept of a plot of G_{fi}^E against E (eq. 2). These plots are linear at low E, then curve towards the E axis and asymptotically approach zero slope as G_{fi}^E approaches G_{tot} at very high fields. It can be seen from eqs. 2 and 3 that the field strength at which deviation from linearity becomes significant is smaller for larger values of y. This also implies that deviation from linearity will be observed at lower fields for liquids that have higher values of G_{fi}^0.

The preceding was given to facilitate understanding. However, the model is more conveniently programmed for a computer in the following way (7). For values of y greater than a certain value y_c eq. 4 applies.

$$[4]\quad \frac{\phi(y)^E}{\phi(y)^0} = e^{r/y}\left[1 - e^{-r/y}\,\frac{2r}{My}\sum_{i=1}^{M/2} e^{-2\beta y x_i^2}\sum_{n=0}^{\infty}\frac{(2\beta r)^n \gamma_n x_i^{2n}}{(n!)^2}\right] \qquad y \geqslant y_c$$

where

$$x_i = \cos\,[(2i-1)\pi/2M] \qquad \text{and} \qquad \gamma_n = \sum_{k=1}^{\infty}\frac{(r/y)^{k-1}}{(n+1)(n+2)\ldots(n+k)}$$

It was more than sufficient to take $M = 13$ and to vary n from 0 to 16. The computer ceased adding terms to the summation in γ_n when the $(k+1)$th term was less than 10^{-10} times as large as the sum of the first k terms.

To average eq. 4 over a distribution of y values the distribution function was broken into about

Can. J. Chem. Downloaded from www.nrcresearchpress.com by 210.87.254.5 on 09/05/12
For personal use only.

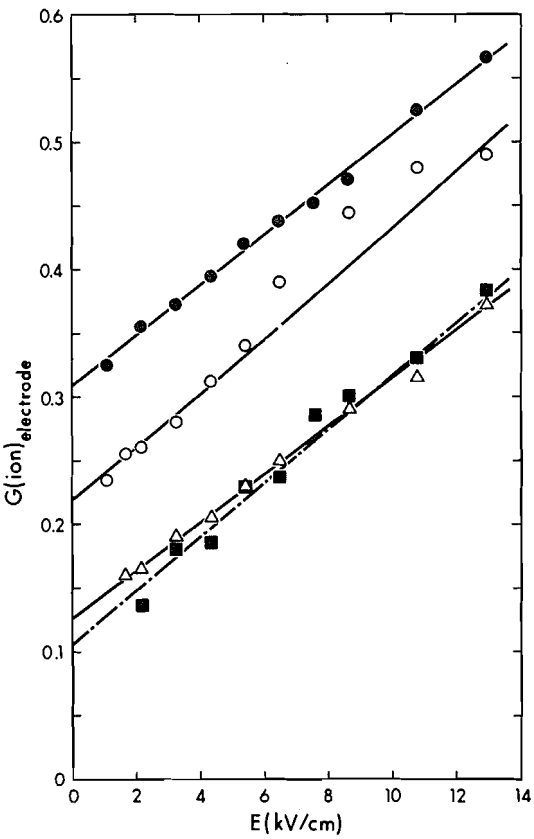

FIG. 3. Yield of ions collected at each electrode as a function of applied field strength in 2-methylpropane. Temperature: ●, 294; ○, 233; △, 183; ■, 148 °K. The curves through the points were calculated using the y distribution function YG1 at 294 and 233 °K, and the function YP with $x = 3.0$ at 183 °K and $x = 2.5$ at 148 °K.

twenty convenient steps, with $F(y_i)$ representing the fraction of ion–electron pairs in the i'th step, in which the average value of y is y_i. The free ion yield at field strength E is then

$$[5] \qquad G_{fi}^{E} = G_{tot} \sum_{i} F(y_i)\, e^{-r/y_i} \frac{\phi(y_i)^E}{\phi(y_i)^0}$$

Equation 4 becomes indeterminate for values of y less than y_c; the value of y_c increases with decreasing temperature and dielectric constant and is about 35 Å in liquid hydrocarbons at 300 K. However, eq. 6 can be derived from the Onsager model for the special case of $y = 0$ (7).

$$[6] \qquad \phi(0)^E/\phi(0)^0 = \sum_{j=0}^{\infty} (\beta r/2)^j (2j)!/(j!)^4$$

This series was summed up to $j = 17$.

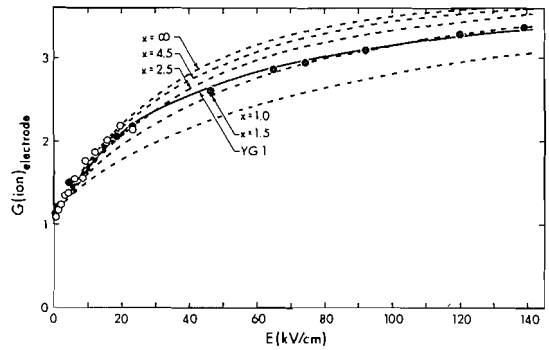

FIG. 4. Yield of ions collected at each electrode as a function of applied field strength in 2,2-dimethylpropane. ○, present results at 294 °K; ●, Schmidt's results (12) at 296 °K. The curves were calculated using the following y distribution functions: —, YG1; ---, YP with the value of x indicated.

The field effect expressed by $\phi(y)^E/\phi(y)^0$ is maximum for $y = 0$ and decreases continuously with increasing y (see later).

The negative term in the square brackets on the right hand side of eq. 4 equals zero at $y = \infty$ and approaches unity at small values of y. For practical purposes we allowed the value of the negative term to go as high as 0.99990, and the value of y that gave this value was taken as y_c. When the y distribution function contained y values less than y_c an interpolation was made between eqs. 4 and 6 using eq. 7.

$$[7] \qquad \frac{\phi(y)^E}{\phi(y)^0} = \frac{\phi(y_c)^E}{\phi(y_c)^0} + \frac{(y_c - y)}{y_c}\left[\frac{\phi(0)^E}{\phi(0)^0} - \frac{\phi(y_c)^E}{\phi(y_c)^0}\right] \qquad y < y_c$$

where $\phi(y_c)^E/\phi(y_c)^0$ is calculated from eq. 4.

In summary, values of G_{fi}^{E} were calculated from eq. 5, using eqs. 4 and 7 to determine $\phi(y)^E/\phi(y)^0$ over the appropriate ranges of y.

Discussion

Initial Slopes and Values of G_{fi}^{0}

The ratios of the initial slopes of the curves in Figs. 1–4 to their intercepts should equal $9.69/\varepsilon T^2$, according to eq. 3. Empirical values of the ratio $(dG/dE)/G_{fi}^{0}$ are given for the three hydrocarbons in Table 1. The empirical values agree satisfactorily with those of $9.69/\varepsilon T^2$ in all cases, at temperatures from 123 to 294 °K (Table 1).

Can. J. Chem. Downloaded from www.nrcresearchpress.com by 210.87.254.5 on 09/05/12
For personal use only.

The values of G_{fi}^0 in the present work agree with the free ion yields measured by applying an electric field after the radiation pulse (22), within experimental error (Table 1).

Curvature in the ion yield plot for 2,2-dimethylpropane was detectable at about 5 kV/cm (Fig. 4), whereas the plot for propane was linear up to at least 26 kV/cm (Fig. 2). The free ion yield, and hence the mean value of y, is greater in 2,2-dimethylpropane than in propane. The curvature at lower field strength for fluids in which the y values are higher is predicted by eq. 3.

y Distributions

The true y distribution in a liquid is not known. Several types of distribution function have been assumed by different workers (a comprehensive list is given in ref. 23) and it is of interest to test four of them in eq. 5. The four functions are

(*a*) A power function designated YP (23–25)

$$[8a] \qquad \begin{aligned} F(>y) &= y_{min}^{x} y^{-x} && y \geqslant y_{min} \\ F(>y) &= 1 && y \leqslant y_{min} \end{aligned}$$

where

$$F(>y) = \int_{y}^{\infty} F(y)\, dy$$

and therefore

$$[8b] \qquad \begin{aligned} F(y) &= x y_{min}^{x} y^{-(x+1)} && y \geqslant y_{min} \\ F(y) &= 0 && y \leqslant y_{min} \end{aligned}$$

(*b*) A delta function YD (7, 23, 26, 27), which is simply eq. 8 with $x = \infty$, so $y = y_{min}$ for all ion electron pairs.

(*c*) A single parameter, three dimensional Gaussian function designated YG1 (23, 26, 27)

$$[9] \qquad F(y) = (4y^2/\pi^{\frac{1}{2}} b^3) \exp(-y^2/b^2)$$

where b is the dispersion parameter.

(*d*) The semi-empirical function YSE that has been used in charge scavenging calculations for liquids that contain distinctly non-spherelike molecules (23, 28–30).

Effects of y and E on $\phi(y)^E/\phi(y)^0$

Values of $\phi(y)^E$ in propane at 183 °K are plotted against y for $E = 0$, 10, and 100 kV/cm in Fig. 5. Although $\phi(y)^E$ increases with increasing y at any given field strength, the ratio $\phi(y)^E/\phi(y)^0$ decreases with increasing y (Table 2). The decrease in the ratio with y is more marked at higher field strengths.

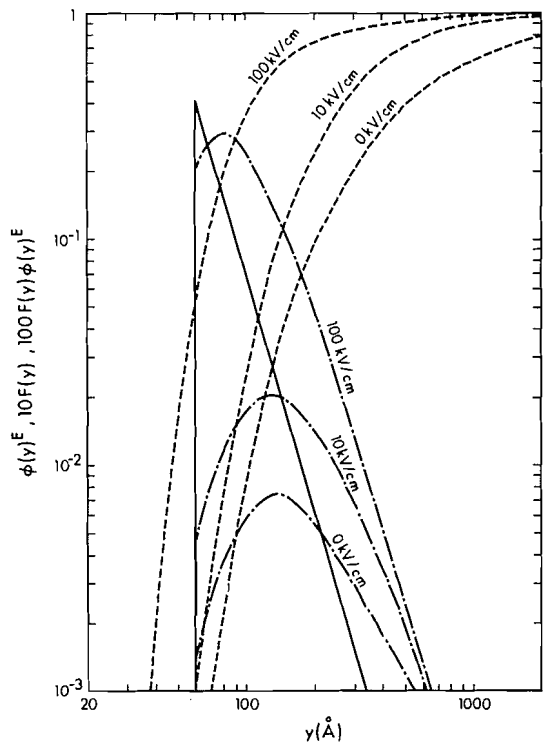

FIG. 5. Values of $\phi(y)^E$, $F(y)$, and $F(y)\phi(y)^E$ as functions of y in propane at 183 °K. $E = 0$, 10, and 100 kV/cm. ---, $\phi(y)^E$; —, $F(y) \propto y^{-3.5}$ (see text); -·-·-·, $F(y)\phi(y)^E$. The $F(y) \propto y^{-3.5}$ curve corresponds to the same function as the $F(>y) \propto y^{-2.5}$ curve shown in Fig. 6.

TABLE 2. Influence of y and E on $\phi(y)^E/\phi(y)^0$ in propane at 183 °K

y (Å)	$\phi(y)^0$	$\phi(y)^{10}/\phi(y)^{0*}$	$\phi(y)^{100}/\phi(y)^{0*}$
0†	0†	3.7†	1900†
70	0.001	3.2	100
200	0.090	2.6	8.2
600	0.45	1.7	2.1

*E is given in kV/cm.
†Hypothetical, eq. 6.

To illustrate the operation of $\phi(y)^E$ on a y distribution, a function $F(y) \propto y^{-3.5}$ (*i.e.* YP with $x = 2.5$) and the product $F(y)\phi(y)^E$ are also shown in Fig. 5. This $F(y)$ for propane at 183 °K gives values of G_{fi}^E that agree with experiment (see later). The product $F(y)\phi(y)^E$ passes through a maximum of 7.6×10^{-5} at $y = 140$ Å for $E = 0$. The value of the product increases and

Can. J. Chem. Downloaded from www.nrcresearchpress.com by 210.87.254.5 on 09/05/12
For personal use only.

the value of y at the maximum decreases with increasing E, reaching 2.9×10^{-3} and 80 Å, respectively, at 100 kV/cm.

Propane

Calculations using all four of the above mentioned types of y distribution were made for propane at 183 °K.

When YP was used, the values of the parameters x and y_{min} were varied to find the pair that gave the minimum mean difference between the calculated and the experimental ion yields over the field strength range studied. The best values for propane at 183 °K were $x = 2.5$ and $y_{min} = 60$ Å, corresponding to $G_{fi}^0 = 0.073$. The calculated ion yields are shown by the curve marked $x = 2.5$ in Fig. 2.

To illustrate the effect of the breath of the y distribution on the field effect, YP functions with $x = 1.0$–4.5 in steps of 0.5 and $x = \infty$ were chosen such that each gave $G_{fi}^0 = 0.073$. Some of the distributions are shown in Fig. 6. A lower value of x corresponds to a broader distribution. The field dependencies expected for several of the distributions are displayed by the curves in Fig. 2. Although the initial slopes of all the curves are the same, the magnitude of the field effect at higher fields increases with increasing x. It is the ion–electron pairs with the larger y values in a given distribution that have the greatest probability of becoming free ions (Fig. 5). The larger the value of x the lower is the average value of y of the pairs that become free ions (Fig. 6). The lower the value of y of these pairs, the greater the field effect (Table 2).

The YP distribution with $x = \infty$ corresponds to the delta function (23) mentioned in (*c*) above. It predicts the largest field effect of all the distributions, and is not suitable for the present system.

The Gaussian distribution also predicts too great a field dependence of the ion yield (Fig. 2). The value of b used was 90 Å. The excessively large predicted field dependence indicates that the tail of the Gaussian distribution towards high y values is too short.

The distribution YSE for propane at 183 °K was obtained by multiplying that for *n*-hexane at 293 °K (28) by the inverse ratio of the liquid densities; $d(\text{hexane})/d(\text{propane}) = 0.660/0.637 = 1.03$. The free ion yields calculated from eq. 5 using YSE are shown as the dashed line in Fig. 2.

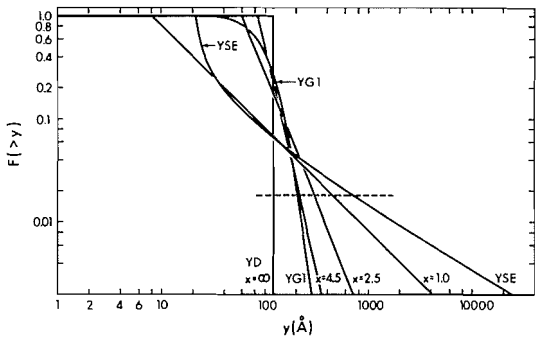

FIG. 6. Integrated y distributions for propane at 183 °K. $F(>y) = \int_y^\infty F(y)\,dy$. All these distributions except YSE give $G_{fi}^0 = 0.073$; YSE gives $G_{fi}^0 = 0.083$. Distributions YP are shown for $x = 1.0$, 2.5, and 4.5. The value of b in YG1 is 90 Å. The horizontal, dashed line marks the fraction that corresponds to $G_{fi}^0 = 0.073$.

The calculated field dependence of the ion yield is too low, which implies that the tail of the distribution YSE at high y values is too long.

The most suitable type of distribution for the treatment of field effects in propane at 183 °K is apparently YP. This function was therefore used in the analysis of the ion yields at the other temperatures. At each temperature the best value of x was found to be 2.5, with an estimated uncertainty of ± 0.5. The best-fit curves are drawn in Fig. 1 and the function parameters are listed in Table 3. The calculated values of G_{fi}^0 (Table 3) agree with the empirically extrapolated values within experimental error (Table 1).

Other things being equal, electron ranges are inversely proportional to the density of the medium (31). The product of the liquid density and the median y value in the best propane y distribution is independent of temperature (Table 3). This suggests that electron energy loss and localization processes are independent of temperature in propane at temperatures between 123 and 233 °K.

2-Methylpropane

Values of G_{fi}^E were calculated from eq. 5 using YP functions with several values of x. By contrast with propane where the best value of x was 2.5 at all temperatures, in 2-methylpropane the best value of x increased from 2.5 at 148 °K to 4.5 at 233 °K (Table 3). The behavior of the calculated curves at 148 and 294 °K is shown in Fig. 7. Increasing the temperature decreases the relative effect of E on G_{fi}.

TABLE 3. Parameters for the best y distribution functions and calculated values of G^0_{fi}

Liquid	T (°K)	Function	Parameters			y_{med}* (Å)	$y_{med}d$† (10^{-8}g/cm^2)	$G^0_{fi,calcd}$
			x	y_{min} (Å)	b (Å)			
C_3H_8	123	YP	2.5	54		71	50	0.024
	148	YP	2.5	56		74	50	0.041
	183	YP	2.5	60		79	51	0.073
	233	YP	2.5	66		87	50	0.139
$(CH_3)_3CH$	148	YP	2.5	78		103	74	0.11
	183	YP	3.0	81		102	70	0.13
	233	YP	4.5	99		115	72	0.22
		YG1			107	118	74	0.22
	294	YP	4.5	96		112	62	0.31
		YG1			105	116	64	0.31
$(CH_3)_4C$	294	YG1			215	237	140	1.10

*y_{med} is the median value of y.
†d is the density of the liquid.

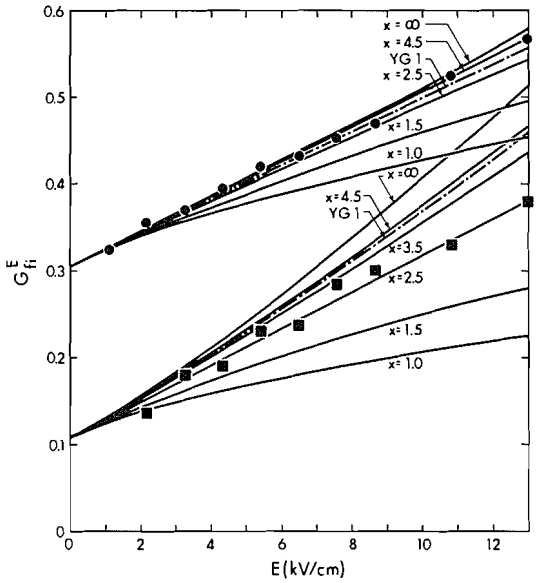

FIG. 7. Calculated values of G^E_{fi} for 2-methylpropane at 148 (●) and 294 °K (■), using different y distributions. —, YP with the value of x shown; -·-·-·, YG1.

The Gaussian distribution leads to too large a field effect at 148 and 183 °K, but gives reasonable agreement with experiment at 233 and 294 °K (Fig. 7). The Gaussian function was used to calculate the curves shown in Fig. 3 for the two higher temperatures.

The parameters for the best y distribution functions are listed in Table 3.

2,2-Dimethylpropane

Values of G^E_{fi} calculated from eq. 5 using a Gaussian y distribution agree with the present experimental results and those of Schmidt (12) over the range of field strength from zero to 140 kV/cm (Fig. 4). The YP distributions with values of $x \geqslant 3$ also gave satisfactory results at $E < 25$ kV/cm, but none of the YP functions was satisfactory over the entire range of E (Fig. 4).

Comparison of the Hydrocarbons

Within the framework of the present model it appears that the Gaussian distribution of y values provides the best interpretation of the field effects when $G^0_{fi} > 0.2$ and that a distribution YP with $x < 4$ is best when $G^0_{fi} < 0.2$ (Table 3). The Gaussian has a steeper slope at high y values than does YP with $x < 4$ (Fig. 6).

Perhaps a better description of all the distributions would be a Gaussian core with a more gently sloping tail.

An alternative interpretation is that the distribution is more Gaussian-like in liquids in which the electron range is greater.

Argon–Oxygen Systems

Ion yields reported elsewhere (22) for liquid argon, argon–oxygen solutions, and liquid oxygen have now been analyzed according to eq. 5. The best-fit calculated ion yields at different field strengths are displayed along with the experimental results in Fig. 8. The y distribution functions that gave the best calculated yields are listed in Table 4.

The results are consistent with those obtained with the different hydrocarbons. When the free

Can. J. Chem. Downloaded from www.nrcresearchpress.com by 210.87.254.5 on 09/05/12
For personal use only.

TABLE 4. Argon and oxygen systems at 87 °K

Mol% O_2	G_{fi}^{0}*	G_{tot}	Best y function	Parameters x	Parameters y_{min} (Å)	Parameters b (Å)
0	2.0±0.3	5.4±0.2*	YG1			1300
1.5	0.7	5†	YG1			570
13	0.3	5†	YG1			380
			YP	2.5	270	
28	0.2	5†	YP	1.5	120	
100	0.013	4†	YP	1.5	23	

*Obtained by fitting eq. 5 to data in Fig. 8.
†Assumed. In the gas phase G (total ionization) = 3.8 in pure argon and 3.2 in pure oxygen (ref. 39).

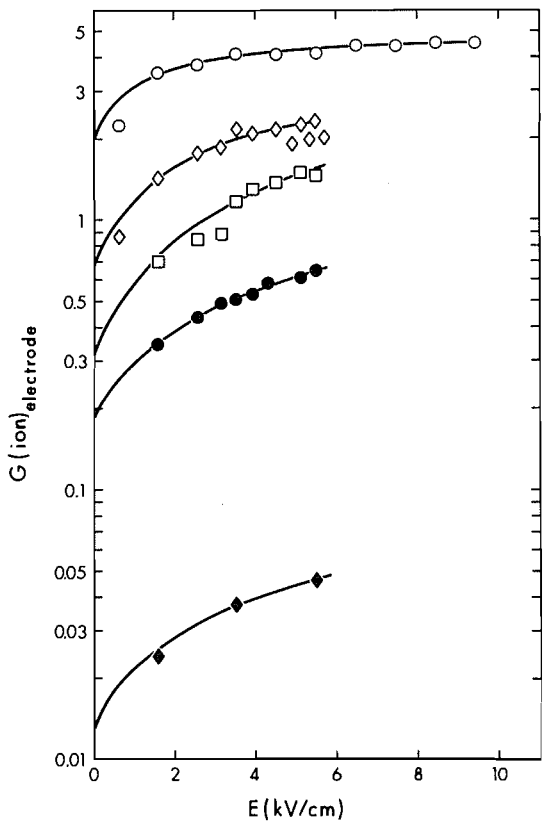

FIG. 8. Yield of ions collected at each electrode as a function of applied field strength at 87 °K in liquid Ar (○), Ar + 1.5 mol% O_2 (◇), Ar + 13 mol% O_2 (□), Ar + 28 mol% O_2 (●), and pure liquid O_2 (◆). The curves were calculated using the y distribution functions in Table 4.

ion yield is large the Gaussian y distribution gives the best results within the framework of the present model. However, when G_{fi} is small a distribution with a gentler slope, such as YP with $x < 3$, is required to fit the field dependence of the ion yield.

One may conclude that the tail of a relatively tight distribution, *i.e.* one for which G_{fi} is small, has a relatively gentle slope, and that the core of a relatively loose distribution has a Gaussian-like shape. The present experiments do not give information about the shape of the core of a tight distribution or the tail of a loose one. When the free ion yield is large the y values in the tail of the distribution may be so large that reaction 11 cannot compete with reaction 12 even in the absence of an applied field.

[10] $M \rightsquigarrow [M^+ + e^-]$

[11] $[M^+ + e^-] \rightarrow M^*$ (geminate neutralization)

[12] $[M^+ + e^-] \rightarrow M^+ + e^-$ (free ions)

The field effect on reaction 11 would then be only important for the ion pairs in the core of the y distribution, and the apparent shape determined from the field effect would apply only to the core. Conversely, information obtained about the shape of the tail in the systems with small free ion yields cannot be extrapolated to the core.

G_{fi} and Secondary Electron Ranges in Liquid Argon

The present analysis of the electric field effect has shown that, contrary to earlier belief (16, 32), not all the ion pairs in liquid argon become free ions. The facts that the monatomic molecules of argon do not possess internal energy levels between the ground state and the lowest excited electronic state at 11.6 eV, and that low energy electrons do not form a localized state in liquid argon (33) led one to expect that the ranges of the secondary electrons in argon would be so large that nearly all of the electrons would escape geminate neutralization. In reality only 37% of the electrons become free ions in X-irra-

Can. J. Chem. Downloaded from www.nrcresearchpress.com by 210.87.254.5 on 09/05/12
For personal use only.

diated pure argon, and the most probable range of the secondary electrons is only $b = 1300$ Å (Table 4). This argon was sufficiently pure to permit the measurement of the rate constant $k(e^- + Ar_2^+)$ and the mobility of electrons in the liquid (22), so the low value of b is probably not due to the presence of impurities. The oxygen had been removed to $\ll 1$ p.p.m. and the nitrogen was < 5 p.p.m. One can estimate from Fig. 4 of ref. 22 that if b equalled infinity in pure argon the addition of 10 p.p.m. of oxygen or nitrogen would only reduce b to 40 000 Å. The observed $b = 1300$ Å therefore appears to be due to electron energy loss interactions with the liquid argon itself.

Methane molecules have excited electronic energy levels down to 8 eV above the ground state (34) and vibrational levels down to 0.2 eV (CH_2 bending). In spite of this gross difference from the internal energy levels of argon, the value of b in liquid methane is 500 Å (35), about 40% of the value in argon. The similarity of the secondary electron energy loss interactions in these two liquids is worthy of theoretical investigation. Phonon emission by the electrons in liquid argon may be much more efficient than had been expected and might involve transient states of the type Ar_2^*.

The authors are grateful to the staff of the Radiation Research Center for aid with the electronics.

1. G. JAFFÉ. Ann. Physik, **25**, 257 (1908); Ann. Physik, **32**, 175 (1910).
2. G. JAFFÉ. Ann. Physik, **42**, 303 (1913).
3. W. MIES and M. CURIE. Quoted on p. 332 of ref. 2.
4. A. N. GERRITSEN and J. KOLHAAS. Physica, **10**, 49 (1943).
5. A. N. GERRITSEN. Physica, **14**, 381, 407 (1948).
6. H. A. KRAMERS. Physica, **18**, 665 (1952).
7. G. R. FREEMAN. J. Chem. Phys. **39**, 1580 (1963).
8. M. CHYBICKI. Acta Physica Polonica, **30**, 927 (1966).
9. A. JAHNS and W. JACOBI. Z. Naturforsch. **21a**, 1400 (1966).
10. R. GIBAUD. J. Chim. Phys. **64**, 521 (1967).
11. A. HUMMEL and A. O. ALLEN. J. Chem. Phys. **46**, 1602 (1967).
12. W. F. SCHMIDT. Rad. Res. **42**, 73 (1970).
13. L. ONSAGER. Phys. Rev. **54**, 554 (1938).
14. W. F. SCHMIDT and A. O. ALLEN. Science, **160**, 301 (1968); J. Phys. Chem. **72**, 3730 (1968).
15. P. H. TEWARI and G. R. FREEMAN. J. Chem. Phys. **49**, 4394 (1968).
16. P. H. TEWARI and G. R. FREEMAN. J. Chem. Phys. **51**, 1276 (1969).
17. W. F. SCHMIDT and A. O. ALLEN. J. Chem. Phys. **52**, 2345 (1970).
18. R. W. GALLANT. Physical properties of hydrocarbons. Vol. 1. Gulf Publishing Co., Houston, 1968.
19. Handbook of chemistry and physics, 50th ed. Chemical Rubber Publishing Co., Cleveland, 1969.
20. R. D. NELSON, JR., D. R. LIDE, JR., and A. A. MARYOTT. Selected values of electric dipole moments for molecules in the gas phase. NSRDS-NBS 10 (1967).
21. (*a*) P. E. PARISOT and E. F. JOHNSON. J. Chem. Eng. Data, **6**, 263 (1961). (*b*) J. TIMMERMANS. Physico-chemical constants of pure organic compounds. Elsevier Publishing Co., Amsterdam, Vol. 1 (1950); Vol. 2 (1965).
22. P. G. FUOCHI and G. R. FREEMAN. J. Chem. Phys. **56**, 2333 (1972).
23. (*a*) J.-P. DODELET and G. R. FREEMAN. Can. J. Chem. **49**, 2643 (1971). (*b*) J.-P. DODELET and G. R. FREEMAN. Can. J. Chem. In press.
24. L. G. WALKER. Ph.D. Thesis. University of Alberta, Edmonton, Alberta, 1967.
25. J. A. LEONE and W. A. HAMILL. J. Chem. Phys. **49**, 5304 (1968).
26. A. MOZUMDER. J. Chem. Phys. **48**, 1659 (1968); **50**, 3153 (1969); **50**, 3162 (1969).
27. P. LUDWIG. J. Chem. Phys. **50**, 1787 (1969).
28. G. R. FREEMAN. J. Chem. Phys. **46**, 2822 (1967).
29. J. C. RUSSELL and G. R. FREEMAN. J. Chem. Phys. **48**, 90 (1968).
30. K. N. JHA and G. R. FREEMAN. J. Chem. Phys. **51**, 2846 (1969).
31. D. E. LEA. Actions of radiations on living cells. University Press, Cambridge, 1955. Chapter 1.
32. M. G. ROBINSON, P. G. FUOCHI, and G. R. FREEMAN. Can. J. Chem. **49**, 984 (1971).
33. B. E. SPRINGETT, J. JORTNER, and M. H. COHEN. J. Chem. Phys. **48**, 2720 (1968).
34. R. L. PLATZMAN. Vortex **23**, 372 (1962).
35. M. G. ROBINSON, P. G. FUOCHI, and G. R. FREEMAN. Can. J. Chem. **49**, 3657 (1971).
36. G. G. MEISELS. J. Chem. Phys. **41**, 51 (1964).
37. P. ALDER and H. K. BOTHE. Z. Naturforsch. **20a**, 1700 (1965).
38. R. COOPER and R. M. MOORING. Aust. J. Chem. **21**, 2417 (1968).
39. U. FANO. *In* Studies in penetration of charged particles in matter. N.A.S.–N.R.C. Publication 1133, 1964. Appendix A.

Can. J. Chem. Downloaded from www.nrcresearchpress.com by 210.87.254.5 on 09/05/12
For personal use only.

Some Thermodynamic Properties of Lithium Chlorate in Water and Dioxane–Water mixtures

A. N. CAMPBELL AND O. N. BHATNAGAR

Department of Chemistry, University of Manitoba, Winnipeg R3T 2N2, Manitoba

Received November 4, 1971

Heats of solution and heats of dilution of lithium chlorate in water and dioxane–water mixtures have been determined experimentally. From these data apparent molal heat content, ϕ_L, and relative partial molal heat contents of solvent, $\bar{L}_1$, and of solute $\bar{L}_2$ have been calculated. The values of ΔG^0, ΔH^0, and ΔS^0 are also calculated.

Nous avons déterminé expérimentalement les chaleurs de solution et de dilution du chlorate de lithium dans l'eau et dans des mélanges eau-dioxanne. Nous avons calculé, à partir de ces résultats, la quantité de chaleur molale apparente, ϕ_L et les quantités de chaleur relatives molales partielles, $\bar{L}_1$ du solvant et du soluté $\bar{L}_2$. Nous avons aussi calculé les valeurs ΔG^0, ΔH^0, et ΔS^0.

Canadian Journal of Chemistry, **50**, 1627 (1972)

Can. J. Chem. Downloaded from www.nrcresearchpress.com by 210.87.254.6 on 09/05/12
For personal use only.

Introduction

Lithium chlorate is one of the least studied inorganic compounds from the point of view of thermodynamic and electrochemical properties. Scatchard *et al.* (1) reported the activity coefficients ($\gamma_\pm$) of potassium, sodium, and lithium chlorates and perchlorate in water from freezing point measurements. Some earlier work on lithium chlorate from this laboratory comprehends phase equilibrium studies (2) and conductance density and viscosity measurements in dioxane–water mixtures (3, 4). Recently, Campbell and Oliver (5) reported the activity coefficients of sodium and lithium chlorates in water and dioxane–water mixtures, from vapor pressure measurements. In a recent paper (6) we have reported the thermodynamic properties of sodium chlorate in water and dioxane–water mixtures. The present paper is a similar study of lithium chlorate in water and dioxane–water mixtures.

Experimental

Lithium chlorate was prepared as described by Campbell and Griffiths (2). Our purification of dioxane is described elsewhere (5), where the methods of measuring heats of solution and heats of dilution are also given. Since lithium chlorate is extremely hygroscopic, all samples were measured out in a vacuum dry box under dry nitrogen atmosphere and sealed under vacuum. In order to determine the initial and final concentration for heat of dilution measurements, duplicate samples of lithium chlorate in water and dioxane–water mixtures were analyzed by both volumetric and gravimetric methods, but later on, a gravimetric method was adopted. All analyses of duplicate samples agreed within 0.2%. When determining the lithium chlorate in dioxane–water mixtures, special care was taken to see that the dioxane content was less than 10%, otherwise the lithium chlorate could decompose as observed by Campbell *et al.* (7).

Calculations and Results

The heats of solution, heats of dilution, and derived heats of solution in water, 44.5 wt.% dioxane–water and 64.5 wt.% dioxane are given in Tables 1–3. These data were utilized to calculate the apparent molal heat content, ϕ_L. From these values of ϕ_L the relative partial molal heat contents of solvent $\bar{L}_1$ and of solute $\bar{L}_2$ were calculated as follows:

$$[1] \qquad \bar{L}_1 = \frac{-M_1 m^{3/2}}{2000} \cdot \frac{d\phi_L}{dm^{1/2}}$$

$$[2] \qquad \bar{L}_2 = \phi_L + \frac{m^{1/2}}{2} \cdot \frac{d\phi_L}{dm^{1/2}}$$

where m is the molality of solution and M_1 is the molecular weight of the solvent.

In order to calculate the values of $\bar{L}_1$ and $\bar{L}_2$ the smoothed values of ϕ_L *vs.* $m^{1/2}$ were fitted to a least squares polynomial equation and the best curve fit was obtained on our IBM 360/65 computer. This equation, which is of the form

$$[3] \qquad \phi_L = Am^{1/2} + Bm + Cm^{3/2} + Dm^2 + \ldots$$

was differentiated with respect to $m^{1/2}$ to give the values of $d\phi_L/dm^{1/2}$. A second program was written to do this which also gave the values of ϕ_L, $\bar{L}_1$, and $\bar{L}_2$ at various concentrations. These data are given in Table 4.

The activity coefficients ($\gamma_\pm$) of lithium chlorate in the concentration range 1.0 m to satura-

TABLE 1. Heat of solution, heat of dilution, and derived heat of solution of $LiClO_3$ in water

m*	$m^{1/2}$	$-\Delta H_{solution}$ (kcal/mol)	Initial concentration m_1*	Final concentration m_2*	$-\Delta H_{dilution}$ (cal/mol)	$-\Delta H_{solution}$ (derived) (kcal/mol)
0.0000	0.0000	3.1700	2.1058	1.5730	60.0	2.0300
0.0263	0.1621	3.0628	3.7767	2.1058	200.0	1.9700
0.0471	0.2171	2.9906	5.2971	3.7767	180.0	1.7900
0.0771	0.2776	2.8764	7.0321	5.2971	190.0	1.5300
0.1075	0.3279	2.7616	9.6775	7.0321	320.0	1.2100
0.1366	0.3696	2.6298	10.6628	9.6775	70.0	1.1400
0.1841	0.4291	2.5921	12.4181	10.6628	235.0	0.9050
0.2602	0.5101	2.4812	13.9376	12.4181	165.0	0.7400
0.2914	0.5398	2.4720	17.2198	13.9376	380.0	0.3600
0.4428	0.6654	2.3800	19.2520	17.2198	220.0	0.1400
0.5471	0.7396	2.3163				
0.6749	0.8215	2.2724				
0.7954	0.8918	2.2756				
1.1589	1.0765	2.2001				
1.5730	1.2542	2.1652				
1.7019	1.3045	2.1486				
2.0774	1.4413	2.1063				

*In mol/kg.

TABLE 2. Heat of solution, heat of dilution, and derived heat of solution of $LiClO_3$ in 44.5% dioxane + 55% water

m*	$m^{1/2}$	$-\Delta H_{solution}$ (kcal/mol)	Initial concentration m_1*	Final concentration m_2*	$-\Delta H_{dilution}$ (cal/mol)	$-\Delta H_{solution}$ (derived) (kcal/mol)
0.0000	0.0000	3.8000	2.2971	1.0694	292.0	2.7900
0.0115	0.1072	3.7513	3.7855	2.2971	288.0	2.5020
0.0233	0.1526	3.7096	5.6200	3.7855	300.0	2.2010
0.0310	0.1760	3.6978	7.9205	5.6200	461.0	1.7400
0.0537	0.2317	3.5787	10.0169	7.9205	361.0	1.3790
0.0734	0.2709	3.5501	12.4012	10.0169	459.0	0.9200
0.1195	0.3456	3.4650	15.4635	12.4012	622.0	0.2980
0.1478	0.3844	3.4301				
0.1613	0.4016	3.4202				
0.2221	0.4712	3.3809				
0.3582	0.5984	3.2896				
0.5048	0.7105	3.2201				
0.6667	0.8165	3.1814				
0.7510	0.8666	3.1652				
0.8955	0.9463	3.1200				
1.0694	1.0341	3.0820				

*In mol/kg.

tion have been reported by Campbell and Oliver (5). The $\gamma_\pm$ values of lithium chlorate in the concentration 0.1 to 1.0 m have been calculated by an empirical method proposed by the authors (8). According to this method, a reference electrolyte is chosen which is similar in molecular size and is of the same valence type as the unknown salt (in this case lithium chlorate), whose $\gamma_\pm$ values are known in the range 0.1–1.0 m as well as 1.0–2.0 m at various intervals. The ratios of $\gamma_\pm$ values of unknown and reference salt between 1.0 and 2.0 m are plotted against the concentrations. Since at $m = 0$ (infinite dilution) the $\gamma_\pm$ of all electrolytes becomes unity, this

Can. J. Chem. Downloaded from www.nrcresearchpress.com by 210.87.254.6 on 09/05/12
For personal use only.

TABLE 3. Heat of solution, heat of dilution, and derived heat of solution of $LiClO_3$ in 64.5% dioxane + 35.5% water

m*	$m^{1/2}$	$-\Delta H_{solution}$ (kcal/mol)	Initial concentration m_1*	Final concentration m_2*	$-\Delta H_{dilution}$ (cal/mol)	$-\Delta H_{solution}$ (derived) (kcal/mol)
0.0000	0.0000	5.2300	2.5339	1.4073	295.0	2.8530
0.0139	0.1179	5.1513	4.2524	2.5339	572.0	2.2810
0.0382	0.1954	5.0750	5.5554	4.2524	775.0	1.5060
0.0528	0.2299	5.0551	7.0330	5.5554	776.0	0.7300
0.0589	0.2426	5.0334				
0.1304	0.3607	4.8702				
0.2070	0.4450	4.7168				
0.2948	0.5429	4.5702				
0.3863	0.6215	4.4200				
0.4933	0.7023	4.2508				
0.8001	0.8951	3.8203				
0.9012	0.9490	3.6952				
1.4073	1.1863	3.0801				

*In mol/kg.

TABLE 4. Apparent molal and relative partial molal heat contents of lithium chlorate

	100% water			44.5% dioxane + 55.5% water			64.5% dioxane + 35.5% water		
$m^{1/2}$	ϕ_L	$\bar{L}_1$	$\bar{L}_2$	ϕ_L	$\bar{L}_1$	$\bar{L}_2$	ϕ_L	$\bar{L}_1$	$\bar{L}_2$
0.1	185	−0.01	272	143	−0.02	209	56	−0.01	93
0.2	347	−0.11	499	264	−0.12	376	147	−0.17	256
0.3	490	−0.32	689	367	−0.35	508	272	−0.74	481
0.5	722	−1.13	974	528	−1.20	699	601	−4.59	1066
0.7	897	−2.35	1164	648	−2.59	837	998	−14.01	1721
1.0	1085	−4.62	1342	797	−6.72	1037	1602	−36.96	2536
1.2	1177	−6.46	1427	896	−12.37	1203	1940	−50.99	2835
1.4	1255	−8.94	1508	1004	−21.98	1404	2197	−59.06	2958
1.6	1325	−12.72	1601	1125	−36.90	1640	2387	−70.18	3080
1.8	1395	−18.76	1716	1261	−58.15	1902	2569	−119.02	3498
2.0	1469	−28.23	1861	1410	−86.43	2181	2833	−266.11	4514
2.5	1699	−75.73	2373	1826	−195.50	2944			
3.0	2012	−172.00	3073	2315	−410.07	3942			
3.5	2401	−324.14	3871	3080	−846.52	5404			
4.0	2839	−516.17	4631	3682	−1290.64	6563			
4.5	3281	−704.00	5213						

curve is interpolated to unity at $m = 0$. From this curve the values of the ratio at various concentrations are chosen between 0.1 and 1.0 m. From the known values of $\gamma_\pm$ of the reference electrolyte we can obtain the activity coefficient of our unknown salt. In our case, we chose $NaClO_3$ as reference electrolyte for calculating the $\gamma_\pm$ values of lithium chlorate in water. Since the $\gamma_\pm$ values of hydrochloric acid are the only ones known in 45% dioxane–water and 65% dioxane–water mixtures (ref. 9, pp. 717, 718) we were obliged to use HCl as reference electrolyte for calculations of $\gamma_\pm$ for lithium chlorate in dioxane–water mixtures. We have assumed that the $\gamma_\pm$ values of HCl in 44.5 and 45.0% are essentially the same and similarly in 64.5 and 65% dioxane–water mixtures. These derived values of the $\gamma_\pm$ of lithium chlorate are given in Table 5. As mentioned above, for concentrations greater than 1 m, experimental activity coefficients were used. The $\gamma_\pm$ values were used to calculate the free energy of solution at various concentrations.

Can. J. Chem. Downloaded from www.nrcresearchpress.com by 210.87.254.6 on 09/05/12
For personal use only.

Can. J. Chem. Downloaded from www.nrcresearchpress.com by 210.87.254.6 on 09/05/12
For personal use only.

TABLE 5

(*a*). Summary of thermodynamic properties of the process: $LiClO_3$ (crystal) → $LiClO_3$ (solution, *m*)

	100% water				44.5% dioxane + 55.5% water				64.5% dioxane + 35.5% water			
m (mol/kg)	$\gamma_\pm$*	$-\Delta G$ (kcal/mol)	$-\Delta H$ (kcal/mol)	$T\Delta S$ (kcal/mol)	$\gamma_\pm$	$-\Delta G$ (kcal/mol)	$-\Delta H$ (kcal/mol)	$T\Delta S$ (kcal/mol)	$\gamma_\pm$	$-\Delta G$ (kcal/mol)	$-\Delta H$ (kcal/mol)	$T\Delta S$ (kcal/mol)
0.10	0.803	10.772	2.790	7.982	0.522	7.902	3.350	4.552	0.210	6.748	4.922	1.826
0.20	0.776	10.264	2.570	7.694	0.452	7.228	3.390	3.838	0.144	6.373	4.740	1.633
0.30	0.767	9.524	2.500	7.024	0.415	6.844	3.330	3.514	0.123	6.080	4.560	1.520
0.50	0.768	8.917	2.390	6.524	0.366	6.376	3.240	3.136	0.109	5.617	4.228	1.389
0.70	0.779	8.502	2.300	6.220	0.332	6.106	3.170	2.936	0.109	5.218	3.940	1.278
1.00	0.809	8.034	2.230	5.804	0.326	5.708	3.090	2.618	0.119	4.692	3.610	1.082
1.50	0.886	7.449	2.160	5.289	0.365	5.093	2.960	2.133	0.148	3.952	3.370	0.582
2.00	0.988	6.976	2.110	4.866	0.422	4.581	2.850	1.731	0.184	3.354	3.132	0.222
2.50	1.088	6.597	2.060	4.537	0.495	4.127	2.740	1.387	0.215	2.904	2.890	0.014
3.00	1.193	6.272	2.000	4.272	0.573	3.738	2.640	1.098	0.260	2.463	2.650	−0.187
3.50	1.306	5.985	1.930	4.055	0.655	3.397	2.540	0.857	0.290	2.152	2.418	−0.266
4.00	1.428	5.718	1.880	3.838	0.758	3.066	2.440	0.626	0.334	1.826	2.180	−0.354

*The activity coefficients from 0.1 to 1.0 *m* are calculated by the empirical rule and the activity coefficient from 1.0 to 4.0 *m* are those reported by Campbell and Oliver (5).

(*b*). Summary of thermodynamic properties of the process $NaClO_3$ (crystal) → $NaClO_3$ (solution, *m*)

	100% water				44.5% dioxane + 55.5% water				64.5% dioxane + 35.5% water			
m (mol/kg)	$\gamma_\pm$*	$-\Delta G$ (kcal/mol)	ΔH (kcal/mol)	$T\Delta S$ (kcal/mol)	$\gamma_\pm$†	$-\Delta G$ (kcal/mol)	ΔH (kcal/mol)	$T\Delta S$ (kcal/mol)	$\gamma_\pm$†	$-\Delta G$ (kcal/mol)	ΔH (kcal/mol)	$T\Delta S$ (kcal/mol)
0.00			5.280				4.920				3.000	
0.01	0.915	−7.379	5.190	12.569	0.755	−5.810	4.860	10.670	0.526	−3.826	3.220	7.046
0.05	0.825	−5.593	5.070	10.663	0.579	−4.217	4.770	8.987	0.288	−2.630	3.470	6.100
0.10	0.772	−4.870	4.980	9.850	0.500	−3.570	4.710	8.280	0.207	−2.202	3.650	5.852
0.30	0.688	−3.686	4.760	8.446	0.392	−2.555	4.550	7.105	0.107	−1.681	3.960	5.641
0.50	0.645	−3.157	4.600	7.757	0.355	−2.068	4.440	6.508	0.096	−1.205	3.980	5.185
0.70	0.617	−2.811	4.670	7.481	0.334	−1.741	4.350	6.091	0.084	−0.963	3.900	4.863
1.00	0.589	−2.443	4.320	6.763	0.313	−1.395	4.240	5.635	0.074	−0.690	3.740	4.430
1.50	0.555	−2.032	4.130	6.162	0.286	−1.022	4.080	5.102	0.063	−0.401	3.560	3.961
2.00	0.538	−1.729	3.960	5.689	0.264	−0.776	3.950	4.726	0.058	−0.159	3.440	3.599
2.50	0.525	−1.493	3.820	5.313	0.248	−0.585	3.850	4.435				
3.00	0.515	−1.301	3.690	4.991	0.239	−0.423	3.760	4.183				
3.50	0.508	−1.133	3.580	4.713	0.239	−0.230	3.700	3.930				
4.00	0.506	−0.981	3.500	4.481	0.251	−0.014	3.630	3.881				

*Data taken from ref. 13.
†Data taken from ref. 5.

TABLE 6. Values of ΔG, ΔH, and ΔS for the processes of Table 5 (*a*) and (*b*) at standard state

Solvent	$NaClO_3$			$LiClO_3$		
	ΔG^0 (kcal/mol)	ΔH^0 (kcal/mol)	ΔS^0 (e.u.)	ΔG^0 (kcal/mol)	ΔH^0 (kcal/mol)	ΔS^0 (e.u.)
100% water	−1.816	5.280	23.79	−7.738	−3.170	15.32
44.5% dioxane + 55.5% water	−0.019	4.920	16.78	−4.380	−3.800	1.95
64.5% dioxane + 35.5% water	2.394	3.000	2.07	−2.169	−5.230	−10.26

From the $\gamma_\pm$ of lithium chlorate at saturation concentrations, we can calculate the standard free energy, ΔG^0, of solutions

$$[4] \qquad \Delta G^0 = 2RT \ln m\gamma_\pm$$

knowing the value of ΔG^0 we can calculate ΔG values at various concentrations. The ΔG values, along with ΔH values, were used to calculate $T\Delta S$ values. The values of $\gamma_\pm$, ΔG, ΔH, and $T\Delta S$ are given in Table 5*a*. The values of ΔG^0, ΔH^0, and ΔS^0 for sodium and lithium chlorates are given in Table 6.

Discussion

The heats of solution and heats of dilution are negative in all three systems; the exothermicity increases in passing from 100% water to 44.5% dioxane–water to 64.5% dioxane–water mixtures. This could be explained on the assumption that, in water, some of the heat energy is consumed in breaking the hydrogen bonding. In 44.5% dioxane–water and 64.5% dioxane–water the hydrogen bonding decreases with increasing dioxane content and hence the heat effects are greater in mixtures. A similar trend was observed for sodium chlorate in dioxane–water mixtures, though the ΔH values were all positive there.

If we look at the rate of increase in ΔH^0 values from 100% water to 64.5% dioxane–water mixtures we find that there is little change in passing from pure water to 44.5% dioxane–water mixture, but from 44.5% dioxane to 64.5% dioxane–water mixtures, the change in ΔH^0 value is much greater; this is true for both $NaClO_3$ and $LiClO_3$. The reason for this may be that the addition of a small amount of dioxane to water initially increases the water structure, by making the hydrogen bonds stronger as compared to pure water, because dioxane is a better proton acceptor than water itself and consequently the increased structure breaking on addition of an electrolyte would result in a smaller change in ΔH^0 value. As more dioxane is added, a point will be reached when dioxane molecules can no longer be accommodated in the water structure and thus the solvent structure will break down again. Somewhat similar observations were made by Feakins *et al.* (10) when they compared the viscosity B coefficients of NaCl, KCl, and $MgCl_2$ in various dioxane–water mixtures, ranging from 10 to 50% dioxane. They found that the B coefficients increase with the increasing proportion of dioxane content. This kind of behavior is to be expected if the dioxane–water mixtures have less structure than water. The dioxane content, however, must be greater than 10%. Feakins' measurements of ΔH^0 for various alkali metal halides, in 20% dioxane–water mixtures, show that the heats of transfer, at infinite dilution, from 20% dioxane–water to 100% water, are negative, agreeing with our observations in 44.5 and 64.5% dioxane–water mixtures. Further support for this is given by the ΔS^0 values of $NaClO_3$ and $LiClO_3$ in 100% water, 44.5% dioxane, and 64.5% dioxane–water mixtures. In water, which has a three dimensional structure and is the most structurally complex solvent, the entropies are largest for both salts, and smallest in 64.5% dioxane–water mixtures.

The values of $\bar{L}_1$ and $\bar{L}_2$ given in Table 4 can be used to calculate $\gamma_\pm$ of lithium chlorate at any temperature, assuming $\bar{L}_2$ remains constant, because the $\gamma_\pm$ of lithium chlorate at 25 °C is known. Using the following equation

$$[5] \qquad \log \frac{\gamma_{25}}{\gamma'} = \frac{\bar{L}_2}{4.576v}\left[\frac{1}{T_{25}} - \frac{1}{T'}\right]$$

where γ_{25} and γ' are the mean ionic activity coefficients at T_{25} (*i.e.* 25 °C) and T' and v is the total number of ions resulting from a solute molecule, we attempted to calculate the γ' at

Can. J. Chem. Downloaded from www.nrcresearchpress.com by 210.87.254.6 on 09/05/12
For personal use only.

0 °C in water, and compared the results with those obtained by Scatchard *et al.* (1). On the whole our calculated values of $\gamma_{\pm}$ at the freezing point are higher by almost 5–7% in the concentration range 0.1–1.0 *m*. However, when we considered hygroscopic electrolytes like LiBr, LiCl, NaOH, etc., and using the literature values (ref. 9, pp. 708–710) of $\gamma_{\pm}$ and $\bar{L}_2$ at 25 °C, calculated back $\gamma_{\pm}$ for these electrolytes at 0 °C, we found that in certain cases these calculated values were also higher by as much as 6% than those reported by Scatchard *et al.* (1). This implies that the results of Scatchard may be somewhat inaccurate even if we take into account the change in $\bar{L}_2$ with temperature. On the other hand, their results for non-hygroscopic salts are in good agreement with the calculated values (say within 2%). Tables of the $\bar{L}_1$ and $\bar{L}_2$ values have made possible the calculation of the relative partial molal entropy functions used by various authors (11, 12).

We have discovered some inconsistencies in the calculations of the Table 2 of our last paper (6) on $NaClO_3$. We give the corrected results in Table 5*b*.

We would like to thank Mr. B. Arya, M.Sc., of the Department of Mechanical Engineering for his help in computer programming.

1. G. SCATCHARD, S. S. PRENTISS, and P. T. JONES. J. Am. Chem. Soc. **56**, 805 (1934).
2. A. N. CAMPBELL and J. E. GRIFFITHS. Can. J. Chem. **34**, 1647 (1956).
3. A. N. CAMPBELL, E. M. KARTZMARK, and B. G. OLIVER. Can. J. Chem. **44**, 925 (1966).
4. B. G. OLIVER and A. N. CAMPBELL. Can. J. Chem. **47**, 4207 (1969).
5. A. N. CAMPBELL and B. G. OLIVER. Can. J. Chem. **47**, 2671 (1969).
6. A. N. CAMPBELL and O. BHATNAGAR. Can. J. Chem. **49**, 217 (1971).
7. A. N. CAMPBELL, E. M. KARTZMARK, and W. B. MARYK. Can. J. Chem. **44**, 935 (1966).
8. O. N. BHATNAGAR and A. N. CAMPBELL. Unpublished results.
9. H. S. HARNED and B. B. OWEN. The physical chemistry of electrolyte solutions. 3rd ed. Reinhold Publishing Co., New York, 1957.
10. D. FEAKINS, B. C. SMITH, and L. THAKUR. J. Chem. Soc. (A), 714 (1966).
11. R. H. WOOD. J. Phys. Chem. **63**, 1367 (1959).
12. F. R. JONES and R. H. WOOD. J. Phys. Chem. **67**, 1576 (1963).
13. R. A. ROBINSON and R. H. STOKES. Electrolyte solutions. 2nd ed. Butterworths, London, 1959.

Can. J. Chem. Downloaded from www.nrcresearchpress.com by 210.87.254.6 on 09/05/12
For personal use only.

Peptides de l'acide djenkolique. II. Une nouvelle méthode de synthèse du glutathion oxydé[1]

BERNARD MARINIER[2] ET MICHÈLE BÉRUBÉ[3]

Research Laboratories, Frank W. Horner Limited, Montréal, Québec

Reçu le 17 septembre 1971

Cette publication montre qu'il est possible de passer d'un peptide protégé contenant de l'acide djenkolique au peptide correspondant contenant de la cystine. Ainsi, le tripeptide **8** et le pentapeptide **9** ont été convertis aux peptides **10** et **11** respectivement par traitement avec le brome en milieu anhydre suivi d'une hydrolyse. Les pentapeptides **9** et **11** ont par la suite été débarrassés de leurs groupes protecteurs et purifiés par filtration sur Sephadex G-10 pour donner le pentapeptides bis-γ-L-glutamyl-L-djenkolyl-bis-glycine (**7**) et le glutathion oxydé (**2**) avec des rendements globaux respectifs de 57 et 38% à partir de l'acide djenkolique (**1**).

This paper shows that it is possible to convert a protected peptide containing djenkolic acid to the corresponding peptide containing cystine. Thus, the tripeptide **8** and the pentapeptide **9** were converted to peptides **10** and **11** respectively by treatment with bromine in anhydrous medium followed by an hydrolysis. The pentapeptides **9** and **11** were then deprotected and purified by filtration through Sephadex G-10 to give respectively the pentapeptide bis-γ-L-glutamyl-L-djenkolyl-bis-glycine (**7**) and oxidized glutathione (**2**) with overall respective yields of 57 and 38% from djenkolic acid (**1**).

Canadian Journal of Chemistry, **50**, 1633 (1972)

Dans la publication précédente (2), on a montré que l'acide djenkolique (**1**) est un acide aminé stable qui forme les dérivés usuels utilisés en synthèse peptidique. Comme cet acide est à la fois l'homologue supérieur de la cystine et le mercaptal de la cystéine avec la formaldéhyde, il sembla intéressant de voir si l'on pouvait passer directement des peptides de l'acide djenkolique à ceux de la cystine ou de la cystéine par élimination du CH_2 central. Cela impliquait tout d'abord la mise au point d'une méthode d'élimination du CH_2 central dans l'acide djenkolique ou ses dérivés, puis la synthèse d'un peptide simple de l'acide djenkolique que l'on transformerait au peptide correspondant de la cystine. On choisit de préparer par cette méthode le glutathion oxydé (**2**).

Il était évident, au départ, qu'une hydrolyse ne pourrait être utilisée pour éliminer le méthylène central car l'acide djenkolique est tellement stable que les conditions nécessaires à cette hydrolyse aurait provoqué rapidement un scission des liaisons peptidiques. Une réaction connue depuis 1887 (3) et étudiée plus récemment par Gauthier (4) retint notre attention: il s'agit de l'oxydation des mercaptals par le brome en milieu aqueux pour donner les disulfures correspondants (éq. 1). Cependant, le disulfure lui-même pouvant être oxydé en bromure de sulfonyle par un excès de brome selon l'éq. 2, la réaction générale se produit selon l'éq. 3 qui est l'addition des deux premières et elle utilise 6 équivalents de brome. L'équation 2 illustre la méthode de Siggia et Edsberg pour le titrage des disulfures (5).

$$[1]\quad (RS)_2CHR' + Br_2 + H_2O \rightarrow RSSR + R'CHO + 2HBr$$

$$[2]\quad RSSR + 5Br_2 + 4H_2O \rightarrow 2RSO_2Br + 8HBr$$

$$[3]\quad (RS)_2CHR' + 6Br_2 + 5H_2O \rightarrow 2RSO_2Br + R'CHO + 10HBr$$

On entreprit une étude de la réaction du brome sur les dérivés de l'acide djenkolique afin de déterminer les conditions conduisant exclusivement aux disulfures, c'est-à-dire aux dérivés correspondants de la cystine. On constata d'abord, qu'en présence d'eau, l'addition d'un seul équivalent de brome provoquait la formation de toute la gamme des produits d'oxydation, depuis le disulfure jusqu'à l'acide sulfonique, ce qui signifie que la première réaction (éq. 1) n'est pas plus rapide que les suivantes. On nota aussi que les sulfures (6) et même les bis-sulfures (7) peuvent donner des produits d'addition stables en milieu anhydre par réaction avec un seul équivalent de brome ou d'iodure de méthyle

[1]Ce travail a été présenté au 36° Congrès de l'ACFAS à Ottawa le 8 novembre 1968 et a également fait l'objet d'une communication (1).

[2]Adresse actuelle: Université du Québec, 300 avenue des Ursulines, Rimouski, Québec.

[3]Adresse actuelle: Direction des Aliments et des Drogues, 400 Carré Youville, Montréal, Québec.

Can. J. Chem. Downloaded from www.nrcresearchpress.com by 210.87.254.5 on 09/05/12
For personal use only.

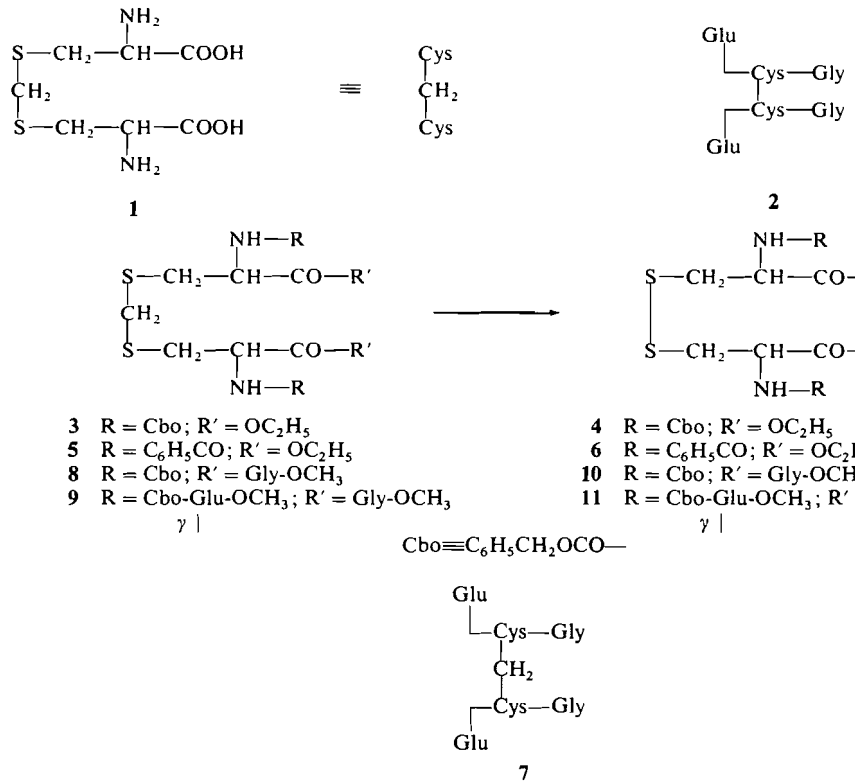

par exemple. On imagina alors que l'addition d'une seule molécule de brome en milieu anhydre donnerait un produit d'addition sans qu'il y ait de brome en excès dans la solution. Par la suite, l'addition d'eau provoquerait la décomposition ou l'hydrolyse du produit d'addition en disulfure et la réaction s'arrêterait à ce stade. Ce serait, en fait, une façon d'assurer la réaction d'une seule molécule de brome avec une seule molécule de mercaptal.

En appliquant ce principe, on put transformer le dicarbobenzoxy-L-djenkolate de diéthyle (**3**) en dicarbobenzoxy-L-cystinate de diéthyle (4) avec un rendement de 76.3% tandis qu'en prolongeant le temps d'hydrolyse, le dibenzoyl-L-djenkolate de diéthyle (**5**) fut converti en dibenzoyl-L-cystinate de diéthyle (**6**) avec un rendement de 76.7%. Il restait à démontrer que la réaction pouvait s'appliquer aux peptides de l'acide djenkolique. La synthèse du peptide de l'acide djenkolique correspondant au glutathion oxydé, le bis-γ-L-glutamyl-L-djenkolyl-bis-glycine (7), fut alors entreprise.

L'acide dicarbobenzoxy-L-djenkolique (2) fut d'abord condensé avec 2 équivalents de glycinate de méthyle en utilisant le réactif de Woodward (8). On obtint une huile difficile à purifier et qui fournit le tripeptide dicarbobenzoxy-L-djenkolyl-bis-(glycinate de méthyle) (**8**) avec des rendements de 50 à 70%. Par contre, l'utilisation des anhydrides mixtes (9) donna très facilement un produit cristallisé avec un rendement de près de 95%. L'enlèvement des groupes carbobenzoxy par l'acide bromhydrique dans l'acide acétique sec (10) donna un dibromhydrate très hygroscopique qui fut condensé avec le carbobenzoxy-L-glutamate d'α-monométhyle préparé selon Nefkens et Nivard (11). Grâce à la méthode des anhydrides mixtes, le pentapeptide bis-γ-[*N*-carbobenzoxy-L-glutamyl-α-(*O*-méthyl)]-L-djenkolyl-bis-(glycinate de méthyle) (**9**) fut obtenu avec un rendement de 84%.

La synthèse de l'analogue 7 fut interrompue à ce point afin de transformer les peptides protégées **8** et **9** en leurs analogues contenant de la cystine. On effectua d'abord la conversion du

Can. J. Chem. Downloaded from www.nrcresearchpress.com by 210.87.254.5 on 09/05/12
For personal use only.

Can. J. Chem. Downloaded from www.nrcresearchpress.com by 210.87.254.5 on 09/05/12
For personal use only.

tripeptide **8** en dicarbobenzoxy-L-cystinyl-bis-(glycinate de méthyle) (**10**) qui est un tripeptide connu (12). Après quelques essais peu encourageants, on prolongea le temps d'hydrolyse jusqu'à 24 h et réussit la conversion avec un rendement de 45%. En utilisant les mêmes conditions, il fut facile de transformer le pentapeptide **9** en son analogue contenant de la cystine, le bis-γ-[*N*-carbobenzoxy-L-glutamyl-α-(*O*-méthyl)]-L-cystinyl-bis-(glycinate de méthyle) (**11**) avec un rendement de 68.5%. Ce peptide, qui est le glutathion oxydé portant des groupes protecteurs, a le même point de fusion que le peptide **9** mais il donne un abaissement de point de fusion en mélange avec ce dernier, montre un R_f différent à la chromatographie sur couche mince, possède un indice de rotation plus négatif et donne un test positif pour les disulfures (13).

Les pentapeptides **9** et **11** furent débarrassés de leurs groupes protecteurs par une saponification d'une durée de 5 h suivie d'une scission des groupes carbobenzoxy par HBr dans l'acide acétique sec (10). Un filtration sur Sephadex G-10 de la solution aqueuse de chacun des bromhydrates permit d'obtenir le peptide **7** et le glutathion oxydé **2** avec des rendements respectifs de 76 et 68.5%, d'où des rendements globaux respectifs de 57 et 38% à partir de l'acide djenkolique.

L'analyse du peptide **7** selon Spackman *et al.* (14) donna lieu à certaines difficultés car, dans les conditions d'hydrolyse préalable, l'acide djenkolique est presque totalement détruit. En fait, un échantillon de cet acide aminé soumis à une hydrolyse identique montra quatre pics à l'analyse: le pic de l'acide djenkolique, celui de la cystine, un pic faible en position proline et un autre entre la thréonine et la sérine. On trouva que ce dernier pic est celui de la thioproline ou acide thiazolidine-carboxylique-4, résultat de la condensation d'une mole de cystéine avec une mole de formaldéhyde (15). Quant au pic en position proline, sa position et son faible facteur "C", calculé par différence, indiquèrent qu'il s'agissait probablement de cystéine (16). L'hydrolysat du peptide **7** donna évidemment ces quatre pics pour l'acide djenkolique en plus de ceux de la glycine et de l'acide glutamique mais l'addition de ces quatre pics permit d'obtenir le rapport théorique pour ces acides aminés. L'analyse du glutathion oxydé **2** ne donna évidemment que les trois pics Glu, Cys_2, et Gly dans le rapport attendu sans aucune trace d'acide djenkolique ou de ses produits d'hydrolyse.

L'indice de rotation du pentapeptide **7** dans l'eau est de $-34.2°$ à comparer à $-94°$ pour le glutathion oxydé. Ceci est conforme aux résultats obtenus tout au long de ce travail, à savoir que les indices de rotation des dérivés ou peptides de l'acide djenkolique sont toujours moins négatifs que les dérivés ou peptides correspondants de la cystine. Par contre, le peptide **7** est très soluble dans l'eau tout comme le glutathion oxydé et les deux peptides ont des R_f identiques dans tous les solvants utilisés en chromatographie sur papier.

Cette synthèse montre donc que l'on peut convertir un peptide de l'acide djenkolique au peptide correspondant de la cystine au moyen d'une réaction extrêmement simple et sans qu'il y ait racémisation. Il est évident qu'une telle méthode n'est pas toujours utile ou nécessaire mais elle peut rendre de très grands services dans certains cas particuliers.

Partie expérimentale

Les points de fusion ne sont pas corrigés et furent déterminés en tubes capillaires avec un appareil électrique de marque Gallenkamp. Les chromatographies sur couche mince furent effectuées sur silicagel (Eastman Chromagram Sheet, 5 × 20 cm) dans un des mélanges suivants: (A) chloroforme/acétone (8:2); (B) chloroforme/acétate d'éthyle (5:5); (C) cyclohexane/acétate d'éthyle (2:8). Les chromatographies sur papier Whatman No. 1 furent effectuées dans le mélange *n*-butanol/pyridine/acide acétique/eau (15:10:3:12). La révélation des taches fut faite par des vapeurs d'iode pour les peptides protégés et avec la ninhydrine pour les peptides libres.

Les analyses élémentaires furent effectuées par le Dr. C. Daesslé, Organic Microanalysis, 5757, rue Decelles, Montréal, Québec. Les échantillons furent d'abord séchés à 80–100° sous 0.1 mm de mercure durant au moins 18 h. Les analyses d'acides aminés furent effectuées dans un appareil Beckman-Spinco.

*Dicarbobenzoxy-L-djenkolyl-bis-(glycinate de méthyle) (**8**)*

On dissout 10.46 g (0.02 mol) d'acide dicarbobenzoxy-L-djenkolique dans 100 ml de chloroforme sec et on ajoute 4.46 ml (0.04 ml) de *N*-méthyl-morpholine à la solution. On refroidit à $-5°$, ajoute 5.22 ml (0.04 mol) de chloroformiate d'isobutyle et agite la solution durant 10 min. On ajoute alors 5.02 g (0.04 mol) de chlorhydrate du glycinate de méthyle presque complètement dissout dans 75 ml de chloroforme sec et froid (0°) contenant 5.55 ml (0.04 mol) de triéthylamine. Une autre portion de 75 ml de chloroforme sec est ajoutée et on agite la solution durant 4 h à tempéra-

Can. J. Chem. Downloaded from www.nrcresearchpress.com by 210.87.254.5 on 09/05/12
For personal use only.

ture ambiante, puis on la lave avec H_2O, $NaHCO_3$ 5%, H_2O, HCl dilué, et H_2O (trois fois). Après séchage sur Na_2SO_4 et évaporation sous vide, on obtient un solide p.f. 139–140° qui est recristallisé dans le nitrométhane après traitement au charbon actif: 11.95 g (90%), p.f. 139–140°, $[\alpha]_D^{25}$ −62.6°(*c*, 1 dans la diméthylformamide), R_f 0.53, 0.26 et 0.6 dans les mélanges A, B, et C respectivement. Les eaux-mères donnent une deuxième récolte, 0.64 g, p.f. 139–140°, d'où un rendement total de 94.7%.

Anal. calc. pour $C_{29}H_{36}N_4O_{10}S_2$: C, 52.39; H, 5.46; N, 8.43; S, 9.65. Trouvé: C, 52.47; H, 5.58; N, 8.49; S, 9.49.

Traitement du tripeptide **8** *par HBr/AcOH*

On met 6 g de peptide **8** en suspension dans 60 ml de HBr 4.2 *N* dans l'acide acétique sec. On agite de temps en temps jusqu'à dissolution complète ($\frac{1}{4}$ h) puis laisse au repos $\frac{1}{2}$ h. On ajoute 600 ml d'éther anhydre, filtre le solide sous vide, et le lave avec 600 ml d'éther anhydre. On le sèche durant une nuit sous vide dans un dessicateur en présence de NaOH solide et de P_2O_5. Ce produit est hygroscopique et doit être gardé sous vide dans un dessicateur.

*Bis-γ-[N-carbobenzoxy-*L*-glutamyl-α-(O-méthyl)]-*L*-djenkolyl-bis-(glycinate de méthyle) (***9***)*

On dissout 5.9 g (0.02 mol) de *N*-carbobenzoxy-L-glutamate d'α-monométhyle (11) dans 20 ml de diméthylformamide, ajoute 2.23 ml (0.02 mol) de *N*-méthyl-morpholine, et refroidit la solution à −5°. On ajoute 2.61 ml (0.02 mol) de chloroformiate d'isobutyle, agite 10 min puis ajoute 5.58 g (0.01 mol) du dibromhydrate du L-djenkolyl-bis-(glycinate de méthyle), et 2.23 ml (0.02 mol) de *N*-méthyl-morpholine dissoute dans 25 ml de diméthylformamide. On agite 4 h à température ambiante, puis verse cette solution dans 700 ml d'eau et laisse cristalliser durant $1\frac{1}{2}$ h. Le peptide est filtré sous vide, lavé sur le filtre avec de l'eau, et séché à l'air: il pèse 8.64 g (91%) et son p.f. est 177–180°. Par recristallisation dans l'éthanol absolu, on obtient 8 g (84%) de produit, p.f. 180–182°, $[\alpha]_D^{25}$ −52.7° (*c*, 1 dans la diméthylformamide), R_f 0.1 dans le mélange A. L'échantillon analytique obtenu après plusieurs cristallisations fond à 181–184°.

Anal. calc. pour $C_{41}H_{54}N_6O_{16}S_2$: C, 51.78; H, 5.72; N, 8.84; S, 6.74. Trouvé: C, 51.44; H, 5.48; N, 8.85; S, 6.81.

*Bis-γ-*L*-glutamyl-*L*-djenkolyl-bis-glycine (***7***)*

On dissout 0.237 g (0.00025 mol) de pentapeptide **9** dans 2 ml de diméthylformamide, on refroidit la solution à 0° et, sous agitation, on ajoute 1.1 ml de NaOH 1 *N* goutte à goutte sur une période de 10 min. On continue l'agitation durant 1 h à 0° puis à température ambiante durant 4 h. On acidifie jusqu'au virage du Congo rouge par addition de 1.2 ml de HCl 1 *N*, ajoute 15 ml d'eau et extrait le peptide par l'acétate d'éthyle. La solution organique est séchée sur Na_2SO_4, évaporée sous vide et le résidu est séché sous vide durant la nuit.

Ce résidu est dissout dans 2 ml d'acide acétique sec, puis on ajoute 2 ml d'une solution d'acide bromhydrique 5.4 *N* dans l'acide acétique et on agite durant 1 h: il y a un précipité à la fin. On ajoute 40 ml d'éther sec, filtre le précipité sous vide et le lave rapidement sur le filtre avec 40 ml d'éther sec. Ce dibromhydrate hydroscopique est séché dans un dessicateur en présence de P_2O_5 durant 3 h (poids 0.231 g), puis il est dissout dans 1.5 ml d'eau et la solution est ajustée au p*H* 2.85 avec NaOH 6 *N*. Cette solution est versée sur une colonne de Sephadex G-10 de 2.5 cm de diamètre par 90 cm de hauteur qui est ensuite éluée avec de l'eau. La vitesse d'élution est maintenue constante à 14 ml/h (2.85 ml/cm²/h) au moyen d'une pompe péristatique et des fractions de 2 ml sont recueillies. Les peptides présents sont détectés quantitativement par réaction avec la ninhydrine selon Moore et Stein (17) sur 0.1 ml de solution. La quantité de bromure de sodium est déterminée par titrage du brome selon la méthode de Volhard (18).

Les fractions 94 à 102 ne montrent qu'une seule tache R_f 0.06 à la chromatographie sur papier tandis que la fraction 104 est très légèrement impure. Les fractions 94 à 103 réunies et lyophilisées donnent 0.119 g (76%) de solide incolore, $[\alpha]_D^{25}$ −34.2° (*c*, 1 dans l'eau). Un échantillon hydrolysé dans HCl 6 *N* en tube scellé à 120° durant 24 h donne les acides aminés dans le rapport suivant: Glu, 2.06; Gly, 2.00; Dje (somme de quatre pics), 0.97.

*Dicarbobenzoxy-*L*-cystinate de diéthyle (***4***)*

*(a) A partir de la dicarbobenzoxy-*L*-cystine*

Préparé selon Baganz et Dransch (19), p.f. 86°, $[\alpha]_D^{22}$ −142° (*c*, 1 dans la diméthylformamide).

*(b) A partir du dicarbobenzoxy-*L*-djenkolate de diéthyle (***3***)*

On dissout 0.289 g (0.0005 mol) de dicarbobenzoxy-L-djenkolate de diéthyle (2) dans 3 ml de chloroforme et ajoute 1 ml d'une solution 0.5 *M* de brome dans le même solvant. Après 10 min d'agitation, on ajoute 2 ml de $NaHCO_3$ 10% et agite fortement: il y a décoloration partielle. On verse la solution dans une ampoule à décantation, ajoute quelques ml de chloroforme et agite fortement: la couleur disparaît. On sépare les couches, lave la couche chloroformique avec de l'eau, sèche, évapore le chloroforme sous vide, ajoute un peu d'éthanol 95%, et évapore à sec avec léger chauffage. Le résidu solide est cristallisé dans l'éthanol absolu: 0.176 g (62.2%) de cristaux p.f. 85°, sans abaissement avec le produit préparé en (*a*) et donnant un abaissement à environ 70° en mélange avec le produit de départ; $[\alpha]_D^{22}$ −139° (*c*, 1 dans la diméthylformamide). L'addition de quelques gouttes d'eau aux eaux-mères donne une autre récolte de 0.040 g, p.f. 82–82.5°, d'où un rendement total de 76.3%.

*Dibenzoyl-*L*-djenkolate de diéthyle (***5***)*

On dissout 3.22 g (0.007 mol) d'acide dibenzoyl-L-djenkolique (20) dans 40 ml d'éthanol absolu puis on sature avec HCl sec durant $\frac{1}{2}$ h. On chauffe à reflux 2 h puis évapore sous vide et recristallise le résidu dans l'éthanol absolu, d'où l'on tire 1.8 g (49.6%) de cristaux p.f. 156–158°, $[\alpha]_D^{22}$ −122° (*c*, 1 dans la diméthylformamide).

Anal. calc. pour $C_{25}H_{30}N_2O_6S_2$: C, 57.94; H, 5.83; N, 5.40; S, 12.36. Trouvé: C, 57.53; H, 5.88; N, 5.23; S, 12.11.

*Dibenzoyl-*L*-cystinate de diéthyle (***6***)*

*(a) A partir de la dibenzoyl-*L*-cystine*

On dissout 0.75 g de dibenzoyl-L-cystine (21) dans 10 ml d'éthanol absolu, sature la solution avec HCl sec durant $\frac{1}{2}$ h, chauffe à reflux durant 2 h puis laisse refroidir, et filtre. On obtient 0.61 g (72%) de produit p.f. 183°, $[\alpha]_D^{22}$ − 216° (*c*, dans la diméthylformamide). La littérature (22) rapporte p.f. 183–185.5°, $[\alpha]_D$ +13.3° (*c*, 0.5 dans EtOH 99%).

*(b) A partir du dibenzoyl-*L*-djenkolate de diéthyle (***5***)*

On dissout 0.259 g (0.0005 mol) de dibenzoyl-L-djenkolate de diéthyle dans 10 ml de chloroforme sec et ajoute 1 ml

Can. J. Chem. Downloaded from www.nrcresearchpress.com by 210.87.254.5 on 09/05/12
For personal use only.

d'une solution 0.5 *M* de brome dans le même solvant. Après 10 min d'agitation, on ajoute à la solution jaune foncé 5 ml de $NaHCO_3$ 5% et quand la décoloration est complète, on ajoute 20 ml d'éther de pétrole 30–60° et agite le mélange durant $22\frac{1}{2}$ h. Les solvants sont évaporés partiellement, les couches sont séparées et la couche organique est lavée avec de l'eau, séchée, et évaporée. Le résidu recristallisé dans l'éthanol absolu donne 0.193 g (76.7%) de cristaux p.f. 181–183° sans dépression avec le produit préparé en (*a*) et $[\alpha]_D$ −217° (*c*, 1 dans la diméthylformamide).

*Dicarbobenzoxy-*L*-cystinyl-bis-(glycinate de méthyle) (**10**)*

*(a) A partir de la dicarbobenzoxy-*L*-cystine*

A une solution de 0.25 g (0.002 mol) du chlorhydrate du glycinate de méthyle et de 2.8 ml de triéthylamine dans 6 ml de $CHCl_3$, on ajoute 0.523 g (0.001 mol) de dicarbobenzoxy-L-cystine. On refroidit dans la glace et ajoute 0.412 g (0.002 mol) de dicyclohexylcarbodiimide sous bonne agitation. Après $\frac{1}{2}$ h, le bain de glace est enlevé et l'agitation à température ambiante est poursuivie durant 18 h. On ajoute quelques gouttes d'acide acétique 50%, filtre la dicyclohexylurée (0.418 g, 93.5%), lave le filtrat avec HCl dilué, $NaHCO_3$ 10%, et H_2O, sèche et évapore sous vide. Le résidu blanc fond à 164.5–165° mais après une cristallisation dans l'acétate d'éthyle, il fond à 156–156.5°. Une recristallisation dans le méthanol ramène le p.f. à 169–169.5° avec un rendement de 61%, un $[\alpha]_D^{25}$ −150° (*c*, 1 dans la diméthylformamide) et des R_f de 0.59, 0.29, et 0.63 dans les solvants A, B et C respectivement. La littérature (12) rapporte: p.f. 172–172.5° et $[\alpha]_D^{25}$ −146° (*c*, 1 dans la diméthylformamide).

*(b) A partir du dicarbobenzoxy-*L*-djenkolyl-bis-(glycinate de méthyle) (**8**)*

A une solution de 0.665 g (0.001 mol) du tripeptide **8** dans 20 ml de chloroforme, on ajoute 2 ml d'une solution 0.5 *M* de brome dans $CHCl_3$. Après 10 min d'agitation, on ajoute 20 ml de $NaHCO_3$ 5% et poursuit l'agitation durant toute la nuit. On sépare alors les couches, lave la couche aqueuse avec du chloroforme puis les couches organiques réunies avec de l'eau, sèche, et évapore le chloroforme sous vide. On obtient un solide un peu collant qu'on recristallise dans le méthanol pour obtenir 0.293 g (45%) de cristaux blancs, p.f. 168–169.5° sans abaissement avec le produit préparé en (*a*), $[\alpha]_D^{25}$ −145.5° (*c*, 1 dans la diméthylformamide) et donnant des R_f identiques à ceux obtenus en (*a*).

*Bis-γ-[N-carbobenzoxy-*L*-glutamyl-α-(O-méthyl)]-*L*-cystinyl-bis-(glycinate de méthyle) (**11**)*

Par chauffage, on dissout 0.475 g (0.0005 mol) du pentapeptide **9** dans 20 ml de chloroforme sec, puis on refroidit à température ambiante et ajoute 1 ml d'une solution 0.5 *M* de brome dans $CHCl_3$. Après 1 min d'agitation, on ajoute 10 ml de $NaHCO_3$ 5% et 10 ml d'eau et on agite violemment durant 2–3 min. On ajoute ensuite 60 ml d'acétate d'éthyle et poursuit l'agitation durant 24 h. Les solvants organiques sont alors évaporés et le solide qui précipite est filtré sous vide et lavé avec de l'eau. Après séchage sous vide, on obtient 0.370 g (79%) de solide blanc p.f. 176–178° donnant un abaissement de p.f. à 165–169° avec le produit de départ. Un cristallisation dans l'éthanol absolu donne 0.321 g (68.5%) de cristaux p.f. 178–181°. $[\alpha]_D^{25}$ −76.9° (*c*, 1 dans la diméthylformamide), R_f 0.23 dans le solvant A. L'échantillon analytique obtenu après plusieurs cristallisations fond à 182–183°.

Anal. calc. pour $C_{40}H_{52}N_6O_{16}S_2$: C, 51.27; H, 5.59; N, 8.97; S, 6.84. Trouvé: C, 51.06; H, 5.61; N, 8.95; S, 7.12.

*Glutathion oxydé (**2**)*

On dissout 0.234 g (0.00025 mol) de pentapeptide **11** dans 2 ml de diméthylformamide, on refroidit la solution à 0° et, sous agitation, on ajoute 1.1 ml de NaOH 1 *N* goutte à goutte sur une période de 15 min. On continue l'agitation durant 1 h à 0° et $2\frac{1}{2}$ h à température ambiante. On acidifie jusqu'au virage du Congo rouge, ajoute 15 ml d'eau, et extrait le peptide avec de l'acétate d'éthyle. La solution organique est séchée sur Na_2SO_4, évaporée sous vide, et le résidu est séché sous vide poussé durant la nuit.

Ce résidu est dissout dans 2 ml d'acide acétique sec, puis on ajoute 2 ml d'une solution d'acide bromhydrique 5.4 *N* dans l'acide acétique et on agite 1 h. On ajoute 40 ml d'éther sec et une gomme précipite. On décante la solution surnageante, lave la gomme plusieurs fois par trituration dans l'éther et sèche sous vide en présence de P_2O_5. Le résidu gommeux (0.259 g) est alors dissout dans 2 ml d'eau et la solution est ajustée au p*H* 2.85 avec NaOH 6 *N*. Cette solution est versée sur une colonne de Sephadex G-10 de 2.5 cm de diamètre par 90 cm de hauteur qui est éluée avec de l'eau tel que décrit précédemment. Les fractions 96 à 106 ne montrent qu'une seule tache R_f 0.07 à la chromatographie sur papier tandis que les fractions 107–108 sont légèrement impures. Les fractions 94 à 106 réunies et lyophilisées donnent 0.106 g (68.5%) de solide incolore, $[\alpha]_D$ −94° (*c*, 1 dans l'eau). Un échantillon hydrolysé dans HCl 6 *N* en tube scellé à 120° durant 24 h donne les acides aminés dans le rapport suivant: Glu, 1.03; Gly, 1.00; Cys, 0.9.

Nous remercions le Conseil National de Recherches du Canada qui a subventionné ce travail. Nos remerciements vont également au Dr. F. L. Chubb pour de nombreuses et utiles discussions, au Dr. L. Eric pour ses suggestions concernant la purification finale du peptide et au Dr. N. A. Attallah autrefois de l'Université McGill qui a effectué les analyses d'acides aminés.

1. B. MARINIER et M. BERUBE. Can. J. Chem. **47**, 4507 (1969).
2. B. MARINIER et P. PENEV. Can. J. Chem. **45**, 1253 (1967).
3. H. FASBENDER. Chem. Ber. **20**, 460 (1887).
4. B. GAUTHIER. Ann. pharm. franç. **12**, 281 (1954).
5. S. SIGGIA et R. L. EDSBERG. Anal. Chem. **20**, 938 (1948).
6. F. BOBERG, G. WINTER, et G. R. SCHULTZE. Chem. Ber. **89**, 1160 (1956).
7. C. W. CRANE et H. N. RYDON. J. Chem. Soc. 766 (1947).
8. R. B. WOODWARD, R. A. OLOFSON, et H. MAYER. J. Am. Chem. Soc. **83**, 1010 (1961).
9. J. R. VAUGHAN et R. L. OSATO. J. Am. Chem. Soc. **74**, 676 (1952).
10. D. BEN-ISHAI et A. BERGER. J. Org. Chem. **17**, 1564 (1952).
11. G. H. L. NEFKENS et R. J. F. NIVARD. Rec. Trav. chim. Pays-Bas. **83**, 199 (1964).
12. L. ZERVAS, I. PHOTAKI, et N. GHELIS. J. Am. Chem. Soc. **85**, 1337 (1963).
13. G. TOENNIES et J. J. KOLB. Anal. Chem. **23**, 823 (1951).

14. D. H. SPACKMAN, W. H. STEIN, et S. MOORE. Anal. Chem. **30**, 1190 (1958).
15. S. RATNER et H. T. CLARKE. J. Am. Chem. Soc. **59**, 200 (1937).
16. S. BLACKBURN. Amino acid determination, methods and techniques. Marcel Dekker Inc., 1968. p. 127.
17. S. MOORE et W. H. STEIN. J. Biol. Chem. **211**, 907 (1954).
18. A. I. VOGEL. A textbook of quantitative inorganic analysis. 2e Edition. Longmans, Green and Co., New York, 1951. p. 258.
19. H. BAGANZ et G. DRANSCH. Chem. Ber. **93**, 784 (1960).
20. V. DU VIGNEAUD et W. I. PATERSON. J. Biol. Chem. **114**, 533 (1936).
21. R. A. GORTNER et W. F. HOFFMAN. J. Biol. Chem. **72**, 433 (1927).
22. T. KANEKO *et al.* Bull Chem. Soc. Japan, **37**, 242 (1964).

Can. J. Chem. Downloaded from www.nrcresearchpress.com by 210.87.254.5 on 09/05/12
For personal use only.

The Alkaloids of *Ormosia semicastrata*: (−)-Ormosanine, (±)-Piptanthine, (−)-18-Epiormosanine, and (−)-Ormocastrine

STEWART MCLEAN AND MARIE LESSARD ROY
Department of Chemistry, University of Toronto, Toronto, Ontario
AND
H.-J. LIU AND D. T. CHU
Department of Chemistry, University of New Brunswick, Fredericton, New Brunswick

Received December 15, 1971

The alkaloids of *Ormosia semicastrata* have been shown to be (−)-ormosanine, (±)-piptanthine, (−)-18-epiormosanine, and (−)-ormocastrine. The structure and relative configuration shown in **1** have been assigned to ormocastrine on the basis of its 220 MHz n.m.r. spectrum and its conversion to ormosanine, among other products, on hydrogenation.

Les alcaloïdes de *Ormosia semicastrata* sont la (−)-ormosanine, la (±)-piptanthine, la (−)-18-épiormosanine, et la (−)-ormocastrine. La structure et la configuration relative représentées par **1** ont été attribuées à l'ormocastrine sur la base de son spectre r.m.n. à 220 MHz et par sa transformation en ormosanine, entre autre, par hydrogénation.

Canadian Journal of Chemistry, **50**, 1639 (1972)

We have recently reported (1) the isolation of four alkaloids from the seeds of *Ormosia semicastrata*: ormosanine, (±)-piptanthine, 18-epiormosanine, and one, $C_{20}H_{33}N_3$, which we will now call ormocastrine. Although our evidence indicated that ormocastrine was a stereoisomer of dihydroormojanine (2), it was not sufficiently conclusive to establish this unequivocally. We now present evidence that allows us to assign to ormocastrine the structure and stereochemistry (relative configuration) shown in **1**.[1]

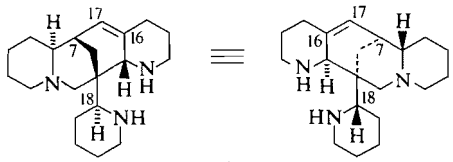

1

The structural ambiguity was primarily concerned with the location of the double bond, which was tentatively assigned the position shown since at 100 MHz the n.m.r. spectrum of the alkaloid provided evidence for the presence of only one vinyl proton, and this was associated with a doublet, $J = 6$ Hz, (broadened by further weak coupling) at τ 4.35. The most probable explanation for this signal was that the vinyl proton had one neighboring proton and therefore should be placed at C-17, adjacent to the bridgehead proton at C-7. However, as Deslongchamps *et al.* (2) pointed out in the case of dihydroormojanine, the double bond could be in one of a small number of alternative locations in the molecule if the steric constraints caused the vinyl proton to couple relatively strongly ($J = 6$ Hz) with one proton of an adjacent methylene group and very weakly ($J \simeq 0$ Hz) with the other. We have now shown that the latter possibility can be excluded since a careful examination of the n.m.r. spectrum of ormocastrine at 220 MHz has allowed us to locate the signal arising from the proton to which the vinyl proton is coupled. This signal appears at τ 8.00 as an unresolved multiplet (its width at half-height is 16 Hz) with an area corresponding to one proton. This proton and the vinyl proton can be decoupled from one another; irradiation at τ 8.00 causes the vinyl signal at τ 4.35 to collapse to a slightly broadened singlet, while irradiation at τ 4.35 causes the signal at τ 8.00 to sharpen; although it is still a multiplet, its width indicates that the other

[1]In previous publications the Toronto and New Brunswick authors have differed in the manner in which they have represented structural formulae and, in order to assist the reader who may wish to compare formulae shown here with those in other papers, we have shown both conventions explicitly. In no case is an assignment of the absolute configuration implied by these representations.

Can. J. Chem. Downloaded from www.nrcresearchpress.com by 210.87.254.105 on 09/05/12
For personal use only.

Can. J. Chem. Downloaded from www.nrcresearchpress.com by 210.87.254.105 on 09/05/12
For personal use only.

coupling constants associated with it are smaller in magnitude than that with the vinyl proton and it is highly improbable that a geminal coupling is present. It follows that **1** represents the true structure of ormocastrine.

The stereochemical question that remained was answered by first treating ormocastrine with phosgene and converting it to the urea, referred to as the homoxy derivative, in which the two secondary amine functions are joined by a carbonyl bridge. When homoxyormocastrine, which shows the vinyl proton as a doublet, $J = 6$ Hz, at τ 4.45 in its n.m.r. spectrum, was subjected to hydrogenation in the presence of platinum in glacial acetic acid, three products were isolated. Two were reduction products, one of which was identified as homoxyormosanine and the other was consequently deduced to be homoxy-16-epiormosanine. The third product resulted from isomerization of homoxyormocastrine and is assigned formula **2**; it is

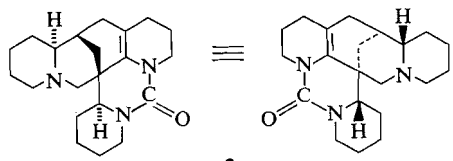

2

identical with a synthetic product obtained by the group at the University of New Brunswick (3). Hydrogenation of ormocastrine itself afforded in good yield equal amounts of two products, the first identified as ormosanine and the second deduced to be 16-epiormosanine. The homoxy derivative of 16-epiormosanine produced in this way was identical with the material obtained by hydrogenation of homoxyormocastrine. Since ormosanine possesses all of the chiral centers present in ormocastrine, it follows that the relative configuration of ormocastrine is that shown in **1**, provided that no epimerization has occurred during the hydrogenation, and experience with the behavior of this class of compounds indicates that epimerization is unlikely in the present case (2, 3).

Ormocastrine proved to be laevorotatory, $[\alpha]_D$ $-29°$ in methanol, with a plain negative dispersion curve down to 250 mμ at least. This optical activity led us to examine more carefully the other alkaloids isolated from the plant since it might have been anticipated that either all would be active or all would be inactive. However, the piptanthine which we had previously described as racemic because of its melting point (1), did in fact prove to be optically inactive. On the other hand, we were surprised to find that our ormosanine is weakly laevorotatory, $[\alpha]_D$ $-9°$, with a plain negative dispersion curve. As we pointed out previously (1), we had expected the ormosanine to be inactive since it appeared that this alkaloid has always been isolated as a racemic modification, with the only exception being the early report of Lloyd and Horning (4) that their sample was very weakly dextrorotatory in chloroform. Our 18-epiormosanine is also weakly laevorotatory, $[\alpha]_D$ $-10°$, with a plain negative dispersion curve. In conclusion then, three of the four alkaloids are laevorotatory and one is racemic; the plant which provided the first natural (±)-piptanthine has also provided the first natural (−)-ormosanine.

Experimental

A Perkin–Elmer Infracord spectrophotometer and a Hitachi Perkin–Elmer RMU-6D mass spectrometer were used. The 220 MHz spectrum was recorded on a Varian HR-220 at the Canadian 220 MHz N.M.R. Center; decoupling experiments were carried out under track-field sweep decoupling conditions. Optical rotatory dispersion curves were recorded on a Jasco ORD/UV-5 instrument and $[\alpha]_D$ values were obtained on a Perkin–Elmer Model 141 Polarimeter with samples dissolved in methanol.

Hydrogenation of Homoxyormocastrine

Homoxyormocastrine (**1**) (12 mg) in glacial acetic acid (2 ml) was hydrogenated over Adams catalyst (10 mg) at room temperature under a hydrogen atmosphere overnight. The catalyst was filtered and washed thoroughly with glacial acetic acid and chloroform. The filtrate was basified with aqueous sodium hydroxide and extracted with chloroform. After it had been dried over magnesium sulfate, filtered, and evaporated, the extract gave an oil (10 mg) consisting of three products. Silica gel preparative t.l.c. using ether containing 15% methanol as eluent led to their separation and isolation as homoxy-16-epiormosanine (3 mg), homoxyormosanine (3 mg), and an isomer (1 mg) of ormocastrine, assigned structure **2**.

Homoxy-16-epiormosanine shows a molecular ion peak at *m/e* 343 in its mass spectrum and an urea absorption band at 6.21 μ (1610 cm^{-1}) in its i.r. spectrum. Homoxyormosanine and compound **2** thus obtained were found to be identical with authentic samples (3) by comparison of their i.r. and mass spectra and t.l.c. characteristics.

Hydrogenation of Ormocastrine

Ormocastrine (13 mg) was hydrogenated in the manner

described above. The reduction product (10 mg) obtained was shown to be a mixture of equal parts of ormosanine and 16-epiormosanine, which were isolated by preparative t.l.c. on alumina with elution by ether containing 10% methanol. The ormosanine obtained had i.r., t.l.c., and mass spectral characteristics identical with those of an authentic sample. The 16-epiormosanine showed a parent ion at *m/e* 317 in its mass spectrum and reacted with phosgene (5) to afford a quantitative yield of the homoxy derivative, identical with that obtained by the hydrogenation of homoxyormocastrine.

Discussions with Professor Z. Valenta during the course of this work have been of great value to us. Financial support from the National Research Council of Canada is gratefully acknowledged.

1. S. McLEAN, P. K. LAU, S. K. CHENG, and D. G. MURRAY. Can. J. Chem. **49**, 1976 (1971).
2. P. DESLONGCHAMPS, Z. VALENTA, and J. S. WILSON. Can. J. Chem. **44**, 2539 (1966).
3. D. T. CHU, H.-J. LIU, T. T. J. YU, and Z. VALENTA. Can. J. Chem. To be published.
4. H. A. LLOYD and E. C. HORNING. J. Am. Chem. Soc. **80**, 1506 (1958).
5. Z. VALENTA, P. DESLONGCHAMPS, M. H. RASHID, R. H. WIGHTMAN, and J. S. WILSON. Can. J. Chem. **44**, 2525 (1966).

Can. J. Chem. Downloaded from www.nrcresearchpress.com by 210.87.254.105 on 09/05/12
For personal use only.

Adsorption of Co^{2+} by Oxides from Aqueous Solution

P. H. TEWARI, A. B. CAMPBELL, AND WOON LEE

Research Chemistry Branch, Whiteshell Nuclear Research Establishment, Atomic Energy of Canada Limited, Pinawa, Manitoba

Received November 22, 1971

The adsorption of Co(II) by Fe_3O_4, Al_2O_3, and MnO_2 has been studied as a function of Co(II) concentration, solution-pH, and temperature. It is observed that the adsorption of cobalt increases markedly with the solution pH between pH 5 and 7.5. Above pH 8 adsorption becomes increasingly masked by precipitation of $Co(OH)_2$ and no resolution of these two contributions to the loss of Co(II) from solution is possible. A $\log \theta/(1-\theta)$ *vs.* pH plot is found to be linear between pH 5 and 7.5, where θ is the fraction of occupied adsorption sites. The presence of 0.1 m Ba^{2+} and Mg^{2+} in the solution does not seem to affect the hydrogen ion dependence of the adsorption of Co(II) on alumina.

The adsorption results have been analyzed by the Langmuir adsorption isotherm over a wide range of Co(II) concentration (10^{-6}–10^{-3} m). The adsorption of Co(II) is found to be an endothermic process and increases markedly with temperature between 30 and 100 °C. The heat of adsorption decreases with increasing surface coverage of the oxides. At saturation coverage, the heats of adsorption for Co(II) on Al_2O_3, MnO_2, and Fe_3O_4 are −14.9, −14.3, and −6.3 kcal/mol, respectively. Hydrolysis of Co(II) is suggested as a possible mechanism for the marked dependence of adsorption on pH and temperature.

L'adsorption de Co(II) sur Fe_3O_4, Al_2O_3, et MnO_2 a été étudiée en fonction de la concentration en Co(II), du pH de la solution et de la température. On observe que l'adsorption du cobalt croît fortement avec le pH de la solution entre 5 et 7.5. Au delà de pH 8, l'adsorption est de plus en plus marquée par la précipitation de $Co(OH)_2$; il n'est plus possible alors d'estimer la perte de Co(II) de la solution à l'une de ces deux contributions. La courbe $\log \theta/(1-\theta)$ en fonction du pH est linéaire entre pH 5 et 7.5, θ étant la fraction de sites d'adsorption occupés. La présence de 0.1 M de Ba^{2+} et de Mg^{2+} dans la solution, ne semble pas affecter la relation existant entre l'adsorption de Co(II) sur l'alumine en fonction de l'ion hydrogène.

Les résultats de l'adsorption ont été analysés selon l'isotherme d'adsorption de Langmuir dans un grand intervalle de concentration en Co(II) (de 10^{-6} à 10^{-3} m). L'adsorption de Co(II) est un processus endothermique et croît fortement avec la température entre 30 et 100 °C. La chaleur d'adsorption décroît lorsque la surface recouverte en oxydes croît. Lorsque celle-ci atteint la saturation, les chaleurs d'adsorption de Co(II) sur Al_2O_3, MnO_2, et Fe_3O_4 sont respectivement de −14.9, −14.3, et −6.3 kcal/mol. On pense que l'hydrolyse de Co(II) est un mécanisme possible expliquant la dépendance marquée de l'adsorption en fonction du pH et de la température.

Canadian Journal of Chemistry, **50**, 1642 (1972)

Introduction

The adsorption of metal ions from aqueous solutions is of considerable practical importance in many areas. Our interest in the study of adsorption from solution lies in its possible role in the transport of radioactivity in water cooled nuclear reactors. In particular, the transport of cobalt adsorbed on corrosion product oxides seems to be an important factor in the growth of reactor radiation fields. The adsorption of Co(II) from solution by metal oxides is reported here as a function of solution pH, concentration and temperature.

Experimental

In this study small concentration changes due to adsorption were determined by counting γ-ray emissions from ^{60}Co tracer using a sodium iodide detector. A ^{60}Co solution of high specific activity, in the form of $Co(NO_3)_2$ was used as tracer. This was mixed with known amounts of inactive cobalt nitrate to give cobalt concentrations in the range of 10^{-7}–10^{-2} m. A count rate *vs.* concentration graph was found to be linear over a concentration range of four to five orders of magnitude. The concentrations of cobalt used for the calibration were also verified by atomic absorption spectroscopy. The precision of the cobalt determination in the concentration range $<10^{-5}$ m was ±10% and in concentrations $>10^{-5}$ m was ±5% (2σ).

Fe_3O_4 was synthesized by addition of ferrous sulfate to a solution of sodium hydroxide containing KNO_3 and was purified by repeated washing with conductivity water as described by Benton and Horsfall (1). Emission spectrographic analysis showed the following impurity concentrations in μg/g oxide: 17 Co, 19 Si, 5 Ni, and 100 Mn. Aluminum and magnesium were less than 1 μg/g. X-Ray diffraction data gave characteristic magnetite peaks.

The Al_2O_3 and MnO_2 used in the experiment were analytical grade reagents (Fisher Scientific Company) and were thoroughly washed with conductivity water to remove trace impurities. Analytical grade HNO_3, KNO_3, $BaCl_2$, and $Mg(NO_3)_2$ were used. The NaOH used was CO_2 free and was stored in plastic bottles.

Can. J. Chem. Downloaded from www.nrcresearchpress.com by 210.87.254.105 on 09/05/12
For personal use only.

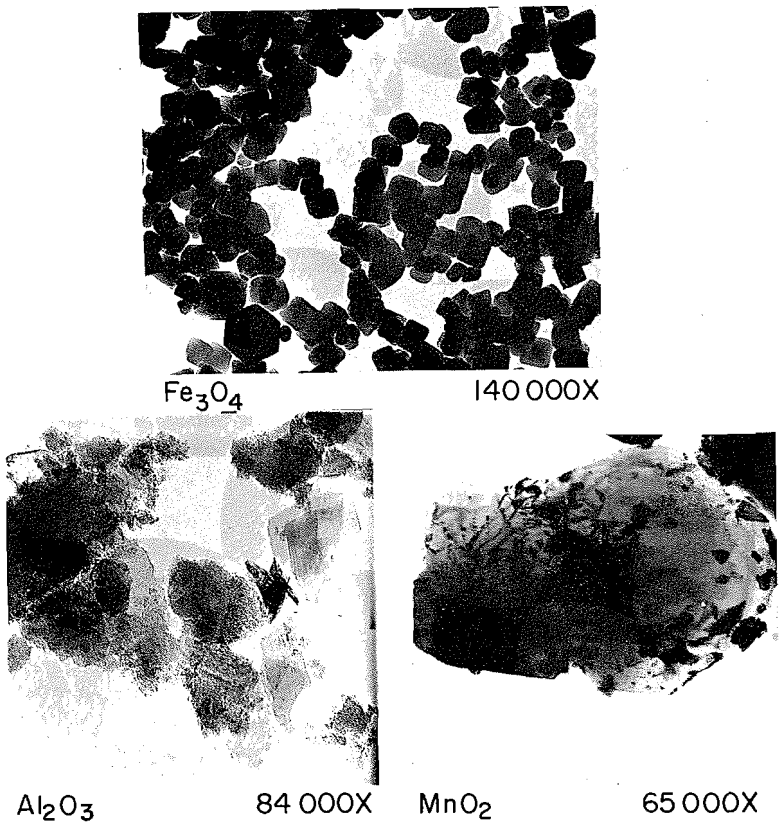

FIG. 1. Electron micrograph of: (*a*) Fe_3O_4, (*b*) Al_2O_3, (*c*) MnO_2.

Surface area measurements were obtained by the B.E.T. nitrogen adsorption method. The surface areas for Al_2O_3, Fe_3O_4, and MnO_2 were 247, 15, and 0.6 m^2/g, respectively.

Electron micrographs of the oxides were also obtained to further characterize the surfaces of the adsorbents. As evident from Fig. 1, the synthesized Fe_3O_4 was always a well formed crystalline material in contrast to Al_2O_3 and MnO_2 which showed ill-defined features.

When a known amount of the oxide was shaken with a Co^{2+} solution, the p*H* changed quite markedly due to the acidic or basic nature of the oxides. To avoid this, an automatic titrimeter (Fisher model 36) was used to maintain a constant p*H* during the adsorption experiments. HNO_3 was added to counteract basic reactions with Al_2O_3 and NaOH was added in acidic reactions for Fe_3O_4 and MnO_2. By these means the p*H* was maintained within ± 0.02 unit. Attempts to use chemical buffers to maintain the solution p*H* were not successful. In phosphate buffer, a significant portion of the activity was lost on centrifugation due to formation of highly insoluble cobalt phosphate and with borax buffer the capacity was exceeded.

A nitrogen atmosphere was maintained throughout the experiment. The temperature was controlled to ± 0.2 °C. Adsorption was continued for about 12 h for runs at temperatures up to 60 °C and for only about 6 h at 80 to 100 °C. Tests showed that these times were sufficient for equilibrium. The solution (including the oxide) was then centrifuged for half an hour at 15 000 r.p.m. The supernatant solution was analyzed for cobalt by determining the count rate for a 5 g sample.

In all adsorption experiments blank runs were performed to correct for any loss of activity due to adsorption on the reaction vessel or centrifugation tube. Glass vessels were found to adsorb a significant percentage of the Co^{2+} at lower concentrations. Polyethylene vessels were found to be satisfactory and were therefore used in all experiments.

Results

A marked increase in adsorption of cobalt on MnO_2 was observed with increasing p*H* as shown in Fig. 2. The percent of cobalt adsorbed on MnO_2 increased rapidly between p*H* 5 and 8. At p*H* values higher than 8 the percent of adsorption apparently levelled off. However, beyond this p*H*, activity losses due to $Co(OH)_2$ precipitation and adsorption could not be separated. A similar strong p*H* dependence for the adsorption of cobalt was exhibited by Fe_3O_4 and Al_2O_3.

Can. J. Chem. Downloaded from www.nrcresearchpress.com by 210.87.254.105 on 09/05/12
For personal use only.

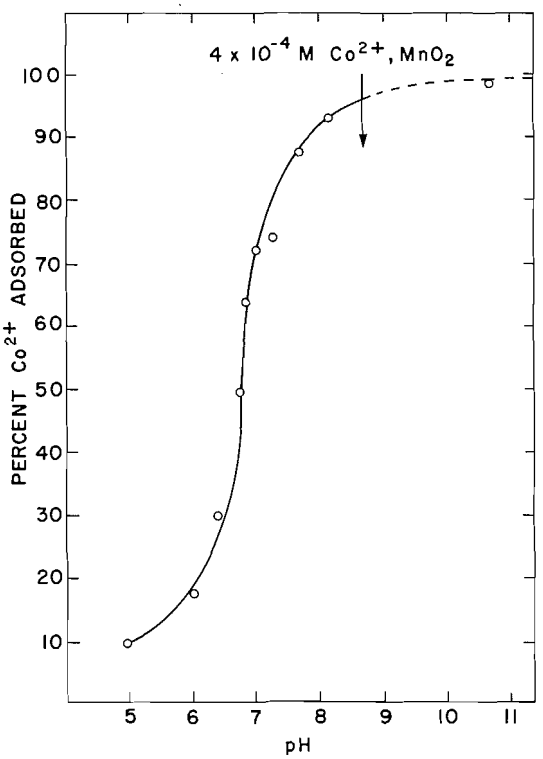

FIG. 2. Percentage of cobalt adsorbed on MnO_2 from solution (4×10^{-4} *m* Co^{2+}).

Experiments were also carried out to see the effect of ions such as Ba^{2+} and Mg^{2+} on the adsorption of cobalt. The presence of 0.1 *m* Ba^{2+} and Mg^{2+} in the solution did not have any significant effect on the hydrogen ion dependence of the adsorption of cobalt on alumina as shown in Fig. 3. The concentration of cobalt solutions in all the runs of this set was 4×10^{-4} *m* compared to 0.1 *m* of the competing Ba^{2+} and Mg^{2+} ions.

The adsorption results were analyzed by the Langmuir adsorption isotherm

$$[1] \qquad \theta = \frac{ac}{1 + ac}$$

where θ is the fraction of occupied adsorption sites, c is the equilibrium solution concentration and a is a constant related to the intensity of adsorption. For the case of adsorption in solutions eq. 1 may be represented as (2, 3)

$$[2] \qquad \frac{c}{w} = \frac{c}{M} + \frac{1}{aM}$$

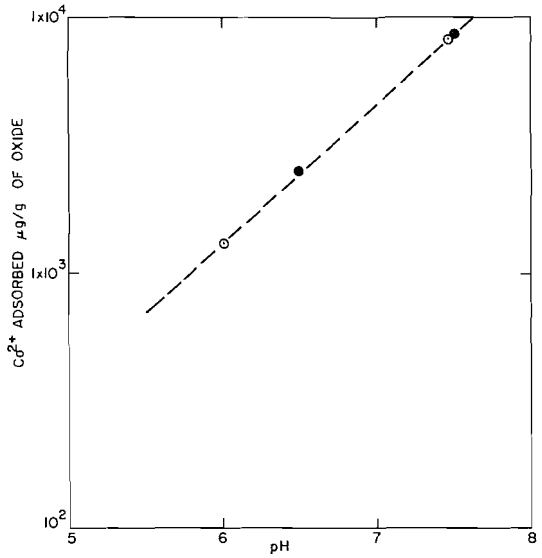

FIG. 3. Effect of competing Ba^{2+} and Mg^{2+} ions (0.1 *m*) on the hydrogen ion dependence of adsorption of cobalt on Al_2O_3 at 30 °C. Dashed line: adsorption of cobalt *vs.* p*H* without competing ions, Co(II) concentration 4×10^{-4} *m*. ○, Adsorption of cobalt in presence of 0.1 *m* Ba^{2+} ions; ●, adsorption of cobalt in presence of 0.1 *m* Mg^{2+}.

where c is the equilibrium concentration, w is the amount of absorbate per unit amount of adsorbent for a given concentration, M is the saturation amount of adsorbate per unit amount of the adsorbent and a is the same constant as in eq. 1. A Langmuir plot showing conformity of the data with eq. 2 is presented in Fig. 4.

From the slopes of the linear plots of c/w *vs.* c, the value of M, the capacity for adsorption for the oxides has been determined. The saturation values M for cobalt adsorption for Al_2O_3 and MnO_2 at p*H* 6 are 6.6×10^{-4} and 4.2×10^{-2} $\mu g/cm^2$, respectively. For Fe_3O_4 at p*H* 6.5 the M value is 3.7×10^{-2} $\mu g/cm^2$.

Discussion

Effect of Temperature

The adsorption process for cobalt on the oxides studied here is markedly endothermic. An endothermic adsorption of Co^{2+} on montmorillonite is also reported by Hodgson (4) between 25 and 55 °C. However, Chester (5) has found that while adsorption of Co^{2+} from sea water on illite increases with increasing temperature, the adsorption of Zn^{2+} decreases. Dyck (6) found no change in adsorption of

Can. J. Chem. Downloaded from www.nrcresearchpress.com by 210.87.254.105 on 09/05/12
For personal use only.

Can. J. Chem. Downloaded from www.nrcresearchpress.com by 210.87.254.105 on 09/05/12
For personal use only.

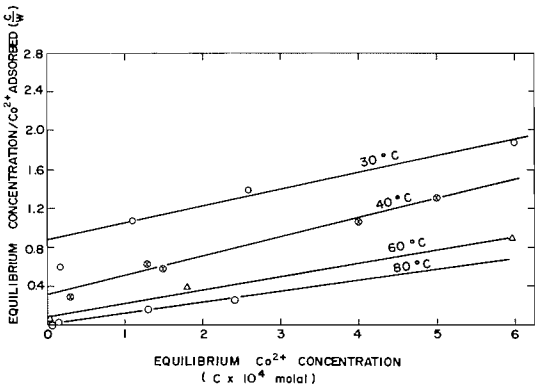

FIG. 4. Langmuir adsorption isotherm of Co on Al_2O_3 at pH 6.

silver ion on ferric oxide over the temperature range 25 to 50 °C. Endothermic adsorption of a colloidal dye on solid surfaces in aqueous solutions is reported by Giles *et al.* (7–9) and aggregation of the dye is thought to be responsible for the increased adsorption. An increase in adsorption with temperature has also been found for polymers on metal powders (10), and for some metal ions on glass, steel, and polyvinyl chloride (11).

Calculation of Heat of Adsorption

From the linear plots of c/w *vs.* c of eq. 2 M is derived from the slope. The ratio of slope/intercept determines the value of a. a is related to the heat of adsorption ΔH as follows (2, 3)

$$[3] \qquad a = a' \, e^{\Delta H/RT}$$

Thus from ln a *vs.* $1/T$ plots, the value of ΔH is calculated for saturation adsorption. Such a plot for Al_2O_3 is given in Fig. 5. The heats of adsorption calculated for Al_2O_3, MnO_2, and Fe_3O_4 from the above procedure are -14.9, -14.3, and -6.3 kcal/mol, respectively.

The heat of adsorption, ΔH_x, may also be calculated from the integrated form of the Clausius–Clapeyron relationship,

$$[4] \qquad \Delta H_x = R \left(\frac{\partial \ln c}{\partial (1/T)} \right)$$

The heat of adsorption calculated in this manner is always a function of surface coverage x. The value of ΔH_x may be obtained from the linear plot of log c *vs.* $1/T$ for a fixed coverage of the solid (Fig. 6). Table 1 gives the ΔH_x values for the oxides at different coverages.

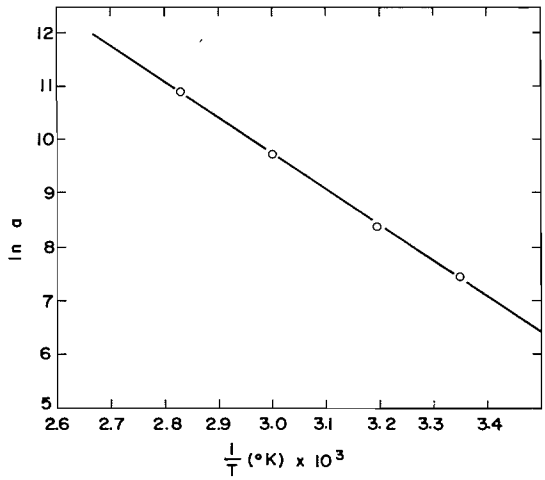

FIG. 5. Plot of ln a *vs.* $1/T$ for cobalt adsorption on Al_2O_3 at pH 6.

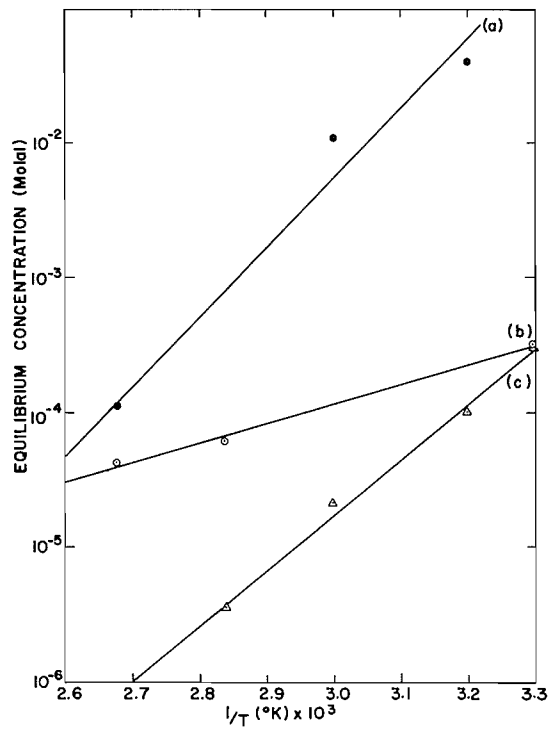

FIG. 6. Clausius–Clapeyron plot of log c *vs.* $1/T$: (a), MnO_2, surface coverage 1.67×10^{-2} μg/cm^2 at pH 6; (b), Fe_3O_4, surface coverage 3.3×10^{-2} μg/cm^2 at pH 6.5; (c), Al_2O_3, surface coverage 2×10^{-4} μg/cm^2 at pH 6.

It is seen from Table 1 that the value of ΔH_x decreases with surface coverage. A steady decrease of heat of adsorption with increasing

TABLE I. ΔH_x values for the oxides at different coverages

Oxide	pH	Coverage $\mu g/cm^2$	ΔH_x (kcal/mol)
MnO_2	6.0	1.0×10^{-2}	−22.2
		2.0×10^{-2}	−20.8
		*4.2×10^{-2}	−14.3
Al_2O_3	6.0	8.0×10^{-5}	−20.5
		2.0×10^{-4}	−18.7
		*6.6×10^{-4}	−14.9
Fe_3O_4	6.5	2.2×10^{-2}	−7.3
		3.3×10^{-2}	−6.6
		*3.7×10^{-2}	−6.3

*Saturation value.

amount of adsorption has been reported in the literature (12). The values of ΔH_x at saturation, for Al_2O_3 and MnO_2 are almost the same, −14.9 and −14.3 kcal/mol respectively. The above values compare favorably with the value of −16 kcal/mol for Co^{2+} adsorption on montmorillonite reported by Hodgson (4). The saturation ΔH_x value for Fe_3O_4 is only −6.3 kcal/mol. The reason for this low value of ΔH_x for Fe_3O_4 is not known. Fe_3O_4 was synthesized in the laboratory. It had well defined crystalline features (Fig. 1) and was probably much more hydrated because it had not been subjected to temperatures higher than 80 °C. Al_2O_3 and MnO_2, on the other hand, were commercial samples. The synthetic Fe_3O_4 might be easily hydroxylated which might facilitate the surface reaction.

Effect of pH

The adsorption of Co^{2+} on the oxides increases with increasing pH. A similar increased adsorption of metal ions by oxides with increasing pH has been reported by Kurbatov *et al.* (13), Von Grimme (14), Stryker and Matijevic (15 and references therein) and others (16–18). In general the hydrolysis of the adsorbing metal ions has been assumed to be responsible for the enhanced adsorption, although the use and the meaning of the term hydrolysis is not always consistent (15).

Hodgson *et al.* (16) point out that the enhanced adsorption of metal ions on clay mineral surfaces with increasing pH may be explained either by a mechanism involving prior hydrolysis of the metal ions in solution (reaction 5) to give a hydrolysis product which is more strongly adsorbed (reaction 6) or by a mechanism involving direct exchange of the unhydrolyzed ion (reaction 7) with a specific group on the adsorbing surface

$$[5] \qquad [M^{2+}] + [H_2O] \rightleftarrows [MOH^+] + [H^+]$$

$$[6] \qquad [MOH^+] + [X^-] \rightleftarrows [XMOH]$$

$$[7] \qquad [M^{2+}] + [HX] \rightleftarrows [M^+X] + [H^+]$$

where X represents the adsorbing surface and $[M^{2+}]$ and $[MOH^+]$ represent $[Co^{2+}]$ and $[CoOH^+]$, respectively.

Hodgson *et al.* (16) have shown that the two hypotheses cannot be distinguished on the basis of variations in θ with $[H^+]$, as both mechanisms exhibit the same type of pH dependence. However, the two mechanisms may be differentiated if a non-hydrolyzable bivalent competing ion is used. They have derived equations showing that θ for the adsorption process represented by reaction 7 will be independent of $[H^+]$ in the presence of a large concentration of nonhydrolyzable competing ions. Conversely, for the hydrolysis mechanism θ will still depend inversely on the hydrogen ion concentration.

In experiments, where Ba^{2+} and Mg^{2+} ions (0.1 m concentration) have been used, there seems to be no noticeable effect of the competing ions on the $[H^+]$ dependence of θ, *i.e.*, the slopes of the θ *vs.* pH plot for the adsorption of Co^{2+} on alumina both in the presence and absence of the competing ions are identical as shown in Fig. 3. This suggests hydrolysis as the dominant mechanism. It may be pointed out here that Ba^{2+} and Mg^{2+} ions have been shown (19) to remain unhydrolyzed above the pH values that have been used in this work.

To further test the hydrolysis mechanism eq. 1 may be rearranged on the consideration of the equilibria of the cobalt in solution (20). If C is the total concentration of cobalt in solution, then

$$C = [Co^{2+}] + [CoOH^+]$$

$$[Co^{2+}] = \frac{C[H^+]}{[H^+] + K}$$

and

$$[CoOH^+] = \frac{CK}{[H^+] + K}$$

where K is the hydrolysis constant of reaction 5. Substituting this value of $[CoOH^+]$ in eq. 1 the Langmuir adsorption isotherm reduces to

Can. J. Chem. Downloaded from www.nrcresearchpress.com by 210.87.254.105 on 09/05/12
For personal use only.

Can. J. Chem. Downloaded from www.nrcresearchpress.com by 210.87.254.105 on 09/05/12
For personal use only.

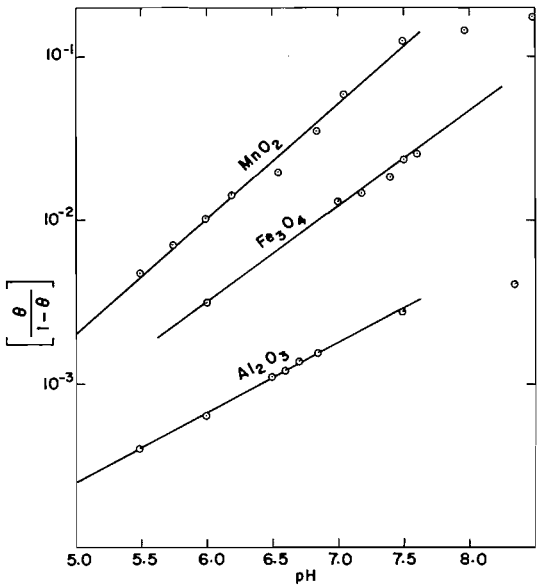

FIG. 7. Plot of log $\theta/(1-\theta)$ *vs.* p*H* plot at 30 °C for cobalt adsorption on Al_2O_3, MnO_2, and Fe_3O_4.

$$\theta = \frac{aKC}{[H^+] + K + aKC} \quad [8]$$

or

$$\frac{1}{\theta} = \frac{[H^+]}{aKC} + \frac{1}{aC} + 1 \quad [9]$$

The above equation predicts that a plot of $1/\theta$ *vs.* $[H^+]$ at a constant C will be linear. As the H^+ concentration used in the experiment varies many orders of magnitude, a more convenient plot will be log $\theta/(1-\theta)$ *vs.* p*H*. In a log form eq. 9 reduces to

$$\log \theta/(1-\theta) = \log aKC + pH - \log (1 + K/[H^+]) \quad [10]$$

Equation 10 predicts that under conditions of $K \ll [H^+]$ a plot of log $\theta/(1-\theta)$ *vs.* p*H* is linear. In the present case $K \ll [H^+]$. The plots as predicted are linear as shown in Fig. 7. The linearity is not obeyed above p*H* 7.5. Equation 10 predicts non-linearity at higher p*H*.

Equation 9 can be further rearranged to give

$$\frac{1}{\theta} = \frac{1}{C}\left[\frac{[H^+]}{aK} + \frac{1}{a}\right] + 1 \quad [11]$$

Equation 11 predicts that at constant $[H^+]$, a plot of $1/\theta$ *vs.* $1/C$ will be linear. For Al_2O_3 at p*H* 6, a plot of $1/\theta$ *vs.* $1/C$ is found to be linear over a wide range of concentration, as predicted, and is shown in Fig. 8. The results for Fe_3O_4 exhibit a similar plot. These results are consistent with the hydrolysis mechanism for the enhanced adsorption of Co^{2+} with increasing p*H*.

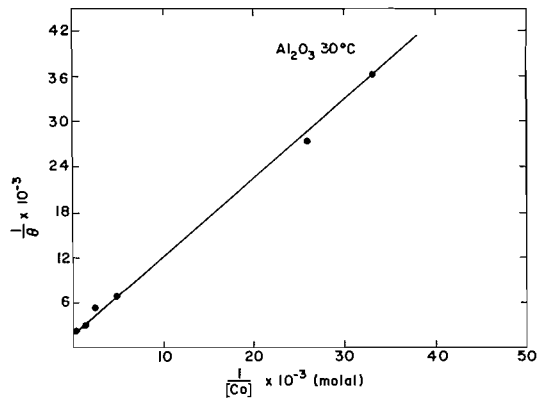

FIG. 8. Plot of $1/\theta$ *vs.* $1/C$ plot for Al_2O_3 at p*H* 6, temperature 30 °C.

The values of K were calculated from the slopes of the linear plots of eq. 11 and by substituting the values of a from the plots of eq. 2. The pK values thus calculated decreased with increasing temperature. (It decreased from 9.4 at 30 °C to 8.9 at 80 °C.) A decrease in pK or an increase in K with temperature was also reported by Bolzan and Arvia (21) (a decrease from 9.8 at 25 °C to 9.5 at 45 °C). However, the calculated pK values are lower than the reported values by 0.3 to 0.4 unit.

Matijevic *et al.* (22) found that the adsorption of thorium on AgI increased above p*H* 3.82, (equivalent to pK) where the ratio of hydrolyzed thorium to TH^{4+} also increased markedly. Between p*H* 5.5 and 7 the dominant species calculated from the pK is Co^{2+} and not $CoOH^+$. The adsorption increase thus does not correspond to the p*H* where the $[CoOH^+]/[Co^{2+}]$ ratio increases, based on the known pK (20). However, it is not necessary that the ratio $[Co(OH)^+]/[Co^{2+}]$ has to be greater than one for the adsorption of hydrolysis products on the surface. The hydrolysis products formed at p*H* values lower than pK may be adsorbed and the increased adsorption may be noticeable at p*H* values much lower than pK. A similar increase of Co^{2+} adsorption has been reported on silica (18) and for Cu^{2+}, Zn^{2+}, Mn^{2+}, and

Co^{2+} on goethite (14) at pH values much below the value of pK. Furthermore, at interfaces the pH for hydrolysis reactions may not correspond to the pH in the bulk solution. It has been reported (15) that hydrolysis products may be formed at solid–liquid interfaces at concentrations well below those for saturation or precipitation in the solution. The formation of a polymeric cobalt hydroxide has been reported (18) at a silica surface at concentrations below those for saturation or precipitation of cobalt. Ragland and Coleman (23) have also reported that hydrolysis of aluminum chloride can occur at pH values as low as 3.4 in presence of large interfacial surfaces, compared to a pK of 5.5.

Though quantitative agreement between the known hydrolysis constant of cobalt and the pH range over which the enhanced adsorption takes place is lacking, the hydrolysis mechanism satisfactorily explains the results of the adsorption studies and the increased adsorption of cobalt on the oxides with pH.

The assistance of our colleagues in the Analytical Science Branch for the surface area measurements of the oxides, for emission-spectrographic and atomic absorption analysis, and of Messrs. A. M. Duclos and E. E. Sexton for X-ray diffraction and electron-micrograph work is gratefully acknowledged. The authors thank Mr. G. W. A. Claus for the literature survey.

1. D. P. Benton and G. A. Horsfall. J. Chem. Soc. 3899 (1962).
2. A. W. Adamson. Physical chemistry of surfaces. 2nd ed. Interscience Publishers, N.Y. 1967. p. 401.
3. D. N. Misra. J. Colloid and Interface Sci. **28**, 24 (1968).
4. J. F. Hodgson, H. R. Geering, and Martha Fellows. Soil Sci. Soc. Am. Proc. **28**, 39 (1964).
5. R. Chester. Nature, **206**, 884 (1965).
6. W. Dyck. Can. J. Chem. **46**, 1441 (1968).
7. C. H. Giles, J. J. Greczek, and S. N. Nakhwa. J. Chem. Soc. 93 (1961).
8. J. J. Kipling. Adsorption from solutions of non-electrolyte. Academic Press. 1965. p. 264.
9. J. H. De Boer. Advan. Catal. **9**, 427 (1957).
10. J. Koral, R. Ullman, and F. R. Elrich. J. Phys. Chem. **62**, 541 (1958); referred in ref. 8, p. 158.
11. F. Kepak. Chem. Rev. **4**, 357 (1971).
12. A. W. Adamson. Physical chemistry of surfaces. 2nd ed. Interscience Publishers, N.Y. 1967. p. 617.
13. M. H. Kurbatov, G. B. Wood, and J. D. Kurbatov. J. Phys. Chem. **55**, 1170 (1951).
14. Von H. Grimme. Z. Pflanzenernach, Bodenk, **121** (1), 58 (1968).
15. L. J. Stryker and E. Matijevic. Advances in chemistry, series 79, 1968, p. 45.
16. J. F. Hodgson, K. G. Tiller, and M. Fellows. Soil Sci. Soc. Am. Proc. **28**, 42 (1964).
17. R. G. Menzel and M. L. Jackson. Soil Sci. Soc. Am. Proc. **15**, 122 (1951).
18. T. W. Healy, R. O. James, and R. Cooper. Advances in chemistry series 79, 1968, p. 62.
19. R. H. Ottewill and J. N. Shaw. Discuss. Faraday Soc. **42**, 154 (1966).
20. J. Bjerrum, G. Schwarzenback, and L. G. Sillen. Stability constants. London Chem. Soc., London. 1956.
21. J. A. Bolzan and A. J. Arvia. Electrochim. Acta, **17**, 589 (1962).
22. E. Matijevic, M. B. Abramson, R. H. Ottewill, K. F. Schulz, and M. Kerker. J. Phys. Chem. **65**, 1724 (1961).
23. J. L. Ragland and N. T. Coleman. Soil Sci. Soc. Am. Proc. **24**, 457 (1960).

Can. J. Chem. Downloaded from www.nrcresearchpress.com by 210.87.254.105 on 09/05/12
For personal use only.

Equilibrium Constants for 2,3-Dihydroxypyridine and its Complex with Iron(III) in 1 *M* Hydrochloric Acid

K. E. CURTIS AND G. F. ATKINSON

Department of Chemistry, University of Waterloo, Waterloo, Ontario

Received November 4, 1971

Improved values for two acidity constants of 2,3-dihydroxypyridine have been computed using program PITMAP. The composition of the complex with iron(III) and its conditional and overall stability constants in 1 *M* hydrochloric acid have been evaluated.

On a calculé par ordinateur les valeurs améliorées des deux constantes d'acidité du 2,3-dihydroxypyridine en utilisant le programme PITMAP. On a évalué aussi la composition du complexe avec le fer(III) et ses constantes de stabilité globales dans l'acide chlorhydrique 1 *M*.

Canadian Journal of Chemistry, **50**, 1649 (1972)

Can. J. Chem. Downloaded from www.nrcresearchpress.com by 210.87.254.5 on 09/05/12
For personal use only.

In a previous report from this laboratory (1), 2,3-dihydroxypyridine (DHP) was shown to react with iron(III) in mineral acid media 1.0 *M* in hydrogen ion to form blue complex species of metal-to-ligand ratios of 1:1. A spectrophotometric procedure for the analysis of iron(III) in 1.0 *M* hydrochloric acid has been developed (2). This work reinvestigates the acidity constants of DHP and reports on the complex composition and the conditional and overall stability constants of the complex with iron(III) in 1.0 *M* hydrochloric acid solution.

Experimental

Reagents

Iron(III) chloride solutions were prepared by dilution with 1.0 *M* hydrochloric acid solution from a 9.110×10^{-2} *M* stock solution prepared and standardized as before (1). Solutions of DHP were prepared by dissolving accurately weighed amounts of the sublimed reagent in a known volume of the appropriate solvent. Other chemicals were reagent grade and were tested as necessary for the absence of interfering impurities. Water used was deionized, distilled, and deaerated with nitrogen.

Apparatus

Absorbance measurements were made at 25 °C with a double beam Cary 14 recording spectrophotometer using fused quartz cells (10 mm) throughout. An Orion Model 801 p*H* meter with a glass and calomel electrode pair calibrated as a concentration probe was used to measure hydrogen ion concentration (3). All volumetric ware was Class A and all pipettes were calibrated.

Computations were performed on an IBM 360/75 computer with graphical output plotted by a Calcomp 763 digital incremental plotter.

Determination of the Acidity Constants of DHP

The p*H* of twenty-two solutions of DHP concentration 1.500×10^{-4} *M* was adjusted with standardized potassium hydroxide and/or hydrochloric acid solutions to give a range of $[H^+] = 9.50$ *M* to a p*H* of 13.12. The ionic strength of solutions between p*H* 0 and 14 was maintained at 1.0 by means of potassium chloride solution but constancy was sacrificed at higher acidities in order to determine the "approximate protonation constant" (4) of DHP. The spectrum of each of these solutions was recorded between 220 and 315 nm against a reference solution of a solvent blank, corrected for baseline, and absorbance values at every 5 nm tabulated. The p*H* of each solution between 0 and 14 was measured while the spectrum was being recorded, while those of the solutions of higher acidities were calculated from known hydrogen ion concentrations. These data were then submitted to the computer program PITMAP (5).

Investigations of the DHP–Iron(III) Complex

Two procedures were used:

(*a*) Following the method of Heller and Schwarzenbach (6) as modified by Budesinsky and Haas (7, 8) and the method of proportional absorbances of Budesinsky (9, 10), three sets of solutions were prepared so that while iron and DHP were kept equimolar in all cases, the iron and DHP, the chloride ion, and the hydrogen ion concentrations respectively were varied within each set. The hydrogen ion concentration was altered or kept constant at 1.0 *M* as required, with standardized perchloric acid solution, while the chloride ion concentration was similarly controlled by means of a standard sodium chloride solution. Details of all solutions are given in Table 1.

The spectrum of each solution was recorded from 700 to 500 nm against an appropriate solvent blank, corrected for baseline and absorbance values digitized every 50 nm.

(*b*) Eight spectra were recorded from 700 to 500 nm against the appropriate solvent blanks, for solutions of constant iron(III) concentration 7.916×10^{-4} *M* but with varying DHP concentrations. In this way, metal-to-ligand molar ratios of 0.5, 1.0, 2.5, 5.0, 10.0, 15.0, 20.0, and 25.0 in 1.0 *M* hydrochloric acid solution were obtained. After correction for baseline, the absorbance was digitized at 5 nm intervals. The p*H* of each solution was measured and these data, along with other known information, were submitted to PITMAP for computation of the overall stability constant of the complex.

Can. J. Chem. Downloaded from www.nrcresearchpress.com by 210.87.254.5 on 09/05/12
For personal use only.

TABLE 1. Composition of solutions used for the method of Budesinsky (7–10).

Set 1			Set 2			Set 3		
$C_{Fe} = C_{DHP}$ ($M \times 10^3$)	C_{H^+} (M)	C_{Cl^-} (M)	$C_{Fe} = C_{DHP}$ ($M \times 10^3$)	C_{H^+} (M)	C_{Cl^-} (M)	$C_{Fe} = C_{DHP}$ ($M \times 10^3$)	C_{H^+} (M)	C_{Cl^-} (M)
4.157	0.950	0.950	2.772	1.013	0.502	2.772	0.494	1.064
2.079	0.950	0.950	1.386	1.013	0.502	1.386	0.494	1.064
3.464	0.950	0.950	2.772	1.013	0.754	2.772	0.734	1.064
1.732	0.950	0.950	1.386	1.013	0.754	1.386	0.734	1.064
2.772	0.950	0.950	2.772	1.013	1.005	2.772	0.974	1.064
1.386	0.950	0.950	1.386	1.013	1.005	1.386	0.974	1.064
2.079	0.950	0.950	2.772	1.013	1.257	2.772	1.214	1.064
1.039	0.950	0.950	1.386	1.013	1.257	1.386	1.214	1.064
1.386	0.950	0.950	2.772	1.013	1.508	2.772	1.454	1.064
0.693	0.950	0.950	1.386	1.013	1.508	1.386	1.454	1.064

Can. J. Chem. Downloaded from www.nrcresearchpress.com by 210.87.254.5 on 09/05/12
For personal use only.

Results and Discussion

The Acidity Constants of DHP

The accepted mechanism for the stepwise deprotonation of DHP:

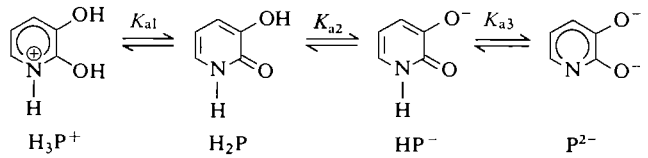

Evidence has been produced to support this order of proton removal, especially the tautomeric shift to the lactam structure for H_2P (11). Comparison with the known pK_a values for similar reagents also lends weight to the mechanism. In an extensive study of the spectral properties and ionization constants of substituted 2-hydroxypyridines, Spinner and White (11) have given values for pK_{a1} and pK_{a2} for DHP, with the third constant being reported as inaccessible. However, the value for pK_{a1}, of the order of 0.2, was reported with a rather large degree of uncertainty. The study of the reagent in media 1.0 *M* in hydrogen ion made it necessary to obtain a better value. Consequently, the computer program PITMAP, written by Metzler (12) and extensively modified in our laboratory (5) was used to compute a new set of pK_a values. The results are shown in Table 2, along with the wavelengths of maximum absorbance for each species. No evidence for the dissociation of the third proton was found up to a p*H* of 14.

PITMAP also supplies molar absorptivities of the individual species over the wavelength range, which may be plotted as shown in Fig. 1. When these values, along with the constants obtained, are submitted to program PLOT (5), spectra based on the optimized mathematical model are derived and compared graphically with the experimental input absorbances. Five such comparisons are shown in Fig. 2 and excellent agreements were also obtained with the other seventeen spectra.

The complex with iron(III) in 1.0 M hydrochloric acid solution

The general equation for the formation of the complex may be written as

[1] $$Fe_mCl_i + H_jP_n \rightleftharpoons Fe_mCl_iH_jP_n$$

It was already known from previous work (1) that the ratio of m:n was 1:1. The absolute values of m, i, j, and n were found and the overall stability constant determined by the method of Budesinsky and Haas (7–9), taking into account the side reactions of the ligand with hydrogen ion and of the metal with chloride ion. It was assumed that HP^- rather than P^{2-} was the most deprotonated species of the ligand, a valid assumption when working in acidities of 1.0 *M*. The overall stability constant was therefore represented by β^*_{mijn} to indicate this modification. The conditional stability constant was determined by the method of proportional absorbances (9, 10) supplemented by a table of computed values for log y and x_{mn} (13).

The mathematical treatment of the various relationships in these procedures gave the expression

[2] $$\log \beta^*_{mijn} = \log K_{mn} + m \log \alpha_{Fe(Cl)} + n \log \alpha_{HP(H)} + i\mathrm{p[Cl]} + (j-1)\mathrm{p[H]}$$

where

α represents the coefficient of a side reaction (14)

$$\beta^*_{mijn} = \frac{[Fe_mCl_iH_jP_n]}{[Fe]^m[Cl]^i[H]^{j-n}[HP]^n}$$

$$K_{mn} = \frac{[Fe_mCl_iH_jP_n]}{(C_{Fe} - m[Fe_mCl_iH_jP_n])^m(C_P - n[Fe_mCl_iH_jP_n])^n}$$

During the determination of K_{mn}, the absolute values of m and n were found to be unity, as shown in Table 3. Equation 2 then became

[3] $$\log \beta^*_{1ij1} = \log K_{11} + \log \alpha_{Fe(Cl)} + \log \alpha_{HP(H)} + i\mathrm{p[Cl]} + (j-1)\mathrm{p[H]}$$

TABLE 2. pK_a values for the deprotonation of DHP

Species	λ_{max} (nm)	pK_a	σ
H_3P^+	227, 291	0.107	0.007
H_2P	234, 297	8.694*	0.007
HP^-	255, 311		
P^{2-}	not observed		

*Value of $pK_a = 8.7$ found by potentiometric titration.

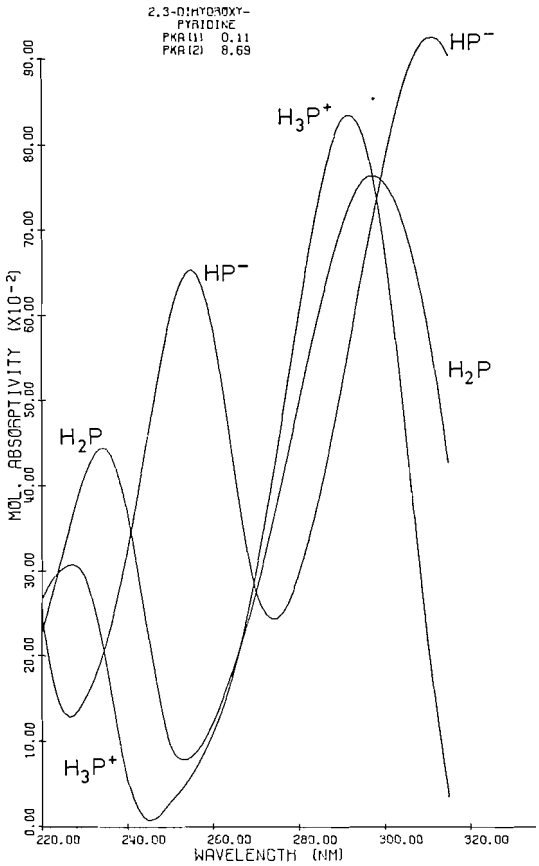

FIG. 1. Computed spectra of DHP species.

Then, at constant C_{Fe}, C_{DHP}, and $[H^+]$, eq. 3 reduced to

$$[4] \qquad \log K_{11}\alpha_{Fe(Cl)} = \text{constant} - i\text{p[Cl]}$$

The calculated dependence of $\log K_{11}\alpha_{Fe(Cl)}$ on p[Cl] was plotted in Fig. 3, in which the slope of the curve indicated a value of $-i = -1$, making the complex composition $FeClH_jP$. Similarly, at constant C_{Fe}, C_{DHP}, and $[Cl^-]$, eq. 3 became

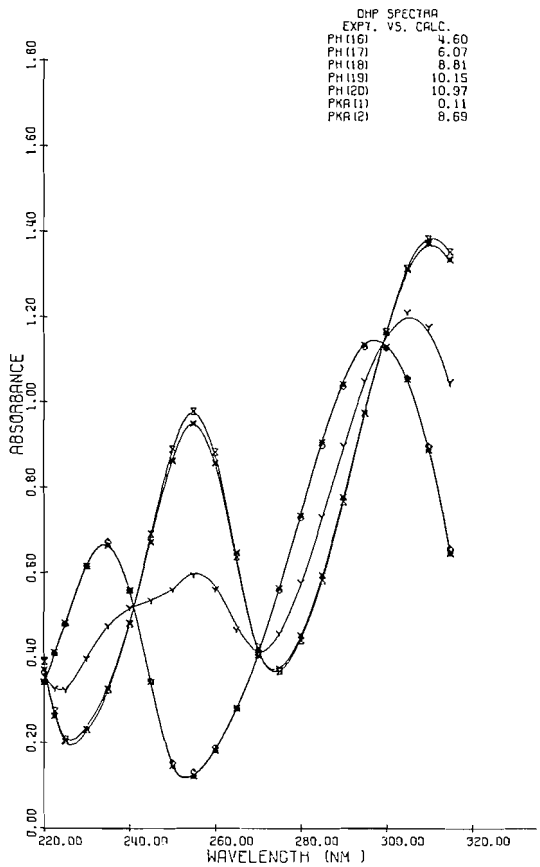

FIG. 2. Experimental (symbols) *vs.* calculated (solid lines) spectra of DHP solutions. Symbols for various p*H* values are ⁎, 4.60; ◇, 6.07; Y, 8.81; □, 10.15; ⧖, 10.97.

TABLE 3. Determination of m and n and the conditional stability constant

$-\log C_{Fe}$	x_{mn}*	$-\log y_{11}$	$\log K_{11}$†	$-\log y_{22}$	$\log K_{22}$†
2.38	1.539	−0.25	2.13	1.03	8.17
2.46	1.574	−0.33	2.13	0.97	8.35
2.56	1.621	−0.43	2.13	0.92	8.59
2.68	1.681	−0.56	2.12	0.79	8.83
2.86	1.749	−0.73	2.13	0.69	9.26

*$\lim_{y\to\infty} x_{11} = 2.00$ and $\lim_{y\to\infty} x_{22} = 8.00$ under the experimental conditions. The observed variation of x_{mn} therefore indicates $m = n = 1$.
†By inspection, $\log K_{11}$ values are more constant than those for $\log K_{22}$, confirming $m = n = 1$.

$$[5] \qquad \log K_{11}\alpha_{HP(H)} = \text{constant} - (j-1)\text{p[H]}$$

This plot is also shown in Fig. 3, a slope of $-(j-1) = 0$ being obtained. The final complex composition was thus FeClHP. Introducing this

Can. J. Chem. Downloaded from www.nrcresearchpress.com by 210.87.254.5 on 09/05/12
For personal use only.

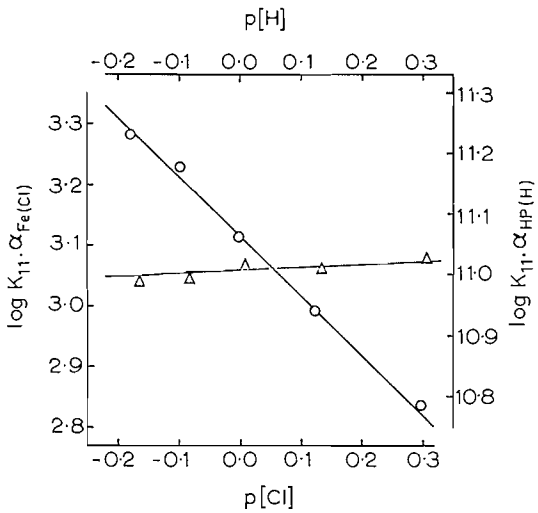

FIG. 3. Determination of the coefficients i and j in the complex $FeCl_iH_jP$. ○, left and lower scales show $i = 1$; △, right and upper scales show $(j - 1) = 0$.

information into eq. 3 gave

$$[6] \quad \log \beta^*_{1111} = \log K_{11} + \log \alpha_{Fe(Cl)} + \log \alpha_{HP(H)} + p[Cl]$$

Calculations then gave $\log \beta^*_{1111} = 12.13$ with a standard deviation of 0.06.

Using this value as an initial estimate of the true answer, program PITMAP was used to compute a value for the overall constant.[1] Subroutine EQUIL, which calculates concentrations of the individual species present, was rewritten for the proposed model FeClHP. Other input data for the program included molar absorptivities for all the metal and ligand species present (conveniently zero in all cases as neither absorbed in the wavelength region studied), the pK_a values computed above, $\log \beta$ values for the iron(III) chloride system (15), and for each solution, the pH, concentration of iron and DHP, and the digitized spectrum. An answer of $\log \beta^*_{1111} = 12.127$ with a standard deviation of 0.002 was obtained, in satisfactory agreement with the previous value found. Figure 4 shows the experimental *vs.* calculated spectra.

[1]More recent and convenient versions of the computer programs used may be obtained by requesting "Computer Programs for the Analysis of Electronic Absorption Spectra" from Dr. J. A. Thomson, Department of Biochemistry and Biophysics, Iowa State University, Ames, Iowa 50010, U.S.A.

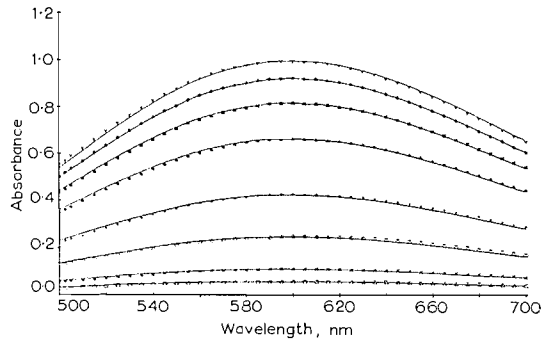

FIG. 4. Experimental (symbols) *vs.* calculated (solid lines) spectra of the complex FeClHP at various concentrations of DHP. Symbol for various [L]/[M] ratios are □, 0.5; ×, 1.0; ○, 2.5; +, 5.0; △, 10.0; ✳, 15.0; ◇, 20.0; Y, 25.0.

Summary

Improved values for two of the acidity constants of 2,3-dihydroxypyridine have been computed using program PITMAP.

Using these values, the overall stability constant of the complex with iron(III) in 1.0 *M* hydrochloric acid solution has been evaluated by two different procedures. One of these procedures also shows the composition of the complex to be FeClHP and gives a value of the conditional stability constant.

The values for the constants found are

$$pK_{a1} = 0.10_7 \quad \sigma = 0.007 \quad \text{for} \quad H_3P^+ \rightarrow H_2P + H^+$$

$$pK_{a2} = 8.69_4 \quad \sigma = 0.007 \quad \text{for} \quad H_2P \rightarrow HP^- + H^+$$

$$\log K_{11} = 2.13$$

$$\log \beta^*_{1111} = 12.12_7 \quad \sigma = 0.002$$

This work was supported in part by a National Research Council of Canada grant. One of us (K.E.C.) also acknowledges with thanks the award of an American Chemical Society Analytical Fellowship sponsored by the Society for Analytical Chemists of Pittsburgh, and of an N.R.C.C. Scholarship. We wish to thank Dr. J. A. Thomson for making the computer programs available and for his assistance in their use, and Dr. B. Budesinsky for valuable discussions.

1. K. E. CURTIS, J. A. THOMSON, and G. F. ATKINSON. Anal. Chim. Acta, **49**, 351 (1970).
2. K. E. CURTIS and G. F. ATKINSON. Presented at the Pittsburgh Conference on Analytical Chemistry and Applied Spectroscopy, Cleveland, Ohio, 2nd March 1971.

Can. J. Chem. Downloaded from www.nrcresearchpress.com by 210.87.254.5 on 09/05/12
For personal use only.

3. W. A. E. McBryde. Analyst (London), **94**, 337 (1969).
4. W. A. E. McBryde. Can. J. Chem. **43**, 3472 (1965).
5. J. A. Thomson and G. F. Atkinson. Talanta, **18**, 817 (1971).
6. J. Heller and G. Schwarzenbach. Helv. Chim. Acta, **34**, 1876 (1951).
7. B. Budesinsky and K. Haas. Acta Chim. Acad. Sci. Hung. **39**, 7 (1963).
8. B. Budesinsky. Z. anal. Chem. **195**, 244 (1963).
9. B. Budesinsky. Z. anal. Chem. **209**, 379 (1965).
10. B. Budesinsky. J. Inorg. Nucl. Chem. **31**, 1345 (1969).
11. E. Spinner and J. C. B. White. J. Chem. Soc. B, 991 (1966).
12. K. Nagano and D. E. Metzler. J. Am. Chem. Soc. **89**, 289 (1967).
13. D. J. Leggett and B. Budesinsky. Unpublished results.
14. G. Schwarzenbach. Complexometric titrations. Interscience, New York, 1957.
15. E. Rabinowitch and W. H. Stockmayer. J. Am. Chem. Soc. **64**, 335 (1942).

Can. J. Chem. Downloaded from www.nrcresearchpress.com by 210.87.254.5 on 09/05/12
For personal use only.

Evaluation of Unbonded O—H Groups for HDO in Liquid D_2O from Infrared Absorptivity Measurements[1]

E. C. W. CLARKE AND D. N. GLEW

Research Department, Dow Chemical of Canada, Limited, Sarnia, Ontario

Received October 18, 1971

Wyss and Falk's infrared absorptivities between 10 and 85 °C for HDO in liquid D_2O in the fundamental O—H stretch region have been analyzed numerically and show a statistically significant weak band near 3600 cm^{-1} at each temperature. This band, the Raman analog of which was reported earlier, confirms the presence of HDO species with unbonded O—H groups in the liquid state. The percentage of HDO species with unbonded O—H groups is found to be 4.6, 6.1, 10.1, and 11.9, respectively, at 10, 35, 60, and 85 °C.

The four predominant HDO species in equilibrium at low temperatures are defined together with their equilibrium constant for the O—H---O bond-rupturing process. A standard enthalpy change of $\Delta H° = 6800 \pm 1100$ cal is found for the rupture of one mole of O—H---O bonds. This is in contrast with the apparent enthalpy change of 2900 ± 500 cal, as usually derived from the temperature dependence of the equilibrium quotient. Approximate mole fractions for each of twelve differently bonded HDO species are derived from a model for random H- and D-bond statistics. Results show that the four predominant HDO species give a full interpretation of the absorptivities at 10, 35, and 60 °C but that additional minor species contribute slightly to the absorptivity at 85 °C.

Nous avons analysé numériquement les absorbances infrarouges de Wyss et Falk entre 10 et 85 °C pour HDO dans D_2O liquide dans la région fondamentale d'élongation O—H; elles montrent une bande faible près de 3600 cm^{-1} à chaque température. Cette bande, dont l'analogue Raman a été rapportée précédemment, confirme la présence d'espèces HDO avec des groupes O—H non-liés à l'état liquide. On trouve que le pourcentage d'espèces HDO avec des groupes O—H nonliés est de 4.6, 6.1, 10.1, et 11.9, respectivement, à 10, 35, 60, et 85 °C.

Nous définissons les quatre espèces HDO prédominantes à l'équilibre à basses températures, de même que leur constante d'équilibre pour le procédé de rupture de la liaison O—H---O. Nous trouvons un changement d'enthalpie standard $\Delta H° = 6800 \pm 1100$ cal pour la rupture d'une mole deliens O—H---O. Cette valeur contraste avec le changement d'enthalpie apparen de 2900 ± 500 cal, tel que dérivé habituellement à partir de la dépendance de la température du quotient d'équilibre. Les fractions molaires approximatives pour chacune des douze espèces HDO différemment liées sont tirées d'un modèle pour les statistiques des liens H et D aléatoires. Les résultats montrent que les quatre espèces HDO prédominantes donnent une pleine interprétation des absorbances à 10, 35, et 60 °C, mais que d'autres espèces mineures contribuent légèrement à l'absorbance à 85 °C.

Canadian Journal of Chemistry, **50**, 1655 (1972)

Introduction

Wyss and Falk (1) recently published infrared molar absorptivities for HDO in liquid water and deuterium oxide between 10 and 85 °C. Strong, wide, single-peaked absorptions were shown for the O—H and O—D stretch modes, ν_3 and ν_1, respectively, with weak absorption for the angular deformation overtone mode, $2\nu_2$. In that work it was reasserted, as earlier (2), that the ν_3 and ν_1 absorptions were single bands, deriving from continuous distributions of H-bonded O—H and D-bonded O—D groups, and that these single ν_3 and ν_1 bands showed no evidence for unbonded O—H and O—D groups of HDO molecules with broken H- and D-bonds. This interpretation of the infrared measurements was inconsistent with Walrafen's Raman contours (3, 4, 30) which showed definite high-frequency shoulders on the O—H and O—D stretch bands of HDO. In this work we show a statistically significant decomposition of Wyss and Falk's O—H stretch absorption contours at each temperature into component bands which correspond with the observed Raman shoulders.

[1]Contribution No. 193.

Statement of Problem and Selection of Model

Predominant Species in Liquid Water

Many studies of the properties of liquid water and aqueous nonelectrolyte solutions indicate that at low temperature water is nearly completely H-bonded (1, 2, 5–14) and that the predominant and most stable molecular species

Can. J. Chem. Downloaded from www.nrcresearchpress.com by 210.87.254.40 on 09/05/12
For personal use only.

is that in which the H_2O molecules maintain four, tetrahedrally oriented H-bonds with near water neighbors. These H-bonds are being ruptured continually in the liquid state and must have lifetimes of at least 10^{-12} s in order to show discrete quantized bands at 60 cm^{-1} (15, 16). Thus an H_2O molecular species with a given H-bond configuration may be reasonably assumed to exist for at least 10^{-12} s before its H-bond configuration changes, a time sufficient for 55 complete vibrations of the intramolecular O—H stretch modes at 3400 cm^{-1}. After the most probable H_2O species with four H-bonds, the next most probable species will be those maintaining three H-bonds with near neighbors, with progressively decreasing fractions of the less stable species forming two, one, and zero H-bonds with neighbors.

Similarly, if we consider a dilute solution of HDO in liquid deuterium oxide at low temperature, we anticipate that the predominant HDO species is the four-bonded species I, and that the next most common species are the three-bonded species II, III, and IV.

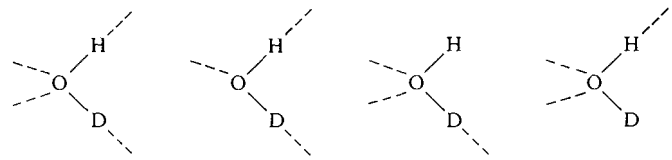

Species	I	II	III	IV
Mole fraction	[I]	[III] + [IV]	[III]	[IV]

Those HDO species forming two or less bonds occur at lower concentrations and will be disregarded until later discussion. If a mole fraction [III] of HDO is present as the three-bonded species III, a fraction [IV] must exist as the three-bonded species IV, then a fraction [III] + [IV] must be present as the three-bonded species II. In postulating the existence of species II, III, and IV we mean that these are equilibrium species which have life-times of at least 10^{-12} s. Thus if the O—H stretch absorption contour is not a single band due to a single species I, it must be a composite of at least four bands due to the four different major species I, II, III, and IV.

H-bond Dissociation Equilibria

Spectroscopic determination of the concentration of unbonded HDO species in the liquid state raises the problem of the proper definition of the HDO species present and of their appropriate equilibrium constant.

Earlier spectroscopic determinations (17–19) have used a concentration quotient, q, equivalent to [HDO, unbonded]/[HDO, bonded], to define the equilibrium between the bonded and unbonded HDO species. This implies that the bond-rupturing and bond-forming reactions are opposed first order processes. Such an equilibrium quotient ignores the fact that the formation of species with unbonded O—H or O—D groups leads to the concomitant formation of an equal concentration of independent species with unbonded lone-pair electrons.

It is more realistic to expect that successful H-bond formation occurs with the bimolecular encounter between an HDO molecule with an unbonded O—H group and one with an unbonded lone pair. Indirect support for a second order rate dependence of the H-bond-forming reaction is provided by the fact that the addition of polyvinylpyrrolidone to HDO solutions suppresses the concentration of unbonded O—H groups (17). Some part of the concentration reduction of unbonded O—H groups derives from the structure-making effect (17), as described elsewhere for aqueous nonelectrolyte solutions (20). However, the addition of the pyrrolidine groups, with lone-pair electrons on the ring nitrogen and carbonyl oxygen atoms, provides additional bonding sites for the unbonded O—H and O—D groups, the concentration of which is thereby diminished. Any bonding of HDO to the pyrrolidine groups leads to an attendant increase of concentration of HDO species with unbonded lone-pair electrons.

Additional evidence for a second order rate dependence of the H-bond-forming reaction is provided by the analogous ionization equilib-

Can. J. Chem. Downloaded from www.nrcresearchpress.com by 210.87.254.40 on 09/05/12
For personal use only.

TABLE 1. Parameters for single-band representation of O—H stretch absorptivities

Temperature (°C)	ν_0 (cm^{-1})	w (cm^{-1})	ε_0 (10^3 cm^2 mol^{-1})	Gaussian (%)	Asymmetry factor (μm)	Band area (10^3 cm mol^{-1})
10	3393±1	243±2	73.0±0.3	47±2	0.1±0.7	19 620
35	3413±1	252±3	66.9±0.3	47±2	5.5±0.8	18 670
60	3429±1	261±4	60.6±0.4	49±3	7.7±1.0	17 460
85	3445±1	272±9	54.6±0.3	59±5	9.2±0.9	16 130

Temperature (°C)	Degrees of freedom	Q	$\sigma(\varepsilon)$ (10^3 cm^2 mol^{-1})
10	32	12.34	0.62
35	32	15.40	0.69
60	32	24.18	0.87
85	32	18.43	0.76

rium of water. There the ionization reaction is pseudounimolecular giving OH^- and H_3O^+ and these two independent, three-bonded species exist in water for sufficient time that their recombination reaction rate is second order, proportional to their concentration product, $[OH^-][H_3O^+]$. In this case the independent lifetimes of given OH^- and H_3O^+ species are probably considerably shorter than those for the unbonded water species, due to their ionic charges promoting recombination.

The existence of species III and II as independent entities requires that the first H-bond dissociation constant, K_H, for liquid HDO be defined by the equation

$$[1] \qquad K_H = \frac{[III][II]}{[I]}$$

in which a pseudounimolecular bond-rupturing process for species I is opposed by a second order bond-forming reaction between species III and II. Similarly, the first D-bond dissociation equilibrium constant, K_D, is defined by

$$[2] \qquad K_D = \frac{[IV][II]}{[I]}$$

in which a unimolecular D-bond rupturing process for species I is opposed by a second order D-bond-forming reaction between IV and II.

Numerical Treatment of Absorptivities

Decomposition of Infrared Band Contours

As a necessary modification of earlier work (21) to allow for the possibility of band asymmetry (22), we represent the absorption contours of single bands by the Gauss–Cauchy (Lorentz) product function

$$[3] \qquad \varepsilon = \varepsilon_0 \frac{\exp[-G^2 Y^{-2}(\nu - \nu_0)^2 A]}{[1 + (1-G)^2 Y^{-2}(\nu - \nu_0)^2 A]}$$

with an asymmetry function defined by

$$[4] \qquad A = 1 + a(\nu - \nu_0) + a^2(\nu - \nu_0)^2/2,$$

where ε_0 is the peak extinction, ν_0 is the peak frequency, Y is proportional to the bandwidth w at half-extinction, G is the fraction Gaussian and $(1 - G)$ the fraction Cauchy (Lorentzian), and a is the asymmetry factor.

To decompose overlapped multiple-band contours into self-consistent sets of single bands we derive the band parameters using Pitha and Jones' non-linear least-squares method V (21). The errors on the parameters are evaluated by standard methods (23) from the inverse matrix elements of the linearized normal equations. The present work summarizes the final results from approximately 250 non-linear least-squares fits of absorptivity data using an IBM 360/40 computer. From Wyss and Falk's very accurate HDO absorptivities we represented their 37 values between 3720 and 3200 cm^{-1} at each temperature first by a single band, then by two bands, and finally by four bands.

Single-band Representation

Table 1 shows the five parameters together with their standard errors for the best single bands representing the measurements at each temperature. The residuals, plotted in Fig. 1 as the small dots joined by the fine lines, are seen to be conspicuously similar and non-random at all four temperatures. Significant positive resid-

Can. J. Chem. Downloaded from www.nrcresearchpress.com by 210.87.254.40 on 09/05/12
For personal use only.

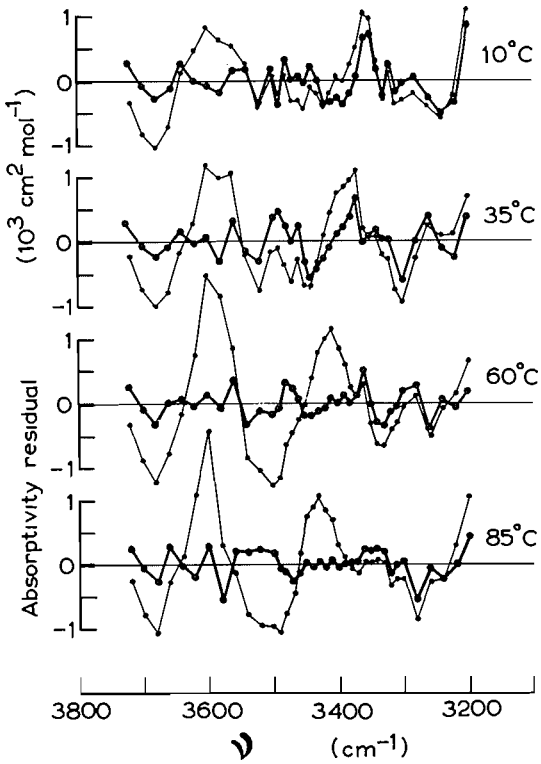

FIG. 1. Frequency distribution in the O—H stretch region of the absorptivity residuals at 10, 35, 60, and 85 °C. Small dots joined by fine lines show residuals from single-band representations. Large dots joined by heavy lines show residuals from four-band representations.

uals (absorptivity residual = absorptivity observed − absorptivity calculated) are invariably shown near 3600 cm^{-1} indicating the probable occurrence of a band. Consequently the sums of the squares of the residuals, Q, and the assessments of the standard error on a single absorptivity measurement, $\sigma(\varepsilon)$, shown in Table 1 are systematically too large. As the temperature increases the weakening of the H-bonds is indicated by the increase of the peak frequency, ν_0, and by the decrease of the integrated band area (24). Also with increasing temperature the single bands become wider and more Gaussian, and the representation of the measurements by a single band becomes poorer with larger Q values. The bands are never completely Gaussian and become more asymmetric with increasing low-frequency tails at higher temperatures.

Two-band Representation

Table 2 shows the parameters together with their standard errors for the two-band representation of the measurements at each temperature. In this approximation band I derives from all HDO species in which the O—H group is H-bonded, while band III near 3600 cm^{-1} derives from all species in which the O—H group is unbonded. Because it was impossible to obtain meaningful values for the percentage Gaussian and the asymmetry factor for band III, these parameters were made equal to those for the main band I. Preliminary fits of the data at 35, 60, and 85 °C showed that band III had widths at half-extinction of 119 ± 28, 93 ± 8, and 97 ± 14 cm^{-1}, respectively, which give a weighted mean value of 99 cm^{-1}. Since these half-widths were not well defined, even at the highest temperatures, we refitted the measurements taking a constant half-width of 100 cm^{-1} for band III at all temperatures. The two-band representations given in Table 2 are statistically unique in the sense that they are the only pairs of bands that properly fit the measurements.

The Q values for the two-band representations in Table 2 are considerably smaller than those for the single-band representations in Table 1. The variance ratio F-test (23) shows that the improvement of the seven-parameter, two-band representation over the five-parameter, single-band representation is statistically significant, occurring by chance alone at the 1×10^{-5}, 7×10^{-9}, 5×10^{-18}, and 2×10^{-11} probability levels at 10, 35, 60, and 85 °C, respectively. The overall probability that band III arises by chance alone is 10^{-41}. Thus the infrared absorptivity measurements of Wyss and Falk exhibit a real band near 3600 cm^{-1}.

We assign this HDO infrared band III near 3600 cm^{-1} mainly to the three-bonded species III, with the band area giving a direct measure of the species III concentration. The analogous HDO Raman band found at 3628 cm^{-1} (4, 30) was assigned earlier to the same three-bonded species (24). The existence of measurable concentrations of species III for liquid HDO chemically requires the simultaneous coexistence of equilibrium concentrations of species II and IV, as discussed above.

Four-band Representation

The use of four bands to represent the infrared

Can. J. Chem. Downloaded from www.nrcresearchpress.com by 210.87.254.40 on 09/05/12
For personal use only.

TABLE 2. Parameters for two-band representation of O—H stretch absorptivities

Temperature (°C)	ν_0 (cm^{-1})	w (cm^{-1})	ε_0 (10^3 cm^2 mol^{-1})	Gaussian (%)	Asymmetry factor (μm)	Band area (10^3 cm mol^{-1})
Band I						
10	3394±1	240±2	73.2±0.2	49±2	2.3±0.7	19 320
35	3412±1	243±2	67.3±0.2	46±1	8.4±0.6	18 320
60	3427±1	245±1	61.3±0.1	45±1	12.1±0.4	16 950
85	3441±1	256±3	55.1±0.2	50±2	12.5±0.6	15 650
Band III						
10	3583±6	100	2.5±0.5			280
35	3578±5	100	3.7±0.4			407
60	3584±2	100	5.8±0.3			649
85	3595±3	100	5.2±0.5			576

Temperature (°C)	Degrees of freedom	Q	$\sigma(\varepsilon)$ (10^3 cm^2 mol^{-1})
Bands I and III			
10	30	5.79	0.44
35	30	4.39	0.38
60	30	1.70	0.24
85	30	3.55	0.34

absorptivity measurements is dictated by the existence of the four instantaneously distinct species I to IV, each of which contributes its characteristic O—H absorption band. The introduction of the four bands is thus made subject to a number of constraints which are defined by information external to the infrared data. Subject to the systematic application of these constraints, which are described below, the four-band representations of the infrared measurements are statistically unique.

Table 3 shows the parameters and their standard errors for the four-band representations of the measurements. The residuals, plotted in Fig. 1 as the large dots joined by the heavy lines, are seen to be nearly randomly distributed and nearer to the zero ordinate than those for the single-band representations. Figure 2 illustrates the total absorptivity contour at 85 °C and its decomposition into four bands. To define the four-band representation the twenty undetermined parameters were reduced to nine by imposing reasonable constraints on the values of those parameters which were least well defined. The main band I for species I was represented by five undetermined parameters, while the smaller bands II–IV for species II–IV were represented by fewer undetermined parameters, the balance being constrained parameters.

Preliminary fits of the measurements at 10, 35, 60, and 85 °C showed that band III had half-widths of 105±36, 104±3, 86±8, and 97±7 cm^{-1}, respectively, which give a weighted mean of 102 cm^{-1}. Since these half-widths were not well defined we initially took a constant half-width of 100 cm^{-1} for band III at all temperatures. Band II was taken with a half-width of 150 cm^{-1} at all temperatures, the mean value from preliminary fits. Band IV was taken with a frequency 95 cm^{-1} lower than band I, with half-width equal to band I. The Gaussian and asymmetry parameters for bands II–IV were taken equal to those of band I. Two additional constraints were made so that the area of band IV gave a species IV concentration equal to that of species III, and the area of band II gave a species II concentration equal to the sum of the concentrations of species III and IV. Equal concentrations were taken for species III and IV because the Raman study of Walrafen (30) showed the same fraction of unbonded O—H and O—D groups in liquid deuterium oxide at 25 °C. Further, the best representations of the infrared absorptivities were invariably obtained when the concentrations of species III and IV were taken as equal.

Walrafen (30) has also shown it necessary to use four component bands to adequately represent his Raman O—H stretch band contours for HDO at 25 °C. In the near-infrared Luck

Can. J. Chem. Downloaded from www.nrcresearchpress.com by 210.87.254.40 on 09/05/12
For personal use only.

TABLE 3. Parameters for four-band representation of O—H stretch absorptivities

Temperature (°C)	ν_0 (cm^{-1})	w (cm^{-1})	ε_0 (10^3 cm^2 mol^{-1})	Gaussian (%)	Asymmetry factor (μm)	Band area (10^3 cm mol^{-1})
Band I						
10	3391±1	220±4	68.3±1.2	43±1	2.2±1.0	16 811
35	3407±1	218±4	59.8±1.6	38±2	7.7±0.9	15 004
60	3422±1	195±4	49.1±0.9	31±1	13.8±1.0	11 532
85	3437±1	190±4	41.9±0.9	31±2	17.0±1.6	9 631
Band II						
10	3496±10	150	7.5±1.4			1 256
35	3497±8	150	9.8±1.6			1 686
60	3507±3	150	15.3±1.0			2 745
85	3522±3	150	16.5±1.0			2 969
Band III						
10	3595±7	97±5	3.1±0.6			335
35	3583±5	97±5	4.5±0.7			498
60	3588±2	97±5	7.1±0.5			817
85	3599±2	97±5	7.5±0.5			869
Band IV						
10	3296±1	220±4	5.0±0.9			1 226
35	3312±1	218±4	6.3±1.0			1 586
60	3327±1	195±4	11.1±0.7			2 617
85	3342±1	190±5	12.8±0.8			2 934

Temperature (°C)	Degrees of freedom	Q	$\sigma(\varepsilon)$ (10^3 cm^2 mol^{-1})
Bands I–IV			
10	28	3.85	0.37
35	28	3.08	0.33
60	28	1.62	0.24
85	28	2.18	0.28

and Ditter (25) have used three component bands, one of which was anomalously wide compared with the other two.

The Q values for the four-band representations in Table 3 are considerably smaller than those for the single bands in Table 1, and are smaller than those for the two-band representations in Table 2. The variance ratio F-test (23) shows that the improvement of the nine-parameter, four-band representation over the seven-parameter, two-band representation is statistically significant, occurring by chance alone at the 3×10^{-3}, 7×10^{-3}, 5×10^{-1}, and 1×10^{-3} probability levels at 10, 35, 60, and 85 °C, respectively. The values for the assessment of the standard error $\sigma(\varepsilon)$ given in Table 3 are probably characteristic of the experimental reproducibility of the absorption measurements (1).

It is recognized that the constraints applied in the data treatment may lead to slight systematic bias in the values of the undetermined parameters, but such bias will be comparable for each temperature. The errors shown for the constrained parameters do not reflect the uncertainties of the assumed constraints.

However, the necessity for band III near 3600 cm^{-1} at each temperature was unaffected by any constraints which were applied to the parameters. For our final calculations Fig. 3(*a*) shows the dependence of the values for the sums of the squares of the residuals, Q, on the constrained value of the band III half-width. The minimum of Q defines the best value for the half-width at each temperature. The final best values for the band III half-widths and their standard errors are 106 ± 37, 105 ± 28, 88 ± 8, and 102 ± 7 cm^{-1}, respectively, at 10, 35, 60, and 85 °C. The smaller standard errors directly reflect the larger curvatures at the minima of Q. Figure 3(*b*) shows the aggregate sum of squares for all temperatures as a function of the band

Can. J. Chem. Downloaded from www.nrcresearchpress.com by 210.87.254.40 on 09/05/12
For personal use only.

Can. J. Chem. Downloaded from www.nrcresearchpress.com by 210.87.254.40 on 09/05/12
For personal use only.

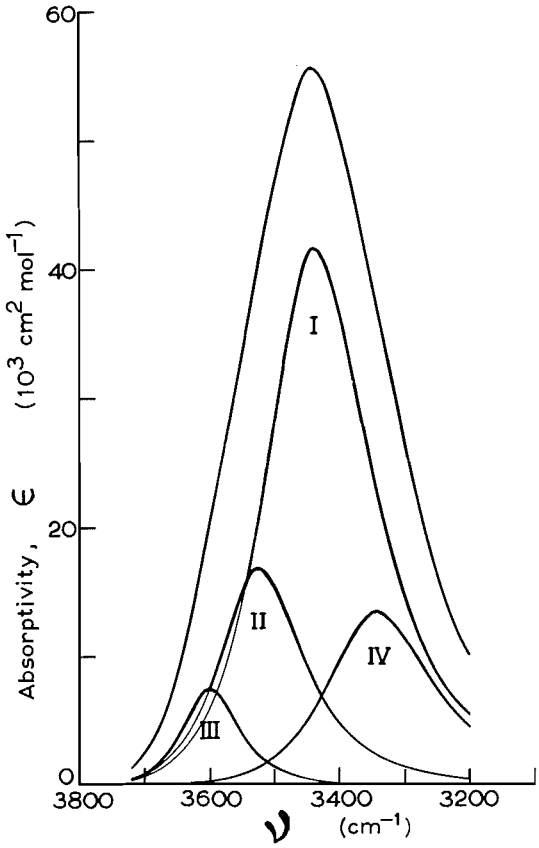

FIG. 2. The infrared O—H stretch contour of HDO at 85 °C showing its decomposition into four component bands.

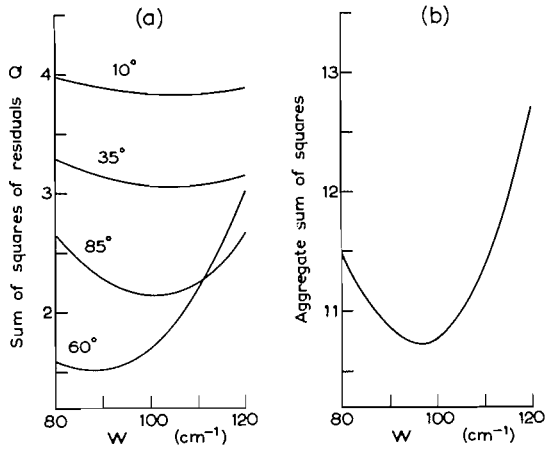

FIG. 3. The variation of (*a*) the sum of the squares of the residuals at each temperature and (*b*) the aggregate sum of squares for all temperatures with the constrained band III half-width.

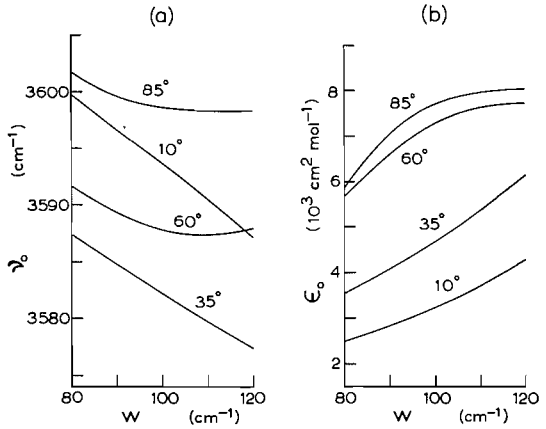

FIG. 4. The variation of (*a*) the band III frequency and (*b*) the band III peak extinction with the constrained band III half-width.

III half-width. This curve has a sharp minimum at 97 cm^{-1} and gives a best overall value of 97 $\pm$ 5 cm^{-1} for the band III half-width between 10 and 85 °C.

Figure 4 shows the variation of the band III frequency and peak extinction with the constrained band III half-width: a 1 cm^{-1} increase of half-width causes a 0.006% decrease of frequency and a 1.2% increase of extinction.

Results for final calculations in Table 3 show that the band III frequency is almost temperature invariant, as required for an O—H group which is not directly perturbed by any bonding neighbor. The band III half-width of 97 cm^{-1} is anomalously wide for an unbonded O—H group of HDO (24). This width for the three-bonded species III derives from the indirect inductive perturbations from the other bonds to the lone-pair electrons and to the O—D group (24). The most significant feature of band III is its monotonous increase of peak extinction, ε_0, with temperature.

Band II, with frequency about 3500 cm^{-1}, is assigned to the HDO species II since earlier work (24) indicates that the H-bond for species I should be stronger than that for species II, due to the increased induced charge polarization from the bonding of both lone pairs of electrons for species I. Band IV, with frequency lower than band I, is assigned to species IV because its H-bond is stronger than that for species I, due to the decreased repulsion from the unbonded O—D group of species IV. The monotonous

TABLE 4. HDO fraction with unbonded O—H and H-bond-rupture equilibrium constant

Temperature (°C)	[III]			K_H		
	Observed	Calculated	Error	Observed	Calculated	Error
0		0.036	0.008		0.0030	0.0014
10	0.046	0.044	0.007	0.0051	0.0047	0.0017
25		0.058	0.006		0.0086	0.0022
35	0.061	0.068	0.006	0.0098	0.0125	0.0024
50		0.083	0.005		0.0209	0.0028
60	0.101	0.094	0.004	0.0345	0.0287	0.0035
85	0.119	0.122	0.007	0.0535	0.0586	0.0103
100		0.138	0.010		0.0858	0.0200

increases of ε_0 for bands II and IV result from the imposed constraints on the species II and IV concentrations.

Band I, with highest extinction, which decreases with temperature, moves between 3391 and 3437 cm^{-1} and is assigned to the predominant species I, for which the concentration must decrease with temperature. The half-width and Gaussian percentage for band I are significantly smaller than for the other representations, and these parameters agree well with the values found for dilute solutions of HDO in dimethyl sulfoxide and in the substituted pyridines (24, 26). Both of these parameters decrease at higher temperatures. Values for the asymmetry factor also agree with those found for HDO in dimethyl sulfoxide and in the substituted pyridines (26).

Band Frequencies and Half-widths

The infrared frequencies of band III, with a weighted mean value of 3593 cm^{-1}, and of band I, with a value of 3400 cm^{-1} at 25 °C, are both 35 cm^{-1} lower than the corresponding Raman bands at 3628 and 3435 cm^{-1} (4, 30). These differences are real and beyond the combined experimental errors. Half of this frequency difference can be explained by the H-bonding intensification of infrared bands at lower frequencies (24). Convolution of the intensity–frequency relationship [5] with symmetric 35% Gaussian bands at 3625 cm^{-1} of 100 cm^{-1} half-width and at 3435 cm^{-1} of 200 cm^{-1} half-width gives transformed asymmetric 45% Gaussian bands at 3608 cm^{-1} of 98 cm^{-1} half-width and at 3414 cm^{-1} of 198 cm^{-1} half-width, respectively. The half-widths are little changed by the convolution and we find good agreement between our 97 cm^{-1} half-width for band III and the 100 and 110 cm^{-1} values from Raman measurements (30).

Band III for HDO in liquid deuterium oxide has a lower frequency and larger half-width than the unbonded infrared O—H bands reported in polyelectrolyte salt membranes with low water contents (31), indicating a less extensively H-bonded environment (24) within the substituted polystyrene ion-exchange membranes.

Determination of Species Concentrations

Concentration of Predominant HDO Species

The recent infrared study of HDO in a wide range of basic solvents (24) has shown that the O—H stretch band area is directly proportional to the band frequency shift from the 3707 cm^{-1} value in the gas phase (27). Thus the band area A_0 for one mole of HDO in 1000 cm^3 is given by

$$[5] \qquad A_0 = D(3707 - \nu_0)$$

in which ν_0 is the peak frequency and D is a constant. In the earlier study D was found to be $66.3 \pm 1.7\ 10^3$ cm^2 mol^{-1} for all solvents, including deuterium oxide. When eq. 5 is applied to the four-band representations in Table 3 we find the D values of 65.1, 66.1, 67.9, and 67.8 10^3 cm^2 mol^{-1} at 10, 35, 60, and 85 °C, respectively. The small variation of these values with temperature and their good agreement among themselves and with the earlier value for all other solvents, provides an *a posteriori* justification for this treatment. An unknown concentration c mol 10^{-3} cm^{-3} of a species is evaluated from the species band area A using the equation

$$[6] \qquad c = \frac{A}{D(3707 - \nu_0)}$$

Table 4 presents the species III mole fractions $[III]_{obsd}$ derived from the final four-band repre-

Can. J. Chem. Downloaded from www.nrcresearchpress.com by 210.87.254.40 on 09/05/12
For personal use only.

Can. J. Chem. Downloaded from www.nrcresearchpress.com by 210.87.254.40 on 09/05/12
For personal use only.

sentations. The $K_{H\ obsd}$ values were evaluated from eq. 1 with [III] and with [IV] = [III], [II] = 2 [III], and [I] = 1 − 4 [III]. The best (28) weighted equation for the temperature dependence of K_H is

$$[7] \qquad \log_{10} K_H = 2.896 - 1478/T$$

which gives a standard error of 26% on a K_H determination of unit weight. The back-calculated $K_{H\ calc}$ values from eq. 7 together with their standard errors are shown in the final two columns of Table 4. The back-calculated $[III]_{calc}$ values and their standard errors were evaluated from the corresponding K_H values. The relative errors on the $[III]_{calc}$ values are two to three times smaller than on the $K_{H\ calc}$ values. The standard enthalpy and entropy changes together with their standard errors, determined from eq. 7, for the rupture of one mole of O—H---O bonds are $\Delta H^0 = 6800 \pm 1100$ cal and $\Delta S^0 = 13.2 \pm 3.3$ cal deg^{-1}. This ΔH^0 value for the H-bond dissociation equilibrium [1] is in good agreement with the 6800 ± 200 cal value derived for the low temperature bond-rupturing pre-equilibrium in the nuclear relaxation of D_2O (29). At low temperatures our species I is identified with the "lattice" water and the three-bonded species II, III, and IV with the "free" water of that work.

The temperature dependence of the concentration quotient, q, defined by

$$[8] \qquad q = \frac{[III]}{1 - [III]}$$

is represented by the weighted equation

$$[9] \qquad \log_{10} q = 0.912 - 632/T$$

which gives a standard error of 11% on a determination of q of unit weight (23). This yields an apparent enthalpy change of 2900 ± 500 cal for the process defined by eq. 8: the temperature dependence of q in eq. 9 agrees reasonably with earlier studies which give 2400 cal for H-bond rupture (17), and 2500 ± 600 (3) and 2300 ± 400 cal (19) for D-bond rupture.

The concentration of unbonded O—H groups derived from our treatment is some 60% lower than indicated by near-infrared measurements (25). However, recent Raman measurements (30) showed 5 and 7% unbonded O—H groups at 25 °C, which agree well with the 5.8 ± 0.6% given in Table 4 for HDO in liquid D_2O.

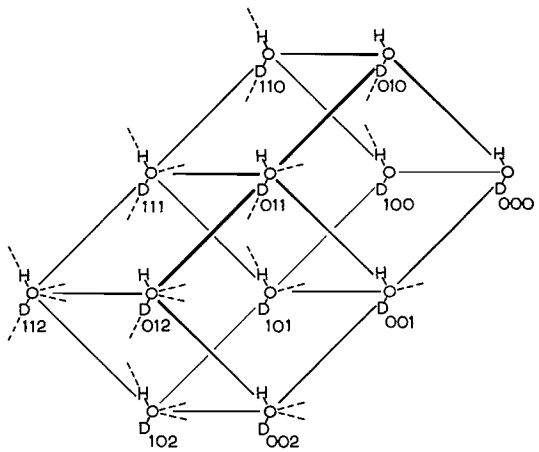

FIG. 5. Representation of the H-bonding interrelationship of the twelve HDO species, in which three dashes indicate H- or D-bonds, and the three-element array indicates the bonding configuration of the species.

Many and wide variations of the constraints have been investigated to determine their effect on the mole fraction $[III]_{obsd}$ and we found that $[III]_{obsd}$ was only slightly changed. Thus, we conclude that our values for $[III]_{obsd}$ in Table 4 represent realistic estimates for the unbonded O—H group mole fractions based on the infrared absorptivities of Wyss and Falk (1).

Estimation of the Concentrations of the Twelve HDO Species

In all earlier sections to maintain clarity of treatment we have disregarded the small concentrations of less stable HDO species which form two or less H- or D-bonds with near neighbors. We now present order of magnitude calculations for the concentrations of these minor species based on the gross assumptions that the H- and D-bonds of all species are equally likely to rupture and that there is no isotope effect. This reduces the statistical treatment for HDO to the case of simple random hydrogen-bond statistics which has been treated for water earlier by Levine and Perram (32).

For HDO in the liquid state there are twelve formally distinct bonding configurations which are indicated at the rhombic vertices in Fig. 5. Species with the same number of H- or D-bonds are shown in the same vertical column, while the species joined by a line differ from each other by the rupture of a single bond. Then, if H- or D-bond rupture is stepwise the fully or four-bonded species I at the leftmost vertex of the

TABLE 5. Temperature dependence of mole fractions of the twelve HDO species

Species	Mole fraction at 0 °C	25 °C	50 °C	100 °C
112	0.8634	0.7884	0.7055	0.5512
111	0.0646	0.0965	0.1285	0.1770
012	0.0323	0.0483	0.0643	0.0885
102	0.0323	0.0483	0.0643	0.0885
011	0.0024	0.0059	0.0117	0.0284
101	0.0024	0.0059	0.0117	0.0284
110	0.0012	0.0030	0.0059	0.0142
002	0.0012	0.0030	0.0059	0.0142
001	0.00009	0.00036	0.0011	0.0046
010	0.00005	0.00018	0.00053	0.0023
100	0.00005	0.00018	0.00053	0.0023
000	0.000002	0.00001	0.00005	0.0004

diagram must pass through the progressively less stable, three-bonded, two-bonded, and one-bonded configurations in order to form the fully unbonded HDO species at the rightmost vertex. We identify the bonding configuration of each species by a linear three-element array, *fgh*, in which *f* is 1 if the O—H group is bonded or 0 if unbonded, *g* is 1 if the O—D group is bonded or 0 if unbonded, and *h* is 2 if both lone pairs are bonded, 1 if a single lone pair is bonded, or 0 if no lone pair is bonded. Thus our major species I, II, III, and IV are shown in Fig. 5 represented by the arrays 112, 111, 012, and 102, respectively.

Table 5 presents the mole fractions for the twelve HDO species existing in liquid deuterium oxide at 0, 25, 50, and 100 °C, as evaluated from eq. 7 for random H-bond statistics (32) assuming that the fraction of unbonded species III is properly equal to the sum of the fractions for the species 012, 011, 002, 010, 001, and 000, each of which has an unbonded O—H group.

The completely unbonded species 000 comprises 0.0002% of the total HDO at 0 °C increasing to 0.04% at 100 °C, so that this species is spectroscopically negligible in the infrared over the temperature range. Species forming two and fewer H- or D-bonds comprise less than 1% of the total at 0 °C increasing to about 10% at 100 °C, so that these species are spectroscopically insignificant at 0 °C but just become significant near 100 °C. This *a posteriori* justifies our neglect of these minor species in treating the absorptivities at 10, 35, and 60 °C and shows that more than the four major species I–IV (112, 111, 012, and 102) make a small contribution to the absorptivity at 85 °C.

The species fractions in Table 5 clearly show that any two-state model (14, 29, 33, 34) for liquid HDO water is a gross oversimplification, even at low temperatures. If we consider a two-state water model, the completely H-bonded lower state of HDO "lattice" water must be comprised entirely of species 112, while the upper state of "free" water is comprised of a mixture of the three three-bonded species 111, 012, and 102 at low temperatures. At higher temperatures, near and above 100 °C, the upper state is comprised of a mixture of predominantly three-bonded species together with significant fractions of the two-bonded species 011, 101, 110, and 002. To what extent the pyramidally bound three-bonded species are orientationally free in the upper state is questionable on purely geometrical structural grounds: Hindman *et al.* (29) have indicated that in their "free" upper state the water molecules are not completely free at low temperatures. The fractions of the species in Table 5 appear to be generally consistent with the findings of Hindman *et al.* (29) and their proposed two-state relaxational model for $H_2^{17}O$ and D_2O, in which few "free" molecules exist at low temperatures and H-bond rupture precedes the relaxation process, while at higher temperatures above 100 °C many "free" molecules exist and the relaxation process can proceed without the necessity of prior H-bond rupture.

1. H. R. WYSS and M. FALK. Can. J. Chem. **48**, 607 (1970).
2. M. FALK and T. A. FORD. Can. J. Chem. **44**, 1699 (1966).
3. G. E. WALRAFEN. J. Chem. Phys. **48**, 244 (1968).
4. G. E. WALRAFEN. J. Chem. Phys. **50**, 560 (1969).
5. J. D. BERNAL and R. H. FOWLER. J. Chem. Phys. **1**, 515 (1933).
6. J. MORGAN and B. E. WARREN. J. Chem. Phys. **6**, 666 (1938).
7. J. A. POPLE. Proc. Roy. Soc. A**205**, 163 (1951).
8. D. N. GLEW. J. Phys. Chem. **66**, 605 (1962).
9. D. P. STEVENSON. J. Phys. Chem. **69**, 2145 (1965).
10. T. T. WALL and D. F. HORNIG. J. Chem. Phys. **43**, 2079 (1965).
11. M. S. JHON, J. GROSH, T. REE, and H. EYRING. J. Chem. Phys. **44**, 1465 (1966).
12. E. U. FRANCK and K. ROTH. Disc. Faraday Soc. **43**, 108 (1967).
13. J. SCHIFFER and D. F. HORNIG. J. Chem. Phys. **49**, 4150 (1968).
14. D. EISENBERG and W. KAUZMANN. The structure and properties of water. Clarendon Press, Oxford. 1969.

Can. J. Chem. Downloaded from www.nrcresearchpress.com by 210.87.254.40 on 09/05/12
For personal use only.

15. K. E. LARSSON and V. DAHLBORG. Physica, **30**, 1561 (1964).
16. G. E. WALRAFEN. J. Chem. Phys. **40**, 3249 (1964).
17. J. D. WORLEY and I. M. KLOTZ. J. Chem. Phys. **45**, 2868 (1966).
18. G. E. WALRAFEN. *In* Hydrogen-bonded solvent systems. *Edited by* A. K. Covington and P. Jones. Taylor and Francis Limited, London. 1968.
19. W. A. SENIOR and R. E. VERALL. J. Phys. Chem. **73**, 4242 (1969).
20. D. N. GLEW, H. D. MAK, and N. S. RATH. *In* Hydrogen-bonded solvent systems. *Edited by* A. K. Covington and P. Jones. Taylor and Francis Limited, London. 1968.
21. J. PITHA and R. N. JONES. Can. J. Chem. **44**, 3031 (1966).
22. A. CABANA and C. SANDORFY. Spectrochim. Acta, **16**, 335 (1960).
23. N. R. DRAPER and H. SMITH. Applied regression analysis. John Wiley and Sons, Inc., New York, N.Y. 1966.
24. D. N. GLEW and N. S. RATH. Can. J. Chem. **49**, 837 (1971).
25. W. A. P. LUCK and W. DITTER. J. Phys. Chem. **74**, 3687 (1970).
26. E. C. W. CLARKE and D. N. GLEW. Unpublished work.
27. W. S. BENEDICT, N. GAILAR, and E. K. PLYLER. J. Chem. Phys. **24**, 1139 (1956).
28. E. C. W. CLARKE and D. N. GLEW. Trans. Faraday Soc. **62**, 539 (1966).
29. J. C. HINDMAN, A. J. ZIELEN, A. SVIRMICKAS, and M. WOOD. J. Chem. Phys. **54**, 621 (1971).
30. G. E. WALRAFEN. J. Chem. Phys. **50**, 567 (1969).
31. G. ZUNDEL. Hydration and intermolecular interaction. Academic Press, Inc., New York, N.Y. 1969.
32. S. LEVINE and J. W. PERRAM. *In* Hydrogen-bonded solvent systems. *Edited by* A. K. Covington and P. Jones. Taylor and Francis Limited, London. 1968.
33. A. H. NARTEN and H. A. LEVY. Science, **165**, 447 (1969).
34. H. S. FRANK. Science, **169**, 635 (1970).

Can. J. Chem. Downloaded from www.nrcresearchpress.com by 210.87.254.40 on 09/05/12
For personal use only.

Heterogeneous Interactions of Methylamines on Porous Adsorbents. Part I. The Adsorption of Monomethylamine on Silica Gels and Silica–Alumina

W. G. Cook and R. A. Ross

Department of Chemistry, Lakehead University, Thunder Bay, Ontario

Received December 29, 1971

The adsorption of monomethylamine has been studied near its boiling point, 266 °K, on silica–alumina and on a wide range of silica gels by measurement of adsorption–desorption isotherms and isothermal calorimetric heats of adsorption. In addition, surface areas and pore-size distributions have been determined by low-temperature nitrogen adsorption. Heats of adsorption on Davison "923" silica gel varied from around 33.0 kcal/mol at $\theta = 0.01$ to 6.2 kcal/mol at monolayer completion. Maxima were observed in this heat curve in the regions of $\theta = 0.15$, 0.28, and 0.40. These phenomena are believed to be related to interactions among the adsorbed species in pores of diameters approaching molecular dimensions. Heats of adsorption on silica–alumina fell smoothly from 39.5 kcal/mol at $\theta = 0.03$ to 13.0 kcal/mol at $\theta = 1.00$. Adsorption–desorption characteristics of methylamine were also examined on a series of silica gels with widely different pore structures. The variations in the heats of adsorption with surface coverage are discussed in terms of both the nature of the adsorbed surface species and lateral interactions among the adsorbed molecules.

L'adsorption de la monométhylamine a été étudiée au voisinage de son point d'ébullition, 266 °K, sur silice–alumine et sur plusieurs silica gels en mesurant les isothermes d'adsorption–désorption et les chaleurs d'adsorption isothermes calorimétriques. De plus les aires de la surface ainsi que les distributions dans la taille des pores ont été déterminées par adsorption de l'azote à basse température. Les chaleurs d'adsorption sur le silica gel Davison "923" varient de 33.0 kcal/mol à $\theta = 0.01$ à 6.2 kcal/mol à la saturation monocouche. Des maxima ont été observés sur la courbe de chaleur dans les régions $\theta = 0.15$, 0.28, et 0.40. On pense que ces phénomènes sont en relation avec les interactions entre les espèces adsorbées dans les pores dont les diamètres sont proches des dimensions de la molécule. Les chaleurs d'adsorption sur silica–alumine chutent lentement de 39.5 kcal/mol à $\theta = 0.03$ jusqu'à 13.0 kcal/mol pour $\theta = 1.00$. Les caractéristiques de l'adsorption–désorption de la méthylamine ont été également examinées sur une série de silica gels de structures de pore largement différentes. Les variations dans les chaleurs d'adsorption avec la surface recouverte sont discutées en tenant compte à la fois de la nature des espèces adsorbées sur la surface et des interactions latérales entre les molécules adsorbées.

Canadian Journal of Chemistry, **50**, 1666 (1972)

Introduction

Most adsorption studies of amines and basic vapors on siliceous adsorbents have been concerned with the estimation of the "acid strength" of the adsorbent (1–3). Such investigations are often activated by industrial interest in the properties of cracking catalysts, while certain other studies, using ammonia mainly, have provided fundamental data on surface complexes and gas/solid interactions through measurements of isosteric (4) and calorimetric (5, 6) heats of adsorption. Work in this general area has therefore both applied and basic connotations.

In previous papers (7, 8) the possible modes of the interaction of ethylamine on silica and silica xerogels have been deduced from studies of adsorption–desorption isotherms, rates of desorption, and isosteric heats of adsorption. However, many problems remain to be solved, particularly in regard to the general nature of the adsorption process up to 0.1 to 0.2 of a monolayer. With this aim and with the additional need to obtain comparative and comprehensive data on the adsorption of other amines, a study of the adsorption of monomethylamine vapor has been made from 246 to 286 °K, mainly through the measurement of isotherms and isothermal calorimetric heats of adsorption.

Experimental

Materials

The physical and chemical properties of the adsorbents other than silica–alumina have been specified (8) previously. The low temperature nitrogen adsorption–desorption isotherm for silica–alumina is shown in Fig. 1 with a B.E.T. plot inset. This material contained 13% w/w alumina, surface area 610 m^2/g and mercury "lump" density 0.445 g/cc after treatment at 240 °C for 3 h. Any other necessary data regarding these materials are included in the Results section.

Monomethylamine (Matheson) was vacuum distilled over three columns of sodium hydroxide into a cold trap. The

Can. J. Chem. Downloaded from www.nrcresearchpress.com by 210.87.254.42 on 09/05/12
For personal use only.

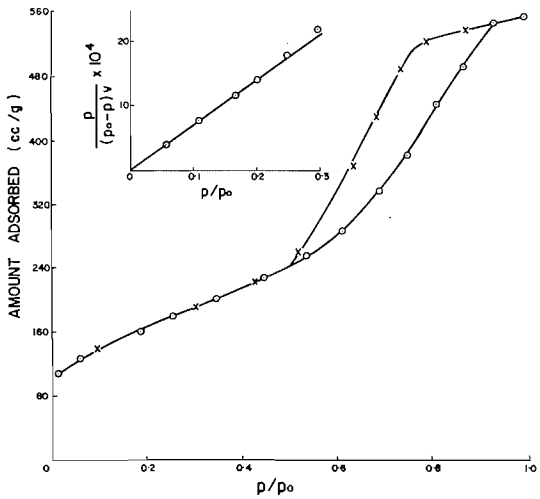

FIG. 1. Low temperature nitrogen adsorption–desorption isotherm for silica–alumina. Inset, B.E.T. plot.

first and last fractions were discarded while the acceptable fraction was outgassed thrice immediately prior to admission to the adsorbent. The final purity, determined by gas–liquid chromatography, was 99.6%, principal impurity was dimethylamine.

n-Butane (Matheson) and nitrogen (British Oxygen Co.) were both >99.90% pure.

Apparatus and Method

Details of the sorption balance have been described (7). The apparatus used to determine "lump" densities by mercury displacement was adapted from that used by Jepson (9). The calorimeter was operated isothermally (10) and was similar to that detailed earlier (10) with slight design modifications to the sample holder, calibration heater and thermistor assembly. Sample temperature control was $\pm 0.05°$ over the refrigeration bath range of -30 to $+60$ °C and the least detectable heat input from the internal heater was 0.2 cal.

Results

Monomethylamine Adsorption/Desorption Isotherms and Isosteric Heats of Adsorption

Figure 2 shows the complete adsorption–desorption isotherm of methylamine on Davison "923" silica gel at 266 °K, boiling point, after activation of the gel at 513 °K for 3 h. Adsorption equilibrium was achieved within 5–10 min up to about 160 mg/g methylamine adsorbed. The equilibrium time gradually increased to a maximum of 60 min at the highest relative pressures while the monolayer coverage value obtained from a B.E.T. plot, inset Fig. 2, was 157.5 mg/g. The reversibility of adsorption was

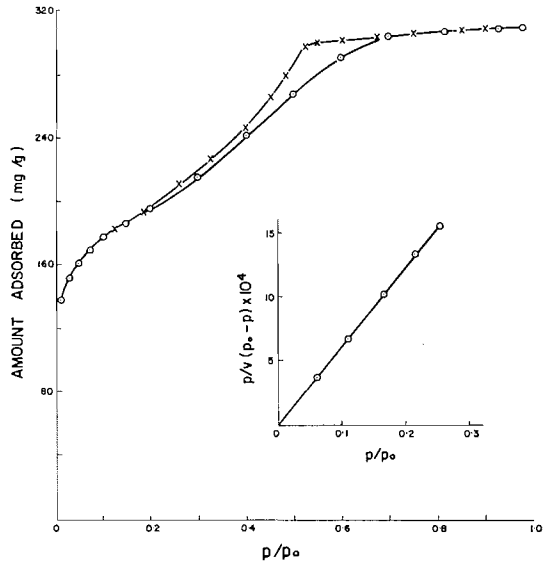

FIG. 2. Adsorption–desorption isotherm for monomethylamine at 266 °K on "923" gel. Inset, B.E.T. plot.

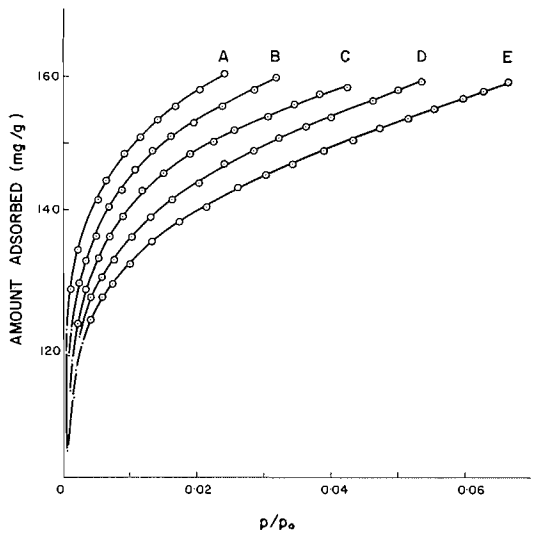

FIG. 3. Monolayer region isotherms for monomethylamine on "923" gel. Range 246–286 °K. *A*, 246 °K; *B*, 256 °K; *C*, 266 °K; *D*, 276 °K; *E*, 286 °K.

tested at four points along the isotherm in the usual fashion (7) for temperature switches between 266 and 338 °K. At each point complete reversibility of the system was found.

A series of monolayer isotherms was determined in the temperature region 246 to 286 °K at 10° intervals (Fig. 3). It can be seen from the proximity of the isotherms that the construction

Can. J. Chem. Downloaded from www.nrcresearchpress.com by 210.87.254.42 on 09/05/12
For personal use only.

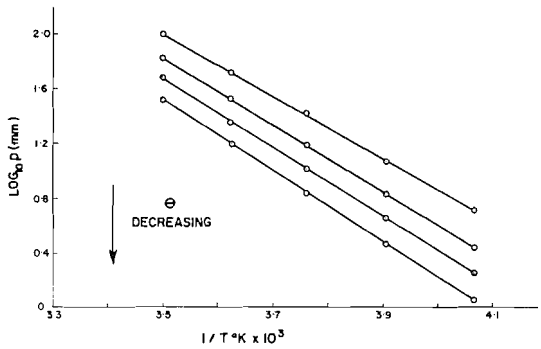

FIG. 4. Adsorption isosteres for monomethylamine on "923" gel. Surface coverage, 0.88 to 1.00 θ.

of adsorption isosteres was not possible below 140 mg/g. Figure 4 shows adsorption isosteres derived from isotherm data for the range $\theta =$ 0.88 to 1.00. For this range, isosteric heats calculated using the logarithmic form of the Clausius/Clapeyron equation (11) were of the order of 10 kcal/mol.

When the pressure of monomethylamine was increased after partial desorption in the region of the lower portion of the hysteresis loop, $p/p_0 = 0.42$ to 0.20, a new path was followed by the adsorption isotherm parallel to the original at a difference of about 4.5 mg/g above it. This new path coincided with the original at about $p/p_0 = 0.70$, the point of inception of the hysteresis loop (Fig. 5).

A series of partial adsorption/desorption isotherms was measured to ascertain the pressure at which hysteresis was initiated. Figure 6(*a*)–(*d*) shows the development of the lower part of the hysteresis loop as the isotherm was determined to increasingly higher relative pressures. The adsorption and desorption paths are coincident until p/p_0 exceeds 0.45 on adsorption and the hysteresis loop does not develop to its fullest extent until desorption from $p/p_0 = 0.60$, Fig. 6(*d*).

Monomethylamine isotherms were determined at 266 °K on a series of silica gels with different pore structures after pretreatment of these at 513 °K for 3 h. The measurements are shown in Fig. 7(*a*)–(*d*) with the B.E.T. plots inset. The adsorption characteristics of the materials are summarized in Table 1 along with the comparative information for Davison "923" gel.

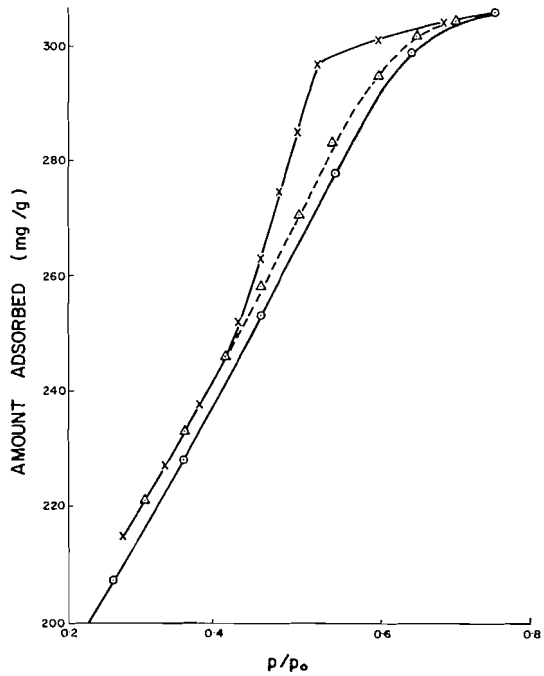

FIG. 5. Monomethylamine hysteresis loop on "923" gel. ○, Adsorption points; ×, desorption points; △, re-adsorption points.

Isothermal Calorimetric Heats of Adsorption

The heat curve from $\theta = 0.01$ to 1.00 at 266 °K for monomethylamine on "923" gel after activation at 513 °K for 3 h followed by outgassing the sample at 363 °K for 1 h at $> 10^{-5}$ mm is shown in Fig. 8, curve *A*. The three minima and maxima which occur between $\theta = 0.10$ to about 0.40 were particularly striking, they were repeated and carefully checked. To test further the validity of these results, a heat curve for *n*-butane was determined which would be expected to exclude any surface effects which might be due to acid site and/or polar interactions in the amine experiments, but would include any characteristics of the methylamine heat curve possibly related to instrumental functions. No maxima or minima were observed in the butane heat curve as shown in Fig. 8, curve *B*.

Since the "high surface area" silica gel gave a similar low temperature nitrogen adsorption/desorption isotherm to that of Davison "923" gel, calorimetric heats were determined on this material for comparative purposes. The results are shown in Fig. 9 along with the heat curve for

Can. J. Chem. Downloaded from www.nrcresearchpress.com by 210.87.254.42 on 09/05/12
For personal use only.

Can. J. Chem. Downloaded from www.nrcresearchpress.com by 210.87.254.42 on 09/05/12
For personal use only.

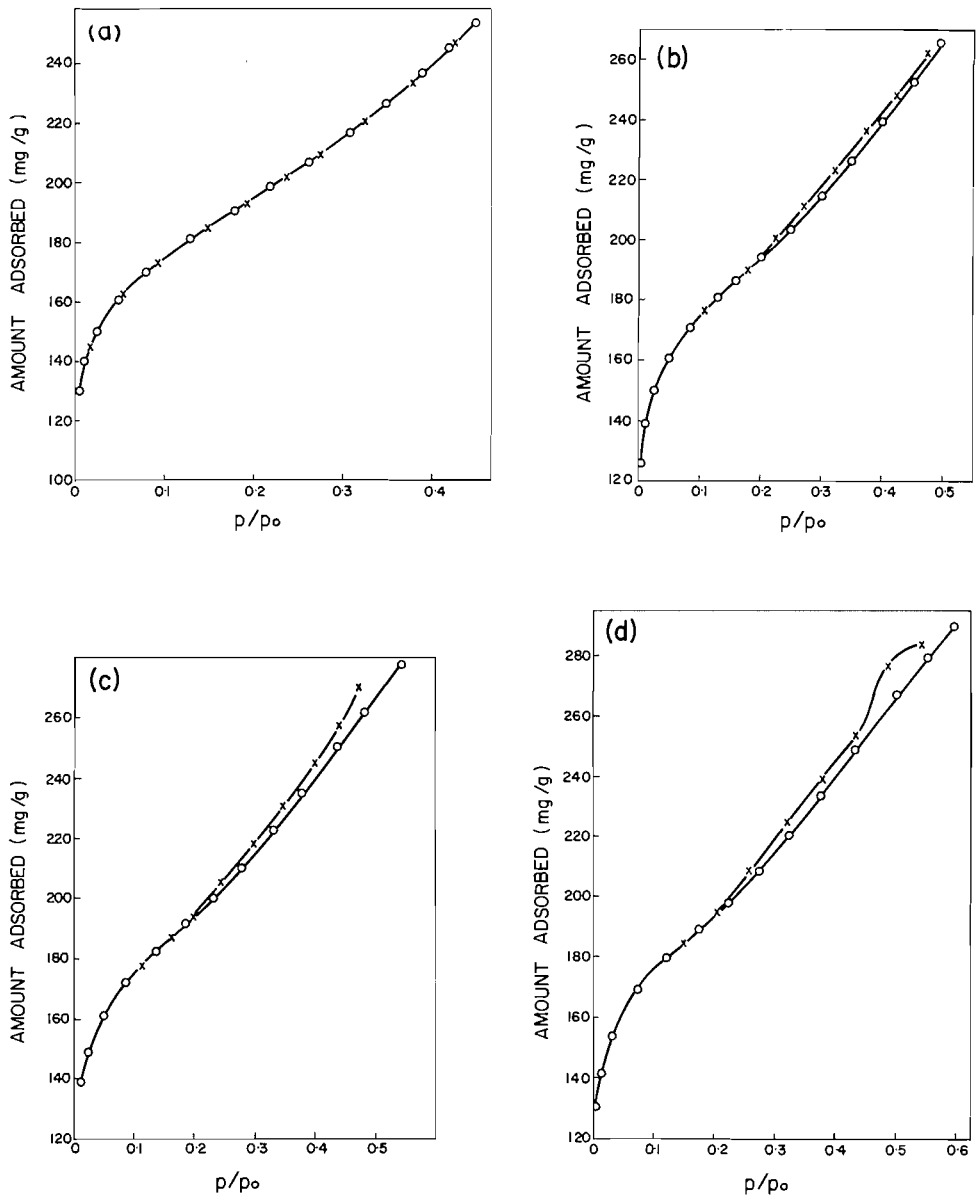

FIG. 6. Development of the lower portion of the hysteresis loop on adsorption to, and desorption from (*a*) $p/p_0 = 0.450$, (*b*) $p/p_0 = 0.500$, (*c*) $p/p_0 = 0.545$, and (*d*) $p/p_0 = 0.600$.

silica–alumina. Both of these materials were activated in the same fashion as the Davison "923" gel prior to the experiments.

A summary of the isothermal calorimetric heats for monomethylamine obtained with the various adsorbents for three standard values of surface coverage is presented in Table 2.

Discussion

Adsorption of methylamine on "923" gel was initially rapid with about one-third of the total adsorbed amount adsorbed below $p/p_0 \sim 0.001$. Equilibrium times were short and even after pumping to 10^{-5} mm at a temperature of 353 °K small amounts, ~4 mg/g, of the amine

Can. J. Chem. Downloaded from www.nrcresearchpress.com by 210.87.254.42 on 09/05/12
For personal use only.

TABLE 1. Summary of surface areas, pore distributions, mercury densities, and monomethylamine adsorption characteristics of the adsorbents

Adsorbent	Surface area (m^2/g)	Complete range of pore diameters (Å)	Main distribution of pore diameters (Å)	Mercury density (g/cc)	Monolayer coverage value (mg/g)	Monolayer coverage pressure (p/p_0)	Hysteresis loop properties			Amount adsorbed at $p/p_0 = 0.950$ (mg/g)
							Opened (p/p_0)	Closed (p/p_0)	Maximum width of loop (mg/g)	
Davison "923"	650	<20–110	<20–80	1.163	157.5	0.038	0.73	0.26	24.0	308.5
"High surface area"	840	<20–120	<20–80	1.120	173.4	0.030	0.80	0.46	31.5	330.5
"Microporous"	730	<20–120	<20–30	1.217	157.0	0.036	—	—	—	239.2
"Macroporous"	215	60–300	200–240	0.336	43.8	0.033	—	0.50	20.6	—
"Neosyl F.X."	690	<20–110	<20–80	0.258	142.8	0.026	0.82	—	9.0	276.0
Silica/alumina	610	<20–300	<20–120	0.445	127.3	0.030	—	0.02	50.0	670.0

Can. J. Chem. Downloaded from www.nrcresearchpress.com by 210.87.254.42 on 09/05/12
For personal use only.

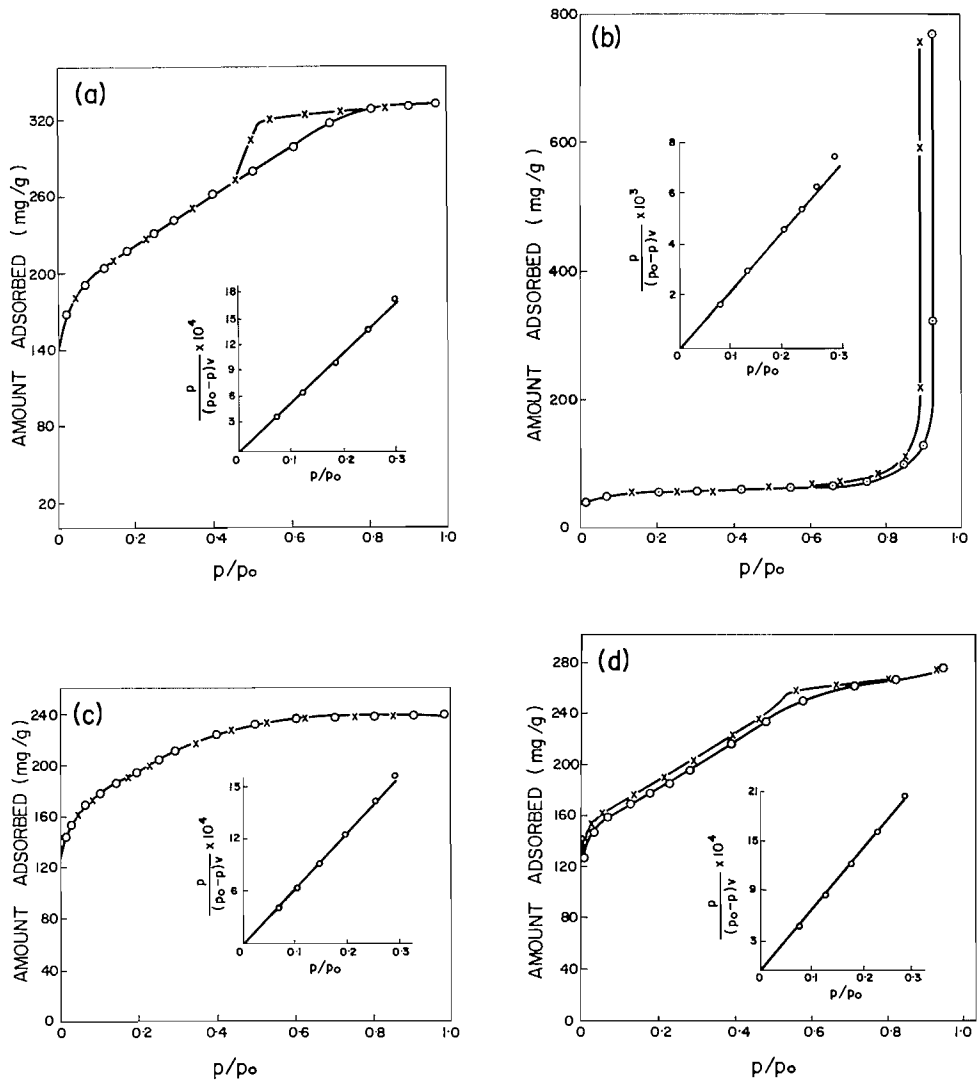

FIG. 7. Adsorption–desorption isotherms for methylamine on (*a*) "high surface area" gel, (*b*) "macroporous" gel, (*c*) "microporous" gel, (*d*) "neosyl F.X." silica. Inset B.E.T. plots.

were still retained by the gel on desorption from $p/p_0 = 0.90$. All of these factors (8) are indicative of strong adsorbate/adsorbent interactions in the initial steep adsorption region of the isotherm, which involve forces considered to be at least partly "chemical" in nature. Similar preliminary observations and conclusions have been made in previous studies concerning aliphatic amines (7, 12).

From the monolayer coverage amount of 157.5 mg/g on "923" gel and the B.E.T. surface area, 650 m^2/g, the average concentration of adsorbed methylamine molecules can be shown to be 47 per 1000 $Å^2$ of surface. This indicates that generally one methylamine molecule is adsorbed for every OH group on the gel surface since the hydroxyl group concentration, determined as previously described (7) was 49 per 1000 $Å^2$. Other workers (13) quote a concentration of 48 hydroxyl groups per 1000 $Å^2$ for similarly treated silica gels. From Livingstone's equation for cross-sectional areas of adsorbed molecules (14) and assuming two dimensional close packing, the cross-sectional area of an

Can. J. Chem. Downloaded from www.nrcresearchpress.com by 210.87.254.42 on 09/05/12
For personal use only.

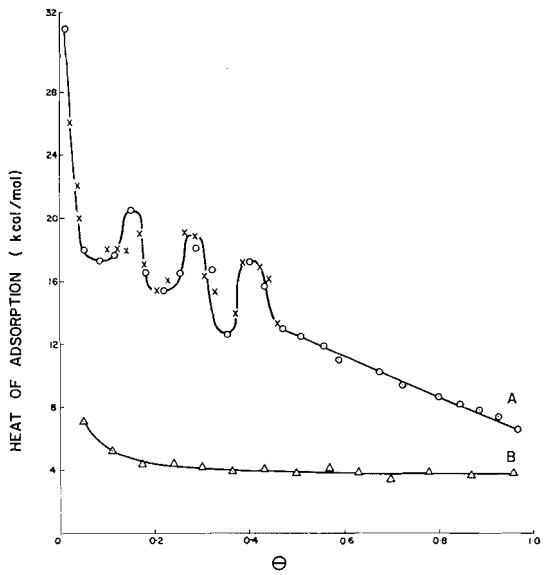

FIG. 8. Variation of isothermal calorimetric heat of adsorption with θ for Davison "923" gel. *A*, methylamine adsorption; *B*, butane adsorption.

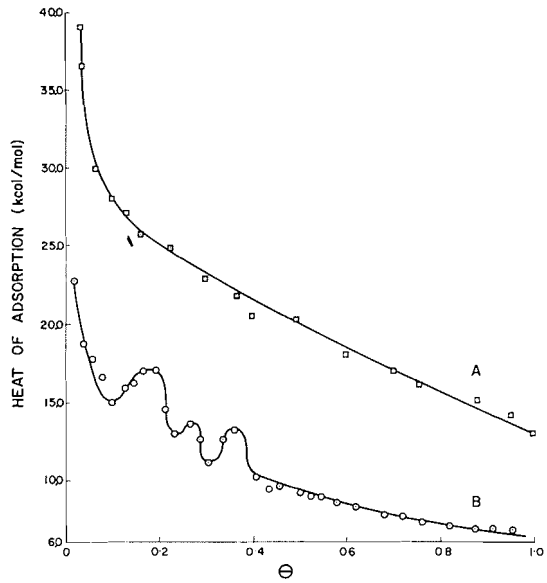

FIG. 9. Variation of calorimetric isothermal heat of adsorption with θ for methylamine on (*A*) silica–alumina and (*B*) "high surface area" silica gel.

adsorbed methylamine molecule was calculated as 19 to 20 Å^2. This alternative statistical approach yields an approximate figure of around 920 Å^2 for the total area occupied by 47 adsorbed molecules and adds evidence to the view

TABLE 2. Monomethylamine calorimetric isothermal heats of adsorption at various surface coverages on siliceous adsorbents

	Heat evolved at various surface coverages (kcal/mol)		
Adsorbent	$\theta = 0.010$	$\theta = 0.500$	$\theta = 1.000$
Davison "923"	33.0	13.5	6.2
"High surface area"	24.2	9.0	6.1
Silica–alumina	39.5 (θ = 0.030)	19.6	13.0

that the hydroxyl groups are directly involved in methylamine adsorption.

The general shape of the hysteresis loop given by methylamine on "923" gel falls between loop types "D" and "E" in de Boer's nomenclature (15). However, the tendency for the desorption branch to run nearly parallel with the adsorption branch at p/p_0 values from about 0.4 to 0.2 and also the path followed by the adsorption scanning-curve indicate that the pore shapes are largely of the "ink-bottle" type (16). Similar conclusions have been advanced previously for "923" gel from results obtained by electron microscopy and low-temperature nitrogen adsorption (17).

From the partial adsorption–desorption isotherms, Fig. 6, it can be observed that the partial hysteresis loop between $p/p_0 = 0.42$ to 0.20 is linked to adsorption which occurs between $p/p_0 = 0.45$ to 0.60. Pores filling in this region are from 37 to 53Å diameter (18). Molecules desorbing through the narrow passages in these "ink-bottle" pores where the cross-section approaches molecular dimensions would have a slow rate of outward diffusion, possibly involving a series of adsorption/desorption hops along the pore walls (7). This phenomenon is clearly linked to pore shape and structure since it was not observed with the other gels.

Figure 7(*a*)–(*d*) shows the isotherms for the other gels. The isotherm determined on "high surface area" material is best classified as type "E" (15). "Microporous" gel has a pore size distribution largely from 20 to 30Å diameter (11) and gave no hysteresis effects. The asymptotic rise in adsorption above $p/p_0 = 0.90$ with the "macroporous" gel is probably due to condensation of methylamine in macropores >200 Å diameter as the pore distribution of the

Can. J. Chem. Downloaded from www.nrcresearchpress.com by 210.87.254.42 on 09/05/12
For personal use only.

material ranges mainly from 200 to 240 Å diameter (11). The hysteresis loop obtained with "Neosyl F.X." remains open to below $p/p_0 = 0.01$. This material is finely divided silica with a lump density, 0.258 g cc^{-1}, much lower than that of "923" gel, 1.163 g cc^{-1}, but with a pore range comparable to that of "923" gel (11). The failure of the hysteresis loop to close is probably due to a small measure of irreversible adsorption within the interior pore matrix of this extremely porous material.

The calorimetric heat curve for methylamine on "923" gel, Fig. 8, indicates a high initial heat of 33 kcal/mol at $\theta = 0.01$. This compares with previously estimated values of 30 to 40 kcal/mol for the isosteric heat of adsorption of ethylamine on the same gel at surface coverages below $\theta = 0.10$ (8) and with a value of around 38 kcal/mol (19) for the isosteric heat of adsorption of ammonia on silica gel, heat-treated at 500 °C for 1 h under high vacuum, at a surface coverage of less than two adsorbed molecules per 1000 $Å^2$. Such heat values point to the formation of a linkage between the adsorbed molecule and surface silanol groups which is "chemical" in nature (8). The silanol groups may be expected to act as Brønsted acid sites (7) with the possibility of proton displacement to the adsorbed amine taking place such that, in the limit, a charge-transfer or ionic type of adsorbed complex may be formed on the surface. A similar possibility has been suggested previously to explain the adsorption of triethylamine on silica gel (20).

The initial heat falls rapidly to 17.0 kcal/mol at $\theta \sim 0.10$ on "923" gel, Fig. 8, and similarly to 15.0 kcal/mol with "high surface area" gel, Fig. 9, at the same surface coverage. Then, with both of these gels distinct heat rises amounting to about 2 kcal/mol were observed up to $\theta = 0.50$. This phenomenon has not been observed previously with such systems to the same extent, although single heat maxima beginning in similar surface coverage regions have been recorded in studies of the heats of adsorption of *n*-butylamine on kaolin (21), triethylamine on silica/alumina (4), and ammonia on silica/alumina and silica (5, 22). In the particular instance of ammonia adsorbed on silica (22) the heat rise of about 2 kcal/mol in the region of 5% coverage was not observed in later experiments (6). In view of the latter difference particular attention was given to the verification of the present results.

The explanation of the phenomenon seems most probably linked to the pore structure of the adsorbents. Thus the heat rises occur at similar coverages, $\theta = 0.15$, 0.28, and 0.40 with "923" gel and at $\theta = 0.18$, 0.27, and 0.36 with "high surface area" gel. These regions of surface coverage are most likely to correspond to adsorption in pores of monomolecular dimensions since monolayer coverages at about $p/p_0 = 0.04$ corresponds to the filling of pores of less than 20 Å diameter as determined by nitrogen adsorption methods (18). The interactions of adsorbing methylamine molecules at $\theta = 0.10$, with the previously formed ionic-type adsorbed species in molecular size capillaries could be expected to lead to a temporary rise in heat liberated. This possibility would be enhanced by the existence of some of the adsorbing hydroxyl groups in dense "islands" (23), thereby increasing the likelihood of the occurrence of lateral interactions among the adsorbed molecules.

The existence of three heat rises may indicate that molecular access to all such species does not occur at the same time but depends on increase of pressure allowing the occupation of slightly larger pores, thus bringing further adsorbing molecules into intimate contact with further charged species. It is especially noticeable that in the case of "923" gel the peaks are of approximately equal distance, 2 kcal/mol, above the base of the heat curve. As increasing numbers of methylamine molecules are adsorbed around the charged complexes their sphere of influence will decrease by virtue of the increase in distance, thereby causing a decrease in the heat liberated. This situation could cause the falls in the heat curve observed after the initial rise in each case.

From $\theta = 0.50$ to monolayer coverage with "923" gel the heat curve falls almost linearly from 13.5 to 6.2 kcal/mol, and for "high surface area" gel from 9.0 to 6.1 kcal/mol. These final heats are substantially higher than the latent heat of condensation for methylamine, 0.199 kcal/mol (24), and may indicate that the formation of bonds of the N---H—O type (8) is still likely even at monolayer completion.

The heat curve for methylamine adsorption on silica–alumina, Fig. 9, shows no irregulari-

ties and falls smoothly from 39.5 kcal/mol at $\theta = 0.03$ to 13.0 kcal/mol at $\theta = 1.00$. The general form of the curve is similar to that found previously for ammonia on silica–alumina (6, 19). The curve shows higher heat values at all points than either of the methylamine heat curves determined on "923" or "high surface area" silica gels. Thus at $\theta = 0.10$, 0.50, and 1.00 heats for silica–alumina were about 29.0, 19.6, and 13.0 kcal/mol while at these coverages the average values for the gels were 14.5, 11.3, and 6.2 kcal/mol, respectively. The higher heats may be explained by the adsorption of methylamine molecules through coordination of the lone-pair electrons of the nitrogen atoms to electron deficient aluminum atoms exposed on the gel surface as has been suggested previously to explain methylamine adsorption on alumina (25). The higher heat values over the entire range of coverage for silica–alumina are certainly indicative of the presence of a much greater number of strongly adsorbing sites than is present on the gels.

1. O. JOHNSON. J. Phys. Chem. **59**, 827 (1955).
2. G. A. MILLS, E. R. BELDEYER, and A. C. OBLAD. J. Am. Chem. Soc. **72**, 1559 (1950).
3. H. PINES and W. O. HAAG. J. Am. Chem. Soc. **82**, 2411 (1960).
4. Y. TEZEUKA and T. TAKEUCHI. Bull. Chem. Soc. Jap. **38**, (3), 485 (1965).
5. P. Y. HSIEH. J. Catal. **2**, 211 (1963).
6. F. S. STONE and L. WHALLEY. J. Catal. **8**, 173 (1967).
7. R. A. ROSS and A. H. TAYLOR. Proc. Brit. Ceram. Soc. **5**, 167 (1965).
8. R. A. ROSS and A. H. TAYLOR. J. Catal. **9**, 104 (1967).
9. W. B. JEPSON. J. Sci. Inst. **36**, 319 (1959).
10. E. ROBINSON and R. A. ROSS. J. Chem. Soc. (A), 2521 (1969).
11. R. A. ROSS and A. H. TAYLOR. J. Chem. Eng. Data, **14**, (3), 347 (1969).
12. F. E. BARTELL and D. G. DOBAY. J. Am. Chem. Soc. **72**, 4388 (1950).
13. L. T. ZHURALEV and A. V. KISELEV. Zhur. Fiz. Khim. (Engl. Transl.) **39**, (2), 236 (1965).
14. H. K. LIVINGSTONE. Z. Colloid. Sci. **4**, 450 (1949).
15. J. H. DE BOER. Colston papers. Vol. 10. Butterworths Scientific Publications, London. 1958. p. 68.
16. D. H. EVERETT. The solid–gas interface. *Edited by* E. A. Flood. Marcel Dekker, Inc., New York. Vol. 2. 1967. pp. 1055, 1063.
17. E. ROBINSON and R. A. ROSS. Can. J. Chem. **48**, 14 (1970).
18. R. W. CRANSTON and F. A. INKLEY. Adv. Catal. **9**, 143 (1957).
19. A. CLARK, V. C. F. HOLM, and D. M. BLACKBURN. J. Catal. **1**, 244 (1962).
20. A. V. KISELEV and V. V. KULICHENKO. Dokl. Akad. Nauk. S.S.S.R. **93**, 101 (1953).
21. A. C. ZETTLEMOYER and J. J. CHESSICK. J. Phys. Chem. **64**, 1131 (1960).
22. V. KERVORKIAN and R. G. STEINER. J. Phys. Chem. **67**, 545 (1962).
23. A. V. KISELEV. Infrared spectra of adsorbed species. Academic Press Inc. New York. 1966. p. 276.
24. Matheson gas data book. The Matheson Company, Inc. 353 (1966).
25. K. HIROTA, K. FEUKI, and T. SAKAI. Bull. Chem. Soc. Jap. **35**, 1545 (1962).

Can. J. Chem. Downloaded from www.nrcresearchpress.com by 210.87.254.42 on 09/05/12
For personal use only.

Réaction du sulfure de bore avec quelques composés difonctionnels

S. JERUMANIS, P. A. BEGIN, ET D. VU CONG
Département de chimie, Université de Sherbrooke, Sherbrooke, Québec

Reçu le 6 octobre 1971

Les auteurs ont étudié la réaction du sulfure de bore avec le catéchol, l'acide salicylique, l'acide succinique, l'acide maléique, et l'acide phtalique. La réaction du catéchol avec le sulfure de bore donne l'*o*-phénylènedioxy-2,2′ bis-(benzodioxa-1,3 borole-2) (**1**) tandis que l'acide salicylique réagit seulement par sa fonction hydroxyle pour donner le tris(*o*-carboxylphénoxy) borane (**3**). Les acides succinique et maléique ne réagissent pas, mais l'acide phtalique subit une déshydratation et se transforme quantitativement en anhydride.

Catechol reacts with boron sulfide to give 2,2′-*o*-phenylenedioxybis-(1,3,2-benzodioxaborole) (**1**) while only the hydroxyl function of salicylic acid reacts to give a quantitative yield of tris(*o*-carboxylphenoxy)borane (**3**). Phthalic acid is dehydrated to phthalic anhydride, but succinic acid and maleic acid have been found inert to the action of the boron sulfide.

Canadian Journal of Chemistry, **50**, 1675 (1972)

Can. J. Chem. Downloaded from www.nrcresearchpress.com by 210.87.254.42 on 09/05/12
For personal use only.

La réaction du sulfure de bore avec divers types de molécules monofonctionnelles possédant un hydrogène mobile, tels que les amines (1), les mercaptans (2), les alcools (3), et les acides (4) a été déjà étudiée. Par contre la réaction avec les molécules hydroxylées polyfonctionnelles n'a pas encore été rapportée. Nous avons étudié cette réaction avec l'acide salicylique, l'acide phtalique, l'acide maléique, l'acide succinique, et le catéchol.

Le catéchol réagit avec le sulfure de bore pour donner de l'*o*-phénylènedioxy-2,2′ bis-(benzodioxa-1,3 borole-2) (**1**), éq. 1.

On admet que le biborate de tricatéchol **1** est linéaire, la forme bicyclique **2** proposée par

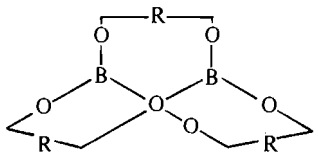

2

Dupire (5) pour les biborates des 1,2- et 1,3-diols étant considérés comme peu probable en raison de l'instabilité (6).

Même, si la formation de la liaison B—O est confirmée par une forte absorption à 1460 cm^{-1}, la spectroscopie i.r., la r.m.n., et l'analyse centésimale ne permettent pas une distinction très nette entre ces deux formes du biborate. Par contre, en analysant le spectre de masse de cette substance on peut établir plus clairement cette distinction. En effet, l'ion moléculaire à $m/e = 346$ indique que la réaction du sulfure de bore avec le catéchol donne un monomère et la présence des fragments:

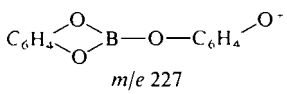

m/e 227

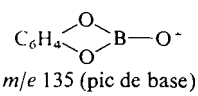

m/e 135 (pic de base)

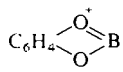

m/e 119

confirme que le biborate obtenu existe sous la forme linéaire.

L'acide salicylique réagit avec le sulfure de bore seulement par son groupement hydroxyle pour donner la naissance au tris(*o*-carboxylphénoxy)borane (**3**), éq. 2.

Les spectres d'absorption dans l'i.r. des com-

[1] 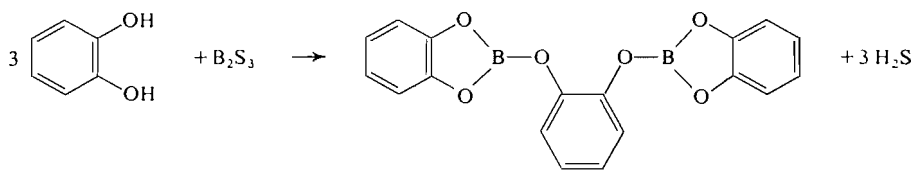

1

[2] 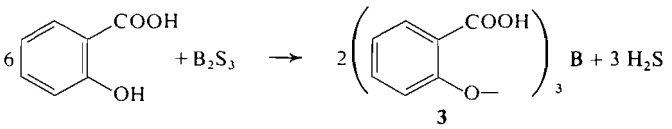

3

posés **1** et **3** montrent la présence de bore différemment hybridé (7) et sont compatibles avec leurs structures (voir partie expérimentale).

Avec l'acide phtalique on n'observe pas la formation de la liaison B—O mais une simple déshydratation. Même à la température ambiante l'acide phtalique en présence du sulfure de bore est quantitativement transformé en anhydride phtalique. Par contre, l'acide maléique ne se déshydrate pas. Dans le benzène à reflux l'acide maléique s'isomérise en acide fumarique et on n'observe aucune réaction avec le sulfure de bore. Egalement l'acide succinique reste inerte en présence du sulfure de bore.

Partie expérimentale

Les spectres i.r. ont été pris sur le spectrophotomètre Perkin–Elmer modèle 257.

Les spectres de r.m.n. ont été obtenus avec un appareil Varian A60, en se servant de tétraméthylsilane comme référence interne.

Les points de fusion (p.f.) ont été déterminés en tubes capillaires au moyen d'un appareil Büchi et ne sont pas corrigés. Les analyses élémentaires furent effectuées par "Schwarzkopf Microanalytical Laboratory" de New York.

Les spectres de masse ont été enregistrés sur un appareil Hitachi–Perkin–Elmer, modèle RMU-6D.

Le pourcentage de bore a été déterminé par la méthode de Thomas (8).

(1) Réaction du catéchol avec le sulfure de bore

Une solution de 18 g (0.16 mol) de catéchol dans 500 ml de benzène anhydre et 6.4 g (0.054 mol) de sulfure de bore est refluée sous atmosphère d'azote jusqu'à ce que cesse le dégagement du sulfure d'hydrogène. Durant cette réaction le sulfure de bore est maintenu en suspension par une agitation magnétique. Au terme de ce contact, le mélange réactionnel est filtré à chaud sur un filtre d'amiante et le filtrat concentré par évaporation sous pression réduite. On obtient ainsi une poudre légèrement jaunâtre, p.f. 71–104 °C. Ce produit brut est repris dans l'éther anhydre pour éliminer le soufre et la solution éthérée est évaporée sous vide. Le produit obtenu est traité par le sulfure de carbone pour séparer le catéchol qui n'a pas réagit. Après la filtration, le sulfure de carbone est évaporé sous vide. Cette opération est répétée plusieurs fois. On obtient ainsi une poudre blanche, p.f. 91–93 °C (litt. 99–104 (8); 104 (9); 71–73.5 (10); 72–74° (11)), représentant 50% du poids de substance mis en expérience. Spectre i.r. (KBr): bandes à 1460 et 1235 (fortes), 3050, 1600 (faibles), 735 cm^{-1} (large). Spectre de r.m.n. (dans l'acétone-d_6): absorption aromatique dans la région 2.6–3.3 τ.

Anal. calc. pour $C_{18}H_{12}O_6B_6$: C, 62.49; H, 3.47; B, 6.25. Trouvé: C, 62.44; H, 3.70; B, 6.40.

Spectre de masse, *m/e*: 346, 227, 135, 119, 109, 93, 65, 27.

(2) Réaction de l'acide salicylique avec le sulfure de bore

A une suspension de 6.62 g (0.05 mol) du sulfure de bore dans 500 ml de benzène anhydre 20 g (0.14 mol) d'acide salicylique est ajouté et la réaction est effectuée suivant le protocole donné pour le catéchol. Le produit obtenu après l'évaporation du solvant est lavé à l'éther sec. On obtient ainsi les cristaux blancs, p.f. 258–260 °C, avec un rendement quantitatif. Spectre i.r. (KBr): bandes à 3000 (large), 1700 (forte), 1615 et 1580 (moyennes), 1348 et 1225 (fortes), 775 cm^{-1} (épaulement). Spectre de r.m.n. (dans l'acétone-d_6): multiplet entre 1.90 et 3.00 τ.

Anal. calc. pour $C_{21}H_{15}O_9B$: C, 59.74; H, 3.58; B, 2.56. Trouvé: C, 59.47; H, 3.38; B, 2.35.

Spectre de masse, *m/e*: 285, 121, 120 (pic de base), 45.

(3) Réaction de l'acide succinique avec le sulfure de bore

A une suspension de 2 g (0.017 mol) du sulfure de bore dans 300 ml d'acétone, 6 g (0.051 mol) d'acide succinique est ajouté et le mélange chauffé et agité durant 6 jours sous atmosphère d'azote. Par la filtration on retrouve le sulfure de bore inchangé et un filtrat qui après décoloration et évaporation met en liberté la quantité initiale d'acide succinique, p.f. 144–146 °C.

(4) Réaction de l'acide maléique avec le sulfure de bore

Une solution de 20 g (0.17 mol) d'acide maléique dans 500 ml de dioxane anhydre est refluée pendant 6 jours en présence de 10 g (0.084 mol) du sulfure de bore en suspension. La solution chaude est ensuite filtrée et décolorée sur le charbon actif. Après évaporation sous vide le résidu est recristallisé dans le mélange de dioxane–éther. Le produit final est un solide blanc qui est identifié par les méthodes spectroscopiques (i.r. et r.m.n.) et d'après son p.f. (299–301 °C) comme étant l'acide fumarique.

(5) Réaction de l'acide maléique avec le sulfure de bore

Une solution de 20 g (0.12 mol) d'acide phtalique dans 500 ml de dioxane anhydre à 25 °C est agitée pendant 12 jours en présence de 5.64 g (0.046 mol) du sulfure de bore, sous atmosphère d'azote. La masse réactionnelle est filtrée. Le filtrat est évaporé sous vide et le produit solide lavé au sulfure de carbone, et puis repris dans l'éther anhydre. On obtient ainsi, après évaporation de l'éther, 17.5 g d'un produit incolore, sous formes d'aiguilles brillantes, p.f. 131 °C. Décrit pour l'anhydride phtalique, p.f. 130.8 °C. Les spectres i.r. d'un échantillon authentique de l'anhydride phtalique et de substance obtenue sont identiques.

Les auteurs remercient le Conseil National de Recherches du Canada pour le subside de recherche accordé.

1. S. JERUMANIS et J.-M. LALANCETTE. J. Org. Chem. **31**, 1531 (1966).

Can. J. Chem. Downloaded from www.nrcresearchpress.com by 210.87.254.42 on 09/05/12
For personal use only.

2. J. BRAULT et J.-M. LALANCETTE. Can. J. Chem. **42**, 2903 (1964).
3. J.-M. LALANCETTE. Can. J. Chem. **42**, 2356 (1964).
4. J.-M. LALANCETTE, F. BESSETTE, et J.-M. CLICHE. Can. J. Chem. **44**, 1577 (1966).
5. A. DUPIRE. Compt. Rend. **202**, 2086 (1936).
6. A. J. HUBERT, B. HARGITAY, et J. DALE. J. Chem. Soc. 931 (1961).
7. J. A. BLAU, W. GERRARD, M. F. LAPPERT, B. A. MOUNTFIELD, et H. PYSZORA. J. Chem. Soc. 380 (1960).
8. L. H. THOMAS. J. Chem. Soc. 820 (1946).
9. W. GERRARD, M. F. LAPPERT, et B. A. MOUNTFIELD. J. Chem. Soc. 1529 (1959).
10. J. PROCHAZKA. Czech. Pat. 84 283 (1955).
11. J. F. WILLEMS et A. E. VAN HOOF. Brit. Pat. 812673 (1959).

Can. J. Chem. Downloaded from www.nrcresearchpress.com by 210.87.254.42 on 09/05/12
For personal use only.

Photolysis of 2,5- and 2,4-Dimethylpyrrole Vapors at Room Temperature[1]

E. CHUNG WU[2] AND JULIAN HEICKLEN

Department of Chemistry and Center for Air Environment Studies, The Pennsylvania State University, University Park, Pennsylvania 16802

Received December 6, 1971

Both 2,5- and 2,4-dimethylpyrrole vapors at pressures from 0.05 to 0.70 Torr were irradiated at 2139 and 2288 Å at room temperature. The products were H_2, CH_4, C_2H_6, and polymer. No ring cleavage products were found. $\Phi\{H_2\}$ and $\Phi\{CH_4\}$ were remarkably insensitive to which pyrrole was used, its pressure, I_a, or the wavelength of the incident radiation. They were ~0.10–0.15 and ~0.01–0.02, respectively. $\Phi\{C_2H_6\}$ was comparable to $\Phi\{CH_4\}$ and was also invariant to which substrate was used or the incident wavelength. However $\Phi\{C_2H_6\}$ did increase at low pressure or as I_a was reduced.

The effect of scavengers showed that the products were produced mainly from free radical precursors. The main primary steps are:

$$\begin{aligned} DMP + h\nu &\rightarrow DMP^* \\ DMP^* &\rightarrow H + F_a \\ &\rightarrow CH_3 + F_b \\ &\rightarrow DMP \end{aligned}$$

where DMP* is an electronically excited state of the dimethylpyrrole and F_a and F_b are radical fragments. Experiments with quenching gases showed that DMP* could be quenched, but that this reaction was less important than the first-order steps below 1 Torr.

Les vapeurs de diméthyl-2,5 et diméthyl-2,4 pyrrole ont été irradiées toutes deux à 2139 et 2288 Å à la température ambiante sous un vide de 0.05 à 0.70 Torr. Les produits obtenus sont H_2, CH_4, C_2H_6 et du polymère, à l'exclusion de produits d'ouverture de cycle. $\Phi\{H_2\}$ et $\Phi\{CH_4\}$ sont remarquablement indépendants du pyrrole utilisé, de sa pression, I_a, ou de la longueur d'onde de la radiation incidente; ils sont respectivement de ~0.10–0.15 et ~0.01–0.02. $\Phi\{C_2H_6\}$, comparable à $\Phi\{CH_4\}$ est aussi indépendant du substrat utilisé ou de la radiation incidente. Cependant $\Phi\{C_2H_6\}$ croît pour de basse pression ou lorsque I_a décroît.

L'effet des inhibiteurs montre que les produits découlent principalement de précurseurs radicalaires libres. Les étapes primaires principales sont:

$$\begin{aligned} DMP + h\nu &\rightarrow DMP^* \\ DMP^* &\rightarrow H + F_a \\ &\rightarrow CH_3 + F_b \\ &\rightarrow DMP \end{aligned}$$

où le DMP* est un état électronique excité de diméthylpyrrole et F_a, F_b des fragments radicalaires. Les expériences en présence de gaz inhibiteurs montrent que le DMP* peut être capté mais que cette réaction est moins importante que les étapes du premier ordre en dessous de 1 Torr.

Canadian Journal of Chemistry, **50**, 1678 (1972)

Introduction

Previously we have examined the photolysis of pyrrole vapor (1). We found that ring cleavage occurs, though the quantum yields were small. In this paper we extend our studies to the 2,5- and 2,4-dimethylpyrroles.

Earlier work in solution has shown that the substituted pyrroles undergo valence isomerization only. Thus the thermal (2) and photochemical (3) 1–2 and 1–3 valence isomerizations

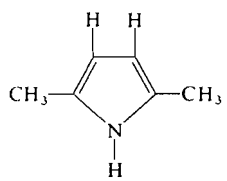

2,5-dimethylpyrrole

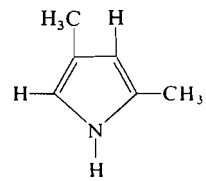

2,4-dimethylpyrrole

[1]CAES Report No. 225-71.

[2]Present address: Department of Chemistry, Texas A & M University, College Station, Texas 77843.

Can. J. Chem. Downloaded from www.nrcresearchpress.com by 210.87.254.40 on 09/05/12
For personal use only.

Can. J. Chem. Downloaded from www.nrcresearchpress.com by 210.87.254.40 on 09/05/12
For personal use only.

of benzylpyrroles have been reported. However the 2-isomer is not the precursor to the 3-isomer in the photochemical reaction, because the 2-isomer does not photoisomerize to its 3-isomer, though it does so thermally. Hiraoka (4) showed that the irradiation of 2-cyanopyrrole in methanol yielded 3-cyanopyrrole as a major product, but that the reaction was not reversible, *i.e.* irradiation of 3-cyanopyrrole did not produce 2-cyanopyrrole.

We were interested to see if the ring cleavage reactions would occur in the vapor phase for the substituted pyrroles, or whether ring isomerization would dominate. To our surprise we found that other processes were important which produced H_2, CH_4, and C_2H_6, and this paper reports the production of these products.

Experimental

2,4-Dimethylpyrrole and 2,5-dimethylpyrrole from K & K Laboratories, Inc. showed no impurity peaks on the gas chromatograms from a 20-ft long column packed with 10% tricresyl phosphate on Chromosorb G. After degassing at −64 °C, these compounds were distilled *in vacuo* from trap to trap at room temperature to remove the dark color. All gases were from the Matheson Co. HBr was distilled *in vacuo* at −130° and NO was distilled *in vacuo* at −186° after degassing at −196°. Extra dry grade O_2 and C.P. grade C_2H_4 were introduced into the reaction cell directly. Both *i*-C_4H_{10} (Instrument Grade 99.5% pure) and C_2F_6 (99.6% pure) were used as received.

The experimental apparatus and procedure were the same as described in our previous report (1), except that one additional light source, a Phillips Type 93107E Cd lamp, was used. The photochemically effective emission of this lamp is the spectral line at 2288 Å, though weak lines at 2144 and 2265 Å are also present.

The reaction mixture was passed through a trap in an acetone slush (−90 °C) after irradiation. The gaseous products were collected in a Toepler pump and analyzed on the 10-ft Porapak Q gas chromatographic column as described previously (1).

Room temperature extinction coefficients (to base 10) were found on a Cary 14 spectrophotometer to be 0.370, 0.299, and 5.5×10^{-3} $Torr^{-1}$ cm^{-1} at 2139 Å and 0.152, 0.138, and 1.17×10^{-3} $Torr^{-1}$ cm^{-1} at 2288 Å for 2,4-dimethylpyrrole, 2,5-dimethylpyrrole, and HBr, respectively.

An attempt to investigate the photoisomerization of 2,5-dimethylpyrrole was also tried. Various lengths (1-ft to 10-ft long) of coiled copper columns (1/4-in. in diameter) with 10% by weight of tricresyl phosphate, dinonylphthalate, or 15% diethyleneglycol succinate on Chromosorb W were tried for this purpose. The column temperature was varied from 100 to 170 °C and the flow rate of He gas changed from 40 to 100 cm^3/min. A 6-ft long glass column (i.d. 1/8 in.) packed with 15% of diethyleneglycol succinate at 130 °C was also tried. A single peak with very broad tailing was observed with either 2,5- or 2,4-dimethylpyrrole, and the retention times of both compounds were similar on all the columns.

Results

The dimethylpyrrole (DMP) vapors were irradiated at room temperature with 2139 or 2288 Å radiation. The substrate pressures ranged from 0.05 to 0.70 Torr, the lower limit being imposed by experimental and analytical considerations, and the upper limit corresponding to the vapor pressure. The principal product of the reaction was H_2, though CH_4 and C_2H_6 were also produced. There was also evidence for polymeric material, since the transmission of the reaction cell to the incident radiation decreased after continued irradiation of the samples. Flaming and pumping the reaction cell would return the transmission to its original value.

Of special interest was the absence of the ring cleavage products. In particular no C_2H_2, CH_2CCH_2, or CH_3CCH were produced, except in trace amounts for very extended exposures of 2,5-DMP only. Four-carbon hydrocarbons were never produced. Consequently the presence of two methyl groups on the ring completely stabilizes pyrrole against ring decomposition. We have no evidence regarding the importance of CH_3 group migration during photolysis. Several attempts were made to study the isomerization, but the separation of the isomers was so poor on all of our chromatographic columns that we could not obtain meaningful results. Therefore we studied the photodecomposition only.

Initially the effect of irradiation time on the gaseous products was examined. Such studies are shown in Table 1 for conditions where a time effect should be most pronounced, *i.e.* at high intensities. With 2,5-DMP at 0.5–0.7 Torr, and the absorbed intensity, I_a, ~31–36 μ/min (μ/min can be converted to einstein/l min by dividing by 1.86×10^7) at either 2139 or 2288 Å, the quantum yields are constant for up to 20 min irradiation, but then fall off for longer exposures. As the absorbed light intensity decreased ~30% after a 2-h run, the fall-off at high conversions is attributed to the polymer build-up on the windows which reduces the incident intensity. With 2,4-DMP at 2139 Å, the time effect is unimportant. Also some runs were done for different exposure times with

Can. J. Chem. Downloaded from www.nrcresearchpress.com by 210.87.254.40 on 09/05/12
For personal use only.

TABLE 1. Effect of irradiation time on product quantum yields

Irradiation time (min)	$\Phi\{H_2\}$	$\Phi\{CH_4\}$	$\Phi\{C_2H_6\}$
[2,5-DMP] = 0.70 Torr, I_a = 31.2 μ/min, λ = 2139 Å			
5.00	0.148	0.0218	0.0258
10.00	0.148	0.0193	0.0219
20.00	0.134	0.0160	0.0180
30.00	0.118	0.0144	0.0157
[2,4-DMP] = 0.64 Torr, I_a = 22.8 μ/min, λ = 2139 Å			
5.00	0.090	0.0142	0.0112
10.00	0.089	0.0168	0.0113
20.00	0.084	0.0162	0.0111
30.00	0.078	0.0153	0.0105
40.00	0.071	0.0135	0.0112
[2,5-DMP] = 0.50 Torr, I_a = 36.5 μ/min, λ = 2288 Å			
6.00	0.126	0.0119	0.0081
11.00	0.119	—	0.0065
20.00	0.097	0.0086	0.0063
65.00	0.0535	0.0055	0.0040

TABLE 2. Quantum yields of H_2 formation in the photolysis of dimethylpyrroles at 25 °C

[DMP] (Torr)	I_a (μ/min)	Irradiation time (min)	$\Phi\{H_2\}$
	2,5-DMP, λ = 2139 Å		
0.08	9.0	5.00	0.184
0.085	2.66	6.00	0.208
0.08	1.28	21.00	0.208
0.165	17.5	5.00	0.164
0.155	4.75	5.00	0.177
0.15	2.2	21.00	0.157
0.31	26.7	5.00	0.141
0.295	7.7	6.00	0.131
0.32	3.81	21.00	0.130
0.48	29.6	5.00	0.143
0.50	8.8	5.00	0.131
0.50	8.8	5.00	0.121
0.50	4.23	20.00	0.133
0.70	33.0	5.00	0.140
0.70	9.2	10.00	0.121
0.70	9.2	5.00	0.125
0.69	4.41	20.0	0.152
			average = 0.152 ±0.023
	2,4-DMP, λ = 2139 Å		
0.055	6.9	5.00	0.190
0.10	2.52	15.00	0.124
0.13	22	5.00	0.125
0.20	30.7	5.00	0.178
0.25	5.1	10.00	0.109
0.30	35.7	5.00	0.102
0.40	38.0	5.00	0.105
0.40	5.52	10.00	0.111
0.50	39.1	7.00	0.108
0.50	5.68	10.00	0.115
0.58	5.85	17.00	0.118
0.60	40.2	5.00	0.113
			average = 0.113 ±0.006
	2,5-DMP, λ = 2288 Å		
0.05	7.3	7.00	0.117
0.10	13.3	6.00	0.146
0.10	2.08	22.00	0.151
0.20	21.8	6.00	0.131
0.20	3.42	20.00	0.167
0.30	28.0	10.00	0.166
0.30	4.38	20.00	0.167
0.41	33.3	8.00	0.129
0.39	5.07	21.00	0.148
0.50	36.5	6.00	0.132
0.50	5.70	21.00	0.156
			average = 0.146 ±0.014
	2,4-DMP, λ = 2288 Å		
0.05	7.8	5.00	0.155
0.06	1.47	30.00	0.094
0.10	2.23	20.00	0.117
0.11	15.3	5.00	0.098
0.20	23.2	6.00	0.100
0.20	3.63	21.00	0.103
0.30	29.6	11.00	0.090
0.29	4.53	20.00	0.093
0.38	33.6	6.00	0.093
0.40	5.4	20.00	0.102
0.50	38.2	7.00	0.104
0.50	6.0	20.00	0.099
0.50	2.46*	21.00	0.117
0.66	43	5.00	0.107
			average = 0.101 ±0.007

*NO filter present to remove the weak 2265 and 2144 Å lines.

2,4-DMP at 2288 Å and these results (for CH_4 and C_2H_6 only) are interspersed in Table 5. While these results are badly scattered, there is no obvious trend.

Because of the analytical procedures employed, one set of experiments was done to measure H_2 production, and another set to

TABLE 3. Quantum yields of H_2 formation in the photolysis of dimethylpyrroles at 25 °C in the presence of O_2

$[O_2]$ (Torr)	Irradiation time (min)	$\Phi\{H_2\}$	$[O_2]$ (Torr)	Irradiation time (min)	$\Phi\{H_2\}$
[2,5-DMP] = 0.50 Torr, λ = 2139 Å, I_a = 29.8 μ/min			[2,4-DMP] = 0.50 Torr, λ = 2139 Å, I_a = 34 μ/min		
0.0	5.00	0.127	0.0	—	0.113*
0.185	5.00	0.109	0.16	12.00	0.0630
0.425	5.00	0.088	0.24	14.00	0.0575
0.685	6.50	0.076	0.40	10.00	0.0557
1.30	5.00	0.066	1.08	13.00	0.0307
1.99	5.00	0.053	1.625	10.00	0.0295
[2,5-DMP] = 0.10 Torr, λ = 2139 Å, I_a = 9.95 μ/min			[2,4-DMP] = 0.30 Torr, λ = 2139 Å, I_a = 25.4 μ/min		
0.0	15.00	0.189	0.0	—	0.113*
0.24	13.00	0.0518	0.58	10.00	0.0396
0.53	15.00	0.0314	0.945	11.00	0.0267
0.61	10.00	0.0397	1.495	10.00	0.0210
0.96	10.00	0.0334			
1.38	10.00	0.0294			
2.04	10.00	0.0256			
[2,5-DMP] = 0.50 Torr, λ = 2288 Å, I_a = 36.5 μ/min			[2,4-DMP] = 0.10 Torr, λ = 2139 Å, I_a = 14.5 μ/min		
0.0	10.00	0.134	0.0	—	0.113*
0.20	10.00	0.10	0.24	12.00	0.0238
0.45	10.00	0.086	0.50	10.00	0.0172
0.72	20.00	0.051	0.79	10.00	0.0146
1.02	10.00	0.067	1.04	10.00	0.0129
1.83	10.00	0.0505	1.35	10.00	0.0093
			1.72	10.00	0.00903
			[2,4-DMP] = 0.50 Torr, λ = 2288 Å, I_a = 38.2 μ/min		
			0.0	—	0.101*
			0.25	7.00	0.0695
			0.675	6.00	0.0579
			0.89	9.00	0.0418
			0.97	7.00	0.0470
			1.4	6.00	0.0395
			2.09	6.00	0.0301

*Average value from Table 2.

measure CH_4 and C_2H_6 production. The results for H_2 production alone, in the presence of O_2, and in the presence of other gases, are given respectively in Tables 2, 3, and 4. Likewise similar experiments for the CH_4 and C_2H_6 yields are given in Tables 5–7. All the results reported in these tables are for short irradiation times, and the quantum yields may be considered initial values.

Table 2 shows that in the absence of added gases $\Phi\{H_2\}$ is remarkably insensitive to which pyrrole is used, its pressure, I_a, or the wavelength of the incident radiation. There is some indication that $\Phi\{H_2\}$ may rise at very low substrate pressures, but this effect is not pronounced, if indeed it occurs at all. Average values are listed in Table 2 and $\Phi\{H_2\}$ is $\sim$0.10–0.15.

The effect of added O_2 on $\Phi\{H_2\}$ is shown in Table 3. The presence of O_2 markedly reduces $\Phi\{H_2\}$, and the amount of reduction depends on the DMP pressure. Thus about 1.6 Torr of O_2 drops $\Phi\{H_2\}$ from 0.113 to 0.030 with 0.50

Can. J. Chem. Downloaded from www.nrcresearchpress.com by 210.87.254.40 on 09/05/12
For personal use only.

Can. J. Chem. Downloaded from www.nrcresearchpress.com by 210.87.254.40 on 09/05/12
For personal use only.

TABLE 4. Quantum yields of H_2 formation in the photolysis of dimethylpyrroles (0.50 ± 0.02 Torr) at 25 °C and 2139 Å in the presence of added gases

[X] (Torr)	Irradiation time (min)	$\Phi\{H_2\}$	[X] (Torr)	Irradiation time (min)	$\Phi\{H_2\}$
2,5-DMP, X = NO, $I_a = 29.8$ μ/min			2,4-DMP, X = NO, $I_a = 34$ μ/min		
0.0	5.00	0.127	0.0	5.00	0.0952
0.085	8.00	0.103	0.08	5.00	0.0890
0.085	5.00	0.105	0.18	5.00	0.0844
0.17	5.00	0.111	0.35	5.00	0.0773
0.20	5.50	0.105	0.47	5.00	0.0750
0.268	5.50	0.129	1.01	11.00	0.0487
0.31	7.00	0.111	1.79	11.00	0.0371
0.495	5.50	0.113			
0.92	5.00	0.095			
1.775	6.50	0.085			
2,5-DMP, X = C_2H_4, $I_a = 29.8$ μ/min			2,5-DMP, X = C_2F_6, $I_a = 29.8$ μ/min		
0.0	5.00	0.127	0.0	5.00	0.127
0.19	5.50	0.112	0.7	6.00	0.082
0.33	5.00	0.078	1.08	10.00	0.072
1.435	7.00	0.040	2.67	6.00	0.046
4.75	5.00	0.019	5.1	6.00	0.035
13.5	9.00	0.0044	9.0	6.00	0.020
17.5	5.00	0.0048	27.0	6.00	0.008

Torr of 2,4-DMP at 2139 Å, but the drop is to 0.0090 for 0.10 Torr of 2,4-DMP. The addition of NO, C_2H_4, and C_2F_6 also reduces $\Phi\{H_2\}$, though all these gases were less efficient than O_2. The results are in Table 4.

With CH_4 and C_2H_6, the results are similar though somewhat more complex than for H_2. Table 5 shows the results in the absence of added gases. $\Phi\{CH_4\}$ is nearly invariant to changes in substrate, substrate pressure, I_a, or incident wavelength, being between 0.01 and 0.02 except at low pressures at 2288 Å, where it falls to about 0.006. $\Phi\{C_2H_6\}$ is comparable in magnitude to $\Phi\{CH_4\}$. It is reasonably invariant to substrate or incident wavelength. However it does increase at low pressure, the increase being more pronounced at 2139 than 2288 Å. The most remarkable result, though, is that $\Phi\{C_2H_6\}$ *increases* noticeably as I_a is reduced.

The effect of O_2 is shown in Table 6. Only small amounts of O_2 reduce $\Phi\{C_2H_6\}$ to zero showing that all the C_2H_6 comes from CH_3 radical combination. $\Phi\{CH_4\}$ is reduced less rapidly by the addition of O_2, but about 95% of the CH_4 is suppressed by the addition of one or more Torr of O_2.

TABLE 5. Quantum yields of CH_4 and C_2H_6 formation in the photolysis of dimethylpyrroles at 25 °C

[DMP] (Torr)	I_a (μ/min)	Irradiation time (min)	$\Phi\{CH_4\}$	$\Phi\{C_2H_6\}$
		2,5-DMP, $\lambda = 2139$ Å		
0.08	9.0	5.00	0.0149	0.0286
0.085	2.66	10.00	0.0117	0.070
0.16	17.3	5.00	0.0159	0.0264
0.15	4.6	11.00	0.0127	0.0360
0.15	2.2	20.00	0.0114	0.0672
0.31	26.7	5.00	0.019	0.022
0.30	7.8	11.50	0.0123	0.0190
0.31	3.79	20.00	0.0168	0.0272
0.48	29.6	5.00	0.0149	0.0153
0.485	8.75	13.00	0.0136	0.0155
0.50	29.8	5.00	0.0178	0.0145
0.50	8.8	5.00	0.0130	0.0173
0.50	4.23	20.00	0.0143	0.0268
0.52	29.9	5.00	0.0154	0.0126
0.635	9.1	5.00	0.0129	0.0191
0.70	4.42	20.00	0.0192	0.0215
		2,4-DMP, $\lambda = 2139$ Å		
0.06	10.2	6.00	0.0112	0.0383
0.06	1.49	15.00	0.0134	0.0630
0.11	17.3	5.00	0.0156	0.0297
0.115	2.88	10.00	0.0112	0.0390
0.205	30.7	6.00	0.0141	0.0133
0.24	4.87	10.00	0.0131	0.0262
0.33	36.5	5.00	0.0208	0.0151

Can. J. Chem. Downloaded from www.nrcresearchpress.com by 210.87.254.40 on 09/05/12
For personal use only.

TABLE 5. (*Concluded*)

[DMP] (Torr)	I_a (μ/min)	Irradiation time (min)	$\Phi\{CH_4\}$	$\Phi\{C_2H_6\}$
0.40	38.0	5.00	0.0169	0.0122
0.40	5.62	10.00	0.0151	0.0173
0.48	39.0	5.00	0.0172	0.0122
0.49	5.71	10.00	0.0133	0.0212
0.50	35.3	5.00	0.0184	0.0121
0.50	36.7	5.00	0.0180	0.0125
0.56	5.80	10.00	0.00965	0.0195
0.60	40.1	5.00	0.0143	0.0109
		2,5-DMP, $\lambda = 2288$ Å		
0.05	7.3	6.00	0.00575	0.0233
0.10	13.3	6.00	0.00685	0.0211
0.10	2.48	22.00	0.00378	0.0213
0.20	21.8	6.00	0.00810	0.0142
0.20	3.42	22.00	0.0086	0.0216
0.29	27.4	6.00	0.0117	0.0091
0.30	4.38	20.00	0.0062	0.0203
0.40	32.8	7.00	0.0099	0.00765
0.41	5.23	21.00	0.00995	0.0120
0.51	37	7.00	0.00905	0.0073
0.52	5.84	21.00	0.0071	0.0073
		2,4-DMP, $\lambda = 2288$ Å		
0.06	9.4	6.00	0.00691	0.01685
0.10	14.3	21.00	0.009	0.0282
0.13	17.4	6.00	0.01395	0.01725
0.19	22.4	20.00	0.00715	0.0203
0.25	26.5	6.00	0.0136	0.0108
0.30	29.6	20.00	0.0108	0.0188
0.35	32.2	6.00	0.0142	0.00842
0.41	34.8	25.00	0.0110	0.0132
0.50	38.2	6.00	0.0138	0.00615
0.50	38.2	7.00	0.01375	0.0055
0.50	38.2	20.00	0.0109	0.0116
0.50	1.52	20.00	0.00817	—
0.66	43	8.00	0.0123	0.0047

Table 7 shows the results with added NO, i-C_4H_{10}, and C_2H_4. Both CH_4 and C_2H_6 are readily suppressed by NO, and both are reduced by i-C_4H_{10}, but considerably less efficiently. $\Phi\{CH_4\}$ is reduced by the addition of C_2H_4, but $\Phi\{C_2H_6\}$ is enhanced, thus demonstrating the presence of H atoms in the system. The peak increase in $\Phi\{C_2H_6\}$ corresponds roughly to the drop in $\Phi\{H_2\}$.

Discussion

The results clearly indicate the presence of both H atoms and CH_3 radicals. Thus the simplest scheme to explain the primary process is

[1] $$DMP + h\nu \rightarrow DMP^*$$

[2a] $$DMP^* \rightarrow H + F_a$$

[2b] $$\rightarrow CH_3 + F_b$$

[2c] $$\rightarrow DMP$$

The H atoms ultimately become H_2, but whether this occurs on the wall, by interaction with the fragments F_a and F_b, or by an abstraction reaction with DMP is not clear. For simplicity let us assume that the abstraction reaction with pyrrole predominates.

[3] $$H + DMP \rightarrow H_2 + F_a$$

In support of this hypothesis is the fact that the peak increase in $\Phi\{C_2H_6\}$ when C_2H_4 is added corresponds to the loss in $\Phi\{H_2\}$. This would be the case if each C_2H_5 radical produced by H addition to C_2H_4 produced a C_2H_6 molecule, whereas each H not scavenged produced an H_2 molecule.

The above simple reaction scheme leads to the rate law

[I] $$\Phi\{H_2\} = k_{2a}/k_2$$

which conforms with the results in the absence of added gases with $k_{2a}/k_2 \sim 0.10$–0.15. In the presence of a scavenger, such as O_2, the H atoms can be removed via

[4] $$H + S + M \rightarrow HS + M$$

where S is the scavenger. The reaction is written as third order since at the low pressures used here a chaperone is required, especially with O_2 or NO as scavengers. The rate law then becomes

[II] $$\Phi\{H_2\}^{-1} = \frac{k_2}{k_{2a}}\left(1 + \frac{k_4[S][M]}{k_3[DMP]}\right)$$

If $[M] \sim [DMP]$, then eq. II predicts that $\Phi\{H_2\}^{-1}$ should be linear with the scavenger pressure. Appropriate plots are shown in Figs. 1–5.

Figure 1 shows the scavenging by O_2 when 0.50 Torr of DMP is irradiated at 2288 Å, and good straight-line plots are obtained. In Fig. 2 the data are for 2,4-DMP with 2139 Å radiation. For 0.50 or 0.30 Torr the same results are obtained and the plot is linear as expected. However with 0.10 Torr of 2,4-DMP, the data points lie higher and the plot has curvature at

Can. J. Chem. Downloaded from www.nrcresearchpress.com by 210.87.254.40 on 09/05/12
For personal use only.

TABLE 6. Quantum yields of CH_4 and C_2H_6 formation in the photolysis of dimethylpyrroles at 25 °C in the presence of O_2

$[O_2]$ (Torr)	Irradiation time (min)	$\Phi\{CH_4\}$	$\Phi\{C_2H_6\}$	$[O_2]$ (Torr)	Irradiation time (min)	$\Phi\{CH_4\}$	$\Phi\{C_2H_6\}$
[2,5-DMP] = 0.50 Torr, λ = 2288 Å, I_a = 36.5 μ/min				[2,4-DMP] = 0.50 Torr, λ = 2139 Å, I_a = 35.3 μ/min			
0.0	5.00	0.0119	0.0081	0.0	5.00	0.0184	0.0121
0.12	17.00	0.0034	0.00422	0.11	10.00	0.00675	0.00805
0.23	15.00	0.000945	0.00130	0.16	10.00	0.00412	0.00400
0.26	15.00	0.000715	Trace	0.215	10.00	0.00174	Trace
0.37	15.00	0.000546	0.0	0.375	10.00	0.00088	0.0
0.73	15.00	0.000365	0.0	0.64	11.00	0.00083	0.0
1.32	15.00	0.000365	0.0	0.87	11.00	0.00102	0.0
[2,4-DMP] = 0.50 Torr, λ = 2288 Å, I_a = 38.2 μ/min				[2,4-DMP] = 0.10 Torr, λ = 2139 Å, I_a = 12.55 μ/min			
0.0	6.00	0.0138	0.00615	0.0	11.00	0.00932	0.0301
0.075	10.00	0.00747	0.0049	0.06	10.00	0.00287	0.0080
0.145	7.00	0.000825	Trace	0.10	11.00	0.00191	0.0023
0.32	7.00	0.000677	0.0	0.20	10.00	0.00111	0.0
0.48	7.00	0.000524	0.0	0.62	11.00	0.00061	0.0
0.95	6.00	0.000670	0.0	1.10	10.00	0.00040	0.0

TABLE 7. Quantum yields of CH_4 and C_2H_6 formation in the photolysis of dimethylpyrroles at 25 °C and 2139 Å in the presence of added gases

[X] (Torr)	Irradiation time (min)	$\Phi\{CH_4\}$	$\Phi\{C_2H_6\}$
[2,5-DMP] = 0.50 Torr, X = NO, I_a = 29 μ/min			
0.0	5.00	0.0178	0.0145
0.08	6.00	0.0147	0.0057
0.09	5.00	0.0181	0.0049
0.25	5.50	0.0061	0.0
0.47	5.00	0.0031	0.0
1.005	6.50	0.0015	0.0
6.0	5.00	Trace	0.0
[2,5-DMP] = 0.10 Torr, X = NO, I_a = 9.95 μ/min			
0.0	10.00	0.0110	0.0343
0.08	10.00	0.0335	0.0
0.205	10.00	0.0197	0.0
0.35	10.00	0.0083	0.0
0.49	10.00	0.0045	0.0
0.95	10.00	0.0023	0.0
[2,4-DMP] = 0.49 Torr, X = NO, I_a = 37 μ/min			
0.0	5.00	0.0180	0.0125
0.08	12.00	0.0067	0.0127
0.095	10.00	0.0076	0.0121
0.16	10.00	0.0118	0.0061
0.22	10.00	0.0124	0.0031
0.26	10.00	0.0110	Trace
0.30	11.00	0.0100	Trace
0.39	13.00	0.0056	0.0
0.94	10.00	0.00075	0.0
[2,5-DMP] = 0.50 Torr, X = i-C_4H_{10}, I_a = 29.8 μ/min			
0.0	5.00	0.0178	0.0145
0.255	5.00	0.0104	0.0086
0.52	8.00	0.0096	0.0032
1.03	5.00	0.0081	0.0024
2.09	5.00	0.0054	0.0012
5.9	5.00	0.0024	—
13.0	5.00	0.0005	—
[2,5-DMP] = 0.50 Torr, X = C_2H_4, I_a = 29.8 μ/min			
0.0	5.00	0.0178	0.0145
0.175	8.00	0.0085	0.0146
0.52	8.00	0.0052	0.0231
1.03	8.00	0.0031	0.0258
1.92	6.00	0.0019	—
2.28	8.00	0.0014	0.0265
6.4	20.00	0.0004	0.0198

low O_2 pressures; 2,5-DMP shows the same behavior as seen in Fig. 3. Apparently at low DMP pressures other processes are occurring. Perhaps H_2 formation is from the interaction of H atoms with the fragments

[5] $$H + F_a, F_b \rightarrow H_2 +$$

Then [DMP] would disappear from the denominator of the last term in eq. II and the rise in $\Phi\{H_2\}^{-1}$ should be rapid with increasing O_2 pressure. Of course the rise might be quadratic since [M] is now $[O_2]$. On the other hand some H_2 could be produced molecularly

[2*d*] $$DMP^* \rightarrow H_2 + F_d$$

Then $\Phi\{H_2\}^{-1}$ would reach some upper limiting value. However this value is large and reaction 2*d* cannot account for more than 10% of the H_2 produced.

Figure 4 shows the scavenging effect of NO with 0.50 Torr of DMP. Again good straight line plots are obtained.

In addition to the scavenging of H atoms, an added gas might also quench DMP*

[6] $$DMP^* + M \rightarrow DMP + M$$

That this occurs is shown by the addition of C_2F_6 which cannot scavenge H atoms. For no scavenging of H atoms the mechanism predicts

[III] $$\Phi\{H_2\}^{-1} = \frac{k_2}{k_{2a}}\left(1 + \frac{k_6[M]}{k_2}\right)$$

Figure 5 shows that eq. III is followed for both

Can. J. Chem. Downloaded from www.nrcresearchpress.com by 210.87.254.40 on 09/05/12
For personal use only.

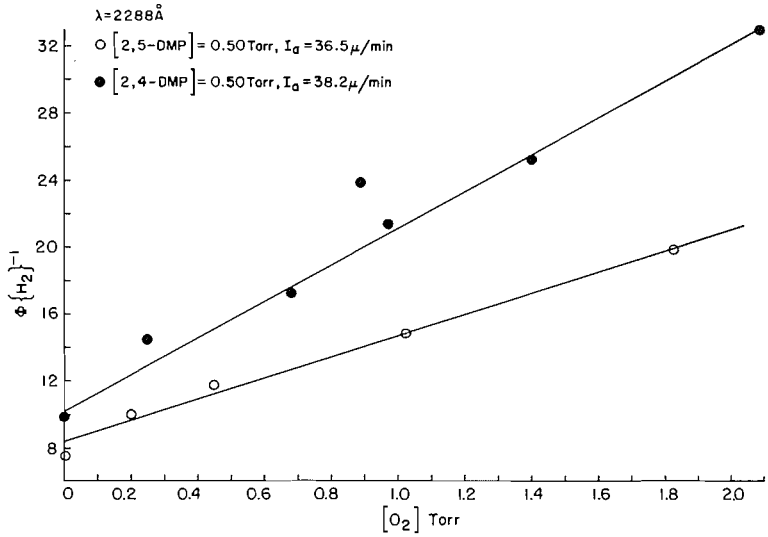

FIG. 1. Plot of $\Phi\{H_2\}^{-1}$ *vs.* O_2 pressure in the photolysis of dimethylpyrroles at 0.50 Torr pressure at 2288 Å and room temperature in the presence of O_2.

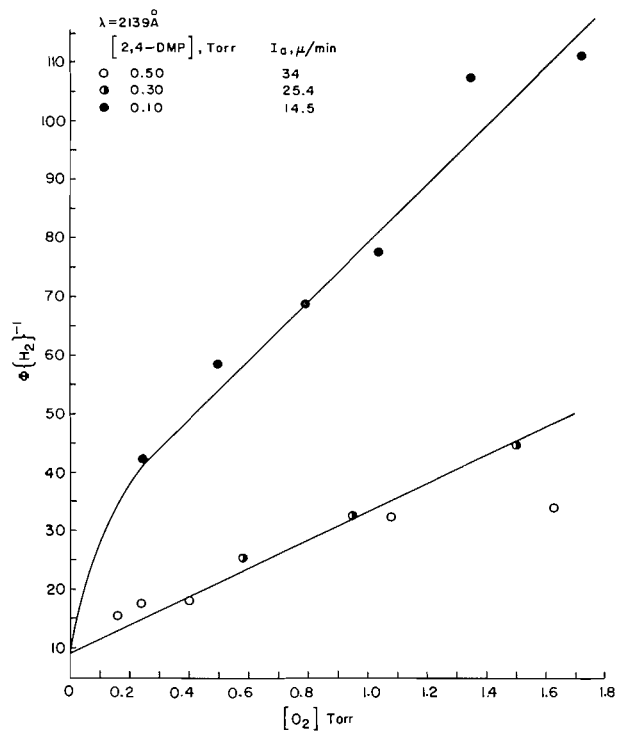

FIG. 2. Plot of $\Phi\{H_2\}^{-1}$ *vs.* O_2 pressure in the photolysis of 2,4-DMP at 2139 Å and room temperature in the presence of O_2.

Can. J. Chem. Downloaded from www.nrcresearchpress.com by 210.87.254.40 on 09/05/12
For personal use only.

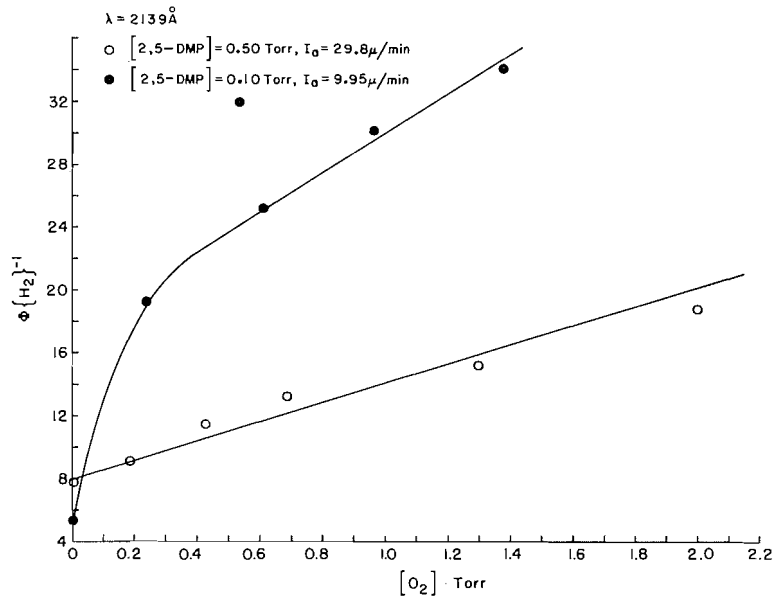

FIG. 3. Plot of $\Phi\{H_2\}^{-1}$ *vs.* O_2 pressure in the photolysis of 2,5-DMP at 2139 Å and room temperature in the presence of O_2.

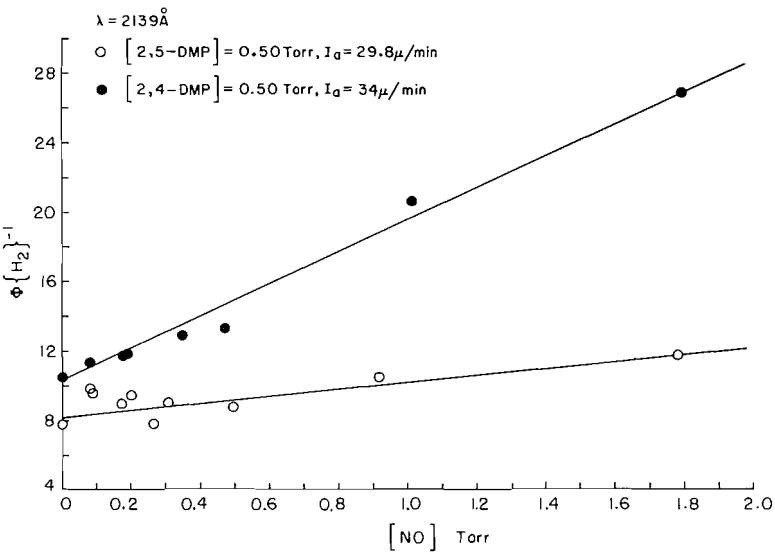

FIG. 4. Plot of $\Phi\{H_2\}^{-1}$ *vs.* NO pressure in the photolysis of dimethylpyrroles at 0.50 Torr pressure at 2139 Å and room temperature in the presence of NO.

C_2H_4 and C_2F_6. The ratio of slope to intercept gives $k_6/k_2 = 0.52$ and 1.45 $Torr^{-1}$, respectively, for C_2F_6 and C_2H_4. Of course in the case of C_2H_4, scavenging of H atoms is also occurring so that both effects may be important. However the C_2H_6 results (Table 7, X = C_2H_4) show that the scavenging of H atoms is essentially complete with 1 Torr of C_2H_4, so that the quenching effect is what is observed at higher pressures. Because of its greater molecular complexity,

Can. J. Chem. Downloaded from www.nrcresearchpress.com by 210.87.254.40 on 09/05/12
For personal use only.

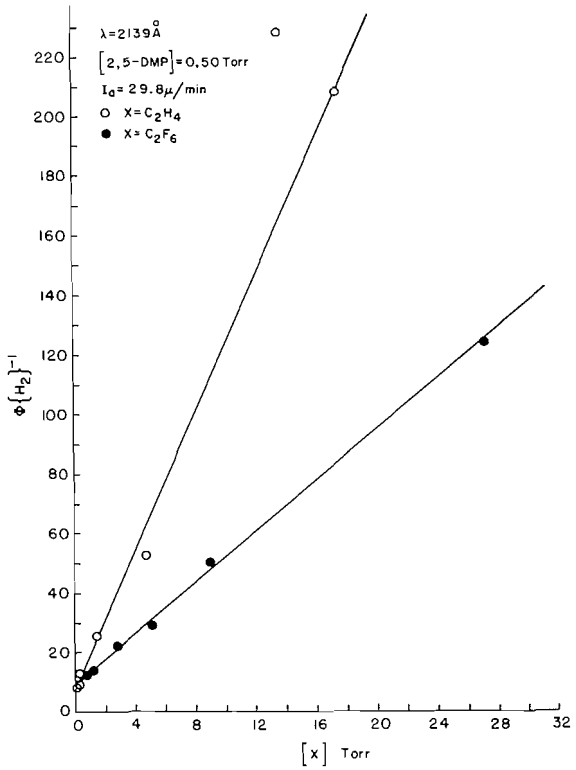

FIG. 5. Plot of $\Phi\{H_2\}^{-1}$ *vs.* the pressure of added gas in the photolysis of 2,5-DMP at 0.50 Torr at 2139 Å and room temperature in the presence of either C_2H_4 or C_2F_6.

C_2F_6 should be a more efficient quencher of DMP* than O_2 or NO (unless a triplet state is involved). Thus the quenching of DMP* by O_2 or NO at the pressures used is negligible.

The production of C_2H_6 comes from CH_3 radical recombination.

[7] $$2CH_3 \rightarrow C_2H_6$$

The CH_4 comes mainly from CH_3 radical abstraction reactions. If the sole process were

[8] $$CH_3 + DMP \rightarrow CH_4 + C_6H_8N$$

then

[IV] $$I_a^{1/2}\Phi\{CH_4\}/(\Phi\{C_2H_6\})^{1/2}[DMP] = k_8/k_7^{1/2}$$

Only a cursory examination of Table 5 will show that eq. IV is not obeyed, *i.e.* the quantity on the left hand side is not constant. Consequently the chief source of CH_4 is

[9] $$CH_3 + F_a, F_b \rightarrow CH_4 + ?$$

Some CH_4 might also come from the molecular process

[2e] $$DMP^* \rightarrow CH_4 + F_e$$

though the scavenging experiments in Tables 6 and 7 show that step 2*e* can account for no more than 5% of the CH_4.

The most unusual effect observed is that $\Phi\{C_2H_6\}$ *increases* as I_a drops. This can be explained if the fragments F_a and F_b are removed at the wall to form polymer. Then as the intensity is reduced, this wall removal reaction becomes more important relative to reaction 9, relatively fewer CH_3 radicals are removed in reaction 9, and $\Phi\{C_2H_6\}$ goes up. The pressure effect on $\Phi\{C_2H_6\}$ would be explained the same way, *i.e.* at lower pressures the wall removal reaction for F_a and F_b is enhanced, and $\Phi\{C_2H_6\}$ is reduced. Relatively little effect is seen on $\Phi\{CH_4\}$ since its production depends on the interaction of CH_3 and either F_a or F_b. As one reactant is reduced in

Can. J. Chem. Downloaded from www.nrcresearchpress.com by 210.87.254.40 on 09/05/12
For personal use only.

relative importance, the other is enhanced, and little change results.

This work was supported by the Environmental Protection Agency through the Office of Air Programs under Grant No. 1 RO1 AP00718, for which we are grateful.

1. E. C. Wu and J. Heicklen. J. Am. Chem. Soc. **93**, 3432 (1971).
2. J. M. Patterson, L. T. Burka, and M. R. Boyd. J. Org. Chem. **33**, 4033 (1968).
3. J. M. Patterson and L. T. Burka. Tetrahedron Lett. 2215 (1969).
4. H. Hiraoka. IBM research report. RC 2928 (1970).

Can. J. Chem. Downloaded from www.nrcresearchpress.com by 210.87.254.40 on 09/05/12
For personal use only.

Microwave Spectrum of 1,3-Dioxane

R. KEWLEY[1]

Department of Chemistry, Queen's University, Kingston, Ontario

Received November 29, 1971

The microwave spectrum of 1,3-dioxane has been studied within the region 8 to 40 GHz. The rotational constants of the molecule in its ground vibrational state are, in MHz, $A = 4999.94(0.05)$, $B = 4807.61(0.05)$, and $C = 2757.12(0.05)$. The dipole moment components are, in Debye units, $\mu_b = 1.61(0.02)$, $\mu_c = 1.29(0.01)$, and $\mu = 2.06(0.03)$. The values of the above quantities are consistent with a chair form structure. Rotational spectra due to five excited vibrational states of 1,3-dioxane have been assigned.

Le spectre micro-onde du dioxane-1,3 a été étudié dans l'intervalle de 8 à 40 GHz. Les constantes de rotation de la molécule dans son état de vibration fondamental sont, en MHz, $A = 4999.94(0.05)$, $B = 4807.61(0.05)$, et $C = 2757.12(0.05)$. Les composantes du moment dipolaire sont, en unités Debye, $\mu_b = 1.61(0.02)$, $\mu_c = 1.29(0.01)$, et $\mu = 2.06(0.03)$. Les valeurs précédentes sont en accord avec une structure de forme chaise. Les spectres de rotation, dues à cinq états excités de vibration du dioxane-1,3, ont été attribués.

Canadian Journal of Chemistry, **50**, 1690 (1972)

Can. J. Chem. Downloaded from www.nrcresearchpress.com by 210.87.254.42 on 09/05/12
For personal use only.

Introduction

In earlier studies of the microwave spectra of the molecules piperidine (1), tetrahydropyran (2), morpholine (3), and *sym*-trioxane (4), the chair form structure of the ring atoms was in each case the only one for which a spectrum could be detected. This is expected for tetrahydropyran and morpholine on account of the boat form being energetically unfavorable because of repulsions between eclipsed hydrogen atoms attached to adjacent carbon atoms.

For 1,3-dioxane the possibility of hydrogen eclipsing is somewhat reduced. In the diagrams, the oxygen lone pair electrons are indicated by the dashed lines. In the form boat A a flagpole repulsive interaction between hydrogens on C-2 and -5 would be present together with C—H bond pair – oxygen lone pair repulsion for O_1—C_6 and O_3—C_4. In boat B the flagpole interaction between the O-3 lone pair and the C-6 hydrogen could be weakly attractive. An ordinary eclipsing of hydrogens would occur between C-4 and -5 hydrogens. Also possible are two twist forms. One of these, which relates two identical boat B forms, has C_2 symmetry and just one dipole moment component directed along the C_2 axis, which would also be a principal inertia axis. The other twist form relates the boat A form to either of the mirror image boat B forms, has no symmetry and would have sizeable dipole moment components along all three principal inertia axes. Each twist form has a mirror image form. The boat B form also lacks symmetry and would have three non-zero dipole components. The chair and boat A forms would each have just two dipole components and these would be directed in the molecular symmetry plane. It is expected that the chair form will be the lowest energy conformation, because of staggering of C—H bonding pairs and oxygen lone pairs and also by comparison with the results for *sym*-trioxane (4).

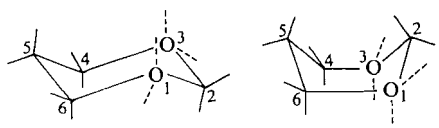

Chair

Boat A

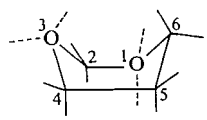

Boat B

An additional point of interest for the chair form of 1,3-dioxane is the possibility that because of repulsion between the axial oxygen lone pair electrons the $O_1C_2O_3C_4C_6$ section of the molecule might be flattened towards a half chair structure.

The above considerations suggested that a

[1]On sabbatical leave September 1, 1971 to August 31, 1972 at Department of Chemistry, Rice University, Houston, Texas 77001.

Can. J. Chem. Downloaded from www.nrcresearchpress.com by 210.87.254.42 on 09/05/12
For personal use only.

study of the microwave spectrum of 1,3-dioxane should be of interest. In addition, the quite large reported dipole moment of 2.134 (in benzene) and 2.145 D (in cyclohexane) (5) indicated that the spectrum would be intense, and favorable for the observation of satellite spectra from vibrationally excited states of the molecule.

Experimental

The sample of 1,3-dioxane was purchased from the Aldrich Chemical Company and used without further purification. All observations were taken at room temperature with sample pressures in the range 5 to 100 μ.

The spectrum was observed initially at Queen's University using the 100 kHz Stark modulation spectrometer described previously (2, 3). Direct monitoring of the variable 5 MHz output of the Micronow model 101D frequency standard was effected, using a Hewlett Packard model 5245M frequency counter. This counter was equipped with a model 5256A plug-in unit which was particularly useful when conducting survey frequency sweeps in the 13 to 18 GHz region. Almost all of the frequency measurements for the ground vibrational state of the molecule were taken with this spectrometer and are accurate to within 0.1 MHz. The majority of the Stark effect and vibrational satellite frequency and intensity measurements were made at Rice University using a Hewlett Packard model 8460A MRR spectrometer in the range 26.5 to 40 GHz. Such frequency measurements are accurate to 0.05 MHz or better.

Results

Rotational Spectrum

The rotational spectrum of only one conformer of the molecule could be detected. As in the molecules piperidine (1), tetrahydropyran (2), and morpholine (3) the dominant feature of the spectrum is a set of double Q-branch series. The branch heads occur at intervals of 4.29 GHz, see Table 1. For 1,3-dioxane the observed lines are due to transitions of the type ${}^{b}Q_{-1,J}$. The series to which the most attention was given was that with the branch head $J = 4$–4 very close to 15 GHz. In this case the sub-branch with $K_{-1} + K_{+1} = J$ proceeds continuously to lower frequency with increasing J but the $K_{-1} + K_{+1} = J + 1$ sub-branch decreases frequency for $J = 4$ to $J = 8$ and thereafter increases frequency starting at $J = 9$. A careful study of these lines was required to show that they are in fact due to b-type and not a-type transitions. The value of the asymmetry parameter κ of 0.82849 is very close to that of 0.82776 for tetrahydropyran (2). This facilitated further analysis. The R-branch assignment was obtained by identifying the superimposed transitions 3_{03}–4_{14} and 3_{13}–4_{04} by means of the expected first order Stark effect, due to oblate near degenerate asymmetry doublets. Thereafter other b-type and also c-type R-branch lines were observed. None of the c-type lines showed any evidence of splitting due to inversion of the molecule. The rotational constants were determined by a least squares fit to the 19 $J = 0$–1, 1–2, and 2–3 transitions given in Table 2. The standard deviation, σ, of the fit was 0.22 MHz. The resulting rotational con-

TABLE 1. Q-branch b-type transitions of 1,3-dioxane, ground vibrational state

Transition	$\nu_{obsd.}$ (MHz)	$\nu_{obsd.} - \nu_{calcd.}$ (MHz)
5_{24}–5_{33}*	14 992.87	−1.41
5_{14}–5_{23}	14 978.76	−0.61
6_{34}–6_{43}	14 980.46	−0.76
6_{24}–6_{33}	14 937.08	−0.14
7_{44}–7_{53}	14 967.20	−1.39
7_{34}–7_{43}	14 861.24	0.10
8_{54}–8_{63}	14 961.47	−0.84
8_{44}–8_{53}	14 732.82	−0.76
9_{64}–9_{73}	14 970.16	−1.00
9_{54}–9_{63}	14 533.25	−0.69
10_{74}–10_{83}	15 005.66	−0.83
10_{64}–10_{73}	14 241.64	−0.94
11_{84}–11_{93}	15 079.95	−1.63
11_{74}–11_{83}	13 846.63	−0.95
12_{94}–$12_{10,3}$	15 208.90	−1.86
12_{84}–12_{93}	13 351.00	−1.55
5_{15}–5_{24}	19 292.90	−0.38
6_{25}–6_{34}	19 280.89	−1.05
7_{35}–7_{44}	19 263.18	−1.26
8_{45}–8_{54}	19 238.39	−1.10
8_{35}–8_{44}	19 229.53	−0.91
9_{55}–9_{64}	19 205.06	−1.30
9_{45}–9_{54}	19 182.60	−0.63
10_{65}–10_{74}	19 163.72	−1.60
10_{55}–10_{64}	19 111.51	−1.00
11_{75}–11_{84}	19 116.27	−1.94
11_{65}–11_{74}	19 006.66	−1.48
12_{85}–12_{94}	19 066.75	−2.10
12_{75}–12_{84}	18 855.02	−1.38
6_{16}–6_{25}	23 582.82	−0.13
7_{26}–7_{35}	23 572.80	−0.47
8_{36}–8_{45}	23 557.98	−0.85
9_{46}–9_{55}	23 537.45	−0.88
10_{56}–10_{65}	23 508.07	−2.30
11_{66}–11_{75}	23 471.67	−1.88
11_{56}–11_{65}	23 468.43	−0.57
12_{76}–12_{85}	23 425.96	−0.68
12_{66}–12_{75}	23 414.31	−1.47

*The $J = 4$–4 lines were unresolved due to the proximity of the transition 10_{74}–10_{83}.

Can. J. Chem. Downloaded from www.nrcresearchpress.com by 210.87.254.42 on 09/05/12
For personal use only.

TABLE 2. R-branch transitions of 1,3-dioxane, ground vibrational state

Transition	$\nu_{obsd.}$ (MHz)	$\nu_{obsd.} - \nu_{calcd.}$ (MHz)
b-type		
$1_{11}-2_{02}$	13 066.22	0.15
$1_{01}-2_{12}$	13 271.14	−0.16
$1_{10}-2_{21}$	17 756.90	−0.04
$2_{12}-3_{03}$	18 680.86	−0.16
$2_{02}-3_{13}$	18 694.75	0.28
$1_{11}-2_{20}$	21 679.11	0.63
$2_{21}-3_{12}$	22 630.14	0.10
$2_{11}-3_{22}$	23 271.11	−0.07
$2_{20}-3_{31}$	27 847.82	−0.07
$2_{21}-3_{30}$	31 344.83	−0.11
$3_{03}-4_{14}$	24 201.47	−0.68
$3_{30}-4_{41}$	38 012.81	−0.31
$4_{04}-5_{15}$	29 715.53	−0.57
c-type		
$0_{00}-1_{10}$	9 807.58	0.03
$1_{01}-2_{11}$	19 422.74	−0.02
$1_{10}-2_{20}$	19 627.83	−0.17
$1_{11}-2_{21}$	19 807.45	0.03
$2_{11}-3_{21}$	29 142.27	−0.23
$2_{02}-3_{12}$	29 371.21	−0.19
$2_{12}-3_{22}$	29 422.64	0.00
$2_{20}-3_{30}$	29 473.73	−0.14
$2_{21}-3_{31}$	29 719.25	0.30

stants are given in Table 3. Centrifugal distortion was neglected. However this effect is probably the reason why the majority of the calculated Q-branch frequencies in Table 1 are above the observed ones.

Dipole Moment

Since first order Stark shifts are easily observed in this spectrum in addition to the usual second order shifts, the value of μ_c was determined independently of other dipole components from the splittings $\Delta\nu\pm$ between + and − M components of transitions involving asymmetry doublets, see Table 4.

Values for μ_a and μ_b were then obtained by least squares fitting to the observed second order Stark shifts. When this was done the value of μ_a was found to be close to zero. As a check on the value of μ_a two methods of calculation were used. In the first μ_c was calculated from the seven $\Delta\nu\pm/EM$ values by weighted averaging with weights proportional to (standard error in $\Delta\nu\pm/EM)^{-2}$ and a value $\mu_c = 1.29_0$ D obtained. Averaging with equal weights given to the values of $\Delta\nu\pm/EM$ yielded $\mu_c = 1.29_6$ D. After the least squares fitting the results were

	$\mu_a^2(D^2)$	$\mu_b^2(D^2)$
$\mu_c = 1.29_0(0.01)$ D	0.00305	2.59165
$\mu_c = 1.29_6(0.01)$ D	−0.00180	2.66073

A value of μ_c of about 1.29_4 D, which is entirely possible within the experimental error in μ_c, would bring μ_a to zero. It is thus considered highly probable that μ_a is in fact zero. The values of μ_a, μ_b, and μ_c quoted in Table 4 correspond to the weighted average procedure for μ_c. With such a low value of μ_a^2 no meaningful observations can be made concerning the definite presence or absence of *a*-type transitions in the rich spectrum of 1,3-dioxane. It is estimated that μ_a would have to be larger than about 0.25 D for *a*-type lines to be observable. Even then it would be difficult to distinguish the *a*-type lines from the many other small lines which are present.

Stark cell calibrations were made on the basis of $\mu_{ocs} = 0.71521(0.00020)$ D (6). The molecule methyl acetylene (7), with a dipole moment of 0.784(0.001) D, when corrected to the value of μ_{ocs} just quoted, was a very useful secondary standard for the 26.5 to 40 GHz region. Methyl acetylene has easily measurable first and second order Stark shifts for the $J = 1$–2 transition whereas for the ground vibrational state of OCS in the $J = 2$–3 transition the Stark lobes are not well separated from the line at low voltages.

The observed gas phase dipole moment of 2.06(0.03) D is in good agreement with the solution values of 2.134(0.03) (benzene) and 2.145(0.03) D (cyclohexane), quoted above (5).

Conformation

From the considerations given in the introduction it is expected that 1,3-dioxane exists very largely in the chair form. This has been stated to be the case in work in which the n.m.r. spectrum was recorded (8). No supporting evidence was given however. In the present work the observation of only μ_b and μ_c dipole components (taking μ_a to be zero) rules out the possibility that the spectrum is due to either the boat B or a twist form of the molecule. It

TABLE 3. Rotational constants and principal moments of inertia* of 1,3-dioxane, ground vibrational state

Rotational constant	Value (MHz)	Principal moment of inertia	Value (u Å^2)	κ
A	4999.94(0.05)	I_a	101.076_6	
B	4807.61(0.05)	I_b	105.120_6	0.82849(0.00005)
C	2757.12(0.05)	I_c	183.298_8	

*Conversion factor 505 377 MHz u Å^2.

TABLE 4. Stark effect coefficients and dipole moment components of 1,3-dioxane

First order Stark effects		$10^2 \times \Delta\nu_{\pm}/EM$ (MHz cm V^{-1})	
Transition	M	Observed	Calculated
$3_{03}-4_{14}$	±1	6.53(0.26)	6.44
and	±2	6.49(0.19)	6.44
$3_{13}-4_{04}$	±3	6.49(0.12)	6.44
$4_{04}-5_{15}$	±1	4.37(0.07)	4.33
and	±2	4.34(0.04)	4.33
$4_{14}-5_{05}$	±3	4.31(0.05)	4.33
	±4	4.31(0.03)	4.33
Second order Stark effects		$10^5 \times \Delta\nu/E^2$ (MHz cm^2 V^{-2})	
Transition	M	Observed	Calculated
$1_{10}-2_{21}$	1	−4.19(0.06)	−3.98
$2_{20}-3_{30}$	1	−1.19(0.08)	−1.18
$2_{20}-3_{30}$	2	−4.74(0.13)	−4.71
$3_{30}-4_{41}$	0	0.0489(0.008)	0.0517
$3_{30}-4_{41}$	1	−0.664(0.003)	−0.665
$3_{30}-4_{41}$	2	−2.79(0.03)	−2.81
$3_{30}-4_{41}$	3	−6.35(0.04)	−6.40
Dipole moment components			
Dipole moment		Value (D)	
μ_a		$\leq$0.06(0.10)	
μ_b		1.61(0.02)	
μ_c		1.29(0.01)	
μ		2.06(0.03)	

remains to decide between the chair and boat A forms. For tetrahydropyran a comparison of the observed and calculated angles between the total dipole moment and the principal a-axis was sufficient to identify the chair form (2). This was easily done because the chair form of tetrahydropyran was calculated to have only μ_a and μ_c dipole components over a reasonable range of variation in structural parameters, whereas the boat form was calculated to have μ_b and μ_c components. When the same approach is tried for 1,3-dioxane it is found that a clear decision cannot be reached on this basis alone. Calculations of the moments of inertia of chair and boat forms were made using the assumed parameters: C—H = 1.108, C—C = 1.533 Å, as quoted by Hendrickson (9), tetrahedral angles at carbon, C—O = 1.410 Å, and an angle C—O—C = 111°43′ as in dimethyl ether (10). The total dipole moment was assumed to be

Can. J. Chem. Downloaded from www.nrcresearchpress.com by 210.87.254.42 on 09/05/12
For personal use only.

TABLE 5. Comparison of calculated and observed planar principal moments for 1,3-dioxane and tetrahydropyran

Conformation	$\sum_i m_i a_i^2$ (u Å^2)	$\sum_i m_i b_i^2$ (u Å^2)	$\sum_i m_i c_i^2$ (u Å^2)
1,3-Dioxane			
Observed	93.671	89.628	9.949
Chair, calcd. ($\phi = 57°18'$)	91.344	89.737	11.728
Boat, calcd. ($\phi = -57°18'$)	91.344	81.140	16.142
Flattened chair, calcd. ($\phi = 45°$)	94.664	91.344	9.779
Half chair, calcd. ($\phi = 0°$)	98.158	91.344	10.213
Tetrahydropyran			
Observed	99.285	94.992	13.145
Chair, calcd.	96.982	94.183	13.876
Boat, calcd.	94.183	88.946	17.694

given solely by the vector sum of the two COC group moments, each directed along a C—O—C angle bisector. These calculations predicted that both conformers should have μ_b and μ_c components. Also the calculated angle between μ and the b principal axis was 55°3′ for the chair form and 35°40′ for the boat form. The observed angle is 38°38′, seemingly favoring the boat form. However it is considered that the inherent errors in both the assumed structural parameters and the simple bond moment approach are such that the above angle comparison does not furnish any real evidence for the boat form.

More useful comparisons can be made between the calculated and observed moments of inertia and this is best done in terms of the quantities $\sum_i m_i a_i^2$, $\sum_i m_i b_i^2$ and $\sum_i m_i c_i^2$ where $\sum_i m_i a_i^2 = 1/2\ (I_b + I_c - I_a)$, for example. These quantities are given in Table 5. The corresponding values are given for tetrahydropyran which has been shown previously to be in chair form (2). It can be seen that for each molecule the observed value of $\sum_i m_i b_i^2$ is in very good agreement with that calculated for the chair but not for the boat form. More significant still is that for each molecule the observed $\sum_i m_i c_i^2$ is much closer to the chair, calculated than the boat, calculated value. It is therefore considered that these comparisons show that the observed conformer for 1,3-dioxane must be the chair form. Although the observed planar moments are also consistent with a flattened chair or even a half chair structure (see Table 5), these forms are ruled out by the dipole moment data (see below).

As a check on the assignment of the correct conformer and also to investigate the possibility of flattening of the molecule by oxygen lone pair repulsions, calculations were also made of the way in which the moments of inertia and dipole components would vary with the angle ϕ, between the $O_1C_2O_3$ and $O_1O_3C_4C_6$ planes.

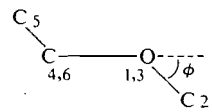

$\phi = 57°18'$ (chair) and $-57°18'$ (boat) are the values obtained from the parameters assumed initially, see above. Figure 1 shows the variation of I_a and I_b and also the ratio μ_c/μ with ϕ. The observed moments of inertia are given in Table 3 and the observed value of μ_c/μ is 0.621. The most important result of these calculations is to show that for $-32° < \phi < 55°$ 1,3-dioxane is predicted to have only μ_a and μ_c dipole moments. The observation of just μ_b and μ_c components thus indicates that ϕ is outside the $-32°$ to 55° range. Taken together with the planar principal moment information of Table 5 this puts $\phi > 55°$ indicating little flattening of the molecule, if any. It should be borne in mind that these calculations are based on assumed parameters which almost certainly differ from the true values. Even so the conclusion reached is considered to be a firm one.

One further piece of empirical evidence for the chair conformation is that if the ratio $(A+B+C)_{\text{obsd.}}/(A+B+C)_{\text{chair,calcd.}}$ is evalu-

Can. J. Chem. Downloaded from www.nrcresearchpress.com by 210.87.254.42 on 09/05/12
For personal use only.

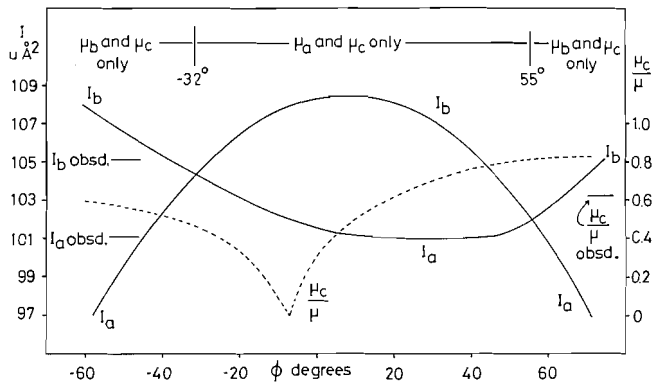

FIG. 1. Solid curves: calculated variation of the moments of inertia I_a and I_b with ϕ, the angle between the $O_1C_2O_3$ and $O_1O_3C_4C_6$ planes of 1,3-dioxane. Dashed curve: calculated variation of the ratio μ_c/μ. For the assumptions involved in the calculations, see text.

TABLE 6. R-branch transitions for five excited states of 1,3-dioxane

	$\nu_{obsd.}$ (MHz) for excited state				
Transition	1	2	3	4	5
b-type					
$1_{01}-2_{12}$	13 198.48				
$1_{10}-2_{21}$	17 727.44				
$2_{02}-3_{13}$	18 572.35				
$2_{12}-3_{21}$		35 212.30		35 260.95	
$2_{11}-3_{22}$	23 193.80				
$3_{03}-4_{14}$	24 032.82	24 338.84	24 273.70		24 148.99
$3_{12}-4_{23}$		28 615.67	28 582.42		28 457.02
$3_{22}-4_{13}$		28 551.49	28 512.25	28 235.33	28 300.46
$3_{21}-4_{32}$			33 411.16		33 302.26
$3_{30}-4_{41}$			38 042.06		
$4_{04}-5_{15}$	29 501.10	29 892.80	29 806.03	29 371.41	29 652.97
$4_{13}-5_{24}$		34 137.44	34 082.27	33 713.15	33 921.91
$4_{23}-5_{14}$		34 133.38	34 077.70	33 708.22	33 917.17
$4_{22}-5_{33}$		38 489.78	38 470.24	38 178.55	
$4_{32}-5_{23}$			38 259.87		
c-type					
$1_{10}-2_{20}$	19 611.18				
$1_{11}-2_{21}$	19 794.22				
$2_{02}-3_{12}$	29 343.95	29 349.76	29 375.12		
$2_{12}-3_{22}$	29 396.00	29 398.59	29 428.18	29 348.09	29 319.46
$2_{11}-3_{21}$	29 110.98	29 125.46			
$2_{21}-3_{31}$	29 700.06	29 687.18	29 729.61	29 662.56	
$2_{20}-3_{30}$	29 450.50	29 447.46	29 481.63	29 404.64	29 376.82
$3_{03}-4_{13}$		39 170.71			
$3_{13}-4_{22}$		39 173.82			
$3_{12}-4_{22}$			39 117.89		
$3_{22}-4_{32}$		39 207.49			
$3_{21}-4_{31}$		38 848.86	38 876.22	38 754.85	
$3_{31}-4_{41}$		39 596.25		39 564.47	
$3_{30}-4_{40}$		39 319.22			39 233.55
σ	0.43	0.47	0.71	0.29	0.48

Can. J. Chem. Downloaded from www.nrcresearchpress.com by 210.87.254.42 on 09/05/12
For personal use only.

TABLE 7. Ground and vibrationally excited states of 1,3-dioxane

State	A(MHz)	B(MHz)	C(MHz)	κ	Relative intensity	ν(cm^{-1})	$\Delta\nu$(cm^{-1}) Raman
Ground	4999.94	4807.61	2757.12	0.82849	1.00		
1	4997.65	4801.27	2733.89	0.82650	0.28_9	257(25)	273
2	4993.46	4806.02	2777.24	0.83085	0.24_6	290(25)	273
3	5002.20	4807.21	2767.13	0.82547	0.12_4	432(50)	421
4	4993.09	4789.69	2720.25	0.82102	0.12_0	439(50)	421
5	4998.39	4784.78	2752.14	0.81790	0.10_2	472(50)	468

ated for each of 1,3-dioxane and tetrahydropyran the similar quantities 0.991322 and 0.990794 are obtained. The corresponding values for $(A+B+C)_{\text{obsd.}}/(A+B+C)_{\text{boat,calcd.}}$ are 0.979578 and 0.979523. Since these two molecules have similar structures and the same assumed parameters were used in each calculation it is probably not accidental that the two chair forms give closely similar ratios. It would be advisable to make a check on this procedure by carrying out the corresponding calculations for *sym*-trioxane. Unfortunately a value for the C rotational constant of this molecule has not yet been reported in the literature.

Excited Vibrational States

Each ground vibrational state Q-branch series was seen to have two vibrational satellite series towards higher frequencies. The $J = 6$–6 Q-branch heads for these satellites are at 23 788.88 and 23 849.68 MHz. The corresponding ground vibrational state line 6_{16}–6_{25} occurs at 23 582.82, see Table 1. These observations prompted a search for vibrational satellites of R-branch lines and a total of five vibrational states were identified. The assigned R-branch lines are given in Table 6 and the derived rotational constants in Table 7.

Table 7 also contains the vibrational frequencies estimated on the basis of relative intensities of the lines in the coincident transitions 4_{04}–5_{15} and 4_{14}–5_{05}, see Fig. 2. Additional lines at 29 607 and 29 640 MHz may be noticed which probably represent two other excited states. The corresponding lines in other transitions could not be positively identified, however. Calculating from the peak heights, good agreement is obtained with the observed Raman displacements in the 200 to 500 cm^{-1} region (11) provided that the displacements at 273 and 421 cm^{-1} each correspond to an unresolved

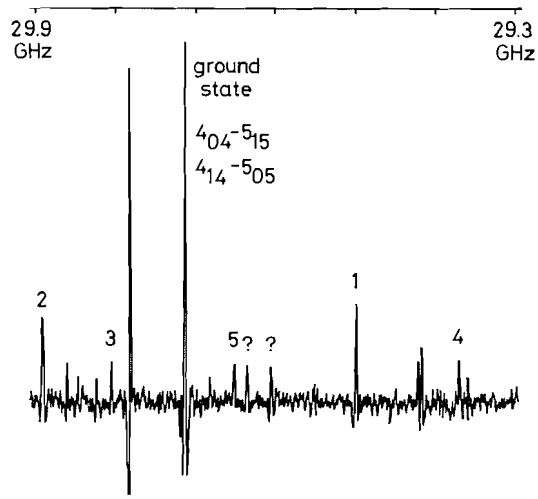

FIG. 2. Vibrational satellite pattern for an R-branch transition of 1,3-dioxane. The assigned satellites are labelled 1 through 5. The additional peaks at 29 607 and 29 640 MHz, denoted by ?, could also be due to excited vibrational states of the molecule. The diagram is a trace of a spectrum recorded with the Hewlett Packard 8460A spectrometer at a Stark voltage of 40 V cm^{-1} and a sample pressure of 15 μ.

doublet. The calculated frequencies of Voetler and Wollrab (12), 189, 221, 421, 450, and 468 cm^{-1} are in good agreement in the 400 to 500 cm^{-1} region. The present work shows conclusively that the lowest vibrational frequency of the molecule is the one corresponding to 273 cm^{-1} in the Raman work (11) and that calculated values of 189 and 221 (12) are in considerable error.

The fact that the lower vibrational frequencies of 1,3-dioxane are quite comparable to those of 242, 276, 402, 432, and 460 cm^{-1} for tetrahydropyran (13) and that 1,3-dioxane is found to be in the chair form indicates that repulsions between C—H bonding electron pairs and oxygen lone pair electrons do not allow any

Can. J. Chem. Downloaded from www.nrcresearchpress.com by 210.87.254.42 on 09/05/12
For personal use only.

marked increase in freedom of movement in this molecule compared to one which is restrained in the chair form by repulsions between C—H hydrogens only.

The author thanks Professor R. F. Curl and the Robert A. Welch Foundation for the use of computing and instrumental facilities at Rice University. Mrs. S. Leavell, C. D. Le Croix, Dr. H. Takeo, and Dr. H. Jones were all very helpful with spectroscopic equipment and computing. The support of this work by the National Research Council of Canada through operating grants is gratefully acknowledged.

1. P. J. Buckley, C. C. Costain, and J. E. Parkin. Chem. Commun. 668 (1968).
2. V. M. Rao and R. Kewley. Can. J. Chem. **47**, 1289 (1969).
3. J. J. Sloan and R. Kewley. Can. J. Chem. **47**, 3453 (1969).
4. T. Oka, K. Tsuchiya, S. Iwata, and Y. Morino. Bull. Chem. Soc. Jap. **37**, 4 (1964).
5. R. Walker and D. W. Davidson. Can. J. Chem. **37**, 492 (1959).
6. J. S. Muenter. J. Chem. Phys. **48**, 4544 (1968).
7. J. S. Muenter and V. W. Laurie. J. Chem. Phys. **45**, 855 (1966).
8. C. Barbier, J. Delmau, and J. Ranft. Tetrahedron Lett. 3339 (1964).
9. J. B. Hendrickson. J. Am. Chem. Soc. **83**, 4537 (1961).
10. U. Blukis, P. H. Kasai, and R. J. Myers. J. Chem. Phys. **38**, 2753 (1963).
11. M. J. Murray and F. F. Cleveland. J. Chem. Phys. **12**, 156 (1944).
12. H. Voetter and F. Wollrab. Acta Phys. Aust. **5**, 529 (1952).
13. P. A. Akishin, N. G. Rambidi, I. K. Korobitsyna, G. Y. Krondrat'eva, and Y. K. Yur'ev. Chem. Abstr. **50**, 8330*d* (1956).

Can. J. Chem. Downloaded from www.nrcresearchpress.com by 210.87.254.42 on 09/05/12
For personal use only.

Reactions of Ethylene with Rhodium(III) Chloride. Part III.[1] The Catalytic Oxidation of Ethylene to Acetaldehyde in Aqueous Hydrochloric Acid Solutions Containing Pentachloroaquorhodate(III)

B. R. JAMES AND M. KASTNER

Department of Chemistry, University of British Columbia, Vancouver 8, British Columbia

Received January 7, 1972

In the presence of iron(III) or other oxidants, aqueous acid chloride solutions of $RhCl_5(H_2O)^{2-}$ catalyze under mild conditions the oxidation of ethylene to acetaldehyde. The kinetics of the reaction measured by gas-uptake techniques indicate the presence of both ethylene dependent and independent paths. Besides fully protonated anions, hydroxy species such as $RhCl_5(OH)^{3-}$ and $RhCl_4(OH)(H_2O)^{2-}$, although present in very small concentrations, are significantly reactive towards ethylene. A mechanism, based on that postulated for a similar palladium(II) system in the well-known Wacker process, is presented. Under our reaction conditions the slow steps in the rhodium system involve formation of π-complexes in the ethylene dependent paths and the formation of tetrachlororhodate(III) complexes in the ethylene independent paths. Iron(III) regenerates the rhodium(III) catalyst by oxidation of the rhodium(I). Rate constants are estimated for the various reaction paths.

En présence de fer(III) ou d'autres oxydants, les solutions chlorhydriques aqueuses de $RhCl_5(H_2O)^{2-}$ catalysent dans des conditions douces, l'oxydation de l'éthylène en acétaldéhyde. Les cinétiques de la réaction, mesurées par des techniques d'absorption gazeuse, indiquent à la fois une certaine indépendance et dépendance vis-à-vis de l'éthylène. A côté des anions complètement protonés, des espèces hydroxylées telles que $RhCl_5(OH)^{3-}$ et $RhCl_4(OH)(H_2O)^{2-}$, bien que présentes en très faibles concentrations, réagissent de façon significative avec l'éthylène. Un mécanisme basé sur celui postulé pour le système voisin Pd(II) dans le processus bien connu de Wacker, a été présenté. Dans nos conditions de réaction, les étapes lentes dans le système rhodium dépendant de l'éthylène impliquent la formation de complexes π alors que c'est la formation de complexes tétrachlororhodate(III) qui expliquent l'indépendance vis-à-vis de l'éthylène. Le fer(III) regénère le catalyseur Rh(III) par oxydation du Rh(I). Les constantes de vitesse sont évaluées pour les diverses voies réactionnelles.

Canadian Journal of Chemistry, **50**, 1698 (1972)

Introduction

We have reported previously (1) on the reaction between ethylene and aqueous solutions containing rhodium(III) chloride trihydrate, $RhCl_3.3H_2O$, at 1 atm and ambient temperatures. The ethylene catalyzes the production of $RhCl_2(H_2O)_4^+$ species via a mechanism involving trace amounts of chlororhodate(I) species formed according to a reaction such as 1.

$$[1] \qquad Rh^{III} + C_2H_4 \xrightarrow{H_2O} Rh^{I} + CH_3CHO + 2H^+$$

Subsequent formation of a bridged Rh^{III}—Rh^{I} intermediate, followed by a 2 electron transfer and cleavage of a labile Rh^{I}—Cl bond, leads to rapid formation of $RhCl_2(H_2O)_4^+$ which is unreactive towards ethylene at the ambient conditions. At temperatures of *ca.* 50°, reaction 1 results in the production of metal via disproportionation of Rh^{I}, and the catalytic substitution is not observed.

Reaction between ethylene and $RhCl_3.3H_2O$ in *N,N'*-dimethylacetamide solution at 60–80° has also been shown (2) to give complete reduction to Rh^{I}, basically according to the stoichiometry of reaction 1, although 2 further moles of ethylene coordinate rapidly to stabilize Rh^{I} as the $RhCl_2(C_2H_4)_2^-$ complex.

It seemed highly likely that in the presence of an excess of a suitable oxidizing agent the Rh^{I} formed via reaction 1 could be rapidly reconverted to Rh^{III}, and an overall catalytic oxidation of ethylene to acetaldehyde achieved with consumption of the added oxidant. Such a system is closely akin to the well-known Wacker process (3) which employs a $Pd^{II} \rightarrow Pd^0 \rightarrow Pd^{II}$ cycle, the oxidant being a Cu^{II}/oxygen system.

The rhodium(III) chloride complexes $RhCl_n(H_2O)_{6-n}^{(n-3)-}$ have been characterized in aqueous acid solutions (4), and hence we studied these systems for ethylene oxidation. This paper

[1]Presented at the XIIIth International Conference on Coordination Chemistry. Cracow-Zakopane, 1970. Part II is ref. I.

Can. J. Chem. Downloaded from www.nrcresearchpress.com by 210.87.254.6 on 09/05/12
For personal use only.

Can. J. Chem. Downloaded from www.nrcresearchpress.com by 210.87.254.6 on 09/05/12
For personal use only.

reports on a detailed kinetic study under mild conditions using $RhCl_5(H_2O)^{2-}$ as catalyst and iron(III) to regenerate the rhodium(III), although a number of other oxidants, including molecular oxygen on its own, can be used.

Osipov and co-workers (5) have briefly mentioned the use of acid chloride solutions containing $RhCl_6^{3-}$ for the catalytic oxidation of ethylene to acetaldehyde, and noted that the activity was some 150 times less than that of $PdCl_4^{2-}$ solutions under the same conditions (90°, < 1 atm pressure and using Cu^{II}/oxygen to regenerate the catalyst).

Experimental

Rhodium(III) trichloride was obtained as the trihydrate $RhCl_3.3H_2O$ from Johnson Matthey Limited. Other materials used and the procedure used for following C_2H_4 uptake at constant pressure have been described earlier (6, 7). All uptake measurements were made on 2 ml of solution. Ferric solutions were standardized by reduction to the ferrous state using a Jones Reductor, and then reoxidized using standard dichromate solution.

Solutions of $RhCl_3.3H_2O$, in 0.1–3.0 *M* HCl and containing up to 3 *M* total chloride, equilibrated quite rapidly on heating, and showed absorption maxima at 400 nm ($\varepsilon \sim 85$) and 505 nm ($\varepsilon \sim 75$); the predominant species is $RhCl_5(H_2O)^{2-}$ (4).

Acetaldehyde from Eastman Organic Chemicals was distilled immediately before use. Liquid organic products were analyzed by use of a Beckman GC-2A chromatograph with a dinonyl phthalate column, and by a Varian T-60 NMR spectrometer.

Visible and ultraviolet absorption spectra were recorded in a Perkin–Elmer 202 spectrophotometer with matched silica cells of 1 mm path length.

Total pressures of 330–950 mm Hg were employed; the partial pressures of ethylene were obtained after correcting for the vapor pressures of the HCl solutions (8), and the ethylene solubilities were extrapolated values from those listed in ref. 7.

Results

Stoichiometry

When excess iron(III) was added to a solution of 0.1 *M* $RhCl_3.3H_2O$ in 3 *M* HCl and then the mixture exposed at 80° to ethylene at 1 atm, gas was absorbed at a linear rate. The reaction rate exhibited inverse chloride and acid dependences, and for kinetic convenience detailed studies were carried out mainly using solutions 0.1 *M* in HCl and 2.0 *M* in LiCl. Since protons are a product of the catalytic reaction (*cf.* reaction 1), some of the uptake plots (depending on the conditions) showed, after an initial linear region, a slightly decreasing rate presumably due to the inverse acid dependence. Eventually, all the uptake plots showed a sharp upward break at a point where metallic rhodium appeared. Just prior to metal production, the solutions gave absorption spectra almost identical to that of $RhCl_5(H_2O)^{2-}$; at this stage the spectrum shows none of the more intense absorption of iron(III) chloride (λ_{max} 422 nm) which has been consumed in the reaction. The iron(III) is converted entirely to iron(II), as shown by a potentiometric titration with standard dichromate (a solution initially 0.19 *M* in Fe^{III} analyzed finally for 0.18 *M* Fe^{II}). Ferrous chloride in the acid chloride media gave practically no absorption between 350 and 550 nm. In the absence of any added Fe^{III}, the $RhCl_5(H_2O)^{2-}$ solutions were immediately reduced to metal.

At the end of reactions when 0.19 *M* Fe^{III} had been consumed, the organic products were separated by distillation and analyzed by gas chromatography and n.m.r. Acetaldehyde corresponding to a 0.08 ± 0.01 *M* solution was the only product detected. Comparison with standard solutions showed no presence of acetic acid, ethylene glycol or paraldehyde. The distillate from a corresponding reaction using a 0.1 *M* DCl/2 *M* LiCl/D_2O solution yielded by n.m.r. a doublet at 8.1 τ showing that no deuterium is present in the acetaldehyde molecule.

The noted Fe:acetaldehyde stoichiometry (*ca.* 2:1) and the spectrophotometric data may be rationalized in terms of reaction 1 followed by reaction 2.

$$[2] \qquad Rh^{I} + 2Fe^{III} \rightarrow Rh^{III} + 2Fe^{II}$$

The net reaction is

$$[3] \qquad 2Fe^{III} + C_2H_4 \xrightarrow[H_2O]{Rh^{III}} 2Fe^{II} + CH_3CHO + 2H^+$$

However, the ethylene uptake plots using variable iron(III) concentrations and ethylene concentrations showed an apparent consumption of ethylene and iron(III) at the end of the reaction, when metal forms, in mole ratios of $1:3.7 \pm 0.5$ (approx. 1:4) instead of the anticipated 1:2. This apparent discrepancy arises from the fact that approximately one half of the acetaldehyde product appears in the gas phase, and hence the measured total uptake of ethylene is about one half the true uptake. This factor of

TABLE 1. Kinetic data for the $RhCl_5(H_2O)^{2-}$ system (0.1 *M* HCl, 2 *M* LiCl, 0.19 *M* $FeCl_3$, unless stated otherwise).

$[Rh^{III}]$ (*M*)	C_2H_4 (mm)	$[C_2H_4] \times 10^4$ (*M*)	Temperature (°C)	Linear rate $\times 10^6$ ($M\ s^{-1}$)
0.0	400	8.0	80	0.0
0.01	400	8.0	80	0.7
0.05	400	8.0	80	4.5
0.10	400	8.0	80	8.1*
0.10	400	8.0	80	7.9†
0.15	400	8.0	80	13.6
0.10	20	0.4	80	2.9
0.10	50	1.0	80	3.3
0.10	170	3.4	80	5.1
0.10	290	5.8	80	6.8
0.10	490	9.8	80	10.0
0.10	590	11.8	80	10.5
0.10	35	0.75	75	2.2
0.10	115	2.5	75	3.6
0.10	230	5.0	75	4.6
0.10	465	10.2	75	7.5
0.10	555	12.1	75	8.5
0.10	35	0.6	85	3.3
0.10	100	1.8	85	4.6
0.10	165	3.0	85	6.5
0.10	320	5.8	85	9.1
0.10	410	7.4	85	11.1

*Independent of $[Fe^{III}]$ up to 0.60 *M*.
†Using 0.1 *M* DCl/2*M* LiCl/D_2O.

TABLE 2. Kinetic data at 80° for the $RhCl_5(H_2O)^{2-}$ system (0.1 *M* $RhCl_3$, 2 *M* LiCl, 0.19 *M* $FeCl_3$)

[HCl] (*M*)	C_2H_4 (mm)	$[C_2H_4] \times 10^4$ (*M*)	Linear rate $\times 10^6$ ($M\ s^{-1}$)
0.05	48	1.0	5.4
0.05	198	4.0	7.3
0.05	398	8.0	10.2
0.20	53	1.1	1.4
0.20	203	4.1	3.3
0.20	403	8.1	5.3

0.5 is for our particular apparatus (which has a dead-space volume of about 50 ml) using 2 ml of reactant solution, and is calculated using a literature value (9) of 380 mm Hg for the partial pressure of acetaldehyde over a 0.55 *M* aqueous acetaldehyde solution at 82°. It should be noted also that measured ethylene uptake rates at 82° would therefore be one half the true absorption rates. This factor is independent of the ethylene pressure but can become dependent on temperature. Using other data given in ref. 9, the factor is calculated to be 0.7 at 63° but is again 0.5 at 93.5°; a factor of 0.6 will be assumed for data at 75°. Under the conditions noted in Table 1, the acetaldehyde formed in the gas phase never contributes more than *ca.* 5% to the total pressure above the solution, *i.e.* the ethylene partial pressure is affected little during a kinetic uptake experiment in the constant pressure apparatus. That some of the observed rates are linear is consistent with this.

There was no sign of production of rhodium carbonyls via decarbonylation of acetaldehyde (*cf.* ref. 10) during the kinetic studies.

Kinetics

The kinetics of the catalyzed ethylene oxidation were readily determined from the linear plots or else the initially linear rates of the uptake plots. Tables 1 and 2 summarize the kinetic data for the $RhCl_5(H_2O)^{2-}$ system. The rates listed are the measured linear ones and are not corrected (see above). As anticipated from the linear uptake plots, no dependence of the rate on $[Fe^{III}]$ was found; there is a good first-order dependence on $[Rh^{III}]$ up to 0.15 *M*. The rate is linearly dependent on the ethylene concentration, but each plot at 3 different acidities at 80° and *ca.* 2 *M* chloride and at 3 different temperatures for 0.1 *M* HCl/2 *M* LiCl solutions

Can. J. Chem. Downloaded from www.nrcresearchpress.com by 210.87.254.6 on 09/05/12
For personal use only.

Can. J. Chem. Downloaded from www.nrcresearchpress.com by 210.87.254.6 on 09/05/12
For personal use only.

TABLE 3. Kinetic data at 80° showing the dependence of the reaction rate on $[H^+]$ and $[Cl^-]$ (0.1 *M* $RhCl_3$, 0.19 *M* $FeCl_3$, 8×10^{-4} *M* C_2H_4)

[HCl] (*M*)	[LiCl] (*M*)	$[Cl^-]_{total}$* (*M*)	Linear rate $\times 10^6$ ($M\,s^{-1}$)
0.1	2.9	3.0	6.3
0.2	2.8	3.0	3.4
0.5	2.5	3.0	1.1
1.0	2.0	3.0	0.9
3.0	0.0	3.0	0.6
0.05	2.0	2.05	10.2
0.1	2.0	2.1	8.2
0.2	2.0	2.2	5.3
1.0	1.0	2.0	5.0
0.1	0.0	0.1	10.8
0.1	0.5	0.6	9.3
0.1	1.0	1.1	8.7
0.1	3.0	3.1	5.8
0.1	1.0	1.1 (+1.0 *M* $LiClO_4$)	9.7
0.1	1.0	1.1 (+2.0 *M* $LiClO_4$)	9.3
0.1 *M* $HClO_4$	2.0	2.0	12.8 (ref. 12)

*Excludes chloride added as rhodium(III) and iron(III) trichloride (see text).

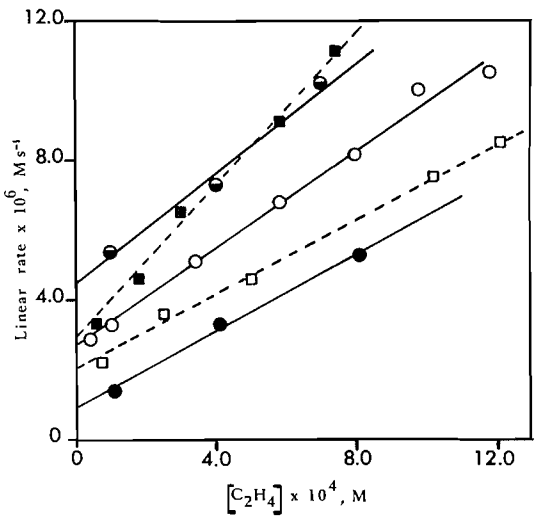

FIG. 1. Rates of ethylene absorption as a function of ethylene concentration with 0.1 *M* $RhCl_3$, 0.19 *M* $FeCl_3$, 2.0 *M* LiCl; ● at 80°, 0.2 *M* HCl; ○ at 80°, 0.1 *M* HCl; ◒ at 80°, 0.05 *M* HCl; □ at 75°, 0.1 *M* HCl; ■ at 85°, 0.1 *M* HCl.

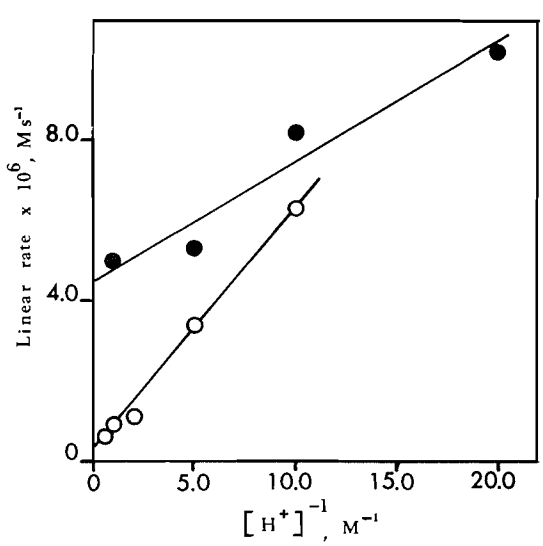

FIG. 2. Rates of ethylene absorption at different acidities at 80°, with 0.1 *M* $RhCl_3$, 0.19 *M* $FeCl_3$; ● at *ca.* 2 *M* chloride; ○ at 3.0 *M* chloride.

shows an intercept on the ordinate axis corresponding to zero ethylene (Fig. 1).

In order to establish the dependences of the rate on $[H^+]$ and on $[Cl^-]$, ethylene uptakes were studied at several acid and chloride concentrations. The results are summarized in Table 3. The [HCl] was varied in two sets of experiments in which the total chloride was kept essentially constant (3.0 and *ca.* 2 *M*) by addition of LiCl; plots of rate *vs.* $[H^+]^{-1}$ are reasonably linear (Fig. 2). A less pronounced inverse chloride dependence was noted for experiments performed using 0.1 *M* HCl solutions with different concentrations of added LiCl; these data refer to solutions with different

Can. J. Chem. Downloaded from www.nrcresearchpress.com by 210.87.254.6 on 09/05/12
For personal use only.

TABLE 4. Summary of rates with various oxidants; 0.1 *M* $RhCl_3$, 0.1 *M* HCl, 2 *M* LiCl, 80°, 1 atm total pressure

Oxidant	C_2H_4 (mm)	Linear rate × 10^6 ($M\ s^{-1}$)
0.2 *M* $FeCl_3$	400	8.2
	100	3.4
0.2 *M* $CuCl_2$	400	14.3
0.2 *M* $K_2Cr_2O_7$	400	9.7
300 mm O_2	100	1.2

ionic strengths although such variations appear relatively unimportant considering the little effect addition of $LiClO_4$ has on the rates of reactions carried out at 0.1 *M* HCl and 1.0 *M* LiCl. There is no obvious relationship between the rate and the chloride concentration.

It should be noted that the total chloride concentration listed in Table 3 does not include consideration of equilibria involving the metal chloride complexes. Using the stability constants for ferric chloride complexes in 1 *M* $HClO_4$, $K_1 = 4.2$, $K_2 = 1.3$, $K_3 = 0.04\ M^{-1}$ at 27° (11), 0.19 *M* $FeCl_3$ in solution yields 0.24 *M* free chloride; 0.1 *M* $RhCl_3$ will require 0.2 *M* chloride to form the pentachloroaquo species.

The spectra of the various pre-equilibrated rhodium solutions used for the studies summarized in Tables 1–3 were essentially identical and all corresponded approximately to that for $RhCl_5(H_2O)^{2-}$.

Several other oxidants besides Fe^{III} were investigated for the catalyzed ethylene oxidation. The initially linear rates are given in Table 4 together with those for Fe^{III} for comparison. No rhodium metal was formed during these experiments, thus showing that the oxidants are efficient for removing Rh^I; as expected, the Cu^{II} system precipitated metallic copper.

Discussion

The Activity of the Pentachloro Species

The kinetic dependences on rhodium and ethylene may be expressed by eq. 4

$$[4] \quad -d[C_2H_4]/dt = k_a[Rh^{III}] + k_b[Rh^{III}][C_2H_4]$$

where k_a and k_b are pseudo first- and second-order rate constants containing all dependences except those of rhodium and ethylene, and $[Rh^{III}]$ refers to the total rhodium concentration. k_b refers to a rate determining step of the overall

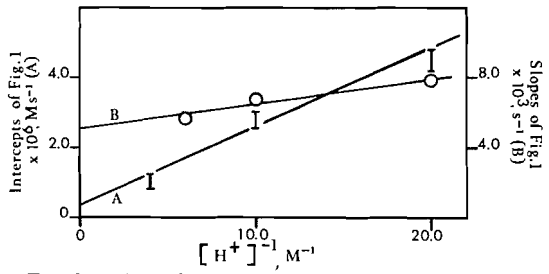

FIG. 3. Plots of the intercepts (*A*) and slopes (*B*) of the solid lines of Fig. 1 (the 80° data) *vs.* the inverse of the acid concentration.

reaction shown in reaction 3; the independence of the rate on $[Fe^{III}]$ is consistent with reaction 2 being fast. k_a for the ethylene independent step must refer to some relatively slow substitution reaction of the initial rhodium complex, which competes with the k_b process, to give a species which then reacts with ethylene in a more rapid step than the substitution; an aquation reaction would yield a tetrachloro complex while chloride substitution would give the hexachloro species. The small inverse effect of added chloride on the rate argues against formation of more active $RhCl_6^{3-}$ since the k_a path would then be expected to show a direct first-order dependence on chloride (13). Other studies using the series of $RhCl_n(H_2O)_{6-n}^{(n-3)-}$ complexes have in fact shown that solutions containing $RhCl_4(H_2O)_2^-$ are generally more active than those containing $RhCl_5(H_2O)^-$ while $RhCl_6^{3-}$ is completely inactive (12), thus confirming that k_a refers to production of a tetrachloro complex.

The kinetic data give information only about the ways of forming the Rh^{III}–ethylene intermediates. The slow steps shown in reactions 5–8 are thought to be involved. The analysis given below was done to some extent on a trial and error basis to give internal consistency in the estimated rate constants; the lines plotted in Figs. 1–3 are drawn to give this consistency.

Figure 1 for $[H^+] = 0.1\ M$ gives $k_a = 2.8 \times 10^{-5}\ s^{-1}$ and $k_b = 6.7 \times 10^{-2}\ M^{-1}\ s^{-1}$ at 80°. The ethylene independent rate (k_a) is acid dependent since the intercepts of Fig. 1 for the 80° data are unequal; an inverse acid dependence is noted and a plot of these intercepts versus $[H^+]^{-1}$ goes close to the origin as shown in Fig. 3*A*. This shows that the major contribution to the k_a path is one involving hydroxy species:

$$[5] \quad RhCl_5(OH)^{3-} + H_2O \xrightarrow{k_1} RhCl_4(OH)(H_2O)^{2-} + Cl^-$$

Can. J. Chem. Downloaded from www.nrcresearchpress.com by 210.87.254.6 on 09/05/12
For personal use only.

The possibility that a small contribution involves an aquo species (eq. 6) cannot be excluded completely, since this acid independent step requires that Fig. 3*A* shows a positive intercept on the ordinate axis.

[6] $RhCl_5(H_2O)^{2-} + H_2O \xrightarrow{k_2} RhCl_4(H_2O)_2^- + Cl^-$

The slopes of Fig. 1 for the data at 80° are not very different showing that the ethylene-dependent rate (k_b) is essentially acid independent. Figure 3*B* shows a plot of these slopes *vs.* $[H^+]^{-1}$; the intercept (*ca.* 5.2×10^{-3} s^{-1}) results from a contribution of the aquo species (eq. 7), while the slope (*ca.* 1.3×10^{-4} $M\ s^{-1}$) refers to a possible small contribution from hydroxy species (eq. 8).

[7] $RhCl_5(H_2O)^{2-} + C_2H_4 \xrightarrow{k_3} \text{products}$

[8] $RhCl_5(OH)^{3-} + C_2H_4 \xrightarrow{k_4} \text{products}$

Writing K_5 for the acid dissociation constant of $RhCl_5(H_2O)^{2-}$, eq. 4 can be expanded to include the acid dependence and the relevant rate constants k_1, k_2, k_3, and k_4.

$$[9]\quad \text{Rate} = \left\{\frac{k_1K_5}{[H^+]} + k_2\right\}[RhCl_5(H_2O)^{2-}] + \left\{k_3 + \frac{k_4K_5}{[H^+]}\right\}[RhCl_5(H_2O)^{2-}][C_2H_4]$$

At 80° and 0.1 M $[H^+]$, the k_a and k_b values estimated from Fig. 1 are thus identified with the constants involved in eq. 9:

$$[10]\quad k_a = k_1K_5[H^+]^{-1} + k_2 \qquad k_b = k_3 + k_4K_5[H^+]^{-1}$$

Equation 9 can also be rearranged to describe the plots of rate versus $[H^+]^{-1}$ shown in Fig. 2:

$$[11]\quad \text{Rate} = \{k_2 + k_3[C_2H_4]\}[RhCl_5(H_2O)^{2-}] + \frac{K_5\{k_1 + k_4[C_2H_4]\}[RhCl_5(H_2O)^{2-}]}{[H^+]}$$

For the line drawn for the 80° data at *ca.* 2 M chloride, the intercept gives for the reaction rate involving the aquo species,

$$[12]\quad 4.5 \times 10^{-6}\ M\ s^{-1} = \{k_2 + k_3[C_2H_4]\}[RhCl_5(H_2O)^{2-}]$$

As discussed above, the k_2 path is not important compared to the k_3 path and hence, on neglecting k_2 in eq. 12, k_3 is calculated to be $5.6 \times 10^{-2}\ M^{-1}\ s^{-1}$. Using the value for k_b defined by eq. 10, and the estimated k_3 value, k_4K_5 is calculated to be $1.1 \times 10^{-3}\ s^{-1}$. The intercept and slope of Fig. 3*B* noted above give the values $k_3 = 5.2 \times 10^{-2}\ M^{-1}\ s^{-1}$ and $k_4K_5 = 1.3 \times 10^{-3}\ s^{-1}$.

TABLE 5. Rate constant data at 80° in 2 M LiCl

k_1K_5 ($M\ s^{-1}$)	k_2 (s^{-1})	k_3 ($M^{-1}\ s^{-1}$)	k_4K_5 (s^{-1})
2.2×10^{-6}	0.6×10^{-5}	5.6×10^{-2}	1.1×10^{-3}

According to eq. 11 again, the slope of the line in Fig. 2 (80°, 2 M chloride) gives the reaction rate involving the hydroxy species, namely,

$$[13]\quad 3.1 \times 10^{-7}\ M^2\ s^{-1} = K_5\{k_1 + k_4[C_2H_4]\}[RhCl_5(H_2O)^{2-}]$$

Using the k_4K_5 value of $1.1 \times 10^{-3}\ s^{-1}$, eq. 13 gives $k_1K_5 = 2.2 \times 10^{-6}\ M\ s^{-1}$; the same value is also calculated directly by the slope of Fig. 3*A*. Lastly, using the k_a value defined by eq. 10 and the estimated k_1K_5 value, k_2 is calculated to be $0.6 \times 10^{-5}\ s^{-1}$ (this requires an intercept of $0.6 \times 10^{-6}\ M\ s^{-1}$ on Fig. 3*A*).

The above analysis of the kinetic data gives values for k_1K_5, k_2, k_3, and k_4K_5 for the system at 80° and 2 M LiCl; these are summarized in Table 5. The relative contribution to the total reaction rate at any acidity is readily estimated by use of eq. 9. At 0.1 M $[H^+]$, the relative contributions to the total rate of $8.1 \times 10^{-6}\ M\ s^{-1}$ for paths 5, 6, 7, and 8 are about 30, 7, 55, and 8%, respectively.

Robb and Steyn (13) have determined a value of k_2 directly to be $8 \times 10^{-5}\ s^{-1}$ at 30° in HCl–$HClO_4$ media at an acid concentration of 4 M. It is somewhat difficult to make too meaningful a comparison with the k_2 value estimated here. In our work the exact solubility of the ethylene is not known; we observed somewhat higher rates when using $HClO_4$ in place of HCl (Table 3) and this could be attributed to differences in ethylene solubility. Our estimation of k_2 from eq. 10 is subject to considerable error since it depends on the difference between two quite similar numbers 2.8×10^{-6} and 2.2×10^{-6}, and the latter is estimated through eqs. 12, 13 with some uncertainty; further, the k_2 value in Table 5

is uncorrected for the stoichiometry problem (see above), and should be multiplied by a factor of 2. The data of Robb and Steyn were measured at only one acidity and involved spectrophotometric studies; the possibility of an undetected contribution via a path involving reaction 5 cannot be excluded.

Acetaldehyde Production

The kinetic data show that both aquo and hydroxy complexes of rhodium(III) react with ethylene. $RhCl_5(H_2O)^{2-}$ and $RhCl_5(OH)^{3-}$ react with rates governed by k_3 and k_4 (reactions 7, 8), while reactivity with tetrachloro species can be represented by reactions 14 and 15 which are faster steps than reactions 5 and 6, respectively

[14] $RhCl_4(OH)(H_2O)^{2-} + C_2H_4 \xrightarrow{k_5}$ products

[15] $RhCl_4(H_2O)_2^- + C_2H_4 \xrightarrow{k_6}$ products

On analogy with the oxidation of ethylene by Pd^{II} (3), and Rh^{III} in non-aqueous solvents (2), reaction 7 probably involves the following steps, although the present kinetic data concern only the production of **1**:

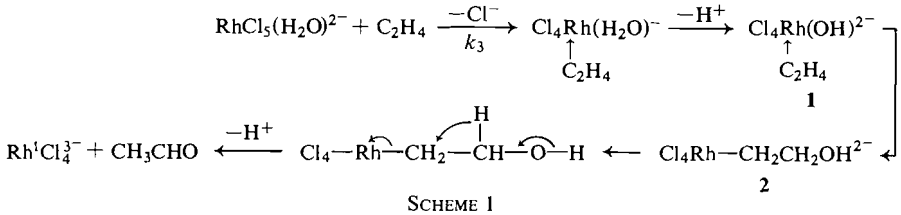

SCHEME 1

Reaction 8 will produce the hydroxyl intermediate **1** directly. Migration of the hydroxy ligand would result in formation of the σ-bonded Rh^{III} hydroxyethyl intermediate **2**. Decomposition of **2** is unlikely to involve a carbonium ion since no ethylene glycol product was detected; the rhodium, after a 2-electron transfer, probably assists a 1,2 hydrogen shift which yields acetaldehyde and a proton (3). Reactions 14 and 15 presumably follow similar paths to those outlined in the scheme although it is not obvious whether ethylene will initially replace a coordinated water or chloride, *e.g.*,

[16] $RhCl_4(OH)(H_2O)^{2-} + C_2H_4 \rightarrow Cl_4Rh(C_2H_4)(OH)^{2-}$
or $Cl_3Rh(C_2H_4)(OH)(H_2O)^-$

Rhodium(I) complexes are labile (14), and $RhCl_n(H_2O)_{4-n}^{(n-1)-}$ seems the likely product from the various rhodium(III) complexes considered. The occurrence of some linear rates and spectrophotometric data indicate that the subsequent rapid redox reaction with ferric regenerates the rhodium(III) as $RhCl_5(H_2O)^{2-}$.

In a related study on the hydration of acetylene catalyzed by rhodium chloride complexes, the activity of $RhCl_5(H_2O)^{2-}$ was much greater than that of $RhCl_6^{3-}$ which was essentially inactive (15). The initial part of the reaction scheme follows that given above and it was concluded that a *ligand* water molecule was necessary for the hydration process. Similar reasoning seems likely for the ethylene reaction; in particular, the slight inverse chloride effect noted at higher chloride could be due to production of the relatively inactive $RhCl_6^{3-}$ complex (12).

The finding that no deuterium is incorporated into the acetaldehyde molecule on using DCl/D_2O solutions is consistent with the hydrogen shift shown in Scheme 1. The same result, that all the hydrogen atoms of the acetaldehyde come from the ethylene, has been observed for the Pd^{II} system (3). The small isotope effect shown in Table 1 (8.1:7.9) is probably significant. The corresponding isotope effect measured in the Pd^{II} system was 4.0; this was attributed to the difference in K_a values for the complex $PdCl_2(C_2H_4)(H_2O)$ in H_2O and D_2O, and showed that ionization to a hydroxy species was prior to the rate determining step which in this system is thought to be decomposition of the π-complex to the σ-complex (*cf.* **1** → **2**). In the present work, the low isotope effect indicates that ionization is subsequent to the rate determining step at the conditions of measurement (0.1 *M* HCl, 2 *M* LiCl); our analysis shows that this is true for about 62% of the reaction (reactions 6 and 7). Spectrophotometric and gas uptake measure-

Can. J. Chem. Downloaded from www.nrcresearchpress.com by 210.87.254.6 on 09/05/12
For personal use only.

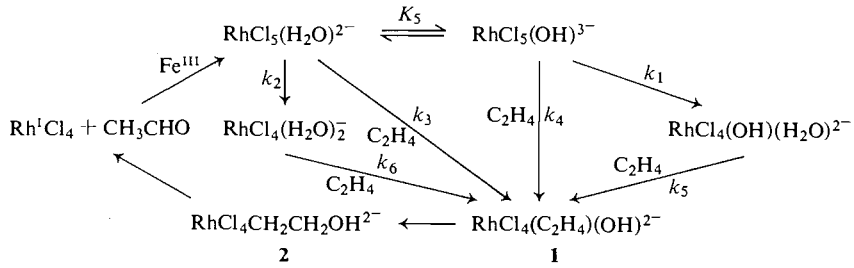

(H_2O, H^+, and Cl^- as reactants and products are not shown)

SCHEME 2

ments showed no evidence for a rapid initial equilibrium process to form an ethylene π-complex via a reaction such as 17, as

$$[17]\quad RhCl_5(H_2O)^{2-} + C_2H_4 \overset{K}{\rightleftharpoons} RhCl_4(C_2H_4)(H_2O)^- + Cl^-$$

for the Pd^{II} system (3). If K is very small, such a process followed by ionization and slow decomposition of the π-complex would still give a linear dependence on ethylene. However, a direct inverse dependence on both proton and chloride would be anticipated for the ethylene dependent path. These were not observed and, considering also the measured isotope effect, the pre-equilibrium can be ruled out, at least at the conditions studied.[2]

We find that solutions of $PdCl_2$ at 0.1 M HCl and 2 M LiCl using ferric as oxidant are about twice as active as corresponding solutions of $RhCl_3$; it should be noted that the rate law reported for the Pd system shows an inverse second-order dependence on chloride (3) in contrast to the slight inverse dependence we observe for the Rh system, and undoubtedly conditions may be chosen in which the rhodium chlorides show higher activity than the palladium chlorides.

Further General Discussion

The rhodium in the 0.1 M HCl/2 M LiCl solutions seems to be present almost entirely as $RhCl_5(H_2O)^{2-}$. However, there are clearly kinetically significant quantities of other active catalysts. Assuming that all the various paths lead eventually to **1** shown in Scheme 1, the entire reaction may be outlined as shown in Scheme 2.

The acidity of $RhCl_5(H_2O)^{2-}$ will be much less than that of the $Rh(H_2O)_6^{3+}$ species (K_a *ca.* 10^{-3}, ref. 16) and somewhat greater than that of the $IrCl_5(H_2O)^{2-}$ complex (K_a *ca.* 10^{-10}, ref. 17). The concentration of hydroxy complexes in the acid solutions is clearly very low. A value of 10^{-8} M for K_5 gives $k_1 = 2.2 \times 10^2$ s^{-1} and $k_4 = 1.1 \times 10^5$ M^{-1} s^{-1}. Comparison of k_1 with k_2 shows that $RhCl_5(OH)^{3-}$ undergoes aquation with loss of a chloride some 10^7 times faster than $RhCl_5(H_2O)^{2-}$. The strong labilizing effect of the hydroxy group in octahedral coordination chemistry is well known (18). In the cobalt(III) system shown in eq. 18,

$$[18]\quad Co(en)_2LCl^+ + H_2O \rightarrow Co(en)_2L(H_2O)^{2+} + Cl^-$$

the rate constants for L = *cis*- or *trans*- OH are 10^3–10^4 times that for the corresponding aquo complexes (18). The data are rationalized in terms of the strong π-donor ability of OH^- to stabilize 5-coordinate intermediates formed by initial dissociation of the chloride in reaction 18. A similar conclusion could be drawn for the mechanism of the k_1 path. Swaminathan and Harris (16) have shown that the conjugate base cation of $Rh(H_2O)_6^{3+}$ is 6000 times more reactive towards chloride anation than the fully protonated cation. Comparison of k_4 with k_3 shows that C_2H_4 reacts *ca.* 10^6 times more rapidly with $RhCl_5(OH)^{3-}$ than with $RhCl_5(H_2O)^{2-}$. Assuming the same K_5 value, the hydroxy species is also some 10^8 times more reactive than the aquo complex towards carbon monoxide (19); after correcting for the stoichiometry problem, the k_3 value at 80° is *ca.* 0.1 M^{-1} s^{-1},

[2]As pointed out by a referee, the equilibrium concentration of an olefin complex commonly decreases with increasing temperature while the rate of its subsequent decomposition increases; also the palladium system (3) was studied at ambient temperatures at conditions when all of the metal was present as $PdCl_4^{2-}$.

Can. J. Chem. Downloaded from www.nrcresearchpress.com by 210.87.254.6 on 09/05/12
For personal use only.

TABLE 6. Temperature dependence of rate constants k_a and k_b; data from Fig. 1 at 0.1 *M* HCl and 2 *M* LiCl

T (°C)	$10^5 k_a$ (s^{-1})	$10^5 k_a$* (s^{-1})	$10^2 k_b$ ($M^{-1}\,s^{-1}$)	$10^2 k_b$* ($M^{-1}\,s^{-1}$)
75	~2.1	~3.5	5.6	9.3
80	~2.8	~5.6	6.7	13.4
85	~3.2	~6.4	11.2	22.4

*Corrected for the stoichiometry problem.

which is comparable to the value of 0.2 $M^{-1}\,s^{-1}$ for the corresponding reaction with carbon monoxide at 80°.

Values of k_a and k_b at 70, 80, and 85° can be estimated from the intercepts and slopes, respectively, of Fig. 1. The data are summarized in Table 6. The measured values have been converted to the true values by correcting for the stoichiometry problem as described above; a correction factor of 0.5 was used at 80–85°, and a factor of 0.6 at 75°. The k_b values (corrected or not) give a good Arrhenius plot, and an activation energy of 17.5 ± 1.0 kcal mol^{-1}; this ethylene dependent path occurs to the extent of *ca.* 85% via reaction 7, and the $\Delta H^{\ddagger}$ value must refer to the rate constant k_3. An activation energy of 22 kcal mol^{-1} was reported for the reaction between $RhCl_5(H_2O)^{2-}$ and acetylene (15). The k_a values cannot be determined with any accuracy but the data do show a smaller dependence on temperature, implying a lower activation energy; this $\Delta H^{\ddagger}$ value would refer to reaction 5 since this step contributes about 80% of the ethylene independent step under these conditions.

The present study gives no data on the fast reaction between Rh^{I} and Fe^{III}. In the reaction medium there are aquo, hydroxy, and chloride ligands, all of which are suitable for bridging so that an inner or outer sphere electron transfer process is possible (20). The mechanism may be similar to that suggested for Rh^{I}–Rh^{III} reactions involving chloro-bridged intermediates (1, 14, 19).

Table 4 shows that some variation in the reaction rate is observed on using different oxidants to regenerate the Rh^{III} catalyst. The variation on using Fe^{III}, Cu^{II}, and Cr^{VI} is less than a factor of 2 and is probably not significant. The rate using O_2 seems low; the measured uptake rate includes the half mole O_2 required for the oxidation of one mole per Rh^{I}, and so the ethylene uptake would in fact be 0.8×10^{-6} $M\,s^{-1}$, some 4 times lower than using Fe^{III} oxidant under corresponding conditions.

In conclusion, the kinetics of the Rh^{III} reaction with ethylene in acid chloride solutions proved to be much more complex than anticipated, since the overall reaction involved contributions from an ethylene independent path as well as the expected ethylene dependent one. Studies on the acid dependence of the contributing paths have shown that hydroxy species, although present in very small concentrations, are significant kinetically. The data also imply that solutions containing tetrachlororhodate(III) species are more active than those containing pentachlororhodate(III) species, at least at 0.1 *M* acidity.

The results are considered significant since they suggest that more efficient rates of conversion of C_2H_4 to CH_3CHO would be observed in less acid conditions where higher concentrations of Rh^{III} hydroxy complexes would be present; efficient oxidants would be required in these conditions to prevent accumulation of Rh^{I} and its disproportionation to metal. Oxygen is appealing since the process would then be somewhat simpler than the Wacker process where O_2 and Cu^{II} are needed to regenerate Pd^{II} from Pd metal; oxygen is probably not very efficient as an oxidant at ordinary pressures in aqueous solution because of its low solubility, and its oxidation power does decrease with decreasing acidity (21). However, the use of higher O_2 pressures and some other non-aqueous solvent system, where the O_2 solubility is higher and Rh^{I} is less likely to disproportionate (*e.g.* in *N*,*N*′-dimethylacetamide (22)), seems worthy of study.

Grateful acknowledgment is made to the National Research Council of Canada for financial support, and to Johnson Matthey Limited for loan of the rhodium.

1. B. R. JAMES, M. KASTNER, and G. L. REMPEL. Can. J. Chem. **47**, 349 (1969).
2. B. R. JAMES and G. L. REMPEL. Can. J. Chem. **46**, 571 (1968).
3. A. AGUILO. Adv. Organomet. Chem. **5**, 321 (1967); P. M. HENRY. J. Am. Chem. Soc. **86**, 3246 (1964).
4. W. C. WOLSEY, C. A. REYNOLDS, and J. KLEINBERG. Inorg. Chem. **2**, 463 (1963).
5. A. M. OSIPOV, K. I. MATVEEV, and N. N. SHUL'TS. Russ. J. Inorg. Chem. **12**, 993 (1967).

Can. J. Chem. Downloaded from www.nrcresearchpress.com by 210.87.254.6 on 09/05/12
For personal use only.

6. B. R. JAMES and G. L. REMPEL. Can. J. Chem. **44**, 233 (1966).
7. B. R. JAMES and J. HALPERN. Can. J. Chem. **44**, 495 (1966).
8. International Critical Tables. Vol. III. McGraw-Hill, New York, 1928. p. 301.
9. International Critical Tables. Vol. III. McGraw-Hill, New York. 1928. p. 310.
10. M. J. CLEARE and W. P. GRIFFITH. J. Chem. Soc. A, 372 (1969).
11. E. RABINOWITCH and W. H. STOCKMAYER. J. Am. Chem. Soc. **64**, 335 (1942).
12. B. R. JAMES and M. KASTNER. Can. J. Chem. This issue.
13. W. ROBB and M. M. DE V. STEYN. Inorg. Chem. **6**, 616 (1967).
14. For example, J. V. RUND. Inorg. Chem. **7**, 24 (1968).
15. B. R. JAMES and G. L. REMPEL. J. Am. Chem. Soc. **91**, 863 (1969).
16. K. SWAMINATHAN and G. M. HARRIS. J. Am. Chem. Soc. **88**, 4411 (1966).
17. C. K. JORGENSEN. Acta Chem. Scand. **11**, 151 (1957).
18. F. BASOLO and R. G. PEARSON. Mechanisms of inorganic reactions. 2nd ed. Wiley, New York. 1967. p. 170.
19. B. R. JAMES and G. L. REMPEL. J. Chem. Soc. A, 78 (1969).
20. A. G. SYKES. Chem. Brit. **6**, 159 (1970).
21. F. A. COTTON and G. WILKINSON. Advanced inorganic chemistry. 2nd ed. Interscience. 1966. p. 366.
22. F. T. T. NG. Ph.D. thesis. University of British Columbia, Vancouver, British Columbia. 1970.

Can. J. Chem. Downloaded from www.nrcresearchpress.com by 210.87.254.6 on 09/05/12
For personal use only.

Reactions of Ethylene with Rhodium(III) Chloride. Part IV.[1] Relative Activity of Tetra-, Penta-, and Hexa-chlororhodate(III) Complexes for the Oxidation of Ethylene to Acetaldehyde in Aqueous Acid Solutions

B. R. JAMES AND M. KASTNER

Department of Chemistry, University of British Columbia, Vancouver 8, British Columbia

Received January 7, 1972

The catalytic oxidation of ethylene to acetaldehyde using the rhodium(III) chloride complexes, $RhCl_n(H_2O)_{6-n}^{(n-3)-}$, in the presence of iron(III) has been studied kinetically in aqueous acid solutions under mild conditions. $RhCl_6^{3-}$ is inactive due to the absence of a coordinated water (hydroxide) ligand. Solutions containing tetrachloro species are generally more reactive than those containing pentachloro species because of the presence of a greater concentration of highly reactive hydroxy species. The neutral and cationic chloro-complexes are inactive due to their substitution inertness.

L'oxydation catalytique de l'éthylène en acétaldéhyde par un complexe chloré de rhodium(III), $RhCl_n(H_2O)_{6-n}^{(n-3)-}$, en présence de fer(III), a été étudiée cinétiquement en solution aqueuse et acide et sous des conditions douces. L'inactivité de $RhCl_6^{3-}$ est due à l'absence de ligand hydroxyle (eau) coordonné. Les solutions contenant des espèces tétrachloro sont, d'une façon générale, plus réactive que celles contenant des espèces pentachloro et ceci par suite d'une concentration plus élevée en espèces hydroxyles hautement réactives. Les complexes chloro, neutres et cationiques, sont inactifs par suite de leur inertie à la substitution.

Canadian Journal of Chemistry, **50**, 1708 (1972)

Introduction

We recently reported (1) on the use of aqueous hydrochloric acid solutions of pentachloro-aquorhodate(III) for the oxidation of ethylene to acetaldehyde; the rhodium(III) is reduced to rhodium(I). The reaction becomes catalytic with respect to rhodium in the presence of a suitable oxidant such as iron(III), which re-oxidizes rhodium(I) to the trivalent state.

An observed 2 term rate-law showed the existence of an ethylene independent path, and this was rationalized in terms of a slow aquation to more reactive tetrachlororhodate(III) complexes. The reactions involved were summarized in Scheme 1.

Values of k_1K_5, k_2, k_3, and k_4K_5 at 80° were estimated from an analysis of the kinetic data; a small inverse chloride dependence was tentatively attributed to the formation of less active hexachlororhodate(III) species (1).

This paper describes studies to investigate the relative activities of the tetra-, penta-, and hexachloro complexes, in particular the estimation of the k_5 and k_6 rate constants of Scheme 1. The activities of the lower chloride complexes were studied also.

Experimental

The materials used and the procedure for following the C_2H_4 uptake at constant pressure have been described

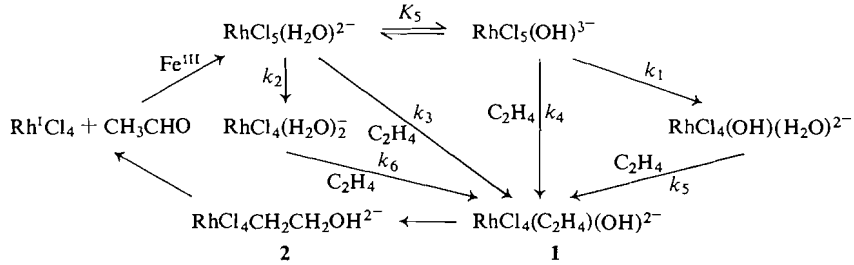

(H_2O, H^+, and Cl^- as reactants and products are not shown)

SCHEME 1

[1]Presented at the XIIIth International Conference on Coordination Chemistry. Cracow-Zakopane, 1970. Part III is ref. 1.

Can. J. Chem. Downloaded from www.nrcresearchpress.com by 210.87.254.42 on 09/05/12
For personal use only.

Can. J. Chem. Downloaded from www.nrcresearchpress.com by 210.87.254.42 on 09/05/12
For personal use only.

TABLE 1. Rates of ethylene absorption at 80° and 1 atm total pressure; $[HCl] + [HClO_4] = 6.0\ M$, $[C_2H_4] \approx 8 \times 10^{-4}\ M$, $[Fe^{III}]^* = 0.1\ M$

Main species	$[Rh^{III}]^*$ (M)	[HCl] (M)	Rate $\times 10^6$ ($M\ s^{-1}$)
$RhCl_6^{3-}$	0.05	6.0	0.0
$RhCl_5(H_2O)^{2-}$	0.07	2.0	metal ppts. (see text)
$RhCl_4(H_2O)_2^-$	0.07	0.30	metal ppts. (see text)
$RhCl_3(H_2O)_3$	0.07	0.20	0.8
—	—	0.20	0.8
$RhCl_2(H_2O)_4^+$	0.07	0.15	0.85
$RhCl(H_2O)_5^{2+}$	0.07	0.07	0.8
$Rh(H_2O)_6^{3+}$	0.07	0.0	0.8

*Present initially as perchlorate.

(see ref. 1). Aqueous solutions containing the complexes $RhCl_n(H_2O)_{6-n}^{(n-3)-}$ were made generally in HCl–$HClO_4$ mixtures from perchloric acid solutions of $Rh(H_2O)_6^{3+}$ (2), based on the methods of Wolsey and co-workers (3); the total acidity in these solutions was always 6.0 M, and the species were characterized by their absorption spectra (2, 3). We also found that equilibration (120° for 2 weeks) of 0.1–0.2 M perchloric acid solutions of 0.1 M $RhCl_3.3H_2O$ in the presence of 2 M LiCl and 0.2 M LiCl gave solutions containing predominantly $RhCl_5(H_2O)^{2-}$ and $RhCl_4(H_2O)_2^-$, respectively. In order to maintain more effective control over the chloride concentration in some of the experiments, the iron(III) reoxidant was added as the perchlorate rather than the chloride.

Other relevant experimental details are given in the previous paper (1).

The ethylene uptake rates reported are the measured "gas uptake" rates; no correction has been made for the presence of acetaldehyde product in the gas phase (see ref. 1).

Results and Discussion

Reactivity in 6 M Acid Solutions

The $RhCl_n(H_2O)_{6-n}^{(n-3)-}$ complexes ($n = 0$ to 6) were characterized earlier by Wolsey and co-workers in perchloric acid – hydrochloric acid mixtures of 6 M acidity (3). We used such a series of solutions to investigate the relative activity of the complexes towards ethylene. The data at 80° are summarized in Table 1.

Solutions containing mainly cationic or neutral species absorbed ethylene extremely slowly at a linear rate which was followed for about 8 h. The visible spectra of the final solutions were identical with those of the respective starting solutions; no ferric had been reduced and the rhodium species were unchanged. That this slow rate (*ca.* $0.8 \times 10^{-6}\ M\ s^{-1}$) was a "blank" reaction was confirmed by a run in which no rhodium was present. This blank reaction was not studied further but is presumably a slow hydration reaction in the perchloric acid medium, since all the solutions showing this blank reaction are close to 6 M in $HClO_4$. No such reaction was observed in the aqueous hydrochloric acid – chloride media (1), and also in the present work, a 6 M HCl solution containing $RhCl_6^{3-}$ showed no reactivity whatsoever towards ethylene.

The inactivity of the hexachloro complex is significant since the complexes $RhCl_n(H_2O)_{6-n}^{(n-3)-}$ show increasing lability with increasing number of coordinated chlorides (2–4). The conclusion drawn is that the presence of a coordinated water (hydroxide) is essential for the production of hydroxyethyl species (**2**) in the reaction scheme outlined above. In effect this means the reverse of reaction 1 competes effectively with any subsequent aquation reaction in this high chloride medium. Earlier studies (5) have reported a quite similar finding of inactivity for the hexachloro complex as a catalyst for the hydration of acetylenes. The slight inverse chloride effect measured for the rate of oxidation of ethylene by acid chloride solutions of $RhCl_5(H_2O)^{2-}$ (1) could therefore be explained qualitatively by the production of small amounts of the inactive $RhCl_6^{3-}$ complex.

$$[1] \qquad RhCl_6^{3-} + C_2H_4 \rightleftharpoons RhCl_5(C_2H_4)^{2-} + Cl^-$$

The solutions containing mainly $RhCl_5(H_2O)^{2-}$ or $RhCl_4(H_2O)_2^-$ were reactive towards ethylene but unfortunately metal was precipitated almost immediately, and it was impossible to make any quantitative measurements. The uptake plots were autocatalytic in nature and were most irreproducible, both these effects presumably due to production of metal. Semi-quantitatively, by measuring rates at corresponding reaction times, the system containing the tetrachloro complex appeared to be 2–4 times more active than that containing the pentachloro complex but no such definite conclusion can be drawn from the studies on these essentially heterogeneous systems. The studies on the activity of $RhCl_5(H_2O)^{2-}$ in HCl–LiCl solutions (1) show that at 6 M acid the k_3 path of the reaction scheme would predominate with a small contribution from the k_2 path, and an expected rate of *ca.* $4 \times 10^{-6}\ M\ s^{-1}$ can be estimated for the 0.07 M $RhCl_5(H_2O)^{2-}$ solution listed in Table 1; the measured rate in the presence of metal ranged from

Can. J. Chem. Downloaded from www.nrcresearchpress.com by 210.87.254.42 on 09/05/12
For personal use only.

an initial value of *ca.* 0.6×10^{-6} M s^{-1} to the maximum measured of *ca.* 6.0×10^{-6} M s^{-1}.

Metal is almost certainly formed by disproportionation of rhodium(I)

$$[2] \quad Rh^{III} + C_2H_4 \xrightarrow{H_2O} Rh^{I} + CH_3CHO + 2H^+$$

$$[3] \quad 2Rh^{I} \rightleftharpoons Rh^{0} + Rh^{II}$$

In contrast to the system in HCl–LiCl (1), the rhodium(I) is apparently not oxidized rapidly enough to rhodium(III) by iron(III) to prevent the disproportionation reaction. We have not studied the possible reasons for the differences in the two media which could depend on a number of factors. The iron(III) was added as perchlorate in the present work and as trichloride in the other work (1), and the nature of the iron(III) species present could play an important role in the non-equivalent 2 electron transfer process. However, the difference in the acidities used in the two systems is certainly a more critical factor. Pertinent data for the HCl–LiCl systems were obtained at much lower acidities of 0.05–1.0 M; further, reoxidation of Rh^{I} by Fe^{III} was found to be effective in 0.1–0.2 M perchloric acid solutions (see below). Higher acidities could inhibit the Rh^{I}–Fe^{III} reaction by kinetic factors (*e.g.*, if some hydroxy species plays a significant role) or thermodynamic factors (*e.g.*, depending on the reduction potentials of the Fe^{III}/Fe^{II} and Rh^{III} (or Rh^{II})/Rh^{I} couples). There are no quantitative data on the disproportionation reaction (reaction 3). Some recent studies (6) on the oxidation of ethylene by rhodium(III) in acid chloride solutions, in the absence of any reoxidant, have shown that the rhodium is reduced to metal and a pale yellow filtrate, which gives an e.s.r. signal, possibly due to a monomeric paramagnetic rhodium(II) species.

In conclusion, the studies in the 6 M acid medium show that ethylene is unreactive towards the $RhCl_n(H_2O)_{6-n}^{(n-3)-}$ complexes with $n = 1$, 2, 3, and 6. The inactivity of the cationic and neutral species is consistent with their substitution inertness, while that of the hexachloro complex is attributed to lack of a ligand water molecule. The complexes with $n = 4$ and 5 are reactive towards ethylene, some semiquantitative data indicating possibly higher reactivity for the tetrachloro complex.

TABLE 2. Kinetic data at 80° for the reaction of ethylene with $RhCl_4(H_2O)_2^-$; 0.1 M $RhCl_3$, 0.2 M $Fe(ClO_4)_3$, 0.2 M LiCl

$[HClO_4]$ (M)	C_2H_4 (mm)	$[C_2H_4] \times 10^4$ (M)	Linear rate $\times 10^6$ (M s^{-1})
0.1	50	1.0	7.0
0.1	200	4.0	23.0
0.1	400	8.0	43.0*
0.2	53	1.1	4.2
0.2	203	4.1	15.0
0.2	403	8.1	23.0

*For a solution containing 0.1 M Rh as $RhCl_5(H_2O)^{2-}$ under corresponding conditions (but with 2.0 M LiCl), the linear rate was 12.8×10^{-6} M s^{-1}.

Reactivity in 0.1–0.2 M Acid Solutions

Conditions were found for the formation of perchloric acid solutions of lower acidities containing mainly $RhCl_5(H_2O)^{2-}$ or mainly $RhCl_4(H_2O)_2^-$ (see Experimental). These solutions now reacted at 80° with ethylene (up to 1 atm) in the presence of excess iron(III) in a manner quite analogous to that described for the pentachloro species in aqueous hydrochloric acid solutions (1). Catalytic oxidation of the ethylene to acetaldehyde occurs at the rhodium with the consumption of iron(III); the intermediate rhodium(I) is efficiently reoxidized by iron(III) and no metal production is apparent until the ferric concentration approaches zero. Spectrophotometric studies show that there is essentially no change in the equilibrium composition of the chlororhodate(III) complexes during the reaction; the $RhCl_5(H_2O)^{2-}$ solutions gave absorption maxima at 397 nm ($\varepsilon \sim 85$) and 500 nm ($\varepsilon \sim 85$), while the $RhCl_4(H_2O)_2^-$ solutions gave maxima at 375 nm ($\varepsilon \sim 70$) and 475 nm ($\varepsilon \sim 75$).

The initially linear rates of the uptake plots were readily measured; the rates were first order in rhodium to 0.1 M and were independent of the ferric concentration. Table 2 summarizes some kinetic data at 80° for the $RhCl_4(H_2O)_2^-$ system and shows the dependences on ethylene and proton concentrations.

Figure 1 demonstrates a reasonable first-order dependence on ethylene at 0.1 and 0.2 M $HClO_4$ for the reaction involving $RhCl_4(H_2O)_2^-$. In contrast to the previous studies (1) involving $RhCl_5(H_2O)^{2-}$, there is no *significant* contribution from an ethylene-independent path which

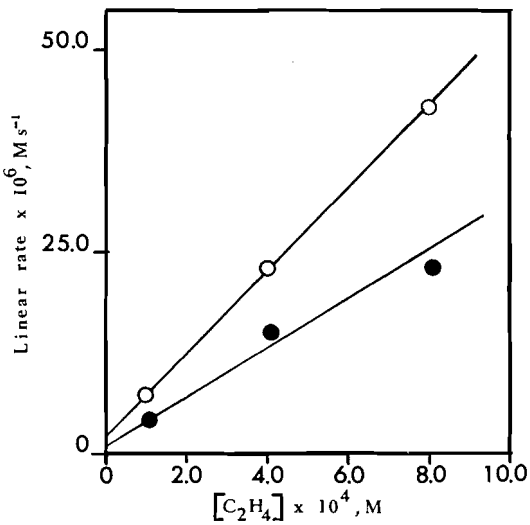

FIG. 1. Rate of ethylene absorption as a function of ethylene concentration with 0.1 *M* $RhCl_3$, 0.2 *M* $Fe(ClO_4)_3$, 0.2 *M* LiCl at 80°; ○ at 0.1 *M* $HClO_4$; ● at 0.2 *M* $HClO_4$.

would be evident as an intercept on the ordinate axis at zero ethylene concentration. However, there may be quite small such intercepts, and they could result from a contribution to the rate by some pentachloro species in the equilibrated and so-called $RhCl_4(H_2O)_2^-$ solutions. Some estimation of the probable magnitude of such intercepts can be made. The rate given in footnote * of Table 2 for the $RhCl_5(H_2O)^{2-}$ solution in 0.1 *M* $HClO_4$ (12.8×10^{-6} *M* s^{-1}) is some 50% higher than that observed previously for the analogous system in 0.1 *M* HCl (8.2×10^{-6} *M* s^{-1}, ref. 1), possibly attributable to differences in the solubility of ethylene in the two media; assuming 50% higher rates in the perchloric acid media, the intercepts of a plot such as shown in Fig. 1 for the system containing mainly $RhCl_5(H_2O)^{2-}$ would be about 6×10^{-6} *M* s^{-1} at 0.1 *M* acidity and about 2×10^{-6} at 0.2 *M* acidity (*cf.* Fig. 1 in ref. 1). Hence the intercepts in Fig. 1 would be some fraction of this depending on the fraction of the rhodium present as the pentachloro complex.

An important conclusion is that 0.1 and 0.2 *M* acid solutions containing $RhCl_4(H_2O)_2^-$ are about 3 times more reactive than corresponding solutions containing $RhCl_5(H_2O)^{2-}$.

The kinetic data in Fig. 1 will be analyzed neglecting possible intercepts on the ordinate axis. The data show an inverse acid dependence and thus, as previously (1), the ethylene reactions must involve both aquo and hydroxy species (see also Scheme 1):

$$[4]\quad RhCl_4(OH)(H_2O)^{2-} + C_2H_4 \xrightarrow{k_5} RhCl_4(C_2H_4)(OH)^{2-}$$

$$[5]\quad RhCl_4(H_2O)_2^- + C_2H_4 \xrightarrow{k_6} RhCl_4(C_2H_4)(OH)^{2-}$$

The rate-law can be written as

$$[6]\quad \frac{-d[C_2H_4]}{dt} = \left\{\frac{k_5K_4}{[H^+]} + k_6\right\}[RhCl_4(H_2O)_2^-][C_2H_4]$$

where K_4 is the acid dissociation constant of $RhCl_4(H_2O)_2^-$. Using eq. 6 the slopes of Fig. 1 (5.2×10^{-2} s^{-1} and 3.1×10^{-2} s^{-1}) may be used to calculate the value of k_5K_4 as 4.2×10^{-2} s^{-1}, and the value of k_6 as 0.1 M^{-1} s^{-1} at 80°. A value of *ca.* 10^{-8} *M* was assumed for the acid dissociation constant (K_5) for the $RhCl_5(H_2O)^{2-}$ complex (1). $RhCl_4(H_2O)_2^-$ will be a somewhat stronger acid, and K_4 is likely to be *ca.* 10^{-6}–10^{-7}. Thus, although present in very small concentrations, the hydroxy complex is kinetically very significant, *e.g.*, at 0.1 *M* acidity it contributes some 80% of the total reactivity and is some 10^5 times more reactive towards ethylene than the aquo complex. A similar conclusion was reached for the pentachlororhodate(III) complexes (1).

The rate constant data determined previously at 80° in HCl–LiCl solutions for the various reaction paths shown in Scheme 1 in the introduction are: $k_1K_5 = 2.2 \times 10^{-6}$ *M* s^{-1}, $k_2 = 6.0 \times 10^{-6}$ s^{-1}, $k_3 = 5.6 \times 10^{-2}$ M^{-1} s^{-1}, and $k_4K_5 = 1.1 \times 10^{-3}$ s^{-1} (1). There will be small differences in ethylene solubility in the somewhat different media, although the rate constants were estimated assuming the same solubility in each (8.0×10^{-4} *M* at 400 mm pressure). However, it seems clear from the rate constant data that rate paths showing no dependence on the ethylene concentration are indeed possible for the pentachloro complex. This requires that the aquation of $RhCl_5(H_2O)^{2-}$ to $RhCl_4(H_2O)_2^-$ is slower than the subsequent reaction of the latter with ethylene, and that aquation of $RhCl_5(OH)^{3-}$ to $RhCl_4(OH)(H_2O)^{2-}$ is slower

Can. J. Chem. Downloaded from www.nrcresearchpress.com by 210.87.254.42 on 09/05/12
For personal use only.

Can. J. Chem. Downloaded from www.nrcresearchpress.com by 210.87.254.42 on 09/05/12
For personal use only.

than subsequent reaction of the latter with ethylene. These two requirements are met if $k_2 < k_6[C_2H_4]$ and $k_1K_5 < k_5K_4[C_2H_4]$, respectively, and the above data satisfy these conditions.

The finding of higher activity for acid solutions of $RhCl_4(H_2O)_2^-$ compared with corresponding solutions of $RhCl_5(H_2O)^{2-}$, which is initially surprising considering that lability increases with increasing number of coordinated chlorides, is readily rationalized on consideration of the various reaction paths involved. For example, at 0.1 *M* acidity and 1 atm pressure, the major contribution to the rate for the tetrachloro system is reaction 4 involving $RhCl_4(OH)(H_2O)^{2-}$ and C_2H_4 for which $k_5K_4 = 4.2 \times 10^{-2}\ s^{-1}$; the major contribution to the rate for the pentachloro system is the reaction involving $RhCl_5(H_2O)^{2-}$ and C_2H_4 for which $k_3 = 5.6 \times 10^{-2}\ M^{-1}\ s^{-1}$ (1). Thus, although hydroxy species are present in very small amounts in both systems, more kinetically significant amounts are present in the tetrachloro system and this is reasonable since $K_4 > K_5$. The rates of reaction between C_2H_4 and the hydroxy species are governed by k_5K_4 and k_4K_5, and the former is larger by a factor probably of about 25 to 40. The actual rate constants k_5 and k_4 are probably quite similar; on lability grounds, k_4 for $RhCl_5(OH)^{3-}$ is expected to be somewhat greater than k_5 for $RhCl_4(OH)(H_2O)^{2-}$ which requires that $K_4/K_5 > 25$–40, and this is quite reasonable.

At very high acidities, the ethylene-independent step for the pentachloro system becomes negligible (1), and the reaction rate will be governed purely by the rate constant k_3 for the reaction between $RhCl_5(H_2O)^{2-}$ and C_2H_4. Similarly, the rate for the tetrachloro system would be governed purely by the rate constant k_6 for the reaction between $RhCl_4(H_2O)_2^-$ and C_2H_4. As above, a somewhat greater value would be anticipated for k_3 and solutions of the pentachloro complex would be expected to have higher reactivity (k_3/k_6 for reactivity towards H_2 is reported elsewhere (2) as 1.5). The present data give k_3/k_6 *ca.* 0.6, and this will be somewhat higher if allowance is made for the higher rates measured in perchloric acid media (see above); within the errors of experiment and kinetic analysis, our data suggest very similar reactivity of the two aquo complexes towards ethylene.

The possible path for acetaldehyde production via faster steps following the rate determining formation of the rhodium(III)–ethylene intermediates (reactions 4, 5) was considered in the previous paper (1). The present work confirms the previous findings that the process is more efficient in less acid solutions where higher concentrations of the kinetically important hydroxy species are present, and shows that such solutions of the tetrachloro complex are more reactive than solutions of the pentachloro complex due to the higher acid dissociation constant of the tetrachlorobisaquorhodate(III) complex compared to that of the pentachloroaquorhodate(III) complex. These studies are being extended to other Group VIII metal systems.

Grateful acknowledgment is made to the National Research Council of Canada for financial support, and to Johnson Matthey Limited for loan of the rhodium.

1. B. R. JAMES and M. KASTNER. Can. J. Chem. This issue.
2. B. R. JAMES and G. L. REMPEL. Can. J. Chem. **44**, 233 (1966).
3. W. C. WOLSEY, C. A. REYNOLDS, and J. KLEINBERG. Inorg. Chem. **2**, 463 (1963).
4. W. ROBB and M. M. DE V. STEYN. Inorg. Chem. **6**, 616 (1967).
5. B. R. JAMES and G. L. REMPEL. J. Am. Chem. Soc. **91**, 863 (1969).
6. B. R. JAMES and M. KASTNER. Unpublished results.

High Resolution Nuclear Magnetic Resonance Investigation of the Structure of the Adducts Formed by the Interaction of Benzylidenemalononitriles with Trialkylphosphines[1]

C. A. FYFE AND M. ZBOZNY
Chemistry Department, University of Guelph, Guelph, Ontario

Received December 2, 1971

High resolution n.m.r. has been used to determine unambiguously the structure of the adducts formed by the action of trialkylphosphines on para-substituted benzylidenemalononitriles[2] as a zwitterionic species formed by attack of the phosphine on the α-carbon atom of the alkene. The relation of this result to possible mechanisms of nucleophilic alkene substitution reactions is discussed.

La r.m.n. à haute résolution a été utilisée pour déterminer sans ambiguité possible la structure des produits d'addition formés lors de l'action des trialkylphosphines sur les benzylidènemalononitriles substitués en para; il s'agit de zwitterions formés par l'attaque de la phosphine sur le carbone-α de l'alcène. Les résultats sont discutés en termes de mécanismes de réactions de substitution nucléophile sur l'alcène.

Canadian Journal of Chemistry, **50**, 1713 (1972)

Introduction

The initial product formed in nucleophilic attack on alkenes is postulated as an ionic intermediate of general formula **1**, eq. [1], (1).

[1] 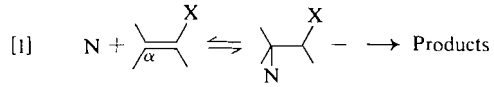

1

(X = electron withdrawing group)

Few attempts have been made to characterize intermediates of this general type formed by nucleophilic attack on alkenes until very recently (2–4). Stewart and Kroeger using u.v. spectroscopy and Fyfe, using high resolution n.m.r. have characterized the intermediates formed by the attack of methoxide ion (2–4) and other nucleophiles (2) on activated stilbene systems where further reaction was prevented by the use of aprotic solvents.

A special case occurs if the nucleophile is neutral, where a zwitterionic species will be formed. One case where 1:1 adducts of neutral nucleophiles with alkenes are known to be formed is the reaction of benzylidenemalononitriles with trialkylphosphines (11).

These adducts were originally described as zwitterions with structure **2**, but, as pointed out by Rappoport (5), since they dissociate in solution, 'chemical' tests of their structures are quite invalid. A variety of other structures have been considered, **3**–**5** (5). In addition, one should also consider structure **6**, produced by attack of the phosphine on the β-carbon atom and **7**, a phosphorane structure, analogous to the ylides proposed formed by the attack of triphenyl phosphine on maleic anhydride (6, 7), since

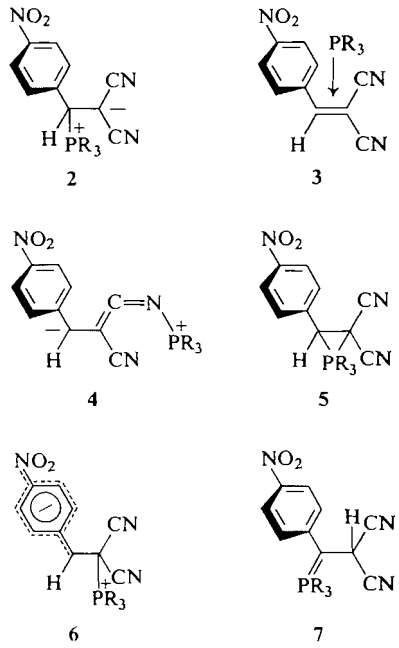

2 **3** **4** **5** **6** **7**

R = Et; *n*-Bu

[1]Presented at the 54th Chemical Institute of Canada Conference, Halifax, Nova Scotia, June, 1971.

[2]Hereafter referred to as X-BMN.

Can. J. Chem. Downloaded from www.nrcresearchpress.com by 210.87.254.42 on 09/05/12
For personal use only.

Can. J. Chem. Downloaded from www.nrcresearchpress.com by 210.87.254.42 on 09/05/12
For personal use only.

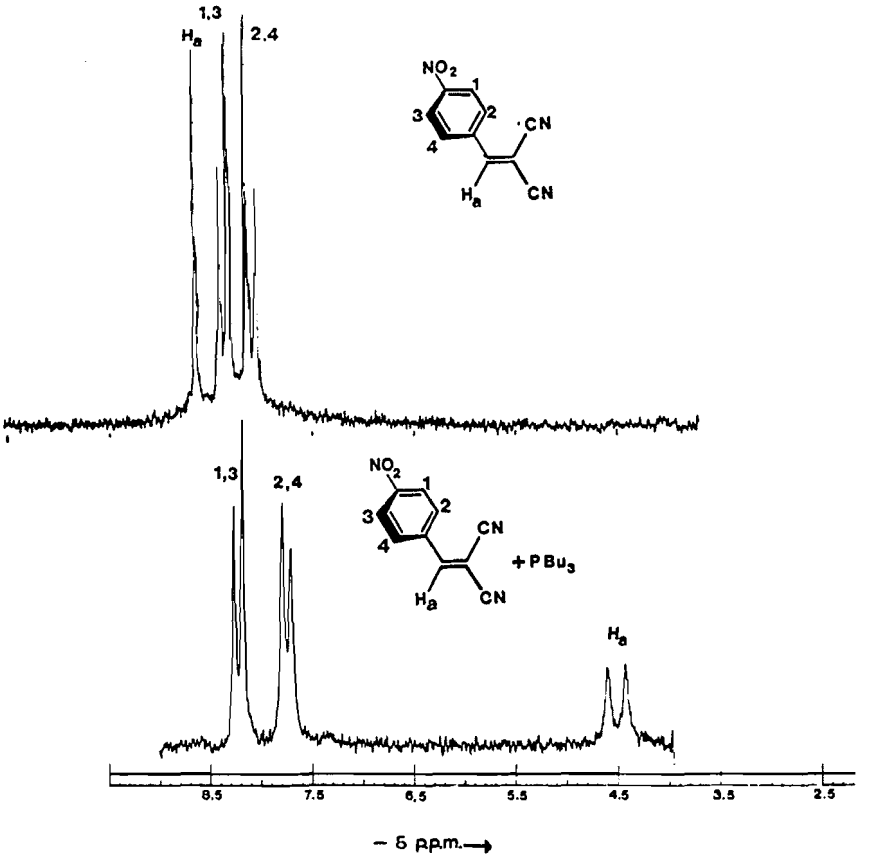

FIG. 1. The 100 MHz n.m.r. spectra in DMSO solution *p*-NO_2-BMN at probe temperature (31°) and the adduct formed from the attack of tri-*n*-butyl phosphine on *p*-NO_2-BMN (31°).

they too analyze as 1:1 adducts. There is indirect evidence in support of structure **2** in that the structures of closely related species formed by the action of trivalent phosphorous compounds on α,β unsaturated ketones (8, 9) have been recently established as being zwitterions.[3]

Because of their direct relevance to the postulated mechanism of nucleophilic substitution reactions of alkenes, an attempt has been made in the present work to define absolutely the structure of these adducts, with a view to ultimately determining the kinetic parameters for their formation and decomposition and the dependence of both these parameters on substituents and on solvents.

[3]The authors would like to acknowledge the help of a referee in bringing this work to their attention and pointing out its relevance to the present study.

Experimental

The ^{1}H n.m.r. spectra were recorded at 100 MHz on a Varian H.A. 100 spectrometer. Chemical shifts are reported in p.p.m. from an internal TMS reference. The ^{31}P n.m.r. spectra were recorded at 23.5 MHz and chemical shifts are quoted w.r.t. an external H_3PO_4 reference (see acknowledgments). The u.v. spectra were recorded on a Unicam S.P. 800 spectrophotometer using 1 cm matched cells.

All chemicals used were prepared by literature methods and were purified until their m.p.'s were in agreement with published values. The BMN's were prepared by the general method of Corson and Stoughton (10) and the tri-alkyl phosphine adducts as described by Horner and Klupfel (11).

Results and Discussion

The low field portion of the proton n.m.r. spectrum of *p*-NO_2-BMN in DMSO solution and that of the adduct formed from it by the addition of tri-*n*-butylphosphine are shown in Fig. 1. The spectrum of the alkene, (Fig. 1

TABLE 1. Chemical shift data ($-\delta$ p.p.m.) and coupling constants (Hz) from the low field region* of the proton n.m.r. spectra of adducts formed by the action of PBu_3 on BMN's of general structure **8** in DMSO-d_6 solution at probe temperature and CD_3CN solution at -20 °C

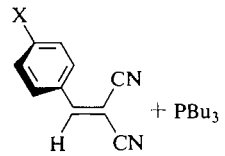

8

X	Aromatic†	H_a (product)	J_{P-H_a}	Solvent
H	multiplet at 7.50 ± .02	4.32 ±0.02	—	DMSO-d_6
NO_2	A_2X_2 at 8.01 ± .01	4.52 ±0.01	18.2±0.1	DMSO-d_6
Cl	A_2X_2 at 7.45 ± .01	4.30 ±0.01	16.6±0.1	DMSO-d_6
H	multiplet at 7.43 ± .02	4.019±0.01	16.2±0.1	CD_3CN
NO_2	A_2X_2 at 7.99 ± .01	4.289±0.01	16.9±0.1	CD_3CN
Cl	A_2X_2 at 7.48 ± .01	4.063±0.01	16.7±0.1	CD_3CN

*In addition, all show large resonances at $\delta = -2.2$, -1.4, and -0.9 due to the butyl groups.
†Denotes multiplet center.

upper), consists of a sharp resonance at $\delta = -8.69$ (relative intensity 1) due to the alkene hydrogen H_a, and an A_2X_2 pattern (relative intensity 4) centered at $\delta = -8.26$ assigned to the phenyl ring hydrogens. With the addition of tri-*n*-butylphosphine to form the adduct, we see a change in the spectrum: the singlet absorption due to H_a is no longer present at low field and the A_2X_2 pattern of the phenyl ring has shifted slightly upfield to $\delta = -8.0$ ($J_{1,2} = J_{3,4} \simeq 8.4$ Hz, $V_0\delta \simeq 45.1$ Hz). The spectrum of the adduct has a doublet absorption, ($J_{H-P} = 18.2$ Hz) (relative intensity 1), at higher field. (Although the room temperature spectra of several of the adducts show evidence of an exchange process (see below) this is not important in the present instance.)

From this spectrum one can eliminate possibilities **3**, **4**, and **6**. The charge-transfer structure can be eliminated since one would expect a singlet absorption due to the alkene hydrogen H_a; but such a low field singlet is absent. One would also expect a shift in the absorption due to changes in concentration but no concentration dependence is observed. Nor should a phosphorous–hydrogen coupling be observed, as such equilibria are usually fast (12). (The extreme case where a strong localized charge-transfer complex between phosphorous and carbon is formed, might show a slower exchange, but would in fact be the zwitterion **2**.)

Structure **4** can be eliminated since its spectrum should also show a singlet absorption for H_a. Structure **6** may be eliminated since one would expect a larger upfield shift for the phenyl ring protons because of the delocalization of the negative charge into the ring and onto the NO_2 group as is observed for the intermediates formed by nucleophilic attack on activated stilbenes (2). Further, compounds known to have similar electronic structures to structure **6** give rise to intense purple colors ($\lambda_{max} \sim 580$ mμ) on formation. Instead, the 1:1 adducts show absorptions <400 mμ and are orange–colorless. This eliminates all but possibilities **2**, **5**, and **7**.

A tabulation of chemical shifts and coupling constant data at room temperature in DMSO solution as well as in deuteroacetonitrile solution at -20 °C, for a series of BMN's and their PBu_3 adducts is given in Table 1. There is little variation in the chemical shift values of H_a in either solution, as would be expected if the structure is a zwitterion. Differences in P–H couplings and the non-observation of a P–H coupling for the unsubstituted BMN in DMSO-d_6 solution at room temperature and the presence of a P–H coupling in CD_3CN solution at -20 °C is attributed to an exchange process (see on). The data in Table 1 are in good agreement with the zwitterion structure, but, since information about compounds which are struc-

Can. J. Chem. Downloaded from www.nrcresearchpress.com by 210.87.254.42 on 09/05/12
For personal use only.

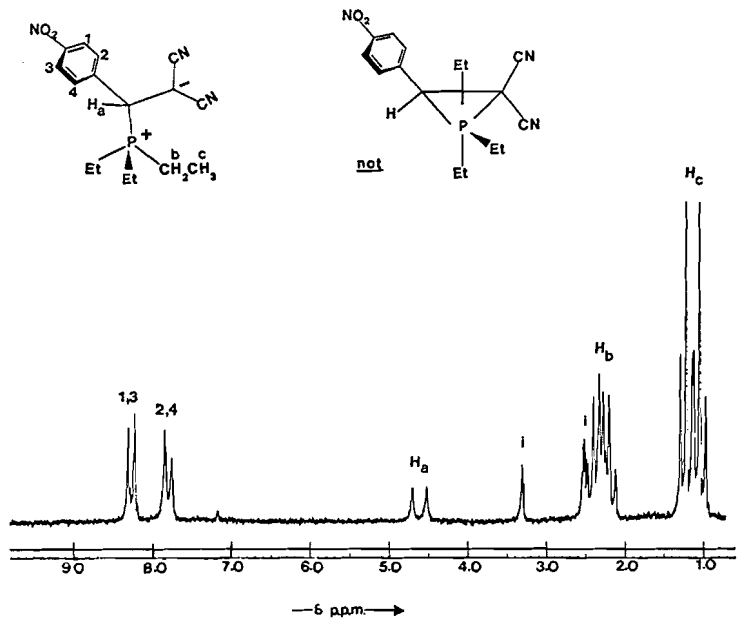

FIG. 2. The 100 MHz n.m.r. spectrum of the triethyl adduct of p-NO_2 at 34 °C in DMSO-d_6 solution.

turally related to **5** and **7** is lacking, they can not be dismissed on this basis.

However, when tri-ethylphosphine is used as the nucleophile, complete interpretation of the n.m.r. spectrum of the adduct formed is possible, resulting in the elimination of structure **5**. The spectrum in DMSO-d_6 of the adduct thus formed from p-NO_2-BMN is shown in Fig. 2. The A_2X_2 pattern centered at $\delta = -9.00$ p.p.m. ($J_{3,4} \simeq 8.8$ Hz, $V_0\delta \simeq 47$ Hz), can be assigned to the phenyl ring protons. H_a is a doublet centered at $\delta = -4.63$, $J_{P-H} = 18.3$ Hz (relative intensity 1) due to coupling with phosphorous and, as noted above, occurs at a field strength characteristic of protons attached to sp^3 hybridized carbons. Peaks marked i are impurities due to traces of H_2O ($\delta = -3.3$) and DMSO-d_5 impurity ($\delta = -2.54$ p.p.m.). The absorption of the methylene hydrogens of the ethyl groups, which are coupled both to the phosphorous and the methyl protons, appears as a multiplet; centered at $\delta = -2.3$ p.p.m. The absorption due to the methyl hydrogens is centered at $\delta = -1.1$ and appears as a multiplet due to coupling with the methylene hydrogens and the phosphorous. The coupling constants are ($J_{P-H_a} = 18.3$, $J_{P-CH_2} = 17.3$, $J_{CH_2-CH_3} = 8.0$ Hz). If structure **5** were correct, the proton n.m.r. spectrum should show an absorption due to the two types of ethyl groups as indicated in the stereo drawing, Fig. 2, which shows two "axial" ethyl groups and one "equatorial" ethyl group. As indicated above, the spectrum can be interpreted fully in terms of a single type of ethyl group, eliminating structure **5**, leaving only possibilities **2** and **7** to be considered. The spectrum is unchanged at $-30°$ in CD_3CN solution, ruling out the possibility that the equivalence of the ethyl groups is due to an exchange process.

The proton n.m.r. spectrum is thus compatible with either of structures **2** or **7**. However, ^{31}P n.m.r. should indicate which 1:1 adduct is actually formed, since ylides involving tri-phenylphosphine groups, analogous to structure **7**, have a phosphorous absorption at different field strengths from (approximately 15–20 p.p.m. upfield) the corresponding quadruply connected phosphorous compounds (13–15). One would expect a similar behavior pattern with tri-n-butylphosphine adducts.

The adducts show ^{31}P absorptions at -36.8 p.p.m. (p-Cl) and -37.2 p.p.m. (p-NO_2) from external phosphoric acid when the spectra are measured in DMSO solution. The proton spectra under these conditions indicate that there is no detectable exchange, and these shifts

Can. J. Chem. Downloaded from www.nrcresearchpress.com by 210.87.254.42 on 09/05/12
For personal use only.

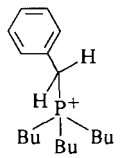

9

$Bu_3P{=}CH_2$

10

are thought to be close to the true values for the complexes. The shifts are close to the value found for the closely related compound **9**, *known* to contain positively charged phosphorous, namely −31 p.p.m. (8).

Ylides, of similar structure, have a correspondingly higher chemical shift; in particular compound **10** absorbs at −16 p.p.m. (16). The general agreement between the ^{31}P chemical shifts of the adducts with that of the ion **9**, is taken as strong evidence for the zwitterionic structure **2** and against the proposed ylide structure **7**.

Thus it is thought that n.m.r. has allowed us to determine the structure of this adduct unambiguously as being the zwitterion in the solvents used, independent of any equilibrium processes in solution.

The u.v. spectra do not change appreciably when the solvent is varied, having λ_{max} values of 418, 405, and 428 mμ in acetone, acetonitrile, and DMSO respectively, indicating that the species is the same in *all* solvents studied, although substantial changes in the n.m.r. spectra may be observed.

The relatively sharp doublet obtained for the phosphorous—hydrogen coupling of **2** (p-NO_2) in DMSO solution (Figs. 1, 2) compared to the broad doublets in other less basic solvents prompted us to investigate the possibility of an exchange process involving the phosphines. Figure 3 shows the temperature dependence of the H_a resonance of **2** (p-NO_2) in CD_3COCD_3 solution, which at low temperature approximates to a simple two-site exchange process with equal population of the two sites, indicating that the equilibrium is well in favor of the adduct at these temperatures. However the spectra at higher temperatures are unsymmetrical, indicating an appreciable effect from the population of the third site, the parent alkene.

This aspect is currently under investigation, together with stopped flow measurements of the kinetics of the formation of the adducts, and it is hoped that both methods will give values for the activation energies of the forward and reverse steps in the equilibria. It is hoped that the theoretical interpretation of these parameters will eventually yield a model for calculations applicable to nucleophilic alkene substitutions in general.

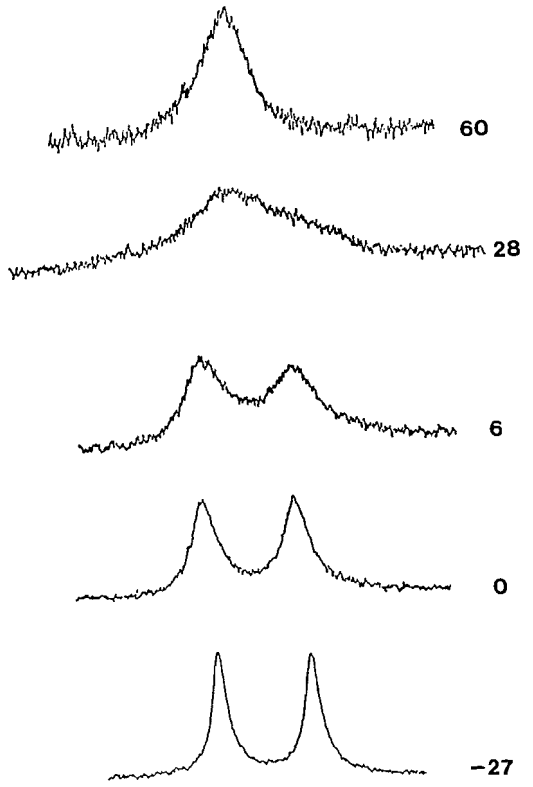

FIG. 3. The temperature dependence of the H_a resonance of the adduct **2**, (p-NO_2) in CD_3COCD_3 solution.

The authors would like to acknowledge the financial support of the National Research Council of Canada for a grant in aid of research (C.A.F.) and for a Major Equipment Grant for the purchase of the spectrometer. They would also like to acknowledge the help of the Department of Chemistry, McMaster University, Hamilton, Ontario, in recording the ^{31}P n.m.r. spectra quoted.

1. S. PATAI and Z. RAPPOPORT. *In* The chemistry of alkenes. *Edited by* S. Patai. Interscience Publishers, Inc., London. 1964.
2. C. A. FYFE. Can. J. Chem. **47**, 2331 (1969).
3. R. STEWART and D. J. KROEGER. Can. J. Chem. **45**, 2172 (1967).
4. D. J. KROEGER and R. STEWART. Can. J. Chem. **45**, 2136 (1967).

Can. J. Chem. Downloaded from www.nrcresearchpress.com by 210.87.254.42 on 09/05/12
For personal use only.

5. Z. RAPPOPORT and S. GERTLER. J. Chem. Soc. 1260 (1964).
6. R. F. HUDSON and P. A. CHOPARD. Helv. Chim. Acta, **46**, 2178 (1963).
7. C. OSUCH, J. E. FRANZ, and F. B. ZIENTY. J. Org. Chem. **29**, 3721 (1964).
8. F. RAMIREZ, O. P. MADAN, and C. P. SMITH. Tetrahedron, **22**, 567 (1966).
9. F. RAMIREZ, J. F. PILOT, and C. P. SMITH. Tetrahedron, **24**, 3735 (1968).
10. B. B. CORSON and R. W. STOUGHTON. J. Am. Chem. Soc. **50**, 2825 (1928).
11. L. HORNER and K. KLUPFEL. Ann. Chem. **591**, 69 (1955).
12. R. FOSTER. Organic charge-transfer-complexes. Academic Press, 1969.
13. V. MARK, C. H. DUNGAN, M. M. CRUTCHFIELD, and J. R. VAN WAZER. Topics in phosphorous chemistry. **5**, 227 (1967).
14. M. J. GALLAGHER. Aust. J. Chem. **21**, 1197 (1969).
15. H. J. BESTMANN and J. P. SNYDER. J. Am. Chem. Soc. **89**, 3936 (1967).
16. R. KÖSTER, D. SIMIÉ, and M. A. GRASSBERGER. Ann. Chem. **739**, 211 (1970).

Can. J. Chem. Downloaded from www.nrcresearchpress.com by 210.87.254.42 on 09/05/12
For personal use only.

Circular Dichroism of Nitrate Esters: A Planar Symmetry Rule for the Nitrato Chromophore[1]

R. E. BARTON AND L. D. HAYWARD

Department of Chemistry, University of British Columbia, Vancouver 8, British Columbia

Received December 9, 1971

Conformational analysis of nitrate esters based on X-ray and spectroscopic data showed the nitrato group to be coplanar with the α carbon atom and, in the preferred rotamer, the nitro moiety to be antiperiplanar to the β carbon atom. Three optically active absorption bands not apparent in the isotropic electronic spectra were resolved in the circular dichroism spectra. Band I (270 nm) reflected nitrato group libration changing sign and magnitude with changes in temperature and solvent polarity. Differences in rotatory strength of band III (210 nm) for *cis*- and *trans*-dinitrates indicated transition moment coupling. A planar symmetry rule for chromophores in the C_s point group correlated the molecular geometry and sign of band II for 42 nitrate esters: when the lowest-energy rotamer of the nitrate ester is viewed down the O—C bond with the nitro group uppermost rotatory contributions to band II (230 nm) are positive for perturbing atoms to the right and negative for those to the left of the nitrato symmetry plane.

L'analyse conformationnelle des esters nitriques, basée sur les données de la spectroscopie et des rayons-X, montre que le groupe nitrate est coplanaire avec l'atome de carbone en α et que, dans le rotamère privilégié, le fragment nitro est antipériplanaire à l'atome de carbone en β. Trois bandes d'absorption optiquement actives, non apparentes sur le spectre électronique isotrope, ont été résolues dans le spectre de dichroisme circulaire. La bande I (270 nm) reflète la vibration du groupe nitro et change de signe et d'amplitude lorsque la température et la polarité du solvant changent. Les différences dans le pouvoir rotatoire de la bande III (210 nm) pour les dinitrates *cis* et *trans* indiquent un couplage du moment de transition. Une règle de symétrie plane pour les chromophores du groupe C_s relie la géométrie moléculaire au signe de la bande II pour 42 esters nitriques: lorsque le rotamère de plus basse énergie de l'ester nitrique est regardé le long de la liaison O—C avec le groupe nitro, les contributions rotatoires décisives pour la bande II (230 nm) sont positives lorsque les atomes sont situés à droite du plan de symétrie du nitrate et négatives lorsqu'ils sont à gauche.

Canadian Journal of Chemistry, **50**, 1719 (1972)

Can. J. Chem. Downloaded from www.nrcresearchpress.com by 210.87.254.40 on 09/05/12
For personal use only.

Introduction

A correlation of the absolute configuration (chirality) of nitrate esters with their accessible c.d. spectra was sought in the present work. Such a symmetry rule (1, 2) would permit assignment of unknown configurations and contribute to understanding of the bonding, electronic spectra, and conformational equilibria of these explosive and physiologically reactive compounds.

Early o.r.d. spectra of hexose nitrates (3–7) included background rotation due to other chromophores and only the transition of the nitrato group at 270 nm (band I) was identified with the aid of c.d. spectra (5, 6). The sign of band I was positive for nitrato groups in α- (or D) configuration and negative for those with β- (or L) configuration in α-glucosides, the signs being reversed for the corresponding β-anomers. Band I was reported to be red-shifted by steric crowding of the chromophore and to decrease in rotatory strength with location on the hexose chain in the order C-2 > C-3 > C-4 > C-5. It was also concluded from o.r.d. data that (*R*)- and (*S*)-α-nitrato-carboxylic acids showed positive and negative Cotton effects, respectively, at *ca.* 265 nm (5).

Our preliminary c.d. studies on a series of 1,4;3,6-dianhydrohexitol nitrates (8) revealed a new transition at 230 nm (band II) which was positive for *endo*-(*R*)- and negative for *exo*-(*S*)-nitrato groups at locations 4 and 8 on the *cis*-2,6-dioxabicyclo[3.3.0]octane skeleton. In this series of nitrates the sign of band I was positive throughout and was insensitive to changes in configuration at the α-carbon atom.

A third dichroitic band at 210 nm (band III) was detected in nitrato steroids (9). Exciton splitting as the source of band III was considered improbable since its rotatory strength varied independently of that of band II. Although the sign patterns of bands I–III were characteristic

[1]Taken in part from the thesis submitted by R. E. Barton in partial fulfilment of the requirements for the Ph.D. degree. This is Part III of a series on stereochemistry of nitrate esters. For part II, see ref. 24.

Can. J. Chem. Downloaded from www.nrcresearchpress.com by 210.87.254.40 on 09/05/12
For personal use only.

of location on the steroid skeleton, rotational mobility of the nitrato group precluded complete configurational analysis (9).

A fourth nitrato absorption band at 200 nm (band IV, ε 5800) was found in the isotropic spectrum of ethyl nitrate (10) but has not so far been reported in c.d. spectra. Band I has been identified with the $n \rightarrow \pi^*$ transition (11), and bands III and IV with the $\pi \rightarrow \pi^*$ transition (10) of the nitrato chromophore whereas the identity of the transition associated with band II is unknown.

The nitrato group, $-ONO_2$, with four coplanar atoms (12–16) belongs to the C_s point group with symmetry elements E and σ. The molecular orbitals of the nitro moiety probably resemble those of the nitroalkanes (17, 18); however, there is uncertainty concerning participation of the alkoxyl oxygen in π bonding (16). The scatter of the available values for the RO—NO_2 bond length (1.36 to 1.53 Å) (13–16) leaves open the question of electron delocalization over the entire $-ONO_2$ group.

From the C_s character table the pseudoscalar part of the $-ONO_2$ potential is the A'' representation and hence, according to Schellman's analysis (2), there should exist a planar symmetry rule for nitrate esters based on the symmetry plane. This approach specifies only the minimum number of spatial regions in which perturbing groups generate rotational strength (19); other nodal surfaces not determined by symmetry may lead to further spatial subdivisions. In view of the uncertainty in the bonding and orbitals in $-ONO_2$, however, only a planar rule was considered as a first approximation. The problem was then to establish the most probable position of σ in the molecular framework; once this was known examination of molecular models would reveal the distribution of polarizable groups with respect to the fiducial plane for comparison with c.d. spectra.

The investigation involved the following steps: (*a*) synthesis of model nitrate esters with known configurations and restricted molecular conformations, (*b*) measurement of isotropic and c.d. spectra to establish the preferred conformations, (*c*) analysis of the c.d. spectra in terms of the molecular geometry in an attempt to assign rotatory contributions from spatial regions of the intramolecular environment, and (*d*) generalization of the pictorial model through tests on nitrate esters with more varied patterns and degrees of substitution and greater degrees of molecular flexibility.

Experimental

Circular dichroism spectra were taken on JASCO J5 and J20 spectrophotometers calibrated for wavelength and dichroic absorption with 5α-cholestan-3-one in 1,4-dioxan ($\Delta\varepsilon + 1.13$ at 295 nm (20)). Low temperature measurements (21) were corrected for volume contraction from published solvent data (22). Ultraviolet spectra were run on a Cary 15 spectrophotometer with slit widths less than 1 mm and absorbance below 1.0. All solvents were of spectral grade or were purified by standard procedures to give satisfactory ultraviolet absorption spectra.

The nitrate esters were synthesized from the corresponding chiral alcohols (Table 3) (7, 24, 28–32) either with anhydrous nitric acid in acetic acid – acetic anhydride at 0° (23, 24) or via the corresponding chloroformate and silver nitrate (25) and were purified by distillation (*ca.* 0.5 Torr) or chromatography on columns of silica gel developed with chloroform (26). Purification was monitored by t.l.c. (26) and by the u.v., c.d., n.m.r., (27) and i.r. (24) spectra which agreed with the constitutional assignments. Elemental analyses of new nitrate esters are shown in Table 1.

Results and Discussion

The isotropic electronic absorption spectra of the nitrate esters in solvents of different polarity showed no maxima; however, the molar extinction coefficients of the band envelope were measured at wavelengths corresponding to bands I–IV (Table 2). These were generally larger in acetonitrile than in cyclohexane at 270 and 230 nm and the reverse was true at 210 and 200 nm. This trend of ε with solvent polarity was confirmed in the u.v. spectra of (−)-menthyl nitrate (**19**) in four additional solvents and suggested the presence of different unresolved transitions.

*Oxolanyl Nitrates (**1–11**)*

The restricted, approximately V-shaped conformation of the fused oxolane rings in the parent 4,8-dihydroxy-*cis*-2,6-dioxabicyclo-[3.3.0]octanes (**1–4, 8–10**) is known from X-ray data (14) and has been shown by n.m.r. measurements not to be significantly altered by intramolecular hydrogen bonding or esterification (28). The restricted nonplanar conformation of oxolan-2-one (**6, 7**) was established by microwave spectroscopy (29).

The barrier to rotation on the O—C bond in methyl nitrate is 2.3 kcal mol^{-1} and to rotation on the O—N bond, 9.1 kcal mol^{-1} (16), the

TABLE 1. Analyses of nitrate esters

Nitrate ester	Melting point/boiling point	Analysis (%) Calculated C	H	N	Found C	H	N
3-Nitrato-4,4-dimethyl-oxolan-2-one (**7**)	90°/0.5 mm	41.14	5.18	8.00	41.28	5.16	8.07
3,4-Dinitratooxolane (**11**)	43.7°	24.75	3.12	14.43	24.78	3.01	14.58
2-*exo*,3-*exo*-Dinitrato-bornane (**15**)	73.8–75.0°	46.15	6.20	10.77	46.31	6.25	10.65
1-Nitrato-2-isopropyl-5-methylcyclohexane (**19**)	62.5–63.0°/0.5 mm	59.67	9.52	6.96	59.39	9.72	6.92
1-Nitrato-2-methyl-5-isopropylcyclohexane (**21**)	82–90°/1 mm	59.67	9.52	6.96	59.99	9.70	6.91
1-Nitrato-2-methylene-5-isopropylcyclohexane (**23**)	60–74°/1 mm	60.28	8.60	7.03	60.15	8.51	7.10
1-Nitrato-3-methylcyclo-hexane (**24**)	48–53°/1 mm	52.81	8.23	8.80	52.92	8.20	8.85

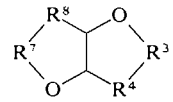

	R^3	R^4	R^7	R^8
1	CH_2	$CHONO_2$(*endo*)	CH_2	CHOH(*exo*)
2	CH_2	$CHONO_2$(*exo*)	CH_2	CHOH(*endo*)
3	CH_2	$CHONO_2$(*endo*)	CH_2	CHOH(*endo*)
4	CH_2	$CHONO_2$(*exo*)	CH_2	CHOH(*exo*)
5	CHR*	$CHONO_2$(*exo*)	$C(CH_3)_2$	O
8	CH_2	$CHONO_2$(*exo*)	CH_2	$CHONO_2$(*exo*)
9	CH_2	$CHONO_2$(*endo*)	CH_2	$CHONO_2$(*endo*)
10	CH_2	$CHONO_2$(*endo*)	CH_2	$CHONO_2$(*exo*)

R* = 1,3-dioxa-2,2-dimethyl-4-cyclopentyl

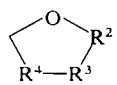

	R^2	R^3	R^4
6	C=O	$CHONO_2(\beta)$	$C(CH_3)_2$
7	C=O	$CHONO_2(\alpha)$	$C(CH_3)_2$
11	CH_2	$CHONO_2(\alpha)$	$CHONO_2(\beta)$

former value being comparable to the barriers restricting overall molecular rotation in various solvents (30). Our calculations from the atom coordinates of six nitrate ester groups in different chemical and crystal environments (12–15) showed that the carbon atom α to the nitrato group lies in or close to the symmetry plane of the group in every case as was also found for methyl nitrate by microwave spectroscopy (16).

The *endo*-nitrato groups at C-4 of the 2,6-dioxabicyclo[3.3.0]octane skeleton (14) was found to be also coplanar with the methylene β carbon atom, C-3, and to be antiperiplanar to it on the O—C bond (rotamer *anti*-C_β). This conformation brings the *endo*-nitrato group into proximity with the oxygen atom in the ad-

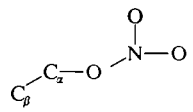

anti-C_β

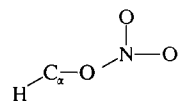

anti-H

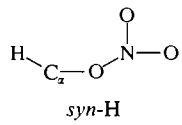

syn-H

Can. J. Chem. Downloaded from www.nrcresearchpress.com by 210.87.254.40 on 09/05/12
For personal use only.

Can. J. Chem. Downloaded from www.nrcresearchpress.com by 210.87.254.40 on 09/05/12
For personal use only.

TABLE 2. Ultraviolet absorption of nitrate esters at 25°

Nitrate ester	Solvent	ε(mol l^{-1} cm^{-1})* 270 nm	230 nm	210 nm	200 nm
7	CH_3CN	25	670	2100	3400
	C_6H_{12}	25	642	2200	3600
11†	CH_3CN	28	700	4700	7700
	C_6H_{12}	28	550	5200	8900
12	CH_3CN	37	1100	3800	4500
	C_6H_{12}	30	830	3900	5100
13	CH_3CN	34	1140	3800	4400
	C_6H_{12}	26	800	3900	4100
14	CH_3CN	60	1600	3200	4100
	C_6H_{12}	37	1200	3200	4400
15†	CH_3CN	65	1700	5900	7600
	C_6H_{12}	58	1300	6700	9700
17†	CH_3CN	52	1400	5100	6700
	C_6H_{12}	47	1200	6000	8700
18†	CH_3CN	59	1860	7200	9500
	C_6H_{12}	50	1260	7400	9900
19	CH_3CN	30	940	3900	4900
	C_6H_{12}	25	650	3800	5300
23	CH_3CN	38	860	3900	7700
24	CH_3CN	28	336		
25	CH_3CN	35			

*At four selected points on the smoothly rising absorption envelope.
†Dinitrate esters.

jacent ring (O....N 2.85 Å (14)) in compounds **1**, **3**, **9**, and **10** and causes an increase in the symmetric stretching frequency of the NO_2 group in acetonitrile solutions (24). The *exo*-nitrato group in compounds **2**, **4**, **8**, and **10**, on the other hand, does not show this frequency shift and cannot interact with the oxygen atom of the adjacent ring. Models show that rotamer *anti*-C_β, C_β=CH_2 is probably also preferred for the *exo*-nitrato group but with a somewhat greater degree of librational freedom. Rotamer *anti*-H is precluded by steric hindrance from the oxolane ring and rotamer *syn*-H may be ruled out on the basis of the microwave spectrum of methyl nitrate which showed the methyl hydrogens to be staggered with respect to the nearest oxygen of the NO_2 group (16). Models permitted selection of *anti*-C_β as the preferred rotamer in compounds **5**, **6**, **7**, and **11** (Table 4) with the choice of C_β being governed by steric crowding.

The sign of c.d. band I was found to be dependent on nitrato rotamer populations for other nitrate esters (*vide infra*) but did not change for compounds **6**–**11** on going from acetonitrile to cyclohexane as solvent (Table 3) thus confirming that rotamer *anti*-C_β persists in these solutions. The positive sign of band II for **7** distinguished it from the negative lactone band observed for the parent hydroxylactone (31). The rotatory strength of band II increased moderately ($I^{+5}_{-90} = -47\%$ (32)) and that of band I was drastically decreased ($I^{+5}_{-90} = +150\%$) on cooling a methanol solution of **7**. This result suggested that partial rotation (libration) of the nitrato group on the O—C bond alters an interaction of the lactone and nitrato chromophores.

Resolution of band II for the oxolanyl dinitrate, **11**, was achieved through variation of solvent and temperature. In nonpolar solvents it apparently was hidden under bands I and III but in polar solvents a negative peak appeared near 238 nm (Fig. 1). In methanol solution the intensity of both bands I and II decreased with temperature and in EPA solution band I passed through a minimum negative value between $-115°$ and $-145°$. These results are most readily understood as due to libration of nitrato rotamers leading to interaction of contiguous nitrato groups (13, 27) in the less polar solvents (24) and at the lower temperatures. In the absence of this attractive interaction in polar solvents the dihedral angle between the planes of the nitrato groups in **11** would increase to approximately 180° to give the rotamer conformation shown in Table 4.

The sign of band II was characteristic of the configuration of the nitrate esters **1**–**11** and was found to depend on the distribution of perturbing atoms with respect to the plane of the nitrato group according to the following rule

When the nitrate ester in the anti-C_β conformation is viewed down the O—C bond with the NO_2 group uppermost the rotatory contribution to band II is positive for atoms lying to the right of the plane of the nitrato group and is negative for atoms to the left of that plane.

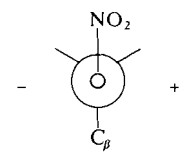

In applying the rule only atoms other than hydrogen were counted and atoms lying in the

TABLE 3. Circular dichroism spectra of nitrate esters*

Nitrate Ester			$[\theta]_{max} \times 10^{-3}$		
Formula	Configuration	Parent alcohol	Band I (270 nm)	Band II (230 nm)	Band III (200–210 nm)
1	1*R*4*R*5*R*8*S*	D-Isosorbide(24)	+2.41	+11.0	
2	1*R*4*S*5*R*8*R*	D-Isosorbide(24)	+0.10	−1.91	
3	1*R*4*R*5*R*8*R*	D-Isommanide(24)	+1.82	+10.3	
4	1*R*4*S*5*R*8*S*	L-Isoidide(24)	+0.40	−2.08	
5	1*R*3*R*4*S*5*R*(4*R*)	1,2;5,6-di-*O*-Isopropylidene-α-D-glucose (6, 8)	+0.59	−4.13	+1.66
6	3*S*	L-Pantolactone	−0.60(−0.50)	−6.50(−3.50)	+17.0(+7.0)
7	3*R*	D-Pantolactone	+0.60(−0.48)	+6.50(+3.50)	−17.0(−6.2)
8†	1*R*4*S*5*R*8*S*	L-Isoidide(23)	+0.43(+0.15)	−4.46(−1.35)	+19.8
9†	1*R*4*R*5*R*8*R*	D-Isommanide(23)	+2.48(+2.97)	+18.4(+16.2)	−1.18
10†	1*R*4*S*5*R*8*R*	D-Isosorbide(23)	+1.58(+1.75)	+7.26(+8.42)	−6.84
11†	3*S*4*S*	L-Threitan	−0.52(−0.69)	−0.57§	+16.0(+16.0)
12	1*R*2*R*4*R*	Isoborneol(28)	+0.13(−0.09)	−1.65‖	−2.20(−1.80)
13	1*S*2*R*4*S*	Borneol(28)	−0.26(−0.25)	−3.30(−3.40)	+2.90
14	1*R*2*R*4*S*	D-α-Fenchol(28)	−0.74(−0.48)	+11.2(+10.5)	−12.7(−9.8)
15†	1*R*2*S*3*R*4*S*	Camphane-2,3-diol	−0.59(−0.43)	−0.30‖	+0.92
16†	1*R*2*S*3*S*4*S*	Camphane-2,3-diol	+0.10	−5.10	+7.20
17†	1*R*2*R*3*S*4*S*	Camphane-2,3-diol	+0.40(+0.30)	+4.10(+3.60)	−2.00
18†	1*R*2*R*3*R*4*S*	Camphane-2,3-diol	+0.20(−0.15)	+9.00(+7.10)	−9.00
19‡	1*R*2*S*5*R*	Menthol	+1.23(+0.91)	−3.26(−3.23)	+7.30(+5.80)
20‡	1*R*2*R*5*R*	Carvomenthol	+0.63	−0.87	+5.00
21	1*S*2*S*5*R*	Isocarvomenthol	+0.06(−0.03)	+0.87(+1.10)	
22	1*R*5*R*	*p*-Menth-1(7)-ene-2-ol	+0.92	+0.25‖	+9.20
23	1*S*5*R*	*p*-Menth-1(7)-ene-2-ol	−0.61(−1.09)	+6.40(+6.34)	−12.0(−9.30)
24‡	1*R*3*S*	3-Methylcyclohexanol	+0.07(+0.01)	+0.06(+0.20)	
25‡	1*S*3*S*	3-Methylcyclohexanol	+0.03(−0.01)	−0.07(−0.04)	
26‡	2*R*	Lactic acid	−0.22	+0.36	−2.30
27‡	2*S*	Diethyl malate(7)	+0.17	−2.10	+4.00
28†	2*R*3*R*	Diethyl tartrate(7)	+0.44	+0.66	−11.00

*At 30° in acetonitrile solution. Numbers in parentheses refer to solution in cyclohexane.
†Dinitrate esters.
‡Additional bands for **19**: 320 nm, −0.010(−0.018); **20**: 318 nm, −0.009; **24**: 298 nm, −0.004; **25**: 292 nm, (−0.004); **26**: 292 nm, +0.022; **27**: 310 nm, −0.010.
§At 238 nm in polar solvents.
‖Estimated from unresolved bands.

C_s plane were considered to make no rotatory contribution. For dinitrates the distribution of the perturbing atoms was examined for each nitrato group in turn and the algebraic sum of their contributions was used to predict the sign of band II. In Table 4 colums 2 and 3 show the *anti*-C_β rotamer conformations by means of the location numbers for the carbon atoms α and β to the nitrato groups. The distribution of perturbing atoms is shown in column 4 as left-of-plane, in-plane, and right-of-plane, respectively. For dinitrate **10** where the atom distributions for the *endo*- and *exo*-groups are equal and opposite a positive sign for band II was predicted from the greater magnitude of the positive band of the *endo*-group.

The agreement of predicted and observed signs is consistent with the known configurations and the conformational analysis, and permits extension of the symmetry rule to both vicinal and non-vicinal dinitrates.

*Alkylbicyclo[2.2.1]heptyl Nitrates (**12**–**18**)*

The rigid bridged bicyclic skeleton sterically hinders rotation of the nitrato group in this series. Models show that both *endo*- and *exo*-nitrato groups at C-2 are restricted to libration of about ±45° from the conformer *anti*-C_β with C_β = C-1. The C-3 nitrato group in the dinitrates also adopts rotamer *anti*-C_β with C_β = C-2 (Table 4). Nitrato group librational freedom decreases in the order **13** > **12** > **14** for the

Can. J. Chem. Downloaded from www.nrcresearchpress.com by 210.87.254.40 on 09/05/12
For personal use only.

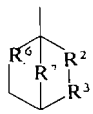

	R^2	R^3	R^6	R^7
12	$CHONO_2$(*exo*)	CH_2	CH_2	$C(CH_3)_2$
13	CH_2	CH_2	$CHONO_2$(*endo*)	$C(CH_3)_2$
14	$CHONO_2$(*endo*)	$C(CH_3)_2$	CH_2	CH_2
15	$CHONO_2$(*exo*)	$CHONO_2$(*exo*)	CH_2	$C(CH_3)_2$
16	$CHONO_2$(*exo*)	$CHONO_2$(*endo*)	CH_2	$C(CH_3)_2$
17	$CHONO_2$(*endo*)	$CHONO_2$(*endo*)	CH_2	$C(CH_3)_2$
18	$CHONO_2$(*endo*)	$CHONO_2$(*exo*)	CH_2	$C(CH_3)_2$

TABLE 4. Conformations and chirality of nitrate esters **1**–**28**

Compound	Conformation*		Perturbing atoms†	Sign of band II	
	C_α	C_β		Predicted	Observed
1	4	3	0/6/7	+	+
2	4	3	7/6/0	−	−
3	4	3	0/6/7	+	+
4	4	3	7/6/0	−	−
5	4	3	8/6/7‡	−	−
6	3	4	4/7/1	−	−
7	3	4	1/7/4	+	+
8	4,8	3,7	10/6/0,10/6/0	−	−
9	4,8	3,7	0/6/10,0/6/10	+	+
10	4,8	3,7	10/6/0,0/6/10	+§	+
11	3,4	4,3	4/6/3,4/6/3	−	−
12	2	1	6/6/2	−	−
13	2	1	6/7/1	−	−
14	2	1	1/6/7	+	+
15	2,3	1,2	10/6/2,8/7/3	−	−
16	2,3	1,2	10/6/2,4/7/7	−	−
17	2,3	1,2	1/7/10,3/8/7	+	+
18	2,3	1,2	1/7/10,8/6/4	+	+
19	1	2	4/7/3	−	−
20	1	2	6/7/1	−	−
21	1	2	1/10/3	+	+
22	1	6	1/6/7	+	+
23	1	2	0/7/7	+	+
24	1	2	1/6/7	+	+
25	1	6	5/6/0	−	−
26	2‖	3‖	0/6/3	+	+
27	2‖	3‖	5/11/0	−	−
28	2,3‖	3,2‖	4/11/5,4/11/5	+	+

*Anti-C_β, C_α and C_β are identified by location numbers of carbon atoms in formulae **1** to **28**
†Numbers of nonhydrogen atoms left/in plane/right of plane of nitrate group.
‡Rotation of the substituent on C-3 would reduce the + value.
§Assigned from the relative rotatory strengths of *endo* (+) and *exo* (−) bands.
‖Assigned on the basis of the planar chirality rule.

mononitrates and **17** > **18** > **16** > **15** for the dinitrates.

The intensity of the isotropic absorption envelope at 230 nm (Table 2) increased with steric hindrance for the mononitrates, and, among the dinitrates, the most sterically hindered, **15**, had the largest ε value at this wavelength.

The sign of c.d. band I was reversed with change of solvent for nitrates **12** and **18** (Table 3). It was positive for compound **12** in four solvents and negative in seven. The rotatory

Can. J. Chem. Downloaded from www.nrcresearchpress.com by 210.87.254.40 on 09/05/12
For personal use only.

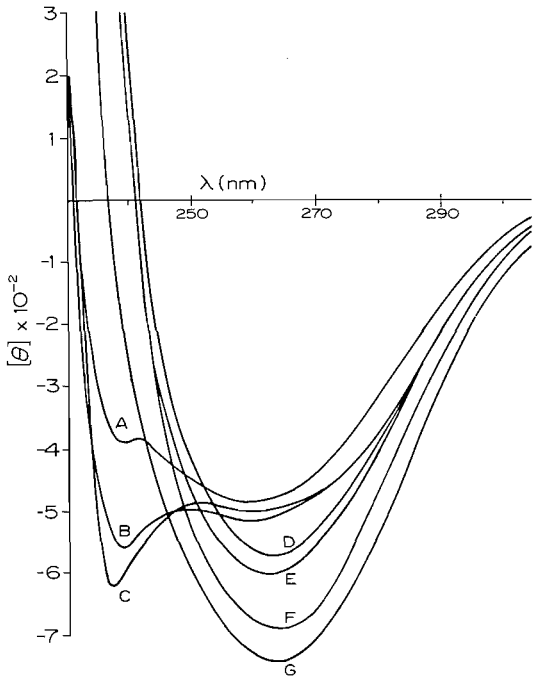

FIG. 1. Effect of solvent on the c.d. spectrum of L-threitan dinitrate (**11**). *A*, 2,2,2-trifluoroethanol; *B*, acetonitrile; *C*, methanol; *D*, pentane; *E*, heptane; *F*, cyclohexanes; *G*, tetrahydrofuran/cyclohexane (14:86, v/v).

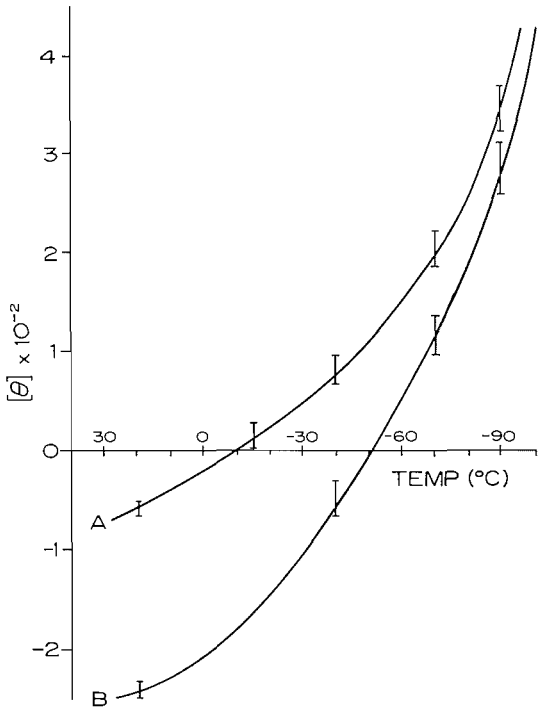

FIG. 2. Effect of temperature on band I (*A*) for isobornyl nitrate (**12**) and (*B*) for bornyl nitrate (**13**) in methanol.

strength of band I for compound **14** showed no correlation with the usual solvent parameters of refractive index, dipole moment, dielectric constant, *Z*-value, or the relation $K - 1/K + 2$ (33) of the eleven solvents. On cooling methanol solutions of **12–18**, band I showed no appreciable change in frequency but reversed sign for compounds **12**, **13**, (Fig. 2), **16**, and **17** and increased in intensity for **14**. Similar temperature effects were observed in other solvents, the smallest changes being observed for a chloroform solution of **13** and for a methanol solution of **15**. Varying the concentration of **12** from 0.036 to 0.1 *M* in methanol did not appreciably alter the molecular ellipticity *vs.* temperature plot for band I (Fig. 2).

The intensity of band III for the *trans*-dinitrates **16** and **18** was 5–8 times greater than for the *cis*-dinitrates **15** and **17** in acetonitrile solutions whereas the magnitudes of band II showed only 2-fold differences between the *cis*- and *trans*-isomers (Table 3). Since band III is a strong transition ($\varepsilon > 10^3$) and therefore probably allowed, electric dipole–electric dipole transition coupling could be expected (2, 34) which would lead to the observed lower rotatory strength for the approximately parallel *cis*-nitrato groups as compared to the more nearly orthogonal *trans*-nitrato groups (34, 35). The exciton splitting would not be evident because of overlap with band II.

The sign of band II was not altered by changes in solvent or temperature and, on application of the planar symmetry rule, was again found to be a reliable indicator of the molecular configuration (Table 4).

Alkylcyclohexyl Nitrates (19–25)

Conformational freedom in these nitrate esters includes the possibility of ring inversion as well as nitrato group rotation. The parent alcohols of **19** and **20** have *ca.* 100% and that of **21** *ca.* 70% population of the conformer with equatorial hydroxyl at 25° (36). Since cyclohexyl nitrate is 73% equatorial (37) and cyclohexanol 65% equatorial (38) at 25°, ring conformations with equatorial nitrato groups would be expected to predominate in compounds **19**, **20**, **22**,

Can. J. Chem. Downloaded from www.nrcresearchpress.com by 210.87.254.40 on 09/05/12
For personal use only.

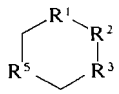

	R^1	R^2	R^3	R^5
19	$CHONO_2$(e)	$CHCH(CH_3)_2$(e)	CH_2	$CHCH_3$(e)
20	$CHONO_2$(e)	$CHCH_3$(e)	CH_2	$CHCH(CH_3)_2$(e)
21	$CHONO_2$(e)	$CHCH_3$(e)	CH_2	$CHCH(CH_3)_2$(a)
22	$CHONO_2$(e)	$C{=}CH_2$	CH_2	$CHCH(CH_3)_2$(e)
23	$CHONO_2$(a)	$C{=}CH_2$	CH_2	$CHCH(CH_3)_2$(e)
24	$CHONO_2$(e)	CH_2	$CHCH_3$(e)	CH_2
25	$CHONO_2$(a)	CH_2	$CHCH_3$(e)	CH_2

and **24**. All substituents in compounds **21**, **23**, and **25** cannot be equatorial; however, estimates from conformational free energy differences for these groups (39) suggest that the nitrato group would be equatorial in **21** and axial in **23** and **25**. Similar estimates for the related methyl ethers correctly predicted axial and equatorial methoxyl groups (40). The n.m.r. spectrum of **23** indicated an axial nitrato group since the α-proton resonance, a distorted triplet, had a half-height band width of 10 Hz. This ring conformation of **23** also permitted maximum separation of the π orbitals of the exocyclic double bond and the nitrato group. The preferred ring conformations in this series are shown in formulae **19**–**25**.

The preferred nitrato rotamer was also *anti*-C_β in this series with C_β = C-2 for **19**–**21** and **23**, and C_β = C-6 for **22**, **24**, and **25** (Table 4). Ring inversion in **23** and **25** did not alter the rotamer preference.

The c.d. spectra of nitrates **19**–**25** showed bands I–III and, in addition, very weak new bands appeared in the region 292–320 nm (Table 3) which did not correspond to any previously reported nitrate ester transitions. Similar bands were found in the spectra of the acyclic nitrates **26** and **27** but not in those of more conformationally rigid nitrates. The new band was negative for compound **19** in 15 different solvents and as the neat liquid ($[\theta]_{max}$ −6.4 to −18 at 322 ± 2 nm). Its intensity rapidly approached zero as the temperature of a methanol solution was lowered to −90° while that of bands I and II increased more slowly. These results suggest that the new band may be a component of the n–π* transition, similar to the 350 nm band of nitro-compounds (17), or that it may be the resultant of partially-overlapped, oppositely-signed 270 nm bands from different conformers. In the latter case the conformers probably arise from nitrato group libration rather than from ring inversion since the energy barrier for the latter process is estimated to be *ca.* 4.4 kcal mol^{-1} for **19** and **20** and (+)-3-methyl-cyclohexyl nitrate (**24**), which could be expected to have a larger population of the axial conformer, had the weakest of these bands near 298 nm (Table 3).

Band I was even more sensitive to changes in temperature and solvent polarity for **19**–**25** than for the more conformationally rigid nitrate esters. It was positive in acetonitrile solution for all members of the series except **23** and changed sign for compounds **21** and **25** on going to cyclohexane solutions. It appeared at 270 ± 2 nm for compound **19** in 15 different solvents, as the vapor, and as the neat liquid, and was most intense in highly polar solvents such as hexafluoroisopropanol ($[\theta]_{max}$ + 1590) and weakest in cyclohexane (Table 3). There was no clear correlation of the molecular ellipticity of band I with the usual solvent parameters (33), and, as noted above, it increased linearly in magnitude with decreasing temperature.

Nitrates **22** and **23** showed greater intensity in band III than other members of the series and this might be attributed to transition moment coupling of the olefinic and nitrato chromophores.

Again in this series band II was relatively insensitive to changes in solvent and temperature showing no change in sign or wavelength and only ±3% differences in $[\theta]_{max}$ among eight solvents and an increase of only 13% in $[\theta]_{max}$ between +30° and −90° for compound **19**. Band II for compound **22** was partially obscured by band III but was clearly positive in sign. The agreement between the observed signs of band II and those predicted by the planar rule from

Can. J. Chem. Downloaded from www.nrcresearchpress.com by 210.87.254.40 on 09/05/12
For personal use only.

TABLE 5. Conformations and chirality of steroid nitrates

Nitrate	Conformations*		Perturbing atoms†	Sign of band II	
	C_α	C_β		Predicted	Observed (8,9)
3β-Cholesteryl	3	4	0/6/25	+	+
3β-Acetoxycholestane-6-one-5α-yl	5	10	8/7/21	+	+
3β,6β-Diacetoxycholestane-5α-yl	5	10	8/7/29	+	+
6α-Fluoro-21-acetoxy-16α-methyl-1,4-pregnadiene-3,20-dione-11α-yl	11	9	15/8/10	−	−
3α,17β-Diacetoxy-5β-androstane-11β-yl	11	9	11/7/13	+	+
6α-Fluoro-21-acetoxy-16-methyl-1,4-pregnadiene-3,20-dione-11β-yl	11	9	8/8/17	+	+
4-Androstene-3-one-17β-yl	17	13	4/10/10	+	+
17α-Ethynyl-4-estrene-3-one-17β-yl	17	13	6/10/9	+	+
5α-Androstane-3β-ol-17β-yl	17	13	4/10/10	+	+
5α-Androstane-3-one-17β-yl	17	13	4/10/10	+	+
3β-Acetoxy-5α-androstane-17β-yl	17	13	4/13/10	+	+
19-*nor*-4-Pregnene-3,20-dione-17α-yl	17	16	3/6/17	+	+
4-Pregnene-3,20-dione-17α-yl	17	16	3/6/18	+	+
21-Acetoxy-4-pregnene-3,20-dione-17α-yl	17	16	7/6/18	+	+

*Anti-C_β, C_α, and C_β are identified by carbon atom location numbers.
†Numbers of nonhydrogen atoms left/in plane/right of plane of nitrato group.

the preferred conformations was excellent (Table 4).

Steroid Nitrates

The planar rule was further tested on 20 nitrate esters of secondary steroid alcohols for which the nitrato c.d. bands have previously been reported (8, 9). The conformational analyses followed the procedure outlined above, the results, and the predicted and observed signs of band II are shown in Table 5. Agreement between observed and predicted signs for fourteen of these steroidal nitrates is very good. Six cholestane and androstane derivatives with 3α- or 3β-nitrato groups (compounds numbered **1**–**6** by Snatzke and co-workers (9)) could not be conformationally analyzed since molecular models showed no preference for one nitrato rotamer in the 3-position on ring A. Conformational lability is suggested by the absence of a detectable band I in the spectra of the 3-equatorial nitrates and the weakly negative band I found for the axial chromophores (7). The conformational preference of this nitrato group probably could be determined through variable temperature and solvent studies. The rule could not be applied to the c.d. spectra of hexose nitrates published by Tsuzuki *et al.* (5, 6) since only band I has been reported.

*Acyclic Nitrates (**26**–**28**)*

Since no skeletal constraint was apparent from models of these compounds, the planar symmetry rule was applied to predict molecular conformations.

Rotamer *anti*-C_β was assumed to predominate and selection of C_β as methyl, methylene, and methine carbons, respectively, in compounds **26**–**28** yielded agreement of predicted and observed signs for band II (Table 4). Nitrates **26** and **27** gave bands I–III and an additional, weak, long wavelength bands at 292 nm and 310 nm respectively which, as noted earlier, may be due to the presence of different rotamers in solution. The additional band did not appear

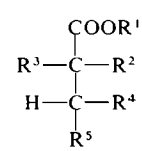

	R^1	R^2	R^3	R^4	R^5
26	H	ONO_2	H	H	H
27	C_2H_5	H	ONO_2	H	$COOC_2H_5$
28	C_2H_5	H	ONO_2	ONO_2	$COOC_2H_5$

Can. J. Chem. Downloaded from www.nrcresearchpress.com by 210.87.254.40 on 09/05/12
For personal use only.

in the spectrum of the dinitrate of diethyl-L-tartrate (**28**). The o.r.d. data for **26–28** which suggested that nitrates of α-D-hydroxy acids have positive Cotton effects while those of α-L-hydroxy acids have negative Cotton effects (7) probably reflected the sign of band III only since the weaker bands I and II would have been obscured in the background rotation.

The acyclic nitrate esters of the primary steroid alcohols, 3β-acetoxy-5α-cholestane-19-ol and 3β-acetoxy-5β-cholestane-19-ol (9) when assigned *anti*-C_β conformations (C_α = C-19, C_β = C-10) showed a further degree of conformational freedom, namely rotation on the C_α—C_β bond. Assignment of the conformation with C-9 antiperiplanar to the nitrato group gave agreement of the predicted (+) and observed (+) signs for band II whereas similar assignments for C-1 or C-5 were less favored according to the molecular models of these compounds and predicted (+) and (−) signs for band II, respectively.

In general the application of the symmetry rule to the acyclic nitrate esters led to molecular conformations which appeared to be plausible from molecular models.

We are grateful to Professor S. J. Angyal, Dr. D. F. Dong, Dr. S. Schroeter, Dr. A. H. Sommers, and Dr. R. N. Totty for gifts of chiral compounds, and to the National Research Council of Canada for financial support.

1. W. KLYNE. Advanced study institute on fundamental aspects and recent developments in optical rotatory dispersion and circular dichroism, Tirrenia (Pisa), Italy. September 5–18, 1971. Abstracts p. 20.
2. J. A. SCHELLMAN. J. Chem. Phys. **44**, 55 (1966).
3. Y. TSUZUKI, K. TANABE, and K. OKAMOTO. Bull. Chem. Soc. Jap. **38**, 274 (1965).
4. Y. TSUZUKI, K. TANABE, and K. OKAMOTO. Bull. Chem. Soc. Jap. **39**, 761 (1966).
5. Y. TSUZUKI, K. TANABE, K. OKAMOTO, and N. YAMADA. Bull. Chem. Soc. Jap. **39**, 1391 (1966).
6. Y. TSUZUKI, K. TANABE, K. OKAMOTO, and N. YAMADA. Bull. Chem. Soc. Jap. **39**, 2269 (1966).
7. Y. TSUZUKI, K. TANABE, K. OKAMOTO, and M. FUKUBAYASHI. Bull. Chem. Soc. Jap. **39**, 1387 (1966).
8. L. D. HAYWARD and S. CLAESSON. Chem. Commun. 302 (1967).
9. G. SNATZKE, H. LAURENT, and R. WIECHERT. Tetrahedron, **25**, 761 (1969).
10. K. KAYA, K. KUWATA, and S. NAGAKURA. Bull. Chem. Soc. Jap. **37**, 1055 (1964).
11. I. G. CSIZMADIA and L. D. HAYWARD. Photochem. Photobiol. **4**, 657 (1965).
12. J. TROTTER. Acta Cryst. **16**, 698 (1963).
13. T. C. W. MAK and J. TROTTER. Acta Cryst. **17**, 367 (1964).
14. A. CAMERMAN, N. CAMERMAN, and J. TROTTER. Acta Cryst. **19**, 449 (1965).
15. F. H. ALLEN and J. TROTTER. J. Chem. Soc. (B), 1551 (1970).
16. W. B. DIXON and E. B. WILSON, JR. J. Chem. Phys. **35**, 191 (1961).
17. G. SNATZKE. J. Chem. Soc. 5002 (1965).
18. G. SNATZKE, H. RIPPERGER, C. HORSTMANN, and K. SCHREIBER. Tetrahedron, **22**, 3103 (1966).
19. C. W. DEUTSCHE, D. A. LIGHTNER, R. W. WOODY, and A. MOSCOWITZ. Ann. Rev. Phys. Chem. **20**, 407 (1969).
20. L. VELLUZ, M. LEGRAND, and M. GROSJEAN. Optical circular dichroism. Academic Press, New York, 1965.
21. L. D. HAYWARD and R. N. TOTTY. Can. J. Chem. **49**, 624 (1971).
22. (*a*) R. PASSERINI and I. G. ROSS. J. Sci. Instrum. **30**, 274 (1953). (*b*) E. W. WASHBURN. (*Editor*) International Critical Tables **3**, 27 (1928).
23. M. JACKSON and L. D. HAYWARD. Can. J. Chem. **38**, 496 (1960).
24. L. D. HAYWARD, D. J. LIVINGSTONE, M. JACKSON, and V. CSIZMADIA. Can. J. Chem. **45**, 2191 (1967).
25. R. BOSCHAN. J. Am. Chem. Soc. **81**, 3341 (1959).
26. L. D. HAYWARD, R. A. KITCHEN, and D. J. LIVINGSTONE. Can. J. Chem. **40**, 434 (1962).
27. L. D. HAYWARD and I. G. CSIZMADIA. Tetrahedron, **19**, 2111 (1963).
28. F. J. HOPTON and G. H. S. THOMAS. Can. J. Chem. **47**, 2395 (1969).
29. A. C. LEGON. Chem. Commun. 838 (1970).
30. C. M. SHEPPERD, T. SCHAEFER, B. W. GOODWIN, and J. T'RAA. Can. J. Chem. **49**, 3158 (1971).
31. A. KIKKAWA, H. MEGURO, and K. TUZIMURA. Agr. Biol. Chem. **33**, 80 (1969).
32. G. SNATZKE. Proc. Roy. Soc. **A297**, 43 (1967).
33. D. KIRK, W. KLYNE, and S. R. WALLIS. J. Chem. Soc. (C), 350 (1970).
34. H. THOMAS and K. MISLOW. J. Am. Chem. Soc. **92**, 6292 (1970).
35. H. EYRING, H. LIU, and D. CALDWELL. Chem. Rev. **68**, 525 (1968).
36. H. FELTKAMP and N. FRANKLIN. Tetrahedron, **21**, 1541 (1965).
37. A. E. ALLAN, E. PREMUZIC, and L. W. REEVES. Can. J. Chem. **41**, 204 (1963).
38. E. L. ELIEL, N. L. ALLINGER, S. J. ANGYAL, and G. A. MORRISON. Conformational analysis. Interscience Publishers Inc., New York, 1965, p. 147.
39. J. A. HORSCH. Topics Stereochem. **1**, 199 (1967).
40. D. VOISIN and B. GASTAMBIDE. Bull. Soc. Chim. France, 2643 (1971).

Can. J. Chem. Downloaded from www.nrcresearchpress.com by 210.87.254.40 on 09/05/12
For personal use only.

Meisenheimer Complex Formation Between 1,3,5-Trinitrobenzene and Hydroxide Ion. Equilibrium Constants for the Dimethylformamide–Water Solvent System

E. A. SYMONS AND E. BUNCEL

Department of Chemistry, Queen's University, Kingston, Ontario

Received January 4, 1972

Sigma-complex formation between 1,3,5-trinitrobenzene (TNB) and hydroxide ion has been studied quantitatively as a function of medium composition for part of the dimethylformamide (DMF)–water solvent system by spectrophotometric methods. Only a 1 : 1 complex is detected under the conditions of measurement, with [TNB] ≥ [OH^-]. The equilibrium constant (K_{eq}) for complex formation in 22 mol % DMF has the value 3×10^3 l mol^{-1}, compared with 3 l mol^{-1} in purely aqueous medium. Further increases in K_{eq} occur as the DMF content of the medium is raised; in 50 mol % DMF $K_{eq} \approx 10^5$, but reliable K_{eq} values could not be obtained in this region of medium composition. The increase in K_{eq} with increasing DMF content is interpreted largely on the basis of hydroxide ion desolvation.

La formation d'un complexe-σ entre le trinitro-1,3,5 benzène (TNB) et l'ion hydroxyle a été étudiée quantitativement en fonction de la composition du milieu, constitué d'un mélange diméthylformamide (DMF)–eau, au moyen de méthodes spectrophotométriques. Dans les conditions des mesures, avec [TNB] ≥ [OH^-], seul un complexe 1:1 a été détecté. La constante d'équilibre (K_{eq}), pour la formation du complexe dans une solution à 22% en mol de DMF, a la valeur de 3×10^{-3} l mol^{-1}, comparée à 3 l mol^{-1} dans un milieu purement aqueux. La valeur de K_{eq} augmente si la teneur du milieu en DMF augmente; avec 50% en mol de DMF, $K_{eq} \approx 10^5$, mais dans ce cas, des valeurs fidèles de K_{eq} ne peuvent pas être obtenues dans cette zone de composition. L'augmentation de la valeur de K_{eq} avec la teneur du milieu en DMF est interprétée surtout sur la base d'une désolvatation des ions hydroxyles.

Canadian Journal of Chemistry, **50**, 1729 (1972)

The formation of Meisenheimer (σ) complexes between aromatic nitro compounds and bases is well documented (1–8). The present study was undertaken as part of a program aimed at elucidating the relationship between hydrogen–deuterium exchange (9, 10) and σ-complex formation in trinitrobenzene–base systems. Results of equilibrium measurements for reaction 1 as a function of medium composition for part of the dimethylformamide–water composition range are now reported.

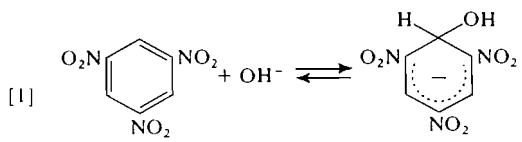

[1]

1

Experimental

Reagents

1,3,5-Trinitrobenzene (Eastman) was purified by recrystallization; spectral absorption in 96% ethanol: λ_{max} 225 mμ, ε_{max} 25 700 l mol^{-1} cm^{-1}. The solvent DMF (Fisher Certified Reagent) was purified by the method of Ritchie and Megerle (11). Sodium hydroxide solutions (Fisher Scientific) and tetramethylammonium hydroxide solutions (Matheson, Coleman, and Bell) were stored in polyethylene bottles. The distilled water used was carbon dioxide-free.

Procedures

The main consideration with respect to the procedures employed was to avoid any serious complication arising from the reaction of hydroxide ion with the solvent, *i.e.* the basic hydrolysis of DMF (12). This problem was minimized by operating generally under the conditions [TNB] ≥ [OH^-], thus effectively reducing the concentration of free hydroxide ion as a result of complex formation. Extensive complexing of the hydroxide ion occurred in solvents even moderately rich in DMF ($K_{eq} \approx 10^3$ in *ca.* 20 mol % DMF). In the more aqueous media, where K_{eq} was considerably smaller, the irreversible loss of hydroxide ion (12) resulted in a decrease in absorbance with time, necessitating the observation of absorbance at a fixed wavelength and extrapolation back to the time of mixing. At 25° the typical decay in absorbance after 10 min was within 4% of the extrapolated zero time value for solvent mixtures containing more than 30 mol % DMF, but reached a maximum of about 40% in the region of 10 mol % DMF for the same period. Initial absorbance readings were taken about 1 min after mixing.

The possible problem of limited base solubility in media rich in DMF (12) did not arise since most of the hydroxide ion is present in complexed form in these TNB–OH^- systems.

Solutions for spectral examination were prepared by addition of standard hydroxide to a solution of TNB in DMF–water. Spectral measurements were made in quartz cells in

Can. J. Chem. Downloaded from www.nrcresearchpress.com by 210.87.254.6 on 09/05/12
For personal use only.

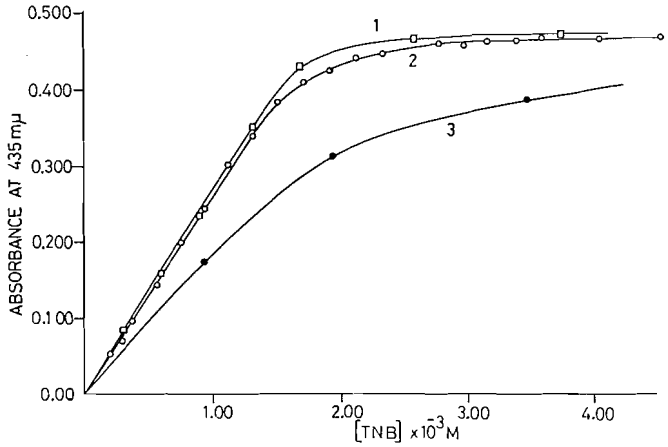

FIG. 1. Plot of absorbance *vs.* trinitrobenzene concentration at constant (1.92×10^{-3} *M*) NaOH concentration for various solvent compositions (0.1 mm cell, 25°). Curve 1, 45.3 mol % DMF; 2, 33.1 mol % DMF; 3, 18.2 mol % DMF.

the thermostatted ($25.0 \pm 0.1°$) cell compartment of a Unicam SP800 spectrophotometer or a Bausch and Lomb spectronic 600 spectrophotometer coupled to a Sargent SRL Recorder. The cuvettes used varied in pathlength between 0.1 and 10 mm, depending on the medium composition.

Results and Discussion

Spectral Characterization and Medium Dependence

The visible region spectrum of the colored solution formed between trinitrobenzene and hydroxide ion in aqueous DMF, consisting of a major peak at 435 nm and a minor, broader, peak centred near 500 nm, is ascribed to the σ-complex (Meisenheimer adduct) **1**. Under the conditions employed, with excess TNB and a moderately high DMF content, most of the hydroxide ion is present in complexed form. The molar extinction coefficient of the complex is thus readily obtained by measuring the absorbance at a given wavelength (λ_{max}) as a function of trinitrobenzene concentration, while keeping the base concentration constant (0.002 *M*). The application of this "overload" method to several solvent compositions is shown in Fig. 1. The curves level off at a progressively lower ratio of [TNB]:[NaOH] as the media become richer in DMF, indicating the trend in the magnitude of the equilibrium constant with changing solvent composition. However, this limiting absorbance method was not applicable to media containing less than *ca.* 20 mol % DMF because of the limited solubility of TNB in these more aqueous solutions, combined with the lower magnitude of the equilibrium constant.

The extinction coefficient data and the absorption maxima for media covering the range 18–80 mol % DMF, determined in the manner described above, are presented in Table 1. The usual relationship between the absorbance (A), molar extinction (ε), concentration (c), and cell pathlength (b), was used in the calculations ($A = \varepsilon cb$). It is apparent that there is a slight but definite increase in the extinction coefficients as the DMF content increases, though the ratio of the extinctions at the primary and secondary maxima remains constant. This relationship between the extinction coefficients at the two maxima and the medium composition, expressed as mol %, is approximately linear. Also, whereas the primary spectral maximum is independent of solvent composition, the secondary maximum exhibits a shift to longer wavelengths as the DMF content is increased.

The stoichiometry of the complex, determined by application of the method of continuous variations (13), was found to be 1:1 for 45 and 13 mol % DMF. Application of the slope-ratio method (13) also gave results indicating a 1:1 complex in these systems. The above methods do not distinguish whether or not there is more than a single 1:1 complex present. However, there have been numerous n.m.r. studies in recent years (1–5, 14–17), involving trinitrobenzene (albeit in other solvent systems and with other bases) which have given conclusive

Can. J. Chem. Downloaded from www.nrcresearchpress.com by 210.87.254.6 on 09/05/12
For personal use only.

TABLE 1. Spectral characteristics of the trinitrobenzene–hydroxide ion σ-complex as a function of solvent composition at 25°

DMF in water (mol %)	λ^1_{max} (mμ)	λ^2_{max} (mμ)	$\varepsilon_{\lambda 1}$ (l mol^{-1} cm^{-1})	$\varepsilon_{\lambda 2}$ (l mol^{-1} cm^{-1})	$\varepsilon_{\lambda 1}/\varepsilon_{\lambda 2}$	[TNB]/[NaOH]*
0.75	435	490–510	‡	‡	—	2
1.2	435	490–510	‡	‡	—	2
2.5	435	490–510	‡	‡	—	1
8.9	435	500	‡	‡	—	1
13.0	435	500	‡	‡	—	10†
18.2	435	504	25 700	16 800	1.53	10
22.1	435	—	25 900	—	—	10§
24.8	435	507	26 300	17 500	1.50	20†
33.1	435	509	26 400	17 300	1.53	50
38.2	435	510	26 900	17 600	1.53	50
44.7	435	—	27 400	—	—	2.5§
45.2	435	—	26 900	—	—	10§
45.3	435	511	27 600	18 100	1.52	50
61.7	435	—	27 600	—	—	2.5§
65.1	435	512	28 900	18 800	1.54	50
75.8	435	—	28 800	—	—	20§
80.5	435	514	29 400	19 300	1.52	50

*For DMF = 0.75, 1.2, and 2.5 mol %, [NaOH] was 1.00×10^{-3} *M*, otherwise 1.95×10^{-3} *M*.
†Saturated with trinitrobenzene.
‡K_{eq} was not large enough in this solvent region to allow direct measurement of ε.
§Measurements made with Me_4NOH.

evidence for formation of complexes such as **1**. It is reasonable then to conclude that there is only one such complex formed in the aqueous DMF system and that its structure is given by **1**.

Equilibrium Constants and Medium Dependence

Two methods were utilized to evaluate the equilibrium constants for σ-complex formation between trinitrobenzene and hydroxide ion as a function of DMF content. In the first, K_{eq} was calculated by means of eq. 2 which

$$[2] \quad K_{eq} = \frac{A}{\varepsilon b}([TNB]_{stoich} - A/\varepsilon b)^{-1} \times ([NaOH]_{stoich} - A/\varepsilon b)^{-1}$$

is obtained by substituting in the usual expression $K_{eq} = [TNB{\cdot}OH^-]/[TNB]_{eq}\,[NaOH]_{eq}$ for the equilibrium concentration of complex, *i.e.* $[TNB{\cdot}OH^-] = A/\varepsilon b$. The absorbances, A, corresponding to cell pathlengths, b, are given in Table 2. The results were determined as described in the previous section but equal concentrations of trinitrobenzene and sodium hydroxide (2×10^{-3} *M*) were used, in accord with recommended procedure (13). The extinction coefficient values, ε, for media containing less than 20 mol % DMF were obtained by extrapolation of the linear plot of ε *vs.* mol % DMF derived from Table 1. The error in K_{eq}, as estimated from eq. 2 based on an error of ± 3% in the measured absorbance value, is about ± 10% for $K_{eq} \leqslant 10^3$ but increases to about ± 100% for $K_{eq} \geqslant 10^4$. The limit of applicability of the method was hence taken as corresponding to $K_{eq} \approx 10^4$.

The second procedure, proposed by Foster and Matheson (18), is based on use of eq. 3.

$$[3] \quad \frac{b[TNB]_{stoich}}{A} = \frac{1}{\varepsilon} + \frac{1}{K_{eq}^{1/2}\varepsilon^{1/2}}\left(\frac{b}{A}\right)^{1/2}$$

The method involved measurement of the absorbance of solutions containing equal but variable concentrations of TNB and base (*ca.* 5×10^{-4} to 5×10^{-3} *M*). For this work Me_4NOH was the base used. In the graphical analysis of the data (18), plots of $b[TNB]_{stoich}/A$ *vs.* $(b/A)^{1/2}$ should be linear with slope $1/(K^{1/2}\varepsilon^{1/2})$ and intercept $1/\varepsilon$. In practise it was found that satisfactory plots could not be obtained for media containing more than *ca.* 30 mol % DMF; the reason was the appearance of a distinct upward curvature in these graphs at the lower concentrations of each set of data, combined with considerable scatter, arising at least in part from the great magnitude of K_{eq}.

Can. J. Chem. Downloaded from www.nrcresearchpress.com by 210.87.254.6 on 09/05/12
For personal use only.

TABLE 2. Equilibrium constants (K_{eq}) for trinitrobenzene–hydroxide ion σ-complex formation as a function of solvent composition at 25°

DMF in water (mol %)	Absorbance* at 435 mμ	Cell path length (cm)	K_{eq} (l mol^{-1})
0.75	0.385 ± 0.008	1.000	4.1
1.2	0.475 ± 0.011	1.000	4.9
2.5	0.763 ± 0.011	1.000	8.1
8.9	0.606 ± 0.009	0.100	7.83×10^1
10.9	—	—	1.53×10^2†
13.0	1.537 ± 0.020	0.100	3.15×10^2
18.2	0.279 ± 0.006	0.0104	1.16×10^3
22.1	—	—	3.30×10^3†
24.8	0.380 ± 0.008	0.0104	3.86×10^3
33.1	0.436 ± 0.006	0.0104	9.8×10^3
33.8	—	—	*ca.* 2×10^4†

*Stoichiometric [TNB] = 2.00×10^{-3} *M*, stoichiometric [NaOH] = 1.98×10^{-3} *M*; absorbance given is mean of triplicate runs.
†Determined by the method of Foster and Matheson (18), Me_4NOH was the base.

However, where acceptable plots were obtained, the K_{eq} calculated from the slope plus the appropriate ε value from Table 1 was in good agreement with the values obtained by the first method, as seen in Table 2. However, qualitatively, K_{eq} appears to be at least 10^5 by 50 mol % DMF.

The K_{eq} data in the region of low DMF composition may be extrapolated to the pure aqueous medium to yield the value $K_{eq} = 3.0 \pm 0.2$ l mol^{-1}. In a study of the trinitrobenzene–hydroxide ion system in aqueous solution, Abe (19) obtained the value $K_{eq} = 2.7$ l mol^{-1} by using a low (*ca.* 10^{-5} *M*) concentration of trinitrobenzene and excess of hydroxide. A revised value of 3.2 l mol^{-1} is obtained from the data of Gold and Rochester (20)[1]. (Both Abe (18) and Gold and Rochester (20) found evidence for a significant 2:1 OH^-:TNB interaction at very large ratios ($>10^3$) of hydroxide ion to trinitrobenzene.) Bernasconi (21) reports the value $K_{eq} = 3.7 \pm 0.4$ l mol^{-1} at 25°, as obtained from kinetic studies by fast reaction techniques of the forward and reverse reaction rates for eq. 1, with NaOH in excess over TNB and an ionic strength (NaCl) of 1.0 *M*.

The observed increase in K_{eq} with increasing DMF content is large indeed, covering over three powers of ten just over the range 0–25 mol (60 vol) % DMF. In previous studies (22, 23) of the effect of medium on Meisenheimer complex formation by trinitrobenzene (using other anions and different media) large increases in K_{eq} were also observed. It was concluded (23) that the dominant factor was desolvation of the small anionic reagent upon complex formation. In the present case, the increase in K_{eq} is thus ascribed to progressive desolvation of the small ("hard" in HSAB theory (24)) hydroxide ion, aided by some increased solvation of the large, polarizable ("soft") σ-complex as the aqueous component is replaced by the dipolar aprotic component (25, 26). This is in agreement with the conclusion drawn in an H_- study of proton abstraction equilibria by hydroxide ion in DMF–water mixtures (27), that DMF is a poor hydrogen-bond donor toward hydroxide ion but a strong hydrogen-bond acceptor from solvent water. In these properties DMF closely resembles DMSO and similar dipolar aprotic solvents (25–27).

[1]Gold and Rochester (20) quoted the value 2.7 l mol^{-1} using an approximate extinction coefficient of 30 000 for the complex. However, the current work yields, through extrapolation of the data in Table 1, a value of 24 700 for ε. A recalculation of the data of Gold and Rochester then leads to $K_{eq} = 3.2$.

Financial support of this work by the National Research Council of Canada is gratefully acknowledged. E.A.S. was the holder of a NRCC scholarship. Discussions with Drs. A. R. Norris and K. E. Russell are also acknowledged.

1. M. J. STRAUSS. Chem. Rev. **70**, 667 (1970).
2. M. R. CRAMPTON. Adv. Phys. Org. Chem. **7**, 211 (1969).
3. P. BUCK. Angew. Chem. Int. Ed. **8**, 120 (1969).

Can. J. Chem. Downloaded from www.nrcresearchpress.com by 210.87.254.6 on 09/05/12
For personal use only.

4. E. BUNCEL, A. R. NORRIS, and K. E. RUSSELL. Quart. Rev. London, **22**, 123 (1968).
5. R. FOSTER and C. A. FYFE. Rev. Pure Appl. Chem. (Australia), **16**, 61 (1966).
6. F. TERRIER and F. MILLOT. Tetrahedron Lett. No. 31, 2933 (1971).
7. E. J. FENDLER, D. M. CAMAIONI, and J. H. FENDLER. J. Org. Chem. **36**, 1544 (1971).
8. C. F. BERNASCONI and R. G. BERGSTROM. J. Org. Chem. **36**, 1325 (1971).
9. E. BUNCEL and E. A. SYMONS. Can. J. Chem. **44**, 771 (1966).
10. E. BUNCEL and E. A. SYMONS. Chem. Commun. 771 (1967).
11. C. D. RITCHIE and G. H. MEGERLE. J. Am. Chem. Soc. **89**, 1447 (1967).
12. E. BUNCEL and E. A. SYMONS. Chem. Commun. 164 (1970); E. BUNCEL, S. KESMARKY, and E. A. SYMONS. Chem. Commun. 120 (1971).
13. M. M. JONES. Elementary coordination chemistry. Prentice Hall, Englewood Cliffs, N.J., 1964. Chapt. 8.
14. M. R. CRAMPTON and V. GOLD. J. Chem. Soc. B, 893 (1968); 23 (1967); M. R. CRAMPTON. J. Chem. Soc. B, 1341 (1967).
15. K. L. SERVIS. J. Am. Chem. Soc. **89**, 1508 (1967).
16. R. FOSTER and C. A. FYFE. Tetrahedron, **22**, 1831 (1966).
17. E. BUNCEL, A. R. NORRIS, and W. PROUDLOCK. Can. J. Chem. **46**, 2759 (1968).
18. R. FOSTER and I. B. C. MATHESON. J. Chem. Soc. B, 1713 (1970).
19. T. ABE. Bull. Chem. Soc. Japan, **33**, 41 (1960).
20. V. GOLD and R. ROCHESTER. J. Chem. Soc. 1710 (1964).
21. C. F. BERNASCONI. J. Am. Chem. Soc. **92**, 4682 (1970).
22. M. R. CRAMPTON. J. Chem. Soc. B, 1208 (1968).
23. E. BUNCEL, A. R. NORRIS, K. E. RUSSELL, and W. PROUDLOCK. Can. J. Chem. **47**, 4129 (1969).
24. R. G. PEARSON. J. Am. Chem. Soc. **85**, 3433 (1963); **89**, 1827 (1967).
25. A. J. PARKER. Chem. Rev., **69**, 1 (1969); Quart. Rev. London, **16**, 163 (1962).
26. C. D. RITCHIE. Solute–solvent interactions. *Edited by* J. F. Coetzee and C. D. Ritchie. Marcel Dekker, New York, 1969. Chapt. 4.
27. E. BUNCEL, E. A. SYMONS, D. DOLMAN, and R. STEWART. Can. J. Chem. **48**, 3354 (1970).

Can. J. Chem. Downloaded from www.nrcresearchpress.com by 210.87.254.6 on 09/05/12
For personal use only.

Reactions of Thiyl Radicals. VIII. Photolysis of Methyl Ethyl Sulfide Vapor[1]

D. R. TYCHOLIZ AND A. R. KNIGHT

Department of Chemistry and Chemical Engineering, University of Saskatchewan, Saskatoon, Saskatchewan

Received November 12, 1971

Methyl ethyl sulfide has been photolyzed in the vapor phase with wavelengths between 2000 and 2350 Å and the effects of pressure, temperature, and exposure time investigated. The vapor phase absorption spectrum of the sulfide has been determined and the variation in the nature and rates of formation of products in the presence of CO_2, CF_4, propylene, and 2-pentene measured. Quantum yields of products from the decomposition of the pure substrate were determined at 2288 Å.

The products of the reaction are, in order of decreasing importance, C_2H_6, $CH_3SSC_2H_5$, $C_2H_5SSC_2H_5$, CH_4, CH_3SCH_3, $C_2H_5SC_2H_5$, C_3H_8, C_2H_4, CH_3SSCH_3, C_4H_{10}, C_2H_5SH, and CH_3SH. A carbon/sulfur mass balance is obtained at all substrate pressures at 25 °C, and at the single substrate pressure examined at 120 °C. In the presence of propylene four additional products, n-C_5H_{12}, $CH_3S(CH_2)_2CH_3$, $(CH_3CH_2CH_2)_2S$, and $CH_2{=}CH{-}CH_2SC_2H_5$, were found.

Only a small fraction of photochemically excited methyl ethyl sulfide molecules undergoes chemical decomposition. The two primary processes

[3*a*] $$CH_3SC_2H_5 + h\nu \rightarrow CH_3 + C_2H_5S$$

[3*b*] $$CH_3SC_2H_5 + h\nu \rightarrow CH_3S + C_2H_5$$

and subsequent reactions of the radicals so formed account for the observed products. R_{3a}/R_{3b} has a value of 1.32 at 25 °C.

Le sulfure d'éthyle et de méthyle a été photolysé en phase vapeur avec des longueurs d'onde comprises entre 2000 et 2350 Å et les effets de la pression, température, et durée d'exposition ont été examinés. Le spectre d'absorption en phase gazeuse du sulfure a été déterminé et la variation, dans la nature et dans les vitesses de formation des produits en présence de CO_2, CF_4, propylène, et pentène-2, mesurée. Les rendements quantiques en produits, à partir de la décomposition du substrat pur, ont été déterminés à 2288 Å.

Les produits de la réaction sont, par ordre d'importance décroissante, C_2H_6, $CH_3SSC_2H_5$, $C_2H_5SSC_2H_5$, CH_4, CH_3SCH_3, $C_2H_5SC_2H_5$, C_3H_8, C_2H_4, CH_3SSCH_3, C_4H_{10}, C_2H_5SH, et CH_3SH. Une balance en masse carbone/soufre est obtenue pour toutes les pressions du substrat à 25 °C et pour une seule à 120 °C. En présence de propylène quatre produits supplémentaires ont été obtenus: n-C_5H_{12}, $CH_3S(CH_2)_2CH_3$, $(CH_3CH_2CH_2)_2S$, et $CH_2{=}CH{-}CH_2SC_2H_5$. Seule une petite fraction de sulfure d'éthyle et de méthyle photochimiquement excitée, subit une décomposition chimique. Les deux processus primaires

[3*a*] $$CH_3SC_2H_5 + h\nu \rightarrow CH_3 + C_2H_5S$$

[3*b*] $$CH_3SC_2H_5 + h\nu \rightarrow CH_3S + C_2H_5$$

et les réactions ultérieures des radicaux ainsi formés, rendent compte des produits observés. R_{3a}/R_{3b} a une valeur de 1.32 à 25 °C.

Canadian Journal of Chemistry, **50**, 1734 (1972)

Introduction

There has been only one reported investigation of the photochemistry of methyl ethyl sulfide. Milligan *et al.* (1) irradiated liquid $CH_3SC_2H_5$ at 2537 Å for 48 h. They reported CH_4, C_2H_6, and C_2H_4 in the ratio 60:35:5 along with CH_3SSCH_3, $C_2H_5SSC_2H_5$, $CH_3SSC_2H_5$, and trace amounts of CH_3SCH_3.

The photolysis of dimethyl sulfide vapor has recently been studied (2) and it was found that the main products of the reaction were CH_4, C_2H_6, CH_3SSCH_3, and CH_3SH. The thiol was a minor product indicating that disproportionation of RS radicals was relatively unimportant in that system. Evidence was also obtained that indicated the formation of hot CH_3 and CH_3S radicals in the primary process which involves scission of the S—C bond.

As part of a continuing series of investigations of the photochemical kinetics and mechanism of compounds that yield thiyl radicals on photolysis, we have examined in detail, and report on here, the vapor phase photolysis of methyl ethyl sulfide. This substrate has the advantage of

[1]From the Ph.D. Thesis of D. R. Tycholiz to be submitted to the University of Saskatchewan, Saskatoon, Saskatchewan.

Can. J. Chem. Downloaded from www.nrcresearchpress.com by 210.87.254.6 on 09/05/12
For personal use only.

Can. J. Chem. Downloaded from www.nrcresearchpress.com by 210.87.254.6 on 09/05/12
For personal use only.

allowing the reactions of both methylthiyl and ethylthiyl radicals to be examined simultaneously.

Experimental

The photolyses were conducted in a conventional high vacuum system described previously (3). The light source was a Hanovia 30620 medium pressure mercury lamp filtered to remove wavelengths less than 2000 Å. The demountable reaction cell was a quartz cylinder, 5 cm o.d. and 10 cm in length with plane windows. The absorption spectrum of the substrate was determined using a Zeiss Model PMQ-II spectrophotometer fitted with a 1 m path length gas cell connected to the vacuum system.

Methyl ethyl sulfide (99.96 ± 0.04% purity American Petroleum Institute standard sample) was degassed and used without further purification after g.c. analysis indicated the absence of detectable impurities. Carbon dioxide (Canlab), carbon tetrafluoride (Matheson), and 2-pentene (Matheson, Coleman, and Bell) were degassed and purified by trap-to-trap distillation. Gas chromatographic analysis of samples of each of these addends confirmed the absence of detectable impurities.

Reaction products were identified initially by comparison of g.c. retention times and each identification was subsequently confirmed by mass spectrometric analysis of each product trapped from the g.c. effluent.

At the conclusion of reactions involving only the substrate, CH_4 was removed at −196 °C and determined in a gas burette, C_2H_6 and C_2H_4 were removed at −160 °C and analyzed on a 6 ft Poropak Q column, and the remaining fraction, including unreacted substrate, was analyzed using a 12 ft tricresyl phosphate column. When CO_2 was present, CH_4, C_2H_6, and C_2H_4 were removed first and then CO_2 was pumped off, along with C_3H_8, C_4H_{10}, and CH_3SH (products not analyzed in that series) at −130 °C and the remaining products analyzed as before. In experiments with added CF_4, the addend was pumped off at −183 °C along with CH_4 and C_2H_4 which were not determined, and the remainder of the analyses carried out as in pure substrate experiments. When propylene was added, it was removed at the end of the reaction, along with the undetermined products CH_4, C_2H_4, C_2H_6, C_3H_8, and C_4H_{10}, at −130 °C before the remaining products were analyzed on the g.c. The only products analyzed in the experiments with added 2-pentene were CH_4 in the gas burette and C_2H_4, C_2H_6, and C_3H_8, which were removed at −130 °C.

For the actinometry experiments, the light source was fitted with a Baird Atomic interference filter which had a 60 Å pass band centered at 2288 Å. The photolysis of diethyl ketone at 165 °C was used to determine the light intensity, taking Φ(CO) as unity at a ketone pressure of 29 Torr. The percent absorption by both substrate (100%) and actinometer (1.5%) was determined using the Zeiss spectrophotometer and the reaction cell employed in the actinometry experiments. The absorbed light intensity was found to be 6.7×10^{-6} μeinsteins/s and thus 40 h runs were required to obtain sufficient products for analysis.

Results

The absorption spectrum of methyl ethyl sulfide vapor is shown in Fig. 1. The band centered at 2225 Å would correspond to the principal photochemically effective absorption with the filtered light source used here. The absorption may be ascribed, by analogy with the interpretation of the dimethyl sulfide spectrum (4), to excitation of a non-bonding electron from the S-atom to an antibonding orbital of a C—S bond.

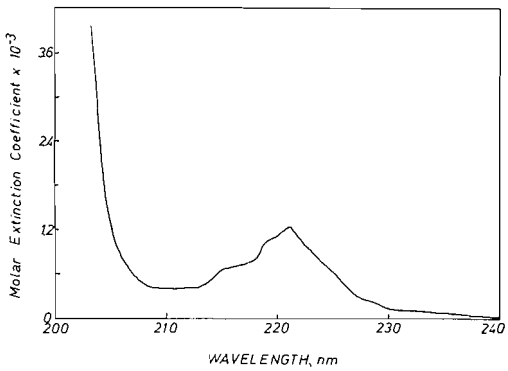

FIG. 1. The u.v. absorption spectrum of methyl ethyl sulfide vapor. The units of the molar extinction coefficient are l/mol cm.

It is apparent from Fig. 1 that although there is some suggestion of structure that might be observable at higher resolution, the spectrum does not exhibit the pronounced vibrational structure reported (5) and analyzed (4) for dimethyl sulfide and found in the present investigation when the CH_3SCH_3 spectrum was redetermined for comparison. The general similarity of the two spectra, however, would suggest that the same kind of bound state is involved in both compounds, but that the larger number of degrees of vibrational freedom in $CH_3SC_2H_5$ has the effect of increasing vibrational band overlap complexity to the extent that the fine structure could be discerned only under high resolution.

The room temperature photolysis of $CH_3SC_2H_5$ in the vapor phase yields the following detectable products, listed in order of decreasing rate of formation: C_2H_6, $CH_3SSC_2H_5$, $C_2H_5SSC_2H_5$, CH_4, CH_3SCH_3, $C_2H_5SC_2H_5$, C_3H_8, C_2H_4, CH_3SSCH_3, C_4H_{10}, C_2H_5SH, and CH_3SH. To test observed yields for a mass balance in carbon and sulfur, a rate for carbon containing products, R_C, may be evaluated on the basis of eq. 1, while a rate for sulfur con-

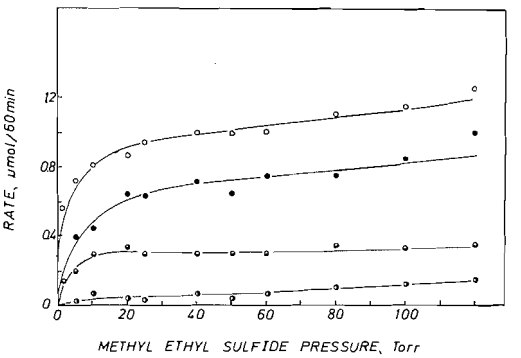

FIG. 2. Rate of formation of C_2H_6, ○; CH_4, ●; C_2H_4, ◒; and CH_3SH, ◑; in the photolysis of $CH_3SC_2H_5$ vapor at 25 °C for 60 min, as a function of substrate pressure.

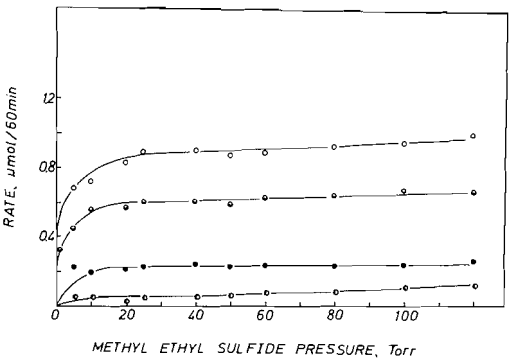

FIG. 3. Rate of formation of $CH_3SSC_2H_5$, ○; CH_3SCH_3, ◒; CH_3SSCH_3, ●; and C_2H_5SH, ◐; in the photolysis of $CH_3SC_2H_5$ vapor at 25 °C for 60 min as a function of substrate pressure.

$$[1]\quad R_C = 2R_{C_2H_6} + 3R_{CH_3SSC_2H_5} + 4R_{C_2H_5SSC_2H_5} + R_{CH_4} + 2R_{CH_3SCH_3} + 4R_{C_2H_5SC_2H_5} + 3R_{C_3H_8} + 2R_{C_2H_4} + 2R_{CH_3SSCH_3} + 4R_{C_4H_{10}} + 2R_{C_2H_5SH} + R_{CH_3SH}$$

taining products, R_S, may be calculated from eq. 2. For total rates defined in this way, the

$$[2]\quad R_S = 2R_{CH_3SSC_2H_5} + 2R_{C_2H_5SSC_2H_5} + R_{CH_3SCH_3} + R_{C_2H_5SC_2H_5} + 2R_{CH_3SSCH_3} + R_{C_2H_5SH} + R_{CH_3SH}$$

stoichiometry of $CH_3SC_2H_5$ decomposition requires that $R_C = 3\ R_S$. This test would, however, be insensitive to products in which the C:S ratio is 3:1, for example, the dimer of the substrate radical formed by H-atom abstraction, $C_2H_5SC_2H_4SC_2H_5$ and its isomers.

Figs. 2, 3, and 4 show the rates of formation of the 12 products from the photolysis at 25 °C as a function of methyl ethyl sulfide pressure. The most significant alteration in rates occurs in the 0–25 Torr range, and this may be ascribed to increasing absorption in the cell. The changes that occur in product rates at higher pressures are considerably less pronounced. Calculation of R_C and R_S at 25 Torr sulfide and at 100 Torr sulfide indicates that there is an acceptable mass balance among the analyzed products. Thus at $P(CH_3SC_2H_5) = 25$ Torr, $R_C = 13.9$ μmol/h while $3\ R_S = 14.3$ μmol/h; at $P(CH_3SC_2H_5) = 100$ Torr, $R_C = 16.5$ μmol/h, and $3\ R_S = 15.9$ μmol/h. Considering the experimental error in the determination of individual product yields,

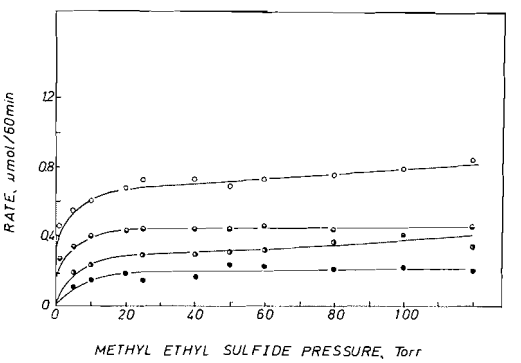

FIG. 4. Rate of formation of $C_2H_5SSC_2H_5$, ○; $C_2H_5SC_2H_5$, ◒; C_3H_8, ◑; and C_4H_{10}, ●; in the photolysis of $CH_3SC_2H_5$ vapor at 25 °C for 60 min as a function of substrate pressure.

inordinate significance should not be attached to the agreement in the carbon–sulfur balance, although the data do indicate that there are no additional major volatile products that were not detected and analyzed.

A series of experiments was carried out in which the yields of all products were determined as a function of exposure time. A representative graph giving the amount of $C_2H_5SSC_2H_5$, C_3H_8, C_4H_{10}, and C_2H_5SH formed at each exposure time studied is given in Fig. 5.[2] The yields of CH_3SCH_3, $C_2H_5SC_2H_5$, CH_3SSCH_3, and C_2H_4 were found to be linearly dependent on time. The products CH_4 and C_2H_6 appear to

[2]The yield curves for the other products have been placed in and may be obtained from the Depository of Unpublished Data, National Science Library, National Research Council of Canada, Ottawa, Canada K1A 0S2.

Can. J. Chem. Downloaded from www.nrcresearchpress.com by 210.87.254.6 on 09/05/12
For personal use only.

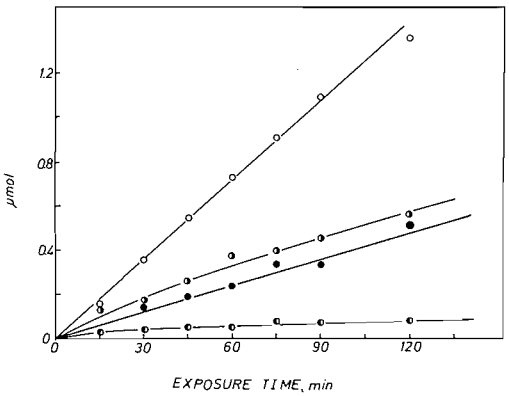

FIG. 5. Yields of $C_2H_5SSC_2H_5$, ○; C_3H_8, ◑; C_4H_{10}, ●; and C_2H_5SH, ◐; as a function of exposure time in the photolysis of 25 Torr methyl ethyl sulfide.

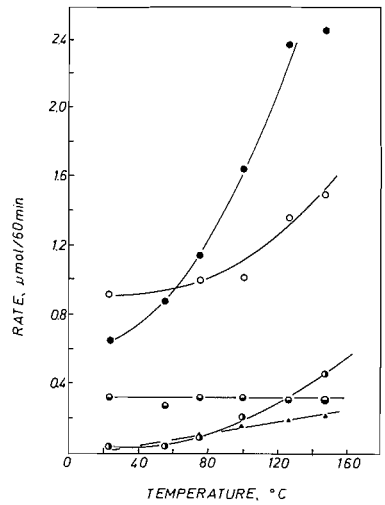

FIG. 6. Rate of formation of C_2H_6, ○; CH_4, ●; C_2H_4, ◒; CH_3SH, ◑; and $CH_3SCH(CH_3)_2$, ▲; as a function of temperature for the photolysis of 25 Torr methyl ethyl sulfide for 60 min.

be formed at a slightly increased rate after the first 30 min of reaction, while $CH_3SSC_2H_5$ shows a slight decrease in rate at longer exposure times. Ethanethiol exhibits the same behavior as CH_3SH, its rate increasing very slowly in the later stages of the reaction. This trend may result from H-atom abstraction reactions involving consumption of these products with labile hydrogen atoms by the various radicals in the system, which reactions would be expected to become more important at longer exposure times. The increase in C_3H_8 yield with time appears to drop off somewhat with time, to an extent comparable to the change in methane and ethane yields. The calculated percent decomposition in this run indicated that at 60 min, 2.03% of the substrate has reacted.

When the photolysis was studied as a function of temperature two additional products, $CH_3SCH(CH_3)_2$ and $CH_3SC_2H_4SCH_3$ were found in measurable quantities. Because of its relatively small yield it is not possible to determine definitely if methyl isopropyl sulfide is formed in the room temperature reaction. Although the yield of 2,5-dithiahexane is larger, its g.c. retention time is 2 h on the temperature programmed tricresyl phosphate column and accurate area determination is difficult. Therefore there was considerable scatter in the rate values obtained, but an extrapolation of an approximate rate *vs.* temperature plot for this product indicates that its rate at room temperature is finite.

The rates of product formation as a function of temperature were determined and a representative graph of these results is given in Fig. 6[3] for C_2H_6, CH_4, C_2H_4, CH_3SH, and $CH_3SCH(CH_3)_2$. The only other product that shows a significant increase in rate as the temperature is raised is C_2H_5SH. The stoichiometric calculations described by eqs. 1 and 2, modified to include the rate of $CH_3SCH(CH_3)_2$ formation, but not that of 2,5-dithiahexane, show that at 120 °C, $R_C = 12.9$ and $3R_S = 11.6$. The data for 2,5-dithiahexane were rather scattered; however, if a value of 0.32 μmol/60 min is taken for R(2,5-dithiahexane), the observed values being 0.21 at 99 °C and 0.39 at 147 °C, and eqs. 1 and 2 further modified to include that product, $R_C = 14.2$ and $3R_S = 13.5$.

The stoichiometric calculations show that the net effect of temperature is to alter product distribution without appreciably affecting the total rate of product formation. Thus at 25 °C and 25 Torr substrate the mean R_C, $3R_S$ value is 14.1 compared to the value of 13.8 at 25 Torr substrate and 120 °C. Again the uncertainty in these values must be considered, but the agreement obtained indicates the strong likelihood of a reasonable actual mass balance in the analyzed products.

[3]The rate *vs.* temperature plots for the other products have been placed in and may be obtained from the Depository of Unpublished Data, National Science Library, National Research Council of Canada, Ottawa, Canada K1A 0S2.

Can. J. Chem. Downloaded from www.nrcresearchpress.com by 210.87.254.6 on 09/05/12
For personal use only.

TABLE 1. Effect of carbon tetrafluoride on the photolysis of methyl ethyl sulfide*

$P(CF_4)$ (Torr)	Rate (μmol/60 min)									
	C_2H_6	C_3H_8	C_4H_{10}	CH_3SH	C_2H_5SH	$(CH_3)_2S$	$(C_2H_5)_2S$	$(CH_3S)_2$	$CH_3S_2C_2H_5$	$(C_2H_5S)_2$
0	0.930	0.285	0.203	0.035	0.063	0.583	0.442	0.228	0.848	0.705
250	†	0.285	0.160	0.032	0.063	0.583	0.415	0.210	0.727	0.630
500	0.156	0.200	0.110	0.041	0.063	0.620	0.420	0.260	0.795	0.609
700	0.205	0.210	0.184	0.043	0.063	0.620	0.440	0.225	0.730	0.668
900	0.095	0.230	0.180	0.046	0.090	0.640	0.446	0.255	0.718	0.595

*Exposure time, 60 min; temperature, 25 °C; methyl ethyl sulfide pressure, 25 Torr.
†Not determined.

TABLE 2. Effect of CO_2 on photolysis of methyl ethyl sulfide*

$P(CO_2)$ (Torr)	Rate (μmol/60 min)						
	CH_4	C_2H_5SH	$(CH_3)_2S$	$(C_2H_5)_2S$	$(CH_3S)_2$	$CH_3S_2C_2H_5$	$(C_2H_5S)_2$
0	0.635	0.063	0.585	0.442	0.228	0.848	0.705
100	0.350	0.065	0.575	0.465	0.215	0.795	0.655
200	0.350	0.068	0.642	0.502	0.230	0.924	0.767
300	0.299	0.072	0.685	0.462	0.237	0.810	0.675
400	0.299	0.065	0.640	0.455	0.210	0.793	0.670
500	0.299	0.063	0.600	0.493	0.225	0.800	0.698
600	0.150	0.042	0.572	0.470	0.184	0.797	0.665
700	0.299	0.080	0.655	0.465	0.208	0.792	0.662
900	0.249	0.080	0.652	0.532	0.208	0.770	0.660

*Exposure time, 60 min; temperature, 25 °C; methyl ethyl sulfide pressure, 25 Torr.

For the four products arising from primary radicals and whose rate increases with temperature the Arrhenius plots are linear[4] and apparent activation energies have been determined as follows: CH_4, 2.75; C_2H_6, 1.10; CH_3SH, 6.22 and C_2H_5SH, 3.55 kcal/mol.

To assess the possible participation in this system of excited species susceptible to collisional deactivation, two series of experiments were carried out with inert addends. Because of the wide range of vapor pressures among the products it was not possible to study the effect of a single addend on all products. In the first series for which the results are summarized in Table 1, the effect of CF_4 on the yields of all products except CH_4 and C_2H_4 was determined. Table 2 lists the results of a series of runs in which the sulfur containing products, and CH_4, were determined as a function of pressure of added CO_2. The data indicate that there is a pronounced dependence on addend pressure of CH_4 and C_2H_6 rates. The rates of formation of other products are affected as well but to a much smaller extent. Stoichiometric analysis of the data shows, however, that there is a relatively small decrease in the total detectable product yields. The experimental error in determining product yields is larger here than in other runs where the separation of a large amount of addend was not required. In applying eqs. 1 and 2, therefore, average values for product rates in the addend pressure range 500 to 900 Torr were employed. These data give $R_C = 11.6$ and 3 $R_S = 11.7$, compared to $R_C = 14.1$ for 25 Torr of substrate alone, and thus indicate that at the highest pressure examined the total amount of detectable decomposition might be decreased by up to about 20%.

Because of the evident production of both CH_3 and C_2H_5 radicals in this system, and the possibility of production of sulfur atoms in either the primary process or from the decomposition of excited sulfide molecules formed in radical recombination processes, the nature of products and, to a limited extent, rates of product forma-

[4]The value for $R(CH_4)$ at 147 °C would appear to be in error, since the other five values from Fig. 6 lie on a straight line in the Arrhenius plot.

Can. J. Chem. Downloaded from www.nrcresearchpress.com by 210.87.254.6 on 09/05/12
For personal use only.

TABLE 3. Effect of propylene on the photolysis of methyl ethyl sulfide*

$P(C_3H_6)$ (Torr)	Rate (μmol/60 min)						
	CH_3SH	C_2H_5SH	$(CH_3)_2S$	$(C_2H_5)_2S$	$(CH_3S)_2$	$CH_3SSC_2H_5$	$(C_2H_5S)_2$
0	0.035	0.063	0.583	0.442	0.228	0.848	0.705
100	0.035	0.060	0.428	0.367	0.185	0.495	0.535
200	0.065	0.080	0.416	0.395	0.184	0.498	0.538
300	0.065	0.060	0.387	0.440	0.175	0.508	0.543
400	0.065	0.098	0.369	0.448	0.163	0.445	0.460
500	0.062	0.106	0.350	0.400	0.163	0.418	0.425
584	0.070	0.107	0.355	0.382	0.185	0.320	0.346
700	0.087	0.167	0.351	0.385	0.193	0.442	0.357
900	0.093	0.120	0.303	0.374	0.203	0.428	0.324

*Exposure time, 60 min; temperature, 25 °C; methyl ethyl sulfide pressure, 25 Torr.

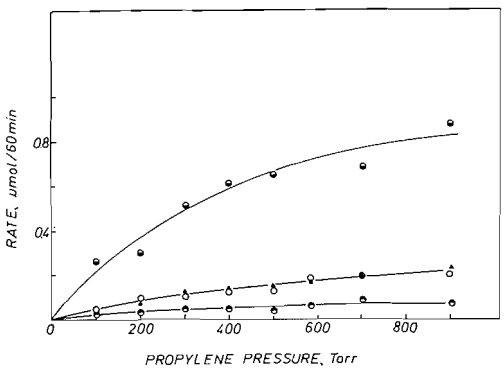

FIG. 7. Rate of formation of $CH_2{=}C_2H_3SC_2H_5$, ●; n-C_5H_{12}, ○; $CH_3S(CH_2)_2CH_3$, ▲; $(CH_3CH_2CH_2)_2S$, ◓, as a function of pressure of added propylene in the photolysis at 25 °C of 25 Torr methyl ethyl sulfide for 60 min.

tion were studied in the presence of olefins. If sulfur atoms are formed in either the triplet or singlet state, their presence would be manifested by the production of episulfides via the well established S—atom–olefin addition raction (6).

The most detailed investigations were done with propylene where the rates for all sulfur containing products were determined. The formation of propylene episulfide was not observed. Four additional analyzable products, however, were found, n-C_5H_{12}, $CH_3S(CH_2)_2CH_3$, $(CH_3CH_2CH_2)_2S$, and a product tentatively identified as $CH_2{=}CH{-}CH_2SC_2H_5$. The latter product exhibited a mass spectrum that is also consistent with methyl ethyl ethylene episulfide. The identification of this product as the unsaturated sulfide is based on the relatively large yield of this material in the presence of propylene combined with the fact that a rather complex series of reactions, involving initially propylene episulfide formation (which should therefore have been detected), would be required to explain the formation of

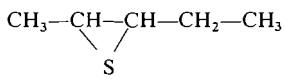

The rates of formation of these new products are shown in Fig. 7, as a function of olefin pressure. Table 3 lists the rates of the other sulfur containing products.

To investigate the effect of olefin on the hydrocarbon products of the reaction, the rates of CH_4, C_2H_4, C_2H_6, and C_3H_8 formation were determined in the presence of 2-pentene. These results are listed in Table 4. No search was made for additional products with this olefin.

Finally, utilizing filtered light at 2288 ± 30 Å the quantum yields of formation of the products whose yields are sufficiently large for accurate

TABLE 4. Effect of added 2-pentene on the photolysis of methyl ethyl sulfide*

$P(2\text{-}C_5H_{10})$ (Torr)	Rate (μmol/60 min)			
	CH_4	C_2H_4	C_2H_6	C_3H_8
0	0.635	0.325	0.930	0.285
10	0.872	0.231	1.038	0.204
25	0.997	0.168	1.139	0.151
50	1.246	0.151	1.170	0.132
100	1.370	0.107	1.168	0.118
200	1.395	0.090	1.173	0.041
300	1.296	0.055	1.168	0.047
427	1.395	0.059	1.075	0.021

*Exposure time, 60 min; temperature, 25 °C; methyl ethyl sulfide pressure, 25 Torr.

Can. J. Chem. Downloaded from www.nrcresearchpress.com by 210.87.254.6 on 09/05/12
For personal use only.

TABLE 5. Quantum yields of products of photolysis of methyl ethyl sulfide*

Pressure $CH_3SC_2H_5$ (Torr)	Quantum yields × 10^3								
	C_2H_4	C_2H_6	C_3H_8	C_4H_{10}	$(CH_3)_2S$	$(C_2H_5)_2S$	$(CH_3S)_2$	$CH_3SSC_2H_5$	$(C_2H_5S)_2$
50	0.54	3.98	0.39	0.38	0.89	0.83	1.11	1.75	1.76
120	0.78	5.91	0.47	0.24	0.90	†	1.10	1.68	1.86

*Exposure time, 40 h; temperature, 165 °C; $I_a = 6.7 \times 10^{-6}$ μeinsteins/s.
†Not determined.

analysis in the small percent conversion runs involved in the low intensity actinometry runs, were determined at two substrate pressures. The results are listed in Table 5. The observed quantum yields follow the same general trend as the rates determined with the full lamp spectrum at appreciably higher effective intensity. Of the products determined, only ethane shows a significant increase in quantum yield as the substrate pressure is increased from 50 to 120 Torr.

Discussion

The low quantum yields observed in the decomposition, together with the observation of a mass balance among the products of the reaction and the spectroscopic indications of a bound state attained on absorption suggest that energy dissipation in the methyl ethyl sulfide molecule occurs primarily by routes other than photochemical decomposition. Elucidation of these processes will require further investigation of the photophysical aspects of the system.

The nature of the observed products is evidence for the occurrence of two primary processes (eqs. 3*a* and *b*) involving C—S bond cleavage. Assuming that no products involving RS radicals

[3*a*] $CH_3SC_2H_5 + h\nu \rightarrow CH_3 + C_2H_5S$

[3*b*] $CH_3SC_2H_5 + h\nu \rightarrow CH_3S + C_2H_5$

other than those detected in this study are formed, the observed rates for sulfur containing products can be utilized to estimate the relative importance of the two primary steps via eq. 4. The equation is set up on the assumption that the thiols, whose rates represent the maximum contribution from thiyl radical disproportionation, arise solely from H-atom abstraction. These rates are relatively minute, however, and even if both thiols were formed solely by disproportionation, the resulting error in calculated R_{3a}/R_{3b} values would be less than 1%. The two terms in eq. 4 that cannot be determined experimentally are the rates of the substrate reforming reactions, eqs. 5 and 6. In the absence of the

[5] $CH_3 + C_2H_5S \rightarrow CH_3SC_2H_5 \qquad R_{[5]} = R'_{CH_3SC_2H_5}$

[6] $CH_3S + C_2H_5 \rightarrow CH_3SC_2H_5 \qquad R_{[6]} = R''_{CH_3SC_2H_5}$

required data, it is assumed that R_5 and R_6 are the same, and are equal to the average of the rates of the combination of CH_3 and CH_3S radicals, $R_{CH_3SCH_3}$, and the combination of C_2H_5 and C_2H_5S radicals, $R_{C_2H_5SC_2H_5}$.

With these assumptions and calculating from the data presented in Figs. 2, 3, and 4 and the rate data determined at 120 °C the values obtained for R_{3a}/R_{3b} are 1.31 and 1.33 at substrate pressures of 25 and 100 Torr at 25 °C, and 1.10 for 25 Torr substrate at 120 °C. Thus at room temperature reaction 3*a* accounts for 57% of the primary decomposition, while 43% proceeds via 3*b*. Presumably the more equal rates for the two primary steps observed at 120 °C reflect a decrease in specificity associated with increased energy input to the system.

The four radicals produced in the primary processes all apparently undergo, in addition to other processes to be considered below, abstraction reactions involving the substrate and it is useful to consider these reactions separately. Representing CH_3, CH_3S, C_2H_5, and C_2H_5S as X, the three possible abstraction processes can be written as eqs. 7*a–c*. The observation that as

[7*a*] $X + CH_3SC_2H_5 \rightarrow \dot{C}H_2SC_2H_5 + XH$

[7*b*] $X + CH_3SC_2H_5 \rightarrow CH_3S\dot{C}HCH_3 + XH$

[7*c*] $X + CH_3SC_2H_5 \rightarrow CH_3SCH_2\dot{C}H_2 + XH$

[4] $$\frac{R_{3a}}{R_{3b}} = \frac{R_{C_2H_5SH} + R_{C_2H_5SC_2H_5} + 2R_{(C_2H_5S)_2} + R_{CH_3SSC_2H_5} + R'_{CH_3SC_2H_5}}{R_{CH_3SH} + R_{CH_3SCH_3} + 2R_{(CH_3S)_2} + R_{CH_3SSC_2H_5} + R''_{CH_3SC_2H_5}}$$

Can. J. Chem. Downloaded from www.nrcresearchpress.com by 210.87.254.6 on 09/05/12
For personal use only.

Can. J. Chem. Downloaded from www.nrcresearchpress.com by 210.87.254.6 on 09/05/12
For personal use only.

$$[8]\qquad \frac{R_{3a}}{R_{3b}} = \frac{R_{CH_4} + 2R^{c}_{C_2H_6} + R_{C_3H_8} + R_{CH_3SCH_3} + R'_{CH_3SC_2H_5}}{R^{ad}_{C_2H_6} + R_{C_2H_4} + 2R_{C_4H_{10}} + R_{C_3H_8} + R_{C_2H_5SC_2H_5} + R''_{CH_3SC_2H_5}}$$

reaction temperature is increased the product that appears in measureable quantities first is $CH_3SCH(CH_3)_2$ is evidence that reaction 7*b* may be the most important. This is consistent with the expectation that on energetic grounds the methylene H-atom would be most susceptible to abstractive attack.

Methyl isopropyl sulfide, however, is the only observed product formed by substrate radicals. Comparing its yield to the total yield of XH type products indicates that only a small fraction of CH_3SCHCH_3 and its isomers produced in reaction 7 are accounted for. As indicated in the discussion of the stoichiometric calculations, the recombination products would not affect the mass balance, nor would they likely be detected in the present system. In addition, there may be yields, below the detection limit, of the recombination or disproportionation of substrate radicals with other radicals in the system.

Some information about the relative contributions of the various processes, including reactions 7*a–c*, giving rise to the important products methane and ethane can be obtained from the stoichiometry and the values of R_{3a}/R_{3b} calculated from the yields of sulfur containing products. The primary process rate ratio may also be calculated from the rates for products consuming CH_3 and C_2H_5 radicals using eq. 8, where $R'_{CH_3SC_2H_5}$ and $R''_{CH_3SC_2H_5}$ are defined and estimated as outlined for eq. 4. The indicated rates of formation of ethane are related by eq. 9, which represents the observed rate of

$$[9]\qquad R^{t}_{C_2H_6} = R^{c}_{C_2H_6} + R^{ad}_{C_2H_6}$$

ethane formation, $R^{t}_{C_2H_6}$, as the sum of the rate of methyl recombination, $R^{c}_{C_2H_6}$, and the combined rates of ethane formation in reactions 7*a–c* and the disproportionation of C_2H_5 radicals with themselves and other radicals in the system, $R^{ad}_{C_2H_6}$. Again using the appropriate rate values along with the corresponding R_{3a}/R_{3b} values calculated above, eqs. 8 and 9 can be solved for $R^{ad}_{C_2H_6}$. The values calculated are 0.46 and 0.55 μmol/h for 25 and 100 Torr substrate at 25 °C. If the rate of disproportionation reactions involving ethyl radicals is independent of substrate pressure, the increase in $R^{ad}_{C_2H_6}$ would be consistent with the expected higher rate of H-atom abstraction as the concentration of substrate increases. From the data at 120 °C, the calculation indicates that $R^{c}_{C_2H_6}$ is zero within experimental error. The observed ethane yield at the higher temperature would thus apparently arise virtually in total from abstraction and disproportionation, consistent with the expected increase in abstraction with increasing temperature. The effect is of sufficient magnitude to be reflected in a decrease in the rate of C_4H_{10} as an increasing proportion of C_2H_5 radicals are involved in reactions 7*a–c*. The decline of $R^{c}_{C_2H_6}$ to zero within experimental error at 120 °C indicates that H-atom abstraction by CH_3 radicals is the most important source of methane at this temperature.

Production of C_3H_8 involves presumably CH_3 and C_2H_5 radicals and its decrease in rate from 0.30 μmol/h at 25 °C to 0.05 μmol/h at 120 °C is further evidence for an increase, in the case of both radicals, of the rate of abstractive processes compared to radical–radical reactions.

The observed deactivating effect of inert addends and the apparent activation energies determined from the temperature studies indicate the presence of excited species in this system. The average energy of incident quanta in the photolysis is *ca.* 125 kcal/mol, about 50 kcal/mol in excess of C—S bond energies in the methyl sulfide molecule. With the possible exception of E_a for CH_3SH formation, the apparent activation energies for XH type products formed in reactions 7*a–c* are appreciably less than would be expected for thermalized species. However, energy partitioning is evidently not on a simple mass basis since activation energies for the formation of C_2H_6 and C_2H_5SH are less than those for CH_4 and CH_3SH.

The approximately 20% decrease in total observable decomposition found at the highest addend pressures studied may be due to a limited contribution from a process in which the electronic excited state of the substrate attained in the absorption process is deactivated.

The formation of the observed reaction products can be explained on the basis of reactions 7*a–c* and radical–radical reactions, eqs. 10–20.

Can. J. Chem. Downloaded from www.nrcresearchpress.com by 210.87.254.6 on 09/05/12
For personal use only.

[10] $CH_3 + CH_3 \rightarrow C_2H_6$

[11] $CH_3 + C_2H_5 \rightarrow C_3H_8$

[12] $CH_3 + C_2H_5 \rightarrow CH_4 + C_2H_4$

[13] $CH_3 + CH_3S \rightarrow CH_3SCH_3$

[14] $C_2H_5 + C_2H_5 \rightarrow C_4H_{10}$

[15] $C_2H_5 + C_2H_5 \rightarrow C_2H_6 + C_2H_4$

[16] $C_2H_5 + C_2H_5S \rightarrow C_2H_5SC_2H_5$

[17] $CH_3S + CH_3S \rightarrow CH_3SSCH_3$

[18] $CH_3S + C_2H_5S \rightarrow CH_3SSC_2H_5$

[19] $C_2H_5S + C_2H_5S \rightarrow C_2H_5SSC_2H_5$

[20] $CH_3 + CH_3SCHCH_3 \rightarrow CH_3SCH(CH_3)_2$

On the basis that a satisfactory mass balance is obtained among the reaction products, the disproportionation processes that would be alternatives to reactions 13 and 16, leading to the thioaldehyde and hydrocarbon, and to reactions 17, 18, and 19, leading to thioaldehyde and thiol, have not been included as significant reactions in the system. Although the small contribution that might be made by the former two reactions cannot be determined from the data available, the relative yields of RSH and RSSR products give an upper limit for the contribution from thiyl radical disproportionation. Thus comparing the total thiol yields with those of the three disulfides at 25 °C gives maximum R_d/R_c ratios of 0.067 at 25 Torr methyl ethyl sulfide and 0.12 at 100 Torr substrate pressure. In view of the evidence in favor of H-atom abstraction as an important source of RSH at room temperature, the actual extent of radical disproportionation is likely appreciably less than suggested by the calculated R_d/R_c ratios. This is in accord with evidence obtained in the photolysis of dimethyl sulfide (2) and methyl disulfide (3) for a minor role for thiyl radical disproportionation. At 120 °C, the thiol:disulfide rate ratio is 0.55, but this reflects the increased importance of RS abstraction since the disproportionation process will be temperature insensitive.

The additional products found in the presence of propylene may be explained in part on the basis of reactions 21–26, where X is any of the primary radicals in the system and RH is any H-atom source, including the substrate. The mechanism of dipropyl sulfide formation is not immediately apparent.

[21] $C_3H_6 + C_2H_5 \rightarrow C_5H_{11}$

[22] $C_5H_{11} + RH \rightarrow n\text{-}C_5H_{12}$

[23] $C_3H_6 + X \rightarrow C_3H_5 + XH$

[24] $C_3H_5 + C_2H_5S \rightarrow CH_2{=}CHCH_2SC_2H_5$

[25] $C_3H_6 + CH_3S \rightarrow CH_3SC_3H_6$

[26] $CH_3SC_3H_6 + RH \rightarrow CH_3S(CH)_2CH_3 + R$

Fig. 7 shows that the rates for the additional products are proportional to olefin pressure and that within experimental error, the rates extrapolate to zero in the absence of olefin, indicating that these products are not formed in the decomposition of the pure substrate. The data in Tables 3 and 4 illustrate that products for which formation via H-atom abstraction is important, CH_4, C_2H_6, CH_3SH, and C_2H_5SH, exhibit increases in rate as the olefin concentration, particularly in the case of 2-pentene, is increased, while other products that result from radical–radical reactions show diminished rates when the olefin is present.

The details of the reaction mechanism in the presence of olefin would require further study to elucidate the source of dipropyl sulfide and to rationalize the appearance of only a small number of the products that could possibly result from the interaction of the primary and secondary radicals with the addend. Stoichiometric calculations indicate that there are almost certainly other, higher molecular weight products that were not detected. However, the limited results with added olefin obtained here are of considerable value in providing definitive evidence against the formation of sulfur atoms in the decomposition of pure substrate.

The authors are grateful for the financial support of the research by the National Research Council of Canada. We are also indebted to Dr. P. J. Smith of this Department for assistance in the mass spectrometric analyses.

1. B. MILLIGAN, D. E. RIVETT, and W. E. SAVIGE. Aust. J. Chem. **16**, 1020 (1960).
2. P. M. RAO and A. R. KNIGHT. Can. J. Chem. **50**, 844 (1972).
3. P. M. RAO, J. A. COPECK, and A. R. KNIGHT. Can. J. Chem. **45**, 1369 (1967).
4. S. D. THOMPSON, D. G. CARROLL, F. WATSON, M. O'CONNELL, and S. P. MCGLYNN. J. Chem. Phys. **45**, 1367 (1966).
5. J. G. CALVERT and J. N. PITTS, JR. Photochemistry. Wiley, 1966. p. 489.
6. H. E. GUNNING and O. P. STRAUSZ. Advances in photochemistry. Vol. 4, Interscience Publishers, 1966. p. 143.

Cavitation-induced Reactions in Pure Substituted Benzenes[1]

G. K. Diedrich, P. Kruus, and L. M. Rachlis
Department of Chemistry, Carleton University, Ottawa, Canada K1S 5B6

Received January 5, 1972

The formation of polymers has been observed on exposure of pure substituted benzenes to ultrasound intense enough to cause cavitation. The products have some of the characteristics of the char obtained from low temperature pyrolysis of hydrocarbons. They are difficult to dissolve, melt above 300 °C, and give a large broad e.p.r. signal. A crude correlation between bond dissociation energy and the reaction rate suggests that the initiation reaction is a thermal decomposition in a cavitation bubble. The phenomenon is compared to radiolysis and thermal reactions.

La formation de polymères a été observée lorsque des composés purs, du type benzénique substitués, sont exposés à des ultrasons suffisamment intenses pour provoquer des cavités. Les produits obtenus ont certaines des caractéristiques des produits de carbonisation provenant de la pyrolyse à basse température d'hydrocarbures. Ils sont difficiles à solubiliser, fondent au-dessus de 300 °C, et donnent en r.p.e. un signal très large. Une corrélation grossière entre l'énergie de dissociation de liaison et la vitesse de réaction, suggère que la réaction d'initiation est une décomposition thermique dans une cafité en forme de bulle. Le phénomène est comparé aux réactions thermiques et de radiolyse.

Canadian Journal of Chemistry, **50**, 1743 (1972)

Introduction

There have been numerous studies of chemical reactions in liquids exposed to ultrasonic waves of high enough intensity to cause cavitation. El'piner (1) gives a comprehensive review of such work up to 1963. More recent reviews are given by LeBras (2) and Margulis (3). Nearly all the systems studied have been aqueous solutions. Reports of studies of cavitation-induced chemical reactions in pure organic liquids are few (4).

The mechanisms by which cavitation in a liquid could give rise to chemical reactions are reviewed by Flynn (5). When a liquid is subjected to an intense sound field, then at the rarefaction sites, holes or cavities can be formed, usually about some cavitation nucleus. The cavitation bubbles may then fill with the vapor of the liquid or dissolved gases.

The results of experiments examining variation of the chemical reaction rate with the thermal conductivity of gases saturating the liquid suggest that the chemical reactions are of a thermal origin (6, 7). On the collapse of cavitation bubbles, a high local temperature is developed, leading to chemical reactions and luminescence. An increase in the thermal conductivity in the bubble due to the presence of gas will lower the temperature which can be achieved (up to thousands of degrees (6)), and hence the rate of reaction. Other workers have only recently concluded, however, that electrical effects within the cavitation bubbles are of primary importance (8, 9).

Reactions can occur in places other than in the cavitation bubbles. Some reactions may occur due to the shock waves produced on collapse of the bubble, and products of any reaction in the cavitation bubble can cause further reactions in the bulk of the liquid. It has also been suggested that at higher frequencies, mechanisms other than cavitation may be partially responsible for chemical reactions (10).

Experimental

The following is a description of the experimental equipment and procedure used generally. Differences from this general experimental procedure will be described under the appropriate section in presentation of the results.

A Fisher–Blackstone Ultrasonic Generator (20 kc.p.s.) Model SS-2, together with a Probe, Model BP-2, were used in the cavitation experiments. The probe had a head on it which, in the case of most runs, was inserted into a glass cell as shown in Fig. 1. The whole assembly was set up in a darkened fume hood.

In most cases the runs were made with the oscillator power set on 70 (on a scale of 100) after a warm-up time of 20 min with tap water circulating through the cooling jacket. Argon gas which had passed through a P_2O_5 drying column was slowly bubbled through the cell in order to promote cavitation by providing nuclei for the formation of cavitation bubbles, and also to keep a positive pressure in the cell.

The rate of reaction was followed by withdrawing samples from the liquid at regular intervals with a syringe. Absorption

[1]Taken in part from the thesis submitted by L. M. Rachlis in partial fulfilment of the B.Sc. (Honors) degree.

Can. J. Chem. Downloaded from www.nrcresearchpress.com by 210.87.254.40 on 09/05/12
For personal use only.

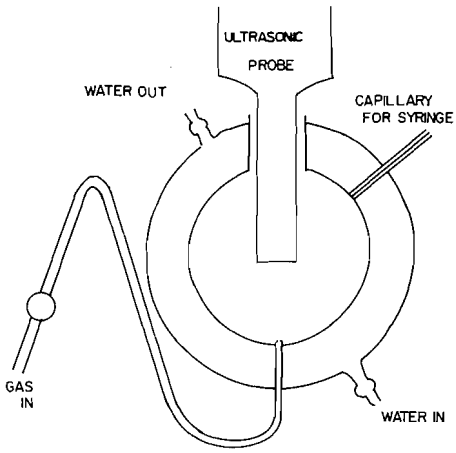

FIG. 1. Diagram of the cell.

was measured on a Perkin–Elmer 202 u.v.–visible spectrophotometer with the original liquid as both the diluent and the reference. Plots of the absorption of the wavelength of maximum absorption, corrected assuming a linear dilution relation, *vs.* the time usually showed a reasonable linear relationship. An example of such a plot is shown in Fig. 2. The scatter of the points from the straight-line relationship is typical of the runs made. Although up to 15 samples were taken for some systems to check the linearity, the rate of reaction in most cases was monitored by taking absorption measurements on only five samples. There seemed to be no change in the shape of the absorption bands as the absorption intensity increased. Plots of the area under the absorption curves *vs.* the time were also linear.

The liquids used were in most cases Fisher reagent grade which had been in storage over grade 4A molecular sieves.

Results

(a) Power Calibration

In order to estimate the acoustic power used in the experiments, measurements were made of the rate of formation of chlorine through cavitation in a saturated aqueous solution of carbon tetrachloride (11). The concentration of Cl_2 in water was determined spectrophotometrically using *o*-tolidine reagent (12).

When, for the above system, a value of 0.095 is used for the sonochemical G (11) (molecules produced per 100 eV energy absorbed), then the power level in the cavitation experiments was estimated to be about 6 acoustic W. This corresponds to an intensity level at the probe of the order of 5 W cm^{-2}.

Power levels of the same magnitude were also obtained using a far more simple technique. The temperature of a known amount of water in a dewar flask was followed for 10 min while cavitation was going on. A plot of temperature versus time was linear in all cases. The power delivered by the probe could then easily be calculated. As the temperature *vs.* time curve became sharply horizontal when the cavitation was stopped, then conduction of heat from the probe could be neglected.

Such power measurements were carried out regularly after every important run. This was necessary as the effectiveness of the probe decreased with use. After some use, the probe also did not always deliver constant power during the long periods (7 h) used for some runs. This, together with errors in dilution of the small (< 1 ml) samples withdrawn and in reading the spectrophotometer charts would seem to be the main causes of the scatter in the plots illustrated in Fig. 2.

The effect of the level of acoustic power on the rate of reaction was examined by making a series of runs with different power settings. The rate of darkening of nitrobenzene (dry, with dried argon bubbling through, at 23 ± 3 °C) was measured as well as the power delivered at the settings. The results of one series of runs indicate that there is a variation of less than 10% in the rate of reaction with power in the 5 to 8 W region, but that there is a decrease at lower power levels. Comparison with the other runs suggests, however, that unless runs are made in the same series, there may be an error of up to 20% introduced in making relative comparisons of rates. This error seemed to be due primarily to wearing out of the probe. All the runs discussed in the following sections were taken at power levels of 4.7 to 7 W with no corrections made for the differences in power levels.

(b) Effect of Water

Because it has been reported (1) that the presence of water is necessary to obtain cavitation-induced chemical reactions in most liquids, the effect of water on the rate of cavitation was examined.

Dry nitrobenzene was prepared by refluxing Fisher Reagent Grade material over barium oxide and then distilling it. The cell was filled in a dry box, and enclosed throughout the run in a plastic bag in which a considerable positive pressure of dry argon was kept. Water-saturated nitrobenzene was prepared by rapidly stirring

Can. J. Chem. Downloaded from www.nrcresearchpress.com by 210.87.254.40 on 09/05/12
For personal use only.

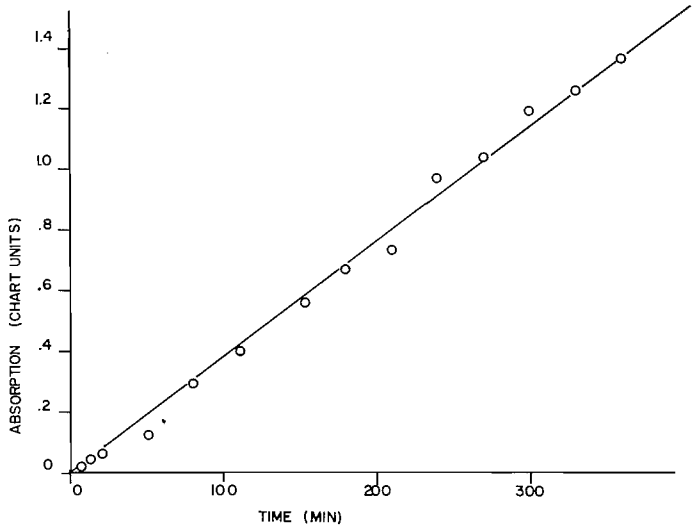

FIG. 2. Absorption at 430 mμ *vs.* time for nitrobenzene undergoing cavitation.

a water–nitrobenzene mixture overnight and then allowing a complete phase separation to take place. A solution of nitrobenzene half-saturated with water was prepared by mixing equal proportions of the dry and saturated.

The rate of darkening of dry nitrobenzene was measured to be 8.8 units, of half-saturated as 7.9 units, and of water-saturated as 6.5 units. Thus water is not essential to have a darkening occur. As the three runs were made consecutively, the decrease in the darkening with increasing water content is likely to be real and not just due to changes in experimental conditions.

(c) Effect of Temperature

A series of runs was made to test the sensitivity of the rate of reaction to the bulk temperature of the liquid under cavitation. Differences in temperature were obtained by adjusting the temperature of the water flowing through the cooling jacket of the cell.

Using nitrobenzene under the usual conditions, the following rates of darkening were obtained: at 12°, 8.8; at 27°, 6.2; at 43°, 5.1; at 75°, 2.0. Such a decrease in the rate of reaction with an increase in temperature occurs in other cavitation-induced reactions (12).

The temperature in the liquid undergoing cavitation in other series of runs was constant to within $\pm 3°$. However, depending upon the season, the average temperature in a series varied from 15 to 25 °C. As comparisons were made inside series of runs, and as the rate was relatively insensitive to the temperature (*cf.* 13), no improvements were made in the thermostatting.

(d) Effect of Solid Impurities

In some experiments, traces of metal powder were found in the solution arising from erosion of the probe due to cavitation. There may also have been some erosion of the reaction vessel. As solid impurities can act as nuclei for the formation of cavitation bubbles (14) and hence alter the rate of reaction, the effect of iron powder on the rate of reaction was investigated.

Two runs, one using nitrobenzene and the other nitrobenzene with iron powder added, were made under the usual conditions. The rate of darkening in the two runs differed only by 6%. This difference is within the experimental error. Thus the presence of iron powder has little if any effect on the rate of reaction.

(e) Effect of Bubbling Gas

Gas was bubbled through the cell in order to keep a positive pressure above the solution and thus to prevent entry of water vapor into the solution. It was also used in preliminary experiments in attempts to flush more volatile reaction products into a trap. A significant increase was noted in the reaction rate, however, when bubbling gas was present.

Can. J. Chem. Downloaded from www.nrcresearchpress.com by 210.87.254.40 on 09/05/12
For personal use only.

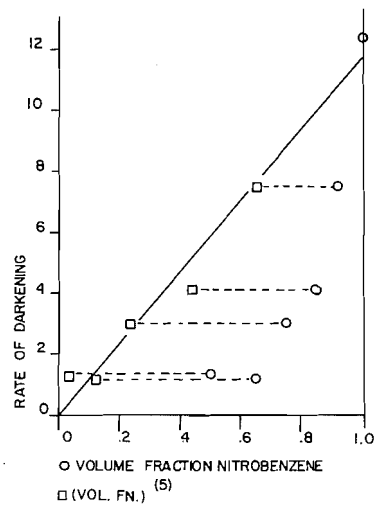

FIG. 3. Rate of darkening *vs.* volume fraction of nitrobenzene in benzene: ○ plotted *vs.* volume fraction to the first power; □ plotted *vs.* volume fraction to the fifth power.

With no bubbling gas present, the rate was measured as 2.6, as compared to 4.8 in the presence of dried nitrogen, 6.7 in the presence of dry air, and 9.4 in the presence of dry argon. Besides providing cavitation nuclei, the presence of gas also affects the cavitation phenomenon by changing the ionization potential and the thermal conductivity (6). The observations that the rate is greater with argon than with air than with nitrogen is in agreement with previous work (6, 7).

(f) Effect of Concentration

Figure 3 shows the effect of concentration on the reaction rate. The conditions for this series of runs were dry nitrobenzene, diluted by benzene, with argon bubbled through. The rate of darkening of benzene is negligible as compared to that of nitrobenzene (see section g).

The rate of darkening decreases rapidly as the nitrobenzene is diluted with benzene. In fact, the rate seems to vary as approximately the fifth power of the volume fraction, *i.e.* the concentration, of nitrobenzene. The absorption band shapes showed no change with the concentration of nitrobenzene.

(g) Effects of Substituents

A series of runs was made to observe the relative rates of reaction of different substituted benzenes. The results are shown in Table 1. Each run was for a 7 h period in order to make it possible to recover some of the product. The length of the runs and the difficulties in separating the product quantitatively introduce some measure of uncertainty into the results. The acetophenone was therefore run before, in the middle, and at the end of the series to test the reproducibility; this was found to be $\pm 10\%$.

The liquids used were all Fisher Reagent Grade except for benzene (Matheson, Coleman, and Bell Spectroquality Reagent), nitrobenzene (Baker and Adamson), and iodobenzene (Eastman Organic Chemicals). All were used as the commercially available product stored under 4A molecular sieves except iodobenzene, which was used directly, and aniline, which was distilled just prior to use.

The solutions resulting from the cavitation were concentrated to a small volume through vacuum distillation, transferred to a weighed clay dish, and dried at room temperature. All distillates had refractive indices within 0.0007 of the value of the initial reagent. The weight of the iodobenzene product is not very reliable, as some molecular iodine distilled over during the separation procedures. When the residue was heated, then crystals of iodine appeared on the cover. The presence of molecular iodine was not noted in the pure iodobenzene used, even when its temperature was raised above 85 °C for more than 5 min.

The plots of absorption of λ_{max}, the wavelength of maximum absorption, *vs.* time were generally all linear. However, the bromobenzene and the iodobenzene showed a more than linear increase in the intensity. The rates of darkening and λ_{max} are also given in Table 1. It was not possible to trap any volatile products with the apparatus and experimental methods used.

(h) Electron Paramagnetic Resonance Measurements

Some of the cavitation-induced reactions were run in a specially designed reaction vessel which fitted into the cavity of an e.p.r. machine (Varian V4502). Even though noise due to the presence of the ultrasonic generator made detection difficult, the growth of a broad signal was observed after some minutes. The solid product also gave a broad e.p.r. signal.

The e.p.r. signals from samples of the solid

Can. J. Chem. Downloaded from www.nrcresearchpress.com by 210.87.254.40 on 09/05/12
For personal use only.

TABLE 1. Rates of cavitation-induced reaction for substituted benzenes

Liquid	λ_{max} (mμ)	Absorption at λ_{max} after 2 h	Rate of reaction* (mol $h^{-1} \times 10^4$)	Dissociation energy (kcal mol^{-1})
Benzene	280	0.04	0.17	102.0
Toluene	285	0.12	0.15	78.0‖
Chlorobenzene	290	3.0	1.0‡	85.6
Bromobenzene	295	5.3	2.0	71.0
Iodobenzene	370	19.0	2.8§	57.0
Aniline	340†	11.0	3.8	75.0¶
Nitrobenzene	430	5.2	5.6	57.3¶
Acetophenone	390	1.0	1.8	75.0¶
Anisole	300	4.6	1.1	77.0¶

*Assuming an energy input of 5 W, the G value for the reactions is 5.4×10^{-3} times the values in the column.
†A weaker absorption maximum was noted at 460 mμ.
‡This is an estimate, as some of the product was lost on weighing. The results of two preliminary sets of runs are in good agreement with this figure.
§This figure may be somewhat low, as some of the iodine lost during distillation may not have been recovered.
‖This is for the formation of a benzyl radical. The dissociation energy for formation of a phenyl radical is 88.6 kcal mol^{-1}.
¶Figures for the CH_3—R bond (ref. 15). The extra resonance energy (~6 kcal mol^{-1}) in C_6H_5—R could make these bonds up to that much stronger. The corresponding differences for R = H, CH_3, Cl, Br, and I are 0, 4, 5, 4, and 4 kcal mol^{-1}, respectively.

products of benzene, iodobenzene, and nitrobenzene were examined. The mean G value was 2.0028 ± 0.0008 for the three samples, and the peak to peak width 3.3 ± 0.8 G. It was found impossible to find a solvent for the products, but a suspension could be formed which gave a weak decaying e.p.r. signal with the same spectrum as the solid.

(i) Other Properties of Products

The product of nitrobenzene cavitation was investigated by several methods. It was not found to be soluble in any solvent so that several physico-chemical measurements, *e.g.* n.m.r., were not possible.

No change is observed in the product when heated to above 350 °C in the absence of oxygen. A sample used for mass spectrometry at 250 °C also was unchanged. The only peaks showing in the mass spectrum were a strong nitrobenzene peak and fragments from nitrobenzene. These could be accounted for by residual nitrobenzene present in the sample after drying.

When heated in a Pyrex test tube over a Bunsen flame, some dense yellowish-white vapor is given off. Some dark-brown coloring appears on the sides of the test tube, but even after minutes at red heat, the greater part of the sample remains as a dark solid.

An elemental analysis of the sample gives 66.30% C, 3.88% H, 6.66% N, with 3% of the original material remaining as ash. Assuming the remaining 23.16% as O gives a formula of $C_6H_{4.1}N_{0.51}O_{1.56}$ for the product. It is thus deficient in H, N, and O relative to C. Volatile products containing primarily these three elements must thus have been produced. There is some possibility of material coming from erosion of the reaction vessel, the probe, and even from diffusion in against the positive pressure of argon.

(j) Cavitation in Other Liquids

A series of other liquids was exposed to cavitation under the same conditions as the substituted benzenes. No reaction was observed in the case of acetone, which decomposes on photolysis to give, among other things, biacetyl. There seemed also to be no acceleration of the rate of decomposition of di-*t*-butyl peroxide, which undergoes slow thermal decomposition even at room temperature. After hours of cavitation, its n.m.r. and v.p.c. (10% FFAD at 70 °C) was the same as that of a non-cavitated sample. The thermal decomposition of trimethylene oxide was also not accelerated by cavitation in a cyclohexane solution. No changes (v.p.c.) were observed in a sample of cyclohexane after 7 h exposure to cavitation.

A reaction similar to that for the aromatics was noted for acrylonitrile, however. The rate of formation of product was more than linear, varying as nearly the square of the time under cavitation. The acrylonitrile cavitation product

Can. J. Chem. Downloaded from www.nrcresearchpress.com by 210.87.254.40 on 09/05/12
For personal use only.

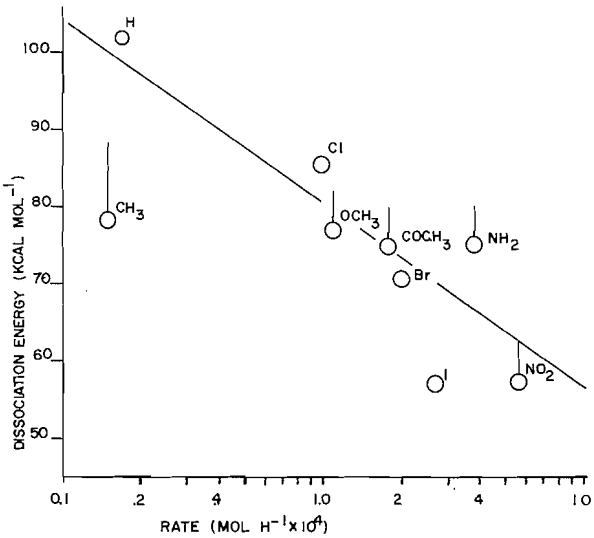

FIG. 4. Dissociation energy (from Table 1) *vs.* the logarithm of the rate of reaction (Table 1).

and a sample of polyacrylonitrile absorb at the same wavelength (275 mμ) in the u.v. While polyacrylonitrile is white, however, the cavitation product was yellowish-brown. The weight of product formed after 7 h was 0.03 g as compared to 0.08 g for anisole, for example.

Discussion

The effect of gas and temperature on the reaction indicate that the reactions must be due to cavitation. The reactions are also not critically dependent upon the presence of traces of water or solid impurities.

In the cavitation-induced reactions of most of the substituted benzenes, there is no indication that the reactions are autocatalytic, as the rate of darkening is constant with time. The nature of the products seem also independent of the degree of advancement of the reaction, as no change was observed in the shape of the absorption spectrum in the visible and u.v. region.

The non-linear changes in the intensity of iodobenzene and bromobenzene may well be due to the formation of highly colored charge-transfer complexes. The deviation from linearity became marked only after the reaction has proceeded for 1 h, and some molecular iodine or bromine may have been formed by that time. Molecular iodine was found in the distillate when reaction products from iodobenzene were recovered, but tests for molecular bromine or chlorine in the corresponding cases were negative.

An explanation for the concentration dependence of the reaction (Fig. 3) can be found by considering the vapor pressures of the compounds involved. Assuming that the primary reaction occurs in the cavitation bubble (6), then the composition of the vapor in the cavity is important. As benzene has a vapor pressure far greater than that of nitrobenzene (by a factor of 200 at 20 °C), then there would be greater amounts of benzene than nitrobenzene in the vapor even at mole fractions of nitrobenzene greater than 0.95 according to Raoult's law. The presence of the benzene would facilitate translational–vibrational energy transfer, and increase the instantaneous heat capacity in the cavitation bubble. This would moderate the final temperature which can be reached on compression of the bubble. The higher vapor pressure of benzene would also shorten the life-time of the bubble and slow the reaction.

Figure 4 shows a plot of the dissociation energy of the weakest bond (in most cases the C_6H_5–R bond) *vs.* the logarithm of the rate of formation of solid product. There is a crude correlation between these quantities. Some explanations can be suggested for the lack of better correlation in the data. Volatile products were not trapped, and may make up a variable and non-negligible part of the total product in

Can. J. Chem. Downloaded from www.nrcresearchpress.com by 210.87.254.40 on 09/05/12
For personal use only.

Can. J. Chem. Downloaded from www.nrcresearchpress.com by 210.87.254.40 on 09/05/12
For personal use only.

the nine systems, especially in the case of iodobenzene. The inaccuracies in obtaining product recovery can be substantial, especially in cases such as toluene and benzene, where only 0.009 g of product were obtained after 7 h.

Even with completely accurate data, a better correlation may not be present. The thermal conductivity of the compounds does not vary much and would not be expected to be an important factor. However, the vapor pressure does vary significantly, and could be an important factor. The chemical nature of the substituent group and the ionization potential could also play an important part. Nevertheless, the correlation between the rate and the dissociation energy as shown in Fig. 4 is considerably better than other correlations tried.

Such a correlation suggests that it is reasonable to assume the primary process in the reaction to be a thermal decomposition in the cavitation bubble. When aromatic compounds are involved, such a decomposition would result in radicals, for benzene C_6H_5 and C_6H_7, formed by having H combine with C_6H_6 (16). Such radicals can then initiate polymerization in the bulk liquid (17, 18).

An estimate of the temperature present can be obtained from Fig. 4 if some questionable assumptions are made. The concept of temperature itself is not valid in such gross dis-equilibrium situations. Nevertheless, if a first order thermal decomposition is assumed, and if the concentration, pre-exponential factor, and temperature are taken to be the same in all cases, then from the slope of the line drawn in Fig. 4, the "temperature" can be calculated to be of the order of 5000 °C. This is at least of the order of magnitude suggested by Fitzgerald *et al.* (6).

The reason why cavitation-induced reactions occur in aromatic liquids and not in liquids such as di-*t*-butyl peroxide may lie in the relative stability of aromatic radicals (19). The radicals formed in the case of di-*t*-butyl peroxide would have a greater tendency to recombine as soon as formed, and would not produce any reactions in the bulk liquid. It may also be that no reaction was observed in the case of di-*t*-butyl peroxide, as without polymerization, the conversion to product is too small to be detected, especially if volatile products are not trapped.

The product of the reaction seems to be a high molecular weight polymer, as suggested by the insolubility and the high melting point. The e.p.r. spectrum is similar to the spectrum obtained in low temperature (500 °C) pyrolysis of carbohydrates (20), or in some natural substances such as coal.

The mechanism for the formation of the polymer would seem to be analogous to the mechanism for polymerization which occurs on the radiolysis of benzene (17, 18). The difference in the two radiolysis mechanisms suggested is that in the one, a hexatrienyl radical is postulated as an intermediate (17) forming a polymer $R(C_6H_6)_nR$, while in the other, it is a cyclohexadienyl (18), which may then react to form a phenylcyclohexadienyl.

In this case, the radical polymerization which occurs does not stop in many cases by combination with another radical. It may be that the concentration of radicals in this case is too low for such termination. Instead, some of the polymer molecules remain with an unpaired electron.

The element analysis of the nitrobenzene residue indicated a deficiency in H, in agreement with radiolysis work. A deficiency of N and O, and a deficiency of N with respect to O shows that volatile products from the substituent group must have been produced. The low N:O ratio may be due to a greater amount of N in the volatile products. However, even with a positive pressure of argon, there may be some diffusion of air into the reaction vessel to introduce some oxygen.

There are some interesting comparisons between the cavitation phenomena observed and radiolysis reactions. The *G* value for the formation of polymer for liquid benzene by radiolysis is 0.75 (19); the *G* value for cavitation-induced reactions is 0.001 (Table 1). The *G* value for cyclohexane by radiolysis is greater than for benzene, 1.7, while no reaction is observed in cavitation-induced reaction. For ultrasonic cavitation, a *G* value of 0.001 as for benzene is quite low; for nitrobenzene it is 0.03; 0.095 for $CCl_4 \rightarrow Cl_2$ (11); 0.0045 for $H_2O \rightarrow H_2O_2$ (11).

It would seem that in radiolysis the stability of excited aromatic molecules acts to make them "sponge-type protectors." In cavitation-induced reactions the stability of the radicals formed from decomposition of aromatics seems to make it possible for these to survive the collapse of the cavitation bubbles and initiate polymerization

in the liquid. The differences in such behavior are presumably due to the much greater energies concentrated in the case of radiolysis.

The thermal decomposition of benzoyl peroxide in aromatic solvents and the subsequent reactions would also seem to have some relation to this work. An analysis (21) indicates that phenylcyclohexadiene radicals form quickly when this reaction takes place in benzene, and that such radicals are fairly stable. High molecular weight residues are also found.

Conclusions

The formation of polymers in pure substituted benzenes has been observed on exposure to ultrasound intense enough to cause cavitation. The product has some of the characteristics of the char obtained from low temperature pyrolysis of carbohydrates.

A free-radical mechanism similar to that suggested for polymerization from radiolysis seems probable. A crude correlation between bond dissociation energy and the reaction rate suggests that the initiation reaction is a thermal decomposition in a cavitation bubble.

The mechanism for such reactions could quite certainly be clarified by extending the experiments to liquid mixtures and solutions. This may also lead to some practical applications. It would seem advisable to extend such work using a more sophisticated apparatus than that used in these experiments, so that reaction conditions can be better controlled. It also seems advisable to do the experiments both at high and at low frequencies.

The authors thank Mr. D. G. Fecchio and Mr. N. F. Feiner for technical assistance, Dr. P. M. Laughton and Dr. R. H. Wightman for helpful discussions, and Dr. J. R. Morton and Dr. A. H. Reddoch of the National Research Council of Canada for making e.p.r. examinations of the samples. This research was supported by grants from the Ontario Department of University Affairs, the National Research Council of Canada, and Carleton University.

1. I. E. EL'PINER. Ultrasound, physical, chemical, and biological effects. Consultants Bureau. New York, N.Y., 1964.
2. A. LE BRAS. Rev. Chim. Miner. **4**, 283 (1967).
3. M. A. MARGULIS. Akust. Zh. **15**, 153 (1969); Soviet Physics-Acoustics, **15**, 135 (1969).
4. A. WEISSLER, I. PECHT, and M. ANBAR. Sci. **150**, 1288 (1965).
5. H. G. FLYNN. Physics of acoustic cavitation in liquids. *In* Physical acoustics. Vol. I, Part B. *Edited by* W. P. Mason. Academic Press. New York, N.Y., 1964.
6. M. E. FITZGERALD, V. GRIFFING, and J. SULLIVAN. J. Chem. Phys. **25**, 926 (1956).
7. F. R. YOUNG. 6th International Congress on Acoustics, Tokyo, 1968. Paper H-5-3, H-169.
8. M. DEGROIS and P. BALDO. C. R. Acad. Sc. Paris, Ser. C, **271**, 13 (1970).
9. L. A. SPURLOCK and S. B. REIFSNEIDER. J. Am. Chem. Soc. **92**, 6112 (1970).
10. R. M. G. BOUCHER. Brit. Chem. Eng. **15**, 363 (1970).
11. A. WEISSLER. J. Acoust. Soc. Am. **32**, 283 (1960).
12. C. SNELL and F. SNELL. Colorimetric methods of analysis. Vol. II. 3rd ed. Van Nostrand. New York, N.Y., 1949.
13. M. IBISI and B. BROWN. J. Acoust. Soc. Am. **41**, 568 (1967).
14. C. D. MESSINO, D. SETTE, and F. WANDERLINGH. J. Acoust. Soc. Am. **41**, 573 (1967).
15. C. WALLING. Free radicals in solution. John Wiley and Sons. London, 1957.
16. S. OHNISHI, T. TANEI, and I. NITTA. J. Chem. Phys. **37**, 2402 (1962).
17. W. N. PATRICK and M. BURTON. J. Am. Chem. Soc. **76**, 2626 (1954).
18. S. GORDON, A. R. VAN DYKEN, and T. F. DOUMANI. J. Phys. Chem. **62**, 20 (1958).
19. A. J. SWALLOW. Radiation chemistry of organic liquids. Pergamon, Oxford, 1960.
20. R. S. ALGER. Electron paramagnetic resonance: techniques and applications. Interscience. New York, N.Y., 1967.
21. D. F. DE TAR. J. Am. Chem. Soc. **89**, 4058 (1967).

Can. J. Chem. Downloaded from www.nrcresearchpress.com by 210.87.254.40 on 09/05/12
For personal use only.

Radiation-induced Oxidation of 2-Propanol by Nitrous Oxide in Alkaline Aqueous Solution

C. E. BURCHILL AND G. P. WOLLNER[1]

Department of Chemistry, University of Manitoba, Winnipeg, Manitoba R3T 2N2

Received December 30, 1971

The radiation-induced oxidation of 2-propanol to acetone by N_2O in alkaline aqueous solution proceeds via a free radical chain mechanism independent of p*H* above 12.5. The results are explained by abstraction of H from 2-propanol by O^- at both the α and β positions (85% α attack). Chain propagation is by reaction of the α radical anion, $(CH_3)_2\dot{C}O^-$, with N_2O with a rate constant of $(3.8 \pm 0.4) \times 10^4\ M^{-1}\ s^{-1}$, and by reaction of the β radical, $\dot{C}H_2(CH_3)CHOH$, with 2-propanol to give the α radical with a rate constant of $430 \pm 30\ M^{-1}\ s^{-1}$.

The conclusions are supported by the demonstration of kinetic isotope effects for selectively deuterated alcohols.

La réaction d'oxydation, induite par les radiations, du propanol-2 en acétone par N_2O, en solution aqueuse et basique, se fait par un mécanisme radicalaire en chaîne qui est indépendant du p*H* au-dessus de 12.5. Les résultats sont expliqués par une abstraction d'H du propanol-2 par O^- et ceci sur les positions α et β (85% d'attaque α). La propagation de chaîne se fait par réaction du radical anion α, $(CH_3)_2\dot{C}O^-$, avec N_2O et ceci avec une constante de vitesse de $(3.8 \pm 0.4) \times 10^4\ M^{-1}\ s^{-1}$, ainsi que par la réaction du radical β, $\dot{C}H_2(CH_3)CHOH$, avec le propanol-2 pour conduire au radical α selon une constante de vitesse de $430 \pm 30\ M^{-1}\ s^{-1}$.

Les conclusions s'appuient sur l'existence d'effets isotopiques cinétiques dans le cas d'alcools sélectivement deutérés.

Canadian Journal of Chemistry, **50**, 1751 (1972)

There have been several fragmentary reports of a radiation-induced chain oxidation of 2-propanol by N_2O in alkaline aqueous solution (1–3) but the only detailed study of this reaction has been for the case in which the solvent was the pure alcohol (4, 5). Few quantitative data are available for aqueous solutions.

Scholes *et al.* (1) reported only that the yields of acetone and N_2 were high, implicating a chain reaction. They suggested the sequence of reactions 1–3 to explain the chain yields.

[1] $$\dot{O}H + (CH_3)_2CHO^- \rightarrow H_2O + (CH_3)_2\dot{C}O^-$$

[2] $$(CH_3)_2\dot{C}O^- + N_2O + H_2O \rightarrow (CH_3)_2CO + OH^- + N_2 + \dot{O}H$$

[3] $$2\,(CH_3)_2\dot{C}O^- + H_2O \rightarrow (CH_3)_2CO + (CH_3)_2CHOH + OH^-$$

Allan and Beck (2) found that the N_2 yields, while showing an inverse dose rate effect did not fit the simple kinetic expression (eq. 4) which could be derived from this mechanism.

[4] $$G(N_2) = G_{e_{aq}^-} + k_2\left(\frac{G_R}{2k_3D}\right)^{1/2}[N_2O]$$

They suggested that this failure could be attributed to the incomplete acid dissociation of 2-propanol at p*H* 13 and the non-selective abstraction of H from 2-propanol by OH to give a finite yield of $\dot{C}H_2(CH_3)CHOH$. 2-Propanol was said to be 87% dissociated at p*H* 13 on the basis of an equilibrium constant proposed by Wells (6) from a change in the rate of photochemical autoxidation in this p*H* range. More recently Murto (7) has estimated pK_a for 2-propanol to be 17.1 so that it is unlikely that the anion plays any role in the reactions of 2-propanol in aqueous solution. However the radical $(CH_3)_2\dot{C}OH$ has been shown to undergo acid dissociation with $pK_a = 12.2$ (8) and it is probable that this is the controlling factor in both the radiation-induced reaction and the autoxidation. Non-selective abstraction of H from 2-propanol by OH has been demonstrated to be a significant factor in its free radical oxidation by H_2O_2 as a consequence of the differences in reactivity of the radicals formed (9–12).

Dainton *et al.* (3) observed that in the radiation-induced reaction of 2-propanol with N_2O in alkaline aqueous solution the yield of N_2 increased with increasing concentrations of both N_2O and alcohol. The latter effect is similar to that observed in the chain reaction of 2-propanol with H_2O_2 in neutral solution (9, 10) and suggests that reaction 5 may be significant.

[5] $$\dot{C}H_2(CH_3)CHOH + (CH_3)_2CHOH \rightarrow (CH_3)_2CHOH + (CH_3)_2\dot{C}OH$$

As part of a continuing study of radiation-

[1]University of Manitoba Graduate Fellowship, 1970–71.

Can. J. Chem. Downloaded from www.nrcresearchpress.com by 210.87.254.105 on 09/05/12
For personal use only.

induced oxidations in aqueous solutions we have carried out an investigation of this particular reaction.

Experimental

Aqueous solutions were prepared with triply-distilled water. 2-Propanol and NaOH (Fisher, Certified Reagent) were used as received. Deuterium labelled alcohols ($(CD_3)_2$-CHOH and $(CH_3)_2CDOH$) were from Merck, Sharpe and Dohme and were used without further purification. N_2O (Matheson) was passed through a column of KOH pellets to remove CO_2 and was freed of permanent gases by repeated freeze–pump–thaw cycles on a vacuum line.

Samples, of 5 ml volume in Pyrex bulbs, were degassed by the freeze–pump–thaw method. An appropriate quantity of N_2O (measured manometrically in a side-bulb) was then condensed into the bulb using liquid nitrogen and the sample sealed off under vacuum. The samples were then thawed and equilibrated at 26 °C until immediately before irradiation. The N_2O concentration in the solution was calculated from the quantity of N_2O introduced and the volumes of the liquid and gas space. It was assumed that the solubility of N_2O in the alkaline solutions used was the same as for water containing the same concentrations of NaOH (13) (the concentration of 2-propanol was, for most experiments, $\leqslant 0.1$ *M*).

Irradiations were carried out in a ^{60}Co Gammacell 220 (AECL) at the ambient temperature of the unit. Because most of the irradiations were short (< 1 min) it was assumed that neither the temperature nor the N_2O concentration would change significantly during an irradiation. Dosimetry was based on $G(Fe^{3+}) = 15.6$ for the Fricke dosimeter (14) and the absorbed dose was assumed to be directly proportional to the electron density of the samples.

Acetone, the only product determined quantitatively, was measured spectrophotometrically using salicylaldehyde (15). The majority of *G* values reported were calculated from a minimum of four points on linear yield-dose plots. In a few cases, noted in Fig. 2, *G* values were calculated from single irradiations.

Results and Discussion

In irradiated alkaline aqueous solutions of 2-propanol containing N_2O the yield of acetone was found to depend upon the p*H* and the concentrations of N_2O and alcohol. Figure 1 shows the p*H* dependence of *G*(acetone) for solutions containing 2-propanol (0.105 *M*) and two different concentrations of N_2O. In both cases the yield showed a marked increase in the p*H* range 10.5–12.5. Further work on this system used solutions containing 0.3 *M* NaOH (p*H* 13.5).

In solutions containing N_2O, all e^-_{aq} will react with N_2O (reaction 6) and oxidation of 2-propanol is initiated by abstraction of H from 2-propanol by OH (or O^-). The α radical, $(CH_3)_2\dot{C}OH$, has been shown to undergo an acid dissociation at high p*H* (8, 16) and the

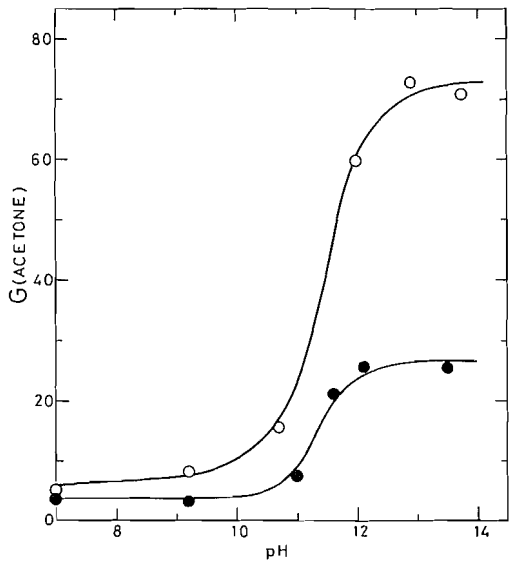

FIG. 1. Variation of *G*(acetone) with p*H*; [2-propanol] = 0.105 *M*, average dose rate = 1.13×10^{19} eV l^{-1} s^{-1}; ○, $[N_2O] = 1.04 \times 10^{-1}$ *M*; ●, $[N_2O] = 7.4 \times 10^{-3}$ *M*.

p*H* dependence of the yield may be understood on the basis of the equilibrium system represented by eq. 9 *if* only the anionic form of the radical undergoes the chain propagating reaction 10, as previously proposed (1–5). The mid-point of the rise in the yield curves of Fig. 1 (p*H* ~ 11.4) is significantly less than the pK_a estimated for the radical (~ 12.2) by Asmus *et al.* (8) but it may be that in both cases the points of inflection are determined by kinetic, rather than equilibrium, conditions.

[6] $e^-_{aq} + N_2O \rightarrow N_2 + \dot{O}^-$ $\quad (\dot{O}^- + H_2O \rightleftharpoons \dot{O}H + OH^-)$

[7] $\dot{O}H\ (\dot{O}^-) + (CH_3)_2CHOH \rightarrow H_2O\ (OH^-) + (CH_3)_2\dot{C}OH$

[8] $\dot{O}H\ (\dot{O}^-) + (CH_3)_2CHOH \rightarrow H_2O\ (OH^-) + \dot{C}H_2(CH_3)CHOH$

[9] $(CH_3)_2\dot{C}OH + OH^- \rightleftharpoons (CH_3)_2\dot{C}O^- + H_2O$

[10] $(CH_3)_2\dot{C}O^- + N_2O \rightarrow (CH_3)_2CO + N_2 + \dot{O}^-$

For fixed concentrations of base (0.3 *M*) and 2-propanol (0.105 *M*) the variation of *G*(acetone) with N_2O concentration is shown in Fig. 2. The yield approached a maximum limiting value at $[N_2O] > 9 \times 10^{-2}$ *M*. This effect is attributed to the formation of two different radicals, $(CH_3)_2\dot{C}OH$ and $\dot{C}H_2(CH_3)$-CHOH (reactions 7, 8), by abstraction of H from 2-propanol. Of these, only the α radical

Can. J. Chem. Downloaded from www.nrcresearchpress.com by 210.87.254.105 on 09/05/12
For personal use only.

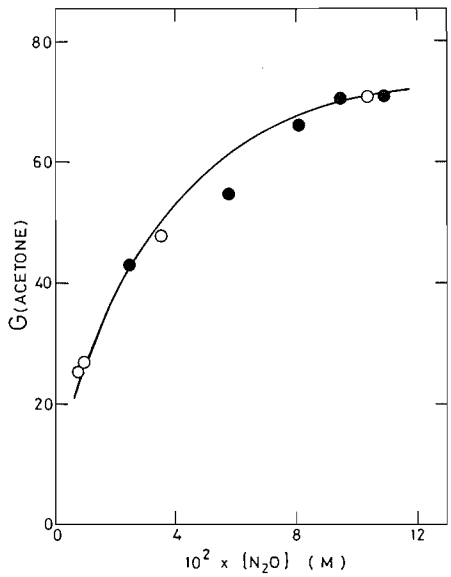

FIG. 2. Variation of G(acetone) with $[N_2O]$; [2-propanol] = 0.105 M, pH = 13.5, average dose rate = 1.13 × 10^{19} eV l^{-1} s^{-1}; ○, calculated from a yield–dose plot; ●, calculated from a single irradiation.

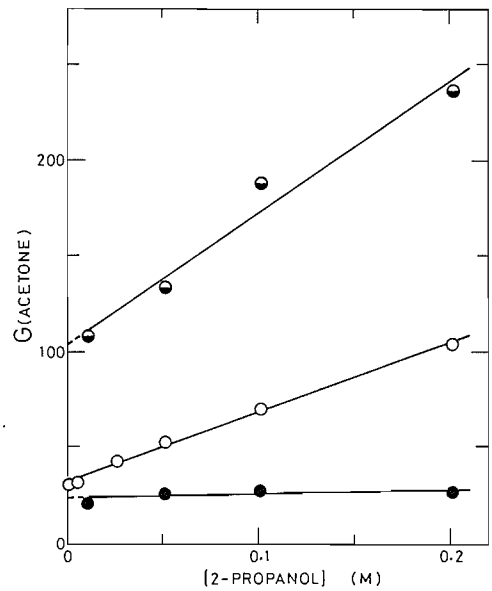

FIG. 3. Variation of G(acetone) with [2-propanol]; $[N_2O]$ = 0.104 M, pH = 13.5, average dose rate = 1.12 × 10^{19} eV l^{-1} s^{-1}; ○, $(CH_3)_2CHOH$; ◒, $(CD_3)_2CHOH$; ●, $(CH_3)_2CDOH$.

is assumed to ionize and undergo the chain propagating reaction with N_2O (eqs. 9, 10). (No acid dissociation of the radical from t-butyl alcohol, formally similar to the β radical above, was observed in pulse radiolysis studies (17).) However both radicals may undergo bimolecular termination, as in reactions 11–13. With increasing N_2O concentration the rate of reaction 10 would be increased and the steady state concentration of $(CH_3)_2\dot{C}O^-$ decreased until only reaction 13 would be a significant terminating process. At this point the yield of acetone would become independent of $[N_2O]$.

[11] $2\,(CH_3)_2\dot{C}O^- \rightarrow$ non-radical products

[12] $(CH_3)_2\dot{C}O^- + \dot{C}H_2(CH_3)CHOH \rightarrow$ non-radical products

[13] $2\,\dot{C}H_2(CH_3)CHOH \rightarrow$ non-radical products

At fixed concentrations of NaOH (0.3 M) and N_2O (0.104 M, corresponding to an equilibrium pressure of about 4.5 atm), where G(acetone) was essentially independent of their value, the yield was found to vary linearly with alcohol concentration, as shown in Fig. 3. This effect, similar to that observed in neutral solution for radiation-induced oxidation by H_2O_2, is ascribed to the reaction of the β radical with the alcohol as the rate-determining propagating step (eq. 5).

The overall mechanism proposed for high base and N_2O concentrations may be represented by eqs. 5–10, 13–16. It is assumed that

[14] $H_2O \rightsquigarrow e^-_{aq}, \dot{H}, \dot{O}H, H_2, H_2O_2, H_3O^+$

[15] $\dot{H} + OH^- \rightarrow e^-_{aq}$

[16] $\dot{O}H + OH^- \rightarrow H_2O + \dot{O}^-$

[6] $e^-_{aq} + N_2O \rightarrow N_2 + \dot{O}^-$

[7] $\dot{O}^- + (CH_3)_2CHOH \rightarrow OH^- + (CH_3)_2\dot{C}OH$

[8] $\dot{O}^- + (CH_3)_2CHOH \rightarrow OH^- + \dot{C}H_2(CH_3)CHOH$

[9] $(CH_3)_2\dot{C}OH + OH^- \rightarrow H_2O + (CH_3)_2\dot{C}O^-$

[10] $(CH_3)_2\dot{C}O^- + N_2O \rightarrow (CH_3)_2CO + N_2 + \dot{O}^-$

[5] $\dot{C}H_2(CH_3)CHOH + (CH_3)_2CHOH \rightarrow (CH_3)_2CHOH + (CH_3)_2\dot{C}OH$

[13] $2\,\dot{C}H_2(CH_3)CHOH \rightarrow$ non-radical products

Can. J. Chem. Downloaded from www.nrcresearchpress.com by 210.87.254.105 on 09/05/12
For personal use only.

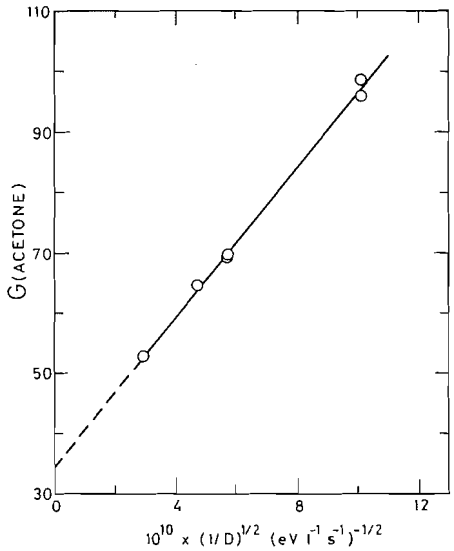

FIG. 4. Variation of G(acetone) with dose rate (D). [2-propanol] = 0.052 M, [N_2O] = 0.104 M, pH = 13.5.

at these high (0.3 M) base concentrations reactions 15, 16, and 9 are sufficiently rapid that all H atoms are converted to e^-_{aq}, all OH to O^-, and all $(CH_3)_2\dot{C}OH$ to $(CH_3)_2\dot{C}O^-$ before further reaction. It is also assumed that at the high concentration of N_2O (0.104 M) reaction 10 is the only reaction of $(CH_3)_2\dot{C}O^-$ (*i.e.* only reaction 13 is a significant termination step). Under these conditions a steady state kinetic analysis leads to eq. 17 ($G_R = G_{e^-_{aq}} + G_H + G_{OH}$, and D is the dose rate in units of 6.02×10^{25} eV l^{-1} s^{-1}).

$$[17] \quad G(\text{acetone}) = \frac{k_7}{k_8} G_R + \left(1 + \frac{k_7}{k_8}\right) k_5 \times \left(\frac{G_R}{2k_{13}D}\right)^{1/2} [\text{2-propanol}]$$

Equation 17 is in good agreement with the form of the experimental results shown in Fig. 3. The extrapolated non-zero intercept (32.0 ± 1.0) for G(acetone) at [2-propanol] = 0 corresponds to $k_7 G_R/k_8$ and, taking $G_R = 5.9$ (18), gives $k_7/k_8 = 5.4 \pm 0.2$. Equation 17 also predicts a linear dependence of the yield on $D^{-1/2}$, extrapolating to the same non-zero intercept at $D^{-1/2} = 0$. Figure 4 shows the dose rate dependence for fixed alcohol (0.052 M) and N_2O (0.104 M) concentrations. The extrapolated intercept (34.2 ± 1.2) is in good agreement with that found from the alcohol dependence and corresponds to $k_7/k_8 = 5.8 \pm 0.2$. Using these values of k_7/k_8, and assuming $2k_{13} = 2 \times 10^9$ M^{-1} s^{-1} (typical of bimolecular rate constants for termination of neutral alcohol radicals (17)), values of $k_5 = 445 \pm 20$ and 420 ± 20 M^{-1} s^{-1} may be calculated from the slopes of the lines in Figs. 3 and 4 respectively.

Strong support for this interpretation is obtained from the results for selectively deuterated alcohols, shown also in Fig. 3. If $(CD_3)_2$-CHOH is substituted for $(CH_3)_2CHOH$, reaction 8 would be expected to show a normal primary kinetic isotope effect ($k_{8(H)} > k_{8(D)}$). This would have the effect of increasing both the extrapolated intercept and the slope of the line in Fig. 3, which is the observed effect. From the ratio of the intercepts for the deuterated and undeuterated alcohols $k_{8(H)}/k_{8(D)} = 3.26 \pm 0.23$. Substitution of $(CH_3)_2CDOH$ for $(CH_3)_2CHOH$ would be expected to give $k_{7(H)} > k_{7(D)}$, and $k_{5(H)} > k_{5(D)}$, and to decrease both the intercept and the slope of the line in Fig. 3. The ratio of the intercepts gives $k_{7(H)}/k_{7(D)} = 1.35 \pm 0.10$ and, assuming no secondary isotope effects, the change in slope corresponds to $k_{5(H)}/k_{5(D)} = 11 \pm 6$.

The values for k_7/k_8, and the magnitudes of the kinetic isotope effects, are very similar to those obtained by Burchill and co-workers (9, 10) (and independently confirmed by Walling and Kato (11)) for reactions of OH with 2-propanol. The total rate constant for reaction of O^- with 2-propanol has been found to be very similar to that for reaction of OH (19). These results support the suggestion by Rabani (20) that O^- and OH are about equally efficient in hydrogen abstraction reactions.

The mean value for k_5 reported here (430 ± 30 M^{-1} s^{-1}) is much larger than that found by Burchill and co-workers (52 ± 3 M^{-1} s^{-1}) in neutral solution (9, 10). The latter value was suggested to be a lower limit (9) but it seems unlikely to be in error by such a large amount. A possible explanation for the higher value in alkaline solution is that reactions 5 and 9 represent a concerted or base-catalyzed reaction (eq. 18). This would, however, require a form

$$[18] \quad \dot{C}H_2(CH_3)CHOH + (CH_3)_2CHOH + OH^- \rightarrow (CH_3)_2CHOH + H_2O + (CH_3)_2\dot{C}O^-$$

Can. J. Chem. Downloaded from www.nrcresearchpress.com by 210.87.254.105 on 09/05/12
For personal use only.

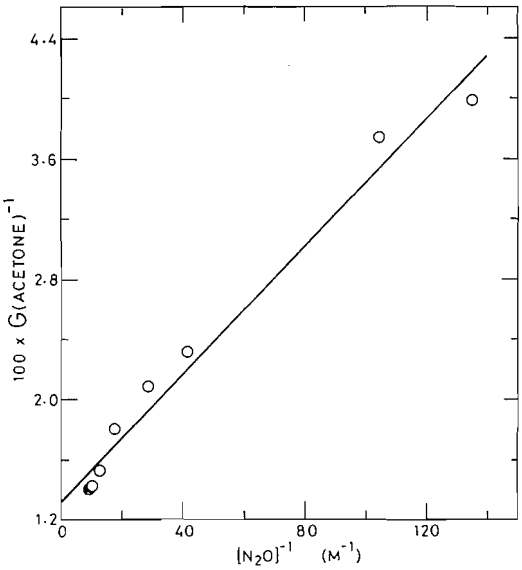

FIG. 5. Data of Fig. 2 replotted according to eq. 19.

of termolecular reaction which seems rather unlikely.

The kinetic analysis presented above was for high concentrations of N_2O, where the reaction of $(CH_3)_2\dot{C}O^-$ with N_2O was assumed to be stoichiometric and only reaction 13 was considered as a terminating step. If reactions 11–13 can be represented by a composite rate constant such that $k_t = 2k_{11} = k_{12} = 2k_{13}$ the results for lower N_2O concentrations may also be considered. A steady state solution leads to eq. 19.

$$[19]\quad G(\text{acetone})^{-1} = \left[\frac{k_7 G_R}{k_7 + k_8} + k_5\left(\frac{G_R}{k_t D}\right)^{1/2}[\text{2-propanol}]\right]^{-1} \times \left[\frac{k_8}{k_7 + k_8} + \frac{(G_R D k_t)^{1/2} + k_5[\text{2-propanol}]}{k_{10}[N_2O]}\right]$$

On the basis of the proposed mechanism, for a sufficiently high base concentration and a fixed concentration of alcohol, $G(\text{acetone})^{-1}$ should be a linear function of $[N_2O]^{-1}$. Figure 5 shows the data of Fig. 2 replotted in this way. The best straight line has been drawn but the experimental results suggest a systematic curvature. This probably arises from the fact that there is not a simple algebraic relationship among the three rate constants for the terminating reactions. However, using the values previously derived for k_7/k_8, k_5, and assuming $k_t = 2 \times 10^9\ M^{-1}\ s^{-1}$, an approximate value of $k_{10} = (3.8 \pm 0.4) \times 10^4\ M^{-1}\ s^{-1}$ may be calculated from the slope and intercept of the line drawn. The results reported by Sherman (5) suggest that reaction 10 may be considerably faster in 2-propanol as solvent. If the chain is terminated by bimolecular radical reactions having rate constants *ca.* $10^9\ M^{-1}\ s^{-1}$ the very high yields reported by Sherman would require $k_{10} > 10^5\ M^{-1}\ s^{-1}$. The variation of acetone yields with N_2O concentration may be fitted to eq. 19, giving a value for k_{10} of $\simeq 8 \times 10^5\ M^{-1}\ s^{-1}$. There are, moreover, reasons to believe that this rate constant may increase in going from water to an alcohol as solvent. Experiments with water–methanol mixtures (21) indicated that the rate constant for reaction of $\dot{C}H_2O^-$ with N_2O increased with increasing methanol content. Moelwyn-Hughes (22) has proposed that for the reaction of an ion with an uncharged species a major portion of the activation energy is associated with the solvation energy of the ion. The decreased solvation energy of the anion, $(CH_3)_2\dot{C}O^-$, in going from aqueous to alcoholic solution could thus lead to a decrease in activation energy and an increase in the specific rate constant.

In his study of the radiation-induced oxidation of alkaline 2-propanol by N_2O Sherman (5) found a significant chain yield of methane and that the reaction was inhibited by small amounts of acetone added prior to irradiation. We have examined the gaseous products from our experiments in aqueous solution by mass spectrometry and were unable to detect methane. In our experiments the addition of $\simeq 10^{-3}$ M acetone (approximately the concentration formed during the longest irradiations) to the solutions before irradiation had no measurable effect on G(acetone).

Summary

A self-consistent mechanism has been proposed for the radiation-induced oxidation of 2-propanol by N_2O in alkaline aqueous solution. The mechanism is based on the acid dissociation of the α radical of 2-propanol followed by electron transfer from the anion to N_2O as the propagating step. This may be contrasted with the chain oxidation of 2-propanol by H_2O_2 in that only the α radical anion

Can. J. Chem. Downloaded from www.nrcresearchpress.com by 210.87.254.105 on 09/05/12
For personal use only.

TABLE 1. Rate constant data derived from oxidation of 2-propanol by N_2O in alkaline aqueous solution

k_7/k_8	5.6 ± 0.3
$k_{7(H)}/k_{7(D)}$	1.35 ± 0.10
$k_{8(H)}/k_{8(D)}$	3.26 ± 0.23
k_5	$430 \pm 30\ M^{-1}\ s^{-1}$
$k_{5(H)}/k_{5(D)}$	11 ± 6
k_{10}	$(3.8 \pm 0.4) \times 10^4\ M^{-1}\ s^{-1}$

reacts with N_2O whereas the undissociated radical will react with H_2O_2 in neutral or acid solution (9, 12). The β radical is unreactive toward either N_2O or H_2O_2 but may react with the parent alcohol to give an α radical in a secondary propagating reaction. The ratio of $\alpha:\beta$ abstraction from 2-propanol by O^- in alkaline solution is very similar to that for OH in neutral solution. The principal numerical conclusions are summarized in Table 1.

Financial support for this research was provided in part by the National Research Council of Canada and in part by Atomic Energy of Canada Limited, Commercial Products Division.

1. G. SCHOLES, M. SIMIC, and J. J. WEISS. Discuss. Faraday Soc. **36**, 214 (1963).
2. J. T. ALLAN and C. M. BECK. J. Am. Chem. Soc. **86**, 1483 (1964).
3. F. S. DAINTON, A. R. GIBBS, and D. SMITHIES. Trans. Faraday Soc. **62**, 3170 (1966).
4. W. V. SHERMAN. Chem. Commun. 250 (1966).
5. W. V. SHERMAN. J. Phys. Chem. **71**, 1695 (1967).
6. C. F. WELLS. Discuss. Faraday Soc. **29**, 219 (1960).
7. J. MURTO. Acta Chem. Scand. **18**, 1043 (1964).
8. K. D. ASMUS, A. HENGLEIN, A. WIGGER, and G. BECK. Ber. Bunsenges. Phys. Chem. **70**, 756 (1966).
9. C. E. BURCHILL and I. S. GINNS. Can. J. Chem. **48**, 1232 (1970).
10. C. E. BURCHILL and G. F. THOMPSON. Can. J. Chem. **49**, 1305 (1971).
11. C. WALLING and S. KATO. J. Am. Chem. Soc. **93**, 4275 (1971).
12. C. E. BURCHILL and P. W. JONES. Can. J. Chem. **49**, 4005 (1971).
13. International critical tables. Vol. 3. McGraw-Hill, New York, 1928.
14. H. A. J. B. BATTAERD and G. W. TREGEAR. Rev. Pure Appl. Chem. **16**, 83 (1966).
15. S. BERNTSSON. Anal. Chem. **28**, 1337 (1956).
16. K. EIBEN and R. FESSENDEN. J. Phys. Chem. **75**, 1186 (1971).
17. M. SIMIC, P. NETA, and E. HAYON. J. Phys. Chem. **73**, 3794 (1969).
18. I. G. DRAGANIĆ, M. T. NENADOVIĆ, and Z. D. DRAGANIĆ. J. Phys. Chem. **73**, 2564 (1969).
19. G. V. BUXTON. Trans. Faraday Soc. **66**, 1656 (1970).
20. J. RABANI. *In* Radiation chemistry of aqueous solutions. G. Stein, ed. Interscience, New York, 1968. p. 229.
21. G. P. WOLLNER. M.Sc. Thesis. University of Manitoba, Winnipeg, Manitoba, 1971.
22. E. A. MOELWYN-HUGHES. Physical chemistry. Pergamon Press, Oxford, 1961. p. 1285.

Can. J. Chem. Downloaded from www.nrcresearchpress.com by 210.87.254.105 on 09/05/12
For personal use only.

Terpolymerization of Methacrylonitrile, Styrene, and α-Methylstyrene

ALFRED RUDIN, SCHUMANN S. M. CHIANG, H. KIRK JOHNSTON, AND PAUL D. PAULIN
Department of Chemistry, University of Waterloo, Waterloo, Ontario

Received January 31, 1972

The free radical copolymerization of methacrylonitrile, styrene, and α-methylstyrene was studied at 60 °C in toluene solution. Copolymer composition was calculated from the composition of the unreacted monomers, as measured by g.l.c. Reactivity ratios measured previously for the three monomer pairs involved were used with the simple terpolymerization equation to predict polymer composition. Agreement between predicted and experimental polymer compositions was satisfactory. The behavior of α-methylstyrene can be described by a simple model without reference to ceiling temperature or penultimate effects because sequence lengths of this monomer in the terpolymers are short.

A true azeotropic feed composition was not investigated, but several monomer mixtures produced copolymers with compositions which varied so little from that of the feed that the systems could be considered to be azeotropic for practical synthetic purposes. This behavior is in accord with expectations.

Analytical accuracy of the gas chromatographic techniques was examined and means are suggested to make the best use of this method in copolymerization studies.

La copolymérisation par radicaux libres de méthacrylonitrile, styrène, et α-méthylstyrène a été étudiée à 60 °C en solution dans le toluène. La composition du copolymère a été calculée à partir de celle des monomères restants par c.g.l. Les rapports de réactivité précédemment mesurés pour les trois monomères impliqués pris deux à deux, ont été utilisés dans la simple équation de terpolymérisation pour prévoir la composition du polymère. Un accord satisfaisant entre les compositions calculée et trouvée a été obtenu. Le comportement de l'α-méthylstyrène peut être décrit par un modèle simple sans faire référence à la température "de plafond" ou à des effets préterminaux car les longueurs des séquences de ce monomère dans les terpolymères sont courtes. La composition d'une alimentation azéotropique vraie n'a pas été recherchée car de nombreux mélanges de monomères ont donné des copolymères dont la composition diffère tellement peu de celle de l'alimentation, qu'il est possible de considérer ces systèmes comme étant azéotropiques, à des fins de synthèse pratique. Cette attitude est conforme aux prévisions.

La précision analytique des techniques de chromatographie en phase gazeuse a été examinée et des moyens ont été proposés afin de faire le meilleur usage de cette méthode à des études de copolymérisation.

Canadian Journal of Chemistry, **50**, 1757 (1972)

Can. J. Chem. Downloaded from www.nrcresearchpress.com by 210.87.254.5 on 09/05/12
For personal use only.

Introduction

This paper reports the free radical copolymerization at 60 °C in toluene solution of methacrylonitrile, styrene, and α-methylstyrene. Previous communications from this laboratory have reported copolymerization behavior of the three binary pairs which can be chosen from this trio of monomers (1–4). Reactivity ratios were determined from loss of monomers measured by gas–liquid chromatographic analysis of the reaction mixtures. Values obtained differed somewhat from those reported by earlier workers, with the major difference being that α-methylstyrene copolymerizations were found to conform to simple copolymer behavior (5) even at reaction temperatures near or higher than the ceiling temperature of poly(α-methylstyrene). This result can be explained on the grounds that short sequence lengths of this monomer in the copolymer have greater enthalpies of polymerization and correspondingly higher ceiling temperatures than high molecular weight homopolymer (2, 3). Other discrepancies between the results reported and those found by other workers can be ascribed to use of more modern analytical procedures and data-handling methods (3, 4, 6).

The articles cited are not the first examples of use of gas chromatographic analyses in copolymerization studies, but the methods used to handle the raw data are novel. It was of interest to extend the investigation to simultaneous copolymerization of the three monomers involved to test the application of the analytical method to this more complicated system. This study also provided a test of the binary reactivity ratios which had been reported previously. Six reactivity ratios are required to determine the composition of the polymer formed from given concentrations of three monomers. Reactivity ratios cannot be measured at present directly in multicomponent systems, but values deter-

mined in two-component studies appear to be generally applicable in more complicated copolymerizations (7–10), although there have been reports in which the predicted and experimental copolymer compositions do not agree very well (11, 12).

Experimental

Materials

The middle third of the reduced pressure distillates of the monomers was retained and stored in the cold until polymerization. Toluene was dried over sodium and the middle third of the distillate at atmospheric pressure was used as a solvent. The azodiisobutyronitrile (AIBN) initiator was recrystallized from methanol. Hydroquinone used to terminate the free radical polymerizations was used as received.

Polymerization

Copolymerizations of styrene (S), methancrylonitrile (MAN), and α-methylstyrene (AMS) were carried out in toluene solution at 60 °C. Reaction mixtures contained 10 ml toluene and a total of 15 ml monomers. These quantities were pipetted into 75 ml capacity reaction bottles equipped with ground glass tapered necks. The same pipet was used for all liquid deliveries. Eight replicate mixtures were prepared for each polymerization. Two of these mixtures were retained as gas chromatographic standards and were not reacted. One standard solution was degassed with the six polymerization samples and one was used without degassing. The gas chromatographic analyses of the standards did not differ much, but preference was always given to the data from the degassed sample.

The solutions were degassed by freezing and thawing twice under "vacuum" and the reaction vessels were then flushed with nitrogen and sealed with rubber septum stoppers. Mixtures to be polymerized were warmed for 10 min in a 60 °C constant temperature bath before addition of 2 ml toluene solution containing 20 mg/ml AIBN initiator. The reaction bottles were then returned to the bath for times between 2 and 24 h. These polymerization schedules served to convert up to 15 weight percent of the monomer charge.

A syringe was used to bleed gas from the vapor spaces above the warmed mixtures and reduce the pressure in the reaction vessels to atmospheric or slightly less.

Samples were removed from the bath after the required reaction times and polymerization was terminated by addition of 15 ml toluene saturated with hydroquinone. Each vessel was then flushed with nitrogen, resealed and stored in the cold until analysis, which was always within 48 h.

The two standard solutions, which were not heated, were treated with 2 ml initiator solution followed immediately (or sometimes preceded) by 15 ml saturated inhibitor mixture. All solutions thus contained the same volume of solvent, within the limits of precision of pipet delivery.

Six different feed compositions were used. The volumes (totalling 15 ml) of monomers for these mixtures are given in Table 2.

Analysis

A Carle model 9000 gas chromatograph, with a hydrogen flame ionization detector and integrating recorder, was used to analyze for unreacted monomers and solvent. The column, which was packed with 8% dinonylphthalate on Anakron ABS, was operated at 93–96 °C with gas flow rates of 5 ml/15 s and 5 ml/7.2 s for helium and helium plus hydrogen, respectively.

A 1 μl syringe equipped with Chaney adaptor was used to inject 0.2–0.3 μl samples of the reaction mixtures directly into the column. A glass wool plug in the column inlet trapped the polymer and inhibitor. The only peaks observed with reacted samples were identical to those of the monomers and solvent in the standard samples. The pre-column unit was changed after analysis of the six reacted mixtures and two standards for each composition. This prevented excessive polymer build-up in the glass wool plug and consequent distortion of the gas chromatographic peaks.

The standard sample which had not been degassed was analyzed first. The degassed standard was analyzed immediately before and after the reacted mixtures. This checked that the detector sensitivity had remained constant over the course of the measurements. Reacted samples were analyzed in order of polymerization times, to minimize polymer loading on the pre-column plug. At least four replicate analyses were made for each reacted mixture and six for standard samples.

Analytical Accuracy

The accuracy of the analysis is determined by the limitations of the gas–liquid chromatographic technique. The accuracy with which the compositions of the standard solutions can be estimated from the make-up volumes is also a factor in the present application, because the solvent serves as an internal calibration standard (1). Systematic errors which have been troublesome in chemical analyses of nitrile-containing copolymers (10, 13) are unlikely in the present case because the monomers serve as calibration standards for detector sensitivity (4).

Five monomer mixtures were made to assess the accuracy of the gas chromatographic analysis and the metering of liquids in the initial feed compositions. All samples were analyzed in quadruplicate. One sample, containing 5 ml of each of the three monomers, was chosen as the standard and the ratios of its peak areas to those of the other mixtures were used to estimate the compositions of the other four solutions. All peak areas were normalized on the mean solvent peak area of the standard mixture, as described by Rudin and Yule (4).

The results of this experiment are shown in Table 1. It can be seen that the analytical technique used appears to be accurate to within 2% of the nominal make-up volumes of the monomer feeds. The coefficients of variation of peak areas of individual monomers appear to be independent of the concentration of the monomer. The reliability found here is generally as expected for gas chromatographic analyses and is probably at least as good as can be achieved by isolation and chemical analysis of polymer formed in the reaction mixture.

Analytical uncertainties of this order of magnitude make it impossible, however, to derive reliable reactivity ratios from measurements of a few polymer compositions at low conversions. This conclusion is probably valid for all analytical methods in current use, and is a factor in the lack of agreement which is often noted between results from different laboratories (6).

Can. J. Chem. Downloaded from www.nrcresearchpress.com by 210.87.254.5 on 09/05/12
For personal use only.

TABLE 1. Analysis of monomer feed composition (standard 5:5:5 MAN:S:AMS*)

Make-up volume (ml)	Experimental volume (ml)	Deviation (%)	Mean peak area†‡	Coefficient of variation of peak area
MAN – 5	—	—	499	0.0079
S – 5	—	—	1779	0.0152
AMS – 5	—	—	3492	0.0196
toluene 10	—	—	1100	§
MAN – 5	5.010	0.20	500	0.0051
S – 3	3.004	0.15	1069	0.0080
AMS – 7	7.103	1.47	4961	0.0065
MAN – 6	6.042	0.70	603	0.0042
S – 6	6.116	1.90	2176	0.0071
AMS – 3	3.011	0.37	2103	0.0073
MAN – 5	5.030	0.60	496	0.0111
S – 7	7.097	1.38	2525	0.0044
AMS – 3	2.997	−0.11	2093	0.0100
MAN – 6	6.032	0.53	602	0.0063
S – 3	2.999	−0.04	1067	0.1080
AMS – 6	6.137	2.28	4268	0.0035

*MAN = methacrylonitrile, S = styrene, AMS = α-methylstyrene.
†Mean of four analyses.
‡Arbitrary units.
§Each analysis normalized to a solvent peak area of 1100 units.

For this reason, gas chromatographic analysis of unreacted monomer concentrations is most reliable if a relatively large number of data points are obtained at various extents of reaction. These results are plotted against total percent conversion of monomers and the values for estimation of polymer composition are taken from the corresponding best-fit least squares line. The most accurate experimental points are those obtained at the highest conversions because the difference between the measured initial and final monomer concentrations is greatest under these conditions. The linear least squares fit gives these data the heaviest weighting. This procedure would appear to provide better estimates than those from the same number of analyses clustered at low conversions, because the uncertainty in the difference between two gas chromatographic analyses is independent of the magnitude of this difference. As pointed out below, this procedure does not prevent use of a differential form of the copolymer equation under some circumstances.

Calculations

The basic calculations used to obtain unreacted weight fractions of monomers from the raw data have been described previously, for copolymerization of styrene and methacrylonitrile (4). Figures 1–3 show plots of weight fraction monomer against reaction times for one of the feed compositions. The best-fit lines are obtained by a linear least squares fit to the mean values at each time.

The best-fit lines in such plots extrapolated to the feed composition at zero reaction time in previous studies of binary copolymerizations (2–4). This was not so, however, in the terpolymerizations reported here. The extrapolated value for initial weight fraction of MAN in Fig. 1 is lower than the value computed from the initial monomer volumes and densities. The converse situation is observed for AMS in Fig. 3. The deviations between make-up compositions and the corresponding extrapolated zero reaction time values are within the reliability limits indicated by the experiment summarized in Table 1. The differences could not be dismissed on these grounds, however, because they were systematic. The extrapolated initial values for methacrylonitrile tended to be lower than the figures estimated from volume make-up, styrene figures generally coincided, and the extrapolated α-methylstyrene values matched or exceeded the make-up counterparts.

These variations can be attributed to losses by volatilization from the reaction vessels and could have occurred when gases were removed by syringe to reduce pressure in the vapor phase at the beginning of the reaction or, less probably, when the septum cap was removed for addition of terminator solutions after the reaction

Can. J. Chem. Downloaded from www.nrcresearchpress.com by 210.87.254.5 on 09/05/12
For personal use only.

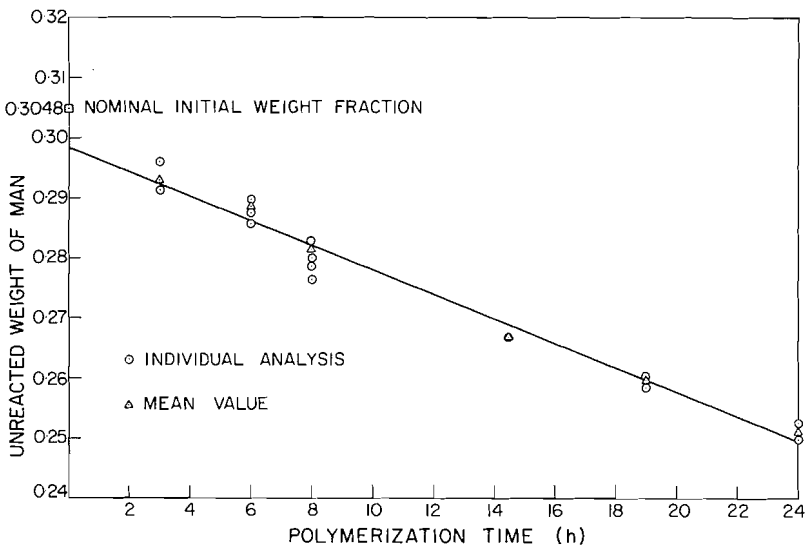

FIG. 1. Unreacted methacrylonitrile in 1 g initial total monomers as a function of reaction time. Feed composition: MAN/S/AMS = 5/5/5 ml.

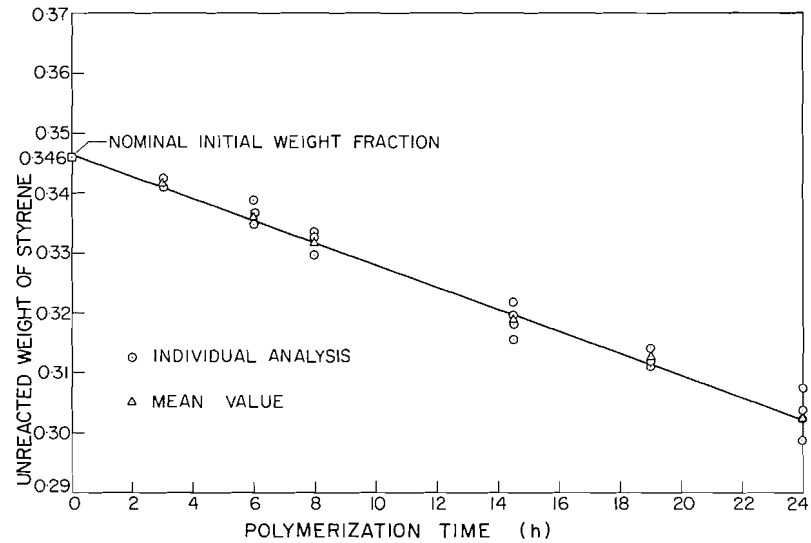

FIG. 2. Unreacted styrene in 1 g initial total monomers as a function of reaction time. Feed composition: as in Fig. 1.

periods. The boiling points of the reaction mixture ingredients are: MAN 90, toluene 110.6, S 145, and AMS 163 °C. The deviations between initial feeds and zero-time extrapolation values can be accounted for if the vapor pressure of the liquids at 60° are in approximately the same ratios as their boiling points. No clear reason can be seen for the difference between the present work and previous experience with the same technique, although it is possible that it may be connected with a change of operators. The method used requires consistent manual technique; and even variations in the drainage of the pipet used to make the monomer feed mixtures can result in a noticeable increase in scatter of data. In retrospect, the estimates of initial feed compositions from relative volumes of monomers should have been verified by weighings.

For the reasons outlined above, the initial feed compositions were taken from the zero-time extrapolated values of the best-fit lines through the concentration reaction time plots (as

Can. J. Chem. Downloaded from www.nrcresearchpress.com by 210.87.254.5 on 09/05/12
For personal use only.

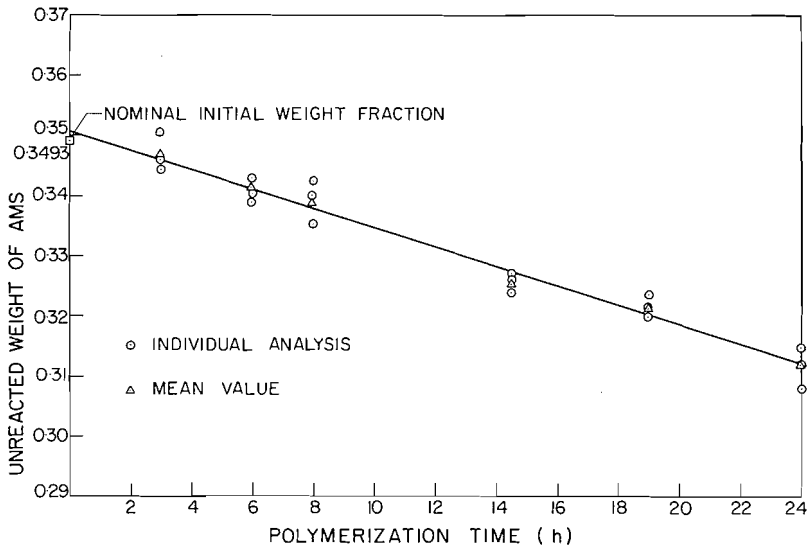

FIG. 3. Unreacted α-methylstyrene in 1 g initial total monomers as a function of reaction time. Feed composition: as in Fig. 1.

in Figs. 1–3) rather than from the make-up volumes. This procedure is consistent with the use of these lines to estimate relative monomer losses.

The experimental copolymer composition was compared to that calculated using the binary reactivity ratios reported previously for the three monomer pairs involved in these experiments (2–4). The instantaneous copolymer composition is given by the differential equation of Alfrey and Goldfinger (7): (eqs. 1 and 2) where the M_i are the molar concentrations of monomer i ($i = 1, 2, 3$) and r_{ij} ($i \neq j$) are the appropriate binary reactivity ratios. In the present case the monomer subscripts 1, 2, 3 refer to MAN, S, and AMS, respectively and the definitions of r_{ij} are the ones in standard use (14).

The terpolymer equation was integrated numerically, with a digital computer, using the method of Crescentini *et al.* (15) which assumes constant volume of reaction mixture. Integration was performed in increments of 0.001 mol change in M_3. The corresponding changes in M_1 and M_2 were calculated from eqs. 1 and 2 and the final monomer concentrations ($M_i - \mathrm{d}M_i$) were used as the initial values in the next iterative step. Fifty iterations accounted for about 15 weight percent conversion of monomers. The total weight percent conversion, conversion of each monomer and mean copolymer composition were calculated for each incremental change in M_3. The latter parameter is given by (15) eq. 3,

$$[3] \quad \bar{C}_{i\mu} = \frac{100 P_i \sum_{v=1}^{\mu} \delta M_{iv} \qquad i = 1, 2, 3}{\sum_{i=1}^{3} \sum_{v=1}^{\mu} P_i \delta M_{iv} \qquad P = 1, 2, \ldots}$$

where $\bar{C}_{i\mu}$ is the weight fraction of component i in the copolymer produced during μ iterative calculations, P_i is the formula weight of this monomer and δM_{iv} is the decrease in concentration of monomer i during the v'th iteration (from eqs. 1 and 2).

Reactivity Ratios

The binary ratios used in the foregoing calculations were reported previously (2–4). It should be noted in this connection that the reporting of a reactivity ratio as a single value with a standard deviation is not sound practice

$$[1] \quad \frac{\mathrm{d}M_1}{\mathrm{d}M_3} = \frac{M_1(M_1 r_{23} r_{32} + M_2 r_{31} r_{23} + M_3 r_{32} r_{21})(M_1 r_{12} r_{13} + M_2 r_{13} + M_3 r_{12})}{M_3(M_1 r_{12} r_{23} + M_2 r_{13} r_{21} + M_3 r_{12} r_{21})(M_3 r_{31} r_{32} + M_1 r_{32} + M_2 r_{31})}$$

$$[2] \quad \frac{\mathrm{d}M_2}{\mathrm{d}M_3} = \frac{M_2(M_1 r_{32} r_{13} + M_2 r_{13} r_{31} + M_3 r_{12} r_{31})(M_2 r_{21} r_{23} + M_1 r_{23} + M_3 r_{21})}{M_3(M_1 r_{12} r_{23} + M_2 r_{13} r_{21} + M_3 r_{12} r_{21})(M_3 r_{31} r_{32} + M_1 r_{32} + M_2 r_{31})}$$

Can. J. Chem. Downloaded from www.nrcresearchpress.com by 210.87.254.5 on 09/05/12
For personal use only.

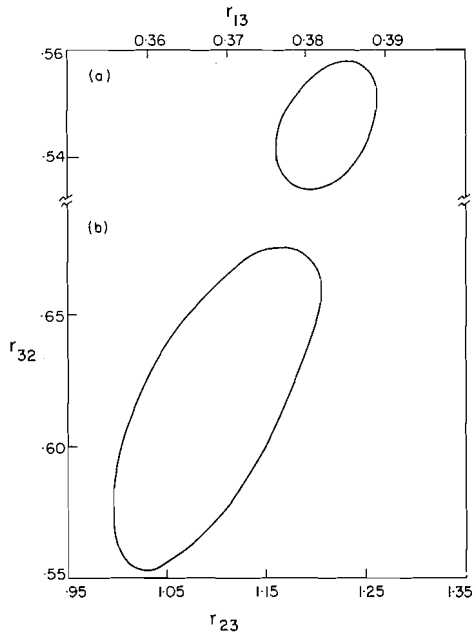

FIG. 4. Joint confidence limits for (*a*) methacrylonitrile (monomer 1) and α-methylstyrene (monomer 3) reactivity ratios, (*b*) styrene (monomer 2) and α-methylstyrene (monomer 3) reactivity ratios.

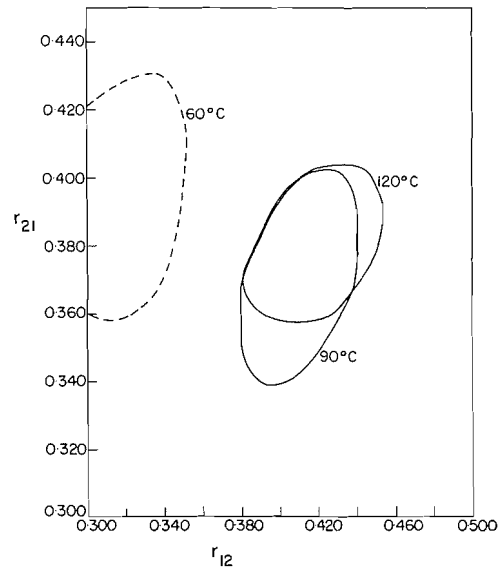

FIG. 5. Joint confidence limits for methacrylonitrile (monomer 1) and styrene (monomer 2) reactivity ratios.

because reactivity ratios are determined in pairs, and the corresponding experimental uncertainties are coupled. A better procedure involves calculation of joint confidence limits within which the correct values are believed to coexist with stated probability. Figure 4 shows the joint 95% confidence limits for MAN–AMS and S–AMS. These plots, which are combined from another report (3), were calculated by the method of Tidwell and Mortimer (16). Any point within the loops shown represents an equally likely ordered pair of reactivity ratios.

Joint confidence limit loops are shown in Fig. 5 for the methacrylonitrile–styrene pair. These calculations, which have not been reported before, are from the data of a previous study (4) of effects of temperature in this copolymerization. The data at 90 and 120 °C overlap and differ from those at 60 °C. It is expected theoretically that the temperature dependence of these reactivity ratios should be slight (17), and preliminary calculations did indeed show that calculated and experimental terpolymer compositions agreed better with r_{12} and r_{21} values from the overlapping elipses in Fig. 5 than from the 60 °C loop shown. This is further evidence, then, for the conclusion (4) that the reactivity ratios in this system are not significantly affected by reaction temperature in this range. The reasons for the deviation of the 60° copolymerization data are not clear.

Results

Table 2 compares the experimental and calculated mean terpolymer compositions at 5 weight percent total conversion of monomers. The reactivity ratios used were selected from the plots in Figs. 4 and 5 and are listed in Table 2. Other combinations of the six reactivity ratios could have been selected, of course, but a systematic study did not seem to be worthwhile, as a number of random selections of values from the joint confidence limit loops did not affect the agreement between experimental and calculated compositions very strongly.

The concordance between calculated and experimental copolymer compositions in Table 2 is about as close as those reported in studies of free radical terpolymerizations (8, 10, 15). The results indicate that the simple copolymerization model (7) is satisfactory, without allowance for penultimate effects or depropagation of sequences of α-methylstyrene units.

Prediction of copolymer composition is a

Can. J. Chem. Downloaded from www.nrcresearchpress.com by 210.87.254.5 on 09/05/12
For personal use only.

TABLE 2. Experimental and calculated copolymer compositions*

Feed composition MAN:S:AMS		Copolymer composition (mole fraction)					
		MAN		S		AMS	
Volumes (ml)	Mole fractions	Calcd.	Exp.	Calcd.	Exp.	Calcd.	Exp.
5:5:5	0.420:0.307:0.273	0.436	0.485	0.303	0.284	0.261	0.231
7:5:3	0.555:0.290:0.155	0.525	0.544	0.306	0.332	0.169	0.123
3:7:5	0.264:0.450:0.286	0.334	0.330	0.419	0.412	0.247	0.259
5:7:3	0.414:0.424:0.162	0.443	0.452	0.403	0.389	0.154	0.162
2:8:5	0.180:0.527:0.293	0.264	0.265	0.491	0.464	0.245	0.271
2:5:8	0.184:0.337:0.480	0.256	0.287	0.339	0.309	0.405	0.405

*Reactivity ratios: r_{12} 0.44, r_{21} 0.37, r_{13} 0.38, r_{31} 0.53, r_{23} 1.124, r_{32} 0.627.

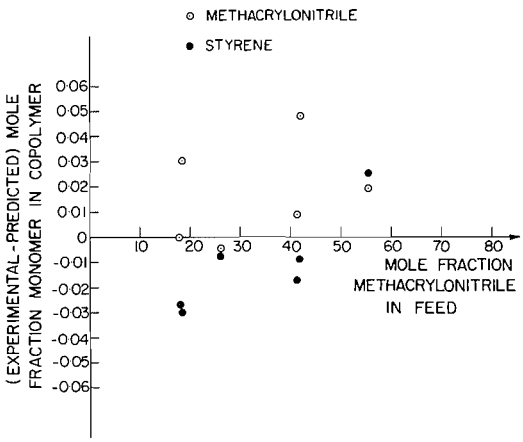

FIG. 6. Errors in prediction of copolymer composition as a function of methacrylonitrile content in feed.

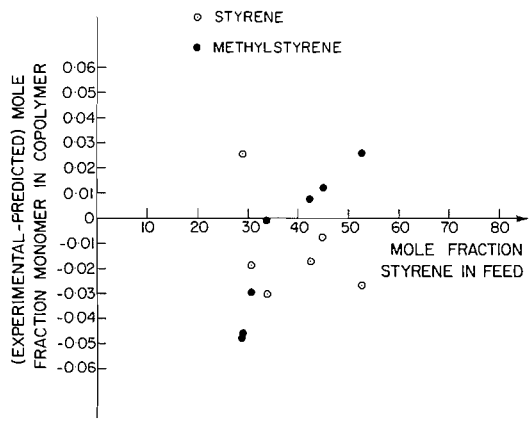

FIG. 7. Predictive errors as a function of styrene in feed.

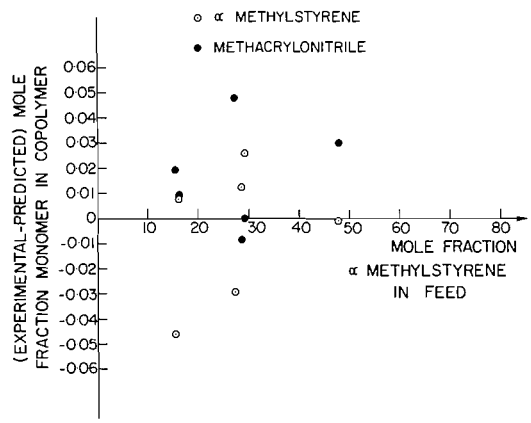

FIG. 8. Predictive errors as a function of α-methylstyrene content in feed.

necessary, but not sufficient condition to show that a particular copolymerization model describes a system. The model should also be shown to give estimates which are independent of extent of reaction or feed composition (6). In this connection, Figs. 6–8 show the deviations between experimental and calculated copolymer compositions plotted against methacrylonitrile and styrene feed compositions, respectively. No particular trend is noticeable with varying feed composition in these figures. Similar plots against percent conversion of monomers would be trivial in the present case, for reasons discussed below.

Differential and Integrated Copolymer Equations

Analytical errors are reduced if the reaction is carried to as high a conversion as possible, since the content of a given monomer in the polymer equals the difference between its initial and final measured contents in the feed mixture. The uncertainty in the copolymer analysis is thus a smaller proportion of the estimated quantity, the greater the magnitude of the decrease in

Can. J. Chem. Downloaded from www.nrcresearchpress.com by 210.87.254.5 on 09/05/12
For personal use only.

TABLE 3. Copolymer composition as a function of monomer conversion

Mole conversion (%)	Weight conversion (%)	Copolymer composition (mole fraction) MAN	S	AMS
(a) Mole fractions in feed: MAN 0.180, S 0.527, AMS 0.293				
0.31	0.30	0.266	0.490	0.244
1.24	1.19	0.266	0.490	0.244
4.01	3.86	0.264	0.491	0.245
8.30	8.00	0.262	0.492	0.246
15.28	14.75	0.259	0.494	0.247
(b) Mole fractions in feed: MAN 0.184, S 0.337, AMS 0.480				
0.19	0.18	0.258	0.338	0.404
1.15	1.11	0.258	0.338	0.404
6.10	5.88	0.256	0.339	0.405
9.50	9.17	0.255	0.339	0.406

monomer concentration in the feed (4). It seems appropriate under these circumstances to estimate reactivity ratios by fitting the data to an integrated form of the copolymer equation.

It should be noted, however, that straight-line representations, as in Figs. 1–3, imply that the copolymer composition does not vary significantly during the experiment. The ordinate in such a plot is the unreacted mass of a given polymer, with the intercept at zero reaction time being the mass of this monomer in unit total mass of monomers (weight fraction). The linear plot can then be expressed as:

$$[4] \qquad W_i = W_{0i} + S_i t$$

where W_i and W_{0i} are the mass of monomer i (in unit initial total mass of monomers) at reaction times equal to zero and t, respectively, and S_i is the slope of the line. The number of moles, P_i, of a given monomer in the polymer formed to time t is then:

$$[5] \qquad P_i = \frac{W_{0i} - W_i}{m_i} = \frac{S_i t}{m_i}$$

where m_i is the formula weight of monomer i. The corresponding mole fraction of this monomer in the polymer, f_i, is:

$$[6] \quad f_i = \left(\frac{S_i t}{m_i}\right) \Big/ \sum_i \left(\frac{S_i t}{m_i}\right) = \left(\frac{S_i}{m_i}\right) \Big/ \sum_i \left(\frac{S_i}{m_i}\right)$$

Thus f_i does not vary as long as the analytical data can be represented as shown in Figs. 1–3, by a line with constant slope, S. Conversely, a linear experimental relation shows that the copolymer composition does not vary significantly. Both the differential and integrated forms of the copolymer equation are then equally reliable in this range of monomer conversions. (The linearity observed cannot be expected to continue to complete conversion of monomers, except for azeotropic feed compositions (4).)

To illustrate this point, Table 3 lists integrated copolymer compositions calculated from the reactivity ratios listed in Table 2, for various conversions within our experimental range and at two of the more extreme feed compositions. The copolymer composition is seen to be almost invariant under these conditions if the simple copolymerization model describes the polymerization.

The predicted and experimental copolymer compositions could have been compared in the present case equally as well with a differential copolymer equation (eqs. 1 and 2) as with the integrated form which was actually used. Other factors must be taken into account, however, if the object of the experiments is the calculation of reactivity ratios from the analytical data. The best procedure then involves use of a non-linear least squares fit to a differential equation or use of an integrated form of the copolymer equation. A linear least squares fit of reactivity ratios to analytical data in a differential copolymer equation can lead to errors even when the polymer composition does not vary over the experimental range of monomer conversions (3, 4, 6, 16).

These considerations suggest that it might be possible to estimate reactivity ratios directly

Can. J. Chem. Downloaded from www.nrcresearchpress.com by 210.87.254.5 on 09/05/12
For personal use only.

Can. J. Chem. Downloaded from www.nrcresearchpress.com by 210.87.254.5 on 09/05/12
For personal use only.

from gas chromatographic analyses of multicomponent polymerizations in some cases. If the plots of unreacted monomer against polymerization time are linear a sufficient number of analyses should be made to establish the slope of these lines accurately. A least-squares fit to eqs. 1 and 2 can then be made by computer iterations starting with approximate reactivity ratio values (as from Q–e calculations) to obtain the best values of the reactivity ratios. This procedure is being investigated and will be reported separately if it should prove to be mathematically tractable.

Azeotropy in Ternary Copolymerizations

The question of azeotropy in ternary copolymerization has been discussed extensively (18–22). Tarasov and coworkers (22) suggest that a necessary and sufficient condition for existence of an azeotrope is that S, Q, and R (eqs. 7*a–c*) have the same sign and are different from zero. The azeotropic feed composition is given by eq. 8. Substitution of the reactivity ratios listed in Table 2 into eq. 8 gives the azeotropic feed as 0.471, 0.320, and 0.209 in terms of mole fractions of MAN, S, and AMS, respectively.

$$[7a]\quad S=\left(1-\frac{1}{r_{13}}\right)\left(\frac{1}{r_{32}}-1\right)-\left(\frac{1}{r_{12}}-\frac{1}{r_{13}}\right)\left(\frac{1}{r_{31}}-1\right)$$

$$[7b]\quad Q=\left(\frac{1}{r_{21}}-\frac{1}{r_{23}}\right)\left(\frac{1}{r_{12}}-\frac{1}{r_{13}}\right)-\left(1-\frac{1}{r_{23}}\right)\left(1-\frac{1}{r_{13}}\right)$$

$$[7c]\quad R=\left(\frac{1}{r_{31}}-1\right)\left(1-\frac{1}{r_{23}}\right)-\left(\frac{1}{r_{32}}-1\right)\left(\frac{1}{r_{21}}-\frac{1}{r_{23}}\right)$$

$$[8]\quad M_1:M_2:M_3=R\left(\frac{Q}{r_{13}r_{32}}+\frac{S}{r_{12}r_{23}}+\frac{R}{r_{12}r_{13}}\right):S\left(\frac{S}{r_{21}r_{23}}+\frac{Q}{r_{23}r_{31}}+\frac{R}{r_{21}r_{13}}\right):Q\left(\frac{Q}{r_{31}r_{32}}+\frac{S}{r_{21}r_{32}}+\frac{R}{r_{12}r_{31}}\right)$$

None of the experimental feeds listed in Table 2 has exactly the same composition as that calculated for the azeotropic mixture. The listed mixtures which resemble the azeotrope to the extent that the mole fraction of MAN is greater than 0.4 do, however, yield polymers with compositions sufficiently close to that of the feed to qualify as azeotropic reactions, for practical synthetic purposes.

Slocombe (23) proposed an empirical rule for prediction of the occurrence of high clarity terpolymers. Termonomer systems which form two azeotropic copolymers were found to give clear products frequently when the ratio of monomers in the feed was taken from values on a line joining the azeotropic compositions in a triangular diagram. An example given was the acrylonitrile–styrene – α-methylstyrene system, which is formally similar to the monomer trio in this report. (It should be noted, however, that the reactivity ratios Slocombe used for the styrene – α-methylstyrene pair are quite different from those found in this laboratory (2).)

In binary systems, an azeotropic composition is defined by eq. 9. Both reactivity ratios must

$$[9]\quad \frac{M_i}{M_j}=\frac{1-r_{ji}}{1-r_{ij}}$$

be less than unity for occurrence of an azeotrope. In the present case, binary azeotropes can be formed by the styrene–methacrylonitrile and methacrylonitrile – α-methylstyrene monomer pairs. A plot of the data according to Slocombe's rule suggests that termonomer feeds containing about 0.5 mol fraction of methacrylonitrile and various corresponding combinations of styrene and α-methylstyrene concentrations would yield clear copolymers. This is consistent with the conclusions from the results in Table 2 that the experimental feeds with higher methacrylonitrile content gave copolymers with compositions quite close to that of the monomer mixture. The products of such reaction mixtures can evidently not vary much in composition as the monomer charge is depleted.

While no true azeotrope has been demonstrated in this work, it is clear nevertheless that a number of monomer mixtures gave products which are close enough to the azeotropic state to be so treated for all practical purposes. In this case, also, both the expression of Tarasov *et al.* (22) and Slocombe's rule (23) apparently predict

the azeotropic composition with an accuracy suitable for most purposes. (Slocombe's rule must be interpreted in this context as implying that optical clarity of the copolymer product indicates an invariant, azeotropic composition.)

Discussion

The results of this work support the conclusions of previous studies (2, 3) that free radical copolymerization behavior of α-methylstyrene is described by the conventional simple model in which the reactivity of a given polymer radical is determined only by the natures of the terminal unit in the radical and the adding monomer. The sequence lengths of this monomer in binary copolymers with styrene and methacrylonitrile are sufficiently short that their ceiling temperatures (24) are considerably higher than that of high molecular weight poly(α-methylstyrene). This difference stems from the inverse relation between enthalpy of polymerization and degree of polymerization, at low poly(α-methylstyrene) molecular weights (25). That is to say, the composition of binary copolymers was indicated to be controlled by kinetic rather than by possible thermodynamic (ceiling temperature) or steric (penultimate unit) effects.

Kinetic control would be expected to be even more pronounced in terpolymerizations than in binary copolymerizations. The average sequence length in high molecular weight terpolymers is smaller than in any one of the corresponding three binary copolymers made from the same feed ratio (26). It is not surprising, then, that the simple copolymer model which was found to apply in the binary cases also describes the terpolymerization.

Free radical polymerization of α-methylstyrene tends to be comparatively slow. This presumably reflects the existence of a normal bimolecular termination rate and slow propagation rate due to steric hindrances at the doubly substituted vinyl carbon atom. (Transfer of an allylic hydrogen from the α methyl could also be a factor.) Qualitatively, we note that polymerization rates are faster in a termonomer system than in binary polymerizations. Feeds (Table 2) with relatively low α-methylstyrene concentrations gave conversions of about 15% total monomers in 24 h at 60 °C. The conversion for higher α-methylstyrene contents was about 9%, but both polymerization rates are considerably faster than those noted previously in binary systems (2, 3). This would be expected to parallel the lower mean sequence lengths of terpolymers.

The authors thank the Defence Research Board of Canada for financial support.

1. H. K. JOHNSTON and A. RUDIN. J. Paint Technol. **42**, 430 (1970).
2. H. K. JOHNSTON and A. RUDIN. J. Paint Technol. **42**, 435 (1970).
3. H. K. JOHNSTON and A. RUDIN. Macromol. 4, 661 (1971).
4. A. RUDIN and R. G. YULE. J. Polym. Sci. A-1, **9**, 3009 (1971).
5. F. R. MAYO and F. M. LEWIS. J. Am. Chem. Soc. **66**, 1594 (1944).
6. P. W. TIDWELL and G. A. MORTIMER. J. Macromol. Sci.-Revs. C4, 281 (1970).
7. T. ALFREY, JR. and G. GOLDFINGER. J. Chem. Phys. **12**, 322 (1944).
8. C. WALLING and E. R. BRIGGS. J. Am. Chem. Soc. **67**, 1774 (1945).
9. R. G. FORDYCE, E. C. CHAPIN, and G. E. HAM. J. Am. Chem. Soc. **70**, 2489 (1948).
10. C. SIMEONESCU, N. ASANDIE, and A. LIGA. Makromol. Chem. **110**, 278 (1967).
11. S. L. AGGARWAL and F. A. LONG. J. Polym. Sci. **11**, 127 (1953).
12. K. TAKEMOTO, Y. KIKUCHI, and M. IMOTO. Chem. High Polym. (Tokyo). **23**, 459 (1966).
13. G. G. CAMERON, D. H. GRANT, N. GRASSIE, J. E. LAMB, and I. C. MCNEIL. J. Polym. Sci. **36**, 173 (1959).
14. T. ALFREY, JR., J. J. BOHRER, and H. MARK. Copolymerization. Interscience, 1952.
15. L. CRESCENTINI, G. B. GECHELE, and A. ZANELLA. J. Appl. Polym. Sci. **9**, 1323 (1965).
16. P. W. TIDWELL and G. A. MORTIMER. J. Polym. Sci. A3, 369 (1965).
17. K. F. O'DRISCOLL. J. Macromol. Sci. A3, 307 (1969).
18. W. RING. Europ. Polym. J. **4**, 413 (1968).
19. K. F. O'DRISCOLL and G. E. HAM. J. Macromol. Sci.-Chem. A1, 1365 (1967).
20. G. E. HAM. J. Macromol. Chem. **1**, 93 (1966).
21. R. K. S. CHAN and V. MEYER. J. Macromol. Sci.-Chem., A1, 1089 (1967).
22. A. I. TARASOV, V. A. TSAI, and S. S. SPASKII. Vysokomolekul. Soedin. **2**, 1601 (1900).
23. R. J. SLOCOMBE. J. Polym. Sci. **26**, 9 (1957).
24. F. S. DAINTON and K. IVIN. Quart. Rev. (London), **12**, 61 (1958).
25. D. E. ROBERTS and R. S. JESSUP. J. Res. Natl. Bur. Stand. **46**, 11 (1951).
26. C. TOSI. Europ. Polym. J. **6**, 161 (1970).

Can. J. Chem. Downloaded from www.nrcresearchpress.com by 210.87.254.5 on 09/05/12
For personal use only.

Thermolysis of γ-Phenylazo-γ-valerolactone

H. LUI AND J. WARKENTIN
Department of Chemistry, McMaster University, Hamilton, Ontario
Received January 20, 1972

γ-Phenylazo-γ-valerolactone decomposed at 230° to 4,5-dihydro-6-methyl-2-phenyl-3(2*H*)-pyridazinone and to 6-methyl-2-phenyl-3(2*H*)-pyridazinone.

La γ-phénylazo-γ-valérolactone se décompose à 230° pour donner la 4,5-dihydro-6-méthyl-2-phényl-3(2*H*)-pyridazinone et la 6-méthyl-2-phényl-3(2*H*)-pyridazinone.

Canadian Journal of Chemistry, **50**, 1767 (1972)

Can. J. Chem. Downloaded from www.nrcresearchpress.com by 210.87.254.42 on 09/05/12
For personal use only.

Introduction

A γ-phenylazo-γ-lactone (**1**) and a δ-phenylazo-δ-lactone (**2**) were synthesized recently by oxidation of appropriate phenylhydrazones with lead tetraacetate (1, 2). The chemistry of these

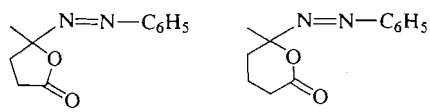

1 2

unsymmetrical azo compounds is of interest because they are potential sources of the corresponding γ- and δ-lactonyl radicals, the chemistry of which has not been explored. For example, the reactions of eq. 1 might occur; acyl radicals and α-alkoxyalkyl radicals being well known intermediates in other reactions. Accordingly we pyrolyzed **1**, both neat and as a solution in cumene.

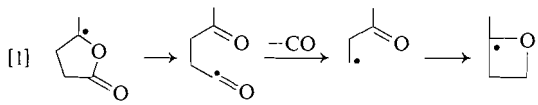

Results and Discussion

The azo compound, **1**, was found to be surprisingly stable, with a half life at 230° (neat) near $3\frac{1}{2}$ h. For comparison, phenylazo-1,1-dimethylethane is reported (3) to be extensively decomposed on distillation at 56–58° (2.3 mm). Therefore substitution of ester oxygen for carbon, depicted below, appears to increase the stability of an azo compound substantially.

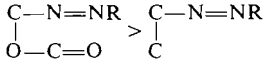

The products of thermolysis of **1** were also surprising. Analysis and molecular weight revealed that the major non-volatile products differ from starting material by one oxygen atom or by one oxygen and two hydrogen atoms. Their spectra suggested that appropriate structures might be **3** and **4**, respectively; an assignment that was confirmed by independent synthesis. The ratio (**3**:**4**) was 1.75:1, from pyrolysis of neat **1**, and the combined yield (estimated by n.m.r.) was greater than 80%. Gaseous products, which comprised about 0.5 mol per mol of **1** decomposed, consisted mainly of N_2 (and/or CO) and CO_2. Oxygen was also present but the amount of the latter varied from one run to another, presumably because it reacts at 230° with the organic materials present. Water and benzene were also detected.

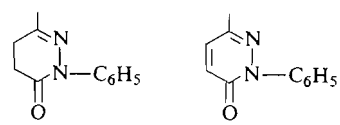

3 4

It is fairly clear from the product composition that the major reaction pathway does not involve homolytic C—N bond-breaking characteristic of the high temperature chemistry of azo compounds. In view of this unexpected course, it became important to attempt rationalization of the reactions that do occur. An attractive first step is intramolecular nucleophilic addition to the carbonyl group, to form a bicyclo-[2.2.1]-system, which could open to a six-membered ring, eq. 2. If **6** were formed it might undergo an intramolecular addition of the Michael type, leading to **7** which in turn could open to the nitrone (**8**), eq. 3. Tautomerization of **8**, possibly by the action of the basic oxygen atom

Can. J. Chem. Downloaded from www.nrcresearchpress.com by 210.87.254.42 on 09/05/12
For personal use only.

[2] 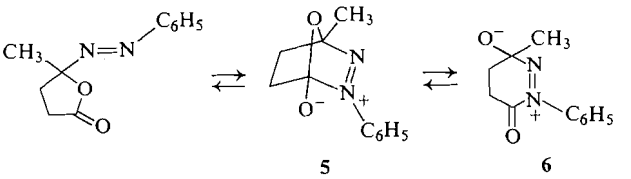

5 6

[3] 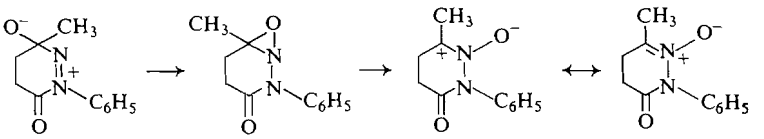

6 7 8

[4] 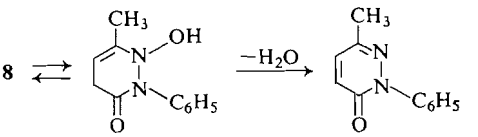

9 4

[5] 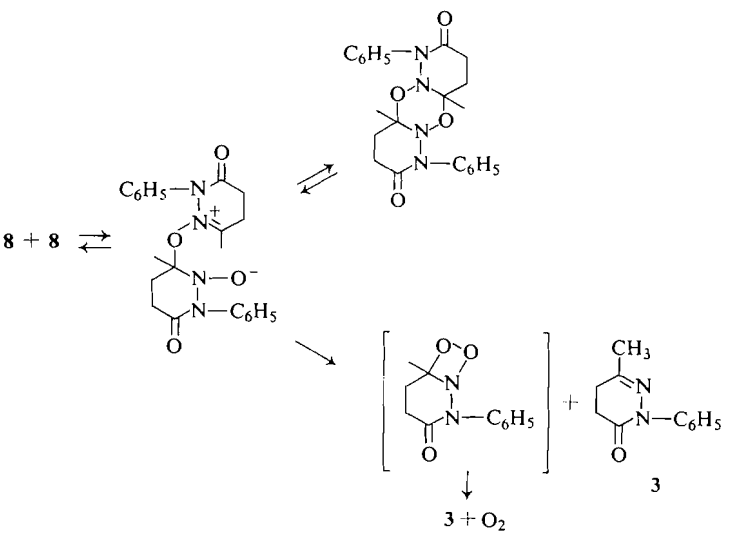

of one molecule on the acidic ring protons of another (4), to hydroxylamine system **9**, is analogous to enolization (5). Finally, loss of water by 1,4-elimination (eq. 4) could lead to **4**.

It is more difficult to devise a reasonable route to the major product **3**, which differs from the substrate by one oxygen atom. Although organic reactions which liberate oxygen are rare, we considered the possibility that two molecules of **3**, and one of O_2, are formed in a bimolecular process from isomers of **1**. One such scheme is shown as eq. 5. We tentatively propose this mechanism because of the known tendency of nitrones to dimerize (5) and because, in invoking **8** as intermediate, it is consistent with the proposed mechanism for forming **4**.

In an attempt to change the reaction course through capture of an intermediate, **1** was heated at 230° in cumene. Again **3** and **4** were obtained, in approximately 1.3:1 ratio. A control experiment showed that **4** is not reduced to **3** by cumene under those conditions. The product ratio from pyrolysis of **1** in cumene is therefore about the same as that from pyrolysis of

neat **1** and provides no information about mechanism.

Experimental

γ-Phenylazo-γ-valerolactone (**1**, 1.9242 g, 0.0094 mol) was heated at 230° under nitrogen for 7 h. The crude product was placed on alumina (Fisher A950, 28 × 1.5 cm column) from which fractions were eluted with ether.

The first fraction (100 ml) contained a reddish-brown solid, m.p. 100–102°, which was recrystallized from a solution of alcohol in petroleum ether (1:1) to yield a white solid (0.97 g, 55%), m.p. 104–106°, identified as 4,5-dihydro-6-methyl-2-phenyl-3(2*H*)-pyridazinone (**3**) (lit.[1] (6) m.p. 107°), p.m.r. (CCl_4) δ 2.04 (s, 3, CH_3), 2.65 (s, 4, CH_2CH_2), 7.35 (m, 5, C_6H_5); i.r. ($CHCl_3$) 1670 cm^{-1} (C=O); u.v. (C_2H_5OH) λ_{max} 235 nm, log ε 4.02; mass spectrum (*m/e*, relative intensity in brackets) 189(14), 188(100), 186(12), 185(8), 160(8), 159(14), 119(62), 105(8), 93(12), 92(24), 91(30), 77(50), 65(8), 64(10), 53(8), 51(18).

The second 100 ml fraction from the column yielded a yellow semi-solid which was crystallized from ethanol in petroleum ether (1:1) to give 0.35 g (20%) of colorless plates identified as 6-methyl-2-phenyl-3(2*H*)-pyridazinone (**4**), m.p. 77.5–78° (lit. (6) m.p. 79–80°). Identity of this compound was confirmed by analysis, through its formation from **3** (see below), and from its spectra: p.m.r. (CCl_4) δ 2.28 (s, 3, CH_3); 6.88 (q, 2, vinyl); 7.48 (m, 5, C_6H_5); i.r. (CCl_4) 1675 cm^{-1} (C=O); u.v. (C_2H_5OH) λ_{max} 312 nm, log ε 3.64; mass spectrum (*m/e*, relative intensity in brackets) 188(20), 187(14), 186(100), 185(46), 158(22), 157(20), 119(12), 118(6), 117(8), 93(10), 92(12), 77(52), 53(30), 52(8), 51(20), 50(8).

Anal. Calcd. for $C_{11}H_{10}N_2O$ (mol. wt. 186): C, 70.96; H, 5.38; N, 15.05. Found (199 (vaporimetric)): C, 70.94; H, 5.32; N, 15.10.

Further fractions from the column gave small amounts of colored materials which were not identified.

4,5-Dihydro-6-methyl-2-phenyl-3(2H)-pyridazinone from Levulinic Acid Phenylhydrazone

Levulinic acid phenylhydrazone (31.5 g) was stirred for 24 h at room temperature with 150 ml of concentrated H_2SO_4 (6). The solution was diluted to 1600 ml with crushed ice and the white precipitate which settled was collected. It was washed several times with cold dilute bicarbonate solution and with water before it was dried. Crystallization from methanol gave the title compound (70%), m.p. 105–106°, with spectra identical to those of **3** obtained from **1** by pyrolysis. The mixture m.p. was 105–106°.

Thermolysis of 1 in Cumene

The lactone (**1**, 0.57 g, 2.8 mmol) and freshly-distilled cumene (1 ml), in an evacuated, sealed tube, were heated at 230° for 7 h. Cumene was then removed by vacuum distillation. The n.m.r. spectrum of a portion of the residue indicated roughly 50% of starting material still present, together with **3** and **4** in the ratio 1.3:1, respectively. Chromatography on neutral alumina (Fisher A950, 20 × 1.5 cm column) yielded **3** and **4** in the ratio 1.2:1 and unreacted **1**.

In a control experiment, **4** was heated with cumene at 230° for 7 h. The residue left after distillation showed only **4**, and no trace of **3**, by n.m.r.

Oxidation of 3 with DDQ

4,5-Dihydro-6-methyl-2-phenyl-3(2*H*)-pyridazinone (2.0 g, 0.01 mol) was treated with 2,3-dichloro-5,6-dicyano-1,4-benzoquinone (DDQ, 2.4 g, 0.01 mol) in refluxing dioxane (80 ml). The color of the solution changed from green to brown during the sixth hour and crystals of the hydroquinone settled out. After 40 h had elapsed, the mixture was filtered and dioxane was removed from the filtrate by vacuum distillation. The residue was placed on a column (30 × 2.5 cm) of neutral (A 950) alumina. Elution with petroleum ether (2 l), followed by 50% ether in petroleum ether gave **4** which was obtained as colorless plates by recrystallization from CCl_4, m.p. 77.5–78°. Spectra of this material matched those of material, labelled **4**, originating from pyrolysis of **1**.

Gaseous Products

A sample of **1** (0.174 g, 0.85 mmol) was heated neat at 230° for 7 h in an evacuated tube fitted with a breakseal. The tube was fitted to a Hitachi RMU-6A mass spectrometer where the quantity of gas was found by expanding it from the cold tube into a calibrated section of the instrument. The volume was 141 cc at 52.5 mm and 293 °K; 0.41 mmol or 48%, based on one to one stoichiometry. Composition was estimated from the peak intensities at *m/e* 28, 32, and 44 to be $N_2:O_2:CO_2 = 1.7:1.9:1$; assuming that *m/e* 28 was primarily from N_2 and not from CO. The ratios varied greatly from run to run, with CO_2 apparently dominating in some cases, and with O_2 much less prominent. They have no quantitative significance.

The residue in the tube was dissolved in CCl_4 and the solution was filtered. A p.m.r. spectrum of the material showed primarily two products, **3** and **4**, in the ratio 1.75:1, and no trace of starting material.

[1]The authors (6) named **3** incorrectly as 2-phenyl-6-methyl-3-pyridazinone.

1. G. B. Gubelt and J. Warkentin. Can. J. Chem. **47**, 3983 (1969).
2. J. Warkentin. Synth. 279(1970).
3. D. Y. Curtin and J. L. Tveten. J. Org. Chem. **26**, 1764 (1961).
4. H. K. Kim and P. M. Weintraub. J. Org. Chem. **35**, 4282 (1970).
5. Reviews of nitrone chemistry. J. Hamer and A. Macaluso. Chem. Rev. **64**, 473 (1964); G. R. Delpierre and M. Lamchen. Quart. Rev. (London), **19**, 329 (1965).
6. W. G. Overend and L. F. Wiggins. J. Chem. Soc. 549 (1947).

Can. J. Chem. Downloaded from www.nrcresearchpress.com by 210.87.254.42 on 09/05/12
For personal use only.

Mechanisms of S_Ni Reactions. The Kinetics of the Decomposition of Aralkyl Carbonates[1]

J. M. PROKIPCAK AND T. H. BRECKLES
Department of Chemistry, University of Guelph, Guelph, Ontario

Received August 19, 1971[2]

Anisylic phenyl carbonates decomposed at elevated temperatures to give CO_2 and the corresponding anisylic phenyl esters. The decomposition follows first order kinetics very similar to those found for alkyl chloroformates. The decompositions involve the heterolysis of the aralkyl oxygen bond followed by the breakdown of the subsequent ion pair via a cyclic mechanism. The dependence of the decomposition rates on the nature of the solvent and structural changes of the starting carbonates is discussed.

Les carbonates d'anisyle et de phényle se décomposent à hautes températures pour donner du CO_2 et les oxydes correspondants d'anisyle et de phényle. La décomposition obéit à une loi cinétique du premier ordre, très semblable à celle trouvée dans le cas des chloroformates d'alkyle. La décomposition implique l'hétérolyse de la liaison aralkyle-oxygène, suivie d'une dissociation de la paire d'ions par un mécanisme cyclique. L'influence sur les vitesses de décomposition de la nature du solvant et de modifications structurales dans les carbonates de départ, est discutée.

Canadian Journal of Chemistry, **50**, 1770 (1972)

Introduction

Previous work (1) indicated that the decomposition under investigation could follow one of the two paths as shown in Scheme 1. The overall reaction scheme applies to two analogous reactions. One is the thermal decomposition of thiocarbonates (2, 3) which involves a path 1 mechanism, whereas similar experiments on alkyl chloroformates (4, 5) show that the path 2 mechanism (or path 1 with $k_2 \gg k_{-1}$) may be operative. The basic difference in the two reaction paths is the timing of the various bond scissions.

All the carbonates studied decomposed reasonably fast at 150 °C to give excellent yields of the corresponding ethers. The variation in decomposition rates due to structural changes in R and R^1 as well as solvents of different dielectric constants was examined. This report gives the result of the investigation and a mechanism is proposed with particular attention being given to the question of timing of the various bond scissions.

Experimental

Synthesis and Decomposition of Carbonates

The synthesis, physical constants, etc. of the carbonates

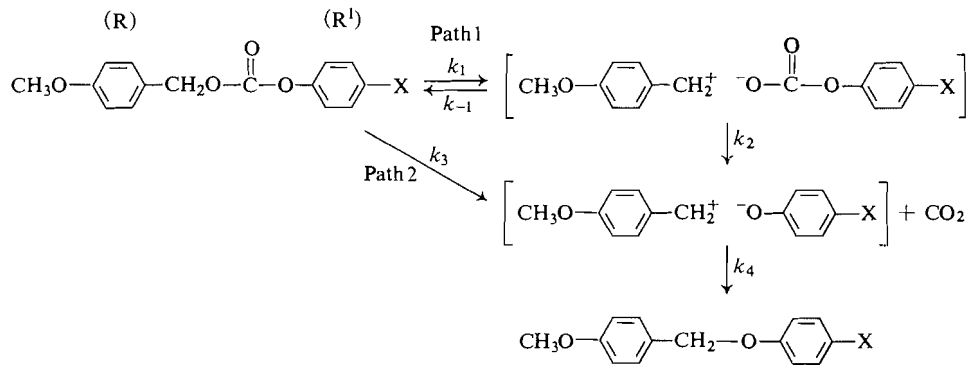

SCHEME I

[1]Taken from the thesis of T. H. Breckles presented to the Faculty of Graduate Studies, University of Guelph, Guelph, Ontario, as part of the requirements for the degree of Master of Science.

[2]Revision received February 23, 1972.

Can. J. Chem. Downloaded from www.nrcresearchpress.com by 210.87.254.105 on 09/05/12
For personal use only.

TABLE 1. Kinetics of the decomposition* of anisylic phenyl carbonates† at 150°

R	R^1	k_1 (s^{-1})
Anisyl (*p*-methoxybenzyl)	*p*-Methylphenyl	1.50×10^{-4}
	p-Methoxyphenyl	1.61×10^{-4}
	Phenyl	1.74×10^{-4}
	p-Chlorophenyl	8.37×10^{-4}
	p-Cyanophenyl	4.97×10^{-3}
	p-Nitrophenyl	1.36×10^{-2}
3,4-Dimethoxybenzyl	*p*-Methylphenyl	1.59×10^{-4}
	p-Methoxyphenyl	1.93×10^{-4}
	Phenyl	3.02×10^{-4}
	p-Chlorophenyl	1.31×10^{-3}
	p-Cyanophenyl	7.45×10^{-3}
	p-Nitrophenyl	1.49×10^{-2}

*Decompositions carried out using hexamethylphosphoramide as solvent.

†General structure is R—O—C(=O)—O—R^1.

used in this study can be found in previous work (*1*). Similarly their decomposition temperatures, the identification of phenolic side products, the characterization of the major products (anisylic phenyl ethers) along with their physical constants and elemental analysis are reported.

Kinetics of the Decompositions

The decompositions of all the carbonates were followed by means of n.m.r. using a Varian A 60A instrument. A typical kinetic run will be outlined. A solution of the carbonate (5.0 g) in hexamethylphosphoramide (4 cc) was made and equal aliquots (0.5 ml) of this solution were put into a series of n.m.r. tubes. These tubes were placed in an equilibrated (constant temperature) oil bath at 150°. These tubes were then removed at proper time intervals and immediately quenched in a Dry Ice–acetone mixture. Equivalent amounts of diglyme (1.0 ml) were added to each tube to act as a standard and the carbonate methylene peak and the diglyme standard peak were measured. The relative integrated areas gave the carbonate concentration changes. Diglyme was used as a standard for three reasons: (*1*) diglyme did not have numerous peaks in the critical region of the n.m.r. spectrum which was being used; (*2*) diglyme had a singlet near the carbonate methylene peak which meant that only a small portion of the n.m.r. spectrum had to be integrated; (*3*) all reaction components were soluble in diglyme.

Results and Discussion

Using the aforementioned method, the decompositions were found to exhibit good first order kinetics over at least 90% of the reaction. The first order rate constants were obtained by plotting log concentration *vs.* time. Table 1 summarizes the results of the various kinetic runs for the anisyl *p*-substituted phenyl series. The method of least squares was used in order to determine the slopes of the lines and in all cases regression coefficients of at least 0.990 were obtained.

In order to get as complete a picture as possible, the influence of both R and R^1 on the decomposition rates was investigated. First the effect of structural changes of the aralkyl group (R) was examined. This group would form the carbonium ion in the reaction if indeed it formed and any variation in rate of decomposition would indicate just how dependent the reaction is on this carbonium ion formation. The results in Table 2 indicate that the mechanism involves at least in part the heterolysis of the aralkyl–oxygen bond with the formation of an aralkyl carbonium ion. The relative decomposition rates are very similar to what one would expect on the basis of carbonium ion stability. For example, the addition of a methoxy group which has the ability to stabilize an electron deficient center by its inductive effect causes an increase in decomposition rate. This is shown to be the case in going from the benzhydryl to the *p*-methoxybenhydryl as well as from the anisyl to the 3,4-dimethoxybenzyl compounds. Furthermore when one adds a benzene ring to the aralkyl group, one adds resonance stability to any carbonium ion that may be forming and an increase in rate should be observed. This occurred when a comparison of decomposition rates was made between the anisyl phenyl and *p*-methoxybenzhydryl phenyl carbonates. The variation in decomposition rates with the variation of the aralkyl group's ability to stabilize an electron deficient center by resonance or an inductive effect would seem to indicate at least partial carbonium ion formation is occurring.

Further support for the heterolysis of the aralkyl–oxygen bond is drawn from the influence of solvents of different ionizing powers. In order to make the solvent comparisons as valid as possible, all kinetic runs were carried out at 150°. At this temperature, the decomposition in diphenyl ether did not, practically speaking, occur. The decomposition reactions did occur more rapidly in solvents of high ionizing power. This very marked difference in rate upon going to solvents of the high ionizing power indicates that under the reaction conditions, the decomposition reaction does involve an ionization process (6). However, how complete this ionization actually is is not known at this time.

Can. J. Chem. Downloaded from www.nrcresearchpress.com by 210.87.254.105 on 09/05/12
For personal use only.

TABLE 2. Decomposition rates of aralkyl phenyl carbonates*

Aralkyl group (R)	Solvent (dielective constant)	k_1 (s^{-1})	Relative rate
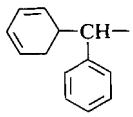	Hexamethylphosphoramide (HMP)	1.61×10^{-5}	0.05
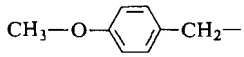	HMP	1.74×10^{-4}	0.57
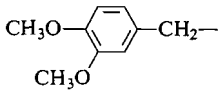	Dimethylformamide (38.9)	3.29×10^{-4}	1.09
	HMP (30.0)	3.02×10^{-4}	1.00
	Benzonitrile (25.2)	5.42×10^{-5}	0.18
	Diphenyl ether (3.65)	Too slow to measure	
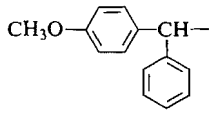	HMP	3.37×10^{-2}	112

*General structure is 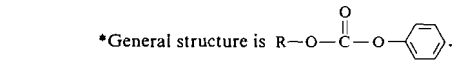 .

The dependence of the decomposition rates on the nature of the substituted phenoxy group (R^1) was next investigated. Whether the actual mechanism involved path 1 or 2, there should be a correlation between the decomposition rate and the electron-withdrawing character of the phenoxy group. One should observe an enhancement in rate by an electron-withdrawing group since this should stabilize the negative charge of the carboxylate ion or the R^1O^- anion. This was in fact what was found when a plot of log k/k_0 *vs.* σn (7) was made for the two series. Figure 1 shows the plots for the anisyl and 3,4-dimethoxybenzyl series. Both series yielded a ρ value of +2.11. As in the case of the kinetic runs, the method of least squares was used to determine the slope of the two Hammett plots. The positive ρ values obtained would indicate that the decomposition of the transition state requires the dispersal of a negative charge which has accumulated adjacent to the benzene ring carrying the substituent, *i.e.* the phenoxy group. These results are in accord with results from studies of urethanes (8), thiocarbonates (2), and thiosulfonates (9). The fact that both series investigated have the same positive value is not surprising since the only difference between the anisyl phenyl and 3,4-dimethoxybenzyl phenyl carbonate is the additional methoxy group on the benzyl portion of the molecule. This could help to stabilize the positive charge when formed but would have no effect on the dispersal of the negative charge on the anion portion of the molecule.

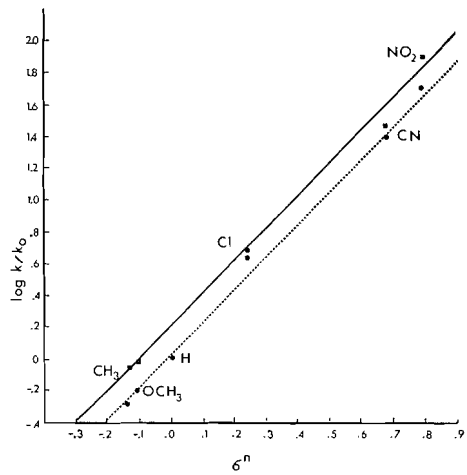

FIG. 1. Log k/k_0 for carbonates plotted against Hammett σ^n values, solid line for anisyl phenyl carbonates and dashed line for 3,4-dimethoxybenzyl phenyl carbonates. The ρ values for both plots were + 2.11

An interesting aspect of the decomposition was found when the rates of decomposition of the various anisyl phenyl carbonates were plotted against the pK_A values of the corresponding substituted phenols (Fig. 2). It can

Can. J. Chem. Downloaded from www.nrcresearchpress.com by 210.87.254.105 on 09/05/12
For personal use only.

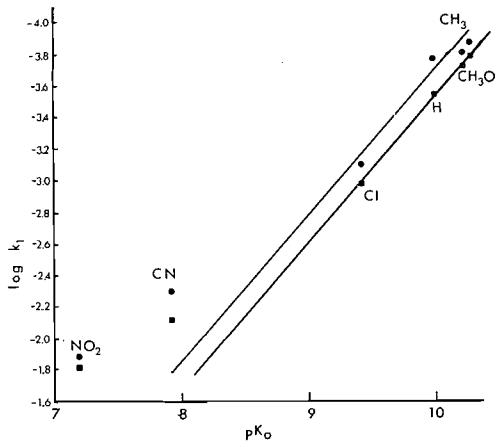

FIG. 2. First order rate constants for the anisyl (●) and 3,4-dimethoxybenzyl (■) phenyl carbonates *vs.* the pK_A values of *p*-substituted phenols H—O—C$_6$H$_4$—X.

be seen from Fig. 2 that *p*-cyano and *p*-nitrophenol deviate from the straight line and these two rates are appreciably slower than would be expected on the basis of pK_A values. The observed deviation could be explained by a transition state of anionic character in which the *p*-CN and *p*-NO_2 groups can only interact partially with the full negative charge. Such would be the case if the anionic species in the transition state were the carboxylate anion. Here the negative charge is removed from the phenolic portion of the molecule and thus only a part of this charge can interact mesomerically with the *p*-CN or *p*-NO_2 group. If the negative charge which is to be dispersed in the transition state were on the phenolic oxygen, the *p*-CN and *p*-NO_2 groups would be able to exert their full influence and the relative decomposition rates should coincide with the pK_A values of the corresponding substituted phenols. This effect has been previously observed for thiocarbonate decompositions (2).

Another possible explanation would be to consider a transition state such as below where the initial ion pair intermediate resulting from the aralkyl–oxygen bond cleavage can break down via a cyclic mechanism.

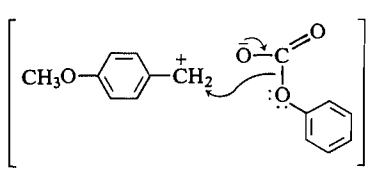

The electrons on the phenolic oxygen are needed for the reaction to occur and any substituent such as cyano or nitro which could effectively remove these electrons by resonance would inhibit the decomposition to a certain extent. The chloro substituent, though electron-withdrawing, cannot remove electrons by resonance and so no appreciable deviation occurs. Cyclic intermediates have been proposed for chloroformate (10) and carboxylic thiolcarbonic anhydride (11) decompositions.

From the completed work, a path 1 mechanism seems to best explain the experimental results. The initial ion pair formed may then break down via a cyclic manner to give the products. The breakdown of the ion pair would seem to depend primarily on the ability of the phenoxy group to stabilize the negative charge on the anionic portion of the ion pair. It is doubtful if any appreciable separation of this ion pair occurs for if it did, electrophilic substitution of the phenolic portion by the anisylic carbonium ion should be substantial (12). This would result in a much lower yield of ethers than was actually obtained.

The experimental results obtained thus far do not permit us to distinguish whether in this path 1 mechanism $k_2 \gg k_{-1}$ or $k_2 < k_{-1}$. The data are consistent with either interpretation. Stereochemical work would indicate whether racemization (k_{-1}) of an optically active starting carbonate occurs faster or slower than its decomposition (k_2). This information along with activation parameters would do much to help in elucidating further on the mechanism of the decomposition and experiments in this line are now in progress.

The authors wish to thank the National Research Council of Canada for financial support of this research and the Department of University Affairs for the award of an Ontario Graduate Fellowship to T. H. Breckles. We also wish to thank Dow Chemical of Canada Ltd. for a generous supply of HMP.

1. J. M. PROKIPCAK and T. H. BRECKLES. Can. J. Chem. **49**, 914 (1971).
2. J. L. KICE, R. A. BARTSCH, M. A. DANKLEFF, and S. L. SCHWARTZ. J. Am. Chem. Soc. **87**, 1734 (1965).
3. J. L. KICE, R. L. SCRIVEN, E. KOUBEK, and M. BARNES. J. Am. Chem. Soc. **92**, 5608 (1970).
4. K. B. WIBERG and T. M. SHRYNE. J. Am. Chem. Soc. **77**, 2774 (1955).
5. J. L. KICE and G. C. HANSON. Tetrahedron Lett. 2927 (1970).

Can. J. Chem. Downloaded from www.nrcresearchpress.com by 210.87.254.105 on 09/05/12
For personal use only.

6. K. L. OLIVER and W. G. YOUNG. J. Am. Chem. Soc. **81**, 5811 (1959).
7. P. R. WELLS. Linear free energy relationships. Academic Press. New York, N.Y. 1968. p. 14, 29.
8. T. MUKAIYAMO and M. IRWANAMI. J. Am. Chem. Soc. **79**, 73 (1957).
9. J. L. KICE, F. M. PARHAM, and R. M. SIMONS. J. Am. Chem. Soc. **82**, 834 (1960).
10. E. S. LEWIS and W. C. HERNDON. J. Am. Chem. Soc. **83**, 1955 (1961); **83**, 1959 (1961); **83**, 1961 (1961).
11. L. WEI and D. S. TARBELL. J. Org. Chem. **33**, 1884 (1968).
12. G. A. RUSSELL and R. C. WILLIAMSON, JR. J. Am. Chem. Soc. **86**, 2357 (1964).

Can. J. Chem. Downloaded from www.nrcresearchpress.com by 210.87.254.105 on 09/05/12
For personal use only.

Can. J. Chem. Downloaded from www.nrcresearchpress.com by 210.87.254.5 on 09/05/12
For personal use only.

NOTES

Triazine Intermediates in the Decomposition of 1-(*o*-Carbethoxyphenyl)-3-(*o*-cyanophenyl)-triazene in Aqueous Ethanol

KEITH VAUGHAN

Department of Chemistry, St. Mary's University, Halifax, Nova Scotia

Received December 14, 1971

The thermal decomposition of 1-(*o*-carbethoxyphenyl)-3-(*o*-cyanophenyl)-triazene (**4**) in aqueous ethanol has been found to give 2-phenylquinazolin-4(3*H*)-one (**8**); the formation of triazine intermediates in the reaction has been established.

La décomposition thermique du (*o*-carbéthoxyphényl)-1 (*o*-cyanophényl)-3 triazène (**4**) dans l'éthanol aqueux conduit à la 3 *H*-phényl-2 quinazolinone-4 (**8**); la formation intermédiaire de triazine dans la réaction a été établie.

Canadian Journal of Chemistry, **50**, 1775 (1972)

In a previous report (1), the thermal decomposition of 1,2,3-benzotriazin-4(3*H*)-one (**1**) was found to give quinazolino[3,2-*c*][1,2,3]benzotriazin-8-one (**2**). An extensive study by Stevens and his co-workers (2–4) has shown that the imino-analogue of **2** is an intermediate in the conversion of 1,3-di-*o*-cyanophenyltriazene (**3**) to 4-amino-2-phenylquinazoline in aqueous ethanol. It was thus of interest to study the reactions of 1-(*o*-carbethoxyphenyl)-3-(*o*-cyanophenyl)-triazene (**4**), which, by analogy, would be expected to provide an alternative route to the triazinoquinazolone (**2**).

The coupling reaction of aromatic diazonium salts with primary aromatic amines is a general method of synthesis of diaryltriazenes (diazoamino compounds) (5), but the triazene **4** required for this study had not previously been reported. Diazotization of ethyl anthranilate, followed by coupling of the cold diazonium salt solution with anthranilonitrile, gave a 50% yield of 1-(*o*-carbethoxyphenyl)-3-(*o*-cyanophenyl)-triazene (**4**); the spectroscopic properties of this product are in accord with either of the tautomeric structures **4***a* ⇌ **4***b*.

Prolonged refluxing (2–3 weeks) of the triazene **4** in 70% aqueous ethanol gave an 80% yield of 2-phenylquinazolin-4(3*H*)-one (**8**), which was identical with an authentic sample (6). Shorter reaction times in the same solvent medium gave mixtures of unchanged starting material (varying from 70% recovery after 2 h reflux to 10% after 100 h), the quinazolone **8**, and quinazolino[3,2-*c*][1,2,3]benzotriazin-8-one (**2**) (maximum yield 20% after 15 h reflux). The latter product, **2**, was identical with the product of thermolysis of 1,2,3-benzotriazin-4(3*H*)-one (**1**) (1). These results are summarized in Table 1.

The quinazolone **8** may arise from the triazene **4** by either route *i* or *ii*, as shown in Scheme 1. Nucleophilic addition at the nitrile group in tautomer **4***a*, a characteristic reaction of *o*-cyanophenyltriazenes (2), would lead to the formation of the 3-aryl-4-iminobenzotriazine **5**, which could cyclize directly to the quinazolino-[1,2-*c*][1,2,3]benzotriazine (**7**; route *ii*). Alternatively, the intermediate ester **5** could undergo Dimroth rearrangement to the isomeric 4-aryliminotriazine **6**, followed by cyclization at the ortho-ester group to give the triazinoquinazolone (**2**; route *i*). A less likely source of the triazinoquinazolone **2** is the isomerization **7** → **2**. Reductive loss of nitrogen from either of the isomeric triazinoquinazolones, **2** or **7**, would then yield the observed product, 2-phenylquinazolin-4(3*H*)-one (**8**).

The available evidence almost overwhelmingly supports route *i* as the more likely mechanism. The triazinoquinazolone **2** is a minor product when the triazene **4** is refluxed in aqueous ethanol for short periods, and has been shown in a previous report (1) to undergo conversion to the quinazolone **8** after 15 h refluxing in aqueous ethanol. Stevens has shown (2*b*) that

TABLE I. Product distribution for the decomposition of the triazene **4** in refluxing aqueous ethanol

Reaction time	Yield (%)		
	Triazene (**4**) (recovered)	Quinazolino[3,2-*c*][1,2,3]-benzotriazin-8-one (**2**)	2-Phenylquinazolin-4(3*H*)-one (**8**)
2 h	70	12	—
15 h	32	20	6
100 h	10	—	20
3 weeks	—	—	81

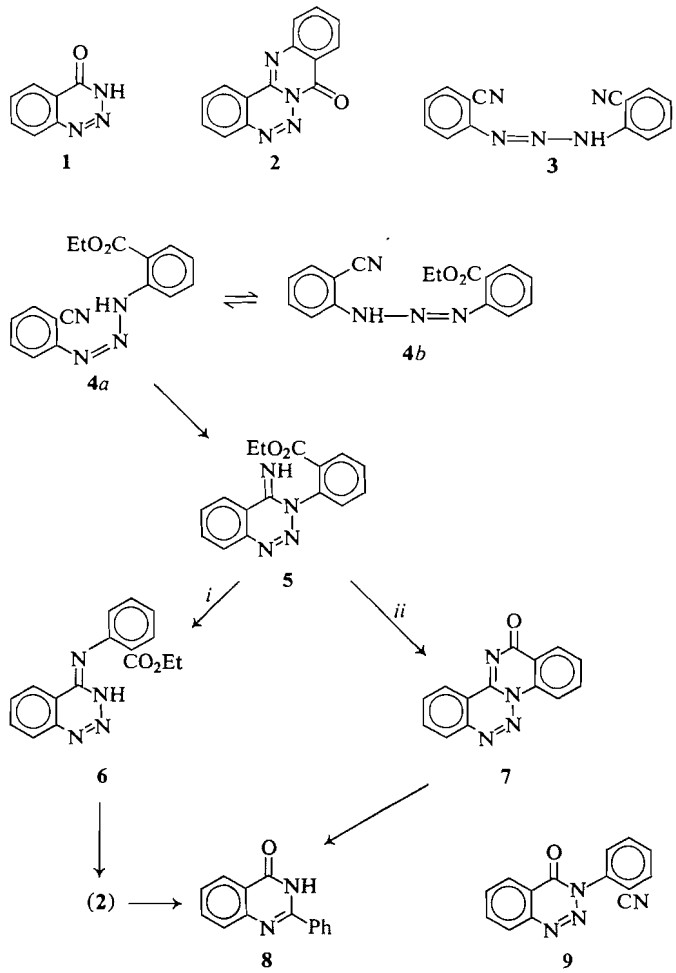

SCHEME I

3-aryl-4-imino-1,2,3-benzotriazines undergo facile Dimroth rearrangement to the isomeric 4-arylimino-1,2,3-benzotriazines (such as **5** → **6**), and that the rearrangement is accelerated in triazines bearing electron-attracting substituents (*e.g.* **5**). It has also been established that the conversion of 1,3-di-*o*-cyanophenyltriazene (**3**) to 4-amino-2-phenylquinazoline (**4**) most likely proceeds in a manner analogous to route *i*.

The long reflux time required for complete

Can. J. Chem. Downloaded from www.nrcresearchpress.com by 210.87.254.5 on 09/05/12
For personal use only.

Can. J. Chem. Downloaded from www.nrcresearchpress.com by 210.87.254.5 on 09/05/12
For personal use only.

decomposition of the triazene **4** indicates an unusually low reactivity compared with compounds of similar structure. The cyclizations of *o*-cyanophenyltriazenes (2) and *o*-carbalkoxyphenyltriazenes (7) to the corresponding 1,2,3-benzotriazines require only 1–2 h reflux in 70% aqueous ethanol, and the conversion of the dinitrile **3** to 4-amino-2-phenylquinazoline is quantitative in 95% ethanol at 20° after 48 h (3*a*). These cyclizations cannot take place unless the triazene is in the less stable *cis*-configuration about the N=N bond, and in all reactions of this type there is probably a *trans* → *cis* isomerization prior to cyclization (2*b*). Inspection of models of the *cis*-configurations of triazenes **3** and **4** shows that, in the nitrile-ester (tautomer **4***a*), there is considerable steric interaction between the nitrile and ester groups, whereas in the dinitrile **3**, there is no interaction at all between the nitrile groups. Thus the low reactivity of the nitrile-ester **4** is probably a result of the instability of the *cis*-isomer due to steric factors. The models do not reveal any difference in the stability of the tautomers **4***a* and *b*, and thus do not explain why the expected product of cyclization of tautomer **4***b*, 3-(*o*-cyanophenyl)-1,2,3-benzotriazin-4-one (**9**), is not found in any of the reaction mixtures. The latter observation may be interpreted as a difference in reactivity of nitrile and carbethoxy groups towards nucleophilic addition of amino nitrogen.

Stevens (3*a*) found that decomposition of 1,3-di-*o*-cyanophenyltriazene (**3**) on alumina afforded quickly the imino-analogue of the triazinoquinazolone **7**, and by analogy alumina-catalyzed decomposition of the triazene **4** would be expected to give rise to **7**. However, the triazene **4** was found to decompose very slowly in the presence of alumina and a low yield of the triazinoquinazolone **2** was obtained. Evidently, if isomer **7** is formed in this reaction, it must isomerize readily to **2**.

Experimental

Melting points were obtained on a Fisher–Johns apparatus and are corrected. The i.r. spectra were recorded with liquid paraffin mulls on a Perkin–Elmer Infracord spectrophotometer, and the n.m.r. spectrum with a Varian A-60A spectrometer using tetramethylsilane as the internal standard. Mass spectral data were obtained with a Dupont–C.E.C. model 21-491 spectrometer. Merck grade alumina was obtained from Brinkmann Instruments (Canada) Limited.

1-(o-Carbethoxyphenyl)-3-(o-cyanophenyl)-triazene (4)

Ethyl anthranilate (3.3 g) was dissolved in concentrated hydrochloric acid (5.0 ml) and the solution diluted with water (100 ml), cooled to 0 °C, and diazotized to starch-iodide end-point with aqueous sodium nitrite (1.4 g in 10 ml). After the cold diazonium salt solution had been stirred for 15 min, a solution of *o*-aminobenzonitrile (2.1 g) in 2 *M* hydrochloric acid (20 ml) was added dropwise with constant agitation. The mixture was then made alkaline with an excess of sodium acetate, stirred for 2.0 h, and then filtered to yield the triazene **4** (2.4 g, 50%), m.p. 156–157 °C (yellow needles from ethanol), ν_{max} 3220 (NH), 2220 (C≡N), 1675 (C=O), and 1410 (N=N) cm^{-1}; δ ($CDCl_3$) 6.90–8.10 (8H, m, aromatic), 4.42 (2H, q, methylene), and 1.42 (3H, t, methyl) p.p.m.; *m/e* 294 (P, $C_{16}H_{14}N_4O_2$), 266 ($C_{16}H_{14}N_2O_2$).

Decomposition of the Triazene 4 in Aqueous Ethanol

General Procedure

1-(*o*-Carbethoxyphenyl)-3-(*o*-cyanophenyl)-triazene (**4**) (0.001 mol) was refluxed in 70% aqueous ethanol (50 ml) for times varying from 2 h to 3 weeks. Unreacted starting material was recovered from the cooled reaction mixture by filtration. Evaporation of the filtrate gave a yellow solid residue, which upon recrystallization from absolute ethanol afforded quinazolino[3,2-*c*][1,2,3]benzotriazin-8-one (**2**), m.p. and mixed m.p. 215–216 °C, ν_{max} 1720, 1660, and 1605 cm^{-1}, identical with an authentic sample (1).

Evaporation of the mother liquor from the recrystallization afforded 2-phenylquinazolin-4(3*H*)-one (**8**), m.p. 238–239 °C (needles, from ethanol), ν_{max} 1665 cm^{-1}, identical with an authentic sample (6). Table 1 shows the yields of these products obtained after different durations of refluxing.

Alumina-catalyzed Decomposition of the Triazene 4 in Anhydrous Benzene

Basic alumina (Merck, activity I, untreated) (3.0 g) was added to a solution of the triazene **4** (0.2 g) in anhydrous benzene (50 ml), and the suspension was stirred at room temperature for 42 h. The alumina was separated by filtration and washed with 10 × 20 ml aliquots of anhydrous benzene. The combined benzene filtrate and washings afforded, on evaporation, a yellow gummy solid, which, after repeated recrystallization from benzene/petroleum ether and subsequently from benzene, yielded the quinazolinobenzotriazinone **2** (8 mg, 5%), identical with a sample from the previous reaction. Evaporation of the combined mother liquors from the recrystallizations gave unreacted starting material (0.13 g, 65%).

The financial support of the National Research Council of Canada is gratefully acknowledged. I am also grateful to Drs. W. D. Jamieson and A. W. McCulloch of the Atlantic Regional Laboratory, NRCC, for mass spectral and n.m.r. data respectively.

1. A. W. Murray and K. Vaughan. J. Chem. Soc. C, 2070 (1970).
2. (*a*) M. W. Partridge and M. F. G. Stevens. J. Chem. Soc. 3663 (1964). (*b*) H. N. E. Stevens and M. F. G. Stevens. J. Chem. Soc. C, 765 (1970).
3. (*a*) M. F. G. Stevens. J. Chem. Soc. C, 1096 (1967). (*b*) J. Chem. Soc. C, 348 (1968).

4. H. N. E. STEVENS and M. F. G. STEVENS. J. Chem. Soc. C, 2289 (1970).
5. H. ZOLLINGER. Diazo and azo chemistry. Interscience Publishers Inc., New York, N.Y. 1961. pp. 177–180.
6. M. M. ENDICOTT, E. WICK, M. L. MERCURY, and M. L. SHERRILL. J. Am. Chem. Soc. **68**, 1299 (1946).
7. H. MEHNER. J. prakt. Chem. **63**, 241 (1901(2)); F. D. CHATTAWAY and A. J. WALKER. J. Chem. Soc. 329 (1927); P. GRAMMATICAKIS. Compt. Rend. **243**, 2094 (1956); P. GRAMMATICAKIS. Bull. Soc. Chim. Fr. **26**, 480 (1959).

Can. J. Chem. Downloaded from www.nrcresearchpress.com by 210.87.254.5 on 09/05/12
For personal use only.

The Interception of *N*-Dibenzylaminonitrene Generated from *N*-Azido Dibenzylamine

RIAZ AHMED AND J.-P. ANSELME[1]

Department of Chemistry, University of Massachusetts, Boston, Massachusetts 02116

Received October 26, 1971

N-Dibenzylaminonitrene (**6**) has been shown to be generated from the decomposition of *N*-azido dibenzylamine (**9**) by its interception with 4-phenyl-1,2,4-triazoline-3,5-dione, as the azimine (**8**).

On a montré que le *N*-dibenzylaminonitrène (**6**) est issu de la décomposition de la *N*-azidodibenzylamine (**9**) par son interception avec la phényl-4 triazoline-1,2,4 dione-3,5, en tant qu'azimine (**8**).

Canadian Journal of Chemistry, **50**, 1778 (1972)

The concept of *N*-nitrenes (**1**) has gradually come of age (1) through a slow accumulation of results most conveniently rationalized via such intermediates, in particular, the formation of products resulting from nitrogen extrusion. Although the isolation of adducts such as **2** and **3** (2, 3) can be formally viewed as resulting from the trapping of *N*-nitrenes, it has not been established that such adducts did not arise from "prenitrene" precursors. Similarly, although the participation of **6** in the formation of **8**[2]

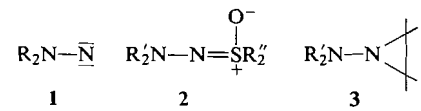

was suggested, it is also conceivable that **8** might have arisen via the oxidation of an initial tetrazane (**7**), without the intervention of **6** (4) (see eq. 1).

Earlier we had presented evidence for the

[1]

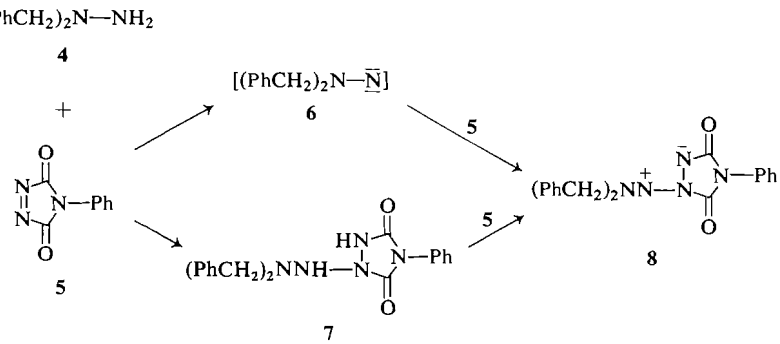

[1]Fellow of the Alfred P. Sloan Foundation. To whom inquiries should be addressed.

[2]In a recent private communication, Prof. Fahr has informed us that X-ray analysis of the adduct formed between 1,1-diphenylhydrazine and **5**, has confirmed the azimine structure.

4. H. N. E. STEVENS and M. F. G. STEVENS. J. Chem. Soc. C, 2289 (1970).
5. H. ZOLLINGER. Diazo and azo chemistry. Interscience Publishers Inc., New York, N.Y. 1961. pp. 177–180.
6. M. M. ENDICOTT, E. WICK, M. L. MERCURY, and M. L. SHERRILL. J. Am. Chem. Soc. **68**, 1299 (1946).
7. H. MEHNER. J. prakt. Chem. **63**, 241 (1901(2)); F. D. CHATTAWAY and A. J. WALKER. J. Chem. Soc. 329 (1927); P. GRAMMATICAKIS. Compt. Rend. **243**, 2094 (1956); P. GRAMMATICAKIS. Bull. Soc. Chim. Fr. **26**, 480 (1959).

Can. J. Chem. Downloaded from www.nrcresearchpress.com by 210.87.254.105 on 09/05/12
For personal use only.

The Interception of *N*-Dibenzylaminonitrene Generated from *N*-Azido Dibenzylamine

RIAZ AHMED AND J.-P. ANSELME[1]

Department of Chemistry, University of Massachusetts, Boston, Massachusetts 02116

Received October 26, 1971

N-Dibenzylaminonitrene (**6**) has been shown to be generated from the decomposition of *N*-azido dibenzylamine (**9**) by its interception with 4-phenyl-1,2,4-triazoline-3,5-dione, as the azimine (**8**).

On a montré que le *N*-dibenzylaminonitrène (**6**) est issu de la décomposition de la *N*-azidodibenzylamine (**9**) par son interception avec la phényl-4 triazoline-1,2,4 dione-3,5, en tant qu'azimine (**8**).

Canadian Journal of Chemistry, **50**, 1778 (1972)

The concept of *N*-nitrenes (**1**) has gradually come of age (1) through a slow accumulation of results most conveniently rationalized via such intermediates, in particular, the formation of products resulting from nitrogen extrusion. Although the isolation of adducts such as **2** and **3** (2, 3) can be formally viewed as resulting from the trapping of *N*-nitrenes, it has not been established that such adducts did not arise from "prenitrene" precursors. Similarly, although the participation of **6** in the formation of **8**[2]

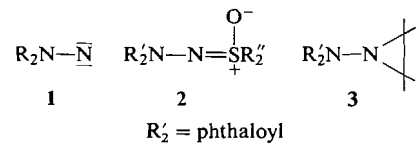

was suggested, it is also conceivable that **8** might have arisen via the oxidation of an initial tetrazane (**7**), without the intervention of **6** (4) (see eq. 1).

Earlier we had presented evidence for the

[1]

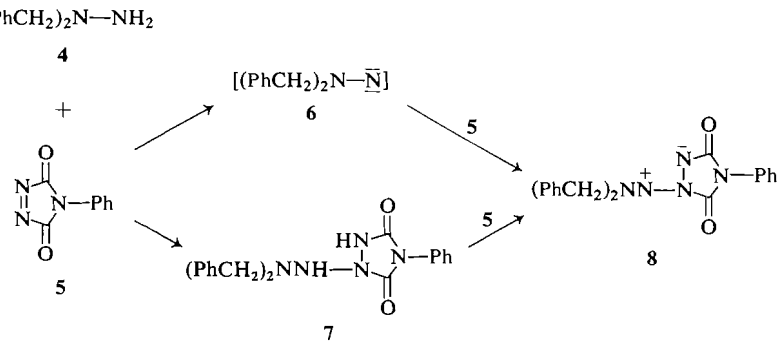

[1]Fellow of the Alfred P. Sloan Foundation. To whom inquiries should be addressed.

[2]In a recent private communication, Prof. Fahr has informed us that X-ray analysis of the adduct formed between 1,1-diphenylhydrazine and **5**, has confirmed the azimine structure.

Can. J. Chem. Downloaded from www.nrcresearchpress.com by 210.87.254.105 on 09/05/12
For personal use only.

formation of *N*-azido dibenzylamine (**9**) from the *diazo transfer* of tosyl azide to 1,1-dibenzylhydrazine anion (**4***a*) and suggested that **9** was a precursor of **6** (5) (eq. 2). During the course of our investigation of some of the reaction of 4-phenyl-1,2,4-triazoline-3,5-dione (**5**), it was discovered that azides, in contrast to diazoalkanes (6, 8), do not react with **5** (PTD) at room temperature. This finding prompted us to attempt to demonstrate the formation of **6** from **9**. Indeed, if adduct **8** could be isolated from the reaction of **9** with PTD, this would constitute evidence for the direct interception of **6** with PTD since presumably, as with other azides (6), **9** would not react with PTD.

$$[2]\quad \underset{\mathbf{4}a}{(PhCH_2)_2N\bar{\underline{N}}H} \xrightarrow[-60^\circ]{TosN_3} \underset{\mathbf{9}}{[(PhCH_2)_2N{-}N_3]} \xrightarrow[-10^\circ]{-N_2} [\mathbf{6}] \rightarrow \text{Products}$$

1,1-Dibenzylhydrazine monoanion (10 mmol) was prepared as previously described and then treated with a 1.2 equiv of tosyl azide at −60°. The reaction mixture was stirred for 15 min at that temperature. No apparent reaction took place when a solution of 2 equiv of **5** in tetrahydrofuran was added at −60°. The flask was removed from the cooling bath and allowed to warm up. The vigorous evolution of nitrogen which had begun slowly at about −20°, was accompanied by a slow fading of the red color above 0°. After 1 h at room temperature, the initial red color of the reaction mixture had completely disappeared and a yellow solid had precipitated. After addition of ether and water and work-up of the organic phase, **8** was isolated in 65% yield[3] as a yellow solid, m.p. 154–155° (dec.); it was identical to the product obtained from the reaction of 1,1-dibenzylhydrazine and **5** (4).

The interaction of **4***a* with **5** as the source of **8** was ruled out in control runs. When the above described experiment was repeated with less than an equivalent amount of tosyl azide, *immediate* reaction occurred upon addition of **5** as evidenced by the precipitation of **8** at −60°; as expected, *immediate* reaction was again evident when **5** was added to a solution of dibenzylhydrazine anion (**4***a*) at −60° *in the absence* of tosyl azide. These results are to be contrasted with the original experiment in which *no* reaction occurred until much higher temperatures (−10 to 10°) were reached. Both **8** and the triphenylphosphine adduct of tosyl azide (7) were isolated and characterized[4] by consecutive treatment of the mixture of **9** and tosyl azide (*freed from 1,1-dibenzylhydrazine*) (5) with **5** and triphenylphosphine. These results quite clearly indicate that in our reaction, **8** did *not* arise by the reaction of **4** or of **4***a* with **5**.

The alternative possibility that *N*-azido dibenzylamine reacted initially with **5** to give a primary adduct which decomposed to the azimine (**8**) was discussed above. Coupled with our finding that in contrast with diazoalkanes (6, 8), azides are completely inert toward **5**, the fact that the disappearance of the deep red color of **5** was concomitant with the evolution of nitrogen, did not support the formation of intermediates such as **10***a* or *b*. In order to establish this, the rate of the decomposition of **9** was measured in the absence of PTD and in the presence of 0.5 and 1 equiv of PTD. Within the limits of experimental error, there was no difference in the rate of nitrogen evolution between these three experiments.

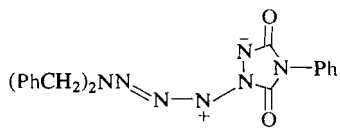

10*a*

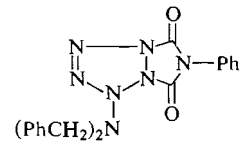

10*b*

In view of these results, the formation of **8** in our reaction can be most rationally regarded as the direct interception of *N*-dibenzylaminonitrene with **5** and further supports the validity of our original suggestion as depicted in eq. 2.

[3]In our initial experiment, only 1 equiv of **5** was used. Only a 28% yield of the adduct in addition to 4-phenyl urazole (0.7 mmol) and *p*-toluenesulfonamide (21%) were isolated. A 100% excess of **5** was used because we anticipated that **5** could be consumed via alternate reactions such as with *p*-toluenesulfonamide anion and with unreacted 1,1-dibenzylhydrazine anion.

[4]Bibenzyl and dibenzylbenzalhydrazone (5) were detected by t.l.c. from the filtrate of the reaction mixture.

The support of this work by the National Institute of Health, Grant GM 13689 and of the Alfred P. Sloan Foundation is hereby acknowledged with deep appreciation.

1. For a recent review see D. Lemal *In* Nitrenes. W. Lwowski, Ed., Interscience Publishers, New York, N.Y. 1970. p. 345 *ff.*
2. D. J. ANDERSON, T. L. GILCHRIST, D. C. HORWELL, and C. W. REES. Chem. Commun. 146 (1969). *N*-carbazoyl nitrene has also been trapped with olefins (D. J. Anderson and C. W. Rees, private communication).
3. T. L. GILCHRIST, C. W. REES, and E. STANTON. Chem. Commun. 801 (1971).
4. K.-H. Koch and E. Fahr. Angew. Chem. Int. Ed. **9**, 634 (1970).
5. G. KOGA and J.-P. ANSELME. J. Org. Chem. **35**, 960 (1970).
6. R. AHMED and J.-P. ANSELME. Unpublished results.
7. H. BOCK and M. SCHNÖLLER. Chem. Ber. **102**, 38 (1969).
8. G. F. BETTINETTI and L. CAPRETTI. Gazz. Chim. Ital. **95**, 33 (1965).

Branched-chain Nitro Sugars. Methyl 4,6-*O*-Benzylidene-2,3-dideoxy-3-*C*-nitromethyl-α-D-*ribo*-hexopyranoside

ALEX ROSENTHAL AND GÜNTER SCHÖLLNHAMMER

Department of Chemistry, The University of British Columbia, Vancouver, British Columbia

Received December 9, 1971

The preparations of methyl 3-*O*-acetyl-4,6-*O*-benzylidene-2-deoxy-3-*C*-nitromethyl-α-D-*ribo*-hexopyranoside (**4**) and the *arabino*-epimer (**5**) are described. Schmidt–Rutz degradation of **4** and **5** afforded a *cis–trans* mixture of the branched-chain carbohydrate nitroolefins **6** which were stereoselectively reduced with sodium borohydride to yield methyl 4,6-*O*-benzylidene-2,3-dideoxy-3-*C*-nitromethyl-α-D-*ribo*-hexopyranoside (7). The utility of circular dichroism studies in determining the configuration of nitro sugars is discussed.

Les préparations des méthyl 3-*O*-acétyl-4,6-*O*-benzylidène-2-déoxy-3-*C*-nitrométhyl-α-D-*ribo*-(**4**) (et *arabino* **5**) hexopyranosides sont décrites. La dégradation de Schmidt–Rutz sur **4** et **5** conduit à un mélange *cis–trans* de nitrooléfines ramifiées **6** qui par réduction par le borohydrure de sodium, conduisent stéréosélectivement au méthyl-4,6-*O*-benzylidène-2,3-didéoxy-3-*C*-nitrométhyl-α-D-*ribo*-hexopyranoside (7). L'utilisation du dichroisme circulaire dans la détermination des configurations des nitro sucres est discutée.

Canadian Journal of Chemistry, **50**, 1780 (1972)

In a previous communication (1) we have described the synthesis of methyl 4,6-*O*-benzylidene-2-deoxy-3-*C*-nitromethyl-α-D-*ribo*-(and *arabino*-)hexopyranoside (**2** and **3**) by application of the nitromethane synthesis (2) to methyl 4,6-*O*-benzylidene-2-deoxy-α-D-*erythro*-hexopyranosid-3-ulose (**1**). Acetylation of **2** with acetic anhydride and *p*-toluenesulfonic acid monohydrate gave an impure 3-*O*-acetate which underwent decomposition upon attempted purification on silica gel. Baer and co-workers (2) have warned about the difficulties encountered during acetylation and work-up of some nitro sugars.

In this communication we wish to report the successful preparation of the 3-acetates of **2** and **3** and their subsequent conversion via a Schmidt–Rutz degradation (3) followed by stereoselective sodium borohydride reduction of the nitroolefin to afford a 2,3-dideoxy branched-chain nitro sugar.

Acetylation of **2** and **3** was achieved with acetic anhydride and *p*-toluenesulfonic acid as catalyst under careful surveillance by t.l.c. monitoring. As soon as the reaction was complete the reaction was quenched by pouring the reaction mixture into a mixture of ice and water followed by immediate neutralization with sodium hydrogen carbonate. Extraction of the acetylation products of **2** and **3** with dichloromethane gave pure crystalline methyl 3-*O*-acetyl-4,6-*O*-benzylidene-2-deoxy-3-*C*-nitromethyl-α-D-*ribo*-(and *arabino*-)hexopyranoside (**4** and **5**) in good yields. Conversion of the latter compounds, via a Schmidt–Rutz reaction (3), into the expected carbohydrate nitroolefin **6** revealed

Can. J. Chem. Downloaded from www.nrcresearchpress.com by 210.87.254.105 on 09/05/12
For personal use only.

The support of this work by the National Institute of Health, Grant GM 13689 and of the Alfred P. Sloan Foundation is hereby acknowledged with deep appreciation.

1. For a recent review see D. Lemal *In* Nitrenes. W. Lwowski, Ed., Interscience Publishers, New York, N.Y. 1970. p. 345 *ff.*
2. D. J. ANDERSON, T. L. GILCHRIST, D. C. HORWELL, and C. W. REES. Chem. Commun. 146 (1969). *N*-carbazoyl nitrene has also been trapped with olefins (D. J. Anderson and C. W. Rees, private communication).
3. T. L. GILCHRIST, C. W. REES, and E. STANTON. Chem. Commun. 801 (1971).
4. K.-H. Koch and E. Fahr. Angew. Chem. Int. Ed. **9**, 634 (1970).
5. G. KOGA and J.-P. ANSELME. J. Org. Chem. **35**, 960 (1970).
6. R. AHMED and J.-P. ANSELME. Unpublished results.
7. H. BOCK and M. SCHNÖLLER. Chem. Ber. **102**, 38 (1969).
8. G. F. BETTINETTI and L. CAPRETTI. Gazz. Chim. Ital. **95**, 33 (1965).

Can. J. Chem. Downloaded from www.nrcresearchpress.com by 210.87.254.6 on 09/05/12
For personal use only.

Branched-chain Nitro Sugars. Methyl 4,6-*O*-Benzylidene-2,3-dideoxy-3-*C*-nitromethyl-α-D-*ribo*-hexopyranoside

ALEX ROSENTHAL AND GÜNTER SCHÖLLNHAMMER

Department of Chemistry, The University of British Columbia, Vancouver, British Columbia

Received December 9, 1971

The preparations of methyl 3-*O*-acetyl-4,6-*O*-benzylidene-2-deoxy-3-*C*-nitromethyl-α-D-*ribo*-hexopyranoside (**4**) and the *arabino*-epimer (**5**) are described. Schmidt–Rutz degradation of **4** and **5** afforded a *cis–trans* mixture of the branched-chain carbohydrate nitroolefins **6** which were stereoselectively reduced with sodium borohydride to yield methyl 4,6-*O*-benzylidene-2,3-dideoxy-3-*C*-nitromethyl-α-D-*ribo*-hexopyranoside (7). The utility of circular dichroism studies in determining the configuration of nitro sugars is discussed.

Les préparations des méthyl 3-*O*-acétyl-4,6-*O*-benzylidène-2-déoxy-3-*C*-nitrométhyl-α-D-*ribo*-(**4**) (et *arabino* **5**) hexopyranosides sont décrites. La dégradation de Schmidt–Rutz sur **4** et **5** conduit à un mélange *cis–trans* de nitrooléfines ramifiées **6** qui par réduction par le borohydrure de sodium, conduisent stéréosélectivement au méthyl-4,6-*O*-benzylidène-2,3-didéoxy-3-*C*-nitrométhyl-α-D-*ribo*-hexopyranoside (7). L'utilisation du dichroisme circulaire dans la détermination des configurations des nitro sucres est discutée.

Canadian Journal of Chemistry, **50**, 1780 (1972)

In a previous communication (1) we have described the synthesis of methyl 4,6-*O*-benzylidene-2-deoxy-3-*C*-nitromethyl-α-D-*ribo*-(and *arabino*-)hexopyranoside (**2** and **3**) by application of the nitromethane synthesis (2) to methyl 4,6-*O*-benzylidene-2-deoxy-α-D-*erythro*-hexopyranosid-3-ulose (**1**). Acetylation of **2** with acetic anhydride and *p*-toluenesulfonic acid monohydrate gave an impure 3-*O*-acetate which underwent decomposition upon attempted purification on silica gel. Baer and co-workers (2) have warned about the difficulties encountered during acetylation and work-up of some nitro sugars.

In this communication we wish to report the successful preparation of the 3-acetates of **2** and **3** and their subsequent conversion via a Schmidt–Rutz degradation (3) followed by stereoselective sodium borohydride reduction of the nitroolefin to afford a 2,3-dideoxy branched-chain nitro sugar.

Acetylation of **2** and **3** was achieved with acetic anhydride and *p*-toluenesulfonic acid as catalyst under careful surveillance by t.l.c. monitoring. As soon as the reaction was complete the reaction was quenched by pouring the reaction mixture into a mixture of ice and water followed by immediate neutralization with sodium hydrogen carbonate. Extraction of the acetylation products of **2** and **3** with dichloromethane gave pure crystalline methyl 3-*O*-acetyl-4,6-*O*-benzylidene-2-deoxy-3-*C*-nitromethyl-α-D-*ribo*-(and *arabino*-)hexopyranoside (**4** and **5**) in good yields. Conversion of the latter compounds, via a Schmidt–Rutz reaction (3), into the expected carbohydrate nitroolefin **6** revealed

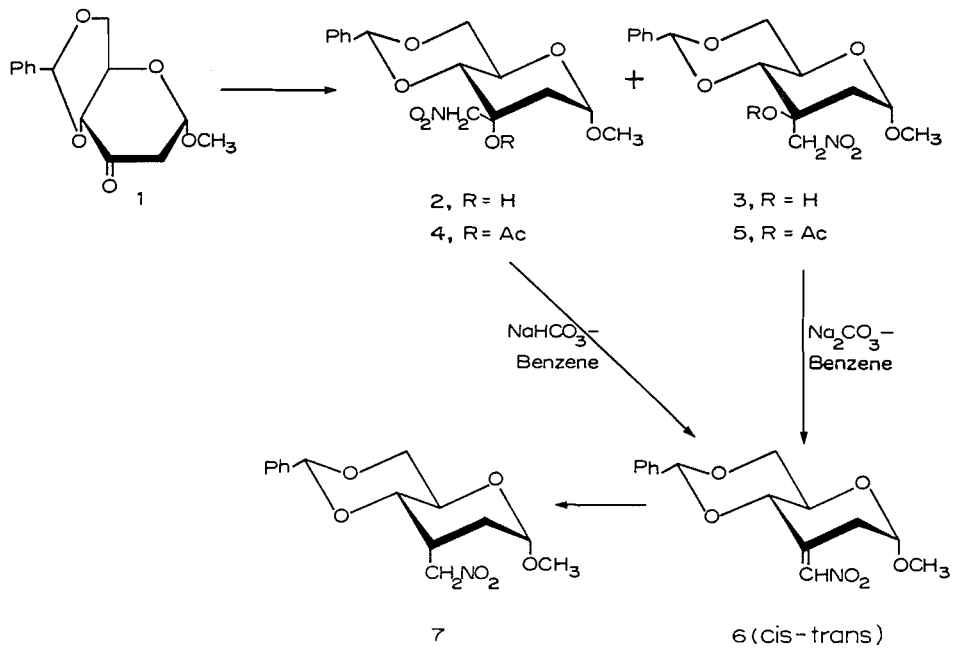

a remarkable difference in chemical reactivity of **4** and **5** towards sodium hydrogen carbonate; the *ribo*-acetate **4** readily underwent dehydroacetylation, whereas the epimeric *arabino*-isomer **5** was inert under the same conditions. This difference in chemical reactivity might be attributed to conformational and steric factors. Although both epimers possess an axial anomeric methoxyl group, **4** has an equatorially oriented nitromethyl group and **5** contains an axially oriented nitromethyl group. Since it is presumed that dehydroacetylation is first initiated by an abstraction of an α-H from the carbon bearing the nitro group followed by β-elimination of the acetoxy group (4), it can be surmised that the approach of sodium hydrogen carbonate ion to the equatorially oriented nitromethyl group of **4** is not hindered by the axial methoxyl group and thus the formation of the nitromethine anion is easy whereas the access of the same nucleophile to the axially oriented nitromethyl group of **5** is restricted by the axially oriented methoxyl group. Other workers (4) have also reported that the ease of elimination of acetic acid from nitro sugar *O*-acetates can be expected to depend upon structural and steric factors. For example, the α-methyl glycoside of 2-*O*-acetyl-4,6-*O*-benzylidene-3-deoxy-3-nitro-D-glucoside exhibited much slower chemical reactivity to base than the corresponding anomeric β-methyl glycoside (5). On the basis of the n.m.r. spectrum of the carbohydrate nitroolefin **6** obtained from **4** it is suggested that a 1:4 mixture (*cis* and *trans* isomers) of **6** was formed since the ratio of the two low field ($\tau \sim 2.7$) multiplets was approximately 1:4. Although these geometrical isomers exhibited slightly different R_f's, attempts to separate them in pure form by preparative t.l.c. on silica gel were unsuccessful. Jones and coworkers (6) have successfully prepared and isolated both *cis* and *trans* nitroolefins during the course of their work on the synthesis of the carbohydrate moiety in lincomycin. Configurational assignments of the *cis* and *trans* unsaturated nitroolefins were made on the basis of their n.m.r. spectra. When the epimeric *arabino*-nitro compound **5** was subjected to a more rigorous treatment using sodium carbonate in refluxing benzene the same unsaturated nitro sugar **6** was produced, and in addition, an unstable carbohydrate nitroolefin which could not be separated from **6**. A possible similar rearrangement of a nitroolefin was encountered during studies of the dehydroacetylation of nitromethylcyclohexylacetate (7).

Reduction of methyl 4,6-*O*-benzylidene-3-*C*-nitromethylene-2,3-dideoxy-α-D-*erythro*-hexopyranoside (**6**) with sodium borohydride in

Can. J. Chem. Downloaded from www.nrcresearchpress.com by 210.87.254.6 on 09/05/12
For personal use only.

Can. J. Chem. Downloaded from www.nrcresearchpress.com by 210.87.254.6 on 09/05/12
For personal use only.

ethanol (8) proceeded stereoselectively to afford a 2,3-dideoxy branched-chain nitro sugar **7**. The structure of the latter compound was readily deduced from its n.m.r. spectrum (see Experimental). Although the resonance of H-4 (two doublets having $J = 4$ and 10 Hz) and H-6 overlapped at τ 6.25, irradiation of H-3 at τ 7.0 removed the coupling of H-4 and -3 leaving a doublet for H-4 and -5 having a value of 10 Hz. Thus the much narrower doublet having $J = 4$ Hz at approximately τ 6.25 is attributed to coupling of the axial H-4 with an equatorial hydrogen on C-3. Therefore the nitromethyl group is axially oriented and **7** must be methyl 2,3-dideoxy-3-*C*-nitromethyl-α-D-*ribo*-hexopyranoside. This assignment, however, was not substantiated by circular dichroism (c.d.) studies (9). Possibly, Satoh's empirical rules (9) apply only to deoxy nitro carbohydrates having an asymmetric center adjacent to the carbon having the nitro or nitromethyl group and do not apply to dideoxy nitro carbohydrates. Indirect support for the assignment of structure is provided by the fact that reduction of an analogous unsaturated branched-chain ester obtained by a Wittig reaction on the same ketose **1** also proceeded stereoselectively to afford a 2,3-dideoxy *ribo* compound (10).

Experimental

General Consideration

The n.m.r. spectra were obtained in chloroform-*d* solution with tetramethylsilane as the internal standard (set at τ 10) by using a Varian HA-60 or 100 spectrometer (s, singlet, d, doublet, t, triplet, q, quartet, m, multiplet). The c.d. spectra were measured with a JASCO model ORD/UV-5 spectropolarimeter. The optical rotations were determined using a Perkin–Elmer model 141 automatic polarimeter. All melting points (micro hot stage) are corrected. Elemental analyses were performed by the microanalytical laboratory of the University of British Columbia, Vancouver, B.C.

*Methyl 3-O-Acetyl-4,6-O-benzylidene-2-deoxy-3-C-nitromethyl-α-D-ribo-hexopyranoside (**4**) and Methyl 3-O-Acetyl-4,6-O-benzylidene-2-deoxy-2-C-nitromethyl-α-D-arabino-hexopyranoside (**5**)*

Methyl 4,6-*O*-benzylidene-2-deoxy-3-*C*-nitromethyl-α-D-*ribo*-hexopyranoside (**2**) (0.57 g) (1) was acetylated with acetic anhydride (25 ml) and *p*-toluenesulfonic acid monohydrate (0.200 g) at room temperature. The progress of the reaction was monitored by t.l.c. on silica gel using 10:1 benzene–ethyl acetate as developer. When the reaction was complete the reaction mixture was poured into ice-water, neutralized with sodium hydrogen carbonate, and the product extracted with dichloromethane (5 × 50 ml). The dichloromethane extract was washed with aqueous sodium hydrogen carbonate, followed by water, then dried over sodium sulfate, filtered, and evaporated under reduced pressure to yield 0.465 g (74%) of crystalline **4** which was recrystallized from ethyl acetate–light petroleum ether (b.p. 30–60°); m.p. 138–148°; $[\alpha]_D^{23} + 90°$ (*c* 1, chloroform); c.d. (*c* 0.0004, methanol): $[\theta]_{285} -4170$; τ ($CDCl_3$) 2.5 (aromatic H), 4.4 (s, CHPh), 4.9 (d, CH_2NO_2), 5.2 (q, H-1, $J_{1,2e} = 1$, $J_{1,2a} = 4$ Hz), 5.4–6.4 (m), 6.60 (s, OCH_3), 7.70–8.1 (two m, H_{2e} and H_{2a}), 7.90 (Ac).

Anal. of **4** Calcd. for $C_{17}H_{21}NO_8$: C, 55.6; H, 5.8; N, 3.8. Found: C, 55.77; H, 5.76; N, 3.80.

The *arabino*-epimer **3** was acetylated by the same procedure used to prepare **4** to afford methyl 3-*O*-acetyl-4,6-*O*-benzylidene-2-deoxy-3-*C*-nitromethyl-α-D-*arabino*-hexopyranoside (**5**); m.p. 145°; $[\alpha]_D^{22} + 38°$ (*c* 1, chloroform); c.d. (*c* 0.0004, methanol): $[\theta]_{285} + 4110$; τ ($CDCl_3$) 4.70 (d, CH_2NO_2), 5.2 (q, H-1, $J_{1,2e} = 1$, $J_{1,2a} = 4.5$ Hz), 5.35–6.32 (m), 6.65 (s, OCH_3), 7.12 (2-d, H_{2e}, $J_{2e,1} = 2$, $J_{2e,2a} = 13$ Hz), 7.60 (2-d, H_{2a}, $J_{2a,1} = 4$, $J_{2a,2e} = 13$ Hz), 7.95 (Ac).

Anal. of **5** Calcd. for $C_{17}H_{21}NO_8$: C, 55.8; H, 5.8; N, 3.8. Found: C, 55.35; H, 5.70; N, 4.0.

*Application of Schmidt–Rutz Reaction to **4** and to **5** to Yield cis–trans Methyl 4,6-O-Benzylidene-3-C-nitromethylene-2,3-dideoxy-α-D-erythro-hexopyranoside (**6**)*

To the acetate **4** (0.195 g) in anhydrous benzene (30 ml) was added finely powdered anhydrous sodium hydrogen carbonate (0.800 g) and the resulting mixture was refluxed for 15 h (or until all starting material was consumed as evidenced by t.l.c. on silica using 10:1 benzene–ethyl acetate). Both the *cis* and *trans* elimination products (1:4 ratio) having R_f's of 0.55 and 0.52 were formed. The solids were removed by filtration and washed with benzene. The combined benzene filtrate was evaporated under reduced pressure to yield 0.130 g of crystalline residue which was recrystallized from ethyl acetate–light petroleum ether: m.p. 134–136°; τ ($CDCl_3$) 2.60–2.68 (m, due to $C{=}CHNO_2$), 2.68–2.84 (m, due to $C{=}CHNO_2$ of other isomer; ratio 1:4), 4.40 (s, CHPh), 5.05 (d, H-1), 5.50–6.35 (m), 6.67 (s, OCH_3), 6.5–6.7 (m, overlapping OCH_3 peak), 7.4 and 7.63 (two q = 1 H).

Anal. Calcd. for $C_{15}H_{17}NO_6$: C, 58.7; H, 5.6; N, 4.6. Found: C, 58.74; H, 5.37; N, 4.40.

The acetate **5** was resistant to elimination of acetic acid using sodium hydrogen carbonate. Treatment of **5** with potassium carbonate in benzene under reflux for 12 h yielded compound **6** and another unstable unsaturated compound in about equal amounts. Attempts to isolate the second nitroolefin by preparative t.l.c. were unsuccessful.

*Methyl 4,6-O-Benzylidene-2,3-dideoxy-3-C-nitromethyl-α-D-ribo-hexopyranoside (**7**)*

Compound **6** (0.150 g) dissolved in ethanol (10 ml) was reduced with sodium borohydride (0.100 g) at room temperature for 1 h. The excess sodium borohydride was consumed by the addition of acetone. After addition of water (5 ml) the solution was acidified with acetic acid and then extracted with dichloromethane (3 × 20 ml). The dichloromethane extract was evaporated to dryness under reduced pressure to afford a product which was recrystallized from ethyl acetate–light petroleum ether to give pure **7** (0.084 g), m.p. 110–111°; $[\alpha]_D^{22} + 58°$ (*c* 1, chloroform); c.d. (*c* 0.0004, methanol): $[\theta]_{270} + 2740$; τ ($CDCl_3$) 2.7 (aromatic H), 4.5

(CHPh), 5.20 (CH_2NO_2), 5.36 (t, H-1), 5.8 (m, H-5), 6.25 (m, H-4, H-6, $J_{4,3} = 4$, $J_{4,5} = 10$ Hz), 6.70 (OCH_3), 6.83–7.05 (m, H-3), 7.96–8.10 (5 peaks, H-2a, H-2e). Irradiation at τ 8.0 (H-2) collapsed the H-1 signal to a singlet and altered the H-3 multiplet. Irradiation at τ 5.36 (H-1) collapsed the multiplet at τ 8.0 to three peaks. Irradiation at τ 7.0 (H-3) changed the multiplet at τ 8 to a broad singlet and altered the signals at τ 6.25 showing $J_{4,5} =$ 10 Hz.

Anal. Calcd. for $C_{15}H_{19}NO_6$: C, 58.2; H, 6.2; N, 4.5. Found: C, 58.18; H, 6.0; N, 4.35.

1. Alex Rosenthal and Khong-Seng Ong. Can. J. Chem. **48**, 3034 (1970).
2. (*a*) H. H. Baer. Adv. Carbohydr. Chem. and Biochem. **24**, 67 (1969); (*b*) H. H. Baer, F. Kienzle, and F. Rajabalee. Can. J. Chem. **46**, 80 (1968).
3. E. Schmidt and G. Rutz. Ber. **61**, 2142 (1928).
4. H. H. Baer and L. Urbos. The chemistry of the nitro and nitroso groups. Part 2. Interscience Publishers, New York, N.Y., 1970. p. 75.
5. H. H. Baer and F. Kienzle. Can. J. Chem. **45**, 983 (1967).
6. (*a*) G. B. Howarth, D. G. Lance, W. A. Szarek, and J. K. N. Jones. Can. J. Chem. **47**, 75 (1969); (*b*) G. B. Howarth, D. G. Lance, W. A. Szarek, and J. K. N. Jones. Can. J. Chem. **47**, 81 (1969).
7. (*a*) Z. Eckstein, T. Urbanski, and H. Wojnowska. Rocz. Chem. **31**, 1177 (1959); (*b*) Z. Eckstein, T. Urbanski, and H. Wojnowska. Bull. Acad. Pol. Sci. Ser. Sci. Chim. Geol. Geograph. **5**, 219 (1957).
8. (*a*) H. Shechter, D. E. Ley, and E. B. Roberson, Jr. J. Am. Chem. Soc. **78**, 4984 (1956); (*b*) H. H. Baer and W. Rank. Abstract of papers (CARBO, No. 12). Joint Conference of the Chem. Inst. of Can. and the Amer. Chem. Soc. Toronto, Ontario, May, 1970.
9. C. Satoh, A. Kujomoto, and T. Okuda. Carbohydr. Res. **5**, 140 (1967).
10. A. Rosenthal and P. Catsoulacos. Can. J. Chem. **46**, 2868 (1968).

A Simple Synthesis of 2-Methoxy and 2-Ethoxytetrahydrofuran

Daniel Frehel and Pierre Deslongchamps[1]

Laboratoire de Synthèse organique, Département de chimie, Université de Sherbrooke, Sherbrooke, Québec

Received January 17, 1972

Ozonolysis of dihydropyran gives 4-formyloxybutyraldehyde which is then easily converted into 2-methoxy or 2-ethoxytetrahydrofuran.

L'ozonolyse du dihydropyranne conduit au formyloxy-4-butyraldehyde qui se transforme facilement en méthoxy-2- ou éthoxy-2-tétrahydrofuran.

Canadian Journal of Chemistry, **50**, 1783 (1972)

In connection with our recent investigation on the ozonolysis of acetals (1), we required a certain quantity of 2-methoxytetrahydrofuran (**1***a*). A search in the chemical literature revealed that the standard method to prepare 2-alkoxytetrahydrofuran is the addition of alcohols to 2,3-dihydrofuran in presence of mineral acid (2). However, 2,3-dihydrofuran is not very readily available (2–5). The alternative synthesis of 2-alkoxytetrahydrofuran (6) from tetrahydrofuran and *t*-butyl perbenzoate in the presence of alcohols is not more convenient (2).

We wish to report a new two-step synthesis of 2-methoxytetrahydrofuran from a readily available starting material while using simple experimental procedures.

Ozonolysis of dihydropyran in methanol at −78° followed by the addition of methyl sulfide (7) gave 4-formyloxybutyraldehyde (**2**) in 95% yield (see Scheme 1). The next operation was to convert **2** into 2-methoxytetrahydrofuran (**1***a*). One possible route for such a transformation was the hydrolysis of **2** to **3** and then the conversion **3** into **1***a*. We felt that such a two-step procedure should be avoided because we were expecting experimental difficulties in the isolation of the water-soluble 2-hydroxytetrahydrofuran (**3**) (8). Also, the use of methanol as solvent in the final step was not desirable since 2-methoxytetrahydrofuran (**1***a*) has a low boiling

[1]A. P. Sloan Fellow, 1970–1972.

Can. J. Chem. Downloaded from www.nrcresearchpress.com by 210.87.254.6 on 09/05/12
For personal use only.

(CHPh), 5.20 (CH_2NO_2), 5.36 (t, H-1), 5.8 (m, H-5), 6.25 (m, H-4, H-6, $J_{4,3} = 4$, $J_{4,5} = 10$ Hz), 6.70 (OCH_3), 6.83–7.05 (m, H-3), 7.96–8.10 (5 peaks, H-2a, H-2e). Irradiation at τ 8.0 (H-2) collapsed the H-1 signal to a singlet and altered the H-3 multiplet. Irradiation at τ 5.36 (H-1) collapsed the multiplet at τ 8.0 to three peaks. Irradiation at τ 7.0 (H-3) changed the multiplet at τ 8 to a broad singlet and altered the signals at τ 6.25 showing $J_{4,5} =$ 10 Hz.

Anal. Calcd. for $C_{15}H_{19}NO_6$: C, 58.2; H, 6.2; N, 4.5. Found: C, 58.18; H, 6.0; N, 4.35.

1. Alex Rosenthal and Khong-Seng Ong. Can. J. Chem. **48**, 3034 (1970).
2. (*a*) H. H. Baer. Adv. Carbohydr. Chem. and Biochem. **24**, 67 (1969); (*b*) H. H. Baer, F. Kienzle, and F. Rajabalee. Can. J. Chem. **46**, 80 (1968).
3. E. Schmidt and G. Rutz. Ber. **61**, 2142 (1928).
4. H. H. Baer and L. Urbos. The chemistry of the nitro and nitroso groups. Part 2. Interscience Publishers, New York, N.Y., 1970. p. 75.
5. H. H. Baer and F. Kienzle. Can. J. Chem. **45**, 983 (1967).
6. (*a*) G. B. Howarth, D. G. Lance, W. A. Szarek, and J. K. N. Jones. Can. J. Chem. **47**, 75 (1969); (*b*) G. B. Howarth, D. G. Lance, W. A. Szarek, and J. K. N. Jones. Can. J. Chem. **47**, 81 (1969).
7. (*a*) Z. Eckstein, T. Urbanski, and H. Wojnowska. Rocz. Chem. **31**, 1177 (1959); (*b*) Z. Eckstein, T. Urbanski, and H. Wojnowska. Bull. Acad. Pol. Sci. Ser. Sci. Chim. Geol. Geograph. **5**, 219 (1957).
8. (*a*) H. Shechter, D. E. Ley, and E. B. Roberson, Jr. J. Am. Chem. Soc. **78**, 4984 (1956); (*b*) H. H. Baer and W. Rank. Abstract of papers (CARBO, No. 12). Joint Conference of the Chem. Inst. of Can. and the Amer. Chem. Soc. Toronto, Ontario, May, 1970.
9. C. Satoh, A. Kujomoto, and T. Okuda. Carbohydr. Res. **5**, 140 (1967).
10. A. Rosenthal and P. Catsoulacos. Can. J. Chem. **46**, 2868 (1968).

Can. J. Chem. Downloaded from www.nrcresearchpress.com by 210.87.254.5 on 09/05/12
For personal use only.

A Simple Synthesis of 2-Methoxy and 2-Ethoxytetrahydrofuran

Daniel Frehel and Pierre Deslongchamps[1]

Laboratoire de Synthèse organique, Département de chimie, Université de Sherbrooke, Sherbrooke, Québec

Received January 17, 1972

Ozonolysis of dihydropyran gives 4-formyloxybutyraldehyde which is then easily converted into 2-methoxy or 2-ethoxytetrahydrofuran.

L'ozonolyse du dihydropyranne conduit au formyloxy-4-butyraldehyde qui se transforme facilement en méthoxy-2- ou éthoxy-2-tétrahydrofuran.

Canadian Journal of Chemistry, **50**, 1783 (1972)

In connection with our recent investigation on the ozonolysis of acetals (1), we required a certain quantity of 2-methoxytetrahydrofuran (**1***a*). A search in the chemical literature revealed that the standard method to prepare 2-alkoxytetrahydrofuran is the addition of alcohols to 2,3-dihydrofuran in presence of mineral acid (2). However, 2,3-dihydrofuran is not very readily available (2–5). The alternative synthesis of 2-alkoxytetrahydrofuran (6) from tetrahydrofuran and *t*-butyl perbenzoate in the presence of alcohols is not more convenient (2).

We wish to report a new two-step synthesis of 2-methoxytetrahydrofuran from a readily available starting material while using simple experimental procedures.

Ozonolysis of dihydropyran in methanol at −78° followed by the addition of methyl sulfide (7) gave 4-formyloxybutyraldehyde (**2**) in 95% yield (see Scheme 1). The next operation was to convert **2** into 2-methoxytetrahydrofuran (**1***a*). One possible route for such a transformation was the hydrolysis of **2** to **3** and then the conversion **3** into **1***a*. We felt that such a two-step procedure should be avoided because we were expecting experimental difficulties in the isolation of the water-soluble 2-hydroxytetrahydrofuran (**3**) (8). Also, the use of methanol as solvent in the final step was not desirable since 2-methoxytetrahydrofuran (**1***a*) has a low boiling

[1]A. P. Sloan Fellow, 1970–1972.

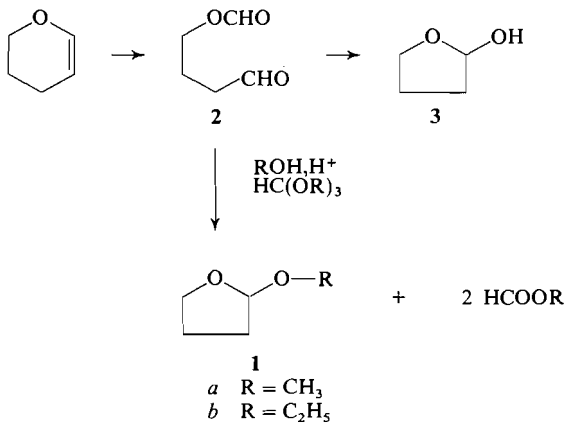

SCHEME 1

point. Consequently, we directed our effort in the development of a one-step procedure from **2**.

Treatment of **2** with 1 mol-equiv of trimethyl orthoformate containing a drop of methanol and a catalytic amount of *p*-toluenesulfonic acid at room temperature gave 2-methoxytetrahydrofuran (**1***a*) in 80% yield after distillation. During this reaction, 2 mol-equiv. of the low boiling methyl formate are formed. Using similar experimental conditions, and triethyl orthoformate, **2** was transformed into 2-ethoxytetrahydrofuran (**1***b*) in 84% yield after distillation.

Experimental

The i.r. spectra were taken on a Perkin–Elmer 257 Spectrophotometer. The n.m.r. spectra (τ value) were recorded on a Varian A-60 Spectrometer in solvent indicated and with TMS as internal standard. The ozonized oxygen was produced by a Welsbach T-816 Laboratory Ozonator. Microanalyses were performed by Schwarzkopf Microanalytical Laboratory, Woodside, N.Y.

*4-Formyloxybutyraldehyde (**2**)*

Dihydropyran (63 g, 0.75 mol) was dissolved in reagent grade methanol (100 ml) and cooled at −78°. Ozonized oxygen (3.7%-O_3/O_2, 1.5 l/min) was passed through the solution and the end of the reaction was indicated by the appearance of the characteristic blue color of ozone. The excess ozone was swept away with a stream of nitrogen, methyl sulfide (80 ml) was added to the reaction mixture which was allowed to be warmed up at −10° (bath temperature) for 1 h, then at 0° for 1 h, and finally at room temperature for 3 h. The solvent was removed *in vacuo* and water (300 ml) was added. The aqueous phase was extracted with ether (4 × 50 ml) and with dichloromethane (4 × 50 ml). The combined organic phase was dried over magnesium sulfate, filtered, and evaporated to dryness yielding crude **2** (85.1 g, 97%). Distillation *in vacuo* (b.p. 55°, 2 mm) gave pure 4-formyloxybutyraldehyde (82.5 g, 95%). The i.r. ν (max) 1720 cm^{-1}; n.m.r.: τ ($CDCl_3$) 0.27 (1H, triplet, J = 1.0 Hz, CHO), 1.97 (1H, singlet, —OCHO), 5.82 (2H, triplet, J = 7.0 Hz, —CH_2—OCHO), 7.24–7.64 (2H, multiplet, —CH_2—CHO), and 7.79–8.27 (2H, multiplet, CH_2—CH_2—CHO).

Anal. Calcd. for $C_5H_8O_3$: C, 51.72; H, 6.94; O, 41.34. Found: C, 51.48; H, 7.20; O, 41.32.

*2-Methoxytetrahydrofuran (**1***a*)*

Trimethyl orthoformate (2.12 g, 0.02 mol) was slowly added (exothermic reaction) to a cooled mixture (0°) of 4-formyloxybutyraldehyde (2.32 g, 0.02 mol), *p*-toluenesulfonic acid (2 mg), and one drop of methanol. The reaction mixture was then left at room temperature for 36 h. Anhydrous sodium carbonate (100 mg) was added and the reaction mixture was magnetically stirred for 1 h. The inorganic salt was filtered and methyl formate was removed by distillation at normal pressure. Water (2 ml) was added to the reaction mixture which was extracted with ether (4 × 50 ml). Distillation of the dried (magnesium sulfate) organic phase gave pure 2-methoxytetrahydrofuran (1.63 g, 80%, b.p. 106–107°, lit. (8) b.p. 105–107°). The n.m.r.: τ ($CDCl_3$) 5.1 (1H, multiplet, C*H*OCH_2), 6.00–6.65 (2H, multiplet, CH_2O), 6.75 (3H, singlet, OCH_3), and 7.85–8.40 (4H, multiplet).

Anal. Calcd. for $C_5H_{10}O_2$: C, 58.80; H, 9.87; O, 31.33. Found: C, 58.90; H, 9.81; O, 31.29.

*2-Ethoxytetrahydrofuran (**2***b*)*

2-Ethoxytetrahydrofuran (**2***b*, 1.95 g, 84%, b.p. 125°, lit. (9) b.p. 125°) was obtained by utilizing an identical experimental procedure as the one described above with the exception that trimethyl orthoformate was replaced by triethyl orthoformate (2.964 g, 0.02 mol) and methanol by ethanol (one drop). The n.m.r.: τ ($CDCl_3$) 4.92 (1H, multiplet, C*H*OC_2H_5), 5.95–6.80 (4H, multiplet, OCH_2 and OCH_2CH_3), 8.35–7.90 (4H, multiplet), and 8.85 (3H, triplet, J = 7.0 Hz, CH_3CH_2O).

Anal. Calcd. for $C_6H_{12}O_2$: C, 62.04; H, 10.41; O, 27.55. Found: C, 61.86; H, 10.41; O, 27.73.

Support for this work by the National Research Council of Canada and by the "Ministère de l'Education" (Québec) is gratefully acknowledged.

1. P. Deslongchamps and C. Moreau. Can. J. Chem. **49**, 2465 (1971).
2. E. L. Eliel, B. E. Nowak, R. A. Daignault, and V. G. Badding. J. Org. Chem. **30**, 2441 (1965) and references quoted therein.
3. H. Normand. C.R. Acad. Sci. Paris, **228**, 102 (1949).
4. D. A. Barr and J. B. Rose. J. Chem. Soc. 3766 (1954).
5. G. Sosnovsky. Tetrahedron, **13**, 241 (1961).
6. S. O. Lawesson and C. Burglund. *Arkiv. Kemi*, **17**, 475 (1961); G. Sosnovsky. J. Org. Chem. **25**, 874 (1960). Tetrahedron, **13**, 241 (1961).
7. J. J. Pappas, W. P. Keaveney, E. Gancher, and M. Berger. Tetrahedron Lett. 4273 (1966).
8. R. Paul and S. Tchelitcheff. Bull. Soc. Chim. Fr. 197 (1948).
9. S. O. Lawesson and C. Burglund. Acta Chem. Scand. **14**, 1854 (1960).

Can. J. Chem. Downloaded from www.nrcresearchpress.com by 210.87.254.5 on 09/05/12
For personal use only.

Anomalous Rate Laws in the Halogenation of Carbon Tetrahalides

B. K. DUNNING AND H. O. PRITCHARD
Centre for Research in Experimental Space Science, York University, Downsview, Ontario

Received January 7, 1972

The initial rate of bromination of carbon tetrachloride is independent of surface-to-volume ratio and can be fitted to a rate law which assumes that the rate-determining step is $Br + CCl_4 \rightarrow BrCl + CCl_3$; however, the overall temperature coefficient of the rate is inconsistent with the known thermochemistry of the system. The same anomaly has been reported recently in the fluorination of trichlorofluoromethane by Foon and Tait, and similar inconsistencies occur in the fluorination of carbon tetrachloride and the chlorination of bromotrichloromethane.

La vitesse initiale de bromation du tétrachlorure de carbone est indépendante du rapport surface-sur-volume et peut être exprimée par une loi de vitesse qui suppose que l'étape de vitesse déterminante est: $Br + CCl_4 \rightarrow BrCl + CCl_3$; cependant, le coefficient global de température de la vitesse est incompatible avec la thermochimie connue du système. La même anomalie a récemment été rapportée par Foon et Tait, lors de la fluoration du trichlorofluorométhane, et les mêmes contractions se retrouvent lors de la fluoration du tétrachlorure de carbone et de la chloration du bromotrichlorométhane.

Canadian Journal of Chemistry, **50**, 1785 (1972)

Can. J. Chem. Downloaded from www.nrcresearchpress.com by 210.87.254.42 on 09/05/12
For personal use only.

To complement our recent investigation of the equilibria between carbon tetrachloride and bromotrichloromethane in the presence of bromine and chlorine (1) we undertook to study the kinetics of the bromination of carbon tetrachloride in the temperature range 500–540 °K and the chlorination of bromotrichloromethane in the range 370–430 °K. Experiments were carried out in 300 ml Pyrex flasks, which were thoroughly flamed under vacuum before filling and sealing off, to prevent the formation of spurious HCl or HBr: initial amounts of carbon tetrachloride and of halogen were each in the range $2–5 \times 10^{-5}$ mol, and reaction times (t) were such that 1–5% of the reactants were consumed; further details will be made available elsewhere (2). Since the reaction rate was unchanged when the reaction vessels were packed with short lengths of glass tubing, it is natural to assume that the reactions are homogeneous and that, for example, the bromination of carbon tetrachloride can be represented by Reactions 1–3, with other less important fates

$$[1] \qquad Br_2 \rightleftharpoons Br + Br$$

$$[2] \qquad Br + CCl_4 \rightarrow BrCl + CCl_3$$

$$[3] \qquad CCl_3 + Br_2 \rightarrow CCl_3Br + Br$$

of the CCl_3 radical being combination to C_2Cl_6, combination with Br atoms to form CCl_3Br and abstraction from BrCl to reform CCl_4. Similar reaction schemes have been proposed by Clark and Tedder (3) and by Foon and Tait (4) for the fluorination of carbon tetrachloride and trichlorofluoromethane respectively. In our experiment there was also some secondary bromination (about 10%) of the CCl_3Br to give CCl_2Br_2, but nevertheless plots of the total amount of product ($CCl_3Br + CCl_2Br_2$) against $[Br_2]^{1/2}[CCl_4]t$ were good straight lines, passing through the origin, as required by reactions 1–3.[1] The overall rates can be represented by the expression $2.0 \times 10^7 \exp(-24\,000/RT)$ $cc^{1/2}$ $mol^{-1/2}$ s^{-1}, whence, since $\frac{1}{2}D(Br_2) \approx 23$ kcal/mol, $E_2 \approx 1$ kcal/mol. However, despite uncertainties in the heat of formation of carbon tetrachloride (5), the known thermochemistry (6) implies that E_2 cannot be less than about 20 kcal/mol. Our results for the chlorination of bromotrichloromethane (which of course does not suffer from the complication of secondary halogenation) are less extensive, but equally unsatisfactory.

Foon and Tait (4) have recently performed extensive experiments on the fluorination of

[1]At 500 °K, the equilibrium constant for the reaction between Br_2 and CCl_4 is about 0.1, so that (for example) using equal quantities of reactant, 25% consumption of each would represent equilibrium (2); hence in the 1–5% reactant consumption range, the reverse reaction will not cause a severe perturbation in the rate law.

trichlorofluoromethane, reporting identical conclusions to those described above, and although it was not recognized at the time, the experiments of Clark and Tedder (3) on the fluorination of carbon tetrachloride appear to be equally inconsistent (4, 7) in that their proposed activation energy for the abstraction from CCl_4 by a fluorine atom is much too low. Foon and Tait suggest that these observations can be explained by assuming that both the chain initiation and termination are heterogeneous, in such a way that the overall rate is independent of surface-to-volume ratio, and it is our purpose here to note that the occurrence of such anomalous rate laws is common to many of the halogenations of carbon tetrahalides.

1. B. K. DUNNING and H. O. PRITCHARD. J. Chem. Thermodyn. **4**, 213 (1972).
2. B. K. DUNNING. Ph.D. Thesis. York University, Toronto, Ontario. To be submitted.
3. D. T. CLARK and J. M. TEDDER. J. Phys. Chem. **68**, 2018 (1964).
4. R. FOON and K. B. TAIT. Trans. Faraday Soc. **67**, 3038 (1971).
5. A. LORD and H. O. PRITCHARD. J. Chem. Thermodyn. **1**, 495 (1969).
6. JANAF Thermochemical Tables. Dow Chemical Co., Midland, Michigan. 1965.
7. A. S. RODGERS. J. Phys. Chem. **72**, 3400 (1968).

Nuclear Magnetic Resonance Spectra of Methyl Substituted 6-Aryl[1,2,4]triazolo[4,3-*d*]tetrazoles

R. N. BUTLER
Department of Chemistry, University College, Galway, Ireland

Received November 19, 1971

The n.m.r. spectral properties of a range of the title compounds are reported and discussed.

Les caractéristiques des spectres r.m.n. d'une série de 6-aryl[1,2,4]triazolo[4,3-*d*]tétrazoles sont rapportées et discutées.

Canadian Journal of Chemistry, **50**, 1786 (1972)

Of the six theoretically possible triazolotetrazole ring systems (1) only one such fused heterocyclic ring is known, namely the 1,2,4-triazolo[4,3-*d*]tetrazole systems **1** and **2** (2, 3). By classifying the azide–tetrazole ring closure as an electrocyclic 1,5-dipolar cyclization, which obeys the rules of orbital symmetry, Reimlinger (1) has explained the special stability of this system and has predicted that at least one of the other possible triazolotetrazole systems should have comparable stability. The isomeric materials **1** and **2** were obtained by cyclization of the corresponding hydrazones **3** and **4** (2, 3). The presence of the methyl group had an important stabilizing influence on the fused bicyclic system. With the unmethylated analog, cleavage of the tetrazole ring occurred and triazolyl azides were formed (2, 4). The influence of heterocyclic rings on the n.m.r. shifts of adjacent aryl protons has been used to advantage in elucidating the nature of electronic effects operating between the ring systems and studies of different isomeric modifications have led to the detection of resonance interactions in such systems (5). Hence the n.m.r. spectra of the different isomeric modifications **1** and **2** were studied with view to obtaining information on the properties of this new ring system.

The n.m.r. spectra of the materials **1** and **2** (Table 1) exhibit downfield shifts in the ortho and meta protons of the phenyl group. The ortho protons (H_A) are deshielded by an extra 0.7 p.p.m. relative to the meta protons (H_B). Columns 3 and 4 of Table 1 contain the shifts of the ortho and meta protons of the phenyl substituent in the materials. Columns 5 and 6 contain the difference between these shifts and those of the corresponding protons of the substituted benzene.

The deshielding nature and relative magnitudes of the shifts are of interest. Deshielding shifts have been observed for the ortho protons

Can. J. Chem. Downloaded from www.nrcresearchpress.com by 210.87.254.42 on 09/05/12
For personal use only.

trichlorofluoromethane, reporting identical conclusions to those described above, and although it was not recognized at the time, the experiments of Clark and Tedder (3) on the fluorination of carbon tetrachloride appear to be equally inconsistent (4, 7) in that their proposed activation energy for the abstraction from CCl_4 by a fluorine atom is much too low. Foon and Tait suggest that these observations can be explained by assuming that both the chain initiation and termination are heterogeneous, in such a way that the overall rate is independent of surface-to-volume ratio, and it is our purpose here to note that the occurrence of such anomalous rate laws is common to many of the halogenations of carbon tetrahalides.

1. B. K. DUNNING and H. O. PRITCHARD. J. Chem. Thermodyn. **4**, 213 (1972).
2. B. K. DUNNING. Ph.D. Thesis. York University, Toronto, Ontario. To be submitted.
3. D. T. CLARK and J. M. TEDDER. J. Phys. Chem. **68**, 2018 (1964).
4. R. FOON and K. B. TAIT. Trans. Faraday Soc. **67**, 3038 (1971).
5. A. LORD and H. O. PRITCHARD. J. Chem. Thermodyn. **1**, 495 (1969).
6. JANAF Thermochemical Tables. Dow Chemical Co., Midland, Michigan. 1965.
7. A. S. RODGERS. J. Phys. Chem. **72**, 3400 (1968).

Nuclear Magnetic Resonance Spectra of Methyl Substituted 6-Aryl[1,2,4]triazolo[4,3-*d*]tetrazoles

R. N. BUTLER
Department of Chemistry, University College, Galway, Ireland

Received November 19, 1971

The n.m.r. spectral properties of a range of the title compounds are reported and discussed.

Les caractéristiques des spectres r.m.n. d'une série de 6-aryl[1,2,4]triazolo[4,3-*d*]tétrazoles sont rapportées et discutées.

Canadian Journal of Chemistry, **50**, 1786 (1972)

Of the six theoretically possible triazolotetrazole ring systems (1) only one such fused heterocyclic ring is known, namely the 1,2,4-triazolo[4,3-*d*]tetrazole systems **1** and **2** (2, 3). By classifying the azide–tetrazole ring closure as an electrocyclic 1,5-dipolar cyclization, which obeys the rules of orbital symmetry, Reimlinger (1) has explained the special stability of this system and has predicted that at least one of the other possible triazolotetrazole systems should have comparable stability. The isomeric materials **1** and **2** were obtained by cyclization of the corresponding hydrazones **3** and **4** (2, 3). The presence of the methyl group had an important stabilizing influence on the fused bicyclic system. With the unmethylated analog, cleavage of the tetrazole ring occurred and triazolyl azides were formed (2, 4). The influence of heterocyclic rings on the n.m.r. shifts of adjacent aryl protons has been used to advantage in elucidating the nature of electronic effects operating between the ring systems and studies of different isomeric modifications have led to the detection of resonance interactions in such systems (5). Hence the n.m.r. spectra of the different isomeric modifications **1** and **2** were studied with view to obtaining information on the properties of this new ring system.

The n.m.r. spectra of the materials **1** and **2** (Table 1) exhibit downfield shifts in the ortho and meta protons of the phenyl group. The ortho protons (H_A) are deshielded by an extra 0.7 p.p.m. relative to the meta protons (H_B). Columns 3 and 4 of Table 1 contain the shifts of the ortho and meta protons of the phenyl substituent in the materials. Columns 5 and 6 contain the difference between these shifts and those of the corresponding protons of the substituted benzene.

The deshielding nature and relative magnitudes of the shifts are of interest. Deshielding shifts have been observed for the ortho protons

Can. J. Chem. Downloaded from www.nrcresearchpress.com by 210.87.254.6 on 09/05/12
For personal use only.

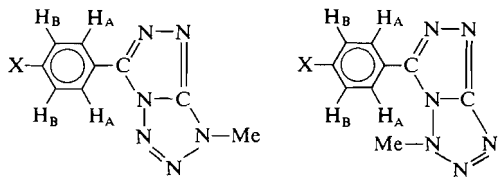

1 2

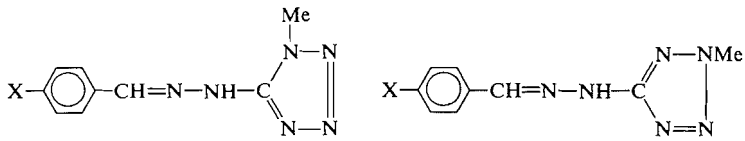

3 4

X = (*a*) Me, (*b*) H, (*c*) Br, (*d*) Cl

TABLE 1. Proton magnetic resonance spectra of triazolotetrazoles

Compound	τ *N*-Me	τ H_A	τ H_B	Δτ H_A*	Δτ H_B†
1*a*	5.83	1.89‡ (1.88)§	2.67‡ (2.58)§	−0.94	−0.16
1*b*	5.80	1.78‖	2.48¶	−0.95	−0.25
1*c*	5.80	—	—	—	—
2*b*	5.40	1.80‖	2.49¶	−0.93	−0.24
2*d*	5.40	1.84‡ (1.80)§	2.49‡ (2.49)§	−0.89	−0.24
2*c*	5.39	—	—	—	—

*$\tau H_A - \tau H_{meta}$ in XC_6H_5.
†$\tau H_B - \tau H_{ortho}$ in XC_6H_5.
‡Doublets (J = 8 Hz). The weaker features of the A_2X_2 system were not observed.
§Figures in parentheses represent shifts calculated on the basis of additivity of X and triazolotetrazole substituent effects.
‖Doublet (J = 3 Hz).
¶Overlapping doublets containing para H signal (spread 7–8 Hz).

in a number of other heterocyclic biaryls (6–9) and a very similar deshielding of the ortho protons relative to the meta protons has been observed for 5-aryltetrazoles by Fraser and Haque (5). The deshielding of the ortho protons has been attributed to (*a*) anisotropy of the heterocyclic ring (6, 8, 9); (*b*) a combination of ring anisotropy, nitrogen anisotropy, and a Van der Waals interaction with the nitrogen lone pair (7, 10); (*c*) the above factors combined with a resonance interaction of the heterocyclic ring system (5). Calculations of deshielding, based on the factors mentioned in (*b*), indicate that the ring anisotropic effect may account for less than half of the total effect (7, 10). Mayo and Goldstein (11) have reported the deshielding of the ortho protons in biphenyl to be 0.24 p.p.m.[1] Hence anisotropic effects alone may not account for an extra deshielding of 0.7 p.p.m. It is significant that the ortho protons of the hydrazones **3** are deshielded by only 0.29–0.37 p.p.m. relative to benzene. Furthermore, evidence has been cited that the contribution of the Van der Waals interaction to the deshielding is unimportant (12). A comparison of the shifts of the ortho ($\tau = 1.79 \pm 0.01$) and meta ($\tau = 2.485 \pm 0.00_5$) protons of compounds **1***b* and **2***b* with those of 5-phenyltetrazole (5) ($\tau_{ortho} = 1.90$ and $\tau_{meta} = 2.49$) shows a considerable similarity between the effects of both the tetrazole and triazolotetrazole ring systems on these protons.[1] Hence, from the present data it is concluded that effects, which result in an overall electron

[1]The deshielding of the ortho protons occurs only if coplanarity of the rings is not sterically forbidden. Information on the rotational barriers in these systems is not readily available. It is assumed here that energy differences between the conformations are small and comparable and that large population differences do not exist.

Can. J. Chem. Downloaded from www.nrcresearchpress.com by 210.87.254.6 on 09/05/12
For personal use only.

withdrawing influence, are present in the triazolotetrazole ring system in addition to anisotropic effects. It is not possible, however, to quantify individual contributions from resonance and inductive effects because the balance of these, as detected by the n.m.r. of the phenyl protons, is not altered in the different isomeric modifications **1** and **2**. The available synthetic routes to the compounds **1** and **2** do not allow for the introduction of labile substituents such as OH and NH_2 which could be useful for this purpose. The rather small deshielding of the meta protons together with the relatively small discrepancy between the predicted and observed shifts (Table 1) for the ortho and meta protons may, however, be indicative of a weak electron donating resonance effect.

The net shielding experienced by the *N*-methyl substituents (Table 1) varies in the different isomers **1** and **2**, in contrast with that of the parent hydrazones (13), thus affording a means of distinguishing between such alkyl substituted isomeric triazolotetrazoles.[2] Differences in *N*-methyl resonances have been used previously as a useful basis for distinguishing between isomeric *N*-substituted tetrazoles (14–16).

[2]Professor Brian M. Lynch, Chemistry Department, St. Francis Xavier University, Antigonish, Nova Scotia, has informed the author that methyl proton shifts in *N*-methylazoles often correlate very well with the calculated charge density at the pyrrole-type nitrogen as evaluated by HMO or SCF methods. Calculations, carried out by Professor Lynch, on the parent systems of **1** and **2** (*i.e.* lacking the phenyl group) indicate charge densities at the methyl-bearing nitrogen of 1.527 and 1.490 respectively in agreement with the observed chemical shifts for the methyl groups.

Experimental

The n.m.r. spectra were measured on a Varian Associates A60 n.m.r. spectrometer at 38° with deuteriochloroform as solvent and tetramethylsilane as internal reference. Concentrations were approximately 0.1 *m*. Because of insolubility the aromatic region of the *p*-bromo species could not be studied, even with saturated solutions.

The range of compounds **1**–**4** were prepared as previously described by us (2, 3, 13).

1. H. Reimlinger. Chem. Ber. **103**, 1900 (1970).
2. R. N. Butler and F. L. Scott. J. Chem. Soc. C, 239 (1967).
3. R. N. Butler and F. L. Scott. J. Chem. Soc. C, 1711 (1968).
4. F. L. Scott, D. A. Cronin, and J. K. O'Halloran. J. Chem. Soc. C, 2769 (1970).
5. R. R. Fraser and K. E. Haque. Can. J. Chem. **46**, 2855 (1968).
6. I. Crossland. Acta Chem. Scand. **20**, 258 (1966).
7. H. Gunther and S. Castellano. Ber. Bunsenges Physik. Chem. **70**, 913 (1966).
8. B. M. Lynch and Y. Y. Hung. Can. J. Chem. **46**, 1605 (1964).
9. L. G. Tensmeyer and C. Ainsworth. J. Org. Chem. **31**, 1878 (1966).
10. S. Castellano, H. Gunther, and S. Ebersole. J. Phys. Chem. **69**, 4166 (1965).
11. R. E. Mayo and J. H. Goldstein. Mol. Phys. **10**, 301 (1966).
12. T. M. Spotswood and C. I. Tanzer. Australian J. Chem. **20**, 1227 (1967).
13. R. N. Butler and F. L. Scott. J. Org. Chem. **32**, 1224 (1967) and **31**, 3182 (1966).
14. F. L. Scott, R. N. Butler, and J. Feeney. J. Chem. Soc. B, 919 (1967).
15. R. Raap and J. Howard. Can. J. Chem. **47**, 813 (1969).
16. R. Raap. Can. J. Chem. **47**, 3677 (1969).

Aqueous Reactions of Sparingly Soluble Tellurites I. Silver Tellurite[1]

M. C. Mehra and S. M. Kahn

Department of Chemistry, University of Moncton, Moncton, New Brunswick

Received October 5, 1971

The aqueous interactions of the sparingly soluble silver tellurite show that in a controlled ionic medium and at a constant temperature, an aqueous complex, $Ag(TeO_3)_2^{3-}$ is formed in presence of free tellurite ions. The solubility product of silver tellurite and the stability constant of the complex species have been evaluated from the experimental data.

On a trouvé que le composé tellurite d'argent, forme un complexe $Ag(TeO_3)_2^{3-}$ dans un milieu aqueuse de force ionique constante en présence des ions tellurites libres. Le produit de solubilité de tellurite d'argent et la constante de formation du complexe ont été calculés à partir des données expérimentales.

Canadian Journal of Chemistry, **50**, 1788 (1972)

[1]Presented in part at the 54th Annual meeting of C.I.C., Halifax, Nova Scotia.

Can. J. Chem. Downloaded from www.nrcresearchpress.com by 210.87.254.6 on 09/05/12
For personal use only.

withdrawing influence, are present in the triazolotetrazole ring system in addition to anisotropic effects. It is not possible, however, to quantify individual contributions from resonance and inductive effects because the balance of these, as detected by the n.m.r. of the phenyl protons, is not altered in the different isomeric modifications **1** and **2**. The available synthetic routes to the compounds **1** and **2** do not allow for the introduction of labile substituents such as OH and NH_2 which could be useful for this purpose. The rather small deshielding of the meta protons together with the relatively small discrepancy between the predicted and observed shifts (Table 1) for the ortho and meta protons may, however, be indicative of a weak electron donating resonance effect.

The net shielding experienced by the *N*-methyl substituents (Table 1) varies in the different isomers **1** and **2**, in contrast with that of the parent hydrazones (13), thus affording a means of distinguishing between such alkyl substituted isomeric triazolotetrazoles.[2] Differences in *N*-methyl resonances have been used previously as a useful basis for distinguishing between isomeric *N*-substituted tetrazoles (14–16).

Experimental

The n.m.r. spectra were measured on a Varian Associates A60 n.m.r. spectrometer at 38° with deuteriochloroform as solvent and tetramethylsilane as internal reference. Concentrations were approximately 0.1 *m*. Because of insolubility the aromatic region of the *p*-bromo species could not be studied, even with saturated solutions.

The range of compounds **1**–**4** were prepared as previously described by us (2, 3, 13).

[2]Professor Brian M. Lynch, Chemistry Department, St. Francis Xavier University, Antigonish, Nova Scotia, has informed the author that methyl proton shifts in *N*-methylazoles often correlate very well with the calculated charge density at the pyrrole-type nitrogen as evaluated by HMO or SCF methods. Calculations, carried out by Professor Lynch, on the parent systems of **1** and **2** (*i.e.* lacking the phenyl group) indicate charge densities at the methyl-bearing nitrogen of 1.527 and 1.490 respectively in agreement with the observed chemical shifts for the methyl groups.

1. H. Reimlinger. Chem. Ber. **103**, 1900 (1970).
2. R. N. Butler and F. L. Scott. J. Chem. Soc. C, 239 (1967).
3. R. N. Butler and F. L. Scott. J. Chem. Soc. C, 1711 (1968).
4. F. L. Scott, D. A. Cronin, and J. K. O'Halloran. J. Chem. Soc. C, 2769 (1970).
5. R. R. Fraser and K. E. Haque. Can. J. Chem. **46**, 2855 (1968).
6. I. Crossland. Acta Chem. Scand. **20**, 258 (1966).
7. H. Gunther and S. Castellano. Ber. Bunsenges Physik. Chem. **70**, 913 (1966).
8. B. M. Lynch and Y. Y. Hung. Can. J. Chem. **46**, 1605 (1964).
9. L. G. Tensmeyer and C. Ainsworth. J. Org. Chem. **31**, 1878 (1966).
10. S. Castellano, H. Gunther, and S. Ebersole. J. Phys. Chem. **69**, 4166 (1965).
11. R. E. Mayo and J. H. Goldstein. Mol. Phys. **10**, 301 (1966).
12. T. M. Spotswood and C. I. Tanzer. Australian J. Chem. **20**, 1227 (1967).
13. R. N. Butler and F. L. Scott. J. Org. Chem. **32**, 1224 (1967) and **31**, 3182 (1966).
14. F. L. Scott, R. N. Butler, and J. Feeney. J. Chem. Soc. B, 919 (1967).
15. R. Raap and J. Howard. Can. J. Chem. **47**, 813 (1969).
16. R. Raap. Can. J. Chem. **47**, 3677 (1969).

Aqueous Reactions of Sparingly Soluble Tellurites I. Silver Tellurite[1]

M. C. Mehra and S. M. Kahn

Department of Chemistry, University of Moncton, Moncton, New Brunswick

Received October 5, 1971

The aqueous interactions of the sparingly soluble silver tellurite show that in a controlled ionic medium and at a constant temperature, an aqueous complex, $Ag(TeO_3)_2^{3-}$ is formed in presence of free tellurite ions. The solubility product of silver tellurite and the stability constant of the complex species have been evaluated from the experimental data.

On a trouvé que le composé tellurite d'argent, forme un complexe $Ag(TeO_3)_2^{3-}$ dans un milieu aqueuse de force ionique constante en présence des ions tellurites libres. Le produit de solubilité de tellurite d'argent et la constante de formation du complexe ont été calculés à partir des données expérimentales.

Canadian Journal of Chemistry, **50**, 1788 (1972)

[1]Presented in part at the 54th Annual meeting of C.I.C., Halifax, Nova Scotia.

Can. J. Chem. Downloaded from www.nrcresearchpress.com by 210.87.254.105 on 09/05/12
For personal use only.

Can. J. Chem. Downloaded from www.nrcresearchpress.com by 210.87.254.105 on 09/05/12
For personal use only.

Introduction

The increasing number of potential applications of the heavy metal compounds of selenium and tellurium as semiconductors has resulted in a revived interest in the chemistry of metal chalcogens as a whole. The reactions of metal sulfur compounds appear to have been investigated in some detail in the past couple of decades, whereas very little seems to have been contributed to the solution chemistry of metal selenium or tellurium compounds (1).

In recent publications the authors have shown that sparingly soluble compounds of sulfur and selenium with heavy metal cations give rise to aqueous complexes of definite stoichiometries (2–6). This complexation behavior extends to the oxy-anions of sulfur and selenium as well (7–9). Although numerous metal tellurites have been prepared (10–13), the aqueous reactions of sparingly soluble compounds of tellurium or its oxygenated anions have been studied to a very limited extent. It was, therefore, thought worthwhile to explore the aqueous interactions of metallic tellurites and the present communication describes the aqueous reactions of silver tellurite.

Experimental

All the reagents employed were of analytical grade; doubly distilled deionized water was used throughout. Silver tellurite was produced *in situ* by mixing radioactive silver nitrate and sodium tellurite at the desired acidity, tellurite concentration, or ionic strength. The system was equilibrated for a period of 5 days before analyses. The radiotracer Ag-110 was obtained from AECL Chalk River, Ontario. Experimental details and the method of analysis were similar to one adopted in an earlier study on silver selenide (4). The radiometric solubility represents the total solubility of the system, while the potentiometric solubility represents the ionic solubility of silver tellurite. The measurements were made at unit molar ionic strength and 25 °C.

Results

Because of the limited solubility of sodium tellurite in water and also its decomposition to TeO_2 in slightly acid media, this study was restricted to the pH 8 to 12. Furthermore, it is only in alkaline condition that the system is composed of tellurite or bitellurite ions (13).

The experimental data of this system show that total solubility remains far superior to the ionic solubility, thereby indicating the formation of some complex species in the aqueous phase in equilibrium with the precipitated compound. Furthermore, the experimental solubility was also found to remain independent of pH of the medium, though it varied as a function of tellurite concentration. The average $[Ag]_{tot}$ for 19 experimental points in the pH range 8–12.5 was computed to be $10^{-6.2}$ M at ~ 0.02 M TeO_3^{2-} concentration, while the corresponding average $[Ag^+]$ was only $10^{-8.02}$ M. The data for another 16 experimental points at a higher ~ 0.125 M TeO_3^{2-} concentration were similarly $10^{-5.13}$ M and $10^{-8.49}$ M respectively.

The solubility pattern of Ag_2TeO_3 as a function of tellurite concentration has an interesting feature (Fig. 1); the solubility slope changes from 0 to 1.5 in the acidity region (p$H \simeq 9.5$) far removed from the second ionization constant of the so-called tellurous acid (H_2TeO_3). The experimental curve clearly indicates the formation of two complex species conformating to two distinct solubility slopes. Obviously one remains independent of pH or the tellurite concentration (slope 0) while the other, though independent of pH, increases its concentration progressively with increasing tellurite concentration. These species are identified by comparing the experimentally observed solubility slopes with the theoretical possibilities as discussed in detail earlier (4). Analysis of the experimental data indicates the presence of Ag^+, $Ag_2TeO_3(aq)$, and $Ag(TeO_3)_2^{3-}$ in the equilibrated supernatant phase.

Solubility Product of Silver Tellurite

The solubility product constant is derived from the potentiometric data utilising the following expressions

$$[1] \qquad [Ag^+]^2[TeO_3^{2-}] = K_{sp}$$

$$[2] \quad [TeO_3]_{tot} = [H_2TeO_3] + [HTeO_3^-] + [TeO_3^{2-}]$$

where $[TeO_3]_{tot}$ is the analytical concentration of tellurite in the medium.

Introduction of the two ionization constants K_1, K_2 of the acid H_2TeO_3 and rearrangement of eq. 2 above gives

$$[3] \qquad [TeO_3^{2-}] = \frac{[TeO_3]_{tot} K_1 K_2}{[H^+]^2 + K_1[H^+] + K_1 K_2}$$

The logarithmic numerical values of K_1 and K_2 have been reported as -2.52 and -7.70, respectively, which suggest that the species

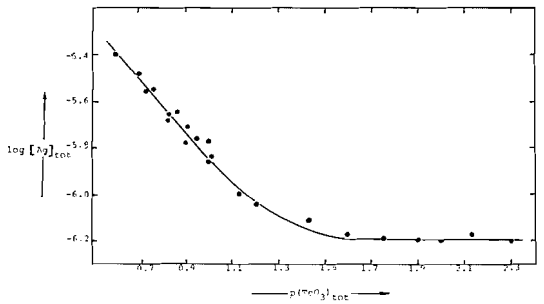

FIG. 1. Radiometric solubility curve of Ag_2TeO_3 as a function of $[TeO_3]_{tot}$, pH (9.4–9.8); $^{110}Ag_{tot}$ (original) = 0.001 M.

TeO_3^{2-} will become the predominant species in the medium only when pH is greater than 8, otherwise, the last two terms in the denominator in eq. 3 will remain significant (1). Hence the concentration of species TeO_3^{2-} at any required acidity is obtained by using the appropriate form of eq. 3 and the solubility product of the compound is obtained by inserting this in eq. 1. An average value of the solubility product of Ag_2TeO_3 from 26 experimental points was calculated to be

$$pK_{sp} = 17.85 \pm 0.11$$

The Formation Constant of Species $Ag(TeO_3)_2^{3-}$

As mentioned earlier, this species makes its appearance felt when the solubility of silver tellurite conforms to a distinct slope of 1.5 (*cf.* Fig. 1). However, one may still regard the experimentally observed $[Ag]_{tot}$ as the sum of all species in any appreciable concentration in solution *i.e.*

$$[4] \quad [Ag]_{tot} = [Ag^+] + [Ag_2TeO_3]_{aq} + [Ag(TeO_3)_2]^{3-}$$

It is assumed that the region of constant solubility (slope 0, Fig. 1) represents the inherent solubility of the compound or the average $[Ag]_{tot}$ here represents the concentration of the species $Ag_2TeO_3(aq)$. The species Ag^+, on the other hand, may even be neglected in eq. 4 since its concentration evaluated from the solubility product of Ag_2TeO_3 at the two different tellurite concentrations will remain inferior to concentration of $Ag_2TeO_3(aq)$. Hence, the concentration of the complex $Ag(TeO_3)_2^{3-}$ is derived by applying appropriate corrections to eq. 4 above and this may be expressed as

$$[5] \quad [Ag(TeO_3)_2^{3-}] = [Ag_{complex}] = [Ag]_{tot} - 10^{-6.19}$$

The stability constant of the complex is obtained from the expression below. The appropriate calculations are recorded in Table 1.

$$[6] \quad \beta_{12} = \frac{[Ag(TeO_3)_2^{3-}]}{[Ag^+][TeO_3^{2-}]^2} = \frac{[Ag_{complex}]}{K_{sp}^{1/2}[TeO_3]_{tot}^{3/2}}$$

$$[7] \quad p\beta_{12} = p[Ag_{complex}] - \tfrac{1}{2}pK_{sp} - \tfrac{3}{2}p[TeO_3]_{tot} = -4.34 \pm 0.05$$

Discussion

The low solubility product value of Ag_2TeO_3 as compared to values of the parallel Ag_2SO_3 and Ag_2SeO_3 under more or less similar experimental conditions reflects that in the series S, Se, and Te, the solubilities of the ionic compounds decrease as a function of atomic weight (1).

This is further borne out by the fact that the complexation reaction in the case of silver tellurite terminates with the formation of only one aqueous complex $Ag(TeO_3)_2^{3-}$ whereas the other two systems do form several aqueous species (7–9). Furthermore the tellurite complex is formed only at a higher ligand concentration, which confirms that the coordinating tendency of tellurite ligand is weaker than the corresponding sulfite and selenite ligands.

Lenher and Wolesensky (10) have reported by a gravimetric analysis that only the compound Ag_2TeO_3 is formed by the interaction of silver nitrate and sodium tellurite. In this study by pH titration of the inherently alkaline sodium tellurite with silver nitrate, the stoichiometry of 2:1 for Ag^+ and TeO_3^{2-} ions has been reconfirmed for the precipitated compound. It has been further shown that up to pH 12, the alkalinity of the medium does not influence the composition of the precipitate. It may, thus, be inferred confidently from the experimental data that OH^- ions do not participate in the complexation reaction or in other words mixed complex formation with OH^- as ligand is totally absent under the controlled experimental conditions described earlier in the text.

It is tacitly assumed in the present work that the tellurite system stems from a diprotic acid the same way as sulfite or selenite systems origi-

Can. J. Chem. Downloaded from www.nrcresearchpress.com by 210.87.254.105 on 09/05/12
For personal use only.

TABLE 1. Stability constant for complex $Ag(TeO_3)_2^{3-}$ at unit molar ionic strength and 25 °C

pH	$p[Ag]_{tot}$	$p[TeO_3]_{tot}$	$p[Ag_{complex}]$	$-p\beta_{12}$
9.82	5.40	0.60	5.48	4.33
9.66	5.48	0.70	5.57	4.39
9.72	5.49	0.70	5.59	4.37
9.76	5.52	0.73	5.63	4.37
9.80	5.55	0.76	5.66	4.39
9.63	5.66	0.82	5.83	4.31
9.56	5.68	0.82	5.84	4.30
9.74	5.64	0.86	5.78	4.42
9.62	5.72	0.90	5.90	4.36
9.48	5.78	0.90	5.99	4.27
9.58	5.76	0.95	5.96	4.37
9.50	5.86	1.00	6.13	4.28
				Mean 4.34 ± 0.05

nate from sulfurous or selenous acids. However, there is a general lack of agreement in the literature on the existence of the species H_2TeO_3 (1, 14). On the other hand, formation of two series of salts, bitellurites and tellurites has been generally accepted (13). Although it is beyond the scope of this note to comment on the formation of tellurous acid, this study does lend support to the argument that sodium tellurite may be treated in much the same manner as sodium sulfite or sodium selenite. This is very important since eq. 3 and the argument leading to the identification of complex species depend on such a behavior. Assuming that the two reported ionization constants of the so called tellurous acid, K_1 ($10^{-2.52}$) and K_2 ($10^{-7.70}$) are true, then the compound Na_2TeO_3 will dissociate in such a manner that in pH region beyond the value of K_2 it will essentially be ionized as Na^+ and TeO_3^{2-} ions. If sodium tellurite under a condition $pH > pK_2$ is reacted with a cation forming a sparingly soluble compound with tellurite ions, the ionic solubility of the compound formed will theoretically remain independent of pH. This aspect has actually been discussed in detail in an earlier publication for a system involving a diprotic acid (4). The experimental results for the system silver tellurite do show such a behavior, where one observes that the potentiometric and radiometric solubilities remain independent of pH, though these vary as a function of tellurite concentration. Therefore, the mathematical equations derived for a diprotic acid system for the identification of aqueous complex species originating through heterogeneous system remain valid for the tellurite system as well. The formation of the complex species $Ag(TeO_3)_2^{3-}$ thus appears justified both on theoretical and experimental grounds. There is, however, no report available in the literature on the complexation of reactions of tellurite ion.

Financial support from the National Research Council of Canada (grant A-5782) and the University of Moncton is gratefully acknowledged.

1. L. C. SILLEN and A. E. MARTELL. Stability constants of metal ions. Chem. Soc. Spec. Publ. No. 17, London, 1964.
2. J. STE-MARIE, A. E. TORMA, and A. O. GUBELI. Can. J. Chem. **42**, 662 (1964).
3. A. O. GUBELI and J. STE-MARIE. Can. J. Chem. **45**, 2101 (1967).
4. M. C. MEHRA and A. O. GUBELI. Can. J. Chem. **48**, 3491 (1970).
5. M. C. MEHRA and A. O. GUBELI. J. Less Common Metals, **22**, 281 (1970).
6. M. C. MEHRA and A. O. GUBELI. J. Less Common Metals, **25**, 221 (1971).
7. H. CHATEAU, M. DUARANTE, and B. HERVIER. Sc. Indust. Phot. **27**, 81 (1956).
8. H. CHATEAU, M. DUARANTE, and B. HERVIER. Sc. Indust. Phot. **27**, 257 (1956).
9. M. C. MEHRA and A. O. GUBELI. Radiochem. Radioanal. Letters, **2** (2), 61 (1969).
10. V. LENHER and E. WOLESENSKY. J. Am. Chem. Soc. **35**, 718 (1913).
11. M. J. REDMAN and W. W. HARVEY. J. Less Common Metals, **12**, 395 (1967).
12. W. A. DUTTON. Tellurium. *Edited by* Charles W. Cooper. Van Nostrand Reinhold, New York. 1971. Chap. 4.
13. K. W. BAGNALL. The chemistry of selenium, tellurium and polonium. Elsevier, Amsterdam. 1966.
14. W. A. DUTTON and W. C. COOPER. Chem. Rev. **66**, 657 (1966).

Can. J. Chem. Downloaded from www.nrcresearchpress.com by 210.87.254.105 on 09/05/12
For personal use only.

Can. J. Chem. Downloaded from www.nrcresearchpress.com by 210.87.254.5 on 09/05/12
For personal use only.

Canadian Journal of Chemistry

Published by THE NATIONAL RESEARCH COUNCIL OF CANADA

VOLUME 50 JUNE 15, 1972 NUMBER12

The Hydrogenation of Allene. IV. The Reaction of Allene with Hydrogen Catalyzed by Palladium, Platinum, Iridium, Rhodium, Ruthenium, and Osmium Catalysts

R. S. MANN AND A. M. SHAH

Department of Chemical Engineering, University of Ottawa, Ottawa K1N 6N5, Canada

Received July 9, 1971[1]

The reaction between allene and hydrogen over unsupported palladium, platinum, iridium, rhodium, ruthenium, and osmium catalysts has been investigated in a static constant volume system between 70 and 149 °C for a wide range of reactant ratios. The orders of reaction with respect to hydrogen and allene were one and zero, respectively, and temperature independent. The overall apparent activation energies for unsupported platinum, iridium, palladium and rhodium were 17.7, 9.1, 6.4, and 17.4 kcal/mol, respectively. The catalytic activities of the unsupported metals were in the sequence Pd > Ir > Rh > Pt > Ru, Os. Selectivity was highest with palladium and rhodium, and least with iridium. The polymerization was highest with platinum and least with iridium.

Nous avons étudié la réaction entre l'allène et l'hydrogène sur des catalyseurs non-supportés de palladium, platine, iridium, rhodium, ruthénium, et osmium, dans un système de volume statique constant entre 70 et 149 °C et dans un large domaine de rapports des réactifs. Les ordres de réaction par rapport à l'hydrogène et à l'allène étaient respectivement un et zéro et indépendants de la température. Les énergies totales d'activation apparentes pour le platine, l'iridium, le palladium et le rhodium sans support sont respectivement de 17.7, 9.1, 6.4, et 17.4 kcal/mole. Les activités catalytiques des métaux sans support étaient dans l'ordre: Pd > Ir > Rh > Pt > Ru, Os. La sélectivité était plus élevée pour le palladium et le rhodium et plus faible avec l'iridium. La polymérisation était plus élevée avec le platine et plus faible avec l'iridium.

Canadian Journal of Chemistry, **50**, 1793 (1972)

Introduction

In Parts I, II, and III of this series, the kinetics and products obtained from the reaction of allene with hydrogen catalyzed by pumice supported metals of the eighth group (1), unsupported nickel, iron, and cobalt (2), and nickel, copper, and their alloys (3) were reported. In this concluding paper of the series, we report the kinetics of allene hydrogenation over palladium, platinum, iridium, rhodium, ruthenium, and osmium.

Experimental

The apparatus, experimental procedure and method of product analysis were the same as described earlier (3, 4). The unsupported palladium, platinum, iridium, rhodium, ruthenium, and osmium catalysts were prepared by evaporating the solutions containing $(NH_4)_2PdCl_6$, $(NH_4)_2PtCl_2$, $(NH_4)_2IrCl_6$, $(NH_4)_2RhCl_6$, $(NH_4)_2RuCl_6$, and $(NH_4)_2OsCl_6$, respectively. The catalysts were reduced in a hydrogen stream for 24 h at 400 °C. The amount of polymers formed (allene lost) was calculated as the difference between the initial allene pressure and the pressure of hydrocarbons in the products. The pressure of hydrocarbons was the sum of the unreacted allene, propylene, and propane in the products.

Results

Unsupported platinum, palladium, iridium, and rhodium catalysts were found to be quite active and did not get poisoned when allene or hydrogen was admitted first into the reactor. The activity remained fairly constant for several days. Though ruthenium and osmium were found to be active at the beginning, they lost their activity after a few hours, and no measur-

[1]Revision received March 1, 1972.

TABLE 1. Order of reaction and activation energies

Catalyst	Weight of metal (g)	Temperature range (°C)	Order with respect to Hydrogen (±0.005)	Order with respect to Allene (±0.04)	k, specific rate at 60 °C (min^{-1} g $metal^{-1}$)	E, activation energy (kcal/mol)
Platinum	0.03054	120–149	1.00	0.00	0.0034	17.7
Iridium	0.02940	93–141	1.00	0.02	0.0981	9.1
Palladium	0.01933	70–142	0.996	0.00	0.3853	6.4
Rhodium	0.03232	80–115	0.995	0.00	0.0553	17.4
Ruthenium	0.21810	20–140	Catalyst deactivated after few runs			
Osmium	0.32560	20–194				

able rates were observed at high temperatures. The loss of activity of ruthenium and osmium was not due to mercury poisoning. While studying the reaction over palladium, a few drops of silicone oil were placed over the mercury in the manometer connected to the reactor to avoid the poisoning of the palladium catalyst, and the catalyst was isolated by closing the valve connected to the manometer when the reaction was not being studied.

A. Kinetics

The pressure–time curves observed during the study of allene hydrogenation over unsupported platinum, palladium, iridium, and rhodium catalysts were of Type III (4), regardless of (*i*) the initial reactant ratio, (*ii*) the order of admission of the reactants, and (*iii*) the temperature.

The orders of reaction were determined by the method of initial rates, the partial pressure of allene or hydrogen being varied while the other was kept constant at 50 mm. The orders of reaction with respect to hydrogen and allene were one and zero respectively and were temperature independent (Table 1).

Plots of $\log_{10}$ specific reaction rate against the reciprocal of absolute temperatures were good straight lines over a wide range of temperatures for unsupported platinum, palladium, iridium, and rhodium catalysts, satisfying the Arrhenius equation. The derived apparent activation energies are given in Table 1.

B. Selectivity

The course of the reaction and the dependence of the selectivity upon pressure fall was studied for hydrogen/allene ratios of 1 and 2, by analyzing the reaction products at different pressure falls. The selectivity (S) has been defined as the ratio of propylene to propylene plus propane.

The dependence of the selectivity upon pressure fall for hydrogen/allene ratio of 1 is shown in Fig. 1. Selectivity was independent of pressure fall for palladium and rhodium. While the selectivity increased with pressure fall for platinum, it decreased with the progress of the reaction in the case of iridium. The amount of allene polymerized increased with pressure fall, irrespective of the reactant ratio or the catalyst.

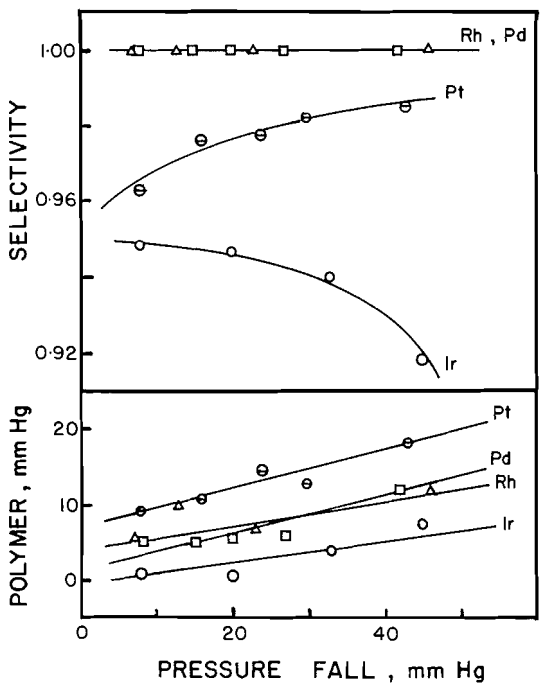

FIG. 1. Dependence of selectivity upon pressure fall, $P_{H_2} = 50$ mm Hg, $P_{C_3H_4} = 50$ mm Hg. Ir powder, ○, $T =$ 132.5 °C; Rh powder, Δ, $T = 107.0$ °C; Pd powder, □, $T = 128.5$ °C; Pt powder, 0, $T = 143.0$ °C.

Can. J. Chem. Downloaded from www.nrcresearchpress.com by 210.87.254.5 on 09/05/12
For personal use only.

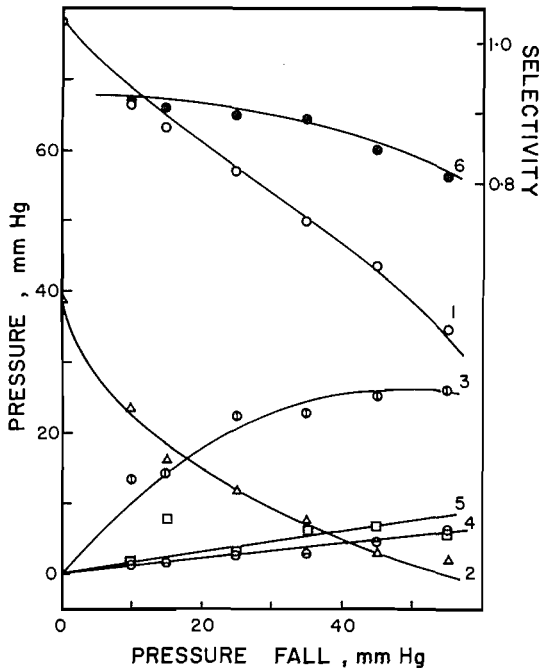

FIG. 2. Distribution of products during the course of reaction over Ir-powder catalyst at 132.5 °C. $P_{H_2} = 100$ mm Hg, $P_{C_3H_4} = 50$ mm Hg, Curve *1*, hydrogen; curve *2*, allene; curve *3*, propylene; curve *4*, propane; curve *5*, polymer; curve *6*, selectivity.

The product distribution during the course of the reaction for iridium catalyst is shown in Fig. 2. Similar results were obtained for platinum, palladium, and rhodium catalysts.

Measurements were made of the selectivity of the catalysts as a function of initial hydrogen pressure at several temperatures by using a fixed allene pressure (50 mm) and varying the hydrogen pressure (40–170 mm). The products were analyzed when the total pressure fall was equal to 30 mm. While the selectivity was independent of initial hydrogen pressure for rhodium and palladium, it decreased with increased hydrogen pressure for platinum and iridium catalysts. The extent of allene polymerization was nearly independent of hydrogen pressure for all catalysts.

The dependence of selectivity upon initial allene pressure was studied by using a fixed hydrogen pressure and varying the allene pressure (40–150 mm). The products were analyzed at a fixed pressure fall (20 mm for Ir, Pd, and Rh, and 30 mm for Pt). The selectivity was independent of allene pressure for palladium, rhodium, and iridium catalysts. However, the selectivity of platinum increased with increased allene pressure up to 80 mm, and thereafter remained constant. While the amount of allene polymerized increased with allene pressure for platinum, iridium, and rhodium catalysts, it was independent of allene pressure for palladium catalysts.

The temperature dependence of the selectivity for hydrogen/allene ratio of 2 was studied by analyzing the products at several temperatures at a pressure fall of 20 mm in the case of iridium, rhodium, and palladium, and 30 mm for platinum catalyst. While the selectivity was independent of the temperature for rhodium and palladium catalysts, it decreased with increasing temperatures for platinum and iridium catalysts. While the extent of polymerization was independent of temperature for platinum and rhodium catalysts, it increased with increased temperatures for palladium and iridium.

Discussion

The pressure–time curves (Type III) observed in the present study were similar to those observed earlier in the study of allene hydrogenation over nickel–copper alloys (3). The pressure–time curves of Type III were also observed in the study of allene hydrogenation over pumice supported transition metals of the eighth group (1) and unsupported iron, cobalt, and nickel catalysts (2).

The orders of the reaction with respect to hydrogen and allene were one and zero, respectively. Similar orders were observed for allene hydrogenation by other investigators (1–3, 5). Mann and Khulbe (6) in the study of methylacetylene hydrogenation over unsupported palladium, platinum, iridium, rhodium, and osmium catalysts observed that order with respect to hydrogen was one, and zero to slightly negative with respect to methylacetylene.

The order of relative activities of the various unsupported metals observed for the hydrogenation of allene (Table 1) in the present investigation is

(*a*) Pd > Ir > Rh > Pt ≫ Ru, Os

as compared to

(*b*) Pd > Ir > Pt > Rh > Ru > Os

Can. J. Chem. Downloaded from www.nrcresearchpress.com by 210.87.254.5 on 09/05/12
For personal use only.

observed by Mann and Khulbe (6) for methylacetylene hydrogenation over unsupported metal catalysts. Since no studies have been made of the catalytic activities of various unsupported metals for allene hydrogenation, by any other investigator, no direct comparison of the present work can be made with any published work. The catalytic activities of pumice supported metals for allene hydrogenation were reported by Mann and To (1) to be in the sequence

(*c*) $$Pt > Pd > Rh > Ir > Ru > Os$$

The results of the present investigations show close similarity in the catalytic activities of unsupported metals to those obtained by Mann and Khulbe (6) for methylacetylene hydrogenation over the same metals. Palladium was found to be the most active catalyst for allene and methylacetylene hydrogenation. Comparing (*a*) and (*c*), the relative activities of the unsupported and supported metals, it is seen that the activity of the catalyst depends on the form (supported or unsupported) of the catalyst. Thus pumice supported platinum (*c*) was more active than supported palladium, as compared to unsupported palladium being more active than unsupported platinum (*a*). It has been found that irrespective of the fact whether the catalysts were supported or unsupported, the metals having the face centered cubic structure (Pd, Pt, Ir, and Rh) were found to be active catalysts, whereas those having close packed hexagonal structure (Ru, Os) were not active at all.

The unsupported metals can be placed in the following sequence of decreasing selectivity for allene hydrogenation:

(*d*) $$Pd \approx Rh > Pt > Ir$$

The order of the sequence found in this investigation compares well with the order of the selectivities derived for methylacetylene (6). It is important to note that the selectivity exhibited is primarily a function of the particular metal and is substantially independent of the hydrocarbon undergoing reaction and of the conditions under which the reaction is carried out.

The results of the present investigation largely confirm the expected resemblance between the hydrogenation of allene and acetylenes. Since the dependence of the selectivity on temperature and pressures of the reactants and the kinetics of the reaction of hydrogen with allene and acetylene are very similar, it can be assumed that the reaction mechanism for these may be similar, and that the allene hydrogenation reaction is the one in which gaseous allene and hydrogen are adsorbed on the surface to form the half hydrogenated state

$$H_2C{=}C{-}CH_3$$
$$\quad\quad\quad

Studies of β-Diketone Complexes of Rhenium. Part II. Physical Studies of Dihalobis(pentane-2,4-dionato)rhenium(IV) Compounds

W. D. COURRIER, C. J. L. LOCK,[1] AND G. TURNER

Department of Chemistry and Institute for Materials Research, McMaster University, Hamilton, Ontario

Received October 1, 1971

Studies on *trans*-$Re(acac)_2Cl_2$ in the solid state, solution, and gas phases by spectroscopic and classical physical methods show that the compound is a monomer and not a dimer as previously claimed (2). *cis*-$Re(acac)_2Cl_2$, $Re(acac)_2Br_2$, $Re(acac)_2I_2$, and $Re(dbm)_2Cl_2$ have been prepared for the first time and corresponding physical measurements are reported.

Les études effectuées sur le *trans*-$Re(acac)_2Cl_2$, en phase solide, en solution et en phase gazeuse au moyen des méthodes spectroscopiques et physiques classiques, montrent que ce composé est un monomère et non un dimère comme cela avait été annoncé (2). Les composés nouveaux, *cis*-$Re(acac)_2Cl_2$, $Re(acac)_2Br_2$, $Re(acac)_2I_2$, et $Re(dbm)_2Cl_2$, ont été préparés et les mesures physiques correspondantes sont rapportées.

Canadian Journal of Chemistry, **50**, 1797 (1972)

Introduction

Several β-diketone complexes of rhenium have been described (1, 2). One of the compounds prepared was described as $Re_2(acac)_4Cl_4$ in which two acetylacetonate ions, bonding through the oxygen atoms bridged two rhenium atoms.[2] The structure was suggested on the basis of analysis, molecular weight determinations, and spectroscopic results. It has been shown (3) that in the solid state the compound is a monomer, *trans*-dichlorobis(pentane-2,4-dionato)rhenium(IV). It seemed appropriate, therefore, to reexamine spectroscopic results for this compound, and for the corresponding bromide and iodide complexes which had not been prepared previously.

Experiments

Analyses were performed by Galbraith Laboratories, Inc., Knoxville Tennessee, A. B. Gygli, Toronto, Canada and Meade Microchemical Laboratories, Amherst, Mass. Infrared spectra were recorded on Perkin–Elmer 337, 521, and 301 machines. Samples were ground into a mull with Nujol and mounted between potassium bromide or polyethylene plates. Raman spectra were excited by the 6328 Å line of a helium–neon laser and were recorded on a Czerny–Turner-type Spex laser Raman recording spectrograph. Samples were powders contained in Pyrex melting-point tubes. Ultraviolet and visible spectra were recorded on a Cary 14 instrument. Samples were solutions of the compound in benzene contained in 1 cm quartz cells. Measurements of the magnetic susceptibilities of powdered, solid samples were made by the Gouy method on an apparatus described previously (4). To minimize packing errors, the samples, in 3 mm o.d. quartz tubes, were placed in the vibrator of a Hoover (Philadelphia, Pa.) Unimelt apparatus and shaken to a constant 10 cm length. Calibration of the magnetic apparatus was accomplished using mercury thiocyanatocobaltate(II), obtained from Eastman Organic Chemicals, Rochester, New York. Magnetic susceptibilities were measured at four different field strengths to check for ferromagnetic behavior of either the sample or any impurities present. Corrections for diamagnetism of ligands and metal ions were taken from Selwood (5) and Föex (6). Mass spectra[3] were recorded on a Consolidated Electrodynamics Corporation mass spectrometer Model 21-110B. The samples were injected directly at 200 °C. X-Ray diffraction photographs of powdered samples were recorded on a Debye–Scherrer camera using nickel-filtered CuKα radiation. The samples were sealed inside quartz tubes. Line intensities were measured from the photographs with a Joyce–Loebl microdensitometer.

Dielectric constants and refractive indices of dilute benzene solutions of the dihalobis(pentane-2,4-dionato)-rhenium(IV) isomers were measured at 25.0 ± 0.1 °C. Dielectric constants were measured using a Wissenschaftlich-Technische Werkstätten dipolemeter Type DMO1, and a measuring cell Type DFL1. The measuring condenser was calibrated with air, *n*-hexane, carbon tetrachloride, benzene, carbon disulfide, and diethyl carbonate. The calibrating liquids were all Fisher Scientific A.R. grade, and were dried over Lindeman molecular sieve type 4A. Refractive indices were determined at the sodium D line with a Bausch and Lomb dipping refractometer which was calibrated with benzene. The dipole moments were calculated using the Guggenheim method (7). The results are presented in Table 4.

Calculations

Dipole moments were determined by the equation

$$\mu^2 = \frac{9kT}{4\pi N}\left[\frac{3}{(\varepsilon_1 + 2)(n_1^2 + 2)}\right] \times (a_\varepsilon - a_n) \times \frac{M_2}{d_1}$$

d_1, ε_1, n_1 are density, dielectric constant, and refractive index of solvent; M_2 is molecular weight of solute; a_ε is the slope of

[1]To whom correspondence should be addressed.

[2]acac is the 2,4-pentanedionate ion, $C_5H_7O_2^-$; dbm is the anion derived from the enol form of dibenzoylmethane, $C_6H_5.CO.CH.CO.C_6H_5^-$; dik is the anion of any β-diketone.

[3]Mass spectra were obtained through the courtesy of Professor D. B. MacLean.

Can. J. Chem. Downloaded from www.nrcresearchpress.com by 210.87.254.42 on 09/05/12
For personal use only.

TABLE 1. Analyses and properties of compounds of the type $ReX_2(dik)_2$

Compound	Analysis (%) C Calcd.	C Found	H Calcd.	H Found	Halogen Calcd.	Halogen Found	Solubility in C_6H_6	Solubility in CH_2Cl_2	Decomposition temperature
trans-$ReCl_2(acac)_2$	26.4	26.4	3.1	3.1	15.6	15.3	VSS*	SS	~275°
cis-$ReCl_2(acac)_2$	26.4	27.2	3.1	3.1	15.6	15.9	S	S	~255°
$ReBr_2(acac)_2$	22.1	21.6	2.6	2.8	29.4	30.6	SS	SS	~265°
$ReI_2(acac)_2$	18.8	18.9	2.2	2.6	39.8	38.4	SS	S	>325°
$ReCl_2(dbm)_2$	51.3	50.7	3.2	3.0	10.1	10.2	VSS	VSS	>325°

*S = soluble, SS = slightly soluble, VSS = very slightly soluble.

TABLE 2. Mass spectral data for $ReX_2(acac)_2$

Fragment	*trans*-Cl *m/e*	*trans*-Cl *I*	*cis*-Cl *I*	Br *m/e*	Br *I*	I *m/e*	I *I*
$ReX_2(acac)_2^+$	*P**	100	100	*P*	100	*P*	86
$ReX(acac)_2^+$	*P* − 35	6	4	*P* − 79	7	*P* − 127	69
$Re(acac)_2^+$	*P* − 70	3	2	*P* − 158	74	*P* − 254	100
$ReX(acac)C_3H_4O^+$	*P* − 78	—	4	—	—	—	—
$ReOX_2(acac)^+$	*P* − 83	<2	5	—	—	—	—
$ReX_2(acac)^+$	*P* − 99	<2	2	—	—	—	—
$ReOX(acac)^+$	*P* − 118	63	62	*P* − 162	30	*P* − 210	10
$ReX(acac)^+$	*P* − 134	<2	5	—	—	—	—
$ReOH(acac)^+$	—	—	—	*P* − 240	3	*P* − 336	23
$ReO(acac)^+$	*P* − 153	2	2	*P* − 241	2	*P* − 337	10
$ReOX_2^+$	*P* − 182	5	7	*P* − 182	6	*P* − 182	5
$ReX(acac)_2^{2+}$	—	—	—	*P* − 310	7	*P* − 382	17

**P* is the mass of the lowest isotopic component of the parent peak. All masses refer to the lowest mass isotopic component.

the line obtained by plotting $e_{solution} - e_{solvent}$ *vs.* w_2; a_n is the slope of the line $n^2_{solution} - n^2_{solvent}$ *vs.* w_2; w_2 is the "weight in" quantity of solute = weight of solute/weight of solution. Conductivities were determined on an Industrial Instruments, N. J. Model RC1632 conductivity bridge as distributed by Fisher Scientific. The molar conductance of *cis*-$Re(acac)_2Cl_2$ in acetonitrile at 25 °C was 0.767 ohm^{-1} cm^2 at 5.25×10^{-3} *M* and 0.456 ohm^{-1} cm^2 at 2.1×10^{-3} *M*. The molar conductance of *trans*-$Re(acac)_2Cl_2$ in acetonitrile at 25 °C was 0.241 ohm^{-1} cm^2 at 1.8×10^{-4} *M* and 0.218 ohm^{-1} cm^2 at 1.1×10^{-4} *M*.

The Measurement of Molecular Weight

Molecular weight measurements in solution were made on a Hitachi–Perkin–Elmer 113 molecular weight apparatus. The apparatus was calibrated using benzil as a solute in benzene and dichloromethane solvents. It was established that to obtain reproducible results carefully purified and dried chemicals had to be used. The calibration curve for benzene solvent was obtained using benzil (mol. wt. 210) recrystallized from benzene to a m.p. of 95 °C, and A.C.S. Standard benzene which had been sodium dried (density 0.8787 g ml^{-1} at 22 °C). Measurements were made with a main oven temperature 40.8 °C, a sub oven temperature of 35.2 °C, and room temperature of 22.2 °C. Calibration was made over a range 0.02–0.0034 mol solute/kg of solvent. The time to reach equilibrium was 2 min. Repeat calibrations showed that the extreme error which could exist was ±7%. The instrument specification claims ±15% in the range $1 \times 10^{-4} - 5 \times 10^{-2}$ mol/kg and ±3% for $3 \times 10^{-2} - 2 \times 10^{-2}$ mol/kg for a benzene solvent. The calibration was checked with recrystallized triphenylphosphine (mol. wt. 262) and the results are shown in Table 3. The calibration for dichloromethane used benzil in dichloromethane (A.C.S. AR reagent, molecular sieve dried, density 1.327 g ml^{-1} at 22 °C). The main oven temperature was 25.2 °C and both the sub oven and room temperatures were 22.2 °C. Greater variation was observed in calibration (±10–15%) and equilibrium time was taken at 4 min, the maximum allowable according to the manual. Calibration was made over a range $2.43 \times 10^{-2} - 2 \times 10^{-3}$ mol/kg. A check was made using triphenylphosphine and the results are presented in Table 3. Measurements of the molecular weight of *cis*-$Re(acac)_2Cl_2$ were then made in both dichloromethane and benzene and of *trans*-$Re(acac)_2Cl_2$ in dichloromethane. The results are presented in Table 3.

Subsequently, the molecular weight of *trans*-$Re(acac)_2Cl_2$ was determined by Meade Microchemical Laboratories,

Can. J. Chem. Downloaded from www.nrcresearchpress.com by 210.87.254.42 on 09/05/12
For personal use only.

TABLE 3. Molecular weight measurements

Solute	Solvent	Concentration mol solute/kg solvent	Molecular weight
$(C_6H_5)_3P$	C_6H_6	2.9×10^{-2}	257
		1.43×10^{-2}	261
		1.4×10^{-3}	267
		5×10^{-4}	373
$(C_6H_5)_3P$	CH_2Cl_2	1.96×10^{-2}	273
		2.3×10^{-3}	233
cis-$Re(acac)_2Cl_2$	C_6H_6	7.3×10^{-3}	450
		5.2×10^{-3}	498
		2.3×10^{-3}	561
cis-$Re(acac)_2Cl_2$	CH_2Cl_2	5.9×10^{-3}	440
		2.0×10^{-3}	513
trans-$Re(acac)_2Cl_2$	CH_2Cl_2	1.2×10^{-3}	421
		0.8×10^{-3}	593
		0.6×10^{-3}	553
trans-$Re(acac)_2Cl_2$* (sample 1)	CH_2Cl_2	—	468
			463
trans-$Re(acac)_2Cl_2$* (sample 2)	$C_6H_4Cl_2$	—	464

*Determined by Meade Microchemical Laboratories, Amherst, Mass. using a Mechrolab osmometer.

Amherst, Mass. using a Mechrolab Osmometer, in both dichloromethane and *o*-dichlorobenzene as solvents. These results are also shown in Table 3.

Rhenium metal was obtained from the Rhenium Division, Chase Brass and Copper Co. Inc., Solon, Ohio. Perrhenic acid was obtained as an aqueous solution from S. W. Shattuck Chemical Co., Denver, Colorado. All solvents and reagents used were reagent grade. Solvents were dried, when necessary, by treatment with freshly regenerated molecular sieves (Linde Type 4A) and were deoxygenated by bubbling dry nitrogen through them using a dispersion bubbler.

Preparation of Compounds

trans-Dichlorobis(pentane-2,4-dionato)rhenium(IV), $ReCl_2(acac)_2$

This compound was made by a number of methods. The products from the various reactions were identical. (*a*) The compound was prepared by the method of Grove *et al.* (2) for tetrachlorobis(pentane-2,4-dionato)-μ_2-bis(pentane-2,4-dionato)dirhenium(IV). (*b*) $ReOCl_2(acac)P(C_6H_5)_3$ (0.6 g) (2) was refluxed in acetylacetone (5 ml) for 4 h under an atmosphere of nitrogen. The solution was cooled and the orange crystals collected by filtering the solution; yield 0.25 g (58%). (*c*) $ReCl_2(acac)(P(C_6H_5)_3)_2$ (2) or $ReCl_2(acac)(OP(C_6H_5)_3)P(C_6H_5)_3$ (9) when refluxed with acetylacetone in air overnight gave fair yields of $ReCl_2(acac)_2$ on cooling (39 and 69%, respectively).

cis-Dichlorobis(pentane-2,4-dionato)rhenium(IV), $ReCl_2(acac)_2$

The filtrates of several preparations of *trans*-$ReCl_2(acac)_2$ were combined and evaporated slowly. A small amount of a reddish-brown crystalline compound was isolated.

Dibromobis(pentane-2,4-dionato)rhenium(IV), $ReBr_2(acac)_2$

$ReO(OCH_3)Br_2\{P(C_6H_5)_3\}_2$ (1 g) (8) was refluxed with 50 ml of acetylacetone for 48 h in air. The solution was cooled and the red crystals collected by filtering the solution. Yield, 0.69 g(33%).

Diiodobis(pentane-2,4-dionato)rhenium(IV), $ReI_2(acac)_2$

The dark red compound was prepared in ~29% yield from $ReOI_2(OCH_3)\{P(C_6H_5)_3\}_2$ (8) in a way similar to the bromo-compound.

Dichlorobis(1,3-diphenylpropane-1,3-dionato)rhenium-(IV), $ReCl_2(dbm)_2$

$ReO(OCH_3)Cl_2\{P(C_6H_5)_3\}_2$ (2 g) was fused with dibenzoylmethane (10 g), at a minimum temperature necessary to keep the mixture molten, for 48 h in a nitrogen atmosphere. Dark red needles of the compound were isolated by dissolving excess ligand in acetone. Yield 0.8 g (47%). Analyses and properties for all compounds are summarized in Table 1. None of the compounds was soluble in methanol, diethyl ether, or 30–60° petroleum ether, nor did they show any sign of halogen exchange when boiled in dichloromethane.

Results and Discussion

Previous work (3) has shown that $ReCl_2(acac)_2$ is not dimeric in the solid state. In order to see whether any dimerization occurred in the gas phase we have made mass spectral measurements on four of the compounds described in

Can. J. Chem. Downloaded from www.nrcresearchpress.com by 210.87.254.42 on 09/05/12
For personal use only.

TABLE 4. Measurement of dipole moments of $ReX_2(acac)_2$

(*a*) Calibration*

Compound	$\varepsilon_{25\,°C}$†	Capacity (βF)
"Air"	~1	430.5
n-Hexane	1.882	2418.7
Carbon tetrachloride	2.228	3195.5
Benzene	2.274	3293.5
Carbon disulfide	2.628	4111.8
Diethyl carbonate	2.81	about 4500 (limit of cell)

*Slope of calibration curve, $\Delta\varepsilon$/capacity = 4.65×10^{-4}. All dielectric and refractometric measurements were done in dilute benzene solutions.
†Data from ref. 24.

(*b*) Measurement of dipole moments

Compound	$w_2 \times 10^4$	$(\varepsilon_{soln} - \varepsilon_{benzene}) \times 10^3$	$\eta_{25\,°C}$	$(\eta_{soln}^2 - \eta_{benzene}^2) \times 10^3$
cis-$Re(acac)_2Cl_2$*	2.987	29.75	1.5090	27.68
	2.688	26.69	1.5081	25.00
	2.419	23.40	1.5073	22.55
	1.936	18.80	1.5058	18.03
	1.355	13.09	1.5040	12.62
trans-$Re(acac)_2Cl_2$†	1.80	3.90	1.5011	3.91
	1.10	1.50	1.5003	1.46
$Re(acac)_2Br_2$‡	4.94	3.845	1.5022	3.90
	3.90	3.564	1.5821	3.60
	2.75	3.283	1.5020	3.30
	1.49	2.814	1.5019	3.00
$Re(acac)_2I_2$§	9.27	1.844	1.5015	1.802
	5.38	1.501	1.5014	1.502

*$\eta_{25\,°C}$ benzene measured at 1.4998; literature value is 1.5005. a_ε = slope of $(\varepsilon_{soln} - \varepsilon_{benzene})$ *vs.* $w_2 = 9.96 \pm 0.02$. a_n = slope of $(n^2_{soln} - n^2_{benzene})$ *vs.* $w_2 = 9.28 \pm 0.01$.
†$n_{25\,°C}$ benzene measured at 1.4998.
‡$n_{25\,°C}$ benzene measured at 1.5009. $a_\varepsilon = 2.93 \pm 0.07$. $a_n = 2.55 \pm 0.02$.
§$n_{25\,°C}$ benzene measured at 1.5009.

(*c*) Calculated values of dipole moment

Compound	Calculated dipole moment (D)
cis-$Re(acac)_2Cl_2$	5.5(5)
trans-$Re(acac)_2Cl_2$	0.0(5)
$Re(acac)_2Br_2$	4.4(6)
$Re(acac)_2I_2$	0.0(5)

this work: it was not possible to obtain a mass spectrum of $ReCl_2(dbm)_2$ because of its low volatility. The results are presented in Table 2. In all cases the fragment with the highest *m/e* value was $ReX_2(acac)_2^+$ and there was no evidence of $Re_2X_4(acac)_4^+$ or any derived dimeric fragments.

A comparison of the relative intensities of the $ReX_2(acac)_2^+$ and $ReX(acac)_2^+$ fragments suggests that the difficulty of removal of the halogen group is Cl > Br > I, in line with the expected rhenium–halogen bond strengths. It is not clear, however, why the proportion of $ReBr(acac)_2^+$ is so low when compared to the iodide. The pattern of break up of the compounds is very similar to that observed for $Re(acac)_3$ (12). There is some tendency to form oxo- and hydroxo-containing species, but little tendency to form ions con-

Can. J. Chem. Downloaded from www.nrcresearchpress.com by 210.87.254.42 on 09/05/12
For personal use only.

Can. J. Chem. Downloaded from www.nrcresearchpress.com by 210.87.254.42 on 09/05/12
For personal use only.

taining other fragments of the acetylacetone group. Indeed, the most characteristic feature of the breakup of *cis*-$ReCl_2(acac)_2$ is the formation of the ion $ReCl(acac)(C_3H_4O)^+$. Otherwise the differences between the *cis*- and *trans*-isomers are very slight, which is to be expected since after the first chlorine atom is lost, the remaining ions will have the same structure. This makes us suggest that $ReCl_2(acac)(C_3H_4O)^+$ must have been formed directly from the parent ion $ReCl_2(acac)_2^+$.

Although it proved easy to establish that $Re(acac)_2Cl_2$ was monomeric in the solid state (3) and gas phases, it was far more difficult to test the claims that the material was dimeric in solution (2, 10). We were unable to get high enough solubilities to check the molecular weight of *trans*-$Re(acac)_2Cl_2$ using either ebullioscopic methods or a Mechrolab osmometer. Two commercial analysts also found the same problem with the osmotic method. Recently, however, using the Hitachi–Perkin–Elmer isopiestic molecular weight apparatus we have obtained results (Table 3), which although varying considerably because we were working close to the concentration limit of the instrument, are consistent only with the monomeric formulation for *trans*-$Re(acac)_2Cl_2$. Subsequently Meade Microchemical Laboratories determined the molecular weight of two different samples of *trans*-$Re(acac)_2Cl_2$ using an osmometer and have confirmed our results. Thus previous reports (2, 10) that *trans*-$Re(acac)_2Cl_2$ is dimeric in solution are clearly in error.

The isolation of a second form of $Re(acac)_2Cl_2$ suggested that this material might have been responsible for previous reports of a dimeric species. It was possible that this second form of $Re(acac)_2Cl_2$ was (*a*) an ionic compound such as $[Re(acac)_3]_2ReCl_6$ or $[Re(acac)_2Cl]Cl$; (*b*) a dimer, trimer, or polymer; (*c*) a different crystal form of the *trans*-isomer; (*d*) the *cis*-isomer. Clearly our results are only consistent with (*d*). The negligible conductivity eliminates (*a*) and the molecular weight eliminates (*b*). The dipole moment of 5.5(5) D (Table 4) is somewhat smaller than 6.3 D for *cis*-$Sn(acac)_2Cl_2$ (11) but clearly eliminates (*c*). Again there is no evidence of a dimeric form of $Re(acac)_2Cl_2$ in solution (Table 3).

The interconversion of the *trans*- and *cis*-isomers of $Re(acac)_2Cl_2$ must occur extremely slowly. Once we had separated the materials, in all subsequent operations there was no evidence of formation of the opposite isomer. In particular the *trans*-isomer is much less soluble and the *cis*-isomer was prepared by collecting the supernatant solutions and concentrating them. After the *trans*-isomer had been removed, subsequent concentration of the solutions yielded negligible amounts of *trans*-isomer, but ultimately good crystals of the *cis*-isomer could be obtained. The two forms are extremely easy to distinguish by color (*trans*, orange; *cis*, orange-brown) and crystal habit (*trans*, needles or plates; *cis*, truncated spheres). We have made detailed studies of the physical properties of both compounds in order to compare them.

TABLE 5. Electronic spectral data for $ReX_2(dik)_2$ compounds

Compound	Wavenumber (cm^{-1})	$\varepsilon_{max} \times 10^{-3}$
trans-$ReCl_2(acac)_2$	36 230	4.8
	30 100	1.6
	23 600	0.81
	19 900	0.26
cis-$ReCl_2(acac)_2$	39 050	7.8
	30 300	3.1
	25 000	1.6
$ReBr_2(acac)_2$	36 350	5.1
	27 800	3.2
	22 750	1.4
	20 000	0.68
$ReI_2(acac)_2$	34 000	7.2
	28 100	2.8
	24 050	4.2
	18 200	2.5
$ReCl_2(dbm)_2$	35 450	2.6
	29 400	8.6
	20 750	3.0
	19 600	3.1

The electronic spectra for the compounds are presented in Table 5. The electronic spectra in no way resemble those of the best-studied Re(IV) compound, K_2ReCl_6. The absorption coefficients are high enough to correspond to charge transfer or ligand bands. It is possible, because of the low solubility of the materials, that lower energy weaker bands were not observed. There are some superficial resemblances to the spectrum of $Re(acac)_3$ (12) and the observed bands do not vary regularly with the halogen suggesting that the transitions are associated with the β-diketone ring. The transition at 34 000–39 000

TABLE 6. Magnetic data for $ReX_2(dik)_2$*

$ReCl_2(acac)_2$		$ReBr_2(acac)_2$		$ReI_2(acac)_2$		$ReCl_2(dbm)_2$	
T (°K)	χ'_m (c.g.s.u. × 10^5)	T (°K)	χ'_m (c.g.s.u. × 10^5)	T (°K)	χ'_m (c.g.s.u. × 10^5)	T (°K)	χ'_m (c.g.s.u. × 10^5)
95	1174	85	1169	82	882	86	1180
100	1116	93	1079	96	800	96	1127
113	998	111	944	103	765	108	1070
121	936	125	863	113	721	124	1004
144	814	145	766	124	679	139	951
160	764	159	715	135	655	153	908
170	718	177	675	144	624	171	858
180	683	191	630	159	597	185	825
189	657	206	597	174	566	202	788
210	605	222	560	190	539	215	763
226	572	238	534	205	514	231	735
242	543	255	505	221	491	247	710
265	508	268	485	238	474	260	691
271	499	286	455	255	456	276	670
294	471			269	443		
310	457			286	425		

*χ'_m is the molar susceptibility after correction for the diamagnetism of the ligands.

TABLE 7. Magnetic constants for $ReX_2(dik)_2$ and K_2ReX_6

Compound	Constants 1*				Constant 2†	Constant 3‡
	C	θ (°K)	α (c.g.s.u. × 10^6)	r.m.s. deviation	θ (°K)	θ (°K)
trans-$ReCl_2(acac)_2$	1.003	2	1315	1.3%	<18	3
$ReCl_2(dbm)_2$	1.660	85	2100	0.8%	135	—
K_2ReCl_6	1.633	55	65	—	—	—
$ReBr_2(acac)_2$	1.004	12	1295	1.2%	<25	13
K_2ReBr_6	1.548	76	75	—	—	—
$ReI_2(acac)_2$	1.005	55	1380	1.0%	<80	43
K_2ReI_6	1.84	100	<50	—	—	—

*Obtained by fit of data to $\chi = c/(T + \theta) + \alpha$.
†Obtained by linear extrapolation of $1/\chi$ against T after 100 × 10^{-6} c.g.s.u. subtracted from each value of χ.
‡Value obtained by linear extrapolation of magnetometer data (CI) or fit to Kamimura *et al.* (18) plot. These are the preferred values.

cm^{-1} is in the region assigned by Cotton *et al.* to a ligand $\pi \rightarrow \pi^*$ transition (13), although ε_{max} is low for such a transition.

The magnetic data for the compounds are presented in Table 6. No data were obtained for *cis*-$ReCl_2(acac)_2$ because of the small amount of sample available. We have attempted to fit the magnetic data for our complexes to an expression of the type

$$\chi = \frac{C}{T + \theta} + \alpha$$

used by Eisenstein (14) to explain the magnetic susceptibility of K_2ReCl_6 and K_2ReBr_6. It is possible using the constants listed as constants 1 in Table 7 to get an excellent fit for the data with the r.m.s. deviation of ~1% being of the order of the experimental error. It is clear, however, that despite the excellent fit, the derived constants are nonsense, since as Griffith (15) has shown, one would expect α to be ~100 × 10^{-6} c.g.s.u. In addition our magnetic susceptibility data are very similar to those for $M^I_2ReX_6$ compounds (16, 17) where an excellent treatment of the data has been made by Eisenstein (14) using a value of $\alpha \approx 100 \times 10^{-6}$ c.g.s.u.

Can. J. Chem. Downloaded from www.nrcresearchpress.com by 210.87.254.42 on 09/05/12
For personal use only.

TABLE 8. Plot of μ_{eff} vs. I

Compound	μ_{eff} at 0° K (extrapolated)	100 °K	300 °K
$Re(acac)_2Cl_2$	2.87	2.99	3.32
$Re(acac)_2Br_2$	2.55	2.87	3.21
$Re(acac)_2I_2$	2.05	2.50	3.11

Our first consideration was to show that the data were reliable. Re^{III} compounds such as $Re(acac)X_2(PPh_3)_2$ (9) from which our compounds were made and $Re(acac)_3$ (12) show large ($\sim$1000–1400 $\times 10^{-6}$ c.g.s.u.), essentially temperature-independent paramagnetism (t.i.p.), and if present as impurities might appear to give rise to t.i.p. in our compounds. We find no evidence of any impurity in our samples using such techniques as analysis and infrared spectroscopy, and susceptibility data from different samples agree within experimental error.

The second point was to show that antiferromagnetic interactions were small. If our data are corrected by about 100×10^{-6} c.g.s.u. to allow for a reasonable value of α, plots of $1/\chi$ against T are curved and extrapolation of $1/\chi$ to 0 is not good; nevertheless, the maximum possible values for θ for the Cl, Br, and I compounds are 18, 25, and 60°, respectively. As a check we have measured the susceptibility of $Re(acac)_2Cl_2$ to 10 °K using a vibrating magnetometer and see no point of a Néel point; furthermore a plot of $1/\chi$ extrapolates to give $\theta = 3°$.

An attempt was made to correlate the data using the method of Kamimura *et al.* (18)[4] by plotting μ_{eff} $(2.84\sqrt{\chi T})$ against T. The values of μ_{eff} are shown in Table 8.

The curves were of the form calculated by Kamimura *et al.* but the variation with halide should not be present. A much better plot was obtained using the alternative plot suggested by Kamimura *et al.*, namely, $\mu_{eff} = (2.84\sqrt{\chi(T+\theta)})$ against T. Using values for θ of 3, 13, and 43° for Cl, Br, and I, respectively, which are consistent with extrapolations of our $1/\chi$ against T plots, the values of μ_{eff} at given T for all halides are very similar (2.88 at 0 °K, 3.04 at 100 °K, and $\sim$3.35 at 300 °K). The spin–orbit coupling parameter, ζd, can be obtained from these plots; unfortunately the values obtained lie outside the range calculated by Kamimura *et al.* Attempts have been made to estimate the values of $\eta = \zeta d/(3B + c)$ and the slope of μ_{eff} against T (since Kamimura *et al.* plot μ_{eff} against $KT/\zeta d$) by extrapolation of the published curves. Because our data lie well outside the range of values calculated by Kamimura *et al.* our extrapolated values for η and ζd, which were obtained graphically, are very rough indeed. Values of η of 1.6–2.0 are obtained depending on the extrapolation, and assuming $3B + C \sim 2000$ cm^{-1}, ζd is $\sim$3200–4000 cm^{-1}. A fit of the slope of the curve gives $\zeta d \sim 1000$ cm^{-1}. We feel that the true value of ζd probably lies closer to the higher value since we have more faith in our extrapolation to find η. Clearly, however, the value of η is greater than 1.3, the value found previously for K_2ReCl_6. Thus, despite the excellent fit of our original calculations we feel that our compounds are behaving much like K_2ReCl_6 (14). The values of θ obtained for our compounds are smaller than those obtained for K_2ReX_6 (see Table 7) and are consistent with superexchange being smaller. For *trans*-$Re(acac)_2Cl_2$ (3) superexchange through chlorine atoms can take place in one direction rather than three for K_2ReCl_6 (14). In addition the increase in θ from chloride to iodide is consistent with the observation that the superexchange is increased as the electronegativity of the anion decreases (19).

The vibrational spectra for $Re(acac)_2X_2$ compounds are presented in Table 9. It was only possible to obtain a Raman spectrum for *trans*-$Re(acac)_2Cl_2$ as the other compounds absorbed the laser beam and decomposed. The vibrational transitions were assigned by comparison with the work of Fay *et al.* (20) and following the arguments we have used previously (12).

The spectra bear considerable resemblance to those of $Zr(acac)_2X_2$ and $Hf(acac)_2X_2$(X = Cl, Br) (20) except in the region above 1450 cm^{-1} where there are some small differences. The spectra of *cis*- and *trans*-$Re(acac)_2Cl_2$ are also quite similar, although there are small but significant variations in intensity and band wave number. The most important differences occur in the Re—Cl stretching region where, as expected the *cis*-compound has two strong bands in the infrared spectrum at 336 and 346 cm^{-1}, whereas only one band is observed in the infrared spectrum of *trans*-$Re(acac)_2Cl_2$ at 309 cm^{-1}.

Fay *et al.* (20) have argued that the coinci-

[4]The symbols used in this section are defined in ref. 18.

Can. J. Chem. Downloaded from www.nrcresearchpress.com by 210.87.254.42 on 09/05/12
For personal use only.

TABLE 9. Vibrational spectral data for $ReX_2(acac)_2$ compounds

cis-$ReCl_2(acac)_2$	*trans*-$ReCl_2(acac)_2$		$ReBr_2(acac)_2$	$ReI_2(acac)_2$	
Infrared	Infrared	Raman	Infrared	Infrared	Assignment
	1620w		1630w	1630w	$\nu(C\cdots O)$
1540sh	1535vs		1540vs	1535vs	$\nu_s(C\cdots C)$
1515vs					
	1480sh		1490sh	1490sh	?
1450m	1440sh		1440sh		?
1405w	1420s		1430s	1420s	$\delta_d CH_3$
1380m	1385sh		1390sh	1380s	
1360m	1375s	1368m	1380s	1360s	$\delta_s CH_3$
1320s	1318s		1320s	1319s	$\nu_{as}(C\cdots O)$
	1296sh	1299s	1295sh	1293sh	$\nu_s(C\cdots C)$
1285s	1287s		1287s	1285s	
	1193w	1204w	1191w	1190vw	δ(C—H)
	1189sh		1188sh		
1027s	1031s	1025w	1031s	1029s	ρCH_3
1015sh	1021sh		1020sh	1021sh	
938s	938s	948m	937s	935s	$\nu(C—CH_3)$
906w					?
808s	812s		810s	804s	π(C—H)
	760vw		755vw		?
	744w		747sh		?
			742w		?
720vw	720vw		720vw	720vw	?
	698sh		697sh		
684s	686s	694m	685s	681s	ν(Re—O) + (δ(C—CH_3) or δ(ring))
650w	650w	653vw	646vw	644vw	
604s	610s	607w	606s	603s	ν(Re—O) + (δ(C—CH_3) or δ(ring))
	584vw		582vw	584vw	Ring mode?
		554w			
	526sh		523sh		—
	520w		516w	515vw	—
	510w		507w		—
	501sh		500sh		—
472sh					
460s	464s	479vw	462s	460s	ν_{as}(Re—O)
		448vw			
416vw	422m	422w	420m	417m	π ring?
346s, 333s					ν(Re—Cl)
	309vs	320vw			ν_{as}(Re—Cl)
		301s			ν_s(Re—Cl)?
	286sh				
259m	253s	262vw	255s	251sh, 245s	ν(Re—O)
	245s	245vw	248sh		
		221w			
		207m			?
			208m, 190m		ν(Re—Br)
				170s	ν(Re—I)

dences in the infrared and Raman spectra of $Zr(acac)_2X_2$ and $Hf(acac)_2X_2$ show that these compounds had *cis*-conformations (other evidence is presented elsewhere (21)). Examination of the infrared and Raman data for *trans*-$Re(acac)_2Cl_2$ shows at least as many coincidences. The explanation is that while *trans*-$Re(acac)_2Cl_2$ does have a center of symmetry (3), the

Can. J. Chem. Downloaded from www.nrcresearchpress.com by 210.87.254.42 on 09/05/12
For personal use only.

TABLE 10. X-Ray diffraction data for powdered samples of $ReX_2(acac)_2$

trans-$ReCl_2(acac)_2$		*cis*-$ReCl_2(acac)_2$		$ReBr_2(acac)_2$		$ReI_2(acac)_2$	
d	*I*	*d*	*I*	*d*	*I*	*d*	*I*
6.92	70	8.37	<5	10.18	70	7.50	45
6.25	80	6.80	100	7.87	55	6.54	90
5.79	75	6.41	90	7.43	35	6.24	100
5.52	80	5.71	90	7.03	50	5.87	70
5.25	80	5.21	15	6.19	100	3.85	70
4.11	10	4.46	10	5.85	35	3.56	90
3.98	65	3.98	80	5.41	25	3.42	60
3.81	55	3.78	10	4.82	20	3.26	40
3.66	70	3.62	10	4.09	30	2.94	10
3.50	75	3.42	75	3.94	35	2.80	10
3.31	100	3.26	<5	3.83	40	2.50	10
3.22	60	3.14	5	3.72	40	1.956	30
3.09	65	3.09	5	3.64	40	1.881	10
2.88	30	2.92	5	3.44	40	1.777	15
2.75	10	2.83	15	3.38	10		
2.64	35	2.72	<5	3.16	20		
2.54	75	2.62	15	2.92	4		
2.47	80	2.57	15	2.84	6		
2.40	60	2.52	20	2.75	12		
2.34	10	2.33	15	2.63	25		
2.27	30	2.28	15	2.49	20		
2.25	50	2.24		2.44	10		
2.08	10	2.09		2.37	5		
2.00	25	1.973		2.32	5		
1.940	25	1.932		2.26	10		
1.913	30	1.894		2.22	5		
1.863	20	1.726					
1.826	45	1.703					
1.801	30	1.481					
1.756	25						
1.714	20						
1.654	10						
1.605	30						

vibrations under consideration are ligand modes and the ligands do not have a center of symmetry. The arguments about coincidence and the center of symmetry apply only to the coupled vibrations of the ligands. If this coupling is very weak the coupled symmetric and asymmetric modes will be shifted very little, if at all, from the uncoupled modes and we shall get apparent coincidence. Thus, the presence of coincidences of ligand vibrations in the spectra of compounds of the type $M(acac)_2X_2$ does not allow one to decide whether the compound has the *cis*- or *trans*-conformation; the coincidence test should only be applied to modes which should be strongly coupled such as ν(M—O) and ν(M—Cl).

The infrared spectrum of $Re(acac)_2Br_2$ shows two bonds assigned to Re—Br stretches suggesting this is the *cis*-form and $Re(acac)_2I_2$ shows one bond in the Re—I region suggesting a *trans*-isomer. The X-ray data are also consistent with this interpretation.

The X-ray data were recorded for powdered samples of $Re(acac)_2X_2$ compounds, primarily for identification purposes, and the results are presented in Table 10. It has not proved possible to index the powder films, but this is hardly surprising since we know that *trans*-$Re(acac)_2Cl_2$ is triclinic (3). A comparison of our X-ray data with that of Fay *et al.* (21–23) for the series $M(acac)_2X_2$ (M = Ti, Zr, Hf; X = Cl, Br, I)[5] shows that data for *trans*-$Re(acac)_2Cl_2$ bear little resemblance to those for $M(acac)_2Cl_2$. However, there are some similarities in both *d*

[5]M is used to mean Ti, Zr, and Hf unless a metal is mentioned specifically.

Can. J. Chem. Downloaded from www.nrcresearchpress.com by 210.87.254.42 on 09/05/12
For personal use only.

value and intensity for *cis*-$Re(acac)_2Cl_2$ and $M(acac)_2Cl_2$.

There is an even higher correspondence between the data for $Re(acac)_2Br_2$ and $M(acac)_2Br_2$, the major difference being extra lines in the powder pattern of the rhenium compound. Since $M(acac)_2Br_2$ compounds are claimed to be *cis*-isomers we suggest that our material is principally *cis*-isomer with some small amount of *trans*-isomer. This result is consistent with the infrared data and the dipole moment which is somewhat lower than would be expected for the pure *cis*-isomer. The value obtained corresponds to about 70% *cis*-isomer.

Similarities in the X-ray data for $Re(acac)_2I_2$ and $Ti(acac)_2I_2$ which is postulated to be the *trans*-isomer suggest that $Re(acac)_2I_2$ was isolated as the *trans*-isomer and again this is borne out by the infrared data and the dipole moment.

We conclude that we have prepared and characterized what we have shown unambiguously to be *monomeric trans*-$Re(acac)_2Cl_2$, *cis*-$Re(acac)_2Cl_2$, a mixture of isomers of $Re(acac)_2Br_2$ which is primarily the *cis*-isomer, and *trans*-$Re(acac)_2I_2$. However, at this point we are unable to say what factors are important in deciding which isomer is formed.

We thank the National Research Council of Canada and the International Nickel Company for support of this work and the grant of scholarships to two of us (W.D.C. and G.T.).

1. R. Colton, R. Levitus, and G. Wilkinson. J. Chem. Soc. 4121 (1960).
2. D. E. Grove, N. P. Johnson, C. J. L. Lock, and G. Wilkinson. J. Chem. Soc. 490 (1965).
3. C. J. L. Lock and C. Wan. Chem. Commun. 1109 (1967).
4. P. W. Frais, A. Guest, and C. J. L. Lock. Can. J. Chem. **47**, 1069 (1969).
5. P. W. Selwood. Magnetochemistry. Interscience Publishers, Inc., New York, 1956. pp. 78, 92–95.
6. G. Föex, C-J. Gorter, et L. J. Smits. Constantes selectionées: diamagnétisme et paramagnétisme, relaxation paramagnétique. Masson et Cie, Paris, 1957.
7. E. A. Guggenheim. Trans. Faraday Soc. **45**, 714 (1949).
8. N. P. Johnson, C. J. L. Lock, and G. Wilkinson. Inorg. Synth. **9**, 145 (1966).
9. W. D. Courrier. Ph.D. Thesis, McMaster University, Hamilton, Ontario, 1971.
10. G. Rouschias and G. Wilkinson. J. Chem. Soc. (A), 465 (1966).
11. N. Serpone and R. C. Fay. Inorg. Chem. **8**, 2379 (1969).
12. W. D. Courrier, W. Forster, C. J. L. Lock, and G. Turner. Can. J. Chem. **50**, 8 (1972).
13. R. H. Holm and F. A. Cotton. J. Am. Chem. Soc. **80**, 5658 (1958).
14. J. C. Eisenstein. J. Chem. Phys. **34**, 1628 (1961).
15. J. S. Griffith. Theory of transitional metal ions. Methuen and Co., Ltd. London, 1961. pp. 277–280.
16. B. N. Figgis, J. Lewis, and F. E. Mabbs. J. Chem. Soc. 3138 (1961).
17. R. H. Busey and E. Sonder. J. Chem. Phys. **36**, 93 (1962).
18. H. Kamimura, S. Koide, H. Sekiyama, and S. Sugano. J. Phys. Soc. Jap. **15**, 1264 (1960).
19. J. H. Van Vleck. J. Phys. Radium, **12**, 262 (1951).
20. R. C. Fay and T. J. Pinnavaia. Inorg. Chem. 7, 508 (1968).
21. T. J. Pinnavaia and R. C. Fay. Inorg. Chem. **7**, 502 (1968).
22. R. C. Fay and R. N. Lowry. Inorg. Chem. **6**, 1512 (1967).
23. R. C. Fay and R. N. Lowry. Inorg. Chem. **9**, 2048 (1970).
24. National Bureau of Standards. Circular 514. Table of dielectric constants of pure liquids.

Can. J. Chem. Downloaded from www.nrcresearchpress.com by 210.87.254.42 on 09/05/12
For personal use only.

Technetium Chlorides and Oxochlorides

A. GUEST
Department of Chemistry, University of the West Indies, Mona, Jamaica
AND
C. J. L. LOCK[1]
Institute for Materials Research, McMaster University, Hamilton, Ontario

Received October 27, 1971

We have been unable to prepare $TcCl_6$ by the method published previously even though our reaction between Tc and Cl_2 gave products which appeared the same. TcO_3Cl and $TcOCl_4$ have been prepared and fully characterized for the first time.

Il a été impossible de préparer $TcCl_6$ par la méthode précédemment publiée, même si la réaction entre Tc et Cl_2 conduit à des produits qui semblent les mêmes. Les composés TcO_3Cl et $TcOCl_4$ ont été préparés et caractérisés sans ambiguïté pour la première fois.

Canadian Journal of Chemistry, **50**, 1807 (1972)

Introduction

Rhenium hexachloride and technetium hexachloride were reported in notes published in 1962 (1, 2) but almost no further data were published on these compounds. Recently there has been a report of $ReCl_6$ prepared by a different method and with significantly different magnetic properties (3). In addition we have published our investigations of the original method for preparing $ReCl_6$ in which we show that the product we obtained in all cases was impure $ReOCl_4$ (4).

Because $ReCl_6$ and $TcCl_6$ were originally prepared by essentially the same method it became of interest to reinvestigate the Tc–Cl system. In this paper we report our studies.

Experimental

Precautions used in handling air-sensitive materials have been described previously (4). All operations involving handling more than 50 mg of technetium were performed in a "hot-lab". ^{99}Tc was purchased from Oak Ridge National Laboratories as powdered metal and was not purified further except for certain experiments indicated below where the metal was vacuum dried and heated in hydrogen to reduce surface oxides. All other reagents were purified by methods described previously (4).

Analyses were performed on hydrolyzed samples of compounds. Chloride was determined gravimetrically as silver chloride. Technetium was determined by counting. A diluted sample solution was evaporated on a planchet (about 1 μg ^{99}Tc per analysis) and the β-activity compared with that of a standard sample. The standard solution was prepared by dissolving an accurately weighed amount of ^{99}Tc metal in concentrated nitric acid and diluting. Counting was performed on a Nuclear Chicago windowless proportional flow counter. Oxidation number of the technetium was determined by hydrolysis with dilute ammonia solution. The precipitate was dissolved in nitric acid, and samples of this solution and of the filtrate were evaporated and counted to give the Tc^{IV}: Tc^{VII} ratio (1).

Infrared spectra were recorded on a Perkin–Elmer 521 grating spectrometer as Nujol mulls between KBr plates or in the vapor phase in a cell described previously (5). Ultraviolet–visible spectra were recorded on a Cary 14 recording spectrometer in the vapor phase in a 10 cm path length quartz cell.

The Chlorination of Technetium Metal

All reactions were carried out in the same type of apparatus. This consisted of a Pyrex tube about 50 cm long and 2 cm i.d. One end was fitted with a three way stopcock to allow gas to be admitted and the other end was connected to a train of U-traps made of Pyrex glass (8 mm i.d.). The traps were generally 20 cm in depth and the arms were about 5 cm apart. Each U-trap was fitted with a breakseal. The 2 cm tube could be heated with a tube furnace.

Reaction Scheme (a)

A sample of technetium metal was placed in the 2 cm tube. The tube was flushed with a dried deoxygenated nitrogen stream while the metal was heated to about 150 °C for 2 h to remove water. The metal was cooled in the nitrogen stream, the flow stopped and then chlorine was passed through the tube while the metal was heated to temperatures from 300–550 °C depending on the experiment. In all cases reaction occurred and at the beginning of the reaction a volatile material distilled off and was condensed as a blue solid in a trap cooled in an ice–salt mixture. Subsequent reaction produced red-brown technetium tetrachloride (confirmed by X-ray diffraction), which condensed in the tube at the point it emerged from the tube furnace. It was found that the blue material was very sensitive to light, but could be separated by trap-to-trap distillation under vacuum in the dark using slush baths in the -30 to -60 °C range, into purple $TcOCl_4$ and very pale yellow TcO_3Cl (see below).

Reaction Scheme (b)

Reaction (*a*) was repeated, but the technetium metal was vacuum dried, and reduced in hydrogen for 3 h at 200 °C and

[1]To whom correspondence should be addressed.

Can. J. Chem. Downloaded from www.nrcresearchpress.com by 210.87.254.42 on 09/05/12
For personal use only.

Can. J. Chem. Downloaded from www.nrcresearchpress.com by 210.87.254.42 on 09/05/12
For personal use only.

then 3–4 h at 550 °C before chlorination. Chlorination was carried out as in (*a*) but the chlorine was purified as in ref. 4. The amount of volatile blue material produced was very small and the major product was $TcCl_4$.

Reaction Scheme (c)

Technetium metal was converted to pertechnic acid in cold concentrated nitric acid. The solution was then evaporated to near dryness and neutralized with 2 *M* ammonia solution. The solution was diluted to about 10 ml with water, and pieces of broken porous pot were dropped into the solution and the mixture slowly evaporated to dryness. The bits of pot were transferred to the reaction tube and heated (24 h at 200 °C/24 h at 550 °C) in a hydrogen stream. The pot was then cooled, and chlorination was carried out at 300–500 °C (depending on the run) as in method (*b*). The major product of chlorination was a volatile material which condensed in a U-trap cooled in ice-water as a green solid (>90%). The other material produced was $TcCl_4$ which condensed in the reaction tube at the point where it left the furnace. The green material was easily decomposed by light, but could be separated by trap-to-trap distillation under vacuum in the dark at −30 to −60 °C into $TcOCl_4$ and TcO_3Cl (see below).

Chlorotrioxotechnetium(VII), Pertechnyl Chloride, TcO_3Cl

This was prepared by (*a*) vacuum distillation from the mixture of oxochlorides produced on chlorination of technetium metal. (*b*) placing technetium tetrachloride in a Carius tube fitted with a breakseal which was then filled with oxygen and sealed. The tube was heated to 450 °C for a few hours. On cooling the tube was connected to a vacuum line via the breakseal and the product distilled out. A quantitative yield of TcO_3Cl was obtained. TcO_3Cl is a very pale yellow liquid boiling at 25 °C.

Anal. Calcd. for ClO_3Tc: Cl, 19.5; Tc, 54.2. Found: Cl, 19.4; Tc, 54.1.

Tetrachloroxotechnetium(VI), $TcOCl_4$

This was separated from the mixture of oxochlorides produced on chlorination of technetium metal by trap-to-trap distillation *in vacuo*, in the dark. The pure product is a purple crystalline solid (m.p. ~ 35 °C), which is photodecomposed.

Anal. Calcd. for Cl_4OTc: Cl, 52.3; Tc, 38.5. Found: Cl, 52.6; Tc, 38.2.

Trichloroxotechnetium(V), $TcOCl_3$

This was prepared by decomposition of $TcOCl_4$. The $TcOCl_4$ was allowed to decompose to involatile $TcOCl_3$ and chlorine in sunlight and the chlorine removed under vacuum. It was not even necessary to purify the $TcOCl_4$ before use, if it was distilled off the mixture obtained on chlorinating technetium, since the other volatile oxochloride TcO_3Cl was removed with the chlorine. $TcOCl_3$ is a brown solid indentical to the physical and spectral properties to the compound described previously (6).

Technetium Tetrachloride, $TcCl_4$

This was the major product of the chlorination of technetium metal and was identical to the product described previously (7).

Discussion

Direct chlorination of powdered technetium metal at 550 °C did not produce the green compound described previously (1) but gave initially a bright blue "compound", the other product being technetium tetrachloride. By taking great care to reduce oxygen contamination of the reactants it was possible to reduce the amount of blue material to a very minor product, but never to eliminate it entirely. However, if the chlorination was of a metal film on porous pot, a reaction almost entirely like Colton's was observed. A green "compound" was formed in much higher yield than the blue product described above and in this case technetium tetrachloride was the minor product. Vacuum distillation in the dark of the blue and green "compounds" has shown that both are mixtures of a very pale yellow volatile liquid and a volatile purple crystalline solid.

The liquid has been shown to be pertechnyl chloride (TcO_3Cl). TcO_3Cl was hydrolyzed by dilute ammonia to give a colorless pertechnate solution thus proving the oxidation number of seven and chlorine and technetium elemental analyses confirm our formulation. The vapor-phase infrared spectrum, the liquid phase Raman spectrum and the vapor phase ultraviolet–visible spectrum have been recorded and are very similar to those of perrhenyl chloride. (Infrared Tc=O stretch at 955 cm^{-1} (broad), u.v.–visible bands at 1920, 2280, and 3150 Å (band has vibrational structure)). Detailed analyses of the spectra will be reported elsewhere (8, 9). We note, however, that the previously reported spectrum (12) for "TcO_3Cl" is incorrect. Strong bands at 3450, 3900, and 5950 Å are not consistent with a pale yellow compound and differ markedly from our results.

Colton and Tomkins (7) have speculated that the volatile blue compound formed on chlorination of TcO_2 was technetium oxotetrachloride, but reported that the compound was too thermally unstable to isolate. We have found that $TcOCl_4$ appears to be blue when some impurity TcO_3Cl is present but when pure is a purple color and forms large crystals similar in all but color to $ReOCl_4$. Contrary to previous reports $TcOCl_4$ is stable at room temperature for months (we have a sample over a year old) if kept out of the light but decomposes rapidly even at −78 °C if left in sunlight or artificial fluorescent light. Hydrolysis by dilute ammonia solution gave a TcO_2/TcO_4^- ratio of 1:2 proving an oxidation number of VI and chloride and technetium analysis results are consistent with the $TcOCl_4$ formulation. An infrared spectrum, taken as rapidly as possible of a cell of vapor which had

Can. J. Chem. Downloaded from www.nrcresearchpress.com by 210.87.254.42 on 09/05/12
For personal use only.

been filled in the dark, showed only a peak at 998 cm^{-1}. This is considerably lower than the metal–oxygen stretching frequency of gaseous $ReOCl_4$ which occurs at 1040 cm^{-1}. The lowering of frequency may be caused by a lowering of force constant associated with a weakening of the Tc=O bond when compared to Re=O. This is not unexpected since the Tc 4d orbitals are less extended than the Re 5d orbitals and there will be less $p\pi$–$d\pi$ overlap. A similar lowering of Tc=O stretch frequencies is seen in TcO_3Cl (955 cm^{-1}) compared to those for ReO_3Cl (1003, 971 cm^{-1}).

After exposure to the globar source a brown compound deposited on the cell windows, the peak at 998 cm^{-1} disappeared and a peak at 1016 cm^{-1} appeared. The new peak arises from the Tc=O stretching vibration in $TcOCl_3$ which has a reported value of 1017 cm^{-1} (10). The chlorine produced in the photochemical reaction

$$2TcOCl_4 \xrightarrow{h\nu} 2TcOCl_3 + Cl_2$$

was identified by its ultraviolet spectrum.

Below we summarize previous work on the Tc–Cl system and compare it with our results. Previous results have suggested

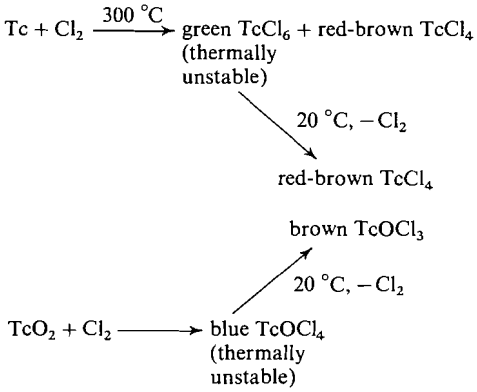

Our results are

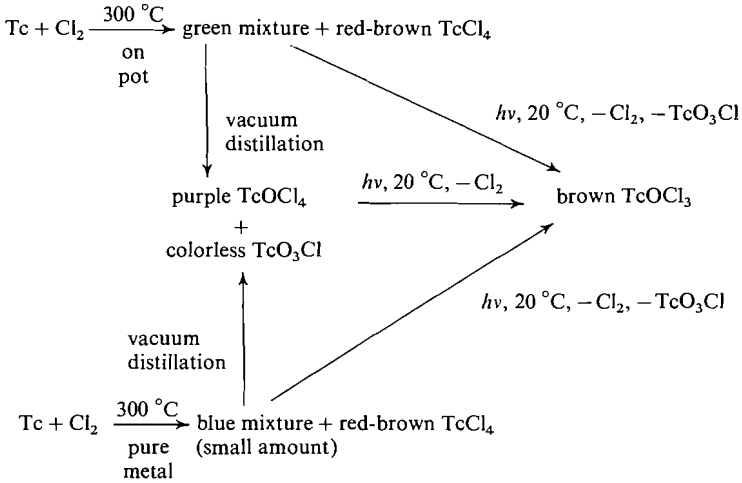

We show that we have not prepared $TcCl_6$ by the action of chlorine on technetium metal, but we have isolated and fully characterized TcO_3Cl and $TcOCl_4$ for the first time. We note that there is a great similarity between our experimental observations and those of previous workers although our interpretation is quite different. Because of the small amount of previously published data useful for identification we cannot show that the two reaction schemes are the

same. However, our scheme is more satisfactory than one which postulates the preparation at 300 °C in a chlorine stream of a compound which is thermally unstable at room temperature *even in a chlorine atmosphere* and which decomposes rapidly "even on very gentle warming" (1, 11). Indeed, the only positive evidence for $TcCl_6$ is the Tc:Cl ratio of 1:6 (1) and an oxidation state of VI, but it has been noted elsewhere (11) that "chlorine is quite soluble in $TcCl_6$" and is difficult to remove. In the light of this and our previous results on the rhenium system we suggest that the existence of technetium hexachloride has not been proved.

We thank the National Research Council of Canada and the Canadian International Development Agency for support of this work and the award of a C.I.D.A. Visiting Fellowship to A.G.

1. R. COLTON. Nature, **193**, 872 (1962).
2. R. COLTON. Nature, **194**, 374 (1962).
3. J. H. CANTERFORD. Inorg. Nucl. Chem. Lett. **7**, 395 (1971).
4. A. GUEST and C. J. L. LOCK. Can. J. Chem. **49**, 603 (1971).
5. A. GUEST and C. J. L. LOCK. Rev. Sci. Instrum. **39**, 780 (1968).
6. R. COLTON and I. B. TOMKINS. Aust. J. Chem. **21**, 1981 (1968).
7. M. ELDER and B. R. PENFOLD. Inorg. Chem. **5**, 1197 (1966).
8. A. GUEST, H. E. HOWARD-LOCK, and C. J. L. LOCK. J. Mol. Spectrosc. In press.
9. A. GUEST, H. E. HOWARD-LOCK, and C. J. L. LOCK. Unpublished results.
10. J. H. CANTERFORD, R. COLTON, and I. B. TOMKINS. Inorg. Nucl. Chem. Lett. **4**, 471 (1968).
11. J. H. CANTERFORD and R. COLTON. Halides of the second and third row transition metals. Wiley, London. 1968. p. 284.
12. C. L. RULFS, R. A. PACER, and R. F. HIRSCH. J. Inorg. Nucl. Chem. **29**, 681 (1967).

Can. J. Chem. Downloaded from www.nrcresearchpress.com by 210.87.254.42 on 09/05/12
For personal use only.

The Preparation, Physical Properties, and Structure of Oxotetrachloroaquorhenium(VI), $ReOCl_4(OH_2)$

P. W. FRAIS AND C. J. L. LOCK[1]

Institute for Materials Research, McMaster University, Hamilton, Ontario

Received January 5, 1972

Oxotetrachloroaquorhenium(VI), $ReOCl_4 \cdot H_2O$, has been prepared and characterized for the first time by analysis, infrared spectroscopy and single crystal X-ray diffraction. The crystals were orthorhombic, $a = 10.834(8)$, $b = 11.089(8)$, $c = 5.517(4)$ Å, $Pn2_1a$, $Z = 4$. Intensity data were recorded by integrating film methods and measured with a Joyce–Loebl microdensitometer, and 624 observable of the 704 measured independent reflections were given non-zero weight in the final cycle of full matrix least-squares refinement where $R_1 = 0.0572$ and $R_2 = 0.0687$.[2] The molecular structure is based on a very distorted octahedron with a strongly bonded oxo-group (Re—O, 1.63(2) Å) *trans* (177(2)°) to a weakly bonded aquo-group (Re—O, 2.27 (2) Å). The Re—Cl distances do not differ significantly (2.29(1) Å av). The chlorine atoms are bent away from the oxo-group (angles vary from (94–102°(1)).

L'oxotétrachloroaquorhénium(VI), $ReClO_4 \cdot H_2O$, a été préparé et caractérisé pour la première fois par analyse, spectroscopie infra-rouge et diffraction des rayons-X. Les cristaux sont orthorhombiques, $a = 10.834(8)$, $b = 11.089(8)$, $c = 5.517(4)$ Å, $Pn2_1a$, $Z = 4$. Les intensités des tâches de diffraction ont été enregistrées sur film (intégration) et évaluées avec un microdensimètre Joyce–Loebl. Des 704 réflections indépendantes mesurées, 624 furent considérées comme observées au cours du dernier cycle d'affinement par moindres carrés (matrice complète). L'accord final est indiqué par $R_1 = 0.0572$ et $R_2 = 0.0687$.[2] La structure moléculaire est basée sur un octaèdre très déformé avec un groupe oxo fortement lié (Re—O = 1.63(2) Å) en *trans* (177(2)°) d'un groupe *aquo* faiblement lié (Re—O = 2.27(2) Å). Les distances Re—Cl ne diffèrent pas d'une manière significative (moyenne 2.29(1) Å). Les atomes de chlore tendent à s'éloigner du groupe oxo (angles variant entre 94 et 102(1)°).

Canadian Journal of Chemistry, **50**, 1811 (1972)

Introduction

We have reported previously some of the products obtained from the reaction of $ReO_3 + ReCl_5$ (1). One product, which was observed on several occasions but isolated only once, was a red crystalline material. Although the crystals were stable in an evacuated tube, the compound was unstable even in a good dry box. Nevertheless, it was possible to isolate several single crystals and do a single crystal X-ray structure analysis. The only other chemical experiment done on these crystals was neutron activation analysis (2). The combined results showed a molecular compound containing a rhenium atom, four chlorine atoms, and two other light atoms, probably oxygen atoms. The results suggested a compound of the type $ReOCl_4 \cdot OH$ or $ReOCl_4(OH_2)$ but we were unable to determine which was correct because of lack of material.

The formulations did suggest alternative methods of preparation and we subsequently prepared the compound by the reaction of water and $ReOCl_4$. We have shown that the two products are identical and that the stoichiometry is $ReOCl_4 \cdot OH_2$. The crystal and molecular structure of $ReOCl_4(OH_2)$ as well as some physical and chemical properties are described in this paper.

Experiments

Analyses for rhenium and chlorine, as well as determination of the oxidation state of rhenium by the alkaline hydrolysis method were performed using the neutron activation method described previously (2). Infrared spectra were recorded on Perkin–Elmer 337 and 521 spectrometers. Solid samples were either the solid powder ground between two potassium bromide discs or were solid ground into a mull with dry Nujol and mounted between potassium bromide plates. The Nujol was dried by refluxing over phosphorus pentoxide and vacuum distilled. Gas samples were contained in a heated gas cell with silver chloride windows (3). Solution samples were prepared in the manner described previously (4) and were contained in standard solution cells with potassium bromide windows. Raman spectra were excited by the 6328 Å line of a helium–neon laser and were recorded on a Czerny–Turner-type Spex laser Raman recording spectrograph, which contained a double monochromator. Solid samples were mounted in melting point tubes and maintained at a temperature of −100 °C. X-Ray diffraction photographs of powdered samples were recorded on a Debye–Scherrer

[1]To whom correspondence should be addressed.

[2] $R_1 = \dfrac{\Sigma||F_o| - |F_c||}{\Sigma|F_o|}$; $\quad R_2 = \left\{\dfrac{\Sigma\omega|F_o^2 - F_c^2|}{\Sigma\omega F_o^2}\right\}^{1/2}$

Can. J. Chem. Downloaded from www.nrcresearchpress.com by 210.87.254.6 on 09/05/12
For personal use only.

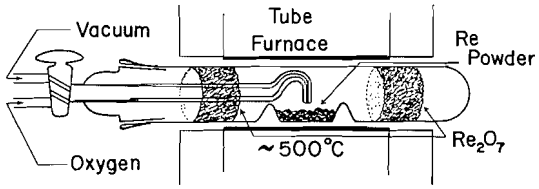

FIG. 1. Apparatus for the preparation of Re_2O_7.

camera using nickel-filtered CuKα radiation. Samples were sealed inside quartz tubes. All X-ray film intensities were measured using a Joyce–Loebl microdensitometer.

Preparation and Purification of Starting Materials

Powdered rhenium metal, rhenium trioxide, rhenium oxotetrachloride, oxygen, and chlorine were obtained and purified as described previously (4). Rhenium heptoxide was prepared from vacuum dried rhenium metal and dry oxygen using a method similar to that of Melaven *et al.* (5), but using a modified apparatus (Fig. 1) that greatly increases the rate of reaction. In the modified apparatus, the excess pressure of oxygen gas is forced directly onto the surface of the metal and this displaces the very dense vapors of Re_2O_7 which provide a blanket in the conventional apparatus and slow the reaction.

Rhenium pentachloride was prepared in a similar apparatus using a modification of normal methods (6, 7) and purified by the method we have described previously (4).

Preparation of Oxotetrachloroaquorhenium (VI)

(*a*) Rhenium pentachloride (91 mg) and rhenium trioxide (65 mg) were heated in an evacuated Pyrex reaction vessel, fitted with a breakseal, at 445 °C for 3 days. The vessel was cooled slowly and sealed to a vacuum line, which was evacuated and allowed to degas for some hours. The breakseal was broken and volatile products of the reaction were allowed to sublime into a U-trap cooled in liquid nitrogen, while the reaction vessel was submerged in an oil bath at 80 °C. After 24 h, the evacuated reaction vessel and U-trap system were separated by sealing under vacuum, and the involatile black residue in the reaction vessel was analyzed by X-ray powder photography. It was the orthorhombic phase of rhenium dioxide with small amounts of an impurity which was not rhenium metal, Re_3Cl_9, $ReCl_4$, or $ReCl_5$.

The bright red sublimate was kept at room temperature, while an adjacent U-trap was cooled in ice–water. After a week the evacuated traps were separated by sealing the neck between them. The ice–water trap contained small amounts of a yellow liquid, probably impure ReO_3Cl. The room-temperature U-trap contained a very fine red coating, which after standing at room temperature for several weeks developed plates of dark red crystals, usually away from the bulk of the starting material. The U-trap was opened in a dry box cooled to 10 °C, and several crystals were isolated and sealed in quartz capillary tubes. The bulk of the material changed to a black residue within hours. Neutron activation analysis of one of the crystals gave a Cl:Re atom ratio of 4.07 (calculated value 4.00), but because of surface decomposition and the size of the sample, an oxidation state analysis was not attempted. The preparation (but not purification) described above was not reproducible and in many experiments, other products were obtained (see ref. 1). This is hardly surprising since it is evident that the formation of the compound is dependent on water impurity being present.

(*b*) A known amount of $ReOCl_4$ (estimated from the volume of the melt) was distilled into a tube fitted with a breakseal and which was cooled in liquid nitrogen. An equimolar amount of water vapor was then distilled into the reaction tube. (The amount of water was obtained by connecting an evacuated calibrated vessel to a source of water and varying the vapor pressure of the water by varying the temperature.) The reaction vessel was isolated by sealing and placed in a tube furnace at 350 °C for 24 h, care being taken to avoid a temperature gradient. The furnace was cooled very slowly to room temperature. The reaction vessel contained bright red crystals in the form of long rectangular plates. The tube was transferred to a dry box before opening and subsequent experiments on the crystals. Three independent analyses gave an average chlorine to rhenium atom ratio of 3.92(9) (calculated value 4.00) and a ReO_4^-/ReO_2 ratio on hydrolysis of 2.2(1) (calculated value 2.0).

Crystallography

Single crystal X-ray studies were done on a crystal prepared by method *a*. The crystal was sealed in a fused silica capillary tube. All crystal data were obtained from a triangular plate crystal with sides 0.4, 0.5, 0.5 mm and thickness 0.11 mm.

Weissenberg photographs of the crystal showed that it was orthorhombic with systematic absences $0kl, k + l =$ odd, and $hk0, h =$ odd suggesting the space groups $Pnma$, or $Pn2_1a$. Precession photographs of the ($hk0$) and ($0kl$) layers taken with CuKα radiation were calibrated with a crystal of TiO_2 (rutile) and accurate cell parameters were obtained using the parameters for TiO_2, $a = 4.5929(5)$, $c = 2.9591(3)$ Å (8). Crystal data were

$H_2Cl_4O_2Re$ f.w. = 362.1

Orthorhombic, $a = 10.834(8)$, $b = 11.089(8)$, $c = 5.517(4)$ Å, $V = 662.8$ Å^3, $Pn2_1a$, ρ_o not determined, see text, $Z = 4$, $\rho_c = 3.62$ (22 °C; CuKα, $\lambda = 1.5418$ Å). Because of the instability of $ReOCl_4(OH_2)$ it was not possible to obtain an experimental value for the density.

Intensity data were obtained from films recorded on a precession camera using MoKα radiation. The (nkl), $n =$ 0–4 and (hkm), $m = 0, 1, 2$ layers were recorded. The intensities were measured using a Joyce–Loebl microdensitometer and then corrected for Lorentz and polarization effects. No absorption corrections were made because of the irregular shape of the crystal.

Standard errors, σ, were assigned to each intensity measured and weights $w = 1/\sigma^2$ were used throughout the refinement. For each reciprocal lattice layer measured, a minimum value of σ was estimated from the accumulated relative errors of the factors used to scale different films and different wedges on the densitometer. To this minimum value of σ was added an additional value which took account of the intensity of the spot, the intensity profile of each spot, irregular background, intensity of the background, edges of the beam stop or layer screen, and average reproducibility of each measured intensity. Smallest values of σ were therefore assigned to well-defined spots of uniform integrated intensity, whose intensity could be measured on three or more films. For unobserved reflections, weights calculated from $\sigma = 0.5\ F_{min}$ were used only when the calculated structure factor $|F_c| > 0.8\ F_{min}$, where F_{min} was the local minimum of

Can. J. Chem. Downloaded from www.nrcresearchpress.com by 210.87.254.6 on 09/05/12
For personal use only.

TABLE 1. Final parameters (estimated standard deviations in parentheses)
T.F. = $\exp\{-2\pi^2(a^{*2}h^2U_{11} + \ldots + 2a^*b^*hkU_{12} + \ldots +)\}$

Atom	x	y	z	U_{11}	U_{22}	U_{33}	U_{12}	U_{13}	U_{23}
Re	0.1474(1)	0.2558(6)	0.3936(1)	0.0146(5)	0.0288(4)	0.0245(5)	−0.000(1)	−0.0026(4)	0.0023(6)
Aq	−0.005(2)	0.266(6)	0.676(4)	0.03(1)	0.07(2)	0.06(1)	0.00(2)	0.04(1)	−0.02(2)
O	0.252(2)	0.244(3)	0.182(4)	0.013(7)	0.03(1)	0.05(1)	0.00(1)	0.02(1)	0.00(1)
Cl1	0.0189(7)	0.3969(6)	0.224(2)	0.036(4)	0.027(3)	0.066(5)	0.002(3)	−0.011(4)	0.014(3)
Cl2	0.0235(7)	0.1083(6)	0.233(1)	0.018(4)	0.045(4)	0.031(3)	−0.002(3)	−0.015(4)	−0.003(3)
Cl3	0.2226(6)	0.1072(6)	0.645(1)	0.022(3)	0.038(3)	0.027(3)	0.003(2)	−0.006(4)	0.004(2)
Cl4	0.2324(8)	0.3939(6)	0.649(1)	0.032(4)	0.030(3)	0.050(4)	0.002(3)	−0.011(4)	−0.005(2)

the observed structure factor; otherwise they were given zero weights.

Atomic scattering factors used for rhenium, oxygen, and chlorine were obtained from Cromer and Waber (9) and anomalous dispersion corrections for rhenium and chlorine were obtained from Cromer (10).

Solution of the Structure

The systematic absences indicated the space groups *Pnma* or $Pn2_1a$. The two dimensional Patterson maps for the $(h0l)$ and $(0kl)$ layers were readily soluble for the x and y coordinates of the single rhenium atom in the asymmetric unit. Assuming the centrosymmetric space group *Pnma*, the y coordinate was fixed at 0.25. The large reduction in value of the R factor, as well as the reasonable value of U_{iso} indicated that the chosen coordinates for rhenium were approximately correct. The large interatomic Re–Re distances excluded the possibility of any oxygen or chlorine bridging, so an octahedral arrangement around each Re atom was assumed. The position of the remaining atoms were found from electron density and difference synthesis maps phased on the heavy atom positions.

Since only a few crystals of the material were available at this stage, and a neutron activation analysis had not yet been done, the compound was assumed to be $ReOCl_5$ from the similarity of the unit cell parameters with $OsOF_5$ (11) and from the stoichiometry of the reaction; *i.e.*

$$ReO_3 + ReCl_5 \rightarrow ReO_2 + ReOCl_5$$

With an unweighted R value of 0.09, four chlorine atoms were stable at Re—Cl distances of ~2.3 Å, and one oxygen at Re=O of ~1.6 Å, with reasonable isotropic temperature factors. The fifth chlorine, *trans* to the terminal oxygen was found at a distance of ~2.2 Å from the rhenium atom, a distance much shorter than that expected for a terminal chlorine opposite a double bonded oxygen (12). In addition the temperature factor for this atom was much larger than expected, and chlorine–chlorine non-bonded distances to the other four chlorine atoms were unreasonably short.

If the atom *trans* to the terminal oxygen was assumed to be oxygen, the Re-atom distance was now reasonable, and a much more satisfactory value for U_{iso} was obtained. At this point, neutron activation was carried out on another crystal of the same batch, and the rhenium to chlorine ratio of 1:4 was confirmed. Unfortunately the small size of the crystal, and the surface decomposition made a meaningful oxidation state analysis impractical, and it was not attempted.

Refinement was continued assuming both *Pnma* and $Pn2_1a$ space groups, and of the 704 independent reflections used, 624 were given non-zero weights in the last cycle of the least squares refinement, where convergence occurred at $R_2 = 0.0687$ for $Pn2_1a$ and $R_2 = 0.0716$ for *Pnma*. The Hamilton significance test (22) was applied to these refinements, and the conclusion was reached that to a 90% confidence level, the noncentrosymmetric space group $Pn2_1a$ fits the data better than the centrosymmetric space group *Pnma*. The choice of $Pn2_1a$ as the space group for $ReOCl_4(OH_2)$ was based on the Hamilton test alone, since the geometry of the molecules or the presence of hydrogen bonding (see Discussion) did not provide any basis for choosing either space group.

The observed structure factors are compared with those calculated in Table 4.[3] In the final cycle of refinement no parameter changed by more than 1/3 of its estimated standard deviation. A difference synthesis obtained had no peaks higher than 1.2 e/Å^3 or lower than 0.8 e/Å^3.

Observations and Discussion

The Structure of $ReOCl_4(OH_2)$

The final atomic parameters, including the estimated standard deviations, are listed in Table 1. Bond distances and bond angles are shown in Table 2, and intra- and intermolecular non-bonded distances less than 3.50 Å are listed in Table 3.

It is not possible to attribute any real chemical significance to the nonisotropic temperature factors listed in Table 1 because of absorption and the highly irregular shape of the crystal. Attempts were indeed made to approximate the shape of the crystal by cylinders of appropriate thicknesses for each of the two orientations of the crystal on the precession camera used to gather the data. On this basis, the data were corrected, and subsequent refinement yielded atomic parameters that were, within error, unchanged from those obtained from the uncorrected data, with the exception of the temperature factors, which were uniformly larger. In

[3]Table 4 is available from the Depository of Unpublished Data, National Science Library, National Research Council of Canada, Ottawa, Canada, K1A 0R6.

Can. J. Chem. Downloaded from www.nrcresearchpress.com by 210.87.254.6 on 09/05/12
For personal use only.

Can. J. Chem. Downloaded from www.nrcresearchpress.com by 210.87.254.6 on 09/05/12
For personal use only.

TABLE 2.
(*a*) Bond distances (Å) in $ReOCl_4(OH_2)$

Bond	Distance	Bond	Distance
Re—O	1.63(2)	Re—Aq	2.27(2)
Re—Cl1	2.30(1)	Re—Cl3	2.29(1)
Re—Cl2	2.29(1)	Re—Cl4	2.28(1)

(*b*) Bond angles (deg) in $ReOCl_4(OH_2)$, angles subtended at Re by

Atom pair	Angle	Atom pair	Angle
O–Cl1	100(1)	Cl1–Cl4	91.9(4)
O–Cl2	94(1)	Cl2–Aq	83(1)
O–Aq	177(2)	Cl2–Cl3	86.2(3)
O–Cl3	97(1)	Cl2–Cl4	162.8(3)
O–Cl4	102(1)	Aq–Cl3	83(1)
Cl1–Cl2	88.5(3)	Aq–Cl4	80(1)
Cl1–Aq	79(1)	Cl3–Cl4	88.1(3)
Cl1–Cl3	161.8(3)		

TABLE 3. Non-bonded distances* (Å) in $ReOCl_4(OH_2)$
(*a*) Intramolecular

Atoms	Distance	Atoms	Distance
Aq–Cl1	2.90(4)	O–Cl3	2.98(3)
Aq–Cl2	3.02(4)	O–Cl4	3.07(3)
Aq–Cl3	3.03(4)	Cl1–Cl2	3.20(1)
Aq–Cl4	2.94(4)	Cl1–Cl4	3.29(1)
O–Cl1	3.05(3)	Cl2–Cl3	3.13(1)
O–Cl2	2.91(3)	Cl3–Cl4	3.18(1)

(*b*) Intermolecular

Atoms	Symmetry relationship†	Distance
Aq–O′	$(x-1/2, y, 1/2-z)$	3.31(3)
Aq–Cl′1	$(x, y, z+1)$	3.36(4)
Aq–Cl′4	$(x-1/2, y, 3/2-z)$	3.32(4)
O–Cl′3	$(x, y, z-1)$	3.35(3)
O–Cl′4	$(x, y, z-1)$	3.39(3)
O–Cl′1	$(1/2+x, y, -1/2-z)$	3.40(3)
O–Cl′2	$(1/2+x, y, -1/2-z)$	3.33(3)
Cl1–Cl′2	$-(-1-x, 1/2+y, -1-z)$	3.47(1)

*Distances > 3.50 Å are not included.
†Atoms indicated with a prime mark are related to the atoms listed in Table 1 (x, y, z) by the symmetry relationships listed in column 2.

addition, the R factor was found to be ~2% larger than in the case of uncorrected data. Using the uncorrected data, plots were made of $|F_o - F_c|$ *vs.* $\sin\theta/\lambda$ as well as F_o/F_c *vs.* $\sin\theta/\lambda$ for each layer measured, and no systematic trend was found in these graphs that could be attributed directly to absorption.

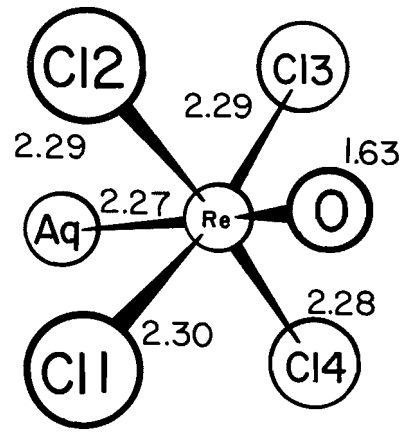

FIG. 2. Geometry of a single molecule of $ReOCl_4(OH_2)$ with bond distances in Å.

Because of these facts, the data were left uncorrected for absorption. Since the thin part of the crystal lies along the x axis, one would expect that the values obtained for U_{11} should be smaller than expected if no adsorption had taken place, and those for U_{22} and U_{33} should be larger than expected. This effect is indeed observed for the rhenium atoms.

The geometry of a single molecule of $ReOCl_4(OH_2)$ viewed along the c axis is shown in Fig. 2. As expected, the rhenium atom has a distorted octahedral environment with the four chlorine atoms bent away from the terminal oxygen atom, and toward the loosely bound aquo group.

A careful examination of the aquo groups (shown in Fig. 3 as double circles) reveals that the intermolecular environment of this group includes one terminal oxygen and four chlorine atoms, to which the possibility of hydrogen bonding exists. Examination of Table 3 shows that the terminal oxygen is 3.31(3) Å from the oxygen of the aquo group, while two of the four chlorines are 3.32(4) and 3.36(4) Å away and the remaining two more than 3.50 Å away (actually 3.55(4) and 3.58(4) Å). These distances are very large for even very weak hydrogen bonding (13). The acceptor angles for the three combinations of the terminal oxygen and two chlorines at 3.32 and 3.36 Å are 129° (O—Aq—Cl1), 61.4° (O—Aq—Cl4), and 67.8° (Cl1—Aq—Cl4). These values are on the upper and lower extremes of the acceptor angle variation found in hydrates (13).

It seems probable that any hydrogen bonding

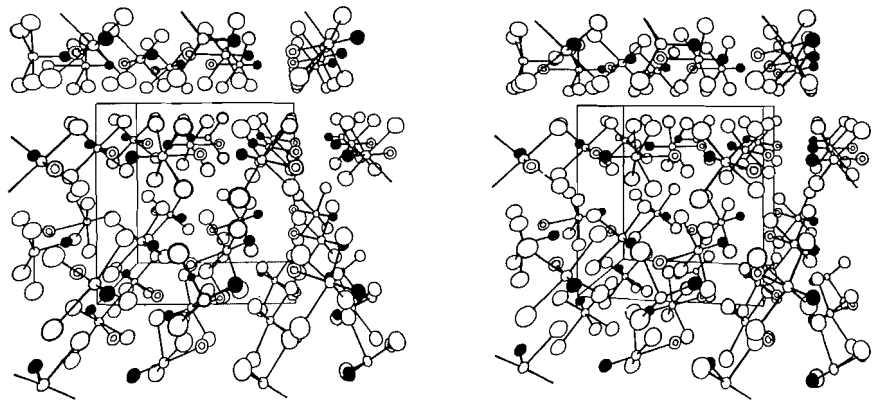

FIG. 3. Stereogram (stereoscopic pair of perspective projections) of $ReOCl_4(OH_2)$ viewed down the *c* axis, with the origin at the upper right hand corner, and the *a* and *b* axes parallel to the horizontal and vertical directions of the page. Open circles are chlorine or rhenium atoms, double circles are aquo groups and filled circles are terminal oxygen atoms.

is weak. Nevertheless, hydrogen bonding to neighboring groups probably occurs, and such bonding would cause changes in the structure. It seems probable that these small changes are concealed by disorder and the present parameters represent an average position. Such an effect may explain the difficulty in determining the correct space group. Unfortunately, because of the errors in the temperature factors caused by the absorption problem mentioned above, the disorder cannot be detected from anomalies in the temperature factors.

Although $ReOCl_4(OH_2)$ represents the first molecular species of the type $MOX_4(OH_2)$ (M = transition metal, X = halogen), several salts containing the species $MOX_4(OH_2)^{n-}$ have been studied by X-ray diffraction techniques. A comparison of the bond distances, bond angles, and non-bonded distances of $ReOCl_4(OH_2)$ (Tables 2 and 3) with those of $MoOBr_4(OH_2)^-$ (14), $ReOBr_4(OH_2)^-$ (15), and $VOCl_4(OH_2)^{2-}$ (16) shows that the intramolecular parameters for these compounds are comparable.

Figure 3 gives a three-dimensional view of how the molecules of $ReOCl_4(OH_2)$ are packed in the structure relative to the unit cell. An approximate depth of three unit cell distances along the *c* axis as well as two unit cell distances in the *a* and *b* directions are shown in the diagram. The structure is made up of chains of molecules stacked in the *c* direction, and these chains are arranged to give clearly defined layers parallel to the *ac* plane. Contact between molecules in the *c* direction is between the aquo and two chloro groups of each molecule and the oxo and two chloro groups of the next. In the *a* direction the oxo and two chloro groups of one molecule in a chain interleave with the aquo and two chloro groups of two molecules (one higher, one lower along *c*) in the adjacent chain. Thus all the oxo groups are on one side of each chain. In the next layer of chains in the *b* direction the oxo groups are on the other side of the chains. In the *b* direction contact between layers of chains is only between chlorine atoms.

To ensure that the crystals isolated from the reaction of ReO_3 and $ReCl_5$ were the same as those prepared subsequently by the aquation of $ReOCl_4$, single crystals of the latter product were mounted and precession photographs compared with those obtained from the former. In addition, a powder photograph was taken on a sample of powder, prepared by grinding some crystals (method *b*) in the dry box at 10 °C, sealed in a fused silica capillary tube. The unit cell parameters, space group, and atom parameters listed in Table 1 were used to calculate *d* spacings as well as theoretical intensities. The agreement between observed and calculated powder data (Table 5) is moderately good.

Physical and Chemical Properties of $ReOCl_4(OH_2)$

$ReOCl_4(OH_2)$ is a bright red volatile solid, which forms rectangular plate crystals. It is completely soluble in $ReOCl_4$, and a mixture of the two compounds is very similar in appearance to pure $ReOCl_4$ itself. If a solution of the two com-

Can. J. Chem. Downloaded from www.nrcresearchpress.com by 210.87.254.6 on 09/05/12
For personal use only.

TABLE 5. A comparison of the powder X-ray diffraction pattern of $ReOCl_4(OH_2)$ with values calculated from the crystal data for the product of the reaction of ReO_3 and $ReCl_5$

d_{obs}	d_{calc}	hkl	I_{obs}	I_{calc}	d_{obs}	d_{calc}	hkl	I_{obs}	I_{calc}
5.539	5.544	020	57	154*		2.458	202		2
	5.417	200		11	2.423	2.434	420	23	26
	4.939	011		52*†		2.415	141		9
	4.916	101		29*†	2.406	2.408	122	23	23
4.874‡	4.867	210	100	264*		2.400	212		1
4.500	4.494	111	63	102*	2.378	2.375	411	<8	8
	3.875	220		10	2.345	2.339	331	<8	9
3.862	3.865	201	23	24	2.252	2.253	241	10	11
3.673	3.678	121	26	25	2.226	2.227	421	<8	5
	3.650	211		1	2.190	2.192	302	<8	6
3.170	3.171	221	19	27		2.185	430		7
	3.071	031		10		2.166	132		10
3.050	3.053	230	30	41	2.155	2.150	312	17	22
3.015	3.022	301	22	24		2.058§	051		4
2.952	2.954	131	8	9	2.054‡	2.052§	250	22	18
	2.915	311		1		2.047§	232		2
	2.772	040		6		2.043§	341		7
	2.758	002		2		2.039§	322		2
	2.673	102		2		2.031§	431		7
2.669‡	2.671§	231	43	42		2.022§	151		6
	2.653§	321		21	1.984	1.984	511	9	12
	2.631§	410		15		1.955	042		3
2.596	2.599	112	8	8	1.936	1.937	440	24	28
	2.470	022		1		1.933	402		4
	2.468	240		3	1.924	1.924	142	24	17

*Probably has extinction errors.
†Observed as shoulders on the 4.874 Å peak, but not measurable.
‡Very broad peak.
§All would fall under the 2.669 or 2.054 Å peak.

pounds is allowed to sit at room temperature under vacuum (for a period of weeks), crystals of $ReOCl_4(OH_2)$ slowly form at the far extremes of the vessel, away from the bulk of the material. When heated under nitrogen, pure $ReOCl_4(OH_2)$ begins to decompose to a yellow-green liquid at $\sim 120\,^{\circ}C$, and appears to melt at $\sim 160\,^{\circ}C$.

The oxygen atom *trans* to the terminal oxygen was characterized as belonging to an aquo group rather than a hydroxo group by the oxidation state analysis as well as the i.r. spectrum. Table 6 summarizes the i.r. data, and some of the spectra obtained are illustrated in Fig. 4.

Solid $ReOCl_4(OH_2)$ is characterized in its i.r. spectrum by a broad peak in the 3600–3300 cm^{-1} region, corresponding to the stretching modes of water, a sharp peak at 1580 ($\pm$ 5) cm^{-1}, arising from a bending mode of water, and a strong peak at 1016.5 ($\pm$ 1.0) cm^{-1}, corresponding to an Re=O stretching mode. The bending mode at 1580 cm^{-1} is slightly lower than the corresponding vibrational mode in $[Et_4N][ReOBr_4(OH_2)]$ which was found at 1605 cm^{-1} (15), but comparable to that found in $[RuCl_5(OH_2)]^{2-}$ at 1570 cm^{-1} (17). The occurrence of the terminal oxygen stretching frequency at 1016.5 cm^{-1} compared to that in $ReOCl_4$ at 1033 cm^{-1} is similar to that observed in $ReOCl_4 \cdot OPCl_3$, recently reported by Guest and Lock (4) at 1020 cm^{-1}. The far i.r. spectrum shows only one broad peak centered at $\sim 350\ cm^{-1}$, a little lower than the 372 cm^{-1} reported for $ReOCl_4$ (4). Since some attack on polyethylene occurred, the assignment of this peak as νRe—Cl for $ReOCl_4(OH_2)$ may be invalid.

The gas phase i.r. spectrum of $ReOCl_4 \cdot OPCl_3$ showed that decomposition into $ReOCl_4$ and $POCl_3$ had occurred, but this is not the case with $ReOCl_4(OH_2)$. As shown in Fig. 4 and Table 5, $ReOCl_4$ does appear to be one of the products (1033 cm^{-1}), but the liberated water quickly hydrolyzes the rest of the material to yield ReO_3Cl (1003, 971 cm^{-1}), and at least one other

Can. J. Chem. Downloaded from www.nrcresearchpress.com by 210.87.254.6 on 09/05/12
For personal use only.

TABLE 6. Infrared spectral data for $ReOCl_4(OH_2)$

Infrared (cm^{-1})			
Powder	Nujol mull	Heated in gas cell*	Assignment
	3600–3300 m†, vbr		H—O str
1575 w	1580 s		HOH bend
		1038 m 1033 sh	Re=O stretch of $ReOCl_4$
1025 w, sharp	1025 vw, sharp		Impurity
1015 m	1016 vs	1013 vw	Re=O stretch of $ReOCl_4(OH_2)$
		1003 w 971 sbr	Re=O stretch of ReO_3Cl or $ReOCl_4 \cdot ReO_3Cl$
		936 m	Re=O stretch of $ReOCl_4 \cdot ReO_3Cl$?
Not recorded below 400			
	~ 350 s, vbr		Re—Cl stretch of $ReOCl_4(OH_2)$

*Sample obviously decomposed on heating before spectrum was recorded.
†w = weak, m = medium, s = strong, br = broad, sh = shoulder, v = very.

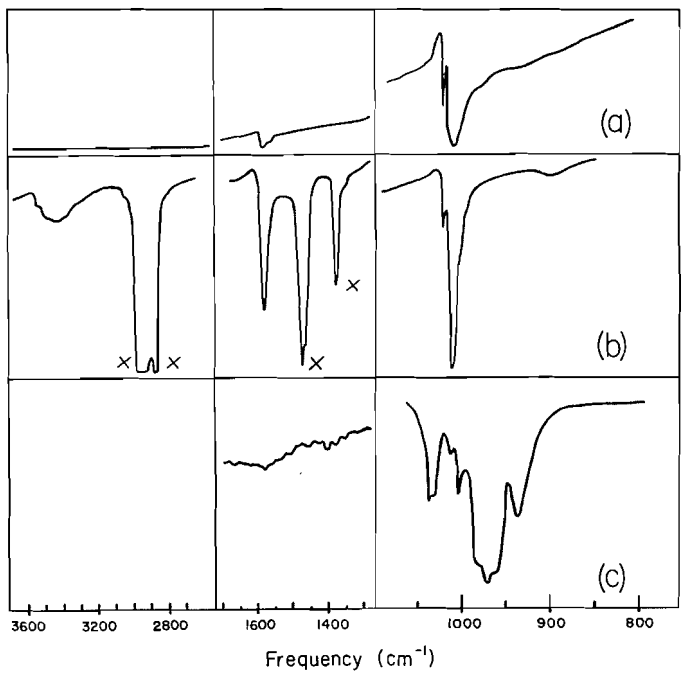

FIG. 4. Infrared spectra of $ReOCl_4(OH_2)$. × indicates a Nujol absorption peak. (*a*) Powder sample of $ReOCl_4 \cdot OH_2$. (*b*) Nujol mull sample of $ReOCl_4 \cdot OH_2$. (*c*) Heated sample of $ReOCl_4 \cdot OH_2$ in gas cell. Decomposition had occurred.

material characterized by the peak at 936 cm^{-1}. It is possible that this peak arises from the formation of the adduct $ReOCl_4 \cdot ReO_3Cl$ (21). This could account for the splitting observed in the 1033 cm^{-1} peak.

In Nujol, as well as for the pure powder ground between KBr plates, a weak, very sharp peak of very variable intensity relative to that of the 1016.5 cm^{-1} peak was always observed at ~1025 cm^{-1}. One would expect only one Re=O stretch for $ReOCl_4 \cdot OH_2$, and the variability suggests it is caused by an impurity. It

Can. J. Chem. Downloaded from www.nrcresearchpress.com by 210.87.254.6 on 09/05/12
For personal use only.

may arise from the surface coating which always forms when handling $ReOCl_4 \cdot OH_2$. We have been unable to characterize this impurity at this stage of our investigations.

An attempt was made to measure the Raman spectrum of $ReOCl_4(OH_2)$ at room temperature, but decomposition occurred immediately. At $-120\,^{\circ}C$, several absorptions were observed, but as the sample had at least partially decomposed, no attempt was made to assign these peaks.

Several authors (18–21) have reported absorptions at ~ 1033 and $\sim 1016\ cm^{-1}$ in the i.r. spectrum of $ReOCl_4$ in Nujol. We have observed only a single strong peak at $1033\ cm^{-1}$ for $ReOCl_4$ in Nujol consistent with our previous observations of $ReOCl_4$ in the gas phase and in $TiCl_4$ and CCl_4 solutions (4). Since $ReOCl_4(OH_2)$ is completely soluble in $ReOCl_4$, and the solution of these compounds has properties very similar to those of $ReOCl_4$ itself, we suggest that the peak at $\sim 1016\ cm^{-1}$ arises from $ReOCl_4(OH_2)$ impurity formed by the reaction of $ReOCl_4$ with traces of water.

$ReOCl_4(OH_2)$ is stable in vacuum in the absence of a temperature gradient. The compound could be distilled under vacuum, but partial decomposition always occurred. The decomposition products include $ReOCl_4$, ReO_3Cl, and an involatile black residue. $ReOCl_4(OH_2)$ is insoluble in CCl_4 and $TiCl_4$, but slowly decomposes to form a green solution of $ReOCl_4$. When $ReOCl_4(OH_2)$ is handled in a dry box at $10\,^{\circ}C$, a black surface coating forms within hours. The powder photograph shows these decomposition products as impurity lines at $d = 7.39$ and 6.65 Å. The exact nature of the various decomposition reactions of $ReOCl_4(OH_2)$ is being studied further.

We thank the National Research Council of Canada for financial support of this work and the grant of a scholarship to P.W.F.

1. P. W. Frais, C. J. L. Lock, and A. Guest. Chem. Commun. 75 (1971).
2. W. D. Courrier, A. Guest, C. J. L. Lock, and R. H. Tomlinson. Can. J. Chem. **46**, 2965 (1968).
3. A. Guest and C. J. L. Lock. Rev. Sci. Instrum. **39**, 780 (1968).
4. A. Guest and C. J. L. Lock. Can. J. Chem. **49**, 603 (1971).
5. A. D. Melaven, J. N. Fowle, W. Brickell, and C. F. Hiskey. Inorg. Synth. **3**, 188 (1950).
6. K. Knox, S. Y. Tyree, R. D. Srivastava, V. Norman, J. Y. Bassett, and J. H. Holloway. J. Am. Chem. Soc. **79**, 3358 (1957).
7. L. C. Hurd and E. Brimm. Inorg. Synth. **1**, 180 (1939).
8. D. T. Cromer and K. Herrington. J. Am. Chem. Soc. **77**, 4708 (1955).
9. D. T. Cromer and J. T. Waber. Acta Cryst. **18**, 104 (1965).
10. D. T. Cromer. Acta Cryst. **18**, 17 (1965).
11. N. Bartlett, N. K. Jha, and J. Trotter. Proc. Chem. Soc. 277 (1962).
12. L. O. Atovmyan, O. A. D'yachenko, and E. B. Lobkovskii. J. Struct. Chem. **11**, 429 (1970).
13. W. C. Hamilton and J. A. Ibers. Hydrogen bonding in solids. W. A. Benjamin, Inc., New York. 1968.
14. J. G. Scane. Acta Cryst. **23**, 85 (1967).
15. F. A. Cotton and S. J. Lippard. Inorg. Chem. **4**, 1621 (1965).
16. L. O. Atovmyan and Z. G. Aliev. J. Struct. Chem. **11**, 728 (1970).
17. K. I. Petrov, V. V. Kravchenko, and N. M. Sinitryn. Zh. Neorgan. Khim. **15**, 2732 (1970).
18. K. W. Bagnall, D. Brown, and R. Colton. J. Chem. Soc. 3017 (1964).
19. B. J. Brisdon and D. A. Edwards. Inorg. Chem. **7**, 1898 (1968).
20. J. H. Canterford, R. Colton, and I. B. Tomkins. Inorg. Nucl. Chem. Lett. **4**, 471 (1968).
21. K. I. Petrov, V. V. Kravchenko, D. V. Drobot, and V. A. Aleksandrova. Russ. J. Inorg. Chem. **16**, 928 (1971).
22. W. C. Hamilton. Acta Cryst. **18**, 502 (1965).

Can. J. Chem. Downloaded from www.nrcresearchpress.com by 210.87.254.6 on 09/05/12
For personal use only.

The Total Synthesis of (±) Ochrobirine

B. NALLIAH, Q. A. AHMED, AND R. H. F. MANSKE
Department of Chemistry, University of Waterloo, Waterloo, Ontario
AND
R. RODRIGO
Waterloo Lutheran University, Waterloo, Ontario
Received February 10, 1972

The total synthesis of (±) ochrobirine is described.

La synthèse totale de la (±) ochrobirine est décrite.

Canadian Journal of Chemistry, **50**, 1819 (1972)

Can. J. Chem. Downloaded from www.nrcresearchpress.com by 210.87.254.40 on 09/05/12
For personal use only.

Ochrobirine was first isolated by Manske (1) in 1936 from *Corydalis sibirica* (L.) Pers. and has since been found in other species of Corydalis (2, 3). Recently (4), the spirobenzylisoquinoline structure **1** was assigned to the alkaloid almost entirely on the basis of its p.m.r. spectrum.

Since no rational degradations of ochrobirine could be found it was decided to attempt a synthesis of the alkaloid in order to confirm its structure. Many syntheses of spirobenzylisoquinoline alkaloids have been successfully achieved (5) by Pictet–Spengler condensation of suitable β-phenethylamines with various 1,2-indanediones. Consequently, it was decided to attempt the synthesis of ochrobirine by an extension of this method using 4,5-methylenedioxyindanetrione in a similar Pictet–Spengler condensation. Preliminary experiments, carried out in this laboratory, demonstrated that such a condensation between homopiperonylamine (**2**) and ninhydrin (**3**) produced a spirodione **4** in excellent yield (6) thus verifying the applicability of this route to ochrobirine. In the latter case the synthesis would entail the elaboration of the methylenedioxy ninhydrin **5**, a similar Pictet–Spengler condensation, *N*-methylation, and reduction of the resulting spirodione **6** to produce a mixture of diastereomers which should contain (±) ochrobirine.

The synthesis of **5** thus becomes the major task of this undertaking and predictably enough, was tedious, time-consuming, and beset with poor yields. Two approaches were explored. The first, illustrated in Scheme 1, was based on the

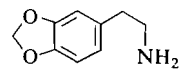

2

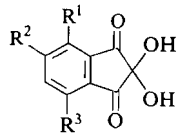

3 $R^1 = R^2 = R^3 = H$
5 $R^1 + R^2 = O{-}CH_2{-}O$; $R^3 = H$
13 $R^1 + R^2 = OCH_2O$; $R^3 = Br$

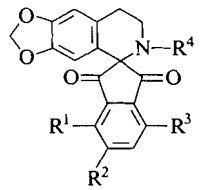

4 $R^1 = R^2 = R^3 = R^4 = H$
6 $R^1 + R^2 = OCH_2O$; $R^3 = R^4 = H$
16 $R^1 + R^2 = OCH_2O$; $R^3 = Br$, $R^4 = H$
17 $R^1 + R^2 = OCH_2O$; $R^3 = Br$, $R^4 = CO_2Et$
19 $R^1 + R^2 = OCH_2O$; $R^3 = H$, $R^4 = Me$

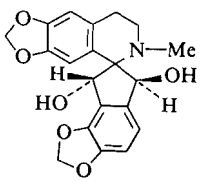

1

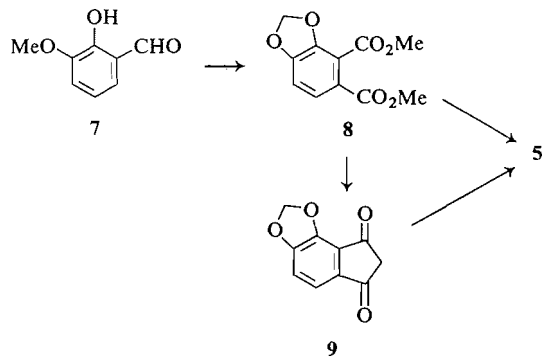

SCHEME 1

use of *o*-vanillin (7) as the starting material and on the demonstration that diethyl phthalate is readily converted into ninhydrin in high yield by condensation with dimethyl sulfoxide under basic catalysis (7). The dimethyl phthalate **8** was prepared by standard methods in an overall yield of 6% from *o*-vanillin. However, the condensation of **8** with dimethyl sulfoxide produced a red gum lacking methylenedioxy resonance in its p.m.r. spectrum but possessing a broad peak at δ 9.0 (exchangeable with D_2O) and providing a deep blue–black color with neutral ferric chloride. Use of irreversibly formed methylsulfinyl carbanion (8) gave similar results. An alternative method for effecting the required conversion of **8** to **5** was also investigated. This involved the sodium hydride condensation of **8** with ethyl acetate (9) to the 1,3-indanedione **9** which could be oxidized with selenium dioxide (10) to **5**. Again, a red gum was obtained in the ester condensation and only a very small amount of **9** could be isolated. It therefore appears that the methylenedioxy group is unstable under the strongly basic conditions, probably undergoing nucleophilic displacement in the course of the reaction.

An alternative starting material, piperonal (**10**), has the advantage of possessing the required methylenedioxy group, and the problem of the unsuitable meta situation of the aldehyde group could be overcome by modifying the synthetic target to the bromoindanetrione **13** so as to accommodate a blocking bromine atom. Piperonal was converted by standard procedures to the bromoacid **11** which was cyclized with phosphorus pentoxide (11) to the bromoindanone **12** (Scheme 2). This cyclization was found to be a most temperamental reaction and the yield at the best of times was only about 20%. Moreover the product was accompanied by a significant impurity, which could only be removed by several crystallizations or repeated chromatography. The nature of this impurity was investigated and it was shown to be the enol ester **14**. This structure was supported by the i.r. and p.m.r. spectra (see Experimental) and also by the fact that alkaline hydrolysis of it afforded **11** and **12**. A similar product has been identified in the PPE cyclization of a substituted phenylpropionic acid (20). In subsequent runs of this experiment the crude solid product was therefore saponified with aqueous methanolic potassium carbonate before isolation of the indanone. In this manner a purer product was obtained.

Several other methods of cyclization of this acid were also attempted. Concentrated sulfuric acid, fluorosulfonic acid, and hydrofluoric acid caused charring; the sulfur trioxide dimethylformamide complex (12) gave an excellent yield of the *N*,*N*-dimethylamide **15**, probably by amide exchange. The structure of **15** was evident from its i.r. and p.m.r. spectra and from the fact that it could be obtained by reaction between the acid chloride of **11** and dimethylamine. Attempts were made to cyclize the acid chloride. It was treated with aluminum chloride at temperatures ranging from -15 to $+20°$ but only traces of the desired indanone were obtained. Results were similar with stannic chloride as the catalyst.

Nonetheless, the indanone **12** was available and now had to be converted to the indanetrione **13** and here there was a choice of two methods. The first which was Ruhemann's classical synthesis of ninhydrin (13) was known to give a poor yield. The second method (14), more recent, consisted of oxidation of 1-indanone with selenium dioxide directly to ninhydrin in 79% yield, but in our case it furnished the trione **13** in only 15% yield.

The Pictet–Spengler reaction of **13** with homopiperonylamine (**2**) was now carried out to afford the spirodione **16**. It was decided to *N*-methylate this compound via the urethane **17** in view of a recent report (15) that stereospecific reduction of a carbonyl group in a closely related

Can. J. Chem. Downloaded from www.nrcresearchpress.com by 210.87.254.40 on 09/05/12
For personal use only.

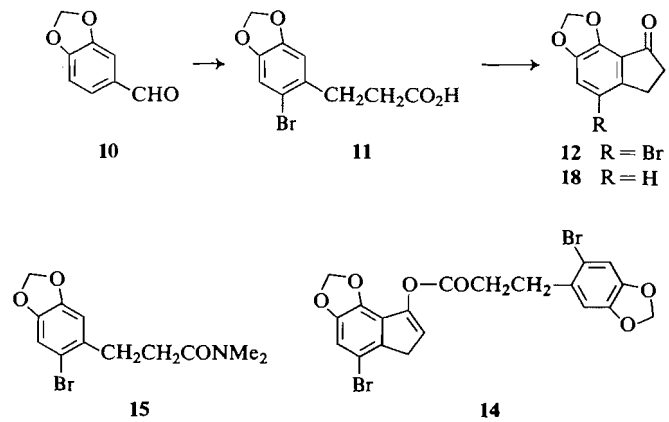

SCHEME 2

spiro compound was achieved in a like manner. The urethane thus obtained from the reaction of **16** with ethylchloroformate was then reduced with lithium aluminum hydride to a product which was a mixture of two compounds, presumably diastereomers, of which the preponderant component was identical with natural ochrobirine (i.r., p.m.r., and t.l.c.). The hydrogenolysis of the bromide was not entirely unexpected (18) and could be regarded as a nucleophilic substitution favored by the presence of the ortho carbonyl group. Alternatively, if this carbonyl group was reduced initially, an intramolecular hydride transfer via a cyclic alkoxide intermediate may be envisaged by analogy with the earlier work (18).

A short while after the completion of this synthesis a communication claiming the total synthesis of (±) ochrobirine by a similar route appeared (16). The sodium borohydride reduction of the dione **6**, contrary to previous reports with similar systems (*5b*, *5c*, 6) and to our own experience with **17**, was claimed to take place stereospecifically to give (±) ochrobirine exclusively. Furthermore, the melting point of the product as reported was 23° lower than that of our synthetic compound. This synthesis was therefore repeated in our laboratory starting from the bromoindanone **12** which was catalytically hydrogenated (palladium–charcoal) to **18**, oxidized with selenium dioxide to **5**, and condensed with homopiperonylamine to give **6**, which was *N*-methylated with formic acid and formalin to the *N*-methyl dione **19**. Reduction of this compound by sodium borohydride in methanol yielded a mixture of two compounds of very similar R_f (t.l.c.) which were separable by preparative thick-layer chromatography. The preponderant product was (±) ochrobirine identical with our previous synthetic sample. An independent synthesis of (±) ochrobirine (17) via a Pomeranz–Fritsch cyclization involved, in its penultimate stages, intermediates **6** and **19** which were identical with ours. A mixture similar to ours resulted in the final borohydride reduction of **19**.

TABLE 1. Melting points recorded for ochrobirine and some synthetic intermediates

Compound	Melting point (°C)		
	Present synthesis	Reference 16	Reference 17
5	222	208–210	—
6	198–200	167–171	198–199
19	194–196	118–122	195–196
1	210	185–187	210–212

Furthermore, there were surprising discrepancies in the reported melting points of these intermediates (Table 1).

We have also observed that the melting point of synthetic (±) ochrobirine increased on standing to about 225° after *ca.* 4 months. In later preparations, the product obtained melted at 235°. As all these products were structurally identical (i.r. in chloroform solution, t.l.c.) the differences in melting point can only be attributed to the existence of two crystalline modifications of (±) ochrobirine.

Can. J. Chem. Downloaded from www.nrcresearchpress.com by 210.87.254.40 on 09/05/12
For personal use only.

Can. J. Chem. Downloaded from www.nrcresearchpress.com by 210.87.254.40 on 09/05/12
For personal use only.

Experimental

Melting points were determined using a Fisher Meltemp unit and are uncorrected. The p.m.r. spectra, unless otherwise specified, were recorded using the frequency sweep mode of a Varian HA-100 spectrometer. Spectra at 60 MHz were recorded on a Varian T-60 instrument. Samples were dissolved in $CDCl_3$, unless otherwise specified, using TMS as the internal locking signal. Chemical shifts were measured relative to TMS. The i.r. spectra were recorded on a Perkin–Elmer 457 spectrometer and a Coleman–Hitachi EPS-3T spectrophotometer was used for the u.v. spectra.

*Dimethyl-3,4-methylenedioxyphthalate (**8**)*

3,4-Methylenedioxyphthalic acid (19) (0.7 g) in methanol (25 ml) was treated with excess ethereal diazomethane and the mixture allowed to stand overnight. The brownish gum obtained after removal of the solvents was purified by column chromatography (alumina, Brockman Activity I, 80–200 mesh) in methylene chloride. The colorless thick oil crystallized upon standing and was washed with ligroin (40–60°) (0.6 g) and the solid recrystallized from methylene chloride – ligroin m.p. 57–59°.

The i.r. spectrum: ν_{max} ($CHCl_3$) 1720 cm^{-1}. The 60 MHz p.m.r. spectrum (δ): 3.83 (3H, s); 3.87 (3H, s); 6.40 (2H, s); 6.83 (1H, d); 7.47 (1H, d) (J_{AB} = 8 Hz).

Anal. Calcd. for $C_{11}H_{10}O_6$: C, 55.47; H, 4.23. Found: C, 55.70; H, 4.26.

*3,4-Methylenedioxyindan-1,3-dione (**9**)*

A solution of **8** (0.5 g) in dry ethyl acetate (1 ml) was added to sodium hydride (0.148 g, 50% dispersion in mineral oil) contained in 5 ml round-bottomed flask fitted with a condenser and calcium chloride guard tube. The mixture was refluxed on a steam bath for 4 h, after which the dark red gum was washed with ether and filtered. It was treated with 3 *N* hydrochloric acid (8 ml) and heated on a water bath at 80–85° for 1 h. The mixture was extracted with methylene chloride, washed, and dried ($MgSO_4$). After removal of the solvent the resulting red product was chromatographed (silica gel) in ethyl acetate, and a small amount of **9** obtained and recrystallized from benzene, m.p. 198–200°.

The i.r. spectrum: ν_{max} ($CHCl_3$) 1710 and 1740 cm^{-1}. The 60 MHz p.m.r. spectrum (δ): 3.23 (2H, s); 6.31 (2H, s); 7.27 (1H, d); 7.57 (1H, d); (J_{AB} = 8 Hz).

*4-Bromo-6,7-methylenedioxyindan-1-one, (**12**) and 1-(4′,5′-Methylenedioxy-2′-bromo)hydrocinnamoyloxy-4-bromo-6,7-methylenedioxyindene (**14**)*

Compound **12** was prepared by the method of Haworth *et al.* (11). The crude solid obtained consisted of two compounds (t.l.c. silica, benzene–acetone 4:1). The faster moving component **14** was separated from the slower **12** by column chromatography using the same system and crystallized from methanol m.p. 163°.

The i.r. spectrum of **14**: ν_{max} ($CHCl_3$) 1762 cm^{-1}. The 60 Hz p.m.r. spectrum (δ): 3.00 (4H, m); 3.33 (2H, d); 6.27 (1H, t) (J_{AX} = 2 Hz); 6.00 (2H, s); 6.03 (2H, s); 6.90 (1H, s); 6.93 (1H, s); 7.07 (1H, s).

Anal. Calcd. for $C_{20}H_{14}Br_2O_6$: C, 47.16; H, 2.77. Found: C, 47.65; H, 2.85.

*Hydrolysis of **14***

Compound **14** (200 mg), potassium carbonate (100 mg), methanol (15 ml), and water (2 ml) were heated on a steam bath for 2 h. The mixture was diluted with water and extracted with ether. The ethereal extract was washed with water and dried (Na_2SO_4) to leave a residue which was crystallized from benzene (80 mg). The product was identical with **12** (p.m.r., i.r., and m.p.).

The aqueous extract on acidifying with concentrated HCl deposited a precipitate which was dissolved in ether, dried (Na_2SO_4), and evaporated to dryness to leave a residue which crystallized from chloroform (94 mg). This product was identical with 6-bromo-3,4-methylenedioxy hydrocinnamic acid (p.m.r., i.r., and m.p.).

*N,N-Dimethyl-3,4-methylenedioxy-6-bromohydrocinnamamide (**15**)*

3,4-Methylenedioxy-6-bromohydrocinnamic acid (1 g) was heated with sulfur trioxide – dimethylformamide complex (12) (20 ml) at 160° for 30 min. The solution was poured into crushed ice and the white precipitate which separated extracted with chloroform. The chloroform extract was washed (10% aqueous sodium carbonate), dried ($MgSO_4$), evaporated to dryness, and the residue crystallized from benzene (780 mg), m.p. 77°.

The u.v. spectrum: λ_{max} (MeOH) 238 and 294 nm (log ε 3.63 and 3.63). The i.r. spectrum: ν_{max} ($CHCl_3$) 1630 cm^{-1}. The 60 MHz p.m.r. spectrum (δ): 7.0 (1H, s); 6.8 (1H, s); 5.97 (2H, s); 2.97 (6H, s); 2.9–3.2 (2H, m).

Anal. Calcd. for $C_{12}H_{14}BrNO_3 \cdot \frac{1}{2}H_2O$: C, 46.60; H, 4.54; N, 4.54. Found: C, 46.43; H, 4.89; N, 4.53.

*4-Bromo-6,7-methylenedioxyindan-1,3-dione-2,2-diol (**13**)*

Compound **12** (5.3 g) was added to a solution of selenium dioxide (4.4 g) in peroxide free dioxane (60 ml) and water (0.5 ml). The mixture was heated at 95–100° for 6 h. The black precipitate of selenium was filtered. The red filtrate was concentrated under reduced pressure to half its volume. Water (50 ml) was added, and the solution was brought to boiling and filtered. The hot filtrate was decolorized (charcoal), and on cooling deposited pale yellow prisms (800 mg), recrystallized from water, m.p. 230–233°.

The u.v. spectrum: λ_{max} (MeOH) 253, 315, and 358 nm (log ε 4.37, 3.70, and 3.63). The i.r. spectrum: ν_{max} ($CHCl_3$) 1728, 1753 cm^{-1}. The p.m.r. spectrum (acetone-d_6, δ): 6.37 (2H, s); 7.47 (1H, s).

Anal. Calcd. for $C_{10}H_5BrO_6 \cdot \frac{1}{2}H_2O$: C, 39.35; H, 1.97. Found: C, 39.43; H, 2.03.

*6,7-Methylenedioxy-1,2,3,4-tetrahydroisoquinoline-1-spiro-2′-(4′bromo-6′,7′-methylenedioxy-1′,3′-indanedione) (**16**)*

A solution of homopiperonylamine (**2**) (200 mg), in absolute ethanol (5 ml) was placed in a 100 ml two-necked flask equipped with a magnetic stirrer, pressure-equalizing dropping funnel, and a calcium chloride guard tube. The flask was cooled in an ice bath and a solution of **13** (200 mg) in absolute ethanol (20 ml) was added dropwise over a period of 15 min. The solution was stirred for another 25 min. The solution on further cooling (Dry Ice – acetone) deposited a white precipitate which dissolved to an orange solution when dry hydrogen chloride was bubbled through the mixture (15 min). The temperature was now raised to 25° and the solution poured into crushed ice, basified with concentrated ammonia solution, and extracted with ether. The ether was removed to yield a yellow residue which crystallized from acetone–methanol (180 mg), m.p. 219–221°.

Can. J. Chem. Downloaded from www.nrcresearchpress.com by 210.87.254.40 on 09/05/12
For personal use only.

The u.v. spectrum: λ_{max} (MeOH) 251, 304, 352 nm (log ε 4.38, 3.86, 3.78). The i.r. spectrum: ν_{max} ($CHCl_3$) 1714 and 1743 cm^{-1}. The p.m.r. spectrum (δ): 1.78 (1H, s exchangeable with D_2O); 2.78 (2H, t); 3.4 (2Ht) ($J_{AX} = 6$ Hz); 5.84 (2H, s); 6.02 (1H, s); 6.32 (2H, s); 6.62 (1H, s); 7.36 (1H, s).

Anal. Calcd. for $C_{19}H_{12}BrNO_6$: C, 53.04; H, 2.81; N, 3.25. Found: C, 52.48; H, 2.81; N, 3.21.

Mol. Wt. Calcd. for $C_{19}H_{12}{}^{79}BrNO_6$: 428.985. Found (h.r.m.s.): 428.987.

*2-Carbethoxy-6,7-methylenedioxy-1,2,3,4-tetrahydroisoquinoline-1-spiro-2′-(4′-bromo-6′,7′-methylenedioxy-1′,3′-indanedione) (**17**)*

A solution of ethyl chloroformate (200 mg) in chloroform (10 ml) was added to a stirred suspension of **16** (150 mg) in 20% aqueous sodium carbonate solution (20 ml) maintained between 0 and 10°. The mixture was stirred for 1 h, the chloroform layer was separated and washed with 1 *M* hydrochloric acid, dried (Na_2SO_4), and the chloroform removed under reduced pressure. The residue was crystallized from methanol (120 mg), m.p. 225–226°.

The u.v. spectrum: λ_{max} (MeOH) 251, 303, and 362 nm (log ε 4.51, 3.93, 3.80). The i.r. spectrum: ν_{max} ($CHCl_3$) 1681, 1726, 1758 cm^{-1}. The p.m.r. spectrum (δ): 1.26 (3H, t); 4.10 (2H, q) ($J_{AX} = 8$ Hz); 3.0 (2H, t); 3.90 (2H, t) ($J_{A'X'} = 5$ Hz); 5.88 (2H, s); 6.18 (1H, s); 6.30 (2H, d) (2′,3′-O—CH_2—O); 6.68 (1H, s); 7.36 (1H, s).

Anal. Calcd. for $C_{22}H_{16}BrNO_8$: C, 52.61; H, 3.21; N, 2.78. Found: C, 52.42; H, 3.26; N, 2.88.

The molecular formula was confirmed by h.r.m.s.

Mol. Wt. Calcd. for $C_{22}H_{16}{}^{79}BrNO_8$: 501.006. Found (h.r.m.s.): 500.999.

Mol. Wt. Calcd. for $C_{22}H_{16}{}^{81}BrNO_8$: 503.004. Found (h.r.m.s.): 503.002.

*(±) Ochrobirine (**1**)*

A solution of the urethane, **17** (200 mg) and lithium aluminum hydride (150 mg) in dry tetrahydrofuran (40 ml) was refluxed for 13 h. The excess reagent was decomposed with water and the mixture extracted with ether. The ethereal extract was washed with water, dried ($MgSO_4$), and evaporated to dryness. The residue on t.l.c. (silica gel) showed two spots of similar R_f, from which (±) ochrobirine the major component, was isolated by column chromatography (silica gel; benzene, acetone, methanol (65:15:20)) and crystallized from methanol (52 mg), m.p. 210°. In subsequent preparations the product melted at 235°.

All these samples had identical i.r., p.m.r. spectra with natural ochrobirine and on t.l.c. (silica gel) had similar R_f values in the following solvent systems: benzene, acetone, methanol (65, 15, 20); benzene, ethyl acetate, methanol (30, 10, 10); benzene, ether, methanol (30, 10, 10).

*4,5-Methylenedioxyindan-1,3-dione-2,2-diol (**5**)*

6,7-Methylenedioxyindan-1-one (5*c*) (3.5 g) was added to a solution of selenium dioxide (4.4 g) in peroxide free dioxane (50 ml) and water (0.5 ml). The mixture was heated at 95–100° for 6 h. The black precipitate of selenium was filtered. The red filtrate was concentrated under reduced pressure to 20 ml, water (50 ml) was added, and the solution was brought to boiling and filtered. The hot filtrate was decolorized (charcoal), and on cooling deposited pale yellow prisms (850 mg), crystallized from water, m.p. 221–222°.

The u.v. spectrum: λ_{max} (MeOH) 247, 295, and 347 nm (log ε 4.48, 3.73, 3.64). The i.r. spectrum: ν_{max} ($CHCl_3$) 1710 and 1740 cm^{-1}. The 60 MHz p.m.r. spectrum in MeOH (δ): 6.01 (2H, s); 7.07 (1H, d); 7.27 (1H, d) ($J_{AX} = 8$ Hz).

Anal. Calcd. for $C_{10}H_6O_6$: C, 54.05; H, 2.70. Found: C, 54.00; H, 2.97.

*6,7-Methylenedioxy-1,2,3,4-tetrahydroisoquinoline-1-spiro-2′-(4′,5′-methylenedioxy-1′,3′-indanedione) (**6**)*

A solution of homopiperonylamine (**2**) (200 mg), in absolute ethanol (5 ml) was placed in a 100 ml, two-necked flask equipped with a magnetic stirrer, pressure-equalizing dropping funnel, and a calcium chloride guard tube. The flask was cooled in an ice bath and a solution of **5** (200 mg) in absolute ethanol (35 ml) was added dropwise over a period of 15 min and the solution stirred for another 45 min. The solution on cooling (Dry Ice – acetone) deposited a white precipitate which dissolved to an orange solution when dry hydrogen chloride was bubbled through the mixture (15 min). The temperature was raised to 40°, the solution was poured into crushed ice, basified with concentrated ammonia solution, and extracted with ether. The yellow residue obtained on removal of the ether crystallized from methanol–chloroform (230 mg), m.p. 199–201°.

The u.v. spectrum: λ_{max} (MeOH) 245, 297, and 348 nm (log ε 4.55, 3.97, and 3.80). The i.r. spectrum: ν_{max} ($CHCl_3$) 1711 and 1743 cm^{-1}. The p.m.r. spectrum (δ): 1.95 (1H, s); 2.81 (2Ht); 3.42 (2Ht); ($J_{AX} = 6$ Hz); 5.83 (2H, s); 6.03 (1H, s); 6.31 (2H, s); 6.63 (1H, s); 7.27 (1H, d) 7.67 (1H, d) ($J_{AB} = 8$ Hz).

Anal. Calcd. for $C_{19}H_{13}NO_6$: C, 64.91; H, 3.70; N, 3.99. Found: C, 65.17; H, 3.91; N, 3.80.

*2-Methyl-6,7-methylenedioxy-1,2,3,4-tetrahydroisoquinoline-1-spiro-2′-(4′,5′-methylenedioxy-1′,3′-indanedione) (**19**)*

A solution of the amine **6**, (100 mg), in 90% formic acid (1.5 ml) and 37% formaldehyde (1.5 ml) was heated on a steam bath for 6 h. The solution was poured into crushed ice and basified with concentrated ammonia solution. The mixture was extracted with ether, dried ($MgSO_4$), and evaporated to dryness. The yellow residue crystallized from methanol (60 mg), m.p. 194–196°.

The u.v. spectrum: λ_{max} (MeOH) 245, 297, and 348 nm (log ε 4.57, 3.96, and 3.80). The i.r. spectrum: ν_{max} ($CHCl_3$) 1710 and 1741 cm^{-1}. The p.m.r. spectrum (δ): 2.39 (3H, s); 2.99 (2H, m); 3.31 (2H, m); 5.81 (2H, s); 5.96 (1H, s); 6.32 (2H, s); 6.63 (1H, s); 7.30 (1H, d); 7.64 (1H, d) ($J_{AB} = 8$ Hz).

Anal. Calcd. for $C_{20}H_{15}NO_6$: C, 65.75; H, 4.11. Found: C, 65.81; H, 4.28.

*(+) Ochrobirine (**1**)*

Sodium borohydride (150 mg) was added to a solution of **19** (60 mg) in methanol (20 ml). The solution was stirred for 24 h. The solution was acidified with acetic acid and solvent was removed under reduced pressure. The residue was basified with concentrated ammonia solution and was extracted with ether. The ether extract was dried ($MgSO_4$) and evaporated to dryness. The residue on t.l.c. (silica gel) showed two spots of similar R_f, from which (±) ochrobirine the major component, was isolated by preparative t.l.c. (silica gel; benzene, acetone, methanol (65:15:20)) and crystallized from methanol (31 mg), m.p. 235°.

The i.r. and p.m.r. spectra were identical with that of the natural ochrobirine and on t.l.c. (silica gel) had similar R_f values in the same solvent systems as before.

We wish to thank Prof. D. B. MacLean for the high resolution mass spectra of **16** and **17**. Generous support from the National Research Council of Canada is gratefully acknowledged.

1. R. H. F. MANSKE. Can. J. Res. **14B**, 354 (1936).
2. R. H. F. MANSKE. Can. J. Res. **17B**, 89 (1939).
3. R. H. F. MANSKE. Can. J. Res. **17B**, 95 (1939).
4. R. H. F. MANSKE, R. G. A. RODRIGO, D. B. MACLEAN, D. E. F. GRACEY, and J. K. SAUNDERS. Can. J. Chem. **47**, 3589 (1969).
5. (*a*) S. MCLEAN, M.-S. LIN, and J. WHELAN. Can. J. Chem. **48**, 948 (1970). (*b*) H. IRIE, T. KISHIMOTO, and S. UYEO. J. Chem. Soc. C, 3051 (1968). (*c*) T. KISHIMOTO and S. UYEO. J. Chem. Soc. C, 2600 (1969) and 1644 (1971). (*d*) B. A. BECKETT and R. B. KELLY. J. Heterocycl. Chem. **5**, 685 (1968) and Can. J. Chem. **47**, 2501 (1969).
6. R. H. F. MANSKE and Q. A. AHMED. Can. J. Chem. **48**, 1280 (1970).
7. H.-D. BECKER and G. A. RUSSELL. J. Org. Chem. **28**, 1896 (1963).
8. G. A. RUSSELL, E. T. SABOURIN, and G. HAMPRECHT. J. Org. Chem. **34**, 2339 (1969).
9. H. GRUEN and B. E. NORCORSS. J. Chem. Ed. **42**, 268 (1965).
10. A. I. VOGEL. Practical organic chemistry: 3rd Ed. John Wiley and Sons Inc., New York, N.Y. 1966. p. 995.
11. R. D. HAWORTH, W. H. PERKIN, JR., and T. S. STEVENS. J. Chem. Soc. 1764 (1926).
12. E. BALTAZZI and A. J. WYSOCKI. Chem. and Ind. 1080 (1963).
13. S. RUHEMANN. J. Chem. Soc. 1438 (1910).
14. M. E. NEUZIL, A. LIERMAIN, H. JENSEN, and J. HERVIEU. Bull. Soc. Pharm. Bordeaux, **107**, 105 (1968); Chem. Abstr. **71**, 112672*t* (1969).
15. H. IRIE, S. TANI, and H. YAMANE. Chem. Commun. 1713 (1970).
16. T. KAMETANI, S. HIBINO, and S. TAKANO. Chem. Commun. 925 (1971).
17. Personal communication from DR. D. B. MACLEAN, Chemistry Department, McMaster University, Hamilton, Ontario. N. E. CUNDASWAMY and D. B. MACLEAN. Can. J. Chem. In press.
18. G. J. KARABATSOS, R. L. SHONE, and S. E. SCHEPPELE. Tetrahedron Lett. 2113 (1964).
19. E. SPÄTH, F. KUFFNER, and T. MEINHARD. Ber. **74**, 1557, (1941).
20. D. W. BROWN, C. DENMAN, and H. O. DONNELL. J. Chem. Soc. C, 3195 (1971).

Can. J. Chem. Downloaded from www.nrcresearchpress.com by 210.87.254.40 on 09/05/12
For personal use only.

An Electron Spin Resonance Examination of Ferrocenylalkyl- and Aryl Ketyls

G. BIGAM, JOHN HOOZ,[1] SIEGFRIED LINKE,[2] R. E. D. MCCLUNG,[1]
MELVYN W. MOSHER,[3] AND DENNIS D. TANNER[1]

Department of Chemistry, University of Alberta, Edmonton, Alberta

Received October 25, 1971

Several ferrocenylalkyl- and aryl ketyls were generated and their e.s.r. spectra were recorded. Pentadeuteriobenzoylferrocene and benzoyl perdeuterioferrocene were synthesized. Analysis of the e.s.r. spectra of their corresponding ketyls enabled the determination of the hyperfine splitting constants of benzoylferrocene ketyl, and allowed an assignment of the electron densities at various positions in the molecule.

A comparison of the magnitudes of the *g*-values for the ketyls derived from benzophenone (2.0034), benzoylferrocene (2.0062), and 2,2-dimethylpropanoylferrocene (2.0126), combined with the proton hyperfine splittings, gave some insight into the nature of the interaction of the free electron with the ferrocene system.

Plusieurs ferrocenylalkyl- et arylcétyles ont été engendrés et leurs spectres r.p.e. enregistrés. Le benzoylferrocène pentadeutérié et le benzoylferrocène perdeutérié ont été synthétisés. L'analyse des spectres r.p.e. de leurs cétyles correspondants rend possible la détermination des constantes de multiplicité hyperfine du benzoylferrocène cétyle et permet une attribution des densités électroniques sur les différentes positions de la molécule.

Une comparaison des grandeurs des valeurs *g* pour les cétyles dérivés de la benzophénone (2.0034), du benzoylferrocène (2.0062) et du diméthyl-2,2 propanoylferrocène (2.0126), combinée avec les multiplicités hyperfines du proton, a permis de pénétrer la nature de l'interaction de l'électron libre avec le système ferrocène.

Canadian Journal of Chemistry, **50**, 1825 (1972)

Introduction

The nature of the bonding in α-ferrocenyl carbonium ions (1–11) and radicals (12–15) has been the subject of conjecture by a number of workers. The bonding interactions in these intermediates have been interpreted in a variety of ways. One view is that π-bonding between the cyclopentadienyl ring and the α-carbon atom confers extra stability; the new π-bond being formed at the expense of a carbon–iron bond. Another view is one in which there is significant d–p bonding due to the interaction of doubly occupied iron d-orbitals with the unoccupied p-orbital on the α-carbon atom.

In order to study the interactions of the atomic orbitals which impart stability to these α-ferrocenyl intermediates, we have investigated the ketyls derived from some ferrocenyl ketones. In going from the carbonium ion to the ketyl, the character of the iron–carbon bonding, hopefully, would not be drastically different and consequently any information which we could obtain about bonding in the ketyls would likewise be useful in the description of the bonding in the carbonium ion.

Results

The ketyls derived from benzoylferrocene (**1**), pentadeuteriobenzoylferrocene (**2**), benzoylperdeuterioferrocene (**3**), and 2,2-dimethylpropanoylferrocene (**4**) were generated by reduction of the parent ketones with potassium metal, using tetrahydrofuran (THF) as the solvent.

The e.s.r. spectrum of **1** consists of 15 incompletely resolved lines as shown in Fig. 1. A computer simulation of this spectrum, using the proton hyperfine splittings given in Table 1, is also shown in Fig. 1. These proton splittings agree reasonably well with those previously reported (12) although, as discussed later, we have assigned unequal splittings to the ortho-protons in the phenyl group. An unambiguous assignment of the hyperfine splittings to the protons in the ketyl could not be made without further information. A study of the e.s.r. spectra of the ketyls **2** and **3** was therefore undertaken.[4]

The e.s.r. spectrum of **2** consists of a single line with a peak-to-peak derivative width of 2.4 G.

[1]Authors to whom inquiries should be directed.

[2]University of Alberta Postdoctoral Research Fellow, 1967–1968.

[3]University of Alberta Postdoctoral Research Fellow, 1967–1969.

[4]Since the completion of our work, but prior to its submission, some of the deuteration experiments which we describe have been reported by other workers (15), although no experimental or computational details were given. The values of the hyperfine splittings which they report are sufficiently different from ours that the spectrum simulated with their splittings does not agree with the observed spectrum.

Can. J. Chem. Downloaded from www.nrcresearchpress.com by 210.87.254.105 on 09/05/12
For personal use only.

TABLE 1. Hyperfine splitting constants of ferrocenyl ketyls

Ketyl	Proton hyperfine splitting constants (G)
Benzoylferrocene 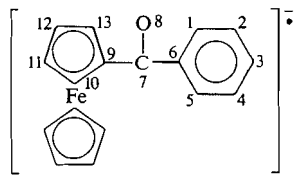 **1**	a_1,a_5* = 3.30, 2.91 a_2,a_4 = 0.89 a_3 = 4.34 a_{10},a_{13} = 0.89
Pentadeuteriobenzoylferrocene 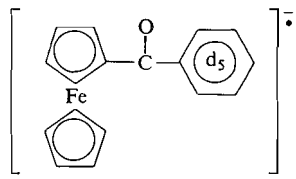 **2**	No splittings observed in a single line of width 2.4 G
Benzoylperdeuterioferrocene 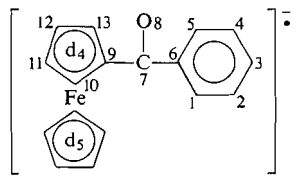 **3**	a_1a_5* = 3.30, 2.91 a_2,a_4 = 0.89 a_3 = 4.34
2,2-Dimethylpropanoylferrocene 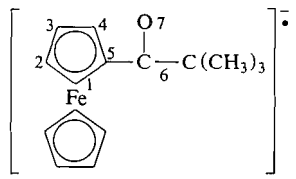 **4**	No splittings observed in a single line of width 5.8 G

*The specific assignment of the different proton splittings to positions 1,5 has not been attempted.

No hyperfine splitting due to the protons in the ferrocenyl group was discernible.

The ketyl **3** has the e.s.r. spectrum shown in Fig. 2. The computer simulation of this spectrum, using the proton hyperfine splittings given in Table 1, is also presented in Fig. 2. The assignment of the proton hyperfine splittings to the *o*-, *p*-, and *m*-positions on the benzene ring was made by analogy to the assignments in benzophenone (16, 17) ketyl and was in agreement with the spin density calculations described in the Discussion. The deuteration of **3** was incomplete (85.3% as indicated from the mass spectrum). Since the ketyl molecules which have protons at the 10 or 13 positions in the cyclopentadiene ring will give a different e.s.r. spectrum from that due to ketyl molecules with deuteriums at these positions, a computer simulation of a mixture of 75% dideuterated and 25% monodeuterated (at the 10 and 13 positions) was performed. This simulation is shown as the dashed curve in Fig. 2. This

Can. J. Chem. Downloaded from www.nrcresearchpress.com by 210.87.254.105 on 09/05/12
For personal use only.

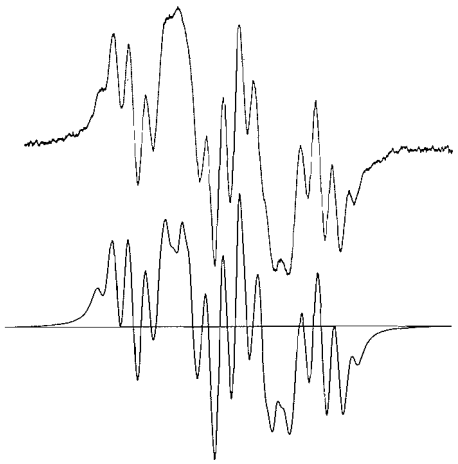

FIG. 1. Comparison of experimental (upper) and computed (lower) e.s.r. spectra for benzoylferrocene ketyl (**1**) in THF solution. Hyperfine splittings used in the computed spectra are given in Table 1.

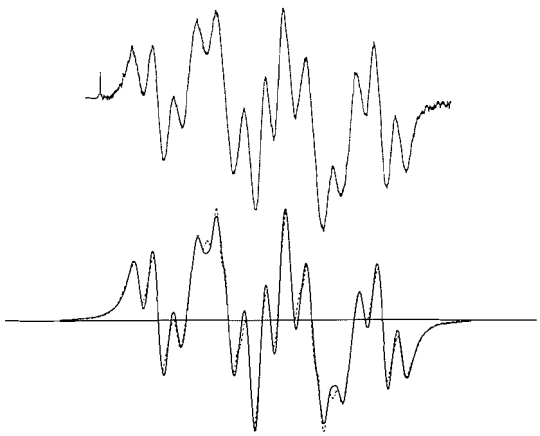

FIG. 2. Comparison of experimental (upper) and computed (lower) e.s.r. spectra for benzoylperdeuterioferrocene ketyl (**3**) in THF solution. Hyperfine splittings used in the computed spectra are given in Table 1. The dotted curve in the computed spectrum corresponds to a mixture of ketyls, 75% dideuterated and 25% monodeuterated at the 10 and 13 positions.

simulated spectrum resembles very closely the spectrum calculated assuming 100% dideuteration at the 10 and 13 positions.

The ketyl **4** exhibited an e.s.r. spectrum consisting of a single line of width 5.8 G. No experimental conditions were found which permitted resolution of the hyperfine structure to be expected from the interaction of the unpaired electron with the ferrocenyl protons.

The g-values of the ketyls **1** and **4** and those of related ketyls, nitroxides, and nitroanions are given in Table 2.

Discussion

The g-values of the ketyls studied in this work, together with those for related systems, form a basis for the discussion of the participation of iron orbitals in the π-electron molecular orbitals of substituted ferrocenes. It is apparent, from a comparison of the g-values of benzophenone (18) and benzoylferrocene (**1**), that the replacement of a phenyl group by a ferrocenyl moiety causes a substantial increase in the g-value which can be directly attributed to the participation of iron orbitals in the π-system. A further increase in g-value occurs when the phenyl group (**1**) is replaced by a t-butyl group (**4**) because the iron orbitals are even more important in this ketyl since the π-system is less delocalized than in benzoylferrocene. These increases in g-value are very good evidence for a significant degree of participation of the iron orbitals in the π-system, in particular for the orbital containing the unpaired electron. Significant contributions of iron orbitals to the π-electron systems in the nitroferrocene anion (12) and t-butyl ferrocenyl nitroxide (13) are also evident from the comparison of their g-values with those of the analogous phenyl compounds (19, 20).

It has been pointed out (15) that the g-value of the benzoylruthenocene ketyl (2.0035) is close to that for the benzophenone ketyl (2.0036), which could be interpreted as evidence against significant metal orbital participation in the π-system of benzoyl ruthenocene. The evidence presented in Table 2 for the ferrocene systems unequivocally indicates significant iron participation in those systems.

However, the interplanar distances in ruthenocene and ferrocene differ by 0.36 Å (22), and the nature of the interactions between the benzoyl and metallocene are undoubtedly quite different. The observation that the proton hyperfine splittings in the benzoylferrocene and benzoylruthenocene are identical is most unexpected and more detailed work on the ruthenocenes is required before the e.s.r. parameters in that system can be interpreted correctly.

In order to gain a better understanding of the π-electron system in the ketyls **1** and **4**, we performed McLachlan semiempirical calculations

Can. J. Chem. Downloaded from www.nrcresearchpress.com by 210.87.254.105 on 09/05/12
For personal use only.

Can. J. Chem. Downloaded from www.nrcresearchpress.com by 210.87.254.105 on 09/05/12
For personal use only.

TABLE 2. Comparison of g-values of ferrocenyl ketyls with other paramagnetic species

Radical or ion radical	g-Value	Reference
Benzoylferrocene ketyl (**1**)	2.0063	This work
Benzophenone ketyl	2.00359	18
2,2-Dimethylpropanoylferrocene ketyl (**4**)	2.0127	This work
Hexamethylacetone ketyl	2.003	21
t-Butyl ferrocenyl nitroxide	2.0149	13
t-Butyl phenyl nitroxide	2.006	20
Nitroferrocene anion	2.0133	12
Nitrobenzene anion	2.005	19

TABLE 3. Calculated and observed spin densities of ferrocenyl ketyls and cyclopentadienide ketyls

Radical ion	Spin density	Source
Benzoylferrocene ketyl (**1**)*	$\rho_1,\rho_5 = 0.123, 0.139$†	Observed $\rho_i = a_i/23.7$‡
	$\rho_2 = \rho_4 = 0.038$	
	$\rho_3 = 0.183$	
	$\rho_{10} = \rho_{13} = 0.038$	
Benzoylcyclopentadienide	$\rho_1 = \rho_5 = 0.144$	McLachlan calculation
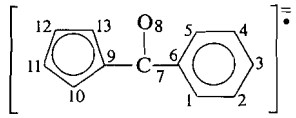	$\rho_2 = \rho_4 = 0.045$	with‡,§
	$\rho_3 = 0.182$	$\alpha_O = \alpha_C + 1.4\beta_{CC}$
	$\rho_6 = 0.020$	$\beta_{CO} = 1.2\beta_{CC}$
	$\rho_7 = 0.375$	
	$\rho_8 = 0.119$	
	$\rho_9 = -0.048$	
	$\rho_{10} = \rho_{13} = 0.073$	
	$\rho_{11} = \rho_{12} = 0.004$	
2,2-Dimethylpropanoyl ferrocene ketyl (**4**)*	$\rho_1,\rho_4 < 0.1$	Estimated from observed e.s.r. spectrum
2,2-Dimethylpropanoylcyclopentadienide ketyl	$\rho_1 = \rho_4 = 0.148$	McLachlan calculation
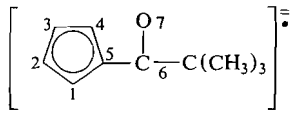	$\rho_2 = \rho_3 = -0.016$	with‡,§
	$\rho_5 = 0.106$	$\alpha_O = \alpha_C + 1.4\beta_{CC}$
	$\rho_6 = 0.682$	$\beta_{CO} = 1.2\beta_{CC}$
	$\rho_7 = 0.160$	

*See Table 1 for numbering of centers.
†No specific assignment of the different spin densities was attempted.
‡The value of $Q = 23.7$ G is that found to give best results for aromatic ketones (19).
§This choice of integrals is consistent with those used for benzophenone, see ref. 16.

(23) of the spin densities in the benzoylcyclopentadienide (**5**) and 2,2-dimethylpropanoylcyclopentadienide (**6**) ketyls using the values of the resonance and coulomb integrals given in Table 3. These integrals were used by previous investigators (16) for benzophenone ketyl. The calculated spin densities for **5** and **6** are compared with the observed spin densities of **1** and **4** in Table 3. In both cases, the calculated spin densities at the ortho carbon atoms in the cyclopentadienide ring are much larger than those observed in the corresponding ferrocenyl ketyl. This is what one would expect if there were participation of the iron atom in the π-system.

We have assigned different values to the hyperfine splittings of the two ortho-protons in the phenyl group of the benzoyl ferrocenyl ketyl because much closer agreement between computed and observed e.s.r. spectra was obtained than in attempts to fit the observed spectra with

Can. J. Chem. Downloaded from www.nrcresearchpress.com by 210.87.254.105 on 09/05/12
For personal use only.

equal ortho-proton splittings. Rieger and Fraenkel (17) investigated several ketyls including benzophenone ketyl (where no difference in ortho splittings is observed), but were not able to explain satisfactorily the occurrence of "locked" planar structures or "unlocked" structures on theoretical grounds. The calculated bond order between the ring carbon atom and the carbonyl carbon is larger in benzoylcyclopentadienide ketyl (**5**) than in benzophenone but not so large that one could state conclusively that one should expect a "locked" planar structure for **1** on this basis.

The results of our e.s.r. investigation of the ferrocenyl ketyls and those of other workers (12–15) clearly indicate that the iron orbitals contribute significantly to the occupied molecular orbitals of highest energy, which are the orbitals of greatest importance in the chemistry of the ferrocenes.

Experimental

Melting points were determined with a Fisher–Johns apparatus and are uncorrected. The i.r. spectra were recorded with a Perkin–Elmer grating spectrophotometer Model 421. Mass spectra were measured by Dr. A. M. Hogg and his associates using an A.E.I. MS-9 spectrometer at an ionization potential of 70 eV; n.m.r. spectra were recorded on a Varian A-60 spectrometer using tetramethylsilane as internal reference and $CDCl_3$ as solvent.

Materials

Benzoylferrocene (24), m.p. 107–108°; n.m.r. τ 1.9–2.8 (5H, phenyl protons), 5.08 (2H, t), 5.41 (2H, t), 5.79 (5H, s, unsubstituted cyclopentadienyl ring protons); i.r. ($CHCl_3$) 1632, 1102, 995 cm^{-1}.

Ferrocene-d_{10} was prepared by a modification of the method of Little and co-workers (25), m.p. 170–173°, from ferrous chloride and cyclopentadiene-d_6 (obtained by repeated exchanges of cyclopentadiene with NaOD–CH_3OD (26)).

Benzoylperdeuterioferrocene was prepared from ferrocene-d_{10} and benzoyl chloride by the method of Weliky and Gould (24), m.p. 107–108°; n.m.r. 2.0–2.7 τ (phenyl protons); the sample contained approximately 13% protons in the ferrocenyl moiety; i.r. ($CHCl_3$) 1632, 995 cm^{-1}, and the "9μ" band corresponding to the "9,10μ Rule" of monosubstituted ferrocenes (27) was missing; *m/e* 299.0950 (calcd. for $C_{17}D_9H_5FeO$: 299.0959), and also indicated 14.7% of undeuterated ferrocene moieties, in excellent accord with the n.m.r. results.

Pentadeuteriobenzoylferrocene was prepared by a Friedel–Crafts reaction between ferrocene and benzoyl-d_5-chloride (Merck, Sharp and Dohme of Canada, Ltd.) according to the method of Weliky and Gould (24), m.p. 107–108°; n.m.r. τ 5.13 (2H, t), 5.47 (2H, t), 5.84 (5H, s, unsubstituted cyclopentadienyl ring protons); i.r. ($CHCl_3$) 1628, 1098, 995 cm^{-1}; *m/e* 295.0699 (calcd. for $C_{17}D_5H_9FeO$: 295.0708), and a maximum of 3% of d_4 species.

2,2-Dimethylpropanoylferrocene, m.p. 90–92°; n.m.r. τ 5.19 (2H, t), 5.59 (2H, t), 5.86 (5H, s, unsubstituted cyclopentadienyl ring protons), 8.69 (9H, s, CH_3); i.r. ($CHCl_3$) 1650, 1375, 1362, 1102, 999; *m/e* 270.0707 (calcd. for $C_{15}H_{18}FeO$: 270.0709).

Tetrahydrofuran was purified by successive reflux periods over potassium hydroxide pellets, sodium metal, and lithium aluminum hydride, prior to being distilled from lithium aluminum hydride under a dry nitrogen atmosphere. The purified tetrahydrofuran was stored in degassed sealed ampoules containing clean slivers of potassium metal, and distilled into the tube containing the appropriate ketone immediately prior to ketyl formation.

The Electron Spin Resonance Sample Preparation and Measurements

The ferrocenyl ketyls were generated by reduction of the corresponding ketones in tetrahydrofuran solution. The procedure used to prepare samples for e.s.r. studies involved double distillation of freshly cut potassium under vacuum into a clean glass bulb separated from a tube containing a degassed solution of the ketone (10^{-3} *M*) by a break-seal. Just prior to spectral examination, the break-seal was broken and the ketone solution was shaken with the potassium metal. The formation of the ketyl was accompanied by a change in the color of the solution.

The e.s.r. spectra were recorded with a Varian V-4502 spectrometer system. The magnetic field was calibrated using a Harvey–Wells Magnion model G-502 proton gaussmeter and the microwave frequency was measured with a Hewlett–Packard model X532 wavemeter. *g*-Value measurements were made relative to an aqueous solution of potassium peroxylamine disulfonate, which has $g = 2.00550$ (28), using a Varian V-4532 dual cavity accessory. We estimate the precision of our *g*-value measurements to be ± 0.0005. In order to obtain optimum spectral resolution, the temperature of the sample was varied using a Varian V-4557 variable temperature accessory.

1. J. H. Richards and E. A. Hill. J. Am. Chem. Soc. **81**, 3484 (1959).
2. E. A. Hill and J. H. Richards. J. Am. Chem. Soc. **83**, 3840 (1961).
3. E. A. Hill and J. H. Richards. J. Am. Chem. Soc. **85**, 4216 (1963).
4. M. Cais, J. J. Dannenberg, A. Eisenstadt, M. I. Levenberg, and J. H. Richards. Tetrahedron Lett. 1695 (1966).
5. E. A. Hill. J. Org. Chem. **28**, 2586 (1963).
6. D. S. Trifan and R. Bacskai. Tetrahedron Lett. No. 13, 1 (1960).
7. D. S. Trifan and R. Bacskai. J. Am. Chem. Soc. **82**, 5010 (1960).
8. T. G. Traylor and J. C. Ware. J. Am. Chem. Soc. **89**, 2304 (1967).
9. G. R. Buell, W. E. McEwer, and J. Kleinberg. Tetrahedron Lett. No. 5, 16 (1959).
10. J. C. Ware and T. G. Traylor. Tetrahedron Lett. No. 15, 1965 (1966).
11. T. T. Tidwell and T. G. Traylor. J. Am. Chem. Soc. **88**, 3442 (1966).
12. C. Eischenbroich and M. Cais. J. Organomet. Chem. **18**, 135 (1969).

13. A. R. FORRESTER, S. P. HEPBURN, R. S. DUNLOP, and H. H. MILLS. Chem. Commun. 698 (1969).
14. W. C. DANEN and C. T. WEST. Tetrahedron Lett. 219 (1970).
15. J. J. MCDONNELL. Tetrahedron Lett. 2039 (1969). J. J. MCDONNELL, G. CAPEN, and R. MICHEALSON. Tetrahedron Lett. 4251 (1969). J. J. MCDONNELL and D. J. POCHOPIEN. J. Org. Chem. **36**, 2092 (1971).
16. P. S. GILL and E. WARHURST. Trans. Faraday Soc. **64**, 293 (1968).
17. P. RIEGER and G. K. FRAENKEL. J. Chem. Phys. **37**, 2811 (1961).
18. M. S. BLOIS, H. W. BRAUN, and J. E. MALING. Arch. Sci. (Geneva), **13**, 243 (1960).
19. G. BIGAM. Unpublished results.
20. A. CALDER and A. R. FORRESTER. Chem. Commun. 682 (1967).
21. N. HIROTA and S. I. WEISSMAN. J. Am. Chem. Soc. **84**, 4424 (1960).
22. J. D. DUNITZ, L. E. ORGEL, and A. RICH. Acta Crystallogr. **9**, 373 (1956). P. L. HARDGROVE and D. H. TEMPLETON. Acta Crystallogr. **12**, 28 (1959).
23. A. D. MCLACHLAN. Mol. Phys. **3**, 233 (1960).
24. N. WELIKY and E. S. GOULD. J. Am. Chem. Soc. **79**, 2742 (1957).
25. W. F. LITTLE, R. C. KOESTLER, and R. EISENTHAL. J. Org. Chem. **25**, 1435 (1960).
26. S. MCLEAN and P. HAYNES. Tetrahedron, **21**, 2329 (1965).
27. M. ROSENBLUM and R. B. WOODWARD. J. Am. Chem. Soc. **80**, 5443 (1958).
28. S. H. GLARUM and J. H. MARSHALL. J. Chem. Phys. **41**, 2182 (1964).

Can. J. Chem. Downloaded from www.nrcresearchpress.com by 210.87.254.105 on 09/05/12
For personal use only.

The Structure of Nupharolutine, an Alkaloid of *Nuphar luteum*

J. T. WROBEL AND A. IWANOW
Department of Chemistry, University of Warsaw, Warsaw, Poland
AND
C. BRAEKMAN-DANHEUX, T. I. MARTIN, AND D. B. MACLEAN
Department of Chemistry, McMaster University, Hamilton, Ontario

Received January 5, 1972

A new alkaloid, nupharolutine, ($C_{15}H_{23}NO_2$) has been isolated from the basic extract of the rhizomes of *Nuphar luteum*. By spectroscopic and chemical methods it is shown to be a hydroxy derivative of deoxynupharidine. The mass spectra of the new base and several isomers are reported.

Un nouvel alcaloïde, la nupharolutine ($C_{15}H_{23}NO_2$) a été isolé à partir des extraits basiques de rhizomes du *Nuphar luteum*. Au moyen de méthodes spectroscopiques et chimiques il a été montré qu'il s'agit d'un dérivé hydroxylé de la désoxynupharidine. Les spectres de masse de cette nouvelle bas et de plusieurs isomères sont rapportés.

Canadian Journal of Chemistry, **50**, 1831 (1972)

Several structural types have so far been identified among the alkaloids of *Nuphar* species (1, and references cited therein) exemplified by deoxynupharidine (**1**), nuphamine (**2**), and neothiobinupharidine (**3**). Whereas deoxynupharidine and its relatives have a quinolizidine system, nuphamine and its structural analogues are piperidine derivatives formally derived by fission of the N—C_6 bond of **1**. Neothiobinupharidine and other C_{30} alkaloids have two deoxynupharidine units joined through carbon and sulfur linkages as illustrated. All of the *Nuphar* alkaloids are characterized by the presence of one or more furan rings in their structure and are apparently terpenoid in origin.

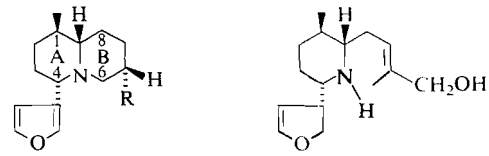

1 Deoxynupharidine, R = CH_3 **2** Nuphamine
5 Nupharidine = *N*-oxide of **1**
6 Castoramine, R = CH_2OH

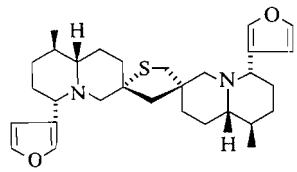

3 Neothiobinupharidine

During the examination of the alkaloids of *N. luteum* a new base (**4**) was isolated to which the trivial name, nupharolutine, has been assigned. Its composition ($C_{15}H_{23}NO_2$), determined by elemental analysis and high resolution mass spectrometry, is identical with that of nupharidine (**5**) (1) and castoramine (**6**) (2, 3). On comparison of the properties of **4** with those of **5** and **6** it is evident that nupharolutine is isomeric with both of the known alkaloids. Only small quantities of **4** were isolated and therefore it was necessary to rely mainly on physical methods in the study of its structure.

The i.r. spectrum of **4** in carbon tetrachloride shows the presence of bonded and non-bonded hydroxyl absorption. The former shifts upon dilution indicating that the hydrogen bonding is intermolecular. The i.r. spectrum also shows the presence of Bohlmann bands (4) suggesting the presence of a *trans*-quinolizidine system similar to that known to be present in deoxynupharidine. Attempts to acetylate the new alkaloid with acetic anhydride–pyridine at 20° for 24 h or at 100° for 2 h led only to the recovery of starting material indicating that the hydroxyl function was tertiary.

The 100 MHz p.m.r. spectrum of **4** was similar to that of deoxynupharidine (5) but there was one major difference. Deoxynupharidine shows two doublets attributed to $>CHCH_3$ groups centered at 0.89 and 1.01 δ while the new alkaloid has a doublet centered at 0.92 and a singlet (3H)

Can. J. Chem. Downloaded from www.nrcresearchpress.com by 210.87.254.105 on 09/05/12
For personal use only.

Can. J. Chem. Downloaded from www.nrcresearchpress.com by 210.87.254.105 on 09/05/12
For personal use only.

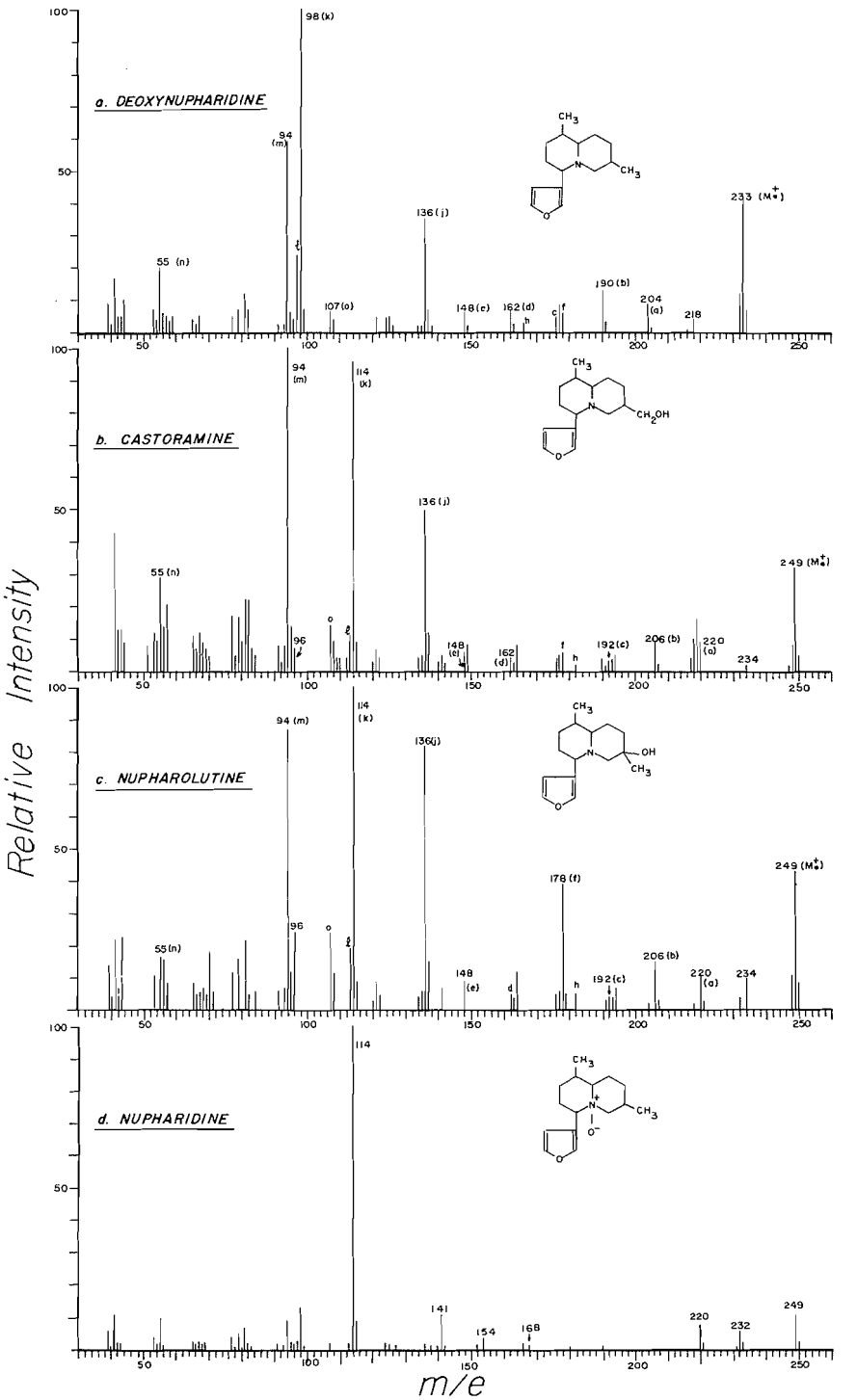

FIG. 1. The mass spectra of (*a*) deoxynupharidine; (*b*) castoramine; (*c*) nupharolutine, and (*d*) nupharidine.

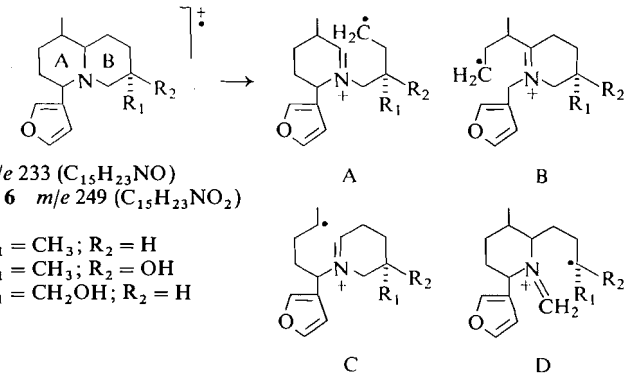

1 *m/e* 233 ($C_{15}H_{23}NO$)
4 and **6** *m/e* 249 ($C_{15}H_{23}NO_2$)

1 $R_1 = CH_3$; $R_2 = H$
4 $R_1 = CH_3$; $R_2 = OH$
6 $R_1 = CH_2OH$; $R_2 = H$

SCHEME 1

at 1.21 δ. The singlet nature of this peak and its chemical shift are compatible with the grouping

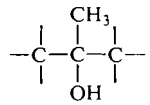

in the molecule. The presence of a tertiary hydroxyl function was deduced also from the acetylation studies. Like deoxynupharidine the spectrum of **4** has signals attributed to three protons in a furan ring at 7.22 (2H, α-protons) and 6.34 δ (1H, β-protons). A poorly resolved quartet of area one centered at 3.03 δ ($J = 8.3$ and 6.0 Hz) resembles a similar signal in the spectrum of deoxynupharidine attributed to C_4H (axial), the proton α to nitrogen and α to the furan ring, which is reported to appear at 2.88 δ ($J = 8.0$ and 6.2 Hz). A doublet of doublets (1H) centered at 2.67 δ ($J = 11.0$ and 2.0 Hz) is assigned by analogy with the spectrum of deoxynupharidine to C_6H_α (equatorial). In **1** this signal appeared as a quartet centered at 2.70 δ ($J = 12.5$ and 2.5 Hz). The remaining protons are present as a complex multiplet between 1.0 and 2.0 δ.

These data suggested that nupharolutine has one of the following structures:

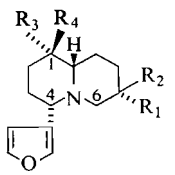

4(*i*) $R_1 + R_2 = CH_3 + OH$
$R_3 + R_4 = CH_3 + H$
4(*ii*) $R_1 + R_2 = CH_3 + H$
$R_3 + R_4 = CH_3 + OH$

To resolve the structural problem we resorted to mass spectrometry. The spectrum of **4** was recorded and compared with that of deoxynupharidine, nupharidine, and castoramine. From the spectra shown in Fig. 1, it is obvious that the spectrum of **4** resembles those of **1** and **6** but is distinctly different from that of **5**. An interpretation of the spectra follows.

The mass spectrum of deoxynupharidine was first reported in 1964 (6). Our spectrum is identical with that reported earlier showing intense peaks at *m/e* 233 (M^+) and at *m/e* 136, 98, and 94. High resolution studies have enabled us to confirm the composition assigned to the intense ions in the original work and to determine the composition of less intense ions, thereby gaining further insight into the fragmentation process. In all cases measured masses agreed with the calculated values within ± 3 milli mass units.

There are four positions β to nitrogen in **1** that may undergo fission to yield the molecular ions designated A, B, C, and D in Scheme 1. Of these C and D should be more stable than the others and they are used to explain the subsequent fragmentation of the molecule. Thus the homologous ions shown in Scheme 2 at *m/e* 204 (*a*), 190 (*b*), and 176 (*c*) are considered to form from **1**C by the loss of the hydrocarbon fragments, C_2H_5, C_3H_7, and C_4H_9, respectively, processes accompanied by hydrogen rearrangement and the ions *m/e* 162 (*d*) and 148 (*e*) through retro Diels–Alder loss of propylene from *m/e* 204 and 190, respectively. The ion at *m/e* 178 (*f* or *g*) may arise from **1**D or **1**C, respectively, by the processes shown in Scheme

Can. J. Chem. Downloaded from www.nrcresearchpress.com by 210.87.254.105 on 09/05/12
For personal use only.

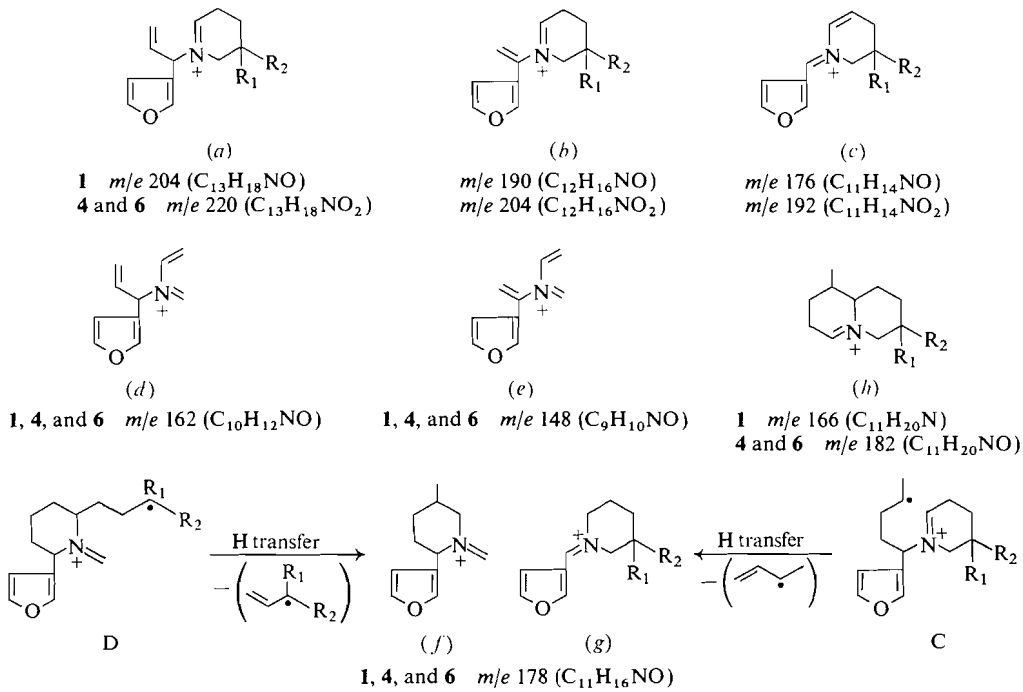

SCHEME 2

2 but the former is favored (compare with the spectrum of castoramine below). An ion at *m/e* 166 (*h*) has the composition $C_{11}H_{20}N$ and must be formed by cleavage of the furan ring as illustrated in Scheme 2.

The major ions in the spectrum of **1** appear at *m/e* 136 (*j*), 98 (*k*), 97 (*l*), 94 (*m*) and 55 (*n*) and a less intense but significant ion at *m/e* 107 (*o*). In Scheme 3 a proposal for their derivation is outlined. Their compositions have been established and all may be considered to arise from the molecular ion **1**C. Recent labelling studies are in harmony with the structure proposed for *m/e* 98 (7). In fragmentation by route 3*a* the charge is retained on the furan-containing fragment to give the ion at *m/e* 136 (*j*), and in route 3*b* on the nitrogen-containing fragment to give *m/e* 97 (*l*), which by a retro Diels–Alder process (route 3*c*) leads to *m/e* 55 (*n*). When fragmentation proceeds with hydrogen transfer as in route 3*d* the ion at *m/e* 98 (*k*) results. (Hydrogen transfer from C-2 is shown but there is no evidence that the hydrogen actually arises from this site.) The further fragmentation of *m/e* 136 via processes 3*e* and 3*f*, leads to the ions at *m/e* 107 (*o*) and 94 (*m*), respectively.

Analysis of the spectrum of castoramine shows that it fragments in a manner analogous to deoxynupharidine. Thus ions *a*, *b*, *c*, and *h* of Scheme 2 contain one oxygen more than those derived from **1** but are deemed to have the same carbon framework. The ions *d* and *e* are the same in **6** as in **1** and the ion at *m/e* 178 has the composition $C_{11}H_{16}NO$ and can be represented as *f*. Of the ions of Scheme 3, *j*, (*m/e* 136) *m*, (*m/e* 94) *n*, (*m/e* 55), and *o* (*m/e* 107) are identical in composition in both **1** and **6** but *k* and *l* appearing at *m/e* 114 and 113, respectively are shifted upwards by 16 mass units in **6** from their position in **1** reflecting the presence of the OH group.

Recent work of ours (8) on the spectra of neothiobinupharidine (**3**) and related systems shows that the dimeric compounds have many ions in their spectra whose formation may be interpreted through the schemes suggested here. The fact that the fragmentation of **1** and **6** and many of the fragmentations of **3** may be interpreted through Schemes 2 and 3 lends credibility to them.

The hydroxyl group present in **6** leads to new ions in its spectrum not present in the spectrum

Can. J. Chem. Downloaded from www.nrcresearchpress.com by 210.87.254.105 on 09/05/12
For personal use only.

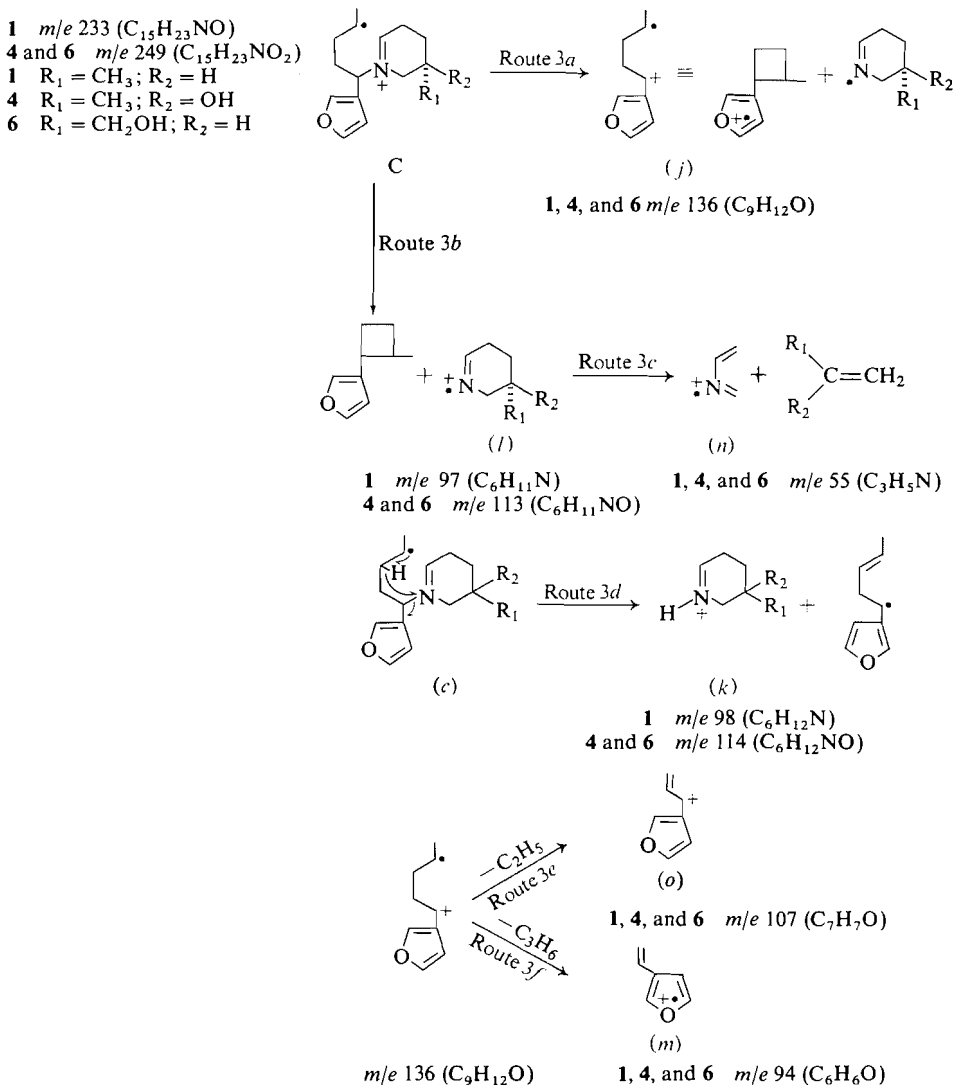

SCHEME 3

of **1**. Thus a strong ion at *m/e* 96 can be ascribed to **6***k*—H_2O and an ion at *m/e* 164 to **6***h*—H_2O and the ions at *m/e* 218 and 219 to loss of CH_2O and CH_2OH from the molecule as shown in Scheme 4. The spectrum of nupharolutine **4** has many features in common with that of castoramine but it is distinctly different from that of nupharidine. There seems little doubt, therefore, that nupharolutine must have an OH group in ring B and may be represented as **4**(*i*).

The differences between the spectra of **4** and **6** are compatible with the structural differences. Thus the loss of CH_3 and OH would be predicted to be favored more in **4** than in **6** as would the formation of ion *f*. The spectra bear this out. It is interesting to note that the loss of H_2O from *m/e* 114 to form *m/e* 96 is more pronounced in **4**, the tertiary alcohol, than it is in **6**, the primary alcohol.

The spectrum of nupharidine (**5**) is discussed briefly below. Like other *N*-oxides it suffers loss of oxygen and OH with peaks at *m/e* 232 and 231 (9). The peak at *m/e* 220 results not from loss of an ethyl fragment but from loss of CHO, a frag-

Can. J. Chem. Downloaded from www.nrcresearchpress.com by 210.87.254.105 on 09/05/12
For personal use only.

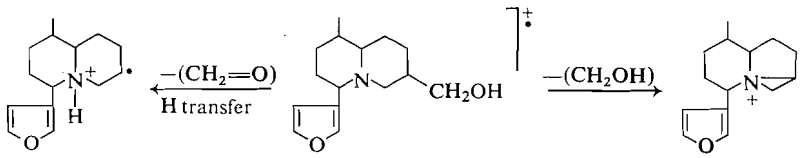

SCHEME 4

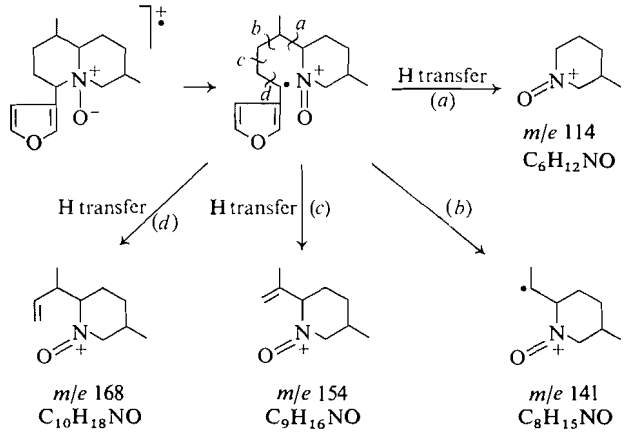

SCHEME 5

mentation characteristic of furans (10). In Scheme 5 proposals are put forward for the derivation of the major ion at *m/e* 114 and related fragments, based upon a determination of their compositions by high resolution studies.

The spectroscopic and other evidence presented points to structure **4**(*iii*) $R_1 + R_2 = CH_3 + H$ below for nupharolutine. The Bohlmann bands in the i.r. point to a *trans*-quinolizidine system and since the tertiary hydroxyl is not internally hydrogen bonded it must occupy the equatorial position at C-7. The p.m.r. evidence discussed earlier points to an equatorial position for the furan ring. The coupling of C_6H_α in **4** requires comment since it is almost identical with the corresponding proton in **1** where the two couplings were explained on the basis of a large geminal coupling and a smaller coupling to C_7H_β. A geminal coupling is still possible and present in **4** but the smaller coupling must be a "w" type (11) coupling with the equatorial proton at C-8 since C-7 is quaternary. The only structural feature remaining unsolved is the configuration of methyl at C-1 and although the p.m.r. evidence suggests that it is the same as in **1** it is not convincing. Accordingly we set out to convert **4** to **1**. Treatment of **4** with $POCl_3$–pyridine gave a chloro compound **7**,

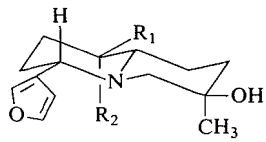

4(iii)

separated from the reaction mixture by t.l.c., which was reduced over Pt to a substance identical with **1** by t.l.c. and on two g.l.c. columns. Thus nupharolutine must be **4**(*iii*), $R_1 = CH_3$, $R_2 = H$. A spectroscopic comparison was not possible because of a lack of material.

The mass spectrum of **7**, determined at low resolution is worthy of comment. It shows the intense ions observed at *m/e* 136, 107, and 94 in **1**, **4**, and **6**. Ion *k*, Scheme 3, appears as an isotopic doublet at *m/e* 132 and 134 which, through loss of HCl, leads to an ion at *m/e* 96 also observed in the spectra of **4** and **6**. Aside from the isotopic molecular ions at *m/e* 267 and 269 the only intense ion in the high mass region appears at *m/e* 232 (M^+—Cl).

Experimental

Apparatus, Methods and Materials

Mass spectra were determined on a C.E.C. 21-110B double-focusing mass spectrometer. Samples were intro-

Can. J. Chem. Downloaded from www.nrcresearchpress.com by 210.87.254.105 on 09/05/12
For personal use only.

Can. J. Chem. Downloaded from www.nrcresearchpress.com by 210.87.254.105 on 09/05/12
For personal use only.

duced through a direct inlet system. Spectra are plotted in terms of relative abundance, with the most intense peak (base peak) taken as 100%. Only those peaks with an intensity equal to or greater than 3% of the most intense peak have been recorded.

The high resolution mass spectra (h.r.m.s.) were recorded on Ilford Q-2 photographic plates, which were developed in the usual manner. The spectra were then recorded on magnetic tape, using a Gaertner comparator-densitometer linked to a Datex system. They were processed on a CDC-6400 computer using a modified version of the HIRES program of Tunnicliff and Wadsworth (12).

The 100 MHz spectra were recorded using the frequency sweep mode of a Varian HA-100 spectrometer. Samples were dissolved in $CDCl_3$ using added TMS as the internal locking signal. Chemical shifts were measured relative to TMS using a V4315 frequency counter incorporated in the instrument. Double irradiation was achieved by employing a Hewlett–Packard 201C audiogenerator at the desired frequency.

A Perkin–Elmer 337 grating i.r. spectrometer was used to record i.r. spectra.

Melting points were determined on a Kofler hot stage and are uncorrected.

Isolation of Nupharolutine

The crude bases derived from the rhizomes of *N. luteum* harvested in Poland were adsorbed on a column of alumina (activity III) and eluted successively with benzene, ether, chloroform, and methanol.[1] The methanol fraction was subjected to a 50 transfer counter current distribution using 1-butanol and a citrate–phosphate buffer (p*H* 4). Fractions 20–35 were combined, the basic fraction recovered, and subjected to chromatography on silica gel with $CHCl_3$: acetone = 1:1. The middle fractions were collected and combined. The crystalline residue obtained on removal of solvent was recrystallized from methanol–acetone, m.p. 96–98°; $[\alpha]_D^{22°}$ ($CHCl_3$) −105°.

Anal. Calcd. for $C_{15}H_{23}NO_2$ (mol. wt. 249.173): C, 72.3; H, 9.3; N, 5.6. Found (249.173 (h.r.m.s.)): C, 72.4; H, 9.5; N, 5.9.

Preparation of 7-Chlorodeoxynupharidine

Nupharolutine (10 mg) was treated with 1 ml of a solution of $POCl_3$ in dry pyridine (1:4) and the mixture allowed to stand at 0° for 24 h with occasional shaking. The resultant light brown solution was added to ice water (5 ml), basified by addition of 1 *M* NaOH, and extracted with CH_2Cl_2 (4 × 10 ml). The extract was dried over anhydrous sodium sulfate and then taken to dryness under reduced pressure. The residue was separated into two components (R_f = 0.60 and 0.45) on a t.l.c. plate (0.5 mm, silica gel) using benzene–acetone = 3:1 as developer. The major component (R_f = 0.60) was recovered by extraction of the silica gel with methylene chloride; yield 3.7 mg. The mass spectrum of this product showed isotopic molecular ions at 267 and 269 in approximate ratio, 3:1.

Reduction of 7-Chlorodeoxynupharidine

The chloro compound prepared above (3.4 mg) was dissolved in absolute ethanol (10 ml) and to the solution 50 mg of solid KOH and 25 mg of 30% Pd on $CaCO_3$ were added and the whole was shaken with hydrogen at 45 p.s.i.g. for 30 min. The reduction mixture was neutralized with ethanolic HCl, the catalyst separated by filtration, and washed with CH_2Cl_2. The ethanolic and methylene chloride solutions were combined and evaporated to dryness under reduced pressure. The residue was separated by t.l.c. (silica gel, 0.5 mm) into a major component (R_f = 0.25) and a minor component (R_f = 0.45) with $CHCl_3$–acetone = 5:4. The band, R_f = 0.25, was removed from the plate and extracted with CH_2Cl_2 yielding 2 mg of colorless product which had the same R_f value on t.l.c. as an authentic sample of deoxynupharidine. The mass spectrum was identical with that of deoxynupharidine and this product had the same retention time on g.l.c. on two different columns as authentic deoxynupharidine. The g.l.c. columns used were (*a*) 5% SE 30 on 60/80 Chromosorb W (5 ft × 1/8 in. column, 175°, 35 p.s.i.g. He), and (*b*) 20% DEGS on 60/80 Chromosorb W (5 ft × 1/8 in. column, 180°, 35 p.s.i.g. He).

This work was supported at McMaster University through a grant from the National Research Council of Canada. We thank Professor Z. Valenta for a sample of castoramine hydrochloride. One of us, C. Braekman-Danheux, wishes to thank the Canada Council for the award of a fellowship.

[1]Full details of the separation procedure will be published elsewhere.

1. J. T. WROBEL. Alkaloids, **9**, 441 (1967).
2. Z. VALENTA and A. KHALEQUE. Tetrahedron Lett. **12**, 1 (1959).
3. F. BOHLMANN, E. WINTERFIELD, H. LAURENT, and W. UDE. Tetrahedron, **19**, 195 (1963).
4. F. BOHLMANN. Chem. Ber. **91**, 2157 (1958).
5. C. F. WONG, E. AUER, and R. T. LALONDE. J. Org. Chem. **35**, 517 (1970).
6. O. ACHMATOWICZ, H. BANASEK, G. SPITELLER, and J. T. WROBEL. Tetrahedron Lett. 927 (1964).
7. R. T. LALONDE, C. F. WONG, and W. P. CULLEN. Tetrahedron Lett. 4477 (1970).
8. J. T. WROBEL, A. IWANOW, J. SZYCHOWSKI, J. POPLAWSKI, C. K. YU, T. I. MARTIN, and D. B. MACLEAN. Can. J. Chem. This issue.
9. R. GRIGG and B. G. ODELL. J. Chem. Soc. B, 218 (1966).
10. H. BUDZIKIEWICZ, C. DJERASSI, and D. H. WILLIAMS. Mass spectrometry of organic compounds. Holden-Day Inc., San Francisco, 1967. p. 615.
11. S. STERNHELL. Quart. Rev. **23**, 259 (1969).
12. D. D. TUNNICLIFF and P. A. WADSWORTH. Anal. Chem. **40**, 1826 (1968).

Relative Rate of Reaction of $O(^1D_2)$ with N_2O [1]

G. PARASKEVOPOULOS, V. B. SYMONDS,[2] AND R. J. CVETANOVIĆ

Division of Chemistry, National Research Council of Canada, Ottawa, Canada K1A 0R9

The rate of reaction of $O(^1D_2)$ with N_2O relative to the rate of its reaction with neopentane has been determined by a competitive method. The value obtained, $k_{N_2O}/k_{neop.} = 0.145 \pm 0.010$, is in good agreement with several values in the literature. It is also found that N_2O does not deactivate $O(^1D_2)$ to $O(^3P)$ but reacts with it to form products.

La vitesse de réaction de $O(^1D_2)$ avec N_2O par rapport à la vitesse de sa réaction avec le néopentane a été déterminée par une méthode compétitive. La valeur obtenue, $k_{N_2O}/k_{neop.} = 0.145 \pm 0.010$, est en bon accord avec plusieurs valeurs de la littérature. Il a également été trouvé que N_2O ne désactive pas $O(^1D_2)$ en $O(^3P)$ mais qu'il réagit avec $O(^1D_2)$ pour former des produits.

Canadian Journal of Chemistry, **50**, 1838 (1972)

Can. J. Chem. Downloaded from www.nrcresearchpress.com by 210.87.254.40 on 09/05/12
For personal use only.

Introduction

The photolysis of N_2O at 1850–2300 Å gives electronically excited oxygen atoms, mainly in the $O(^1D_2)$ state (1). At 2139 Å, in particular, reaction 1 is the only primary process (1, 2).

[1] $$N_2O + h\nu \rightarrow N_2 + O(^1D)$$

The $O(^1D)$ atoms can react further with N_2O to give O_2, N_2, and NO

[2a] $$O(^1D) + N_2O \rightarrow N_2 + O_2$$

[2b] $$\rightarrow 2NO$$

Although the value of the ratio k_{2a}/k_{2b} has been subject to some controversy (3, 4) (discordant values of 0.6 and 1.0 have been reported), Preston and co-workers (4) have recently established by three different experimental techniques that $k_{2a}/k_{2b} = 1.0$.

The photolysis of N_2O has been used extensively in this and other laboratories for the production of $O(^1D)$ atoms. Moreover, the yield of N_2 from reaction 2*a* has also been used for the measurement of relative rates of $O(^1D)$ reactions in experiments in which various added gases compete with N_2O for $O(^1D)$ (5, 6). However, the published values of the rate of reaction of $O(^1D)$ with N_2O (5–13), usually expressed relative to the rate of the $O(^1D)$ reaction with CO_2, differ by a factor of about 2. As a result of this large uncertainty, comparison of the relative values obtained by the N_2O technique with other measurements of relative rates of $O(^1D)$ atoms is difficult and uncertain. Further determinations of k_{N_2O}, using independent techniques, are therefore necessary.

In the present work a relative rate of the N_2O reaction was obtained in competitive experiments with neopentane. This technique is based on the measurements of the decrease in the yield of neopentanol, the main product of the reaction of $O(^1D)$ with neopentane, when other gases compete with neopentane for $O(^1D)$. The technique, described in detail elsewhere (2), has been used successfully in this laboratory to measure relative rates for a number of $O(^1D)$ reactions (2, 6, 14). The relative value of k_{N_2O} now obtained permits interconversion and thus direct comparison of the $O(^1D)$ rates expressed relative to N_2O with the rates expressed relative to neopentane and vice versa.

The neopentane technique also permits direct identification and measurement of any $O(^3P)$ formed during the reaction (2). In the case of N_2O it is thus possible to distinguish between the chemical reaction steps (2*a* and 2*b*) and the electronic deactivation step (2*c*),

[2c] $$O(^1D) + N_2O \rightarrow O(^3P) + N_2O$$

Although previous work (3, 4) has indicated that reaction 2*c* is not important, the more direct test for $O(^3P)$ atoms by the neopentane technique (2) has been applied in the present work and a very low upper limit for potential occurrence of reaction 2*c* has been established. This information was necessary since it appears from recent

[1] NRCC No. 12559.

[2] Summer student 1971.

Can. J. Chem. Downloaded from www.nrcresearchpress.com by 210.87.254.40 on 09/05/12
For personal use only.

literature (15) that there is still some confusion[3] in this respect.

Experimental

The $O(^1D)$ atoms were formed by photolysis of N_2O with the 2139 Å zinc resonance line. The light was provided by two 93106 E Philips zinc lamps and was focused by two Ultrasil lenses. The cylindrical photolysis cell had a volume of 195.6 ml and suprasil quartz windows 5 cm in diameter.

The N_2 generated in reactions 1 and 2*a* was measured in every experiment by gas–solid chromatography on a 18 ft 13X Molecular Sieve column. Neopentanol was separated from the unreacted reactants and measured on a 300 ft long, 0.015 in. i.d. stainless steel capillary column coated with β,β'-thiodipropionitrile and equipped with a flame ionization detector. The vacuum systems used and the experimental and analytical techniques have been described elsewhere (16). In the present experiments a solid nitrogen trap (−220 °C), capable of trapping NO, was added before the Toepler pump. Neopentane and N_2O were of the same grade and purified in the same manner as described before (17).

Results and Discussion

The experiments were made at 25 ± 2 °C and at about 240 Torr, *i.e.* above the pressure at which the neopentanol is essentially completely stabilized (17). The ratio of neopentane/N_2O was varied from about 0.05 to about 1.

The following reaction scheme represents the main features of the reaction of $O(^1D)$ produced by photolysis of N_2O with N_2O and neopentane

$$[1] \quad N_2O + h\nu \xrightarrow{2139\ \text{Å}} N_2 + O(^1D)$$

$$[2a] \quad O(^1D) + N_2O \longrightarrow N_2 + O_2$$

$$[2b] \quad \longrightarrow 2NO$$

$$[2c] \quad \longrightarrow O(^3P) + N_2O$$

$$[3] \quad O(^1D) + RH \longrightarrow \alpha ROH + (1-\alpha)(R^{\cdot} + OH)$$

where RH and ROH are neopentane and neopentanol, respectively, α is the fraction of the $O(^1D)$ atoms interacting with neopentane which form neopentanol.

It has been shown in detail previously (6) that, when the extent of reaction is small, molecular oxygen does not affect the neopentanol yield from reaction 3 in any way other than by competing with neopentane for the $O(^1D)$. Under the conditions of the present experiments the neopentanol yield was entirely unaffected by the small amount of O_2 produced in reaction 2*a*. On the other hand the NO produced in reaction 2*b* was found to affect the yield of N_2. It is well known (18, 19) that NO reacts with alkyl radicals to form alkyl nitroso compounds which then react further with NO. In the presence of excess NO, alkyl radicals catalyze disproportionation of NO to N_2 and NO_2 according to the following stoichiometric equation

$$[4] \quad 4NO(+R) \rightarrow N_2 + 2NO_2(+R)$$

It has been shown by Christie and co-workers (19) that one free alkyl radical can lead to the disproportionation of several hundred molecules of NO and that at low concentrations of nitrosoalkanes the reaction of alkyl radicals with NO_2 is the important chain breaking step. In the present system neopentyl radicals, formed to the extent of about 25% of the $O(^1D)$ (17), are expected to catalyze the disproportionation of NO (18). It is also possible that NO_2 may react with neopentanol although it is more likely that it will be consumed in reactions with neopentyl radicals. Since the yields of N_2 and neopentanol are the experimental parameters used in the calculation of the relative rate, a number of experiments were made to establish the role of NO in the present system, *i.e.*, how NO affects the ratio neopentanol/N_2. In these experiments a mixture of neopentane/N_2O at a ratio of ≈4 was photolyzed in the absence and presence of NO. At this ratio practically all the $O(^1D)$ formed reacts with neopentane (17). The results are given in Table 1 and are plotted in Fig. 1.

In the absence of NO the N_2 yield is equivalent to the $O(^1D)$ produced in reaction 1. The average value of α = neopentanol/N_2 = 0.63, given in the first row of Table 1, agrees well with previous determinations (2, 17). When NO is added, the neopentanol/N_2 ratio decreases and it may be seen in Fig. 1 that the decrease is linear. The NO reacted was also measured in these experiments and the N_2 produced in reaction 4 may be calculated from the measured total N_2, the neopentanol yield and the value of neopentanol/N_2 when no NO is added (*i.e.* 0.63). The values of (NO reacted)/(N_2 produced in

[3]Bradley *et al.* (15) have assumed in a recent publication that reaction 2*c* is efficient and quote a paper by Preston and Cvetanović (8) in support of this assumption. However, in this latter paper (8) reference is clearly made to the *total* reaction of $O(^1D)$ with N_2O, *i.e.* to reactions 2*a*, 2*b*, and 2*c* combined, and *not* to deactivation (reaction 2*c*) separately. In fact, with the technique used by Preston and Cvetanović (8) it was not possible to distinguish between steps 2*a*, 2*b*, and 2*c*.

TABLE 1. Effect of the addition of NO on the ratio of neopentanol/N_2

Neopentane / N_2O	Total N_2 (μmol)	NO added		Neopentanol / N_2	NO reacted (μmol)	NO (reacted) / N_2 (produced in reaction 4)
		Torr	μmol			
4.18*	2.3–5.8*	none		0.633*	—	—
4.17	3.98	0.57	5.95	0.540	2.39	4.19
5.44	3.46	1.19	12.44	0.520	2.65	4.17
4.04	4.19	1.88	19.75	0.400	5.85	3.89
						Average = 4.08

*Average of four experiments.

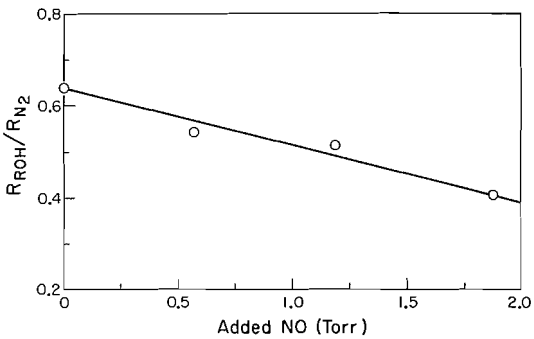

FIG. 1. Change of R_{ROH}/R_{N_2} with added NO.

reaction 4), calculated in this manner, are given in the last column of Table 1. The average value of 4.1 agrees very well with the reported (18, 19) stoichiometry of reaction 4. These results also suggest that in these experiments neopentanol is not consumed in reactions with NO_2, which is probably removed in reactions with neopentyl radicals.

If reaction 4 is neglected for the moment and taking[4] $k_{2a} = k_{2b}$ (4), the usual steady state assumption for $O(^1D)$, applied to reactions 1, 2*a*, 2*b*, and 3, leads to the following expression

$$\text{apparent}\ \frac{k_2}{k_3} = \frac{2}{3}\left(\alpha\frac{R_{N_2}}{R_{ROH}} - 1\right)\frac{[RH]}{[N_2O]}$$

where R_{N_2} is the rate of production of N_2 and R_{ROH} is the rate of production of neopentanol, R_{N_2}/R_{ROH} is the ratio of the yields of N_2 and neopentanol, and $\alpha = 0.633$ (see first row of Table 1). The ratio k_2/k_3 is called apparent because it is not expected to be constant, since reaction 4 has been neglected, but to decrease

[4]As was mentioned in the introduction, it has been established recently that $k_{2a}/k_{2b} = 1$ (4). However, if the previously reported (3) value of $k_{2a}/k_{2b} = 0.59$ is used, our results are increased only by about 10%.

TABLE 2. Values of the apparent k_2/k_3 from the photolysis of various mixtures of neopentane and N_2O at 2139 Å

Neopentane (Torr)	N_2O (Torr)	N_2 (μmol)	N_2 / Neopentanol	Apparent k_2/k_3
117	112	2.15	1.90	0.141
116	155	5.97	2.14	0.177
66.7	166	2.80	2.41	0.141
54.5	164	1.93	2.88	0.182
41.3	189	2.42	3.48	0.175
32.7	200	2.69	4.64	0.212
26.4	205	2.70	5.04	0.188
23.0	196	1.96	6.08	0.223
20.3	231	4.98	8.66	0.263
14.0	205	2.56	10.32	0.252
14.0	217	2.04	10.57	0.247
11.7	209	2.70	14.59	0.307
10.7	211	2.52	14.24	0.272
10.1	205	2.31	18.05	0.342

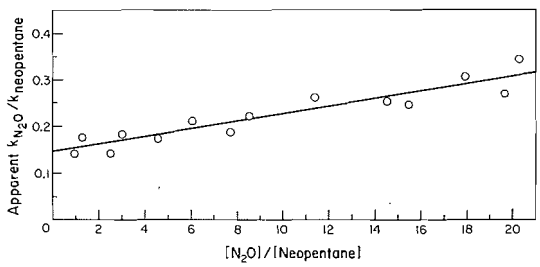

FIG. 2. Plot of the apparent $k_{N_2O}/k_{neopentanol}$ against $[N_2O]/[neopentane]$.

linearly with decreasing N_2O/neopentane, *i.e.*, with decreasing production of NO in accordance with the results presented in Table 1 and Fig. 1. The values obtained for the apparent k_2/k_3 are given in Table 2 and are plotted against N_2O/neopentane in Fig. 2. It may be seen that indeed the apparent k_2/k_3 decreases linearly with decreasing N_2O/neopentane. The intercept of the straight line at zero N_2O/neopentane, *i.e.*, zero NO production, should give the true value of

Can. J. Chem. Downloaded from www.nrcresearchpress.com by 210.87.254.40 on 09/05/12
For personal use only.

Can. J. Chem. Downloaded from www.nrcresearchpress.com by 210.87.254.40 on 09/05/12
For personal use only.

TABLE 3. Test for the formation of $O(^3P)$ atoms in the reaction $O(^1D) + N_2O$

Compound	Amount
N_2O	742 Torr
1-Butene	1.17 Torr
N_2 formed	4.00 μmol
$O(^1D)$	2.67 μmol*

Rate of product formation (per $O(^1D)$)

Product	Rate
1,2-Butene oxide	0.012
n-Butyraldehyde	0.008
Methylethyl ketone	Trace

*The total $O(^1D)$ generated, taken as $O(^1D) = N_2/1.5$ (for $k_{2a}/k_{2b} = 1$, the quantum yield of N_2 in the photolysis of N_2O is 1.5).

k_2/k_3. The least square value of the intercept is $k_2/k_3 = 0.145 \pm 0.010$. The error quoted is the standard deviation.

The possibility of deactivation of $O(^1D)$ to $O(^3P)$ by N_2O was examined in an experiment in which about 1 atm of N_2O was photolyzed in the presence of about 1 Torr of 1-butene, and the characteristic products of the addition of $O(^3P)$ to 1-butene (1,2-butene oxide, *n*-butyraldehyde, and methylethyl ketone) were measured as described in detail elsewhere (2). The results are given in Table 3, and it may be seen that the total amount of $O(^3P)$ characteristic products is about 2% of the $O(^1D)$ reacted.[5] This places an upper limit of 2% on the fraction of $O(^3P)$ in the system. The same limit of about 2% has been found with all the gases that react but do not deactivate $O(^1D)$, (*i.e.* H_2, CH_4, *iso*-C_4H_{10}, *neo*-C_5H_{12}, and H_2O) (2, 14, 16), and with those that apparently do not interact at all with $O(^1D)$ (*i.e.* SF_6 and He) (2). In the previous work (2, 14) N_2O and neopentane have always been present together with the other gas and it was not possible to distinguish between the reactions that may form $O(^3P)$. The present result tentatively suggests that the small amount of $O(^3P)$ may perhaps be formed in all cases in the initial photolysis of N_2O by the spin-forbidden reaction 1*a*.

$$[1a] \qquad N_2O + h\nu \xrightarrow{2139\ \text{Å}} N_2 + O(^3P)$$

However, the data are not sufficiently accurate and reaction 1*a* may be considered as merely a possibility.

The relative rates from this and other determinations are listed in Table 4. All the rates in this table are expressed relative to CO_2. For the present value use was made of the rate of CO_2 relative to that of neopentane determined previously by the same technique (2). It appears from the table that the lower value for k_{N_2O}/k_{CO_2} is favored by the greater number of determinations. If we ignore the last five values in the table, the first five values give an average $k_{N_2O}/k_{CO_2} = 1.15 \pm 0.04$ which is an excellent agreement in

TABLE 4. Comparison of the relative rates of the $O(^1D) + N_2O$ reaction determined by different techniques with $O(^1D)$ from different sources

Source of $O(^1D)$*	$\frac{k_{N_2O}}{k_{CO_2}}$	Reference
Photolysis of N_2O (2139 Å)	1.15	This work
Photolysis of NO_2 (2288 Å)	1.24	6
Photolysis of NO_2 (2288 Å)	1.11†	8†
Photolysis of N_2O (2139 Å) and O_3 (3132 Å)	1.10	12
Photolysis of O_3 (2537 Å)	1.14	11
Photolysis of O_2 (1470 Å)	0.76	10
Photolysis of O_2 (1470 Å)	0.98†	9†
Flash photolysis of O_3 (continuum > 2100 Å)	1.84	5
Photolysis of N_2O (1849 Å)	1.6‡	7‡
Flash photolysis of N_2O (1750–2200 Å)	1.6	13

*It should be noted that in addition to the sources of $O(^1D)$ used, the techniques by which $O(^1D)$ atoms were monitored are also of interest. These include a variety of physical and chemical methods identifying and measuring products of the reactions of $O(^1D)$. For details on these techniques the individual references should be consulted.

†The data of refs. 8 and 9 corrected for the more recent value (4) $k_{2a}/k_{2b} = 1.0$.

‡The value of 1.6 quoted here is obtained from the data in ref. 7 assuming free exchange of ^{18}O with NO formed in reaction 2*b*. In ref. 7 the value of 1.6 was tentatively ascribed only to k_{2a}/k_{CO_2} by neglecting the ^{18}O exchange with NO. In ref. 8 a value of 2.4 was indirectly inferred for $(k_{2a} + k_{2b})/k_{CO_2}$ from the same data, again without allowance for ^{18}O exchange with NO. The present value takes this exchange into account and therefore supersedes both these earlier values (7, 8).

[5]The possibility that the small yields of the characteristic products were not formed by addition of $O(^3P)$ to 1-butene but in another process was considered. These products may be formed to some extent in the presence of O_2, alkyl radicals, and 1-butene (6). Small amounts of O_2 are formed in reaction 2*a*, and it is possible although not very likely that minute amounts of alkyl radicals may be formed by photolysis of 1-butene. (Absorption of the 2139 Å light by 1-butene is very small (20) and in the present experiment the ratio N_2O/1-butene has been about 650.) In a separate experiment 1.2 Torr of butene and 0.3 Torr of O_2 were irradiated with light of 2139 Å under conditions exactly the same as those of the experiment in Table 3. No 1,2-butene oxide and *n*-butyraldehyde were detectable in the mixture.

view of the diverse experimental techniques used and the errors involved in them. If all the values in Table 4 are taken, the mean $k_{N_2O}/k_{CO_2} = 1.25 \pm 0.25$.

1. K. F. PRESTON and R. F. BARR. J. Chem. Phys. **54**, 3347 (1971).
2. G. PARASKEVOPOULOS and R. J. CVETANOVIĆ. J. Am. Chem. Soc. **91**, 7572 (1969).
3. R. I. GREENBERG and J. HEICKLEN. Int. J. Chem. Kinet. **2**, 185 (1970).
4. P. M. SCOTT, K. F. PRESTON, R. J. ANDERSEN, and L. M. QUICK. Can. J. Chem. **49**, 1808 (1971).
5. P. M. SCOTT and R. J. CVETANOVIĆ. J. Chem. Phys. **54**, 1440 (1971).
6. G. PARASKEVOPOULOS, K. F. PRESTON, and R. J. CVETANOVIĆ. J. Chem. Phys. **54**, 3907 (1971).
7. H. YAMAZAKI and R. J. CVETANOVIĆ. J. Chem. Phys. **40**, 582 (1964).
8. K. F. PRESTON and R. J. CVETANOVIĆ. J. Chem. Phys. **45**, 2888 (1966).
9. P. WARNECK and J. O. SULLIVAN. Ber. Bunsenges. Phys. Chem. **72**, 159 (1968).
10. R. A. YOUNG, G. BLACK, and T. G. SLANGER. J. Chem. Phys. **49**, 4758 (1968).
11. W. B. DEMORE. J. Chem. Phys. **52**, 4309 (1970).
12. H. YAMAZAKI. Can. J. Chem. **48**, 3269 (1970).
13. R. J. DONOVAN, D. HUSAIN and L. J. KIRSCH. Chem. Phys. Lett. **6**, 488 (1970).
14. G. PARASKEVOPOULOS and R. J. CVETANOVIĆ. Chem. Phys. Lett. **9**, 603 (1971).
15. J. N. BRADLEY, A. D. EDWARDS and J. R. GILBERT. J. Chem. Soc. 326 (1971).
16. G. PARASKEVOPOULOS and R. J. CVETANOVIĆ. J. Chem. Phys. **50**, 590 (1969).
17. G. PARASKEVOPOULOS and R. J. CVETANOVIĆ. J. Chem. Phys. **52**, 5821 (1970).
18. O. P. STRAUSZ and H. E. GUNNING. Can. J. Chem. **41**, 1207 (1963).
19. M. I. CHRISTIE, C. GILLBERT and M. A. VOISEY. J. Chem. Soc. 3147 (1964).
20. Ultraviolet Spectral Data, American Petroleum Institute, Research Project 44.

Can. J. Chem. Downloaded from www.nrcresearchpress.com by 210.87.254.40 on 09/05/12
For personal use only.

The Synthesis and Structural Studies of some Dialkyltin(IV) Salts of Strong Monobasic Acids

T. H. TAN, J. R. DALZIEL, P. A. YEATS, J. R. SAMS, R. C. THOMPSON, AND F. AUBKE[1]

Department of Chemistry, The University of British Columbia, Vancouver 8, British Columbia

Received September 28, 1971

A number of dialkyltin(IV)-bisfluorosulfates, -bistrifluoromethanesulfonates, and -bisdifluorophosphates are synthesized by solvolysis of dialkyltin(IV) chlorides in an excess of the corresponding acid according to $R_2SnCl_2 + 2HX \xrightarrow{25\ ^\circ C} R_2SnX_2 + 2HCl$; R = CH_3, C_2H_5, *n*-C_3H_7, *n*-C_4H_9, and *n*-C_8H_{17}; X = SO_3F, SO_3CF_3, and PO_2F_2. The structural proposals, hexacoordination for tin with the alkyl groups in *trans*-octahedral position and bidentate bridging anionic groups with coordination through oxygen, are based on ^{119}Sn Mössbauer, infrared and, where obtainable, Raman spectra. The vibrational spectra of the difluorophosphates are discussed in detail. Variations in isomer shift and quadrupole splitting values with different alkyl groups in all three groups of compounds follow the same regular pattern as in the series R_2SnF_2. The results of point charge calculations are reported.

Un certain nombre de bisfluorosulfates, bistrifluorométhanesulfonates et bisdifluorophosphates de dialkyl-étain(IV) a été synthétisé par solvolyse des chlorures de dialkyl-étain(IV) dans un excès correspondant d'acide selon: $R_2SnCl_2 + 2HX \xrightarrow{25\ ^\circ C} R_2SnX_2 + 2HCl$; R = CH_3, C_2H_5, *n*-C_3H_7, *n*-C_4H_5, et *n*-C_8H_{17}; X = SO_3F, SO_3CF_3, et PO_2F_2. Les propositions de structure, c'est-à-dire hexacoordination pour l'étain avec les groupes alkyles dans une position octaédrale *trans* et les groupes anioniques formant un pont bidentique se coordinant par l'oxygène, sont basées sur les spectres infrarouge, Mössbauer de ^{119}Sn et Raman lorsque cela était possible. Le spectre vibrationnel des difluorophosphates est discuté en détail. Les variations dues au changement d'isomère et les valeurs des multiplicités quadrupolaires avec divers groupes alkyles dans les trois séries de composés, suivent le même schéma régulier que dans les séries R_2SnF_2. Les résultats de calculs de charge ponctuelle sont rapportés.

Canadian Journal of Chemistry, **50**, 1843 (1972)

Introduction

The solvolysis of methyltin(IV)–chlorine compounds of the type $(CH_3)_nSnCl_{4-n}$ with *n* ranging from 1 to 4, in strong protonic acids such as HSO_3F (1–3), HSO_3CF_3 (1–4) and anhydrous HF (5) has been found recently to be a simple and convenient synthetic route to either binary tin(IV) compounds of the type $(CH_3)_nSnX_{4-n}$ or ternary derivatives of the type $(CH_3)_nSnCl_mX_{4-(n+m)}$, with X = SO_3F, SO_3CF_3 or F and *n* or *m* = 1, 2, or 3. A systematic study in these solvents has revealed that with the acid in moderate excess, disubstitution occurs at room temperature under evolution of CH_4 and/or HCl with preferential cleavage of the tin–chlorine over the tin–carbon bond. Consequently dimethyltin(IV) derivatives can be synthesized in three different ways as shown below:

$$\left.\begin{matrix}(CH_3)_4Sn\\(CH_3)_3SnCl\\(CH_3)_2SnCl_2\end{matrix}\right\} + 2HX \rightarrow (CH_3)_2SnX_2 + \left\{\begin{matrix}2CH_4\\CH_4 + HCl\\2HCl\end{matrix}\right.$$

with X = SO_3F, SO_3CF_3 or F.

As evidenced by infrared, Raman and ^{119}Sn Mössbauer spectra (1, 3, 5), a common structural type is found for all three dimethyltin(IV) derivatives. In sheet type polymers, the central tin atom has achieved hexacoordination, with the two methyl groups in *trans*-octahedral positions and the X groups acting as bidentate bridging ligands. These conclusions were in agreement with X-ray diffraction studies of $(CH_3)_2SnF_2$ (6) and $(CH_3)_2Sn(SO_3F)_2$ (7). The reported ^{119}Sn Mössbauer data (1, 3) for both $(CH_3)_2Sn(SO_3F)_2$ and $(CH_3)_2Sn(SO_3CF_3)_2$ are rather unusual, both the isomer shifts (~1.8 mm/s) and the quadrupole splittings (~5.5 mm/s) being the largest values yet reported for organotin(IV) derivatives. The vibrational spectra allowed assignments of fundamentals for bidentate bridging fluorosulfate and trifluoromethanesulfonate.

It became interesting to extend our work in two directions: (*a*) the use of other organyltin(IV) chlorides, primarily of the type R_2SnCl_2 as solutes, and, (*b*) the use of difluorophosphoric acid, HPO_2F_2, as solvent, in order to get some idea about the limitations of the synthetic route.

[1]To whom correspondence should be addressed.

Can. J. Chem. Downloaded from www.nrcresearchpress.com by 210.87.254.105 on 09/05/12
For personal use only.

Can. J. Chem. Downloaded from www.nrcresearchpress.com by 210.87.254.105 on 09/05/12
For personal use only.

The expected compounds of the type R_2SnX_2 with $X = SO_3F$, SO_3CF_3, F, and PO_2F_2 are of structural interest. Vibrational spectra of difluorophosphates have only been reported for simple ionic salts $M^IPO_2F_2$, with M^I = Li, Na, K, Rb, Cs, or NH_4 (8). The fact that the SO_3F and the PO_2F_2 groups are isoelectronic leads one to expect some structural similarity for the diorganyltin(IV) compounds. Vibrational assignment for this group should be feasible.

A comparison of all vibrational spectra should allow for the oxyacid derivatives the detection of structural changes within a given series by using the fundamental frequencies of the anionic group as criteria.

For isostructural compounds, all trends of the ^{119}Sn Mössbauer parameters in a series of compounds should reflect primarily changes in the electron distribution around tin as affected by the change in R. A number of comparative studies for diorganyltin(IV) derivatives of the type R_2SnY_2, with Y as a polyatomic anionic group were reported previously. These include diorganotin(IV) thiocyanides (9), cyanates (10), and oxinates (11–13); however, no clear pattern seems to emerge, which at least in part is due to the different molecular structures suggested for the three anionic groups. The thiocyanates appear to show *trans*-octahedral coordination for tin (9), the oxinates are *cis*-octahedral complexes (11–16), and for the cyanates a distorted tetrahedral configuration was proposed (10). Of the dialkyltin(IV) halides only the fluorides can be safely included, since the *trans*-octahedral configuration for tin is present (5, 6). We have recently reported Mössbauer data for the series R_2SnF_2, with R = CH_3, C_2H_5, *n*-C_3H_7, *n*-C_4H_9, and *n*-C_8H_{17} (5).

Experimental

I. Chemicals

Technical grade fluorosulfuric acid (Baker and Adamson) was doubly distilled under atmospheric pressure as described before (17). Trifluoromethane sulfonic acid was obtained from $Ba(SO_3CF_3)_2$ (3M Company) and sulfuric acid with subsequent purification by a reduced pressure distillation. Difluorophosphoric acid (Ozark-Mahoning Chemical Company) was purified by repeated distillations at reduced pressure (10 cm of mercury) in a Pyrex system as reported previously (8).

The dialkyltin(IV) chlorides $(CH_3)_2SnCl_2$, $(C_2H_5)_2SnCl_2$, $(n\text{-}C_3H_7)_2SnCl_2$, $(n\text{-}C_4H_7)_2SnCl_2$, and $(n\text{-}C_8H_{17})_2SnCl_2$ were all obtained from Alfa Inorganic Chemicals. Their purity was checked by melting points. Purification was carried out by vacuum sublimation or by recrystallization from petroleum ether where necessary. Freon 11, $CFCl_3$, was dried over Linde's Molecular sieve.

II. Instrumentation

Infrared spectra were recorded on a Perkin–Elmer 457 grating spectrophotometer. Silver chloride, cesium iodide, and KRS-5 windows (all from Harshaw Chemicals) were used either with Nujol or without any mulling agent.

Raman spectra on the solid samples were obtained with a Cary 81 spectrometer, equipped with a model 125 He–Ne gas laser (Spectra Physics Corp.). The 6328 Å wavelength line was used as exciting light. The samples were contained in 5 mm o.d. Pyrex tubes with flat bottoms.

The Mössbauer spectrometer has been described before in detail (18). Measurements were made with the absorber either at 80 or 298 °K and the Ba $^{119m}SnO_3$ source at 298 °K. All isomer shifts are reported relative to SnO_2 absorber at 80 °K. The confidence limit for both isomer shifts and quadrupole splittings is judged to be ± 0.03 mm/s.

All manipulations of solid materials were carried out in a Vacuum Atmosphere Corp. "Dri-Lab" model no. He-43-2 filled with purified dry nitrogen and equipped with "Dri-Train" model no. HE-93B.

III. Preparations

All preparations were carried out in about 100 ml two-part reaction flasks, fitted with Teflon coated magnetic stirring bars and Teflon stem stopcocks (Fisher and Porter). In all instances a small excess of the acid was added to a known amount of substrate either at atmospheric pressure (HSO_3F), reduced pressure (HPO_2F_2), or by transfer in an inert atmosphere box, resulting in instantaneous HCl evolution. In order to avoid side reactions and subsequently dark-colored substances, about 20–25 ml $CFCl_3$ were added to the reactions of the *n*-propyl and *n*-butyl compounds with the sulfonic acids.

After removal of all volatile products under vacuum and at room temperature, the dialkyltin(IV) salts were isolated as rather high-melting white crystalline solids. The remaining traces of acids were removed by prolonged pumping at slightly elevated temperatures (50–60 °C). All reactions were followed by weight. The obtained products were handled inside the dry box.

The previously reported (19) compounds $(CH_3)_2Sn(PO_2H_2)_2$ and $(CH_3)_2Sn(PO_2H(C_6H_5))_2$ were synthesized from aqueous solution as described.

Compounds of the type R_2SnF_2 were obtained from the solvolysis of the corresponding chlorides in aqueous HF solution. Details are described elsewhere (5).

IV. Analytical Results

All products were identified by C and H microanalysis, performed by Borda of this department. The results together with the melting or decomposition points are listed in Table 1.

More detailed analysis was carried out for $(CH_3)_2Sn(SO_3F)_2$ (3), $(CH_3)_2Sn(SO_3CH_3)_2$ (3), and $(n\text{-}C_3H_7)Sn(PO_2F_2)_2$ by Alfred Bernhardt, Microanalytical Laboratory, Elbach, West Germany. The results for the latter compound are listed below.

Anal. Calcd. for $(n\text{-}C_3H_7)_2Sn(PO_2F_2)_2$: P, 15.23; F, 18.68. Found: P, 15.36; F, 18.68.

TABLE 1. Analytical data for the series R_2SnX_2 with R = CH_3, C_2H_5, n-C_3H_7, n-C_4H_9, and n-C_8H_{17} and X = SO_3F, SO_3CF_3, and PO_2F_2

	Compound	Melting point* (°C)	Analysis (%) C Calculated	C Found	H Calculated	H Found
1	$(C_2H_5)_2Sn(SO_3F)_2$	249 (d)	12.81	12.69	2.69	2.84
2	$(n\text{-}C_3H_7)_2Sn(SO_3F)_2$	215 (d)	17.89	17.59	3.47	3.65
3	$(n\text{-}C_4H_9)_2Sn(SO_3F)_2$	198 (d)	22.28	22.13	4.22	4.49
4	$(C_2H_5)_2Sn(SO_3CF_3)_2$	330 (d)	15.17	14.86	2.13	2.40
5	$(n\text{-}C_3H_7)_2Sn(SO_3CF_3)_2$	318 (d)	19.10	18.14	2.81	3.06
6	$(n\text{-}C_4H_9)_2Sn(SO_3CF_3)_2$	250 (d)	22.62	21.95	3.42	3.71
7	$(CH_3)_2Sn(PO_2F_2)_2$	204 (d)	6.85	6.93	1.72	2.62
8	$(C_2H_5)_2Sn(PO_2F_2)_2$	262 (d)	12.68	12.53	2.66	2.71
9	$(n\text{-}C_3H_7)_2Sn(PO_2F_2)_2$	245 (d)	17.71	17.64	3.47	3.44
10	$(n\text{-}C_4H_9)_2Sn(PO_2F_2)_2$	235 (d)	22.09	22.09	4.17	4.05
11	$(n\text{-}C_8H_{17})_2Sn(PO_2F_2)_2$	114	35.12	35.42	6.26	6.25

*(d) denotes decomposition.

Results

The new dialkyltin(IV) salts are easily obtained by solvolysis of the corresponding dialkyltin(IV) dichlorides in the acids HSO_3F, HSO_3CF_3, and HPO_2F_2. All are moderately hygroscopic white solids, showing decomposition points generally higher than 200 °C.

Infrared spectra for all compounds were obtained in the region 4000–250 cm^{-1}. However, the discussion will be restricted to the region of 2000–250 cm^{-1}, and to the $R_2Sn(PO_2F_2)_2$ compounds only. Raman spectra on solid samples could be obtained only for the methyl derivatives and even here not all expected vibrational modes could be found.

The vibrational frequencies found for the dialkyltin(IV) bisdifluorophosphates are listed in Table 2 together with the frequencies for KPO_2F_2 (8) and a suggested assignment for the PO_2F_2 group in these compounds.

Well resolved ^{119}Sn Mössbauer spectra could be obtained for all compounds at 80 °K and for some also at room temperature. An example is shown in Fig. 1. The observed isomer shift, quadrupole splitting, and line-width values are listed in Table 3 together with data for some related compounds, *e.g.*, for the series R_2SnF_2 (5).

Discussion

I. Synthesis

As the results indicate, solvolysis proceeds readily for all three monobasic acids according to the general scheme: $R_2SnCl_2 + 2HX \xrightarrow{25\ °C} R_2SnX_2 + 2HCl$ for R = CH_3, C_2H_5, n-C_3H_7, and n-C_4H_9, and X = SO_3F, SO_3CF_3, and PO_2F_2 under cleavage only of the tin–chlorine bonds. It appears that the reactions in HPO_2F_2 proceed slightly more slowly than in the two sulfuric acids. On the other hand discolorations and slightly brownish products are more readily formed in HSO_3F and HSO_3CF_3, necessitating the use of $CFCl_3$ as a dilutant. The fact that only in HPO_2F_2 a n-octyltin(IV) salt could be obtained indicates that side reactions appear to decrease in the weaker acid. Whereas in HSO_3F and HSO_3CF_3 it is possible to form the corresponding dimethyltin(IV) salts also from $(CH_3)_3SnCl$ with the acid in a slight excess (1, 3) indicating the cleavage of both an Sn—Cl and Sn—C bond, the analogous reaction in HPO_2F_2 does not proceed. Neither HCl nor CH_4 evolution could be noted at room temperature. It appears HPO_2F_2 is less capable of cleaving Sn—C bonds than the stronger sulfonic acids, thus reducing the chances for side reactions as mentioned above. The behavior of $(CH_3)_3SnCl$ in HPO_2F_2 is reminiscent of the solvolysis of this substrate in some carboxylic acids (20) where no reaction is noted at room temperature but cleavage of one Sn—C bond occurs at about 100 °C.

Attempts to extend the reaction to other solutes such as divinyl-, dibenzyl-, and diphenyltin(IV) dichloride failed for all three acids. Extensive side reactions and the formation of

Can. J. Chem. Downloaded from www.nrcresearchpress.com by 210.87.254.105 on 09/05/12
For personal use only.

TABLE 2. Vibrational spectra of dialkyltin bisdifluorophosphates $R_2Sn(PO_2F_2)_2$ and KPO_2F_2 (cm^{-1})*

KPO_2F_2			$R = CH_3$		Infrared			
Infrared	Raman	Assignment	Infrared	Raman	$R = C_2H_5$	$R = n\text{-}C_3H_7$	$R = n\text{-}C_4H_9$	$R = n\text{-}C_8H_{17}$
			1298sh					
						1424w	1425w	1422vw
					1370sh	1370sh	1356vw	1370sh
					1330sh	1330sh	1290w	1290sh
					1300sh			1278sh
1310s	1314w	$\nu_{as}PO_2(B_1)\nu_6$	1258s		1267s	1270s	1260s	1258s
					1235vw	1207w	1200vw	1227vw
						1184w	1180w	1220vw
			1218w	1230w				
					1210w	1162sh		
1148s	1144s	$\nu_sPO_2(A_1)\nu_1$	1168s	1169m	1158s	1158s	1157s	1175s
			1128sh		1128sh	1080s	1089m	1150s
			1050vw		1027m	1027sh	1053vw	1138sh
			1018vw		1007vw	1010s	1033m	1113sh
					978m			1047w
								1027w
								987w
850s	—	$\nu_{as}PF_2(B_2)\nu_8$	928s	927w	926s	918s	920s	922s
832s	825s	$\nu_sPF_2(A_1)\nu_2$	888s	887m	886s	885s	884s	882s
			858vw					851w
								830w
							772vw	770w
			808s			812m		
					725w	738sh	752vw	737sh
					700m	725w		720m
					670vw	694s	723w	693s
			740vw			670sh	693s	670vw
			725vw					
								645w
		$\nu_{as}SnC_2$	603m			638m	644w	584w
		ν_sSnC_2		535s		600vw		
	518m	PO_2 bend $(A_1)\nu_3$	540m		560w	536m	533m	532m
503s		rocking $(B_1)\nu_7$	506m		510sh	517m	501w	502w
495s	503w	rocking $(B_2)\nu_9$	485s		493s	490s	484s	487s
—	356w	PF_2 bend $(A_1)\nu_4$	350m		350w	350w	—	350w

*s = strong, m = medium, w = weak, sh = shoulder, v = very; ν_s = symmetric stretch, ν_{as} = asymmetric stretch.

black-brown products were observed. Microanalysis indicated the additional cleavage of Sn—C bonds in these reactions. This is not totally unexpected and was observed also in anhydrous hydrogen fluoride (5). An empirical series relating to the ease of cleavage of the Sn—C bond in tetraorganyltin(IV) compounds (21) suggests the order: phenyl > benzyl > vinyl > methyl > ethyl > propyl > butyl > hexyl > octyl. Assuming the correctness of this order, it appears that preferential cleavage of the Sn—Cl bonds in solutes of the type R_2SnCl_2 is found for methyl and the higher homologues C_nH_{2n+1} but not for the more labile C_2H_3-, $C_6H_5CH_2$-, and C_6H_5-derivatives.

II. Vibrational Spectra

Since the vibrational frequencies for a number of methyltin(IV) fluorosulfates and trifluoromethanesulfonates have been assigned and discussed extensively elsewhere (1–3), this part will be concerned primarily with the interpretation of the infrared spectra for the dialkyltin(IV) difluorophosphates. Infrared spectra of compounds in the series $R_2Sn(SO_3X)_2$ with R = C_2H_5, n-C_3H_7, and n-C_4H_9 and X = F and CF_3 are found to agree quite well with the spectra of the methyl compounds in respect to the SO_3X vibrations.

As pointed out before the SO_3F^- and the $PO_2F_2^-$ ions are isoelectronic but the free ions

Can. J. Chem. Downloaded from www.nrcresearchpress.com by 210.87.254.105 on 09/05/12
For personal use only.

TABLE 3. ^{119}Sn Mössbauer data of R_2SnX_2-type compounds at 80 °K*

No.	Compound	δ (mm/s)	Δ (mm/s)	Γ (mm/s)		$R = \Sigma^{298}/\Sigma^{80}$
1	$(CH_3)_2Sn(SO_3F)_2$†	1.82	5.54			0.09
2	$(C_2H_5)_2Sn(SO_3F)_2$	1.94	5.32	1.05	1.05	§
3	$(n\text{-}C_3H_7)_2Sn(SO_3F)_2$	1.98	5.35	0.93	0.94	0.07
4	$(n\text{-}C_4H_9)_2Sn(SO_3F)_2$	1.97	5.42	0.91	1.01	0.11
5	$(CH_3)_2Sn(SO_3CF_3)_2$†	1.79	5.51			0.13
6	$(C_2H_5)_2Sn(SO_3CF_3)_2$	2.01	5.47	0.87	1.07	§
7	$(n\text{-}C_3H_7)_2Sn(SO_3CF_3)_2$	1.94	5.29	0.94	1.04	weak
8	$(n\text{-}C_4H_9)_2Sn(SO_3CF_3)_2$	1.96	5.40	0.91	1.01	weak
9	$(CH_3)_2Sn(PO_2F_2)_2$	1.53	5.13	0.90	0.92	0.05
10	$(C_2H_5)_2Sn(PO_2F_2)_2$	1.67	4.91	1.10	1.10	weak
11	$(n\text{-}C_3H_7)_2Sn(PO_2F_2)_2$	1.64	5.00	0.97	0.95	§
12	$(n\text{-}C_4H_9)_2Sn(PO_2F_2)_2$	1.67	5.03	1.04	1.06	§
13	$(n\text{-}C_8H_{17})_2Sn(PO_2F_2)_2$	1.62	4.79	1.01	1.26	§
14	$(CH_3)_2Sn(PO_2H_2)_2$	1.23	4.34	0.93	1.03	0.19
15	$(CH_3)_2Sn(PO_2H(C_6H_5))_2$	1.14	4.30	1.01	1.02	0.09
16	$(CH_3)_2SnF_2$‡	1.23	4.52	1.08	1.20	0.45
17	$(C_2H_5)_2SnF_2$‡	1.40	4.43	1.21	1.19	0.37
18	$(n\text{-}C_3H_7)_2SnF_2$‡	1.38	4.40	1.07	1.07	0.21
19	$(n\text{-}C_4H_9)_2SnF_2$‡	1.42	4.48	1.05	1.12	0.16
20	$(n\text{-}C_8H_{17})_2SnF_2$‡	1.42	4.50	1.17	1.19	0.32

*δ = Isomer shift rel. to SnO_2; Δ = quadrupole splitting; Γ = linewidth at half peak height; R = room temperature effect; Σ^T = magnitude of the Mössbauer effect at temperature T.
†Reference 1.
‡Reference 5.
§Not observed.

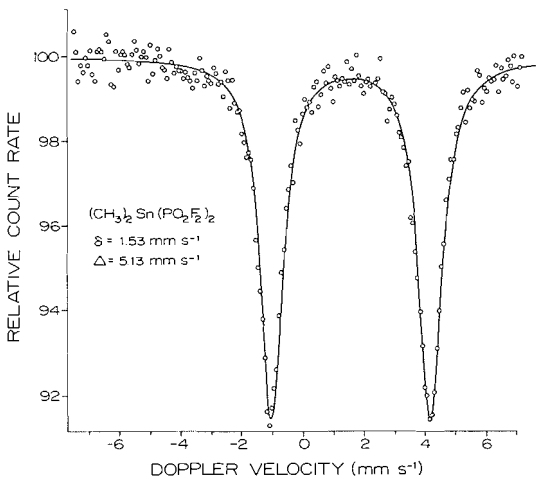

FIG. 1. An example of ^{119}Sn Mössbauer spectra.

have different symmetry: C_{3v} for SO_3F^- and C_{2v} for $PO_2F_2^-$ (22). For a bidentate bridging group the symmetry for the SO_3F group will be reduced to C_s whereas the PO_2F_2 group still retains C_{2v} symmetry, provided bridging occurs through oxygen in both instances. Following the assignment for bridging SO_3F groups (2), frequency shifts for the bridging PO_2F_2 groups are expected, notably in the stretching frequency region.

The nine expected modes (approximately described as PO_2 and PF_2 symmetric and asymmetric stretches, PO_2 and PF_2 bending, two POF rocking modes, and a torsion mode) have all been observed before except for the last one, which belongs to the group A_2 and should occur only in the Raman spectrum. Buehler and Bues (23) suggest an assignment of a Raman band in molten KPO_2F_2 at 300 °C as $\nu_5(A)_2$ found at 365 cm^{-1}, whereas the reported infrared spectra of all alkali difluorophosphates (8) suggest that $\delta PF_2(A_1)$ occurs in the same region. Since only one band is observed in the Raman spectrum at 360 cm^{-1}, it is impossible to make an unambiguous assignment for the missing torsion mode.

As can be seen from Table 2, assignment of the remaining eight fundamentals is possible for all $R_2Sn(PO_2F_2)_2$. Internal modes of the R groups are identified by comparison with the infrared spectra for the corresponding R_2SnCl_2 compounds. No attempt is made to interpret these modes in detail. The following features are interesting: (*a*) only one type of PO_2F_2 group seems to be present in the *n*-alkyltin(IV) bisdi-

Can. J. Chem. Downloaded from www.nrcresearchpress.com by 210.87.254.105 on 09/05/12
For personal use only.

Can. J. Chem. Downloaded from www.nrcresearchpress.com by 210.87.254.105 on 09/05/12
For personal use only.

fluorophosphates; (*b*) the narrow range for each fundamental within the series indicates the PO_2F_2 is relatively unaffected by the increasing size of R; and (*c*) positional changes have occurred when compared to the ionic $PO_2F_2^-$ in KPO_2F_2. This point merits further comment. It appears that in particular the stretching modes are affected to a different degree. As found for the corresponding fluorosulfates, the symmetric and asymmetric P—F (S—F) stretching modes are found at higher frequencies. Of the P—O stretching modes, the asymmetric one is lowered by about 40–50 cm^{-1} whereas the symmetric mode is slightly raised, resulting in a weak net lowering for the average P—O stretch throughout the series.

Since most certainly coordination through oxygen occurs, the expected lowering of νPO_{ave} can be explained partly by charge withdrawal from the P—O into the Sn—O bond region. Similar effects are observed for organyltin(IV) carboxylates (24) affecting here $\nu C{=}O$. However, back donation from lone electron pairs on oxygen and fluorine towards phosphorus can compensate the charge withdrawal at least partially, and can account for the observed increase in the P—F stretching frequency. A suitable model involving the empty 3d orbitals on phosphorus and sulfur has been introduced by Cruickshank (25).

Further structural information is obtained from the tin–carbon stretching modes for dimethyltin(IV) bisdifluorophosphate. The asymmetric Sn—C stretch at 603 cm^{-1} is found only in the infrared spectrum, and νSn—C sym at 535 cm^{-1} is found in the Raman spectrum only as a strong band. Similar band positions are found for $(CH_3)_2Sn(SO_3F)_2$ (1, 3), $(CH_3)_2Sn(SO_3CF_3)_2$ (1, 3), and $(CH_3)_2SnF_2$ (26). As for all these compounds, the validity of the mutual exclusion rule for $(CH_3)_2Sn(PO_2F_2)_2$ means that the molecule has a center of symmetry with the carbon–tin–carbon group in a linear or nearly linear arrangement.

The structural model most consistent with our observations is identical to the ones observed or suggested for the dimethyltin(IV) sulfonates (3, 7) and for $(CH_3)_2SnF_2$ (6): hexacoordination for tin with the methyl groups in *trans*-octahedral positions and the PO_2F_2 groups acting as bidentate bridging ligands, thus resulting in chain, or more likely, sheet-like polymers.

A monomeric model with bidentate chelating PO_2F_2 groups can not be ruled out on the basis of the vibrational spectra, but the observed high melting points and insolubility in non-polar solvents seem to favor a polymeric structure.

TABLE 4. Measured and calculated quadrupole splittings for some dialkyltin(IV) compounds

Compound	Δ^* (mm s^{-1}) Observed	Predicted
$(C_2H_5)_2Sn(SO_3CF_3)_2$	5.47	+5.36
$(n\text{-}C_3H_7)_2Sn(SO_3CF_3)_2$	5.29	+5.32
$(n\text{-}C_4H_9)_2Sn(SO_3CF_3)_2$	5.42	+5.48
$(C_2H_5)_2Sn(PO_2F_2)_2$	4.91	+4.98
$(n\text{-}C_3H_7)_2Sn(PO_2F_2)_2$	5.00	+4.94
$(n\text{-}C_4H_9)_2Sn(PO_2F_2)_2$	5.03	+5.10
$(C_2H_5)_2SnF_2$	4.43	+4.37
$(n\text{-}C_3H_7)_2SnF_2$	4.40	+4.33
$(n\text{-}C_4H_9)_2SnF_2$	4.48	+4.49

*All values assume axial symmetry. The sign is the sign of the quadrupole coupling constant, eQV_{zz}.

III. ^{119}*Sn Mössbauer Spectra*

The Mössbauer data listed in Table 4 support the general conclusion derived earlier that no structural change within any of the three series of oxyacid derivatives has occurred, when substituting CH_3 by C_2H_5, $n\text{-}C_3H_7$ and $n\text{-}C_4H_9$. This is not unexpected, since structural changes such as the breakdown of a polymeric structure and a change in the coordination number of tin caused by steric crowding will be more evident for triorganotin(IV) derivatives (9, 27, 28) where the C—Sn—C bond angles are expected to be between 109.5° and 120°.

For all compounds discussed here, a *trans*-octahedral coordination is evident from the quadrupole splitting values. For a distorted tetrahedral or *cis*-octahedral configuration, much smaller Δ values would be observed. Although the probable upper limits of Δ for the latter geometries are open to question (27, 29), the largest value yet recorded for a supposedly tetrahedral organotin(IV) compound is 3.06 mm s^{-1} (30) and *cis*-octahedral species show $\Delta < \sim 2.4$ mm s^{-1} (11). The expected bond angle for *trans*-octahedrally coordinated tin of 180° makes steric crowding less likely.

The oxyacid derivatives show at best only a weak room temperature resonance absorption, indicating stronger dependence of the recoilless fraction on temperature than is observed in many other organyltin(IV) polymers, *e.g.*,

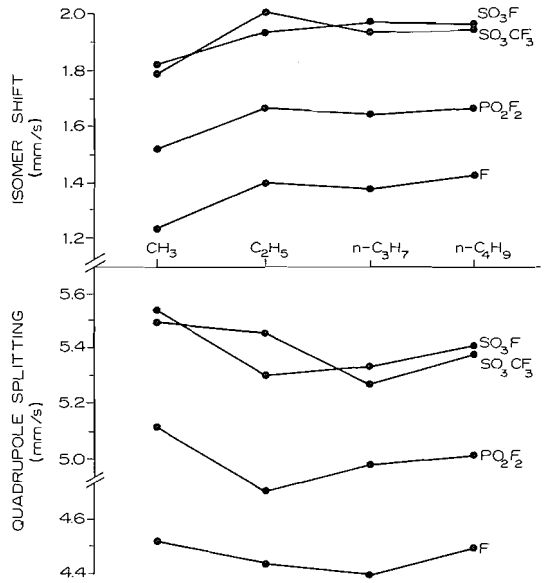

FIG. 2. Comparison of Mössbauer parameters of dialkyltin(IV) difluorides, bisdifluorophosphates, bisfluorosulfates, and bistrifluoromethylsulfonates.

$(CH_3)_2SnF_2$. (Since no effort was made to control carefully the absorber thickness, the R values in Table 4 are of semi-quantitative significance only.) There can be little question, however, that all the compounds are associated in the solid state and are essentially isostructural with $(CH_3)_2Sn(SO_3F)_2$ (7) and $(CH_3)_2SnF_2$ (6). It is of interest that whereas $(CH_3)_2SnF_2$ shows a strong anisotropy of the recoilless fraction (Gol'danskii–Karyagin effect) (31), no appreciable integral asymmetry of the quadrupole doublet lines was observed for any of the oxyacid derivatives. As illustrated by Fig. 2, the observed ^{119}Sn Mössbauer parameters show three rather interesting trends for both the dialkyltin(IV)oxyacid salts and the fluorides: (*1*) The numerical values for both δ and Δ decrease in the following order: $R_2Sn(SO_3F)_2 \approx R_2Sn(SO_3CF_3)_2 > R_2Sn(PO_2F_2) > R_2SnF_2$ for compounds with identical R; (*2*) The isomers shift values (δ) are found to increase from R = CH_3— to C_2H_5— and then stay relatively constant for R = n-C_3H_7— and n-C_4H_9— within each series; (*3*) The quadrupole splitting values (Δ) decrease from CH_3— to C_2H_5— within each series and again remain relatively constant for R = n-C_3H_7— and n-C_4H_9— even though here the pattern seems less regular than the one observed for δ.

The discussion will center mainly around these three points.

To explain the uncommonly high values of δ and Δ in $(CH_3)_2Sn(SO_3F)_2$ and $(CH_3)_2Sn(SO_3CF_3)_2$, we have proposed (3) a model involving essentially linear $(CH_3)_2Sn^{2+}$ cations interacting covalently with the SO_3X^- anions via rather weak polar 3-center–4-electron bonds, utilizing the p_x and p_y orbitals on tin.[2] This model, consistent with the results of the X-ray structure determination of $(CH_3)_2Sn(SO_3F)_2$ (7), and KSO_3F (22), is extensively discussed elsewhere (3) together with the effect on δ and Δ.

The decrease in both Mössbauer parameters in the series R_2SnX_2 with $X = PO_2F_2$, SO_3F, SO_3CF_3, and F, appears to be parallel to the decrease in acid strength of the parent acid, at least for the oxyacids. From conductivity studies in various protonic acids (32–34) the order $HSO_3F \approx HSO_3CF_3 > HPO_2F_2$ emerges, but for anhydrous HF while being a weaker acid than the two sulfuric acids, the position in respect to HPO_2F_2 is uncertain (34). It must be assumed that in $(CH_3)_2SnF_2$ appreciable charge density will remain in $5p_x$ and $5p_y$ on tin because F is monoatomic and electronic charge cannot be dissipated to the same extent that is possible for the oxyacid salts.

Substitution of CH_3— by C_2H_5— results as noted in increased isomer shifts. The observed value for $(C_2H_5)_2Sn(SO_3CF_3)_2$ is the highest reported value for any organotin(IV) derivatives (35), with the possible exception of some organotin(IV) transition metal compounds. Since no significant structural changes seem to occur, this increase can only be due to a decrease in electronegativities from CH_3 to C_2H_5. Reported values of group electronegativities (36) (CH_3 = 2.30 and C_2H_5 = 2.01) support this assumption, and other isostructural pairs of CH_3 and C_2H_5 organotin compounds show the same trend (35, 37). Since no significant change in δ occurs when going from C_2H_5 to n-C_3H_7 and n-C_4H_9 one can assume that the group electronegativities for these two groups will not be very different from the value for C_2H_5; however, no numerical values seem to be reported (36).

Whereas the trend in δ values within each series is therefore expected and certainly not unprecedented, the trend in Δ is somewhat

[2]The z-axis is assumed to coincide with the C—Sn—C bond axis.

Can. J. Chem. Downloaded from www.nrcresearchpress.com by 210.87.254.105 on 09/05/12
For personal use only.

surprising. According to the bonding model presented here, increased electron donation into the $5sp_z$ hybrid orbital should also result in an even greater asymmetry of the electronic charge distribution between p_z and the pair p_x, p_y, thus increasing Δ. Moreover, the decrease in Taft's inductive constants, σ^* (38) from CH_3— to C_2H_5— leads one also to expect larger Δ values. From the observed trend for all four groups, it must be concluded that some of the additional electronic charge will go into the p_x and p_y orbitals on tin as well, thereby reducing the charge asymmetry. Previously reported Δ values for pairs of dimethyl- and diethyltin(IV) (or dibutyltin(IV) compounds, where far more data are published) show both increases and decreases in their Δ values when going from CH_3— to C_2H_5— (or *n*-C_4H_9—) (9–13, 35, 39); however, as pointed out before, these examples are not directly comparable because different structural types are encountered. The variations of Δ for different R within the four groups result in a slightly more irregular pattern than is observed for variations in δ, as mentioned before. This is not very surprising since the quadrupole splitting is far more sensitive to small distortions from ideal geometries than is the isomer shift. Such small distortions are evident from the reported crystal structure for $(CH_3)_2Sn(SO_3F)_2$ (7).

Finally it is interesting that a point-charge formalism (3, 11, 30) yields predicted quadrupole splitting values in excellent agreement with those observed. To calculate Δ values we have assumed a positive quadrupole coupling constant eQV_{zz} throughout, as found for $(CH_3)_2SnF_2$ (31). For *trans*-R_2SnX_4, $V_{zz} = 4[R] - 4[X]$, where [L] is the partial quadrupole splitting (p.q.s.) value for ligand L. We have previously derived (3) p.q.s. values for CH_3 (-0.93 mm s^{-1}) and SO_3CF_3 ($+0.45$ mm s^{-1}). These, with the above expression for V_{zz}, enable us to obtain p.q.s. values for C_2H_5, *n*-C_4H_9, PO_2F_2, and F from the observed splittings for compounds **2**–**4**, **9**, and **16**, respectively. Predicted Δ values for the remaining compounds are given in Table 4. Although based on a point-charge approach, the results in Table 4 are actually of much broader significance and show that the additivity condition, which is required in *any* general theory of Mössbauer quadrupole coupling constants (40), is closely followed by the present series of compounds.

Whether such subtle changes in the electron distribution around tin, responsible for the effects discussed above, can be detected by X-ray diffraction methods appears doubtful because the limits of error introduce considerable uncertainty.

Financial support by the National Research Council of Canada is gratefully acknowledged. We are also thankful to the 3M Company for a gift of $Ba(SO_3CF_3)_2$ and Mrs. B. Krizsan and Mrs. A. Sallos for technical assistance.

1. P. A. YEATS, B. F. E. FORD, J. R. SAMS, and F. AUBKE. Chem. Commun. 791 (1969).
2. P. A. YEATS, J. R. SAMS, and F. AUBKE. Inorg. Chem. **10**, 1877 (1971).
3. P. A. YEATS, J. R. SAMS, and F. AUBKE. Inorg. Chem. Submitted for publication.
4. M. SCHMMEISSER, P. SARTORI, and B. LIPPSMEIER. Chem. Ber. **103**, 868 (1970).
5. L. E. LEVCHUK, J. R. SAMS, and F. AUBKE. Inorg. Chem. **11**, 43 (1972).
6. E. O. SCHLEMPER and W. C. HAMILTON. Inorg. Chem. **5**, 995 (1966).
7. F. A. ALLEN, J. LERBSCHER, and J. TROTTER. J. Chem. Soc. (A), 2507 (1971).
8. R. C. THOMPSON and W. REED. Inorg. Nucl. Chem. Lett., **5**, 581 (1969), and references therein.
9. B. GASSENHEIMER and R. H. HERBER. Inorg. Chem. **8**, 1120 (1969).
10. K. L. LEUNG and R. H. HERBER. Inorg. Chem. **10**, 1020 (1971).
11. B. W. FITZSIMMONS, N. J. SEELEY, and A. W. SMITH. J. Chem. Soc. (A), 143 (1969).
12. R. C. POLLER and J. N. R. RUDDICK. J. Chem. Soc. (A), 2273 (1969).
13. K. M. ALI, D. CUNNINGHAM, M. J. FRAZER, J. D. DONALDSON, and B. J. SENIOR. J. Chem. Soc. (A), 2836 (1969).
14. E. O. SCHLEMPER. Inorg. Chem. **6**, 2012 (1967).
15. B. A. GOODMAN and N. N. GREENWOOD. J. Chem. Soc (A), 1862 (1971).
16. R. V. PARISH and C. E. JOHNSON. J. Chem. Soc. (A), 1906 (1971).
17. J. BARR, R. J. GILLESPIE, and R. C. THOMPSON. Inorg. Chem. **3**, 1149 (1964).
18. P. A. YEATS, B. L. POH, B. F. E. FORD, J. R. SAMS, and F. AUBKE. J. Chem. Soc. (A), 2188 (1970).
19. D. SEYFERTH and F. G. A. STONE. J. Am. Chem. Soc. **79**, 515 (1959).
20. C. S. WANG and J. M. SHREEVE. Chem. Commun. 151 (1970).
21. R. K. INGHAM, S. D. ROSENBERG, and H. GILMAN. Chem. Rec. **60**, 478 (1960).
22. K. O'SULLIVAN, R. C. THOMPSON, and J. TROTTER. J. Chem. Soc. (A), 2024 (1967).
23. K. BUEHLER and W. BUES. Z. Anorg. Allg. Chem. **308**, 62 (1961).
24. R. OKAWARA and M. WADA. *In* Advances in organometallic chemistry. Vol. 5. Academic Press, New York, 1967. p. 137.
25. D. W. J. CRUIKSHANK. J. Chem. Soc. 5486 (1961).

Can. J. Chem. Downloaded from www.nrcresearchpress.com by 210.87.254.105 on 09/05/12
For personal use only.

26. M. GOLDSTEIN and W. D. UNSWORTH. J. Chem. Soc. (A), 2121 (1971).
27. A. G. MADDOCK and R. H. PLATT. J. Chem. Soc. (A), 1191 (1971).
28. B. F. E. FORD and J. R. SAMS. J. Organometal. Chem. **31**, 47 (1971).
29. J. ENSLING, Ph. GÜTLICH, K. M. HASSELLBACH, and B. W. FITZSIMMONS. J. Chem. Soc. (A), 1940 (1971).
30. B. V. LIENGME, M. J. NEWLANDS, and J. R. SAMS. Inorg. Nucl. Chem. Lett. Submitted for publication.
31. R. H. HERBER and S. CHANDRA. J. Chem. Phys. **52**, 6045 (1970).
32. J. BARR, R. J. GILLESPIE, and E. A. ROBINSON. Can. J. Chem. **39**, 1266 (1961).
33. A. M. QURESHI and F. AUBKE. Unpublished results.
34. W. REED. Ph.D. thesis, University of British Columbia, Vancouver, British Columbia. 1968.
35. P. J. SMITH. Organometal. Chem. Rev. (A), 373 (1970).
36. J. HINZE. Fortschr. Chem. Forsch. **9**, 448 (1968).
37. R. V. PARISH and R. H. PLATT. Inorg. Chim. Acta, **4**, 598 (1970).
38. R. W. TAFT. *In* Steric effects in organic chemistry. *Edited by* M. S. Newman. John Wiley and Sons Inc., New York, 1956. p. 556.
39. R. V. PARISH and R. H. PLATT. Inorg. Chim. Acta, **4**, 65 (1970).
40. M. G. CLARK. Mol. Phys. **20**, 257 (1971).

Can. J. Chem. Downloaded from www.nrcresearchpress.com by 210.87.254.105 on 09/05/12
For personal use only.

INDO Molecular Orbital Calculations on the Conformational Dependence of Long-range Spin–Spin Coupling of Methyl Protons in Toluene, *p*-Fluorotoluene, and the Xylenes

R. WASYLISHEN[1] AND T. SCHAEFER

Chemistry Department, University of Manitoba, Winnipeg, Manitoba R3T 2N2

Received December 29, 1971

The conformational dependence of the nuclear spin–spin coupling from methyl protons to ring protons, to the fluorine nucleus, and to protons of other methyl groups in toluene, *p*-fluorotoluene, and the xylenes is computed by the finite perturbation technique in the INDO approximation of molecular orbital theory. The calculated coupling over six bonds to the proton in the para position agrees quantitatively with experiment and its predicted dependence on the rotational angle of the methyl group supports a commonly assumed π electron mechanism for the transmission of spin information between the nuclei. Similar remarks apply to the fluorine nucleus in *p*-fluorotoluene. The couplings over five and four bonds to the protons in the meta and ortho positions display a more complex angular dependence and the former can be interpreted in terms of a dominant σ electron mechanism. The coupling between protons in different methyl groups in the ortho and meta xylenes is calculated as rather larger than the values observed in their derivatives and in the main shows the behavior expected from a π electron mechanism. Those conformations of ortho xylene in which the coupled protons are in close proximity yield computed values plausibly attributable to "direct" and/or "through-space" mechanisms. The preferred conformation of the methyl group in toluene is predicted to have a C—H bond eclipsing the plane of the aromatic ring and the calculated barriers to rotation of 0.013 kcal/mol in toluene and of 0.014 kcal/mol in *p*-fluorotoluene are in quantitative accord with microwave data.

Nous avons compilé la dépendance conformationnelle du couplage nucléaire spin–spin des protons méthyle aux protons du cycle, aux noyaux de fluor, et aux protons des autres groupes méthyle dans le toluène, le *p*-fluorotoluène, et les xylènes, par la technique de perturbation finie dans l'approximation INDO de la théorie des orbitales moléculaires. Le couplage calculé de six liens au proton en position para concorde quantitativement avec l'expérience et sa dépendance prédite sur l'angle de rotation du groupe méthyle supporte un mécanisme d'électron π qu'on suppose communément pour la transmission d'information de spin entre les noyaux. On peut appliquer les mêmes remarques dans le cas du noyau de fluor dans le *p*-fluorotoluène. Les couplages au travers de cinq et quatre liaisons à partir des protons en position méta et ortho occasionnent une dépendance angulaire plus complexe et le premier cas peut être interprété en termes d'un mécanisme à électron sigma (σ) dominant. Nous avons calculé que le couplage entre les protons des différents groupes méthyle des xylènes ortho et méta est plus grand que les valeurs observées chez leurs dérivés et le principal d'entre eux possède le comportement qui laisserait soupçonner un mécanisme d'électron π. Les conformations de l'ortho-xylène pour lequel les protons couplés sont rapprochés nous amènent à des valeurs compilées qu'on pourrait vraisemblablement attribuer à des mécanismes "directs" et/ou "à travers l'espace". Nous prédisons que la conformation la plus favorable du groupe méthyle dans le toluène possède une liaison C—H éclipsant le plan du noyau aromatique et les barrières à la rotation calculées de 0.013 kcal/mol dans le toluène et de 0.014 kcal/mol dans le *p*-fluorotoluène sont en accord quantitatif avec les résultats venant des microondes.

Canadian Journal of Chemistry, **50**, 1852 (1972)

Introduction

The "methyl group replacement" technique (1, 2) is often used (2–7) in estimating the π electron contribution to spin–spin coupling constants between protons and protons or other nuclei in conjugated systems. It is based on the idea (2), derived from arguments about proton–electron hyperfine coupling in organic radicals, that a replacement of a hydrogen atom in a C—H bond by a methyl group (under conditions where approximately free rotation of the methyl group occurs) yields a new coupling constant of the same magnitude as, but of different sign to, the original coupling of the replaced proton. This will be roughly true if a π electron mechanism operates to the exclusion of a σ electron mechanism of coupling. For example, in toluene the coupling over six bonds between the methyl protons and the para ring proton, ${}^6J_p^{H,CH_3}$ is 0.62 ± 0.02 Hz (8) while it is 0.62 ± 0.03 Hz in a derivative of *p*-xylene (6).

Such a result is encouraging but extension to the coupling between methyl and ring protons over four and five bonds is problematical in that

[1]Holder of an NRCC Scholarship, 1971–1972.

Can. J. Chem. Downloaded from www.nrcresearchpress.com by 210.87.254.105 on 09/05/12
For personal use only.

Can. J. Chem. Downloaded from www.nrcresearchpress.com by 210.87.254.105 on 09/05/12
For personal use only.

a σ electron contribution is now more difficult to exclude on theoretical grounds (9–11). Another view (8) holds that the ring–methyl proton coupling constants are transmitted by a mechanism independent of that operating to couple the ring protons themselves. This view is based on the fact that coupling between ring protons is markedly substituent dependent while this is not true of the ring–methyl proton couplings. It is then held that the methyl–ring couplings are propagated by a π electron mechanism.

The general success of the INDO molecular orbital calculations of nuclear spin–spin coupling constants (12–15), particularly in reproducing the observed substituent dependence of ring proton couplings in monosubstituted benzenes (15), encourages their extension to ring–methyl proton couplings in toluene and to the fluorine–methyl proton coupling in *p*-fluorotoluene for which accurate experimental data (7, 8) are available. Experimental methyl–methyl proton couplings are also known for derivatives of the xylenes (6). In this paper such couplings are computed as a function of the rotational angle of the methyl group with the intention of elucidating to some extent the mechanism of coupling and in the hope of their use in future conformational studies by n.m.r.

The discussion takes the view that computed numbers shall be related as closely as possible to the common concepts of the experimentalist, such as the separability of σ and π electron systems, conjugation, hyperconjugation and the like; which are used, for example, in the interpretation of chemical shifts, intensities of i.r. spectra of benzene derivatives, and of nuclear quadrupole frequencies (16). The INDO formulation, of course, treats all valence electrons on an equal footing but this is not to say that the semiquantitative concepts are no longer necessary or at least useful.

Computational Procedure

(1) Toluene and p-Fluorotoluene

Standard geometrics (17, 18) are used to calculate atomic coordinates. The finite perturbation method (12, 18) at the INDO level of approximation (18, 19) is employed with the convergence requirement that for all i

$$[1] \qquad 10^{-5} \leqslant (\rho_{ii}^{\text{old}} - \rho_{ii}^{\text{new}})/\rho_{ii}^{\text{old}}$$

where ρ_{ii} are diagonal elements of the spin density matrix. Such a criterion allows an estimate of the error in the computed coupling constant, J_{AB}, because J_{AB} is directly proportional to ρ_{AA}/h or ρ_{BB}/h depending on whether nucleus A or B is perturbing, h being the perturbation parameter. For example, in the parameterization given by Pople and Beveridge (18) one has

$$[2] \qquad J_{H,H} = 105.0447246\ \rho_{H,H}/h$$

Consider the error in a calculated coupling of 1 Hz. Then since h is 10^{-3} one has $\rho_{H,H} \sim 10^{-5}$ and eq. 1 becomes

$$[3] \qquad 10^{-10} \leqslant \rho_{ii}^{\text{old}} - \rho_{ii}^{\text{new}}$$

Therefore ρ_{ii} is not changing by more than 10^{-10} in one SCF cycle and the change in $J_{H,H}$ is less than 0.0000105 Hz in that cycle.

When convergence is not reached in 90 SCF cycles, 100 cycles are carried out and the coupling constants are usually not changing by more than 10^{-3} Hz per cycle at that stage. It is felt that the present convergence criterion is more stringent (but also more costly) than one using all elements of the spin density matrices.

All coupling constants are computed in Hz for the conformations **1**, **2**, and **3** of the methyl group

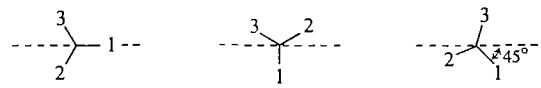

1 **2** **3**

(the dashed lines representing the plane of the aromatic ring). The method can be checked by computing all coupling constants to one of the ring protons situated ortho to the methyl group. Satisfactory agreement with literature values is found (15).

In Table 1 the coupling constants are given as a function of the angle θ, defined as the $H_1C_4C_5C_6$ dihedral angle in **4***a* and *b*.

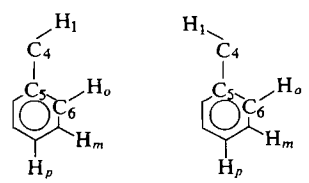

4*a* ($\theta = 0°$) **4***b* ($\theta = 180°$)

TABLE 1. Computed long-range coupling constants in Hz of the methyl protons in toluene, A, and in *p*-fluorotoluene, B

θ* (degrees)	$^4J_o^{H,CH_3}$		$^5J_m^{H,CH_3}$		$^6J_p^{H,CH_3}$	$^6J_p^{F,CH_3}$
	A	B	A	B		
0	−0.345	−0.343	0.234	0.242	−0.075	−0.008
15	−0.414	−0.416	0.266	0.276	−0.151	0.117
30	−0.606	−0.617	0.358	0.373	−0.357	0.463
45	−0.875	−0.898	0.493	0.515	−0.642	0.935
60	−1.154	−1.189	0.646	0.673	−0.929	1.406
75	−1.370	−1.412	0.786	0.816	−1.141	1.750
90	−1.467	−1.511	0.889	0.918	−1.219	1.872
105	−1.424	−1.464	0.943	0.964		
120	−1.264	−1.294	0.946	0.956		
135	−1.036	−1.052	0.917	0.912		
150	−0.806	−0.807	0.876	0.857		
165	−0.637	−0.627	0.843	0.814		
180	−0.575	−0.562	0.831	0.798		

*The angle θ is defined in **4***a* and *b* of the text.

TABLE 2. Computed long-range coupling constants in Hz of the methyl protons in *p*-xylene

	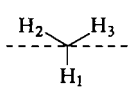	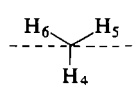	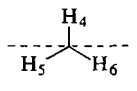	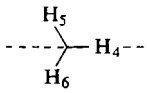
Coupling*	**5**		**6**	**7**
$^4J_o^{H_1,H}$	−1.484		−1.483	−1.491
	−1.484		−1.483	−1.476
$^5J_m^{H_1,H}$	0.920		0.931	0.924
	0.921		0.931	0.927
$^7J^{H_1,H_4}$	2.881		2.914	0.141
$^7J^{H_1,H_5}$	0.834		0.815	2.218
$^7J^{H_1,H_6}$	0.836		0.814	2.187

*The couplings to the ring protons over four and five bonds can be compared to those in Table 1 for $\theta = 90°$. The plane of the aromatic ring lies perpendicular to the plane of the paper and is indicated by dashed lines in **5**, **6**, and **7**.

(2) The Xylenes

Again, standard geometries are employed but the convergence parameter in eq. 1 is changed from 10^{-5} to 10^{-4}. Because of computational costs the coupling constants are calculated for a limited number of conformations, given in Tables 2–5. All computations were performed on an IBM 360/65 computer.

Results and Discussion

The computed couplings in Tables 1–5 are quoted to three decimal places in accord with the convergence criteria; experimental values are known to a precision of a few hundredths of a Hz. Note that there are checks on the internal consistency of the calculations; thus conformations **5** and **6** in Table 2 should and do show almost identical couplings from H_1 to the ring protons, H_4, H_5, and H_6. Similar checks can be found in the other tables.

Note also that a second methyl group does not appreciably change the magnitude of the ring–methyl proton couplings: compare, for example, Tables 1 and 2. This result may be in part due to the use of standard geometries but is also consistent with the observed insensitivity

Can. J. Chem. Downloaded from www.nrcresearchpress.com by 210.87.254.105 on 09/05/12
For personal use only.

TABLE 3. Computed long-range coupling constants in Hz of the methyl protons in *m*-xylene

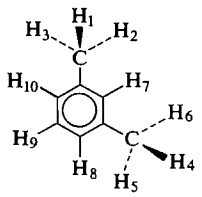

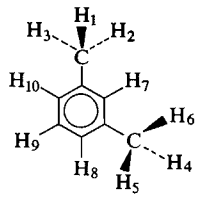

Coupling*	8	9
$^4J^{H_1,H_7}_o$	−1.501	−1.502
$^4J^{H_1,H_{10}}_o$	−1.484	−1.483
$^5J^{H_1,H_9}_m$	0.897	0.899
$^6J^{H_1,H_8}_p$	−1.246	−1.243
$^6J^{H_1,H_4}$	−1.936	−1.927
$^6J^{H_1,H_5}$	−0.582	−0.596
$^6J^{H_1,H_6}$	−0.584	−0.580

*In both **8** and **9**, C—H_1 and C—H_4 lie in a plane perpendicular to the plane of the ring. In **8**, C—H_4 lies above the plane and lies below the plane in **9**. The couplings to the ring protons can be compared with those for $\theta = 90°$ in Table 1.

TABLE 4. Computed long-range coupling constants in Hz of the methyl protons in *o*-xylene for two conformations

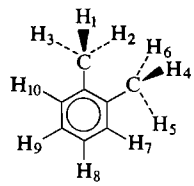

10

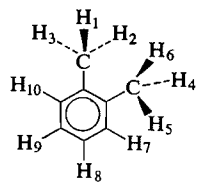

11

Coupling*	X =	1	2	3	1	2	3
$^4J^{H_x,H_{10}}_o$		−1.479	−0.800	−0.626	−1.473	−0.802	−0.629
$^5J^{H_x,H_9}_m$		0.913	0.908	0.358	0.919	0.901	0.361
$^5J^{H_x,H_7}_m$		0.910	0.405	0.881	0.901	0.390	0.899
$^6J^{H_x,H_8}_p$		−1.223	−0.360	−0.364	−1.221	−0.358	−0.366
$^5J^{H_x,H_4}$		2.714	0.931	0.773	2.727	0.701	0.874
$^5J^{H_x,H_5}$		0.773	0.214	0.256	0.875	0.033	0.283
$^5J^{H_x,H_6}$		0.931	−0.164	0.214	0.700	−0.259	0.277

*The conformations of the methyl groups are as described in Table 3.

(3, 6, 8, 20, 21) of the ring–methyl proton coupling constants to substituent effects.

(1) Ring–Methyl Proton Couplings in Terms of a π Electron Mechanism

By analogy to the McConnell–Heller equation (22) for the hyperfine interaction of methyl protons with the unpaired spin density in the π orbital of the contiguous carbon atom in the conjugated system, a π electron mechanism for the ring-methyl proton coupling suggests that the coupling may be written as

$$J = J_0 + J_1 \sin^2 \theta \qquad [4]$$

The angle θ is defined in **4** and J_0 is presumably small compared to J_1. Therefore J has its largest magnitude when the C—H bond of the methyl group containing the coupled proton lies in a plane perpendicular to the aromatic ring. For

Can. J. Chem. Downloaded from www.nrcresearchpress.com by 210.87.254.105 on 09/05/12
For personal use only.

TABLE 5. Computed long-range coupling constants in Hz of the methyl protons in *o*-xylene for three conformations in which two of the methyl protons lie in the plane of the benzene ring

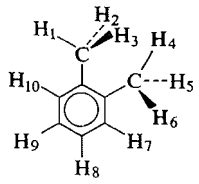

12

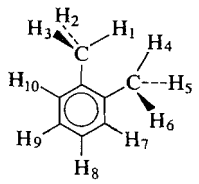

13

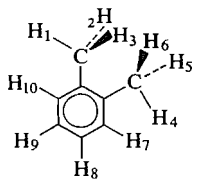

14

Coupling*	$X=$	1	2	1	2	1	2
${}^4J^{H_x,H_9}_o$		−0.380	−1.256	−0.557	−1.179	−0.356	−1.269
${}^5J^{H_x,H_9}_m$		0.277	0.976	0.861	0.662	0.226	0.974
${}^5J^{H_x,H_7}_m$		0.841	0.672	0.280	0.965	0.841	0.673
${}^6J^{H_x,H_8}_p$		−0.091	−0.923	−0.069	−0.936	−0.086	−0.936
${}^5J^{H_x,H_4}_o$		−0.400	−0.297	−0.691	0.040	0.060	0.135
${}^5J^{H_x,H_5}$		0.121	1.740	0.040	1.605	0.135	1.448
${}^5J^{H_x,H_6}$		0.121	1.529	0.040	1.649	0.135	1.883

*The C—H_1 and C—H_4 bonds lie in the plane of the aromatic ring in each of **11**, **12**, and **13**.

free rotation of the methyl group one has $\langle \sin^2\theta \rangle = 1/2$, a good assumption for toluene (and by implication for meta and para xylene) in which the barrier to rotation of the methyl group is 0.014 kcal/mol in the gas phase (23). J_1 is known from the computed value of J at $\theta = 90°$ (J_0 small).

(a) Toluene and p-Xylene

Considering now ${}^6J_p^{H,CH_3}$ one has from Table 1 that its average value is $-1.22/2 = -0.61$ Hz, in excellent agreement with the known value of -0.62 Hz (8). Alternatively, $\langle {}^6J_p^{H,CH_3} \rangle = \{-1.219 - (-0.075)\}/2 - 0.075 = -0.65$ Hz if one assumes that -0.075 Hz ($\theta = 0°$) corresponds to a J_0 term in eq. 4, present at all angles θ. Note also that the computed values of ${}^6J_p^{H,CH_3}$ in Table 1 quite closely obey a $\sin^2\theta$ dependence.

It follows that in *p*-xylene (Table 2) the coupling between the protons in the two different methyl groups should be $\langle {}^7J^{CH_3,CH_3} \rangle = 0.25(2.881 + 2.914)/2 = 0.72$ Hz where the mean is taken of the computed values at $\theta = 90°$ for conformations **5** and **6**. Or, in terms of a J_0 term, $\langle {}^7J^{CH_3,CH_3} \rangle = 0.25(2.898 - 0.141) + 0.140 = 0.83$ Hz (note that $0.141 \sim 2|0.075|$). The experimental value in *p*-xylene itself is unknown but in a *p*-xylene derivative it is 0.62 ± 0.03 Hz (6).

(b) Toluene and m-Xylene and o-Xylene

From the values of ${}^4J_o^{H,CH_3}$ and ${}^5J_m^{H,CH_3}$ for toluene in Table 1 it is likely that the computations are not in agreement with a sole π mechanism for these couplings. Each should then have equal magnitudes at $\theta = 0°$ and 180°, they do not, and they should have a maximum magnitude at $\theta = 90°$, but ${}^5J_m^{H,CH_3}$ has a maximum near 120°.

Nevertheless, application of the same argument as for *p*-xylene yields $\langle {}^5J_m^{H,CH_3} \rangle = 0.889/2 = 0.45$ Hz (Table 1) and $\langle {}^6J_m^{CH_3,CH_3} \rangle = -1.931/4 = -0.48$ Hz for *m*-xylene (Table 3). Similarly, $\langle {}^4J_o^{H,CH_3} \rangle = -1.467/2 = -0.73$ Hz (Table 1) and $\langle {}^5J_o^{CH_3,CH_3} \rangle = 2.720/4 = 0.68$ Hz for *o*-xylene (Table 4). These numbers compare with ${}^4J_o^{H,CH_3} = -0.75$ and ${}^5J_m^{H,CH_3} = 0.36$ Hz observed in toluene (8) and ${}^5J_o^{CH_3,CH_3} = 0.40$ and ${}^6J_m^{CH_3,CH_3} = -0.19$ Hz found in xylene derivatives (6).

One may conclude that on the basis of the "methyl group replacement" model and taking only those conformations where $\theta = 90°$, the computations imply a π electron mechanism for the ring–methyl proton couplings insofar[2] as $-\langle {}^4J_o^{H,CH_3} \rangle \sim \langle {}^5J_o^{CH_3,CH_3} \rangle$ and $-\langle {}^5J_m^{H,CH_3} \rangle \sim \langle {}^6J_m^{CH_3,CH_3} \rangle$, remembering that these averages are obtained by taking $\langle \sin^2\theta \rangle = 1/2$. The experimental data, on the other hand, imply that only a fraction of ${}^4J_o^{H,CH_3}$ and ${}^5J_m^{H,CH_3}$ are accounted for by a π mechanism.

[2]Valence bond studies (11), when calibrated on the experimental value of ${}^6J_p^{H,CH_3}$ in toluene, give precisely these equalities for a π electron mechanism.

Can. J. Chem. Downloaded from www.nrcresearchpress.com by 210.87.254.105 on 09/05/12
For personal use only.

Can. J. Chem. Downloaded from www.nrcresearchpress.com by 210.87.254.105 on 09/05/12
For personal use only.

One may now find the mean values over θ of the ring–methyl coupling constants in Table 1, a reasonable approximation to the true mean because numbers are given at 15° intervals. In this way one finds $^6J_p^{H,CH_3} = -0.64$, $^5J_m^{H,CH_3} = 0.69$, and $^4J_o^{H,CH_3} = 0.92$ Hz. Comparison of these close approximations to the true calculated mean with those obtained from $\theta = 90°$ indicates agreement of the computations with a sole π electron mechanism for $^6J_p^{H,CH_3}$ but disagreement for the other two couplings. It also suggests that the computed approximate equalities in the magnitudes of the ring–methyl and methyl–methyl proton couplings ($\theta = 90°$) is fortuitous for *o*-xylene and *m*-xylene. The observed values of the methyl–methyl proton couplings also imply as much. The matter is discussed further in sections 2 and 3.

(c) Ratio of Q_{CH} and Q_{CCH} from $^6J_p^{H,CH_3}$ and $^7J_p^{CH_3,CH_3}$

The McConnell formulation of π electron coupling between ring and methyl protons predicts that (24, 25)

$$[5] \qquad J^{\pi} \propto Q_{CH}Q_{CCH}$$

where Q_{CH} and Q_{CCH} are isotropic hyperfine coupling constants corresponding to the interaction between a π electron in carbon atomic orbital and the ring and methyl protons, respectively. If $^6J_p^{H,CH_3}$ and $^7J_p^{CH_3,CH_3}$ are dominated by π electron propagation of spin information then one may write

$$Q_{CH}/Q_{CCH} = (^6J_p^{H,CH_3}/^7J_p^{CH_3,CH_3})_{\theta=90°} = -1.219/1.449 = -0.84$$

from the computations in Tables 1 and 2 and as

$$Q_{CH}/Q_{CCH} = {}^6J_p^{H,CH_3}/{}^7J_p^{CH_3,CH_3} = -0.62/0.62 = -1.0$$

from experimental coupling. The e.s.r. data (26–29) suggest the former ratio as more reasonable, however. INDO methods are markedly successful in calculating unpaired spin distributions in free radicals (30). Of course, the ratios above assume the invariance of other parameters like mobile bond order to the insertion of a second methyl group into toluene.

(d) Methyl Proton Couplings in p-Fluorotoluene

An inappreciable substituent effect on $^4J_o^{H,CH_3}$ and $^4J_m^{H,CH_3}$ may be inferred from the computed values in Table 1 and these parameters are indeed equal to within experimental error in toluene (8) and *p*-fluorotoluene (7).

The mean value of $^6J_p^{F,CH_3}$ is 0.94 Hz in Table 1 while a π mechanism ($\theta = 90°$) yields $1.872/2 = 0.94$ Hz, hence in correspondence with such a mechanism. The experimental value is 1.15 ± 0.02 Hz (7). As the theory takes into account only the contact contribution to spin–spin coupling, the close agreement between experiments and theory suggests a minor contribution from magnetic dipole–dipole and orbital–dipole interactions between electron and nucleus.

(2) Angular Dependence of $^5J_m^{H,CH_3}$

Available experimental evidence (31–36) indicates that a proton on a sidechain, *e.g.*, an amino, hydroxyl, or aldehydic group, couples by 0.5–0.8 Hz over five bonds to a ring proton when $\theta = 180°$ as in **15***a* but does not couple by more than 0.1 Hz when $\theta = 0°$ as in **15***b*. For the

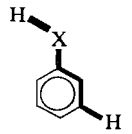

15*a* ($\theta = 180°$)

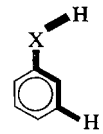

15*b* ($\theta = 0°$)

methyl group itself no direct evidence is available, of course, but in **16**, $^5J_m^{H,H}$ is 0.5–0.6 Hz while in **17**, $^5J_m^{H,H}$ is less than 0.1 Hz (37, 38).

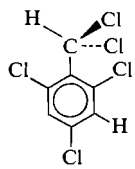

16

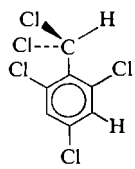

17

$^5J_m^{H,CH_3}$ in Table 1 is computed as 0.234 Hz when $\theta = 0°$, suggesting an overestimate of about 0.2 Hz. A similar situation is found for benzaldehyde (36) where $^5J_m^{H,CHO}$ is calculated to be 0.20 Hz when $\theta = 0°$. Subtraction of 0.234 Hz from the computed value at $\theta = 180°$ yields 0.597 Hz, in better agreement with what is known experimentally. Subtraction of 0.234 Hz from each of the values of $^5J_m^{H,CH_3}$ in Table 1 yields a mean coupling of 0.46 Hz considerably closer to the experimental value of 0.36 Hz than

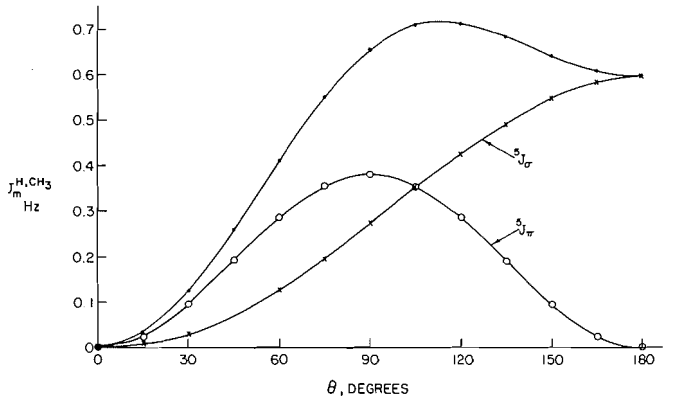

FIG. 1. The coupling over five bonds between ring and methyl protons in toluene $^5J_m^{H,CH_3}$, as adjusted by the procedure described in section 2 of the text, is plotted as closed circles *vs.* the dihedral angle θ defined in **4***a* and *b* of the text. The open circles give the π electron contribution to $^5J_m^{H,CH_3}$ as estimated in the text. The crosses give the resultant σ electron contribution to the coupling.

the mean of 0.69 Hz found without the subtraction.

These considerations allow a reasonable if somewhat arbitrary estimate of the actual angular dependence of $^5J_m^{H,CH_3}$ and, by implication, of the analogous coupling for protons on other sidechains. In Fig. 1 the empirically adjusted $^5J_m^{H,CH_3}$ numbers are plotted as a function of θ (closed circles) and it is clear that about 70% of the mean value of the coupling is accounted for by the region between 90 and 180° (this is also true, of course, for the unadjusted numbers). A reasonable check of the plot in Fig. 1 is available from data (39) on **18**, where $^5J_m^{H,CH_2X}$ is almost independent of the nature of

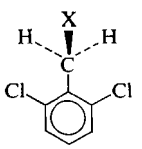

18

X and has a value of 0.35 Hz, the same as in toluene. From Fig. 1 the predicted value of 0.39 Hz is extracted, the average of $^5J_m^{H,CH_3}$ at $\theta = 30$ and 150°, to which the experimental value in **18** corresponds.

The shape of the plot in Fig. 1 is compatible with π mechanism ($\sin^2\theta$ curve) superimposed on a σ mechanism. An attempt at decomposing this plot into those of the two mechanisms could be undertaken by use of the data in Table 3 on $^6J_m^{CH_3,CH_3}$ were it not for the high probability that they would yield an overestimate of the π contribution (see section 1*b*). Consequently we take the experimental value of $^6J_m^{CH_3,CH_3} = -0.19$ Hz in an *m*-xylene derivative (6) and write $^5J_\pi^{H,CH_3} = 0.38 \sin^2\theta$. This function is plotted in Fig. 1 as open circles. The σ electron dependence of the coupling is obtained by difference as the plot consisting of crosses. Its period is twice that of the π dependence and it quite closely follows a $\sin^2(\theta/2)$ function. Such a dependence has not been predicted for coupling over five bonds in saturated systems (10).

(3) Angular Dependence of $^6J_m^{CH_3,CH_3}$

The computed coupling over six bonds between methyl protons in *m*-xylene is dominated by a π electron mechanism (Table 3) as can be seen from its θ dependence. Thus $^6J_m^{CH_3,CH_3} = -0.585$ Hz when $\theta_1 = 90$ and $\theta_2 = 30°$ for the two methyl groups. Therefore $4 \times 0.585 = -2.340$ Hz, not much larger than the -1.931 Hz for consistency with a π mechanism; the latter representing 80% of the former. Apparently theory overestimates the magnitude of the coupling substantially but qualitatively agrees with the "methyl group replacement" model.

(4) Angular Dependence of $^4J_o^{H,CH_3}$

Although in contrast to $^5J_m^{H,CH_3}$ the computed magnitude of $^4J_o^{H,CH_3}$ reaches a maximum at $\theta = 90°$ and although $-1.47/2 = -0.73$ Hz coincides with the measured datum in toluene, the substantial and different magnitudes at

Can. J. Chem. Downloaded from www.nrcresearchpress.com by 210.87.254.105 on 09/05/12
For personal use only.

Can. J. Chem. Downloaded from www.nrcresearchpress.com by 210.87.254.105 on 09/05/12
For personal use only.

$\theta = 0$ and 180° again indicate that a π mechanism is modified by a σ electron contribution; albeit to a lesser extent than for $^5J_m^{H,CH_3}$. The mean value for $^4J_o^{H,CH_3}$ of -0.92 Hz in Table 1 can be brought into agreement with the observed value of 0.75 Hz by subtraction of -0.17 Hz from each calculated value. This may well be a reasonable procedure but there exists no unequivocal experimental data with which to test the computed values at $\theta = 0$ and 180°. The only data are for **19** and **20** where $^4J_o^{H,CHCl_2}$ is -0.4 Hz

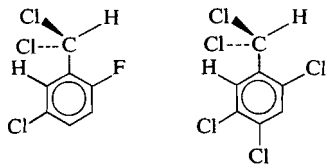

19 **20**

(40), corresponding to $\theta = 180°$ and consistent with a subtraction of -0.17 Hz from the computed value. However, there probably exists an appreciable substituent effect from the chlorine atoms on the sidechain. In addition there probably occurs an appreciable torsional oscillation of the dichloromethyl group about the indicated conformation.

In any event the σ electron contribution to $^4J_o^{H,CH_3}$ is apparently negative at all angles θ but its numerical angular dependence depends on whether one takes the π contribution as $-2.720/2 = -1.36$ Hz from $\theta = 90°$ (*o*-xylene in Table 4) or as $-0.40 \times 2 = -0.80$ Hz from $\theta = 90°$ using the measured value of $^5J_o^{CH_3,CH_3}$ in an *o*-xylene derivative. One objection to these estimates recognizes the possibility of a significant σ contribution to the methyl–methyl proton coupling over five bonds, as implied by four different values of the computed coupling between H_1 and H_5 or H_6 in Table 4, ranging from 0.70–0.93 Hz. These couplings should be nearly equal in the event of a π mechanism, as is found in Table 3 for $^6J_m^{CH_3,CH_3}$. Another objection to the estimates cites an appreciable barrier of 2 kcal/mol to rotation of the methyl group (41) in *o*-xylene; arising from mutual hindrance of the two groups and thereby vitiating a simple averaging procedure based on free rotation.

It therefore appears unwise to attempt a numerical separation into σ and π mechanisms in the manner undertaken above for $^5J_m^{H,CH_3}$. One may note, however, that the computed curve implies a dominant π mechanism and, when adjusted by subtraction of -0.17 Hz from each value, predicts significant couplings for $\theta = 0$ and 180°. This contrasts with $^6J_p^{H,CH_3}$ and implies that a π mechanism operating by spin polarization, *i.e.*, along the H—C—C fragment and then into the π system by a one-center two electron exchange interaction, is unimportant for nuclear spin–spin coupling in toluene derivatives. The hyperconjugative π electron mechanism, involving interaction of the C—H bond of the methyl group with the π system and obeying a $\sin^2\theta$ relationship, is therefore implied by the INDO formulation. In consequence the computed values of $^4J_o^{H,CH_3}$ values at $\theta = 0$ and 180° may be accepted as σ electron effects.

(5) Comparison of the Computed $^4J_o^{H,CH_3}$ in Toluene and Propene

It is interesting to compare $^4J_o^{H,CH_3}$ in toluene in Table 1, with the analogous *cisoid* allylic coupling in propene, recently computed in the INDO approximation (42). Both couplings display a maximum magnitude at $\theta = 90°$ but the asymmetry about $\theta = 90°$ in propene is the reverse of that in toluene (Table 4 and Fig. 4 of ref. 42) in that the magnitude at $\theta = 0°$ is larger than at $\theta = 180°$ for propene. In addition the allylic coupling in propene is calculated to be larger in magnitude at all angles than is $^4J_o^{H,CH_3}$ in toluene, confirming the valence bond results (43) which characterize the aromatic π electron system as less effective than a linear polyene in transmitting spin information; as found experimentally (8, 44).

(6) Coupling Mechanism of $^5J_o^{CH_3,CH_3}$ in o-Xylene

In addition to the propagation of coupling via some or all of the intervening bonds, the close proximity of two methyl protons in some conceivable conformations of *o*-xylene can lead to "direct" interactions in the sense that *only* the two C—H bonds containing the coupled protons are involved. Normally such interactions are important in coupling over two or three bonds (10). If the proximity is high enough a "through-space" mechanism, proportional to an interaction integral between the two hydrogen 1s orbitals, also becomes possible (10). These two mechanisms need not be considered in the other compounds of this paper and they introduce a

Can. J. Chem. Downloaded from www.nrcresearchpress.com by 210.87.254.105 on 09/05/12
For personal use only.

further complication into the use of $^5J_o^{CH_3,CH_3}$ as a measure of the π electron contribution to $^4J_o^{H,CH_3}$.

Consequently three other conformations of *o*-xylene, shown in Table 5, were examined in the hope of elucidating the matter. In each of **12**, **13**, and **14**, two of the methyl protons (H_1 and H_4) lie in the plane of the aromatic ring and the coupling is computed between two protons on one methyl group and the three protons on the other group. For symmetry reasons this yields six couplings for each conformation. The striking points about the computed couplings in **10** to **14** are that (*i*) they have a maximum when the C—H bonds containing the coupled protons lie in planes perpendicular to the ring, *e.g.*, 2.7 Hz in **10** and **11**; (*ii*) they have a minimum and are often almost zero when one or both of the coupled protons are situated in the ring plane, *e.g.*, J^{H_1,H_5} is 0.1 Hz in **12** to **14** and J^{H_1,H_4} is 0.1 Hz in **14**; but (*iii*) they may also be negative when both coupled protons lie in the aromatic plane or if they are spatially proximate, e.g., J^{H_2,H_6} is -0.2 Hz in **10** and **11**, J^{H_2,H_4} is -0.3 Hz in **12**; (*iv*) the most negative coupling occurs when the coupled protons are nearest one another, viz., J^{H_1,H_4} is -0.7 Hz in **13**.

Now the π mechanism does not operate if one of the coupled protons is coplanar with the ring. By analogy with the available valence bond formulation for a saturated hydrocarbon (10) a maximum positive σ contribution to the coupling between H_1 and H_4 is expected in **14**, the magnitude evidently being independent of the dihedral angle about the aromatic C—C bond (10). Yet J^{H_1,H_4} is computed as only 0.06 Hz in **14**. Therefore the observed negative couplings can probably be attributed to the "direct" and/or the "through-space" mechanism.[3] Their actual magnitude in *o*-xylene remains in doubt because unknown and unconsidered distortion of the molecule could in fact bend the methyl groups significantly away from a regular geometry.

[3]An exception may be the coupling of -0.4 Hz between H_1 and H_4 in **12** where the C—H_4 bond might interact with C—H_3 and C—H_2. As a point of interest, INDO calculations in which we bring a hydrogen or methane molecule to within van der Waals distances of a methane molecule predict negative couplings between protons in different molecules and imply that there two mechanisms yield negative couplings, at least for some configurations.

In general the computed couplings in Tables 4 and 5 support the dominance of the π mechanism in the methyl–methyl couplings in *o*-xylene (points *i* and *ii*), but in any event overestimate their magnitude. Thus the average of 45 values known from the calculations is 0.75 Hz whereas the observed value is 0.40 Hz in a derivative of *o*-xylene.

There remains the question whether such a simple averaging procedure is justified for *o*-xylene. Hot bands in the u.v. spectrum of *o*-xylene (41), heat capacities in the gas phase (45), neutron scattering results (46), far i.r. spectra (47*a*), and carbon-13 spin relaxation times (47*b*) agree in finding a barrier of 2 kcal/mol to rotation of the methyl group. The equilibrium structure is not known although **14** is assumed in the u.v. work. According to INDO the most stable of the five conformations, **10** to **14**, is indeed **14**, being more stable than **12** by 0.9 kcal/mol and more stable than **10** and **11** by 1.1 kcal/mol; while conformation **13** is less stable than **14** by 4.8 kcal/mol. At room temperature **14** is therefore weighted about 4 to 1 relative to **10**, **11**, or **12** while **13** need not be considered, probably because of strong nonbonded repulsion between H_1 and H_4. Perusal of the data in Tables 4 and 5, however, demonstrates that this weighing procedure will not change the computed $^5J_o^{CH_3,CH_3}$ appreciably from that obtained by a simple average. Even if **14** is more stable than all other conformations by 2 kcal/mol this conclusion stands.

(7) Barrier to Methyl Group Rotation in Toluene

The present calculations predict that **1** is lower in energy than **2** by 0.013 kcal/mol and that **3** is of intermediate stability. The experimental barrier is 0.014 kcal/mol (23). For *p*-fluorotoluene the calculations similarly give 0.0138 kcal/mol in exact agreement with the experimental barrier (48). The chemical shifts of the alkyl protons in a series of alkylarenes are best interpreted in terms of a preferred conformation in which a C—H bond of the side-chain eclipses the aromatic plane, in qualitative agreement with the INDO predictions (49).

(8) Geminal Couplings between Methyl Protons, $^2J_g^{H,H}$

The experimental value of $J_g^{H,H}$ in methane is -12.4 Hz (50) while INDO calculates -6.13

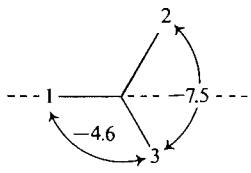

21

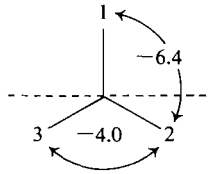

22

Hz (18). In toluene $J_g^{H,H}$ is expected to depend on the conformation of the molecule (51). Present calculations are summarized in **21** and **22** where the dashed lines indicate the plane of the ring and for example, $J^{H_2H_3}$ is -7.5 Hz in **21**. Relative to methane a positive shift in the calculated J_g occurs when the line joining the coupled protons is parallel to the ring plane or when one of the coupled protons lies in this plane. A negative shift occurs when the joining line is perpendicular to the ring plane or when one of the C—H bonds containing the proton lies in a plane perpendicular to the ring. Experimental data (52) suggest that the observed negative shift in J_g in the presence of a π system is largest when the joining line is perpendicular to the ring plane, qualitatively bearing out the calculated value of -7.5 Hz in **21**.

In terms of an earlier molecular orbital theory (51) the negative shift in J_g arises from hyperconjugative withdrawal of electrons from the methyl group by the aromatic nucleus. The INDO calculations predict that the charge in the hydrogen orbital of the C—H bond of the methyl group decreases by 0.01 electron units (from -0.024 to -0.013 units) as θ goes from 0 to 90°; this change accurately following a $\sin^2\theta$ dependence and in agreement with a hyperconjugative effect. The earlier theory is not in qualitative agreement with the calculated coupling of -4.6 Hz between H_1 and H_3 in **21** because it predicts a negative shift from the methane value when one proton is situated in the ring plane. On the other hand, the earlier theory agrees with the positive shift calculated for the coupling between H_2 and H_3 in **22**.

Summary and Conclusions

The calculations by molecular orbital theory in the INDO approximation are in quantitative agreement with experiment for $^6J_p^{H,CH_3}$ in toluene and are in accord with a π mechanism for the propagation of the spin information; similarly for $^6J_p^{F,CH_3}$ in *p*-fluorotoluene. The calculations for $^5J_m^{H,CH_3}$ can be interpreted in terms of a predominant σ electron mechanism which, however, apparently makes a much smaller relative contribution to the calculated $^4J_o^{H,CH_3}$.

The calculated methyl–methyl proton couplings in the xylenes are dominated by a π electron mechanism but are rather larger in magnitude than the observed values in xylene derivatives. The computations indicate the likelihood of negative values for $^5J_o^{CH_3,CH_3}$, caused by "direct" or even "through space" mechanisms, in conformations where the coupled protons are in close proximity.

An earlier molecular orbital theory of the conformational dependence of geminal proton coupling in the methyl group of toluene is in rough qualitative agreement with the INDO formulation.

The calculated barriers to rotation of the methyl group in toluene and *p*-fluorotoluene are in quantitative accord with experiment. The preferred conformation is one in which a C—H bond of the methyl group eclipses the plane of the aromatic nucleus.

We are grateful to the National Research Council of Canada for financial support.

1. R. A. HOFFMAN. Mol. Phys. **1**, 326 (1958).
2. R. A. HOFFMAN and S. GRONOWITZ. Acta Chem. Scand. **13**, 1477 (1959).
3. D. J. BLEARS, S. S. DANYLUK, and T. SCHAEFER. J. Chem. Phys. **47**, 5037 (1967).
4. J. B. ROWBOTHAM, R. WASYLISHEN, and T. SCHAEFER. Can. J. Chem. **49**, 1799 (1971).
5. R. HOFFMAN and S. GRONOWITZ. Arkiv Kemi, **16**, 471 (1960).
6. C. J. MACDONALD and W. F. REYNOLDS. Can. J. Chem, **48**, 1002 (1970).
7. R. WASYLISHEN and T. SCHAEFER. Can. J. Chem. **49**, 94 (1971).
8. M. P. WILLIAMSON, R. KOSTELNIK, and S. M. CASTELLANO. J. Chem. Phys. **49**, 2218 (1968).
9. H. FRISCHLEDER and G. BÄR. Mol. Phys. **11**, 359 (1966).
10. M. BARFIELD and M. KARPLUS. J. Am. Chem. Soc. **91**, 1 (1969).
11. M. BARFIELD and B. CHAKRABARTI. J. Am. Chem. Soc. **91**, 4346 (1969).
12. J. A. POPLE, J. W. MCIVER, JR., and N. S. OSTLUND. J. Chem. Phys. **49**, 2960, 2965 (1968).
13. G. E. MACIEL, J. W. MCIVER, JR., N. S. OSTLUND, and J. A. POPLE. J. Am. Chem. Soc. **92**, 1 (1970).
14. M. BARFIELD, C. J. MACDONALD, I. R. PEAT, and W. F. REYNOLDS. J. Am. Chem. Soc. **93**, 4195 (1971).
15. G. E. MACIEL, J. W. MCIVER, JR., N. S. OSTLUND, and J. A. POPLE. J. Am. Chem. Soc. **92**, 4506 (1970).

Can. J. Chem. Downloaded from www.nrcresearchpress.com by 210.87.254.105 on 09/05/12
For personal use only.

16. A. R. KATRITZKY and R. D. TOPSOM. Angew. Chem. Int. Ed. **9**, 87 (1970).
17. J. A. POPLE and M. S. GORDON. J. Am. Chem. Soc. **89**, 4253 (1967).
18. J. A. POPLE and D. L. BEVERIDGE. Approximate molecular orbital theory. McGraw-Hill Book Company, New York, N. Y., 1970.
19. P. A. DOBOSH. Program number 141. Quantum chemistry program exchange. University of Indiana, Bloomington, Indiana.
20. G. KOTOWYCZ and T. SCHAEFER. Can. J. Chem. **44**, 2743 (1966).
21. D. GAGNAIRE and TRINH-HUU-ICH. Bull. Chem. Soc. Fr. 3763 (1966).
22. C. HELLER and H. M. MCCONNELL. J. Chem. Phys. **32**, 1535 (1960).
23. H. RUDOLPH, H. DREIZLER, A. JAESCHKE, and P. WENDLING. Z. Naturforsch. **22***a*, 940 (1967).
24. H. M. MCCONNELL. J. Chem. Phys. **30**, 126 (1959).
25. M. J. S. DEWAR and R. C. FAHEY. J. Am. Chem. Soc. **85**, 2704 (1963).
26. J. V. ACRIVOS. Mol. Phys. **5**, 1 (1962).
27. R. A. HOFFMAN. Arkiv Kemi, **17**, 1 (1961).
28. A. D. MCLACHLAN. Mol. Phys. **2**, 223 (1959).
29. T. M. MCKINNEY and D. H. GESKE. J. Am. Chem. Soc. **89**, 2806 (1967).
30. J. A. POPLE, D. L. BEVERIDGE, and P. A. DOBOSH. J. Am. Chem. Soc. **90**, 4201 (1968).
31. J. A. WEIL, A. BLUM, A. H. HEISS, and J. K. KINNAIRD. J. Chem. Phys, **46**, 3132 (1967).
32. R. WASYLISHEN and T. SCHAEFER. Can. J. Chem. **48**, 1263, 1343 (1970).
33. S. FORSÉN and R. A. HOFFMAN. J. Mol. Spectrosc. **20**, 168 (1966).
34. T. SCHAEFER and G. KOTOWYCZ. Can. J. Chem. **46**, 2865 (1968).
35. G. J. KARABATSOS and F. M. VANE. J. Am. Chem. Soc. **85**, 3886 (1963).
36. R. WASYLISHEN and T. SCHAEFER. Can. J. Chem. **49**, 3216 (1971).
37. T. SCHAEFER, R. SCHWENK, C. J. MACDONALD, and W. F. REYNOLDS. Can. J. Chem. **46**, 2187 (1968).
38. B. J. FUHR, B. W. GOODWIN, H. M. HUTTON, and T. SCHAEFER. Can. J. Chem. **48**, 1558 (1970).
39. A. F. JANZEN and T. SCHAEFER. Can. J. Chem. **49**, 1818 (1971).
40. H. M. HUTTON, J. B. ROWBOTHAM, B. H. BARBER, and T. SCHAEFER. Can. J. Chem. **49**, 2033 (1971).
41. K. C. INGHAM and S. J. STRICKLER. J. Chem. Phys. **53**, 4313 (1970).
42. M. BARFIELD. J. Am. Chem. Soc. **93**, 1066 (1971).
43. M. BARFIELD and B. CHAKRABARTI. Chem. Rev. **69**, 757 (1969).
44. A. A. BOTHNER-BY and C. NAAR-COLIN. J. Am. Chem. Soc. **83**, 231 (1961).
45. W. J. TAYLOR, D. D. WAGMAN, M. G. WILLIAMS, K. S. PITZER, and F. D. ROSSINI. J. Res. Natl. Bur. Std. **37**, 95 (1946).
46. J. J. RUSH. J. Chem. Phys. **47**, 3936 (1967).
47. (*a*) G. W. F. PARDOC, S. J. LARSON, H. A. GEBBIE, S. J. STRICKLER, K. C. INGHAM, and D. G. JOHNSON. J. Chem. Phys. **52**, 6426 (1970). (*b*) K. F. KUHLMANN and D. M. GRANT. J. Chem. Phys. **55**, 2998 (1971).
48. H. D. RUDOLPH and H. SEILER. Z. Naturforsch. **20***a*, 1682 (1965).
49. R. J. OUELLETTE, B. K. SINHA, J. STOLFO, C. LEVIN, and S. WILLIAMS. J. Am. Chem. Soc. **92**, 7145 (1970).
50. M. KARPLUS, D. H. ANDERSON, T. C. FARRAR, and H. S. GUTOWSKY. J. Chem. Phys. **27**, 597 (1957).
51. J. A. POPLE and A. A. BOTHNER-BY. J. Chem. Phys. **42**, 1339 (1965).
52. M. BARFIELD and D. M. GRANT. J. Am. Chem. Soc. **85**, 1899 (1963).

Can. J. Chem. Downloaded from www.nrcresearchpress.com by 210.87.254.105 on 09/05/12
For personal use only.

Proton Magnetic Resonance Spectrum of 1-Penten-3-yne. INDO and CNDO/2 Molecular Orbital Calculations on Long-Range Spin–Spin Coupling Constants in Enynes

L. ERNST,[1] H. M. HUTTON,[2] AND T. SCHAEFER

Department of Chemistry, University of Manitoba, Winnipeg, Manitoba R3T 2N2

Received January 11, 1972

The high resolution p.m.r. spectra of 1-penten-3-yne in carbon disulfide and in benzene solution are analyzed. Long-range spin–spin coupling constants are discussed in terms of σ and π electron contributions. Comparisons are made with the isomeric 2-methyl-1-buten-3-yne and the parent compound, vinylacetylene. The results of INDO and CNDO/2 molecular orbital calculations are compared to the experimental coupling constants. It is concluded that the π electron contribution to ^5J in enyne systems is $+0.6$ to 0.7 Hz and that σ electron contributions are rather small, the *transoid* ("pseudo-zig–zag") being larger than the *cisoid* one. Observed allylic coupling constants in the propene derivative are compared with the calculated values, including those for propene and 2-cyanopropene, available in the literature.

Nous avons analysé le spectre à haute résolution de r.m.p. du 1-pentène-3-yne en solution dans le disulfure de carbone et dans le benzène. Nous avons discuté des constantes de couplage à longue distance spin–spin en termes de contributions électroniques σ et π. Nous avons fait la comparaison entre l'isomère 2-méthyl-1 butène-3-yne et le composé voisin vinylacétylène. Nous avons comparé les résultats des calculs d'orbitales moléculaires INDO et CNDO/2 aux constantes de couplage expérimentales. Nous concluons que la contribution de l'électron π à ^5J dans les systèmes enyne est de $+0.6$ à 0.7 Hz et que les contributions de l'électron σ sont plutôt petites, la *transoide* ("pseudo-zig–zag") étant plus grande que la *cisoide*. Nous comparons aussi les constantes de couplage allyliques observées pour le dérivé du propène aux valeurs calculées, incluant celles pour le propène et le 2-cyanopropène, qu'on peut d'ailleurs retrouver dans la littérature.

Canadian Journal of Chemistry, **50**, 1863 (1972)

Introduction

In view of the current interest in the mechanism of long-range spin–spin coupling in both aromatic (1–4) and nonaromatic (5–9) compounds, we analyze the p.m.r. spectrum of 1-penten-3-yne (**1**) to get further information on σ and π electron contributions to long-range couplings in enyne systems. Whereas considerable work has been done on diene systems (5–10), this seems to be less so for the enyne case (11–14). Encouraged by recent successful applications of INDO molecular orbital methods to calculations of long-range coupling constants (2, 3, 15), we apply them to some of the compounds which are relevant to the present study.

Experimental

1-Penten-3-yne was obtained from K & K Laboratories and used without further purification. A 5 mol % solution in carbon disulfide and a 10 mol % solution in benzene were prepared, both containing a small quantity of tetramethylsilane (TMS) as internal reference and locking substance. The samples were degassed by the usual freeze–pump–thaw technique. The p.m.r. spectra were taken on a Varian HA-100 D spectrometer operating in the frequency sweep mode at a probe temperature of 30 ± 1 °C. Sweep rates were 0.01 or 0.02 Hz/s. Peak positions were calibrated four times at intervals of less than 5 Hz using a Hewlett–Packard 5323A frequency counter. The resolution obtained was 0.11 Hz. Spin tickling experiments (16) were performed on the CS_2 solution, yielding the relative signs of the coupling constants. These experiments were straightforward since all multiplets had line separations exceeding 0.5 Hz, thus easily permitting the irradiation of certain lines without affecting neighboring ones. The spectra were analyzed using the iterative computer program LAME (17) on the IBM/360-65 computer of the University of Manitoba. The spectra were of the $ABCX_3$ type with the one in CS_2 solution somewhat more tightly coupled due to the smaller range of chemical shifts.

[1]Postdoctoral Fellow, 1971–72.

[2]Department of Chemistry, University of Winnipeg, Winnipeg, Manitoba.

Results and Discussion

(1) Analysis of Proton Magnetic Resonance Spectra

The spectral parameters for **1** obtained in the iterative calculations are given in Table 1. Of the 113 calculated transitions, 95 were assigned for the benzene solution; for the CS_2 solution the corresponding figures are 115 and 92. The r.m.s. deviations between observed and calculated frequencies were 0.0200 Hz for the CS_2 solution

Can. J. Chem. Downloaded from www.nrcresearchpress.com by 210.87.254.5 on 09/05/12
For personal use only.

TABLE 1. Chemical shifts and coupling constants for 1-penten-3-yne

Parameter	10 mol % in C_6H_6	5 mol % in CS_2
ν_1*‡	512.570 (0.005)	524.493 (0.005)
ν_2	549.129 (0.006)	539.053 (0.007)
ν_3	569.406 (0.006)	562.342 (0.006)
ν_4	158.753 (0.004)	187.571 (0.004)
$J(1,2)$†‡	2.279 (0.008)	2.331 (0.008)
$J(1,3)$	11.105 (0.008)	11.064 (0.007)
$J(1,4)$	−0.562 (0.004)	−0.567 (0.004)
$J(2,3)$	17.494 (0.006)	17.440 (0.008)
$J(2,4)$	−0.714 (0.005)	−0.730 (0.005)
$J(3,4)$	2.305 (0.005)	2.314 (0.005)

*Shifts in Hz at 100 MHz relative to internal TMS.
†Coupling constants in Hz relative to $J(1,2)$ as positive.
‡Figures in brackets represent standard deviations as given by the computer program. Probable errors are believed to be *ca.* four times as high.

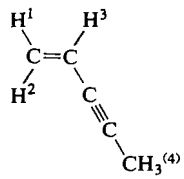

1

and 0.0203 Hz for the benzene solution. There are small differences between the coupling constants measured for **1** in benzene and the corresponding values in CS_2 solution. Although these differences are mostly somewhat larger than the calculated standard deviations they are probably not significant as they are smaller than the accuracy to which the line positions can be measured using a ruler. As analyses for the different solutions were carried out independently, the two sets of coupling constants indicate their reliability.

(2) Couplings via the Triple Bond

The long-range couplings[3] from the methyl group to the olefinic protons ${}^6J'_t(1,4) = -0.56$, ${}^6J'_c(2,4) = -0.72$, and ${}^5J'(3,4) = 2.31$ Hz may be compared to the acetylenic proton vinylic proton coupling constants in the parent compound vinylacetylene (**2**): ${}^5J_t(1,4) = 0.92$, ${}^5J_c(2,4) = 0.70$, and ${}^4J(3,4) = -2.17$ Hz (11). The reversal of sign and approximate retention of magnitude in going from **2** to **1**, Hoffman's "methyl group replacement technique" (18), suggests the π coupling to be the prevailing mechanism of these spin interactions. There are, however, small but significant differences between ${}^6J'_t$ and ${}^6J'_c$ in **1** and between ${}^5J_t$ and ${}^5J_c$ in **2** of 0.16 and 0.22 Hz, respectively, the *transoid* coupling being larger (less negative and more positive) in both cases. As coupling constants consisting entirely of π contributions should be independent of such geometric isomerism, according to Karplus' theory (19), this suggests a σ contribution of about 0.2 Hz to ${}^6J'_t$ and ${}^5J_t$. This can be easily rationalized since the path for these couplings bears some resemblance to the famous "zig–zag path" associated with high σ electron coupling (20). Both here and in the zig–zag case the C—H bonds of the coupling protons are parallel to each other. A similar situation holds for the five-bond couplings in 2-methyl-1-buten-3-yne (**3**), studied earlier in this laboratory (13). Here ${}^5J_t = 0.67$ and ${}^5J_c = 0.59$ Hz, the difference between these values being outside the error limits of the analysis. Their smaller magnitudes compared to **2** are possibly related to the mobile bond order of the intervening bonds calculated to be smaller for **3** than for **2** (or **1**) by the INDO procedure (described in section 3).

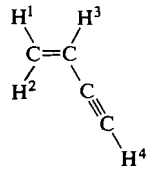

2

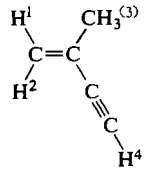

3

A striking feature in the comparison of **1**, **2**, and **3** is the following: as already mentioned, reversal of sign and approximate retention of magnitude is observed in replacing the acetylenic proton of **2** by a methyl group, *i.e.* ${}^4J(3,4) \simeq -{}^5J'(3,4)$; replacing the olefinic proton H^3 by methyl, however, decreases the coupling by a factor of 7, *i.e.* ${}^5J'(3,4)$ is only 0.3 Hz in **3**. This behavior can be understood in terms of the hyperconjugative model often applied to explain the so-called σ,π exchange mechanism. A valence bond structure **1***a* can be written for **1** involving hyperconjugation between the methyl group and both the double and the triple bonds,

[3]Notations for the coupling constants across multiple bonds are termed ${}^nJ_c$ or ${}^nJ_t$ where n gives the number of intervening bonds; c and t indicate whether the olefinic proton under consideration is *cis* or *trans* with respect to the acetylenic group. Primes indicate couplings involving a methyl group.

Can. J. Chem. Downloaded from www.nrcresearchpress.com by 210.87.254.5 on 09/05/12
For personal use only.

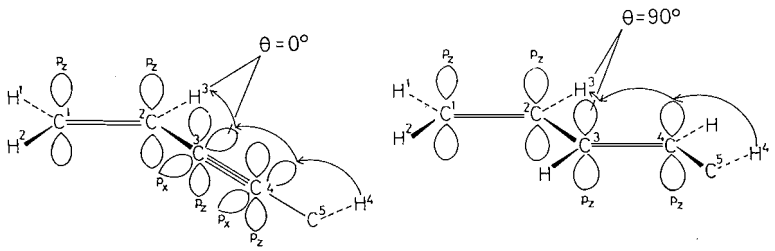

FIG. 1. Transfer of spin information through the π system in 1-penten-3-yne (left) and *trans*-pentadien-1,3 (right). The p_z orbitals are in the plane of the paper.

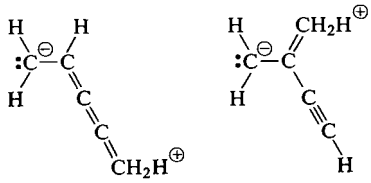

1*a* 3*a*

whereas the only hyperconjugative canonical structure for **3** is **3***a*, involving the methyl group and the double but not the triple bond. A structure for **3** comparable to **1***a* would be a very unfavorable one and would require the =C—C≡ bond to be broken. A more explicit rationalization is given further on in this section.

Another illustrative comparison is the one between 1-penten-3-yne and the corresponding diene compound *trans*-pentadiene-1,3 (**4**) which has been studied by Harris and co-workers (9). Including *cis*-pentadiene-1,3 is not useful because of rather different steric requirements in this molecule. The long-range coupling constants in **4** relevant to the present discussion are: ${}^6J'_{tt}(1,4) = -0.74$, ${}^6J'_{ct}(2,4) = -0.76$, and ${}^5J'_t(3,4) = 0.45$ Hz, respectively. It is evident that the six-

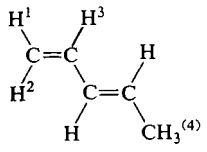

4

bond couplings are similar in both sign and magnitude for the diene and enyne systems. The same does not hold for the five-bond coupling which has the same sign in both compounds, but shows a considerable decrease in magnitude in **4** relative to **1**. Using a simplifying picture of how the spin information is transferred from the methyl protons to H^3 (Fig. 1), this can be accounted for in the following manner: The spin information of the methyl group in **1** can get through the π system of the triple bond either via the carbon p_z or p_x orbitals. Only the latter case, however, is favorable since the C^2—H^3 bond forms an "allylic" dihedral angle θ of 0° with the p_x orbitals. As shown by the well known $\cos^2\theta$ dependence of allylic coupling, this arrangement represents the most effective way of spin information transfer. On the other hand, the coupling has to go through the p_z orbitals of C^4 and C^3 in **4** which form a θ of 90° with the C^2—H^3 bond because the s-*trans*-conformation is the most stable: therefore ${}^5J'(\text{enyne}) \gg {}^5J'(\text{diene})$. The same kind of argument is not valid in discussing the six-bond couplings. Here the coupling path is only through the p_z orbitals in both **1** and **4**, spin information transfer from the C^3-p_x via C^3-p_z into the C^2-p_z orbital being forbidden because of the orthogonality of C^3-p_x and C^3-p_z. This rationalizes the fact that ${}^6J'(\text{enyne}) \simeq {}^6J'(\text{diene})$. Comparison of vinylacetylene (11) with butadiene (7) shows analogous features for the couplings over four and five bonds.

The scheme shown for **1** in Fig. 1 also rationalizes the small coupling of 0.3 Hz observed between the methyl protons and the acetylenic proton in **3**. When H^3 in **1** is replaced by a methyl group the β-interaction (in the language common in electron spin resonance) between the C^2—H^3 bond and the C^3-p_x orbital in **1** is replaced by a γ-interaction between the C—H bond of the methyl group and the C^3-p_x orbital in **3**. As in radicals, the latter interaction is expected to be a good deal smaller than the former.

(3) INDO and CNDO/2 Molecular Orbital Calculations

The bond lengths and angles used in the

Can. J. Chem. Downloaded from www.nrcresearchpress.com by 210.87.254.5 on 09/05/12
For personal use only.

TABLE 2. Observed and calculated long-range coupling constants via the triple bond for **1**, **2**, and **3** in Hz

	1			**2**			**3**		
	Obs.	INDO	CNDO/2	Obs.	INDO	CNDO/2	Obs.	INDO	CNDO/2
$J(1,4)$	−0.56	−0.84	0.08	0.92	1.09	0.39	0.67	1.17	0.44
$J(2,4)$	−0.72	−1.03	−0.07	0.70	0.73	0.13	0.60	0.77	0.17
$J(3,4)$	2.31	3.53	2.10	−2.17	−1.67	0.23	0.31	0.59	0.12

molecular orbital calculations were taken from the literature. The molecular geometry of **1** was obtained by electron diffraction (ref. 21*a*), those of **2** and **3** by microwave spectroscopy (ref. 21*b*, 22). Since the data were not quite complete, a few assumptions concerning bond angles had to be made. Furthermore, coupling constants in **3** were only calculated for the conformation known to be the most stable one, *viz.* with one of the methyl protons eclipsing the double bond (22). This does not seem to be a very satisfactory solution, but no information concerning stabilities of other possible conformations was available. For **1** free rotation about the C^4—CH_3 bond was assumed and possible small energy differences between the three different conformers were neglected. Coupling constants for these were calculated and averaged with regard to their statistical weights. A qualitative argument used in section 2 about the differences between the five-bond couplings in **1** and **4** is supported nicely by these calculations. The coupling in **1** of a methyl proton to H^3 is predicted by INDO to reach a maximum if the dihedral angle θ, H^4—C^5···C^2—H^3, is near 0 or near 180°, *i.e.* if the H^4—C^5 bond eclipses the p_x orbital of C^4, and has its minimum value at $\theta = 90°$ with the H^4—C^5 bond eclipsing the p_z orbital (see Fig. 1).

A summary of the results of the calculations (23) is given in Table 2. If one compares the calculated coupling constants with the experimental ones, it is obvious that the agreement is by no means quantitative, the absolute INDO values being too large by *ca.* 30–70% for all J's except $J(3,4)$ in **2**. Qualitatively, however, the INDO calculations in Table 2 give the correct sequence of the magnitudes of $J(1,4)$, $J(2,4)$, and $J(3,4)$ in each of **1**, **2**, and **3**. In all but one case in Table 2 the CNDO/2 results are much smaller than the observed ones, indicating the importance of π electron contributions to these coupling constants (15).

Taking $J(\text{INDO}) - J(\text{CNDO})$ as an approximate measure of the π contribution to the coupling constants (15) and considering the differences between observed and calculated couplings, one may arrive at a fairly constant $^5J_\pi$ for ^5J_c and ^5J_t in **2** and **3** of about +0.6 Hz and a $^6J'_\pi$ for $^6J'_c$ and $^6J'_t$ in **1** of about −0.6 Hz. These values compare to a $^5J_\pi$ of +0.7 Hz in diene systems as proposed by Harris and coworkers (7).

(4) The Allylic Couplings between Methyl and Olefinic Protons in **3**

These couplings over four bonds are measured (13) as $^4J'_c = -1.60$ and $^4J'_t = -1.08$ Hz. Following the procedure of Barfield in his analogous calculations for propene (24), the present calculations yield $^4J'_c = -1.83$ and $^4J'_t = -1.61$ Hz in the INDO approximation but $^4J'_c = 0.05$ and $^4J'_t = 0.39$ Hz in the CNDO/2 approximation. These results bear out the contention (24) that the *cisoid* is larger in magnitude than the *transoid* coupling because of a larger positive σ electron contribution to the *transoid* coupling. The INDO predictions for **3** have the same qualitative relationship to propene as do those for 2-cyanopropene (24), in that $^4J'_c$ is calculated to be larger in **3** than in propene but $^4J'_t$ smaller in **3** than in propene.

(5) Calculated and Observed Dipole Moments

The dipole moment of **1** is calculated to be 0.29 D by the INDO, and 0.42 D by the CNDO/2 approximation. The experimental value is unknown. For **2** we calculate 0.14 (INDO) and 0.20 D (CNDO/2) while the experimental value is 0.44 D in the gas phase (25). The calculated dipole moment of **3** in the conformation with one methyl C—H bond eclipsing the double bond is 0.32 (INDO) and 0.46 D (CNDO/2)

Can. J. Chem. Downloaded from www.nrcresearchpress.com by 210.87.254.5 on 09/05/12
For personal use only.

while the experimental value is 0.51 D in the gas phase (22). The computed moments are somewhat smaller than the observed moments, as found previously for other hydrocarbons (15).

We are grateful to Dr. J. B. Rowbotham and Mr. R. Wasylishen for help with the computer program and to the National Research Council of Canada for financial support.

1. C. J. MACDONALD and W. F. REYNOLDS. Can. J. Chem. **48**, 1002 (1970).
2. M. BARFIELD, C. J. MACDONALD, I. R. PEAT, and W. F. REYNOLDS. J. Am. Chem. Soc. **93**, 4195 (1971).
3. R. WASYLISHEN and T. SCHAEFER. Can. J. Chem. **49**, 3216 (1971).
4. J. B. ROWBOTHAM, R. WASYLISHEN, and T. SCHAEFER. Can. J. Chem. **49**, 1799 (1971).
5. R. T. HOBGOOD and J. H. GOLDSTEIN. J. Mol. Spectrosc. **12**, 76 (1964).
6. A. A. BOTHNER-BY and R. K. HARRIS. J. Am. Chem. Soc. **87**, 3445 (1965).
7. A. A. BOTHNER-BY and R. K. HARRIS. J. Am. Chem. Soc. **87**, 3451 (1965).
8. A. V. CUNLIFFE and R. K. HARRIS. Mol. Phys. **13**, 269 (1967).
9. P. ALBRIKTSEN, A. V. CUNLIFFE, and R. K. HARRIS. J. Magn. Res. **2**, 150 (1970).
10. A. L. SEGRE, L. ZETTA, and A. DI CORATO. J. Mol. Spectrosc. **32**, 296 (1969).
11. E. I. SNYDER, L. J. ALTMAN, and J. D. ROBERTS. J. Am. Chem. Soc. **84**, 2004 (1962).
12. J. C. HIRST and D. M. GRANT. J. Am. Chem. Soc. **84**, 2009 (1962).
13. H. M. HUTTON and T. SCHAEFER. Can. J. Chem. **45**, 1165 (1967).
14. R. M. LEQUAN and M. P. SIMONNIN. Compt. rend. Acad. Sci. Paris (C) **266**, 825 (1968).
15. D. L. BEVERIDGE and J. A. POPLE. Approximate molecular orbital theory. McGraw-Hill Book Company, New York. N.Y., 1970.
16. R. FREEMAN and W. A. ANDERSON. J. Chem. Phys. **37**, 2053 (1962).
17. C. W. HAIGH and J. M. WILLIAMS. J. Mol. Spectrosc. **32**, 398 (1969).
18. R. A. HOFFMAN. Mol. Phys. **1**, 326 (1958).
19. M. KARPLUS. J. Chem. Phys. **33**, 1842 (1960).
20. S. STERNHELL. Quart. Rev. Chem. Soc. **23**, 236 (1969).
21. Tables of interatomic distances and configuration in molecules and ions. The Chemical Society, Special Publication No. 11, London, 1958. (*a*) p. 181; (*b*) p. 161.
22. S. L. HSU and W. H. FLYGARE. J. Mol. Spectrosc. **32**, 375 (1969).
23. Program 141. Quantum Chemistry Program Exchange. Indiana University, Bloomington, Indiana.
24. M. BARFIELD. J. Am. Chem. Soc. **93**, 1066 (1971).
25. G. A. SOBOLEV, A. M. SHCHERBAKOV, and P. A. AKISHIN. Opt. Spectrosc. **12**, 58 (1962).

Can. J. Chem. Downloaded from www.nrcresearchpress.com by 210.87.254.5 on 09/05/12
For personal use only.

A Kinetic Study of the Oxidative Addition of Substituted Benzenethiols Towards *trans*-Halocarbonylbis(triphenylphosphine)iridium(I)[1]

J. R. GAYLOR AND C. V. SENOFF[2]

Department of Chemistry, University of Guelph, Guelph, Ontario

Received January 13, 1972

The kinetics of the oxidative addition of a series of para-substituted benzenethiols, HSC_6H_4Y, where Y = 4-NO_2, 4-Br, 4-Cl, 4-F, 4-H, 4-CH_3, or 4-CH_3O towards the complexes, *trans*-$IrX(CO)(Ph_3P)_2$ where X = Cl, Br, or I have been studied in benzene between 15 and 45°. These reactions follow simple second order kinetics, rate = $k_2[IrX(CO)(Ph_3P)_2][HSC_6H_4Y]$. The two principal factors which influence the rates of these reactions are the mesomeric and inductive effects of the para-substituent and the nature of the ligand, X, coordinated to iridium. The rate of reaction increases as the substituent becomes more electron withdrawing and as X varies from Cl to Br to I. The kinetic data together with spectroscopic data (i.r. and n.m.r.) suggest that oxidative addition proceeds via a three-centered activated complex to give the *cis*-product.

Les cinétiques de l'addition oxydante d'une série de benzènethiols parasubstitués, HSC_6H_4Y avec Y = NO_2-4, Br-4, Cl-4, F-4, H-4, CH_3-4 ou OCH_3-4, sur les complexes $IrX(CO)(Ph_3P)_2$-*trans* avec X = Cl, Br ou I, ont été étudiées dans le benzène entre 15 et 45°. Ces réactions suivent une cinétique de second ordre simple dont la vitesse est $k_2[IrX(CO)(Ph_3P)_2][HSC_6H_4Y]$. Les deux facteurs principaux qui influent sur les vitesses de ces réactions sont les effets mésomère et inductif du substituant en para et la nature du ligand X coordiné à l'iridium. La vitesse de la réaction croît à mesure que le substituant devient plus électroattracteur et à mesure que X passe de Cl à Br puis à I. Les données cinétiques et spectroscopiques (i.r. et r.m.n.) font penser que l'addition oxydante passe par un complexe activé à trois centres pour conduire ensuite au produit *cis*.

Canadian Journal of Chemistry, **50**, 1868 (1972)

The activation of small covalent molecules by the complexes, *trans*-$[IrX(CO)(Ph_3P)_2]$ (X = Cl, Br, I, or a pseudohalogen) via oxidative addition has been the subject of numerous investigations in recent years (1–3). Several kinetic studies have been carried out in order to ascertain the mechanism of the oxidative addition towards these particular substrates (4–8). Previous work from this laboratory as well as others has shown that substituted benzenethiols will oxidatively add to *trans*-$[IrCl(CO)(Ph_3P)_2]$ to form $[IrHCl(SAr)(CO)(Ph_3P)_2]$ where ^-SAr is a substituted benzenethiolato ligand (9–11). As part of a general program investigating the reactivity of aromatic thiols towards low valent transition metal complexes, we have undertaken a kinetic study of reaction 1

[1] *trans*-$[IrX(CO)(Ph_3P)_2] + HSC_6H_4Y \rightarrow [IrHX(SC_6H_4Y)(CO)(Ph_3P)_2]$

where X = Cl, Br, or I and Y = a para-substituent, NO_2, F, Cl, Br, H, CH_3, or CH_3O. The results of this investigation are reported at this time.

[1]Taken from the M.Sc. Thesis of J.R.G., August, 1971.

[2]To whom correspondence should be addressed.

Results and Discussion

The products of reaction 1 when X = Cl have been previously isolated and characterized (10). During the course of this kinetic study, the corresponding products when X = Br or I were isolated and characterized. Infrared and ^1H n.m.r. data are summarized in Tables 1 and 2. Examination of these data indicates that the spectral characteristics of $[IrHX(SAr)(CO)(Ph_3P)_2]$ (X = Br or I) follow the same pattern established for $[IrHCl(SAr)(CO)(Ph_3P)_2]$, *i.e.*, ν_{CO} is a linear function of the Hammett substituent parameter, σ_p, and τ(Ir—H) for a given ligand, X, is invariant to the nature of the para-substituent associated with the benzenethiolato-ligand, ^-SAr (10). These results indicate that the mode of addition of the para-substituted benzenethiols is *cis*- for all three substrates. It may also be noted that ν_{Ir-H} decreases with increasing *trans*- influence of the halogen, X (12). Also, the changes in τ(Ir—H) as X is varied follow the general trend noted recently in the literature (13).

Representative kinetic data for reaction 1 in benzene at 25° are given in Table 3. Kinetic data at various temperatures are summarized in Table 4. These data indicate that the rates of

Can. J. Chem. Downloaded from www.nrcresearchpress.com by 210.87.254.40 on 09/05/12
For personal use only.

Can. J. Chem. Downloaded from www.nrcresearchpress.com by 210.87.254.40 on 09/05/12
For personal use only.

TABLE 1. Infrared data for the complexes, $IrHX(SC_6H_4Y)(CO)(Ph_3P)_2$*

Y	ν_{CO} Nujol	ν_{CO} $CHCl_3$	ν_{Ir-H} Nujol	ν_{Ir-H} $CHCl_3$
(*a*) X = Br				
NO_2	2058s	2045s	2241w	2244w
Br	2045s	2040s	2233w	2242w
Cl	2033s	2040s	2206w	2241w
F	2037s	2039s	2265w	2244w
H	2031s	2037s	2253w	2241w
CH_3	2030s	2037s	2258w	2242w
CH_3O	2027s	2035s	2258w	2239w
(*b*) X = I				
NO_2	2056s	2045s	2214w	2230w
Br	2043s	2040s	2217w	2228m
Cl	2045s	2040s	2213w	2228w
F	2037s	2039s	2236w	2228m
H	2027s	2036s	2226w	2232w
CH_3	2042s	2037s	2211w	2228w
CH_3O	2043s	2037s	2208w	2226w

*s = strong; m = medium; w = weak.

TABLE 2. ^1H n.m.r. data for the complexes, $IrHX(SC_6H_4Y)(CO)(Ph_3P)_2$*

Y	τ(Ir—H) (p.p.m.)	$^3J_{P-H}$ (Hz)
(*a*) X = Br		
NO_2	25.04	12.2
Br	25.33	12.4
Cl	25.21	12.0
F	25.38	12.2
H	25.51	12.0
CH_3	25.40	12.2
CH_3O	25.34	12.4
(*b*) X = I		
NO_2	23.04	12.4
Br	23.25	12.2
Cl	23.28	12.3
F	23.33	12.1
H	23.33	12.3
CH_3	23.31	12.3
CH_3O	23.37	12.0

*Recorded in $CDCl_3$ with TMS as internal reference.

reaction are dependent on the concentration of the substrate, $[IrX(CO)(Ph_3P)_2]$, and the incoming substituted benzenethiol. The rates are also dependent on the nature of the substrate and the substituted benzenethiol. Plots of the pseudo first-order rate constant, k_{obs}, *vs.* $[HSC_6H_4Y]$ were linear with zero intercepts. Representative plots for the substrate, *trans*-$[IrCl(CO)(Ph_3P)_2]$ are shown in Fig. 1. Hence, reaction 1 obeys the simple second-order rate law, eq. 2

TABLE 3. Kinetic data for reaction *trans*-$[IrCl(CO)(Ph_3P)_2] + HSC_6H_4Y \rightarrow [IrHCl(SC_6H_4Y)(CO)(Ph_3P)_2]$ in benzene at 25°

HSC_6H_4Y	$[HSC_6H_4Y]$ (*M*)	$10^2 k_{obs}$ (s^{-1})	k_2 ($M^{-1}s^{-1}$)
$HSC_6H_4NO_2$	0.005	0.77	1.5
	0.017	2.7	1.6
	0.020	3.1	1.6
	0.028	4.3	1.5
HSC_6H_4Br	0.204	6.8	0.33
	0.230	8.1	0.35
	0.281	9.9	0.35
	0.306	11	0.36
	0.384	13	0.35
HSC_6H_4Cl	0.240	7.5	0.31
	0.292	8.8	0.30
	0.362	12	0.33
	0.640	21	0.33
HSC_6H_4F	0.228	5.0	0.22
	0.571	12	0.21
	0.686	14	0.20
	0.914	18	0.20
HSC_6H_4H	0.195	1.6	0.082
	0.292	2.5	0.086
	0.390	3.2	0.082
	0.487	4.0	0.082
	0.580	4.7	0.081
	0.600	5.0	0.083
$HSC_6H_4CH_3$	0.126	0.87	0.069
	0.190	1.4	0.074
	0.280	1.9	0.068
	0.346	2.4	0.069
	0.443	3.1	0.070
$HSC_6H_4OCH_3$	0.325	2.6	0.080
	0.489	4.1	0.084
	0.650	5.4	0.083
HSC_6H_4D	0.30	2.0	0.067
	0.75	5.1	0.068

$$[2] \quad \frac{-d[IrX(CO)(Ph_3P)_2]}{dt} = k_2[IrX(CO)(Ph_3P)_2][HSC_6H_4Y]$$

This rate law is similar to that commonly found for oxidative addition reactions of *trans*-$[IrX(CO)(Ph_3P)_2]$ (4–8).

As mentioned above, the rates of reaction are dependent on the nature of X; the second-order rate constants increase in the order Cl < Br < I. In fact, the reactions when X = I

TABLE 4. Second-order rate constants for reaction *trans*-[IrX(CO)(Ph_3P)$_2$] + HSC_6H_4Y → [IrHX(SC_6H_4Y)(CO)(Ph_3P)$_2$] in benzene

X = Cl			X = Br		
T (°C)	Y	k_2 ($M^{-1}s^{-1}$)	T (°C)	Y	k_2 ($M^{-1}s^{-1}$)
15	NO_2	0.79	15	NO_2	5.9
25		1.6	25		11
35		2.3	35		18
45		3.7	45		29
15	Br	0.16	15	Br	1.1
25		0.35	25		1.9
35		0.52	35		3.3
45		0.89	45		5.1
15	Cl	0.17	15	Cl	1.2
25		0.32	25		1.8
35		0.53	35		3.5
45		0.89	45		4.9
15	F	0.12	15	F	0.67
25		0.21	25		1.3
35		0.35	35		2.7
45		0.75	45		3.4
15	H	0.043	15	H	0.38
25		0.082	25		0.66
35		0.12	35		1.0
45		0.18	45		1.8
15	CH_3	0.036	15	CH_3	0.33
25		0.070	25		0.72
35		0.12	35		1.2
45		0.19	45		1.9
15	CH_3O	0.040	15	CH_3O	0.37
25		0.082	25		0.65
35		0.15	35		1.0
45		0.24	45		2.4

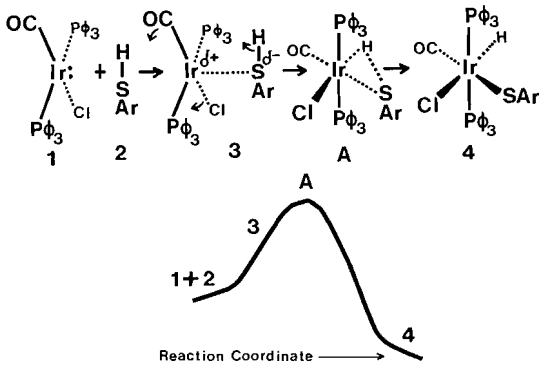

FIG. 1. Plot of k_{obs} *vs.* [HSC_6H_4Y] for *trans*-[IrCl(CO)(Ph_3P)$_2$] at 25°.

were too fast to be reliably monitored with the available instrumentation. This order of reactivity parallels that observed for the reactions of H_2 and O_2 with these iridium(I) complexes (4, 6, 7). The rates of reaction also varied with the nature of the para-substituent on the benzenethiol; the trend is towards an increase in rate as the acidity of the substituted benzenethiol increases (14). For a given substrate the rates of reaction increase as the electron withdrawing ability of Y increases and *vice versa* for electron releasing substituents. A Hammett plot of ln k_2 versus σ_p for *trans*-[IrCl(CO)(Ph_3P)$_2$] is shown in Fig. 2 having a slope, $\rho = +3.2$. The corresponding Hammett plot for *trans*-[IrBr(CO)(Ph_3P)$_2$] had a ρ value of +2.8. The somewhat larger slope for the chlorocomplex suggests that it can better discriminate between the different substituent effects.

Activation parameters were calculated using the Eyring eq. 3 and are given in Table 5.

Can. J. Chem. Downloaded from www.nrcresearchpress.com by 210.87.254.40 on 09/05/12
For personal use only.

TABLE 5. Activation parameters*

X = Cl			X = Br		
Y	ΔH^* (kcal mol^{-1})	ΔS^* (cal mol^{-1} deg^{-1})	Y	ΔH^* (kcal mol^{-1})	ΔS^* (cal mol^{-1} deg^{-1})
NO_2	8.4	−30	NO_2	8.9	−24
Br	9.4	−29	Br	8.7	−28
Cl	9.3	−30	Cl	8.2	−30
F	10	−27	F	9.5	−26
H	7.8	−37	H	8.6	−31
CH_3	9.4	−32	CH_3	9.8	−26
CH_3O	10	−29	CH_3O	10	−25

*Estimated uncertainties are ±1 kcal mol^{-1} for ΔH^* and ±3 cal mol^{-1} deg^{-1} for ΔS^*.

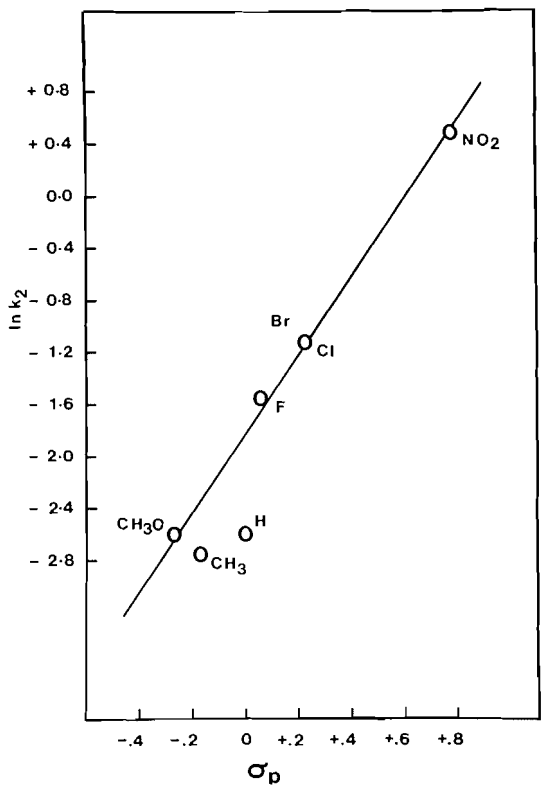

FIG. 2. Hammett plot for *trans*-[IrCl(CO)(Ph_3P)$_2$].

$$[3] \qquad k_2 = \frac{kT}{h} \exp\left(-\frac{\Delta H^*}{RT}\right) \exp\left(\frac{\Delta S^*}{R}\right)$$

The change in ΔH^* as X and Y are varied for reaction 1 is small. The change in ΔS^* is somewhat larger but there appears to be no simple correlation between these two parameters. The large negative entropies of activation suggest a highly constrained three-center transition state, A, comparable to that proposed when O_2 and

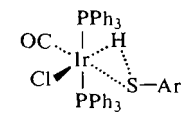

A

H_2 react with these iridium(I) substrates (4, 6–8). The rate of reaction of S-deuterated benzenethiol with *trans*-[IrCl(CO)(Ph_3P)$_2$] was also measured and these kinetic data are included in Table 3. The ratio, $k_2^H/k_2^D = 1.2$ represents a small kinetic isotope effect.

It is then apparent that the two major factors which influence the rate of formation of the oxidative addition product in reaction 1 are (*i*) the inductive and mesomeric effects of the para-substituent associated with the benzenethiol and (*ii*) the nature of the ligand, X, coordinated to iridium(I). Since the rates of reaction 1 are related to the acidity of HSC_6H_4Y, the kinetic data presented herein substantiate Vaska's "acid–base" concept for the oxidative addition reactions of *trans*-[IrX(CO)(Ph_3P)$_2$] (2). The breaking of the H—S bond may then be considered to be the "dominant inertial factor" in reaction 1 for a given X. The variation in rate as X is changed for a given substituent suggests that bond making must be the driving force in reaction 1 since iridium formally loses a pair of electrons to the incoming substituted benzenethiol. These changes in rate as X is varied also reflect the change in "basicity" of the substrate as well as the significant dependence of bond formation on the nature of X.

In view of the fact that the enthalpies of activation are ~8–10 kcal mol^{-1} and the average strength of the sulfur–hydrogen bond is ~80 kcal mol^{-1} (15), it is unlikely that the mechanism for reaction 1 involves dissociation

Can. J. Chem. Downloaded from www.nrcresearchpress.com by 210.87.254.40 on 09/05/12
For personal use only.

TABLE 6. Analytical data

Complex	Calculated		Found	
	C	H	C	H
$IrHBr(SC_6H_4NO_2)(CO)(Ph_3P)_2$	52.72	3.57	53.35	3.92
$IrHBr(SC_6H_4Br)(CO)(Ph_3P)_2$	50.96	3.45	51.58	3.28
$IrHBr(SC_6H_4Cl)(CO)(Ph_3P)_2$	53.29	3.61	53.19	3.94
$IrHBr(SC_6H_4F)(CO)(Ph_3P)_2$	54.22	3.67	54.40	3.69
$IrHBr(SC_6H_4H)(CO)(Ph_3P)_2$	55.26	3.85	55.32	3.92
$IrHBr(SC_6H_4CH_3)(CO)(Ph_3P)_2$	55.71	4.01	55.76	4.43
$IrHBr(SC_6H_4OCH_3)(CO)(Ph_3P)_2$	54.79	3.94	55.14	4.13
$IrHI(SC_6H_4NO_2)(CO)(Ph_3P)_2$	50.30	3.41	50.65	3.49
$IrHI(SC_6H_4Br)(CO)(Ph_3P)_2$	48.69	3.30	48.94	3.50
$IrHI(SC_6H_4Cl)(CO)(Ph_3P)_2$	50.82	3.44	51.22	3.58
$IrHI(SC_6H_4F)(CO)(Ph_3P)_2$	51.65	3.50	52.06	3.77
$IrHI(SC_6H_4H)(CO)(Ph_3P)_2$	52.60	3.67	52.97	3.85
$IrHI(SC_6H_4CH_3)(CO)(Ph_3P)_2$	53.07	3.82	53.29	3.79
$IrHI(SC_6H_4OCH_3)(CO)(Ph_3P)_2$	52.23	3.76	51.63	3.96

of the sulfur–hydrogen bond as a distinguishable step. This notion is also supported by the small kinetic isotope effect which was observed.

In conclusion, the kinetic data presented herein are consistent with a non-dissociative mechanism for reaction 1 which involves an activated complex similar to that previously proposed for the activation of O_2 and H_2 by *trans*-$[IrX(CO)(Ph_3P)_2]$ (4, 6, 7). The overall proposed mechanism is schematically shown below.

The initial step leading to the activated complex, **A**, may be regarded as a nucleophilic attack by the iridium(I) complex, **1**, at the sulfur atom of the thiol, **2** (or an electrophilic attack by the sulfur at iridium) accompanied by some electron transfer from iridium to sulfur, **3**, with concomitant formation of the iridium–hydrogen bond yielding the activated complex, **A**. Bond making and bond breaking then proceed further in the latter to eventually form the observed product, **4**.

Experimental

(1) Materials

Triphenylphosphine was purchased from Eastman Organic Chemicals, Inc., and was recrystallized from ethanol prior to use. Other chemicals were reagent grade unless otherwise indicated.

trans-Halocarbonylbis(triphenylphosphine)iridium(I), $IrX(CO)(Ph_3P)_2$

These complexes were prepared according to literature procedures (4, 16).

S-Deuterated Benzenethiol, C_6H_5SD

This reagent was prepared according to the method of Ellgen and Gregory (17). The extent of S-deuteration was determined by n.m.r. using a Varian A60 spectrometer. The product was found to be 96.6% deuterated.

(2) Isolation of Reaction Products

The products, $[IrHBr(SC_6H_4Y)(CO)(Ph_3P)_2]$ and $[IrHI(SC_6H_4Y)(CO)(Ph_3P)_2]$, were isolated by the procedure used to prepare $[IrHCl(SC_6H_4Y)(CO)(Ph_3P)_2]$ (10). Analytical data are given in Table 6.

(3) Kinetic Measurements

The kinetics of reaction 1 were followed spectrophotometrically by monitoring the consumption of the iridium(I) substrate at a fixed wavelength with a Bausch and Lomb 505 spectrophotometer. The absorption peaks used were 439 nm ($\varepsilon = 7.68 \times 10^2$ l mol^{-1} cm^{-1}) for *trans*-$[IrCl(CO)(Ph_3P)_2]$ and 444 nm ($\varepsilon = 7.33 \times 10^2$ l mol^{-1} cm^{-1}) for *trans*-$[IrBr(CO)(Ph_3P)_2]$. This procedure was modified when 4-nitrothiophenol was used as the incoming addendum since the spectrum of the product masked the absorption peaks at 439 and 444 nm for the iridium(I) substrates. However, the products of reaction with this particular thiol absorbed strongly at 420 nm ($\varepsilon \sim 14.5$ l mol^{-1} cm^{-1}) when X = Cl and at 424 nm ($\varepsilon \sim 14.5$ l mol^{-1} cm^{-1}) when X = Br. The corresponding substrates exhibited absorption minima at these wavelengths. Hence, the rate of appearance of product was monitored when 4-nitrobenzenethiol was the addendum.

All kinetic runs were carried out in benzene which had been dried over sodium, degassed, and then saturated with nitrogen. Individual solutions of substrate and thiol were thermostated for approximately 1 h prior to mixing. An aliquot (1.0 ml) of the solution containing the thiol was placed in a quartz cell in the thermostated cell compartment of the spectrophotometer and then an equal volume of the solution containing the appropriate substrate was quickly added by means of a hypodermic syringe to ensure rapid and complete mixing of the two solutions. The rate of reaction was then followed at a fixed wavelength as described above.

The concentration of *trans*-$[IrCl(CO)(Ph_3P)_2]$ used for the kinetic runs was 1.0×10^{-3} *M* and the concentration of the incoming thiol was varied from 0.01–0.75 *M* (at least a

Can. J. Chem. Downloaded from www.nrcresearchpress.com by 210.87.254.40 on 09/05/12
For personal use only.

10-fold excess) in order to maintain pseudo first-order kinetic conditions. The corresponding concentration of *trans*-[IrBr(CO)(Ph_3P)$_2$] was 2.5×10^{-5} *M* and 1.0×10^{-3}–2.5×10^{-3} *M* for the incoming thiol. The pseudo first-order rate constants, k_{obs}, were obtained from plots of $\ln (A_t - A_\infty)$ or $\ln (A_\infty - A_t)$ *vs.* time where A_t is the absorbance at time t, and A_∞ is the absorbance at infinite time. Pseudo first-order rate constants were reproducible to $\pm 10\%$ or better.

Microanalyses were determined by A. G. Gygli, Toronto. Infrared spectra were recorded on a Beckman IR-12 spectrophotometer in $CHCl_3$ with 0.2 mm NaCl cells or as Nujol mulls between NaCl plates. Proton n.m.r. spectra were recorded on a Varian HA100 or A60 spectrometer.

We wish to acknowledge financial support from the National Research Council of Canada in the form of an operating grant to C.V.S. We are indebted to Mr. B. G. Sayer for obtaining the n.m.r. spectra and the Department of Chemistry, McMaster University, Hamilton, for the use of the Varian HA100 spectrometer. We also thank Dr. R. K. Boyd for helpful discussions throughout the course of this work and Dr. L. Vaska for providing some of his results prior to publication.

1. J. P. COLLMAN and W. R. ROPER. Adv. Organomet. Chem. **7**, 63 (1968).
2. L. VASKA. Accts. Chem. Res. **1**, 335 (1968).
3. J. HALPERN. Accts. Chem. Res. **3**, 386 (1970).
4. P. B. CHOCK and J. HALPERN. J. Am. Chem. Soc. **88**, 3511 (1966).
5. J. A. SMITH, M. GREEN, and D. C. WOOD. J. Chem. Soc. A, 1847 (1970).
6. L. VASKA and M. F. WERNEKE. Trans. N.Y. Acad. Sc. **33**, 70 (1971).
7. L. VASKA, L. S. CHEN, and C. V. SENOFF. Science, **174**, 587 (1971).
8. L. VASKA and L. S. CHEN. Chem. Commun. 1080 (1971).
9. H. SINGER and G. WILKINSON. J. Chem. Soc. A, 2516 (1968).
10. C. V. SENOFF. Can. J. Chem. **48**, 2444 (1970).
11. M. H. B. STIDDARD and R. E. TOWNSEND. J. Chem. Soc. A, 2719 (1970).
12. F. BASOLO and R. G. PEARSON. Mechanisms of inorganic reactions. John Wiley, N.Y. 1967. p. 351.
13. E. R. BIRNBAUM. Inorg. Nucl. Chem. Lett. 7, 233 (1971).
14. G. CHUCHANI and A. FROHLICH. J. Chem. Soc. B, 1417 (1971).
15. W. E. DASENT. Nonexistent compounds. Marcel Dekker, Inc., N.Y. 1965. Chap. 1.
16. L. VASKA and J. W. DILUZIO. J. Am. Chem. Soc. **84**, 679 (1962).
17. P. C. ELLGEN and C. D. GREGORY. Inorg. Chem. **10**, 980 (1971).

Can. J. Chem. Downloaded from www.nrcresearchpress.com by 210.87.254.40 on 09/05/12
For personal use only.

The Concentration Dependence at 1 atm Pressure and 300 °K of the Binary Diffusion Coefficients of the Systems Helium–Carbon Dioxide, Helium–Nitrous Oxide, and Helium–Sulfur Hexafluoride

KENNETH R. HARRIS AND T. N. BELL

Department of Chemistry, Simon Fraser University, Burnaby 2, British Columbia

AND

PETER J. DUNLOP

Department of Physical and Inorganic Chemistry, University of Adelaide, South Australia

Received December 30, 1971

Binary diffusion coefficients are reported for the systems He–CO_2, He–N_2O, and He–SF_6. In agreement with the Chapman–Enskog theory the concentration dependence of the diffusion coefficient of each system increases with the mole fraction of the heavier component.

Les coefficients de diffusion binaire sont rapportés pour les systèmes He–CO_2, He–N_2O, et He–SF_6. En accord avec la théorie de Chapman–Enskog, la dépendance du coefficient de diffusion de chaque système par rapport à la concentration, augmente avec la fraction molaire du composé le plus lourd.

Canadian Journal of Chemistry, **50**, 1874 (1972)

Giddings and Seager (1) have reported data at approximately 300 °K for the concentration dependence of the binary diffusion coefficient, D_{12}, of the systems He–N_2 and He–CO_2. Their results, obtained by a chromatographic technique, indicated that, while the binary diffusion coefficient for the former system *increased* with the mole fraction of the heavier component, D_{12} actually *decreased* with the mole fraction of CO_2 for the latter system. Since the Chapman–Enskog theory (2) for transport in dilute gases predicts that D_{12} should increase with the mole fraction of the heavier component (3–5), it seemed worthwhile to remeasure D_{12} for the system He–CO_2 with a technique we have developed (6), but which was originally proposed by Onsager (7) and used by Harned and co-workers (7, 8) to study transport in dilute electrolyte solutions.

In addition we have measured the concentration dependence of D_{12} for the systems He–N_2O and He–SF_6. N_2O was chosen as a component for the former system since like CO_2 it is a linear molecule, it is isoelectronic with CO_2, and it has a mass almost identical with that species; however, it differs in its polar characteristics and therefore probably in its interaction potential. SF_6 was chosen as a component for the latter system because it was a spherically symmetrical polyatomic molecule with a mass much greater than CO_2 and N_2O.

Experimental

The method used to measure the concentration dependence of D_{12} for each system has been previously described in detail (6). It is suggested that that paper be read in conjunction with this article. The temperature of the water-thermostat, in which the diffusion cell was placed, was controlled to approximately $\pm 0.001°$ at 300 °K, and we believe that this feature of our apparatus was mainly responsible for the precision of our measurements.

The purities of He, CO_2, N_2O, and SF_6 were stated by the suppliers to be better than 99.99, 99.99, 99.9, and 99.8%, respectively.

Since the above gases and their mixtures are non-ideal at 300 °K and 1 atm pressure, virial coefficient data for He–CO_2 in the literature (9) were used for the calculation of concentrations for that system. Similar data are not available for the systems He–N_2O and He–SF_6.

Results

Table 1 summarizes the experimental data for each system. In this table are given the experiment number; the mole fraction, x_2, of the heavy component in each experiment; the total pressure, P; the corresponding experimental value of D_{12} and that corrected to 1 atm pressure. The data may be represented by the following equations, where x_2 is the mole fraction of the heavy component and s the standard deviation:

Can. J. Chem. Downloaded from www.nrcresearchpress.com by 210.87.254.6 on 09/05/12
For personal use only.

TABLE 1. Diffusion coefficients for the systems He–CO_2, He–N_2O and He–SF_6 at 300 °K and 1 atm

Expt. No.	x_2	P (atm)	D_{12} (cm²/s) Experimental	D_{12} (cm²/s) Corrected to 1 atm
		[He–CO_2]		
103	0.052_2	0.984_9	0.613_1	0.603_9
104	0.055_8	0.992_2	0.609_8	0.605_0
105	0.060_4	0.995_7	0.606_2	0.603_6
102	0.446_8	0.988_6	0.617_3	0.610_3
109	0.482_8	1.012_4	0.603_3	0.610_8
110	0.508_2	1.009_6	0.605_2	0.611_0
108	0.508_4	0.995_7	0.609_6	0.607_0
111	0.751_6	0.998_5	0.614_7	0.613_7
106	0.940_2	0.956_3	0.644_0	0.615_8
107	0.940_8	0.950_6	0.649_8	0.617_7
101	0.941_5	1.006_3	0.614_0	0.617_8
		[He–N_2O]		
113	0.055_6	0.995_9	0.596_6	0.594_1
114	0.111_9	1.059_0	0.560_6	0.593_7
117	0.497_7	1.000_3	0.598_4	0.598_6
118	0.500_5	1.001_0	0.600_6	0.601_2
116	0.501_6	0.998_7	0.602_4	0.601_6
119	0.940_4	0.988_3	0.612_1	0.604_9
115	0.940_5	0.992_9	0.611_3	0.607_0
		[He–SF_6]		
120	0.057_4	0.731_3	0.533_7	0.390_3
126	0.062_9	0.667_7	0.584_9	0.390_5
121	0.119_4	0.782_7	0.499_2	0.390_7
130	0.302_3	0.663_4	0.593_6	0.393_8
128	0.401_1	0.667_3	0.590_0	0.393_7
131	0.500_1	0.663_8	0.596_5	0.396_0
129	0.699_8	0.663_8	0.599_1	0.397_8
127	0.786_8	0.675_7	0.589_0	0.398_0
123	0.937_8	0.666_9	0.600_0	0.400_2
125	0.940_4	0.663_7	0.606_6	0.402_6

$$D_{12}\ (\mathrm{cm^2/s, He\text{–}CO_2}) = 0.603_1 + 0.014_5\ x_2;\quad s = 0.0014$$

$$D_{12}\ (\mathrm{He\text{–}N_2O}) = 0.593_0 + 0.014_4\ x_2;\quad s = 0.0014$$

$$D_{12}\ (\mathrm{He\text{–}SF_6}) = 0.389_5 + 0.012_1\ x_2;\quad s = 0.0008$$

The data in Table 1 are shown in Fig. 1 where one can see, in contrast to similar data for binary mixtures of rare gases (6), that all the experimental diffusion coefficients are linear in x_2 within the estimated experimental error of 0.1 to 0.2%. This linear dependence was also noted previously (6) for the system H_2–N_2 at

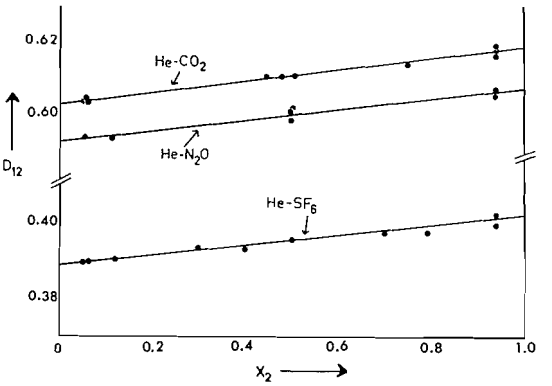

FIG. 1. Diffusion coefficients for the systems He–CO_2, He–N_2O and He–SF_6.

TABLE 2. Diffusion data for the systems He–CO_2 and He–SF_6 for comparison with the results in Table 1 and Fig. 1

x_2	D_{12} (cm² s⁻¹)*	Reference
	[He–CO_2]	
0.5	0.601	10
0.5	0.622	1
0.5	0.606	11
0.5	0.616	12
~0	0.623	13
~0	0.617	14
	[He–SF_6]	
~0	0.431	15
0.5	0.410	12

*Corrected to 300 °K and 1 atm.

300 °K. Thus it would appear that, if the data in Table 1 are correct, the Chapman–Enskog theory may not be sufficient (at least to the second Kihara approximation) to describe the concentration dependence of D_{12} where one or both components possess internal degrees of freedom. In addition it seems that the Chapman–Enskog theory does indeed give the correct sign for the concentration dependence of the system He–CO_2.

Figure 1 indicates that the experimental technique employed in this study easily distinguishes between the systems He–CO_2 and He–N_2O. Because CO_2 and N_2O molecules are isoelectronic and have essentially identical masses, the observed differences in the diffusion coefficients of these two systems are due to differences in the collision cross-sections.

Can. J. Chem. Downloaded from www.nrcresearchpress.com by 210.87.254.6 on 09/05/12
For personal use only.

The data in the literature for the systems He–CO_2 and He–SF_6 have been corrected to 300 °K and 1 atm and listed in Table 2. We were unable to find data for the system He–N_2O.

This work was supported by the Australian Research Grants Committee, the National Research Council of Canada, and the President's Research Grant (S.F.U.).

1. J. C. GIDDINGS and S. L. SEAGER. I EC Fundam. **1**, 277 (1962).
2. S. CHAPMAN and T. G. COWLING. The mathematical theory of non-uniform gases. Cambridge University Press, New York. 1952.
3. T. KIHARA. Imperfect gases. Asakura Bookstore, Tokyo. 1949; Rev. Mod. Phys. **25**, 831 (1953).
4. J. O. HIRSCHFELDER, C. F. CURTISS, and R. B. BIRD. Molecular theory of gases and liquids. Wiley, New York. 1954. p. 1210.
5. E. A. MASON. J. Chem. Phys. **27**, 75 (1957); **27**, 782 (1957).
6. P. J. CARSON, T. N. BELL, and P. J. DUNLOP. J. Chem. Phys. **56**, 531 (1972).
7. H. S. HARNED and D. M. FRENCH. Ann. N.Y. Acad. Sci. **46**, 267 (1945).
8. H. S. HARNED. Chem. Rev. **40**, 461 (1947).
9. R. C. HARPER, JR. and J. G. MILLER. J. Chem. Phys. **27**, 36 (1957).
10. B. K. ANNIS, A. E. HUMPHREYS, and E. A. MASON. Phys. Fluids, **12**, 78 (1969).
11. J. N. HOLSEN and M. R. STRUNK. I EC Fundam. **3**, 143 (1964).
12. B. A. IVAKIN and P. E. SUETIN. Soviet Phys. Tech. Phys. **9**, 866 (1964) (Zh. Tekh. Fiz. **34**, 1115 (1964)).
13. S. L. SEAGER, L. R. GEERTSON, and J. C. GIDDINGS. J. Chem. Eng. Data, **8**, 168 (1963).
14. R. E. WALKER, N. DEHAAS, and A. A. WESTENBERG. J. Chem. Phys. **32**, 1314 (1960).
15. E. V. EVANS and C. N. KENNEY. Proc. Roy. Soc. **A284**, 540 (1965).

Can. J. Chem. Downloaded from www.nrcresearchpress.com by 210.87.254.6 on 09/05/12
For personal use only.

Analysis of ^{134}Cs Isomer Ratios in the Fission of ^{237}Np with Protons in the Energy Range 20–85 MeV[1]

C. L. RAO[2] AND L. YAFFE

Department of Chemistry, McGill University, Montreal 101, Quebec

Received February 1, 1972

An analysis has been made of the isomer ratio, $\sigma_m/(\sigma_m + \sigma_g)$ for ^{134}Cs isomers formed in the fission of ^{237}Np by protons of energies 20–85 MeV. Compound nucleus formation was assumed up to a bombarding energy of 50 MeV, with direct interaction as the mechanism at higher energies. Values of the root-mean-square angular momentum of $12\hbar$ at 20 MeV and $16–18\hbar$ at 60–85 MeV bombarding energy agree with the experimental results. The results are consistent with the hypothesis that angular momentum is generated in the fission process.

On a fait l'analyse du rapport $\sigma_m/(\sigma_m+\sigma_g)$ pour les isomères ^{134}Cs formés lors de la fission du ^{237}Np par des protons d'énergie de 20 à 85 MeV. La formation du noyau du composé est supposée jusqu'à une énergie de bombardement de 50 MeV, pour des énergies plus élevées le mécanisme est du type interaction directe. Le valeurs des racides carrées moyennes du moment angulaire de $12\hbar$ à 20 MeV et $16–18\hbar$ à 60–80 MeV sont en accord avec les résultats expérimentaux. Les résultats sont compatibles avec l'hypothèse que le moment angulaire est produit dans le processus de fission.

Canadian Journal of Chemistry, **50**, 1877 (1972)

Introduction

Studies of isomer ratios formed in nuclear reactions on various elements (1–5) and by nuclear fission of heavy elements (6–14) by particles with thermal, low, and medium energies have been carried out. These have been particularly helpful in the understanding of angular momentum effects in these various reactions.

In a number of cases these studies were made as a function of bombarding energy. In the simple nuclear reactions it was shown that the formation of the higher spin state is enhanced as the particle energy is increased (1) owing to a larger transfer of angular momentum. A similar trend is also observed in low and medium energy fission (7).

Huizenga and Vandenbosch (15, 16) used the following expression, based on a statistical model, to determine the dependence of the nuclear level density on the spin

$$[1] \quad \rho(J) = \rho(0)(2J+1)\exp[-(J+1/2)^2/2\sigma^2]$$

where $\rho(0)$ and $\rho(J)$ are respectively the densities of states with spin 0 and J, and σ is the spin cut-off factor which describes the angular momentum distribution of the level density and is related to the moment of inertia and temperature of the nucleus. The isomer ratio depends initially on the spin distribution of the compound nucleus which is subsequently altered by the emission of particles and the accompanying gamma cascade. Equation 1 has been used to calculate the angular momentum distribution after each of the above steps.

In the fission process the first step, which determines the initial spin distribution, is not easy to calculate since it involves a calculation of the angular momentum distribution of the pairing fragments formed in the fission process. According to Warhanek and Vandenbosch (8) the angular momentum distribution in fission can be described by the following functional form

$$[2] \quad F(J) = (2J+1)\exp(-J(J+1)/B^2)$$

where B, a factor similar to the spin cut-off parameter σ, is related to J, the root-mean-square angular momentum. The de-excitation steps which follow, *i.e.* particle and gamma emission, are treated as in the case of simple nuclear reactions, assuming some energy-dependent factor of σ, the spin cut-off parameter, and I, the nuclear moment of inertia.

The isomers of ^{134}Cs offer a convenient way of determining the formation cross sections of

[1]This research was supported by a grant from the National Research Council of Canada.

[2]Present address: Department of Radiology, Albert Einstein College of Medicine of Yeshiva University, 1300 Morris Park Ave., Bronx, N.Y. 10461.

Can. J. Chem. Downloaded from www.nrcresearchpress.com by 210.87.254.5 on 09/05/12
For personal use only.

TABLE 1. Experimental cross sections of $^{134}Cs^{m}$ and $^{134}Cs^{m+g}$ and their ratios in the fission of ^{237}Np with protons in the energy range 20–85 MeV

Proton energy (MeV)	σ		
	$^{134}Cs^{m}$	$^{134}Cs^{m+g}$	σ_m/σ_{m+g}
20	2.8±0.4	4.6±0.9	0.61±0.09
40	9.9±1.5	16.0±3.2	0.62±0.08
50	11.1±1.7	17.2±3.4	0.65±0.09
60	12.7±1.9	16.3±3.3	0.78±0.10
72	12.6±1.9	17.7±3.5	0.71±0.10
85	10.3±1.6	13.8±2.8	0.75±0.10

independently-formed isomers in fission, and these have been determined in the fission of a number of heavy nuclides (8, 10, 11). The present study deals with the analysis of data on isomer ratios in the fission of ^{237}Np by protons with energies 20–85 MeV, enabling this system to be compared with other fissioning systems.

Experimental

The experimental procedures are described elsewhere (17) and only a very brief outline is given here. Mixtures of NpO_2 and CuO were irradiated at various energies in the internal proton circulating beam of the McGill synchrocyclotron. The beam was monitored by the $^{65}Cu(p,pn)^{64}Cu$ reaction (18). After chemical separation of the cesium the activities of $^{134}Cs^{m}$ and $^{134}Cs^{g}$ were measured with a 30-cc Ge(Li) detector coupled to a 1600-channel pulse-height analyzer. Photo-peaks at 127 and 605 keV were used to measure the activities of the former and latter, respectively (19). The 605-keV peak was measured several months after the end of irradiation so that no serious interference from ^{136}Cs resulted. Corrections were made for chemical yields, branching ratios, and counting efficiencies to calculate the formation cross sections which are given in Table 1, along with the isomer ratio values.

Analysis of Data

The data were analyzed according to the energy-dependent model proposed by Saha and Yaffe (10). A brief outline of the method follows. The compound or residual cascade nuclei formed by the bombardment of the target nucleus with protons at different energies, undergo fission or neutron evaporation, depending on fission width, Γ_f, neutron emission width, Γ_n, and excitation energy. The fission branching ratios, $G_i = \Gamma_f/(\Gamma_f + \Gamma_n)$, of successive residual nuclei determine the fission probability at each step of the chain. The primary fragments formed from the fissioning nucleus have a wide spectrum of excitation energies and de-excite by neutron emission, followed by gamma emission. Angular momentum is thus carried off, the initial spin distribution of the fragments being changed at each step. The isomer ratio is calculated from the following expression

$$[3] \quad \frac{\sigma_m}{\sigma_g} = \frac{\sum_i G_i \sum_{A_iZ_i} P_{m_i} F_i(Z_i) Y_i(A_i) W_i(A_iZ_i)}{\sum_i G_i \sum_{A_iZ_i} P_{g_i} F_i(Z_i) Y_i(A_i) W_i(A_iZ_i)}$$

where G = fission probabilities of the i successive residual nuclei leading to the fragment (A,Z); P_m and P_g = formation probabilities of the metastable and ground states, respectively, from the fragment (A_iZ_i) through neutron and gamma emission; $F(Z)$ and $Y(A)$ = formation probabilities of the fragment of charge Z and mass A, respectively; $W(A,Z)$ = formation probability of the isomer from the primary fragment by neutron emission, and taken to be unity in this energy range.

The values of G used were those of Huizenga and Vandenbosch (20). In the energy range 20–50 MeV the excitation energy was determined by assuming compound nucleus formation. In the energy range 60–85 MeV the Vegas cascade calculation (21) was used. From the Step No model the average deposition energies were obtained, assuming these for the present system to be the same as those for protons interacting with ^{238}U. The average residual nucleus for ^{238}U in this energy range was found to be ^{238}Np, and in the present case, by analogy, ^{237}Pu was assumed. Successive excitation energies of the fissioning nuclei were obtained by subtracting the binding energy of the neutron, B_n, plus its kinetic energy, $2T$, from that of the preceding nucleus. The nuclear temperature, T, was obtained from the relationship

$$[4] \quad U' = aT^2 - 4T$$

where U' = effective excitation energy of the residual nucleus (22), a = level-density parameter, taken as 10.5 MeV^{-1}. Correction for the odd–even nature of the fissioning nucleus was made with a pairing energy value of 1.1 MeV (20). The values of G_i were all normalized so that their sum was unity. Values of B_n and those for fission barriers were taken from Myers and Swiatecki (23). The fission yields $Y(A)$ in the mass region 134–139 have not been determined for the present system, other than by summing

Can. J. Chem. Downloaded from www.nrcresearchpress.com by 210.87.254.5 on 09/05/12
For personal use only.

Can. J. Chem. Downloaded from www.nrcresearchpress.com by 210.87.254.5 on 09/05/12
For personal use only.

from the charge dispersion curves. These values show that the mass–yield curve is relatively flat in this very narrow mass region. The assumption of constant fission yield was made, with the further implicit assumption that the mass distribution for the products and fragments has the same shape for different fissioning nuclei, and varies only with excitation energy. Similarly the fractional yields, $F(Z)$, for various mass numbers are not known, since the charge dispersion for the primary fragments has not been determined. The Gaussian expression relating the fractional yields to the most probable charge, Z_p, and width d was used to calculate $F(Z)$ values. Values of Z_p were calculated on the basis of the u.c.d. postulate (24) and values of d obtained from the charge dispersion studies in the fission of ^{237}Np (17).

The total average excitation energy of the fragment is obtained by energy balancing:

$$[5] \quad \bar{E}^* = \Delta M^*(A,Z) - (\Delta M_L + \Delta M_H) - KE_{av}$$

where $\Delta M^*(A,Z)$ = mass excess of the excited compound nucleus (equal to the ground state mass excess plus the excitation energy due to the bombarding energy); and ΔM = mass excesses of the light, L, and heavy, H, complementary fragments (23). The average total kinetic energy of the two fragments was taken as the average value obtained from ^{237}Pu (25), considered constant at all energies. The excitation energy, $\bar{E}^*$, was assumed to be shared between the two fragments in proportion to their masses. A number of complementary fragment pairs, with cesium isotopes of masses 134–140 on the heavy side, were selected for each fissioning nucleus, and the excitation energies determined as outlined above. Neutron emission from these heavy fragments was followed, as outlined earlier, and those leading to ^{134}Cs as the final fragment were selected, the residual excitation energy being dissipated by a cascade of gamma rays. The average energy, E_γ, carried off by each γ-ray was based on the empirical relation given by Vonach *et al.* (22). When the residual energy is less than, or equal to, 1 MeV the isomer-deciding γ-ray is emitted. With these data on the numbers of neutrons and γ-rays emitted from each fragment leading to the isomer, the computer code of Hafner *et al.* (26) was used to calculate the formation probabilities of the metastable and ground state isomers, P_m and P_g, respectively. The transmission coefficient values, $T_l(E)$, for neutron emission from different fragments were calculated for a diffuse-edge, surface-absorption optical potential of Bjorklund and Fernbach (27) using Auerbach's ABACUS code (28). The photons were assumed to be dipole.

The primary spin distribution was taken to be of the form given by eq. 2, the value of B defining the width of the distribution, and for large values, $B = \sqrt{\overline{J^2}}$, the average root-mean-square angular momentum of the primary fragment. The spin cut-off factor, σ, is equated to the thermodynamic temperature through the moment of inertia, I_{eff}, of the excited nucleus (29). The value of I_{eff} has been shown to increase with excitation energy of the nucleus, approaching I_r, the rigid body value as an upper limit, where

$$[6] \quad I_r = \tfrac{2}{5}MAR^2$$

M = mass of a nucleon; A = mass number; and R = nuclear radius. From the work of Dudey and Sugihara (30) at energies about 10–15 MeV, the ratio $I_{eff}/I_r = 1$, the value decreasing with decreasing energy. Since neutron emission occurs in the higher excitation energy range and gamma emission at lower energies, the following spin cut-off values were used:

$$\sigma_n^2 = (I_r t/\hbar^2)$$

and

$$\sigma_\gamma^2 = (I_{eff} t/\hbar^2)\,,$$

values of I_{eff}/I_r being interpolated from the data of Dudey and Sugihara (30). Calculations for σ_n were also made with $I_{eff}/I_r = 0.75$ at one value to check the effect of a reduced moment of inertia on the isomer ratio predictions. Similarly, at one value of B, fixed values of $\sigma_n = 4$ and $\sigma_\gamma = 3$ were taken. As done by others (8, 10) the spin distribution following the emission of the final γ-ray was assumed to divide midway between the two isomeric states, ^{134}Cs^m(8−) and ^{134}Cs^g(4+).

Discussion

The calculated and experimental isomer ratios, $\sigma_m/(\sigma_m + \sigma_g)$ for ^{134}Cs are shown in Fig. 1 as a function of bombarding energy. The calculated results for different values of B, σ_n, and σ_γ are shown. The experimental values show a slight increase with energy initially and tend

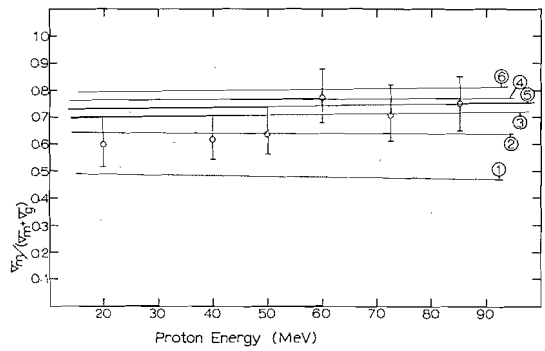

FIG. 1. ^{134}Cs isomer ratios in ^{237}Np fission with protons: ○, experimental values; solid lines are calculated values with different parameters as follows: (*1*) $B = 12$, $\sigma_n = 4$, $\sigma_\gamma = 3$; (*2*) $B = 12$, $\sigma_n^2 = I_r t/\hbar^2$, $\sigma_\gamma^2 = I_{eff} t/\hbar^2$; (*3*) $B = 14$, $\sigma_n^2 = I_r t/\hbar^2$, $\sigma_\gamma^2 = I_{eff} t/\hbar^2$; (*4*) $B = 16$, $\sigma_n^2 = I_r t/\hbar^2$, $\sigma_\gamma^2 = I_{eff} t/\hbar^2$; (*5*) $B = 16$, $\sigma_n^2 = 0.75 I_r t/\hbar^2$, $\sigma_\gamma^2 = I_{eff} t/\hbar^2$; (*6*) $B = 18$, $\sigma_n^2 = I_r t/\hbar^2$, $\sigma_\gamma^2 = I_{eff} t/\hbar^2$.

to level off at higher energies as observed for other fissioning systems (8, 10, 11). The isomer ratios obtained with different targets, in this energy range, are about the same at a given bombarding energy, irrespective of the spin of the target.

The underlying assumptions for each of the factors used in the above calculations have been discussed by Saha and Yaffe (10), who pointed out the difficulty involved in investigating the variation in calculated ratios with changes in all the parameters, owing to the wide spectrum of fissioning nuclei. However, some generalizations follow from the present calculations. For the same value of B the ratio $P_m/(P_m + P_g)$ varies from fragment to fragment, and increases with increased value of B for each fragment. With a reduced moment of inertia, reflected in smaller values of σ_n, for the same value of B the isomer ratio values drop (lines 4 and 5, Fig. 1). Dipole radiation only for γ-emission has been considered in these calculations, since cascade γ-rays of the pure quadrupole type have been shown to reduce the calculated isomer ratios greatly. It is possible that some admixture dipole and quadrupole radiations might be closer to reality, but it is difficult to take such an admixture into consideration in these calculations. The root-mean-square angular momentum, $\sqrt{\overline{J^2}}$, (equal to B for large values), for best agreement between experimental and calculated values is $12\hbar$ at 20 MeV and 16–$18\hbar$ at 60–85 MeV bombarding energy. Similar high values of angular momentum have been reported for ^{134}Cs isomers in the fission of several other heavy nuclides (8, 10, 11).

From the optical model calculations of proton transmission into a neptunium nucleus, with the parameters of Fricke *et al.* (31), it has been found that at 20 MeV only $6\hbar$ units of root-mean-square angular momentum are brought in. At 85 MeV the calculations of Chen *et al.* (21) give an average value of $12\hbar$. Vandenbosch *et al.* (32) have pointed out that a major fraction of the initial angular momentum is retained as the intrinsic spin of the primary fragments, and only a small amount as the orbital angular momentum. It is difficult to account, however, for a value of $\sqrt{\overline{J^2}} = 12\hbar$ at 20 MeV, as found in this work and by previous authors (7, 10) unless as Strutinski (33) has suggested, considerable intrinsic angular momentum is generated in the fission process itself.

From the Halpern and Strutinski model (34), the fission fragments are emitted along the symmetry axis of the fissioning nucleus and their intrinsic spins add vectorially to give the vector K, which is the projection of the spin of the fissioning nucleus along the symmetry axis. Following the above model, the average value of $\sqrt{\overline{K^2}}$, weighted with the fission probability of each fissioning nucleus in the fission chain, gave a value of $11.3\hbar$, as against a value of $12\hbar$ for $\sqrt{\overline{J^2}}$ at 20 MeV, associated with a single fragment. Accordingly, the spins of the fragments must be so oriented that only partial cancellation of spins of the complementary fragments occurs, and not entirely cancelled as would be the case if they were oriented antiparallel to each other. Hoffman (35) found the latter to be the case in the thermal fission of ^{235}U.

1. J. WING. U.S. Atomic Energy Commission Rept., ANL-6598. 1962.
2. R. VANDENBOSCH, L. HASKIN, and J. C. NORMAN. Phys. Rev. **137**, 1134 (1965).
3. T. MATSUO, J. M. MATSUZEK, JR., N. D. DUDEY, and T. T. SUGIHARA. Phys. Rev. **139**, B886 (1965).
4. D. R. SACHDEV and L. YAFFE. Can. J. Chem. **45**, 2711 (1967).
5. D. R. SACHDEV and L. YAFFE. Can. J. Chem. **47**, 1667 (1969).
6. I. F. CROALL and H. H. WILLIS. J. Inorg. Nucl. Chem. **24**, 221 (1962).
7. D. G. SARANTITES, G. E. GORDON, and C. D. CORYELL. Phys. Rev. **138**, B353 (1965).
8. H. WARHANEK and R. VANDENBOSCH. J. Inorg. Nucl. Chem. **26**, 669 (1964).
9. J. H. FORSTER and L. YAFFE. Can. J. Chem. **46**, 1763 (1968).

Can. J. Chem. Downloaded from www.nrcresearchpress.com by 210.87.254.5 on 09/05/12
For personal use only.

10. G. B. SAHA and L. YAFFE. J. Inorg. Nucl. Chem. **31**, 189 (1969).
11. G. B. SAHA, I. TOMITA, and L. YAFFE. J. Inorg. Nucl. Chem. **31**, 3731 (1969).
12. E. HAGEBØ. J. Inorg. Nucl. Chem. **25**, 1201 (1963).
13. E. HAGEBØ. J. Inorg. Nucl. Chem. **27**, 927 (1965).
14. E. HAGEBØ. J. Inorg. Nucl. Chem. **29**, 2515 (1967).
15. J. R. HUIZENGA and R. VANDENBOSCH. Phys. Rev. **120**, 1305 (1960).
16. R. VANDENBOSCH and J. R. HUIZENGA. Phys. Rev. **120**, 1313 (1960).
17. T. MCGEE, C. L. RAO, and L. YAFFE. J. Inorg. Nucl. Chem. In press.
18. S. MEGHIR. Ph.D. Thesis, McGill University, Montreal, Quebec. 1962.
19. C. M. LEDERER, J. M. HOLLANDER, and I. PERLMAN. Table of isotopes. John Wiley and Sons, Inc., N.Y. 1967.
20. J. R. HUIZENGA and R. VANDENBOSCH. Nuclear reactions. *Edited by* P. M. Endt. and P. B. Smith. North Holland, Amsterdam. 1962.
21. K. CHEN, Z. FRAENKEL, G. FRIEDLANDER, J. R. GROVER, J. M. MILLER, and Y. SHIMAMOTO. Phys. Rev. **166**, 949 (1968).
22. H. K. VONACH, R. VANDENBOSCH, and J. R. HUIZENGA. Nucl. Phys. **60**, 70 (1964).
23. W. D. MYERS and W. J. SWIATECKI. U.S. Atomic Energy Commission Rept. UCRL-11980. 1965.
24. L. YAFFE. Symposium on Physics and Chemistry of Fission. IAEA, Vienna (1969), paper SM/122/3.
25. J. E. GINDLER and J. R. HUIZENGA. Nuclear chemistry, Vol. II. *Edited by* L. Yaffe. Academic Press, N.Y. 1968. Chap. 7.
26. W. L. HAFNER, JR., J. R. HUIZENGA, and R. VANDENBOSCH. U.S. Atomic Energy Rept., ANL-6662. 1962.
27. F. BJORKLUND and J. FERNBACH. Phys. Rev. **109**, 1296 (1958).
28. E. H. AUERBACH. ABACUS-2, U.S. Atomic Energy Commission Rept., BNL-6562. 1962.
29. T. ERICSON. Adv. Phys. **9**, 425 (1960).
30. N. D. DUDEY and T. T. SUGIHARA. Phys. Rev. **139**, B896 (1965).
31. M. P. FRICKE, E. E. GROSS, B. J. MORTON, and A. ZUCKER. Phys. Rev. **156**, 1207 (1967).
32. R. VANDENBOSCH, H. WARHANEK, and J. R. HUIZENGA. Phys. Rev. **124**, 846 (1961).
33. V. M. STRUTINSKI. J. Exp. Theoret. Phys. **10**, 613 (1960).
34. I. HALPERN and V. M. STRUTINSKI. Proc. 2nd Intl. Conf. on Peaceful Uses of Atomic Energy, Vol. 15. United Nations, Geneva. 1958. p. 408.
35. M. M. HOFFMAN. Phys. Rev. **133**, B714 (1964).

Can. J. Chem. Downloaded from www.nrcresearchpress.com by 210.87.254.5 on 09/05/12
For personal use only.

Synthesis of 1-Methyl-tricyclo[5.2.2.0^{2,6}]undec-2(6)-ene-8-one

C. MERCIER,[1] A. R. ADDAS, AND P. DESLONGCHAMPS[2]

Laboratoire de Synthèse organique, Département de chimie, Université de Sherbrooke, Sherbrooke, Québec

Received January 20, 1972

Synthesis of the tricyclic ketone **1** is reported.

La synthèse de la cétone tricyclique **1** est rapportée.

Canadian Journal of Chemistry, **50**, 1882 (1972)

Can. J. Chem. Downloaded from www.nrcresearchpress.com by 210.87.254.42 on 09/05/12
For personal use only.

Our recent studies toward the synthesis of ryanodine (1) led us to consider and develop different routes for the synthesis of compounds having a tricyclic skeleton such as **1**. We wish now to report a successful synthesis of the tricyclic ketone 1.[3]

Condensation of sodiomalonate in dimethylformamide with α-chloroacetone during 18 h at room temperature gave the ketone ester **2** (2) in 55% yield which was converted into ketal ester **3**. The sodium salt of **3** dissolved in dimethoxyethane was then condensed with 2-chlorocyclopentanone yielding crude substituted cyclopentanone **4** in 90% yield.

Experimental conditions were then sought in order to transform **4** into **5** in a single operation. We selected a strong acidic medium and heat so the hydrolysis of the esters and ketal functions would certainly occur as well as the decarboxylation of the substituted malonic acid and it was hoped that under those conditions, aldol condensation followed by dehydration would also be observed. We found that when **4** was heated in a mixture of dioxane and 15% aqueous sulfuric acid for 52 h, the enone acid **5** was obtained in 80% yield. The crude acidic product **5** was esterified with diazomethane and the corresponding enone ester **6** was purified by distillation (80% yield). Ketalization of **6** with ethylene glycol gave the ketal ester **7** in 80% yield.

The introduction of a methyl group at the alpha position of the carbomethoxy group was then realized. Treatment of **7** in dry dimethoxyethane containing methyl iodide and sodium hydride at 35 °C during 12 h gave the desired compound **8** in 82% yield. The ketal alcohol **9** obtained in 95% yield by reduction of **8** with lithium aluminum hydride in ether was further oxidized with Collins reagent (3) giving the unstable ketal aldehyde **10** in 90% yield. Wittig condensation (4) of **10** with methoxymethylenetriphenylphosphorane gave in 65% yield a mixture of the *cis* and *trans* isomeric enol ether **11** in a ratio of 7:3. Mild hydrolysis of **11** with acetone and *p*-toluenesulfonic acid yielded the unstable ketal acetaldehyde **12** in 95% yield.

The crude ketal aldehyde **12** was then reduced with lithium aluminum hydride in ether (90% yield) to the ketal alcohol **13** which was then converted to the ketal mesylate **14** (95% yield) by reaction with methanesulfonylchloride and pyridine in dichloromethane. Hydrolysis of ketal mesylate **14** with a mixture of acetone and aqueous hydrochloric acid (3 *N*) during 2 h at room temperature gave the enone mesylate **15** in quantitative yield.

Treatment of crude enone mesylate **15** with sodium hydride in dimethoxyethane containing a small quantity of ethanol gave a major product which was isolated by v.p.c. (60% yield). It was shown to have structure **1** by analytical and spectral analysis.

The tricyclic ketone **1** is a liquid, its DNP derivative melts at 172–173 °C. Its i.r. spectrum exhibits an absorption at 1720 cm^{-1} for the six-membered ring ketone and its n.m.r. spectrum, a multiplet at 6.83 τ (1H) for the bridgehead proton and a singlet at 8.77 τ (3H) for the methyl group. Its mass spectrum shows a strong molecular ion at *m/e* 176.

Experimental

The i.r. spectra were taken on a Perkin–Elmer 257 spectrophotometer. The n.m.r. spectra (τ value) were recorded on a Varian A-60 spectrometer in solvent indicated and with TMS as internal standard. Mass spectra (m.s.) were

[1]Holder of an NRCC Studentship (Canada), 1970–1971.
[2]A. P. Sloan Fellow, 1970–1972.
[3]For another successful synthesis of this type of tricyclic compound, see ref. 1.

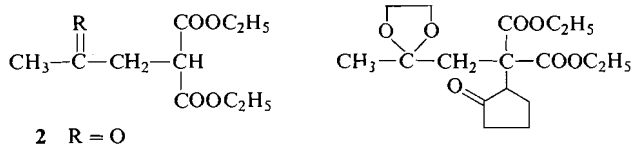

2 R = O
3 R = OCH_2—CH_2O

4

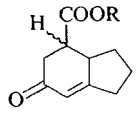

5 R = H
6 R = CH_3

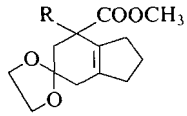

7 R = H
8 R = CH_3

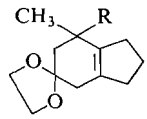

9 R = CH_2OH
10 R = CHO
11 R = CH=$CHOCH_3$
12 R = CH_2—CHO
13 R = CH_2—CH_2OH
14 R = CH_2—CH_2—OSO_2CH_3

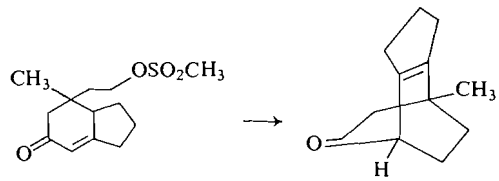

15 **1**

obtained on a Hitachi–Perkin–Elmer RMU-6 spectrometer. The u.v. spectra were measured on a Beckman DB-6 Grating spectrophotometer. The vapor phase chromatographic purification and analysis were done on a Hewlett–Packard 5750 Research chromatograph. Organic solutions were dried over anhydrous magnesium sulfate and Florisil was used in all the column and preparative layer chromatography. Microanalyses were performed by Schwarzkopf Microanalytical Laboratory, Woodside, N.Y.

Commercially available α-chloroacetone (Eastman Organic Chemicals) and 2-chlorocyclopentanone (Aldrich Chemical Co.) was used in this work.

Ketone Ester **2**

Ethyl malonate (160 g, 1 mol) was added in small portions to dimethylformamide (1 l) containing sodium hydride (32 g, 1.32 mol) in suspension under an atmosphere of nitrogen. The mixture was then heated at 85° for 1 h. It was cooled to room temperature and α-chloroacetone (111 g, 1.2 mol) was slowly added and the reaction mixture was left for 18 h at room temperature. Water (6 l) was then added, the mixture was acidified with hydrochloric acid (3 *N*) and extracted several times with ether. The organic phase was washed twice with water, dried, and evaporated to dryness (180 g). Fractional distillation gave ketone ester **2** (118 g, 55% yield; b.p. 102–104° at 0.9 mm; lit. (2) b.p. 145–155° at 20 mm).

Ketal Ester **3**

A mixture containing ketone ester **2** (65 g, 0.306 mol), ethylene glycol (285 ml, 6.0 mol), and *p*-toluenesulfonic acid (2.6 g, 15 mmol) in benzene (3.5 l) was heated at reflux for 15 h with continuous azeotropic removal of water by means of a Dean–Stark trap. The cooled mixture was washed with saturated aqueous sodium carbonate and brine. The dried organic phase was evaporated to give crude ketal ester **3** (79 g, 98% yield). The analytical sample was obtained by distillation *in vacuo* (b.p. 118° at 0.9 mm). The i.r.: ν_{max} ($CHCl_3$) 1745 cm^{-1}; n.m.r.: τ ($CDCl_3$) 5.78 (4H, quadruplet, J = 7.0 Hz, —OCH_2CH_3) 6.06 (4H, singlet, OCH_2—CH_2O), 6.45 (1H, triplet, J = 7.0 Hz, methine hydrogen), 7.69 (2H, doublet, J = 7.0 Hz, methylene hydrogen), 8.67 (3H, singlet, CH_3), and 8.74 (6H, triplet, J = 7.0 Hz, —OCH_2CH_3).

Anal. Calcd. for $C_{12}H_{20}O_6$: C, 55.37; H, 7.74. Found: C, 55.28; H, 7.53.

Substituted Cyclopentanone **4**

Ketal ester **3** (75 g, 0.29 mol) dissolved in dry dimethoxyethane (85 ml) was slowly added under nitrogen to a suspension of sodium hydride (7.4 g, 0.30 mol) in dimethoxyethane (450 ml). The mixture was refluxed for ½ h, cooled to room temperature and 2-chlorocyclopentanone (40 g, 0.37 mol) dissolved in dimethoxyethane (85 ml) was slowly added. At the end of the addition, the reaction mixture was heated at reflux overnight. A portion of the dimethoxyethane (300 ml) was removed from the reaction mixture by evaporation *in vacuo*, water (2 l) was added and the mixture was thoroughly extracted with ether. Evaporation of the dried extract gave crude **4** (90 g, 90% yield). This product was found unstable on distillation *in vacuo*, an analytical sample was not prepared. The i.r.: ν_{max} ($CHCl_3$) 1745 cm^{-1};

Can. J. Chem. Downloaded from www.nrcresearchpress.com by 210.87.254.42 on 09/05/12
For personal use only.

Can. J. Chem. Downloaded from www.nrcresearchpress.com by 210.87.254.42 on 09/05/12
For personal use only.

n.m.r.: τ ($CDCl_3$) 5.80 (4H, quadruplet, $J = 7.0$ Hz, OCH_2—CH_3), 6.13 (4H, singlet, OCH_2CH_2O), 8.67 (3H, singlet, CH_3), and 8.75 (6H, triplet, $J = 7.0$ Hz, OCH_2CH_3).

Enone Acid **5** *and Enone Ester* **6**

A solution of the substituted cyclopentanone **4** (80 g, 0.234 mol) in dioxane (240 ml) was mixed with water (400 ml) containing concentrated sulfuric acid (62 g) and heated at reflux for 52 h. The cooled solution was made alkaline (p*H* 8–9) with aqueous sodium hydroxide (2 *N*) and extracted with ether which was discarded. The aqueous phase was acidified and thoroughly extracted with ether. The dried organic phase was evaporated to dryness giving the liquid enone acid **5** (35 g, 80% yield). The i.r.: ν_{max} ($CHCl_3$) 1720 and 1680 cm^{-1}; n.m.r.: τ ($CDCl_3$) 4.0 (1H, broad singlet, olefinic hydrogen); m.s.: *m/e* 180 (M^+).

Crude enone acid **5** (35 g, 0.194 mol) dissolved in ether (200 ml) was mixed with an excess of an ethereal solution of diazomethane for $\frac{1}{2}$ h at room temperature. Evaporation of the solvent gave a crude product which was purified by distillation giving pure enone ester **6** (33 g, 80% yield, b.p. 145° at 0.8 mm). The i.r.: ν_{max} ($CHCl_3$) 1740 and 1680 cm^{-1}; u.v.: λ_{max} (EtOH) 236 m (ε 10 280); n.m.r.: τ ($CDCl_3$) 4.0 (1H, broad singlet, olefinic hydrogen) and 6.25 (3H, singlet, OCH_3); m.s.: *m/e* 194 (M^+). The 2,4-dinitrophenylhydrazone had m.p. 141–142° (methanol).

Anal. Calcd. for $C_{17}H_{18}O_6N_4$: C, 54.54; H, 4.84; N, 14.98. Found: C, 54.67; H, 5.01; N, 15.12.

Ketal Ester **7**

A mixture containing enone ester **6** (16 g, 0.082 mol), ethylene glycol, and *p*-toluenesulfonic acid (1.3 g) in benzene (800 ml) was heated at reflux for 15 h with continuous azeotropic removal of water by means of a Dean–Stark trap. The cooled mixture was washed with saturated aqueous sodium carbonate and brine. The dried organic phase was evaporated to dryness and the resulting oil was purified by distillation (14 g, 80% yield). The analytical sample was obtained by distillation *in vacuo* (b.p. 100° at 0.3 mm). The i.r.: ν_{max} ($CHCl_3$) 1730 cm^{-1}; n.m.r.: τ ($CDCl_3$) 6.02 (4H, singlet, OCH_2CH_2O) and 6.30 (3H, singlet, OCH_3).

Anal. Calcd. for $C_{13}H_{18}O_4$: C, 65.53; H, 7.61. Found: C, 65.63: H, 7.65.

Methylated Ketal Ester **8**

The oily ketal ester **7** (29.5 g, 0.124 mol) was slowly added under nitrogen to dry dimethoxyethane (300 ml) containing sodium hydride (5.5 g, 0.124 mol) in suspension. Iodomethane (35.2 g, 0.248 mol) was then added by portion and the reaction was kept at 35° for 5 h. Sodium hydride (5.5 g, 0.124 mol) in suspension in dimethoxyethane (300 ml) was then added followed by a second addition of iodomethane (35.2 g, 0.248 mol) and the reaction mixture was kept again at 35° overnight. Excess sodium hydride was destroyed by careful addition of water. Most of the solvent was removed by evaporation, brine (1 l) was added, and the mixture was thoroughly extracted with ether. The dried organic phase was evaporated yielding the crude oily ketal ester **8** (25 g, 82% yield). The analytical sample was obtained by preparative t.l.c. The i.r.: ν_{max} 1730 cm^{-1}; n.m.r.: τ ($CDCl_3$) 6.04 (4H, multiplet, OCH_2CH_2O), 6.32 (3H, singlet, OCH_3), and 8.70 (3H, singlet, CH_3).

Anal. Calcd. for $C_{14}H_{20}O_4$: C, 66.64; H, 7.99. Found: C, 66.48; H, 8.16.

Ketal Alcohol **9**

Lithium aluminum hydride (8 g) added to an ethereal solution (200 ml) of ketal ester **8** (15.8 g, 0.063 mol) and the mixture was refluxed overnight. The excess hydride was carefully destroyed with a small quantity of water in order to get a precipitate. Magnesium sulfate was added, the solution was filtered and evaporated to dryness. The resulting oil was filtered through Florisil (13 g, 95% yield).

The analytical sample was obtained by preparative t.l.c. of the corresponding benzoate derivative (benzoyl chloride: pyridine). The i.r.: ν_{max} ($CHCl_3$) 1715 cm^{-1}; n.m.r.: τ ($CDCl_3$) 2.0 (2H, multiplet, benzoate hydrogens), 2.55 (3H, multiplet, benzoate hydrogens), 5.75 (2H, singlet, $—CH_2O$), 6.08 (4H, singlet, OCH_2CH_2O), and 8.82 (3H, singlet, CH_3); m.s.: *m/e* 224 (M^+).

Anal. Calcd. for $C_{13}H_{20}O_3$: C, 73.15; H, 7.37. Found: C, 72.88; H, 7.50.

Ketal Aldehyde **10**

A solution of ketal alcohol **9** (2 g, 9 mmol) in dry dichloromethane (10 ml) was added to a suspension of chromium trioxide–pyridine complex (11.5 g, 0.045 mol) (3) in dry dichloromethane (20 ml) and the mixture was stirred for 10 min at room temperature. Water (150 ml) was added and the mixture was extracted with dichloromethane. The organic phase was dried, filtered through celite, and evaporated to dryness yielding crude ketal aldehyde **10** (1.8 g, 90% yield) as an oil which decomposed on standing at room temperature. The i.r.: ν_{max} ($CHCl_3$) 2740 and 1720 cm^{-1}; n.m.r.: τ ($CDCl_3$) 0.4 (1H, singlet, CHO), 6.00 (4H, singlet, OCH_2CH_2O), and 8.84 (3H, singlet, CH_3); m.s.: *m/e* 222 (M^+).

Wittig Reaction on **10**

Sodium hydride (1.0 g, 0.04 mol) was mixed with dimethylsulfoxide (40 ml) and heated at 75° for $1\frac{1}{2}$ h. To the cooled solution was added dry (under P_2O_5) methoxymethyltriphenylphosphonium chloride (13.2 g, 0.042 mol) dissolved in dimethylsulfoxide (40 ml). After 30 min, ketal aldehyde **10** (1.8 g, 8.4 mmol) in dimethylsulfoxide (10 ml) was added dropwise and the reaction mixture was maintained at 45° during 15 h. Water (100 ml) was added and the mixture was thoroughly extracted with pentane. The dried organic phase was filtered and evaporated to dryness. The residue was purified by column chromatography with Florisil. Elution with pentane gave triphenylphosphine, elution with benzene gave the isomeric *cis* and *trans* enol ether **11** in a ratio of 7:3 as judged by n.m.r. (1.05 g, 63% yield). The i.r.: ν_{max}($CHCl_3$) 1650 cm^{-1}; n.m.r.: τ ($CDCl_3$) 3.68 (0.35 H, doublet, $J = 12.0$ Hz, $CH{=}CHOCH_3$ *trans*), 5.02 (0.35 H, doublet, $J = 12.0$ Hz, $CH{=}CHOCH_3$ *trans*), 4.27 (0.65 H, doublet, $J = 7.0$ Hz, $CH{=}CHOCH_3$ *cis*), 5.60 (0.65 H, doublet, $J = 7.0$ Hz, $CH{=}CHOCH_3$ *cis*).

The analytical sample was obtained on the *trans* isomer which was obtained pure by preparative t.l.c. followed by molecular distillation. The i.r.: ν_{max} ($CHCl_3$) 1650 cm^{-1}; n.m.r.: τ ($CDCl_3$) 3.68 (1H, doublet, $J = 12.0$ Hz, $—CH{=}CHOCH_3$) 5.02 (1H, doublet, $J = 12.0$ Hz, $—CH{=}CHOCH_3$), 6.02 (4H, singlet, $O—CH_2CH_2O$), 6.48

(3H, singlet, OCH_3), and 8.84 (3H, singlet, CH_3); m.s.: *m/e* 250 (M^+).

Anal. Calcd. for $C_{15}H_{22}O_3$: C, 71.97; H, 8.86. Found: C, 71.13; H, 8.95.

Ketal Acetaldehyde **12**

The isomeric *cis* and *trans* enol ether **11** (932 mg, 3.7 mmol) was dissolved in acetone (250 ml) containing *p*-toluenesulfonic acid (4 mg) and two drops of water. The mixture was left for 6 h at room temperature. Water was added and the mixture extracted with ether. The dried organic phase was evaporated to dryness yielding crude ketal acetaldehyde (836 mg, 95%) which was used directly for the next operation. This product was found to decompose rapidly at room temperature. The i.r.: ν_{max} ($CHCl_3$) 2740 and 1715 cm^{-1}; n.m.r.: τ ($CDCl_3$) 0.4 (1H, triplet, $J = 2.0$ Hz, CHO), 6.05 (4H, singlet, OCH_2CH_2O), and 8.78 (3H, singlet, CH_3); m.s.: *m/e* 236 (M^+).

Ketal Alcohol **13**

Lithium aluminum hydride (197 mg, 5.2 mmol) was added to an ethereal solution (50 ml) of ketal acetaldehyde **12** (981 mg, 4.1 mmol) and the reaction was left at room temperature for 1 h. Excess lithium aluminum hydride was carefully destroyed by a small amount of water, magnesium sulfate was added, and the dried solution was filtered and evaporated to dryness. The resulting oil was purified by column chromatography with Florisil (elution with benzene–ether) (896 mg, 90% yield). The analytical sample was obtained by preparative t.l.c. The i.r.: ν_{max} ($CHCl_3$) 3610 and 3500 cm^{-1}; n.m.r.: τ ($CDCl_3$) 5.97 (4H, singlet, OCH_2CH_2O), 6.30 (2H, triplet, $J = 7.0$ Hz, CH_2O), and 8.87 (3H, singlet, CH_3); m.s.: *m/e* 238 (M^+).

Anal. Calcd. for $C_{14}H_{22}O_3$: C, 70.55; H, 9.31. Found: C, 70.46; H, 9.11.

Ketal Mesylate **14**

Methanesulfonyl chloride (0.40 ml, 5.3 mmol) was added to a cold solution of ketal alcohol **13** (601 mg, 2.1 mmol) in methylene chloride (50 ml) containing pyridine (6 ml) and the reaction mixture was left at 5° for 2 days. Methylene chloride (200 ml) and a saturated sodium bicarbonate solution (25 ml) were added and the mixture was stirred for 15 min. The organic phase was separated, washed twice with water, dried, and evaporated to dryness yielding crude ketal mesylate **14** as an oil (840 mg, 95% yield). This product decomposed by distillation *in vacuo*. The i.r.: ν_{max} ($CHCl_3$) 1360 and 1170 cm^{-1}; n.m.r.: τ ($CDCl_3$) 5.70 (2H, triplet, $J = 7.0$ Hz, CH_2O), 5.98 (4H, singlet, OCH_2CH_2O), 6.97 (3H, singlet, CH_3SO_2O), and 8.84 (3H, singlet, CH_3); m.s.: *m/e* 272 (M).

Enone Mesylate **15**

A mixture of ketal mesylate **14** (665 mg, 2.1 mmol), acetone (150 ml), and aqueous hydrochloric acid (3 *N*, 4.2 ml) was left at room temperature for 2 h. Most of the acetone was then evaporated *in vacuo*, water was added and the aqueous phase was extracted with dichloromethane. The organic phase was washed with a saturated solution of sodium bicarbonate, water, dried, and evaporated to dryness. The resulting crude enone mesylate **15** (572 mg, ~100%) was not purified further and was used directly in the next operation. The i.r.: ν_{max} ($CHCl_3$) 1670, 1360, and 1170 cm^{-1}; n.m.r.: τ ($CDCl_3$) 3.95 (1H, broad singlet, olefinic proton), 5.60 (2H, triplet, $J = 7.0$ Hz, CH_2O), 6.94 (3H, singlet, CH_3SO_2O), and 9.07 (3H, singlet, CH_3); m.s.: *m/e* 272 (M^+).

Tricyclic Ketone **1**

Enone mesylate **15** (122 mg, 0.45 mmol) was added to a suspension of sodium hydride (13 mg, 0.56 mmol) in dry dimethoxyethane (15 ml) containing two drops of ethanol and the mixture was refluxed for 15 h under nitrogen. Water (15 ml) was added and the mixture was extracted with ether. The organic phase was dried and evaporated to dryness yielding an oil (71 mg). The v.p.c. analyses revealed the presence of two products in a ratio of 7:3. The major product was obtained pure by preparative v.p.c. (3 ft, 10% Carbowax 20 *M* column, 150°). It is a liquid. The i.r.: ν_{max} ($CHCl_3$) 1720 cm^{-1}; n.m.r.: τ ($CDCl_3$) 6.84 (1H, multiplet, bridgehead hydrogen) and 8.77 (3H, singlet, CH_3); m.s.: *m/e* 176 (M^+). The analytical sample was obtained on the 2,4-dinitrophenylhydrazone derivative (m.p. 172–173°, methanol).

Anal. Calcd. for $C_{18}H_{20}O_4$: C, 60.66; H, 5.66; N, 15.72. Found: C, 60.55; H, 5.69; N, 15.83.

1. D. BERNEY and P. DESLONGCHAMPS. Can. J. Chem. **47**, 515 (1969).
2. H. GAULT and T. SALOMON. Ann. Chim. **2**, 133 (1924).
3. J. C. COLLINS. Tetrahedron Lett. 3363 (1968).
4. R. GREENWALD, M. CHAYKOVSKY and E. J. COREY. J. Org. Chem. **28**, 1128 (1963).

Can. J. Chem. Downloaded from www.nrcresearchpress.com by 210.87.254.42 on 09/05/12
For personal use only.

Studies in Solvolysis. Part IV.[1] Substituent and Solvent Isotope Effects in the Solvolysis of a Series of Benzyl Trifluoroacetates

JUNE G. WINTER AND J. M. W. SCOTT
Chemistry Department, Memorial University, St. John's, Newfoundland

Received December 17, 1971

The rates of neutral hydrolysis of a series of 4-substituted benzyl trifluoroacetates 4-X-$C_6H_4CH_2OCOCF_3$, X = NO_2, Cl, H, CH_3, and OCH_3 have been studied in water and deuterium oxide, both solvents containing 0.012 mol fraction of acetone. The alteration of the rates with the nature of the 4-substituent and the kinetic solvent isotope effect ($k(H_2O)/k(D_2O)$) are consistent with the proposal that the esters with X = NO_2, Cl, H, and CH_3 all react by an acyl–oxygen $B_{Ac}2$ mechanism. On the other hand, the same mechanistic criteria indicate that the 4-methoxybenzyl ester reacts by both the $B_{Ac}2$ and the S_N1 alkyl–oxygen fission paths in equal amounts.

Les vitesses de l'hydrolyse neutre d'une série de trifluoroacétates de benzyle substitués en 4-(X-4-$C_6H_4CH_2$-$OCOCF_3$ avec X = NO_2, Cl, H, CH_3, et OCH_3) ont été étudiées dans l'eau et dans l'eau lourde contenant toutes deux 0.012 fraction molaire d'acétone. La modification des vitesses avec la nature du substituant en 4 et l'effet isotopique du solvant sur la cinétique ($k(H_2O/k(D_2O)$) sont compatibles avec le mécanisme $B_{Ac}2$ proposé selon lequel les esters avec X = NO_2, Cl, H, et CH_3 réagissent tous par l'oxygène de l'acyle. De plus, ce même mécanisme montre que l'ester méthoxy-4 benzyle réagit à la fois par le schéma $B_{Ac}2$ et par le schéma S_N1 correspondant à la rupture de la liaison alkyl–oxygène, dans le même rapport.

Canadian Journal of Chemistry, 50, 1886 (1972)

Introduction

Using ^{18}O tracer studies Bunton and Hadwick (2) have deduced that the neutral hydrolysis of methyl trifluoroacetate takes place by a $B_{Ac}2$ acyl–oxygen fission reaction. On the other hand Moffat and Hunt (3) cite the extent of olefin formation in the solvolysis of *t*-butyl trifluoroacetate and conclude that the neutral hydrolysis of this substrate is mechanistically similar to *t*-butyl chloride, *i.e.*, the tertiary carboxylic ester is considered to react via an S_N1 carbonium ion mechanism involving alkyl–oxygen fission.

These views have been amply confirmed in more extended studies (4, 5) of the α-methylated series CF_3COOR (R = Me, Et, *i*-Pr, and *t*-Bu) using the kinetic solvent isotope effect (k.s.i.e. $k(H_2O)/k(D_2O)$), the thermodynamic parameters $\Delta H^{\ddagger}$, $\Delta S^{\ddagger}$, and $\Delta C_p^{\ddagger}$ and secondary C—H/C—D isotope effects as mechanistic criteria. The summarized data from these studies are reported in Table 1 and the mechanistic conclusions to be derived from it are clear cut; the primary and secondary esters react by the $B_{Ac}2$ path and the tertiary ester reacts by an S_N1 route. A comparison of *t*-butyl chloride parameters with those for the corresponding trifluoroacetate is again useful (*c.f.* ref. 3).

The reasons for the change in mechanism $B_{Ac}2 \rightarrow S_N1$ in the α-methylated series must be energetic but even a qualitative analysis of the contributing factors is difficult. These factors are presumably a blend of electronic, steric, and solvation effects which alter as the structure of the alkyl group is varied. In the alkyl–oxygen fission reaction the alkyl group is the reaction seat and hence the S_N1 path must display greater sensitivity to the structure of the alkyl group than the competitive $B_{Ac}2$ process in which the same structural alterations are relatively remote from the reaction center. A combination of two reaction paths ($B_{Ac}2$ and S_N1) of widely disparate sensitivity to structural alterations is an ideal situation for mechanistic changes but in the α-methylated series does not provide the possibility of assessing the relative importance of the contributing factors mentioned above. On the other hand a sequence of 4-substituted benzyl trifluoroacetates provides a more tractable series of reactants in which solvation and steric factors remain constant to a first approximation, leaving the residual electronic factors as paramount in the emergence of the S_N1 process. The facility of heterolytic fission in the gas phase as measured by the enthalpy change

[1]Reference 1 is to be considered as Part III of the present series.

Can. J. Chem. Downloaded from www.nrcresearchpress.com by 210.87.254.105 on 09/05/12
For personal use only.

TABLE 1. Thermodynamic parameters, solvent isotope effects, and secondary isotope effects for the solvolysis of a series of alkyl trifluoroacetates and *t*-butyl chloride*

Mechanism	Ester or chloride	$\Delta H^*(H_2O)$ (kcal/mol)	$\Delta S^*(H_2O)$ (e.u.)	$\frac{k(H_2O)\dagger}{k(D_2O)}$	$\frac{k(H)\S}{k(D)}$
$B_{Ac}2$	CF_3COOCH_3	10.60	−32.3	3.54	1.050 (d_3)
	$CF_3COOCH_2CH_3$	10.53	−35.1	3.67	1.036 (d_5)
	$CF_3COOCH(CH_3)_2$	10.51	−37.1	3.83	1.026 (d_6)‖
S_N1	$CF_3COOC(CH_3)_3$	25.44	13.7	1.24	2.175 (d_9)
	$(CH_3)_3CCl$	23.79¶	14.41¶	1.38**	2.45†† (d_9)

*Except where stated otherwise the figures are from ref. 4. The errors in the values of ΔH^* are considered slightly less than ± 0.1 kcal/mol and the errors in ΔS^* about ± 0.5 e.u. on average.
†Average values at 4.98 °C except for *t*-butyl chloride which is at 4.00 °C.
§From ref. 5. Average values at 10 °C except for *t*-butyl chloride and trifluoroacetate which are at 25 °C.
‖Deuteration on methyl groups, *i.e.*, $-CH(CD_3)_2$.
¶From ref. 6.
**From ref. 7.
††From ref. 8.

Can. J. Chem. Downloaded from www.nrcresearchpress.com by 210.87.254.105 on 09/05/12
For personal use only.

(ΔH_g^i) associated with the reaction

[1] $4\text{-X-}C_6H_4CH_2OCOCF_3 \rightarrow 4\text{-X-}C_6H_4CH_2^+ + CF_3COO^-$

should provide a useful guide as to which structures are likely to react by the S_N1 path. Unfortunately such data are not available for the trifluoroacetates. However, the values for the related series of benzyl chlorides in which the enthalpies of ionization are expected to parallel those of the related trifluoroacetates can be calculated from available thermochemical information. The data for the chlorides are recorded in Table 2 and the relatively low values for the 4-MeO and 4-CH_3 compounds suggest that the related trifluoroacetates would be likely candidates for the S_N1 reaction.

We proposed to detect such a change in mechanism via the k.s.i.e. (see Table 1) and also using the Hammett equation on the assumption that deviations from a linear free energy plot ($\log k$ *vs.* σ) would characterize any shift in mechanism $B_{Ac}2 \rightarrow S_N1$. The results of such experiments are reported below.

Experimental

General

Nuclear magnetic resonance spectra were recorded on a Varian A-60 spectrometer using carbon tetrachloride as solvent and tetramethylsilane as internal standard. Infrared

TABLE 2. Estimated gas phase enthalpies of ionization (ΔH_g^i) for a series of 4-substituted benzyl chlorides

X (4-X-$C_6H_4CH_2Cl$)	Ionization potential (kcal/mol)	ΔH_g^{i*} (kcal/mol)
NO_2	201	179
Cl	183	161
H	179	157
CH_3	172	150
OCH_3	157	135

*The gas phase enthalpies of ionization (ΔH_g^i) for the series of benzyl chlorides were calculated using the relationship $\Delta H_g^i = D(R—Cl) + I_p(R^\cdot) + E_f(Cl^\cdot)$ where D is the dissociation energy of the R—Cl band, I_p is the ionization potential of $R^\cdot$ and E_f is the electron affinity of $Cl^\cdot$. Bond dissociation energies for the chlorides were calculated from those for the bromides (9) with reference to the heats of formation (ΔH_f^0).

$$D(R—Cl) = \Delta H_f^0(R^\cdot) + \Delta H_f^0(Cl^\cdot) - \Delta H_f^0(RCl)$$
$$D(R—Br) = \Delta H_f^0(R^\cdot) + \Delta H_f^0(Br^\cdot) - \Delta H_f^0(RBr)$$

which gives on subtraction,

$$D(R—Cl) - D(R—Br) = \Delta H_f^0(Cl^\cdot) - \Delta H_f^0(Br^\cdot) - \Delta H_f^0(RCl) - \Delta H_f^0(RBr)$$

Reported heats of formation for several chlorides and bromides (10) lead to the average value of $D(R—Cl) - D(R—Br) = 13 \pm 2$ kcal/mol. Values of $D(R—Cl)$ that were calculated for the above series were constant to within the error reported below and an average value of 62 ± 2 kcal/mol was employed. The electron affinity for Cl was taken as 84 kcal/mol (11). The most significant contribution to changes in ΔH_g^i is the ionization potential of the $R^\cdot$ group. The values of ionization potentials quoted above are from the work of Lossing and co-workers (12), the value for the 4-nitrobenzyl radical being extrapolated from a least squares calculation of ionization potential *vs.* the Brown σ^+ parameter for a series of twelve 3- and 4-substituted benzyl radicals. The gas phase enthalpies of ionization are considered accurate to ± 4 kcal/mol.

TABLE 3. Physical properties of some esters derived from trifluoroacetic acid

Ester ($X\text{-}C_6H_4\text{-}CH_2OCOCF_3$)	Nuclear magnetic resonance (τ)	Infrared ν(C=O) (cm^{-1})	Saponification* value	B.p.† (°C)
NO_2	1.49, 2 4, 4.50	1790	240 (249)	134–136 m.p. 47–48 Lit. 47 (13)
Cl	2.72, 4.74	1784	240 (238)	33–36
H	2.69, 4.75	1790	202 (204)	63–64
CH_3	2.87, 4.80, 7.00	1780	217 (218)	30
OCH_3	2.74, 3.14, 4.77, 6.26	1780	234 (234)	39–41
CF_3COOCH_3	6.05	1790	133 (128)	42–42.5 at 760 mm Lit. 43 (14)

*Theoretical value in brackets.
†Boiling point values quoted for vacuum of 0.05–0.1 mm unless stated otherwise.

spectra were recorded on a Perkin–Elmer model 237B grating spectrophotometer using a liquid cell technique with carbon tetrachloride as solvent. Mass spectra were recorded on a Hitachi Perkin–Elmer RMU6E spectrometer at 50 °C using an ionizing potential of 70 V with no appreciable difference between initial and final total ion current.

Materials

Esters were prepared by the usual method, either from trifluoroacetic anhydride/alcohol or silver trifluoroacetate/bromide and were distilled under vacuum. 4-Nitrobenzyl trifluoroacetate was recrystallized several times from petroleum ether (40–60 °C). All the esters were stored at 0 °C in a desiccator. The 4-methoxybenzyl trifluoroacetate was very unstable and tended to polymerize to a deep red tar if left at room temperature for more than 2–3 h before distillation and, consequently, this material was vacuum distilled immediately after preparation.

All kinetic measurements were made soon after purification. Purity was established by saponification, mass spectra, n.m.r., and infrared measurements. The excellent first order plots also vindicated the purity of the esters. The analytical and spectral data are recorded in Table 3.

Deuterium oxide was obtained from Atomic Energy of Canada and was used several times without appreciable loss of purity. The solvent was recovered after each kinetic run and was distilled, any acid present having been neutralized before hand with dried sodium carbonate. The first fraction containing acetone was discarded. The concentration of deuterium oxide was never less than 97%, determined by using n.m.r. spectrometry with purified acetonitrile as an internal standard.

Acetone was purified by treatment with small amounts of potassium permanganate until the pink color persisted. After drying with anhydrous potassium carbonate the material was distilled at 55.5–56 °C.

Kinetics

Rates were determined conductimetrically using apparatus described elsewhere (5). The concentration of ester in the kinetic determinations was *ca.* 10^{-4} *M* and the solvent systems used were water/acetone or deuterium oxide/acetone mixtures containing 0.012 mol fraction of acetone to facilitate dissolution of the ester. All rates were measured at 5.05 °C. A stock solution of the ester in acetone was prepared (*ca.* 0.002 *M*) and cooled to 5.05°. An aliquot (2 ml, 1.65 ± 0.02 g) of this solution was added, using a 2 ml syringe, to a measured volume of backing electrolyte (41 ml, 40.72 ± 0.06 g) at 5.05° in a stirred cell. The backing electrolyte was prepared by allowing a suitable amount of the appropriate ester to react with distilled water so as to reduce the initial resistance of the solution to a convenient value. The two weights quoted above, 1.65 ± 0.02 and 40.72 ± 0.06 g, are both averages of eight weight determinations. The backing electrolyte was introduced into the cell at room temperature using a 50 ml burette, the cell having been rinsed three times with backing electrolyte and then cleared of as much liquid as possible before refilling. The residual liquid on the sides of the cell weighed 0.2 g and did not vary from run to run. The amount of residual liquid is included in the weight of backing electrolyte quoted above.

For kinetic runs with deuterium oxide as the solvent, the volume of backing electrolyte used was adjusted so that the final reaction mixture contained 0.012 mol fraction of acetone.

Resistance readings were taken over approximately three half-lives and when the reaction was complete the infinity resistance was measured. At least four rate determinations were made for each ester and solvent combination.

The pseudo first order rate constants and k.s.i.e.'s are quoted in Table 4 for the 4-substituted benzyl esters along with those values for the methyl trifluoroacetate in the same solvent system for comparison. The k.s.i.e. of 3.4 for hydrolysis of this last ester in 0.012 mol fraction of acetone in water is in close agreement with the k.s.i.e. of 3.5 measured (4) in pure water. Therefore comparisons between the two solvent systems are considered legitimate.

Can. J. Chem. Downloaded from www.nrcresearchpress.com by 210.87.254.105 on 09/05/12
For personal use only.

Can. J. Chem. Downloaded from www.nrcresearchpress.com by 210.87.254.105 on 09/05/12
For personal use only.

TABLE 4. Rates of solvolysis of a series of trifluoroacetates in 0.012 mol fraction acetone in water and deuterium oxide at 5.05 °C

Ester (CF_3COOR)	k_{H_2O} ($\times 10^3$ s^{-1})*	k_{D_2O} ($\times 10^3$ s^{-1})*	k_{H_2O}/k_{D_2O}
4-Nitrobenzyl	7.996(7) ±0.065	2.030(4) ±0.029	3.9
4-Chlorobenzyl	3.305(9) ±0.065	0.8731(4) ±0.0112	3.8
Benzyl	2.448(10) ±0.035	0.6563(4) ±0.0109	3.7
4-Methylbenzyl	1.939(5) ±0.028	0.5356(4) ±0.0058	3.6
4-Methoxybenzyl	3.212(8) ±0.038	1.794(4) ±0.013	1.8
Methyl	1.934(4) ±0.026	0.5644(4) ±0.0024	3.4

*Number of rate determinations in parentheses.

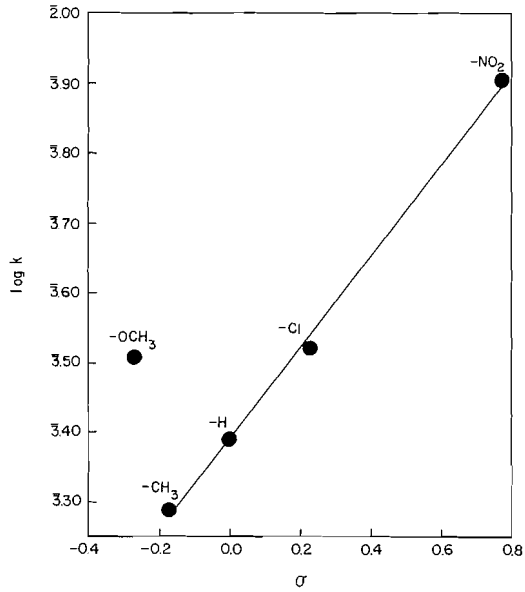

FIG. 1. Correlation of the rates of hydrolysis at 5.05 °C of 4-substituted benzyl trifluoroacetates with the Hammett σ parameter.

Discussion

We propose a useful rule which states that if the members of a series of substrates can each conceivably react by two distinct paths, A and B, and if both paths can be correlated by a linear free energy relationship using a common substituent scale, then deviations from the separate correlations, caused by a change in mechanism from A to B or vice versa, must be positive. This rule follows from the principle that if two reaction paths exist the path of minimum free energy will be the most important. The above rule is in accord with experience in the present study since the rate of solvolysis for the 4-methoxybenzyl trifluoroacetate deviates positively from a Hammett plot for which the remaining points are satisfactorily linear (see Fig. 1). From the sign of the ρ parameter we assume that this line corresponds to the $B_{Ac}2$ mechanism which is in agreement with the k.s.i.e's for the 4-CH_3 → 4-NO_2 compounds (see Table 4) and consistent with the fact that the sign of ρ for S_N1 reactions is always negative.

The deviation of the 4-OCH_3 compound from the $B_{Ac}2$ linear free energy correlation and the magnitude of the k.s.i.e. for this substance indicate that it reacts by a route different from that followed by the other structures but the relatively high value of the k.s.i.e. (1.8) is greater than those usually observed for S_N1 processes extensively studied by Laughton and Robertson (15). This possibly indicates "mixed kinetics", *i.e.*, the observed rate is the sum of $B_{Ac}2$ and S_N1 components. Indeed the results for the k.s.i.e. and the Hammett plot provide methods of calculating the relative contributions of the $B_{Ac}2$ and S_N1 processes to the observed rate for the 4-methoxybenzyl ester.

On the basis that the k.s.i.e. for S_N1 reactions is *ca.* 1.2 and for $B_{Ac}2$ reactions *ca.* 3.6 such a calculation can be made in the following way. Let k_S be the rate of the S_N1 reaction and k_B the rate of the $B_{Ac}2$ reaction; then if k_o is the observed rate we have,

$$[2] \qquad k_o = k_S + k_B$$

and hence for 4-methoxybenzyl trifluoroacetate

$$[3] \qquad \frac{k_o(H_2O)}{k_o(D_2O)} = \frac{k_S(H_2O) + k_B(H_2O)}{k_S(D_2O) + k_B(D_2O)} = 1.8$$

But

$$[4] \qquad \frac{k_S(H_2O)}{k_S(D_2O)} = 1.2 \text{ (average value)}$$

and

$$[5] \qquad \frac{k_B(H_2O)}{k_B(D_2O)} = 3.6 \text{ (average value)}$$

which, on combining eqs. 3, 4, and 5 gives

$$[6] \qquad k_S(H_2O) = k_B(H_2O)$$

i.e., the two paths are of equal importance for the 4-OCH_3 ester.

From the linear free energy relationship (Fig. 1) the extrapolated $B_{Ac}2$ rate for the 4-OCH_3 compound is 1.64×10^{-3} s^{-1} whereas the observed rate is 3.21×10^{-3} s^{-1} giving k_S equal to 1.57×10^{-3} s^{-1}. Thus both methods of calculation lead to the same conclusion, *i.e.*, $k_S(H_2O) = k_B(H_2O)$ for 4-methoxybenzyl trifluoroacetate.

Thanks are due to the Technical Services Department at Memorial University of Newfoundland for their continued care of the apparatus used in this work. We are grateful to Miss Marion Baggs and Mr. Earl Benson for measuring mass and n.m.r. spectra and to our colleagues for many useful discussions. We also express our thanks to the N.R.C.C. for their support of this work.

1. J. M. W. Scott and R. E. Robertson. Can. J. Chem. **50**, 167 (1972).
2. C. A. Bunton and T. Hadwick. J. Chem. Soc. 3248 (1958).
3. A. Moffat and H. Hunt. J. Am. Chem. Soc. **80**, 2985 (1958).
4. J. G. Winter and J. M. W. Scott. Can. J. Chem. **46**, 2887 (1968).
5. S. Lobo. M.Sc. Thesis. Memorial University of Newfoundland, St. John's, Newfoundland. 1970.
6. E. A. Moelwyn-Hughes, R. E. Robertson, and S. Sugamori. J. Am. Chem. Soc. **87**, 2097 (1965).
7. P. M. Laughton and R. E. Robertson. Can. J. Chem. **34**, 1714 (1957).
8. L. Hakka, A. Queen, and R. E. Robertson. J. Am. Chem. Soc. **87**, 161 (1965).
9. M. Szwarc, C. H. Leigh, and A. H. Sehon. J. Chem. Phys. **19**, 658 (1951).
10. H. A. Skinner. Modern aspects of thermochemistry. The Royal Institute of Chemistry, Lectures, Monographs and Reports. No. 3, 1958. p. 24.
11. R. S. Berry, C. W. Reimann, and G. N. Spokes. J. Chem. Phys. **37**, 2278 (1962).
12. A. G. Harrison, P. Kabarle, and F. P. Lossing. J. Am. Chem. Soc. **83**, 777 (1961).
13. E. J. Bourne, C. E. M. Tatlow, and J. C. Tatlow. J. Chem. Soc. 1367 (1950).
14. A. Moffat and H. Hunt. J. Am. Chem. Soc. **79**, 54 (1957).
15. P. M. Laughton and R. E. Robertson. *In* Solute–solvent interactions. *Edited by* J. F. Coetzee and Calvin D. Ritchie. Marcel Dekker, New York. 1969. p. 400.

Can. J. Chem. Downloaded from www.nrcresearchpress.com by 210.87.254.105 on 09/05/12
For personal use only.

L'effet d'anions sur l'oxydation anodique du méthanol

GUY BELANGER
Institut de Recherche de l'Hydro-Québec, Varennes, Québec

Reçu le 13 décembre 1971

L'oxydation anodique du méthanol en milieu acide (1 *N* H_2SO_4) est passée brièvement en revue avec la présentation de courbes de polarisation et de courbes potentiodynamiques. Le mécanisme possible d'oxydation est présenté: on illustre le phénomène d'inhibition de l'oxydation par la formation d'oxydes à la surface du platine. La présence d'anions à faible concentration (10^{-3} à 10^{-4} *N*) modifie parfois le courant d'oxydation du méthanol. On tente de relier cet effet inhibiteur de certains anions à des valeurs théoriques de force de liaison, d'énergie du réseau cristallin et de chaleur d'hydratation. Une certaine corrélation sommaire peut s'établir entre l'importance de l'effet d'inhibition et la classification des anions en bases douces ou dures.

Anodic oxidation of methanol in acidic medium (1 *N* H_2SO_4) is briefly reviewed with the presentation of polarization and potentiodynamic curves. The possible mechanism of oxidation is presented: the inhibition phenomenon of oxidation is illustrated by the formation of oxides on the surface of platinum. The oxidation current of methanol is sometimes modified by the presence of anions in a low concentration (10^{-3} to 10^{-4} *N*). An attempt is made to relate the inhibitor effect of some anions to theoretical values of binding strength, crystal lattice energy, and heat of hydration. A succinct correlation can be set up between the importance of the inhibition effect and the classification of the anions in hard or soft bases.

Canadian Journal of Chemistry, **50**, 1891 (1972)

Introduction

Dans la mise au point d'une pile à combustible économique et fiable, l'oxydation anodique du combustible demeure un élément de recherche: le mécanisme de la réaction, le rôle d'oxydes à la surface des électrodes et leur participation à la réaction, l'effet du milieu réactionnel, l'effet des anions sont différents problèmes qui ne sont pas tout à fait résolus.

Plusieurs travaux ont été accomplis dans le domaine de l'oxydation anodique du méthanol en milieu aqueux (1–5). Il est à noter que le mécanisme de la réaction, quoique assez bien établi dans ses grandes lignes, pose encore quelques problèmes (6).

Un des aspects qui retiennent de plus en plus l'attention est l'effet de la présence de différents anions lors de l'oxydation anodique du méthanol et d'autres combustibles (7–10). Une étude mécanistique de l'effet des anions (autres que les halogénures) s'avère importante quant à la compréhension globale du mécanisme d'oxydation.

Partie expérimentale

Les mesures furent effectuées dans une cellule en Pyrex à trois compartiments isolés par des robinets non graissés. L'électrode de référence à hydrogène sur platine–platiné dans la solution fut utilisée. L'électrode de travail (platine) opérait sous atmosphère d'hélium (Grade Electrolytique de la compagnie Liquid Carbonic). L'hydrogène était désoxygéné par un catalyseur de palladium ("Dexo" de la compagnie Engelhard), l'hélium (Grade A, de la compagnie Liquid Carbonic) était désoxygéné sur du cuivre chauffé à environ 500 °C. Les lignes de gaz étaient en verre. Les autres aspects du montage et de la purification des gaz furent déjà décrits (11).

Le méthanol de meilleure qualité ("Fisher certified") fut employé directement de même que les sels de sodium ou de potassium des différents anions.

La solution de référence (1 *N* H_2SO_4) fut purifiée par une pré-électrolyse (environ 48 h minimum à 100 mA/cm^2) avec une anode de platine–platiné (2 cm^2) et une cathode de platine; ces deux électrodes étaient remplacées par de nouvelles électrodes de platine pour les mesures.

Les courbes de polarisation furent enregistrées comme nous l'avons décrit précédemment (12). Les différents instruments utilisés furent les suivants: le potentiostat Tacusel modèle PRT 10–20x, le potentiomètre motorisé Servovit 9B de Tacusel, l'amplificateur logarithmique Logalex 100B de Tacusel et un enregistreur *X*–*Y* de Honeywell modèle 550. L'intervalle de temps entre les mesures fut établi à 2 min.

Résultats

(a) Méthanol + 1 N H_2SO_4

Comme notre référence sera le système méthanol–1 *N* H_2SO_4, nous présenterons en premier lieu quelques données sur celui-ci. Notre "référence" est quelque peu arbitraire; nous l'avons choisie à cause du peu d'adsorption des sulfates. Les diminutions de courant illustrant l'effet des anions seront référées à ce système de base.

La fig. 1 illustre une courbe de polarisation typique pour une telle solution. On notera l'aspect quelque peu complexe de la relation courant–potentiel. Dans la partie ascendante

Can. J. Chem. Downloaded from www.nrcresearchpress.com by 210.87.254.6 on 09/05/12
For personal use only.

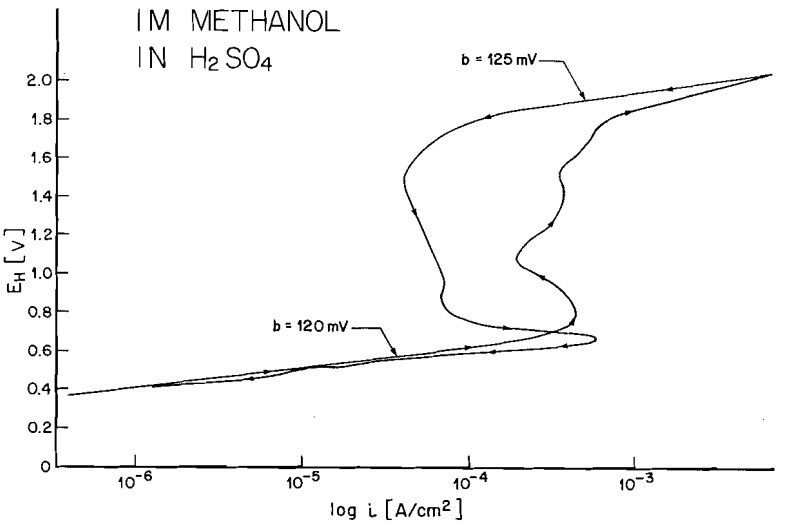

FIG. 1. Courbe de Tafel du méthanol dans l'acide sulfurique sur une électrode de platine: parties ascendantes et descendantes des valeurs de potentiel.

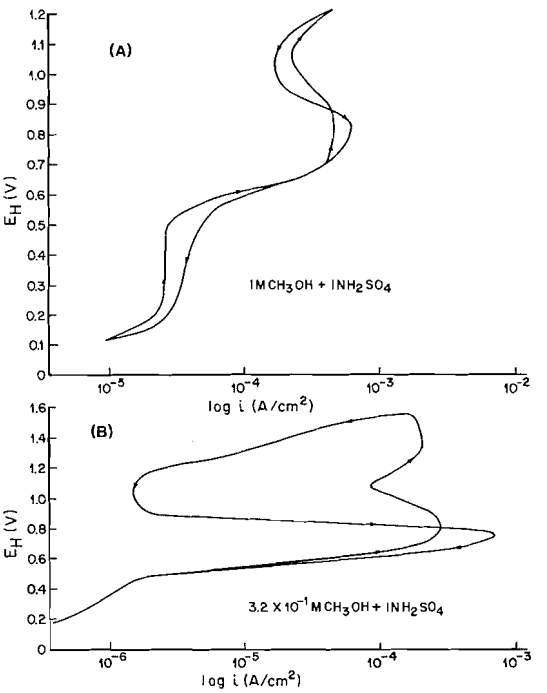

FIG. 2. (*a*) Courbe de Tafel de 0.1 à 1.2 V pour le méthanol dans l'acide sulfurique. (*b*) Courbe de Tafel de 0.2 à 1.6 V pour le méthanol dans l'acide sulfurique.

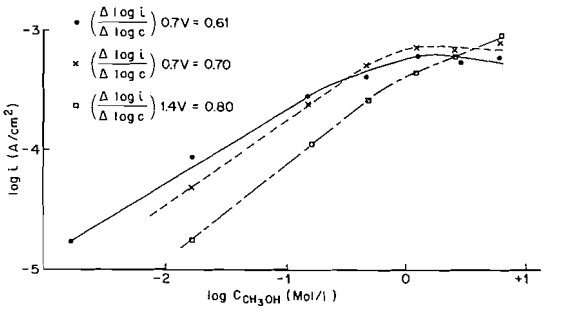

FIG. 3. Variation du courant à différents potentiels pour une série de concentrations de méthanol dans 1 *N* H_2SO_4; ●, 0.7 V pour la partie descendante de la courbe de Tafel; ×, 0.7 V, et □, 1.4 V pour la partie ascendante de la courbe.

(0.4 à 2.0 V) plusieurs aspects méritent d'être mentionnés. Le premier maximum de courant se manifeste à environ 0.75 V et correspond assez bien aux valeurs déjà observées pour ce système (3) et d'autres oxydations anodiques de composés organiques sur les électrodes de platine (2, 12, 13). A potentiel plus anodique, le courant décroît illustrant un phénomène d'inhibition. Il est maintenant reconnu que cette inhibition trouve son origine dans la présence d'oxydes de platine à la surface de l'électrode (3, 13, 14). Le même phénomène se reproduit à 1.4 V. La pente ($\Delta E/\Delta \log i$) pour l'intervalle entre 0.5 et 0.7 V est de 120 mV et se compare très bien avec la valeur rapportée par Bagotsky et Vasilyev (3): nous élaborerons plus en détail cette valeur au prochain chapitre.

L'influence d'une forme quelconque d'oxyde à la surface de l'électrode et son rôle dans le mécanisme d'oxydation sont illustrés par l'hystérésis très prononcée de la courbe. En effet, la

Can. J. Chem. Downloaded from www.nrcresearchpress.com by 210.87.254.6 on 09/05/12
For personal use only.

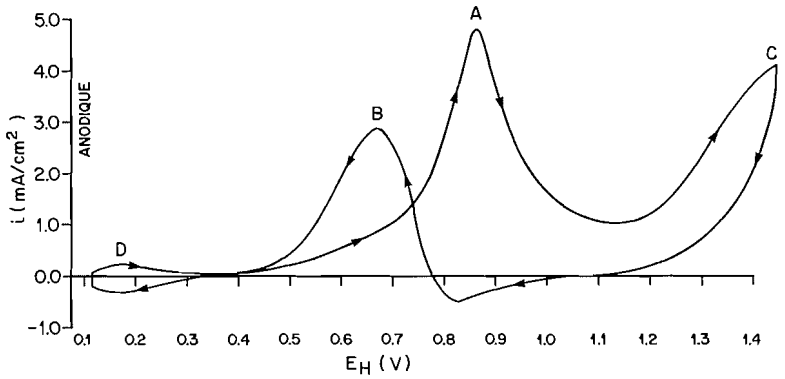

FIG. 4. Courbe potentiodynamique: vitesse de balayage de 260 mV/s. Concentration de méthanol 4.7×10^{-1} *M* dans 1 *N* H_2SO_4.

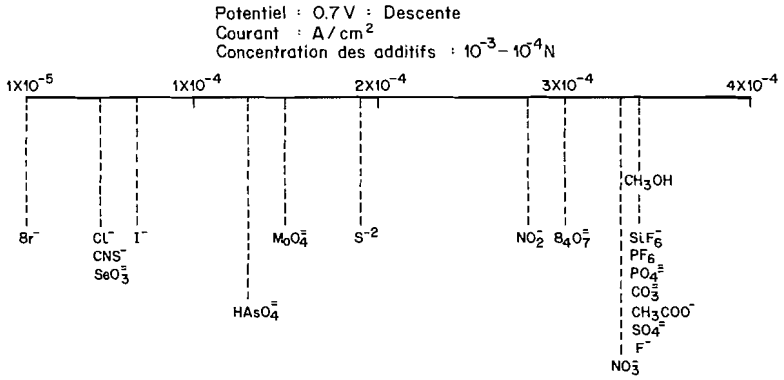

FIG. 5. Courant du pic à 0.7 V de la partie descendante de la courbe de Tafel en présence de différents anions.

partie descendante (2.0 à 0.4 V) de la courbe de polarisation, diffère grandement de la partie ascendante (fig. 1). L'aspect de la courbe est aussi différent. Le pic d'oxydation est beaucoup plus fin pour la partie descendante de la courbe illustrant le caractère d'adsorption du méthanol sur l'électrode. Une discussion plus élaborée sera reprise au prochain chapitre en utilisant la théorie d'inhibition de Gilroy et Conway (15).

Le rôle de la nature de la surface est illustré à la fig. 2*a*, où l'électrode est polarisée de 0.1 à 1.2 V. Pour cet intervalle de potentiel, on notera l'absence à toute fin pratique d'hystérésis: les pics d'oxydation ne sont pas tout à fait symétriques mais la différence est beaucoup moins grande que pour un balayage plus complet (figs. 1 et 2*b*). La fig. 2*b* indique le rétablissement de l'effet de surface même si le potentiel anodique ne dépasse pas 1.6 V.

La fig. 3 illustre la relation entre la densité de courant à l'équilibre et la concentration globale du méthanol et ceci à différents potentiels. On observe un ordre de réaction fractionnel et aussi à plus forte concentration, la vitesse de la réaction devient indépendante de la concentration globale du méthanol. Une explication plus approfondie sera tentée plus loin.

Pour compléter cette revue sur l'oxydation du méthanol en milieu acide, la fig. 4 montre la courbe potentiodynamique pour ce système. On note les deux pics d'oxydation, le pic du balayage anodique A et celui du balayage cathodique B. En C, c'est le deuxième pic anodique à environ 1.4 V, identique à celui observé pour les courbes à équilibre (fig. 1). Les pics en D illustrent l'adsorption et la désorption de l'hydrogène. Cette courbe potentiodynamique reproduit assez bien celle obtenue par Gilman et Breiter (16) et par Bagotsky et Vasilyev (2). Ici encore l'effet d'inhibition est très marqué.

(b) Méthanol + anions

La fig. 5 illustre d'une façon schématique l'influence de la présence d'anions (10^{-3}–10^{-4} *N*) sur le pic d'oxydation de la partie descendante de la courbe de Tafel. Ce pic à 0.7 V fut choisi car

Can. J. Chem. Downloaded from www.nrcresearchpress.com by 210.87.254.6 on 09/05/12
For personal use only.

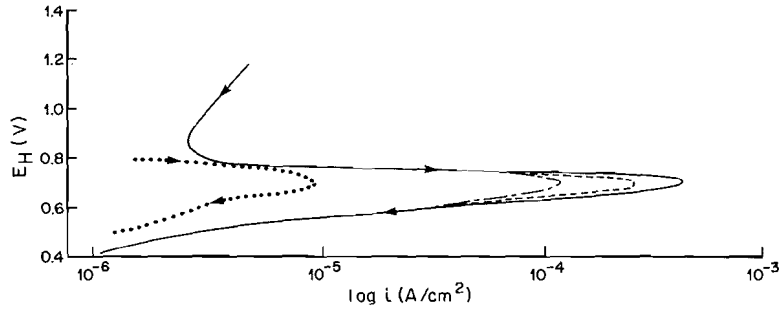

FIG. 6. Partie descendante de la courbe de Tafel avec différents anions; — 1 M CH_3OH + 10^{-3} N SiF_6^-; --- 1 M CH_3OH + 10^{-3} N NO_2^-; -·- 1 M CH_3OH + 10^{-3} N S^{2-}; ●●● 1 M CH_3OH + 10^{-3} N Br^-

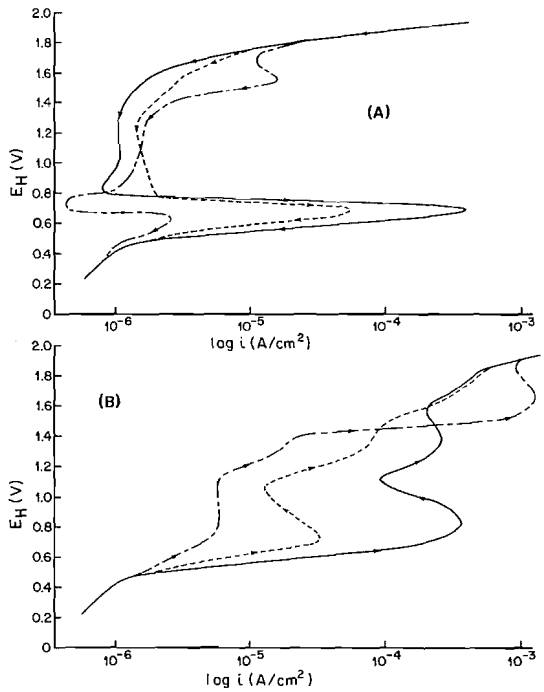

FIG. 7. (*a*) Partie descendante de la courbe de Tafel pour solution de 3×10^{-1} M CH_3OH dans 1 N H_2SO_4 avec différentes concentrations de NaCl: — 0 M NaCl; --- 2×10^{-4} M NaCl; --- 1×10^{-1} M NaCl. (*b*) Partie ascendante de la courbe de Tafel pour les mêmes solutions.

il est le mieux défini et le plus libre d'interférences par le recouvrement d'autres pics.

De la série des anions étudiés, il y a toute la gamme des activités. Certains n'ont aucune influence sur l'oxydation (*e.g.* SiF_6^-, F^-, CH_3COO^-, PO_4^{3-}), d'autres par contre inhibent presque totalement la réaction (*e.g.* Br^-, Cl^-, CNS^-) et enfin certains ont un effet intermédiaire (*e.g.* S^{2-}, $HAsO_4^{2-}$).

La fig. 6 fait voir d'une façon plus détaillée les courbes expérimentales en l'absence et en présence de différents anions avec des pouvoirs d'inhibition variés.

La fig. 7*a* et *b* montre l'effet de la concentration du chlorure sur la courbe complète de polarisation. On notera la variation des intensités de courant en fonction de la concentration du chlorure. A une concentration importante (0.1 N NaCl), la présence d'un pic à 1.6 V illustre le dégagement du chlore.

Discussion

Mécanisme d'oxydation du méthanol

(a) Courbes de polarisation

Comme nous l'avons mentionné précédemment, une pente de Tafel de 120 mV a été observée pour la partie ascendante de la courbe entre 0.5 et 0.7 V. On peut mettre de l'avant différents mécanismes de réaction qui nous mèneront à cette valeur de pente. Il faut en plus que d'autres résultats expérimentaux concordent avec ce mécanisme proposé.

Le mécanisme suivant a été proposé (2–4):

[1] $$4Pt + CH_3OH \rightleftharpoons Pt\{COH\} + 3Pt\{H\}$$

Cette première étape conduit à une déshydrogénation rapide de la molécule de méthanol (3, 17). L'hydrogène absorbé sur l'électrode est libéré grâce à la réaction suivante:

[1*a*] $$Pt\{H\} \rightarrow Pt + H^+ + e$$

Une autre réaction qui peut être considérée à l'équilibre (quasi-équilibre) implique la molécule d'eau et peut se formuler ainsi:

[2] $$Pt + H_2O \underset{i_{-2}}{\overset{i_2}{\rightleftharpoons}} Pt\{OH\} + H^+ + e$$

Can. J. Chem. Downloaded from www.nrcresearchpress.com by 210.87.254.6 on 09/05/12
For personal use only.

Can. J. Chem. Downloaded from www.nrcresearchpress.com by 210.87.254.6 on 09/05/12
For personal use only.

La réaction qui peut être considérée comme l'étape déterminante est la suivante:

[3] $\quad Pt\{OH\} + Pt\{COH\} \rightarrow 2Pt\{H\} + CO_2$

Les espèces $Pt\{OH\}$ et $Pt\{COH\}$ sont des entités transitoires et de nature mal définie. Les lois de Temkin (19) gouvernent l'adsorption de ces espèces à l'électrode. On peut dériver la relation courant–potentiel pour un tel système (13, 18, 19).

L'équation 1 peut être représentée comme suit:

$$[4] \qquad \ln K_1' + \ln C_{MeOH} = \frac{r\theta_{COH}}{RT}$$

où K_1' groupe une série de constantes de la réaction, C_{MeOH} est la concentration du méthanol, θ_{COH} est la fraction de l'électrode qui est recouverte par l'espèce $\{COH\}$, R et T sont la constante des gaz et la température respectivement. Le symbole r représente le paramètre de Temkin et tient compte de l'hétérogénéité de la surface ou des interactions entre les différentes espèces adsorbées (19).

Aussi réaction 2 peut être transcrite de la même manière:

$$[5] \qquad \ln K_2' + \ln C_{H_2O} + \frac{FV}{RT} = \frac{r\theta_{OH}}{RT}$$

où F est la constante de Faraday, V est le potentiel de l'électrode et θ_{OH} est le recouvrement de l'électrode par l'espèce $\{OH\}$. On peut, à titre d'exemple dériver de façon plus explicite cette dernière relation 5.

Le courant dans une direction pour l'éq. 2 est donné par la relation suivante (19):

$$[5a] \quad i_2 = k_2(1-\theta)C_{H_2O}\exp\left[\frac{\alpha F}{RT}V\right] \times \exp\left[-\frac{\alpha r}{RT}\theta_{OH}\right]$$

Le courant dans la direction opposée est donné comme suit (19):

$$[5b] \quad i_{-2} = k_{-2}\theta_{OH}C_{H^+}\exp\left[-\frac{(1-\alpha)}{RT}FV\right] \times \exp\left[\frac{(1-\alpha)}{RT}r\theta_{OH}\right]$$

Comme [2] est considéré étant à l'équilibre alors $i_2 = i_{-2}$ et donc

$$[5c] \quad \ln\frac{k_2}{k_{-2}} + \ln(1-\theta) + \ln C_{H_2O} - \ln\theta_{OH} - \ln C_{H^+} + \frac{FV}{RT} = \frac{r}{RT}\theta_{OH}$$

où k_2 et k_{-2} sont des constantes de la vitesse de la réaction, $1-\theta$ est la fraction de la surface qui est libre et α est coefficient de transfert qui est de l'ordre de 0.5 (19). En groupant les différents termes définis comme K_2', on obtient la relation 5.

De même on peut écrire pour la réaction 3, l'équation suivante:

$$[6] \quad \ln i_3 = \ln k_3 + \ln\theta_{OH} + \ln\theta_{COH} + \frac{r\alpha}{RT}(\theta_{OH} + \theta_{COH})$$

Ici les paramètres d'adsorption de Temkin ont été posés égaux comme cela se fait habituellement (19, 13). Il est certain cependant qu'ils sont différents mais pour la simplification de la dérivation des équations le même symbole a été utilisé. Il est à noter cependant que les conclusions générales tirées de ces équations ne seront pas modifiées car les valeurs de r n'apparaissent pas dans la pente de Tafel ou dans le calcul de l'ordre de la réaction.

Des éqs. 4 et 5, 6 peut se réécrire:

$$[7] \quad \ln i_3 = \ln k_3 + \ln\theta_{OH} + \ln\theta_{COH} + \alpha\ln K_1' + \alpha\ln K_2' + \alpha\ln C_{H_2O} + \alpha\ln C_{MeOH} + FV/RT$$

La relation 7 nous permet de tirer les conclusions suivantes: (*a*) la pente de Tafel: $\Delta V/\Delta\log i = 2.303\ RT/\alpha F = 120$ mV; (*b*) l'ordre de la réaction par rapport au méthanol: $\Delta\log i/\Delta\log C_{MeOH} = \alpha = 0.5$.

Expérimentalement, on observe une pente de 120 mV dans la région où la relation de Tafel est suivie. L'ordre de la réaction se situe aux environs de 0.6 (c.f. fig. 3) pour plusieurs potentiels.

La confirmation directe du mécanisme n'a pas été réalisée: des expériences avec le méthanol contenant de l'oxygène 18 pourrait indiquer plus exactement l'origine d'un des oxygènes dans le produit final, le CO_2. Il faut remarquer cependant que les évidences indirectes sont assez convaincantes pour justifier le mécanisme global (1 et les références incluses).

L'étape réaction 2 pourrait être l'étape déterminante et donnerait une pente de 120 mV mais

Can. J. Chem. Downloaded from www.nrcresearchpress.com by 210.87.254.6 on 09/05/12
For personal use only.

dans ce cas-là, la relation courant–concentration de méthanol serait inexistante: la réaction serait d'ordre zéro ce qui n'est pas le cas. A forte concentration, l'ordre de la réaction par rapport à la concentration du méthanol devient d'ordre zéro ce qui est normal. Le mécanisme plus haut concorde assez bien dans ses grandes lignes avec celui proposé par Bagotsky et Vasilyev (2).

(b) Mécanisme d'inhibition

Comme nous l'avons déjà mentionné, la partie ascendante de la courbe de polarisation illustre le phénomène d'inhibition. Cet aspect de l'oxydation anodique de composé organique a été traité d'une façon extensive par Gilroy et Conway (15). Comme nous l'avons vu, l'étape réaction 2 fournit une espèce active du genre Pt—OH. Cependant, lorsque le potentiel de l'électrode augmente, une réaction subséquente se produit:

$$[8] \qquad Pt\{OH\} \rightarrow Pt\{O\} + H^+ + e$$

Cette dernière espèce Pt{O}, agit comme inhibiteur et empêche la réaction 3 de se produire. Dans la partie descendante de la courbe de polarisation de 2 à environ 0.8 V, il n'y a que l'oxyde Pt{O} sous une forme cristallographique inactive. A potentiel plus bas, il y a formation de l'espèce active Pt{OH}. C'est le cas (*iii*) dans cette publication: pour cette situation, les prédictions théoriques du traitement (15) prévoient une pente de 2 RT/F pour la partie non-inhibée et après le maximum de courant celui-ci décroît avec une pente de 2 $RT/3F$. Nous avons donc, un pic asymétrique. Ces valeurs de pentes sont valables pour le cas où les espèces adsorbées obéissent aux lois de Langmuir. Pour les isothermes de Temkin, la pente positive ne varie pas mais la pente négative peut varier selon la valeur du paramètre r dans les éqs. (4–6). La relation courant–potentiel obtenue par ces auteurs est de la forme suivante:

$$[9] \qquad \frac{i}{i_{max}} = [2 \exp \beta F \Delta V/RT] \Big/ \left(1 + \exp\left[\frac{3\beta F \Delta V}{RT}\right]\right)$$

où i_{max} est le courant maximum (à 0.75 V pour le méthanol) et $\Delta V = V - V_{max}$.

Un autre aspect lié au phénomène d'inhibition est l'hystérésis très prononcée des courbes de polarisation (figs. 1 et 2) et des courbes potentiodynamiques (fig. 4). Ce phénomène est lié à la présence d'oxyde sous forme cristallographique différente. En effet, comme nous l'avons noté à la fig. 2*a*, cette hystérésis est très légère si le maximum anodique ne dépasse pas 1.2 V. Cependant à 1.6 V, l'hystérésis est complète. Il semble qu'entre la forme d'oxyde dans la partie ascendante de la courbe et celle qui se manifeste pour la partie descendante, il y ait une différence catalytique très importante. Il semble donc y avoir un changement de phase entre ces potentiels.

Oxydation du méthanol en présence d'anions

Comme nous l'avons vu lors de la présentation des résultats, nous pouvons noter toute une gamme d'effets de différents anions sur la vitesse d'oxydation du méthanol.

Généralement on explique l'inhibition par les anions en invoquant une adsorption préférentielle de ceux-ci sur l'électrode par rapport à la molécule organique, (8–10). Le mécanisme exact d'adsorption des anions n'est pas encore très bien connu et les raisons qui militent en faveur d'une adsorption importante pour certains anions et négligeable pour d'autres portent aussi à controverse.

Graham (20) utilise la notion de liaison covalente entre l'anion et le métal (le mercure en l'occurence) comme critère d'adsorption. Pour Lévine, Bell et Calvert (21) c'est dans l'énergie d'image qu'il faut rechercher l'origine de l'adsorption: c'est un concept impliquant des forces électrostatiques. Bockris *et al.* (22) invoquent l'énergie de solvatation comme critère d'adsorption pour un ion donné.

Enfin, une autre façon d'aborder le problème fut présentée par Barclay (23) et repose sur les concepts d'acides ou de bases douces ou dures de Pearson (24) ("soft or hard acids or bases"). Sous cette classification les anions qui sont fortement adsorbés sont les bases douces et ceux qui ne sont pas adsorbés sont des bases dures. Les anions durs sont relativement petits, non polarisables et leurs électrons de valence ne sont pas facilement enlevés (*e.g.* F^-). Les anions doux par contre, sont relativement gros et facilement polarisables (*e.g.* S^{2-}). Il a été montré (23) qu'il existait une corrélation assez juste entre le déplacement du potentiel de charge zéro du mercure et le degré d'adsorption des différents anions. Ce déplacement est peu important pour

Can. J. Chem. Downloaded from www.nrcresearchpress.com by 210.87.254.6 on 09/05/12
For personal use only.

TABLEAU 1

Anion	Classification	% inhibition
S^{2-}	Doux	55
I^-	Doux	80
CNS^-	Doux	85
Br^-	Intermédiaire	97
Cl^-	Intermédiaire	85
NO_2^-	Intermédiaire	20
NO_3^-	Dur	0
CH_3COO^-	Dur	0
F^-	Dur	0

des anions non-adsorbés mais il acquiert une valeur importante en présence d'anions fortement adsorbés (*e.g.* le p.c.z. est de 437 mV par rapport à l'électrode de calomel standard en présence de fluorure et il est de 880 mV en présence de sulfure, un déplacement de 443 mV). Bien que cette classification ait été faite que pour le mercure qui est un métal unique, on peut tenter une approche similaire pour le platine. Ici c'est l'effet inhibiteur qui sera notre critère. Le tableau 1 illustre cette classification entre certains anions doux ou durs et le degré d'inhibition. Ce pourcentage d'inhibition est calculé en posant le courant à 0.7 V de la courbe descendante (fig. 1) à 100% pour le méthanol 1 *M* en milieu 1 *N* H_2SO_4. Le courant à ce potentiel est lu en présence des différents anions et la différence entre cette valeur et le 100% est prise comme degré d'inhibition, c'est-à-dire:

$$[10] \quad \%\ \text{d'inhibition} = \frac{(i_{CH_3OH+1\ N\ H_2SO_4} - i_{CH_3OH+1\ N\ H_2SO_4+Anion}) \times 100}{i_{CH_3OH+1\ N\ H_2SO_4}}$$

La classification de Barclay (23) s'applique dans ses grandes lignes: les anions durs ont un effet négligeable sur l'oxydation du méthanol et les anions doux ou intermédiaires ont des effets variables sur la vitesse d'oxydation. Cette classification est loin d'être parfaite mais c'est déjà un pas de fait dans une tentative d'explication des résultats expérimentaux.

La chaleur d'hydratation est un deuxième type de corrélation possible avec le pourcentage d'inhibition. Cette valeur thermodynamique donne une idée de la stabilisation d'un anion par le solvant. Si cette stabilisation est faible, l'ion sera porté à être adsorbé sur l'électrode pour acquérir un état d'énergie minimum (22). La

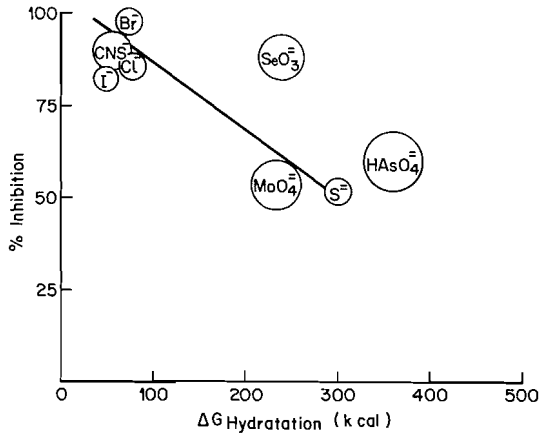

FIG. 8. Pourcentage d'inhibition du courant à 0.7 V de la partie descendante de la courbe de Tafel en fonction de la chaleur d'hydratation de différents anions.

chaleur d'hydratation est donnée par la relation suivante (25)

$$[11] \quad \Delta G_{HYD} = \frac{-164Z^2}{(r^- + 0.35)}$$

où ΔG_{HYD} est en kcal/mol, Z et r^-, sont la charge et le rayon ionique de l'anion, 0.35 est un facteur empirique tenant compte du rayon d'hydration des anions et 164 est un facteur de conversion incluant différentes constantes fondamentales. La fig. 8 illustre cette corrélation pour différents anions montrant une activité d'inhibition. Il existe un certain degré de dépendance entre cette valeur thermodynamique et le pourcentage d'inhibition. Il faut cependant noter que plusieurs anions ayant une valeur de ΔG_{HYD} relativement faible (donc ils seraient stabilisés par une adsorption sur l'électrode) n'influent pas sur l'oxydation du méthanol. Ce critère de faible valeur de ΔG_{HYD} n'est donc pas unique mais semble très important (23).

La force de la liaison covalente entre le métal et l'atome adsorbé (*e.g.* Pt—F, Pt—O—PO_3^{3-}, etc.) est une autre indication du degré d'adsorption d'un anion. On peut calculer une valeur d'énergie de liaison covalente en utilisant l'équation de Pauling (26):

$$[12] \quad D_{Pt-X} = 1/2\{D_{Pt-Pt} + D_{X-X}\} + 23\,(\chi_{Pt} - \chi_X)^2$$

où D_{Pt-Pt} et D_{X-X} sont les énergies de dissociation des liaisons simples platine—platine et

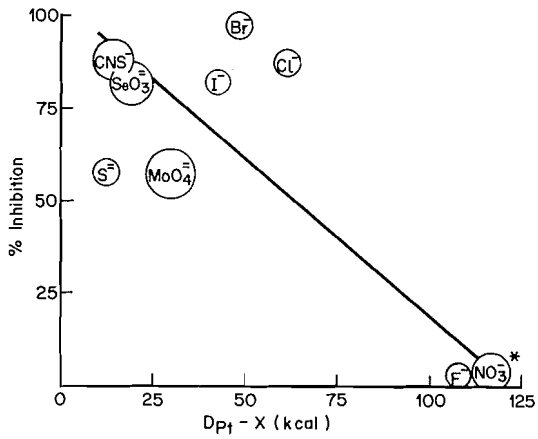

FIG. 9. Pourcentage d'inhibition du courant à 0.7 V de la partie descendante de la courbe de Tafel en fonction de l'énergie covalente de liaison platine–anion.
*Valeur pour la liaison Pt—O.

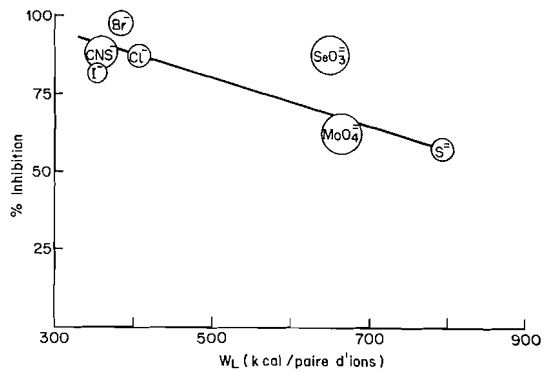

FIG. 10. Pourcentage d'inhibition du courant à 0.7 V de la partie descendante de la courbe de Tafel en fonction du réseau cristallin.

X—X respectivement, χ_{Pt} et χ_X sont les électronégativités. Toutes les valeurs utilisées pour ces déterminations sont tirées du volume de Sanderson (26). La fig. 9 indique la corrélation résultante entre cette énergie de liaison covalente et le pourcentage d'inhibition. Pour les anions composés de plusieurs atomes, le point d'ancrage de cet anion avec le platine est l'oxygène ou le fluore pour les cas suivants (NO_3^-, PO_4^{3-}, PF_6^-, SiF_6^-). Pour ces anions, le degré de saturation est complet et aucune liaison ne peut s'établir entre l'atome central et le platine.

La corrélation obtenue à la fig. 9 pose quelques problèmes d'interprétation: en effet une valeur d'énergie plus grande entre le platine et un anion donné impliquerait une stabilité accrue pour ce composé et causerait donc une inhibition plus marquée. Cependant cette relation ne se retrouve pas expérimentalement. Le problème d'une liaison du type Pt—F pour un anion comme le PF_6^- limite quelque peu la valeur de ce genre de corrélation. En effet, le fluore est déjà engagé dans une liaison covalente avec le phosphore et peut difficilement formé une liaison avec le métal car il est déjà dans son état de valence maximum. On peut calculer une interaction électrostatique entre les anions et l'électrode pour palier à la limitation de la méthode précédente. L'énergie du réseau cristallin, W_L entre un cation Pt(IV) et différents anions a été calculé à l'aide de la méthode de Kapustinski (27):

$$[13] \quad W_L = \frac{287.2\ (nn')}{r_c + r_a} \times \left[1 - \frac{0.345}{r_c + r_a}\right] \text{kcal/paire d'ion}$$

où n et n' sont les charges des ions, r_c et r_a sont les rayons ioniques du cation et de l'anion. La fig. 10 nous montre la corrélation possible entre certains anions étudiés et le pourcentage d'inhibition. Comme pour la comparaison avec les valeurs pour l'énergie de liaison covalente, la corrélation se situe dans le mauvais sens. Nous avons omis délibérément les anions qui ne montraient aucun effet d'inhibition pour toutes ces corrélations. Il est à noter que pour les valeurs de ΔG_{HYD} et W_L, les résultats sont très proches car la méthode de calcul est très semblable: les valeurs cherchées sont proportionnelles à la charge et inversement proportionnelles au rayon ionique.

Pour résumer ces différentes corrélations, on peut dire que celles impliquant le calcul des liaisons covalentes ou ioniques ne sont pas valables. La conclusion préliminaire qui s'impose est l'importance du facteur de stabilisation de l'anion par le solvant et non la stabilisation sur l'électrode. Cependant, une faible valeur de l'énergie de solvatation n'est pas l'unique critère d'adsorption. Klopman (28) a mis au point une méthode théorique où il fait intervenir à la fois l'énergie de solvatation et l'énergie de l'orbital de l'anion adsorbé. Le traitement théorique donné par cet auteur est relativement complexe mais offre des possibilités d'application pour les cas qui nous occupent. Cependant

Can. J. Chem. Downloaded from www.nrcresearchpress.com by 210.87.254.6 on 09/05/12
For personal use only.

il n'entre pas dans le cadre de cet article d'élaborer cette théorie.

Le mécanisme d'inhibition est surtout par adsorption, c'est-à-dire, par blocage des sites actifs. C'est ainsi que l'on a expliqué les phénomènes d'interaction entre l'oxydation de composés organiques et différents anions (9, 10, 29–31). Les facteurs régissant cette adsorption ne sont pas entièrement élucidés mais il semble qu'il y ait toujours une série de paramètres à considérer (chaleurs d'hydration, énergie d'interaction anion-électrode, stabilité des espèces dans les solvants, etc.). Taylor *et al.* (8) ont montré qu'il y a plus qu'une simple adsorption d'anion inhibiteur qui réduit la vitesse oxydation de l'acide formique. En effet, pour un recouvrement très faible de l'électrode par le chlorure, ($\theta \simeq 0.1$), il y a une réduction de 80% dans le courant d'oxydation. Il semble donc qu'il y ait d'autres facteurs qui jouent lors de ces inhibitions.

Une étude plus approfondie par différentes techniques s'impose pour les anions qui montrent une certaine activité d'inhibition. Il est important de déterminer quelles espèces sont présentes sur l'électrode et quel est le mécanisme de blocage de la réaction.

L'auteur tient à remercier d'une façon particulière Monsieur Ashok K. Vijh pour la direction générale, les échanges de vue et l'encouragement au cours du présent travail.

Des remerciements s'adressent aussi à Messieurs P. Lenfant, J.-P. Randin et I. Morcos pour les discussions intéressantes lors de la réalisation de ce travail.

1. E. GILEADI et B. PIERSMA. Modern aspects of electrochemistry. Vol. 4, *Edited by* J. O'M. Bockris. Plenum (1966).
2. V. S. BAGOTSKY et YU. B. VASILYEV. Electrochim. Acta, **9**, 869 (1964).
3. V. S. BAGOTSKY et YU. B. VASILYEV. Electrochim. Acta, **12**, 1323 (1967).
4. T. BIEGLER et D. F. A. KOCH. J. Electrochem. Soc. **114**, 904 (1967).
5. L. D. BURKE et A. MOYNIHAN. Electrochim. Acta, **16**, 167 (1971).
6. S. GILMAN. Electroanalytical chemistry. Vol. 2, *Edited by* A. J. Bard (1967). Vol. 2.
7. V. S. BAGOTSKY, YU. B. VASILYEV, J. WEBER, et J. N. PIRTSKHALAVA. J. Electroanal. Chem. **27**, 31 (1970).
8. A. H. TAYLOR, R. D. PEARCE, et S. B. BRUMMER. Trans. Faraday Soc. **66**, 2076 (1970).
9. B. I. PODLOVCHENKO, V. E. KAZARINOV, et V. F. STENIN. Elektrokhim. **6**, 252 (1970).
10. J. N. PIRTSKHALAVA, YU. B. VASILYEV, et V. S. BAGOTSKY. Elektrokhim. **6**, 1144 (1970).
11. A. BÉLANGER, G. BÉLANGER, et A. K. VIJH. J. Electrochem. Soc. **118**, 1543 (1971).
12. G. BÉLANGER. J. Electrochem. Soc. **118**, 583 (1971).
13. A. K. VIJH. Can. J. Chem. **49**, 78 (1971).
14. J. WOJTOWICZ, D. GILROY, et B. E. CONWAY. Electrochim. Acta, **14**, 1119 (1969).
15. D. GILROY et B. E. CONWAY. J. Phys. Chem. **69**, 1259 (1965).
16. S. GILMAN et M. W. BREITER. J. Electrochem. Soc. **119**, 1099 (1962).
17. S. S. BESKOROVAINAYA, YU. B. VASILYEV, et V. S. BAGOTSKY. Elektrokhim. **2**, 167 (1966).
18. B. E. CONWAY, E. J. RUDD, et L. G. M. GORDON. Discuss. Faraday Soc. **45**, 87 (1968).
19. B. E. CONWAY. Theory and principles of electrode processes. The Ronald Press Co., New York. 1967.
20. D. C. GRAHAM. Chem. Rev. **41**, 441 (1947).
21. S. LEVINE, G. M. BELL, et D. CALVERT. Can. J. Chem. **40**, 518 (1960).
22. J. O'M. BOCKRIS, M. A. V. DEVANATHAN, et K. MULLER. Proc. Roy. Soc. London, **274** A, 55 (1963).
23. D. J. BARCLAY. J. Electroanal. Chem. **19**, 318 (1968).
24. R. G. PEARSON. J. Am. Chem. Soc. **85**, 3533 (1963).
25. D. A. JOHNSON. J. Chem. Ed. **45**, 236 (1968).
26. R. T. SANDERSON. Inorganic chemistry. Reinhold Publishing Corp. (1967).
27. T. W. WADDINGTON. Advances in inorganic and radiochemistry. Vol. 1, *Edited by* H. J. Emeleus et A. G. Sharge. Academic Press, New York. 1959.
28. G. KLOPMAN. J. Am. Chem. Soc. **90**, 223 (1968).
29. J. A. SHROPSHIRE. J. Electrochem. Soc. **112**, 465 (1965).
30. J. A. SHROPSHIRE. J. Electrochem. Soc. **114**, 773 (1967).
31. K. J. CATHRO. Electrochem. Technol. **5**, 441 (1967).

Can. J. Chem. Downloaded from www.nrcresearchpress.com by 210.87.254.6 on 09/05/12
For personal use only.

Isotopic Exchange Between Hydrogen and Water Vapor over Supported Metal Catalysts. Part I. Kinetics of the Exchange[1,2]

J. H. ROLSTON AND J. W. GOODALE

Physical Chemistry Branch, Chalk River Nuclear Laboratories, Chalk River, Ontario

Received January 4, 1972

Some rate data for the transfer of a deuterium atom tracer between hydrogen and water vapor, catalyzed by platinum supported on γ-alumina, are reported. Above 100 °C the transfer rate measured at 1 atm total pressure is shown to be free of mass transfer effects, and obeys an initial first order dependence on water vapor for vapor pressures less than 10 Torr. A near zero order dependence is observed at higher water vapor pressures. At temperatures below 100 °C the transfer rate is essentially independent of water vapor pressure between 5 and 100 Torr suggesting that surface adsorbed water is involved in the rate limiting transfer step.

Nous rapportons quelques résultats de vitesse pour le transfert d'un atome de deutérium traceur entre l'hydrogène et la vapeur d'eau, catalysé par le platine sur un support d'alumine-γ. Nous montrons qu'au-delà de 100 °C, la vitesse de transfert mesurée à une pression totale d'une atmosphère est exempte d'effets de transfert de masse et obéit à une dépendance initiale de premier ordre de la vapeur d'eau pour des pressions de vapeur de moins de 10 Torr. Nous observons une dépendance d'ordre presque zéro à de plus fortes pressions de vapeur d'eau. A des températures au-dessous de 100 °C, la vitesse de transfert est essentiellement indépendante de la pression de vapeur d'eau entre 5 et 100 Torr, suggérant que l'eau adsorbée à la surface est impliquée dans l'étape limitante de la vitesse de transfert.

Canadian Journal of Chemistry, **50**, 1900 (1972)

Introduction

At moderate temperatures the partitioning of deuterium between water vapor and hydrogen,

$$[1] \qquad HDO(v) + H_2(g) \overset{K}{\rightleftarrows} HD(g) + H_2O(v)$$

is such that the equilibrium position favors concentration of the deuterium in the water with calculated values (1) of the equilibrium constant, K, varying between 0.239 at 0 °C and 0.412 at 125 °C. As this represents a substantial isotope fractionation the reaction has received consideration (2, 3) as the basis of chemical exchange processes for the recovery of deuterium from natural water. The success of such a process depends to a large extent upon the rate of isotope transfer between the two chemical species and it is clear from early studies (4, 5) that rapid exchange rates, at moderate temperatures, can only be achieved in the presence of a catalyst.

A search for a suitable catalyst under the auspices of the Manhattan Project (2) led to the adoption of platinum on charcoal and of chromia-promoted nickel as the two most promising catalysts for large scale operations. Both catalysts appear to lose catalytic activity when liquid water contacts the surface (6, 7) and with nickel-chromia catalysts (8) this has been attributed to the ease of vapor condensation in the catalyst pores. In the absence of such effects a surface reaction would appear to govern the exchange kinetics (9) although diffusion effects often complicate the observed exchange rates (10–12). Thus it has been necessary to show that the exchange rate is not limited by such effects before attempting to assess the role of vapor composition on this isotope exchange reaction and accordingly a single pass flow reactor has been constructed and used to define the necessary reaction conditions for characterizing the exchange rate over a supported platinum catalyst.

Experimental

Catalyst

A commercially available catalyst[3] consisting of a nominal 0.5 wt. % loading of platinum on alumina was used. This was supplied in the form of 3.2 mm diameter right cylinders with the metal impregnated only on the outer 0.3 mm layer of the pellets (13). The pellets were crushed in a mortar and sieved through standard screens to provide catalyst particles of known diameters, generally 0.05 mm. Clean Pyrex glass was crushed and sieved to a particle diameter between 0.10 and 0.15 mm for use as an inert diluent in maintaining a catalyst bed of fixed geometry.

[1]A.E.C.L. No. 4191.

[2]Presented in part at the 4th Canadian Symposium on Catalysis, Halifax, Nova Scotia, June, 1971.

[3]Obtained from Engelhard Industries Ltd., New Jersey.

Can. J. Chem. Downloaded from www.nrcresearchpress.com by 210.87.254.6 on 09/05/12
For personal use only.

Can. J. Chem. Downloaded from www.nrcresearchpress.com by 210.87.254.6 on 09/05/12
For personal use only.

Materials

The hydrogen source was Matheson Gold Label Hydrogen which was passed through a "Deoxo" unit[3] and a liquid nitrogen trap to minimize trace impurities. Water of natural isotopic abundance (10^6 D/H = 143) was triply distilled from sodium dichromate prior to use and was enriched with measured volumes of 99.48% deuterium oxide to provide saturator liquid of known isotopic abundance (nominal atom ratio: 10^6 D/H = 3000). The mole fraction of HDO present in the vapor was calculated from the known isotope content of the saturator liquid and the liquid–vapor separation factor (14). Dissolved gases were removed from the saturator liquid by a prior purge of the liquid with purified hydrogen.

Method

The stream of hydrogen was bubbled through the enriched water contained in the thermostated saturator column and the humidified stream was passed downward through a weighed amount of catalyst particles (5–25 mg). The latter was mixed with the Pyrex chips (950 mg) and supported in the reactor over a porous glass frit, forming a catalyst bed 9.0 mm in length and 10.5 mm diameter. A 2 mm deep layer of glass chips was placed on top of the catalyst bed to aid in establishing a uniform flow pattern. The catalytic activity of the crushed Pyrex was checked and shown to be negligible below 200 °C.

The temperature of the catalyst was measured by a thermocouple enclosed in a thin-walled glass tube located immediately above the catalyst bed and attached to the sealed end of a 21 cm section of 25 mm Pyrex tubing. The latter fitted concentrically over the open end of the inner 13 mm diameter Pyrex tube supporting the catalyst bed and provided an enclosed volume for preheating of the gas stream prior to its entry into the catalyst chamber. The outer chamber was surrounded by a length of copper tubing and the assembly was placed in a cylindrical electrical heater which was controlled by an electronic relay.[4] The control thermocouple was placed between the copper sheath and the outer glass tube and conditions were adjusted to maintain both thermocouples to within 1 °C of each other.

The effluent hydrogen flow was determined with a soap-film flowmeter after removal of the water vapor in a condenser and calcium chloride drying tube. The deuterium content of the hydrogen was measured on a Thompson-Houston 202 mass spectrometer, modified (15) to permit on-line deuterium analysis at near natural abundance levels with a precision of 0.1%. The calibration of the spectrometer was repeatedly checked against hydrogen standards of known isotopic content.

Catalysts were initially reduced in a stream (1 cm^3/s) of dry hydrogen over a period of 17 h at 300 °C and cooled to operating temperatures under hydrogen. A flow of partially humidified hydrogen was initiated and kinetic measurements were taken at temperatures between 75 and 200 °C with the quantity of deuterium transferred varying between 5 and 90% of the equilibrium value. The ratio of the partial pressures of hydrogen and water was varied from 150:1 to 7:1 by altering the temperature of the saturator liquid. Values of the equilibrium deuterium content in the effluent gas were determined by increasing the quantity of catalyst in the bed and reducing the flow rate. These were in good agreement with values calculated assuming conservation of deuterium between the two components and known values of K (1).

[4]Temperature Controller Model 5626, Bach Simpson, Toronto, Ontario.

Treatment of Data

With mixtures of hydrogen and water vapor of low deuterium content the exchange activity of a catalyst was characterized by a transfer coefficient k_r, as the moles of HD transferred per second per gram of catalyst. An expression for k_r was developed by considering a volume element of the reactor dV, of cross section A (cm^2) and height dz (cm) through which the hydrogen and the vapor streams flow co-currently (8). The increase in the flow of deuterium as HD, in the volume element is given as the product of the hydrogen flow F_{H_2} (mol/s) and the incremental change in the mole fraction dn, of HD. The rate at which deuterium is transferred to the hydrogen stream is equal to the rate at which it is depleted from the water stream as the total deuterium content of the volume element is conserved. Thus

$$[2] \qquad F_{H_2}\,dn + F_{H_2O}\,dN = 0$$

where F_{H_2O} is the molar flow of water vapor and dN the corresponding change in the mole fraction of HDO. The ratio of the partial pressure of water to hydrogen is π, hence $F_{H_2O} = \pi F_{H_2}$ and eq. 2 can be integrated to give

$$[3] \qquad N = N_0 - \frac{(n - n_0)}{\pi}$$

where n_0, N_0 and n, N are the mole fractions of HD and HDO in the hydrogen and water vapor streams which enter and leave the volume V of the catalyst bed. For a volume increment dV the rate of isotope transfer per unit volume has the form (16)

$$[4] \qquad \frac{1}{dV} F_{H_2}\,dn = k_r \rho (N - K^{-1} n)$$

where k_r is the transfer coefficient denoting the rate of isotope transfer per gram of catalyst, ρ is the number of grams of catalyst per cm^3 of reactor volume, K^{-1} is the reciprocal of the equilibrium constant of the exchange reaction and the term $(N - K^{-1}n)$ is the displacement from the equilibrium isotopic distribution. Substitution of eq. 3 and the expression $dV = A\,dz$ into eq. 4 and integrating over the length, z (cm), of catalyst bed leads to

$$[5] \qquad \log_e \left\{ \frac{\left(N_0 + \frac{n_0}{\pi}\right) - n_0\left(K^{-1} + \frac{1}{\pi}\right)}{\left(N_0 + \frac{n_0}{\pi}\right) - n\left(K^{-1} + \frac{1}{\pi}\right)} \right\} = \left(K^{-1} + \frac{1}{\pi}\right) k_r \rho \frac{Az}{F_{H_2}}$$

Simplification of eq. 5 is achieved in terms of the equilibrium isotope contents n_e and N_e which are related by

$$[6] \qquad (1 - n_e)N_e = K^{-1}(1 - N_e)n_e$$

Integration of eq. 2 between the initial and equilibrium

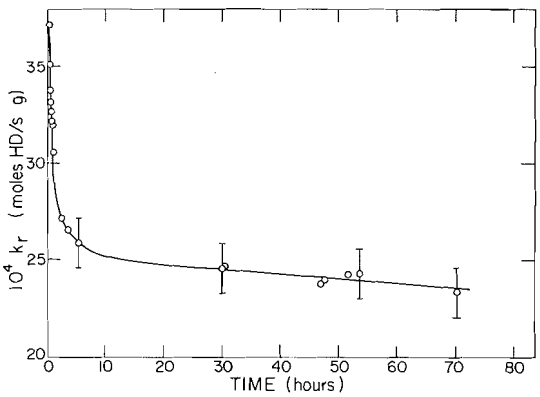

FIG. 1. Dependence of transfer coefficient upon time. $F_{H_2} = 3.5$ cm^3 S.T.P./s; $P_{H_2}/P_{H_2O} = 22.0$; $T = 125$ °C.

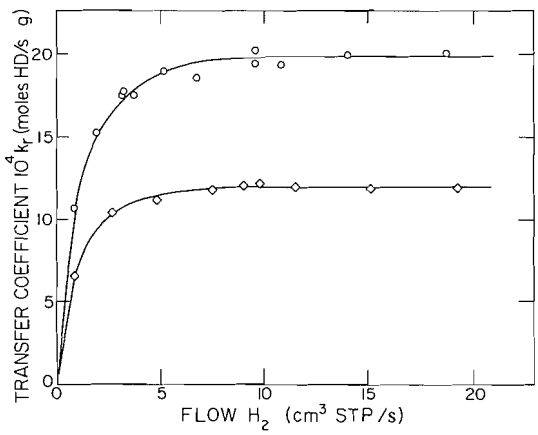

FIG. 2. Dependence of transfer coefficient upon hydrogen flow rate. (◇) 80 °C, ordinate ×2; (○) 180 °C.

boundary conditions leads to

$$[7] \qquad n_e = n_0 - \pi(N_e - N_0)$$

In streams of low deuterium concentration $n_e \ll 1$, $N_e \ll 1$ thus $N_e = K^{-1}n_e$ to a good approximation and eq. 7 can be written as

$$[8] \qquad \left(N_0 + \frac{n_0}{\pi}\right) = n_e\left(K^{-1} + \frac{1}{\pi}\right)$$

Substitution of eq. 8 into eq. 5 and recalling that the weight W(g) of catalyst in the reactor volume is ρAz results in the following expression for the transfer coefficient k_r

$$[9] \qquad k_r = \left(\frac{1}{K^{-1} + \frac{1}{\pi}}\right)\frac{F_{H_2}}{W}\log_e\left(\frac{n_e - n_0}{n_e - n}\right)$$

Results

The initial phase of this study was confined to an investigation of the conditions under which the effects of mass transfer on the isotope transfer rate could be eliminated. Preliminary studies indicated the exchange rate, as defined by the transfer coefficient k_r (mol HD/s g) in eq. 9 decreased rapidly over the first 2 h of operation (Fig. 1) after which rates were constant to within ±5% as indicated by the error bars. It was therefore necessary to "condition" the catalyst for 2–3 h before attempting further experiments with different flow rates. With hydrogen flows greater than 10 cm^3/s S.T.P. the transfer rate is independent of the gas velocity for catalyst temperatures less than 200 °C, (Fig. 2). The calculated transfer coefficient was also found to be independent of both the quantity of catalyst loaded in the reactor bed and of the deuterium content of the liquid water used to humidify the hydrogen (Table 1).

TABLE 1. Dependence of transfer coefficient k_r on weight of catalyst and deuterium concentration

Isotope ratio in liquid water (10^6 D/H)	Weight of catalyst (mg)	Transfer coefficient, $10^4 k_r$ (mol HD/s g)
3135	12.8	19.1*
3135	12.8	20.2*
3135	12.8	20.6*
3135	12.8	19.0*
3135	17.6	18.6*
3135	17.6	18.4*
3135	25.3	21.4*
943	12.8	18.2†
2135	12.8	17.4†
3130	12.8	20.4†
5310	12.8	18.2†

*$P_{H_2O} = 31.4$ Torr, $P_{H_2} = 729$ Torr with H_2 flow = 10.5 cm^3/s and $T = 126$ °C using 0.5% platinum–alumina catalyst.
†$P_{H_2O} = 34.5$ Torr, $P_{H_2} = 727$ Torr with H_2 flow = 10.5 cm^3/s and $T = 123$ °C using 0.5% platinum–alumina catalyst.

Although the measured transfer rates would appear to be free of external mass transport effects (Fig. 2), it was necessary to test for the absence of internal transport effects within the catalyst particles. This was accomplished by varying the average diameter of the particles of crushed catalyst over a ten-fold range. The data for two temperatures, plotted in Fig. 3, show that the transfer rates approach maximum values as the particle size decreases below 0.1 mm and decrease significantly with particles of larger size. This indicates that at these temperatures, internal mass transfer effects are not

Can. J. Chem. Downloaded from www.nrcresearchpress.com by 210.87.254.6 on 09/05/12
For personal use only.

Can. J. Chem. Downloaded from www.nrcresearchpress.com by 210.87.254.6 on 09/05/12
For personal use only.

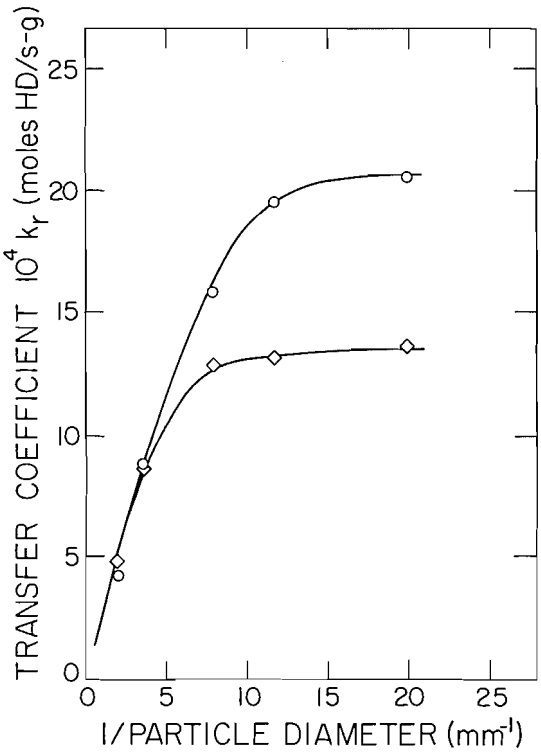

FIG. 3. Dependence of transfer coefficient upon diameter of catalyst particle. (◇) 80 °C, ordinate ×2; (○) 123 °C.

governing the transfer rate in particles with an average diameter of 0.05 mm. As a consequence of increased reaction rates at higher temperatures somewhat smaller particles appear necessary to achieve this condition at 123 °C than at 80 °C.

The dependence of the transfer coefficient upon the vapor composition was investigated by varying the partial pressure of water by a factor of 20 at four different temperatures (Fig. 4) with the total pressure fixed at 1 atm. This restriction reduces systematically the partial pressure of hydrogen as the water vapor pressure increases. The rate changes rapidly from first to zero order with respect to water vapor with the transition being most pronounced at temperatures below 100 °C, where the rate becomes independent of the water vapor pressure when the relative humidity exceeds 10%. Operation at 173 °C, with the relative humidity less than 2%, produces a near linear increase through the initial range of water vapor pressures studied.

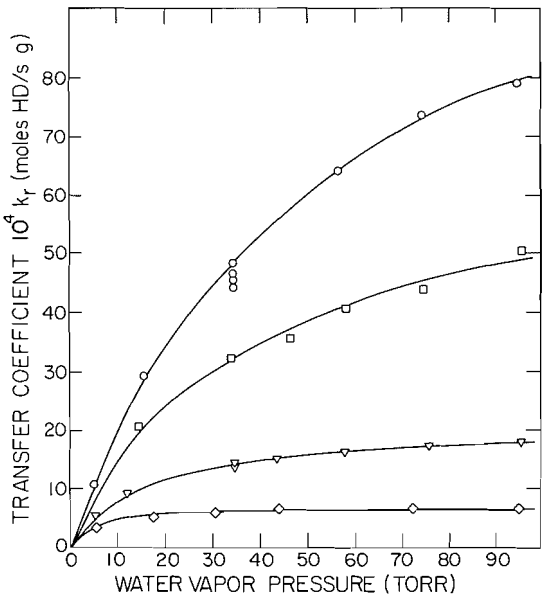

FIG. 4. Dependence of transfer coefficient upon partial pressure of water. (◇) 74 °C; (▽) 92 °C; (□) 126 °C; (○) 173 °C.

To assess the sensitivity of the transfer rate to changes in the partial pressure of hydrogen, a series of experiments was done under increased hydrogen partial pressures, with total pressures in excess of 1 atm and flow rates sufficient to ensure that the isotope transfer rates were independent of the hydrogen flow. The results are recorded in Table 2 and confirm that the measured transfer coefficients plotted in Fig. 4 are not significantly affected by the 100 Torr decrease in hydrogen partial pressure which accompanies the increases in the water vapor pressure. At 171 °C the transfer coefficient is not expected to decrease by more than 6% as a result of a drop in the hydrogen partial pressure from 750 to 650 Torr. Under these conditions the observed transfer rate is essentially independent of the hydrogen pressure.

The data in Table 2 also show that the transfer rates are not entirely independent of the hydrogen over pressure at higher temperatures. Thus a 30% increase in rate was obtained by doubling the hydrogen over pressure at 171 °C. Under these conditions the relative humidity of the gas mixture is less than 2% and the transfer rate is a function of both the hydrogen and water vapor pressures. In contrast at 80 °C the transfer rate is independent of the hydrogen over

Can. J. Chem. Downloaded from www.nrcresearchpress.com by 210.87.254.6 on 09/05/12
For personal use only.

TABLE 2. Dependence of transfer coefficient on partial pressure of hydrogen

P_{H_2O} (Torr)	Temperature (°C)	P_{H_2} (Torr)	$10^4 k_r$* (mol HD/s g)
34.0	80	714	6.70
		853	6.65
		1052	6.65
		1228	6.71
		1448	7.14
94.0	80	655	5.88
		771	6.05
		974	6.47
		1173	6.47
		1385	6.62
30.0	171	708	16.3
		835	16.4
		1024	17.5
		1240	18.5
		1462	18.7
87.0	171	649	23.5
		805	25.3
		975	26.7
		1180	28.8
		1399	30.4

*H_2 flow 9.8 cm^3 S.T.P./s, 0.5% platinum–alumina catalyst.

pressure within the limits of experimental uncertainty ($\pm 5\%$) for water vapor pressures of 34.0 and 94.0 Torr which correspond to relative humidities of 9.6 and 26.5%, respectively.

Discussion

Measurement of the rate of isotope exchange in terms of the transfer coefficient k_r, permits assessment of catalyst activity as the moles of HD transferred to the hydrogen stream per unit weight of catalyst. The freshly reduced 0.5% platinum–alumina catalyst showed a rapid initial drop in activity of about 30% (Fig. 1), which suggests that the catalyst surface must be stabilized with respect to a flow of the mixture of hydrogen and water vapor. Since the commercial catalyst is extremely effective in catalyzing the exchange, special attention was taken to obtain transfer rates free of external mass transfer and diffusion effects. Thus hydrogen flows of 10 cm^3/s S.T.P. (Fig. 2) and a particle diameter of 0.05 mm (Fig. 3) are necessary to eliminate these effects over the temperature range 75 to 125 °C. Rate data obtained under these conditions can therefore be used in an assessment of the influence of the vapor composition on the exchange reaction.

Fig. 4 shows the dependence of the transfer coefficient upon the partial pressure of water and indicates that for temperatures below 100 °C the transfer rate is essentially independent of the water vapor pressure when the relative humidity exceeds 10%. With temperatures greater than 100 °C the transfer rate is initially first order with respect to water vapor but again approaches zero order as the relative humidity approaches 10%. In contrast the effect of hydrogen over pressures on the transfer rate is much less pronounced. The data in Table 2 show that hydrogen over pressures have a negligible effect on the transfer rates when the relative humidity exceeds 10% (80 °C) but increased transfer rates are noted at 171 °C when the relative humidity is less than 2%. This marked dependence of the transfer rate upon the partial pressure of water suggests that adsorbed water is involved in the rate limiting step. It would appear that the transfer rate is dependent upon the hydrogen partial pressure only when the humidity and the surface coverage of adsorbed water are low, $<10\%$. With a high surface coverage of water the rate is independent of the hydrogen partial pressure. Under conditions of low relative humidity the hygroscopic alumina can be expected to acquire a partial coverage of physically adsorbed water and the rate of isotope transfer will vary in proportion to the extent of surface coverage. The data presently available on the platinum alumina catalyst suggests that a rate limiting surface coverage is achieved at a relative humidity of about 10%.

A possible alternative explanation follows from observations of the exchange over nickel–chromia catalysts (8) in which condensation of water vapor in the pores of the catalyst is claimed to limit the exchange. If it is assumed that adsorbed water wets the walls of the capillaries then application of the Kelvin equation (17) predicts that only pores of radii less than 0.3 nm will be filled at a relative humidity of 10% at 75 °C. Mercury penetration studies indicate that the present catalyst has less than 10% of the total pore volume associated with pores of less than 1.5 nm. Capillary condensation does not therefore play a major role in limiting the transfer rates under these conditions even if the extreme assumption is taken that the catalytic surface of pores filled with condensate is totally inactive in isotope transfer and hence this explanation cannot be valid. We conclude that the major

Can. J. Chem. Downloaded from www.nrcresearchpress.com by 210.87.254.6 on 09/05/12
For personal use only.

portion of the active catalytic surface resides in pores with radii greater than 0.5 nm which are not filled by liquid condensate under the low relative humidities studied here.

The complex dependence of the exchange rate upon water vapor pressure can be explained satisfactorily in terms of a kinetic model involving surface exchange between hydrogen chemisorbed on the metal crystallites and mobile physically adsorbed water. Water vapor is not expected (18) to prevent hydrogen chemisorption on platinum crystallites. Thus the exchange can be viewed as the following sequence with the surface adsorbed species denoted by the subscript, a, and gas and vapor molecules by (g) and (v) respectively. Hydrogen is assumed to adsorb dissociatively on platinum (Type I) sites while water is physically bound on neighboring alumina (Type II) sites.

[10] $$H_2(g) + 2(I) \rightleftarrows 2H_a$$

[11] $$HDO(v) + (II) \rightleftarrows HDO_a$$

[12] $HDO_a + H_a \rightleftarrows$ 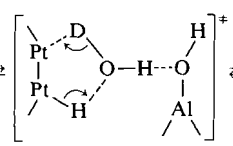 $\rightleftarrows H_2O_a + D_a$

[13] $$D_a + H_a \rightleftarrows HD(g) + 2(I)$$

[14] $$H_2O_a \rightleftarrows H_2O(v) + (II)$$

If it is assumed that the transfer rate per gram of catalyst can be expressed in terms of the fractional coverages θ_i of the surface sites available to species i, then it follows from eq. 4 that

[15] $$k_r(N - K^{-1}n) = k_{12}\theta_{HDO}\theta_H - k_{-12}\theta_{H_2O}\theta_D$$

where k_{12} and k_{-12} are the kinetic constants for the forward and reverse steps of the surface exchange occurring at the exposed interfaces between crystallite and hydrated alumina support. As equilibria between the gas and surface phases are established throughout the course of the reaction

$$\theta_{HDO} = \theta_{H_2O}K_{11}K_{14}\frac{P_{HDO}}{P_{H_2O}}$$

and

$$\theta_D = \frac{\theta_H}{K_{10}K_{13}}\frac{P_{HD}}{P_{H_2}}$$

Since $P_{HDO} = NP_{H_2O}$ and $P_{HD} = nP_{H_2}$ it follows that

[16] $$k_r = k_{12}K_{11}K_{14}\theta_{H_2O}\theta_H$$

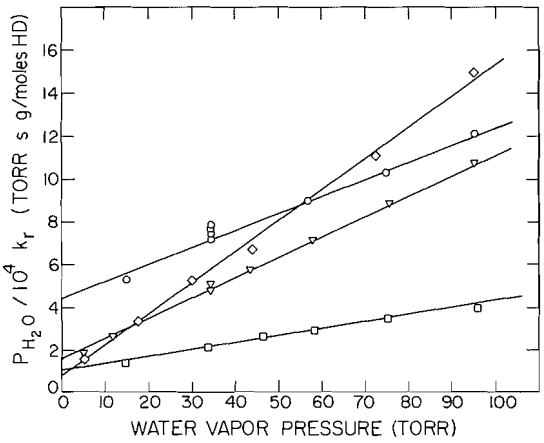

FIG. 5. Test of equation 18. (◇) 74 °C; (▽) ordinate ×2, 92 °C; (□) ordinate ×2, 126 °C; (○) ordinate ×10, 173 °C.

The data plotted in Fig. 4 were obtained under conditions in which the transfer rate was essentially independent of hydrogen pressure. In these circumstances it is assumed that θ_H is constant and that the coverage of Type II sites by water vapor is given by a Langmuir isotherm of the form

[17] $$\theta_{H_2O} = \frac{K_{14}^{-1}P_{H_2O}}{1 + K_{11}P_{HDO} + K_{14}^{-1}P_{H_2O}}$$

Since $K_{11}N \ll K_{14}^{-1}$ the dependence of the transfer rate on the water vapor pressure is given by the linear eq. 18

[18] $$\frac{P_{H_2O}}{k_r} = \frac{1}{k_{12}K_{11}\theta_H}\{1 + K_{14}^{-1}P_{H_2O}\}$$

The implied dependence of the exchange velocity upon the water vapor pressure is reasonably well obeyed by the data throughout the temperature and pressure range examined (Fig. 5). However, it is not possible at this stage to exclude entirely a second scheme suggested from the studies of Temkin (19) which involves dissociation of water vapor to hydrogen gas and a surface oxide. The latter has been suggested (9) as a scheme to rationalize the exchange over the chromia promoted nickel catalysts but it offers no advantage over that involving isotopic exchange between physically adsorbed water and dissociatively adsorbed hydrogen in accounting for the exchange over alumina supported platinum.

We would like to thank Mr. Warren Thurston, General Chemistry Branch, CRNL for his assistance and advice in the analysis of the hydrogen streams and Mr. Murray James, Chemical Engineering Branch, CRNL for maintenance and calibration of the spectrometer.

1. I. KIRSHENBAUM and H. G. UREY. Physical properties and analysis of heavy water. McGraw-Hill, New York. 1951. p. 48.
2. G. M. MURPHY, H. G. UREY, and I. KIRSHENBAUM. Production of heavy water. McGraw-Hill, New York. 1955.
3. J. A. AYRES. Production of heavy water. Status report BNWL-884. Battelle Memorial Institute, Pacific Northwest Laboratory, Richland, Washington. 1969.
4. J. HORIUTI and M. POLANYI. Nature, **132**, 819 (1933).
5. A. FARKAS. Trans. Faraday Soc. **32**, 922 (1936); **33**, 678 (1937).
6. H. G. UREY and A. V. GROSSE. United States Patent 2,690,379 (1954).
7. H. S. TAYLOR. United States Patent 2,690,380 (1954).
8. N. MARAZAN, P. MARGINEANU, and A. OLARIU. Abhandl. Deut. Akad. Wiss. Berlin, K1. Chem. Geol. Biol. **7**, 793 (1964).
9. V. MERCEA. Énergie Nucléaire, **10**, 367 (1968).
10. N. PALIBRODA, A. OLARIU, and P. MARGINEANU. J. Catal. **12**, 347 (1968).
11. N. MARAZAN, P. MARGINEANU, and A. OLARIU. Abhandl. Deut. Akad. Wiss. Berlin, K1. Chem. Geol. Biol. **7**, 783 (1964).
12. E. S. NEDUMOVA, G. K. BORESKOV, and M. G. SLINKO. Kinet. Catal. **6**, 53 (1965).
13. J. C. KEMPLING and R. B. ANDERSON. Ind. Eng. Chem. Process Des. Develop. **9**, 116 (1970).
14. L. MERLIVAT, R. BOTTER, and G. NIEF. J. Chim. Phys. **60**, 56 (1960).
15. W. M. THURSTON. Rev. of Sci. Instr. **41**, 963 (1970).
16. K. COHEN. Theory of isotope separation. McGraw-Hill, New York. 1951. p. 130.
17. S. J. GREGG and K. S. W. SING. Adsorption, surface area and porosity. Academic Press, New York. 1967. p. 136.
18. M. A. VANNICE, J. E. BENSON, and M. BOUDART. J. Catal. **16**, 348 (1970).
19. M. I. TEMKIN. Zhur. Fiz. Khim. **31**, 1 (1957).

Can. J. Chem. Downloaded from www.nrcresearchpress.com by 210.87.254.6 on 09/05/12
For personal use only.

Bond Scission in Sulfur Compounds. V.[1] A Kinetic Study of Sulfur–Oxygen and Sulfur–Chlorine Bond Scission in the Methanolysis of *p*-Nitrophenyl Chlorosulfate

E. BUNCEL AND A. RAOULT

Department of Chemistry, Queen's University, Kingston, Ontario

Received December 29, 1971

A kinetic study of the reaction of *p*-nitrophenyl chlorosulfate with methoxide ion in methanol has been carried out over the temperature range 5–35°. The results are discussed in terms of two bond scission processes, S—O and S—Cl scission. A stereo-electronic factor is considered dominant in discussion of activation entropies.

L'étude cinétique de la réaction du chlorosulfate de *p*-nitrophényle avec l'ion méthylate en milieu méthanolique entre 5 et 35°, a permis de mettre en évidence la coupure des liaisons S—O et S—Cl. Les paramètres d'activation ont été mesurés pour chaque mode de coupure. Les entropies d'activation sont examinées en fonction d'un facteur stéréo-electronique.

Canadian Journal of Chemistry, **50**, 1907 (1972)

Can. J. Chem. Downloaded from www.nrcresearchpress.com by 210.87.254.5 on 09/05/12
For personal use only.

Reaction of phenyl chlorosulfate with methoxide ion in methanol yields products resulting from S—O bond scission and from S—Cl bond scission (1). Nucleophilic substitution at sulfur in $C_6H_5OSO_2Cl$ hence is associated with leaving group tendencies of phenoxy and chlorine which are approximately equal, in contrast to the situation for substitution at aliphatic carbon (2). To substantiate this unusual order of leaving group tendencies (3), study has been extended to *p*-nitrophenyl chlorosulfate, in which system it was anticipated that the reaction proceeding with S—O bond scission would become relatively more important. Further, with this substrate it appeared possible that yet another process might occur, namely nucleophilic substitution at aromatic carbon (4–7) with OSO_2Cl as the leaving group. The results of the investigation are now reported.

Experimental

p-Nitrophenyl chlorosulfate was prepared from *p*-nitrophenol and sulfuryl chloride in anhydrous ether in presence of pyridine and purified by treatment with boron trichloride according to the method of Gerrard (8). The product obtained on final distillation, b.p. 137–138°/5 mm, slowly crystallized when kept in the refrigerator. The solid material was recrystallized twice from methanol – petroleum ether to yield pale yellow crystals, m.p. 28°; λ_{max} 254 nm (ε 10150) in methanol.

Anal. Calcd. for $C_6H_4O_5ClNS$: C, 30.33; H, 1.70; Cl, 14.92; N, 5.90; S, 13.50. Found: C, 30.84; H, 1.76; Cl, 15.02; N, 5.69; S, 13.27.

Methyl *p*-nitrophenyl sulfate was prepared from *p*-nitrophenyl diazonium fluoroborate and dimethyl sulfate by the method of Whiting and co-workers (9). The product was recrystallized from CCl_4, m.p. 45°; λ_{max} 258 nm (ε 9350) in ether.

Anal. Calcd. for $C_7H_7O_6NS$: C, 36.07; H, 3.03; N, 6.01; S, 13.76. Found C, 35.86; H, 2.59; N, 6.05; S, 13.70.

p-Nitrophenyl sulfate was obtained as the potassium salt from Sigma Chemicals. It was analyzed spectrophotometrically after complete acid hydrolysis to *p*-nitrophenol, which was obtained in 98% yield. (The commercial material was first shown to be free of *p*-nitrophenol.)

Preparation of reaction solutions and the details of the kinetic method were as described previously (1).

Results

Reaction of *p*-nitrophenyl chlorosulfate with methoxide ion in methanol as followed spectrophotometrically results in the appearance of an absorption at 390 nm due to the liberation of *p*-nitrophenoxide ion. However, the 390 nm absorption does not reach the maximum value corresponding to 100% formation of *p*-nitrophenoxide ion based on the initial stoichiometric concentration of substrate. At a given temperature the yield of *p*-nitrophenoxide ion remains constant as the methoxide ion concentration is varied but on increasing the temperature this yield increases (Table 1). Plots of log $(A_\infty - A_t)$ *vs.* time, where A_∞ is the experimental absorbance value at 390 nm on completion of reaction, are linear and yield the pseudo first-order rate constants (k_{obs}) at given methoxide ion concentrations (Table 1).

The probable identity of the second reaction product was considered to be methyl-*p*-nitrophenyl sulfate, resulting from concurrent S—Cl

[1]For part IV in series, see ref. 1.

TABLE 1. Rate data for reaction of *p*-nitrophenyl chlorosulfate ($5 \times 10^{-5} M$) with sodium methoxide in methanol

Temperature (°C)	$[CH_3ONa]$ ($\times 10^3 M$)	$10^3 k_{obs}$ (s^{-1})	% yield ArO^-	k_{tot}* ($l\ mol^{-1}\ s^{-1}$)	k_{ArO^-}† ($l\ mol^{-1}\ s^{-1}$)	k_{Cl^-}‡ ($l\ mol^{-1}\ s^{-1}$)
5.69	1.30	0.575	67.9	0.443	0.302	0.142
	2.61	1.16	68.1			
	5.22	2.37	68.1			
	7.83	3.48	67.6			
	10.44	4.62	68.8			
			68.1 ± 0.4§			
15.04	1.30	1.54	76.3	1.27	0.963	0.310
	2.61	3.40	75.0			
	5.22	6.90	75.6			
	7.83	9.97	76.2			
	10.44	13.2	75.8			
			75.8 ± 0.4§			
25.00	1.30	5.48	80.6	4.10	3.35	0.750
	2.61	11.2	82.2			
	5.22	20.7	81.7			
	7.83	33.9	81.9			
	10.44	42.2	81.7			
			81.6 ± 0.5§			
34.84	1.30	13.2	85.0	11.16	9.30	1.86
	2.61	28.2	84.3			
	5.22	53.2	82.0			
	7.83	84.7	82.6			
	10.44	115.7	82.8			
			83.3 ± 1.1§			

*Computed slope in plot of k_{obs} *vs.* $[CH_3O^-]$ using a least-squares program.
†$k_{ArO^-} = k_{tot} \times$ % yield *p*-nitrophenoxide ion.
‡$k_{Cl^-} = k_{tot} - k_{ArO^-}$.
§Standard deviation.

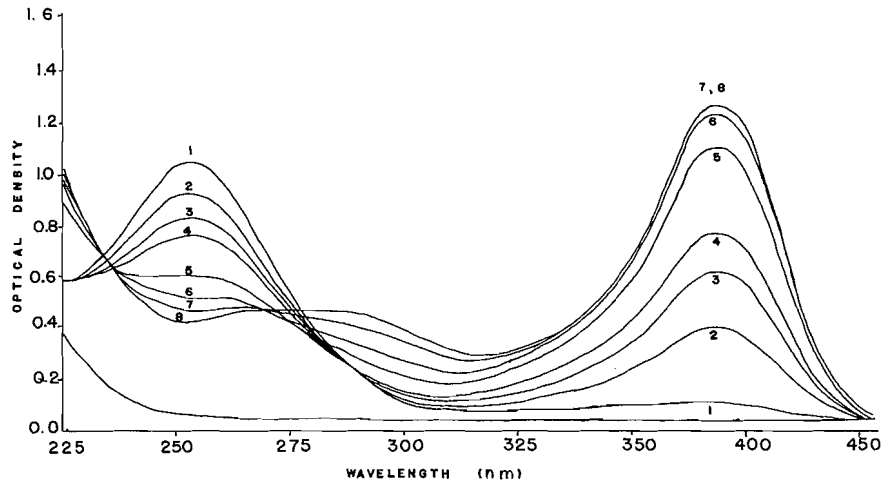

FIG. 1. Spectral scans for reaction of *p*-nitrophenyl chlorosulfate ($5.00 \times 10^{-5} M$) with methanolic sodium methoxide ($1.31 \times 10^{-3} M$) at 5.68°. Spectra taken at various times: no. 1, 1 min; no. 4, 10 min; no. 7, 30 min; no. 8, 1200 min.

scission, by analogy with the phenyl chlorosulfate–methoxide reaction (1). An alternative possibility would be *p*-nitroanisole, the product of substitution at aromatic carbon. In fact spectra of "mock infinity" solutions prepared from calculated amounts of *p*-nitrophenol and methyl-*p*-nitrophenyl sulfate in methanolic sodium methoxide correspond within experimental

Can. J. Chem. Downloaded from www.nrcresearchpress.com by 210.87.254.5 on 09/05/12
For personal use only.

Can. J. Chem. Downloaded from www.nrcresearchpress.com by 210.87.254.5 on 09/05/12
For personal use only.

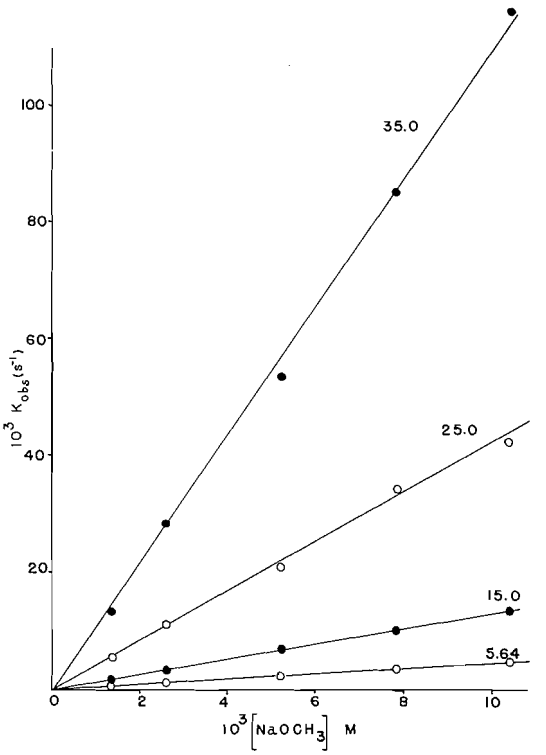

FIG. 2. Plots of k_{obs} *vs.* $[CH_3O^-]$ at various temperatures for reaction of *p*-nitrophenyl chlorosulfate with methoxide ion.

error with spectra of solutions resulting on completion of reaction between *p*-nitrophenyl chlorosulfate and methoxide. When *p*-nitroanisole was substituted for methyl-*p*-nitrophenyl sulfate (20% *p*-nitroanisole/80% *p*-nitrophenoxide), the spectrum was significantly different in the 300 nm region from that of the experimental infinity solution (in methanolic sodium methoxide *p*-nitroanisole has λ_{max} at 305 nm (ε 12 000) whereas methyl-*p*-nitrophenyl sulfate has λ_{max} at 260 nm (ε 9400) and only small absorption at 305 nm (ε 930)).

Further evidence indicating that the second reaction product was methyl-*p*-nitrophenyl sulfate was found in the consecutive solvolysis of the latter yielding *p*-nitrophenyl sulfate. This secondary reaction was detected spectrally in the *p*-nitrophenyl chlorosulfate–MeO^- reaction as a continuing increase in absorption in the 275–325 nm region once the absorption at 390 nm had reached *ca.* 90% of its maximum value. *p*-Nitrophenyl sulfate absorbs at 283 nm (ε 9200), it has negligible absorption at 390 nm, and is stable in the methanolic methoxide solutions (*cf.* refs. 10, 11). The increase in absorption was also seen in the "mock infinity" solution spectra prepared from *p*-nitrophenol and methyl-*p*-nitrophenyl sulfate. In contrast, the solutions containing *p*-nitrophenoxide and *p*-nitroanisole showed no spectral change, as expected.

Selected spectra obtained in a kinetic run with *p*-nitrophenyl chlorosulfate and methoxide ion are shown in Fig. 1 to illustrate the various spectral changes. It is seen that the reasonably good isosbestic behavior, which is maintained during most of the primary reaction, becomes progressively more poorly defined as the secondary solvolysis reaction takes over.

The evidence presented above is fully consistent with the occurrence of two parallel processes in the reaction of *p*-nitrophenyl chlorosulfate with methoxide ion: S—O scission yielding *p*-nitrophenoxide ion and S—Cl scission yielding methyl-*p*-nitrophenyl sulfate.

The dissected rate constants for the two parallel processes are obtained by standard methods (12, 13). The total second-order rate constant, $k_{tot} = k_{ArO^-} + k_{Cl^-}$, is obtained from the linear plot of k_{obs} *vs.* $[CH_3O^-]$, Fig. 2. The constituent rate constants, k_{ArO^-} and k_{Cl^-}, are then obtained from the fractional yields of the products. The resulting data at various temperatures are given in Table 1, while Table 2 contains the derived activation parameters. The Arrhenius plots for the two processes are presented in Fig. 3.

Discussion

The parallel reactions representing S—O bond scission and S—Cl bond scission are given by reactions 1 and 2. Nucleophilic displacement

[1] 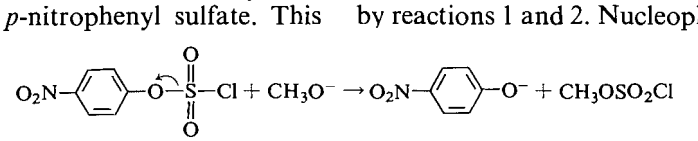

[2] 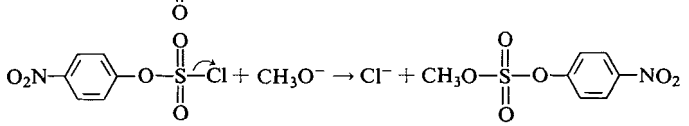

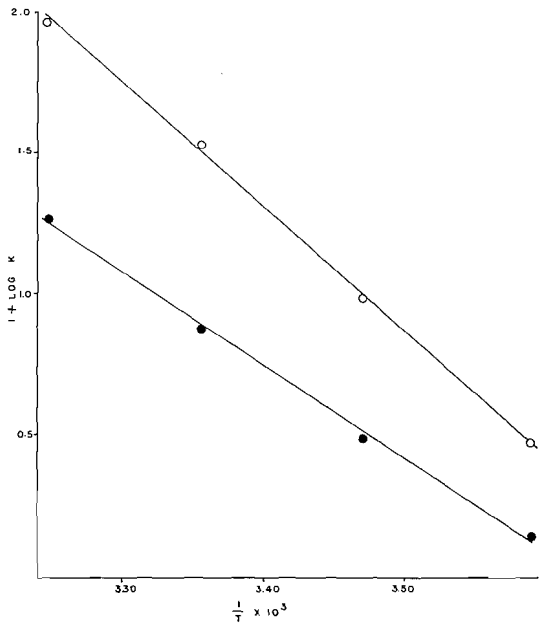

FIG. 3. Arrhenius plots for the two bond scission processes in the methanolysis of *p*-nitrophenyl chlorosulfate: *p*-nitrophenoxide ion leaving (open circles) and chloride ion leaving (full circles).

at aromatic carbon has not been detected. Reactions 1 and 2 are both followed by secondary processes. The methyl chlorosulfate formed in reaction 1 will undergo rapid solvolysis yielding dimethyl ether (14) (OSO_2Cl^- leaving group). The methyl-*p*-nitrophenyl sulfate produced in reaction 2 undergoes relatively slow solvolysis as described above (*p*-nitrophenyl sulfate leaving group).

Comparison with the phenyl chlorosulfate–methoxide system shows that S—O scission is relatively more important in the nitro-substituted case. For instance the 82% yield of *p*-nitrophenoxide ion at 25° (Table 1) compares with only 39% yield of phenoxide ion at this temperature (1). This observation is in accord with *p*-nitrophenoxide being the better leaving group compared to phenoxide. It is interesting that for S—O scission the rate constant ratio $(k'/k)_{S-O}$ at 25° for the two systems is 93, whereas for S—Cl scission the $(k'/k)_{S-Cl}$ ratio is 13, where k' and k are the constituent rate constants at 25° in reaction of *p*-nitrophenyl chlorosulfate and of phenyl chlorosulfate respectively. At the other temperatures the rate ratios take on somewhat different values, though the orders of magnitude remain unchanged. In energy terms S—O scission is favored for *p*-nitrophenyl chlorosulfate over the unsubstituted compound by a $\Delta\Delta F^{\ddagger}$ value of 2.8 kcal/mol, whereas the S—Cl scission process is favored in the same direction by a $\Delta\Delta F^{\ddagger}$ value of only 1.5 kcal/mol.

Clearly the sulfur center is more positively charged in *p*-nitrophenyl chlorosulfate than in the unsubstituted isomer, which should lead to a greater extent of bond formation between methoxide ion and sulfur in the transition state for the *p*-nitrophenyl chlorosulfate reaction. The resulting gain in bond energy is expected to make $\Delta H^{\ddagger}$ smaller in the case of *p*-nitrophenyl chlorosulfate for both S—O and S—Cl scissions, as observed experimentally (Table 2). Similarly, the concomitant greater desolvation of MeO^- in the *p*-nitrophenyl chlorosulfate case will result in a more positive $\Delta S^{\ddagger}$ value in that system compared with the phenyl chlorosulfate case, as observed.

It will be noted (Table 2) that a striking dissimilarity exists between the $\Delta S^{\ddagger}$ values for the S—O and the S—Cl pathways, the former being associated with a rather large positive entropy of activation. In the case of S—Cl scission, the entropy of activation is negative, as reported for the hydrolysis of sulfonyl chlorides (15–17). Though the greater solvation of the incipient chloride ion, compared with the aryloxide ion, in the transition state will tend to lead to a more negative $\Delta S^{\ddagger}$ in the former case, it appears unlikely that such differential solvation would account for a difference in $\Delta S^{\ddagger}$ of about 20 e.u. The positive $\Delta S^{\ddagger}$ for S—O scission is hence ascribed largely to a stereo-electronic effect.

The ground state conformation of aryl chlorosulfates (18), with the chlorine atom above the plane of the benzene ring, is associated with considerable internal strain and restricted rotation about the aryloxy–sulfur bond as well as about the carbon–oxygen bond. In the transition states (**1** and **2**) for nucleophilic attack by CH_3O^- at sulfur (trigonal bipyramidal configurations resulting from backside nucleophilic attack with respect to the departing ligand), S—O cleavage (**1**) will result in a relief of internal strain but S—Cl cleavage (**2**) does not lead to such relief of strain. Further, partial rupture of the S—O bond is accompanied by a

Can. J. Chem. Downloaded from www.nrcresearchpress.com by 210.87.254.5 on 09/05/12
For personal use only.

TABLE 2. Activation parameters for reactions of *p*-nitrophenyl chlorosulfate and phenyl chlorosulfate with methoxide ion in methanol*

	Value			
	S—O scission		S—Cl scission	
Parameter	p-$NO_2.C_6H_4.OSO_2Cl$	$C_6H_5OSO_2Cl$	p-$NO_2.C_6H_4.OSO_2Cl$	$C_6H_5OSO_2Cl$
ΔH^* (kcal mol^{-1})	19.5	21.5	14.4	15.1
ΔS^* (cal deg^{-1} mol^{-1})	9.3	7.0	−10.8	−13.8
ΔF^* (kcal mol^{-1}) at 25°	16.8	19.6	17.7	19.2

*Data for phenyl chlorosulfate are taken from ref. 1.

gain in vibrational and rotational degrees of freedom, an effect absent in S—Cl bond weakening. The combined result of these effects will be to yield a considerably more positive $\Delta S^{\ddagger}$ for aryloxide displacement.

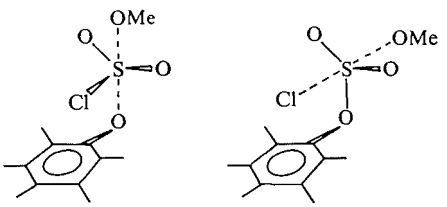

1 2

The *p*-nitrophenyl chlorosulfate–methoxide ion reaction has been considered only within the framework of the two parallel processes mechanism. An alternative possibility, that a pentacoordinate intermediate (19–22) is formed which then partitions along two paths with *p*-nitrophenoxy and chlorine departing, is considered to be unlikely as has been discussed for the phenyl chlorosulfate–methoxide ion system (1).

We thank the National Research Council of Canada for a grant. The award of a Fellowship to A.R. from the Canada Council, as part of the Franco-Canadian Cultural Exchange Program, is gratefully acknowledged.

1. E. BUNCEL, L. I. CHOONG, and A. RAOULT. J. C. S. Perkin II. In press.
2. E. R. THORNTON. Solvolysis mechanisms. The Ronald Press Company, N.Y. 1964. p. 163–166.
3. E. BUNCEL. Chem. Rev. **70**, 323 (1970).
4. J. F. BUNNETT. Quart. Rev. **12**, 1 (1958).
5. S. D. ROSS. Prog. Phys. Org. Chem. **1**, 31 (1963).
6. J. MILLER. Aromatic nucleophilic substitution. Elsevier, Amsterdam. 1968.
7. (*a*) E. BUNCEL, A. R. NORRIS, and K. E. RUSSELL. Quart. Rev. **22**, 123 (1968). (*b*) P. BUCK. Angew. Chem. Int. Edit. **8**, 120 (1969).
8. W. GERRARD. J. Chem. Soc. 5480 (1964).
9. G. R. CHALKLEY, D. J. SNODIN, G. STEVENS, and M. C. WHITING. J. Chem. Soc. (C), 682 (1970).
10. S. J. BENKOVIC and P. A. BENKOVIC. J. Am. Chem. Soc. **88**, 5504 (1966).
11. E. J. FENDLER and J. H. FENDLER. J. Org. Chem. **33**, 3852 (1968).
12. A. A. FROST and R. G. PEARSON. Kinetics and mechanism. Wiley, New York. 1961. p. 161.
13. W. P. JENCKS. Catalysis in chemistry and enzymology. McGraw-Hill Co., New York. 1969. p. 569.
14. E. BUNCEL and J. P. MILLINGTON. Can. J. Chem. **47**, 2145 (1969).
15. M. L. TONNET and A. N. HAMBLY. Aust. J. Chem. **23**, 2427 (1970); F. E. JENKINS and A. N. HAMBLY. Aust. J. Chem. **14**, 190, 205 (1961).
16. O. ROGNE. J. Chem. Soc. (B), 1294 (1968).
17. R. E. ROBERTSON and B. ROSSALL. Can. J. Chem. **49**, 1441 (1971); R. E. ROBERTSON, B. ROSSALL, S. E. SUGAMORI, and L. TREINDL. Can. J. Chem. **47**, 4199 (1969).
18. O. EXNER, P. DEMBECH, and P. VIVARELLI. J. Chem. Soc. (A), 620 (1971).
19. W. A. PRYOR and U. TONELLATO. J. Am. Chem. Soc. **89**, 3379 (1967).
20. J. L. KICE and G. J. KASPEREK. J. Am. Chem. Soc. **91**, 5510 (1969).
21. E. T. KAISER. Accounts Chem. Res. **3**, 145 (1970).
22. E. CIUFFARIN and A. FAVA. Prog. Phys. Org. Chem. **6**, 81 (1968).

Can. J. Chem. Downloaded from www.nrcresearchpress.com by 210.87.254.5 on 09/05/12
For personal use only.

Conformational Studies on the 1,2;5,6-Di-*O*-isopropylidene-D-hexoses

L. D. HALL
University of British Columbia, Vancouver 8, British Columbia
AND
S. A. BLACK, K. N. SLESSOR,[1] AND A. S. TRACEY
Simon Fraser University, Burnaby, British Columbia
Received January 28, 1971[2]

Nuclear magnetic resonance studies on the 1,2;5,6-di-*O*-isopropylidene-D-hexofuranose sugars have provided information on the conformational preferences of the five-membered rings in these molecules. They appear to have strong conformational preferences rather than existing as freely pseudorotating systems. The furanose rings of the 3-deoxy-*ribo* and *lyxo* derivatives are found to preferentially exist in an envelope conformation in which C-4 is displaced from the plane of the ring. The *arabino* and *xylo* derivatives are found to be much less distorted, with preferred conformations approaching twist forms involving displacements of C-1 and -2. Substitution of various *endo* and *exo* groups at C-3 appears to have only minor influence on the parent furanose conformation.

Les études r.m.n. sur les sucres de la série des di-*O*-isopropylidène-1,2;5,6-D-hexofuranoses ont fourni des renseignements sur les conformations privilégiées des cycles à cinq dans ces molécules. Plutôt que d'être en pseudo-rotation libre, ces systèmes apparaissent sous des conformations nettement préférentielles. Les cycles furanoses des dérivés déoxy-3 *ribo* et *lyxo* existent préférentiellement dans la conformation enveloppe dans laquelle le C-4 est au dehors du plan du cycle. Les dérivés *arabino* et *xylo* sont nettement moins tordus et adoptent la conformation privilégiée proche des formes "twist" impliquant les déplacements des C-1 et -2. La substitution des divers groupes *endo* et *exo* sur le C-3 semble n'avoir qu'une influence mineure sur la conformation du furanose parent.

Canadian Journal of Chemistry, **50**, 1912 (1972)

Introduction

The importance of 1,2;5,6-di-*O*-isopropylidene-D-hexoses as synthetic intermediates as well as an interest in conformational problems inherent in molecules containing a heterocyclic five-membered ring has prompted us to investigate the stereochemistry of these compounds and their 3-deoxy, 3-*O*-acetyl, and 3-keto analogues. Several specifically deuterated derivatives were prepared (1) since these allowed unambiguous assignment of proton resonance positions and thus aided in computer analysis of the n.m.r. spectra.

The inclusion of the 3-deoxy derivatives in this study is particularly important since the conformational properties of these compounds may be studied with the use of Dihedral Angle Estimation by the Ratio Method (DAERM) (2). DAERM is based on the assumption that the $\cos^2\theta$ term of the Karplus equation (3) is not significantly affected by various atomic and molecular parameters such as ring size and electronegativity. These perturbations would then have their major effect on the size of the Karplus constants. Using this approach, a consistent and complete solution of the conformations of the four furan rings (**1**, **4**, **7**, **10**) has been obtained (see Fig. 1). The preferred conformations of the di-*O*-isopropylidene-D-hexoses were obtained from correspondence in couplings between the deoxy sugars and their parent sugar derivatives.

In the following discussion, the section of the furan ring (*a*) is the focal point of the conformational discussions. In DAERM, ω is the projection angle of the methylene protons along the C_2—C_3 or C_4—C_3 bond (*b*). In a perfect tetrahedral system, ω is 120°. Internal angles between carbon atoms involved in a furan ring are known (4) to be smaller than the regular tetrahedral value of 109.5°. Assuming constant p-character in the carbon bonding, the angle subtended by the hydrogens on a methylene function of a furan ring will necessarily be greater than the tetrahedral angle (5). Recognizing this

[1]To whom correspondence should be addressed.
[2]Revision received February 7, 1972.

Can. J. Chem. Downloaded from www.nrcresearchpress.com by 210.87.254.40 on 09/05/12
For personal use only.

Can. J. Chem. Downloaded from www.nrcresearchpress.com by 210.87.254.40 on 09/05/12
For personal use only.

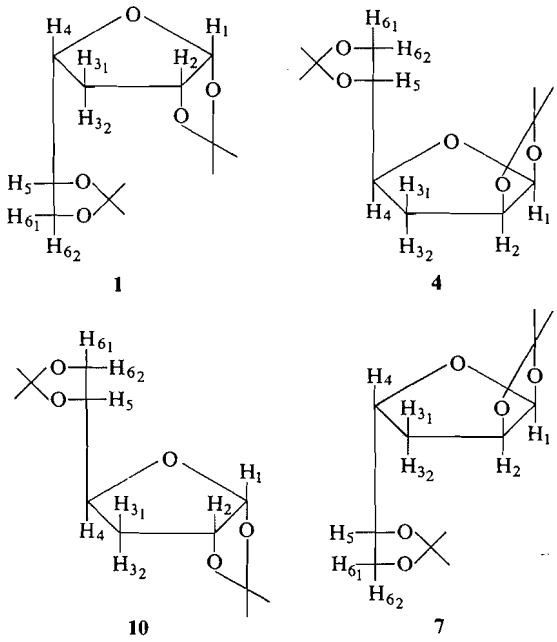

FIG. 1. **1**, 1,2;5,6-Di-*O*-isopropylidene-3-deoxy-α-D-*xylo*-hexose. **4**, 1,2;5,6-Di-*O*-isopropylidene-3-deoxy-β-D-*arabino*-hexose. **7**, 1,2;5,6-Di-*O*-isopropylidene-3-deoxy-β-D-*lyxo*-hexose. **10**, 1,2;5,6-Di-*O*-isopropylidene-3-deoxy-α-D-*ribo*-hexose.

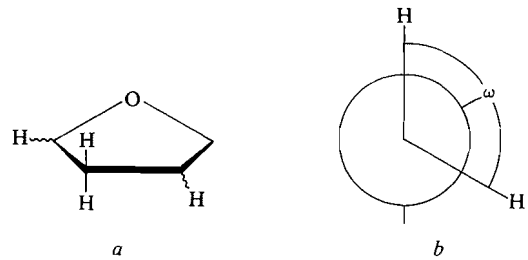

effect, an ω value of 124° has been selected for the DAERM calculations as has a ratio k_1/k_2 of 0.9. Evidence is presented to show that considerable deviations of either the ratio or ω from their assigned values has minimal effect on conformational arguments.

Results

Spectral assignments were made on the basis of the easily recognized H-1 and -2 resonances at low field with assignment of the remaining protons being made by general procedures. Assignment of configuration to the methylene protons was made from the n.m.r. data and in one instance a specifically deuterated analogue was prepared to confirm these assignments. All n.m.r. spectra were computer simulated from first order data and an iterative fit to experimental data was performed using the LAOCN III program of Bothner-By and Castellano (6). The necessity of computer-analyzed data is indicated by a comparison of the first order (Fig. 2A), fitted (Fig. 2B), and experimental (Fig. 2C) spectra for 3-deoxy-1,2;5,6-di-*O*-isopropylidene-β-D-*arabino*-hexose (**4**).

From a consideration of the general appearance of the n.m.r. spectra and their molecular architecture, the di-*O*-isopropylidene-hexoses are dealt with as four sets of compounds. These are the families derived from 3-substitution of the 3-deoxy-α-D-*ribo*-, -α-D-*xylo*-, -β-D-*lyxo*-, and -β-D-*arabino*-hexose derivatives. The chemical shift results which have not been published elsewhere (7, 8) are listed in Table 1 and the vicinal proton coupling parameters are listed in Table 2 (see also Fig. 3).

Conformational Assignments

1,2;5,6-Di-O-isopropylidene-α-D-xylo-hexose Derivatives

Considering first 3-deoxy-1,2;5,6-di-*O*-isopropylidene-α-D-*xylo*-hexose (**1**), four solutions for the couplings from H-2 to -3's are obtained from DAERM. In Table 3 and all subsequent discussion, *J*-1 is taken to be the *cis* coupling and θ-1 the corresponding angle.

Cases *i* and *iii* are both solutions for which few steric interactions within the molecule would be expected whereas cases *ii* and *iv* do not seem to be reasonable solutions since they represent conformations in which there is a large torsional twist on the C_2—C_3 bond. This places the "tail" (C-5, -6, and their substituents) in a position where large steric interactions with the 1,2-*O*-isopropylidene group would be expected. The rather large values for the calculated Karplus constants also indicate that solutions *ii* and *iv* are not valid. DAERM analysis of the $J_{3_1,4}-J_{3_2,4}$ couplings indicates that cases *vi* and *viii* can be eliminated since the Karplus constants are unacceptably large. As only very severe distortions of the furan ring could possibly make *ii* and *iv* compatible with any but cases *vi* and *viii*, cases *ii* and *iv* now must be eliminated and only *i* and *iii*, and *v* and *vii* remain as acceptable solutions.

The remaining problem is to decide which set

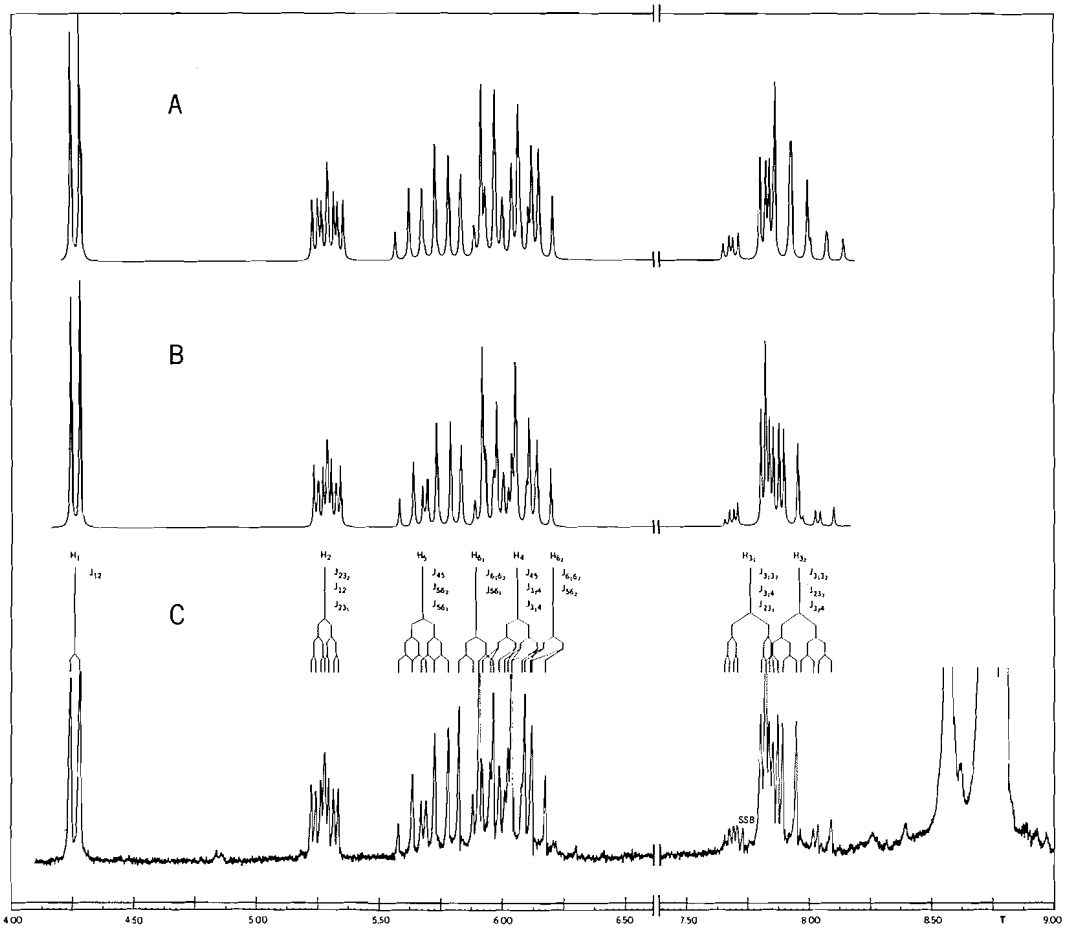

FIG. 2. The n.m.r. spectra for 3-deoxy-1,2;5,6-di-*O*-isopropylidene-β-D-*arabino*-hexose (**4**). A, Computer drawn spectrum on first order data. B, Computer drawn spectrum on computer fitted data. C, 100 MHz experimental spectrum.

of solutions is valid, *i.e.*, *i/v* or *iii/vii*. The former (*i/v*) indicates a conformation in which the "tail" involves less steric interactions but requires a rather severe distortion towards the envelope ^{2}V form. The latter solution (*iii/vii*) appears less distorted although there are eclipsing interactions between the furan ring substituents.

To establish unequivocally the conformation of **1**, deuteration at the H_{3_1} position was carried out and the resulting disappearance of the large coupling (6.30 Hz) rather than the smaller (1.35 Hz) clearly indicates the conformation *iii/vii* is correct (see Fig. 4). This follows from the definition of *J*-1 and θ-1 as the *cis* coupling and dihedral angle respectively.

If the torsional twists of two adjacent bonds within a five-membered ring are defined, the geometry of the complete ring, within the limits of bond distortion, must be uniquely defined. Assignment of torsional angles between C-2, -3, and -4 thus indicates the position of C-1 and the ring oxygen. On this basis, the conformation of compound **1** has been assigned. 3-Deoxy-1,2;5,6-di-*O*-α-D-*xylo*-hexose (**1**) prefers a conformation $V_0 \rightleftarrows {}^1T_0 \rightleftarrows {}^1V$, where the conformational symbols are those defined by Hall *et al.* (9). The degree of distortion from planarity is slight in this molecule and inspection of a molecular model indicates that the H_1—H_2 dihedral angle is probably not more than 10° and may well be closer to 0°.

Since the value of $\omega = 124°$ has been estimated, the effect of varying ω over a 20° range was investigated. Evidence is presented in Table

Can. J. Chem. Downloaded from www.nrcresearchpress.com by 210.87.254.40 on 09/05/12
For personal use only.

TABLE 1. Proton chemical shifts*

1,2;5,6-Di-*O*-isopropylidene	No.	H_1	H_2	H_3	H_4	H_5	H_{6_1}	H_{6_2}
-α-D-gulose	**2**	4.23	5.35	5.73	6.09	5.49	6.32	6.37
-α-D-galactose	**3**	4.13	5.45	5.90	6.13	5.64	5.93	6.16
-β-D-altrose	**5**	4.11	5.46	5.60	6.18	5.74	5.90	6.08
-β-D-mannose	**6**	4.30	5.33	5.71	6.14	5.43	5.88	6.03
-β-D-idose	**8**	4.03	5.50	5.81	5.88	5.55	5.85	6.07
-β-D-talose	**9**	4.20	5.43	6.13	6.24	5.81	5.95	6.04
-α-D-allose	**11**	4.21	5.40	5.98	6.17	5.71	5.95	6.01
-α-D-glucose	**12**†	4.17	5.51	5.84	5.96	5.69	5.97	6.11
3-*O*-Acetyl-α-D-gulose	**13**	4.20	5.19	4.92	5.93	5.39	5.91	6.45
3-*O*-Acetyl-α-D-galactose	**14**	4.11	5.42	5.10	6.15	5.55	5.97	6.17
3-*O*-Acetyl-β-D-altrose	**15**	4.13	5.44	4.68	6.02	5.68	5.91	6.05
3-*O*-Acetyl-β-D-mannose	**16**	4.29	5.24	4.83	5.98	5.50	5.92	6.03
3-*O*-Acetyl-β-D-idose	**17**	4.04	5.50	4.82	←	5.70 to 6.35		→
3-*O*-Acetyl-β-D-talose	**18**	4.17	5.21	5.21	←	5.80 to 6.13		→
3-*O*-Acetyl-α-D-allose	**19**	4.22	5.16	5.16	—	5.75	5.96	6.14
3-*O*-Acetyl-α-D-glucose	**20**	4.16	5.54	4.77	←	5.75 to 6.05		→
α-D-*xylo*-hexos-3-ulose	**21**	3.94	5.49	—	5.85	5.66	5.90	6.03
β-D-*arabino*-hexos-3-ulose	**22**	3.99	5.53	—	5.82	5.65	← 6.0	→
β-D-*lyxo*-hexos-3-ulose	**23**	3.88	5.61	—	←	5.56 to 6.03		→
α-D-*ribo*-hexos-3-ulose	**24**	3.88	5.62	—	6.0	5.68	5.94	6.04
α-D-*ribo*-hexos-3-ulose-hydrate	**25**	4.18	5.72	—	6.08	5.57	5.86	5.91

*$CDCl_3$ solution with TMS as internal standard (10.0 τ).
†Measured in acetone-d_6 solution.

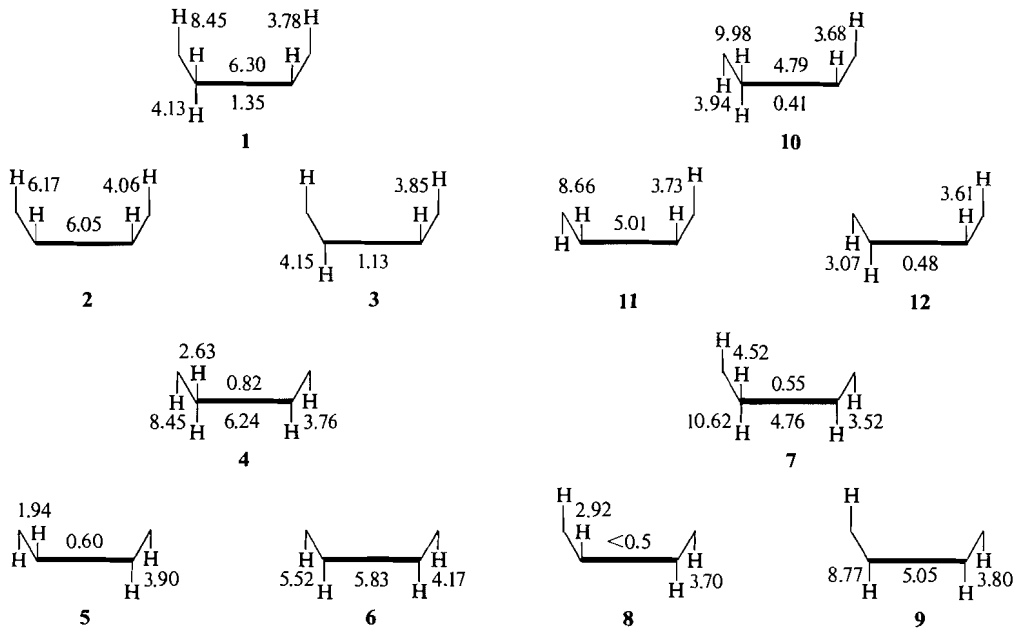

FIG. 3. Observed couplings in Hz for the furanose ring hydrogens of the 3-deoxy and 1,2;5,6-di-*O*-isopropylidene-D-hexoses (read from right to left C-1, C-2, C-3, and C-4).

4 which indicates that conformational assignments are not appreciably changed by varying ω through reasonable limits. Similarly, variation of the value k_1/k_2, as has been indicated before (2), results only in small changes in dihedral angle. Molecular models conveniently show that small changes in ω and the ratio result in little difference in the conformational assignment.

Can. J. Chem. Downloaded from www.nrcresearchpress.com by 210.87.254.40 on 09/05/12
For personal use only.

Can. J. Chem. Downloaded from www.nrcresearchpress.com by 210.87.254.40 on 09/05/12
For personal use only.

TABLE 2. Proton coupling constants*

1,2;5,6-Di-*O*-isopropylidene	No.	$J_{1,2}$	$J_{2,3_1}$	$J_{2,3_2}$	$J_{3_1,3_2}$	$J_{3_1,4}$	$J_{3_2,4}$	$J_{4,5}$	$J_{5,6_1}$	$J_{5,6_2}$	$J_{6_1,6_2}$	J_{H_3OH}†
-3-Deoxy-α-D-*xylo*-hexose	**1**	3.78	6.30	1.35	−14.20	8.45	4.13	8.14	6.71	6.91	−8.27	
-α-D-gulose	**2**	4.06	6.05			6.17		8.80	6.64	7.30	−8.66	6.3
-α-D-galactose	**3**	3.85	1.13			4.15		7.48	6.70	7.15	−8.67	4.0
-3-Deoxy-β-D-*arabino*-hexose	**4**	3.76	0.82	6.24	−14.74	2.63	8.45	9.65	6.13	5.61	−9.08	
-β-D-altrose	**5**	3.90	0.60			1.94		9.51	6.25	5.49	−8.94	4.0
-β-D-mannose	**6**	4.17	5.83			5.52		8.36	6.41	5.69	−8.76	5.2
-3-Deoxy-β-D-*lyxo*-hexose	**7**‡	3.52	0.55	4.76	−13.11	4.52	10.62	5.51	6.56	6.81	−8.28	
-β-D-idose	**8**	3.70	<0.5			2.92		5.31	6.89	6.93	−8.37	4.1
-β-D-talose	**9**	3.80	5.05			8.77		4.97	6.50	7.61	−8.26	9.0
-3-Deoxy-α-D-*ribo*-hexose	**10**	3.68	4.79	0.41	−13.41	9.98	3.94	—	—	—	—	
-α-D-allose	**11**	3.73	5.01			8.66		4.55	6.61	6.68	−8.57	7.3
-α-D-glucose	**12**§	3.61	0.48			3.07		7.27	6.46	5.95	−8.60	4.3
3-*O*-Acetyl-α-D-gulose	**13**	4.11	5.58			6.66		9.04	6.55	7.19	−8.30	
3-*O*-Acetyl-α-D-galactose	**14**	3.8	~0.7			2.56		7.84	6.66	6.92	−8.66	
3-*O*-Acetyl-β-D-altrose	**15**	3.78	0.70			1.16		9.67	6.14	4.80	−9.03	
3-*O*-Acetyl-β-D-mannose	**16**	4.02	5.75			5.92		8.48	6.50	5.22	−8.42	
3-*O*-Acetyl-β-D-idose	**17**	3.8	0.6			2.3		—	—	—	—	
3-*O*-Acetyl-β-D-talose	**18**	3.8	—			—		—	—	—	—	
3-*O*-Acetyl-α-D-allose	**19**	3.7	—			—		—	6.5	5.8	−8.6	
3-*O*-Acetyl-α-D-glucose	**20**	3.7	~0.5			~2.0		—	—	—	—	
α-D-*xylo*-hexos-3-ulose	**21**	4.4	N.C.			N.C.		6.08	6.39	6.91	−8.50	
β-D-*arabino*-hexos-3-ulose	**22**	4.3	N.C.			N.C.		~6.0	—	—	—	
β-D-*lyxo*-hexos-3-ulose	**23**	4.40	N.C.			N.C.		1.85	7.62	6.95	−8.41	
α-D-*ribo*-hexos-3-ulose	**24**	4.4	N.C.			N.C.		—	—	—	—	
α-D-*ribo*-hexos-3-ulose-hydrate	**25**	3.80	N.C.			N.C.		6.66	6.58	6.04	−8.90	

*All spectra run in $CDCl_3$ at 100 MHz; J's in Hz; iterative computer analyzed couplings to second decimal. N.C. indicates no coupling present.
†J_{H_3OH} not computer analyzed.
‡Measurements obtained from 220 MHz spectrum.
§Acetone-d_6 solution.

TABLE 3. DAERM analysis* of couplings in **1**

Protons coupled	Case	Obsd. J-1	Obsd. J-2	Calcd. θ-1	Calcd. θ-2	Calcd. k_1	Calcd. k_2
H_2, H_{3_1}, H_{3_2}	*i*	1.35	6.30	58	182	5.93	6.59
	ii	1.35	6.30	72	52	17.27	19.19
	iii	6.30	1.35	6	118	6.65	7.39
	iv	6.30	1.35	52	72	17.27	19.19
H_{3_1}, H_{3_2}, H_4	*v*	4.13	8.45	43	167	8.27	9.19
	vi	4.13	8.45	67	57	29.21	32.46
	vii	8.45	4.13	8	132	8.90	9.89
	viii	8.45	4.13	57	67	29.21	32.46

*$\omega = 124°$; $k_1/k_2 = 0.9$.

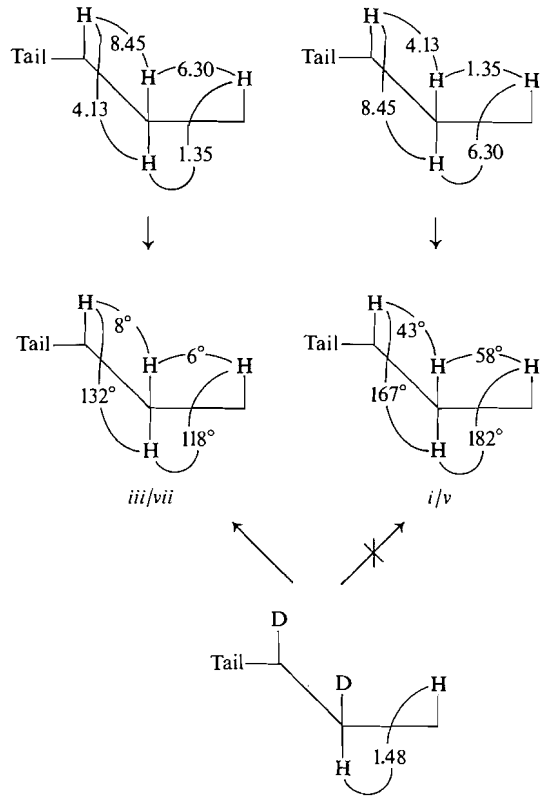

FIG. 4. DAERM analysis of 3-deoxy-1,2;5,6-di-*O*-isopropylidene-α-D-*xylo*-hexose (**1**).

1,2;5,6-Di-*O*-isopropylidene-α-D-gulose (**2**) and -α-D-galactose (**3**) are assigned the same conformational preferences as the 3-deoxy analogue (**1**) on the basis of the close correspondence in n.m.r. coupling parameters for these three compounds. A large coupling of about 8 Hz for the $J_{4,5}$ couplings observed for this family indicates a rotational preference for the

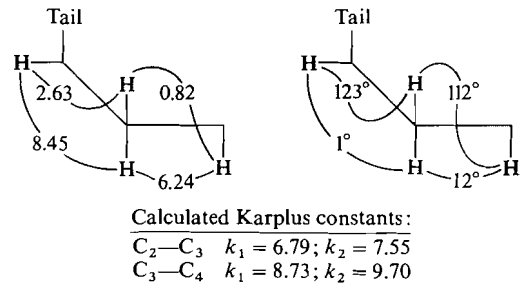

Calculated Karplus constants:

C_2—C_3	$k_1 = 6.79$; $k_2 = 7.55$
C_3—C_4	$k_1 = 8.73$; $k_2 = 9.70$

FIG. 5. Conformation of 3-deoxy-1,2;5,6-di-*O*-isopropylidene-β-D-*arabino*-hexose (**4**).

"tail". Obviously this preference is not regulated by hydrogen bond formation to the "tail" since the deoxy *xylo*-hexose (**1**) and galactose (**2**) derivatives cannot form such a bond.

1,2;5,6-Di-O-isopropylidene-β-D-arabino-hexose Family

The DAERM solutions for 3-deoxy-1,2;5,6-di-*O*-isopropylidene-β-D-*arabino*-hexose (**4**) are shown in Fig. 5 and suggest the conformational preferences ${}^0T_1 \rightleftarrows V_1 \rightleftarrows {}^2T_1$. The distortion from planarity, as in the *xylo*-hexose case, is only slight. Again the 1,2 dihedral angle is probably less than 10–12°.

The coupling results, displayed in Table 2, strongly suggest that the conformational preferences of 1,2;5,6-di-*O*-isopropylidene-β-D-altrose (**5**) and -β-D-mannose (**6**) are not different from the 3-deoxy analogue (**4**). It is again clear that the "tail" prefers an orientation independent of possible hydrogen bonding interactions.

1,2;5,6-Di-O-isopropylidene-β-D-lyxo-hexose Derivatives

DAERM analysis of the 2,3 and 3,4 couplings of 3-deoxy-1,2;5,6-di-*O*-isopropylidene-β-D-

Can. J. Chem. Downloaded from www.nrcresearchpress.com by 210.87.254.40 on 09/05/12
For personal use only.

TABLE 4. Variation of ω and k_1/k_2 in dihedral angle estimation*

$\omega°$	k_1/k_2	$J_{2,3_1}$	$J_{2,3_2}$	$\theta_{2,3_1}$	$\theta_{2,3_2}$	k_1	k_2
130	0.9	6.30	1.35	13	117	6.9	7.7
124	0.7	6.30	1.35	10	114	6.8	9.7
124	0.8	6.30	1.35	8	116	6.7	8.4
124	0.9	6.30	1.35	6	118	6.6	7.4
124	1.0	6.30	1.35	4	120	6.6	6.6
120	0.9	6.30	1.35	2	118	6.6	7.3
110	0.9	6.30	1.35	8	118	6.7	7.4
		$J_{3_1,4}$	$J_{3_2,4}$	$\theta_{3_1,4}$	$\theta_{3_2,4}$		
130	0.9	8.45	4.13	2	132	8.7	9.7
124	0.7	8.45	4.13	2	126	8.7	12.5
124	0.8	8.45	4.13	5	129	8.8	11.0
124	0.9	8.45	4.13	8	132	8.9	9.9
124	1.0	8.45	4.13	10	134	9.0	9.0
120	0.9	8.45	4.13	11	131	9.1	10.1
110	0.9	8.45	4.13	19	129	9.8	10.9

*DAERM analysis of couplings into the methylene function of 3-deoxy-1,2;5,6-di-*O*-isopropylidene-α-D-*xylo*-hexose (**1**).

TABLE 5. DAERM analysis* of couplings in 3-deoxy-1,2;5,6-di-*O*-isopropylidene-β-D-*lyxo*-hexose (**7**)

Protons coupled	Case	Obsd. *J*-1	Obsd. *J*-2	Calcd. θ-1	Calcd. θ-2	Calcd. k_1	Calcd. k_2
H_2, H_{3_1}, H_{3_2}	*i*	0.55	4.76	65	189	4.65	5.17
	ii	0.55	4.76	75	49	11.87	13.19
	iii	4.76	0.55	12	112	5.26	5.85
	iv	4.76	0.55	49	75	11.87	13.19
H_{3_1}, H_{3_2}, H_4	*v*	4.52	10.62	46	170	10.09	11.21
	vi	4.52	10.62	68	56	34.61	38.46
	vii	10.62	4.52	5	129	10.98	12.20
	viii	10.62	4.52	56	68	34.61	38.46

*$\omega = 124°$; $k_1/k_2 = 0.9$.

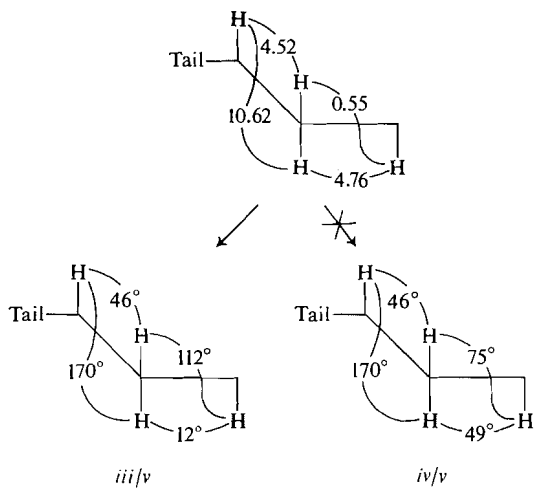

FIG. 6. DAERM analysis of 3-deoxy-1,2;5,6-di-*O*-isopropylidene-β-D-*lyxo*-hexose (**7**).

lyxo-hexose (**7**) are found in Table 5. Case *ii* can be rejected as a reasonable solution on the basis of the extreme distortion of the furan ring necessary to satisfy the angles. Cases *vi* and *viii* can be rejected because of their unacceptably large Karplus constants. Rejection of cases *vi* and *viii* leaves case *i* as an unacceptable solution as no reasonable conformation is possible from the solution of case *i* with *vii*. Similarly, case *vii* is not compatible with *iii* or *iv* as a *trans* coupling from H_2 to an H_3 proton must have a corresponding *cis* coupling from that H_3 proton to H_4. There remain two reasonable solutions, *iii*/*v*, or *iv*/*v* (Fig. 6). Conformation *iii*/*v* is taken as the correct conformation because *iv*/*v* requires a severe twisting in the furan ring and also the Karplus constants calculated for *iii*/*v* agree well with those calculated for the *xylo* (**1**) and *arabino* (**4**) derivatives at these positions. Thus,

Can. J. Chem. Downloaded from www.nrcresearchpress.com by 210.87.254.40 on 09/05/12
For personal use only.

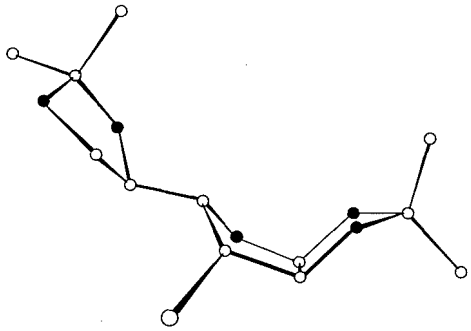

FIG. 7. Conformation of 3-chloro-3-deoxy-1,2;5,6-di-*O*-isopropylidene-β-D-idose in the crystalline state.

having defined the torsional angles about C-2, -3, and -4, the conformation of **7** must be $^4T_3 \rightleftarrows {}^4V \rightleftarrows {}^4T_0$. As in the previous cases the correspondence in couplings (Table 2) strongly suggests that replacement of hydrogen by hydroxyl at position 3 has little effect on the conformational preference.

The i.r. studies (1) indicate that a strong hydrogen bond between the "tail" and 3-OH of the idose derivative (**8**) is possible. The 4.1 Hz coupling into the hydroxyl group is consistent with formation of such a bond and in fact, such a bond would effectively lock the conformation into that proposed. The 9.0 Hz coupling into the hydroxyl group of 1,2;5,6-di-*O*-isopropylidene-β-D-talose (**9**) is consistent with hydrogen bond formation to the 2-oxygen of the 1,2-*O*-isopropylidene ring. All members of the β-D-*lyxo*-hexose family are thus expected to have the $^4T_3 \rightleftarrows {}^4V \rightleftarrows {}^4T_0$ conformational preference. A recently completed crystal structure (10) of 3-chloro-3-deoxy-1,2;5,6-di-*O*-isopropylidene-β-D-idose (Fig. 7) clearly shows C-4 to be out of the plane. A computer drawn representation of the atomic coordinates clearly indicates the ^4V conformation in the crystalline state.

1,2;5,6-Di-O-isopropylidene-α-D-ribo-hexose Derivatives

The DAERM calculations on the n.m.r. results obtained from this compound indicate that 3-deoxy-*ribo*-hexose (**10**) has the $^3T_4 \rightleftarrows V_4 \rightleftarrows {}^0T_4$ conformational preference. The similarity of the couplings reported in Table 2 indicates that the *endo* (**11**) and *exo* (**12**) hydroxylated derivatives of 3-deoxy-*ribo*-hexose (**10**) have

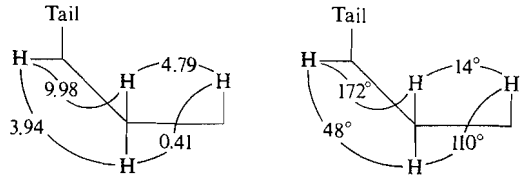

Calculated Karplus constants:

C_2—C_3	$k_1 = 5.39$; $k_2 = 5.99$
C_3—C_4	$k_1 = 9.42$; $k_2 = 10.46$

FIG. 8. Conformation of 3-deoxy-1,2;5,6-di-*O*-isopropylidene-α-D-*ribo*-hexose (**10**).

a conformational preference identical to the parent compound. The 7.3 Hz coupling into the hydroxyl group of 1,2;5,6-di-*O*-isopropylidene-α-D-allose (**11**) is in agreement with an *anti* arrangement of H_3 and hydroxyl proton (11). This orientation of the hydroxyl group and the suggested conformation are completely consistent with the proposed hydrogen bond formation between the C-3 hydroxyl and the C-2 oxygen of the 1,3-dioxolane ring (1). In the allose compound the coupling constant $J_{4,5}$ of 4.55 Hz may reflect freedom of rotation of the "tail" whereas in glucose the coupling constant, $J_{4,5}$ of 7.3 Hz, indicates a more preferred conformer. All observations are in complete agreement with the assignment of $^3T_4 \rightleftarrows V_4 \rightleftarrows {}^0T_4$ for the conformational preferences of these *ribo*-hexose derivatives (Fig. 8).

Acetyl and Keto Derivatives

The 3-*O*-acetyl- and 3-keto-derivatives of the 1,2;5,6-di-*O*-isopropylidene-D-hexoses yield much more complex spectra than those obtained from the parent compounds. Complete analysis was not achieved in several cases. The results that were obtained are given in Table 1 (chemical shifts) and Table 2 (coupling constants).

Comparisons of the coupling data in Table 2 and the values presented in Fig. 3 appear to indicate that there is little change in conformation of the furan ring on acetylation of the C-3 hydroxyl group. It should be noted, however, that on acetylation of 1,2;5,6-di-*O*-isopropylidene-α-D-galactose (**3**), the position 3 to 4 coupling drops from 4.15 to 2.56 Hz. At the same time the position 2 to 3 coupling goes from 1.13 to 0.7 Hz. Comparison of these couplings with those obtained from the *arabino*-hexose family (**4**, **5**, **6**) indicates that the molecule shifts

Can. J. Chem. Downloaded from www.nrcresearchpress.com by 210.87.254.40 on 09/05/12
For personal use only.

TABLE 6. Long-range couplings*

1,2;5,6-Di-*O*-isopropylidene	No.	$J_{1,3}$	$J_{2,4}$
β-D-altrose	**5**	—	~0.4
α-D-glucose	**12**	—	~0.
3-*O*-acetyl-β-D-altrose	**15**	0.64	0.41
3-*O*-acetyl-β-D-idose	**17**	—	~0.
α-D-*xylo*-hexos-3-ulose	**21**	N.C.	0.8
β-D-*arabino*-hexos-3-ulose	**22**	N.C.	0.9
β-D-*lyxo*-hexos-3-ulose	**23**	N.C.	1.15

*Measured in $CDCl_3$, values in Hz; N.C., no coupling observed; (—) indicates a coupling not measured.

its conformational preference after acetylation, from the $V_0 \rightleftarrows {}^1T_0 \rightleftarrows {}^1V$ of the parent to ${}^1T_0 \rightleftarrows {}^1V \rightleftarrows {}^1T_2$ of the derivative. Similar results are obtained for the benzoylated derivative, but not for 3-fluoro-3-deoxy-1,2;5,6-di-*O*-isopropylidene-α-D-galactose (12).

Little information can be gained from the sparse results on the 3-keto compounds. A significant increase in the coupling $J_{1,2}$ to about 4.4 Hz in these compounds (**21**–**24**) can be attributed to the effect of carbonyl group electronegativity (J_2^V) as described by Cohen and Schaefer (13). The ketones (**21**–**24**) exhibited rather large long-range couplings from H_2–H_4 across the carbonyl function. Long-range couplings were found to be a general phenomenon in the 1,2;5,6-di-*O*-isopropylidene-D-hexose system. Both H_1–H_3 *cis* and H_1–H_3 *trans* couplings were observed with the latter being generally larger. Double resonance experiments were used to confirm some of the assignments and in one case, the H_1–H_3 *trans* coupling in 3-deoxy-3,4-dideutero-1,2;5,6-di-*O*-isopropylidene-α-D-galactose (Fig. 4) of −0.55 Hz was determined. Sign determination was simplified by deuterium decoupling. *trans* H_2–H_4 couplings were not observed, although H_2–H_4 *cis* couplings were quite common. Since both *trans* and *cis* H_2–H_4 long-range couplings were observed for the 3-keto-derivatives it seems likely that the preceding results are simply a reflection of the difference in ring conformations for the two ring systems. Table 6 lists some of the long range couplings which were observed.

"Tail" Conformational and Rotational Preference

In order to better evaluate the possible influence of hydrogen bonding on the orientation of the "tail" the temperature dependence of

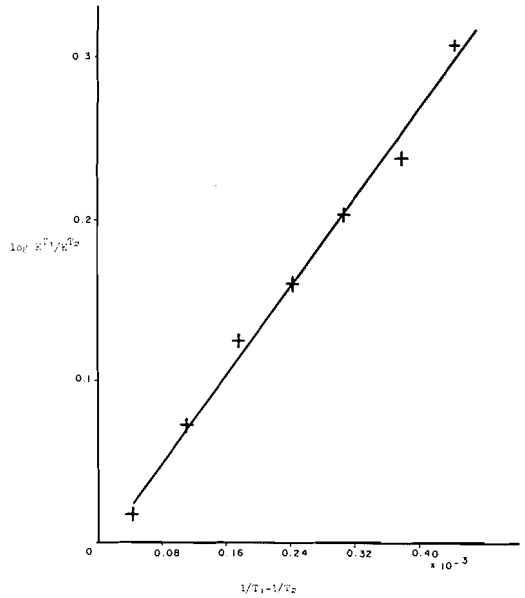

FIG. 9. Plot of log K^{T_1}/K^{T_2} *vs.* $1/T_1 - T_2$ for 1,2;5,6-di-*O*-isopropylidene-α-D-glucose (**12**) in the temperature range −14.1 to +19.5°; slope = 693.

hydrogen bond formation was investigated for several di-*O*-isopropylidene derivatives. The i.r. spectra of 1,2;5,6-di-*O*-isopropylidene-β-D-mannose (1) (**6**) and -β-D-idose (**8**) revealed no observable shift in equilibrium upon varying the temperature from −30 to +50°. The spectrum of 1,2;5,6-di-*O*-isopropylidene-α-D-glucose (**12**) indicated a continuous change with temperature. A ΔH of -3.1 ± 0.2 kcal/mol was calculated (Fig. 9) for this process, a value typical of H—O...H systems (14). The presence of free hydroxyl in the *gluco* derivative (**12**) and in the *ribo*-hexofuranos-3-ulose *gem* diol (**25**) and the presence of a second possible hydrogen bond in the *manno* derivative (**6**) indicate the presence of alternate forces which may provide some rotameric preference to the "tail". That such forces are present is indicated by many of the $J_{4,5}$ couplings, the magnitude of which cannot possibly represent freely rotating systems.

DAERM (2) calculations were performed on the position 5 to 6 couplings in order to evaluate the twist in the dioxolane ring of the "tail". The results are seen in Table 7 and indicate that the "tail" is distorted from planarity and that this distortion is 21–25° for all the compounds investigated. The X-ray crystal structure of 3-

Can. J. Chem. Downloaded from www.nrcresearchpress.com by 210.87.254.40 on 09/05/12
For personal use only.

TABLE 7. DAERM* calculations on the 5,6-*O*-isopropylidene group analysis of $J_{5,6_1}$, $J_{5,6_2}$ couplings

1,2;5,6-Di-*O*-isopropylidene	No.	Obsd. *J*-1	Obsd. *J*-2	Calcd. θ-1	Calcd. θ-2	Calcd. k_1	Calcd. k_2
-3-deoxy-α-D-*xylo*-hexose	**1**	6.91	6.72	24	148	8.7	9.6
-α-D-gulose	**2**	7.20	6.50	23	147	8.8	9.7
-α-D-galactose	**3**	7.15	6.70	23	147	8.8	9.8
-3-deoxy-β-D-*arabino*-hexose	**4**	5.70	5.71	25	149	7.3	8.1
-β-D-altrose	**5**	6.25	5.50	22	146	7.6	8.4
-β-D-mannose	**6**	6.41	5.70	22	146	7.8	8.7
-β-D-idose	**8**	6.93	6.89	25	149	8.8	9.8
-β-D-talose	**9**	7.61	6.50	21	145	9.1	10.1
-α-D-allose	**11**	6.68	6.61	25	149	8.5	9.4
-α-D-glucose	**12**	6.50	5.95	23	147	8.0	8.9

*$\omega = 124°$, $k_1/k_2 = 0.9$.

chloro-3-deoxy-1,2;5,6-di-*O*-isopropylidene-β-D-idose (Fig. 7) shows a twist of 25° in the O_5—C_5—C_6—O_6 dihedral angle. Calculations on X-ray data from 3-deoxy-3,4-*C*-(dichloromethylene)-1,2;5,6-di-*O*-isopropylidene-α-D-galactofuranose (15), shows a twist of 24.9° for the "tail". Both these results are in excellent agreement with the n.m.r. conclusions.

Inspection of Table 7 reveals a surprising variation in the Karplus constants, particularly since ring size and substitution patterns in the "tail" are identical for all ten compounds. Recognizing that the n.m.r. spectra of D and L isomers are identical then these derivatives may be compared as five sets of C-5 isomers (D-C_5 D-C_4 *vs.* L-C_5 D-C_4). The sets are *gluco*/*ido*; *allo*/*talo*; *altro*/*galacto*; *manno*/*gulo*; and 3-deoxy-*arabino*/3-deoxy-*xylo*, and in each case the first member of each set has the lower Karplus constant. Inspection of the DAERM results for couplings from H_4 to the H_{3_1}, H_{3_2} protons in the 3-deoxy derivatives shows an identical pattern, indicating a proximity effect due to a preferential orientation of the "tail". The effect of solvent on Karplus constants, suggested in a previous paper (2), may well be a more general example of such proximity effects.

The magnitude of the coupling, $J_{4,5}$, for the *xylo*- and *arabino*-hexose derivatives (**13**–**16**), indicates that the rotameric preference of the "tail" is probably not significantly affected by the presence of the acetoxy group at C-3. It should be noted, though, that a change of rotameric preference from *anti* to eclipsed or vice versa would not have an appreciable effect on the n.m.r. couplings observed. H_4 to H_5 couplings for the 3-uloses (**21**, **22**, **25**) of 6–7 Hz indicate a reasonable degree of conformational purity of an eclipsed or *anti* nature. The $J_{4,5}$ (1.85 Hz) coupling in the *lyxo* ketone (**23**) is the only coupling observed for this position definitive enough to indicate a preferred rotamer other than the eclipsed or *anti* configurations previously discussed.

Discussion

The n.m.r. parameters obtained from spectra of flexible molecules represent a weighted average of the parameters of all individual conformers present. This allows two interpretations of a conformation assigned to a potentially flexible molecule from n.m.r. data. Either the molecule has a strong preference for the pseudorotational segment predicted or two or more conformations exist whose coupling parameters time-average to give the observed values resulting in a time-averaged conformational assignment.

In the case of the *ribo* and *lyxo* derivatives it is difficult to see how the presence of a significant percentage of conformations other than those predicted could provide *trans* H_2–H_3 couplings of about 0.5 Hz and at the same time retain large *trans* couplings H_3–H_4 of about 10 Hz.

This question is not so easily resolved in the case of the *xylo* and *arabino* derivatives. The presence of the large *cis* position 3 to 4 couplings (8.5 Hz) indicates a high percentage of a single conformer since alternate conformers could only reduce this value. It should be noted that if this value is already partially reduced from some higher value the conformational assignment would not be altered. Low temperature n.m.r. studies on the 3-deoxy-*xylo* and *arabino*

Can. J. Chem. Downloaded from www.nrcresearchpress.com by 210.87.254.40 on 09/05/12
For personal use only.

Can. J. Chem. Downloaded from www.nrcresearchpress.com by 210.87.254.40 on 09/05/12
For personal use only.

derivatives ($\sim -60°$) showed no significant deviations from the spectra obtained at room temperature. It seems unlikely, then, that the spectra of any of these compounds represent any significant degree of conformational averaging.

In this work the dihedral angle between H_1 and H_2 has been assigned a value of 10–12° or less based on the assigned conformational preference. Previous studies (16) have assigned values of from 40–50° on the basis of coupling constants. The smaller value of 0–12° is in excellent agreement with X-ray crystal structures exhibiting this structural feature. The crystal structure of the chloroidose derivative, previously mentioned, indicated a torsional angle of about 4° for the O_1—C_1—C_2—O_2 dihedral angle. Without gross deformation of the tetrahedral geometry about carbons one and/or two, the H_1—H_2 dihedral angle must be of this order. The chloro derivative exhibits a typical coupling, $J_{1,2}$ of 3.6 Hz in deuterochloroform solution. Other X-ray structure determinations confirm this work with O_1—C_1—C_2—O_2 dihedral angles of 4.6 (15) and 9.0° (17).

It is difficult to ascertain whether the differences in ring conformation for the two systems (*cis* or *trans* ring substitution) are important chemically since the overriding effect is undoubtedly that of *cis* or *trans* substitution. On the other hand it does appear that the "tail" can have a significant effect on the chemistry of these compounds. This is indicated in that the times required for enol acetate formation from the parent ketones (7) are faster for the D-C_5, D-C_4 configuration than for the D-C_5, L-C_4 configuration.

This effect is readily explained if it is assumed that the preferred rotamer of the "tail" is one in which the C-5 oxygen preferably sits on the same side of the molecule as the C-1 and ring oxygens, that is, O_5 prefers to sit *gauche* to the ring oxygen. The large H_4–H_5 couplings mean, then, that the C-4 and -5 protons are near eclipsed in the D-C_5, D-C_4 case and near *anti* in the D-C_5, L-C_4 case. The small 1.85 Hz coupling observed for the *lyxo* ketone (**23**) indicates a situation in which the *gauche* interaction puts the C_4—C_5 protons in a near 90° relationship. Thus both *gauche* rotamers are suggested from n.m.r. evidence. A *gauche* interaction of this type would leave the C-4 position more open to attack by base in the D-C_5, D-C_4 case and provide more steric interaction to the approach of base in the alternate case.

The i.r. spectra of ref. 1 are completely in accord with the above explanation. The gulose and idose derivatives at first sight seem anomalous with complete hydrogen bonding to the "tail" being indicated by the i.r. spectra. This hydrogen bonding is, of course, not possible if the *gauche* O_5–ring oxygen configuration is present. Optical rotatory dispersion studies of the gulose derivative in various solvents indicate a major change in conformation on going from a solvent such as chloroform to water. The positive curve of the former case $[\alpha]_D^{20}$ +10° (*c*, 0.4 $CHCl_3$) being replaced by a strongly negative curve in the second case $[\alpha]_D^{20}$ −34° (*c*, 0.4 H_2O) (18). Interestingly enough the n.m.r. spectrum changes very little in D_2O indicating that the "tail", now no longer forming a hydrogen bond to the C-3 oxygen, has simply rotated to the conformation preferred in the absence of such a bond (*i.e.*, from an eclipsed to an *anti* configuration of the C-4 and -5 protons). Optical rotatory dispersion studies of the idose derivative (**8**) showed a similar effect. Although the curve did not change sign when the solvent was changed to water, it went from a moderately positive curve to a very strongly positive curve, an effect in accord with the above explanation.

Conclusions

The studies on the conformations of the 1,2;5,6-di-*O*-isopropylidene-D-hexoses demonstrate clearly that the furan ring conformation is determined by the substitution pattern of the 1,2-*O*-isopropylidene unit and the "tail". If these units are substituted on the furan ring in a *cis* fashion, the furan ring tends to be flattened with one or two of the atoms C-1, -2, and the ring oxygen slightly displaced from the mean plane. Thus the *xylo* and *arabino* derivatives have conformational preferences most readily described as $V_0 \rightleftarrows {}^1T_0 \rightleftarrows {}^1V$ and ${}^0T_1 \rightleftarrows V_1 \rightleftarrows {}^2T_1$, respectively. If, however, the units are substituted on the furan ring in a *trans* fashion, the ring is considerably distorted with one or two of the atoms C-3, -4, or the ring oxygen displaced in the preferred conformers. Thus the *ribo* and *lyxo* derivatives have as conformation preferences the ${}^3T_4 \rightleftarrows V_4 \rightleftarrows {}^0T_4$ and ${}^4T_3 \rightleftarrows {}^4V \rightleftarrows {}^4T_0$ conformations respectively. Two X-ray crystal structures of compounds exhibiting this

Can. J. Chem. Downloaded from www.nrcresearchpress.com by 210.87.254.40 on 09/05/12
For personal use only.

trans arrangement (10, 17) show C-4 to be the atom displaced. This work indicates an H_1–H_2 dihedral angle less than 10 to 12°, a result also in accord with X-ray analysis of related molecules.

Substitution of *endo* or *exo* groups at the C-3 position does not strongly influence the conformational preference of the furan ring. These derivatives generally show the same conformational preference exhibited by their parent deoxy analogues, although the *cis* substituted (*xylo* and *arabino*) derivatives seem more susceptible to influence from a substituent at C-3.

DAERM calculations on the "tail" (C_5—C_6 and substituents) have also been informative. The "tails" of the compounds investigated were twisted in the same manner and to the same extent (~24°). The sense and extent of this twist have been confirmed by two crystal structures (15, 10). The H_4–H_5 coupling parameters also indicate that the "tails" of these compounds have definite preferred rotamers. The n.m.r. results can be explained in terms of rotamers in which the ring oxygen and C-5 oxygen are preferably *gauche* to one another. This explanation correlates well with rates of enol acetate formation (7), with hydrogen bond formation, and with optical rotatory dispersion studies (18). This work lends strong support to the recently proposed "*gauche* effect" (19) and is in complete agreement with it.

Experimental

Melting points were determined on a Fisher–Johns apparatus and are uncorrected.

All compounds except 3-deoxy-1,2;5,6-di-*O*-isopropylidene-D-*lyxo*-hexose (**7**) gave spectra from a Varian HA-100 MHz spectrometer which were analyzable. Compound **7** was run on the Varian HR-220 MHz spectrometer of the National Research Council of Canada in Toronto, Ontario. All spectra were measured in deuterochloroform solution with TMS as an internal reference.

All spectra were analyzed using the LAOCN III n.m.r. program of Bothner-By and Castellano (6). Hydrogen bonding studies were performed in matched, jacketed cells of 1 cm path length on a Beckman IR 12. The absorbance traces were resolved on a Dupont 310 Curve Resolver to obtain the fraction of bonded and non-bonded material present.

Preparation of compounds **1**, **4**, **13**, and **16** has been described in ref. 7, **7** and **10**, in ref. 8, and **2**, **3**, **5**, **6**, **8**, **9**, **11**, **12**, **21**–**25** in ref. 1 and refs. therein.

cis-3,4-Dideutero-3-deoxy-1,2;5,6-di-O-isopropylidene-α-D-xylo-hexose

3-Deoxy-1,2;5,6-di-*O*-isopropylidene-α-D-*erythro*-hex-3-enose (2 g), prepared by the method of Weygand and Wolz (20) was dissolved in 95% ethanol (75 ml) and reduced over palladium black with deuterium at atmospheric pressure. After uptake of deuterium had ceased, t.l.c. (ethyl ether : toluene, 2:1) indicated the reaction complete. The reaction mixture was filtered and evaporated to a sirup which crystallized spontaneously. Recrystallization from petroleum ether (65–110°) yielded long needles (1.8 g), m.p. 79–80°, $[\alpha]_D^{22}$ −27° (*c*, 0.82 $CHCl_3$), lit. (7, 20) m.p. 81°, $[\alpha]_D$ −38.1° (*c*, 4.11 ethanol).

*3-O-Acetyl-1,2;5,6-di-O-isopropylidene-α-D-glucose (**20**)*

1,2;5,6-di-*O*-isopropylidene-α-D-glucose (**12**) (1 g) was dissolved in a mixture of pyridine (5 ml) and acetic anhydride (2 ml). The solution was kept overnight at room temperature. Repeated co-evaporation of the solution with toluene gave a slightly orange sirup free of acetylating reagents. The sirup was dissolved in chloroform (75 ml) treated with charcoal, filtered, and evaporated. The residue crystallized readily and was recrystallized from petroleum ether (65–110°) to yield 950 mg of product melting at 59–60°; $[\alpha]_D^{22}$ −38.4 (*c*, 1.07 $CHCl_3$), lit. (21) m.p. 62°, $[\alpha]_D^{24}$ −38.5 (*c*, 1.3 $CHCl_3$).

*3-O-Acetyl-1,2;5,6-di-O-isopropylidene-α-D-allose (**19**)*

Prepared from **11** in the same way as **20**; m.p. 74–75°, $[\alpha]_D^{22}$ +100.6° (*c*, 0.73 $CHCl_3$), lit. (22) m.p. 75.5–76.5°, $[\alpha]_D^{20}$ +107.6 (*c*, 1.0 $CHCl_3$).

*3-O-Acetyl-1,2;5,6-di-O-isopropylidene-β-D-idose (**17**)*

Prepared from **8** in the same way as **20**; m.p. 75.5–76.5°, $[\alpha]_D^{22}$ +16.6 (*c*, 0.67 $CHCl_3$), lit. (23) for the -L-isomer, m.p. 77–78°, $[\alpha]_D^{15}$ −12° (*c*, 0.75 $CHCl_3$).

Anal. Calcd. for $C_{14}H_{22}O_7$: C, 55.63; H, 7.28. Found: C, 55.82; H, 7.30.

*3-O-Acetyl-1,2;5,6-di-O-isopropylidene-β-D-talose (**18**)*

Prepared from **9** in the same way as **20** except that **18** did not crystallize, $[\alpha]_D^{22}$ −7.4° (*c*, 0.38 $CHCl_3$).

Anal. Calcd. for $C_{14}H_{22}O_7$: C, 55.63; H, 7.28. Found: C, 55.84; H, 7.32.

*3-O-Acetyl-1,2;5,6-di-O-isopropylidene-α-D-galactose (**14**)*

Prepared from **3** in the same way as **20** except that **14** did not crystallize, $[\alpha]_D^{22}$ −7.5° (*c*, 1.47 $CHCl_3$).

Anal. Calcd. for $C_{14}H_{22}O_7$: C, 55.63; H, 7.28. Found: C, 55.50; H, 7.15.

*3-O-Acetyl-1,2;5,6-di-O-isopropylidene-β-D-altrose (**15**)*

Prepared from **5** in the same way as **20**. The m.p. 92–93°, $[\alpha]_D^{22}$ +14.4° (*c*, 0.68 $CHCl_3$).

Anal. Calcd. for $C_{14}H_{22}O_7$: C, 55.63; H, 7.28. Found: C, 55.48; H, 7.37.

We are pleased to acknowledge the financial support of the National Research Council of Canada in the form of operating grants to L.D.H. and K.N.S.

1. K. N. Slessor and A. S. Tracey. Can. J. Chem. **47**, 3989 (1969).
2. K. N. Slessor and A. S. Tracey. Can. J. Chem. **49**, 2874 (1971).
3. M. Karplus. J. Chem. Phys. **30**, 11 (1959).
4. J. B. Hendrickson. J. Am. Chem. Soc. **83**, 4537 (1961).

5. E. L. ELIEL, N. L. ALLINGER, S. J. ANGYAL, and G. A. MORRISON. Conformational analysis. Interscience Publishers, Inc. New York, N.Y. 1965. p. 448.
6. A. A. BOTHNER-BY and S. M. CASTELLANO. Computer programs for chemistry. Vol. 1. *Editor* D. F. DeTar. W. A. Benjamin Inc. New York, N.Y. 1968. p. 10.
7. K. N. SLESSOR and A. S. TRACEY. Can. J. Chem. **48**, 2900 (1970).
8. C. R. HAYLOCK, L. D. MELTON, K. N. SLESSOR, and A. S. TRACEY. Carbohydr. Res. **16**, 375 (1971).
9. L. D. HALL, P. R. STEINER, and C. PEDERSEN. Can. J. Chem. **48**, 1155 (1970).
10. F. W. B. EINSTEIN and K. N. SLESSOR. Can. J. Chem. **50**, 93 (1972).
11. R. R. FRASER, M. KAUFMAN, P. MORAND, and G. GOVIL. Can. J. Chem. **47**, 403 (1969).
12. J. S. BRIMACOMBE, A. B. FOSTER, R. HEMS, J. H. WESTWOOD, and L. D. HALL. Can. J. Chem. **48**, 3946 (1970).
13. A. D. COHEN and T. SCHAEFER. Molec. Phys. **10**, 209 (1966).
14. L. P. KUHN and R. A. WIRES. J. Am. Chem. Soc. **86**, 2161 (1964).
15. J. S. BRIMACOMBE, P. A. GENT, and T. A. HAMOR. J. Chem. Soc. B, 1566 (1968).
16. R. J. ABRAHAM, L. D. HALL, L. HOUGH, and K. A. MCLAUCHLAN. J. Chem. Soc. 3699 (1962).
17. J. S. BRIMACOMBE, J. G. H. BRYAN, and T. A. HAMOR. J. Chem. Soc. B, 514 (1970).
18. C. R. HAYLOCK. Optical rotary dispersion of the 1,2;5,6-di-*O*-isopropylidene-D-hexofuranoses. B.Sc. Thesis. Simon Fraser University, Burnaby, B.C. 1969.
19. S. WOLFE, A. RAUK, L. M. TEL, and I. G. CSIZMADIA. J. Chem. Soc. (B), 136 (1971).
20. F. WEYGAND and H. WOLZ. Chem. Ber. **85**, 256 (1952).
21. I. E. MUSKAT. J. Am. Chem. Soc. **56**, 2449 (1934).
22. M. HAGA, M. TAKANO, and S. TEJIMA. Carbohydr. Res. **14**, 237 (1970).
23. N. BAGGETT and R. W. JEANLOZ. J. Org. Chem. **28**, 1845 (1963).

Can. J. Chem. Downloaded from www.nrcresearchpress.com by 210.87.254.40 on 09/05/12
For personal use only.

The Synthesis of Delphinine: A Stereoselective Total Synthesis of an Optically Active Advanced Relay Compound

K. WIESNER, E. W. K. JAY, T. Y. R. TSAI, C. DEMERSON, LIZZIE JAY, T. KANNO, J. KŘEPINSKÝ, A. VILÍM, AND C. S. WU

Natural Products Research Center, University of New Brunswick, Fredericton, N.B.

Received February 2, 1972

A stereoselective total synthesis of the optically active delphinine degradation product 3*b* is described.

La synthèse totale et stéréosélective du produit 3*b* optiquement actif et issu de la dégradation de la delphinine, est décrite.

Canadian Journal of Chemistry, **50**, 1925 (1972)

Can. J. Chem. Downloaded from www.nrcresearchpress.com by 210.87.254.42 on 09/05/12
For personal use only.

Some time ago we deduced the structure **1***a* for the alkaloid delphinine (1). Among various degradative studies which led to this structure proposal a simple and comparatively high yield conversion of delphinine into the aromatization product **2** was discovered (2). It is clear that this aromatic degradation product or its derivatives constitute an extremely favorable advanced relay for the synthesis of delphinine. We wish to describe in the present paper in detail our total synthesis of this relay compound, the resolution of the synthetic racemate into optical antipodes, and the rigorous identification of one enantiomer with the naturally derived material of the same structure (3).

It will be seen in the sequel that the synthetic compounds which turned out to be identical with their "natural" counterparts had the configurations **2***b*, **3***b*, and **4***b* rather than **2***a*, **3***a*, and **4***a*. Thus, it is clear that the configuration of the ring A methoxyl in delphinine has to be reversed and this alkaloid has to be represented by the formula **1***b*.

The starting material for our synthesis was the methoxy tetralone **5** (4). This compound was converted by the Stork pyrrolidine–enamine procedure (5) to the allyl tetralone **6**[1] in a yield of 89%. A second alkylation with benzyl chloromethyl ether (6) and sodium hydride in benzene gave 70% of the geminally disubstituted tetralone **7** after purification by chromatography. Compound **7** was subjected to a catalytic osmylation with osmic acid – sodium chlorate in tetrahydrofuran (7). The two diastereoisomeric diols **8** (A, m.p. 108–109 °C; B, m.p. 125–130 °C) were obtained in equal amounts and practically quantitative yield. The absence of carbonyl absorption in the i.r. spectra of both products indicated that they existed as the hemiketal tautomers. The diastereoisomers **8** were treated with an excess of metaperiodate in aqueous tetrahydrofuran. The aldehyde **9** (i.r.: 1726, 1715 cm^{-1} (—CH=O, $\diagdown$C=O); n.m.r.: broad singlet (1H) τ 0.49 p.p.m. (—CH=O)) was obtained in both cases in a quantitative yield.

The next step which is actually the crucial operation of the synthesis involved a base-catalyzed aldol condensation portrayed by the arrows in formula **9***b*. The hydroxy ketone **10** obtained quantitatively in this manner was oily, but homogeneous in t.l.c. and sufficiently pure for further work. It showed a carbonyl maximum in the i.r. spectrum at 1755 cm^{-1} typical for the keto group in the apex of the benzobicyclooctane system. The cyclization **9** → **10** is thermodynamically controlled and thus the hydroxyl in compound **10** may be assigned the more stable *exo*-configuration. This is borne out by the n.m.r. spectrum of **10** which shows the hydrogen unshielded by the hydroxyl as a clean quadruplet centered at τ 5.7 p.p.m. The dihedral angle of this *endo*-hydrogen and the bridgehead hydrogen is 90° and consequently coupling occurs only with the methylenic protons on the other side of the hydroxyl.

We have now constructed three of the five rings of our target compound by an extremely simple reaction sequence. It should be pointed out that compound **10** was assembled in such a

[1]All spectral data and properties of all compounds are recorded in the Experimental. They are mentioned in the Theoretical only in specially relevant cases.

Can. J. Chem. Downloaded from www.nrcresearchpress.com by 210.87.254.42 on 09/05/12
For personal use only.

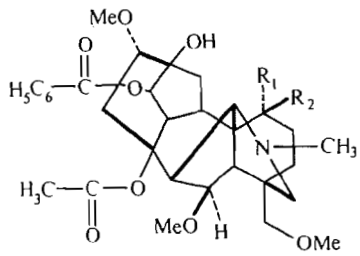

1*a* $R_1 = OMe$; $R_2 = H$
1*b* $R_1 = H$; $R_2 = OMe$

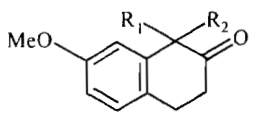

5 $R_1 = H$; $R_2 = H$
6 $R_1 = H$; $R_2 = -CH_2-CH=CH_2$
7 $R_1 = -CH_2-O-CH_2-C_6H_5$; $R_2 = -CH_2-CH=CH_2$
8 $R_1 = -CH_2-O-CH_2-C_6H_5$; $R_2 = -CH_2-\underset{OH}{CH}-\underset{OH}{CH_2}$
9 $R_1 = -CH_2-O-CH_2-C_6H_5$; $R_2 = -CH_2-C(=O)H$

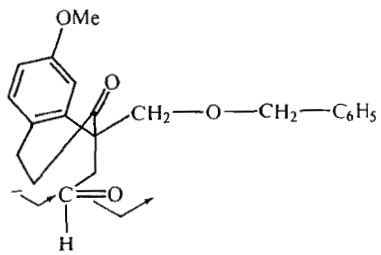

9*b*

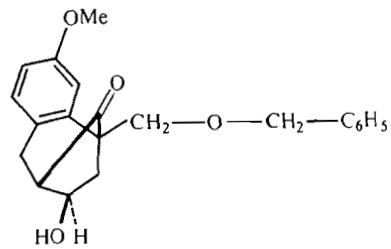

10

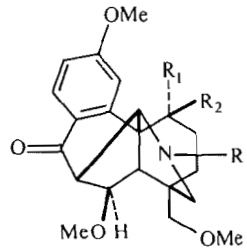

2*a* $R = -C(=O)H$; $R_1 = OMe$; $R_2 = H$
2*b* $R = -C(=O)H$; $R_1 = H$; $R_2 = OMe$
3*a* $R = H$; $R_1 = OMe$; $R_2 = H$
3*b* $R = H$; $R_1 = H$; $R_2 = OMe$
4*a* $R = -C(=O)-CH_3$; $R_1 = OMe$; $R_2 = H$
4*b* $R = -C(=O)-CH_3$; $R_1 = H$; $R_2 = OMe$

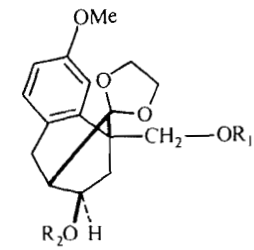

11 $R_1 = -CH_2-C_6H_5$; $R_2 = H$
12 $R_1 = -CH_2-C_6H_5$; $R_2 = -C(=O)-CH_3$
13 $R_1 = H$; $R_2 = -C(=O)-CH_3$
14 $R_1 =$ 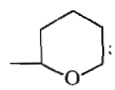 ; $R_2 = -C(=O)-CH_3$
15 $R_1 =$ 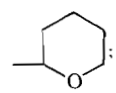 ; $R_2 = H$
16 $R_1 =$ 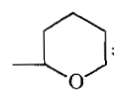 ; $R_2 = -CH_2-C_6H_5$
17 $R_1 = H$; $R_2 = -CH_2-C_6H_5$

SCHEME 1

Can. J. Chem. Downloaded from www.nrcresearchpress.com by 210.87.254.42 on 09/05/12
For personal use only.

manner that the functional groups which are needed either for the continuation of the synthesis or as part of the functionality of the final product **2** automatically materialized in the correct positions. The hydroxy ketone **10** was converted to the ketal **11** (m.p. 95–97 °C) by treatment with ethylene glycol and *p*-toluenesulfonic acid in refluxing benzene. The yield of the recrystallized compound **11** was 88%.

The next operation which had to be executed was the transfer of the benzyl blocking group from the primary to the secondary alcoholic function, *i.e.* compound **11** had to be converted to its isomer **17**. While this process required a number of steps, it has to be emphasized that these were simple and nearly quantitative and thus *the overall yield was finally raised to 65%*.[2]

Acetylation of **11** with acetic anhydride and pyridine gave the acetoxy derivative **12** (m.p. 81–82 °C). Compound **12** was subjected to hydrogenolysis in ethanol with 10% palladium–charcoal. The oily product **13** was homogeneous in t.l.c. and immediately used for further work. The alcoholic function in **13** was now blocked by tetrahydropyranylation with dihydropyran in dry chloroform and a drop of hydrochloric acid. The product **14** was purified by chromatography and was homogeneous in t.l.c. The acetoxy group of **14** was cleaved by reduction with lithium aluminum hydride and the oily alcohol **15** was purified by chromatography on silica gel. The secondary alcoholic group in **15** was now benzylated in dry dioxane with sodium hydride and benzyl chloride at reflux temperature. Chromatography on silica gel yielded the pure oily compound **16**. The tetrahydropyranyl group was selectively removed by treating **16** with a large volume of methanol containing 1% concentrated hydrochloric acid at room temperature. The product **17** was purified by chromatography on silica gel and it was an oil homogeneous in t.l.c. The n.m.r. and i.r. spectra of **11** and **17** clearly showed the presence of an identical functional group system.

[2]Since the overall yield **11** → **17** was good, it did not seem worth while to start from the beginning with a modified starting material which would allow a much more direct conversion of **11** to **17**. One such modification which comes to mind would be the use of the acid sensitive *p*-methoxybenzyl group as R_1 in compound **11**. It would have been necessary to go back to step **6** → **7** to implement this modification.

The primary alcohol **17** was oxidized by chromium trioxide in pyridine and the aldehyde **18** was obtained after chromatography on silica gel as an oil homogeneous in t.l.c. in a yield of 85% (i.r.: 2700, 1725 cm^{-1}; n.m.r.: singlet (1H) τ 0.17 p.p.m. (—CH=O)).

At this point the stage was set to attach the substituted butane derivative destined to form ring A. The synthesis of this element was carried out as follows.

1-Methoxy-3-cyano-2-propene (8) (mixture of *cis*- and *trans*-isomers) was added to a solution of sodium in benzyl alcohol and the mixture was stirred for a week at room temperature. The crude product **19** was purified by distillation and the pure material was obtained in a yield of 32%. Compound **19** was heated at reflux for 50 h with 10% sulfuric acid in methanol. The methyl ester **20** was obtained in a yield of 72%. Reduction of the ester **20** with lithium aluminum hydride in ether gave the alcohol **21** in a yield of 68%. Finally, tosylation of **21** with tosyl chloride and pyridine followed by exchange of the tosyl group with lithium bromide in acetone gave the bromo derivative **22** in a 75% yield.

Both moieties of the convergent synthesis (**18** and **22**) were now ready and it was possible to couple them and proceed with the construction of ring A with its substituents.

One mole of the aldehyde **18** in THF was added to 5 mol of the Grignard reagent prepared from the bromide **22** in the same solvent. Work-up and chromatography on silica gel gave the alcohol **23** in a yield of 91%. While compound **23** had an uncontrolled asymmetric center (benzyloxy group in the side chain), it was homogeneous in t.l.c., and all subsequent transformations (especially after the conversion of the side chain benzyloxy group into a ketone) proved that it was sterically homogeneous with respect to the R_1R_2 asymmetric center. It was thus clear that the Grignard reaction was stereospecific and produced only one of the two epimeric alcohols at the position of the future delphinine ring A methoxyl. At this point there was no completely reliable way to determine the configuration of this alcohol and to predict whether it corresponded (at the R_1R_2 asymmetric center) to the natural configuration of delphinine. It finally turned out that the configuration of **23** was in fact *epimeric* to the

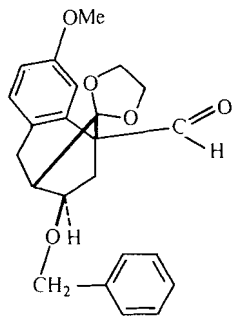

18

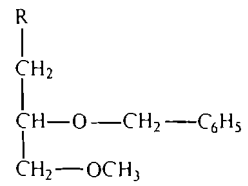

19 R = —C≡N
20 R = —$COOCH_3$
21 R = —CH_2—OH
22 R = —CH_2—Br

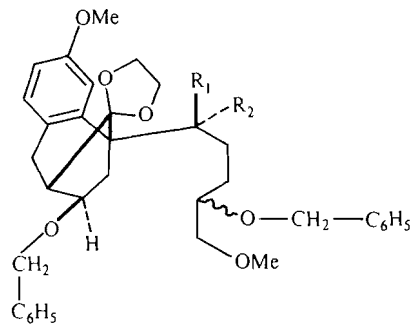

23 $R_1 = H; R_2 = OH$
24 $R_1R_2 = =O$
25 $R_1 = OH; R_2 = H$
26*a* $R_1 = H; R_2 = OMe$
26*b* $R_1 = OMe; R_2 = H$

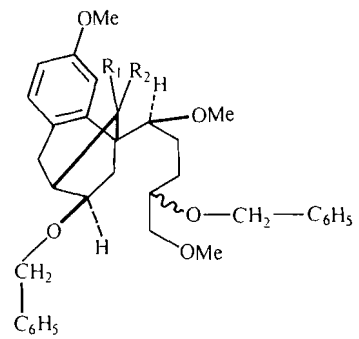

27*b* $R_1R_2 = =O$
28*b* $R_1 = H; R_2 = NH_2$

SCHEME 2

natural configuration of delphinine and as given in the formula.

With this knowledge we may now interpret the stereospecificity of the Grignard reaction by the assumption that the aldehyde group is fixed in a single conformation by a magnesium complex involving the carbonyl oxygen and one or both of the dioxolane oxygens. In this complex the carbonyl group is attacked by the Grignard carbanion from the less hindered side. With the large benzyloxy group providing effective steric hindrance the less hindered approach is clearly from the side of the flat anisole ring.

The epimer of the Grignard alcohol **23**, *i.e.* compound **25**, was prepared as follows. The alcohol **23** was oxidized to the ketone **24** by the Jones' reagent in a yield of 94%. The product was homogeneous in t.l.c. without purification. Reduction of compound **24** with lithium aluminum hydride in dioxane at 90 °C (the stereochemical outcome is temperature dependent) gave a mixture (yield 97%) of the alcohols **25** and **23** in a ratio 7:3. The products were acetylated for 8 h with acetic anhydride and pyridine at room temperature. Only the epimer **25** acetylated under these conditions. The acetate was separated by chromatography on silica gel and the pure epimer **25** was obtained by saponification with methanolic potassium hydroxide. The recovered epimer **23** was added to the next oxidation run and thus the entire material was ultimately converted to **25**.

Both alcohols **23** and **25** were methylated in refluxing dioxane with sodium hydride and an excess of methyl iodide. The corresponding methyl ethers **26***a* and *b* were obtained in almost quantitative yield. The n.m.r. peaks of the three methoxy groups in compounds **26***a* and *b* (τ 6.29, 6.47, 6.67 and 6.27, 6.59, 6.62 p.p.m. respectively) were all narrow singlets and sufficiently

Can. J. Chem. Downloaded from www.nrcresearchpress.com by 210.87.254.42 on 09/05/12
For personal use only.

Can. J. Chem. Downloaded from www.nrcresearchpress.com by 210.87.254.42 on 09/05/12
For personal use only.

different to insure that the materials were completely homogeneous with respect to the R_1R_2 asymmetric center. Moreover, both compounds differ very strongly in t.l.c. and are easily separable by chromatography.

Since, as we already stated, there was no way to ascertain at this point which of the two compounds **26***a* and *b* corresponded to the natural configuration of the delphinine ring A methoxyl, we have decided to carry out the synthesis first with **26***a*.[3]

Proceeding via steps which will be outlined in the sequel we have synthesized the beautifully crystalline derivative **4***a* (m.p. 177 °C) and fully characterized it by high resolution mass spectrum and elemental analysis. While this synthetic racemate was very similar to the corresponding optically active delphinine derivative there were clear differences in t.l.c., i.r., and n.m.r. which made it certain that the two materials were not identical. On the other hand the synthetic and "natural" compound gave *identical* mass spectra and thus we concluded that the only difference between them was the configuration of the ring A methoxyl.

It was evident that, true to the proverb, the bread fell again on the buttered side, and it was necessary to repeat the synthesis starting with the epimer **26***b*. This time as expected the synthesis resulted in end-products which were identical with the naturally derived materials in every detail.

Since the individual steps in both series were performed in exactly the same manner, we shall describe only the sequence starting with **26***b*.[4] The conversion of compound **26***b* into the final products was executed as follows. The ketal was hydrolyzed under reflux with aqueous acetic acid and the product **27***b* was obtained in quantitative yield. It showed an i.r. maximum at 1755 cm^{-1}, typical for the keto group in the apex of the bicyclic system.

[3]It must be remembered that the configurations of the ring A methoxyl given in the formulae became known only after the completion of the synthesis.

[4]The description of both series may be found in the Experimental. For the sake of simplicity of the formula schemes we do not reproduce the structures of the intermediates belonging to the **26***a* series. In the Experimental these compounds are referred to by numbers with the subscript "a". Their structural formulae may be derived by inverting the configuration of the "ring A methoxyl" in the formula with the same number and the subscript "b".

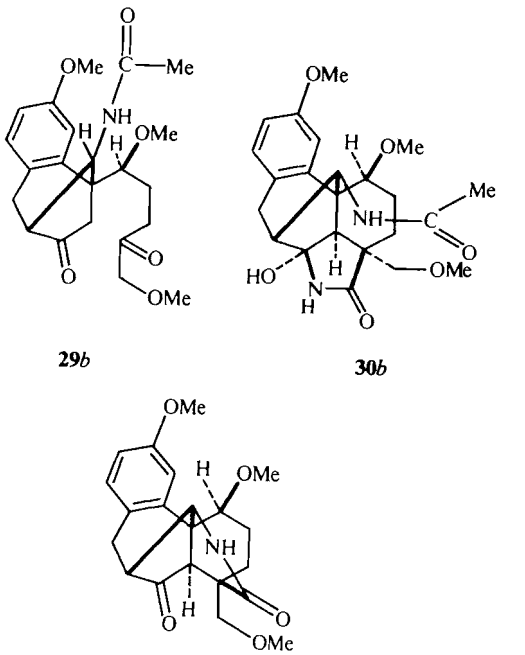

29*b* **30***b*

31*b*

SCHEME 3

Compound **27***b* was now subjected to amination with Raney nickel in methanolic ammonia exactly as worked out in our model experiments (3, 9). However, in the present case the desired *anti*-isomer **28***b* was obtained stereoselectively (ratio *anti*:*syn* 10:1, overall yield 97%). The crude amine **28***b* was acetylated with acetic anhydride–pyridine, the benzyl groups removed by hydrogenolysis, and the two liberated alcoholic functions oxidized by chromium trioxide in pyridine.

The diketone **29***b* (m.p. 100–102 °C) was separated by chromatography on silica gel from the small amount of the undesired *syn*-epimer and purified by crystallization; (i.r.: 1745, 1720 cm^{-1} (ketones), 1660 cm^{-1} (amide); n.m.r.: singlets (3H each) τ 6.23, 6.52, 6.57 (3 OCH_3), singlet (2H) 5.93 p.p.m. (—CO—CH_2—O—)). The overall yield of pure **29***b* from the crude amine **28***b* was 50%.

The diketone **29***b* was now heated for 6 h with 5 mol of potassium cyanide in aqueous ethanol. The lactamol **30***b* (m.p. 238 °C) resulted stereospecifically in a yield of 91%.

While this reaction may seem remarkable it was fully anticipated from our extensive model

Can. J. Chem. Downloaded from www.nrcresearchpress.com by 210.87.254.42 on 09/05/12
For personal use only.

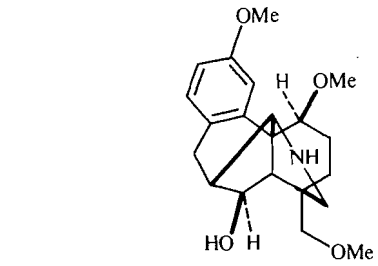

32*b*

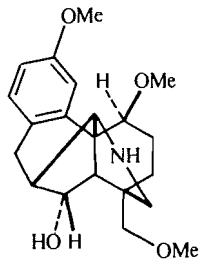

33*b*

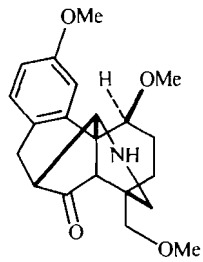

34*b*

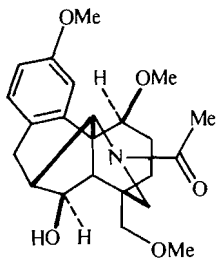

35*b*

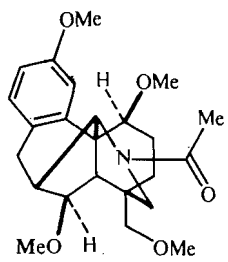

36*b*

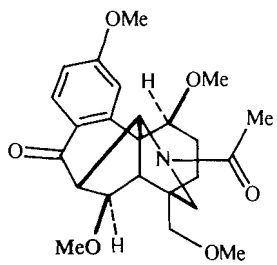

4*b*

SCHEME 4

studies (9, 3). It is actually a sequence of simple steps all of which were part of our original plan. Thus, the only noteworthy feature of the transformation was the fact that conditions were found where all these steps occurred in high yield stereospecifically and in one reaction solution.

The mechanism of the conversion **29***b* → **30***b* may be visualized as follows. Base-catalyzed aldol condensation of **29***b* yielded first an $\alpha\beta$-unsaturated ketone. This intermediate, which we have not isolated, then added cyanide axially, in a thermodynamically controlled reaction. The nitrile group was subsequently hydrolyzed to a primary amide, which tautomerized to the lactamol **30***b*.

The conversion of the lactamol to the ketolactam **31***b* (m.p. 268 °C) was accomplished by heating in a mixture of methanol and concentrated hydrochloric acid in a yield of 64%; (i.r.: 1740 cm^{-1} (ketone), 1670 cm^{-1} (lactam); n.m.r.: singlets (3H each) τ 6.20, 6.57, 6.63 p.p.m. (3 OCH_3)).

With the synthesis of the ketolactam **31***b* accomplished, it remained only to modify the functional group system. This task was easy, since it required merely the reduction of the lactam group, the conversion of the ring B ketone into an *exo*-methoxy group, and the introduction of a keto group into the benzylic position. All these operations have been worked out previously in our model studies (3). The keto lactam **31***b* was reduced with lithium aluminum hydride in refluxing dioxane. The mixture of the two products **32***b* and **33***b* was separated by chromatography on alumina. The ratio of the two compounds was 1:1 and the yield was 76%.

The *exo*-alcohol **32***b* was crystalline (m.p. 228 °C); the *endo*-epimer **33***b* remained oily and it was converted to the ketone **34***b* by Jones oxidation. This last compound was subjected without purification to a reduction with sodium in refluxing absolute ethanol. The alcohols **32***b* and **33***b* were again obtained (yield 74%), but in this thermodynamically controlled reduction the desired *exo*-alcohol **32***b* predominated (ratio 7:3).

The *exo*-alcohol **32***b* was now acetylated with acetic anhydride in pyridine and the product hydrolyzed by heating with dilute methanolic potassium hydroxide. The crystalline alcohol **35***b* (m.p. 183 °C) was obtained in a yield of 95%.

Compound **35***b* was methylated in refluxing dioxane with sodium hydride and methyl iodide. The crystalline methoxy derivative **36***b* (m.p. 157 °C) was obtained in a yield of 87%. The n.m.r. spectrum of this material showed a singlet (11H) at τ 6.70 p.p.m. which includes

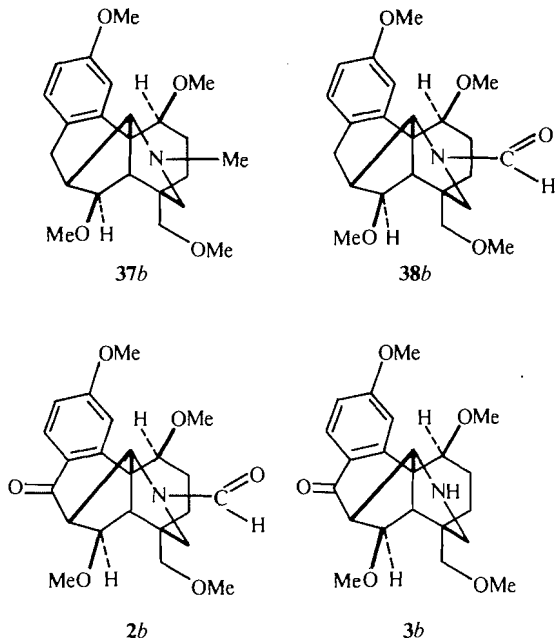

SCHEME 5

the three aliphatic methoxyls and the two hydrogens unshielded by the primary methoxyl. We have pointed out previously (3) that the ring B *endo*-methoxyl is located in the shielding region of the benzene ring and is consequently shifted upfield to τ 6.93 p.p.m. Thus, the n.m.r. spectrum of **36***b* is in agreement with the configuration portrayed in the formula. Compound **36***b* was converted into the final product **4***b* by Jones' oxidation in a yield of 89%. The racemate **4***b* was a crystalline sharply melting material (m.p. 188–190°C) and it was characterized by a high resolution mass spectrum and elemental analysis.

The i.r., n.m.r., u.v., and mass spectra of the synthetic racemate and the naturally derived compound of the same structure were superimposable. The two materials were also indistinguishable in several t.l.c. systems.

Since we wished to synthesize also the formyl derivative **2***b* and the secondary base **3***b* and since it turned out that the *N*-acetyl group of **4***b* is exceedingly difficult to hydrolyze, we have worked out a second variant of the final stages of the synthesis.

The *exo*-alcohol **32***b* was methylated in refluxing dioxane with sodium hydride and methyl iodide. The oily tetramethoxy *N*-methyl derivative **37***b* was obtained in a yield of 96%.

The conversion of **37***b* to the *N*-formyl derivative **38***b* was accomplished in a yield of 95% by oxidation with potassium permanganate in acetone at room temperature. Compound **38***b* was a highly crystalline, sharply melting solid (m.p. 158–160°C) and it was transformed into the final "delphinine aromatization product" **2***b* by Jones oxidation in a yield of 67%. A direct conversion of **37***b* to **2***b* was also accomplished by a prolonged oxidation with an excess of potassium permanganate in acetone acetic acid (yield 82%). The synthetic racemate **2***b* remained oily, but it was homogeneous in several t.l.c. systems and indistinguishable from the "natural" delphinine derivative. Both materials also gave identical i.r., n.m.r., and mass spectra.

The formyl derivative **2***b* was finally smoothly hydrolyzed to the secondary base **3***b* (m.p. 176°C, yield 94%) by refluxing with dilute hydrochloric acid. The synthetic racemate **3***b* was characterized by elemental analysis and high resolution mass spectrometry and it was found to be indistinguishable from the optically active "natural" derivative of the same structure by t.l.c., i.r., n.m.r., and mass spectrometry.

Thus, the stereoselective total synthesis of the racemic relay compound **3***b* was complete. In spite of the stereoselectivity of the entire process (including the setting up of the configuration of the ring A methoxyl) the synthesis did not provide any reliable information about the configuration of the ring A methoxy group.

The only point rigorously established about this asymmetric center was that its configuration in the synthetic products was the same as in the natural alkaloid and its derivatives.

The configuration **1***a* (Scheme 1) of the ring A methoxyl in delphinine was assigned (1*c*) on the basis of a direct correlation (10) of delphinine with aconitine, in the course of which this asymmetric center remained undisturbed. The corresponding ring A methoxyl of aconitine in turn was tentatively assigned the configuration *trans* to the nitrogen bridge on the basis of a conformational argument (11). A similar conformational argument seemed also to hold when this substituent was studied directly in delphinine (1*c*). It was quite clear to us that these assignments were not completely secure, since there was some uncertainty about the conformation of ring A in alkaloids of the delphinine type.

While our synthetic objective was reached, we

Can. J. Chem. Downloaded from www.nrcresearchpress.com by 210.87.254.42 on 09/05/12
For personal use only.

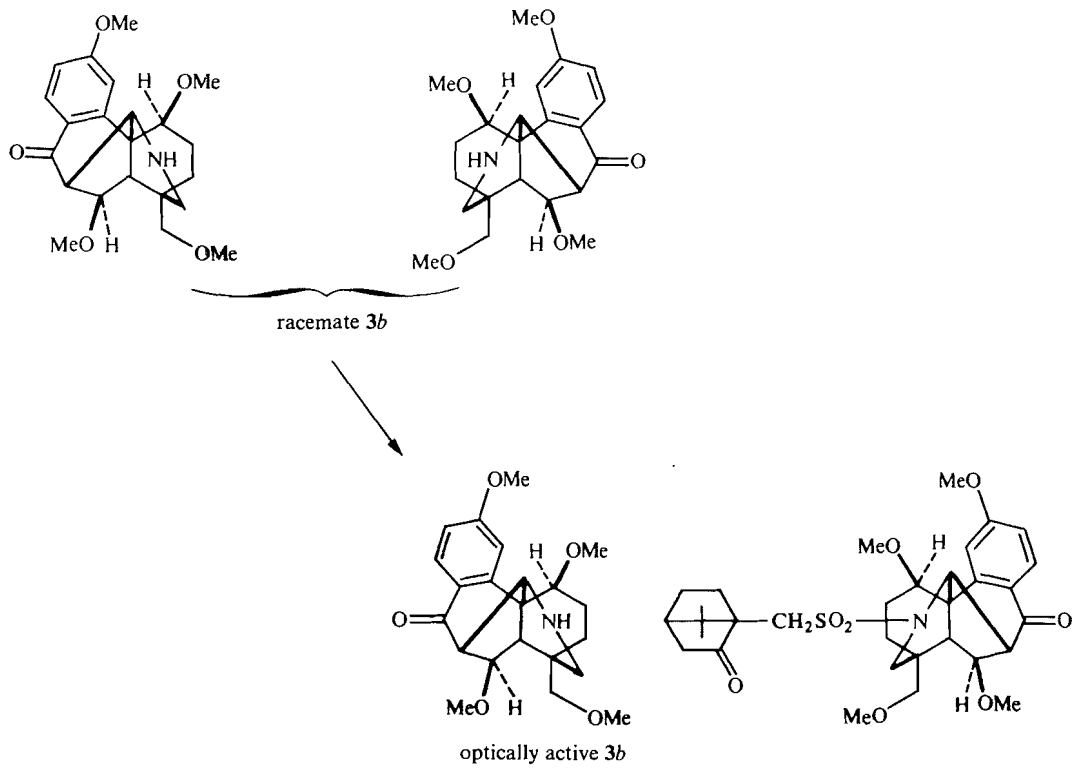

SCHEME 6

felt that we wished to know the configuration of the ring A methoxyl in the synthetic compounds directly and not merely by correlation with a natural derivative. Consequently we have prepared the beautifully crystalline acid oxalate of the *racemate*[5] **3***b* [m.p. 189–192 °C] and submitted it for X-ray crystallography to Dr. Maria Przybylska at the National Research Council of Canada Laboratories, Ottawa, Canada. The structure determination performed by Dr. Karin Bjåmer Birnbaum (12) corroborated all the features of the molecule and revealed the configuration of the ring A methoxyl to be as portrayed in formula **3***b*.

Since we wished to use **3***b* as a relay compound and draw our supplies of this material for the continuation of the synthesis from natural sources it was imperative to resolve the racemate into optical antipodes.

After numerous unsuccessful attempts at resolution by conventional methods, we have noticed that if the racemate was allowed to react with D-camphor–sulfonyl chloride in pyridine, the reaction stopped when approximately 50% of the secondary amine was consumed. Isolation of the unreacted free base yielded material which was optically active and showed an optical rotatory dispersion (o.r.d.) curve antipodal to the o.r.d. recorded for the natural degradation product.

Consequently, we have achieved the preparation of the totally synthetic optically active antipode **3***b* with the natural absolute configuration in the following manner. The racemate **3***b* was dissolved in dry pyridine and treated with 1 mol of L-camphor–sulfonyl chloride at 0 °C. The temperature was allowed to rise to 20 °C and the mixture was kept overnight. The unreacted free base was converted to the acid

[5]The X-ray structure determination of the synthetic *racemate* is also important as an independent verification of the synthesis. Since long laborious total syntheses unlike other work may never be repeated in independent laboratories and since X-ray methods are increasingly fast and effective it seems to the authors that an X-ray of the synthetic *racemate* in a synthesis like the present one should be almost a requirement.

Can. J. Chem. Downloaded from www.nrcresearchpress.com by 210.87.254.42 on 09/05/12
For personal use only.

Can. J. Chem. Downloaded from www.nrcresearchpress.com by 210.87.254.42 on 09/05/12
For personal use only.

oxalate, which was recrystallized to a constant melting point of 195–196 °C. This melting point was identical with the melting point of the "natural" degradation base oxalate and the two products did not show melting point depression. Both materials gave also superimposable i.r. and n.m.r. spectra and o.r.d. curves. The totally synthetic optically active oxalate was decomposed and the synthetic optically active base **3***b* was recrystallized to a melting point of 144.5 °C. This melting point was undepressed by admixture of the "natural" base which had the same melting point. Both materials showed superimposable i.r., n.m.r., and mass spectra and t.l.c. behavior.

Thus, our objective has been fully achieved and a stepping stone created for the synthesis of alkaloids of the delphinine type. It should be pointed out that while compound **3***b* is structurally complex, it is operationally very simple. After suitable blockade of the nitrogen the entire system is solid saturated and unreactive, all except the *p*-methoxy acetophenone group which must be used for building up the CD ring system. Thus, the obstacles in the remaining part of the synthesis are more financial than chemical in nature.

Experimental

Allyl Tetralone **6**

Distilled pyrrolidine (135 ml, 1.65 mol) was added to a stirred solution of 7-methoxy-2-tetralone (164 g, 0.93 mol) in benzene (1500 ml). The solution was refluxed under nitrogen until all the water produced by the reaction had been removed by a Dean Stark trap (3 h). The reaction mixture was then cooled to room temperature and allyl bromide (195 ml, 2.28 mol) was added dropwise. The mixture was refluxed for 17 h, at the end of which, water (2000 ml) was added and the reflux continued for another period of 3 h.

The organic phase was separated, washed with water (3 × 500 ml), dried over anhydrous magnesium sulfate, and taken to dryness *in vacuo*. The crude product (193 g) was distilled *in vacuo* and gave 178 g of the pure allyl tetralone **6** (b.p. 118–120 °C, 0.05 mm Hg); yield 89%.

I.r. (CCl_4): 1715 (C=O); 915 cm^{-1} (C=CH_2).

N.m.r. ($CDCl_3$): multiplet (3H) τ 2.80–3.50 (aromatic protons of the anisole ring); multiplet (3H) 4.20–5.20 (vinylic protons); singlet (3H) 6.28 p.p.m. (methoxyl protons).

Mass spectrum Calcd. for $C_{14}H_{16}O_2$: *m/e*, 216. Found: 216.

Disubstituted Tetralone **7**

The allyl tetralone **6** (66 g, 0.30 mol) was dissolved in dry benzene (500 ml). Sodium hydride (12.6 g, 0.31 mol; 60% suspension in mineral oil) was added and the resulting mixture was stirred under nitrogen at room temperature for 15 h then at 60° for 6 h. The mixture was cooled in an ice-water bath, and benzyloxymethyl chloride (59.4 g, 0.36 mol) in dry benzene (250 ml) was added dropwise. The mixture was then allowed to warm up to room temperature and stirring was continued for 18 h.

After addition of water (250 ml), the organic phase was separated and the aqueous phase was extracted with benzene (3 × 75 ml). The benzene extracts were combined, washed with water (3 × 150 ml), and dried over anhydrous magnesium sulfate. Evaporation of the solvent *in vacuo* gave the crude disubstituted tetralone **7** (112 g). Chromatography on silica gel (3 Kg) in benzene gave the pure compound **7** (67.5 g); yield 68%.

I.r. (CCl_4): 1715 (C=O); 915 cm^{-1} (C=CH_2).

N.m.r. ($CDCl_3$): multiplet (8H) τ 2.81–3.14 (aromatic protons of the anisole ring and the benzyl group); multiplet (3H) 4.50–5.50 (vinylic protons); singlet (2H) 5.70 (benzylic methylene protons); singlet (5H) 6.26 p.p.m. (aromatic methoxyl and the methylene protons deshielded by the benzyloxyl group).

Mass spectrum Calcd. for $C_{22}H_{24}O_3$: *m/e*, 336.1726. Found: 336.1719.

Diols **8**

A solution of compound **7** (51.9 g, 0.17 mol) in tetrahydrofuran (250 ml) was combined with osmic acid (0.25 g, 0.001 mol) in tetrahydrofuran (25 ml) and stirred at room temperature for 10 min. A solution of sodium chlorate (26.6 g, 0.25 mol) in water (250 ml) was added in several portions, and the stirring was continued for 16 h at 60°.

After distilling off most of the tetrahydrofuran under reduced pressure, water (200 ml) was added and the solution was extracted with ether (3 × 150 ml). The combined ether extracts were washed with water (3 × 150 ml), dried over anhydrous magnesium sulfate, and evaporated to dryness *in vacuo* to give the crude diols. The dark viscous product was chromatographed on silica gel (2 Kg). Elution with a 2:8 ether–benzene mixture gave two epimeric diols (A, 22.4 g, m.p. 108–109 °C; B, 23.0 g, m.p. 125–130 °C). Both compounds were recrystallized from benzene; yield 79%.

I.r. of A and B (KBr pellet): 3200–3500 cm^{-1} (hydroxyl); no carbonyl absorption.

N.m.r. ($CDCl_3$): A and B multiplet (8H) τ 2.80–3.50 (aromatic protons); singlet (2H) A, 5.55, B, 5.58 (benzylic methylene protons); singlet (5H) A, 6.26, B, 6.34 p.p.m. (protons deshielded by the benzyloxyl and the aromatic methoxyl protons).

Mass spectrum Calcd. for $C_{22}H_{26}O_5$: *m/e*, 370. Found: 352 ($M^+ - H_2O$).

Anal. Calcd. for $C_{22}H_{26}O_5$: C, 71.33; H, 7.07. Found for Diol A: C, 71.37; H, 7.00. Found for Diol B: C, 71.13; H, 6.86.

Keto Aldehyde **9**

The epimeric diols **8** (46.4 g, 0.14 mol) were dissolved in a 1:1 THF–water mixture (660 ml). Sodium metaperiodate (232 g, 1.08 mol) was added over a period of 15 min and the mixture was stirred at room temperature under nitrogen for 8 h. The resulting white precipitates were filtered off and washed well with ether. Water (300 ml) was added and the filtrate was extracted with ether (5 × 200 ml). The combined ethereal extracts were washed with water (2 × 200 ml) and dried over anhydrous magnesium sulfate. The crude keto-aldehyde **9** (41 g) was obtained after evaporation of the

Can. J. Chem. Downloaded from www.nrcresearchpress.com by 210.87.254.42 on 09/05/12
For personal use only.

solvent *in vacuo*, and was used for the next step without further purification.

I.r. (CCl_4): 2720 (C—H, aldehyde); 1726 (C=O, aldehyde); 1715 cm^{-1} (C=O, ketone).

N.m.r. ($CDCl_3$): singlet (1H) τ 0.49 (aldehydic proton); multiplet (8H) 2.60–3.28 (aromatic protons of the anisole ring and the benzyl group); singlet (2H) 5.62 (benzylic methylene protons); singlet (5H) 6.21 p.p.m. (aromatic methoxyl and methylene protons deshielded by the benzyloxy group).

Hydroxy Ketone ***10***

A solution of the keto-aldehyde **9** (41 g, 0.12 mol) in methanol (3500 ml) was added to sodium hydroxide (5.32 g, 0.13 mol) in water (138 ml). The resulting brown solution was stirred at 55 °C under nitrogen for 30 h. Water (2000 ml) was added and the solution was neutralized with 20% hydrochloric acid. The methanol was partially evaporated *in vacuo* until the mixture just became cloudy. The mixture was extracted with ether (5 × 800 ml) and the combined ethereal extracts were washed with water (2 × 1000 ml), dried over anhydrous magnesium sulfate and evaporated to dryness *in vacuo* to give the crude hydroxy-ketone **10** (34.8 g). This material was purified by chromatography on silica gel (1 kg). Elution with benzene–ether gave the pure hydroxy ketone **10** (28.2 g).

I.r. (CCl_4): 3600, 3475 (O—H); 1755 cm^{-1} (five membered ketone).

N.m.r. ($CDCl_3$): singlet (5H) τ 2.78 (aromatic protons of the benzyl group); multiplet (3H) 3.25–3.50 (aromatic protons of anisole ring); singlet (2H) 5.42 (benzylic methylene protons); quadruplet (1H) centered at 5.70 (proton deshielded by the hydroxyl); singlet (2H) 6.08 (methylene protons deshielded by the benzyloxy group); singlet (3H) 6.31 p.p.m. (aromatic methoxyl protons).

Mass spectrum Calcd. for $C_{21}H_{22}O_4$: *m/e*, 338. Found: 338.

Both compounds **9** and **10** were rather unstable and had to be characterized by a derivative. The crystalline ketal **11** was used for this purpose.

Hydroxy Ketal ***11***

A mixture of the hydroxy ketone **10** (54.1 g, 0.16 mol), ethylene glycol (17.1 g, 0.27 mol), and *p*-toluenesulfonic acid (4.57 g, 0.034 mol) in benzene (1000 ml) was heated under reflux for 2 h using a Dean Stark water separator to remove the water produced by the reaction. The reaction mixture was cooled, washed with water (2 × 200 ml), then with 5% aqueous sodium bicarbonate (3 × 200 ml) and with water (2 × 200 ml). The organic phase was dried over anhydrous magnesium sulfate and evaporated to dryness under reduced pressure. The pure ketal **11** was obtained by crystallization from ether (53.2 g, m.p. 97–99 °C), yield: 88%.

I.r. (KBr pellet): 3600–3200 cm^{-1} (hydroxyl); no carbonyl absorption.

N.m.r. ($CDCl_3$): singlet (5H) τ 2.74 (aromatic protons of the benzyl group); multiplet (3H) 3.25–3.30 (aromatic protons of the anisole ring); singlet (2H) 5.48 (benzylic methylene protons); broad singlet (6H) 6.18 (ketal methylenes and methylene protons deshielded by the benzyloxy group); singlet (3H) 6.43 p.p.m. (aromatic methoxyl).

Mass spectrum Calcd. for $C_{23}H_{26}O_5$: *m/e*, 382. Found: 382.

Anal. Calcd. for $C_{23}H_{26}O_5$: C, 72.23; H, 6.85. Found: C, 72.25; H, 6.83.

Acetoxy Ketal ***12***

The hydroxy-ketal **11** (50 g, 0.13 mol) dissolved in pyridine (100 ml) and acetic anhydride (100 ml) was allowed to stand at room temperature overnight. The solvent was evaporated *in vacuo*, and ether (1000 ml) was added. The ether solution was washed with 10% aqueous sodium bicarbonate (3 × 500 ml), then with water (2 × 300 ml), dried over anhydrous magnesium sulfate, and evaporated to dryness *in vacuo*. The crude product was crystallized from ether to give a quantitative yield of the pure acetoxy-ketal **12** (56 g, m.p. 81–82 °C).

I.r. (KBr pellet): 1725 cm^{-1} (acetoxyl carbonyl).

N.m.r. ($CDCl_3$): singlet (5H) τ 2.68 (aromatic protons of the benzyl group); multiplet (3H) 2.70–3.40 (aromatic protons of the anisole ring); multiplet (1H) centered at 5.15 (proton deshielded by the acetoxyl); broad singlet (6H) 6.07 (ketal methylenes and protons deshielded by the benzyloxyl); singlet (3H) 6.30 (aromatic methoxyl); singlet (3H) 7.95 p.p.m. (acetoxyl methyl protons).

Mass spectrum Calcd. for $C_{25}H_{28}O_6$: *m/e*, 424. Found: 424.

Anal. Calcd. for $C_{25}H_{28}O_6$: C, 70.81; H, 6.66. Found: C, 71.16; H, 6.78.

Acetoxy Alcohol ***13***

The acetoxy-ketal **12** (54.5 g, 0.13 mol) was dissolved in ethanol (2000 ml), 10% palladium-on-charcoal (20 g) was added, and the reaction mixture was hydrogenated (room temperature, 1 atm) for 5 h. The catalyst was filtered off and the solvent evaporated *in vacuo* to yield the acetoxy-alcohol **13** (41.3 g, 96%) which was homogeneous on t.l.c.

I.r. ($CHCl_3$): 3550 (hydroxyl); 1726 cm^{-1} (acetoxyl carbonyl).

N.m.r. ($CDCl_3$): multiplet (3H) τ 2.90–3.45 (aromatic protons of the anisole ring); quadruplet (1H) centered at 5.17 (proton deshielded by the acetoxyl); multiplet (4H) centered at 5.95 (ketal methylenes); singlet (5H) 6.27 (aromatic methoxyl and methylene protons deshielded by the primary hydroxyl); singlet (3H) 7.95 p.p.m. (acetoxy methyl protons).

Mass spectrum Calcd. for $C_{18}H_{22}O_6$: *m/e*, 334.1430. Found: 334.1426.

Tetrahydropyranyl Acetate ***14***

The acetoxy alcohol **13** (40 g, 0.12 mol) was dissolved in dry chloroform (2000 ml). Dihydropyran (25.5 g, 0.3 mol) and one drop of concentrated hydrochloric acid were added. The solution was stirred at room temperature for 18 h. The mixture was then washed with 10% aqueous sodium bicarbonate (2 × 500 ml), and with water (3 × 500 ml), dried over anhydrous magnesium sulfate, and finally, evaporated to dryness *in vacuo*. The crude product (60 g) was chromatographed on silica gel (1200 g). Elution with 4% ether in benzene gave the pure tetrahydropyranyl acetate **14** (43.3 g, 86%).

I.r. ($CHCl_3$): no hydroxyl absorption; 1725 cm^{-1} (acetoxyl carbonyl).

N.m.r. ($CDCl_3$): multiplet (3H) τ 2.80–3.45 (aromatic protons of the anisole ring); multiplet (4H) centered at 6.05 (ketal methylenes); singlet (5H) 6.24 (aromatic methoxyl and methylene protons deshielded by the primary oxygen),

Can. J. Chem. Downloaded from www.nrcresearchpress.com by 210.87.254.42 on 09/05/12
For personal use only.

singlet (3H) 7.92 (acetoxy methyl protons), broad singlet (6H) 8.33 p.p.m. (methylene protons of the tetrahydropyran ring).

Mass spectrum Calcd. for $C_{23}H_{30}O_7$: *m/e*, 418. Found: 418.

Tetrahydropyranyl Alcohol **15**

The tetrahydropyranyl acetate **14** (42.2 g, 0.10 mol) was dissolved in dry ether (2000 ml). Lithium aluminum hydride (3.95 g, 0.10 mol) was added and the resulting suspension was stirred at room temperature for 1 h. The reaction mixture was poured into wet ether (2000 ml) and a few drops of water were added. The solid material was filtered off and the filtrate was dried over anhydrous magnesium sulfate and evaporated to dryness. The crude product was chromatographed on silica gel (1.5 kg). The pure tetrahydropyranyl alcohol **15** (38.3 g, 98%) was eluted with 10% ether in benzene.

I.r. ($CHCl_3$): 3500 cm^{-1} (hydroxyl); no carbonyl absorption.

N.m.r. ($CDCl_3$): multiplet (3H) τ 2.80–3.50 (aromatic protons of the anisole ring); broad singlet (1H) 5.30 (proton deshielded by the hydroxyl); multiplet (4H) centered at 6.00 (ketal methylenes); singlet (3H) 6.24 (aromatic methoxyl); broad singlet (6H) 8.33 p.p.m. (methylene protons of the tetrahydropyran ring).

Mass spectrum Calcd. for $C_{21}H_{28}O_6$: *m/e*, 376.1885. Found: 376.1882.

Tetrahydropyranyl Benzyl Ketal **16**

The tetrahydropyranyl alcohol **15** (37.6 g, 0.10 mol) was dissolved in absolute dioxane (1000 ml); sodium hydride (6.5 g, 0.15 mol, 56% suspension in mineral oil) and benzyl chloride (25.6 g, 0.15 mol) were added and the mixture was heated at reflux for 18 h. The suspension was then cooled to room temperature and filtered through Celite. The filtrate was partially evaporated (about 100 ml remained), water (200 ml) was added, and the solution was extracted with chloroform (4 × 300 ml). The chloroform extracts were washed with water (3 × 200 ml), dried over anhydrous sodium sulfate, and evaporated to dryness. The crude product was chromatographed on silica gel (1.5 kg). Elution with 2% ether in benzene gave the pure benzyl derivative **16** (37.5 g, 81%).

I.r. ($CHCl_3$): no hydroxyl absorption.

N.m.r. ($CDCl_3$): singlet (5H) τ 2.64 (aromatic protons of the benzyl group); multiplet (3H) 2.70–3.50 (aromatic protons of the anisole ring); multiplet (4H) centered at 6.00 (ketal methylenes); singlet (3H) 6.22 (aromatic methoxyl); broad singlet (6H) 8.32 p.p.m. (methylene protons of the tetrahydropyran ring).

Mass spectrum Calcd. for $C_{28}H_{34}O_6$: *m/e*, 466. Found: 466.

Hydroxy Ketal **17**

The benzyloxy compound **16** (46.6 g, 0.1 mol) was dissolved in a mixture of concentrated hydrochloric acid and methanol (1:99, 500 ml) and stirred at room temperature for 1 h. After neutralization with 5% aqueous sodium bicarbonate, the methanol was partially evaporated *in vacuo*, water (500 ml) was added, and the solution was extracted with chloroform (3 × 500 ml). The organic phase was washed with water (2 × 300 ml), dried over anhydrous sodium sulfate, and evaporated to dryness *in vacuo*. The crude alcohol was purified by chromatography on silica gel (1.5 kg). Elution with 15% ether in benzene gave the pure hydroxy ketal **17** (34.4 g, 90%).

I.r. (CCl_4): 3550 cm^{-1} (hydroxyl).

N.m.r. ($CDCl_3$): singlet (5H) τ 2.64 (aromatic protons of the benzyl group); multiplet (3H) 2.90–3.40 (aromatic protons of the anisole ring); singlet (2H) 5.50 (benzylic methylene protons); multiplet (4H) centered at 5.90 (ketal methylene protons); singlet (3H) 6.21 p.p.m. (aromatic methoxyl).

Mass spectrum Calcd. for $C_{23}H_{26}O_5$: *m/e*, 382.1780. Found: 382.1772.

Aldehyde **18**

A solution of the primary alcohol **17** (12 g, 0.03 mol) in dry dichloromethane (100 ml) was added in 1 min to a solution of chromium trioxide–pyridine complex (50.4 g) in dichloromethane (1000 ml). The resulting mixture was stirred at room temperature for 10 min. Ether (2000 ml) was added, the solid material was filtered off, and the filtrate was evaporated *in vacuo*. The crude product was chromatographed on silica gel (800 g). Elution with 5% ether in benzene gave the pure aldehyde **18** (12.7 g, 85%).

I.r. (CCl_4): 2720 and 1725 cm^{-1} (aldehyde), no hydroxyl absorption.

N.m.r. ($CDCl_3$): singlet (1H) τ 0.17 (aldehydic proton); doublet (5H) centered at 2.67 (aromatic protons of the benzyl group); multiplet (3H) 2.70–3.80 (aromatic protons of the anisole ring); singlet (2H) 5.50 (benzylic methylene protons); multiplet (4H) centered at 6.00 (ketal methylene protons), singlet (3H) 6.30 p.p.m. (aromatic methoxyl).

Mass spectrum Calcd. for $C_{23}H_{24}O_5$: *m/e*, 380.1619. Found: 380.1623.

1-Methoxy-2-benzyloxy-3-cyano Propane **19**

Benzyl alcohol (300 g, 2.78 mol) and sodium (3.5 g, 0.155 mol) were stirred at room temperature until all the sodium was dissolved and then 1-methoxy-3-cyano-2-propene (8) (150 g, 1.55 mol) was added dropwise. The solution was stirred for a week at room temperature. After neutralization with acetic acid, ether (100 ml) and water (100 ml) were added and the mixture was extracted into ether (3 × 200 ml). The organic layer was washed with water (3 × 200 ml), dried over anhydrous magnesium sulfate, and finally the ether was evaporated *in vacuo*. The crude compound was distilled to give pure 1-methoxy-2-benzyloxy-3-cyano propane (102 g, b.p. 115–120 °C/0.3 mm Hg); yield: 32%.

I.r. (CCl_4) 2240 cm^{-1} (nitrile).

N.m.r. ($CDCl_3$): singlet (5H) τ 2.90 (aromatic protons of the benzyl group); singlet (2H) 5.39 (benzylic methylene protons); multiplet (1H) centered at 6.05 (proton deshielded by the benzyloxyl); doublet (2H) centered at 6.56 (protons deshielded by the methoxyl); singlet (3H) 6.65 (—OCH_3); doublet (2H) centered at 7.44 p.p.m. (C_3 methylene protons).

Mass spectrum Calcd. for $C_{12}H_{15}O_2N$: *m/e*, 205.1103. Found: 205.1102.

1-Methoxy-2-benzyloxy-3-carbomethoxy Propane **20**

A solution of 1-methoxy-2-benzyloxy-3-cyano propane (36 g, 0.175 mol) in methanol (1000 ml) and sulfuric acid (100 ml) was heated under reflux for 50 h. The excess of methanol was then evaporated *in vacuo*. The reaction mixture was poured into water (500 ml) and the product was extracted into ether (3 × 500 ml). The ethereal layer was

Can. J. Chem. Downloaded from www.nrcresearchpress.com by 210.87.254.42 on 09/05/12
For personal use only.

washed with 5% sodium carbonate in water (3 × 200 ml), then with water (3 × 500 ml), and dried over anhydrous magnesium sulfate. After evaporation of the ether *in vacuo*, the crude ester was purified by distillation (29.5 g, 71.5%, b.p. 115–125 °C/0.01 mm Hg).

I.r. ($CHCl_3$): 1735 cm^{-1} (ester carbonyl).

N.m.r. ($CDCl_3$): doublet (5H) centered at τ 2.80 (aromatic protons of the benzyl group); singlet (2H) 5.40 (benzylic methylene protons); multiplet (1H) centered at 6.00 (proton deshielded by the benzyloxyl); singlet (3H) 6.37 (carbomethoxy methyl protons); doublet (2H) centered at 6.57 (protons deshielded by the methoxyl); singlet (3H) 6.70 (—OCH_3); doublet (2H) centered at 7.65 p.p.m. (C_3 protons).

Mass spectrum Calcd. for $C_{13}H_{18}O_4$: *m/e*, 238. Found: 238.

1-Methoxy-2-benzyloxy-4-hydroxybutane **21**

A suspension of lithium aluminum hydride (953 mg, 0.025 mol) in dry ether (200 ml) was stirred in an ice-water bath for 10 min. A solution of the ester **20** (5.0 g, 0.021 mol) in dry ether (80 ml) was added slowly and the reaction was stirred for 1.5 h at room temperature. The reaction mixture was then poured into wet ether (500 ml), the solid material was filtered off, the filtrate was dried over anhydrous magnesium sulfate, and finally, the solvent was evaporated *in vacuo*. The crude alcohol (5.0 g) was purified by chromatography on silica gel (200 g). Elution with 10–20% ether in benzene gave pure 1-methoxy-2-benzyloxy-4-hydroxybutane (2.0 g); yield 68%.

For large scale preparations, distillation was used as a purification method. The alcohol distilled at 120–125 °C/1 mm Hg.

I.r. ($CHCl_3$): 3600 cm^{-1} (OH); no carbonyl absorption.

N.m.r. ($CDCl_3$): singlet (5H) τ 2.65 (aromatic protons of the benzyl group); doublet (2H) centered at 5.37 (benzylic methylene protons); triplet (2H) centered at 6.28 (protons deshielded by the hydroxyl); doublet (2H) centered at 6.59 (protons deshielded by the methoxyl); singlet (3H) 6.70 (—OCH_3); broad singlet (1H) 7.24 (OH); quadruplet (2H) centered about 8.22 p.p.m. (C_3 methylene protons).

Mass spectrum Calcd. for $C_{12}H_{18}O_3$: *m/e*, 210.2156. Found: 210.2157.

1-Methoxy-2-benzyloxy-4-bromobutane **22**

The alcohol **21** (30.0 g, 0.143 mol) was dissolved in dry pyridine (30 ml) and the solution was stirred in an ice-water bath for 30 min, after which *p*-toluenesulfonyl chloride (32.8 g, 0.172 mol) was added and stirring was continued with cooling for 3 h. The reaction mixture was then poured into ice water (150 ml) and the product was extracted into ether (3 × 200 ml). The combined ethereal layers were washed with water (5 × 200 ml), dried over anhydrous magnesium sulfate, and finally the ether was evaporated *in vacuo* giving 1-methoxy-2-benzyloxy-4-tosyloxybutane (45.2 g) which was homogeneous on t.l.c.; yield: 87%.

I.r. ($CHCl_3$): 1364, 1179 cm^{-1}, no hydroxyl absorption.

N.m.r. ($CDCl_3$): two doublets (2H each) centered at τ, 2.23 and 2.76 (aromatic protons of the tosyl group; singlet (5H) 2.74 (aromatic protons of the benzyl group); doublet (2H) centered at 5.55 (benzylic methylene protons); triplet (2H) centered at 5.89 (protons deshielded by the tosyloxyl); multiplet (1H) centered at 6.42 (proton deshielded by the benzyloxyl); doublet (2H) centered at 6.65 (protons deshielded by the methoxyl); singlet (3H) 6.71 (—OCH_3); singlet (3H) 7.62 (tosyl methyl protons); quadruplet (2H) centered about 8.12 p.p.m. (C_3 methylene protons).

The tosylate (43.2 g, 0.124 mol) was dissolved in acetone (750 ml, distilled over potassium permanganate) and lithium bromide (43.0 g, 0.476 mol) was added. The resulting solution was heated under reflux for 3 h. The reaction mixture was cooled, excess acetone was evaporated, and water (1500 ml) was added. After extraction into ether (3 × 500 ml) the combined ethereal layers were washed with water (3 × 500 ml), and dried over anhydrous magnesium sulfate. Evaporation of the ether *in vacuo* gave the crude bromide (34 g) which was purified by chromatography on silica gel (1200 g). Elution with benzene gave 1-methoxy-2-benzyloxy-4-bromobutane **22** (33 g, 83.5%).

N.m.r. ($CDCl_3$): singlet (5H) τ 2.67 (aromatic protons of the benzyl group); doublet (2H) centered at 5.38 (benzylic methylene protons); multiplet (1H) 6.21 (proton deshielded by the benzyloxyl); doublet (2H) centered at 6.53 (protons deshielded by bromine); doublet (2H) centered at 6.58 (protons deshielded by the methoxyl); singlet (3H) 6.65 (—OCH_3); quadruplet (2H) centered at 7.95 p.p.m. (C_3 methylene protons).

Mass spectrum Calcd. for $C_{12}H_{17}O_2Br$: *m/e*, 272, 274. Found: 272, 274.

High resolution mass spectrum Calcd. for $C_{12}H_{17}O_2Br$ (lower isotope): *m/e*, 272.0412. Found: 272.0411.

Grignard Alcohol **23**

To a mixture of fine magnesium turnings (8.55 g, 0.35 mol) and a small grain of iodine in absolute tetrahydrofuran (700 ml), one third of a solution of 1-methoxy-2-benzyloxy-4-bromobutane **22** (95.5 g, 0.35 mol) in absolute tetrahydrofuran (700 ml) was introduced and the mixture was refluxed at 70° (bath temperature) under nitrogen. As soon as the color of the iodine had disappeared the remaining solution was added dropwise. The reaction mixture was then heated to 70 °C for 4 h, at the end of which most of the magnesium was dissolved and the mixture was cooled to room temperature. The benzyloxy-aldehyde **18** (22.8 g, 0.06 mol) in absolute tetrahydrofuran (180 ml) was added dropwise and the solution was stirred overnight.

The reaction mixture was poured into a saturated ammonium chloride solution (1000 ml) and extracted with chloroform (5 × 500 ml). The chloroform extract was washed with water (3 × 500 ml) and dried over anhydrous sodium sulfate. The solvent was evaporated *in vacuo* and the crude product was chromatographed on silica gel (1.2 kg). Elution with a 2:8 ether–benzene mixture gave the pure Grignard alcohol **23** (31.3 g, 91%).

I.r. (CCl_4): 3510 cm^{-1} (hydroxyl); no carbonyl absorption.

N.m.r. ($CDCl_3$): singlet (10H) τ 2.68 (aromatic protons on two benzyl groups); two singlets (2H each) 5.38 and 5.52 (methylene protons of two benzyl groups); multiplet (4H) centered at 6.00 (ketal methylene protons), and two singlets (3H each) 6.31 and 6.66 p.p.m. (two methoxyls).

Mass spectrum Calcd. for $C_{35}H_{42}O_7$: *m/e*, 574.2933. Found: 574.2944.

Methylation **23** → **26a**

Sodium hydride (13 g, 50% oil suspension (0.26 mol)) was added to the alcohol **23** (27.2 g, 0.047 mol) in absolute dioxane (1500 ml) and the solution was refluxed for 3 h. After cooling to room temperature, excess methyl iodide

Can. J. Chem. Downloaded from www.nrcresearchpress.com by 210.87.254.42 on 09/05/12
For personal use only.

(100 ml) was added and the solution was stirred at room temperature for 1 h and then refluxed for 5 h. The solution was filtered, the filtrate was washed with water (3 × 600 ml), dried over anhydrous sodium sulfate, and evaporated to dryness. The crude product (28.9 g) was chromatographed on silica gel. Elution with 15% ether in benzene gave the pure methylation product **26***a* (25.4 g, 92%).

I.r. (CCl_4): no hydroxyl absorption.

N.m.r. ($CDCl_3$): singlet (10H) τ 2.68 (aromatic protons of the two benzyl groups); multiplet (3H) 3.0–3.50 (aromatic protons of the anisole ring); two singlets (2H each) 5.37 and 5.50 (protons of two benzylic methylene groups); multiplet (4H) centered at 6.00 (ketal methylene protons); three singlets (3H each) 6.27, 6.59, and 6.62 (three methoxyls); singlet (2H) 6.50 p.p.m. (methylene protons deshielded by the primary side chain methoxyl).

Mass spectrum Calcd. for $C_{36}H_{44}O_7$: *m/e*, 588.3075. Found: 588.3087.

Ketone **27***a*

Compound **26***a* (25.4 g, 0.043 mol) was dissolved in 75% aqueous acetic acid (850 ml) and heated under reflux for 18 h. The acetic acid was evaporated *in vacuo* and chloroform (500 ml) was added. The solution was washed with 10% sodium bicarbonate (3 × 300 ml) and with water (2 × 300 ml), dried over anhydrous sodium sulfate, and evaporated to dryness. The ketone **27***a* (23 g) which was homogeneous on t.l.c. was obtained in quantitative yield.

I.r. (CCl_4): 1755 cm^{-1} (five-membered ketone).

N.m.r. ($CDCl_3$): two singlets (5H each) τ 2.68 and 2.70 (aromatic protons of the two benzyl groups); two singlets (2H each) 5.40 and 5.52 (benzylic methylene protons); three singlets (3H each) 6.27, 6.49, 6.67 p.p.m. (three methoxyls).

Mass spectrum Calcd. for $C_{34}H_{40}O_6$: *m/e*, 544.2824. Found: 544.2818.

Conversion of **27***a to the Diketone* **29***a*

The ketone **27***a* (23 g, 0.042 mol) was dissolved in methanol (90 ml) and cooled in a methanol – Dry Ice bath. Raney nickel (9.5 g) and liquid ammonia (125 ml) were added. The mixture was hydrogenated (165 °C, 4000 p.s.i. H_2) for 10 h. The catalyst was removed by filtration through Celite and washed thoroughly with methanol. The filtrate was evaporated to dryness and yielded the amine **28***a* (20.5 g, 90%) which was used without purification for the subsequent step.

I.r. (CCl_4): 3400 cm^{-1} (N—H), no carbonyl band.

N.m.r. ($CDCl_3$): two singlets (5H each) τ 2.70 and 2.77 (aromatic protons of the two benzyl groups); multiplet (3H) 3.0–3.40 (aromatic protons of the anisole ring); doublet (2H) centered at 5.42 (benzylic methylene protons); singlet (2H) 5.60 (benzylic methylene protons); three singlets (3H each) 6.30, 6.51, and 6.67 p.p.m. (three methoxyl).

Mass spectrum Calcd. for $C_{34}H_{43}O_5N$: *m/e*, 545.3141. Found: 545.3128.

The amine **28***a* (20 g, 0.036 mol) was dissolved in pyridine (60 ml) and acetic anhydride (60 ml). The mixture was allowed to remain at room temperature for 10 h. The pyridine and acetic anhydride were evaporated in high vacuum, chloroform (200 ml) was added, and the solution was washed with 5% aqueous sodium bicarbonate (3 × 150 ml), water (2 × 150 ml), dried over anhydrous sodium sulfate, and evaporated to dryness. The product (20 g, 95%) was homogeneous on t.l.c. and was used without further purification.

I.r. (CCl_4): 3395 (N—H); 1670 cm^{-1} (acetyl amino carbonyl).

N.m.r. ($CDCl_3$): multiplet (13H) τ 2.70–3.42 (aromatic protons of the two benzyl groups and the anisole ring); doublet centered at 5.74 (apex proton of *anti*-epimer); multiplet centered at 5.24 (apex proton of *syn*-epimer); singlet 8.05 (N—CO—CH_3, *anti*), singlet 8.24 p.p.m. (N—CO—CH_3, *syn*).

The above material (20 g, 0.034 mol) was dissolved in ethanol (1000 ml) and 10% palladium-on-charcoal (10 g) was added. The mixture was hydrogenated (1 atm H_2; room temperature) for 16 h. The catalyst was removed by filtration through Celite and washed thoroughly with ethanol. The ethanol was evaporated *in vacuo* and the crude diol (14 g), was purified by chromatography on silica gel (800 g). Elution with 2% methanol in chloroform yielded the pure material (12.5 g, 90%).

I.r. (CCl_4): 3645, 3435, and 3390 (O—H, N—H); 1660 cm^{-1} (acetylamino carbonyl).

Mass spectrum Calcd. for $C_{22}H_{33}O_6N$: *m/e*, 407.2308. Found: 407.2304.

The above material (12.25 g, 0.03 mol) in dry dichloromethane (100 ml) was added over 1 min to a stirred solution of the chromium trioxide – pyridine complex (100.8 g) in dry dichloromethane (2000 ml). The resulting mixture was stirred at room temperature for 20 min. It was then poured into ether (2000 ml) and the precipitate was removed by filtration. The filtrate was evaporated to dryness in high vacuum and the crude product was purified by chromatography on silica gel (1 kg). Elution with 2% methanol in chloroform gave the pure diketone **29***a*. After crystallization from ether the compound melted at 154–156 °C (7.85 g, 65%).

I.r. (KBr pellet): 3390 (N—H); 1740 (five-membered ketone); 1721 (ketone); 1666 cm^{-1} (*N*-acetyl).

N.m.r. ($CDCl_3$): multiplet (3H) τ, 2.9–3.36 (aromatic protons of the anisole ring); doublet (1H) 5.70 (apex proton); singlet (2H) 5.99 (—CO—CH_2—OCH_3); three singlets (3H each) 6.15 (aromatic methoxyl), 6.42 (side chain methoxyl at C_1), 6.57 (primary methoxyl); singlet (3H) 8.03 p.p.m. (N—CO—CH_3).

Mass spectrum Calcd. for $C_{22}H_{29}O_6N$: *m/e*, 403.1995. Found: 403.1995.

Anal. Calcd. for $C_{22}H_{29}O_6N$: C, 65.49; H, 7.24; N, 3.47. Found: C, 65.46; H, 6.82; N, 3.37.

Lactamol **30***a*

The diketone **29***a* (4.44 g, 0.011 mol) was dissolved in ethanol (520 ml). Potassium cyanide (3.7 g, 0.056 mol) in water (120 ml) was added and the mixture was heated under reflux for 6 h. Most of the ethanol was then evaporated *in vacuo* and water (100 ml) was added. The mixture was extracted with chloroform (5 × 100 ml), and the combined chloroform extracts were washed with water (2 × 100 ml), dried over anhydrous magnesium sulfate, and evaporated to dryness. The crude product (4.6 g) was crystallized from methanol and gave the pure lactamol **30***a* (4.04 g, 85.5%), m.p. 246.5 °C.

I.r. (KBr pellet): 3450 (hydroxyl), 3345 (acetylamino N—H), 3280 (lactamol N—H), 1700 (five-membered lactam), 1675 cm^{-1} (N—CO—CH_3).

N.m.r. ($CDCl_3$): multiplet (3H) τ 2.87–3.40 (aromatic protons of the anisole ring); singlet (3H) 6.22 (aromatic

Can. J. Chem. Downloaded from www.nrcresearchpress.com by 210.87.254.42 on 09/05/12
For personal use only.

methoxyl); singlet (8H) 6.7 (two methoxyls and the protons deshielded by the primary methoxyl); singlet (3H) 8.03 p.p.m. (N—CO—CH_3).

Mass spectrum Calcd. for $C_{23}H_{30}O_6N_2$: *m/e*, 430.2104. Found: 430.2104.

Anal. Calcd. for $C_{23}H_{30}O_6N_2$: C, 64.15; H, 7.02; N, 6.50. Found: C, 64.08; H, 6.82; N, 6.82.

Ketolactam 31a

The crystalline lactamol **30***a* (3.5 g, 0.008 mol) was dissolved in a 1:1 concentrated hydrochloric acid–methanol mixture (200 ml) and the solution was heated under reflux for 24 h. After cooling to room temperature, water (100 ml) was added and the methanol was evaporated *in vacuo*. The aqueous solution was extracted with chloroform (5 × 50 ml), and the chloroform extract was washed with 10% aqueous hydrochloric acid (2 × 50 ml) and with water (2 × 100 ml). The organic phase was dried over anhydrous sodium sulfate and evaporated to dryness. The crude product **31***a* crystallized from a chloroform–ether mixture was recrystallized from methanol to a constant melting point of 244–248 °C (463 mg). The mother liquor and the aqueous phase were evaporated to dryness and dissolved in methanol–HCl for further reaction under exactly the same conditions. The yield was 846 mg of **31***a* in the first re-run and 470 mg in the second. The overall conversion into the ketolactam in three successive runs was 1.78 g (60%).

I.r. (KBr pellet): 3190, 3084 (lactam N—H), 1745 (five-membered ketone), 1665 cm^{-1} (six-membered lactam).

N.m.r. ($CDCl_3$): three singlets (3H each) τ 6.24 (aromatic methoxyl), 6.70 (ring A methoxyl), 6.80 (primary methoxyl), singlet (2H) 6.67 p.p.m. (methylenic protons deshielded by primary methoxyl).

Mass spectrum Calcd. for $C_{21}H_{25}O_5N$: *m/e*, 371.1733. Found: 371.1732.

Anal. Calcd. for $C_{21}H_{25}O_5N$: C, 67.92; H, 6.78; N, 3.71. Found: C, 67.72; H, 6.67; N, 3.89.

Hydroxy Amines 32a and 33a

Lithium aluminum hydride (380 mg, 10 mmol) was added to the keto lactam **31***a* (371 mg, 1 mmol) dissolved in dry dioxane (50 ml). After stirring at room temperature for 15 min, the solution was heated under reflux for 3 h. The reaction mixture was cooled, poured into wet ether (300 ml), and a few drops of water were added. The precipitate was removed by filtration and the filtrate was evaporated to dryness. The product was a mixture of the α-hydroxy amine **33***a* and the β-hydroxy amine **32***a*. The two compounds were separated and purified by preparative t.l.c. on neutral alumina, with 10% methanol in chloroform as solvent. The pure α-hydroxy amine **33***a* (157 mg, crystallized from ether–chloroform, m.p. 155–156 °C) and the β-hydroxy amine **32***a* (145 mg, crystallized from methanol, m.p. 196–198 °C) were obtained in an 84% yield.

I.r. (KBr pellet) α-hydroxy amine **33***a*: 3580, 3375, 3160 (N—H, O—H), 1575 cm^{-1} (N—H bending); β-hydroxy amine **32***a*: 3600, 3390, and 3140 (N—H, O—H), 1565 cm^{-1} (N—H bending).

N.m.r. ($CDCl_3$) α-hydroxy amine **33***a*: singlet (3H) τ 6.20 (aromatic methoxyl), singlet (3H) 6.67 (ring A methoxyl at C_1), singlet (2H) 6.84 (protons deshielded by the primary methoxyl), singlet (3H) 6.93 p.p.m. (primary methoxyl); β-hydroxy amine **32***a*: singlet (3H) τ 6.22 (aromatic methoxyl), singlet (5H) 6.68 (ring A methoxyl at C_1 and the protons deshielded by the primary methoxyl), singlet (3H) 6.90 p.p.m. (primary methoxyl).

Mass spectrum Calcd. for $C_{21}H_{29}O_4N$: *m/e*, 359.2097. Found for **32***a*: 359.2090.

Anal. Calcd. for $C_{21}H_{29}O_4N$: C, 70.18; H, 8.13; N, 3.90. Found for **33***a*: C, 70.11; H, 8.08; N, 3.86. Found for **32***a*: C, 70.15; H, 8.08; N, 3.91.

The N-Acetyl Alcohol 35a

The β-hydroxy amine **32***a* (143.6 mg, 0.4 mmol) was dissolved in pyridine (1 ml) and acetic anhydride (1 ml) and the resulting mixture was allowed to stand at room temperature for 24 h. The pyridine and acetic anhydride were evaporated in high vacuum and the residue was dried at 60 °C in high vacuum for 5 h. The *N,O*-diacetyl derivative was obtained in a quantitative yield (175 mg) and it was homogeneous on t.l.c.

I.r. (CCl_4): 1745 (ester), 1645 cm^{-1} (amide).

N.m.r. ($CDCl_3$): multiplet (3H) τ 2.20–3.34 (aromatic protons of the anisole ring), singlet (3H) 6.20 (aromatic methoxyl), doublet (6H) 6.67, 6.70 (ring A methoxyl and the primary methoxyl), singlet (2H) 6.78 (protons deshielded by the primary methoxyl), singlet (3H) 7.84 (N—CO—CH_3), singlet (3H) 7.92 p.p.m. (O—CO—CH_3).

The *N,O*-diacetate (145 mg, 0.35 mmol) was dissolved in 5 ml of methanol and 5 ml of 0.2 *N* aqueous potassium hydroxide were added. The reaction mixture was heated to 50 °C for 2 h. The mixture was then cooled, extracted with chloroform (4 × 10 ml), the chloroform extracts were washed with water (2 × 10 ml), dried over anhydrous magnesium sulfate, and evaporated to dryness *in vacuo*. Compound **35***a* (130.5 mg, 93%) was recrystallized from ether–chloroform to a m.p. 229–231 °C.

I.r. (CCl_4): 3615, 3400 (O—H), 1640 cm^{-1} (amide).

N.m.r. ($CDCl_3$): singlet (3H) τ 6.20 (aromatic methoxyl); singlet (6H) 6.67 (ring A methoxyl and the primary methoxyl); singlet (2H) 6.78 (protons deshielded by the primary methoxyl); singlet (3H) 7.87 p.p.m. (N—CO—CH_3).

Mass spectrum Calcd. for $C_{23}H_{31}O_5N$: *m/e*, 401.2202. Found: 401.2196.

Compound 36a

A solution of compound **35***a* (125 mg, 0.31 mmol) and sodium hydride (89.68 mg, 1.86 mmol, 50% mineral oil suspension) in absolute dioxane was heated under reflux for 1 h. The reaction mixture was cooled, methyl iodide (1.5 ml) was added and the mixture was refluxed for another 3 h. The solution was cooled again, the precipitate was removed by filtration through Celite and the filtrate was evaporated to dryness. The crude product was purified by preparative t.l.c. on silica gel (5% methanol in chloroform). The pure compound **36***a* (110 mg, 85%) was crystallized from ether, m.p. 137–139 °C.

I.r. (CCl_4): 1650 cm^{-1} (amide), no hydroxyl absorption.

N.m.r. ($CDCl_3$): singlet (3H) τ 6.21 (aromatic methoxyl), doublet (9H) 6.68, 6.73 (ring A methoxyl, primary methoxyl and ring B methoxyl), singlet (2H) 6.76 (protons deshielded by the primary methoxyl), singlet (3H) 7.86 p.p.m. (N—CO—CH_3).

Mass spectrum Calcd. for $C_{24}H_{33}O_5N$: *m/e*, 415.2359. Found: 415.2351.

Anal. Calcd. for $C_{24}H_{33}O_5N$: C, 69.37; H, 8.01; N, 3.37. Found: C, 69.09; H, 7.83; N, 3.20.

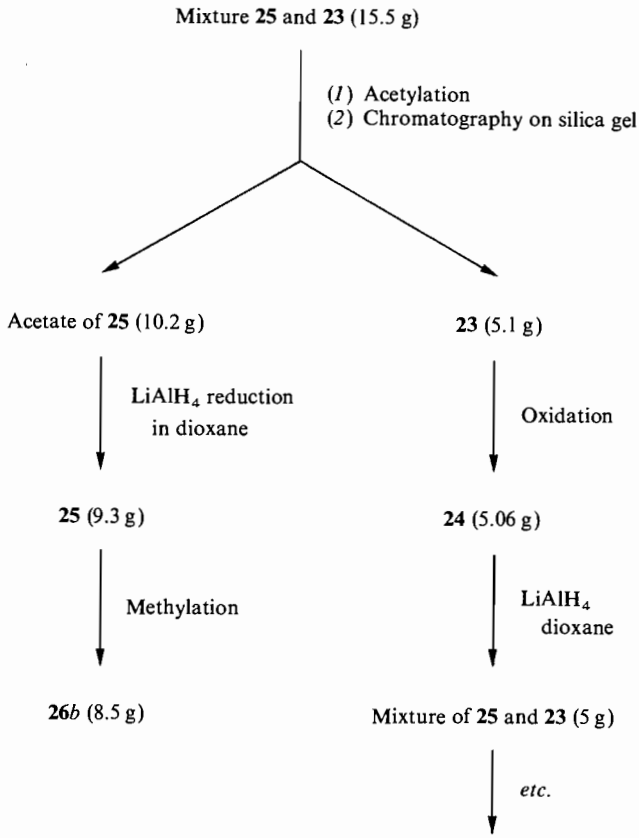

SCHEME 7

Compound 4a

Compound **36***a* (100 mg, 0.24 mmol) was dissolved in acetone (30 ml, distilled over $KMnO_4$) and Jones' reagent was added dropwise to the solution over a period of 6 h. Methanol (1.6 ml) was then added, the mixture was neutralized with 10% aqueous sodium bicarbonate and filtered. The filtrate was partially evaporated, saturated aqueous sodium chloride (15 ml) was added, and the aqueous solution was extracted with chloroform (4 × 15 ml). The chloroform extracts were dried over anhydrous sodium sulfate and evaporated to dryness. The crude product was purified by preparative t.l.c. on silica gel (5% methanol in chloroform). The pure *N*-acetyl ketone **4***a* (86.5 mg, 84%) was crystallized from ether to a m.p. 174–177 °C.

I.r. (CCl_4): 1690 (conjugated ketone), 1655 cm^{-1} (amide).

N.m.r. ($CDCl_3$): doublet (1H) τ 2.05 (aromatic proton deshielded by the benzylic ketone), multiplet (2H) 2.66–3.06 (aromatic protons), singlet (3H) 6.13 (aromatic methoxyl), doublet (11H) 6.68, 6.73 (three methoxyls and methylene protons deshielded by the primary methoxyl), singlet (3H) 7.90 p.p.m. (N—CO—CH_3).

Mass spectrum Calcd. for $C_{24}H_{31}O_6N$: *m/e*, 429.2151. Found: 429.2141.

Anal. Calcd. for $C_{24}H_{31}O_6N$: C, 67.11; H, 7.28; N, 3.26. Found: C, 66.97; H, 7.23; N, 3.68.

Ketone 24

The Grignard alcohol **23** (30 g, 0.052 mol) dissolved in acetone (1.5 l, distilled over potassium permanganate) was cooled in an ice bath. Jones' reagent (18 ml) was added dropwise over a period of 15 min. After 10 min stirring, methanol (10 ml) was added to destroy the excess of Jones' reagent. The inorganic precipitate was removed by filtration and the filtrate was neutralized with 10% aqueous sodium bicarbonate. Most of the acetone was evaporated under reduced pressure, water (500 ml) was added, and the solution was extracted with chloroform (4 × 400 ml). The chloroform extracts were washed with water (2 × 400 ml), dried over anhydrous sodium sulfate, and evaporated to dryness *in vacuo*. The ketone **24** (28 g, 94%) was homogeneous on t.l.c.

I.r. ($CHCl_3$): 1700 cm^{-1} (C=O), no hydroxyl absorption.

N.m.r. ($CDCl_3$): singlet (10H) τ 2.70 (aromatic protons of two benzyl groups); two singlets (2H each) 5.40, 5.53 (protons of two benzylic methylene groups); broad singlet (4H) 6.03 (ketal methylene protons), two singlets (3H each) 6.33 (aromatic methoxyl); 6.66 p.p.m. (primary methoxyl).

Mass spectrum Calcd. for $C_{35}H_{40}O_7$: *m/e*, 572.2774. Found: 572.2766.

Reduction of the Ketone 24

The ketone **24** (28 g, 0.049 mol) in absolute dioxane

Can. J. Chem. Downloaded from www.nrcresearchpress.com by 210.87.254.42 on 09/05/12
For personal use only.

Can. J. Chem. Downloaded from www.nrcresearchpress.com by 210.87.254.42 on 09/05/12
For personal use only.

(200 ml) was added dropwise to a suspension of lithium aluminum hydride (11 g, 0.24 mol) in absolute dioxane (2000 ml) which had been preheated to 90 °C. The reaction mixture was stirred at 90 °C for 1 h, cooled, and poured into wet ether (2000 ml, saturated with water). The inorganic precipitate was removed by filtration and the filtrate was evaporated under reduced pressure to dryness. The mixture (27.2 g, 97%) of alcohols **25** and **23** was homogeneous on t.l.c. and it was shown in the next methylation step to be in a ratio of 7:3.

I.r. (CCl_4): 3550 cm^{-1} (hydroxyl).

N.m.r. (CCl_4): singlet (10H) τ 2.70 (aromatic protons of the two benzyl groups); multiplet (3H) 2.80–3.40 (aromatic protons of the anisole ring); two singlets (2H each) 5.38, 5.52 (four benzylic methylene protons); multiplet (4H) centered at 6.07 (ketal methylene protons); two singlets (3H each) 6.32 (aromatic methoxyl), 6.67 p.p.m. (primary methoxyl).

Methylation of Alcohols **25** *and* **23**

The mixture of the alcohols **25** and **23** (25.8 g, 0.045 mol) was methylated under the same conditions used in the preparation of compound **26***a*. Work-up and chromatography on silica gel (1.5 kg, elution with 10–15% ether in benzene) gave compound **26***b* (17.5 g) (larger R_f) and compound **26***a* (7.7 g) (smaller R_f) in an overall yield of 95%.

I.r. (CCl_4): no hydroxyl absorption.

N.m.r. ($CDCl_3$): (for compound **26***b*) singlet (10H) τ 2.69 (aromatic protons of the two benzyl groups); multiplet (3H) 2.50–3.50 (aromatic protons of the anisole ring); doublet (2H) 5.39 (benzylic methylene protons); singlet (2H) 5.51 (benzylic methylene protons); multiplet (4H) centered at 6.10 (ketal methylene protons); three singlets (3H each) 6.29 (aromatic methoxyl), 6.47 (side chain methoxyl at C_1), 6.67 (primary methoxyl); singlet (2H) 6.55 p.p.m. (methylenic protons deshielded by the primary methoxyl).

Mass spectrum (**26***b*) Calcd. for $C_{36}H_{44}O_7$: *m/e*, 588.3075. Found: 588.3086.

Compound **26***b* was also obtained by the method shown in Scheme 7. While this process increased the stereoselectivity of the preparation of **26***b*, we have used the simpler less stereoselective method described in detail to supply large amounts of material with less effort.

Ketone **27***b*

Compound **26***b* (17.5 g, 0.03 mol) was deketalized under the same conditions used in the preparation of compound **27***a*. Work-up gave the ketone **27***b* (16.2 g) in a quantitative yield.

I.r. (CCl_4): 1755 cm^{-1} (ketone).

N.m.r. ($CDCl_3$): two singlets (5H each) τ 2.68, 2.70 (aromatic protons of the two benzyl groups); two singlets (2H each) 5.40 and 5.52 (benzylic methylene protons); three singlets (3H each) 6.27 (aromatic methoxyl); 6.48 (side chain methoxyl at C_1); 6.64 p.p.m. (primary methoxyl).

Mass spectrum Calcd. for $C_{34}H_{40}O_6$: *m/e*, 544. Found: 544.

Diketone **29***b*

The ketone **27***b* (16.2 g, 0.03 mol) was dissolved in 70 ml of methanol and subjected to reductive amination under the same conditions which were used in the preparation of compound **29***a*. Work-up gave the crude amine **28***b* (16 g, 97%) which was used without purification for the subsequent step.

I.r. (CCl_4): 3400 cm^{-1} (N—H); no carbonyl absorption.

N.m.r. ($CDCl_3$): two singlets (5H each) τ 2.63 and 2.66 (aromatic protons of the two benzyl groups); multiplet (3H) 2.40–3.50 (aromatic protons of the anisole ring); doublet (2H) centered at 5.41 (benzylic methylene protons); singlet (2H) 5.52 (benzylic methylene protons); three singlets (3H each) 6.28, 6.47, and 6.66 p.p.m. (three methoxyls).

The crude amine **28***b* (16 g, 0.029 mol) was acetylated under the same conditions used in the preparation of compound **29***a*. Work-up gave the *N*-acetyl derivative (16.4 g, 96%) which was homogeneous on t.l.c. and was used without further purification for the subsequent step.

I.r. (CCl_4): 3400 (N—H), 1675 cm^{-1} (N—CO—CH_3).

N.m.r. ($CDCl_3$): multiplet (13H) τ 2.40–2.70 (aromatic protons of the two benzyl groups and the anisole ring); doublet (1H) centered at 3.64 (—HN—CO—); doublet (2H) centered at 5.40 (benzylic methylene protons); singlet (2H) 5.50 (benzylic methylene protons); three singlets (3H each) 6.30, 6.47, and 6.64 (three methoxyls); singlet 8.05 (N—CO—CH_3 of the *anti*-epimer); singlet at 8.19 p.p.m. (N—CO—CH_3 of the *syn*-epimer).

The above material (16 g, 0.027 mol) was subjected to hydrogenolysis under the same conditions used in the "a" series. Work-up and chromatography on silica gel (600 g, 2% methanol in chloroform) gave the corresponding diol (10.1 g, 92%).

I.r. (CCl_4): 3400 (O—H, N—H), 1655 cm^{-1} (N—CO—CH_3).

N.m.r. ($CDCl_3$): multiplet (3H) τ 3.00–3.50 (aromatic protons of the anisole ring); two singlets (3H each) 6.26 and 6.48 (two methoxyls); singlet (5H) 6.63 (methoxyl and the protons deshielded by the primary methoxyl); singlet 7.95 (N—CO—CH_3 of the *anti*-epimer); singlet 8.15 p.p.m. (N—CO—CH_3 of the *syn*-epimer).

Mass spectrum Calcd. for $C_{22}H_{33}O_6N$: *m/e*, 407.2308. Found: 407.2313.

The above diol (9.8 g, 0.024 mol) was oxidized with the chromium trioxide – pyridine complex under the same conditions used in the preparation of the diketone **29***a*. Work-up gave the crude product which was purified by chromatography on silica gel (1 kg). Elution with 2% methanol in chloroform gave the pure diketone **29***b* which was crystallized from benzene–ether to a constant m.p. of 100–102 °C (6.5 g, 58%).

I.r. (KBr pellet): 3600–3300 (N—H), 1745 (five-membered ketone), 1720 (side chain ketone), 1660 cm^{-1} (N—CO—CH_3).

N.m.r. ($CDCl_3$): doublet (1H) centered at τ 2.47 (—NH—CO—); multiplet (3H) 2.90–3.30 (aromatic protons of the anisole ring); singlet (2H) 5.93 (—CO—CH_2—OCH_3); three singlets (3H each) 6.23, 6.51, and 6.56 (3—OCH_3); singlet (3H) 7.92 p.p.m. (N—CO—CH_3).

Mass spectrum Calcd. for $C_{22}H_{29}O_6N$: *m/e*, 403.1995. Found: 403.1990.

Anal. Calcd. for $C_{22}H_{29}O_6N$: C, 65.49; H, 7.24; N, 3.47. Found: C, 65.03; H, 7.08; N, 3.34.

Lactamol **30***b*

The diketone **29***b* (4.068 g, 0.010 mol) was converted to the lactamol **30***b* under the same conditions used in the preparation of the lactamol **30***a*. Work-up of the reaction mixture gave 4.2 g of crude product which was crystallized from chloroform–ether to a constant m.p. of 235–238 °C (3.85 g, 90%).

Can. J. Chem. Downloaded from www.nrcresearchpress.com by 210.87.254.42 on 09/05/12
For personal use only.

I.r. (KBr pellet): 3550–3200 (O—H, N—H), 1720 (five-membered lactam), 1665 cm^{-1} (N—CO—CH_3).

N.m.r. ($CDCl_3$): multiplet (3H) τ 2.80–3.40 (aromatic protons); three singlets (3H each) 6.18, 6.60, and 6.67 (3 —OCH_3); singlet (3H) 8.07 p.p.m. (N—CO—CH_3).

Mass spectrum Calcd. for $C_{23}H_{30}O_6N_2$: *m/e*, 430.2104. Found: 430.2100.

Anal. Calcd. for $C_{23}H_{30}O_6N_2$: C, 64.15; H, 7.02; N, 6.50. Found: C, 64.08; H, 6.94; N, 6.82.

Keto Lactam 31b

The pure lactamol **30***b* (3.44 g, 0.008 mol) was subjected to an acid-catalyzed cyclization under the same conditions used in the preparation of the ketolactam **31***a*. Work-up and crystallization in the same manner gave the pure ketolactam **31***b*, m.p. 266–268 °C (3.32 g) in a yield of 64%.

I.r. (KBr pellet): 3455 and 3335 (N—H), 1738 (ketone), 1670 cm^{-1} (lactam).

N.m.r. ($CDCl_3$): multiplet (3H) τ 3.00–3.50 (aromatic protons); three singlets (3H each) 6.20, 6.57, and 6.63 p.p.m. (3 —OCH_3).

Mass spectrum Calcd. for $C_{21}H_{25}O_5N$: *m/e*, 371.1733. Found: 371.1736.

Anal. Calcd. for $C_{21}H_{25}O_5N$: C, 67.92; H, 6.78; N, 3.71. Found: C, 67.62; H, 6.67; N, 3.89.

The Hydroxy Amines 32b and 33b

The pure ketolactam **31***b* (1.484 g, 0.004 mol) was converted to the hydroxy amines **32***b* and **33***b* by exactly the same procedure used in the "a" series. Crystallization of the crude products from methanol gave the pure crystalline β-hydroxy amine **32***b* (442 mg). The mother liquor was purified by chromatography on neutral alumina (120 g). Elution with chloroform gave the oily α-hydroxy amine **33***b* (610 mg) and more of the β-hydroxy amine (150 mg), which was recrystallized from methanol to a constant melting point of 226–228 °C. The overall yield of recrystallized β-hydroxy amine was 625 mg.

I.r. ($CHCl_3$) α-hydroxy amine **33***b*: 3600–3400 cm^{-1} (N—H, O—H); β-hydroxy amine **32***b*: 3500–3320 cm^{-1} (N—H, O—H).

N.m.r. ($CDCl_3$) α-hydroxy amine **33***b*: singlet (3H) τ 6.22 (aromatic methoxyl); doublet (6H) 6.66, 6.70 (ring A methoxyl and primary methoxyl); singlet (2H) 6.87 p.p.m. (protons deshielded by the primary methoxyl); β-hydroxy amine **32***b*: singlet (3H) τ 6.28 (aromatic methoxyl); singlet (8H) 6.70 p.p.m. (two methoxyls and protons deshielded by the primary methoxyl).

Mass spectrum Calcd. for $C_{21}H_{29}O_4N$: *m/e*, 359. Found for α-hydroxy amine **33***b*: 359. Found for β-hydroxy amine **32***b*: 359.

Anal. Calcd. for $C_{21}H_{29}O_4N$ **32***b*: C, 70.18; H, 8.13; N, 3.90. Found: C, 70.29; H, 8.23; N, 3.90.

The N-Acetyl-β-alcohol 35b

Compound **32***b* (359 mg, 1 mmol) was acetylated with acetic anhydride (2.5 ml) and pyridine (2.5 ml) as in the "a" series. The *N*-acetyl-β-acetate was obtained in a quantitative yield (441 mg).

I.r. (CCl_4): 1745 (—O—CO—CH_3), 1645 cm^{-1} (N—CO—CH_3).

N.m.r. ($CDCl_3$): multiplet (3H) τ 2.80–3.40 (aromatic protons); singlet (3H) 6.20 (aromatic methoxyl); singlet (8H) 6.72 (two methoxyls and the protons deshielded by the primary methoxyl); singlet (3H) 7.87 (N—CO—CH_3); singlet (3H) 7.95 p.p.m. (O—CO—CH_3).

The above material (400 mg, 0.9 mmol) was saponified exactly as in the "a" series. The *N*-acetyl-β-alcohol **35***b* (350 mg, 95%) was crystallized from ether to a m.p. of 182–183 °C.

I.r. (CCl_4): 3600–3200 (O—H), 1620 and 1645 cm^{-1} (N—CO—CH_3).

N.m.r. ($CDCl_3$): multiplet (3H) τ 2.87–3.30 p.p.m. (aromatic protons); singlet (3H) 6.20 (aromatic methoxyl); doublet (8H) 6.67, 6.72 (two methoxyls and the protons deshielded by the primary methoxyl); singlet (3H) 7.85 p.p.m. (N—CO—CH_3).

Mass spectrum Calcd. for $C_{23}H_{31}O_5N$: *m/e*, 401.2202. Found: 401.2298.

Anal. Calcd. for $C_{23}H_{31}O_5N$: C, 68.82; H, 7.78; N, 3.47. Found: C, 69.02; H, 7.84; N, 3.75.

Compound 36b

The alcohol **35***b* (200 mg, 0.5 mmol) was methylated exactly as in the "a" series. Crystallization from hexane–ether gave compound **36***b* which melted at 155–157 °C in a yield of 87%.

I.r. (CCl_4): no hydroxyl absorption; 1640 cm^{-1} (N—CO—CH_3).

N.m.r. ($CDCl_3$): multiplet (3H) τ 2.89–3.33 (aromatic protons); singlet (3H) 6.20 (aromatic methoxyl); singlet (11H) 6.70 (three methoxyls and protons deshielded by the primary methoxyl); singlet (3H) 7.87 p.p.m. (N—CO—CH_3).

Mass spectrum Calcd. for $C_{24}H_{33}O_5N$: *m/e*, 415.2359. Found: 415.2358.

Anal. Calcd. for $C_{24}H_{33}O_5N$: C, 69.37; H, 8.01; N, 3.37. Found: C, 69.39; H, 8.00; N, 3.39.

Compound 4b

The above material (120 mg, 0.29 mmol) was oxidized exactly as in the "a" series. Crystallization from *n*-hexane–ether gave compound **4***b* which melted at 188–190 °C in a yield of 89%.

I.r. (CCl_4): 1685 (ketone); 1650 cm^{-1} (N—CO—CH_3).

N.m.r. ($CDCl_3$): doublet (1H) τ 2.00 (aromatic proton deshielded by the benzylic ketone); multiplet (2H) 2.90–3.20 (aromatic protons); singlet (3H) 6.11 (aromatic methoxyl); doublet (11H) 6.70–6.72 (three methoxyls and protons deshielded by the primary methoxyl); singlet (3H) 7.90 p.p.m. (N—CO—CH_3).

Mass spectrum Calcd. for $C_{24}H_{31}O_6N$: *m/e*, 429.2151. Found: 429.2151.

Anal. Calcd. for $C_{24}H_{31}O_6N$: C, 67.11; H, 7.28; N, 3.26. Found: C, 67.17; H, 7.37; N, 3.66.

The Amino Ketone 34b

Concentrated hydrochloric acid (five drops) was added to the α-hydroxy amine **33***b* (30 mg, 0.084 mol) in 5 ml of methanol and the solution was evaporated to dryness *in vacuo*. The residue was redissolved in acetone (25 ml, distilled over potassium permanganate) and cooled in an ice-water bath for 10 min. A slight excess of Jones' reagent was added and the solution was stirred for 10 min. Saturated aqueous sodium chloride (20 ml) was added, the solution was basified with bicarbonate and extracted with chloroform (3 × 10 ml). The chloroform extracts were washed with water (1 × 10 ml), dried over anhydrous sodium sulfate, and evaporated to dryness. The amino ketone **34***b* (29 mg) which

Can. J. Chem. Downloaded from www.nrcresearchpress.com by 210.87.254.42 on 09/05/12
For personal use only.

was homogeneous in t.l.c. was obtained in a quantitative yield.

I.r. (CCl_4): 1740 cm^{-1} (ketone).

N.m.r. (CCl_4): multiplet (3H) τ 3.00–3.50 (aromatic protons); two singlets (3H each) 6.27 and 6.61 (2 —OCH_3), singlet (5H) 6.74 p.p.m. (OCH_3 and protons deshielded by the primary methoxyl).

Mass spectrum Calcd. for $C_{21}H_{27}O_4N$: *m/e*, 357. Found: 357.

Hydroxy Amines 32b and 33b from the Amino Ketone 34b

Sodium (about 20 mg) was added in 0.5 h intervals to the amino ketone **34***b* (29 mg, 0.084 mmol) in refluxing absolute ethanol (2 ml). After 4 h under reflux, methanol (1 ml) was added followed by water (8 ml). The solution was extracted with chloroform (4 × 10 ml), and the combined chloroform extracts were washed with water (2 × 10 ml), dried over anhydrous sodium sulfate, and evaporated to dryness. The crude hydroxy amines were separated by preparative t.l.c. on silica gel (12% methanol in chloroform) to yield pure **33***b* (6.5 mg) and **32***b* (15.3 mg) in a ratio of 3:7.

Both materials were identical (m.p., i.r., and mass spectra) with the samples described above.

The Tertiary Amine 37b

Sodium hydride (202 mg, 4.2 mmol) was added to the solution of compound **32***b* (250 mg, 0.7 mmol) in absolute dioxane (50 ml) and the mixture was heated under reflux for 1 h. Methyl iodide (1 ml) was added and reflux was continued for another 3 h. The reaction mixture was cooled and filtered through Celite. The filtrate was evaporated to dryness, chloroform (50 ml) was added, and the solution was washed with water (3 × 20 ml). The organic phase was dried over anhydrous sodium sulfate and evaporated to dryness to yield the crude methylated compound **37***b*. The crude product was purified by chromatography on silica gel (2% methanol in chloroform) and the pure tertiary amine **37***b* (260.5 mg) was obtained in a yield of 96%.

I.r. (CCl_4): no N—H and O—H absorption.

N.m.r. ($CDCl_3$): multiplet (3H) τ 2.90–3.40 (aromatic protons); four singlets (3H each) 6.23, 6.68, 6.73, and 6.77 (4 —OCH_3); singlet (3H) (7.73 p.p.m. (—N—CH_3).

Mass spectrum Calcd. for $C_{23}H_{33}O_4N$: *m/e*, 387.2410. Found: 387.2405.

The N-Formyl Compound 38b

A solution of the tertiary amine **37***b* (200 mg, 0.52 mmol) and potassium permanganate (200 mg) in acetone (40 ml, distilled over permanganate) and acetic acid (2 ml) was stirred at room temperature for 24 h. The precipitate was removed by filtration and washed thoroughly with chloroform. The filtrate was evaporated to dryness *in vacuo*, chloroform (50 ml) was added, and washed with water (2 × 30 ml), dried over anhydrous sodium sulfate, and evaporated to dryness. The crude product was purified by preparative t.l.c. on silica gel (5% methanol in chloroform) to give the pure *N*-formyl compound **38***b* (198 mg) which was crystallized from ether (m.p. 158–160 °C).

I.r. (CCl_4): 1662 cm^{-1} (—N—CH=O).

N.m.r. ($CDCl_3$): broad singlet (1H) τ 2.17 (—N—CH=O); multiplet (3H) 3.00–3.50 (aromatic protons); singlet (3H) 6.26 (aromatic —OCH_3); broad singlet (11H) 6.77 p.p.m. (3 —OCH_3 and protons deshielded by the primary —O—CH_3).

Mass spectrum Calcd. for $C_{23}H_{31}O_5N$: *m/e*, 401.2202. Found: 401.2200.

Anal. Calcd. for $C_{23}H_{31}O_5N$: C, 68.81; H, 7.78; N, 3.49. Found: C, 68.72; H, 7.69; N, 3.40.

The N-Formyl Ketone 2b

Compound **38***b* (180 mg, 0.45 mmol) was dissolved in acetone (50 ml, distilled over potassium permanganate). Jones' reagent was added dropwise over a period of 6 h. The reaction mixture was stirred at room temperature and a slight excess of the Jones' reagent was maintained during the entire period. A few drops of methanol were added and the precipitate was removed by filtration. Saturated aqueous sodium chloride (50 ml) was added to the filtrate and the solution was extracted with chloroform (3 × 40 ml). The organic layer was dried over anhydrous sodium sulfate and evaporated to dryness. The crude product was purified by t.l.c. on silica gel (5% methanol in chloroform) to yield the pure *N*-formyl ketone **2***b* (120 mg, 67%) which was identical with the corresponding derivative obtained from delphinine by i.r., n.m.r., and mass spectra. Identity was also established by t.l.c. in several systems.

I.r. (CCl_4): 1690 (—N—CH=O); 1655 cm^{-1} (ketone).

N.m.r. ($CDCl_3$): singlet (1H) τ 1.93 (N—CH=O); doublet (1H) centered at 1.96 (aromatic proton deshielded by the benzylic ketone); multiplet (2H) 3.00–3.50 (aromatic protons); four singlets (3H each) 6.12, 6.72, 6.74, and 6.77 p.p.m. (4 OCH_3).

Mass spectrum Calcd. for $C_{23}H_{29}O_6N$: *m/e*, 415.1995. Found: 415.1995.

Direct Conversion of Compound 37b to the N-Formyl Ketone 2b

A mixture of compound **37***b* (25 mg, 0.064 mmol) and potassium permanganate (250 mg) in acetone (15 ml, distilled over potassium permanganate) and acetic acid (0.75 ml) was stirred at room temperature for 5 days. Acetone (10 ml) was added and the precipitate was removed by filtration. The filtrate was evaporated to dryness *in vacuo*, the residue dissolved in chloroform (30 ml) and washed with water (2 × 10 ml). The chloroform was dried over anhydrous sodium sulfate and evaporated to dryness. The crude product was purified by preparative t.l.c. on silica gel (5% methanol in chloroform) to yield the *N*-formyl ketone **2***b* (21 mg, 82%) which was identical by its i.r., n.m.r., and mass spectra with the material obtained via the compound **38***b*.

The Amino Ketone 3b

The *N*-formyl ketone **2***b* (100 mg, 0.24 mmol) dissolved in a 1:9 concentrated hydrochloric acid methanol solution (30 ml) was heated under reflux for 24 h. The solution was evaporated to dryness, taken up in 5% sodium bicarbonate (20 ml), and extracted with chloroform (4 × 20 ml). The chloroform extracts were dried over anhydrous sodium sulfate and evaporated to dryness *in vacuo*. The crude product (98 mg) was crystallized from ether to yield 72 mg of the pure amino ketone **3***b* (m.p. 176 °C). The mother liquor was purified by preparative t.l.c. on silica gel (5% methanol in chloroform) and gave another 19 mg of the amino ketone. This material was identical with the delphinine degradation product of the same structure by i.r., n.m.r., and mass spectroscopy and t.l.c. in several systems.

I.r. (CCl_4): 3400–3200 (N—H); 1683 cm^{-1} (ketone).

N.m.r. ($CDCl_3$): doublet (1H) centered at τ 2.04 (aro-

matic proton deshielded by the conjugated ketone); multiplet (2H) 2.80–3.30 (aromatic protons); four singlets (3H each) at 6.11, 6.68, 6.70, and 6.73 (4 —OCH_3).

Mass spectrum Calcd. for $C_{22}H_{29}O_5N$: *m/e*, 387.2046. Found: 387.2040.

Anal. Calcd. for $C_{22}H_{29}O_5N$: C, 68.19; H, 7.54; N, 3.62. Found: C, 68.22; H, 7.37; N, 3.68.

Resolution of 3b

The synthetic racemic ketone **3b** (125 mg, 0.32 mmol) was dissolved in absolute pyridine and the solution was cooled in an ice-water bath. L-camphor–sulfonyl chloride (69.7 mg, 0.32 mmol) was added and the solution was allowed to stand overnight. Water (0.5 ml) was added and the mixture was stirred for 0.5 h. The mixture was then evaporated to dryness and the products were separated and purified by preparative t.l.c. on silica gel (5% methanol in chloroform) to give 78 mg of sulfonamide and 56 mg of the unreacted amino ketone. This last material (56 mg) was dissolved in ether, a large excess of oxalic acid in ether was added, and the oxalate precipitated. The mixture was kept in the refrigerator overnight, and the ethereal solution was decanted. The oxalate was recrystallized from methanol ether five times until a constant m.p. of 195–196 °C was reached (34 mg). The resolved synthetic oxalate and the corresponding oxalate derived from the degradation of delphinine were compared as follows: (*1*) melting ranges (°C) 195–196 synthetic, 194–196 "natural", 194–196 mixture; (*2*) identical i.r. spectra in KBr and in $CHCl_3$; (*3*) identical optical rotatory dispersion curves, $[\alpha]^{26}_{295} = +1 \times 10^5$, $[\alpha]^{26}_{250} = -7 \times 10^4$.

Anal. Calcd. for $C_{24}H_{31}O_9N$: C, 60.36; H, 6.54; N, 2.93. Found: C, 60.38; H, 6.57; N, 2.82.

Synthetic Optically Active 3b Free Base

The optically active oxalate (28 mg) was dissolved in chloroform (2 ml) and passed through a short column of basic alumina (1 g). The free amine was obtained by eluting the column with 5% methanol in chloroform (50 ml). After evaporation *in vacuo* to dryness, absolute ether (1.5 ml) was added, and the mixture was kept in the refrigerator for 4 days. The mother liquor was removed by a pipette and the crystals were washed with ether and dried in high vacuum. The crystalline free base **3b** was recrystallized to a constant m.p. of 144.5 °C from ether.

Identity with compound **3b** prepared from delphinine was established as follows: (*1*) m.p. (°C) 144.5 synthetic, 143 "natural", 144 mixture; (*2*) identical i.r. (KBr and $CHCl_3$) spectra; (*3*) identical mass spectra; (*4*) identical n.m.r. spectra; (*5*) identical R_f in several t.l.c. systems.

Mass spectrum Calcd. for $C_{22}H_{29}O_5N$: *m/e*, 387.2040. Found: 387.2046.

Racemic Oxalate of 3b for X-Ray Analysis

The synthetic racemic compound **3b** (58 mg) was converted to the racemic oxalate by treating with a large excess of oxalic acid under the same conditions which were employed for the preparation of the optically active oxalate **3b**.

The salt was recrystallized from ether–methanol until a constant melting point (189–193 °C) was reached (32 mg).

Anal. Calcd. for $C_{24}H_{31}O_9N$: C, 60.36; H, 6.54; N, 2.93. Found: C, 60.52; H, 6.45; N, 2.90.

We wish to thank the National Research Council of Canada, Ottawa, Canada, and Hoffmann La-Roche Inc., Nutley, New Jersey and Dorval, Quebec, for continuous financial support in the course of this study.

1. (*a*) K. WIESNER, F. BICKELHAUPT, and D. R. BABIN. Experientia, **15**, 93 (1959); (*b*) K. WIESNER, F. BICKELHAUPT, D. R. BABIN, and M. GÖTZ. Tetrahedron Lett. No. 3, 11 (1959), Tetrahedron, **9**, 254 (1960); (*c*) K. WIESNER, D. L. SIMMONS, and R. H. WIGHTMAN. Tetrahedron Lett. No. 15, 23 (1960).
2. K. WIESNER, M. GÖTZ, D. L. SIMMONS, and L. R. FOWLER. Coll. Czech. Chem. Commun. **28**, 2462 (1963).
3. For model experiments *c.f.* K. WIESNER, WEN-LING KAO, and J. ŠANTROCH. Can. J. Chem. **47**, 2431 (1969). For preliminary communications K. WIESNER, E. W. K. JAY, C. DEMERSON, T. KANNO, J. KŘEPINSKÝ, LIZZIE POON, T. Y. R. TSAI, A. VILÍM, and C. S. WU. Experientia, **26**, 1030 (1970); K. WIESNER, E. W. K. JAY, and LIZZIE (POON) JAY. Experientia, **27**, 363 (1971).
4. M. D. SOFFER, J. C. CAVAGNOL, and H. E. GELLERSON. J. Am. Chem. Soc. **71**, 3857 (1949).
5. G. STORK, A. BRIZZOLARA, H. LANDESMAN, J. SZMUSZKOVICZ, and R. TERRELL. J. Am. Chem. Soc. **85**, 207 (1963).
6. C. L. GRAHAM and F. J. MCQUILLIN. J. Chem. Soc. 4634 (1963).
7. K. WIESNER, K. K. CHAN, and C. DEMERSON. Tetrahedron Lett. 2893 (1965).
8. C. F. KOELSCH. J. Am. Chem. Soc. **65**, 2461 (1943).
9. K. WIESNER and J. ŠANTROCH. Tetrahedron Lett. 5939 (1966).
10. K. WIESNER, D. L. SIMMONS, and L. R. FOWLER. Tetrahedron Lett. No. 18, 1 (1959).
11. F. W. BACHELOR, R. F. C. BROWN, and G. BÜCHI. Tetrahedron Lett. No. 10, 1 (1960).
12. KARIN BJÅMER BIRNBAUM, K. WIESNER, E. W. K. JAY, and LIZZIE JAY. Tetrahedron Lett. No. 13, 867 (1971).

Can. J. Chem. Downloaded from www.nrcresearchpress.com by 210.87.254.42 on 09/05/12
For personal use only.

Approaches to the Synthesis of Triterpenoids. II. Some Tetracyclic Precursors Suitable for Conversion into Pentacyclic Triterpenoids[1]

J. W. ApSimon, P. Baker, J. Buccini, J. W. Hooper, and S. Macaulay
Department of Chemistry, Carleton University, Ottawa, Canada K1S 5B6

Received January 11, 1972

The stereoselective total synthesis of several partially reduced chrysene derivatives, suitable as precursors for a variety of triterpenoids, is described. The key reaction in the most efficient route involves the highly stereoselective reductive alkylation of a cyclic α,β-unsaturated ketone with allyl bromide in lithium–ammonia, using water as a proton donor.

La synthèse totale et stéréosélective de plusieurs dérivés partiellement réduits du chrysène est décrite; ces dérivés sont utilisés en tant que précurseurs d'un certain nombre de composés triterpéniques. La réaction cruciale, par la méthode la plus efficace, implique une alkylation par réduction hautement stéréosélective d'une cétone α,β-insaturée par le bromure d'allyle dans un mélange lithium–ammoniaque et en utilisant l'eau comme source de protons.

Canadian Journal of Chemistry, **50**, 1944 (1972)

Despite the many recorded total syntheses of natural products, relatively few of pentacyclic triterpenoids (1) have been reported (2). Recently, Ireland *et al.* (3, 4) and Stork *et al.* (5) have reported elegant highly stereoselective routes to some members of this class and the shortcomings as well as the general considerations involved in the total synthesis of such compounds have been summarized (3*a*). In this paper we report the completion of the first phase of our approach to the total synthesis of such compounds, a route designed to give intermediates that can be converted to several structural types. We describe routes to the tetracyclic compounds **1***a* and *b* (Schemes 1 and 2) containing two 1,3-diaxially disposed methyl groups and a *trans–transoid* arrangement of two carbocyclic rings,[2] both features being common to many triterpenoids. Scheme 1 indicates the possible utility of such compounds (*e.g.* 1*b*) taking advantage of the existing stereochemistry and the varied functionality at the termini leading to several structural types.

Our first route was based on the observations of previous workers (6) that alkylation of the dienolate anions of α,β-unsaturated ketones of type **3** occur with high stereoselectivity, yielding products, **4**, resulting from "equatorial" alkylation (see Scheme 3).

The tricyclic enone **3***a* was prepared by the Robinson annelation of **2** (7) with ethyl vinyl ketone.

The β-tetralone **2** preparation described herein (see Experimental) appears to be an improvement on the published procedure (2*a*). Base-catalyzed alkylations of **3***a* were performed using the known compounds **5***a* (8), *b* (8), and *c* (9) in order to produce compounds capable of conversion to tetracyclic species. Reaction with **5***a* and *b* gave less than 20% of unstable alkylation products, a reflection perhaps of the low nucleophilicity of the dienolate anions (10) and the low reactivity of the alkylating agents. When tosylate **5***c* was used and the anion of **3***a* was generated using potassium *t*-amyloxide in benzene, a 48% yield of diketone **6***a*[3] was obtained by direct crystallization after acidic hydrolysis of the ethylene ketal group.

Hydrogenation of the 10,10*a*-double bond[2] was expected to lead to the required *trans*-dihydrodiketone **7***a*, in accord with precedents

[1]Presented in part at the 53rd Canadian Chemical Conference, Toronto, Ontario, May 1970 and at the 54th Canadian Chemical Conference, Halifax, Nova Scotia, June 1971.

[2]Structural formulae of synthetic materials containing asymmetric carbon atoms depict one enantiomer only but refer to racemic compounds throughout. In the text the (±)-prefix is omitted and all intermediates are assumed to be racemic. Tricyclic materials are described using phenanthrene nomenclature and each racemate is arbitrarily represented by that enantiomer having the 4*a*-methyl group in the β configuration. Likewise the tetracyclic compounds are considered as chrysene derivatives.

[3]This material is stable in crystalline form but slowly decomposes in solution with the formation of polar substances. These appear to be products of autoxidation at the benzylic–allylic position.

Can. J. Chem. Downloaded from www.nrcresearchpress.com by 210.87.254.42 on 09/05/12
For personal use only.

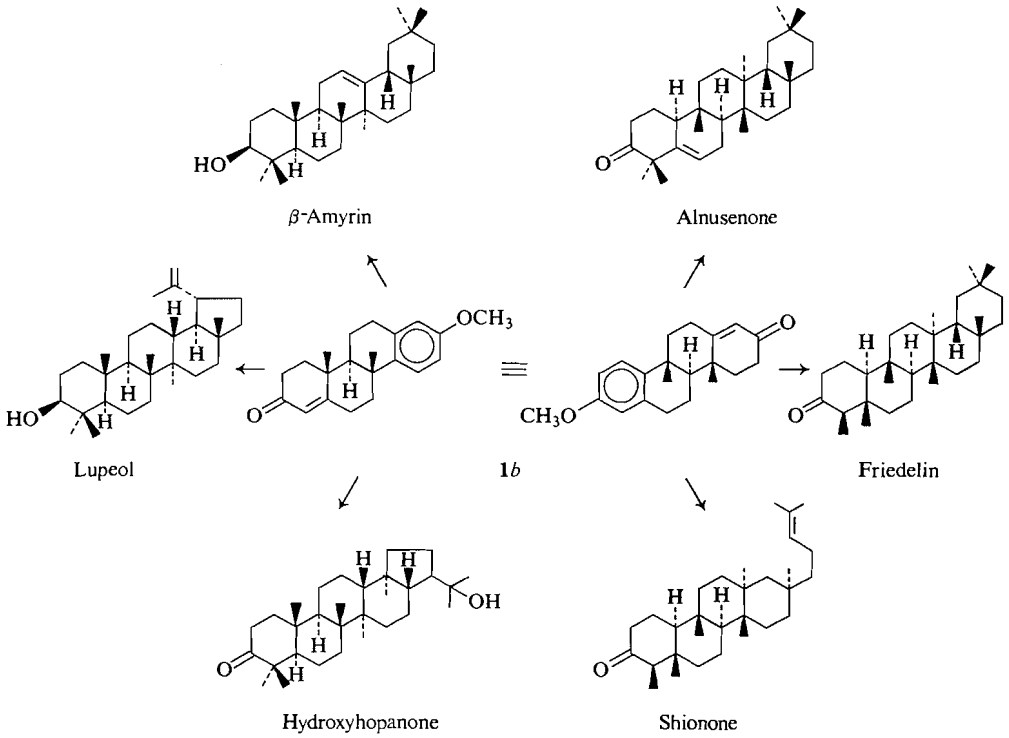

SCHEME 1

(2*a*, 6, 11). However, Ireland *et al.* (3*a*) have recently pointed out that these examples may be special cases and that for C-1α side chains longer than one carbon atom, one cannot make confident predictions of the stereochemistry of hydrogenation based on the "ease of approach to catalyst" argument (see footnote 5). Fortuitously, our parallel studies on the hydrogenation of **6***a* and *b* indicated that in fact our conditions led to behavior in accord with precedent. Thus, attempts at hydrogenation of **6***a* in acetic acid – sulfuric acid mixtures led to complex mixtures. In one case a low yield of crystalline material was obtained that appeared from spectral evidence to be a mixture of ketols **9***a* (12). These observations suggested the use of non-acidic solvents for the hydrogenation and since no hydrogen uptake was observed in boiling ethanol, the use of higher-boiling, non-polar solvents was investigated. At 100–110° in toluene using a palladium catalyst, **6***a* was slowly reduced to the dihydro-derivative **7***a* (55%). Boiling *p*-xylene as solvent gave rapid hydrogenation to **7***a* in 72% yield. The alternative *cis*-fused formulation **8***a* was discarded for the major reduction product on the basis of benzene-induced solvent shifts of the methyl peaks in the n.m.r. spectrum (3, 13). Throughout this work we have used benzene-induced solvent shifts as a probe for methyl group stereochemistry (14). Our observations are summarized in Table 1.[4] The shifts observed

[4]An obvious objection to this approach is our assignment of methyl signals. In general the lowest-field methyl signal attached to an aliphatic center is assigned to the C-4*a* methyl in the reduced phenanthrenes. Support for this assumption comes from the n.m.r. spectrum of **12** where the C-4*a* methyl singlet resonates at 1.35 δ while the C-1α methyl doublet appears at 1.10 δ. We assume that no signal crossover occurs. These working rules are supported by the nuclear Overhauser effects described in this paper and by the correlation established between our compounds and a compound whose stereochemistry is known from X-ray studies (*vide infra*). Thus the results in Table 1 are self-consistent and apparently the assignments are correct.

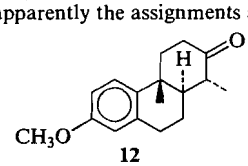

12

Can. J. Chem. Downloaded from www.nrcresearchpress.com by 210.87.254.42 on 09/05/12
For personal use only.

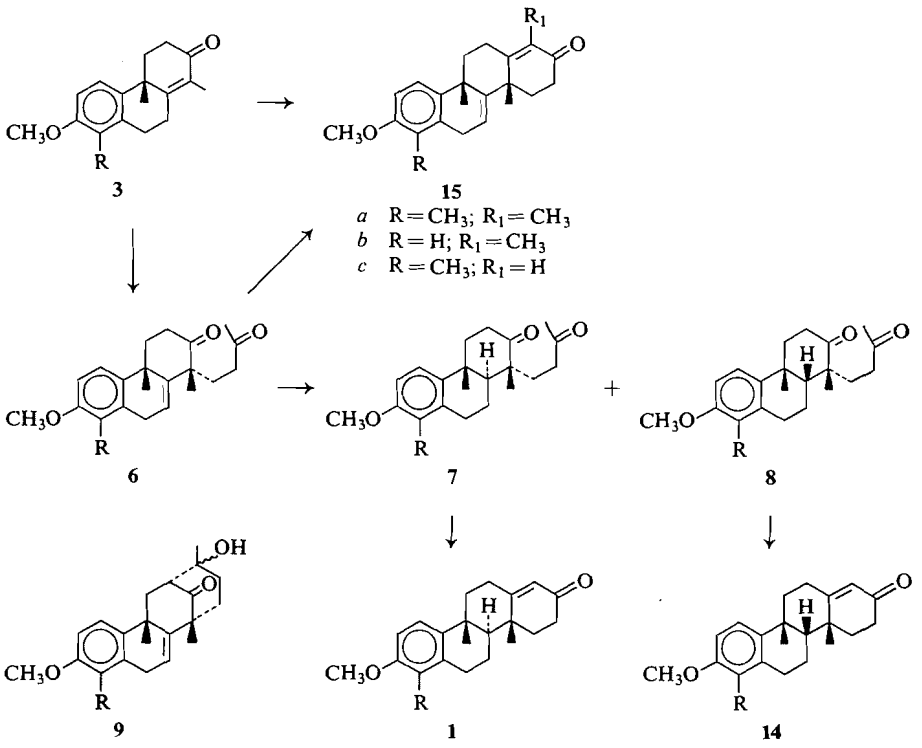

SCHEME 2. Series *a*, R = CH_3; series *b*, R = H

for **7***a* were +9 Hz for the C-1 methyl group and +12 Hz for the C-4*a* methyl group. These values can only be accommodated by a *trans* ring junction and axial methyl groups as in **10**. In the case of a *cis* ring fusion, molecular models indicate that the preferred conformation would be **11** with an equatorial C-1 methyl group which would show a small, negative benzene-induced solvent shift, if any.

Several compounds were hydrogenated using our conditions and the results are summarized in Table 2. These reactions proceeded in very high yield to give, in each case, a mixture of only two products (usually not separated), the major component of which was identified as the *trans*-fused isomer **10** on the basis of benzene-induced solvent shifts (Table 1). The minor components were assumed to be the *cis*-fused species **11**. These results are in direct contrast to those of Ireland *et al.* (3*a*) where hydrogenation of the olefinic ketone **13** gave mixtures in which the *cis*-fused isomer predominated (3:1 to 8:1). The reasons for our observations are unclear but could be a con-

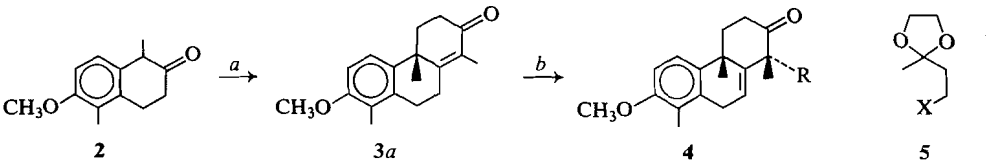

SCHEME 3. Reagents: *a*, $CH_3CH_2COCH{=}CH_2$, KOH, MeOH; *b*, (*i*) base, (*ii*) RX.

Can. J. Chem. Downloaded from www.nrcresearchpress.com by 210.87.254.42 on 09/05/12
For personal use only.

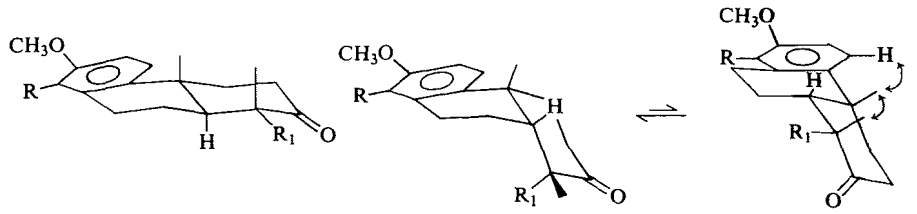

10 11

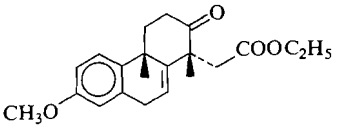

13

sequence of ring C conformational differences at higher temperatures in non-polar solvents.[5] It is interesting to note that our optimum conditions for the hydrogenation of **6***a* and similar compounds include a high catalyst:substrate ratio, a minimum of solvent, and high temperatures, all of which are quoted as leading to lower stereoselectivity (15).

Treatment of diketone **7***a* with aqueous methanolic potassium hydroxide gave the *trans–transoid* tetracyclic enone **1***a* in 90% yield. When the crude product of a hydrogenation of **6***a* (toluene 105°, non-optimum conditions) was subjected to base treatment, a mixture resulted from which was isolated an enone isomeric to **1***a*. This we consider to be the *cis–cisoid* isomer **14***a* arising from the cyclization of the *cis* isomer **8***a*. The n.m.r. spectra of **1***a* and **14***a* support the stereochemical assignments. The chemical shifts of their C-4*a* angular methyl groups together with those of two analogous steroids are listed in Table 3. In *cis–cisoid* steroids the C-19 methyl protons resonate at lower field than those of the *trans–transoid* series (16). The same behavior is noted for **1***a* and **14***a*. In the case of **14***a* a nuclear Overhauser effect of $13 \pm 2\%$ was detected between the C-10*b* methyl protons and the C-10 aromatic proton, whereas for **1***a* a negligible effect was detected. These data are only consistent with a BC-*cis* fused ring system (17) for **14***a*. The benzene-induced solvent shifts also support this assignment of stereochemistry (see Table 1).

When olefinic diketone **6***a* was treated with base an unstable substance was obtained whose spectral characteristics were consistent with the expected tetracyclic dienone **15***c*. The methyl analog **15***a* had previously been obtained as a by-product of the annelation of β-tetralone **2** with ethyl vinyl ketone. This stable, crystalline compound could also be obtained by reaction of **3***a* with ethyl vinyl ketone in boiling aqueous methanolic potassium hydroxide.[6] A similar sequence of reactions starting from enone **3***b* provided the non-crystalline tetracyclic compound **15***b*.

Tetracyclic enone **1***b* was prepared from **3***b* by the above route but in this series the compounds could not be completely purified and characterization was only possible by spectroscopic means. The alkylation product **6***b* proved particularly difficult to separate from unreacted tosylate **5***c* and very prone to autoxidation. This difference in stability compared to **6***a* is possibly due to easier access to the benzylic-allylic C-9 position in the absence of a methyl substituent on the aromatic ring. The best route, although not adjustable to large scale work, involved alkylation of **3***b* with **5***c* and chromatography to yield a fraction rich in olefinic diketone **6***b* which was hydrogenated without further purification (see Table 2) and then treated with base. The product was a mixture of the tetracyclic enones **1***b* and **14***b* (80:20 v.p.c.). Preparative t.l.c. afforded a pure sample of the *trans–transoid* isomer **1***b* as a colorless glass, identical in spectral properties to a crystalline sample

[5]Ireland's argument (3*a*) was that the bulky C-1α substituent ($-CH_2COOC_2H_5$) is eclipsed with the carbonyl group in the expected chair-like conformation of **13** thus leading to a preferred conformation with a β-face more available for catalyst approach. In this case the solvent was acetic acid and possibly solvation at the carbonyl group makes this even bulkier, favoring the conformational changes proposed.

[6]This double-annelation is an interesting reaction *per se* but incomplete studies in this laboratory indicate that this route is not a practical synthetic route to tetracyclic materials.

Can. J. Chem. Downloaded from www.nrcresearchpress.com by 210.87.254.42 on 09/05/12
For personal use only.

TABLE 1. Benzene-induced solvent shifts in the n.m.r. spectra* of some synthetic tri- and tetracyclic compounds ($\Delta = \delta_{CDCl_3} - \delta_{C_6D_6}$)

Compound		R	R_1	Methyl	δ_{CDCl_3}	$\delta_{C_6D_6}$	Δ
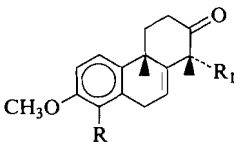	**6***a*	CH_3	$CH_2CH_2COCH_3$	C-1	71	64	+7
				C-4*a*	80	79	+1
		H	$CH_2CH_2COOCH_3$	C-1	70	58	+12
				C-4*a*	80	76	+4
		H	CH_2COOCH_3	C-1	79	74	+5
				C-4*a*	82	67	+15
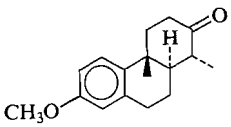	**12**			C-1	66	64	+2
				C-4*a*	81	59	+22
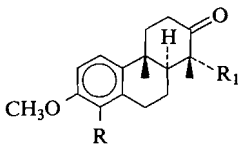	**7***a*	CH_3	$CH_2CH_2COCH_3$	C-1	67	58	+9
				C-4*a*	77	65	+12
		H	$CH_2CH_2COOCH_3$	C-1	67	56	+11
				C-4*a*	74	59	+15
		H	CH_2COOCH_3	C-1	67	55	+12
				C-4*a*	78	64	+14
	16	CH_3	CD_3	C-1β	68	60	+8
				C-4*a*	80	68	+12
	17	H	$CH_2CH{=}CH_2$	C-1	67	55	+12
				C-4*a*	82	70	+12
	19	H	CH_2CH_2COOH	C-1	69	56	+13
				C-4*a*	76	61	+15
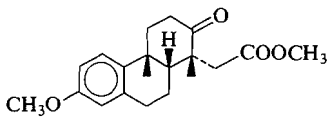				C-1	72	76	−4
				C-4*a*	72	59	+13
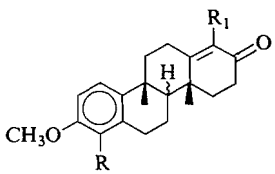	**1***a*	CH_3	H(4bα-H)	C-4*a*	74	48	+26
				C-10*b*	82	68	+14
	1*b*	H	H(4bα-H)	C-4*a*	76	49	+27
				C-10*b*	82	66	+16
	1*c*	H	CH_3(4bα-H)	C-4*a*	74	50	+24
				C-10*b*	82	70	+12
	14*a*	CH_3	H(4bβ-H)	C-4*a*	89	69	+20
				C-10*b*	91	82	+9
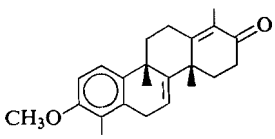	**15***a*			C-4*a*	93	75	+18
				C-10*b*	79	74	+5

*Determined at 60 MHz. Shifts are given in Hz downfield from internal TMS.

prepared by annelation of the enol-lactone **20** described below.

It is apparent that the routes described so far, whilst providing tetracyclic species, do not lend themselves to relatively large scale work or to pure materials except for **1***a* and **15***a*. Thus, alternate routes were sought.

Our most successful route involves the reductive alkylation of **3***b*[7] which allows us to take advantage of the structural integrity of the

[7]Model studies on the Birch reduction and catalytic hydrogenation of ring A of **3***a* were disappointing (P. Baker, unpublished), thus we turned our attention to the demethyl series.

Can. J. Chem. Downloaded from www.nrcresearchpress.com by 210.87.254.42 on 09/05/12
For personal use only.

TABLE 2. The stereochemistry of hydrogenation of various alkylation products*

Substrate		R	R_1	Product composition† *cis*-BC fusion	*trans*
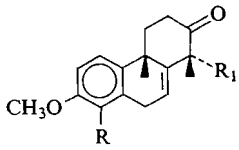	6*a*	CH_3	$CH_2CH_2COCH_3$	14	86
	6*b*	H	$CH_2CH_2COCH_3$	20	80
		H	$CH_2CH_2COOCH_3$‡	20	80
		H	CH_2COOCH_3§	19	81

*Conditions: 0.5 g substrate and 0.2 g 10% Pd/C in xylene at 140° for 4 h, 1 atm of hydrogen.
†Estimated by g.l.c. (±2%).
‡Prepared by alkylation of 3*b* with ethyl β-bromopropionate, followed by hydrolysis and methylation.
§Prepared by methylation of the corresponding acid, the synthesis of which has been reported (3*a*).

lithium enolate formed by the Birch reduction of the α,β-unsaturated ketone group (18) and its subsequent reaction with reactive alkylating agents (5). The attractiveness of such a route is that one reaction produces two asymmetric centers in the required orientation. In our case, the best conditions for formation of the enolate involved the use of one equivalent of water as the proton donor for the first formed radical anion (19), followed by reaction with a large excess of alkylating agent. The use of trideuteriomethyl iodide and enone 3*a* gave ketone **16** (Scheme 4) in which alkylation had occurred from the α-face (>90%) as indicated by the benzene-induced solvent shifts (Table 1) (5, 14, 20). Reductive alkylation of 3*b* with allyl bromide led to a non-crystalline product **17** containing over 80% of mono-alkylated species (v.p.c.). Ketalization of the crude reaction mixture with neat ethylene glycol yielded crystalline **18** (74% yield from 3*b*). Hydroboration–oxidation using disiamylborane (21) gave the terminal alcohol which, after oxidation with Jones reagent (22) and deketalization in acetone-

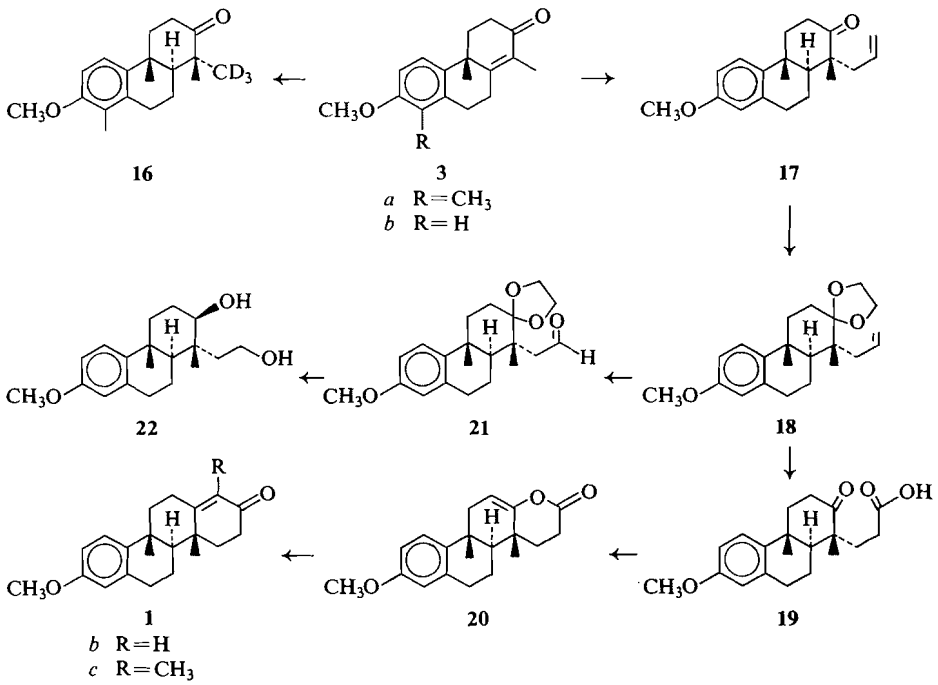

SCHEME 4

Can. J. Chem. Downloaded from www.nrcresearchpress.com by 210.87.254.42 on 09/05/12
For personal use only.

TABLE 3. Chemical shifts of angular methyl groups γ to the carbonyl in tetracyclic enones*

Compound	R	*cis–cisoid* isomer	*trans–transoid* isomer
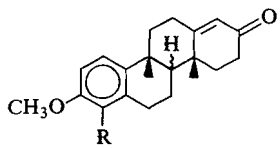	CH_3	(**14***a*) 1.50	(**1***a*) 1.23
	H		(**1***b*) 1.27
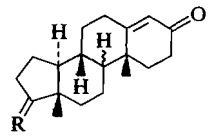	O	1.35	1.23
	H, OH	1.30	1.20

*Determined in $CDCl_3$ solutions and expressed in the δ scale. The values for the steroids were obtained from the data in ref. 16.

dilute sulfuric acid, yielded the crystalline keto-acid **19** in 72% yield from **18**. Conversion to the enol-lactone **20** was accomplished in two steps. Treating **19** with trifluoroacetic anhydride in acetonitrile led to the expected (23) ketone-mixed anhydride. The addition of a trace of 70% perchloric acid to this mixed anhydride in carbon tetrachloride (24) gave the crystalline enol-lactone **20** in 92% yield from **19**. Reacting **20** with methyl and ethyl Grignard reagents followed by base-catalyzed cyclization gave good yields of tetracyclic enones **1***b* and *c*, respectively.[8] The overall yield of tetracyclic species from the tricyclic enone **3***b* is 35%, making this a viable route to such intermediates.

As mentioned before, the one weak point in all of the above syntheses was the assignment of stereochemistry to our intermediates (*e.g.* **17**) based on solvent shift data and precedent. We have recently been able to establish that our proposals were correct by correlating **17** and **22**.[9] The synthesis of **22** has been reported (26) and its stereochemistry is known from X-ray studies of a conversion product (3). Reacting **18** with osmium tetroxide/sodium periodate gave the crystalline ketal-aldehyde **21** in 70% yield. This compound was reduced with sodium borohydride in ethanol, deketalized with acetone – dilute sulfuric acid, and again treated with sodium borohydride/ethanol to give the crystalline diol **22** as the major product. The sample of **22** prepared from **18** was identical in all respects to the authentic sample, thus verifying our stereochemical assignments.

[8]Attempting to form **1***b* using methyllithium instead of the Grignard gave only the carbinol **i** and unreacted **20**. Similar results were obtained under a variety of conditions with the ethylene ketal of **19** and the corresponding ketal-methyl ester (25).

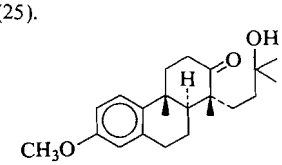

i

[9]We thank Prof. R. E. Ireland for a generous sample of this compound.

Experimental

Melting points were determined on a Kofler hot stage and are corrected. The n.m.r. spectra were obtained on a JEOLCO C-60 or a Varian T-60 spectrometer with tetramethylsilane as internal standard. Chemical shifts are expressed in the δ scale and the following abbreviations apply: s, singlet; d, doublet; t, triplet; q, quartet; m, multiplet. The i.r. spectra were determined on a Perkin–Elmer 237B grating spectrophotometer. The g.l.c. was carried out on a Hewlett–Packard 402 gas chromatograph using 5% OV-210 on Diatoport S and 5% SE-54 on Chromosorb W columns at 265°. Mass spectra were obtained on an AEI MS 12 instrument. Combustion analyses were performed by the Spang Microanalytical Laboratory, Ann Arbor, Michigan. The t.l.c. was performed using pre-coated plates obtained from E.M. Reagents (silica gel F-254, 0.25 or 2.0 mm). The term "work-up" refers to the separation of an organic phase from an aqueous one, followed by drying with sodium or magnesium sulfate, and rotary evaporation of the volatile organic solvents to yield the organic product.

1,5-Dimethyl-6-methoxy-2-tetralone (2)

The method is due to Stork *et al.* (2*a*). Methyl magnesium iodide was prepared from magnesium (60 g) and methyl iodide (400 g) in ether (1 l) and allowed to react with 6-methoxy-5-methyl-1-tetralone (150 g) in benzene (500 ml)

Can. J. Chem. Downloaded from www.nrcresearchpress.com by 210.87.254.42 on 09/05/12
For personal use only.

Can. J. Chem. Downloaded from www.nrcresearchpress.com by 210.87.254.42 on 09/05/12
For personal use only.

for 2 h at room temperature. The addition of water and work-up gave crude 3,4-dihydro-1,5-dimethyl-6-methoxynaphthalene (157 g). A solution of this material (157 g) in ether (250 ml) was added to a solution of monoperphthalic acid (174 g) in ether (1200 ml) over 1.5 h and then stored at 5° for 16 h. The absence of starting material in the reaction mixture was confirmed by t.l.c. The solid deposit was dissolved by the careful addition of 10% aqueous sodium bicarbonate while stirring over a 4–8 h period. The organic layer and two ether extracts were combined, washed twice with water, and then stirred with 10% hydrochloric acid (500 ml) overnight. Work-up and distillation afforded the β-tetralone **2** (108 g, 67%) as a yellow viscous oil (b.p. 128–150°/0.4 Torr) which rapidly solidified, m.p. 46–50° (lit. (*2a*) 50°); ν_{max} (Nujol) 1720 cm^{-1}; n.m.r. ($CDCl_3$) δ 1.40 (d, $J = 7$ Hz, 3H, —CH—CH_3), 2.15 (s, 3H, $ArCH_3$), 3.72 (s, 3H, —OCH_3).

1,4a,8-Trimethyl-7-methoxy-4,4a,9,10-tetrahydro-2(3H)-phenanthrone (3a)

A solution of the β-tetralone **2** (15.2 g) in methanol (70 ml) was added to a stirred solution of potassium hydroxide (5.7 g), water (10 ml), and methanol (30 ml) at 0° under nitrogen. The mixture was cooled to −20° and freshly distilled ethyl vinyl ketone (7.9 g, 1.25 equiv) in methanol (10 ml) was added dropwise with stirring. The temperature was allowed to rise to −5° and kept at $-3 \pm 2°$ for 2 h. After standing at room temperature overnight the mixture was refluxed for 4 h, cooled, and poured onto an ice/dilute sulfuric acid mixture. The organic materials were extracted with ether and work-up yielded a red oil (21 g) which crystallized from methanol in two crops affording the tricyclic enone **3a** as yellow needles (14.1 g, 70%) m.p. 123–124°; ν_{max} (Nujol) 1665 (C=O), 1625 (C=C), and 810 cm^{-1}; n.m.r. ($CDCl_3$) δ 1.52 (s, 3H, C_{4a}—CH_3), 1.85 (s, 3H, C_1—CH_3), 2.13 (s, 3H, $ArCH_3$), 3.77 (s, 3H, —OCH_3).

Anal. Calcd. for $C_{18}H_{22}O_2$: C, 79.97; H, 8.20. Found: C, 80.31; H, 8.32.

1,4aβ,7,10bβ-Tetramethyl-8-methoxy-4,4a,6,10b,11,12-hexahydro-2(3H)-chrysenone (15a)

Repeating the preceding preparation using large amounts of the β-tetralone **2** (122 g) and ethyl vinyl ketone (63 g, 1.25 equiv) gave the crystalline tricyclic ketone **3a** in 63% yield (104 g). Chromatography of the mother liquors on silica gel using increasing proportions of ether in hexane as eluent gave further **3a** (5.2 g) and then the tetracyclic ketone **15a** (6.6 g), crystallizing as pale yellow needles from methanol, m.p. 131–132°; ν_{max} (Nujol) 1660 (C=O), 1615 (C=C), and 785 cm^{-1}; n.m.r. ($CDCl_3$) δ 1.31 (s, 3H, C_{10b}—CH_3), 1.55 (s, 3H, C_{4a}—CH_3), 1.75 (s, 3H, C_1—CH_3), 2.17 (s, 3H, $ArCH_3$), 3.77 (s, 3H, OCH_3), and 5.98 (q, $J_1 = J_2 = 3$ Hz, 1H, C-5 vinyl H).

Anal. Calcd. for $C_{23}H_{28}O_2$: C, 82.12; H, 8.39. Found: C, 82.34; H, 8.63.

1α-(3-Oxobutyl)-1β,4aβ,8-trimethyl-7-methoxy-3,4,4a,9-tetrahydro-2(1H)-phenanthrone (6a)

A mixture of potassium (1.83 g), *t*-amyl alcohol (10 ml) and benzene (200 ml) was refluxed under a nitrogen atmosphere to give a solution of potassium *t*-amyloxide. The tricyclic ketone **3a** (12.1 g) was added to the cooled solution and, while fresh benzene was being added, the reaction mixture was heated for 5 h to distil off a mixture of benzene–*t*-amyl alcohol. The resulting green–brown suspension of the potassium salt of **3a** was cooled to 0° and a 30% solution of the tosylate **5c** (9) (1 equiv) in toluene was added over a 10 min period. This mixture was stirred for 12 h at room temperature and then refluxed for 2 h, cooled, and acidified with 5% sulfuric acid. The organic materials were isolated with ether in the usual way to yield a red oil. A solution of this oil in acetone (250 ml) and 0.2 *N* sulfuric acid (25 ml) was refluxed for 2 h and, after removal of most of the acetone, extracted twice with dichloromethane. Routine work-up of the organic layers and crystallization of the residue from ether gave the olefinic diketone **6a** as yellow plates, m.p. 134–136° (7.05 g, 48%); ν_{max} (Nujol) 1715 (—$COCH_3$) and 1700 (ring C=O) cm^{-1}; n.m.r. ($CDCl_3$) δ 1.18 (s, 3H, C_1—CH_3), 1.33 (s, 3H, C_{4a}—CH_3), 2.05 (s, 3H, —$COCH_3$), 2.15 (s, 3H, $ArCH_3$), 3.80 (s, 3H, OCH_3), and 5.89 (m, 1H, C-10 H).

Anal. Calcd. for $C_{22}H_{28}O_3$: C, 77.57; H, 8.29. Found: C, 77.81; H, 8.49.

1α-(3-Oxobutyl)-1β,4aβ,8-trimethyl-7-methoxy-3,4,4a,9,10,10aα-hexahydro-2(1H)-phenanthrone (7a)

Olefinic diketone **6a** (0.50 g) in *p*-xylene (5 ml) was hydrogenated for 4 h at atmospheric pressure and 140° over (prehydrogenated) 10% Pd/C (0.20 g). The product obtained had two constituents (86:14) as judged by g.l.c. The diketone **7a** crystallized from ethanol as colorless needles, m.p. 147–149°, 97% pure by g.l.c. (0.35 g, 70%). Two recrystallizations from acetone/hexane gave the analytical sample, m.p. 158–159°; ν_{max} (Nujol) 1716 (C=O) and 790 cm^{-1}; n.m.r. ($CDCl_3$) δ 1.12 (s, 3H, C_1—CH_3), 1.28 (s, 3H, C_{4a}—CH_3), 2.12 (s, 6H, —$COCH_3$ and $ArCH_3$), and 3.80 (s, 3H, OCH_3).

Anal. Calcd. for $C_{22}H_{30}O_3$: C, 77.13; H, 8.83. Found: C, 77.06; H, 9.07.

4aβ,7,10bβ-Trimethyl-8-methoxy-4,4a,4bα,5,6,10b,11,12-octahydro-2(3H)-chrysenone (1a)

A suspension of the diketone **7a** (0.265 g), methanol (25 ml), water (4 ml), and potassium hydroxide (1.5 g) was refluxed under nitrogen for 2.5 h. The solid gradually dissolved and was later replaced by pale yellow prisms of the tetracyclic enone **1a** (0.190 g), m.p. 184–185°. Further crystalline **1a** (0.038 g) was obtained by dilution of the mother liquors, extraction with dichloromethane, and crystallization of the product from acetone/methanol (total yield 0.228 g, 90%); ν_{max} (Nujol) 1670 (C=O), 1625 (C=C), and 790 cm^{-1}; n.m.r. ($CDCl_3$) δ 1.23 (s, 3H, C_{4a}—CH_3), 1.37 (s, 3H, C_{10b}—CH_3), 2.10 (s, 3H, $ArCH_3$), 3.77 (s, 3H, OCH_3), and 5.82 (broad s, 1H, C-1 vinyl proton).

Anal. Calcd. for $C_{22}H_{28}O_2$: C, 81.39; H, 8.70. Found: C, 81.48; H, 8.93.

4aβ,7,10bβ-Trimethyl-8-methoxy-4,4a,4bβ,5,6,10b,11,12-octahydro-2(3H)-chrysenone (14a)

The olefinic diketone **6a** (15.0 g) in toluene (100 ml) was hydrogenated for 6 days at atmospheric pressure and 110° over 10% Pd/C (1.0 g). The complex mixture obtained was dissolved in a solution of methanol (200 ml), water (20 ml), and potassium hydroxide (6.0 g) and refluxed under nitrogen for 3 h. The solution was cooled, diluted with water and extracted twice with dichloromethane to yield

Can. J. Chem. Downloaded from www.nrcresearchpress.com by 210.87.254.42 on 09/05/12
For personal use only.

an orange gum on work-up. The previously characterized enone **1***a* crystallized from methanol (2.6 g). The mother liquors were chromatographed on silica gel using increasing proportions of ether in hexane as eluent. This gave further impure **1***a* and fractions containing mixtures of **1***a* and an unidentified substance, and then fractions rich in the enone **14***a*. Several recrystallizations of these fractions from methanol gave pure **14***a* (1.2 g) as small, yellow needles, m.p. 142–144°; ν_{max} (Nujol) 1665 (C=O), 1605 (C=C), and 790 cm^{-1}; n.m.r. ($CDCl_3$) δ 1.51 and 1.53 (two s, 6H, C_{4a} and C_{10b}—CH_3), 2.05 (s, 3H, $ArCH_3$), 3.85 (s, 3H, OCH_3), and 5.71 (s, 1H, vinyl H); mass spectrum: M^+ at 324.

Anal. Calcd. for $C_{22}H_{28}O_2$: C, 81.39; H, 8.70. Found: C, 80.73; H, 8.89.

4aβ,7,10bβ-Trimethyl-8-methoxy-4,4a,6,10b,11,12-hexahydro-2(3H)-chrysenone (15c)

A solution of the diketone **6***a* (0.500 g), methanol (27 ml), water (3 ml), and potassium hydroxide (1.50 g) was refluxed under nitrogen for 16 h. The mixture was diluted with water, acidified (H_2SO_4), extracted with ether and worked-up to a brown gum which was shown to be a complex mixture by t.l.c. Chromatography on silica gel (40 g) using increasing proportions of ether in hexane as eluent gave various mixtures of unidentified substances and several fractions (total 0.12 g) containing essentially one substance (by g.l.c. and t.l.c.); ν_{max} 1670 (C=O) cm^{-1}; n.m.r. ($CDCl_3$) δ 1.33 (s, 3H, C_{10b}—CH_3), 1.52 (s, 3H, C_{4a}—CH_3), 2.16 (s, 3H, $ArCH_3$), 3.77 (s, 3H, OCH_3), 5.77 (s, 1H, C-1 vinyl proton), and 5.97 (m, 1H, C-5 vinyl proton). This appeared to be crude tetracyclic ketone **15***c* but it could not be purified further and deteriorated on standing.

4aβ,10bβ-Dimethyl-8-methoxy-4,4a,4bα,5,6,10b,11,12-octahydro-2(3H)-chrysenone (1b) from Tricyclic Enone 3b

A mixture of potassium (1.2 g, 30.7 mmol), *t*-amyl alcohol (5 ml), and benzene (50 ml) was refluxed under a nitrogen atmosphere to give a solution of potassium *t*-amyloxide. The tricyclic enone **3***b* (26) (6.0 g, 23.4 mmol) was added to the cooled solution and, while fresh benzene was being added, the reaction mixture was heated for 5 h to distil off a mixture of benzene – *t*-amyl alcohol. The resulting green–brown suspension of the potassium salt of **3***b* was cooled to 0° and a solution of the tosylate **5***c* (8.0 g, 30 mmol) in benzene (10 ml) was slowly added. This mixture was stirred for 18 h at room temperature, acidified with 1 *N* sulfuric acid (20 ml), and extracted twice with ether. Work-up of the organic extracts gave a red oil (12.6 g) which was refluxed for 24 h with a mixture of methanol (150 ml) and 10% sodium hydroxide (10 ml). The organic product was isolated and subjected to two more methanol/sodium hydroxide treatments to finally yield the alkylated product (6.6 g) free of tosylate **5***c*. A solution of this material in acetone (175 ml) and 0.2 *N* sulfuric acid (25 ml) was refluxed for 1 h and, after removal of most of the acetone, extraction with ether and work-up yielded a red oil (5.2 g). This was chromatographed on silica gel (260 g) using increasing proportions of ether in benzene as eluent. Non-crystalline diketone **6***b* (1.3 g, 17% from **3***b*) was eluted with 10% ether in benzene and appeared homogeneous on t.l.c. and g.l.c.; ν_{max} (neat) 1705 (C=O), 1660 (C=C), 1610 (Ar C=C) cm^{-1}; n.m.r. ($CDCl_3$) δ 1.17 (s, 3H, C_1—CH_3), 1.32 (s, 3H, C_4—CH_3), 2.02 (s, 3H, CO—CH_3), 3.40 (d, $J = 4$ Hz, 2H, C-9 protons), 3.74 (s, 3H, OCH_3), 5.87 (t, $J = 4$ Hz, 1H, C-10 vinyl H).

Non-crystalline olefinic diketone **6***b* (0.50 g, 1.53 mmol) in *p*-xylene (5 ml) was hydrogenated for 1 day at atmospheric pressure and 140° over (prehydrogenated) 10% Pd/C (0.15 g). The product obtained had two constituents (80:20) as judged by g.l.c. The absorptions for the olefinic bond in the i.r. (1660 cm^{-1}) and n.m.r. (5.87 δ) spectra of **6***b* were not found in the spectra of the product. As the product could not be crystallized or separated into its constituents on t.l.c., the product mixture was refluxed with methanol (50 ml), water (5 ml), and potassium hydroxide (1.5 g) for 3 h under a nitrogen atmosphere. The cooled reaction mixture was diluted with water and extracted with ether. Work-up gave non-crystalline tetracyclic material (0.37 g, 79% from **6***b*) which was greater than 90% **1***b* (g.l.c.). The spectra of this sample of **1***b* were almost identical to those of the crystalline sample of **1***b* obtained from the enol–lactone **20**.

1,4aβ,10bβ-Trimethyl-8-methoxy-4,4a,6,10b,11,12-hexahydro-2(3H)-chrysenone (15b)

To a refluxing solution of methanol (3 ml), water (1 ml), and potassium hydroxide (0.56 g) were added a solution of the tricyclic enone **3***b* (26) (2.0 g) in methanol (7 ml) and then a solution of ethyl vinyl ketone (1.45 g) in methanol (1.5 ml). The reaction mixture was refluxed under a nitrogen atmosphere for 1.5 h and then cooled, poured into dilute sulfuric acid, and extracted with ether. The g.l.c. showed the product to be a 5:2 mixture of the tetracycle **15***b* and starting material. Excess tricycle **3***b* was distilled off at 120°/0.5 Torr to yield a residue which was over 90% tetracycle **15***b* by g.l.c. (0.79 g); ν_{max} (neat) 1660 (C=O) cm^{-1}; n.m.r. ($CDCl_3$) δ 1.30 (s, 3H, C_{10b}—CH_3), 1.52 (s, 3H, C_{4a}—CH_3), 1.73 (s, 3H, C_1—CH_3), 3.35 (broad d, 2H, C-6 protons), 3.74 (s, 3H, OCH_3), 5.95 (broad t, 1H, C-5 vinyl proton).

1α-Trideuteromethyl-1β,4aβ,8-trimethyl-7-methoxy-3,4,4a,9,10,10aα-hexahydro-2(1H)-phenanthrone (16)

A solution of tricyclic enone **3***a* (540 mg, 2 mmol) in anhydrous tetrahydrofuran (25 ml) was added to a stirred mixture of lithium (170 mg, 24.3 mmol) and anhydrous liquid ammonia (50 ml). The resulting solution was stirred for 25 min and then quenched with a solution of trideuteromethyl iodide (5 g, 34.5 mmol) in anhydrous ether (10 ml). The ammonia was allowed to evaporate overnight. Saturated sodium chloride solution was added to the residue and the resulting mixture was extracted with ether. Work-up of the organic layer gave a mixture of **3***a* and **16** (40:60) as judged by g.l.c. The product was crystallized from methanol to give **16** as small clusters of yellow needles, m.p. 85–89°; ν_{max} (Nujol) 1700 cm^{-1} (C=O); n.m.r. ($CDCl_3$) δ 1.13 (s, 3H, C_1—CH_3), 1.33 (s, 3H, C_{4a}—CH_3), 2.13 (s, 3H, $ArCH_3$), 3.84 (s, 3H, OCH_3); mass spectrum: M^+ at 289.

1′α-Allyl-1′β,4′aβ-dimethyl-7′-methoxy-3′,4′,4′a,9′,10′,10′aα-hexahydro-spiro [1,3-dioxolane-2,2′(1′H)-phenanthrene] 18

A solution of tricyclic enone **3***b* (2.05 g, 8.0 mmol), water (143 mg, 7.9 mmol), and anhydrous tetrahydrofuran

Can. J. Chem. Downloaded from www.nrcresearchpress.com by 210.87.254.42 on 09/05/12
For personal use only.

(150 ml) was added to a stirred mixture of lithium (320 mg, 46 mmol) and anhydrous liquid ammonia (150 ml). The blue solution was allowed to stir for 10 min and then quenched with a large excess of freshly distilled allyl bromide (14.5 g, 0.12 mol). *Caution*: this addition of allyl bromide can result in a very violent reaction! The ammonia was allowed to evaporate overnight. Saturated sodium chloride solution was added to the residue and the resulting mixture was extracted with ether. Work-up of the organic layer gave **17** as a colorless oil; ν_{max} (neat) 1700 (C=O), 1635 (vinyl C=C)cm^{-1}; n.m.r. ($CDCl_3$) δ 1.12 (s, 3H, C_1—CH_3), 1.37 (s, 3H, C_4—CH_3), 3.77 (s, 3H, OCH_3), 4.7–6.4 (m, 3H, —CH=CH_2).

A mixture of crude **17**, ethylene glycol (250 ml), and *p*-toluenesulfonic acid (100 mg) was heated and the bulk of the ethylene glycol was distilled off at 70°/0.05 Torr. The residue was diluted with benzene and washed successively with saturated sodium bicarbonate and aqueous sodium chloride. Work-up of the organic layer gave a colorless oil which yielded crystalline **18** upon the addition of methanol. Recrystallization from methanol gave the ketal–olefin **18** as colorless plates, m.p. 121–123° (2.02 g, 73.5% from **3***b*); ν_{max} (Nujol) 1630 (vinyl C=C), 1612 (aromatic C=C) cm^{-1}; n.m.r. ($CDCl_3$) δ 1.03 (s, 3H, C_1—CH_3), 1.20 (s, 3H, C_4—CH_3), 3.73 (s, 3H, OCH_3), 3.83–4.07 (m, 4H, O—CH_2CH_2—O), 4.7–6.4 (m, 3H, —CH=CH_2); M^+ at 342.

Anal. Calcd. for $C_{22}H_{30}O_3$: C, 77.16; H, 8.83. Found: C, 77.26; H, 8.67.

*1β,4aβ-Dimethyl-7-methoxy-2-oxo-1,2,3,4,4a,9,10,10aα-octahydro-1α-phenanthrenepropionic Acid (**19**)*

Disiamylborane (21) was prepared by stirring a mixture of sodium borohydride (0.661 g, 17.5 mmol), 2-methyl-2-butene (5.00 ml, 47.3 mmol), and boron trifluoride etherate (2.92 ml, 23.2 mmol) in anhydrous tetrahydrofuran (THF) (75 ml) for 2 h at 0°. Then a solution of the ketal–olefin **18** (2.15 g, 6.3 mmol) in anhydrous THF (30 ml) was quickly added to the disiamylborane solution and the reaction mixture allowed to stir at room temperature for 3 h. The mixture was again cooled to 0°, followed by the cautious addition of 3 *N* sodium hydroxide (30 ml) and then 30% hydrogen peroxide (15 ml). The THF was removed by rotary evaporation and the resulting mixture extracted with ether. Work-up of the organic extract gave the ketal–primary alcohol as a colorless oil. ν_{max} (neat) 3400 cm^{-1} (OH); n.m.r. ($CDCl_3$) δ 3.55 (broad t, J = 6 Hz, 2H, CH_2—OH), 3.77 (s, 3H, OCH_3), 3.94 (m, 4H, —OCH_2-CH_2O—).

The crude alcohol was dissolved in acetone (50 ml), cooled to 0°, and oxidized with an excess of Jones reagent (22). Acetone was removed and the resulting mixture diluted with water and extracted (3 ×) with ether. The ether layer was extracted with 1 *N* sodium hydroxide (3 × 35 ml) and discarded. The alkaline solution was acidified with dilute hydrochloric acid and extracted with chloroform. Work-up of the chloroform extract gave ketal–acid as an oil. This material was refluxed with a mixture of acetone (30 ml) and 1 *N* sulfuric acid (10 ml) for 1 h and then diluted with water and extracted with chloroform. Work-up of the organic extract gave the keto-acid **19** as an oil which was crystallized from methanol as colorless needles, m.p. 171–173° (1.50 g, 4.53 mmol, 72% from **18**); ν_{max} (Nujol) 3200–2500 (acid OH), 1705–1690 (acid, ketone C=O) cm^{-1}; n.m.r. ($CDCl_3$) δ 1.15 (s, 3H, C_1—CH_3), 1.27 (s, 3H, C_4—CH_3), 3.80 (s, 3H, OCH_3), 9.04 (broad s, 1H, acid —OH); M^+ at 330.

Anal. Calcd. for $C_{20}H_{26}O_4$: C, 72.70; H, 7.93. Found: C, 72.63; H, 8.02.

*Enol–Lactone (**20**)*

A mixture of the keto–acid **19** (1.18 g, 3.59 mmol), acetonitrile (20 ml), and trifluoroacetic anhydride (3 ml) was stirred at room temperature for 0.5 h to give a clear solution. The solvents were removed and the resulting oil dissolved in carbon tetrachloride (15 ml) and cooled to 0°. One drop of 70% perchloric acid was added and the reaction mixture stirred for 20 min and then extracted twice with cold, saturated sodium bicarbonate (25 ml). Work-up of the organic layer gave a clear oil which slowly crystallized. Recrystallization from ether gave the enol–lactone **20** as colorless needles, m.p. 163–165° (0.85 g, 2.73 mmol, 76%); ν_{max} (Nujol) 1750 (C=O), 1680 (enol C=C) cm^{-1}; n.m.r. ($CDCl_3$) δ 1.17, 1.30 (two s, 3H each, angular CH_3), 3.77 (s, 3H, OCH_3), 5.36 (pair of d, 1H, —CH=C—O, J = 6, 2.5 Hz, unequal coupling to allylic H's); M^+ at 312.

Anal. Calcd. for $C_{20}H_{24}O_3$: C, 76.89; H, 7.74. Found: C, 76.96; H, 7.73.

The sodium bicarbonate extracts were acidified, extracted with chloroform, and worked-up to give crystalline keto–acid **19** (201 mg, 0.61 mmol, 17%). Thus, allowing for the recovered starting material, the yield of **20** from **19** is 92%.

*4aβ,10bβ-Dimethyl-8-methoxy-4,4a,4bα,5,6,10b,11,12-octahydro-2(3H)-chrysenone (**1b**) from Enol–Lactone **20***

A solution of the enol–lactone **20** (200 mg, 0.64 mmol) in anhydrous tetrahydrofuran (8 ml) was cooled to 0° and placed under a dry nitrogen atmosphere. A 1.8 *N* ethereal solution of methyl magnesium iodide (0.80 ml, 1.44 mmol) was then added by syringe and the reaction mixture left to warm to room temperature and stirred for 16 h. To this mixture were added saturated ammonium chloride (5 ml), water (10 ml), and ether (10 ml). Work-up of the organic layer gave a clear oil which was then refluxed for 24 h with a mixture of potassium hydroxide (460 mg), methanol (12 ml), and water (12 ml) under a nitrogen atmosphere. The cooled reaction mixture was extracted with ether and work-up gave an oil which was purified by t.l.c. on silica gel (benzene/ether = 3/1) and recrystallized from methanol to give the tetracyclic enone **1***b* as colorless plates, m.p. 137–139° (139 mg, 0.45 mmol, 70%); ν_{max} (Nujol) 1655 (C=O), 1602 (C=C) cm^{-1}; n.m.r. ($CDCl_3$) δ 1.26 (s, 3H, C_{4a}—CH_3), 1.37 (s, 3H, C_{10b}—CH_3), 3.78 (s, 3H, OCH_3), 5.84 (d, J = 2 Hz, 1H, C-1 vinyl proton); M^+ at 310.

Anal. Calcd. for $C_{21}H_{26}O_2$: C, 81.25; H, 8.44. Found: C, 81.02; H, 8.31.

*1,4aβ,10bβ-Trimethyl-8-methoxy-4,4a,4bα,5,6,10b,11,12-octahydro-2(3H)-chrysenone (**1c**)*

Reacting ethereal ethyl magnesium bromide with the enol–lactone **20** under the same conditions used to prepare **1***b*, a 66% yield of **1***c* was obtained as colorless plates from methanol, m.p. 135–137°; ν_{max} (Nujol) 1675 (C=O), 1610 (C=C) cm^{-1}; n.m.r. ($CDCl_3$) δ 1.23 (s, 3H, C_{4a}—CH_3),

Can. J. Chem. Downloaded from www.nrcresearchpress.com by 210.87.254.42 on 09/05/12
For personal use only.

1.37 (s, 3H, C_{10b}—CH_3), 1.82 (s, 3H, C_1—CH_3), 3.78 (s, 3H, OCH_3); M^+ at 324.

Anal. Calcd. for $C_{22}H_{28}O_2$: C, 81.44; H, 8.70. Found: C, 81.59; H, 8.65.

*1′β,4′aβ-Dimethyl-7′-methoxy-3′,4′,4′a,9′,10′,10′aα-hexahydro-spiro [1,3-dioxolane-2,2′(1′H)-phenanthrene]-1′α-acetaldehyde (**21**)*

Sodium periodate (748 mg, 3.50 mmol) was added in portions over a 20 min period to a stirred suspension of the ketal–olefin **18** (512 mg, 1.50 mmol), osmium tetroxide (38 mg, 0.15 mmol), saturated sodium bicarbonate solution (1 ml), dioxane (18 ml), and water (6 ml). This mixture was stirred for 2.5 h at room temperature, poured into saturated sodium bicarbonate solution, and extracted with chloroform (3 × 50 ml). The combined chloroform extracts were washed with saturated sodium sulfite solution (2 × 50 ml) and then with saturated sodium bicarbonate (25 ml). Work-up of the chloroform layer gave a clear oil which proved to be a mixture of the desired ketal–aldehyde **21** and uncleaved ketal–diol. This crude product was dissolved in dioxane (10 ml) and reacted with a solution of periodic acid dihydrate (732 mg, 3.21 mmol) in water (2 ml). The reaction mixture was stirred for 2.5 h at room temperature, diluted with water, and extracted with chloroform. Work-up gave a clear oil which slowly crystallized. Recrystallization from ether gave the ketal–aldehyde **21** as clusters of colorless needles, m.p. 125–127° (358 mg, 1.04 mmol, 70%); ν_{max} (Nujol) 2740 (aldehyde C—H), 1710 (C=O), 1612 (Ar C=C) cm^{-1}; n.m.r. ($CDCl_3$) δ 1.15 (s, 3H, C_1—CH_3), 1.22 (s, 3H, C_4—CH_3), 2.18 (d, $J = 3$ Hz, 2H, —CH_2CHO), 3.67–4.00 (m, 4H, OCH_2CH_2O), 3.70 (s, 3H, OCH_3), 9.60 (t, $J = 3$ Hz, 1H, —CHO); M^+ at 344.

Anal. Calcd. for $C_{21}H_{28}O_4$: C, 73.23; H, 8.19. Found: C, 73.31; H, 8.25.

*1α-(Hydroxyethylene)-1β,4aβ-dimethyl-2β-hydroxy-7-methoxy-1,2α,3,4,4a,9,10,10aα-octahydrophenanthrene (**22**)*

The ketal–aldehyde **21** (147 mg, 0.427 mmol) was dissolved in ethanol (5 ml), stirred with sodium borohydride (160 mg, 4.21 mmol) for 4 h at room temperature, and then diluted with water, and extracted with chloroform to yield a clear oil on work-up. This ketal–alcohol was immediately dissolved in acetone (50 ml) and 1 *N* sulfuric acid (5 ml) and warmed on a steam bath for 30 min to hydrolyze the ketal group. Removal of acetone followed by ether extraction and work-up gave the ketone–alcohol as an oil; ν_{max} (film) 3375 cm^{-1} (OH), no C=O absorption, indicating that this compound exists in the hemi-ketal form. The crude ketone–alcohol was dissolved in ethanol (5 ml), stirred with sodium borohydride (160 mg, 4.21 mmol) for 4 h at room temperature, and then diluted with water, and extracted with ether. Work-up gave a clear oil which was separated into two fractions by t.l.c. chromatography on silica gel (chloroform:methanol = 100:3). The minor component just separated from the major one (lower R_f). The major fraction was eluted and crystallized from acetone/hexane to give the diol **22** as tiny clusters of colorless needles, m.p. 135–137°. The authentic sample[9] of **22** had m.p. 131–133° and a mixture of the two samples had m.p. 132–134°. The i.r. and mass spectra of the authentic and synthetic samples of **22** were identical and the samples had the same R_f value on t.l.c. silica gel plates.

The minor component isolated from the t.l.c. plate had an i.r. spectrum very similar to that of **22** and a similar mass spectrum (M^+ at 304). It is presumed to be the 2α-OH isomer of **22**.

We thank the National Research Council of Canada for generous financial assistance. Professor R. A. Bell, McMaster University, Hamilton, Ontario kindly determined the nuclear Overhauser effects.

1. J. Simonsen and W. C. J. Ross. The terpenes. Vol. V. Cambridge University Press, Cambridge, England. 1957. T. G. Halsall and R. T. Aplin. *In* Fortschritte der Chemie Organisher Naturstoffe. Vol. XXII. L. Zechmeister, *Editor*. Springer–Verlag, New York. 1964. p. 153.
2. (*a*) G. Stork, A. Meisels, and J. E. Davies. J. Am. Chem. Soc. **85**, 3419 (1963). (*b*) E. E. van Tamelen, M. A. Schwartz, E. J. Hessler, and A. Storni. Chem. Commun. 409 (1966); E. J. Corey, H. J. Hess, and S. Proskow. J. Am. Chem. Soc. **81**, 5258 (1959); J. A. Barltrop, J. D. Littlehailes, J. D. Rushton, and N. A. J. Rogers. Tetrahedron Lett. 429 (1962); E. Ghera and F. Sondheimer. Tetrahedron Lett. 3887 (1964); D. H. R. Barton, E. F. Lier, and J. F. McGhie. J. Chem. Soc. C, 1031 (1968).
3. (*a*) R. E. Ireland, D. A. Evans, D. Glover, G. M. Rubottom, and H. Young. J. Org. Chem. **34**, 3717 (1969). (*b*) R. E. Ireland, D. A. Evans, P. Löliger, J. Bordner, R. H. Stanford, Jr., and R. E. Dickerson. J. Org. Chem. **34**, 3729 (1969).
4. R. E. Ireland, S. W. Baldwin, D. J. Dawson, M. I. Dawson, J. E. Dolfini, J. Newbould, W. S. Johnson, M. Brown, R. J. Crawford, P. F. Hudrlik, G. H. Rasmussen, and K. K. Schmiegel. J. Am. Chem. Soc. **92**, 5743 (1970); R. E. Ireland and S. C. Welch. J. Am. Chem. Soc. **92**, 7232 (1970).
5. G. Stork, S. Uyeo, T. Wakamatsu, P. Grieco, and J. Labovitz. J. Am. Chem. Soc. **93**, 4945 (1971).
6. G. Stork and J. W. Schulenberg. J. Am. Chem. Soc. **84**, 284 (1962); E. Wenkert, A. Afonso, J. B. Bredenberg, G. Kaneko, and A. Tahara. J. Am. Chem. Soc. **86**, 2038 (1964); R. E. Ireland and R. C. Kierstead. J. Org. Chem. **31**, 2543 (1966); C. L. Graham and F. J. McQuillin. J. Chem. Soc. 4521 (1964).
7. A. Barco, A. A. Bothner-By, G. P. Pollini, and G. Traverso. Gazz. Chim. Ital. **96**, 1186 (1966).
8. G. Stork. Pure Appl. Chem. **9**, 131 (1964).
9. E. Wenkert, K. G. Dave, and R. V. Stevens. J. Am. Chem. Soc. **90**, 6177 (1968); J. P. Yardley, R. W. Rees, and H. Smith. J. Med. Chem. **10**, 1088 (1967); K. Wiesner, J. G. McCluskey, J. K. Chang, and V. Šmůla. Can. J. Chem. **49**, 1092 (1971).
10. M. E. Kuehne and J. A. Nelson. J. Org. Chem. **35**, 161 (1970).
11. U. R. Ghatak, D. K. Datta, and S. C. Ray. J. Am. Chem. Soc. **82**, 1728 (1960); A. Ogiso and S. W. Pelletier. Chem. Commun. 94 (1967).

12. W. S. JOHNSON, J. J. KORST, R. A. CLEMENT, and J. DUTTA. J. Am. Chem. Soc. **82**, 614 (1960).
13. J. E. BRIDGEMAN, P. C. CHERRY, A. S. CLEGG, J. M. EVANS, E. R. H. JONES, A. KASAL, V. KUMAR, G. D. MEAKINS, Y. MORISAWA, E. E. RICHARDS, and P. G. WOODGATE. J. Chem. Soc. C, 250 (1970) and references therein.
14. R. S. MATTHEWS, P. K. HYER, and E. A. FOLKERS. Chem. Commun. 38 (1970); R. S. MATTHEWS, S. J. GIRGENTI, and E. A. FOLKERS. Chem. Commun. 708 (1970) and references therein.
15. R. L. AUGUSTINE. Catalytic hydrogenation. Edward Arnold (Publishers) Ltd., London. 1965. Chapt. II.
16. S. J. HALKES and E. HAVINGA. Rec. Trav. Chim. **84**, 889 (1965).
17. R. A. BELL and J. K. SAUNDERS. Can. J. Chem. **48**, 1114 (1970).
18. G. STORK, P. ROSEN, N. GOLDMAN, R. V. COOMBS, and J. TSUJI. J. Am. Chem. Soc. **87**, 275 (1965); D. CAINE and B. J. L. HUFF. Tetrahedron Lett. 4695 (1966); 3399 (1967).
19. H. A. SMITH, B. J. L. HUFF, W. J. POWERS, III, and D. CAINE. J. Org. Chem. **32**, 2851 (1967); L. E. HIGHTOWER, L. R. GLASGOW, K. M. STONE, D. A. ALBERTSON, and H. A. SMITH. J. Org. Chem. **35**, 1881 (1970) and references therein.
20. M. E. KUEHNE and J. A. NELSON. J. Org. Chem. **35**, 161 (1970); M. J. GREEN, N. A. ABRAHAM, E. B. FLEISCHER, J. CASE, and J. FRIED. Chem. Commun. 234 (1970) and references therein; H. O. HOUSE, R. W. GIESE, K. KRONBERGER, J. P. KAPLAN, and J. F. SIMEONE. J. Am. Chem. Soc. **92**, 2800 (1970).
21. G. ZWEIFEL and H. C. BROWN. Org. React. **13**, 1 (1963).
22. L. F. FIESER and M. FIESER. Reagents for organic synthesis. John Wiley and Sons, Inc. New York, N.Y. 1967. p. 142.
23. W. D. EMMONS, K. S. MCCULLUM, and A. F. FERRIS. J. Am. Chem. Soc. **75**, 6047 (1953).
24. D. H. R. BARTON, R. M. EVANS, J. C. HAMLET, P. G. JONES, and T. WALKER. J. Chem. Soc. 747 (1954).
25. E. PIERS, R. W. BRITTON, and W. DE WAAL. Can. J. Chem. **47**, 4307 (1969); J. WEILL-RAYNAL. Synth. **1**, 49 (1969).
26. D. A. EVANS. Ph.D. Thesis. California Institute of Technology. Pasadena, California. 1968.

Can. J. Chem. Downloaded from www.nrcresearchpress.com by 210.87.254.42 on 09/05/12
For personal use only.

Can. J. Chem. Downloaded from www.nrcresearchpress.com by 210.87.254.5 on 09/05/12
For personal use only.

^{13}C Nuclear Magnetic Resonance of Oximes. I. Solvent and Isotope Effects on the ^{13}C Chemical Shifts of Acetoxime

N. GURUDATA

Department of Chemistry, Sir George Williams University, Montreal, Quebec

Received November 15, 1971

The ^{13}C n.m.r. spectrum of acetoxime has been obtained in five representative solvents and the chemical shifts of the three carbon atoms measured. The solvent effects on the chemical shifts are found to reflect specific solute–solvent interactions. The effect of deuteration of the α-protons on the chemical shift of the oximino carbon is also discussed.

Le spectre r.m.n. de ^{13}C de l'acétoxime a été obtenu dans cinq solvants judicieux, et les déplacements chimiques des trois atomes de carbone ont été mesurés. Les effets des solvants sur les déplacements chimiques rendent compte des interactions spécifiques soluté–solvant. Il est également discuté de l'influence d'une deutération des protons en α sur le déplacement chimique du carbone oximinique.

Canadian Journal of Chemistry, **50**, 1956 (1972)

Introduction

The stereochemistry of oximes has been investigated by a number of physical techniques including i.r. spectroscopy (1), n.m.r. spectroscopy (2–7), and X-ray spectrometry (8). The p.m.r. studies of Lustig (2) and Karabatsos and Taller (3) demonstrated the dependence of the chemical shift on the topography of the protons relative to the hydroxyl group. The shielding of the hydroxyl group is also sensitive (4) to the stereochemistry of the oxime, as are the $^{15}N–H$ coupling constants (5). Even with the aid of solvent effects (2, 3), however, the differences involved are comparatively small. Some enhancement of the chemical shift differences has been achieved by the addition of HCl (6) and, more recently, a lanthanide shift reagent has been used (7) to provide sufficiently large separations for direct examination of *syn* and *anti* isomers of a number of oximes. Unfortunately, there appears to be a considerable discrepancy between the reports of Wolkowski (*7a*) and Berlin (*7b*). For example, while the former author (*7a*) gives a $Eu(DPM)_3$-induced shift of 21.2 p.p.m. for the α-methyl group in *syn* methyl ethyl ketoxime, Berlin (*7b*) reports a relative shift of only 0.26 p.p.m. Since different solvents were used and Wolkowski's data are "after extrapolation to an equimolar ratio of $Eu(DPM)_3$ to oxime", some disagreement is expected. A difference approaching two orders of magnitude does, however, demand some clarification before this technique can be of general use.

Because of the well established large range of chemical shift values in ^{13}C magnetic resonance (^{13}C.m.r.) and the sensitivity of this parameter to molecular geometry, it can be expected that configurational differences will cause appreciable chemical shift differences in formally similar carbon atoms of oximes. In addition, a major reactive site of ketoximes, the sp^2 hybridized carbon atom, is accessible to ^{13}C.m.r. investigation. Further, while geminal deuterium isotopic shifts in p.m.r. are about 0.013 p.p.m. (9), an isotopic shift of 0.28 p.p.m. (0.047 p.p.m. per deuteron) has been found for the carbonyl carbon of acetone (10, 11).

In the present work acetoxime is used as a model to determine the magnitude of chemical shift changes due to configurational, solvent, and isotope effects, and to establish the feasibility of employing natural abundance ^{13}C.m.r. in investigating oximes.

Experimental

Acetoxime was prepared from acetone by standard techniques and recrystallized from 30–60° petroleum spirit. A sample of acetoxime-α,α'-d_6 with $95 \pm 1\%$ deuteration (12) was kindly provided by Dr. T. J. Adley.

The p.m.r. spectra were obtained in dilute CCl_4 solution

Can. J. Chem. Downloaded from www.nrcresearchpress.com by 210.87.254.5 on 09/05/12
For personal use only.

TABLE 1. ^{13}C Chemical shift* data (p.p.m.)

Solvent	C=N	CH_3(*anti*)	CH_3(*syn*)	$\Delta\delta(CH_3)$†
CCl_4	38.61	171.13	177.64	6.51
Benzene	38.44	171.93	178.50	6.57
$CHCl_3$	37.27	171.09	177.71	6.62
CH_3OH	37.71	172.39	179.08	6.69
$(CH_3)_2SO$	39.88	170.91	177.75	6.84
ΔBenzene	+0.17	−0.80	−0.86	−0.06
$\Delta CHCl_3$	+1.34	+0.04	−0.07	−0.11
ΔCH_3OH	+0.90	−1.26	−1.44	−0.18
$\Delta(CH_3)_2SO$	−1.28	+0.22	−0.11	−0.33

*From CS_2. Precision estimated to be better than ±0.04 p.p.m.
†$\Delta\delta = \delta(syn) - \delta(anti)$; $\Delta = \delta$ in $CCl_4 - \delta$ in other solvent.

on a Varian HA100 Spectrometer operated in the "frequency sweep" mode. Proton decoupled ^{13}C.m.r. spectra were run at 25.15 MHz using the above spectrometer equipped with a VK-3512-1 Heteronuclear Noise Decoupler and a V-3530 wide sweep accessory. A C-1024 Computer of Averaged Transients was used for accumulation. Spectra for solvent effects were obtained from 3.0 *M* solutions. Isotope effects were measured in saturated benzene solution containing equimolar amounts of acetoxime and acetoxime-α-α′-d_6.

Results and Discussion

The observed proton chemical shifts ($\delta = 1.85$ and 1.86 p.p.m. for the methyl groups and 10.01 p.p.m. for the hydroxyl proton) are consistent with previous reports. Table 1 summarizes the ^{13}C.m.r. chemical shift data. The relative shifts of the methyl groups and the solvent effects are also shown. (A positive solvent effect indicates that the carbon atom is less shielded in the particular solvent than in carbon tetrachloride.) The oximino carbon atom absorbs in the range 37.27 to 37.88 p.p.m. (from CS_2). Of the methyl resonances, the higher field signal is assigned to the *cis* methyl group because of the screening effect of a neighboring hydroxyl group (13, 14). This can be rationalized in terms of sterically induced polarization of electronic charge (14–16). It is noteworthy that the relative shifts of the methyl groups are of similar magnitude ($\simeq$6.8 p.p.m.) to the shielding of a γ-carbon atom in cyclohexane by an axial hydroxyl group (14). The distance between the oxygen and carbon atoms is estimated to be approximately 3.0 Å in each case. Roberts' suggestion (14) that the C_β—C_γ bond in "axial cyclohexanol" is elongated seems unlikely in view of the known *compression* of the *syn* C—C bond in acetoxime (8).

Although the trend in the relative chemical shifts of the methyl groups [$\Delta\delta(CH_3)$] is in the same direction as that of the dielectric constants of the solvents, there is no simple correlation with this parameter. The solvent effects are best explained in terms of specific solvation.

The proton of chloroform can hydrogen bond to the oximino nitrogen. By comparison with analogous hydrogen bonding effects on the carbonyl carbon (17, 18), the deshielding of the oximino carbon is readily understood in terms of a contribution from structure **1**. The smaller

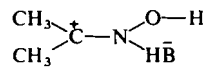

1

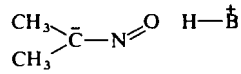

2

net deshielding effect of methanol at this carbon atom may be due to simultaneous solvation at nitrogen (deshielding) and at the oximino hydrogen as in **2** (shielding). Structure **2** also represents the type of species expected in dimethyl sulfoxide, and explains its shielding effects on the sp^2 carbon atom. The methyl carbon atoms are screened in methanol. One possible contributor to this effect is a solvent molecule oriented as in **3**. Steric perturbation

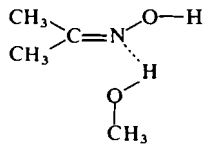

3

by the oxygen atom shields the *anti* methyl group. The high field shift of the *syn* methyl carbon reflects the compression of the C—C—N angle and consequent increased charge polarization by the oximino oxygen.

The effect of benzene can be explained in terms of previous models proposed (3, 19) for aromatic solvation of oximes and oxime ethers. Electron donation by benzene to the oximino carbon depolarizes the C=N bond giving a low field shift of 0.17 p.p.m. This is reasonable in comparison to the deshielding of the carbonyl group of acetone by 0.5 p.p.m. (18). Although Roberts has suggested (20) that anisotropy effects may be negligible at the carbon nucleus of the solute, there is ample evidence of appreciable ring current effects on carbon chemical shifts (21). The shielding of both methyl carbon

atoms may well be of this origin, with the small difference in relative shielding reflecting the asymmetric orientation of the solvent molecules necessitated by lone pair repulsions of the oximino oxygen.

Isotope Effects

Because of the wide application of deuterated species in organic chemistry, appreciable effort has been expended in elucidating deuterium isotope effects. Although accessible with modern instrumentation, the effect on H-1 chemical shifts and coupling constants is very small and not readily observable. The greater sensitivity of ^{13}C chemical shifts to structural features holds the hope of more tractable changes on deuteration. Surprisingly little work has been reported on isotope effects on ^{13}C spectra despite the extensive use of deuterated compounds as secondary references and the fact that deuterated compounds have been used to provide evidence critical to the assignment of carbon resonances (22). Maciel *et al.* (10) have reported a downfield shift of 0.28 p.p.m. for the carbonyl carbon of acetone-d_6 relative to the parent compound. In addition to confirming this result Reilly (11) measured appreciable deuterium induced shielding of the methyl carbon of acetone-d_6, dimethyl sulfoxide-d_6, and acetonitrile-d_3. While these findings are consistent with the dominance of an inductive effect, the absence of an observable effect on the sp carbon of acetonitrile (11) and the screening of the sp^2 carbon in acetoxime-α,α'-d_6 (0.08 ± 0.02 p.p.m.) found in the present study indicates clearly the need for a careful evaluation of the nature and magnitude of such perturbations.

The author wishes to thank Dr. T. J. Adley of this Department for a sample of acetoxime-α,α'-d_6, Dr. K. Berlin of Oklahoma State University for a preprint of his paper, and Dr. C. A. Reilly of Shell Development Company for his permission to quote his unpublished data.

1. A. Ossart, H. Sauvaitre, and P. Pineau. J. Chim. Phys. **64**, 953 (1967).
2. E. Lustig. J. Phys. Chem. **65**, 491 (1961).
3. G. J. Karabatsos and R. A. Taller. Tetrahedron, **24**, 3347 (1968).
4. G. G. Kleinspehn, J. A. Jung, and S. A. Studniarz. J. Org. Chem. **32**, 460 (1967).
5. D. Crépaux, J. M. Lehn, and R. R. Dean. Mol. Phys. **16**, 225 (1969).
6. B. L. Fox, J. E. Reboulet, R. E. Roudeau, and H. M. Rosenberg. J. Org. Chem. **35**, 4234 (1970).
7. (*a*) Z. W. Wolkowski. Tetrahedron Lett. 825 (1971). (*b*) K. D. Berlin and S. Rengaraju. J. Org. Chem. **36**, 2912 (1971).
8. T. K. Bierlein and E. C. Lingafelter. Acta Cryst. **4**, 450 (1951).
9. R. A. Bernheim and H. Batiz-Hernandez. J. Chem. Phys. **45**, 2261 (1966).
10. G. E. Maciel, P. D. Ellis, and D. C. Hofer. J. Phys. Chem. **71**, 2161 (1967).
11. C. A. Reilly. Unpublished results.
12. T. A. Schulz. M.Sc. Thesis. Sir George Williams University, Montreal, Quebec, 1971.
13. G. W. Buchanan and J. B. Stothers. Can. J. Chem. **47**, 3605 (1969).
14. J. D. Roberts, F. J. Weigert, J. I. Kroschwitz, and H. J. Reich. J. Am. Chem. Soc. **92**, 1338 (1970).
15. D. M. Grant and B. V. Cheney. J. Am. Chem. Soc. **89**, 5315 (1967).
16. B. V. Cheney and D. M. Grant. J. Am. Chem. Soc. **89**, 5319 (1967).
17. J. B. Stothers and P. C. Lauterbur. Can. J. Chem. **42**, 1563 (1964).
18. G. E. Maciel and J. J. Natterstad. J. Chem. Phys. **42**, 2752 (1965).
19. N. E. Alexandrou and A. G. Varvoglis. Org. Mag. Res. **3**, 293 (1971).
20. R. L. Lichter and J. D. Roberts. J. Phys. Chem. **74**, 913 (1970).
21. See, for example, A. J. Jones, T. D. Alger, D. M. Grant, and W. M. Litchman. J. Am. Chem. Soc. **92**, 2386 (1970) and references therein.
22. For example, H. J. Koch and A. S. Perlin. Carbohydr. Res. **15**, 403 (1970).

Can. J. Chem. Downloaded from www.nrcresearchpress.com by 210.87.254.5 on 09/05/12
For personal use only.

Nature de la luminescence de la colchicine

H. ROIGT ET R. M. LEBLANC

Université du Québec à Trois-Rivières, Département de chimie-biologie, C.P. 500, Trois-Rivières, Québec

Reçu le 29 décembre 1971

Des mesures de décroissance et de polarisation d'émission ainsi que des observations d'effet de solvant et d'atome lourd permettent de conclure aux multiplicités des états excités d'absorption et d'émission de la colchicine.

Measurements of the emission decrease and polarization, as well as solvent and heavy-atom effect observations, have led us to determine the excited states multiplicity of absorption and emission in colchicine.

Canadian Journal of Chemistry, **50**, 1959 (1972)

Can. J. Chem. Downloaded from www.nrcresearchpress.com by 210.87.254.42 on 09/05/12
For personal use only.

Récemment, Aronson et Inoué (1) ont déterminé un rendement photochimique de dégradation relativement faible pour la colcémide (**1**).

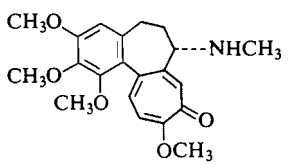

1

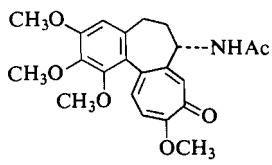

2

Notre étude qui porte sur la colchicine (**2**) montre également un rendement du même ordre de grandeur soit $\Phi_{366\,nm} = 3 \times 10^{-3}$ en solution aqueuse ($pH = 5.8$). Compte tenu de cette dégradation photochimique très faible, nous avons envisagé l'existence d'une luminescence comme autre mode de désactivation. Ainsi des mesures de fluorescence à température ambiante et dans différents solvants se sont avérées négatives, mais à 77 °K une importante luminescence a été décelée. Plusieurs résultats nous permettent de caractériser cette émission.

Partie expérimentale

Les solvants tels le 3-méthylpentane (Aldrich, "puriss."), l'iodure d'éthyle (Fisher, "Certified"), et le mélange diéthyléther, isopentane, éthanol, 5:5:2, (EPA mixed solvent, American Instrument Co. Inc.) ont été utilisés sans autre purification.

La colchicine (Sigma) a été purifiée par chromatographie sur couche mince et possédait les critères suivants: (*a*) $R_F = 0.60$ avec le méthanol (Fisher "spectrograde") comme éluant, chambre saturée, couches de gel de silice, 250 μ (Machrey, Nagel, et Co.). Le révélateur était en l'occurence le réactif de Dragendorff suivi d'une vaporisation d'acide sulfurique concentré (2). Les taches apparaissaient jaune–orange sur fond brun. (*b*) Point de fusion situé entre 145 et 150 °C (analyse différentielle thermique, et appareil de fusion de Fisher). (*c*) Coefficients d'absorption moléculaire dans l'éthanol, 95%, $\varepsilon_{351\pm1\,nm} = 16\,550\,1\ mol^{-1}\,cm^{-1}$ et $\varepsilon_{243\pm.5\,nm} = 29\,300\,1\ mol^{-1}\,cm^{-1}$, calculés par la méthode des moindres carrés, se comparent relativement bien aux valeurs de référence, soient $\varepsilon_{350\,nm} = 16\,740$, $\varepsilon_{244\,nm} = 30\,000$ (3); $\varepsilon_{350.5\,nm} = 16\,600$, $\varepsilon_{243\,nm} = 29\,600$ (4).

Les solutions de colchicine ont été préparées dans l'obscurité et dégazées par la technique du vide obtenu par pompage à la température de l'azote liquide, *i.e.* cycles "gel-dégel".

Les spectres d'absorption sont pris à l'aide d'un spectrophotomètre Unicam SP 1800 et ceux de luminescence avec un spectrofluorimètre Perkin–Elmer MFP 2A, équipé des accessoires de phosphorescence et de polarisation.

La phosphorescence est détectée au moyen d'un photomultiplicateur HTV R 106. Pour la mesure du temps de vie, nous utilisons une cellule photoélectrique du type "pin-diode, MRD 500" reliée à un oscilloscope au moyen d'un amplificateur différentiel (l'impédance d'entrée diode-amplificateur est supérieure à 20 MΩ), et la lampe du spectrofluorimètre est remplacée par une lampe éclair au Xénon de 100 W (Nihon–Kohden) donnant des éclairs de 10 μs.

Le temps de vie de phosphorescence est calculé par méthode graphique en posant le logarithme de l'intensité en fonction du temps.

Résultats et discussion

Par excitation de la colchicine à 370 nm, une bande d'émission relativement large est décelée à la température de 77 °K (fig. 1). La différence de 20 nm entre le maximum d'absorption et celui d'excitation est due au changement d'état du solvant. Il est à noter qu'aucune fluorescence n'a été détectée à la température ambiante dans les solvants tels que l'EPA, l'eau, l'éthanol, et le benzène.

A priori, la luminescence observée peut aussi bien être de la fluorescence à basse température que de la phosphorescence.

Il est à noter que le maximum d'absorption à 350 nm subit un déplacement bathochrome lorsque la polarité du solvant augmente. De plus compte tenu du coefficient d'absorption moléculaire élevé ($\varepsilon_{351} \sim 16\,000\,1\ mol^{-1}\ cm^{-1}$)

Can. J. Chem. Downloaded from www.nrcresearchpress.com by 210.87.254.42 on 09/05/12
For personal use only.

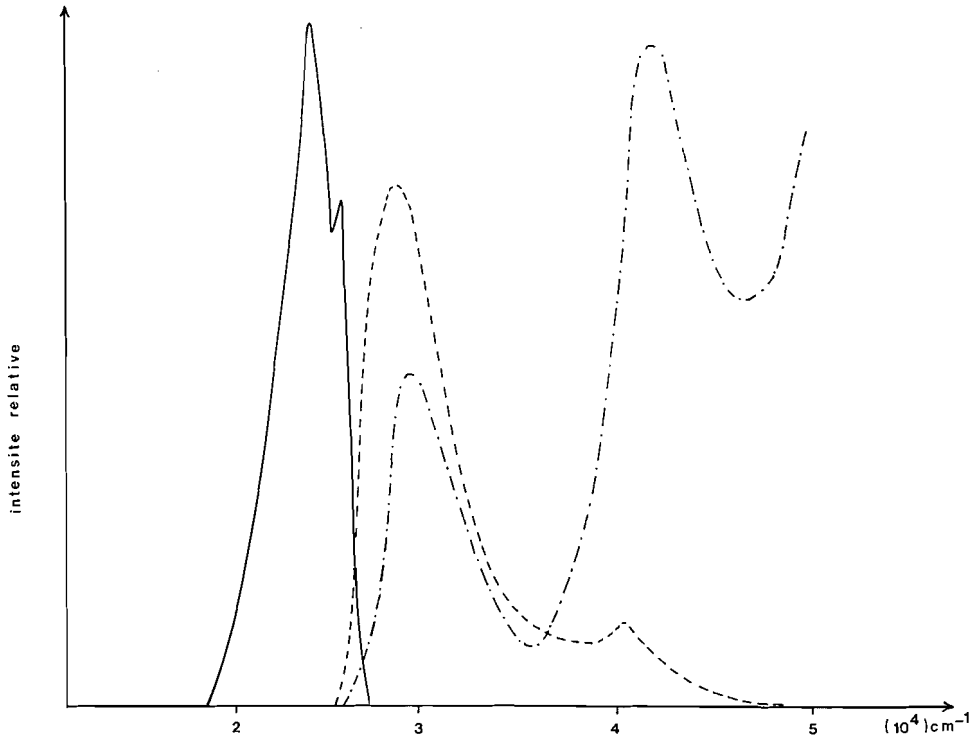

FIG. 1. Spectres d'absorption (—·—·—) à 25 °C, d'excitation (---) et d'émission (—) à −196 °C de la colchicine dans l'EPA.

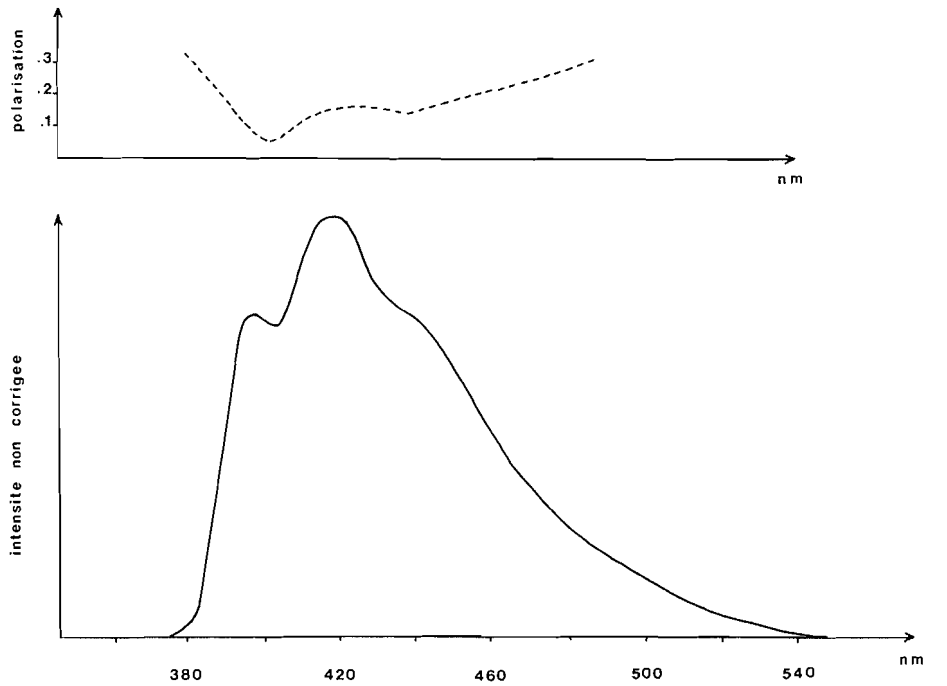

FIG. 2. Spectres d'émission et de polarisation de l'émission de la colchicine dans l'EPA à −196 °C.

la bande est identifiée comme étant une bande $\pi-\pi^*$ d'un état singulet.

En ce qui a trait à la bande de luminescence, on observe par contre un effet hypsochrome par augmentation de la polarité du solvant. D'autre part, l'augmentation du couplage spin-orbite par dissolution de la colchicine dans l'iodure d'éthyle n'apporte aucun changement du spectre. Un tel résultat a été commenté par McGlynn et coll. (5). Enfin des mesures de polarisation aux différentes longueurs d'onde de l'émission, il découle une valeur moyenne $P = +0.2$ (fig. 2).

Chacun de ces résultats présente une preuve directe de la présence d'une bande $n-\pi^*$ (probablement dûe à la délocalisation des électrons du groupement carbonyle de l'anneau tropolone) (6, 7).

Puisque la bande d'absorption à 350 nm possède un caractère $\pi-\pi^*$ et que celle d'émission revêt un caractère $n-\pi^*$, c'est qu'il existe une absorption $n-\pi^*$. Il nous a été cependant impossible de détecter la présence de cette bande, du fait de son faible coefficient d'extinction molaire ($\varepsilon_{n-\pi^*} < 2000$). De plus, la position de la bande 0–0 d'émission se situe à 402 nm, ce qui impliquerait une absorption vers la même longueur d'onde, absorption qui disparaît donc sous la bande $\pi-\pi^*$.

Afin de déterminer la multiplicité de l'état excité de la colchicine, le temps de vie a été mesuré, soit 2×10^{-4} s ce résultat permet d'identifier l'émission comme étant de la phosphorescence (8).

L'existence de cette forme de dégradation de l'état excité par émission de phosphorescence laisse entrevoir, pour la molécule de colchicine en particulier, de nombreuses possibilités d'explication de son mode d'action sur l'appareil mitotique cellulaire.

Nous remercions le Conseil National de Recherches du Canada de leur aide financière.

1. J. Aronson et S. Inoué. J. Cell Biol. **45**, 470 (1970).
2. H. Potěšilová, J. Wiedermannová, et F. Šantavý. Coll. Czech. Chem. Commun. **34**, 3642 (1969).
3. R. M. Horowitz et G. E. Ullyot. J. Am. Chem. Soc. **74**, 587 (1952).
4. Index Merck. 8ième ed. Merck & Cie Inc., Rahway, N.J. 1968.
5. S. P. McGlynn, T. Azumi, et M. Kasha. J. Chem. Phys. **40**, 507 (1964).
6. S. Hotchandani et A. C. Testa. J. Chem. Phys. **54**, 4508 (1971).
7. M. Kasha. Light and life. *Edited by* W. D. McElroy and B. Glass. Johns Hopkins Press, Baltimore, Md. 1961. p. 31.
8. C. A. Parker. Photoluminescence of solutions. Elsevier, London. 1968. p. 38.

Pyrrole Chemistry. XIV. Some Chemical and Physical Properties of 3-Pyrrolecarbaldehyde and 1-Methyl-3-pyrrolecarbaldehyde

Hugh J. Anderson and H. Nagy

Department of Chemistry, Memorial University of Newfoundland, St. John's, Newfoundland

Received January 31, 1972

3-Pyrrolecarbaldehyde (1) has been prepared on an increased scale. A general survey of the physical and chemical properties of the 3-aldehyde and 1-methyl-3-pyrrolecarbaldehyde has been carried out. The results indicate similar chemical properties to those of the corresponding 2-aldehydes. The physical properties are generally predictable on the basis of earlier studies.

Le pyrrolecarbaldéhyde-3 (1) a été préparé sur une plus grande échelle. Une revue générale des propriétés physiques et chimiques de l'aldéhyde-3 et du méthyl-1 pyrrolecarbaldéhyde-3 a été menée à bien. Les résultats indiquent des propriétés chimiques semblables à celles des aldéhydes-2 correspondants. Les propriétés physiques sont en général prévisibles en se fondant sur les études précédentes.

Canadian Journal of Chemistry, **59**, 1961 (1972)

The availability of 3-pyrrolecarbaldehyde (1) has permitted an examination of some of its physical and chemical properties. These properties have been compared with those of 1-methyl-3-pyrrolecarbaldehyde, 2-pyrrolecarbaldehyde, and the 1-methyl-2-aldehyde. The last two com-

Can. J. Chem. Downloaded from www.nrcresearchpress.com by 210.87.254.42 on 09/05/12
For personal use only.

la bande est identifiée comme étant une bande $\pi-\pi^*$ d'un état singulet.

En ce qui a trait à la bande de luminescence, on observe par contre un effet hypsochrome par augmentation de la polarité du solvant. D'autre part, l'augmentation du couplage spin-orbite par dissolution de la colchicine dans l'iodure d'éthyle n'apporte aucun changement du spectre. Un tel résultat a été commenté par McGlynn et coll. (5). Enfin des mesures de polarisation aux différentes longueurs d'onde de l'émission, il découle une valeur moyenne $P = +0.2$ (fig. 2).

Chacun de ces résultats présente une preuve directe de la présence d'une bande $n-\pi^*$ (probablement dûe à la délocalisation des électrons du groupement carbonyle de l'anneau tropolone) (6, 7).

Puisque la bande d'absorption à 350 nm possède un caractère $\pi-\pi^*$ et que celle d'émission revêt un caractère $n-\pi^*$, c'est qu'il existe une absorption $n-\pi^*$. Il nous a été cependant impossible de détecter la présence de cette bande, du fait de son faible coefficient d'extinction molaire ($\varepsilon_{n-\pi^*} < 2000$). De plus, la position de la bande 0–0 d'émission se situe à 402 nm, ce qui impliquerait une absorption vers la même longueur d'onde, absorption qui disparaît donc sous la bande $\pi-\pi^*$.

Afin de déterminer la multiplicité de l'état excité de la colchicine, le temps de vie a été mesuré, soit 2×10^{-4} s ce résultat permet d'identifier l'émission comme étant de la phosphorescence (8).

L'existence de cette forme de dégradation de l'état excité par émission de phosphorescence laisse entrevoir, pour la molécule de colchicine en particulier, de nombreuses possibilités d'explication de son mode d'action sur l'appareil mitotique cellulaire.

Nous remercions le Conseil National de Recherches du Canada de leur aide financière.

1. J. Aronson et S. Inoué. J. Cell Biol. **45**, 470 (1970).
2. H. Potěšilová, J. Wiedermannová, et F. Šantavý. Coll. Czech. Chem. Commun. **34**, 3642 (1969).
3. R. M. Horowitz et G. E. Ullyot. J. Am. Chem. Soc. **74**, 587 (1952).
4. Index Merck. 8ième ed. Merck & Cie Inc., Rahway, N.J. 1968.
5. S. P. McGlynn, T. Azumi, et M. Kasha. J. Chem. Phys. **40**, 507 (1964).
6. S. Hotchandani et A. C. Testa. J. Chem. Phys. **54**, 4508 (1971).
7. M. Kasha. Light and life. *Edited by* W. D. McElroy and B. Glass. Johns Hopkins Press, Baltimore, Md. 1961. p. 31.
8. C. A. Parker. Photoluminescence of solutions. Elsevier, London. 1968. p. 38.

Pyrrole Chemistry. XIV. Some Chemical and Physical Properties of 3-Pyrrolecarbaldehyde and 1-Methyl-3-pyrrolecarbaldehyde

Hugh J. Anderson and H. Nagy

Department of Chemistry, Memorial University of Newfoundland, St. John's, Newfoundland

Received January 31, 1972

3-Pyrrolecarbaldehyde (1) has been prepared on an increased scale. A general survey of the physical and chemical properties of the 3-aldehyde and 1-methyl-3-pyrrolecarbaldehyde has been carried out. The results indicate similar chemical properties to those of the corresponding 2-aldehydes. The physical properties are generally predictable on the basis of earlier studies.

Le pyrrolecarbaldéhyde-3 (1) a été préparé sur une plus grande échelle. Une revue générale des propriétés physiques et chimiques de l'aldéhyde-3 et du méthyl-1 pyrrolecarbaldéhyde-3 a été menée à bien. Les résultats indiquent des propriétés chimiques semblables à celles des aldéhydes-2 correspondants. Les propriétés physiques sont en général prévisibles en se fondant sur les études précédentes.

Canadian Journal of Chemistry, **59**, 1961 (1972)

The availability of 3-pyrrolecarbaldehyde (1) has permitted an examination of some of its physical and chemical properties. These properties have been compared with those of 1-methyl-3-pyrrolecarbaldehyde, 2-pyrrolecarbaldehyde, and the 1-methyl-2-aldehyde. The last two com-

Can. J. Chem. Downloaded from www.nrcresearchpress.com by 210.87.254.5 on 09/05/12
For personal use only.

Can. J. Chem. Downloaded from www.nrcresearchpress.com by 210.87.254.5 on 09/05/12
For personal use only.

pounds have provided considerable discussion over the years (2–4).

The necessary modifications for optimum yield in larger scale preparation of the 3-aldehyde are described in the Experimental. Standardization trials for the decarbonylation step were tedious and the best means of product analysis was careful filtration of an aliquot, evaporation, and p.m.r. examination of the residue for the various possible products (1). The readily available 1-methyl-2-aldehyde (5) could be formylated by the Friedel–Crafts method to the 1-methyl-2,4-dialdehyde but the yield was only 26%. Thus, although the subsequent decarbonylation step appeared to go satisfactorily, this method was not used to prepare the 1-methyl-3-aldehyde. Instead, this substance was isolated in about 6% yield as a by-product of the Vilsmeier preparation of the 1-methyl-2-aldehyde[1] being used in other work.

Herz and Brasch (3) compared the physical and chemical properties of the 2-aldehyde and its 1-methyl derivative and concluded that a resonance hybrid:

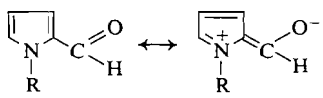

R=H or CH_3

best accounted for the observations made. Similar forms:

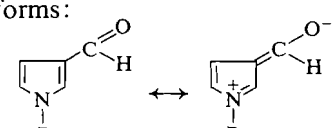

R=H or CH_3

may be drawn for the 3-aldehydes.

The 3-aldehyde carbonyl stretching frequency in carbon tetrachloride was found to be at 1683 cm^{-1} (6) while we find that of the 1-methyl derivative to be at 1685 cm^{-1}. The most recent values for the carbonyl bands of the 2-aldehyde and its 1-methyl derivative are 1667 and 1671.5 cm^{-1}, respectively, in the same solvent (7). These values support the usual statement that electron release is easier through the 2- than through the 3-position. However, the small, and similar, effect of the 1-methyl group on the carbonyl band positions makes it difficult to see that intramolecular hydrogen bonding is important to the low frequency of the 2-aldehyde carbonyl absorption (8).

In a footnote, Herz and Brasch (3) reported that the u.v. spectrum of the 2-aldehyde did not obey Beer's Law. However, we found no deviation greater than experimental error:[2] λ_{max} 290 nm (ε 16 500 $\pm$ 2.5%) in the range from 3.3×10^{-2} to 1.1×10^{-5} M in 95% ethanol, and λ_{max} 281 nm (ε 16 000 $\pm$ 6%) from 5.8×10^{-2} to 1.1×10^{-4} M in methylcyclohexane. Our spectra of the 2-aldehyde and its 1-methyl derivative in alcohol agree well with those reported by Andrisano *et al.* (9). The 3-aldehyde also obeys Beer's Law over a wide range of concentration in ethanol. Insolubility of the 3-aldehydes prevents u.v. measurement in hydrocarbon solvent. In ethanol there does not seem to be any consistent spectral change arising from the introduction of the 1-methyl group in these two aldehydes. Eisner and Gore (10) observed that the longer wavelength absorption band of 3-substituted compounds is much less intense than that of the 2-substituted ones. This is true here, although that band is a shoulder in the 3-aldehyde spectra and measurement is not precise. Also this band is 15–18 nm lower for the 3- than for the corresponding 2-derivative as noted before (10) in more highly substituted examples.

The p.m.r. spectra of the 3-aldehyde and 1-methyl-3-aldehyde of pyrrole showed no observable coupling of the aldehyde and ring protons at probe temperature. This contrasts with the spectra of the 3-aldehyde of furan (11) and of thiophene (12) where —C*H*O to H-5 and to H-4 coupling was observed. In both 2,4-pyrroledicarbaldehyde and its 1-methyl derivative the 2-C*H*O is coupled to H-5, but the 4-C*H*O signal is again a singlet.

The mass spectra of the four aldehydes were found to be entirely as expected on the basis of earlier work (13)[3]. In each, the important peaks are M^+, M − 1, M − CHO, as well as the peak at *m/e* 39 and, for the 1-methyl derivatives, the peak at *m/e* 53.

[1]Observed by Dr. C. E. Loader of this Department. In large scale preparations of 2-pyrrolecarbaldehyde, he also obtained about 1/2% of the 3-aldehyde from the residue.

[2]In a personal communication Professor Herz agrees that their observation may have been an effect of stray light at high absorbance.

[3]Under the instrument conditions we used, the spectrum of the 2-aldehyde showed good agreement with ref. 13 for higher masses but was less satisfactory for lower masses.

Can. J. Chem. Downloaded from www.nrcresearchpress.com by 210.87.254.5 on 09/05/12
For personal use only.

It has been reported (2, 3) that 2-pyrrolecarbaldehyde does not show positive Schiff's, Fehling's, or Tollen's tests. Herz and Brasch (3) stated that the 1-methyl-2-aldehyde also failed these tests. As the usual Fehling's test generally fails for aromatic aldehydes (14) that result is not surprising. We confirmed that the Schiff test fails for both the 2- and 3-aldehydes as well as their 1-methyl derivatives. However, Tollen's reagent with either the 2- or the 3-aldehyde gave a silver mirror rapidly on warming or within 5 min in the dark at room temperature. Surprisingly, neither 1-methyl derivative reacted within several hours, nor on warming. All four aldehydes may be converted to their acids using fresh silver oxide in the method of Hodge and Rickards (15).

Attempts to convert the 2- or the 3-aldehyde to its acetal failed. However, the ethylene acetal of the 3-aldehyde, 3-(1,3-dioxolan-2-yl)-pyrrole, could be made by conversion of ethyl 4-formyl-2-pyrrolethiolcarboxylate to its ethylene acetal followed by removal of the ethyl thiolcarboxylate group by Raney nickel. Both acetals were highly unstable toward light and to the most weakly acidic conditions. Similar instability of the ethylene ketal of methyl 4-acetyl-2-pyrrolecarboxylate has been observed (16). Attempts to convert the 3-acetal to a pyrrole Grignard reagent were unsuccessful.

It has been reported (17) that in Wittig reactions with the 2-aldehyde and with its 1-methyl derivative the yields are very sensitive to relative basicities and reaction conditions. We found that the yield of 1-methyl-3-styrylpyrrole from the 1-methyl-3-aldehyde was low under a variety of conditions and that the only apparently successful reaction of 3-pyrrolecarbaldehyde with triphenylbenzylphosphonium chloride could not be repeated.

Although the Knoevenagel reaction with ethyl malonate succeeded with the 3-aldehyde, the benzoin and Perkin condensations failed. The lithium aluminum hydride reduction was also unsuccessful, but Wolff–Kischner reduction to 3-methylpyrrole worked well. We have already reported the direct Wolff–Kischner conversion of ethyl 4-formyl-2-thiolcarboxylate to 3-methylpyrrole (18).

In general, the chemical reactivities of the 3-aldehyde of pyrrole and its 1-methyl derivative are not greatly different from those of the corresponding 2-aldehydes. In both simple aldehydes the N—H is decidedly acidic and this complicates some base-catalyzed reactions.

Experimental

Melting points (uncorrected) were determined on a Fisher–Johns apparatus. Elemental analyses were by Alfred Bernhardt, West Germany. The i.r. spectra were recorded on a Perkin–Elmer 237B grating spectrophotometer using potassium chloride discs, while u.v. spectra were recorded on a Perkin–Elmer 202 spectrophotometer. The p.m.r. spectra were determined using a Varian A-60 or HA100 instrument. Values are given using the τ scale with tetramethylsilane as internal reference. Mass spectra were recorded on a Hitachi–Perkin–Elmer RMU-6E spectrometer using the direct inlet system. Spectra were normalized when the variation of total ion current was less than 6% peak. Peak intensities are given as a percentage of the base peak.

3-Pyrrolecarbaldehyde[4]

(a) Ethyl 4-Formyl-2-thiolcarboxylate

The dichloromethyl methyl ether was fractionated through a 50 cm Widmer column prior to use. The crude reaction product was extracted 48 h in a Soxhlet using petroleum (80–100°); yield about 88% starting from 10–25 g thiol ester.

(b) Raney Nickel W-5

The literature method (19) could be increased fourfold in scale by increasing the diameter of the washing chamber to 10 cm while other dimensions remained the same. A Teflon paddle gave good agitation of the nickel. Deionized water (40 l) was used for washing the catalyst.

(c) 3-Pyrrolecarbaldehyde

On the larger scale a short-path distillation of the product (132–142° at 1 mm) was more convenient than column chromatography for initial product isolation. Storage of the purified material in the dark over sodium hydroxide pellets was found most satisfactory; λ_{max} (ethanol) 246 (ε 10 800), 272 nm (sh ε 6500).

3-Pyrrolecarboxylic Acid

The 3-aldehyde was oxidized by the method of Hodge and Rickards (15) to the 3-acid (75%), m.p. 144–144.5°, lit. (20) m.p. 144.5–145.5°.

1-Methyl-3-pyrrolecarboxylic Acid (by N. C. Wang)

The 1-methyl-3-aldehyde was oxidized in the same manner to give 1-methyl-3-pyrrolecarboxylic acid (72%), m.p. 145–145.5° (benzene–hexane); λ_{max} (ethanol) 233 (ε 9160), 246 nm (sh ε 7250); p.m.r. ($CDCl_3$) τ 1.02 (s, 1H), 2.66 (m, 1H), 3.40 (m, 2H), 6.30 (s, 3H).

Anal. Calcd. for $C_6H_7NO_2$: C, 57.60; H, 5.60; N, 11.20. Found: C, 57.74; H, 5.69; N, 11.36.

1-Methyl-2,4-pyrroledicarbaldehyde

1-Methyl-2-pyrrolecarbaldehyde (2.75 g, 25 mmol) was dissolved in methylene chloride (25 ml). Nitromethane (3 ml) in methylene chloride (75 ml) was added, with stirring, followed by aluminum chloride (15.6 g, 117 mmol) and dichloromethyl methyl ether (7.6 g, 66 mmol) in methylene

[4]Modifications to method of ref. 1 for larger scale synthesis.

Can. J. Chem. Downloaded from www.nrcresearchpress.com by 210.87.254.5 on 09/05/12
For personal use only.

chloride (25 ml). The mixture was stirred at room temperature 1 h, then refluxed 10 min, cooled, and poured onto ice. The organic phase was separated and the aqueous phase extracted with chloroform. The combined organic phase was washed with water and dried ($MgSO_4$). Vacuum evaporation of the solvent was followed by distillation of unreacted starting material (680 mg). The black residue was chromatographed on neutral alumina using chloroform as eluant. The solid product was recrystallized from petroleum (80–100°) to give light yellow crystals (980 mg, 26%), m.p. 95°; λ_{max} (ethanol) 237 (ε 24 700), 260 (sh ε 9600), 290 nm (ε 15 400); p.m.r. ($CDCl_3$) τ 0.18 (s, 1H), 0.33 (d, 1H); 2.5 (m, 1H), 2.7 (m, 1H), 5.99 (s, 3H).

Anal. Calcd. for $C_7H_7NO_2$: C, 61.31; H, 5.15. Found: C, 61.30; H, 5.20.

1-Methyl-3-pyrrolecarbaldehyde

Following the Vilsmeier synthesis of 1-methyl-2-pyrrolecarbaldehyde on a 2-mol scale (4), the principal product was distilled at 45°/1 mm. The residue was then distilled at 75°/1 mm and was found to consist mainly of the 1-methyl-3-aldehyde. After redistillation the yield was 10.4 g (~6%). The material was dissolved in ether and chilled to −70° producing crystals from which the ether was decanted. The crystals melted well below 0° to a colorless oil that gave a single peak on the gas chromatograph; λ_{max} (ethanol) 254 (ε 12 000), 274 nm (sh, ε 8600); p.m.r. ($CDCl_3$) τ 0.25 (s, 1H), 2.72 (m, 1H), 3.37 (m, 2H), 6.32 (s, 3H).

Anal. Calcd. for C_6H_7NO: C, 66.03; H, 6.47. Found: C, 65.72; H, 6.42.

Ethyl 4-(1,3-Dioxolan-2-yl)-2-pyrrolethiolcarboxylate

Ethyl 4-formyl-2-pyrrolethiolcarboxylate (11.7 g, 0.075 mol) and ethylene glycol (192 ml) were added to benzene (940 ml) containing *p*-toluenesulfonic acid (768 mg). "Molecular Sieves" (10 g) were added and the mixture was refluxed, using a Dean and Stark separator, for 72 h. The benzene solution was washed with sodium bicarbonate solution and dried ($MgSO_4$). Evaporation gave a yellow solid which was recrystallized from petroleum (40–60°) to give pale yellow needles (12 g, 83%), m.p. 61–61.5°, λ_{max} (ethanol) 227 (ε 25 000), 260 (sh, ε 9900), 270 (ε 10 800), 298 nm (ε 20 600); p.m.r. ($CDCl_3$) τ 2.76 (m, 1H), 2.81 (m, 1H), 4.04 (s, 1H), 5.88 (m, 4H), 6.91 (q, 2H), 8.68 (t, 3H).

Anal. Calcd. for $C_{10}H_{13}NO_3S$: C, 52.86; H, 5.77. Found: C, 52.68; H, 5.77.

3-(1,3-Dioxolan-2-yl)pyrrole

W-5 Raney nickel (32 g) was washed with acetone (3 × 100 ml). Ethyl 4-(1,3-dioxolan-2-yl)-2-pyrrolethiolcarboxylate (2.0 g, 8.8 mmol) in acetone (125 ml) was added and the mixture stirred 70 min. After the Raney nickel was filtered off and washed well with acetone the filtrate was evaporated to give 950 mg oil. Solution in ether and cooling to −70° induced crystallization. The ethylene acetal of 3-pyrrolecarbaldehyde (650 mg, 53%), m.p. 63–63.5° (ether), p.m.r. ($CDCl_3$) τ 3.28 (m, 1H), 3.44 (m, 1H), 3.71 (m, 1H), 4.18 (s, 1H), 6.03 (m, 4H).

Anal. Calcd. for $C_7H_9NO_2$: C, 60.42; H, 6.52. Found: C, 60.41; H, 6.64.

1-Methyl-3-styrylpyrrole

Potassium (234 mg, 6 mmol) was dissolved in *t*-butyl alcohol (7 ml) under nitrogen. Ether (5 ml) was added, with stirring, followed by benzyltriphenylphosphonium chloride (1.94 g, 5 mmol). The mixture was cooled and 1-methyl-3-pyrrolecarbaldehyde (444 mg, 4 mmol) in ether (5 ml) was added dropwise to the mixture. The stirring was continued at room temperature for 3 h. The mixture was poured into water (30 ml), the phases separated and the aqueous layer extracted with ether. The combined organic phase was then washed with water and dried ($MgSO_4$). After evaporation, the crude product was chromatographed on silica gel (BDH) with benzene. The early fractions gave an oil which was crystallized from petroleum (80–100°) and then sublimed. Colorless crystals (130 mg, 13%), m.p. 95°, λ_{max} (ethanol) 314 (ε 28 300), 303 (sh, ε 26 600), 236 (sh, ε 12 700), 230 nm (ε 13 300); p.m.r. ($CDCl_3$) τ 2.5–2.8 (m, 5H), 3.09 (d, 2H), 3.27 (m, 1H), 3.41 (m, 1H), 3.51 (m, 1H), 6.39 (s, 3H).

Anal. Calcd. for $C_{13}H_{13}N$: C, 85.20; H, 7.15. Found: C, 85.01; H, 7.12.

Attempted Preparation of 3-Styrylpyrrole

The procedure used to prepare the 1-methyl derivative was applied to 3-pyrrolecarbaldehyde. Although a small amount of crystalline material with the expected p.m.r. and mass spectrum was obtained on one occasion the preparation could not be repeated. Several variations of the method were equally unsuccessful.

Ethyl 1-Carbethoxy-3-(3-pyrrolyl)acrylate

3-Pyrrolecarbaldehyde (200 mg, 2.1 mmol) was dissolved in a few drops of ethanol. Ethyl malonate (600 mg, 3.7 mmol), methylammonium chloride (100 mg, 1.3 mmol), and anhydrous potassium carbonate (200 mg, 1.5 mmol) were added. After 4 days at room temperature the mixture was poured into water and extracted with ether. The ether layer was washed with water and dried ($MgSO_4$). It was then evaporated giving 190 mg of yellow oil. Chromatography on neutral alumina (benzene) gave several fractions, one of which crystallized 3 months later. The product (89 mg, 18%) was pale yellow m.p. 62–63° (ether–petroleum (60–80°)), λ_{max} 314 nm (ε 15 100); p.m.r. ($CDCl_3$) τ 2.22 (s, 1H), 2.85 (m, 1H), 3.18 (m, 1H), 3.58 (m, 1H), 5.70 (m, 4H), 8.68 (m, 6H).

Anal. Calcd. for $C_{12}H_{15}NO_4$: C, 60.75; H, 6.37. Found: C, 60.56; H, 6.29.

Mass Spectra

2-Pyrrolecarbaldehyde: M^+ 95(100%), 94(63), 66(43), 39(16). *3-Pyrrolecarbaldehyde*: M^+ 95(100%), 94(72), 66-(43), 39(24). *1-Methyl-2-pyrrolecarbaldehyde*: M^+ 109(100), 108(76), 80(23), 53(28), 39(16). *1-Methyl-3-pyrrolecarbaldehyde*: M^+ 109(100), 108(99), 80(16), 53(22), 39(18).

The authors gratefully acknowledge the continued financial assistance of the National Research Council of Canada. They also thank Dr. C. E. Loader and Dr. J. K. Groves for many helpful discussions.

1. C. E. Loader and H. J. Anderson. Tetrahedron, **25**, 3879 (1969).
2. H. Fischer and H. Orth. Die Chemie des Pyrrols. Vol. 1. Akad. Verlaggesellschaft, Leipzig, 1943. p. 150.
3. W. Herz and J. Brasch. J. Org. Chem. **23**, 1513 (1958).

4. K. SCHOFIELD. Hetero-aromatic nitrogen compounds. Butterworths, London, 1967. p. 92.
5. E. E. RYSKIEWICZ and R. M. SILVERSTEIN. J. Am. Chem. Soc. **76**, 5802 (1954).
6. M. K. A. KHAN, K. J. MORGAN, and D. P. MORREY. Tetrahedron, **22**, 2095 (1966).
7. R. A. JONES and P. H. WRIGHT. Tetrahedron Lett. 5495 (1968).
8. R. A. JONES. Adv. Heterocycl. Chem. **11**, 457 (1970).
9. R. ANDRISANO, G. PAPPALARDO, and L. BOLOGNARI. Gazz. Chem. Ital. **85**, 1430 (1955).
10. U. EISNER and P. H. GORE. J. Chem. Soc. 922 (1958).
11. S. GRONOWITZ, G. SÖRLIN, B. GESTBLOM, and R. A. HOFFMAN. Arkiv Kemi, **19**, 483 (1962).
12. S. GRONOWITZ, B. GESTBLOM, and B. MATHIASSON. Arkiv Kemi, **20**, 407 (1963).
13. W. BUDZIKIEWICZ, C. DJERASSI, A. H. JACKSON, G. W. KENNER, D. J. NEWMAN, and J. M. WILSON. J. Chem. Soc. 1949 (1964).
14. R. DANIELS, C. C. RUSH, and L. BAUER. J. Chem. Ed. 37, 205 (1960).
15. P. HODGE and R. W. RICKARDS. J. Chem. Soc. 468 (1963).
16. J. ELGUERO, R. JACQUIER, and B. SHIMIZU. Bull. Soc. Chim. Fr. 1585 (1970).
17. R. A. JONES, T. POJARLIEVA, and R. J. HEAD. Tetrahedron, **24**, 2013 (1968).
18. J. K. GROVES, H. J. ANDERSON, and H. NAGY. Can. J. Chem. **49**, 2427 (1971).
19. R. MOZINGO. Organic syntheses. Coll. Vol. 3. *Edited by* E. C. Horning. J. Wiley and Sons, Inc., New York, 1947. p. 176.
20. H. RAPOPORT and C. D. WILLSON. J. Am. Chem. Soc. **84**, 630 (1962).

The Conformational Enthalpy, Entropy, and Free Energy of The Formyl Group Determined by Low Temperature Proton Magnetic Resonance

G. W. BUCHANAN AND A. R. MCCARVILLE
Department of Chemistry, Carleton University, Ottawa, Canada

Received January 7, 1972

The low temperature proton n.m.r. peak area method has been applied to the formyl proton of cyclohexanecarboxaldehyde. The conformational enthalpy and entropy of the CHO group have been measured for the first time. The results indicate that the axial conformation has the higher entropy and $-\Delta G^0$ for the CHO function is about 0.8 kcal/mol.

La méthode de la surface des pics par r.m.n. à basse température a été appliquée au proton formyle du cyclohexanecarboxaldéhyde. L'enthalpie et l'entropie conformationnelle du groupe CHO ont été mesurées pour la première fois. Les résultats indiquent que la conformation axiale possède l'entropie la plus élevée et que $-\Delta G^0$ pour la fonction CHO est environ de 0.8 kcal/mol.

Canadian Journal of Chemistry, **50**, 1965 (1972)

Introduction

Considerable discrepancy exists between the published results for the conformational energy ($-\Delta G^0$) of the formyl group. Based on room temperature ^{1}H n.m.r. chemical shifts and couplings for the aldehyde proton of cyclohexanecarboxaldehyde and its *cis*- and *trans*-4-*t*-butyl derivatives, a value of 1.35 kcal/mol has been obtained (1, 2). A subsequent report by Eliel *et al.* gives a range of 0.56 to 0.78 kcal/mol as determined from equilibration experiments (3).

The n.m.r. procedure employing model compounds contains the inherent assumption that the 4-*t*-butyl group does not affect appreciably the properties of the axial and equatorial formyl groups respectively. In other substituted cyclohexanes, this method has been shown to be sometimes inaccurate for C-1 methine ring protons (4). No doubt similar perturbations exist for exocyclic protons although they are spatially further from the *t*-butyl group. This factor may be particularly important in these aldehydes, where the chemical shift difference between formyl protons in the *cis*- and *trans*-4-*t*-butylcyclohexyl compounds is only *ca.* 0.1 p.p.m.

The formyl group is not ideally suited for equilibration studies. Under some of the conditions employed in the previous work, condensation reactions occur and some doubt is cast on the assumption that true equilibrium was attained (3).

In view of the above data and assumptions in

Can. J. Chem. Downloaded from www.nrcresearchpress.com by 210.87.254.5 on 09/05/12
For personal use only.

4. K. SCHOFIELD. Hetero-aromatic nitrogen compounds. Butterworths, London, 1967. p. 92.
5. E. E. RYSKIEWICZ and R. M. SILVERSTEIN. J. Am. Chem. Soc. **76**, 5802 (1954).
6. M. K. A. KHAN, K. J. MORGAN, and D. P. MORREY. Tetrahedron, **22**, 2095 (1966).
7. R. A. JONES and P. H. WRIGHT. Tetrahedron Lett. 5495 (1968).
8. R. A. JONES. Adv. Heterocycl. Chem. **11**, 457 (1970).
9. R. ANDRISANO, G. PAPPALARDO, and L. BOLOGNARI. Gazz. Chem. Ital. **85**, 1430 (1955).
10. U. EISNER and P. H. GORE. J. Chem. Soc. 922 (1958).
11. S. GRONOWITZ, G. SÖRLIN, B. GESTBLOM, and R. A. HOFFMAN. Arkiv Kemi, **19**, 483 (1962).
12. S. GRONOWITZ, B. GESTBLOM, and B. MATHIASSON. Arkiv Kemi, **20**, 407 (1963).
13. W. BUDZIKIEWICZ, C. DJERASSI, A. H. JACKSON, G. W. KENNER, D. J. NEWMAN, and J. M. WILSON. J. Chem. Soc. 1949 (1964).
14. R. DANIELS, C. C. RUSH, and L. BAUER. J. Chem. Ed. 37, 205 (1960).
15. P. HODGE and R. W. RICKARDS. J. Chem. Soc. 468 (1963).
16. J. ELGUERO, R. JACQUIER, and B. SHIMIZU. Bull. Soc. Chim. Fr. 1585 (1970).
17. R. A. JONES, T. POJARLIEVA, and R. J. HEAD. Tetrahedron, **24**, 2013 (1968).
18. J. K. GROVES, H. J. ANDERSON, and H. NAGY. Can. J. Chem. **49**, 2427 (1971).
19. R. MOZINGO. Organic syntheses. Coll. Vol. 3. *Edited by* E. C. Horning. J. Wiley and Sons, Inc., New York, 1947. p. 176.
20. H. RAPOPORT and C. D. WILLSON. J. Am. Chem. Soc. **84**, 630 (1962).

The Conformational Enthalpy, Entropy, and Free Energy of The Formyl Group Determined by Low Temperature Proton Magnetic Resonance

G. W. BUCHANAN AND A. R. MCCARVILLE
Department of Chemistry, Carleton University, Ottawa, Canada

Received January 7, 1972

The low temperature proton n.m.r. peak area method has been applied to the formyl proton of cyclohexanecarboxaldehyde. The conformational enthalpy and entropy of the CHO group have been measured for the first time. The results indicate that the axial conformation has the higher entropy and $-\Delta G^0$ for the CHO function is about 0.8 kcal/mol.

La méthode de la surface des pics par r.m.n. à basse température a été appliquée au proton formyle du cyclohexanecarboxaldéhyde. L'enthalpie et l'entropie conformationnelle du groupe CHO ont été mesurées pour la première fois. Les résultats indiquent que la conformation axiale possède l'entropie la plus élevée et que $-\Delta G^0$ pour la fonction CHO est environ de 0.8 kcal/mol.

Canadian Journal of Chemistry, **50**, 1965 (1972)

Introduction

Considerable discrepancy exists between the published results for the conformational energy ($-\Delta G^0$) of the formyl group. Based on room temperature ^{1}H n.m.r. chemical shifts and couplings for the aldehyde proton of cyclohexanecarboxaldehyde and its *cis*- and *trans*-4-*t*-butyl derivatives, a value of 1.35 kcal/mol has been obtained (1, 2). A subsequent report by Eliel *et al.* gives a range of 0.56 to 0.78 kcal/mol as determined from equilibration experiments (3).

The n.m.r. procedure employing model compounds contains the inherent assumption that the 4-*t*-butyl group does not affect appreciably the properties of the axial and equatorial formyl groups respectively. In other substituted cyclohexanes, this method has been shown to be sometimes inaccurate for C-1 methine ring protons (4). No doubt similar perturbations exist for exocyclic protons although they are spatially further from the *t*-butyl group. This factor may be particularly important in these aldehydes, where the chemical shift difference between formyl protons in the *cis*- and *trans*-4-*t*-butylcyclohexyl compounds is only *ca.* 0.1 p.p.m.

The formyl group is not ideally suited for equilibration studies. Under some of the conditions employed in the previous work, condensation reactions occur and some doubt is cast on the assumption that true equilibrium was attained (3).

In view of the above data and assumptions in

Can. J. Chem. Downloaded from www.nrcresearchpress.com by 210.87.254.105 on 09/05/12
For personal use only.

Can. J. Chem. Downloaded from www.nrcresearchpress.com by 210.87.254.105 on 09/05/12
For personal use only.

the methods, it is desirable to determine the conformational preferences of the CHO group by a more direct procedure. The low temperature n.m.r. peak area method offers this alternative. When ring inversion is slow on the n.m.r. time scale, integration of peak areas under non-saturating radiofrequency conditions allows determination of the equilibrium constant K directly.

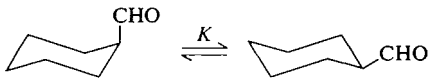

Extensive work has been done on other monosubstituted cyclohexanes using the C-1 methine proton for this purpose (5, 6). In cyclohexanecarboxaldehyde the C-1 methine proton shift is not sufficiently different from that of other ring protons to permit such a study. It is possible, however, to employ the aldehyde proton and the present report is believed to be the first case in which protons on exocyclic carbons have been utilized in this way. From the temperature dependence of the equilibrium constant, estimates of the enthalpy difference, ΔH^0, and the entropy difference, ΔS^0, between axial and equatorial formyl groups have been obtained for the first time. The equilibrium has been studied in four representative solvent media.

Results and Discussion

Figure 1 shows the temperature dependence of the formyl proton resonance of cyclohexanecarboxaldehyde in solvent CD_2Cl_2. The axial and equatorial formyl proton resonances are clearly separated below -85 °C. The chemical shift difference observed (*ca.* 0.1 p.p.m.) is similar to that between the *cis*- and *trans*-4-*t*-butylcyclohexanecarboxaldehydes, with the axial formyl proton appearing at lower field. From examination of the spectra it can be seen that the equilibrium constant K increases as the temperature decreases. In solvents CD_2Cl_2, CS_2, and THF–MeOD, K was measured over a temperature range of about 30 °C. Such a study was prevented by viscosity broadening in toluene-d_8 below $-95°$. Accordingly we report only a free energy difference at low temperature for the formyl group in this medium.

A typical plot of ln K *vs.* $1/T$ is illustrated in Fig. 2 for the formyl group in CD_2Cl_2 solution. Computer analysis of the data via an unweighted least squares procedure gives a slope, $-\Delta H^0/R$, of 483.59 and an intercept, $\Delta S^0/R$, of -0.39. Multiplication by the constant R yields $-\Delta H^0 = 0.96$ kcal/mol and $\Delta S^0 = -0.77$ cal/deg mol. From these data, the conformational free energy of the formyl group at 25 °C can be calculated using the equation $\Delta G^0 = \Delta H^0 - T\Delta S^0$, and the results are summarized in Table 1. In toluene-d_8, the equilibrium constant at -93 °C is 8.8 ± 0.3 and the conformational energy is thus obtained using the equation $-\Delta G^0 = RT \ln K$. Errors quoted are standard deviations.

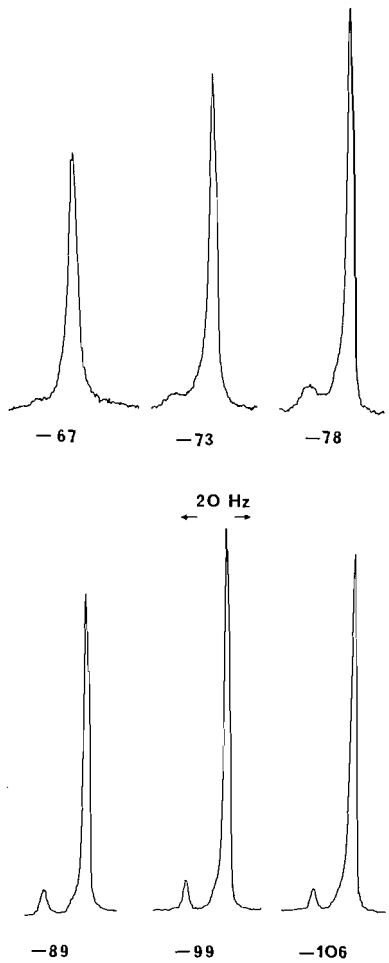

FIG. 1. Temperature dependence of the formyl proton resonance of cyclohexanecarboxaldehyde in CD_2Cl_2.

Clearly the precision of these measurements does not allow distinction between small differential solvent effects. These results suggest, however, that no dramatic solvent effects are opera-

Can. J. Chem. Downloaded from www.nrcresearchpress.com by 210.87.254.105 on 09/05/12
For personal use only.

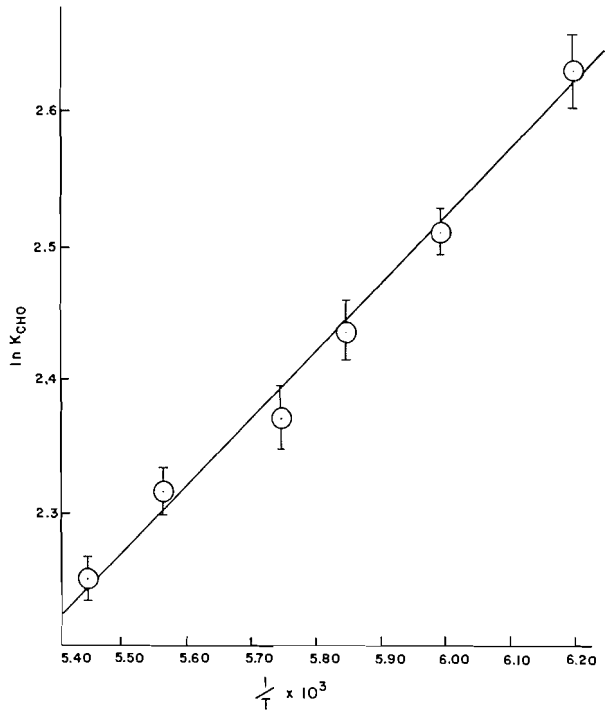

FIG. 2. Plot of ln K *vs.* $1/T$ for the formyl group in CD_2Cl_2.

TABLE 1. Conformational enthalpy, entropy, and free energy of the formyl group

Solvent	$-\Delta H^0$ (kcal/mol)	ΔS^0 (cal/degree mol)	$-\Delta G^0_{25}$ (kcal/mol)
CD_2Cl_2	0.96±0.06	−0.77±0.15	0.73±0.11
CS_2	0.90±0.08	−0.36±0.17	0.79±0.13
THF–MeOD	1.02±0.09	−0.47±0.18	0.88±0.14
C_7D_8			0.77±0.04*

*Value for −93 °C.

tive, in agreement with the earlier work (1–3). The two striking features, however, emerge from the data. Firstly, it is apparent that the formyl group has a negative conformation entropy in these three media. In general, one would predict that an equatorial substituent would have a larger number of populated rotamers than an axial one and would have, therefore, the higher entropy (7). Experimentally it has been found for related groups that equatorial $COOCH_3$, $COOC_2H_5$, and $COCH_3$ do indeed have higher entropies than their axial counterparts (8). In contrast, axial COO^-, COOH, and COCl groups are found to have substantially larger entropies (0.6 – 0.9 cal/deg mol) than the respective equatorial functions. It has been suggested that solvation and self-association are responsible for the latter findings (8). The more accessible equatorial isomer should be more strongly associated (or solvated) than its more sterically hindered axial counterpart. This restricted translational motion will cause a decrease in the entropy of the equatorial form. Presumably this rationale is correct for COO^- and COOH, but the situation is less clear for the COCl and now the CHO moieties.

The second important feature of the data concerns the observed free energy differences, which are smaller by *ca.* 0.5 kcal/mol than the values obtained using the *cis*- and *trans*-4-*t*-butylcyclohexanecarboxaldehydes as models for pure axial and equatorial CHO groups respectively. The present results are in reasonable accord with those obtained via equilibration, although the precision of the equilibration measurements was not reported (3). Since the present work involves no assumptions, we re-

gard the values presented in Table 1 as accurately representing the conformational thermodynamic parameters of the formyl group.

Experimental

Cyclohexanecarboxaldehyde was purchased from Frinton Laboratories, South Vineland, New Jersey. Degassed 0.2 *M* solutions were employed.

Spectra were recorded with a Varian XL-100-12 n.m.r. spectrometer equipped with a variable temperature probe. The temperatures were calibrated using a dummy n.m.r. tube containing a copper–constantan thermocouple and are believed to be accurate to ± 2 °C.

To ensure that non-saturating radiofrequency conditions were employed, spectra were initially recorded at widely different r.f. powers, and the relative peak areas were measured. Final conditions were then chosen where the slope of the relative peak area *vs.* r.f. power graph was zero. Integration of the areas under the peaks was done by the cutting and weighing procedure. Each value represents an average of six determinations at a given temperature.

Least squares analysis of the data was carried out with the aid of an XDS SIGMA 6 computer. Errors in $-\Delta G^0$ were calculated from the equation $\Delta\Delta G^0 = \Delta\Delta H^0 + T\Delta\Delta S^0 + \Delta T\Delta S^0$. Contributions from the last term are negligibly small since ΔT is ± 2 °C.

The standard deviations in the equilibrium constants measured at low temperature are depicted in Fig. 2. The computer program calculated the deviations in the slopes and the intercepts by standard statistical methods (9).

We thank the National Research Council of Canada for financial support of this work.

1. G. W. BUCHANAN and J. B. STOTHERS. Chem. Commun. 179 (1967).
2. G. W. BUCHANAN, J. B. STOTHERS, and S-T. WU. Can. J. Chem. **45**, 2955 (1967).
3. E. L. ELIEL, D. G. NEILSON, and E. C. GILBERT. Chem. Commun. 360 (1968).
4. F. R. JENSEN and B. H. BECK. J. Am. Chem. Soc. **90**, 3251 (1968).
5. C. H. BUSHWELLER and J. W. O'NEIL. J. Org. Chem. **35**, 276 (1970).
6. C. H. BUSHWELLER, J. A. BEACH, J. W. O'NEIL, and G. U. RAO. J. Org. Chem. **35**, 2086 (1970).
7. E. L. ELIEL, N. L. ALLINGER, S. J. ANGYAL, and G. A. MORRISON. Conformational analysis. Interscience Division of John Wiley and Sons, Inc., New York, N.Y. 1965. pp. 60–62.
8. E. L. ELIEL and M. C. REESE. J. Am. Chem. Soc. **90**, 1560 (1968).
9. H. MARGENAU and G. M. MURPHY. The mathematics of physics and chemistry. D. Van Nostrand Co., Inc., Princeton, N.J. 1956. p. 519.

Neothiobinupharidine Sulfoxide, a New Alkaloid of *Nuphar luteum*

J. T. WRÓBEL, A. IWANOW, J. SZYCHOWSKI, AND J. POPLAWSKI
Department of Chemistry, University of Warsaw, Warsaw, Poland

AND

C. K. YU, T. I. MARTIN, AND D. B. MACLEAN
Department of Chemistry, McMaster University, Hamilton, Ontario

Received January 19, 1972

A new alkaloid ($C_{30}H_{42}N_2O_3S$), isolated from *Nuphar luteum*, is shown to be neothiobinupharidine sulfoxide. The mass spectra of neothiobinupharidine and the new alkaloid are discussed.

Un nouvel alcaloïde ($C_{30}H_{42}N_2O_3S$), isolé a partir du *Nuphar luteum*, s'est avéré être le néothiobinupharidine sulfoxyde. Les spectres de masse du néothiobinupharidine et du nouvel alcaloïde sont discutés.

Canadian Journal of Chemistry, **50**, 1968 (1972)

Several sulfur-containing alkaloids of Nuphar species have been described but for only one of them, neothiobinupharidine (**1**) has the structure and relative configuration been completely resolved. Neothiobinupharidine was isolated and studied in Poland (1) and some years later its structure was elucidated by X-ray analysis (2). An isomer of **1**, thiobinupharidine (3, 4), is also known. Recently, two alkaloids related in structure to **1** have been reported (5). The two alkaloids are bis-carbinolamines that on reduction give dideoxy compounds, isomeric with one

Can. J. Chem. Downloaded from www.nrcresearchpress.com by 210.87.254.105 on 09/05/12
For personal use only.

gard the values presented in Table 1 as accurately representing the conformational thermodynamic parameters of the formyl group.

Experimental

Cyclohexanecarboxaldehyde was purchased from Frinton Laboratories, South Vineland, New Jersey. Degassed 0.2 *M* solutions were employed.

Spectra were recorded with a Varian XL-100-12 n.m.r. spectrometer equipped with a variable temperature probe. The temperatures were calibrated using a dummy n.m.r. tube containing a copper–constantan thermocouple and are believed to be accurate to ± 2 °C.

To ensure that non-saturating radiofrequency conditions were employed, spectra were initially recorded at widely different r.f. powers, and the relative peak areas were measured. Final conditions were then chosen where the slope of the relative peak area *vs.* r.f. power graph was zero. Integration of the areas under the peaks was done by the cutting and weighing procedure. Each value represents an average of six determinations at a given temperature.

Least squares analysis of the data was carried out with the aid of an XDS SIGMA 6 computer. Errors in $-\Delta G^0$ were calculated from the equation $\Delta\Delta G^0 = \Delta\Delta H^0 + T\Delta\Delta S^0 + \Delta T\Delta S^0$. Contributions from the last term are negligibly small since ΔT is ± 2 °C.

The standard deviations in the equilibrium constants measured at low temperature are depicted in Fig. 2. The computer program calculated the deviations in the slopes and the intercepts by standard statistical methods (9).

We thank the National Research Council of Canada for financial support of this work.

1. G. W. BUCHANAN and J. B. STOTHERS. Chem. Commun. 179 (1967).
2. G. W. BUCHANAN, J. B. STOTHERS, and S-T. WU. Can. J. Chem. **45**, 2955 (1967).
3. E. L. ELIEL, D. G. NEILSON, and E. C. GILBERT. Chem. Commun. 360 (1968).
4. F. R. JENSEN and B. H. BECK. J. Am. Chem. Soc. **90**, 3251 (1968).
5. C. H. BUSHWELLER and J. W. O'NEIL. J. Org. Chem. **35**, 276 (1970).
6. C. H. BUSHWELLER, J. A. BEACH, J. W. O'NEIL, and G. U. RAO. J. Org. Chem. **35**, 2086 (1970).
7. E. L. ELIEL, N. L. ALLINGER, S. J. ANGYAL, and G. A. MORRISON. Conformational analysis. Interscience Division of John Wiley and Sons, Inc., New York, N.Y. 1965. pp. 60–62.
8. E. L. ELIEL and M. C. REESE. J. Am. Chem. Soc. **90**, 1560 (1968).
9. H. MARGENAU and G. M. MURPHY. The mathematics of physics and chemistry. D. Van Nostrand Co., Inc., Princeton, N.J. 1956. p. 519.

Neothiobinupharidine Sulfoxide, a New Alkaloid of *Nuphar luteum*

J. T. WRÓBEL, A. IWANOW, J. SZYCHOWSKI, AND J. POPLAWSKI
Department of Chemistry, University of Warsaw, Warsaw, Poland

AND

C. K. YU, T. I. MARTIN, AND D. B. MACLEAN
Department of Chemistry, McMaster University, Hamilton, Ontario

Received January 19, 1972

A new alkaloid ($C_{30}H_{42}N_2O_3S$), isolated from *Nuphar luteum*, is shown to be neothiobinupharidine sulfoxide. The mass spectra of neothiobinupharidine and the new alkaloid are discussed.

Un nouvel alcaloïde ($C_{30}H_{42}N_2O_3S$), isolé a partir du *Nuphar luteum*, s'est avéré être le néothiobinupharidine sulfoxyde. Les spectres de masse du néothiobinupharidine et du nouvel alcaloïde sont discutés.

Canadian Journal of Chemistry, **50**, 1968 (1972)

Several sulfur-containing alkaloids of Nuphar species have been described but for only one of them, neothiobinupharidine (**1**) has the structure and relative configuration been completely resolved. Neothiobinupharidine was isolated and studied in Poland (1) and some years later its structure was elucidated by X-ray analysis (2). An isomer of **1**, thiobinupharidine (3, 4), is also known. Recently, two alkaloids related in structure to **1** have been reported (5). The two alkaloids are bis-carbinolamines that on reduction give dideoxy compounds, isomeric with one

Can. J. Chem. Downloaded from www.nrcresearchpress.com by 210.87.254.42 on 09/05/12
For personal use only.

Can. J. Chem. Downloaded from www.nrcresearchpress.com by 210.87.254.42 on 09/05/12
For personal use only.

another and with neothiobinupharidine. Here we report the isolation and structure of a new sulfur alkaloid, **2**, $C_{30}H_{42}N_2O_3S$. Since only small quantities of the compound were available for structural study, physical methods, particularly mass spectrometry, was used to deduce the structure. Chemical methods were then used to confirm it.

The mass spectra of **1** and **2** were examined and compared. An earlier report of the mass spectrum of **1** appeared before its structure was established (6) and it is appropriate, therefore, to reexamine and reinterpret its spectrum in the light of the revised structure and to compare it with that of deoxynupharidine, **3** (6, 7). In the earlier report it was recognized that many of the ions present in the spectrum of deoxynupharidine were also prominent in the spectrum of **1** indicating that both alkaloids had structural features in common despite the disparity in their molecular weights.

In the high mass region of the spectrum of **1** there are peaks of low intensity corresponding to the loss of CH_3, C_2H_5, and C_3H_7 from the molecular ion just as there are in the spectrum of deoxynupharidine. Ions at *m/e* 461 and 447,

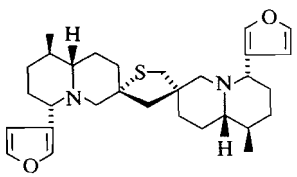

1 Neothiobinupharidine

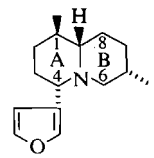

3 Deoxynupharidine

which have no counterparts in the spectrum of **3**, owe their origin to the loss of SH and CH_2SH, respectively, from the molecular ion. An ion at *m/e* 359 formed by loss of $C_9H_{11}O$ from the molecular ion may be represented as in Scheme 1. The analogous ion in **3** appears at *m/e* 98. If hydrogen transfer does not occur and the charge remains with the furan moiety an ion at *m/e* 136 results of the same mass and composition as in the spectrum of **3**.

In the low and medium mass region the spectrum shows ions at *m/e* 230, 178, 107, and 94 besides that at *m/e* 136 already discussed. The ions at *m/e* 94 and 107 are also found in **3** and can be formed in this system in a similar way. The ions at *m/e* 230 and 178, however, deserve

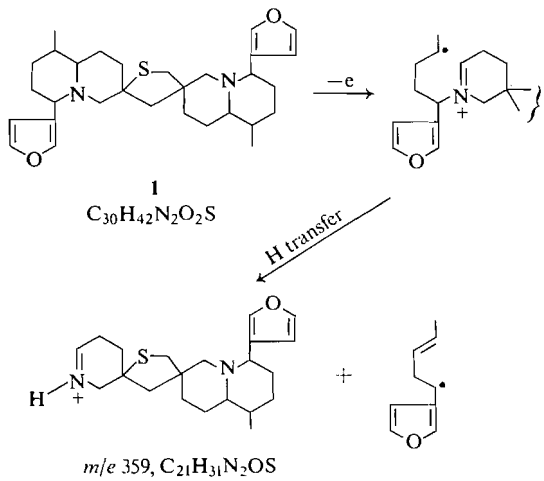

1
$C_{30}H_{42}N_2O_2S$

m/e 359, $C_{21}H_{31}N_2OS$

SCHEME 1

further comment. The former, of composition $C_{15}H_{20}NO$, can be formulated and derived as shown in Scheme 2. If a hydrogen is transferred to the sulfur-containing fragment and charge is retained on this fragment one can account for the ion observed at *m/e* 264, ($C_{15}H_{22}NOS$) which is of low intensity compared to *m/e* 230. The most intense ion of the spectrum is found at *m/e* 178 corresponding in composition to $C_{11}H_{16}NO$. A proposal for its derivation is found in Scheme 3. Charge is also carried by the residual fragment, for a peak of low intensity is also present at *m/e* 316 ($C_{19}H_{26}NOS$). An ion of *m/e* 178 is present in **3** but its intensity is

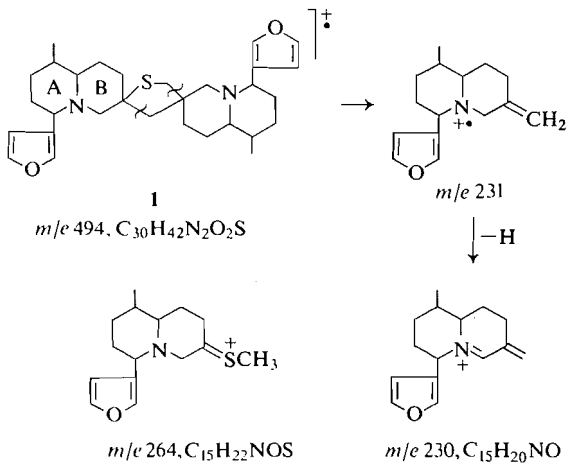

1
m/e 494, $C_{30}H_{42}N_2O_2S$

m/e 231

m/e 264, $C_{15}H_{22}NOS$

m/e 230, $C_{15}H_{20}NO$

SCHEME 2

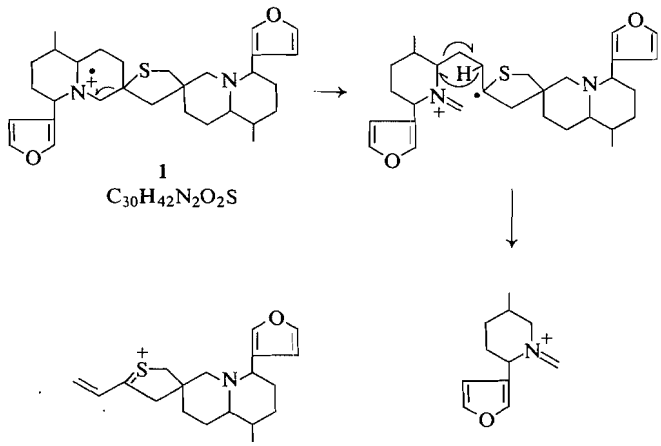

1
$C_{30}H_{42}N_2O_2S$

m/e 316, $C_{19}H_{26}NOS$ *m/e* 178, $C_{11}H_{16}NO$

SCHEME 3

relatively weak. The quaternary center present in **1** may be responsible for promoting fission in ring B thereby leading to the formation of this ion.

In their study of the reduction products of the thionuphlutines, Lalonde *et al.* (5) came to the same conclusion regarding the derivation of the ions at *m/e* 178 and 230.

The mass spectrum of the new alkaloid **2** shows losses of SOH and CH_3SO from the molecular ion at *m/e* 461 and 447 paralleling the losses of SH and CH_2SH from neothiobinupharidine. The spectrum shows an intense peak at *m/e* 493 corresponding to the loss of OH, a transformation supported by the presence of a metastable peak. Sulfoxides are known to lose OH from the molecular ion (8) and this fact coupled with the evidence that the oxygen is lost with sulfur on electron impact suggested that the alkaloid was a sulfoxide.

The rest of the spectrum of **2** is similar to that of neothiobinupharidine. Thus, the peaks at *m/e* 230, 178, 136, 107, and 94 are all present and have compositions identical with those found in the spectrum of **1**. Ions of low intensity are also present at *m/e* 280 ($C_{15}H_{22}NO_2S$), 262 (280-H_2O), 375 ($C_{21}H_{31}N_2O_2S$), and 357 (375-H_2O). The *m/e* 280 ion is cognate to *m/e* 230 while *m/e* 375 is cognate to *m/e* 136-H. Thus the mass spectral evidence indicates that the new alkaloid is a sulfoxide of a compound related in structure to neothiobinupharidine.

Chemical studies have confirmed that the new alkaloid is neothiobinupharidine sulfoxide for it has been both prepared from and converted to **1**. The configuration at sulfur has not been established, however, by these studies.

When **1** was treated with H_2O_2 in glacial acetic acid it yielded a compound identical with the natural base **2**. Their identity was established by comparison of their i.r., p.m.r., and mass spectra, their melting points, and a mixture melting point determination. The i.r. spectrum showed a band at 1020 cm^{-1} which is just below the region reported for sulfoxides (9) but considerably above that reported for *N*-oxides (10). An *N*-oxide structure is unlikely on the basis of the mass spectral evidence. The mass spectrum of deoxynupharidine is very different from its *N*-oxide, nupharidine (7), whereas the spectra of **1** and **2** are similar. Compound **2** is remarkably stable to reducing agents which argues further against its being an *N*-oxide. For example it is recovered unchanged after treatment with Zn in acetic acid, sulfur dioxide in aqueous solution, and sodium borohydride in alcohol. Nupharidine is converted, however, to deoxynupharidine with aqueous SO_2.

The natural base yielded **1** upon treatment with phosphorus trichloride in ethyl acetate, a reagent known to convert sulfoxides to sulfides (11). Thus, there seems little doubt that the new compound is a sulfoxide. It is the first representative of its class among the sulfur-containing

Can. J. Chem. Downloaded from www.nrcresearchpress.com by 210.87.254.42 on 09/05/12
For personal use only.

alkaloids of Nuphar species. Its structure is represented in **2** below.

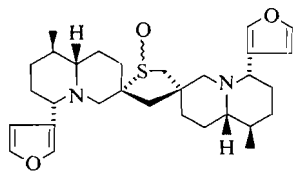

2

$C_{30}H_{42}N_2O_3S$

Experimental

Apparatus, Methods, and Materials

Mass spectra were determined on a C.E.C. 21-110B double-focusing mass spectrometer. Samples were introduced through a direct inlet system. The high resolution mass spectra (h.r.m.s.) were recorded on Ilford Q-2 photographic plates, which were developed in the usual manner. The spectra were then recorded on magnetic tape, using a Gaertner comparator-densitometer linked to a Datex system. They were processed on a CDC-6400 computer using a modified version of the HIRES program of Tunnicliff and Wadsworth (12). The composition of all ions discussed in this paper was established by high resolution measurements and agreed with calculated values within the limits, ±5 milli mass units.

A Perkin–Elmer 337 grating i.r. spectrometer was used to record i.r. spectra.

Melting points were determined on a Kofler hot stage and are uncorrected.

Isolation of Neothiobinupharidine Sulfoxide

The crude bases extracted from the rhizomes of *N. luteum* were adsorbed on neutral alumina (activity III) and the column eluted progressively with benzene, ether, chloroform, and methanol. The chloroform fraction was rechromatographed on a cellulose column using a citrate–acetate buffer of p*H* 4 and 1-butanol.[1] The sulfoxide, after separation from other bases, was recrystallized from methanol–acetone yielding colorless crystals melting at 240–242°.

Anal. Calcd. for $C_{30}H_{42}N_2O_3S$ (mol. wt. 510.291): C, 70.6; H, 8.2; N, 5.5. Found (510.286 (h.r.m.s.)): C, 70.2; H, 8.3; N, 5.3.

Mass spectrum (relative intensities in brackets): 511(5), 510(15), 495(10), 494(30), 493(66), 492(3), 461(2), 447(3), 375(1), 357(5), 280(1), 262(4), 231(20), 230(100), 179(4), 178(24), 136(5), 107(15), 94(31).

[1]Full details of the isolation procedure will be published elsewhere.

Oxidation of Neothiobinupharidine

A solution of neothiobinupharidine (110 mg) in glacial acetic acid (4 ml) was treated with 30% hydrogen peroxide (54 mg) at 20° for 1.5 h. The mixture was poured into water (20 ml), made alkaline with potassium hydroxide, and extracted repeatedly with benzene. Evaporation of the benzene gave a colorless oil which showed three spots on t.l.c. The mixture was separated by chromatography on alumina (25 g). The column was eluted successively with benzene–chloroform (9:1), followed by benzene–chloroform (1:1). The first solvent system gave neothiobinupharidine (22 mg) and the second gave first an oil (20 mg), not further investigated, and then a crystalline fraction (70 mg), m.p. 240–242°, identical with natural neothiobinupharidine sulfoxide.

Treatment of Neothiobinupharidine Sulfoxide with Phosphorus Trichloride

A solution of **2** (4 mg) in ethyl acetate (4 ml) was treated with PCl_3 (3–4 drops) and the mixture heated under reflux for 15 min, poured into water (5 ml), and made alkaline with aqueous KOH. The organic layer was separated and evaporated, and the crystalline residue obtained proved to be identical with an authentic sample of neothiobinupharidine.

This work was supported at McMaster University by the National Research Council of Canada.

1. O. Achmatowicz and J. T. Wróbel. Tetrahedron Lett. 129 (1964).
2. G. I. Birnbaum. Tetrahedron Lett. 4149 (1965).
3. O. Achmatowicz and Z. Bellen. Roczniki Chem. **36**, 1815 (1962).
4. O. Achmatowicz and Z. Bellen. Tetrahedron Lett. 112 (1962).
5. R. T. Lalonde, C. F. Wong, and W. P. Cullen. Tetrahedron Lett. 4477 (1970).
6. O. Achmatowicz, H. Banasek, G. Spiteller, and J. T. Wróbel. Tetrahedron Lett. 927, (1964).
7. J. T. Wróbel, A. Iwanow, C. Braekman-Danheux, T. I. Martin, and D. B. MacLean. Can. J. Chem. This issue.
8. H. Budzikiewicz, C. Djerassi, and D. H. Williams. Mass spectrometry of organic compounds. Holden–Day Inc., San Francisco, 1967. p. 552.
9. K. Nakanishi. Infrared absorption spectroscopy. Holden–Day Inc., San Francisco, 1962. p. 54.
10. K. Nakanishi. Infrared absorption spectroscopy. Holden–Day Inc., San Francisco, 1962. p. 51.
11. I. Branoth, A. Kalir, and Z. Pelah. J. Chem. Soc. C, 2424 (1969).
12. D. D. Tunnicliff and P. A. Wadsworth. Anal. Chem. **40**, 1826 (1968).

Can. J. Chem. Downloaded from www.nrcresearchpress.com by 210.87.254.42 on 09/05/12
For personal use only.

Les équilibres solide–liquide dans des systèmes binaires formiate d'alcalin-formiate d'alcalino-terreux

G. BERCHIESI, A. CINGOLANI, D. LEONESI ET G. PIANTONI

Istituto Chimico dell'Università, 62032 Camerino (MC), Italy

Reçu le 8 novembre, 1971

Les températures d'équilibre entre la phase liquide et la phase solide des systèmes binaires $(HCOOMe)_2 + (HCOO)_2Me'$ (Me = Na, K, Tl; Me' = Mg, Ca, Sr, Ba) ont été déterminées. Les déviations de la courbe idéale $T = \Delta H_{fus}/(\Delta S_{fus} - R \ln x)$ ont été interprétées sur la base de l'effet de polarisation des cations.

The liquid–solid equilibrium temperatures of the $(HCOOMe)_2 + (HCOO)_2Me'$ (where Me = Na, K, Tl; Me' = Mg, Ca, Sr, Ba) binary systems were determined. The deviations from the ideal curve $T = \Delta H_{fus}/(\Delta S_{fus} - R \ln x)$ are explained by the polarization effect of the ions.

Canadian Journal of Chemistry, 50, 1972 (1972)

Can. J. Chem. Downloaded from www.nrcresearchpress.com by 210.87.254.105 on 09/05/12
For personal use only.

Introduction

Les formiates de Mg, Ca, Sr, Ba sont notoirement thermolabiles, mais les mélanges avec les formiates de Na, K, Tl ont montré une bonne stabilité jusqu'à des concentration de $(HCOO)_2$-Me, Me = Mg, Ca, Sr, Ba, supérieures à la concentration de mélange eutectique.

Nous avons mesuré les températures de première cristallisation des mélanges binaires des formiates de Na, K, et Tl avec les formiates de Mg, Ca, Sr, et Ba dans l'intervalle de concentration dans lequel la stabilité thermique permettait une bonne reproductibilité des mesures. Seul le système $(HCOONa)_2 + (HCOO)_2Mg$ n'a pas été étudié, à cause de la grande instabilité dans tout l'intervalle de concentration. La méthode expérimentale employée est largement décrite dans des notes publiées precédemment (1, 2). Les produits employés sont: HCOONa, HCOOK, et $(HCOO)_2Ca$, C. Erba R.P., HCOO-Tl, BDH, et $(HCOO)_2$ Mg, $(HCOO)_2Sr$, $(HCO-O)_2Ba$, K & K, dont le degré de pureté était au minimum de 99%.

Résultats et discussion

Les courbes d'équilibre entre la phase liquide et la phase solide, pour les 11 systèmes étudiés, sont représentées à la Fig. 1, et les coordonnées des points invariants sont données au Tableau 1.

Si les deux composants ont une solubilité négligeable à l'état solide et si la solution est idéale, les propriétés thermodynamiques de fusion ΔH et ΔS, fixent la température de fusion d'un mélange selon la formule

$$[1] \qquad T = \frac{\Delta H_{fus\,i}}{\Delta S_{fus\,i} - R \ln x_i}$$

où $\Delta H_{fus\,i}$ et $\Delta S_{fus\,i}$ représentent l'enthalpie et l'entropie molaires de fusion du corps pour i à la température T_i, et x_i la fraction molaire des corps i, qui pour tous les systèmes est représentée par une ligne continue; ΔH_{fus} et ΔS_{fus} relatifs aux formiates de Na, K, et Tl sont connus (3–5). ΔH_{fus} est connu à une précision de 2% et T_{fus} à une précision de 1%.

Comme on peut le remarquer, les systèmes binaires $(HCOOK, Na)_2 + (HCOO)_2Me$, Me = Mg, Ca, Sr, Ba s'écartent négativement de l'idéalité. Il est donc bien probable que ces mélanges binaires ne forment pas de cristaux mixtes. Au contraire les systèmes $(HCOOTl)_2 + (HCOO)_2Me$, Me = Ca, Sr, Ba s'écartent assez peu de l'idéalité et de façon positive tandis que le système $(HCOOTl)_2 + (HCOO)_2Mg$ montre un minimum de température de fusion et non un eutectique à cause de la formation probable de cristaux mixtes.

Pour les systèmes contenant les formiates de sodium et de potassium on a cherché une équation $T_{observée} = (\Delta H_{fus\,i} + A)/(\Delta S_{fus\,i} - R \ln x_i)$ pour les mélanges riches en formiate de Na ou K, où A est un terme correctif qui rend compte de la déviation négative de ces systèmes (3, 4). La dépendence de A (qui est toujours négatif) de la fraction molaire est répresentée sur la Fig. 2. Dans les systèmes $(HCOONa)_2 + (HCOO)_2Me$,

Can. J. Chem. Downloaded from www.nrcresearchpress.com by 210.87.254.105 on 09/05/12
For personal use only.

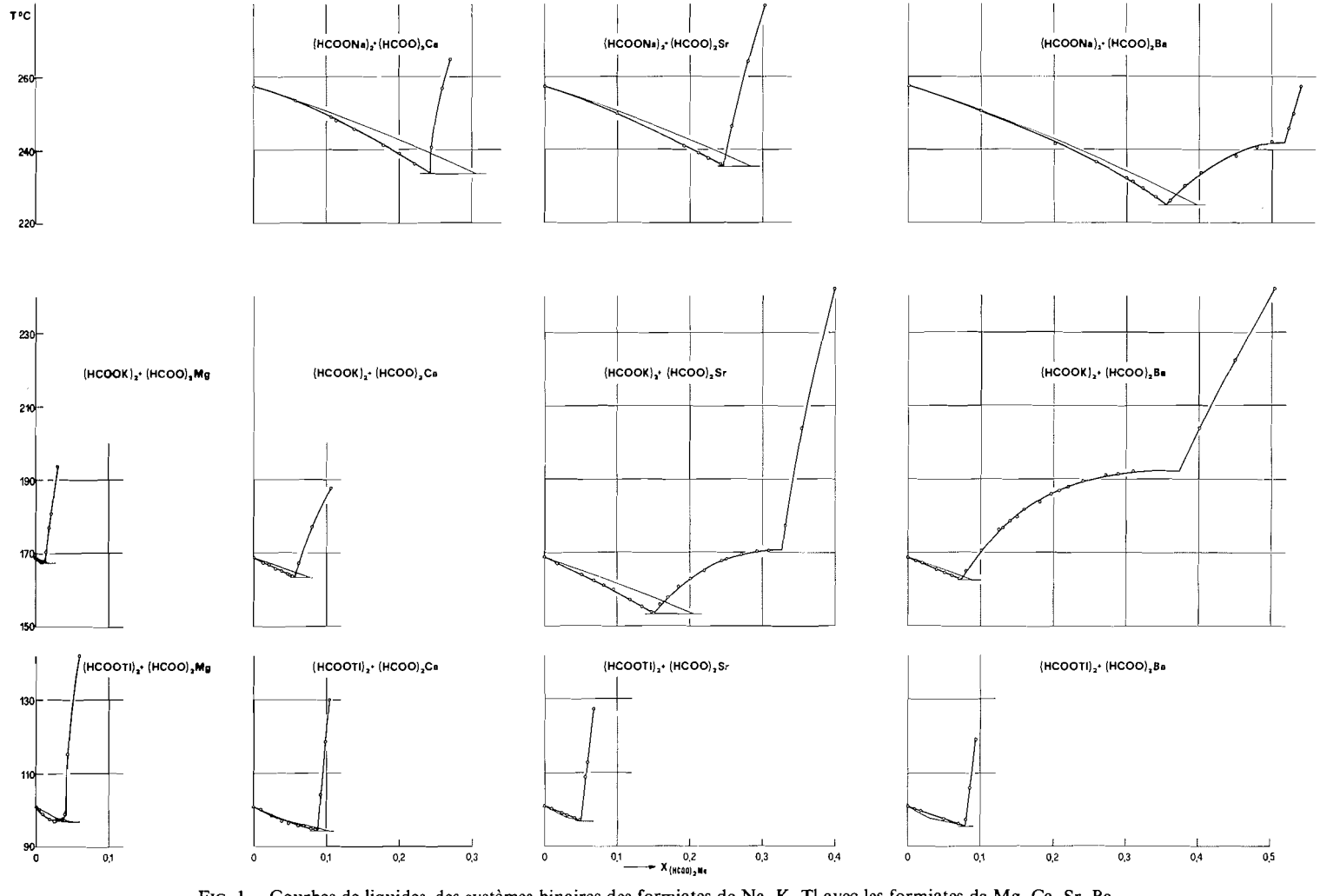

FIG. 1. Courbes de liquides des systèmes binaires des formiates de Na, K, Tl avec les formiates de Mg, Ca, Sr, Ba.

TABLEAU 1. Température de cristallisation et composition des mélanges eutectiques et péritectiques

	Paramètre	Valeur $(HCOOK)_2$	$(HCOONa)_2$	$(HCOOTl)_2$	
$(HCOO)_2Mg$	T	167.4		97.0	
	$X_{(HCOO)_2Mg}$	0.013		0.030	minimum
$(HCOO)_2Ca$	T	163.2	233.4	94.2	
	$X_{(HCOO)_2Ca}$	0.057	0.243	0.088	
$(HCOO)_2Sr$	T_{Eut}	153.2	235.4	96.8	
	$x_{(HCOO)_2Sr}$	0.150	0.246	0.051	
	T_{Per}	170.8			
	$X_{(HCOO)_2Sr}$	0.327			
$(HCOO)_2Ba$	T_{Eut}	162.6	224.8	95.4	
	$X_{(HCOO)_2Ba}$	0.074	0.354	0.079	
	T_{Per}	192.2	242.0		
	$X_{(HCOO)_2Ba}$	0.373	0.518		

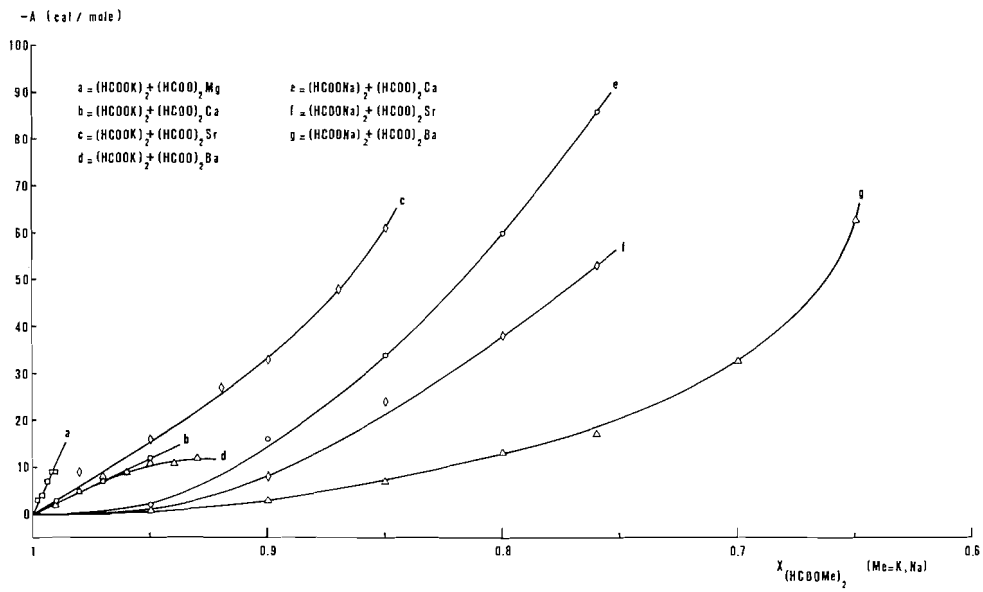

FIG. 2. Facteur correctif A, rélatif aux formiates de sodium et de potassium.

Me = Ca, Sr, Ba le terme de non idéalité A est plus petit que dans les systèmes $(HCOOK)_2 + (HCOO)_2Me$, Me = Mg, Ca, Sr, Ba. En effet, les ions sodium, plus petits que les ions potassium, ont une plus grande intensité de champ électrique et sont, en conséquence, plus polarisants que les ions potassium. A cause de la différence de pouvoir polarisant plus grande pour le couple K^+–Me^{2+} que pour le couple Na^+–Me^{2+} (6), le terme A est plus important dans les systèmes contenant le formiate de potassium que ceux contenant le formiate de sodium. Pour la même raison dans la série de systèmes $(HCOONa)_2 + (HCOO)_2Me$, Me = Ca, Sr, Ba,

Can. J. Chem. Downloaded from www.nrcresearchpress.com by 210.87.254.105 on 09/05/12
For personal use only.

A (en valeur absolue) diminue dans le sens Ca, Sr, Ba.

Dans les systèmes $(HCOOK)_2 + (HCOO)_2$-Me, Me = Mg, Ca, Sr, Ba, on a observé encore cette regularité sauf une exception: en effet A rélatif au système $(HCOOK)_2 + (HCOO)_2Ca$ est intermédiaire entre ceux rélatifs aux systèmes $(HCOOK)_2 + (HCOO)_2Sr$ et $(HCOOK)_2 + (HCOO)_2Ba$. Dans d'autres classes de systèmes (7, 8), une relation entre la composition eutectique et le rayon ionique avait été remarquée. Dans ces familles, cette régularité $X_{Eut} \propto r_{Me^{2+}}$ n'a pas été remarquée.

1. M. BRAGHETTI, D. LEONESI, et P. FRANZOSINI. Ric. Sci. **38**, 116 (1968).
2. A. CINGOLANI, G. BERCHIESI, et G. PIANTONI. J. Chem. Eng. DATA, sous presse (1971).
3. D. LEONESI, G. PIANTONI, G. BERCHIESI, et. P. FRANZOSINI. Ric. Sci. **38**, 702 (1968).
4. M. BRAGHETTI, G. BERCHIESI, et P. FRANZOSINI. Ric. Sci. **39**, 576 (1969).
5. G. BERCHIESI et M. LAFFITTE. J. Chim. Phys. **6**, 877 (1971).
6. T. FØRLAND. Norg. Tek. Vitenskapsakad. Series 2, No. 4 (1957).
7. G. PIANTONI, M. BRAGHETTI, et P. FRANZOSINI. Z. Naturforsch. **23a**, 2069 (1968).
8. D. LEONESI, M. BRAGHETTI, A. CINGOLANI, et P. FRANZOSINI. Z. Naturforsch. **25a**, 52 (1970).

^{13}C-Nuclear Magnetic Resonance Spectrum of Tropolone

LARRY WEILER

Department of Chemistry, University of British Columbia, Vancouver 8, British Columbia

Received December 20, 1971

The ^{13}C-n.m.r. spectrum of tropolone has been obtained and it clearly shows that there is a rapid tautomeric equilibrium at room temperature. The peaks have been tentatively assigned using calculated π charge densities and nuclear Overhauser enhancements.

Le spectre r.m.n. du ^{13}C du tropolone a été obtenu; celui-ci indique clairement qu'à la température de la pièce, il se fait un équilibre tautomérique rapide. Les pics ont été provisoirement attribués en se servant des densités de charge π calculées et de l'exaltation de l'effet nucléaire Overhauser.

Canadian Journal of Chemistry, **50**, 1975 (1972)

Recently there has been a great upsurge of interest in ^{13}C-n.m.r. spectroscopy (1). To date ^{13}C-n.m.r. has been utilized in many ways similar to ^{1}H-n.m.r.; for example, use of chemical shifts, coupling constants, and partial decoupling in structural assignments, heteronuclear decoupling, and the use of shift reagents (2) have been applied successfully in both cases. Anet *et al.* have recently used ^{13}C-n.m.r. to study a conformational equilibrium and they were able to freeze out the two conformers of methylcyclohexane at low temperature (3). We would like to report the use of ^{13}C-n.m.r. for studying systems in which there is an equilibrium between two tautomeric forms and to show the useful simplification of these problems by ^{13}C-n.m.r. The ^{1}H-n.m.r. spectrum of tropolone (**1**) has been recorded and even at 100 MHz the spectrum contains over 20 lines (4). The computer analysis of this spectrum does fit an AA'BB'C system and this indicated that there is a rapid equilibrium between two tautomers, reaction 1. The electron diffraction data on

[1] 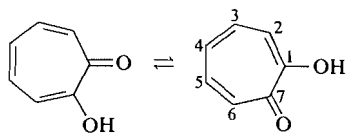

1

tropolone are consistent with a symmetric structure (5). The barrier to interconversion of the two tautomers must be low since it could not be frozen out in the n.m.r. spectrum and also in light of the electron diffraction results.

The proton-decoupled ^{13}C-n.m.r. spectrum of tropolone is shown in Fig. 1. This spectrum consists of only four singlets (*cf.* ^{1}H-n.m.r. spectrum

Can. J. Chem. Downloaded from www.nrcresearchpress.com by 210.87.254.105 on 09/05/12
For personal use only.

A (en valeur absolue) diminue dans le sens Ca, Sr, Ba.

Dans les systèmes $(HCOOK)_2 + (HCOO)_2$-Me, Me = Mg, Ca, Sr, Ba, on a observé encore cette regularité sauf une exception: en effet A rélatif au système $(HCOOK)_2 + (HCOO)_2Ca$ est intermédiaire entre ceux rélatifs aux systèmes $(HCOOK)_2 + (HCOO)_2Sr$ et $(HCOOK)_2 + (HCOO)_2Ba$. Dans d'autres classes de systèmes (7, 8), une relation entre la composition eutectique et le rayon ionique avait été remarquée. Dans ces familles, cette régularité $X_{Eut} \propto r_{Me^{2+}}$ n'a pas été remarquée.

1. M. BRAGHETTI, D. LEONESI, et P. FRANZOSINI. Ric. Sci. **38**, 116 (1968).
2. A. CINGOLANI, G. BERCHIESI, et G. PIANTONI. J. Chem. Eng. DATA, sous presse (1971).
3. D. LEONESI, G. PIANTONI, G. BERCHIESI, et. P. FRANZOSINI. Ric. Sci. **38**, 702 (1968).
4. M. BRAGHETTI, G. BERCHIESI, et P. FRANZOSINI. Ric. Sci. **39**, 576 (1969).
5. G. BERCHIESI et M. LAFFITTE. J. Chim. Phys. **6**, 877 (1971).
6. T. FØRLAND. Norg. Tek. Vitenskapsakad. Series 2, No. 4 (1957).
7. G. PIANTONI, M. BRAGHETTI, et P. FRANZOSINI. Z. Naturforsch. **23a**, 2069 (1968).
8. D. LEONESI, M. BRAGHETTI, A. CINGOLANI, et P. FRANZOSINI. Z. Naturforsch. **25a**, 52 (1970).

^{13}C-Nuclear Magnetic Resonance Spectrum of Tropolone

LARRY WEILER

Department of Chemistry, University of British Columbia, Vancouver 8, British Columbia

Received December 20, 1971

The ^{13}C-n.m.r. spectrum of tropolone has been obtained and it clearly shows that there is a rapid tautomeric equilibrium at room temperature. The peaks have been tentatively assigned using calculated π charge densities and nuclear Overhauser enhancements.

Le spectre r.m.n. du ^{13}C du tropolone a été obtenu; celui-ci indique clairement qu'à la température de la pièce, il se fait un équilibre tautomérique rapide. Les pics ont été provisoirement attribués en se servant des densités de charge π calculées et de l'exaltation de l'effet nucléaire Overhauser.

Canadian Journal of Chemistry, **50**, 1975 (1972)

Recently there has been a great upsurge of interest in ^{13}C-n.m.r. spectroscopy (1). To date ^{13}C-n.m.r. has been utilized in many ways similar to ^{1}H-n.m.r.; for example, use of chemical shifts, coupling constants, and partial decoupling in structural assignments, heteronuclear decoupling, and the use of shift reagents (2) have been applied successfully in both cases. Anet *et al.* have recently used ^{13}C-n.m.r. to study a conformational equilibrium and they were able to freeze out the two conformers of methylcyclohexane at low temperature (3). We would like to report the use of ^{13}C-n.m.r. for studying systems in which there is an equilibrium between two tautomeric forms and to show the useful simplification of these problems by ^{13}C-n.m.r. The ^{1}H-n.m.r. spectrum of tropolone (**1**) has been recorded and even at 100 MHz the spectrum contains over 20 lines (4). The computer analysis of this spectrum does fit an AA'BB'C system and this indicated that there is a rapid equilibrium between two tautomers, reaction 1. The electron diffraction data on

[1] 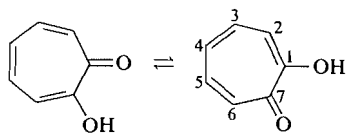

1

tropolone are consistent with a symmetric structure (5). The barrier to interconversion of the two tautomers must be low since it could not be frozen out in the n.m.r. spectrum and also in light of the electron diffraction results.

The proton-decoupled ^{13}C-n.m.r. spectrum of tropolone is shown in Fig. 1. This spectrum consists of only four singlets (*cf.* ^{1}H-n.m.r. spectrum

Can. J. Chem. Downloaded from www.nrcresearchpress.com by 210.87.254.105 on 09/05/12
For personal use only.

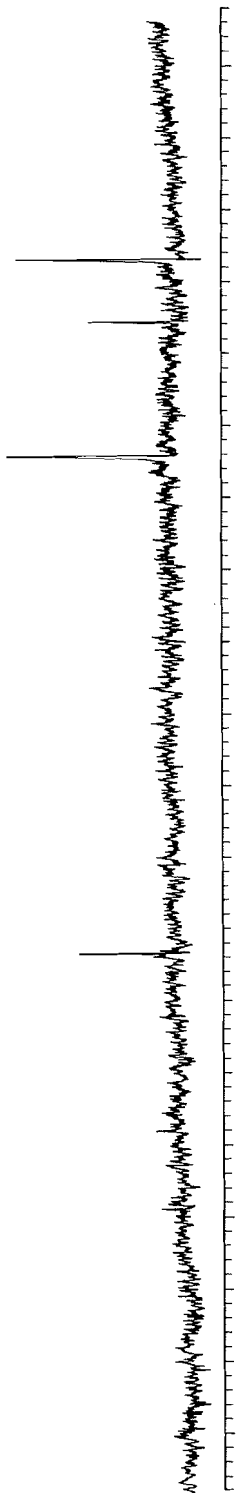

FIG. 1. The ^{13}C-n.m.r. spectrum of tropolone in $CDCl_3$; single scan at 2500 MHz sweep width.

Can. J. Chem. Downloaded from www.nrcresearchpress.com by 210.87.254.105 on 09/05/12
For personal use only.

TABLE 1. ^{13}C-n.m.r. data for tropolone

δ (p.p.m.)*	δ (p.p.m.)†	Assignment	ρ_π‡
0	−44.1	C-1, C-7	0.8489
34.6	−8.6	C-3, C-5	0.9491
44.0	+0.40	C-4	1.0230
48.2	+5.0	C-2, C-6	1.0375

*Relative to lowest field singlet, taken in $CDCl_3$.
†Relative to benzene, in C_6H_6–C_6D_6 (1:1).
‡Average of charge densities from ref. 6 (*vide infra*).

of over 20 lines), and the shifts and assignments are given in Table 1. The assignments for the C-2,3,5 and 6 resonances are based on the calculated π charge densities (6). These calculations are for one of the tautomers in the equilibrium hence the charges given in the table are the average of the calculated values for the tautomerically related carbons. There is a good correlation between the observed ^{13}C chemical shifts and the calculated π charge densities; this is shown in Fig. 2. One might expect even better agreement when calculations including the σ electrons are used.

Note that there is a solvent effect on the relative chemical shifts in Table 1. The three high field singlets have a relative intensity ratio of 2:1:2 which indicated a similar nuclear Overhauser enhancement for carbons 2–6. The relative intensity of the low field singlet is *ca.* 1.3 indicating a much lower nuclear Overhauser enhancement which is in accord with the assignment of this signal to a carbon which is not directly connected to a proton. Clearly the simplicity of the ^{13}C-n.m.r. spectrum compared to the very complex ^{1}H-n.m.r. spectrum shows another advantage of ^{13}C-n.m.r. in studying problems of this type.

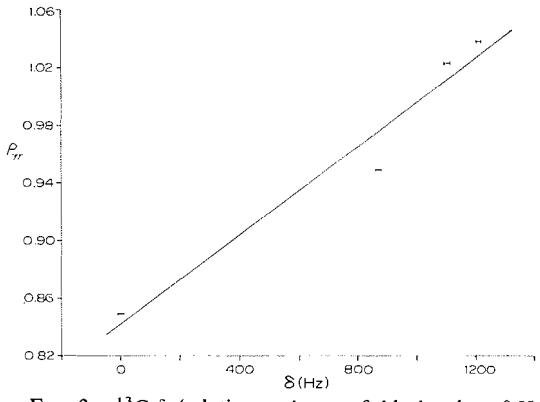

FIG. 2. ^{13}C-δ (relative to lowest field signal at 0 Hz) *vs.* π-electron charge density (ρ).

Experimental

The ^{13}C-n.m.r. spectra were recorded on a Varian XL-100 spectrometer using $CDCl_3$ or C_2D_6 as internal lock and 15 mm diameter n.m.r. tubes. The spectra were obtained using single scan at 2500 MHz sweep width. The n.m.r. solutions contained 1 g of tropolone in 5 ml of solvent.

The tropolone was recrystallized several times from petroleum ether to give white needles, m.p. 49.5–50.5°.

I am grateful to Roland Burton for running the ^{13}C-n.m.r. spectra and to the National Research Council of Canada and the University of British Columbia for financial support.

1. E. W. RANDALL. Chem. Brit. **7**, 371 (1971) and references therein.
2. J. BRIGGS, F. A. HART, G. P. MOSS, and E. W. RANDALL. Chem. Commun. 364 (1971).
3. F. A. L. ANET, C. H. BRADLEY, and G. W. BUCHANAN. J. Am. Chem. Soc. **93**, 258 (1971).
4. D. J. BERTELLI, T. G. ANDREWS, JR., and P. O. CREWS. J. Am. Chem. Soc. **91**, 5286 (1969).
5. E. HEILBRONNER and K. HEDBERG. J. Am. Chem. Soc. **73**, 1386 (1951).
6. H. KURODA and T. KUNI. Theoret. Chim. Acta, **7**, 220 (1967).

Can. J. Chem. Downloaded from www.nrcresearchpress.com by 210.87.254.105 on 09/05/12
For personal use only.

Vapor–Liquid Equilibria of Cyclohexane–*cis*-Decalin Mixtures at 25 °C[1]

TOMÁS BOUBLÍK

Institute of Chemical Process Fundamentals, Czechoslovak Academy of Science, Prague, Czechoslovakia

AND

G. C. BENSON

Division of Chemistry, National Research Council of Canada, Ottawa, Canada K1A 0R6

Received January 7, 1972

Vapor–liquid equilibria of cyclohexane–*cis*-decalin mixtures were determined at 25 °C in a circulation still. Excess Gibbs free energies derived from the experimental results are in reasonable agreement with values calculated from the theory of Flory.

Les équilibres vapeur–liquide de divers mélanges cyclohexane–*cis*-décaline furent déterminés a 25 °C dans un ébuillioscope à circulation. Les énergies libres d'excès de Gibbs, dérivant des résultats expérimentaux, sont en assez bon accord avec les valeurs calculées selon la théorie de Flory.

Canadian Journal of Chemistry, **50**, 1978 (1972)

Can. J. Chem. Downloaded from www.nrcresearchpress.com by 210.87.254.105 on 09/05/12
For personal use only.

This note reports results for the vapor–liquid equilibria of cyclohexane–*cis*-decalin mixtures at 25 °C. The work is an extension of a previous investigation (1) in which enthalpies and volumes of mixing were studied.

The component materials were cyclohexane (Lachema) which had been rectified in a 60-plate column, and *cis*-decalin (Fluka) which had been purified chromatographically. Values of their refractive indices measured at 20 °C and of their vapor pressures determined ebulliometrically at 25 °C, are compared with data from the literature (2, 3) in Table 1.

The design and operation of the still used for studying the vapor–liquid equilibria has been described previously (4). Values of the equilibrium pressure were obtained from measurements of the temperature of a water ebullioscope connected to the same manostat as the still. Estimates of the error in the values of the pressure vary from 0.02 mm Hg at low pressures to 0.05 mm Hg at the highest pressure encountered. Compositions of the equilibrium liquid and condensed vapor phases were obtained from measurements of their refractive indices using the relation

$$[1]\quad n_D^{20}(x_1) = 1.42622x_1 + 1.48100(1 - x_1) + x_1(1 - x_1)[0.02230 - 0.00629(1 - 2x_1) - 0.00077(1 - 2x_1)^2]$$

where x_1 is the mole fraction of cyclohexane. This equation represents the results for a series of mixtures of known composition with a standard error of estimate of 0.00004. The corresponding error in the estimate of the mole fraction from eq. 1 varies from 0.0004 to 0.0010 depending on the value of the mole fraction.

Experimental results obtained for the vapor–liquid equilibria of cyclohexane(1)–*cis*-decalin(2) mixtures, when the still was operated at a head temperature of 25.00 ± 0.01 °C, are summarized in Table 2. There, p is the total pressure; x_1 and y_1 are the mole fractions of cyclohexane in the liquid and vapor phases, respectively. No results are given for mixtures dilute in cyclohexane since it was impossible to obtain reproducible equilibria for $x_1 < 0.35$.

The activity coefficients of the components in the liquid phase are related to the vapor–liquid equilibria by the equation

$$[2]\quad \ln \gamma_i = \ln (y_i p/x_i p_i^0) + [(B_{ii} - V_i^0)(p - p_i^0) + (2B_{12} - B_{11} - B_{22})(1 - y_i)^2 p]/RT$$

where p_i^0 and V_i^0 are the vapor pressures and molar volumes of the pure components. The quantities B_{ij} are the second virial coefficients describing the deviation of the vapor phase from ideality. For cyclohexane at 25 °C, $B_{11} = -1650$ cm^3 mol^{-1} (5); values of $B_{22} = -8320$ and $B_{12} = -3510$ cm^3 mol^{-1} were estimated from an empirical correlation (6).

The molar excess Gibbs free energy of the

[1]NRCC No. 12543.

TABLE 1. Properties characterizing the pure component liquids

Component	Refractive index, n_D^{20}			Vapor pressure, p^{25} (mm Hg)		
	Experimental	Literature	Reference	Experimental	Literature	Reference
Cyclohexane	1.42622	1.42623	2	97.48	97.58	2
cis-Decalin	1.48100	1.48098	3	0.84	0.78*	3

*Calculated from Antoine coefficients obtained from experimental results measured above 90 °C.

TABLE 2. Vapor–liquid equilibria of cyclohexane(1)–*cis*-decalin(2) mixtures at 25.00 °C

x_1	y_1	p (mm Hg)	Δy_1 calc. – obs.	Δp (mm Hg) calc. – obs.
0.3714	0.9805	37.61	0.0050	−0.27
0.4526	0.9880	45.11	0.0015	−0.09
0.4810	0.9894	47.59	0.0011	0.11
0.5606	0.9938	55.07	−0.0008	0.15
0.5848	0.9927	57.53	0.0010	−0.01
0.6034	0.9946	59.48	−0.0005	−0.20
0.6930	0.9950	67.86	0.0010	−0.05
0.7397	0.9962	72.23	0.0006	0.05
0.8109	0.9977	79.28	0.0002	−0.15
0.9056	0.9990	88.55	0.0000	−0.26
0.9527	0.9991	92.86	0.0004	0.01
0.9951	0.9999	96.72	0.0001	0.28

mixture can be calculated from

$$[3] \qquad G^E = RT(x_1 \ln \gamma_1 + x_2 \ln \gamma_2)$$

if values of the activity coefficients are available. However, eq. 2 is unsuitable for the direct evaluation of $\ln \gamma_2$ from the present experimental results, since the values of y_2 are small and are subject to relatively large errors. In order to obtain values of the excess Gibbs free energy from the vapor–liquid equilibria, it was assumed that the concentration dependence of G^E could be represented by the form

$$[4] \qquad G^E = x_1 x_2 \sum_{r=1}^{n} c_r (1 - 2x_1)^{r-1}$$

It follows from eq. 4 that

$$[5] \quad \ln \gamma_1 = (x_2^2/RT) \sum_{r=1}^{n} c_r (1 - 2rx_1)(1 - 2x_1)^{r-2}$$

Values of the coefficients c_r were determined by a weighted least squares calculation in which eq. 5 was fitted to values of $\ln \gamma_1$ obtained from eq. 2. This calculation led to the representation

$$[6] \quad G^E/\text{J mol}^{-1} = x_1 x_2 [163.2 + 53.8(1 - 2x_1)]$$

with a standard error of estimate equal to 6.5 J mol^{-1}. The values of the coefficients were not altered significantly by the use of other reasonable estimates for the virial coefficients B_{22} and B_{12}. Furthermore, a statistical analysis indicated that the use of more than 2 coefficients was unjustifiable. Adopting eq. 6, the values of y_1 and p were computed at the experimental values of x_1. Differences between the observed and calculated vapor phase compositions are given in the fourth column of Table 2; in most cases, these are of the same order as the uncertainty in y_1. Differences between observed and calculated total pressures are listed in the last column of the table; the average deviation of the pressures is somewhat larger than the estimated experimental error.

A plot of G^E, calculated from eq. 6, is given in Fig. 1. It can be seen from the latter that at 25 °C G^E is positive for all mole fractions. At higher temperatures (from 80 to 120 °C) the work of Dutta (7) indicates that the curves for G^E have a sigmoid shape and vary in a rather complicated way with temperature.

Previously (1), we used the theory of Flory (8)

Can. J. Chem. Downloaded from www.nrcresearchpress.com by 210.87.254.105 on 09/05/12
For personal use only.

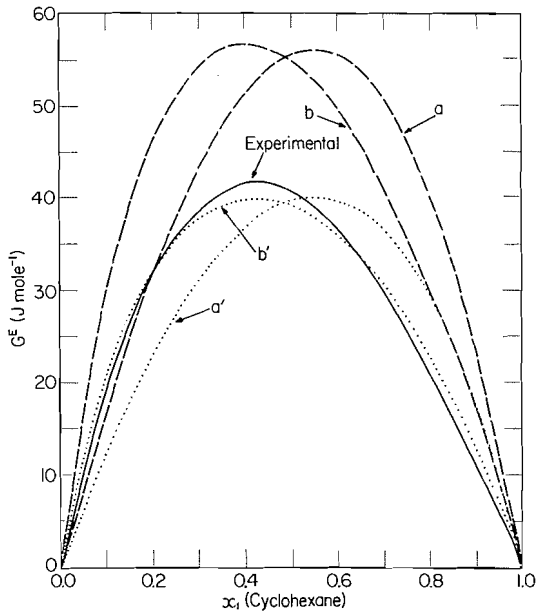

FIG. 1. Molar excess Gibbs free energy at 25 °C. Solid curve represents the experimental results. Broken and dotted curves were calculated from the theory of Flory using the following values of the parameters. Curve a: $s_1/s_2 = 1.147$, $X_{12} = 2.365$ J cm^{-3}, $Q_{12} = 0$. Curve b: $s_1/s_2 = 4.60$, $X_{12} = 5.351$ J cm^{-3}, $Q_{12} = 0$. Curve a': $s_1/s_2 = 1.147$, $X_{12} = 2.365$ J cm^{-3}, $Q_{12} = 2.19 \times 10^{-3}$ J cm^{-3} K^{-1}. Curve b': $s_1/s_2 = 4.60$, $X_{12} = 5.351$ J cm^{-3}, $Q_{12} = 5.06 \times 10^{-3}$ J cm^{-3} K^{-1}.

to correlate the excess enthalpies and volumes of cyclohexane–*cis*-decalin mixtures. Two calculations, (*a*) and (*b*), were described. In both of these, the energy parameter, X_{12}, was adjusted by the method of least squares to give the best fit between theoretical and experimental values of the excess enthalpy. In calculation (*a*), the ratio of the numbers of intermolecular contact sites, s_1/s_2, was estimated from the hard core molecular volumes of the two species; in (*b*), it was treated as a further adjustable parameter.

It is interesting to extend the calculations outlined above to estimate the excess free energy. In Fig. 1, the two broken curves marked *a* and *b* were computed from formulae given by Flory (8) and correspond to calculations (*a*) and (*b*), respectively. The numerical values used for the characteristic temperatures, pressures, and volumes were taken from ref. 1, and a polymer-type combinatorial term (8) was assumed. Both calculations lead to nearly the same maximum value of G^E (~ 56 J mol^{-1}). This is larger than the experimental result (~ 43 J mol^{-1}), but the discrepancy is only twice the standard error of estimate of the latter. Curve *b* reproduces the asymmetry of the experimental curve more closely than does curve *a*. This finding is in agreement with the better fit of the excess enthalpy obtained in calculation (*b*) (see ref. 1).

Orwoll and Flory (9) have added to the formula for G^E, an empirical term which allows for the fact that interactions between neighboring species may contribute to the entropy of mixing as well as to the enthalpy. The term, as formulated, contains another adjustable parameter Q_{12}.

Our calculations described so far correspond to setting Q_{12} equal to zero in the augmented formula for G^E. However, the theoretical estimates of G^E for both calculations can be brought into better agreement with the experimental results by using non-zero values of Q_{12}, as illustrated by the curves marked a' and b' in Fig. 1. The standard deviations of these curves from the experimental curve are 6.0 and 1.4 J mol^{-1}, respectively, for curves a' and b'.

1. G. C. BENSON, S. MURAKAMI, V. T. LAM and J. SINGH. Can. J. Chem. **48**, 211 (1970).
2. American Petroleum Institute. Research Project 44. Selected values of properties of hydrocarbons and related compounds. Chemical Thermodynamics Properties Centre. A. and M. College of Texas, College Station, Texas.
3. D. L. CAMIN and F. D. ROSSINI. J. Phys. Chem. **59**, 1173 (1955).
4. T. BOUBLÍK and G. C. BENSON. Can. J. Chem. **47**, 539 (1969).
5. J. H. DYMOND and E. B. SMITH. The virial coefficients of gases. Oxford University Press, Oxford. 1969.
6. J. P. O'CONNELL and J. M. PRAUSNITZ. Ind. Eng. Chem. Process Des. Develop. **6**, 245 (1967).
7. M. DUTTA. Ph.D. Thesis. Ohio State University 1969; see also Dis. Abst. **30**, 1654B (1969).
8. P. J. FLORY. J. Am. Chem. Soc. **87**, 1833 (1965).
9. R. A. ORWOLL and P. J. FLORY. J. Am. Chem. Soc. **89**, 6822 (1967).

Can. J. Chem. Downloaded from www.nrcresearchpress.com by 210.87.254.105 on 09/05/12
For personal use only.

Electron Spin Resonance Spectrum of the *tert*-Butylperoxy Radical, $B^{16}O^{17}O^{\cdot}$ [1]

J. A. HOWARD

Division of Chemistry, National Research Council of Canada, Ottawa, Canada K1A OR9

Received February 7, 1972

A *tert*-butylperoxy radical specifically labelled with ^{17}O on the terminal oxygen has been prepared by photolysis of di-*tert*-butyl peroxide in perdeuterocyclopentane containing ^{17}O enriched oxygen. The value of the ^{17}O hyperfine coupling constant is 23.45 G.

Un radical *tert*-butylperoxy, spécifiquement marqué par du ^{17}O sur l'oxygène terminal, a été préparé par photolyse du peroxyde de di-*tert*-butyle dans le perdeutérocyclopentane contenant de l'oxygène enrichi en ^{17}O. La valeur de la constante hyperfine de couplage est de 23.45 G.

Canadian Journal of Chemistry, **50**, 1981 (1972)

Can. J. Chem. Downloaded from www.nrcresearchpress.com by 210.87.254.42 on 09/05/12
For personal use only.

Introduction

Photolysis of di-*tert*-butyl peroxide (BOOB) in oxygen-saturated alkanes (RH) has been used to prepare alkylperoxy radicals (ROO·) *in situ* in the sample cavity of an e.s.r. spectrometer (1). These radicals are generated by the following reaction sequence

$$[1] \qquad BOOB \xrightarrow{h\nu} 2BO^{\cdot}$$

$$[2] \qquad BO^{\cdot} + RH \longrightarrow BOH + R^{\cdot}$$

$$[3] \qquad R^{\cdot} + O_2 \longrightarrow ROO^{\cdot}$$

Monitoring the variation of the radical signal with time after interruption of the initiating light enables absolute termination rate constants, $2k_t$, for tertiary and secondary peroxy radicals to be measured (1).

$$[4] \qquad ROO^{\cdot} + ROO^{\cdot} \xrightarrow{2k_t} \text{Molecular products}$$

Photolysis of BOOB in air-saturated cyclopropane does not give detectable concentrations of cyclopropylperoxy radicals (2). Bennett and Summers (2) have, however, made the very interesting observation that when irradiation of this reaction is interrupted at 140 °K, a stable single line spectrum grows and is destroyed immediately upon re-photolysis. This spectrum was attributed to the *tert*-butylperoxy radical.

In this note we report the preparation of the *tert*-butylperoxy radical specifically labelled with ^{17}O on the terminal oxygen by photolysis of BOOB in perdeuterocyclopentane in the presence of ^{17}O enriched oxygen.

[1]NRCC No. 12564.

Experimental

Perdeuterocyclopentane (Merck, Sharpe and Dohme of Canada, Ltd.) was trap-to-trap distilled before use. Enriched oxygen (47% ^{17}O) was obtained from Yeda Inc., Israel. Di-*tert*-butyl peroxide was distilled and percolated through basic alumina to remove any adventitious hydroperoxidic impurity. Cyclopropane and Freon 11 were used as inert solvents to obtain liquid phase spectra at temperatures below the melting point of cyclopentane.

Electron spin resonance spectra were recorded on a Varian E-3 spectrometer at temperatures between 183 and 143 °K. The sample temperature was altered with a V-4557 variable temperature accessory. To improve spectra resolution solutions were degassed several times using the freeze (77 °K)–thaw (173 °K) technique. This is possible for the *tert*-butylperoxy radical because it does not decay irreversibly at 173 °K.

Results and Discussion

Photolysis of BOOB in air-saturated perdeuterocyclopentane at 183 °K generates perdeuterocyclopentylperoxy radicals by reactions 1 to 3. When the initiating light is interrupted these radicals decay *immediately* with a bimolecular decay constant of $\sim 3 \times 10^5\ M^{-1}\ s^{-1}$. Warming up to room temperature a reaction mixture that has been through the reaction sequence 1 to 4 generates a substantial concentration (*ca.* $10^{-5}\ M$) of *tert*-butylperoxy radicals. This radical is relatively easy to characterize by e.s.r. spectroscopy. It has a single line spectrum, a *g*-value of 2.0146 and is almost completely stable at 183 °K. No other radicals with these characteristics could possibly be generated by photolysis of BOOB, perdeuterocyclopentane and oxygen.

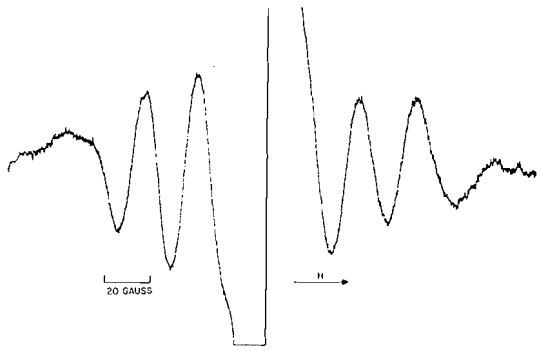

FIG. 1. Electron spin resonance spectrum of $B^{16}O^{16}O^{\cdot}$ and $B^{16}O^{17}O^{\cdot}$ in Freon 11 at 163 °K.

When this reaction is performed in the presence of ^{17}O enriched oxygen the *tert*-butylperoxy radical specifically labelled on the terminal oxygen with ^{17}O, $B^{16}O^{17}O^{\cdot}$, is produced. The e.s.r. spectrum of this species is given in Fig. 1.

There have been several recent reports of e.s.r. spectra of peroxy radicals enriched with ^{17}O (3–6). These spectra contain contributions from $R^{16}O^{17}O^{\cdot}$, $R^{17}O^{16}O^{\cdot}$, and $R^{16}O^{16}O^{\cdot}$ (where R is an alkyl group, F or CF_3O) which results in rather poor resolution of the ^{17}O hyperfine lines. Two ^{17}O hyperfine coupling constants have been determined, $|a'_O| = 22.17$ to 23.0 G and $|a''_O| = 14.5$ to 18.0 G and consequently the two O atoms are not equivalent. Because of the similarity of the values of the two coupling constants it has not been possible to assign positively the constants to the two positions. Adamic, Ingold, and Morton (6), however, deduced from their study of ^{17}O enriched *tert*-alkylperoxy radicals that $R^{16}O^{17}O^{\cdot}$ has the larger hyperfine interaction.

Only four of the six ^{17}O hyperfine lines of $B^{16}O^{17}O^{\cdot}$ are well resolved because the other two lines are obscured by the zero spin line. Within experimental error the widths of the 4 resolvable hyperfine lines in $B^{16}O^{17}O^{\cdot}$ are 12 G. The spectrum is slightly asymmetric with respect to position of the ^{17}O lines, the low field 5/2 line is 59.0 G down field from the zero spin line while the high field 5/2 line is 58.2 G up field from the zero spin line. The hyperfine splitting constant $|a_O| = 23.45 \pm 0.10$ G $(0.2 \times 117.2$ G) and is very similar to Adamic, Ingold, and Morton's corrected value[2] of $|a'_O| = 24.0$ G and Fessenden and Schuler's (3, 4) value of $|a'_O| = 23.0$ G for the peroxy radical produced by irradiation of 2,2,4-trimethylpentane containing ^{17}O enriched oxygen.

We can, therefore, conclude with certainty from this work that the larger ^{17}O hyperfine splitting obtained previously (3–6) from ^{17}O enriched peroxy radicals is produced by the $R^{16}O^{17}O^{\cdot}$ species and that the smaller hyperfine splitting is produced by the $R^{17}O^{16}O^{\cdot}$ species.

Bennett and Summers (2) have suggested that *tert*-butylperoxy radicals are formed when photolysis of BOOB in air-saturated cyclopropane is ceased, by decomposition of an unsymmetric trioxide, BOOOR. This trioxide can be produced by combination of a *tert*-butoxy radical, formed in the initiation step, and a *sec*-alkylperoxy radical derived from either cyclopropane or a trace hydrocarbon impurity.

[5] $$BO^{\cdot} + ROO^{\cdot} \rightleftharpoons BOOOR$$

BOOOR can decompose to the original radicals or it can decompose to give a *tert*-butylperoxy radical and an alkoxy radical, $RO^{\cdot}$,

[6] $$BOOOR \rightarrow BOO^{\cdot} + RO^{\cdot}$$

Bennett and Summers also observed a further production of *tert*-butylperoxy radicals at 200 °K which they attributed to the decomposition of di-*tert*-butyl trioxide (7), BOOOB, formed at low temperatures by the reaction

$$BO^{\cdot} + BOO^{\cdot} \rightarrow BOOOB$$

The production of $B^{16}O^{17}O^{\cdot}$ from photolysis of a mixture of perdeuterocyclopentane, BOOB and ^{17}O enriched oxygen confirms that trioxides are indeed formed during photolysis at low temperatures. This is because a specifically labelled radical can only be formed by the reaction sequence

[1] $$BOOB \xrightarrow{h\nu} 2BO^{\cdot}$$

[2] $$BO^{\cdot} + RH \longrightarrow BOH + R^{\cdot}$$

[3] $$R^{\cdot} + O_2 \text{ (enriched)} \longrightarrow R^{16}O^{16}O^{\cdot},\ R^{17}O^{17}O^{\cdot},\ R^{16}O^{17}O^{\cdot},\ R^{17}O^{16}O^{\cdot}$$

[2]The hyperfine splittings reported by Adamic, Ingold, and Morton (6) are low by ~10% because of an error in the sweep of the magnetic field.

Can. J. Chem. Downloaded from www.nrcresearchpress.com by 210.87.254.42 on 09/05/12
For personal use only.

$$[5]\quad \left.\begin{matrix} R^{16}O^{16}O^{\cdot} \\ R^{17}O^{17}O^{\cdot} \\ R^{16}O^{17}O^{\cdot} \\ R^{17}O^{16}O^{\cdot} \end{matrix}\right\} + BO^{\cdot} \longrightarrow \left\{\begin{matrix} R^{16}O^{16}O^{16}OB \\ R^{17}O^{17}O^{16}OB \\ R^{16}O^{17}O^{16}OB \\ R^{17}O^{16}O^{16}OB \end{matrix}\right.$$

$$[6]\quad \begin{matrix} R^{16}O^{16}O^{16}OB \longrightarrow R^{16}O^{\cdot} + B^{16}O^{16}O^{\cdot} \\ R^{17}O^{17}O^{16}OB \longrightarrow R^{17}O^{\cdot} + B^{16}O^{17}O^{\cdot} \\ R^{16}O^{17}O^{16}OB \longrightarrow R^{16}O^{\cdot} + B^{16}O^{17}O^{\cdot} \\ R^{17}O^{16}O^{16}OB \longrightarrow R^{17}O^{\cdot} + B^{16}O^{16}O^{\cdot} \end{matrix}$$

The yield of trioxide and hence the yield of $BOO^{\cdot}$ will of course depend on the strength of the labile hydrogen in RH. If it is too weak all the $BO^{\cdot}$ radicals will react with RH while if it is too strong $BO^{\cdot}$ will not react with RH. In either case a trioxide will not be formed.

The author thanks Dr. J. R. Morton for measuring the magnetic fields and the microwave frequency.

1. J. E. BENNETT, D. M. BROWN, and B. MILE. Trans. Faraday Soc. **66**, 386 (1970); **66**, 397 (1970).
2. J. E. BENNETT and R. SUMMERS. Presented at the Autumn Meeting of the Chemical Society at York, 28–30 September, 1971. Abstract E 17.
3. R. W. FESSENDEN and R. H. SCHULER. J. Chem. Phys. **44**, 434 (1966).
4. R. W. FESSENDEN and R. H. SCHULER. Adv. Radiat. Chem. **2**, 1 (1970).
5. R. W. FESSENDEN. J. Chem. Phys. **48**, 3725 (1968).
6. K. ADAMIC, K. U. INGOLD, and J. R. MORTON. J. Am. Chem. Soc. **92**, 922 (1970).
7. P. D. BARTLETT and G. GUARALDI. J. Am. Chem. Soc. **89**, 4799 (1967).

Can. J. Chem. Downloaded from www.nrcresearchpress.com by 210.87.254.42 on 09/05/12
For personal use only.

Can. J. Chem. Downloaded from www.nrcresearchpress.com by 210.87.254.105 on 09/05/12
For personal use only.

Stereochemistry of the Cycloaddition of Singlet Excited β-Substituted Styrenes to Olefins[1]

O. L. CHAPMAN, R. D. LURA,[2] R. M. OWENS, E. D. PLANK,[3] AND S. C. SHIM

Department of Chemistry, Iowa State University, Ames, Iowa 50010

AND

D. R. ARNOLD[4] AND L. B. GILLIS

Union Carbide Research Institute, P.O. Box 278, Tarrytown, New York 10591

Received March 14, 1972

The photocycloaddition of β-substituted styrenes (*trans*-cinnamic acid (**1***b*), methyl *trans*-cinnamate (**1***c*), *trans*-cinnamonitrile (**1***d*), and *cis*-cinnamonitrile) to olefins occurs with retention of stereochemistry and involves the S_1 state. In certain cases (**1***b*, *c*) a photoene reaction competes with the cycloaddition. The triplet states of the β-substituted styrenes produced by sensitization give only *cis* ⇄ *trans* isomerization. Neither cycloadduct nor photoene reaction is observed from the triplet states. It is thus likely that both addition and photoene reactions involve the S_1 state of the β-substituted styrene.

La photocycloaddition des styrènes β substitués (acide *trans* cinnamique (**1***b*), cinnamate de méthyle *trans* (**1***c*), cinnamonitrile *trans* (**1***d*), et cinnamonitrile *cis*) aux oléfines se fait avec rétention de stéréochimie et passe par l'état S_1. Dans certains cas (**1***b*, *c*) la réaction photoène entre en compétition avec la cycloaddition. Les états triplets des styrènes substitués obtenus par sensibilisation, ne conduisent qu'à l'isomérisation *cis* ⇄ *trans*. La cycloaddition ainsi que la réaction photoène n'ont pas été observées à partir des états triplets. Il est donc probable que la réaction photoène et l'addition passent toutes deux par l'état S_1 du styrène β substitué.

Canadian Journal of Chemistry, **50**, 1984 (1972)

The mechanism of the photocycloaddition of *trans*-stilbene to tetramethylethylene involves reversible reaction of S_1 *trans*-stilbene with ground state tetramethylethylene giving an exciplex which demotes to the adduct with retention of the *trans*-stereochemistry (1). We now report that photocycloaddition of other β-substituted styrenes (**1***b–d*) occurs with retention

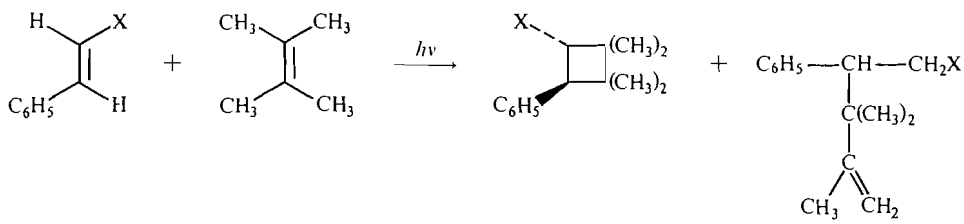

1 **2** **3**

a, X = C_6H_5; *b*, X = CO_2H; *c*, X = CO_2CH_3; *d*, X = CN

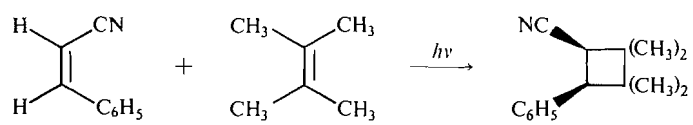

[1]Photochemical transformations. LX.

[2]National Defense Education Act Fellow, 1967–1970.

[3]National Institutes of Health Postdoctoral Fellow, 1-F2-GM-20, 937, 1965–1966.

[4]Present address: The Photochemistry Unit, Department of Chemistry, University of Western Ontario, London 72, Ontario.

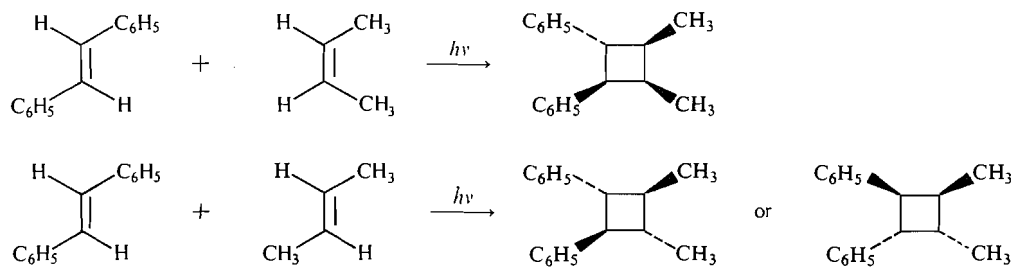

of stereochemistry and involves the S_1 state. In certain cases (**1***b*, *c*) a photoene reaction competes with the cycloaddition. The triplet states of the *β*-substituted styrenes produced by sensitization give only *cis* ⇄ *trans* isomerization. Neither cycloadduct nor photoene reaction is observed from the triplet states. It is thus likely that both addition and photoene reactions involve the S_1 state of the *β*-substituted styrene.[5]

Irradiation of benzene solutions of *trans*-stilbene (**1***a*), *trans*-cinnamic acid (**1***b*), methyl *trans*-cinnamate (**1***c*), and *trans*-cinnamonitrile (**1***d*) in the presence of tetramethylethylene give in each case an adduct (**2**) in which the *trans*-stereochemistry is maintained.[6] The corresponding *cis*-*β*-substituted styrenes, with the exception of *cis*-cinnamonitrile, do not add to tetramethylethylene sufficiently rapidly to compete effectively with *cis* → *trans* isomerization. Irradiation of *cis*-cinnamonitrile in the presence of tetramethylethylene gives an adduct in which the phenyl and nitrile groups are *cis*. Both *trans*- and *cis*-cinnamonitrile give linear $1/\Phi_{add}$ *vs.* 1/[olefins] plots. Irradiation of solutions of either nitrile and sensitizers (benzophenone, 2-acetylnaphthalene)[7] gives only *cis* ⇄ *trans* isomerization. The cycloaddition of these S_1 *β*-substituted styrenes is stereospecific with respect to the excited enophile.

Irradiation of *trans*-stilbene in the presence of *cis*-2-butene gives a single adduct which shows two methyl resonances in the n.m.r. spectrum.[8] In similar fashion, *trans*-stilbene in the presence of *trans*-2-butene gives a single, different adduct in which the n.m.r. spectrum shows equivalent methyl groups.[8] These photocycloadditions clearly occur with retention of stereochemistry on both the excited (S_1) enophile and the ground state olefin.

In the irradiation of *trans*-cinnamic acid and methyl *trans*-cinnamate in the presence of tetramethylethylene a second product was obtained in addition to the cycloadduct (**2**). The additional product in each was shown to be the terminal olefin expected from a photoene reaction to which we tentatively assign structure **3***b*, *c*. The ratio of cycloadduct to photoene product in neat tetramethylethylene was **2***c*/**3***c* = 1.5 and in benzene **2***b*/**3***b* = 5 and **2***c*/**3***c* = 1.6. In the other cases studied (**1***a* and *d*) photoene products were not observed. Polar solvents favored the photocycloaddition to a small extent (**2***c*/**3***c* = 3.2 in ethanol and 3.4 in acetic acid). The ratio of cycloadduct to photoene was insensitive to variation in light intensity. In the

[5]The fact that the triplet states do not give either the adduct or the photoene is consistent with reaction via either S_1 or vibrationally excited S_0. Rapid thermal equilibration of vibrationally excited species in solution makes reaction of an S_0 state unlikely. Furthermore, it has been shown that cycloaddition of *trans*-stilbene involves the S_1 state (1).

[6]Irradiations were carried out with a 450 W Hanovia medium pressure mercury vapor lamp through a Pyrex filter. The adducts all gave satisfactory element analyses and spectra consistent with the cyclobutane adduct structures (**3***b*–*d*). Saponification of the adduct from methyl *trans*-cinnamate gave the adduct (m.p. 129–130°) from *trans*-cinnamic acid. This adduct was converted by methyl lithium to the corresponding methyl ketone. The ketone did not epimerize under conditions which led to exchange of four protons for deuterium and hence must have the thermodynamically more stable *trans* arrangement of phenyl and acetyl groups. Oxidation of the methyl ketone gave the adduct from *trans*-cinnamic acid which thus must have *trans* phenyl and carboxyl groups. The adduct from *trans*-cinnamic acid was converted via the amide to the nitrile which was identical to the adduct obtained from *trans*-cinnamonitrile.

[7]The irradiation of solutions of 2-acetylnaphthalene with methyl cinnamate under these conditions leads to the adduct described previously (2).

[8]The adduct from *cis*-2-butene shows n.m.r. bands at *δ* 7.25 (10H, aromatic protons), 3.2–4.0 (2H, benzyl methine protons), 2.2–2.9 (2H, m, methine protons), 1.15 (3H, d, methyl protons), and 0.80 (3H, d, methyl protons). The adduct from *trans*-2-butene shows n.m.r. bands at *δ* 7.20 (10H, aromatic protons), 4.10 (2H, m, benzyl methine protons), 2.1–2.5 (2H, m, methine protons), and 0.95 (6H, d, methyl protons).

Can. J. Chem. Downloaded from www.nrcresearchpress.com by 210.87.254.105 on 09/05/12
For personal use only.

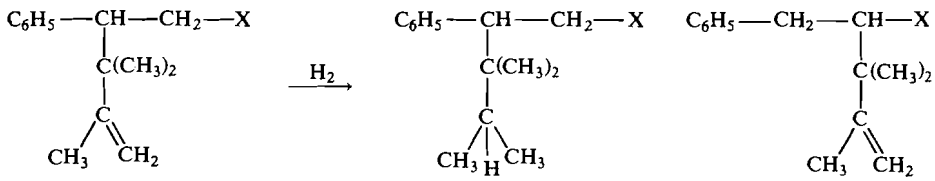

3 7 6

sensitized reactions neither cycloadduct nor photoene was observed. Heating methyl *trans*-cinnamate with tetramethylethylene at 200° for 24 h gave no detectable reaction.

The tentative structural assignment (**3***b*, *c*) for the photoenes rests primarily on the n.m.r. spectrum. The alternative structure **6** has not been rigorously excluded. The n.m.r. spectrum of the photoene (m.p. 114.5–115.5°) from *trans*-cinnamic acid shows non-equivalent methyl groups (δ 0.82 and 0.95), a vinyl methyl group (δ 1.78), and ABX pattern for the methylene and methine protons (AB centered at δ 2.51, X at 3.21), terminal methylene protons (δ 4.72), aromatic protons (5, δ 7.33), and a carboxyl proton (δ 11.25). The mixture of esters (**2***c* and **3***c*) from methyl *trans*-cinnamate is difficult to separate, but hydrolysis of the mixture and repeated crystallizations from heptane gave the acids **2***b* (25%) and **3***b*(7%). Catalytic reduction of the mixture of esters and v.p.c. separation gave **7***c*.

The demonstration that singlet addition of β-substituted styrenes to tetramethylethylene is a general phenomenon, the demonstration that the photocycloaddition of S_1 *trans*-stilbene to tetramethylethylene proceeds via an exciplex (1), and the demonstration that these photocycloadditions are stereospecific on both the excited enophile and the ground state olefin place stringent limits on the mechanisms which can be considered. The most probable mechanism is concerted decay of an exciplex to the adduct. If an intermediate such as a singlet 1,4-biradical is formed, the lifetime of this intermediate must be short with respect to the reciprocal of the rate constant for rotation about a single bond. This seems unlikely in view of the known behavior of singlet 1,4-biradicals (3, 4). It may be that unsymmetrically substituted olefins or olefins with radical stabilizing substituents will favor formation of long-lived biradicals. Studies directed to this point are in progress.

The stereospecificity of the addition of singlet excited styrenes to olefins together with the observed retention of stereochemistry in the dimerization of the isomeric 2-butenes upon direct irradiation (5) suggests that singlet cycloaddition may provide a useful tool for stereospecific synthesis of complex molecules.

This research was supported at Iowa State University by grants from the National Science Foundation (GP 6704), the National Institute of General Medical Sciences (GM 14305), and the National Institute of Arthritis and Metabolic Disease (AM 14624).

1. O. L. CHAPMAN and R. D. LURA. J. Am. Chem. Soc. **92**, 6352 (1970); J. SALTIEL, J. T. D'AGOSTINO, O. L. CHAPMAN, and R. D. LURA. J. Am. Chem. Soc. **93**, 2804 (1971).
2. D. R. ARNOLD, L. B. GILLIS, and E. B. WHIPPLE. Chem. Commun. 918 (1969).
3. P. D. BARTLETT and N. A. PORTER. J. Am. Chem. Soc. **90**, 5317 (1968).
4. K. R. KOPECKY and S. EVANI. Can. J. Chem. **47**, 4041 (1969).
5. H. YAMAZAKI and R. J. CVETANOVIC. J. Am. Chem. Soc. **91**, 520 (1969).

Can. J. Chem. Downloaded from www.nrcresearchpress.com by 210.87.254.105 on 09/05/12
For personal use only.

Can. J. Chem. Downloaded from www.nrcresearchpress.com by 210.87.254.6 on 09/05/12
For personal use only.

V. 50
p. 1987-3 00
1972
546 c

Canadian Journal of Chemistry

Published by THE NATIONAL RESEARCH COUNCIL OF CANADA

VOLUME 50 JULY 1, 1972 NUMBER 13

Coupling of Amino Acids and Amino Sugars with Cyanuric Chloride (2,4,6-Trichloro-*s*-triazine)[1]

A. S. CHAUDHARI[2] AND C. T. BISHOP

Biochemistry Laboratory, National Research Council of Canada, Ottawa, Canada K1A 0R6

Received January 5, 1972

2,4,6-Trichloro-*s*-triazine (cyanuric chloride) has been used to couple glycine ethyl ester with seven carbohydrate derivatives that contain amino groups. The reactions proceed in high yield under mild conditions. The compounds serve as models for the coupling of carbohydrates to proteins by well-defined linkages through amino groups.

La 2,4,6-trichloro-*s*-triazine (chlorure cyanurique) a été utilisée pour coupler l'ester éthylique de la glycine avec sept dérivés de carbohydrates contenant des groupes amines. Les réactions se font avec d'excellent rendement et sous des conditions douces. Les composés sont utilisés en tant que modèles pour les couplages de carbohydrates avec des protéines au moyen de liaisons bien définies par l'intermédiaire de groupes amines.

Canadian Journal of Chemistry, **50**, 1987 (1972)

A recent preliminary communication (1) described the preparation of an antigenic polysaccharide–protein conjugate by the use of 2,4,6-trichloro-*s*-triazine (cyanuric chloride) as a coupling reagent. Gel electrophoresis and the production of antibody to the carbohydrate moiety showed that the polysaccharide and the protein were covalently linked. The linkage must have occurred through hydroxyl groups in the nitrogen-free polysaccharide and amino groups in the protein, but the extent and location of the cross-linkages were not determined. In the absence of amino groups in the polysaccharide, the cyanuric chloride must have reacted with hydroxyl groups at random. These factors are not important for the simple preparation of polysaccharide antigens. However, the introduction of specific determinant groups into a peptide or protein requires conjugates in which linkages are more closely defined. The present paper describes the preparation of some model compounds representing carbohydrate–protein conjugates in which the linkages are well-characterized.

It is known that replacement of one chlorine atom in 2,4,6-trichloro-*s*-triazine by an amino, or substituted amino, group deactivates the remaining two so that stepwise reactions can be obtained by temperature control (2–5). However, the deactivating effects of alkoxy- or aryloxy-groups are weaker and the reaction of chlorotriazines with hydroxylated compounds yields mixtures from which it is difficult to isolate and characterize any product (4). This observation was confirmed during the present work by unsuccessful attempts to isolate characterizable products from the reaction of 2,4,6-trichloro-*s*-triazine with 2,3,4,6-tetra-*O*-acetyl-β-D-glucose or with methyl α-D-glucopyranoside. Furthermore, it has been established that 2,4,6-trichloro-*s*-triazine reacts preferentially with amino groups when both amino groups and hydroxyl groups are present in the same substrate molecule (4, 5).

From these results it was clear that successive replacement of two chlorine atoms from 2,4,6-trichloro-*s*-triazine by amino substituents offered the best possibilities for preparing well-defined, carbohydrate–protein conjugates. As there are several ways to introduce amino groups into

[1]NRCC No. 12561.
[2]NRCC Postdoctorate Fellow, 1970–1972.

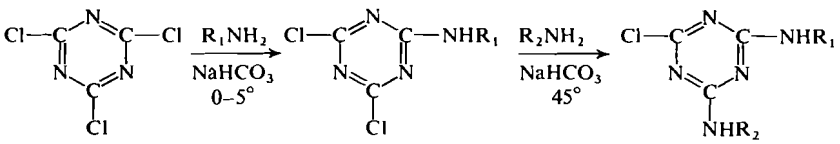

A B

Compounds type **A**

1	NHR_1 = ethoxycarbonylmethylamino
5	= 2-amino-2-deoxy-D-glucopyranose
6	= 2-amino-2-deoxy-D-galactopyranose
7	= 2-hydroxyethylamino

Compounds type **B**

	NHR_1 = ethoxycarbonylmethylamino
2	NHR_2 = amino
3	= 2-hydroxyethylamino
4	= 2-ethoxycarbonylmethylamino
8	= 2-amino-2-deoxy-D-glucopyranose
9	= 2-amino-2-deoxy-D-galactopyranose
10	= 2-amino-2-deoxy-D-mannopyranose
11	= 1-amino-1-deoxy-D-glucitol
12	= 1-amino-1-deoxy-D-mannitol
13	= 1-amino-1-deoxy-D-galactitol
14	= 2-amino-2-deoxy-D-glucosediethyl-dithioacetal

SCHEME 1

carbohydrates the method should be of general applicability.

The coupling of amino acids and amino sugars with cyanuric chloride according to Scheme 1, can be achieved in two ways by using either the amino sugar or the amino acid derivative in the first step, *i.e.* the introduction of NHR_1. Thus, replacement at 0 °C of one of the chlorine atoms of cyanuric chloride by the amino groups of glucosamine and galactosamine gave compounds **5** and **6** respectively. Further reaction of these compounds at 45 °C with glycine ethyl ester gave the disubstituted products **8** and **9**. The same compounds could also be prepared by the initial reaction of cyanuric chloride with the amino acid derivative to give compound **1**, and subsequent reaction of this at 45 °C with the amino sugars to give compounds **8** and **9**. Overall yields of these compounds were better by the latter route, probably because of the ease with which compound **1** can be made in high yield.

Compounds **2**, **3**, and **7** were prepared with the intention of having amino or hydroxyl groups available for subsequent reaction with acetobromo sugars. However, the difficulty with which these compounds (**2**, **3** and **7**) dissolve in organic solvents precluded attempts to extend the reaction sequence in that direction.

The 1-amino-1-deoxy alditols (NHR_2 on compounds **11**, **12**, and **13**) were prepared by the method of Kagan *et al.* (6) in which *N*-benzyl aminitols were formed by the reductive alkylation of benzylamine with the appropriate sugar. The *N*-benzyl-1-amino-1-deoxy-alditols were then hydrogenolyzed to the 1-amino-1-deoxy alditols which, on reaction with compound **1** yielded compounds **11**, **12**, and **13**. The *N*-benzyl-1-amino-1-deoxy-D-mannitol that was prepared for this series of reactions does not seem to have been reported previously; it was therefore characterized further as a crystalline acetate. The 2-amino-2-deoxy-D-glucose diethyldithioacetal was prepared by methods described (7); condensation of this derivative with compound **1** gave compound **14**. The other starting compounds were available commercially and were used without further purification.

The structures of these compounds follow from the method of synthesis because it is known that 2,4,6-trichloro-*s*-triazine or a monosubstituted dichloro-*s*-triazine reacts preferen-

Can. J. Chem. Downloaded from www.nrcresearchpress.com by 210.87.254.6 on 09/05/12
For personal use only.

Can. J. Chem. Downloaded from www.nrcresearchpress.com by 210.87.254.6 on 09/05/12
For personal use only.

tially with the amino group of hydroxylamines (4, 5). However, some of the compounds were examined in further detail to confirm that this generalization held for the carbohydrate derivatives used in the present study.

The structure of compound **1** was confirmed by the analysis that showed two atoms of chlorine remaining in the molecule and by n.m.r. spectroscopy that accounted for all of the protons as follows: N—H (singlet; one proton; δ, 7.2), C—CH_3 (triplet; three protons; δ, 1.32), 2 × CH_2 (quartet; four protons; δ, 4.30). Compound **4**, the disubstituted analogue of compound **1**, gave a similar n.m.r. spectrum with two nitrogen protons, eight methylene protons, and six C—methyl protons accounted for by integration.

With the structure of compound **1** established it was clear from the method of synthesis and from the chlorine analyses that the compounds of type B had to be disubstituted monochloro-*s*-triazine derivatives. The location of the linkage through the amino group in the carbohydrate moiety was confirmed for **8** and **14** as representative examples of these compounds. Thus, the n.m.r. spectrum of **14** showed nine C—CH_3 protons (δ, 1.3), five C—H protons (δ, 2.5–2.8), four OH protons (δ, 3.77), ten CH_2 protons (δ, 4.0–4.5), and two NH protons (δ, 7.2). The presence of four hydroxyl groups showed that the linkage must have been through the amino group of the diethyldithioacetal. Acetylation of **8** and **14** introduced four *O*-acetyl groups into each of them as determined by analysis and by the ratio of *C*-methyl to acetyl protons in the n.m.r. spectra. The method of acetyl analysis (8) and the absence of any absorption at 1618–1665 cm^{-1} in the i.r. established that all of the acetyl groups were *O*-acetyl and that no *N*-acetyls were present. These results prove that all of the hydroxyl groups in **8** and **14** were free and that the linkages were through the amino groups of the carbohydrate moieties. Compounds **8**, **9**, and **10**, were probably anomeric mixtures and it is likely that they were in the pyranose ring form.

The present results show that cyanuric chloride (2,4,6-trichloro-*s*-triazine) can be used for the selective coupling of compounds that contain amino groups. The reaction takes place preferentially with amino groups and any hydroxyl groups present need not be blocked. The condensations proceed in high yield (66–88%) and under mild conditions that makes the method amenable for use with sensitive compounds. In particular, this method of coupling would seem to offer an attractive alternative to diazotization (9–11) for introduction of determinant groups into peptides or proteins for use as artificial antigens or as immunoabsorbents.

Experimental

Solutions were evaporated under reduced pressure at bath temperatures not exceeding 40°. A Perkin–Elmer 140 polarimeter was used to measure optical rotations which are equilibrium values unless otherwise specified. Melting points were determined on a Fisher–Johns hot stage and are uncorrected. The t.l.c. was done on glass plates coated with silica gel G using the following solvent mixtures: (A) chloroform:ethanol, 3:1; (B) ethyl acetate:acetic acid:water, 9:2:2. Unless stated otherwise, compounds containing amino sugars were homogeneous by t.l.c. in both solvent systems. The u.v. spectra were recorded on aqueous solutions using a Cary Recording spectrophotometer. All of the compounds showed the same spectral characteristics due to the triazine absorption; λ_{max} 261 mμ, $\varepsilon = 3150 \rightarrow 3400$. The i.r. spectra were recorded with a Perkin–Elmer Infracord spectrophotometer using chloroform solutions of the compounds. The n.m.r. spectra were obtained in deuterochloroform solution using a Varian HA-60 spectrometer with tetramethylsilane as a standard.

*N-Benzyl-1-amino-1-deoxy-*D*-mannitol*

This compound does not seem to have been reported before. It was prepared in 76% yield by the method of Kagan *et al.* (5). The crystalline product, m.p. 162–163 °C, was recrystallized from methanol to a constant melting point of 164–165 °C; $[\alpha]_D^{22}$ +9.0° (*c*, 1.0 in water).

Anal. Calcd. for $C_{13}H_{21}O_5N$: C, 57.55; H, 7.80; N, 5.16. Found: C, 57.39; H, 7.90; N, 5.33.

*N-Benzyl-1-amino-1-deoxy-2,3,4,5,6-penta-O-acetyl-*D*-mannitol*

The *N*-benzyl-1-amino-1-deoxy-D-mannitol (1 g) was acetylated in acetic anhydride:pyridine (1:1, 20 ml) at room temperature. The product was recrystallized from ethanol: m.p. 76–77 °C, $[\alpha]_D^{22}$ +20° (*c*, 1.0 in chloroform).

Anal. Calcd. for $C_{23}H_{31}O_{10}N_1$: C, 57.38; H, 6.44; N, 2.91. Found: C, 57.73; H, 6.73; N, 2.65.

2,4-Dichloro-6-(ethoxycarbonylmethylamino)-s-triazine (1)

Cyanuric chloride (2,4,6-trichloro-*s*-triazine) (5.3 g) was dissolved in hot acetone (10–12 ml) and poured into well-stirred ice water (20 ml). To this stirred solution was added a cold (0–5 °C) aqueous solution (20 ml) of glycine hydrochloride ethyl ester (4.0 g) and sodium bicarbonate (4.82 g). The mixture was stirred at 0 °C for 1 h. The white, crystalline product was filtered, washed with ice-cold water, and dried. The compound (85% yield) required no further purification because recrystallization from acetone did not change its properties: m.p. 85–86 °C.

Anal. Calcd. for $C_7H_8O_2N_4Cl_2$: C, 33.48; H, 3.21; N,

Can. J. Chem. Downloaded from www.nrcresearchpress.com by 210.87.254.6 on 09/05/12
For personal use only.

22.32; Cl, 28.24. Found: C, 33.20; H, 3.04; N, 22.10; Cl, 28.44.

2-Chloro-4-amino-6-(ethoxycarbonylmethylamino)-s-triazine (2)

Compound **1** (12 g) was dissolved in hot acetone (50 ml) and this solution was added with stirring to water (75 ml) through which ammonia gas was passed continuously. The temperature of the reaction was maintained at 45 °C. After 15–20 min the white, crystalline product was filtered off and dried; yield 10.2 g, 88%. Recrystallized from acetone: nitromethane (1:1), the product had m.p. 235–237 °C.

Anal. Calcd. for $C_7H_{10}O_2N_5Cl_1$: C, 36.28; H, 4.31; N, 30.23; Cl, 15.33. Found: C, 35.91; H, 4.57; N, 30.5; Cl, 15.18.

2-Chloro-4-(2-hydroxyethylamino)-6-(ethoxycarbonylmethylamino)-s-triazine (3)

Compound **1** (3 g) in hot acetone (20 ml) was added with stirring to water (10 ml) at 0–5 °C. A solution of ethanolamine (0.75 ml) in acetone (10 ml) was then added and the reaction mixture was allowed to warm up to room temperature (22 °C). An aqueous solution (5 ml) of sodium bicarbonate (1 g) was then added slowly to the stirred reaction mixture over a period of 30 min. The reaction was stirred at 45 °C for 1.5 h after which the product was filtered and dried; yield, 2.2 g, 85%. Recrystallized from acetone:ethanol (1:1), the compound had m.p. 197–199 °C.

Anal. Calcd. for $C_9H_{14}O_3N_5Cl$: C, 39.20; H, 5.08; N, 25.40; Cl, 12.88. Found: C, 39.08; H, 5.04; N, 25.18; Cl, 12.91.

6-Chloro-(2,4-di-ethoxycarbonylmethylamino)-s-triazine (4)

Cyanuric chloride (2,4,6-trichloro-*s*-triazine) (1.84 g) was condensed with glycine hydrochloride ethyl ester (2.8 g) in the presence of sodium bicarbonate (3.36 g) as described for compound **1** except that the temperature of the reaction was maintained at 45 °C instead of 0–5 °C. The disubstituted product which precipitated out in the reaction was filtered and dried; yield 2.3 g, 72%. When recrystallized from acetone it had m.p. 182–183 °C.

Anal. Calcd. for $C_{11}H_{16}O_4N_5Cl$: C, 41.58; H, 5.04; N, 22.04; Cl, 11.18. Found: C, 41.48; H, 5.08; N, 22.2; Cl, 11.27.

2-(2,4-Dichloro-s-triazin-6-yl)amino-2-deoxy-D-glucopyranose (5)

Cyanuric chloride (2,4,6-trichloro-*s*-triazine) (1.84 g) was condensed with 2-amino-2-deoxy-D-glucopyranose hydrochloride (2.16 g) in the presence of sodium bicarbonate (1.68 g) at 0–5 °C for 1.5 h as described for compound **1**. The solid product which precipitated out in the reaction was filtered, dried, and recrystallized from acetone; yield, 2.2 g, 67%; the compound decomposed with charring above 200 °C; $[\alpha]_D^{22}$ +45° (*c*, 1.4 in methanol).

Anal. Calcd. for $C_9H_{12}O_5N_4Cl_2$: C, 33.02; H, 3.67; N, 17.12; Cl, 21.71. Found: C, 32.60; H, 3.74; N, 17.50; Cl, 21.39.

2-(2,4-Dichloro-s-triazin-6-yl)amino-2-deoxy-D-galactopyranose (6)

The condensation of cyanuric chloride (2,4,6-trichloro-*s*-triazine) (0.925 g) and 2-amino-2-deoxy-D-galactopyranose hydrochloride (1.08 g) in the presence of sodium bicarbonate (0.84 g) was performed in the same way as for compound **5**. The product was recrystallized from acetone; yield, 1.03 g, 62%; the compound decomposed with charring above 200 °C; $[\alpha]_D^{22}$ +56.5° (*c*, 1.2 in methanol).

Anal. Calcd. for $C_9H_{12}O_5N_4Cl_2$: C, 33.02; H, 3.67; N, 17.12; Cl, 21.71. Found: C, 32.76; H, 3.44; N, 17.37; Cl, 21.42.

2,4-Dichloro-6-(2-hydroxyethylamino)-s-triazine (7)

Cyanuric chloride (2,4,6-trichloro-*s*-triazine) (1.84 g), ethanolamine (0.61 ml), and sodium bicarbonate (0.84 g) were stirred in acetone:water at 0–5 °C as described for compound **1**. The reaction mixture was clarified by filtration and the filtrate was evaporated leaving a solid residue. Recrystallization from methanol yielded compound **7**, 1.12 g, 53%; m.p. 113–115 °C.

Anal. Calcd. for $C_5H_6ON_4Cl_2$: C, 28.70; H, 2.86; N, 26.79; Cl, 33.97. Found: C, 28.84; H, 2.99; N, 26.64; Cl, 33.59.

2-(4-Chloro-2-ethoxycarbonylmethylamino-s-triazin-6-yl)-amino-2-deoxy-D-glucopyranose (8)

Compound **1** (3.23 g) in hot acetone (15 ml) and 2-amino-2-deoxy-D-glucopyranose hydrochloride (3.76 g) in water (10 ml) were added to well-stirred ice water at 0.5 °C. The temperature of the reaction mixture was allowed to rise to room temperature and then an aqueous solution (15 ml) of sodium bicarbonate (2.52 g) was added slowly over a period of 30 min. The reaction was stirred continuously for 1 h at 45 °C and was then clarified by filtration. The filtrate was evaporated to dryness and extracted with methanol. Evaporation of the methanol extract yielded compound **8** which was recrystallized from water, yield, 4.2 g, 71%; m.p. 125–127°; $[\alpha]_D^{22}$ +24° (*c*, 1.0 in ethanol).

Anal. Calcd. for $C_{13}H_{20}O_7N_5Cl$: C, 39.64; H, 5.08; N, 17.78; Cl, 9.02. Found: C, 39.46; H, 5.04; N, 17.66; Cl, 8.83.

2-(4-Chloro-2-ethoxycarbonylmethylamino-s-triazin-6-yl)-amino-2-deoxy-D-galactopyranose (9)

This compound was prepared from compound **1** (3 g), 2-amino-2-deoxy-D-galactopyranose hydrochloride (2.59 g), and sodium bicarbonate (2 g) as described for compound **8**. The product (4.8 g) was not homogeneous on t.l.c. and required purification by column chromatography on silica gel using solvent A; a large portion of the major product was lost due to overlap with the impurity. The purified compound, 2.5 g, 51%, was recrystallized from ethanol:water (1:1); m.p. 118-120 °C, $[\alpha]_D^{22}$ +25° (*c*, 1.0 in ethanol).

Anal. Calcd. for $C_{13}H_{20}O_7N_5Cl$: C, 39.64; H, 5.08; N, 17.78; Cl, 9.02. Found: C, 39.51; H, 5.01; N, 17.89; Cl, 8.92.

2-(4-Chloro-2-ethoxycarbonylmethylamino-s-triazin-6-yl)-amino-2-deoxy-D-mannopyranose (10)

Compound **1** (2.1 g), 2-amino-2-deoxy-D-mannopyranose hydrochloride (1.8 g), and sodium bicarbonate (1.4 g) were reacted as described for compound **8**. The reaction product (2.8 g) was purified on silica gel as for compound **9** to yield compound **10**, 2.4 g, 73%. Crystallized from ethanol this compound had m.p. 108–111 °C and $[\alpha]_D^{22}$ −2° (*c*, 1.0 in ethanol).

Anal. Calcd. for $C_{13}H_{20}O_7N_5Cl$: C, 39.64; H, 5.08; N, 17.78; Cl, 9.02. Found: C, 39.79; H, 5.14; N, 17.58; Cl, 8.88.

Can. J. Chem. Downloaded from www.nrcresearchpress.com by 210.87.254.6 on 09/05/12
For personal use only.

*1-(4-Chloro-2-ethoxycarbonylmethylamino-s-triazin-6-yl)-amino-1-deoxy-D-glucitol (**11**)*

Compound **1** (2.51 g) in acetone (15 ml) and 1-amino-1-deoxy-D-glucitol (6) (1.81 g) in water (12 ml) were mixed together with continuous stirring in a further 10 ml of water. An aqueous solution (10 ml) of sodium bicarbonate (0.84 g) was added slowly during 30 min. The reaction mixture was stirred at 45 °C for 1 h. The insoluble product was filtered and washed with cold water and cold acetone; yield, 2.5 g, 63%; m.p. 192–194 °C.; $[\alpha]_D^{22}$ −21° (*c*, 1.0 in ethanol:water (1:1)).

Anal. Calcd. for $C_{13}H_{22}O_7N_5Cl$: C, 39.44; H, 5.56; N, 17.69; Cl, 8.98. Found: C, 39.12; H, 5.84; N, 17.44; Cl, 9.4.

*1-(4-Chloro-2-ethoxycarbonylmethylamino-s-triazin-6-yl)-amino-1-deoxy-D-mannitol (**12**)*

Compound **1**, 1-amino-1-deoxy-D-mannitol, and sodium bicarbonate were reacted in the same quantities and under the same conditions as for compound **11**. However, in this instance the product was soluble so the reaction mixture was filtered and concentrated to a syrup which then crystallized. The crystalline product was filtered, washed with cold ethanol, and recrystallized from methanol; yield 2.68 g, 67%; m.p. 174–175 °C; $[\alpha]_D^{22}$ +15° (*c*, 1.2 in ethanol:water (1:1)).

Anal. Calcd. for $C_{13}H_{22}O_7N_5Cl$: C, 39.44; H, 5.56; N, 17.69; Cl, 8.98. Found: C, 39.41; H, 5.74; N, 17.69; Cl, 9.27.

*1-(4-Chloro-2-ethoxycarbonylmethylamino-s-triazin-6-yl)-amino-1-deoxy-D-galactitol (**13**)*

Compound **1** (2.51 g) in acetone (15 ml), 1-amino-1-deoxy-D-galactitol (6) (1.81 g) in water (15 ml), and sodium bicarbonate (0.84 g) in water (12 ml) were reacted as described for **11**. The reactants were dissolved by addition of ethanol (30–40 ml) and the solution was heated at 50° for 1.5 h. The solution was concentrated and the product crystallized when most of the acetone and ethanol had been removed. It was recrystallized from acetone:water (1:3); yield 3.1 g, 78%; m.p. 187–188 °C; $[\alpha]_D^{22}$ −18.5° (*c*, in ethanol:water (1:1)).

Anal. Calcd. for $C_{13}H_{22}O_7N_5Cl$: C, 39.44; H, 5.56; N, 17.69; Cl, 8.98. Found: C, 39.19; H, 5.68; N, 17.68; Cl, 8.81.

*2-(4-Chloro-2-ethoxycarbonylmethylamino-s-triazin-6-yl)-amino-2-deoxy-D-glucose Diethyl Dithioacetal (**14**)*

Compound **1** (3 g) in acetone (15 ml), 2-amino-2-deoxy-D-glucose diethyl dithioacetal hydrochloride (7) (3.8 g) in water (15 ml), and sodium bicarbonate (1 g) in water (10 ml) were reacted as described for compound **11**. The mixture was clarified by filtration and the filtrate was evaporated to dryness. The residue was extracted with ethanol and evaporation of the extract yielded a syrupy product that was purified by chromatography on silica gel in solvent A. The pure compound was crystallized from ether:light petroleum (1:1); yield, 3.5 g, 58%; m.p. 56–58 °C; $[\alpha]_D^{22}$ −25° (*c*, 1.0 in ethanol).

Anal. Calcd. for $C_{17}H_{30}O_6N_5ClS_2$: C, 40.84; H, 6.00; N, 14.01; Cl, 7.10; S, 12.81. Found: C, 40.98; H, 5.87; N, 13.69; Cl, 7.13; S, 12.61.

*Acetylation of Compounds **8** and **14***

The compound (100 mg) was added slowly to a heated mixture of acetic anhydride (5 ml) and anhydrous sodium acetate (75 mg). The mixture was heated under reflux for 1 h and was then poured into ice water (50 ml). The product was extracted into chloroform (2 × 25 ml); the extract was washed successively with saturated aqueous sodium bicarbonate and water, dried (anhydrous sodium sulfate), and evaporated. The acetates of both compounds crystallized spontaneously and were analyzed without recrystallization.

The acetate of compound **8** had m.p. 90–93 °C, $[\alpha]_D^{22}$ +29° (*c*, 2% in chloroform), and *O*-acetyl, 30.10%; calcd. *O*-acetyl, 30.66%. Integration of the well-resolved signals for C—CH_3 and C(=O)—CH_3 protons at 1.32 and 2.0–2.3 δ respectively in the n.m.r. spectrum gave a ratio of 3:12 in agreement with the proposed structure. There was strong absorption at 1740 cm^{-1} in the i.r. spectrum of this compound indicative of *O*-acetyl group; no absorption attributable to acetamido groups could be detected in the range 1618–1665 cm^{-1}.

The acetate of compound **14** had m.p. 52–54 °C and $[\alpha]_D^{22}$ 0° (*c*, 2% in chloroform). Integration of the signals for the C—CH_3 and C(=O)—CH_3 protons as before gave a ratio of 9:12 in agreement with the proposed structure.

Anal. Calcd. for $C_{25}H_{38}N_5O_{10}ClS_2$: C, 44.98; H, 5.70; N, 10.50; *O*-acetyl, 25.8. Found: C, 45.04; H, 5.86; N, 10.47; *O*-acetyl, 25.48.

We are grateful to Mr. H. Seguin for the microanalyses and to Mr. F. Cooper for the u.v. spectra of these compounds.

1. R. J. Fielder, C. T. Bishop, S. F. Grappel, and F. Blank. J. Immunol. **105**, 265 (1970).
2. J. T. Thurston, J. R. Rudley, D. W. Kaiser, I. Hechenbleikner, F. C. Schaefer, and D. Holm-Hansen. J. Am. Chem. Soc. **73**, 2981 (1951).
3. S. Horrobin. J. Chem. Soc. 4130 (1963).
4. W. F. Beech. J. Chem. Soc. 466 (1967).
5. C. K. Banks, O. M. Gruhzit, E. W. Tillitson, and J. Controulis. J. Am. Chem. Soc. **66**, 1771 (1944).
6. F. Kagan, M. A. Rebenstorf, and R. V. Heinzelman. J. Am. Chem. Soc. **79**, 3541 (1957).
7. M. W. Whitehouse, P. W. Kent, and C. A. Pasternak. J. Chem. Soc. 2315 (1954).
8. A. L. Steyermark. Quantitative organic microanalysis. Academic Press Inc., London. 1961.
9. K. Landsteiner. The specificity of serological reactions. Harvard University Press, Cambridge, Mass. 1945.
10. W. F. Goebel and O. T. Avery. J. Exp. Med. **50**, 521 (1929).
11. P. Z. Allen, I. J. Goldstein, and R. N. Iyer. Biochem. **6**, 3029 (1967).

The Hydration of Ketones in Mixtures of Water and Polar Aprotic Solvents[1]

ROSS STEWART AND JOHN D. VAN DYKE[2]

Department of Chemistry, University of British Columbia, Vancouver 8, British Columbia

Received February 7, 1972

The hydration of a series of ring-substituted trifluoroacetophenones (Z) has been studied by means of u.v. and n.m.r. spectroscopy in DMSO–water and sulfolane–water mixtures. The W_0 function is defined as $W_0 = pK_d + \log [Z]/[ZH_2O] = -\log (f_Z/f_{ZH_2O} \cdot a_{H_2O})$, where K_d is the equilibrium constant for the reaction $ZH_2O \rightleftarrows Z + H_2O$.

Mixtures of water and sulfolane in all proportions have a dehydrating effect compared to water but mixtures of water and DMSO down to 15 mol % water are more hydrating with respect to the carbonyl group of trifluoroacetophenones than is pure water. An analysis of activity coefficient behavior indicates that the diol, ZH_2O, has a higher requirement for solvation by water molecules than does water itself.

The rate of the uncatalyzed hydration in aqueous sulfolane drops drastically as the water content of the medium decreases, whereas the rate of the acid-catalyzed reaction is not greatly affected by changes in the solvent composition; a plot of log k for both catalyzed and uncatalyzed reactions is approximately linear in W_0.

L'hydratation d'une série de trifluoroacétophénones substituées sur le cycle, a été étudiée par u.v. et r.m.n. dans des mélanges DMSO–eau et sulfolane–eau. La fonction W_0 est définie par $W_0 = pK_d + \log [Z]/[ZH_2O] = -\log (f_Z/f_{ZH_2O} \cdot a_{H_2O})$, où K_d est la constante d'équilibre pour la réaction $ZH_2O \rightleftarrows Z + H_2O$.

Les mélanges en toute proportion d'eau et de sulfolane ont un effet déshydratant comparé à l'eau mais les mélanges d'eau et de DMSO (limite inférieure 15% molaire en eau) sont plus hydratants vis-à-vis du carbonyle des trifluoroacétophénones que l'eau pure. L'analyse du comportement du coefficient d'activité indique que le diol, ZH_2O, est plus exigeant dans la solvatation par les molécules d'eau que ne le ferait l'eau elle-même.

La vitesse de l'hydratation non-catalysée dans le sulfolane aqueux tombe considérablement lorsque la teneur en eau décroît tandis que la réaction acidocatalysée n'est pas affectée de façon notable par des changements dans la composition du solvant; la courbe log K à la fois pour les réactions catalysée et non-catalysée est approximativement une droite dans W_0.

Canadian Journal of Chemistry, **50**, 1992 (1972)

Introduction

The first study of the hydration of aldehydes and ketones was made in 1886 by Ramsay and Young (1), who discovered that acetaldehyde and water mix with considerable heat and diminution of volume. With the advent of u.v. spectroscopy it was possible to show that this hydration involved a chemical reaction between water and the carbonyl compound, since the carbonyl absorption is almost zero in aqueous solution, whereas it is of normal intensity in solvents such as hexane. It is furthermore possible to isolate crystalline hydrates of certain aldehydes and ketones containing strongly electronegative substituents and n.m.r. and Raman (2) spectra provide direct evidence for the *gem*-diol formula, $R_2C(OH)_2$ (3).

A number of studies have been made of carbonyl hydration using u.v. spectroscopy to measure the concentration of unhydrated compound. Difficulties arise with regard to determining the exact extinction coefficient (ε) of the carbonyl compound since the rate of hydration in water may be very fast. Many ketones which are not appreciably hydrated show considerable variation in their ε values from solvent to solvent so that when dealing with a compound which undergoes partial hydration one cannot simply take the ε value in an inert solvent and apply it to aqueous systems.

$$R_2C{=}O + H_2O \rightleftarrows R_2CH(OH)_2$$

Bell and Clunie (4) have estimated ε values in water by combining calorimetric and spectroscopic data and Bloch and Rumpf (5) have used a kinetic method for the same purpose. Solvent correction parameters have also been used with considerable success, as indicated by the correspondence of equilibrium values based on such estimated ε values with the equilibrium values obtained by n.m.r. measurements (6). The advantage of n.m.r. in determining equilibrium values for hydration is that one can determine the concentration of both the *gem*-diol and the

[1]Taken from the Ph.D. thesis of J. D. Van Dyke, University of British Columbia, 1970.

[2]Present address: Polymer Corporation, Sarnia, Ontario.

Can. J. Chem. Downloaded from www.nrcresearchpress.com by 210.87.254.42 on 09/05/12
For personal use only.

Can. J. Chem. Downloaded from www.nrcresearchpress.com by 210.87.254.42 on 09/05/12
For personal use only.

carbonyl compound. Its only disadvantage is that larger concentrations are required for accurate measurements than with u.v. spectroscopy.

Kinetics of hydration have been studied using dilatometry (7), u.v. (8) and n.m.r. spectroscopy (9), ^{18}O exchange (10), polarography (11), chemical scavenging (12), and thermal methods (13). The carbonyl hydration reaction is subject to both general acid and general base catalysis; in the case of acetaldehyde, the Brønsted coefficient for acid catalysis, α, is equal to 0.54; for base catalysis, the Brønsted coefficient, β, is equal to 0.45. The corresponding numbers for formaldehyde are 0.24 and 0.40 and for *s*-dichloroacetone, they are 0.27 and 0.53. It appears that the coefficient α is more influenced by the structure of the carbonyl compound than is β.

Eigen (14) has suggested that the spontaneous hydration reaction (the contribution to the overall rate that is independent of acid or base) occurs by way of a cyclic hydrogen-bonded transition state containing two or more water molecules as, for example, in the structure below.

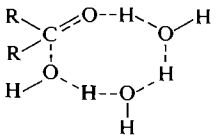

Kurz and Coburn's work (15) supports such an interpretation. For example, the entropy of activation for the spontaneous hydration of acetaldehyde is -38 e.u. compared to values of -4 and -7 e.u. for the routes catalyzed by hydrogen and hydroxide ions, respectively. Bell *et al.* (8) found that in aqueous dioxan and aqueous acetonitrile the order with respect to water molarity was close to three for hydration and two for dehydration. It is surprising that integral orders in water molarity are maintained over a fairly wide concentration range since freezing-point and vapor-pressure measurements reveal the presence of large deviations from ideal solution behavior.

It is known that polar aprotic solvents such as dimethyl sulfoxide (DMSO) and tetramethylene sulfone (sulfolane) cause drastic increases in the effective basicity of hydroxide ion, largely as a result of the solvents' inability to effectively hydrate such a small, "hard", ion. DMSO is considerably more effective than sulfolane in this regard (16).

DMSO appears to form strong hydrogen bonds with water molecules (17) as indicated by thermodynamic, dielectric, and viscometric data (18). Indeed, the value of the partial heat-of-mixing of water term at infinite dilution ΔH_w^∞, in DMSO, -1.28 kcal/mol, (19) indicates that the sulfoxide group is a strong acceptor of protons. Data for the activity of water at 70° (20) in DMSO–water mixtures show that, as the water content decreases and the DMSO content increases, both the activity of water and the activity coefficient of water, f_{H_2O}, steadily decrease. This indicates negative deviations from Raoult's law ($\Delta G < 0$). Thus DMSO–water interactions are stronger than the intermolecular association of water.

Sulfolane interacts quite differently with water. Here the partial heat of mixing at infinite dilution, ΔH_w^∞, is $+1.6$ kcal/mol (19). The activity coefficient of water, f_{H_2O}, increases rather than decreases as water is replaced by sulfolane in the solution. Thus, there are positive deviations from Raoult's law ($\Delta G > 0$) in sulfolane–water solutions.

The present study was undertaken to see if a hydration scale (W_0), analogous to the acidity function H_0, could be developed in solvents such as DMSO and sulfolane. Such scales would allow hydration equilibrium constants to be determined in media whose hydrating properties are far different from that of the standard state, water. We have previously shown in a brief communication that such scales can be used to generate K values for a series of ring-substituted trifluoroacetophenones,

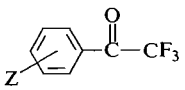

and have shown that these values are correlated by the Hammett σ^+ substituent constant (21). In the present work we examine the factors that determine the hydrating and dehydrating properties of aqueous DMSO and aqueous sulfolane solutions with respect to these ketones and the effect of changing media on the spontaneous and acid-catalyzed hydration and dehydration reactions.

Can. J. Chem. Downloaded from www.nrcresearchpress.com by 210.87.254.42 on 09/05/12
For personal use only.

Experimental

Materials

Most of the α,α,α-trifluoroacetophenones were obtained either from commercial sources or prepared as previously described (21, 22, 26).

4-Dimethylamino-α,α,α-trifluoroacetophenone was prepared by slowly adding trifluoroacetic anhydride to a one-fold excess of *N,N*-dimethylaniline. Crystallization and sublimation gave a product of m.p. 75.5–77° (lit. (23), 76.5–77°).

2-Trifluoromethyl-2-(4′-methoxyphenyl)-1,3-dioxolane (**1**) was prepared by heating together 1 g (0.0049 mol) of 4-methoxy-α,α,α-trifluoroacetophenone, 0.78 g (0.0126 mol) ethylene glycol, and 0.22 g (0.00129 mol) 4-toluenesulfonic acid at 110° in a flask fitted with a total reflux separating head. When droplets of water were observed to form in the column, petroleum ether (60–100°) was introduced, and the mixture was refluxed for 24 h. The refluxing was then discontinued and 0.22 g sodium acetate was introduced. After stirring for 1 h, the solution was filtered and concentrated. The precipitated crystals were collected and recrystallized twice from petroleum ether, m.p.: 52–53°.

The purity was checked by dissolving the compound in ether and analyzing the solution by g.l.c.

The identity of the compound was established by i.r. and n.m.r. spectroscopy.

Anal. Calcd. for $C_{11}H_{11}O_3F_3$: C, 52.23; H, 4.43; F, 22.96. Found: C, 53.35; H, 4.63; F, 22.72.

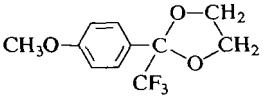

1

Solvent–water mixtures were prepared and stored as previously described (16) and the water content determined by Karl Fischer titration. Owing to the hygroscopic nature of these systems each solution was tested for water content immediately prior to dissolving the ketones for n.m.r. measurements. For u.v. measurements Karl Fischer titrations were carried out directly on the solutions being measured.

Equilibrium and Kinetic Measurements

Equilibrium constants were determined both by ^{19}F n.m.r. and by u.v. spectroscopy whereas only the latter was used in the rate studies. Equilibrium measurements were made in the presence of 0.1 *M* methanesulfonic acid, except in the case of the 4-dimethylamino ketone. The sealed n.m.r. tubes containing about 0.1 *M* substrate were kept for 2 days at the the appropriate temperature to allow equilibrium to be reached before the ^{19}F absorptions of the ketone and the hydrate were measured. To establish the W_0 scale, all measurements, both n.m.r. and ultraviolet, were made at 31.4°, the temperature within the n.m.r. probe at room temperatures, as measured by chromel–alumel thermocouple. For thermodynamic studies temperatures were adjusted to temperatures above 31.4° and measured in the same way. In the case of the 4-dimethylamino compound, where very little hydrate was found to be present, time averaging (28 n.m.r. scans) was carried out to facilitate measurement of the small hydrate peak.

The u.v. measurements, which were done on much more dilute solutions of substrate, require that the extinction coefficients (ε_0) at the carbonyl absorption maximum be known of the ketone and hydrate (for the latter these are close to zero). The extinction coefficients of the ketones measured were generally very large requiring a stock solution of the ketone to be prepared, which upon dilution in an u.v. cell would give a measurable concentration.

The procedure consisted of measuring the carbonyl absorbance of the two ketones whose equilibrium constants were measured by u.v. spectroscopy (the 4-methoxy- and 4-dimethylamino trifluoroacetophenones) in the appropriate solvent mixture. The extinction coefficient so obtained was due to hydrate and ketone. The absolute extinction coefficient of the ketone in this mixture was determined through the use of model compounds. First the extinction coefficient of the ketone was measured in 100% sulfolane or DMSO. This was always done after preparing the ketone stock solution so that small amounts of water that might be present would not be able to hydrate the ketone. (The rate of reaction is slow in 100% solvent.) Then the absorbance of a non-hydrating model compound (4-methoxyacetophenone or 4-dimethylaminoacetophenone) was measured both in 100% solvent and in the solvent mixture in which ε_0 was desired, and the change in absorbance noted. Assuming the same relative change to be applicable to the trifluoro ketone, the ketone absorbance measured in 100% inert solvent was corrected to give ε_0 for the solvent mixture.

For 4-methoxytrifluoroacetophenone, an experiment was conducted to see if any significant tailing of the small aromatic absorptions at 277 and 271 mμ lay at 299 mμ, the position of carbonyl absorbance. For this purpose, the ethylene glycol ketal of 4-$CH_3OC_6H_4COCF_3$ (2-trifluoromethyl-2-(4′-methoxyphenyl)-1,3-dioxolane) was prepared in order to simulate its hydrate. For the dioxolane, zero absorbance was observed at 299 mμ with retention of absorbance at 277 and 271 mμ. Thus, it could be assumed that the hydrate molecule had neither any carbonyl absorbance nor any tailing of phenyl peaks at 299 mμ in the specific case of the 4-CH_3O compound. The entire absorbance at 299 mμ is then due to the ketone. For the 4-$(CH_3)_2N$ compound, the carbonyl absorbance occurs far removed from the phenyl absorptions, rendering it unnecessary to prepare the comparable ketal.

The u.v. results were compared with the n.m.r. results wherever possible. Using the above technique for determining u.v. equilibrium constants, comparable results were obtained by the two techniques. For example, Fig. 1 contains a comparison of u.v. and n.m.r. equilibrium constants for the 4-CH_3O compound. In another experiment with the 4-dimethylamino compound, 28 time-averaging n.m.r. runs carried out on a dilute solution of the ketone in 80 mol % water yielded a value of 15 for $[Z][ZH_2O]$, compared to the u.v. result of 14.5.

Rate Constants

The rate of disappearance of the u.v. carbonyl absorption peak of the ketone Z was followed and the rate coefficients k_h and k_d for hydration and dehydration, respectively, were calculated as follows. Equation 1 on integration gives eq. 2 which can be used in the form of eq. 3. The rate constant for the hydration reaction, k_h, a pseudo first order rate constant, can be obtained from the experimental rate constant, k_{obs}, by using the relation given in eq. 4. (This

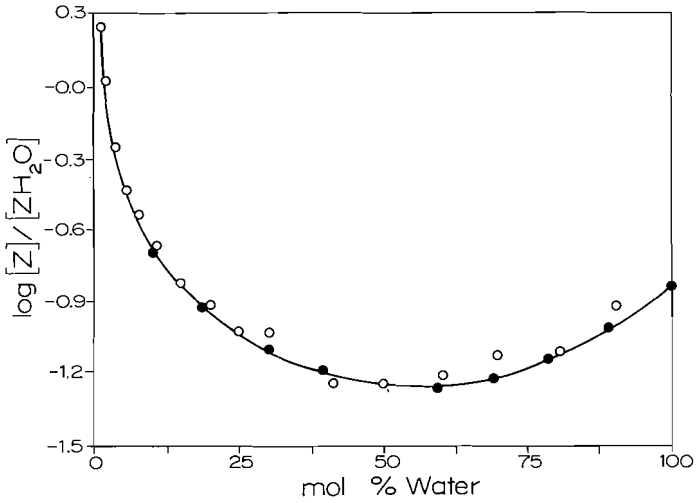

FIG. 1. A comparison of results determined by u.v. and n.m.r. techniques for the equilibrium hydration of 4-$CH_3OC_6H_4$-$COCF_3$ in DMSO; ○ n.m.r. values (0.1 *M* methanesulfonic acid present), ● u.v. values (no acid present).

relation can be shown to be valid at all solution compositions.)

$$[1] \qquad \frac{-\mathrm{d}[Z]}{\mathrm{d}t} = k_h[Z] - k_d[ZH_2O]$$

$$[2] \qquad \ln\left\{\frac{[Z]-[Z]_\infty}{[Z]_0-[Z]_\infty}\right\} = -(k_h + k_d)t$$

$$[3] \qquad \ln\left\{\frac{A-A_\infty}{A_0-A_\infty}\right\} = -(k_h + k_d)t$$

$$[4] \qquad k_h/k_d = [ZH_2O_\infty]/[Z_\infty]$$

The slopes were obtained by plots of ln $(A - A_\infty)$ against time, using the method of least squares. Excellent first-order plots were obtained.

Results and Discussion

The W_0 Function

When the Hammett stepwise technique (24) is applied to the hydration of ketones in a manner analogous to that applied to the ionization of weak acids or bases the equilibrium constant for dehydration, K_d, can be written as

$$[5] \qquad K_d = \frac{[Z]}{[ZH_2O]} \cdot \frac{f_Z}{f_{ZH_2O}} \cdot a_{H_2O}$$

If the negative logarithm of each side of eq. 5 is taken the following expression is obtained:

$$[6] \qquad pK_d = -\log\left(\frac{[Z]}{[ZH_2O]}\right) - \log\left(\frac{f_Z}{f_{ZH_2O}} \cdot a_{H_2O}\right)$$

From this, W_0 and w_0 can be defined as follows:

$$[7] \qquad W_0 = -\log\left(\frac{f_Z}{f_{ZH_2O}} \cdot a_{H_2O}\right)$$

$$[8] \qquad w_0 = \frac{f_Z}{f_{ZH_2O}} \cdot a_{H_2O}$$

Thus, for two ketones, Z_1 and Z_2, in the same solution

$$[9] \qquad pK_d^{Z_1} - pK_d^{Z_2} = \log\frac{[Z_2]}{[Z_2H_2O]} - \log\frac{[Z_1]}{[Z_1H_2O]} + \log\frac{f_{Z_2}f_{Z_1H_2O}}{f_{Z_2H_2O}f_{Z_1}}$$

If the Hammett treatment is successful for ketones in mixtures of water and polar aprotic solvents, the last quantity in eq. 9 will be zero regardless of the solvent composition, and eq. 9 will reduce to

$$[10] \qquad pK_d^{Z_1} - pK_d^{Z_2} = \log\frac{[Z_2]}{[Z_2H_2O]} - \log\frac{[Z_1]}{[Z_1H_2O]}$$

The relative pK_s's for two ketones that are partially hydrated in the same solution can be obtained by measuring the two quantities on the right-hand side of eq. 10. If the thermodynamic pK_d value for one ketone is known, the pK_d values for ketones with a wide range of pK_d's can

Can. J. Chem. Downloaded from www.nrcresearchpress.com by 210.87.254.42 on 09/05/12
For personal use only.

Can. J. Chem. Downloaded from www.nrcresearchpress.com by 210.87.254.42 on 09/05/12
For personal use only.

TABLE 1. W_0-Values for sulfolane–water and DMSO–water*†

Water (mol %)	W_0	
	Sulfolane	DMSO
1.0	2.72‡	1.09§
2.0	2.31	—
3.0	2.03	—
5.0	—	0.46
6.0	1.63	—
10.0	1.36	0.15
20.0	1.00	−0.11
30.0	0.81	−0.27
40.0	0.66	−0.36
60.0	0.47	−0.42
80.0	0.31	−0.31
90.0	0.21	−0.18
95.0	0.12	—
100.0	0‖	0‖

*$T = 31.4°$; all measurements of W_0 in sulfolane–water were made in the presence of 0.1 M methanesulfonic acid. In DMSO–water only the measurements at 1.02 and 5% were obtained in the presence of acid.
†The pK_d values (21) for the substituted trifluoroacetophenone indicators used to determine these values of W_0 are: 4-$(CH_3)_2N$, −0.86; 4-CH_3O, 0.84; 4-CH_3, 1.46; 3-CH_3, 1.77; unsubstituted, 1.89; 4-F, 1.91; 3-CH_3O, 1.99; 3-F, 2.50; 3-NO_2, 3.15.
‡Exact solvent composition, 1.05 mol % water.
§Exact solvent composition, 1.02 mol % water.
‖By definition.

TABLE 2. Activity coefficient ratio of ketone to hydrate in sulfolane–water and in DMSO–water

Water (mol %)	f_{H_2O}		f_Z/f_{ZH_2O}*	
	Sulfolane†	DMSO‡	Sulfolane	DMSO
10	3.07	0.47	0.14	15.0
20	2.68	0.55	0.19	11.8
30	2.18	0.59	0.24	10.5
40	1.86	0.68	0.29	8.5
50	1.62	0.77	0.35	6.5
60	1.44	0.87	0.39	5.0
70	1.28	0.96	0.44	3.8
80	1.14	1.05	0.54	2.4
90	1.05	1.06	0.65	1.6
100	1.00	1.00	1.00	1.00

*Calculated using eq. 6 and using activities for water in sulfolane and DMSO given in refs. 19 and 20 and adjusted in the case of DMSO to 31.4° using data kindly supplied by Professor R. L. Benoit.
†Reference 19.
‡See*.

be determined depending on how effective the inert solvents are at reducing the extent of hydration.

The function, W_0, is determined from the same measurements of $[Z]/ZH_2O]$ that are used to determine the pK_d's (21) of the ketones. From eqs. 6 and 7 eq. 11 can be obtained. It can be

$$[11] \qquad W_0 = pK_d + \log \frac{[Z]}{[ZH_2O]}$$

seen that positive values of W_0 indicate a solution which is less hydrating than pure water; for negative values of W_0 the opposite is true. Furthermore, a plot of $\log [Z]/[ZH_2O]$ *vs.* W_0 will give a straight line of unit slope. This fact was used to test the validity of the Hammett postulate for ketones in polar aprotic solvents.

The W_0 values for sulfolane and DMSO mixtures with water are given in Table 1. It can be seen that sulfolane has a much larger dehydrating effect on *gem*-diols than does DMSO. Indeed aqueous solutions of the latter are *more* hydrating over most of the solvent composition range than is pure water (see Fig. 1). These results are surprising in view of the way that sulfolane and DMSO, particularly the latter, raise the activity of hydroxide ion and produce powerfully basic systems. The greater effect of DMSO in this regard has been ascribed to its ability to interact with water and lower the latter's activity. In Table 2 the activity coefficient of water, f_{H_2O}, is given as a function of solvent composition for aqueous sulfolane and DMSO. The changes in W_0 are in the *opposite* direction to what would be predicted on the basis of changes in the activity coefficient of water. The water system becomes more dehydrating as sulfolane is added yet f_{H_2O} rises (although a_{H_2O} decreases somewhat). On the other hand, water becomes a better hydrating medium as DMSO is added, even though both f_{H_2O} and a_{H_2O} decrease.

By using eq. 8 and the known values of the activity of water in DMSO–water and sulfolane–water systems we can determine the effect of changing media on the activity coefficient ratio of the ketone and its hydrate, f_Z/f_{ZH_2O} (Table 2).

It can be seen from the activity coefficient ratios in Table 2 how differently the two solvents, sulfolane and DMSO, behave. Carbonyl compounds are generally more soluble in sulfolane and DMSO than in water and hence we can assume that f_Z will decrease somewhat as the amount of water in the system decreases. This conclusion can only be reconciled with the trend in the values of f_Z/f_{ZH_2O} found in DMSO if the

Can. J. Chem. Downloaded from www.nrcresearchpress.com by 210.87.254.42 on 09/05/12
For personal use only.

activity coefficient of the hydrate decreases drastically as the amount of water in the system falls. Presumably the hydrate is very much more effectively solvated by DMSO than it is by water.

In the case of sulfolane a different situation emerges. If f_Z is assumed to decrease as the water content of the system decreases (in line with the generally greater solubility of ketones in sulfolane than in water) then the decrease in f_Z/f_{ZH_2O} shown in Table 2 can be attributed, at least partly, to this factor. This, in turn, means that sulfolane, unlike DMSO, is not particularly efficient at solvating the hydrate. These results can be rationalized by assuming that the activity coefficient of the diol is affected by changing media in the same way as is that of water, only more so. This is presumably a consequence of the similarity in hydrogen-bonding requirements of the two hydroxylic molecules, water, and the diol, although the latter's appears to be the greater.

The variations in activity coefficient described above raise the suspicion that a hydration parameter such as W_0 may be a function not only of the solvent system but also of the type of substrate used. Although further work is needed to settle this question results with *s*-dichloroacetone are indicative. A plot of log $[Z]/[ZH_2O]$ for the hydration of this compound in sulfolane–water against W_0 values from Table 1 gives a roughly linear relation of unit slope only between 10 and 45 mol % water and a straight line of considerably higher slope (1.56) between 45 and 95 mol % water (correlation coefficient 0.9988).

Thermodynamic Parameters

The values of ΔH and ΔS for hydration of 4-methoxy-α,α,α-trifluoroacetophenone in water were determined to be -6.7 kcal mol^{-1} and -18.1 e.u., respectively. These values change to slightly more negative values as sulfolane is added to the system. For example, in 68.1 mol % water $\Delta H = -7.1$ kcal mol^{-1} and $\Delta S = -19.4$ e.u. These results are in line with the observations of Bell and McDougall (25) that both ΔH and ΔS for the hydration of *s*-dichloroacetone in dioxan–water are little affected by changes in solvent composition ($\Delta H = -5.7$ kcal, $\Delta S = -14.8$ e.u., in water in this case). The fairly large negative value of -18.1 for entropy of hydration reflects the reduction in the number of molecules from two to one and also, presumably, the higher solvation requirements of the diol than of the ketone.

TABLE 3. Rate of hydration of 4-$CH_3OC_6H_4COCF_3$ in sulfolane–water mixtures in the absence of added acid

Water (mol %)	a_{H_2O}*	$10^4 k_h$ (s^{-1})	k_h/a_{H_2O}	k_d (s^{-1})
17.0	0.480	0.140	0.291	0.258
21.8	0.560	0.345	0.616	0.473
26.3	0.618	0.803	1.30	0.892
30.8	0.661	1.57	2.37	1.42
32.9	0.686	2.17	3.16	1.82
35.9	0.710	3.38	4.77	2.51
40.3	0.744	5.70	7.67	3.62
45.7	0.781	10.6	14.6	5.80
50.1	0.810	17.5	21.5	8.63
54.5	0.831	28.1	33.8	13.0
60.6	0.864	42.4	49.0	18.1
65.0	0.875	67.9	77.6	27.4
69.9	0.894	105	117	38.7
75.0	0.904	178	197	60.0
79.7	0.910	299	328	91.0
83.6	0.925	434	469	119

*Interpolated from the data in ref. 19.

Kinetics of Hydration

In Table 3 the rate constants, k_h and k_d, for hydration and dehydration respectively, are listed for mixtures of sulfolane and water, together with the activity of water in the various systems. It can be seen that the rate of hydration decreases drastically as water is removed from the system and that this decrease is much more marked than is the decrease in the activity of water. (A plot of log k_h against log a_{H_2O} gives a curved line whose slope rises from approximately 7 at 20 mol % water to over 20 at 80 mol % water; it is clear that water activity is not a useful parameter for correlating hydration and dehydration rates in this case, a conclusion Bell *et al.* (8) have also come to in connection with the hydration of *s*-dichloroacetone in dioxan–water mixtures.)

A plot of log k_h against the solvation parameter W_0 gives a reasonably linear relation (Fig. 2) suggesting that the transition state of the uncatalyzed hydration reaction has some of the character of the diol molecule. The slope of the line in Fig. 2 is -4.56. This indicates a much higher requirement for water solvation in the transition state than in the diol, although the number of solvating water molecules cannot simply be identified with the slope of the line.

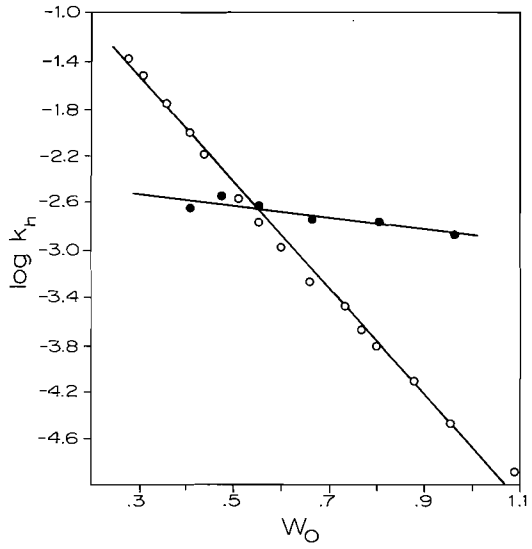

FIG. 2. The rate constants k_h^0 and $k_h^{H^+}$ for the spontaneous and acid-catalyzed hydration of 4-$CH_3OC_6H_4COCF_3$ in sulfolane–water as a function of the hydration parameter W_0; ○ no acid present, ● 0.025 *M* methanesulfonic acid present.

A plot of log k_h against the molar concentration of water in the manner of Bell *et al.* (8) yields a slope of 3.1 with a correlation coefficient of 0.9990 (Fig. 3). Bell *et al.* found that uncatalyzed carbonyl hydration and dehydration reactions in acetonitrile and dioxan give slopes near 3 and 2, respectively, when log *k* is plotted against water molarity and they conclude that three molecules of water are involved in the transition state for hydration and two for dehydration. (The fact that water molarity appears to give better correlations with hydration rates than does water activity can only be due to cancellation of activity coefficient effects.) In our case a plot of log k_d against water molarity for the dehydration reaction gives a straight line of slope 2.4 (correlation coefficient of 0.9998).

The acid-catalyzed hydration reaction in sulfolane–water is strikingly different from the uncatalyzed reaction in terms of its dependence on W_0. Figure 2 reveals that k_h for the reaction in the presence of 0.1 *M* methanesulfonic acid is only slightly dependent on W_0 over a considerable range of solvent composition.[3]

One can conclude that the transition state for spontaneous hydration of carbonyl compounds has a much higher requirement for water molecules than does the diol but that the transition state for the acid-catalyzed hydration has similar solvation requirements to the diol.

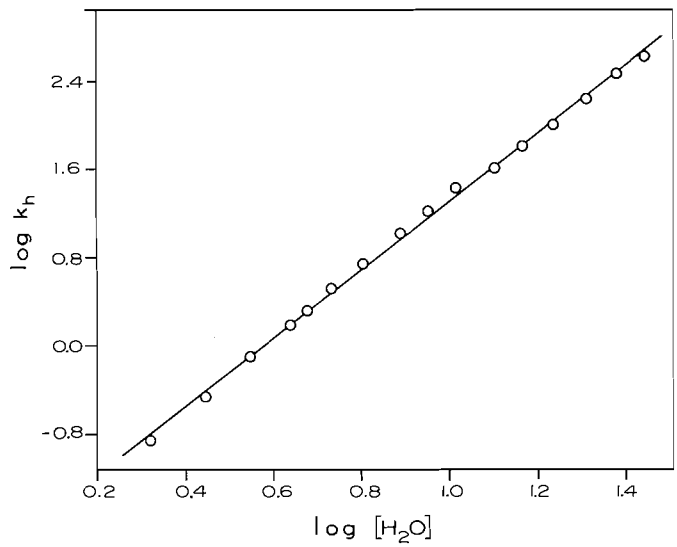

FIG. 3. The logarithm of the rate of the spontaneous hydration reaction of 4-$CH_3OC_6H_4COCF_3$ in sulfolane–water as a function of the logarithm of the water molarity.

[3]The values of k_h used in Fig. 2 for the acid-catalyzed reaction, that is $k_h^{H^+}$, are obtained by subtracting the rate for the spontaneous reaction in the same medium, that is k_h^0, from the overall rate. They thus are in the units of s^{-1}. Experiments at different methanesulfonic acid concentrations show that the acid-catalyzed rate is, in fact, directly proportional to the concentration of acid present in a given medium.

Can. J. Chem. Downloaded from www.nrcresearchpress.com by 210.87.254.42 on 09/05/12
For personal use only.

The financial support of the National Research Council of Canada is gratefully acknowledged as is a fellowship granted by the H. R. MacMillan Foundation to J.V.D.

1. W. RAMSAY and S. YOUNG. Phil. Trans. **177**, 71 (1886).
2. E. O. BISHOP and R. E. RICHARDS. Trans. Faraday Soc. **55**, 1070 (1959); J. H. HIBBEN. J. Am. Chem. Soc. **53**, 2418 (1931).
3. R. P. BELL. Advan. Phys. Org. Chem. **4**, 1 (1966).
4. R. P. BELL and J. C. CLUNIE. Trans. Faraday Soc. **48**, 439 (1952).
5. C. BLOCH and P. RUMPF. Compt. Rend. **237**, 619 (1953).
6. P. GREENZAID, Z. RAPAPORT, and D. SAMUEL. Trans. Faraday Soc. **63**, 2131 (1967).
7. R. P. BELL and W. C. E. HIGGINSON. Proc. Roy. Soc. A**197**, 141 (1949); R. P. BELL and B. DE B. DARWENT. Trans. Faraday Soc. **46**, 34 (1950).
8. R. P. BELL, J. P. MILLINGTON, and J. M. PINK. Proc. Roy. Soc. A**303**, 1 (1968); Y. POCKER and J. E. MEANY. J. Phys. Chem. **71**, 1857 (1969).
9. J. HINE and J. G. HOUSTON. J. Org. Chem. **30**, 1328 (1965); G. SOCRATES. J. Org. Chem. **34**, 2958 (1969); P. GREENZAID, Z. LUZ, and D. SAMUEL. Trans. Faraday Soc. **64**, 2787 (1968).
10. M. BYRN and M. CALVIN. J. Am. Chem. Soc. **88**, 1916 (1966).
11. P. VALENTA. Coll. Czech. Chem. Commun. **25**, 853 (1960).
12. P. G. EVANS, M. M. KREEVOY, and R. G. MILLER. J. Phys. Chem. **69**, 4325 (1965); P. LEHENAFF. Compt. Rend. C**263**, 1205 (1966).
13. R. P. BELL, V. GOLD, J. HILTON, and M. H. RAND. Disc. Faraday Soc. **17**, 151 (1954); L. C. GRUEN and P. T. MCTIGUE. J. Chem. Soc. 5224 (1963).
14. M. EIGEN. Disc. Faraday Soc. **39**, 7 (1965).
15. J. L. KURZ and J. I. COBURN. J. Am. Chem. Soc. **89**, 3528 (1967).
16. D. DOLMAN and R. STEWART. Can. J. Chem. **45**, 911 (1967); R. STEWART and J. P. O'DONNELL. Can. J. Chem. **42**, 1681 (1964).
17. R. FUCHS, G. E. MCCRARY, and J. J. BLOOMFIELD. J. Am. Chem. Soc. **83**, 4281 (1961); E. TOMMILA and M.-L. MURTO. Acta Chem. Scand. **17**, 1947 (1963).
18. A. J. PARKER. Quart. Rev. **16**, 163 (1962); D. MARTIN, A. WEISE, and H.-J. NICLAS. Angew. Chem. Int. Ed. **6**, 318 (1967).
19. R. L. BENOIT and G. CHOUX. Can. J. Chem. **46**, 3215 (1968).
20. J. KENTTAMAA and J. J. LINDBERG. Suomen. Kemi. B**33**, 98 (1960).
21. R. STEWART and J. D. VAN DYKE. Can. J. Chem. **48**, 3961 (1970).
22. R. STEWART and R. VAN DER LINDEN. Can. J. Chem. **38**, 399 (1960).
23. W. A. SHEPHERD. J. Am. Chem. Soc. **87**, 2410 (1965).
24. L. P. HAMMETT. Physical organic chemistry. McGraw Hill Book Co. New York, N.Y. 1970.
25. R. P. BELL and A. O. MCDOUGALL. Trans. Faraday Soc. **56**, 1281 (1960).
26. E. T. MCBREE, S. RESCONICH, L. R. BELOHLAV, and H. P. BRAENDLIN. J. Org. Chem. **28**, 3579 (1963).

Can. J. Chem. Downloaded from www.nrcresearchpress.com by 210.87.254.42 on 09/05/12
For personal use only.

The Oxidation of 2-Propanol by Ruthenium Tetroxide

DONALD G. LEE AND MATTHIJS VAN DEN ENGH[1]

Department of Chemistry, The University of Saskatchewan Regina Campus, Regina, Saskatchewan, S4S 0A2

Received January 6, 1972

The kinetics of the oxidation of 2-propanol by ruthenium tetroxide in aqueous perchloric acid solutions have been investigated. The results indicate that the two mechanisms pertain; at moderate acidities (1–6.5 *M* $HClO_4$) the rate determining step involves hydride abstraction while at very high acid concentrations the rate determining step becomes carbonium ion formation.

Les cinétiques de l'oxydation du propanol-2 par le tétroxyde de ruthénium dans des solutions aqueuses d'acide perchlorique ont été étudiées. Les résultats indiquent que deux mécanismes sont concernés; à une acidité modérée (1–6.5 *M* $HClO_4$), l'étape qui détermine la vitesse implique un arrachement d'hydrure alors qu'à une concentration élevée en acide l'étape qui détermine la vitesse correspond à la formation d'un ion carbonium.

Canadian Journal of Chemistry, **50**, 2000 (1972)

Introduction

Ruthenium tetroxide is currently finding extensive use as an oxidant for alcohols (1), particularly carbohydrates (2), and steroids (3). With simple alcohols the reaction proceeds according to reaction 1 giving quantitative yields of ketone.

$$[1]\quad 2R{-}\underset{\displaystyle OH}{\underset{|}{C}}H{-}R' + RuO_4 \rightarrow 2R{-}\overset{\displaystyle O}{\overset{\|}{C}}{-}R' + RuO_2 + 2H_2O$$

Water and carbon tetrachloride are the most commonly used solvents. Since it is a vigorous reagent, even under very mild conditions, ruthenium tetroxide has found particular application with alcohols which are normally resistant to oxidation (4).

The reaction can be carried out using a stoichiometric quantity of ruthenium tetroxide or by use of a catalytic amount of ruthenium dioxide in conjunction with a co-oxidant such as sodium periodate (3, 5). In the latter procedure, the co-oxidant continuously regenerates the tetroxide from the dioxide as in reaction 2.

$$[2]\quad RuO_2 + 2ClO_4^- \rightarrow RuO_4 + 2ClO_3^-$$

Despite its wide utility very little is known concerning the mechanisms of these and related reactions of ruthenium tetroxide. Consequently, we have undertaken an extensive study of the oxidation of organic compounds by ruthenium tetroxide and wish to report here the results obtained for the oxidation of 2-propanol in aqueous perchloric acid solutions.

[1]N.R.C.C. Scholarship holder 1969–1971.

Experimental

Reagents

Ruthenium tetroxide was prepared by the oxidation of hydrated ruthenium dioxide (0.5 g) obtained from Engelhard Industries Inc., with a solution of sodium periodate (2 g) in 25 ml of water. The mixture was shaken until the reaction was complete (as evidenced by the disappearance of the insoluble black ruthenium dioxide). The bright yellow product of this reaction, ruthenium tetroxide, was extracted into carbon tetrachloride and stored over sodium periodate. Just prior to a kinetic experiment an aliquot of the solution was removed and the ruthenium tetroxide extracted into an aqueous perchloric acid solution of the desired molarity.

2-Propanol was distilled from calcium oxide and a middle fraction boiling at 81.9–82.0° was collected and used in the kinetic experiments. 2-Propanol-2-*d* was prepared following the procedure of Leo and Westheimer (6) by reduction of acetone with lithium aluminum deuteride. The deuterium incorporation was verified by n.m.r. spectroscopy. 2-Propanol-2-C-14 was prepared in a similar way by the reduction of acetone-2-C-14 with lithium aluminum hydride. 1,1,1-Trifluoro-2-propanol and 2-butanol were both obtained commercially and purified via preparative gas chromatography prior to use.

Perchloric acid solutions were prepared by the dilution of 70% $HClO_4$ with doubly distilled water (7).

Kinetic Method

In a typical kinetic experiment 3.0 ml of a perchloric acid solution containing a specified amount of ruthenium tetroxide were pipetted into a cuvet which was placed in a thermostated cuvet holder for about 20 min. Then the desired quantity of 2-propanol was added using a microsyringe. The timer was started immediately and the absorption at either 386 or 310 nm was recorded periodically using a Unicam SP500 Spectrophotometer. As the reaction proceeded the color of the solution changed from bright yellow to brown.

Two different methods were used for analysis of the data. The differential method, which involves the use of initial rates as determined from the initial slopes of the plots of absorbance against time, was used to determine the order of the reaction with respect to each of the reactants (8). (A

Can. J. Chem. Downloaded from www.nrcresearchpress.com by 210.87.254.5 on 09/05/12
For personal use only.

Can. J. Chem. Downloaded from www.nrcresearchpress.com by 210.87.254.5 on 09/05/12
For personal use only.

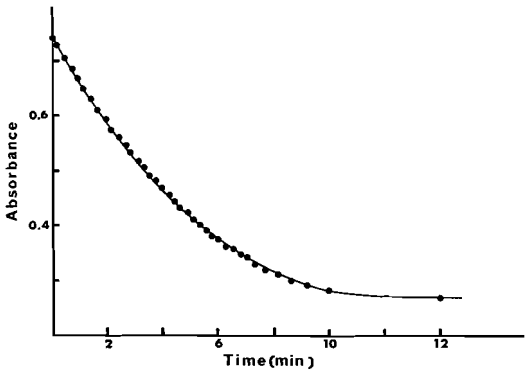

FIG. 1. Rate plot for the oxidation of 2-propanol by RuO_4 in 2.96 *M* $HClO_4$.

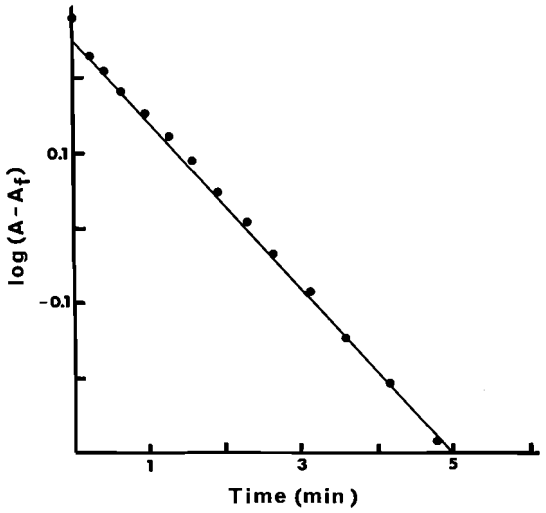

FIG. 2. Pseudo first order plot for the oxidation of 2-propanol by Ruo_4 in 1.86 *M* $HClO_4$.

typical plot of absorbance *vs.* time has been reproduced in Fig. 1.) Under conditions where the alcohol/oxidant ratio was high integral methods were used to verify the order with respect to ruthenium tetroxide; below about 7 *M* $HClO_4$ plots of log (absorbance – final absorbance) *vs.* time gave straight lines (Fig. 2) while above 9 *M* $HClO_4$ plots of absorbance *vs.* time were linear (Fig. 3), thus indicating that the order with respect to ruthenium tetroxide changes from unity to zero at high acid concentrations.

All rates and rate constants reported herein are the average of at least two determinations which agreed to within ± 5% or less.

Product Analysis

Ruthenium(III) was identified as one of the products of this reaction by an analysis of the ultraviolet spectrum of the final solution and from the observation that this solution would not oxidize iodide (9). The latter fact rules out ruthenium(IV) as a product because it is known to be reduced to ruthenium(III) by iodide. Consequently, it appears

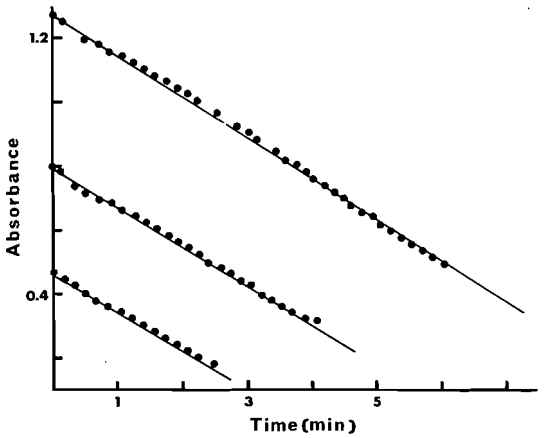

FIG. 3. Rate plots for the oxidation of 2-propanol by RuO_4 in 9.95 *M* $HClO_4$.

that under aqueous acidic conditions, the reaction involves a five electron change as indicated in reaction 3.

$$[3]\quad 5R{-}\underset{\displaystyle OH}{\underset{|}{C}}H{-}R' + 2RuO_4 \xrightarrow{H^+/H_2O} 5R{-}\overset{\displaystyle O}{\overset{\|}{C}}{-}R' + 2Ru^{3+}$$

The organic products of the reaction were identified by use of isotope dilution techniques (10), which permitted the analysis to be carried out under conditions identical to those used in the kinetic experiments. 2-Propanol-2-C-14 was added to a solution of ruthenium tetroxide and allowed to react for 1 h. The product solution was divided into three portions and unlabelled acetone was added to the first portion, unlabelled acetaldehyde to the second, and unlabelled acetic acid to the third. Acetone and acetaldehyde were isolated as the 2,4-dinitrophenylhydrazones and acetic acid as the *S*-benzylthiuronium salt. Each derivative was repeatedly recrystallized to constant activity and compared with the activity of the starting material (2-propanol) which was counted as the 3,5-dinitrobenzoate derivative. Counting was accomplished by the planchet method using a Bechman Lowbeta counter (9). From the results, which are summarized in Table 1, it can be seen that a single product, acetone, was obtained in a quantitative yield in 3.0 *M* $HClO_4$ while in 10.2 *M* $HClO_4$ two products, acetone and acetaldehyde, were produced.

Results

Order of the Reaction with Respect to Ruthenium Tetroxide

The rate of the reaction at a particular acidity can be expressed as in eq. 4.

$$[4]\quad \frac{-d[RuO_4]}{dt} = k_2[RuO_4]^x[Alc]^y$$

When the concentration of 2-propanol is in excess eq. 4 can be restated as eqs. 5 and 6.

$$[5]\quad \frac{-d[RuO_4]}{dt} = k_{obs}[RuO_4]^x$$

TABLE 1. Product analysis

$[HClO_4]$ (M)	RuO_4 (mmol)	Specific activity of reactant and products	mmol of product* (Actual/theoretical)	Yield (%)
10.2	0.375	2-Propanol-2-C^{14} (122400 c.p.m./mmol)		
		Acetone-2-C^{14} (2158 c.p.m./mmol)	0.72/0.94	77
		Acetaldehyde-C^{14} (431 c.p.m./mmol)	0.21/0.94	22
		Acetic acid-C^{14} (0 c.p.m./mmol)	0/0.94	0
3.0	0.23	2-Propanol-2-C^{14} (94900 c.p.m./mmol)		
		Acetone-2-C^{14} (3937 c.p.m./mmol)	0.58/0.58	100

*Actual yields were calculated from the formula $x/(x+n) = A_1/A_2$, where n is the number of mmol of product added as diluent, x is the number of mmol of product formed, and A_1 and A_2 are the specific activities of the products and reactants respectively (10). Theoretical yields were calculated assuming that RuO_4 undergoes a loss of 5 electrons and that formation of the product involves a gain of 2 electrons by 2-propanol.

TABLE 2. Calculation of the order with respect to RuO_4 in the oxidation of 2-propanol at acid concentrations from 0.41 to 6.62 M $HClO_4$

[2-Propanol] $M \times 10^2$	$[HClO_4]$ (M)	N*	Order†	Correlation coefficient
1.29	1.25	3	1.06±0.01	1.00
1.71	1.25	3	1.19±0.02	1.00
1.71	1.08	6	1.08±0.01	1.00
1.71	1.86	3	1.14±0.01	1.00
1.71	0.41	3	1.07±0.04	0.97
1.71	0.76	3	1.08±0.01	1.00
1.71	1.50	3	1.13±0.02	1.00
1.71	6.62	3	1.16±0.07	0.96
2.12	3.22	3	1.02±0.01	1.00
2.13	3.22	3	1.16±0.01	1.00

*Number of points plotted.
†From the slope obtained by plotting log (absorbance) against log (initial slope).

$$[6] \qquad k_{obs} = k_2[\text{Alc}]^y$$

Since any absorbance due to products would be negligible during the initial stages of the reaction, it is convenient to express eq. 5 in terms of absorbance and extinction coefficients as in eqs. 7 or 8.

$$[7] \qquad \frac{-\mathrm{d}(A/\varepsilon)}{\mathrm{d}t} = k_{obs}(A/\varepsilon)^x$$

$$[8] \qquad \log\frac{-\mathrm{d}A}{\mathrm{d}t} = \log A + (1-x)\log\varepsilon + \log k_{obs}$$

Hence the order of the reaction with respect to ruthenium tetroxide can be determined from a plot of the logarithm of the initial slopes against the logarithm of the initial absorbances.

Ten such plots were prepared for acid concentrations varying from 0.41 to 6.62 M $HClO_4$. A summary of the results (presented in Table 2) indicates that below 6.62 M $HClO_4$ the order of the reaction with respect to ruthenium tetroxide is unity.

TABLE 3. Variation of initial rates with ruthenium tetroxide concentration in 9.95 M $HClO_4$, $T = 25.0 \pm 0.1$ °C

$[RuO_4]$ ($M \times 10^3$)	[2-Propanol] (M)	Initial rate ($M\ s^{-1} \times 10^6$)
1.35	0.338	1.96
1.84	0.338	2.07
0.50	0.338	2.00

At acidities greater than 9 M $HClO_4$ the initial rates of the reaction were found to be independent of the initial concentration of ruthenium tetroxide (Table 3) and straight lines were obtained for plots of absorbance against time (Fig. 3). Hence it is apparent that under highly acidic conditions the order of the reaction with respect to oxidant is zero.

Order of the Reaction with Respect to 2-Propanol

By making use of the observation that the order with respect to ruthenium tetroxide is unity at low acidities and zero at high acidities it is possible to combine eqs. 6 and 8 to give eqs. 9 and 10 for the reaction under conditions of "low" and "high" acidity respectively.

$$[9] \qquad \log\frac{-\mathrm{d}A}{\mathrm{d}t} = \log A + \log k_2 + y\log[\text{Alc}]$$

$$[10] \qquad \log\frac{-\mathrm{d}A}{\mathrm{d}t} = y\log[\text{Alc}] + \log k_2 + \log\varepsilon$$

The order of the reaction with respect to alcohol, y, can then be determined from a plot of the logarithm of the initial slope divided by the initial absorbance against the logarithm of

Can. J. Chem. Downloaded from www.nrcresearchpress.com by 210.87.254.5 on 09/05/12
For personal use only.

TABLE 4. Determination of the order with respect to 2-propanol

$[HClO_4]$ (M)	N*	Order	Correlation coefficient
1.05	18	1.05±0.02†	0.99
1.25	30	0.91±0.01†	1.00
3.22	18	0.89±0.02†	1.00
9.95	13	0.99±0.05‡	0.99

*Number of points.
†From the slope obtained by plotting log (initial slope/initial absorbance) against log [2-propanol].
‡From the slope obtained by plotting log (initial slope) against log [2-propanol].

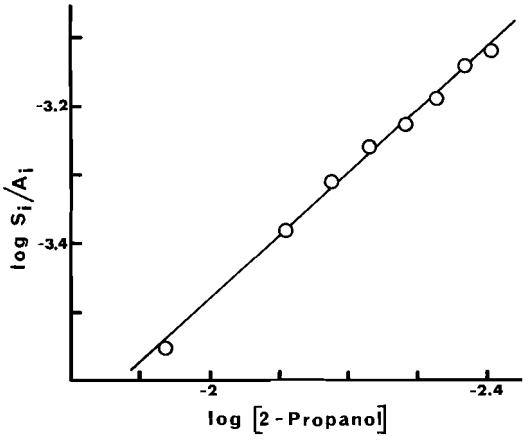

FIG. 4. Plot for calculation of the order with respect to 2-propanol for oxidations in 1.25 M $HClO_4$. Slope = 0.91.

the concentration of alcohol at low acidities, or a plot of the logarithm of the initial slope against the logarithm of the concentration of alcohol at high acidities.

When this method of analysis was applied to four sets of results obtained at different acidities, ranging from 1.05 to 9.95 M $HClO_4$, it was clear that the order of the reaction with respect to alcohol is unity (see Table 4). Typical plots have been reproduced in Figs. 4 and 5.

Dependence of the Reaction on the Acidity of the Medium

The reaction was also found to be dependent on the acidity of the medium; below 7.5 M $HClO_4$ the second order rate constants decreased as the acidity of the medium increased as indicated by the data in Table 5. This is rather surprising since the converse is observed for most other oxidation reactions involving the use of transition metal oxides. In Fig. 6, log k_2 has

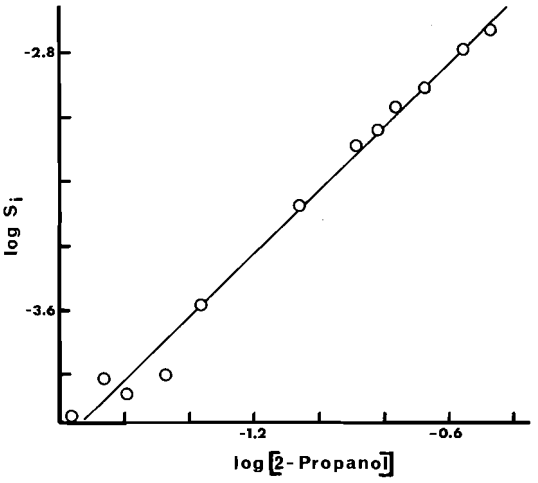

FIG. 5. Plot for calculation of the order with respect to 2-propanol for the oxidations in 9.95 M $HClO_4$. Slope = 0.99.

TABLE 5. Dependence of k_2 on acidity in the oxidation of 2-propanol by RuO_4

$[HClO_4]$ (M)	$-H_0$*	$k_2 \times 10^2$ (M^{-1} s^{-1})
0.93	0.27	1.58
1.05	0.35	1.91
1.07	0.35	1.97
1.86	0.80	1.33
2.96	1.30	0.89
3.22	1.43	0.98
3.80	1.70	0.66
4.73	2.15	0.42
5.86	2.80	0.28
6.41	3.13	0.21
6.62	3.25	0.18
7.47	3.77	0.13

*The H_0 values as a function of the molarity of perchloric acid have been reported by Yates and Wai (21).

been plotted against the Hammett acidity function, $-H_0$ (11, 12), and although a reasonably good straight line is obtained, the nonintegral value, −0.35, for the slope suggests that the explanation for this inverse dependence on acidity may be complex.

Under more highly acidic conditions (8.5 M $HClO_4$ or greater), where the reaction is zero order with respect to ruthenium tetroxide, the rate of reaction increases with increasing acidity (Table 6). However, it is again found that a plot of log k_1 against $-H_0$ gives a straight line with a nonintegral slope of 0.68 (Fig. 7).

Can. J. Chem. Downloaded from www.nrcresearchpress.com by 210.87.254.5 on 09/05/12
For personal use only.

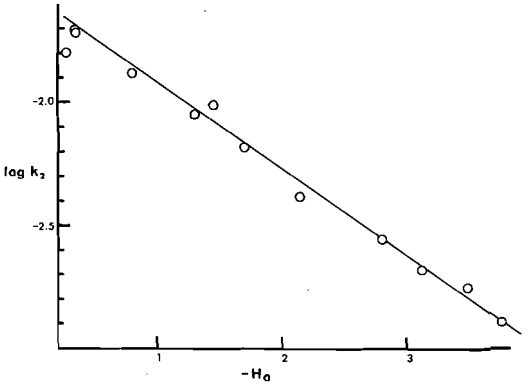

FIG. 6. Dependence of rate on acidity for the oxidation of 2-propanol by RuO_4 in 1–6.5 M $HClO_4$. Slope = −0.35.

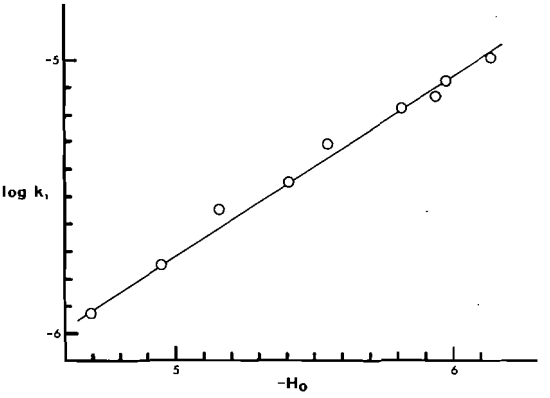

FIG. 7. Dependence of rate on acidity for the oxidation of 2-propanol by RuO_4 in 8.5–10 M $HClO_4$. Slope = 0.68.

TABLE 6. Dependence of k_1 on acidity in the oxidation of 2-propanol by RuO_4

$[HClO_4]$ (M)	$-H_0$*	$k_1 \times 10^6$ (s^{-1})
8.52	4.70	1.17
8.81	4.95	1.76
8.83	5.00	1.40
9.03	5.16	2.30
9.09	5.20	2.21
9.31	5.41	3.56
9.47	5.55	4.92
9.72	5.82	6.58
9.84	5.94	7.32
9.90	5.98	8.40
10.07	6.14	9.89

*The H_0 values as a function of the molarity of perchloric acid have been reported by Yates and Wai (21).

Isotope Effects

The oxidation of 2-propanol-2-*d* was carried out at three different acidities, 1.94, 8.47, and 9.52 M $HClO_4$. The observed rates were then compared with those for the oxidations of 2-propanol to determine a kinetic isotope effect. The results, summarized in Table 7, indicate that at 1.94 M $HClO_4$ a substantial primary kinetic isotope effect is observed ($k_H/k_D = 4.6 \pm 0.2$). Hence the C—H bond is broken in the rate determining step. However, at 9.52 M $HClO_4$ the isotope effect is unity (within experimental error), suggesting that cleavage of the C—H bond is not involved in the rate determining step. At 8.47 M $HClO_4$ an isotope effect of intermediate magnitude ($k_H/k_D = 1.9 \pm 0.1$) is observed, probably because of a contribution from two different mechanisms at this acidity.

TABLE 7. Isotope effects for the oxidation of $CH_3CROHCH_3$ in aqueous $HClO_4$

R	$[HClO_4]$ (M)	$k_2 \times 10^2$ (M^{-1} s^{-1})	$k_1 \times 10^6$ (s^{-1})	k_H/k_D
H	1.94	1.55±0.03		
D	1.94	0.34±0.01		4.6±0.2
H	8.47		0.73±0.02	
D	8.47		0.39±0.02	1.9±0.1
H	9.52		4.2 ±0.4	
D	9.52		3.2 ±0.3	1.3±0.3

TABLE 8 Oxidation of $RCHOHCH_3$ by RuO_4 in 1.94 M $HClO_4$ at 25.0°

R	[Alcohol] ($M \times 10^2$)	$k_2 \times 10^2$ (M^{-1} s^{-1})
Et	4.72	2.13
Me	4.36	1.58
CF_3	3.59	~0.1

Substituent Effects

The rates of oxidation of 2-butanol and 1,1,1-trifluoro-2-propanol by ruthenium tetroxide were determined and compared with those for 2-propanol in an attempt to determine the effect of substituents on the rate of the reaction. The resulting rate constants are presented in Table 8.

At high acidity (10.0 M $HClO_4$) it was impossible to obtain a meaningful initial slope for 2-butanol and 1,1,1-trifluoro-2-propanol, although it was evident that the oxidation of 2-butanol was faster and that the oxidation of 1,1,1-trifluoro-2-propanol was slower than the oxidation of 2-propanol.

Can. J. Chem. Downloaded from www.nrcresearchpress.com by 210.87.254.5 on 09/05/12
For personal use only.

Can. J. Chem. Downloaded from www.nrcresearchpress.com by 210.87.254.5 on 09/05/12
For personal use only.

TABLE 9. Data for determination of the activation parameters for the oxidation of 2-propanol by ruthenium tetroxide

$[HClO_4]$ (M)	Temperature (°C)	$k \times 10^2$
2.89	9.9	0.347*
2.89	20.0	0.818*
2.89	30.0	1.84*
2.89	40.0	4.09*
2.89	50.0	8.46*
9.10	10.0	0.0373†
9.10	20.0	0.131†
9.10	30.0	0.554†
9.10	40.0	1.76†
9.10	50.0	5.04†

*Second order rate constants (M^{-1} s^{-1}).
†First order rate constants (s^{-1}).

These results indicate that electron donating substituents increase the rate of the reaction, while electron withdrawing substituents decrease the rate of the reaction in the oxidation of secondary alcohols by ruthenium tetroxide.

Activation Parameters

From a knowledge of the way in which the rate of a reaction varies with changes in temperature, it is possible to calculate the activation parameters, $\Delta H^{\neq}$ and $\Delta S^{\neq}$ (8). The former is obtained from the slope and the latter from the intercept of a plot of $\ln k_2/T$ against $1/T$. When this was done for the oxidation of 2-propanol in 2.89 M $HClO_4$ $\Delta H^{\neq}$ and $\Delta S^{\neq}$ were calculated to be 14.0 ± 0.1 kcal/mol and -20.3 ± 0.2 e.u. while in 9.10 M $HClO_4$ they were found to be 21.9 ± 0.4 kcal/mol and 2.8 ± 1.4 e.u., respectively. The data on which these calculations were based are found in Table 9 and the plots have been reproduced in Fig. 8.

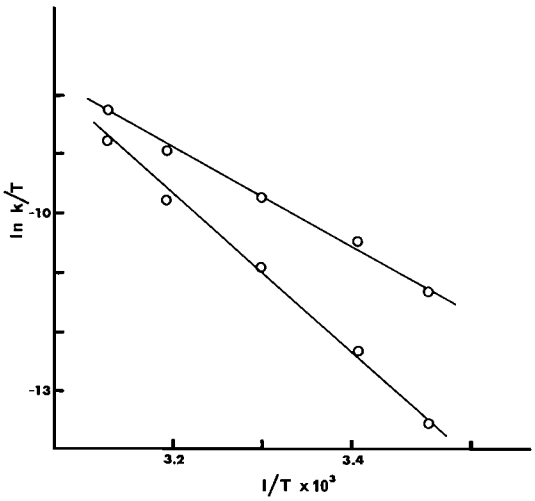

FIG. 8. Plots for calculating activation parameters. The top line is for k_2(M^{-1} s^{-1}) constants obtained in 2.89 M $HClO_4$ while the bottom line is for k_1(s^{-1}) constants obtained in 9.10 M $HClO_4$.

Influence of Oxygen on the Rate of Reaction

In order to determine if the presence of oxygen has any influence on the rate of oxidation several experiments were carried out in which different gases were bubbled through the solution at the start of the reaction. The results indicated that solutions flushed with helium, nitrogen, and oxygen all reacted at the same rate within the limits of experimental error. Since oxygen has no appreciable effect on the rate, it is not likely that the reaction involves formation of free radicals.

Discussion

It is apparent from the summary of results presented in Table 10 that two different reaction mechanisms pertain. The results obtained in the less acidic region are most easily explained in terms of a hydride transfer mechanism. The rate law, the isotope effect, and the effect of substituents are all consistent with this suggestion. The activation parameters are very similar to those obtained for other hydride transfer oxidation reactions (13) and the absence of any effect by oxygen on the rate eliminates a free radical mechanism. In addition it should be noted that ruthenium tetroxide oxidizes alcohols and ethers with approximately equal ease (9, 4); this property is also observed for other oxidants which are known to be reduced by hydride abstraction reactions (13).

The most unexpected of the results obtained in the lower acid region is the observation that the rate of reaction decreases as the acidity increases whereas most other oxidation reactions are subject to acid catalysis. Any possible explanation of this rather unique observation must be made while bearing in mind the fact that increasing the acid concentration of a solution has two effects, (*i*) it increases the hydrogen ion activity and (*ii*) it decreases the water concentration. Either or both of these effects might have an influence on the reaction rate.

The most likely consequence of an increase in

Can. J. Chem. Downloaded from www.nrcresearchpress.com by 210.87.254.5 on 09/05/12
For personal use only.

TABLE 10. Summary of results obtained for the oxidation of 2-propanol by RuO_4 in aqueous $HClO_4$ solutions

	1–6.5 *M* $HClO_4$	9–10.5 *M* $HClO_4$
Products	Acetone (100%)	Acetone (77%) Acetaldehyde (22%)
Rate law	$v = k_2[RuO_4][2\text{-Propanol}]$	$v = k_1[2\text{-Propanol}]$
Acidity dependence	$v \propto h_0^{-0.35}$	$v \propto h_0^{0.68}$
Isotope effect	$k_H/k_D = 4.6 \pm 0.2$	$k_H/k_D = 1.3 \pm 0.3$
Activation parameters	$\Delta H^{\ddagger} = 14.0 \pm 0.1$ kcal/mol $\Delta S^{\ddagger} = -20.3 \pm 0.2$ e.u.	$\Delta H^{\ddagger} = 21.9 \pm 0.4$ kcal/mol $\Delta S^{\ddagger} = 2.8 \pm 1.4$ e.u.
Substituent effects	Electron donating substituents increase the rate of reaction	Electron donating substituents increase the rate of reaction

acidity would be to shift the alcohol protonation equilibrium [11] to the left.

$$[11] \quad CH_3-\overset{+OH_2}{\overset{|}{C}}H-CH_3 \overset{K}{\rightleftharpoons} CH_3-\overset{OH}{\overset{|}{C}}H-CH_3 + H^+$$

If the protonated alcohol were unreactive (as might be expected for a hydride transfer reaction) the rate would be decreased as the solution became more acidic. A somewhat similar explanation for the inverse acidity dependence was given for the oxidation of ascorbic acid by osmium tetroxide (14).

The protonation of 2-propanol should be defined by an acidity function H_{ROH}, which has been recently proposed by Lee and Cameron (15). Although such a function has not been firmly established it appears from the available evidence (15, 16) that it is approximately equal to 0.25 H_0 in both sulfuric and perchloric acid solutions, and thus the pK_{BH^+} for equilibrium [11] which has been reported to be -5.16 in H_0 units (16) would be approximately -1.3 in H_{ROH} units.

The concentration of unprotonated alcohol can then be calculated as indicated in eqs. 12–15.

$$[12] \quad K = \frac{[ROH]h_{ROH}}{[ROH_2^+]}$$

$$[13] \quad [ROH] + [ROH_2^+] = [ROH]_{total}$$

$$[14] \quad [ROH] + \frac{[ROH]h_{ROH}}{K} = [ROH]_{total}$$

$$[15] \quad [ROH] = \frac{[ROH]_{total}}{1 + h_{ROH}/K} = \frac{K[ROH]_{total}}{K + h_{ROH}}$$

Hence if the rate of oxidation of 2-propanol is very fast compared with its conjugate acid the rate law would be given by eqs. 16 and 17

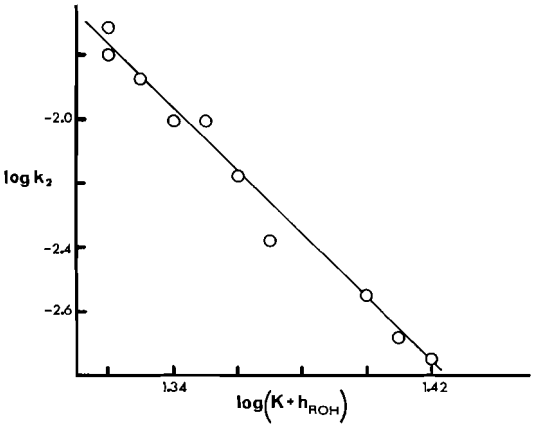

FIG. 9. Dependence of rate on acidity for the oxidation of 2-propanol by RuO_4 in 1–6.5 *M* $HClO_4$. Slope = -10.0.

$$[16] \quad \frac{-d[RuO_4]}{dt} = \frac{kK[RuO_4][ROH]}{K + h_{ROH}}$$

$$[17] \quad k_2 = \frac{kK}{K + h_{ROH}}$$

which suggests that a plot of log k_2 against log $(K + h_{ROH})$ should be linear with slope of -1. From Fig. 9, it can be seen that the magnitude of the slope is much greater than this (-10) suggesting that other factors are contributing to the decrease in rate; *i.e.*, the decrease in the activity of water may also be reponsible for part of the rate diminution. This would be so if the complete rate law were of the form given in eq. 18.

$$[18] \quad \frac{-d[RuO_4]}{dt} = \frac{kK[RuO_4][ROH]}{K + h_{ROH}} a^n_{H_2O}$$

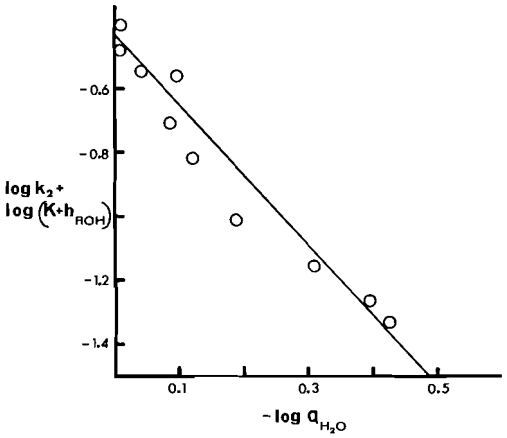

FIG. 10. Plot used for calculating the extent to which water is involved in the transition state for the oxidation of 2-propanol by RuO_4. Slope = 2.2.

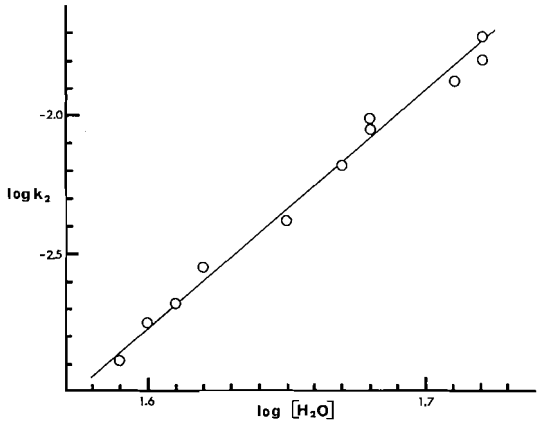

FIG. 11. Plot of log k_2 against log $[H_2O]$. Slope = 8.8.

If eq. 18 is, in fact, an accurate description of the rate law for the reaction it should be possible to estimate n, the order with respect to water activity, since the reported rate constants, k_2, would be given in eq. 19 from which eq. 20 can be derived.

$$[19] \qquad k_2 = \frac{kK}{K + h_{ROH}} a_{H_2O}^n$$

$$[20] \quad \log k_2 + \log (K + h_{ROH}) = n \log a_{H_2O} + \log (kK)$$

It then follows that a plot of log k_2 + log $(K + h_{ROH})$ against log a_{H_2O} should be linear with a slope equal to n. This plot has been reproduced in Fig. 10 and although there is some scatter, possibly because the abscissa is the difference between two fairly large numbers, it is obvious that the slope of the best straight line is positive (approx. 2). Consequently, the empirical rate law for this reaction under conditions of "low" acidity can be approximated by eq. 21.

$$[21] \qquad \frac{-d[RuO_4]}{dt} = \frac{kK[RuO_4][ROH]}{K + h_{ROH}} a_{H_2O}^2$$

This rate law indicates that the transition state of the reaction has a greater demand for solvation by water than do the reactants, thus suggesting that it may be quite polar. Furthermore it is not likely that RuO_4 is highly solvated, as indicated by the fact that it has the same spectral characteristics in the vapor state, in carbon tetrachloride solutions, and in aqueous acids (17), but it is known that reduced forms of ruthenium are highly solvated in water (18). Consequently, it is not unlikely that a polar transition state containing ruthenium in one of the lower oxidation states would require additional solvation.

It should be noted here that Bunnett has previously suggested an analogous approach for acid catalyzed reactions (19). He proposed that the role of water in a reaction mechanism could be determined by plotting log $k + H_0$ (or log k − log [HX]) against log a_{H_2O}. The slopes (ω or ω^*) of the resulting plots are thought to indicate the way in which water is involved in the rate determining steps (20). The principal difference between Bunnett's approach and the present one is simply that he was dealing with acid catalyzed reactions whereas in the present case the reaction is subject to acid inhibition.

As indicated in Fig. 11 a plot of log k_2 *vs.* log $[H_2O]$ also gives a straight line with a slope of 8.8 for the oxidation of 2-propanol and although such plots are not conventional it shows empirically that the transition state has a high demand for water. This is also indicated by a plot of log k_2 against log a_{H_2O} (see Fig. 12).

Now turning to a consideration of the reaction under highly acidic conditions, the observation that no primary isotope effect was observed indicates that the α-carbon—hydrogen bond is not broken in the rate determining step. This result is also consistent with the fact that the concentration of ruthenium tetroxide does not appear in the rate law. Evidently the rate determining step involves a reaction of 2-propanol prior to the transfer of electrons to ruthenium

Can. J. Chem. Downloaded from www.nrcresearchpress.com by 210.87.254.5 on 09/05/12
For personal use only.

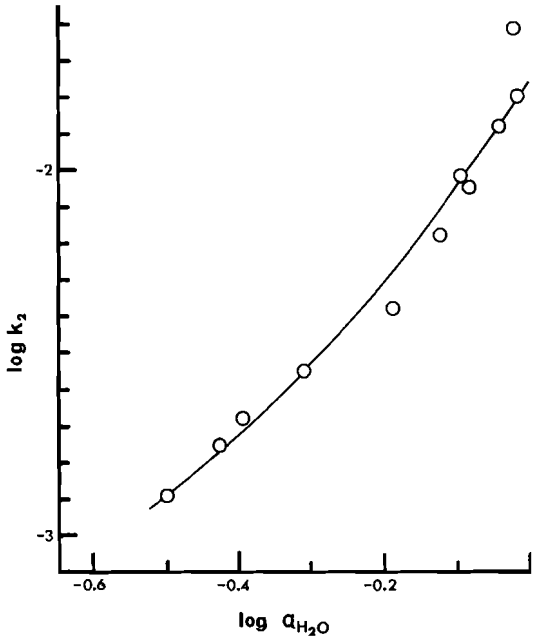

FIG. 12. Plot of log k_2 against log a_{H_2O}.

tetroxide. The substituent effects indicate an electron deficient reaction center, and thus suggest the probability of a carbonium ion intermediate.

The observation that the rate of reaction, under these conditions, is subject to acid catalysis (Fig. 7) is also consistent with rate determining carbonium ion formation, and the change in activation parameters verifies that hydride transfer is no longer the rate determining step.

The presence of acetaldehyde amongst the products of the reaction suggests that oxidation of the carbonium ion might be in competition with propene formation; the carbonium ion would be oxidized to acetone while propene would give acetaldehyde (1) as indicated in reaction 22.

$$[22]\quad CH_3\overset{OH}{\overset{|}{C}}HCH_3 + H^{\oplus} \xrightarrow[-H_2O]{\text{slow}}$$

$$CH_3\overset{\oplus}{C}HCH_3 \rightleftharpoons CH_3CH{=}CH_2$$
$$\downarrow RuO_4 \qquad\qquad \downarrow RuO_4$$
Acetone Acetaldehyde

The rate law for this reaction would be expressed by eq. 23 and a steady state approximation for the reactive intermediate (R^+) gives eq. 24

$$[23]\quad \text{rate} = k_2[RuO_4][R^+]$$

$$[24]\quad \text{rate} = \frac{k_1k_2[RuO_4][ROH]h_{R'}}{k_{-1} + k_2[RuO_4]}$$

where $h_{R'}$ is an acidity function defined by the equilibrium between aliphatic alcohols and the corresponding carbonium ions.

If $k_2[RuO_4] > k_{-1}$ then rate $= k_1[ROH]h_{R'}$. This expression is similar to the experimentally observed rate law, and the mechanism is also in accordance with the substituent effects, since electron donating substituents will increase k_1 with the converse being true for electron withdrawing substituents.

The observed value of k_H/k_D (1.3 ± 0.3) indicates that there might be a small isotope effect; however, on the basis of the proposed mechanism this could be attributed to a secondary isotope effect.

Summary

The reaction mechanism appears to involve a hydride transfer to the oxidant in the rate determining step under conditions of "low" acidity. Since protonated alcohols would be less reactive towards hydride transfer and because the transition state apparently requires added solvation by water the rate of the reaction decreases as the acidity of the medium increases. However, under conditions of very high acidity, carbonium ions and alkenes, which are very readily attacked by ruthenium tetroxide, begin to form and the reaction rate increases with the acidity of the solution. The rate determining step then becomes carbonium ion formation.

The authors are grateful to the National Research Council of Canada for the award of an operating grant (D.G.L.) and a scholarship (M.E.).

1. D. G. LEE. *In* Oxidation, techniques and applications in organic synthesis. *Edited by* R. L. Augustine. Marcel Dekker, Inc., New York. 1969.
2. R. F. BUTTERWORTH and S. HANESSIAN. Synthesis, 70 (1971).
3. H. NAKATA. Tetrahedron, **19**, 1959 (1963).
4. R. M. MORIARTY, H. GOPAL, and T. ADAMS. Tetrahedron Lett. 4003 (1970). K. C. RAMEY, D. C. LINI, R. M. MORIARTY, H. GOPAL, and H. G. WELSH. J. Am. Chem. Soc. **89**, 2401 (1967). J. A. CAPUTO and R. FUCHS. Tetrahedron Lett. 4729 (1967).

Can. J. Chem. Downloaded from www.nrcresearchpress.com by 210.87.254.5 on 09/05/12
For personal use only.

5. P. N. RYLANDER. Elgelhard Industries Technical Bulletin, **9**, 135 (1969). F. G. OBERENDER and J. A. DIXON. J. Org. Chem. **24**, 1226 (1959). S. WOLFE, S. K. HASAN, and J. R. CAMPBELL. J. Chem. Soc. D, 1420 (1970).
6. A. LEO and F. WESTHEIMER. J. Am. Chem. Soc. **74**, 4383 (1952).
7. I. M. KOLTHOFF and E. B. SANDELL. Textbook of quantitative inorganic analysis. The MacMillan Company, New York. 1952. p. 181.
8. K. J. LAIDLER. Chemical kinetics. McGraw-Hill Book Company, New York. 1965.
9. M. VAN DEN ENGH. Ph.D. Thesis, The University of Saskatchewan Regina Campus, Regina, Saskatchewan. 1971.
10. M. CALVIN, C. HEIDELBERGER, J. C. REID, B. M. TOLBERT, and P. F. YANKWICH. Isotopic carbon. John Wiley and Sons, Inc., New York. 1949. p. 278.
11. L. P. HAMMETT. Physical organic chemistry. 2nd ed. McGraw-Hill, New York. 1970.
12. C. H. ROCHESTER. Acidity functions. Academic Press, New York. 1970.
13. R. M. BARTER and J. S. LITTLER. J. Chem. Soc. B, 205 (1967). E. J. STROJNY, R. T. IWAMASA, and L. K. FREUEL. J. Am. Chem. Soc. **93**, 1171 (1971).
14. U. S. MEHROTRA and S. P. MUSHRAN. Can. J. Chem. **48**, 1148 (1970).
15. D. G. LEE and R. CAMERON. J. Am. Chem. Soc. **93**, 4724 (1971).
16. R. E. WESTON, S. EHRENSON, and K. HEINZINGER. J. Am. Chem. Soc. **89**, 481 (1967).
17. G. B. BARTON. Spectrochim. Acta, **19**, 1619 (1963).
18. R. E. CONNICK and D. A. FINE. J. Am. Chem. Soc. **82**, 4187 (1960).
19. J. F. BUNNETT. J. Am. Chem. Soc. **83**, 4956 (1961); **83**, 4968 (1961); **83**, 4973 (1961); **83**, 4978 (1961). J. F. BUNNETT and F. P. OLSEN. Can. J. Chem. **44**, 1899 (1966); **44**, 1917 (1966).
20. K. B. WIBERG. Physical organic chemistry. John Wiley and Sons, Inc., New York. 1964. p. 435.
21. K. YATES and H. WAI. J. Am. Chem. Soc. **86**, 5408 (1964).

Can. J. Chem. Downloaded from www.nrcresearchpress.com by 210.87.254.5 on 09/05/12
For personal use only.

Photosensitization by $Cd(^3P_1)$ Atoms. II. Gas Phase Decomposition of Cyclohexane[1]

B. L. KALRA AND A. R. KNIGHT

Department of Chemistry and Chemical Engineering, University of Saskatchewan, Saskatoon, Saskatchewan

Received December 2, 1971

The photodecomposition of cyclohexane sensitized by $Cd(^3P_1)$ atoms has been studied in the vapor phase at 355 °C. The primary decomposition gives hydrogen atoms and cyclohexyl radicals. The volatile products of the decomposition are H_2, cyclohexene, propylene, ethane, ethylene, methane, propane, butadiene, and methylcyclopentane. Products other than H_2 and cyclo-C_6H_{10} arise from unimolecular reactions of cyclohexyl radicals, the most important such process being the production of propylene and allyl radicals. Hydrogen yields decrease rapidly with time because of H-atom scavenging reactions involving olefinic products. The quantum yield of molecular hydrogen formation at the shortest exposure time examined is 0.53.

La photodécomposition du cyclohexane sensibilisée par des atomes de $Cd(^3P_1)$ a été étudiée en phase vapeur à 355 °C. La décomposition initiale donne des atomes d'hydrogène et des radicaux cyclohexyles. Les produits volatils de la décomposition sont H_2, le cyclohexène, le propylène, l'éthane, l'éthylène, le méthane, le propane, le butadiène et le méthylcyclopentane. Les produits différents de H_2 et du cyclo-C_6H_{10} proviennent de réactions unimoléculaires à partir des radicaux cyclohexyles; le processus le plus important étant la formation de radicaux propylènes et allyles. Les rendements en hydrogène diminuent rapidement avec le temps par suite des réactions qui piègent les atomes d'H et qui impliquent des produits oléfiniques. Le rendement quantique correspondant à la formation d'hydrogène moléculaire pendant le temps d'exposition examiné le plus court est de 0.53.

Canadian Journal of Chemistry, **50**, 2010 (1972)

Introduction

The decomposition of cyclohexane vapor by triplet cadmium atoms has not been investigated previously. In the present investigation we have utilized the techniques employed previously to study the acetone decomposition, to examine the reaction between cyclohexane and $Cd(^3P_1)$ atoms. Unlike the analogous reaction with triplet mercury atoms, the energy required for C—H bond cleavage with this substrate is larger than the excitation energy of the sensitizer and thus the formation of CdH may be involved if the decomposition occurs.

The mercury photosensitized decomposition of cyclo-C_6H_{12} has been examined previously in both the liquid and vapor phase. Gunning and co-workers (2) studied the vapor phase system at 30 °C, while Arai *et al.* (3) carried out an investigation over the temperature range 60 to 400 °C. The liquid phase decomposition has been studied by Cramer (4) and by Klots and Johnsen (5). In every case the data obtained indicated that the primary step is rupture of the C—H bond giving cyclohexyl radicals and hydrogen atoms. At temperatures in excess of 250 °C, cyclohexyl radicals decompose giving olefins and alkyl radicals (3). The results of a study of the Hg-sensitized decomposition of cyclopentane at temperatures up to 376 °C by Gunning and Stock (6) are also relevant to this investigation.

Experimental

The essential details of the apparatus and procedures have been given previously (1). In the present work the light source was a Model 1500 Spectroline cadmium spectral lamp, filtered to remove 2288 Å radiation, so that only the 3261 Å resonance line, giving rise to $Cd(^3P_1)$ atoms is absorbed in the cell. The reaction cell assembly was operated at 355 ± 2 °C, while the side-arm cadmium metal reservoir was maintained at 315 °C. At the latter temperature, the vapor pressure of cadmium is 140 μ. The percent absorption by cadmium vapor in the reaction cell was determined using a Zeiss Model PMQ-II monochromator and photocell module to be 60%. The cadmium metal employed was Alpha Inorganics, Inc. 99.9999% purity.

Cyclohexane (British Drug Houses, reagent) was purified by distillation at atmospheric pressure through a glass helix packed column, retaining the fraction distilling at 81 °C at 710 Torr. The substrate was degassed and further fractionated at low temperature in the vacuum line. Gas chromatographic analysis confirmed the absence of impurities. The maximum cyclohexene impurity that would remain undetected is 0.001%.

Nitric oxide (Matheson) was pre-purified by the method of Hughes (7) and subsequently fractionated between −161 °C and −196 °C in the vacuum line. The NO for each run was distilled once, immediately prior to use, from −161 °C to remove any traces of NO_2 formed in storage. Carbon

[1]From the Ph.D. thesis of B. L. Kalra to be submitted to the University of Saskatchewan, Saskatoon.

Can. J. Chem. Downloaded from www.nrcresearchpress.com by 210.87.254.40 on 09/05/12
For personal use only.

Can. J. Chem. Downloaded from www.nrcresearchpress.com by 210.87.254.40 on 09/05/12
For personal use only.

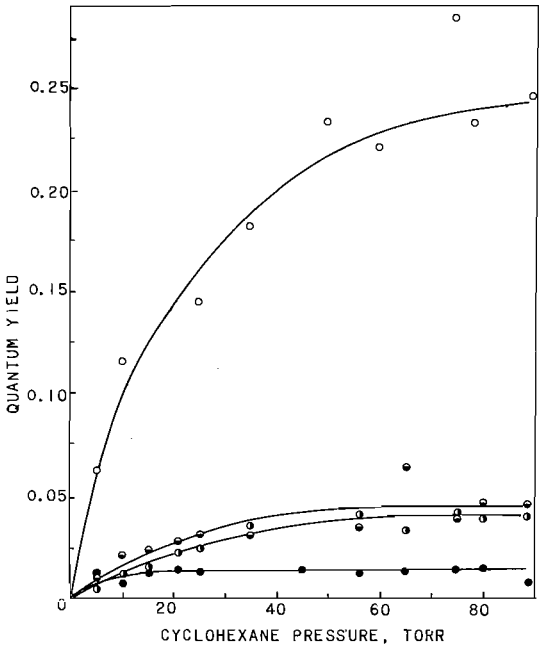

FIG. 1. Quantum yield of H_2, ○; cyclo-C_6H_{10}, ◒; cyclo-$C_5H_9CH_3$, ◑; and CH_4, ●; as a function of substrate pressure in the cadmium-photosensitized decomposition of cyclohexane at 355 °C for 8 h.

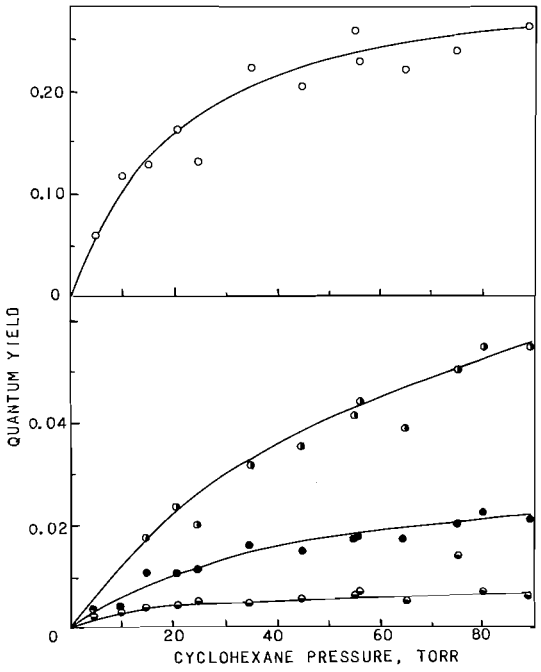

FIG. 2. Quantum yield of C_3H_6, ○; C_2H_6, ◑; C_2H_4, ●; and C_3H_8, ◒; as a function of substrate pressure in the cadmium photosensitized decomposition of cyclohexane at 355 °C for 8 h.

tetrafluoride (Matheson) was degassed and purified by low temperature distillation. *cis*-Butene-2 and *trans*-butene-2 (Matheson) were freed from impurities by distillation in the vacuum line before storage, and the appropriate amount of butene-2 purified by preparative gas chromatography before each actinometry experiment.

Products non-condensable at −196 °C, H_2 and CH_4, were measured together in a gas burette and analyzed by gas chromatography using a 5 Å molecular sieve column and helium carrier gas for CH_4 or nitrogen carrier for H_2. The fraction volatile at −117 °C, principally lower molecular weight hydrocarbons, was analyzed on an 8 ft silica gel column operated at 100 °C. The remaining condensable products and unreacted substrate were eluted on a 12 ft dimethylsulfolane column. Identification of products was by mass spectrometric analysis of the compounds trapped from the g.c. effluent.

In runs with added CF_4 the fraction non-condensable at liquid oxygen temperature was removed before further separation of products. The butene-2 isomers were separated on a 15 ft ethylene glycol – silver nitrate column.

Light intensities were determined by measuring the initial rate of *cis–trans* isomerization of butene-2 (8) at pressures of 6.5 and 10 Torr for exposure times of 60 min, taking a value of $\Phi = 0.50$ for the process (9). A small amount of thermal isomerization occurred in the reaction cell and therefore thermal blanks were run concurrently with each sensitized reaction. The absorbed intensity determined in this way was 4.0×10^{-3} μeinstein min^{-1}. Because the extent of the thermal reaction was not particularly reproducible, there may be an error in the absolute magnitude of the reported quantum yields of ±10%.

Results

The products of the reaction of cyclohexane with $Cd(^3P_1)$ atoms at 355 °C are H_2, C_3H_6, cyclo-C_6H_{10}, C_2H_6, C_2H_4, CH_4, cyclo-$C_5H_9CH_3$, and C_3H_8. Small amounts of butadiene were also observed but the yields were too minute for accurate analysis. The possible product bicyclohexyl would not have been detected in the analytical procedures used here. Because of the relatively high temperatures at which this study was conducted, the possibility of direct thermal decomposition of the substrate was investigated. Thermal blanks were run with the substrate itself and with the various substrate–addend combinations used. No detectable dark reactions were found.

Figures 1 and 2 give the quantum yields of product formation as a function of substrate pressure for exposure times of 8 h. Because of the low absorbed intensity long exposure times were required to produce sufficient product for

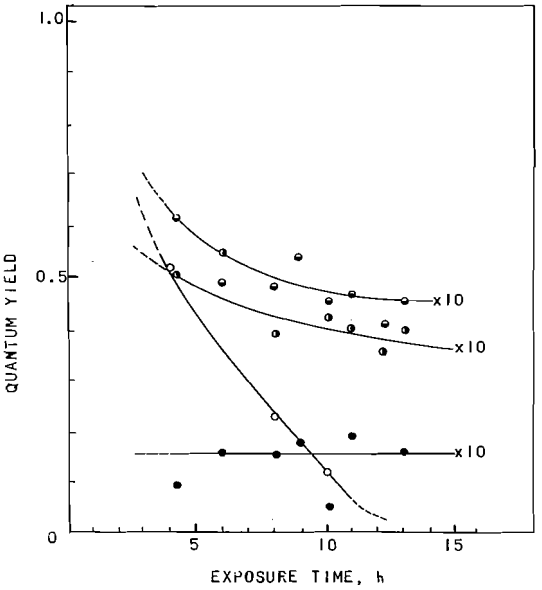

FIG. 3. Quantum yield of H_2, ○; cyclo-C_6H_{10} (× 10), ◒; cyclo-$C_5H_9CH_3$ (× 10), ◑; and CH_4 (× 10), ●; as a function of exposure time for the cadmium sensitized decomposition of cyclohexane at a pressure of 80 Torr and a temperature of 355 °C.

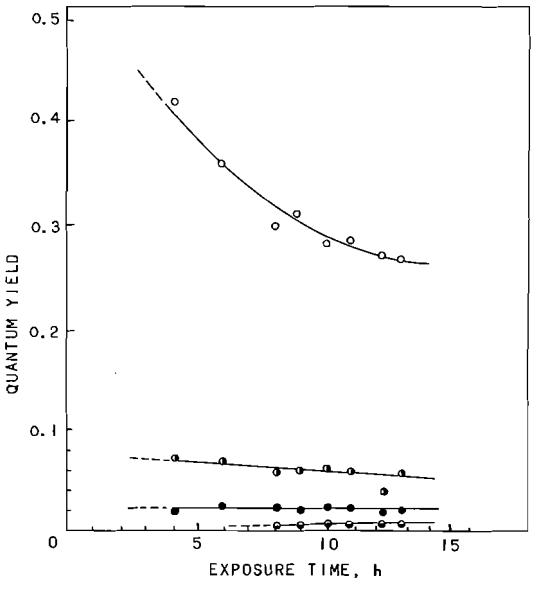

FIG. 4. Quantum yield of C_3H_6, ○; C_2H_6, ◑; C_2H_4, ●; and C_3H_8, ◒; as a function of exposure time in the cadmium sensitized decomposition of cyclohexane at a pressure of 80 Torr and a temperature of 355 °C.

analysis. At the highest substrate pressure examined, the amount of H_2 formed corresponds to 0.1% decomposition of the substrate.

Although there is some scatter in the observed hydrogen yields, it would appear that at 80 Torr substrate pressure the system is in, or very close to the substrate concentration region where there is complete quenching of $Cd(^3P_1)$ atoms. With the exception of C_2H_6, the products attain a constant rate of formation at lower pressures. The number of data for hydrogen is less than that for the other products since H_2 was determined separately in a second set of experiments.

Figures 3 and 4 show the results of a series of experiments in which the rate of formation of reaction products was determined as a function of exposure time. It is apparent that the yield of hydrogen is quite strongly dependent on time, as is that of cyclohexene and, to a lesser extent, methylcyclopentane. The rates for the other minor products appear to be constant within experimental error.

To assess the effects of radical scavenger on the reaction a series of runs was performed in the presence of nitric oxide. The observed quantum yields for products that could be analyzed are listed in Table 1. No attempt was made to identify or analyze products that may have resulted from the radical–NO reactions that are likely occurring in such a system. The data are a clear indication that the decomposition in general is free radical in character, although it is to be noted that the rate of formation of cyclohexene appears to be decreasing appreciably less rapidly than that of other products.

The possibility that the decomposition proceeds through a relatively long lived excited substrate molecule capable of being collisionally deactivated was explored in a series of experiments in which the effect of added carbon tetrafluoride as inert addend was determined. The results are listed in Table 2. Propylene, cyclohexene, and methylcyclopentane continue to be formed at the same rate. The reported ethane yields are subject to some uncertainty because of the mechanical difficulties in quantitatively separating this product from the large amount of addend.

Because of the indication from the radical scavenger studies that cyclohexene might be formed, along with H_2, in a molecular process, the rates of formation of products as a function

Can. J. Chem. Downloaded from www.nrcresearchpress.com by 210.87.254.40 on 09/05/12
For personal use only.

TABLE 1. Effect of nitric oxide on the Cd-sensitized decomposition of cyclohexane vapor*

P(NO) (Torr)	Quantum yield				
	C_2H_6	C_2H_4	C_3H_6	cyclo-C_6H_{10}	cyclo-$C_5H_9CH_3$
0	0.058	0.024	0.30	0.048	0.040
2	0.038	0.013	0.184	0.061	0.027
4	0.007	0	0.058	0.061	0.026
6	0.012	0	0.140	0.055	0.015
8	0	0	0	0.017	0

*Cyclohexane pressure = 80 Torr; exposure time = 8 h; yields not corrected for competitive quenching; see text.

TABLE 2. Effect of carbon tetrafluoride on the Cd-sensitized decomposition of cyclohexane vapor*

P(CF_4) (Torr)	Quantum yield			
	C_2H_6	C_3H_6	cyclo-C_6H_{10}	cyclo-$C_5H_9CH_3$
0	0.058	0.30	0.047	0.040
9	0.032	0.25	0.045	0.038
21	0.015	0.29	0.047	0.035
103	0.015	0.33	0.047	0.045
422	0.020	0.31	0.043	0.047

*Cyclohexane pressure = 80 Torr; exposure time = 8 h. Quenching cross section of CF_4 assumed to be negligible.

of added propylene, intended primarily as a scavenger of H-atoms, were determined. The quantum yield data are tabulated in Table 3. With the exception of the experiment at $P(C_3H_6) = 14$ Torr, where the addend is responsible for 65% of the quenching, *vide infra*, the yields of all products, apart from propane, decrease as the pressure of addend is increased. The rate of formation of propane increases as a result of H-atom abstraction by propyl radicals which result from the addition of hydrogen atoms, formed in the primary process, to propylene. Of particular interest in this series is the fact that the rate of H_2 formation becomes indetectably small at propylene pressures of 7 Torr or greater. The cadmium photosensitized decomposition of propylene itself has been investigated recently (10) and no chemical decomposition is observed, although there is detectable *cis–trans* isomerization of propylene-d_4.

For experiments with added gases it is necessary to correct the observed yields for competitive quenching of triplet cadmium atoms by

TABLE 3. Effect of propylene on the Cd-sensitized decomposition of cyclohexane vapor*

P(C_3H_6) (Torr)	Quantum yield					
	H_2	C_2H_6	C_2H_4	C_3H_8	cyclo-C_6H_{10}	cyclo-$C_5H_9CH_3$
0	0.125	0.06	0.025	0.006	0.046	0.040
0.19	0.032	0.018	0.014	0.007	0.015	†
1.2	0.014	0.015	†	0.027	0.016	†
7	0	0.042	0.001	0.150	†	†
14	0	0.151	0.051	0.445	†	‡

*Cyclohexane pressure = 50 Torr; exposure time = 10 h. Yields corrected for competitive quenching; see text.
†Trace amount, too minute for analysis.
‡Not determined.

Can. J. Chem. Downloaded from www.nrcresearchpress.com by 210.87.254.40 on 09/05/12
For personal use only.

Can. J. Chem. Downloaded from www.nrcresearchpress.com by 210.87.254.40 on 09/05/12
For personal use only.

the addend. In the absence of a value for the quenching cross section of the substrate, σ^2(cyclohexane) was calculated from an additivity rule proposed by Darwent (11), using the measured cross section for cyclopropane, 0.71 Å^2 (12), as follows: σ for cyclo-C_3H_6 = 0.84 Å, and thus σ^2 for cyclo-$C_6H_{12} = (6 \times 0.84/3)^2 = 2.8$ Å^2. Thus the results obtained in the presence of propylene were corrected using that value of σ^2(cyclohexane) and the value of 29.1 Å^2 for σ^2(propylene) determined by Steacie and LeRoy (12).

Quenching cross sections have not been determined for NO or CF_4. The data obtained with added nitric oxide have therefore not been corrected for competitive quenching, and quantitative interpretation of those results is thus not possible. For CF_4 it has been assumed that, as in the case of Hg($^3P_1$)atoms, its quenching cross section for triplet cadmium is negligibly small. That assumption is consistent with our observation here that added CF_4 has virtually no effect on the rates of product formation.

Discussion

The nature of the observed reaction products indicates that the net result of the primary process is the production of H-atoms and cyclo-C_6H_{11} radicals, and that the products formed in lesser amounts arise from unimolecular decomposition of the latter species.

Two alternatives must be considered for the primary process: the decomposition giving H-atoms directly,

[1*a*] $Cd(^3P_1) + \text{cyclo-}C_6H_{12} \rightarrow Cd(^1S_0) + \text{cyclo-}C_6H_{11} + H$

or a sequence of two steps involving the intermediate formation of cadmium hydride,

[1*b*] $Cd(^3P_1) + \text{cyclo-}C_6H_{12} \rightarrow CdH + \text{cyclo-}C_6H_{11}$

[1*c*] $CdH \rightarrow Cd + H$

Energetic considerations do not give a clear indication of the relative importance of these two possibilities. Unlike the case of mercury photosensitization of hydrocarbons in general, cadmium hydride formation has been observed (13). The excitation energy of Cd($^3P_1$) atoms is 87.3 kcal/mol (3261 Å). The formation of CdH in the primary energy transfer process would make available an additional 15.5 kcal/mol, and the carbon–hydrogen bond energy in the substrate is 94 kcal/mol (14). Assuming classical vibrational energy contributions to the energy of cyclohexane at 355 °C, there would be available a total of *ca.* 15 kcal/mol vibrational energy in excess of that at 25 °C. If the usual assumption that about half of this energy would be available for rupture of an individual bond is made, there would be just sufficient energy for reaction 1*a* to occur. On the other hand, if the energy transfer process occurs through an abstractive type intermediate such as cyclo-C_6H_{12}····H···Cd, the vibrational energy partitioning may be appreciably altered in a way that reduces the net energy available for C—H bond rupture. Therefore, although there are attendant experimental difficulties, it would be instructive with respect to elucidating the role of reaction 1*b* to examine this system at lower temperatures where the contribution from thermal excitation is reduced.

The possibility of a primary process in which there is molecular hydrogen formation can be ruled out on the basis that this product is reduced to zero in the presence of sufficient propylene to scavenge the hydrogen atoms from whose abstraction reaction H_2 evidently arises.

A primary process of the excited molecule type in which cyclohexane molecules are formed in an excited state of sufficient longevity to be susceptible to collisional deactivation can also be excluded on the evidence that the overall extent of decomposition is unaffected by the addition of CF_4 up to 422 Torr.

Although their interpretation is complicated by the possible reactions of RNO type products that are involved and the absence of cross section data to permit competitive quenching corrections, the results obtained in the presence of nitric oxide strongly suggest that the decomposition proceeds via free radical rather than molecular reactions, and indeed the formation of all reaction products may be explained on that basis. Thus reaction 1 would be followed by

[2] $H + \text{cyclo-}C_6H_{12} \rightarrow H_2 + \text{cyclo-}C_6H_{11}$

[3] $2\ \text{cyclo-}C_6H_{11} \rightarrow \text{cyclo-}C_6H_{10} + \text{cyclo-}C_6H_{12}$

[4] $2\ \text{cyclo-}C_6H_{11} \rightarrow \text{bicyclohexane}$

The major product propylene arises via the unimolecular decomposition of cyclohexyl radicals,

[5] $\text{cyclo-}C_6H_{11} \rightarrow C_3H_6 + C_3H_5$

Can. J. Chem. Downloaded from www.nrcresearchpress.com by 210.87.254.40 on 09/05/12
For personal use only.

which would be followed by

[6] $C_3H_5 + \text{cyclo-}C_6H_{12} \rightarrow C_3H_6 + \text{cyclo-}C_6H_{11}$

and other radical–radical reactions of the resonance stabilized allyl radical. The activation energy for process 6 is likely rather high, the analogous process for H-atom abstraction from cyclopentane has an activation energy of 32 kcal/mol (15), and thus radical–radical reactions would be more important. Furthermore, if reaction 6 were important reactions 5 and 6 would give rise to a chain reaction and appreciably larger yields of propylene than were observed.

The strong dependence of rate of production of H_2, propylene, and cyclohexene indicates that H-atom scavenging reactions by olefinic products, a well established phenomenon in sensitized alkane decompositions in general (16, 17), is occurring to an appreciable extent here. Propylene is the olefin present in largest concentrations and therefore the most important reaction of this type will be

[7] $H + C_3H_6 \rightarrow C_3H_7$

The propyl radicals so formed account, via reaction 8,

[8] $C_3H_7 + \text{cyclo-}C_6H_{12} \rightarrow C_3H_8 + \text{cyclo-}C_6H_{11}$

for the observed production of propane. Propyl radicals also account, in part, for the formation of ethylene and products arising from CH_3 radicals, through the unimolecular decomposition process

[9] $C_3H_7 \rightarrow CH_3 + C_2H_4$

The reaction analogous to [7] with cyclohexene evidently occurs to a lesser extent, while ethylene, the olefin present in smallest concentrations, does not appear to compete successfully for H-atoms, as suggested by the time independence of its quantum yield.

Three other possible modes of unimolecular decomposition of the substrate radical should be considered in connection with the formation of the minor products CH_4, C_2H_6, and C_2H_4.

[10] $\text{cyclo-}C_6H_{11} \rightarrow C_4H_7 + C_2H_4$

[11] $\text{cyclo-}C_6H_{11} \rightarrow CH_3 + C_5H_8$

[12] $\text{cyclo-}C_6H_{11} \rightarrow C_2H_5 + C_4H_6$

Butene would have been detected here and its absence indicates that either reaction 10 is not occurring to a measurable extent, or that C_4H_7 radicals also undergo thermal decomposition at 355 °C, giving rise to additional ethylene via the sequence

[13] $C_4H_7 \rightarrow C_2H_4 + C_2H_3$

[14] $C_2H_3 + \text{cyclo-}C_6H_{12} \rightarrow C_2H_4 + \text{cyclo-}C_6H_{11}$

Pentadiene would be obscured by the large substrate peak in the g.c. analysis and thus the yield of CH_4 can be interpreted only as an upper limit for the contribution of reaction 11, since CH_3 radicals are also formed in process 9.

Ethane is produced in amounts greater than the trace quantities of butadiene found. The latter would be highly reactive towards H-atoms, but its small concentration suggests that the inequality $R(C_2H_6) > R(C_4H_6)$ arises because of an additional ethane source, for example CH_3 recombination, rather than significant C_4H_6 consumption. The mode of methylcyclopentane formation is not immediately apparent.

The quantum yields observed at the shortest exposure times that could be examined here, together with evidence for secondary consumption of H-atoms by olefins, suggests that the primary process likely occurs with unit efficiency, although precise measurements of quantum yields at short exposure times would be required to establish that characteristic.

Finally, comparison of the results obtained in this study with those reported previously for the Hg-sensitized decomposition of cyclohexane (3) and cyclopentane (6) at similar temperatures indicates that the decomposition proceeds through essentially the same mechanism despite the significant difference in the energy available from the sensitizer.

The authors gratefully acknowledge the financial support of the National Research Council of Canada for this research and the University of Saskatchewan for provision of a Graduate Scholarship to B.L.K.

1. B. L. KALRA and A. R. KNIGHT. Can. J. Chem. **44**, 1333 (1970).
2. P. W. BECK, D. V. KNIEBES, and H. E. GUNNING. J. Chem. Phys. **22**, 672 (1954).
3. S. ARAI, S. SATO, and S. SHIDA. Nippon Kagaku Zassi, **81**, 1790 (1960); Chem. Abstr. **55**, 7007 (1962).
4. W. A. CRAMER. J. Phys. Chem. **71**, 1112 (1967).
5. C. E. KLOTS and R. H. JOHNSEN. Can. J. Chem. **41**, 2702 (1963).

6. H. E. GUNNING and R. L. STOCK. Can. J. Chem. **42**, 357 (1964).
7. E. E. HUGHES. J. Chem. Phys. **35**, 1531 (1961).
8. S. TSUNASHIMA and S. SATO. Bull. Chem. Soc. Jap. **41**, 284 (1968).
9. H. E. HUNZIKER. J. Chem. Phys. **50**, 1294 (1969).
10. S. HIROKAMI and S. SATO. Bull. Chem. Soc. Jap. **43**, 2389 (1970).
11. B. DEB. DARWENT. J. Chem. Phys. **18**, 1532 (1959).
12. E. W. R. STEACIE and D. J. LEROY. J. Chem. Phys. **11**, 164 (1943).
13. E. W. R. STEACIE and D. J. LEROY. J. Chem. Phys. **12**, 34 (1944).
14. J. G. CALVERT and J. N. PITTS, JR. Photochemistry. John Wiley and Sons Inc. 1960. p. 93, 824.
15. A. S. GORDON, J. R. SMITH, and J. R. MCNESBY. J. Am. Chem. Soc. **81**, 5059 (1959).
16. R. A. BACK. Trans. Faraday Soc. **54**, 512 (1958).
17. R. A. BACK. Can. J. Chem. **37**, 1824 (1959).

Can. J. Chem. Downloaded from www.nrcresearchpress.com by 210.87.254.40 on 09/05/12
For personal use only.

The Photolysis of Benzoic Acid in the Vapor Phase

FRANCIS CHAU, CYRIL GIBBONS, AND DONALD BARTON

Department of Chemistry, Memorial University of Newfoundland, St. John's, Newfoundland

Received February 24, 1971[1]

The photolysis of benzoic acid in the vapor phase has been investigated in a flow system at temperatures ranging from 110–305 °C, pressures from 0.06–1.73 Torr, and at various incident light intensities. Carbon dioxide and benzene are the main products and carbon monoxide is a minor product. The rate of formation of carbon dioxide is proportional to the first power of the light intensity and is independent of benzoic acid concentration at pressures from 0.29–1.73 Torr. The activation energy for carbon dioxide formation is approximately 3 kcal per mol. A radical chain mechanism has been suggested, in which initiation results from decomposition of vibrationally excited ground state benzoic acid molecules, and termination occurs at the wall. A molecular mechanism is a possibility if the rate of formation of vibrationally excited ground state is a function of temperature.

La photolyse de l'acide benzoïque en courant gazeux a été examinée à des températures s'échelonnant de 110–305 °C, à des pressions de 0.06–1.73 Torr et pour diverses intensités de lumière incidente. Les produits majeurs sont le gaz carbonique et le benzène, l'oxyde de carbone est le produit mineur. La vitesse de formation du CO_2 est proportionnelle à la puissance première de l'intensité lumineuse et est indépendante de la concentration en acide benzoïque pour des pressions allant de 0.29–1.73 Torr. L'énergie d'activation pour la formation du gaz carbonique est approximativement de 3 kcal/mol. Un mécanisme en chaîne radicalaire a été suggéré dans lequel l'initiation résulte de la décomposition des molécules d'acide benzoique dont l'état fondamental est vibrationnellement excité et la terminaison se produit sur les parois. Un mécanisme moléculaire reste possible si la vitesse de formation de l'état fondamental vibrationnellement excité, dépend de la température.

Canadian Journal of Chemistry, **50**, 2017 (1972)

Can. J. Chem. Downloaded from www.nrcresearchpress.com by 210.87.254.6 on 09/05/12
For personal use only.

Introduction

The primary reactions 1, 1*a*, 2, 3, and 4 have been shown to occur during the photolysis of organic acids in the vapor phase. The intra-

[1] $RCOOH \rightarrow RCO + OH$

[1*a*] $RCOOH \rightarrow RCO_2 + H$

[2] $R_2CHCR_2CR_2COOH \rightarrow R_2C=CR_2 + HCR_2COOH$

[3] $RCOOH \rightarrow RH + CO_2$

[4] $RCOOH \rightarrow R + COOH$

molecular process [3] accounted for a part of the CO_2 produced in the photolysis of acetic acid. Reactions 1 and 1*a*, variations of the Norrish type I split, as well as [4], were also suggested (1). Reaction 1 was proposed as the major primary reaction in the photolysis of formic acid (2). The primary reactions for *n*-butyric acid were found to be reaction 2, the Norrish type II split, and the variations of the type I split, reactions 1 and 1*a* (3).

The first absorption band of the aliphatic organic acids, a weak band lying in the near u.v., is thought to be due to an $n \rightarrow \pi^*$ singlet–singlet transition of a non-bonding electron of the oxygen atom (4). The absorption of radiation in this region is responsible for reactions 1–4 of the aliphatic acids. For benzoic acid, an intense absorption band ($\varepsilon \sim 10^4$ 1 mol^{-1} cm^{-1}) is observed in the near u.v. (5). This band is attributed not to an $n \rightarrow \pi^*$ transition but to a $\pi \rightarrow \pi^*$ transition of the phenyl ring, which is conjugated with the carboxyl group (6, 7).

As a contribution to the understanding of the photochemistry of the aromatic acids in the vapor phase, we report the results of an exploratory study of the photolysis of benzoic acid.

Experimental

Since the relevant extinction coefficient is large the pressure was maintained at ~0.06 Torr during the preliminary experiments, but the restriction was relaxed after the order with respect to light intensity had been observed (8). The vapor was composed substantially of monomeric benzoic acid over the selected temperature and pressure ranges (9). A flow system, composed of a reservoir of benzoic acid, cylindrical vitreosil reaction vessel (length 10 cm, diameter 5 cm), trap, mercury diffusion pump, toepler pump, and gas buret, was used. Analyses were carried out by gas buret, mass spectrometer, titration, and gas chromatograph. Reported gas temperatures are considered to be reliable within 2 °C (10, 11).

The light source was a Hanovia type A S-500 medium

[1]Revision received March 15, 1972.

TABLE 1. Product yields in preliminary experiments

Temperature (°C)	Time (s)	Products (mol × 10^6) CO_2	CO	H_2	C_6H_6	C_6H_5COOH transferred (mol × 10^6)
151	7510	1.78	0.25	0.046	2.00	143
150	7670	1.61	0.19	0.032	1.73	107
150	7570	1.70	0.21	0.037	1.43	111
151	7590	1.71	0.21	0.034	1.86	144
150	7570	1.59	0.16	0.029	1.53	135
150	7570	1.49	0.16	0.024	1.43	98
150	7590	1.55	0.17	0.028	1.72	150
150*	7570	0.08	0.02	0.017	—	119

*Thermal reaction only. The other results are not corrected for thermal reaction.

pressure mercury arc. Neutral density filters of 50.0 and 31.6% (Oriel Optics Corp.), and Corning filters CS 9-54 (7910) and CS 7-54 (9863) were used. Pressures were measured by means of a capacitance manometer (Granville–Phillips Co.).

Benzoic acid (McArthur Chemical Co.) was melted, cooled, ground, and evacuated on the line at 0 °C.

Results

Products

The results of some preliminary experiments are summarized in Table 1. The yields of CO_2, averaging $(1.63 \pm 0.08) \times 10^{-6}$ mol, are moderately reproducible with a thermal contribution of the same order of magnitude as the average deviation. The yield of CO is less reproducible and the thermal contribution is relatively larger. There is no evidence for photochemically produced H_2. The yield of C_6H_6 is rather more erratic than was expected from tests of the procedure for recovery and analysis. Although unsuccessful attempts were made to identify biphenyl and phenol, small amounts of these and other products may be present; in fact, the presence of CO (and H_2, although no doubt a thermal contribution) is consistent with the presence of aromatic compounds in addition to C_6H_6.

The results of detailed studies reported below centered upon the rate of formation of CO_2, and to a smaller extent upon CO. The experiments were performed at a slightly different lamp intensity than was used in the preliminary experiments.

Effective Radiation

The near u.v. absorption bands of benzoic acid are reported to be, in ethanol–water solution for example, at 2020, 2280, and 2790 Å with extinction coefficients of 8000, 11 000, and 5501 $mol^{-1}\ cm^{-1}$ respectively (6). The mercury lamp emits radiation at intensities of the same order of magnitude over both of the longer wavelength bands. Two experiments were performed using a Corning CS 9-54 filter, which transmits from 75–85% of the radiation in the range 2600–2900 Å, ~5% at 2200, ~25% at 2300 and ~45% at 2400 Å. The results are compared in Table 2 with experiments performed without the filter and with some thermal reactions. A preliminary experiment in a static system at a benzoic acid pressure of ~40 mm, with no filter, resulted in a yield similar to those reported in Table 2. When a Corning CS 7-54 filter was used, which transmits ~0% of the radiation up to 2300 Å and ~15% at 2400 Å, no products were detected. The radiation responsible for the formation of CO and CO_2 in this study clearly corresponds to the intense absorption band near 2280 Å which is attributed to a $\pi \rightarrow \pi^*$ transition. This is not surprising, since the intensity of light

TABLE 2. Effect of Corning CS 9-54 filter on yields at 205 °C

Pressure (mm)	Filter	Rate (mol × $10^6\ h^{-1}$) CO_2	CO	H_2
0.091	None	1.37	0.24	0.012
0.095	None	1.49	0.33	0.019
0.107	None	1.85	0.31	0.017
0.095	CS 9-54	0.31	0.09	0.013
0.093	CS 9-54	0.31	0.08	0.011
0.125*		0.04	‡	‡
0.065†		0.07	0.04	0.011

*Thermal reaction only at 215 °C.
†Thermal reaction only at 208 °C.
‡No analysis performed.

Can. J. Chem. Downloaded from www.nrcresearchpress.com by 210.87.254.6 on 09/05/12
For personal use only.

Can. J. Chem. Downloaded from www.nrcresearchpress.com by 210.87.254.6 on 09/05/12
For personal use only.

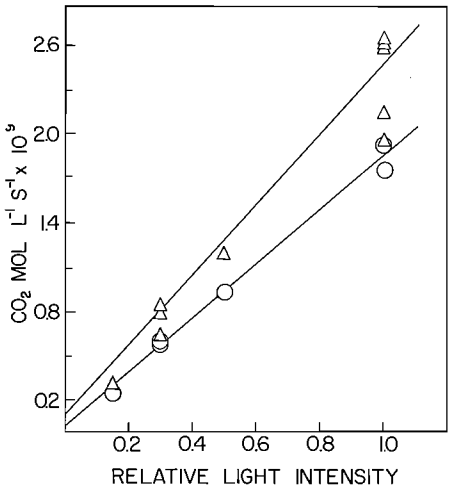

FIG. 1. The rate of formation of CO_2 as a function of light intensity; ○ at 150 °C; △ at 205 °C.

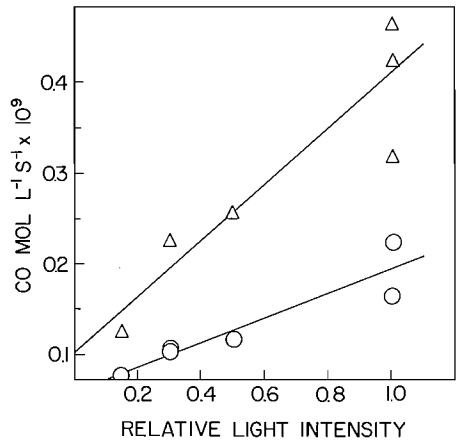

FIG. 2. The rate of formation of CO as a function of light intensity; ○ at 150 °C; △ at 250 °C.

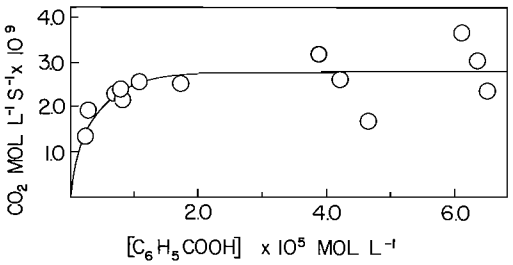

FIG. 3. The rate of formation of CO_2 as a function of benzoic acid concentration at 153 °C.

absorbed is very small over the longer wavelength band.

Light Intensity

The effect upon the rate of formation of CO_2 of changing the light intensity is shown in Fig. 1. The order for CO_2 formation with respect to light intensity is 1.06 ± 0.05 at 150° and 1.00 ± 0.05 at 205 °C. Results are similar for CO formation, shown in Fig. 2, although the thermal reaction makes a relatively large contribution. The experiments on the effect of light intensity were carried out before the installation of the capacitance manometer. Consequently the exact pressure is unknown, but was fixed at ~0.06 Torr for all experiments by regulating the temperature of the solid benzoic acid.

Order of Reaction for CO_2 Formation

The rates of formation of CO_2 were measured at various pressures of benzoic acid at 152 °C and the results are plotted in Fig. 3. Although the points are scattered it is apparent that the rate is insensitive to the concentration of benzoic acid over the range 1.0×10^{-5} to 6.5×10^{-5} mol l^{-1}. After making approximate corrections to the five results at the lowest pressures, at which the absorption of light is incomplete, by dividing by $(1 - \exp [C_6H_5COOH] \times 11\,000 \times 10)$, the slope of the log–log plot was found to be 0.02 ± 0.05. Comments on the scatter in the results will be found below.

Activation Energy

From the slopes of the plots in Fig. 1, the activation energy for CO_2 formation was estimated to be 2700 ± 600 cal mol^{-1}. Some additional data were obtained at temperatures of 110, 153, 209, and 305 °C and concentrations of 1.16, 1.09, 0.86, and 1.28×10^{-5} mol l^{-1} respectively. Since the rate of formation of CO_2 was shown to be insensitive to pressure, an Arrhenius plot of these data is justified. The results from a number of thermal reactions which were carried out at various temperatures and pressures showed that the thermal reaction rate was usually less than 5% of the photochemical rate, but was variable. Although corrections for the thermal reaction were not applied to the rates at the four temperatures, any such corrections up to ≈10% would not alter the conclusion reached regarding the temperature dependence of the

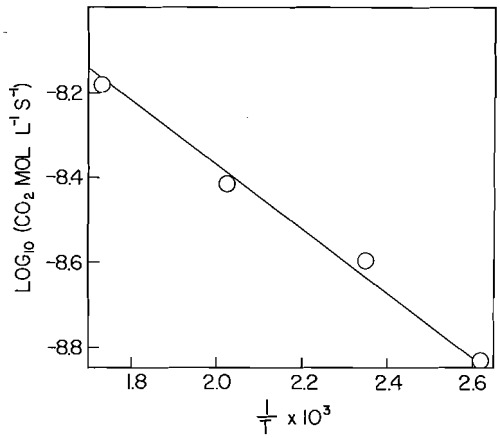

FIG. 4. Arrhenius plot for CO_2 formation.

photochemical reaction. The Arrhenius plot, from which the activation energy was found to be 3500 ± 400 cal mol^{-1}, is shown in Fig. 4.

An appreciable activation energy was also found in the reaction producing CO, as is apparent in Fig. 2.

Following exposure of the reaction vessel to air a fast thermal reaction was observed, up to 20 times as fast as the thermal contributions already reported. This phenomena had been observed previously during a study of the thermal reactions of benzoic acid in the gas phase (12).

Discussion

The effect of temperature on the rate probably rules out direct formation from the excited singlet state as the major reaction yielding CO and CO_2 (13). Chain mechanisms, which were adapted from those discussed by Noyes and Leighton (14), were at first considered. Reac-

[5] $C_6H_5COOH + h\nu \rightarrow C_6H_5 + COOH$

[6] $C_6H_5 + C_6H_5COOH \rightarrow C_6H_6 + C_6H_5CO_2$

[7] $C_6H_5CO_2 \rightarrow C_6H_5 + CO_2$

[8] $C_6H_5 + \text{wall} \rightarrow \text{products}$

[9] $2C_6H_5 \rightarrow (C_6H_5)_2$

tions 5–7 with the homogeneous termination reaction 9 yield the rate expression:

$$d[CO_2]/dt = (k_6/k_9)I_a^{1/2}[C_6H_5COOH]$$

and with the heterogeneous reaction 8 yield

$$d[CO_2]/dt = (2k_6/k_8)I_a[C_6H_5COOH]$$

The evidence favors the wall termination reaction 8 since the rate depends upon I_a, not upon $I_a^{1/2}$. The observed scatter in the results may reflect the variation in efficiency of reaction 8 due to changes in the condition of the wall of the reaction vessel.

Since the order with respect to benzoic acid is approximately zero, a modification of the mechanism is required. This order would be observed if the absorption of a photon is followed mainly by collisional deactivation by benzoic acid molecules rather than by reaction. Reaction 5 would be replaced by [10], [11], and [12]. The electronically excited state is repre-

[10] $C_6H_5COOH + h\nu \rightarrow C_6H_5COOH^*$

[11] $C_6H_5COOH^* \rightarrow C_6H_5 + COOH$

[12] $C_6H_5COOH^* + M \rightarrow C_6H_5COOH + M$

sented by $C_6H_5COOH^*$ and, in pure benzoic acid, M represents a molecule of benzoic acid. The radiative lifetime of the excited molecule would however be rather short, since the extinction coefficient is large. Using the expression

$$\tau \sim \frac{10^{-4}}{\varepsilon_{max}}$$

the radiative lifetime is estimated to be $\sim 10^{-8}$ s. The collision frequency at the pressures used would be such that radiative decay would be 10^2 or 10^3 more probable than collisional deactivation, and the radiative lifetime is too short to allow the molecule to undergo deactivating collisions. This problem has been discussed by Srinivasan (15). Since there is a large energy difference between the first excited singlet state and the first excited triplet state (16), the probability of intersystem crossing is small (17). For purposes of discussion the possibility of the existence of other triplet states below the first excited singlet state has been neglected.

We therefore propose that internal conversion is rapid, and that reaction takes place from the vibrationally excited ground state. A reasonable mechanism, which can serve as a basis for future work and discussion, is given.

[10] $C_6H_5COOH + h\nu \rightarrow C_6H_5COOH^*$

[13] $C_6H_5COOH^* \rightarrow C_6H_5COOH'$

[14] $C_6H_5COOH' + M \rightarrow C_6H_5COOH + M$

[15] $C_6H_5COOH' \rightarrow C_6H_5 + COOH$

[6] $C_6H_5 + C_6H_5COOH \rightarrow C_6H_6 + C_6H_5CO_2$

Can. J. Chem. Downloaded from www.nrcresearchpress.com by 210.87.254.6 on 09/05/12
For personal use only.

[7] $C_6H_5CO_2 \rightarrow C_6H_5 + CO_2$

[8] $C_6H_5 + \text{wall} \rightarrow \text{products}$

The vibrationally excited ground state is represented as C_6H_5COOH'. The rate expression is

$$d[CO_2]/dt = (k_6k_{15}/k_{14}k_8)I_a,$$

if $k_{14}[M] \gg k_{15}$. The inequality may be rationalized by making a rough estimate of the rates of the two steps. The collision frequency was used to calculate the rate of deactivation, with an efficiency of one and a molecular diameter of 7 Å. The rate of decomposition was estimated by means of the classical expression, $-d[C_6H_5COOH']/dt = A(1 - E^*/E)^{s-1}[C_6H_5COOH']$, with $A = 10^{14}\ s^{-1}$, $E^* = 97$ kcal, $E = 125$ kcal, and $s = 20$. E^* is ΔH for reaction 15 (18–20) and E is the energy of the absorbed photon. The two calculated rates are equal at $\sim 10^{-3}$ mm, suggesting that deactivation predominates over the range of pressure used in this study.

The rate of reaction 15 is not strongly dependent upon temperature because the energy delivered by the photon is ~ 30 kcal greater than the heat of reaction. Since the rates of reactions 8 and 14 are also not strongly dependent upon temperature, the activation energy according to this mechanism, can be attributed largely to reaction 6.

Mechanisms which do not involve radicals may be invoked. If, for example, the internal conversion process [13] is affected by temperature a mechanism in which fluorescence competes with internal conversion is possible.

[10] $C_6H_5COOH + h\nu \rightarrow C_6H_5COOH^*$

[16] $C_6H_5COOH^* \rightarrow C_6H_5COOH + h\nu$

[13] $C_6H_5COOH^* \rightarrow C_6H_5COOH'$

[17] $C_6H_5COOH' \rightarrow C_6H_6 + CO_2$

The rate expression is

$$d[CO_2]/dt = (k_{13}I_a)/(k_{13} + k_{16})$$

Similar but more intricate mechanisms may be written.

The CO formation data suggest analogous mechanisms, although the effect of benzoic acid pressure was not obtained and the thermal contribution is rather large.

Clearly the system is an interesting one and further research into the quantum yields, effect of inert gases, and into the photophysical processes is in order.

We thank Dr. J. F. Ogilvie for his advice and the interest which he has shown in this work, and a referee for suggestions. Financial support from the National Research Council of Canada is gratefully acknowledged.

1. P. Ausloos and E. W. R. Steacie. Can. J. Chem. **33**, 1530 (1955).
2. R. Gorden and P. Ausloos. J. Phys. Chem. **65**, 1033 (1961).
3. P. Borrell and R. G. W. Norrish. Proc. Roy. Soc. **A262**, 19 (1961).
4. J. G. Calvert and J. N. Pitts, Jr. Photochemistry. John Wiley and Sons, Inc., New York. 1967. p. 427.
5. C. M. Moser and A. I. Kohlenberg. J. Chem. Soc. 804 (1951).
6. S. Nagakura and J. Tanaka. J. Chem. Phys. **22**, 236 (1954).
7. S. Nagakura. J. Chem. Phys. **23**, 1441 (1955).
8. W. A. Noyes, Jr. and P. A. Leighton. The photochemistry of gases. Dover Publications, Inc., New York. 1966. p. 200.
9. G. Opel and U. V. Weber. Z. Chem. **6**, 349 (1966).
10. H. Melville and B. G. Gowenlock. Experimental methods in gas reactions. MacMillan and Co. Ltd., New York. 1964. p. 24.
11. F. Chau. M.Sc. Thesis. Memorial University of Newfoundland, 1970.
12. K. Winter. M.Sc. Thesis. Memorial University of Newfoundland, 1968; K. Winter and D. Barton. Can. J. Chem. **48**, 3797 (1970).
13. Reference 4. p. 646.
14. Reference 8. p. 195.
15. R. Srinivasan. Advances in photochemistry. Vol. 4. *Edited by* W. A. Noyes, Jr., G. S. Hammond, and J. N. Pitts, Jr. Interscience Publishers, Inc., New York. 1966. p. 113.
16. R. L. Flurry, Jr., E. W. Stout, and J. J. Bell. Theoret. Chim. Acta, **8**, 203 (1967).
17. M. Gouterman. J. Chem. Phys. **36**, 2846 (1962).
18. J. D. Cox. Tetrahedron, **18**, 1337 (1962).
19. S. W. Benson. J. Chem. Educ. **42**, 502 (1965).
20. A. S. Rodgers, D. M. Golden, and S. W. Benson. Ber. Bunsenges. Physik. Chem. **72**, 253 (1968).

Can. J. Chem. Downloaded from www.nrcresearchpress.com by 210.87.254.6 on 09/05/12
For personal use only.

A New Synthesis of "Schöpf's Base VI" and Related 10*H*-Isoindolo[2,3-*c*]benzazepines

S. TEITEL, W. KLÖTZER,[1] J. BORGESE, AND A. BROSSI

Chemical Research Department, Hoffmann-La Roche Inc., Nutley, New Jersey 07110

Received January 24, 1972

The 10*H*-isoindolo[2,3-*c*][3]benzazepines, "Schöpf's base VI" (**4***a*) and its 4-methoxy derivative **4***b*, have been prepared by a new and facile synthesis which utilized intermediates derived from phthalideisoquinoline alkaloids.

Les 10*H*-isoindole[2,3-*c*][3]benzazépines, la base VI (**4***a*) de Schöpf et son 4-méthoxy dérivé **4***b*, ont été préparés par une nouvelle synthèse et facile qui a utilisé des produits intermédiaires dérivés des alcaloïdes phthalideisoquinoléniques.

Canadian Journal of Chemistry, **50**, 2022 (1972)

The tetracyclic base, obtained as a minor product by reduction of neooxyberberine[2] with zinc and acetic acid (1), was shown by Schöpf and Schweickert (2) to be 8,9-dimethoxy-2,3-methylenedioxy-5,5*a*,12,13-tetrahydro-10*H*-isoindolo[2,3-*c*][3]benzazepine (**4***a*). Commonly referred to as "Schöpf's base VI", **4***a* is of interest because of its relationship with the papaverrubine alkaloids (3). We now describe a novel and facile synthesis of **4***a* as well as its 4-methoxy derivative **4***b*. This was accomplished by reaction sequences which utilized the dihydrobenzazepine sodium salts **1** previously obtained from the phthalide alkaloids (−)-β-hydrastine and (−)-α-narcotine (4, 5). The key intermediate lactams **3** were prepared from the saturated amino acids **2** by *N*-demethylation and cyclization with acetic anhydride (6, 7).[3]

Consecutive treatment of the dihydrobenzazepine sodium salt **1***a* (4) with acetic acid[4] and lithium borohydride in tetrahydrofuran afforded the saturated benzazepine carboxylic acid **2***a*. Reaction of **2***a* with refluxing acetic anhydride formed the lactam **3***a* which was reduced with diborane in tetrahydrofuran to provide the tetracyclic base **4***a*. The physical and spectral properties of **4***a* were identical with an authentic sample[5] of "Schöpf's base VI" (2). By the same reaction sequences, the methoxy-substituted dihydrobenzazepine sodium salt **1***b* (5) was transformed into the corresponding substituted tetracyclic base **4***b*.

[1]Visiting Professor, Institute of Organic and Pharmaceutical Chemistry, University of Innsbruck, Austria.

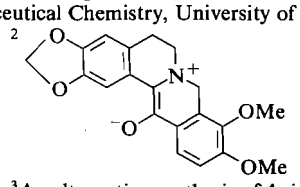

[3]An alternative synthesis of **4***a* involving photocyclization was recently reported (8).

[4]Mineral acid effects conversion to the phthalideisoquinoline (5).

Experimental

Melting points were taken on a Kofler microscope hot stage and are uncorrected. The u.v. spectra were measured in ethanol with a Cary recording spectrophotometer Model 14M and the i.r. spectra were determined with a Beckman Infrared Model IR-9 in KBr, unless otherwise noted. The n.m.r. spectra were obtained on a Varian HA-100 spectrophotometer using tetramethylsilane as internal reference. Chemical shifts are reported in δ with the following abbreviations: (s) singlet, (d) doublet, (m) multiplet, (b) broad. The mass spectra were taken with a CEF 21–110 mass spectrometer at 70 eV using a direct insertion probe. Extracts of products in organic solvents were washed with water and dried over anhydrous sodium sulfate prior to evaporation. Water of crystallization in compounds **2***a*, hydrobromide of **4***a*, **2***b*, and hydrochloride of **2***b* was determined with the Karl Fischer reagent.

*6-(7,8-Methylenedioxy-3-methyl-1,2,4,5-tetrahydro-3H-3-benzazepin-2-yl)-o-veratric Acid Hemihydrate (**2***a*)*

A solution of 6-(4,5-dihydro-7,8-methylenedioxy-3-methyl-3*H*-3-benzazepin-2-yl)-*o*-veratric acid sodium salt (**1***a*) (4) (20 g, 0.049 mol) in water (480 ml) was adjusted to p*H* 5 with acetic acid (12 ml), extracted with methylene chloride (three 80 ml portions) and the combined extracts evaporated. The residual oil was dissolved in tetrahydrofuran

[5]We are grateful to Professor G. Habermehl, Technische Hochschule Darmstadt, Germany, for providing us with a sample.

Can. J. Chem. Downloaded from www.nrcresearchpress.com by 210.87.254.105 on 09/05/12
For personal use only.

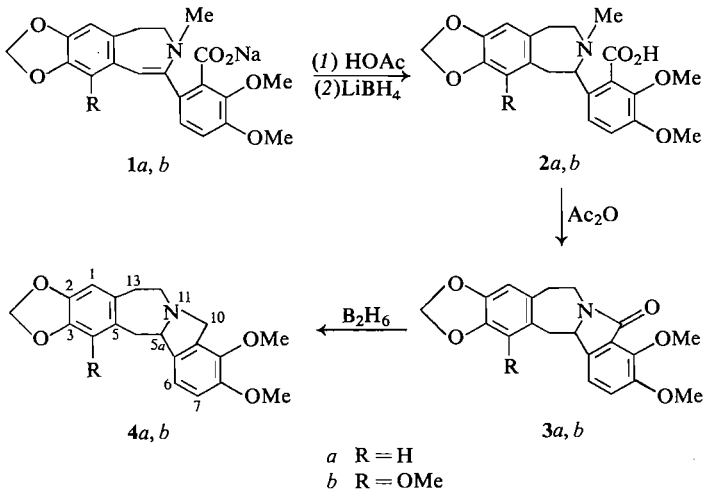

(200 ml), cooled to 4°, and a solution of lithium borohydride (4.4 g, 0.202 mol) in tetrahydrofuran (100 ml) added over 15 min. The reaction mixture was allowed to warm to room temperature, stored for 2 h, and evaporated under reduced pressure. The residual oil was dissolved in water (160 ml), acetic acid (26 ml) added, the resulting suspension heated at 95° for 30 min and cooled. The crystals were collected to give **2***a* (17.1 g, 90%), m.p. 230–231°. An analytical sample prepared from methanol exhibited: m.p. 234–236°; u.v. max 235 (ε 12 500) (infl), 289 nm (6020); i.r. 2700–2400, 1700, 1575 cm^{-1}; n.m.r. (MeOD) δ 2.52 (s, 3, NCH_3), 2.75–3.50 (m, 6, 3 CH_2), 3.83 (s, 6, 2 OCH_3), 4.50 (m, 1, CH), 5.88 (s, 2, OCH_2O), 6.70 (s, 2, arom), 6.96, 7.07 (2d, 2, *J* (ortho) = 8 Hz, arom).

Anal. Calcd. for $C_{21}H_{23}NO_6 \cdot 0.5\ H_2O$ (394.42): C, 63.96; H, 6.13; N, 3.55. Found: C, 64.09; H, 5.99; N, 3.61.

8,9-Dimethoxy-2,3-methylenedioxy-5,5a,12,13-tetrahydro-10H-isoindolo[2,3-c][3]benzazepin-10-one (3a)

A mixture of the saturated benzazepine carboxylic acid **2***a* (9.8 g, 0.0256 mol) in acetic anhydride (140 ml) was refluxed in a nitrogen atmosphere for 1 h, water (250 ml) added, and allowed to cool to room temperature. The resulting crystals were filtered, washed with water, and dried to give **3***a* (5.8 g, 64%), m.p. 228–229°. An analytical specimen prepared from methanol exhibited: m.p. 228–229°; u.v. max 202 (ε 62 600), 213 (44 500) (infl), 233 (18 500) (infl), 293 nm (9500); i.r. 2780, 1678, 1290, 1265, 1590, 1492, 1480 cm^{-1}; n.m.r. ($CDCl_3$) δ 2.90 (m, 4, 2 CH_2), 3.95, 4.09 (2s, 6, 2 OCH_3), 4.1–5.0 (m, 3, CH + CH_2N), 5.81 (s, 2, OCH_2O), 6.65, 6.72, 7.11 (3s, 3, arom).

Anal. Calcd. for $C_{20}H_{19}NO_5$ (353.36): C, 67.98; H, 5.42; N. 3.96. Found: C, 67.79; H, 5.36; N, 3.95.

8,9-Dimethoxy-2,3-methylenedioxy-5,5a,12,13-tetrahydro-10-H-isoindolo[2,3-c][3]benzazepine ("Schöpf's base VI") (4a)

A mixture of the lactam **3***a* (5 g, 0.014 mol) in tetrahydrofuran (250 ml) and a solution of 1 *M* diborane in tetrahydrofuran (25 ml) was refluxed for 48 h, cooled, and evaporated under reduced pressure. The residue was suspended in water (100 ml), extracted with chloroform (three 100-ml portions), the combined extracts evaporated, the residue dissolved in methanol (415 ml), refluxed for 2 h, and cooled. The crystals were filtered and dried to give **4***a* (3.58 g, 75%), m.p. 176–177°. An analytical specimen prepared by sublimation exhibited: m.p. 177–179° (lit. (2): m.p. 180–181°); i.r. 2815, 2760, 2745, 1618, 1500, 1263 cm^{-1}; n.m.r. ($CDCl_3$) δ 2.5–3.5 (m, 7, 3 CH_2 + CH), 2.62 (d'd, 1, *J* = 13, 3Hz, CH of CH_2), 3.84, 3.86 (2s, 6, 2 OCH_3), 4.35 (d, 1, *J* = 13 Hz, CH of CH_2), 5.90 (s, 2, OCH_2O), 6.65, 6.74 (2s, 2, arom), 6.80, 6.88 (2d, 2, *J* (ortho) = 8 Hz, arom); mass spectrum *m/e* (relative intensity) 339 (100), 337 (10), 324 (29), 322 (4), 191 (5), 176 (6), 163 (35), 162 (23); identical in mixed m.p., t.l.c., and mass spectrum with an authentic sample[5] of "Schöpf's base VI" (2).

Anal. Calcd. for $C_{20}H_{21}NO_4$ (339.38): C, 70.78; H, 6.24; N, 4.13. Found: C, 70.62; H, 6.33; N, 4.03.

The hydrobromide of **4***a* was prepared in the usual manner and crystallized from 2% hydrobromic acid, m.p. 212–215° (lit. (2): m.p. 212–214°).

Anal. Calcd. for $C_{20}H_{21}NO_4 \cdot HBr \cdot 0.5\ H_2O$ (429.29): C, 55.96; H, 5.40; N, 3.26. Found: C, 55.83; H, 5.43; N, 3.16.

6-(9-Methoxy-7,8-methylenedioxy-3-methyl-1,2,4,5-tetrahydro-3H-3-benzazepin-2-yl)-o-veratric Acid Sesquihydrate (2b)

By the procedure described for **2***a*, 6-(4,5-dihydro-9-methoxy-7,8-methylenedioxy-3-methyl-3*H*-3-benzazepin-2-yl)-*o*-veratric acid sodium salt (**1***b*) (5) (19 g, 0.043 mol) afforded **2***b* (15.6 g, 88%), m.p. 160–165° (from methanol).

Anal. Calcd. for $C_{22}H_{25}NO_7 \cdot 1.5\ H_2O$ (442.44): C, 59.73; H, 6.38; N, 3.17. Found: C, 59.93; H, 6.53; N, 3.17.

The hydrochloride of **2***b* exhibited: m.p. 220–225° (from a mixture of methanol and 1 *N* hydrochloric acid); u.v. max 212 (ε 67 000), 239 (15 000) (infl), 285 nm (4000); i.r. 3400, 2670, 2620, 2520, 1714, 1270, 1227 cm^{-1}; n.m.r. (DMSO-d_6) δ 2.44 (s, 3, CH_3N) 3.82 (s, 6, 2 OCH_3), 3.92 (s, 3, OCH_3), 6.00 (s, 2, OCH_2O), 6.62 (s, 1, arom), 7.28, 8.03 (2d, 2, *J* (ortho) = 9 Hz, arom), 12.35 (b, 1, N^+H).

Anal. Calcd. for $C_{22}H_{25}NO_7 \cdot HCl \cdot 0.25\ H_2O$ (456.42): C, 58.00; H, 5.84; N, 3.07. Found: C, 58.02; H, 5.96; N, 3.05.

Can. J. Chem. Downloaded from www.nrcresearchpress.com by 210.87.254.105 on 09/05/12
For personal use only.

2,3-Methylenedioxy-4,8,9-trimethoxy-5,5a,12,13-tetrahydro-10H-isoindolo[2,3-c][3]benzazepin-10-one (3b)

Treatment of the saturated benzazepine carboxylic acid **2b** (6 g, 0.0143 mol) with acetic anhydride according to the procedure given for the preparation of **3a** afforded **3b** (4.68 g, 86%): m.p. 204–206° (from methanol); u.v. max 279 (ε 4900) (infl), 289 (5250), 305 nm (3900) (infl); i.r. 1680, 1617, 1598, 1278 cm^{-1}; n.m.r. ($CDCl_3$) δ 2.85 (m, 4, 2 CH_2), 3.90, 3.97, 4.08 (3s, 9, 3 OCH_3), 4.26 (m, 3, CH + CH_2N), 5.90 (s, 2, OCH_2O), 6.42 (s, 1, arom), 7.14 (s, 2, arom).

Anal. Calcd. for $C_{21}H_{21}NO_6$ (383.39): C, 65.79; H, 5.52; N, 3.65. Found: C, 65.88; H, 5.44; N, 3.55.

2,3-Methylenedioxy-4,8,9-trimethoxy-5,5a,12,13-tetrahydro-10H-isoindolo [2,3-c] [3]benzazepine (4b)

Reduction of the lactam **3b** (3.83 g, 0.01 mol) according to procedure given for the preparation of **4a** afforded **4b** (3.25 g, 88%): m.p. 175–176° (from methanol); i.r. ($CHCl_3$) 2790, 1625, 1595, 1270 cm^{-1}; u.v. max 205 (ε 58 000), 230 (11 000) (infl), 283 nm (3000); n.m.r. ($CDCl_3$) δ 3.76 (s, 6, 2 OCH_3), 4.05 (s, 3, OCH_3), 5.84 (s, 2, OCH_2O), 6.18 (s, 1, arom), 6.69, 6.90 (2d, 2, *J* (ortho) = 8 Hz, arom); mass spectrum *m/e* (relative intensity) 369 (100), 354 (25), 270 (10), 193 (47), 192 (34), 176 (20), 162 (8), 132 (14), 105 (10), 91 (12), 77 (15).

Anal. Calcd. for $C_{21}H_{23}NO_5$ (369.42): C, 68.28; H, 6.28; N, 3.79. Found: C, 68.10; H, 5.99; N, 3.81.

The hydrobromide of **4b** melted at 202–204° (from 2% hydrobromic acid).

Anal. Calcd. for $C_{21}H_{23}NO_5 \cdot HBr$ (450.31): C, 56.01; H, 5.37; N, 3.11. Found: C, 56.20; H, 5.39; N, 3.15.

We wish to thank the following members of our Physical Chemistry Department (Director, Dr. R. P. W. Scott): Dr. F. Scheidl for the microanalyses, Mr. S. Traiman for the i.r. spectra, Dr. V. Toome for the u.v. spectra, Dr. T. Williams for the n.m.r. spectra, and Dr. W. Benz for the mass spectra.

1. T. Takemoto, Y. Kondo, and K. Kondo. J. Pharm. Soc. (Japan), **83**, 162 (1963).
2. C. Schöpf and M. Schweickert. Chem. Ber. **98**, 2566 (1965).
3. F. Sǎntavý. *In* The alkaloids. Vol. XII, R. H. F. Manske, *Editor*. Academic Press, New York, N.Y. 1970. pp. 412–414.
4. W. Klötzer, S. Teitel, and A. Brossi. Helv. Chim. Acta, **54**, 2057 (1971) give the preparation of a closely related dihydrobenzazepine sodium salt. Details will be reported in Monatsh. Chem.
5. W. Klötzer, S. Teitel, J. F. Blount, and A. Brossi. J. Am. Chem. Soc. **93**, 4321 (1970). Details will be reported in Helv. Chim. Acta.
6. (*a*) J. C. Sheehan, R. L. Young, and P. A. Cruickshank. J. Am. Chem. Soc. **82**, 6147 (1960). (*b*) P. A. Cruickshank and J. C. Sheehan. J. Am. Chem. Soc. **83**, 2891 (1961).
7. (*a*) L. J. Dolby and S. Sakai. J. Am. Chem. Soc. **86**, 1890 (1964). (*b*) J. Harley-Mason and Atta-ur-Rahman. Chem. Commun. 1048 (1967).
8. H. O. Bernhard and V. Snieckus. Tetrahedron Lett. 4867 (1971).

Can. J. Chem. Downloaded from www.nrcresearchpress.com by 210.87.254.105 on 09/05/12
For personal use only.

The Synthesis of Two Phenacetin Metabolites

A. FOCELLA, P. HESLIN, AND S. TEITEL
Chemical Research Department, Hoffmann–La Roche Inc., Nutley, New Jersey 07110

Received January 24, 1972

A new metabolite of phenacetin was identified as 4-hydroxy-3-methylthioacetanilide (**11**). The synthesis of **11** and the isomeric 4-hydroxy-2-methylthioacetanilide (**4**) as well as that of the previously reported phenacetin metabolite 3-[(5-acetamido-2-hydroxyphenyl)thio]alanine (**18**) is described.

Un nouveau métabolite de phénacétine a été identifiée comme 4-hydroxy-3-méthylthioacétanilide (**11**). La synthèse de **11** et celle du 4-hydroxy-2-méthylthioacétanilide isomérique sont décrites, aussi bien que celle du métabolite préalablement rapporté de phénacétine, 3-[(5-acétamido-2-hydroxyphényl)thio]alanine (**18**).

Canadian Journal of Chemistry, **50**, 2025 (1972)

In connection with a recent study on the metabolism of phenacetin (*p*-ethoxyacetanilide), a new metabolite isolated from dog urine[1] (1) exhibited n.m.r. and mass spectra[2] compatible with either 4-hydroxy-2-methylthioacetanilide (**4**) or 4-hydroxy-3-methylthioacetanilide (**11**). It therefore became necessary, in order to establish unequivocally the structure of this metabolite, to synthesize in an unambiguous manner both isomers.

The 2-methylthio isomer **4** was prepared (Scheme 1) as follows. Reduction of the known 4-nitrothioether **1** (2) with sodium hydrosulfite in alkaline solution provided the substituted aniline **2**. Conversion of **2** with acetic anhydride into the acetoxyacetanilide **3** followed by *O*-deacetylation with boron trichloride afforded 4-hydroxy-2-methylthioacetanilide (**4**).

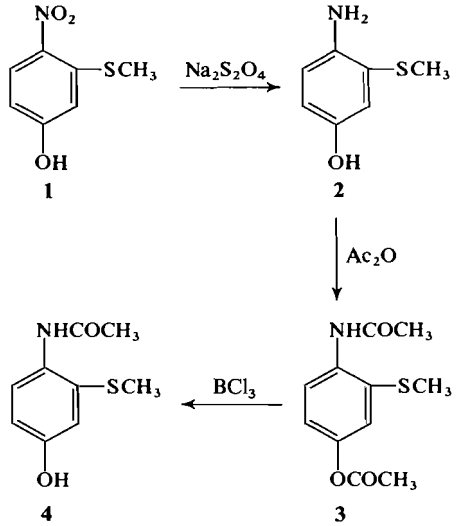

SCHEME 1. Synthesis of 4-hydroxy-2-methylthioacetanilide (**4**).

The isomeric 4-hydroxy-3-methylthioacetanilide (**11**) was prepared (Scheme 2) from the key intermediate **9** which was obtained by two methods. Diazotization of the aminonitrophenol **5** in fluoboric acid gave the known (3)[3] diazooxide **6** which was converted by a Sandmeyer reaction with sodium thiomethylate to the thioether **7**. Subsequent reduction of the nitro group with sodium hydrosulfite afforded **9**. Alternatively, treatment of the thiophenol **8** with diazotized sulfanilic acid followed by sodium hydrosulfite reduction yielded **9** more directly. Treatment of **9** with acetic anhydride in the presence of *p*-toluenesulfonic acid gave a separable mixture of the desired hydroxyacetanilide **11** and its *O*-acetoxy derivative **10**. Saponification of **10** with aqueous alkali also afforded **11**.

A comparison of the pertinent n.m.r. and m.s. data for the metabolite and the synthesized isomers **4** and **11** (Table 1) indicates that the metabolite and compound **11** are identical. The data for the metabolite and **4** are unlike; there are large differences in the chemical shifts of the aromatic protons in the n.m.r. and in the relative intensities for the three major peaks in the mass spectra.

Having established the structure of this metabolite as 4-hydroxy-3-methylthioacetani-

[1]Made available by Dr. A. Klutch of Burroughs Wellcome & Co.

[2]We are grateful to Dr. F. Vane and Mr. R. Pitcher of our Physical Chemistry Department for these determinations.

[3]Previously characterized only by a thermal decomposition study.

Can. J. Chem. Downloaded from www.nrcresearchpress.com by 210.87.254.6 on 09/05/12
For personal use only.

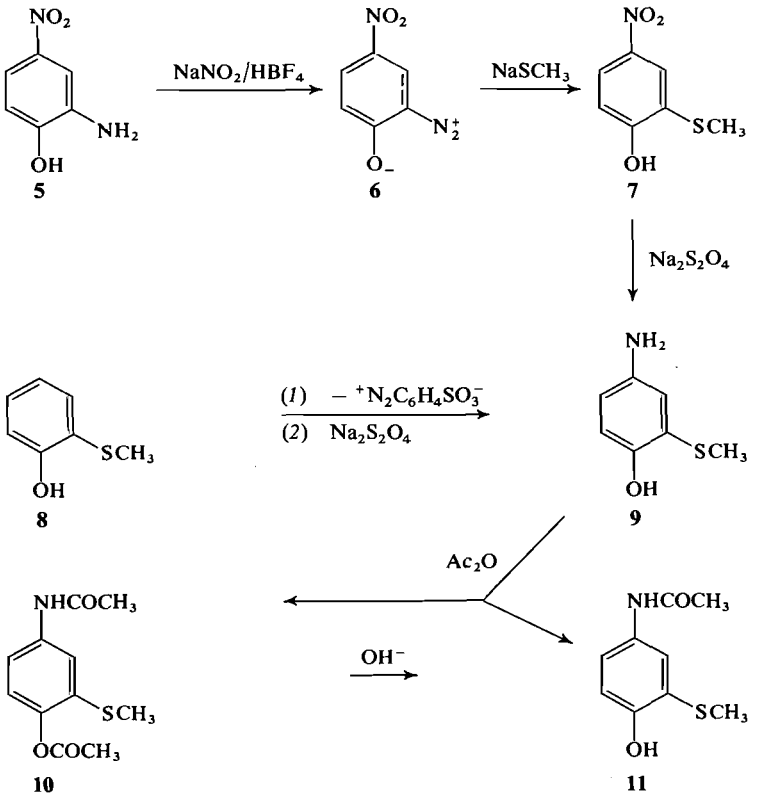

SCHEME 2. Synthesis of 4-hydroxy-3-methylthioacetanilide (**11**).

TABLE 1. Comparison of n.m.r. and mass spectrum data for the metabolite (1) with **4** and **11**

	Nuclear magnetic resonance (δ)*						Mass spectrum (m/e)‡		
			Aromatic protons†			NH or			
Compound	$COCH_3$	SCH_3	H_1	H_2	H_3	OH	197 (M^+]	155 [$M-C_2H_2O$]	140 [$M-C_2H_2O$, CH_3]
Metabolite (1)	2.15	2.35	6.90	—	~7.70	~6.48	100	70–72	68–75
4	2.20	2.38	7.85	6.65	6.83	5.06	75–100	88–97	94–100
11	2.16	2.36	6.93	7.22	7.67	6.41	100	70–90	67–92

*Obtained in chloroform-*d* solutions with a Varian HA-100 spectrometer using a C-1024 time averaging computer.
†H_1, H_2, and H_3 correspond to the following protons:

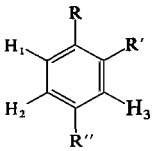

H_2 of the metabolite was obscured by a chloroform impurity peak.
‡The low resolution mass spectra were obtained with a CEC 21–110 mass spectrometer operating at 70 eV. The large range in the relative intensities observed for the three major peaks in the mass spectra of the metabolite and the two isomers **4** and **11** may be a temperature effect. Intensities are given in % base peak.

lide (**11**), it appeared reasonable that another phenacetin metabolite previously identified as *S*-(1-acetamido-4-hydroxyphenyl)cysteine (**4**) was probably related to **11** and therefore should be 3-[(5-acetamido-2-hydroxyphenyl)thio]alanine (**18**). To prove this hypothesis, we synthe-

Can. J. Chem. Downloaded from www.nrcresearchpress.com by 210.87.254.6 on 09/05/12
For personal use only.

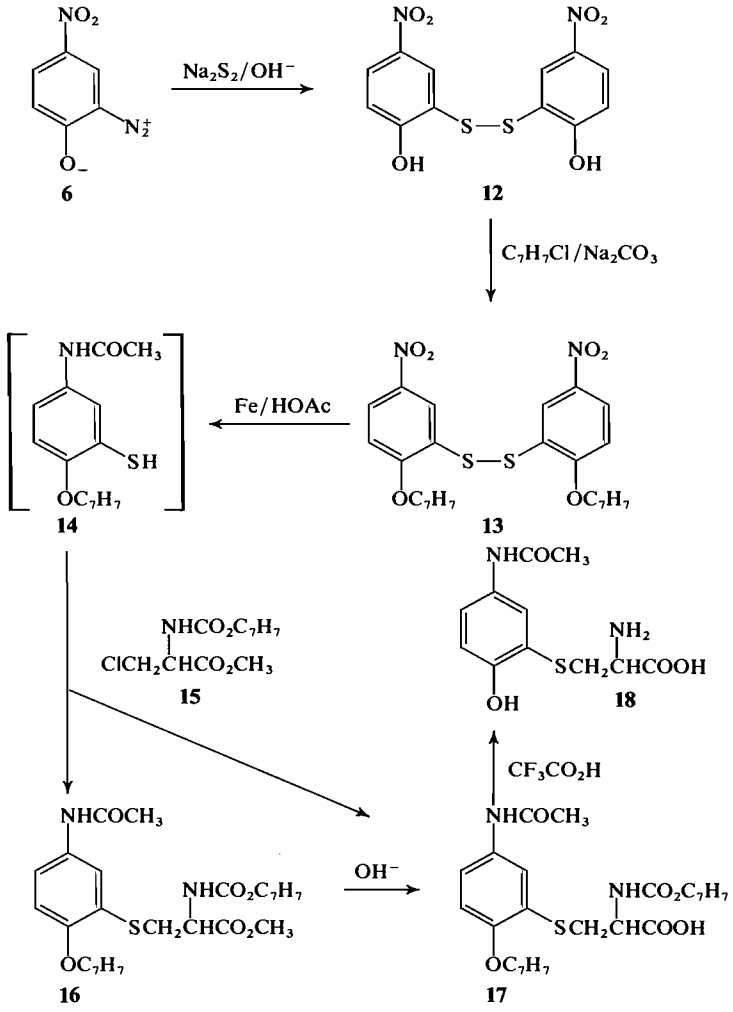

SCHEME 3. Synthesis of 3-[(5-acetamido-2-hydroxyphenyl)thio]alanine (**18**).

sized **18** as follows (Scheme 3). A Sandmeyer reaction carried out by treating the diazo-oxide **6** with sodium polysulfide provided the disulfide **12** which was converted into the di-*O*-benzyl derivative **13**. Reaction of **13** with iron[4] in acetic acid effected simultaneously reduction, acetylation, and cleavage of the disulfide to afford the unstable thiophenol **14**. *S*-Alkylation of **14** in ethyl acetate[5] with α-benzyloxycarbonylamino-β-chloropropionic acid methyl ester (**15**), obtained from 3-chloroalanine methyl ester, yielded a separable mixture of the methyl ester **16** and a minor amount of the corresponding acid **17**. Saponification of **16** also provided the acid **17** which was selectively debenzylated and decarbobenzylated with trifluoroacetic acid to the desired compound **18**.

Comparison of the physical data reported for the metabolite *S*-(1-acetamido-4-hydroxyphenyl)cysteine (4) and those exhibited by **18** (Table 2) indicates their similarity in these respects. However, we could not unequivocally establish their identity since a sample of the metabolite was not available for a more direct correlation.

[4]In contrast to iron, zinc reductively cleaved the disulfide **13** in very poor yield.

[5]Attempts to *S*-alkylate the unstable **13** in other conventional solvents gave mainly the corresponding disulfide.

Can. J. Chem. Downloaded from www.nrcresearchpress.com by 210.87.254.6 on 09/05/12
For personal use only.

TABLE 2. Physical data of metabolite *S*-(1-acetamido-4-hydroxyphenyl)cysteine and **18**

Compound	Melting point (°C)	Ultraviolet absorption (λ_{max}, nm) 0.1 *N* HCl	0.1 *N* KOH	Infrared absorption (μ) Amine	Amide	Paper chromatography* (R_f) Ascending	Descending
Metabolite (4)	187–188 (needles)	203 243 295	270 313	6.2	6.0 6.5	0.70	0.28
18	192–193 (needles)	200 240 292	268 312	6.2	6.0 6.5	0.68	0.26

*Paper chromatography was carried out according to the conditions described (4) using Whatman No. 1 chromatography paper employing butan-1-ol : acetic acid : water (4:1:1) for ascending development and phenol : water : concentrated ammonium hydroxide (800:200:1) for descending development and detected with ninhydrin.

Experimental

All melting points (uncorrected) were taken in open capillary tubes in a Thomas–Hoover melting point apparatus. The i.r. spectra were determined with a Beckman IR-5 or IR-9 recording spectrophotometer and the u.v. spectra with a Carey 14 spectrophotometer. The n.m.r. spectra were obtained with either a Varian A-60A, Varian HA-100, or a Jeolco C-60H spectrometer using tetramethylsilane as internal standard.

4-Amino-3-methylthiophenol (2)

To a stirred solution of 3-methylthio-4-nitrophenol (**1**) (27 g, 0.146 mol) in 10% NaOH (250 ml) at 60°, sodium hydrosulfite (75 g, 0.430 mol) was cautiously added. The mixture was stirred and heated at 95° for 40 min, allowed to cool to room temperature, and the crystalline precipitate collected to give 20 g (88%) of **2**, m.p. 145–148°. An analytical sample prepared from ethyl acetate exhibited: m.p. 148–150°; i.r. (KBr) 3330, 3300 (NH_2), 2780–2570 cm^{-1} (associated OH of phenol); n.m.r. (DMSO-d_6) δ 2.31 (s, 3, CH_3), 4.40 (br. s, 2, NH_2), 6.66 (br. s, 1, H_2), 6.53 (br. s, 2, $H_{5,6}$), 8.50 (s, 1, OH).

Anal. Calcd. for C_7H_9NOS: C, 54.17; H, 5.84. Found: C, 54.25; H, 5.55.

4-Acetoxy-2-methylthioacetanilide (3)

A mixture of the substituted aniline **2** (15 g, 0.0965 mol), *p*-toluenesulfonic acid (15 g), and acetic anhydride (200 ml), was stirred overnight at room temperature. The excess acetic anhydride was distilled under reduced pressure and the residue partitioned between water and ethyl acetate. The organic phase was washed successively with water, two 100-ml portions of 1% NaOH, 0.1 *N* HCl, and evaporated under reduced pressure. The crystalline residue of **3** weighed 15.5 g (67%) and melted at 103–106°. An aliquot prepared from ether exhibited: m.p. 100–102°; i.r. ($CHCl_3$) 3380 (NH), 1760 (phenolic ester), 1685, 1510 cm^{-1} (amide); n.m.r. ($CDCl_3$) δ 2.20, 2.30, 2.40 (s, 9, 3 CH_3), 7.00 (d of d), 7.20 (d), 8.30 (d) (ABX, 3, J_{AB} meta 2.5, J_{AX} ortho 7 Hz, aromatic), 8.05 (br. s, 1, NH).

Anal. Calcd. for $C_{11}H_{13}NO_3S$: C, 55.21; H, 5.47. Found: C, 55.17; H, 5.65.

4-Hydroxy-2-methylthioacetanilide (4)

To a solution of the acetanilide **3** (2 g, 84 mmol) in methylene chloride (100 ml) at −78° was slowly added with stirring a methylene chloride solution (21 ml) containing boron trichloride (10 mmol). The mixture was allowed to stir 4 h at room temperature, methanol (4 ml) added dropwise, washed with water and 1 *N* hydrochloric acid, and extracted with 2% sodium hydroxide. Neutralization of the alkaline solution with dilute hydrochloric acid precipitated 1.1 g (67%) of crystalline **4**, m.p. 147–149°. A sample crystallized from acetone gave: m.p. 148–149°; i.r. (KBr) 3230 (OH + NH), 1626, 1520 cm^{-1} (amide); n.m.r. (DMSO-d_6) δ 1.95, 2.32 (s, 6, 2 CH_3), 6.61 (d of d), 6.48 (d), 6.98 (d) (ABX, 3, J_{AB} meta 2.5, J_{AX} ortho 7 Hz, aromatic), 8.95, 9.33 (s, 2, NH + OH); mass spectrum (70 eV) *m/e* (relative intensity) 197 (75–100), 155 (88–97), 140 (94–100).

Anal. Calcd. for $C_9H_{11}NO_2S$: C, 54.80; H, 5.67. Found: C, 54.94; H, 5.85.

4-Nitrobenzene-2-diazo-1-oxide (6)

To a stirred suspension of 20 g (0.130 mol) of 2-amino-4-nitrophenol (**5**) (20 g, 0.13 mol) in 48% fluoboric acid (50 mol), maintained at 4°, a cold solution of sodium nitrite (9 g, 0.13 mol) in water (18 ml) was added dropwise. The mixture was stirred for 30 min at room temperature, the solid collected, washed once with cold fluoboric acid solution (10 ml), then with two 15-ml portions of cold water, and sucked dry. The solids were suspended in acetone (200 ml), collected, and dried under P_2O_5 to yield 15 g (70%) of **6**, m.p. 120° (with violent decomposition[3]). A sample recrystallized from water and acetone had m.p. 120°; u.v. max (2-propanol) 238 (ε 11 620), 259 (12 610), 324 (11 350), 400 (6650), 490–500 nm (1000) (sh); n.m.r. (MeOD + DCl) δ 7.22 (d, 1, *J* ortho 10 Hz, aromatic), 8.60 (d of d, 1, *J* meta 3, *J* ortho 10 Hz, aromatic), 9.27 (d, 1, *J* meta 3 Hz, aromatic).

Anal. Calcd. for $C_6H_3N_3O_3$: C, 43.63; H, 1.83; N, 25.45. Found: C, 43.62; H, 1.68; N, 25.45.

4-Hydroxy-3-methylthionitrobenzene (7)

To a vigorously stirred mixture of sodium hydroxide (20 g), copper powder (3 g), and methanethiol (25 g, 0.52 mol) in water (70 ml) was added slowly[6] at about 4° a suspension of the diazo-oxide **6** (15 g, 0.091 mol) in ice water (60 g). The reaction mixture was stirred at room temperature for 1 h, filtered, and the cake washed with 5% sodium hydroxide (50 ml). The combined filtered material was acidified to p*H* 5 with 6 *N* hydrochloric acid and the resulting precipitate was filtered, washed with water, and purified by means of semi-dry column chromatography (5) as follows.

[6]Ether was added as necessary to control the foaming.

Can. J. Chem. Downloaded from www.nrcresearchpress.com by 210.87.254.6 on 09/05/12
For personal use only.

Can. J. Chem. Downloaded from www.nrcresearchpress.com by 210.87.254.6 on 09/05/12
For personal use only.

The solids were dissolved in ethyl acetate (100 ml), 35 g of chromatographic grade silica gel (0.05–0.02 mesh) deactivated with 8% of water was added and the mixture evaporated to dryness. The residue was deposited on top of a column (20 × 3 in.) packed with 300 g of the deactivated silica gel, followed by the addition of a 1:1 mixture of ethyl acetate and benzene (70 ml). The column was eluted with benzene (200 ml) and the eluate evaporated to give 7 g (42%) of **7** of m.p. 58–62°. An analytical sample prepared from petroleum ether showed: m.p. 64–65°;[7] i.r. (KBr) 3330 (bonded OH of phenol), 1510, 1335 cm^{-1} (NO_2); n.m.r. ($CDCl_3$) δ 2.44 (s, 3, CH_3), 8.43 (d), 8.16 (d of d), 7.09 (d) (ABX, 3, J_{AB} meta 2.5, J_{BX} ortho 9 Hz, aromatic), 7.30 (s, 1, OH).

Anal. Calcd. for $C_7H_7NO_3S$: C, 45.38; H, 3.81. Found: C, 45.63; H, 4.13.

*4-Hydroxy-3-methylthioaniline (**9**)*

(a) Preparation from 7

A stirred solution of 35 g (0.190 mol) of the thioether **7** (35 g, 0.19 mol) in 10% sodium hydroxide (200 ml) was heated to 45–50° and sodium hydrosulfite (76 g, 0.44 mol) was added cautiously in two portions. The mixture was heated on a steam bath for 25 min and allowed to cool to room temperature. The crystals were filtered, washed with water, and dried in a vacuum oven at 60° to give 22 g (75%) of **9**, m.p. 170–175°. An analytical sample prepared from ethyl acetate exhibited: m.p. 190–192°; i.r. (KBr) 3356, 3300 (NH_2), 2500 cm^{-1} (associated phenolic OH); n.m.r. (DMSO-d_6) δ 2.28 (s, 3, CH_3), 4.28 (br, 2, NH_2), 6.42, (d of d), 6.25 (d), 6.53 (d) (ABX, 3, J_{AB} meta 2.5, J_{AX} ortho 8 Hz, aromatic), 8.40 (br. s, 1, OH).

Anal. Calcd. for C_7H_9NOS: C, 54.17; H, 5.84; N, 9.03. Found: C, 54.51; H, 5.92; N, 8.93.

(b) Preparation from 8

To a stirred mixture of 2-(methylmercapto)phenol (**8**) (20 g, 0.14 mol) and sodium hydroxide (32 g) in water (210 ml) was added at 7–12° a diazonium salt suspension prepared by diazotization (6) of sulfanilic acid (41 g, 0.21 mol). The stirred mixture was allowed to warm to room temperature, heated to 45–50° and sodium hydrosulfite (130 g, 0.74 mol) was added in two portions. The mixture was stirred and heated on a steam bath for 45 min, allowed to cool to room temperature, and the resulting crystalline precipitate collected and recrystallized from ethyl acetate to give 16.4 g (74%) of **9**, identical in mixed m.p. and n.m.r. with **9** obtained from **7**.

*4-Acetoxy-3-methylthioacetanilide (**10**)*

A mixture of 4-hydroxy-3-methylthioaniline (**9**) (15.5 g, 0.1 mol), *p*-toluenesulfonic acid (15.5 g), and acetic anhydride (200 ml) was stirred at room temperature overnight. The excess acetic anhydride was distilled under reduced pressure and the residue partitioned between water and ethyl acetate. The organic phase was washed with water, with two 75-ml portions of 1% sodium hydroxide (this alkaline solution contained **11**), and with water until neutral p*H*. The ethyl acetate solution was dried (Na_2SO_4), the solvent evaporated, and the residue crystallized from ethyl acetate to give 14.4 g (58%) of **10**: m.p. 146–147°; i.r. (KBr) 3280 (NH), 1765 (ester CO), 1653, 1550 (amide), 1212, 1180 cm^{-1} (C—O—C of ester).

[7]Dimorphic; another crystalline form exhibited m.p. 93–94°.

Anal. Calcd. for $C_{11}H_{13}NO_3S$: C, 55.21; H, 5.47. Found: C, 55.53; H, 5.54.

*4-Hydroxy-3-methylthioacetanilide (**11**)*

(a) Preparation from 9

The alkaline phase from the preparation of **10** was neutralized with dilute hydrochloric acid and the resulting crystals, recrystallized from ethyl acetate, gave 2.8 g (14%) of **11**: m.p. 130–131°; i.r. ($CHCl_3$) 3230 (OH, NH) 2400 (associated OH of phenol), 1690, 1570 cm^{-1} (amide); u.v. max (2-propanol) 234 (ε 19 850), 301 nm (4450); u.v. max (0.1 *N* HCl) 227 (ε 18 650), 294 nm (3750); u.v. (0.1 *N* KOH) 222 (ε 19 730), 265 (9320); 309 nm (6400); n.m.r. ($CDCl_3$) δ 2.16 (s, 3, CH_3CO), 2.32 (s, 3, CH_3S), 7.22 (d of d), 6.93 (d), 7.67 (d) (AMX, 3, J_{AM} ortho 8, J_{AX} meta 2.5 Hz, aromatic); mass spectrum (70 eV) *m/e* (relative intensity) 197 (100), 155 (70–90), 140 (67–92).

Anal. Calcd. for $C_9H_{11}NO_2S$: C, 54.88; H, 5.62. Found: C, 54.89; H, 5.50.

(b) Preparation from 10

A suspension of the acetanilide **10** (6 g, 0.025 ml) in 2.5% sodium hydroxide (100 ml) was stirred at 50° for 30 min, cooled, and extracted with two 75-ml portions of ethyl acetate. The aqueous layer was acidified to p*H* 5 with dilute hydrochloric acid, re-extracted with two 100-ml portions of ethyl acetate, dried (Na_2SO_4), and the extracts evaporated. The residue was crystallized from ethyl acetate to give 3.0 g (61%) of **11**, m.p. 129–131°; identical in mixed m.p. with **11** obtained from **9**.

*Bis(2-hydroxy-5-nitrophenol)disulfide (**12**)*

To a vigorously stirred solution, maintained at 0–10°, of sodium polysulfide (prepared by dissolving a mixture of sodium sulfide monohydrate (130 g, 1.35 mol) and sulfur powder (17 g, 0.53 mol) in 40% sodium hydroxide (50 ml) and water (140 ml) and heating on a steam bath) was added portionwise over 45 min a suspension of the diazo-oxide **6** (55.9 g, 0.39 mol) in ice water (150 ml). The resulting solution was allowed to warm to room temperature and stirred overnight. The reaction mixture was cooled, acidified with concentrated hydrochloric acid, ethyl acetate (600 ml) added, stirred for 45 min, and the amorphous solids filtered. The organic extract was concentrated to about 350 ml and stirred overnight with a solution of sodium carbonate (53 g, 0.5 mol) in water (200 ml). The precipitate was filtered, washed with two 100-ml portions of ethyl acetate, and dried (Na_2SO_4) to give 90 g (68.5%) of **12** as the disodium salt which was used for the next step. An aliquot was acidified with 1 *N* hydrochloric acid, extracted with ethyl acetate, and the extracts evaporated. The residue was crystallized from ethyl acetate to give yellow crystals of **12**: m.p. 174–176°; i.r. (KBr) 3375 (OH), 1602, 1474 (aromatic), 1510, 1330 cm^{-1} (NO_2); n.m.r. (MeOD) δ 6.93 (d), 8.00 (d of d), 8.36 (d) (AMX, 3, J_{AM} meta 2.5, J_{MX} ortho 9 Hz, aromatic).

Anal. Calcd. for $C_{12}H_8N_2O_6S_2$: C, 42.35; H, 2.37; N, 8.23; S, 18.84. Found: C, 42.67; H, 2.70; N, 8.00; S, 18.86.

*Bis(2-benzyloxy-5-nitrophenyl)disulfide (**13**)*

A mixture of the crude disodium salt of **12** (60 g, 0.155 mol), sodium carbonate (40 g, 0.38 mol), and benzyl chloride (60 g, 0.48 mol) in ethanol (600 ml) was stirred and refluxed for 24 h. The yellow crystals were filtered, washed with cold ethanol (35 ml), and then with water until the washings were neutral to litmus paper and dried to give

60 g (74.4%) of **13**, m.p. 172–174°. An analytical sample prepared from ethyl acetate exhibited: m.p. 176–177°; u.v. max (2-propanol) 207 (ε 42 400), 225 (21 500) (infl), 258 (21 800), 293 (18 350), 330 nm (10 800) (sh); i.r. (KBr) 1596, 1474 (aromatics), 1510, 1335 (NO_2), 1270 cm^{-1} (C—O—C).

Anal. Calcd. for $C_{26}H_{20}N_2O_6S_2$: C, 59.99; H, 3.87; N, 5.38; S, 12.32. Found: C, 60.12; H, 3.89; N, 5.32; S, 12.43.

α-Benzyloxycarbonylamino-β-chloropropionic Acid Methyl Ester (15)

To a vigorously stirred mixture of 3-chloroalanine methyl ester hydrochloride (30 g, 0.173 mol), ethyl acetate (300 ml), and saturated sodium bicarbonate solution (100 ml) was added benzyl chloroformate (60 g, 0.35 mol). The mixture was maintained at 5° and rendered slightly alkaline by the addition of saturated sodium bicarbonate as needed. The mixture was stirred at room temperature for 2 h, cooled to 5°, and a solution of piperidine (25 g, 0.29 mol) in water (50 ml) was added dropwise. The reaction was allowed to warm to room temperature, the organic phase separated, washed with two 75-ml portions of 3 *N* hydrochloric acid, then with water, dried (Na_2SO_4), and evaporated under reduced pressure. The oily residue was crystallized from petroleum ether to give 35 g (75%) of **15**, m.p. 51–52°. An analytical sample prepared from petroleum ether gave: m.p. 51–52°; i.r. (KBr) 3445 (NH), 1760 (ester CO), 1730 (urethane), 1520 cm^{-1} (amide).

Anal. Calcd. for $C_{12}H_{14}ClNO_4$: C, 53.05; H, 5.19; Cl, 13.05. Found: C, 53.04; H, 5.14; Cl, 13.15.

rac-3-[(5-Acetamido-2-benzyloxyphenyl)thio]-N-benzyloxycarbonylalanine Methyl Ester (16)

A mixture of the di-*O*-benzyl derivative **13** (14 g, 0.027 mol), glacial acetic acid (200 ml), and iron powder (30 g) was stirred and refluxed for 3 h, cooled to 60°, and filtered through a thin pad of Hyflo. The cake was washed with acetic acid (50 ml) and the combined filtrates were evaporated under reduced pressure. The residue was partitioned between ethyl acetate (120 ml) and 2% hydrochloric acid (50 ml) and the organic extract washed with water (30 ml), dried (Na_2SO_4), decanted and redried (anhydrous $CaSO_4$). To the ethyl acetate solution in a nitrogen atmosphere, the methyl ester **15** (15 g, 0.055 mol) was added. The mixture was stirred and slowly heated to reflux under N_2 while maintaining the p*H* between 7 and 8 by addition of a solution of 17% of sodium methoxide in methanol as needed. After stirring and refluxing for a total of 6 h, the mixture was allowed to stand overnight at room temperature. The resulting crystals were filtered, washed with water, and dried to give 12 g of **16**, m.p. 133–135°. The organic filtrate was extracted with two 100 ml portions of sodium carbonate solution and the aqueous extract acidified to precipitate 2.4 g (9%) of **17**, m.p. 188–192°. The spent ethyl acetate solution was evaporated under reduced pressure and the residue crystallized from ethyl acetate to give an additional 3 g (total 52.1%) of crude **16**, m.p. 132–134°. An analytical sample of **16** prepared from ethyl acetate exhibited: m.p. 141–142°; i.r. (KBr) 3300, 3280 (NH), 1730 (ester), 1717 (urethane), 1650, 1530 cm^{-1} (amide); n.m.r. (DMSO-d_6) δ 2.03 (s, 3, CH_3CO), 3.67 (s, 3, CH_3O), 4.22 (m, 1, CH), 5.06, 5.16 (s, 4, 2 CH_2O), 6.90–7.70 (m, 13, aromatic), 9.84 (s, 1, NH).

Anal. Calcd. for $C_{27}H_{28}N_2O_6S$: C, 63.76; H, 5.55; N, 5.51. Found: C, 63.62; H, 5.57; N, 5.46.

rac-3-[(5-Acetamido-2-benzyloxyphenyl)thio]-N-benzyloxycarbonylalanine (17)

A mixture of rac-3-[5-acetamido-2-benzyloxyphenyl)-thio]-*N*-benzyloxycarbonylalanine methyl ester (**16**) (5 g, 0.01 mol), 5% sodium hydroxide (100 ml) was heated on a steam bath for 20 min, Norit added, and the solution filtered hot through a thin pad of Hyflo. The cake was washed with 5% sodium hydroxide (20 ml) and the combined filtrates neutralized with 1 *N* hydrochloric acid. The mixture was allowed to stand for 4 h, the precipitate filtered, washed with water, and dried to give 3.46 g (70%) of **17**, m.p. 188–190°. An analytical sample prepared from ethyl acetate exhibited: m.p. 198–200°; i.r. (KBr) 3320 (NH, OH), 2700–2600 (acid OH), 1730–1705 (acid CO), 1670, 1550 cm^{-1} (amide); n.m.r. (DMSO-d_6) δ 2.03 (s, 3, CH_3CO), 3.28 (d, 2, $J = 6$ Hz, CH_2S), 4.12 (m, 1, CH), 5.04, 5.14 (s, 4, $2CH_2O$), 6.90–7.70 (m, 13, aromatic), 9.78 (s, 1, NH).

Anal. Calcd. for $C_{26}H_{26}N_2O_6S$: C, 63.14; H, 5.30; N, 5.66. Found: C, 63.36; H, 5.37; N, 5.67.

rac-3-[(5-Acetamido-2-hydroxyphenyl)thio]alanine (18)

A mixture of the acid **17** (4 g, 0.008 mol), trifluoroacetic acid (100 ml), and boron trifluoride etherate (12 drops) was stirred at reflux under N_2 for 4 h and then at room temperature overnight. The solvent was evaporated under reduced pressure, the oily residue dried by azeotropic distillation with benzene, the semi-solid residue was suspended in warm ethyl acetate (20 ml), and the mixture stored at room temperature for 2 h. The supernatant solution was decanted, and the residue crystallized from a mixture of methanol (20 ml) and benzene (50 ml) to give 0.78 g of **18**, m.p. 184–186° dec. From the mother liquor, a second crop of 0.25 g, m.p. 178–182° (dec.) (total 47%) was obtained. An analytical sample prepared from a mixture of water and ethanol exhibited: m.p. 192–193°; u.v. max (0.1 *N* KOH) 268 (ε 9580), 312 nm (6200); i.r. (KBr) 3200 (OH, NH), 3070–2600 (NH_3^+), 1650 (amide), 1610 (COO^-), 1500 (amide), 1410 cm^{-1} (COO^-); n.m.r. (DMSO-d_6) δ 1.99 (s, 3, CH_3CO), 2.80–3.40 (m, 2, CH_2), 6.82, (d), 7.35 (d of d), 7.59 (d) (AMX, 3, J_{AM} ortho 8.5, J_{MX} meta 2.5 Hz, aromatic), 9.84 (s, 1, NH); mass spectrum, thermal decomposition.

Anal. Calcd. for $C_{11}H_{14}N_2O_4S$: C, 48.88; H, 5.22; N, 10.36; S, 11.86. Found: C, 48.55; H, 5.08; N, 10.11; S, 11.67.

We are indebted to our Physical Chemistry Department for the analytical and spectral data. We are particularly grateful to Dr. F. Vane and Mr. R. Pitcher for the mass spectral and n.m.r. comparisons.

1. A. KLUTCH, R. CHANG, W. LEVIN, and A. H. CONNEY. To be published. For other phenacetin metabolites, see B. B. BRODIE and J. AXELROD. J. Pharmacol. **97**, 58 (1949).
2. H. PELSTER and R. EEISS. Fr. Pat. 1 377 649. Chem. Abstr. **62**, 10376*h* (1965).
3. J. VAUGHAN and L. PHILLIPS. J. Chem. Soc. 1560 (1947).
4. O. R. JAGENBURG and K. TOCZKO. Biochem. J. **92**, 639 (1964).
5. B. LOEV and R. M. SNODER. Chem. and Ind. 15 (1965).
6. Org. Syn. Coll. Vol. II. John Wiley and Sons. New York, N.Y. p. 35.

Can. J. Chem. Downloaded from www.nrcresearchpress.com by 210.87.254.6 on 09/05/12
For personal use only.

Dielectric Relaxation of Bromoalkanes in Cyclohexane Solution

SING PIN TAY AND JOHN CROSSLEY
Department of Chemistry, Lakehead University, Thunder Bay, Ontario
Received February 7, 1972

Mean relaxation times, Cole–Cole distribution parameters and apparent dipole moments, obtained from dielectric constant and loss measurements at 2 MHz and 1.5, 2.0, 2.5, 9.3, 16, 24, 35, 70, and 145 GHz, are reported for 1-, 2-, and 4-bromooctane, 1-bromodecane, 1-bromododecane, 1-bromohexadecane, 1-bromooctadecane, and 1,10-dibromodecane in cyclohexane solution at 25 °C.

Les temps de relaxation moyens, les paramètres de distribution de Cole–Cole et les moments dipolaires apparents, obtenus à partir des constantes diélectriques et des mesures de perte à 2 MHz et 1.5, 2.0, 2.5, 9.3, 16, 35, 70 et 145 GHz sont rapportés pour les bromooctanes 1, 2, et 4, le bromo-1 décane, le bromo-1 dodécane, le bromo-1 hexadécane, le bromo-1 octadécane et le dibromo-1,10 décane en solution dans le cyclohexane à 25 °C.
Canadian Journal of Chemistry, **50**, 2031 (1972)

Introduction

Dipole reorientation by the intramolecular rotation of polar groups has been extensively investigated for substituted benzenes and naphthalenes (1). Aliphatic molecules are far more flexible, intramolecular rotation may occur about many bonds and involve molecular segments of different size, and their dielectric behavior has not been studied in such great detail. This paper presents results which form part of a systematic investigation of the dielectric relaxation of aliphatic compounds in solution. Our initial studies (2, 3) revealed that dipole reorientation in 1-aminoalkanes ($R—NH_2$) and 2-alkanones ($R—COCH_3$) occurs primarily by the intramolecular rotation of the polar end group. Rotational orientation of the whole molecule makes a significant contribution to the absorption of secondary and tertiary amines, but only becomes evident for relatively long ketones in which the carbonyl group is well removed from the chain end. The results indicate that whole molecule rotation only makes a significant contribution to the dispersion of ketones and amines when the intramolecular process is sterically restricted.

The interpretation of the comparatively large amount of dielectric absorption data for pure liquid haloalkanes has been complicated by the viscosity, internal field and molecular interaction effects and some conflict has arisen regarding the nature of their distribution function (4–12). The former problems may be largely eliminated in dilute solution but little data has been available. In *n*-heptane solution the dielectric absorption of 1-bromooctane has been satisfactorily represented by a symmetrical distribution function (13). However, the absorptions, at only three microwave frequencies, of some α,ω-dibromoalkanes in dilute solution have been represented by a skewed arc function and discussed in terms of a superposition of two Debye-type dispersions (14).

The present study examines the dielectric relaxation of eight alkylbromides in cyclohexane solution. As before (2, 3), the position of the polar group and the length of the hydrocarbon chain are varied.

Experimental

The apparatus and procedure used to determine dielectric constants (ε') and dielectric losses (ε'') at 1–2.5 (15), 9–35 (16), and 70–145 GHz (17) have been described previously. Refractive index measurements at the sodium D-line were made with an Abbe refractometer. Static dielectric constants (ε_0) were measured at 2 MHz using a WTW Dipolmeter.

Results

The experimental $\varepsilon'(\pm 0.5\%)$ and $\varepsilon''(\pm 5.0\%)$ values measured at 25 °C are given in Table 1. For all the systems it is possible, within experimental error, to draw smooth depressed center semicircular arcs through the experimental points, when plotted in the complex plane. The data for each system were analyzed for a most probable relaxation time (τ_0), Cole–Cole distribution parameter (α), and very high frequency dielectric constant (ε_∞) using a computer fit to the Cole–Cole equations (18). Apparent dipole

Can. J. Chem. Downloaded from www.nrcresearchpress.com by 210.87.254.5 on 09/05/12
For personal use only.

Can. J. Chem. Downloaded from www.nrcresearchpress.com by 210.87.254.5 on 09/05/12
For personal use only.

TABLE 1. Dielectric constants and losses for bromoalkanes at mole fraction f_2 in cyclohexane at 25 °C

Frequency (GHz)	1-Bromooctane $f_2 = 0.0780$		2-Bromooctane $f_2 = 0.0697$		4-Bromooctane $f_2 = 0.0700$		1-Bromodecane $f_2 = 0.0703$	
	ε'	ε''	ε'	ε''	ε'	ε''	ε'	ε''
145	2.06	0.031	2.05	0.038	2.05	0.034	2.06	0.027
70.6	2.07	0.050	2.06	0.054	2.06	0.048	2.07	0.035
35.1	2.09	0.066	2.09	0.085	2.07	0.075	2.08	0.054
24.0	2.11	0.081	2.12	0.107	2.10	0.100	2.10	0.071
16.2	2.13	0.089	2.16	0.128	2.13	0.127	2.12	0.082
9.32	2.16	0.089	2.21	0.126	2.19	0.143	2.16	0.089
2.45	2.26	0.073	2.32	0.072	2.33	0.076	2.24	0.067
1.95	2.26	0.070	2.33	0.061	2.34	0.060	2.25	0.062
1.45	2.28	0.057	—	—	—	—	2.26	0.060
0.002	2.299	—	2.337	—	2.338	—	2.293	—

Frequency (GHz)	1-Bromododecane $f_2 = 0.0698$		1-Bromohexadecane $f_2 = 0.0698$		1-Bromooctadecane $f_2 = 0.0701$		1,10-Dibromodecane $f_2 = 0.0700$	
	ε'	ε''	ε'	ε''	ε'	ε''	ε'	ε''
145	2.06	0.023	2.07	0.023	2.07	0.021	2.10	0.050
70.6	2.06	0.032	2.07	0.032	2.07	0.030	2.12	0.080
35.1	2.08	0.046	2.09	0.046	2.08	0.040	2.14	0.101
24.0	2.09	0.058	2.10	0.058	2.10	0.052	2.18	0.128
16.2	2.11	0.073	2.11	0.071	2.10	0.064	2.21	0.163
9.32	2.14	0.082	2.14	0.082	2.13	0.077	2.30	0.189
2.45	2.22	0.063	2.23	0.067	2.23	0.061	2.49	0.116
1.95	2.23	0.057	2.24	0.064	—	—	2.50	0.100
1.45	2.24	0.055	2.25	0.058	2.24	0.055	2.52	0.085
0.002	2.279	—	2.296	—	2.280	—	2.527	—

TABLE 2. Mean relaxation time τ_0 (ps), distribution parameter α square of refractive index n_D^2, and apparent dipole moment μ (in D units) data for some bromoalkanes at mol fraction f_2 in cyclohexane solution at 25 °C

Solute	f_2	τ_0	α	μ	ε_∞	n_D^2
1-Bromooctane	0.0707	16	0.24	1.96	2.027	2.034
2-Bromooctane	0.0697	14	0.11	2.08	2.033	2.034
4-Bromooctane	0.0700	16	0.04	2.06	2.038	2.032
1-Bromodecane	0.0703	20	0.21	1.92	2.040	2.036
1-Bromododecane	0.0698	23	0.21	1.86	2.046	2.039
1-Bromohexadecane	0.0698	26	0.24	1.95	2.051	2.046
1-Bromooctadecane	0.0701	27	0.22	1.87	2.057	2.048
1,10-Dibromodecane	0.0700	19	0.08	2.68	2.093	2.051

moments (μ) were calculated from

$$[1] \qquad \mu^2 = \frac{9kT}{4\pi N} \frac{(\varepsilon_0 - \varepsilon_\infty)(2\varepsilon_0 + \varepsilon_\infty)}{\varepsilon_0(\varepsilon_\infty + 2)^2}$$

in which N is the number of solute molecules per ml of solution.

Table 2 lists the values of τ_0, μ, ε_∞, and n_D^2 for each of the alkylbromides at mol fraction f_2 in cyclohexane solution at 25 °C.

Discussion

Figure 1, which is typical of all the systems, shows that the experimental dielectric constant and loss data are adequately described by a Cole–Cole symmetrical distribution function. There is no evidence of the skewed arc behavior which has been reported for pure liquid haloalkanes (11) and dibromoalkanes in solution (13). Furthermore, the ε_∞ and n_D^2 values, Table 2,

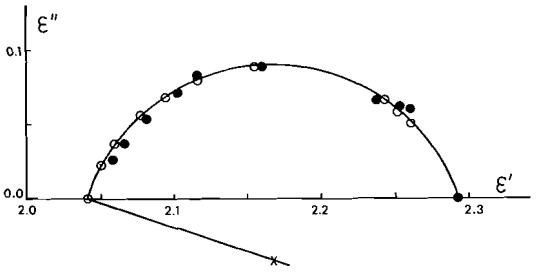

FIG. 1. Cole–Cole plot for 1-bromodecane in cyclohexane at 25 °C. Solid circles represent experimental points and the hollow circles represent points calculated from the parameters given in Table 2.

are similar and the apparent dipole moments compare favorably with those obtained by classical methods (19). We were unable to obtain any sensible analyses of the data in terms of two discrete relaxation times.

The τ_0 values in Table 2 are considerably longer than those for analogous amines and ketones which, under the same conditions, have values of about 3 and 7×10^{-12} s, respectively, almost independent of the size of the alkyl group (2, 3). These results suggest that polar end group rotation is not as dominant a mechanism of dipole reorientation for bromoalkanes as it is for primary amines and 2-alkanones. However, the mean relaxation times in Table 2 only lengthen slightly with increased molecular size and the contribution from intramolecular rotation, especially for the larger molecules, is not negligible. Potential barriers to rotation of the polar group in CH_3—NH_2, CH_3—$COCH_3$, and CH_3—CH_2Br of 1.94, 0.78, and 3.57 kcal mol^{-1}, respectively, have been reported (20). The values for the amine and ketone are considerably smaller than the barrier height in saturated aliphatic hydrocarbons, about 3 kcal mol^{-1}, and rotation of the polar end group in 1-amino alkanes and 2-alkanones should be faster than any segmental rotations within their hydrocarbon chain. Consequently, dipole reorientation by intramolecular rotation will be dominated by the former process with little or no contribution from longer segments. Conversely, rotation of the terminal CH_2Br group may be slightly slower than segmental rotations for alkylbromides, and dipole reorientation about the long axis of these molecules is likely to involve a variety of segments which contain the CH_2Br group. The dielectric absorption of the pure liquids has been considered in these terms (7). The relaxation times of the pure liquids are longer, and lengthen much more markedly with increased molecular size, than those for the dilute solutions. This is probably due to differences in viscosity; curves for macroscopic viscosity and τ_0, for the pure liquids, plotted against the number of carbon atoms are very similar (4). The viscosities of all the systems under investigation are essentially the same, *i.e.*, the viscosity of cyclohexane at 25 °C.

It is interesting to observe that the relaxation times for 1,10-dibromodecane and 1-bromodecane are almost the same. Furthermore, the location of the dipole has little effect on the relaxation times for bromooctanes, which is also the case for the nonanones and nonylamines. However, the α values for 1,10-dibromodecane and 2- and 4-bromooctane are significantly smaller than those for the 1-bromoalkanes. This may be due to a reduction in the number of molecular segments of different length which have a terminal CH_2Br group. The α values for the 1-bromoalkanes do not display any significant increase with increased chain length, and the relaxation times for the C_{16} and C_{18} bromides are essentially the same. These results suggest that intramolecular reorientation is dominated by the smaller segments. In addition, increased coiling will occur with increased chain length and the molecular relaxation time may not lengthen appreciably with increased molecular size for the longer molecules.

1. C. P. SMYTH. Adv. Mol. Relaxation Processes. **1**, 1 (1967–68).
2. S. P. TAY and J. CROSSLEY. J. Chem. Phys. **56**, 4303 (1972).
3. J. CROSSLEY. J. Chem. Phys. **56**, 2549 (1972).
4. W. M. HESTON, JR., E. J. HENNELLY, and C. P. SMYTH. J. Am. Chem. Soc. **70**, 4093 (1948), **70**, 4102 (1948).
5. H. L. LAQUER and C. P. SMYTH. J. Am. Chem. Soc. **70**, 4097 (1948).
6. F. H. BRANIN, JR., and C. P. SMYTH. J. Chem. Phys. **20**, 1121 (1952).
7. K. HIGASI, K. BERGMANN, and C. P. SMYTH. J. Phys. Chem. **64**, 880 (1960).
8. W. E. VAUGHAN, W. S. LOVELL, and C. P. SMYTH. J. Chem. Phys. **36**, 753 (1962).
9. D. J. DENNEY. J. Chem. Phys. **27**, 259 (1957).
10. S. H. GLARUM. J. Chem. Phys. **33**, 639 (1960).
11. F. I. MOPSIK and R. H. COLE. J. Chem. Phys. **44**, 1015 (1966).
12. S. CHANDRA and J. PRAKASH. J. Chem. Phys. **54**, 5366 (1971).

Can. J. Chem. Downloaded from www.nrcresearchpress.com by 210.87.254.5 on 09/05/12
For personal use only.

13. G. P. JOHARI, J. CROSSLEY, and C. P. SMYTH. J. Am. Chem. Soc. **91**, 5197 (1969).
14. S. CHANDRA and J. PRAKASH. J. Phys. Chem. **75**, 2616 (1971).
15. S. E. KEEFE and E. H. GRANT. Rev. Sci. Instrum. **39**, 1800 (1968).
16. W. F. HASSELL, M. D. MAGEE, S. W. TUCKER, and S. WALKER. Tetrahedron, **20**, 2137 (1964).
17. S. K. GARG, H. KILP, and C. P. SMYTH. J. Chem. Phys. **43**, 2341 (1965).
18. K. S. COLE and R. H. COLE. J. Chem. Phys. **9**, 341 (1941).
19. A. L. MCCLELLAN. Tables of experimental dipole moments. W. H. Freeman, U.S.A. 1963.
20. E. L. ELIEL. Stereochemistry of carbon compounds. McGraw-Hill. 1962.

Can. J. Chem. Downloaded from www.nrcresearchpress.com by 210.87.254.5 on 09/05/12
For personal use only.

An Investigation of Long-range Proton–Proton Coupling Constants in Phenylacetylene Derivatives

C. J. MACDONALD
Department of Chemistry, Brandon University, Brandon, Manitoba
AND
G. K. HAMER,[1] I. R. PEAT,[2,3] AND W. F. REYNOLDS
Department of Chemistry, University of Toronto, Toronto 5, Ontario

Received November 30, 1971

Signs and magnitudes of long-range coupling constants in three phenylacetylene derivatives have been determined. Values of the coupling constants are discussed in terms of the McConnell formulation and compared with results of MO–INDO–FPT calculations. Coupling constants are dominated by π contributions. Estimated values of hyperfine interaction constants for acetylene and methylacetylene groups are respectively $Q_{CC\equiv CH} = -12$ and $Q_{CC\equiv CCH} = +12$ G. The theoretical calculations are in excellent agreement with experimental results. Both approaches allow quantitative estimation of nine bond couplings in 4-vinylphenylacetylene.

Les signes et les amplitudes des constantes de couplage à longue distance de trois dérivés du phénylacétylène ont été déterminés. Les valeurs des constantes de couplage sont discutées en terme de la formulation de McConnell et comparées avec les résultats des calculs MO–INDO–FPT. Les constantes de couplage sont dominées par les contributions π. Les valeurs estimées des constantes d'interaction hyperfine pour les groupes acétylène et méthylacétylène sont respectivement $Q_{CC\equiv CH} = -12$ et $Q_{CC\equiv CCH} = +12$ G. Les calculs théoriques sont en excellent accord avec les résultats expérimentaux. Les deux approches permettent une estimation quantitative des couplages de neuf liaisons dans le vinyl-4 phénylacétylène.

Canadian Journal of Chemistry, **50**, 2035 (1972)

Introduction

The observed magnitudes and signs of long-range couplings between side chain protons and ring protons in styrenes (1) and benzaldehydes (2) are well predicted by theoretical computations using MO–INDO wave functions (3) and finite perturbation theory (MO–INDO–FPT) (4). McConnell's conceptually similar, but much simpler, MO formulation for alternate hydrocarbons (5) has been found to give good agreement with experiment for acenaphthenes (6), toluenes (7, 8), fluorobenzenes (9), pyridines (10), benzaldehydes (11), and xylenes (12). This latter method gives coupling constants in terms of mobile bond orders, mean excitation energies to triplet states, and proton hyperfine interaction constants. Its simplicity makes it attractive when considering more extended coupling paths. However, little data is available to test this extension. Experiments which yielded the signs and magnitudes of long-range coupling constants in the substituted phenylacetylenes **1**, **2**, and **3** are described below. The results are interpreted in terms of the McConnell formulation and are compared with MO–INDO–FPT calculations.

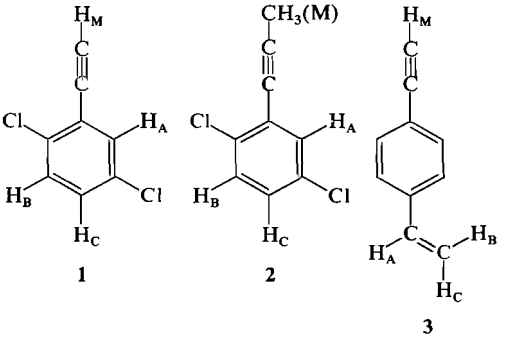

1 **2** **3**

Experimental

(a) Preparation of Compounds

(2,5-Dichlorophenyl)-acetylene

This compound was synthesized using the method of Drehfahl and Plotner (13). Bromination of the vinyl group of 2,5-dichlorostyrene yielded 1-(2,5-dichlorophenyl)-1,2-dibromoethane. Dehydrobromination using potassium hydroxide in *t*-butanol (13) gave crude (2,5-dichlorophenyl)-acetylene (**1**). Chromatography of the crude product on neutral alumina followed by vacuum sublimation gave **1** as

[1]NRCC Scholarship Holder, 1967–1970.
[2]NRCC Scholarship Holder, 1968–1971.
[3]Gulf Oil Fellowship Holder, 1971–1972.

Can. J. Chem. Downloaded from www.nrcresearchpress.com by 210.87.254.6 on 09/05/12
For personal use only.

Can. J. Chem. Downloaded from www.nrcresearchpress.com by 210.87.254.6 on 09/05/12
For personal use only.

white plates, m.p. 40 °C. The structure of **1** was confirmed by its characteristic n.m.r. spectrum. The latter showed a one proton singlet (at low resolution) at δ 3.25 in CCl_4 (δ 4.4 in C_5D_5N), characteristic of an acetylenic proton, and a three proton ABC spectrum in the phenyl region. Detailed analysis in C_5D_5N (see below) showed the presence of one ortho (8.68 Hz), one meta (2.58 Hz), and one para (0.37 Hz) ring proton coupling constant, confirming retention of the 1,2,5-trisubstitution pattern of the phenyl group. These three coupling constants are almost identical with those for the parent 2,5-dichlorostyrene (8.54, 2.53, and 0.34 Hz (1)). The structure was further confirmed by the magnitudes of the long-range coupling constants to the acetylenic proton which are nearly identical to those for phenylacetylene (14) (see below).

1-(2,5-Dichlorophenyl)-propyne

This compound was prepared using standard procedures (13, 15). Acylation of *p*-dichlorobenzene with $AlCl_3$/propionyl chloride gave 2,5-dichloropropiophenone. Reaction with PCl_5, followed by dehydrochlorination using potassium hydroxide in *t*-butanol gave 1-(2,5-dichlorophenyl)-propyne (**2**) and other products. Preparative t.l.c. followed by vacuum sublimation gave a small yield of pure **2** as white needles, m.p. 28–30 °C. The compound was characterized by its n.m.r. spectrum which showed a three proton singlet (at low resolution) at δ 2.0 due to the propyne methyl group and a three proton ABC multiplet in the phenyl region. The latter multiplet showed ortho (8.64 Hz), meta (2.59 Hz), and para (0.38 Hz) coupling constants. These are identical, within experimental error, to the values for **1** and confirm the 1,2,5-trisubstitution pattern of the phenyl group.

4-Vinylphenylacetylene

This compound was synthesized as one of a series of 4-substituted styrenes. Full details are provided elsewhere (16).

(b) Nuclear Magnetic Resonance Experiments

Ten mole percent solutions of **1** and **2** in pyridine-d_5 and a 5 mol % solution of **3** in acetone-d_6 (with 3 mol % TMS for lock and reference signal) were degassed by several freeze–pump–thaw cycles and sealed under vacuum in n.m.r. tubes. Pyridine-d_5 was chosen for **1** and **2** since it gave nearly first order spectra. Acetone-d_6 was used for **3** since it collapsed the AA′BB′ spectrum of the ring protons to a sharp singlet (line width $\approx$ 0.3 Hz), allowing complete decoupling of the ring protons at moderate power levels.

Single, double, and triple resonance spectra (frequency sweep, internal lock) were obtained using Varian HA-100 and HA-100D spectrometers and one or more Hewlett–Packard 4204A oscillators. Techniques used were identical to those previously reported (1, 12). Spectra were recorded at a sweep rate of 0.01 Hz/s and calibrated at <5 Hz intervals with a frequency counter. Line widths of non-degenerate peaks were 0.10–0.12 Hz. The ambient temperature was 30 ± 1 °C.

(c) CNDO/2 and MO–INDO–FPT Calculations

Calculations were performed on an IBM 360/65 computer, using the Quantum Chemistry Program Exchange program no. 141 and standard parameters (17). For the finite perturbation calculations, the program was modified to give a more rigorous convergence criterion (4). The modified program reproduced published results (4).

Results

Proton labelling schemes for **1**, **2**, and **3** have been shown above. They are labelled conventionally, in order of increasing field (decreasing frequency). Final parameters are shown in Table 1. The signs and magnitudes of the long-range coupling constants for **1** are in good agreement with previously reported results for phenylacetylene (14). In that report, signs were determined by analysis. We have confirmed the signs by double-irradiation experiments.

The relative signs of the long-range coupling constants in **1** and **2** were established relative to the known positive signs of intra-ring coupling constants in benzene derivatives (18) and in **3** relative to the known positive signs of the vinyl proton coupling constants in styrene (19). For **1**, the sign determinations involved observation of Overhauser effects caused by very weak "tickling" double irradiation (20, 11*a*),[4] showing $J_{AM}, J_{CM} > 0, J_{BM} < 0$. For **2**, double resonance experiments analogous to those used to determine signs in 2-bromo-5-chlorotoluene (21) were employed, showing $J_{AM}, J_{CM} < 0, J_{BM} > 0$. In **3**, triple irradiation was employed: strong irradiation to decouple the ring protons and very weak irradiation yielding Overhauser effects (20, 11*a*) or decoupling (12). These showed J_{BM}, $J_{CM} > 0$, with no information about J_{AM}. Slight broadening of the A peaks suggested $|J_{AM}| \approx 0.05$ Hz. A typical experiment for sign determination is shown in Fig. 1. Irradiation of peak B_1 (low field peak of the B octet) decreased C_1 and increased C_3 while irradiation of B_2 decreased C_2 and increased C_4. This experiment proved that J_{BM} and J_{CM} had the same sign. Figure 1 illustrates the usefulness of the Overhauser "tickling" technique for determination of signs of small couplings since B_1 and B_2 are separated by only 0.11 Hz.

Spectra were analyzed by the iterative computer programs LAOCN3 (22) and LAME (23), giving the parameters in Table 1. The only point worthy of note concerns **1**. Proton B gave sharp peaks with no observed coupling to M. (The line width at half height was $\approx$0.12 Hz, almost identical to that for known singlet peaks.) However, the iterative computer fit gave $J_{BM} = -0.07$ Hz. In calculations where J_{BM} was fixed

[4]A typical H_2 power level was 2 mV under load (measured on the oscilloscope).

Can. J. Chem. Downloaded from www.nrcresearchpress.com by 210.87.254.6 on 09/05/12
For personal use only.

TABLE 1. The n.m.r. parameters of 2,5-dichlorophenylacetylene (**1**), 1-(2,5-dichlorophenyl)-propyne (**2**), and 4-vinylphenylacetylene (**3**)*

Parameter	Compound 1	2	3
δA	7.549	7.455	6.744
δB	7.304	7.297	5.838
δC	7.226	7.170	5.290
δM	4.428	1.989	3.621
J_{AB}	+0.37	+0.38	+17.64
J_{AC}	+2.58	+2.59	+10.96
J_{BC}	+8.68	+8.64	+0.89
J_{AM}	+0.29 (+0.27)†	−0.30	<0.10‡
J_{BM}	−0.07 (−0.11)	+0.15	+0.11
J_{CM}	+0.33 (+0.24)	−0.26	+0.14
Program	LAOCN3	LAME	LAOCN3
No. of peaks fitted	32	52	32
Worst fit (Hz)	0.030	0.016	0.023
R.m.s. deviation (Hz)	0.011	0.007	0.009
Probable errors of parameters	0.006–0.011	—	0.003–0.004
Standard deviation of parameters	—	0.001–0.002	—

*Chemical shifts on δ scale, coupling constants in Hz (±0.03 Hz).
†Results from ref. 14.
‡Magnitude only.

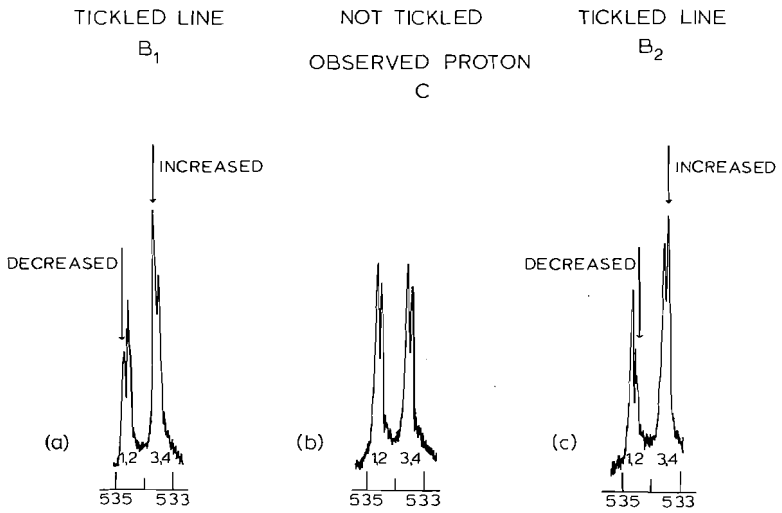

FIG. 1. Triple resonance Overhauser experiments used to determine relative signs of J_{BM} and J_{CM} in 4-vinylphenylacetylene. Ring protons are decoupled in all three spectra. (*a*) Lowfield quartet (C_1–C_4) of C proton octet with triple resonance frequency at B_1 (592.28 Hz); (*b*) C_1–C_4 without triple resonance; (*c*) C_1–C_4 with triple resonance frequency at B_2 (592.17 Hz).

at 0.00 Hz or +0.07 Hz, the fit between calculated and experimental spectra was significantly worse, particularly in the M proton region. The computed sign is consistent with the double resonance experiments and with previous results for phenylacetylene (14).

Results of MO–INDO–FPT calculations of long-range coupling constants are given in

TABLE 2. Long-range coupling constants (in Hz) obtained from MO–INDO–FPT calculations

Coupling constant*	Compound		
	Phenylacetylene	1-Phenylpropyne	4-Vinylphenylacetylene (3)
J_{AM}	+0.46	−0.38	−0.08
J_{BM}	−0.09	+0.27	+0.11
J_{CM}	+0.20	−0.26	+0.11

*Labelling of protons is identical to that previously given for 1, 2, and 3.

Table 2. For **1** and **2**, calculations were performed for the parent compounds, phenylacetylene and 1-phenylpropyne, for reasons of computational economy. For **1** and **2**, the perturbation was placed on the acetylenic proton. A repetition of the calculation for **1** with the perturbation on the four proton, C, gave a value of J_{CM} which differed by less than 0.001 Hz from the original value. For **2**, four calculations were performed for two conformations of the methyl group (see Fig. 2). The results in Table 2 are a weight average (allowing for the number of equivalent protons) of the four calculations.

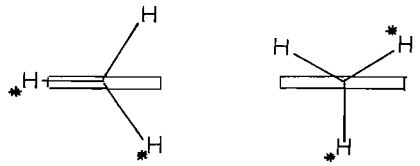

FIG. 2. Conformations of methyl group in 1-phenylpropyne for which MO–INDO–FPT calculations were performed. Protons on which pertubations were placed are marked with asterisks.

TABLE 3. Bond orders (CNDO/2 calculations) between carbon to which substituent is attached and carbon para to substituent

Compound	Bond order $\rho_{NN'}$
Toluene	−0.3266
p-Xylene	−0.3206
Styrene	−0.3193
Phenylacetylene	−0.3225
1-Phenylpropyne	−0.3212
4-Vinylphenylacetylene	−0.3089

Discussion

The McConnell relationship for calculation of π contributions to coupling constants in benzene is (5):

$$[1] \qquad J_{HH'} = \beta^2 \rho^2_{NN'} Q_{CH} Q_{CH'} / h\Delta E$$

where β = Bohr magneton, $\rho_{NN'}$ = mobile bond order between carbon atoms to which hydrogens are bonded, Q_{CH} is the proton hyperfine splitting constant, and ΔE is an average excitation energy to low-lying triplet states. This approach has been extended to several benzene derivatives (6–12). For example, for toluene, [1] may be written (6, 10)

$$[2] \qquad J_{H,CH_3} \propto Q_{CH} Q_{CCH}$$

where Q_{CCH} is the methyl hyperfine splitting constant.

If it is assumed that the same proportionality constant can be used for different compounds, then possible σ and π contributions to long-range coupling constants can be discussed in terms of equations of the same type as [2] (9–12). This assumption requires that $\rho^2_{NN'}/\Delta E$ must be constant for the compounds under investigation. Bond orders for a series of compounds which are relevant to this discussion have been estimated by CNDO/2 MO calculations (see Table 3). $\rho_{NN'}$ is nearly constant. The observation that J_{H,CH_3} values in toluene derivatives are nearly substituent independent (19, 21) suggests that the variation in $1/\Delta E$ must also be small. Therefore, it is reasonable to use the same proportionality constant for different compounds.

The McConnell relationship applies specifically to π electron contributions. For toluene, $J^{\pi}_{H,CH_3} = -0.6$ Hz (21, 24) while $Q_{CCH} = +25$ G (10). It has been shown that J^{π}_{H,CH_3} contains a negligible σ contribution (12). If it is assumed that J_{CM} for **1** also contains only π contributions, then $Q_{CC\equiv CH}/Q_{CCH} = J_{CM}/J^{\pi}_{H,CH_3}$. The average of J_{CM} from the two sets of experimental results is +0.28 Hz. Consequently, the estimated value of

Can. J. Chem. Downloaded from www.nrcresearchpress.com by 210.87.254.6 on 09/05/12
For personal use only.

Can. J. Chem. Downloaded from www.nrcresearchpress.com by 210.87.254.6 on 09/05/12
For personal use only.

$Q_{CC\equiv CH}$ is $(0.28 \times 25/(-0.6)) = -12$ G. This value can be checked by calculating the long-range coupling constants for **3**. The corresponding long-range coupling constants for the para proton to the vinyl group in styrene derivatives are $J^p_A = -0.24$, $J^p_B = +0.26$, and $J^p_C = +0.28$ Hz. Assuming $Q_{CH} = -23$ G (10), $Q_{CC\equiv CH}/Q_{CH} = 12/23$ and estimated coupling constants for **3** are $J_{AM} = -0.12$, $J_{BM} = +0.13$, and $J_{CM} = +0.14$ Hz. The magnitude of J_{AM} is slightly overestimated but J_{BM} and J_{CM} are in excellent agreement with the experimental values. This strongly suggests that the estimated value of $Q_{CC\equiv CH}$ is accurate and that J_{CM} for **1** is dominated by π effects. Consequently the acetylenic linkage appears to be about half as effective as a methyl group in transmitting spin information from a phenyl π electron system. It is almost equal in effectiveness to a vinyl group since in the latter case, the corresponding para to β hydrogen coupling constants (which are also dominated by π effects (1)) are identical in sign and magnitude to J_{CM} for **1** (see above).

Further information concerning π contributions to coupling constants can be obtained by the methyl group replacement technique (25). If a coupling constant to a proton is transmitted through the π system, then replacement of the proton by a methyl group should give a coupling constant opposite in sign but nearly equal in magnitude (since $Q_{CH} \approx -Q_{CCH}$). For example, J^p_{H,CH_3} in toluene $= -0.6$ Hz while $J^p_{CH_3,CH_3}$ in *p*-xylene $= +0.6$ Hz (12). It is not obvious, *a priori*, that the methyl group replacement technique will work when the methyl group is bonded to an acetylenic linkage rather than directly to a phenyl group. However, the averaged values for the two sets of coupling constants for **1** ($J_{AM} = +0.28, J_{BM} = -0.09, J_{CM} = +0.28$ Hz are nearly identical in magnitude and opposite in sign to those for **2**. This strongly suggests that the methyl group replacement technique can be applied to this system and that the observed long-range coupling constants in **1** and **2** are all transmitted primarily through the π system. All of the determined signs of coupling constants are entirely consistent with π contributions.

Assuming $Q_{CC\equiv CH} = -12$ G, the observed coupling constants for **2** indicate that $Q_{CC\equiv CCH} = +12$ G. By comparing hyperfine e.p.r. coupling constants for γ-phenylpropargyl and benzyl radicals, Kochi and Krusic (26) concluded that the interposition of an acetylenic linkage reduced the transmission of spin density from a methylene group to a phenyl group by 47%. Since this corresponds to $Q_{CC\equiv CCH} = (0.47 \times 25) = +12$ G, our conclusions are in quantitative agreement with those obtained from e.p.r. measurements.

The MO–INDO–FPT calculations were performed to determine whether they could reproduce the long-range coupling constants for **1**–**3** and consequently provide insight into the mechanism of transmission of these coupling constants. For **1**, J_{CM} and J_{AM} are respectively under- and overestimated but the overall agreement between calculation and experiment is very good. The agreement is even better for **2** although J_{AM} and J_{BM} are slightly overestimated. The agreement for **3** is excellent, assuming that J_{AM} has the expected negative value. The overall agreement for the three compounds is extremely good with four of the eight long-range coupling constants whose signs were determined estimated within the probable experimental error (0.03 Hz).

The conformational dependence of the calculated long-range coupling constants for **2** provides insight into the mechanism of transmission of these interactions. J_{CM} varied from -0.05 Hz for the C—H bond coplanar to the phenyl group to -0.46 Hz for the C—H bond perpendicular to the phenyl group with a $\sin^2 \phi$ dependence (defining ϕ as the projection angle between the C—H bond and the phenyl group). Similar behavior has been noted for α C—H bonds in toluene (27), styrene (1), and benzaldehyde (11) and attributed to a σ–π configuration interaction (27). The fact that the same behavior is noted for a methyl group bonded to an acetylenic linkage suggests that the spin information is only transmitted through the extended π system. This could account for both the success of the methyl group replacement technique for **2** and the conclusion that vinyl and acetylenic linkages are equally effective in transmitting spin information.

J_{AM} and J_{BM} showed similar, although less marked conformational dependence. For the planar forms ($\phi = 0°$), J_{BM} was predicted to have a slightly larger value for conformation I ($+0.24$ Hz) than for conformation II ($+0.17$ Hz). For α proton couplings, an enhanced positive con-

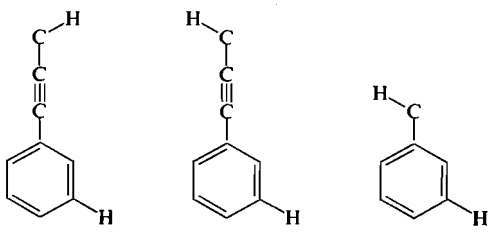

I II III

tribution has been found for the all-*trans* conformation III (28, 29, 1). It would be difficult to check the prediction concerning I and II.

In summary, the McConnell formulation has proved useful for extended coupling paths, since starting from results for a six bond coupling constant in toluene it has proved possible to derive Q values which quantitatively predict the nine bond couplings, J_{BM} and J_{CM} in **3**. MO–INDO–FPT also predict these couplings accurately. Even more extended coupling paths are under investigation.

C.J.M. and W.F.R. acknowledge financial support from the National Research Council of Canada. We thank Professor T. Schaefer for allowing the use of the HA-100D spectrometer on which some of the measurements were made. We are also indebted to Professor M. Barfield for first demonstrating to us the great usefulness of MO–INDO–FPT calculations in investigations of long-range coupling constants. I.R.P. thanks Gulf Oil Canada Limited for a Fellowship.

1. M. Barfield, C. J. Macdonald, I. R. Peat, and W. F. Reynolds. J. Am. Chem. Soc. **93**, 4195 (1971).
2. R. Wasylishen and T. Schaefer. Can. J. Chem. **49**, 3216 (1971).
3. J. A. Pople, D. L. Beveridge, and P. A. Dobosh. J. Chem. Phys. **47**, 2026 (1967).
4. J. A. Pople, J. M. McIver Jr., and N. S. Ostlund. J. Chem. Phys. **49**, 2960, 2965 (1968).
5. H. M. McConnell. J. Mol. Spectrosc. **1**, 11 (1957).
6. M. J. S. Dewar and R. C. Fahey. J. Am. Chem. Soc. **85**, 2704 (1963).
7. J. V. Acrivos. Mol. Phys. **5**, 1 (1962).
8. D. Gagnaire and Tri-Huu-ICH. Bull. Chem. Soc. Fr. 3763 (1966).
9. D. J. Blears, S. S. Danyluk, and T. Schaefer. J. Chem. Phys. **47**, 5037 (1967).
10. T. Schaefer, S. S. Danyluk, and C. L. Bell. Can. J. Chem. **47**, 1507 (1969).
11. (*a*) C. L. Bell, S. S. Danyluk, and T. Schaefer. Can. J. Chem. **47**, 3529 (1969). (*b*) T. Schaefer and S. S. Danyluk. Can. J. Chem. **47**, 4289 (1969).
12. C. J. Macdonald and W. F. Reynolds. Can. J. Chem. **48**, 1002 (1970).
13. G. Drehfahl and G. Plotner. Chem. Ber. **91**, 1280 (1958).
14. S. Castellano and J. Lorenc. J. Phys. Chem. **69**, 3552 (1965).
15. T. L. Jacobs. Org. React. **5**, 1 (1949).
16. G. K. Hamer. Ph.D. Thesis, University of Toronto, Toronto, Ontario, 1972.
17. D. L. Beveridge and J. A. Pople. Approximate molecular orbital theory. McGraw–Hill. New York, N.Y. 1970.
18. A. A. Bothner-By. Advances in magnetic resonance. Vol. 1. *Edited by* J. S. Waugh. Academic Press. New York, N.Y. 1965.
19. (*a*) P. C. Lauterbur and R. J. Kurland. J. Am. Chem. Soc. **84**, 3405 (1962). (*b*) Gurudata, J. B. Stothers, and J. D. Talman. Can. J. Chem. **45**, 731 (1967).
20. R. Kaiser. J. Chem. Phys. **39**, 2435 (1963).
21. G. Kotowycz and T. Schaefer. Can. J. Chem. **44**, 2743 (1966).
22. S. Castellano and A. A. Bothner-By. Mellon Institute Publication. Pittsburgh, Pa., 1967.
23. C. W. Haigh and J. M. Williams. J. Mol. Spectrosc. **32**, 398 (1969).
24. M. P. Williamson, R. Kostelnik, and S. M. Castellano. J. Chem. Phys. **49**, 2218 (1968).
25. R. Hoffman. Ark. Kem. **17**, 1 (1961).
26. J. K. Kochi and P. J. Krusic. J. Am. Chem. Soc. **92**, 4110 (1970).
27. For a summary of evidence see M. Barfield and B. Chakrabarti. Chem. Rev. **69**, 759 (1969).
28. T. Schaefer, R. Schwenk, C. J. Macdonald, and W. F. Reynolds. Can. J. Chem. **46**, 2187 (1968).
29. D. G. DeKowalewski and S. Castellano. Mol. Phys. **16**, 567 (1969).

Can. J. Chem. Downloaded from www.nrcresearchpress.com by 210.87.254.6 on 09/05/12
For personal use only.

Benzene Radical Cation Formation on Hydrogen Mordenite. The Role of Adsorbed Oxygen[1,2]

N. H. SAGERT, R. M. L. POUTEAU, M. G. BAILEY, AND F. P. SARGENT

Research Chemistry Branch, Whiteshell Nuclear Research Establishment, Atomic Energy of Canada Limited, Pinawa, Manitoba R0E 1L0

Received February 21, 1972

The e.p.r. spectrum of benzene on hydrogen mordenite (Zeolon H) has been studied as a function of coverage, degassing temperature, and hydrogen and oxygen treatment. The initial spectrum observed was that due to the benzene cation radical dimer. The maximum number of spins was formed when the solid was completely saturated with benzene. Large yields were obtained only when the zeolitic water and water of hydration of the protons were removed. The largest yields were observed where significant dehydroxylation had occurred. Chemisorbed oxygen was essential, and there was a 1:1.2 ratio between the maximum number of spins observed in the presence of excess oxygen and the amount of oxygen chemisorbed. The largest concentration of radical cations noted (2×10^{18}/g) was much smaller than the number of acid sites known to be present (10^{21}/g). In fact, only one unit cell of the hydrogen mordenite in 100 had a site capable of oxidizing benzene to the cation. Hence these sites must be in special positions in the solid.

Le spectre r.p.e. du benzène sur l'hydrogène mordenite (Zeolon H) a été étudié en fonction du recouvrement de la température de dégazage et du traitement à l'hydrogène et à l'oxygène. Le spectre initialement observé est celui du radical cation dimère. Le nombre maximum de spins est produit lorsque le solide est complètement saturé en benzène. Les rendements élevés ne sont obtenus qu'après élimination des eaux zéolitique et d'hydratation des protons. Les rendements les plus élevés ont été observés là où une des hydroxylations significatives s'est produite. L'oxygène chimisorbé est essentiel et il existe un rapport de 1 à 1.2 entre le nombre maximum de spins observés en présence d'oxygène en excès et la quantité d'oxygène chimisorbé. La concentration la plus élevée en radical cation (2×10^{18}/g) est beaucoup plus petite que le nombre de sites acides connus pour être présents (10^{21}/g). En fait seule une unité d'hydrogène mordenite sur cent possède un site capable d'oxyder le benzène en cation. En conséquence ces sites doivent occuper des positions spéciales dans le solide.

Canadian Journal of Chemistry, **50**, 2041 (1972)

Introduction

The species formed when various substances are adsorbed on alumino-silicates have been studied by e.p.r. techniques (1–3). Stanmires and Turkevich (1) observed cation radicals of triphenylamine on Y-type zeolites, and Rooney and Pink (2) observed e.p.r. signals from both anthracene and perylene cation radicals on silica–alumina. They did not observe signals from benzene or methyl substituted benzenes adsorbed on silica–alumina. Hirschler *et al.* (3) reported signals from benzene on calcium and rare earth exchange Y zeolites and cerium exchanged X zeolites. However, their spectra were poorly resolved. More recently Corio and Shih (4) and Kurita *et al.* (5) observed better resolved spectra from benzene adsorbed on hydrogen mordenite. They identified the initial spectrum as the benzene radical cation dimer.

It has been generally agreed that, for silica–aluminas, treatment with hydrogen suppresses the e.p.r. signals (6–8). Initially it was reported that oxygen decreased the signals (2, 9), but Dollish and Hall (8) showed that this is due to a physical interaction which broadens the lines and changes their shape. Porter and Hall (7) then showed that radical ion concentrations on silica–alumina increased on adding oxygen and Dollish and Hall (10) demonstrated that chemisorbed oxygen is actually essential for the generation of radical ions from perylene on NH_4^+Y zeolites, NH_4^+X zeolites, and $Ca^{2+}Y$ zeolites.

The work presented here examines the effect of hydrogen, oxygen, and evacuation temperature on the benzene cation radical dimer formation over hydrogen mordenite. This was done to obtain more information about the sites responsible for the one-electron oxidation.

Experimental

The synthetic hydrogen mordenite, trade name Zeolon H,

[1]AECL No. 4197.

[2]Presented in part at the 55th Chemical Institute of Canada Conference, Quebec City, Quebec, June, 1972.

Can. J. Chem. Downloaded from www.nrcresearchpress.com by 210.87.254.40 on 09/05/12
For personal use only.

Can. J. Chem. Downloaded from www.nrcresearchpress.com by 210.87.254.40 on 09/05/12
For personal use only.

was obtained from Norton Chemical Products. Emission spectrographic analysis revealed 100 p.p.m. of iron, 5 p.p.m. of nickel, 10 p.p.m. of chromium, and 150 p.p.m. of titanium. It was heated in air at 500 °C for 16 h to remove carbonaceous material and was then re-hydrated by exposure to atmospheric moisture for several days. As a standard treatment, about 0.5 g was weighed out into a 6 mm (o.d.) e.p.r. tube. The tube was attached to a mercury and grease-free vacuum line and the mordenite was evacuated while the temperature was raised to the desired level. It was continuously evacuated at this temperature for 16 h, reaching pressures below 2×10^{-6} Torr. This was the normal treatment. Samples designated "hydrogen treated" were then contacted with 1 atm of hydrogen for 15 min at the evacuation temperature, and the hydrogen was pumped out. This was repeated twice, followed by evacuation at the same temperature for about 3 h. The tubes were then allowed to cool under vacuum.

The Reagent Grade benzene was degassed by the freeze–pump–thaw technique. It was then distilled under vacuum through a P_2O_5 bed onto the zeolite which was kept at 77 °K. The tube was sealed off under vacuum and kept at 77 °K until 10 min before the e.p.r. measurements were made.

The e.p.r. measurements were normally made at room temperature with a Varian V-4500 series X-band spectrometer operating at about 9.3 GHz with a modulation frequency of 100 KHz. The power level was 0.4 ± 0.1 mW. Spectra were obtained as the first derivative of the absorption, and concentrations were obtained by doubly integrating the spectra numerically, using the method of Wyard (11). The minimum detectable concentration of benzene radical cation dimers was less than 10^{15}/g. A Varian high concentration pitch standard, placed in the back cavity of the Varian dual cavity accessory, was used as a working standard. The peak height of this standard was related to the number of spins in the hydrogen mordenite by doubly integrating the signals from solid mixtures of finely ground 1,1-diphenyl-2-picrylhydrazyl (DPPH) with hydrogen mordenite. These mixtures were contained in tubes identical to those used for samples and were placed in the front cavity. The amount of DPPH in them was adjusted to give first derivative peak heights similar to those obtained from samples being studied. The DPPH was re-crystallized twice before use, and its purity was determined spectrophotometrically (12).

The surface areas were measured by nitrogen adsorption at 77 °K using the B.E.T. technique, taking the area of the nitrogen molecule as 16.2 Å^2. The amount of nitrogen adsorbed was measured by the pulse desorption method using a Perkin–Elmer 212D Sorptometer. Benzene and oxygen adsorption isotherms at 28 °C were measured with a grease-free volumetric adsorption apparatus incorporating a quartz spiral manometer capable of measuring pressure changes to $\pm 3\ \mu$.

Results

The spectra obtained are shown in Fig. 1 and are similar to those obtained by Corio and Shih (4) and Kurita *et al.* (5). After 3 min at room temperature a spectrum shown as 1*a* was obtained with line spacings of 2.2 G. This spectrum has been identified as due to the benzene cation radical dimer (4, 5). After 1 h

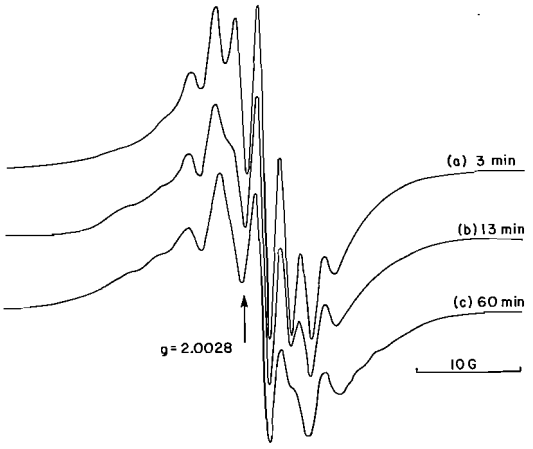

FIG. 1. The e.p.r. spectra of benzene on hydrogen mordenite degassed at 550 °C (*a*) after 3 min, (*b*) after 13 min, and (*c*) after 60 min. The spectra are displaced along the *Y*-axis for clarity.

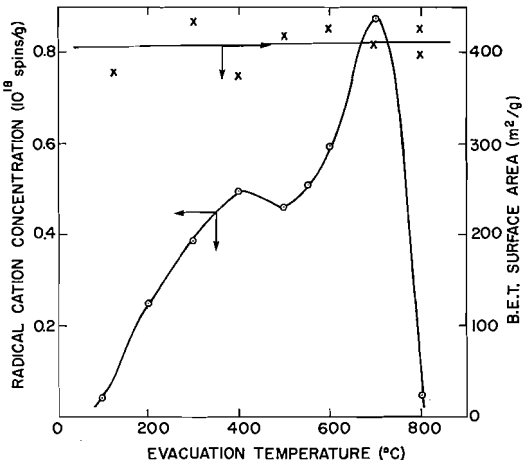

FIG. 2. Spin concentrations in the presence of 0.5 ml/g benzene (○), and B.E.T. surface areas (×) for hydrogen mordenites evacuated at different temperatures.

the spectrum shown as 1*c* was obtained. It has been identified by Kurita *et al.* (5) as the biphenyl cation radical. The total number of spins in Fig. 1*a* and 1*c* is the same to within 8%. The method of integration is only claimed to be accurate to within 5% (11), and other uncertainties probably increase this error considerably. Our reproducibility was about 10%. Thus, to within the error of our measurements, the spin concentration remained constant while the spectrum changed during the 60 min.

Figure 2 shows the number of spins per gram

Can. J. Chem. Downloaded from www.nrcresearchpress.com by 210.87.254.40 on 09/05/12
For personal use only.

as a function of the degassing temperature of the hydrogen mordenite. The B.E.T. surface area, measured by nitrogen adsorption at 77 °K is given on the same figure as a function of degassing temperature. The number of spins per gram increased up to 700 °C, and then fell rapidly. The apparent maximum at 400 °C may be a result of experimental scatter as the reproducibility of our spin concentrations was at best ±10%. However, there was some evidence, as mentioned below, that samples degassed at 300 and 600 °C behaved differently when treated with hydrogen.

Experiments with varying benzene concentrations on hydrogen mordenite degassed at 500 °C showed that the maximum number of spins was obtained using about 0.1 ml of liquid benzene per gram. Smaller spin concentrations were obtained with smaller amounts and no changes (±10%) were obtained with larger amounts. The 0.1 ml of benzene corresponds to 6.8×10^{20} molecules, but only 6×10^{17} spins/g were produced, *i.e.*, about 0.1% of the benzene was converted. Benzene adsorption experiments indicated that the full adsorption capacity of benzene corresponded to 0.083 ml/g at 28 °C, in agreement with the 0.09 ml/g at 25 °C obtained by Barrer and Peterson (13). Thus the full adsorption capacity appears necessary to develop the maximum number of spins, and benzene is not selectively adsorbed on the sites capable of oxidizing it. The amount of adsorbed benzene (0.083 ml/g) if adsorbed as a monolayer would correspond to a surface area of 232 m^2/g if the area of benzene molecule is taken as 41 $Å^2$ (14). As the surface areas measured by nitrogen adsorption are about 400 m^2/g, over half the total area seems accessible to benzene.

To assess the role of oxygen, samples degassed at 550 °C were prepared with from 2–11 Torr of oxygen present. The spin concentration quadrupled (Table 1) compared to the spin concentration from a normal sample degassed at 550 °C (Fig. 2). When 6.0 Torr of oxygen was added to a sample degassed at 800 °C, a very large increase in spin concentration compared to that in the absence of oxygen was noted. Some samples were then treated with hydrogen to remove chemisorbed oxygen completely. This decreased the number of spins by a factor of 4 in the case of a sample degassed at 300 °C and to an undetectable level in the case of a sample degassed at 500 °C (Table 1). Thus samples prepared at higher temperatures seem more susceptible to hydrogen treatment.

TABLE 1. Effect of hydrogen treatment and oxygen pressure on the yield of radical ions

Evacuation temperature (°C)	Hydrogen treatment	Oxygen pressure (Torr)	Radical concentration (10^{17} spins/g)
550	no	2.7	21.0
550	no	9.5	17.5
550	no	11.0	20.4
800	no	6.0	6.1_9
300	yes	0	1.1_8
500	yes	0	<0.01

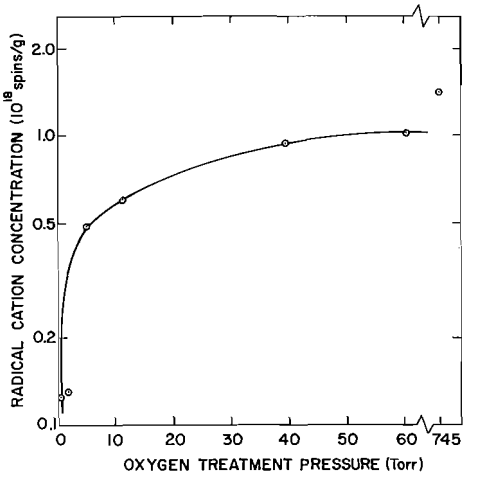

FIG. 3. Increase in spin concentration when a sample given the "hydrogen treatment" at 550 °C is exposed to varying oxygen pressures.

Finally, a series of hydrogen mordenites degassed at 550 °C and given the hydrogen treatment was allowed to contact oxygen at various pressures for 15 min. The oxygen was pumped out at room temperature, and benzene added in the usual way. Figure 3 shows the results obtained, plotting the number of spins produced against the pressure of oxygen used. About 5 Torr of O_2 restored the spin concentration to its normal value obtained without hydrogen treatment. High pressures gave yields of the order of those obtained in the actual presence of oxygen gas. An oxygen adsorption isotherm after hydrogen treatment (Fig. 4) showed that at 28 °C 2.5×10^{18} molecules of O_2 were chemisorbed per gram after hydrogen treatment. This was estimated by extrapolating

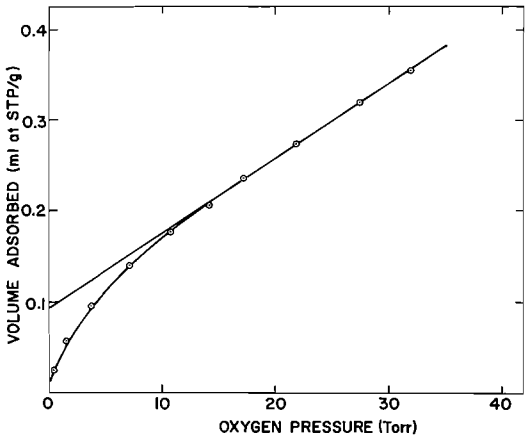

FIG. 4. Adsorption isotherm of O_2 on hydrogen mordenite given the "hydrogen treatment" at 550 °C; $T = 28$ °C.

the high pressure part of the isotherm to zero pressure, and is to be compared with the 1.45×10^{18} spins/g maximum obtained in Fig. 3 and the 2.0×10^{18} spins/g measured in the presence of oxygen gas (Table 1).

No spins were observed when perylene was adsorbed from *n*-hexane solution onto hydrogen mordenite degassed at 550 °C, and the *n*-hexane distilled off.

Discussion

(i) General Features

Ordinary silica–alumina cracking catalysts are not capable of oxidizing benzene (2). As the gas phase ionization potential of benzene is 9.24 eV (15), strong oxidation sites of about this energy are probably required to form cations. Both Corio and Shih (4) and Kurita *et al.* (5) have observed that hydrogen mordenite can oxidize benzene. Both groups agree that the initially observed seven-line spectrum with a line spacing of 2.2 G is from the benzene radical cation dimer, formed by the removal of a π electron from benzene. They also agree that this converts into a different radical ion with a line spacing of 3.8 G within 1 h. Corio and Shih assumed an equilibrium was formed between the radical cation dimer and the monomer. On the other hand Kurita *et al.* presented strong evidence that the final product was the biphenyl cation radical. Our spectra are quite similar to those obtained by both groups and we have nothing to add to this controversy. Our results indicate that the conversion of cation dimer to the other species occurs without decrease in the total number of radical ions, since there is no significant decrease in the total number of spins as the spectrum changes. Peak heights, of course, vary considerably in 1 h but the doubly integrated first derivative spectrum measured after 10 min seems to be a reasonable measure of the number of oxidizing sites on the hydrogen mordenite.

(ii) Water Content of the Zeolite

The formation of sites able to abstract electrons from benzene can be related to the removal of strongly held water from the hydrogen mordenite. Hydrogen mordenite is made from sodium mordenite by ion-exchanging with ammonium and heating. Ammonia is eliminated leaving most of the sodium exchanged for H_3O^+. The unit cell of the sodium mordenite mineral is $Na_8 \cdot (AlO_2)_8 \cdot (SiO_2)_{40} \cdot 24H_2O$ (16). In making hydrogen mordenite, almost one aluminum ion is lost from the unit cell along with the cations (13, 17), leading to an approximate formula for hydrogen mordenite:

$$(H_3O)_{7-n}Na_nAl_7Si_{40}O_{92}(OH)_4 \cdot 15H_2O$$

where $0.5 < n < 1$. This formula identifies four sources or potential sources of water. Zeolitic water, the $15H_2O$, accounts for 7.4% of the formula weight, and is removed between room temperature and 360 °C (13). The water of hydration of the protons, the $(H_2O)_{7-n}$, accounts for about a 3.6% weight loss and is also removed by 360 °C (13). Much of the hydroxyl water, the $(OH)_4$, may be removed by 360 °C as well. A 2% weight loss between 500 and 900 °C has been ascribed to the attack of bare protons, $(H^+)_{7-n}$, on the alumino-silicate structure (13), and some hydroxyl water was thought to be lost at these temperatures as well. Attack of protons on the alumino-silicate structure presumably initially forms anion and cation vacancy pairs (10). Dollish and Hall (10), suggest that this structure readjusts to a system of lower energy. Kerr (18) has proposed that, for hydrogen Y zeolite, some of the alumina lost from the unit cell is present as $Al(OH)_3$ and the positive vacancy may be located on this aluminum hydroxide as $Al(OH)_2^+$. A significant amount of this dehydroxylation (eq. 1) may occur at lower temperatures as well since Lefrancois and

Can. J. Chem. Downloaded from www.nrcresearchpress.com by 210.87.254.40 on 09/05/12
For personal use only.

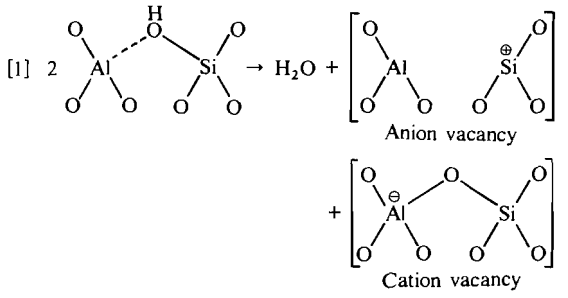

Malbois (19) have shown that on hydrogen mordenite the number of Lewis acid sites increases between 200 and 450 °C.

Our results as a function of degassing temperature (Fig. 2) suggest that removal of water, and the accompanying formation of Lewis acid sites, is necessary to create the site capable of oxidizing benzene. Because the spin concentration begins to increase again at degassing temperature higher than 550 °C, it appears that some of the vacancy sites created by this treatment (eq. 1) can oxidize benzene also. Thus there may be two types of sites capable of oxidizing benzene. The existence of two types of sites is also suggested by the resistance to hydrogen treatment: the sites formed at 300 °C seem more resistant to hydrogen than those formed at 500 °C (Table 1). The drop in spin concentration at the highest temperatures probably results from removal of chemisorbed oxygen, as discussed below. It does not result from a loss of surface area. Analogous observations by Flockhart *et al.* (20) have led them to suggest that amorphous silica–alumina also has two types of sites capable of oxidizing perylene.

(iii) Role of Chemisorbed Oxygen

The results of Table 1 and Fig. 3 show that chemisorbed oxygen is necessary to develop the sites capable of oxidizing benzene. We found a 1:1.2 ratio between the maximum number of spins produced (2.1×10^{18}/g) and the amount of oxygen chemisorbed after hydrogen treatment (2.5×10^{18} molecules/g). The hydrogen treatment probably removes most of the chemisorbed oxygen present after a normal treatment. Thus there is almost a 1:1 ratio between spins produced and chemisorbed oxygen. This suggests that a molecule of oxygen must be chemisorbed at, or close to, a special site in the solid, and that this combination of original site and oxygen molecule forms a new electron accepting site capable of oxidizing benzene. As the ionization potential of benzene is 9.24 eV, the new site is probably almost this strong.

Oxygen is likewise needed for the oxidation of perylene on X and Y zeolites (10) and on silica–alumina (6). Dollish and Hall (10) also showed that on NH_4^+Y zeolite, one oxygen molecule was required to form the oxidizing site because they obtained a 1:1 ratio between the number of spins produced and the number of molecules of oxygen added.

In our experiments pumping off oxygen adsorbed at 745 Torr at room temperature prior to adding benzene reduced the cation dimer yield by only 30%, compared to the yield observed in the presence of excess oxygen (Table 1 and Fig. 3). This confirms that chemisorbed and not physically adsorbed oxygen is needed for cation dimer formation.

(iv) Number and Nature of Sites

For a sample exposed to 745 Torr oxygen at room temperature and then evacuated, a yield of 1.45×10^{18} spins/g was obtained. With NH_4^+Y zeolite, Dollish and Hall (10) obtained a yield of 5.8×10^{18} spins/g for perylene oxidation under comparable conditions. Thus fewer oxidizing sites are available in the hydrogen mordenite than in the NH_4^+Y zeolite.

A measure of the total number of acid sites is obtained from the ammonia adsorption work of Eberly *et al.*, (21). They showed that, at 371 °C and 8 Torr, 9.4×10^{20} molecules of NH_3 were adsorbed per gram, and that this adsorption was a measure of the acidity of the surface. This number of sites is almost 500 times larger than the largest number of spins which we observed. A number of explanations are possible for this large discrepancy.

The hydrogen mordenite consists of tubes with an elliptical cross section of about 7 × 6 Å connected by side pockets which have diameters of 3–4 Å. Thus benzene, which has a diameter of 6.6 Å (13) could conceivably be barred from access to the interior of the solid. Adsorption isotherms measured by us and by others (13, 22, 23) show that this is not the case. Benzene is adsorbed throughout the large channels, although it is excluded from the small side pockets of the main channels (13).

It is most likely that radical cation formation

Can. J. Chem. Downloaded from www.nrcresearchpress.com by 210.87.254.40 on 09/05/12
For personal use only.

is limited by the amount of chemisorbed oxygen which is available. A sample evacuated at 500 °C and given the hydrogen treatment chemisorbed 2.5×10^{18} molecules O_2/g at 28 °C. This corresponds to 0.012 molecules per unit cell, assuming the unit cell for dehydrated hydrogen mordenite (Zeolon H) to be

$$8.42\{Na_{0.08}H_3O^+_{0.75}Al_{0.83}Si_{4.75}O_{10.82}OH_{0.68}\}$$

as determined by Barrer and Murphy (17). Thus only about one unit cell in 80 has a site capable of chemisorbing oxygen. The maximum number of spins formed under any conditions was 2.1×10^{18}/g. Therefore only about one unit cell in 100 has a site capable of oxidizing benzene. These sites must correspond to special positions possibly at the edge of crystal faces or at points of special strain in the lattice. Their exact nature has yet to be determined. However, it is well established that benzene is excluded from the side pockets of the mordenite. Therefore the sites are likely located in the main channels. Furthermore, no spins were observed from perylene on the hydrogen mordenite. As perylene is known to be more easily oxidized (2) but is probably excluded from the main channels of the mordenite, it is likely that the oxidizing sites are not on the exterior surface of the solid. The exterior area is almost 20% of the total area (23), so that if perylene was oxidized on the exterior of the solid, it should have been observed.

We would like to thank A. G. Wikjord and C. F. Musick of the Analytical Science Branch of our laboratory for measuring the nitrogen surface areas. Helpful discussions on the structure of mordenites with E. V. T. Murphy are also gratefully acknowledged. E. V. T. Murphy and M. Tomlinson are thanked for their frank comments on earlier versions of this manuscript.

1. D. N. Stanmires and J. Turkevich. J. Am. Chem. Soc. **86**, 749 (1964).
2. J. J. Rooney and R. C. Pink. Trans. Faraday Soc. **58**, 1632 (1962).
3. A. E. Hirschler, W. C. Neikam, D. S. Barmby, and R. L. James. J. Catal. **4**, 628 (1965).
4. P. L. Corio and S. Shih. J. Catal. **18**, 126 (1970).
5. Y. Kurita, T. Sonoda, and M. Sato. J. Catal. **19**, 82 (1970).
6. J. K. Fogo. J. Phys. Chem. **65**, 1919 (1961).
7. R. P. Porter and W. K. Hall. J. Catal. **5**, 366 (1966).
8. F. R. Dollish and W. K. Hall. J. Phys. Chem. **69**, 4402 (1965).
9. H. Imai, Y. Ono, and T. Keii. J. Phys. Chem. **69**, 1082 (1965).
10. F. R. Dollish and W. K. Hall. J. Phys. Chem. **71**, 1005 (1967).
11. S. J. Wyard. J. Sci. Instrum. **42**, 769 (1965).
12. J. W. Eastman, G. M. Androes, and M. Calvin. J. Chem. Phys. **36**, 1197 (1962).
13. R. M. Barrer and D. L. Peterson. Proc. R. Soc. London, Ser. A **280**, 446 (1964).
14. R. N. Smith, C. Pierce, and H. Cordes. J. Am. Chem. Soc. **72**, 5595 (1950).
15. V. I. Vedeneyev, L. V. Gurvich, V. N. Kondrat'yev, V. A. Medvedev, and Ye L. Frankevich. Bond energies, ionization potentials and electron affinities. Edward Arnold (Publishers) London. 1966. p. 157.
16. W. M. Meier. Z. Kristallogr. **115**, 439 (1961).
17. R. M. Barrer and E. V. T. Murphy. J. Chem. Soc. A, 2506 (1970).
18. G. T. Kerr. J. Phys. Chem. **71**, 4155 (1967).
19. M. Lefrancois and G. Malbois. J. Catal. **20**, 350 (1971).
20. B. D. Flockhart, J. A. N. Scott, and R. C. Pink. Trans. Faraday Soc. **62**, 730 (1966).
21. P. E. Eberly Jr., C. N. Kimberlin Jr., and A. Voorhies Jr. J. Catal. **22**, 419 (1971).
22. P. E. Eberly, Jr. J. Phys. Chem. **67**, 2404 (1963).
23. M. M. Dubinin, E. G. Zhukovskaya, V. M. Luk'yanovich, K. O. Murdmaa, E. F. Polstyanov, and E. E. Senderov. Izvest. Akad. Nauk SSSR, Ser. Khimicheskaya, **8**, 1500 (1965).

Can. J. Chem. Downloaded from www.nrcresearchpress.com by 210.87.254.40 on 09/05/12
For personal use only.

Ceric Ammonium Nitrate Oxidation of Cyclic Ketones

P. SOUCY, TSE-LOK HO, AND P. DESLONGCHAMPS[1]

Laboratoire de Synthèse Organique, Département de chimie, Université de Sherbrooke, Sherbrooke, Québec

Received January 13, 1972

Ceric ammonium nitrate oxidation of cyclohexanone, cyclopentanone, and norbornanone gives nitrato-carboxylic acids, oxidation of adamantanone and adamantan-2-ol gives the lactone **14**.

Par oxydation avec le nitrate cérique d'ammonium, la cyclohexanone, la cyclopentanone, et la norbornanone donnent des acides nitrato-carboxyliques correspondants. L'oxydation de l'adamantanone ou de l'adamantanol-2 conduit à la lactone **14** correspondante.

Canadian Journal of Chemistry, **50**, 2047 (1972)

Can. J. Chem. Downloaded from www.nrcresearchpress.com by 210.87.254.6 on 09/05/12
For personal use only.

Ceric ion in various coordinated forms is a strong oxidizing agent. Numerous reports of utilizing Ce(IV) to oxidize organic compounds have appeared in the literature (1). In particular, Ce(IV) oxidation of alcohols has received much attention in recent years, as an outgrowth of the colorimetric detection and quantitative determination of these substrates. It is known that Ce(IV) ion forms 1:1 complexes with alcohols which rapidly collapse to the products.

The studies by Trahanovsky and coworkers, *inter alia*, on ceric ammonium nitrate (CAN) oxidation of a number of organic compounds have uncovered some useful applications. Thus, benzylic and cyclopropylcarbinyl alcohols are oxidized to the corresponding aldehydes (2) in good yields, α-glycols are cleaved (3) in analogy to the lead tetraacetate reaction and cycloheptatriene has been oxidized to benzaldehyde, benzene, and carbon monoxide (4). CAN also oxidizes benzylic methylene groups to the carbonyl derivatives (5) and it has also been used in regeneration of the parent ketones from their oximes and semicarbazones (6). More recently, oxidative cleavages of bicyclo-[2.2.1]-2-heptanols and bicyclo[2.2.2]-2-octanol (7), of alkylphenylcarbinols (8), of 1,2-diaryl-ethanols and 1-aryl-2,3-diphenylpropan-2-ols (9) have also been reported.

Under more drastic conditions, carbonyl compounds such as aliphatic aldehydes and ketones are attacked by Ce(IV) ions to yield formic acid and carbon dioxide as ultimate products (1). Consequently, almost all the pertinent investigations have been limited to reaction kinetics and mechanistic aspects, without probing into the synthetic utility of these oxidations.

In connection with a certain synthetic program, we have been interested in the oxidation of cyclic ketones with ceric salts, specifically with CAN. At present, we wish to report the results of such oxidation performed on a few representative cyclic ketones.

Results and Discussion

Our standard conditions of oxidation involve the treatment of ketone with 4 mol equiv of CAN at 60° in aqueous acetonitrile, until discoloration of the orange solution is complete. The major fractions isolated from oxidation of cyclohexanone, cyclopentanone, and norbornanone are acidic in nature. The combined yields of these products are of *ca.* 50%.

Cyclohexanone gave a mixture of 6- and 5-nitratohexanoic acids in a ratio of 3:2. The structures of these compounds were deduced from the i.r., n.m.r., and mass spectra, and have been verified by comparison of their methyl esters **1***a* and **2***a* with authentic specimens prepared by unambiguous routes.

Cyclopentanone yielded a more complex mixture of acidic products. The v.p.c. analysis of the derived methyl esters indicated the presence of four major components in the ratio of 24:16:34:26 identified as **3**, **4**, **5**, and **6** respectively, on basis of spectral data. Authentication of **3** has been made by its preparation from methyl 5-hydroxypentanoate.

Next we focused our attention to the oxidation of 2-norbornanone. Two nitrato-carboxylic acids **7** and **8** were obtained. The v.p.c. analysis of the derived methyl esters (**7***a* and **8***a*) indicated that the *trans*-epimer was present in larger

[1]A. P. Sloan Fellow, 1970–1972.

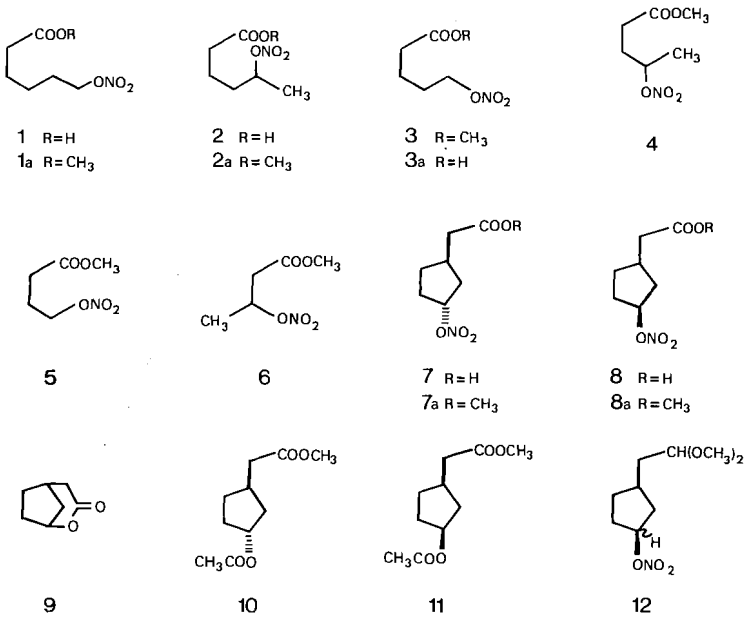

quantity (ratio of 3:2). Hydrolysis of the crude acidic products (**7** and **8**) furnished a mixture of hydroxyacids which was subsequently esterified and oxidized by Collins reagent (10) to methyl 3-oxocyclopentane acetate, identical with a sample prepared from 2-oxabicyclo[3.2.1]octan-3-one (**9**). Characterization and stereochemical assignments of the oxidation products were carried out as the following. Saponification of **7***a* and **8***a* and treatment with *p*-toluenesulfonic acid in benzene gave a mixture of lactone **9** and *trans*-3-hydroxycyclopentane acetic acid, which were readily separated. The *trans*-acid has been converted to the acetoxyester **10**; the lactone **9** was similarly transformed into the epimeric *cis*-acetoxyester **11**.

It was reported that the *exo*- or *endo*-norbornanol probably gives only *cis*-3-nitratocyclopentane acetaldehyde besides two cyclopentene acetaldehydes (7). We have, therefore, repeated the oxidation and converted the higher boiling aldehyde fraction into the dimethyl acetal **12**, thence to the methyl ester by ozonolysis (11). This ester sample has been shown by v.p.c. to contain two components corresponding to **7***a* and **8***a*, the *trans*-epimer being slightly predominant.

The rates of CAN oxidation of all three ketones mentioned above are similar; the reaction is generally complete within 1–1.5 h at 60°. However, camphor was found to be stable under the same conditions for at least 20 h, during which time CAN was slowly consumed (solvent oxidation). This observation led us to believe that the oxidation requires a close approach of the ketone and CAN, perhaps a complex formation is involved. Since Ce(IV) is coordinated by 8 to 12 atoms and thus the cerium species is fairly bulky, complex formation with camphor must be difficult. The success of isoborneol in undergoing CAN oxidation (7) is somewhat understandable, if one takes into consideration the great stability difference between a Ce(IV) alkoxide and a weakly coordinated (C=O → Ce(IV)) complex in judging the relative reactivities.

We envision that nitratocarboxylic acids arise from electron-transfer from the carbonyl oxygen to Ce(IV) within the CAN–ketone complex to generate a cation-radical **A** (Scheme 1). This cation-radical would then suffer a C—C bond fission (**A** → **B**) and react with water in the medium (**B** → **C**); the free radical can be further oxidized by electron transfer (**C** → **D**) or by ligand-transfer (12) to yield the final products. Generation of nitrato derivatives *via* this mechanism has previously been discussed by Trahanovsky *et al.* (7).

In order to account for the formation of acids having a secondary nitrato group, a

Can. J. Chem. Downloaded from www.nrcresearchpress.com by 210.87.254.6 on 09/05/12
For personal use only.

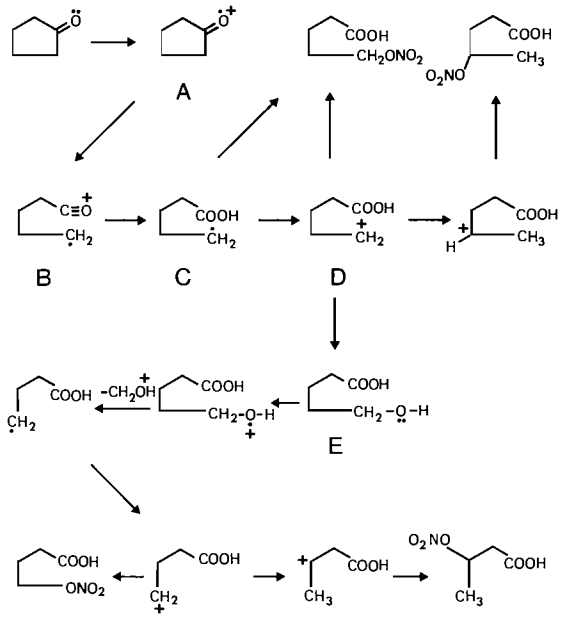

SCHEME 1

competitive oxidation of **C** by an electron-transfer process is proposed. The incipient carbonium ion **D** could undergo 1,2-hybride shift prior to its capture by the nitrate anion.

Degradation of one-carbon fragment observed during CAN oxidation of cyclopentanone poses an interesting problem. 5-Nitratopentanoic acid (*3a*) was recovered unchanged when exposed to CAN, hence it is not a precursor of the other three nitratocarboxylic acids. A similar result was obtained with δ-valerolactone. However, oxidation of the sodium salt of 5-hydroxypentanoic acid with CAN gave γ-butyrolactone in 50% yield. Consequently, loss of a one-carbon fragment might be explained by partial capture of the carbonium ion **D** to give **E** which can then be further oxidized and fragmented as outlined in Scheme 1.

We have also studied the CAN oxidation of adamantanone (**13**)[2] which is structurally unique with respect to its rigid and nonenolizable nature. Thus adamantanone was allowed to react with 4 equiv of CAN in aqueous acetonitrile at 60°; discoloration (orange to faintly yellow) was observed at the end of 3 h. The rate of the reaction is slower than those of the ordinary ketones such as cyclopentanone and cyclohexanone; yet the reaction was quite clean, for only a single spot was detected by t.l.c. The product was isolated in 73% yield after sublimation, and was shown to be identical with the lactone **14** (13) obtained from *m*-chloroperbenzoic acid oxidation of adamantanone.

It is instructive to consider the above finding in light of a similar reaction of norbornanone. Whereas the result of adamantanone oxidation may be interpreted as illustrated in Scheme 2, in the case of norbornanone, lactonization of a possible intermediate such as **F** would be discouraged by the introduction of strain in reforming a bridged ring system. Furthermore, the entropy factor must play an important role in suppressing lactone formation. Consequently, monocyclic nitrato-carboxylic acids resulted.

Structurally constrained ketones are expected to behave in analogy to adamantanone; thus the present work may indicate a welcoming alternative to the classical Baeyer–Villiger oxidation, particularly where peracid-sensitive groupings such as olefinic linkages are present in the molecule.

CAN oxidation of adamantan-2-ol also afforded the lactone **14** in 50% yield. Adaman-

[2]In our laboratories, this reaction has been named "CANADA" reaction.

Can. J. Chem. Downloaded from www.nrcresearchpress.com by 210.87.254.6 on 09/05/12
For personal use only.

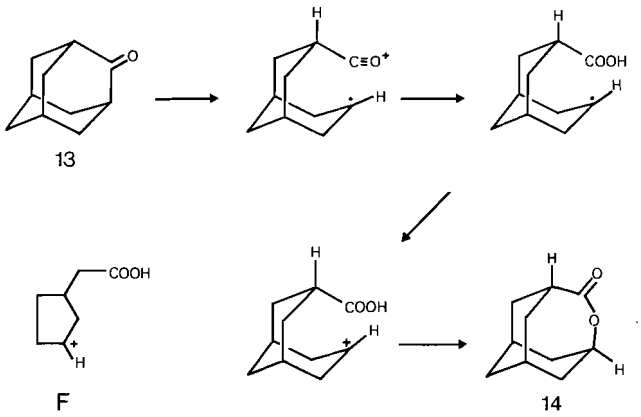

SCHEME 2

tanone was shown to be the intermediate (v.p.c.). In sharp contrast to the oxidation of bicyclic alcohols (7) which led to exclusively ring cleavage products at a fast rate, the conversion of adamantan-2-ol into the ketone, even in the presence of excess oxidizing agent, was not complete before a considerable amount of the lactone had been accumulated. In other words, the reaction cannot be stopped cleanly at the ketone stage for further oxidation takes place at a competitive rate.

From the foregoing results, one might conclude that CAN oxidations of bridged bicyclic alcohols are rather special cases (7). In general, CAN oxidations of secondary alcohols give rise to ketones which are susceptible to oxidative cleavage. Hintz and Johnson (14) reported the oxidations of cyclopentanol and cyclohexanol to the corresponding ketones with ceric sulfate.

Experimental

The i.r. spectra were taken on a Perkin–Elmer 257 Spectrophotometer; n.m.r. spectra (τ-value) were recorded on a Varian A-60 spectrometer in solvent indicated and with TMS as standard. The m.s. were run in a Hitachi–Perkin Elmer RMU-6 Spectrometer. The v.p.c. analyses were done on a Hewlett–Packard 5750 Research Chromatograph. Organic solutions were dried over anhydrous magnesium sulfate and Florisil was used in all the column chromatography. Microanalyses were performed by Schwarzkopf Microanalytical Laboratory, Woodside, N.Y.

CAN Oxidation of Cyclohexanone

A solution of cyclohexanone (4.0 g, 40 mmol) in acetonitrile (100 ml) was treated with ceric ammonium nitrate (87.7 g, 160 mmol) in water (300 ml). The resulting solution was heated at 60° with stirring for 1 h. It was saturated with sodium chloride and extracted with chloroform. The acidic products (2.33 g) were isolated from the chloroform solution by extraction with aqueous sodium bicarbonate followed by reacidification and extraction with ether. From the chloroform layer, cyclohexanone (1.54 g) was recovered. The crude acidic mixture (2.33 g) was esterified with ethereal diazomethane and separated by preparative v.p.c. (6 ft, 10% Carbowax 20 M column, 165°).

Compound **1***a*, retention time 19.0 min; i.r.: ν_{max} ($CHCl_3$) 1735, 1635, and 1280 cm^{-1}; n.m.r.: τ ($CDCl_3$) 5.45 (2H, triplet, $J = 6.0$ Hz, CH_2ONO_2), 6.28 (3H, singlet, $COOCH_3$), 7.62 (2H, triplet, $J = 6.0$ Hz, CH_2COO), and 7.95–8.70 (6H, multiplet, CH_2); m.s.: *m/e* 160 ($M^+ - OCH_3$) and 129 ($M^+ - ONO_2$).

Anal. Calcd. for $C_7H_{13}NO_5$: C, 43.98; H, 6.80. Found: 44.25; H, 7.05.

Compound **2***a*, retention time 11.6 min; i.r.: ν_{max} ($CHCl_3$) 1735, 1630, and 1280 cm^{-1}; n.m.r.: τ ($CDCl_3$) 4.90 (1H, multiplet, —CH-ONO_2), 6.31 (3H, singlet, $COOCH_3$), 7.62 (2H, multiplet, CH_2COO), 8.27 (4H, multiplet, CH_2), and 8.63 (3H, doublet, $J = 6.0$ Hz, CH_3); m.s.: *m/e* 160 ($M^+ - OCH_3$) and 129 ($M^+ - ONO_2$).

Anal. Calcd. for $C_7H_{13}NO_5$: C, 43.98; H, 6.80. Found: C, 44.25; H, 6.98.

Methyl 6-Nitratohexanoate (1a)

To the nitrating agent (15) prepared from 70% nitric acid (40 ml, 0.96 mol) and acetic anhydride (304 ml, 3.2 mol) at −5° was added methyl 6-hydroxyhexanoate (3.5 g, 24 mmol) during 20 min. The excess reagent was carefully destroyed with water and the resulting mixture was extracted with chloroform. The organic phase was separated, washed with water until neutral to litmus, dried, and evaporated. Short-path distillation gave **1***a* (3.88 g, 84.3%).

Methyl 5-Nitratohexanoate (2a)

The nitrating agent (15) was prepared from 70% nitric acid (20 ml, 0.48 mol) and acetic anhydride (152 ml, 1.6 *M*) at −5°. Treatment of methyl 5-hydroxyhexanoate (1.70 g, 12 mmol) with the nitrating agent for 20 min, and work-up as described in the preceding paragraph furnished the crude ester **2***a*. Column chromatography yielded the pure ester (1.68 g, 76%).

CAN Oxidation of Cyclopentanone

Cyclopentanone (8.4 g, 0.1 mol) in acetonitrile (200 ml) was oxidized with CAN (219.3 g, 0.4 mol) in water (600 ml)

Can. J. Chem. Downloaded from www.nrcresearchpress.com by 210.87.254.6 on 09/05/12
For personal use only.

Can. J. Chem. Downloaded from www.nrcresearchpress.com by 210.87.254.6 on 09/05/12
For personal use only.

at 60° for 4 h. Chloroform extraction of the reaction mixture saturated with sodium chloride, yielded a mixture of acidic and neutral products. The acidic material (4.8 g) was isolated by extraction with aqueous sodium bicarbonate followed by acidification and extraction with ether. Esterification of the acids with ethereal diazomethane followed by column chromatography gave a mixture of methyl esters (4.8 g). The v.p.c. analysis (6 ft, 10% Carbowax 20 M column, 130°) showed the presence of four major compounds which were isolated by preparative v.p.c.

Ester **3**, 24%, retention time 52.5 min; i.r.: ν_{max} ($CHCl_3$), 1735, 1635, and 1280 cm^{-1}; n.m.r.: τ (CCl_4) 5.55 (2H, diffuse triplet, $J = 6.0$ Hz, CH_2ONO_2), 6.38 (3H, singlet, $COOCH_3$), 7.68 (2H, diffuse triplet, $J = 6.0$ Hz, CH_2COO), and 8.1–8.5 (4H, multiplet, CH_2); m.s.: *m/e* 146 ($M^+ - OCH_3$) and 115 ($M^+ - ONO_2$).

Anal. Calcd. for $C_6H_{11}NO_5$: C, 40.67; H, 6.21. Found: C, 40.80; H, 6.25.

Ester **4**, 16% (>92% pure) retention time 26.7 min; i.r.: ν_{max} ($CHCl_3$) 1735, 1635, and 1280 cm^{-1}; n.m.r.: τ (CCl_4) 4.93 (1H, sextet, $J = 6.0$ Hz, $CHONO_2$), 6.37 (3H, singlet, $COOCH_3$), 7.3–8.4 (4H, multiplet, CH_2), and 8.62 (3H, doublet, $J = 6.0$ Hz, CH_3); m.s.: *m/e* 146 ($M^+ - OCH_3$) and 115 ($M^+ - ONO_2$).

Ester **5**, 34% (97% pure), retention time 30.0 min; i.r.: ν_{max} ($CHCl_3$) 1735, 1635, and 1280 cm^{-1}; n.m.r.: τ (CCl_4) 5.50 (2H, triplet, $J = 6.0$ Hz, CH_2ONO_2), 6.34 (3H, singlet, $COOCH_3$), and 7.4–8.2 (4H, multiplet, CH_2); m.s.: *m/e* 132 ($M^+ - OCH_3$) and 101 ($M^+ - ONO_2$).

Ester **6**, 26%, retention time 15.0 min; i.r.: ν_{max} ($CHCl_3$) 1740, 1640, and 1280 cm^{-1}; n.m.r.: τ (CCl_4) 4.59 (1H, sextet, $J = 6.5$ Hz, $CHONO_2$), 6.33 (3H, singlet, $COOCH_3$), 7.40 (2H, octet, $J_{AB} = 16$, $J_{AX} = J_{BX} = 6.5$ Hz, CH_2COO), and 8.57 (3H, doublet, $J = 6.5$ Hz, CH_3); m.s.: *m/e* 132 ($M^+ - OCH_3$) and 101 ($M^+ - ONO_2$).

*Methyl 5-Nitratopentanoate (**3**)*

The nitrating agent (15) prepared from 70% nitric acid (13.3 ml, 0.32 mol) and acetic anhydride (101 ml, 1.06 mol) at −5° was mixed thoroughly with methyl 5-hydroxypentanoate (1.05 g, 8 mmol) for 20 min. After addition of water, the reaction mixture was extracted with chloroform to give the crude nitrato ester. Column chromatography yielded methyl 5-nitratopentanoate (**3**, 1.20 g, 85%).

CAN Oxidation of Sodium 5-Hydroxypentanoate

δ-Valerolactone (1.009 g, 0.01 mol) was heated to reflux with an aqueous solution (20 ml) of sodium hydroxide (400 mg, 0.01 mol) during 48 h. Ceric ammonium nitrate (21.93 g, 0.04 mol) was dissolved in water (10 ml), acetonitrile (60 ml) then added, and the mixture was heated at 60° for 18 h. Sodium chloride was then added and the mixture was extracted with ether. The organic phase was washed with an aqueous solution of sodium bicarbonate, dried, and evaporated to dryness yielding a neutral substance (486 mg) which was identified as γ-butyrolactone by comparison (i.r., n.m.r., and v.p.c.) with an authentic sample.

Acidification of the aqueous phase and extraction with ether gave a small quantity (10 mg) of acidic material which was not further investigated.

Methyl 3-Nitratocyclopentane Acetate (7a and 8a)

(a) CAN Oxidation of Norbornan-2-one

A solution of norbornanone (1.1 g, 10 mmol) in acetonitrile (20 ml) was warmed at 60° with CAN (22.0 g, 40 mmol) in water (60 ml), for 1.5 h. It was cooled, saturated with sodium chloride, extracted with chloroform. An acidic mixture was obtained from the chloroform extract. Esterification of this mixture with diazomethane gave the crude methyl esters 7*a* and 8*a* (935 mg). The v.p.c. analysis (6 ft, 10% Carbowax 20 M column, 165°) showed the presence of two compounds (retention time: 28.0 and 29.4 min) in a ~3:2 ratio; i.r.: ν_{max} ($CHCl_3$) 1735, 1635, and 1280 cm^{-1}; n.m.r.: τ ($CDCl_3$) 4.50 (1H, multiplet, $CHONO_2$), 6.27 (3H, singlet, $COOCH_3$), 7.56 (2H, multiplet, CH_2COO), and 7.70–8.90 (7H, multiplet); m.s.: *m/e* 172 ($M^+ - OCH_3$) and 141 ($M^+ - ONO_2$).

*(b) Ozonolysis of 3-Nitratocyclopentane Acetaldehyde Dimethyl Acetal (**12**)*

A mixture of 3-nitratocyclopentane acetaldehyde (7) (2.08 g, 12 mmol), trimethyl orthoformate (1.27 g, 12 mmol), *p*-toluenesulfonic acid (40 mg) in anhydrous methanol (5 ml) was kept under reflux for 4 h. It was cooled, diluted with ether (300 ml) and washed with water. Evaporation of the dried ethereal solution gave an oil which was further purified by column chromatography to give the dimethyl acetal **12** (2.02 g, 77%); i.r.: ν_{max} ($CHCl_3$) 1630 and 1280 cm^{-1}; n.m.r.: τ ($CDCl_3$) 4.55 (1H, multiplet, $CHONO_2$), 5.56 (1H, triplet, $J = 5.5$ Hz, $CH(OMe)_2$), 6.65 (6H, singlet, OCH_3), and 7.2–8.9 (9H, multiplet); m.s.: *m/e* 188 ($M^+ - OCH_3$).

The dimethyl acetal **12** (1.0 g, 4.5 mmol) in ethyl acetate (100 ml) was ozonyzed at 0° for 2h. The solvent was stripped off and the residue was dissolved in ether, washed with aqueous sodium carbonate and water. The dried ethereal solution was evaporated *in vacuo* and the product was chromatographed to give the methyl esters 7*a* and 8*a* (850 mg, 91%). The v.p.c. analysis indicated a mixture of two compounds in a ~3:2 ratio.

*2-Oxabicyclo[3.4.1]octan-3-one (**9**) and Methyl trans-3-Acetoxycyclopentane Acetate (**10**)*

A mixture of esters 7*a* and 8*a* (5.0 g) and aqueous sodium hydroxide (200 ml, 0.75 *N*) was refluxed for 15 h. It was cooled, acidified, and extracted with ether. On evaporation of the dried organic phase a yellow oil (2.7 g) was obtained. This oil was dissolved in benzene (175 ml) containing a trace of *p*-toluenesulfonic acid, and heated for 3 h under a Dean–Stark trap to convert the *cis*-hydroxy acid into the lactone **9**. The benzene solution was extracted with sodium bicarbonate which upon reacidification and ether extraction yielded *trans*-3-hydroxycyclopentane acetic acid (1.4 g). The neutral compound obtained by concentration of the benzene layer was shown to be 2-oxabicyclo[3.3.1]octan-3-one (**9**) (0.8 g).

An ethereal solution of *trans*-3-hydroxycyclopentane acetic acid (1.4 g) described in the preceding paragraph, was treated with an excess diazomethane to afford the methyl ester (1.41 g); i.r.: ν_{max} ($CHCl_3$) 3710, 3470, and 1730 cm^{-1}; n.m.r.: τ ($CDCl_3$) 5.73 (1H, multiplet, CHOH), 5.93 (1H, singlet, OH), and 6.34 (3H, singlet, $COOCH_3$). Acetylation of the crude product with acetic anhydride (10 ml) and pyridine (10 ml) at room temperature for 24 h yielded methyl *trans*-3-acetoxycyclopentane acetate (6 ft, 10% SE-30 column, 150°, retention time 9.5 min); i.r.: ν_{max} ($CHCl_3$) 1735 cm^{-1}; n.m.r.: τ ($CDCl_3$) 4.75 (1H, multiplet, CHOAc), 6.28 (3H, singlet, $COOCH_3$), and 7.97 (3H, singlet, $OCOCH_3$); m.s.: *m/e* 169 ($M^+ - OCH_3$), 157 ($M^+ - CH_3CO$), and 140 ($M^+ - CH_3COOH$).

Can. J. Chem. Downloaded from www.nrcresearchpress.com by 210.87.254.6 on 09/05/12
For personal use only.

Anal. Calcd. for $C_{10}H_{16}O_4$: C, 60.00; H, 8.00. Found: C, 60.25; H, 8.08.

Methyl cis-3-Acetoxycyclopentane Acetate (11)

2-Oxabicyclo [3.2.1]octan-3-one (**9**) (2.44 g, 19 mmol) dissolved in anhydrous methanol (50 ml) was stirred with sodium methoxide (1.04 g, 19 mmol) at room temperature for 2 h. The solvent was removed *in vacuo* and the residue was distributed between chloroform and water. Acidification of the alkaline solution followed by extraction with ether yielded the starting lactone **9** (1.06 g). Concentration of the chloroform solution gave methyl *cis*-3-hydroxycyclopentane acetate (1.82 g); i.r.: ν_{max} ($CHCl_3$) 3610, 3460, and 1735 cm^{-1}; n.m.r.; τ (CCl_4) 5.73 (1H, quintet, $J = 5.0$ Hz, CHOAc), 5.93 (1H, singlet, OH), and 6.34 (3H, singlet, $COOCH_3$). Acetylation of the hydroxy ester (0.80 g) with acetic anhydride and pyridine furnished methyl *cis*-3-acetoxycyclopentane acetate (**11**) (0.85 g, 84%). The analytical sample was collected from v.p.c. (6 ft, 10% SE-30 column, 150°, retention time 8.72 min); i.r.: ν_{max} ($CHCl_3$) 1735 cm^{-1}; n.m.r.: τ ($CDCl_3$) 4.86 (1H, multiplet, CHOAc), 6.35 (3H, singlet, $COOCH_3$), and 8.04 (3H, singlet, $OOCH_3$); m.s.: *m/e* 157 ($M^+ - CH_3CO$) and 140 ($M^+ - CH_3CO_2H$).

Anal. Calcd. for $C_{10}H_{16}O_4$: C, 60.00; H, 8.00. Found: C, 59.78; H, 8.09.

Methyl 3-Oxocyclopentane Acetate

(a) From Methyl cis-3-Hydroxycyclopentane Acetate

To an ice cooled Collins reagent (10) (9.75 g, 38 mmol) in dry methylene chloride (200 ml) was added a solution of methyl *cis*-3-hydroxycyclopentane acetate (1.0 g, 6.3 mmol) in methylene chloride (20 ml). After stirring at room temperature for 20 min, water was added. The organic phase was treated with activated charcoal and dried. Removal of solvent and short-path distillation (bath temperature 105°/0.1 mm) of the residue afforded methyl 3-oxocyclopentane acetate (862 mg, 86%); i.r.: ν_{max} ($CHCl_3$) 1745 and 1740 cm^{-1}; n.m.r.: τ (CCl_4) 6.30 (3H, singlet, $COOCH_3$), and 7.20–8.70 (9H, multiplet); m.s.: *m/e* 156 (M^+).

Anal. Calcd. for $C_8H_{12}O_3$: C, 61.54; H, 7.69. Found: C, 61.34; H, 7.83.

(b) From cis- and trans-3-Hydroxycyclopentane Acetic Acid

A mixture of the 3-hydroxycyclopentane acetic acid (*cis*-, *trans*-epimers) (1.12 g, 7.8 mmol), potassium carbonate (1.33 g, 9.6 mmol) and iodomethane (6 ml) in acetone (40 ml) was kept under reflux (16). An additional quantity (6 ml) of iodomethane was added after 1.5 h and the total heating time was 5 h. Acetone was removed, the residue was taken up with chloroform and washed with water. The dried chloroform solution was evaporated to give the epimeric methyl 3-hydroxycyclopentane acetates (926 mg, 75%). Oxidation of a portion of the crude product (690 mg, 4.3 mmol) with Collins reagent (6.66 g, 25.8 mmol) in methylene chloride (150 ml) at room temperature gave a ketoester (552 mg, 86%) identical with methyl 3-oxocyclopentane acetate described above.

CAN Oxidation of Adamantanone

To a solution of adamantanone (1.0 g, 6.6 mmol) in acetonitrile (15 ml) was added ceric ammonium nitrate (15.0 g, 27.3 mmol) in water (30 ml). The resulting solution was stirred magnetically at 60° for 3 h during which time the orange color faded to faintly yellow. It was cooled, poured into brine, and extracted with chloroform. The extracts were dried and evaporated to give a soft solid mass (t.l.c. homogeneous). Sublimation of this material at 130–150° (bath temperature) under water aspirator pressure furnished lactone **14** (815 mg, 73.4% yield, m.p. 285–287°; lit. (13) m.p. 288–290°); i.r.: ν_{max} ($CHCl_3$) 1718 cm^{-1}; n.m.r.: τ ($CDCl_3$) 5.43 (1H, quintet, $J = 3.0$ Hz), 6.88 (1H, quintet, $J = 3.5$ Hz), and 7.8–8.3 (12 H, multiplet).

CAN Oxidation of Adamantan-2-ol

Adamantanol (475 mg, 3.2 mmol) in acetonitrile (10 mg) was treated with CAN (14.25 g, 26 mmol) in water (30 ml) during 3 h at 60°. After cooling to room temperature, the reaction mixture was extracted with chloroform. Evaporation of the dried extracts yielded a yellowish waxy solid which was sublimed to give lactone **14** (250 mg, 50% yield).

Support for this work by the National Research Council of Canada and by the "Ministère de l'Education" (Québec) is gratefully acknowledged.

1. W. H. Richardson. Oxidation in organic chemistry. *Edited by* K. B. Wiberg. Part A. Academic Press, 1965. Chapt. IV.
2. (*a*) W. S. Trahanovsky, L. B. Young, and G. L. Brown. J. Org. Chem. **32**, 3865 (1967); (*b*) L. B. Young and W. S. Trahanovsky. J. Org. Chem. **32**, 2349 (1967).
3. W. S. Trahanovsky, L. H. Young, and M. H. Bierman. J. Org. Chem. **34**, 869 (1969).
4. W. S. Trahanovsky, L. B. Young, and M. D. Robbins. J. Am. Chem. Soc. **91**, 7084 (1969).
5. L. Syper. Tetrahedron Lett. 4493 (1966).
6. J. W. Bird and D. G. M. Diaper. Can. J. Chem. **47**, 145 (1969).
7. W. S. Trahanovsky, P. J. Flash, and L. M. Smith. J. Am. Chem. Soc. **91**, 5068 (1969).
8. W. S. Trahanovsky and J. Cramer. J. Org. Chem. **36**, 1890 (1971).
9. P. M. Nave and W. S. Trahanovsky. J. Am. Chem. Soc. **93**, 4536 (1971).
10. J. C. Collins, W. W. Hess, and F. J. Frank. Tetrahedron Lett. 3363 (1968).
11. C. Moreau and P. Deslongchamps. Can. J. Chem. **49**, 2465 (1971).
12. R. A. Sheldon and J. K. Kochi. J. Am. Chem. Soc. **90**, 6688 (1968), and ref. therein.
13. A. C. Udding, H. Wynberg, and J. Strating. Tetrahedron Lett. 5719 (1968).
14. H. L. Hintz and D. C. Johnson. J. Org. Chem. **32**, 556, (1967).
15. D. Djerassi. Steroid reactions. Holden-Day, Inc. San Francisco, 1963. p. 75.
16. R. E. Ireland, D. A. Evans, D. Glover, G. M. Rubottom, and H. Young. J. Org. Chem. **34**, 3717 (1969).

Evaluation of Some of the Factors Involved in the Selective Hydrolysis of Aromatic Ester Protecting Groups by α-Chymotrypsin[1]

J. Bryan Jones and Yong Yeng Lin

Department of Chemistry, University of Toronto, Toronto 181, Ontario

Received January 27, 1972

Studies have been carried out which delineate some of the factors involved in the exploitation of α-chymotrypsin as a catalyst for the specific hydrolysis of selected aromatic ester protecting groups under mild conditions with a specificity not achievable by non-enzymic reagents. The reactions can be carried out under heterogeneous conditions and examination of a series of diesters has shown dihydrocinnamyl to be the most satisfactory of the hydroxyl protecting groups evaluated so far. The degree of specificity achievable is demonstrated by the fact that α-chymotrypsin-catalyzed hydrolysis of 2-acetoxyethyl dihydrocinnamate at p*H* 7.8 stops when the latter function has been cleaved. In addition, some guidelines have been developed regarding the application of literature specificity data for predicting the course and rate of preparative scale reactions.

Des études ont été menées en vue de délimiter quelques uns des facteurs liés à l'exploitation de l'α-chymotrypsine en tant que catalyseur dans l'hydrolyse spécifique de groupes protecteurs constitués par certains esters aromatiques, avec une sélectivité non-réalisable par des réactifs non enzymatiques. Les réactions peuvent être faites dans des conditions hétérogènes et l'examen d'une série de diesters montre que le dihydrocinnamyle est le groupe protecteur de l'hydroxyle le plus satisfaisant jusqu'ici. Le degré de spécificité réalisable est démontré dans l'hydrolyse à p*H* 7.8 catalysée par l'α-chymotrypsine du dihydrocinnamate d'acétoxy-2 éthyle, qui s'arrête après clivage de cette fonction. De plus, quelques exemples ont été développés concernant l'application des données de la littérature sur la spécificité, pour prévoir le cours et la vitesse des réactions à l'échelle préparative.

Canadian Journal of Chemistry, **50**, 2053 (1972)

Although the capacity of α-chymotrypsin (α-CT) for preferential and stereospecific hydrolysis of a broad range of acyclic and cyclic aliphatic and aromatic esters and amides, and also some hydroxamides and hydrazides, is well documented (1–5), preparative exploitation of α-CT's properties has so far been relatively limited in scope. From the organic chemical viewpoint one of the most obvious areas for α-CT application is in the selective removal of protecting groups from hydroxyl and amino functions and in the latter connection the use of α-CT to catalyze the hydrolytic cleavage of acyl protecting groups has already been explored in the nucleotide field (6–8).

The above data (1–8) encouraged us to consider that selective hydrolysis by α-CT might be usefully applied during synthetic and other studies on a broad range of organic compounds and accordingly, a systematic investigation of the preparative advantages and limitations of the approach was initiated. This communication is primarily concerned with some of the experimental factors concerned with the protecting group aspect and with developing guidelines for the application of literature specificity data to competitive preparative scale reactions.

The acetate esters **3** were selected for the preparative scale specificity comparisons. Diesters of this type were considered superior to the monofunctional compounds usually employed (1) since, while they continued to allow easy analysis of α-CT specificity towards the various aromatic functions, the presence of the acetate ester provided an internal reference standard. Aliphatic acetates are hydrolyzed very sluggishly by α-CT (9) and it was considered that the extent of α-CT-catalyzed acetate hydrolysis of **3***a–f* would provide a measure of the practicability of achieving selective cleavage of the various aromatic acyl functions when the method was applied to compounds in which other relatively α-CT-insensitive ester groups were present. Furthermore, since the k_{-OH} values for each of the ester moieties of compounds **3** should not differ significantly (10), the degrees of differential hydrolysis observed were expected to be a direct reflection of the preparative α-CT specificity (9, 10) for each of the acyl groups.

[1]This work was presented in part at the 54th Canadian Chemical Conference, Halifax, Nova Scotia, June 1, 1971.

Can. J. Chem. Downloaded from www.nrcresearchpress.com by 210.87.254.6 on 09/05/12
For personal use only.

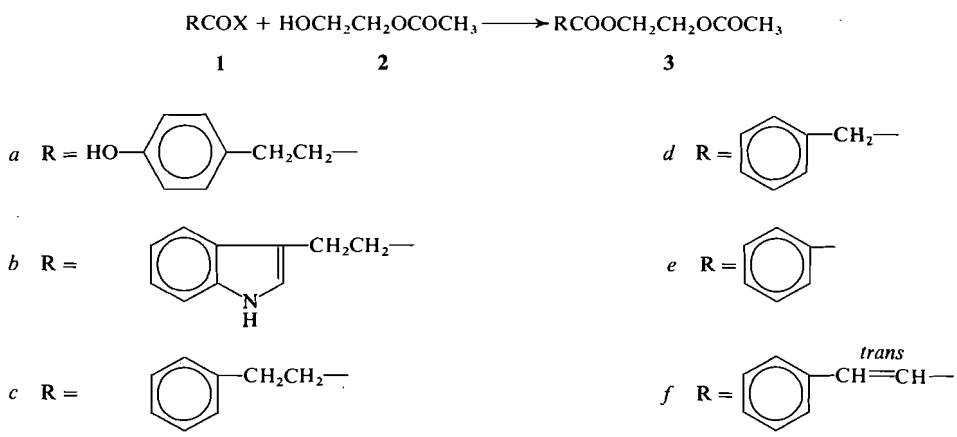

The predilection of α-CT for aromatic L-amino acid derivatives (1) suggests that their application as acyl protecting groups for alcohols and amines should afford the highest degree of hydrolytic specificity. However, in the nucleotide studies referred to previously (6, 7) practical difficulties were encountered with L-phenylalanyl esters and use of the dihydrocinnamyl analogues was found to be more satisfactory (8). In view of this it was assumed that α-CT would exhibit a still greater preference for the corresponding β-(*p*-hydroxyphenyl)-propionyl and β-indolylpropionyl analogues of the even better (1) tyrosyl and tryptophan substrates.[2] Accordingly, attention was directed initially towards the preparation of the diesters **3***a* and *b*. The presence of phenolic —OH and indolyl —NH functions precluded attempts to prepare **3***a* and *b* by condensation of **2** with the acid chlorides **1***a* and *b*, X = Cl; and, although some of the desired diesters were formed during a survey of acid-catalyzed (14) and dicyclohexylcarbodiimide (15, 16) mediated esterifications of 2-hydroxyethyl acetate (**2**) with the acids **1***a* and *b*, X = OH, only low yields of impure **3***a* and *b* could be isolated. In view of the above difficulties it was decided that the feasibility of employing β-(*p*-hydroxyphenyl)-propionyl and β-indolylpropionyl functions for the protection of hydroxyl groups was too limited to warrant their further consideration at this time.

In contrast, preparation of the diester **3***c* incorporating the dihydrocinnamyl group of proven value (8) was accomplished without complication.[3] The compound was immiscible with the types of aqueous media preferred for α-CT-catalyzed hydrolysis (1) but became readily soluble in water containing 30% of methanol or acetonitrile. Although α-CT kinetics have been studied in aqueous solutions containing these and even higher levels of organic solvents (4, 5), marked reductions in hydrolysis rates on addition of organic solvents[4] are well documented (1) and for **3***c*, the rates of reaction in the above homogeneous solutions were found to be too slow to be of preparative value. However, in view of the preparative scale resolutions successfully effected by α-CT on aqueous suspensions of racemates (3–5, 19, 20) it was decided to study the hydrolysis of **3***c* in the absence of organic solvents under heterogeneous conditions. It was found that under such conditions, α-CT-catalyzed hydrolysis of **3***c* proceeded extremely readily with specific cleavage of the dihydrocinnamate ester function. A range of reaction conditions was surveyed and optimum results were obtained at p*H*

[2]The correspondence in α-CT specificity towards the dihydrocinnamyl and phenylalanyl groups probably reflects their identity of interaction with the hydrophobic aromatic binding locus, ρ_{ar}, of the active site (1, 3, 11, 12) and the situation with respect to the tyrosine and tryptophan side chains and their analogues would be expected to be similar. The X-ray data available (13) support this view.

[3]All of the diesters **3***c–f* were readily purified and were obtained in good (*ca.* 80%) yields either by acid-catalyzed esterification of 2-hydroxyethyl acetate (**2**) with **1***c–f*, X = OH or via the acid chlorides **1***c–f*, X = Cl.

[4]Some of the organic solvent disadvantages of this and other enzymes are overcome by their stabilization on insoluble supports (17, 18) and studies are being carried out on the preparative applications of insolubilized α-CT.

Can. J. Chem. Downloaded from www.nrcresearchpress.com by 210.87.254.6 on 09/05/12
For personal use only.

Can. J. Chem. Downloaded from www.nrcresearchpress.com by 210.87.254.6 on 09/05/12
For personal use only.

7.8 (1) in aqueous 0.1 *M* potassium chloride at 25° with a substrate to enzyme ratio (w/w) of ~40:1. Satisfactory rates of hydrolysis were achievable using solutions containing 0.5–2 mg/ml of α-CT and little loss of activity was observed when enzyme solutions of this concentration were kept under the above reaction conditions for extended periods (> 24 h). As the reaction proceeded, the degree of heterogeneity gradually diminished and a clear solution was obtained when all of the dihydrocinnamyl moiety had been hydrolyzed.

From the preparative point of view the specificity of hydrolysis at p*H* 7.8 is virtually absolute and, as Fig. 1 illustrates, the reaction almost stops when 96–98% of the dihydrocinnamyl acyl group has been removed. The rate of hydroxide ion catalyzed hydrolysis of **3***c* at p*H* 7.8 was found to be negligibly small. Unfortunately, owing to its water solubility, 40–50% yields only of the 2-hydroxyethylacetate (**2**) product could be recovered. It was hoped that the latter situation would be improved using the slightly more hydrophobic 1,3-propyleneglycol analogue of **3***c* but, although the specificity of cleavage paralleled that of **3***c*, again the solubility of the 3-hydroxypropyl acetate product posed similar analytical and isolation problems.[5]

The specificity data in the literature (1, 22, 23) indicate that the dimensions of the dihydrocinnamyl group are close to the optimum for good binding in the ρ_{ar} locus and that an increase or decrease in chain length is reflected in raised K_m (or K_i of analogous inhibitors (24)) and/or lower k_{cat} values (1, 22, 23). That this was also broadly applicable to the preparative aspects of α-CT specificity and hydrolysis rates was confirmed by comparison of the homologous series of diesters, **3***c–e*. As Table 1 shows, decreasing the size of the aromatic function in the progression dihydrocinnamyl (**3***c*), phenylacetyl (**3***d*), and benzoyl (**3***e*) results in dramatic reductions in the hydrolysis rates for each methylene group

[5]Use of other α,ω-glycols of sufficiently high CH_2 content to ensure satisfactory recovery of the monoacetate from the aqueous reaction media was considered. However, in view of the adverse effect to be expected on the already low water-solubility of the types of diesters being evaluated, this aspect was not pursued further. In subsequent applications of the method for the selective hydrolysis of a selection of higher molecular weight esters of structural interest to organic chemists, 90%-quantitative yields of the alcohol moieties were isolated (21).

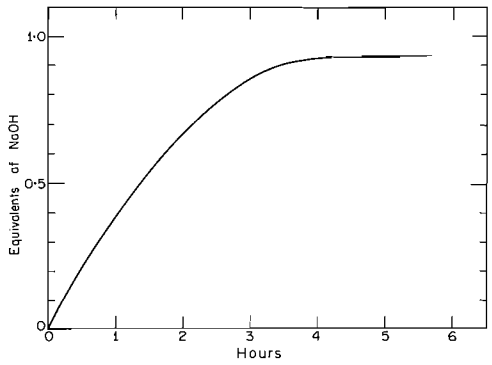

FIG. 1. A typical preparative scale p*H*-stat plot for the α-CT-catalyzed hydrolysis of dihydrocinnamate acetate diesters at p*H* 7.8. The termination of the reaction following uptake of ≃1 equiv of base illustrates the effectively absolute specificity of the cleavage with respect to the dihydrocinnamyl moiety. The above plot was recorded for a hydrolysis at 25° under nitrogen of **3***c* suspended in 0.1 *N* KCl containing 1.25 mg/ml of α-CT. The base used to maintain the p*H* at 7.8 was 1 *N* NaOH.

TABLE 1. Apparent rate constants for preparative scale α-CT-catalyzed hydrolyses of compounds **3***c–f*

Compound	k_{app} ($s^{-1} \times 10^3$)*
3*c*	96
$C_6H_5(CH_2)_2COO(CH_2)_3OCOCH_3$	113
3*d*	13.0
3*e*	<0.002
3*f*	7.9

*The rates of reactions were measured at 25° at p*H* 7.8 on stirred heterogeneous mixtures of 0.5×10^{-3} mol of substrate and aqueous 0.1 *N* KCl (10 ml) containing 0.5×10^{-6} mol (1.25 mg/ml) of α-CT. k_{app} values were calculated by dividing the observed initial velocity by the enzyme concentration.

lost. Although for the benzoyl derivative **3***e* the extent of hydrolysis observable during a preparative run was negligibly small, selective hydrolysis was still observed for the phenylacetyl ester **3***d*. However, with the latter compound some competitive acetate cleavage of the water-soluble 2-hydroxyethyl acetate initial product also occurred and preferential hydrolysis of the phenylacetyl moiety was achievable to a maximum extent of only 78%.

From the K_m and k_{cat} values of its ester derivatives (1, 9) the cinnamyl group would be expected to be a fairly good α-CT-sensitive protecting group (7). Surprisingly, however, the cinnamate acetate diester **3***f* proved to be a poor substrate under preparative conditions having a k_{app} (Table 1) more than an order of magnitude

Can. J. Chem. Downloaded from www.nrcresearchpress.com by 210.87.254.6 on 09/05/12
For personal use only.

smaller than that of **3***c*. Furthermore, subsequent cleavage of the 2-hydroxyethyl acetate produced initially became significant and accordingly, no further consideration was given to cinnamyl as a hydroxyl protecting group.

From the above and previous data (6–8) it is evident that of the α-CT-sensitive protecting groups surveyed so far the dihydrocinnamyl function is the most attractive, and the results of our studies on its applicability to a selection of compounds of general organic chemical interest will be reported shortly (21).

The above results also allow some preliminary conclusions to be drawn regarding application of the α-CT literature specificity and kinetic data for predicting the rate and course of a preparative scale hydrolysis. It is obviously unrealistic to expect that data usually obtained on homogeneous solutions under Michaelis–Menten conditions (*i.e.*, $[S] \gg [E]$, and often with $[S] \simeq 0.1\text{–}10\ K_m$) would be directly extrapolatable to preparative reactions of the types described above where the reaction media are heterogeneous and, in the aqueous layer, [S] is unlikely to be much, if at all, greater than [E]. In addition, at the concentrations of α-CT used, the significant proportion ($\simeq 10\%$) of oligomeric enzyme expected to be present cannot be ignored in any truly quantitative kinetic analysis (25, 26). Thus the variations in the values of k_{app} (Table 1), which is a composite rate constant in which the influence of solubility, specificity, and rates of acylation and deacylation are all reflected, cannot be regarded as being meaningful in any physical-organic or enzyme-kinetic sense. Nevertheless, analysis of the total data revealed certain encouraging correlations with some of the literature constants.

The two constants regarded as being most meaningful for α-CT-catalyzed hydrolyses of esters are k_{cat}/K_m, and k_3 or k_{cat} (the deacylation rate constant) (9). Unfortunately, the data on ester substrate analogues of **3***c–f* are too limited to permit an evaluation of the feasibility of using literature k_{cat}/K_m values for forecasting of the course of preparative reactions. In contrast, many k_3 constants of esters comparable with **3***c–f* are available and are found to parallel the rate and selectivity results observed in the preparative scale experiments. For example, the relative k_3's for the *p*-nitrophenyl esters of dihydrocinnamic acid, phenylacetic acid, cinnamic acid, and acetic acid are in the ratios 18:1.9:1.26:1 (9, 23). A similar pattern emerges for the corresponding methyl esters (9). These ratios are broadly consistent with the preparative scale observations that (*a*) **3***c* is hydrolyzed specifically at the dihydrocinnamyl group at a rate 7.5 times greater than that of **3***d*, (*b*) selective cleavage of the phenylacetyl function of **3***d* is possible but that competitive hydrolysis of the acetate ester begins to become important, and (*c*) as a result of the further reduction in hydrolysis rate of **3***f* (1.6 times slower than **3***d*) selective removal of the cinnamyl group without significant concomitant hydrolysis of the acetate ester is not a practical proposition. Although the correlation of the literature k_3's with the rates and selectivities of the preparative experiments appears to deny the importance of binding factors, for each of **3***c*, *d*, and *f*, good, predominantly productive binding would be expected (1, 11) and in such cases reliance on literature k_3 data seems justified. Further evaluations of the predictive value of literature k_3 and k_{cat}, and k_{cat}/K_m constants for preparative applications of α-CT are in progress.

Experimental

Each of the commercially available compounds used was recrystallized or redistilled before use. In addition, 2-hydroxyethylacetate was purified by column chromatography on Florisil prior to the final redistillation. All distillations were carried out using Nester–Faust spinning band columns. All liquids were purified until <1% impurity could be detected by spectroscopic and t.l.c. (on silica gel G) and g.l.c. analyses. The g.l.c. analyses were performed on an F and M 400 chromatograph equipped with 3.8% SE 30 or 1% QF-1 on Chromosorb G glass columns and n.m.r. spectra were determined on $CDCl_3$ (TMS internal standard) solutions with a Varian T-60 instrument. Solvent removals were effected by rotary evaporation. α-Chymotrypsin (crystallized three times) was purchased from the Worthington Biochemical Corp.

Preparation of the Diesters 3c–f

Each of the diesters was prepared from 2-hydroxyethylacetate (0.1 mol) by reaction with the appropriate acid chloride (0.1 mol), or acid (0.1 mol) in the presence of toluene-*p*-sulfonic acid (200 mg). Approximately eighty percent yields were obtained and the products were purified by spinning band distillation. The properties recorded for each were as follows:

2-Acetoxyethyl dihydrocinnamate (3c), b.p. 92–93°/0.05 Torr; n.m.r. δ 2.02 (3H, s), 2.80 (4H, A_2B_2 m), 4.25 (4H, apparent s), and 7.23 p.p.m. (5H, s).

Can. J. Chem. Downloaded from www.nrcresearchpress.com by 210.87.254.6 on 09/05/12
For personal use only.

Anal. Calcd. for $C_{13}H_{16}O_4$: C, 66.12; H, 6.77. Found: C, 66.37; H, 6.72.

2-Acetoxyethyl phenylacetate (3d), b.p. 88–89°/0.03 Torr; n.m.r. δ 2.03 (3H, s), 3.67 (2H, s), 4.31 (4H, apparent s), and 7.35 p.p.m. (5H, s).

Anal. Calcd. for $C_{12}H_{14}O_4$: C, 64.85; H, 6.34. Found: C, 64.97; H, 6.51.

2-Acetoxyethyl benzoate (3e), b.p. 104–105° (lit. (27) b.p. 110–115°/2 Torr); n.m.r. δ 2.03 (3H, s), 4.43 (4H, m), and 7.43–8.06 p.p.m. (5H, m).

Anal. Calcd. for $C_{11}H_{12}O_4$: C, 63.45; H, 5.81. Found: C, 63.56; H, 5.75.

2-Acetoxyethyl cinnamate (3f), b.p. 110–111°/0.025 Torr; n.m.r. δ 2.07 (3H, s), 4.4 (4H, apparent s), 6.5 and 7.74 (2H, ABq, J_{AB} = 16 Hz), and 7.44 p.p.m. (5H, m).

Anal. Calcd. for $C_{13}H_{14}O_4$: C, 66.65; H, 6.02. Found: C, 66.84; H, 6.20.

3-Acetoxypropyl dihydrocinnamate was prepared similarly from 3-hydroxypropyl acetate (28) (0.1 mol). It had b.p. 123–124°/0.08 Torr; n.m.r. δ 1.92 (2H, quintet, J = 6 Hz), 2.03 (3H, s), 2.78 (4H, A_2B_2 m), 4.12 (2H, t, J = 6 Hz), 4.17 (2H, t, J = 6 Hz), and 7.23 p.p.m. (5H, s).

Anal. Calcd. for $C_{14}H_{18}O_4$: C, 67.18; H, 7.24. Found: C, 67.06; H, 7.35.

Selective α-Chymotrypsin-catalyzed Hydrolyses of the Diesters on a Preparative Scale

Kinetic Runs

The relative rates of hydrolysis of each diester surveyed were measured on heterogeneous reaction mixtures containing 0.5 mmol of diester, 0.5×10^{-6} mol (12.5 mg) of α-CT and 0.1 *M* aqueous KCl (10 ml). The kinetic measurements were made at 25° with stirring under a nitrogen atmosphere using a Radiometer p*H*-stat (comprised of a TTTlc p*H*-meter, SBR2c titrigraph, SBUla syringe burette, and GK2024c combination electrode) to maintain the p*H* at 7.8. The base used was Fisher certified 1.0 *N* aqueous sodium hydroxide which had been freshly standardized by titration against potassium hydrogen phthalate. Initial velocities, v_0, taken directly from the p*H*-stat traces were used to calculate the apparent rate constants, k_{app} ($= v_0/[E]$). Each kinetic run was carried out at least in duplicate and the initial velocities were reproducible to within ±10% for any one diester. The k_{app} data recorded in Table 1 are mean values.

Preparative Procedure and Product Analysis

The procedure described below for 2-acetoxyethyl dihydrocinnamate (**3***c*) is representative of the analytical and product isolation method applied to each diester studied. The conditions described have been found satisfactory for quantities up to 2 g of diester.

2-Acetoxyethyl dihydrocinnamate (**3***c*, 795 mg, 3.4 mmol), 0.1 *M* aqueous KCl (40 ml), and aqueous α-CT (10 ml, containing 50 mg α-CT) were placed in a 60 ml p*H*-stat reaction vessel fitted with a rubber stopper through which the combination electrode, the needle of a 5 ml syringe (filled with 1 *N* aqueous NaOH), and a nitrogen line were introduced. The p*H*-stat was set to maintain a p*H* of 7.8 and the heterogeneous reaction mixture was magnetically stirred (avoiding cavitation of the liquid) at room temperature under a nitrogen atmosphere (with the nitrogen passing *over*, not through, the mixture in order to avoid enzyme denaturation) until base uptake (≃0.95 equiv) had almost stopped (≃6 h). The reaction mixture, which had gradually become homogeneous during this time, was then washed with ether (3 × 25 ml). The ether washings were extracted with saturated aqueous sodium bicarbonate (25 ml) and the combined aqueous solutions acidified to p*H* 2 with 2 *N* aqueous HCl and extracted with ether (3 × 25 ml). Quantitative g.l.c. analysis of the latter solution showed it to contain 3.1 mmol (98% of base consumption) of dihydrocinnamic acid. Isolation of the latter acid followed by distillation afforded a pure sample (100 mg), b.p. 105°/0.2 Torr, m.p. 47–48°, identical in all respects with an authentic sample. The g.l.c. analysis of the initial ether washings showed them to contain some of the diester **3***c* (< 5% of starting material used) together with 1.5 mmol (44% of theoretical[6]) of 2-hydroxyethyl acetate (**2**). The identity of the latter compound was confirmed by comparisons of its i.r. and n.m.r. spectra with those of authentic material.

p*H*-Stat control of the hydrolysis provided the most convenient means for monitoring the course of the reaction. However, in view of the fact that the hydrolysis was so selective for the dihydrocinnamyl group, use of a p*H*-meter, and a burette for periodic adjustment of the p*H* to 7.8 until hydrolysis ceased, also proved quite satisfactory.

The rate and specificity of hydrolysis of 3-acetoxypropyl dihydrocinnamate, and yields of products isolated, were virtually identical with those recorded for **3***c*. For 2-acetoxyethyl phenylacetate (**3***d*) slow hydrolysis up to the consumption of 1 equiv of base was only 78% specific for the phenylacetate group and for the still more sluggishly hydrolyzed cinnamate ester **3***f*, the effective selectivity of cinnamate cleavage was of an even lower order (< 50%). Phenylacetic acid, b.p. 104–105°/0.4 Torr, m.p. 73–74° and cinnamic acid, m.p. 134–135° (both identical with authentic samples) were isolated from the latter two reactions. Hydrolysis of **3***e* proceeded so slowly that kinetic studies only were carried out.

We are grateful to Mr. D. N. Palmer for his contributions to the studies on compound **3***a–c*. Financial support for this work was provided by the National Research Council of Canada.

1. L. Cunningham. *In* Comprehensive biochemistry. Vol. 16. *Edited by* M. Florkin and E. H. Stotz. Elsevier, New York. 1965. pp. 85–138.
2. B. Belleau and R. Chevalier. J. Am. Chem. Soc. **90**, 6864 (1968).
3. S. G. Cohen and L. W. Lo. J. Biol. Chem. **245**, 5718 (1970).
4. M. S. Silver, M. Stoddard, T. Sone, and M. S. Malta. J. Am. Chem. Soc. **92**, 3151 (1970) and previous papers.
5. Y. Hayashi and W. B. Lawson. J. Biol. Chem. **244**, 4158 (1969) and previous papers; Abstracts, 160th A.C.S. National Meeting, 1970. Biol. 12.
6. Z. A. Shabarova, N. I. Sokolova, and M. A. Prokov'ev. Doklady Akad. Nauk SSR **128**, 740 (1959); N. I. Sokolova, L. A. Borkova, and M. A. Prokof'ev. Zhur. Obshchei Khim, **29**, 2917 (1959).

[6]The low recovery of this material is a direct reflection of its solubility in water.[5]

7. D. H. RAMMLER and H. G. KHORANA. J. Am. Chem. Soc. **85**, 1997 (1963).
8. H. S. SACHDEV and N. A. STARKOVSKY. Tetrahedron Lett. 733 (1969).
9. M. L. BENDER and F. J. KEZDY. Ann. Rev. Biochem. **34**, 49 (1965); M. L. BENDER, F. J. KEZDY, and C. R. GUNTER. J. Am. Chem. Soc. **86**, 3714 (1964).
10. Tables of chemical kinetics. U.S. National Bureau of Standards Circular 510.
11. G. HEIN and C. NIEMANN. Proc. Nat. Acad. Sci. U.S. **47**, 1341 (1961); J. Am. Chem. Soc. **84**, 4495 (1962).
12. K. J. STEPHENSON and L. B. SMILLIE. Can. J. Biochem. **46**, 1357 (1968).
13. J. J. BIRKTOFT, D. M. BLOW, R. HENDERSON, and T. A. STEITZ. Phil. Trans. Roy. Soc. (London), B**257**, 67 (1970); R. HENDERSON. J. Mol. Biol. **54**, 341 (1970) and refs. therein.
14. *cf.* J. H. LOOKER and D. N. THATCHER. J. Org. Chem. **19**, 785 (1954).
15. *cf.* S. NEELAKANTAN, R. PADMASANI, and T. R. SESHADRI. Tetrahedron, **21**, 3531 (1965).
16. *cf.* J. C. HART, E. M. MATHESON, and O. HUTZINGER. Can. J. Chem. **48**, 177 (1970).
17. I. H. SILMAN and E. KATCHALSKI. Ann. Rev. Biochem. **35**, 873 (1966).
18. *e.g.* L. GOLDSTEIN. *In* Methods in enzymology. Vol. 19. *Edited by* S. F. Colowick and N. O. Kaplan. Academic Press, New York. 1970. pp. 935 *et seq.*
19. E. J. COREY, R. J. MCCAULLY, and H. S. SACHDEV. J. Am. Chem. Soc. **92**, 2476 (1970).
20. J. H. TONG, C. PETITCLERK, A. D'IORIO, and N. L. BENOITON. Can. J. Biochem. **49**, 877 (1971).
21. J. B. JONES and Y. Y. LIN. To be published.
22. J. B. JONES, T. KUNITAKE, C. NIEMANN, and G. E. HEIN. J. Am. Chem. Soc. **87**, 1777 (1965).
23. A. DUPAIX, J. J. BECHET, and C. ROUCOUS. Biochem. Biophys. Res. Commun. **41**, 404 (1970).
24. H. T. HUANG and C. NIEMANN. J. Am. Chem. Soc. **74**, 5963 (1952).
25. K. A. BOOMAN and C. NIEMANN. Biochim. Biophys. Acta, **26**, 439 (1957).
26. L. D. FALLER and R. E. LAFOND. Biochem. **10**, 1033 (1971).
27. E. JIRAT and F. VONASEK. Czech. Pat. 108 786. Chem. Abstr. **60**, 9205*b* (1964).
28. S. A. BALLARD, B. P. GEYER, and R. H. MORTHEIMER. U.S. Pat. 2 515 108; Chem. Abstr. **44**, 8944*h* (1950).

Can. J. Chem. Downloaded from www.nrcresearchpress.com by 210.87.254.6 on 09/05/12
For personal use only.

A Transient Intermediate in the Bimolecular Reaction of Hydrated Electrons

N. Basco, G. A. Kenney-Wallace,[1] S. K. Vidyarthi, and D. C. Walker

Chemistry Department, University of British Columbia, Vancouver

Received December 24, 1971

Further studies are reported which attempt to identify the transient species (X) produced from hydrated electrons which may be photodissociated to re-form e^-_{aq}. The method used involves the production of e^-_{aq} by u.v. flash photolysis of aqueous OH^-/H_2 solutions followed, after any specified delay, by a second and third photoflash of restricted wavelengths. Photoregeneration of e^-_{aq} is effected by light in the spectral range 320 to 400 nm, not at $\lambda > 700$ nm as earlier reported (1). The species X is much longer lived than e^-_{aq}, having a mean lifetime of ~ 5 ms at pH 11, but this is very dependent on the lifetime of e^-_{aq} in the system. Two conditions seem to be necessary in order to detect the presence of X, (*i*) e^-_{aq} must decay to a considerable extent through the bimolecular dimerisation reaction and (*ii*) the lifetime of e^-_{aq} with respect to all other reactions must be $>$ *ca.* 200 μs. Thus it is not expected to be observable in most pulse radiolysis studies. Its extinction coefficient in that part of its absorption band which leads to photodissociation (320–400 nm) is estimated to average $>2000\ M^{-1}\ cm^{-1}$, may be as high as $6000\ M^{-1}\ cm^{-1}$ at 347 nm but does not exceed $12\,000\ M^{-1}\ cm^{-1}$ at any wavelength. Its identity is discussed and it is concluded that X is probably the hydrated electron dimer, $(e_2^{2-})_{aq}$, or a product formed therefrom by association with a cation.

Des études plus poussées sont rapportées en vue d'identifier l'espèce transitoire (X) produite à partir d'électrons hydratés qui pourraient être photodissociés pour redonner e^-_{aq}. La méthode employée met en oeuvre la production de e^-_{aq} par photolyse flash u.v. de solutions aqueuses OH^-/H_2 suivie, après un temps déterminé, d'une seconde puis d'une troisième photolyse flash de longueurs d'onde réduites. La photoregénération de e^-_{aq} est effectuée par la lumière dans l'intervalle 320–400 nm et non pour $\lambda > 700$ nm comme il a été précédemment rapporté (1). L'espèce X a une durée de vie supérieure à e^-_{aq} (environ 5 ms à pH 11) et dépend étroitement de la durée de vie de e^-_{aq} dans le système. Deux conditions semblent nécessaires à la détection de la présence de X, (*i*) la disparition de e^-_{aq} par une réaction de dimérisation bimoléculaire doit être considérable. (*ii*) la durée de vie de e^-_{aq} par rapport à toutes les autres réactions doit être $>$ ca. 200 μs. Aussi ne doit-on pas s'attendre à l'observer dans la plupart des études de radiolyse par impulsion. Son coefficient d'extinction dans la zone de la bande d'absorption qui conduit à la photodissociation (320–400 nm) est estimé à une moyenne $>2000\ M^{-1}\ cm^{-1}$ pouvant atteindre $6000\ M^{-1}\ cm^{-1}$ à 347 nm mais en tout cas $< 12\,000\ M^{-1}\ cm^{-1}$ quelle que soit la longueur d'onde. L'identité de X est discutée, il s'agit probablement de l'électron hydraté dimère, $(e_2^{2-})_{aq}$, ou d'un produit qui en découle par association avec un cation.

Canadian Journal of Chemistry, **50**, 2059 (1972)

Introduction

In a previous communication (1) we reported evidence for a comparatively long-lived species whose precursor was the hydrated electron. This species was postulated to be $(e_2^{2-})_{aq}$, a hydrated electron dimer. In these experiments $\sim 10^{-6}\ M$ concentrations of hydrated electrons were produced by u.v. flash photolysis of $\sim 10^{-3}\ M$ NaOH in very pure water saturated with H_2 gas. This is a particularly "clean" chemical system because there is no overall chemical change and, apart from trace amounts of impurities, the only chemical species present are Na^+, OH^-, H_2, e^-_{aq}, and OH together with their reaction products. This long-lived intermediate could be of some interest from the point of view of radiation chemistry, particularly in the context of intra-spur reactions; perhaps also in the reaction of alkali metals with water and in cathodic electrolytic decompositions at high pH, in which e^-_{aq} could be involved in comparable reaction schemes (2).

For these reasons we built an improved and more versatile double-flash photolysis arrangement for this study and have examined the intermediate in more detail. One of our new findings concern the wavelength band responsible for the photoregeneration of e^-_{aq}. Contrary to our earlier report, for reasons we shall discuss, we believe this to be $320 < \lambda < 400$ nm rather than $\lambda > 700$ nm. Our data are largely consistent with some recent results of Gopinathan *et al.* (3) in a related type of experiment (but using considerably lower concentrations of e^-_{aq}) and it is highly probable that the same

[1]Present address: Radiation Laboratory, University of Notre Dame, Indiana 46556.

Can. J. Chem. Downloaded from www.nrcresearchpress.com by 210.87.254.40 on 09/05/12
For personal use only.

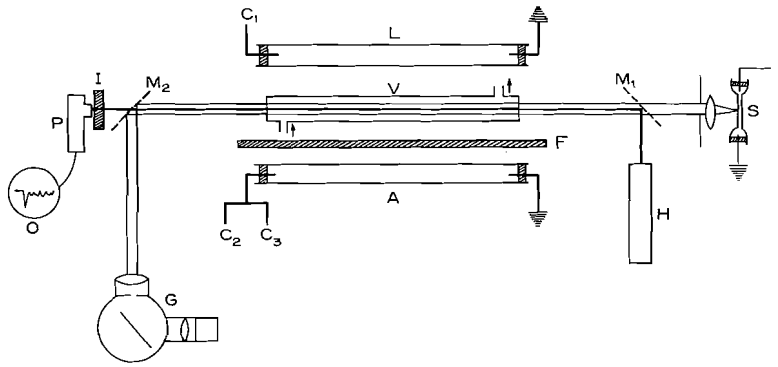

FIG. 1. Schematic drawing of the apparatus. V, reaction vessel; L, Main flash lamp; A, Auxiliary flash lamp; C_1, C_2, and C_3, capacity–spark gap assemblies shown in Fig. 2; F, light filters; S, spectroflash lamp; G, spectrograph; H, He/Ne laser; I, interference filter (narrow band pass at 632.8 nm); P, photomultiplier detector; O, oscilloscope; M_1 and M_2, plane mirrors. For spectrographic studies M_1 was removed; for photometric work M_2 was removed.

species is involved. However, our results would not support the species they propose.

Experimental

Experiments were performed with the apparatus shown schematically in Fig. 1. The reaction vessel, V, was 42.5 cm long made of Suprasil quartz and carried filling and emptying ports at its extremities. Quartz windows were fused onto the vessel. Aqueous solutions were prepared in an all-glass, sealed system where they were deoxygenated by continuous bubbling with H_2 or He and flowed through the reaction vessel under slight pressure when required. Adjacent to and on either side of V were two 50 cm long Suprasil quartz flash photolysis lamps; L and A. L will be described as the Main lamp and A as the Auxiliary lamp. These lamps were discharged typically at 4 to 8 kV, through 33 or 50 μF capacitors, thus yielding from 300 to 1000 J energy flashes having a width at half-height of about 20 μs. The lamps and reaction vessel were encased in a close-fitting metal reflector within a cylindrical container. A variety of Corning Color Glass light filters F, held in an aluminum frame which fitted snugly in a slot in the outer container, restricted the wavelength range of light from the Auxiliary lamp entering the reaction vessel.

Lamps L and A could be fired with any preselected time interval from 1 μs to 100 ms by means of electronic delay circuits, or at longer times by manual firing (4). An additional feature of this double-flash apparatus permitted the Auxiliary lamp to be discharged twice with any interval between consecutive flashes. This was achieved by connecting the lamp in parallel to two isolated capacitors each held off by a spark gap as indicated in Fig. 2. A capillary spectroflash Lamp S could also be fired at any time after any of the three photoflashes, and the absorption spectra of transient absorbing species recorded on a low dispersion spectrograph G. Various spectrographs were used including "Medium" and "Small" Hilger and Watts quartz prism instruments and a grating spectrograph built on the design of Bass and Kessler (5) in conjunction with a 35 mm camera. Two types of photographic films and plates were used covering different spectral regions, Ilford HP3 plates (320–650 nm), and Kodak Fast Infrared film (500–850 nm).

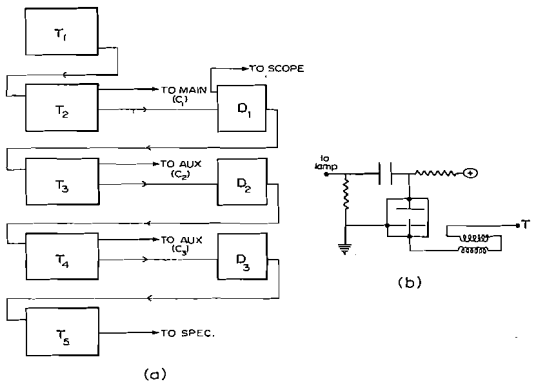

FIG. 2. (*a*) Triggering and time delay sequence for three photoflashes and a spectroflash. T_1 is a manually operated trigger pulse generator; T_2, T_3, T_4, and T_5 are trigger pulse generators for the Main, Auxiliary (first flash), Auxiliary (second flash), and spectroflash, respectively. D_1, D_2, and D_3 are variable time delays. Any unit may be bypassed. (*b*) Capacitor–spark gap assembly circuits for the Main and Auxiliary lamps (C_1, C_2, and C_3 in Fig. 1). T is the trigger pulse input.

For kinetic photometry studies at $\lambda = 632.8$ nm (where e^-_{aq} absorbs strongly, $\varepsilon = 1.2 \times 10^4\ M^{-1}\ cm^{-1}$ (6)) a 9 mW He/Ne CW laser, H, was used. Transient changes in the transmitted laser beam intensity were monitored by a photomultiplier, P, (either RCA 1P28 or Hamamatsu R213, using load resistances typically of 1 or 10 kΩ) coupled to an oscilloscope O. An advantage of using the laser as a light source is that there is sufficient intensity at 632.8 nm to employ a very narrow band-pass ($\sim$3 nm) interference filter as a window to the detector and virtually eliminate scattered light from the flash lamps. In this way the concentration of e^-_{aq} could be monitored *during* the photoflashes.

Figure 3 shows the transmission characteristics (7) of the various color glass filters used in F.

The solutions were prepared from distilled water which had been redistilled from dilute acidified dichromate solution, γ-irradiated with a dose of 2 Mrad and then refluxed

Can. J. Chem. Downloaded from www.nrcresearchpress.com by 210.87.254.40 on 09/05/12
For personal use only.

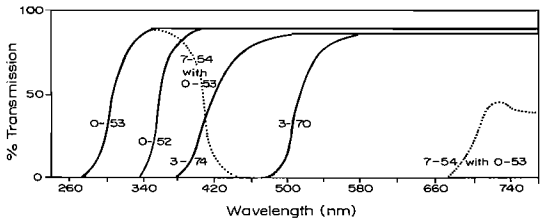

FIG. 3. Transmission curves for the various Corning Glass filters used at F in Fig. 1 (7).

continuously from very dilute alkaline permanganate solution until just prior to use. The NaOH, $NaClO_4$, $Ba(OH)_2$, HCOONa and isopropanol were Analar grade chemicals. As much of the residual carbonate content as possible was removed from the alkaline solutions by precipitating out carbonate in the concentrated stock supply. The NH_3 gas was 99.8% pure (Matheson), the H_2 was Matheson Prepurified grade and was passed through an activated Pd catalyst to remove traces of oxygen.

Results

(a) Chemical System

Following some preliminary experiments using the photolysis of I^- as the source of hydrated electrons and various alcohol scavengers to remove the oxidizing radical species, the OH^-/H_2 system was found to be the most satisfactory and nearly all the work reported was done with these solutions. In the iodide system other molecular and ionic photolysis products absorb in the visible which make interpretations of the spectral data ambiguous. The hydroxyl ion absorbs light of $\lambda < 220$ nm to produce e^-_{aq} and OH radicals according to reaction 1

$$[1] \qquad OH^- \xrightarrow[\lambda < 220\ nm]{h\nu} OH + e^-_{aq}$$

with a fairly low quantum yield within the accessible and useful wavelength range ($\sim$185 to 220 nm). The concentration of e^-_{aq} produced can be adjusted somewhat by altering the energy of the Main flash and by choosing the appropriate $[OH^-]$. If the latter is too high the absorption of the u.v. light occurs predominantly near the edge of the reaction vessel and a nonuniform concentration of e^-_{aq} results. One further advantage of using the laser therefore is that the analyzing light beam is very narrow (<2 mm diameter) and providing it is parallel to the axis of the vessel the kinetic measurements will not be seriously complicated by a concentration gradient across the cell diameter (10 mm). In all the experiments reported, the beam passed down the long axis of the cell.

A further consideration in the choice of hydrated electron concentration to be used arises from the lifetime of this species. For reasons which will become evident later we required that e^-_{aq} reacted predominantly by reaction 2

$$[2] \quad e^-_{aq} + e^-_{aq} \rightarrow [X] \xrightarrow{2H_2O} H_2 + 2\ OH^-, \qquad k_2 = 5 \times 10^9\ M^{-1}\ s^{-1}$$

rather than with either OH or with the inevitable low concentration of impurities present.[2] The extent to which this was achieved is indicated by the lifetime of e^-_{aq}. To avoid reaction 3

$$[3] \quad e^-_{aq} + OH \rightarrow OH^-_{aq}, \qquad k_3 = 3 \times 10^{10}\ M^{-1}\ s^{-1}$$

as much as possible the solution was saturated with H_2 gas, which converts OH to e^-_{aq} by reactions [4] and [5].

$$[4] \quad OH + H_2 \rightarrow H + H_2O, \qquad k_4 = 5 \times 10^7\ M^{-1}\ s^{-1}$$

$$[5] \quad H + OH^-_{aq} \rightarrow e^-_{aq}, \qquad k_5 = 2 \times 10^7\ M^{-1}\ s^{-1}$$

Reaction 3 nevertheless imposes the upper limit on the concentration of e^-_{aq} which may be used because of the comparatively low values of k_4 and k_5 and the fact that the apparatus was limited to H_2 pressures of 1 atm ($[H_2] = 7 \times 10^{-4}\ M$). At this $[H_2]$, however, there should be no serious complications arising from H_2O_2 which could otherwise be formed in reaction 6

$$[6] \quad OH + OH \rightarrow H_2O_2, \qquad k_6 = 5 \times 10^9\ M^{-1}\ s^{-1}$$

From these considerations we chose $(OH^-]$ in the range 10^{-3} to $3 \times 10^{-3}\ M$, $[H_2] = 7 \times 10^{-4}\ M$ and Main flash energies $\sim$500 J. This combination created e^-_{aq} at up to $2 \times 10^{-6}\ M$ with mean lifetimes of 200 to 100 μs. Although reaction 2 should be the dominant reaction of e^-_{aq} under these conditions, reaction 3 will contribute to some extent. Furthermore reaction 7

$$[7] \quad e^-_{aq} + H \rightarrow [H^-_{aq}], \qquad k_7 = 2.5 \times 10^{10}\ M^{-1}\ s^{-1}$$

cannot be entirely ignored because of H produced in reaction 4. In order to examine the role of reactions 3 and 7 some experiments are reported in which the OH radicals were scavenged using low concentrations of sodium formate or 2-propanol.

Most experiments were performed with OH^-/H_2 solutions because this is a particularly "clean" system in which to study e^-_{aq} (9) and is

[2]All rate constants are taken from the Tables presented in ref. 8.

Can. J. Chem. Downloaded from www.nrcresearchpress.com by 210.87.254.40 on 09/05/12
For personal use only.

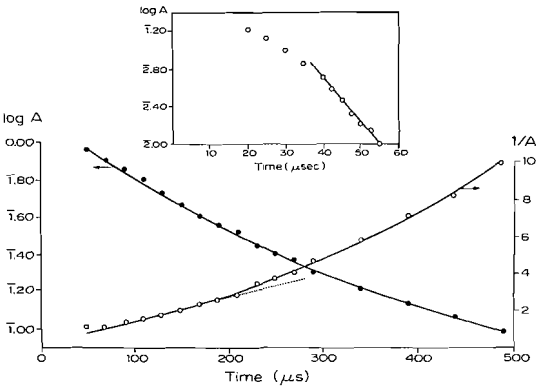

FIG. 4. First- and second-order kinetic plots for the decay of e^-_{aq} following the Main flash. Insert shows first-order plot for a solution containing 1.1×10^{-5} *M* $NaNO_3$, 10^{-4} *M* HCOONa at p*H* 11.5.

essentially unchanged (even cleaned up) by repeated flashing.

(b) Decay of e^-_{aq} Following the Main Flash

Figure 4 shows typical first- and second-order kinetic plots for the decay of absorbance due to e^-_{aq} at 632.8 nm following the Main flash in a OH^-/H_2 solution. The first 70 μs are complicated both by the tail of the light flash and by the occurrence of reactions 4 and 5. For times longer than 70 μs the decay was treated according to a method of combined first- and second-order reactions (10) by plotting $A_{t+\theta}^{-1}$ against A_t^{-1}, where θ is a constant time interval. Straight lines were obtained for these plots. Using a value of $\theta = 200$ μs the line obtained had a slope of 1.67 ± 0.02 and an intercept of 2.53 ± 0.1, from which one calculates a second-order rate constant (k_s) of $(4.9 \pm 0.2) \times 10^9$ M^{-1} s^{-1} and a first-order rate constant (k_f) of $(2.5 \pm 0.1) \times 10^3$ s^{-1}. This value of k_s (defined by $-dc/dt = k_s c^2 + k_f c$), which approximates the limiting slope in Fig. 4 (6.5×10^9 M^{-1} s^{-1}), should be compared with the published values of $2k_2$. In this experiment e^-_{aq} was produced at $\sim 2 \times 10^{-6}$ *M* so that, from k_s and k_f, one calculates that 60% of e^-_{aq} reacted by the bimolecular combination reaction 2. (For experiments in which e^-_{aq} was produced at 1×10^{-6} *M* reaction 2 would consume only 45% of e^-_{aq}.)

The mean lifetime of e^-_{aq} with respect to the pseudo first-order component, given by k_f, is thus 400 μs. This reaction is only 2.8 times faster than the slowest reaction computed for the decay of e^-_{aq} at nanomolar concentrations by pulse radiolysis and attributed to the reaction of e^-_{aq} with H_2O (11). We must presume that k_f represents reaction with an impurity which we could not eliminate. For that reaction to be reasonably well described by a pseudo first-order rate the impurity must be present at greater than ~ 2 times the initial $[e^-_{aq}]$ and consequently its concentration must be $> 4 \times 10^{-6}$ *M* and its reaction with e^-_{aq} must have a rate constant $< 6 \times 10^8$ M^{-1} s^{-1}.

The absorption spectrum presented later shows that the absorption monitored at 632.8 nm is due to e^-_{aq}. This is confirmed by the decay data at 632.8 nm shown as the insert on Fig. 4 which pertains to an aqueous solution at p*H* 11.5 containing 1.1×10^{-5} *M* $NaNO_3$, 10^{-4} *M* sodium formate, and deoxygenated by saturating with He gas. Under these conditions the $HCOO^-$ scavenges the OH radical and the NO_3^- reacts with e^-_{aq}. The first 40 μs are complicated because of the tail of the Main flash but thereafter a good first-order decay is obtained, from the slope of which one obtains $k(e^-_{aq} + NO_3^-) = 1.1 \times 10^{10}$ M^{-1} s^{-1}. This compares most favourably with published values for this reaction which range from (0.92 to 1.1) $\times 10^{10}$ M^{-1} s^{-1}.

In experiments conducted on various very low NO_3^- solutions, at concentrations where e^-_{aq} still decayed largely by pseudo first-order kinetics, no absorption at all could be detected when the Auxiliary lamp was flashed at any delay with the 0–53 filter placed in F. This verifies that either the occurrence of reaction 2 or a long-lived e^-_{aq} is a prerequisite for photoregeneration of e^-_{aq}. Apparently both conditions are necessary, though this is not easy to test directly.

(c) Light Filter Experiments

Figure 5 shows three typical oscilloscope traces for the double flash photolysis of OH^-/H_2 solutions, monitored at 632.8 nm, in which a Pyrex glass filter (0–53) was incorporated between the Auxiliary lamp and reaction vessel. The position of the arrow indicates the moment at which the Auxiliary lamp (photolyzing only at $\lambda > 260$ nm) was fired. A second absorption signal was recorded in Fig. 5 (*a*), (*b*), and (*c*). As the delay time was increased the second absorption signal decreased and was barely detectable for times greater than ~ 20 ms. Figure 5(*d*)

Can. J. Chem. Downloaded from www.nrcresearchpress.com by 210.87.254.40 on 09/05/12
For personal use only.

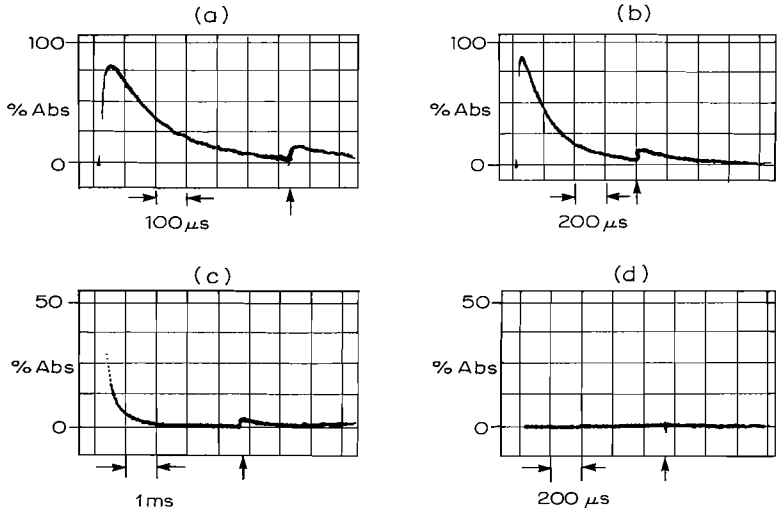

FIG. 5. Reproductions of oscilloscope traces showing the absorption at 632.8 nm as a function of time in an OH^-/H_2 solution as described in the text. The arrows indicate when the Auxiliary flash ($\lambda > 260$ nm) occurred. In (*d*) the Main lamp was not fired.

shows a trace in which the Main flash was not fired but the oscilloscope time-base triggered by the Main lamp's triggering circuit. In this case no absorption was created by the Auxiliary lamp at $\lambda > 260$ nm.

It is clear then that hydrated electrons must be created by the u.v. flash before a second peak may be observed. Kinetic plots of the absorbance created by the Auxiliary flash indicate neither simple first- nor second-order decays for the species responsible. The absorbances measured for the Auxiliary-induced peak have never exceeded 20% of the absorbance due to e_{aq}^- in the Main peak. Furthermore the height of the Auxiliary peak depends strongly on both the $[e_{aq}^-]$ produced initially by the Main lamp and on the lifetime of e_{aq}^-, increasing as the lifetime increases. When the lifetime of e_{aq}^- was $< 10^{-4}$ s with respect to the first-order component no Auxiliary-induced absorbance could be detected at all.[3] For these reasons it is impossible for us to quote a lifetime for the intermediate species X which is very meaningful. In a good "clean" system it is certainly > 1 ms and may typically be ~ 5 ms. There are experimental indications that X was being both formed and decomposed during the lifetime of e_{aq}^- and that its maximum concentration is reached when the e_{aq}^-, and the OH, H, and H_2O_2, have been largely destroyed at about 500 μs after the Main flash.

Less than a 20% change in the Auxiliary absorption peak was obtained on changing from one to two layers of the 0–53 filter in F. This suggests that X does not have a strong narrow absorption band between 280 and 320 nm (or that there is enough light and absorption at other wavelengths to dissociate X completely). On exchanging the 0–53 light filter for the other filters shown in Fig. 3 we find the following results. One layer of 0–52 reduces the Auxiliary peak to about 70% of that obtained with 0–53 and 2 layers reduces it further. Filters 3–74 and 3–70 eliminate the Auxiliary absorption peak completely. This finding is contrary to data reported in our previous communication (1). At that time we concluded from the use of filter 7–54 that it must be wavelengths > 700 nm that were responsible for the second peak, rather than the "window" of that filter at 260–420 nm, because we also saw the second absorption peak using filter 3–70. We cannot explain the erroneous results obtained with the 3–70

[3]Czapski and Peled (12) have shown that, in the pulse radiolysis of an alkaline aqueous solution containing 10^{-2} *M* alcohol, there was no evidence for a species which was *both* long-lived and absorbed light in the region 600–1100 nm. This conclusion is consistent with our present filter data indicating the different wavelength range. However, it should be noted that it could equally well have arisen from the requirement of a long-lived e_{aq}^- because in their system (12) e_{aq}^- itself decayed through ~ 14 half-lives in 200 μs by reaction with other solutes present (Czapski and Peled suggest these may be H_2O_2 or aldehydes).

Can. J. Chem. Downloaded from www.nrcresearchpress.com by 210.87.254.40 on 09/05/12
For personal use only.

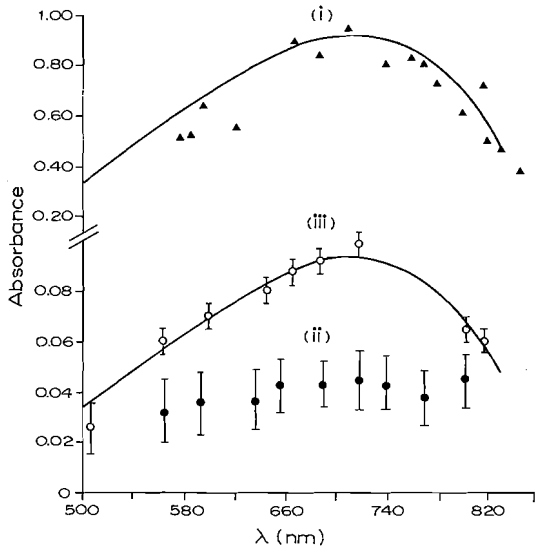

FIG. 6. Absorption spectra of an OH^-/H_2 solution: (*i*) 70 μs after the Main flash; (*ii*) 600 μs after the Main flash; (*iii*) 55 μs after the Auxiliary flash ($\lambda > 260$ nm) which was fired 600 μs after the Main flash.

filter at that time except by concluding that some stray u.v. light must have by-passed that filter in those experiments, which were performed on another flash photolysis apparatus.

It is evident then that the Auxiliary absorption peak is produced by wavelengths largely in the range 320 to 400 nm. In this respect our observations are in reasonable accord with results recently reported by Gopinathan *et al.* who found that $\sim 10^{-9}$ *M* e^-_{aq} may be generated by flash photolysis using similar wavelengths when a H_2-saturated solution at p*H* 11 was concurrently exposed to the u.v. light from a Hg lamp (3). It seems highly probable that the same intermediate is produced in these two experiments (but not the one they suggest).

(d) Absorption Spectra

The absorption spectra of species present at any preselected time after either photoflash may be measured spectrographically using the spectroflash lamp S as a white light source. The film or plate densities were converted to solution absorbance data using characteristic curves constructed for each wavelength. Figure 6 shows the absorbance of the solution between 500 and 850 nm, (*i*) 70 μs after the Main flash, (*ii*) 600 μs after the Main flash (no Auxiliary flash), and (*iii*) 55 μs after the Auxiliary flash (with 0–53 filter in F) which was fired 600 μs after the Main flash. These data were recorded on Kodak Fast Infrared film using the Bass-Kessler spectrograph.

The wavelength range 300 to 500 nm was investigated using the Hilger spectrographs and Ilford HP3 photographic plates. For this wavelength range the scatter in the background plate density resulting from small fluctuations in the spectroflash lamp intensity was more severe and placed a lower limit of absorbance ~ 0.1 on the sensitivity for detection of absorbing species. The same three experiments yielded the following information: in (*i*) the tail of the band shown in Fig. 6 decreased continuously from 500 to 300 nm; in (*ii*) and (*iii*) no absorbance could be detected.

Several conclusions may be drawn from the data in Fig. 6. Firstly, in (*i*) the absorption band determined corresponds very closely to the known spectrum of the hydrated electron. In conjunction with the kinetic evidence this enables us to attribute the absorbance measured using the He/Ne laser to e^-_{aq}. Secondly, the weak absorption observed in (*iii*) also resembles that of e^-_{aq}, thus strongly suggesting that hydrated electrons are being regenerated by the Auxiliary flash. Thirdly, no absorption could be detected ($A < 0.1$) for species X in (*ii*). This fact will be used later to place an upper limit of $\sim 1.2 \times 10^4$ M^{-1} cm^{-1} on the absorption coefficient of this species over the range 300 to 850 nm.

(e) Triple-flash Experiments

Why could only 20% of the hydrated electrons be regenerated even under the most favorable circumstances within our experimental limitations? Was it because the extinction coefficient of X was small or flash intensity was too low, or did only 20% of the initial e^-_{aq} generated by the Main flash form X? To try to answer this we discharged the Auxiliary lamp twice, at about the same energy, with 100–400 μs separation. Figure 7(*a*) shows the oscilloscope trace using laser photometry at 632.8 nm when there was no light filter present between the Auxiliary lamp and reaction vessel. This indicates that the u.v. light intensity was comparable in the two Auxiliary flashes. Figure 7(*b*) shows a trace taken under similar conditions, but with the 0–53 filter in F. Evidently the second Auxiliary flash regenerates <20% as much e^-_{aq} as is pro-

Can. J. Chem. Downloaded from www.nrcresearchpress.com by 210.87.254.40 on 09/05/12
For personal use only.

Can. J. Chem. Downloaded from www.nrcresearchpress.com by 210.87.254.40 on 09/05/12
For personal use only.

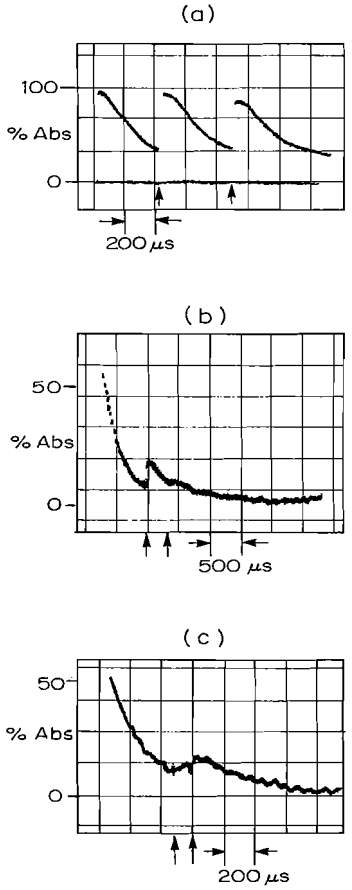

FIG. 7. Reproductions of oscilloscope traces showing the absorption at 632.8 nm in the triple flash experiments described in the text on an OH^-/H_2 solution: (*a*) no filter in F; (*b*) filter 0–53 in F. Arrows indicate the times at which the Auxiliary lamp was fired (Auxiliary lamp fired at 7 kV both times); (*c*) as in (*b*) except that the Auxiliary lamp was fired at 3 kV first time and at 7 kV 110 μs later.

duced by the first Auxiliary flash. This does not however arise from the normal decay of X during the extra 340 μs delay from the Main flash, as indicated by the relative magnitudes of peaks obtained from single Auxiliary flashes at 530 and 870 μs delays. This latter point is further corroborated by the trace shown in Fig. 7(*c*). In this experiment the Auxiliary was fired at 3 kV, 630 μs after the Main flash then fired again 110 μs later but this time at 7 kV charging voltage. The difference in light intensities produced in the range 300–400 nm by these two flashes should be more than the factor of 5.5 calculated simply from $(7/3)^2$. Absorption produced by the first Auxiliary flash in this case is barely detectable.

We interpret these triple flash experiments to mean that ~80% of X is normally photodissociated by the Auxiliary flash and thus that less than 24% of the hydrated electrons initially formed yield X molecules which can survive 600 μs in our system.

Therefore, in a typical experiment, the concentration of X after 600 μs must be only $\sim 2 \times 10^{-7}$ *M*. When combined with the absorbance limit, $A < 0.1$, this yields an upper limit of $1.2 \times 10^4\ M^{-1}\ cm^{-1}$ on the absorption coefficient over the wavelength range where it is photodissociated to give e^-_{aq}, and also over the whole visible region of the spectrum.

From these results it may be argued as well that the mean extinction coefficient ($\bar{\varepsilon}$) within the wavelength range 320 to 400 nm cannot be very small. Since the absorbance of the solution across the cell is very small, the fraction of incident light absorbed by X following the discharge of the Auxiliary lamp may be approximated to

$$\Delta I/I = 2.3\ \bar{\varepsilon} l[X]$$

where *l* is the mean optical path length traversed in the solution by light originating from the Auxiliary lamp. A reasonable value for *lI* may be obtained from the measured extent of photolysis of gaseous bromine at 1 Torr pressure (13) using the previously described apparatus (1). From the known absorption spectrum of bromine it could then be calculated that $2.3lI \approx 6 \times 10^{-6}$ einstein cm nm^{-1}. Assuming the same output for the range 320–400 nm, similar efficiency for the apparatus, and putting $\Delta I \approx [X]$, one calculates $\bar{\varepsilon}$ for X to be $\sim 2 \times 10^3\ M^{-1}\ cm^{-1}$. In fact this is probably a lower limit because the new apparatus is somewhat larger (to accommodate the filters in F).

Within the wavelength range responsible for photodissociation X appears to have a mean extinction coefficient $> 2000\ M^{-1}\ cm^{-1}$; but it does not exceed 12 000 $M^{-1}\ cm^{-1}$ at any λ.

(f) Frequency-doubled Ruby Laser Data

Some further evidence that these solutions contain a relatively long-lived intermediate species X comes from experiments performed using the frequency-doubled Ruby laser line at 347 nm. The He/Ne laser was replaced by a

Can. J. Chem. Downloaded from www.nrcresearchpress.com by 210.87.254.40 on 09/05/12
For personal use only.

Q-switched ruby laser incorporating a frequency doubling crystal which converted about 1% of the 75 MW pulse of 20 ns duration at 694.3 nm to 347.1 nm light. In these experiments the 694 nm flux was eliminated by the use of a $CuSO_4$ absorber and the 347 line was attenuated with a $K_2Cr_2O_7$ filter to an intensity level where it would not cause photodissociation of X. Unfortunately this laser could be fired only up to delay times of 500 μs after the Main flash because of the triggering mechanism. Absorbance measurements were made by comparison of the transmitted 347 nm light from the Main flash with that obtained at various time delays after the Main flash. Because of the small absorbance and slight variations in the laser light from pusle to pulse there is considerable scatter in the data obtained. Nevertheless, the absorbance seemed to be ~ 0.1 at all delay times up to 500 μs. These data are given in Fig. 8, together with the time dependence of the absorbance measured separately for the particular solution and Main flash energy used in this experiment as monitored at 632.8 nm by the He/Ne laser. Also shown in Fig. 8 is the absorbance that would be expected at 347 nm due to e^-_{aq}, calculated from the measured absorbance at 632.8 nm by multiplying the latter by the ratio of extinction coefficients of e^-_{aq} at 347 and 632 (*i.e.* multiplied by 0.11 (6)).

The initial concentration of e^-_{aq} was $\sim 2 \times 10^{-6}$ M in these experiments, so that if we assume 20% conversion to X then the extinction coefficient of X at 347 nm must be ~ 6000 M^{-1} cm^{-1}.

(g) Added Solutes

Experiments performed on different chemical systems using laser photometry and typically an 800 μs delay between the u.v. and Auxiliary flash (only $\lambda > 260$ nm) led to the following observations:

(i) Excess Na^+

When the $[Na^+]$ was varied from 10^{-3} to 1 M by adding $NaClO_4$ to the $NaOH/H_2$ system, no marked change could be detected in the height of the Auxiliary absorption peak.

However, we did note the following. When H_2 saturated water (p$H \sim 7$) was flash photolyzed no absorption at all was observed at 632.8 nm either following the Main flash (u.v.) or Auxiliary flash ($\lambda > 260$ nm). When 1 M $NaClO_4$ at p$H \sim 7$ was photolyzed some aborption at 632.8 nm could be detected ($\sim 10\%$ that found at pH 11) following the Main flash but again none following the Auxiliary flash. This suggests that direct u.v. photolysis of our $NaClO_4$ solutions produced small concentrations of e^-_{aq}. Similar effects may have been observed in the experiments of Gopinathan *et al.* (3) who found $NaClO_4$ increased the concentration of photogenerated e^-_{aq} to $\sim 10^{-8}$ M. The presence of $NaClO_4$ in their experiments may have increased the steady state concentration of e^-_{aq}, thus yielding more X to be photodissociated, and thereby placing a different interpretation on the role of Na^+ ions.

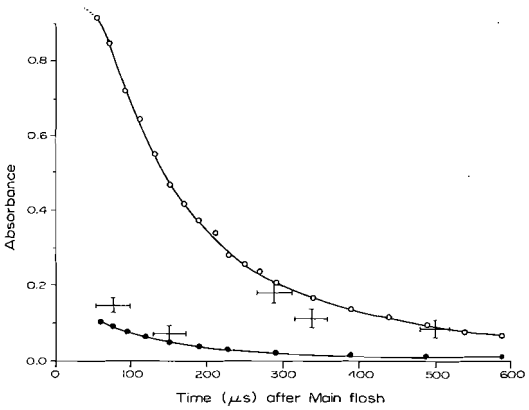

FIG. 8. Absorbance as a function of time: +, absorbance measured at 347 nm using the Ruby Laser (see text); ○, absorbance measured at 632.8 nm using the He/Ne laser; ●, absorbance calculated for e^-_{aq} at 347 nm from the He/Ne data using $\varepsilon_{633}/\varepsilon_{347} = 0.11$.

(ii) NH_4OH Solutions

When metal ions were eliminated from the system by using a solution containing only NH_4OH saturated with H_2 the Auxiliary peak was formed in comparable yield to that obtained in NaOH solutions of the same pH.

(iii) Ba^{2+} Ions

A solution made of $Ba(OH)_2$ and H_2 also gave similar results, confirming that the same effects can be observed with various cations. This further shows that the carbonate radical anion, CO_3^-, which could be formed by attack of OH on any CO_3^{2-} present in the NaOH solutions, is not responsible for the absorption at 632.8 nm.

(iv) H_2O_2 Solutions

When various concentrations of H_2O_2 in the range 10^{-5} to 10^{-3} M were added to the

Can. J. Chem. Downloaded from www.nrcresearchpress.com by 210.87.254.40 on 09/05/12
For personal use only.

$NaOH/H_2$ solutions no Auxiliary-induced absorption signal was detected. This indicates that the second absorption peak does not arise by photolysis of H_2O_2 or HO_2^- formed in these solutions by reaction 6. Furthermore, this corroborates our earlier conclusion that if the lifetime of e_{aq}^- is curtailed by the presence of an e_{aq}^- scavenger then no Auxiliary peak could be observed.

(v) Formate Ions and 2-Propanol as OH Scavengers

In most of the experiments discussed so far the OH radicals produced in the u.v. photolysis of OH^- were scavenged by H_2 at 7×10^{-4} *M* and converted to e_{aq}^- by reactions 4 and 5 only rather slowly (mean lifetimes of OH and H being about 30 μs each). In order to establish whether OH or H were involved in the formation of X, some experiments were performed using sodium formate or isopropanol to reduce the lifetime of OH to ~ 1 μs and exclude the formation of H. These solutions consisted of 2×10^{-3} *M* NaOH, 3×10^{-5} *M* HCOONa (or 3×10^{-4} *M* 2-propanol) and deoxygenated by bubbling with pure He gas. Following the Main flash the initial absorption at 632.8 nm was smaller than in the OH^-/H_2 solutions (as would be expected since none was formed via reactions 4 and 5) and the decay rate somewhat faster. However, in both cases Auxiliary-induced absorption was obtained in yields quite similar to that found in OH^-/H_2 solutions having the same initial $[e_{aq}^-]$ and comparable decay rates. Furthermore, light filter 3–70 eliminated the Auxiliary peak and 0–52 reduced it markedly, as in the H_2/OH^- systems. It was clear, however, that by adding much higher concentrations ($\sim 10^{-2}$ *M*) of alcohols or formate the lifetime of e_{aq}^- was curtailed (presumably due to impurities introduced with these solutes) and no Auxiliary-induced photodissociation of X was observed.

Summary of Results

A transient species, X, is produced from hydrated electrons under conditions where e_{aq}^- is itself quite long-lived (greater than ~ 200 μs with respect to pseudo first-order processes including impurities and added solutes) and when it decays predominantly in the bimolecular combination reaction 2. Species X is photodissociated to regenerate e_{aq}^- by light largely in the range 320 to 400 nm. Filter experiments indicate that the absorption band responsible for photodissociation is fairly broad, perhaps covering most of this range. Absorption measurements suggest that the mean extinction coefficient between 320 and 400 nm is at least 2000 M^{-1} cm^{-1}, that it may be as high as 6000 M^{-1} cm^{-1} at 347 nm but that it does not exceed 12 000 M^{-1} cm^{-1} at any wavelength.

From the measured concentration of e_{aq}^- regenerated by the Auxiliary flash at various delay times, it is deduced that the life-time of X is very sensitive to the yield and lifetime of e_{aq}^- created initially and that in a "good" experiment its half-life is ~ 5 ms. However, its decay rate cannot be described by simple first- or second-order kinetics and a 20% yield of regenerated hydrated electrons was the largest ever found. Triple flash experiments showed that there was enough light in the first Auxiliary flash to dissociate 80% of the X molecules present 600 μs after the Main flash.

Similar results were obtained when the OH radical was scavenged by H_2 (7×10^{-4} *M*), 2-propanol (3×10^{-4} *M*) or $HCOO^-$ (3×10^{-5} *M*), thereby proving that the OH radical is not involved in the formation of X. Furthermore, different cations (vast excess of added Na^+ ions or the use of NH_4OH or $Ba(OH)_2$ as the source of OH^-) had almost no effect on the yield of photoregenerated e_{aq}^-.

Spectral measurements have confirmed the kinetic evidence that the species responsible for absorption at 632.8 nm in the Main and Auxiliary flashes are hydrated electrons. However, the absorption spectrum of X could not be detected spectrographically; thus on upper limit of 1.2×10^4 M^{-1} cm^{-1} may be placed on its extinction coefficient over the spectral range 300 to 850 nm.

Discussion

Our previous postulate that the comparatively long-lived species found in these systems was a hydrated electron dimer, formed in reaction 8,

[8] $$e_{aq}^- + e_{aq}^- \rightarrow (e_2^{2-})_{aq}$$

which could be photodissociated in the process

$$(e_2^{2-})_{aq} \xrightarrow{h\nu} 2e_{aq}^-$$

This was based partly on the kinetic information but largely on the understanding that this species absorbed light of wavelengths > 700 nm. For such a species to in fact absorb strongly in the

Can. J. Chem. Downloaded from www.nrcresearchpress.com by 210.87.254.40 on 09/05/12
For personal use only.

range 320 to 400 nm does not immediately gain credence from comparisons with F' centers in alkali halide crystals (14) and other dielectron species in solids (15), where the dimers have broad bands which are red-shifted with respect to the monomeric species. However, it should be noted that in the case of solids the size of the cavity constituting the F or F' center is fixed by the lattice parameters, whereas for liquids the cavity may adjust its size to the constraints imposed by the presence of two electrons (in either singlet or triplet state, the latter presumably requiring a large cavity). The polarization of the medium could then correspond to the solvation of a doubly charged species. Indeed calculations by Fueki on trapped dielectron species predict a small blue-shift for λ_{max} in liquid water (16).

It is interesting (and perhaps significant) that the photon energy found for the regeneration of e^-_{aq} from X ($\sim$3.5 eV) is about twice the solvation energy of e^-_{aq} (1.7 eV (17), which also equals the photon energy of the absorption band maximum). ΔG for reaction 8 will be governed by the small change in entropy expected for the reaction as written but mainly by the difference in heats of solvation of the species involved. (This assumes of course that the bond energy of e_2 is negligible.) Reaction 8 would thus be quite endoergic if the dimeric species had a lower solvation energy than the monomeric species; *i.e.* if the e_2 species had a red-shifted absorption band maximum. On this basis a solvation energy for $(e_2^{2-})_{aq}$ of $\sim$3.5 eV is consistent, thermodynamically, with its formation in reaction 8. In solids, the e_2 species which have been observed did not arise from a "chemical reaction" such as reaction 8; but rather by trapping of a free electron (from a comparatively high energy state) at a site already containing a trapped electron.

It might be argued that an e_2 species would be expected to have a much broader absorption band than our filter experiments indicate. However, it should be recalled that the 320 to 400 nm range only represents that wavelength range which is observed to lead to photoionization. This may be merely the high energy tail of a much broader band involving bound–bound transitions at longer wavelengths.

It has not been possible for us to establish the identity of X. As indicated above we feel that a hydrated electron dimer is still a strong candidate. The kinetic evidence suggests that X is either $(e_2^{2-})_{aq}$ or a species formed therefrom; perhaps by proton abstraction from water, reaction 9

$$[9] \qquad (e_2^{2-})_{aq} + H_2O \rightarrow H^-_{aq} + OH^-_{aq}$$

or association with a cation according to reaction 10.

$$[10] \qquad (e_2^{2-})_{aq} + M^{n+} \rightarrow M^{(n-2)+}_{aq}$$

H^-_{aq} seems to be a likely possibility since it is merely the conjugate acid of $(e_2^{2-})_{aq}$ as given by equilibrium [11]

$$[11] \qquad (e_2^{2-})_{aq} + H^+_{aq} \rightleftarrows H^-_{aq}$$

but, because the pH was $\sim$11 in our experiments, it would have to be formed by reaction 9 rather than reaction 11. H^-_{aq} should also be formed from OH radicals by reactions 4, 5, and 7 when H_2 was used as the OH scavenger. Calculations show that 10 to 20% of e^-_{aq} could be consumed by reaction 7 in a typical OH^-/H_2 experiment. When 2-propanol or formate ions were used to scavenge OH, reaction 7 was excluded and yet we observed very comparable photoregeneration of e^-_{aq}. Thus it may be stated that if H^-_{aq} is formed in both reactions 7 and 9 then X is not H^-_{aq}. As a rider to this one should add that, although it is generally accepted that the reaction between H_2 and OH may be written as reaction 4, if it in fact proceeds by the one-step reaction 12 at pH 11,

$$[12] \qquad H_2 + O^-_{aq} \rightarrow e^-_{aq}$$

or through the formation of H_3O rather than H by reaction [4], then H^-_{aq} cannot be discounted.

In the presence of Na^+, NH_4^+, or Ba^{2+} dielectrons may undergo reaction 10 to form $(e^-.M^{n+}.e^-)_{aq}$ species. It is conceivable that the absorption band of such species is not influenced much by the nature of the cation and that they all absorb in the 320 to 400 nm range with comparable extinction coefficients. It is also possible that X may be Na^-_{aq} in all these systems since the solutions were deoxygenated in Pyrex glass vessels and therefore probably all contained $\sim 10^{-5}$ M of Na^+ ions. For solutions of Na in various amines (18) and hexamethylphosphoramide (19) evidence has been presented for the occurrence of Na_s^- having fairly strong absorption bands centered at

Can. J. Chem. Downloaded from www.nrcresearchpress.com by 210.87.254.40 on 09/05/12
For personal use only.

photon energies about twice that of the maximum in the solvated electron band.

If X is to be attributed to the analogous aqueous species, Na^-_{aq}, then we must conclude from our experiments with added Na^+ that it is formed in sequence 13

$$[13] \qquad 2e^-_{aq} \rightarrow (e_2^{2-})_{aq} \xrightarrow{Na^+} Na^-_{aq}$$

with the first step being rate determining. Our data is not consistent with the intermediate formation of a simple $(Na^+e^-)_{aq}$ complex formed by direct reaction of e^-_{aq} with Na^+ (3).

We cannot of course eliminate the possibility that the effects observed arise from the formation of a transient species produced by the reaction of e^-_{aq} with a trace impurity. However, we would have to conclude that this impurity has always been present in our especially purified water at about the *same concentration* throughout this entire study. Furthermore, it is not consistent with our qualitative observation that the fraction of e^-_{aq} regenerated by the Auxiliary flash decreases as the fraction of initial e^-_{aq} reacting by the pseudo first-order component decreases following the Main flash.

Another possibility for X is the product of the reaction of e^-_{aq} with water, reaction 14,

$$[14] \qquad e^-_{aq} + H_2O \rightarrow ? \qquad k_{14} = 16\ M^{-1}\ s^{-1}\ (11)$$

or an adduct formed therefrom. If this spontaneous decomposition reaction of e^-_{aq} has the value k_{14} attributed to it (11) then 10–20% of the original e^-_{aq} could undergo that reaction following the Main flash, and its yield would increase with the mean lifetime of e^-_{aq}, as observed. However, we can conclude that X does not arise from reaction 14 if the product of that reaction is an H-atom, as postulated (11), because of the results obtained with added H-atom scavengers such as OH^-, 2-propanol, and sodium formate.

The possibility of e^-_{aq} being formed during the second flash from long-lived triplet states of H_2O or OH^- is discarded on the basis of the following factors: (*i*) e^-_{aq} cannot be detected by photolysis of pure water during the Main or Auxiliary flashes; (*ii*) solutes other than OH^- (specifically I^- or SO_4^{2-}) show comparable results; and (*iii*) very small concentrations of NO_3^- and H_2O_2, which are good e^-_{aq} scavengers, eliminate the formation of a second absorption peak indicating that e^-_{aq} is a necessary precursor.

As indicated earlier it is not possible to alter the p*H* significantly because the OH^- ions are involved in the primary photolysis 1 and in reaction 5. Nevertheless, the p*H* probably has an important influence on the lifetime of species X. This would certainly be expected if X is $(e_2^{2-})_{aq}$, H^-_{aq}, or Na^-_{aq}.

It is not clear which of the following possibilities imposes the 20% maximum on the observed regeneration of e^-_{aq}. (N.B. This represents ~30% of e^-_{aq} reacting by reaction 2.) (*i*) This constitutes the yield of X initially formed; (*ii*) under all conditions only a fraction of X survive the multifarious reactions which occur following the Main flash; (*iii*) photolysis of X has alternative decomposition paths so that the quantum yield for dissociation to give e^-_{aq} is substantially less than unity; or (*iv*) X is formed in more than one spin state (e_2, for instance, could be a singlet or triplet), only one of which is photodissociated by the light used. It should be noted with regard to (*iii*) that all wavelengths >400 nm were also illuminating the solution during the Auxiliary flash. It is conceivable that a bound photoexcited state e_2, for instance, may abstract a proton from the solvation shell.

Our experiments indicate that in order to observe the photoregeneration of e^-_{aq} from X in this system it is necessary to have two conditions fulfilled: (*a*) e^-_{aq} must decay to a considerable extent by the bimolecular combination reaction 2; and (*b*) the mean lifetime of e^-_{aq} with respect to all *other* reactions (with solutes, impurities, reaction products, etc.) must exceed ~200 μs. This latter requirement suggests that X is quite as reactive towards reducible solutes as is e^-_{aq}. Consequently, if X is formed by intra-spur reactions in the radiolysis of aqueous solutions it will be destroyed by other radiolysis products, such as OH radicals, H^+_{aq} ions and H_2O_2, and by reducible solutes. Thus it may be rather short-lived in a radiolysis system and not easily detected by pulse radiolysis methods, especially in the presence of $\sim 10^{-2}\ M$ alcohols at high p*H* (12, 20). In 1965 Dorfman concluded that if a dielectron species is formed in pulse-irradiated water it either has a lifetime <0.2 μs or its absorption band is not in the same region of the spectrum as e^-_{aq} (21). The flash photolysis of OH^-/H_2 solutions seems to be much more favorable to the formation and longevity of X than is a radiation chemical system. Conse-

quently its probable role in molecular H_2 formation by radiolysis is not easy to deduce.

The effect of added e_{aq}^- scavengers on X is ambiguous. They could interfere with the formation of X; but they could also be quite reactive towards X. Indeed one might expect an e_2 species (even if it is protonated or associated with other cations) to be about as strong a reducing agent as is e_{aq}^-. It has been suggested that e_2 may be more effective than e_{aq}^- in reducing solutes, such as Tl^{3+}, which can readily accommodate two electrons (22); but unfortunately that cannot be tested in the present system because of the p*H*, concentrations, and timescales to which we are restricted.

If these conclusions are correct then, in the absence of e_{aq}^- scavengers, X is apparently more stable with respect to the solvent and itself than is e_{aq}^-. Consequently X probably plays an important role in any chemical or physical process by which water is reduced to H_2 through the creation of hydrated electrons in high local concentrations.

The authors are most grateful to Mr. Eric Fisher for technical assistance and to the National Research Council of Canada and the Defense Research Board of Canada for financial support of this research.

1. N. Basco, G. A. Kenney, and D. C. Walker. Chem. Commun. 917 (1969).
2. (*a*) D. C. Walker. Adv. Chem. Ser. **81**, 49 (1968). (*b*) G. A. Kenney and D. C. Walker. *In* Electroanalytical chemistry. Ed. A. J. Bard. Vol. V. Marcel Dekker, N.Y. 1971. Chapter 1.
3. C. Gopinathan, E. J. Hart, and K. H. Schmidt. J. Phys. Chem. 74, 4169 (1970).
4. N. Basco and S. K. Dogra. Proc. Roy. Soc. **A323**, 401 (1971).
5. A. M. Bass and K. G. Kessler. J. Opt. Soc. Am. **49**, 1223 (1959).
6. J. P. Keene. Rad. Res. **22**, 1 (1964).
7. Corning Glass Filters. Corning, N.Y. (C.S. numbers).
8. M. Anbar and P. Neta. Int. J. Appl. Rad. Isot. **18**, 493 (1967).
9. (*a*) J. Jortner and J. Rabani. J. Am. Chem. Soc. **83**, 4868 (1961). (*b*) S. Gordon and E. J. Hart. J. Am. Chem. Soc. **86**, 5343 (1964). (*c*) J. Rabani, W. A. Mulac, and M. S. Matheson. J. Phys. Chem. **69**, 53 (1965). (*d*) K. H. Schmidt and E. J. Hart. Adv. Chem. Ser. **81**, 267 (1968).
10. M. S. Matheson and L. M. Dorfman. Pulse radiolysis. M.I.T. Press, Cambridge. 1967.
11. E. J. Hart, S. Gordon, and E. M. Fielden. J. Phys. Chem. **70**, 150 (1966).
12. G. Czapski and E. Peled. Chem. Commun. 1303 (1970).
13. Gwen H. Thomas. Unpublished results.
14. J. J. Markham. *F*-centers in alkali halides. Academic Press, N.Y. 1966.
15. (*a*) O. F. Khodzhaev, B. G. Ershov, and A. K. Pikaev. Izv. Akad. Nauk SSSR, Ser. Khim, 1882, 2253 (1967). (*b*) L. Kevan, D. R. Renneke, and R. J. Friauf. Solid State Comm. **6**, 469 (1968).
16. K. Fueki. J. Chem. Phys. **50**, 5381 (1969).
17. J. H. Baxendale. Rad. Res., Suppl. **4**, 139 (1964).
18. (*a*) E. Arnold and A. Patterson. J. Chem. Phys. **41**, 3089 (1964); **41**, 3098 (1964). (*b*) S. Golden, C. Guttman, and T. R. Tuttle. J. Chem. Phys. **44**, 3791 (1966). (*c*) I. Hurley, T. R. Tuttle, and S. Golden. J. Chem. Phys. **48**, 2818 (1968). (*d*) S. Matalon, S. Golden, and M. Ottolenghi. J. Phys. Chem. **73**, 3098 (1969). (*e*) D. Huppert and K. H. Bar-Eli. J. Phys. Chem. **74**, 3285 (1970). (*f*) J. L. Dye. Accts. Chem. Res. **1**, 306 (1968).
19. J. M. Brooks and R. R. Dewald. J. Phys. Chem. **72**, 2655 (1968).
20. B. D. Michael, E. J. Hart, and K. H. Schmidt. J. Phys. Chem. **75**, 2798 (1971).
21. L. M. Dorfman. Adv. Chem. Ser. **50**, 36 (1965).
22. G. B. Porter. Private communication.

Can. J. Chem. Downloaded from www.nrcresearchpress.com by 210.87.254.40 on 09/05/12
For personal use only.

Synthesis and Ion Exchange Properties of Thermally Stable Titanium(IV) Vanadate: Separation of Sr^{2+} from Ca^{2+}, Ba^{2+}, and Mg^{2+}

MOHSIN QURESHI, K. G. VARSHNEY, AND S. K. KABIRUDDIN

Z.H. College of Engineering and Technology,
and
Department of Chemistry, Aligarh Muslim University, Aligarh (U.P.) India

Received August 10, 1971

A new, thermally stable, and highly strontium-specific inorganic ion exchanger, titanium(IV) vanadate, has been prepared by mixing 0.5 *M* solution of titanic chloride and sodium vanadate at p*H* 0–1. Its ion exchange capacity is 0.65 mequiv./g at 400 °C. Separation factors of Sr^{2+} with respect to Ba^{2+}, Ca^{2+}, and Mg^{2+} are 8, 11.8, and 33.3, respectively. Binary mixtures of Sr^{2+} with Ba^{2+}, Ca^{2+}, and Mg^{2+} have been separated. Calcium and magnesium are eluted with 0.001 *M* HNO_3. Barium and strontium are eluted with 0.01 and 0.1 *M* HNO_3, respectively. A new parameter $\Delta C/\Delta T$ is proposed for the study of structural changes in inorganic ion exchangers.

Un échangeur d'ion inorganique nouveau, thermiquement stable et hautement spécifique pour le strontium et le vanadate de titane(IV) a été préparé en mélangeant une solution 0.5 *M* de chlorure de titane et de vanadate de sodium à p*H* 0–1. Sa capacité d'échange d'ion est de 0.65 mequiv./g à 400 °C; les facteurs de séparation du Sr^{2+} par rapport à Ba^{2+}, Ca^{2+}, et Mg^{2+} sont respectivement de 8, 11.8 et 33.3. Les mélanges binaires de Sr^{2+} avec Ba^{2+}, Ca^{2+}, et Mg^{2+} ont été séparés. Le calcium et le magnésium sont élués par HNO_3 0.001 *M*, le strontium et le barium par HNO_3 0.01 et 0.1 *M*, respectivement. Un nouveau paramètre $\Delta C/\Delta T$ est proposé pour étudier les changements de structure dans les échangeurs d'ion inorganique.

Canadian Journal of Chemistry, **50**, 2071 (1972)

Introduction

The selectivity of an ion exchange material depends considerably on the specific interaction of the counter ions with the exchanger. This interaction varies with the chemical composition of the exchanger which can be altered with greater ease and facility in inorganic materials than in the organic ones. The synthesis of new inorganic ion exchangers is therefore of outstanding analytical interest.

Of the various inorganic ion exchangers studied earlier the vanadates are probably the least well investigated. Some studies have been made on the vanadates in connection with their use as a catalyst (1). Alkali vanadates have been used for the amperometric titrations of uranyl (2) and thorium (3) ions. The probable species formed in solution have also been postulated. However, the first mention of the ion exchange properties of vanadates is in the work of Phillips and Kraus (4) who made a cursory study of the vanadates of uranium, thorium, thallium, niobium, zirconium etc., and reported their selectivity for cesium and rubidium. Weiss and co-workers (5, 6) studied the exchange behavior of the mineral uranite and determined the crystal structure of tetrathiovanadate. Shichko and Biochinova (7) synthesized an inorganic ion exchanger based on zirconium and vanadium and concluded that its ion exchange capacity depends on the chemical composition of the samples, thermal treatment, and size of the grains. However, a detailed and systematic study on the ion exchange properties of titanium(IV) vanadate is lacking. Bishop and co-workers (8, 9), synthesized it only when they investigated the mixed oxides of groups III, IV, and V as selective ion exchangers for incorporation into electrodialysis membranes. We have therefore synthesized titanium(IV) vanadate and are reporting the ion exchange properties, sorption behavior, and thermal dehydration results.

Experimental

Reagents

Titanium dioxide and a 15% (w/v) solution of titanium(IV) chloride were obtained from B.D.H., England while vanadium pentoxide was a Reidel product. All other chemicals used in this study were of reagent grade.

Apparatus

The various instruments used for spectrophotometry, X-ray studies, i.r. studies, p*H* measurements, and thermogravimetry were the Bausch and Lomb Spectronic-20 colorimeter, the Philips X-ray unit, the Perkin–Elmer model-137 spectrophotometer, the ELICO (India) p*H*-meter model LI-10 and a Stanton thermobalance type-H4, respectively. A temperature controlled shaker from SICO, India was used for equilibrium studies.

Can. J. Chem. Downloaded from www.nrcresearchpress.com by 210.87.254.5 on 09/05/12
For personal use only.

TABLE 1. Condition of preparation and some properties of titanium(IV) vanadate samples

Serial No.	Concentration of mixing solution (*M*)	Volume ratio of mixing	Adjusted p*H*	Reagent used to adjust p*H*	Appearance	Ion exchange capacity mequiv./g
1	0.5	1:1	0	NaOH	Dark brown shiny	0.68
2	0.5	1:2	0	NaOH	Dark brown shiny	0.69
3	0.05	1:1	1.0	Urea	Orange-yellow	0.70
4	0.05	1:1	0.5	Urea	Yellow	0.60
5	0.05	1:1	0	Urea	Yellow + heating	0.60

Preparation of Reagent Solutions

Dilute (0.5 *M*) solution of titanium(IV) chloride was prepared from the stock solution by diluting with 1.5 *M* HCl. The 0.5 *M* vanadium(V) solution was prepared by dissolving vanadium pentoxide in 1 *M* NaOH and then neutralizing the excess alkali with nitric acid. Stock titanium sulfate solution was prepared by dissolving 8 g of titanium dioxide in 250 ml of hot concentrated H_2SO_4 containing 100 g ammonium sulfate with constant stirring.

Preparation of Titanium(IV) Vanadates

(a) Using Titanium(IV) and Vanadium(IV) Solutions

Four samples were prepared by mixing in the cold the *M*/40 solution of titanium(IV) sulfate and vanadyl sulfate in the volume ratio 1:1 at p*H* values 10, 6.8, 4.8, and 2.7. The p*H* value was adjusted with ammonia or sodium hydroxide. The gels were digested at room temperature for 48 h. They were filtered and washed with demineralized water until the p*H* of the washings was about 6. They were dried at 40 °C in an oven and immersed in water to yield small granules. The granules were then dried and placed in 1–2 *M* HNO_3 or HCl for 24 h, occasionally replacing the supernatant liquid, to convert them into the hydrogen form. During this operation the samples prepared at p*H* 4.8, 6.8, and 10 dissolved completely. The gel prepared at p*H* 2.7 produced brown shiny particles which dissolve slightly in 1–2 *M* HNO_3. Its ion exchange capacity for Na^+ was 0.34 mequiv./g.

Some samples were also prepared by heating the precipitates in the presence of oxidizing agents such as HNO_3 and H_2O_2. The procedures are summarized below:

(*i*) A mixture of 500 ml of *M*/40 titanium(IV), 500 ml of *M*/40 vanadium(IV) solution, and 100 ml of 1 *M* HNO_3 was refluxed for 12 h. Only a small amount of yellow precipitate was obtained which dissolved readily in 1 *M* HNO_3 when kept for 24 h.

(*ii*) 500 ml of *M*/40 titanium(IV) sulfate and 500 ml of *M*/40 vanadyl sulfate were heated in presence of 100 ml of 4 *M* HNO_3 for 4 h. The p*H* was then adjusted to 2.7 by the addition of NaOH. A yellow colored sample which was slightly soluble in HNO_3 was obtained. Its ion exchange capacity for Na^+ was 0.32 mequiv./g of dry exchanger.

(*iii*) 400 ml of *M*/40 vanadyl sulfate were heated with 50 ml of 4 *M* HNO_3 till the solution became yellowish indicating the oxidation of V(IV) to V(V). Now, 450 ml of *M*/40 titanium(IV) sulfate were added and the p*H* was adjusted to 2.7. A yellowish muddy precipitate was obtained which was soluble in HNO_3 on keeping for 24 h.

(*iv*) 50 ml of H_2O_2 (20 vol) were added to a mixture of 500 ml of *M*/40 titanium(IV) sulfate and 500 ml of *M*/40 vanadyl sulfate solution. The contents were refluxed for 8 h. The yellow precipitates obtained were soluble in HNO_3.

(b) Using Titanium(IV) and Vanadium(V) Solution

0.5 *M* solutions of titanium(IV) chloride and of vanadium(V) were mixed in two volume ratios (1:1 and 1:2). The p*H* (0) was adjusted by adding NaOH. The precipitates thus obtained were digested at room temperature for 24 h, washed and decanted several times and filtered. They were washed again with demineralized water until the filtrate was free from titanium and vanadium. After drying at 40 °C in an oven, the material was immersed in water to crack it into small uniform particles. They were then sieved to obtain particles of appropriate mesh size. The ion exchanger, thus prepared, was converted into H^+ form with 1–2 *M* HNO_3 as usual and subjected to ion exchange studies after washing with demineralized water and drying at 40 °C. Three samples were also prepared by adjusting the p*H* (1, 0.5, and 0) with urea instead of NaOH. Urea gives ammonia on slow hydrolysis. Table 1 summarizes the conditions of preparation and some properties of these samples.

Chemical Stability

Out of the five samples listed in Table 1 sample No. 1 was found to be fairly stable in water and mineral acids. Other samples dissolved continuously on prolonged standing with these solvents. Further ion exchange studies were, therefore, performed on sample 1.

Chemical stability of titanium(IV) vanadate (sample 1) heated to different temperatures was determined in water and 0.5 *M* HNO_3. For this purpose 500 mg of the sample were heated to the specified temperature and then shaken in 50 ml of the solvent for 6 h at room temperature. A shaking period of 6 h was chosen because it is the maximum time usually required in a column operation during separations. The dissolved amounts of titanium and vanadium were determined simultaneously (10) by spectrophotometry. Table 2 summarizes the results.

Composition

100 mg of the exchanger were dissolved in 10 ml of concentrated HCl and diluted to about 100 ml with water. Titanium was separated from vanadium by the sodium peroxide method (11). The precipitate of titanium peroxyhydroxide so obtained was redissolved in 10 ml of concentrated HCl; titanium was determined volumetrically with ferric ammonium sulfate (ref. 12, p. 1104). The filtrate containing vanadium was made acidic by adding HCl followed by 10 ml of 10% H_2SO_4. Vanadium(V) was reduced

Can. J. Chem. Downloaded from www.nrcresearchpress.com by 210.87.254.5 on 09/05/12
For personal use only.

TABLE 2. Chemical stability of titanium(IV) vanadate heated to different temperatures

Serial No.	Temperature (°C)	Amount dissolved (%) in 0.5 *M* HNO_3 Ti(mg)	in 0.5 *M* HNO_3 V(mg)	In water Ti(mg)	In water V(mg)
1	40	0.94	1.76	0.00	0.00
2	100	0.92	1.55	0.00	0.00
3	200	1.52	1.28	0.00	0.00
4	300	0.76	2.38	0.026	0.06
5	400	0.22	6.5	0.004	0.04
6	500	1.76	15.95	0.02	1.09
7	700	0.25	1.64	0.04	0.45

to vanadium(IV) by passing SO_2 into the solution at room temperature. Excess of SO_2 was completely removed by heating the solution for a long time and bubbling CO_2 through it to hasten the removal. Vanadium was determined volumetrically (ref. 12, p. 1212) with $KMnO_4$. Repetition of experiments showed that the results were consistent and reproducible. Thus, the Ti:V mole ratio in the titanium vanadate was observed to be 1:3.9 as determined on the basis of this elemental analysis.

Physical Properties

Titanium(IV) vanadate is in the form of darker brown opaque particles which can be used for column operations. They suffer no change in physical appearance when immersed in dilute mineral acid solution (up to 0.5 *M*). The material is unstable in 1 *N* NaOH. Strong acid solutions also dissolve it to some extent.

(a) Ion Exchange Properties. Ion exchange capacity of the exchanger for Na^+, K^+, Ba^{2+}, and Mg^{2+}, determined as usual by the column method, was found to be 0.65, 0.72, 0.61, and 0.42 mequiv./g, respectively. The initial p*H* values of Na^+, K^+, Ba^{2+}, and Mg^{2+} solutions were 6–7, 6–7, 5–6, and 5–6, respectively.

(b) Concentration and Elution Curves. It was observed that the elution of hydrogen ions from a column of the exchanger depends upon the eluent concentration. As the eluent (KCl) concentration increased, so were the milliequivalents of hydrogen ions eluted, attaining a maximum value with 1 *M* KCl. On taking a column of 1 g titanium vanadate in H^+ form and eluting it with 1 *M* KCl it was found that almost all H^+ ions are eluted in the first 60 ml of the KCl solution.

(c) pH-Titration. The p*H* titrations were performed by the method of Topp and Pepper (13).

(d) Thermogravimetry. Figure 1 shows the thermograms for titanium(IV) vanadate in the hydrogen as well as in the potassium form. The heating rate was kept at 4 °C per min.

(e) X-Ray Studies. The X-ray diffraction pattern of titanium vanadate reveals the fact that the exchanger is noncrystalline.

(f) Infrared Spectroscopy. This study was made by the KBr disk method. The spectrum is shown in Fig. 2.

(g) Distribution Coefficients. Distribution studies on the exchanger were performed by taking 0.5 g of the exchanger and shaking it with 100 ml of the solution containing 0.5 ml of the stock solution of the cation concerned for 6 h. Equilibrium is attained within 6 h since the K_d value does not change on shaking the exchanger with the solution of the cation concerned for more than 6 h. The amount of the cation present in the solution did not exceed 3% of the total ion exchange capacity of the exchanger. The amount of the

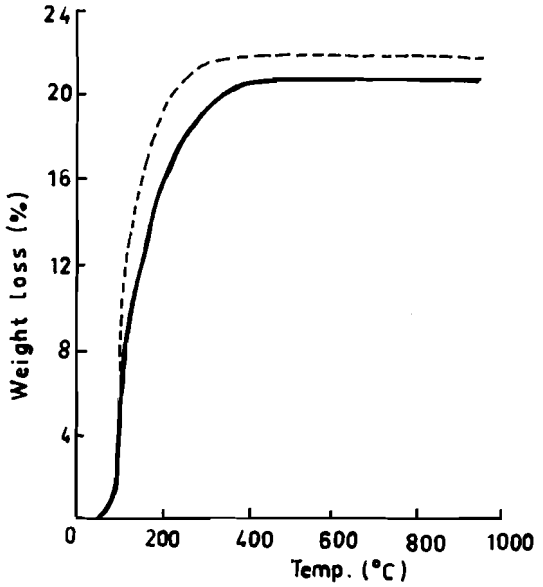

FIG. 1. Thermogram of titanium vanadate.

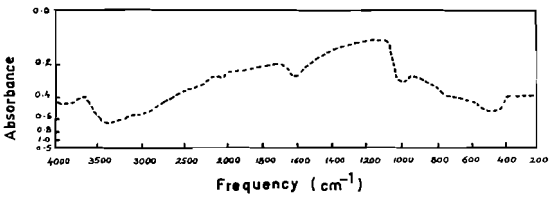

FIG. 2. Infrared spectrum of titanium vanadate.

Can. J. Chem. Downloaded from www.nrcresearchpress.com by 210.87.254.5 on 09/05/12
For personal use only.

TABLE 3. K_d values of different metal ions on titanium(IV) vanadate

Serial No.	Metal ion	K_d (ml g^{-1})	Serial No.	Metal ion	K_d (ml g^{-1})
1	Zn(II)	4 088	8	Mn(II)	2 500
2	Cd(II)	3 630	9	In(III)	587
3	Mg(II)	576	10	Y(III)	3 800
4	Ca(II)	1 693	11	La(III)	8 800
5	Sr(II)	20 400	12	Sm(III)	12 400
6	Ba(II)	2 560	13	Zr(IV)	377.7
7	Pb(II)	25 800	14	Th(IV)	944

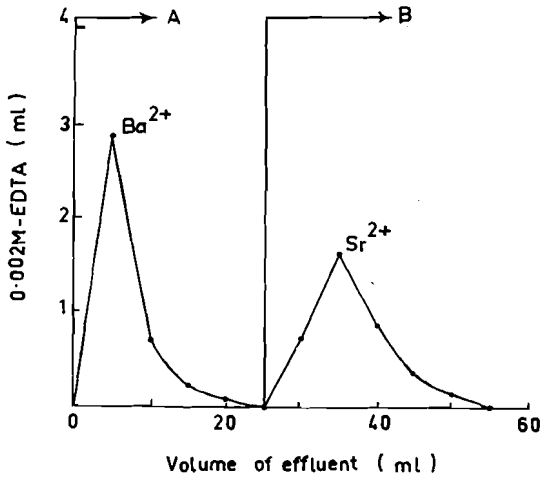

FIG. 3. Separation of Ba^{2+}–Sr^{2+}. *A*, 0.01 *M* HNO_3; *B*, 0.1 *M* HNO_3.

cations before and after equilibrium were determined by titrating with 0.002 *M* EDTA. The distribution coefficients were then calculated by the formula:

$$K_d = \frac{I - F}{F \times W} \times 100$$

where I = volume of EDTA used before equilibrium; F = volume of EDTA used after equilibrium, W = weight of the exchanger taken in g.

Table 3 lists the K_d values.

Separations

Depending upon the K_d values the following quantitative separations were achieved on a 3.9 mm (i.d.) column taking 2 g of the exchanger. A constant flow rate of 4–5 drops per min was maintained.

(a) Separation of Ba^{2+} from Sr^{2+}. A mixture of 308.4 μg of Sr^{2+} and 533.0 μg of Ba^{2+} was applied to the column. Ba^{2+} and Sr^{2+} were eluted using 0.01 and 0.1 *M* HNO_3, respectively (Fig. 3).

(b) Separation of Mg^{2+} from Sr^{2+}. 190.7 μg of Mg^{2+} with 308.4 μg of Sr^{2+} were applied to the column. 0.001 *M*

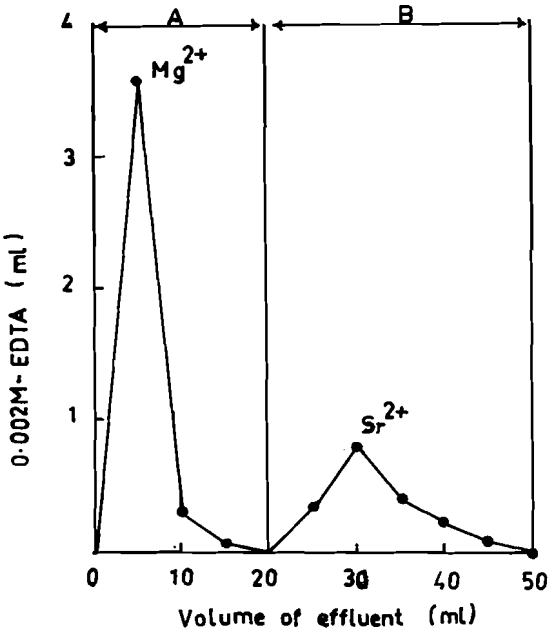

FIG. 4. Separation of Mg^{2+}–Sr^{2+}. *A*, 0.001 *M* HNO_3; *B*, 0.1 *M* HNO_3.

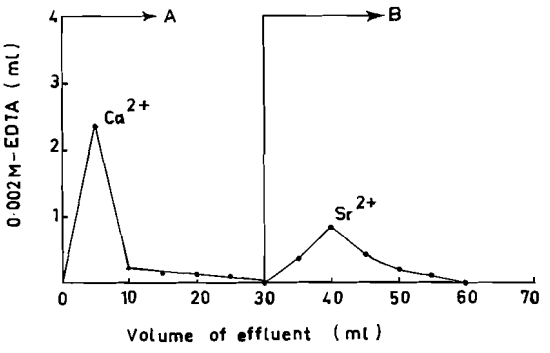

FIG. 5. Separation of Ca^{2+}–Sr^{2+}. *A*, 0.001 *M* HNO_3; *B*, 0.1 *M* HNO_3.

Can. J. Chem. Downloaded from www.nrcresearchpress.com by 210.87.254.5 on 09/05/12
For personal use only.

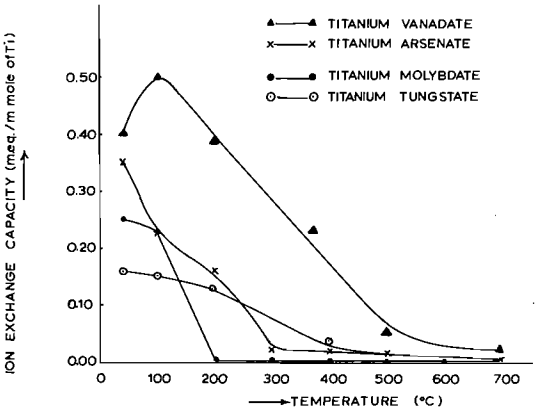

FIG. 6. Ion exchange capacity as a function of temperature for some titanium-based ion exchangers.

HNO_3 and 0.1 *M* HNO_3 were used as eluents for Mg^{2+} and Sr^{2+}, respectively (Fig. 4).

(c) Separation of Ca^{2+} from Sr^{2+}. A mixture of 229.25 μg of Ca^{2+} and 308.4 μg of Sr^{2+} was applied. Ca^{2+} and Sr^{2+} were eluted with 0.001 and 0.1 *M* HNO_3, respectively (Fig. 5).

Effect of Temperature on Ion Exchange Capacity

The sample previously dried at 40 °C was heated to different temperatures and the ion exchange capacity of the substances obtained was determined as usual. Figure 6 shows the effect of heating on the ion exchange capacity of some ion exchangers based on titanium.

Results and Discussion

The high thermal stability and the specificity for strontium are two unique features of titanium vanadate and in these aspects it stands out from other titanium based exchangers. Figure 7 compares the separation factors of Mg^{2+}, Ca^{2+}, and Ba^{2+} with respect to Sr^{2+} on titanium vanadate, arsenate (14), molybdate (15), antimonate (16) and tungstate (17). It is very interesting to see that the general trend is the same *i.e.*, the separation factor first decreases and then increases as we go from vanadate to tungstate. The values of α^{Sr}_{Mg} and α^{Sr}_{Ba} are highest for titanium vanadate and show the specificity of the exchanger for strontium. The α^{Sr}_{Ca} is greater for titanium arsenate than for vanadate. This is misleading, however, since the actual K_d values of Sr and Ca on titanium arsenate are low (Fig. 8) and do not have much significance. In fact strontium could not be separated from calcium on its columns. Titanium vanadate, on the other hand, is highly selective for Sr^{2+} and therefore strontium has been easily separated from Mg^{2+}, Ca^{2+}, and Ba^{2+} on this ion exchanger (Figs. 3–5). The unusually strong adsorption of Sr^{2+} on titanium vanadate can be explained on the basis of the solubility of the

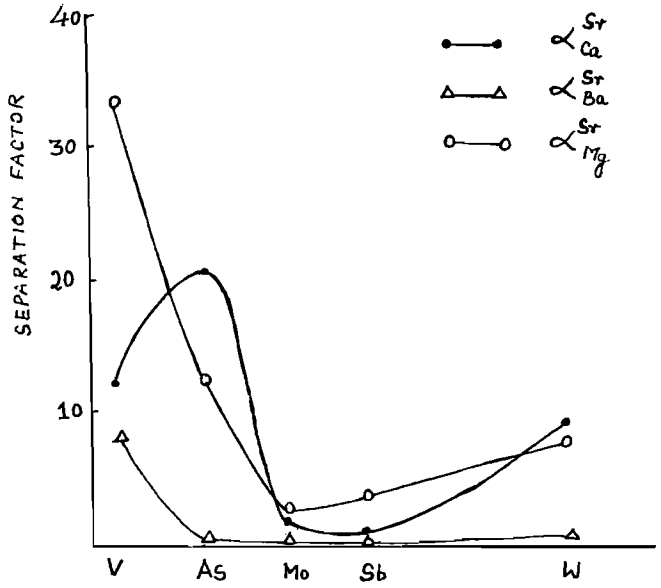

FIG. 7. Separation factors *vs.* atomic number of the main acidic element in the exchanger.

Can. J. Chem. Downloaded from www.nrcresearchpress.com by 210.87.254.5 on 09/05/12
For personal use only.

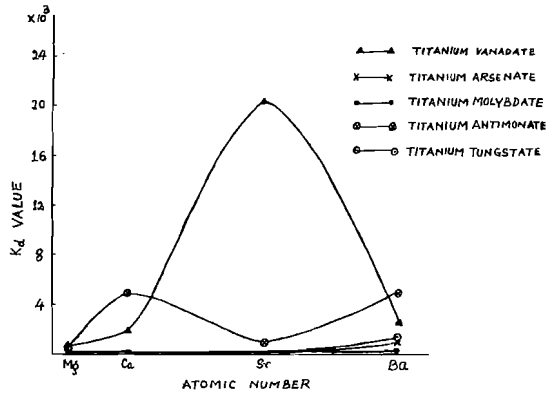

FIG. 8. K_d values of alkaline earths on some titanium-based ion exchangers.

alkaline earth vanadates. Accurate solubility data are not available. The records (18) show, however, that strontium metavanadate is sparingly soluble in water while calcium metavanadate is more soluble than the strontium salt. Barium and magnesium metavanadates are described as soluble and freely soluble. The K_d values faithfully correspond to the solubility data. It appears probable that the high K_d value of strontium is due to the specific interaction of Sr^{2+} ions with the exchanger resulting in ion-pair formation. However, further studies are in progress to prove this point.

Distribution coefficients of metal ions on an ion exchanger depend upon their ionic radii. Thus, the normal sequence for K_d values of alkaline earths should be

$$Ba^{2+} > Sr^{2+} > Ca^{2+} > Mg^{2+}$$

A comparative study of the K_d values on the most stable samples of different titanium-based ion exchangers shows that the molybdate, tungstate, and arsenate follow the above sequence. On titanium antimonate calcium has a higher K_d value than strontium. This exchanger has been used for the separation of Mg^{2+} from Ca^{2+} and Sr^{2+}. On titanium vanadate the K_d value of strontium is greater than that of barium while other ions follow the normal sequence. The unique feature of this exchanger is that this is the only exchanger on which strontium has a higher K_d value than barium, calcium, and magnesium. In fact the K_d value for Sr^{2+} is unusually high and its separation from Ba^{2+}, Ca^{2+}, and Mg^{2+} has been practically achieved.

The titanium(IV) vanadate exchanger is prepared at p$H < 1$. The elemental analysis indicates that the product has the Ti/V ratio 1:4 although the solutions were mixed in 1:1 mole ratio. The excess of titanium is washed out during filtration and the acid treatment of the exchanger. The following equilibrium is known to exist (ref. 19, p. 812) for vanadium at the pH of the preparation of titanium(IV) vanadate:

$$3[VO_3(OH)]^{2-} + 3H^+ \rightleftharpoons V_3O_9^{3-} + 3H_2O \quad (K = 10^{-30.7})$$

The trimeric species may be considered to be built up from VO_2^+ ions and the following equilibrium probably exists

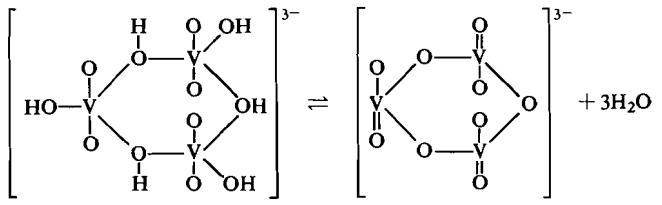

Also, in 1 M acid the titanium species in the solution would be basic consisting of $(TiO)_n^{2+}$ or $Ti(OH)^{3+}$ chains (ref. 19, p. 803). Since the Ti:V ratio is 1:4 in the sample a tentative formula may be suggested on the basis of the possible aqueous species in acidic media:

$$[Ti_3(V_3O_9.1.5\ H_2O)_4.13\ H_2O]_n$$

The number of external water molecules per mole of the exchanger has been calculated by the method of Alberti *et al.* (20) from thermogravimetric analysis (Fig. 1). These molecules are lost from the exchanger when it is heated to 180 °C (% wt loss at this temperature = 14.4). Above this temperature condensation begins. This process continues up to 370 °C when six more water molecules are lost. After 370 °C the weight becomes constant due to the formation of

Can. J. Chem. Downloaded from www.nrcresearchpress.com by 210.87.254.5 on 09/05/12
For personal use only.

Can. J. Chem. Downloaded from www.nrcresearchpress.com by 210.87.254.5 on 09/05/12
For personal use only.

anhydrous titanium vanadate (21) in which the weight loss continues up to 371 °C when anhydrous barium vanadate [$Ba(VO_3)_2$] is obtained. In amperometric studies on thorium vanadate, Saxena and co-workers (3) also found Th:V ratio of 1:4 in acidic medium and suggested the formula [$ThO_2.2V_2O_5$] for the metavanadate formed. The pH titration curve shows only one break. The exchanger is therefore a monofunctional weak cation exchanger like other ion exchangers reported from this laboratory. The exchange reactions are reversible and the resolution of the cation occurs with consequent regeneration of titanium vanadate on washing with acid.

The effect of temperature on the ion exchange capacity of some titanium based exchangers has been plotted in Fig. 6. The ion exchange capacity of all exchangers is calculated in terms of mequiv./mmol of Ti per fixed weight of the exchanger taking into consideration different chemical transformations based on thermogravimetric studies. These curves clearly show that in comparison with other ion exchangers of this class, titanium vanadate has the highest ion exchange capacity and thermal stability. There is an increase in ion exchange capacity when the sample is heated to 100 °C owing to the irreversible loss of some external water molecules. If we assume that the unbridged hydroxyl groups are the exchangeable groups, then the ion exchange capacity would approach 1 mequiv./mmol of Ti. However, the observed value at 100 °C is 0.5. After this temperature the capacity decreases and at ~200 °C it becomes 0.43 mequiv./mmol of Ti which is equal to the value at room temperature. Thus, the removal of external water molecules does not, obviously, effect the ion exchange capacity. Above this temperature, the capacity decreases, probably because of the loss of exchangeable hydroxyl groups during condensation. At 370 °C the capacity is 0.23 mequiv./mmol of Ti although all of the exchangeable sites have been lost at this temperature according to the following chemical transformation

$$Ti_3(V_3O_9.1.5H_2O)_4 \rightarrow 3[TiO_2.2V_2O_5] + 6H_2O$$

The exchange capacity further decreases until it becomes negligibly small (0.05 at 500 °C). The persistance of the ion exchange capacity even after the exchanger has been heated to a

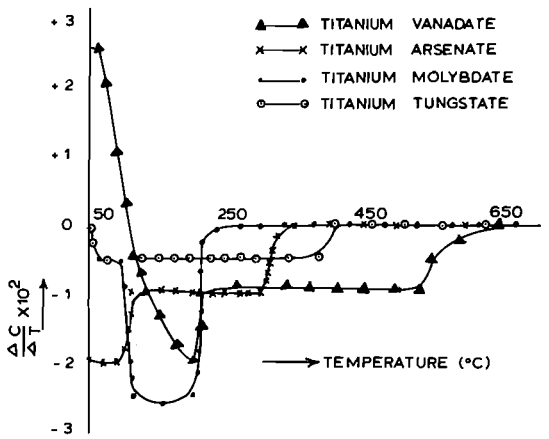

FIG. 9. Plot of $\Delta C/\Delta T$ *vs.* temperature.

temperature when the condensation has taken place can be explained on the basis of the surface hydroxyl groups present on the $(TiOH)^{3+}$ chains. After heating, the surface can rehydrate in water to re-establish these groups, thus showing the ion exchange capacity. Other ion exchangers lose their ion exchange capacity almost completely at much lower temperatures (Fig. 6). The unique thermal behavior of titanium vanadate is made clearer by considering Fig. 9. $\Delta C/\Delta T$ is defined as the rate of change of capacity with temperature, the capacity being measured in mequiv./mmol of Ti per fixed weight of the exchanger. It is quite interesting to note that except for titanium vanadate all the ion exchangers based on titanium suffer a loss in ion exchange capacity on heating as the negative value of $\Delta C/\Delta T$ suggests, the rate of loss being maximum for titanium molybdate at 100 °C. For titanium vanadate $\Delta C/\Delta T$ becomes zero at 100 °C indicating the maximum ion exchange capacity at this temperature.

Contrary to our earlier experience with titanium tungstate (17) there is no significant increase in stability on heating the exchanger to higher temperatures. When the exchanger is heated to 500 °C it dissolves more in water than if it is heated to either 400 or 700 °C (Table 2). It is difficult to explain this behavior satisfactorily. The thermogram shows that on heating, the exchanger in K^+ form suffers a greater weight loss than the one in H^+ form. This is probably because the sample is more hydrated in K^+ form. This behavior is similar to that of stannic molybdate (22).

From i.r. spectrum of the titanium vanadate (Fig. 2) we draw the following conclusions:

There are four peaks observed in the spectrum at the frequency ranges ~ 3400, ~ 1600, ~ 1000, and $\sim 500\ cm^{-1}$. The strong but broad peak at $3400\ cm^{-1}$ is characteristic (23) of free water and OH groups. The strong peak at $1600\ cm^{-1}$ also represents the free water molecules. Vanadate has its characteristic frequency (24) between 800 and $1000\ cm^{-1}$. It is therefore represented by the third sharp peak at $1000\ cm^{-1}$. The last strong peak at $\sim 500\ cm^{-1}$ is due to the presence of Ti—O bonds (25) in the structure.

The authors thank Dr. S. M. F. Rahman for research facilities. Dr. B. Rama Rao (RRL, Hyderabad) and Dr. H. V. K. Udupa (C.E.C.R.I. Karaikudi, Madras) are thanked for their help in X-ray and thermogravimetric studies. Financial assistance to S.K.K. by the National Science Talent Search Department, India, is gratefully acknowledged.

1. A. D. KAGARLITSKII, B. V. SUVOROV, and S. R. RAFIKOV. Zhur. Obshchel Khim. **29**, 157 (1959).
2. M. L. MITTAL and R. S. SAXENA. J. Inorg. Nucl. Chem. **27**, 2553 (1965).
3. R. S. SAXENA and O. P. SHARMA. J. Inorg. Nucl. Chem. **28**, 195 (1966).
4. H. O. PHILLIPS and K. A. KRAUS. U.S.A.E. Comm. Report ORNL-3320. 1962. p. 81.
5. A. WEISS and K. J. HIKE. Angew. Chem. **77**, 347 (1965).
6. H. SCHAEFER, P. MORITZ, and A. WEISS. Z. Naturforsch, **20b(6)**, 603 (1965).
7. V. A. SHICHKO and E. S. BIOCHINOVA. Zh. Prik. Khim. **41**, 526 (1968).
8. G. A. GUTER, H. K. BISHOP, J. A. HUNTER, W. S. GILLAM, and H. E. PODALL. U.S. Office Saline Water Res. Develop. Rep. **278**, 189 (1967).
9. H. K. BISHOP, J. A. BITTLES, and G. A. GUTER. Desalination, **6**, 369 (1969).
10. A. WEISSLER. Ind. Eng. Chem. (Anal. Ed.). **17**, 694 (1945).
11. G. E. F. LUNDELL, H. A. BRIGHT, and J. I. HOFFMAN. Applied inorganic analysis. 2nd ed. John Wiley and Sons, Inc., New York, 1953. p. 579.
12. N. H. FURMAN. Scott's standard methods of chemical analysis. 6th ed., Vol. 1. D. Van Nostrand Co., Inc., Princeton, New Jersey, 1962.
13. N. E. TOPP and K. W. PEPPER. J. Chem. Soc. 3299 (1949).
14. M. QURESHI and S. A. NABI. J. Inorg. Nucl. Chem. **32**, 2059 (1970).
15. M. QURESHI and H. S. RATHORE. J. Chem. Soc. (A), 2515 (1969).
16. M. QURESHI and V. KUMAR. J. Chem. Soc. (A), 1488 (1970),
17. M. QURESHI and J. P. GUPTA. J. Chem. Soc. (A), 1755 (1969).
18. J. W. MELLER. A comprehensive treatise on inorganic and theoretical chemistry. Vol. IX, p. 768–773.
19. F. A. COTTON and G. WILKINSON. Advanced inorganic chemistry. 2nd ed. Interscience Publishers, U.S.A. 1966.
20. G. ALBERTI, P. C. GALLI, U. COSTANTINO, and E. TORRACCA. J. Inorg. Nucl. Chem. **29**, 571 (1967).
21. C. DUVAL. Inorganic thermogravimetric analysis. Elsevier Publishing Co., New York, 1953. p. 171.
22. M. QURESHI, K. HUSAIN, and J. P. GUPTA. J. Chem. Soc. (A), 29 (1971).
23. S. R. YOGANARASIMHAN. Indian J. Chem. **18**, 360 (1963).
24. F. A. MILLER and C. H. WILKINS. Anal. Chem. **24**, 1253 (1952).
25. C. H. WIRGUIN and A. A. YARON. J. Inorg. Nucl. Chem. **28**, 2379 (1966).

Can. J. Chem. Downloaded from www.nrcresearchpress.com by 210.87.254.5 on 09/05/12
For personal use only.

An Electron Paramagnetic Resonance Study of a fast Lewis Acid–Base Reaction between Copper(II) bis(Diethyldithiocarbamate) and Pyridine in Benzene

J. B. FARMER, F. G. HERRING,[1] AND R. L. TAPPING

Department of Chemistry, University of British Columbia, Vancouver 8, British Columbia

Received February 4, 1972

The fast Lewis acid–base reaction between copper(II) bis(diethyldithiocarbamate) and pyridine

$$Cu(DDC)_2 + \text{pyridine} \rightleftharpoons Cu(DDC)_2.\text{pyridine}$$

has been studied from 280 to 320 °K in benzene. The method employed is the analysis of electron paramagnetic resonance line positions and line widths using the solutions of the modified Bloch equations in the fast exchange limit. Arrhenius plots, over the temperature range employed, gave values for the thermodynamic data of the process.

La réaction rapide acide de Lewis acid–base entre le bis(diéthyldithiocarbamate) de cuivre(II) et la pyridine

$$Cu(DDC)_2 + \text{pyridine} \rightleftharpoons Cu(DDC)_2.\text{pyridine}$$

a été étudiée dans le benzène entre 280 et 320 °K. La méthode utilisée est l'analyse par résonance paramagnétique électronique des positions de raies et des largeurs de raies en utilisant les solutions des équations modifiées de Bloch dans la limite d'un échange rapide. Les courbes d'Arrhenius, sur l'échelle de température utilisée, donnent les valeurs qui se rapportent aux données thermodynamiques du processus.

Canadian Journal of Chemistry, **50**, 2079 (1972)

Introduction

The effects of adduct formation on the electronic and magnetic properties of neutral bis chelates of the cupric ion have been the subject of recent investigations (1–10). Of particular interest here is the interaction of Lewis bases with four coordinate square planar Cu(II) chelates to form five coordinate adducts in solution.

Adduct formation is often characterized by an equilibrium of the type

$$[1] \qquad ML_2 + B \underset{k_r}{\overset{k_f}{\rightleftharpoons}} ML_2B$$

where ML_2 is the metal bis chelate and B the Lewis base. If both the species ML_2 and ML_2B are paramagnetic and the forward (k_f) and back (k_r) reaction rates are in the range 10^7 to 10^9 s^{-1} then such an equilibrium can be treated as a two jump system on the e.p.r. time scale. An e.p.r. line width variation can therefore be expected if there is sufficient difference between the spin Hamiltonian parameters of ML_2 and ML_2B. Provided that these various conditions are met and if the system is studied over a temperature range the equilibrium constant (K), the rate constants (k_f and k_r), and thermodynamic data can be extracted from the line positions and line widths using the solutions to the Bloch equations in the fast or near-fast exchange limit (11–14). Some complications may arise due to rotational correlation times and non-secular terms (15) in the expression for $1/T_2$; these are discussed later.

The work of Aasa *et al.* (6) suggested that the interaction between copper(II) bis(diethyldithiocarbamate) [$Cu(DDC)_2$] and various organic bases in suitable solvents would be an appropriate system to study the applicability of the approach outlined in the previous paragraph. Aasa *et al.* noted line position and line width shifts that varied with ligand concentration but did not interpret them in terms of a Lewis acid–base equilibrium. Whilst this work was in progress two other studies appeared in the literature by Corden and Rieger (9) and Shklyaev and Anufrienko (10). The former workers studied the e.p.r. of copper(II) bis(di-*n*-butyldithiocarbamate) with a number of bases and obtained equilibrium constants, rate constants, and thermodynamic data but also observed certain inconsistencies in the interpretation of their experimental data. Shklyaev and Anufrienko studied $Cu(DDC)_2$ and pyri-

[1]To whom all correspondence should be addressed.

Can. J. Chem. Downloaded from www.nrcresearchpress.com by 210.87.254.40 on 09/05/12
For personal use only.

Can. J. Chem. Downloaded from www.nrcresearchpress.com by 210.87.254.40 on 09/05/12
For personal use only.

dine in toluene (10); their results will be compared to ours later.

Experimental

The determination of equilibrium and reaction rate constants requires an analysis of line positions and line widths. To avoid the complication of the two naturally occurring isotopes of copper (^{63}Cu and ^{65}Cu) in such an analysis, copper(II) bis(diethyldithiocarbamate) was prepared from isotopically pure ^{63}Cu, this being obtained from UKAEA, Harwell, England. The pure copper metal was converted to copper(II) nitrate by reaction with nitric acid. The nitrate anions were replaced by chloride anions by repeated reaction with hydrochloric acid. The pure $CuCl_2.2H_2O$ so obtained was then added to an excess of sodium diethyldithiocarbamate in absolute ethanol. The resultant crude $Cu(DDC)_2$ was recrystallized several times from benzene, yielding shiny dark green – brown needles.

The solvents, benzene and pyridine, used in the study were of spectro-grade quality and were kept under nitrogen. Gas chromatographic analysis showed no trace of impurity. It is important to note here that benzene and pyridine are miscible in all proportions and that $Cu(DDC)_2$ is soluble in both of them. Further, since the results were to be least-squares fitted, the number of solutions (usually about 12) was always three times greater than the number of parameters to be fitted. A series of solutions containing the required solvent mixture and a weighed amount of $^{63}Cu(DDC)_2$ were prepared. These solutions were placed in silica sample tubes suitable for an e.p.r. machine and then degassed on a vacuum line. All e.p.r. spectra were recorded within 1–2 h of sample preparation; no decomposition was apparent. Typically the copper ion concentration was 10^{-4} M, exchange broadening being absent at such concentrations.

Spectra were recorded on a Varian E-4 spectrometer, equipped with a Varian (V6040) variable temperature accessory. Figure 1 shows the effect on the line widths upon adding pyridine to a sample of $Cu(DDC)_2$ in benzene. Field calibration was made with a proton resonance magnetometer. The microwave frequency was monitored with a Hewlett–Packard 5425L counter equipped with an X-band plug-in unit. Absolute field position measurements were accurate to ± 0.2 G and the frequency reproducible to ± 20 kHz in 9 GHz. The g-value measurements are reliable to ± 0.0002 and hyper-fine splittings to ± 0.05 G. Calibration of the thermocouple used in temperature measurement indicated that the maximum absolute error in the thermocouple was less than 0.02 °C and that the temperature variation over a particular spectrum was never more than ± 0.2 °C. The error in actual sample temperature as compared to the thermocouple reading was usually $\leqslant \pm 0.5$ °C.

The calculations reported in this work were carried out on an IBM360/67 using programs written in this laboratory.

The line widths measured in the present study were corrected for the effect of modulation amplitude using Wahlquist's equation (16).

Results

The chemical equilibrium considered here

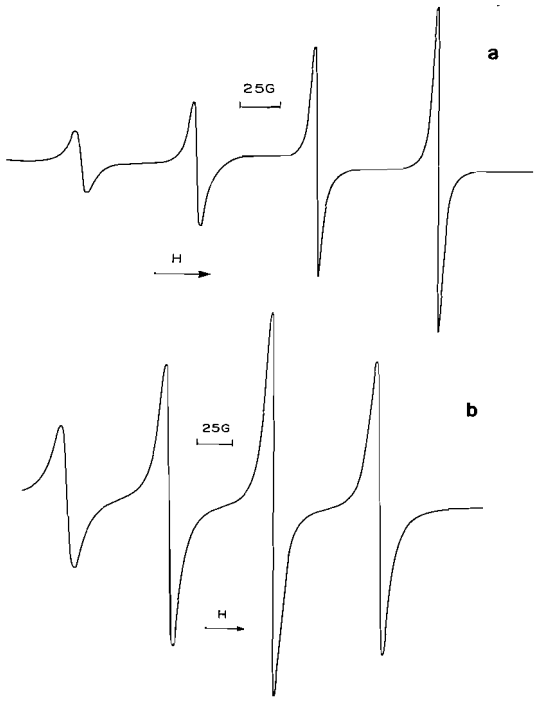

FIG. 1. (*a*) Electron paramagnetic resonance spectrum of $Cu(DDC)_2$ in benzene at 300 °K; (*b*) e.p.r. spectra of $Cu(DDC)_2$ with approximately 1 M pyridine in benzene at 300 °K.

can be treated by the modified Bloch equations as a two jump problem between the two inequivalent sites ML_2 and ML_2B, designated A and B, respectively. The general solution to this problem (13) yields the total complex magnetic moment

$$[2] \quad G = G_A + G_B = \frac{-i\gamma H_1 M_0[\tau_A + \tau_B + \tau_A\tau_B(\alpha_A P_A + \alpha_B P_B)]}{(1 + \alpha_A\tau_A)(1 + \alpha_B\tau_B) - 1}$$

where $\alpha_A = T_{2A}^{-1} - i(\omega_A - \omega)$, ω_A is the Larmor frequency of site A, T_{2A}^{-1} is the inverse of the transverse relaxation time of site A, τ_A is the mean lifetime for a stay on the site A, and P_A is the fractional population of site A ($P_A = 1 - P_B = \tau_A/(\tau_A + \tau_B)$).

When τ_A and τ_B are small compared to the inverse of the difference between the respective Larmor frequencies then eq. 2 has the solution

$$[3] \quad G = \frac{-i\gamma H_1 M_0}{P_A\alpha_A + P_B\alpha_B}$$

Can. J. Chem. Downloaded from www.nrcresearchpress.com by 210.87.254.40 on 09/05/12
For personal use only.

which corresponds to the limit of fast exchange. The absorption line shape is proportional to the imaginary part of eq. 3, v, and is specifically

$$[4]\quad v = -\gamma H_1 M_0 \times \frac{T_2}{1 + (T_2)^2(P_A\omega_A + P_B\omega_B - \omega)^2}$$

i.e., we have a Lorentzian line shape. Equation 3 represents a single exchange signal centered at a mean frequency

$$[5a]\quad \langle\omega\rangle = P_A\omega_A + P_B\omega_B$$

with a mean line width

$$[5b]\quad T_2^{-1} = P_A T_{2A}^{-1} + P_B T_{2B}^{-1}$$

Experimentally it is nearly always impossible to reach the extreme fast exchange limit represented by eq. 4 and in general the observed line may not be completely collapsed so that the observed width will be greater than that given by eq. 5*a*. The line will still be centered at $\langle\omega\rangle$, however. To take this fact into account an effective transverse relaxation time can be given (13, 18, 19)

$$[6a]\quad T_2^{-1} = P_A T_{2A}^{-1} + P_B T_{2B}^{-1} + P_A^2 P_B^2(\tau_A + \tau_B)(\omega_A - \omega_B)^2$$

$$[6b]\quad = P_A T_{2A}^{-1} + P_B T_{2B}^{-1} + P_A^2 P_B \tau_B(\omega_A - \omega_B)^2$$

Consider first the determination of the equilibrium constant $K = (k_f/k_r)$. Let T_{ML_2} and T_B be the total concentrations of complex and base respectively, then $K = C/(T_{ML_2} - C)(T_B - C)$ where C is the equilibrium concentration of the adduct. Under the present experimental conditions $T_{ML_2} \ll T_B$, consequently $T_B \gg C$; whence $K = C/T_B(T_{ML_2} - C)$. Remembering that $\tau_B = 1/k_r$ and $\tau_A = 1/k_f(T_B - C) \simeq 1/k_f T_B$ we have $P_A = 1/(1 + KT_B)$ and $P_B = KT_B/(1 + KT_B)$; thus

$$[7]\quad \langle\omega\rangle = \frac{1}{(1 + T_B K)}\omega_A + \frac{KT_B}{(1 + KT_B)}\omega_B$$

using eq. 5*a*.

The $\langle\omega\rangle$ values for each hyperfine line as a function of ligand concentration were obtained by carrying out a least-squares fit of the isotropic form of Bleaney's equation (up to second order in the hyperfine coupling constant (A_0) and the **g**-tensor ($\mathbf{g}_0$))

$$[8]\quad \mathrm{H}(m_I) = H_0 - A_0 m_I - \frac{A_0^2}{2H_0}[I(I+1) - m_I^2]$$

in the usual notation (17).

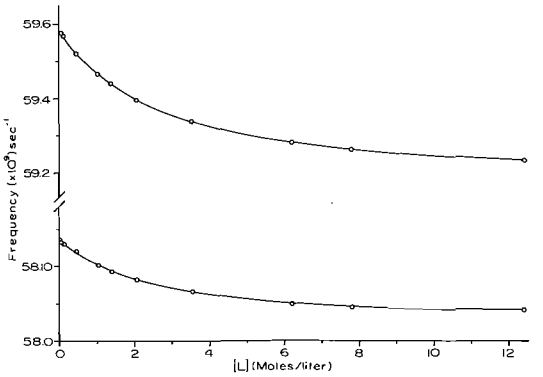

FIG. 2. Variation of e.p.r. line position with pyridine concentration [L]. The top and bottom curves correspond to +3/2 line and +1/2 lines, respectively, at 300 °K.

With these exchange averaged values of A_0 and $\mathbf{g}_0$ the frequency of any hyperfine line could be computed for any chosen microwave frequency. The variation of the position of the +3/2 and +1/2 lines is shown in Fig. 2. These plots confirm that eq. 5*a* is applicable to the present investigation. It should be noted here that only the high fields +3/2 and +1/2 ($A_0 < 0$) were employed in the line position and line width analysis since the other two lines are often considerably broadened and tend to overlap.

The equilibrium constant and the values of ω_A and ω_B were obtained from the line position data by means of a three parameter least-squares fit of eq. 7 with T_B as the independent variable and $\langle\omega\rangle$ as the dependent variable. This procedure obviates any necessity of determining ω_A and ω_B from measurements in pure solvents (benzene and pyridine in this case). A rigorous test of this procedure, and its efficacy, is that the determined values of ω_A and ω_B could be used in the estimation of the rate constants (see later); Corden and Rieger (9) found this impossible. In addition these workers found it necessary to constrain $(\omega_A - \omega_B)$ to be constant over the range of temperatures they studied; obviously, we did not find this necessary. The free variation of ω_A and ω_B in the analysis of the line position and line width data gives internally consistent results in the present work.

TABLE 1. Parameters obtained from a least-squares fit of the line position data and obtained from measurements in heat solvents

Temperature (°K)	Hyperfine line position (10^{-9} s^{-1}) +3/2 ω_A*	+3/2 ω_A†	+3/2 ω_B*	+3/2 ω_B†	+1/2 ω_A*	+1/2 ω_A†	+1/2 ω_B*	+1/2 ω_B†	K‡ (mol l^{-1})
280	59.612	59.483	59.133	59.196	58.143	58.108	58.010	58.024	0.64
285	59.607	59.478	59.146	59.211	58.143	58.106	58.010	58.029	0.58
290	59.601	59.474	59.156	59.205	58.141	58.105	58.013	58.027	0.53
295	59.594	59.469	59.163	59.232	58.139	58.104	58.015	58.035	0.45
300	59.587	59.465	59.156	59.223	58.137	58.102	58.013	58.032	0.38
305	59.579	59.460	59.144	59.230	58.135	58.101	58.009	58.034	0.32
310	59.577	59.455	59.158	59.252	58.134	58.099	58.013	58.041	0.30
315	59.569	59.451	59.164	59.255	58.132	58.098	58.015	58.042	0.29
320	59.559	59.446	59.150	59.255	58.129	58.097	58.011	58.042	0.24
325	59.554	59.441	59.145	59.262	58.128	58.096	58.010	58.044	0.23

*Value obtained from least-squares fit.
†Value obtained from measurement in neat solvent.
‡The value of K is the average between the values for the two hyperfine line studies; uncertainty ± 0.02.

The results of fitting the line position data, for the particular temperature 300 °K, to eq. 7 are shown in Fig. 2 as an example. The fit is seen to be excellent. The line position measurements were carried out over the temperature range 280 to 325 °K. The determined values of ω_A, ω_B, and K for this temperature range are given in Table 1; also contained in this table are the values of ω_A and ω_B obtained from measurements on the pure solvents. Table 2 contains the thermodynamic data, for the temperature of 300 °K, obtained from the Arrhenius plot for the equilibrium constant; see Fig. 3.

We note here that it is also possible to obtain K from a similar fit to the expression

$$\langle A \rangle = P_A A_A + P_B A_B$$

for the average value of the isotropic hyperfine splitting. This was in fact carried out and entirely consistent results for K were obtained. This is the method employed by Shklyaev and Anufrienko (10). The values of A_A and A_B are given in Table 3 together with the corresponding equilibrium constants.

We turn now to a discussion of the determination of the rate constant k_r. The estimation of a rate constant requires the analysis of line width data in conjunction with an equation of the type given in eq. 6. It was found, however, that eq. 6 does not adequately fit the line width behavior observed in the present case. An order of magnitude calculation indicated that the non-secular terms included by Atherton and Luckhurst (15) become important at low pyridine concentrations. The reason for this can be seen if we consider the equation for T_2^{-1} given by Atherton and Luckhurst (15).

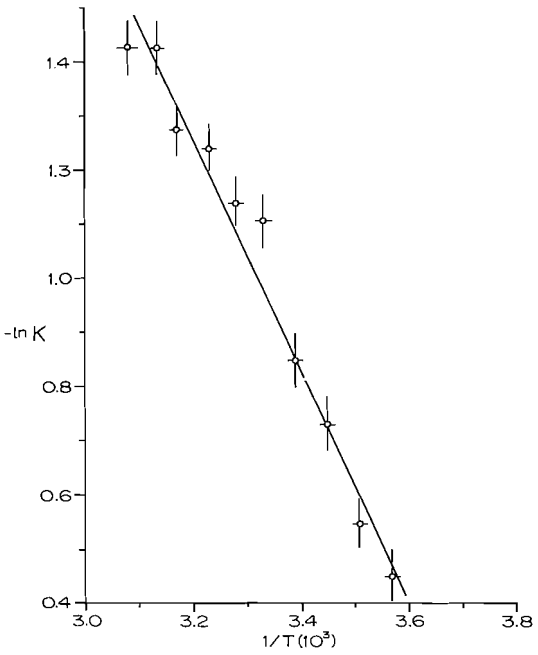

FIG. 3. Arrhenius plot for the equilibrium constant (K).

[9] $$T_2^{-1} = P_A T_{2A}^{-1} + P_B T_{2B}^{-1} + P_A^2 P_B \tau_B \times \left\{ (\omega_A - \omega_B)^2 + \frac{\Delta A}{2} \frac{[I(I+1) - m^2]}{(1 + \omega_0^2 P_A^2 \tau_B^2)} \right\}$$

Can. J. Chem. Downloaded from www.nrcresearchpress.com by 210.87.254.40 on 09/05/12
For personal use only.

Can. J. Chem. Downloaded from www.nrcresearchpress.com by 210.87.254.40 on 09/05/12
For personal use only.

TABLE 2. Thermodynamic data*

Complex	Solvent	Base	Temperature (°K)	K (l/mol)	ΔH^0 (kcal/mol)	ΔS^0 (e.u.)	k_r ($\times 10^8$)	ΔH_f^* (kcal/mol)	ΔS_f^* (e.u.)	ΔH_r^* (kcal/mol)	ΔS_r^* (e.u.)	Reference
$Cu(DnBDC)_2$	$C_6H_{11}CH_3$	Piperidine	298	3.9	−7.5	−22	3.7	—	—	7.4	5	9
		n-Hexylamine	298	2.1	−7.3	−23	13.	—	—	6.6	5	9
		Pyridine	298	0.40	−5.	−19	20.	~0	—	5	−1	9
$Cu(DDC)_2$	$C_6H_5CH_3$	Pyridine	298	0.49	−4.9	—	3.4	+3.7	—	8.6	—	10
$Cu(DDC)_2$	C_6H_6	Pyridine	300	0.38 (±0.02)	−4.8 (±0.5)	−16 (±5)	5.8	−2.9 (±0.5)	−30 (±5)	+2.1 (±0.5)	−12 (±5)	Present work

*The errors correspond to least-squares r.m.s. errors multiplied by 5.

TABLE 3. Parameters obtained from a least-squares fit of the hyperfine parameters

Temperature (°K)	Isotropic hyperfine constants (10^{-8} s^{-1})					K (± 0.02) (mol l^{-1})
	A_A*	A_A†	A_B*	A_B†	ΔA (10^{-8} s^{-1})	
280	14.333	13.441	11.063	11.424	3.274	0.62
285	14.283	13.409	11.081	11.531	3.202	0.60
290	14.247	13.378	11.063	11.486	3.184	0.51
295	14.211	13.348	11.207	11.675	3.004	0.47
300	14.175	13.315	11.189	11.612	2.986	0.33
305	14.121	13.283	11.099	11.666	3.022	0.34
310	14.081	13.252	11.153	11.819	2.932	0.30
315	14.040	13.222	11.243	11.837	2.806	0.30
320	13.995	13.189	11.207	11.837	2.788	0.26
325	13.959	13.157	11.225	11.891	2.734	0.24

*Value obtained from least-squares fit.
†Values obtained from measurements in neat solvent.

TABLE 4. Parameters obtained from the line width data

Temperature (°K)	Line widths for the +3/2 line (10^{-6} s^{-1})				k_r ($\times 10^{-8}$ s^{-1})	k_f ($=Kk_r$) ($\times 10^{-8}$ s^{-1})	τ_B (10^9 s)
	T_{2A}*	T_{2A}†	T_{2B}*	T_{2B}†			
280	51.27	57.87	63.66	62.34	4.13	2.56	2.42
285	46.73	58.20	66.19	62.86	4.76	2.62	2.10
290	46.76	58.81	61.36	64.99	5.24	2.52	1.91
295	47.84	59.67	54.43	67.31	5.55	2.36	1.80
300	50.13	60.76	52.25	69.66	5.85	2.17	1.71
305	51.86	62.00	50.58	71.98	6.25	2.13	1.60
310	51.77	63.56	53.54	74.31	6.62	1.99	1.51
315	55.57	63.87	59.80	76.65	6.99	1.89	1.43
320	60.86	67.30	57.46	79.45	7.52	1.88	1.33
325	66.82	69.48	59.66	81.31	8.55	1.79	1.17

*Value obtained from the least-squares fit.
†Value obtained from measurement in neat solvent.

where $\Delta A = A_A - A_B$. At low temperatures ΔA increases to the point where this non-secular contribution approaches 20% of the transverse relaxation time for the system under study here.

Corden and Rieger, however, found it necessary to include extra terms derived from eq. 2. We have found that these terms afforded only a small improvement which did not warrant their inclusion since this greatly increased the computational time involved. In any event these corrections are certainly smaller than the errors introduced by neglecting non-secular, pseudo-secular, and rotational terms (14, 15).

Accordingly, the line width data were fitted by applying the least-squares techniques to eq. 9 with T_{2A}, T_{2B}, and τ_B as parameters, the values of A_A, A_B, ω_A, and ω_B having been determined previously from the line position data. The values of T_{2A}, T_{2B}, and k_r obtained in this way are given in Table 4. A comparison of the experimental and fitted line width data is given in Fig. 4 and it is seen that the overall fit is quite satisfactory. The rate constants were obtained at various temperatures; the Arrhenius plot that can be constructed from this data is shown in Fig. 5. The thermochemical data estimated, for the temperature 300 °K, from the temperature variation of the rate constants are given in Table 2. Line widths were also measured in neat solvents and are reported in Table 4.

Discussion

The results of the least-squares fitting of the line position data, given in Table 1, show that the line positions measured in pure benzene are somewhat less than those obtained by the fit; similarly those measured in neat pyridine are

Can. J. Chem. Downloaded from www.nrcresearchpress.com by 210.87.254.40 on 09/05/12
For personal use only.

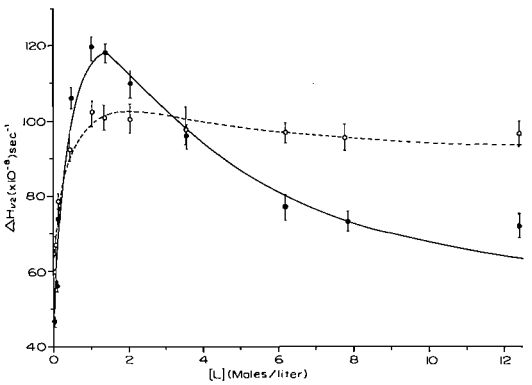

FIG. 4. Variation of e.p.r. linewidth data at 300 °K for the +3/2 line (solid) and +1/2 (dotted) line.

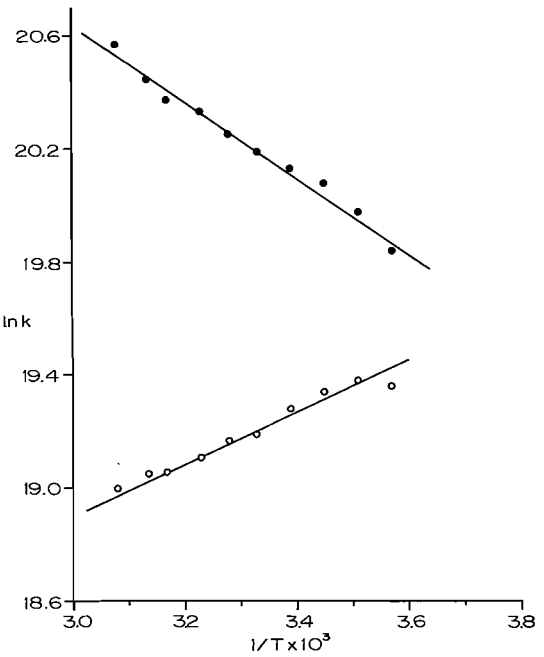

FIG. 5. Arrhenius plots for the forward (open circles) and reverse (solid circles) rate constants.

less than the fitted values. The latter result is readily understood when one appreciates that even in pure pyridine the equilibrium concentration of ML_2B is only 80% of that of ML_2, *i.e.*, fast exchange is still in evidence. The fitted value of $\langle\omega\rangle$ at 12.4 M pyridine is 63.76×10^6 s^{-1} at 285 °K which is well within experimental error of that measured in neat pyridine (62.86×10^6 s^{-1}). This result suggests that it is inappropriate to fix the value of ω_B to that measured in the pure solvent and that fitting involving a free variation of ω_B (and ω_A) is the preferred procedure.

The fact that ω_A measured in pure benzene is less than that obtained by the least-squares technique would imply that there is indeed an interaction between the benzene solvent molecules and the $Cu(DDC)_2$. The pure benzene results were checked several times, always with the same finding. In order to check the behavior of the curve shown in Fig. 2, line position measurements were carried out at very low pyridine concentration (5×10^{-4} M). It was found that the measured line position fell on the extrapolation of the curve toward zero base concentration, *i.e.*, the curve did not turn down toward the value of ω_A measured in pure benzene. Thus it would appear that there is a small change in the solvation of $Cu(DDC)_2$ effected by the addition of pyridine. This result does not appear to have been observed by other workers (9, 10) who used ω_A measured in pure solvent. This finding supports the contention that ω_A and ω_B should be regarded as solvent interaction free parameters valid only in the fast exchange region and in fact are unattainable experimentally.

The isotropic hyperfine coupling, as expected, since the isotropic g-value varies little, exhibits a similar "anomalous" behavior. The difference between A_B measured in pure pyridine and least squares fitted can be explained in the same way as for ω_B. The fact that A_A in benzene is less than the fitted value suggests that the interaction between the solute and the solvent is such as to reduce the spin density on the copper atom; this in turn implies a delocalization of spin density into the benzene solvent molecules. It is tempting to suggest that there is in fact a fast exchange between the benzene solvent molecules and $Cu(DDC)_2$ but the line width data shown in Table 3 indicate that the temperature dependence of the line widths T_{2A} is dominated by a spin-rotational term (21, 22) so this can be discounted.

The results given in Table 4 show that fitting line width data to eq. 9 leads to values of T_{2A} and T_{2B} which vary over the temperature range studied in a manner that is quite consistent with what might be expected for the line widths based on the theory of Kivelson (22, 23). This fact lends support to the approach taken in analyzing the trends in line width data over varying ligand concentration. We note that

Can. J. Chem. Downloaded from www.nrcresearchpress.com by 210.87.254.40 on 09/05/12
For personal use only.

Can. J. Chem. Downloaded from www.nrcresearchpress.com by 210.87.254.40 on 09/05/12
For personal use only.

there are differences between the T_{2A}'s measured in neat benzene and those fitted; again this may be indicative of some sort of solute–solvent interaction but is more likely a result of the approximation inherent in our method of analysis.

The application of the Bloch equations to the study of chemical exchange is not always possible. Atherton and Luckhurst (15) have shown that when any of the lifetimes in an exchanging process become comparable to the rotational reorientation time of the complex in solution, then a relaxation matrix analysis of the reorientation–exchange problem does not reduce to a solution of the Bloch equations. The Bloch equations are generally valid, when the reorientational correlation time, τ_c, is much smaller than the exchange lifetime τ_{ex}, except for non-secular and pseudo-secular terms that can become important under certain conditions (14).

In the present case, analysis of our line width data in terms of the parameters derived by Kivelson suggests that the rotational reorientation time is $\sim 10^{-11}$ s, thus being several orders of magnitude shorter than τ_{ex} ($\sim 10^{-9}$ s). This result supports our use of the modified Bloch equation. In viscous solvents, or for reactions involving large molecules great care must be exercised to ensure the validity of any approximate procedures employed.

The viscosity dependence of line widths is well known and it is implicit in the present work that the variation in viscosity as the base concentration varies is small. This assumption, as pointed out by Corden and Rieger (9) means that the value of T_{2B} obtained corresponds to some average value and this may well be the reason for the discrepancy between T_{2A} fitted and measured in neat benzene.

The results of previous work (9, 10) and our own are collected in Table 2. The results for the equilibrium constants for the reactions

$$\text{Cu(DnBDC)}_2 + \text{pyridine} \rightleftharpoons \text{Cu(DnBDC)}_2\text{.pyridine}$$

$$\text{Cu(DDC)}_2 + \text{pyridine} \rightleftharpoons \text{Cu(DDC)}_2\text{.pyridine}$$

are in reasonable agreement. The amount of data reported so far is too small to reach any conclusions as to the acid-strength of the two copper complexes studied or as to the different solvent effects between benzene and toluene (10). The temperature dependence of the equilibrium constants is also similar and consequently leads to comparable values of ΔH^0 and ΔS^0.

The value of the reverse rate constant (k_r) will depend critically on the method of analysis of the line width data. The difference in the method employed by Corden and Rieger and the present work is quite marked. Thus for their study of the reaction between Cu(DnBDC)_2 and pyridine they (*a*) assumed that $(\omega_A - \omega_B)$ does not vary with temperature and (*b*) used the value for piperidine as they were unable to get a realistic fit of the line width data with pyridine; no such problems were met in the present work. We therefore feel that we cannot reasonably compare their lifetime data with ours except to say that theirs appear to be quite low in comparison with that measured here. The work of Shklyaev and Anufrienko (10) gave a rate of reaction in the reverse direction very similar to that obtained here (see Table 2).

The forward rate at 25 °C measured is about 2.2×10^8 s, and the question arises whether or not this reaction is diffusion controlled. Clarke and Wanye (20) indicate that diffusion considerations can only be safely ignored if $k_{obs} < 10^7$. The rates here are of the order of 10^8; consequently a diffusion controlled mechanism cannot be ruled out. This is the conclusion reached by Shklyaev and Anufrienko.

One interesting aspect of the present results is the fact that ΔH_f^* is negative. Corden and Rieger (9) obtained a value of approximately zero and felt that this result contradicted the idea of a diffusion controlled mechanism. The fact that k_f, measured here, decreases with increasing temperature also does not appear to correspond to a diffusion controlled mechanism since a diffusion controlled rate constant should increase with increasing temperature. The existence of an apparent negative energy of activation may reflect either an artifact of the approximations involved in the determination of $k_f(Kk_r)$, or may indicate that ΔS^* is varying over the temperature range studied. The reliability of the present result can only be established by further studies and these are being embarked upon.

Implicit throughout this work has been the assumption that only a 1:1 adduct is formed. Corden and Rieger (9) consider the possibility of 1:2 adduct formation (CuL_2B_2), but consideration of previous results (24–28) indicates

that a 1:2 adduct is not formed to an extent sufficient to affect the e.p.r. results, even in neat pyridine solution.

The formation of two adducts is very likely to be a step-wise process (24), involving a very fast 1:1 followed by a relatively slow 1:2 adduct formation. Stereochemical arguments have been invoked to show that in solution the addition of a sixth ligand is extremely unfavorable for planar Cu(II) complexes (25–28) and undoubtedly the second stepwise formation constant will be much less than the first (24), so that very little, if any, 1:2 adduct would be formed. The effects of such a slow modulation on an existing fast exchange e.s.r. spectrum would not be evident unless the concentration of the 1:2 adduct was a significant fraction of the 1:1 adduct concentration, in which case two distinct spectra would be observable. This has not been observed here, but if it were, the effect of the second equilibrium process on the fast exchange situation would simply be a very small additional line broadening proportional to the lifetime of the 1:2 adduct.

Further, several authors have demonstrated that square planar complexes of copper(II), while definitely showing penta-coordination in solution with appropriate ligands, do not show any evidence of the formation of a hexa-coordinate complex in solution (25, 27, 28). It is likely, also, that any hexa-coordinate Cu(II) species would have properties significantly different from a penta-coordinate adduct, and would thus be readily observable by the methods utilized so far.

We thank the National Research Council of Canada for financial support.

1. D. P. GRADDON. Coord. Chem. Rev. **4**, 1 (1969).
2. D. P. GRADDON and K. B. HENG. Aust. J. Chem. **24**, 1781 (1971).
3. B. L. LIBUTTI, B. B. WAYLAND, and A. F. GARITO. Inorg. Chem. **8**, 1510 (1969).
4. A. F. GARITO and B. B. WAYLAND. J. Am. Chem. Soc. **91**, 866 (1969).
5. T. VÄNNGÅRD and S. AKERSTROM. Nature, London, **184**, 183 (1959).
6. T. AASA, R. PETTERSON, and T. VÄNNGÅRD. Nature, London, **190**, 258 (1961).
7. J. F. GIBSON. Trans. Faraday Soc. **66**, 2105 (1965).
8. K. E. FALK, E. IVANOVA, B. ROOS, and T. VÄNNGÅRD. Inorg. Chem. **9**, 556 (1970).
9. B. J. CORDEN and P. H. RIEGER. Inorg. Chem. **10**, 263 (1971).
10. A. A. SHKLYAEV and V. F. ANUFRIENKO. Zhurnal Strukt. Khimii, **12**, 601 (1971).
11. H. S. GUTOWSKY, D. W. MCCALL, and C. P. SLICHTER. J. Chem. Phys. **21**, 279 (1953).
12. H. M. MCCONNELL. J. Chem. Phys. **28**, 430 (1958).
13. J. A. POPLE, W. G. SCHNEIDER, and H. J. BERNSTEIN. High resolution nuclear magnetic resonance. McGraw-Hill Inc., New York. 1959.
14. G. K. FRAENKEL. J. Phys. Chem. **71**, 139 (1967).
15. N. M. ATHERTON and G. R. LUCKHURST. Mol. Phys. **13**, 145 (1967).
16. H. WAHLQUIST. J. Chem. Phys. **35**, 1708 (1961).
17. B. BLEANEY. Phil. Mag. 441, **42** (1951).
18. H. S. GUTOWSKY and C. H. HOLM. J. Chem. Phys. **25**, 1228 (1956).
19. S. MEIBOOM, Z. LUZ, and D. GILL. J. Chem. Phys. **27**, 1411 (1957).
20. I. D. CLARKE and R. P. WANYE. Comprehensive chemical kinetics. Vol. 2. *Edited by* C. H. Bamford and C. F. H. Tipper. Elsevier. 1969. p. 308.
21. G. NYBERG. Mol. Phys. **12**, 69 (1967).
22. R. WILSON and D. KIVELSON. J. Chem. Phys. **44**, 4440 (1966).
23. R. WILSON and D. KIVELSON. J. Chem. Phys. **44**, 4445 (1966).
24. F. A. COTTON and G. WILKINSON. Advanced inorganic chemistry. Interscience, New York. 1962. Chap. 25.
25. V. ROMANO and J. BJERRUM. Acta Chem. Scand. **24**, 1551 (1970).
26. L. E. ORGEL and J. S. GRIFFITH. Quart. Rev. **11**, 381 (1957).
27. D. P. GRADDON and E. C. WATTON. J. Inorg. Nucl. Chem. **21**, 49 (1961).
28. D. P. GRADDON. Nature, **183**, 1610 (1959).

Can. J. Chem. Downloaded from www.nrcresearchpress.com by 210.87.254.40 on 09/05/12
For personal use only.

The Ultraviolet Absorption Spectrum of Furazan

B. J. FORREST AND A. W. RICHARDSON

Chemistry Department, Bishop's University, Lennoxville, Quebec

Received March 1, 1972

The ultraviolet absorption spectrum of furazan (1,2,5-oxadiazole) in the region 2500–2300 Å has been recorded and analyzed as a $\pi \rightarrow \pi^*$ transition from the planar ground state to a non-planar excited state having a potential barrier to planarity of about 215 cm^{-1}.

Le spectre d'absorption ultraviolet du furazane (1,2,5-oxadiazole) a été enregistré dans la région de 2500 à 2300 Å. L'analyse indique qu'il s'agit d'une transition $\pi \rightarrow \pi^*$ de l'état planaire fondamental vers un état excité non planaire ayant une barrière de potentiel de 215 cm^{-1} environ vis à vis de la planéité.

Canadian Journal of Chemistry, **50**, 2088 (1972)

Introduction

Furazan (1,2,5-oxadiazole) (**1**, X = O) has been shown by a microwave spectroscopic study (1) to be a planar molecule of C_{2v} symmetry with some aromatic character, and study of its infrared and Raman spectra (2, 3) has lead to assignments for all 15 normal modes of vibration. This paper reports the results of an investigation of the 2430 Å absorption spectrum of furazan. This study is of particular interest in light of a recent report of an investigation of the first u.v. absorption spectrum of 1,2,5-thiadiazole (**1**, X = S) which showed that, although the ground state is planar, the excited state is non-planar and has a barrier to planarity of about 460 cm^{-1} (4).

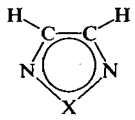

1

Experimental

Furazan was prepared by heating a mixture of solid glyoxime and succinic anhydride to 150–170 °C, as described by Olofson and Michelman (5), and purified by triple distillation. The i.r. spectrum of the liquid and vapor showed no signs of impurities and g.l.c. indicated a purity in excess of 99%.

The majority of the spectra were recorded on a Hitachi–Perkin–Elmer model 139 single beam spectrometer (modified for scanning and equipped with a photomultiplier) at a slit width giving a band pass of about 20 cm^{-1}. Some spectra were also recorded on a Bausch and Lomb 1.5 m grating spectrograph using a 150 W high pressure xenon lamp and Spectrum Analysis No. 1 film. Measurements of these spectra were made from prints enlarged about 15 times by interpolation between iron standards.

The spectra were obtained for the vapor in a 1 m fused silica absorption cell at sample pressures ranging from the vapor pressure at 0 °C to that at about 100 °C. Spectra were also taken with the sample pressure equal to the vapor pressure at 25 °C but with the vapor at a number of temperatures between 25 and 200 °C on the Hitachi–Perkin–Elmer spectrometer.

Results and Assignments

A tracing of the u.v. absorption spectrum of furazan obtained with the Hitachi–Perkin–Elmer spectrometer is shown in Fig. 1, and the vacuum wavenumbers of the bands are given in Table 1. The listed wavenumbers of almost all bands are the averages of measurements from at least four spectrometer traces. The precision of the measurements ranges from ± 5 to ± 10 cm^{-1} because of the weakness or diffuseness of most of the bands. The spectra taken on the Bausch and Lomb spectrograph (theoretical resolution < 1 cm^{-1}) show that only the bands at 40 497, 41 105, 41 296, 41 751, 41 879, and 42 042 cm^{-1} have sharp band heads; the bands at low wavenumber were too weak to observe clearly, and the bands at high wavenumber are definitely diffuse.

Comparison of the spectrometer traces obtained for a fixed pressure of vapor at temperatures between 25 and 200 °C indicates that all bands at wavenumbers less than 41 105 cm^{-1} are hot, thus placing the origin band at 41 105 cm^{-1}. All but two hot bands can be related to bands at higher wavenumber by use of the ground state vibration $\nu_5'' = 1006$ cm^{-1}, a symmetric ring in-plane bending mode (2), as shown in Table 1. This is completely in accord with the observations in 1,2,5-thiadiazole where the strongest hot bands involve the analogous vibration $\nu_5'' = 805$ cm^{-1} (4).

Can. J. Chem. Downloaded from www.nrcresearchpress.com by 210.87.254.40 on 09/05/12
For personal use only.

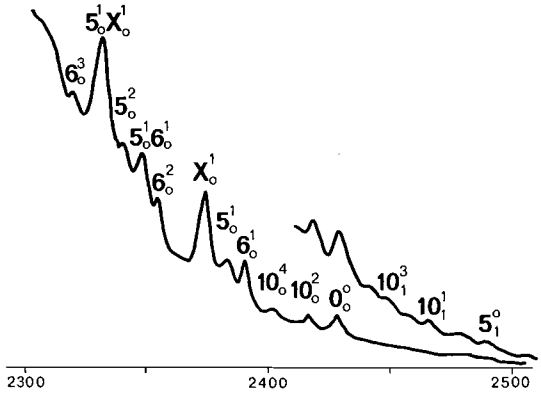

FIG. 1. Ultraviolet absorption spectrum of furazan as recorded on the Hitachi–Perkin–Elmer model 139 spectrometer. Lower trace, vapor at 25 °C; upper trace, vapor at about 150 °C.

All but three bands to high wavenumber of 41 105 cm^{-1} can be explained using three excited state vibrations of frequencies 646, 774, and 937 cm^{-1}. The 646 and 774 cm^{-1} vibrations occur in progressions and therefore must be totally symmetric A_1 modes. Since 774 cm^{-1} is the most active excited state vibration, it seems reasonable to correlate it with $\nu_5'' = 1006$ cm^{-1}, the only totally-symmetric vibration giving hot bands. This is supported by the fact that the decrease going from the ground to excited state is about 25%, which is about the same as in 1,2,5-thiadiazole where ν_5 decreases from 805 to 604 cm^{-1} (4). A possible assignment for 646 cm^{-1} is ν_6' since $\nu_6'' = 872$ cm^{-1} (2).

The 937 cm^{-1} vibration occurs only as a single quantum with a progression in ν_5' based on it. This suggests that 937 cm^{-1} may be due to a non-totally symmetric vibration active in Herzberg–Teller intensity stealing (6).[1] This vibration is most likely one of the b_2 in-plane vibrations (7–9) probably correlating with $\nu_{13}'' = 1177$ cm^{-1}, a C—H in-plane bend, or $\nu_{14}'' = 952$ cm^{-1}, a ring in-plane bend (2). Since nothing definite can be said about this on the basis of the evidence available, the 937 cm^{-1} vibration has been denoted by X in Table 1. It is interesting to note

TABLE 1. Observed bands in the 2430 Å absorption system of furazan

Intensity	ν_{obs} (cm^{-1})	Assignment†	ν_{calc} (cm^{-1})‡
0.6	38 869	5_2^1	39 867
0.8	40 088	5_1^0	40 099
0.6	40 292	$5_1^010_0^2$	40 290
0.8	40 497	10_1^1	—
0.4	40 636	5_2^2	40 641
0.7	40 780	10_1^3	—
0.6	40 886	5_1^1	40 873
1	41 030 sh	$5_1^0X_0^1$	41 036
7	41 105	0_0^0	—
4	41 296	10_0^2	—
0.9	41 584	10_0^4	—
17	41 751	6_0^1	—
13	41 879	5_0^1	—
40	42 042	X_0^1	—
16	42 394	6_0^2	42 397
33	42 512	$5_0^16_0^1$	42 525
28	42 649	5_0^2	42 653
100	42 816	$5_0^1X_0^1$	42 816
19	43 027	6_0^3	43 043
47	43 229 sh	—	—
47	43 295	$5_0^26_0^1$	42 299
71	43 442	5_0^3	43 427
150	43 600	$5_0^2X_0^1$	43 590
47	43 806	$5_0^16_0^3$	43 817

*The listed intensities are only approximate. Errors may be large especially for bands at higher wavenumbers which are diffuse and seem to be superimposed on continuous absorption.
†A $v'-v''$ transition in the Kth normal mode is labelled $K_{v''}^{v'}$.
‡$\nu_5'' = 1006$ cm^{-1}, $\nu_{10}'' = 631$ cm^{-1} (2), $\nu_5' = 774$ cm^{-1}, $\nu_6' = 646$ cm^{-1}, $\nu_x' = 937$ cm^{-1}.

that the bands due to the 937 cm^{-1} vibration and the ν_5' progression based on it are stronger than other bands near them. This implies that the forbidden component of the spectrum is about as strong as or stronger than the allowed component. Similar observations have been made in the spectra of ethynylbenzene (9) and naphthalene (10) where the forbidden component is estimated to be about three and ten times, respectively, as intense as the allowed component.

At this stage, there are only four important bands left unassigned, namely those at 40 497, 40 780, 41 296, and 41 584 cm^{-1}. By analogy to the assignments made for 1,2,5-thiadiazole (4), these bands may be given the assignments 10_1^1, 10_1^3, 10_0^2, and 10_0^4, respectively, where ν_{10} is a b_1 out-of-plane ring bending vibration.[2] That is, the excited state of furazan is taken to be nonplanar as shown in 1,2,5-thiadiazole (4). With

[1]In the spectra taken on the Bausch and Lomb spectrograph, the origin band at 41 105 cm^{-1} has a definite double-headed appearance while the band at 42 042 cm^{-1} (= 41 105 + 937) does not. However, with these spectra, it is not possible to tell whether this difference is due to a different band contour, as the assignment requires, or to the onset of diffuseness.

[2]In ref. 4, the b_1 out-of-plane ring bending vibration was designated ν_{15} instead of ν_{10} as it should have been.

Can. J. Chem. Downloaded from www.nrcresearchpress.com by 210.87.254.40 on 09/05/12
For personal use only.

Can. J. Chem. Downloaded from www.nrcresearchpress.com by 210.87.254.40 on 09/05/12
For personal use only.

TABLE 2. Observed and calculated term values $G_0'(v_{10}')$ for v_{10}' (cm^{-1})

	v_{10}' (cm^{-1})			
		Calculated		
Term	Observed	(*i*)	(*ii*)	(*iii*)
0	0	0	0	0
1	23±2	22.9	23.0	23.0
2	190±2	190.0	190.0	190.0
3	313±10	314.4	306.7	298.2
4	479±10	480.9	464.6	447.6
5	—	659.1	628.7	597.5

	Calculated value		
Parameter	(*i*)	(*ii*)	(*iii*)
$G(0)$	113.9	111.1	108.7
ρ	0.60	0.90	1.20
B	0.8406	1.0664	1.2781
v_0	255.72	204.26	173.87
b	214.96	217.82	222.22

these assignments and the value $v_{10}'' = 631$ cm^{-1} from the i.r. (2), the vibrational term values $G_0'(v_{10}')$ can be calculated. Table 2 lists these values together with estimated uncertainties. The uncertainties in $G_0'(1)$ and $G_0'(2)$ are relatively small since the appropriate bands are relatively strong and have sharp heads, and so could be measured to about ± 1 cm^{-1} on spectra taken with the Bausch and Lomb spectrograph; the uncertainties in $G_0'(3)$ and $G_0'(4)$ are much greater because the bands are weaker and could not be as accurately measured.

The origin band at 41 105 cm^{-1} has a definite double-headed appearance consisting of a sharp narrow feature at high wavenumber separated by about 13 cm^{-1} from, and having a relative intensity about twice that of, a broader feature at low wavenumber. The appearance of this band is very similar to that of the origin band of 1,2,5-thiadiazole (4). This suggests that the transition is $\pi \rightarrow \pi^*$ in nature as is that for 1,2,5-thiadiazole.

Calculations

The $G_0'(v_{10}')$ term values have been fitted to a double-minimum potential function of the form

$$V(Q) = \tfrac{1}{2}\lambda Q^2 + A \exp\{-a^2Q^2\}$$

using tables of eigenvalues in the literature (11). Because of their smaller uncertainties, the term values $G_0'(1)$ and $G_0'(2)$ have been used to determine the parameters. The term values calculated for several sets of parameters are compared to the observed values in Table 2. The agreement of the observed and calculated values is as good as expected in light of the uncertainties in the observed $G_0'(v_{10}')$ values. The values indicate that the barrier to planarity in furazan is in the order of 215 cm^{-1} which is rather less than the values of 460 cm^{-1} determined for 1,2,5-thiadiazole (4).

Discussion

Microwave studies of furazan (1) and 1,2,5-thiadiazole (12) have shown that although both molecules have significant electron delocalization (aromatic character) in the ground electronic state, it is greater in 1,2,5-thiadiazole than in furazan, presumably as the result of sulfur atom d orbital participation in the π bonding of the ring (13). The observation that the first $\pi \rightarrow \pi^*$ excited state in both molecules is non-planar indicates that the change in electronic structure is sufficient to destroy the aromatic π bonding of these cyclic compounds.

The increase in the excited state barrier to planarity in going from furazan to 1,2,5-thiadiazole shows the same trend as observed in the ground states of trimethylene oxide (14) and trimethylene sulfide (15) where the barriers are about 15 and 274 cm^{-1}, respectively. The change in the four-membered rings is explained in terms of two opposing forces in the molecules. One is the torsional interaction between adjacent methylene groups which favors a non-planar configuration and is about the same in trimethylene oxide and sulfide. The second is the ring strain which tends to favor a planar configuration since puckering the ring decreases the ring angles and increases the ring strain. The latter is smaller for trimethylene sulfide since normal angles for sulfides are smaller than for corresponding ethers, thus leading to a more non-planar equilibrium position and a higher barrier to planarity in the sulfide. In the five-membered rings discussed here, there are no torsional (non-bonded) interactions to consider and so it must be a purely electronic effect which leads to non-planarity. Presumably as in the four-membered rings, the ring strain is less for 1,2,5-

thiadiazole than for furazan and leads to a larger barrier to planarity in the former than in the latter.

The authors thank the National Research Council of Canada for financial support of this work. One of us (B.J.F.) thanks Hoffman-LaRoche Ltd. for the Professor A. L. Keuhner Memorial Scholarship. The authors thank Miss E. Crepeau who prepared the sample of furazan used for this investigation and recorded some preliminary spectra.

1. E. SAEGEBARTH and A. P. COX. J. Chem. Phys. **43**, 166 (1965).
2. G. SBRANA, M. GINANNESCHI, and M. MARXOCCHI. Spectrochim. Acta, A**23**, 1757 (1967).
3. E. BORELLO, A. ZECCHINA, and E. GUGLIELMINOTTI. Gazz. Chim. Ital. **96**, 852 (1966).
4. E. FIRKINS and A. W. RICHARDSON. Chem. Commun. 1368 (1971).
5. R. A. OLOFSON and J. S. MICHELMAN. J. Org. Chem. **30**, 1854 (1965).
6. G. HERZBERG. Molecular spectra and molecular structure. Vol. III. Electronic spectra and electronic structure of polyatomic molecules. Van Nostrand, Princeton, N.J. 1967. pp. 177–178.
7. H. D. BIST, J. C. D. BRAND, and D. R. WILLIAMS. J. Mol. Spectry. **21**, 76 (1966).
8. R. D. GORDON and R. F. YANG. J. Mol. Spectry. **39**, 295 (1971).
9. G. W. KING and S. P. SO. J. Mol. Spectry. **33**, 376 (1970).
10. D. P. CRAIG, J. M. HOLLAS, M. F. REDIES, and S. C. WAIT, JR. Phil. Trans. Roy. Soc. London, Ser. A**253**, 543 (1961).
11. J. B. COON, N. W. NAUGLE, and R. D. MCKENZIE. J. Mol. Spectry. **20**, 107 (1966).
12. SR. V. DOBYNS and L. PIERCE. J. Am. Chem. Soc. **85**, 3553 (1963).
13. L. M. WEINSTOCK and P. I. POLLAK. Adv. Heterocyclic Chem. **9**, 161 (1968).
14. S. I. CHAN, T. R. BORGERS, J. W. RUSSELL, H. L. STRAUSS, and W. D. GWINN. J. Chem. Phys. **44**, 1103 (1966).
15. T. R. BORGERS and H. L. STRAUSS. J. Chem. Phys. **45**, 947 (1966).

Can. J. Chem. Downloaded from www.nrcresearchpress.com by 210.87.254.40 on 09/05/12
For personal use only.

Studies of Organophosphorus Derivatives. Part I. Nuclear Magnetic Resonance Studies of the 2-Oxo-1,3,2-dioxaphosphorinane System[1]

L. D. HALL AND R. B. MALCOLM[2]

Department of Chemistry, The University of British Columbia, Vancouver 8, British Columbia

Received July 19, 1971[3]

The n.m.r. spectra of a series of simple derivatives of the 2-oxo-1,3,2-dioxaphosphorinane system are discussed in terms of the favored conformations of the derivatives and the stereospecific dependencies of *vicinal* $^{31}P—O—C—^{1}H$ couplings. Attention is drawn to a type of "deceptively-simple" ABX spectrum which is commonly found for the n.m.r. spectra of substances containing one or more heteronuclear species.

Les spectres r.m.n. d'une série de dérivés simples du système 2-oxo-1,3,2-dioxaphosphorinane sont discutés à la lumière des conformations priviligiées des dérivés et des dépendances stéréospécifiques des couplages *vicinaux* $^{31}P—O—C—^{1}H$. L'accent est mis sur un type de spectre ABX "anormalement simple" que l'on retrouve dans les substances qui contiennent une ou plusieurs espèces hétéronucléaires.

Canadian Journal of Chemistry, **50**, 2092 (1972)

Introduction

Organophosphate esters are a fundamentally important class of compounds. Especially, they play key roles in many biosynthetic pathways and comprise structural sub-units of many physiologically important materials. Although the conformational analysis of such molecules is of considerable interest, a satisfactory method for studying the conformational properties intrinsically associated with the phosphate moiety has not yet been developed. High-resolution n.m.r. studies associated with the ^{31}P nucleus have not yet been thoroughly investigated to this end, and in the present paper we describe some model studies.

For several derivatives of the synthetically available 2-oxo-1,3,2-dioxaphosphorinane system (**A**), we have been able to relate heteronuclear magnetic resonance coupling constants to geometrical properties via both established ^{1}H n.m.r. parameter dependencies and an X-ray structure determination for 2-oxo-2-phenoxy-1,3,2-dioxaphosphorinane (**1**). In particular, we have determined the partial angular dependencies of $^{31}P—O—C—^{1}H$ and $^{31}P—O—C—C—^{1}H$ coupling constants. A number of these derivatives gave interesting examples of a class of deceptively-simple ABX spectra which appears not to have been widely recognized so far; an analysis of this type of spectrum is given separately elsewhere.[4]

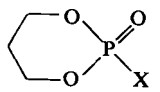

A

TABLE 1. Structural parameters of 2-oxo-2-phenoxy-1,3,2-dioxaphosphorinane (from ref. 6)

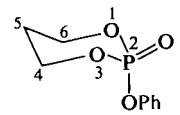

1

Central bond	Dihedral angle (°)
$P_2—O_1$	43
$O_1—C_6$	54
$C_6—C_5$	59
$C_5—C_4$	59
$C_4—O_3$	52
$O_3—P$	42

Since these studies were completed, a number of other workers (2–5) have shared our interest in $^{31}P—O—C—^{1}H$ coupling constant stereo-

[1]A full account of this work was given at the 155th meeting of the American Chemical Society, San Francisco, March 31–April 5, 1968 and in the M.Sc. thesis of R. B. Malcolm, University of British Columbia, 1969. For preliminary accounts see ref. 1.

[2]Recipient of a British Columbia Sugar Refining Co. Scholarship, 1968–1970.

[3]Revision received January 25, 1972.

[4]The original draft of this manuscript included, as an Appendix, a detailed account of the explicit analysis of this important class of deceptively-simple spectra. This analysis is now available from the Depository of Unpublished Data, National Science Library, National Research Council of Canada, Ottawa, Canada K1A 0S2. It includes a table of transition frequencies and relative intensities together with a series of computer simulated illustrative examples.

Can. J. Chem. Downloaded from www.nrcresearchpress.com by 210.87.254.5 on 09/05/12
For personal use only.

TABLE 2. The n.m.r. parameters for derivatives of 2-oxo-2-phenoxy-1,3,2-dioxaphosphorinane*

Structure	Chemical shifts (τ-values, δ-values)						
	4a(6a)	4e(6e)	5a	5e	Me_a	Me_e	^{31}P
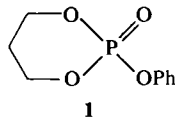 **1**	5.49	5.57	7.75†	8.25†	—	—	126.0
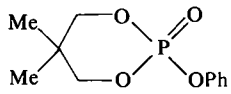 **3**	5.78	6.05	—	—	8.74	9.16	126.5

	Coupling constants (Hz)						
	4a,P	4e,P	5e,P	5a,P	4a,6a	4a,6e	5a,5e
1	2.9 ± 0.8	21.9 ± 0.8	2.7‡	0.9‡	§	§	−15.3†
3	1.7	22.5	—	—	§	§	—
	4a,4e	4e,6e	4a,5a	4a,5e	4e,5a	4e,5e	$4a,Me_a$
1	−10.9	§	11.4‖	2.7	5.2‖	2.7	—
3	−10.9	3.0	—	—	—	—	<1.0¶

*Data for $CDCl_3$ solutions.
†First-order values.
‡Estimated from $^1H-\{^{31}P\}$ decoupling experiment, assuming similar signs.
§Assumed zero to facilitate assignment of spectrum.
‖Probable error 0.5 Hz, LAOCN3 program.
¶Estimated from $^1H-\{^1H\}$ decoupling experiment.

specificities and, where appropriate, discussion of their results accompanies our own. As we shall mention later, further detailed n.m.r. studies are required before the present results can be extended to determine more general ^{31}P n.m.r. stereospecific dependencies.

Discussion

Geise (6) has reported an X-ray study of 2-oxo-2-phenoxy-1,3,2-dioxaphosphorinane (**1**) and has shown that in the solid state, this molecule favors a slightly flattened chair conformation having the phenoxy substituent axially oriented. The pertinent data from that study are summarized in Table 1.

The magnitudes of the *vicinal* $^1H-^1H$ coupling constants of **1**, listed in Table 2, suggest that this derivative favors one chair form almost exclusively. Thus the 4a,5a coupling (11.4 Hz) is well within the range anticipated (7) for a *trans–diaxial* disposition of the two protons. The remaining $^1H-^1H$ couplings are also consistent with the chair conformation.

If we assume that the activation energy associated with the conformational inversion process **B** ⇄ **C**, is available at room temperature in

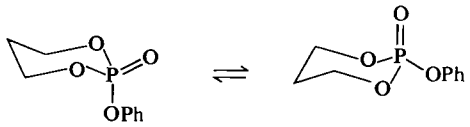

B **C**

solution, it follows that the measured couplings of **1**, and of the other derivatives described here, are weighted, time-averaged values. Our results for **1** thus imply a greater than 95% predominance of one chair form over the other. All attempts to confirm the presence of other conformations by low temperature measurements have so far been unsuccessful.

It is important to note that the analysis of the n.m.r. spectrum of **1** suggests a partial angular

Can. J. Chem. Downloaded from www.nrcresearchpress.com by 210.87.254.5 on 09/05/12
For personal use only.

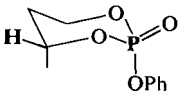

J_{trans} *ca.* 22 Hz

D

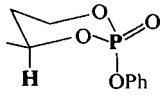

J_{gauche} *ca.* 2 Hz

E

dependence of *vicinal* $^{31}P—O—C—^{1}H$ coupling constants as depicted in **D**, **E**. We shall discuss this later. The ^{4}J, $^{31}P—O—C—C—^{1}H$ couplings also exhibit a stereospecific dependence as depicted in **F**, **G**.

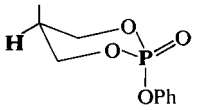

$|^{4}J| = 2.7$ Hz

F

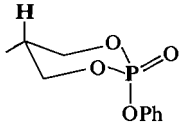

$|^{4}J| = 0.9$ Hz

G

We have assumed that the predominant chair conformation of **1** is that depicted in **B**, having the phenoxy group axially oriented. This *tentative* assignment is in accord with the result for the solid state (6). Furthermore, it has the merit of effectively minimizing any dipolar interactions between the P—O(Ph) bond and the $C_6—O_1$, $C_4—O_3$ bonds, should such interactions determine conformational preferences in this system.[5] Until a satisfactory method of configurational assignment at phosphorus is perfected this assignment must remain tentative. However, it is important at this juncture to recognize that, whatever the correct configurational assignment, the phosphorus moiety of **1** has a conformational preference of at least 1.8 Kcal/mol.

The ^{1}H n.m.r. spectrum of **2**, the cyclic phenyl phosphate of *o*-hydroxybenzyl alcohol, is shown in Fig. 1. It is a deceptively-simple type of ABX spectrum as discussed elsewhere.[4] Results of the analysis of this spectrum are given in Table 3. Both direct analysis and spin-tickling experiments confirmed that both *vicinal* $^{31}P–^{1}H$ couplings had the same sign, a result we assume is reasonable also for **1**. Presumably these couplings are absolutely positive in sign, in accord with the established result for acyclic systems (10).

[5]This type of interaction, or a version thereof, has been invoked previously to rationalize the conformational preference of certain carbohydrate derivatives when it is familiarly termed the "anomeric effect" (8). Similar dipolar interactions have been considered to govern the conformational preference in a number of other organic systems (9).

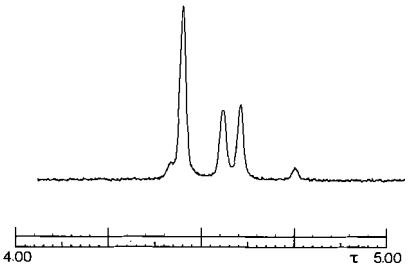

FIG. 1. Partial ^{1}H n.m.r. spectrum (100 MHz) of the cyclic, phenylphosphate ester of *o*-hydroxybenzyl alcohol in $CDCl_3$ solution.

TABLE 3. The n.m.r. parameters for the cyclic phenyl phosphate (**2**) of 2-hydroxybenzyl alcohol

Chemical shifts (τ-values, δ ^{31}P)		
H_A	H_B	^{31}P
4.49	4.55	147.5
Coupling constants (Hz)		
J_{AB}	J_{AP}	J_{BP}
−14.4	6.8*	19.6*

*± 1 Hz.

Inspection of the n.m.r. parameters given in Tables 4 and 5 shows that the 2-phenoxy-(**3**) and 2-chloro-(**4**) derivatives of 5,5-dimethyl-2-oxo-1,3,2-dioxaphosphorinane also have a marked conformational preference. Thus their *vicinal* $^{31}P–^{1}H$ couplings show a similar, marked steric dependence. Again it is not possible to assign unequivocally the configuration at phosphorus although rationales, similar to that applied for **1**, can be given.

The 60 MHz ^{1}H n.m.r. spectrum of **4** in $CDCl_3$ solution, is of the deceptively-simple type observed for **2**. At 100 MHz a "normal" AA′-BB′X spectrum, similar to that obtained for **3** is observed. Both types can be analyzed independently to give a set of identical chemical shifts and coupling constants. That $^{3}J_{trans}$[6] (~28 Hz) is significantly larger than that for **1** and **3** (~22 Hz), is not readily explained. A

[6]For simplicity throughout the remaining discussion, we shall refer to the *vicinal* $^{31}P—O—C—^{1}H$ coupling constants in these systems as J_t and J_g for equatorial and axial protons respectively. The terms J_{180} and J_{60} will be used to denote similar couplings referred to P—O—C—H dihedral angles of 180 and 60° respectively.

Can. J. Chem. Downloaded from www.nrcresearchpress.com by 210.87.254.5 on 09/05/12
For personal use only.

TABLE 4. Chemical shift values (p.p.m.) for 2-oxo-1,3,2-dioxaphosphorinanes

Structure	Chemical shifts* (τ-values, δ-values) 4a	4e	Me_a	Me_e	^{31}P
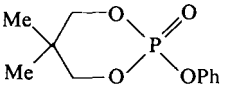 **3**	5.78	6.05	8.74	9.16	126.5
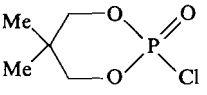 **4**	5.69	5.93	8.70	9.09	115.0
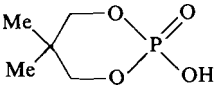 **5**	6.00†	6.00†	8.94†	8.94†	119.5
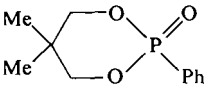 **6**	5.76	6.16	8.89†	8.89†	98.0

*$CDCl_3$ solution except CD_3COCD_3 solution for **5**.
†Conformationally "time-averaged" values.

greater "anomeric effect" associated with the chloro substituent could result in a significantly lower population of the inverted conformer, a larger P—O—C—H dihedral angle in the preferred conformer, or both. A direct effect of substituent electronegativity on these couplings may also be operative; unfortunately no direct distinction[7] between these alternatives is possible at this juncture.

The n.m.r. spectrum of 5,5-dimethyl-2-hydroxy-2-oxo-1,3,2-dioxaphosphorinane (**5**) suggests that this derivative undergoes rapid interconversion at room temperature between equally populated chair conformers of the type **B**, **C**. Thus the observed ^{31}P–^1H coupling constant of 12.0 Hz corresponds almost precisely to the average of J_t and J_g for **1** (12.4 Hz) and for **3** (12.1 Hz).

[7]In this regard, however, the ^1H–^1H couplings of **1** are not compatible with significant time-averaging and a recent X-ray study (11) of a 2-bromo-derivative, which similarly has a very large J_t (12), is similar to that for **1**.

We were somewhat surprised, however, to find that 5,5-dimethyl-2-oxo-2-phenyl-1,3,2-dioxaphosphorinane (**6**) similarly had nearly equal ^3J couplings of 11.0 and 12.6 Hz. Subsequent analysis at −80 °C provided values of 7.8 and 15.9 Hz respectively. These changes reflect, at least in part, the expected change in relative populations of the two conformers **H**, **I**

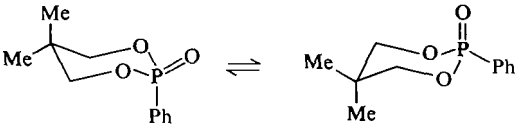

H **I**

on decreasing temperature. Unfortunately, as yet, we have been unable to "freeze-out" this interconversion process. We hope to return to this type of experiment in future.

While it is evident from our n.m.r. results for **1** and **3** that *vicinal* ^{31}P—O—C—^1H coupling constants show a marked steric dependence, it is also evident from our results for **4** that a careful

Can. J. Chem. Downloaded from www.nrcresearchpress.com by 210.87.254.5 on 09/05/12
For personal use only.

TABLE 5. Coupling constants (Hz) for 2-oxo-1,3,2-dioxaphosphorinanes

Structure	Coupling constants* (Hz) 4a,P	4e,P	4a,4e	4a,6a	4a,6e	4e,6e	4a,Me_a
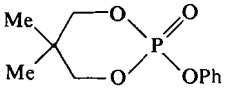 **3**	1.7	22.5	−10.9	†	†	3.0	<1.0‡
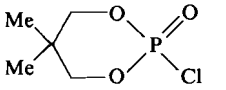 **4**	2.9	28.5	−11.1	†	†	3.4	§
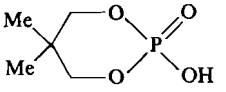 **5**	12.0	12.0	—	†	†	—	—
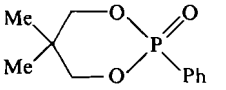 **6**	11.0	12.6	−11.1	†	†	‖	§

*$CDCl_3$ solution, except CD_3COCD_3 solution for **5**.
†Assumed zero to facilitate assignment of spectrum.
‡Estimated from $^1H-\{^{31}P\}$ decoupling experiment.
§Broadening due to long-range coupling.
‖Not detected.

consideration of specific substituent effects on these coupling constants must be made before this dependence can be widely extended outside the cyclic phosphate system. Further studies in this series will attempt to systematically extend our present results and apply them to pertinent conformational problems. At this time, however, it does seem appropriate to discuss some of the apparent inconsistencies that have developed in the literature and offer some clarification of these in light of our own results and other established data.

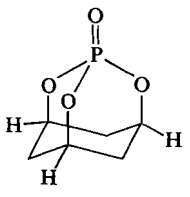

$J_{180} = 20$ Hz
J

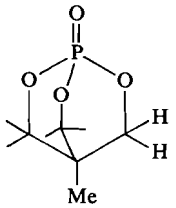

$J_{120} = 6$ Hz
K

The original n.m.r. data **J**, **K**, that should have elucidated a *vicinal* $^{31}P—O—C—^1H$ coupling constant stereospecific dependence was published (13) in 1962. Unfortunately, this result[8] was not used in considering the conformational properties of a series of derivatives of the type **L**, **M**, which seem to be undergoing a greater or lesser amount of conformational "time-aver-

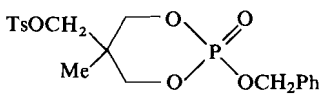

L

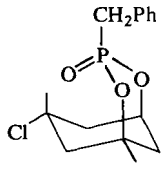

M

[8]The J_{120} value is as later corrected (14). Our J_t values for **1** and **3** clearly do not agree *quantitatively* with the above J_{180}; presumably some special effect attributable to the polycyclic structure, previously discussed (2) in the trivalent phosphorus series, is responsible.

Can. J. Chem. Downloaded from www.nrcresearchpress.com by 210.87.254.5 on 09/05/12
For personal use only.

Can. J. Chem. Downloaded from www.nrcresearchpress.com by 210.87.254.5 on 09/05/12
For personal use only.

aging" by analogy with **6** of the present study.[9] Thus equal, 11.6 Hz (15), ^3J couplings for **L** indicate a nearly equal proportion of the two chair conformers in solution. Molecules of this type had also previously (16) been thought to exist in a single chair conformation. The 17.5 Hz $^{31}P—O—C—^1H$ coupling observed for **M** in solution is comparable to our J_t for **1** and **3** and suggests that this compound exists *predominantly* in the chair–chair conformation illustrated above rather than the boat–chair conformation rationalized (17) from other data.

Derivatives of the type **L**, **M** were unfortunately later chosen as model systems for a survey (18) of data pertinent to the conformational sensitivity of the i.r., phosphoryl bond, stretching frequency. It was concluded at that time that "... $\nu_{P=O}$ suffers little from conformational environment". It thus seems quite likely that more recent i.r. studies (19, 20) of 2-oxo-1,3,2-dioxaphosphorinane ring systems *in solution,* could lead to the establishment of a general dependence of $\nu_{P=O}$ on conformational preference at the phosphorus moiety. Such a dependence, combined with an n.m.r. conformational analysis of the ring system, could be a valuable aid in assigning configuration at phosphorus in these derivatives.

Another laboratory (5) has recently shared our interest in developing stereospecific dependencies of ^{31}P n.m.r. parameters with a view to their subsequent application to polynucleotide conformational analysis in solution.

We feel it is appropriate to point out some of the very important problems that can arise from premature quantitative application of an incompletely determined $^{31}P—O—C—^1H$ coupling constant–dihedral angle dependence, similar to that we have suggested for **1**, **3**.

The ^1H n.m.r. spectrum of **N** exhibited (21) a 1.5 Hz splitting due to coupling with the phosphorus nucleus. This value of J_g was combined with the fully time-averaged value ($J_{av} = 10.4$ Hz)[10] for an acyclic methyl phosphate group, to predict[11] a J_{180} value of 28.2 Hz. A more complete analysis (22) of the n.m.r. spectrum of **N** later resulted in observed $J_t = 22.1$ and $J_g = 2.3$ Hz values.[12] In the same study, the ^{31}P n.m.r. spectra of inosine-5′-monophosphate and guanosine-5′-monophosphate were found to exhibit 4.5 Hz triplets due to coupling between the ^{31}P and $^1H_{5'}$ nuclei. Using the J_t, J_g values for **N** and these J_{av} values[13] for the mononucleotides, the relative populations of the rotamers around the $O–C_{5'}$ bond were calculated.[14] Thus a_t, the fraction of the rotameric population having a *trans* orientation with respect to the $P—O—C_{5'}—C_{4'}$ bond, was calculated to be 0.78 (22). In a subsequent publication (24), the n.m.r. parameters for **N** were revised[15] to give $J_t = 22.3$ and $J_g = 1.9$ Hz, and some account of the anticipated difference between these values and J_{180}, J_{60} values was taken. Unfortunately, the suggested, revised couplings, $J_{180} = 23.5$, $J_{60} = 4.5$ Hz,[16] led to contradictory implications in their subsequent application via an assumed type of "Karplus curve" (7) to the study (5) of a dinucleotide conformation in solution. Clearly, an experimental coordinate pair used to derive a ^3J *vs.* dihedral angle curve must be consistent with data derived from the curve. The co-ordinate pair, $J_{65} = 1.9$ Hz from **N** (24), should thus be consistent with the co-ordinate pair, $J_{64} = 3.4$ Hz (5), derived.[17]

Unfortunately, the first, incorrect $J_t = 28.2$

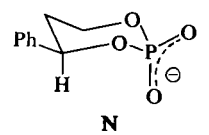

N

[9]Throughout this discussion we have made the implicit assumption that our J_t, J_g stereospecific dependence for **1** and **3** is general for both the phosphate and phosphonate series. Although subtle differences undoubtedly occur, sufficient data exist at this time (*vide infra*) to justify this assumption in the present context.

[10]Actually the averaged value between sodium methyl phosphate and barium dimethyl phosphate (21).

[11]Thus $J_{av} = (J_{180} + 2J_{60})/3$. The assumption that $J_g = J_{60}$ has been made by the authors. Our own values of J_t and J_g did not adequately *quantitatively* predict J_{av} when we made (1) the assumption that $J_t = J_{180}$ and $J_g = J_{60}$; this is also not strictly compatible with the X-ray data (6) for **1**.

[12]Coupling with the H_6 protons. The $^1H–^1H$ couplings are compatible with a single predominant chair conformation.

[13]A triplet X resonance of an ABX spin system implies equal AX and BX coupling constants only if the chemical shift difference between the A and B nuclei is significant (23).

[14]The choice made between the two different J_g values in the same molecule has not been rationalized.

[15]Presumably as a result of proper ABX treatment of the spin system.

[16]It was assumed that, since the mononucleotides above had equal couplings of 4.5 Hz, these couplings must correspond directly to J_{60}. This assumes $a_t = 1.0$, in contrast to the previously determined value of 0.78 (22).

[17]Clearly the $J_{60} = 4.5$ Hz co-ordinate point is unjustified and leads to serious uncertainty in the J *vs.* dihedral angle plot, being one of the only two co-ordinate pairs used.

Can. J. Chem. Downloaded from www.nrcresearchpress.com by 210.87.254.5 on 09/05/12
For personal use only.

and $J_g = 1.5$ Hz values derived for **N**, have been used recently by other workers (25, 26) to justify particular choices of J_{av} for acyclic derivatives and a further study (27) has depended on one of these choices. Thus it has been suggested (25) that fully time-averaged J_{av} values for *ethyl* derivatives of the type **O** are more appropriate

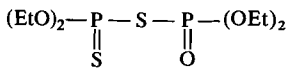

O

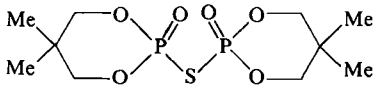

P

than J_{av} values for *methyl* derivatives, when considering the particular choice of J_t and J_g that is expected to correctly predict the conformer populations of derivatives of the type **P** in solution.[18]

A wealth of n.m.r. data related to cyclic *phosphonate* derivatives of the type **6** and **L** has been published (12, 27–29) more recently. The suggestion, based on ^{1}H chemical shift data, that several derivatives were essentially conformationally homogeneous in solution (29), was later revised (27) and clarified by other workers (25). It does seem appropriate however that calculations of conformer populations for these derivatives should be based on J_t and J_g values directly observed for conformationally *homogeneous* derivatives, rather than the somewhat unsatisfactory assumption that $J_t = J_{180}$ and $J_g = J_{60}$. In this regard, the n.m.r. results $J_t = 20.2$ and $J_g = 4.14$ Hz, have recently been published (30) for the thermodynamically stable isomer **Q**.

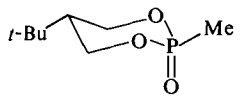

Q

Two other recent results are pertinent to this study. A conformationally stable phosphate isomer, *cis*-5-*t*-butyl-2-methoxy-2-oxo-1,3,2-dioxaphosphorinane (**R**), has $J_t = 22.8$ and $J_g = 1.14$ Hz (30) and 2-*t*-butoxy-5,5-dimethyl-

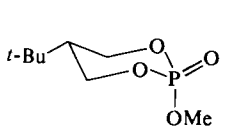

R

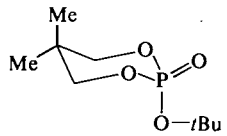

S

2-oxo-1,3,2-dioxaphosphorinane (**S**) has $J_t = 21.0$ and $J_g = 3.3$ Hz (12). The ^{1}H–^{1}H coupling constants of **Q** and **R** are consistent with the presence of one dominant chair conformer in solution, similar to our results for **1**.

In summary, several important statements relating to the conformational properties of cyclic phosphate and cyclic phosphonate derivatives *in solution*, can be derived from the above considerations of our own results in relation to those of other laboratories.

It is clear that the sum of the observed *vicinal* ^{31}P—O—C—^{1}H couplings in phosphate derivatives (24.1 Hz[19]) and the sum in cyclic phosphonate derivatives (22.4 Hz[20]) are quite similar. This is consistent with the suggestion that these derivatives exist as equilibrium mixtures of two rapidly interconverting, "flattened-chair" conformations as generally depicted by several X-ray determinations (6, 31–33) for crystalline derivatives.

In general, the conformational preference associated with a *phosphate* moiety is considerably greater than that associated with a *phosphonate* moiety. This difference is sufficient that the former tend to exist in one predominant conformer in contrast to the latter.

For *phosphate* derivatives, J_t and J_g are in the range 21.0–22.8 and 1.2–3.3 Hz respectively. For *phosphonate* derivatives, J_t and J_g are in the range 18.2–20.2 and 3.2–4.7 Hz respectively.

It is not yet clear whether the slight variations in the ^3J parameters indicated above are due to subtle conformational changes, to specific substituent effects on the coupling constants, or to both.

A sufficient range of n.m.r. data does not yet exist for compounds of known or readily predictable geometry to warrant quantitative definition of a function relating ^3J to dihedral angle in these systems. The n.m.r. and X-ray data that do exist for the *phosphates* **1**, **5**, *trans*-**R**, and

[18]These authors seem to have failed to realize that their justification for choosing *ethyl* derivative models rests on the choice of *methyl* derivative models by the workers who derived the above values for *N*.

[19]Average over eight derivatives, ^3J range 23.4–24.8 Hz (12, 24, 30, this study).

[20]Average over 29 derivatives, ^3J range 20.6–23.6 Hz (12, 27–30, this study).

Can. J. Chem. Downloaded from www.nrcresearchpress.com by 210.87.254.5 on 09/05/12
For personal use only.

the *phosphonate cis*-**Q**, are however, consistent with the suggestion that such a function would be qualitatively similar to that derived (7) by Karplus for ^{1}H—C—C—^{1}H couplings.

Coupling constants, J_{180} and J_{60}, corresponding to idealized rotameric conformations, are not directly determined by these systems. However, if the above suggestion relating ^3J *vs.* dihedral angle is correct, then $J_{180} > J_t$ and $J_{60} > J_g$. It also seems likely that $J_{180} + 2J_{60} =$ 31–33 Hz, from considerations of acyclic methyl derivative couplings.

Clearly, the above statements reveal a sufficiently self-consistent, sensitive dependence of *vicinal* ^{31}P—O—C—^{1}H coupling constants on dihedral angle to justify their *semi-quantitative* use in 1,3,2-dioxaphosph(V)orinane conformational problems of chemical significance.

The interested reader is referred to leading references (3, 4, 34) of similar studies in the 1,3,2-dioxaphosph(III)orinane series.[21]

Although several other n.m.r. laboratories have evidenced (35) an awareness of the type of deceptively-simple ABX spectrum (referred to elsewhere[4]), these articles have been overlooked by some workers in the organophosphorus area. The n.m.r. spectra of several derivatives, which are of this deceptively-simple form, have been reported (24, 28) to be unsuitable for ABX analysis and in other instances have been incorrectly assigned (22, 36). We have derived approximate n.m.r. parameters from two of the published spectra that have appeared. Thus 2-chloro-2-oxo-4-phenyl-1,3,2-dioxaphosphorinane (24) has $J_t = 26.6$ and $J_g = 6.3$ Hz, and 5,5-dimethyl-2-isopropoxy-2-oxo-1,3,2-dioxaphosphorinane (28) has $J_t = 20.6$ and $J_g = 4.3$ Hz. Although not very accurate as we have derived them, these parameters compare favorably with those of similar derivatives we have discussed previously.

This type of deceptively-simple system also occurs frequently as a sub-spectrum of more complex spin systems when its characteristic pattern can be a very valuable simplifying feature. The n.m.r. spectrum of **1** is just one of the many examples that we have encountered in measuring the spectra of derivatives containing a ^{31}P or ^{19}F heteronucleus.

Experimental

All melting points were measured on a Fischer–Johns heating stage and are uncorrected. Satisfactory microanalyses, performed by Mr. P. Borda of this Department, were obtained for all compounds.

The 100 MHz ^{1}H n.m.r. spectra were measured with a modified Varian HA-100 spectrometer operating in the "locked" frequency-sweep mode. The 60 MHz ^{1}H n.m.r. spectra were measured with a Varian A-60 spectrometer. Tetramethylsilane was used as internal reference. All ^{31}P n.m.r. spectra were measured at 40.477 MHz with a Varian HA-100 spectrometer operating in the "extended-offset locked" field sweep mode. The ^{31}P chemical shifts are reported in p.p.m. relative to an internal capillary of P_4O_6.

Heteronuclear double resonance experiments in which the ^{31}P resonance was strongly irradiated while observing the ^{1}H resonances, were carried out routinely to assist in spectral assignment. The equipment consists (37) of a double-tuned probe adaptor, a Hewlett Packard Frequency Synthesizer, and a Hewlett Packard Power Amplifier (Model 230A).

With the exception of those for **1**, the n.m.r. parameters for all derivatives were derived from the spectra both by "long-hand" direct analysis and also using a modified version of the LAOCN3 computer program. A plotting program SCRIBE was used both directly and coupled to LAOCN3 to simulate the results of the analyses for comparison with the experimental spectra. The plot program was also used to provide the simulated spectra of Fig. 2.[22]

The methylene proton resonances of **3** and **4** were assigned using the established (38) steric dependence of long-range H—C—C—CH_3 coupling constants. Thus the low field (axial) methylene resonances were noticeably sharpened on irradiation of the downfield (axial) methyl resonances. This method was also applied to **6** but with less observable result.

*2-Oxo-2-phenoxy-1,3,2-dioxaphosphorinane (**1**)*

This compound was prepared by the method of Meston (39) in good yield (m.p. 75 °C). Although the n.m.r. spin system associated with **1** is quite complex (AA′BB′MNX), assignment of the H_5 region was quite straightforward. The H_4, H_6 region is very complex but exhibits four very intense single resonances which are characteristic of deceptively-simple ABX sub-spectra.[4] The presence of these sub-spectra was a valuable aid to analysis in that certain quantitative

[21]A referee pointed out that our discussion had not included detailed comparisons of our results with those related from the laboratory of Professor J. G. Verkade. Studies from that laboratory are, however, cited as references 2, 3, 12–15, 17, and detailed comparisons were not made because of space restrictions. It seems worthwhile commenting here that Professor Verkade's laboratory and our own appear to have followed independently, and simultaneously (see ref. 1) closely similar lines and both laboratories appear to have reached closely similar conclusions. The same referee drew our attention to an X-ray study of a derivative related to **M**, which was shown (42) to have the chair–boat conformation. We do not feel able to comment on the relevance of this observation.

[22]A copy of Fig. 2 may be obtained on request from the Depository of Unpublished Data, National Science Library, National Research Council of Canada, Ottawa, Canada K1A 0S2.

Can. J. Chem. Downloaded from www.nrcresearchpress.com by 210.87.254.5 on 09/05/12
For personal use only.

relationships between the n.m.r. parameters are implied. Assignment was further aided by homonuclear and heteronuclear double resonance experiments and a set of "guess", first-order n.m.r. parameters was obtained. These parameters were iterated using LAOCN3 with as many experimental transition frequencies as could be assigned. The parameter set of Table 2 was obtained as a result of several cycles of the iterative procedure, spanning the uncertainty limits in assignment of the experimental frequencies. A SCRIBE plot of the transitions associated with the final parameter set was in close agreement with the experimental spectrum. Despite this "good-fit", however, the spectrum proved relatively insensitive to changes in some of the parameters. The error limits of Table 2 reflect either the accuracy problems associated with the deceptively-simple subspectrum[4] or those associated with assigning transition frequencies in the very complex "normal" sub-spectrum.

o-Hydroxybenzyl Alcohol Cyclic Phenyl Phosphate (2)

Phenyl phosphorodichloridate (4.0 g) was added dropwise, with stirring to a cooled (ice bath) solution of *o*-hydroxybenzyl alcohol (2.0 g) in anhydrous pyridine (40 ml). The mixture was left to stand *ca.* 20 h at ~4 °C. Water (40 ml) was added to dissolve precipitated pyridinium hydrochloride and the solution was extracted with $CHCl_3$ (3 × 20 ml). The combined $CHCl_3$ extracts were washed repeatedly with water (5 × 20 ml), dried over anhydrous Na_2SO_4, and concentrated under reduced pressure to give highly crystalline **2** (1.80 g, 69%, m.p. 79.5–81.0 °C).

5,5-Dimethyl-2-oxo-2-phenoxy-1,3,2-dioxaphosphorinane (3)

Structure **3** was prepared by the methods for **1** and **2** and had m.p. 132–133 °C.

2-Chloro-5,5-dimethyl-2-oxo-1,3,2-dioxaphosphorinane (4) and 5,5-Dimethyl-2-hydroxy-2-oxo-1,3,2-dioxaphosphorinane (5)

Structures **4** and **5** were prepared by the methods of Edmundson (40).

5,5-Dimethyl-2-oxo-2-phenyl-1,3,2-dioxaphosphorinane (6)

Structure **6** was prepared by the method of McConnell and Coover (41).

It is a pleasure to thank the National Research Council of Canada for their generous financial support of this work via regular operating grants (A 1905), a special operating grant (A 5456) and an equipment grant (E 1338). We would also like to thank Professor C. A. McDowell for his interest in this work.

1. (*a*) L. D. Hall and R. B. Malcolm. Chem. Ind. (London), 92 (1968). (*b*) R. B. Malcolm. B.Sc. Thesis. University of British Columbia, 1966.
2. D. W. White and J. G. Verkade. J. Mag. Res. **3**, 111 (1970).
3. R. D. Bertrand, J. G. Verkade, D. W. White, D. Gagnaire, J. B. Robert, and J. Verrier. J. Mag. Res. **3**, 494 (1970).
4. M. Kainosho and A. Nakamura. Tetrahedron, **25**, 4071 (1969).
5. M. Tsuboi, S. Takahashi, Y. Kyogoku, H. Hayatsu, and T. Ukita. Sci. **166**, 1504 (1969).
6. H. J. Geise. Rec. Trav. Chim. **86**, 362 (1967).
7. (*a*) M. Karplus. J. Chem. Phys. **30**, 11 (1959). (*b*) M. Karplus. J. Phys. Chem. **64**, 1793 (1961). (*c*) M. Karplus. J. Am. Chem. Soc. **85**, 2870 (1963).
8. (*a*) R. U. Lemieux. *In* Molecular rearrangements. Part 2. *Edited by* P. de Mayo. Interscience, New York, 1964. p. 735–743. (*b*) S. J. Angyal, *In* Conformational analysis. E. L. Eliel, N. L. Allinger, S. J. Angyal, and G. A. Morrison. Interscience, New York, 1965. Chapt. 6. (*c*) J. T. Edward. Chem. Ind. (London), 1102 (1955).
9. E. L. Eliel. Stereochemistry of carbon compounds. McGraw–Hill, New York, 1962 and references therein. See also reference 8*b* and references therein.
10. E. Duval and E. A. C. Lucken. Mol. Phys. **10**, 499 (1966).
11. T. A. Beineke. Acta Cryst. **B25**, 413 (1969).
12. D. W. White, G. K. McEwen, R. D. Bertrand, and J. G. Verkade. J. Mag. Res. **4**, 123 (1971).
13. J. G. Verkade and R. W. King. Inorg. Chem. **1**, 948 (1962).
14. E. J. Boros, R. D. Compton and J. G. Verkade. Inorg. Chem. **7**, 165 (1968).
15. J. G. Verkade, T. J. Huttemann, M. K. Fung, and R. W. King. Inorg. Chem. **4**, 83 (1965).
16. W. S. Wadsworth, Jr. and W. D. Emmons. J. Am. Chem. Soc. **84**, 610 (1962).
17. K. D. Berlin, C. Hildebrand, A. South, D. M. Hellwege, M. Peterson, E. A. Pier, and J. G. Verkade. Tetrahedron, **20**, 323 (1964).
18. R. S. Edmundson. Tetrahedron, **20**, 2781 (1964).
19. M. Kainosho, T. Morofushi, and A. Nakamura. Bull. Chem. Soc. Jap. **42**, 845 (1969).
20. J.-P. Majoral and J. Navech. Bull. Soc. Chim. Fr. 1331 (1971).
21. M. Tsuboi, F. Kuriyagawa, K. Matsuo, and Y. Kyogoku. Bull. Chem. Soc. Jap. **40**, 1813 (1967).
22. M. Tsuboi, M. Kainosho, and A. Nakamura. *In* Recent developments of magnetic resonance in biological systems. S. Fujiwara and L. H. Piette, *editors*. Hirokawa Publishing Co. Inc., Tokyo, 1968. pp. 43–49.
23. R. J. Abraham and H. J. Bernstein. Can. J. Chem. **39**, 216 (1961).
24. M. Kainosho, A. Nakamura, and M. Tsuboi. Bull. Chem. Soc. Jap. **42**, 1713 (1969).
25. A. R. Katritzky, M. R. Nesbit, J. Michalski, Z. Tulimowski, and A. Zwierzak. J. Chem. Soc. B, 140 (1970).
26. A. A. Bothner-by and W.-P. Trautwein. J. Am. Chem. Soc. **93**, 2189 (1971).
27. R. S. Edmundson and E. W. Mitchell. J. Chem. Soc. C, 752 (1970).
28. K. D. Bartle, R. S. Edmundson, and D. W. Jones. Tetrahedron, **23**, 1701 (1967).
29. R. S. Edmundson and E. W. Mitchell. J. Chem. Soc. C, 2091 (1968).
30. W. G. Bentrude and J. H. Hargis. Chem. Commun. 1113 (1969).
31. W. Murayama and M. Kainosho. Bull. Chem. Soc. Jap. **42**, 1819 (1969).
32. Mazhar-ul-haque, C. N. Caughlan, J. H. Hargis, and W. G. Bentrude. J. Chem. Soc. A, 1786 (1970).
33. Mazhar-ul-Haque, C. N. Caughlan, and W. L. Moats. J. Org. Chem. **35**, 1446 (1970).

34. (*a*) D. GAGNAIRE, J. B. ROBERT, and J. VERRIER. Bull. Soc. Chim. Fr. 2392 (1968). (*b*) J.-P. ALBRAND, D. GAGNAIRE, J. B. ROBERT, and M. HAEMERS. Bull. Soc. Chim. Fr. 3496 (1969).
35. (*a*) P. DIEHL. Helv. Chim. Acta, **47**, 1 (1964). (*b*) C. N. BANWELL. *In* Nuclear magnetic resonance for organic chemists. *Edited by* D. W. Mathieson. Academic Press, London, 1967. Chapt. 6. (*c*) F. A. BOVEY. Nuclear magnetic resonance spectroscopy. Academic Press, New York, 1969. pp. 105–113.
36. R. S. EDMUNDSON. Tetrahedron Lett. 1905 (1969).
37. R. BURTON and L. D. HALL. Can. J. Chem. **48**, 59 (1970).
38. L. M. JACKMAN and S. STERNHELL. Applications of nuclear magnetic resonance spectroscopy in organic chemistry. 2nd Ed. Pergamon Press, 1969. pp. 337–338 and references therein.
39. A. M. MESTON. J. Chem. Soc. 6059 (1963).
40. R. S. EDMUNDSON. Tetrahedron, **21**, 2379 (1965).
41. R. L. MCCONNELL and H. W. COOVER, JR. J. Org. Chem. **24**, 630 (1959).
42. D. M. NIMROD, D. R. FITZWATER, and J. G. VERKADE. Inorg. Chim. Acta, **2**, 149 (1968).

Can. J. Chem. Downloaded from www.nrcresearchpress.com by 210.87.254.5 on 09/05/12
For personal use only.

A Novel Class of Isomeric Phosphate Esters[1]

L. D. HALL AND R. B. MALCOLM[2]

Department of Chemistry, The University of British Columbia, Vancouver 8, British Columbia

Received August 20, 1971

Reaction of phenyl phosphorodichloridate with pentane-2,4-diol affords a mixture of isomeric cyclic phosphates. These have been separated and characterized. Analysis of the ^1H and ^{31}P n.m.r. spectra of these derivatives has confirmed the stereospecificity of several sets of ^{31}P–^1H coupling constants.

La réaction du phosphorodichloridate de phényle avec le pentanediol-2,4 conduit à un mélange de phosphates cyclique isomères. Ceux-ci ont été séparés et caractérisés. Les analyses r.m.n. des spectres ^1H et ^{31}P de ces dérivés ont confirmé la stéréospécificité de plusieurs groupes de constantes de couplage ^{31}P–^1H.

Canadian Journal of Chemistry, **50**, 2102 (1972)

Introduction

During the course of a study of phosphate esters (1–3) we had found that reaction between propane-1,3-diol and phenyl phosphorodichloridate afforded a single, crystalline, cyclic phenylphosphate[3] (**1**) in high yield. We were surprised,

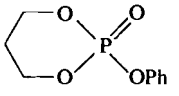

1

therefore, to find that reaction of phenyl phosphorodichloridate with pentane-2,4-diol afforded a mixture of *three* products. We now describe the separation and characterization of these substances.

Results and Discussion

Reaction of phenyl phosphorodichloridate with a commercially available sample of pentane-2,4-diol afforded a syrupy material (**2**),

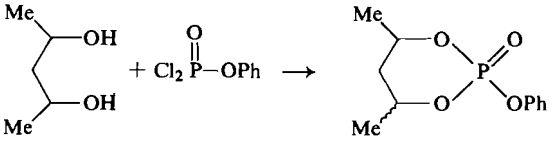

2

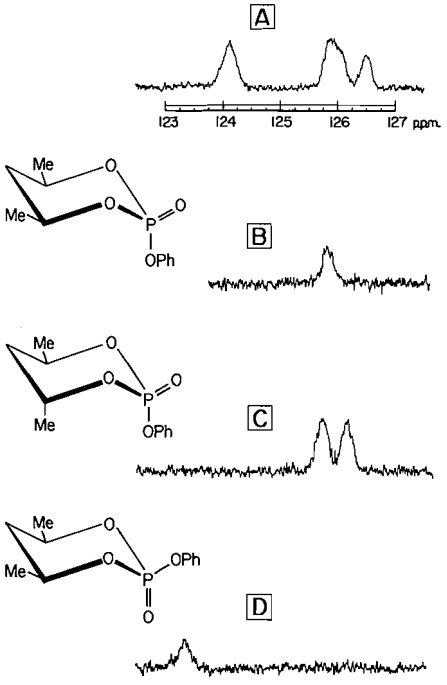

FIG. 1. The ^{31}P n.m.r. spectra (40.5 MHz) of the isomeric 4,6-dimethyl-2-oxo-2-phenoxy-1,3,2-dioxaphosphorinanes in $CDCl_3$ solutions. [A], spectrum of the unseparated mixture of isomers; [B], isomer **2***a*; [C], isomer **2***b*; [D], isomer **2***c*.

shown by t.l.c. to have three components. The ^{31}P n.m.r. spectrum of the mixture (Fig. 1) showed three separate resonances, one of these having a large, $\simeq$17 Hz, splitting. Column chromatography (silica gel/ethyl acetate) of the syrupy mixture, monitored by t.l.c., provided an efficient means of separating the three components, labelled **2***a*, *b*, and *c*, in order of de-

[1]A full account of this study was given at the 155th meeting of the American Chemical Society, San Francisco, March 31–April 5, 1968. For a preliminary communication, see ref. 1. Descriptions have also been given by R. B. Malcolm, see ref. 2. This paper constitutes Part 2 of a series entitled "Studies of organophosphorus derivatives". For Part 1 see ref. 3.

[2]Recipient of a British Columbia Sugar Refining Co. Scholarship, 1968–1970.

[3]Strictly this should be referred to as 2-oxo-2-phenoxy-1,3,2-dioxaphosphorinane.

Can. J. Chem. Downloaded from www.nrcresearchpress.com by 210.87.254.40 on 09/05/12
For personal use only.

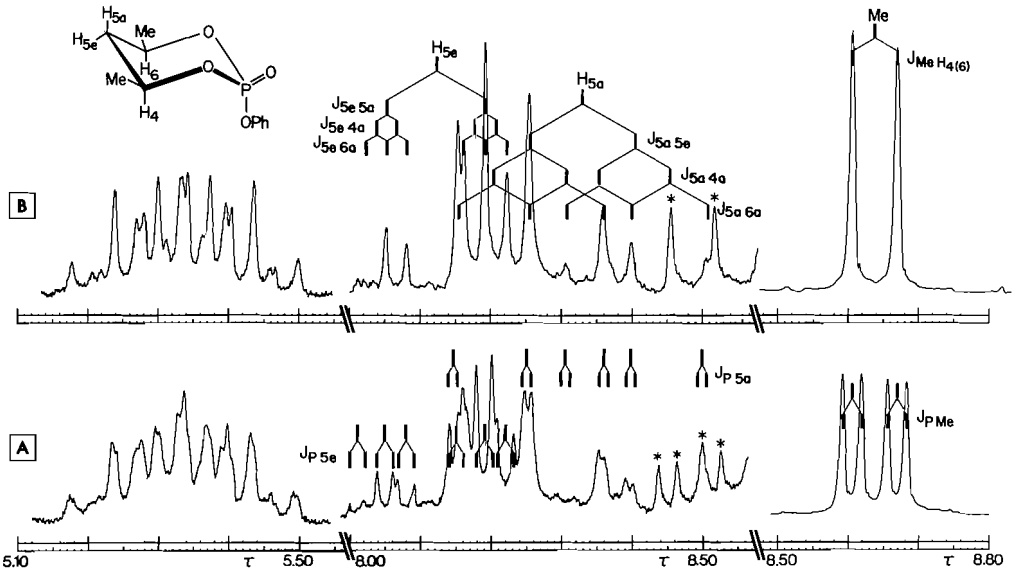

FIG. 2. Partial ^{1}H n.m.r. spectrum (100 MHz) of isomer **2***a* in $CDCl_3$ solution. [A], normal spectrum; [B], spectrum obtained with continuous-wave irradiation at the phosphorus frequency. The peaks marked with an asterisk are spinning side-bands from the methyl peaks. The first-order assignment provides an approximate indication of the multiplet structures.

creasing R_f value. The resulting, crystalline component **2***a* had m.p. 94° and δ ^{31}P chemical shift +125.8 p.p.m. (relative intensity *ca.* 1) while the syrupy components **2***b* and *c* had ^{31}P +126.0 (relative intensity *ca.* 1) and +123.6 p.p.m. (relative intensity *ca.* 1), respectively. These phosphorus chemical shifts are consistent with those of phosphate triesters in general. The elemental analyses of all three components are identical and consistent with that expected for structure **2**.

The 100 MHz p.m.r. spectra (Figs. 2–4) of all three components are very similar and the general features of these spectra are also consistent with assignment of the three components to the three possible *geometrical* isomers of 4,6-dimethyl-2-oxo-2-phenoxy-1,3,2-dioxaphosphorinane depicted below. Two of these are derived from *meso*-pentane-2,4-diol and one from *d,l*-pentane-2,4-diol. Thus the spectra of all three products show a complex multiplet centered in the τ 5.2–5.4 range, of relative intensity 2, due to protons on C-4 and -6 being coupled to virtually every other magnetic nuclear species present. A further complex multiplet centered in the range τ 8.0–8.2, of relative intensity 2, due to the methylene ring protons, is followed by methyl proton resonances of relative intensity 6 centered in the range τ 8.5–8.7. The phenyl resonances at *ca.* τ 2.8 of relative intensity 5, have not been illustrated. The complete assignment of these p.m.r. spectra was facilitated by heteronuclear decoupling and the spectra obtained while irradiating the phosphorus resonances (4) demonstrate, in comparison with the normal spectra, removal of extensive long-range, ^4J coupling of this nucleus into the methyl and methylene protons. Detailed spectral data for each of the isomers has been obtained in part, by a first order analysis, and in part with the aid of computer-simulated spectra. This data is presented in Table 1.

The appearance of a large, $\simeq$17 Hz splitting in the ^{31}P n.m.r. resonance of isomer **2***b* implies a *trans* POCH coupling in accord with the result

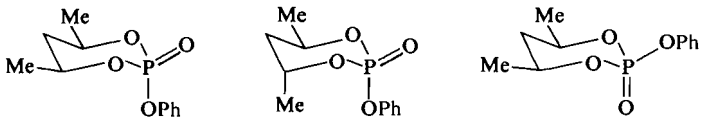

2*a* **2***b* **2***c*

Can. J. Chem. Downloaded from www.nrcresearchpress.com by 210.87.254.40 on 09/05/12
For personal use only.

Can. J. Chem. Downloaded from www.nrcresearchpress.com by 210.87.254.40 on 09/05/12
For personal use only.

TABLE 1. The n.m.r. data for the isomeric 4,6-dimethyl-2-oxo-2-phenoxy-1,3,2-dioxaphosphorinanes in $CDCl_3$ solutions

	Chemical shifts (τ-values, δ-values)									
Structure	4e	4a	6e	6a	5e	5a	Me_e	Me_a	Ph	$\delta^{31}P$
2a	—	5.331	—	5.331	8.130	8.132	8.639	—	*ca.* 2.8	+125.8
2b	5.160	—	—	5.200	8.161	7.935	8.562	8.527	*ca.* 2.8	+126.0
2c	—	5.259	—	5.259	8.154	8.347	8.659	—	*ca.* 2.8	+123.6

	Coupling constants (Hz)															
Structure	4e,5a	4e,5e	4e,6a 4a,6e	4a,6a	4a,5e 6a,5e	4a,5a 6a,5a	5e,5a	P,4e	P,4a P,6a	P,5e	P,5a	P,Me_e	P,Me_a	$4e,Me_a$	$6a,Me_e$	$4a,Me_e$ $6a,Me_e$
2a	—	—	—	0.0	2.9	10.3	−13.2	—	2.9	2.4	0.8	2.7	—	—	—	6.4
2b	5.0	3.2*	0.0	—	4.3*	8.6	−14.7	17.0	~4.0	2.0	1.3	2.3	0.8	6.5	6.9	—
2c	—	—	—	0.0	2.4	11.3	−14.2	—	3.1	2.4	0.7	2.3	—	—	—	6.4

*Unequivocal assignment has not been possible. Interchange of these values has been assumed for the discussion of this molecule in the text.

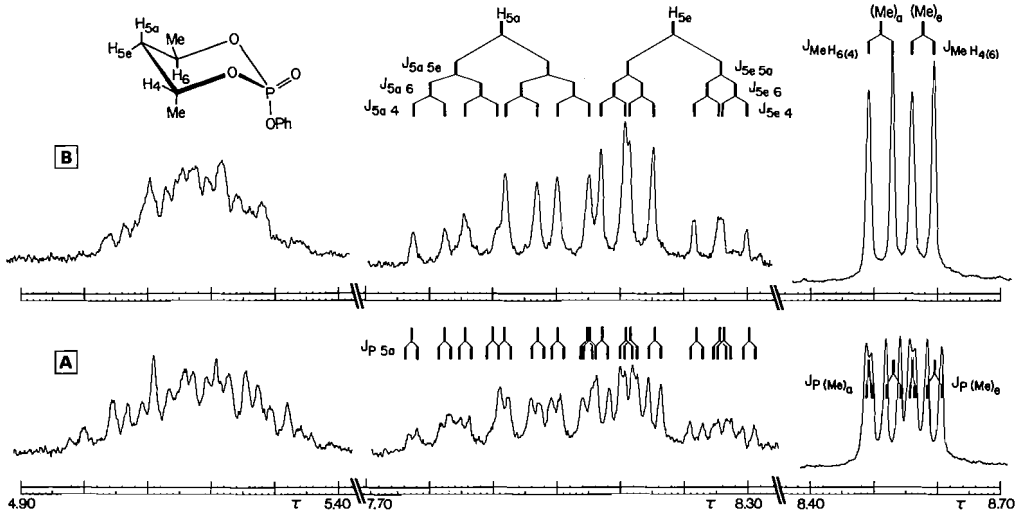

FIG. 3. Partial ^{1}H n.m.r. spectrum (100 MHz) of isomer **2***b* in $CDCl_3$ solution. [A], the normal spectrum; [B], the spectrum obtained with continuous-wave irradiation at the phosphorus frequency. An approximate, first-order, peak assignment is given.

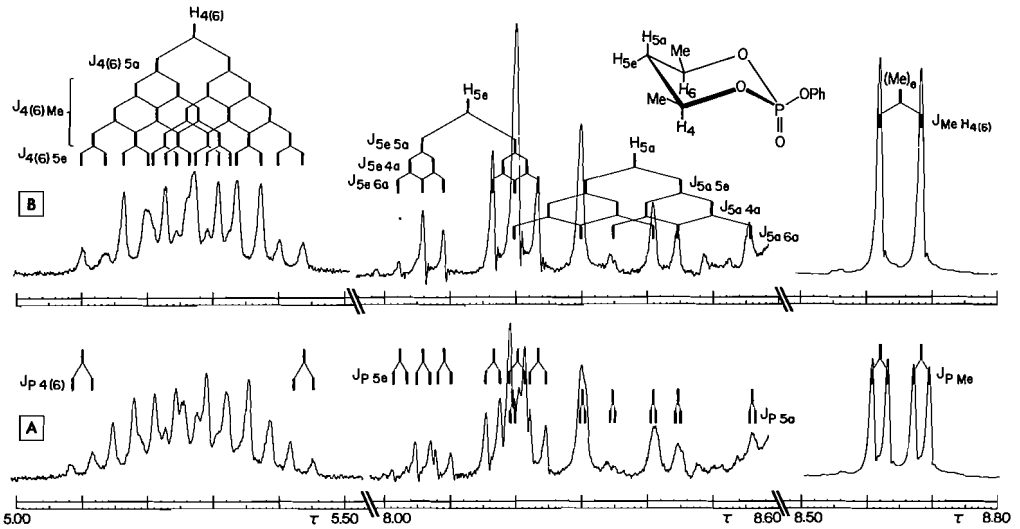

FIG. 4. Partial ^{1}H n.m.r. spectrum (100 MHz) of isomer **2***c* in $CDCl_3$ solution. [A], normal spectrum; [B], spectrum obtained with continuous-wave irradiation at the phosphorus frequency. An approximate, first-order assignment is given.

from compound **3**, Table 2. This enables assignment of the structure **2***b*, the cyclic phenyl phosphate ester of *d,l*-pentan-2,4-diol, to this product. The presence of *two*, non-equivalent methyl resonances in the p.m.r. spectrum confirms this assignment.

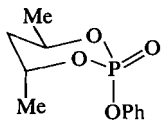

The absence of any large splittings in the ^{31}P resonances of components **2***a* and *c* suggests *gauche* POCH coupling relationships (3) for these isomers. The p.m.r. spectra of these two isomers are virtually identical and the single methyl resonance is consistent with the structures **2***a* and *c*, which have isomeric configurations at the phosphorus.

It is not possible at this time to assign unequivocally the configuration *at phosphorus* for any of these derivatives. However, some circum-

Can. J. Chem. Downloaded from www.nrcresearchpress.com by 210.87.254.40 on 09/05/12
For personal use only.

Can. J. Chem. Downloaded from www.nrcresearchpress.com by 210.87.254.40 on 09/05/12
For personal use only.

TABLE 2. The n.m.r. parameters for derivatives of 2-oxo-2-phenoxy-1,3,2-dioxaphosphorinane*

Structure	Chemical shifts (τ-values, δ-values)						
	4a(6a)	4e(6e)	5a	5e	Me_a	Me_e	^{31}P
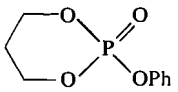 **1**	5.49	5.57	7.75†	8.25†	—	—	126.0
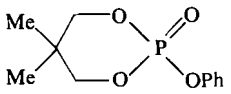 **3**	5.78	6.05	—	—	8.74	9.16	126.5

Structure	Coupling constants (Hz)													
	4a,P	4e,P	5e,P	5a,P	4a,6a	4a,6e	5a,5e	4a,4e	4e,6e	4a,5a	4a,5e	4e,5a	4e,5e	4a,Me_a
1	2.9 ± 0.8	21.9 ± 0.8	2.7‡	0.9‡	—	—	−15.3†	−10.9	§	11.4‖	2.7	5.2‖	2.7	—
3	1.7	22.5	—	—	—	—	—	−10.9	3.0	—	—	—	—	<1.0¶

*Data for $CDCl_3$ solutions.
†First-order values.
‡Estimated from ^1H-{^{31}P} decoupling experiment, assuming similar signs.
§Assumed zero to facilitate assignment of spectrum.
‖Probable error 0.5 Hz, LAOCN3 program.
¶Estimated from ^1H-{^1H} decoupling experiment.

Can. J. Chem. Downloaded from www.nrcresearchpress.com by 210.87.254.40 on 09/05/12
For personal use only.

stantial data can be cited. An X-ray study (5) of **1** has shown that this derivative exists in a slightly flattened, chair conformation having the phenoxy group axially oriented. As in our previous discussion (3), we have assumed for the present that this steric preference also pertains to **1** in solution. *With this sole assumption*, assignment of configuration at phosphorus necessitates only the relationship of **1** with the other derivatives. This can be established by comparison of ^{31}P chemical shifts. Two of the derivatives (**2***a* and *b*) derived from pentane-2,4-diol have chemical shifts close to those of **1** and **3**, whereas that of **2***c* is *ca.* 2.5 p.p.m. to low field. This suggests that the configuration of **2***c* differs from those of **1**, **2***a*, **2***b*, or **3**. Insofar as the configuration, having the phosphoryl oxygen substituent equatorially oriented and the phenoxy group axially oriented, appears to be the more stable in the crystal state, it seems reasonable to assign the phosphorus configurations of **2***a*, *b*, and *c* as outlined above.

Clearly an unequivocal evaluation of this point must await an X-ray crystallographic evaluation of **2***a*.[4] However, at this time we can comment on the conformations in solution of several of these derivatives. It should be appreciated at the outset of this discussion that we have assumed that the same flattening of the six-membered ring observed for **1** in the solid state, occurs for all of these derivatives. This seems reasonable in view of the length of the ring, P—O bonds (1.56 Å). We anticipate also that the activation energy for "chair–chair" conformational inversion is sufficiently low that this process is accessible at room temperature. Thus all of the compounds to be discussed will have a greater, or lesser, degree of conformational time-averaging. As we shall see, most of these derivatives have a remarkable preference for one particular "chair" conformation (*vide infra*).

Isomers **2***a* and **2***c* have very similar n.m.r. spectra and the data of Table 1 are similar for each isomer. The differences which do exist for $J_{4a,5e}$ and $J_{4a,5a}$ are not sufficiently significant, beyond experimental error, to attribute to any difference in the conformations of the two molecules. In comparison with the data for **1**, Table 2, it is seen that only the *geminal*, 5e–5a, coupling constant does not agree within experimental error. Since the 4a–5e and 4a–5a coupling constants of **2***a* and *b* agree well with those of **1**, the conformation of the C_4—C_5—C_6 parts of these molecules is taken to be the same. The similarity of the J_{POCH} *gauche* couplings (P,4a) is taken to mean that the P—O—C—H dihedral angles are similar. Thus, isomers **2***a* and *c* exist predominantly in the flattened-chair conformation (5) typical of **1**. A satisfactory measure of the accuracy of this statement, based on other similar applications would be a $\pm 5\%$ limit on possible changes in dihedral angle for the relevant bonds.

The p.m.r. data for isomer **2***b* is perhaps more interesting, since there are more comparisons possible due to asymmetry of the molecule. The *trans*-diaxial 4e–5a coupling constant for **2***b* is smaller than for **1** (by *ca.* 2.5 Hz), $J_{4e,5e}$ is larger (by *ca.* 1.6 Hz) as is, perhaps, $J_{6a,5e}$ (by *ca.* 0.5 Hz). The *trans* POCH coupling of 17.0 Hz is somewhat smaller than for **1** and **3** (by *ca.* 3 Hz). Such data can usually be explained in one of three ways. Either the molecule is undergoing a rapid conformational inversion as in **A1** $\rightleftharpoons$ **A2**, or it exists in a distorted conformation, or both. For **A**, in which the molecule exists in two now "typical", flattened chair conformations which differ only in the configuration at the phosphorus atom, the room temperature n.m.r. data is expected to be the weighted average of that for each conformation. The observed n.m.r. coupling constants for **2***b* are consistent with

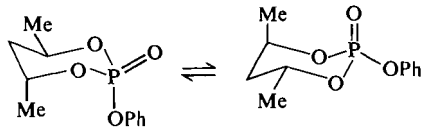

A1 **A2**

conformational "time-averaging" between the two "typical" conformations as in **A**. The 4a–5a coupling constant (8.6 Hz) would be expected to be somewhere between the values of 4e–5e (2.7 Hz) and 4a–5a (11.4 Hz) for **1**, depending on the relative populations of the two conformers. Similarly, the value for 4e–5e is somewhere between that of 4e–5e and 4a–5a for **1**. The experimental values for $J_{4e,5a}$ and $J_{4a,5e}$ as well as those for J_{POCH} and J_{POCCH} also agree well with the suggestion of a conformationally inverting system.

By assuming that the configuration at the

[4]So far we have not obtained a suitable crystal of **2***a*.

Can. J. Chem. Downloaded from www.nrcresearchpress.com by 210.87.254.40 on 09/05/12
For personal use only.

phosphorus atom does not affect seriously the magnitudes of the individual couplings,[5] the relative populations at room temperature of the two conformations of **2***b* may be calculated.

The expression $J_{average} = \alpha J_{A1} + (1 - \alpha)J_{A2}$, where α is the fraction of the population in conformation **A1**, J_{A1} is the value of the coupling constant for **A1**, and J_{A2} is the value of the coupling constant for conformation **A2**, can be used. For the conformational equilibrium between **A1** and **A2**, the value for α can be calculated using five different sets of coupling constants. The results, using **1** as the standard are as follows:

	J_{POCH}	J_{P,CH_3}[6]	J_{P,H_5}[6]	$J_{5a,6a}$	$J_{4e,5a}$
$\alpha =$	0.74	0.78	0.74	0.75	0.86

It is felt that the variation of these values is mainly due to the variation in the accuracies of the proton–proton coupling constants as determined for **1** and **2***b*. That the values calculated from the two phosphorus couplings agree well, can be taken as a measure of the sensitivity with which these couplings depend on dihedral angles. Fortunately, the phosphorus–hydrogen coupling constants can often be accurately determined in systems for which the remaining p.m.r. analysis is difficult.

The low temperature n.m.r. spectrum (−80°) of **2***b* was not entirely satisfactory[7] and values for $J_{4e,5e}$ and $J_{6a,5e}$ were not significantly different from the room temperature values given in Table 1.

At this time it is not possible to firmly decide that **2***b* is conformationally time-averaging though the above observations tend to suggest this. The isomer **A1**, having the same configuration at phosphorus as **3**, **2***a*, and **1**, is expected to be the preferred one.

If **2***b* is undergoing a rapid, chair–chair inversion process it is necessary to offer some rationalization for the fact that **1**, for example, appears to be conformationally homogeneous. It is necessary to postulate that the interaction between the axial methyl group and the phenoxy group of conformer **A1** is now sufficiently large to partially destabilize **A1** with respect to **A2**. Furthermore, it is a necessary condition that the interaction of the axial methyl group and the phosphoryl oxygen of conformer **A2** does not further destabilize an already unfavorable situation.

A considerable number of long-range ^{31}P–^{1}H couplings were observed for these derivatives. The magnitude of the ^4J coupling from ^{31}P, through oxygen, to a methyl group is dependent on the dihedral angle between the P—O and C—CH_3 bonds. Thus compounds **2***a* and *c*, which have the stereo-relationship depicted in **B** in which the P—O and C—Me bonds are

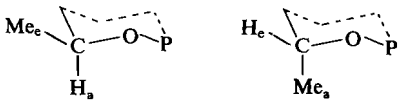

B **C**

trans anti-planar, give a coupling of *ca.* 2.5 Hz. In contrast, a coupling of less than 0.8 Hz[8] is observed for compound **2***b* which has a *gauche* relationship between the P—O and C—Me bonds, as in **C**.

The ^4J couplings between phosphorus and the C-5 methylene protons of **1**, **2***a*, and **2***c* also exhibit a marked stereospecificity, where coupling into the equatorially oriented proton, as in **D**, ranges from 2.4–2.7 Hz while coupling into

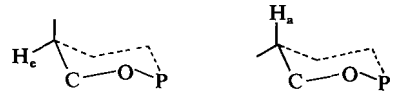

D **E**

the axially oriented proton, **E**, ranges from 0.7 to 0.9 Hz. The couplings for **2***b* are, as we now would anticipate, intermediate between these ranges. Presumably the sign of all of these long range couplings is positive, in accordance with the result (6) for acylic derivatives. It is also interesting that the coupling between the phosphorus and the methyl protons corresponds to the average of the phosphorus couplings to H_{5e} and H_{5a}.

[5]A good approximation in view of the similarity of the couplings for **2***a* and *c*.

[6]See later for a discussion of these couplings. The values of J_{P,CH_3} for isomer **2***a* were used for these calculations. Except for the value derived from J_{POCH}, the values of α are the average of the values derived from the two couplings available.

[7]The spectra were measured in CH_2Cl_2 solution. At low temperatures the Varian HA-100 does not give the best resolution, and in this case the situation was further aggravated by the increased viscosity of the solution.

[8]Likely zero in the absence of conformational time-averaging.

Can. J. Chem. Downloaded from www.nrcresearchpress.com by 210.87.254.40 on 09/05/12
For personal use only.

The formation of just the three products **2***a*, **2***b*, and **2***c* from the commercially available mixture of *meso*- and *d,l*-pentane-2,4-diols can now be rationalized. Both alcohols give rise to the two products which are isomeric at phosphorus. The products from the *meso* alcohol, **2***a* and *c*, have no tendency to invert conformation because this would introduce a severe non-bonded interaction between the methyl groups attached to C-4 and -6 (as in **F**).

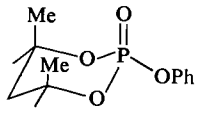

F

The initially formed products from the *d,l*-alcohol are depicted in **G**, **H**, **J**, and **K**. Derivatives **G** and **H** are indistinguishable by normal n.m.r. means; similarly, the pair **J** and **K** cannot

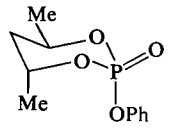

G

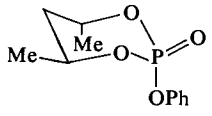

H

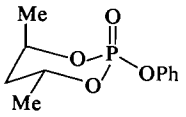

J

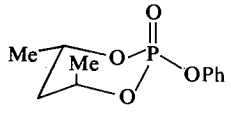

K

be differentiated. Inversion of conformation is now possible in this system, since it no longer introduces any serious non-bonded interactions. Hence, the conformational preference of the phosphate moiety can become effective and the product **2***b* is thus a racemic mixture of two derivatives, with the populations of conformers **G** and **H** favored to an extent of approximately 70%.

Geometric isomerism of the type we have described here has also been detected by other workers (7–9). In some instances isomeric mixtures have been separated (8) and some derivatives have been prepared by stereospecific syntheses (9).

Experimental

The general methods used in this study have been summarized previously (3).

The n.m.r. spectra for compounds **2** were iterated using the LAOCOON III computer program to best fit. The only parameters that could not be iterated were the P,4e and P,4a coupling constants. These couplings, as estimated from the phosphorus spectra and the band-widths of the 4,6 protons, are thought to be accurate to within 0.5 Hz for **2***a* and *c* and within 1.0 Hz for **2***b*. The assignment of 4e,5e and 4a,5e for **2***b* is not unambiguous. These numbers could be reversed. Unfortunately, homonuclear double resonance experiments in which the methyl resonances are irradiated, have not been successful due to the proximity of the methylene protons. The removal of the methyl coupling into the C_4,C_6 protons would have permitted assignment of these couplings. The remaining coupling constants for **2***b* and **2***c* are thought to be well within the stated limits above. For **2***a* the coupling constants from the computer program are slightly less accurate but should be within 0.2 Hz for the smaller couplings. $J_{4a,5a}$ and $J_{5e,5a}$ are probably within 0.5 Hz, having "probable errors" of 0.34 and 0.53 Hz respectively. The chemical shift assignment for 4e and 6a of **2***b* may also be reversed.

Reaction between Phenyl Phosphorodichloridate and Pentane-2,4-diol

Phenyl phosphorodichloridate[9] (3.0 g) was added dropwise with stirring to a solution of pentane-2,4-diol (1.0 g)[10] dissolved in anhydrous pyridine (40 ml) cooled in an ice-bath. The reaction mixture was left to stand in a refrigerator (*ca.* 3°) overnight. A small quantity of water (*ca.* 10 ml) was added to the reaction mixture to dissolve precipitated pyridinium hydrochloride and the entire solution was added to water (*ca.* 100 ml) in a separatory funnel. The resulting solution was extracted with chloroform (5 × 20 ml). The combined chloroform extracts were dried (Na_2SO_4) and concentrated to a syrupy residue (2.1 g, 90%). This material showed three spots on t.l.c. corresponding to the three isomers **2***a*, *b*, and *c* in order of decreasing R_f value.

Column chromatography of 0.5 g of the mixture was carried out using a silica gel column[11] (45 × 1.6 cm). Ethyl acetate was used as eluant and 2 ml fractions were collected. The fractions were monitored by t.l.c. and appropriate series of fractions were combined, and evaporated to give pure (t.l.c., ^1H and ^{31}P n.m.r.) samples of the three isomeric 4,6-dimethyl-2-oxo-2-phenoxy-1,3,2-dioxaphosphorinanes. Isomer **2***a* crystallized spontaneously, m.p. 93.0–95.5°; the other isomers have failed to crystallize over the past three years. The ^{31}P chemical shifts of the isomers **2***a*, *b*, and *c* were respectively, +125.8, +126.0, and +123.6 p.p.m.

Anal. Calcd. for $C_{11}H_{15}O_4P$: C, 54.6; H, 6.2. Found: **2***a*: C, 54.3; H, 6.4. **2***b*: C, 54.3; H, 6.3. **2***c*: C, 54.4; H, 6.3.

The proof of structure of these derivatives is discussed in the text.

It is a pleasure to thank the National Research Council of Canada for their generous support of this study. In particular the award of a Special Grant (no. A 5456) and an equipment grant (No. E 1338) greatly facilitated our progress.

1. L. D. HALL and R. B. MALCOLM. Chem. Ind. (London), 92 (1968).

[9]Aldrich Chemical Co., Milwaukee, Wisconsin.
[10]Frinton Laboratories, South Vineland, N.J.
[11]Mallinckrodt, Silicar CC-7.

2. R. B. MALCOLM. B.Sc. Thesis. University of British Columbia, 1966. M.Sc. Thesis, University of British Columbia, 1969.
3. L. D. HALL and R. B. MALCOLM. Can. J. Chem. This issue.
4. R. BURTON and L. D. HALL. Can. J. Chem. **48**, 59 (1970).
5. H. J. GEISE. Rec. Trav. Chim. **86**, 362 (1967).
6. E. DUVAL and E. A. C. LUCKEN. Mol. Phys. **10**, 499 (1966).
7. (*a*) F. RAMIREZ, A. V. PATWARDHAN, N. B. DESAI, and S. R. HELLER. J. Am. Chem. Soc. **87**, 549 (1965). (*b*) AV. BOGAT-SKII, A. A. KOLESNIK, YU. YU. SAMITOV, and T. D. BUTOVA. J. Gen. Chem. U.S.S.R. Eng. Trans. **37**, 1048 (1967). (*c*) J. DEVILLERS, LE TRANG TRAN, and J. NAVECH. Bull. Soc. Chim. Fr. 182 (1970). (*d*) J.-P. MAJORAL, R. KRAEMER, J. DEVILLERS, and J. NAVECH. Bull. Soc. Chim. Fr. 3917 (1970). (*e*) J. DEVILLERS and J. NAVECH. Bull. Soc. Chim. Fr. 4341 (1970). (*f*) J.-P. MAJORAL and J. NAVECH. Bull. Soc. Chim. Fr. 95 (1971). (*g*) J.-P. MAJORAL and J. NAVECH. Bull. Soc. Chim. Fr. 1331 (1971).
8. (*a*) D. Z. DENNEY and D. B. DENNEY. J. Am. Chem. Soc. **88**, 1830 (1966). (*b*) G. AKSNES, R. ERIKSEN, and K. MELLINGEN. Acta Chem. Scand. **21**, 1028 (1967). (*c*) J.-P. MAJORAL, A. MUNOZ, and J. NAVECH, C.R. Acad. Sci. Paris, Ser. C, **266**, 235 (1968). (*d*) J.-P. MAJORAL and J. NAVECH. C.R. Acad. Sci. Paris, Ser. C, **268**, 2117 (1969). (*e*) M. MIKOLAJCZYK and H. M. SCHIEBEL. Angew. Chem. Int. Edit. **8**, 511 (1969). (*f*) M. MIKOLAJCZYK. Chem. Commun. 1221 (1969). (*g*) D. Z. DENNEY, G. Y. CHEN, and D. B. DENNEY. J. Am. Chem. Soc. **91**, 6838 (1969). (*h*) J. H. FINLEY and D. B. DENNEY. J. Am. Chem. Soc. **92**, 362 (1970).
9. (*a*) W. S. WADSWORTH, JR., and W. D. EMMONS. J. Am. Chem. Soc. **84**, 610 (1962). (*b*) K. D. BERLIN, C. HILDEBRAND, J. G. VERKADE, and O. C. DERMER. Chem. Ind. (London), 291 (1963). (*c*) K. D. BERLIN, C. HILDEBRAND, A. SOUTH, D. M. HELLWEGE, M. PETERSON, E. A. PIER, and J. G. VERKADE. Tetrahedron, 323 (1964). (*d*) J. G. VERKADE, T. J. HUTTEMANN, M. K. FUNG, and R. W. KING. Inorg. Chem. **4**, 83 (1965). (*e*) R. S. EDMUNDSON and E. W. MITCHELL. Chem. Commun. 482 (1966). (*f*) W. S. WADSWORTH, JR. J. Org. Chem. **32**, 1603 (1967). (*g*) R. S. EDMUNDSON and E. W. MITCHELL. J. Chem. Soc. (*c*), 3033 (1968). (*h*) M. MIKOLAJCZYK. Angew. Chem. Int. Edit. **8**, 511 (1969). (*i*) C. BODKIN and P. SIMPSON. Chem. Commun. 829 (1969). (*j*) W. G. BENTRUDE and J. H. HARGIS. Chem. Commun. 1113 (1969). (*k*) W. WADSWORTH, JR., and H. HORTON. J. Am. Chem. Soc. **92**, 3785 (1970). (*l*) W. G. BENTRUDE and J. H. HARGIS. J. Am. Chem. Soc. **92**, 7136 (1970).

Can. J. Chem. Downloaded from www.nrcresearchpress.com by 210.87.254.40 on 09/05/12
For personal use only.

Conformational Studies of Acyclic Organophosphate Esters using Nuclear Magnetic Resonance Spectroscopy[1]

BRUCE DONALDSON AND L. D. HALL[2]

Department of Chemistry, The University of British Columbia, Vancouver 8, British Columbia

Received December 3, 1971

The *vicinal* $^{31}P—O—C—^{1}H$ couplings of a series of acyclic phosphate esters have been measured and rationalized in terms of varying populations of individual rotamers. Variable temperature measurements have been interpreted in terms of the enthalpy and entropy differences between *gauche* and *trans* rotational isomers.

Les couplages *vicinaux* $^{31}P—O—C—^{1}H$ d'une série de phosphate esters acyliques ont été mesurés et rationalisés en termes de populations variables pour des rotomères donnés. Les mesures à températures variables ont été interprétées en termes de différences d'enthalpie et d'entropie entre les isomères de rotation *gauche* et *trans*.

Canadian Journal of Chemistry, **50**, 2111 (1972)

Introduction

Previous studies from this (1, 3) and other (4, 8) laboratories have recognized the potential of *vicinal* $^{31}P—O—C—^{1}H$ couplings as a basis for conformational studies of organophosphate esters. Many such studies have made the *a priori* assumption that cyclic systems such as the 2-oxo-1,3,2-dioxaphosphorinanes (Scheme 1) can serve as acceptable models for acyclic phosphates (Scheme 2). The experimental data available in the literature clearly indicates that there is indeed a semi-quantitative relationship between the coupling constants of these two systems; however the data also imply that a simple quantitative relationship does not exist.

In the present paper we review briefly the coupling constants available in the literature for derivatives of the 2-oxo-1,3,2-dioxaphosphorinane system, and compare these with data from series of specifically prepared acyclic phosphates. The couplings observed for the acyclic compounds are interpreted in terms of the populations of the *gauche* (**A** and **B**) and *trans* (**C**) rotational isomers, and in terms of the free energy differences between these isomers. The changes in the observed coupling with temperature for selected representatives of these compounds are studied and interpreted in terms of the enthalpy and entropy differences between the rotational isomers. Since this study was completed another group has published n.m.r. data for some acyclic phosphates (5); we shall discuss their work later on in this paper because we disagree with some of their interpretations.

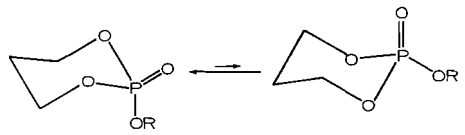

SCHEME 1. Conformational isomers of 2-oxo-1,3,2-dioxaphosphorinane.

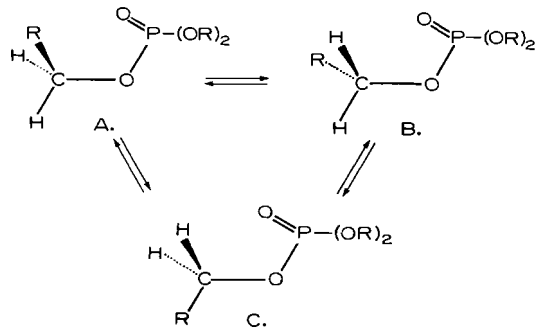

SCHEME 2. Rotational isomerism in acyclic phosphates.

Results and Discussion

The *vicinal* $^{31}P—O—C—^{1}H$ coupling data for three series of acyclic phosphotriester derivatives are shown in Table 1. The monotonic decrease in these values with increasing size of the alkyl group **R** is attributed to an increasing population of the rotational isomer having the R group *trans* to the phosphate moiety (as in **C**, Scheme 2).

[1]Part 3 of a series "Studies of Organophosphorus Derivatives". For part 2 see ref. 1.

[2]Alfred P. Sloan Foundation Research Fellow.

Can. J. Chem. Downloaded from www.nrcresearchpress.com by 210.87.254.5 on 09/05/12
For personal use only.

TABLE 1. Observed couplings (Hz) for acyclic phosphate rotamers

R	Compound: $R{-}CH_2O{-}\overset{\overset{O}{\|}}{P}{-}(OPh)_2$ Set 1	Compound: $(R{-}CH_2O)_2{-}\overset{\overset{O}{\|}}{P}{-}OPh$ Set 2	Compound: $(R{-}CH_2O)_3{-}P{=}O$ Set 3
H	11.5	11.3	11.0
Me	8.7	8.4	8.1
Et	7.8	7.6	7.4
iso-Pr	6.6	6.5	6.4
tert-Bu	5.1	5.0	4.85

TABLE 2. $^{31}P{-}O{-}C{-}^{1}H$ couplings (Hz) and percentage time-averaging in 2-oxo-1,3,2-dioxaphosphorinane systems

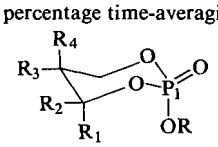

No.	Compound R	R_1	R_2	R_3	R_4	Experimental values J_g	J_t	J_{sum}	Calculated values J_g real	J_t real	% time-averaging	ΔG (cal)	Reference
1	Ph	H	H	Ph	H	1.4	22.8	24.2	1.4	22.8	0.0	∞	*
2	Ph	H	H	H	H	2.8	21.3	24.1	1.35	22.7	6.9	1570	1, 2
3	Ph	H	H	CH_3	CH_3	1.7	22.5	24.2	1.38	22.8	1.4	3945	1, 2
4	Ph	H	H	H	Ph	3.8	20.2	24.0	1.4	22.6	11.7	1215	*
5	H	H	H	CH_3	CH_3	12.0	12.0	24.0	1.4	22.6	50.0	0.0	4*h*
6	H	H	H	H	Ph	5.6	17.9	23.5	1.3	22.2	21.3	787	*
7	K	H	Ph	H	H	1.9	22.3	24.2	1.36	22.9	2.3	2240	4*d*
8	CH_3	H	H	Bu^t	H	1.2	22.8	24.0	1.2	22.8	−0.5	∞	10

*Private communication. J. Campbell of this laboratory.

In order to place these observations on a quantitative basis it is necessary to know the magnitudes of the couplings corresponding to dihedral angles between the P—O and C—H bonds, of 180 and 60° ($J_{180°}$ and $J_{60°}$, respectively). These two values, or an estimate thereof, may be obtained from the *vicinal* $^{31}P{-}O{-}C{-}^{1}H$ couplings of derivatives of the 2-oxo-1,3,2-dioxaphosphorinane system; a summary of the data available in the literature for such derivatives is given in Table 2.

It is evident that although there is a considerable spread in the values for J_{trans} (J_t) and J_{gauche} (J_g), the sum of the couplings is nearly constant. This suggests that the variations in the observed values are due to averaging of the couplings arising from varying populations of the different conformations of the phosphorinane ring. Assuming that only chair conformations are involved, a conformational inversion process will cause the observed *trans* coupling value, J_t (obs), to be lower than the true value J_t (real) and the observed *gauche* coupling value, J_g (obs), to be larger than the true value J_g (real).

These values are related to the extent of population time averaging by the expressions

$$\alpha J_t\,(\text{real}) + (1-\alpha)J_g\,(\text{real}) = J_t\,(\text{obs})$$

$$\alpha J_g\,(\text{real}) + (1-\alpha)J_t\,(\text{real}) = J_g\,(\text{obs})$$

where α is the population of one conformer and $(1-\alpha)$ the population of the other. This process would however leave the sum of the two observed couplings unchanged.

We believe that compound **1** undergoes only a very small amount of conformational inversion because it contains both the axial electronegative substituent on the phosphorous atom (such a substituent favours an axial configuration, with a ΔG of *ca.* 1500 cal (compound **2**, Table 2;

Can. J. Chem. Downloaded from www.nrcresearchpress.com by 210.87.254.5 on 09/05/12
For personal use only.

Can. J. Chem. Downloaded from www.nrcresearchpress.com by 210.87.254.5 on 09/05/12
For personal use only.

see also X-ray data ref. 6) and the equatorial substituent on C-5. Hence the experimental values of J_t 22.8 and J_g 1.4 Hz from this compound approximate J_t (real) and J_g (real).[3] These values in conjunction with the observed couplings can therefore be used to calculate the extent of time-averaging $(100 - \alpha)$ and hence the free energy difference (ΔG) between the two conformers: all of these data are listed in Table 2.

Using the percentage time-averaging we have approximated what the couplings would be for these compounds if no time-averaging were to occur. These calculated, non time-averaged couplings are seen to differ from those for compound **1** only in so far as their J_{sum} values differ; and thus support our premise that $^{31}P—O—C—^{1}H$ couplings in 2-oxo-1,3,2-dioxaphosphorinanes are largely independent of the ring substituents, but vary mainly as a function of conformational time-averaging.

It now remains to take these values of J_t (real) and J_g (real) and relate them to the required couplings $J_{180°}$ and $J_{60°}$.

X-Ray studies on compound **1** (6) have shown that the P—O—C_6—C_5 and P—O—C_4—C_5 dihedral angles are 54° rather than the 60° that would occur for an "ideal" cyclohexane geometry. Assuming that C-6 and -4 are tetrahedral centers, the P—O—C—H dihedral angles become 120° − 54° = 66° for the axial proton and 120° + 54° = 174° for the equatorial proton (Scheme 3).

It is well established that the $\cos^2 \phi$ relationship between the magnitude of the vicinal

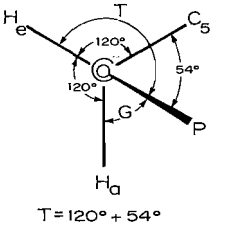

T = 120° + 54°
G = 120° − 54°

SCHEME 3. P—O—C—H dihedral angles in 2-oxo-1,3,2-dioxaphosphorinane.

[3]Compound **8** in Table 2 of Bentrude and Hargis (10) has slightly more extreme couplings, however we calculate that compound **8** time averages to an extent only 0.5% less than compound **3** and it may therefore be taken as good supporting evidence for our choice of J_t and J_g.

coupling constant and the dihedral angle, suggested by Karplus (7) exists for H—C—C—H couplings. *Assuming that a similar relationship also exists for* $^{31}P—O—C—^{1}H$ *vicinal couplings* we can calculate $J_{180°}$ and $J_{60°}$ from J_t (real) and J_g (real). Thus:

$$J_{180°} = J_t \text{ (real)} \times \cos^2 180/\cos^2 174 = 22.9 \text{ Hz}$$

$$J_{60°} = J_g \text{ (real)} \times \cos^2 60/\cos^2 66 = 2.1 \text{ Hz}$$

Using these data, and assuming that they are applicable to acyclic phosphate rotamers we can calculate the coupling exhibited by methyl phosphates.

$$J_{av} = 1/3(J_{180°} + 2J_{60°}) = 9.0 \text{ Hz}$$

The observed values, however, lie in the range 11.0 to 11.5 Hz.

Thus it is not possible to compare directly data from cyclic phosphates with that from acyclic phosphates. Several possible reasons for this lack of quantitative agreement have been considered:

(*a*) That the phosphorinane ring system is flatter in solution than in the crystalline phase. The P—O—C—H_{ax} dihedral angle would thus be increased, causing the calculated $J_{60°}$ to be increased; the P—O—C—H_{eq} dihedral angle would decrease causing the calculated $J_{180°}$ to increase; thus J_{av} would increase. However, the calculated J_{av} for methyl rotamers is still less than the observed value when $J_{60°}$ (the more rapidly changing quantity) reaches the lowest observed coupling for the acyclic rotamers (trineopentyl phosphate 4.05 Hz at 185 °K) a coupling that still contains some *trans* contribution. This value therefore acts as a maximum limit for $J_{60°}$.

(*b*) That the energy minima for the acyclic rotamers do not occur at P—O—C—H dihedral angles of 60 and 180°, but at $(60 + \phi)°$ and $(60 - \phi)°$ and at $(180 \mp \phi)°$. The observed coupling J_{obs} is then given by $1/3(J_t + 2J_g)$, where

$$J_t = J_{180°} \times \cos^2 (180 \pm \phi)°/\cos^2 180°$$

$$2J_g = J_{60°} \times \cos^2 (60 + \phi)°/\cos^2 60° + (J_{60°} \times \cos^2 (60 - \phi)°/\cos^2 60°$$

From which it follows that J_t is less than $J_{180°}$ and J_g is less than $J_{60°}$, and hence that J_{obs} is less than J_{av}. The J_{obs} in the phosphorinanes 11–11.5

Can. J. Chem. Downloaded from www.nrcresearchpress.com by 210.87.254.5 on 09/05/12
For personal use only.

Hz is in fact more than the calculated 9.0 Hz and indicates that such asymmetric rotational isomers are not the cause of the inconsistency in the data.

(*c*) That the electronegative phosphoryl oxygen selectively reduces the coupling into the equatorial proton by 8–10 Hz due to the all *trans* transmission pathway; no similar effect being operable for the axial proton. If this effect were to operate, conformers with an axial phosphoryl oxygen would have to show a J_t of *ca.* 30 Hz. The axial preference of OR substituents on phosphorus precludes direct observation of these conformers; however any phosphorinane which significantly time-averages should show an increase in both J_t and J_{sum}. Inspection of the data in Table 2 shows no evidence of such an effect.

(*d*) That a significant amount of twist conformation is present in the phosphorinane ring; in this case both dihedral angles are 120° and exhibit small *vicinal* couplings. The presence of twist conformations would thus produce a decrease in J_{sum}. The observed constancy of J_{sum} indicates that the population of twist conformers either is constant for all the compounds studied or more reasonably that it is zero.

None of these approaches is able to account for the only semi-quantitative agreement between the data obtained from the two sources. The only obvious difference between these systems is that free rotation about the P—O bond can occur in the acyclic rotors but not in the phosphorinanes; it seems likely that this is in some way responsible for the discrepancy.

We have therefore calculated the populations of the *trans* rotational isomers of the compounds in Table 1 using, first the derived values for $J_{180°}$ and $J_{60°}$ (lines A_1, A_2, and A_3, Fig. 1) and second using the ratio of $J_{180°}/J_{60°}$ and the observed coupling value for the methyl representative of each set of compounds. In this case a different set of J_t and J_g values, J_T and J_G, have been derived for each set of compounds. These normalized data which all fall very close to line B, are given in Table 3.

Assuming that a $\cos^2$ relationship exists between dihedral angle and *vicinal* coupling, the rate of change of the coupling with angle will be greatest for the *gauche* angle of 60°. Thus J_g, the parameter upon which the calculated rotamer

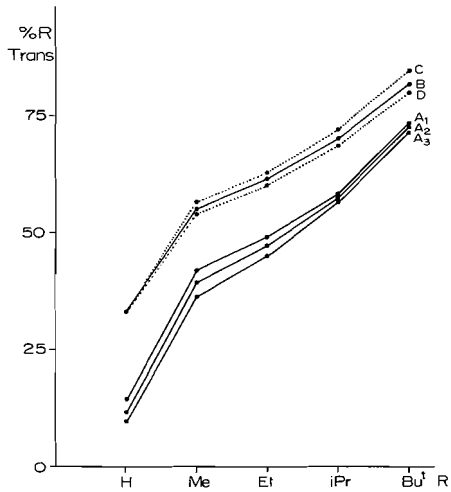

FIG. 1. *trans*-Populations of acylic rotamers as a function of substituent size R.

Line A_1 (compound set 1, $RCH_2O—\overset{\overset{O}{\|}}{P}—(OPh)_2$), line A_2 (compound set 2, $(RCH_2O)_2\overset{\overset{O}{\|}}{P}—OPh$), and line A_3 (compound set 3 $(RCH_2O)_3P{=}O$) obtained using J_{180} and J_{60} values derived from the 2-oxo-1,3,2-dioxaphosphorinane system. Line B using J_T and J_G values normalized to give a 33.3% rotameric population for the methyl phosphate of each compound set; set 1, J_T 29.0, J_G 2.7; set 2, J_T28.6, J_G 2.6; set 3, J_T 27.9, J_G 2.55. Lines C and D for compounds of set 2. Using the likely extreme values of J_G; C, J_T +28.6, J_G 2.1; D, J_T +28.6, T_G 3.1.

populations are most sensitive, is the one with the greatest uncertainty. The lines C and D in Fig. 1 represent the calculated *trans* rotamer populations for the likely extremes of J_g ($\pm$0.5 Hz). The uncertainties in J_T and the sensitivity of the populations toward it are considerably smaller and are ignored. The derivation of the relationships that we have used to calculate the *trans* rotamer population and the equilibrium constants are given in the Appendix.

Regardless of the J_t and J_g values used, the observed monotonic decrease in J_{obs} with increasing bulkiness of the substituent R is reflected in a considerable increase of the *trans* rotamer population. We would point out that the differences between the rotamer populations calculated using the normalized and unnormalized data decreases with increasing population of the *trans* rotamer, thus in studying systems of potential biochemical interest for which this

TABLE 3. Thermodynamic properties of acyclic rotamers

Compound R	*	% population of rotamer having R *trans* C	Equilibrium constant for *gauche–trans* interconversions	Free energy differences between *gauche–trans* states (cal)
H	I	33.3	1.0	0.0
	II	33.3	1.0	0.0
	III	33.3	1.0	0.0
Me	I	54.3	2.38	512
	II	55.5	2.50	541
	III	56.3	2.57	557
Et	I	61.2	3.16	678
	II	61.6	3.21	688
	III	61.7	3.23	692
iso-Pr	I	70.2	4.72	915
	II	70.1	4.69	911
	III	69.9	4.66	908
tert-Bu	I	81.6	8.97	1295
	II	81.6	8.97	1295
	III	81.8	9.02	1300

*I, $ROP(OPh)_2$, J_T 29.0, J_G 2.67; II, $(RO)_2POPh$, J_T 28.6, J_G 2.62; III, $(RO)_3P{=}O$, J_T 27,9, J_G 2.56.

present work acts as a model study, the R groups encountered are usually large enough to give *trans* rotamer populations not seriously altered in a semi-quantitative way by the choice of J_t and J_g.

The data represented by line B, Fig. 1 are, we believe, the best available at present. Using these parameters we have calculated the *trans–gauche* interconversion equilibrium constants and also the free energy differences between the *gauche* and *trans* rotational isomers (Table 3).

The quantitative agreement between the data from the three sets of acylic rotamers is excellent and exemplifies the independence of J $^{31}P—O—C—^{1}H$ upon phosphorus substituents in phosphotriesters. Thus we discount the rationale of Axtmann *et al.* (11) that decreases in couplings arise from electronegativity effects. We also discount the attempt by Katritsky *et al.* (8) to rationalize the data from cyclic and acyclic compounds by assuming that the steric effect of the R group is zero and hence that no nonequivalent rotational isomers occur.

Temperature Studies

Invariance of J_{obs} with temperature, observed for methyl diphenyl phosphate is the behavior expected from the assumption of the equivalence of the rotational isomers in methyl phosphates. The decrease of J_{obs} with decreasing temperature observed for the ethyl and neopentyl derivatives arises from an increasing proportion of the *trans* rotamer at lower temperatures. (Table 4, columns 1 and 2).

It is convenient to express the J_{obs} temperature relationship as a plot of J_{obs} *vs.* $1/T$ (Fig. 2). Over the temperature range experimentally accessible the relationship between J_{obs} and $1/T$ appears linear, and has been so reported (5). However, from the expression for the equilibrium constant K derived in the Appendix to this paper it can be seen that at very high temperatures when the rotational isomers tend to equivalence and K approaches unity, J_{obs} approaches J_{av}. At low temperatures when the *trans* rotamer becomes populated exclusively K becomes very large and then J_{obs} asymptotically approaches J_g. Combining the expression for K and the expression relating the equilibrium constant with temperature it can be seen that the relationship between J_{obs} and $1/T$ is indeed non-linear except when J_{obs} is equal to J_{av}. The conclusions drawn by the workers in ref. 5, that with increasing temperature compounds such as tri-neopentyl phosphate will never attain equal populations of the rotational isomers, are based on a linear relation-

Can. J. Chem. Downloaded from www.nrcresearchpress.com by 210.87.254.5 on 09/05/12
For personal use only.

TABLE 4. Thermodynamic parameters as a function of temperature for acyclic phosphate esters

	MeO—P(=O)—(OPh)$_2$				(EtO)$_2$—P(=O)—OPh				*neo*-Pentyl O—P(=O)—(OPh)$_2$			
Temperature (°K)	J_{obs} (Hz)	Population *trans* (%)	K	ΔG (cal)	J_{obs} (Hz)	Population *trans* (%)	K	ΔG (cal)	J_{obs} (Hz)	Population *trans* (%)	K	ΔG (cal)
185									4.05	89.8	17.5	1050
193									4.15	89.0	16.2	1063
203									4.3	87.9	14.5	1095
233	11.5	33.3	1.0	0.0	7.7	61.0	3.13	528	4.6	85.6	11.9	1145
253					7.95	59.0	2.88	532				
273					8.15	57.3	2.69	536	4.9	83.3	9.9	1240
298	11.5	33.3	1.0	0.0	8.4	55.4	2.49	540	5.1	81.8	9.0	1308
335	11.5	33.3	1.0	0.0	8.65	53.5	2.30	553	5.45	78.2	7.9	1370
370	11.5	33.3	1.0	0.0	8.9	51.6	2.13	555				
393	11.5	33.3	1.0	0.0	9.0	50.7	2.05	560	5.7	77.3	6.85	1500

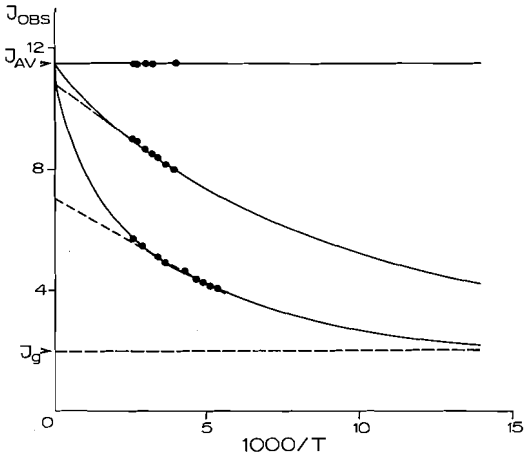

FIG. 2. Variation of the observed rotamer coupling J_{obs} with $1000/T$ for (A) methyl diphenyl phosphate, (B) diethyl phenyl phosphate, (C) *neo*-pentyl diphenyl phosphate. The dashed straight lines passing through the data points of B and C represent interpretation of similar data made in the study, ref. 5.

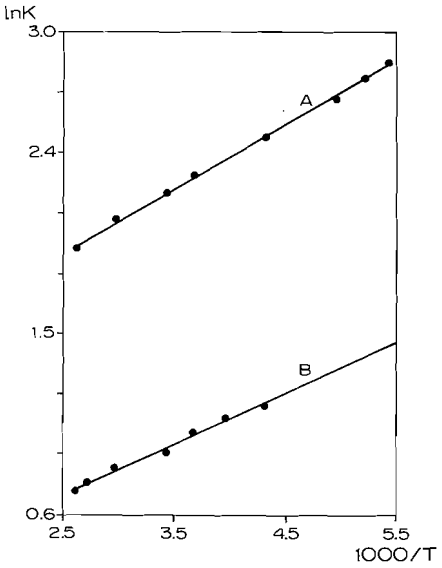

FIG. 3. Plot of log of the rotameric equilibrium constant ln K against the reciprocal of the absolute temperature T. (A) *neo*-pentyl diphenyl phosphate, (B) diethyl phenyl phosphate.

ship between J_{obs} and $1/T$, and are therefore incorrect.

By plotting ln K *vs.* $1/T$ and ΔG *vs.* T (Figs. 3 and 4) we have estimated the enthalpy and entropy differences between the rotational states about the O—C bond. The ln K *vs.* $1/T$ plots have correlations greater than 0.996 and yield values of ΔH of 650 cal for neopentyl diphenyl phosphate and 500 cal for diethyl phenyl phosphate. The plots ΔG *vs.* T have correlations of 0.999 for neopentyl diphenyl phosphate, 0.988 for diethyl phenyl phosphate and >0.999 for methyl diphenyl phosphate yielding values of 650, 480, and 0 cal respectively for ΔH and 2.2, 0.2 and 0 cal/degree mol for the entropies.

In summary then, we have confirmed that a qualitative relationship exists between the *trans* and *gauche* $^{31}P—O—C—^{1}H$ couplings of derivatives of the 2-oxo-1,3,2-dioxaphosphorinane system and the couplings of acyclic phosphate esters. This relationship accords with variations of rotamer populations which follow conven-

Can. J. Chem. Downloaded from www.nrcresearchpress.com by 210.87.254.5 on 09/05/12
For personal use only.

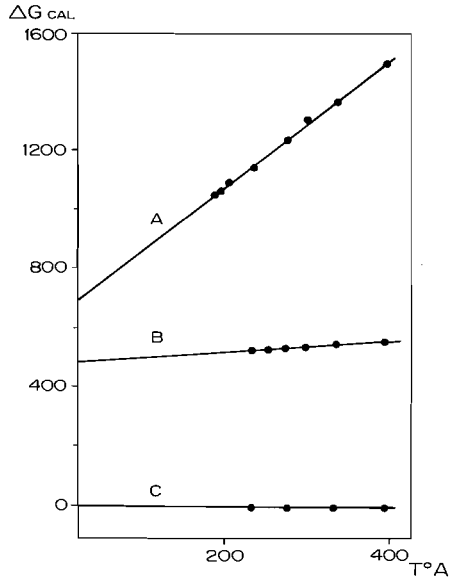

FIG. 4. Plot of the free energy differences between rotameric states, ΔG as a function of the absolute temperature T. (A) *neo*-Pentyl diphenyl phosphate, (B) diethyl phenyl phosphate, (C) methyl diphenyl phosphate.

tional conformational tenets. However, it must be emphasized that a precise quantitative relationship does not exist and we can at present offer no acceptable reason as to why this should be.

Experimental

The following general method was used for the preparation of the acyclic phosphate esters. Phosphorus oxychloride, phenylphosphorodichloridate, or diphenylphosphorochloridate as appropriate (1 equiv) was added slowly to a solution of the alcohol (1.2 equiv) in pyridine solvent, the rate of addition being adjusted to keep the temperature below 40°. After standing for 2 h, unreacted phosphorochloridate was destroyed by the addition of 5 volumes of water. After a further 30 min the mixture was extracted into chloroform and evaporated to a small volume and traces of pyridine were removed as the toluene azeotrope. The crude alkyl phosphate was purified by vacuum distillation (180–220° at 0.1 mm). Yields of crude product in excess of 80% were obtained. Compounds in set 1 (Table 1) were characterized by elemental micro-analysis in addition to the n.m.r. measurements. The remaining compounds were shown to be pure by t.l.c. and were characterized by comparison of the n.m.r. spectra with the appropriate compound of set 1.

Room temperature n.m.r. spectra were run on *ca.* 15% solutions in $CDCl_3$ using a Varian HA 100 spectrometer in the frequency sweep mode. Spectral assignment was simplified by means of phosphorus decoupling experiments (9) and true couplings obtained using the LAØCQØN-3 iterative computer programme. Variable temperature studies were conducted in *ca.* 5% solutions in CH_2Cl_2 for temperatures below 25° and on neat oils at high temperatures using a Varian XL-100 spectrometer.

The t.l.c. experiments were on silica gel G plates in 5% methanol in chloroform solvent.

Measurements were not made with diethyl phosphate below 233 °K because the magnitude of the phosphorus coupling approached that of the proton vicinal coupling.

The plots shown in Figs. 3 and 4 are least squares analyses made with a Hewlett Packard model 9100 programmed calculator and model 9125A plotter.

Appendix

This gives the derivation of expressions for the *trans* population and the *trans–gauche* rotamer equilibrium constants in terms of $J_{180°}$ and $J_{60°}$.

The observed coupling for the rotational isomers shown in Scheme 2 which interconvert rapidly on the n.m.r. time scale is given by the weighted sum of the coupling occurring in each isomer:

$$J_{obs} = J_C[C] + J_A[A] + J_B[B]$$

where [C] is the concentration of the *trans* rotamer (C); [B] = [A] concentrations of the *gauche* rotamers (A and B); and [C] + [B] + [A] = 1.

The couplings occurring in each rotational isomer are given by:

$$J_C = \frac{J_G + J_G}{2} \qquad J_A = J_B = \frac{J_G + J_T}{2}$$

thus

$$J_{obs} = J_G[C] + (J_G + J_T)[A]$$

and hence

$$J_{obs} = J_G[C] + (J_G + J_T)\left(\frac{1 - [C]}{2}\right)$$

Rearranging this equation yields the percentage concentration of the *trans* rotamer:

$$[C] = \frac{J_T + J_G - 2J_{obs}}{J_T - J_G} \times 100$$

The equilibrium constant is given by:

$$\frac{[C]}{[A]} = \frac{2[C]}{1 - [C]}$$

Yielding

$$K = \left[\frac{J_T - J_{obs}}{J_{obs} - J_G}\right] - 1$$

It is a pleasure to thank the National Research Council of Canada for their generous financial support via operating grants (A-1905), via a special grant (A-5456) and an equipment grant (E-1338).

Can. J. Chem. Downloaded from www.nrcresearchpress.com by 210.87.254.5 on 09/05/12
For personal use only.

1. L. D. HALL and R. B. MALCOLM. Can. J. Chem. This issue.
2. L. D. HALL and R. B. MALCOLM. Can. J. Chem. This issue.
3. L. D. HALL and R. B. MALCOLM. Chem. Ind. (London), 92, (1968).
4. For detailed list of references see those quoted in ref. 1 above: a selected list is given here. (*a*) D. W. WHITE, G. K. MCEWEN, R. D. BERTRAND, and J. G. VERKADE. J. Mag. Res. **4**, 123 (1971). (*b*) D. W. WHITE and J. G. VERKADE. J. Mag. Res. **3**, 111 (1970). (*c*) R. D. BERTRAND, J. G. VERKADE, D. W. WHITE, D. GAGNAIRE, J. B. ROBERT, and J. VERRIER. J. Mag. Res. **3**, 494 (1970). (*d*) M. KAINOSHO and A. NAKAMURA. Tetrahedron, **25**, 4071 (1969). (*e*) M. TSUBOI, S. TAKAHASHI, Y. KYOGOKU, H. HAYATSU and T. UKITA. Science, **166**, 1504 (1969). (*f*) R. S. EDMUNDSON and E. W. MITCHELL. J. Chem. Soc. C, 752 (1970). (*g*) D. W. WHITE, G. MCEWEN, R. O. BERTRAND, and J. G. VERKERDE. J. Chem. Soc. B, 1454 (1971). (*h*) M. KAINOSHO, A. NAKAMURA, and M. TSUBOI. Bull. Chem. Soc. Jap. **42**, 1713 (1969).
5. A. A. BOTHNER-BY and W. P. TRAUTWEIN. J. Am. Chem. Soc. **93**, 2189 (1971).
6. H. J. GIESE. Rec. Trav. Chim. **86**, 362 (1967).
7. M. KARPLUS. J. Chem. Phys. **30**, 11 (1959). J. Phys. Chem. **64**, 1793 (1961). J. Am. Chem. Soc. **85**, 2870 (1963).
8. A. R. KATRITSKY, M. R. NESBIT, J. MICHALSKY, Z. TUMILOWSKI, and A. ZWIENZAK. J. Chem. Soc. B, 140 (1970).
9. R. BURTON and L. D. HALL. Can. J. Chem. **49**, 59 (1970).
10. W. G. BENTRUDE and J. H. HARGIS. Chem. Commun. 1113 (1969).
11. R. C. AXTMANN, W. E. SHULER and J. H. EBERLY. J. Chem. Phys. **31**, 850 (1959).

Can. J. Chem. Downloaded from www.nrcresearchpress.com by 210.87.254.5 on 09/05/12
For personal use only.

Evaluation of the Binding Constants, Bound Chemical Shifts, and Stoichiometry of Lanthanide–Substrate Complexes[1]

IAN ARMITAGE,[2] G. DUNSMORE, L. D. HALL,[3] AND A. G. MARSHALL

Department of Chemistry, The University of British Columbia, Vancouver 8, British Columbia

Received November 4, 1971

A theoretical analysis of the equilibrium between a lanthanide shift reagent, L, and a substrate, S, is presented. When $[S]_0 \gg [L]_0$, then a plot of $[S]_0$ *vs.* $(1/\delta)$ at constant $[L]_0$ gives a straight line whose slope is $[L]_0\Delta_B$ and whose *y*-intercept is $-\{(1/K_B) + [L]_0\}$, where K_B is the equilibrium binding constant, δ is the induced chemical shift, and Δ_B is the bound chemical shift. A more general and accurate solution using a computer programme is applicable for all ratios of $[L]_0/[S]_0$. It is also shown that the conventional procedure for evaluating Δ_B leads to varying values for Δ_B that are generally too small, even under the most optimal conditions. $Eu(DPM)_3$[4] has a K_B of *ca.* 34.2 l mol^{-1} with *n*-propylamine and K_B of *ca.* 9.7 l mol^{-1} with *neo*-pentanol. These values increase by at least 10-fold (to $\geqslant$100 l mol^{-1}) for the corresponding complexes with $Eu(FOD)_3$[4] shift reagent. However, the bound chemical shifts for the $Eu(FOD)_3$ complexes are nearly the same as for the $Eu(DPM)_3$ complexes. Finally, it is shown *definitively* that the association between $Eu(DPM)_3$ and either *n*-propylamine or *neo*-pentanol has 1:1 stoichiometry; with $Eu(FOD)_3$ a *tentative* assignment of 1:1 stoichiometry can be made.

Une analyse théorique est présentée sur l'équilibre entre un réactif lanthanide shift L et un substrat S. Pour $[S]_0 \gg [L]_0$, la courbe de $[S]_0$ en fonction de $(1/\delta)$ pour différents $[L]_0$ constants, est une droite dont la pente est $[L]_0\Delta_B$ et l'ordonnée à l'origine $-\{(1/K_B) + [L]_0\}$ où K_B est la constante d'équilibre de liaison, δ le déplacement chimique induit, et Δ_B le déplacement chimique de liaison. Une solution plus générale et plus précise utilisant un programme, est applicable pour tout rapport $[L]_0/[S]_0$. On a également montré que le procédé conventionnel pour évaluer Δ_B conduit à des valeurs variables généralement trop petites, même dans les conditions les plus optimales. L'$Eu(DPM)_3$ a un K_B de 34.2 l mol^{-1} avec la *n*-propylamine et un K_B de 9.7 l mol^{-1} avec le *néo*-pentanol. Ces valeurs croissent au moins de 10 fois (jusqu'à $\geqslant$ 100 l mol^{-1}) pour les complexes correspondants avec l'$Eu(FOD)_3$. Cependant les déplacements chimiques de liaison pour les complexes avec l'$Eu(FOD)_3$ et l'$Eu(DPM)_3$ sont pratiquement les mêmes. En définitive on a montré que l'association entre l'$Eu(DPM)_3$ et la *n*-propylamine ou le *néo*-pentanol est de stoéchiométrie 1:1; avec l'$Eu(FOD)_3$ cette stoéchiométrie possible peut être avancée.

Canadian Journal of Chemistry, **50**, 2119 (1972)

Introduction

The extraordinary surge of interest which has followed from Hinckley's discovery (3) of the lanthanide "shift-reagents" attests to the great importance of this area. Indeed it is already clear that applications using these substances will revolutionize ^1H n.m.r. studies of complex organic systems, at least for those which are soluble in a suitable organic solvent. For the vast majority of these present applications, the details of the mechanism by which the shift-reagent acts are unimportant — it suffices that such changes make a spectral assignment or analysis possible. Nevertheless, beyond the intrinsic interest which would follow from a fundamental description of the binding process, knowledge of the binding stoichiometry and equilibrium constants provides for an unequivocal determination of the "bound" chemical shift for each proton of an organic substrate (S) bound to a lanthanide shift reagent (L). When reliable bound chemical shifts have been determined for such complexes, it should be possible to establish with some confidence the conformation of the complex and hence of the organic moiety itself.

The present paper contains a detailed analysis of the equilibrium process which occurs when a lanthanide shift reagent combines with a substrate molecule having a suitable binding site. In particular, we show how to calculate the equilibrium binding constant (K_B) and stoichiometry, as well as the bound chemical

[1]This paper forms Part 3 of a series, "Nuclear Magnetic Resonance Studies of Paramagnetic Species"; for a preliminary communication, see ref. 1; for Part 2, see ref. 2.

[2]F. J. Nicholson Scholar; H. R. MacMillan Family Fellowship, 1971–1972.

[3]Alfred P. Sloan Foundation Research Fellow.

[4]Abbreviations: $Eu(DPM)_3$ for tris(dipivalomethanato)-europium(III); $Eu(FOD)_3$ for tris(2,2-dimethyl-6,6,7,7,-8,8,8-heptafluoro-3,5-octanedionato)europium(III).

Can. J. Chem. Downloaded from www.nrcresearchpress.com by 210.87.254.6 on 09/05/12
For personal use only.

Can. J. Chem. Downloaded from www.nrcresearchpress.com by 210.87.254.6 on 09/05/12
For personal use only.

shift (Δ_B) of the substrate molecule when it is associated with the lanthanide. Predictions based on this theory are subjected to rigorous experimental test.

As a consequence of the theory, it will be evident that the slope of a plot of observed shift *vs.* $[L]_0/[S]_0$ gives an empirical number (4) which can differ greatly from the actual Δ_B, and that the error can even be different for different protons in the same molecule.

Theory

(I) Fast Exchange Limit

The first step in analyzing the chemical shifts for the system,

$$[1] \qquad L + S \underset{k_{-1}}{\overset{k_1}{\rightleftharpoons}} LS,$$

(in which L denotes lanthanide, S denotes ligand or substrate, and LS is the lanthanide–substrate complex whose chemical shift we would like to obtain) is to establish whether the exchange rates are fast or slow on the n.m.r. time scale (5).

If k_{-1}, $k_1[L] \gg (\delta_{LS} - \delta_S)$, the fast-exchange limit, then there will be a single resonance centered at

$$[2] \qquad \delta_{obs} = f_S\delta_S + f_{LS}\delta_{LS}$$

where δ_S and δ_{LS} are the respective chemical shifts for S and LS, and f_S and f_{LS} are the respective concentration fractions of S at the two sites. But $f_S = 1 - f_{LS}$, so an "induced chemical shift", δ, may be defined as

$$[3] \qquad \delta = \delta_{obs} - \delta_S = f_{LS}(\delta_{LS} - \delta_S)$$

or simply

$$[4] \qquad \delta = f_{LS}\Delta_B$$

where Δ_B is the chemical shift for the LS complex relative to the chemical shift for free S.

Experimentally, the observation of a single resonance whose chemical shift varies linearly with the fraction of substrate present as complex is direct evidence that the fast-exchange limit applies. Using this criterion, it was found that the fast-exchange limit was valid for all data reported in this paper.

(II) Experiments in which $[L]_0$ is Varied at Constant $[S]_0$

Let $[L]_0$ and $[S]_0$ be the initial concentrations of lanthanide and substrate (see Experimental for mixing procedure). Then

$$[5] \qquad \delta = \frac{[LS]\Delta_B}{[LS] + [S]} = \frac{[LS]}{[S]_0}\Delta_B$$

Next, let the binding constant for process [1] be K_B:

$$[6] \qquad K_B = \frac{[LS]}{[L][S]} = \frac{[LS]}{([L]_0 - [LS])([S]_0 - [LS])}$$

It is now necessary to solve eq. 6 for [LS] and then substitute for [LS] in eq. 5, so as to determine the desired quantity Δ_B in terms of the measured parameters $[L]_0$, $[S]_0$, and δ. In order to avoid solving the quadratic eq. 6, it is convenient simply to restrict the experiments to the range,

$$[7] \qquad [S]_0 \gg [L]_0,$$

thus guaranteeing that $([S]_0 - [LS]) \simeq [S]_0$ in eq. 6. Using [7] to solve [6] for [LS], and substituting for [LS] in [5] gives,

$$[8] \qquad \delta = \frac{K_B[L]_0\Delta_B}{1 + K_B[S]_0}$$

Equation 8 is the principal result of this section. The immediate question now becomes, what will happen if one plots δ *vs.* $[L]_0/[S]_0$? The answer is clear for two simple limits:

(*a*) $K_B[S]_0 \gg 1$, *i.e.*, strong binding or high substrate concentration. In this limit, eq. 8 reduces to

$$[9] \qquad \delta = \Delta_B[L]_0/[S]_0$$

so that a plot of δ *vs.* $[L]_0/[S]_0$ will be a straight line through the origin, with slope, Δ_B.

(*b*) $K_B[S]_0 \ll 1$, *i.e.*, weak binding or low substrate concentration. In this limit, eq. 8 reduces to

$$[10] \qquad \delta = K_B\Delta_B[S]_0\left(\frac{[L]_0}{[S]_0}\right)$$

In other words, a plot of δ *vs.* $[L]_0/[S]_0$ will give a straight line whose slope is proportional to $[S]_0$.

Results *a* and *b* from eq. 8 suggest that in carrying out several sets of experiments (each set at a different $[S]_0$ level), then for low $[S]_0$ the slope of a plot of δ *vs.* $[L]_0/[S]_0$ will be proportional to $[S]_0$, while for large $[S]_0$ the

Can. J. Chem. Downloaded from www.nrcresearchpress.com by 210.87.254.6 on 09/05/12
For personal use only.

slope will simply be Δ_B independent of $[S]_0$. Therefore, *only at high substrate concentrations* is it permissible to take the slope of a plot of δ *vs.* $[L]_0/[S]_0$ as Δ_B. This conclusion is of quite practical significance, as shown in the Results section.

(III) Experiments in which $[S]_0$ is Varied at Constant $[L]_0$

Since it is now clear that there is no simple way to extract Δ_B from a single plot of δ *vs.* $[L]_0/[S]_0$ at constant $[S]_0$, one is led to seek out some other simple experiment which will yield the bound chemical shift. Returning to eq. 6, suppose that only the $[LS]^2$ term is neglected (6), then

$$[11] \qquad \delta = \frac{K_B[L]_0\Delta_B}{1 + K_B[S]_0 + K_B[L]_0}$$

which may be re-grouped to give

$$[12] \quad [S]_0 = [L]_0\Delta_B(1/\delta) - ((1/K_B) + [L_0])$$

Equation 12 gives the important fact that a plot of $[S]_0$ *vs.* $(1/\delta)$ gives a straight line whose slope is $[L]_0\Delta_B$ and whose *y*-intercept is $-((1/K_B) + [L]_0)$. Such a plot thus yields both Δ_B and K_B unambiguously.

However, as pointed out by Dahlquist and Raftery for analogous enzyme kinetics experiments (6), the approximations, $(1/K_B) \geqslant [S]_0$ and $\delta \ll \Delta_B$, are necessary to reach eq. 12. The safest procedure is therefore to solve the full quadratic eq. 6 according to the following computerized procedure first suggested by Sykes (7). First, guess a value for K_B and use this value to compute [LS] from eq. 6; this gives [LS] expressed as a function of $[L]_0$ and $[S]_0$. Next, perform experiments in which $[L]_0$ is fixed and $[S]_0$ is varied. Use the expression for [LS] to compute [LS] for each of the experimental $[S]_0$ values. Next, plot δ *vs.* $[LS]/[L]_0$ to obtain Δ_B from eq. 5. This plot (since the wrong value of K_B was probably guessed in the first place) will usually give a curve rather than a straight line. Thus, as a criterion of how well K_B was chosen, let the computer calculate a least mean square slope for the plot and also the standard deviation for the slope. This whole procedure is now repeated for say, 100 values of K_B spanning three powers of 10 in magnitude, and the standard deviation of the slope is plotted as a function of K_B. The correct value of K_B is then taken as the one which gives the smallest standard deviation in the plots of δ *vs.* $[LS]/[L]_0$.

For practical purposes, we have found that for low $[S]_0$ concentrations (see Discussion) the graphical treatment based on eq. 12 gives reasonable agreement with the full computer treatment outlined above, and may often be preferable, inasmuch as precise values for K_B from the computer treatment seem to require quite accurate shift measurements.

All values of K_B and Δ_B reported in this paper were taken from low-concentration experiments in which $[S]_0$ was varied at constant $[L]_0$. In principle, one might hope to extract K_B and Δ_B from experiments in which $[L]_0$ is varied at constant $[S]_0$, based on the slopes of plots of δ *vs.* $[L]_0$ according to eq. 8. There are two reasons why this procedure is impractical. First, the slope of such a plot depends on $[S]_0$, so one would have to carry out several series of experiments at different $[S]_0$ values, necessitating many more experimental measurements than a single "run" in which $[S]_0$ is plotted *vs.* $(1/\delta)$. Second, when $[L]_0$ is changed, substantial changes in the bulk magnetic susceptibility of the solution are introduced, and even an internal standard may not compensate properly for them.

(IV) Stoichiometry

In this section, the implications of a one-step binding process,

$$[13] \qquad L + 2S \underset{k_{-1}}{\overset{k_1}{\rightleftharpoons}} LS_2$$

are discussed. The actual binding process might involve several steps; in writing [13], it is simply assumed that there is a single step which is associated with the large change in chemical shift between "free" and "bound" substrate. It is only this step which will affect n.m.r. measurements (5). It is easy to imagine multi-step binding phenomena which will not satisfy eq. 13 even on an n.m.r. basis — such phenomena are not treated here, because it will be not possible in general to obtain separate binding parameters for even a two-step process, when the n.m.r. data fall in the fast-exchange limit.

For the one-step 2:1 binding model, [13], the criterion for fast exchange is readily shown to be the same as for the case of 1:1 binding; thus an observed proportionality between δ and f_{LS_2}

Can. J. Chem. Downloaded from www.nrcresearchpress.com by 210.87.254.6 on 09/05/12
For personal use only.

is direct evidence that the fast-exchange limit is satisfied.

The equilibrium binding constant for process [13] is

$$[14] \qquad K = \frac{[LS_2]}{[L][S]^2}$$

and it follows that

$$[15] \qquad \delta = \frac{[LS_2]}{[S]_0}\Delta_B$$

if we assume that both S molecules have the same chemical shift when bound to the lanthanide. Solving [15] for $[LS_2]$ and substituting into [14] as in section III, and again restricting experiments to the range $[S]_0 \gg [L]_0$ (so that $(\delta/\Delta) \ll 1$), yields

$$[16] \qquad [S]_0^2 - \frac{\Delta}{\delta}[L]_0[S]_0 + (1/K) = 0$$

(It may be noted that eq. 16 has the same form as eq. 12 if one makes the correspondence, $K[S]_0 = K_B$; the $[L]_0$ term in eq. 12 is usually negligible.)

A criterion for stoichiometry is now available. One need simply specify $[L]_0$, Δ_B, and K, and then use eq. 16 to compute a set of δ-values from a given range of $[S]_0$-values; the values may then be used to construct a plot of $[S]_0$ *vs.* $(1/\delta)$ as shown in Fig. 1. The figure shows the result for several choices of K_B which span the range of K_B-values actually determined in the present experiments. To facilitate comparison with the result for 1:1 binding, a plot of $[S]_0$ *vs.* $(1/\delta)$ for 1:1 binding is also shown; to make the comparison as direct as possible, values of $K_B = 0.1K$ were chosen since typical experimental $[S]_0$ values were about 0.1 *M*. The plots clearly show that for either large K_B (strong binding) or large $[S]_0$, one cannot distinguish between 1:1 binding and 2:1 binding from a plot of this type. On the other hand, when K_B is small enough to be measurable, there are readily observable differences between 1:1 and 2:1 binding. Since our present $[S]_0$ *vs.* $(1/\delta)$ plots (*vide infra*) are linear, it is evident at once that the binding is either strong and/or 1:1. If the experimental extrapolations to $(1/\delta) = 0$ give a *y*-intercept which is more negative than $-[L]_0$, then a straight-line experimental plot is definitive proof that the binding is 1:1 rather than 2:1.

When K_B is large (strong binding), there are no well-controlled measures of stoichiometry. However, some information may be obtained from (high-concentration) experiments in which δ is determined as a function of $[L]_0$ at constant $[S]_0$, and the data are displayed in a plot of δ *vs.* $[L]_0/[S]_0$. If either K_B or $[S]_0$ were infinitely large, such a plot would simply be a straight line from the origin to the end point, $\delta = \Delta_B$ at $[L]_0/[S]_0 = 1$. For smaller $[S]_0$, there will no longer be a sharp end point and one will observe a family of curves which converge for large $[S]_0$ (see Results). Experimentally, then, one need construct several such plots at increasing $[S]_0$ until the lines begin to converge; extrapolation of the limiting line to $\delta = \Delta_B$ (where Δ_B has been determined reliably from low-concentration data according to the method of section III) will then give an *x*-intercept of $(1/n)$.[5]

In conclusion, the most critical test for 1:1 stoichiometry is the linearity of a plot of $[S]_0$ *vs.* $(1/\delta)$, where the range of $[S]_0$ values should cover an order of magnitude in concentration, and include the lowest accessible concentrations for best results.

Experimental

It must be emphasized that all apparatus and materials used in these experiments were carefully dried before use. Any lapse in such precautions has always led to poor results.

Materials Used

Tris(dipivalomethanato)europium(III) was prepared from europium oxide[6] (99.99%) following the method of Eisentraut and Sievers (8). The material from the reaction was stored in a vacuum desiccator over phosphorus pentoxide. A small sample was vacuum sublimed at 145° immediately prior to an experiment. All manipulations after sublimation were carried out in a glove-bag which had been flushed several times with dry nitrogen. Tris(2,2-dimethyl-6,6,7,7,8,8,8-heptafluoro-3,5-octanedionato)europium(III) was also prepared from europium oxide, but by the method of Springer *et al.* (9). The complex was recrystallized twice from methylene chloride and was thereafter stored in a vacuum desiccator as described above. This is important because it has been reported (10) that this compound can absorb 1 mol equiv of water from the atmosphere. *n*-Propyl-

[5]In principle, one might hope to obtain K_B in strong-binding situations by fitting the δ *vs.* $[L]_0/[S]_0$ curve of the preceding paragraph. In the Discussion, it is shown that this method may not work, even if an independently determined Δ_B is used for the fit.

[6]Purchased from Alfa Inorganics, Inc.

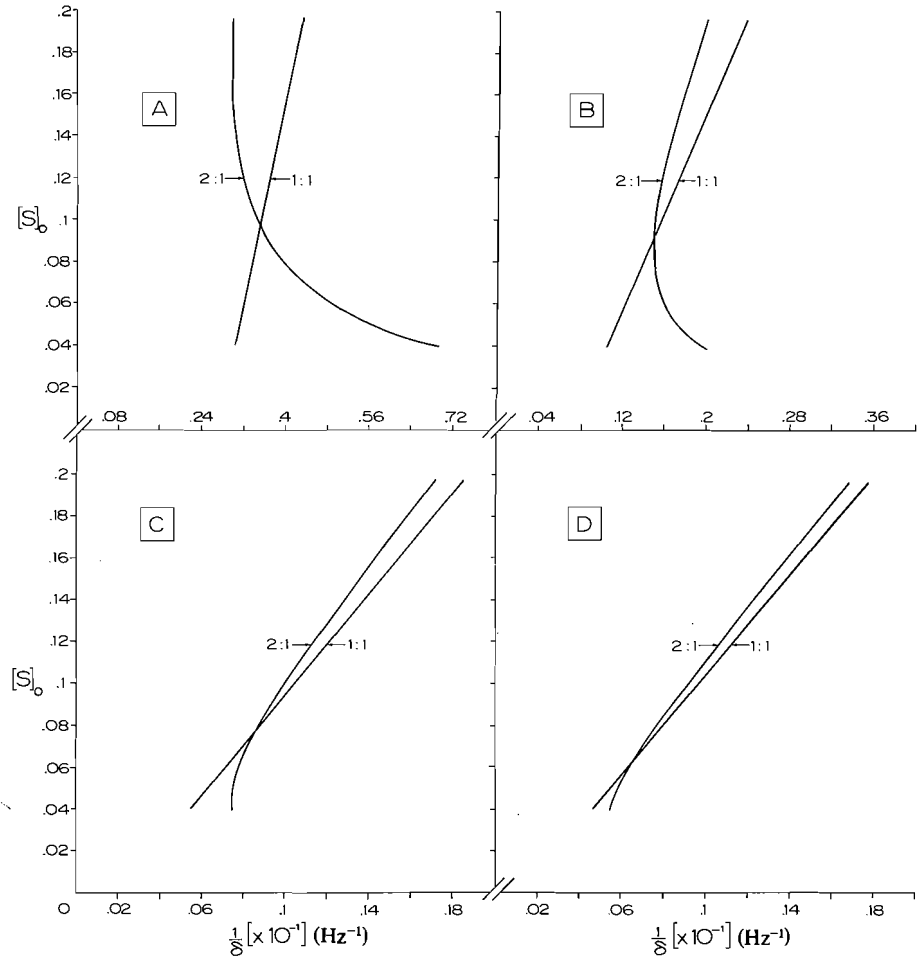

FIG. 1. Graphs of initial substrate concentration $[S]_0$ *vs.* $(1/\delta)$ for a hypothetical substrate of $\Delta_B = 2000$ Hz in the presence of shift reagent of concentration $[L]_0 = 0.006$ *M*. For each graph, the binding is assumed to be either 1:1 (with corresponding binding constant, K_B or 2:1 with binding constant, K). (A) $K = 32$, $K_B = 3.2$; (B) $K = 126$, $K_B = 12.6$; (C) $K = 501$, $K_B = 50.1$; (D) $K = 1000$, $K_B = 100$.

amine (**1**) from Eastman Organic Chemicals was purified by distillation from KOH pellets into a sealed receiver also containing KOH pellets. The material had b.p. 49.0°. *neo*-Pentanol (**2**) was purchased from Matheson Coleman and Bell and was purified by distillation from calcium hydride. The material had b.p. 114 °C. Deuterochloroform (99.8%) from Merck Sharp and Dohme, Montreal was stored over Linde molecular sieve (4A) which had been heated in an oven at 100° for 24 h.

Nuclear Magnetic Resonance Measurements

All measurements were made with a Varian XL-100 instrument operating in the frequency-swept mode with a probe temperature of 38.8°. Deuterochloroform was used as solvent with tetramethylsilane as the internal reference. The preparation of all solutions was conducted under dry nitrogen in a glove-bag using apparatus that had been baked at 110° immediately prior to use.

Method 1. Constant $[S]_0$, Varying $[L]_0$

A series of standard solutions, each containing a known amount of the substrate (*ca.* 0.6, 0.2, 0.08, 0.04 *M*) was prepared. One particular standard solution was then selected and 1.0 ml of this solution was then used to dissolve a known quantity of the lanthanide reagent (*ca.* 0.015 g, 0.02 *M* of $Eu(DPM)_3$; *ca.* 0.190 g, 0.175 *M* of $Eu(FOD)_3$). The spectrum of this mixture then gave the maximum shift. Further spectra were run after each successive addition of a 0.10 ml aliquot of the standard substrate solution. In each case the observed shift decreased.

Method 2. Constant $[L]_0$, Varying $[S]_0$

The lanthanide reagent (0.042 g, 0.012 *M* of $Eu(DPM)_3$;

Can. J. Chem. Downloaded from www.nrcresearchpress.com by 210.87.254.6 on 09/05/12
For personal use only.

Can. J. Chem. Downloaded from www.nrcresearchpress.com by 210.87.254.6 on 09/05/12
For personal use only.

TABLE 1. Calculated values of bound chemical shifts (Δ_B), binding constants (K_B) and stoichiometry for complexes of organic substrates with either $Eu(DPM)_3$[4] or $Eu(FOD)_3$[4]

Substrate		$Eu(DPM)_3$					$Eu(FOD)_3$			
		Δ_B		K_B			Δ_B	K_B		
		Graph*	Computer†	Graph*	Computer†	Stoichiometry	Graph*	Graph*	Computer†	Stoichiometry‡
n-Propylamine	H_1	12.8	11.0	32.1	40.2	1:1	19.0	⩾100	⩾100	0.7±0.1
	H_2	7.7	6.5	32.9	43.1	1:1	12.7	⩾100	⩾100	—
	H_3	4.1	3.7	37.8	44.6	1:1	6.6	⩾100	⩾100	—
neo-Pentanol	H_1	19.7	18.7	9.7	10.1	1:1	20.8	⩾100	⩾100	0.9±0.1
	H_3	7.6	7.0	9.8	10.5	1:1	8.3	⩾100	⩾100	—

*Values of Δ_B (p.p.m.) and K_B (l mol^{-1}) derived from a least-squares fit of a plot of $[S]_0$ *vs.* $(1/\delta)$; precision of either result is ±10%.
†Values of Δ_B and K_B derived (from the same raw data) by a more exact formula, based on an iterative computer program (see text); precision of either result is ±10%.
‡These values should be regarded with some skepticism (see text).

ca. 0.070 g, 0.012 *M* of $Eu(FOD)_3$) was dissolved in deuterochloroform (4.8 ml) and tetramethylsilane (0.2 ml). The substrate was separately dissolved in 5.0 ml of deuterochloroform. Aliquots (0.50 ml) of the lanthanide solution were then added to each of a series of 5–10 graduated 1.0 ml flasks. To each of these flasks was now added varying amounts of the stock solution of substrate; *e.g.*, vial 1, 0.5 ml; vial 2, 0.4 ml; etc. The content of each flask was then made up to 1.0 ml by further addition of deuterochloroform. Each solution was then placed in a separate n.m.r. tube which was capped and stored in a thermostatted water bath prior to measurement.

All plots of the experimental data were made with a Hewlett–Packard Calculator (model 9100 B) and a Hewlett–Packard Calculator Plotter (model 9125 A). We are indebted to Professor Ross Stewart of this Department for making this equipment available to us.

Results and Discussion

It is convenient first to discuss the methods which we believe provide for general and accurate evaluation of Δ_B and K_B, followed by a demonstration that the slope of a plot of δ *vs.* $[L]_0/[S]_0$ (4) will not in general be a good measure of Δ_B, and that the error can vary even among different protons in the same molecule for those measurements. Finally, determination of the stoichiometry of ligand–lanthanide complexes is indicated, followed by a discussion of the interesting ligand-dependence of the K_B and Δ_B values.

Solutions of *n*-propylamine, **1**, and of *neo*-pentanol, **2**, each with $Eu(DPM)_3$, were prepared according to the procedure outlined in the Experimental as method 2. The chemical shifts of these solutions were then measured, and the results plotted on a graph of $[S]_0$ *vs.* $(1/\delta)$; the plot for *n*-propylamine is shown in Fig. 2. The values of K_B and Δ_B were obtained from these plots following the relationship given in eq. 12; the numerical values for these parameters are shown in Table 1. It is expected that the same value should be obtained for K_B regardless of which proton is used for its determination. This may be confirmed experimentally by noting that the plots for protons H_1, H_2, and H_3 in Fig. 2 all intercept the *y*-axis at the same point. It may also be noted that the Δ_B-values obtained by this method vary inversely with distance from the coordination site, as expected for a pseudo-contact shift.[7]

Similar results were obtained for *neo*-pentanol, and the values of Δ_B and K_B for that substrate are also summarized in Table 1. Again, the high internal consistency between the evaluations of K_B based on different proton resonances is evident.

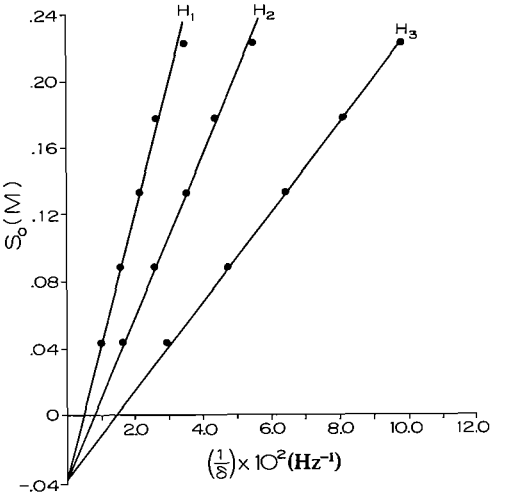

FIG. 2. Graph of $[S]_0$ *vs.* $(1/\delta)$ for the interaction of *n*-propylamine (0.23 to 0.04 *M*) with $Eu(DPM)_3$ (*ca.* 0.006 *M*) in deuterochloroform solution. The separate lines are for protons H_1, H_2, and H_3 of *n*-propylamine. The precision of the K_B evaluation is indicated by the close convergence of the three lines to the same *y*-intercept.

The experimental data obtained for the interaction of **1** and **2** with $Eu(DPM)_3$ were then analyzed by the computer-based method outlined in section III of the Theory. The values of K_B and Δ_B calculated in this way are compared in Table 1 with the values obtained by the more approximate graphical method. The excellent agreement between the two sets of values indicates that the conditions which are implicit in the graphical analysis are satisfied in these experiments; this point will be explored more fully later in this section.

Attention was next directed to the interaction of **1** and **2** with $Eu(FOD)_3$. Following the above methods, attempts were made to process the experimental data by both the graphical and computer-based methods. With either treatment, it was possible to obtain Δ_B, but K_B was too large to be measured. Figure 3 shows why. Δ_B is taken from the slopes of the lines in Fig. 3 and is readily determined. However, the *y*-intercept depends on $(1/K_B)$, and when K_B is large, the *y*-intercept is so close to zero that K_B cannot

[7]However, it must be remembered that an angular dependence is also involved.

Can. J. Chem. Downloaded from www.nrcresearchpress.com by 210.87.254.6 on 09/05/12
For personal use only.

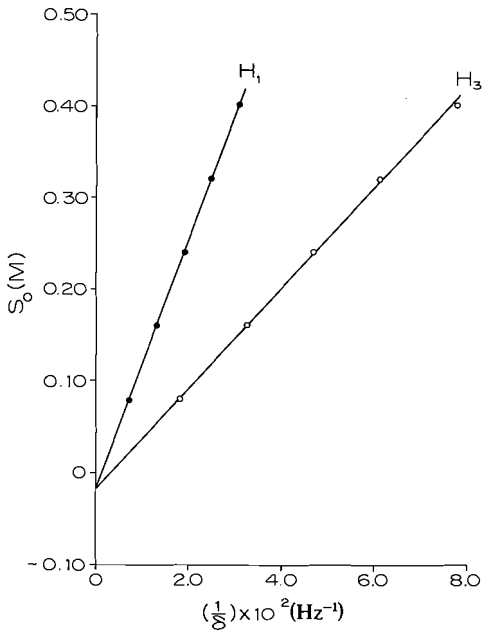

FIG. 3. Plot of $[S]_0$ *vs.* $(1/\delta)$ for the interaction of *neo*-pentanol (0.4 to 0.08 *M*) with $Eu(FOD)_3$ (*ca.* 0.006 *M*) in deuterochloroform solution. The separate lines are for protons H_1 and H_3 of *neo*-pentanol; the different slopes of the two lines are due to the different values of Δ_B for the two respective protons.

be determined with any confidence; in this case only a lower limit for K_B may be deduced. Moreover, the estimate for K_B depends critically on the presence of any inactive shift reagent, as discussed at the end of this section.

It should be appreciated that the graphical method is an approximation which is not expected to be valid when K_B is large. The computer-based method involves no approximations, but simply becomes numerically insensitive when the limit, $(1/K_B) \geqslant [S]_0$, is not satisfied. For the $Eu(FOD)_3$ experiments just mentioned, $(1/K_B) \leqslant 10^{-2}$ mol l^{-1}, while $[S]_0 =$ 0.1 mol l^{-1}, so that even the computer method will yield only a lower limit for K_B.

Similar experiments with *n*-propylamine and $Eu(FOD)_3$ also gave precise linear plots. Again it was possible to obtain the Δ_B values graphically to yield the data listed in Table 1, but again K_B was too large to be measured; all that can be stated with certainty is that K_B is at least 100 l mol^{-1}.

It is now useful to consider the evaluation of Δ_B from plots of δ *vs.* $[L]_0/[S]_0$ according to method 1 of the Experimental to show why the slope of such a plot (4) should not be taken as Δ_B. Recent work by Andersen and Uebel (11), Williams and coworkers (12), and Armitage *et al.* (1) has shown that the slope of such a plot can vary markedly with the *absolute* concentration of substrate in a set of experiments with different $[S]_0$-values. This variation is readily accounted for by reference to two possible limiting cases of eq. 8 of section II of the Theory.

For the interaction of $Eu(DPM)_3$ with **1** and **2**, the limiting condition, $K_B[S]_0 \ll 1$ pertains up to an $[S]_0$ level of at least *ca.* 0.04 *M*, so that eq. 8 reduces to eq. 10 rather than to the anticipated eq. 9. Only for the highest *neo*-pentanol concentration of 0.6 *M*, for which $K_B[S]_0 = 5.8$, is the desired limit of $K_B[S]_0 \gg 1$ effectively reached, since at this concentration the Δ_B-value of 20.5 p.p.m. is within experimental error of the true value of 19.7 p.p.m. (derived from the H_1 proton resonance by the method of section III of the Theory). It is thus neither correct, nor does it suffice to report values of Δ_B for different substrates, even if the molarity of a given substrate is kept constant, unless experimental evidence shows that the molarity of the substrate involved is large enough to satisfy the limit, $K_B[S]_0 \gg 1$, so that eq. 8 reduces to eq. 9. Even under these optimum conditions, K_B cannot be reliably determined (see below).

One issue of continuing concern is the purity of the lanthanide reagent used. It follows from the Theory section that a plot of δ *vs.* $[L]_0$ for any particular fixed concentration of $[S]_0$ should intercept the *x*-axis at the origin if the lanthanide reagent is "pure"; if it is not, then the *x*-intercept of the plot should indicate the amount of "impurity" or "inactive" reagent, as shown clearly for the present experiments in Fig. 4.

With regard to the "activity" of the lanthanide reagent itself, it will be noted that the data listed in Table 1 differ somewhat from those previously reported in a preliminary communication. This is because the lanthanide reagents used in the present study were purified and the solutions prepared under more rigorously anhydrous conditions than were employed[8] during

[8]The present experiments were performed in a polythene glove bag which was continuously flushed with dry nitrogen

Can. J. Chem. Downloaded from www.nrcresearchpress.com by 210.87.254.6 on 09/05/12
For personal use only.

Can. J. Chem. Downloaded from www.nrcresearchpress.com by 210.87.254.6 on 09/05/12
For personal use only.

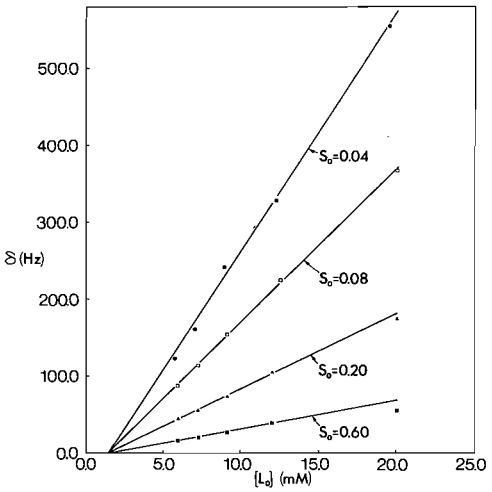

FIG. 4. Plot of δ *vs.* $[L]_0$ for the interaction of *neo*-pentanol (whose concentration was fixed at the value stated for each line) with $Eu(DPM)_3$ (*ca.* 0.02 to 0.005 *M*) in deuterochloroform solution. All shifts are for the H_1 proton of *neo*-pentanol. The lines converge to a point on the *x*-axis which accurately indicates the amount of inactive $Eu(DPM)_3$.

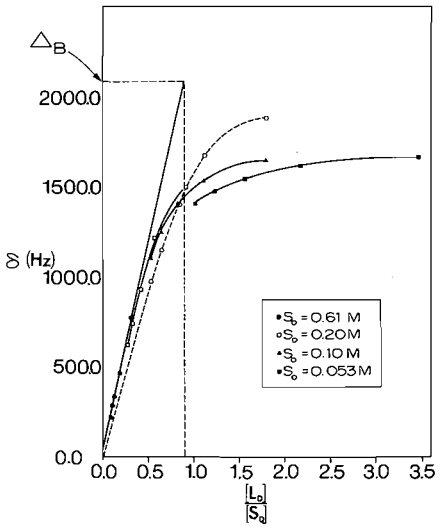

FIG. 5. Plot of δ (induced chemical shift for the H_1 proton) *vs.* ratio of the initial concentration of $Eu(FOD)_3$, $[L]_0$, to *neo*-pentanol, $[S]_0$, in deuterochloroform solvent. The solid lines represent experiments in which $[L]_0$ was varied while keeping $[S]_0$ constant at the value listed for that curve. The dotted line (see text) is a theoretical fit to the $[S]_0 = 0.1$ *M* curve, based on a known value for Δ_B and with K_B magnitude chosen to fit the middle data point of that curve exactly.

the experiments previously described (1). However, it must be emphasized that both the present measurements and those described previously are precisely reproducible. The important conclusion here is that although it is possible to obtain data which are *internally consistent* in a given laboratory, these data may differ significantly from data obtained elsewhere. Our Fig. 4 affords a simple test for the "activity" of a given batch of lanthanide reagent, and such plots may prove useful in standardizing shift reagent results.

It is now appropriate to consider the stoichiometry for the combination of a substrate with a lanthanide shift reagent. Prior to this study, the stoichiometry was unknown, although Rondeau and Sievers' experiments (10) with $Eu(FOD)_3$ leave the impression that the leveling-off of a graph of δ *vs.* $[L]_0/[S]_0$ at a mole ratio of approximately 1:1 might be taken to indicate a 1:1 stoichiometry. In the Theory section, it was shown that such a conclusion is warranted only for cases where K_B and $[S]_0$ are large; Fig. 5 illustrates several such plots determined at different $[S]_0$ levels, for the interaction of *neo*-pentanol with $Eu(FOD)_3$. In this case, the limiting line (the left-most points in Fig. 5) extrapolated to the known Δ_B-value gives a corresponding L/S ratio of 0.9:1, or about 1:1. However, the data points correspond to different $[L]_0$ concentrations, and when $[L]_0$ is changed there will be large changes in the bulk magnetic susceptibility of the solution, and these changes may not be compensated correctly even by an internal standard. Indeed, the poor internal consistency of the results is clearly evident in the dotted line of Fig. 5. This line was obtained by using the middle data point in the $[S]_0 = 0.1$ *M* data set to compute K_B; this value of K_B was then used to obtain the dotted line by using eq. 5 and the full quadratic form of eq. 6. It is evident that the dotted line gives a poor fit to the remaining data points in the $[S]_0 = 0.1$ *M* set. Since it is now obvious that experiments in which $[L]_0$ is varied can give inconsistent results, it is not surprising that for the interaction of *n*-propylamine with $Eu(FOD)_3$, the stoichiometry deduced from similar experiments is not even

and which was located in an airconditioned room. Previously, the glove bag alone was used in an ordinary laboratory. In both instances the apparatus was baked in an oven at 110° and all solvents were rigorously dried.

integral. In conclusion, when the binding is strong (large K_B), these experiments do not reliably predict stoichiometry.

For the weaker binding of **1** or **2** to $Eu(DPM)_3$, the outlook is much improved. As argued in section IV of the Theory, the linearity of a plot of $[S]_0$ *vs.* $(1/\delta)$ is direct proof of 1:1 binding (compare Figs. 1 and 2). Since the range of choices of K_B illustrated in Fig. 1 brackets the observed K_B-values (see Table 1) for binding of **1** or **2** to $Eu(DPM)_3$, there can be no doubt that the binding is 1:1 in each of these two cases.

Practically speaking, then, when the binding is weak ($K_B < 100\ l\ mol^{-1}$), it is possible to obtain reliable, consistent values for Δ_B, K_B, and solution stoichiometry; when the binding is strong ($K_B \geqslant 100\ l\ mol^{-1}$), Δ_B may still be determined accurately, a lower bound for K_B can be proposed, but the stoichiometry may be indicated only approximately.

It is possible that the solvent (chloroform) used in these studies may bind to the shift reagents; if such binding were present, the apparent K_B computed by our methods would be smaller than the K_B which would be observed in a totally inert solvent. This in no way vitiates the fact that our reported K_B-values correctly measure the binding constant for the stated substrates to the stated shift reagent in the stated solvent.

This discussion may be terminated with some comments on the chemical significance of the above findings. When this study was initiated, it was already known (10) that for any particular substrate, a given quantity of $Eu(FOD)_3$ would produce a greater shift than an equal amount of $Eu(DPM)_3$. From the data listed in Table 1, it is clear that the principal source of this enhanced effectiveness is the roughly 10-fold increase in binding constant, since the bound chemical shifts are nearly the same for a given substrate.

A second significant feature derived from the data of Table 1 is that *n*-propylamine has a higher K_B-value (stronger binding) than *neo*-pentanol for association with either $Eu(DPM)_3$ or $Eu(FOD)_3$. In the case of $Eu(DPM)_3$, for which accurate values of K_B are available, the amine binds 3.5 times as strongly as the alcohol. These results suggest that the sequence of observed shifts for various substrates given by Sanders and Williams (13) may be correlated primarily with variation in the binding constants. This speculation may readily be subjected to experimental test, as can also the generality concerning K_B-differences between $Eu(DPM)_3$ and $Eu(FOD)_3$.

Summary

In this paper, we have developed and tested a method for evaluating Δ_B and K_B values as well as stoichiometry for binding of substrates to lanthanide shift reagents. Our results exemplify the potential utility of these parameters in elucidating the mechanism of action of two useful shift reagents; specifically, there is preliminary indication of the effect of changes in either the type of binding site of the substrate or the chelating group attached to the metal. Clearly a number of other chemical variables can now be examined with a perspective not previously possible. Included in this category are the effects which accompany changing either the lanthanide metal or solvent used: these and other possibilities are under investigation.

One final cautionary statement must be reiterated. Much of the quantitative treatment used in this paper is formally analogous to that used in enzyme inhibition studies. Pressing the analogy further, it now seems clear that variations in the "activity" of lanthanide shift-reagents are to be expected, and that these activity differences will be reflected in the calculated K_B and Δ_B. As in enzyme studies, then, one expects consistent results from a given shift-reagent preparation, but one is not alarmed to find differences between results from different preparations. For example, in a previous preliminary communication, (1) we reported data corresponding to some of the numbers in Table 1; in the earlier work, a plot of the type shown in Fig. 4 of this paper showed that the earlier preparation of shift reagent was less pure than that used in the present work. This explains why the present Δ_B-values are smaller while the K_B-values are larger than those obtained with a shift-reagent of lower purity. It was noted in the Discussion that there were *detectable* amounts of "inactive" material in the present shift-reagents; if this impurity can be removed, the Δ_B-values in Table 1 should decrease slightly and the K_B-values increase slightly.

Can. J. Chem. Downloaded from www.nrcresearchpress.com by 210.87.254.6 on 09/05/12
For personal use only.

It is a pleasure for two of us to thank the National Research Council of Canada for financial support (L.D.H., A-1905; A.G.M., A-6178).

1. IAN ARMITAGE, G. DUNSMORE, L. D. HALL, and A. G. MARSHALL. Chem. Commun. 1281 (1971).
2. IAN ARMITAGE, J. R. CAMPBELL, and L. D. HALL. Can. J. Chem. This issue.
3. C. C. HINCKLEY. J. Am. Chem. Soc. **91**, 5160 (1969).
4. P. V. DEMARCO, T. K. ELZEY, R. B. LEWIS, and E. WENKERT. J. Am. Chem. Soc. **92**, 5734, 5737 (1970).
5. W. DEW. HORROCKS, JR. and J. P. SIPE, III. J. Am. Chem. Soc. **93**, 6800 (1971).
6. F. W. DAHLQUIST and M. A. RAFTERY. Biochem. 7, 3269 (1968).
7. B. D. SYKES. J. Am. Chem. Soc. **91**, 949 (1969).
8. K. J. EISENTRAUT and R. E. SIEVERS. J. Am. Chem. Soc. **87**, 5254 (1965).
9. L. S. SPRINGER, JR., D. W. MEEK, and R. E. SIEVERS. Inorg. Chem. **6**, No. 6, 1105 (1967).
10. R. E. RONDEAU and R. E. SIEVERS. J. Am. Chem. Soc. **93**, 1522 (1971).
11. K. K. ANDERSEN and J. J. UEBEL. Tetrahedron Lett. 5253 (1970).
12. D. R. CRUMP, J. K. M. SANDERS, and D. H. WILLIAMS. Tetrahedron Lett. 4419 (1970).
13. J. K. M. SANDERS and D. H. WILLIAMS. J. Am. Chem. Soc. **93**, 641 (1971).

Can. J. Chem. Downloaded from www.nrcresearchpress.com by 210.87.254.6 on 09/05/12
For personal use only.

The Crystalline Structure of Poly-β,D(1→4′)mannose: Mannan I

I. NIEDUSZYNSKI[1] AND R. H. MARCHESSAULT

Département de Chimie, Université de Montréal, C.P. 6128, Montréal, Québec

Received January 24, 1972

The crystallographic structure of mannan I has been examined by X-ray fiber diffraction, polarized i.r. spectroscopy, and computer chain-packing methods. The combination of X-ray intensity data and the chain packing analyses have shown that the overall number of permissible structures is very limited so that van der Waals' forces play a major role in packing. It was concluded that the chain senses are anti-parallel. The interpretation of the polarized i.r. spectra in the OH stretching region is in line with the presence of an intra-molecular hydrogen-bond between O(3)...O(5′). The awkward "knobby" shape of the mannan molecule, largely a result of the axial disposition of O(2)—H, lends itself to a close packing mainly determined by van der Waals' forces. The considerable similarity between X-ray and i.r. data from mannans and glucomannans would indicate that structural conclusions about the former might relate to the latter.

La structure cristallographique du mannan I a été réexaminée par la diffraction aux rayons-x de fibre, par la spectroscopie i.r. en lumière polarisée et par les méthodes de calcul d'entassement des chaînes dans la maille. La combinaison des données sur l'intensité des rayons-x et les analyses des chaînes compactes, ont montré que le nombre global de structures permises est très limité de sorte que les forces de van der Waals jouent un rôle majeur dans l'entassement. On a conclu à l'antiparallélisme des directions des chaînes. L'interprétation du spectre i.r. polarisé, dans la région d'élongation du OH, est conforme à la présence d'une liaison hydrogène intramoléculaire entre O(3)...O(5′). La forme "noueuse et disgracieuse" de la molécule de Mannan, en grande partie due à la disposition axiale de O(2)—H, se prête elle-même à un tassement serré, déterminé surtout par les forces de van der Waals. La grande similitude dans les données des rayons-x et de l'i.r. entre les mannans et les glucomannans, indiquerait que les conclusions sur les structures du premier seraient liées au second.

Canadian Journal of Chemistry, **50**, 2130 (1972)

Introduction

Polymers of β,(1 → 4′)-linked D-mannose residues (1) are abundant in nature: mannan, which comprises solely D-mannose residues is a major constituent of the endosperms of palm (2), date (3), and coffee beans (4) and is also able to replace cellulose as the crystalline structural component in the cell walls of certain green algae (5–6); glucomannans and galactoglucomannans (both containing about 75% of D-mannose) are amongst the principal wood hemicelluloses (7), accounting for approximately 20% of the weight of softwoods.

Ivory-nut mannan is believed to occur in two forms, A and B, which differ in their solubility in dilute alkali. Meier (3) found that while mannan A has a degree of polymerization ($\overline{DP}_n$) of about 20 and appears granular in the electron microscope, mannan B has a $\overline{DP}_n$ of 80 and has a fibrillar structure. Mackie and Sellen (8) determined that the $\overline{DP}_w$ of mannan from the cell wall of the green alga *Codium fragile* ranges from below 20 to above 10 000, the peak in the distribution curve occurring at about 600.

The first X-ray diagram of mannan (9) was observed in 1928, but it was not until 1961 that Frei and Preston (5) reported the first oriented pattern. These authors subsequently assigned the spacings to an orthorhombic unit cell with

$$a = 7.21, \quad b(\text{fiber axis}) = 10.27, \quad c = 8.82 \text{ Å}$$

and proposed a provisional parallel chain structure on the basis of the observed X-ray reflections. They were also able to recrystallize mannan into a different lattice after treatment with alkali, which they characterized and named mannan II by analogy with cellulose. They showed that mannan II has a hydrated structure with an uniplanar orientation. Bittiger and Marchessault (10) have proposed a folded-chain structure for a mannan II prepared from *Tubera salep* by precipitation from an alkaline solution. Recently, Bittiger (11) has shown that when mannan is precipitated from aqueous butanol lamellar structures of mannan I are formed. It seems likely that this is a classical polymer single crystal structure (12) since the lamellae were

[1]Present address: H. H. Wills Laboratory, Department of Physics, Bristol University, Great Britain.

Can. J. Chem. Downloaded from www.nrcresearchpress.com by 210.87.254.40 on 09/05/12
For personal use only.

Can. J. Chem. Downloaded from www.nrcresearchpress.com by 210.87.254.40 on 09/05/12
For personal use only.

about 200 Å thick when material of degree of polymerization of 200–300 was precipitated. Very little i.r. spectroscopy of mannan has been recorded except for the band assignments of ivory-nut mannan (13).

Although D-mannose only differs from D-glucose in the configuration at C(2), mannan differs from cellulose in several respects: it has a considerably lower average degree of polymerization, its microfibrils are much more sensitive to physical and chemical treatment than those of cellulose (14), and in woody plants it is a hetero-copolysaccharide with glucose in the backbone and galactose as side-group (7). Both polymers are positively birefringent but the cellulose X-ray diagram frequently displays evidence of a selective uniplanar orientation which is absent in mannan I (6). The conformational analyses of cellulose and mannan (15–17) have shown that the mannan chain has a slightly larger range of preferred conformations in terms of the conformational angles (ϕ, ψ) which govern rotation at the glycosidic linkage.

In the present investigation the crystallographic structure of mannan I has been examined by X-ray fiber diffraction, polarized i.r. spectroscopy, and computer chain-packing methods.

Materials and Methods

The materials used in this investigation were an oriented mannan from the green alga *Cymopolia barbata*, mannan from ivory-nut (*Phytalephas macrocarpa*), and a glucomannan[2] from white pine (*Pinus strobus*). X-Ray diffraction and i.r. spectroscopy were used to identify the two former as typical β,(1 → 4′)-poly-D-anhydromannose.

The algal cells were first treated with cold 0.1 *N* hydrochloric acid to remove the calcite encrustations and then with successive aliquots of boiling water. The latter treatment diminished the level of diffuse scattering, particularly near the second meridional reflection. The inner wall layers of the basal cells were stretched by about 10–20% before X-ray examination. X-Ray fiber photographs were taken with nickel-filtered CuKα radiation at 40 kV and 20 mA; the humidity being controlled with saturated salt solutions during the exposures.

X-Ray fiber diagrams similar to those presented by Frei and Preston (6) were obtained. In view of the high level of diffuse scattering it was not generally possible to record reliable intensities with the microdensitometer. A Joyce–Loebl Mk. IIIC microdensitometer was, nevertheless, used to monitor a few of the more clearly defined reflections while other intensities were established visually by means of the multiple film method. The observed intensities were corrected for Lorentz and polarization factors, the temperature factor corrections being made on the calculated intensities. Since no uniplanar orientation was observed (nor could it be induced), the intensity values were considered to be cylindrically-averaged.

The i.r. spectra were recorded with a Perkin–Elmer 621 spectrometer equipped with a gold-grid polarizer. Oriented lamellae of the algal mannan walls were aligned on a silver chloride plate which was mounted into a deuteration cell. The specimen was deuterated by bubbling purified nitrogen gas through a solution of 99.7% D_2O and then through the cell.

Given the backbone conformation of the mannan chain (see below), trial chain-packing models were computer-generated for both packing (parallel and anti-parallel chains) by means of two independent chain rotational parameters,[3] α and β, and one translational parameter which moved the center chain along its centroid. The parameters were varied in discrete intervals. The two chains of each packing model were not assumed to be symmetry related. For each generated structure, all of the calculated intensities were compared with the observed ones so that models giving good agreement could be selected. Similarly, for each trial structure the distances between all atoms in neighboring chains were compared with the following contact distances (Å) (18):

Normal limit
C...C 3.2, C...O 2.8, O...O 2.8,
C...H 2.4, O...H 2.4, H...H 2.0

Extreme limit
C...C 3.0, C...O 2.7, O...O 2.7,
C...H 2.2, O...H 2.2, H...H 1.9

In order to establish the most probable conformations of the O(6) hydroxyl group, the intra- and inter-chain close contacts were determined at 10° intervals of rotation (χ)[4] about the C(6)—C(5) bond. Distances (O...O) and angles, related to non-linearity, were calculated for all possible hydrogen-bonds.

Structure Investigation

For convenience in computer programming the unit cell of Frei and Preston was re-indexed as

$$a = 8.82, \quad b = 7.21, \quad c \text{ (fiber axis)} = 10.27 \text{ Å}$$

A schematic of the mannan I diagram is shown

[2]This sample, which had a specific rotation $[\alpha]_D^{19} -32.0°$ in 4 *N* NaOH, was kindly provided by Professor T. E. Timell of the College of Forestry, Syracuse, N.Y. It is a typical softwood glucomannan.

[3]A chain rotation of 0° was defined by superimposing the vector between the axis of rotation of the chain and the C(5) atom on the *x*-axis of the coordinate system; α and ß correspond to central and corner chain rotations respectively, clockwise rotations being positive for parallel chains, *i.e.* looking down the corner chains of the unit cell.

[4]The position where O(6) is *cis* to C(4) is taken to be $\chi = 0°$ and looking down the C(6)—C(5) bond anticlockwise rotation corresponds to positive values of χ.

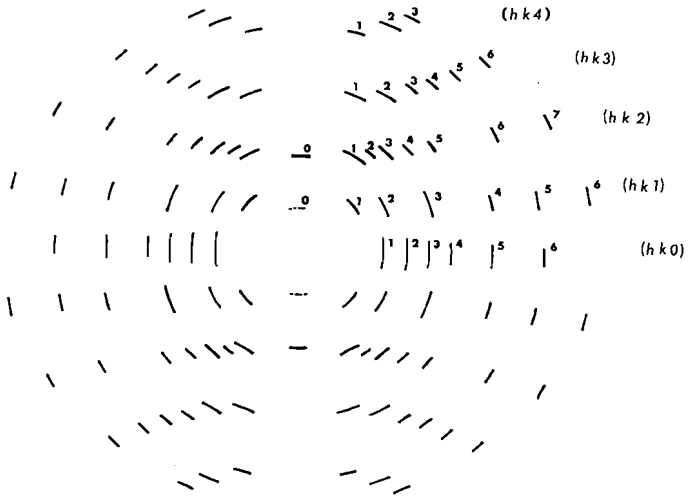

FIG. 1. Schematic of mannan I X-ray fiber diagram. The numbering of the reflections corresponds to the notation in Table 2.

in Fig. 1. Examination of the meridional reflections reveals the presence of an extremely weak (001) and a weak to medium intensity (002), the (003) and (004) being absent. Despite the unpromising nature of these meridionals a twofold screw axis has been incorporated into the mannan backbone conformation as a first approximation, since the fiber repeat of 10.27 Å is very similar to that found for cellulose and chitin in which this symmetry element is believed to occur. It was considered that the presence of the (001) was attributable either to the lack of a twofold screw relationship between O(6) positions in adjacent mannose residues or to the non-stoichiometric occurrence of water within the lattice. The equatorial reflections show systematic absences for (h00) and (0k0) when h and k are odd respectively. This suggests that the chains as projected into the *ab* plane are exactly or very nearly related by two mutually perpendicular twofold screw axes and are anti-parallel. Since the equatorial reflection data terminate at 2.3 Å the resolution is probably insufficient to distinguish between parallel and anti-parallel chain structures on this basis alone.

Following the conformational analysis of Sundararajan and Rao (16), a bridge oxygen angle of 117.5° and (φ, ψ) dihedral angles of (30.1, −30.6°),[5] (that is (38.9, −22.3°) by the convention of the above authors), were selected to give a conformation corresponding to a two-fold screw axis, the required axial repeat and an intra-molecular O(3)...O(5′) hydrogen-bond of length 2.55 Å. The bond lengths and angles used to establish the atomic coordinates corresponds to the average values determined for various β-sugars (18). The O(6) atom was initially positioned *cis* to C(4), ($\chi = 0°$), with a C(6)—O(6) bond length of 1.42 Å and a C(5)—C(6)—O(6) angle of 112°.

The calculated density of dry mannan of 1.65 g cm^{-3} is rather high compared to other polysaccharides (similar to that of algal cellulose) and would make the incorporation of water within the lattice seem improbable. This is the more so since the observed density of mannan was 1.57 g cm^{-3}, in complete agreement with the previously reported value (6).

The approach used in this investigation has been to examine the X-ray data, and then consider the packing merits of all structures which might be consistent with this data. Refinement was then performed from all sterically permissible models. Three structural types may be distinguished (see Fig. 2.) each model representing a group of structures with *ab* projections which would satisfy the equatorial reflection intensities and absences.

(1) Model P1 (as proposed by Frei and Preston (6))

This model involves parallel chains with the

[5]The conformation with (φ, Ψ) = (0, 0°) is chosen as the one in which the C(1)—H(1) bond is *cis* to the O—C(4) bond and the C(4′)—H(4′) bond is *cis* to the C(1)—O bond.

Can. J. Chem. Downloaded from www.nrcresearchpress.com by 210.87.254.40 on 09/05/12
For personal use only.

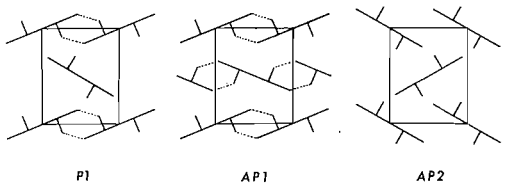

FIG. 2. Three structural types of chain-packing corresponding to *ab* projections in the mannan I unit cell.

corner chains on the (100) plane being bonded via O(6)...O(2) atoms. For the bond to form the O(6) atom may lie at $\chi = 175°$ (*gt* position) or $\chi = 275°$ (*tg* position), however the latter position is not favored by structure factor calculations. Closer examination of the O(6)...O(2) inter-chain hydrogen-bond distance as a function of the corner chain rotation, shows that no satisfactory bond can be formed for $\beta > 69°$ since the hydrogen-bond would be too short and steric hindrance would be encountered between the O(6) of one chain and the H(1) and H(4) atoms of the next. When the corner chain rotation is 69° or less, short contacts between the C(6) and O(6) of this chain and atoms of the central chain are already serious for all chain translations which give a favorable intensity agreement. It is difficult to find any positions for the central chain O(6) atoms which are not sterically hindered. Although a few structures of this type give some measure of intensity agreement, a serious discrepancy arises in that the unobserved (201) reflection is always calculated to be of medium intensity. No completely unhindered structure was found.

(2) Model AP1

This type of structure may correspond to space group $P2_12_12_1$ and involves sheets of chains of similar sense bonded together in the (200) plane via the O(6)...O(2) atoms. The model was readily discarded from consideration since the intensity agreement was generally poor, the unobserved (201) reflection is calculated to be strong and, as with the *P*1 model, whenever the O(6)...O(2) bond is of acceptable length severe short contacts attributable to the C(6) and O(6) atoms arise.

(3) Model AP2

The final model which may also correspond to space group $P2_12_12_1$ does not involve a hydrogen-bond between corner chains. Examination of the chain rotations and relative translations showed very good intensity agreement for a structure which was also favored on packing considerations (see Table 1). This structure has an O(2)...O(5) inter-chain hydrogen-bond between corner and center chains which, although long at 3.03 Å, is very nearly linear. Since there is also an intra-molecular hydrogen-bond wherein O(5) is acceptor, this implies that this atom is a double acceptor. Investigation of all possible positions for the O(6) atoms shows that the least encumbered position is for $\chi = 170–180°$ (*gt* position). No inter-molecular hydrogen-bond can be formed in this position, but it is possible that the O(6) is an acceptor in a bifurcated intra-molecular bond with the O(3) hydrogen atom of the adjacent residue (as recently found in the crystal structure of methyl-β-cellobioside-methanol (19)).

TABLE 1. Mannan close contact map ($\beta - 60°$)

Translation*	α-Rotation (°)						
	−80	−75	−70	−65	−60	−55	−50
1.0	3	3	2	3	2	2	6
0.9	4	2	2	1	2	4	7
0.8	2	1	2	1	4	5	5
0.7	2	3	3	3	2	4	6
0.6	4	3	3	2	4	6	7
0.5	6	5	7	6	6	7	8
0.4	5	4	7	7	8	7	8
0.3	5	4	2	2	2	3	4
0.2	3	2	1	1	0	3	4
0.1	3	3	1	2	2	4	6
0.0	3	3	2	3	2	2	6

*Translation is represented as fractions of the fiber repeat.

The atom O(6) may also be involved in an inter-molecular hydrogen-bond with O(3) of the adjacent chain of the same sense if the position $\chi = 50°$ (*gg* position) is adopted. This position is slightly hindered for the conformation (ϕ, ψ) = (30.1, −30.6°) and gives a poorer level of agreement with the intensity data, but the possibility of its occasional occurrence cannot be eliminated. This would represent an element of disorder in the structure.

Both X-ray intensity and steric considerations strongly support this structure (Figs. 3 and 4), for which the intensity values are given in Table 2 and the coordinates of the asymmetric unit in Table 3. While Fig. 3 and the top section of Fig. 4 represent the same unit cell, the latter

Can. J. Chem. Downloaded from www.nrcresearchpress.com by 210.87.254.40 on 09/05/12
For personal use only.

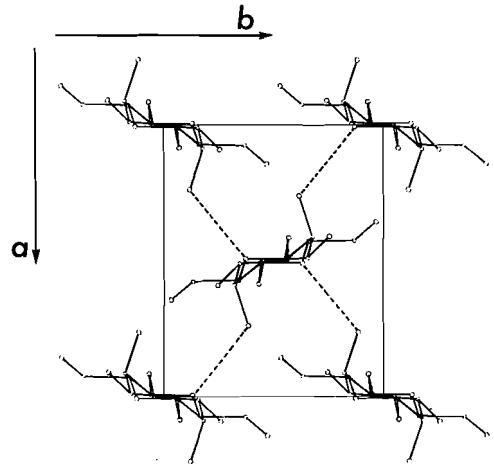

FIG. 3. Projection of mannan I unit cell onto the 001 plane. Inter-molecular hydrogen-bonding scheme between O(2)...O(5′) is shown.

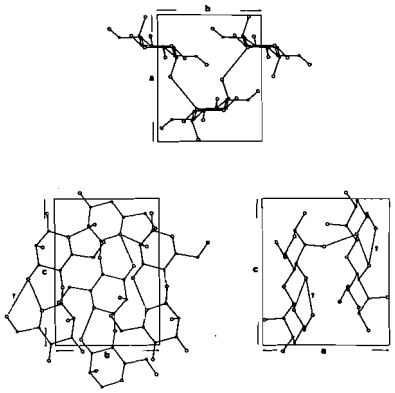

FIG. 4. Three principal projections of mannan I unit cell; origin is halfway between three pairs of non-intersecting screw axes. Inter- and intra-molecular hydrogen-bonds are shown.

corresponds to the correct choice of origin for the space group but the former is included as it shows more clearly how the inter-chain hydrogen-bonding involving O(2) provides cross-sectional cohesion to the mannan crystal.

Infrared Spectroscopy

The spectrum of mannan from *Cymopolia barbata* is almost identical to that from ivory-nut mannan (13), so that only the O—H stretching vibrations will be discussed at present. Comparison of the frequencies of these vibrations in mannan and cellulose indicates that the hydrogen-bonding is much weaker in the former. Also the degree of accessibility of deuterium oxide into the sample suggests that the mannan crystallinity is rather low.

In the spectrum of oriented mannan I (Fig. 5) the following frequencies and polarizations were observed:

TABLE 2. Observed and calculated intensities for mannan I

Reflection		Spacing (Å)	Index	I†	
				Calculated	Observed
E	1	5.58	110	VS	VS
	2	4.41	200	VS	VS
	3	3.76	210	VS	VS
	4	3.34	120	VW	VW
	5	2.72	310	S	S
	6	2.32	130, 320	VW	W
I	0	10.27	001	0	VVW
	1	7.00	101	VVW	VVW
	2	4.90	111	VVW	VW
	3	3.53	211, 021	M	M
	*	2.82	301	VVW	*
	4	2.69	221, 311	W	M
	5	2.34	031	VW	VW
	6	2.07	231	VW	VW
II	0	5.14	002	VVW	VW
	1	4.44	102	VVW	W
	2	4.18	012	VVW	VVW
	3	3.78	112	VVW	VVW
	4	3.34	202	VVW	VVW
	5	3.03	212, 022	VW	VW
	*	2.79	122	VVW	*
	6	2.45	222, 312	VVW	VVW
	*	2.17	032	VW	*
	7	2.11	132, 322	VW	VW
III	0	3.42	003	0	0
	1	3.19	103	VVW	VVW
	2	2.92	113	VW	VW
	3	2.70	203	VVW	VW
	4	2.48	023, 213	VVW	VVW
	5	2.39	123	VVW	VW
	6	2.16	223, 313	VVW	W
IV	0	2.57	004	VVW	0
	1	2.46	104	VVW	VVW
	2	2.33	114	VW	VW
	3	2.21	204	VVW	VVW
	4	2.12	214	VVW	VVW
	5	2.03	124	VVW	VVW
V	0	2.05	005	0	0
	1	2.00	105	VVW	VVW
	2	1.93	115	VW	VVW

*Unobserved reflection whose intensity was taken to be one-half of weakest observed reflection.

†Numerical values have been used during the investigation such that: VS, 75–100; S, 55–75; M, 30–55; W, 20–30; VW, 10–20; VVW, 0–10.

Can. J. Chem. Downloaded from www.nrcresearchpress.com by 210.87.254.40 on 09/05/12
For personal use only.

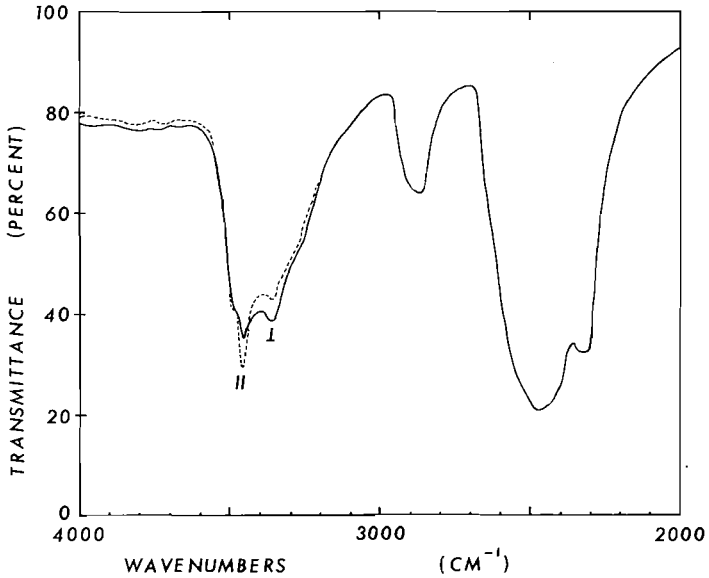

FIG. 5. Polarized i.r. spectrum of partially deuterated and oriented *Cymopolia* cell walls: — electric vector perpendicular to the chain direction; ... electric vector parallel to chain direction.

Frequency (cm^{-1})	Polarization	Interpretation
3497	?	O(6)—H stretching
3462	∥	O(3)—H stretching
3365	⊥	O(2)—H stretching
3280	? weak	(see text)

The first two bands are very similar to those observed in both chitin (20) and cellulose II (21), so that on the basis of its strong parallel dichroism the peak at 3462 cm^{-1} may be assigned to the O(3)—H stretching mode. In the structure proposed for mannan, the O(6)—H does not take part in any inter-molecular hydrogen-bond and it is, therefore, to be expected that the stretching vibration would be of high frequency. The chitin molecule gives rise to two O—H stretching bands at 3447 and 3480 cm^{-1} which presumably correspond to the O(3)—H and O(6)—H vibrations. Therefore, the band at 3497 cm^{-1} can most probably be assigned to the O(6)—H vibration. The perpendicular band at 3365 cm^{-1} can therefore be assigned to the O(2)—H stretching, these atoms forming an inter-molecular hydrogen-bond with O(5) in the proposed structure.

Finally, the band at 3280 cm^{-1} which is rather weak and is even less prominent in some of the spectra recorded, cannot be explained by any structure of mannan which corresponds to the space group $P2_12_12_1$. It is possible that this band relates to the O(6)—H stretching vibration which might arise if certain O(6) atoms were to take up the conformation $\chi = 50°$, (*gg*). In this conformation a short inter-molecular hydrogen-bond of 2.55 Å might be formed with an O(3) atom.

TABLE 3. Fractional atomic coordinates of mannan I*

Atom	*X*	*Y*	*Z*
C(1)	0.2564	0.0600	0.2841
C(2)	0.3372	0.1784	0.1842
C(3)	0.2609	0.1552	0.0534
C(4)	0.2496	−0.0472	0.0156
C(5)	0.1775	−0.1599	0.1253
C(6)	0.1741	−0.3688	0.0998
O(6)	0.1066	−0.4681	0.2038
O(2)	0.4883	0.1166	0.1739
O(3)	0.3405	0.2553	−0.0409
O(4)	0.1656	−0.0693	−0.1000
O(5)	0.2561	−0.1285	0.2430

*Unit cell: $a = 8.82$, $b = 7.21$, c(fiber axis) = 10.27 Å; space group, $P2_12_12_1$.

Discussion

Although the general agreement between

Can. J. Chem. Downloaded from www.nrcresearchpress.com by 210.87.254.40 on 09/05/12
For personal use only.

Can. J. Chem. Downloaded from www.nrcresearchpress.com by 210.87.254.40 on 09/05/12
For personal use only.

observed and calculated intensities is very good and the proposed structure does not involve steric hindrance (a condition which was only met by 1% of the 1500 structures considered), the very weak (001) reflection is not explained by this model and the fourth i.r. hydroxyl stretching frequency is difficult to account for. Evidently the structural differences between the true mannan structure and the one proposed here would need to be such as to destroy the exact twofold screw axis parallel to the fiber direction, and be consistent with a weak fourth hydroxyl stretching band.

The following structural deviations seem possible:

(*i*) The O(6) atoms in contiguous residues may not be screw related; this might be a statistical feature of the structure.

(*ii*) The backbone conformation of mannan does not have a precise twofold screw axis, a situation which might arise if a more stable form of intra-molecular hydrogen-bonding could be achieved, and would involve the presence of a very slow super-helix.

(*iii*) Some non-stoichiometric lattice water be present, although this is unlikely in view of the high density of packing.

(*iv*) The (001) reflection is related to paracrystalline material which is due to the presence of numerous chain ends, folds, or comonomer (6) glucose and galactose included in the main chain.

The latter explanation appears pertinent in view of the abundance of glucomannans in the plant world. Thus mannan in wood has been shown to be a glucomannan with a 1:3 or 1:4 ratio to glucose to mannose. The presence of a small amount of glucose in the mannan I lattice would almost certainly destroy some of the crystalline symmetry which is responsible for systematic absences. Actually the mannan I crystalline structure is quite pertinent to the glucomannan field as will be seen in the following section.

Glucomannan

Glucomannans are typically extracted (22, 23) at 25 °C with 18% NaOH to which 5% H_3BO_3 is added. This material shows very diffuse X-ray scattering so that only two or three reflections may be observed (9, 24–26).

In this investigation we have treated the prepared glucomannan by successively more hydrolytic reagents and monitored the changes in crystallization by X-ray powder diffaction. The following results were obtained:

	Treatment	Interplanar Spacings (Å)
(*i*)	As extracted	4.41
(*ii*)	1 h/70 °C in H_2O	2.68, 4.32, 5.63, 7.7
(*iii*)	1 h/100 °C in H_2O	2.68, 4.34, 5.62, 7.8
(*iv*)	5 h/100 °C in H_2O	2.68, 4.40, 5.60, 7.8
(*v*)	1 h/100°C in 0.2 *N* HCl	2.68, 3.46, 3.72, 4.30, 4.89, 5.58, 7.5

It is clear that except for the reflection at 7.7 Å the data are compatible with the lattice dimensions of mannan I. It is possible that the extra reflection corresponds to a glucomannan phase similar to mannan II (6). The mannan II lattice is sensitive to variation in water content.

Attempts were made to prepare a glucomannan II form by mercerization with alkali and a number of specimens giving crystalline reflections were obtained; however, it is probable that these were soda-glucomannans analogous to the soda-celluloses.

The considerable similarity between both the i.r. spectra and the X-ray data from mannans and glucomannans poses a question. Is there a crystalline glucomannan phase, or are the glucose and mannose residues sufficiently segregated so that only a crystalline mannan phase is involved? At any rate, the presence and development of mannan crystallinity has been shown to be of technological importance (29). A large yield increase in pulping of softwood can be obtained if a mild prehydrolysis precedes the delignification treatment. In view of the now well established crystallizability of glucomannan it seems reasonable to attribute this yield increase to a decrease in accessibility of glucomannan to pulping liquor.

With respect to the above structural investigation it was rather surprising to note that the principal crystalline reflections for glucomannan which were observed in this study and were reported by other workers correspond to mannan I, *i.e.* native mannan. In 1968, Frei and

Can. J. Chem. Downloaded from www.nrcresearchpress.com by 210.87.254.40 on 09/05/12
For personal use only.

Preston clearly showed that a mercerized mannan which they labeled mannan II could be obtained following suitable alkaline treatment of the algal specimen which they were examining. In view of the fact that various workers report crystalline glucomannan X-ray patterns corresponding to mannan I, it would seem that mannan II is much more difficult to prepare than cellulose II. The presence of organic solvents in the precipitating solutions are reported (11) to favor formation of the anhydrous mannan I lattice. Perhaps the presence of borate which is generally used in the extraction schemes for glucomannan influences the formation of mannan I in preference to mannan II, more probably it is the alcoholic system used for precipitating the alkali solved glucomannan. Not investigated so far is the influence of temperature and alkali strength combined which are now well understood for cellulose (27) mercerization.

Conclusion

The crystalline conformation of mannan resembles that of cellulose with respect to screw symmetry along the chain and intra-molecular hydrogen-bonding of the O(3)...O(5′) type. The awkward "knobby" shape of the mannan molecule, largely a result of the axial disposition of O(2)—H, lends itself to a close-packing mainly determined by van der Waals's forces. The high density of the material and the small frequency shift of the O—H stretching bands strongly support this conclusion. It is of interest that the recently proposed structure for poly-β,D(1 → 4′)mannuronic acid (28) also incorporates anti-parallel chains whose rotational and translational parameters are very similar to those proposed here for mannan. The anti-parallel chain structure is consistent with the occurrence of polymer single crystals (11) of mannan I.

The "contact distance" criterion is of great value in the determination of polymer structures where X-ray information is insufficient (see Fig. 6) and the polymer density is high.

The mannan I structure is obtained when glucomannans are precipitated from solution with organic solvents (11) while mannan II is found when crystallization occurs in aqueous alkaline solution (10). This emphasizes the importance of solvation in selection of crystalline polymorphs of polysaccharides.

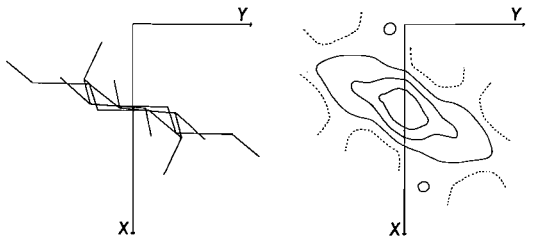

FIG. 6. Fourier synthesis of mannan chain in 001 projection (right); the left side shows the proposed chain orientation arrived at in this study.

The authors are grateful to Dr. P. B. Tomlinson of the Fairchild Tropical Garden, Miami, Florida, for the supply of algae. Mrs. Irene King provided technical assistance in this project and one of us, I.N., was the recipient of financial support from NRCC.

1. Y. IRIKI and T. MIWA. Nature, London, **185**, 178 (1960).
2. G. O. ASPINALL, E. L. HIRST, E. G. V. PERCIVAL and I. R. WILLIAMSON. J. Chem. Soc. 3184 (1953).
3. H. MEIER. Biochim. Biophys. Acta, **28**, 229 (1958).
4. M. L. WOLFROM, M. L. LAVER and D. L. PATIN. J. Org. Chem. **26**, 4533 (1961).
5. E. FREI and R. D. PRESTON. Nature, London, **192**, 939 (1961).
6. E. FREI and R. D. PRESTON. Proc. Roy. Soc. **B169**, 127 (1968).
7. T. E. TIMELL. Wood Sci. Techn. **1**, 45 (1967).
8. W. MACKIE and D. B. SELLEN. Polym. **10**, 621 (1969).
9. K. HESS and M. LUDTKE. Liebigs Ann. Chem. **466**, 18 (1928).
10. H. BITTIGER and R. H. MARCHESSAULT. Private communication.
11. H. BITTIGER. Private communication.
12. A. KELLER. Polym. **3**, 393 (1962).
13. W. J. SCHELL. M.Sc. Thesis. College of Forestry, Syracuse, N. Y., 1966.
14. W. MACKIE and R. D. PRESTON. Planta (Berl.) **79**, 249 (1968).
15. P. R. SUNDARARAJAN. Ph.D. Thesis. University Madras, Madras, India, 1969.
16. P. R. SUNDARARAJAN and V. S. R. RAO. Biopolym. **9**, 1239 (1970).
17. D. A. REES and W. E. SCOTT. J. Chem. Soc. B, 469 (1971).
18. G. N. RAMACHANDRAN, C. RAMAKRISHNAN and V. SASSISEKHARAN. *In* Aspects of protein structure. *Edited by* G. N. Ramachandran. Academic Press, London and New York. 1963. p. 121.
19. J. T. HAM and D. G. WILLIAMS. Acta Cryst. **B26**, 1373 (1970).
20. F. G. PEARSON, R. H. MARCHESSAULT and C. Y. LIANG. J. Polym. Sci. **43**, 71 (1960).

21. R. H. MARCHESSAULT and C. Y. LIANG. J. Polym. Sci. **43**, 71 (1960)
22. R. NELSON. Tappi, **43**, 313 (1960).
23. T. E. TIMELL and A. TYMINSKI. Tappi, **40**, 519 (1957).
24. B. LINDBERG and H. MEIER. Svensk Papperstdn. **60**, 785 (1957).
25. A. J. MORAK and K. WARD. Tappi, **44**, 12 (1961).
26. B. G. RANBY and B. IMMERGUT. Svensk Papperstdn. **60**, 573 (1957).
27. J. O. WARWICKER, R. JEFFRIES, R. L. COLBRAN, and R. N. ROBINSON. Shirley Inst. Pamphlet No. 93. Didsbury, Manchester, 1966.
28. E. D. T. ATKINS, W. MACKIE, K. D. PARKER and E. E. SMOLKO. Polym. Lett. **9**, 311 (1971).
29. G. E. ANNERGREN and S. A. RYDHOLM. Svensk Papperstdn. **62**, 737 (1959).

Can. J. Chem. Downloaded from www.nrcresearchpress.com by 210.87.254.40 on 09/05/12
For personal use only.

Can. J. Chem. Downloaded from www.nrcresearchpress.com by 210.87.254.5 on 09/05/12
For personal use only.

Applications of Lanthanide Shift Reagents to the Identification of ^{13}C Resonances[1]

IAN ARMITAGE,[2] JOHN R. CAMPBELL,[3] AND L. D. HALL[4]

Department of Chemistry, The University of British Columbia, Vancouver 8, British Columbia

Received September 21, 1971

The ^1H and ^{13}C shifts of 2,2-dimethyl-1-propanol (**1**) have been measured by the ^1H–{^{13}C} INDOR technique in the presence of various concentrations of the tris{dipivalomethanato} derivatives of europium (**2**), thulium (**3**), and praseodymium (**4**). All sets of shifts vary with the concentration of added lanthanide; the methylene-^{13}C resonance is shifted more than the methyl-^{13}C resonance. It is shown that tris{dipivalomethanato}gadolinium(III) does not induce chemical shift changes and this further supports the contentation that the pseudo-contact mechanism predominates for lanthanide shift reagents.

Les déplacements chimiques de ^1H et du ^{13}C du diméthyl-2,2 propanol (**1**) ont été mesurés par la technique ^1H–{^{13}C} INDOR en présence de concentrations diverses en tris{dipivalométhanato} d'europium (**2**), de thulium (**3**), et de praseodymium (**4**). Les déplacements chimiques varient avec la concentration de lanthanide ajouté; le pic correspondant à la résonance du méthylène-^{13}C est davantage déplacé que celui correspondant à la résonance du méthyle-^{13}C. On a montré que le tris{dipivalométhanato}gadolinium(III) ne provoque aucun déplacement chimique et ceci confirme le fait d'après lequel le mécanisme de pseudo-contact prédomine avec les réactifs de déplacement.

Canadian Journal of Chemistry, **50**, 2139 (1972)

Introduction

Recent advances in n.m.r. instrumentation have made facile the observation of *natural abundance* ^{13}C n.m.r. spectra of complex organic substances. The principal problem which now inhibits the generality of applications of this technique is the assignment of individual ^{13}C resonances. At present these assignments are generally made on the basis of either "off-resonance" ^{13}C–{^1H} heteronuclear decoupling experiments (2), by the internal consistency of the shifts of a series of closely related derivatives, or by studies of specifically deuterated derivatives. We now report that the lanthanide "shift-reagents", which were first discovered by Hinckley (3) and which have since shown considerable promise in ^1H n.m.r. spectroscopy, may greatly facilitate assignments of ^{13}C n.m.r. spectra. Since this work was completed a preliminary communication has been published (4) that outlines a similar study; we shall discuss this later in this paper.

Discussion

A ^1H–{^{13}C} INDOR spectrometer (5) has been used to measure the ^{13}C shifts of 2,2-dimethyl-1-propanol (**1**) in the presence of varying concentrations of either tris(dipivalomethanato)europium(III) (**2**) or of the related thulium (**3**) or praseodymium (**4**) derivatives. These measurements also provided automatically the ^1H shift changes.

A typical plot of the changes in ^1H and ^{13}C shifts which accompany addition of a lanthanide reagent is given in Fig. 1 and the data are summarized in Table 1. It is quite clear from Fig. 1 that for both ^1H and the ^{13}C resonances a direct relationship exists between the observed shift and the amount of added europium reagent (**2**), at least up to *ca.* 0.15 *M* added lanthanide; the same is also true for the thulium reagent (**3**) up to *ca.* 0.05 *M* and praseodymium reagent (**4**) up to *ca.* 0.15 *M*.

From the standpoint of ^{13}C spectral assignments several points are noteworthy. First, it is encouraging to note that ^{13}C shifts appear to be sufficiently sensitive to added lanthanide for

[1]"Nuclear Magnetic Resonance Studies of Paramagnetic Systems." Part 2. For part 1, see ref. 1.

[2]F. J. Nicholson Scholar; H. R. MacMillan Family Fellowship, 1971–1972.

[3]Recipient of an NRCC Postdoctorate Fellowship, 1969–1971.

[4]Alfred P. Sloan Foundation Research Fellow.

TABLE 1. Summary of the ^1H and ^{13}C chemical shifts of 2,2-dimethyl-1-propanol (**1**) in chloroform solution showing the effect of added tris{dipivalomethanato}europium (**2**), thulium (**3**), or praseodymium (**4**)

Solution* studied	Chemical shifts			
	Proton resonances§		^{13}C resonances‖	
	CH_3	CH_2	$^{13}CH_3$	$^{13}CH_2$
Normal	−0.90	−3.27	−26.26	−73.59
With added **2**†	−1.63	−5.03	−27.38	−77.60
With added **3**‡	−2.37	−7.26	−28.27	−80.00
With added **4**†	0.08	−0.81	*ca.* −24.9	−68.89

*The solutions all contained *ca.* 20% (w/v) of **1** in chloroform solution. Measurements were made at a probe temperature of *ca.* 35°.
†Values for 0.05 mol equiv. of added lanthanide, interpolated from the shift-concentration plots.
‡Values for 0.02 mol equiv. of added thulium reagent.
§δ-values based on tetramethylsilane as an internal reference; error, ±0.02 p.p.m.
‖Values in p.p.m. relative to tetramethylsilane calculated for a magnetic field at which the protons of tetramethylsilane would resonate at precisely 100 MHz; for details see ref. 5; error, ±0.08 p.p.m.

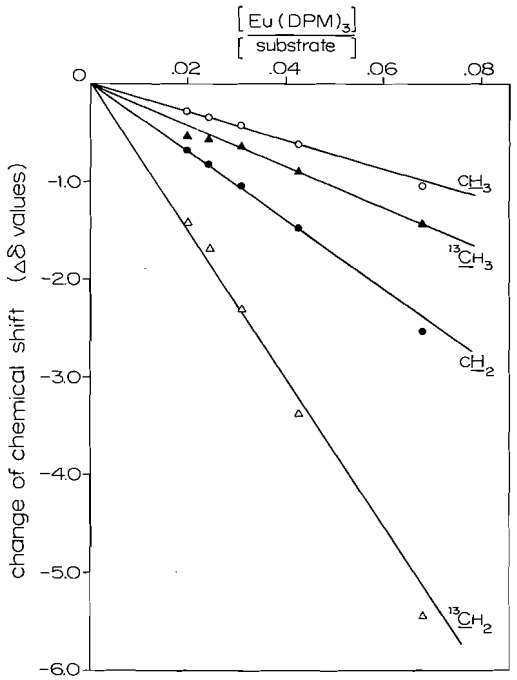

FIG. 1. Plot of the ^1H and ^{13}C chemical shifts of 2,2-dimethyl-1-propanol (**1**) in the presence of varying concentrations of tris{dipivalomethanato} europium(III) (**2**) using chloroform as solvent.

this approach to have some generality. Furthermore, it is important to note that the carbon nearest to the donor function of the organic substrate (C-1 in this case) undergoes a significantly larger shift than the more remote one. However, in the context of cyclic organic substances it must be remembered that *pseudo-contact* shifts have (6) an angular-dependence, and this can be expected to modulate any simple relationships based on distance alone. This is clearly demonstrated by the work of Briggs and co-workers (4); for borneol (**5**), both C-1 and -3 are adjacent to the carbon bearing the hydroxyl function, yet their Δ_{Eu} shift-changes as calculated by Demarco's method (7) are −14.0 and −21.8 p.p.m. respectively.

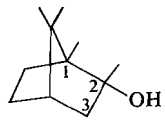

5

Again, from the view of spectral assignments it is important to recognize that whereas both europium (**2**) and thulium (**3**) induce shifts to *lower* field, the praseodymium reagent (**4**) produces *high*-field shifts. Thus it should be possible to use these reagents to remove unwanted degeneracies in ^{13}C spectra. Subsequent extrapolations of suitable shift *vs.* concentration plots can then be used to determine the original positions of individual resonances. This approach should be extremely useful in a number of areas and we are particularly interested in applying it to carbohydrate derivatives.

The use of $Gd(DPM)_3$ in the above study resulted in severe broadening of the resonances for H-1 and -3 which prohibits the detection of the ^{13}C resonance via the INDOR technique, but at the same time no shift was observed for

Can. J. Chem. Downloaded from www.nrcresearchpress.com by 210.87.254.5 on 09/05/12
For personal use only.

the H-1 and -3 resonances of *neo*-pentanol. Applying similar assumptions to those used in previous studies of main group transition metals (8*a*,*b*), this result would seem to further support the evidence that the nature of the shifts induced by lanthanide–$(DPM)_3$ reagents is predominantly pseudo-contact.

Experimental

A sample of 2,2-dimethyl-1-propanol (**1**, *neo*-pentanol) was purified by distillation from calcium hydride.

The tris(dipivalomethanato) derivatives of europium(III) (**2**), thulium(III) (**3**), and praseodymium(III) (**4**) were prepared by the standard literature methods (9).

All n.m.r. measurements were made with a modified (5) Varian HA-100 instrument using internal tetramethylsilane as the lock signal for measurements with **2** and **3**, and chloroform for those with **4**.

It is a pleasure to thank the National Research Council of Canada for their generous financial support via operating grants (A 1905) and two equipment grants (E 1338 and E 1854).

1. IAN ARMITAGE and L. D. HALL. Can. J. Chem. **49**, 2770 (1971).
2. F. J. WEIGERT and J. D. ROBERTS. J. Am. Chem. Soc. **89**, 2967 (1967); D. K. DALLING and D. M. GRANT. J. Am. Chem. Soc. **89**, 6612 (1967).
3. C. C. HINCKLEY. J. Am. Chem. Soc. **91**, 5160 (1969).
4. J. BRIGGS, F. A. HART, G. P. MOSS, and E. W. RANDALL. Chem. Commun. 364 (1971).
5. R. BURTON, L. D. HALL, and P. R. STEINER. Can. J. Chem. **49**, 588 (1971).
6. D. R. EATON. J. Am. Chem. Soc. **87**, 3097 (1965).
7. P. V. DEMARCO, T. K. ELZEY, R. B. LEWIS, and E. WENKERT. J. Am. Chem. Soc. **92**, 5734, 5737 (1970).
8. (*a*) R. W. KLUIBER and W. D. HORROCKS, JR. J. Am. Chem. Soc. **88**, 1399 (1966) and references therein to earlier studies. (*b*) TEIJIRO YONEZAWA, ISAO MORISHIMA, and YOH OHMORI. J. Am. Chem. Soc. **92**, 1267 (1970).
9. K. J. EISENTRAUT and R. E. SIEVERS. J. Am. Chem. Soc. **87**, 5254 (1965).

An Electron Spin Resonance Study of the Radical Cations Derived from Dialkoxybiphenyls

PAUL D. SULLIVAN AND LOUIS J. NORMAN
Department of Chemistry, Ohio University, Athens, Ohio 45701

Received December 24, 1971

The e.s.r. spectra of the cation radicals of various alkyl substituted 4,4′-dihydroxybiphenyls have been studied. These spectra give information regarding the molecular motions occurring in these compounds.

Les spectres e.s.r. des radicaux cationiques de plusieurs 4,4′-dihydroxybiphényles substitués par des groupes alkyles ont été étudiés. Les spectres donnent des informations sur les mouvements moléculaires qui se font dans ces composés.

Canadian Journal of Chemistry, **50**, 2141 (1972)

Radical cations derived from 4,4′-dialkoxybiphenyls belong to the same class of radicals as the Wurster and Weitz radicals, and it has been proposed by Hunig (1) that all radical ions of this type should be termed "violenes". It is the purpose of this note to report on the observation by electron spin resonance of the cation radicals of various alkyl substituted 4,4′-dihydroxybiphenyls, and, in addition, to make a number of suggestions regarding the structure and chemistry of formation of these radicals.

The radicals studied are indicated in Table 1 together with their e.s.r. hyperfine splitting constants and *g* factors. The neutral compounds were either commercially available (**1** and **7**) or were prepared by lead dioxide oxidation of the appropriate phenols (2). The compounds were oxidized with the aluminum chloride–nitromethane system (3). Their behavior in this oxidizing medium could be divided into two types. For compounds **1**, **3**, and **7** when only a slight excess of $AlCl_3$ was used the initial concentrated solution in the e.s.r. tube was dark blue (λ_{max} 800–850 mμ) and exhibited only a broad unresolved e.s.r. signal. Dilution of this concentrated solution at room temperature yielded a green solution (λ_{max} 420–440 and 800–850 mμ) which yielded a well resolved e.s.r. spectrum. On

Can. J. Chem. Downloaded from www.nrcresearchpress.com by 210.87.254.5 on 09/05/12
For personal use only.

the H-1 and -3 resonances of *neo*-pentanol. Applying similar assumptions to those used in previous studies of main group transition metals (8*a*,*b*), this result would seem to further support the evidence that the nature of the shifts induced by lanthanide–$(DPM)_3$ reagents is predominantly pseudo-contact.

Experimental

A sample of 2,2-dimethyl-1-propanol (**1**, *neo*-pentanol) was purified by distillation from calcium hydride.

The tris(dipivalomethanato) derivatives of europium(III) (**2**), thulium(III) (**3**), and praseodymium(III) (**4**) were prepared by the standard literature methods (9).

All n.m.r. measurements were made with a modified (5) Varian HA-100 instrument using internal tetramethylsilane as the lock signal for measurements with **2** and **3**, and chloroform for those with **4**.

It is a pleasure to thank the National Research Council of Canada for their generous financial support via operating grants (A 1905) and two equipment grants (E 1338 and E 1854).

1. IAN ARMITAGE and L. D. HALL. Can. J. Chem. **49**, 2770 (1971).
2. F. J. WEIGERT and J. D. ROBERTS. J. Am. Chem. Soc. **89**, 2967 (1967); D. K. DALLING and D. M. GRANT. J. Am. Chem. Soc. **89**, 6612 (1967).
3. C. C. HINCKLEY. J. Am. Chem. Soc. **91**, 5160 (1969).
4. J. BRIGGS, F. A. HART, G. P. MOSS, and E. W. RANDALL. Chem. Commun. 364 (1971).
5. R. BURTON, L. D. HALL, and P. R. STEINER. Can. J. Chem. **49**, 588 (1971).
6. D. R. EATON. J. Am. Chem. Soc. **87**, 3097 (1965).
7. P. V. DEMARCO, T. K. ELZEY, R. B. LEWIS, and E. WENKERT. J. Am. Chem. Soc. **92**, 5734, 5737 (1970).
8. (*a*) R. W. KLUIBER and W. D. HORROCKS, JR. J. Am. Chem. Soc. **88**, 1399 (1966) and references therein to earlier studies. (*b*) TEIJIRO YONEZAWA, ISAO MORISHIMA, and YOH OHMORI. J. Am. Chem. Soc. **92**, 1267 (1970).
9. K. J. EISENTRAUT and R. E. SIEVERS. J. Am. Chem. Soc. **87**, 5254 (1965).

An Electron Spin Resonance Study of the Radical Cations Derived from Dialkoxybiphenyls

PAUL D. SULLIVAN AND LOUIS J. NORMAN
Department of Chemistry, Ohio University, Athens, Ohio 45701

Received December 24, 1971

The e.s.r. spectra of the cation radicals of various alkyl substituted 4,4′-dihydroxybiphenyls have been studied. These spectra give information regarding the molecular motions occurring in these compounds.

Les spectres e.s.r. des radicaux cationiques de plusieurs 4,4′-dihydroxybiphényles substitués par des groupes alkyles ont été étudiés. Les spectres donnent des informations sur les mouvements moléculaires qui se font dans ces composés.

Canadian Journal of Chemistry, **50**, 2141 (1972)

Radical cations derived from 4,4′-dialkoxybiphenyls belong to the same class of radicals as the Wurster and Weitz radicals, and it has been proposed by Hunig (1) that all radical ions of this type should be termed "violenes". It is the purpose of this note to report on the observation by electron spin resonance of the cation radicals of various alkyl substituted 4,4′-dihydroxybiphenyls, and, in addition, to make a number of suggestions regarding the structure and chemistry of formation of these radicals.

The radicals studied are indicated in Table 1 together with their e.s.r. hyperfine splitting constants and *g* factors. The neutral compounds were either commercially available (**1** and **7**) or were prepared by lead dioxide oxidation of the appropriate phenols (2). The compounds were oxidized with the aluminum chloride–nitromethane system (3). Their behavior in this oxidizing medium could be divided into two types. For compounds **1**, **3**, and **7** when only a slight excess of $AlCl_3$ was used the initial concentrated solution in the e.s.r. tube was dark blue (λ_{max} 800–850 mμ) and exhibited only a broad unresolved e.s.r. signal. Dilution of this concentrated solution at room temperature yielded a green solution (λ_{max} 420–440 and 800–850 mμ) which yielded a well resolved e.s.r. spectrum. On

Can. J. Chem. Downloaded from www.nrcresearchpress.com by 210.87.254.42 on 09/05/12
For personal use only.

TABLE 1. Summary of e.s.r. results for

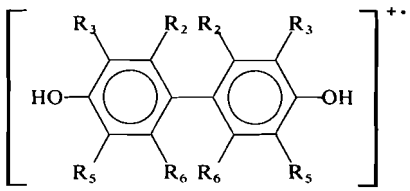

Compound	R_2	R_3	R_5	R_6	a_2	a_3	a_5	a_6	a_{OH}	g-Factor
1*	H	H	H	H	1.98	0.74	0.74	1.98	1.70	2.00305 ± 0.00001
2†	CH_3	CH_3	CH_3	CH_3	1.915	0.620	0.620	1.915	1.549	2.00297 ± 0.00001
3†	H	CH_3	CH_3	H	1.828	0.539	0.539	1.828	1.511	2.00301 ± 0.00001
4‡	H	$CH(CH_3)_2$	$CH(CH_3)_2$	H	1.797	0.513	0.513	1.797	1.519	2.00303 ± 0.00001
5§	H	$C(CH_3)_3$	$C(CH_3)_3$	H	1.827	—	—	1.827	1.461	2.00303 ± 0.00001
6§	H	CH_3	$C(CH_3)_3$	H	1.781	0.588	0.040	1.781	1.465	2.00304 ± 0.00001
7‖	H	CH_3	H	H					1.61	2.00305 ± 0.00001

*Temperature 0°.
†Temperature −40°.
‡Temperature −50°.
§Temperature −30°.
‖Not analyzed in detail, but spectrum is the sum of two species.

lowering the temperature the solution was observed to change color reversibly from green to royal blue and simultaneously the intensity of the e.s.r. spectrum was observed to decrease rapidly being essentially unobservable below −50°. Compound **3**, for example, lost a factor of ten in amplitude over the range −10 to −30°. If these compounds were reacted with an excess of $AlCl_3$ a dark yellow solution was obtained which showed no e.s.r. signal even after dilution.

Compounds **2**, **4**, **5**, and **6** on the other hand, gave a red solution on reaction with a slight excess of $AlCl_3$. Dilution of this solution gave a well resolved e.s.r. spectrum. The intensity of the e.s.r. signal from these compounds did not vary greatly with temperature down to −60°, and no color change was noted on cooling. Addition of a large excess of $AlCl_3$ resulted in the loss of the e.s.r. signal.

The above results are consistent with an equilibrium at room temperature between the radical cation and the dication which depends on the concentration of $AlCl_3$. The change in e.s.r. intensity and color of **1**, **3**, and **7** with temperature can be explained in terms of the formation of a diamagnetic dimer at low temperatures. This interpretation is supported by the absence of an e.s.r. signal in the field range 0–4000 G, from frozen solutions of these compounds. This result is not unexpected when the behavior of other "violene" radicals is considered (4, 5).

The structure of the dimer can be inferred from the observation that the sterically hindered compounds **2**, **4**, **5**, and **6** do not form such a dimer. One can therefore postulate that the dimer results from a stacking of the biphenyl rings on top of each other such that the π systems can interact.

Information on the molecular structure of the cation radicals can also be obtained from their e.s.r. spectra. It has been reported (6) previously that the e.s.r. spectrum of **1** shows line-width alternation effects which appear consistent with a *cis–trans* isomerization. In support of this we observe that the e.s.r. spectrum of **7** is very complex and is apparently interpretable in terms of two species (**1***a* and **1***b*). This indicates a slow rotation about the central C—C bond indicating

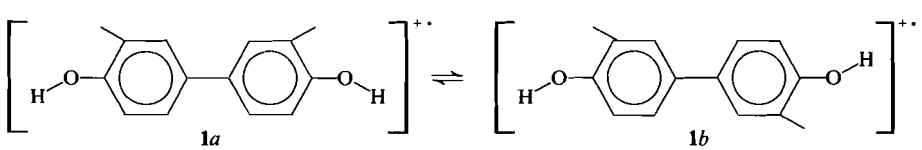

1*a* **1***b*

Can. J. Chem. Downloaded from www.nrcresearchpress.com by 210.87.254.42 on 09/05/12
For personal use only.

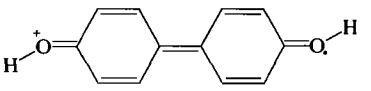

1*c*

a considerable double bond character, undoubtedly due to the importance of structures of the type **1***c*. Molecular orbital calculations using the McLachlan perturbation corrections to HMO theory (7) support this interpretation, since in order to reproduce the experimental spin densities it is necessary to increase the resonance integral of the central C—C bond to a value of 1.25 β_o, where β_o is the standard carbon–carbon resonance integral.

No effects due to rotational isomerism were noted for compounds **2–6**, in the temperature range studied. This is not surprising since in these compounds the potential barrier to rotation for the hydroxyl groups is expected to be decreased considerably (8).

One further observation which merits comment concerns the lifetime of the radical derived from 4,4′-dihydroxyoctamethylbiphenyl (**2**). This radical is considerably shorter lived than the other radicals studied, at 0° it's half-life is approximately 8 min compared to half-lives of several hours for the other radicals at this temperature. If radical **2** is allowed to stand at room temperature for several hours a different e.s.r. signal develops which has been identified as that of the 1,4-dihydroxy 2,3,5,6-tetramethylbenzene (duroquinol) cation radical. Additionally radical **2** also shows strongly temperature dependent hydroxyl and methyl group splitting constants while the other radicals show only temperature dependent hydroxyl group splitting constants. These observations indicate that the torsional oscillations of this molecule manifest themselves in subtle ways in the e.s.r. spectra. Further study of this molecule may be warranted.

Support of this work by a grant from the Petroleum Research Fund of the American Chemical Society is gratefully acknowledged.

1. S. Hunig. Pure and Appl. Chem. **15**, 109 (1967).
2. C. R. H. I. de Jonge, H. M. van Donk, and L. Vollbracht. Tetrahedron Lett. 1881 (1970).
3. W. F. Forbes and P. D. Sullivan. J. Am. Chem. Soc. **88**, 2862 (1966).
4. H. N. Blount and T. Kuwana. J. Am. Chem. Soc. **92**, 5773 (1970).
5. E. M. Kosower and J. L. Cotten. J. Am. Chem. Soc. **86**, 5524 (1964).
6. W. F. Forbes and P. D. Sullivan. Can. J. Chem. **46**, 325 (1968).
7. A. D. McLachlan. Mol. Phys. **3**, 233 (1960).
8. P. D. Sullivan. J. Phys. Chem. **75**, 2195 (1971).

The Thermal Decomposition of *N*-Benzoyl-*N*′-1-cyanocyclohexyl Diimide

Thomas R. Lynch[1] and Frederick N. MacLachlan
Chemistry Department and Scarborough College, University of Toronto, West Hill, Ontario

Received October 19, 1971

N-Benzoyl-*N*′-1-cyanocyclohexyl diimide decomposes in toluene in a first-order manner between 81 and 102°, $k = 10^{15.08}e^{-32.54 \pm 1.35/RT}$. The major product is *N*-benzoyl-*N*-cyclohexane carbonyl imide.

La *N*-benzoyl-*N*′-cyano-1 cyclohexyl diimide se décompose dans le toluène selon une cinétique d'ordre 1 entre 81 et 102°, $k = 10^{15.08}e^{-32.54 \pm 1.35/RT}$. Le produit majeur est la *N*-benzoyl-*N*-cyclohexane carbonyl imide.

Canadian Journal of Chemistry, **50**, 2143 (1972)

We recently reported on the synthesis and spectral properties of a number of acyl alkyl diimides (1). In this paper we report on the kinetics of the thermal decomposition of one of these compounds, namely *N*-benzoyl-*N*′-1-cyanocyclohexyl diimide (**1**), together with a partial study of the products formed. Since the early work of Wieland *et al.* on a variety of triphenylmethyl acyl diimides (2), other accounts of decomposition studies on related diimides

[1]To whom correspondence should be addressed.

Can. J. Chem. Downloaded from www.nrcresearchpress.com by 210.87.254.42 on 09/05/12
For personal use only.

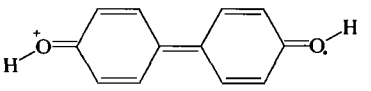

1c

a considerable double bond character, undoubtedly due to the importance of structures of the type **1***c*. Molecular orbital calculations using the McLachlan perturbation corrections to HMO theory (7) support this interpretation, since in order to reproduce the experimental spin densities it is necessary to increase the resonance integral of the central C—C bond to a value of 1.25 β_o, where β_o is the standard carbon–carbon resonance integral.

No effects due to rotational isomerism were noted for compounds **2–6**, in the temperature range studied. This is not surprising since in these compounds the potential barrier to rotation for the hydroxyl groups is expected to be decreased considerably (8).

One further observation which merits comment concerns the lifetime of the radical derived from 4,4′-dihydroxyoctamethylbiphenyl (**2**). This radical is considerably shorter lived than the other radicals studied, at 0° it's half-life is approximately 8 min compared to half-lives of several hours for the other radicals at this temperature. If radical **2** is allowed to stand at room temperature for several hours a different e.s.r. signal develops which has been identified as that of the 1,4-dihydroxy 2,3,5,6-tetramethylbenzene (duroquinol) cation radical. Additionally radical **2** also shows strongly temperature dependent hydroxyl and methyl group splitting constants while the other radicals show only temperature dependent hydroxyl group splitting constants. These observations indicate that the torsional oscillations of this molecule manifest themselves in subtle ways in the e.s.r. spectra. Further study of this molecule may be warranted.

Support of this work by a grant from the Petroleum Research Fund of the American Chemical Society is gratefully acknowledged.

1. S. Hunig. Pure and Appl. Chem. **15**, 109 (1967).
2. C. R. H. I. de Jonge, H. M. van Donk, and L. Vollbracht. Tetrahedron Lett. 1881 (1970).
3. W. F. Forbes and P. D. Sullivan. J. Am. Chem. Soc. **88**, 2862 (1966).
4. H. N. Blount and T. Kuwana. J. Am. Chem. Soc. **92**, 5773 (1970).
5. E. M. Kosower and J. L. Cotten. J. Am. Chem. Soc. **86**, 5524 (1964).
6. W. F. Forbes and P. D. Sullivan. Can. J. Chem. **46**, 325 (1968).
7. A. D. McLachlan. Mol. Phys. **3**, 233 (1960).
8. P. D. Sullivan. J. Phys. Chem. **75**, 2195 (1971).

The Thermal Decomposition of *N*-Benzoyl-*N*′-1-cyanocyclohexyl Diimide

Thomas R. Lynch[1] and Frederick N. MacLachlan
Chemistry Department and Scarborough College, University of Toronto, West Hill, Ontario

Received October 19, 1971

N-Benzoyl-*N*′-1-cyanocyclohexyl diimide decomposes in toluene in a first-order manner between 81 and 102°, $k = 10^{15.08}e^{-32.54 \pm 1.35/RT}$. The major product is *N*-benzoyl-*N*-cyclohexane carbonyl imide.

La *N*-benzoyl-*N*′-cyano-1 cyclohexyl diimide se décompose dans le toluène selon une cinétique d'ordre 1 entre 81 et 102°, $k = 10^{15.08}e^{-32.54 \pm 1.35/RT}$. Le produit majeur est la *N*-benzoyl-*N*-cyclohexane carbonyl imide.

Canadian Journal of Chemistry, **50**, 2143 (1972)

We recently reported on the synthesis and spectral properties of a number of acyl alkyl diimides (1). In this paper we report on the kinetics of the thermal decomposition of one of these compounds, namely *N*-benzoyl-*N*′-1-cyanocyclohexyl diimide (**1**), together with a partial study of the products formed. Since the early work of Wieland *et al.* on a variety of triphenylmethyl acyl diimides (2), other accounts of decomposition studies on related diimides

[1]To whom correspondence should be addressed.

Can. J. Chem. Downloaded from www.nrcresearchpress.com by 210.87.254.105 on 09/05/12
For personal use only.

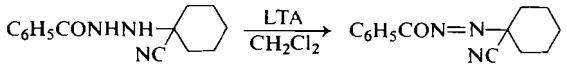

2 1

have been published, but these have been performed in the presence of strong bases (3, 4).

The diimide **1** was obtained by oxidation of the hydrazide **2** (1) with lead tetraacetate in methylene chloride solution. For the kinetic measurements, toluene solutions *ca.* 1.4×10^{-2} *M* in **1** were employed, and the disappearance of **1** was followed by monitoring the decrease of the absorbance of the n–π^* band at *ca.* 400 nm. These decompositions were performed without the exclusion of air. Runs were followed to between one and two half-lives and gave good first-order plots; decompositions at higher concentrations of **1** indicate that the amount of induced decomposition is negligible. Manometric rate constants were in approximate agreement with those obtained as above, but consistent results were difficult to obtain.

The least-squares rate constants thus obtained for the decomposition of **1** at seven temperatures between 81 and 102° are given in Table 1. A plot of $\log_e k$ *vs.* $1/T$ gave an excellent straight line from which the Arrhenius expression $k = 10^{15.08} e^{-32.54 \pm 1.35/RT}$ was obtained. It is notable that at 100.0°, the rate of decomposition of dibenzoyl diimide (7.7×10^{-6} s^{-1} (5)) is *ca.* 13 times slower than that of **1**, while bis-(1-cyanocyclohexyl) diimide at 80.3° decomposes at approximately the same rate (6.5×10^{-6} s^{-1} (6)) as **1** (9.2×10^{-6} s^{-1}).

Removal of the toluene from completely decomposed samples of **1** gave an oil from which a crystalline solid, $C_{14}H_{17}NO_2$, m.p. 159.5–160.5°, was isolated by trituration with pentane followed by crystallization from ether. The mass spectrum of this material (*m/e* 231 (40%) (molecular ion), 122 (100%), 110 (40%), 105 (88%), and 77 (58%)) together with the n.m.r. (δ 1.7 (broad methylene envelope), 3.3 (broad singlet), 9.0 p.p.m. (broad singlet, removed on D_2O was)) and i.r. (ν_{max} 3400 (w, —NH—), 1695 (s, shoulders at 1710 and 1750 cm^{-1}), 1460 (m), 1230 cm^{-1} (m)) spectra of the crude product, suggested this compound to be *N*-benzoyl-*N*-cyclohexane carbonyl imide, **3** (lit. (7) m.p. 157), a compound which has previously been isolated from treatment of 2-phenyl-4-cyclohexylidene-5-oxazolone with sodium azide in aqueous acetic acid (7). Confirmation of the structure **3** was obtained by its independent synthesis from benzamide and cyclohexane carbonyl chloride. The authentic material, m.p. 161.5–163°, had a mass spectrum identical to that of the $C_{14}H_{17}NO_2$ compound and its n.m.r. and i.r. spectra were similar to those of the crude product. Compound **3** is estimated to constitute *ca.* 30% of the crude product, and is presumably formed via addition of water to the acyl ketenimine **4**.

TABLE 1. Least squares rate constants and their standard deviations for the decomposition of **1** in toluene

Concentration ($\times 10^{-2}$ mol l^{-1})	Temperature (°C)	$k \times 10^5$ (s^{-1})
1.44	81.3	1.01±0.05*‡
1.43	88.1	2.42±0.18*
1.41	89.6	2.98±0.08†
8.42	89.6	3.10±0.15†
1.43	91.5	3.86±0.26†
16.68	91.5	3.84±0.17†
1.44	96.2	6.79±0.30*
1.32	99.3	9.49±0.46*
1.43	102.2	13.32±0.30*

*Average of two runs.
†From one run.
‡Taken to 0.6 half-lives.

The g.l.c. analysis of the residue after removal of the toluene showed the product mixture to be complex (*ca.* 19 components); however, it was possible to establish the presence of small amounts of benzaldehyde (**5**), bibenzyl (**6**), 1,1′-dicyano-1,1′-bicyclohexyl (**7**), 1-cyanocyclohexene (**8**), cyanocyclohexane (**9**), cyclohexanone (**10**), and cyclohexanol (**11**), together with a component with the same retention time as biphenyl (**12**), and a possible trace of benzil (**13**).[2]

Decomposition of **1** (200 mg, 8.3×10^{-4} mol) in degassed benzene (2 ml) containing water (28.6 mg, 1.6×10^{-3} mol, to trap the presumed intermediate, the ketenimine **4**, and simplify the products) in an evacuated sealed tube at 104° for 24 h followed by direct g.l.c. analysis led to identification of the following products (approximate mole ratios in parenthesis): cyclohexa-

[2]At the temperatures at which the decompositions were performed, the partial pressure of O_2 in the solvent should be small, thus formation of radical coupling and H-abstraction products is not surprising.

Can. J. Chem. Downloaded from www.nrcresearchpress.com by 210.87.254.105 on 09/05/12
For personal use only.

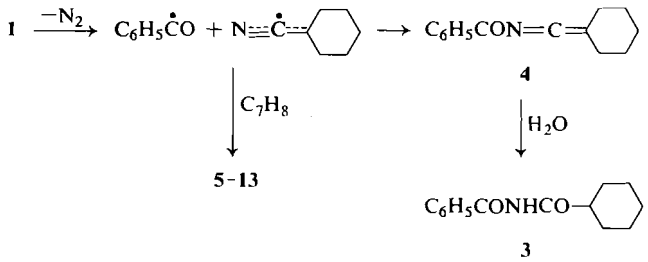

none (1.1), cyanocyclohexane (1.0), benzaldehyde (0.2), 1-cyanocyclohexene (0.3), cyclohexane carboxamide (0.9), 1,1′-dicyano-1,1′-bicyclohexyl (0.1), benzamide (5.6), and the imide **3** (5.2), accounting for *ca.* 65% of the total product observable by g.l.c.; absent were biphenyl, benzil, benzophenone, and cyclohexanol. The amides most probably arise by hydrolysis of the imide by excess water.

Thus both the kinetic and the product studies are consistent with a thermal homolytic fragmentation of **1** to nitrogen and the benzoyl and 1-cyanocyclohexyl radicals which, in turn, react largely by coupling to give the acyl ketenimine **4**.

Experimental

Melting points are uncorrected. Spectroscopic instruments employed were as previously reported (1).

N-Benzoyl-N′-1-cyanocyclohexyl Diimide (1)

A solution of lead tetraacetate (4.35 g, 9.84 mmol) in methylene chloride (125 ml) was poured into a stirred solution of the hydrazide **2** (2.12 g, 8.72 mmol) in methylene chloride (80 ml) cooled to −20°, and the mixture stirred for 30 min at −20°. The yellow orange solution was then poured into water (100 ml), and the layers separated. The organic layer was washed with 5 × 100 ml aliquots of water, once with 100 ml saturated aqueous sodium bicarbonate, and once with water. After drying, the solvent was removed, and the yellow orange solid was recrystallized from pentane (1.92 g, 91%), m.p. 68–69.5°.

Decomposition Studies on 1

The toluene used was dried by standing over sodium wire followed by distillation, and then was stored over molecular sieves. Solutions of **1** in toluene in a 100 ml round-bottomed flask fitted with condenser and a drying tube were then immersed in a Neslab Instruments Inc. Model TE-9HT constant temperature bath, with the bath liquid, ethylene glycol, maintained at the appropriate temperature. Toluene samples were withdrawn at known time intervals and the absorbance of the band at 400 nm measured. First-order rate constants were obtained from the slope of the plot of $\ln (A_0/A)$ *vs.* t(s), where A_0 and A are the absorbances at $t = 0$ and $t = t$ s. respectively. Solutions of **1** in toluene were found to obey Beer's Law.

Isolation of 3 from the Decomposition of 1

Toluene was removed from a completely decomposed sample of **1**, and the residue was triturated with pentane. The pentane was decanted, and the pentane-insoluble material was dissolved in a small quantity of ether. On cooling in the refrigerator overnight, **3** crystallized out and was purified by several further crystallizations from ether, m.p. 159.5–160.5°.

Anal. Calcd. for $C_{14}H_{17}NO_2$: C, 72.70; H, 7.41; N, 6.06. Found: C, 72.78; H, 7.28; N, 6.03.

Synthesis of N-Benzoyl-N-cyclohexane Carbonyl Imide (3)

Cyclohexane carbonyl chloride (13.9 g, 0.095 mol, Eastman Kodak) was added dropwise to a solution of benzamide (11.0 g, 0.091 mol) in pyridine (60 ml). The temperature was maintained at 10–15° throughout the addition. When all the acid chloride had been added, the reaction mixture was stirred for a further 0.5 h at room temperature and then poured on to ice (100 g). The precipitate so obtained was filtered off, digested in ice-cold ether (150 ml), and the aqueous layer was run off. Removal of the solvent after drying gave the crude product (8.5 g, 37%), a sample of which after three crystallizations from ethanol had m.p. 161.5–163°; ν_{max} 3390 (w), 1695 (s, shoulders at 1710 and 1753 cm^{-1}), 1460 (m) and 1230 cm^{-1} (m); n.m.r.: δ 1.7 (broad envelope, 10 H, cyclohexyl —CH_2—), 3.4 (broad singlet, 1 H, methine —C(—H)—), 7.7 (multiplet, 5 H, aromatic =C(—H)—), and 9.0 (broad singlet, 1 H, NH, removed on D_2O wash); λ_{max} (EtOH): 235 (13 600), 274 (sh, 1000) nm.

Miscellaneous

1,1′-diCyano-1,1′-bicyclohexyl (**7**), 1-cyanocyclohexene (**8**), and cyanocyclohexane (**9**) were synthesized by literature methods.

Gas liquid chromatography (g.l.c.) was performed on a Varian Model 1740 Gas Chromatograph, equipped with a flame ionization detector and products were identified by comparison of their retention times with those of authentic samples. Columns used were: A, 5 ft × 1/8 in. 5% DEGSE on acid washed 80/100 mesh Chromosorb W, B, 5 ft × 1/8 in. 3% SE-30 on 100/120 mesh VarAport 30, C, 5 ft × 1/8 in. 5% Carbowax 20M on DMCS treated 80/100 mesh Chromosorb W.

Compounds **5**, **7**, **8**, **9**, and **10**, and the amides were identified on columns B and C, compound **6** on columns A and B, and compound **3** on column B. Positive identification of benzoic and cyclohexane carboxylic acids on columns B and C was not possible due to peak overlap.

Can. J. Chem. Downloaded from www.nrcresearchpress.com by 210.87.254.105 on 09/05/12
For personal use only.

The authors thank the National Research Council of Canada for financial assistance, and Prof. O. Meresz for a sample of biphenyl.

1. T. R. LYNCH, F. N. MACLACHLAN, and Y. K. SIU. Can. J. Chem. **49**, 1598 (1971).
2. H. WIELAND *et al.* Ann. **514**, 145 (1935); Ann. **518**, 166 (1938).
3. R. W. HOFFMANN and K. R. EICKEN. Chem. Ber. **100**, 1465 (1967).
4. G. FRAENKEL and E. PECCHOLD. Tetrahedron Lett. 4821 (1969).
5. J. E. LEFFLER and W. B. BOND. J. Am. Chem. Soc. **78**, 335 (1956).
6. C. G. OVERBERGER, H. BILETCH, A. B. FINESTONE, J. LILKER, and J. HERBERT. J. Am. Chem. Soc. **75**, 2078 (1953).
7. W. I. AWAD, A. F. M. FAHMY, and A. M. A. SAMMOUR. J. Org. Chem. **30**, 2222 (1965).

^{13}C Chemical Shifts of Highly Substituted Bicyclo[2.2.1]heptanes

N. H. WERSTIUK, R. TAILLEFER, R. A. BELL, AND B. G. SAYER

Department of Chemistry, McMaster University, Hamilton, Ontario

Received November 29, 1971

The ^{13}C chemical shifts have been determined for a series of highly substituted norbornanes. A comparison of the observed values with the expected chemical shifts, determined as described by Lippmaa, establishes that ^{13}C shifts may be predicted reasonably accurately even in highly substituted norbornyl systems. Since substituted norbornanes definitely exist in *synchro* or *contra* twist forms as shown by Altona, the results show that Lippmaa's substituted shift parameters must already account for the major part of the increments that arise via hybridization changes resulting from the distortion of the [2.2.1]-skeleton.

Les déplacements chimiques du ^{13}C ont été déterminés pour une série de norbornanes hautement substitués. La comparaison des valeurs observées avec les déplacements chimiques attendus selon Lippmaa, montre que les déplacements chimiques du ^{13}C peuvent être prévus avec une précision raisonnable même pour des systèmes norbornyles hautement substitués. Il a été montré par Altona que les norbornanes substitués existent sous des formes twist *synchro* et *contra*, les résultats montrent que les paramètres de Lippmaa associés aux déplacements chimiques des substituants doivent expliquer le fait que la majeure partie des incréments provient des changements d'hybridation résultant de la distorsion du squelette[2.2.1].

Canadian Journal of Chemistry, **50**, 2146 (1972)

Introduction

Recently, expansion in the application of ^{13}C n.m.r. spectroscopy to organic chemistry has been dramatic (1–7). The accumulated chemical shift data have yielded, in addition to data for the determination of theories of ^{13}C chemical shifts, important information about ground state steric and electronic substituent effects in acyclic and cyclic molecules. Furthermore, ^{13}C–H and ^{13}C–^{13}C coupling constants have been used to gain hybridizational information at the carbon atom (1, 8–10).

Through our interest in the chemistry of the bicyclic diones **2**, **5**, and **9**, and the enones **7** and **11** (11) we have applied ^{13}C.m.r. to determine whether or not the diones and enones, which certainly exist in *synchro* or *contra* twist forms (12) are hybridizationally unusual at the bridgeheads with the angle described by the bonds C_6—C_1—C_2 deviating substantially from the normal 109.5°. Since ^{13}C shifts for sp^3 and sp^2 hybridized carbon are 15–60 and 90–160 p.p.m. (13) downfield from tetramethylsilane respectively, the C-1 and -4 shifts would serve as hybridization probes. The ^{13}C shifts determined experimentally for a series of substituted bicyclic systems are listed in Table 1.

Discussion and Conclusions

In Table 2 a comparison is made between the observed chemical shifts for C-1, -4, -6, and -7 and those predicted by application of Lippmaa's (2) substituent shift parameters. The good agreement indicates that the ^{13}C shifts may be predicted reasonably accurately even in highly substituted systems (*cf.* **9** and **14**, Table 2).

Can. J. Chem. Downloaded from www.nrcresearchpress.com by 210.87.254.105 on 09/05/12
For personal use only.

The authors thank the National Research Council of Canada for financial assistance, and Prof. O. Meresz for a sample of biphenyl.

1. T. R. LYNCH, F. N. MACLACHLAN, and Y. K. SIU. Can. J. Chem. **49**, 1598 (1971).
2. H. WIELAND *et al.* Ann. **514**, 145 (1935); Ann. **518**, 166 (1938).
3. R. W. HOFFMANN and K. R. EICKEN. Chem. Ber. **100**, 1465 (1967).
4. G. FRAENKEL and E. PECCHOLD. Tetrahedron Lett. 4821 (1969).
5. J. E. LEFFLER and W. B. BOND. J. Am. Chem. Soc. **78**, 335 (1956).
6. C. G. OVERBERGER, H. BILETCH, A. B. FINESTONE, J. LILKER, and J. HERBERT. J. Am. Chem. Soc. **75**, 2078 (1953).
7. W. I. AWAD, A. F. M. FAHMY, and A. M. A. SAMMOUR. J. Org. Chem. **30**, 2222 (1965).

^{13}C Chemical Shifts of Highly Substituted Bicyclo[2.2.1]heptanes

N. H. WERSTIUK, R. TAILLEFER, R. A. BELL, AND B. G. SAYER

Department of Chemistry, McMaster University, Hamilton, Ontario

Received November 29, 1971

The ^{13}C chemical shifts have been determined for a series of highly substituted norbornanes. A comparison of the observed values with the expected chemical shifts, determined as described by Lippmaa, establishes that ^{13}C shifts may be predicted reasonably accurately even in highly substituted norbornyl systems. Since substituted norbornanes definitely exist in *synchro* or *contra* twist forms as shown by Altona, the results show that Lippmaa's substituted shift parameters must already account for the major part of the increments that arise via hybridization changes resulting from the distortion of the [2.2.1]-skeleton.

Les déplacements chimiques du ^{13}C ont été déterminés pour une série de norbornanes hautement substitués. La comparaison des valeurs observées avec les déplacements chimiques attendus selon Lippmaa, montre que les déplacements chimiques du ^{13}C peuvent être prévus avec une précision raisonnable même pour des systèmes norbornyles hautement substitués. Il a été montré par Altona que les norbornanes substitués existent sous des formes twist *synchro* et *contra*, les résultats montrent que les paramètres de Lippmaa associés aux déplacements chimiques des substituants doivent expliquer le fait que la majeure partie des incréments provient des changements d'hybridation résultant de la distorsion du squelette[2.2.1].

Canadian Journal of Chemistry, **50**, 2146 (1972)

Introduction

Recently, expansion in the application of ^{13}C n.m.r. spectroscopy to organic chemistry has been dramatic (1–7). The accumulated chemical shift data have yielded, in addition to data for the determination of theories of ^{13}C chemical shifts, important information about ground state steric and electronic substituent effects in acyclic and cyclic molecules. Furthermore, ^{13}C–H and ^{13}C–^{13}C coupling constants have been used to gain hybridizational information at the carbon atom (1, 8–10).

Through our interest in the chemistry of the bicyclic diones **2**, **5**, and **9**, and the enones **7** and **11** (11) we have applied ^{13}C.m.r. to determine whether or not the diones and enones, which certainly exist in *synchro* or *contra* twist forms (12) are hybridizationally unusual at the bridgeheads with the angle described by the bonds C_6—C_1—C_2 deviating substantially from the normal 109.5°. Since ^{13}C shifts for sp^3 and sp^2 hybridized carbon are 15–60 and 90–160 p.p.m. (13) downfield from tetramethylsilane respectively, the C-1 and -4 shifts would serve as hybridization probes. The ^{13}C shifts determined experimentally for a series of substituted bicyclic systems are listed in Table 1.

Discussion and Conclusions

In Table 2 a comparison is made between the observed chemical shifts for C-1, -4, -6, and -7 and those predicted by application of Lippmaa's (2) substituent shift parameters. The good agreement indicates that the ^{13}C shifts may be predicted reasonably accurately even in highly substituted systems (*cf.* **9** and **14**, Table 2).

TABLE 1. ^{13}C Chemical shifts*

Compound	C-1	C-2	C-3	C-4	C-5	C-6	C-7	C-8	C-9	C-10	C-11
1	50.3	217.7	45.6	36.2	27.8	24.9	38.1				
2	47.4	213.7	36.4	47.4	213.7	36.4	33.8				
3	49.8	221.8	46.5	46.2	22.8	24.3	34.6	22.8	21.9		
4	33.9	32.9	41.9	60.2	216.0	24.7	33.4	26.3	25.7		
5	48.5	217.9	44.8	60.2	213.6	38.6	32.6	21.6	21.6		
6	47.8	166.0	41.5	48.4	25.3	28.9	37.1	28.5	23.9	100.0	
7	43.4	162.0	39.1	62.0	215.1	42.3	33.8	24.8	23.7	100.0	
8	53.7	222.4	46.9	45.4	24.9	31.8	41.6	23.1	21.4	14.1	
9	52.8	220.0	45.6	60.0	213.3	45.1	39.1	21.6	21.6	14.4	
10	49.1	160†	42.7	47.6	25.4	35.6	44.3	29.4	25.9	18.1	97.3
11	48.6	160†	42.4	62.1	212.0	50.1	42.4	28.9	27.1	18.2	101.9
12	49.3	85.3	39.6	48.3	25.8	24.9	41.0	30.6	20.6	19.1	
13	47.7	83.1	40.6	63.1	219.4	38.7	42.6	20.7	21.1	18.1	
14	50.1	160†	43.4	52.6	75.4	44.5	43.1	31.8	27.5	18.7	

*In p.p.m. (±0.1) downfield from tetramethylsilane.
†Not determined; estimated from **6** and **7**.

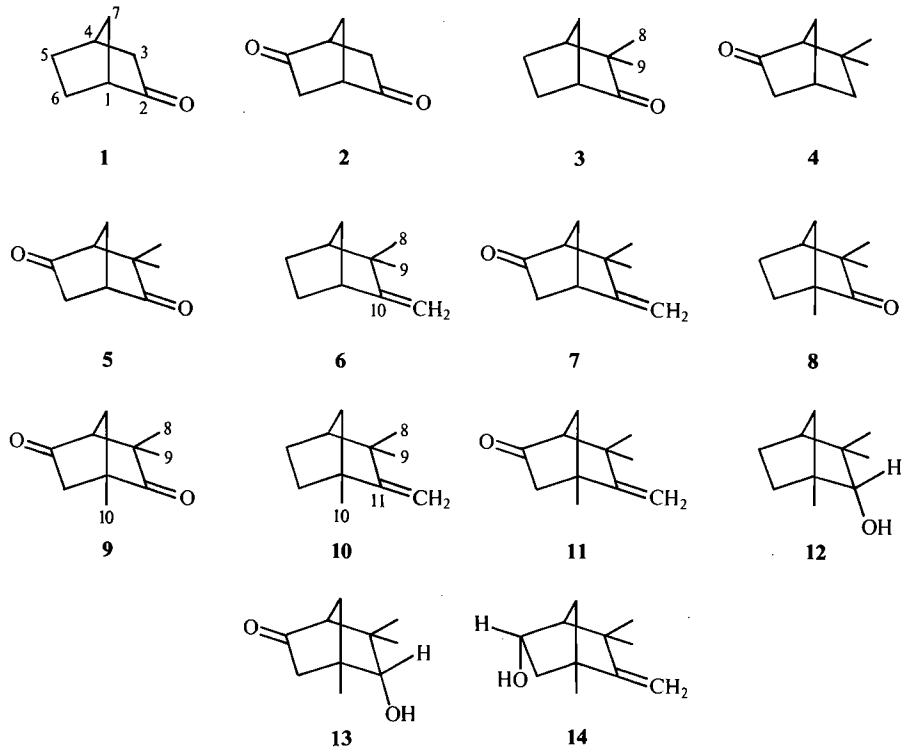

Since the predicted shifts of the diones **2**, **5**, and **9** and the enones **7** and **11** compare favorably with the observed values, several interpretations are possible: (*a*) the diones and enones exist in *synchro* or *contra* twist forms with $90° < \phi < 109.5°$, but that the hybridization change at the bridgeheads is minimal; (*b*) that Lippmaa's parameters account sufficiently for hybridizational changes which arise from distortion of the [2.2.1]-system through incorpora-

TABLE 2. Predicted and observed shifts differences

Compound	Substrate used for prediction	Predicted shifts				Differences from observed shifts*			
		C-1	C-4	C-6	C-7	C-1	C-4	C-6	C-7
2	**1**	49.0	48.2	36.6	37.9	−1.6	−0.8	−0.2	−4.1
3	**1**	50.8	46.2	25.8	37.6	−1.0	0.0	−1.5	−3.0
5	**3**	49.5	58.2	37.5	36.9	−1.0	+2.0	+1.1	−4.3
7	**6**	45.7	60.3	40.6	36.4	−2.3	+1.7	+1.7	−2.6
8	**3**	56.9	46.2	32.3	43.8	−3.2	−0.8	−0.5	−2.2
9	**1**	55.6	60.0	42.8	36.4	−2.8	0.0	+2.3	+2.7
9	**8**	52.4	57.4	43.5	40.9	+0.4	+2.3	+1.6	−1.8
10	**6**	53.1	48.3	35.4	43.3	−3.2	−0.7	+0.2	+1.0
11	**10**	48.6	59.6	47.4	43.6	0.0	+2.5	+2.7	−1.2
13	**12**	48.0	60.3	36.6	40.3	−0.3	+2.8	+2.1	+2.3
14	**MN**†	52.2	56.0	47.2	45.9	−2.1	−3.4	−2.7	−2.8
14	**10**	49.9	54.8	46.9	45.8	+0.2	−2.2	−2.4	−2.7

*Plus and minus indicate upfield and downfield shifts relative to the expected position.
†2-Methylenenorbornane used as substrate.

tion of substituents. That (*b*) is the case can be seen from a consideration of the predicted and observed shift differentials for C-4, -6, and -7. For **5**, **9**, **7**, and **11**, C-4 and -6 are consistently 2.0–2.6 and 1.6–2.7 p.p.m. downfield and C-7, 1.3–3.7 p.p.m. upfield, respectively, from the predicted positions. Carbon-1 appears 1.0–1.6 p.p.m. upfield from the expected position in **2**, **5**, and **7** and at the exact position, within experimental error, in **9** and **11**. Since no consistent upfield–downfield differentials are evident in the other compounds, with special attention drawn to the 2,5-systems **13** and **14**, the shift differentials for **5**, **9**, **7**, and **11** do perhaps indicate the operation of some effect not completely accounted for by the shift parameters. However, to decide conclusively whether or not the 2,5-diones and enones are unusual hybridizationally at the bridgeheads and to determine the magnitude of the effect, requires further studies.

Interestingly, the carbonyl carbons in the 2,5-diones experience a 2.4–4.3 p.p.m. diamagnetic shift relative to the monoketones (*cf.* **1** and **2**, Table 1). A decrease in the dipolar structure of the carbonyl groups due to the 1,4 dipolar interaction of the positive ends of the $\diagdown C{=}O$ dipole would explain this observation.

Also of interest is that C-7 in the diones and enones experiences a diamagnetic shift (1.2–4.3 p.p.m.) relative to the predicted values with a maximum differential of 4.3 in the 5-oxo-camphenilone (**5**). The effect of the carbonyl groups on C-7 contrasts with that of the double bonds in norbornadiene which cause a large paramagnetic shift (2).

Experimental

Apparatus

Spectra were recorded with a Varian Associates HA 100 spectrometer at 23.5 kG and 25.1 MHz. The operating probe temperature was +55 °C. Field frequency stabilization was achieved by use of an external (1.5 mm capillary) $^{13}CS_2$ lock and chemical shift measurements were made initially relative to internal dioxane (67.3 p.p.m.), benzene (129.7 p.p.m.), and then to internal tetramethylsilane. A sample volume of 0.2–0.3 ml was used in a 5 mm o.d. sample tube, with dioxane as solvent where necessary. Normally a signal accumulation of 4–16 scans with a Varian Associates C-1024 time averaging computer, was sufficient to give an adequate signal to noise enhancement. Proton decoupling was carried out using a Varian Associates V-3512-1 noise decoupler. Carbon atom assignments were accomplished by examination of off-resonance decoupled spectra which were obtained by accumulation of 100–300 scans. Deuterium substitution was used in **5** to establish the carbon assignments.

We thank the National Research Council of Canada for financial support.

1. J. B. GRUTZNER, M. JAUTELAT, J. B. DENCE, R. A. SMITH, and J. D. ROBERTS. J. Am. Chem. Soc. **92**, 7107 (1970).
2. E. LIPPMAA, J. PEHK, J. PAASIVIRTA, N. BELIKOVA, and A. PLATE. Org. Mag. Res. **2**, 581 (1970).
3. HANS-JORG SCHNEIDER and W. BREMSER. Tetrahedron Lett. 5197 (1970).
4. E. WENKERT, A. O. CLOUSE, D. W. COCHRAN, and D. DODDRELL. J. Chem. Soc. D, 1433 (1969).
5. H. J. REICH, M. JAUTELAT, M. T. MESSE, F. J. WEIGERT, and J. D. ROBERTS. J. Am. Chem. Soc. **91**, 7445 (1969); J. D. ROBERTS, F. J. WEIGERT, I. J. KROSCHWITZ, and H. J. REICH. J. Am. Chem. Soc. **92**, 1338 (1970);

F. J. WEIGERT and J. D. ROBERTS. J. Am. Chem. Soc. **92**, 1347 (1970); D. E. DORMAN and J. D. ROBERTS. J. Am. Chem. Soc. **92**, 1355 (1970); W. O. CRAIN, JR., W. C. WILDMAN, and J. D. ROBERTS. J. Am. Chem. Soc. **93**, 990 (1971); D. E. DORMAN and J. D. ROBERTS. J. Am. Chem. Soc. **93**, 4463 (1971).
6. B. E. MANN. Chem. Commun. 976 (1971).
7. M. H. CHISHOLM, H. C. CLARK, L. E. MANZER, and J. B. STOTHERS. Chem. Commun. 1627 (1971).
8. G. E. MACIEL, J. W. MCIVER, JR., N. S. OSTLUND, and J. A. POPLE. J. Am. Chem. Soc. **92**, 1 (1970) and references therein.
9. F. J. WEIGERT and J. D. ROBERTS. J. Am. Chem. Soc. **89**, 5963 (1967).
10. W. M. LITCHMAN and D. M. GRANT. J. Am. Chem. Soc. **89**, 6675 (1967).
11. N. H. WERSTIUK and R. TAILLEFER. Can. J. Chem. **40**, 3966 (1970).
12. C. ALTONA and M. SUNDARALINGAM. J. Am. Chem. Soc. **92**, 1995 (1970).
13. J. W. EMSLEY, J. FEENEY, and L. H. SUTCLIFFE. High resolution nuclear magnetic resonance spectroscopy. Vol. II. Pergamon Press, Oxford. 1966. p. 988.

Stereochemistry of 3-Methyl-4-phenylpiperidines Derived from Corresponding 4-Phenyl-4-piperidinols

K. M. J. MCERLANE AND A. F. CASY

Faculty of Pharmacy and Pharmaceutical Sciences, University of Alberta, Edmonton, Alberta

Received October 21, 1971

Catalytic reduction of 3- and 5-methyl-4-phenyl-1,2,5,6-tetrahydropyridines is stereospecific and gives *cis*-3-methyl-4-phenylpiperidines. Hydrogenolysis of 1-*t*-3-dimethyl-4-*r*-hydroxy-4-phenylpiperidine (*β*-prodinol) by Raney nickel also gives a *cis* product. Stereochemical assignments are made on the basis of p.m.r. spectroscopic data. Hot-plate activities in mice of 1-methyl- and 1-phenethyl-*c*-3-methyl-4-phenylpiperidine are reported.

La réduction catalytique des méthyl-3 et -5 phényl-4 tétrahydro-1,2,5,6 pyridines est stéréospécifique et conduit au méthyl-3 phényl-4 pipéridine *cis*. L'hydrogénolyse de la diméthyl-1-*t*-3 hydroxy-4-*r* phényl-4 pipéridine (*β*-prodinol) par le nickel de Raney donne aussi un produit *cis*. Les attributions stéréochimiques sont faites sur la base des données r.m.n. Les activités biologiques sur les souris de la méthyl-1 et phénéthyl-1 méthyl-*c*-3 phényl-4 pipéridine sont rapportées.

Canadian Journal of Chemistry, **50**, 2149 (1972)

A feature common to all narcotic analgesics based on 4-phenylpiperidine is an oxygenated function at C-4; this may be CO_2Et, OCOEt, COEt, or OEt (1). In view of the fact that analgesics of the morphinan and 6,7-benzomorphan class lack a non-aromatic oxygen function as do also certain 3-phenylpiperidine analgesics such as **1**, a series examined by Kugita *et al.* (2), it was of interest to determine if analgesic activity were retained in analogs of reversed esters of pethidine in which the 4-propionyloxy group was replaced by hydrogen as in **2**. Of special interest were the derivatives **2** with *cis* 3-Me/4-Ph geometry, since these isomers are more active than the *trans* forms in the 3-methylpethidine and prodine series (3, 4).[1]

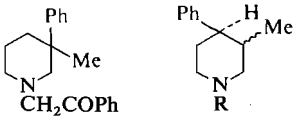

1 **2**

a R = Me
b R = Et
c R = H
d R = $(CH_2)_2Ph$

The first approach to preparing the diastereoisomers **2** was to reduce the acid catalyzed dehydration products of 3-methyl-4-phenyl-4-piperidinols; these were composed of mixtures of the tri- (**3**) and tetra-substituted alkenes (**4**). Single isomeric forms of **2** resulted when the

[1]Pethidine (meperidine) is 4-carbethoxy-1-methyl-4-phenylpiperidine hydrochloride; α- and *β*-prodine (reversed ester analogs of pethidine) are *c*-3-Me- and *t*-3-Me,*r*-4-OCOEt isomers of 1,3-dimethyl-4-phenyl-4-propionyloxypiperidine hydrochloride respectively, while α- and *β*-prodinol are the corresponding 4-piperidinol bases.

F. J. WEIGERT and J. D. ROBERTS. J. Am. Chem. Soc. **92**, 1347 (1970); D. E. DORMAN and J. D. ROBERTS. J. Am. Chem. Soc. **92**, 1355 (1970); W. O. CRAIN, JR., W. C. WILDMAN, and J. D. ROBERTS. J. Am. Chem. Soc. **93**, 990 (1971); D. E. DORMAN and J. D. ROBERTS. J. Am. Chem. Soc. **93**, 4463 (1971).
6. B. E. MANN. Chem. Commun. 976 (1971).
7. M. H. CHISHOLM, H. C. CLARK, L. E. MANZER, and J. B. STOTHERS. Chem. Commun. 1627 (1971).
8. G. E. MACIEL, J. W. MCIVER, JR., N. S. OSTLUND, and J. A. POPLE. J. Am. Chem. Soc. **92**, 1 (1970) and references therein.
9. F. J. WEIGERT and J. D. ROBERTS. J. Am. Chem. Soc. **89**, 5963 (1967).
10. W. M. LITCHMAN and D. M. GRANT. J. Am. Chem. Soc. **89**, 6675 (1967).
11. N. H. WERSTIUK and R. TAILLEFER. Can. J. Chem. **40**, 3966 (1970).
12. C. ALTONA and M. SUNDARALINGAM. J. Am. Chem. Soc. **92**, 1995 (1970).
13. J. W. EMSLEY, J. FEENEY, and L. H. SUTCLIFFE. High resolution nuclear magnetic resonance spectroscopy. Vol. II. Pergamon Press, Oxford. 1966. p. 988.

Stereochemistry of 3-Methyl-4-phenylpiperidines Derived from Corresponding 4-Phenyl-4-piperidinols

K. M. J. MCERLANE AND A. F. CASY

Faculty of Pharmacy and Pharmaceutical Sciences, University of Alberta, Edmonton, Alberta

Received October 21, 1971

Catalytic reduction of 3- and 5-methyl-4-phenyl-1,2,5,6-tetrahydropyridines is stereospecific and gives *cis*-3-methyl-4-phenylpiperidines. Hydrogenolysis of 1-*t*-3-dimethyl-4-*r*-hydroxy-4-phenylpiperidine (β-prodinol) by Raney nickel also gives a *cis* product. Stereochemical assignments are made on the basis of p.m.r. spectroscopic data. Hot-plate activities in mice of 1-methyl- and 1-phenethyl-*c*-3-methyl-4-phenylpiperidine are reported.

La réduction catalytique des méthyl-3 et -5 phényl-4 tétrahydro-1,2,5,6 pyridines est stéréospécifique et conduit au méthyl-3 phényl-4 pipéridine *cis*. L'hydrogénolyse de la diméthyl-1-*t*-3 hydroxy-4-*r* phényl-4 pipéridine (β-prodinol) par le nickel de Raney donne aussi un produit *cis*. Les attributions stéréochimiques sont faites sur la base des données r.m.n. Les activités biologiques sur les souris de la méthyl-1 et phénéthyl-1 méthyl-*c*-3 phényl-4 pipéridine sont rapportées.

Canadian Journal of Chemistry, **50**, 2149 (1972)

A feature common to all narcotic analgesics based on 4-phenylpiperidine is an oxygenated function at C-4; this may be CO_2Et, OCOEt, COEt, or OEt (1). In view of the fact that analgesics of the morphinan and 6,7-benzomorphan class lack a non-aromatic oxygen function as do also certain 3-phenylpiperidine analgesics such as **1**, a series examined by Kugita *et al.* (2), it was of interest to determine if analgesic activity were retained in analogs of reversed esters of pethidine in which the 4-propionyloxy group was replaced by hydrogen as in **2**. Of special interest were the derivatives **2** with *cis* 3-Me/4-Ph geometry, since these isomers are more active than the *trans* forms in the 3-methylpethidine and prodine series (3, 4).[1]

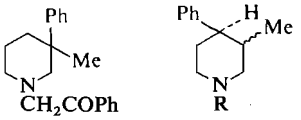

1 **2**

a R = Me
b R = Et
c R = H
d R = $(CH_2)_2Ph$

The first approach to preparing the diastereoisomers **2** was to reduce the acid catalyzed dehydration products of 3-methyl-4-phenyl-4-piperidinols; these were composed of mixtures of the tri- (**3**) and tetra-substituted alkenes (**4**). Single isomeric forms of **2** resulted when the

[1]Pethidine (meperidine) is 4-carbethoxy-1-methyl-4-phenylpiperidine hydrochloride; α- and β-prodine (reversed ester analogs of pethidine) are *c*-3-Me- and *t*-3-Me,*r*-4-OCOEt isomers of 1,3-dimethyl-4-phenyl-4-propionyloxypiperidine hydrochloride respectively, while α- and β-prodinol are the corresponding 4-piperidinol bases.

Can. J. Chem. Downloaded from www.nrcresearchpress.com by 210.87.254.42 on 09/05/12
For personal use only.

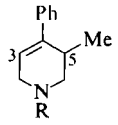

3

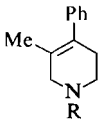

4

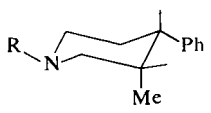

5

alkene hydrochloride salts (R in **3** and **4** = Me, Et, CH_2Ph, $(CH_2)_2Ph$, mixture or pure isomer) were shaken with hydrogen at atmospheric pressure in the presence of palladized charcoal. The isomers **2** were assigned a *cis* 3-Me/4-Ph configuration on the basis of the 3-methyl signals of their p.m.r. spectra undergoing a downfield shift of about 0.3 p.p.m. when the basic center of the molecule was protonated; shifts of these magnitudes in 3-methylpiperidines are evidence for an axial *C*-methyl orientation as in the preferred conformation **5** (3, 5, 6). In the *trans* isomer **2***a* (see later), the 3-methyl shift after *N*-protonation was negligible (0.07 p.p.m.), the substituent being well removed from the deshielding $^+$NH feature of the molecule when it has an equatorial orientation. Assuming that catalytic hydrogenation of **3** and **4** proceeds by *cis* addition from the least hindered side of the molecule (7), the stereospecificity of these reactions may be elaborated as follows. Clearly *cis* addition of hydrogen to the double bond of the 3-methyl-

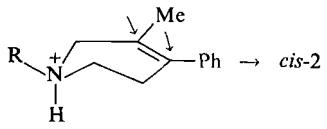

6

tetrahydropyridine **6** must give rise to a *cis* 3-Me/4-Ph product whatever face of the molecule is attacked. The product of *cis* addition to the protonated trisubstituted alkene **3**, however, depends on the conformation of the conjugate acids at the catalyst surface. If it be **7**, a *trans* product results when addition takes place in direction A, and a *cis* derivative if

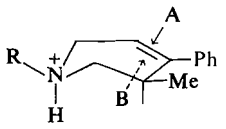

7

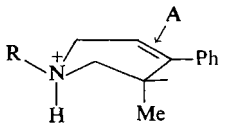

8

approach is from B. If it be **8**, the *cis* product will result (in this case only approach from A need be considered because this is clearly the less hindered route). There is good evidence for the existence of high populations (50% or more) of conformer **8** in solutions of salts of the tetrahydropyridines **3** (8).

In an attempt to obtain the *trans* isomer of **2***a*, hydrogenolysis of the 4-piperidinols **9** by

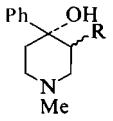

9

a R = H
b R = Me

means of Raney nickel was investigated. Although this method of replacing hydroxyl by hydrogen in benzylic alcohols may occur with inversion of configuration (9), it generally proceeds with retention in the absence of competitive reduction pathways and when high reaction temperatures are avoided (10, 11). The piperidinols **9***a* and 3-*t*-Me,*r*-OH **9***b* (*β*-prodinol) were smoothly hydrogenolyzed by Raney nickel in boiling ethanol, no reaction occurring at room temperature. In the latter case, the product was *cis*-**2***a*, hence the reaction was stereospecific and proceeded with retention. The 3-*c*-Me piperidinol **9***b* (*α*-prodinol) proved resistant to Raney nickel even when the reaction period was extended. This result is attributed to steric hindrance of the hydroxyl function by the gauche 3-methyl group (**10**) whereby ap-

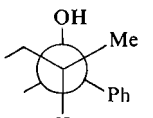

10(*α*)

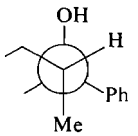

11(*β*)

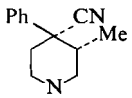

12

proach of the molecule to the catalyst surface is impeded. In *β*-prodinol, the 3-methyl substituent is well removed from the OH function (**11**). Other examples which illustrate the greater accessibility of the hydroxyl group in 3-*t*-Me,*r*-OH prodinol are available (12–15). The *trans*-piperidine **2***a* was finally obtained by cleavage of 4-*r*-cyano-1,3-*c*-dimethyl-4-phenylpiperidine (**12**) with sodamide.

Can. J. Chem. Downloaded from www.nrcresearchpress.com by 210.87.254.42 on 09/05/12
For personal use only.

Can. J. Chem. Downloaded from www.nrcresearchpress.com by 210.87.254.42 on 09/05/12
For personal use only.

The *c*-3-methyl derivative **2***a* was half as active as pethidine in the hot-plate test performed on mice (ED_{50} valves after subcutaneous injection were 8.6 and 4.7 mg/kg respectively). The corresponding 1-phenethyl analogue **2***d* was inactive in this test at a dose level of 100 mg/kg. Hence, since the potency of narcotic analgesics derived from *N*-methyl cyclic bases increases when the *N*-substituent is replaced by 1-phenethyl (1), *c*-3-methyl-**2***a* probably has a general depressant rather than morphine-like action in this test.[2]

Experimental

The p.m.r. spectra were recorded on a Varian A-60D spectrometer at the ambient temperature using $CDCl_3$ or DMSO-d_6 as solvents and TMS as standard. Salts were crystallized from ethanol–ether unless otherwise stated.

Reduction of 3- and 5-Methyl-4-phenyl-1,2,5,6-tetrahydropyridines (3 and 4)

The mixture of **3***a* and **4***a* hydrochlorides (6 g) obtained from α-prodinol (8) was dissolved in ethanol (50 ml) and shaken with 10% palladium-on-charcoal (0.4 g) and hydrogen at room temperature and pressure. When gas absorption ceased the mixture was filtered and the filtrate evaporated. The residue was recrystallized to give *cis (3-Me/4-Ph) 1,3-dimethyl-4-phenylpiperidine hydrochloride* (5 g), m.p. 243–245°, $\delta_{3\text{-Me}}$ 1.14, 0.73 (base) in $CDCl_3$.

Anal. Calcd. for $C_{13}H_{20}ClN$: C, 69.3; H, 8.8. Found: C, 69.2; H, 8.9.

No evidence of a second isomer could be obtained from the mother liquors.

The following analogues of *cis*-**2***a* were similarly prepared from the appropriate alkenes **3** and **4** or alkene mixtures (reduction of the *N*-benzyl derivatives also removed the *N*-substituent).

2*b hydrochloride*, m.p. 260–263°, $\delta_{3\text{-Me}}$ 1.12, 0.8 (base) in $CDCl_3$.

Anal. Calcd. for $C_{14}H_{22}ClN$: C, 70.1; H, 9.25; N, 5.8. Found: C, 70.4; H, 9.1; N, 5.5.

2*c hydrochloride*, m.p. 216–217°, $\delta_{3\text{-Me}}$ 1.05, 0.8 (base) in $CDCl_3$.

Anal. Calcd. for $C_{12}H_{18}ClN$: C, 68.1; H, 8.6; N, 6.6. Found: C, 67.8; H, 8.5; N, 6.8.

2*d hydrochloride*, m.p. 235–236°, $\delta_{3\text{-Me}}$ 1.11, 0.78 (base) in $CDCl_3$.

Anal. Calcd. for $C_{20}H_{26}ClN$: C, 76.05; H, 8.3. Found: C, 76.0; H, 8.5.

Hydrogenolysis of the 4-Piperidinols (9)

A mixture of Raney nickel (5 g) (Grace, Chattanooga, active grade) **9***a* (0.5 g) and ethanol (50 ml) was stirred and heated under reflux for 4 h. The product was cooled, filtered, and the filtrate evaporated to give 1-methyl-4-phenylpiperidine (0.5 g) (in all these experiments completion of hydrogenolysis was checked by the absence of a ν_{OH} band near 3150 cm^{-1} in the i.r. spectrum of the product), isolated as a *hydrochloride*, m.p. 197–198°.

Anal. Calcd. for $C_{12}H_{18}ClN$: C, 68.1; H, 8.6; N, 6.6. Found: C, 68.2; H, 8.6; H, 6.6.

It formed a picrate, m.p. 238° from ethanol, lit. 239–240° (16).

The same treatment of β-prodinol gave *cis*-**2***a*, m.p. and mixed m.p. 242–243°, while α-prodinol was unaffected.

Cleavage of the Isomeric 4-Cyanopiperidines 12 (by K. K. Khullar)

A mixture of 4-*r*-CN,3-*c*-Me **12** (3.1 g) (3), sodamide (5.85 g), and toluene (150 ml) was heated under reflux for 8 h. Water was added to the cooled product and the toluene separated and extracted with dilute hydrochloric acid. The free base was recovered as usual giving *t*-3-Me **2***a* (2.5 g), isolated as a *hydrochloride*, m.p. 232–235°.

Anal. Calcd. for $C_{13}H_{20}ClN$: C, 69.3; H, 8.8; N, 6.2. Found: C, 68.9; H, 9.2; N, 6.3.

It formed a *methiodide*, m.p. 143–146°.

Anal. Calcd. for $C_{14}H_{22}IN$: C, 50.8; H, 6.6; N, 4.2. Found: C, 51.0; H, 6.5; N, 4.2.

The same treatment of 4-*r*-CN,3-*t*-Me **12** gave *c*-3-Me **2***a*, m.p. and mixed m.p. 237–238°.

We thank the Medical Research Council of Canada for financial support, Dr. A. P. Parulkar for samples of **3***b*, **3***c*, **4***b*, and **4***c*, and Dr. K. K. Khullar for carrying out cleavage experiments on the isomers **12**.

[2]We thank Dr. E. L. May, National Institutes of Health, Bethesda, Maryland for these data.

1. A. H. Beckett and A. F. Casy. Prog. Med. Chem. **4**, 171 (1965).
2. H. Kugita, H. Inoue, T. Oine, G. Hayashi, and S. Nurimoto. J. Med. Chem. **7**, 298 (1964).
3. A. F. Casy, L. G. Chatten, and K. K. Khullar. J. Chem. Soc. C, 2491 (1969).
4. A. F. Casy. J. Med. Chem. **11**, 188 (1968), and refs. cited therein.
5. A. F. Casy. Tetrahedron, **22**, 2711 (1966).
6. A. F. Casy. Proton magnetic resonance spectroscopy in medicinal and biological chemistry. Academic Press, London, 1971. p. 203.
7. H. O. House. Modern synthetic reactions. Benjamin, New York, 1965.
8. A. F. Casy, A. H. Beckett, M. A. Iorio, and H. Z. Youssef. Tetrahedron, **21**, 3387 (1965).
9. W. A. Bonner and J. A. Zderic. J. Am. Chem. Soc. **78**, 3218 (1936).
10. E. W. Garbisch. Chem. Commun. 806 (1967).
11. S. Mitsui, Y. Kudo, and M. Yobayashi. Tetrahedron, **25**, 1921 (1969).
12. A. F. Casy. J. Chem. Soc. 5057 (1961).
13. A. F. Casy and P. Pocha. J. Chem. Soc. C, 979 (1967).
14. A. F. Casy, A. H. Beckett, and M. A. Iorio. Tetrahedron, **23**, 1405 (1967).
15. A. F. Casy and K. M. J. McErlane. J. Chem. Soc. 334 (1972).
16. C. J. Schmidle and R. C. Mansfield. J. Am. Chem. Soc. **77**, 5698 (1953).

On the Extent of Transannular Rearrangement in the Formolysis of 1,5-Cyclooctadiene Monoepoxide

JOHN M. MCINTOSH
Department of Chemistry, University of Windsor, Windsor, Ontario
Received January 13, 1972

Formolysis of 1,5-cyclooctadiene monoepoxide (**1**) has been shown to give only *ca.* 25% of products of transannular reactions. The difference between this result and those from the solvolyses of cyclooctene oxide and 4-cyclooctenyl brosylate is attributed to conformational and ring-strain effects.

La formolyse du monoépoxyde (**1**) du cyclooctadiène-1,5 conduit à 25% seulement de produits résultant de réactions trans-annulaire. La différence entre ce résultat et ceux issus de la solvolyse de l'époxyde du cyclooctène et du brosylate du cyclooctényl-4 est attribuée à des effets conformationnels et de tension du cycle.

Canadian Journal of Chemistry, **50**, 2152 (1972)

Transannular reactions involving hydride migrations and π-electron participation in medium-sized ring solvolyses are well-documented (1). Perhaps the most thoroughly investigated case is the formolysis of cyclooctene oxide (2) where the competing reactions of 1,3- and 1,5-hydride migrations have been separated and shown to be in the ratio of 2:3 (3). Attempts to extend the reaction to the migration of other groups have met with limited success (4, 5).

The preparation of 5-cyclooctene-1,2-diol (**2**) in 73% yield by the acid-catalyzed hydroxylation of 1,5-cyclooctadiene has been reported in the patent literature (6). The presumed intermediate in this reaction is 1,5-cyclooctadiene monoepoxide (**1**). The amount of normal epoxide opening reported in this case is surprising when compared with that of cyclooctene oxide (2) since the presence of the double bond might be expected to facilitate 1,3-hydride migrations by stabilization of the developing positive charge. Moreover, transannular π-electron participation might be expected to provide an energetically favorable pathway to bicyclic products. It should be noted that the acetolysis of 4-cyclooctenyl brosylate has been reported (7) to give 74% of rearranged products. Therefore we have reinvestigated the formolysis of 1,5-cyclooctadiene monoepoxide.

When 1,5-cyclooctadiene monoepoxide (**1**) (8) was solvolyzed in either 85 or 98% formic acid, a mixture of hydroxyformates was obtained. Saponification and distillation of the mixture afforded an alcohol fraction and a higher-boiling diol fraction as the only volatile components (Scheme 1). The yields are summarized in Table 1.

The alcohol fraction contained 50% of 3,5-cyclooctadienol (**3**) (9) which was distinguished from its isomer **4** (10) by its u.v. spectrum. The remainder of the fraction was composed of a mixture of bicyclooctenols as was shown by elemental analysis, mass spectrometry, and by integration of the n.m.r. spectrum.

The diol fraction was treated with acetone and the isopropylidene ketal of 5-cyclooctene-1,2-diol (**5**) was separated from the mixture by distillation. The yields are summarized in Table 1. That the residual diol mixture consisted only of saturated bicyclooctanediols was shown by (*a*) the absence of n.m.r. absorptions below $\delta = 5.2$, (*b*) the lack of reaction with dilute bromine solution, and (*c*) the lack of hydrogen absorption in the presence of a palladium catalyst. Acetylation of the mixture gave a mixture of diacetates which contained at least eight components, many of which were incompletely resolved under all v.p.c. conditions utilized. Two of the components were separated and the diols obtained by hydride reduction were identified as bis-*endo*-bicyclo[3.3.0]octan-2,6-diol (**6**) and a mixture of 2,5- and 2,6-epoxycyclooctanol (**7**).

The comparison of the amount of transannular reaction in this case and those of cyclooctene oxide and 4-cyclooctenyl brosylate is shown in Table 2. Clearly the introduction of the π-bond into this cyclooctane ring effectively negates the proclivity for transannular hydride shift reactions found in cyclooctene oxide. The only product isolated compatible with such a

Can. J. Chem. Downloaded from www.nrcresearchpress.com by 210.87.254.6 on 09/05/12
For personal use only.

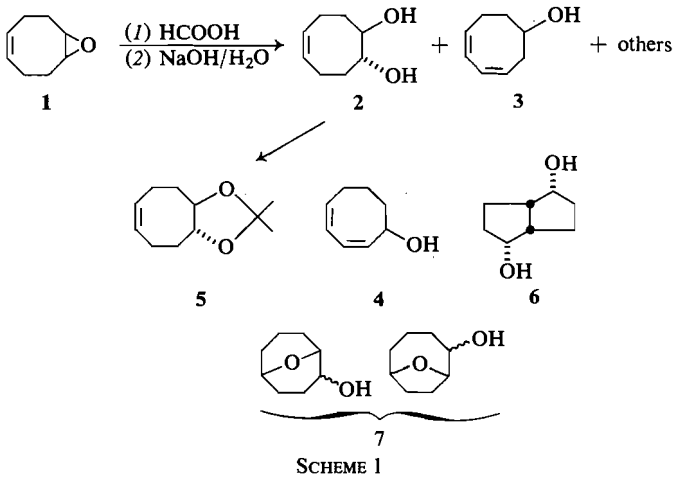

SCHEME 1

TABLE 1. Product distribution in the solvolysis of **1**

Solvolysis medium	Temperature (°C)	Alcohol (%)		Diol **8**‡ (%)		Other diols (%)	
		*	†	*	†	*	†
85% HCOOH§	95	7	4	72.5	45.0	20.0	15.1
95% HCOOH§	60	—	—	74.5	50.7	20.2	13.7

*Based on the total volatile components of the solvolysis.
†Based on **1**.
‡As ketal.
§Average of three runs.

TABLE 2. Comparison of products from cyclooctane compounds

Compound	Medium	Normal reaction (%)*	Hydride shift products (%)*	Bicyclics (%)*
1	85% HCOOH	72.5	7	20.0
	98% HCOOH	74.5	—	20.2
Cyclooctene oxide	85% HCOOH	13	86	<1
4-Cyclooctenyl brosylate	HOAc/NaOAc	26†	—	74

*Based on the total volatile components of the solvolysis.
†Elimination product.

mechanism is dienol **3** (Scheme 2). However, the data do not allow the assignment of this difference to the presence of a preferred pathway involving π-electron participation. Two arguments can be advanced to rationalize these results. Models suggest that (*a*) in a suitable transition state for 1,3-hydride migration, the protons on C-3 and -7 are in very close proximity and (*b*) the conformation required for π-electron participation in the opening of the epoxide ring

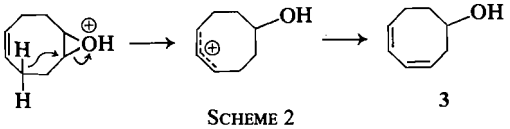

SCHEME 2

also required the eclipsing of the C_3—C_4 and the C_7—C_8 protons. These energetically unfavorable situations may be responsible for the observed increase in the amount of "normal" epoxide opening. Alternately, it has been

Can. J. Chem. Downloaded from www.nrcresearchpress.com by 210.87.254.6 on 09/05/12
For personal use only.

Can. J. Chem. Downloaded from www.nrcresearchpress.com by 210.87.254.6 on 09/05/12
For personal use only.

pointed out that the introduction of one double bond into the cyclooctane ring reduces the ring strain. The experimental evidence on this point has been summarized (7). Although precise thermochemical data are not available, it has been suggested (7) that the ring strain in the bicyclo[3.3.0]octanes and the bicyclo[4.2.0]-octanes (which should be reflected in the transition state leading to them) may be large enough to make their formation from an incipient cyclooctenyl carbonium ion slow relative to the usual epoxide-opening reaction.

If the products from **1** arise by attack of formate directly on the protonated epoxide, the difference in the products from **1** and 4-cyclooctenyl brosylate is understandable since the latter is thought to proceed via a more carbonium ion-like transition state which allows greater flexibility of the ring and thus more π-participation in the product-forming step.

Experimental

Melting points and boiling points are uncorrected; v.p.c. analyses were performed on an F and M Model 720 instrument; i.r. spectra were recorded in chloroform solution; and n.m.r. spectra in deuteriochloroform unless otherwise noted. Microanalyses were performed by Dr. S. M. Nagy and Associates (M.I.T.) and by A. B. Gygli, Microanalysis Laboratory (Toronto).

Solvolysis of 1,5-Cyclooctadiene Monoepoxide (1)

(A) With 85% Formic Acid

To 500 ml of hot (95°) formic acid was added 60 g (0.48 mol) of **1** dropwise with stirring. An exothermic reaction ensued. The temperature was maintained at 95° for 1 h after the final addition and then most of the acid was removed by distillation at 80 mm. The residual brown oil was treated with 150 ml of cold 50% aqueous sodium hydroxide and stirred at room temperature overnight. The thick mass was extracted with four 200 ml portions of chloroform and the extracts were dried, evaporated, and carefully distilled to give an alcohol fraction (2.6 g, 4.3% as dienol), b.p. 45–59° (0.25 mm), a main fraction (48.5 g, 70.1% as cyclooctene diols), b.p. 83–98° (0.23 mm), and a non-distillable residue which was discarded.

(B) With 98% Formic Acid

The reaction was carried out in the same manner except the temperature was maintained at 60°. Fractionation of the saponified mixture gave no alcohol fraction, 47.2 g (68% as cyclooctene diols) of a viscous oil, b.p. 85–100° (0.25 mm), and some residue which was discarded.

The alcohol fraction was separated into two components by preparative v.p.c. (8 ft × 0.25 in. 20% SE30, 150°), one of which was identified as 3,5-cyclooctadienol (**3**) (9) which was distinguished from 2,4-cyclooctadienol (**4**) (10) by its u.v. spectrum: λ_{max} (EtOH) 230 nm (ε 4070).

Anal. Calcd. for $C_8H_{12}O$: C, 77.38; H, 9.74. Found: C, 77.13; H, 9.63.

Catalytic reduction over 10% palladium-on-charcoal resulted in a hydrogen absorption of 2 equiv and furnished cyclooctanol, identical in all respects with an authentic sample.

The n.m.r. spectrum of the remainder of the fraction showed an integrated intensity of 1.4 for the vinyl protons (total of 12) but was otherwise uninformative. Catalytic reduction resulted in a hydrogen absorption of 95% of 1 equiv. Analysis of the product on several v.p.c. columns showed one very broad peak. The n.m.r. spectrum was blank below δ 5.15 and a test with bromine in carbon tetrachloride was negative.

Anal. Calcd. for $C_8H_{12}O$: C, 77.38; H, 9.74. Found: C, 77.37; H, 9.61.

A solution of 40.0 g (0.282 mol) of the fraction of b.p. 83–98° (0.23 mm) in 500 ml of acetone was shaken with 60 g of anhydrous cupric sulfate for 22 h at room temperature. The solution was filtered, the residue washed with acetone and the solvent removed by distillation. Fractionation of the residue afforded 5.8 g (21.2%) of a viscous glycol mixture, b.p. 96–124° (0.4 mm) and 39.4 g (77%) of 5-cyclooctene-*trans*-1,2-diol isopropylidene ketal (**5**), b.p. 66–68° (2.0 mm); n_D^{25} 1.4699; i.r. 3020, 2985, 2940, 2860 1100 cm^{-1}; n.m.r. 5.64 (2H, mult), 3.90 (2H, mult), 2.24 (8H, mult), 1.33 (6H, sing).

Anal. Calcd. for $C_{11}H_{18}O_2$: C, 72.46; H, 9.95. Found: C, 72.50; H, 9.87.

5-Cyclooctene-trans-1,2-diol (2)

Five grams (0.027 mol) of ketal **5** were hydrolyzed with 85% formic acid at reflux for 2 h. After saponification of the product with aqueous sodium hydroxide, distillation gave 3.12 g (80%) of **2**, b.p. 88–89° (0.12 mm); n_D^{25} 1.5110; i.r. 3320 cm^{-1}; n.m.r. 5.59 (2H, trip $J = 4$), 4.38 (2H, broad), 3.53 (2H, mult), 1.1–2.75 (8H, mult).

Anal. Calcd. for $C_8H_{14}O_2$: C, 67.57; H, 9.92. Found: C, 67.72; H, 10.11.

Acetylation of the remainder of the diol in the usual manner afforded a mixture of diacetates. We were unable to completely resolve the mixture under any v.p.c. conditions. There were at least eight components present, none of which corresponded to diol **2**. The lack of reaction of this mixture with dilute bromine solution, the absence of n.m.r. absorptions below δ 5.4 and the absence of a significant peak at *m/e* 224 showed that the mixture was composed of saturated materials only. Two components were isolated, reduced with lithium aluminum hydride, and the products shown to be bis-*endo*-bicyclo[3.3.0]octan-2,6-diol (**6**) identical with an authentic sample (see below) and a mixture of 2,5- and 2,6-epoxycyclooctanol, also identical with an authentic sample (11).

Bis-endo-bicyclo[3.3.0]octan-2,6-diol (6)

Bicyclo[3.3.0]octan-2,6-dione (12) (3.53 g, 0.026 mol) was reduced over prereduced platinum oxide in 75 ml of methanol at 80° and 1450–1300 p.s.i. for 12 h. Filtration and evaporation of the solvent gave residue which was distilled to give **6** (3.36 g, 93%), b.p. 102–103° (0.38 mm); n_D^{25} 1.5095.

Anal. Calcd. for $C_8H_{14}O_2$: C, 67.57; H, 9.92. Found: C, 67.42; H, 9.72.

The bis-phenylurethane had m.p. 196–197°.

Anal. Calcd. for $C_{22}H_{24}O_4N_2$: C, 69.45; H, 6.63; N, 7.37. Found: C, 69.63; H, 6.39; N, 7.12.

The author wishes to express his appreciation to the late Prof. A. C. Cope who initiated these investigations, and to Dr. B. S. Fisher who obtained some of the preliminary results while a student at M.I.T. The technical assistance of Mr. D. Hill and the financial assistance of the National Research Council of Canada is also greatly appreciated.

1. For review see, (*a*) A. C. COPE, M. M. MARTIN, and M. A. MCKERVEY. Quart. Rev. **20**, 119 (1966); (*b*) A. C. COPE. Proc. Robert Welch Foundation Conferences on Chem. Res. **4**, 11 (1960); (*c*) V. PRELOG and J. G. TRAYNHAM. *In* Molecular rearrangements. Vol. 1. *Edited by* P. de Mayo. Interscience. New York, N.Y. 1963. p. 593.
2. A. C. COPE, S. W. FENTON, and C. F. SPENCER. J. Am. Chem. Soc. **74**, 5884 (1952).
3. A. C. COPE, G. A. BERCHTOLD, P. E. PETERSON, and S. H. SHARMAN. J. Am. Chem. Soc. **82**, 6366 (1960).
4. A. C. COPE, P. E. BURTON, and M. L. CASPAR. J. Am. Chem. Soc. **84**, 4855 (1962).
5. J. M. MCINTOSH, M. H. MISKOW, and G. WOOD. Can. J. Chem. **49**, 3243 (1971).
6. P. LAFONT and H. MENAND. Fr. Pat. 1 294 313 (1962); Chem. Abstr. **57**, 16437 (1962).
7. A. C. COPE and P. E. PETERSON. J. Am. Chem. Soc. **81**, 1643 (1959).
8. A. C. COPE, B. S. FISHER, W. FUNKE, J. M. MCINTOSH, and M. A. MCKERVEY. J. Org. Chem. **34**, 2231 (1969).
9. J. K. CRANDALL and L. H. CHANG. J. Org. Chem. **32**, 532 (1967).
10. A. C. COPE, S. MOON, C. H. PARK, and G. L. WOO. J. Am. Chem. Soc. **84**, 4865 (1962).
11. A. C. COPE, M. A. MCKERVEY, and N. M. WEINSHENKER. J. Org. Chem. **34**, 2229 (1969).
12. C. T. BLOOD and R. P. LINSTEAD. J. Chem. Soc. 2255 (1952).

The Magnetic Susceptibilities of Some Oxyhalide Ions

M. B. KENNEDY AND M. W. LISTER

Department of Chemistry, University of Toronto, Toronto 181, Ontario

Received March 3, 1972

Diamagnetic susceptibilities are reported for aqueous sodium hypochlorite, chlorite, hypobromite, and bromite. The results, combined with data from the literature for compounds of general formula $NaXO_n$, show a small increase for $n = 0$ to 2, and a much larger increase thereafter. The interpretation of these results in terms of bond orders is discussed, and comparisons are made with the enthalpies of formation, distances, and force constants of these compounds.

Les susceptibilités diamagnétiques des solutions aqueuses d'hypochlorite, de chlorite, d'hypobromite et de bromite de sodium sont décrites. Les résultats, combinés aux données de la littérature concernant les composés de formule générale $NaXO_n$, montrent un faible accroissement de $n = 0$ à 2 et une croissance plus marquée au-delà. L'interprétation de ces résultats en fonction de l'ordre de liaison est discutée et les comparaisons sont faites avec les enthalpies de formation, les distances et les constantes de force de ces composés.

Canadian Journal of Chemistry, **50**, 2155 (1972)

In an earlier paper (1), one of the present authors attempted to relate the contribution of oxygen atoms to the molar diamagnetic susceptibility with the type of bonding of the oxygen. The compounds then considered contained oxygen linked to nitrogen and phosphorus, and these were considered with special reference to the bond orders of the bonds to oxygen. The present note deals with compounds containing oxygen linked to chlorine or bromine, particularly in the sodium salts of oxyhalide ions.

Since some of the compounds in question are difficult to obtain as pure crystals (*e.g.*, sodium hypobromite), the measurements of susceptibility were made on aqueous solutions. Earlier work (2, 3) has shown that the susceptibilities of salts are not very different depending on whether they are crystals or in solution, at least for uni-univalent salts; typically the susceptibility of the salt in solution is 4 to 5% higher. The susceptibility varies very little with concentration (4), so it was thought to be justifiable to compare salt solutions of different concentrations.

Experimental

Chemicals

Sodium Hypochlorite

A stock solution (about 1.2 *M*) was purified by filtration through sintered glass, and then adding a 5% solution of barium chloride dropwise with stirring, until no more

Can. J. Chem. Downloaded from www.nrcresearchpress.com by 210.87.254.6 on 09/05/12
For personal use only.

The author wishes to express his appreciation to the late Prof. A. C. Cope who initiated these investigations, and to Dr. B. S. Fisher who obtained some of the preliminary results while a student at M.I.T. The technical assistance of Mr. D. Hill and the financial assistance of the National Research Council of Canada is also greatly appreciated.

1. For review see, (*a*) A. C. COPE, M. M. MARTIN, and M. A. MCKERVEY. Quart. Rev. **20**, 119 (1966); (*b*) A. C. COPE. Proc. Robert Welch Foundation Conferences on Chem. Res. **4**, 11 (1960); (*c*) V. PRELOG and J. G. TRAYNHAM. *In* Molecular rearrangements. Vol. 1. *Edited by* P. de Mayo. Interscience. New York, N.Y. 1963. p. 593.
2. A. C. COPE, S. W. FENTON, and C. F. SPENCER. J. Am. Chem. Soc. **74**, 5884 (1952).
3. A. C. COPE, G. A. BERCHTOLD, P. E. PETERSON, and S. H. SHARMAN. J. Am. Chem. Soc. **82**, 6366 (1960).
4. A. C. COPE, P. E. BURTON, and M. L. CASPAR. J. Am. Chem. Soc. **84**, 4855 (1962).
5. J. M. MCINTOSH, M. H. MISKOW, and G. WOOD. Can. J. Chem. **49**, 3243 (1971).
6. P. LAFONT and H. MENAND. Fr. Pat. 1 294 313 (1962); Chem. Abstr. **57**, 16437 (1962).
7. A. C. COPE and P. E. PETERSON. J. Am. Chem. Soc. **81**, 1643 (1959).
8. A. C. COPE, B. S. FISHER, W. FUNKE, J. M. MCINTOSH, and M. A. MCKERVEY. J. Org. Chem. **34**, 2231 (1969).
9. J. K. CRANDALL and L. H. CHANG. J. Org. Chem. **32**, 532 (1967).
10. A. C. COPE, S. MOON, C. H. PARK, and G. L. WOO. J. Am. Chem. Soc. **84**, 4865 (1962).
11. A. C. COPE, M. A. MCKERVEY, and N. M. WEINSHENKER. J. Org. Chem. **34**, 2229 (1969).
12. C. T. BLOOD and R. P. LINSTEAD. J. Chem. Soc. 2255 (1952).

The Magnetic Susceptibilities of Some Oxyhalide Ions

M. B. KENNEDY AND M. W. LISTER

Department of Chemistry, University of Toronto, Toronto 181, Ontario

Received March 3, 1972

Diamagnetic susceptibilities are reported for aqueous sodium hypochlorite, chlorite, hypobromite, and bromite. The results, combined with data from the literature for compounds of general formula $NaXO_n$, show a small increase for $n = 0$ to 2, and a much larger increase thereafter. The interpretation of these results in terms of bond orders is discussed, and comparisons are made with the enthalpies of formation, distances, and force constants of these compounds.

Les susceptibilités diamagnétiques des solutions aqueuses d'hypochlorite, de chlorite, d'hypobromite et de bromite de sodium sont décrites. Les résultats, combinés aux données de la littérature concernant les composés de formule générale $NaXO_n$, montrent un faible accroissement de $n = 0$ à 2 et une croissance plus marquée au-delà. L'interprétation de ces résultats en fonction de l'ordre de liaison est discutée et les comparaisons sont faites avec les enthalpies de formation, les distances et les constantes de force de ces composés.

Canadian Journal of Chemistry, **50**, 2155 (1972)

In an earlier paper (1), one of the present authors attempted to relate the contribution of oxygen atoms to the molar diamagnetic susceptibility with the type of bonding of the oxygen. The compounds then considered contained oxygen linked to nitrogen and phosphorus, and these were considered with special reference to the bond orders of the bonds to oxygen. The present note deals with compounds containing oxygen linked to chlorine or bromine, particularly in the sodium salts of oxyhalide ions.

Since some of the compounds in question are difficult to obtain as pure crystals (*e.g.*, sodium hypobromite), the measurements of susceptibility were made on aqueous solutions. Earlier work (2, 3) has shown that the susceptibilities of salts are not very different depending on whether they are crystals or in solution, at least for uni-univalent salts; typically the susceptibility of the salt in solution is 4 to 5% higher. The susceptibility varies very little with concentration (4), so it was thought to be justifiable to compare salt solutions of different concentrations.

Experimental

Chemicals

Sodium Hypochlorite

A stock solution (about 1.2 *M*) was purified by filtration through sintered glass, and then adding a 5% solution of barium chloride dropwise with stirring, until no more

Can. J. Chem. Downloaded from www.nrcresearchpress.com by 210.87.254.42 on 09/05/12
For personal use only.

Can. J. Chem. Downloaded from www.nrcresearchpress.com by 210.87.254.42 on 09/05/12
For personal use only.

barium carbonate precipitated. The solution contained a little sodium carbonate (from the original sodium hydroxide), and it was known (5) that coprecipitation with barium carbonate removed heavy metal impurities. The solution was then filtered again, and was analyzed as described earlier (6).

Sodium Hypobromite

Stock solutions were prepared by adding bromine slowly to cold sodium hydroxide solutions, and the solutions were purified as for sodium hypochlorite. The analyses of these solutions, and also those of sodium bromite, were carried out by the methods of refs. 7 and 8. In addition, the sodium bromide content was found by adding excess 3% hydrogen peroxide to an aliquot (to destroy sodium hypobromite and bromite), adjustment of the p*H* to about 8, and titration with silver nitrate. This titration measures the total of sodium bromide, hypobromite, and bromite.

Sodium Bromite

Crystals of sodium bromite ($NaBrO_2.3H_2O$) were kindly supplied by la société d'études chimiques pour l'industrie et l'agriculture of Argenteuil, France. These were dissolved in dilute sodium hydroxide to give a stock solution, analyzed as above.

Sodium Chlorite

This was an analytical grade supplied by Matheson, Coleman and Bell Company. It was recrystallized from water and dried before use. It gave the correct equivalent weight, within experimental error, from iodometric titration.

Apparatus

The magnetic susceptibilities were measured as described earlier (1), both benzene and water being used as calibrating liquids. In general three measurements were made on each sample and the average taken. The temperature of the samples was 25 °C, and the density measurements, which are needed to convert the results to molar susceptibilities, were also made at 25 °C. It was assumed that the various components of the solutions contributed to the susceptibility in a simple additive manner. Since some of the solutions very slowly evolve oxygen, they were deoxygenated by bubbling nitrogen through them, and were measured immediately in an atmosphere of nitrogen.

Results

Sodium Hypochlorite

The solution (density 1.156 g/ml) contained 2.102 *M* NaCl, 1.156 *M* NaClO, 0.190 *M* $NaClO_3$, 0.0041 *M* NaOH, and 0.051 *M* Na_2CO_3. Its volume susceptibility was found to be -0.773×10^{-6} e.m.u./ml. If we take the molar susceptibilities of the compounds in solution to be: NaCl, −30.7 (2); $NaClO_3$, −34.6 (9); NaOH, −16.0; Na_2CO_3, −41.0 (10); and H_2O, −12.97 (all $\times 10^{-6}$ e.m.u./mol), then the calculated molar susceptibility of sodium hypochlorite is -31.7×10^{-6} e.m.u./mol. However, the value reported (9) for solid sodium chlorate is −34.7, and the usual difference of about 5% between solid and solution would suggest a value of about −36.4 for the solution. This is supported by the measurements of Trew *et al.* (11) who found a difference of −12.48 (or −6.24 per ion) between the susceptibilities of magnesium chloride and chlorate, both as crystalline hexahydrates. If this difference is correct, aqueous sodium chlorate would have a molar susceptibility of -36.9×10^{-6} e.m.u./mol. These values would lead to a molar susceptibility of -31.5 or -31.4×10^{-6} e.m.u./mol for sodium hypochlorite. Probably the best value to take is -31.5×10^{-6} e.m.u./mol.

Some confirmation of this was obtained from the susceptibility of a sample of crystalline calcium hypochlorite (purified by recrystallization from water) which gave a molar susceptibility of -58.8×10^{-6} e.m.u./mol, after allowing for the presence of small amounts of calcium chloride and chlorate and water, as found by analysis. If the susceptibility in aqueous solution is assumed to be 5% higher, and if the susceptibility of a calcium ion is 2×10^{-6} e.m.u./mol more positive than that of two sodium ions, then the calculated value of aqueous sodium hypochlorite is about -32×10^{-6} e.m.u./mol.

Sodium Chlorite

The molar susceptibility was found to be -31.2×10^{-6} e.m.u./mol for the crystal, and -32.7×10^{-6} e.m.u./mol in solution.

Sodium Hypobromite

Two different solutions were used, and the susceptibilities given are the averages of the measurements on each. The first solution contained NaBr, 1.2487 *M*; NaBrO, 1.259 *M*; NaOH, 0.863 *M*; Na_2CO_3, 0.197 *M*; density 1.2488 g/ml, and had a volume susceptibility of 0.785×10^{-6} e.m.u./ml. The second contained NaBr, 1.799 *M*; NaBrO, 1.810 *M*; NaOH, 0.845 *M*; Na_2CO_3, 0.171 *M*; density 1.3386 g/ml, and had a volume susceptibility of -0.8077×10^{-6} e.m.u./ml. Neither solution contained appreciable amounts of sodium bromate. If we take the molar susceptibility of aqueous sodium bromide to be -41.1×10^{-6} e.m.u./mol, the calculated molar susceptibilities of sodium hypobromite (aqueous) are −41.9 for the first

TABLE 1. Molar susceptibilities for $NaXO_n$

	Molar susceptibility $\times 10^{-6}$ e.m.u./mol	
n	X = Cl (ref. 13)	X = Br (this work)
0	−30.7	−41.1
1	−31.5	−41.7
2	−32.7	−42.5
3	−36.4	−44.2
4	−39.0	—

solution and -41.5×10^{-6} e.m.u./mol for the second; the average value is therefore -41.7×10^{-6} e.m.u./mol.

Sodium Bromite

The solution used contained 1.708 *M* $NaBrO_2$, 0.385 *M* NaBr, 0.045 *M* NaBrO, 0.443 *M* $NaBrO_3$, and 0.109 *M* NaOH; density 1.240 g/ml, and had a volume susceptibility of -0.752×10^{-6} e.m.u./ml. This leads to a value of -42.0×10^{-6} e.m.u./ml for the molar susceptibility of sodium bromite.

Discussion

The results for the molar susceptibilities obtained above, together with results from the literature for the susceptibilities of aqueous $NaXO_n$ may be summarized in Table 1. The possible error is probably around 1% though this depends somewhat on the accuracy of the auxiliary data which were used. The value for sodium perchlorate is a fairly early one, and more recent measurements (11) on $MgCl_2.6H_2O$ and $Mg(ClO_4)_2.6H_2O$ give a difference of −8.96 per ion between chloride and perchlorate ions. The difference in susceptibility between crystalline hexahydrates and solution is only about 1%; hence one would deduce a value of −39.7 to −39.8 for aqueous sodium perchlorate. This is somewhat higher than the value quoted above.

In both series the values rise slowly to $NaXO_2$, and more rapidly thereafter. It is tempting to suggest that this indicates largely double bonding up to XO_2^- (with 12 electrons round X), and that in XO_3^- and XO_4^- the structures involve resonance between single and double bonds, perhaps with no more than 12 electrons round the halogen. If we use observed enthalpies of formation of the aqueous compounds (8, 14, 15) to calculate the mean bond strength of the X—O bond (defined as ΔH for $(1/n)XO_n^-(aq) \rightarrow (1/n)X^-(aq) + O(g)$), we get the values shown in Table 2.

TABLE 2. Mean bond strength of the X—O bond

	Bond strength (kcal/mol)	
n	X = Cl	X = Br
1	44.4	52.0
2	47.3	49.0
3	54.0	54.8
4	56.7	51.0

In both series there is a moderate increase in stability at XO_3^-, perhaps indicating the beginning of a considerably greater degree of electron delocalization. At $n = 2$, there is a much smaller increase for chlorine and a decrease for bromine.

However, this interpretation does not seem to fit the data on bond lengths or force constants (16): the bond lengths decrease steadily in the ClO_n^- series with increasing n, while the force constants increase. These results were interpreted (16) as indicating a steadily increasing bond order with increasing n. At first sight this appears inconsistent with the magnetic results since oxygen in double bonds (as in ketones) makes a very low (or sometimes reverse) contribution to the diamagnetic susceptibility. However this is not true for compounds where other oxygens which are singly bonded to the central atom, as in carboxylic esters and phosphate esters are also present. Presumably XO_3^- and XO_4^- ions fall into this class, and the problem is really why XO^- and XO_2^- species have susceptibilities so little different from the corresponding X^- ions. At present the reason for their magnetic behavior is not clear.

1. M. W. LISTER and R. MASON. Can. J. Chem. **42**, 1817 (1964).
2. G. W. BRINDLEY and F. E. HRARE. Trans. Faraday Soc. **33**, 268 (1937).
3. V. C. G. TREW and S. F. A. HUSSAIN. Trans. Faraday Soc. **57**, 223 (1961).
4. U. VEIEL. Ann. Phys. **24**, 697 (1935).
5. M. W. LISTER. Can. J. Chem. **34**, 465 (1956).
6. M. W. LISTER. Can. J. Chem. **30**, 879 (1952).
7. M. W. LISTER and P. E. MCLEOD. Can. J. Chem. **49**, 1987 (1971).
8. C. L. LEE and M. W. LISTER. Can. J. Chem. **49**, 2822 (1971).

Can. J. Chem. Downloaded from www.nrcresearchpress.com by 210.87.254.42 on 09/05/12
For personal use only.

9. P. PASCAL, A. PACAULT, and C. JAMET. Bull. Soc. Chem. Fr. **15**, 324 (1948).
10. P. PASCAL. C. R. **218**, 175 (1944).
11. V. C. G. TREW, S. F. A. HUSSAIN, and A. J. SIDDIQI. Trans. Faraday Soc. **61**, 1086 (1965).
12. P. W. SELWOOD. Magnetochemistry. 2nd ed. Interscience Publishers. 1956. p. 78.
13. O. E. FRIVOLD and H. SOGN. Ann. Phys. **23**, 413 (1935).
14. F. ROSSINI. Selected values of chemical thermodynamic properties. National Bureau of Standards Circular 500. U.S. Government Printing Office, Washington, 1952.
15. G. K. JOHNSON, P. N. SMITH, E. H. APPELMAN, and W. N. HUBBARD. Inorg. Chem. **9**, 119 (1970).
16. E. A. ROBINSON. Can. J. Chem. **41**, 3021 (1963).

Can. J. Chem. Downloaded from www.nrcresearchpress.com by 210.87.254.42 on 09/05/12
For personal use only.

The Racemization of *trans*-1,2-Divinylcyclopropane

MANNOSUKE ARAI AND ROBERT J. CRAWFORD
Department of Chemistry, University of Alberta, Edmonton 7, Alberta

Received December 7, 1971

The synthesis of (−)-*trans*-1,2-divinylcyclopropane and the kinetics of its racemization and conversion to 1,4-cycloheptadiene, presumably through *cis*-1,2-divinylcyclopropane, are described. It is concluded that the ring opening is not an electrocyclic process.

La synthèse du (−)-*trans*-divinyl-1,2 cyclopropane ainsi que la cinétique de sa racémisation et transformation en cycloheptadiène-1,4, probablement via le *cis*-divinyl-1,2 cyclopropane, sont rapportées. Il en a été déduit que l'ouverture du cycle n'est pas un processus électrocyclique.

Canadian Journal of Chemistry, **50**, 2158 (1972)

Introduction

In attempting to discern whether the *O,O*-trimethylene species (1) is an important intermediate for the isomerization of cyclopropane we have examined the racemization of (*1S:2S*)-*trans*-1,2-divinylcyclopropane (**1**). This compound offers the advantage that the reactivity in thermal processes is primarily confined to the cyclopropane bond situated between the two vinyl groups. While there are numerous possible configurations for diradicals (2) we shall consider two measurable manifestations of diradical formation from **1**; (*a*) racemization and (*b*) geometrical isomerization. Geometrical isomerization of **1** leads to *cis*-1,2-divinylcyclopropane (**2**) which isomerizes rapidly and quantitatively to 1,4-cycloheptadiene (**3**). If there is a preferred mode of ring opening and closing, either dis- or conrotatory, then the rate of racemization should exceed the rate of formation of **3** by more than that expected from steric factors alone. Thus kinetically we would predict that for Scheme 1, $2k_1 > k_2$ (where $k_{rac} = 2k_1$). There remains the possibility of the formation of **3** directly from **1** via either a concerted or diradical process. The former seems unlikely in that *trans-trans*-1,4-cycloheptadiene would result from that conformation in which the termini of the vinyl groups are closest in **1**. There are ten possible *O,O*-trimethylene species resulting from dis- and

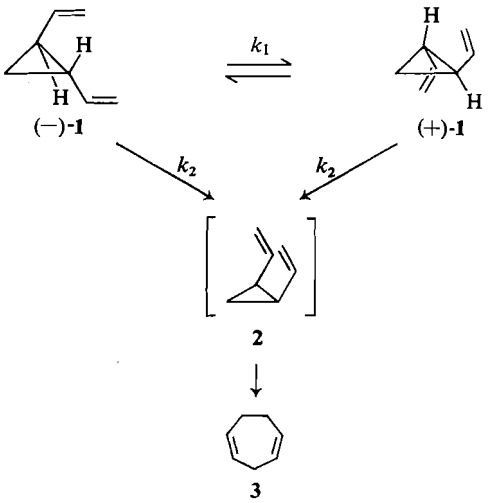

SCHEME 1

9. P. PASCAL, A. PACAULT, and C. JAMET. Bull. Soc. Chem. Fr. **15**, 324 (1948).
10. P. PASCAL. C. R. **218**, 175 (1944).
11. V. C. G. TREW, S. F. A. HUSSAIN, and A. J. SIDDIQI. Trans. Faraday Soc. **61**, 1086 (1965).
12. P. W. SELWOOD. Magnetochemistry. 2nd ed. Interscience Publishers. 1956. p. 78.
13. O. E. FRIVOLD and H. SOGN. Ann. Phys. **23**, 413 (1935).
14. F. ROSSINI. Selected values of chemical thermodynamic properties. National Bureau of Standards Circular 500. U.S. Government Printing Office, Washington, 1952.
15. G. K. JOHNSON, P. N. SMITH, E. H. APPELMAN, and W. N. HUBBARD. Inorg. Chem. **9**, 119 (1970).
16. E. A. ROBINSON. Can. J. Chem. **41**, 3021 (1963).

Can. J. Chem. Downloaded from www.nrcresearchpress.com by 210.87.254.42 on 09/05/12
For personal use only.

The Racemization of *trans*-1,2-Divinylcyclopropane

MANNOSUKE ARAI AND ROBERT J. CRAWFORD
Department of Chemistry, University of Alberta, Edmonton 7, Alberta

Received December 7, 1971

The synthesis of (−)-*trans*-1,2-divinylcyclopropane and the kinetics of its racemization and conversion to 1,4-cycloheptadiene, presumably through *cis*-1,2-divinylcyclopropane, are described. It is concluded that the ring opening is not an electrocyclic process.

La synthèse du (−)-*trans*-divinyl-1,2 cyclopropane ainsi que la cinétique de sa racémisation et transformation en cycloheptadiène-1,4, probablement via le *cis*-divinyl-1,2 cyclopropane, sont rapportées. Il en a été déduit que l'ouverture du cycle n'est pas un processus électrocyclique.

Canadian Journal of Chemistry, **50**, 2158 (1972)

Introduction

In attempting to discern whether the *O,O*-trimethylene species (1) is an important intermediate for the isomerization of cyclopropane we have examined the racemization of (*1S:2S*)-*trans*-1,2-divinylcyclopropane (**1**). This compound offers the advantage that the reactivity in thermal processes is primarily confined to the cyclopropane bond situated between the two vinyl groups. While there are numerous possible configurations for diradicals (2) we shall consider two measurable manifestations of diradical formation from **1**; (*a*) racemization and (*b*) geometrical isomerization. Geometrical isomerization of **1** leads to *cis*-1,2-divinylcyclopropane (**2**) which isomerizes rapidly and quantitatively to 1,4-cycloheptadiene (**3**). If there is a preferred mode of ring opening and closing, either dis- or conrotatory, then the rate of racemization should exceed the rate of formation of **3** by more than that expected from steric factors alone. Thus kinetically we would predict that for Scheme 1, $2k_1 > k_2$ (where $k_{rac} = 2k_1$). There remains the possibility of the formation of **3** directly from **1** via either a concerted or diradical process. The former seems unlikely in that *trans-trans*-1,4-cycloheptadiene would result from that conformation in which the termini of the vinyl groups are closest in **1**. There are ten possible *O,O*-trimethylene species resulting from dis- and

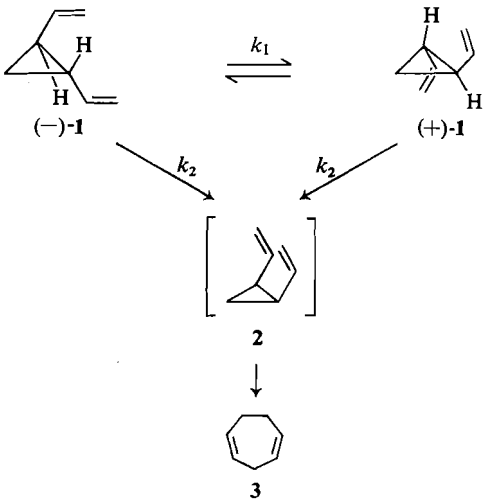

SCHEME 1

conrotatory ring opening of **1**; of these, **4***b*, *c*, and *d* have the requisite configurations such that rotation about a single bond (=CH—CH_2—) will generate the product **3**. Of these, **4***c* and *d* seem unlikely in that the alkyl group has moved inwards, a process known to be unfavorable from the racemization of oxiranes (3). The form **4***b* remains and the consequence of this, and the others if they still pertain, is to overemphasize k_2 and reduce the severity of this test for the *O*,*O*-trimethylene species.

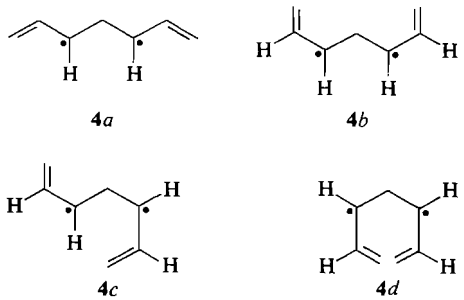

4*a* **4***b* **4***c* **4***d*

Synthesis and Absolute Configuration of **1**

Optically active **1** was prepared by resolving the known *trans*-2-vinylcyclopropanecarboxylic acid via its quinine salt. The resolved acid was then converted to *trans*-1,2-divinylcyclopropane as indicated in Scheme 2. The absolute configuration and optical purity of **1** was ascertained by oxidation to *trans*-1,2-cyclopropanedicarboxylic acid. Thus (*1S:2S*)-*trans*-1,2-divinylcyclopropane of 14% optical purity has a rotation $[\alpha]_{365}^{25}$ −40.2° (*c* 3.70, isopropyl alcohol).

Experimental

(−)-trans-2-Vinylcyclopropanecarboxylic Acid

The method of Vogel *et al.* (4) was used for the preparation of ethyl *cis*- and *trans*-2-vinylcyclopropanecarboxylate from ethyl diazoacetate and butadiene. The *cis* isomer was converted to the *trans* by refluxing the ester (50 g, 0.36 mol) with sodium ethoxide (made by adding 1.0 g of sodium metal to 100 ml absolute ethanol) in ethanol for 60 h. After saponification the acid was then partially resolved via its quinine salt by recrystallization from water. The acid, b.p. 82–83°/2–3 Torr gave $[\alpha]_D^{25}$ −60.0° (*c* 1.49, acetone).

N,N-Dimethyl-trans-2-vinylcyclopropanecarboxamide

trans-2-Vinylcyclopropanecarboxylic acid (28.1 g, 0.25 mol) was added slowly with stirring to freshly distilled thionyl chloride (140 g, 1.0 mol) and dry benzene (15 ml). The solution was maintained at 80° for 3 h and the excess thionyl chloride and benzene was distilled off. The remaining acid chloride was slowly added with stirring to a 25% solution of dimethylamine (180 g). The resulting amide was extracted with ether, washed with water and dilute sulfuric acid, and then dried over anhydrous sodium carbonate. After filtration the ether was removed and the amide distilled, b.p. 79–80°/2.5 Torr; yield 27.7 g, 80%.

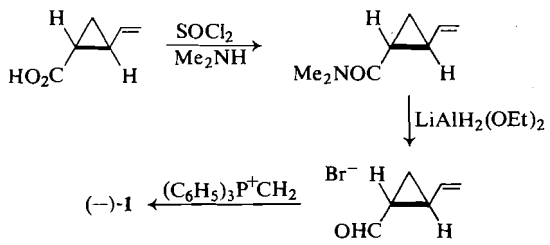

SCHEME 2

trans-2-Vinylcyclopropanecarboxaldehyde

The aldehyde was prepared utilizing lithium diethoxyaluminohydride by the procedure of Brown and Shoaf (5). Ethyl acetate (9.7 g, 0.11 mol) was added slowly to a solution of lithium aluminum hydride (4.2 g, 0.11 mol) in 100 ml of dry ether. The resulting solution was transferred over a period of 30 min to a stirred solution of *N,N*-dimethyl-*trans*-2-vinylcyclopropanecarboxamide (27.2 g, 0.2 mol) in 40 ml of dry ether at 0°. The reaction mixture was stirred for an additional hour and then decomposed, with cooling, by adding to a 10% solution of sulfuric acid. The ether layer was washed, then dried over anhydrous sodium carbonate. The aldehyde distilled at 57.8°/30 Torr; yield 10.6 g, 58%.

trans-1,2-Divinylcyclopropane (1)

A solution of *trans*-2-vinylcyclopropanecarboxaldehyde (10 g, 0.11 mol) in 20 ml ether was added, under nitrogen, to a solution of methylenetriphenylphosphorene, which had been prepared by the addition of methyltriphenylphosphonium bromide (105 g, 0.28 mol) to butyl lithium (0.2 mol) in 100 ml of ether. The resulting complex was refluxed with 100 ml of tetrahydrofuran for 1 h and then the ether soluble portion, after addition to water, was carefully fractionated. The crude product was subjected to preparative gas chromatography using a 10 ft × 3/8 in., β,β′-oxydipropionitrile column operated at 35°. The n.m.r. and i.r. spectra correspond to those described in the literature (3), yield 50%, $[\alpha]_{365}^{25}$ −40.2° (*c* 3.70, isopropyl alcohol).

Oxidation of (−)-1 to (1R:2R)-(−)-trans-1,2-Cyclopropanedicarboxylic Acid

(−)-*trans*-1,2-Divinylcyclopropane (0.47 g, 5 mmol) was added to a 500 ml solution of sodium metaperiodate (15.05 g, 3 mmol) potassium permanganate (0.20 g, 1.2 mmol) in water (6). The reaction mixture was stirred at room temperature for 20 h and then acidified with 10% sulfuric acid. Ether extraction followed by drying and evaporation gave 0.31 g of a solid which upon recrystallization from water gave needles, m.p. 174–175° (lit. value 175° (7)) $[\alpha]_D^{25}$ −34.5° (*c* 2.26, water). The optical purity is thus 14% based on −247° and the absolute configuration is *1R:2R* (8). Thus the absolute configuration of (−)-**1** is *1S:2S*.

Kinetic Measurements

Samples of (−)-**1** (*ca.* 37 mg) were placed in break-seals of 20 ml volume, degassed, sealed, and placed in an air-bath

Can. J. Chem. Downloaded from www.nrcresearchpress.com by 210.87.254.42 on 09/05/12
For personal use only.

TABLE 1. Rate data, at 169.98°, for the conversion of **1** to **3** and the simultaneous racemization of (−)-**1**

t (s)	$-\log \alpha/\alpha_0$	$-\log a/a_0$	$10^5 k_1$ (s^{-1})	$10^4 k_2$ (s^{-1})
1200	0.117	0.074	4.12	1.42
2400	0.263	0.150	5.42	1.44
3600	0.403	0.243	5.11	1.55
5400	0.630	0.372	5.50	1.58
7200	0.903	0.482	6.73	1.54
∞	$\alpha = 0.00$	$a = 0.00$		
			Average 5.38 (0.9)*	1.51 (0.07)*

*Standard deviation.

TABLE 2. Rate constants and activation parameters for Scheme 1

Temperature ±0.03°	$10^6 k_1$ (s^{-1})	$10^6 k_2$ (s^{-1})	Activation parameter
150.03	8.85±0.35	24.5±0.8	$E_a^1 = 33 \pm 2$ kcal mol^{-1}
160.01	22.6 ±0.9	61 ±2	$\log A^1 = 12.1$
169.98	54 ±6	151 ±5	$E_a^2 = 34.3 \pm 0.9$ kcal mol^{-1}
			$\log A^2 = 13.1$

controlled to ±0.03°. The tubes were removed at the appropriate times and quenched in an ice-water bath. The sample was then re-attached to the vacuum line and after a pressure of 10 μ was attained in the manifold the break-seal was opened and the contents transferred to a pre-weighed 1 ml volumetric flask that had been attached to the vacuum line by means of a finely ground 7/16 ⅋ male joint. The stoppered flask was then reweighed and isopropyl alcohol was added up to the 1 ml line. The total solution was weighed and the specific rotation $[\alpha]_t$ at time t was calculated using the expression (9):

$$[\alpha] = \frac{100\alpha}{lpp_s}$$

where α is the observed angle, l is the length of the polarimeter tube in dm, p the concentration of product in g/100 g of solution, and p_s the density of the solution. The density of the solution was not measured as it cancels in the kinetic expression. The rotations were measured using a thermostated polarimeter cell in a Perkin–Elmer 141 Polarimeter set at 365 nm. Infinity tubes were left to greater than ten half-lives and displayed no rotation. A sample corresponding to $t = 0$ was subjected to all of the manipulations except heating. No residual material was observed in any of the break-seals and a sample run using cyclohexane as a standard indicated that the transfer was greater than 95% efficient.

After measuring the rotation the solutions were analyzed by g.c. on a Varian Aerograph 1200 using a 10 ft column of SF-96 on Chromasorb-W. The peaks corresponding to **1** and **3** were integrated using a planimeter. No additional peak other than that of solvent was observed. An example run at 169.98° is given in Table 1. The rate constants were calculated on a point by point basis and the value for k_1 was obtained by using the expression: $k_1 = 2.303/2t(\log a/a_0 - \log \alpha/\alpha_0)$, where a is the fraction of *trans*-1,2-divinylcyclopropane at time t.

Results and Discussion

The rate constants for the interconversion of enantiomers, k_1, and for those assumed to be representative of the *trans* to *cis* isomerization, k_2, are listed in Table 2 along with their probable errors (10) and activation parameters. The precision in determining k_1 is poor since both the errors from the gas chromatographic assessment of the geometrical isomerization and the polarimetric errors for the racemization process are incorporated. The differences between the activation parameters for the two processes cannot be considered to be significant.

Operationally if the racemization is an electrocyclic process and only one mode of rotation (either con- or disrotatory) to the intermediate diradical, **4***a* being the most probable structure, is preferred, then the rate constant for the geometrical isomerization will be infinitely smaller than the rate constant for the racemization process. If however both con- and disrotatory modes are equally accessible, then, invoking the principle of microscopic reversibility, we can state that the racemization rate constant will be twice that of the rate constant

Can. J. Chem. Downloaded from www.nrcresearchpress.com by 210.87.254.42 on 09/05/12
For personal use only.

Can. J. Chem. Downloaded from www.nrcresearchpress.com by 210.87.254.42 on 09/05/12
For personal use only.

TABLE 3. Operative criteria

Path	Predicted k_2/k_1
Only one mode	0
Equivalent dis- and conrotation	2
Smith mechanism	∞

for the geometrical isomerization.[1] If only one chiral center of the reactant (−)-**1** is rotated through 180° (the Smith mechanism (11)) then the starting material is not racemized but is only converted to **3**. This is summarized in Table 3.

The k_2/k_1 ratio observed at 160° for **1** is 2.8. The kinetic data indicate that within the assumptions made in the introduction, the more random diradical process is favored over that wherein only one mode of ring opening and closure is operative.

A problem arises in just what one might expect of a diradical that is free to close to either *cis*- or *trans*-1,2-divinylcyclopropane. If we are to use the definition of Hayes and Siu (12) then from the diradical we are equally likely to get closure to the *cis*-isomer as to the *trans*. This does not take into account the relative thermodynamic stabilities of the *cis*- and *trans*-isomers. If we assume that our diradical has a structure such as **5** where the

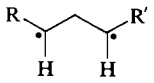

5

alkyl groups R and R′ are in the more stable W-configuration and that it is free to close to either *cis*- or *trans*-dialkylcyclopropane, *sans orbital-symmetry factors*, then it would seem reasonable that those factors which control the relative thermodynamic stability of the ring closure product (*i.e.*, of ΔG_{eq}) will be playing a role in the transition state leading to those products. If, for example, R and R′ are methyl then it is known that the *trans*-isomer is more stable than the *cis* ($\Delta G_{eq} = 1.0$ kcal mol^{-1}) by a factor of 5.5 at 30° (13). Thus if the magnitude of the steric effects were the same for the transition states as for the ground states we would have $\Delta\Delta G^{\ddagger} = \Delta G_{eq}$. This is likely to be too large an estimate and the effect will probably be attenuated. One possible indication of the attenuation is that the ring closure from triplet diradicals (14) gives a 1.55:1 ratio of *trans*- to *cis*-1,2-dimethylcyclopropane and thus $\Delta\Delta G^{\ddagger} = 0.26\ \Delta G_{eq}$. If instead of methyl we consider the case of 1,2-diphenylcyclopropane we find that ΔG_{eq} is 2.34 kcal mol^{-1} at 205° (15, 16). Upon attenuating this value by 0.26 we find that for every mole of substrate going to a diradical 0.65 mol (or the equivalent of $2k_1$ in Scheme 1) will end up as racemic *trans*-1,2-diphenylcyclopropane and 0.35 mol as the *cis*-isomer. This suggests that the analogous k_2/k_1 for the diphenylcyclopropane is such that for any value greater than 1.08 the process is diradical and for smaller values than this that we have some electrocyclic character. The value observed at 205° for the ratio of the rate constants for the loss of optical activity to the rate constant for *trans* to *cis* isomerization (the equivalent of $(2k_1 + k_2)/k_2$ in Scheme 1) is 1.42 (16) which gives a value of k_2/k_1 of 4.8. The divinylcyclopropane may be expected to demonstrate steric effects intermediate between the methyl and phenyl groups, and thus assuming a value of ΔG_{eq} of 1.7 kcal mol^{-1} we get an analogous value for the k_2/k_1 ratio of 1.20. The value observed in this work for 1,2-divinylcyclopropane at 160° is 2.8, again implying that the isomerization has no electrocyclic component.

It has been observed that *cis*- and *trans*-2,3-diaryloxiranes have nearly the same equilibrium value as the diarylcyclopropanes (3). Using these arguments we would expect a value of $k_2/k_1 = 1.08$ or greater for a diradical process. The observed value of 0.0045 for *trans*-2-phenyl-3-*p*-tolyloxirane indicates that it has less than 1% diradical character for the racemization process, and it is thus an electrocyclic process (3). There seems to be little evidence that the thermal isomerization of cyclopropanes is an electrocyclic process for Willcott and Cargle (17) found that while their results were most readily rationalized in terms of simultaneously changing the configuration at two of the ring carbons they were not compatible with a preferred dis- or conrotation. Similarly Berson and Balquist (18) and Bergman and Carter (19) have found that their results are more readily rationalized in terms of competitive free rotation and ring closure from a diradical having no

[1]As indicated in the Introduction this assumes that there is no path by which **1** may be converted directly to **3**.

preference for the mode in which the rotation occurs. We conclude that there is no evidence for the use of the *O,O*-trimethylene species in the thermal reactions of cyclopropanes.

The authors wish to thank the National Research Council of Canada for their financial assistance.

1. R. HOFFMANN. J. Am. Chem. Soc. **90**, 1475 (1968).
2. L. SALEM and C. ROWLAND. Ang. Chem. Int. Ed. **11**, 92 (1972).
3. H. H. J. MACDONALD and R. J. CRAWFORD. Can. J. Chem. **50**, 428 (1972).
4. E. VOGEL, R. ERB, and G. LENZ. Ann. **682**, 1 (1964).
5. H. C. BROWN and C. J. SHOAF. J. Am. Chem. Soc. **86**, 1079 (1964).
6. R. U. LEMIEUX and E. VON RUDOLF. Can. J. Chem. **33**, 1701 (1955).
7. E. BUDNER and R. V. D. HEIDE. Ber. **38**, 3112 (1905).
8. Y. INOUYE, T. SUGITA, and H. M. WALBORSKY. Tetrahedron, **20**, 1695 (1964).
9. W. HELLER. Polarimetry. *In* Technique in organic chemistry. vol. I. pt 3. A. Weissberger, ed. 3rd edit. Interscience Publishers Inc., New York, 1960. p. 2300.
10. K. WIBERG. Physical organic chemistry. J. Wiley and Sons Inc., New York, N.Y. 1964. p. 378.
11. F. T. SMITH. J. Chem. Phys. **29**, 235 (1958).
12. E. F. HAYES and A. K. Q. SIU. J. Am. Chem. Soc. **93**, 2090 (1971).
13. M. C. FLOWERS and H. M. FREY. Proc. Roy. Soc. (London), A**257**, 122 (1960).
14. (*a*) R. MOORE, A. MISHRA, and R. J. CRAWFORD. Can. J. Chem. **46**, 3305 (1968). (*b*) C. MCKNIGHT, P. S. T. LEE, and F. S. ROWLAND. J. Am. Chem. Soc. **89**, 6802 (1967).
15. C. H. DEPUY and L. B. RODEWALD. Tetrahedron Lett. 2951 (1964).
16. R. J. CRAWFORD and T. R. LYNCH. Can. J. Chem. **46**, 1457 (1968).
17. M. R. WILLCOTT and V. H. CARGLE. J. Am. Chem. Soc. **91**, 4310 (1969).
18. J. A. BERSON and J. M. BALQUIST. J. Am. Chem. Soc. **90**, 7343 (1968).
19. R. G. BERGMAN and W. L. CARTER. J. Am. Chem. Soc. **91**, 7411 (1969).

Can. J. Chem. Downloaded from www.nrcresearchpress.com by 210.87.254.42 on 09/05/12
For personal use only.

Can. J. Chem. Downloaded from www.nrcresearchpress.com by 210.87.254.6 on 09/05/12
For personal use only.

Acid-catalyzed Ring Opening of Halo-nortricyclanes[1]

FRANK P. CAPPELLI, GEORGE TIMMINS, AND NICK H. WERSTIUK[2]
Department of Chemistry, McMaster University, Hamilton, Ontario

Received March 23, 1972

The acid-catalyzed ($CH_3COOH-0.1\ M\ H_2SO_4$) opening of the cyclopropyl ring in nortricyclyl chloride and nortricyclyl bromide gives in each case the *anti*-7-, *syn*-7-, *exo*-5-, and *endo*-5-halo-*exo*-2-norbornyl acetates as the major products. When the reactions are carried out in deuterated medium the deuterium is situated *endo* at C-6 in the *anti*- and *syn*-7- haloacetates and establishes that at least 75% of the products arise from *initial edge protonation* of the cyclopropane.

L'ouverture acido catalysée ($CH_3COOH-0.1\ M\ H_2SO_4$) du cycle cyclopropyle dans le chlorure et bromure de nortricyclyle, donne dans chaque cas comme produits majeurs les acétates d'*anti*-7, *syn*-7, *exo*-5, et *endo*-5-halo *exo*-2-norbornyl. Quand les réactions sont faites en milieu deutérié, le deutérium est situé en *endo* sur le C-6 dans les 7-haloacétates *anti* et *syn* et montre ainsi que 75% au moins de produits proviennent d'une protonation initiale sur le site cyclopropane.

Canadian Journal of Chemistry, **50**, 2163 (1972)

The chemistry of protonated cyclopropane has commanded much interest. Electrophilic cleavage of a strained cyclopropane σ bond by the reagents $DOAc-D_2SO_4$, DCl, DBr, and Br_2 (2–6) has been studied extensively to determine the site of attack of the electrophile and the stereochemistry of the addition of the electrophile and nucleophile. The nature of the products and the stereochemical information obtained from the D^+X^- additions were then used to establish the nature of the first formed intermediate resulting either from initial edge or corner protonation. Results from studies on the nortricyclane systems **1***a* (1) and *b* (2) have been interpreted in terms of corner-protonated nortricyclane intermediates but did not establish whether initial protonation occurred cornerwise or edge-wise.

Our interest in the preparation of the 7-halo-*exo*-2-norbornyl brosylates-6-d_1 for γ-deuterium isotope effect studies has led us to a study of the electrophilic cleavage ($HOAc-H_2SO_4$; $DOAc-D_2SO_4$) of the cyclopropane ring in 3-bromo- and 3-chloro-nortricyclane (**1***c* and *d*). We report results which establish that (*a*) the σ bond farthest removed from the electron-withdrawing halogen is cleaved preferentially via initial *edge protonation*, (*b*) the ring opening occurs with retention and inversion at the carbon atoms bearing the electrophile and nucleophile, respectively, and (*c*) the pathways of product formation are as described in Scheme 1.

Reaction of nortricyclyl bromide (**1***c*) in CH_3COOD, 0.1 M D_2SO_4 at 75° for 70 h gives *anti*-7-bromo-*exo*-2-norbornyl acetate-d_1 (49%), *syn*-7-bromo-*exo*-2-norbornyl acetate-d_1 (26%), *exo*-5-bromo-*exo*-2-norbornyl acetate-d_1 (10%), *endo*-5-bromo-*exo*-2-norbornyl acetate-d_1 (8%), 3% of unidentified material,[3-5] and 4% un-

[1]Presented in part at the 54th Annual Meeting of the Chemical Institute of Canada, Halifax, Nova Scotia, June, 1971.

[2]Author to whom enquiries may be addressed.

[3]The *syn*- and *anti*-bromoacetates, obtained from a non-deuterated-run, were identified by spectral comparison and by the melting points of the 2,4-dinitrophenylhydrazones of the corresponding bromoketones (7, 8). The *syn*- and *anti*-chloroacetates were identified by comparison of spectral data to those of authentic samples prepared via addition of HOCl to norbornene (9) followed by acetylation. The *exo*-5-halo-*exo*-2-acetates were identified through the haloketones by comparison of spectral data to authentic samples prepared by the addition of anhydrous HCl and HBr to nortricyclanone in carbon tetrachloride (10). The *endo*-5-halo-*exo*-2-acetates were identified through spectral data comparison of the haloketones to authentic samples prepared by hydroboration of the corresponding *endo*-5-halonorbornene to give the halohydrin followed by chromic acid oxidation.

[4]Reduction of the total chloroacetate and bromoacetate mixtures with sodium in iso-propanol gave a mixture of 97–98% *exo*-norborneol and 2–3% *endo*-norborneol estab-

Can. J. Chem. Downloaded from www.nrcresearchpress.com by 210.87.254.6 on 09/05/12
For personal use only.

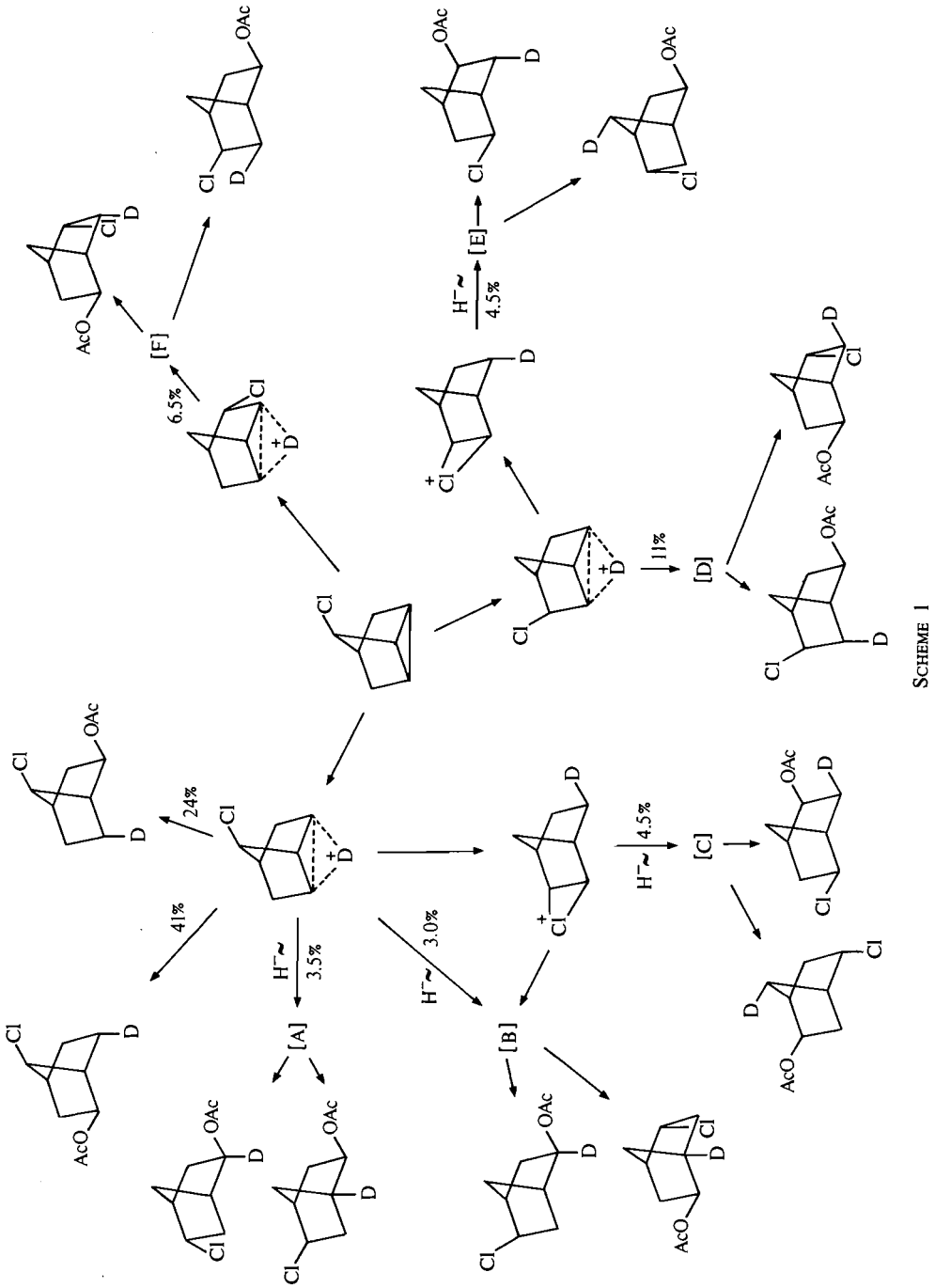

SCHEME 1

Can. J. Chem. Downloaded from www.nrcresearchpress.com by 210.87.254.6 on 09/05/12
For personal use only.

reacted **1***c*. Reaction of nortricyclyl chloride (**1***d*) in CD_3COOD, 0.1 *M* D_2SO_4 at 70° for 500 h gives *anti*-7-chloro-*exo*-2-norbornyl acetate-d_1 (44%), *syn*-7-chloro-*exo*-2-norbornyl acetate-d_1 (26%), *exo*-5-chloro-*exo*-2-norbornyl acetate-d_1 (14%), and *endo*-5-chloro-*exo*-2-norbornyl acetate-d_1 (14%).[3-5]

Infrared fingerprint analysis[6] of the *exo*-norborneols-d_1 obtained from lithium aluminum hydride reduction of the *syn*-7- and *anti*-7-bromo- and chloro-*exo*-2-norbornyl acetates-d_1 showed that the deuterium at C-6 was at least 90% stereochemically pure *endo*. The haloacetates-d_1 obtained from **1***c* and *d* were converted to the corresponding haloketones.[7] Mass spectrometric deuterium assay showed that the 2,5-haloketones contained 8–15% less deuterium than did the 2,7-isomers and thus established the deuterium content at C-2. The norborneols-d_1, obtained from the chloroketones by lithium aluminum hydride reduction, were subjected to n.m.r. (100 MHz, CCl_4) deuterium position analysis (integration) using $Eu(DPM)_3$ (12). The combined mass spectral and n.m.r. data establish that (*a*) the deuterium in the *syn*-7- and *anti*-7-chloro-*exo*-2-norbornyl acetates is situated at C-6 (>90%) with at least 95% *endo* stereochemical purity and (*b*) that the deuterium is positioned at *exo*-6 (0.20 ± 0.05), *endo*-6 (0.20 ± 0.05), C-1 (0.10 ± 0.05), C-2 (0.10 ± 0.05), *exo*-3 (0.20 ± 0.05), *endo*-3 (0.20 ± 0.05) in the *exo*-5-chloro-*exo*-2-norbornyl acetate and at *exo*-6 (0.55 ± 0.05), *endo*-6 (0.25 ± 0.05), C-1 (0.10 ± 0.05), and C-2 (0.15 ± 0.05) in the *endo*-5-chloro-*exo*-2-norbornyl acetate. This establishes the percent contribution (rounded to 0.5%) of the major product-forming pathways as described in Scheme 1.[8]

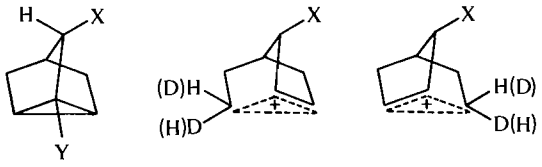

1 **2** **3**

a X = Y = H
b X = H; Y = Me
c X = Br; Y = H
d X = Cl; Y = H

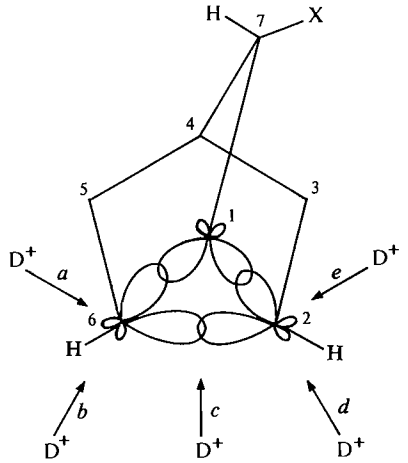

SCHEME 2

These data therefore establish the mechanistic details shown in Scheme 1 for the acid-catalyzed ring opening of nortricyclyl chloride. That a similar scheme operates for nortricyclyl bromide is indicated by the nature of the products and the position and stereochemistry of the deuterium in the *syn*- and *anti*-bromoacetates.

Since there is no significant amount of deuterium at *exo*-6 in the 7-haloacetates, the data establish that corner protonation (via paths *a*, *b*, *d*, *e* (Scheme 2)) to give **2** and **3** is not important unless paths *b* and *d* are preferred stereoelec-

lishing the *exo*- to *endo*-acetate ratio. Control experiments with each of the *syn*- and *anti*-7-haloacetates showed that there is only 3–4% isomerization to the other haloacetates. Also, control experiments with *endo*-5-chloro-*exo*-2-norbornyl acetate under the reaction conditions showed 10–15% isomerization to the *exo*-5-chloro-*exo*-2-norbornyl acetate. Within our limits of detection (2–3%) we did not detect 2,3-haloacetates in the reaction of **1***d*, although the 3% of the unidentified material from **1***c* may be 2,3-compounds. To check for the possibility that 2,3-chloroacetates were formed in quantity from **1***d*, but were not detected due to rearrangement, the *exo*-3-chloro- and *endo*-3-chloro-*exo*-2-norbornyl acetates were prepared via acetylation of the chlorohydrins (11) and subjected to the reaction conditions. Less than 3% isomerization to other acetates occurs.

[5]Mass spectral analysis showed that there was, on the average, only 1–2% of d_2 species in the haloacetates.

[6]We thank Prof. A. Nickon for the spectra of *exo*-norborneol-6-*exo*-*d* and 6-*endo*-*d*.

[7]Control experiments with the deuterio-*exo*-5-chloronorbornan-2-one under the chromic acid oxidation conditions showed no significant amount of deuterium is lost from C-3 via acid-catalyzed enolization.

[8]A, B, C, D, E, and F represent either the norbornonium ion or the appropriate pair of classical ions. Since there is some isomerization of the *endo*-5-chloroacetate to the *exo*-5-chloroacetate (10–15%) the partitioning (of A, B, C, D, E, and F) to the 2,5-systems is not exactly that given by deuterium position analysis, and therefore is represented as totals leading to A, B, C, D, E, and F.

tronically. Possibly, formation of a symmetrical *exo*-chloronium-3-ion (13) could account for such a stereoelectronic preference for path *b*. However, at least 50% of the deuterium in the *syn*-7-haloacetate would be situated at C-5 if this pathway was important and this is not what is observed experimentally. *endo*-Chloronium-3-ion formation for path *d* would not be favorable.

Therefore, at least 75% of the products arise from initial *edge protonation* of the C_2—C_6 bond.[9]

Interestingly, the formation of the *exo*-5-chloroacetates-*exo*-3-d_1 (3.5%) and *endo*-3-d_1 (3.5%) shows that some leakage to the symmetrical chloronium ion occurs. That the *endo*-chloronium-3-ion does not form is shown by the lack of deuterium in the 3-position in the *endo*-5-chloroacetates.

Our study thus should give information on the mechanism of formation of the 2,5-products isolated from the solvolysis of the 7-chloro-*exo*-2-norbornyl tosylates as described by Gassman and Hornback (14) and Goering and Degani (15).

[9]The numbering system employed for the substituted nortricyclanes is used only for clarity to relate to that of the product haloacetates.

We thank the National Research Council of Canada for financial support.

1. A. Nickon and J. Hammons. J. Am. Chem. Soc. **86**, 3322 (1964).
2. J. H. Hammons, E. K. Probasco, L. A. Sanders, and E. J. Whalen. J. Org. Chem. **33**, 4493 (1968).
3. J. B. Hendrickson and R. K. Boeckman, Jr. J. Am. Chem. Soc. **91**, 3269 (1969).
4. J. B. Hendrickson and R. K. Boeckman, Jr. J. Am. Chem. Soc. **93**, 4491 (1971).
5. J. K. Stille and R. D. Hughes. J. Org. Chem. **36**, 340 (1971).
6. S. J. Cristol, W. Y. Lim, and A. R. Dahl. J. Am. Chem. Soc. **92**, 4013 (1970).
7. L. H. Zalkow and A. C. Oehlschlager. J. Org. Chem. **29**, 1625 (1964).
8. A. C. Oehlschlager, C. D. Kennedy, and L. H. Zalkow. J. Org. Chem. **31**, 1682 (1966).
9. J. D. Roberts, F. O. Johnson, and R. A. Carboni. J. Am. Chem. Soc. **76**, 5692 (1954).
10. N. H. Werstiuk and F. P. Cappelli. Unpublished results.
11. E. Tobler, D. E. Battin, and D. J. Foster. J. Org. Chem. **29**, 2834 (1964).
12. N. H. Werstiuk and T. Kadai. Unpublished results.
13. R. D. Bach and H. F. Henneike. J. Am. Chem. Soc. **92**, 5589 (1970) and refs. therein.
14. P. G. Gassman and J. M. Hornback. J. Am. Chem. Soc. **91**, 4290 (1969).
15. H. L. Goering and M. J. Degani. J. Am. Chem. Soc. **91**, 4506 (1969).

Can. J. Chem. Downloaded from www.nrcresearchpress.com by 210.87.254.6 on 09/05/12
For personal use only.

Can. J. Chem. Downloaded from www.nrcresearchpress.com by 210.87.254.105 on 09/05/12
For personal use only.

Canadian Journal of Chemistry

Published by THE NATIONAL RESEARCH COUNCIL OF CANADA

VOLUME 50 JULY 15, 1972 NUMBER 14

Chemistry of the Transition Metals. II. Reaction of Branched Alkyl Chlorides with Titanium[1]

W. R. SUMMERS[2] AND J. F. HARROD

Chemistry Department, McGill University, Montreal, Quebec

Received December 21, 1971

Except for *t*-butyl chloride, the 1- and 2-methyl substituted ethyl chlorides reacted at ambient temperatures with clean titanium surfaces to produce mixtures of the corresponding alkanes and alkenes; *t*-butyl chloride gave only isobutene. At elevated temperatures (80–150 °C depending on reactant) the branched alkyl chlorides underwent clean, catalytic dehydrochlorination on hydrochlorinated titanium films to give gaseous olefin and hydrogen chloride, in contrast to the previously observed dehydrohalogenation of *n*-alkyl halides, where metal was consumed continuously in a non-catalytic fashion.

The kinetics of the dehydrochlorination were exceptionally simple and reproducible for a heterogeneous reaction and all reactions were first order in reactant. The reactivity order was *t*-butyl > *i*-propyl > neopentyl > *i*-butyl (*ca.* $10^6:6:3:1$). Although a slight dependence of activation energy on reactant pressure was observed, all reactants gave a limiting activation energy of 15.5 ± 0.5 kcal/mol and the large variation in activity is attributed to differences in the Arrhenius pre-exponential factor.

It is proposed that the non-catalytic and catalytic dehydrohalogenation reactions proceed by different mechanisms, the former via a dissociative chemisorption of the carbon–halogen bond and the latter via a concerted, surface-assisted HCl elimination.

Sauf pour le chlorure de *t*-butyle, les chlorures d'éthyle substitués en -1 et -2 par un méthyle réagissent à la température ambiante sur les surfaces de titane propres pour conduire à des mélanges d'alcanes et d'alcènes correspondants; le chlorure de *t*-butyle donne seulement l'isobutène.

Aux températures élevées (80–150 °C en fonction du réactant) les chlorures d'alkyles ramifiés subissent une déhydrochloration catalysée et propre, sur des films de titane hydrochloré, en donnant des oléfines gazeuses et de l'HCl, à l'opposé de la déhydrohalogénation précédemment observée pour les halogénures de *n*-alkyle, où le métal était consommé de façon continue et non catalysée.

Les cinétiques de la déhydrochloration sont exceptionnellement simples et reproductibles pour une réaction hétérogène et toutes les réactions sont du premier ordre par rapport au réactant. L'ordre de réactivité est *t*-butyle > *i*-propyle > néopentyle > *i*-butyle (environ $10^6:6:3:1$). Bien qu'on observe une légère influence de la pression du réactant sur l'énergie d'activation, tous les réactants donne une énergie d'activation limitée à 15.5 ± 0.5 kcal/mol et la grande variation dans l'activité est attribuée aux différences du facteur préexponentiel d'Arrhénius.

On propose que les réactions de déhydrohalogénation non catalysées et catalysées procèdent selon des mécanismes différents, la première via une chimisorption dissociative de la liaison carbone–halogène et la seconde, via une élimination concertée d'HCl assistée par la surface métallique.

Canadian Journal of Chemistry, **50**, 2167 (1972)

Introduction

In the first paper of this series we described the reactions of normal alkyl halides with metallic titanium prepared by evaporation under ultra-high vacuum (1). In all cases the reaction observed was a non-catalytic dehydrohalogenation in which the metal scavenged one halogen atom per molecule of alkyl halide reacted, and a fraction of a hydrogen atom, depending on reaction conditions. The hydrogen atoms not

[1]This work was done in partial fulfilment of the requirements for a Ph.D. thesis (W.R.S.).

[2]National Research Council of Canada Scholar 1969–1970.

Can. J. Chem. Downloaded from www.nrcresearchpress.com by 210.87.254.105 on 09/05/12
For personal use only.

scavenged by the metal were consumed in the production of paraffin molecules from alkyl radicals and the gas phase product consisted of an approximately equimolar mixture of alkane and alkene. No other products were detected.

The kinetics of the *n*-alkyl halide reactions were, for a heterogeneous reaction, strikingly consistent and reproducible. *n*-Propyl fluoride was unique in giving a first order rate law; the other halides followed a one-half order rate law. The difference in order of reaction was ascribed to the fact that the scission of the strong C—F bond was rate limiting in the case of the fluoride, whilst in the other cases the various transport processes between phases were rate-limiting.

Since the proposed mechanisms for the *n*-alkyl halide reactions required the elimination of a 2-hydrogen atom from an adsorbed alkyl radical as one of the critical steps, we undertook a systematic study of the reactions of all of the possible derivatives obtainable by substitution of methyl groups at the 1- or 2-carbon atom of ethyl chloride. Although we did not forsee the result at the outset, this group of reactants provided an entirely new class of reaction in addition to providing further support for the mechanism previously proposed for the *n*-alkyl halide reactions.

Experimental

The experimental procedures were the same as described previously (1).

Results

Reactions on Clean Surfaces at Ambient Temperatures

The results are most conveniently discussed by contrasting the 1-methyl with the 2-methyl substituted alkyl chlorides for reactions at ambient temperatures on clean titanium surfaces, and the normal and branched chain alkyl chlorides for reactions at elevated temperatures on pre-reacted surfaces.

(a) The 1-Methyl Series

The reaction of ethyl chloride has previously been described (1). This reaction resulted in the adsorption of approximately one monolayer equivalent of reactant and the liberation of ethane and ethylene in a ratio of *ca.* 30:70. After reaction of about one monolayer the film was completely deactivated and reaction ceased.

Adsorption and reaction of a monolayer equivalent of isopropyl chloride was rapid and complete at 0 °C. The reaction product was a mixture of propane and propene (20:80). After reaction of the first monolayer equivalent the titanium exhibited much reduced, but finite, activity towards subsequent doses of isopropyl chloride. Figure 1 illustrates the course of reaction of second and third monolayer equivalent doses of isopropyl chloride at 0 °C. The rate of reaction of the first dose was too rapid to follow. The function $(P_0 - P)$ in Fig. 1 represents the combined total of isopropyl chloride that had reacted, subsequent to the reaction of the first aliquot, with the virgin metal surface, and it can be seen that the data fit very well the parabolic rate law:

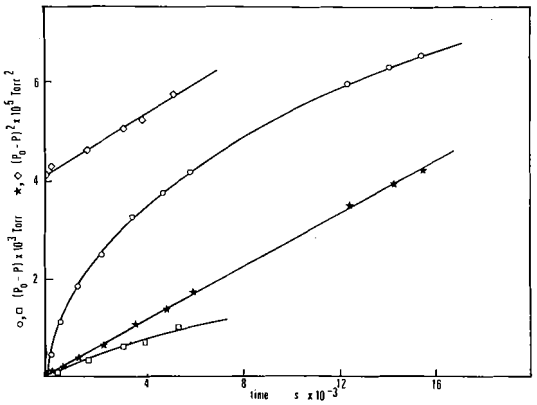

FIG. 1. Reactions of second and third monolayer equivalent doses of isopropyl chloride with a titanium film at 0 °C: P_0 = initial reactant pressure; P = pressure at time t; ○, ★ = second dose; □, ◇ = third dose.

$$[1] \qquad (P_0 - P)^2 = kt + \text{constant}$$

characteristic of a solid phase diffusion controlled reaction.

The adsorption and reaction of a monolayer equivalent of *t*-butyl chloride on a titanium film at 0 °C was rapid and complete. Only isobutene was observed as reaction product. A second dose of *t*-butyl chloride continued to react, but at a considerably enhanced rate compared to the first dose. During the reaction of the second and subsequent doses appreciable amounts of hydrogen chloride appeared in the product.

(b) The 2-Methyl Series

The reactions of ethyl and propyl chlorides have previously been described (1).

The only products detected in the reaction of

TABLE 1. Reactions of alkyl halides with clean titanium films*

Reactant chloride	T (°C)	Product (mol %)			Product ratios
		Adsorbed	Gaseous	Unaffected	
Ethyl	20	23.0	9.0	68.0	ethane:ethylene 30:70
n-Propyl	20	17.5	15.3	67.2	propane:propylene 50:50
i-Propyl	0	21.0	79.0	0.0	propane:propylene 20:80
i-Butyl	0	37.0	10.0	53.0	isobutane:isobutylene 40:60
t-Butyl	0	20.0	80.0	0.0	isobutylene
Neopentyl	0	100.0	trace	0.0	neopentane:isobutylene:methane 90:10:trace

*All measurements made 300 s after admission of reactant to virgin film. Initial pressure 1.0×10^{-2} Torr. Film area *ca.* 400 cm^2.

isobutyl chloride at 0 °C were isobutane and isobutene. Approximately one monolayer equivalent of isobutyl chloride reacted rapidly and completely, but the surface was completely deactivated towards further reaction.

A monolayer equivalent of neopentyl chloride adsorbed rapidly and completely at 0 °C. Only a trace of gaseous reaction product appeared and this consisted primarily of neopentane with a minor amount of isobutene and a trace of methane. Adsorption of approximately one monolayer of neopentyl chloride completely deactivated the surface with respect to further reaction.

Some observations on the behavior of the 1- and 2-methyl series are summarized in Table 1.

Reactions at Elevated Temperatures

At elevated temperatures (*ca.* 200 °C) the *n*-alkyl chlorides underwent reaction to many monolayer equivalents with reproducible rates to give mixtures of alkane and alkene. No hydrogen, or hydrogen chloride was detected and no loss of carbon to the film was observed. The rate laws for these reactions remained strictly half-order in reactant through complete reaction of a given dose and over many monolayer equivalents of reaction (1).

Each of the branched alkyl chlorides investigated in the present study behaved in a quite different way from the *n*-alkyl chlorides. In each case the observed reaction was a *catalytic* dehydrochlorination reaction. After an initial settling down period each of the branched alkyl chlorides reacted to give a stoichiometric mixture of hydrogen chloride and an unsaturated hydrocarbon in the gas phase. In addition, the rate laws for these reactions were all first order.

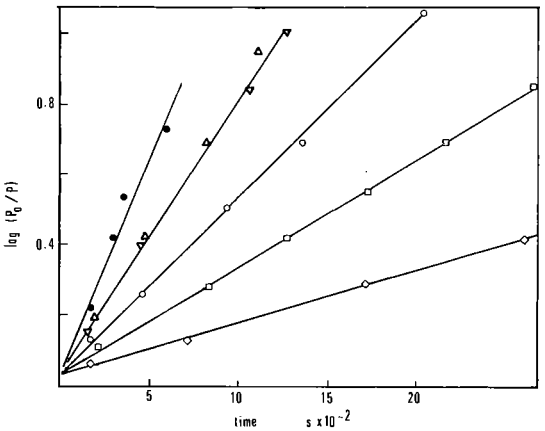

FIG. 2. Reaction of isopropyl chloride with titanium at elevated temperature: ◇, 100°; □, 118°; ○, 134.5°; ▽,△, 157° (duplicate runs performed before and after temperature sweep); ●, 180°.

At elevated temperatures (100–180 °C) the catalytic dehydrochlorination of isopropyl chloride on titanium to give propylene and hydrogen chloride occurred rapidly and in a highly reproducible fashion. The reaction was followed by monitoring the disappearance of reactant and the appearance of products mass spectrometrically and also by simply following the pressure change due to formation of two molecules of product from one of reactant. Both measurements yielded the same results and showed the reaction to be first order in reactant over a wide range of conditions. Figure 2 shows data from runs at several temperatures plotted as a first order reaction.

Can. J. Chem. Downloaded from www.nrcresearchpress.com by 210.87.254.105 on 09/05/12
For personal use only.

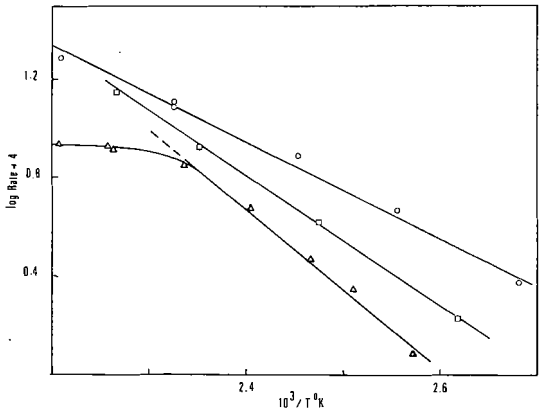

FIG. 3. Arrhenius plots for the reaction of isopropyl chloride on titanium at elevated temperature: ○, $P_0 = 10^{-2}$ Torr; □, 5×10^{-2} Torr; △, 2.5×10^{-1} Torr. The upper curve and points have been displaced upwards by 0.2 log units for purposes of clarity. The ordinate is the logarithm of the slopes of the first order plots shown in Fig. 2.

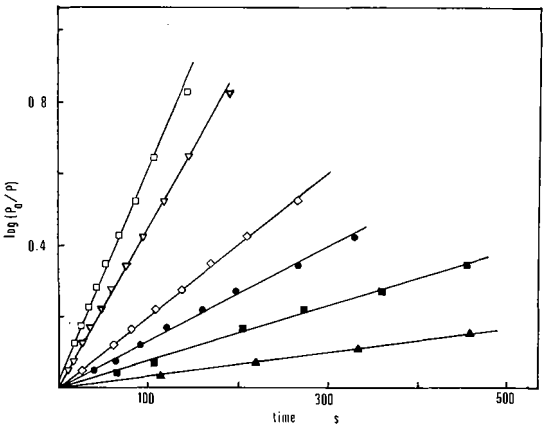

FIG. 4. Catalytic reaction of *t*-butyl chloride on halided titanium surfaces: ▲, 33.5°; ■, 42°; ●, 51.5°; ◇, 56.5°; ▽, 67.5°; □, 80°. $P_0 = 2.8 \times 10^{-2}$ Torr.

Arrhenius plots for three different initial reactant pressures, shown in Fig. 3, show a distinct rise in activation energy with increasing initial reactant pressure. This change in activation energy is well outside the experimental uncertainty, is reproducible over several temperature sweeps, and contrasts with the behavior of *n*-alkyl halides where no change in overall activation energy was observed for a tenfold change in initial reactant pressure. The levelling off of the 2.5×10^{-1} Torr plot at high temperatures in Fig. 3 is an artefact due to the appearance of a rate-controlling diffusion of products from the reactor to the detector. Similar behavior was noted for other reactions where the rates became unduly high, *e.g.*, tertbutyl chloride.

The foregoing description of the isopropyl chloride reaction ceased to be valid above 180 °C. Above this temperature propane and diisopropyl appeared in the gas phase products; the amount of hydrogen chloride produced was less than stoichiometric and the kinetics deviated from strict first order behavior.

Tert-butyl Chloride

The reaction of *t*-butyl chloride followed much the same pattern as isopropyl chloride except that the reaction rate was much greater and hydrogen chloride was produced even at room temperature. Some first order plots for the disappearance of *t*-butyl chloride at several temperatures are shown in Fig. 4. It should be noted that these data span a temperature range some 70–80 °C lower than the comparable set of data for isopropyl chloride shown in Fig. 2.

Because of severe corrosion problems with this reactant in the gauges and mass analyzer, the effect of initial reactant pressure on overall activation energy was not measured. The only reaction products detected throughout the entire experimental range were isobutene and hydrogen chloride.

Isobutyl Chloride

After an initial settling down period, isobutyl chloride underwent smooth catalytic dehydrochlorination in the temperature range 120–220 °C. The kinetics of the catalytic reaction were strictly first order in reactant and only isobutene and hydrogen chloride were detectable in the gas phase.

Like the isopropyl chloride reaction, that of isobutyl chloride gave an activation energy dependent on pressure in the range 1.0 to 5.0×10^{-2} Torr (see Table 2).

Neopentyl Chloride

In the chemistry of transition metal alkyl compounds, the neopentyl compounds show an exceptional stability due to their inability to decompose to olefin and metal hydride by β-hydride elimination from the alkyl group. This stability probably explains the lack of gas phase products in the room temperature reaction. On halided titanium surfaces, neopentyl

Can. J. Chem. Downloaded from www.nrcresearchpress.com by 210.87.254.105 on 09/05/12
For personal use only.

TABLE 2. Kinetic data for reaction of alkyl chlorides with titanium at elevated temperatures

Reactant	Reaction order	Apparent $E_a \pm \sigma$ (kcal)	Gaseous products	$P_0 \times 10^2$ (Torr)	Apparent log A*
Ethyl chloride	Half	23.5±1.5	Ethylene, ethane	1.0	5.7
		21.4±0.4		2.5	4.9
		21.9±0.7		5.0	4.9
n-Propyl chloride	Half	23.4±0.9	Propylene, propane	1.0	6.9
Isopropyl chloride	First	8.7±0.4	Propylene, HCl	1.0	1.3
		12.2±0.1		5.0	3.2
		15.2±0.7		25.0	4.6
Isobutyl chloride	First	12.6±0.3	Isobutylene, HCl	1.0	2.6
		15.9±0.2		5.0	4.2
		15.2±0.8		5.0	3.9
t-Butyl chloride	First	15.4±0.5	Isobutylene, HCl	2.8	7.5
Neopentyl chloride	First	13.9±0.2	2-Methylbutene-2, HCl	1.0	3.9
		15.0±0.5		2.5	4.3

*Apparent Arrhenius pre-exponential factor.

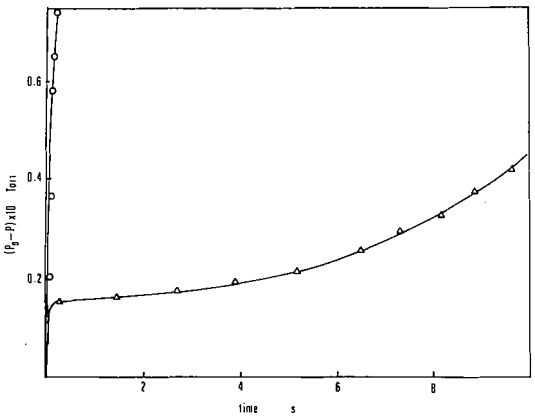

FIG. 5. Comparison of reactions of neopentyl chloride at 200° and 10^{-2} Torr: △, reaction on a virgin film; ○, catalytic reaction on the same film after achievement of constant activity.

chloride showed no reluctance to react in the higher temperature range and underwent facile dehydrochlorination to produce 2-methylbutene-2 and hydrogen chloride. The kinetics of the catalytic reaction were strictly first order after an initial settling down period, and the activation energy was almost identical to that found with the other branched alkyl halides. A rather small change in activation energy with pressure in the range 1.0 to 2.5 × 10^{-2} Torr was observed.

The difference in behavior of the first few monolayer equivalents from that of later doses was more marked with neopentyl chloride than with any of the other reagents investigated in the present study. The reaction of the first dose, after an initial rapid adsorption of reagent, was extremely slow. The disappearance of reactant was, however, autocatalytic and the rate of reaction was augmented by several orders of magnitude before steady first order kinetics and clean stoichiometry were achieved on a well-halided surface. These effects are illustrated in Fig. 5.

Some relevant data for the reactions of branched alkyl chlorides are summarized in Table 2. The data for ethyl and propyl chloride are also included for comparison.

Discussion

Catalytic Reactions

The reaction free energies for dehydrochlorination of the reactants used in our studies follow the sequence isopropyl chloride > *t*-butyl chloride > *n*-propyl chloride > isobutyl chloride > neopentyl chloride.[3] It is thus quite clear that

[3]Free energies for these dehydrochlorination reactions were calculated using standard free energies of formation for reactants and products derived from the following sources: olefins, ref. 10; HCl, ref. 11; alkyl halides, ref. 12. The floor temperatures ($\Delta G^0 = 0$) for some of the dehydrochlorination reactions of the present study at 0.01 Torr were calculated to be: C_2H_5Cl (27 °C); $CH_3{\cdot}CH_2{\cdot}CH_2{\cdot}Cl$ (−18 °C); $CH_3{\cdot}CHCl{\cdot}CH_3$ (35 °C); $(CH_3)_2{\cdot}CH{\cdot}CH_2Cl$ (−43 °C); $(CH_3)_3CCl$ (20 °C).

Can. J. Chem. Downloaded from www.nrcresearchpress.com by 210.87.254.105 on 09/05/12
For personal use only.

Can. J. Chem. Downloaded from www.nrcresearchpress.com by 210.87.254.105 on 09/05/12
For personal use only.

the appearance of gas phase hydrogen chloride through catalytic dehydrohalogenation is not merely dependent on whether or not HCl production is thermodynamically allowed. This being the case, it seems most likely that the two different kinds of reaction proceed by independent mechanisms.

It was previously suggested that the initial step in the reaction of *n*-alkyl halides at elevated temperatures was the dissociative adsorption of the carbon–halogen bond (1). The branched alkyl chlorides used in the present study span the range of primary, secondary, and tertiary carbon–chlorine bonds and neither the stoichiometry nor the kinetics shows a correlation with such structural variation in the substrate. The general reactivity patterns follow those observed for acid, base, and free radical elimination reactions (3).

The activation energies for the catalytic and the non-catalytic reactions fall into two distinct ranges. The former show maximum values in every case within the range 15.5 ± 0.5 kcal/mol and exhibit a dependence on reactant pressure below a critical pressure, whilst the latter are quite independent of pressure over a decade range. The dependence of the activation energy on pressure diminished in the sequence *i*-C_3H_7Cl > *i*-C_4H_9Cl > neo-$C_5H_{11}Cl$. Since the activation energy variation most probably arises from a contribution from the heat of adsorption of the reactant on the surface, the observed sequence may be rationalized on the basis that the heat of adsorption diminishes with increasing bulkiness of the adsorbate.

Since we did not measure the number of active surface sites involved in our reactions we do not have accurate estimates of true rate constants, or of Arrhenius pre-exponential factors. It has been our experience, however, that reaction rates for independent runs under identical conditions are reproducible to within a factor of two and certainly to better than an order of magnitude. Also, activation energies are highly reproducible for both ascending and descending temperature sweeps. In view of this we attach a high level of confidence to the proposition that the extraordinary variations in relative rates of reaction are due primarily to changes in the pre-exponential factors within the two classes of reaction. For example, the eight orders of magnitude difference in relative rate between propyl chloride ($E^{\ddagger} \approx 23$ kcal/mol) and propyl fluoride ($E^{\ddagger} \approx 21$ kcal/mol) arises mostly due to differences in the pre-exponential factors (1); the same is true for the seven orders of magnitude difference between isobutyl chloride and tertiary butyl chloride, both reactions having essentially the same activation energy.

A second assertion that may be made regarding the trends in relative reactivities is that the magnitude of the pre-exponential factor increases significantly in the series: primary < secondary < tertiary chloride, for catalytic reactions. This trend suggests that there are spacial constraints on the transition state that are less severe as the degree of methyl substitution at the α-carbon atom increases. If the pre-exponential factors for the catalytic dehydrochlorination of the *n*-alkyl halides are a few orders of magnitude less than that of isopropyl chloride, the rate for the catalytic mechanism is not competitive with the competing diffusional mechanism previously proposed to explain the non-catalytic dehydrochlorination. Indeed, isopropyl chloride was found to be a borderline case, since at the upper temperature limit of the present study both the order of reaction and the stoichiometry were intermediate between those expected for the catalytic and the non-catalytic reaction.

In the homogeneous gas phase dehydrohalogenation of alkyl halides the behavior of the activation energies and pre-exponential factors is quite different from that observed in the present study (2, 3). For the gas phase reactions the variation in rate for the series ethyl, isopropyl, and tertiary butyl (*ca.* $1:10^2:10^5$) is due almost entirely to a large change in activation energy, whilst the pre-exponential factors vary by less than 10^2 over the series. The same appears to be true of base promoted E2 eliminations, but the difficulty of separating the S_N2 and E2 reactions in this case has resulted in a greater sparsity of reliable kinetic parameters (3). Although acid-catalyzed elimination reactions are well known, we are unaware of any systematic study of activation parameters for such reactions. There seems to be no compelling reason why the large variation in rate between primary, secondary, and tertiary halides in acid-catalyzed elimination should be due to activation entropy, rather than enthalpy differences. In any case, the occurrence of an ionic mechanism in a solvent-free system is most unlikely.

Can. J. Chem. Downloaded from www.nrcresearchpress.com by 210.87.254.105 on 09/05/12
For personal use only.

Reduction of alkyl halide by one-electron transfer to yield a free radical and an adsorbed chlorine atom, reaction 2, is unlikely in view of the complete absence of alkane in the reaction products (S = active surface site).

$$[2] \qquad R\cdot Cl + S \rightarrow R^{\cdot} + S\cdot Cl$$

Solution reactions analogous to [2] are well known and always produce substantial amounts of alkane except in the presence of hydrogen atom scavengers (4, 5). An alternative to reaction 2 would be the immediate capture of the alkyl radical by a second active surface site to yield a surface alkyl species, reaction 3

$$[3] \qquad R\cdot Cl + 2S \rightarrow R\text{-}S + S\text{-}Cl$$

In fact, reaction 3 has already been suggested as the first step in the non-catalytic reactions of primary alkyl halides with titanium (1). If such a mechanism is correct for the non-catalytic reactions, it is difficult to imagine how the catalytic reactions could proceed via similar initial step and yet be so mechanistically different. In particular, it is difficult to explain how reaction 3 could lead to liberation of HCl in one case, but not in another.

In our opinion the catalytic reactions most probably proceed via a mechanism involving concerted elimination of HCl, analogous to an E_i mechanism, but that the weakening of the C—H and C—Cl bonds is in some way assisted by the adsorption process. Such a mechanism is consistent with the observed variation of activation energy with pressure, which can be attributed to a heat of adsorption contribution to the activation energy.

The concerted elimination of HCl from an alkyl halide is a symmetry-forbidden process (7). Almost any strong, low symmetry interaction with such a molecule will reduce the "forbiddeness" and consequently reduce the activation energy for concerted elimination. The ubiquitous catalytic activity of surfaces, a factor which makes studies of homogeneous gas phase eliminations so difficult, may be in part due to the intrinsic asymmetry of the adsorption process (3). It has been recognized that transition metals, and their compounds, may be particularly effective in removing the symmetry forbiddeness of both concerted addition and elimination reactions, by virtue of their possession of orbitals of appropriate symmetry (8). On the basis of such a model, the large variation in Arrhenius pre-exponential factors observed in the present study may be partly explained as a purely statistical effect of the available hydrogen atoms on the 2-carbon atom of the alkyl halide. The details of metal-assisted elimination reactions parallel exactly those previously developed for the cyclobutanation of olefins (9).

The constancy of the limiting activation energies for the catalytic reactions is surprising in view of the considerable structural variations in the reactants. It is in fact difficult to imagine a simple, common transition state that would give rise to a common activation energy. A more likely explanation is that the activation energies are adventitiously constant due to compensating effects.

The organic product resulting from dehydrochlorination of neopentyl chloride, namely 2-methylbutene-2, is the one normally produced from neopentyl eliminations. The similarity of the activation energy to those observed for the other catalytic reactions suggests that the methyl migration is a low energy process having little influence on the overall activation energy.

Reactions on Clean Titanium

Clean titanium reacts rapidly with alkyl halides at room temperature and below. With the exception of neopentyl chloride, any alkyl titanium species produced at the surface are unstable and many of the hydrocarbon groups are rapidly returned to the gas phase as mixtures of alkane and alkene. In the case of neopentyl chloride, although extremely rapid chemisorption occurred at room temperature, almost no gas phase products appeared. Such behavior is in accord with that observed for molecular alkyltitanium compounds (6).

All of the catalytic reactions were preceded by a "settling-down period", during which the behavior of the reactions was intermediate between that of the stoichiometric and catalytic extremes. This period was probably coincidental with a gradual rise in the average effective oxidation state of the surface and the catalytic species was probably titanium in at least oxidation state +2. Studies to allow a clearer definition of the chemical nature of these surface halide phases are presently under way in our laboratory.

Financial support from the National Research Council of Canada for the research reported in this paper is gratefully acknowledged.

1. J. F. HARROD and W. R. SUMMERS. J. Am. Chem. Soc. **93**, 5051 (1971).
2. J. H. S. GREEN, A. MACCOLL, and P. J. THOMAS. J. Chem. Soc. 184 (1960) and references therein.
3. D. V. BANTHORPE. Elimination reactions. Elsevier Publ. Co., Amsterdam. 1963. Chap. 7.
4. J. HALPERN and J. P. MAHER. J. Am. Chem. Soc. **87**, 5361 (1965).
5. J. KWIATEK. Catal. Rev. **1**, 37 (1967).
6. G. A. RAZWAEV and V. N. LATYAEVA. Organomet. Chem. Rev. **2**, 349 (1967).
7. R. B. WOODWARD and R. HOFFMAN. The conservation of orbital symmetry. Academic Press, New York. 1971. Chaps. 2 and 3.
8. R. G. PEARSON. Acc. of Chem. Res. 4, 152 (1971).
9. F. D. MANGO and J. H. SCHACHTSCHNEIDER. J. Am. Chem. Soc. **89**, 2485 (1967).
10. Selected values of the properties of hydrocarbons and other related compounds. American Petroleum Institute, Research Project No. 44.
11. F. P. ROSSINI, D. D. WAGMAN, W. A. EVANS, S. LEVINE, and I. JAFFE. Selected values of chemical and thermodynamic properties. National Bureau of Standards, Circular No. 500.
12. D. R. STULL, E. F. WESTRUM, and G. C. SINKE. The chemical thermodynamics of organic compounds. J. Wiley and Sons, Inc., New York. 1969; Selected values of properties of chemical compounds. Manufacturing Chemists Association Research Project, Chemical Thermodynamics Properties Center, Texas A and M University.

Can. J. Chem. Downloaded from www.nrcresearchpress.com by 210.87.254.105 on 09/05/12
For personal use only.

Studies in Solvolysis. Part V. Further Investigations Concerning the Solvolysis of Primary, Secondary, and Tertiary Trifluoroacetates[1]

D. J. BARNES, M. COLE (née Morrissey), S. LOBO, J. G. WINTER, AND JOHN M. W. SCOTT
Chemistry Department, Memorial University of Newfoundland, St. John's, Newfoundland

Received March 7, 1972

The rate of solvolysis of ethyl trifluoroacetate has been investigated in a series of H_2O/D_2O mixtures at 9.97 °C. The secondary isotope effects related to the hydrolysis of the isotopic pairs, methyl/methyl-d_3, ethyl/ethyl-d_5, *i*-propyl/*i*-propyl-β-d_6 and *t*-butyl/*t*-butyl-d_9 trifluoroacetates have been established as well as the temperature dependence for the hydrolysis of *t*-butyl trifluoroacetate. The significance of all these measurements with respect to the mechanism of these reactions is discussed.

La vitesse de la solvolyse du trifluoroacétate d'éthyle a été étudiée dans divers mélanges H_2O/D_2O à 9.97 °C. Les effets isotopiques secondaires concernant les paires isotopiques des trifluoroacétates de méthyle/méthyl-d_3, d'éthyle/éthyl-d_5, d'*i*-propyle/*i*-propyl-β-d_6 et de *t*-butyle/*t*-butyl-d_9, ont été établis ainsi que l'influence de la température sur l'hydrolyse du trifluoroacétate de *t*-butyle. La signification de toutes ces mesures, quant au mécanisme de ces réactions, est discutée.

Canadian Journal of Chemistry, **50**, 2175 (1972)

Can. J. Chem. Downloaded from www.nrcresearchpress.com by 210.87.254.42 on 09/05/12
For personal use only.

Introduction

In a previous communication (1) the temperature dependence for the rates of uncatalyzed (neutral) hydrolysis of a series of esters CF_3COOR(R = Me, Et, *i*-Pr and *t*-Bu) was reported in water and deuterium oxide. An examination of the thermodynamic parameters $\Delta H^{\neq}$, $\Delta S^{\neq}$, and $\Delta C_p^{\neq}$ which characterize the thermal activation of these molecules suggested that the methyl, ethyl, and *i*-propyl esters all react by a $B_{Ac}2$ acyl–oxygen cleavage mechanism whereas the tertiary ester reacts by an S_N1 alkyl–oxygen fission path or a mechanism which involves mixed kinetics, *i.e.* both the $B_{Ac}2$ and S_N1 routes. The mechanistic pattern based on the thermodynamic parameters was completely substantiated by the kinetic solvent isotope effects (k.s.i.e.) measured in light and heavy water.

The designations $B_{Ac}2$ and S_N1 for these reactions are, however, only partly adequate. The former description merely emphasizes the fact that the "basic" or nucleophilic properties of the solvent are important driving forces for the reaction with at least one water molecule in the transition state for the rate determining step. The latter (S_N1) description offers no indication as to whether the ester itself or the tetrahedral intermediate postulated for the $B_{Ac}2$ reaction reacts further by an alkyl–oxygen fission mechanism and also leaves the question of the incursion of ion pairs etc. unresolved.

[1]For Part IV, see ref. 20.

The inadequacy of the $B_{Ac}2$ description is apparent when a more detailed specification of the overall reaction is attempted. A simplified mechanistic description for the $B_{Ac}2$ process is

$$\text{[I]}\quad \text{Ester} + \text{N} \underset{k_2}{\overset{k_1}{\rightleftarrows}} \text{sp}^3 \text{ intermediate} + \text{E} \xrightarrow{k_3} \text{products}^2$$

where N and E are respectively nucleophilic and electrophilic reagents which, in the case of the uncatalyzed hydrolysis, are provided by the solvent acting in both roles.

In the two step mechanism represented by reaction 1 the observed kinetic behavior for any particular ester will depend on the relative magnitudes of the rate constants associated with the individual steps. With strong nucleophiles *e.g.* the lyate ion, the observed kinetics provide a standard example of a second order reaction and presumably k_1 is the rate determining step. On the other hand, if the nucleophilic strength of N is reduced as is the case when water replaces the hydroxide ion, the kinetic behavior may be modified in such a way as to make k_1, k_2 and k_3 all kinetically significant. In cases where k_3 is kinetically significant the B designation of the $B_{Ac}2$ category will be only partly justified. The indeterminacy of the reaction order with respect to the solvent in the neutral hydrolysis excludes the possibility of locating the rate determining step in the overall process. Indeed, the

[2]We regard reaction 1 as a minimal mechanistic description for the $B_{Ac}2$ process.

Can. J. Chem. Downloaded from www.nrcresearchpress.com by 210.87.254.42 on 09/05/12
For personal use only.

pseudo first order hydrolyses of the trifluoroacetate esters raise all the classical conundrums associated with processes where the reaction medium also provides the attacking reagent or reagents. In spite of these difficulties we hope to show that mixed k.s.i.e.'s and secondary isotope effects provide useful probes to examine these perennial questions. As a prerequisite to some resolution of the problems posed above we report below the rates of hydrolysis of ethyl trifluoroacetate in H_2O/D_2O mixtures as well as the secondary isotope effects for the isotopic ester pairs methyl/methyl-d_3, ethyl/ethyl-d_5, *i*-propyl/*i*-propyl-d_6, and *t*-butyl/*t*-butyl-d_9. A more detailed investigation of the temperature variation of the rate of hydrolysis of *t*-butyl trifluoroacetate is also reported and this particular study suffices to establish the temperature dependence of the enthalpy of activation for this substance.

Experimental

Materials and Methods

The experimental methods for rate determinations were identical to those described in Part I of the present series. The isotopic solvent mixtures were prepared by weight from deuterium oxide of known water content. The ethyl trifluoroacetate used in this study was the same sample used previously (1). Deuterium oxide was obtained from the Atomic Energy of Canada Ltd. and deuterated materials used in the preparation of the esters were obtained from Merck, Sharp, and Dohme Ltd.

The methyl and ethyl trifluoroacetates and their respective deuterated analogs were prepared by reacting the appropriate methyl or ethyl halide with silver trifluoroacetate in purified benzonitrile (1). The *i*-propyl and *t*-butyl trifluoroacetates and the related deuterium compounds were prepared by reacting trifluoroacetic anhydride and the appropriate alcohol in the presence of a small amount of silver trifluoroacetate (2). The *i*-propyl alcohol used was purified with magnesium in the usual way. The *t*-butyl alcohol was purified by fractional freezing and the commercial *t*-butyl alcohol-d_9 was used without further purification. The *i*-propyl alcohol-d_6 was obtained in good yield (*ca.* 90%) by the reduction of acetone-d_6 with lithium aluminum hydride using *n*-butyl carbitol to decompose the alcoholate (3). The usual physical and spectroscopic properties indicated that the eight esters were sufficiently pure for meaningful kinetic studies. The b.p.'s and n.m.r. τ values are recorded in Table 1. When supersaturation of the ester solution was avoided (see below) the excellent Guggenheim plots obtained provided a further check of the homogeneity of the substrates. The rate constants obtained from these studies are recorded in Tables 2, 3, and 4. The rate *vs.* composition profile for ethyl trifluoroacetate reacting in a series of H_2O/D_2O mixtures is illustrated graphically in Fig. 1.

The agreement between the rate constants reported here and those reported previously (1) is generally satisfactory and where minor differences are apparent the new results are to be preferred.

TABLE 1. Some physical properties of esters derived from trifluoroacetic acid

R (CF_3COOR)	Boiling point* (°C at 760 mm)	τ value† (n.m.r.)
CH_3	43 (43)	6.04 (6.02)
CD_3	42.5–43	—
CH_2CH_3	59 (61.3)	8.68, 5.60 (8.58, 5.54)
CD_2CD_3	59.2–60	—
$CH(CH_3)_2$	72.5–73 (73)	8.66, 4.81 (8.64, 4.83)
$CH(CD_3)_2$	73	4.85
$C(CH_3)_3$	84 (45 °C at 145 mm)	8.45 (8.45)
$C(CD_3)_3$	85	—

*Literature values in parentheses are from ref. 4.
†Literature values in parentheses are from ref. 1.

The temperature dependence of the rates of hydrolysis of the methyl, ethyl, and *i*-propyl trifluoroacetates and their deuterated analogs can be represented over a short temperature range by the equation

$$[2] \qquad \log k/T = A/T + B$$

The parameters ΔH^* and ΔS^* were determined from least squares values of A and B in the usual way (1) and the thermodynamic quantities so calculated are reported in Table 5.

For the *t*-butyl trifluoroacetate the temperature dependence of the rates could be expressed by the equation

$$[3] \quad \log k = -10612/T - 38.35 \log T + 127.63$$

The numerical coefficients were determined by a least squares method using the individual rates rather than the average experimental rates quoted in Table 3. The least squares calculation and the evaluation of the thermodynamic parameters from the numerical coefficients in eq. 3 were carried out using a computer program available in Dr. Robertson's laboratory at the University of Calgary.

As mentioned above the supersaturation of the substrate is a bothersome feature in the determination of the rates of hydrolysis of the esters of trifluoroacetic acid. In consequence the yield of reproducible rate constants obtained in the present study is less than that obtained with other substrates such as sulfonates and halides. The supersaturation problem also probably accounts for the relatively large error in the heat capacity of activation reported for *t*-butyl trifluoroacetate.

Discussion

(a) Mixed Solvent Isotope Effects

The theory of rate and equilibrium processes in H_2O/D_2O mixtures has been developed by Kresge, Long, and co-workers and others (4–9) and has been reviewed by Robertson and

TABLE 2. Rate constants and secondary isotope effects for the solvolysis of trifluoroacetates at 5, 10, 15, and 25 °C.

Ester	T (°C)	k(H)* ($\times 10^4$ s^{-1})	k(D)* ($\times 10^4$ s^{-1})	k(H)/k(D)
CF_3COOCH_3	4.963	23.42 ± 0.015 (16)	22.30 ± 0.015 (4)	1.050 ± 0.001
(CD_3—)	10.007	33.45 ± 0.026 (5)	31.74 ± 0.016 (5)	1.054 ± 0.001
	15.001	46.51 ± 0.000 (4)	44.13 ± 0.016 (6)	1.050 ± 0.004
$CF_3COOCH_2CH_3$	5.001	8.837 ± 0.008 (8)	8.531 ± 0.004 (6)	1.036 ± 0.0010
(CD_3—CD_2—)	10.002	12.69 ± 0.013 (6)	12.24 ± 0.015 (4)	1.037 ± 0.0016
	15.000	17.69 ± 0.008 (4)	17.07 ± 0.019 (5)	1.036 ± 0.0012
$CF_3COOCH(CH_3)_2$	5.001	2.465 ± 0.005 (7)	2.402 ± 0.007 (6)	1.026 ± 0.0036
((CD_3)$_2$CH—)	10.000	3.554 ± 0.010 (6)	3.473 ± 0.0003 (5)	1.023 ± 0.0027
	15.001	4.993 ± 0.008 (7)	4.844 ± 0.006 (5)	1.031 ± 0.0021
$CF_3COOC(CH_3)_3$ ((CD_3)$_3$C—)	25.001	14.09 ± 0.007 (7)	6.478 ± 0.053 (11)	2.175 ± 0.018

*Number of rate determinations in parentheses.

TABLE 3. Temperature dependence of the rate of hydrolysis of *t*-butyl trifluoroacetate

T (°C)	k* ($\times 10^4$ s^{-1})
4.986	0.5493 ± 0.0106 (17)
8.919	1.021 ± 0.047 (15)
12.003	1.871 ± 0.044 (8)
15.001	2.970 ± 0.073 (17)
19.082	5.586 ± 0.122 (9)
21.782	8.540 ± 0.162 (12)
24.777	13.20 ± 0.43 (11)
27.509	17.53 ± 1.35 (10)

*Number of rate determinations in parentheses.

TABLE 4. Rates of solvolysis of ethyl trifluoroacetate in H_2O/D_2O mixtures at 9.97 °C

Atom fraction deuterium (n)	k* ($\times 10^4$ s^{-1})	$\frac{k(n)}{k(H)}$
1.000		0.275 (extrapolated)
0.993	3.503 ± 0.006 (7)	0.281
0.892	4.061 ± 0.008 (4)	0.326
0.773	4.821 ± 0.012 (4)	0.387
0.751	5.101 ± 0.015 (4)	0.409
0.543	6.547 ± 0.013 (4)	0.525
0.434	7.498 ± 0.010 (4)	0.601
0.358	7.913 ± 0.018 (4)	0.634
0.225	9.505 ± 0.026 (4)	0.762
0.122	10.532 ± 0.030 (4)	0.844
0.000 (pure H_2O)	12.476 ± 0.021 (4)	1.000

*Number of rate determinations in parentheses.

Laughton (10). The more recent developments in the theory use the fractionation factor (ϕ) formalism which provides a means of considering the variation of the ratios $k(n)/k(H)$ (rates) or $K(n)/K(H)$ (equilibria) in terms of "n", the atom fraction deuterium in the solvent and the fractionation factors (ϕ) mentioned previously. The "n" parameter requires no further discussion but some explanatory remarks concerning the ϕ parameter are helpful.

Essentially the fractionation factors (ϕ) are isotopic equilibrium constants for all the labile protons associated with each equilibrium state, either ground or activated, which define any particular rate or equilibrium process. The fractionation factor for each labile proton is defined by the equation

$$[4] \quad \phi = ([D]/[H])_{substrate}/([D]/[H])_{solvent}$$

In applications of the Kresge–Long theory no attempt is made to relate the various ϕ parameters to the more fundamental statistical quantities (vibrational frequencies etc.) which must ultimately determine their magnitude. Rather, the ϕ's are considered as disposable parameters which can be estimated from the rate or equilibrium constants observed in the pure isotopic solvents. The ϕ values so calculated are then

Can. J. Chem. Downloaded from www.nrcresearchpress.com by 210.87.254.42 on 09/05/12
For personal use only.

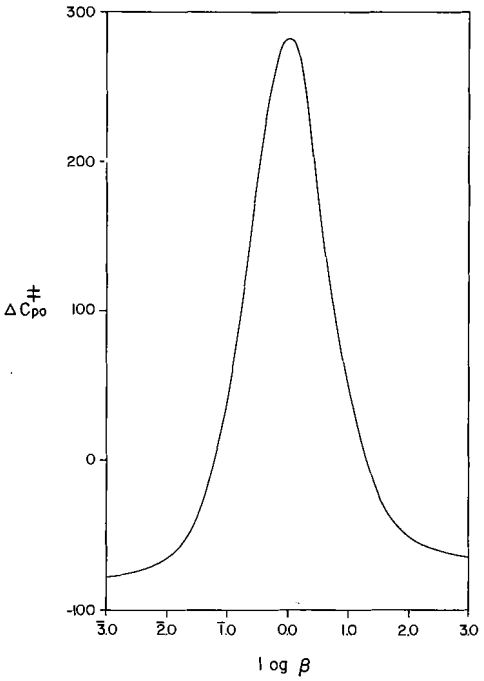

FIG. 1. Correlation between the rate ratios, $k(n)/k(H)$ and the atom fraction, n, of D_2O for the solvolysis of ethyl trifluoroacetate in H_2O/D_2O mixtures.

used to establish the variation of the rate or equilibrium constants as a function of the isotopic composition of the solvent.

Fractionation factors which are less than unity correspond to normal isotope effects and those greater than unity inverse effects.[3] In processes which involve the cooperative attack of several water molecules, and in which both the nucleophilic and hydrogen bonding (electrophilic) properties of the solvent are important, the net weakening of hydrogen–oxygen bonds compared with those of bulk water should lead, on the basis of a simple zero-point treatment (11, 12), to normal effects. This implies that the appropriate fractionation factors will be less than unity.

The application of the Kresge–Long theory requires some assumptions concerning the path between the reactants and products for the chemical reaction studied. In the case of ethyl trifluoroacetate, we have adopted the mechanism

[3]This is a consequence of the fact that the Kresge–Long theory considers isotopic ratios with the light atom quantities in the denominator. The opposite convention is more usual.

TABLE 5. Thermodynamic parameters (at 10 °C) for the solvolysis of deuterated and non-deuterated trifluoroacetates in water

R (CF_3COOR)	ΔH^* (kcal mol^{-1})	ΔS^* (cal mol^{-1} deg^{-1})
CH_3	10.35 ± 0.02	-33.2 ± 0.2
CD_3	10.26 ± 0.02	-33.6 ± 0.2
CH_2CH_3	10.53 ± 0.04	-34.5 ± 0.4
CD_2CD_3	10.49 ± 0.03	-34.7 ± 0.4
$CH(CH_3)_2$	10.68 ± 0.05	-36.5 ± 0.6
$CH(CD_3)_2$	10.62 ± 0.07	-36.7 ± 0.9

represented by reaction 1 with the further assumption that the nucleophile (N) and the electrophile (E) are respectively represented by "p" and "q" water molecules, *i.e.* the bonding of $2p$ labile protons is modified in the first step to give an intermediate containing $2p$ labile protons which then decomposes into the products.

The application of the Kresge–Long theory to this model is straightforward and gives

$$[5] \quad \frac{k(n)}{k(H)} = \frac{(1-n+n\bar{\phi}_1^{\ddagger})^{2p}(1-n+n\bar{\phi}_2^{\ddagger})^{2q}(1+\gamma)}{\gamma(1-n+n\bar{\phi}_1^{\ddagger})^{2p}+(1-n+n\bar{\phi}_2^{\ddagger})^{2q}}$$

in which $\bar{\phi}_1^{\ddagger}$ and $\bar{\phi}_2^{\ddagger}$ are respectively mean fractionation factors for the first and second transition states in reaction 1. The parameter γ is related to the rate constants k_2 and k_3 by the equations

$$[6] \quad k_2/k_3 = \gamma$$

with

$$[7] \quad k_2/(k_2+k_3) = \gamma/(1+\gamma)$$

and

$$[8] \quad k_3/(k_2+k_3) = 1/(1+\gamma)$$

To simplify the present theoretical treatment it was assumed that the fractionation factors are all equal (ϕ), and that $2q = 2p + 2$, *i.e.* one water molecule is involved in the k_3 step. Equation 5 is then reduced to

$$[9] \quad \frac{k(n)}{k(H)} = \frac{(1-n+n\phi)^{2q}(1+\gamma)}{\gamma+(1-n+n\phi)^2} = R$$

Can. J. Chem. Downloaded from www.nrcresearchpress.com by 210.87.254.42 on 09/05/12
For personal use only.

TABLE 6. A comparison of the theoretical and observed dependence of the rate of hydrolysis of ethyl trifluoroacetate in light and heavy water mixtures

	$\delta \times 10^3$ for $\gamma =$						
q	10^{-3}	10^{-2}	10^{-1}	1	10	10^2	10^3
1	432	367	224	81.3	84.0	29.9	29.6
2	29.6	30.3	32.0	23.2	15.4	14.3	14.3
3	14.3	14.3	14.7	13.7	12.8	12.7	12.7
4	12.7	12.7	12.9	13.0	13.4	13.6	13.5
5	13.5	13.6	13.6	13.6	14.2	14.3	14.3

When $\gamma < 10^{-2}$ eq. 9 reduces to

$$[10] \qquad \frac{k(n)}{k(\mathrm{H})} = (1 - n + n\phi)^{2q-2} = R$$

and when $\gamma > 10^2$ eq. 8 becomes

$$[11] \qquad \frac{k(n)}{k(\mathrm{H})} = (1 - n + n\phi)^{2q} = R$$

Equations 10 and 11 are identical in form but are out of phase with respect to the variable q. This has important consequences when eq. 9 is used to analyze the experimental data (see below).

For $n = 1$, which corresponds to the pure isotopic rate ratio $k(D_2O)/k(H_2O)$, values of ϕ were determined for five integral values of q in the range $1 < q < 5$ and six integral values of $\log\gamma$ in the range $-3 < \log\gamma < 3$ together with $\log\gamma = 0$ giving a total of seven different values of γ. This leads to thirty five values of ϕ appropriate to $n = 1$. Each of these values ϕ with the appropriate values of q and γ gives rise to a family of theoretical curves relating $k(n)/k(H_2O)$ to n. The derived theoretical curves may be compared with the experimental curve using a least squares criterion such as

$$[12] \qquad \delta = \{\Sigma(R_{\mathrm{calc}} - R_{\mathrm{obs}})^2\}^{1/2}$$

to search for the best values of γ and q in the γ–q grid (Table 6). Minima in δ are evident in the grid at $q = 4$ and $\gamma = 10^{-2}$ or 10^{-3} and at $q = 3$ with $\gamma = 10^2$ or 10^3. The identity of the values of δ at these minima arises merely from the fact that the exponents of eqs. 10 and 11 are out of phase. Since eq. 9 does not provide a unique minimum, mechanistic conclusions based on this criterion are of limited significance. However, of the two alternatives suggested by the above analysis we find the sequential attack of a total of three water molecules ($q = 3$) on both the substrate and the intermediate involved in a pre-equilibrium mechanism ($\gamma = 10^2$ or 10^3) to be more likely than the attack of four water molecules on the substrate in a unitary step ($q = 4$ and $\gamma = 10^{-2}$ or 10^{-3}). The pre-equilibrium model is also in accord with Bender's mechanistic description of ester hydrolysis involving a tetrahedral intermediate (13).

TABLE 7. Thermodynamic parameters for the hydrolysis of *t*-butyl trifluoroacetate in water at various temperatures

T (°K)	ΔH_T^* (kcal/mol)	ΔS_T^* (e.u.)
273.15	27.20	19.9
298.15	25.24	13.0
323.15	23.29	6.75
348.15	21.33	0.92
373.15	19.38	−4.58

*$\Delta C_{p0}^* = -78 \pm 16$ cal mol^{-1} deg^{-1}. The conversion of the numerical coefficients of eq. 3 to enthalpies, entropies, and heat capacities of activation was made in the usual way (see ref. 1).

(b) The Thermodynamic Parameters

The new thermodynamic parameters reported here include the $\Delta H^{\neq}$ and $\Delta S^{\neq}$ for the deuterated primary and secondary esters and the heat capacity of activation for *t*-butyl trifluoroacetate (see Tables 5 and 7). The $\Delta H^{\neq}$ and $\Delta S^{\neq}$ values for the deuterated esters do not call for any particular comment but the $\Delta C_{p0}^{\neq}$ for the tertiary ester is of considerable interest.

The observed heat capacity of activation $\Delta C_{p0}^{\neq}$ for a process proceeding simultaneously by

Can. J. Chem. Downloaded from www.nrcresearchpress.com by 210.87.254.42 on 09/05/12
For personal use only.

Can. J. Chem. Downloaded from www.nrcresearchpress.com by 210.87.254.42 on 09/05/12
For personal use only.

two distinct mechanisms with rate constants k_1 and k_2 is given by the expression

$$[13]\quad \Delta C_{p0}^{\ddagger} = \frac{1}{1+\beta}\Delta C_{p1}^{\ddagger} + \frac{\beta}{1+\beta}\cdot\Delta C_{p2}^{\ddagger} + \frac{\beta}{(1+\beta)^2}\cdot\frac{(\Delta H_2^{\ddagger} - \Delta H_1^{\ddagger})^2}{RT^2}$$

where $\beta = k_1/k_2$ and $\Delta C_{p1}^{\ddagger}$, $\Delta C_{p2}^{\ddagger}$, $\Delta H_1^{\ddagger}$, and $\Delta H_2^{\ddagger}$ are respectively the heat capacities and enthalpies of activation associated with the individual paths. Thus if a situation exists in which both paths contribute to the observed rate such that[4] $0.01 < \beta < 100$ then the observed heat capacity of activation will be made up of real and spurious terms. The first two terms of the r.h.s. of eq. 13 are real and the final term is spurious (see ref. 14). If the "average" heat capacities of activation for $B_{Ac}2$ and S_N1 processes are respectively -65 and -80 cal mol^{-1} deg^{-1} (1, 15) and the difference in the enthalpies of activation for the two processes is taken as 15 kcal mol^{-1} (1), then the calculated expression for $\Delta C_{p0}^{\ddagger}$ as a function of β *i.e.* mechanism, is illustrated in Fig. 2. The strongly positive heat capacities of activation calculated for the region $0.01 < \beta < 100$ suggest that the *t*-butyl ester reacts primarily by an S_N1 mechanism which agrees with other evidence presented in this paper and elswehere (1).

(c) Secondary Isotope Effects

The secondary isotope effects reported in Table 2 are considered in the light of previous mechanistic conclusions based on other evidence. Since the alkyl group is the reaction seat in the S_N1 process and is relatively remote from the reaction center in the $B_{Ac}2$ process, deuteration of the alkyl group is likely to be more potent in the former reaction. This analysis is consistent with the experimental observations. The rate ratio for the normal and d_9 *t*-butyl trifluoroacetates is very similar to that of the related chlorides and is fully consistent with the S_N1 description based on $\Delta H^{\ddagger}$, $\Delta S^{\ddagger}$, and k.s.i.e. parameters.

The isotope effects observed with the primary esters are more complex. We first draw attention to the fact that deuteration in the methyl groups of the methyl halides or sulfonates leads

[4]These limits define the mixed region. Outside the limits the mechanisms are not mixed. The limits are, of course, quite arbitrary.

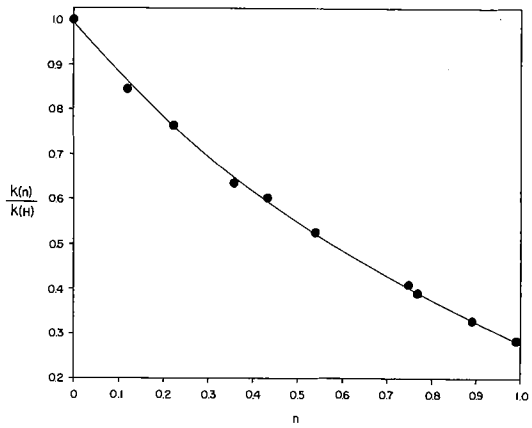

FIG. 2. Variation of the observed heat capacity of activation for a reaction proceeding partly by the $B_{Ac}2$ and S_N1 routes.

to inverse effects (16). Thus the normal effect in the case of methyl trifluoroacetate is entirely consistent with attack at a position other than the methyl group. Any further analysis of the isotope effects observed with the primary and secondary esters must be made in terms of the Bender (13) pre-equilibrium mechanism mentioned above, which is

$$[14]\quad k_o = K_e k_3 \quad \text{where} \quad K_e = k_1/k_2$$

It may be readily shown that the observed isotope effect for the pre-equilibrium mechanism is influenced only by vibrational-force constant changes between the initial state and the second transition state. We assume reasonably that the vibrational changes in the alkyl group of the ester arise primarily from the increasing oxonium character of the alkyl oxygen in the second transition state as a consequence of electrophilic attack at this position. Since bond angles in oxonium compounds are similar to those involving divalent oxygen the isotope effects are primarily a consequence of electronic changes rather than changes which derive from concomitant electronic and geometrical alterations. Differential hydrogen–deuterium inductive electron release (17) to the incipient oxonium center should lead to the increased reactivity of the deuterium compounds in the case of the methyl/methyl-d_3 and the ethyl/ethyl-d_5 esters, assuming that the net isotope effect in the ethyl compounds is dominated by the deuterium atoms on the carbon adjacent to the alkyl oxygen atom. Since

Can. J. Chem. Downloaded from www.nrcresearchpress.com by 210.87.254.42 on 09/05/12
For personal use only.

the isotopic methyl esters demonstrate a normal effect and the net effect in the case of the ethyl esters is also normal, the inductive hypothesis is reasonably rejected. The decreasing isotope effect with increasing homology of the alkyl group in the case of the primary and secondary esters is more consistent with the hyperconjugation hypothesis developed by Shiner and coworkers (17, 18). However, such an interpretation is not clear-cut because γ contributions are present in the case of both the ethyl and *i*-propyl esters and the hyperconjugation hypothesis is only applicable to deuteration which is β to the reaction site.

Isotopic substitution γ to the reacting center has been shown to lead to inverse effects in reactions which involve substitution at a saturated carbon atom (19). In contrast, complete deuteration of the γ positions in the *i*-propyl esters, *i.e.*, deuteration of the two methyl groups, leads to a normal effect. Thus there is no correlation between the influence of γ isotopic substitution in nucleophilic substitution reactions and ester hydrolyses. This is not surprising. Although reacting oxygen and carbon centers become more positive in the transition state in both types of reaction, any further resemblance between the two processes is slight, particularly with respect to geometrical reorganization which is virtually absent in the case of ester hydrolyses (see above).

Clearly the main value of the secondary isotope effects in the present study is to further emphasize the distinction between the primary and secondary esters on the one hand and the tertiary ester on the other. The finer differences displayed within the primary and secondary esters as a group are less amenable to unequivocal theoretical interpretation.

The authors wish to thank Dr. R. E. Robertson for his help in various phases of the present study and Dr. W. J. Albery for some useful advice concerning reactivity in mixed isotopic solvents. We also wish to thank the Technical Services group at Memorial University for their continued assistance. Finally we thank Memorial University and the National Research Council of Canada for financial support.

1. J. M. W. Scott and J. G. Winter. Can. J. Chem. **46**, 2887 (1968).
2. E. J. Bourne, M. Stacey, J. C. Tatlow, and R. Worrall. J. Chem. Soc. 3268 (1958).
3. V. J. Shiner, Jr. J. Am. Chem. Soc. **74**, 5285 (1952).
4. A. Moffat and H. Hunt. J. Am. Chem. Soc. **79**, 54 (1957); **81**, 2082 (1959).
5. A. J. Kresge. *In* Proceedings of the symposium on isotope mass effects in chemistry and biology. Vienna, 1963. International Union of Pure and Applied Chemistry and International Atomic Energy Agency. Butterworths, London. 1964. p. 243.
6. H. H. Huang, R. R. Robinson, and F. A. Long. J. Am. Chem. Soc. **88**, 1866 (1966).
7. P. Gross, H. Steiner, and H. Suess. Trans. Faraday Soc. **32**, 883 (1936).
8. W. J. C. Orr and J. A. V. Butler. J. Chem. Soc. 330 (1937).
9. W. E. Nelson and J. A. V. Butler. J. Chem. Soc. 958 (1938).
10. R. E. Robertson and P. M. Laughton. *In* Solute–solvent interactions. *Edited by* J. F. Coetzee and C. D. Ritchie. Marcel Dekker, New York and London. 1969. Section III, p. 415.
11. A. Streitwieser, Jr., R. C. Fahey, R. H. Jagow, and S. Suzuki. J. Am. Chem. Soc. **80**, 2326 (1958).
12. C. A. Bunton and V. J. Shiner. J. Am. Chem. Soc. **83**, 3207 (1961).
13. M. Bender. Chem. Rev. **60**, 53 (1960).
14. J. M. W. Scott and R. E. Robertson. Can. J. Chem. **50**, 167 (1972).
15. E. A. Moelwyn Hughes, R. E. Robertson, and S. Sugamori. J. Chem. Soc. 1965 (1965).
16. J. A. Llewellyn, R. E. Robertson, and J. M. W. Scott. Can. J. Chem. **38**, 222 (1960).
17. E. A. Halevi. *In* Progress in physical organic chemistry. *Edited by* S. Cohen and A. J. Streitwieser, Jr. Interscience, John Wiley and Sons, New York and London. 1963. p. 137.
18. Indiana conference of hyperconjugation. *Co-chaired by* V. J. Shiner and E. Campaigne. Tetrahedron **5**, 105–274 (1959).
19. R. E. Robertson, J. A. Llewellyn, and K. T. Leffek. J. Am. Chem. Soc. **82**, 6315 (1960).
20. J. M. W. Scott and J. G. Winter. Can. J. Chem. In press.

The Preparation of Iron Carbonyl Complexes of Fluorocarbon-Bridged Ligands

L. S. CHIA, W. R. CULLEN, AND D. A. HARBOURNE

Chemistry Department, University of British Columbia, Vancouver 8, British Columbia

Received February 1, 1972

The reactions of the ligands $L\overline{C{=}CL'(CF_2)_{n/2}}$ ($L = (CH_3)_2As$, $(C_6H_5)_2P$; $L' = (CH_3)_2As$, $(C_6H_5)_2P$; $n = 4$, 6, 8; but not all combinations) with iron carbonyls are described in detail. The nature of the products is discussed as a function of the reaction conditions and the ligands. The mixed ligands yield eight different types of complexes which have been characterized. Two of these types $(L{-}L')_2Fe_2(CO)_4$ and $(L{-}L')_2Fe(CO)_3$ were previously unknown.

Les réactions des ligands $L\overline{C{=}CL'(CF_2)_{n/2}}$ ($L = (CH_3)_2As$, $(C_6H_5)_2P$, $L' = (CH_3)_2As$, $(C_6H_5)_2P$; $n = 4$, 6, 8 mais pas toutes les combinaisons) avec les fer carbonyles sont décrites en détail. La nature des produits est discutée en fonction des conditions de réaction et des ligands. La combinaison des ligands donne huit types de complexes différents qui ont été caractérisés. Deux d'entre eux $(L{-}L')_2Fe_2(CO)_4$ et $(L{-}L')_2Fe(CO)_3$ étaient jusqu'ici inconnus.

Canadian Journal of Chemistry, **50**, 2182 (1972)

Introduction

A number of iron carbonyl derivatives of fluorocarbon-bridged ditertiary arsines and phosphines have been described in recent years (1–4). Of special interest have been the complexes formed by $f_4$fars and $f_4$fos **1***a* and **1***b*. The

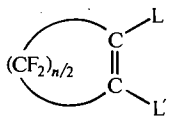

1

a L = $(CH_3)_2As$ = L′, *n* = 4, $f_4$fars
b L = $(C_6H_5)_2P$ = L′, *n* = 4, $f_4$fos
c L = $(CH_3)_2As$, L′ = $(C_6H_5)_2P$, *n* = 4, f_4AsP
d L = $(CH_3)_2As$, L′ = $(C_6H_5)_2P$, *n* = 6, f_6AsP
e L = $(C_6H_5)_2P$ = L′, *n* = 6, $f_6$fos
f L = $(C_6H_5)_2P$ = L′, *n* = 8, $f_8$fos

former has the ability to displace two terminal carbonyl groups from $Fe_3(CO)_{12}$ to give the complex $f_4farsFe_3(CO)_{10}$, **2**, (L′ = $(CH_3)_2As$) (3, 5). Furthermore, this $Fe_3(CO)_{10}$ derivative on mild heating breaks down to a complex of formula $f_4farsFe_3(CO)_9$ in which the ligand has undergone rearrangement **3** (L′ = $(CH_3)_2As$) (3, 6). Complexes of these types are not formed by $f_4$fos or by related ditertiary phosphines with larger bridging fluoroalicyclic groups. A further difference between $f_4$fos and $f_4$fars is that only the former gives a chelated complex $f_4$fos-$Fe(CO)_3$ (1).

Because of these differences and because of the general lack of knowledge about iron carbonyl complexes of mixed ligands, the new ligands f_4AsP **1***c* and f_6AsP **1***d* were synthesized (7, 8) to investigate their reactions with iron carbonyls. In general the results which follow show that the products of the reactions are similar to those obtained from their symmetrical analogues. However, it has been found that f_4AsP behaves more like $f_4$fars than $f_4$fos in yielding $f_4AsPFe_3(CO)_{10}$ and $f_4AsPFe_3(CO)_9$, although it also acts like $f_4$fos in giving the chelate complex $f_4AsPFe(CO)_3$.

In view of critical dependence of the products on the reaction conditions and on the ratio of the reactants, we now give comprehensive lists of the reactions of these ligands, including the ditertiary phosphine **1***f* $f_8$fos (9), with the iron carbonyls and discuss the various trends that are apparent in ligand behavior. In addition we describe some interconversion reactions of the

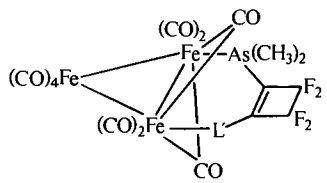

2

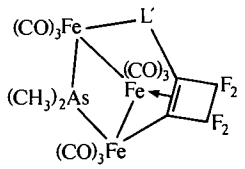

3

Can. J. Chem. Downloaded from www.nrcresearchpress.com by 210.87.254.5 on 09/05/12
For personal use only.

Can. J. Chem. Downloaded from www.nrcresearchpress.com by 210.87.254.5 on 09/05/12
For personal use only.

complexes, especially those of the mixed ligand f_4AsP.

Experimental Section

The preparation of the ligands has been previously described (7–10). Volatile reactants and products were manipulated in a standard vacuum system. Ultra violet irradiations were done with a 200 W Hanovia 654A-36 lamp situated 20 cm from the reaction vessel. The detailed preparations of new complexes described below are selected from a large number of reactions which are given in tabular form in Tables 5–7. The conditions are those found to result in highest yields of the desired compounds coupled with maximum ease of work-up. Tables 5–7 also include bare details of previously unpublished experiments involving the symmetrical ligands $f_4$fars, $f_4$fos, and $f_6$fos. No new techniques were used, most separations being made by chromatography on Florisil (1–3). Qualitative analyses were made by spectroscopic means. When necessary, quantitative analysis of mixtures was made using n.m.r. spectroscopy. Microanalyses were performed by Mr. Peter Borda of this Department.

(1) Preparation of $f_4AsPFe(CO)_4$

A tetrahydrofuran solution (20 ml) containing 4.0 g (9.6 mmol) f_4AsP and 10.0 g (51 mmol) iron pentacarbonyl was heated at 100° in a Carius tube for 4 days. The tube was opened, the brown-red reaction solution filtered, and then the solvent was removed at reduced pressure. The resulting brown-red oil was dissolved in a small volume of diethyl ether and chromatographed on Florisil. Elution with 2% diethyl ether–98% petroleum ether afforded a yellow-orange band of the desired compound ($f_4AsPFe_2(CO)_8$ and $f_4AsPFe(CO)_3$ may contaminate the tail of this band). The $Fe(CO)_4$ derivative was recrystallized from cold petroleum ether to give yellow crystals, m.p. 115° (4.5 g, 78%).

(2) Preparation of $f_4AsPFe_2(CO)_8$

Iron pentacarbonyl (15 g, 76 mmol), f_4AsP (3.0 g, 7.2 mmol), and acetone (30 ml) were sealed under vacuum in a thick-walled Pyrex tube. The tube was irradiated for 120 h with ultraviolet light while shaking. The tube was then opened and the volatile contents were removed. The residue, a brown-red oil, was dissolved in a small volume of methylene chloride and chromatographed on Florisil. Elution with 2–5% diethyl ether–98–95% petroleum ether yielded an orange-red solution. This was concentrated and cooled to give yellow crystals of $f_4AsPFe(CO)_4$ (1.90 g, 45%).

The mother liquors were combined, concentrated, and cooled to give orange-red crystals which were recrystallized from hexane to yield red crystals of $f_4AsPFe_2(CO)_8$, m.p. 98° (1.10 g, 20%).

(3) Preparation of $f_4AsPFe_3(CO)_9$ and $f_4AsPFe_2(CO)_6$

Triiron dodecacarbonyl (5.2 g, 10.3 mmol) and f_4AsP (2.5 g, 6.0 mmol) were refluxed together in cyclohexane (50 ml) under nitrogen for 5 h. The solution was evaporated to dryness and the residue was chromatographed on Florisil. After eluting the initial yellow band which contained traces of $f_4AsPFe(CO)_4$ and $f_4AsPFe_2(CO)_8$ with 2% diethyl ether–98% petroleum ether, a deep violet band was eluted with 2–5% diethyl ether–98–95% petroleum ether. The solvent was removed and a deep violet powder was obtained which was rechromatographed and recrystallized from carbon disulfide to give deep violet crystals of $f_4AsPFe_3(CO)_9$, m.p. 175° (dec.) (1.3 g, 26%). An orange band was eluted with 5–10% diethyl ether–95–90% petroleum ether. The orange solid was purified by rechromatography and/or recrystallization from methylene chloride to give orange-red crystals of $f_4AsPFe_2(CO)_6$, m.p. 212° (dec.) (2.0 g, 51%).

(4) Preparation of $f_4AsPFe_3(CO)_{10}$

Triiron dodecacarbonyl (4.0 g, 8.0 mmol) and f_4AsP (1.0 g, 2.4 mmol) were refluxed together in cyclohexane (50 ml) for 45 min. The resulting solution was evaporated to yield a dark brown oil. This was chromatographed in Florisil. Petroleum ether eluted an initial brown band (traces of $f_4AsPFe(CO)_4$, $f_4AsPFe_3(CO)_9$, etc.) and $Fe_3(CO)_{12}$. A 5% diethyl ether–95% petroleum ether mixture eluted $f_4AsPFe_3(CO)_{10}$ as a gray-green band. The compound was purified by rechromatography and recrystallization from carbon disulfide to give deep green crystals, m.p. 135° (dec.) (1.80 g, 87%).

(5) Preparation of $(f_4AsP)_2Fe(CO)_3$ and $(f_4AsP)_2Fe_2(CO)_4$

Triiron dodecacarbonyl (1.0 g, 2.0 mmol) and f_4AsP (2.5 g, 6.0 mmol) were refluxed together in cyclohexane (60 ml) for 2 h. The cyclohexane was removed. The residue (a brown-red oil) was dissolved in a small volume of methylene chloride and chromatographed on Florisil. Petroleum ether eluted an initial brown-red band (traces of $f_4AsPFe(CO)_4$ and $f_4AsPFe_3(CO)_9$, etc.). 2–5% diethyl ether–98–95% petroleum ether eluted a yellow band which gave a yellow-orange sample of $(f_4AsP)_2Fe(CO)_3$. This was purified by rechromatography and recrystallization from carbon disulfide to give yellow-orange crystals, m.p. 153° (dec.) (0.25 g, 9%).

Diethyl ether–petroleum ether up to 50% eluted a red band which gave a brick-red powder of $(f_4AsP)_2Fe_2(CO)_4$. This was rechromatographed and recrystallized from diethyl ether–petroleum ether to yield brick-red crystals, m.p. 205° (dec.) (0.15 g, 5%).

(6) Preparation of $f_4AsPFe(CO)_3$

Diiron enneacarbonyl (3.0 g, 8.2 mmol), f_4AsP (2.0 g, 4.9 mmol), and acetone (50 ml) were sealed under vacuum in a thick-walled Pyrex tube. After irradiation for 8 days with ultraviolet light while shaking, the tube was opened. The reaction mixture was filtered and the solvent removed. The resulting dark brown oil was dissolved in a small volume of methylene chloride and chromatographed on Florisil. After eluting the initial yellow band ($f_4AsPFe(CO)_4$), a brown-yellow band was eluted with 2–5% diethyl ether–98–95% petroleum ether. This was evaporated and recrystallized from petroleum ether to give brown-yellow crystals of $f_4AsPFe(CO)_3$, m.p. 136° (dec.) (1.00 g, 36%).

(7) Preparation of $f_6AsPFe(CO)_4$

Iron pentacarbonyl (7.0 g, 36 mmol) and f_6AsP (0.46 g, 1.0 mmol) were refluxed together in cyclohexane (30 ml) for 10 h. The volatile contents were then removed and the residue was extracted with petroleum ether. The resulting solution was filtered and evaporated to dryness to give a yellow-brown oil. This was then purified by chromatography. A 2% diethyl ether–98% petroleum ether mixture eluted

$f_6AsPFe(CO)_4$ as a yellow band ($f_6AsPFe(CO)_3$ may contaminate the tail of this band). The compound was recrystallized from *n*-hexane as yellow crystals, m.p. 51° (0.10 g, 16%).

(8) Preparation of $f_6AsPFe(CO)_3$

Iron pentacarbonyl (15 g, 76 mmol) and f_6AsP (0.93 g, 2.0 mmol) were sealed under vacuum with acetone (15 ml) in a Pyrex tube. The tube was irradiated with u.v. light for 2 days while shaking. The tube was opened and the solution was filtered and evaporated to dryness. The dark brown residue was extracted with petroleum ether. This extract was evaporated to dryness, dissolved in a small volume of methylene chloride, and chromatographed on Florisil. Diethyl ether–petroleum ether mixtures eluted a dark brown band which yielded a dark brown powder of $f_6AsPFe(CO)_3$. This was recrystallized from diethyl ether–petroleum ether as dark brown crystals, m.p. 137° (dec.) (0.62 g, 57%).

(9) Preparation of $f_6AsPFe_2(CO)_6$

Triiron dodecacarbonyl (1.0 g, 2.0 mmol) and f_6AsP (0.5 g, 1.1 mmol) were refluxed together in cyclohexane (50 ml) for 4 h. The solvent was removed. The brown residue was extracted with petroleum ether and filtered to remove a brown solid. (The filtrate was evaporated to dryness, dissolved in a small volume of methylene chloride, and chromatographed on Florisil to give $f_6AsPFe(CO)_4$ (~5%) and $f_6AsPFe(CO)_3$ (22%).)

The brown solid was extracted with acetone. The resulting brown-red solution was filtered and evaporated to yield an orange powder of $f_6AsPFe_2(CO)_6$. This was purified by chromatography using diethyl ether as eluent. Recrystallization from methylene chloride–*n*-hexane gave orange crystals, m.p. 215° (dec.) (0.41 g, 50%).

(10) Reaction of cis-$(CH_3)_2AsC(CF_3)$=$C(CF_3)As(CH_3)_2$ with $Fe_3(CO)_{12}$

The ditertiary arsine (1.1 g, 0.30 mmol) and $Fe_3(CO)_{12}$ (1.9 g, 0.38 mmol) in acetone solution (20 ml) were irradiated with ultraviolet light for 24 h. The solvent was removed and chromatography of the solid residue gave two bands which were eluted with petroleum ether. The first band off the column gave a red-brown solid which was identified as $(CH_3)_2AsC(CF_3)$=$C(CF_3)As(CH_3)_2Fe(CO)_3$ (1.0 g, 66%). The mass spectrum showed a parent ion followed by loss of three CO groups. The carbonyl infrared spectrum (C_6H_{12} solution) consisted of the expected pattern of three bands at 2001(8), 1933(7), 1917(10) cm^{-1}.

Anal. Calcd. for $C_{11}H_{12}As_2F_6FeO_3$: C, 25.8; H, 2.3; F, 22.3. Found: C, 25.8; H, 2.3; F, 22.4.

The second band gave a yellow-red solid which was identified as $(CH_3)_2AsC(CF_3)$=$C(CF_3)As(CH_3)_2Fe_2(CO)_6$ (0.1 g, 5%) after purification by sublimation (160°, 10^{-2} mm). The mass spectrum showed a parent ion followed by loss of six CO groups. The carbonyl infrared spectrum showed absorption in the usual pattern as follows: 1956(2), 1968(1), 1986(4), 1996(6), 2024(10), 2062(4) cm^{-1}.

Anal. Calcd. for $C_{14}H_{12}As_2F_6Fe_2O_6$: C, 25.8; H, 1.8. Found: C, 26.0; H, 1.7.

(11) Reaction of f_8fos with $Fe_2(CO)_9$

The ligand (0.36 g, 0.6 mmol) (7) and $Fe_2(CO)_9$ (0.59 g, 1.6 mmol) were stirred in benzene solution (15 ml) for 12 h. The resulting dark solution was filtered and the solvent was evaporated to leave an oil which solidified on trituration with petroleum ether. The brown product was recrystallized from benzene–petroleum ether to give 0.6 g (82%) of $f_8fosFe(CO)_3$, m.p. 158–161 (dec.). The carbonyl infrared spectrum had absorption at 1933(9), 1949(7), and 2009(10) cm^{-1}. The ^{19}F n.m.r. spectrum showed two equal area broad resonances at 134 and 103 p.p.m. upfield from $CFCl_3$.

Anal. Calcd. for $C_{33}H_{20}F_8FeO_3P_2$: C, 54.0; H, 2.8; P, 8.4. Found: C, 54.3; H, 2.8; P, 8.0.

Results and Discussion

Characterization of the Complexes of Unsymmetrical Ligands

The new complexes of the unsymmetrical ligands can be classified into eight groups: (L—L′)$Fe(CO)_4$, (L—L′)$Fe_2(CO)_8$, (L—L′)$Fe(CO)_3$, (L—L′)$_2Fe(CO)_3$, (L—L′)$Fe_2(CO)_6$, (L—L′)$_2Fe_2(CO)_4$, (L—L′)$Fe_3(CO)_{10}$, and (L—L′)$Fe_3(CO)_9$ where (L—L′) is f_4AsP, **1***c*, and/or f_6AsP, **1***d*. All these types except (L—L′)$_2Fe_2(CO)_4$ and (L—L′)$_2Fe(CO)_3$ are known for complexes of the symmetrical ligands f_4fars, **1***a* and f_4fos, **1***b*. The range of known hydrocarbon-bridged ditertiary phosphine and arsine complexes is considerably less (11).

Appropriate analytical and spectroscopic data for the new complexes are listed in Tables 1–4. The mass spectra of all the new compounds showed a parent ion followed by loss of the appropriate number of carbonyl groups. Since the rest of the cracking pattern was not very useful as an aid to the structure determination the spectra are not described further here although fairly complete assignments have been made elsewhere (12).

(1) (L—L′)$Fe(CO)_4$ Complexes

Both f_4AsP and f_6AsP give complexes of this type. The Mössbauer spectra, Table 4, consist of a quadrupole doublet whose isomer shift and quadrupole splitting are characteristic of monosubstituted $Fe(CO)_5$ derivatives (1). The ^1H n.m.r. data, Table 3, indicate that it is the $(C_6H_5)_2P$ moiety that is coordinating since the chemical shift of the $(CH_3)_2As$ group is virtually unchanged on coordination. If the complex were formed by donation of the arsenic lone pair then a downfield shift (~0.5 p.p.m.) of the $(CH_3)_2As$ resonance would be expected. For example, the ^1H n.m.r. spectrum of f_4fars is a singlet at 1.40 p.p.m. The complex $f_4farsFe(CO)_4$ absorbs at 1.90 p.p.m. (coordinated $As(CH_3)_2$ group) and at 1.44 p.p.m. ("free" $(CH_3)_2As$ group) (1).

Can. J. Chem. Downloaded from www.nrcresearchpress.com by 210.87.254.5 on 09/05/12
For personal use only.

TABLE 1. Analytical data for new complexes of unsymmetrical ligands

Complex	m.p. (°C)	Calcd. C	Calcd. H	Calcd. F	Found C	Found H	Found F
$f_4AsPFe(CO)_4$	115	45.4	2.77	13.1	45.4	2.80	12.9
$f_4AsPFe_2(CO)_8$	98	41.6	2.15	10.1	41.7	2.13	9.90
$f_4AsPFe(CO)_3$	136*	45.5	2.91	13.7	45.0	2.85	13.5
$(f_4AsP)_2Fe(CO)_3$	153*	48.4	3.34	16.0	48.1	3.56	15.8
$f_4AsPFe_2(CO)_6$	212*	41.5	2.33	10.9	41.9	2.22	10.6
$(f_4AsP)_2Fe_2(CO)_4$	205*	45.6	3.07	14.5	45.1	3.04	13.8
$f_4AsPFe_3(CO)_{10}$	135*	39.0	1.87	8.82	39.2	1.97	8.80
$f_4AsPFe_3(CO)_9$	175*	38.9	1.94	9.11	38.9	1.94	9.00
$f_6AsPFe(CO)_4$	51	43.7	2.56	18.0	44.1	2.80	17.7
$f_6AsPFe(CO)_3$	137*	43.7	2.68	18.9	44.0	2.59	18.9
$f_6AsPFe_2(CO)_6$	215*	40.4	2.17	15.3	40.3	2.15	15.0

*With decomposition

TABLE 2. Carbonyl infrared spectra of new complexes of unsymmetrical ligands*

Complex	Frequency (cm^{-1})
$f_4AsPFe(CO)_4$	2059(7), 1984(8), 1954(10), 1944(10)
$f_4AsPFe_2(CO)_8$	2064(7), 2059(9), 1992(7), 1984(8), 1975(7), 1961(9), 1954(10), 1942(9)
$f_4AsPFe(CO)_3$	2000(9), 1936(8), 1916(10)
$(f_4AsP)_2Fe(CO)_3$	1986(1), 1913(10), 1898(10)
$f_4AsPFe_2(CO)_6$	2062(7), 2024(10), 1996(8), 1982(5), 1969(4), 1952(3)
$(f_4AsP)_2Fe_2(CO)_4$	1995(9), 1957(10), 1934(5), 1912(4)
$f_4AsPFe_3(CO)_{10}$	2075(7), 2002(10), 1960(4), 1939(3), 1802(w), 1755(w)
$f_4AsPFe_3(CO)_9$	2076(8), 2047(10), 2024(10), 2010(8), 1999(9), 1989(6), 1977(7), 1962(3), 1932(2)
$f_6AsPFe(CO)_4$	2060(8), 1979(8), 1952(10), 1944(10)
$f_6AsPFe(CO)_3$	2005(10), 1941(9), 1919(10)
$f_6AsPFe_2(CO)_6$	2062(8), 2026(10), 2000(8), 1986(7), 1973(4), 1955(4)

*Spectra were run using a Perkin–Elmer model 457 spectrometer. The solvent was cyclohexane and the numbers in parentheses are relative peak heights.

The carbonyl infrared spectra of both compounds show four band patterns. This is probably due to the asymmetry of the ligands causing a splitting of the E mode in the spectrum expected for an axially substituted (C_{3v}) trigonal bipyramidal structure (1, 13). A similar four band spectrum is seen for other (L—L)$Fe(CO)_4$ complexes (1). The predicted structure for $f_4AsPFe(CO)_4$, **4**, has recently been verified by an X-ray investigation (14).

(2) $f_4AsPFe_2(CO)_8$

The suggested structure for this molecule is shown in **5**. The Mössbauer spectrum consists of two quadrupole doublets indicating the presence of iron atoms in two different environments. The only reasonable assignments given in Table 4 result in values δ and Δ which are in the range expected for monosubstituted $Fe(CO)_5$ derivatives (1) such as the analogous f_4fars-$Fe_2(CO)_8$. The iron atom with the greater

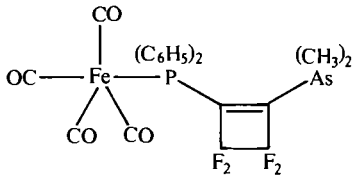

4

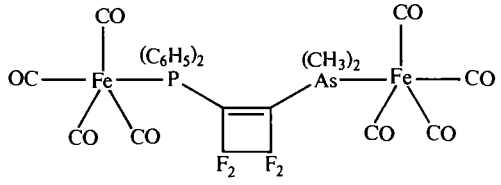

5

Can. J. Chem. Downloaded from www.nrcresearchpress.com by 210.87.254.5 on 09/05/12
For personal use only.

TABLE 3. ^1H and ^{19}F n.m.r. data for new complexes of unsymmetrical ligands*

Complex	^1H Spectrum	^{19}F Spectrum
$f_4AsPFe(CO)_4$	Singlet at 1.25 (area 6), multiplet centered at 7.60 (area 10) (CS_2 solution)	Multiplet with one strong peak at 108.0 ($(CH_3)_2CO$ solution)
$f_4AsPFe_2(CO)_8$	Singlet at 1.98 (area 6), multiplet centered at 7.67 (area 10) (CS_2 solution)	Two multiplets at 106.5 (area 2) and 107.3 (area 2) ($(CH_3)_2CO$ solution)
$f_4AsPFe(CO)_3$	Singlet at 1.80 (area 6), multiplet centered at 7.47 (area 10) (CS_2 solution)	Two multiplets at 108.2 (area 2) and 109.2 (area 2) ($(CH_3)_2CO$ solution)
$(f_4AsP)_2Fe(CO)_3$	Singlet at 1.18 (area 6), multiplet with two strong peaks at 7.60 and 7.63 (total area 10) (CS_2 solution)	Multiplet with one strong peak at 106.5 ($(CH_3)_2CO$ solution)
$f_4AsPFe_2(CO)_6$	Singlets at 1.37 (area 3) and 2.28 (area 3), multiplet with two strong peaks at 7.40 and 7.63 (total area 10) ($CDCl_3$ solution)	Four regions of absorption: (*a*) unsymmetrical doublet ($J = 210$ Hz) centered at 90.2, (*b*) unsymmetrical doublet ($J = 215$ Hz) of multiplets ($J = 40$ Hz) centered at 94.9, (*c*) unsymmetrical doublet ($J = 120$ Hz) of doublets ($J = 30$ Hz) at 106.4, (*d*) unsymmetrical doublet ($J = 125$ Hz) of doublets ($J = 40$ Hz) at 109.8 ($(CH_3)_2CO$ solution)
$(f_4AsP)_2Fe_2(CO)_4$	Singlets at 1.38 (area 3), 1.77 (area 3), 1.88 (area 3), and 2.15 (area 3), multiplet with two strong peaks at 7.33 and 7.52 (total area 20) ($CDCl_3$ solution)	Complex multiplet with two strong peaks at 108.0 and 110.0 (THF solution)
$f_4AsPFe_3(CO)_{10}$	Singlet at 1.87 (area 6), multiplet centered at 7.57 (area 10) ($CDCl_3$ solution)	Two multiplets at 108.0 (area 2) and 108.9 (area 2) ($(CH_3)_2CO$ solution)
$f_4AsPFe_3(CO)_9$	Singlets at 0.10 (area 3), and 1.83 (area 3), multiplet centered at 7.60 (area 10) ($CDCl_3$ solution)	Complex multiplets with four strong peaks at 91.5, 94.7, 99.0, and 101.6 ($(CH_3)_2CO$ solution)
$f_6AsPFe(CO)_4$	Singlet at 1.18 (area 6), multiplet with two strong peaks at 7.58 and 7.61 (area 10) (CS_2 solution)	Complex multiplets at 105.5 (area 2), 106.2 (area 2), and 132.3 (area 2) ($(CH_3)_2CO$ solution)
$f_6AsPFe(CO)_3$	Singlet at 1.85 (area 6), multiplet with two strong peaks at 7.42 and 7.54 (area 10) (CS_2 solution)	Complex multiplets at 106.0 (area 2), 108.2 (area 2), and 126.6 (area 2) ($(CH_3)_2CO$ solution)
$f_6AsPFe_2(CO)_6$	Singlets at 1.18 (area 3) and 2.25 (area 3), multiplet with two strong peaks at 7.38 and 7.58 (area 10) ($CDCl_3$ solution)	Complex multiplets at 72.4, 83.3, 95.9, 100.4, 109.5, and 122.3 (THF solution)

*Spectra were run on a Varian T60 spectrometer. Chemical shifts are reported in p.p.m. downfield from internal TMS (^1H spectra) or upfield from external $CFCl_3$ (^{19}F spectra).

isomer shift is believed to be the one coordinated to the $(CH_3)_2As$ moiety on the grounds that the arsine end would be the weaker π-acceptor. Other spectroscopic properties are in agreement with the proposed structure.

(3) (L—L)Fe(CO)$_3$ Complexes

These are obtained for both f_4AsP and f_6AsP. Again their Mössbauer and infrared spectra indicate a five coordinate iron(0) derivative. The n.m.r. data show that both ends of the ligands are coordinated and that the ligands have the same symmetry in the complexes as in the free ligands. It is probable that, in solution, these derivatives, like the other (L—L)$Fe(CO)_3$ and (L—L)$Ru(CO)_3$ complexes (1, 15) are undergoing positional exchange possibly by the "turnstile" mechanism (16). In the solid the ligands are probably coordinated at an axial and equatorial position giving an L—Fe—L angle of $\sim 90°$ (as is reported for diars$Fe(CO)_3$ (17), diars = 1,2-$((CH_3)_2As)_2C_6H_4$). Angles of $\sim 90°$ are found in the chelate complexes

Can. J. Chem. Downloaded from www.nrcresearchpress.com by 210.87.254.5 on 09/05/12
For personal use only.

TABLE 4. Mössbauer parameters for some new compounds

Complex	Temperature (°K)	δ (mm/s)	Δ (mm/s)	$\bar{\Gamma}$ (mm/s)
$f_4AsPFe(CO)_4$	80	0.18	2.58	0.36
	295	0.11	2.57	0.22
$f_4AsPFe_2(CO)_8$	80	0.21	2.83	0.27
		0.19	2.18	0.26
	295	0.15	2.83	0.21
		0.13	2.12	0.24
$f_4AsPFe(CO)_3$	80	0.22	2.47	0.26
	295	0.13	2.47	0.20
$(f_4AsP)_2Fe(CO)_3$	80	0.17	2.81	0.27
	295	0.10	2.85	0.23
$f_6AsPFe(CO)_4$	80	0.17	2.59	0.26
$f_6AsPFe(CO)_3$	80	0.21	2.61	0.27

*δ: Isomer shift, relative to sodium nitroprusside; Δ: Quadrupole splitting; $\bar{\Gamma}$: Full width at half maximum, average of the two resonance lines. Spectra were determined and processed as described in ref. 1.

$[(f_6fos)_2Rh]^+[Rh(CO)_2Cl_2]^-$ (18) and $f_6fosFe(NO)_2$ (19). In the latter case a P—Fe—P angle closer to 109° might have been expected. Equatorial–equatorial substitution in a trigonal bipyramidal (L—L′)$Fe(CO)_3$ complex would require the ligand to subtend an angle of ~120° at the iron atom.

(4) $(f_4AsP)_2Fe(CO)_3$

The spectroscopic data are consistent with the structure indicated in **6**. In particular the

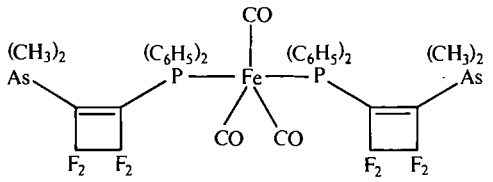

6

n.m.r. spectrum indicates that both ligands are P-bonded. The carbonyl infrared spectrum shows two strong bands of similar frequency (1913, 1898 cm^{-1}) and a weaker band at higher energy (1986 cm^{-1}). An ideal D_{3h} molecule would give just one infrared active band. In the case of **6**, it is probable that the weak band is the A_1' mode which is made weakly infrared active by the asymmetry of the ligand. The two strong frequencies are possibly due to splitting of the E mode for the same reason or, alternatively, they are due to the presence of rotamers in solution corresponding, for example, to "eclipsed" or "staggered" orientations of the ligands with respect to the central planar $Fe(CO)_3$ group. Rotation about other bonds such as the P—cyclobutene could also result in rotamers.

(5) $(L—L')Fe_2(CO)_6$

These compounds were isolated using both ligands. They are orange solids with high (>200°) melting points. The pattern of infrared bands for these complexes is very similar to that described for other complexes of the same formula (2). The Mössbauer spectra, which will be discussed in detail in another publication (20), are also typical showing four equal intensity lines indicating two different iron environments, and the ^1H n.m.r. spectra show two singlet resonances in the As—CH_3 region. Thus the

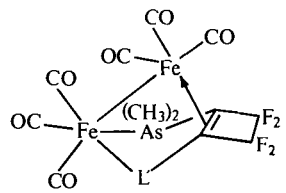

7

structures are analogous to that found for $f_4farsFe_2(CO)_6$ **7** (L′ = $As(CH_3)_2$) (21) and the f_4AsP analogue would have L′ = $P(C_6H_5)_2$.

(6) $(f_4AsP)_2Fe_2(CO)_4$

This complex is also an orange-red solid

Can. J. Chem. Downloaded from www.nrcresearchpress.com by 210.87.254.5 on 09/05/12
For personal use only.

Can. J. Chem. Downloaded from www.nrcresearchpress.com by 210.87.254.5 on 09/05/12
For personal use only.

which suggests that it is a derivative of $f_4AsPFe_2(CO)_6$. This is confirmed by its synthesis from $f_4AsPFe_2(CO)_6$ and f_4AsP when an acetone solution of the two reactants is irradiated (20). The Mössbauer spectrum shows two different iron atoms (20). This and other spectroscopic data are consistent with a structure in which the second f_4AsP ligand is bridging the two iron atoms of **7** ($L' = (C_6H_5)_2P$). An alternative structure with the second ligand chelated to the 6-coordinated iron atom can be eliminated since this has been obtained from other experiments (20) and its structure confirmed by X-ray methods (22).

(7) $f_4AsPFe_3(CO)_{10}$

The structure proposed for this compound is **2** ($L' = P(C_6H_5)_2$). The spectroscopic properties are very similar to those of $f_4farsFe_3(CO)_{10}$ **2** ($L' = As(CH_3)_2$). Thus the $As(CH_3)_2$ moiety in $f_4AsPFe_3(CO)_{10}$ is coordinated and its ^1H n.m.r. resonance is a singlet. The carbonyl infrared spectrum shows the presence of weak bridging carbonyl bands.

(8) $f_4AsPFe_3(CO)_9$

This was believed to have the structure **3** ($L' = P(C_6H_5)_2$) because of the similarity of its spectroscopic properties with those of the known $f_4farsFe_3(CO)_9$ **3** ($L' = As(CH_3)_2$) (6). However, one feature of the ^1H n.m.r. spectrum, an $As—CH_3$ resonance at high field ($\sim$0.10 p.p.m.), seemed to suggest that perhaps the structure was different and that an $Fe—CH_3$ bond was present. A subsequent X-ray investigation (23) has shown that **3** is indeed the correct structure and the origin of the upfield shift of the arsenic–methyl resonance is probably that it is situated directly over a phenyl ring (23).

Preparation of Fluorocarbon-bridged Complexes

In general, the products obtained by reacting the iron carbonyls with fluorocarbon-bridged

TABLE 5. Reactions of ligands with $Fe(CO)_5$

$Fe(CO)_5$ (mmol)	Ligand (mmol)	Conditions	Products	Yield (%)
30	f_4fos(3.0)	reflux, 2 d, benzene (50 ml)	$f_4fosFe(CO)_3$ $f_4fosFe(CO)_4$ $f_4fosFe_2(CO)_6$	~5 72 trace
2.0	f_4fos(1.0)	reflux, 1.5 d, toluene (50 ml)	$f_4fosFe(CO)_4$	low
22	f_4fos(0.8)	u.v., 4.5 d, acetone (10 ml)	$f_4fosFe(CO)_3$ $f_4fosFe(CO)_4$	64 trace
7.7	f_6fos(0.3)	reflux, 1 d, benzene (50 ml)	$f_6fosFe(CO)_3$	90
19	f_6fos(0.9)	u.v., 7 d, acetone (15 ml)	$f_6fosFe(CO)_3$	62
1.0	f_8fos(1.0)	reflux, 1 d, benzene (50 ml)	$f_8fosFe(CO)_3$	low
3.0	f_8fos(1.0)	u.v., 3 h, cyclohexane (10 ml)	$f_8fosFe(CO)_3$	high
23	f_4fars(3.0)	reflux, 4 d, benzene (50 ml)	$f_4farsFe(CO)_4$ $f_4farsFe_2(CO)_8$ $f_4farsFe_2(CO)_6$	good fair trace
38	f_4fars(3.6)	u.v., 4 d, petroleum ether (9 ml)	$f_4farsFe(CO)_4$ $f_4farsFe_2(CO)_8$	57 37
87	f_4AsP(7.2)	reflux, 3 d, benzene (50 ml)	$f_4AsPFe(CO)_4$ $f_4AsPFe_2(CO)_8$	25 4
23	f_4AsP(7.2)	reflux, 5.5 d, cyclohexane (50 ml)	$f_4AsPFe(CO)_4$ $f_4AsPFe_2(CO)_8$	42 trace
20	f_4AsP(2.4)	120°, 2.5 d	$f_4AsPFe(CO)_4$ $f_4AsPFe_2(CO)_6$	55 12
51	f_4AsP(9.6)	100°, 4 d, THF (20 ml)	$f_4AsPFe(CO)_4$ $f_4AsPFe_2(CO)_8$ $f_4AsPFe(CO)_3$	78 trace 11

TABLE 5 (*Concluded*).

$Fe(CO)_5$ (mmol)	Ligand (mmol)	Conditions	Products	Yield (%)
7.6	f_4AsP(4.8)	150°, 6 d, THF (20 ml)	$f_4AsPFe(CO)_4$	32
			$f_4AsPFe(CO)_3$	12
			$f_4AsPFe_2(CO)_6$	45
76	f_4AsP(7.2)	u.v., 5 d, acetone (30 ml)	$f_4AsPFe(CO)_4$	45
			$f_4AsPFe_2(CO)_8$	20
			$f_4AsPFe(CO)_3$	trace
			$f_4AsPFe_2(CO)_6$	trace
13	f_4AsP(3.6)	u.v., 3.5 d, acetone (30 ml)	$f_4AsPFe(CO)_4$	33
			$f_4AsPFe_2(CO)_8$	5
			$f_4AsPFe(CO)_3$	trace
			$f_4AsPFe_2(CO)_6$	trace
76	f_4AsP(3.6)	u.v., 4.5 d, cyclohexane (20 ml)	$f_4AsPFe(CO)_4$	28
			$f_4AsPFe_2(CO)_8$	19
			$f_4AsPFe(CO)_3$	trace
			$f_4AsPFe_2(CO)_6$	trace
36	f_6AsP(1.0)	reflux, 10 h, cyclohexane (30 ml)	$f_6AsPFe(CO)_4$	16
			$f_6AsPFe(CO)_3$	~5
			$f_6AsPFe_2(CO)_6$	~5
61	f_6AsP(3.2)	reflux, 1.5 d, cyclohexane (60 ml)	$f_6AsPFe(CO)_4$	10
			$f_6AsPFe(CO)_3$	15
			$f_6AsPFe_2(CO)_6$	25
28	f_6AsP(3.2)	reflux, 3 d, benzene (50 ml)	$f_6AsPFe(CO)_4$	8
			$f_6AsPFe(CO)_3$	30
			$f_6AsPFe_2(CO)_6$	30
66	f_6AsP(1.7)	100°, 9 h, cyclohexane (20 ml)	$f_6AsPFe(CO)_4$	15
			$f_6AsPFe(CO)_3$	23
			$f_6AsPFe_2(CO)_6$	8
76	f_6AsP(2.0)	u.v., 2 d, acetone (15 ml)	$f_6AsPFe(CO)_4$	8
			$f_6AsPFe(CO)_3$	57
			$f_6AsPFe_2(CO)_6$	14
76	f_6AsP(5.4)	u.v., 3 d, cyclohexane (18 ml)	$f_6AsPFe(CO)_4$	4
			$f_6AsPFe(CO)_3$	50

ligands (Tables 5–7) are very dependent on the reaction conditions. As might be expected, the reactions of $Fe(CO)_5$ mainly produce complexes in which the ligands are monoligate ((L—L′)-$Fe(CO)_4$), biligate bimetallic ((L—L′)Fe_2-$(CO)_8$), or biligate monometallic ((L—L′)Fe-$(CO)_3$), Table 5.

One ligand, $f_4$fars, does not form the chelate complex $f_4$farsFe$(CO)_3$; but when chelate complexes are known their formation seems to be favored by prolonged ultraviolet irradiation. Mild irradiation or reflux conditions usually afford greater yields of the (L—L′)Fe$(CO)_4$ and (L—L′)$Fe_2(CO)_8$ types, respectively, although the yield of the latter is never very high.

The ease of formation of the chelate complexes (L—L′)Fe$(CO)_3$ appears to be in the sequence (L—L′)=$f_4$fars < f_4AsP < f_6AsP ≤ $f_4$fos < $f_6$fos ≈ $f_8$fos. Since the carbonyl infrared spectra of the complexes $f_n$fosM$(CO)_4$ (M = Cr, Mo, W) are little affected by the increasing ring size of the bridging group, it can be concluded (9) that electronic effects are probably not responsible for the absence of $f_4$farsFe$(CO)_3$ and the low yield of f_4AsPFe$(CO)_3$. Instead it seems that the bite of the ligand is the main reason. Thus the donor groups are at their maximum distance apart with a cyclobutene bridging group coupled with longer C—As bonds. In agreement with this notion is the result that

Can. J. Chem. Downloaded from www.nrcresearchpress.com by 210.87.254.5 on 09/05/12
For personal use only.

TABLE 6. Reactions of ligands with $Fe_2(CO)_9$

$Fe_2(CO)_9$ (mmol)	Ligand (mmol)	Conditions	Products	Yield (%)
2.8	$f_4$fos(1.0)	reflux, 1 d, cyclohexane (50 ml)	$f_4$fosFe$(CO)_3$	trace
			$f_4$fosFe$(CO)_4$	~55
			$f_4$fosFe$_2(CO)_6$	~13
2.8	$f_4$fos(1.0)	reflux, 14 h, toluene (50 ml)	$f_4$fosFe$(CO)_4$	low
			$f_4$fosFe$_2(CO)_6$	60
1.4	$f_6$fos(0.9)	reflux, 18 h, toluene (50 ml)	$f_6$fosFe$(CO)_3$	87
3.3	$f_6$fos(0.6)	reflux, 0.5 d, cyclohexane (50 ml)	$f_6$fosFe$(CO)_3$	50
			$f_6$fosFe$_2(CO)_6$	8
			$f_6$fosFe$_2(CO)_7$	32
1.6	$f_8$fos(0.6)	20°, 0.5 d, benzene (15 ml)	$f_8$fosFe$(CO)_3$	82
2.0	$f_8$fos(2.1)	20°, 0.5 d, THF (25 ml)	$f_8$fosFe$(CO)_3$	high
2.8	$f_4$fars(1.5)	reflux, 1 d, benzene (50 ml)	$f_4$farsFe$(CO)_4$	good
			$f_4$farsFe$_2(CO)_8$	fair
			$f_4$farsFe$_2(CO)_6$	trace
10	f_4AsP(4.8)	reflux, 2 d, toluene (80 ml)	f_4AsPFe$(CO)_4$	68
			f_4AsPFe$_2(CO)_6$	trace
			f_4AsPFe$(CO)_3$	trace
8.2	f_4AsP(4.8)	reflux, 3.5 d, cyclohexane (60 ml)	f_4AsPFe$(CO)_4$	53
			f_4AsPFe$_2(CO)_6$	26
8.2	f_4AsP(4.8)	u.v., 8 d, acetone (50 ml)	f_4AsPFe$(CO)_4$	40
			f_4AsPFe$(CO)_3$	36
			f_4AsPFe$_2(CO)_6$	9
2.8	f_6AsP(1.0)	reflux, 1 d, cyclohexane (50 ml)	f_6AsPFe$(CO)_4$	trace
			f_6AsPFe$(CO)_3$	14
			f_6AsPFe$_2(CO)_6$	20
2.1	f_6AsP(1.0)	u.v., 2 d, cyclohexane (20 ml)	f_6AsPFe$(CO)_4$	~5
			f_6AsPFe$(CO)_3$	~40
			f_6AsPFe$_2(CO)_6$	trace

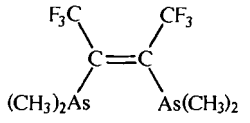

8

$f_6$fars$((CH_3)_2$AsC=CAs$(CH_3)_2(CF_2)_2CF_2)$(8) *does* form $f_6$farsFe$(CO)_3$ (24). Also the ligand **8**[1] (25) which must be electronically similar to $f_4$fars also gives a chelated $Fe(CO)_3$ complex in good yield as described in the Experimental section. Here the acyclic bridging group allows the two arsenic atoms to come closer together.

The only other products from the reaction of the ligands with $Fe(CO)_5$ are the complexes (L—L′)$Fe_2(CO)_6$ where the ligand is acting as a chelating group to one $Fe(CO)_3$ group and is coordinated to the second $Fe(CO)_3$ group through the double bond, the two iron atoms being linked by an Fe—Fe bond as shown in **7** (2, 21).

This type of complex is known for all the ligands except $f_8$fos although $f_6$fos$Fe_2(CO)_6$ is not obtained by reaction with $Fe(CO)_5$. The highest yields of these $Fe_2(CO)_6$ complexes are obtained by reaction of the ligands with $Fe_3(CO)_{12}$. In this way $f_4$fos$Fe_2(CO)_6$ can be prepared in 76% yield. The interconversion reactions (Table 8) indicate that these stable complexes are probably formed from (L—L′)$Fe(CO)_4$ and (L—L′)$Fe_2(CO)_8$.

The ease of formation of the $f_n$fos$Fe_2(CO)_6$ complexes decreases as n increases which suggests that the ring size is a factor, since the

[1]A preliminary communication describing the iron carbonyl complexes of this ligand has appeared (ref. 26).

Can. J. Chem. Downloaded from www.nrcresearchpress.com by 210.87.254.5 on 09/05/12
For personal use only.

Can. J. Chem. Downloaded from www.nrcresearchpress.com by 210.87.254.5 on 09/05/12
For personal use only.

tendency to relieve ring strain in the ring by coordinating the double bond to a second iron atom would then decrease as the size increased. However, the yields of $f_6AsPFe_2(CO)_6$ and $f_4AsPFe_2(CO)_6$ are comparable and are greater than those of $f_6fosFe_2(CO)_6$ which suggests that reduction of steric hindrance by replacing bulky $P(C_6H_5)_2$ groups with $As(CH_3)_2$ groups is an important factor in encouraging the formation of this type of complex. The recent synthesis of $f_6farsFe_2(CO)_6$ and $f_8farsFe_2(CO)_6$ in 70 and 45% yield, respectively (20), lends support to arguments invoking steric hindrance. That ring strain in the starting ligand is not necessary for the formation of $(L—L')Fe_2(CO)_6$ type complexes is shown by the isolation of *cis*-$(CH_3)_2AsCCF_3{=}CCF_3As(CH_3)_2Fe_2(CO)_6$ from the reaction of **8** with $Fe_3(CO)_{12}$.

The use of $Fe_2(CO)_9$ as reagent (Table 6) has much the same result as $Fe(CO)_5$, and the only new complex type is $f_6fosFe_2(CO)_7$ which is unique to this ligand. It is believed to be

TABLE 7. Reactions of ligands with $Fe_3(CO)_{12}$

$Fe_3(CO)_{12}$ (mmol)	Ligand (mmol)	Conditions	Products	Yield (%)
1.6	f_4fos(0.8)	reflux, 5.5 h, benzene (50 ml)	$f_4fosFe(CO)_4$	low
			$f_4fosFe_2(CO)_6$	76
0.8	f_4fos(0.4)	reflux, 1 d, toluene (50 ml)	$f_4fosFe(CO)_4$	low
			$f_4fosFe_2(CO)_6$	35
5.8	f_4fos(3.0)	u.v., 4.5 d, acetone (30 ml)	$f_4fosFe(CO)_3$	33
			$f_4fosFe_2(CO)_6$	13
12.0	f_6fos(2.9)	reflux, 5 h, cyclohexane (50 ml)	$f_6fosFe(CO)_3$	~45
			$f_6fosFe_2(CO)_6$	5
			$f_6fosFe_2(CO)_7$	36
1.7	f_6fos(0.9)	u.v., 3 d, acetone (30 ml)	$f_6fosFe(CO)_3$	~70
2.0	f_8fos(2.0)	20°, 1 d, THF (40 ml)	$f_8fosFe(CO)_3$	~100
2.0	f_8fos(2.0)	reflux, 3 h, benzene (40 ml)	$f_8fosFe(CO)_3$	~50
7.0	f_4fars(3.9)	reflux, 5.5 h, cyclohexane (50 ml)	$f_4farsFe_3(CO)_9$	90
			$f_4farsFe_3(CO)_{10}$	1
			$f_4farsFe_2(CO)_6$	~2
			$As_2(CH_3)_2CH_2Fe_3(CO)_9$	~4
1.0	f_4fars(3.0)	reflux, 3.5 h, cyclohexane (50 ml)	$f_4farsFe(CO)_4$	25
			$f_4farsFe_3(CO)_9$	35
			$f_4farsFe_3(CO)_{10}$	25
3.8	f_4fars(3.0)	u.v., 4.5 d, acetone (20 ml)	$f_4farsFe(CO)_4$	26
			$f_4farsFe_2(CO)_8$	13
			$f_4farsFe_2(CO)_6$	21
			$f_4farsFe_3(CO)_9$	trace
			$f_4farsFe_3(CO)_{10}$	7
10.0	f_4AsP(6.0)	reflux, 5 h, cyclohexane (50 ml)	$f_4AsPFe_3(CO)_9$	26
			$f_4AsPFe_2(CO)_6$	51
			$f_4AsPFe(CO)_4$	trace
8.0	f_4AsP(2.4)	reflux, 45 min, cyclohexane (50 ml)	$f_4AsPFe_3(CO)_{10}$	87
			$f_4AsPFe_3(CO)_9$	trace
			$f_4AsPFe_2(CO)_6$	trace
			$f_4AsPFe(CO)_4$	trace
3.0	f_4AsP(5.6)	reflux, 8 h, cyclohexane (80 ml)	$f_4AsPFe(CO)_4$	trace
			$f_4AsPFe_3(CO)_9$	5
			$(f_4AsP)_2Fe(CO)_3$	8
			$f_4AsPFe(CO)_3$	15
			$f_4AsPFe_2(CO)_6$	13
			$(f_4AsP)_2Fe_2(CO)_4$	4

TABLE 7 (*Concluded*).

$Fe_3(CO)_{12}$ (mmol)	Ligand (mmol)	Conditions	Products	Yield (%)
6.0	$f_4AsP(6.6)$	u.v., 5.5 d, acetone (30 ml)	$f_4AsPFe(CO)_4$	27
			$f_4AsPFe_2(CO)_6$	11
1.0	$f_6AsP(1.0)$	u.v., 1 d, petroleum ether (20 ml)	$f_6AsPFe(CO)_4$	trace
			$f_6AsPFe(CO)_3$	~20
			$f_6AsPFe_2(CO)_6$	~25
3.5	$f_6AsP(2.0)$	20°, 0.5 d, cyclohexane (60 ml)	$f_6AsPFe(CO)_4$	~4
			$f_6AsPFe(CO)_3$	~10
			$f_6AsPFe_2(CO)_6$	trace
2.0	$f_6AsP(1.1)$	reflux, 4 h, cyclohexane (50 ml)	$f_6AsPFe(CO)_4$	~5
			$f_6AsPFe(CO)_3$	22
			$f_6AsPFe_2(CO)_6$	50
3.0	$f_6AsP(6.0)$	reflux, 4 h, cyclohexane (80 ml)	$f_6AsPFe(CO)_4$	trace
			$f_6AsPFe(CO)_3$	25
			$f_6AsPFe_2(CO)_6$	35
2.4	$f_6AsP(1.0)$	reflux, 5 h, benzene (50 ml)	$f_6AsPFe(CO)_4$	trace
			$f_6AsPFe(CO)_3$	20
			$f_6AsPFe_2(CO)_6$	38

bonded through the phosphorus to a $Fe(CO)_4$ group and through the double bond to the $Fe(CO)_3$ moiety (3).

When the ligands are treated with $Fe_3(CO)_{12}$ (Table 7) mild conditions result in the isolation of $(L—L')Fe_3(CO)_{10}$, (L—L')=$f_4$fars, and f_4AsP, where the ligand bridges the two iron atoms that are also carbonyl bridged, **2**. A very surprising result is that when the ligand-to-carbonyl ratio is 1:3 the greatest yield of $f_4farsFe_3(CO)_{10}$ is obtained. Previously we have reported a maximum yield of 7% (3). In the ruthenium carbonyl reaction the same conditions were found to give a maximum yield (63%) of $(f_4fars)_2Ru_3(CO)_8$ (27) whose structure retains the Ru_3 triangle (28).

The high yield of $f_4AsPFe_3(CO)_{10}$, **2** (L' = $P(C_6H_5)_2$), is unexpected and it seems that here the low tendency to chelate coupled with the bite of the ligand is just right to allow the ligand to "clip" on to the Fe_3 fragment. Like $f_4farsFe_3(CO)_{10}$ which is easily converted to $f_4farsFe_3(CO)_9$ in which a $(CH_3)_2As$ group is displaced from the cyclobutene ring as in **3** (L' = $As(CH_3)_2$), f_4AsP also undergoes this reaction to afford $f_4AsPFe_3(CO)_9$ **3** (L' = $P(C_6H_5)_2$). However, although $f_4farsFe_3(CO)_9$ is unstable with respect to loss of fluorocarbon groups giving eventually $(CH_3)_2As_2CH_2Fe_3(CO)_9$ and other products, $f_4AsPFe_3(CO)_9$ is stable under the same condition (Table 8). This indicates that the breakdown of $f_4farsFe_3(CO)_9$ occurs by way of cleavage of the one remaining As–cyclobutene ring in **3** (L' = $As(CH_3)_2$). Cleavage reaction of this type also occurs when $f_4farsMn_2(CO)_8$ is heated (29, 30).

The other ligands, as pointed out above, have a strong tendency to chelate and the main products from their reactions with $Fe_3(CO)_{12}$ are $(L—L')Fe(CO)_3$ and $(L—L')Fe_2(CO)_6$ type complexes, although $f_6$fos does give $f_6fosFe_2(CO)_7$. It is worth noting that since $f_4AsPFe_3(CO)_9$ is moderately stable by itself (Table 8) the formation of derivatives such as $(f_4AsP)_2Fe(CO)_3$ **6**, and $(f_4AsP)_2Fe_2(CO)_4$ (a bridged derivative of $f_4AsPFe_2(CO)_6$ described above) and $f_4AsPFe(CO)_3$ with fewer iron atoms per molecule could well arise through reaction of the $(L—L')Fe_3(CO)_9$ compound with the ligand.

Finally, some of the other interconversion reactions described in Table 8 are worthy of note. Thus the bridged complex $f_4AsPFe_2(CO)_8$ is obtained in moderate yield when $f_4AsPFe(CO)_4$ is treated with $Fe(CO)_5$ and u.v. irradiation. However, if the $Fe(CO)_5$ is omitted, the chelated $f_4AsPFe(CO)_3$ is produced. This shows that f_4AsP, like $f_4$fars, has a strong tendency to bridge rather than chelate. Nevertheless when the bridged complex is heated, an $Fe(CO)_4$ moiety is lost and $f_4AsPFe(CO)_4$ is obtained:

Can. J. Chem. Downloaded from www.nrcresearchpress.com by 210.87.254.5 on 09/05/12
For personal use only.

TABLE 8. Interconversion reactions

	Reactants (g)	Conditions*	Products (% Yield)
1.	$f_4AsPFe(CO)_4$ (0.5)	reflux, 3 d, THF	$f_4AsPFe(CO)_3$ (7) $f_4AsPFe_2(CO)_6$ (30)
2.	$f_4AsPFe(CO)_4$ (0.5)	u.v., 7 d, acetone	$f_4AsPFe(CO)_3$ (22) $f_4AsPFe_2(CO)_6$ (10)
3.	$f_4AsPFe(CO)_4$ (0.8)	150°, 1 d, benzene	$f_4AsPFe_2(CO)_6$ (80)
4.	$f_4AsPFe(CO)_4$ (0.5) + $Fe(CO)_5$ (0.7)	u.v., 5 d, acetone	$f_4AsPFe(CO)_3$ (8) $f_4AsPFe_2(CO)_8$ (25) $f_4AsPFe_2(CO)_6$ (14)
5.	$f_4AsPFe(CO)_4$ (0.8) + $Fe(CO)_5$ (3)	150°, 1 d, benzene	$f_4AsPFe_2(CO)_6$ (85)
6.	$f_4AsPFe(CO)_4$ (0.6) + f_4AsP (0.8)	reflux, 13 h, cyclohexane	$f_4AsPFe(CO)_3$ (~5) $f_4AsPFe_2(CO)_6$ (~5) $f_4AsPFe(CO)_4$ (90)
7.	$f_4AsPFe(CO)_4$ (0.6) + f_4AsP (0.8)	150°, 2 d, benzene	$(f_4AsP)_2Fe(CO)_3$ (~5) $f_4AsPFe_2(CO)_6$ (70)
8.	$f_4AsPFe(CO)_4$ (0.6) + f_4AsP (0.8)	u.v., 6 d, acetone	$f_4AsPFe(CO)_3$ (~70)
9.	$f_4AsPFe_2(CO)_8$ (0.8)	reflux, 2 h, cyclohexane	$f_4AsPFe(CO)_4$ (50) $f_4AsPFe_2(CO)_6$ (~30)
10.	$f_4AsPFe_2(CO)_8$ (0.8)	150°, 1 d, benzene	$f_4AsPFe_2(CO)_6$ (90)
11.	$f_4AsPFe(CO)_3$ (0.5) + $Fe(CO)_5$ (3.0)	150°, 1 d, benzene	$f_4AsPFe_2(CO)_6$ (50)
12.	$f_4AsPFe(CO)_3$ (0.5) + f_4AsP (0.8)	130°, 1 d, cyclohexane	$(f_4AsP)_2Fe(CO)_3$ (15)
13.	$f_4AsPFe_2(CO)_6$ (0.3)	u.v., 9 d, acetone	no reaction
14.	$f_4AsPFe_2(CO)_6$ (1.0) + f_4AsP (1.9)	reflux, 3.5 d, cyclohexane	no reaction
15.	$f_4AsPFe_3(CO)_{10}$ (0.4)	reflux, 1 h, cyclohexane	$f_4AsPFe_3(CO)_9$ (50)
16.	$f_4AsPFe_3(CO)_9$ (0.4)	reflux, 15 h, cyclohexane	no reaction
17.	$f_4AsPFe_3(CO)_9$ (0.8)	u.v., 6 d, acetone	no reaction
18.	$f_6AsPFe_2(CO)_6$ (0.4)	reflux, 3 d, cyclohexane	no reaction
19.	$f_6AsPFe_2(CO)_6$ (0.4)	u.v., 9 d, acetone	no reaction

*The volume of solvent used for all reactions was approximately 40 ml.

stronger heating affords the very stable $f_4AsPFe_2(CO)_6$.

We thank the National Research Council of Canada for financial support. Some reactions involving the ligands **1***f* and **8** were carried out by Drs. J. P. Crow and J. A. J. Thompson. We are indebted to Dr. J. R. Sams for assistance in obtaining the Mössbauer spectra.

1. W. R. CULLEN, D. A. HARBOURNE, B. V. LIENGME, and J. R. SAMS. Inorg. Chem. **8**, 1464 (1969).
2. W. R. CULLEN, D. A. HARBOURNE, B. V. LIENGME, and J. R. SAMS. Inorg. Chem. **8**, 95 (1969).
3. W. R. CULLEN, D. A. HARBOURNE, B. V. LIENGME, and J. R. SAMS. Inorg. Chem. **9**, 702 (1970).
4. J. P. CROW and W. R. CULLEN. Can. J. Chem. **49**, 2948 (1971).
5. P. J. ROBERTS, B. R. PENFOLD, and J. TROTTER. Inorg. Chem. **9**, 2137 (1970).
6. F. W. B. EINSTEIN, A. M. PILOTTI, and R. RESTIVO. Inorg. Chem. **10**, 1947 (1971).
7. J. P. CROW and W. R. CULLEN. Inorg. Chem. **10**, 2165 (1971).
8. L. S. CHIA and W. R. CULLEN. Can. J. Chem. In press.
9. W. R. CULLEN, D. F. DONG, and J. A. J. THOMPSON. Can. J. Chem. **47**, 4671 (1969).
10. W. R. CULLEN, D. S. DAWSON, and P. S. DHALIWAL. Can. J. Chem. **45**, 683 (1967).

Can. J. Chem. Downloaded from www.nrcresearchpress.com by 210.87.254.5 on 09/05/12
For personal use only.

11. W. R. CULLEN and D. A. HARBOURNE. Can. J. Chem. **47**, 3371 (1969).
12. L. S. CHIA. M.Sc. Thesis, University of British Columbia, 1971.
13. F. A. COTTON and R. V. PARISH. J. Chem. Soc. 1440 (1960).
14. F. W. B. EINSTEIN and R. D. G. JONES. J. Chem. Soc. In press.
15. W. R. CULLEN and D. A. HARBOURNE. Inorg. Chem. **9**, 1839 (1970).
16. I. UGI, D. MARQUARDING, H. KLUSACEK, P. GILLESPIE, and F. RAMIREZ. Acc. Chem. Res. **4**, 288 (1971).
17. D. S. BROWN and G. W. BUSHNELL. Acta. Cryst. **22**, 292 (1967).
18. F. W. B. EINSTEIN and C. R. S. M. HAMPTON. Can. J. Chem. **49**, 1901 (1971).
19. W. HARRISON and J. TROTTER. J. Chem. Soc. A, 1542 (1971).
20. L. S. CHIA, W. R. CULLEN, and J. R. SAMS. Unpublished results.
21. F. W. B. EINSTEIN and J. TROTTER. J. Chem. Soc. A, 824 (1967).
22. F. W. B. EINSTEIN and R. D. G. JONES. J. Chem. Soc. In press.
23. F. W. B. EINSTEIN and R. D. G. JONES. To be published.
24. L. S. CHIA and W. R. CULLEN. Unpublished results.
25. J. P. CROW, W. R. CULLEN, F. G. HERRING, J. R. SAMS, and R. L. TAPPING. Inorg. Chem. **10**, 1616 (1971).
26. J. P. CROW, W. R. CULLEN, J. R. SAMS, and J. E. H. WARD. J. Organomet. Chem. **22**, C29 (1970).
27. W. R. CULLEN and D. A. HARBOURNE. Inorg. Chem. **9**, 1839 (1970).
28. P. J. ROBERTS and J. TROTTER. J. Chem. Soc. A, 1479 (1971).
29. J. P. CROW, W. R. CULLEN and F. L. HOU. Inorg. Chem. In press.
30. J. P. CROW, W. R. CULLEN, F. L. HOU, L. Y. Y. CHAN, and F. W. B. EINSTEIN. Chem. Commun. 1229 (1971).

Can. J. Chem. Downloaded from www.nrcresearchpress.com by 210.87.254.5 on 09/05/12
For personal use only.

Attempts at the Synthesis of the Penicillin Ring System by Transannular Reactions[1]

M. H. BENN AND ROBIN E. MITCHELL[2]

Department of Chemistry, The University, Calgary 44, Alberta

Received October 19, 1971

Attempts were made to achieve new syntheses of the penicillin ring system by effecting the transannular cyclization of 3D-carbomethoxy-*N*-chloro-2,2-dimethyl-5-oxoperhydro-6L-phthalimido-1,4-thiazepine sulfone. However the products obtained were those resulting from ring cleavage and elimination reactions.

Des essais ont été entrepris afin d'effectuer une nouvelle synthèse du cycle de la pénicilline par cyclisation trans-annulaire de la 3D-carbométhoxy-*N*-chloro-2,2-diméthyle-5-oxoperhydro-6L-phtalimido-1,4-thiazépine sulfone. Cependant, les produits obtenus sont ceux résultant des réactions d'élimination et de clivage du cycle.

Canadian Journal of Chemistry, **50**, 2195 (1972)

Introduction

Five years ago, Woodward described the problem of achieving direct, highly-efficient routes to totally synthetic penicillins (**1**) as "one of the most challenging and recalcitrant synthetic objectives of our generation" (1). The challenge remains, and continues to fascinate chemists in much the same way that the Matterhorn attracted mountaineers. Although circumstantial evidence suggests that the biosynthesis of penicillins most probably proceeds from an acyclic peptide precursor or monocylic derivative such as **2** (2, 3), synthesis via a transannular bridging of the relatively readily available perhydrothiazepine system **3***a* stands out as a spectacular *diretissima* approach and this was the objective of the work which we describe here.

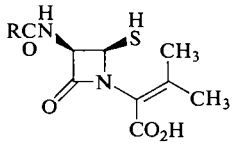

2

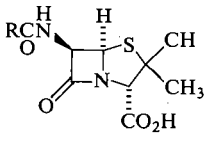

1

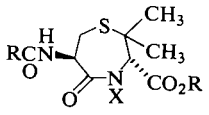

3

a X = R = H
b X = Cl; R = H

The overall concept was not new. The most obvious possibility, transannular nucleophilic displacement of halogen from C-7 by anionic nitrogen, has been attempted by several groups (4–6) but the products were usually tetrahydrothiazepines (**4**). The reverse process involving displacement of a leaving group on nitrogen by anionic C-7 seems to have been attempted only by Lillya, on the compound **5**, and also failed to produce a β-lactam (6). Similarly, various attempts to achieve the photochemical cyclization of tetrahydrothiazepines (**4**) and dihydrothiazepines (**6**) have been unsuccessful (4, 6, 7).

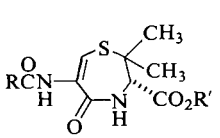

4

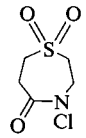

5

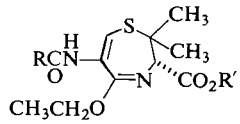

6

Our plan was to attempt to utilize the then recent discovery by Edwards and his co-workers that argentous ion induced the cyclization, albeit in low yield, of the *N*-chloro derivatives of medium-ring lactams to bicyclic lactams with bridgehead nitrogen (8); and also examine the reverse Knunyants reaction: *i.e.*, we would attempt the transformation **3***b* → **1**.

Success or failure appeared to depend on the ability to surmount various obstacles. Critical to

[1]Taken from the Ph.D. thesis of R.E.M., University of Calgary, 1969.

[2]NRCC Pre-doctoral Scholar 1968, 1969; present address Plant Diseases Division, D.S.I.R., Private Bag, Auckland, New Zealand.

Can. J. Chem. Downloaded from www.nrcresearchpress.com by 210.87.254.42 on 09/05/12
For personal use only.

Can. J. Chem. Downloaded from www.nrcresearchpress.com by 210.87.254.42 on 09/05/12
For personal use only.

success by the first approach, and completely unprecedented, the Edwards reaction would have to give reasonable yields of a β-lactam; even then formation of a pair of compounds epimeric at C-7 would be anticipated. The other approach appeared fraught with many dangers, consequent upon the use of bases to generate an anionic center for the transannular nucleophilic displacement reaction; among these were the known base-lability of the penicillin β-lactam system as well as the possibility of base-catalyzed epimerization at C-3 and -6, and elimination to give an acylimine.

Materials

Since we needed a C-6 nitrogen function inert to chlorinations, we decided to carry out our experiments with 3D-carbomethoxy-2,2-dimethyl-5-oxoperhydro-6L-phthalimido-1,4-thiazepine. A mixture of the 6D- and 6L-epimers was obtained by the Woodward K reagent induced condensation and cyclization of D-penicillamine methyl ester and α-phthalimidoacrylic acid, and separated by column chromatography and fractional crystallization.

The C-6 configurations of the diastereomers were deduced from their p.m.r. spectra. Thus, if the stable conformations of the two compounds

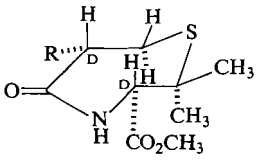

7

a R = phthalimido
b R = phenylacetamido

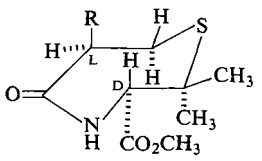

8

a R = phthalimido
b R = phenylacetamido

are the pseudo-chairs **7** and **8** an analysis of the C-6 and -7 proton couplings should provide a method for assigning the stereochemistry at C-6.

In fact, the C-6 proton signal of one isomer revealed couplings of 11.8 and 7.5 Hz consistent with the axial–axial and axial–equatorial couplings expected for **7***a*. Other data, chemical shift and specific rotation, for the two isomers also correlated well with the values recorded for the analogues **7***b* and **8***b* (see Table 1) whose absolute configurations had been established by degradation (9).

The product ratio of the unwanted 3D,6D (**7***a*) to the desired 3D,6L-epimer (**8***a*) was about 2:1.[3]

TABLE 1. Comparison of some data for **7***a*, **7***b*, **8***a*, and **8***b*

Thiazepine	$\tau(CH_3)_2$	(α_D)	Concentration in ethanol	T °C
7*a*	8.75, 8.37	−50.0°	0.12	29
7*b*	8.72, 8.64	−39.7°	0.6	25
8*a*	8.55, 8.55	−90.0°	0.12	29
8*b*	8.62, 8.62	−57.1°	0.6	25

The reaction of **7***a* or **8***a* with chlorine in methylene chloride solution gave the same tetrahydrothiazepine **9**,[4] m.p. 179–182°,[5] thus establishing their C-6 epimeric relationship.

Under mild conditions the reaction of **7***a* with chlorine afforded the 7-chloro derivative **10**[4,6] (under these conditions the product from **8***a* was **9**); **10** readily decomposed to **9**.

A side product from the reaction with **8***a* was a substance assigned[4] structure **11***a*. However,

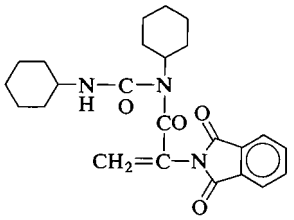

i

[3]A similar ratio was obtained when dicyclohexylcarbodiimide was used instead of the Woodward K-reagent, but the overall yield was lower, and isolation of pure **7***a* and **8***a* was difficult. In addition, a side-product from this reaction was identified as (i) indicating that the known reaction of carboxylic acids with the carbodiimide (10) was a competing process.

[4]See Experimental for the analysis of data which lead to this conclusion.

[5]Sheehan and Cruickshank have described a compound assigned structure **9**, but with m.p. 237–237.5° (11).

[6]The stereochemistry of **10** was revealed by its p.m.r. spectrum which, while similar in some respects to that of **7***a* had in place of the three proton AMX system a two proton AB quartet at τ 4.75 and 3.47 (J = 11.5 Hz) which may be attributed to C-6 and -7 methine protons in a pseudo-*trans*-diaxial relationship. Therefore C-7 bears the chlorine substituent in a pseudo-*trans*-diequatorial relationship to the phthalimido substituent at C-6, which has the D-configuration. Absence of a compound isomeric with **10** in the reaction of the 6L-phthalimido epimer **8***a* seems significant: it is likely that a 7-chlorothiazepine forms in this reaction too, but the C-6 hydrogen and C-7 chlorine substituents probably are able to assume a *trans*-diaxial relationship with ease, thus promoting the elimination which leads to **9**.

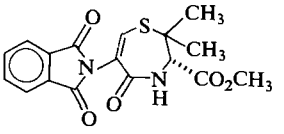

9

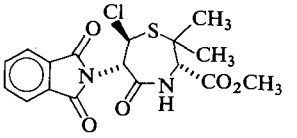

10

sodium periodate oxidation of **8***a* gave a sulfoxide (**11***b*) apparently diastereomeric with **11***a*. We have tentatively designated **11***a* as the α-, and **11***b* as the β-isomer.[7]

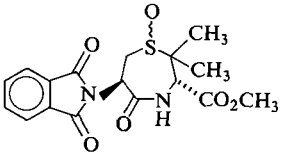

11
a α-sulfoxide
b β-sulfoxide

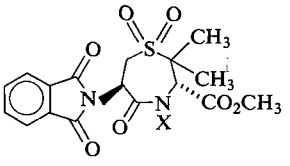

12 X = H
13 X = Cl

Since it was necessary to mask the sulfide function of the tetrahydrothiazepine during preparation of the *N*-chloro derivative, and preliminary chlorination experiments with the sulfoxide **11***b* were unpromising (13), **8***a* was oxidized with potassium permanganate in acetic acid to the sulfone **12**.

The reaction of **12** with *t*-butyl hypochlorite in acetic acid solution gave, after removal of the solvent, a glass completely soluble in benzene (a solvent in which **12** is very sparingly soluble). This product gave a strong "active chlorine" reaction[8] and its i.r. spectrum was devoid of NH absorptions, and when a solution in 2-propanol was boiled for a few minutes, **12** was obtained in *almost quantitative yield*.

In conjunction with the above evidence a p.m.r. spectrum conclusively established the identity of the product as the required *N*-chloro-6L-phthalimido sulfone **13**: particularly significant was the appearance of the C-3 methine as an unsplit singlet.[9]

Results and Discussion

With the completion of the syntheses of **13** the stage was set for our attempts at the transannular cyclization reactions.

We first tried the Edwards reaction. The *N*-chloro substituent of the sulfone **13** was shown to be very labile in "protic" solvents. However, in dry DMF or benzene solution little decomposition occurred over a period of several hours. When a reaction vessel containing a solution of **13** in dry DMF and containing suspended silver carbonate (14) was inserted in an oil-bath held at 45°, a negative active-chlorine analysis was obtained within 3 min. Upon work-up, a 47% yield of the parent thiazepine (**12**) was obtained. The mother liquor remaining after removal of this material contained two major components which proved[4] to be **14**[10] and **15**. No trace of a β-lactam could be found.[11]

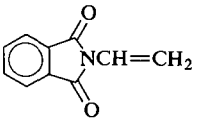

14

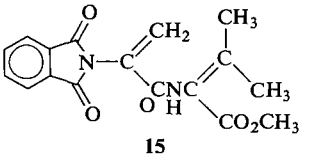

15

When **13** was illuminated with tungsten light in refluxing benzene solution, tests for active chlorine were negative after 7 h. The crude reaction product had no NH band in the i.r. spec-

[7]*Sodium periodate oxidation of various penicillins has* been shown to give exclusively one stereomer: the β-sulfoxide (12).

[8]The presence or absence of "active chlorine" (N—Cl or O—Cl) compounds was determined by a starch–potassium iodide spot-test.

[9]In the cases of all other perhydrothiazepines which we examined, the C-3 methine signal appeared as a doublet (J = 6–7 Hz) if the adjacent lactam nitrogen was unsubstituted.

[10]We did not find a compound corresponding to the fragment lost from the thiazepine during the formation of *phthalimidoethylene; presumably this was lost during the* evaporation of DMF from the reaction mixture.

[11]As judged by the i.r. of the crude reaction product.

Can. J. Chem. Downloaded from www.nrcresearchpress.com by 210.87.254.42 on 09/05/12
For personal use only.

Can. J. Chem. Downloaded from www.nrcresearchpress.com by 210.87.254.42 on 09/05/12
For personal use only.

trum, and apparently no lactam CO band, but a very intense band at 2255 cm^{-1}. The products were identified[4] as **14** and **16**. Again there was no evidence for any β-lactam formation.

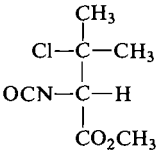

16

At the time of its discovery the Edwards reaction was thought to involve nitrenium ions and a transannular hydride shift; indeed it was this aspect of the reaction which attracted us to it. However under the conditions which we employed homolysis of the N—Cl bond occurs, with subsequent hydrogen atom transfer and the formation of *C*-chloro intermediates.[12]

Presumably the amidyl radical (**17**) generated from **13**, like its analogue **14**, is unable to adopt a conformation which permits intramolecular hydrogen abstraction.[13] Instead, hydrogen atom extraction from solvent, and fragmentation with

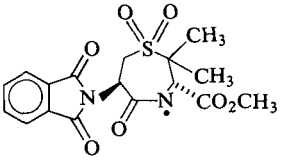

17

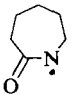

18

[12]Thus we had returned to a Knunyants approach in which the cyclization was to be induced by silver ion rather than strong base.

[13]The next higher homologue of **18** undergoes efficient intramolecular hydrogen transfer (14) and we had hoped that the slight increase in ring size consequent upon replacing a CH_2 unit in **18** by $—SO_2—$ might have permitted sufficient conformational mobility in **17** that it might behave similarly except that, in the absence of δ-, a γ-situated hydrogen (at C-7, or C-2 methyl) might have been abstracted by the amidyl nitrogen. However, models suggested that this was unlikely, and if the abstraction did occur that it would be the undesired one, *i.e.*, from the α-oriented methyl group to give **ii**. In the event we could find no evidence for either attack.

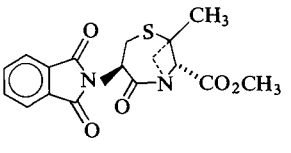

ii

extrusion of sulfur dioxide compete, and are respectively dominant in DMF and benzene.

The oxidation level of sulfur, necessary for the preparation of **13** probably aids the undesirable fragmentations, extrusion of sulfur dioxide being facile. Such an extrusion from **19**, itself produced either from **17** or by heterolysis of **13**, would account for the formation of **15**, while **16** is probably derived from **17** by a radical-chain mechanism.[14]

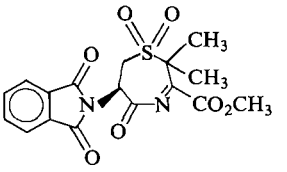

19

Thwarted on the Edwards reaction approach, we turned to the base induced cyclizations of **13** but failed to obtain any β-lactam: with potassium fluoride or sodium carbonate in DMF, the products isolated were the parent lactam **12** and the unsaturated acyclic amide **15**; while with *t*-butyl lithium in anhydrous THF, at Dry Ice–acetone temperature, **13** gave a product mixture from which the lactam **12** was isolated in 50% yield. The residue, which consisted of at least six components but which again failed to exhibit β-lactam i.r. absorption, was not investigated further.

Experimental

Melting points were determined on a Kofler hot stage and are uncorrected. The i.r. spectra were recorded on a Perkin–Elmer Model 327 grating spectrometer. The p.m.r. spectra were measured with Varian A-60 or HA-100 instruments in deuteriochloroform solution with tetramethylsilane as internal standard, unless otherwise specified. The u.v. spectra were recorded with a Perkin–Elmer model 202 spectrometer with ethanol (95%) as solvent. The mass spectra were recorded on an AEI-MS-9 instrument, with a direct inlet, at 70 eV ionization potential, and significant ions at higher *m/e* values as well as ions with a relative abundance of 20% or more of the base peak, are quoted as *m/e* values, with their relative abundance in parentheses. The o.r.d. curves were recorded on a Durrum–Jasco ORD-UV/5 spectro-polarimeter in ethanol (95%) solution and specific rotations were measured from these curves at the sodium D-line (589.5 nm). For t.l.c. and p.l.c. we used Merck silica gel G (0.25 mm thickness) and Merck silica gel PF_{254} (1 mm thickness) respectively and, for column chromatograms, Florisil (Fisher Scientific Co., 100–200 mesh).

[14]The fragmentation of amidyl radicals to yield isocyanates has been observed before (14).

Can. J. Chem. Downloaded from www.nrcresearchpress.com by 210.87.254.42 on 09/05/12
For personal use only.

D-Penicillamine Methyl Ester Hydrochloride

D-Penicillamine (Aldrich, m.p. 208–210°) was esterified according to the patent literature (15). Recrystallization of the crude solid from 2-propanol yielded colorless needles (75–80% yield) m.p. 180–182° (dec.) (lit. (15) 184° (dec.)); ν_{max} (KBr) 3450 (NH), 2495 (SH) and 1750 cm^{-1} (ester CO); τ (D_2O) (TMS external ref.) 8.50 (3H) (s), 8.43 (3H) (s) ($\rangle C(CH_3)_2$), 6.12 (3H) (s) ($—CO_2CH_3$), and 5.78 (1H) (s).

α-Phthalimidoacrylic Acid

This compound was prepared from cysteine (24 g) by the method of Sakakibara (16) in comparable yield. A modified work-up procedure was followed which was much less tedious than the original; the crude fusion product was extracted with boiling ethyl acetate (*ca.* 600 ml), filtered, and the filter-cake washed with boiling ethyl acetate (3 × 100 ml). The combined extracts and washings were washed with saturated aqueous sodium bicarbonate solution (3 × 150 ml) which was then back-washed with ethyl acetate (2 × 100 ml), adjusted to p*H* 1.5 with 2 *N* hydrochloric acid, and extracted with ethyl acetate (3 × 100 ml). The combined ethyl acetate extracts from the acidic aqueous phase were finally washed with brine (3 × 50 ml), dried ($MgSO_4$), and evaporated. The residue was extracted with boiling chloroform (*ca.* 500 ml) and filtered hot. Upon cooling, the filtrate deposited off-white needles, 20 g. Concentration of the mother liquor (to *ca.* 150 ml) afforded a further 8.5 g of material. The total product was recrystallized once from chloroform affording colorless needles, 18.5 g, in 45% yield, m.p. 172–176° raised to 174.5–177.5° upon further recrystallization (lit. (16) 169–171°); ν_{max} (KBr) 3280 (br) (carboxylic acid OH), 1800 (w, sharp) (phthalimido CO asym. str), 1725 (br, st) (phthalimido CO and carboxylic acid CO), 1645 and 885 ($\rangle C{=}CH_2$), and 1615 and 715 cm^{-1} (phthalimido aromatic); τ (CD_3COCD_3) 3.88 (1H) (s), 3.30 (1H) (s) (two vinylic methylene protons), and 2.09 (4H) (s) (aromatic).

3D-Carbomethoxy-2,2-dimethyl-6D- and 6L-Phthalimido-5-oxoperhydro-1,4-thiazepine (7a, 8a)

A solution of phthalimidoacrylic acid (10.71 g, 49.3 m*M*), neutralized with triethylamine (6.83 ml, 49.3 m*M*), in anhydrous acetonitrile (675 ml) was added to *N*-ethyl-5-phenylisoxazolium-3′-sulfonate (Woodward reagent K) (12.49 g, 49.3 m*M*). The mixture was stirred until all the solids had dissolved. A second solution was prepared from D-penicillamine methyl ester hydrochloride (9.85 g, 49.3 m*M*) and triethylamine (6.83 ml, 49.3 m*M*) in acetonitrile (675 ml). Both solutions were filtered, then simultaneously added dropwise to acetonitrile (61) containing Triton B (40% in methanol, 12.3 ml), under a slow steady stream of dry nitrogen at room temperature, agitated with a Vibromixer, over a period of 8 h. Stirring was continued for 12 h after the addition was complete. Removal of the solvent (bath <40°) afforded a residue which was partitioned between chloroform (250 ml) and water (25 ml). The aqueous extract was washed with chloroform (50 ml) and the combined chloroform extracts were washed with 2*N* hydrochloric acid (3 × 50 ml), then with saturated aqueous sodium bicarbonate (4 × 50 ml), and finally dried ($MgSO_4$) and evaporated to afford an off-white glass (16 g). Recrystallization from 95% ethanol afforded colorless needles, 11.25 g, demonstrated by t.l.c. (R_f with methyl formate–benzene, 25:75 (v/v)) to be a mixture of **7***a* (R_f 0.22) and **8***a* (R_f 0.29), in ratio *ca.* 2:1 by subsequent isolation. Evaporation of the mother liquors gave a viscous yellow oil showing several components on t.l.c. (R_f 0.42, 0.35, 0.29, 0.22, 0.15, and 0.02); no more of **7***a* and/or **8***a* could be crystallized from this oil which was not further investigated. The crystalline mixture of **7***a* and **8***a* was separated by multiple recrystallizations, one "cycle" being described as follows. Slow crystallization over 24 h at room temperature, from a solution obtained by dissolving the solid in boiling isopropyl acetate, and one similar recrystallization afforded pure **7***a* homogeneous on t.l.c. at high spotting concentrations. The filtrates were evaporated, the residue dissolved in boiling ethanol, and allowed to crystallize slowly at room temperature over 24 h. One similar recrystallization of the colorless needles so obtained afforded pure **8***a*, also homogeneous on t.l.c. at high spotting concentrations.

Compound **7***a*, colorless prisms, m.p. 205.5–207° had ν_{max} (KBr) 3370 (lactam NH), 1780 and 1745 (sh) (phthalimido CO), 1730 (ester CO), 1670 (lactam CO), 1620 (w) and 720 cm^{-1} (phthalimido aromatic); τ ($CDCl_3$) 8.75 (3H) (s), 8.37 (3H) (s) ($\rangle C(CH_3)_2$), 6.12 (3H) (s) ($—CO_2CH_3$), 7.29 (1H) (q, $J_{AM} = 15$, $J_{AX} = 7.5$ Hz), 6.73 (1H) (q, $J_{AM} = 15$, $J_{MX} = 11.75$ Hz) (A and M quartets for C-7 geminal protons), 4.87 (1H) (q, $J_{AX} = 7.5$, $J_{MX} = 11.75$ Hz) (X quartet for C-6 methine), 5.12 (1H) (d, $J = 6$ Hz) (C-3 methine), 3.29 (1H) (br, mult.), and 2.20 (4H) (mult.) (phthalimido aromatic protons); at 100 MHz, irradiation at τ 4.87 decoupled the A and M quartets to two doublets at 7.31 and 6.76 ($J_{AM} = 15$ Hz); $[\alpha]_D^{29} - 51.3°$ (*c* 0.12) and a negative Cotton effect curve with trough at 368 and peak at 332 nm; *m/e* 362 (M^+) (8), 189 (100), 173 (82), and 74 (48).

Anal. Calcd. for $C_{17}H_{18}N_2O_5S$: C, 56.35; H, 5.09; N, 7.72. Found: C, 56.04; H, 5.24; N, 7.31.

Compound **8***a*, colorless needles, m.p. 206–208° had ν_{max} (KBr) 3380 (lactam NH), 1785 and 1750 (phthalimido CO), 1730 (ester CO), 1680 (lactam CO), 1620 (w) and 720 cm^{-1} (phthalimido aromatic); τ ($CDCl_3$) 8.55 (6H) (s) ($\rangle C(CH_3)_2$), 6.14 (3H) (s) ($—CO_2CH_3$), 7.00 (1H) (q, $J_{AM} = 15.5$, $J_{AX} = 4.5$ Hz), 6.12 (1H) (q, $J_{AM} = 15.5$, $J_{MX} = 8.75$ Hz) (A and M quartets for C-7 geminal protons), 5.31 (1H) (d) (C-3 methine), 4.62 (1H) (q, $J_{AX} = 4.5$, $J_{MX} = 8.75$ Hz) (X quartet for C-6 methine), 3.63 (1H) (br, d, $J =$ *ca.* 7 Hz), and 2.17 (4H) (complex mult.); at 100 MHz, irradiation at τ 4.60 decoupled the A and M quartets to two doublets at 7.09 and 6.22 ($J_{AM} = 15.5$ Hz); $[\alpha]_D^{29} - 90.0°$ (*c* 0.12) and a negative Cotton effect curve with a trough at 334 and a peak at 306 nm; *m/e* 362 (M^+) (11), 330 (13), 189 (86), 173 (100), 104 (34), 76 (32), 74 (54), and 59 (30).

Anal. Calcd. for $C_{17}H_{18}N_2O_5S$: C, 56.35; H, 5.09; N, 7.72. Found: C, 55.95; H, 5.25; N, 7.24.

Alternatively the mixture (4 g) of **7***a* and **8***a* could be separated by chromatography on a column (*ca.* 3 cm diameter) of Florisil (150 g) packed in benzene, by eluting with ether (**7***a* commenced eluting), ether–acetone (99:1 (v/v)) (**7***a* and **8***a* mixture, followed by **8***a* eluting), and finally ethyl acetate. The column was monitored by t.l.c. and appropriate fractions were combined. Thus **8***a* (0.7 g), **7***a* (1.1 g), and a mixture of these (2.2 g), were obtained.

An alternative, but less successful, preparation of **7***a* and

Can. J. Chem. Downloaded from www.nrcresearchpress.com by 210.87.254.42 on 09/05/12
For personal use only.

8*a* utilized dicyclohexylcarbodiimide as the condensing agent. Dicyclohexylcarbodiimide (0.58 g, 2.80 m*M*) in acetonitrile (5 ml) was added dropwise over 12 min to a stirred solution of α-phthalimidoacrylic acid (0.53 g, 2.45 m*M*), penicillamine methyl ester hydrochloride (0.5 g, 2.50 m*M*), and triethylamine (0.38 ml, 2.75 m*M*) in anhydrous acetonitrile (15 ml), at room temperature. After the reaction mixture had been stirred for 7.5 h and cooled in the refrigerator for 4 h the dicyclohexylurea which had precipitated (0.435 g) was filtered off and washed with a small volume of acetonitrile. Evaporation of the combined filtrate and washings gave an amorphous solid which was dissolved in chloroform (*ca.* 25 ml), then washed with 2 *N* hydrochloric acid (2 × 20 ml), saturated brine (20 ml), and aqueous sodium bicarbonate (2 × 20 ml). The chloroform solution was then dried ($MgSO_4$) and evaporated to yield an off-white amorphous solid (1.17 g) which could not be induced to crystallize. The total product dissolved in benzene was entered onto a column (15 × 2.6 cm) of Florisil (35 g) packed in benzene, and the column eluted first with benzene, then with increasing concentrations of ethyl acetate in benzene; 100, then 200 ml (after fraction 8) fractions were collected.

Fractions 11 and 12 eluted with ethyl acetate–benzene (10:90 (v/v)) were combined, evaporated, and the residue recrystallized from ethanol, affording pure **8***a* (by i.r., n.m.r., and t.l.c. R_f, comparison).

Fractions 14–16, eluted with ethyl acetate–benzene (10:90 and 15:85 (v/v)), were combined, evaporated and the residue purified by p.l.c. (two elutions with methyl formate–benzene, 15:85 (v/v)) and subsequent recrystallization from carbon tetrachloride, affording pure 7*a* (by i.r. and t.l.c. comparison).

Fractions 17–21 were a mixture of 7*a* and **8***a* as indicated by t.l.c. The approximate total yield of 7*a* and **8***a* mixture (fractions 11–21 total) was *ca.* 40% in *ca.* 2:1 ratio.

Fractions 6 and 7 were combined and evaporated to yield 12 mg of residue which was recrystallized from ethanol yielding 4 mg colorless needles, m.p. 163.5–165.5°; R_f 0.51 on t.l.c. with methyl formate–benzene (15:85 (v/v)) as eluent. An analysis of the i.r. spectrum of this product led to its formulation as *N*-(α-phthalimido)acrylyl-*N*,*N*′-dicyclohexyl urea, and the i.r. spectrum was superimposable on that of an authentic sample (see below).

*N-(α-Phthalimido)acrylyl-N,N′-dicyclohexyl Urea (**i**)*

To a solution of dicyclohexylcarbodiimide (238 mg, 1.15 m*M*) in pyridine (5 ml), at 80°, a solution of α-phthalimidoacrylic acid (250 mg, 1.15 m*M*) in pyridine (10 ml) was slowly added over the course of 45 min. After stirring at 80–95° for a further 2 h, the solution was cooled to room temperature, diluted with chloroform (25 ml), and extracted with 2 *N* hydrochloric acid until the washings were strongly acidic (*ca.* 6 × 10 ml HCl), then with saturated aqueous sodium bicarbonate solution (3 × 10 ml). The chloroform extract was dried ($MgSO_4$), evaporated, and the residue recrystallized three times from 95% ethanol, affording colorless needles, 230 mg (325 mg after the first recrystallization), m.p. 162.5–165°; ν_{max} (KBr) 3345 (amide NH), 3030 (w) (>C=CH—), 1640 and 885 (>C=CH_2), 1615 and 735 (phthalimido aromatic), 2930 and 2855 (—CH_2—), 1795 (phthalimido asym CO str), 1770 (w), 1720, and 1715 (sh) (carbonyl CO), 1655 (amide CO), 1640 (possibly urea CO with double bond C=C str), and 1530 cm^{-1} (acyclic amide); τ ($CDCl_3$) 9.0–8.0 (2OH) (complex), *ca.* 6.4 (1H) (br, mult.), *ca.* 5.8 (1H) (br, mult.), 4.27 (1H) and 4.14 (1H) (d, d, J = 1.5 Hz) (vinylic methylene protons), 3.08 (1H) (br, d, J = 8 Hz) (NH), and 2.15 (4H) (mult.).

*The Reaction of Chlorine with 7a: Isolation of 3D-Carbomethoxy-2,2-dimethyl-5-oxo-6D-phthalimido-2,3,4,5-tetrahydro-1,4-thiazepine (**9**) and 3D-Carbomethoxy-7L-chloro-2,2-dimethyl-5-oxoperhydro-6D-phthalimido-1,4-thiazepine (**10**)*

(*a*) Under the conditions described by Leonard and Wilson (4), a reaction of 7*a* (200 mg) with chlorine in methylene chloride afforded, after p.l.c. of the product (two successive elutions with methyl formate–benzene, 1:4 (v/v)), a 55% yield of the tetrahydrothiazepine **9**, colorless needles from benzene–ether, m.p. 180–182°, ν_{max} (KBr) 3380 (lactam NH), 1780 and 1740 (phthalimido and ester CO), 1680 (lactam CO), 1620 (w, sh) (aromatic) and 1595 cm^{-1} (w) (—COC(=CH)—); λ_{max} 217 (ε 4.39 × 10^4), 229 (sh) (ε 2.58 × 10^4), 237 (sh) (ε 2.07 × 10^4), and 285 nm (ε 1.30 × 10^4); τ ($CDCl_3$) 8.50 (3H) (s), 8.45 (3H) (s) (>C(CH_3)$_2$), 6.13 (3H) (s) (—CO_2CH_3), 5.42 (1H) (d, J = 7 Hz) (C-3 methine), 3.20 (1H) (d, J = 7 Hz) (NH), 2.95 (1H) (s) (vinylic proton) and 2.17 (4H) (mult.); *m/e* 360 (M^+) (37), 132 (36), 104 (100), 98 (39), 76 (68), and 74 (35).

Anal. Calcd. for $C_{17}H_{16}N_2O_5S$: C, 56.65; H, 4.48; N, 7.77. Found (consistent with **10**): C, 56.84; H, 4.78; N, 7.92.

(*b*) In a second reaction of pure 7*a* (0.5 g, 1.38 m*M*) in methylene chloride (10 ml) with a carbon tetrachloride solution 0.52 *M* in chlorine (2.93 ml, 1.52 m*M*), stirring was maintained for 3 h at a reaction temperature of −77° and then for 1.5 h while the reaction mixture was allowed to warm to 0° when it was immediately evaporated to yield a colorless glass. The t.l.c. examination (R_f after elution with methyl formate–benzene, 1:3 (v/v)) of this crude product indicated the presence of unchanged 7*a* (R_f 0.25) and compound **10** (R_f 0.32), and only a trace of **9** (R_f 0.2). A minor contamination (R_f 0.45) was also present. Rapid chromatography on a column (1.8 × 18 cm) of Florisil (20 g), packed in benzene, and elution with ether–benzene (1:5 (v/v)) (and finally acetone), gave two main fractions.

Fraction 1, upon evaporation yielded a colorless glass, 230 mg, (R_f 0.32, containing a trace of a contaminant, R_f 0.45) which, when triturated with ether afforded colorless glassy crystals. These, after recrystallization from warm ethanol, had m.p. 160–163.5°, gave a positive Beilstein test for halogen, and had ν_{max} (KBr) 3370 (lactam NH), 1780 and 1725 (phthalimido and ester CO), 1670 (lactam CO), and 1610 (w) and 720 cm^{-1} (phthalimido aromatic); τ ($CDCl_3$) 8.81 (3H) (s), 8.20 (3H) (s) (>C(CH_3)$_2$), 6.11 (3H) (s) (—CO_2CH_3), 5.03 (1H) (d, J = 5.5 Hz), (C-3 methine), 4.75 (1H) and 4.47 (1H) (AB quartet, J_{AB} = 11.5 Hz) (C-6 and -7 methines), 3.24 (1H) (br) (NH), and 2.17 (4H) (mult.); *m/e* 396 (M^+) (1), 360 (28), 132 (39), 104 (100), 76 (69), and 74 (40); all consistent with the structure **10**.

Fraction 2 was evaporated to yield a residue, *ca.* 300 mg, which was a mixture (*ca.* 1:1) of 7*a* and **9** as judged by t.l.c. The appearance of **9** after chromatography on Florisil indicated that elimination of HCl had occurred during column chromatography.

Can. J. Chem. Downloaded from www.nrcresearchpress.com by 210.87.254.42 on 09/05/12
For personal use only.

The Reaction of Chlorine with Pure 8a: Isolation and Data on Compound 11a

A reaction, as above, of pure **8***a* (200 mg) with chlorine, led to a reaction mixture which, when cooled and diluted with CCl_4, deposited colorless plates, 20 mg, of **11***a*. The filtrate was subjected to p.l.c. (two successive elutions with methyl formate–benzene, 1:4 (v/v)) and yielded **9**, 41 mg (i.r. spectrum identical to **9** from *7a*), and impure fractions not further purified. Compound **11***a* recrystallized from ethanol as colorless plates, with m.p. 208–210.5° dependent on time of heating;[15] ν_{max} (KBr) 3500–3000 (several w–m bands), 1780 and 1750 (phthalimido CO), 1730 (ester CO), 1695 (lactam CO), 1615 and 715 (phthalimido aromatic), and 1034 cm^{-1} (s) (sulfoxide SO); τ ($CDCl_3$) 8.63 (3H) (s), 8.57 (3H) (s) ($>C(CH_3)_2$), 6.15 (3H) (s) ($—CO_2CH_3$), 6.50 (1H) (complex), 6.13 (1H) (complex), 4.87 (1H) (complex), 5.75 (1H) (d, $J = 7$ Hz, collapsing to a singlet after shaking with D_2O) (C-3 methine), 3.66 (br, d, $J = ca.$ 7 Hz disappearing on shaking with D_2O) (lactam NH), and 2.19 (4H) (mult.) (phthalimido aromatic protons); *m/e* 378 (M^+) (12), 329 (36), 221 (54), 200 (35.5), 173 (100), 172 (44), 130 (31.5), 104 (54), 76 (46), 70 (38), and 51 (40.5); consistent with **11***a* being a sulfoxide of *7a*, diastereomeric with the sulfoxide **11***b* on the basis of different i.r. spectra and t.l.c. behavior, yet closely similar mass spectra.

3D-Carbomethoxy-2,2-dimethyl-5-oxoperhydro-6L-phthalimido-1,4-thiazepine-1-monoxide (11b)

An aqueous solution (10 ml) of sodium periodate (256 mg, 1.2 m*M*) was added to a stirred suspension of 6L-phthalimido perhydrothiazepine **8***a* (400 mg, 1.1 m*M*) in methanol (25 ml) at room temperature. The suspension was stirred for 24 h then extracted with chloroform (4 × 10 ml). The combined chloroform extracts were dried ($MgSO_4$), evaporated, and the residue recrystallized twice from 95% ethanol affording colorless plates, m.p. 221.5–223.5°, 314 mg, in 75% yield; with λ_{max} (KBr) 3325 (lactam NH), 1795 and 1740 (phthalimido and ester CO), 1700 (lactam CO), 1620 and 719 (phthalimido aromatic), and 1040 cm^{-1} (sulfoxide SO); *m/e* 378 (M^+) (16), 360 (2), 329 (44.5), 297 (30), 221 (55), 200 (30.5), 173 (100), 172 (42.5), 104 (52), and 76 (44.5).

Anal. Calcd. for $C_{17}H_{18}N_2O_6S$: C, 53.95; H, 4.79; N, 7.40. Found: C, 53.57; H, 4.84; N, 7.54.

3D-Carbomethoxy-2,2-dimethyl-5-oxoperhydro-6L-phthalimido-1,4-thiazepine-1,1-dioxide (12)

A solution of potassium permanganate (5% w/v), in aqueous 80% (v/v) acetic acid (19 ml), was added quickly to 6L-phthalimidoperhydrothiazepine **8***a* (1 g). After stirring for 30 min excess permanganate was destroyed by the dropwise addition of 30% hydrogen peroxide, and water was added (*ca.* 50 ml). The colorless microneedles which deposited were collected, washed with water, and dried, affording 1.058 g, 97% yield, m.p. 269–274°; t.l.c. homogeneous (R_f 0.35 after elution with methyl formate–benzene, 3:7 (v/v)) with ν_{max} (KBr) 3310 (lactam NH), 1790 and 1750 (phthalimido CO), 1725 (ester CO), 1705 (sh) (lactam CO), 1330 and 1106 cm^{-1} (sulfone SO): *m/e* 394 (M^+) (5.5), 330 (5.5), 174 (58.5), and 173 (100); "metastable" *m/e* 276.5.

[15]The value quoted is optimum, obtained from *ca.* 5 min heating after insertion of sample at *ca.* 200°.

Anal. Calcd. for $C_{17}H_{18}N_2O_7S$: C, 51.77; H, 4.60; N, 7.10. Found: C, 51.07; H, 5.17; N, 6.83.

3D-Carbomethoxy-2,2-dimethyl-5-oxoperhydro-6L-phthalimido-N-chloro-1,4-thiazepine-1,1-dioxide (13)

A solution of **8***a* (0.5 g) in acetic acid (13 ml) containing *t*-butyl hypochlorite (2 ml) was allowed to stand at room temperature for *ca.* 36 h. Evaporation of the reaction mixture, under reduced pressure and finally in a vacuum desicator over KOH pellets and H_2SO_4, yielded a colorless glass, which gave a strongly positive active chlorine test, and had ν_{max} ($CHCl_3$) 1790 and 1770 (phthalimido CO), 1730 (ester and lactam CO), 1615 (w) and 710 cm^{-1} (phthalimido aromatic); τ ($CDCl_3$) 8.43 (3H) (s), 8.25 (3H) (s) ($>C(CH_3)_2$), 6.15 (3H) (s) ($—CO_2CH_3$), 6.60 (1H) (apparent q, $J_{AX} \leqslant 1$ Hz, $J_{AB} = 15$ Hz), 5.57 (1H) (q, $J_{BX} = 11.5$, $J_{AB} = 15$ Hz) (A and B quartets, respectively, for the C-7 geminal protons), 4.27 (1H) (apparent q, $J_{BX} = 11.5$, $J_{AX} \leqslant 1$ Hz) (C-6 methine), 4.60 (1H) (s) (C-3 methine), and 2.20 (4H) (mult.) (phthalimido aromatic protons); irradiation at τ 4.27 or 6.60 decoupled the B quartet centered at 5.57 to doublets $J = 15$ and $J = 11.5$ Hz respectively.

The Protolysis of 13

When **13** (50 mg) was refluxed in 2-propanol (10 ml) for 30 min and the suspension cooled for several hours at 0° then filtered, it afforded **12**, 45.5 mg (i.r. spectrum identical to authentic **12**).

The Reaction of 3D-Carbomethoxy-2,2-dimethyl-5-oxoperhydro-6L-phthalimido-N-chloro-1,4-thiazepine-1,1-dioxide (13) with Silver Carbonate

The *N*-chlorolactam **13** (prepared from 0.5 g of **12**) dissolved in anhydrous DMF (20 ml) was stirred with silver carbonate (2 g) and glass beads and the reaction vessel was inserted in an oil bath held at 45°. Within 3 min a negative active chlorine test was obtained. Filtration (Celite) and evaporation of the reaction mixture afforded a gummy crystalline solid, which was recrystallized from ethanol to give colorless needles, 234 mg, R_f 0.31 (on t.l.c. after elution with methyl formate–benzene, (30:70 v/v)), of **12** (identical t.l.c. R_f and i.r. spectra). The mother liquors had no trace of an i.r. absorption band for a β-lactam, but showed two major components on t.l.c. (R_f 0.75 and 0.29); these were separated by p.l.c. (one elution with methanol–chloroform, 10:90 (v/v)).

The higher R_f component was recrystallized from hexane and obtained as colorless needles, 25 mg, m.p. 83–86°; ν_{max} (KBr) 1780 (m) and 1735 (str) (phthalimido CO), and 1630 cm^{-1} (double bond); τ (CCl_4) 5.05 (1H) (d, $J_{cis} = 10$ Hz), 3.98 (1H) (d, $J_{trans} = 17$ Hz) ($—CH=CH_2$) and 3.17 (1H) (q, $J = 10$; $J = 17$ Hz) ($—CH=CH_2$); *m/e* 173 (M^+) (100), 104 (44), and 76 (57); "metastable" *m/e* 123, 62.5 (w), 55.5 and 33; consistent with the assignment of structure **14** to this product.

The lower R_f component was recrystallized from 95% ethanol to yield colorless needles, 30 mg, m.p. 173.5–176.5°; ν_{max} (KBr) 3260 (—NH), 1795 and 1740 (phthalimido CO), 1725 (ester CO, possibly conjugated), 1680 and 1530 (acyclic amide), 1635 and 884 cm^{-1} (methylene $>C=CH_2$); τ ($CDCl_3$) 8.04 (3H) (s), 7.77 (3H) (s) ($>C=C(CH_3)_2$)

6.23 (3H) (s) ($-CO_2CH_3$), 4.12 (1H) and 3.71 (1H) (2d, $J = 1.4$ Hz) ($>C=CH_2$), and 2.15 (4H) (mult.) (phthalimido protons); *m/e* 328 (M^+) (12), 200 (30.5), 173 (22.5), 172 (100), 128 (42), 104 (50.5), and 76 (31); "metastable" *m/e* 123 and 122–120.5, 93.5, and 50 (w); consistent with the structure **15**.

*The Action of White Light on 3D-Carbomethoxy-2,2-dimethyl-5-oxoperhydro-6L-phthalimido-N-chloro-1,4-thiazepine-1,1-dioxide (**13**)*

The *N*-chlorolactam **13** (prepared from 0.5 g of **12**) in refluxing benzene solution (50 ml) contained in a Pyrex flask was illuminated with a 300 W tungsten filament lamp under a steady stream of dry nitrogen, for 7 h, after which time all active chlorine had been lost. The reaction mixture was cooled to room temperature and then evaporated under reduced pressure to yield a colorless glass, with no ν_{max} ($CHCl_3$) assignable to a β-lactam carbonyl, and no ν_{max} 3050–4000, but ν_{max} 2255 cm^{-1} (isocyanate). The crude product was recrystallized from a small volume of hexane–ether affording colorless crystals, 180 mg, m.p. 76–83° after one further recrystallization from hexane, identified as phthalimidoethylene (**14**) (the i.r. spectrum was identical to that of **14** obtained as described above). The mother liquors from the above recrystallization were evaporated, affording an oil which had ν_{max} ($CHCl_3$) 2255 cm^{-1}. After boiling with ethanol and evaporating an oil was obtained with ν_{max} ($CHCl_3$) 3440 (NH), 1785 (w) and 1750 (sh), 1725 (carbonyl), and 1510 cm^{-1} (possibly acyclic amide band); τ (CCl_4) 8.74 (3H) (t, $J = 7$ Hz) ($-OCH_2CH_3$), 8.38 (3H) (s), 8.30 (3H) (s) ($>C(CH_3)_2$), 6.23 (3H) (s) ($-CO_2CH_3$), 5.90 (2H) (q, $J = 7$ Hz) ($-OCH_2CH_3$), 5.60 (1H) (d, $J = 10$ Hz) ("C-3" methine), and 4.51 (1H) (d, broadened *J ca.* 9 Hz) (NH); *m/e* 275 (0.16), 273 (M^+) (0.5), 180 (15.5), 178 (50), 161 (46), 160 (73), 129 (39.5), 88 (100), 70 (51), 56 (55), 45 (34.5), 43 (38), and 41 (44); consistent with this product being the ethyl urethane corresponding to **16**.

*The Reaction of 3D-Carbomethoxy-2,2-dimethyl-5-oxoperhydro-6L-phthalimido-N-chloro-1,4-thiazepine-1,1-dioxide (**13**) with Some Bases*

A solution of **13** (75 mg, 0.17 m*M*) and anhydrous sodium carbonate (19 mg, 0.185 m*M*) in anhydrous DMF (10 ml) was stirred at room temperature for 1.5 h, then evaporated and the residue extracted into chloroform. Evaporation of the filtered chloroform solution and recrystallization of the residue from 95% ethanol afforded colorless needles; 15 mg of **12**. Evaporation of the mother liquors yielded a residue, 22 mg, which was recrystallized from benzene–petroleum ether (b.p. 65–110°) affording colorless crystals, 8 mg, m.p. 166–170°, identified as **15** (i.r. spectral comparison). No β-lactam carbonyl band was detected in the i.r. spectrum of any of the reaction product fractions, crude or pure.

A similar reaction of **13** with potassium fluoride over 6 h resulted in the isolation of the same products as above.

The work described here was supported in part by an operating grant from the National Research Council of Canada, whom we also thank for the award of a Research Scholarship (1968–1969) to R.E.M.

We are indebted to a referee for drawing our attention to ref. 6, and to Dr. Lillya who most courteously made available to us a copy of his thesis.

1. R. B. WOODWARD. Sci. **153**, 487 (1966).
2. N. J. LEONARD and R. Y. YING. J. Org. Chem. **32**, 677 (1967); B. Y. BYCROFT. Nature, **244**, 595 (1969).
3. R. D. G. COOPER. J. Am. Chem. Soc. **94**, 1018 (1972).
4. N. J. LEONARD and G. E. WILSON, JR. J. Am. Chem. Soc. **86**, 5307 (1964).
5. I. L. KNUNYANTS, O. V. KIL'DISHEVA, M. P. KRASUSKAYA, M. G. LIN'KOVA, V. V. SHOKINA, Z. V. BENEVOLENSKAYA, and L. P. RASTEIKENE. Izvest. Akad. Nauk S.S.R., Ser. Khim., 1777 (1959); Chem. Abstr. **54**, 8843*i* (1960); see also P. BLONDEAU, R. GAUTHIER, C. BERSE, and D. GRAVEL. Can. J. Chem. **49**, 3866 (1971).
6. C. P. LILLYA. Ph.D. Thesis, Harvard University, Cambridge, Mass. 1964.
7. M. F. SEMMELHACK and B. F. GILMAN. Chem. Commun. 988 (1971); M. F. SEMMELHACK, S. KUNKES, and C. LEE. Chem. Commun. 698 (1971).
8. O. E. EDWARDS, D. VOCELLE, J. W. APSIMON, and F. HAQUE. J. Am. Chem. Soc. **87**, 678 (1965).
9. N. J. LEONARD and R. Y. YING. J. Org. Chem. **31**, 3928 (1966).
10. F. KURZER and K. DOURAGHI-ZADEH. Chem. Rev. **67**, 107 (1967).
11. J. C. SHEEHAN and P. A. CRUICKSHANK. J. Am. Chem. Soc. **78**, 3680 (1956).
12. R. D. G. COOPER, P. V. DEMARCO, J. C. CHENG, and N. D. JONES. J. Am. Chem. Soc. **91**, 1408 (1969).
13. R. E. MITCHELL. Ph.D. Thesis. University of Calgary, Calgary, Alberta, 1969.
14. O. E. EDWARDS, J. M. PATON, M. H. BENN, R. E. MITCHELL, C. WATANATADA, and K. N. VOHRA. Can. J. Chem. **49**, 1648 (1971).
15. J. C. SHEEHAN and M. TISHLER. Chem. Abstr. **44**, P3034*h* (1950).
16. S. SAKAKIBARA. Bull. Chem. Soc. Japan, **34**, 171 (1961).

Can. J. Chem. Downloaded from www.nrcresearchpress.com by 210.87.254.42 on 09/05/12
For personal use only.

Base-catalyzed Degradations of Carbohydrates. II. β-Elimination Reactions of 4-*O*-Substituted Methyl (Methyl 2,3-Di-*O*-methyl-β-D-glucopyranosid)uronates[1]

G. O. ASPINALL[2] AND P. E. BARRON

Department of Chemistry, Trent University, Peterborough, Ontario

Received February 21, 1972

The action of various bases on the three hexuronic esters, methyl (methyl 2,3,4-tri-*O*-methyl-β-D-glucopyranosid)uronate (**12**), methyl (methyl 4-*O*-methanesulfonyl-2,3-di-*O*-methyl-β-D-glucopyranosid)uronate (**13**), and methyl (methyl 4-*O*-acetyl-2,3-di-*O*-methyl-β-D-glucopyranosid)uronate (**14**), leading to elimination of the 4-*O*-substituents and formation of methyl (methyl 4-deoxy-2,3-di-*O*-methyl-α-L-*threo*-hex-4-enopyranosid)uronate (**15**) has been studied. It is concluded that effectiveness of 4-*O*-substituents as leaving groups is in the sequence, methanesulfonyloxy > acetoxy > methoxy.

L'action de diverses bases sur trois esters hexuroniques (méthyl tri-*O*-méthyl-2,3,4-β-D-glucopyranoside) uronate de méthyle (**12**), (méthyl *O*-méthanesulfonyl-4 di-*O*-méthyl-2,3-β-D-glucopyranoside) uronate de méthyle (**13**), et le (méthyl *O*-acétyl-4 di-*O*-méthyl-2,3-β-D-glucopyranoside) uronate de méthyle (**14**) qui mène à l'élimination des *O*-substituants en 4 avec formation du (méthyl déoxy-4 di-*O*-méthyl-2,3-α-L-*thréo*-hexèno-4 pyranoside) uronate de méthyle (**15**) a été étudiée. On a conclu que l'ordre d'efficacité des *O*-substituants en 4 en tant que "leaving group" suit la séquence méthanesulfonyloxy > acétoxy > méthoxy.

Canadian Journal of Chemistry, **50**, 2203 (1972)

Neukom (1, 2), Northcote (3, 4), Rees (5, 6), Kiss (7, 8) and their collaborators have shown that esterified hexuronates are susceptible to base-catalyzed degradation with the formation of unsaturated hexuronates and with the exposure of new reducing groups. When reaction is performed in aqueous solution competing ester hydrolysis occurs with loss of the driving force of the carboalkoxy group towards elimination, and only limited degradation is achieved. This difficulty may be partially overcome by using a non-aqueous system such as sodium methoxide in methanol, in which instance the ester function is regenerated by base-catalyzed ester exchange. The value of this approach in obtaining new structural information on polysaccharides has been demonstrated by Rees and co-workers (6) in studies on colanic acid. Nevertheless, the full potential of this type of reaction for the degradation of polysaccharides has not been realized because of the limited solubility of the substrates, unless etherified or esterified, in non-aqueous solvents. 4-*O*-Substituted methyl (methyl 2,3-di-*O*-methyl-β-D-glucopyranosid)-uronates (**12**, **13**, **14**) have been prepared, and the action of bases on these compounds has been studied in order to assess the relative effectiveness of 4-*O*-substituents as leaving groups in the β-elimination reaction. The 4-*O*-acetyl (**14**) and 4-*O*-methyl (**12**) derivatives provide models for the behavior of D-glucuronic acid end groups in acetylated or methylated polysaccharides.

The well-known methyl (methyl 2,3,4-tri-*O*-methyl-β-D-glucopyranosid)uronate (**12**) was most satisfactorily prepared from methyl 6-*O*-trityl-β-D-glucopyranoside (**1**) by successive methylation, de-*O*-tritylation, oxidation with chromium trioxide and sulfuric acid in acetone (9), and esterification with diazomethane. The other hexuronates were prepared from methyl 2,3-di-*O*-methyl-6-*O*-trityl-β-D-glucopyranoside (**3**). Thus, the trityl ether (**3**) was mesylated, de-*O*-tritylated, oxidized with chromium trioxide and sulfuric acid in acetone, and esterified with diazomethane to give methyl (methyl 4-*O*-mesyl-2,3-di-*O*-methyl-β-D-glucopyranosid)uronate (**13**). A similar sequence of reactions furnished methyl (methyl 4-*O*-acetyl-2,3-di-*O*-methyl-β-D-glucopyranosid)uronate (**14**).

Treatment of methyl (methyl 4-*O*-mesyl-2,3-di-*O*-methyl-β-D-glucopyranosid)uronate (**13**) with sodium methoxide in methanol or ethanolic potassium hydroxide, as described by Kiss (10) for the preparation of related unsaturated

[1]Taken from the M.Sc. thesis of P. E. Barron, Trent University, 1972.

[2]To whom enquiries should be addressed.

Can. J. Chem. Downloaded from www.nrcresearchpress.com by 210.87.254.6 on 09/05/12
For personal use only.

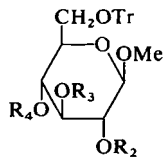

1 $R_2 = R_3 = R_4 = H$
2 $R_2 = R_3 = R_4 = Me$
3 $R_2 = R_3 = Me$; $R_4 = H$
4 $R_2 = R_3 = Me$; $R_4 = Ms$
5 $R_2 = R_3 = Me$; $R_4 = Ac$

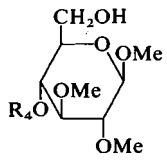

6 $R_4 = Me$
7 $R_4 = Ms$
8 $R_4 = Ac$

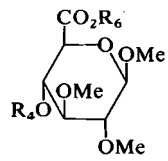

9 $R_4 = Me$; $R_6 = H$
10 $R_4 = Ms$; $R_6 = H$
11 $R_4 = Ac$; $R_6 = H$
12 $R_4 = Me$; $R_6 = Me$
13 $R_4 = Ms$; $R_6 = Me$
14 $R_4 = Ac$; $R_6 = Me$

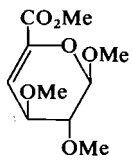

15

esters, gave the crystalline unsaturated ester, methyl (methyl 4-deoxy-2,3-di-*O*-methyl-α-L-*threo*-hex-4-enopyranosid)uronate (**15**), in 84–87% isolated yield. The structure of the ester was fully supported by u.v., i.r., n.m.r., and mass spectra. The ease with which β-elimination of methanesulfonic acid takes place with formation of the unsaturated hexuronate (15) when the mesyl ester (**13**) is treated with base was strikingly emphasized during g.l.c. examination of the mesyl ester (**13**). Whereas g.l.c. of the mesyl ester (**13**) on a column coated with neutral silicone gum SE-30 gave a single peak of substantially higher retention time than that of the unsaturated ester (**15**), g.l.c. on a column coated with the nitrile silicone gum XE-60 as liquid phase gave a single peak of the same retention time as the unsaturated ester (**15**). Gas–liquid chromatography – mass spectrometry supported the conclusion that unsaturated ester had been formed on the g.l.c. column.

Bases chosen for the study of their action on the acetylated (**14**) and methylated (**12**) esters were either those of low nucleophilicity towards ester functions which would catalyze elimination with minimum de-esterification or those which would regenerate hexuronic ester functions by base-catalyzed ester exchange although in the latter case de-*O*-acetylation of the 4-*O*-acetate could take place. The results are summarized in Tables 1 and 2.

Treatment of the acetylated ester (**14**) with DBU (1,5-diazabicyclo[5.4.0]undec-5-ene) in benzene at room temperature afforded the crystalline unsaturated ester (**15**) in 83% isolated yield.[3] The unsaturated ester (**15**) was also isolated in 66% yield as the major detectable product when the acetylated ester (**14**) was treated with sodium hydride in ether. The effect of other bases on the acetylated ester was studied only in small-scale experiments in which products were analyzed by g.l.c. and t.l.c. Treatment of the ester (**14**) with methanolic sodium methoxide resulted in both de-*O*-acetylation and β-elimination. This observation has significance for studies on polysaccharides since the reaction conditions, which are those commonly used for the de-*O*-acylation of acylated derivatives, could result in structural modification of hexuronic ester residues. It was also observed that treatment of the acetylated ester (**14**) with acetic anhydride and potassium acetate at 100° caused some β-elimination. A similar observation was made previously by Schmidt and Neukom (11). Although these conditions are harsher than those which need be used for acetylation it is clear that care should be exercized in the acetylation of carbohydrates containing hexuronic ester units lest inadvertent degradation takes place. Alkali metal fluorides may act as strong bases in dipolar aprotic solvents (12), and some β-elimination was observed on prolonged treatment of the acetylated ester (**14**) with cesium fluoride in methyl sulfoxide at room temperature. In contrast, the unusually strong organic base, 1,8-bis (*N*,*N*-dimethylamino)naphthalene (13), was without effect on the acetylated ester (**14**).

The crystalline unsaturated ester (**15**) was isolated in 58% yield on treatment of the methylated ester (**12**) with methylsulfinyl carbanion in methyl sulfoxide. An unknown substance was formed as a minor reaction product and a substance of similar retention time was also detected amongst the products from the action of potassium *t*-butoxide in methyl sulfoxide on the methylated ester (**12**) but in neither

[3]Recently, Llewellyn and Williams (23) have reported a similar reaction of a 4-*O*-acetyl hexuronic ester with DBU.

Can. J. Chem. Downloaded from www.nrcresearchpress.com by 210.87.254.6 on 09/05/12
For personal use only.

TABLE 1. Action of bases on methyl (methyl 4-*O*-acetyl-2,3-di-*O*-methyl-β-D-glucopyranosid)uronate (**14**)

Base conditions of reaction[a]	Isolated yield (%) of unsaturated ester (**15**)	Relative proportions of products (by g.l.c.)			
		Acetylated ester (**14**)	Unsaturated ester (**15**)	De-*O*-acetylated ester	Others[b]
DBU/benzene, 5 days, r.t.	85		11.0		1.0 (B)
NaH/ether, 24 h, r.t.	66				
NaOMe/MeOH, 90 min, r.t.			1.3	2.1	1.0 (A)
$KOBu_t$/DMSO, 90 min, r.t.			1.0	1.4	
Ac_2O/KOAc, 7 days, r.t.		Unchanged			
Ac_2O/KOAc, 24 h, 100°		5.0	1.0		
bis(DMA)N/benzene, 10 days, r.t.		Unchanged			
bis(DMA)N/DMF, 8 days, r.t.		Unchanged			
CsF/DMSO, 9 days, r.t.		4.5	1.0		

[a]DBU, 1,5-diazabicyclo[5.4.0]undec-5-ene; DMSO, methyl sulfoxide; bis(DMA)N, 1,8-bis(*N*,*N*-dimethylamino)naphthalene.
[b]A and B are unidentified compounds whose relative retention times are quoted in the Experimental.

TABLE 2. Action of bases on methyl (methyl 2,3,4-tri-*O*-methyl-β-D-glucopyranosid)uronate (**12**)

Base/conditions of reaction[a,c]	Isolated yield (%) of unsaturated ester (**15**)	Relative proportions of products (by g.l.c.)		
		Methylated ester (**12**)	Unsaturated ester (**15**)	Others[b]
NaH/DMSO, 4 h, r.t.	58		11.0	1.0 (C)
NaOMe/MeOH, 4 h, r.t.		10.5	1.9	1.0 (D) 2.4 (E)
NaOMe/MeOH, 4 h, 60°		5.9	3.0	1.0 (D) 2.8 (E)
$KOBu_t$/DMSO, 70 min, r.t.			25.6	1.0 (D*) 2.6 (C*)

[a]See footnote to Table 1.
[b]C, D, and E are unidentified compounds whose relative retention times are quoted in the Experimental section; C* and D* have the same relative retention times as C and D respectively but no other criteria of identity are yet available.
[c]No reaction was observed under the following conditions: (*i*) Ac_2O/NaOAc, 9 days, r.t.; (*ii*) Ac_2O/KOAc, 24 h, 100°; (*iii*) bis(DMA)N/benzene, 10 days r.t.; (*iv*) bis(DMA)N/DMF, 7 days, r.t.; (*v*) DBU/benzene, 9 days, r.t.; (*vi*) DBU/DMF, 7 days, r.t.; (*vii*) CsF/DMSO, 7 days, r.t.; (*viii*) MeI/Ag_2O, 3 days, 35°; (*ix*) MeI/Ag_2O/DMF, 8 days, r.t.; (*x*) NaH/benzene, 4 h, r.t.; (*xi*) NaH/ether, 70 min, r.t.

case was it possible to obtain definite evidence for structure. It was noted, however, that the unsaturated ester (**15**) remained unchanged on treatment with methylsulfinyl carbanion in methyl sulfoxide. Of other bases examined only sodium methoxide in methanol caused formation of the unsaturated ester (**15**) from the methylated ester (**12**). Yoshimura and coworkers (14) have shown that when methyl (methyl 2,3,4-tri-*O*-methyl-α-D-glucopyranosid)uronate is treated with sodium methoxide in methanol under a variety of conditions less than 50% conversion into the corresponding unsaturated ester is achieved and that some of the original ester is saponified. In our hands similar treatment of the β-anomer (**12**) with methanolic sodium methoxide in the presence of 2,2-dimethoxypropane to remove traces of water (5) still led to the formation of acidic products. In addition g.l.c. showed that unsaturated ester (**15**) was formed together with two unknown compounds, but under none of the conditions used was methylated ester completely transformed to other products. Treatment of the methylated ester with potassium *t*-butoxide in methyl sulfoxide proceeded to completion with formation of the unsaturated ester as the major product and two unidentified substances as minor products. The absence of detectable β-elimination when the methylated ester (**12**) was treated with silver oxide in methyl iodide alone or with silver oxide and methyl iodide in *N*,*N*-dimethylformamide is significant in view of the widespread use of the Purdie (15) and Kuhn (16) procedures for the methylation of carbohydrates.

The results of these studies on the three 4-*O*-substituted methyl (methyl 2,3-di-*O*-methyl-β-

Can. J. Chem. Downloaded from www.nrcresearchpress.com by 210.87.254.6 on 09/05/12
For personal use only.

Can. J. Chem. Downloaded from www.nrcresearchpress.com by 210.87.254.6 on 09/05/12
For personal use only.

D-glucopyranosid)uronates clearly indicate that mesylate > acetate > methoxide represents the order of effectiveness of leaving groups in base-catalyzed β-eliminations leading to formation of the unsaturated hexuronate (**15**). A full assessment of the potential degradative applications of β-elimination reactions on interior units within acidic polysaccharide chains cannot be made until the effectiveness of 4-*O*-glycosyl substituents has been examined. Model experiments, presently in progress, will assess both the initial elimination and the effect of bases on the reducing sugar residues which may be exposed as a consequence of such eliminations.

Experimental

Melting points are uncorrected. Optical rotations were measured with a Perkin–Elmer model 141 polarimeter at $20 \pm 2°$. The i.r. and u.v. spectra were measured on Unicam SP 200 and SP 800A spectrophotometers. The n.m.r. spectra were recorded on a JEOL C-60HL spectrophotometer with tetramethylsilane as internal standard. The t.l.c. was performed with Kieselgel HF 254 as the adsorbent and the dried plates were sprayed with ethanol containing 5% of sulfuric acid and 5% of 1-naphthol and heated at about 150°. Solvent systems used for t.l.c. were chloroform–acetone (20:1 and 4:1) and benzene – light petroleum (b.p. 30–60°) (5:1). Preparative layer separations were performed using ether – light petroleum (b.p. 30–60°) (5:1). Column chromatography was carried out on silica gel (Davison grade 950, 60–200 mesh). Unless otherwise stated light petroleum refers to the fraction of b.p. 30–60°. Solutions were concentrated below 50° under reduced pressure.

Mass spectra were recorded on an A.E.I. MS 12 mass spectrometer, with an ionization potential of 70 eV. The g.l.c. was performed with a Hewlett–Packard model 5750 chromatograph using columns of dichlorodimethylsilane-treated Celite coated with (*a*) 5% of silicone gum XE-60 (operating temperature 150°) and (*b*) 5% of neopentylglycol adipate polyester (operating temperature 200°). For g.l.c. – mass spectrometry column *a* was used in a Pye 104 chromatograph and attached to the mass spectrometer via a Watson–Biemann separator. The mass spectra were recorded at an inlet temperature of 200°, an ionization temperature of 70 eV, and an ion source temperature of *ca.* 150°. Retention times (R_{Me}) of methyl (methyl glycopyranosid)uronates are quoted relative to methyl (methyl 2,3,4-tri-*O*-methyl-β-D-glucopyranosid)uronate (**12**).

Methyl (Methyl 2,3,4-Tri-O-methyl-β-D-glucopyranosid)-uronate (12)

Sodium hydride (22 g) was added with stirring to methyl 6-*O*-trityl-β-D-glucopyranoside (**1**) (17) (17.15 g) in *N*,*N*-dimethylformamide (350 ml) at 0°, and the mixture was stirred for 20 min. Methyl iodide (90 ml) was added dropwise during 15 min to the cooled solution, and the mixture was kept at room temperature for 18 h. The t.l.c. showed that reaction was complete and methanol was added to destroy excess of sodium hydride. Insoluble material was removed by filtration, the filtrate was concentrated to remove methanol and diluted with chloroform, and the chloroform solution was washed with water, dried, and concentrated to give crude methyl 2,3,4-tri-*O*-methyl-6-*O*-trityl-β-D-glucopyranoside (**2**) (14.4 g, 76.6%), $[\alpha]_D$ −95° (*c*, 2.0 in chloroform); n.m.r. data ($CDCl_3$): τ 2.52–2.97 (15-proton multiplet, trityl), 5.91 (1-proton doublet, splitting 7 Hz, H-1), 6.47 (9-proton singlet, 3 OMe), 6.78 (3-proton singlet, OMe).

Hydrogen bromide (40–45%) in acetic acid (6.5 ml) was added with stirring to the foregoing trityl ether (**2**) (14.1 g) in acetic acid (25 ml). After 3 min trityl bromide was removed by filtration, and the filtrate was poured with stirring into ice-cold, saturated, aqueous solid sodium hydrogen carbonate. Solid material was removed by filtration, the filtrate was extracted with chloroform (3 × 250 ml), and the chloroform solution was washed with saturated sodium hydrogen carbonate solution and twice with water, dried and concentrated to give a crystalline residue. Recrystallization from light petroleum (b.p. 40–65°) – ether (19:1) afforded methyl 2,3,4-tri-*O*-methyl-β-D-glucopyranoside (**6**) (5.29 g, 76%), m.p. 92–94°, $[\alpha]_D$ −24.2° (*c*, 2.0 in methanol) (lit. (18); m.p. 93–94°, $[\alpha]_D$ −22.9° (methanol)); ν_{max} (Nujol) 3520 cm^{-1} (OH); n.m.r. data ($CDCl_3$): τ 5.89 (1-proton doublet, splitting 7 Hz, H-1), 6.43 (3-proton singlet, C-1 OMe), 6.48–6.53 (3 × 3-proton singlets, 3 OMe).

Chromium trioxide (4.21 g) in 3.75 *N* sulfuric acid (20 ml) was added dropwise with stirring to methyl 2,3,4-tri-*O*-methyl-β-D-glucopyranoside (**6**) (3.6 g) in acetone (20 ml) at 5°. After 2 h at room temperature the reaction mixture was poured into ethanol (200 ml) containing ice and the supernatant liquid was decanted from the inorganic deposit into water. The aqueous solution was extracted with chloroform (12 × 100 ml) until the aqueous layer gave only a faint Molisch test. The chloroform extracts were washed once with water, dried, and concentrated to a crystalline residue which was recrystallized from ether – light petroleum (b.p. 30–60°) to yield methyl 2,3,4-tri-*O*-methyl-β-D-glucopyranosiduronic acid (**9**) (2.58 g, 77%), m.p. 132–134°, $[\alpha]_D$ −37.1° (*c*, 1.0 in water) (lit. (19); m.p. 133°, $[\alpha]_D$ −38° (water)); ν_{max} (Nujol) 2800 (broad), 1710 cm^{-1} (CO_2H).

Diazomethane (0.055 g) in ether (20 ml) was added with swirling to the foregoing acid (**9**) (0.25 g) in ether (10 ml). The t.l.c. showed complete disappearance of the acid after a few minutes. Concentration of the solution gave a crystalline mass which was recrystallized from light petroleum to give methyl (methyl 2,3,4-tri-*O*-methyl-β-D-glucopyranosid)uronate (**12**) (0.248 g, 94%), m.p. and mixed m.p. 52–53°, $[\alpha]_D$ −36.4°; ν_{max} (Nujol) 1750 cm^{-1} (ester C=O); n.m.r. data ($CDCl_3$): τ 5.88 (1-proton doublet, splitting 7 Hz, H-1), 6.25 (3-proton singlet, ester OMe), 6.45, 6.50, 6.53, 6.57 (4 × 3-proton singlets, 4 OMe). The g.l.c. showed that the ester was anomerically pure. The mass spectra of the ester by direct insertion on the probe and by g.l.c. – mass spectrometry were identical with that reported by Kováčik *et al.* (20) [M^+, 264].

Methyl 2,3-Di-O-methyl-6-O-trityl-β-D-glucopyranoside (3)

Methyl 2,3-di-*O*-methyl-β-D-glucopyranoside (**21**) (12.7 g) and trityl chloride (16.0 g) in pyridine (100 ml) were heated on a boiling-water bath for 1 h and kept at room temperature for 48 h. Water (3 ml) was added to the

Can. J. Chem. Downloaded from www.nrcresearchpress.com by 210.87.254.6 on 09/05/12
For personal use only.

solution which was kept for 1 h before being poured into ice-water to give a gummy deposit which was dissolved in chloroform. The chloroform solution was washed with water, dried, and concentrated with repeated addition of toluene in order to remove pyridine to give a syrup (28.2 g) which was shown by t.l.c. to contain the desired trityl ether and tritanol. Chromatography of the syrup on silica gel (1000 g) with light petroleum (b.p. 30–60°)–ether (2:1) as eluant to give methyl 2,3-di-*O*-methyl-6-*O*-trityl-β-D-glucopyranoside (**3**) (24.7 g, 93.2%) as a glassy solid, $[\alpha]_D$ −36.7° (*c*, 2.0 in chloroform) (lit. (22); $[\alpha]_D$ −35° (chloroform)) ν_{max} (Nujol) 3600 cm^{-1} (OH); n.m.r. data ($CDCl_3$): τ 2.52–2.97 (15-proton multiplet, trityl), 5.87 (1-proton doublet, splitting 7 Hz, H-1), 6.47, 6.48 (9 protons, 3 OMe).

*Methyl 4-O-Mesyl-2,3-di-O-methyl-6-O-trityl-β-D-glucopyranoside (**4**)*

The trityl ether (**3**) (9.53 g) was treated with methanesulfonyl chloride (2.0 ml) in pyridine (50 ml) for 14 h at room temperature. The mixture was poured into ice-water, saturated aqueous sodium hydrogen carbonate was added with vigorous stirring, the separated syrup was dissolved in chloroform, and the aqueous solution was extracted with chloroform. The combined chloroform extracts were washed with water, dried, and concentrated to a yellow syrup. Chromatography of the syrup on silica gel with chloroform as eluant gave methyl 4-*O*-mesyl-2,3-di-*O*-methyl-6-*O*-trityl-β-D-glucopyranoside (**4**) (10.4 g, 93%) as a syrup, $[\alpha]_D$ −10.8° (*c*, 2.0 in chloroform) (lit. (22); $[\alpha]_D$ −12° (chloroform)); ν_{max} (film) 1335, 1180 cm^{-1} (S=O); n.m.r. data ($CDCl_3$): τ 2.45–3.00 (15-proton multiplet, trityl), 5.87 (1-proton doublet, splitting 7 Hz, H-1), 6.45 (9-proton singlet, 3 OMe), 7.33 (3-proton singlet, mesyl).

*Methyl 4-O-Mesyl-2,3-di-O-methyl-β-D-glucopyranoside (**7**)*

Hydrogen bromide (40–45%) in acetic acid (4.6 ml) was added to the preceding mesyl ester (**4**) (10.22 g) in acetic acid (25 ml) and after 3 min trityl bromide was removed by filtration and the filtrate was worked-up in the usual way to give a crystalline solid (4.79 g) which was recrystallized from ether – light petroleum (b.p. 30–60°) to furnish methyl 4-*O*-mesyl-2,3-di-*O*-methyl-β-D-glucopyranoside (**7**) (4.40 g, 81.1%), m.p. 84.5–85.5°, $[\alpha]_D$ −29.4° (*c*, 2.0 in chloroform) (lit. (22); m.p. 85.5–86.5°, $[\alpha]_D$ −28° chloroform)); ν_{max} (Nujol) 3530 (OH), 1350, 1185 cm^{-1} (S=O); n.m.r. data ($CDCl_3$): τ 5.85 (1-proton doublet, splitting 7 Hz, H-1), 6.42, 6.46, 6.49 (3 × 3-proton singlets, 3 OMe), 6.89 (3-proton singlet, mesyl).

Anal. Calcd. for $C_{10}H_{20}O_8S$: C, 39.9; H, 6.71; S, 10.68. Found: C, 39.88; H, 6.84; S, 10.52.

*Methyl 4-O-Mesyl-2,3-di-O-methyl-β-D-glucopyranosiduronic acid (**10**)*

Chromium trioxide (1.20 g) in 3.75 *N* sulfuric acid was added dropwise with stirring to the mesyl ester (**7**) (1.20 g) in acetone at 5°, and the mixture was kept at room temperature for 2.5 h. The reaction mixture was neutralized with solid sodium hydrogen carbonate and extracted with chloroform (4 × 75 ml). The aqueous solution was acidified to p*H* 2 and extracted with chloroform (10 × 100 ml) until the aqueous layer gave only a faint Molisch test. The dried chloroform extract was concentrated to a crystalline residue which was recrystallized from ether – light petroleum (b.p. 30–60°) to give methyl 4-*O*-mesyl-2,3-di-*O*-methyl-β-D-glucopyranosiduronic acid (**10**) (1.05 g, 83.3%), m.p. 93–95°, $[\alpha]_D$ +10° (*c*, 2.0 in chloroform); ν_{max} (Nujol) 1740 (acid C=O), 1360, 1180 cm^{-1} (S=O); n.m.r. data ($CDCl_3$): τ 2.25 (1-proton, broad, CO_2H), 5.78 (1-proton doublet, splitting 7 Hz, H-1), 6.44, 6.47, 6.52 (3 × 3-proton singlets, 3 OMe), 6.97 (3-proton singlet, mesyl).

Anal. Calcd. for $C_{10}H_{18}O_9S$: C, 38.11; H, 5.77; S, 10.20. Found: C, 37.91; H, 5.82; S, 10.09.

*Methyl (Methyl 4-O-Mesyl-2,3-di-O-methyl-β-D-glucopyranosid)uronate (**13**)*

Diazomethane (0.15 g) in ether (5 ml) was added with swirling to the mesylated acid (**10**) (0.98 g) in ether (20 ml). The t.l.c. showed that reaction was complete after a few min, and work-up of the solution followed by recrystallization from ethanol gave methyl (methyl 4-*O*-mesyl-2,3-di-*O*-methyl-β-D-glucopyranosid)uronate (**13**) (0.96 g, 94%), m.p. 110–112°, $[\alpha]_D$ −31.6° (*c*, 2.0 in chloroform); ν_{max} (Nujol) 1750 (ester C=O), 1340, 1180 cm^{-1} (S=O); n.m.r. data ($CDCl_3$): τ 5.87 (1-proton doublet, splitting 7 Hz, H-1), 6.27 (3-proton singlet, ester OMe), 6.46, 6.50, 6.54 (3 × 3-proton singlets, 3 OMe), 6.99 (3-proton singlet, mesyl); M^+, 328.

Anal. Calcd. for $C_{11}H_{20}O_9S$: C, 40.24; H, 6.14; S, 9.77. Found: C, 40.11; H, 6.16; S, 9.64.

The g.l.c. on a column coated with silicone gum SE-30 at 152° showed that the ester was homogeneous (R_{Me} 3.16) and g.l.c. – mass spectroscopy, using the same column, gave a mass spectrum identical with that obtained by direct insertion on the probe (found: M^+, 328). The g.l.c. on column *a* gave a single peak of the same retention time (R_{Me} 1.31) as the unsaturated ester, methyl (methyl 4-deoxy-2,3-di-*O*-methyl-α-L-*threo*-hex-4-enopyranosid)uronate(**15**). The g.l.c. – mass spectrometry showed that this component gave a mass spectrum identical with that of the unsaturated ester (**15**) (Found: M^+, 232).

*Methyl 4-O-Acetyl-2,3-di-O-methyl-6-O-trityl-β-D-glucopyranoside (**5**)*

Methyl 2,3-di-*O*-methyl-6-*O*-trityl-β-D-glucopyranoside (**3**) (9.36 g) and acetic anhydride (2.3 ml) in pyridine (50 ml) were kept at room temperature for 14 h, when t.l.c. showed that reaction was complete. The mixture was poured into ice-water containing solid sodium hydrogen carbonate and the gummy deposit which separated was dissolved in chloroform. The chloroform solution was washed with saturated sodium hydrogen carbonate solution and with water, dried, and concentrated to give methyl 4-*O*-acetyl-2,3-di-*O*-methyl-6-*O*-trityl-β-D-glucopyranoside (**5**) (9.53 g, 93.4%), $[\alpha]_D$ −2.1° (*c*, 2.0 in chloroform), as a pale yellow syrup; ν_{max} (film) 1745, 1225 cm^{-1} (acetate); n.m.r. data ($CDCl_3$): τ 2.55–3.00 (15-proton multiplet, trityl), 6.43, 6.47, 6.57 (3 × 3-proton singlets, 3 OMe), 8.24 (3-proton singlet, OAc). The sample prepared for analysis crystallized on standing at 0° and had m.p. 92–94°.

Anal. Calcd. for $C_{30}H_{34}O_7$: C, 71.12; H, 6.76. Found: C, 71.16; H, 6.79.

*Methyl 4-O-Acetyl-2,3-di-O-methyl-β-D-glucopyranoside (**8**)*

Hydrogen bromide (40–45%) in acetic acid (4.3 ml) was

Can. J. Chem. Downloaded from www.nrcresearchpress.com by 210.87.254.6 on 09/05/12
For personal use only.

added to the foregoing acetylated trityl ether (**5**) (8.95 g) and after 3 min trityl bromide was removed by filtration and the reaction mixture was worked-up in the usual way to give a crystalline residue (3.90 g). The t.l.c. indicated the presence of a major component and two faster moving minor components. Column chromatography on silica gel with chloroform–ether (2:1) as eluant followed by recrystallization from ether – light petroleum (b.p. 30–60°) afforded methyl 4-*O*-acetyl-2,3-di-*O*-methyl-β-D-glucopyranoside (**8**) (3.48 g, 75%), m.p. 84.0–84.5°, $[\alpha]_D$ −57.1° (*c*, 2.0 in chloroform); ν_{max} (Nujol) 3480 (OH), 1735 cm^{-1} (ester C=O); n.m.r. data ($CDCl_3$): τ 5.84 (1-proton doublet, splitting 7 Hz, H-1), 6.40, 6.46, 6.49 (3 × 3-proton singlets, 3 OMe), 7.91 (3-proton singlet, OAc).

Anal. Calcd. for $C_{11}H_{20}O_7$: C, 50.00; H, 7.63. Found: C, 50.50; H, 7.69.

Methyl 4-O-Acetyl-2,3-di-O-methyl-β-D-glucopyranosiduronic acid (11)

Chromium trioxide (1.80 g) in 3.75 *N* sulfuric acid was added dropwise with stirring to the acetate (**8**) (1.57 g) in acetone (8 ml) at 5° and the mixture was stirred at room temperature for 2 h. The reaction mixture was neutralized with solid sodium hydrogen carbonate and extracted with chloroform. The aqueous solution was acidified to p*H* 2 and extracted with chloroform (10 × 100 ml) until the aqueous layer gave only a faint Molisch test. The chloroform extract was dried and concentrated to a pale yellow syrup which crystallized on standing. Recrystallization from ether – light petroleum (b.p. 30–60°) furnished methyl 4-*O*-acetyl-2,3-di-*O*-methyl-β-D-glucopyranosiduronic acid (**11**) (1.23 g, 75%), m.p. 101–103°, $[\alpha]_D$ −46.8° (*c*, 2.0 in chloroform); ν_{max} (Nujol) 1735, 1235 (acetate), 1700 cm^{-1} (shoulder) (CO_2H); n.m.r. data ($CDCl_3$): τ 0.22 (1-proton singlet, CO_2H), 5.73 (1-proton doublet, splitting 7 Hz, H-1), 6.44, 6.46, 6.49 (3 × 3-proton singlets, 3 OMe), 7.91 (3-proton singlet, OAc).

Anal. Calcd. for $C_{11}H_{18}O_8$: C, 47.28; H, 6.52. Found: C, 47.35; H, 6.51.

Methyl (Methyl 4-O-Acetyl-2,3-di-O-methyl-β-D-glucopyranosid)uronate (14)

Diazomethane (0.105 g) in ether (5 ml) was added with swirling to the foregoing acid (**11**) (0.605 g) in ether (8 ml). The t.l.c. showed that reaction was complete after a few minutes, and work-up of the solution followed by recrystallization from ethanol gave methyl (methyl 4-*O*-acetyl-2,3-di-*O*-methyl-β-D-glucopyranosid)uronate (**14**) (0.588 g, 92.6%), m.p. 97–99°, $[\alpha]_D$ −51.7° (*c*, 2.0 in chloroform); ν_{max} (Nujol) 1750 (broad) (ester C=O), 1240 cm^{-1} (acetate C—O); n.m.r. data ($CDCl_3$): τ 5.85 (1-proton doublet, splitting 7 Hz, H-1), 6.33 (3-proton singlet, ester OMe), 6.47–6.53 (3 × 3-proton singlets, 3 OMe), 7.97 (3-proton singlet, OAc); M^+, 292.

Anal. Calcd. for $C_{12}H_{20}O_8$: C, 49.29; H, 6.90. Found: C, 49.19; H, 6.97.

Methyl (Methyl 4-Deoxy-2,3-di-O-methyl-α-L-threo-hex-4-enopyranosid)uronate (15)

(*a*) Methanolic 1.14 *N* sodium methoxide (0.75 ml) was added with swirling to the mesylated ester (**13**) (0.25 g) in methanol (5 ml). After 5 min sodium methanesulfonate began to precipitate and after 20 min the reaction mixture was only slightly alkaline. Benzene (25 ml) was added and the solution was filtered and concentrated to a syrup which crystallized on standing. Recrystallization from cyclohexane furnished methyl (methyl 4-deoxy-2,3-di-*O*-methyl-α-L-*threo*-hex-4-enopyranosid)uronate (**15**) (0.154 g, 87%), which was homogeneous on g.l.c. and t.l.c. and had m.p. 51–53°, $[\alpha]_D$ +48° (*c*, 2.0 in methanol); ν_{max} (Nujol) 1735 (ester C=O), 1635 cm^{-1} (C=C); λ_{max} (MeOH) 236 nm (ε 6200); n.m.r. data ($CDCl_3$): τ 3.83 (1-proton doublet, splitting 4 Hz, H-4), 5.07 (1-proton doublet, splitting 4 Hz, H-1), 6.26 (3-proton singlet, ester methoxyl), 6.50, 6.53, 6.60 (3 × 3-proton singlets, 3 OMe); M^+, 232; g.l.c. – mass spectrometry of the ester gave a spectrum (M^+, 232) identical to that obtained by direct insertion on the probe.

Anal. Calcd. for $C_{10}H_{16}O_6$: C, 51.72; H, 6.94. Found: C, 51.66; H, 6.99.

(*b*) Ethanolic 0.5 *N* potassium hydroxide (1.1 ml) was added with swirling to the mesylated ester (**13**) (0.156 g) in ethanol (5 ml). After 10 min potassium methanesulfonate had precipitated and after 30 min the reaction mixture was only slightly alkaline. Benzene (20 ml) was added and the solution was filtered, concentrated, and recrystallized from cyclohexane to give the unsaturated ester (**15**) (0.092 g, 83.6%), m.p. and mixed m.p. 51–52°, $[\alpha]_D$ +48.5° (*c*, 2.0 in methanol); ν_{max} (Nujol) 1735 (ester C=O), 1635 cm^{-1} (C=C); λ_{max} 236 nm (ε 6170); M^+, 232.

(*c*) Sodium hydride (11 mg) in ether (5 ml) was added to the acetylated ester (**14**) (0.085 g) in ether (10 ml) and the mixture was stirred vigorously at room temperature for 70 min. A calculated quantity (1.2 *M* excess with respect to hydride) of benzoic acid (1.1 mg/ml) in ether was added to destroy excess of hydride. The solution was shaken with saturated aqueous sodium hydrogen carbonate, dried, and concentrated to a syrup. The t.l.c. showed the presence of a major component with the mobility of the unsaturated ester (**15**), traces of starting material (**13**), and a minor component of lower mobility. The g.l.c. on column *a* showed that the major component had the retention time (R_{Me} 1.32) of the unsaturated ester (**15**) and that a trace of starting material (R_{Me} 4.15) was present while g.l.c. – mass spectrometry of the major component gave a mass spectrum identical with that of the unsaturated ester (**15**). The syrup was separated by preparative layer chromatography to give the unsaturated ester (**15**) (0.044 g, 66%), m.p. and mixed m.p. 51–53°, whose i.r. and n.m.r. spectra were identical with those of previously prepared samples.

(*d*) 1,5-Diazabicyclo[5.4.0]undec-5-ene (0.020 g) was added to the acetylated ester (**14**) (0.130 g) in benzene (2.5 ml), and the solution was kept at room temperature for 5 days when t.l.c. indicated disappearance of starting material and g.l.c. on column *a* showed the presence of unsaturated ester (R_{Me} 1.35) as the major component together with an unknown substance (R_{Me} 1.78). The solution was neutralized by the addition of methanolic hydrogen chloride, diluted with chloroform, washed with water, dried, and concentrated to a syrup (0.094 g). The syrup was separated by preparative layer chromatography and the major fraction was recrystallized from cyclohexane to give the unsaturated ester (**15**) (0.085 g, 83%), m.p. and mixed m.p. 50–52°, which was homogeneous on t.l.c. and g.l.c.

(*e*) Sodium hydride (0.026 g) was dissolved in methyl sulfoxide (10 ml) and the solution of the methylsulfinyl carbanion was added slowly with stirring to the methylated

Can. J. Chem. Downloaded from www.nrcresearchpress.com by 210.87.254.6 on 09/05/12
For personal use only.

ester (**12**) (0.238 g) in methyl sulfoxide (15 ml) and the reaction mixture was kept at room temperature for 4 h when t.l.c. showed complete disappearance of starting material and g.l.c. on column *a* indicated the formation of unsaturated ester (R_{Me} 1.35) and an unknown substance C (R_{Me} 1.54). The reaction mixture was neutralized by the addition of a slight excess of 0.033 *N* hydrochloric acid, excess of acid was destroyed with sodium hydrogen carbonate, and the solution was extracted twice with chloroform. The dried chloroform extract was concentrated to a syrup which was separated by preparative layer chromatography to give a semi-crystalline material which was recrystallized from cyclohexane to give the unsaturated ester (**15**) (0.122 g, 58%), m.p. and mixed m.p. 51–53°, $[\alpha]_D$ +47° (*c*, 2.0 in methanol); ν_{max} (Nujol) 1740 (ester C=O), 1650 cm^{-1} (C=C); λ_{max} 236 nm (ε 6140); whose n.m.r. and mass spectra were identical to those of previously prepared samples.

A sample of the unsaturated ester (**15**) was treated with methylsulfinyl carbanion in methyl sulfoxide under the above conditions. The g.l.c. showed unchanged starting compound and no other detectable product.

*Action of Other Bases on Methyl (Methyl 4-O-Acetyl-2,3-di-O-methyl-β-D-glucopyranosid)uronate (**14**)*

Methanolic 1.42 *N* sodium methoxide (0.30 ml) containing 5% of 2,2-dimethoxypropane was added to acetylated ester (**14**) (0.017 g) in methanol (1 ml) containing 5% of 2,2-dimethoxypropane and the reaction mixture was kept at room temperature. Aliquot portions were withdrawn, neutralized with methanolic hydrogen chloride, and diluted with chloroform, and the chloroform solution was washed with water, dried, concentrated, and examined by g.l.c. and t.l.c. After 90 min starting material had virtually disappeared and g.l.c. on column *a* showed the formation of unsaturated ester (**15**) (R_{Me} 1.33) and an unknown substance A (R_{Me} 2.55) in the relative proportions of 1.3:1. The t.l.c. showed the presence of an immobile component corresponding to acidic products in addition to two mobile components. Since the g.l.c. columns failed to reveal even standard samples of methyl (methyl 2,3-di-*O*-methyl-β-D-glucopyranosid)uronate, the presence of this compound in the reaction mixture was demonstrated by re-acetylation with acetic anhydride in pyridine. The g.l.c. examination of this product on column *a* showed the presence of unsaturated ester (**15**), unknown substance A, and acetylated ester (R_{Me} 4.17) in the relative proportions of 1.3:1:4.1.

Potassium *t*-butoxide (0.012 g) in methyl sulfoxide (0.6 ml) was added with stirring to acetylated ester (**14**) (0.018 g) in methyl sulfoxide (1 ml). The reaction products were examined in the same general way as above and after 90 min starting material had virtually disappeared. Re-acetylation of the reaction product followed g.l.c. on column *b* showed the presence of unsaturated ester (**15**) (R_{Me} 1.10) and acetylated ester (**14**) (R_{Me} 3.70) in the relative proportions of 1:1:4.

The acetylated ester (**14**) was treated with other bases under the conditions summarized in Table 1 and reactions were assessed by g.l.c. and t.l.c.

*Action of Other Bases on Methyl (Methyl 2,3,4-Tri-O-methyl-β-D-glucopyranosid)uronate (**12**)*

Methanolic 1.14 *N* sodium methoxide (0.18 ml) containing 5% of 2,2-dimethoxypropane was added with stirring to methylated ester (**12**) (0.018 g) in methanol (2 ml) containing 5% of 2,2-dimethoxypropane. The reaction mixture was worked-up after 90 min at room temperature and the u.v. spectrum showed a broad band at 236 nm. The g.l.c. examination of the reaction product on column *a* showed the presence of methylated ester (**12**), unsaturated ester (**15**) (R_{Me} 1.32), and unknown substances D (R_{Me} 0.87) and E (R_{Me} 1.22) in the relative proportions of 10.5:1.9:1.0:2.9. When examined by g.l.c. – mass spectrometry the peak of R_{Me} 1.32 gave a mass spectrum identical to that of the unsaturated ester (**15**). The t.l.c. showed a similar mixture of products together with an immobile component characteristic of uronic acids. The reaction was repeated at 60° for 90 min and g.l.c. of the products showed the presence of the same volatile components in the relative proportions of 5.9:2.8:1.0:2.8.

Potassium *t*-butoxide (0.010 g) in methyl sulfoxide (2 ml) was added with stirring under a stream of nitrogen to methylated ester (**12**) (0.015 g) in methyl sulfoxide (2 ml). Starting material had disappeared after 70 min at room temperature and g.l.c. of the reaction product on column *a* showed the presence of unsaturated ester (**15**) and unknown compounds C* (R_{Me} 0.86) and D* (R_{Me} 1.55) in the relative proportions of 25.6:1.0:2.6.

The methylated ester (**12**) was treated with other bases under the conditions summarized in Table 2 and reactions were assessed by g.l.c. and t.l.c.

The authors wish to acknowledge the award of a Province of Ontario Graduate Fellowship (to P.E.B.), a grant from The Institute of Paper Chemistry, Appleton, Wisconsin, under the Pioneering Research Program, and financial support from the National Research Council of Canada.

1. P. Albersheim, H. Neukom, and H. Deuel. Arch. Biochem. Biophys. **90**, 46 (1960).
2. P. Heim and H. Neukom. Helv. Chim. Acta, **45**, 1735, 1737 (1962).
3. A. J. Barrett and D. H. Northcote. Biochem. J. **94**, 617 (1965).
4. R. W. Stoddart, A. J. Barrett, and D. H. Northcote. Biochem. J. **102**, 194 (1967).
5. C. W. McCleary, D. A. Rees, J. W. B. Samuel, and I. W. Steele. Carbohydr. Res. **5**, 492 (1967).
6. C. J. Lawson, C. W. McCleary, H. I. Nakada, D. A. Rees, I. W. Sutherland, and J. F. Wilkinson. Biochem. J. **115**, 947 (1969).
7. J. Kiss. Intern. Symp. Chem. Nat. Prod., 5th, London. Abstracts, E9, 249 (1968).
8. J. Kiss. Tetrahedron Lett. **1983** (1970).
9. E. Zissis and H. G. Fletcher, Jr. Carbohydr. Res. **12**, 361 (1970).
10. J. Kiss. Carbohydr. Res. **10**, 328 (1969).
11. H. W. H. Schmidt and H. Neukom. Tetrahedron Lett. **7**, 2011 (1969).
12. A. J. Parker. Quart. Rev. **16**, 163 (1962).
13. R. W. Alder, P. S. Bowman, W. R. S. Steele, and D. R. Winterman. Chem. Commun. 723 (1968).
14. H. Hashimoto, T. Sekiyama, H. Sakai, and J. Yoshimura. Bull. Chem. Soc. Japan, **44**, 235 (1971).
15. T. Purdie and J. C. Irvine. J. Chem. Soc. **83**, 1021 (1903).

16. R. KUHN, H. TRISCHMANN, and I. LÖW. Angew. Chem. **67**, 32 (1955).
17. B. HELFERICH and J. BECKER. Ann. **440**, 1 (1924).
18. J. C. IRVINE and J. W. H. OLDHAM. J. Chem. Soc. **119**, 1744 (1921).
19. S. W. CHALLINOR, W. N. HAWORTH, and E. L. HIRST. J. Chem. Soc. **258**, (1931).
20. V. KOVÁČIK, Š. BAUER, J. ROSÍK, and P. KOVÁČ. Carbohydr. Res. **8**, 282 (1968).
21. J. W. OLDHAM. J. Am. Chem. Soc. **56**, 1360 (1934).
22. F. W. PARRISH, R. C. CHALK, and L. LONG, JR. J. Org. Chem. **33**, 3165 (1968).
23. J. W. LLEWELLYN and J. M. WILLIAMS. Carbohydr. Res. **22**, 221 (1972).

Can. J. Chem. Downloaded from www.nrcresearchpress.com by 210.87.254.6 on 09/05/12
For personal use only.

An Addition Reaction of Indane with Nitric Acid in Acetic Anhydride

A. FISCHER, C. C. GREIG, A. L. WILKINSON, AND D. R. A. LEONARD
Department of Chemistry, University of Victoria, Victoria, British Columbia

Received February 7, 1972

cis- and *trans*-5-Acetoxy-7*a*-nitro-5,7-dihydroindane are formed as well as the 4- and 5-nitroindanes when indane is reacted with nitric acid and acetic anhydride. These adducts both decompose on standing by loss of nitrous acid forming 5-acetoxyindane. The *cis* isomer is obtained in greater amount and it undergoes elimination less readily than the *trans*.

Les acétoxy-5 nitro-7*a* dihydro-5,7 indanes *cis* et *trans* sont formés ainsi que les nitro-4 et -5 indanes quand l'indane est mis en réaction avec l'acide nitrique et l'anhydride acétique. Ces produits d'addition se décomposent au repos par perte d'acide nitreux en donnant l'acétoxy-5 indane. L'isomère *cis* est obtenu en plus grosse quantité et subit l'élimination moins facilement que le *trans*.

Canadian Journal of Chemistry, **50**, 2211 (1972)

Can. J. Chem. Downloaded from www.nrcresearchpress.com by 210.87.254.6 on 09/05/12
For personal use only.

Reaction of indane with nitric acid and acetic anhydride has been reported to give 5-acetoxyindane as well as the expected 4- and 5-nitroindanes (1). The similar formation of 3,4-xylyl acetate (4-acetoxy-*o*-xylene) and of 3,4,5-trimethylphenyl acetate (5-acetoxyhemimellitene) when *o*-oxylene and 1,2,3-trimethylbenzene (hemimellitene) are treated with nitric acid and acetic anhydride (2) has recently been shown to occur via the 1,4-diene adducts, **1** and **2**, each of which occurs in *cis* and *trans* diastereoisomeric forms (3, 4). It is these dienes, together with the nitroarenes, that are the primary products of the reactions of the arenes. Thermolysis of the dienes, or heating them in acetic acid causes the elimination of nitrous acid and the formation of the aryl acetate which is thus a product of secondary reaction. These results have prompted us to re-examine the reaction of indane.

When indane was reacted with nitric acid in acetic anhydride at temperatures below $-20°$ the product isolated after removal of the anhydride exhibited n.m.r. absorption in the region (τ) 3.5–4.6 p.p.m., indicative of the presence of a diene, as well as absorption in the aromatic region. The predominant diene **3** crystallized when the product was allowed to stand overnight at $-20°$. The diastereoisomer **4** was obtained when the residue was subjected to low temperature chromatography on alumina. The structures assigned to the dienes are based on spectral and chemical evidence. The i.r. absorptions at 1540 and 1380 cm^{-1} and at 1735 and 1230 cm^{-1} establish the presence of nitro and acetoxy groups in **3**. Diene **4** has corresponding i.r. absorptions at 1550 and 1375 and at 1750 and 1225 cm^{-1}. The n.m.r. absorption in the region τ 3.5–4.5 p.p.m., which integrated for four protons, and the absence of absorption in the aromatic region show that **3** and **4** are dienes. That they are 1,4- rather than 1,3-dienes is indicated by the u.v. absorption: λ_{max} is 202 nm (ε 980 m^2 mol^{-1}) for **3** and 199.5 nm (ε 1440 m^2 mol^{-1}) for **4**. 1,3-Cyclohexadienes absorb above 250 nm (5). There are three structurally isomeric 1,4-diene adducts (**3**/**4**, **5**, and **6**), each of which is potentially capable of existing as *cis*–*trans* diastereoisomers, which might be obtained by addition of nitro and acetoxy groups to indane. Structure **6** is not compatible with the coupling constants derived from the n.m.r. spectra (see below) and on chemical grounds is an unlikely structure since it contains an acid proton α to the nitro group. Such a proton would be readily removed by the basic reagents used during work-up with concomitant elimination of the acetate group and formation of 4-nitroindane. Structures **3**/**4** and **5** are consistent with the spectral information, but **5** should readily eliminate acetic acid, like **6**, to form 5-nitroindane. However, elimination of acetic acid does not occur under the strongly basic work-up conditions, and the elimination which does occur on standing results in the loss of nitrous acid and the formation of 5-acetoxyindane. Thus only the structure **3**, and its diastereoisomeric structure **4** are consistent with both the spectral evidence and the chemistry of the dienes.

The assignment of structure **3** to the diene produced in greater amount, *i.e.* that which crystallized preferentially from the reaction product, and of structure **4** to the less easily

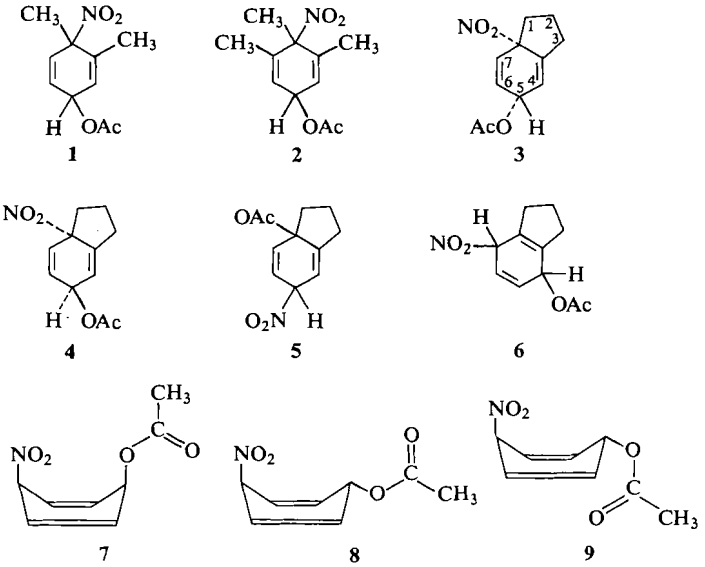

isolated diene is based on the magnitudes and signs of the three- and four-bond vinyl-allylic proton coupling constants of each diene. Agreement between measured and calculated dipole moments provides independent support for these assignments. Dreiding models of the indane adducts show that the five-membered ring locks the six-membered diene ring into a fixed boat conformation.[1] The dihedral angle (ϕ) between the $H_5—C_5—C_6$ and $C_5—C_6—H_6$ planes is $\sim 27°$ in the *cis* adduct **3** and $\sim 93°$ in the *trans* adduct **4**. The dependence of the three-bond and four-bond coupling constants of an allylic system on ϕ are given by Garbisch's equations (8) which are written in the following more simple equivalent forms.

$$\left.\begin{array}{ll}[1] & {}^3J = 4\cos^2\phi + 2.6 \\ [2] & {}^4J = 3.9\cos^2\phi - 2.6\end{array}\right\} 0^0 \leqslant \phi \leqslant 90°$$

$$\left.\begin{array}{ll}[3] & {}^3J = 9\cos^2\phi + 2.6 \\ [4] & {}^4J = 2.6\cos^2\phi - 2.6\end{array}\right\} 90° \leqslant \phi \leqslant 180°$$

[1]Dreiding models of 1,4-cyclohexadiene suggest that there are two rigid boat forms which are interconvertible by a ring flip. The models also suggest that there would be considerable angle strain in planar cyclohexadiene. Although the boat form for 1,4-cyclohexadiene has been supported, or at least assumed, by some authors (6) there is evidence which points to a planar structure (7). In the case of **3** and **4**, where the cyclohexadiene has a cyclopentene ring fused at the 3,4-bond, the requirement of planarity in the cyclopentene ring would force the cyclohexadiene ring into the boat form, even if this were not the preferred form in the unsubstituted 1,4-cyclohexadiene.

For the specified angles, J_{45} and J_{56} (three-bond coupling constants) are predicted to be 5.8 Hz for the *cis* adduct **3** and 2.6 Hz for the *trans* adduct **4**. The four-bond coupling constant J_{57} is predicted to be 0.5 Hz for the *cis* adduct and -2.6 for the *trans*. Comparison of these predicted values and those observed (Table 1) clearly shows that diene **3** is indeed the *cis* adduct and diene **4** is its *trans* isomer. The difference between the J_{45} and J_{56} values of **3**, together with the fact that these values are lower than predicted, may reflect a distortion of the diene ring caused by the repulsion between the diaxial nitro and acetoxy groups. Such distortion may be expected to be larger at C-6 than C-4 because the latter is closer to the restraining fused cyclopentene ring. The structural assignment is not affected by the choice of the particular set of coupling constants for each diene. Although there are two solutions in each case the only significant difference between the two pairs is in the sign of the J_{46} value. In saturated systems coupling constants between protons in the equatorial "W" relationship (as are the H-4 and -6 in **3** and **4**) are positive and in the range 1–2 Hz (9) and we therefore suggest that the first (for **3**) and third (for **4**) solutions in Table 1 are the more likely.

Mention has been made above that structure **6** is inconsistent with the coupling constants of Table 1. For the purposes of the immediately following argument we take the subscripts in the headings of Table 1 as proton labels only and not

Can. J. Chem. Downloaded from www.nrcresearchpress.com by 210.87.254.6 on 09/05/12
For personal use only.

TABLE 1. Computed coupling constants (Hz) and chemical shifts* (τ)

Compound	J_{45}	J_{46}	J_{47}	J_{56}	J_{57}	J_{67}	ν_4	ν_5	ν_6	ν_7	r.m.s.†
3	5.03	1.37	−0.12	4.38	−0.02	9.71	3.94	4.36	3.83	3.60	0.14
3	5.11	−1.42	0.00	4.31	−0.02	9.72	3.94	4.36	3.83	3.60	0.14
4	2.28	1.86	−0.33	2.37	−2.48	9.78	4.08	4.15	3.84	3.75	0.09
4	2.34	−2.00	0.39	2.33	−2.44	9.78	4.08	4.15	3.84	3.75	0.10

*Subscripts are both proton labels and position indicators.
†Deviation (Hz) of the calculated line positions from those observed.

as position indicators and the compound numbers in that table as labels of parameter sets. The large coupling (J_{67}) must be assigned to the vinyl protons of **6**. The other two protons are thus 4 and 5. Either J_{47} or J_{57} must be a three-bond allylic coupling constant the minimum value for which is 2.6 Hz according to Garbisch's equations. This requirement, which is clearly inconsistent with the J_{47} and J_{57} values of Table 1, follows from the structural requirement of **6** that either protons 4 and 7 or 5 and 7 be adjacent. Structure **6** is therefore ruled out.

The measured dipole moment of **3** (2.56 D) is markedly lower than that of **4** (4.09 D). Dipole moments for **3** and **4** were calculated on the assumption that the hexadiene ring is in the rigid boat form. The calculations assume that (*i*) the acetoxy group is in the *s-trans* conformation (10) and that the group moment of the CH—$OCOCH_3$ fragment is the same as the dipole moment of methyl acetate (1.70 D orientated at 66° to the C—O bond with the negative end towards carbon (10)); (*ii*) the group moment of the C—NO_2 fragment is the same as the dipole moment of nitromethane (3.10 D directed along the C—N bond with the positive end towards carbon (10)); (*iii*) the group moment of the rest of the molecule, involving only C—H and C—C bonds, is negligible; (*iv*) the angle between the 1,4-diaxial bonds, estimated from Dreiding models, is 10°. We suggest that the predominant conformation of **3** is as depicted in partial structure **7** with the carbonyl oxygen at the extreme position from the nitro group. Severe steric interactions between carbonyl and nitro oxygens should prevent free rotation above the acetate C—O bond and destabilize structures in which the carbonyl oxygen approaches closely to the nitro group. In contrast conformations **8** and **9** of **4** should both be allowed as there are no marked steric interactions introduced as the acetate group rotates. Thus **4** would be expected to be a free rotation

TABLE 2. Measured and calculated dipole moment values (μ)

Compound	μ*	μ†	μ_{calcd}‡
3	2.56	2.51	2.54
4	4.09	4.04	3.91

*Derived using [6] and [7].
†Derived using [8].
‡Calculated from group moments as described in the text.

mixture. There is excellent agreement between the calculated dipole moments for these conformations and the measured values for **3** and **4** (Table 2) confirming the structural assignments of **3** and **4** based on the n.m.r. coupling constants.

It was possible to detect the presence of each diene in the reaction product by n.m.r. However, because the spectra of the dienes overlap, it was not possible to determine the ratio in which the dienes were produced, although it was obvious that **3** was formed in greater amounts than **4**. The **3**:**4** ratio (4:1) was determined by measurement of the dielectric constant of the product diene mixture, after separation from nitroindanes and a small amount of acetoxyindane by chromatography. Both dienes decompose on standing by elimination of nitrous acid to give 5-acetoxyindane. Decomposition is accelerated by acids. The relative reactivity of **4**:**3** in carbon tetrachloride containing 1% trifluoroacetic acid is 2.6:1. The greater reactivity of the *trans* adduct parallels the observations of Cristol *et al.* (11) on the thermal and base-catalyzed decompositions of *cis*- and *trans*-1,5-dichloro-9,10-dihydro-9,10-anthradiols and their derivatives. Thus, the *trans* diacetate and dibenzoate decomposed at their melting points to give the 1,5-dichloro-9-anthryl acetate and benzoate respectively while the *cis* isomer did not decompose. Similarly, in the base-catalyzed 1,4-conjugate elimination, the *trans* isomer was much more reactive than the *cis*.

It seems likely that the dienes are formed via

Can. J. Chem. Downloaded from www.nrcresearchpress.com by 210.87.254.6 on 09/05/12
For personal use only.

attack of the nitrating electrophile at the position of attachment of the five-membered ring (*ipso* attack). Perrin and Skinner (12) have discussed the possible reaction paths from a σ complex (Wheland) intermediate formed by attack at the *ipso* position, but they have not explicitly recognized the possibility encountered in the present work, *viz.* combination of a nucleophile with the σ complex leading to an overall addition reaction, eq. 5. It is consistent with this two-step

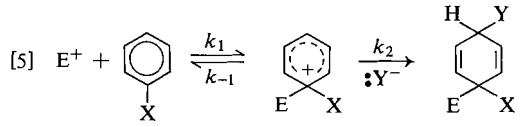

mechanism that a mixture of diastereoisomeric dienes is obtained. What is not obvious is why the *cis* diene should predominate: Dreiding models suggest that steric interactions in **3** (*cf.* partial structure **7**) should be more marked than in **4** (partial structures **8** and **9**) and this should also be true for the respective transition states leading to **3** and **4**. Exclusive formation of *cis* adduct (**3**) could be accounted for by a one-step concerted cycloaddition mechanism but this mechanism cannot account for the formation of the *trans* isomer (**4**). We therefore regard the two-step mechanism, [5], as being the more likely. Earlier work (13) on the kinetics of the acetoxylation reaction of *o*-xylene demonstrated that nitration and acetoxylation (*i.e.* diene formation) have a common intermediate whose formation is rate determining.[2] It is now clear that a nitrating electrophile, and in particular, nitronium ion, the most likely species, would be a common intermediate if the addition followed the two-step path. Addition, by this mechanism, is a nitration which has been diverted in the final step. It would be more difficult to propose a common intermediate if the addition were a concerted process with a mechanism necessarily quite different from that of nitration.

Using the product ratios of Vaughan *et al.* (1) (27 mol % 5-acetoxyindane, 19 mol % 4-nitroindane, and 54 mol % 5-nitroindane) and making the assumption that the fraction of acetoxy product is equal to the fraction of dienes initially formed, the relative reactivity of the 3*a*, 4, and 5 positions of indane to attack by the nitrating electrophile is 1.4:1:2.8. Change of the electrophile will change the relative reactivity of the positions because of change in reaction constant (Hammett ρ) but, unless there are large changes in the relative steric effects, the reactivity order $5 > 3a > 4$ should be the same. Thus a significant fraction of *ipso* attack is to be expected in other electrophilic substitution reactions of indane which give detectable amounts of the 4-substituted indane. Products of *ipso* attack, *e.g.* diene products or products involving diene intermediates, were not observed in the bromination of indane (1). It is possible that such products were formed but not detected but it is more likely that in [5] for bromination $k_{-1} > k_2[Y^-]$ and thus the *ipso* σ intermediate dissociates to reactants before combination with the nucleophile occurs to form an addition product. Bromination, in contrast to nitration, is normally reversible. We attribute the apparent ease with which addition occurs in the course of nitration to the slowness of the reverse reaction of the initial electrophilic attack, *i.e.* $k_2[AcOH] \gg k_{-1}$. Addition does not occur when the electrophile attacks the 4 or 5 positions because in these cases the σ complex is readily deprotonated to give the aromatic substitution product, a reaction pathway not open to the complex formed by *ipso* attack.

Nitrous acid is a weak acid and nitrite anion is not a good leaving group. It is therefore not surprising that the loss of nitrous acid from the diene adduct should be acid-catalyzed. Present information does not allow a distinction to be made between a two-step mechanism involving a σ complex intermediate (E1 type) and a concerted elimination (E2 type).

[2]The kinetics were followed by shaking samples of the reaction mixture with 2 *M* sodium hydroxide solution and extraction of the nitroarenes with carbon tetrachloride. The concentrations of phenoxide ion, in the aqueous phase, and nitroarenes, in the extract, were determined by u.v. spectroscopy. The phenoxide ion was formed by hydrolysis of the phenyl acetate. The latter was presumably formed by elimination of nitrous acid from the diene adduct. The diene adduct could not have eliminated nitrous acid before the sample for analysis was added to the sodium hydroxide since the product, 3,4-dimethylphenylacetate, reacts further with nitric acid to give a nitrodienone (14). Considerable heat was evolved when the sample (acetic anhydride solvent) was added to the sodium hydroxide solution and it is not surprising that decomposition of adduct to phenyl acetate and further hydrolysis of the latter to phenoxide was substantially quantitative. In ref. 13, it is observed that the ratio of the rate of formation of phenyl acetate to that of nitroarenes is constant when the absolute rates vary over a wide range. The observation should be restated that there is a constant ratio of the rate of formation of diene adduct to that of nitroarene.

Can. J. Chem. Downloaded from www.nrcresearchpress.com by 210.87.254.6 on 09/05/12
For personal use only.

Can. J. Chem. Downloaded from www.nrcresearchpress.com by 210.87.254.6 on 09/05/12
For personal use only.

Experimental

The u.v. spectra were determined on a Unicam SP 700 spectrometer. The i.r. spectra were determined on a Perkin–Elmer Model 337 spectrometer calibrated with polystyrene. The n.m.r. spectra were determined on Varian HA-60-IL, Varian XL-100, and Perkin–Elmer R12A spectrometers with tetramethylsilane as internal standard. Molecular weights were determined in methylene dibromide using a Hitachi Perkin–Elmer Model 115 molecular weight apparatus. Microanalyses were by Mr. M. Yang, Simon Fraser University, Burnaby, B.C. Melting points are uncorrected. Alumina was deactivated with 3% of 10% acetic acid.

cis (3) and trans (4) 5-Acetoxy-7a-nitro-5,7-dihydroindane

Fuming nitric acid (300 cm^3) was distilled at 1 mm from urea (10 g) and sulfuric acid (500 cm^3). Distilled nitric acid (3.2 cm^3, 0.075 mol) was added to acetic anhydride (20 cm^3) at −30°. The solution was allowed to warm to 0° to complete the formation of acetyl nitrate (15) and then re-cooled to −30°. This solution was added slowly, with stirring, to a solution of indane (6 cm^3, 0.05 mol) in acetic anhydride (20 cm^3) maintained at a temperature below −60°. The mixture was allowed to warm to −30° and maintained at that temperature for 10 min. It was then cooled in Dry Ice–acetone, ether (100 cm^3) added, and ammonia condensed into the solution. The cooling bath was removed, excess ammonia allowed to evaporate, and the residue poured onto ice and extracted with ether. The ether extract was washed (×6) with water, dried over magnesium sulfate, and the ether evaporated at 14°. The residue was allowed to stand overnight at −20° and the crystals which formed were washed with cold pentane and recrystallized from pentane to give white crystals of **3**, m.p. 61.5–62.5°, u.v. max (CH_3OH) 202 nm (ε 980 m^2 mol^{-1}); i.r. (Nujol) 1735 and 1230 ($OCOCH_3$), 1540 and 1380 cm^{-1} (NO_2); n.m.r. (CCl_4) τ 3.60 (d, 1, H-7), 3.83, 3.94 (m, 2, H-6 and -4), 4.4 (m, 1, H-5), 7.3, 8.2 (m, 6, $CH_2CH_2CH_2$), 7.99 p.p.m. (s, 3, $OCOCH_3$).

Anal. Calcd. for $C_{11}H_{13}NO_4$ (M_r 223): C, 59.19; H, 5.87; N, 6.28. Found (218): C, 59.28; H, 6.03; N, 6.19.

The combined mother liquors were evaporated at 14° and the residue chromatographed on alumina maintained below −30°. Elution with pentane gave a mixture of 4- and 5-nitroindane.

4-Nitroindane has two triplets in the benzylic region (16) with the characteristic lower field one centered at τ 6.7 p.p.m. 5-Nitroindane crystallized from the mixture, i.r. (Nujol) 1550 and 1340 cm^{-1} (NO_2); n.m.r. ($CDCl_3$) τ 2.3 (m, 2, Ar-*H*), 2.92 (m, 1, Ar-*H*), 7.2 (t, 4, $ArCH_2$), 8.0 p.p.m. (m, 2, $CH_2CH_2CH_2$). The benzylic protons were decoupled from the aromatic protons by irradiation at 7.2 p.p.m. Coupling constants and chemical shifts were evaluated for the decoupled spectrum following the procedure described below for the dienes and gave the data $\nu_4 = 2.26$, $\nu_6 = 2.30$, $\nu_7 = 2.95$, $J_{46} = 2.20$, $J_{47} = 0.65$, $J_{67} = 8.15$. The chemical shift values show that there are two low field protons which must therefore be ortho to the nitro group and that the compound must be 5-nitroindane rather than its 4 isomer. The coupling constants show that the aromatic protons are in the *ortho*, *meta*, and *para* relationship which is consistent only with a 5-substituted indane.

Further elution was with ether–pentane mixtures. Trace amounts of 5-acetoxyindane were eluted with 10% ether–pentane, i.r. (film) 1750 and 1220 cm^{-1} ($OCOCH_3$), n.m.r. (CCl_4) τ 3.2 (m, 3, Ar-*H*), 7.2 (t, 4, Ar-CH_2), 7.90 (s, 3, $OCOCH_3$), 7.9 p.p.m. (m, 2, $CH_2CH_2CH_2$). The benzylic protons were decoupled from the aromatic protons by irradiation at 7.19 p.p.m. Coupling constants and chemical shifts were evaluated from the decoupled spectrum and gave $\nu_7 = 2.99$, $\nu_6 = 3.34$, $\nu_4 = 3.22$, $J_{67} = 7.90$, $J_{47} = 0.50$, $J_{46} = 2.15$. The coupling constants show that the three protons are in the *ortho*, *meta*, and *para* relationship and are thus only consistent with a 5-substituted indane.

The dienes **3** and **4** were eluted with 20% ether–pentane. The diene fraction was rechromatographed using an alumina:substrate ratio of 150:1 and pure diene **4** was eluted with 18% ether–pentane. Diene **4** gave white crystals from pentane, m.p. 57.5–58.5°, u.v. max (CH_3OH) 199.5 nm (ε 1440 m^2 mol^{-1}); i.r. (Nujol) 1750 and 1225 ($OCOCH_3$), 1550 and 1375 cm^{-1} (NO_2); n.m.r. (CCl_4) τ 3.75, 3.84 (m, 2, H-7 and -6), 4.08, 4.15 (m, 2, H-4 and -5), 7.4, 8.15 (6, CH_2CH_2-CH_2), 7.97 p.p.m. (s, 3, $OCOCH_3$).

Anal. Calcd. for $C_{11}H_{13}NO_4$: C, 59.19; H, 5.87; N, 6.28. Found: C, 58.76; H, 5.70; N, 6.46.

The n.m.r. spectrum of each diene was taken at 100 MHz with the cyclopentane ring protons decoupled from the diene protons by irradiation at τ 7.50 for **3** and τ 7.52 for **4**. Line positions for the diene protons were measured and corrected for Bloch–Siegert shift (17). The computer program UEAITR (18) was used to refine estimated coupling constants and chemical shifts. Two sets of parameters (Table 1) led to good agreement between the calculated and the observed spectra. Not all of the peaks in the diene region could be resolved and this difficulty was compounded by the broadening of the spectrum caused by the decoupling of the cyclopentane ring protons. For these reasons J_{47} and J_{57} of **3** are not significantly different from 0.

Total yield of reaction products (nitro compounds and dienes) was in the range 75–85%. Gas–liquid chromatography of the decomposition product of each diene (SE 30 column at 200°) showed only 5-acetoxyindane and none of the nitroindanes. Integration of the n.m.r. spectrum of the product mixture in the diene and aromatic regions indicated that about 48% of the mixture was dienes. This is rather larger than the 26% of 5-acetoxyindane obtained by Wright after thermolysis of the reaction product. It is likely that analysis of dienes by n.m.r. is less accurate than Wright's chromatographic analysis of the acetate.

The relative reactivity of **3** and **4**, at 27° in carbon tetrachloride containing 1% trifluoroacetic acid as catalyst, was determined by following the rate of disappearance of the acetate peak of each (7.99 and 7.97 p.p.m., respectively) in the HA 60 spectrometer. At the same time the appearance of the acetate peak (7.90 p.p.m.) in the product 5-acetoxyindane was also followed. First order plots (in which concentration was taken as proportional to measured peak height) gave the rate constants $10^5k_3 = 3.7 \pm 0.6$ s^{-1}; $10^5k_4 = 9.6 \pm 0.9$ s^{-1}; $10^5k_{ArOAc} = 12 \pm 1$ s^{-1}. Within experimental error the rate constant for formation of the acetoxyindane is equal to the sum of the rate constants for disappearance of **3** and **4** and the relative reactivity of **4** to **3** is 2.6:1.

Dielectric Constant Measurements and Dipole Moment Calculations

Dielectric constants of benzene solutions of each diene were determined using a Sargent Chemical Oscillometer Model V with inductive cell-compensator. The compensator was adjusted so that a linear relationship between oscillometer reading (capacitance) and (ε − 1) for benzene, chlorobenzene, and dichloroethane was obtained. Diene (100 mg)

was added in weighed increments (15 mg) to a known weight (7 g) of benzene in the capacitance cell and the instrument reading determined after each addition. The slope and intercept of the linear plot of instrument reading *vs.* mole fraction of diene (n_2) was obtained by a least squares fit and the ratio of these is

$$\frac{1}{\varepsilon_1 - 1} \cdot \frac{\Delta\varepsilon}{\Delta n_2} = \frac{\alpha}{\varepsilon_1 - 1}$$

(subscript 1 refers to solvent benzene and subscript 2 to solute diene). The density of the solution after each addition of diene was measured with a Westphal balance and a plot of specific volume (v) *vs.* n_2 gave the slope β. The dipole moments were then evaluated using the expression (19)

$$[6] \quad \mu = 0.01281\ (P_{2\infty} - P_e - P_a)^{1/2} T^{1/2}$$

where

$$[7] \quad P_{2\infty} = \frac{3\alpha v_1 M_1}{(\varepsilon_1 + 2)^2} + (v_1 M_2 + \beta M_1)\frac{\varepsilon_1 - 1}{\varepsilon_1 + 2}$$

P_e was calculated from bond contributions (20) and P_a was taken as zero (21). The dipole moment was also evaluated from Higasi's simple formula, for benzene solvent at 25° (22, 23).

$$[8] \quad \mu = 0.828\alpha^{1/2}$$

Dipole moments are shown in Table 2. Dipole moments determined in solution are normally reported to ±0.05 to 0.1 D. Values of α were precise to 2% leading to a 1% precision of the derived moment and we therefore believe that the measured moments are within the accepted normal precision. It is to be noted that the values obtained using Higasi's simple expression agree with those evaluated from the more elaborate formula within the accepted precision.

For the mixture of isomers the polarization is related to the polarizations of each isomer by the expression,

$$[9] \quad P = n_3 P_3 + n_4 P_4$$

where n_3 is the mole fraction of **3** in the mixture of **3** and **4**. Since β has the same value for **3** and **4** it follows from [7] that dP/dn is proportional to $d\alpha/dn$ and hence the isomer ratio is given by

$$[10] \quad \frac{n_3}{n_4} = \frac{\alpha - \alpha_4}{\alpha - \alpha_3}$$

Using [10] and the measured values of α for the mixture and for each isomer the ratio $n_3 : n_4$ was found to be 4:1.

We thank the National Research Council of Canada and the University of Victoria for financial support; and Dr. E. J. Wells of Simon Fraser University, Burnaby, B.C., for 100 MHz n.m.r. spectra.

1. J. VAUGHAN, G. J. WELCH, and G. J. WRIGHT. Tetrahedron. **21**, 1665 (1965).
2. A. FISCHER, J. PACKER, J. VAUGHAN, and G. J. WRIGHT. Proc. Chem. Soc. 369 (1961).
3. D. J. BLACKSTOCK, A. FISCHER, K. E. RICHARDS, J. VAUGHAN, and G. J. WRIGHT. Chem. Commun. 641 (1970).
4. D. J. BLACKSTOCK, J. R. CRETNEY, A. FISCHER, M. P. HARTSHORN, K. E. RICHARDS, J. VAUGHAN, and G. J. WRIGHT. Tetrahedron Lett. 2793 (1970).
5. A. E. GILLAM and E. S. STERN. An introduction to electronic absorption spectroscopy in organic chemistry. 2nd ed. Edward Arnold, London, 1957. p. 98.
6. E. L. ELIEL, N. L. ALLINGER, S. J. ANGYAL, and G. A. MORRISON. Conformational analysis. Interscience Publishers, Inc., New York, N.Y., 1965, p. 125.
7. E. W. GARBISCH, JR. and M. G. GRIFFIN. J. Am. Chem. Soc. **90**, 3590 (1968).
8. E. W. GARBISCH, Jr. J. Am. Chem. Soc. **86**, 5561 (1964).
9. M. BARFIELD and B. CHAKRABARTI. Chem. Rev. **69**, 757 (1969).
10. V. I. MINKIN, O. A. OSIPOV, and Y. A. ZHDANOV. Dipole moments in organic chemistry. Plenum Press, New York, N.Y., 1970.
11. S. J. CRISTOL, W. BARASCH, and C. H. TIEMAN. J. Am. Chem. Soc. **77**, 583 (1955).
12. C. L. PERRIN and G. A. SKINNER. J. Am. Chem. Soc. **93**, 3389 (1971).
13. A. FISCHER, A. J. READ, and J. VAUGHAN. J. Chem. Soc. 3691 (1964).
14. D. J. BLACKSTOCK, M. P. HARTSHORN, A. J. LEWIS, K. E. RICHARDS, J. VAUGHAN, and G. J. WRIGHT. J. Chem. Soc. B, 1212 (1971).
15. F. G. BORDWELL and E. W. GARBISCH, JR. J. Am. Chem. Soc. **82**, 3588 (1960).
16. G. J. WRIGHT. Ph.D. Thesis. University of Canterbury, Christchurch, N.Z., 1965.
17. F. BLOCH and A. SIEGERT. Phys. Rev. **57**, 522 (1940).
18. R. B. JOHANNESEN, J. A. FERRITTI, and R. K. HARRIS. J. Mag. Res. **3**, 84 (1970).
19. I. F. HALVERSTADT and W. D. KUMLER. J. Am. Chem. Soc. **64**, 2988 (1942).
20. R. J. W. LE FÈVRE and K. D. STEEL. Chem. Ind. (London), 670 (1961).
21. R. D. NELSON, D. R. LIDE, and A. A. MARYOTT. Selected values of electric dipole moments for molecules in the gas phase. NSRDS–NBS 10. U.S. Government Printing Office, Washington, D.C., 1967.
22. K. HIGASI. Bull. Inst. Phys. Chem. Res. (Tokyo), **22**, 805 (1943).
23. B. KRISHNA and K. K. SRIVASTAVA. J. Chem. Phys. **32**, 663 (1960).

Can. J. Chem. Downloaded from www.nrcresearchpress.com by 210.87.254.6 on 09/05/12
For personal use only.

Direct Photolysis of 2-Propanol Vapor[1]

O. S. HERASYMOWYCH AND A. R. KNIGHT

Department of Chemistry and Chemical Engineering, University of Saskatchewan, Saskatoon, Saskatchewan

Received November 24, 1971

The photolysis of 2-propanol vapor in the 1800–2000 Å wavelength range has been investigated. The volatile products of the reaction and their quantum yields at 80 °C and 200 Torr substrate pressure are H_2 (0.64), CH_3COCH_3 (0.34), CH_4 (0.39), CH_3CHO (0.29), CO (0.15), and C_2H_6 (0.08). A mechanism is proposed that accounts for the observed rate variations with substrate pressure, exposure time, temperature, and pressure of inert addend. Acetone and acetaldehyde undergo significant secondary decomposition and this is the source of CO, CH_4, and C_2H_6. Acetaldehyde is formed in the unimolecular decomposition of C_3H_7O radicals produced in the primary process.

The effects of CO_2 and CF_4 as inert addends have been examined and it has been established that the quantum yield enhancement through collision induced predissociation that has been reported to occur in methanol is not a characteristic of the 2-propanol photolysis.

La photolyse en phase vapeur du propanol-2, dans l'intervalle 1800–2000 Å, a été étudiée. Les produits volatils de la réaction et leurs rendements quantiques à 80 °C, sous une pression de substrat 200 Torr, sont H_2 (0.64), CH_3COCH_3 (0.34), CH_4 (0.39), CH_3CHO (0.29), CO (0.15), et C_2H_6 (0.08). Un mécanisme est proposé qui rend compte des variations observées pour la vitesse avec la pression du substrat, la durée d'exposition, la température et la pression de l'additif inerte. L'acétone et l'acétaldéhyde subissent une décomposition secondaire notable et constituent la source de CO, CH_4, et C_2H_6. L'acétaldéhyde est formé dans la décomposition unimoléculaire des radicaux C_3H_7O issus du processus primaire.

Les effets de CO_2 et CF_4, en tant qu'additifs inertes, ont été examinés et on a établi que l'accroissement du rendement quantique par l'intermédiaire d'une prédissociation due à la collision, qui se produit dans le méthanol, n'est pas une caractéristique de la photolyse du propanol-2.

Canadian Journal of Chemistry, **50**, 2217 (1972)

Introduction

The direct photolysis of 2-propanol vapor in the near vacuum u.v. has not been investigated previously although the mercury photosensitized decomposition at 2537 Å has been studied (1). The methanol system, however, has been examined in both direct photolysis (2–4) and photosensitization (5, 6).

Recently, Hagege *et al.* (7) reported that in the direct photolysis of CH_3OH at 1849 Å, added inert gases increased the decomposition quantum yields. These workers suggested that this enhancement occurs through a collision induced predissociation. There is no evidence, however, that such processes occur in the sensitized reaction (5, 6).

To investigate whether quantum yield increases occur when inert gases are present during the photolysis of other alcohols, we have examined the vapor phase photolysis of 2-propanol in the 1800–2000 Å wavelength region. This substrate was chosen for initial study in perference to methanol itself since the study of methanol photochemistry is complicated by the spontaneous reaction that occurs between methanol vapor and ordinary Pyrex glass giving appreciable amounts of trimethyl borate (6, 8).

Experimental

The photolysis experiments were conducted in a conventional grease- and mercury-free vacuum system with a cylindrical quartz reaction cell. The light source was a Hanovia medium pressure mercury lamp, type 30 620. The effective (with respect to substrate absorption) wavelength range was confined to the *ca.* 1800–2000 Å range by the transmission characteristics of the cell window and the absorption spectrum of the substrate 2-propanol (9). In that spectral region the effective lamp emission is the relatively weak and self-reversed Hg resonance line at 185 nm and a continuum. The region between the photolysis lamp and cell was sealed and continuously flushed with N_2 gas to avoid absorption by atmospheric oxygen. The cell and valve connection to the vacuum system were heated by an aluminum block furnace.

At the end of each experiment the products non-condensable at −196 °C were transferred to an attached vacuum system and determined in a gas burette and subsequently analyzed for H_2 and CH_4, or CO and CH_4, by gas chromatography. In the two procedures, CO and H_2 respectively were determined by difference. Condensable products were

[1]From the M.Sc. Thesis of O. S. Herasymowych, to be submitted to the University of Saskatchewan, Saskatoon, Saskatchewan. Presented in part to the Chemical Institute of Canada Conference, Halifax, N.S., May, 1971.

Can. J. Chem. Downloaded from www.nrcresearchpress.com by 210.87.254.40 on 09/05/12
For personal use only.

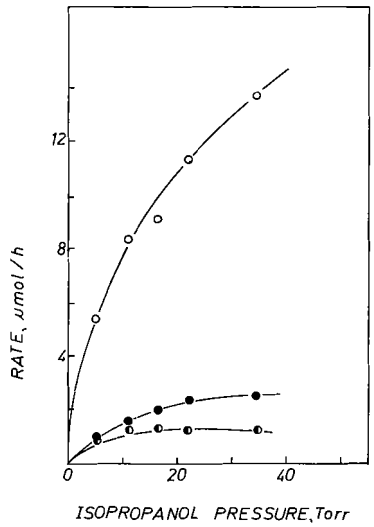

FIG. 1. Rate of formation of H_2, ○; CH_4, ●; and CO, ◐; as a function of pressure in the photolysis of 2-propanol at 30 °C.

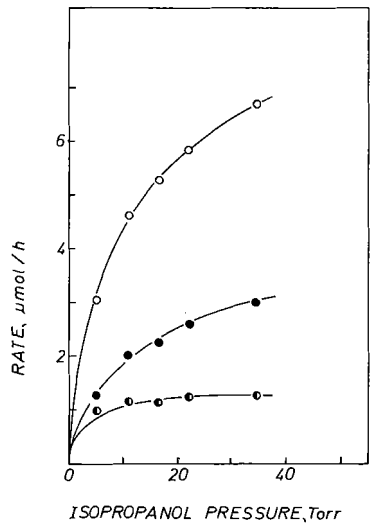

FIG. 2. Rate of formation of CH_3COCH_3, ○; C_2H_6, ◐; and CH_3CHO, ●; as a function of pressure in the photolysis of 2-propanol at 30 °C.

distilled directly into the g.c. sampling volume. Pressures in the system were determined using an N.R.C. Alphatron ion gauge which was calibrated separately for all gases used in this study. Non-condensable products were analyzed using a 5 Å molecular sieve column, while condensables were eluted on a 12 ft Carbowax 20M column. In experiments with added gases the addends were separated from products and unreacted substrate by low temperature distillation. Products were identified by g.c. retention time comparisons and confirmed by mass spectrometric analysis.

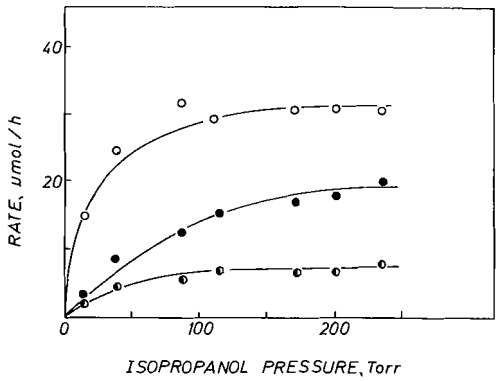

FIG. 3. Rate of formation of H_2, ○; CH_4, ●; and CO, ◐; as a function of pressure in the photolysis of 2-propanol at 80 °C.

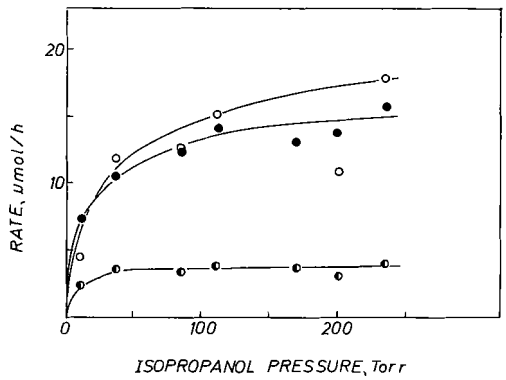

FIG. 4. Rate of formation of CH_3COCH_3, ○; C_2H_6, ◐; and CH_3CHO, ●; as a function of pressure in the photolysis of 2-propanol at 80 °C.

2-Propanol (Shawinigan reagent) was degassed in the vacuum line and had no impurities detectable by g.c. analysis. Carbon tetrafluoride, carbon dioxide, and nitrous oxide (Matheson) were degassed and freed from impurities by successive low temperature fractionations in the vacuum line.

Results

The volatile products of the photolysis of 2-propanol at 30 °C with $\lambda = 1800$–2000 Å are H_2, CH_3COCH_3, CH_3CHO, CH_4, CO, and C_2H_6. After prolonged irradiations very small amounts of pinacol and its isomers were detected by g.c. analysis of ether solutions obtained by successive washings of the reaction cell. The lengthy irradiations required to produce sufficient material for analysis by flame ionization g.c. at maximum sensitivity likely give rise to secondary decomposition of the originally formed C_6 fraction. Stoichiometric

Can. J. Chem. Downloaded from www.nrcresearchpress.com by 210.87.254.40 on 09/05/12
For personal use only.

TABLE 1. Product rates as a function of temperature in the photolysis of 11 Torr 2-propanol for 60 min*

	Rate (μmol/h)					
T (°C)	H_2	CH_4	CO	C_2H_6	CH_3CHO	CH_3COCH_3
30	9.84	1.60	1.04	0.89	2.50	5.22
48.5	11.5	2.70	1.66	1.50	4.14	5.18
74.5	14.1	2.41	2.14	2.00	6.53	4.58
89.5	14.5	3.37	2.85	2.56	6.66	3.90
104.0	16.5	4.06	2.75	2.75	8.78	3.39
142.0	11.7	7.90	3.81	2.87	9.53	4.47
147.0	12.8	8.47	3.74	2.95	9.78	4.85
184.5	13.1	13.4	5.20	2.87	10.6	4.74

*Hydrogen yields were determined by difference in this series. See Experimental. 2-Propanol pressures were measured at 30 °C.

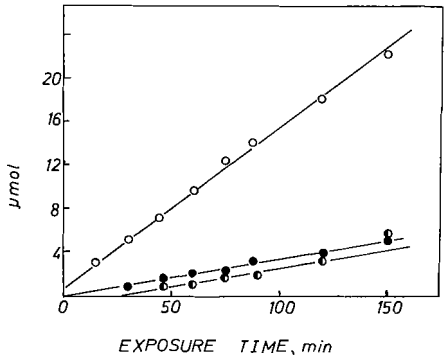

FIG. 5. Yield of H_2, ○; CH_4, ●; and CO, ◐; as a function of exposure time in the photolysis of 11 Torr of 2-propanol at 30 °C.

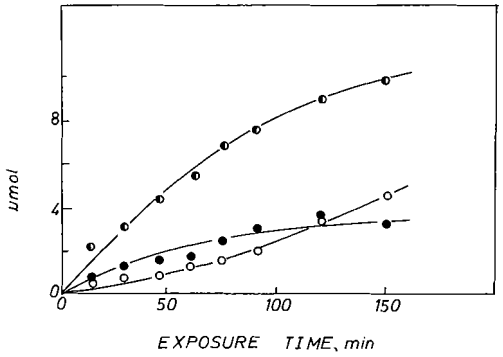

FIG. 6. Yield of CH_3COCH_3, ◐; C_2H_6, ○; and CH_3CHO, ●; as a function of exposure time in the photolysis of 11 Torr of 2-propanol at 30 °C.

calculations of the possible range of values for Φ(pinacol), *vide infra*, do not give a good mass balance. This may be due in part to secondary decomposition and to a minor surface effect since the adequacy of the mass balance has been reported to depend on the shape of the reaction cell in the case of methanol (3). Since actual pinacol yields could not be determined in the present system this effect was not investigated.

Figures 1 and 2 show the rate of formation of the volatile products at 30 °C. It is evident that at the maximum 2-propanol pressure that could be employed at that temperature, absorption of incident radiation is not complete. To permit examination of higher substrate pressures, a series of experiments was carried out at 80 °C where product yields could be determined up to 220 Torr alcohol vapor. The results are shown in Figs. 3 and 4. Under the conditions of these experiments it would appear from the variation in the rate of H_2 formation that absorption is probably complete at around 200 Torr substrate pressure.

To compare these results with others obtained at room temperature, and as well to identify products whose formation is temperature dependent, rates were measured in a series of photolysis of 11 Torr pressure, measured at 30 °C, of 2-propanol from 30 to 185 °C. These data are listed in Table 1. An Arrhenius plot for methane is linear and indicates an apparent activation energy for the formation of this product of 3.8 kcal/mol.

Another series of experiments was conducted at 30 °C to evaluate the effects of exposure time and the results are shown in Figs. 5 and 6. Although there is some uncertainty in determining whether the yield curves are linear at short exposure times, within experimental error the yields of hydrogen, methane, and carbon monoxide are linearly dependent on exposure time. Because of the relatively small amounts of

Can. J. Chem. Downloaded from www.nrcresearchpress.com by 210.87.254.40 on 09/05/12
For personal use only.

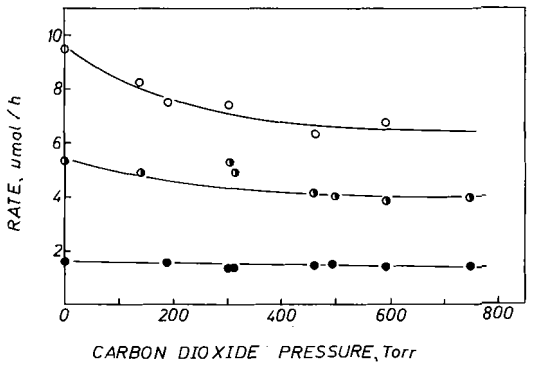

FIG. 7. Rate of formation of H_2, ○; CH_3COCH_3, ◑; and CH_4, ●; as a function of pressure of added carbon dioxide in the photolysis of 11 Torr of 2-propanol at 30 °C.

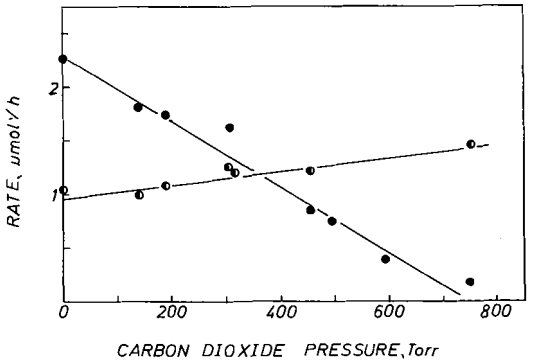

FIG. 8. Rate of formation of CH_3CHO, ●; and CO, ◐; as a function of pressure of added carbon dioxide in the photolysis of 11 Torr of 2-propanol at 30 °C.

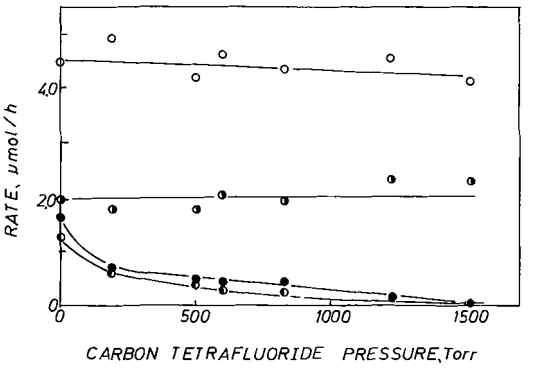

FIG. 9. Rate of formation of CH_4, ●; CO, ◐; CH_3CHO, ◑; and CH_3COCH_3, ○; as a function of pressure of added carbon tetrafluoride in the photolysis of 11 Torr of 2-propanol at 30 °C.

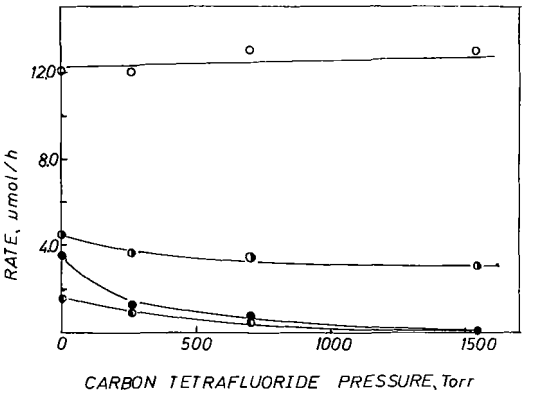

FIG. 10. Rate of formation of CH_4, ●; CO, ◐; CH_3CHO, ◑; and CH_3COCH_3, ○; as a function of pressure of added carbon tetrafluoride for the photolysis of 100 Torr of 2-propanol at 48 °C.

the latter two products it is not possible to determine definitively if their initial rates are zero, although the yield curves suggest that such is the case. For acetone and acetaldehyde, however, it is clear that there is a pronounced decrease in their rate of formation with reaction time, while $R(C_2H_6)$ evidently increases at longer exposure times. An additional series of experiments was carried out with 8.5 Torr substrate pressure and showed the same trends in the yields of all products as found at 11 Torr.

To determine if decomposition rates were enhanced in the presence of inert addends, three sets of runs were conducted. In the first series, 11 Torr of 2-propanol was photolyzed in the presence of up to 1 atm of CO_2. Carbon dioxide was chosen because Hagege *et al.* (7) found that it was the most effective addend in increasing quantum yields in the methanol decomposition. The results obtained in the present study are shown in Figs. 7 and 8. Ethane was not analyzed for in this series. Apart from a slight increase in R(CO) all rates either decline or remain essentially constant. The most significant alteration is the substantial decrease in the rate of acetaldehyde formation.

In the two other series of experiments, rates were determined at substrate pressures of 11 and 100 Torr in the presence of CF_4 examining addend pressures up to 1550 Torr. The results are given in Figs. 9 and 10. Hydrogen was not determined in these runs since it was not possible to separate it quantitatively from the large

Can. J. Chem. Downloaded from www.nrcresearchpress.com by 210.87.254.40 on 09/05/12
For personal use only.

Can. J. Chem. Downloaded from www.nrcresearchpress.com by 210.87.254.40 on 09/05/12
For personal use only.

amount of CF_4 which has a small but finite vapor pressure at -196 °C. Again the rates of formation of all products remain constant within experimental error or decline with the exception of $R(CH_3COCH_3)$, in the case of the photolysis of 100 Torr substrate, which may have increased somewhat at the higher CF_4 pressures.

Because a monochromatic light source was not employed in this study it was not possible to obtain definitive values for the quantum yields. However, it was possible to determine first approximation values because of the coincidence that both the substrate and the nitrous oxide used as actinometer are both essentially transparent at wavelengths greater than 2000 Å and both absorb down to the 1800 Å cutoff. The absorption coefficient of N_2O rises rather slowly in this wavelength region, while that of 2-propanol increases rather sharply with decreasing wavelength, and therefore it is possible to obtain more or less complete absorption in the substrate case at relatively low pressures. The rate of N_2 formation from the photolysis of N_2O was determined as a function of pressure up to 2400 Torr. Consistent with the absorption characteristics outlined above, it was found that at least 800 Torr of actinometer was required for complete absorption as evidenced by the constant $R(N_2)$ value found at this and higher pressures. Taking $\Phi(N_2) = 1.44$ (10, 11) the observed pressure independent rate of nitrogen formation indicated an effective intensity for the system of 0.82 μEinstein min^{-1}. Utilizing the observed rates of product formation at 80 °C and 200 Torr 2-propanol pressure, assuming that there is complete absorption of the same effective intensity by the substrate under these conditions as by the actinometer, the calculated quantum yield values are as follows: H_2, 0.64; CH_4, 0.39; CH_3COCH_3, 0.34; CH_3CHO, 0.29; CO, 0.15; and C_2H_6, 0.08. The data for CH_4, CO, and C_2H_6 are, in effect, rates relative to that of the primary decomposition rather than true Φ values since, as will be demonstrated below, these products arise from secondary photolyses at wavelengths not absorbed by the substrate or the actinometer.

Discussion

The nature of the products observed in this study and the previously determined behavior of this substrate and methanol in direct and sensitized photolysis would indicate that the primary decomposition may proceed by two routes,

[1*a*] $(CH_3)_2CHOH + h\nu \rightarrow C_3H_7O + H$

[1*b*] $(CH_3)_2CHOH + h\nu \rightarrow (CH_3)_2CO + H_2$

where the radical represented as C_3H_7O may be either $(CH_3)_2\dot{C}OH$ or $(CH_3)_2CH\dot{O}$. An investigation of the photolysis of deuterated 2-propanols would be required to distinguish between the three possibilities and to assess their relative contributions to the primary decomposition. The net chemical effect of reaction 1*a*, however, will be the same whether isopropoxy radicals or hydroxyisopropyl radicals are formed in that H-atoms and $(CH_3)_2COH$ radicals will result, the latter from the rapid exchange reaction

[2] $(CH_3)_2CHO + (CH_3)_2CHOH \rightarrow (CH_3)_2CHOH + (CH_3)_2COH$

shown previously to be important in both this substrate (1) and methanol (6).

The results obtained in the present study, however, show that the rate of primary decomposition is not increased by added inert gases, even at relatively high pressures. There is no obvious explanation of why this system does not exhibit the same behavior as methanol. The absorption spectrum of both alcohols in the 1800–2000 Å region is a continuum, although Hagege *et al.* (7) have suggested that there may be fine structure in the CH_3OH spectrum that would be detected only in high resolution and at low pressure. Thus it may be possible that the initially attained electronic excited state of $(CH_3)_2CHOH$ is more dissociative in character than the analogous state proposed as being involved in CH_3OH. One additional factor may be important. The experiments with CH_3OH (7) were carried out in a Pyrex system and it may be possible that the photolysis was complicated by the presence of trimethyl borate. This possibility cannot be ruled out until the phenomenon is demonstrated to occur in a system wherein CH_3OH vapor does not come into contact with boron containing glass.

The observed products and their rate characteristics found in the present investigation of

Can. J. Chem. Downloaded from www.nrcresearchpress.com by 210.87.254.40 on 09/05/12
For personal use only.

2-propanol can be explained on the basis of reactions 1 and 2 followed by reactions 3–12.

[3] $H + (CH_3)_2CHOH \rightarrow H_2 + (CH_3)_2COH$

[4] $2(CH_3)_2COH \rightarrow CH_3COCH_3 + (CH_3)_2CHOH$

[5] $2(CH_3)_2COH \rightarrow (CH_3)_2C(OH)C(OH)(CH_3)_2$

[6] $C_3H_7O \rightarrow CH_3CHO + CH_3$

[7] $CH_3COCH_3 + h\nu \rightarrow CH_3CO + CH_3$

[8] $CH_3CO \rightarrow CH_3 + CO$

[9] $CH_3CHO + h\nu \rightarrow CH_3 + CHO$

[10] $CHO \rightarrow CO + H$

[11] $CH_3 + (CH_3)_2CHOH \rightarrow CH_4 + (CH_3)_2COH$

[12] $2CH_3 \rightarrow C_2H_6$

Reaction 6 is suggested as the source of CH_3CHO. This process has been observed in the photolysis of isopropyl propionate at 2537 Å (12), so that in the present system there should be ample energy from the primary process to have it occur. The dependence of the rate of formation of acetaldehyde on pressure of added CO_2, and to a lesser extent pressure of added CF_4, as well as the marked increase in its rate with temperature, support the proposal that CH_3CHO arises from the unimolecular decomposition of C_3H_7O radicals with energies in excess of thermal excitation. The mechanism, however, does not account for all observations associated with C_3H_7O decomposition. A reduction in the rate of reaction 6 in the presence of inert addends should give rise to a decrease in CO and CH_4 formation. While that is indeed observed with added CF_4, R(CO) and $R(CH_4)$ show an increase or remain constant with added CO_2. There is no obvious explanation of this difference in the effect of the two addends.

The data in Fig. 7 show that $R(H_2)$ declines as $P(CO_2)$ is increased. This may be ascribed to decreasing importance of reaction 3. The H-atoms formed in reaction 1*a* will have, with $\lambda = 1800$–2000 Å as the photolyzing wavelength, some excess energy and the relatively small temperature dependence of $R(H_2)$ is consistent with that expectation. In the presence of addends, these H-atoms will be thermalized and therefore more readily removed in radical–radical reactions, such as, for example the reverse of reaction 1*a*. Furthermore, the production of H-atoms from process 10 would be expected to decrease at higher system pressures.

Acetone and acetaldehyde are both subject to secondary photolysis by lamp emissions at $\lambda > 2000$ Å (principally at 2537 Å) where there is no absorption by the substrate. The marked decrease in the rate of formation of both these products as exposure times are increased is evidence that such secondary decomposition is occurring. The observed rates for CO, CH_4, and C_2H_6 are consistent, within experimental error, with the stoichiometry of the reactions associated with these secondary photolyses. Methyl radicals are formed in reactions 6–9, and the total rate of formation of CH_3 can be computed as follows. The value of $\Phi(CH_3)$ from processes involving formation and secondary photolysis of CH_3CHO will be the sum of $(\Phi(CH_3CHO) + \Phi(CO)_{[10]})$ and $\Phi(CO)_{[10]}$; the former term accounts for CH_3 production in reaction 6, while the latter indicates the extent of CHO formation and consumption and is therefore representative of $\Phi(CH_3)$ in reaction 9. The processes involving acetone also give CH_3 radicals and for these reactions the CH_3 quantum yield is $\Phi(CH_3)_{[7]} + \Phi(CH_3)_{[8]} = 2\Phi(CO)_{[8]}$. Therefore the total $\Phi(CH_3)$ value is given by eq. 13. It is not possible to evaluate the last two

[13] $$\Phi(CH_3) = \Phi(CH_3CHO) + 2\Phi(CO)_{[8]} + 2\Phi(CO)_{[10]}$$

terms directly. However, if it is assumed that CH_3COCH_3 and CH_3CHO undergo secondary photolysis to an extent proportional to their concentrations, then $\Phi(CO)_{[8]} = 1.13\,\Phi(CO)_{[10]}$. Since $\Phi(CO)_{obs.} = \Phi(CO)_{[8]} + \Phi(CO)_{[10]}$, the individual values are $\Phi(CO)_{[8]} = 0.08$ and $\Phi(CO)_{[10]} = 0.07$. Solution of eq. 13 on that basis gives $\Phi(CH_3) = 0.59$. Methyl radicals are consumed in reactions 11 and 12 whence

[14] $$\Phi(-CH_3) = \Phi(CH_4) + 2\Phi(C_2H_6)$$

and the calculated $\Phi(-CH_3)$ value here is 0.56. The formation of methane through abstraction in reaction 11 is consistent with the observed apparent activation energy for CH_4 production considering the lability of the α-hydrogen atom in 2-propanol.

An upper limit for the contribution of reaction 5 can be obtained from stoichiometric calculations involving C_3H_7O radicals. These determinations evidently depend on the contribution of primary process 1*b*.

If that process does occur, the yield on substrate radicals can be determined from their rate of formation in reactions 1*a* and 3 and via

abstraction by CH_3 in reaction 11, so that

[15] $$\Phi(C_3H_7O) = 2\Phi(H_2) + \Phi(CH_4) = 1.67$$

employing quantum yield values at 80 °C and 200 Torr substrate pressure. The value of $\Phi(C_3H_7O)$ can also be obtained from the Φ values for products responsible for the consumption of this radical; that is, pinacol in reaction 5, acetone in reaction 4, and acetaldehyde in reaction 6. It is also necessary to include in the sum the CO yields indicative of the amount of the latter two products that undergo secondary photolysis. On that basis the quantum yield relation is

[16] $$\Phi(C_3H_7O) = 2[\Phi(CH_3COCH_3) + \Phi(CO)_{[8]}] + 2\Phi(\text{pinacol}) + \Phi(CH_3CHO) + \Phi(CO)_{[10]}$$

Calculating the $\Phi(CO)$ values as before, and taking $\Phi(C_3H_7O) = 1.67$ from eq. 15, eq. 16 gives a value of 0.24 for Φ(pinacol). This represents an upper limit.

If reaction 1*b* is included in the stoichiometry and assumed to occur to the same extent as for methanol (25%), eqs. 15 and 16 can be altered to include the appropriate Φ (reaction 1*b*) terms and yield a value of 0.15 for Φ(pinacol).

Finally, it is of interest to compare the main features of the direct and sensitized photolysis of this substrate. Although the products are the same, acetaldehyde and products arising from secondary photolysis of carbonyl compounds are formed in relatively smaller quantities at 2537 Å. The total quantum yield of acetone formation is given by $\Phi(CH_3COCH_3) + \Phi(CO)_{[8]}$ and is equal to 0.42. Thus for the direct photolysis $\Phi(H_2)/\Phi(CH_3COCH_3) = 1.52$. In the mercury photosensitized decomposition, Knight and Gunning (1) found $\Phi(H_2) = 0.72$ and $\Phi(H_2)/\Phi(CH_3COCH_3) = 2.9$, while in a more recent determination of the quantum yields in the 2-propanol–Hg $6(^3P_1)$ reaction, Kato and Cvetanović (13) found $\Phi(H_2) = 0.77$ and $\Phi(H_2)/\Phi(CH_3COCH_3) = 1.29$.

The fundamental difference between the methanol and 2-propanol systems with respect to quantum yield enhancement by inert gases remains unresolved and to that end we have initiated a study of the CH_3OH system in an all-quartz vacuum system.

The authors gratefully acknowledge the financial support of the National Research Council of Canada for this work and also a grant from the Research Corporation for another project which provided much of the apparatus employed in the present study.

1. A. R. KNIGHT and H. E. GUNNING. Can. J. Chem. **40**, 1134 (1962).
2. R. P. PORTER and W. A. NOYES, JR. J. Am. Chem. Soc. **81**, 2308 (1959).
3. J. HAGEGE, S. LEACH, and C. VERMEIL. J. chim. phys. **62**, 736 (1965).
4. J. HAGEGE, P. C. ROBERGE, and C. VERMEIL. J. chim. phys. **65**, 641 (1968).
5. R. F. POTTIE, A. G. HARRISON, and F. P. LOSSING. Can. J. Chem. **39**, 102 (1961).
6. A. R. KNIGHT and H. E. GUNNING. Can. J. Chem. **39**, 1231 (1961).
7. J. HAGEGE, P. C. ROBERGE, and C. VERMEIL. Trans. Faraday Soc. **64**, 3288 (1968).
8. R. P. PORTER. J. Phys. Chem. **61**, 1260 (1957).
9. A. J. HARRISON, P. J. CADERHOLN, and M. TERWILLIGER. J. Chem. Phys. **30**, 355 (1959).
10. M. ZELIKOFF and L. N. ASCHENBRAND. J. Chem. Phys. **22**, 1680 (1954).
11. G. A. CASTELLION and W. A. NOYES, JR. J. Am. Chem. Soc. **79**, 290 (1957).
12. M. H. J. WIJNEN. Can. J. Chem. **36**, 691 (1958).
13. A. KATO and R. J. CVETANOVIĆ. Can. J. Chem. **46**, 235 (1968).

Can. J. Chem. Downloaded from www.nrcresearchpress.com by 210.87.254.40 on 09/05/12
For personal use only.

The Thermal Behavior of Some Resin Acids at 400–500 °C

RAY F. SEVERSON AND WALTER H. SCHULLER
Naval Stores Laboratory,[1] Olustee, Florida 32072

Received October 12, 1971

The hot tube pyrolysis of dehydroabietic acid (**1**) at 400–500 °C was found to produce as major products the three possible A-ring olefins (19-norabieta-4,8,11,13-tetraene (**2**); 19-norabieta-4(18),8,11,13-tetraene (**3**); and 19-norabieta-3,8,11,13-tetraene (**4**)) resulting from the elimination of the carboxylate moiety. The i.r., n.m.r., u.v., and mass spectrum of each olefin was obtained and discussed. The pyrolysis of abietic acid (**7**) and levopimaric acid (**8**) under identical conditions was found to yield A-ring olefins; to isomerize to yield varying mixtures of palustric, **7**, and neoabietic acids; to dehydrogenate to yield **1**; and to eliminate propylene to form deisopropyldehydroabietic acid (**15**). A mechanism to explain the formation of **15** from the dienoic resin acids is given.

On a trouvé que la pyrolyse en tube de l'acide déhydrobiétique (**1**) à 400–500 °C fournit comme produits majeurs les trois oléfines possibles sur le cycle A (nor-19-abiéta tétraène-4,8,11,13 (**2**); nor-19 abiéta tétraène-4(18),8,11,13 (**3**); et nor-19 abiéta tétraène-3,8,11,13 (**4**)) résultant de l'élimination du fragment carboxylate. Les spectres i.r., r.m.n., u.v., et le spectre de masse de chaque oléfine ont été obtenus et discutés. La pyrolyse de l'acide abiétique (**7**) et de l'acide lévopimarique (**8**) dans des conditions identiques donne des oléfines sur le cycle A, des isomérisations conduisant à des mélanges variables d'acides palustrique **7** et néoabiétique, une déshydrogénation conduisant à **1** et une élimination du propylène pour former l'acide desisopropyl-déhydroabiétique (**15**). Un mécanisme expliquant la formation de **15** à partir des acides résines diénoiques est donné.

Canadian Journal of Chemistry, **50**, 2224 (1972)

Our studies on the high temperature (600–800 °C) behavior of dehydroabietic acid (**1**), abietic acid (**7**), and levopimaric acid (**8**) (1, 2) led us to conclude that the elimination of the carboxylate moiety to yield A-ring olefins was the initial primary fragmentation in the thermal decomposition of these acids (or methyl esters). The conjugated dienoic acids were assumed to rapidly isomerize and the dehydrogenation would occur to produce an aromatic C-ring.[2] It thus seemed feasible that under milder conditions, the pyrolysis of resin acids would produce isolatable A-ring olefins.

Because of the recent interest in a facile conversion of resin acids to 19-norabieta-4(18),8,11,-13-tetraene (**3**) (a decarboxylated A-ring olefin) to be used as a possible precursor in steroid synthesis (4) and pyrolytic mechanism considerations, we are reporting in this paper the behavior of **1**, **7**, and **8** under pyrolytic conditions which should minimize further decomposition of the possible initial decarboxylation product.

Experimental

The pyrolysis apparatus was similar to that previously used (2). Five grams of the resin acid in 25 ml benzene were added dropwise over 40 min (N_2 flow 50 ml/min). When the addition was complete, the pyrolysate was quantitatively removed with acetone and stripped to 90 mm Hg at 30° on a rotoevaporator. The product was treated with an ethyl ether – diazomethane solution and analyzed by g.l.c. using a 15 ft × 3/16 in. 10% OV-17 column (60/80 mesh Gas Chrom Q, 120 ml/min He, temperature program 80–280° at 4°/min).

Ethylene and propylene were trapped by means of their 1,2-dibromide derivatives by passing the pyrolysis exhaust gases through a gas dispersion trap containing Br_2 in acetic acid. After extraction with ethyl ether and water, 1,2-dibromoethane and 1,2-dibromopropane were separated by g.l.c. (OV-17 column at 90°) and identified by means of retention time (comparison with authentic compounds) and i.r. data (after collection from g.l.c.).

Methyl palustrate, dehydroabietate, abietate, and neoabietate were identified by means of retention times and u.v. spectra (collected from OV-17 at 260°). The methyl ester of **15** was collected (as a white solid) from the OV-17 column at 260°; i.r. (KBr), 1723 (C=O) and 759 cm^{-1} (four adjacent ArH); n.m.r. δ (CCl_4), 1.21 (s, 3, C_{10}-Me), 1.25 (s, 3, C_4-Me), 3.65 (s, 3, OCH_3), and 7.0 p.p.m. (m, 4, aromatics); λ_{max} (95% EtOH), 264.5 (log ε 2.72) and 272 mμ (log ε 2.70) (lit. (5), 265 (log ε 2.68) and 273 mμ (log ε 2.65)); $[\alpha]_D^{25}$ +54° (*c* 0.25, 95% EtOH) (lit. (5), $[\alpha]_D^{25}$ +60.5°). Mass

[1]One of the laboratories of the Southern Marketing and Nutrition Research Division, Agricultural Research Service, U.S. Department of Agriculture.

[2]Previous work at this laboratory has shown that at 200° the four conjugated dienoic resin acids, neoabietic, palustric, abietic, and levopimaric, thermally isomerize to yield an equilibrium mixture of palustric, abietic, and neoabietic acids and that disproportionation to yield dehydroabietic acid occurs in a very slow irreversible step (3).

Can. J. Chem. Downloaded from www.nrcresearchpress.com by 210.87.254.40 on 09/05/12
For personal use only.

TABLE 1. Percent composition of pyrolysate (g.l.c. volatile portion)

	Pyrolysis temperature							
	Dehydroabietic			Levopimaric		Abietic		Relative* retention time
	500°	450°	400°	400°	500°	500°	400°	
	% of neutral fraction†							
Δ^4-Alkene (2)	2.9	11.3	10.7	2.0	0.0	6.3	11.9	1.50
$\Delta^{4(18)}$-Alkene (3)	23.8	36.7	38.8	8.6	5.3	18.1	26.1	1.54
Δ^3-Alkene (4)	14.1	30.3	31.3	3.6	1.4	3.6	5.3	1.56
Unidentified	59.2	21.7	19.2	87.9	91.2	72.0	56.4	—
	% neutrals‡							
	11.2	8.8	5.8	3.4	9.1	11.3	4.4	
	% of acidic fraction§							
Deisopropyl-dehydroabietic	0.3	0.2	0.1	1.4	15.2	7.8	1.1	1.66
Palustric	—	—	—	33.9	22.3	21.8	19.9	1.78
Dehydroabietic	95.2	97.9	98.7	4.8	18.1	7.8	1.5	1.86
Abietic	—	—	—	47.3	27.0	52.0	69.1	1.89
Neoabietic	—	—	—	2.8	4.4	3.1	3.7	1.98
Unidentified	4.5	1.9	1.2	9.8	13.0	7.5	4.8	—
	% acids‖							
	89.8	91.2	94.2	96.6	90.8	88.7	95.6	
	% recovered¶							
	79.9	98.7	99.8	101.0	60.0	69.2	100.0	

*Relative to 1,5-dimethylnaphthalene (on OV-17, temperature program 80–280 °C. at 5°/min).
†Based on total weight of material in neutral fraction.
‡Total weight of neutrals in pyrolysate.
§Based on total weight of material in acidic fraction.
‖Total weight of acidic material in pyrolysate.
¶Based on total weight of g.l.c. volatile material recovered after pyrolysis.

spectrum *m/e* (relative intensity), 272 (19.3), 257 (22.2), 213 (13.2), and 197 (100).

A-Ring Olefins

A portion of the pyrolysate was placed on neutral alumina (Woelm Activity Grade 1) and eluted with benzene. The neutral material which eluted in a yellow band was collected and the solvent removed under a stream of nitrogen. The A-ring olefins were collected from the OV-17 column and rechromatographed and collected[3] as colorless oils.

Compound **2** (retention time 23.2 min)[4]: i.r. (neat), 1616 and 1498 (C=C, Ar), 880 (isolated ArH), and 820 cm^{-1} (two adjacent ArH); n.m.r. δ (CCl_4), 1.21 (d, 6, $J = 7$ Hz, $(Me)_2CH$), 1.24 (s, 3, C_{10}-Me), 1.33 (s, 3, C_4-Me), 6.80 (s, 1, C_{14}-H), 6.88 (d, 1, $J = 6.5$ Hz, C_{12}-H), and 7.12 p.p.m. (d, 1, $J = 6.5$ Hz, C_{11}-H); λ_{max} (95% EtOH), 266.5 and 274.5 mμ.

Compound **3** (retention time 26.6 min): i.r. (neat), 3070 (=CH_2 stretch), 1648 (C=C, vinylidene), 1612 and 1500 (C=C, Ar), 883 (C=CH_2), 860 (isolated ArH), and 820 cm^{-1} (two adjacent ArH); n.m.r. δ (CCl_4), 0.97 (s, 3, C_{10}-Me), 1.20 (d, 6, $J =$ Hz, $(Me)_2CH$), 4.56 (broad s, =CH, syn), and 4.80 p.p.m. (broad s, 1, =CH, anti) (aromatics as given for **2**); u.v. λ_{max} (95% EtOH), 266.5 and 274.5 mμ.

Compound **4** (retention time 27.8 min): i.r. (neat), 1668 (R_1R_2C=CHR), 1616 and 1500 (C=C, Ar), 886 (isolated ArH), and 820 cm^{-1} (two adjacent ArH); n.m.r. δ (CCl_4), 1.02 (s, 3, C_{10}-Me), 1.20 (d, $J = 7.0$ Hz, $(CH_3)_2CH$), 1.27 (s, 3, C_4-Me), and 5.45 p.p.m. (broad s, 1, C_3-H) (aromatics as given for **2**); λ_{max} (95% EtOH), 267 and 275.0 mμ.

Results and Discussion

Analysis of the products obtained from the pyrolysis runs (400–500°) is shown in Table 1. The three major products in the neutral fraction all had a molecular ion at 254 amu and exhibited

[3]The fact that the pure alkenes were not isomerized under the g.l.c. conditions justifies this method for determining the product ratio in the olefin mixture.

[4]Retention data measured from point of injection.

Can. J. Chem. Downloaded from www.nrcresearchpress.com by 210.87.254.40 on 09/05/12
For personal use only.

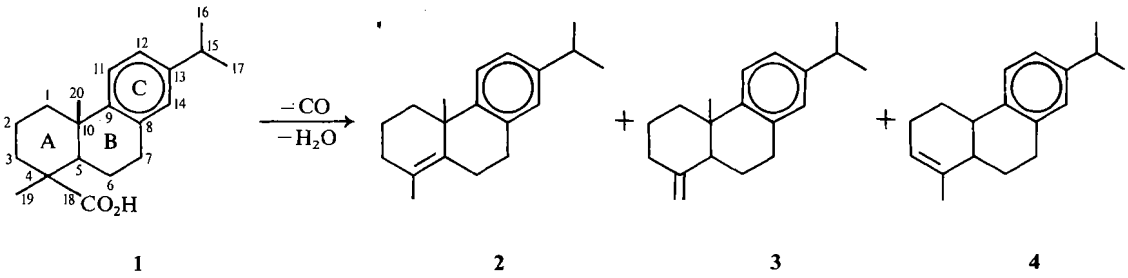

1 2 3 4

SCHEME 1

TABLE 2. Comparison of the fragmentation peaks of A-ring olefins from dehydroabietic acid

	Relative intensity (%)		
m/e	**2**	**3**	**4**
254	43	52.5	70.8
239	100.0	65.5	100.0
211	4.3	8.7	4.2
199	2.9	5.3	36.1
197	7.2	100.0	11.1
169	4.5	10.6	4.2

maxima in the u.v. at 266 and 276 mμ (typical of the aromatic ring system in dehydroabietic acid). Similarly, the 900–675 cm^{-1} region of the i.r. spectrum of each compound indicated the presence of an aromatic system with two adjacent hydrogens (820 cm^{-1}) and an isolated hydrogen (860 cm^{-1}) (6). The above data clearly show that the **B**- and C-rings of the parent molecule are unaltered and suggest that the three isolated olefins are identical to those obtained by Huffman (4) from the lead tetraacetate decarboxylation of **1** (see Scheme 1).

A more detailed study of the i.r., n.m.r., and mass spectra made it possible to assign structure **2** (19-norabieta-4,8,11,13-tetraene) to the most volatile A-ring olefin (relative retention time, 1.50). This compound failed to show any i.r. absorption in the olefin C=C stretching region or vinyl protons in the n.m.r., but did have a deshielded methyl group, as expected for a compound with a tetrasubstituted double bond. The mass spectral fragmentation pattern of **2** is also consistent with the assigned structure (see Table 2). The base peak of **2** found at *m/e* 239 can be readily formed by the loss of the C-10 methyl from the molecular ion to form a benzyl-allyl-stabilized ion (**5**).

The presence of the $=CH_2$ asymmetric stretch (5070 cm^{-1}) and the very strong vinylidine carbon hydrogen wag at 883 cm^{-1} in the i.r. and the presence of two vinyl protons in the n.m.r. of the olefin, with relative retention time of 1.54, are consistent with the structure assigned to compound **3** (19-norabieta-4(18),8,11,13-tetraene). The base peak observed in the mass spectrum of this olefin was found at mass 197 (see Table 2). A metastable at 162 amu indicates that the fragment at mass 197 is the daughter ion of the M-15 peak (*m/e* 239, probably from loss of the C-10 methyl). The work of Genge (7) indicates that the main fragmentation pathway which leads to the base peak does not involve subsequent loss of the aromatic isopropyl group as propylene. However, a reasonable alternate pathway resulting in the loss of propylene from the A-ring to produce an allyl, benzyl, cyclobutyl resonance-stabilized ion (*m/e* 197) (8) which then loses ethylene to yield an isopropylnaphthalene ion (*m/e* 169) can be proposed.[5]

The structure for compound **4** was assigned because of its weak i.r. absorption at 1668 cm^{-1} (consistent with C=C stretch of $C_2C{=}CHC$) and the presence of a vinyl proton and a deshielded methyl group in its n.m.r. spectrum. The high intensity peak (100%) at *m/e* 236 in the mass spectrum of norabieta-3,8,11,13-tetraene (**4**) can be explained by methyl loss followed by double bond migration to yield a vinyl benzyl-

[5]The mass spectral fragmentation mechanism for 19-norabieta-4(18),8,11,13-tetraene may be obtained from the Depository of Unpublished Data, National Science Library, National Research Council of Canada, Ottawa, Canada K1A 0S2.

Can. J. Chem. Downloaded from www.nrcresearchpress.com by 210.87.254.40 on 09/05/12
For personal use only.

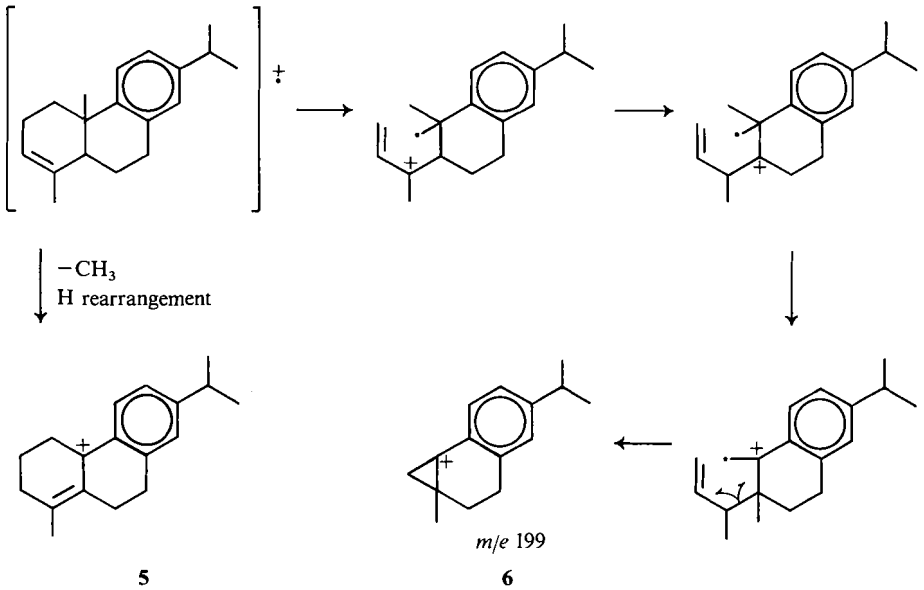

SCHEME 2

stabilized ion **5**. The other major fragment at *m/e* 199 (**6**) may be formed as indicated in Scheme 2.

The A-ring olefins from **1** discussed here have not been previously isolated and characterized in the pure state. They were identified in the olefin mixture by means of n.m.r. spectroscopy (3). The i.r. data reported on **3** and n.m.r. data on the crude mixture (9) are in accord with our findings.

Inspection of the data in Table 1 would appear to indicate that during the thermal decarboxylation of **1**, the formation of the less thermodynamical stable olefins (**3** and **4**) is favored. In contrast to our yield data, one would expect that with increasing pyrolysis temperature the less stable olefins would isomerize to the Δ^4 compound (**2**). However, we feel that since **2** has the structural requirements to undergo a thermal retro-Diels–Alder reaction (10) by the elimination of ethylene, it is probably being decomposed by this reaction at a greatly increased rate at the higher temperatures. The isolation of ethylene (as its 1,2-dibromo derivative) from the pyrolysis exhaust gases substantiates such an argument. Thus, the increased yield of the multi lower molecular weight unidentified neutrals with increasing temperature can be rationalized by the isomerization of the initially formed **3** and **4** to olefin **2** which then thermally decomposes. The constant olefin ratio in the 400 and 450 °C pyrolysates and the failure to isolate any A-ring olefins under higher temperature (600–800 °C) pyrolysis conditions (2) are also consistent with such a mechanism.

The inspection of Table 1 definitely confirms our earlier assumption (2) that the conjugated dienoic acids rapidly isomerize and disproportionation occurs at a much slower rate during hot tube pyrolysis. We also confirmed that in the case of dehydroabietic acid, very little thermal fragmentation occurs until the carboxylate moiety is lost. However, we found that with the conjugated dienoic acids that there are two primary equally important thermal fragmentation pathways. As initially assumed (2), aromatization to dehydroabietic acid does take place along with the unpredicted formation of a lower molecular weight acid (**15**). The strong i.r. absorption at 759 cm^{-1} and a four aromatic proton multiplet in the n.m.r. spectrum of the acid indicated an ortho-disubstituted aromatic ring. Its 264.5 and 272 mμ u.v. absorption maxima, characteristic of a tetralin chromo-

Can. J. Chem. Downloaded from www.nrcresearchpress.com by 210.87.254.40 on 09/05/12
For personal use only.

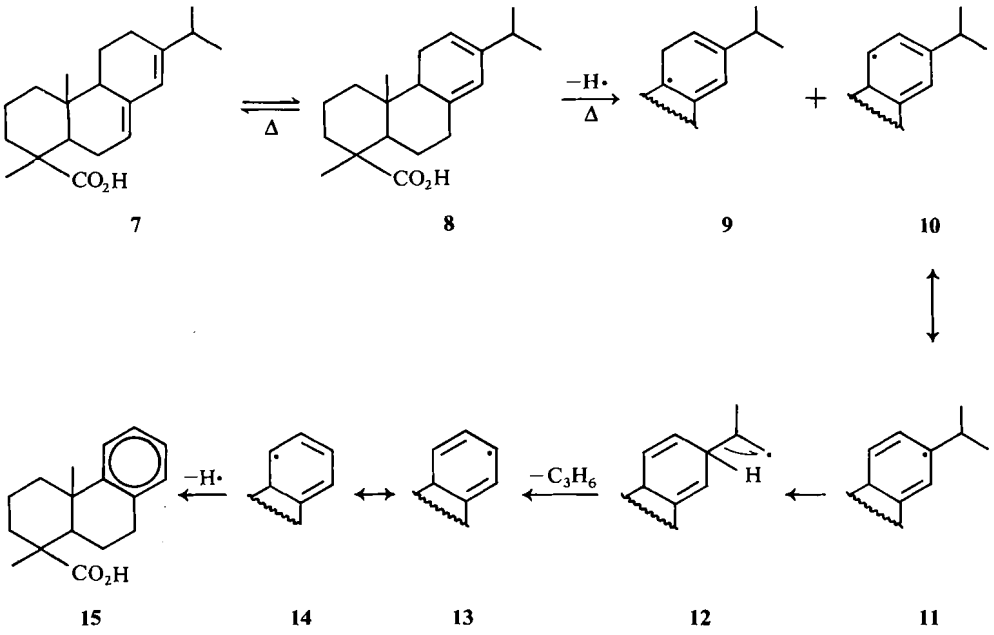

SCHEME 3

phore (11, 12), and its molecular ion at *m/e* 272 suggested that thermal deisopropylation and aromatization of the C-ring had occurred. By comparison of the above data and optical rotation ($[\alpha]_D^{25} + 54°$) with the data given for the minor product formed during the aluminum chloride-induced dialkylation of dehydroabietic acid (5, 13), the identity of **15** was established to be deisopropyldehydroabietic acid.

A somewhat surprising observation is the almost complete lack of formation of the deisopropyl acid during the pyrolysis of dehydroabietic acid. A mechanism which takes this face into acount is given in Scheme 3. Upon heating, levopimaric acid (**8**) would be expected to initially fragment by the loss of one of the allylic hydrogen atoms in the C-ring. A reaction with a previously formed radical would be expected, due to steric considerations (14), to form radical intermediate **10**, while thermal degradation should result in the loss of a hydrogen atom from C-9 to yield **10**. Aromatization could now take place from either **9** or **10** to form the experimentally observed **1**. Resonance stabilization of **10**[6] would be expected to occur to yield the tertiary-diallyl radical **11**. A hydrogen atom rearrangement from one of the isopropyl methyls to the C-13 radical would yield intermediate **12**, which could readily eliminate propylene to produce **13**. Aromatization via **14** would result in the formation of the experimentally observed deisopropyldehydroabietic acid (**15**). This mechanism is substantiated by the isolation of propylene, as 1,2-dibromopropane, from the pyrolysis gases.

The authors wish to thank Mr. James B. Stanley and Mr. Verne W. Tripp of the Southern Regional Research Laboratory, SMNRD, for mass spectral analysis, and Mr. Gordon J. Boudreaux and Mr. Verne W. Tripp of the Southern Regional Research Laboratory, SMNRD, for determining the n.m.r. data.

[6]It is highly probable that **9** and **10** would thermally equilibrate via a hydrogen rearrangement.

1. R. F. SEVERSON, W. H. SCHULLER, and R. V. LAWRENCE. J. Chem. Eng. Data, **17**, 250 (1972).
2. R. F. SEVERSON, W. H. SCHULLER, and R. V. LAWRENCE. Can. J. Chem. **49**, 4027 (1971).
3. H. TAKEDA, W. H. SCHULLER, and R. V. LAWRENCE. J. Org. Chem. **33**, 1683 (1968).
4. J. W. HUFFMANN. J. Org. Chem. **35**, 478 (1970) and references therein.
5. M. OHTA and L. OHMORI. Pharm. Bull. Tokyo, **5**, 91, 96 (1957).
6. N. B. COLTHRUP, L. H. DALY, and S. G. WIBERLEY. Introduction to infrared and raman spectroscopy. Academic Press, New York, N.Y., 1964. p. 226.

Can. J. Chem. Downloaded from www.nrcresearchpress.com by 210.87.254.40 on 09/05/12
For personal use only.

7. C. A. GENGE. Anal. Chem. **31**, 1750 (1959).
8. K. BIEMANN. Mass spectrometry. McGraw-Hill, Inc., New York, N.Y., 1962. p. 337.
9. R. N. SEELYE and W. B. WATKINS. Tetrahedron Lett. 1271 (1968).
10. F. O. RICE and M. T. MURPHY. J. Am. Chem. Soc. **66**, 765 (1944).
11. E. WENKERT and T. E. STEVENS. J. Am. Chem. Soc. **78**, 2318, 5627 (1956).
12. W. E. PARHAM, G. L. WHEELER, and R. M. DODSON. J. Am. Chem. Soc. **77**, 1166 (1955).
13. E. WENKERT, R. W. J. CARNEY, and C. KANEKO. J. Am. Chem. Soc. **83**, 4440 (1961).
14. W. H. SCHULLER and R. V. LAWRENCE. Chem. and Ind. **6**, 203 (1970).

Can. J. Chem. Downloaded from www.nrcresearchpress.com by 210.87.254.40 on 09/05/12
For personal use only.

Kinetics and Rate Constants of Reactions Leading to Hydration of NO_2^- and NO_3^- in Gaseous Oxygen, Argon, and Helium Containing Traces of Water

J. D. PAYZANT, A. J. CUNNINGHAM, AND P. KEBARLE
Chemistry Department, University of Alberta, Edmonton 7, Alberta

Received January 31, 1972

The rate constants for the forward and reverse components of gas phase reactions:

[1] $NO_2^- + H_2O + M \rightleftharpoons NO_2^-(H_2O) + M$

[2] $NO_2^-(H_2O) + H_2O + M \rightleftharpoons NO_2^-(H_2O)_2 + M$

[3] $NO_3^- + H_2O + M \rightleftharpoons NO_3^-(H_2O) + M$

were measured with a pulsed electron beam, time resolved detection high pressure mass spectrometer at 300 °K. O_2, Ar, and He at pressures from 1–7 Torr were used as third gas M. The forward reactions were found to be third order and the reverse reactions second order. Establishment of the equilibria could also be observed.

Les constantes de vitesse des réactions directes et inverses, en phase gazeuse:

[1] $NO_2^- + H_2O + M \rightleftharpoons NO_2^-(H_2O) + M$

[2] $NO_2^-(H_2O) + H_2O + M \rightleftharpoons NO_2^-(H_2O)_2 + M$

[3] $NO_3^- + H_2O + M \rightleftharpoons NO_3^-(H_2O) + M$

ont été mesurées à 300 °K par la spectrométrie de masse utilisant un faisceau d'électrons pulsés et une détection par temps d'envol. On utilise comme troisième gaz M, O_2, Ar, et He sous des pressions de 1 à 7 Torr. Les réactions directes ont été trouvées du troisième ordre et les réactions inverses du deuxième ordre. L'établissement de l'équilibre a pu également être observé.

Canadian Journal of Chemistry, **50**, 2230 (1972)

Introduction

The present work is a continuation of studies dealing with the association of ions with polar molecules. An earlier paper (1) in this journal described measurements of the temperature dependence of hydration equilibria involving: $NO_2^-(H_2O)_n$, $NO_3^-(H_2O)_n$, $CN^-(H_2O)_n$ and $OH^-(H_2O)_n$. These studies led to the evaluation of the enthalpy and entropy changes: $\Delta H_{n,n-1}$ and $\Delta S_{n,n-1}$ for the reactions $(n, n-1)$ where n was generally 1, 2, or 3.

$$(n, n-1) \quad A^-(H_2O)_n = A^-(H_2O)_{n-1} + H_2O$$

The present study deals with the kinetics of the reactions leading to the hydration equilibria of the NO_2^- and NO_3^- ions.

The hydrates of the nitrite and nitrate ions are of particular interest since they are both involved in the negative ion chemistry of the ionosphere. Recent rocket borne mass spectrometer measurements (2, 3) indicate that the $NO_3^-(H_2O)_3$ species is the dominant negative ion at altitudes below 90 km.

Kinetic measurements of the reactions leading to the establishment of ionic equilibria in the gas phase are also of considerable general interest since they provide a useful store of thermochemical data (4). On the basis of such information, unknown rate constants for related reactions can be estimated, and with these, order-of-magnitude time requirements for the achievement of the equilibrium can be obtained. This is an invaluable aid in the selection of proper experimental conditions for the measurement of ionic equilibria. However, the need for careful selection of the experimental conditions ensuring lifetimes of the ions which are longer than the half-lives of the equilibrium reactions, the need for proper sampling conditions, etc., seem not to have been fully appreciated (5).

Experimental

(a) Apparatus and Experimental Conditions

The apparatus used has been described earlier (1, 6); therefore only a brief description will be given here.

A major gas, O_2, Ar, or He at pressures of 1–7 Torr containing known pressures of water (0.8–30 mTorr) was flowed (~ 0.3 l s^{-1} at 4 Torr) through the stainless steel ion source. Ionization was obtained with 2000 V electrons

produced in an electron gun and entering the ion source through a narrow slit (12 μ × 2 mm). The electron beam was pulsed "on" for 10 μs and "off" for 6 ms. Each pulse contained some 10^6 electrons. The resulting ions diffuse through the field free ion source. Some of them come to the vicinity of the molecular flow ion exit slit (12 μ × 2 mm, razor blade edges), escape through the leak into the evacuated region (10^{-4} Torr), and are subjected to magnetic mass analysis (15 cm radius, 90° tube) and electron multiplier detection. The amplified multiplier pulses are collected in a multiscaler whose sweep is triggered by the electron beam "on" pulse. In most runs, the dwell time per channel was 20 μs. The time of flight of ions outside the ion source is short (less than 15 μs for all ions studied) compared to the residence time in the ion source (several ms). The time of flight of ions of different mass was corrected for with a pulse delay circuit. The plane of the electron beam was roughly 2 mm above the ion exit slit.

(b) Measurement of Water Pressure in Ion Source

The achievement of equilibrium for the reaction [4]

[4] $$(2,3)\quad O_2^-(H_2O)_2 + H_2O \rightleftharpoons O_2^-(H_2O)_3$$

could be observed in all runs involving O_2 as a carrier gas (see Results and Discussion section). The observed $O_2^-(H_2O)_3$ and $O_2^-(H_2O)_2$ intensities (normalized ion counts at long reaction times) were substituted in eq. 5 in order to determine the water pressure (Torr) in a given run.

[5] $$K_{2,3} = \frac{O_2^-(H_2O)_3}{O_2^-(H_2O)_2 . P_{H_2O}} = 20 \quad (T = 300.5\,^\circ\mathrm{K})\ \text{(Standard state, 1 Torr)}$$

The value of $K_{2,3}$ was determined in a number of calibration runs involving weight loss based water concentration determinations (7).

The value of $K_{1,2}$ of the NO_2^- ion was found to be reproducible in all runs involving O_2 as the carrier gas. The water concentration in the experiments where Ar and He were used as carrier gas (and where the O_2^- hydrates were not present) was calculated on basis of the $K_{1,2}$ expression for NO_2^- obtained in the oxygen runs.

Results and Discussion

(a) Reactions Leading to NO_2^-, NO_3^-, O_2^-, $C_2H_3O^-$

The NO_2^- and NO_3^- ions were produced by the dissociative electron capture of ethyl nitrate. This method was used in earlier work (1). A few mTorr of ethyl nitrate was added to the major gas (O_2, Ar, or He). When O_2 was the major component, the principle ions observed were NO_2^- and hydrates, O_2^- and hydrates, and $C_2H_3O^-$ and hydrates. The NO_3^- and hydrates were also observed but at somewhat lower yield (~20% of the NO_2^- abundance).

The NO_2^- and $C_2H_3O^-$ are probably produced by reactions 6 and 7.

[6] $$e + C_2H_5ONO_2 \rightleftharpoons NO_2^- + \text{neutral products}$$

[7] $$\rightleftharpoons C_2H_3O^- + \text{neutral products}$$

The electron capture cross section of ethyl nitrate is large only for near thermal electrons (8). The electrons involved in the reactions 6 and 7 are probably secondary electrons brought to near thermal energies by collisions with the major gas. NO_2^- and $C_2H_3O^-$ were the two major ions observed by Kriemler and Butrill (9) in the low pressure mass spectra of ethyl nitrate obtained with low energy electrons. The O_2^- ion and hydrates observed in the present work were probably produced in third body electron capture by oxygen (10), *i.e.*, reaction 8. The ratio of ethyl nitrate

[8] $$2O_2 + e \rightleftharpoons O_2^- + O_2$$

derived ions to O_2^- derived ions could be increased by increasing the ethyl nitrate concentration. Thus in the regime of a few Torr of O_2 and a few mTorr of ethyl nitrate, third body capture by O_2 and dissociative capture by $C_2H_5ONO_2$ proceed at similar rates. The $O_2^-(H_2O)_n$ equilibria were used for calibrations of the water pressure (see Experimental section).

According to Kriemler and Butrill (9), NO_3^- is produced by ion–molecule reactions of $C_2H_3O^-$ (and other minor products of the dissociative electron capture) with ethyl nitrate. Most likely, the NO_3^- observed in the present experiments was due to such a reaction. However, the present observations indicate that an appreciable fraction of $C_2H_3O^-$ does not react with ethyl nitrate, since the sum of the $C_2H_3O^-$ and its hydrates was found to remain a constant proportion of the total ionization after some 50 μs reaction time. Furthermore the NO_2^- and hydrates and the NO_3^- and hydrates each remained a constant proportion of the total ion intensity. The relative negative ion changes in the first 50 μs reaction time were not observed reliably with the present apparatus and conditions, since this is a period of rapid increase of total negative ion intensity (this interval probably corresponds to the time required for the thermalization of the secondary electrons). Since the observed concentration of $C_2H_3O^-$ and hydrates was considerably larger than that of NO_3^- and hydrates, a major part of the $C_2H_3O^-$ does not react with ethyl nitrate.

In the experiments with Ar and He as major gas, $C_2H_3O^-$ and hydrates were the major ion

group, followed by NO_2^- and hydrates. The NO_3^- and hydrates were observed at much lower concentrations. Thus in argon, the intensity of the NO_3^- and hydrates was only 5% of that of the NO_2^- and hydrates while in oxygen the NO_3^- was some 20% of the NO_2^- and hydrates. The dependence of the NO_3^- yield on the nature of the major gas and the inertness of some of the $C_2H_3O^-$ for reactions with ethyl nitrate might be understood if one assumed that two different $C_2H_3O^-$ species are produced in the dissociative electron capture by ethyl nitrate and that one of these is unable to react with ethyl nitrate. The two species might be true isomers or differ only in the degree of internal excitation. It is likely that different proportions of these two species will be present when different major gases are used. Thus the electron thermalization will depend on the nature of the major gas (11) and so electrons of different energies will be captured by the ethyl nitrate and lead to different yields of the fragment ions (8).

Rate Constant Measurements

The determination of the rate constants for the forward and reverse reactions 1, 2, and 3 will be described in this section.

$$[1] \qquad NO_2^- + H_2O + M \underset{-1}{\overset{1}{\rightleftharpoons}} NO_2^-(H_2O) + M$$

$$[2] \qquad NO_2^-(H_2O) + H_2O + M \underset{-2}{\overset{2}{\rightleftharpoons}} NO_2^-(H_2O)_2 + M$$

$$[3] \qquad NO_3^- + H_2O + M \underset{-3}{\overset{3}{\rightleftharpoons}} NO_3^-(H_2O) + M$$

Shown in Fig. 1 is the time dependence of the ion signal for the species NO_2^-, $NO_2^-H_2O$, and $NO_2^-(H_2O)_2$ observed in a typical experiment with oxygen as the major gas. The ion signal for a given ion, such as NO_2^-, has been normalized to the total ion signal for the NO_2^- and hydrates. This is in accordance with the observation (see previous section) that the NO_2^- and hydrates system was independent of the other ions present, *i.e.*, the total relative concentration of the NO_2^- and hydrates remained constant with time. The data in Fig. 1 will be treated as if they represented concentration changes in a reaction vessel in which the total ion concentration is constant with time (12). The figure shows the decrease of NO_2^-, the appearance of the

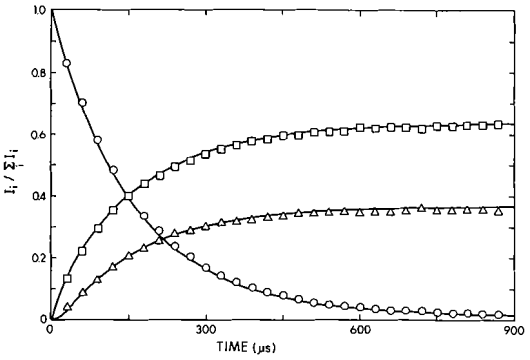

FIG. 1. Time dependence of NO_2^- and hydrates depicting reaction sequence:

$$NO_2^- \rightleftharpoons NO_2^-(H_2O) \rightleftharpoons NO_2^-(H_2O)_2$$

○, NO_2^-; □, $NO_2^-(H_2O)$; △, $NO_2^-(H_2O)_2$. The solid line connecting the experimental points represents a computer fit of reaction system 1–2, see text. $p(O_2) = 2.14$ Torr, $p(H_2O) = 27$ mTorr, $T = 300$ °K.

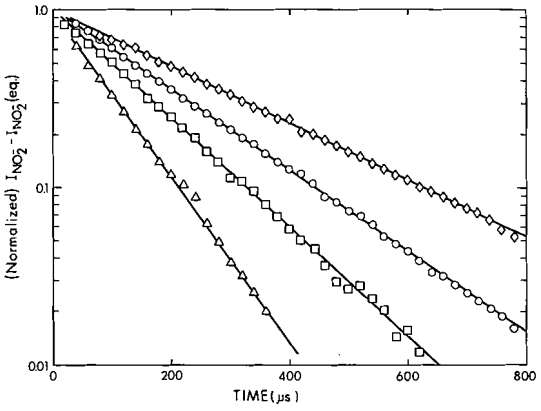

FIG. 2. Determination of k_1 and k_{-1}. Slopes of plots are equal to: $-(\nu_1 + \nu_{-1})/2.3$, where $\nu_1 = k_1[H_2O][O_2]$ and $\nu_{-1} = k_{-1}[O_2]$. In legend below first number given: O_2 pressure in Torr; second number: H_2O pressure in mTorr; third number: $\nu_1 \times 10^{-3}$ in s^{-1}: □, 5.4, 14, 6.53; ○, 1.47, 30.2, 5.16; ◇, 3.8, 9.2, 3.42; △, 3.61, 32.7, 10.67.

hydrate $NO_2^-H_2O$, followed by the dihydrate and the achievement of equilibrium for reaction times longer than ~ 500 μs.

The solid lines connecting the experimental points are analogue computer calculated concentrations obtained by programming the computer to reproduce the reversible reaction system represented by reactions 1 and 2. As can be seen, a very satisfactory fit of the data was obtained. The reactions in an experiment (*e.g.*, Fig. 1), are all first order, so that the computer

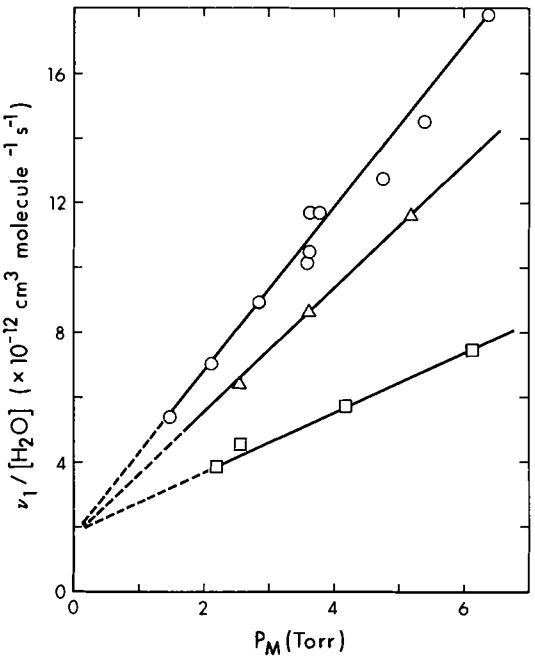

FIG. 3. Plots used to establish whether reaction 1,

$$NO_2^- + H_2O + M \rightleftharpoons NO_2^- H_2O + M$$

obeys relationship $v_1 = k_1[H_2O][M]$. Results indicate that this is correct, *i.e.*, reaction is third order. ○, M = O_2; △, M = Ar; □, M = He.

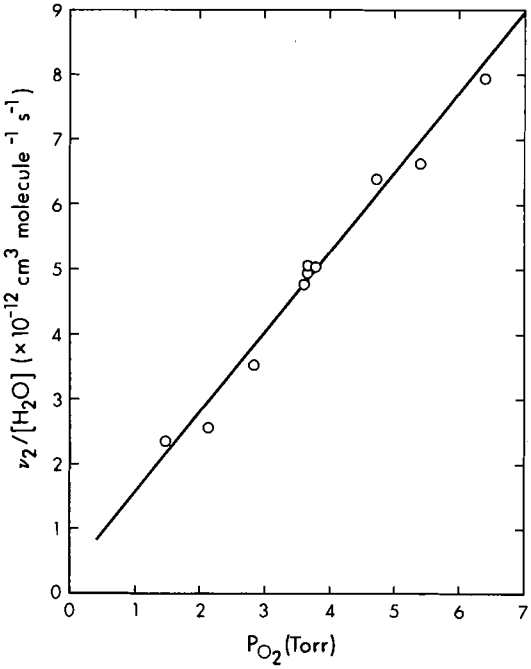

FIG. 4. Plot used to establish whether reaction 2,

$$NO_2^-(H_2O) + H_2O + O_2 \rightleftharpoons NO_2^-(H_2O)_2 + O_2$$

obeys relationship $v_2 = k_2[H_2O][O_2]$. Results show that this is correct, *i.e.*, reaction 2 is third order.

fit provides pseudo first order rate constants (or reaction frequencies) v. Thus, one obtains $v_1 = k_1[M][H_2O]$, $v_{-1} = k_{-1}[M]$, etc. from a given fit. One can then calculate k_i from v_i and the known concentrations of the neutral species. In all, ten runs with O_2 and seven runs with Ar or He as a major gas were made. The pressure of the major gas was varied from 1.5–6.4 Torr and the H_2O pressure from 0.8–30 mTorr. The results are summarized in Figs. 2–4.

Figure 2 illustrates a method by which v_1 and v_{-1} can be evaluated without the use of the computer. For a general reversible reaction:

$$A \underset{v_{-1}}{\overset{v_1}{\rightleftharpoons}} B \underset{v_{-2}}{\overset{v_2}{\rightleftharpoons}} C$$

in which [A] + [B] + [C] = constant, it can be shown (13) that the concentration of reactant A obeys eq. 9.

$$[9] \quad 2.3 \log([A^-] - [A_{eq}^-]) = -(v_1 + v_{-1})t + \text{constant}$$

where $[A_{eq}^-]$ is the equilibrium concentration of A^- and $[A^-]$ is the concentration at time t. The use of eq. 9 for the NO_2^- system is illustrated in Fig. 2. The $[NO_{2eq}^-]$ was determined from time dependence plots similar to those shown in Fig. 1, but extended to much longer reaction times (typically in excess of 2000 μs) where a constant concentration of NO_2^- could be observed over a wide time interval. The four straight lines shown in Fig. 2 are representative of the type of data obtained and the range of concentrations used. The slopes which correspond to $-(v_1 + v_{-1})/2.3$, combined with the measured equilibrium ratio and the relationship: $[NO_2^-(H_2O)_{eq}]/[NO_{2eq}^-] = v_1/v_{-1}$, gave values for v_1 and v_{-1} and thus for k_1 and k_{-1}. These values were very close to those obtained from the computer fit. The computer fit yielded (for the four runs shown in Fig. 2) the values: v_1 = 3.5(3.4), 5.6(5.2), 6.8(6.5), 10.6(10.7) (in units of 10^3 s^{-1}), while the values shown in brackets were obtained from the graphical plot. The linear graphical plot has the advantage of not

TABLE 1. Rate and equilibrium constants for hydration of NO_2^- and NO_3^- at 300 °K

Reactions

$$NO_2^- + H_2O + M \underset{-1}{\overset{1}{\rightleftharpoons}} NO_2^-(H_2O) + M$$

$$NO_2^-(H_2O) + H_2O + M \xrightarrow[-2]{2} NO_2^-(H_2O)_2 + M$$

$$NO_3^- + H_2O + M \underset{-3}{\overset{3}{\rightleftharpoons}} NO_3^-(H_2O) + M$$

Rate or equilibrium constant

$k_1 = 8.4 \times 10^{-29}(O_2)$, 6×10^{-29}(Ar), 2.9×10^{-29}(He) cm^6 molecule^{-2} s^{-1}

$k_1 = 13 \times 10^{-29}$(NO) Puckett and Lineberger (14)

$k_{-1} = 1.6 \times 10^{-15}(O_2)$, 1.1×10^{-15}(Ar), 0.56×10^{-15}(He) cm^3 molecule^{-1} s^{-1}

$K_1 = K_{0,1} = k_1/k_{-1} = 5.2 \times 10^{-14}$ cm^3 molecule^{-1}

$K_1 = 3 \times 10^{-14}$ (previous determination; ref. 1)

$k_2 = 3.8 \times 10^{-29}(O_2)$ cm^6 molecule^{-2} s^{-1}

$k_{-2} = 5.8 \times 10^{-14}(O_2)$ cm^3 molecule^{-1} s^{-1}

$K_2 = K_{1,2} = k_2/k_{-2} = 6.6$ cm^3 molecule^{-1}

$K_2 = 6.5$ cm^3 molecule^{-1} (previous determination; ref. 1)

$k_3 = 7.5 \times 10^{-29}(O_2)$ cm^6 molecule^{-2} s^{-1}

$k_{-3} = 1.4 \times 10^{-14}(O_2)$ cm^3 molecule^{-1} s^{-1}

$K_3 = K_{1,0} = k_3/k_{-3} = 5.3 \times 10^{-15}$ cm^3 molecule^{-1}

$K_3 = 4.9 \times 10^{-15}$ cm^3 molecule^{-1} (previous determination; ref. 1)

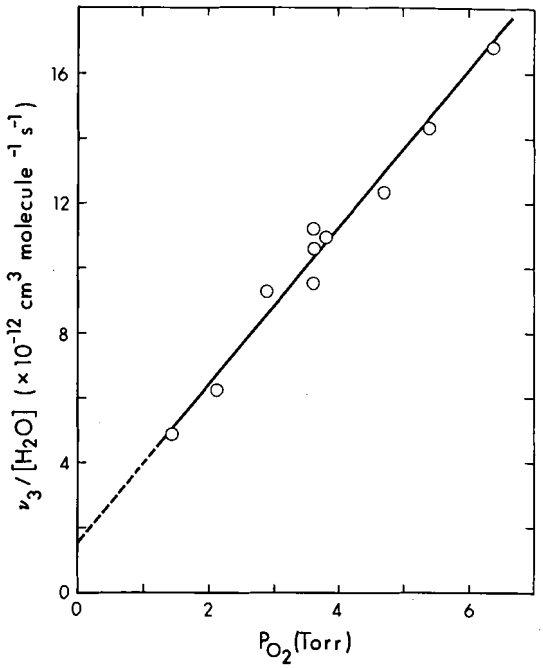

FIG. 5. Plot used to establish whether reaction 3,

$$NO_3^- + H_2O + O_2 \rightleftharpoons NO_3^-(H_2O) + O_2$$

obeys relationship $v_3 = k_3[H_2O][O_2]$. Results indicate that this is correct, *i.e.* reaction 3 is third order.

being affected by subjective error as is the case with the visual fitting of the computer curves to the measured time dependence of the ion concentrations.

Figure 3 shows a plot of $v_1/H_2O]$ *vs.* the pressure of the major gas M. The plots give a linear increase with the pressure of M, but yield a positive intercept. It is not clear whether this effect is real, revealing a complex dependence of reaction on third body pressure, or whether it is due to some insufficiency of the experimental technique. Assuming the latter, values for the third order rate constants $k_1 = v_1/[H_2O][M]$ were obtained from the slopes of the linear portion of the plots. These values are shown in Table 1.

Since reaction 1 appears third order, reaction -1 must be second order, *i.e.*, $v_{-1} = k_{-1}[M]$. The values of k_{-1} obtained from the slope of plots of v_{-1} *vs.* [M] are given in Table 1.

The data for the reaction 3 are summarized in the plot shown in Fig. 4 which gives $v_2/[H_2O]$ plotted against the pressure of the major gas O_2. The v_2 values were obtained from computer fits of the experimental runs. The linear dependence observed in Fig. 4 shows that reaction 2 is third order. The slope of the plot leads to k_2 given in the table. No determinations of k_2 were made with He and Ar as major gas. The second order rate constant k_{-2} given in the table was obtained from the slope of a plot of $v_{-2}/[H_2O]$ *vs.* the oxygen pressure.

The methods applied for the study of reaction 3 and -3 involving the NO_3^- ion and its monohydrate were essentially the same as those used for the analogous reaction 1 involving the NO_2^- ion. The pseudo first order v_3 obtained by graphical plots like those in Fig. 2 are shown in Fig. 5. The plot of $v_3/[H_2O]$ *vs.* the oxygen pressure gives a straight line showing that the reaction is third order. The slope leads to k_3 shown in the table. The second order k_{-3} was evaluated by methods similar to those used for the evaluation of k_{-1}.

The experimental conditions were not favorable for the observation of the higher hydrates of NO_3^- and therefore, the corresponding rate constants were not measured.

The rate and equilibrium constants shown in Table 1 summarize the results of the present work and include previous determinations. Literature information is available only for k_1 which was determined by Puckett and Lineberger (14) with NO as a third body. This value is slightly higher than the present value with O_2. There is no clear *a priori* reason to suggest why NO should be a more efficient third body than O_2. The observed difference between the two values might reflect either a higher efficiency for NO or an experimental error. The lower efficiencies of Ar and He observed in the present work are consistent with previous determinations in similar systems (15).

The forward association rate constants k_1, k_2, and k_3 (Table 1) are seen to be quite close to each other. The binding energies of the hydrates, measured earlier (1), were: $\Delta H_{1,0}(NO_2^-) = 14.3$, $\Delta H_{2,1}(NO_2^-) = 12.9$, and $\Delta H_{1,0}(NO_3^-) = 12.4$ kcal/mol. Thus the formation of the $NO_2^-(H_2O)$ is associated with the largest binding energy, which considered by itself should lead to a higher forward rate constant. The proximity of the observed rate constants indicates that the bond energy effect is at least partially offset by the larger number of degrees of freedom available in the $NO_2^-(H_2O)_2$ and $NO_3^-H_2O$ species.

The equilibrium constants $K_{0,1}$, $K_{1,2}$ for NO_2^- and $K_{0,1}$ for NO_3^- shown in Table 1 are close to those obtained previously (1). The values obtained in the earlier determination were measured with H_2O as the major gas at water pressures in the Torr range, *i.e.*, hundred times higher than the water pressure used in the present work. The lower stability of the $NO_3^-(H_2O)$ and the $NO_2^-(H_2O)$—H_2O relative to the $NO_2^-H_2O$ is reflected in the values of the corresponding equilibrium constants and in the rate constants for the cluster dissociation reactions. The dihydrate of NO_2^- has the highest dissociation rate constant (k_{-2}).

1. J. D. PAYZANT, R. YAMDAGNI, and P. KEBARLE. Can. J. Chem. **49**, 3308 (1971).
2. R. S. NARCISI, A. D. BAILEY, L. DELLA LUCCA, C. SHERMAN, and D. M. THOMAS. J. Atmos. Terr. Phys. **33**, 1147 (1971).
3. F. ARNOLD, J. KISSEL, D. KRANOWSKY, H. WIEDER, and J. ZÄHRINGER. J. Atmos. Terr. Phys. **33**, 1169 (1971).
4. R. YAMDAGNI and P. KEBARLE. J. Am. Chem. Soc. **93**, 7135 (1971).
5. D. P. BEGGS and F. H. FIELD. J. Am. Chem. Soc. **93**, 1576 (1971).
6. M. ARSHADI, R. YAMDAGNI, and P. KEBARLE. J. Phys. Chem. **74**, 1475 (1970). R. YAMDAGNI and P. KEBARLE. J. Am. Chem. Soc. **93**, 7139 (1971).
7. J. D. PAYZANT and P. KEBARLE. J. Chem. Phys. **56**, 3482 (1972).
8. K. JÄGER and A. HENGLEIN. Z. Naturforsch. **22***a*, 700 (1967).
9. PETER KRIEMLER and S. E. BUTTRILL, JR. J. Am. Chem. Soc. **92**, 1123 (1970).
10. J. L. PACK and A. V. PHELPS. J. Chem. Phys. **44**, 1870 (1966).
11. L. G. CHRISTOPHOROU. Progress and problems in contemporary radiation chemistry. Vol. 1. *Edited by* J. L. Teply. Czechoslovak Academy of Sciences, Prague, 1971.
12. D. A. DURDEN, P. KEBARLE, and A. GOOD. J. Chem. Phys. **50**, 805 (1969).
13. J. D. PAYZANT. Ph.D. Thesis, University of Alberta, Edmonton, Alberta. 1972.
14. L. J. PUCKETT and W. C. LINEBERGER. Phys. Rev. A 1, 1635 (1970).
15. D. K. BOHME, D. B. DUNKIN, F. C. FEHSENFELD, and E. E. FERGUSON. J. Chem. Phys. **51**, 863 (1969).

Thermal Decomposition of Stereoisomeric 3-Aroyl- and 3-Carbomethoxyaziridines in Acetonitrile

J. W. LOWN AND M. H. AKHTAR[1]

Department of Chemistry, University of Alberta, Edmonton 7, Alberta

Received August 27, 1971[2]

The thermal decomposition of 1-alkyl-3-benzoyl-2-(*m*-nitrophenyl)aziridines in dry acetonitrile results in a series of autocatalytic hydrolytic cleavages, 1,3-dipolar additions, condensations, and rearrangements to give products including oxazolidines, 1,2-dihydropyrazines, pyrrolo-[3,4-*d*]-4-oxazolines, and α-aminoketones. The marked differences in product type and distribution from *cis*- and *trans*-aziridines are ascribed to preferential hydrolytic opening at the aziridinium ion stage. Complete equilibration of the stereoisomeric azomethine ylides takes place prior to 1,3-dipolar additions.

Thermal decomposition of *cis*- and *trans*-methyl 1-isopropyl-2-(*m*-nitrophenyl)aziridine-3-carboxylates in acetonitrile is not autocatalytic (and can be suppressed) and produces three stereoisomeric oxazolidines in identical yields and ratios, and methyl *N*-isopropylglycine by selective hydrolytic attack at the 2-aziridine position. This result is ascribed to equilibration of the stereoisomeric aziridines prior to hydrolytic cleavage by adventitious moisture only.

La décomposition thermique des alkyl-1 benzoyl-3 *m*-nitrophényl-2 aziridines dans l'acétonitrile sec conduit à une série de clivages hydrolytiques autocatalysés, d'additions dipolaires-1,3, de condensations et de réarrangements donnant des produits comprenant des oxazolidines, des dihydro-1,2 pyrazines, des pyrroles[3,4-*d*] oxazolines-4 et des α-aminocétones. Les différences notables dans le type de produit et leur distribution à partir des aziridines *cis* et *trans* sont attribuées à l'ouverture préférentielle par hydrolyse au stade de l'ion aziridinium. L'équilibration complète des ylures azométhine stéréoisomères se fait avant les additions dipolaires-1,3. La décomposition thermique des carboxylates d'isopropyl-1 *m*-nitrophényl-2 aziridine-3 de méthyle *cis* et *trans*, n'est pas autocatalytique (et peut être supprimée) et conduit à trois oxazolidines stéréoisomères dans des rapports et des rendements identiques et à la méthyl-*N*-isopropylglycine par hydrolyse sélective sur la position-2 de l'aziridine. Ce résultat est attribué à l'équilibration des aziridines stéréoisomères avant clivage par hydrolyse causée seulement par une humidité accidentelle.

Canadian Journal of Chemistry, **50**, 2236 (1972)

The thermal conrotatory and photochemical disrotatory cleavage of the carbon–carbon bond of aziridines to azomethine ylides proceeding according to strict orbital symmetry control is now firmly established (1). Hitherto such reactions and the subsequent 1,3-dipolar additions have been examined largely in nonpolar solvents, *e.g.* benzene or toluene, in which many *cis*- and *trans*-aziridines undergo configurational equilibration without complication (2–6).

For many cycloadditions, particularly with heterocumulene dipolarophiles, more polar solvents, *e.g.* CH_3CN or CH_3NO_2, are desirable for reasons of solubility. It was therefore necessary to examine the controlled decomposition of aziridines in such solvents and elucidate possible side reactions which would be particularly important in cycloadditions of aziridines with less reactive dipolarophiles.

The decomposition of certain aziridines in dry acetonitrile shows a surprisingly facile series of hydrolytic cleavages, 1,3-dipolar additions, condensations, and rearrangements and a marked difference in behavior of *cis*- and *trans*-aziridines is apparent. Configurational assign-

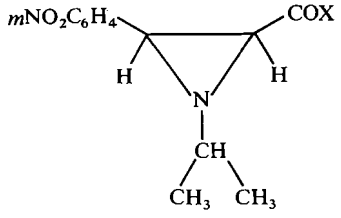

1

a X = C_6H_5
b X = OCH_3

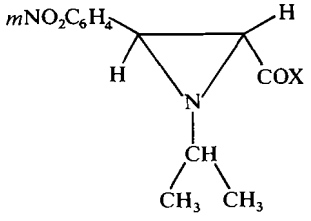

2

a X = C_6H_5
b X = OCH_3

[1]NRCC Postdoctorate Fellow, 1970 to present.

[2]Revision received March 30, 1972.

Can. J. Chem. Downloaded from www.nrcresearchpress.com by 210.87.254.6 on 09/05/12
For personal use only.

Can. J. Chem. Downloaded from www.nrcresearchpress.com by 210.87.254.6 on 09/05/12
For personal use only.

ments of *cis* and *trans* pairs of aziridines in this paper are based on the n.m.r. correlations of Pohland *et al.* (7).

Heating of a solution of pure **1***a* in dry acetonitrile under reflux for 24 h and chromatographic separation of the products afforded (*i*) the stereoisomeric oxazolidines **3***a* and **4***a* in a ratio of (80:20) (one of which could be obtained stereoisomerically pure) in 56% yield, (*ii*) the 1,2-dihydropyrazine derivative **5** in 10% yield,

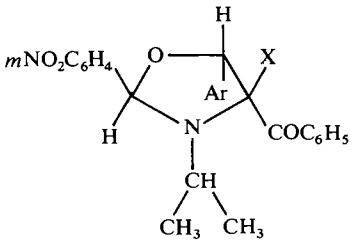

3
a X = H
b X = D

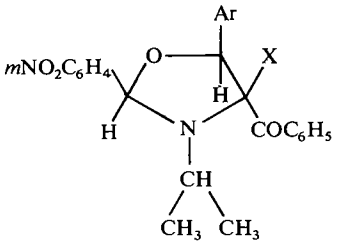

4
a X = H
b X = D

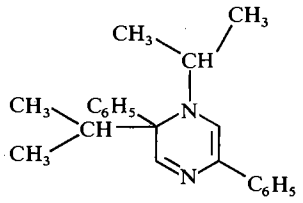

5

(*iii*) *N*-(isopropyl)phenacylamine **6** in 20% yield, and (*iv*) an incompletely characterized basic fraction which probably contains *m*-nitrobenzylisopropylamine **7**, isopropylamine,

$C_6H_5COCH_2NH—CH(CH_3)_2$

6

m-$NO_2C_6H_4CH_2NHCH(CH_3)_2$

7

and other minor basic products to the extent of 10%.

In contrast, reaction of pure **2***a* under precisely the same conditions gave a mixture of products which were separable by column chromatography affording (*i*) the oxazolidines **3***a* and **4***a* in only 5.4% yield, (*ii*) the pyrrolo-[3,4-*d*]-4-oxazoline **8** in 8.5% yield, (*iii*) the 1,2-dihydropyrazine **5** in 12.5% yield, (*iv*) *N*-(isopropyl)phenacylamine **6** in 26.5% yield, (*v*) *m*-nitrobenzaldehyde **9** in 6.3% yield, and (*vi*) a fraction consisting of a mixture of amines in 8% yield, which was very similar to that obtained from **1***a*.

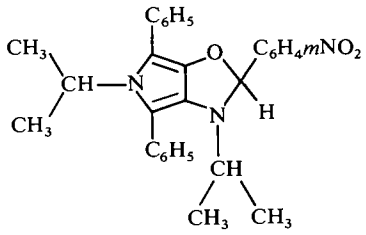

8

It was demonstrated independently that both **1***a* and **2***a* suffer cleavage of the 2–3 carbon–carbon bond in acetonitrile under the reaction conditions since reaction of each separately with an equimolar quantity of *N*-phenylmaleimide gave a single pyrrolidine **10**. Similar products formed in benzene have been reported by Woller and Cromwell (2). The n.m.r. spectrum of **10** closely resembled that of the *N*-cyclohexyl analog **11***a* which was similarly prepared and the full stereochemistry of which was established by examination of the deuterated analog **11***b*, prepared from 1-cyclohexyl-3-benzoyl-3-deutero-2-(*m*-nitrophenyl)aziridine (containing 54% of deuterium label).

Diminution of the 8.5 Hz doublet at 5.30 confirmed the assignment of the 5-pyrrolidine proton. The smaller H_2–H_3 coupling (4.5 Hz) established a *trans* arrangement and proved that the larger groups at the 2- and 5-positions are *trans* related. The assignments of the *cis* and *trans* couplings in these pyrrolidines are based on strong literature analogies (2, 8, 9).

The structures of **3***a* and **4***a* were proven by independent reaction of either **1***a* or **2***a* with an equimolar quantity of *m*-nitrobenzaldehyde. Precisely the same 80:20 ratio of **3***a* to **4***a* was obtained as from the decomposition experiment. The regiospecific cycloaddition of activated

Can. J. Chem. Downloaded from www.nrcresearchpress.com by 210.87.254.6 on 09/05/12
For personal use only.

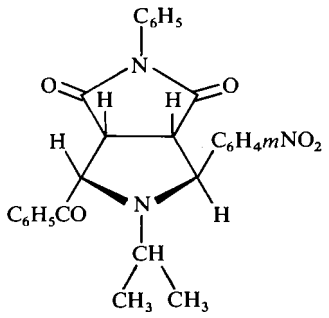

10

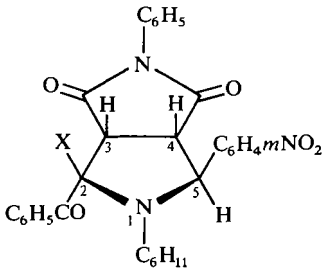

11

a X = H
b X = D

aldehydes to azomethine ylides to form oxazolidines in nonpolar solvents is firmly established (10–12).

The orientation of addition of the *m*-nitrobenzaldehyde was proven by deuterium labelling at the 3-position of the aziridine. The 2-oxazolidine singlets were unaffected while the 4.66 and 5.61 branches of the AB quartets due to the 4,5-protons were diminished. The magnitude of the two 4,5-proton couplings was not sufficiently characteristic to allow for an unambiguous assignment of the position of the 5-*m*-nitrophenyl group relative to the succinimide bridge.

When *cis*-3-benzoyl-1-cyclohexyl-3-deutero-2-(*m*-nitrophenyl)aziridine was heated in acetonitrile it afforded the single oxazolidine **12***b* in 53% yield containing the deuterium label at the 4-position. It is noteworthy that in the experiments involving deuterium labelled aziridines in acetonitrile in this study, quantitative transfer of the deuterium was often observed. This is in contrast to previous work in nonpolar solvents where appreciable leakage of deuterium label was observed (10, 13–16).

The relative positions of the 2 and 4 oxazolidine substituents in **3***a*, **4***a*, and **12** were assigned *trans* by analogy with **10** and **11**, the stereochemistry of which is unambiguous. Aromatic aldehydes are relatively weak dipolarophiles and in the case of addition to *cis*- and *trans*-3-aroylaziridines the corresponding azomethine ylides equilibrate to the more stable *trans*-azomethine ylide prior to cycloaddition. Confirmation is obtained by employing much more reactive dipolarophiles, namely azoesters which even in a 15 *M* equiv excess in acetonitrile are unable to suppress the equilibration of the *cis*-azomethine ylide to the *trans*. The products of these reactions are the 1,2,4-triazolidines **13** consisting of single 3,5-*trans*-configurations in each case.

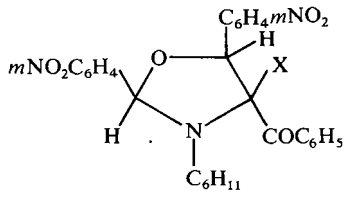

12

a X = H
b X = D

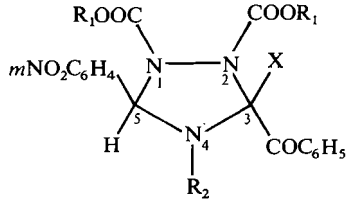

13

a $R_1 = CH_3CH_2$; $R_2 = C_6H_{11}$; X = H
b $R_1 = CH_3CH_2$; $R_2 = C_6H_{11}$; X = D
c $R_1 = CH_3CH_2$; $R_2 = CH(CH_3)_2$; X = H
d $R_1 = C_6H_5$; $R_2 = CH(CH_3)_2$; X = H

Assignment of the 3 and 5 ring protons in **13** is simplified by the observation of significant line broadening of the former due to coupling to the ortho protons of the adjacent *m*-nitrophenyl ring and was confirmed by deuterium labelling.

The deuterated compounds **12***b* and **13***b* did not epimerize nor exchange any deuterium label upon separate refluxing in acetonitrile with either an equivalent of the aziridine or of the corresponding primary amine, isopropylamine, or cyclohexylamine. It is concluded that epimeri-

Can. J. Chem. Downloaded from www.nrcresearchpress.com by 210.87.254.6 on 09/05/12
For personal use only.

zation at the 4-position of these compounds does not occur under the reaction conditions compared with those in **20** despite the greater acidity of the C-4 hydrogen in **3**, **4**, and **12** and **13**. Therefore cycloaddition of the *m*-nitrobenzaldehyde has taken place to the more stable *trans*-azomethine ylide exclusively from either *cis*- or *trans*-aziridine. Even the most stringent precautions to exclude moisture did not suppress formation of the various products indicated above, although examination of the nature of some of the products, *e.g.* **3**, **4**, **6**, **8**, and *m*-nitrobenzaldehyde clearly indicates that hydrolysis is involved. A clue to the course of the reaction in anhydrous acetonitrile is provided by the isolation of the pyrrolo[3,4-*d*]-4-oxazoline **8**. Previous work has shown **8** can arise in the addition of *p*-nitrosophenol to 3-aroylaziridines in two consecutive 1,3-dipolar additions in which the second regiospecific addition is autocatalytic in that the subsequent Paal–Knorr condensation releases 2 equiv of water to further promote hydrolysis in an earlier step (6). The water thus released in the formation of **8** and of **5** (see Scheme 1) becomes available to initiate the hydrolysis of the aziridines. These reactions are interpreted in Scheme 1.

Previous work has shown that uncatalyzed hydrolysis of 2,3-disubstituted aziridines takes place via the aziridinium ion by a predominantly S_N2 process (17–19). Water is sufficiently acidic to provide a very low concentration of the aziridinium ion **14** from most aziridines which initiates attack by the weakly nucleophilic water (20). The nature of the products requires hydrolytic opening at both C-2 and -3 of the aziridinium ion **14** as was found previously by Cromwell and Wankel, in that hydrolysis of *trans*-1-benzyl-2-phenyl-3-*p*-toluoylaziridine results in almost equal attack at these two positions (21).

Water made available in the formation of **5** and **8** therefore, hydrolyzes **14** by attack at C-2 to give *m*-nitrobenzaldehyde **9** and *N*-isopropylphenacylamine **6**. Part of the *m*-nitrobenzaldehyde is trapped regiospecifically by the *trans*-azomethine ylide (which has a low equilibrium concentration relative to the aziridine); the rest of the *m*-nitrobenzaldehyde is isolated.

The structure of **6** was proven by its preparation from phenacyl bromide and isopropylamine and careful neutralization of the salt with base. The n.m.r. spectrum of **6** indicates the presence in solution of a large number of tautomers, the position of equilibrium of which depends on solvent polarity. Such a phenomenon is characteristic of substituted α-aminoketones (22–25). Compound **6** self-condenses very readily at room temperature to a 1,4-dihydropyrazine **15** which is not isolated but rearranges to the 1,2-dihydropyrazine **5**. The latter was identical with the material isolated from the controlled decomposition of the aziridine. Chen and Fowler have recently shown that the 1,4-dihydropyrazine structure previously assumed to be isolated from such dimerizations is incorrect in that the intermediate 1,4-dihydropyrazine suffers a 1,3-alkyl shift to the more stable (*i.e.*, possibly not antiaromatic) 1,2-dihydro form (26).

The n.m.r. spectrum of **5** shows two distinct isopropyl group doublets and two clean septets for the corresponding methines. This discounts the alternative structure **16** which would correspond to migration of the isopropyl group to an unsubstituted position. Chen and Fowler found, for a structure comparable with **16**, appreciable

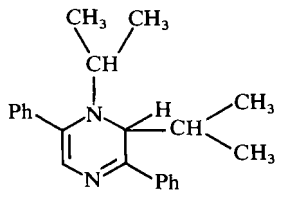

16

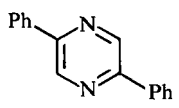

17

coupling between the adjacent methine protons. Additionally no signal ascribable to the N—C*H*—R proton is seen in the n.m.r. spectrum of **5**. Finally pyrolysis of **3** at 280° resulted in elimination of the elements of 2,3-dimethylbutane and afforded the known 2,5-diphenylpyrazine **17**.

Hydrolytic cleavage of the aziridinium ion **14** at C-3 would give rise to phenylglyoxal and *m*-nitrobenzylisopropylamine. It has been demonstrated independently that phenylglyoxal will undergo a regiospecific 1,3-dipolar addition to aziridines to form intermediates like **18** which may in certain cases be isolated and characterized (6). Subsequent treatment with a primary amine results in a rapid Paal–Knorr condensation (28) to form pyrrolo [3,4-*d*]-4-oxazolines like **8** with the release of 2 equiv of water. The source of the isopropylamine in the scheme is

Can. J. Chem. Downloaded from www.nrcresearchpress.com by 210.87.254.6 on 09/05/12
For personal use only.

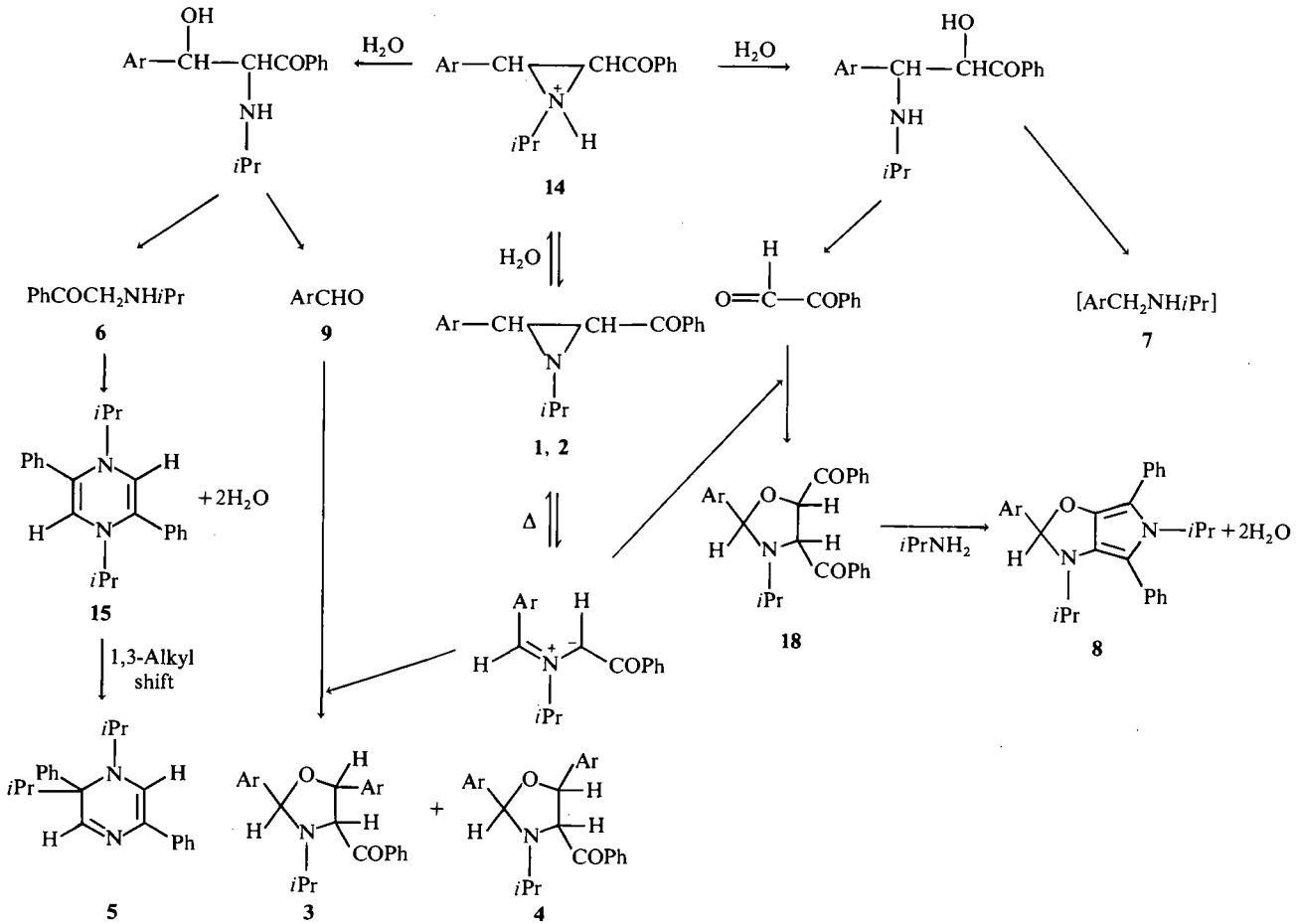

Ar = mNO$_2$C$_6$H$_4$—

SCHEME 1

Can. J. Chem. Downloaded from www.nrcresearchpress.com by 210.87.254.6 on 09/05/12
For personal use only.

not clear at the present time. However it may be noted that often in the direct reaction of phenylglyoxal with aziridines, pyrrolo[3,4-*d*]-4-oxazolines are isolated directly, indicating the aziridine is readily hydrolyzed to provide sufficient primary amine.

A control decomposition of **2***a* in dry acetonitrile at 50° (*i.e.* at a temperature below that at which the 2–3 aziridine bond suffers cleavage indicated by the lack of equilibration of the recovered aziridine) gave rise only to products of hydrolysis, *i.e.* **6** and **9** and not to those of cycloaddition **3**, **4**, and **8**. This suggests, but does not prove, that the primary products of hydrolysis arise from the aziridinium ion **14** and not from the azomethine ylide. Also since it has been shown that the *cis*-azomethine ylide equilibrates rapidly to the *trans* form prior to cycloaddition to form **3**, **4**, and presumably **18**, then the differences in the nature and distribution of the products from *cis*- and *trans*-aziridines result mainly from hydrolysis at the aziridine stage.

Precedents exist for differences in the preferred position of attack and rates of hydrolysis of *cis–trans* pairs of aziridines (18, 21). For example in the case of 1-benzyl-3-*p*-toluoyl-2-phenylaziridine, whereas the *trans* gave rise to hydrolysis at both positions to approximately equal extents, the *cis* isomer resulted in nucleophilic cleavage at C-3 only. In the present work, the *cis*-3-benzoylaziridine shows a marked preference for hydrolytic cleavage at C-2 leading to *ca.* 10 times as much oxazolidine (via *m*-nitrobenzaldehyde) as for the *trans* isomers.

A different situation obtains in the case of 3-carbomethoxyaziridines. Aziridine **1***b*, upon refluxing in acetonitrile, afforded a mixture of three stereoisomeric oxazolidines **20***a*, *b*, and *c*, and methyl *N*-isopropylglycine isolated as the acid. Compounds **20***a*, *b*, *c* were separable and were found in the ratio of 58:35.5:6.5 (*a*:*b*:*c*). Their structures as oxazolidines were proven by independent reaction of the *cis*- or *trans*-aziridines with *m*-nitrobenzaldehyde which afforded **20***a*, *b*, and *c* in virtually the same proportion 54:39:7.0 (*cis*) and 52:40:8.0 (*trans*). The orientation of addition of the aldehyde to the intermediate azomethine ylides was established unambiguously as before by specific deuterium labelling at the 3-position of the aziridine. The fact that all three oxazolidines correspond to the same orientation of addition of the aldehyde requires that in this instance both *cis*- and *trans*-azomethine ylides have been trapped (see below for supporting evidence). The same series of product oxazolidines **20***a*, *b*, and *c* in virtually the same ratio 55:37.5:7.5 are also obtained from **2***b*, implying that the *m*-nitrobenzaldehyde produced by hydrolysis of the aziridines adds to an equilibrium mixture containing both *trans*- and *cis*-azomethine ylides.

The compounds **20***a*, *b*, and *c* did not epimerize upon separate refluxing in acetonitrile with either an equivalent of the corresponding aziridine or isopropylamine, *i.e.* under the conditions of their formation. This confirms that the ratio of products observed is derived by the addition of *m*-nitrobenzaldehyde to the equilibrium mixture of ylides.

The configurational assignments with respect to the aziridine moiety in **20***a*, *b*, and *c* were established by experiments in which aziridines **1***b* and **2***b* were respectively treated with a large excess of *m*-nitrobenzaldehyde to trap the predominant ylide prior to complete equilibration. The pure *trans*-aziridine with 10.5 equiv of *m*-nitrobenzaldehyde in acetonitrile at 115–117° afforded **20***a*, *b*, and *c* in a ratio of 20.5:18:61.5 confirming that **20***c* arises from the predominant *cis*-azomethine ylide.

Similarly the pure *cis*-aziridine reacted with 7.5 *M* equiv of *m*-nitrobenzaldehyde to give

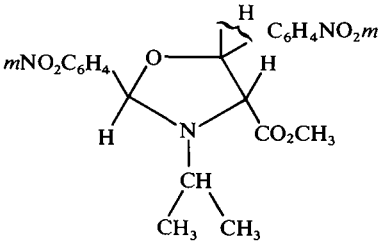

20*a* and *b*

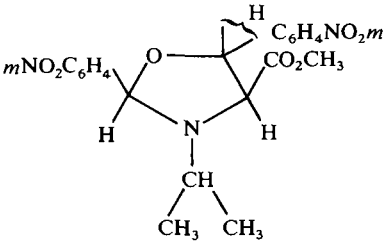

20*c*

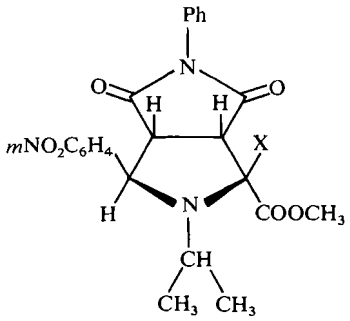

21
a X = H
b X = D

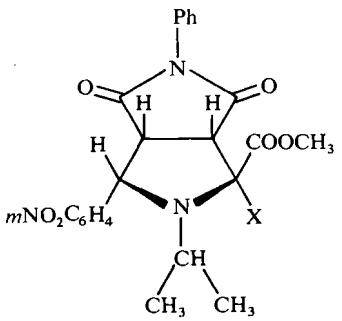

22
a X = H
b X = D

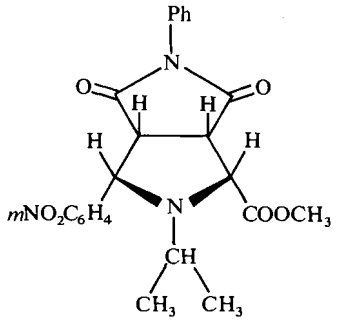

23
a X = H
b X = D

20*a*, *b*, and *c* in the proportion 60:40:0 with no **20***c* detectable. This proves that like **3***a* and **4***a*, both **20***a* and *b* arise from the more stable *trans*-azomethine ylide. A constant orientation of addition of the aldehyde having been established by deuterium labelling, this requires **20***a* and *b* to differ only in the mode of addition of the aldehyde. However the n.m.r. evidence does not allow a distinction between the *trans–cis* and *trans–trans* structures for **20***a* and *b*. Aziridine **1***b* reacted with *N*-phenylmaleimide in refluxing acetonitrile to give a mixture of the two pyrrolidines **21***a* and **22***a* in a ratio of 63:37. The isomeric **2***b* in contrast gave **21***a*, **22***a*, and **23***a* in a ratio of 54:40:6 indicating a small amount of the *cis*-azomethine ylide has been captured.

The n.m.r. line assignments of the methine protons were proven by deuterium labelling at the 3-position of the aziridine ring from which the stereochemical assignments could be made unambiguously. The major product in each case **21***a* corresponded in structural type to that of the sole products **10** and **11***a* obtained from the 3-aroylaziridines. Thus the *N*-phenylmaleimide is only marginally successful in suppressing the equilibration to the *trans*-azomethine ylide. The more reactive dipolarophile dimethyl azodicarboxylate with **1***b* in equimolar proportion gave a mixture of the stereoisomeric triazolidines **24** and **25** in a ratio of 62:38. An experiment performed with 3 equiv of the dipolarophile and **1***b* now gave **24**:**25** in a ratio of 82:18 showing as the concentration of the dipolarophile is increased more of the orbital symmetry controlled *trans*-azomethine ylide is trapped, proving **24** has the stereochemistry shown. Reaction of **2***b* with 1 equiv of dimethyl azodicarboxylate gave **24** and **25** in a ratio of 43:57 while an experiment using 3 equiv of the dipolarophile gave **24** and **25** in a ratio of 25:75. This similarly confirms **25** as having the *cis* geometry of the aziridine moiety.

Control reactions were carried out involving reaction of **1***b* and **2***b* separately with one added equivalent of water in acetonitrile at 115–117° for 24 h. Identical results were obtained, *i.e.* all three stereoisomeric oxazolidines **20***a*, *b*, and *c* were obtained in the proportion of 26:20:54 together with some *m*-nitrobenzaldehyde.

In contrast to the case of the 3-benzoylaziridines stringent exclusion of water from the system succeeded in suppressing the hydrolysis

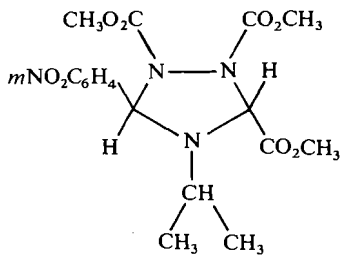

24

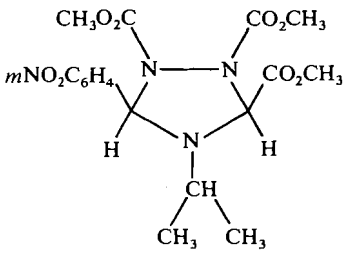

25

Can. J. Chem. Downloaded from www.nrcresearchpress.com by 210.87.254.6 on 09/05/12
For personal use only.

Can. J. Chem. Downloaded from www.nrcresearchpress.com by 210.87.254.6 on 09/05/12
For personal use only.

of the ester aziridines to a great extent. After 24 h refluxing of the *trans* ester aziridine in dry acetonitrile only 15% decomposition occurred whereas the recovered 85% of aziridine had equilibrated to give a *cis–trans* mixture of 63:37, *i.e.* virtually identical with the equilibrium composition obtained in toluene 64:36. Identical results were obtained starting with pure **1***b*. These results are consistent with the scheme in that decomposition of the ester aziridine, since it does not involve autocatalytic condensations and decompositions, is entirely dependent on adventitious moisture. Hydrolysis is therefore slower than for the aroylaziridines, allowing prior equilibration of the stereoisomeric aziridines and accounting for the identity of the products from **1***b* and **2***b* in contrast to the case of **1***a* and **2***a*. Hydrolysis is also more selective in **1***b* and **2***b* than in **1***a* and **2***a* occurring exclusively at the 2-position of the former.

Experimental

Melting points were determined on a Fisher–Johns apparatus and are uncorrected. The i.r. spectra were recorded on a Perkin–Elmer model 421 spectrophotometer, and only the principal, sharply defined peaks are reported. The n.m.r. spectra were recorded on Varian A-60 and A-100 analytical spectrometers. The spectra were measured on approximately 10–15% (W/V) solutions in $CDCl_3$, with tetramethylsilane as a standard. Line positions are reported in p.p.m. from the reference. Mass spectra were determined on an Associated Electrical Industries MS-9 double focusing high resolution mass spectrometer. The ionization energy, in general, was 70 eV. Peak measurements were made by comparison with perfluorotributylamine at a resolving power of 15 000. Kieselgel DF-5 (Camag, Switzerland) and Eastman Kodak precoated sheets were used for t.l.c. Microanalyses were carried out by Dr. C. Daesslé, Organic Microanalysis Ltd., Montreal, Quebec and by Mrs. D. Mahlow of this department.

General Preparation of 3-Aroylaziridines

The 3-aroylaziridines used in this study were prepared by the Gabriel synthesis involving Claisen–Schmidt condensations to form chalcones, addition of bromine to form the dibromochalcones, and treatment of the dibromochalcones with an excess of a primary aliphatic amine to provide 3-aroylaziridines (29).

Synthesis of cis- and trans-Methyl 1-Isopropyl-2-(m-nitrophenyl)-3-aziridinecarboxylate (1b, 2b)

(a) Methyl 2,3-Dibromo-3-(m-nitrophenyl)propionate

This compound, m.p. 87–89°, was obtained in 90% yield by the bromination of methyl *m*-nitrophenyl cinnamate in chloroform.

Anal. Calcd. for $C_{10}H_9Br_2NO_4$ (mol. wt. 364.8888): C, 32.71; H, 2.47; N, 3.81; Br, 43.57. Found (364.8898, mass spectrum): C, 32.89; H, 2.50; N, 3.75; Br, 43.63.

The n.m.r. spectrum δ_{TMS} ($CDCl_3$): 3.92 (s, 3H, CO_2CH_3); 4.83 and 5.43 (d each, 1H, $J = 12.5$ Hz, C_2H and C_3H respectively). The i.r. spectrum ν_{max} ($CHCl_3$): 1745 (C=O); 1525 and 1350 cm^{-1} (NO_2).

(b) Methyl α-Bromo-m-nitrophenylcinnamate

Dehydrohalogenation of methyl 2,3-dibromo-3-(*m*-nitrophenyl)propionate with potassium acetate in refluxing methanol for 18 h gave methyl α-bromo-*m*-nitrophenyl cinnamate in 90% yield, m.p. 97–98.5°.

Anal. Calcd. for $C_{10}H_8BrNO_4$ (mol. wt: 284.9636): C, 42.0; H, 2.85; N, 4.88; Br, 28.30. Found (284.9630, mass spectrum): C, 41.87; H, 3.10; N, 4.81; Br, 28.17.

The n.m.r. spectrum δ_{TMS} ($CDCl_3$): 3.91 (s, 3H, CO_2CH_3); 7.44–8.63 (m, 5H, aromatic protons).

(c) cis- and trans-Methyl 1-Isopropyl-2-(m-nitrophenyl)-aziridine-3-carboxylate

A solution of 18.25 g (0.05 mol) of methyl 2,3-dibromo-3-(*m*-nitrophenyl)propionate in 50 ml of dry benzene containing 17.7 g (0.3 mol) of isopropylamine was stirred at room temperature for 24 h. The reaction mixture was diluted with ether, the precipitated salt collected, and the filtrate washed with water. Removal of the solvent *in vacuo* gave a red oil trituration of which with methanol precipitated pure *trans*-methyl 1-isopropyl-2-(*m*-nitrophenyl)aziridine-3-carboxylate (**2***b*) 6.2 g (48.1% yield), m.p. 87–88.5°.

Anal. Calcd. for $C_{13}H_{16}N_2O_4$ (mol. wt. 264.1110): C, 59.09; H, 6.10; N, 10.57. Found (264.1108, mass spectrum): C, 58.84; H, 6.23; N, 10.23.

The n.m.r. spectrum δ_{TMS} ($CDCl_3$): 1.04, 1.16 (2d, 6H, $J = 6.5$ Hz, $CH(CH_3)_2$); 2.74 (d, 1H, $J = 2.5$ Hz, C_3H); 3.02 (m, 1H, $J = 6.5$ Hz, $CH(CH_3)_2$; 3.33 (d, 1H, $J = 2.5$ Hz, C_2H); 3.79 (s, 3H, CO_2CH_3); 7.35–8.22 (m, 4H, aromatic protons). The i.r. spectrum ν ($CHCl_3$): 1725 (C=O); 1525 and 1343 cm^{-1} (NO_2).

The methanol extract was evaporated and the remaining oil was diluted with benzene–hexane (40:60). Chilling of the solution produced a low melting solid which was recrystallized twice from benzene–hexane to give the pure methyl *cis*-1-isopropyl-2-(*m*-nitrophenyl)aziridine-3-carboxylate (**1***b*) 3.2 g (24.2% yield), m.p. 52–53.5°.

Anal. Calcd. for $C_{13}H_{16}N_2O_4$ (mol. wt. 264.1110): C, 59.09; H, 6.10; N, 10.57. Found (264.1110, mass spectrum): C, 58.82; H, 6.14; N, 10.73.

The n.m.r. spectrum δ_{TMS} ($CDCl_3$): 1.25 (d, 6H, $J = 5.2$ Hz); 1.96 (m, 1H, $CH(CH_3)_2$); 2.61 (d, 1H, $J = 6.5$ Hz, C_3H); 3.06 (d, 1H, $J = 6.5$ Hz, C_2H); 3.49 (s, 3H, CO_2CH_3); 7.25–8.33 (m, 4H, aromatic). The i.r. spectrum ν ($CHCl_3$): 1730 (CO); 1520 and 1342 cm^{-1} (NO_2).

(d) cis- and trans-Methyl 1-Isopropyl-2-(m-nitrophenyl)-3-deuteroaziridine-3-carboxylates

These compounds were prepared by reaction of methyl α-bromo-β-(*m*-nitrophenyl)cinnamate with a 15 fold excess of isopropylamine-*N*-d_2 in ether. The isomeric aziridines were isolated as described above. The integrals of the ring proton spectra indicated 82% deuterium incorporation at C-3.

Thermal Decomposition of cis-3-Benzoyl-1-isopropyl-2-(m-nitrophenyl)aziridine (1a) in Acetonitrile

(a) At Reflux

A solution of 0.932 g (3 mmol) of the pure *cis*-aziridine **1***a* in 50 ml of dry acetonitrile was heated under reflux for 24 h. Removal of the solvent *in vacuo* and trituration of the residue with methanol deposited a white crystalline solid,

TABLE 1. Cycloaddition adducts of aziridines

Adduct no.	Melting point (°C)	Yield (%)	Found C	Found H	Found N	Found Molecular ion (mass spectrum)	Calculated C	Calculated H	Calculated N	Calculated Molecular ion (mass spectrum)
3	158–162	12	—	—	—	310.1321*	—	—	—	310.1317*
4	138–140	44	65.24	4.88	9.47	310.1314*	65.08	4.99	9.11	310.1317*
10	248–249	90	69.20	5.42	8.77	483.1790*	69.55	5.21	8.68	483.1794
11	197–198	91	71.11	5.57	8.23	523.2100	71.10	5.57	8.02	523.2107
12	148–149	50	67.21	5.21	8.37	350.1632*	67.10	5.42	8.41	350.1632*
13*a*	138–139.5	90	62.13	6.56	10.61	419.1935†	61.82	6.15	10.68	419.1931†
13*c*	110–112	89	59.14	5.82	11.66	379.1610†	59.48	5.78	11.56	379.1618†
13*d*	163–164.5	51	66.20	5.08	9.44	475.1610†	66.19	4.86	9.64	475.1618†
20*a,b*	114–115.5	34	57.73	5.11	10.03	415.1374	57.82	5.09	10.11	415.1386
20*a,b*	Liquid		57.62	5.17	10.29	415.1381	57.82	5.09	10.11	415.1386
20*c*	110–112	5	57.78	5.11	10.12	415.1384	57.82	5.09	10.11	415.1386
21	169–171	62	63.13	5.61	9.30	437.1587	63.15	5.25	9.60	437.1586
22	139–140	37	63.08	5.47	9.41	437.1582	63.15	5.25	9.60	437.1586
23	117–119	6	63.21	5.63	9.29	437.1584	63.15	5.25	9.60	437.1586
24	112–113.5	57	49.90	5.42	13.71	410.1459	49.75	5.40	13.65	410.1438
25	105–107	35	49.87	5.28	13.54	410.1439	49.75	5.40	13.65	410.1438

*Parent molecular ion minus *m*-nitrobenzaldehyde ion.
†Parent molecular ion minus benzoyl.

m.p. 148–153°. The t.l.c. and n.m.r. analyses confirmed the presence of the two stereoisomeric oxazolidines **3***a* and **4***a* (80:20), 0.386 g (56% yield).

The solid was subjected to chromatography on 50 g of BDH alumina. Elution with benzene–hexane (40:60) gave a fraction (100 mg) consisting of a 70:30 mixture of **3***a*:**4***a* which crystallized from methanol as a white solid, m.p. 159–162.5°.

Mol. Wt. Calcd. for $C_{25}H_{23}N_3O_6$ (base peak $C_{25}H_{23}N_3O_6$—$C_7H_5NO_3$): 310.1317. Found (mass spectrum): 310.1321.

The n.m.r. spectrum ($CDCl_3$) δ_{TMS} major component (**3***a*) 0.92 (2d, 6H, $CH(CH_3)_2$, $J = 6.5$ Hz); 3.33 (m, 1H, $CH(CH_3)_2$); 5.70 (ABq, 2H, $J = 6.2$ Hz, C_4H and C_5H); 6.30 (s, 1H, C_2H); and 7.18–8.62 (m, 13H, aromatic). The i.r. spectrum ($CHCl_3$) 1667 (C=O), 1530 and 1350 cm^{-1} (NO_2).

Further elution with benzene gave a second fraction (260 mg) of pure **4***a* which crystallized from methanol, m.p. 139–140.5°.

Anal. Calcd. for $C_{25}H_{23}N_3O_6$ (base peak $C_{25}H_{23}N_3O_6$—$C_7H_5NO_3$ = 310.1317): C, 65.08; H, 4.99; N, 9.11. Found (310.1314, mass spectrum): C, 65.24; H, 4.88; N, 9.47.

The n.m.r. spectrum ($CDCl_3$) δ: 1.16 (d, 6H, $CH(CH_3)_2$, $J = 6.5$ Hz); 3.26 (m, 1H, $CH(CH_3)_2$); 4.66 (d, 1H, $J = 6.0$ Hz, C_4H); 5.57 (d, 1H, $J = 6.0$ Hz, C_5H); 6.24 (s, 1H, C_2H); and 7.12–8.64 (m, 13H, aromatic). The i.r. spectrum ν ($CHCl_3$): 1664 (C=O), 1527 and 1345 cm^{-1} (NO_2).

The original filtrate was evaporated and the residue subjected to chromatography on 50 g of BDH alumina. Elution with hexane–benzene (25:75) gave 1,6-diisopropyl-3,6-diphenyl-1,2-dihydropyrazine **5**, 0.043 g (10% yield). The n.m.r. and i.r. spectra of this material were superimposable with those of the independently synthesized material (see below).

Further elution of the column with benzene gave *N*-(isopropyl)phenacylamine **6**, 0.107 g (20% yield), m.p. 71–74°. The n.m.r. and i.r. spectra of this material were superimposable with those of an authentic sample of *N*-(isopropyl)phenacylamine (see below).

Further elution with benzene–chloroform (60:40) gave a red oil, 0.132 g. This basic nitrogen-containing fraction is as yet unidentified but the n.m.r. spectrum shows δ_{TMS} ($CDCl_3$): 1.01–1.86 (m, 6H, $CH(CH_3)_2$); 4.73 (s, 2H); 5.12–5.45 (b, 2H; exchangeable by D_2O, NH_2?); and 7.04–8.35 (m, 12H aromatic).

(b) At 50 ± 1°

A solution of 0.622 g (2 mmol) of the aziridine **1***a* in 40 ml of acetonitrile was heated at 50 ± 1° for 24 h. Removal of the solvent *in vacuo* gave a light orange oil which was subjected to chromatography on 75 g of BDH alumina. Elution with hexane–benzene (75:25) gave some unreacted *cis*-aziridine, 0.341 g (55% yield).

Further elution with hexane–benzene (50:50) gave *m*-nitrobenzaldehyde as an oil which solidified on standing 0.097 g (32% yield), m.p. 51–53°. The n.m.r. and i.r. spectra of this material were superimposable with those of an authentic sample.

Continued elution with benzene gave *N*-(isopropyl)-phenacylamine **6** as an orange oil 0.124 g (35% yield). This material was identical with an authentic sample.

Thermal Decomposition of cis-3-Benzoyl-1-cyclohexyl-3-deutero-2-(m-nitrophenyl)aziridine in Acetonitrile

A solution of 0.350 g (1 mmol) of the labelled aziridine (54% deuterium) in 50 ml of acetonitrile was heated under reflux for 24 h. Work-up of the reaction mixture as described above gave **12***b*, 0.132 g (52.8% yield) of 4-benzoyl-3-cyclohexyl-3-deutero-2,5-di(*m*-nitrophenyl)oxazolidine, m.p. 147–149°.

The n.m.r. spectrum δ_{TMS} ($CDCl_3$): 0.83–2.20 (m, 10H,

Can. J. Chem. Downloaded from www.nrcresearchpress.com by 210.87.254.6 on 09/05/12
For personal use only.

Can. J. Chem. Downloaded from www.nrcresearchpress.com by 210.87.254.6 on 09/05/12
For personal use only.

cyclohexyl CH_2); 2.51–3.17 (m, 1H, cyclohexyl CH); 4.74 (d, 0.57 H, $J = 7$ Hz, C_4H); 5.47 (d, 1H, $J = 7$ Hz, C_5H); 6.23 (s, 1H, C_2H); and 7.25–8.53 (m, 13H, aromatic).

*Thermal Decomposition of trans-3-Benzoyl-1-isopropyl-2-(m-nitrophenyl)aziridine (**2a**) in Acetonitrile*

(a) At Reflux Temperature

A solution of 3.11 g (10 mmol) of the aziridine **2a** in 100 ml of acetonitrile was heated under reflux for 24 h. Removal of the solvent *in vacuo* gave an orange oil, which was subjected to chromatography on 160 g of BDH alumina. Elution with hexane–benzene (75:25) gave 1,6-diisopropyl-3,6-diphenyl-1,2-dihydropyrazine **5** as an oil which solidified on trituration with methanol to an orange solid, m.p. 82–84°, 0.201 g (12.5% yield). The identity of this material was established by comparison with an authentic sample (see below).

Further elution with hexane–benzene (50:50) gave *m*-nitrobenzaldehyde 0.095 g (6.3% yield) as an oil which solidified on standing 48–51°.

Continued elution with benzene gave light orange oil, 0.467 g (26.5% yield) which was identified as *N*-(isopropyl)-phenacylamine **6** by comparison with an authentic sample.

Further elution with benzene–chloroform (90:10) gave a mixture of the stereoisomeric oxazolidines **3a** and **4a** as a solid, m.p. 138–140.5°, 0.124 g (5.4% yield).

Continued elution with benzene–chloroform (75:25) gave a red oil, 0.341 g. This basic nitrogen-containing fraction is as yet unidentified but the n.m.r. spectrum shows δ_{TMS} ($CDCl_3$): 1.04–1.61 (m, 6H); 4.73 (s, 2H); 5.52–5.81 (b, 2H, exchangeable by D_2O, NH_2?).

Further elution with benzene–chloroform (50:50) gave 3,5-diisopropyl-2-(*m*-nitrophenyl)-4,6-diphenylpyrrolo-[3,4-*d*]-4-oxazoline **8** as an orange oil, 0.198 g (8.5% yield) which resisted crystallization. The identity of this compound was established by its independent synthesis by a previously described procedure from the reaction of the aziridine with phenylglyoxal and then treating the 1,3-dipolar addition product with isopropylamine (6).

Anal. Calcd. for $C_{29}H_{29}N_3O_3$ (mol. wt. 467.2209): C, 74.51; H, 6.21; N, 8.99. Found (467.2197, mass spectrum): C, 74.04; H, 6.41; N, 9.21.

The n.m.r. spectrum δ_{TMS} ($CDCl_3$): 1.01 (d, 6H, $CH(CH_3)_2$, $J = 6.0$ Hz); 1.22 (d, $CH(CH_3)_2$, $J = 6.0$ Hz); 2.81–3.22 (septet, 1H, $CH(CH_3)_2$); 3.93–4.21 (septet, 1H, $CH(CH_3)_2$); 6.85–8.03 (m, 15H, aromatic and C-2 proton). The i.r. spectrum ($CHCl_3$): 1530 and 1348 cm^{-1} (NO_2).

(b) At 50 ± 1°

A solution of 1.57 g (5 mmol) of the pure *trans*-aziridine **2a** in 50 ml of dry acetonitrile was heated at 50 ± 1° for 24 h. Removal of the solvent *in vacuo* gave an orange oil which was subjected to chromatography on 80 g of BDH alumina. Elution with hexane–benzene (25:75) gave some unreacted *trans*-aziridine **2a**, 0.98 g (62.5% yield). Further elution with hexane–benzene (50:50) gave *m*-nitrobenzaldehyde as a light yellow oil which solidified on standing, m.p. 53–54°, 0.160 g (20% yield). The n.m.r. and i.r. spectra of this material were superimposable with those of an authentic sample.

Further elution with benzene gave *N*-(isopropyl)phenacylamine **6** as a light orange oil, 0.214 g (24.5% yield) which on trituration with petroleum ether crystallized as yellowish-white needles, m.p. 72–74.5°. This material was identified by comparison with an authentic sample. The mass spectrum of this fraction also exhibits a peak at *m/e* 318 ascribed to 1,6-diisopropyl-3,6-diphenyl-1,2-dihydropyrazine **5** which is expected owing to the facile dimerization and rearrangement of *N*-(isopropyl)phenacylamine recorded below.

General Procedure for Preparation of 1,3-Dipolar Adducts in Acetonitrile

The reactions of aziridines with aldehydes to form oxazolidines and with *N*-phenylmaleimide and diethyl azodicarboxylate to form adducts were carried out according to established procedures. The analytical and spectral data on these compounds are summarized in Tables 1 and 2.

Control Attempted Epimerization/Exchange of 1,3-Dipolar Adducts

Experiments were performed with **12b**, **13a**, **13b**, **24**, and **25** in which solutions of 0.100 g of the adducts in 10 ml of acetonitrile were refluxed for 24 h in the presence of 1 equiv of the corresponding aziridine or primary amine. In all cases examination of the product by n.m.r. showed no detectable evidence of deuterium exchange or epimerization.

*Preparation of N-(Isopropyl)phenacylamine (**6**) and 1,6-Diisopropyl-3,6-diphenyl-1,2-dihydropyrazine (**5**)*

Isopropylamine (5.9 g, 10 mmol) was added to a cold ethereal solution of 10 g (5 mmol) of phenacyl bromide and the mixture allowed to react for 24 h. The precipitated salt was removed and the filtrate washed successively with 10% aqueous potassium carbonate solution, twice with cold water, and dried ($MgSO_4$). Removal of the solvent *in vacuo* afforded an orange oil. Trituration with methanol deposited 1,6-diisopropyl-3,6-diphenyl-1,2-dihydropyrazine (**5**) as an orange solid, m.p. 83–84.5°, 1.42 g (17.9% yield).

Anal. Calcd. for $C_{22}H_{26}N_2$ (mol. wt. 318.2096): C, 82.96; H, 8.22; N, 8.82. Found (318.2101, mass spectrum): C, 82.63; H, 8.14; N, 8.74.

The n.m.r. spectrum δ_{TMS} ($CDCl_3$): 0.79 (d, 3H, $CH(CH_3)_2$, $J = 6.5$ Hz); 1.31 (d, 3H, $CH(CH_3)_2$, $J = 6.5$ Hz); 2.90 (septet, 1H, $CH(CH_3)_2$); 6.81 (s, 1H, C-2 proton); 7.23–7.85 (m, 11H, aromatic and C-5 protons).

Concentration of the methanol filtrate left a red oil which on dilution with petroleum ether (30–60°) and chilling for 2 days deposited *N*-(isopropyl)phenacylamine **6**, m.p. 73–75.5°, 2.64 g (30% yield).

Mol. Wt. Calcd. for $C_{11}H_{15}NO$: 177.1154. Found (mass spectrum): 177.1157.

The i.r. spectrum ($CHCl_3$): 3410 (NH), 1658 cm^{-1} (C=O).

*Thermolysis of 1,6-Diisopropyl-3,6-diphenyl-1,2-dihydropyrazine (**5**)*

The dihydropyrazine **5** (0.500 g) was heated in a sealed tube at 280° for 1 h. The resulting red oil solidified on cooling and was taken up in chloroform. Removal of the solvent *in vacuo* and examination of the oil by n.m.r. revealed the presence of a small amount of unreacted 1,2-dihydropyrazine. The crude reaction mixture was subjected to sublimation at 80°/10 mm to give 2,5-diphenylpyrazine **17** as a light orange solid, m.p. 187–189° (lit. (26) m.p. 192–194°). The melting point of this material was not depressed by admixture with an authentic sample prepared by heating a solution of ω-aminoacetophenone hydrochloride (Aldrich Chemicals, Ltd.) and 10% aqueous potassium carbonate at 100° for 2 h according to a literature procedure (26).

Can. J. Chem. Downloaded from www.nrcresearchpress.com by 210.87.254.6 on 09/05/12
For personal use only.

TABLE 2. The n.m.r. data on adducts

Adduct	*N*-Substituent	Methine chemical shifts and coupling constants; TMS (δ)						
		C_2H	C_3H	C_4H	C_5H	$J_{2,3}$	$J_{3,4}$	$J_{4,5}$
3	1.16(6H) 3.26(1H)	6.24	—	4.66	5.57	—	—	6.0
4	0.93(6H) 3.33(1H)	6.30	—	5.70*	5.70*	—	—	6.2
10	0.87(6H) 2.83(1H)	5.59	3.92	3.42	5.25	8.2	9.5	5.0
11	0.53–2.03(10H) 2.12–2.74(1H)	5.59	3.93	3.37	5.30	8.5	9.5	4.5
12	0.83–2.20(10H) 2.50–3.16(1H)	6.23	—	4.74	5.47	—	—	7.0
13*a*	0.83–1.77(16H)† 2.84–3.34(1H)	—	6.22§	—	6.73	—	—	—
13*c*	0.99(12H) 3.42(1H)	—	6.16§	—	6.66	—	—	—
13*d*	0.99(6H) 3.48(1H)	—	6.36§	—	6.85	—	—	—
20*a,b*	1.06(6H) 3.34(4H)	6.10	—	4.57	5.71	—	—	5.0
20*a,b*	0.96(6H) 3.12(1H) 3.91(ester)	6.01	—	4.26	5.37	—	—	3.0
20*c*	1.13(6H) 3.25(1H) 3.78(ester)	5.93	—	3.75	5.12	—	—	7.0
21	1.05(6H) 2.88(1H) 3.70(ester)	4.59	3.85	3.33	4.93	8.5	10.0	5.5
22	1.07(6H) 2.98(1H) 3.76(ester)	4.65	4.12	3.40	5.15	—	10.0	9.5
23	1.06(6H) 2.97(1H) 3.83(ester)	4.17	3.47‡	3.47‡	4.54	8.5	—	9.5
24	1.16(6H) 3.08(1H) 3.77, 3.82 (ester)	—	5.71	—	5.83§	—	—	—
25	1.25(6H) 3.28(1H) 3.41, 3.68, 3.85 (ester)	—	5.07	—	6.12§	—	—	—

*AB quartet.
†Cyclohexyl and methyl protons of ester groups.
‡Multiplet with identical chemical shift.
§Broad.

Decomposition of cis-Methyl 1-Isopropyl-2-(m-nitrophenyl)-aziridine-3-carboxylate (1b) in Acetonitrile

A solution of 2.64 g (10 mmol) of the aziridine **1***b* in 100 ml of acetonitrile was heated at 115–117° in a pressure vessel for 24 h. Removal of the solvent *in vacuo* gave a red oil. The n.m.r. and t.l.c. analysis of the crude reaction mixture confirmed the formation of three products **20***a*, *b*, and *c* in the ratio of 58:35.5:6.5. Trituration of the oil with methanol

Can. J. Chem. Downloaded from www.nrcresearchpress.com by 210.87.254.6 on 09/05/12
For personal use only.

resulted in the precipitation of a solid **20***c* 0.104 g (5.1% yield), m.p. 110–112°.

Anal. Calcd. for $C_{20}H_{21}N_3O_7$ (mol. wt. 415.1386): C, 57.82; H, 5.09; N, 10.11. Found (415.1366, mass spectrum): C, 57.78; H, 5.11; N, 10.12.

The n.m.r. spectrum δ_{TMS} ($CDCl_3$): 1.13 (d, 6H, $J = 6.5$ Hz, $CH(CH_3)_2$); 3.25 (m, 1H, $CH(CH_3)_2$); 3.75 (d, 1H, $J = 7.0$ Hz, C_4H); 3.78 (s, 3H, OCH_3); 5.12 (d, 1H, $J =$ 7.0 Hz, C_5H); 5.93 (s, 1H, C_2H); and 7.02–8.63 (m, 8H, aromatic). The i.r. spectrum ν ($CHCl_3$): 1730 (C=O), 1525 and 1350 cm^{-1} (NO_2).

Concentration of the methanol filtrate left a red oil which was subjected to chromatography on 80 g of BDH alumina. Elution with benzene–hexane (60:40) gave a pale yellow oil, 1.07 g (51.5% yield) which on trituration with methanol – petroleum ether crystallized to give a white solid **20***a*, *b*, m.p. 114–115.5°.

Anal. Calcd. for $C_{20}H_{21}N_3O_7$ (mol. wt. 415.1386): C, 57.82; H, 5.09; N, 10.11. Found (415.1374, mass spectrum): C, 57.75; H, 5.11; N, 10.03.

The n.m.r. spectrum δ_{TMS} ($CDCl_3$): 1.06 (2d, 6H, $CH(CH_3)_2$, $J = 6.5$ Hz); 3.34 (m, 4H, $CH(CH_3)_2$ and CO_2CH_3); 4.57 (d, 1H, $J = 5.0$ Hz, C_4H); 5.71 (d, 1H, $J =$ 5.0 Hz, C_5H); 6.10 (s, 1H, C_2H); and 7.31–8.62 (m, 8H, aromatic). The i.r. spectrum ($CHCl_3$) ν ($CHCl_3$): 1730 (C=O); 1520 and 1350 cm^{-1} (NO_2).

Further elution with benzene gave light yellow oil of **20***a*, *b*, 0.627 g (30.2%), which resisted crystallization.

Anal. Calcd. for $C_{20}H_{21}N_3O_7$: (mol. wt. 415.1386): C, 57.82, H, 5.09; N, 10.11. Found (415.1391, mass spectrum): C, 57.61; H, 5.21; N, 9.98.

The n.m.r. spectrum δ_{TMS} ($CDCl_3$): 0.95 (2d, 6H, $CH(CH_3)_2$, $J = 6.2$ Hz); 3.12 (m, 1H, $CH(CH_3)_2$); 3.92 (s, 3H, CO_2CH_3); 4.25 (d, 1H, C_4H $J = 3.0$ Hz); 5.36 (d, 1H, C_5H, $J = 3.0$ Hz); 6.02 (s, 1H, C_2H); and 7.50–8.66 (m, 8H, aromatic). The i.r. spectrum ν ($CHCl_3$): 1727 (C=O), 1530 and 1345 cm^{-1} (NO_2).

Similarly the decomposition of *trans*-methyl 1-isopropyl-2-(*m*-nitrophenyl)-3-aziridine carboxylate **2***b* in acetonitrile gave the same compounds in the ratio of 55:37.5:7.5 by n.m.r. analysis.

Decomposition of trans-Methyl 1-Isopropyl-2-(m-nitrophenyl)aziridine-3-carboxylate (2b) in Acetonitrile

A solution of 1.34 g (5 mmol) of the aziridine **2***b* in 50 ml of acetonitrile was heated at 115–117° for 24 h. The bulk of the liquid was distilled into a flask containing 2 ml of concentrated hydrochloric acid. The distillate was allowed to evaporate at room temperature to give methyl *N*-isopropylglycine hydrochloride as a white solid, 0.187 g, m.p. 134–138°. The n.m.r. spectrum of this salt in deuterium oxide showed δ: 1.28 (d, 6H, $J = 6.0$ Hz, $(CH_3)_2CH$); 3.48 (septet, 1H, $(CH_3)_2CH$); 3.78 (s, ester); 3.89 (s, $CH_2CO_2CH_3$); 4.0 (s, CH_2CO_2H). The spectrum suggested that the methyl ester group had been partially hydrolyzed. The hydrolysis was completed by heating an acidified aqueous solution of the salt at 80° for 14 h. Removal of the solvent *in vacuo* gave a white solid which had an n.m.r. spectrum in deuterium oxide δ: 1.27 (d, 6H, $J = 6.0$ Hz, $(CH_3)_2CH$); 3.48 (septet, 1H, $(CH_3)_2CH$); 4.05 (s, 2H, CH_2CO_2H) which was superimposable with that of an authentic sample of *N*-isopropylglycine hydrochloride obtained by the reaction of equimolar quantities of chloroacetic acid and isopropylamine in ether.

Traces of acetonitrile were removed *in vacuo* from the distillation residue to give a mixture of the stereoisomeric oxazolidines **20***a*, *b*, and *c*.

Decomposition of trans-Methyl 1-Isopropyl-2-(m-nitrophenyl)aziridine-3-carboxylate (2b) in Acetonitrile with Water Added

A solution of 0.265 g (1 mmol) of the aziridine **2***b* and 18 mg (1 mmol) of water in 50 ml of acetonitrile was refluxed for 24 h. Removal of the solvent *in vacuo* gave an oil. The n.m.r. analysis of the crude reaction mixture showed the formation of all three oxazolidines **20***a*, *b*, and *c* in the ratio of 26:20:54, and that all the *m*-nitrobenzaldehyde had been trapped.

Thermal Decomposition of trans-Methyl 1-Isopropyl-2-(m-nitrophenyl)aziridine-3-carboxylate (2b) in Absolute Acetonitrile

A solution of 0.790 g (3 mmol) of the aziridine **2***b* in 50 ml of absolute acetonitrile (freshly distilled over calcium hydride) was heated at 115–117° in a sealed vessel for 24 h. Removal of the solvent *in vacuo* gave a red oil, n.m.r. analysis of which showed the isomeric aziridines **1***b* and **2***b* in a ratio of 63:37 to the extent of 85% yield and the oxazolidines **20***a* and *b* in a ratio of 60:40 in 15% yield.

Similarly thermal decomposition of **1***b* in absolute acetonitrile afforded the same products in virtually identical ratios.

In a separate control experiment both **1***b* and **2***b* equilibrated at the reflux temperature of toluene to give a mixture of **1***b*: **2***b* of (64:36).

This research was supported by a National Research Council of Canada grant to J.W.L. We thank Mr. R. Swindlehurst and Dr. A. Hogg for the n.m.r. and mass spectra.

1. R. Huisgen, W. Scheer, and H. Huber. J. Am. Chem. Soc., **89**, 1753 (1967).
2. P. B. Woller and N. H. Cromwell. J. Org. Chem. **35**, 888 (1970).
3. R. Huisgen, W. Scheer, and H. Mader. Angew. Chem. Int. Ed. **8** 602 (1969).
4. R. Huisgen, W. Scheer, G. Szeimies, and H. Huber. Tetrahedron Lett. 397 (1966).
5. J. A. Deyrup. J. Org. Chem. **34**, 2724 (1969).
6. J. W. Lown and M. H. Akhtar. J. Chem. Soc. C, In press.
7. A. E. Pohland, R. C. Badger, and N. H. Cromwell. Tetrahedron Lett. 4369 (1965).
8. J. H. Hall, R. Huisgen, C. H. Ross, and W. Scheer. Chem. Commun. 1188 (1971).
9. H. W. Heine, R. E. Peavy, and A. J. Durbetaki. J. Org. Chem. **31**, 3924 (1966).
10. G. Dallas, J. W. Lown, and J. P. Moser. J. Chem. Soc. C, 2383 (1970).
11. F. Texier and R. Carrie. Compt. Rend. C**269**, 709 (1969).
12. R. Huisgen, V. Martin-Ramos, and W. Scheer. Tetrahedron Lett. 477 (1971).
13. J. W. Lown, J. P. Moser, and R. Westwood. Can. J. Chem. **47**, 4335 (1969).
14. J. W. Lown and K. Matsumoto. Can. J. Chem. **48**, 2215 (1970).

15. J. W. LOWN and K. MATSUMOTO. Can. J. Chem. **48**, 3399 (1970).
16. J. W. LOWN and K. MATSUMOTO. J. Org. Chem. **36**, 1405 (1971).
17. J. F. BUNNETT. J. Amer. Chem. Soc. **83**, 4968 (1961).
18. G. J. BUIST and H. J. LUCAS. J. Am. Chem. Soc. **79**, 6157 (1957).
19. J. E. EARLEY, C. E. O'ROURKE, L. B. CLAPP, J. O. EDWARDS, and B. C. LAWES. J. Am. Chem. Soc. **80**, 3458 (1958).
20. O. C. DERMER and G. E. HAM. Ethylenimine and other aziridines. Academic Press, 1969. p. 219.
21. N. H. CROMWELL and R. A. WANKEL. J. Am. Chem. Soc. **71**, 711 (1949).
22. P. L. JULIAN, E. W. MEYER, A. MAGNANI, and W. COLE. J. Am. Chem. Soc. **67**, 1203 (1945).
23. R. M. COWPER and T. S. STEVENS. J. Chem. Soc. 1041 (1947).
24. F. BROWN and F. G. MANN. J. Chem. Soc. 847, 858 (1948).
25. A. F. CROWTHER, F. G. MANN, and D. PURDIE. J. Chem. Soc. 58 (1943).
26. S-J. CHEN and F. W. FOWLER. J. Org. Chem. **35**, 3987 (1970).
27. P. B. WOLLER and N. H. CROMWELL. J. Heterocycl. Chem. **5**, 579 (1968).
28. (*a*) C. PAAL. Chem. Ber. **17**, 2756 (1884). (*b*) L. KNORR. Chem. Ber. **17**, 2863 (1884).
29. N. H. CROMWELL, N. G. BARKER, R. A. WANKEL, P. J. VANDERHORST, F. W. OLSON, and J. H. ANGLIN. J. Am. Chem. Soc. **73**, 1044 (1951).

Can. J. Chem. Downloaded from www.nrcresearchpress.com by 210.87.254.6 on 09/05/12
For personal use only.

A General Synthesis of 8,2′-Thioanhydropurine Nucleosides[1]

K. K. OGILVIE, L. SLOTIN,[2] J. B. WESTMORE, AND D. LIN
Department of Chemistry, University of Manitoba, Winnipeg, Manitoba

Received January 26, 1972

The synthesis of 8,2′-anhydro-8-mercapto-9-β-D-arabinofuranosyladenine, 8,2′-anhydro-8-mercapto-9-β-D-arabinofuranosylguanine, and 8,2′-anhydro-8-mercapto-9-β-D-arabinofuranosylhypoxanthine is described. The anhydro ring is formed by simultaneous displacement of bromine from position-8 and carbonate from the 2′-position of the parent nucleoside using either sodium hydrogen sulfide or thiourea.

La synthèse de l'anhydro-8,2′ mercapto-8 arabinofuranosyl-9-β-D adénine, de l'anhydro-8,2′ mercapto-8 arabino furanosyl-9-β-D guanine, de l'anhydro-8,2′ mercapto-8 arabinofuranosyl-9-β-D hypoxanthine est décrite. Le cycle anhydro est formé par déplacement simultané du brome de la position-8 et du carbonate de la position-2′ du nucléoside parent, par l'utilisation du bisulfite de sodium et du thiourée.

Canadian Journal of Chemistry, **50**, 2249 (1972)

Can. J. Chem. Downloaded from www.nrcresearchpress.com by 210.87.254.5 on 09/05/12
For personal use only.

Cyclonucleosides are important analogues of natural nucleosides. They are characterized by having in addition to the *N*-glycoside linkage a covalent linkage either directly or via bridging atoms between the 2′, 3′, or 5′ carbons of the sugar and a carbon or nitrogen atom (other than the nitrogen of the glycoside bond) of the purine or pyrimidine ring. Acid or base hydrolysis of the cyclo-linkage normally leads to ribo, arabino, or xylo nucleosides (1). Nucleophilic displacement of the cyclo-linkage leads to nucleosides modified on the sugar moiety (1–3) and sometimes on the base moiety (1, 4–6). Arabino cytidine (7, 8) and cordycepin (6) are but two of the important biologically active compounds obtained from cyclonucleosides. Cyclonucleosides have even been detected as intermediates in proposed prebiotic syntheses (9, 10) and have been used as intermediates in the chemical synthesis of nucleotides (11–13). Investigation of the spectra of cyclonucleosides may lead to useful structural information on nucleic acids (14, 15).

Because of the interest in cyclonucleosides, numerous syntheses have been reported, particularly in the pyrimidine series. Hampton and Nichol (16) developed an exceedingly simple synthesis of O^2,2′-anhydrouridines and other procedures have been developed for the synthesis of 5′- and 3′-cyclouridines (17–19) as well as cycloderivatives of thymidine (20, 21) and cytidine (7, 8, 9, 22). In the purine series, progress has been slower. Ikehara (6) has extensively investigated the cycloadenosines describing syntheses of *O* and *S* 8,2′- (23–26), 8,3′- (6, 25), and 8,5′- (27) cycloderivatives. Recently the synthesis of 8,2′-*N*-cycloadenosine has been described (28).

Cyclonucleosides of purines other than adenosine have received little attention. This probably reflects the complexity of the synthetic methods developed to date. Ikehara has reported syntheses of three derivatives of guanosine cyclonucleosides (29, 30) and we have recently described the first synthesis of 8,2′-thioanhydroguanosine (31). The syntheses of purine cyclonucleosides developed so far are all (*a*) multistep procedures, (*b*) specific for only one nucleoside, (*c*) involve low overall yields or a combination of all three.

We wish to describe a simple, efficient, and general synthetic method for the synthesis of 8,2′-thioanhydropurine nucleosides. A brief preliminary account of this work has appeared (32).

Discussion and Results

The most efficient syntheses of 8,2′-thioanhydropurine nucleosides have employed simultaneous displacement of a halogen from the 8-position of the base and a good leaving group (such as a sulfonate) from the 2′-position of the sugar of the parent nucleoside (26). The difficulty has arisen in the selective introduction of a good leaving group at the 2′-position of the ribose sugar. Unless the 5′-hydroxyl possesses a bulky substituent, sulfonating agents show only a

[1]Part VI in a series on anhydronucleosides. Part V is ref. 31.

[2]NRCC Scholarship Holder, 1970–present.

Can. J. Chem. Downloaded from www.nrcresearchpress.com by 210.87.254.5 on 09/05/12
For personal use only.

slight preference for the 2′-hydroxyl over the 3′-hydroxyl. The combination of a bulky substituent at the 5′-hydroxyl and the use of a sterically hindered sulfonating agent increases the degree of reaction at the 2′-position relative to the 3′-position (26, 31). However, placing a bulky substituent at the 5′-hydroxyl usually introduces several additional steps into the synthesis. Ikehara and Uesugi (33) partially overcame this problem with some adenosine 5′-phosphates by using sodium hydroxide in dioxane with a sulfonating agent. Under these conditions sulfonation appeared to occur exclusively at the 2′-position. However, this still necessitated the blocking of the 5′-position with phosphate since other 5′-protecting groups led to varying degrees of 3′-sulfonation (26).

We had noted that a 2′,3′-carbonate on a pyrimidine nucleoside is readily displaced by nucleophilic groups on the base ring (34). Further it has been found that there is no need to block either the 5′-hydroxyl or amine groups on the base ring in forming 2′,3′-carbonates of purine nucleosides (16, 35). This suggested the possibility of introducing a good leaving group (CO_2) on the 2′-position of any 8-halopurine nucleoside in a single step. Simultaneous displacement of the 8-halogen and the carbonate from the 2′-position should lead to the 8,2′-cyclonucleosides. This would represent an extremely simple general route to such compounds. On this basis we have developed a general procedure (outlined in Scheme 1) for the synthesis of 8,2′-thioanhydropurine nucleosides.

8-Bromopurine nucleosides are readily available by standard procedures. Formation of cyclic carbonates from the 8-bromonucleosides requires a short (30 min) treatment of the 8-bromonucleoside with a slight excess of diphenyl carbonate in DMF at 150 °C in the presence of a small amount of sodium bicarbonate. Yields ranged from slightly above 70% for 8-bromoadenosine 2′,3′-carbonate (**2**) and 8-bromoinosine 2′,3′-carbonate (**5**) to 98% for 8-bromoguanosine 2′,3′-carbonate (**8**). Compounds **2**, **5**, and **8** all possess the characteristic carbonyl absorption at 5.5 μ in the i.r.

The final step in Scheme 1 involves simultaneous displacement of the bromine from the 8-position and the carbonate from the 2′-position. This was accomplished in two ways: method A using sodium hydrogen sulfide in hot DMF and method B using thiourea in refluxing *n*-butanol. We found that method A gave higher yields in all cases.

8,2′-Thioanhydroadenosine (**3**) was obtained in 79% yield from **2** using method A but the yield dropped to 66% using method B. Compound **3** was identical to authentic 8,2′-thioanhydroadenosine prepared by the method of Ikehara and Kaneko (26).

8,2′-Thioanhydroinosine (**6**) was obtained in several ways. From compound **5**, **6** was prepared in 73% yield by method A and 69% by method B. Further, 8,2′-thioanhydroadenosine was readily deaminated by adenosine deaminase (39) to produce **6** quantitatively. These results represent the first reported chemical syntheses of 8,2′-thioanhydroinosine which was further characterized by Raney nickel reduction to 2′-deoxyinosine.

Compound **8** was converted to 8,2′-thioanhydroguanosine (**9**) in 56% yield by method A while the yield was 41% using method B. Compound **9** was identical to authentic 8,2′-thioanhydroguanosine (31) and was converted to 2′-deoxyguanosine using Raney nickel.

This report has described the first simple general route to the 8,2′-thioanhydropurine nucleosides all of which are easily converted to the respective 2′-deoxypurine nucleosides. We will shortly describe the incorporation of these molecules into oligonucleotide chains.

Experimental

General Methods

Descending paper chromatography was carried out on Whatman 3MM paper. The solvent systems employed were: solvent A, *n*-butanol – ethanol – water (3:1:5, organic phase used); solvent B, ethanol–water (7:3). The solvents were prepared on a volume basis. Thin-layer chromatography was carried out at room temperature employing the ascending technique. All t.l.c. was run on Eastman Chromagram Sheets 6060 (silica gel with fluorescent indicator) on strips 10 × 2 cm. Thick-layer chromatography was carried out on glass plates (20 × 20 cm) coated with 2 mm thick layer of silica gel DSF-5 (Mondray Chemicals Ltd.). Nucleosides and their derivatives were detected on paper chromatograms, thin- and thick-layer sheets, using a u.v. source (Mineralite output 254 mm).

The i.r. spectra were obtained on a Perkin–Elmer 337 recording spectrophotometer using KBr disks for sample preparation. The u.v. spectra were obtained on a Cary Model 14 recording spectrophotometer. Mass spectra were obtained on a Hitachi RMU-6D instrument. Melting points were determined on a Fisher–Johns melting point apparatus and are reported uncorrected. Elemental analyses were performed by Galbraith Laboratories Inc., Knoxville, Tenn.

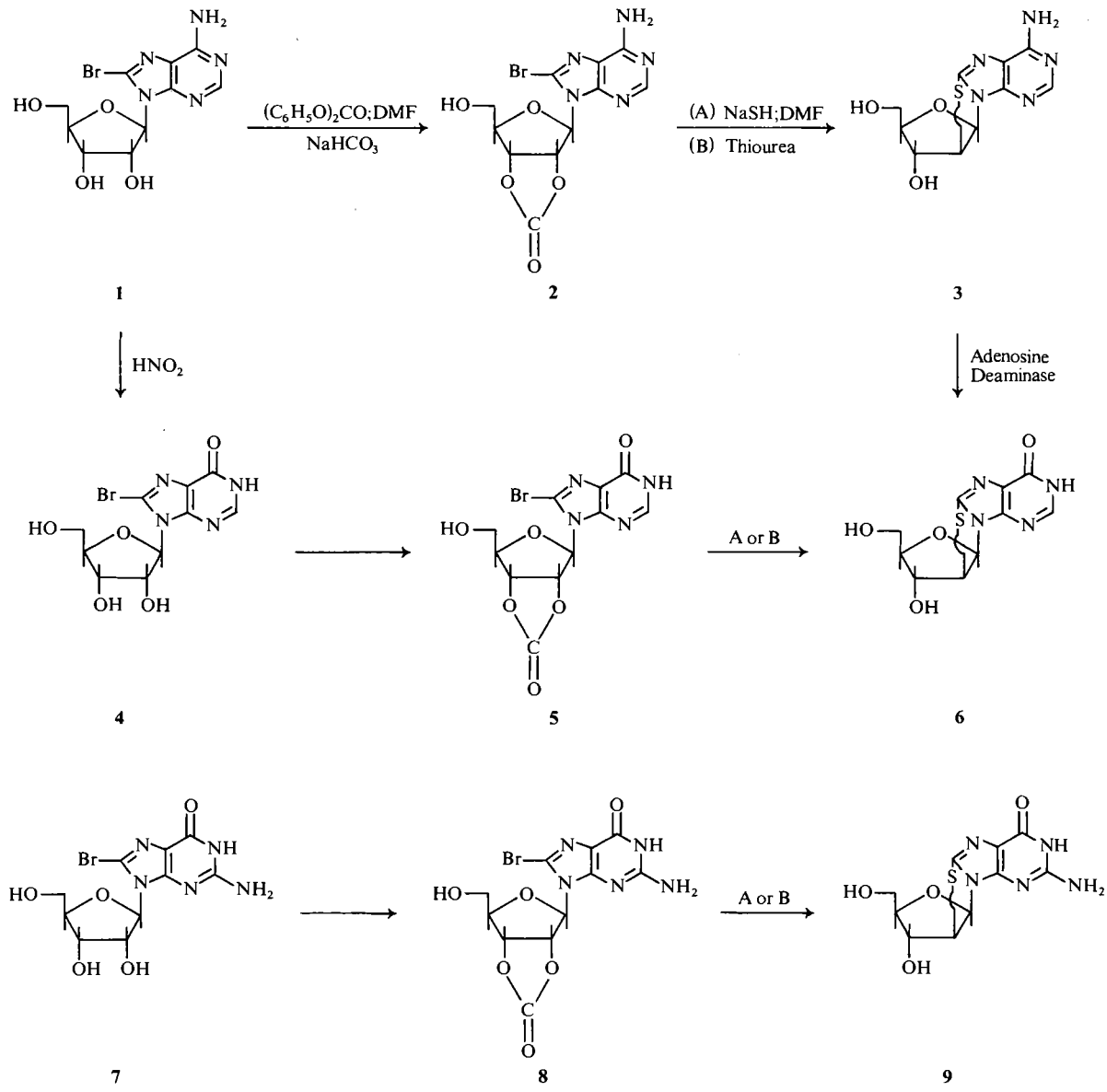

SCHEME 1

Samples submitted to them were prepared by crystallization, lyophilization, or precipitation from tetrahydrofuran with hexane followed by heating in a drying apparatus over P_2O_5. In some cases the molecular formula includes fractional moles of solvent as a correction for the analysis. These corrections were added only when a corresponding weight loss was detected on extensive drying of the sample.

Reagent grade *N,N*-dimethyl formamide (DMF) was dried by distillation from calcium hydride and stored over Linde Molecular Sieve. 8-Bromoadenosine (26, 71%) and 8-bromoguanosine (38, 89%) were prepared as described in the literature. 8-Bromoinosine (37) was obtained by the deamination of **1** using the method of Ikehara (36, 73%).

*8-Bromoadenosine 2',3'-Carbonate (**2**)*

8-Bromoadenosine (1 g, 2.9 mmol), diphenyl carbonate (0.82 g, 3.8 mmol), and sodium bicarbonate (15 mg) were heated in DMF (3 ml) at 150 °C for 30 min. The mixture was cooled to room temperature and applied to eight thick-layer plates which were developed first in ether and then in

Can. J. Chem. Downloaded from www.nrcresearchpress.com by 210.87.254.5 on 09/05/12
For personal use only.

TABLE 1. Properties of nucleoside derivatives

Compound	R_f, paper chromatography		Ultraviolet spectra		
	Solvent A*	Solvent B*	Solvent	λ_{max}, nm (ε)	λ_{min}, nm (ε)
2	0.79	0.81	95% ethanol	263.4 (14 100)	229 (4600)
3	0.30	0.50	water	276.5 (17 000), 222 (15 900)	238 (2500)
5	0.48	0.65	95% ethanol	254 (13 800)	232 (6200)
6	0.28	0.69	water	265 (10 080)	233 (2300)
8	0.57	0.69	95% ethanol	276 (13 600)sh, 263.5 (14 700)	228 (5100)
9	0.23	0.58	water	283 (13 590), 268 (16 630)	230 (4000)

*Solvents described in General Methods.

ethyl acetate. A band at R_f 0.35 was eluted with tetrahydrofuran and on precipitation with hexane yielded 0.75 g (70%, m.p. 159–162 °C) of compound **2** (R_f 0.70 (THF), R_f 0.53 (EtOAC)). Principal bands in the i.r. spectrum occurred at 5.55, 6.80, 8.85, and 9.25 μ. The u.v. and chromatographic properties are shown in Table 1.

Anal. Calcd. for $C_{11}H_{10}N_5O_5Br \cdot 0.2THF$: C, 36.66; H, 3.02; Br, 20.67. Found: C, 36.91; H, 2.94; Br, 21.18.

8-Bromoinosine 2′,3′-Carbonate (5)

Compound **5** was prepared from 8-bromoinosine in the same manner as described for the preparation of **2** above. A 74% yield of **5** (m.p. >218 °C (dec.)) was obtained (i.r. 5.55, 5.75, 8.75, and 11.6 μ). Chromatographic and u.v. properties are shown in Table 1. The compound was not further purified but was used directly to prepare 8,2′-thioanhydroinosine as described below.

8-Bromoguanosine 2′,3′-Carbonate (8)

8-Bromoguanosine (1.0 g, 2.76 mmol), diphenyl carbonate (1.21 g, 5.52 mmol), and sodium bicarbonate (50 mg) were heated in DMF (10 ml) at 150 °C for 30 min. The mixture was cooled to room temperature and poured into ether. A gummy precipitate was obtained which was washed with ether and then precipitated several times from DMF using ether. The solid was then collected and dried to yield 1.03 g (98%) of compound **8** (m.p. >228 °C (dec.)). Compound **8** (R_f 0.14 (THF)) showed principal bands at 5.50, 6.60, 8.65, and 9.25 μ in the i.r. Chromatographic and u.v. properties are shown in Table 1.

Anal. Calcd. for $C_{11}H_{10}N_5O_6Br$: C, 34.04; H, 2.60. Found: C, 33.80; H, 2.59.

8,2′-Thioanhydropurine Nucleosides. General Procedures

Method A

In a typical experiment 1 mmol of the cyclic carbonate dissolved in DMF (2 ml) was added to a 40% solution of sodium hydrogen sulfide (6 equiv of NaSH) and the solution was heated at 70 °C for 18 h. The solution was then either applied directly to thick-layer plates or paper chromatograms.

Method B

In a typical experiment 1 mmol of the cyclic carbonate and 2 equiv of thiourea were refluxed in freshly distilled *n*-butanol (15 ml) for 5 h. The solvent was then removed at reduced pressure and the residue dissolved in ethanol and applied to either thick-layer plates or paper chromatograms.

8,2′-Thioanhydroadenosine (3)

The products from both methods A and B were worked-up in the same way. The reaction products were applied to thick-layer plates which were developed first in ether, then ethyl acetate, and finally tetrahydrofuran. The band at R_f 0.30 was eluted with ethanol, the solvent removed at reduced pressure, and the residue was crystallized from water to yield 8,2′-thioanhydroadenosine (see Table 1) identical to authentic material (26). The yield from method A was 79% and 66% from method B. The mass spectrum had parent peak at *m/e* 281.

8,2′-Thioanhydroguanosine (9)

The reaction products from both methods A and B were separated in the same manner. The reaction products were applied to paper chromatograms which were developed in solvent A. The band at R_f 0.24 was eluted with water which was lyophilized to yield 8,2′-thioanhydroguanosine (Table 1) identical to authentic material (31). The yield was 56% from method A and 41% from method B. The mass spectrum of the trimethylsilyl derivative had a parent peak at *m/e* 585.

8,2′-Thioanhydroinosine (6)

Method A

The reaction mixture was applied to paper chromatograms and developed in solvent A. The band at R_f 0.34 was eluted with water and the product collected by lyophilization to yield **6** (73%, Table 1, m.p. >217 °C (dec.)). Principal bands in the i.r. spectrum occurred at 5.9, 6.3, 9.3, and 12.8 μ. The mass spectrum of the trimethylsilyl derivative had a parent peak at *m/e* 498.

Anal. Calcd. for $C_{10}H_{10}N_4O_4S \cdot 1.2H_2O$: C, 39.52; H, 4.11; S, 10.55. Found: C, 40.07; H, 4.63; S, 9.91.

Method B

The reaction mixture was applied to thick-layer plates which were developed in chloroform–ethanol (7:3). The band at R_f 0.68 was eluted with ethanol, the solvent was removed at reduced pressure, and the residue crystallized from water to yield **6** (69%).

Method C

The procedure for converting 8,2′-thioanhydroadenosine into 8,2′-thioanhydroinosine using adenosine deaminase has been previously described (39).

Raney Nickel Reduction of the 8,2′-Thioanhydronucleosides

The thioanhydronucleosides were dissolved in water and heated at reflux with Raney nickel for 3 h. The products

Can. J. Chem. Downloaded from www.nrcresearchpress.com by 210.87.254.5 on 09/05/12
For personal use only.

were isolated by paper chromatography in solvent A. Compounds **3**, **6**, and **9** led respectively to 2′-deoxyadenosine, 2′-deoxyinosine, and 2′-deoxyguanosine which were identified by comparison to authentic material (40).

We wish to acknowledge financial support from the National Research Council of Canada.

1. J. J. Fox. Pure Appl. Chem. **18**, 223 (1969).
2. M. Imazawa, T. Ueda, and T. Ukita. Tetrahedron Lett. 4807 (1970).
3. J. F. Codington, I. L. Doerr, and J. J. Fox. J. Org. Chem. **29**, 558 (1964).
4. M. Ikehara and K. Muneyama. Chem. Pharm. Bull. **18**, 1196 (1970).
5. T. Ueda and S. Shibuya. Chem. Pharm. Bull. **18**, 1076 (1970).
6. M. Ikehara. Accts. Chem. Res. **2**, 47 (1969).
7. T. Kanai, T. Kojima, O. Maruyama, and M. Ichino. Chem. Pharm. Bull. **18**, 2569 (1970).
8. K. Kikugawa and M. Ichino. Tetrahedron Lett. 867 (1970).
9. C. M. Tapiero and J. Nagyvary. Nature, **231**, 42 (1971).
10. R. A. Sanchez and L. E. Orgel. J. Mol. Biol. **47**, 531 (1970).
11. K. K. Ogilvie and D. Iwacha. Can. J. Chem. **48**, 862 (1970).
12. M. Ikehara, S. Uesugi, and M. Yasumoto. J. Am. Chem. Soc. **92**, 4735 (1970).
13. K. L. Nagpal and M. M. Dhar. Tetrahedron Lett. 47 (1968).
14. M. Ikehara, M. Kaneko, Y. Nakahara, S. Yamada, and S. Uesugi. Chem. Pharm. Bull. **19**, 1381 (1971).
15. D. L. Elder, E. Bunnenberg, C. Djerassi, M. Ikehara, and W. Voelter. Tetrahedron Lett. 727 (1970).
16. A. Hampton and A. W. Nichol. Biochem. **5**, 2076 (1966).
17. D. M. Brown, A. R. Todd, and S. Varadarajan. J. Chem. Soc. 868 (1957).
18. N. C. Yung and J. J. Fox. J. Am. Chem. Soc. **83**, 3060 (1961).
19. S. Tang and J. S. Roth. Tetrahedron Lett. 2123 (1968).
20. G. Kowollik, K. Gaertner, G. Etzold, and P. Langen. Carbohydr. Res. **12**, 301 (1970).
21. G. Kowollik, K. Gaertner, and P. Langen. Tetrahedron Lett. 3863 (1969).
22. J. Zemlicka and J. Smrt. Tetrahedron Lett. 2081 (1964).
23. M. Ikehara, H. Tada, K. Muneyama, and M. Kaneko. J. Am. Chem. Soc. **88**, 3165 (1966).
24. M. Ikehara, H. Tada, and M. Kaneko. Tetrahedron, **24**, 3489 (1968).
25. M. Ikehara and H. Tada. Chem. Pharm. Bull. **15**, 94 (1967).
26. M. Ikehara and M. Kaneko. Tetrahedron, **26**, 4251 (1970).
27. M. Ikehara, M. Kaneko, and M. Sagai. Tetrahedron, **26**, 5675, 5757 (1970).
28. M. Kaneko, B. Shimizu, and M. Ikehara. Tetrahedron Lett. 3113 (1971).
29. M. Ikehara, H. Tada, and K. Muneyama. Chem. Pharm. Bull. **13**, 639 (1965).
30. M. Ikehara and K. Muneyama. J. Org. Chem. **32**, 3039 (1967); Chem. Pharm. Bull. **18**, 1196 (1970).
31. K. K. Ogilvie, L. Slotin, J. B. Westmore, and D. Lin. Can. J. Chem., **50**, 1100 (1972).
32. K. K. Ogilvie and L. Slotin. J. Chem. Soc. D, 890 (1971).
33. M. Ikehara and S. Uesugi. Tetrahedron Lett. 713 (1970).
34. K. K. Ogilvie and D. Iwacha. Can. J. Chem. **47**, 495 (1969).
35. K. K. Ogilvie and L. Slotin. J. Org. Chem. **36**, 2556 (1971).
36. M. Ikehara. Chem. Pharm. Bull. **8**, 367 (1960).
37. R. E. Holmes and R. K. Robins. J. Am. Chem. Soc. **86**, 1242 (1964).
38. R. Shapiro and S. Agarwal. Biochem. Biophys. Res. Commun., **24**, 401 (1966).
39. K. K. Ogilvie, L. Slotin, and P. Rheault. Biochem. Biophys. Res. Commun. **45**, 297 (1971).
40. Sigma Chemical Co., St. Louis, Mo.

Can. J. Chem. Downloaded from www.nrcresearchpress.com by 210.87.254.5 on 09/05/12
For personal use only.

The Measurement of the Activity Coefficient Ratios of Protonated and Neutral Forms of Hammett Indicators in Several Strong Acids

T. R. ESSIG[1] AND J. A. MARINSKY[2]

Chemistry Department, State University of New York at Buffalo, Buffalo, New York 14214

Received October 4, 1971

The activity coefficient ratio for several indicators has been estimated for the protonated and neutral forms of the same indicator molecule over a large range of acidity in H_2SO_4, $HClO_4$, and HCl systems. The activity coefficient (f_B) of the neutral form of a number of Hammett indicators was determined via solubility measurements. The observed linear relationship between $\log f_B$ and $pK_A^{BH^+}$ then permitted estimate by extrapolation of $\log f_B$ not experimentally accessible for the more basic indicators. Solubility studies of the pentacyanopropenide (PCP^-) salts of these more basic protonated indicators were referred to a reference standard, tetraethylammonium pentacyanopropenide (TEA^+PCP^-) according to the method developed by Boyd to obtain the activity coefficient ratio f_{BH^+}/f_{TEA^+}. By synthesizing the term $f_{BH^+}/f_B\ (f_{PCP^-}/f_{TEA^+})^{1/2}$ the approach to a meaningful value of f_{BH^+}/f_B is believed to be facilitated. This function is uniquely related to the water activity of the various acid systems examined to support the suggestion by Hammett that f_{BH^+}/f_B is a constant for primary aniline indicators at a specified acid concentration.

Le rapport du coefficient d'activité pour plusieurs indicateurs a été évalué pour les formes protonée et neutre de la molécule, sur un grand intervalle d'acidité, dans les systèmes H_2SO_4, $HClO_4$, et HCl. Le coefficient d'activité (f_B) de la forme neutre d'un certain nombre d'indicateurs de Hammett a été déterminé par des mesures de solubilité. La relation linéaire observée entre le $\log f_B$ et le $pK_A^{BH^+}$ permet alors d'évaluer par extrapolation le $\log f_B$ non accessible expérimentalement pour les indicateurs plus basiques. Les études de solubilité des sels du pentacyanopropenide (PCP^-) pour ces indicateurs plus basiques sous la forme protonée, ont été rapportées à la référence standard, le tétraéthylammonium pentacyanopropenide (TEA^+PCP^-) selon la méthode de Boyd, pour obtenir le rapport du coefficient d'activité f_{BH^+}/f_{TEA^+}. En construisant le terme $f_{BH^+}/f_B\ (f_{PCP^-}/f_{TEA^+})^{1/2}$, on pense qu'il est plus facile d'approcher une valeur significative de f_{BH^+}/f_B. Cette fonction est uniquement en relation avec l'activité de l'eau dans les divers systèmes acides examinés pour soutenir la suggestion de Hammett que f_{BH^+}/f_B est une constante pour les indicateurs aniline primaire à une concentration acide fixée.

Canadian Journal of Chemistry, **50**, 2254 (1972)

Introduction

The concept of an acidity function (H_0) to measure the ability of a concentrated acid to monoprotonate a neutral Brønsted base was introduced by Hammett and Deyrup (1) in 1932. The general utility of this function has received much investigation in the ensuing years (2–10). Its applicability has been found to be quite limited (5–11) and this has led to the introduction of other acidity functions (12–20). Differences between the various functions have been attributed to hydration effects (21–30) in attempts to generalize the Hammett (H_0) acidity function by identifying its relationship with the others.

Another approach to resolving differences between the different acidity functions and one which has been the subject of this research has concerned itself with the evaluation of activity coefficient terms in the various expressions (31, 32). Solubility measurements as a function of acid concentration have been made for this purpose. For the unprotonated indicator molecule the reference state is the aqueous saturated solution. In the case of the protonated form of the indicator the solubility of the salt has been measured. The 1,1,2,3,3-pentacyanopropenide (PCP^-) anion has been considered by Boyd (32) a most suitable counterion for such studies because of (*1*) the low solubility of its product salt, (*2*) its resistance to protonation over a wide range of acid concentration (33), and (*3*) its absorption maximum in the visible range of the spectrum. The tetraethylammonium (TEA^+) salt of PCP^- is selected as a reference standard in these studies because of its low solubility and resistance to solvent interaction (16). The

[1]Abstracted in part from a dissertation submitted by T.R.E. in partial fulfillment for the requirements of a Ph.D. degree (1970). Present address: E. I. duPont de Nemours and Co., Inc., Spruance Film Plant, P.O. Box 27222, Richmond, Va. 23261.

[2]Visiting Professor 1970–1971, Chemistry Department, McGill University, Montreal, Quebec.

Can. J. Chem. Downloaded from www.nrcresearchpress.com by 210.87.254.105 on 09/05/12
For personal use only.

Can. J. Chem. Downloaded from www.nrcresearchpress.com by 210.87.254.105 on 09/05/12
For personal use only.

activity coefficient of the protonated indicator molecule by this modus operandi is defined as

$$[1] \qquad f^*_{BH^+} = \frac{f^2_{\pm}(BH^+PCP^-)}{f^2_{\pm}(TEA^+PCP^-)}$$

Sweeting and Yates have used this approach to study the activity coefficient behavior of amides in sulfuric acid (34).

One cannot measure directly the activity coefficient of the protonated and neutral form of the same indicator molecule. Only weak bases can be used to measure activity coefficients of the neutral form, f_B, over a large range of acid concentration since the equilibrium must be sufficiently suppressed to avoid excessive protonation of the indicator. Conversely only the stronger bases can be used to measure $f^*_{BH^+}$. As a consequence there is an intrinsic uncertainty in expressing the ratio of the activity coefficient terms, $f^*_{BH^+}/f_B$ since f_B values obtained from different indicator molecules must be used. Boyd's use of this term in this manner in the acidity equations (32) suffers from this serious disadvantage.

In this research it was our objective to circumvent this problem in order to obtain more meaningful $f^*_{BH^+}/f_B$ ratios. An extrapolation technique was developed to deduce f_B values not experimentally accessible and activity coefficient ratios of four indicator molecules were obtained as a function of acid concentration in sulfuric, perchloric, and hydrochloric acid by using the extrapolated f_B values for these indicator molecules. An attempt was made as well to cancel the contribution of the standard TEA^+ ion in this ratio to provide an estimate of f_{BH^+}/f_B.

Experimental

Neutral Indicators

Of the seventeen indicators comprising the set that was used by Hammett and Deyrup in their first paper on acidity functions (1), only the eight substituted primary anilines, *p*-nitroaniline, *o*-nitroaniline, 4-chloro-2-nitroaniline, 2,4-dinitroaniline, 6-bromo-2,4-dinitroaniline, 2,4,6-trinitroaniline, 2,4-dichloro-6-nitroaniline, and 2,5-dinitro-4-methylaniline were considered appropriate for this research. Additional reason for excluding benzalacetophenone, 2-benzoylnaphthalene, 4-benzoylbiphenyl, and anthraquinone arose from the expectation that the ketone functional group would further complicate examination of the class of nitroanilines selected for study in this work. The *N,N'*-dimethyl-2,4,6-trinitroaniline had already been shown to be unsuitable for use in conjunction with substituted anilines (5). Azobenzene and azodiphenylamine were believed capable of the addition of a second proton and 4-nitroazobenzene was too insoluble.

The Hammett indicators were purchased as a set from the Aldrich Chemical Company. Additional indicator, purchased as needed, was recrystallized before use until its absorbance matched that of the indicator in the purified set. Purity was also checked by measuring the melting points of the indicators with a Thomas Hoover melting point apparatus. The melting points of the indicators used agreed with the literature values for the pure compounds.

The maximum absorbance of saturated solutions of the eight indicators chosen for this work were measured. Numerous readings at various time intervals were made to assure reproducibility of results.

Indicator Salts

The salts of *p*-chloroaniline, *m*-nitroaniline, *o*-chloroaniline, and *p*-nitroaniline were prepared by using equimolar solutions of the protonated indicator and sodium pentacyanopropenide (Na^+PCP^-) dissolved in warm water. These mixtures were cooled in an ice bath to precipitate the salt (BH^+PCP^-) which was then washed with acid, filtered, and dried. The standard reference salt, TEA^+PCP^-, was prepared similarly from tetraethylammonium chloride.

The purity of each product was monitored by careful examination of its solution absorption spectrum in the visible and ultraviolet region. Any changes in a product, such as the dissociation of the cation at low acid concentrations, were discernable by this approach as well.

Attempts to prepare the PCP^- salt of *o*-nitroaniline ($pK_A^{BH^+} = -0.29$) and 4-chloro-2-nitroaniline ($pK_A = -1.03$) repeatedly resulted in the dissociation of the cation into neutral base and HPCP upon isolation of the salt. For these mixtures the PCP^- absorption peak at 396 mμ was obscured by the formation of the neutral species which absorbed in the visible region of the spectrum as well. The preparation of salts of weaker bases in the series was not attempted since cation dissociation is more appreciable with decreasing base strength.

Preparation of Na^+PCP^- for use in the isolation of the indicator salts consisted of first converting tetramethylammonium pentacyanopropenide, (TMA^+PCP^-), obtained from Distillation Industries as a custom synthesis, to the acid by passing the salt solution through a bed of BIO-RAD AG 50W-X2 ion-exchange resin in the H^+-ion form. The resin column, prewashed with ethanol to remove impurities, was maintained at a temperature of 80 °C with a steam jacket throughout the operation. The complete removal of tetramethylammonium ion from the product was assured by the absence of precipitate when sodium tetraphenylborate, which forms a white precipitate with quaternary ammonium cations, was periodically added to aliquot portions of the eluant. The acid product, converted next to the sodium salt by potentiometric titration with sodium hydroxide, was evaporated to dryness. Almost quantitative recovery of the sodium pentacyanopropenide (Na^+PCP^-) product was obtained.

Acids

Acid solutions were prepared by dilution of Allied Chemical Reagent C.P. acids with triply distilled water. Concentrations were checked initially and at the end of the testing procedure by titration with Fisher Standard sodium hydroxide.

Can. J. Chem. Downloaded from www.nrcresearchpress.com by 210.87.254.105 on 09/05/12
For personal use only.

Solubility Measurements

After it was experimentally shown that equivalent results were obtained by approaching saturation from the unsaturated and supersaturated condition, saturated solutions of the neutral indicators or salts were prepared by mixing an excess of the powdered solid with approximately 5 ml of the acid solution. The sample, agitated for 1 h, was stored for 24 h at 25.00 ± 0.01 °C in a constant temperature air bath. The constancy of absorbance readings after longer time intervals showed that all of the samples reached equilibrium within the 24 h period.

The samples were then prepared for measurement inside the constant temperature bath by filtering the saturated solutions through a thermostated fritted glass filter into a thermostated vial. A 1 ml sample was then withdrawn from the filtered solution and was diluted when necessary with acid of the same concentration to obtain a convenient optical density. Absorbance readings were made by using a Beckman DU Spectrophotometer fitted with a thermostated cell compartment. The spectrophotometer was checked for accuracy with a set of Beckman Standard Cells and the absorbance cells used for the measurements were corrected to read zero absorbance over the entire spectrum.

Neutral Indicators

All measurements on the neutral indicators were made at λ_{max} which was ascertained by scanning the spectrum at each acidity. Slight shifts in λ_{max} due to the changing medium could not be neglected. The 4-chloro-2-nitroaniline ($pK_A = -1.03$) was the most basic indicator which could be used in a direct measurement over the entire acid concentration range of this study. As pK_A values become more positive than -1.03 protonation increases and the acid concentration range in which a measurable absorbance for the neutral form of the indicator is possible becomes smaller and eventually disappears. For example, *o*-nitroaniline ($pK_A = -0.29$) could be used over a narrow range of acid concentrations to obtain f_B by direct measurement. In the case of *p*-nitroaniline ($pK_A = 0.99$), however, log $[BH^+]/[B]$ is already approximately 2.0 at 20% by weight sulfuric acid. At higher acid concentrations, the absorbance peak at 396 mμ for the neutral molecule is completely obscured.

Indicator Salts

All solubility measurements, except those for the reference state of *p*- and *m*-nitroanilinium pentacyanopropenide, were made by measuring the absorbance peak of the PCP^- ion at 396 mμ. The solubility of these two salts in water was obtained by indirect estimate of absorption at 396 mμ from absorbance readings taken at 245 mμ. This estimate was based upon the ratio $R = \lambda_{max\ vis}/\lambda_{max\ \mu v}$ measured in 10% acid solution. In water the cations of these two salts partially dissociate to the neutral indicator forms which absorb in the visible region of the spectrum to obscure the PCP^- peak. By measuring the ratio, *R*, of the absorption maxima at 396 and 245 mμ for these salts in 10% H_2SO_4 where such dissociation is absent, a true estimate of the relative absorption values for these indicator–salt molecules at these wavelengths was obtained and the absorption readings at 245 mμ in water solution, multiplied by *R*, provide the correct absorption value at 396 mμ.

The reference state of all of the salts was corrected for deviation from ideality by employing a modified form of the Debye–Hückel equation.

TABLE 1. Reference states of indicator salts

PCP^- salt of	log f_1*	A_{396} mμ	
		Experimental	Corrected
p-NO_2^+	−0.084	945†	780
m-NO_2^+	−0.108	1800†	1400
p-Cl^+	−0.075	612	515
o-Cl^+	−0.049	386	345
TEA^+	−0.016	22.9	22.0

*From the Davies modification of the Debye–Hückel equation.
†Corrected for dissociation of the cation into neutral B by: $A_{396\ m\mu} = A_{245\ m\mu} \times R$ where $R = A_{396\ m\mu}/A_{245\ m\mu}$ as measured in 10% H_2SO_4; $A_{396m\mu}(p\text{-}NO_2^+) = 509 \times 1.83 = 945$; $A_{396m\mu}(m\text{-}NO_2^+) = 942 \times 1.93 = 1800$.

$$[2] \qquad \log f_{\pm} = \frac{-A\sqrt{I}}{I + Ba\sqrt{I}} + bI$$

where $b = 0.1\ Z_1Z_2$; $a = 3$ Å; $B = 0.3288$ (36); $A = 0.5065$ (36); and *I*, the ionic strength of the saturated aqueous solution, is obtained from the absorption measurements.

The results of these calculations are shown in Table 1.

The utility of the above method for solubility measurement was carefully documented in preliminary studies with Na^+PCP^-, TEA^+PCP^- and the indicator salts. With Na^+PCP^- it was shown that the visible spectrum of the PCP^- anion exhibited maxima at 396 and 412 mμ, the peak at 396 mμ being the larger of the two, in agreement with the results reported by Middleton (35). A plot of absorbance *vs.* sodium pentacyanopropenide concentration showed that Beer's Law was obeyed over the concentration range tested (1.52×10^{-4} *M* to saturation). In the 24 h interval of the solubility measurements these spectral characteristics persisted in H_2SO_4 and $HClO_4$ solutions less than 40% by weight. Beyond this acid concentration a small increase in absorption in the ultraviolet region of the spectrum was observed: no change in intensity at the longer wavelength ($\varepsilon_{PCP^-} = 2.04 \times 10^{-4}$ at 396 mμ) was detectable to assure the validity of this measurement for quantitative estimate of the solubility of the indicator salts of pentacyanopropenide in these acids. The Na^+PCP^- solution, however, was not stable in concentrated HCl solutions. A new peak appeared at 280 mμ which shifted the maxima at 396 and 245 mμ making accurate absorbance readings at the two wavelengths impossible.

Similar examination of the indicator salts and TEA^+PCP^- in the three acid systems confirmed these observations. The absorption ratio at $\lambda_{max\ vis}$ and $\lambda_{max\ \mu v}$ in sulfuric and perchloric acid in samples up to 50% weight acid did not indicate any gross changes in their composition to substantiate Boyd's observations (33) and the earlier observations with Na^+PCP^- that the PCP^- anion is not protonated in this acid concentration range. At the highest acid concentration greatest change in absorption ratio was observed. This is consistent with the increased absorption observed in the ultraviolet region of the spectrum obtained with Na^+PCP^- in the more concentrated H_2SO_4 and $HClO_4$ solutions. The ratio change was sufficiently small, however, to attest to the fact that the salts tested in sulfuric and perchloric acids have suitable stability. Ratio changes were within acceptable limits

Can. J. Chem. Downloaded from www.nrcresearchpress.com by 210.87.254.105 on 09/05/12
For personal use only.

in up to 20% HCl for most salts to confirm the results obtained with Na^+PCP^- as well. At higher acidities, however, a gross change in sample composition (formation of a new species, $\lambda_{max} = 280$ mμ) occurred. It is due either to the degradation of BH^+PCP^- or to an addition reaction with PCP^- that is catalyzed by the chloride ion. The addition of chlorine to cyanoethylene (35), which is believed to be catalyzed by chloride ion (37), is an example of this kind of reaction. At these higher acidities absorbance readings at 396 or 245 mμ could not be used because of interference from the peak at 280 mμ.

An estimate of the behavior of the activity coefficients of the salts in hydrochloric acid solutions above 20% by weight had to be made by extrapolation of log $f^*_{BH^+}$ *vs.* log a_{H_2O} curves determined at the lower acid concentrations. The data are thus uncertain for salts in HCl solutions greater than 20% by weight and comparison of log f^*_{BH} behavior between the salts in HCl above this acid strength are suspect.

The absorption ratio observed for the *p*-NO_2^+ and *m*-NO_2^+ salts ($R \simeq 1.9$) is smaller than for the other salts ($R \simeq 4.2$). This is due to the fact that their protonated form absorbs in the u.v. The small change in ratio with increasing acid concentration is more pronounced for the salts with cations absorbing near the visible region.

Results

Measurement of f_B

By using the aqueous solution saturated with the indicator as the reference state, the activity coefficient of B at any acid concentration is obtained by the relationship

$$[3] \qquad f_B(\text{acid}) = f_B(H_2O)A_{H_2O}/A_{\text{acid}}$$

This equation gives the activity coefficient as the reciprocal of absorbances (A) of the two saturated solutions since both saturated solutions are at equal activity and $f_B(H_2O)$ is defined as unity in the reference state. The molar concentrations of the saturated aqueous solutions are of the order of 10^{-4}. Since the variation of activity coefficient with concentration of these uncharged species is negligible, the assignment of ideal behavior to these saturated aqueous solutions introduces minimal error in the computation of f_B as a function of acid concentration.

The solubility data obtained with the six most weakly basic indicators employed in this research are presented in Table 2 for the three acid systems studied. In the first column of compilation of data for a particular indicator the wt. % concentration of the acid is presented. The absorbance measurement is given in column 2. The experimentally based log f_B values are listed in column 3. The last column gives an adjusted value of log f_B (at the experimental acid concentration) that is obtained by drawing the best smooth curve through the experimental points (log f_B plotted against acid concentration). Deviations from this smooth curve at high acidities are attributed to uncertainty arising from protonation of some of the indicators.

The variation of the activity coefficient of the neutral species (f_B) behaves in a regular manner for each of the bases studied. Even though the behavior of f_B is different in H_2SO_4 as compared to $HClO_4$ and HCl, the constant variation between members of the class of indicators is maintained. The nature of this negative deviation in activity coefficient has been attributed to the salting-in of the neutral base which is quite sensitive to the structure of the base: Hammett (38) and Deno (31) have suggested the interaction of the nitro group with the solvent as an explanation of this behavior.

When the log f_B obtained at each acid concentration for all but one of the indicators (2,6-dinitro-4-methylaniline) is subtracted from the corresponding log f_B value obtained for the weakest indicator, 2,4,6-trinitroaniline ($pK_A = -9.41$) and this difference (Δ log f_B) is plotted against the difference in base strength (ΔpK_A) for each indicator relative to 2,4,6-trinitroaniline, a family of essentially straight lines that extend over 8.33 pK units appears to describe best the data that are obtained for the three different acids. Even though insufficient data are available to provide a statistical verification of this linear relationship, it appears to provide a reasonable approximation of the real situation to justify extrapolation of these lines over an additional 4.99 pK_A units to estimate f_B for the more basic indicators used in this study. The various values of log f_B that have been estimated for these indicators by such extrapolation for each acid system are given in Table 3. The slope of each of the lines that were drawn for this purpose is presented together with the standard deviation of the experimental values in Table 4.

The uncertainty limits of f_B evaluated by extrapolation as described above is difficult to assess. All solubility measurements of f_B are believed to have had a precision range of 2 to 3% when experimental conditions were optimum. However, the experimental points deviate

TABLE 2. Variation of log f_B

Acid	% by weight of acid	A^*	log f_B	log f_B (adj)	A^*	log f_B	log f_B (adj)	A^*	log f_B	log f_B (adj)
H_2SO_4		4-Chloro-2-nitroaniline			2,4-Dichloro-6-nitroaniline			2,6-Dinitro-4-methylaniline		
	0.00	3.51	0.000	0.000	0.515	0.000	0.000	0.684	0.000	0.000
	10.19	3.25	0.033	0.045	0.503	0.010	0.030	0.680	0.004	0.004
	20.04	3.05	0.061	0.061	0.475	0.035	0.035	0.778	−0.056	−0.056
	30.86	3.29	0.028	0.028	0.587	−0.057	−0.057	1.09	−0.202	−0.202
	40.35	4.89	−0.144	−0.144	0.876	−0.231	−0.231	2.15	−0.498	−0.498
	50.50			−0.332	1.77	−0.536	−0.536	5.38	−0.896	−0.896
	60.77			−0.515	2.55	−0.695	−0.844	13.2	−1.286	−1.286
		2,4-Dinitroaniline			6-Bromo-2,4-dinitroaniline			2,4,6-Trinitroaniline		
	0.00	5.32	0.000	0.000	1.20	0.000	0.000	1.24	0.000	0.000
	10.19	5.51	−0.015	−0.015	1.34	−0.048	−0.038	1.59	−0.108	−0.108
	20.04	6.31	−0.074	−0.074	1.63	−0.133	−0.133	2.41	−0.289	−0.289
	30.86	8.32	−0.194	−0.194	2.37	−0.296	−0.296	4.37	−0.547	−0.547
	40.35	13.9	−0.417	−0.417	4.46	−0.570	−0.570	9.81	−0.898	−0.898
	50.50	29.4	−0.743	−0.743	10.4	−0.938	−0.938	23.5	−1.278	−1.278
	60.77	61.2	−1.061	−1.061	23.0	−1.283	−1.283	53.1	−1.633	−1.633
$HClO_4$		4-Chloro-2-nitroaniline			2,4-Dichloro-6-nitroaniline			2,6-Dinitro-4-methylaniline		
	0.00	3.51	0.000	0.000	0.515	0.000	0.000	0.684	0.000	0.000
	10.33	6.23	−0.249	−0.249	1.05	−0.309	−0.309	1.80	−0.420	−0.420
	20.02	9.82	−0.447	−0.447	1.81	−0.546	−0.546	3.90	−0.757	−0.757
	30.18	15.6	−0.648	−0.634	3.00	−0.765	−0.765	7.68	−1.050	−1.050
	40.13	23.5	−0.826	−0.826	4.68	−0.958	−0.958	14.3	−1.321	−1.321
	50.05			−1.023	7.19	−1.145	−1.160	28.7	−1.623	−1.623
	59.91			−1.200	8.00	−1.291	−1.370	72.9	−2.028	−2.028
		2,4,-Dinitroaniline			6-Bromo-2,4-dinitroaniline			2,4,6-Trinitroaniline		
	0.00	5.32	0.000	0.000	1.20	0.000	0.000	1.24	0.000	0.000
	10.33	13.1	−0.391	−0.391	3.36	−0.447	−0.447	4.15	−0.524	−0.524
	20.02	26.6	−0.699	−0.689	7.50	−0.796	−0.796	13.0	−1.021	−1.021
	30.18	47.6	−0.954	−0.939	14.5	−1.083	−1.083	31.1	−1.399	−1.399
	40.13	82.2	−1.189	−1.189	27.6	−1.362	−1.362	66.9	−1.734	−1.734
	50.05	149.0	−1.447	−1.447	51.0	−1.629	−1.660	143.0	−2.062	−2.062
	59.91	315.0	−1.773	−1.685	106.0	−1.947	−1.947	308.0	−2.395	−2.395
HCl		4-Chloro-2-nitroaniline			2,4-Dichloro-6-nitroaniline			2,6-Dinitro-4-methylaniline		
	0.00	3.51	0.000	0.000	0.515	0.000	0.000	0.684	0.000	0.000
	4.84	4.01	−0.058	−0.058	0.654	−0.104	−0.098	0.859	−0.099	−0.099
	9.68	4.92	−0.147	−0.147	0.880	−0.233	−0.233	1.30	−0.279	−0.279
	14.59	6.42	−0.262	−0.262	1.24	−0.382	−0.382	2.04	−0.475	−0.475
	19.65	9.20	−0.418	−0.418	1.95	−0.578	−0.578	3.34	−0.688	−0.688
	24.62	12.2	−0.541	−0.580	3.12	−0.782	−0.782	5.77	−0.925	−0.925
	29.27			−0.785	4.55	−0.946	−0.980	9.21	−1.129	−1.129
		2,4-Dinitroaniline			6-Bromo-2,4-dinitroaniline			2,4,6-Trinitroaniline		
	0.00	5.32	0.000	0.000	1.20	0.000	0.000	1.24	0.000	0.000
	4.84	7.19	−0.131	−0.131	1.70	−0.151	−0.151	1.82	−0.167	−0.167
	9.68	9.75	−0.263	−0.263	2.65	−0.344	−0.344	3.04	−0.290	−0.390
	14.59	14.0	−0.420	−0.428	4.13	−0.536	−0.536	5.14	−0.618	−0.618
	19.65	21.8	−0.613	−0.613	7.12	−0.772	−0.772	9.17	−0.869	−0.869
	24.62	34.0	−0.806	−0.803	11.8	−0.991	−0.991	15.8	−1.105	−1.105
	29.27	50.1	−0.974	−1.025	18.7	−1.192	−1.192	23.7	−1.281	−1.340

*All absorbances are expressed as that of a 1 cm cell without dilution. Molar concentrations can be calculated from the following extinction coefficients: $\varepsilon = 4.55 \times 10^3$ at 432 mμ, 4-chloro-2-nitroaniline; $\varepsilon = 4.58 \times 10^3$ at 421 mμ, 2,4-dichloro-6-nitroaniline; $\varepsilon = 1.40 \times 10^4$ at 347 mμ, 2,4-dinitroaniline; $\varepsilon = 1.26 \times 10^4$ at 348 mμ, 6-bromo-2,4-dinitroaniline; $\varepsilon = 8.53 \times 10^3$ at 412 mμ, 2,4,6-trinitroaniline.

Can. J. Chem. Downloaded from www.nrcresearchpress.com by 210.87.254.105 on 09/05/12
For personal use only.

TABLE 3. Extrapolated log f_B for strong bases in sulfuric, perchloric and hydrochloric acids

Acid	% by weight of acid	Extrapolated f_B value				
		p-Chloroaniline	*p*-Nitroaniline	*o*-Chloroaniline	*o*-Nitroaniline	*m*-Nitroaniline
H_2SO_4	10.19	0.159	0.099	0.133	0.074	0.129
	20.04	0.361	0.214	0.298	0.151	0.288
	30.86	0.450	0.230	0.356	0.133	0.340
	40.35	0.460	0.160	0.325	0.030	0.310
	50.50	0.245	−0.088	0.102	−0.235	0.082
	60.77	0.067	−0.311	−0.110	−0.473	−0.123
$HClO_4$	10.33	−0.106	−0.202	−0.154	−0.242	−0.154
	20.02	−0.088	−0.298	−0.181	−0.381	−0.191
	30.18	−0.119	−0.404	−0.244	−0.526	−0.262
	40.13	−0.215	−0.549	−0.364	−0.694	−0.384
	50.05	−0.352	−0.725	−0.517	−0.887	−0.540
	59.91	−0.422	−0.852	−0.610	−1.038	−0.638
HCl	4.84	−0.012	−0.047	−0.027	−0.062	−0.030
	9.68	−0.038	−0.119	−0.073	−0.153	−0.080
	14.59	−0.098	−0.215	−0.150	−0.266	−0.156
	19.65	−0.195	−0.346	−0.263	−0.414	−0.271
	24.62	−0.310	−0.492	−0.394	−0.577	−0.403
	29.67	−0.497	−0.692	−0.587	−0.777	−0.597

TABLE 4. Characterization of linear plots ($\Delta pK_A = m\Delta \log f_B$)

Acid	% by weight of acid	Slope of line (m)	Standard deviation
H_2SO_4	10.19	0.020	0.013
	20.04	0.0485	0.034
	30.86	0.0747	0.036
	40.35	0.1013	0.056
	50.50	0.1143	0.021
	60.77	0.1275	0.037
$HClO_4$	10.33	0.0310	0.015
	20.02	0.0700	0.024
	30.18	0.096	0.028
	40.13	0.114	0.049
	50.05	0.1285	0.054
	59.91	0.1485	0.055
HCl	4.84	0.0117	0.013
	9.68	0.0262	0.018
	14.59	0.0387	0.018
	19.65	0.050	0.025
	24.62	0.0587	0.031
	29.27	0.0624	0.021

considerably more than this from the best straight line that can be drawn through them. Dispersion of points by as much as 0.15 log units in the region of measurement far exceeds the projected experimental error range. Additional bias in the extrapolated log f_B values can arise as well from uncertainty in selection of the slope of the line that is drawn through the experimental points. A conservative estimate of the possible uncertainty range in the extrapolated log f_B values is believed to be of the order of 0.2 log units.

TABLE 5. Comparison of experimental and extrapolated log f_B values for *o*-nitroaniline

Acid	% by weight of acid	A	log f_B	
			Experimental	Extrapolated
H_2SO_4	0.00	37.3	0.000	0.000
	10.19	33.3	0.049	0.074
	20.04	32.8	0.058	0.151
	30.86	31.0	0.080	0.133
$HClO_4$	10.33	57.0	−0.184	−0.242
	20.02	98.2	−0.421	−0.381
	30.18	112.0	−0.511	−0.526
HCl	4.84	43.0	−0.063	−0.062
	9.68	49.3	−0.122	−0.153
	14.59	59.9	−0.206	−0.266

To estimate further the reliability of the linear relationships derived by visual inspection of the data extrapolated values of log f_B were compared with the experimental log f_B values obtained for *o*-nitroaniline ($pK_A = -0.29$), the strongest base that could be used to obtain solubility data in a limited acid concentration range. These comparisons are presented in Table 5. Correlation is poorest in the H_2SO_4

Can. J. Chem. Downloaded from www.nrcresearchpress.com by 210.87.254.105 on 09/05/12
For personal use only.

TABLE 6. Values of log $f_{\pm}$ for salts of strong bases in acid

Acid	% acid	p-$NO_2^+PCP^-$		p-Cl^+PCP^-		m-$NO_2^+PCP^-$		o-Cl^+PCP^-		TEA^+PCP^-
		log $f_{\pm}$	log f^*	log $f_{\pm}$	log f^*	log $f_{\pm}$	log f^*	log $f_{\pm}$	log f^*	log $f_{\pm}$
H_2SO_4	10.19	−0.053	0.266	−0.081	0.210	−0.282	−0.192	−0.048	0.276	−0.186
	20.04	0.050	0.812	0.094	0.900	−0.057	0.598	0.158	1.028	−0.356
	30.86	0.156	1.328	0.201	1.418	−0.038	0.940	0.261	1.538	−0.508
	40.35	0.171	2.116	0.269	2.312	−0.204	1.366	0.158	2.090	−0.887
	50.50	0.063	2.728	0.111	2.824	−0.376	1.850	0.031	2.664	−1.301
	60.77	−0.104	3.242	0.050	3.550	−0.381	2.688	−0.229	2.992	−1.725
$HClO_4$	10.33	−0.372	0.730	−0.458	0.558	−0.306	0.862	−0.256	0.962	−0.737
	20.02	−0.537	1.442	−0.605	1.306	−0.700	1.116	−0.439	1.638	−1.258
	30.18	−0.611	2.104	−0.647	2.032	−0.816	1.694	−0.589	2.146	−1.663
	40.13	−0.625	2.786	−0.612	2.812	−0.782	2.472	−0.627	2.780	−2.018
	50.05	−0.648	3.600	−0.682	3.536	−0.886	3.132	−0.716	3.466	−2.450
	59.91	−0.851	3.834	−0.804	3.928	−0.921	3.694	−1.008	3.516	−2.768
HCl	4.84	−0.090	0.598	−0.172	0.434	−0.254	0.278	−0.083	0.611	−0.389
	9.68	−0.081	1.264	−0.173	1.080	−0.062	1.302	−0.154	1.118	−0.713
	14.59	−0.072	1.666	−0.172	1.466	0.050†	1.710	−0.300	1.210	−0.905†
	19.65	−0.030	2.070	−0.152	1.826	0.035†	2.200	−0.233	1.664	−1.065
	24.62	0.000†	2.480	−0.079†	2.322	0.110†	2.700	−0.265†	1.95	−1.240†
	29.27	0.001†	2.732	−0.074†	2.582	0.007†	2.744	−0.280†	2.17	−1.365†

†Obtained by extrapolation and interpolation.

system. However, when the lines to represent this system at the three acid concentrations are redrawn with slopes of 0.0188, 0.0422, and 0.0705 instead of 0.020, 0.0485, and 0.0747 standard deviation of the experimental points from the redrawn lines remain essentially unchanged (0.011, 0.035, and 0.038 as compared to 0.013, 0.034, and 0.036) while prediction and observation are in better agreement (0.049 *vs.* 0.063 instead of 0.074, 0.058 *vs.* 0.095 instead of 0.151, and 0.080 *vs.* 0.096 instead of 0.131).

Though there is a sizeable error in the predictions by this approach, it is within the uncertainty limits that have been projected for the extrapolation procedure. Some satisfaction has to be derived from the fact that f_B values of an indicator as a function of acid concentration that are otherwise completely unaccessible are at least approachable with this kind of treatment. Further investigation to provide sufficient data for a statistically valid analysis of the ΔpK *vs.* $\Delta \log f_B$ relationship is without a doubt desirable to improve the predictive quality of this approach.

The observation that the deviation in log f_B can be linearly related to the pK_A of the base at a fixed water activity in all three acid systems appears to indicate that the substituent effects that determine base strength affect the activity coefficient in a parallel manner.

The 2,6-dinitro-4-methylaniline solubility behavior, since it does not conform, is believed not to be a representative member of the family of indicators under investigation. Possibly it should be considered to belong to a class of substituted *p*-toluidines.

Measurement of $f^*_{BH^+}$

Experimental values of $\log f^{\pm}_{BH^+PCP^-}$ obtained for the reference and indicator salts from the solubility data are presented in Table 6 for the three acid systems studied. The value of $f^{\pm}_{BH^+PCP^-}$ is obtained from the solubility data with eq. 3 modified by multiplying the right hand term of this equation by the $f^{\pm}_{BH^+PCP^-}$ values computed earlier for the saturated aqueous systems. Correction for deviation from ideality in the reference aqueous solution is, by this manner of computation, incorporated in the values listed. Also included in Table 6 is the corresponding log $f^*_{BH^+}$ (*i.e.* log f_{BH^+}/f_{TEA^+}) value obtained from the ratio $f^{\pm 2}_{BH^+PCP^-}/f^{\pm 2}_{TEA^+PCP^-}$ (eq. 3) to provide an estimate of the behavior of f_{BH^+} relative to the standard ion (f_{TEA^+}).

The behavior of $f^*_{BH^+}$ is quite different from that of the neutral species. In all cases there is

Can. J. Chem. Downloaded from www.nrcresearchpress.com by 210.87.254.105 on 09/05/12
For personal use only.

TABLE 7. Calculation of $\log (f_{BH^+}/f_B)(f_{PCP^-}/f_{TEA^+})^{1/2}$

Acid	% by weight of acid	$\log \frac{f_{BH^+}}{f_B}\left(\frac{f_{PCP^-}}{f_{TEA^+}}\right)^{1/2}$			
		p-Chloroaniline	*o*-Chloroaniline	*p*-Nitroaniline	*m*-Nitroaniline
H_2SO_4	10.19	−0.14	−0.05	−0.02	−0.51
	20.04	0.18	0.37	0.24	0.00
	30.86	0.46	0.57	0.66	0.09
	40.35	0.97	0.88	1.07	0.17
	50.50	1.27	1.46	1.42	0.47
	60.77	1.75	1.38	1.83	1.09
$HClO_4$	10.33	−0.08	0.28	0.19	0.28
	20.02	0.13	0.56	0.43	0.05
	30.18	0.58	0.73	0.50	0.29
	40.13	1.01	1.13	1.32	0.84
	50.05	1.41	1.52	1.83	1.22
	59.91	1.58	1.36	1.92	1.56
HCl	4.84	0.06	0.25	0.26	−0.14
	9.68	0.41	0.48	0.67	0.67
	14.59	0.66	0.46	0.98	1.06
	19.65	0.96	0.86	1.35	1.41
	24.65	1.39	1.11	1.73	1.87
	29.27	1.71	1.39	2.06	1.98

first a positive deviation from ideality. This result is undoubtedly due to hydration of the BH^+ cation since the PCP^- contribution has been cancelled and the tetraethylammonium ion is expected to be free of solvent interaction.

The experimental error in measuring the solubility of the various salts is estimated to be less than ± 0.02 log units and the uncertainty range of $f^*_{BH^+}$ is believed to be no more than 0.08 log units. Error in the estimate of deviations from ideality for each indicator salt at the saturation concentration in water is believed to be minimal at the level of salt concentrations that is encountered.

Discussion

It has been the ultimate objective of this research program to obtain f_{BH^+}/f_B ratios for the same indicator molecule. This goal is not fully realized with the $f^*_{BH^+}/f_B$ values listed in Table 6 since all ratios are referred to the standard TEA^+ ion. However if $f^*_{BH^+}/f_B$ is multiplied by $f^{\pm 2}_{BH^+PCP^-}/f_B$ we obtain the expression $(f^2_{BH^+}f_{PCP^-})/(f^2_B f_{TEA^+})$. By taking its square root the term $(f_{BH^+}/f_B)(f_{PCP^-}/f_{TEA^+})^{1/2}$ is resolved and the value of f_{BH^+}/f_B is approached if the ratio of f_{PCP^-}/f_{TEA^+} is not too far removed from unity. For example, if $f_{PCP^-} < 2f_{TEA^+}$ or the reverse is true the value of the above expression is less than 40% different from the value of f_{BH^+}/f_B. This is within the uncertainty limit of the function itself. Both PCP^- and TEA^+ are bulky ions of low charge density and they are not likely to be solvated. It is conceivable that their deviation from ideality may be similar.

The values obtained for $\log (f_{BH^+}/f_B) \times (f_{PCP^-}/f_{TEA^+})^{1/2}$ are presented in Table 7 for the four indicators studied in three different acid systems. By comparing the values of this term for these indicators at each fixed acid concentration it is noticeable that reasonable accord is obtained, in many cases more often than not, falling within the uncertainty limit of about 0.3 log units that is projected to be likely in the evaluation of this term. With the indicator *m*-nitroaniline, however, there is an unusually large discrepancy from the values observed for this term in H_2SO_4 with the three other indicators studied. More careful scrutiny shows as well that this term obtained with the *o*- and *p*-chloroaniline indicators for $HClO_4$ correlates better with each other than does this term derived from the *p*- and *m*-nitroaniline data. Good agreement in this term is obtained for both pairs of indicators in HCl although there is considerable disagreement between the term

Can. J. Chem. Downloaded from www.nrcresearchpress.com by 210.87.254.105 on 09/05/12
For personal use only.

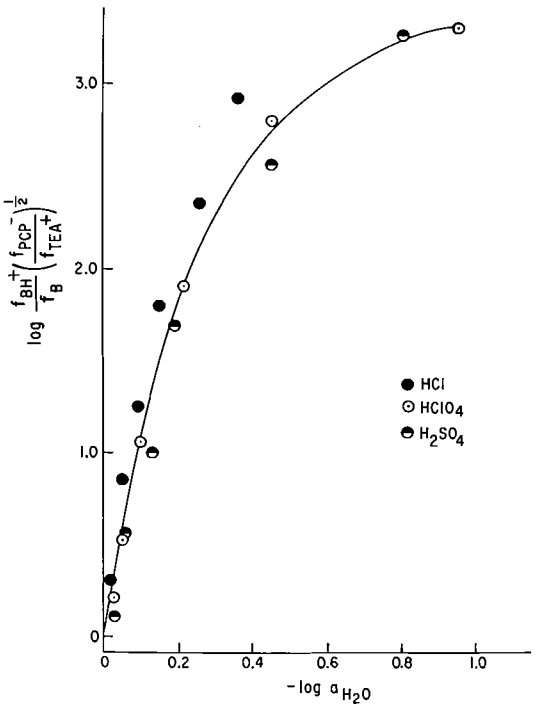

FIG. 1. Plot of $\log (f_{BH^+}/f_B)(f_{PCP^-}/f_{TEA^+})^{1/2}$ *vs.* $-\log a_{H_2O}$.

derived from these indicator pairs. Since the indirect means (dissociation of the nitroanilines obscures the PCP^- peak at 396 mμ) used to measure the absorption of the nitro-substituted anilines in their reference state (saturated aqueous solution) could introduce bias to this solubility measurement, the data obtained with the chloroanilines are believed to provide the more meaningful results. As a consequence, only these data have been used to construct Fig. 1 where the averaged term $\log (f_{BH^+}/f_B) \times (f_{PCP^-}/f_{TEA^+})^{1/2}$ is plotted versus $-\log a_{H_2O}$ for the three systems studied. The term obtained for the HCl system beyond 19.6% by weight concentration is not included in this figure because of the extra uncertainty of the solubility measurements beyond this concentration value.

All of the points in the figure fall within the tolerance limit of ± 0.15 log units that is prescribed for this term. This result indicates that the term is essentially independent of the nature of the acid employed in the system, a result predicted by the pioneer work of Hammett. In addition to this substantiation of the estimate that the ratio of f_{BH^+}/f_B is the same for indicators of similar structure in strong acids at equal water activity it is suggested that evaluation of the term $(f_{BH^+}/f_B)(f_{PCP^-}/f_{TEA})^{1/2}$ for the same indicator molecule markedly improves on the attempt of Boyd to deduce f_{BH^+}/f_B from his construction of $f^*_{BH^+}/f_B$ that is based on two different indicator molecules. The deficiency of his approach is apparent from the large variation of f_B with pK_B that was demonstrated in this research. Even with the considerable uncertainty that is inherent in the extrapolation of f_B values in this research more meaningful values of $f^*_{BH^+}/f_B$ than are reported by Boyd are believed to have been measured here. Also, unless f_{PCP^-} is much different from f_{TEA^+}, computation of this term provides a rather good approximation of f_{BH^+}/f_B. If this is indeed the case the activity of hydrogen ion in strong acids should be calculable from the definition of H_0.

Financial support through Contract No. AT(30-1)-2269 by the U.S. Atomic Energy Commission is gratefully acknowledged.

1. L. P. HAMMETT and A. J. DEYRUP. J. Am. Chem. Soc. **54**, 2721 (1932).
2. L. A. FLEXSER, L. P. HAMMETT, and A. DINGWALL. J. Am. Chem. Soc. **57**, 2103 (1935).
3. L. A. FLEXSER and L. P. HAMMETT. J. Am. Chem. Soc. **60**, 885 (1938).
4. L. ZUCKER and L. P. HAMMETT. J. Am. Chem. Soc. **61**, 2785 (1939).
5. E. M. ARNETT and G. W. MACH. J. Am. Chem. Soc. **88**, 1177 (1966).
6. R. L. HINMAN and J. LANG. J. Am. Chem. Soc. **86**, 3796 (1964).
7. M. J. JORGENSON and D. R. HARTTER. J. Am. Chem. Soc. **85**, 878 (1963).
8. E. M. HEILBRONNER and S. WEBER. Helv. Chem. Acta, **32**, 1513 (1949).
9. J. E. B. RANDLES and J. M. TEDDER. J. Chem. Soc. 1218 (1955).
10. K. N. BASCOMBE and R. P. BELL. J. Chem. Soc. Part 1, 1096 (1959).
11. J. T. EDWARD. Trans. Royal Soc. Can. Vol. II, Section III, 313 (1964).
12. F. H. WESTHEIMER and M. S. KHARASCH. J. Am. Chem. Soc. **68**, 1871 (1946).
13. N. E. DENO, J. J. JARUZELSKI, and A. SCHREISHEIM. J. Am. Chem. Soc. **77**, 3044 (1950).
14. A. M. LOWEN, M. A. MURRY, and G. WILLIAMS. J. Chem. Soc. 3318 (1950).
15. N. C. DENO, P. GROVES, and G. SAINES. J. Am. Chem. Soc. **81**, 5790 (1959).
16. N. C. DENO, P. GROVES, J. J. JARUZELSKI, and M. LUGASCH. J. Am. Chem. Soc. **82**, 4719 (1960).

Can. J. Chem. Downloaded from www.nrcresearchpress.com by 210.87.254.105 on 09/05/12
For personal use only.

17. E. M. ARNETT and G. W. MACH. J. Am. Chem. Soc. **86**, 2671 (1964).
18. K. YATES, J. B. STEVENS, and A. R. KATRITZKY. Can. J. Chem. **42**, 1957 (1964).
19. A. J. KRESGE and Y. CHIANG. Proc. Chem. Soc. 81 (1961).
20. W. F. GIAUQUE, E. W. HORNUNG, J. E. KUNZLER, and T. R. RUBIN. J. Am. Chem. Soc. **82**, 62 (1960).
21. K. N. BASCOMBE and R. P. BELL. Discuss. Faraday Soc. **24**, 158 (1957).
22. P. A. H. WYATT. Discuss. Faraday Soc. **24**, 162 (1957).
23. R. W. TAFT. J. Am. Chem. Soc. **82**, 2965 (1960).
24. J. F. BUNNETT. J. Am. Chem. Soc. **83**, 4956, 4968, 4973, 4978 (1961).
25. J. T. EDWARD and I. C. WANG. Can. J. Chem. **40**, 966 (1962).
26. C. PERRIN. J. Am. Chem. Soc., **86**, 256 (1964).
27. E. HOGFELDT. Acta Chem. Scand. **14**, 1627 (1960).
28. E. HOGFELDT. Acta Chem. Scand. **14**, 1597 (1960).
29. E. HOGFELDT. Acta Chem. Scand. **17**, 785 (1963).
30. J. G. DAUBER. J. Chem. Soc. (A), 1532 (1968).
31. N. C. DENO and C. PERRIZZOLO. J. Am. Chem. Soc. **79**, 1345 (1957).
32. R. H. BOYD. J. Am. Chem. Soc. **85**, 1555 (1963).
33. R. H. BOYD. J. Am. Chem. Soc. **83**, 4288 (1961).
34. L. M. SWEETING and K. YATES. Can. J. Chem. **44**, 2395 (1966).
35. W. J. MIDDLETON, E. L. LITTLE, D. D. COFFMAN, and V. A. ENGLEHARDT. J. Am. Chem. Soc. **82**, 6132 (1960).
36. H. S. HARNED and B. B. OWENS. The physical chemistry of electrolyte solutions. Reinhold Publishing Co., New York. 1943. p. 11.
37. C. L. DICKINSON, D. W. WILEY, and B. C. MCKUSICK. J. Am. Chem. Soc. **82**, 6132 (1960).
38. L. P. HAMMETT and R. P. CHAPMAN. J. Am. Chem. Soc. **56**, 1282 (1934).
39. K. YATES AND H. VOI. J. Am. Chem. Soc. **86**, 5408 (1964).
40. M. E. CARSTEN and H. N. EISEN. J. Am. Chem. Soc. **75**, 4451 (1953).

Can. J. Chem. Downloaded from www.nrcresearchpress.com by 210.87.254.105 on 09/05/12
For personal use only.

Réactions des phosphites triméthylique, triéthylique, et triphénylique avec le cholestérol

CLAUDE BENEZRA ET JEAN-LOUIS BRAVET
Département de Chimie, Université d'Ottawa, Ottawa, Canada K1N 6N5

ET

JEAN RIESS
Département de Chimie, Institut de Mathématiques et Sciences Physiques, Parc Valrose, Université de Nice, 06-Nice, France

Reçu le 11 février 1972

Avec le cholestérol, les phosphites triméthylique et triéthylique conduisent au phosphonate de dicholestéryle $HP(O)(OCholest)_2$ (**6**) et à un phosphonate mixte $HP(O)(OR)(OCholest)$ (**5**, $R = CH_3$ et C_2H_5 respectivement) alors que le phosphite triphénylique donne exclusivement le phosphonate **6**. Ces résultats sont discutés en termes de mécanismes possibles de ces réactions.

With cholesterol, trimethyl and triethyl phosphites afford dicholesteryl phosphonate $HP(O)(OCholest)_2$ (**6**) and an unsymmetrical phosphonate $HP(O)(OR)(OCholest)$ (**5**, $R = CH_3$ and C_2H_5 respectively) while triphenyl phosphite gives exclusively the phosphonate **6**. Those results are discussed in terms of a possible mechanism of these reactions.

Canadian Journal of Chemistry, **50**, 2264 (1972)

Les phosphites de trialcoyle $P(OR)_3$, réagissent sur des alcools aliphatiques pour donner des produits de transestérification (1, 2). Ces réactions sont d'autant plus faciles qu'il y a plusieurs fonctions hydroxyles et qu'un phosphite cyclique à 5 ou 6 chaînons a la possibilité de se former (3). Dans certains cas, les phosphites $P(OR)_3$ peuvent conduire à la formation de phosphonates avec des rendements suffisamment bons pour que ces réactions soient utilisables en synthèse. Ainsi, par exemple, avec le méthanol, le phosphite triéthylique **1** conduit au méthylphosphonate diéthylique **2**, au phosphonate diéthylique **3** et au phosphate triéthylique (4). Pour expliquer la formation du composé **2**, les auteurs proposent un intermédiaire de type quasi-phosphonium $MeP^{+}(OEt)_3$, OH^-.

Le mécanisme de ces réactions est mal connu et il nous a semblé utile d'étudier la réaction de divers phosphites $P(OR)_3$ (R = Me, Et, Ph) avec le cholestérol, une réactivité du type [1] pouvant éventuellement conduire à des stéroylphosphonates, accessibles jusqu'à présent par un nombre limité de méthodes (5).

Résultats

Lorsqu'un mélange de cholestérol **4** et de phosphite triméthylique en excès est chauffé à reflux pendant 24 h, on isole, par chromatographie sur colonne de silice, deux produits principaux auxquels nous avons attribué les

[1] $$P(OEt)_3 + MeOH \rightarrow MeP(O)(OEt)_2 + HP(O)(OEt)_2 + P(OEt)_3$$
1 **2** **3**

[2] 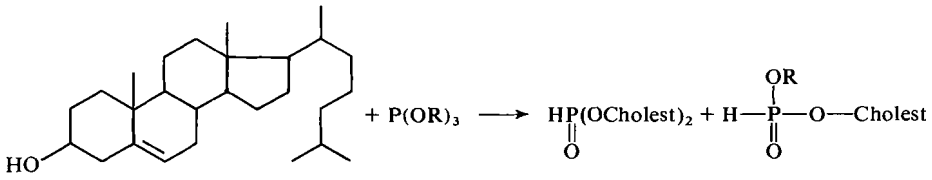

4 **6** **5**

Can. J. Chem. Downloaded from www.nrcresearchpress.com by 210.87.254.6 on 09/05/12
For personal use only.

Can. J. Chem. Downloaded from www.nrcresearchpress.com by 210.87.254.6 on 09/05/12
For personal use only.

structures **5** (R = Me) et **6** (éq. 2).[1] Ces produits sont obtenus avec des rendements de 77 et de 8% respectivement (par rapport au cholestérol qui a réagi). Les structures de ces deux composés ont été déduites de la façon suivante.

Le phosphonate de dicholestéryle (structure **6**) a été identifié (p.f., c.c.m., i.r., r.m.n.) à un échantillon authentique préparé par réaction[2] de PCl_3 sur le cholestérol (6). La liaison P—H est visible en i.r. (2420 cm^{-1} (7)) ainsi, qu'en r.m.n. ou elle apparaît sous forme d'un doublet centré à 6.88 p.p.m. (J_{PH} = 689 Hz)[3]. Ce couplage est compatible avec les valeurs de 630 à 707 Hz décrites dans la littérature (8) pour les phosphonates de type $HP(O)(OR)_2$.

La structure du phosphonate de méthyle et de cholestéryle, **5** (R = CH_3) a pu être établie par analyse centésimale, i.r. (ν_{P-H} 2400, $\nu_{P=O}$ 1265 cm^{-1}) et surtout par r.m.n. Le spectre à 100 MHz montre un doublet à 3.71 p.p.m. attribuable au groupe méthoxy et dont la surface correspond à 3H; l'hydrogène 3α donne un signal très élargi (notamment par couplage *P*—O—C—*H*) et l'hydrogène attaché directement au phosphore donne un doublet centré à 6.80 p.p.m. ($^1J_{PH}$ = 719 Hz).

Lorsque le phosphite de triméthyle est remplacé par du phosphite de triéthyle, on obtient les produits correspondants **5** (R = C_2H_5) et **6** dans des proportions comparables (66 et 15%, respectivement, par rapport au cholestérol qui a réagi).

Les résultats sont très différents avec le phosphite de triphényle et le cholestérol. Dans ce cas, en effet, on ne décèle aucune trace d'un phosphite mixte correspondant à **5** (R = C_6H_5) alors que l'on isole du phosphonate de dicholestéryle (50% par rapport au cholestérol consommé). On isole, outre du phénol, un peu de cyclo-3α,5-cholestène-6 et des produits non identifiés.

Discussion

La formation des phosphonates **5** et **6** est inattendue. Il ne s'agit pas, en effet, d'une simple réaction de transestérification qui aurait conduit à des phosphites trialcoyliques du type $P(OR)_2(OCholest)$, $P(OR)(OCholest)_2$, ou $P(OCholest)_3$. Ce dernier composé ne se forme pas et cela pour des raisons stériques évidentes; dans les conditions habituelles de formation des phosphites trialcoyliques, d'ailleurs (ROH + PCl_3, en présence de pyridine (9)), seuls les phosphonates dialcoyliques se forment, avec le cholestanol (10), comme avec le cholestérol (6).

En gros, deux types de mécanismes peuvent être envisagés: (*a*) transestérification préalable des phosphites puis protonation pour donner les sels d'alcoxyphosphonium **10** et **11** (Schéma 1); ou (*b*) protonation préalable des phosphites par le cholestérol suivie de désalcoylation pour conduire aux phosphonates **12** qui donnent lieu à des réactions de transestérification (Schéma 2).

Dans le Schéma 1, les alcoxyphosphoniums **10** et **11** intermédiaires, du type de ceux postulés par Chopard dans la réaction de $P(OCH_3)_3$ avec les cétones α-halogénées (11), pourraient conduire, par attaque nucléophile de l'alcoolate RO^- sur un reste R, au phosphonate mixte **5** (R = CH_3, C_2H_5, réaction [5]) ou au phosphonate de dicholestéryle **6** (réaction [7]). Une autre possibilité de formation du composé **5** par attaque sur le radical cholestéryle (réaction [6]) peut être écartée parce que d'une part, une substitution nucléophile directe en C-3 est difficile (attaque axiale (12)) d'autre part une attaque de type S_N2 sur les hydrogènes en 7 conduiraient au cyclo-3α,5-cholestène-6 ("isocholestadiène") (**14**) dont nous n'avons pu déceler aucune trace dans le cas où R = CH_3 ou C_2H_5.

Le second type de mécanisme (Schéma 2) suppose la formation d'un éther méthylique (R = CH_3) ou éthylique (R = C_2H_5) du cholestérol. Pour le cas ou R = C_6H_5, ce mécanisme est exclu car il équivaudrait à une substitution *nucléophile* sur un benzène monosubstitué. En revanche, les intermédiaires de type alcoxyphosphonium tels que **10** ou **11**, dans le cas ou R = C_6H_5, sont d'autant plus faciles à former que le phénol est plus acide que le méthanol ou l'éthanol. Le passage au phosphonate de dicholestéryle **6** ne peut se faire que par attaque sur le reste cholestéryle dans une réaction de type [14]: on isole effectivement de l'isocholestadiène **14** dans le cas où R = C_6H_5.

La transestérification, suivie de protonation (Schéma 1) nous semble être favorisée par rap-

[1]Dans la suite de l'article, on représentera le cholestérol sous la forme HOCholest.

[2]Ce phosphonate a été décrit (réf. 6) mais non caractérisé.

[3]Les déplacements chimiques sont exprimés en unités δ et en p.p.m. par rapport au tétraméthylsilane (TMS) pris comme référence interne.

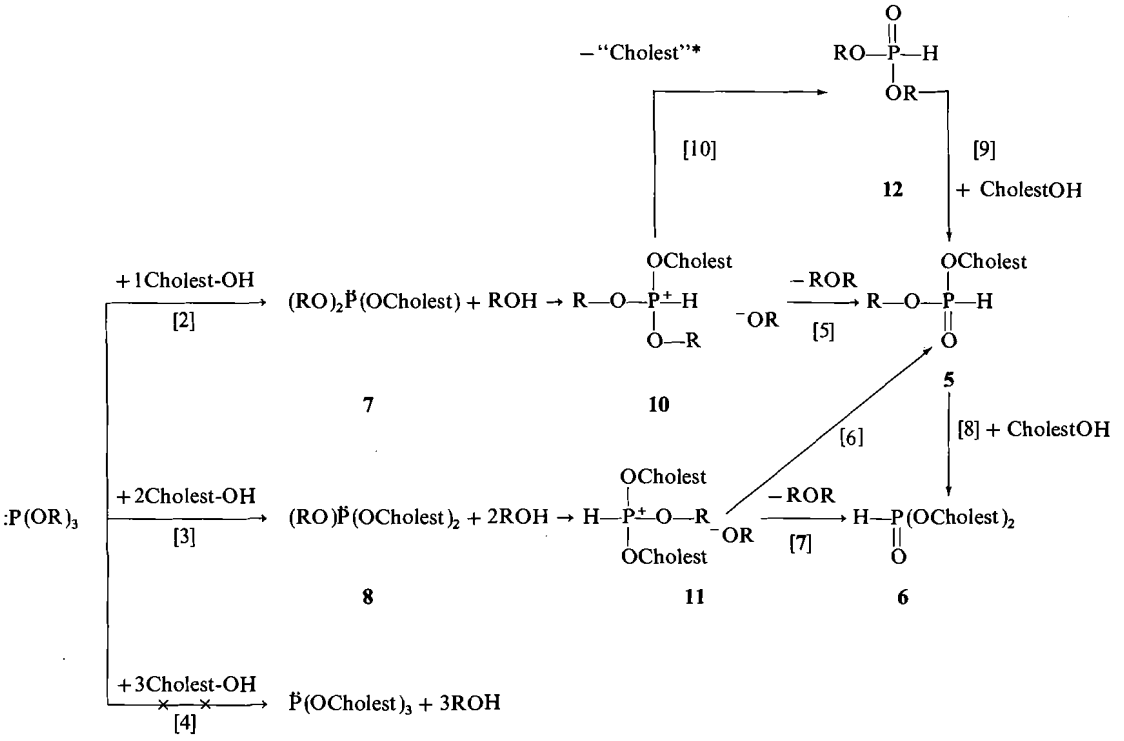

SCHÉMA 1. Formation des composés **5** et **6** par transestérification des phosphites. *Par "cholest", nous entendons perte d'un radical stéroïde: cholestadiène ou cyclo-3α,5-cholestène-6.

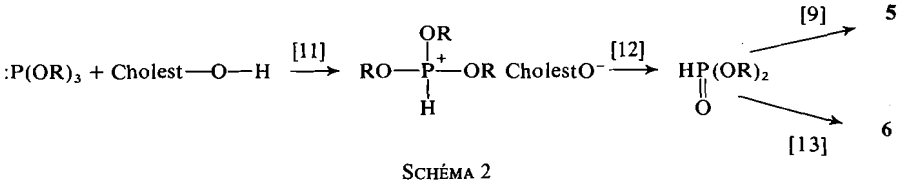

SCHÉMA 2

[14]

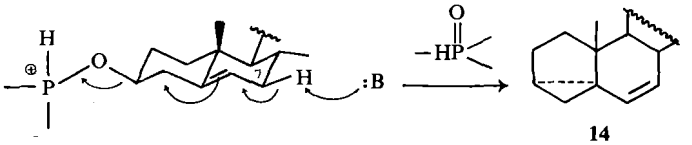

port au Schéma 2 car on n'isole que des traces d'éther ROCholest (R = CH_3 ou C_2H_5) d'une part et que, d'autre part le proton du cholestérol est moins acide que celui du méthanol, de l'éthanol, ou du phénol.

Nous avons pu écarter la possibilité d'une hydrolyse préalable des phosphites selon

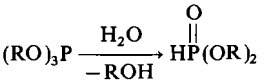

12

en séchant au préalable le cholestérol et en distillant les phosphites avant utilisation.

En conclusion, avec des alcools de haut poids

Can. J. Chem. Downloaded from www.nrcresearchpress.com by 210.87.254.6 on 09/05/12
For personal use only.

Can. J. Chem. Downloaded from www.nrcresearchpress.com by 210.87.254.6 on 09/05/12
For personal use only.

TABLEAU 1. Conditions de réaction et isolement des produits

Phosphite	Cholestérol (mmol)	Solvant	Durée de réaction (h)	Température de réaction (°C)	Produits isolés (mmol)		Eluants utilisés, chromatographie sur colonne (ou autre séparation)*
$P(OCH_3)_3$, 1.2 ml	2.58	—	24	110	**6**	0.09	EP–E^+ 80:20
					Cholestérol	0.16	EP–E 50:50
					5 ($R = CH_3$)	1.86	E
$P(OCH_3)_3$, 0.55 mmol	0.49	Xylène	48	120	**6**	0.06	(Chromatographie en couche mince préparative, élution à l'hexane – acétate d'éthyle 8:2)
					Cholestérol	0.05	
					5 ($R = CH_3$)	0.14	
$P(OC_2H_5)_3$, 6 ml	12.9	—	24	100	**6**	0.75	E
					Cholestérol	2.90	E–MeOH 95:05
					5 ($R = C_2H_5$)	6.57	E–MeOH 90:10
$P(OC_6H_5)_3$, 10.8 mmol	4.57	—	17	110	**14**†	0.06	EP
					$P(OC_6H_5)_3$	3.35	EP–E 80:20
					6	0.71	E
					C_6H_5OH	22.00‡	E
					Cholestérol	1.72	E
$P(OC_6H_5)_3$, 2.83 mmol	2.58	Xylène	70	reflux	**6**	0.35§	Non séparé
					Cholestérol	1.87	

*E, ether; EP, ether de pétrole.
†Identifié (i.r., r.m.n.) à un échantillon authentique préparé en deux étapes à partir du tosylate de cholestéryle (13).
‡Le phénol est élué en même temps que **6**. Pour le séparer on lave une solution éthérée du mélange avec NaOH 2 *N*. La phase éthérée contient **6**. La phase aqueuse est neutralisée (HCl 2 *N*) puis extraite à l'éther pour donner **6** pur.
§Estimation par r.m.n.

Can. J. Chem. Downloaded from www.nrcresearchpress.com by 210.87.254.6 on 09/05/12
For personal use only.

TABLEAU 2. Constantes physiques et caractéristiques spectroscopiques des produits

Produits	p.f. (°C)	$[\alpha]_D^\circ$	i.r. (CCl_4)	r.m.n. ($CDCl_3$, 100 MHz)	Analyse	
					Calculé	Trouvé
$HP(O)(OCholest)_2$ (**6**)	181–182	−27 (*c*, 0.98)	2420, 1460, 1375, 1250, 1030, 960	0.67 (s, 6H, CH_3-18), 0.85 (d, 12H, CH_3-26 et -27, $J = 6$ Hz), 0.91 (d, 6H, CH_3-21, $J = 6$ Hz), 1.00 (s, 6H, CH_3-19), entre 4.01 et 4.52 (m, 2H, —C_3H(OP)—), 5.36 (m, 2H, —C_5=CH—), 6.88 (d, 1H, H—P, $J_{PH} = 689$ Hz)	$C_{54}H_{91}O_3P$ (M = 819.24)	
					C 79.16	79.08
					H 11.19	11.22
					P 3.78	4.02
$HP(O)(OCH_3)$(OCholest) (**5**)	83–84	−29 (*c*, 2.06)	2400, 1460, 1375, 1265, 1180, 1020, 960	0.64 (s, 3H, CH_3-18), 0.82 (d, 6H, CH_3-26 et -27, $J = 6$ Hz), 0.88 (d, 3H, CH_3-21, $J = 6$ Hz), 0.98 (s, 3H, CH_3-19), 3.71 (d, 3H, P—O—CH_3, $J = 11$ Hz), entre 3.94 et 4.50 (m, 1H, —C_3H(OP)—), 5.39 (m, 1H, —C_5=CH—), 6.80 (d, 1H, P—H, $J_{PH} = 719$ Hz)	$C_{28}H_{49}O_3P$ (M = 464.64)	
					C 72.37	72.07
					H 10.65	10.65
					P 6.67	6.59
$HP(O)(OC_2H_5)$(OCholest) (**5**)	48–50	−31 (*c*, 0.76)	2420, 1470, 1380, 1255, 1160, 1035, 960	0.64 (s, 3H, CH_3-18), 0.82 (d, 6H, CH_3-26 et -27, $J = 6$ Hz), 0.88 (d, 3H, CH_3-21, $J = 6$ Hz), 0.97 (s, 3H, CH_3-19), 1.32 (t, 3H, P—O—CH_2—CH_3), entre 3.91 et 4.43 (m, 3H, P—O—CH_2—CH_3 et —C_3H(OP)—), 5.37 (m, 1H, —C_5=CH—), 6.85 (d, 1H, P—H, $J_{PH} = 672$ Hz)	$C_{29}H_{51}O_3P$ (M = 478.67)	
					C 72.76	72.51
					H 10.74	10.56
					P 6.47	6.42

Can. J. Chem. Downloaded from www.nrcresearchpress.com by 210.87.254.6 on 09/05/12
For personal use only.

moléculaire tels que le cholestérol, les phosphites trialcoyliques ($R = CH_3$, C_2H_5) conduisent à des phosphonates dialcoyliques symétrique (composé **6**) ou mixtes (composés **5**).[4] Le phosphite de triphényle donne seulement le phosphonate de dicholestéryle, **6**.

Partie expérimentale

Indications générales

Les spectres de r.m.n. ont été effectués sur spectromètre Varian HA-100 à 100 MHz. Les déplacements chimiques des spectres de r.m.n. sont indiqués en p.p.m., en unités δ par rapport au tétraméthylsilane, pris comme référence interne. Le découplage de ^{31}P a été réalisé à 40 MHz avec un découpleur de spin hétéronucléaire "NMR Specialties". Les absorptions des spectres i.r. sont exprimées en cm^{-1}. Les mesures de pouvoir rotatoire, $[\alpha]_D$, ont été effectuées à 25 °C dans le chloroforme. Les microanalyses ont été faites par "Organic microanalyses", Dr. C. Daesslé, 5757 Décelles Ave., Montréal. Les chromatographies sur colonne ont été effectuées sur gel de silice 0.05–0.2 mm Merck. Les chromatoplaques (c.c.m.) qui ont permis de suivre l'évolution des réactions sont des plaques finies Sil. G. 25 UV 254 de MacRerey-Nagel. Le cholestérol et les phosphites (diméthylique, triméthylique, triéthylique, et triphénylique) sont des produits Aldrich. Les phosphites ont été, selon les cas, distillés ou non avant utilisation.

Les conditions pour la réaction des phosphites avec le cholestérol sont indiquées dans le tableau 1; les propriétés physiques et spectrales des composés obtenus sont résumées dans le tableau 2.

Préparation du phosphonate de dicholestéryle à partir du cholestérol et de PCl_3

A 1.00 g (2.58 mmol) de cholestérol dissous dans 10 ml de pyridine, on ajoute 0.20 g (1.45 mmol) de PCl_3. Le mélange est laissé à température ambiante pendant 1 h, puis il est étendu avec de l'eau et extrait trois fois à l'éther. Les phases éthérées réunies sont lavées successivement avec une solution de HCl 2 *N*, à l'eau, avec une solution saturée de $NaHCO_3$, à l'eau, avec une solution saturée de NaCl, puis séchées sur Na_2SO_4. Par évaporation de l'éther on obtient 0.57 g (0.70 mmol, 54%) de phosphonate de dicholestéryle, le produit obtenu est identifié (r.m.n., i.r., c.c.m., p.f.) au produit **6** obtenu précédemment.

Afin de vérifier la possibilité d'une transestérification du phosphonate de diméthyle, éventuellement formé, la réaction suivante a été effectuée.

Réaction du cholestérol et du phosphonate diméthylique

Le cholestérol (5.00 g; 12.9 mmol) est dissous à chaud dans 10 ml de $HP(O)(OCH_3)_2$. Le mélange obtenu est chauffé à 100 °C pendant 30 h. On décèle en C.C.M. la présence des trois produits habituels ainsi que celle d'un produit que l'on identifie à l'éther méthylique du cholestérol (méthoxy-3β cholestène-5). On évapore sous vide l'excès de phosphite et on chromatographie le résidu sur une colonne de 200 g de silice. On élue successivement: 0.135 g (0.34 mmol, 3%) d'éther méthylique du cholestérol au mélange de 20% d'éther dans l'éther de pétrole, 0.190 g (0.24 mmol, 4%) de phosphonate de dicholestéryle **6** à l'éther, 0.270 g (0.70 mmol) de cholestérol au mélange de 5% de méthanol dans l'éther et enfin 4.020 g (8.65 mmol, 71%) de phosphonate de cholestéryle et de méthyle **5** ($R = CH_3$), au mélange de 10% de méthanol dans l'éther. (Taux de conversion du cholestérol: 95%.) Les phosphonates de dicholestéryle et de cholestéryle et méthyle sont identifiés aux produits obtenus précédemment; l'éther (méthoxy-3β cholestène-5) méthylique du cholestérol est identifié à un échantillon préparé par réaction du cholestérol et de l'orthoformiate de triméthyle en présence de $HClO_4$ (14).

Ce travail a été rendu possible grâce à l'aide financière du Conseil National de Recherches du Canada (octroi A-5596). Une partie de cette étude a été effectuée au laboratoire du Professeur G. Ourisson à Strasbourg.

1. S. R. Landauer et H. N. Rydon. J. Chem. Soc. 2224 (1953).
2. F. W. Hoffmann, R. J. Ess, et R. P. Usinger, Jr. J. Am. Chem. Soc. **78**, 5817 (1956).
3. (*a*) A. J. Kirby et S. G. Warren. The organic chemistry of phosphorus. C. Eaborn et N. B. Chapman, ed. Elsevier, Amsterdam, 1967. p. 238. (*b*) Pour de récents exemples, voir R. S. Edmundson et E. W. Mitchell. J. Chem. Soc. C, 3179 (1971).
4. J. Cason et W. N. Baxter. J. Org. Chem. **23**, 1302 (1958).
5. J. L. Bravet, C. Benezra, et J.-P. Weniger. Steroids, **19**, 101 (1972) et réferences citées.
6. A. W. Dahl, T. L. Fletcher, H. H. Skinner, Jr., et K. A. Merendino. Biochem. Pharmacol. **5**, 231 (1960).
7. L. J. Bellamy. The infra-red spectra of complex molecules. Methuen and Co., London, 1958. p. 311.
8. L. M. Jackman et S. Sternhell. Application of N.M.R. spectroscopy in organic chemistry. Second Edition. Pergamon Press, Oxford, 1969. p. 351.
9. G. M. Kosolapoff. Organophosphorus compounds. John Wiley and Sons, New York, 1950. p. 180–185.
10. C. Kawasaki. J. Pharm. Soc. Japan, **58**, 598 (1938); Chem. Abstr. **32**, 8435 (1938).
11. P. A. Chopard. Helv. Chim. Acta, **50**, 1021 (1967).
12. E. L. Eliel, N. L. Allinger, S. J. Angyal, et G. A. Morrison. Conformational analysis. Interscience, New York, 1967. pp. 86–88.
13. Elsevier's encyclopaedia of organic chemistry. Vol. 14, supplément. F. Radt, ed. Elsevier Publishing Company, Amsterdam, 1954. pp. 1421s et 1724s.
14. J. P. Dusza, J. P. Joseph, et S. Bernstein. Steroids, **8**, 495 (1966).

[4]A propos de ces derniers produits, il faut noter leur particulière instabilité. Ils se conservent difficilement et semblent être très sensibles à l'hydrolyse. C'est le groupe RO ($R = CH_3$ ou C_2H_5) qui part en premier, conduisant probablement à l'acide phosphonique HP(O)(OH)(OCholest); dans le cas où $R = CH_3$, ceci a été vérifié en traitant cet acide avec du diazométhane: on obtient de nouveau le composé **5** ($R = CH_3$).

Effect of Pressure on the Solvolysis of Dimethyl-*t*-butyl Sulfonium Iodide in Ethanol–Water Mixtures

CLAUDE S. DAVIS AND J. B. HYNE

Department of Chemistry, University of Calgary, Calgary, Alberta

Received February 18, 1972

The pressure dependence of the rate of solvolysis of dimethyl-*t*-butyl sulfonium iodide has been studied in ethanol–water mixtures at 60.00 °C. Determination of the partial molal volume of the substrate ions has enabled the volumes of activation to be dissected into initial and transition state components. The solvent composition dependence of the partial molal volumes of the two states provides further details of the nature of the reaction mechanism.

L'influence de la pression sur la vitesse de solvolyse de l'iodure de diméthyl-*t*-butylsulfonium a été étudiée dans des mélanges eau-alcool à 60.00 °C. La détermination du volume molaire partiel des ions substrats a rendu possible la division des volumes d'activation en composantes état initial et état de transition. L'influence de la composition du solvant sur les volumes molaires partiels des deux états fournit des détails supplémentaires sur la nature du mécanisme de la réaction.

Canadian Journal of Chemistry, **50**, 2270 (1972)

Can. J. Chem. Downloaded from www.nrcresearchpress.com by 210.87.254.6 on 09/05/12
For personal use only.

Introduction

The solvent dependence of the partial molal volume of a solvolytic transition state obtained by the dissection of the observed activation volume using the measured partial molal volume of the initial state has been shown to be useful in the characterization of reaction mechanisms (1, 2). Such dissections have been performed on the solvolyses in aqueous ethanol solvents for the substrates *t*-butyl chloride, benzyl chloride, and *p*-chlorobenzyl chloride. These substrates solvolyze by mechanisms which traditionally have been described as varying from S_N1 to S_N2 (1, 3).

The variation of the partial molal volume of the transition state, $\bar{V}_t$, with solvent composition showed a pronounced minimum in $\bar{V}_t$ for *t*-butyl chloride (1). Such a minimum has been shown to be characteristic of the partial molal volume of salts such as Me_4NCl (4) indicating that the transition state in the *t*-butyl chloride solvolysis has considerable charge separation not unlike two oppositely charged ions, *i.e.* an S_N1 type mechanism. The maximum in $\bar{V}_t$ for *p*-chlorobenzyl chloride was similar to that shown by polar substrates such as benzyl fluoride (1) indicating a more polar transition state as a result of the concurrent bond making and breaking, *i.e.* S_N2 type mechanism. Benzyl chloride $\bar{V}_t$ behavior suggested intermediate charge development (1) characteristic of a mechanism lying between the traditionally defined S_N1 and S_N2 limits.

The substrates mentioned above are all non-electrolytes; thus to further test the hypothesis that the behavior of $\bar{V}_t$ in binary solvents is indicative of mechanism (1, 2), the pressure dependence of the solvolysis of an ionic substrate was examined in a similar manner. The solvolysis of the dimethyl-*t*-butyl sulfonium ion, $Me_2tBu\overset{+}{S}$, has been cited as a classic example of a cationic substrate which reacts via a carbonium ion intermediate (5).

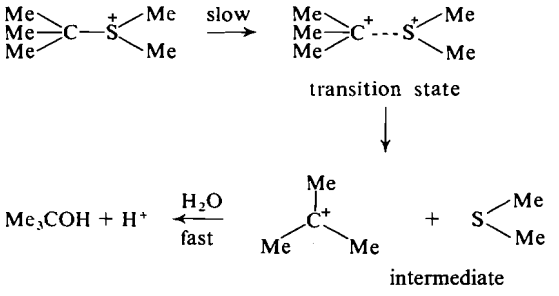

If, as has been claimed previously (1), the partial molal volume behavior of the initial and transition states reflects reaction mechanism in a very specific manner the present study should confirm or dispute the proposed S_N1 type behavior for this cationic solvolysis, and provide, in addition, a more detailed description of

Can. J. Chem. Downloaded from www.nrcresearchpress.com by 210.87.254.6 on 09/05/12
For personal use only.

the process as far as interaction with the solvent environment is concerned.

Experimental

Reagents

Water

Deionized water with a specific conductance no greater than $8 \times 10^{-7}\ \Omega^{-1}\ cm^{-1}$ was used throughout.

Ethanol

Absolute ethanol was dried by distillation from magnesium ethoxide (6). Binary mixtures with water were prepared by weight and stored in well stoppered polythene or glass bottles.

Dimethyl-t-butyl Sulfonium Iodide

The sulfonium salt was prepared from *t*-butylmethyl sulfide and methyl iodide as described by Hyne and Wolfgang (7). Samples were protected from light and stored over ether at −10 °C.

Alkylammonium Salts

Eastman reagent grade tetra-*n*-alkylammonium chlorides R_4NCl (R = Me, Et, *n*-Pr, *n*-Bu) and tetramethylammonium iodide were recrystallized and dried as described by Conway *et al.* (8).

Kinetics

The rates of solvolysis were determined in ethanol–water binaries at 60.00 ± 0.01 °C over the pressure range 1–2746 atm. The solvent compositions used were 0.0, 0.100, 0.200, 0.300, 0.400, and 0.500 mole fraction ethanol. The initial concentration of the sulfonium salt was in the range $1\text{–}4 \times 10^{-4}$ *M*. All solutions were degassed by the conventional freeze–pump–thaw technique before being loaded into the reaction cells. The solvolysis was monitored conductimetrically. The high pressure system, reaction cells, and the conductance measuring equipment used have been described previously (1, 9). Pseudo first-order rate constants were determined graphically by analysis of the conductance data using the Guggenheim method (10).

Partial Molal Volumes

Apparent molal volumes were determined by measuring the densities of solutions of known concentration. The densities were measured with a magnetic float densimeter similar to that described by Millero (11). The design was altered so that the sensitivity of the apparatus could be altered without changing the number of turns on the main solenoid. This was achieved by varying the height of the solution container (and hence the position of the magnetic core of the float in the magnetic field of the solenoid) by supporting the solution container on a threaded brass screw. Because of the wide range in densities of the solvents (0.99–0.83 g/ml) three floats were constructed with the appropriate densities for the various solutions. The system was calibrated as described by Millero. The hold down current was determined by measuring the voltage across a National Bureau of Standards calibrated standard 1 Ω resistor using a Leeds and Northrup Potentiometer. The densities of the solutions are considered accurate to ±2 p.p.m. All solutions (0.005 to 0.15 *M*) were made up by weight. The concentrations were calculated from the known molalities and the measured densities. Apparent molal volumes, ϕ, were calculated using the equation

$$\phi = \frac{M}{d_0} - \frac{1000\Delta d}{d_0 c} \quad [1]$$

where *M* is the molecular weight, d_0 the density of the solvent, and Δd is the difference between the density of the solution and the solvent.

Partial molal volumes, $\bar{V}^0$, were evaluated by extrapolation of ϕ to zero concentration on a plot of ϕ *vs.* $c^{1/2}$ in the relation

$$\phi = \bar{V}^0 + Sc^{1/2} \quad [2]$$

Results

Rates and Activation Parameters

The rate constant for the solvolysis of Me_2tBuS^+ in water and at atmospheric pressure and 60.0 °C is in excellent agreement with the values obtained by Leffek *et al.* at the same temperature (12). The rate constants at the various pressures for different solvent compositions are presented in Table 1. The errors indicated represent average deviations resulting from at least three replicate rate determinations. For each solvent the volume of activation, ΔV^*, and its pressure coefficient, $\partial\Delta V^*/\partial p$, were obtained from the rate-pressure data by a least squares computer fit of the rate-pressure data to the equation

$$\log k = A + Bp + Cp^2 \quad [3]$$

The activation volume in water obtained in this study, 9.9 ± 0.3 ml mol^{-1} (60.00 °C), compares well with values reported by Brower (13) of 9 ± 1 (71.0 °C).

Partial Molal Volumes

In the solvolysis of the sulfonium salt only the cation is involved in the reaction so determining the partial molal volume of the ground state involves an evaluation of the partial molal volume of Me_2tBuS^+, whereas the quantity obtained experimentally is the partial molal volume of the *salt* Me_2tBuSI. The partial molal volume of Me_2tBuS^+ was obtained as follows. The data of Lee and Hyne (4) for the partial molal volumes of tetraalkylammonium chlorides in ethanol–water mixtures were extended to 0.5 mole fraction ethanol. Partial molal volumes of tetramethylammonium iodide were measured in all the aqueous ethanol solvents up to 0.5 mole fraction ethanol. Using the known

TABLE 1. Rate constants for the solvolysis of dimethyl-*t*-butyl sulfonium iodide at 60.00 °C in aqueous ethanol at various pressures

Pressure (atm)	$k \times 10^5$ s^{-1} for mole fraction ethanol =					
	0	0.10	0.20	0.30	0.40	0.50
1	2.789±0.006	2.83 ±0.01	3.254±0.005	3.609±0.013	3.93 ±0.01	4.43 ±0.01
340	2.37 ±0.02	2.47 ±0.02	2.72 ±0.03	2.99 ±0.01	2.38 ±0.02	3.74 ±0.05
663	2.134±0.015					
680		2.128±0.005	2.267±0.006	2.492±0.01	2.78 ±0.01	3.08 ±0.01
1021		1.80 ±0.01				2.610±0.007
1361	1.714±0.008	1.606±0.009	1.64 ±0.01	1.823±0.007	2.09 ±0.01	2.20 ±0.02
2041	1.382±0.014	1.24 ±0.01	1.276±0.004	1.403±0.002	1.58 ±0.01	1.601±0.003
2722		1.024±0.002	1.024±0.005	1.088±0.005	1.191±0.004	
2746	1.085±0.010					
ΔV^* ml mol^{-1}	9.9 ±0.3	13.1 ±0.3	15.6 ±0.2	15.2 ±0.2	13.4 ±0.3	15.0 ±0.4
$-\frac{\partial \Delta V^*}{\partial p} \times 10^3$ ml mol^{-1} atm^{-1}	1.2 ±0.3	4.0 ±0.2	5.9 ±0.2	4.8 ±0.2	2.3 ±0.3	2.5 ±0.7

TABLE 2. Partial molal volumes in aqueous ethanol mixtures of dimethyl-*t*-butyl sulfonium iodide and tetramethylammonium iodide at 25.00 °C

Mole fraction ethanol	Partial molal volume (ml mol^{-1})	
	Me_2tBuSI	Me_4NI
0	162.7±0.2	125.5±0.1(125.75±0.2)*
0.10	158.7±0.2	124.4±0.2
0.20	159.8±0.4	125.4±0.5
0.30	155.7±0.5	122.3±0.3
0.40	151.4±0.5	116.4±0.3
0.50	153.8±0.5	112.9±0.3

*Reference 7.

values for $\bar{V}_{Me_4N^+}$ (4), those for $\bar{V}_{I^-}$ and hence $\bar{V}_{Me_2tBuS^+}$ were determined at each solvent composition by using the relationships shown in eq. 4.

$$[4] \qquad \bar{V}_{Me_2tBuS^+} = \bar{V}_{Me_2tBuSI} - V_{I^-}$$

where $\bar{V}_{I^-} = \bar{V}_{Me_4NI} - \bar{V}_{Me_4N^+}$

Partial molal volumes of dimethyl-*t*-butyl sulfonium iodide and tetramethylammonium iodide in various ethanol–water mixtures are shown in Table 2. The partial molal volume data for the tetra-*n*-alkylammonium chlorides at 0.5 mole fraction ethanol are presented in Table 3.

The partial molal volume of the chloride ion $\bar{V}^0_{Cl^-}$ at 0.5 mole fraction was obtained by the Conway method (8) in which $\bar{V}^0_{R_4NCl}$ is extrapolated to zero cation molecular weight in a linear plot of $\bar{V}^0_{R_4NCl}$ *vs.* molecular weight. Column 2 of Table 4 shows the $\bar{V}^0_{Cl^-}$ values obtained by least-squares fits of the present data at 0.5 mole fraction ethanol along with the data of Lee and Hyne (4) at the other solvent compositions. The other entries in Table 4 were obtained by the appropriate subtractions.

Partial molal volumes for the sulfonium salt were determined at 25.0 °C rather than at 50.0 °C because of the effect the reaction had on the density determinations. In the time required to complete a density measurement (about 1.5 h) some 5–7% of the sulfonium ion would undergo solvolysis at 50.0 °C. The half lives for the reaction at 50.3 °C are ~30 h ($k = 6.3 \times 10^{-6}$ s^{-1}) in water and ~22 h ($k = 8.5 \times 10^{-6}$ s^{-1}) in 0.325 mole fraction ethanol (14). The partial molal volumes of Me_4NI were also determined at 25 °C so that the errors in the value used for V_g, *i.e.* $\bar{V}^0_{Me_2tBuS^+}$, would be minimized. Analysis of the data shows that the difference between the true value for $\bar{V}^0_{Me_2tBuS^+}$ at 50 °C and the value quoted in column 5 of Table 4 is

$$25\left(\frac{(d\bar{V}^0)}{(dT)_{S^+}} - \frac{(d\bar{V}^0)}{(dT)_{Me_4N^+}}\right)$$

where the subscripts S^+ and Me_4N^+ refer to the sulfonium and tetramethylammonium ions, respectively. Since the sign of the temperature dependence of the partial molal volumes of the two ions is the same, the errors will tend to cancel

Can. J. Chem. Downloaded from www.nrcresearchpress.com by 210.87.254.6 on 09/05/12
For personal use only.

Can. J. Chem. Downloaded from www.nrcresearchpress.com by 210.87.254.6 on 09/05/12
For personal use only.

TABLE 3. Partial molal volumes in aqueous ethanol mixtures of tetraalkylammonium chlorides at 50.25 °C

Mole fraction ethanol	$\bar{V}^0$ (ml mol^{-1})			
	Me_4NCl	Et_4NCl	n-Pr_4NCl	n-Bu_4NCl
0	108.1	170.0	237.2	301.0
0.10	98.1	156.0	219.0	286.8
0.20	85.7	153.7	218.3	286.4
0.30	80.7	152.0	219.5	288.5
0.40	88.7	152.8	214.7	277.7
0.50*	96.40±0.3	153.6±0.3	224.0±0.3	287.1±0.4

*This work. All other data ±0.5 ml mol^{-1} (ref. 13).

TABLE 4. Partial molal volume data for various ions in aqueous ethanol mixtures at 50.25 °C

Mole fraction ethanol	$\bar{V}^0$ (ml mol^{-1})			
	Cl^-	Me_4N^+	I^-	Me_2tBuS^+*
0	21.8	86.3	39.2	123.5
0.1	12.5	85.6	38.8	120.0
0.2	−2.1	87.8	37.6	122.3
0.3	−9.8	90.5	31.8	125.9
0.4	6.0	82.7	33.7	117.7
0.5*	9.4	87.0	25.9	127.8

*Data in this row and column this work.

so that the difference between the quoted and true values will be very small.

Discussion

The primary purpose of activation parameters dissection studies of the type reported here is to obtain information on the behavior of some property of the transition state of the reaction with a view to further elucidating the mechanism of the chemical process in question. The dissection of ΔV^* shown in Fig. 1 provides such information on the behavior of the partial molal volume of Me_2tBuS^+ as a function ethanol–water solvent composition. To be of value in revealing the mechanism of the reaction, however, it is necessary to compare the behavior of the partial molal volume of the transition state with that of stable ionic and molecular species as well as the volume behavior of other solvolysis states. Appropriate data for use in such comparisons are available from the earlier work of Mackinnon, Lateef, and Hyne (1) and Lee and Hyne (15) and reproduced schematically in the lower portion of Fig. 1 for convenience.

Before discussing the detailed behavior of

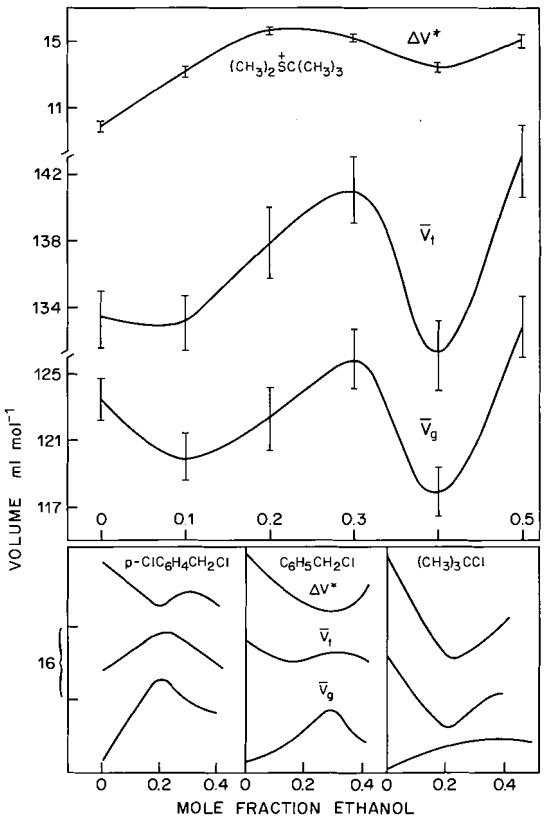

FIG. 1. ΔV^* dissection into initial and transition state components for the solvolyses of Me_2tBuS^+ and some alkyl halides. For details see ref. 1.

$\bar{V}_t$ and $\bar{V}_g$ for the sulfonium salt system shown in Fig. 1, it is worth noting that the overall volume of activation ΔV^* passes through a *maximum* in the 0.2–0.3 mole fraction ethanol region. This behavior contrasts with the minimum in ΔV^* observed in the cases of solvolysis

Can. J. Chem. Downloaded from www.nrcresearchpress.com by 210.87.254.6 on 09/05/12
For personal use only.

of such non-ionic substrates as *t*-butyl chloride, benzyl chloride, and *p*-chlorobenzyl chloride (1). This reversal of behavior of ΔV^* parallels that of ΔH^* as noted by Hyne (16) where the variation of ΔH^* with solvent composition exhibits a maximum for the sulfonium salt solvolysis, but a minimum for alkyl chloride solvolysis. The sign of the pressure coefficient of ΔV^*, *i.e.* $\partial \Delta V^*/\partial P$, is also different for the sulfonium solvolysis compared to the alkyl chloride solvolysis. In both cases, however, the sign of $\partial \Delta V^*/\partial P$ is such that the rate constants tend to a limiting value at high pressure. The reversal is also evident in the sign of ΔV^* being negative, presumably due to electrostriction of solvent in the activation process, in all the alkyl halide cases, but positive for the sulfonium salt solvolysis. The greater volume of the transition state compared with the initial state in the sulfonium salt solvolysis is a clear indication that solvent electrostriction about the transition state is no greater than, and probably less than, that around the ionic initial state. Since the intrinsic volume of the solvolyzing substrate will increase due to bond stretching in the activation process, one cannot state at this stage of the argument that the greater $\bar{V}_t$ value reflects the predominance of solvation shell release, *i.e.* reverse electrostriction. What can be asserted, however, is that *increased* electrostriction on activation sufficient to outweigh the volume increase due to bond stretching does not take place in the sulfonium case as is considered to occur in the alkyl halides. The extent to which the independent carbonium ion is developed in the transition state would appear to be small, and charge *dispersal* between the S and C atoms rather than charge *transfer* from S to C appears to predominate. Despite the fact that the positive charge is dispersed, the transition state will still have an essentially ionic character.

Examination of Fig. 1 immediately reveals that the partial molal volume behavior of the initial and transition states is remarkably similar. This is again in contrast to the corresponding situation for the solvolysis of *t*-butyl chloride and benzyl chloride, although comparable with the behavior of the volume of the kinetic states of *p*-chlorobenzyl chloride. In this latter case the similarity in volume behavior of the two states as a function of solvent composition suggests corresponding similarity in polarity and vice versa. Thus in the sulfonium salt case both the initial and transition states are predominantly ionic in character and in the *p*-chlorobenzyl chloride solvolysis both states are dipolar. In the two alkyl halide systems the initial states are dipolar and the transition states pseudo ionic.

If the kinetic states in the sulfonium salt solvolysis are essentially ionic in character, considerable solvent electrostriction can be expected around both; apart from volume differences due to bond extension on activation, therefore, rather similar values for the partial molal volume of both the initial and transition states might be expected. The similar feature of the two states as a function of solvent composition shows that although the two states are essentially ionic and in the crude sense similar, they differ in detail as a consequence of the interaction with the ethanol–water environment.

It is at this point in the argument that the behavior of $\bar{V}_t$ and $\bar{V}_g$ must be compared with that of stable ionic and dipolar states and other kinetic states. The partial molal volume of the initial state is virtually identical in form to that reported for Et_4N^+, nPr_4N^+, and nBu_4N^+ ions in ethanol–water (4). In particular the characteristic initial decrease in $\bar{V}$ of some 4–8 ml from pure water to 0.1 mole fraction ethanol is present. Many of the initial state volume features are maintained in the behavior of $\bar{V}_t$, but the characteristic initial minimum is almost eliminated. The absence of this minimum is typical of the behavior of polar but non-ionic substrates as illustrated by the $\bar{V}_g$ plots for the benzyl halides and *t*-butyl chloride (Fig. 1). This change in $\bar{V}_t$ behavior therefore supports the argument that while the transition state for the sulfonium salt solvolysis retains its essentially ionic character, its charge density and hence its solvent electrostrictive interaction ability has been weakened.

1. M. J. MACKINNON, A. B. LATEEF, and J. B. HYNE. Can. J. Chem. **48**, 2025 (1970).
2. K. J. LAIDLER and R. MARTIN. Int. J. Chem. Kinet. **1**, 113 (1969).
3. E. T. TOMMILA, E. PAAKKALA, U. K. VIRTANEAU, A. ERVA, and S. VARILA. Ann. Acad. Sci. Fenn. **A11**, 1 (1959).
4. I. LEE and J. B. HYNE. Can. J. Chem. **46**, 2333 (1968).
5. E. D. HUGHES, C. K. INGOLD, and L. T. WOOLF. J. Chem. Soc. 1571 (1933).

6. A. I. VOGEL. A textbook of practical organic chemistry. 3rd ed. Longmans, Green and Co. Ltd., London. 1961. p. 167.
7. J. B. HYNE and R. WOLFGANG. J. Phys. Chem. **64**, 699 (1960).
8. B. E. CONWAY, R. E. VERRALL, and J. E. DESNOYORS. Trans. Faraday Soc. **62**, 2738 (1966).
9. J. B. HYNE, H. S. GOLINKIN, and W. G. LAIDLAW. J. Am. Chem. Soc. **88**, 2104 (1966).
10. E. A. GUGGENHEIM. Phil Mag. **2**(7), 538 (1926).
11. F. J. MILLERO. Rev. Sci. Instr. **38**, 1441 (1967).
12. K. T. LEFFEK, R. E. ROBERTSON, and S. SUGAMORI. J. Am. Chem. Soc. **87**, 2097 (1965).
13. K. R. BROWER. J. Am. Chem. Soc. **85**, 1401 (1963).
14. J. B. HYNE and H. S. GOLINKIN. Can. J. Chem. **41**, 3139 (1963).
15. I. LEE and J. B. HYNE. Can. J. Chem. **47**, 1437 (1969).
16. J. B. HYNE. J. Am. Chem. Soc. **82**, 5129 (1960).

Can. J. Chem. Downloaded from www.nrcresearchpress.com by 210.87.254.6 on 09/05/12
For personal use only.

An Intermediate in the Conversion of an Acetylene to a Vinyl Derivative: The Crystal and Molecular Structure of *trans*-Chloromethylbis(trimethylarsine)-platinum(II) Hexafluorobut-2-yne

BRIAN W. DAVIES, RICHARD J. PUDDEPHATT,[1] AND NICHOLAS C. PAYNE

Department of Chemistry, University of Western Ontario, London, Ontario

Received December 15, 1972

The crystal and molecular structure of *trans*-chloromethylbis(trimethylarsine)platinum(II) hexafluorobut-2-yne has been determined from three dimensional X-ray diffraction data recorded by diffractometric methods. The structure has been refined by full-matrix least-squares methods on F using 1156 reflections to an agreement factor $R = 0.077$. The crystals are monoclinic, space group $P2_1/c, C_{2h}^5$, with $a = 6.803(8)$, $b = 14.93(2)$, $c = 20.20(2)$ Å, $\beta = 104.9(1)°$, and $Z = 4$. The coordination of the platinum atom is trigonal bipyramidal, with the acetylene considered a monodentate ligand, and the two trimethylarsine ligands occupying the equatorial plane. The chlorine atom and the methyl ligand occupy the apical positions, with Pt—Cl and Pt—C distances of 2.47(1) Å and 2.10(4) Å, respectively. The long Pt—Cl bond length indicates the strong *trans*-influence of the methyl ligand. The observed C—C bond length of 1.32(4) Å in the acetylene ligand is lengthened from the value of 1.22(9) Å measured in the free ligand. The geometry of the coordinated ligand is discussed in terms of the bonding scheme proposed by Greaves *et al.*

La structure moléculaire et cristalline du *trans*-chlorométhyl bis(triméthylarsine)platine(II) hexafluorobutyne-2 a été déterminée à partir des données de la diffraction de rayons-X tridimensionnelle enregistrées par les méthodes diffractométriques. La structure a été perfectionnée par la méthode des matrices des moindres carrés sur F utilisant 1156 réflexions jusqu'au facteur d'accord $R = 0.077$. Les cristaux sont monocliniques, de groupe $P2_1/c, C_{2h}^5$, avec $a = 6.803(8)$, $b = 14.93(2)$, $c = 20.20(2)$ Å, $\beta = 104.9(1)°$ et $Z = 4$. La coordination de l'atome de platine est bipyramidale trigonale avec l'acétylène, considéré comme ligand monodentique, et les deux ligands triméthylarsine, occupant le plan équatorial. L'atome de chlore et le ligand méthyle occupent les positions du sommet avec les distances Pt—Cl et Pt—C respectivement de 2.47(1) et 2.10(4) Å. La grande longueur de la liaison Pt—Cl indique la forte influence *trans* du ligand méthyle. La longueur observée pour la liaison C—C de 1.32(4) Å dans le ligand acétylène est allongée par rapport à la valeur de 1.22(9) Å mesurée dans le ligand libre. La géométrie du ligand coordiné est discutée en fonction du schéma proposé par Greaves *et al.*

Canadian Journal of Chemistry, **50**, 2276 (1972)

Introduction

The methylplatinum bond in methylplatinum(II) complexes of the type *trans*-$PtClCH_3L_2$ (L = tertiary phosphine or arsine) can add across the multiple bond of hexafluorobut-2-yne, $CF_3—C{\equiv}C—CF_3$, or tetrafluoroethylene (1, 2). In most cases an intermediate of the reaction in which the acetylene or olefin is complexed to the platinum atom may be isolated allowing an overall reaction mechanism to be proposed (eq. 1).

It was found that the intermediate complexes (**1**) were stabilized by electron releasing groups bound to the platinum atoms and by electron withdrawing substituents on the olefin or acetylene ligand. The relative stabilities of the complexes formed between *trans*-$PtXClL_2$ and the unsaturated compound were found to be

[1]

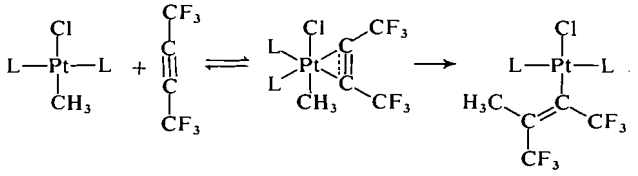

1 **2**

[1]Present address: Department of Inorganic Chemistry, Donnan Laboratories, Grove Street, P.O. Box 147, Liverpool L69 3BX, England.

Can. J. Chem. Downloaded from www.nrcresearchpress.com by 210.87.254.105 on 09/05/12
For personal use only.

Can. J. Chem. Downloaded from www.nrcresearchpress.com by 210.87.254.105 on 09/05/12
For personal use only.

(2, 3) $L = As(CH_3)_3 > As(CH_3)_2C_6H_5 > P(CH_3)_3 > P(CH_3)_2C_6H_5 > P(C_6H_5)_3$; $X = CH_3 \gg Cl$; and the unsaturated ligand = $(CN)_2C{=}C(CN)_2 > CF_3{-}C{\equiv}C{-}CF_3 > CF_2{=}CF_2 > CF_2{=}CFCF_3$, $CF_2{=}CFCl$. This stability sequence, and especially the greater stability of the platinum complexes over similar palladium compounds, which could not be isolated or detected, led to an interpretation of the formation of the complexes by a "partial oxidative addition" reaction (1, 4) indicating that the chief component of the platinum–olefin or platinum–acetylene bond strength was due to the donation of electrons from filled platinum d orbitals into antibonding π^* orbitals of the olefin or acetylene. The same substituent sequence was found for the reactivity towards formation of the addition product (**2**) indicating that the rearrangement (**1**) → (**2**) was favored by a strong platinum–acetylene interaction in the intermediate complex (**1**).

We have completed a three dimensional single crystal X-ray structure analysis of the hexafluorobut-2-yne complex (**1**), where L = $As(CH_3)_3$. The intermediate complexes (**1**) represent a new class of platinum–acetylene complex (5), and structural data can be expected to contribute towards a better understanding of the bond between a transition metal and a π-bonding ligand, and to a clarification of the influence of the ligand L on the stability of the intermediate and the reactivity of (**1**) towards the rearrangement reaction.

Experimental

Crystals of *trans*-chloromethylbis(trimethylarsine)platinum(II)-hexafluorobut-2-yne were prepared by the method of Clark and Puddephatt (2). All crystals examined were mounted in thin-walled glass capillaries. A preliminary photographic examination of reciprocal lattice layers (0–2)*kl*, *h*(0–2)*l*, and *hk*(0–3) showed the crystals to be monoclinic, Laue symmetry 2/*m*. Systematic extinctions for reflections *h*0*l* with *l* odd, and 0*k*0 with *k* odd are consistent with space group $P2_1/c, C_{2h}^5$ (6). The unit cell dimensions, and their estimated standard deviations at 21 °C were determined from a least-squares refinement of the angular settings of 16 reflections centered on a four-circle computer-controlled Picker diffractometer. The density of the crystals was measured by flotation in a mixture of chloroform and ethylene dibromide. The value observed, 2.06(2) g cm^{-3} is only in fair agreement with the calculated value 2.21 g cm^{-3} assuming four molecular units per cell. There are no crystallographic symmetry constraints imposed upon the molecule. Crystal data are as follows:

$PtAs_2ClF_6C_{11}H_{21}$ f.w. = 647.7
Monoclinic, $a = 6.803(8)$, $b = 14.93(2)$, $c = 20.20(2)$ Å, $\beta = 104.9(1)°$, $V = 1982.3$ Å^3, $\rho_o = 2.06(2)$ g cm^{-3}, $Z = 4$, $\rho_c = 2.21$ g cm^{-3}, (21 °C, MoKα_1, $\lambda = 0.70926$ Å).

During the course of the preliminary photographic examination, it became apparent that the crystals suffered from radiation damage. On average one week's continuous photographic exposure resulted in destruction of the crystal lattice.

The sensitivity of the crystal to radiation damage necessitated the collection of data from two crystals in order to obtain sufficient observations. The two data sets were collected under similar conditions. Both crystals were mounted in thin-walled capillaries. Crystal I was of approximate dimensions 0.26 mm × 0.20 mm × 0.09 mm, elongated along [100]. An optical examination identified crystal faces (012), (0$\bar{1}$1), (0$\bar{1}\bar{1}$), (0$\bar{1}$2), (00$\bar{1}$), (01$\bar{2}$), (010), (011), ($\bar{1}\bar{1}$1), (10$\bar{2}$), and those of the form {100}. Crystal II was of dimensions 0.22 mm × 0.17 mm × 0.13 mm, also elongated along [100], with crystal faces (001), and the forms {010}, {100}, and {012}. Both crystals were accurately measured with a filar micrometer eyepiece in preparation for an absorption correction. The linear absorption coefficient for MoKα radiation is $\mu = 105.0$ cm^{-1}.

Intensity data were collected on a Picker computer-controlled four-circle automatic diffractometer using MoKα radiation. Both crystals were mounted with [100] roughly parallel to the diffractometer ϕ axis. The orientation matrix and the refined cell dimensions for Crystal I were obtained from a least-squares refinement of 16 reflections manually centered at 21 °C. Prior to data collection a number of ω-scans of intense, low-angle reflections were performed, using a narrow source and wide-open counter. A mean width at half height of 0.1° was considered suitable (7). The θ–2θ scan technique was employed, with a scan range of 1.4° at a rate of 1° per min. The diffracted beam was filtered through a niobium filter, of thickness 0.08 mm, and collected through an aperture 4 mm × 4 mm placed 32 cm from the crystal. Background counts were made with a stationary crystal, and a stationary counter for ten seconds at the limits of each scan. A take-off angle of 1.3° was employed for the source, under which conditions an intensity of 87% of the maximum attainable for a selected reflection was observed. In view of the crystal decomposition data were collected from Crystal I in the octants *hkl* and *hk*$\bar{l}$ out to a 2θ maximum of 30°. Nine hundred and seventy-nine reflections were recorded. During collection of these data, three intense axial reflections, (400), (040), and (004) were monitored at regular intervals. All three reflections showed a linear decay in intensity, on average 13%.

A second shell of data was then collected from Crystal II under the same conditions. The mosaicity of the crystal, as measured by ω-scans of average width 0.09° was considered acceptable. The orientation matrix was determined as before, and instrumental conditions were unchanged for data collection. The same three reflections were monitored every 100 observations as standards. Linear decay occurred again, to an average extent of 33% after the collection of 1596 data over the 2θ range $25° \leqslant 2\theta \leqslant 40°$. After each data collection, the centering of the crystal was checked, and it was confirmed that the decay of the standards resulted from radiation damage and not from instrumental

Can. J. Chem. Downloaded from www.nrcresearchpress.com by 210.87.254.105 on 09/05/12
For personal use only.

factors, or crystal movement. A correction was applied to each data set assuming a linear decay in intensity with time.

The two data sets were then processed, and corrections applied for background, Lorentz and polarization factors.[2] Standard deviations were assigned to each observation $(\sigma(I))^2 = COUNT + \frac{1}{4}(t_c/t_b)^2(b_1 + b_2) + (pI)^2$ where the total count is given by *COUNT*, measured in a time t_c. b_1 and b_2 are the background counts each measured in a time t_b. The constant p was chosen as 0.05 for each data set, and $I = COUNT - \frac{1}{2}(t_c/t_b)(b_1 + b_2)$. Those reflections with a corrected intensity value greater than three times the estimated standard deviation were considered to be observed; 721 of the 979 reflections from crystal I, and 839 of the 1596 reflections from crystal II. The linear absorption coefficient for MoKα radiation is 105.0 cm^{-1}, and absorption correction trials on both crystals showed transmission factors varying by as much as 46% for crystal I and 50% for crystal II. Accordingly an absorption correction was applied independently to each data set. The two sets of data were then interscaled by a least-squares refinement of scaling factors derived from a comparison of reflections common to both sets in the range $25° \leqslant 2\theta \leqslant 30°$. Reflections of the types *0kl* and *0kl̄*, which are related by symmetry, were not averaged. The data set used in solution and refinement of the structure contained 1165 "observed" reflections.

Structure Solution and Refinement

The position of the platinum atom was located from a three dimensional Patterson synthesis. One cycle of full-matrix least-squares refinement on F, minimizing the function $\sum\omega(|F_o| - |F_c|)^2$ led to agreement factors $R_1 = 0.39$ and $R_2 = 0.47$. $|F_o|$ and $|F_c|$ are the observed and calculated structure amplitudes, the weight assigned an observation is defined as $\omega = 4F_o^2/\sigma^2(F_o^2)$, and $R_1 = \sum(|F_o| - |F_c|)/\sum|F_o|$ and $R_2 = (\sum\omega(|F_o| - |F_c|)^2/\sum\omega F_o^2)^{1/2}$. Atomic scattering factors for Pt, As, Cl, F, and C were taken from Cromer and Waber's tabulation (8), those for H from Stewart *et al.* (9). An anomalous dispersion correction, using the values of $\Delta f'$ and $\Delta f''$ of Cromer (10) for Pt, As, and Cl was included in the calculated structure factors (11). A series of least-squares refinements and difference Fourier syntheses located all 21 non-hydrogen atoms. In subsequent refinement of the structure (89 parameters and 1165 observations) agreement factors $R_1 = 0.089$ and $R_2 = 0.121$ were obtained. At this stage, with anisotropic thermal parameters assigned to the Pt, As, and Cl atoms, and isotropic parameters to the remaining F and C atoms, the geometry of the molecule was considered satisfactory. Attempts were then made to locate the hydrogen atoms using difference Fourier syntheses. The most intense peak, $1.8 \pm 0.2\ e^-$ Å^{-3}, was associated with the Pt atom, and others were observed at the Cl and As positions. A series of difference Fourier planes were then calculated for each of the seven methyl carbon atoms, assuming tetrahedral geometry at each atom (C—H 1.09 Å, H—C—H 109.47°) and examined for evidence of hydrogen atoms. A possible set of peaks was evident for the Pt—CH_3 linkage, but no unequivocal evidence was obtained to warrant the inclusion of the hydrogen atoms in the model. Refinement was continued, using anisotropic thermal parameters for all atoms. Under these conditions non-positive definite thermal parameters were sometimes observed for the carbon atoms; this, and the failure to locate the 21 hydrogen atoms is probably attributable to the effect of the crystal decomposition on the quality of the data. With only the carbon atoms assigned isotropic thermal parameters, two cycles of least-squares refinement (135 parameters, 1165 observations) gave agreement factors $R_1 = 0.062$ and $R_2 = 0.084$. A statistical examination of the structure amplitudes (in terms of F, $\lambda^{-1}\sin\theta$ and indices) showed no major abnormal trends. Seven reflections were discarded at this stage, which were seriously in error, and refinement converged under these conditions at $R_1 = 0.059$ and $R_2 = 0.072$.

A study of the bond distances and bond angles showed this refinement to be subject to errors resulting from crystal decomposition. For example, the platinum–acetylene carbon atom distances of 2.13 and 2.01 Å were significantly different. Also, As—C distances of 1.82, 1.89, and 1.98 Å, with C—As—C angles of 96.9, 103.9, and 106.9° showed greater variation than is to be expected. In particular, the C—C σ-bond lengths in the coordinated acetylene ligand, C(7)—C(8) and C(9)—C(10) (the atom numbering scheme is given in Fig. 2), of 1.57 and 1.39 Å respectively differed considerably from the mean value observed in the free ligand, 1.46(5) Å (12) and markedly from the value of 1.54 Å expected for a σ-bond. An examination of the data suggested these deviations to be due

[2]Computing was carried out on the PDP-10 at the University of Western Ontario, and the CDC6600 at Multiple Access Limited, Toronto. Programs used include versions of Hamilton's GONO absorption correction program, Ibers' NUCLS least-squares program, Busing and Levy's ORFFE function and error program, and Johnson's ORTEP crystallographic illustration program.

Can. J. Chem. Downloaded from www.nrcresearchpress.com by 210.87.254.105 on 09/05/12
For personal use only.

to the quality of data collected, and in order to derive more meaningful geometrical data on the acetylene ligand it was decided to constrain the CF_3 groups in the acetylene ligand to the geometry observed in the electron-diffraction study of the free ligand, and to refine them as groups (C_{3v} symmetry, C—F 1.33 Å, and F—C—F angles of 107.5°) in subsequent least-squares refinements (13). Individual isotropic thermal parameters were assigned to each group atom (anisotropic thermal parameters gave non-positive definite ellipsoids). The refinement on F converged at $R_1 = 0.077$ and $R_2 = 0.081$ (93 parameters, 1156 observations). No evidence for extinction was observed. A total difference Fourier synthesis contained eleven peaks of electron density exceeding 1.0 e^- Å^{-3}, the largest of these, 1.9(2) e^- Å^{-3} at (0.028, 0.335, 0.118) is associated with the Pt atom.

In Table 1 a listing of $|F_o|$ and $|F_c|$ is given in electrons, with the weight assigned to each reflection.[3] The final non-group atom positional and thermal parameters, and the group parameters are listed in Table 2. In Table 3 the derived group atom positional and thermal parameters are presented. The root-mean-square amplitudes of vibration of the Pt, As, and Cl atoms are listed in Table 4. All atomic positional parameters refer to one molecular unit.

Description of the Structure

The crystal decomposition, and the consequent need to collect data from two crystals have affected the determination of accurate bond distances and bond angles. A selection of bond distances and bond angles is given in Table 5, together with estimated standard deviations (e.s.d.'s). The values without e.s.d.'s were constrained to an ideal geometry in the least-squares refinement. The structure consists of discrete molecules of $Cl(CH_3)[As(CH_3)_3]_2Pt.C_4F_6$. The shortest intermolecular non-bonding attraction is 3.16 Å between a methyl carbon atom, C(4), and F(4). The shortest Pt—Pt distance of approach is 6.80 Å.

An overall view of the molecule is given in Fig. 1. The inner coordination sphere geometry at the platinum atom is trigonal bipyramidal.

[3]Photocopies of Table 1 of structure amplitudes may be obtained upon request from the Depository of Unpublished Data, National Science Library, National Research Council of Canada, Ottawa, K1A 0S2.

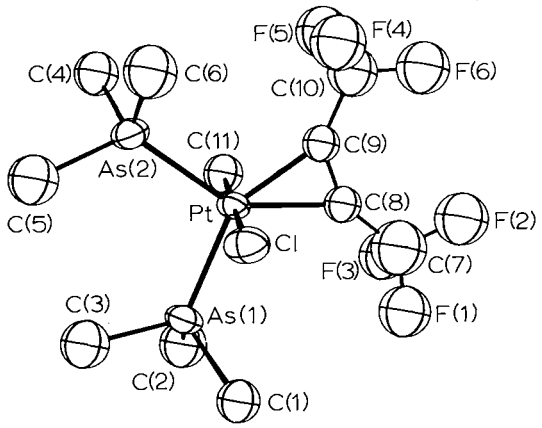

FIG. 1. Overall view of the molecule showing the atom numbering scheme. Hydrogen atoms are omitted. For clarity, thermal ellipsoids are drawn at the 30% probability level.

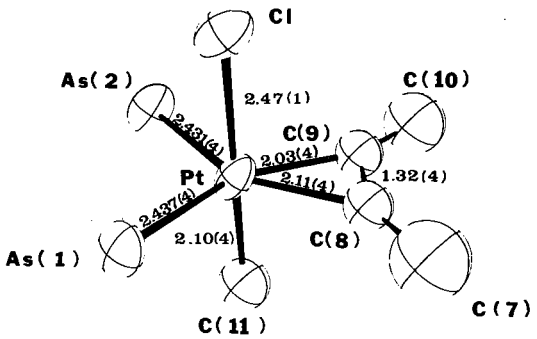

FIG. 2. Inner coordination sphere of the molecule. Thermal ellipsoids are drawn at the 30% probability level.

The *cis*-trimethylarsine ligands and the coordinated acetylene (considered to be unidentate) occupy the equatorial positions. The atom numbering scheme and a view of this geometry are presented in Fig. 2. A least-squares plane containing Pt, As(1), As(2), and the two acetylene carbon atoms, C(8) and C(9), has been calculated and the results are presented in Table 6. All five atoms lie in the plane within experimental error.

The Pt—Cl bond length observed in this structure, 2.47(1) Å, is longer than most other Pt—Cl bond lengths determined. A value of 2.300(2) Å was observed in *trans*-dichloro-(π-di-*t*-butylacetylene)-*p*-toluidine platinum(II) (14), where the chlorine atom is *trans* to another chlorine atom. In the structure of Zeise's salt, $K[Cl_3Pt(C_2H_4)]H_2O$, the Pt—Cl distance *trans*

Can. J. Chem. Downloaded from www.nrcresearchpress.com by 210.87.254.105 on 09/05/12
For personal use only.

TABLE 2. Atomic and group positional and thermal parameters

Atom	x	y	z	U_{11}*	U_{22}	U_{33}	U_{12}	U_{13}	U_{23}
Pt	0.0264(3)†	0.23377(8)	0.11354(7)	991(13)	501(9)	441(8)	−23(11)	126(8)	−51(8)
As(1)	−0.1885(7)	0.2346(3)	−0.0034(2)	1115(37)	868(26)	506(22)	−66(28)	25(24)	−33(21)
As(2)	−0.0539(8)	0.0928(2)	0.1608(2)	1283(43)	654(24)	611(27)	−40(26)	259(28)	77(20)
Cl	0.2830(19)	0.1511(6)	0.0709(5)	1292(106)	788(62)	768(69)	132(70)	311(72)	7(55)

Atom	x	y	z	B(Å^2)
C(1)	−0.037(7)	0.268(3)	−0.072(2)	8.9(11)
C(2)	−0.421(9)	0.322(4)	−0.028(3)	12.1(16)
C(3)	−0.332(8)	0.125(3)	−0.044(3)	11.5(15)
C(4)	−0.231(8)	0.099(3)	0.220(2)	9.7(13)
C(5)	−0.211(8)	−0.001(3)	0.100(3)	11.7(15)
C(6)	0.178(9)	0.039(3)	0.212(3)	12.6(16)
C(8)	0.201(6)	0.352(2)	0.135(2)	6.8(10)
C(9)	0.243(6)	0.296(2)	0.187(2)	6.6(9)
C(11)	−0.190(7)	0.303(3)	0.152(2)	8.4(12)

Group parameters

Group	x_g‡	y_g	z_g	δ	ε	η
CF_3(I)	0.399(3)	0.2991(12)	0.2830(9)	0.405(18)	−2.884(21)	−2.038(22)
CF_3(II)	0.245(3)	0.4670(11)	0.0942(10)	0.289(36)	−2.044(20)	1.924(38)

*The thermal ellipsoid is given by $\exp[-(\beta_{11}h^2 + \beta_{22}k^2 + \beta_{33}l^2 + 2\beta_{12}hk + 2\beta_{13}hl + 2\beta_{23}kl)]$ $U_{ij} = 10^4 \times \beta_{ij}/(2\pi^2 a_i^* \cdot a_j^*)$ Å.

†Values given in parentheses in this and other tables are the estimated standard deviations in the least significant digits.

‡x_g, y_g, and z_g are the fractional coordinates of the group origin, taken as the centroid of the triangle formed by the fluorine atoms, and δ, ε, and η (radians) are the group orientation angles (ref. 13).

TABLE 3. Derived parameters for CF_3 groups

Atom	x	y	z	B (Å^2)
		Group CF_3 (I)		
C(7)	238(3)*	438(1)	104(1)	16.1(21)
F(1)	269(4)	431(1)	42(2)	13.2(9)
F(2)	394(4)	483(2)	143(2)	14.5(10)
F(3)	71(4)	487(1)	98(2)	13.0(9)
		Group CF_3 (II)		
C(10)	362(4)	300(1)	259(1)	11.9(16)
F(4)	471(4)	225(2)	274(1)	14.1(9)
F(5)	237(4)	303(2)	300(1)	13.8(9)
F(6)	490(3)	369(2)	278(1)	13.5(9)

*Positional parameters are given in fractional coordinates × 10^3.

TABLE 4. Root-mean-square amplitudes of vibration (in Å) × 10^3

Atom	Minimum	Median	Maximum
Pt	203(3)	230(2)	320(2)
As(1)	220(5)	294(5)	352(6)
As(2)	231(5)	267(5)	360(6)
Cl	270(10)	280(10)	360(10)

to the olefin ligand is 2.327(5) Å, while a mean Pt—Cl distance of 2.305(9) Å was determined for the two *trans*-Pt—Cl bonds (15). We attribute this difference to the greater *trans* influence of the methyl ligand compared to

TABLE 5. Bond distances and bond angles

Atoms	Distance (Å)	Atoms	Angle (deg)
Pt—As(1)	2.437(4)	As(1)—Pt—As(2)	104.2(2)
Pt—As(2)	2.431(4)	As(1)—Pt—Cl	88.0(3)
Pt—Cl	2.47(1)	As(1)—Pt—C(11)	93(1)
Pt—C(11)	2.10(4)	As(2)—Pt—Cl	87.4(3)
Pt—C(8)	2.11(4)	As(2)—Pt—C(11)	92(1)
Pt—C(9)	2.03(4)	Cl—Pt—C(11)	179(1)
		As(1)—Pt—C(9)	148(1)
		As(2)—Pt—C(8)	144(1)
As(1)—C(1)	1.98(5)		
As(1)—C(2)	2.02(6)	C(1)—As(1)—C(2)	101(2)
As(1)—C(3)	1.97(5)	C(1)—As(1)—C(3)	102(2)
As(2)—C(4)	1.91(3)	C(2)—As(1)—C(3)	100(2)
As(2)—C(5)	1.99(5)	Pt—As(1)—C(1)	113(1)
As(2)—C(6)	1.83(6)	Pt—As(1)—C(2)	118(2)
		Pt—As(1)—C(3)	120(2)
C(7)—C(8)	1.48(4)		
C(8)—C(9)	1.32(4)	C(4)—As(2)—C(5)	95(2)
C(9)—C(10)	1.47(4)	C(4)—As(2)—C(6)	105(2)
		C(5)—As(2)—C(6)	106(2)
C—F	1.33	Pt—As(2)—C(4)	116(1)
		Pt—As(2)—C(5)	121(2)
		Pt—As(2)—C(6)	111(2)
		C(8)—Pt—C(9)	37(1)
		Pt—C(8)—C(9)	68(2)
		C(7)—C(8)—C(9)	150(4)
		Pt—C(8)—C(7)	142(2)
		C(8)—C(9)—Pt	75(2)
		C(8)—C(9)—C(10)	135(4)
		Pt—C(9)—C(10)	149(2)
		C(8)—C(7)—F(1)	115(2)
		C(8)—C(7)—F(2)	113(2)
		C(8)—C(7)—F(3)	107(2)
		C(9)—C(10)—F(4)	108(2)
		C(9)—C(10)—F(5)	110(2)
		C(9)—C(10)—F(6)	116(2)
		F—C—F	107.5

Can. J. Chem. Downloaded from www.nrcresearchpress.com by 210.87.254.105 on 09/05/12
For personal use only.

TABLE 6. Weighted least-squares plane (Equation of plane: $5.680x - 6.745y - 10.482z = 2.617$)

Atom	Deviation (Å)
Pt	0.000(2)
As(1)	0.000(5)
As(2)	0.000(5)
C(8)	−0.03(4)
C(9)	0.04(4)

the chloride ligand. A series of Pt—Cl bond lengths has also been examined by McWeeny *et al.* in planar platinum(II) complexes (16, 17). The longest Pt—Cl bond length observed, 2.45(1) Å, is in the structure of *trans*-[ClPt{P-$(C_6H_5)(CH_3)_2$}$_2${$Si(C_6H_5)_2(CH_3)$}], where the chlorine atom is *trans* to the diphenylmethylsilane ligand (17). Although a direct comparison is hindered by the different geometries at the platinum atoms, it is clear that the *trans* influence of the methyl ligand is considerable. If the covalent radius of Pt(II) in a trigonal bipyramidal environment is assumed the same as that in a square planar arrangement, 1.33 Å, then the Pt—CH_3 bond length of 2.10(4) Å is close to the expected value 2.09 Å calculated for a Pt—C σ-bond.

The mean Pt—As bond length of 2.433(4) Å lies in the expected range, between the sum of the covalent radii, 2.49 Å, and the values of 2.308(2) Å found in di-μ-chloro-[dichlorobis-(trimethylarsine)]platinum(II) (18) and that of 2.375(4) Å determined in the bis(*o*-phenylene-bisdimethylarsine)platinum(II) cation (19).

The decomposition of the crystals appears to have contributed to the variance in the geometries at the As atoms. The mean As—C bond length is 1.95(3) Å, the mean C—As—C angle is 102(2)°. Of the six values averaged three lie outside the estimated standard deviation on the mean, suggesting the data suffers from systematic errors. Comparable means of 1.948(18) Å and 106.0(7)° respectively were observed in $[Cl_2Pt(As(CH_3)_3)]_2$ (18).

The geometry of the coordinated acetylene ligand is of importance in light of the bonding information it supplies. The difference in the Pt—C(8) and Pt—C(9) bond lengths, 0.08(5) Å, is not significant, and the ligand is symmetrically π-bonded. The Pt, As(1), As(2), C(8), and C(9) atoms all lie close to the equatorial plane (Table 6), the largest deviation being that of C(9) of 0.04(4) Å. The carbon–carbon triple bond of the acetylene has apparently lengthened upon coordination to 1.32(4) Å, compared to the value of 1.22(9) Å observed in the free ligand (11). The large standard deviation on the C≡C bond length in the free ligand precludes a more definite comparison. The observed C≡C bond length however is longer than the average value, 1.203(3) Å, quoted for a series of triple bonds observed in simple alkynes (6), at the 3σ level.

The acetylene adopts the *cis*-bent configuration, and the C(10)—C(9)—C(8) and C(7)—C(8)—C(9) angles are observed with values of 135(4) and 150(4)°, respectively. An equivalent configuration was reported in a preliminary communication of the structure of bis(triphenylphosphine)platinum(0)diphenylacetylene, where the analogous angles were 140 and 139°. The platinum, two phosphorous atoms, and one of the acetylene carbon atoms are co-planar, with the other acetylene carbon atom lying out of the plane so that the acetylene carbon–carbon triple bond makes an angle of 14° with the plane (20). No such angle is observed in the present determination. In the di-*t*-butylacetylene complex, the coordinated acetylene C≡C bond makes an angle of 85.2° with the coordination plane of the platinum atom (14). There is a short C≡C bond length, 1.235(18) Å, and the departure from linearity of the acetylene is less, angles of 162(1) and 165(1)° being observed.

The two C—CF_3 bond lengths of 1.48(4) and 1.47(4) Å agree well with the mean value of 1.46(5) Å determined in the free ligand (11).

Discussion

There has been extensive interest of late in the bonding in compounds formed by olefins, acetylenes, and other π-bonding ligands with transition metal complexes, particularly of the nickel triad. To date, although structural information on complexes with simple alkenes as the π-bonding ligand is available, the data on acetylene complexes are more limited. Chatt and his co-workers in their original studies of acetylene complexes (21, 22) characterized two types of complex, using as a criterion the

Can. J. Chem. Downloaded from www.nrcresearchpress.com by 210.87.254.105 on 09/05/12
For personal use only.

Can. J. Chem. Downloaded from www.nrcresearchpress.com by 210.87.254.105 on 09/05/12
For personal use only.

change in $\nu_{C\equiv C}$ which occurred upon coordination. The first type considered, Cl_2LPt(acetylene), where L is Cl^- or an amine, is formally a platinum(II) complex. A decrease in $\nu_{C\equiv C}$ of about 200 cm^{-1} was observed, and a structure was proposed and later confirmed by X-ray analysis (14) of equivalent geometry to the ethylene complex, Zeise's salt. The relatively small frequency decrease was taken to imply a weak metal–acetylene bond, and a small distortion of the acetylene ligand. The second type of complex studied, $(PR_3)_2Pt$(acetylene), formally platinum(0), showed a strong infrared absorption band around 1800 cm^{-1}, which was assigned to the $\nu_{C\equiv C}$ of the coordinated acetylene. The decrease in $\nu_{C\equiv C}$, around 400 cm^{-1}, was considered to represent a much stronger metal–acetylene bond, with a consequent greater distortion of the acetylene geometry. The planar PtP_2C_2 geometry proposed has also been confirmed by X-ray analysis (20). The present analysis therefore represents the first structural analysis of an acetylene complex in which the geometry at the metal atom is trigonal-bipyramidal, and formally platinum(II).

Two bonding schemes were proposed by Chatt to describe the two types of compound. For the first type, a σ- and π-bonding scheme was suggested, in which the metal–acetylene bond consisted of two components. Donation of electrons from π bonding molecular orbitals of the acetylene to empty metal p or d orbitals occurred, forming a σ-bond. This was accompanied by back donation of electron density from filled metal d or dp hybrid orbitals to π^* antibonding orbitals on the acetylene ligand. For the second type of complex a σ-bonding model was proposed, with two Pt—C σ-bonds forming a "metallocyclopropene ring". The possibility that there existed a series of complexes in which the bonding was intermediate between these two types was later suggested by Chatt (23).

Further suggestions on the bonding were combined in an elegant treatment by Greaves *et al.*, who described how these two extreme cases could be discussed in terms of one model (24). From a consideration of the relative energies of the acetylene π and π^* molecular orbitals and the energy of the metal orbitals, and the symmetries of the orbitals, a continuum of bond types was suggested, and five particular relative orbital energy orderings were considered in detail. Firstly, the energy of the metal orbitals could be comparable to that of the π^* molecular orbitals on the acetylene, in which case the bonding would be mainly due to donation of metal electrons into the π^* molecular orbitals of the acetylene. Secondly, the energy of the metal orbitals could be intermediate between the energies of the acetylene π and π^* molecular orbitals, in which case the bonding would be equivalent to the π-bonding scheme first proposed by Chatt. Further lowering of the metal orbital energies, to a value comparable to that of the acetylene π molecular orbitals results in a bond dominated by the σ-bond component. Two further cases were considered, in which the metal orbital energies were first of lower energy than the acetylene π molecular orbitals, but still able to form a bond, and finally much lower, in which case no bond is formed.

The geometry of the coordinated acetylene in the present study is more comparable to that of the diphenylacetylene ligand in $(P(C_6H_5)_3)_2$-Pt(diphenylacetylene) (20), than to that of the di-*t*-butylacetylene ligand. Both acetylenes adopt a *cis*-bent configuration. The mean angular deviation from linearity in the coordinated diphenylacetylene is 40.5(5)°, while values of 30(4) and 45(4)° are observed for the hexafluorobut-2-yne ligand. In contrast, comparable values of 17(1) and 15(1)° were observed in the formally platinum(II) complex *trans*-$Cl_2(CH_3$-$C_6H_4NH_2)$Pt(di-*t*-butylacetylene) (14). Although the precision of the angular measurements in the hexafluorobut-2-yne complex has been hindered by crystal decomposition, it is apparent that there is a close resemblance between the bonding in the trigonal platinum(0) complexes and the present trigonal bipyramidal complex, and we may therefore discuss the bonding of the acetylene ligand in terms of the scheme proposed by Greaves *et al.*. We suggest, on the basis of the structural data, that the present structure is best described by the relative orbital energy ordering in which the metal orbitals used for bonding are intermediate between the acetylene π and π^* molecular orbitals. Thus, as suggested by Greaves *et al.* molecular orbitals containing metal and both π and π^* acetylene character may be written. There is a transfer of electron density from the

Can. J. Chem. Downloaded from www.nrcresearchpress.com by 210.87.254.105 on 09/05/12
For personal use only.

acetylene π orbitals to the metal orbitals, and an accompanying back donation from filled metal orbitals to the acetylene π^* orbitals. This electron transfer results in a reduction of the C≡C bond order, and an angular distortion of the acetylene from linearity.

It is important to elucidate the extent of the electron transfer. Recent ESCA studies (25, 26) indicated that the electron transfer from the platinum atom to the acetylene in $(P(C_6H_5)_3)_2Pt$-(diphenylacetylene) is 0.7 electron (25) although this value has been questioned (26). The extent of transfer in Zeise's salt is lower, 0.3 electron being transferred from the metal to the acetylene, and also from the acetylene to the metal, leaving the acetylene essentially electrically neutral. The extent of the electron transfer should be reflected in both structural and stability changes. Thus, it is interesting that the platinum–olefin bond strength in $(P(C_6H_5)_3)_2Pt$(olefin), as indicated by the C—C bond length, varies as olefin = $C_2H_4 < C_2Cl_4 > C_2F_4 > C_2(CN)_4$. The series is apparently determined by the balance in the metal–ligand bond strength due to σ-donor and π-acceptor components being maximized at C_2Cl_4 (27). However, in platinum(II) compounds the order of bond strength as determined by stability and equilibrium studies (2, 3) is olefin = $C_2(CN)_4 > C_2F_4 > C_2Cl_4$. It appears that a different balance is reached, and that the critical factor in determining the stability is the π-acceptor property of the olefin or acetylene ligand. The different bond strengths are apparent in the greater stability of the platinum(0) complexes. Thus $(As(CH_3)_3)_2Pt$(hexafluorobut-2-yne) can be sublimed *in vacuo* without decomposition at 90°, while *trans*-$Cl(CH_3)(As(CH_3)_3)_2Pt$(hexafluorobut-2-yne) at this temperature readily evolves hexafluorobut-2-yne. The difference is also reflected in the different $\nu_{C\equiv C}$ stretching frequencies for these complexes, being 1765 cm^{-1} for the platinum(0) complex (28) and 1838 cm^{-1} for the platinum(II) complex (2). However, the decrease in $\nu_{C\equiv C}$ of 473 cm^{-1} observed for *trans*-$Cl(CH_3)(P(C_6H_5)_3)_2Pt$-(hexafluorobut-2-yne) is greater than the value of 462 cm^{-1} observed for the arsenic complex, indicating a stronger metal–acetylene bond, a conclusion contradicted by J(Pt—F) measurements (2), and small differences in $\nu_{C\equiv C}$ should therefore be interpreted with care (29). We are initiating further structural studies on platinum—acetylene complexes to explore the dependence of the bonding upon the geometry at, and the formal oxidation state of, the metal atom.

We thank the National Research Council of Canada for financial support.

1. H. C. Clark and R. J. Puddephatt. Inorg. Chem. **9**, 2670 (1970).
2. H. C. Clark and R. J. Puddephatt. Inorg. Chem. **10**, 18 (1971).
3. H. C. Clark and R. J. Puddephatt. Inorg. Chem. **10**, 416 (1971).
4. J. P. Collman and W. R. Roper. Advan. Organomet. Chem. **7**, 53 (1968).
5. T. Theophanides and P. C. Kong. Can. J. Chem. **48**, 1084 (1970).
6. International Tables for X-ray Crystallography. Kynoch Press, Birmingham, England. 1962.
7. T. C. Furnas. Single crystal orienter instruction manual. General Electric Co., Milwaukee, Wis. 1957.
8. D. T. Cromer and J. A. Waber. Acta Cryst. **18**, 104 (1965).
9. R. F. Stewart, E. R. Davidson, and W. T. Simpson. J. Chem. Phys. **42**, 3175 (1965).
10. D. T. Cromer. Acta Cryst. **18**, 17 (1965).
11. J. A. Ibers and W. C. Hamilton. Acta Cryst. **17**, 781 (1964).
12. W. F. Sheenan, Jr. and V. Schomaker. J. Am. Chem. Soc. **74**, 4468 (1952).
13. R. Eisenberg and J. A. Ibers. Inorg. Chem. **4**, 773 (1965).
14. G. R. Davies, W. Hewertson, R. H. B. Mais, P. G. Owston, and C. G. Patel. J. Chem. Soc. A, 1873 (1970).
15. J. A. J. Jarvis, B. T. Kilbourn, and P. G. Owston. Acta Cryst. **B27**, 366 (1971).
16. R. McWeeny, R. Mason, and A. D. C. Towl. Disc. Faraday Soc. **47**, 20 (1969).
17. P. M. Harrison. Ph.D. Thesis, Sheffield University. Sheffield, England.
18. S. F. Watkins. J. Chem. Soc. A, 168 (1970).
19. N. C. Stephenson. Acta Cryst. **17**, 1517 (1964).
20. J. O. Glanville, J. M. Stewart, and S. O. Grim. J. Organomet. Chem. **7**, P9 (1967).
21. J. Chatt, L. A. Duncanson, and R. G. Guy. J. Chem. Soc. 827 (1961).
22. J. Chatt, R. G. Guy, L. A. Duncanson, and D. T. Thompson. J. Chem. Soc. 5170 (1963).
23. J. Chatt. Chimica inorganica. Accad. Nazl. Lincei, Roma, 113 (1961).
24. E. O. Greaves, C. J. L. Lock, and P. M. Maitlis. Can. J. Chem. **46**, 3879 (1968).
25. C. D. Cook, K. Y. Wan, V. Gelius, K. Hamrin, G. Johannson, E. Olsson, H. Siegbahn, C. Nordling, and K. Siegbahn. J. Am. Chem. Soc. **93**, 1904 (1971).
26. D. T. Clark, D. B. Adams, and D. Briggs. Chem. Commun. 602 (1971).
27. J. N. Francis, A. McAdam, and J. A. Ibers. J. Organomet. Chem. **29**, 131 (1971).
28. R. J. Puddephatt. Unpublished results.
29. F. R. Hartley. Chem. Rev. **69**, 799 (1969).

Absolute Rate Constants for Hydrocarbon Autoxidation. XXI. Activation Energies for Propagation and the Correlation of Propagation Rate Constants with Carbon–Hydrogen Bond Strengths[1]

S. KORCEK,[2] J. H. B. CHENIER, J. A. HOWARD, AND K. U. INGOLD

Division of Chemistry, National Research Council of Canada, Ottawa, Canada K1A 0R9

Received January 28, 1972

The rate constants, k_p, for the abstraction of a hydrogen atom from a wide variety of organic substrates at 30° have been correlated with the strengths of the C—H bond that are broken, D[R—H] (in units of kcal/mol). Two empirical relations have been derived, one for tertiary peroxy radicals,

$$\log [k_p^{t\text{-ROO}} \text{ per active hydrogen}/(M^{-1}\ s^{-1})] = 15.4 - 0.2D[\text{R—H}]$$

and one for secondary peroxy radicals,

$$\log [k_p^{s\text{-ROO}} \text{ per active hydrogen}/(M^{-1}\ s^{-1})] = 16.4 - 0.2D[\text{R—H}]$$

These equations hold extremely well for hydrocarbons and reasonably well for substrates containing heteroatoms. The activation energies and pre-exponential factors for the oxidation of some hydrocarbons by *t*-butylperoxy radicals have been measured and the empirical relation

$$E_p^{t\text{-ROO}}/(\text{kcal/mol}) = 0.55(D[\text{R—H}] - 62.5)$$

derived. If D[*t*-ROO—H] is taken as 88 kcal/mol, this yields the Polanyi equation,

$$E_p^{t\text{-ROO}}/(\text{kcal/mol}) = 14 + 0.55\,\Delta H_p^{t\text{-ROO}}$$

where ΔH is the heat of the hydrogen abstraction reaction. These empirical equations permit the calculation of the rate constants for chain propagation in the autoxidation of many organic substrates at 30° and also at other temperatures.

Les constantes de vitesse k_p d'arrachement d'un atome d'hydrogène sur une grande variété de substrats organiques à 30°, ont été reliées aux longueurs de la liaison C—H impliquée D[R—H] (en kcal/mol). Deux relations empiriques ont été déduites, l'une pour les radicaux peroxy tertiaires

$$\log [k_p^{t\text{-ROO}} \text{ par hydrogène actif } (M^{-1}\ s^{-1})] = 15.4 - 0.2D[\text{R—H}]$$

et l'autre pour les radicaux peroxy secondaires

$$\log [k_p^{s\text{-ROO}} \text{ par hydrogène actif}/(M^{-1}\ s^{-1})] = 16.4 - 0.2D[\text{R—H}]$$

Ces équations s'appliquent très bien aux hydrocarbures et de façon raisonnable aux substrats contenant des hétéroatomes. Les énergies d'activation et les facteurs préexponentiels pour l'oxydation de quelques hydrocarbures par les radicaux *t*-butyl peroxy ont été mesurés et la relation empirique

$$E_p^{t\text{-ROO}}/(\text{kcal/mol}) = 0.55\ (D[\text{R—H}] - 62.5)$$

a été déduite. Si on prend D[*t*-ROO—H] égal à 88 kcal/mol, on obtient l'équation de Polanyi

$$E_p^{t\text{-ROO}}/(\text{kcal/mol}) = 14 + 0.55\,\Delta H_p^{t\text{-ROO}}$$

où ΔH est la chaleur de la réaction d'arrachement de l'hydrogène. Ces équations empiriques permettent le calcul des constantes de vitesse de la propagation de chaîne dans l'autooxydation de beaucoup de substrats organiques à 30° et également à d'autres températures.

Canadian Journal of Chemistry, **50**, 2285 (1972)

Introduction

A linear relation between activation energies, E, and exothermicities, ΔH, for bimolecular homolytic substitutions was first proposed in 1938 (1). This relation is referred to as the Polanyi equation and usually takes the form,

$$E = C + \alpha\Delta H$$

where C and α are constants.

Attempts to verify the Polanyi equation have been hindered until recently by a lack of accurate kinetic data and of reliable bond dissociation energies. The equation is obeyed in the gas phase

[1]NRCC No. 12582.

[2]NRCC Postdoctorate Fellow 1968–1970.

Can. J. Chem. Downloaded from www.nrcresearchpress.com by 210.87.254.6 on 09/05/12
For personal use only.

Can. J. Chem. Downloaded from www.nrcresearchpress.com by 210.87.254.6 on 09/05/12
For personal use only.

for hydrogen abstraction by methyl radicals from simple alkanes (2). It also appears to hold for hydrogen abstraction from alkanes by $Br^{\cdot}$, $I^{\cdot}$, and $F_2N^{\cdot}$ radicals, reactions which are all endothermic (3).

The Polanyi equation should only be obeyed if, through a series of reactants, there is no resonance stabilization (or alternatively, an equal amount of stabilization) in the transition state (4) and is therefore only applicable to a series of rather closely related compounds (5). Both simpler (6) and more complex (7) relations between E and ΔH have been proposed but since most exothermic atom abstractions have activation energies of *ca.* 8 ± 3 kcal/mol, it would take a fairly sophisticated rule to be of any predictive value (5).

The Polanyi equation was first applied to hydrogen abstractions in solution in 1950 by Bolland during his study of olefin autoxidation (8). The overall activation energy of an autoxidation, E_0, is related to the activation energies of the individual steps in the chain by the equation,

$$E_0 = E_p + \tfrac{1}{2}E_i - \tfrac{1}{2}E_t$$

where E_p is the activation energy for the chain propagation step,

$$ROO^{\cdot} + RH \rightarrow ROOH + R^{\cdot}$$

E_i is the activation energy for chain initiation (by benzoyl peroxide)

$$PhC(O)OOC(O)Ph \rightarrow \text{radicals}$$

and E_t is the activation energy for chain termination,

$$ROO^{\cdot} + ROO^{\cdot} \rightarrow \text{non-radical products}$$

The activation energy of interest, E_p, was derived from the measured E_0 by assuming that $E_i = 31$ kcal/mol in all the olefins and that $E_t = 0$ for all the olefin peroxy radicals. Unfortunately, neither of these assumptions is justified. It is improbable that E_i will be exactly the same in all olefins since even the "well-behaved" di-*t*-butyl peroxide shows a solvent dependent activation energy for decomposition (9). The assumption that E_t is always zero can often be very far from the truth (10). Bolland correlated his E_p values with the olefin C—H bond strengths available at that time and derived an α value of 0.39 in the Polanyi equation. Although this value must be regarded as being *very* approximate there have been no subsequent attempts to check on whether the Polanyi equation can be applied to the chain propagation step of autoxidations. However, the absence of experimental data has rarely hindered kineticists for long. Two versions of the Polanyi equation have been proposed for hydrogen abstraction by peroxy radicals from alkanes. Benson (11) suggested

$$E_p/(\text{kcal/mol}) = 6.0 + \Delta H_p$$

However, Knox (12) has proposed that α is unlikely to be as large as 1.0 and has suggested that

$$E_p/(\text{kcal/mol}) = 10.0 + 0.60\,\Delta H_p$$

This relationship is based on the reasonable assumption that the electrophilicity of $ROO^{\cdot}$ will be similar to that of $RO^{\cdot}$ in reactions of the same ΔH and therefore E_p should lie on an extension of the curve relating E and ΔH for the $RO^{\cdot}$ radical (12).

Comparatively few direct measurements of autoxidation propagation rate constants have been made over a range of temperature (13). Consequently, there are few directly determined values of E_p. Furthermore, when more than one set of workers have measured E_p for the same hydrocarbon their agreement is generally very poor (*e.g.*, the reported E_p values for tetralin range from 4.5 to 8.3 kcal/mol and for cumene from 6.5 to 12.4 kcal/mol (13)). Such data are obviously unsuited for testing the Polanyi equation and are of little value in predicting propagation rate constants.

During the last few years we have measured absolute rate constants for the reaction of many organic compounds with their peroxy radical (13)

[1] $$ROO^{\cdot} + RH \rightarrow ROOH + R^{\cdot}$$

Rate constants have also been determined for the reaction of organic compounds with the peroxy radical derived from a different substrate

[2] $$R'OO^{\cdot} + RH \rightarrow R'OOH + R^{\cdot}$$

This has been achieved by oxidizing RH in the presence of concentrations of the hydroperoxide R'OOH in the range 0.1–4.0 *M*. Under these conditions all the peroxy radicals derived from RH undergo a fast hydrogen atom transfer reaction with R'OOH.

Can. J. Chem. Downloaded from www.nrcresearchpress.com by 210.87.254.6 on 09/05/12
For personal use only.

[3] $$ROO^{\cdot} + R'OOH \rightarrow ROOH + R'OO^{\cdot}$$

Therefore, only $R'OO^{\cdot}$ radicals are involved in the rate controlling propagation and termination reactions for the oxidation of RH. For example, addition of *t*-butyl hydroperoxide to an autoxidation enables the rate constant for the reaction

[4] $$Bu^tOO^{\cdot} + RH \xrightarrow{k_p^{Bu^tOO}} Bu^tOOH + R^{\cdot}$$

to be determined. This hydroperoxide is ideally suited for measuring "cross" propagation rate constants because it is commercially available and easily purified. Moreover, the rate constant for chain termination by *t*-butylperoxy radicals,

[5] $$2\ Bu^tOO^{\cdot} \xrightarrow{2k_t^{Bu^tOO}} \text{Molecular products}$$

is lower than for any other known alkylperoxy radical. Addition of this hydroperoxide therefore allows many unreactive substrates to be autoxidized at reasonable chain lengths.

Relative "cross" propagation rate constants are generally more accurate than relative homopropagation rate constants because inaccuracies involved in the determination of $2k_t$ are unimportant. We have therefore attempted to measure activation energies for reaction 4 for substrates with labile C—H bond strengths in the range 70–100 kcal/mol so that the Polanyi equation could be put to a proper test for autoxidations.

Experimental

The general experimental procedures employed have been adequately described in previous papers in this series.

Results

Determination of Rate Constants and Arrhenius Parameters

Rates of oxidation and rates of chain initiation have been measured over a range of temperature for seven hydrocarbons in the presence of a sufficient concentration of *t*-butyl hydroperoxide to ensure that the rate controlling chain propagation and chain termination steps involved only the *t*-butylperoxy radical. The oxidations were initiated with azo-bis-isobutyronitrile, AIBN, and the rate of chain initiation, R_i, was determined in each run with 2,6-di-*t*-butyl-4-methoxyphenol, BMeOP. Rates of oxidation, R_s, were obtained from the expression

TABLE 1. AIBN-induced decomposition of Bu^{t}OOH in *o*-dichlorobenzene

Temperature (°C)	$R_i \times 10^7$ ($M\ s^{-1}$)	$\frac{(d[O_2]/dt)_t}{R_i}$ [a]
10	0.02	1.1
20	0.06	1.5
30	0.19	2.6
40	0.8	3.2
50	3.4	3.8
60	11.9	4.8
70	29.3	5.2

[a] $(d[O_2]/dt)_t$ is the rate of oxygen evolved by terminating *and* non-terminating interactions of *t*-butylperoxy radicals and can of course be greater than 1.

[6] $$R_s = -\frac{d[O_2]}{dt} = (R_{O_2})_{net} + \left[\frac{d[N_2]}{dt}\right]_i - \left[\frac{d[O_2]}{dt}\right]_i + \left[\frac{d[O_2]}{dt}\right]_t$$

where $(R_{O_2})_{net}$ is the measured rate of oxygen absorption, $\{d[N_2]/dt\}_i$ and $\{d[O_2]/dt\}_i$ are the rates of nitrogen evolved and oxygen absorbed by the initiator and $\{d[O_2]/dt\}_t$ is the rate of oxygen evolved from the mutual reaction of *t*-butylperoxy radicals (14–17). Values of $\{d[O_2]/dt\}_t$ were determined at each temperature from rates of oxygen evolution for the AIBN induced decomposition of *t*-butyl hydroperoxide in *o*-dichlorobenzene. Values of $\{d[O_2]/dt\}_t/R_i$ found in this work are summarized in Table 1.

The correction term $\{d[O_2]/dt\}_t$ is negligible for the readily oxidized hydrocarbons, *e.g.*, tetralin, oct-1-ene, *p*-xylene and cyclohexa-1,4-diene. However, for paraffinic hydrocarbons this "correction" is about *three* times as large as the measured rates of oxygen absorption. The corrected rates of oxidation of paraffinic hydrocarbons containing *t*-butyl hydroperoxide are therefore about four times as large as their measured rates and, because of the size of the correction, they cannot be determined with high accuracy.

Values of $k_p^{Bu^tOO}$ for highly reactive hydrocarbons such as cyclohexa-1,4-diene are also difficult to measure. This is because at normal substrate concentrations the rate of oxidation is so high that it depends on the partial pressure of oxygen above the liquid. The autoxidation chain length can be reduced by lowering the substrate

TABLE 2. Propagation rate constants and Arrhenius parameters for hydrocarbon oxidation by *t*-butylperoxy radicals

Temperature (°C)	$k_p^{Bu^tOO}$ per H × 10^3 (M^{-1} s^{-1})						
	Cyclohexa-1,4-diene	Tetralin	Oct-1-ene	*p*-Xylene	Hexadecane	Tridecane	Cyclohexane
0	1 850	—	—	—	—	—	—
10	3 650	—	21	4.4	—	—	—
20	7 700	250	42	8.5	—	0.13	0.08
30	20 000	575	92	15	0.30	0.27	0.28
40	—	1000	150	28	0.92	0.86	0.65
50	—	1800	280	47	2.1	—	—
60	—	3100	440	76	4.8	—	—
70	—	—	—	140	11	—	—
$E_p^{Bu^tOO}$ (kcal/mol)	11.3	12.3	11.4	11.0	17.8	~17.8	~17.8
log ($A_p^{Bu^tOO}$ per H/M^{-1} s^{-1})	8.7	8.6	7.1	6.1	9.4	~9.4	~9.4

concentration. However, the concentration of some hydrocarbons has to be lowered so much that the overall rate of oxidation slows down rapidly as oxygen is absorbed because of depletion of the substrate. This leads to difficulties in the accurate determination of $k_p^{Bu^tOO}$.

The rates of oxidation of some compounds which do not oxidize particularly rapidly, *e.g.*, triphenylmethane, depend on the partial pressure of oxygen even at 1 atm. It is not possible to obtain accurate values of $k_p^{Bu^tOO}$ for such compounds.

In spite of these difficulties, the corrected rates of oxidation of all the hydrocarbons studied in this work can be described by the kinetic expression

$$\frac{-d[O_2]}{dt} = \frac{k_p^{Bu^tOO}[RH]\,R_i^{1/2}}{(2k_t^{Bu^tOO})^{1/2}}$$

Values of $k_p^{Bu^tOO}$ at various temperatures were calculated from the ratio $k_p^{Bu^tOO}/(2k_t^{Bu^tOO})^{1/2}$ using values of $2k_t^{Bu^tOO}$ calculated from the expression

$$\log [2k_t^{Bu^tOO}/(M^{-1}\,s^{-1})] = 9.2 - 8.5/\theta$$

where $\theta = 2.3RT$ kcal/mol, which is based on previously published data (18). Measured termination rate constants in *p*-xylene at 10 and 40° and in hexadecane at 40° were found to be in reasonable agreement with the values calculated from this expression. Propagation rate constants per abstractable hydrogen, $k_p^{Bu^tOO}$ per H, for seven hydrocarbons are given in Table 2. Plots of log ($k_p^{Bu^tOO}$ per H) against the reciprocal of the absolute temperature gave excellent straight lines from which the activation energies and pre-exponential factors listed in Table 2 were derived. For the saturated hydrocarbons the correction factor discussed above is so large that systematic errors are not unlikely and so their E and log A values are more uncertain than would be indicated by their Arrhenius plots.

Comparison of Arrhenius Parameters with Previously Published Data for Autoxidations

There are very few Arrhenius parameters in the literature with which the present work may be compared. Our own direct measurements of k_p by the rotating sector method gave for tetralin $E_p = 8.3$ kcal/mol and log (A_p per H/M^{-1} s^{-1}) = 6.1 and for cumene (which presumably is roughly comparable to tetralin or *p*-xylene) $E_p = 12.4$ kcal/mol and log (A_p per H/M^{-1} s^{-1}) = 8.2 (13). Hendry (19) has given $E_p = 10$ kcal/mol and log (A_p per H/M^{-1} s^{-1}) = 6.5 for cumene.

Of considerably more interest are the data of Allara *et al.* on the oxidation of isobutane (20) and *n*-butane (21).

For isobutane (20*a*), $E_p - \frac{1}{2}E_t = 11.3$ kcal/mol and since propagation and termination involve the *t*-butylperoxy radical, $E_p = 15.5$ kcal/mol (based on the E_t value used in this paper). At 50°, $k_p/(2k_t)^{1/2}$ is given as 2.7×10^{-3} (M^{-1} min^{-1})$^{1/2}$. At this temperature $2k_t$ for *t*-butylperoxy radicals is 3.2×10^3 M^{-1} s^{-1} = 1.92×10^5 M^{-1} min^{-1}, from which k_p at 50° is calculated to be 1.2 M^{-1} min^{-1} = 2×10^{-2} M^{-1} s^{-1}.

Can. J. Chem. Downloaded from www.nrcresearchpress.com by 210.87.254.6 on 09/05/12
For personal use only.

Can. J. Chem. Downloaded from www.nrcresearchpress.com by 210.87.254.6 on 09/05/12
For personal use only.

This yields log (A_p per H/M^{-1} s^{-1}) = 8.8 and k_p per H at 30° = 4.2×10^{-3} M^{-1} s^{-1}. Computational modeling studies of alkane oxidation (*20b*) indicate that log (A_p per H/M^{-1} s^{-1}) = 9.4 for this reaction, a value in excellent agreement with that found in the present work for *t*-butylperoxy radical abstraction of secondary hydrogens from saturated hydrocarbons.

For *n*-butane (21) $E_p - \frac{1}{2}E_t = 15.3 \pm 3$ kcal/mol which yields $E_p = 16.3$ kcal/mol if E_t is assumed to have the same value as has been found for *s*-heptylperoxy radicals, *viz.* 1.9 kcal/mol (22). Now *t*-butylperoxy radicals are less reactive in hydrogen atom abstraction than *s*-alkylperoxy radicals by an amount which causes k_p to be lower by a factor of 10 at 30° (see Fig. 1). If this lowered reactivity is ascribed to a higher activation energy, as seems most reasonable, then this factor of 10 corresponds to 1.4 kcal in E_p. That is, the activation energy for the abstraction of a secondary paraffinic hydrogen by a *s*-alkylperoxy radical should, according to our results, be 17.8 − 1.4 = 16.4 kcal/mol in excellent agreement with Allara *et al.*'s (21) value of 16.3 kcal. These workers also give $k_p/(2k_t)^{1/2} = 7.6 \times 10^{-4}$ (M^{-1} min^{-1})$^{1/2}$ at 100°. Taking $2k_t = 4 \times 10^6$ M^{-1} s^{-1} at this temperature yields $k_p = 11.3$ M^{-1} $min^{-1} = 0.19$ M^{-1} s^{-1} from which a value is calculated for log (A_p per H/M^{-1} s^{-1}) = 8.3 and for k_p per H at 30° of 3×10^{-4} M^{-1} s^{-1}. The value of A_p per H is an order of magnitude less than that found in the present work for *t*-butylperoxy radical attack on saturated secondary hydrogens.

Polanyi Relation

Since only a small range in R—H bond strengths could be covered in the present work, a dependable investigation of the Polanyi equation was not possible. However, if it is assumed that this relation is obeyed for the endothermic reactions with the paraffins and the exothermic reactions with tetralin, *p*-xylene and oct-1-ene (*i.e.*, neglecting the activation energy found for cyclohexa-1,4-diene which would appear to be far too large), then plotting $E_p^{Bu^tOO}$ against D[R—H] yields the relation

$$[7] \quad E_p^{Bu^tOO}/(\text{kcal/mol}) = 0.55(D[\text{R—H}] - 62.5)$$

On the assumption that the O—H bond strength in *t*-butyl hydroperoxide is 88 kcal/mol (23) this equation can be rewritten in the form,

$$E_p^{Bu^tOO}/(\text{kcal/mol}) = 14 + 0.55\,\Delta H_p^{Bu^tOO}$$

where $\Delta H_p^{Bu^tOO}$ is the heat of the reaction and is equal to the difference in the C—H and O—H bond strengths of the substrate and the resultant hydroperoxide, respectively,

$$\Delta H_p^{Bu^tOO} = D[\text{R—H}] - D[\text{R'OO—H}]$$

This equation is in surprisingly close agreement with that suggested by Knox (12), *i.e.*

$$E_p/(\text{kcal/mol}) = 10.0 + 0.60\,\Delta H_p$$

If it is assumed that the ten fold greater reactivity of secondary peroxy radicals compared with tertiary peroxy radicals results from a 1.4 kcal/mol smaller activation energy for hydrogen abstractions then

$$[8] \quad E_p^{s\text{-}ROO}/(\text{kcal/mol}) = 0.55(D[\text{R—H}] - 65.0)$$

Although eqs. 7 and 8 are probably the best currently available for predicting E_p values on the basis of R—H bond strengths they should be applied with caution until additional data are available. It is also important to remember that the A factors are not constant in the range where eqs. 7 and 8 were derived. A more sophisticated treatment of our experimental data which would make allowance for this effect seems unwarranted.

Pre-exponential Factors

The pre-exponential factors (per active hydrogen), $A_p^{Bu^tOO}$ per H, listed in Table 2 show a surprisingly large variation. They are all about 2 orders of magnitude lower than the pre-exponential factors, A^1 per H, reported by Golden and Benson (24) for the gas phase reaction of iodine atoms with hydrocarbons of comparable structure (see Table 3).

$$I^{\cdot} + RH \rightarrow IH + R^{\cdot}$$

This holds true over a range of hydrocarbon structures for which the A factors change by 3 orders of magnitude. For both abstraction reactions the higher A factors for the paraffins indicate that these transition states have a less rigidly defined geometry than do the transition states for hydrocarbons yielding resonance stabilized radicals.

The $A_p^{Bu^tOO}$ per H values for the saturated hydrocarbons are unexpectedly large for hydro-

TABLE 3. Comparison of pre-exponential factors[a] for hydrogen atom abstractions by iodine atoms in the gas phase (24) and by *t*-butylperoxy radicals in solution

$RH + I^{\cdot} \rightarrow R^{\cdot} + HI$			$RH + Bu^tOO^{\cdot} \rightarrow R^{\cdot} + Bu^tOOH$		
$R^{\cdot}$	log (A^I per H)	Average log (A^I per H)	RH	log (A^{Bu^tOO} per H)	Average log (A^I per H) − log (A^{Bu^tOO} per H)
Isopropyl	10.9		Hexadecane	9.4	1.5
Isopropyl	10.7	10.9	Tridecane	9.4	1.5
s-Butyl	11.1				
Cyclopentyl[b]	10.9	10.9	Cyclohexane	9.4	1.5
Methylallyl	9.0	9.4	Oct-1-ene	7.1	2.3
Methylallyl	9.7				
Benzyl	7.9	7.9	*p*-Xylene	6.1	1.8
Cyclopentenyl[c]	9.7	9.7	Tetralin	8.6	1.1

[a]In M^{-1} s^{-1}.
[b]Reference 36.
[c]Reference 38.

gen abstractions by a polyatomic, non-linear, free radical (12, 25).[3] Possibly they are in error because of systematic errors in the correction factor (see above). On the other hand, if they are correct they will explain an apparent anomaly in the E_p values for saturated hydrocarbons calculated from gas phase and from liquid phase autoxidations that has been pointed out by Benson (26).

The data of Baldwin *et al.* (27) on the high temperature (400–500°) gas phase oxidation of aldehydes containing small amounts of added hydrocarbons permit rate constants to be calculated for attack on the hydrocarbons by the hydroperoxy radical. For the reaction

$$HOO^{\cdot} + CH_3CH_2CH_3 \rightarrow HOOH + CH_3\dot{C}HCH_3$$

k_p^{HOO} per H = 1×10^5 M^{-1} s^{-1} at 440°. If A_p^{HOO} per H is taken to have the "normal" value of $\sim 2 \times 10^8$ M^{-1} s^{-1} which is typical of many hydrogen abstractions by radicals (25), then E_p^{HOO} for this reaction can be calculated to be ~10 kcal/mol. As discussed above, the liquid phase data yields $E_p^{s\text{-ROO}} \approx 16.4$ kcal/mol for analogous reactions involving *s*-alkylperoxy radicals. This disturbing anomaly can be partially resolved if we assign log (A_p^{HOO} per H/M^{-1} s^{-1}) the "high" value of 9.4 found in this work for the liquid phase reaction. The value of E_p^{HOO} is then calculated to be 14.4 kcal/mol. The remaining difference of 2 kcal/mol is hardly significant in view of the assumptions involved in these calculations, which include the assumption that HOO· radicals and *s*-ROO· radicals have equal reactivities.

[3]Large *A* factors have occasionally been reported by other workers (20*b*), even for hydrogen abstractions from hydrocarbons yielding resonance stabilized radicals. Thus, for the reaction

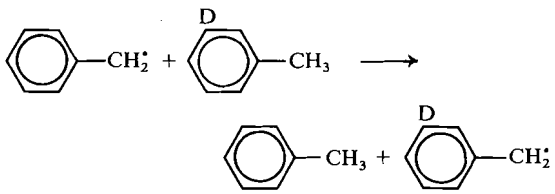

log (A/M^{-1} s^{-1}) = 10.5 and E = 19.9 kcal/mol (53).

Correlations of Propagation Rate Constants with C—H Bond Strengths at 30°

Although the Polanyi equation could not be reliably tested, a simple modification yields another empirical equation that could be tested with some of our previously published rate constants. The Arrhenius equation for chain propagation is

$$\log k_p = \log A_p - E_p/\theta$$

Provided the pre-exponential factors are constant for a series of substrates or, alternatively, vary smoothly with changes in the activation energies, then at any one temperature,

$$\log k_p \propto E_p$$

and hence, if the Polanyi equation is obeyed,

$$\log k_p \propto \Delta H_p$$

i.e.,

$$\log k_p \propto D[\text{R—H}] - D[\text{R'OO—H}]$$

It has been suggested that the O—H bond strength in alkyl hydroperoxides is independent

Can. J. Chem. Downloaded from www.nrcresearchpress.com by 210.87.254.6 on 09/05/12
For personal use only.

Can. J. Chem. Downloaded from www.nrcresearchpress.com by 210.87.254.6 on 09/05/12
For personal use only.

of the nature of the alkyl group (28), and hence we can write

$$\log k_p \propto D[\text{R—H}]$$

Our published propagation rate constants at 30° (13) were found to give two surprisingly good correlations when values of log k_p per active hydrogen (log k_p per H) were plotted against the estimated strength of the weakest C—H bond in the organic substrates. One relation applied to attack by tertiary peroxy radicals and the other, with k_p values for the same substrate about an order of magnitude higher, for attack by secondary (and primary) peroxy radicals. These correlations of already published and of some new, unpublished, values for k_p per H at 30° with estimated values of D[R—H] form the subject of the remainder of this paper.

The C—H bond strengths used to correlate the measured propagation rate constants were obtained principally from the radical stabilization energies, E_s, reported by Golden and Benson (24). More recent work by these authors and by a few others who have used equally accurate techniques were also utilized (29–43). These data, which are listed in Table 4, appear to be internally consistent and to provide the most accurate source of C—H bond strengths that is currently available. Even so, it must be realized that none of these stabilization energies are known to better than ±1 kcal/mol and few are known to this degree of accuracy. In calculating an unknown bond strength it was assumed that stabilization energies were additive unless evidence to the contrary exists. For example

$$D[C_6H_5C(CH_3)H\text{—}H] = D[(CH_3)_2CH\text{—}H] - E_s[C_6H_5\dot{C}H_2]$$
$$= 95 - 13 = 82 \text{ kcal/mol}$$

$$D[C_6H_5CHCl\text{—}H] = D[CH_3CH_2\text{—}H] - E_s[C_6H_5\dot{C}H_2] - E_s[\dot{C}H_2Cl]$$
$$= 98 - 13 + 3 = 88 \text{ kcal/mol}$$

However, for diphenylmethane the assumption that

$$D[(C_6H_5)_2CH\text{—}H] = D[(CH_3)_2CH\text{—}H] - 2E_s[C_6H_5\dot{C}H_2]$$
$$= 98 - 26 = 72 \text{ kcal/mol}$$

is clearly unacceptable since $D[(C_6H_5)_3C\text{—}H]$ is known to be 75 kcal/mol. The C—H bond strength in diphenylmethane was therefore arbitrarily assigned a value of 81 kcal/mol. In a few cases where no E_s values estimated by Benson's methods were available data were taken from Kerr's review (4).

The measured rate constants for chain propagation in the autoxidation of hydrocarbons, RH, at 30° and the estimated R—H bond strengths are given in Table 5. Similar data for organic substrates containing a heteroatom are listed in Table 6. In these tables the rate constants have been statistically corrected for the number of labile hydrogens in the substrate, *i.e.*, for 3 in toluene and for 12 in cyclohexane. The rate constants refer to the following processes

$$ROO\cdot + RH \xrightarrow{k_p^{ROO}} ROOH + R\cdot$$

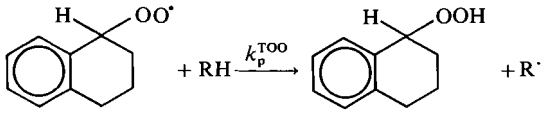

(α-tetralylperoxy)

$$(CH_3)_3COO\cdot + RH \xrightarrow{k_p^{Bu^tOO}} (CH_3)_3COOH + R\cdot$$

$$C_6H_5(CH_3)_2COO\cdot + RH \xrightarrow{k_p^{COO}} C_6H_5(CH_3)_2COOH + R\cdot$$

(cumylperoxy)

Rate constants for reaction of the substrates listed in Tables 5 and 6 with secondary (and primary) peroxy radicals can be approximately described by the equation

[9] $$\log [k_p^{s\text{-}ROO} \text{ per active H}/(M^{-1}\text{ s}^{-1})] = 16.4 - 0.2(D[\text{R—H}] + \Delta)$$

In this equation Δ represents the correction (in kcal/mol) that is required to the assigned R—H bond strength to place the measured log (k_p per H) exactly on the line defined by eq. 9 with Δ = 0. A negative value of Δ means that log (k_p per H) is greater than predicted while a positive value of Δ means that it is less than predicted.

Reaction of the same substrates with tertiary peroxy radicals yields a very similar equation

[10] $$\log [k_p^{t\text{-}ROO} \text{ per active H}/M^{-1}\text{ s}^{-1})] = 15.4 - 0.2(D[\text{R—H}] + \Delta)$$

TABLE 4. Carbon–hydrogen bond dissociation energies, D[R—H] and stabilization energies, E_s, of the parent R˙ radicals (kcal/mol)

R˙	D[R—H]	E_s	Reference
Primary			
$CH_3\dot{C}H_2$	98	0[a]	24
$CH_3CH_2\dot{C}H_2$	98	0	24
$Br\dot{C}H_2$	102	−4	29
$Cl\dot{C}H_2$	101	−3	29
$CH_3CO\dot{C}H_2$	98	0	30, 31
$HO\dot{C}H_2$	94	4	24
$CH_3O\dot{C}H_2$	93	5	24, 32
$CH_2{=}CH\dot{C}H_2$	88	10	33
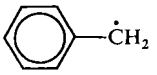	85	13	24
Secondary			
$(CH_3)_2\dot{C}H$	95	0[b]	24
$CH_3CH_2(CH_3)\dot{C}H$	95	0	24
$CH_3CO(CH_3)\dot{C}H$	92	3	34
$CH_2{=}CH(CH_3)\dot{C}H$	83	12	24
$(CH_2{=}CH)_2\dot{C}H$	80	15	24
$CH_3CH_2CH{=}CH(CH_2{=}CH)\dot{C}H$	76.5	18.5	35
	95	0	36, 37
	82	13	38
	92	3	24
	95	0	37
	83	12	25
	71	24	39, 40
	71	24	39, 40
	74	21	41
Tertiary			
$(CH_3)_3C\cdot$	92	0[c]	24
$(CH_3)_2\dot{C}OH$	91	1	24
$CH_3\dot{C}{=}O$	87	5	24
$PhC\cdot{=}O$	87	5	42
$Ph_3C\cdot$	75	17	43

[a]Defined as zero for a primary radical.
[b]Defined as zero for a secondary radical.
[c]Defined as zero for a tertiary radical.

Can. J. Chem. Downloaded from www.nrcresearchpress.com by 210.87.254.6 on 09/05/12
For personal use only.

TABLE 5. Carbon–hydrogen bond strengths, propagation rate constants at 30°, and deviations from the linear free-energy equations for hydrocarbons*

	RH	D[R—H]	k_p^{ROO} per H	Δ^b	k_p^{TOO} per H	Δ^b	$k_p^{Bu^tOO}$ per H[c]	Δ^d	k_p^{COO} per H	Δ^d
1.	Cyclohexane	95	0.004[e]	−1	—	—	0.00026	0	—	—
2.	Tridecane	95	—	—	—	—	0.0031	0	—	—
3.	Hexadecane	95	—	—	—	—	0.00034	0	—	—
4.	Isobutane	92	0.003[f]	−2[d]	—	—	0.003[f]	−2	—	—
5.	Toluene	85	0.08[g]	+2	0.1	+2	0.012	+2	0.011	+2
6.	*p*-Xylene	85	0.14	+1	—	—	0.015	+1	—	—
7.	2,3-Dimethylbut-2-ene	84	0.14	−3[d]	—	—	—	—	0.14	−3
8.	Heptene-3	83	0.35	+1	—	—	0.05	0	—	—
9.	Oct-1-ene	83	0.5	0	—	—	0.084	0	0.13	−1
10.	Dec-5-yne	83	0.7	0	—	—	—	—	0.15	−2
11.	Cyclohexene	83	1.5	−1	—	—	0.75	−7	—	—
12.	Cyclopentene	82	1.7	−1	—	—	0.85	−6	—	—
13.	Bibenzyl	82	0.14	+4	—	—	0.045	+1	0.05	+1
14.	Ethylbenzene	82	0.5[h]	+1	0.25	+3	0.10	0	0.10	0
15.	*n*-Butylbenzene	82	0.28	+3	—	—	—	—	—	—
16.	Indan	82	1.2	0	—	—	0.37	−3	0.42	−3
17.	Tetralin	82	1.6	−1	1.6	−1	0.50	−3	0.4	−3
18.	Diphenylmethane	81	1.0	+1	—	—	0.16	0	0.25	−1
19.	Penta-1,4-diene	80	7.0	−2	—	—	0.23	0	—	—
20.	Phenylcyclohexane	79	0.06	+4[d]	—	—	—	—	—	—
21.	*s*-Amylbenzene	79	0.07	+4[d]	—	—	—	—	0.07	+4
22.	*s*-Butylbenzene	79	0.08	+3[d]	—	—	—	—	0.07	+4
23.	Cumene	79	0.18	+2[d]	0.5	+4	0.16	+2	0.18	+2
24.	Allylbenzene	79	5.0	0	—	—	0.75	−1	—	—
25.	1,1-Diphenylethane	77	0.44	+2[d]	—	—	—	—	0.46	+2
26.	2,5-Dimethylhex-3-ene	77	1.2	0[d]	—	—	—	—	1.1	0
27.	Methyl linoleate	76	31	−1	—	—	—	—	—	—
28.	Methyl linolenate	76	59	−3	—	—	—	—	—	—
29.	Triphenylmethane	75	—[i]	—	—	—	$\geqslant 0.5$[i,j]	$\leqslant +3$	—	—
30.	Cycloheptatriene	74	—[i]	—	—	—	$\geqslant 2.6$[i,j]	$\leqslant +1$	—	—
31.	9,10-Dihydroanthracene	71	80	+1	60	+2	6.0	+2	18	0
32.	Cyclohexa-1,3-diene	71	55[k]	+2	—	—	$\geqslant 1.6$[j,k,l]	$\leqslant +5$	—	—
33.	Cyclohexa-1,4-diene	71	370[l]	−2[l]	—	—	20	0	—	—

[a]Units of D[R—H] and Δ are kcal/mol. Units of k_p per H are M^{-1} s^{-1}. Data are from ref. 13 unless otherwise specified. The D[R—H] values are derived from the E_s values in Table 4.
[b]Deviation from eq. 9 unless otherwise noted.
[c]This work unless otherwise noted.
[d]Deviation from eq. 10.
[e]Calculated from (k_p^{ROO} per H) = 0.044 M^{-1} s^{-1} at 60° (ref. 13) taking log (A_p^{ROO} per H) = 9.4 (see Table 2). This gives E_p^{ROO} = 16.4 kcal/mol and (k_p^{ROO} per H) = 4×10^{-3} M^{-1} s^{-1}.
[f]From data in ref. 20*a*. See text.
[g]Based on an assumed value for $2k_t^{ROO}$, see ref. 13.
[h]Based on an average $2k_t^{ROO} = 2.5 \times 10^7$ M^{-1} s^{-1} at 30°.
[i]Rate dependent on oxygen pressure.
[j]Minimum value for k_p estimated by extrapolation to infinite pressure of values obtained in the range 150–760 mm [O_2].
[k]k_p per H for abstraction. At 30°, 27% of propagating steps are abstractions and 73% are additions.
[l]HOO· radical.

This equation represents a line parallel to that defined by eq. 9 but displaced by 5 kcal/mol in D[R—H] (which is equivalent to an order of magnitude in k_p per H). The two lines and some of the data from Table 5 are shown in Fig. 1.

The excellent correlations of log ($k_p^{t\text{-}ROO}$ per H) and of log ($k_p^{s\text{-}ROO}$ per H) with D[R—H] for hydrocarbons is quite surprising in view of the fact that log (A_p per H) is far from being a constant over the range of structures studied (see Table 2). Presumably there is an approximately linear correlation of log (A_p per H) with E_p which arises because an increase in the resonance stabilization of R·, which decreases D[R—H] and E_p, requires a more rigid geometry of the transition state and hence reduces log

Can. J. Chem. Downloaded from www.nrcresearchpress.com by 210.87.254.6 on 09/05/12
For personal use only.

TABLE 6. Carbon–hydrogen bond strengths, propagation rate constants at 30°, and deviations from the linear free-energy equations for organic substrates that are autoxidized at a carbon adjacent to a heteroatom[a]

RH	D[R—H][b]	k_p^{ROO} per H	Δ[c]	$k_p^{Bu^tOO}$ per H	Δ[d]
2-Nitropropane	—	—	—	0.0003[e]	—
Isopropyl bromide	96	—	—	0.0006[e]	−3
Isopropyl chloride	95	—	—	0.0006[e]	−2
Isopropyl acetate	92	—	—	0.0024[e]	−2
Tetrahydrofuran	92	1.1	−10	0.085	−10
1,4-Dioxan	91	0.12	−4	—	—
Tetrahydropyran	91	0.14	−5	0.006	−3
n-Butyl ether	91	0.3[f]	−6	0.016	−5
Benzyl bromide	89	—	—	0.006	−1
Isopropanol	89	—	—	0.009[e]	−2
Methyl isobutyrate	89	—	—	0.012[e]	−2
Isopropyl ketone	89	—	—	0.026[e]	−4
2,5-Dimethyltetrahydrofuran	89	2.4	−14[d]	0.4	−10
Benzyl chloride	88	1.5	−7	0.008	0
Isopropyl phenyl ether	88	—	—	0.009[e]	−1
Isopropyl *t*-butyl ether	88	0.02	−2[d]	0.02	−2
Isopropyl ether	88	0.055[f]	−5[d]	0.055	−5
Benzaldehyde	87	33 000	−32[d]	0.85	−9
Benzyl acetate	85	2.3	−5	0.008	+2
Benzyl benzoate	85	2.6	−5	0.009	+2
t-Butyl phenylacetate	84	0.8	−1	0.03	+1
Benzylketone	83	—	—	0.045	+1
Benzyl alcohol	83	2.4	−3	0.065	0
Benzyl phenyl ether	81	0.75	+2	0.1	+1
Benzyl ether	81	7.5[f]	−3	0.3	−1
Benzyl *t*-butyl ether	81	5.8	−3	0.55	−3
Phthalan	81	108	−9	—	—
2-Cyanopropane	80	—	—	0.01[e]	+7
α-Methylbenzyl ether	78	—	—	0.042	+6
Benzyl cyanide	73	—	—	⩾0.01[g]	⩽14

[a]Units of D[R—H] and Δ are kcal/mol. Units of k_p per H are M^{-1} s^{-1}. Data are from ref. 13 unless otherwise specified.
[b]Estimates based on E_s values in Table 4 and on data contained in ref. 4. D[R—H] for ethers have been calculated using $E_s = 4$ kcal/mol for the effect of the ethereal oxygen (the mean of the 5 kcal for dimethyl ether and 3 kcal for tetrahydrofuran), except for tetrahydrofuran where D[R—H] was taken directly from Table 4.
[c]Deviation from eq. 9 unless otherwise noted.
[d]Deviation from eq. 10.
[e]This work.
[f]Intermolecular reaction only.
[g]Rate dependent on oxygen pressure.

(A_p per H). Any deviation of a hydrocarbon from this linear log (A_p per H) *vs.* E_p relation would, of course, result in a deviation from the log (k_p per H) *vs.* D[R—H] relation. For example, log (A_p per H) for *p*-xylene (and, presumably, toluene, etc.) is less than for oct-1-ene and tetralin and, in consequence, *p*-xylene and toluene are less reactive towards peroxy radicals than would be predicted from their R—H bond strengths.

Other possible causes of a deviation from the log (k_p per H) *vs.* D[R—H] relations include an error in the measurement of k_p, an incorrect assignment of D[R—H], or some special factor arising from conformational (44), steric or polar effects in the peroxy radical or substrate. However, it must be emphasized that k_p cannot be determined with an absolute accuracy of much better than a factor of two, while even the most accurate C—H bond strengths are uncertain by $\sim \pm 2$ kcal/mol. In consequence, a deviation (Δ) of log (k_p per H) of 2 kcal from eqs. 9 or 10 (Tables 5 and 6) is not significant.

Possible Reasons for Large Deviations from Equations 9 and 10

The difficulty described above in determining values of $k_p^{Bu^tOO\cdot}$ for cyclohexa-1,4-diene is encountered for all highly reactive substrates and only approximate values of $k_p^{Bu^tOO}$ per H can be assigned to these substrates. This problem is not as pronounced with cumene hydroper-

Can. J. Chem. Downloaded from www.nrcresearchpress.com by 210.87.254.6 on 09/05/12
For personal use only.

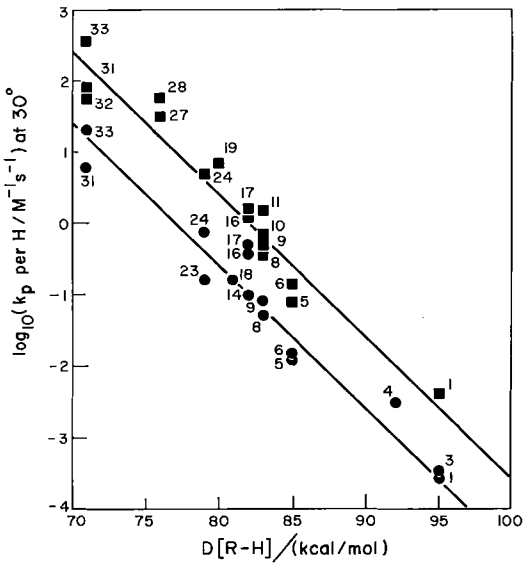

FIG. 1. log [k_p per active H/(M^{-1} s^{-1})] plotted against D[R—H]/(kcal/mol). Equation 10 is represented by the lower line and the circles represent rate constants for tertiary peroxy radicals. Equation 9 is represented by the upper line and the squares represent rate constants for secondary peroxy radicals. The numbers refer to the compounds listed in Table 5 (not all the data in this table have been plotted).

oxide because the stationary state concentration of cumylperoxy radicals is lower ($2k_t^{COO} > 2k_t^{Bu'OO}$). The low reactivity of ethylbenzene and bibenzyl as hydrogen atom donors compared with tetralin or indan is well known and has been related to conformational effects in these molecules (44).

Hydrocarbons yielding *t*-alkyl radicals are less reactive (positive Δ values) than those yielding secondary or primary alkyl radicals. If the correct C—H bond strengths have been assigned a significant steric effect is retarding these reactions.

Ethers are, in general, more reactive to peroxy radicals than eqs. 9 or 10 would predict. The major exception is α-methylbenzyl ether which is relatively unreactive presumably for steric reasons (45). Benzyl phenyl ether is slightly less reactive than would be predicted but the peculiarities which have been noted previously in the oxidation of this ether (45, 46) make the reason for this uncertain. The Δ values for *t*-butylperoxy radicals and for the peroxy radicals derived from the ethers are in excellent agreement (Table 6). The reactivities of α-alkoxyalkylperoxy radicals and alkylperoxy radicals are therefore similar (45). The C—H bond strengths of the ethers were calculated on the basis of a 4 kcal/mol stabilization energy due to the ethereal oxygen (the mean of 5 kcal for dimethyl ether and 3 kcal for tetrahydrofuran, Table 4). If we exclude α-methylbenzyl ether and tetrahydrofuran and its derivatives (2,5-dimethyltetrahydrofuran and phthalan), the Δ values for the remaining ethers average about −3 kcal/mol. That is, the majority of the ethers would fit eqs. 9 and 10 if E_s were 7 kcal/mol for an α-alkoxyalkyl radical. This would give $D[CH_3OCH_2—H] = 91$ kcal/mol rather than the 93 kcal/mol found by the gas phase iodine atom method (32). In view of the reported difficulties arising from surface effects when the iodine atom method is applied to oxygen-containing organic substrates (24), an E_s value of 7 kcal/mol is not altogether unreasonable. However, there is other evidence that α-oxygen substitution imparts relatively little stabilization to alkyl radicals (47, 48) and so an alternative explanation for the enhanced reactivity of ethers is desirable. The most obvious possibility is that the values of A_p per H for ethers are higher than for hydrocarbons of comparable bond strength. However, such an explanation could hardly account for the exceptionally high reactivity of tetrahydrofuran and its derivatives. This ether is also an unexpectedly good hydrogen donor to *t*-butoxy radicals (49) and phenyl radicals (50), so there is a distinct possibility that its C—H bond strength is less than the 92 kcal/mol found by the iodine atom method (24).

The high reactivities of benzyl chloride, benzyl acetate, benzyl benzoate and, particularly, benzaldehyde towards their own peroxy radicals are due to the exceptional reactivities of these radicals which arise from the presence of the electron withdrawing α-substituents (51, 52). Towards the *t*-butylperoxy radical these substrates exhibit a normal pattern of reactivity which implies that polar effects in the hydrogen donor are of less importance in determining k_p than polar effects in the peroxy radical.

Conclusion

The correlation of propagation rate constants for the autoxidation of organic substrates at 30° with the strengths of the weakest C—H bonds in

Can. J. Chem. Downloaded from www.nrcresearchpress.com by 210.87.254.6 on 09/05/12
For personal use only.

the molecule by means of the empirical equations

[9] $\log [k_p^{s\text{-ROO}} \text{ per active H}/(M^{-1}\ s^{-1})] = 16.4 - 0.2\ D[\text{R—H}]$

and

[10] $\log [k_p^{t\text{-ROO}} \text{ per active H}/(M^{-1}\ s^{-1})] = 15.4 - 0.2\ D[\text{R—H}]$

with D[R—H] in kcal/mol, has been surprisingly successful for hydrocarbons and reasonably successful for substrates containing heteroatoms. These equations can be used to predict k_p values not only at 30° but also at other temperatures when combined with the estimated pre-exponential factors and with activation energies calculated from the relations

[7] $E_p^{t\text{-ROO}}/(\text{kcal/mol}) = 0.55\ (D[\text{R—H}] - 65.0)$

and

[8] $E_p^{s\text{-ROO}}/(\text{kcal/mol}) = 0.55\ (D[\text{R—H}] - 62.5)$

Overall rates of oxidation of organic substrates at specified rates of chain initiation are determined by the values of k_p and $2k_t$. Sufficient data now exist (13) for $2k_t$ to be estimated with reasonable certainty provided the structure of the chain terminating peroxy radical is known. Since k_p can be estimated from the above equations it should now be possible to predict the "oxidizability" $(k_p/(2k_t)^{1/2})$ of a hydrocarbon with reasonable accuracy over a wide range of temperature provided D[R—H] is known. Less accurate predictions could be made about organic substrates containing heteroatoms.

1. M. G. Evans and M. Polanyi. Trans. Faraday Soc. **34**, 11 (1938).
2. A. F. Trotman-Dickenson. Quart. Revs. 198 (1953); Chem. Ind. London, 379 (1965).
3. J. A. Kerr. Chem. Rev. **66**, 465 (1966).
4. E. T. Butler and M. Polanyi. Trans. Faraday Soc. **39**, 19 (1943).
5. S. W. Benson and W. B. DeMore. Ann. Rev. Phys. Chem. **16**, 397 (1965).
6. N. M. Semenov. Some problems in chemical kinetics and reactivity. Princeton University Press, Princeton, New Jersey. 1958.
7. H. S. Johnston. Gas phase reaction rate theory. Ronald Press, New York. 1966. Chap. 11. T. Kagiya, Y. Sumida, and T. Inoue. Bull. Chem. Soc. Jap. **42**, 2422 (1969).
8. J. L. Bolland. Trans. Faraday Soc. **46**, 358 (1950); Quart. Rev. **3**, 1 (1949).
9. E. S. Huyser and R. M. Van Scoy. J. Org. Chem. **33**, 3524 (1968). C. Walling and D. Bristol. J. Org. Chem. **36**, 733 (1971).
10. J. R. Thomas and K. U. Ingold. Adv. Chem. Ser. **75**, 258 (1968).
11. S. W. Benson. J. Am. Chem. Soc. **87**, 972 (1965).
12. J. H. Knox. Adv. Chem. Ser. **76**, 1 (1968).
13. J. A. Howard. Adv. Free Radical Chem. **4**, 49 (1972).
14. R. Hiatt, J. Clipsham, and T. Visser. Can. J. Chem. **42**, 2754 (1964).
15. A. Factor, C. A. Russell, and T. G. Traylor. J. Am. Chem. Soc. **87**, 3692 (1965).
16. J. R. Thomas. J. Am. Chem. Soc. **87**, 3935 (1965).
17. J. A. Howard and K. U. Ingold. Can. J. Chem. **47**, 3797 (1969).
18. K. Adamic, J. A. Howard, and K. U. Ingold. Can. J. Chem. **47**, 3803 (1969).
19. D. G. Hendry. J. Am. Chem. Soc. **89**, 5433 (1967).
20. (*a*) D. L. Allara, T. Mill, D. G. Hendry, and F. R. Mayo. Adv. Chem. Ser. **76**, 40 (1968). (*b*) D. L. Allara, D. Edelson, and K. C. Irwin. Int. J. Chem. Kinet. **4**, 345 (1972).
21. D. L. Allara, T. Mill, F. R. Mayo, H. Richardson, and K. Irwin. Division of Petroleum Chemistry, Am. Chem. Soc. Meeting, Los Angeles, 1971. Preprints **16** (1), B31.
22. J. E. Bennett, D. M. Brown, and B. Mile. Trans. Faraday Soc. **66**, 386 (1970).
23. L. R. Mahoney and M. A. DaRooge. J. Am. Chem. Soc. **92**, 4063 (1970).
24. D. M. Golden and S. W. Benson. Chem. Rev. **69**, 125 (1969).
25. S. W. Benson. Thermochemical kinetics. John Wiley and Sons, Inc., New York. 1968.
26. S. W. Benson. Private communication.
27. R. R. Baldwin, D. H. Langford, M. J. Matchan, R. W. Walker, and D. A. Yorke. XIIIth Symp. on Combustion, Salt Lake City, Utah, 1970.
28. S. W. Benson and R. Shaw. Adv. Chem. Ser. **75**, 288 (1968).
29. S. Furuyama, D. M. Golden, and S. W. Benson. J. Am. Chem. Soc. **91**, 7564 (1969).
30. K. D. King, D. M. Golden, and S. W. Benson. J. Am. Chem. Soc. **92**, 5541 (1970).
31. R. K. Solly, D. M. Golden, and S. W. Benson. Int. J. Chem. Kinet. **2**, 11 (1970).
32. F. R. Cruickshank and S. W. Benson. Int. J. Chem. Kinet. **1**, 381 (1969).
33. D. M. Golden, N. A. Gac, and S. W. Benson. J. Am. Chem. Soc. **91**, 2136 (1969).
34. R. K. Solly, D. M. Golden, and S. W. Benson. Int. J. Chem. Kinet. **2**, 381 (1970).
35. K. W. Egger and M. Jola. Int. J. Chem. Kinet. **2**, 265 (1970).
36. S. Furuyama, D. M. Golden, and S. W. Benson. Int. J. Chem. Kinet. **2**, 83 (1970).
37. S. H. Jones and E. Whittle. Int. J. Chem. Kinet. **2**, 479 (1970).
38. S. Furuyama, D. M. Golden, and S. W. Benson. Int. J. Chem. Kinet. **2**, 93 (1970).
39. K. W. Egger and S. W. Benson. J. Am. Chem. Soc. **88**, 241 (1966).

Can. J. Chem. Downloaded from www.nrcresearchpress.com by 210.87.254.6 on 09/05/12
For personal use only.

40. D. G. L. JAMES and R. D. SUART. Chem. Commun. 484 (1966).
41. G. VINCOW, H. J. DAUBEN, JR., F. R. HUNTER, and W. V. VOLLARD. J. Am. Chem. Soc. **91**, 2823 (1969).
42. R. K. SOLLY and S. W. BENSON. J. Am. Chem. Soc. **93**, 1592 (1971).
43. S. W. BENSON. J. Chem. Educ. **42**, 5002 (1965).
44. A. E. EACHUS, J. A. MEYER, J. PEARSON, and M. SZWARC. J. Am. Chem. Soc. **90**, 3646 (1968).
45. J. A. HOWARD and K. U. INGOLD. Can. J. Chem. **47**, 3809 (1969); **48**, 873 (1970).
46. G. A. RUSSELL and R. C. WILLIAMSON, JR. J. Am. Chem. Soc. **86**, 2357 (1964).
47. A. OHNO and Y. OHNISHI. Tetrahedron Lett. 4405 (1969).
48. C. RÜCHARDT. Angew. Chem. Int. Ed. **9**, 830 (1970).
49. C. WALLING and M. J. MINTZ. J. Am. Chem. Soc. **89**, 1515 (1967).
50. G. A. RUSSELL. Private communication.
51. J. A. HOWARD and S. KORCEK. Can. J. Chem. **48**, 2165 (1970).
52. G. E. ZAIKOV, J. A. HOWARD, and K. U. INGOLD. Can. J. Chem. **47**, 3017 (1969).
53. R. A. JACKSON and D. W. O'NEIL. Chem. Commun. 1210 (1969).

Can. J. Chem. Downloaded from www.nrcresearchpress.com by 210.87.254.6 on 09/05/12
For personal use only.

Absolute Rate Constants for Hydrocarbon Autoxidation. XXII. The Autoxidation of some Vinyl Compounds[1]

J. A. HOWARD

Division of Chemistry, National Research Council of Canada, Ottawa, Canada K1A 0R9

Received January 28, 1972

Absolute propagation and termination rate constants have been determined for the autoxidation of some vinyl compounds at 30°. Rates of propagation depend on the structure of both the peroxy radical and the vinyl compound. The reactivity of peroxy radicals towards addition increases as the electron-withdrawing capacity of the α-substituent increases. Rate constants for addition of *t*-butylperoxy radicals to vinyl compounds, $k_{add}^{Bu^tOO}$, fit the equation

$$\log [k_{add}^{Bu^tOO}/(M^{-1}\ s^{-1})] = 0.2\ E_s - 4.3$$

where E_s is the estimated stabilization energy of the β-peroxyalkyl radical (in kcal/mol) formed in the addition reaction.

Les constantes absolues de vitesse de propagation et de terminaison ont été déterminées pour l'autoxydation de quelques composés vinyliques à 30°. Les vitesses de propagation dépendent à la fois de la structure du radical péroxy et du composé vinylique. La réactivité des radicaux peroxy pour l'addition croît avec le pouvoir électroattracteur du substituant en α. Les constantes de vitesse de l'addition des radicaux *t*-butylpéroxy aux composés vinyliques, $k_{add}^{Bu^tOO}$, satisfont l'équation

$$\log\ [k_{add}^{Bu^tOO}/(M^{-1}\ s^{-1})] = 0.2\ E_s - 4.3$$

où E_s est l'énergie de stabilisation mesurée du radical β-peroxyalkyl (en kcal/mol) formé dans la réaction d'addition.

Canadian Journal of Chemistry, **50**, 2298 (1972)

Introduction

Recent work in these laboratories (1) has shown that the magnitude of the rate controlling propagation constant for the autoxidation of α-monosubstituted toluenes, k_p, depends on the nature of the peroxy radical, ROO·, as well as the nature of the toluene, RH.

[1] $$ROO\cdot + RH \xrightarrow{k_p} ROOH + R\cdot$$

Thus it was shown that the reactivity of peroxy radicals increases with the increasing electron-withdrawing capacity of the α-substituent in the order

$C_6H_5C(O)OO\cdot > C_6H_5CH(OC(O)R)OO\cdot > C_6H_5CH(Cl)OO\cdot > C_6H_5CH(CN)OO\cdot > C_6H_5CH(OH)OO\cdot > C_6H_5CH(OR)OO\cdot \sim C_6H_5CH_2OO\cdot$

Vinyl compounds, $CH_2{=}C(X)R$ (where R = CH_3 or H and X = CN, C_6H_5, $OC(O)CH_3$, etc.) react with molecular oxygen at ambient temperatures by a free radical chain process (2). The rate controlling propagation step is

[2] $$-CH_2\overset{R}{\underset{|}{C}}(X)OO\cdot + CH_2{=}\overset{R}{\underset{|}{C}}X \xrightarrow{k_p^{rr}} -CH_2-\overset{R}{\underset{|}{C}}(X)OOCH_2\overset{R}{\underset{|}{C}}X\cdot$$

In order to compare the relative reactivities of α-substituted alkylperoxy radicals towards addition with their relative reactivities towards abstraction we have now measured absolute rate constants for the reaction of a number of vinyl compounds towards their own peroxy radical, k_p^{rr}, and towards the *t*-butylperoxy radical, $k_{add}^{Bu^tOO}$.

[3] $$Bu^tOO\cdot + CH_2{=}\overset{R}{\underset{|}{C}}X \xrightarrow{k_{add}^{Bu^tOO}} Bu^tOOCH_2-\overset{R}{\underset{|}{C}}X\cdot$$

Experimental

Absolute rate constants for the autoxidation of the undiluted vinyl compounds were determined using the rotating sector method (3, 4). Rate constants for reaction of the vinyl compounds with *t*-butylperoxy radicals were determined from autoxidations in the presence of *t*-butyl hydroperoxide

[1]NRCC No. 12583.

Can. J. Chem. Downloaded from www.nrcresearchpress.com by 210.87.254.40 on 09/05/12
For personal use only.

Can. J. Chem. Downloaded from www.nrcresearchpress.com by 210.87.254.40 on 09/05/12
For personal use only.

(1, 5). All the rate constants reported in this work were measured at 30°.

α,α′-Azo-bis-isobutyronitrile and α,α′-azo-bis-cyclohexane carbonitrile were used as thermal and photochemical initiators, respectively. 2,6-Di-*t*-butyl-4-methoxyphenol was the scavenger used to determine rates of chain initiation by the induction period method (6).

The vinyl monomers were, whenever possible, purified by distillation from a sample that was partially polymerized in the absence of oxygen. Non-polymerizable substrates and solvents were purified by fractional distillation and percolation through alumina. *t*-Butyl hydroperoxide was dried and purified by crystallization from pentane.

Results and Discussion

(i) Pure Vinyl Compounds

Steady state rates of oxidation, R_s, of several vinyl compounds at various partial pressures of oxygen, rates of chain initiation, R_i, and substrate concentration, [RH], are summarized in Tables 1 and 2. The values of R_s for vinyl compounds can be approximately described by the usual kinetic expression for autoxidations

$$[4] \qquad R_s = \frac{-d[O_2]}{dt} = \frac{k_p^{rr}[RH]R_i^{1/2}}{(2k_t^{rr})^{1/2}}$$

where k_p^{rr} and $2k_t^{rr}$ are the rate controlling propagation and termination rate constants. However, photochemically initiated oxidations of vinyl acetate, 2,3,3-trimethylbut-1-ene, methyl acrylate, isopropenyl acetate, and ethyl vinyl ether gave values of the ratio of the rate of an oxidation that is subjected to flashes of light of very short duration, *i.e.*, at very fast speeds of sector rotation, to the rate under continuous illumination, R_∞/R_s, of *ca.* 0.4 and eq. 4 is not strictly obeyed for these compounds. Absolute values of k_p^{rr} and $2k_t^{rr}$ in these cases were determined on the basis of the assumption that the oxidation chains are terminated by reactions that are first and second order in the concentration of peroxy radicals (3, 4).

Vinyl compounds can be arranged in the following order of decreasing oxidizability, *i.e.*, decreasing $k_p^{rr}/2k_t^{rr})^{1/2}$)

2,3,3-trimethylbut-1-ene < methyl acrylate < isopropenyl acetate < methyl methacrylate ~ vinyl acetate < acrylonitrile < ethyl vinyl ether < methyl acrylonitrile < styrene < α-methylstyrene

Rate constants for the mutual termination reaction of the peroxy radicals derived from vinyl compounds, $2k_t^{rr}$, lie in the range 6×10^5 to 10^8 M^{-1} s^{-1}. Values of $2k_t^{rr}$ for the radicals with an α-hydrogen atom are similar to rate constants for the secondary peroxy radicals derived from acyclic hydrocarbons, ethers, thioethers, and α-monosubstituted toluenes (7). α-Substitution therefore has very little influence on $2k_t^{rr}$ for the secondary peroxy radicals derived from vinyl compounds. We previously reached the same conclusion from a study of the autoxidation of α-monosubstituted toluenes (1).

Termination rate constants for the peroxy radicals derived from methyl methacrylate, methyl acrylonitrile, isopropenyl acetate, and 2,3,3-trimethylbut-1-ene are in the range $1 \times 10^6 - 1 \times 10^8$ M^{-1} s^{-1}. These rate constants are significantly larger than termination rate constants for the peroxy radicals derived from hydrocarbons, alcohols, and ethers with labile tertiary hydrogens (7). It is well known from the work of Russell (8) that the presence of a small percentage of secondary (or primary) peroxy radicals in the chain drastically reduces the rate of oxidation of a substrate with a labile tertiary hydrogen. This suggests that the relatively high termination rate constants for the α-methyl substituted vinyl compounds are due to peroxy radical attack at the α-methyl group with the consequent production of primary peroxy radicals.

$$[5] \quad ROO^{\cdot} + CH_2{=}C(X)CH_3 \xrightarrow{O_2} ROOH + CH_2{=}C(X)CH_2OO^{\cdot}$$

This reaction is feasible because allylic hydrogens are readily abstracted by peroxy radicals, *e.g.*, k_p^{rr} for oct-1-ene = 1.0 M^{-1} s^{-1} at 30° (7). However, it is also possible that electron-withdrawing α-substituents in peroxy radicals with the structure —CH_2—$C(X)(CH_3)OO^{\cdot}$ directly increase the termination rate constant. For example, the value of $2k_t$ for the 2-cyano-2-propylperoxy radical (9) is *ca.* 3 orders of magnitude larger than for the *t*-butylperoxy radical.

Propagation rate constants, k_p^{rr}, for the vinyl compounds fall in the range 0.6–5.0 M^{-1} s^{-1}. Interpretation of these rate constants is complicated by differences in both peroxy radical and substrate reactivity.

(ii) Autoxidation of Vinyl Compounds in the Presence of t-Butyl Hydroperoxide

The vinyl compounds discussed in the previous section have been oxidized in the presence of *t*-butyl hydroperoxide. At hydroperoxide

Can. J. Chem. Downloaded from www.nrcresearchpress.com by 210.87.254.40 on 09/05/12
For personal use only.

TABLE 1. Kinetic data for the autoxidation of vinyl acetate at 30°

Concentration (M)	Oxygen pressure (Torr)	$R_i \times 10^8$ ($M\,s^{-1}$)	$R_s \times 10^7$ ($M\,s^{-1}$)	$\frac{R_s}{[RH]R_i^{1/2}} \times 10^3$ ($M^{-1/2}\,s^{-1/2}$)	$\frac{R_\infty}{R_s}$	k_p^{rr} ($M^{-1}\,s^{-1}$)	$2k_t^{rr} \times 10^{-7}$ ($M^{-1}\,s^{-1}$)	$k_p^{rr}/(2k_t^{rr})^{1/2} \times 10^3$ ($M^{-1/2}\,s^{-1/2}$)
5.4*	153	20	8.6	0.36		—	—	—
5.4*	334	20	10	0.42		—	—	—
5.4*	700	20	9.5	0.40		—	—	—
10.8	300	20	14.4	0.30		—	—	—
10.8	480	20	11.5	0.24		—	—	—
10.8	700	1.0	2.7	0.25	0.40	1.8	3.2	0.31
10.8	700	3.3	4.8	0.24	0.41	1.9	4.1	0.30
10.8	700	4.0	5.8	0.27	0.41	2.4	4.9	0.34
10.8	700	11.0	11.3	0.31	0.42	3.1	6.7	0.38
10.8	700	16	14.2	0.33	0.43	3.0	6.0	0.38
10.8	700	20	16.3	0.34	0.43	2.9	4.7	0.42

*Diluted with chlorobenzene.

TABLE 2. Kinetic data for the autoxidation of some vinyl compounds at 30°

Vinyl compound	Concentration (M)	$R_i \times 10^8$ ($M\,s^{-1}$)	$R_s \times 10^7$ ($M\,s^{-1}$)	$\frac{R_s}{[RH]R_i^{1/2}} \times 10^3$ ($M^{-1/2}\,s^{-1/2}$)	$\frac{R_\infty}{R_s}$	k_p^{rr} ($M^{-1}\,s^{-1}$)	$2k_t^{rr} \times 10^{-7}$ ($M^{-1}\,s^{-1}$)	$k_p^{rr}/(2k_t^{rr})^{1/2} \times 10^3$ ($M^{-1/2}\,s^{-1/2}$)
2,3,3-Trimethylbut-1-ene*	14.25	10	3.2	~0.07	~0.44	~0.7	~10	~0.07
Methyl acrylate	11.1	20	5.6	0.11	0.40	0.6	1.7	0.14
Isopropenyl acetate	7.45	17.2	9.25	0.24	0.40	0.2	0.16	0.16
Methyl methacrylate	1.9	17	4.5†	0.58	—	—	—	—
Methyl methacrylate	9.4	17	14	0.36	—	—	—	—
Methyl methacrylate	9.4	17	14.5	0.38	0.50	1.0	0.8	0.36
Acrylonitrile	15	23	37	0.51	—	—	—	—
Acrylonitrile	15	7.4	19	0.46	0.50	3.3	6.0	0.47
Acrylonitrile	15	23	33†	0.46	0.50	3.2	4.0	0.46
Ethyl vinyl ether	10.6	17.2	19.4	0.44	0.40	2.74	2.7	0.56
Methyl acrylonitrile	11.9	21	89†	1.6	—	—	—	—
Methyl acrylonitrile	11.9	6.7	44.7	1.45	0.50	4.5	0.96	1.45
Methyl acrylonitrile	11.9	21	83	1.5	0.50	4.5	0.9	1.5
Styrene‡	—	—	—	—	—	41	4.2	6.3
α-Methylstyrene‡	—	—	—	—	—	10	0.06	13

*Rate constants for this compound are very approximate because of the low chain length for autoxidation at 30° and because the rate of oxidation slows down as oxygen is consumed and does not strictly obey equation [4].
†At an oxygen pressure of *ca.* 400 mm Hg.
‡Previously published data (7).

TABLE 3. Kinetic data for the autoxidation of some vinyl compounds in the presence of *t*-butyl hydroperoxide at 30°

Vinyl compound	Concentration (M)	$R_i \times 10^8$ ($M\ s^{-1}$)	$R_s \times 10^7$ ($M\ s^{-1}$)	$k_{add}^{Bu^tOO}/(2k_t^{Bu^tOO})^{1/2} \times 10^3 (M^{-1/2}\ s^{-1/2})$	$k_{add}^{Bu^tOO}$ ($M^{-1}\ s^{-1}$)	$k_p^{rr}/k_{add}^{Bu^tOO}$
Vinyl acetate (1)	8.64	1.6	1.2	0.06	0.002	1258
Isopropenyl acetate (2)	7.45	1.7	3.0	0.31	0.01	20
Acrylonitrile (9)	2.0	2.1	5.3	0.3	0.01	325
Ethyl vinyl ketone (4)	13.5	2.7	8.4	0.38	0.013	—
Methyl acrylate (3)	8.9	1.8	6.6	0.56	0.02	30
Methyl acrylate (3)	8.9	27	28	0.6	0.02	30
Ethyl vinyl ether (5)	8.6	2.3	14.6	1.12	0.04	68.5
Methyl methacrylate (6)	7.5	2.6	27	2.3	0.08	12.5
Methyl acrylonitrile (12)	10	2.3	40	2.7	0.094	48
cis-1,2-Diphenylethylene	1.15	2.26	5.85	3.4	0.12	—
trans-1,2-Diphenylethylene (8)	0.18	1.5	2.72	12.7	0.44	—
Styrene (7)	0.43	4.3	34.5	38.5	1.3	31
β-Methylstyrene	0.12	10	27	71	2.5	20
α-Methylstyrene (10)	0.12	3.8	19.4	83	2.9	3.4
1,1-Diphenylethylene (11)	0.046	1.9	16.6	264	9.2	—

concentrations above *ca.* 1 M, the rate controlling propagation and termination reactions involved in the autoxidation are

$$Bu^tOO^\cdot + CH_2{=}\overset{\overset{R}{|}}{C}{-}X \xrightarrow{k_{add}^{Bu^tOO}} Bu^tOOCH_2{-}\overset{\overset{R}{|}}{C}(X)^\cdot$$

and

$$Bu^tOO^\cdot + Bu^tOO^\cdot \xrightarrow{2k_t^{Bu^tOO}} \text{Molecular products}$$

Measurement of rates of oxidation of vinyl compounds in the presence of *t*-butyl hydroperoxide at known rates of chain initiation enables absolute values of $k_{add}^{Bu^tOO}$ to be calculated. Kinetic data obtained by this procedure are summarized in Table 3.

The last column in Table 3 compares the reactivity of a vinyl compound towards its own peroxy radical and towards the *t*-butylperoxy radical. The following conclusions can be drawn from this comparison.

(a) Peroxy Radical Reactivity

α-Substituted secondary peroxy radicals, R—CH(X)OO$^\cdot$, are significantly more reactive towards addition than the *t*-butylperoxy radical and increase in reactivity in the order

$$—CH(OC(O)CH_3)OO^\cdot > —CH(CN)OO^\cdot > —CH(OC_2H_5)OO^\cdot > —CH(C(O)OCH_3)OO^\cdot \sim —CH(C_6H_5)OO^\cdot$$

This reactivity sequence is identical with the one previously obtained for the reactivity of some α-monosubstituted benzylperoxy radicals towards hydrogen atom abstraction (1). α-Substituted tertiary peroxy radicals $RC(CH_3)(X)OO^\cdot$ are also more reactive than the *t*-butylperoxy radical but are less reactive than the corresponding α-substituted secondary peroxy radicals. These tertiary radicals can be arranged in the following order of increasing reactivity

$$CH_3C(R)(CN)OO^\cdot > CH_3C(R)(OC(O)CH_3)OO^\cdot > CH_3C(R)(C(O)OCH_3)OO^\cdot$$

(b) Substrate Reactivity

The vinyl compounds listed in Table 3 have been arranged in order of increasing reactivity towards the *t*-butylperoxy radical. It is apparent that the reactivity decreases as the electron-withdrawing capacity of the substituent increases. Thus the influence of α-substitution on substrate reactivity is the reverse of the influence of α-substitution on peroxy radical reactivity. For example, the peroxy radical derived from vinyl acetate is the most reactive peroxy radical considered in this work while vinyl acetate is the least reactive vinyl compound towards reaction with the *t*-butylperoxy radical. This effect is analogous to that found in free radical polymerizations where it has been observed that the order of reactivity for polymer radicals is approximately the inverse of that for monomers (10).

It has been proposed (11, 12) for radical addition reactions to olefins

[7] $$R^\cdot + \rangle C{=}C\langle \rightarrow R{-}\overset{|}{\underset{|}{C}}{-}\overset{|}{\underset{|}{C}}^\cdot$$

that changes in the heat of reaction (ΔH) and activation energy (E_a) may be related to the stabilization energies of the attacking radical (R_a), the olefin (R_m), and the radical formed

Can. J. Chem. Downloaded from www.nrcresearchpress.com by 210.87.254.40 on 09/05/12
For personal use only.

Can. J. Chem. Downloaded from www.nrcresearchpress.com by 210.87.254.40 on 09/05/12
For personal use only.

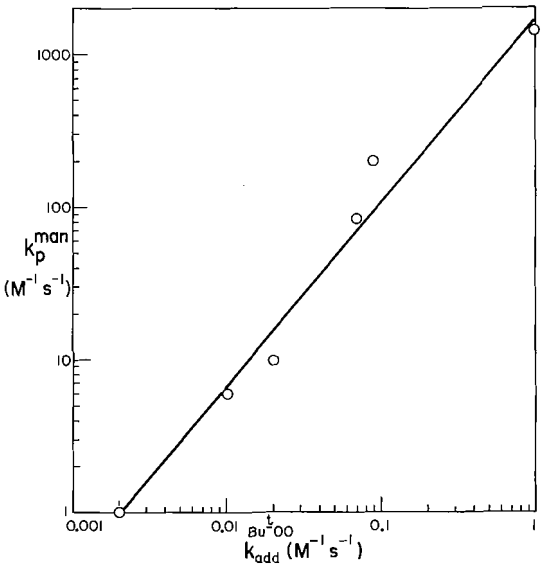

FIG. 1. A free energy plot for the reaction of olefins with the *t*-butylperoxy radical and the poly(methylacrylonitrile) radical.

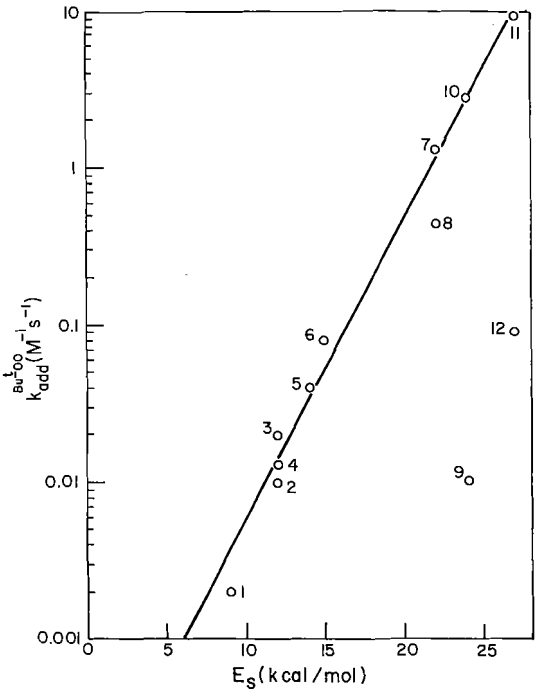

FIG. 2 A plot of the logarithms of the rate constants for addition of *t*-butylperoxy radicals to olefins against estimated stabilization energies of the radical formed upon addition. The numbers refer to the compounds listed in Table 3.

on addition (E_s) by the equation

$$[8] \qquad E_a = \alpha\,\Delta H = \alpha(R_a + R_m - E_s)$$

This equation has been modified (13) for the addition of a given radical to a series of olefins at a constant temperature to give

$$[9] \qquad \log k = A + B[R_m + D[R'\text{—}H]]$$

where k is a relative rate constant for addition, A is a constant providing the pre-exponential factors for the additions are the same, $B = \alpha/2.303\ RT$ and $D[R'\text{—}H]$ is the strength of the $R\overset{|}{\underset{|}{C}}\overset{|}{\underset{|}{C}}$—H bond. Relative rate constants for the addition of methyl radicals to olefins (14–18) correlate quite well with eq. 9 and fit the expression

$$[10] \quad \log k = 11.36 - 0.104\,[R_m + D[R'\text{—}H]]$$

The logarithms of the rate constants for addition of *t*-butylperoxy radicals to olefins do not give a linear free energy correlation with the logarithms of the rate constants for addition of methyl radicals and other electroneutral radicals, *e.g.*, phenyl and polystyryl. This implies that eq. 9 does not hold for the electrophilic *t*-butylperoxy radical. Fairly good correlations are, however, obtained between the *t*-butylperoxy radical and the more polar polymeric radicals from methyl acrylonitrile, methyl methacrylate, acrylonitrile, and methyl acrylate (see, *e.g.*, Fig. 1). The slope of the line shown in this figure can be described by the equation

$$[11] \quad \log\,[k_{add}^{Bu^tOO}/(M^{-1}\ s^{-1})] = 1.2\,\log\,[k^{man}/(M^{-1}\ s^{-1})]$$

where k^{man} represents the rate constant for addition of the poly(methylacrylonitrile) radical to the olefin. This equation indicates that the the *t*-butylperoxy radical is slightly more selective than the poly(methylacrylonitrile) radical towards addition.

Although rate constants for the addition of *t*-butylperoxy radicals to olefins do not obey eq. 9, an excellent correlation is obtained when the logarithms of $k_{add}^{Bu^tOO}$ are plotted against the estimated stabilization energies of the radical formed on addition (Fig. 2). This implies that the rate of addition of the *t*-butylperoxy radical to olefins depends principally on the stability of the incipient radical. The stabilization energies of the β-peroxyalkyl radicals have been assumed to be equal to the stabilization

Can. J. Chem. Downloaded from www.nrcresearchpress.com by 210.87.254.40 on 09/05/12
For personal use only.

TABLE 4. Resonance energies of some α-substituted radicals

Radical*	E_s (kcal/mol)
$CH_3\dot{C}H(OC(O)CH_3)$ (1)	9
$CH_3\dot{C}(CH_3)(OC(O)CH_3)$ (2)	12
$CH_3\dot{C}H(C(O)OCH_3)$ (3)	12
$CH_3\dot{C}(C(O)CH_3)$ (4)	12
$CH_3\dot{C}H(OR)$ (5)	14
$CH_3\dot{C}(CH_3)(C(O)OCH_3)$ (6)	15
$CH_3\dot{C}HC_6H_5$ (7)	22
$C_6H_5CH_2\dot{C}HC_6H_5$ (8)	22
$(CH_3)\dot{C}H(CN)$ (9)	24
$(CH_3)_2\dot{C}C_6H_5$ (10)	25
$(CH_3)\dot{C}(C_6H_5)_2$ (11)	27
$(CH_3)\dot{C}(CH_3)CN$ (12)	27

*Numbers in parentheses identify the radicals with the vinyl compounds listed in Table 3.

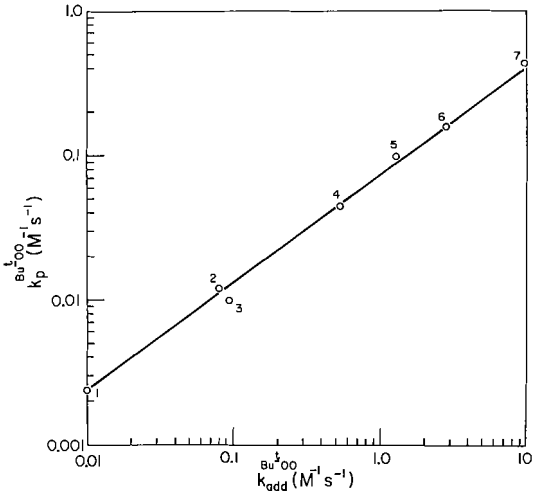

FIG. 3. A plot of log $[k_{add}^{Bu^tOO}/(M^{-1}\,s^{-1})]$ against log $[k_p^{Bu^tOO}/(M^{-1}\,s^{-1})]$ for the reaction of the *t*-butylperoxy radical with olefins and their hydrogenated analogues. The numbers refer to the pairs of compounds listed in Table 5.

energies of the analogous alkyl radical, *e.g.*, E_s for $Bu^tOOCH_2\dot{C}HC_6H_5$ has been assumed to equal E_s for $CH_3\dot{C}HC_6H_5$. The values of E_s used in this work are listed in Table 4 and were calculated from the expression

$$E_s = D[CH_3\text{—}H] - D[XCH_2\text{—}H]$$

using a value of $D[CH_3\text{—}H]$ equal to 104 kcal/mol (19). The values of $D[XCH_2\text{—}H]$ that were used are the most accurate currently available (20). The best line through the points in Fig. 2 fits the equation

$$\log [k_{add}^{Bu^tOO}/(M^{-1}\,s^{-1})] = 0.2\,E_s - 4.3$$

with most of the rate constants lying within a factor of 2 of this line. The obvious exceptions are acrylonitrile and methyl acrylonitrile. We have used Shapiro and Turk's (21) recent E_s value of *ca.* 20 kcal/mol for the $\dot{C}H_2CN$ radical to estimate E_s values for $CH_3\dot{C}H(CN)$ and $(CH_3)_2\dot{C}CN$. Our kinetic data imply that these resonance energies may be too high by *ca.* 10 kcal/mol.

trans-1,2-Diphenylethylene is approximately 4 times as reactive as the *cis*-isomer towards *t*-butylperoxy radicals. This order of reactivity for *cis-trans* isomers of 1,2-disubstituted olefins is often found in free radical co-polymerization reactions despite the fact that the *cis* isomer is the thermodynamically less stable form. Such results have been rationalized by assuming that the radical formed from the *cis*-isomer is less stable than the radical formed from the *trans*-isomer because of steric hindrance to resonance. Our results imply that the *trans*-1,2-diphenylethyl radical is *ca.* 3 kcal/mol more stable than the *cis*-radical.

The reactivity of some olefins, $k_{add}^{Bu^tOO}$, and their hydrogenated analogues, $k_p^{Bu^tOO}$, towards the *t*-butylperoxy radical are compared in Table 5. These rate constants are presented as a linear free energy correlation in Fig. 3 with the

TABLE 5. A comparison of the reactivity of vinyl compounds and their hydrogenated analogues towards *t*-butylperoxy radicals

Vinyl compound	$k_{add}^{Bu^tOO}$ ($M^{-1}\,s^{-1}$)	Saturated analogue	$k_p^{Bu^tOO}$/H ($M^{-1}\,s^{-1}$)
Isopropenyl acetate (1)	0.01	Isopropyl acetate	0.0024
Methyl methacrylate (2)	0.08	Methyl isobutyrate	0.012
Methyl acrylonitrile (3)	0.094	2-Cyanopropane	0.01
trans-1,2-Diphenylethylene (4)	0.44	Bibenzyl	0.045
Styrene (5)	1.3	Ethylbenzene	0.1
α-Methylstyrene (6)	2.8	Cumene	0.16
1,1-Diphenylethylene (7)	9.5	1,1-Diphenylethane	0.45

data fitting the equation

$$\log [k_t^{Bu^tOO}/(M^{-1}\ s^{-1})] = 0.75 \log [k_{add}^{Bu^tOO}/(M^{-1}\ s^{-1})] - 1.14$$

This correlation implies that transition states for addition and abstraction reactions involving peroxy radicals occupy a similar position on the potential energy – reaction co-ordinate curve.

The author wishes to thank Dr. K. U. Ingold for his continued interest and advice throughout the course of this work.

1. J. A. Howard and S. Korcek. Can. J. Chem. **48**, 2165 (1970).
2. F. R. Mayo. Acc. Chem. Res. **1**, 193 (1968).
3. G. M. Burnett and H. W. Melville. Investigation of rates and mechanisms of reactions. *In* Technique of Organic Chemistry. Vol. VIII, Part II. *Edited by* S. L. Friess, E. S. Lewis, and A. Weissberger. Interscience, New York, 1963. Chap. 20.
4. J. A. Howard and K. U. Ingold. Can. J. Chem. **43**, 2729 (1965).
5. J. A. Howard and K. U. Ingold. Can. J. Chem. **46**, 2655 (1968); **48**, 873 (1970). J. A. Howard and S. Korcek. Can. J. Chem. **49**, 2178 (1971).
6. C. E. Boozer, G. S. Hammond, C. E. Hamilton, and J. N. Sen. J. Am. Chem. Soc. **77**, 3233 (1955).
7. J. A. Howard. Adv. Free Radical Chem. **4**, 49 (1972).
8. G. A. Russell. J. Am. Chem. Soc. **77**, 4583 (1955).
9. V. M. Gol'dberg and L. K. Obukhova. Dokl. Akad. Nauk SSSR, **164**, 860 (1965).
10. A. D. Jenkins. Adv. Free Radical Chem. **2**, 139 (1967).
11. M. G. Evans. Discuss. Faraday Soc. **2**, 271 (1947).
12. M. G. Evans, J. Grergely, and E. C. Seaman. J. Polymer Sci. **3**, 866 (1948).
13. C. Walling. J. Phys. Chem. **64**, 166 (1960).
14. M. Szwarc. J. Polymer Sci. **16**, 367 (1955).
15. F. Leavitt, M. Levy, M. Szwarc, and V. Stannett. J. Am. Chem. Soc. **77**, 5493 (1955).
16. R. P. Buckley and M. Szwarc. J. Am. Chem. Soc. **78**, 5696 (1956).
17. R. P. Buckley, F. Leavitt, and M. Szwarc. J. Am. Chem. Soc. **78**, 5557 (1956).
18. A. Rajbenbach and M. Szwarc. J. Am. Chem. Soc. **79**, 6343 (1957).
19. J. A. Kerr. Chem. Rev. **66**, 465 (1966).
20. S. Korcek, J. H. B. Chenier, J. A. Howard, and K. U. Ingold. Can. J. Chem. This issue.
21. R. H. Shapiro and J. Turk. Org. Mass Spectr. **2**, 1067 (1969).

Can. J. Chem. Downloaded from www.nrcresearchpress.com by 210.87.254.40 on 09/05/12
For personal use only.

Hydrogen Atom Recombination on Glass Surfaces

L. W. BADER

Department of Chemistry and Chemical Engineering, University of Saskatchewan, Saskatoon, Saskatchewan

AND

H. D. GESSER

Department of Chemistry, University of Manitoba, Winnipeg, Manitoba R3T 2N2

Received November 17, 1971

The adsorption and recombination of H atoms at temperatures between 77 and 110 °K have been studied on various silicate glass surfaces consisting of fused silica, porous Vycor with surface adsorbed water, and porous Vycor with chemically altered surfaces achieved by replacement of the surface functional hydroxyl group by chlorine, fluorine, and methoxy substituents.

The concentration of adsorbed H atoms was determined by a measurement of the e.s.r. signal and the kinetics of the disappearance of the hydrogen atoms were observed to be second order in mobile atoms, consistent with a diffusion controlled recombination process.

The results require that there be at least two types of surface adsorbed atoms, namely, weakly physically adsorbed atoms that are mobile and immobile. Identification of these adsorbed atom types with a particular surface functional feature leading to the adsorption is proposed.

The activation energy for the second order decay of hydrogen atoms at the surface was found to vary from 1.0 to 2.3 kcal/mol, depending upon the chemical nature of the surface. A correlation between this activation energy and an electronegativity function of the surface group is presented.

L'adsorption et la recombinaison des atomes H, à des températures entre 77 et 110 °K, ont été étudiées sur diverses surfaces de verre au silicate, constituées soit par de la silice fondue, soit par du Vycor poreux ayant adsorbé de l'eau, soit par du Vycor poreux avec des surfaces modifiées chimiquement où les groupes fonctionnels hydroxyles ont été remplacés par du chlore, du fluor et par le groupe méthoxy. La concentration des atomes H adsorbés est déterminée par la mesure du signal RPE, les cinétiques de disparition des atomes d'hydrogène sont du second ordre en atomes mobiles, compatibles avec un processus de recombinaison contrôlé par la diffusion. Ces résultats impliquent l'existence d'au moins deux types d'atomes adsorbés à savoir ceux qui sont physiquement adsorbés de façon faible, mobiles et immobiles. L'identification de ces types d'atomes adsorbés sur une surface fonctionnelle particulière, est proposée.

L'énergie d'activation pour la disparition du 2ième ordre des atomes d'hydrogène de la surface varie de 1.0 à 2.3 kcal/mol, dépendant de la nature chimique de la surface. Une corrélation entre l'énergie d'activation et l'électronégativité de la fonction sur la surface, est présentée.

Canadian Journal of Chemistry, **50**, 2305 (1972)

Introduction

Since the early observations of Wood (1) of the surface catalyzed recombination of hydrogen atoms, and the effect of surface "poisons" on the recombination, the phenomenon has been observed and studied in many atom systems ... H (2), O (3, 4), Cl (5), N (6) ... to list only a few. In particular, the recombination of hydrogen atoms on glass surfaces has been studied by a number of workers (7–11).

Several common features in the reports of these studies can be noted. There is unanimity in the acceptance of the fact that the recombination proceeds via surface adsorbed atoms, S–H.

The Rideal mechanism

[1] $$S + H(g) \rightarrow S{-}H$$

[2] $$S{-}H + H(g) \rightarrow S + H_2$$

is considered to predominate at moderate (−100 to 200 °C) temperatures. The observed activation energy and the observed first order gas phase atom dependence of the reaction result if reaction 2 is the rate determining step.

The Hinshelwood mechanism

[1] $$S + H(g) \rightarrow S{-}H$$

[3] $$2S{-}H \rightarrow 2S + H_2$$

which requires either close proximity or mobility of the adsorbed atoms, would be most evident at extremes of low temperatures (high S—H concentration) and again at high temperatures (greater S—H mobility).

For the Hinshelwood mechanism to be operative at low temperatures with relatively low S—H concentration would require rather weakly adsorbed H atoms as opposed to the strongly adsorbed atoms which only achieve mobility at elevated temperatures.

Can. J. Chem. Downloaded from www.nrcresearchpress.com by 210.87.254.42 on 09/05/12
For personal use only.

Can. J. Chem. Downloaded from www.nrcresearchpress.com by 210.87.254.42 on 09/05/12
For personal use only.

TABLE 1. Glasses, pretreatment of porous Vycor: 300 mm O_2, 500 °C, 2 h

Glass	Treatment	Area (m^2/g)
PV-OH	Evacuate, 800 °C, 4-6 h	145
PV-Cl	PV-OH + 100 mm CCl_4, 450 °C, 4-6 h	115
PV-F	PV-OH + 300 mm CF_4, 650 °C, 4-6 h	120
PV-OCH_3	PV-OH + 100 mm $B(OCH_3)_3$, 25 °C, 30 min	100
PV-H_2O	PV-OH + adsorbed H_2O monolayer coverage	130*
Fused silica	Quartz sample tube, evacuate, 800 °C, 2 h	2 cm^2 in cavity

*Inconsistent area determinations, average quoted.

These two types of adsorbed atoms are used by Wood and Wise (11) in qualitative calculations over a wide range of temperatures.

The existence of these two types of atoms is substantiated by Johnson (7) and, most notably, by Hickmott (10) who assigns adsorptive bond strengths of 25 and 6.6 kcal/mol for the strongly, chemisorbed atoms and the weakly, physically adsorbed atoms, respectively.

A further common feature of the experimental studies to date is that all have been conducted by observation of gas phase phenomena ... pressure changes on adsorption or desorption (7, 8, 10) and gas phase atom decay in flow systems (9, 11). No studies have been conducted by observation of the surface adsorbed state or of the surface itself.

This work undertakes such a study under conditions where the low temperature Hinshelwood mechanism may be observed. The study of the surface adsorbed atoms and their reactions is made possible by their definitive unpaired electron which allows observation by electron spin resonance.

Experimental

Porous Vycor glass (Corning Code #7930) and fused silica were used as the adsorptive surfaces. The surface of the porous Vycor was chemically altered, with resulting changes in specific surface area as outlined in Table 1. Hydrogen atoms were generated for the fused silica study by a 2450 MHz electrodeless discharge in purified H_2 directly in the sample tube. The discharge was maintained about 10 cm above the sample region which was immersed in liquid nitrogen. The H atoms diffused down the tube and were adsorbed on the cold walls.

For the study of porous Vycor the atoms were produced by the ultraviolet photolysis of hydrogen iodide adsorbed on the Vycor samples. The photolyzing radiation was passed through a 2 mm Vycor glass filter and focused on the sample in a 3 mm i.d. quartz sample tube. The photolysis was conducted with the sample immersed in liquid nitrogen in an unsilvered quartz Dewar. The sample tube also contained 10 to 20 Torr pressure of He to prevent desorption of the HI upon cooling in liquid nitrogen and to conduct the photolysis heat away.

The treatment and i.r. absorption of porous Vycor surfaces has recently been reviewed by Hair (13). Table 1 summarizes the experimental procedures followed in preparing the glass surfaces together with pertinent information regarding surface area. The complete replacement of the surface hydroxyl groups was established by the infrared absorption spectra of the porous Vycor samples (13). Surface areas were determined from a B.E.T. adsorption isotherm for N_2 at 77 °K. The porous Vycor samples were prepared and treated on a mercury-free vacuum system and could be connected to the system while in the e.s.r. cavity.

The e.s.r. observations were conducted with a Varian E-3, electron spin resonance spectrometer, with an auxiliary 5 in. strip chart recorder.

Optimum machine parameters for observation of the H atom signal were established at the beginning of the study and, other than amplifier gain, remained constant throughout. The microwave power used, generally 2 mW, was about 80% of the observed signal saturation power, and the modulation amplitude was set at 250 mG (approximately half the observed line-width). The automatic repetitive scan facility of the spectrometer was utilized to record the time variation of the spectrum on the strip chart recorder. The spectrum was scanned through ± 5 G about the high-field line of the H atom doublet. Spectra could be simultaneously recorded on the flat-bed recorder of the instrument for peak-height/area correlations.

Kinetic studies were conducted using liquid nitrogen (-196 °C.), liquid argon (-185° C), and liquid methane (-161 °C) successively in the same e.s.r. cavity Dewar, progressively decaying a given H atom generation at higher and higher temperatures.

Results and Discussion

The observed e.s.r. spectrum (Fig. 1) consisted of two absorption peaks centered about $g = 2.0130$ and separated by 507.5 ± 0.5 G, derivative peak-to-peak line-width $= 475 \pm 50$ mG. These observations are consistent with the spectrum for a relatively unperturbed, ground state H atom and have been noted previously (14, 15). The central, $g = 2$ region of the spectra consisted of several peaks attributable to paramagnetic impurities and glass damage centers in the Dewar and sample system, and other paramagnetic fragments from the HI photolysis. Interest was directed to the high-field peak of the H atom doublet and little attention paid to the central region, except to note that the $g = 2$ spectrum varied from surface to surface.

When observed for an extended period, under stable operating conditions, the H atom

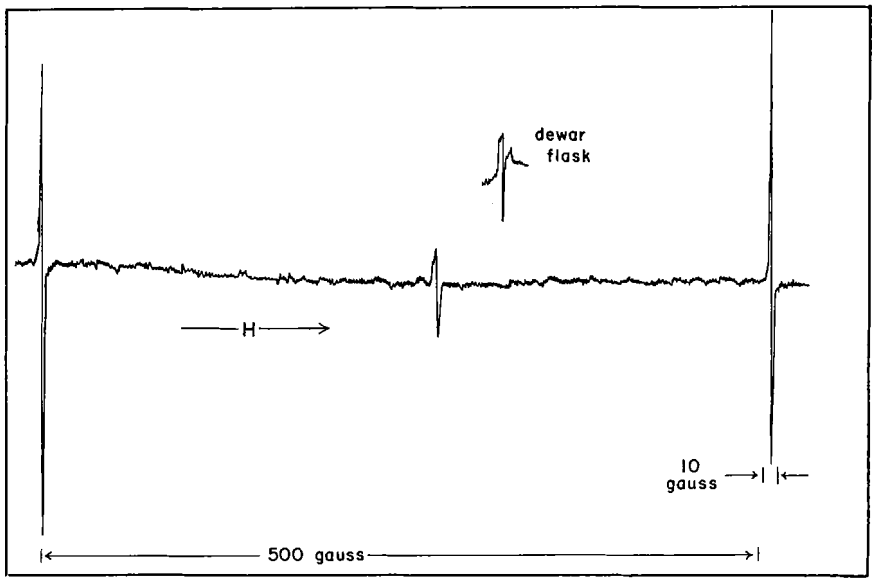

FIG. 1. Electron spin resonance spectrum of H atoms adsorbed on fused silica at 77 °K.

signal was found to decay even at liquid nitrogen temperatures, in direct conflict with the report of Pariiskii and Kazanskii (14). Figure 2 presents a plot of the H atom signal decay at the three temperatures used in this study.

In Fig. 2 it can be seen that in each case the signal does not disappear completely, but rather decays to some finite "steady state" value. (The terminology "steady state" is not meant to imply that there exists a simultaneous atom decay and production. Rather it refers to a constant concentration of non-decayable atoms.) Both the decay rate and the steady state achieved can be seen to be temperature dependent. A study of the atom decay must then be a study of the decayable atoms calculable from $S - H_{ss}$, where S is the total e.s.r. signal and H_{ss} (obtained by extrapolation) is the portion of S attributed to H_{ss} atoms which do not decay at the specified temperatures.

Order determinations showed the decay to be second order in decayable atoms as is evidenced by the second order plot of Fig. 3. The value of the rate constant, k_{obs}, from such plots is in arbitrary chart scale units which are, nonetheless, internally consistent and allow calculation of activation energies.

In the Arrhenius plot of Fig. 4, the k_{obs} data, still in arbitrary units, has been normalized to account for differences in the peak-height/area ratios and differences in scan speeds at the various temperatures. The activation energies thus obtained for the various surfaces are summarized in Table 2 as E_a.

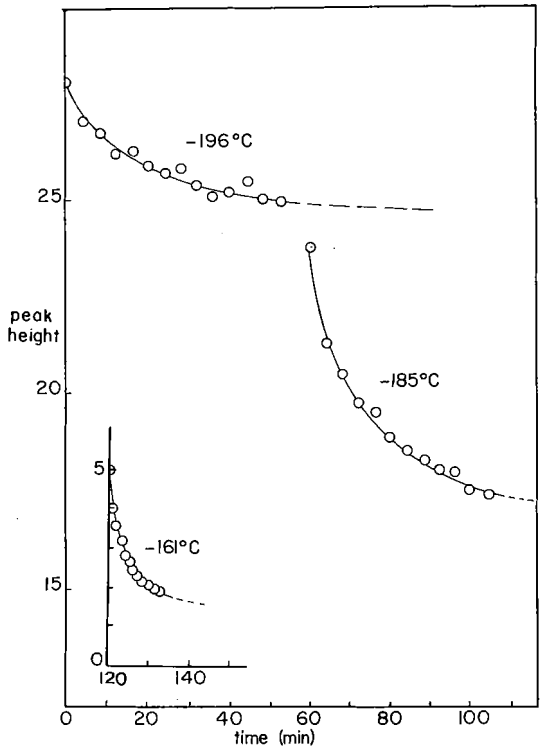

FIG. 2. Decay of H atoms adsorbed on hydroxylated porous Vycor.

Can. J. Chem. Downloaded from www.nrcresearchpress.com by 210.87.254.42 on 09/05/12
For personal use only.

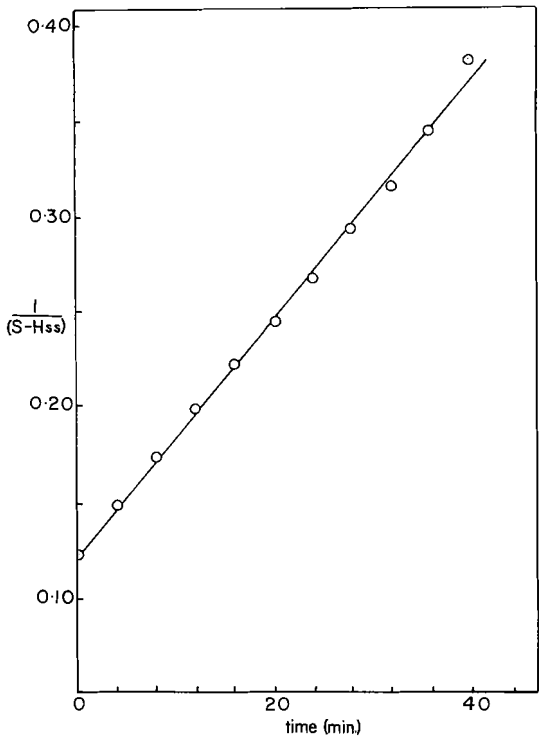

FIG. 3. Second order kinetic plot of decayable adsorbed H atoms (−185 °C decay of Fig. 2).

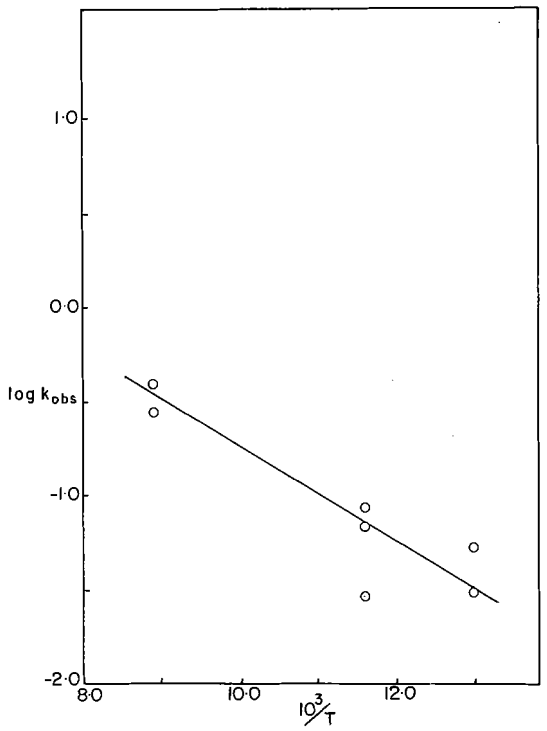

FIG. 4. Arrhenius plot of H atom decay on hydroxylated porous Vycor, PV_{OH}.

The observed temperature dependence of H_{ss} can be related to the decreased adsorption of H_{ss} atoms at successively higher temperatures. A plot of log H_{ss} against $1/T$ is presented in Fig. 5, from which it is possible to determine the heat of adsorption relative to the mobile, decayable atoms. This heat of adsorption data is presented in Table 2 as E_{ss}.

In the course of this study it was noted that the addition of O_2 to the surface adsorbed H atom systems resulted in an increase in the H atom e.s.r. signal. This was previously reported by Pariiskii and Kazanskii (14) who attributed the signal increase to the removal of signal saturation by paramagnetic O_2. Similar enhancement of e.s.r. signals by O_2 addition has been reported (16, 17). More recently (18), it has been shown that the H atom yield from irradiated 1 $M H_2SO_4$ at 77 °K is considerably higher when the matrix is prepared from O_2 saturated solutions than when N_2 saturated. This has been explained by an effective decrease in the relaxation time of the H atom by paramagnetic oxygen.

With an excess of O_2 present the H atom e.s.r. lines were broadened (to about 900 mG) as would be expected for a random perturbation of the resonant magnetic field by a paramagnetic species. The similar addition of He, Ar, N_2, and NO had no such effect. The absence of line broadening by NO or change in spin–lattice relaxation of the H atoms may be explained by the formation of dimeric diamagnetic $(NO)_2$ when NO is adsorbed on some surfaces (19, 20).

Upon evacuation and removal of excess O_2, the H atom signal returned to its former (475 mG) line-width and peak-height/area ratio but retained much of its increased peak-height.

With excess O_2 present several lines were observed in various regions of the e.s.r. spectrum. Upon evacuation these all disappeared except for one peak (now much reduced in size) at $g = 1.9742$ which is attributed to a small amount of residual O_2. The concentration of this residual O_2 is insufficient (or its location inappropriate) to significantly perturb the H atom spectrum or its decay but

Can. J. Chem. Downloaded from www.nrcresearchpress.com by 210.87.254.42 on 09/05/12
For personal use only.

TABLE 2. Decay and adsorption energies for adsorbed H-atoms on various surfaces

Glass	Decay E_a (kcal/mol)	E_{ss} (kcal/mol)	Signal increase with O_2 (%)	k, 77 °K (cm^2/atom s)
PV-OH	1.0	1.6	50–100	1.8×10^{-12}
PV-F	1.7	1.7	50–100	8.2×10^{-13}
PV-Cl	2.0	1.6	50–100	1.9×10^{-12}
PV-OCH_3	2.3	1.7	50–100	1.3×10^{-13}
PV-H_2O	1.9*	1.6	5–10	8.2×10^{-13}
Fused silica	2.0*	1.6*	5–10	1.3×10^{-17}

*Kinetic plots curved.

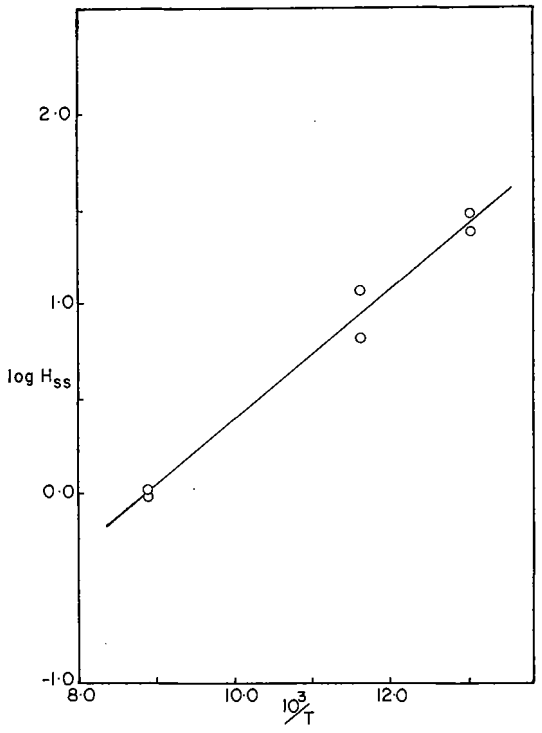

FIG. 5. log H_{ss} against $10^3/T$ for H atoms on PV_{OH}.

is sufficient to affect the relaxation time of the H atom.

The results of this work are consistent with the earlier observations of Johnson (7) and Langmuir (8) and, more recently, that of Hickmott (10) who studied the adsorption and desorption of H atoms. In Hickmott's paper two types of atoms were noted; in his notation these were subscripted "L" for atoms desorbed (pressure recovered) between 77 and 300 °K, and "R" for those desorbed above room temperature. He calculated heats of adsorption of 6.6 and 25 kcal/mol, respectively, consistent with physical and chemical adsorption.

The present study indicates that the weakly bound atoms can be further subdivided as "H" and "H_{ss}" due to adsorption at different physical adsorption sites. E_a, the decay activation energy is variable from glass to glass (Table 2) and would result from adsorption at the chemically altered surface sites. E_{ss}, on the other hand, is constant (± 0.1 kcal/mol) for all the surfaces studied and must result from adsorption at some common surface site.

In the chemical treatment of the porous Vycor all samples started from clean, hydroxylated porous Vycor achieved by evacuation at 800 °C. These conditions not only remove all surface adsorbed contaminants but progressively dehydrate vicinal surface hydroxyl groups, as is evidenced by the narrowing of the infrared adsorption peaks (21). This introduces siloxane bridge structures, $\gtrless$Si—O—Si$\lessgtr$ unaffected by subsequent displacement of the remaining hydroxyl groups. These siloxane bridge sites are thus retained as a common feature of all the glasses (and must also exist at the fused silica surface) and H_{ss} is identified with such sites.

A kinetic scheme can be presented which is consistent with the experimental observations. This is

[4,5] $\quad H \rightleftharpoons H_{ss}$

[6] $\quad H + H \rightarrow H_2$

in which it is to be noted that both H and H_{ss} are surface adsorbed atoms. H is a mobile adsorbed atom. H_{ss} exists as a constant (though temperature dependent) concentration of adsorbed, immobile atoms which are unreactive with H due to their stronger surface adsorptive bond.

E_a is then identifiable with reaction 6 and E_{ss} with reaction 5. Reaction 4, if occurring,

Can. J. Chem. Downloaded from www.nrcresearchpress.com by 210.87.254.42 on 09/05/12
For personal use only.

Can. J. Chem. Downloaded from www.nrcresearchpress.com by 210.87.254.42 on 09/05/12
For personal use only.

would have a very low activation energy and would proceed unobserved.

The existence of an atom decay even at 77 °K, and the observed second order kinetics are both in conflict with the results of Pariiskii and Kazanskii (14) who report no decay at liquid nitrogen temperatures and first order kinetics at higher temperatures. This is probably due to the different technique and the different surface they used. They calculate an activation energy of 2.1 kcal/mol which is not inconsistent with our $E_{ss} = 1.6$ kcal/mol and which may actually be some combination of our E_{ss} and E_a. A further complication (and one which would enhance their first order decay) is the possible reaction between H atoms and paramagnetic glass defects which are a prominent feature of the $g = 2$ region of their published e.s.r. spectra.

In this study, since the primary atom production process has ceased, only reaction 3, the rate determining step of the Hinshelwood mechanism, can be operative and our results may be compared with the Wood and Wise (11) calculations if the adsorbed atom concentrations are known.

By comparison of the H atom e.s.r. signal to that of a standard diphenyl picryl hydrazil sample under identical operating conditions it was possible to establish that there were of the order of 10^{14} to 10^{15} adsorbed atoms in the e.s.r. cavity. In the case of the fused silica this corresponds to a surface atom concentration of about 10^{14} atoms/cm^2, in good agreement with the figure of 10^{15} atoms/cm^2 as calculated by Johnson (7) and others (8, 10). In the case of the porous Vycor samples, due to the large surface area, the concentration was lower by a factor of 10^4.

Wood and Wise (11), in their table of calculated rates of elementary processes of hydrogen atom recombination on glass, quote a value of 7×10^{15} atoms/cm^2 s for the rate of reaction 6 at 77 °K. If we assume a surface saturated with adsorbed hydrogen atoms (at 10^{15} atoms/cm^2) the second order rate constant, k, can be calculated as 7×10^{-15} cm^2/atom s. Calculation of an equivalent rate constant from our results for fused silica gives $k = 1.3 \times 10^{-17}$ cm^2/atom s or, with a "roughness factor" of 10 (22), $k = 1.3 \times 10^{-15}$ cm^2/atom s. Values of this rate constant for the other surfaces are of the order of 10^{-12} cm^2/atom s as presented in Table 2.

In the Wood and Wise calculations for Pyrex an activation energy of 0.75 kcal/mol is used which compares favorably with our value of 1.0 kcal/mol for hydroxylated porous Vycor which, due to its high surface boron content (21*a*, 23), may be presumed to resemble Pyrex.

The disagreement between the Wood and Wise rate constant and our values for the porous Vycor systems can be ascribed to the physical difference in the surfaces. Wood and Wise's Pyrex and our fused silica (for which the rate constants are comparable) are both essentially smooth surfaces. The porous glass surfaces, on the other hand, are tortuously convoluted and may allow adsorbed atom encounters in the third dimension, normal to the surface. The effective atom concentration available for the recombination reaction is thus larger and would result in the larger rate constant which was calculated assuming only two-dimensional, surface encounters. The magnitude of this effect is incalculable though; in the extreme, it could double the effective atom concentration and the observed rate constant would be larger by a factor of four.

A more likely explanation of the discrepancy is that not all of the surface of the porous Vycor sample was being used. The original HI would adsorb preferentially at the first site encountered ... the outer areas of porous Vycor sample. The interior regions and deep pore would not be covered by HI nor subsequently by H atoms.

These discrepancies or uncertainties cannot, however, greatly affect the activation energies determined for these samples. As can be seen from the data in Tables 1 and 2 there is no correlation between specific surface area and activation energy, nor would any be expected if only some fraction of the surface is utilized. These activation energies should, if our assignment of the H atom adsorption site is correct, correlate with some physical or chemical property of the glass surface such as the electronegativity of the surface adsorption site.

While the electronegativity of atoms in simple molecules can be found in virtually any elementary textbook, the electronegativities of polyatomic, or even simple monatomic functional groups as part of a larger structure are not as easily determined. Sanderson (24)

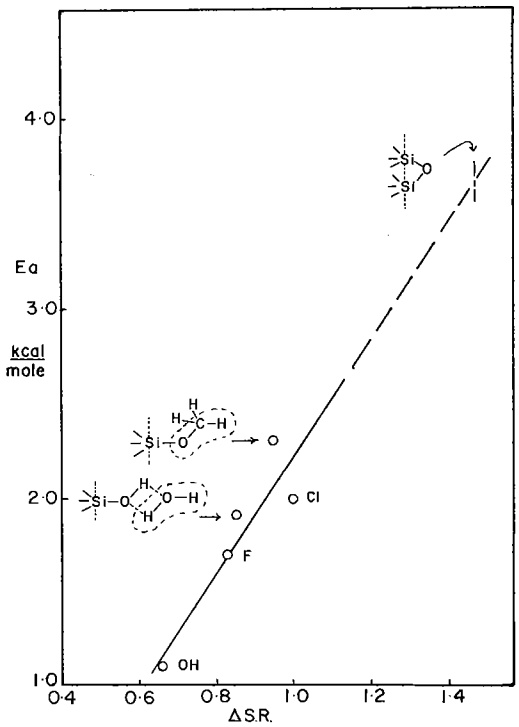

FIG. 6. Plot of the decay activation energy E_a against ΔS.R., the stability ratio difference between the adsorbed H atoms and the surface functional groups.

proposes an electronegativity function, the stability ratio (S.R.) defined as "the ratio of the average electronic density to that of a hypothetical isoelectronic inert element". For atoms and simple molecules there is a linear relationship between Sanderson's S.R. and the more conventional electronegativity scales. In the reference cited Sanderson outlines methods by which the S.R. of molecular fragments may be determined.

Figure 6 presents a plot of the observed activation energies and the S.R. difference ($S.R._H - S.R._{surface}$) for the various glasses studied. The calculation of the S.R. values for $\geq$Si—O—H, $\geq$Si—Cl and $\geq$Si—F are fairly straightforward; however, in the case of $\geq$Si—O—CH_3 and $\geq$Si—OH.H_2O some question exists regarding the exact identity of the effective adsorption site. By judicious choice of a reasonable atomic grouping (outlined in Fig. 6), excellent correlation may be realized.

Also shown in Fig. 6 is the S.R. difference for the siloxane bridge structure, the proposed adsorption site for H_{ss}. Its location would predict an activation energy of 3.6 kcal/mol for a recombination reaction but an activation energy of, very approximately, 1.6 kcal/mol (3.6 − approx. 2.0) for reaction 5. This figure varies slightly from glass to glass but corresponds well to E_{ss} (1.6–1.7 kcal/mol) obtained from the temperature dependence of H_{ss}.

It should be noted too, that the calculated S.R. values are all less than that for the adsorbed H atom, *i.e.*, the H atom is more electronegative than its adsorption site. The increased electron density about the H atom should, therefore be evident from the hyperfine splitting of the H atom doublet in the e.s.r. spectra.

Careful measurement of the splitting showed it to be slightly larger (0.7%) than both the theoretical and the observed splitting for gas phase atoms. The effect was observed for all glasses though no correlation of the magnitude of the effect with glass surface could be observed.

These results substantiate the arguments of Wood and Wise and others regarding the nature of the surface adsorbed species and the relative predominance of the Hinshelwood mechanisms in surface recombination at low temperatures.

This work was supported by the Directorate of Chemical Sciences, U.S. Air Force Office of Scientific Research, Grant No. AF-AFOSR 642-66 and by the National Research Council of Canada.

1. R. W. WOOD. Proc. Roy. Soc. **97**, 455 (1920).
2. B. A. THRUSH. Progress in reaction kinetics. Vol. III. Pergamon Press.
3. F. KAUFMAN. Progress in reaction kinetics. Vol. I. Pergamon Press.
4. D. J. WILLIAMS and M. F. R. MULCAHAY. Aust. J. Chem. **19**, 2163 (1966).
5. L. W. BADER and E. A. ORGYZLO. Nature, **201**, 491 (1964).
6. J. T. HERRON, J. L. FRANKLIN, P. BRADT, and V. H. DIBLLER. J. Chem. Phys. **30**, 879 (1959).
7. M. C. JOHNSON. Proc. Roy. Soc. **123**, 603 (1929); Proc. Roy. Soc. **42**, 490 (1930): Trans. Faraday Soc. **28**, 162 (1932).
8. I. LANGMUIR. J. Am. Chem. Soc. **34**, 1310 (1932); J. Chem. Soc. 511 (1940).
9. W. V. SMITH. J. Chem. Phys. **11**, 110 (1943).
10. T. W. HICKMOTT. J. Appl. Phys. **31**, 128 (1960).
11. B. J. WOOD and H. WISE. J. Phys. Chem. **66**, 1049 (1962).

Can. J. Chem. Downloaded from www.nrcresearchpress.com by 210.87.254.42 on 09/05/12
For personal use only.

12. K. E. SHULER and K. J. LAIDLER. J. Chem. Phys. **17**, 1212 (1949).
13. M. L. HAIR. Infrared spectroscopy in surface chemistry. Marcel Dekker, Inc., New York. 1967.
14. G. V. PARIISKII and V. B. KAZANSKII. Kinet. Katal. **5**, 96 (1964).
15. C. K. JEN, S. N. FONER, E. L. COCHRAN, and V. A. BOWERS. Phys. Rev. **112**, 1169 (1958).
16. R. B. INGALLS and G. A. PEARSON. Anal. Chim. Acta, **25**, 566 (1961).
17. A. J. SARACENS and N. D. COGGESHALL. J. Chem. Phys. **34**, 260 (1961).
18. D. E. HOLMES, N. B. NAZHAT, and J. J. WEISS. Z. Naturforsch. **24**a, 481 (1969).
19. A. LUBEZKY and M. FOLMAN. Trans. Faraday Soc. **67**, 1 (1971).
20. C. L. GARDNER and M. A. WEINBERGER. Can. J. Chem. **48**, 1317 (1970).
21. M. J. D. LOW and N. RAMASUBRAMANIAN. (*a*) J. Phys. Chem. **70**, 2740 (1966); (*b*) J. Phys. Chem. **71**, 730 (1967).
22. P. A. SEWELL. Glass Tech. **8**, 108 (1967).
23. M. L. HAIR and I. D. CHAPMAN. J. Am. Ceram. Soc. **49**, 651 (1966).
24. R. T. SANDERSON. Chemical periodicity. Reinhold Publishing Corp., New York. 1960.

Can. J. Chem. Downloaded from www.nrcresearchpress.com by 210.87.254.42 on 09/05/12
For personal use only.

The Triplet State of Ketene

JOHN S. E. MCINTOSH[1] AND GERALD B. PORTER

Department of Chemistry, University of British Columbia, Vancouver 8, British Columbia

Received October 28, 1971[2]

Ketene quenches the phosphorescence of both biacetyl and hexafluoroacetone. Although the quenching of hexafluoroacetone emission is nearly collision-controlled, that of biacetyl is much less efficient. The large difference in the rate constants is attributed to endothermic energy transfer from triplet biacetyl to ketene and exothermic energy transfer from triplet HFA to ketene. From the endothermicity, the lowest triplet state of ketene is estimated to be at 61 ± 1 kcal/mol above its ground state. No sensitized photodecomposition of ketene occurs as a result of energy transfer from either biacetyl or hexafluoroacetone.

Le cétène arrête la phosphorescence du biacétyle et de l'hexafluoroacétone. Bien que l'extinction de l'émission de l'hexafluoroacétone est pratiquement contrôlée par la collision celle du biacétyle est nettement moins efficace. La grande différence dans les constantes de vitesse est attribuée au transfert d'énergie endothermique du biacétyle triplet au cétène et au transfert d'énergie exothermique du HFA triplet au cétène. A partir de l'endothermicité, l'état triplet le plus bas pour le cétène est évalué à 61 ± 1 kcal/mol au dessus de son état fondamental. Il n'y a pas de photodécomposition sensibilisée du cétène résultant du transfert d'énergie soit du biacétyle soit de l'hexafluoroacétone.

Canadian Journal of Chemistry, **50**, 2313 (1972)

Can. J. Chem. Downloaded from www.nrcresearchpress.com by 210.87.254.40 on 09/05/12
For personal use only.

It is now well established that both singlet and triplet state methylene radicals are produced in the primary photodissociation of ketene (1–5). The fraction of the methylenes formed in the triplet state increases as the wavelength of irradiation is increased (2) and the primary quantum yield decreases, becoming strongly pressure dependent at 366 nm (6).

If the dissociation obeys a spin correlation rule, and there is no reason it should not, the methylenes would arise from the corresponding excited singlet and triplet states of ketene itself (2). However, because no emission has ever been detected from ketene, little is known about the lowest lying singlet and triplet excited states. Dixon and Kirby (7), in a study of the visible and u.v. absorption spectrum of ketene, concluded that two electronic transitions can be seen. They assigned the origin of the *triplet* state as the observed onset of absorption, at *ca.* 61 kcal/mol. In a recent reinvestigation, Laufer and Keller (8) disagreed with Dixon and Kirby and suggested that only one transition is observed, the lowest singlet–singlet absorption. They therefore set an upper limit to the *singlet* state origin as 61 kcal/mol and located the triplet origin at about 55 kcal/mol on the basis of a "normal" singlet–triplet splitting.

The decomposition of ketene can be sensitized by the triplet states of mercury (9) and benzene (10). The fraction of the methylenes then formed in the triplet state is large, which implies that the triplet state of ketene has been formed by energy transfer. In an attempt to locate the triplet state of ketene, Grossman, Semeluk, and Unger (11) tried to sensitize the emission of biacetyl with ketene as donor. Their lack of success can best be interpreted as meaning that the triplet state of ketene is simply too short-lived for such energy transfer to compete with degradation. However, their data do show evidence for energy transfer *from* biacetyl *to* ketene.

We have reinvestigated energy transfer reactions involving ketene, using biacetyl and hexafluoroacetone (HFA) as donors. The results suggest a value for the energy of the ketene triplet state and have important implications about the mechanism of the photochemistry of ketene.

Experimental

Ketene, prepared by the method of Fisher, McLean, and Schnizer (12), was purified by vacuum distillation. Biacetyl (Eastman White Label) was distilled twice and the middle third of each run was retained. Gas chromatographic analysis showed no detectable methane, ethane, or ethylene impurities (less than 1 p.p.m.) in either the biacetyl or the ketene. Both were stored in the dark at -196 °C and were degassed immediately prior to use.

[1]Present address: Cariboo College, P.O. Box 860, Kamloops, British Columbia.

[2]Revision received May 1, 1972.

Can. J. Chem. Downloaded from www.nrcresearchpress.com by 210.87.254.40 on 09/05/12
For personal use only.

HFA, supplied by Dupont, was purified and handled as previously described (13). Hexafluoroethane (Matheson) was degassed at −196 °C by distillation, followed by distillation through a LeRoy–Ward still. The fraction collected at −130 °C was retained.

A completely mercury-free vacuum system was used for all of the experiments. Pressures greater than 10 Torr were measured directly with a calibrated glass spiral gauge. Lower pressures were obtained by expansion into calibrated vessels on the vacuum line. Greaseless metal or glass/Teflon stopcocks were used exclusively on the cells, the expansion vessels, and the ketene storage vessel.

Photolyses were carried out in a 5 cm path Pyrex cell with silica windows attached with epoxy resin. A 1 cm square cuvette was used for both lifetime and steady-state emission measurements. Each of the cells was attached to a magnetically driven glass mixing chamber, which allowed gases to be circulated through the irradiated zones of the cells. A 5 min mixing time was found adequate to ensure a completely homogeneous sample at all pressures used. The volumes of the photolysis and emission systems were 94.3 and 124.9 ml, respectively.

For both photolysis and steady-state emission, the excitation source was a PEK 100 W mercury arc with a Bausch & Lomb u.v. grating monochromator (plus a Corning 7-54 filter for excitation below 400 nm). An RCA 935 phototube, calibrated against the ferrioxalate actinometer, was used to monitor the amount of light absorbed. The technique required to detect and record the emission spectra has been described (13).

Phosphorescence lifetime measurements were made with an argon-filled coaxial capillary flash lamp operated at 4–5 kV. This lamp dissipates 16 to 25 J and has a peak rise time of 3 μs and a half-width of 8 μs. The light was focused at the center of the 1 cm cuvette. Phosphorescence decay from the sample was detected at 90° to the pump light beam with an RCA 1P28 photomultiplier fixed to the exit slit of a Bausch & Lomb visible grating monochromator. The photomultiplier output was displayed on a Tetronix 543B oscilloscope. Correction for scattered light was made by condensing the contents of the cell in a side arm or by evacuating the cell completely.

Analyses were done with an Aerograph Hy-Fi gas chromatograph with a flame ionization detector on a 3 m by 3 mm silica gel column at 25 °C. This column could resolve hydrocarbons up to C_4.

The pressures used with ketene–biacetyl mixtures were high enough to be measured directly with the spiral gauge. The components were then condensed into the reaction vessel and mixed.

For lifetime measurements on the ketene–HFA system, it was necessary to prepare mixtures containing only very small amounts of ketene. At the same time it was not possible to condense the two compounds together.[3] The following procedure was used: the cell and an external cold finger were filled with HFA to the desired pressure. Then the HFA was condensed into the cold finger and isolated while ketene was added to the cell using the expansion volumes to attain the necessary low pressures. The HFA in the cold finger was then vaporized completely and expanded into the cell, where the contents were thoroughly mixed. After a lifetime measurement had been completed, either the cell was evacuated for the next run or the contents of the cell were further diluted with HFA (but no more than once) for another measurement. All experiments were carried out at the ambient temperature, 25 ± 1 °C.

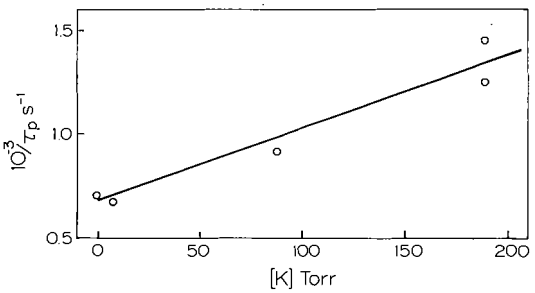

FIG. 1. Lifetime of biacetyl phosphorescence decay in the presence of ketene, with 40 Torr of biacetyl, at 25 °C and excitation at $\lambda > 400$ nm.

Results

Ketene–Biacetyl Mixtures

Lifetime Measurements

For biacetyl excitation, light from the flash lamp was filtered with a Corning 3-75 filter, which is totally absorbing below 370 nm. Therefore only biacetyl was excited directly, and then primarily at wavelengths longer than 400 nm. From the work of Grossman, Semeluk, and Unger (11), it was expected that a relatively high pressure of ketene would be needed to obtain effective quenching. It was first verified, however, that the phosphorescence decay of biacetyl (40 Torr) is unchanged by the addition of 300 Torr of hexafluoroethane as an inert pressurizer.

The effect of ketene on the phosphorescence lifetime of biacetyl is shown in Fig. 1. The quenching rate constant obtained from the least-squares slope is $6.4 \times 10^4\ M^{-1}\ s^{-1}$. This value agrees with that calculated from the data of Grossman *et al.* (11): $k_q = 3$ to $11 \times 10^4\ M^{-1}\ s^{-1}$.

[3]Ketene and HFA have been reported to react in ether solution at −78 °C to form a β-lactone (14). Therefore their compatibility was tested by following the room temperature u.v. absorption spectrum of a mixture of 100 Torr of HFA and 50 Torr of ketene. A slow dark reaction was observed in the gas phase: about 8% of the ketene disappeared over a 2 h period. The reaction was considerably faster when the two were condensed together, presumably occurring during the short interval in which they formed a liquid mixture. At high ketene concentrations, a yellow tar formed in the cold finger where they had been condensed. So long as the two compounds were mixed only in the gas phase and the run times kept short, this reaction between HFA and ketene could be neglected.

Can. J. Chem. Downloaded from www.nrcresearchpress.com by 210.87.254.40 on 09/05/12
For personal use only.

Steady-state Measurements

The phosphorescence and fluorescence yields of biacetyl are known to be independent of total pressure above 5 Torr when excitation is at either 436 or 405 nm (15, 16). As an additional check, the relative quantum yields of phosphorescence and of fluorescence were measured at these two wavelengths with and without 300 Torr of hexafluoroethane. No effect on the quantum yields could be found. However, when 300 Torr of ketene was added to 40 Torr of biacetyl, the phosphorescence yield decreased by a factor of 1.6, in agreement with the lifetime decrease. Ketene at this pressure had no measurable effect on the fluorescence yield of biacetyl.

Photolysis

Biacetyl (25 Torr) and biacetyl–ketene mixtures (25 and 200 Torr, respectively) were irradiated at 436 nm ($I_a = 5 \times 10^{-9}$ einstein s^{-1} cm^{-2}). The only products were small amounts of ethane and methane (carbon monoxide was not measured) from the decomposition of biacetyl. That no ethylene could be detected[4] implies that less than 10^{-10} mol of ethylene was produced and that the quantum yield for ethylene formation was less than 4×10^{-5}.

Ketene–HFA Mixtures

Lifetime Measurements

The flash lamp was used without filters because the first absorption bands of ketene and HFA overlap. As only a small quantity of ketene was present in these experiments, direct absorption by ketene was negligible. The effect of ketene on the lifetime of the triplet state of HFA is shown in Fig. 2. The slope of the line is 8.5×10^9 M^{-1} s^{-1}.

Steady-state Measurements

It was established that with 10 to 50 Torr of ketene added to 600 Torr of HFA, and with 313 nm irradiation, the phosphorescence of HFA was completely quenched but the fluorescence was unaffected.

Photolysis

Mixtures containing 100 Torr of HFA and 2 Torr of ketene were irradiated at 334 nm. This exciting wavelength was chosen to minimize the photochemical dissociation of either HFA itself or of ketene as a result of direct absorption of radiation. At this ketene pressure, however, the phosphorescence of HFA is completely quenched. The only hydrocarbon product detected was a trace of ethylene (7.7×10^{-10} mol). Neither CO nor C_2F_6 were measured quantitatively.

In none of these experiments was any luminescence detected that could be attributed to ketene, either with direct excitation or by sensitization.

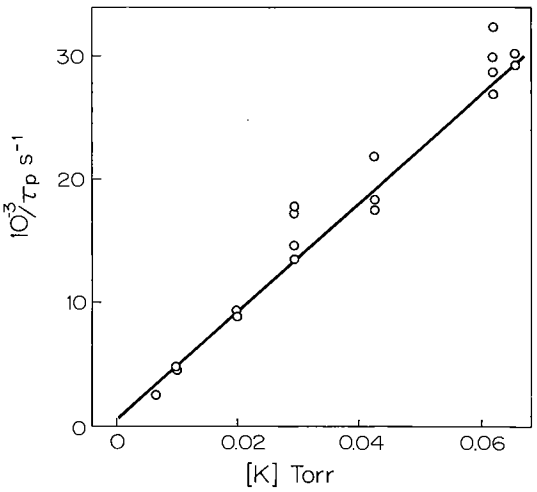

FIG. 2. Lifetime of hexafluoroacetone phosphorescence decay in the presence of ketene, with 100 Torr of HFA, at 25 °C and excitation with unfiltered flash lamp.

Discussion

The quenching data for biacetyl–ketene and HFA–ketene mixtures must be interpreted as the result of energy transfer from an excited state of biacetyl or HFA to one of ketene. Only in this way can the enormous difference in the two rate constants be rationalized. Further, the energy transfer must involve only the triplet states of the two donors because the fluorescence yields of biacetyl and HFA are unaffected by the presence of ketene. By inference then, it is the triplet state of ketene which is populated in the energy transfer. That triplet state is itself too short-lived for either phosphorescence or energy transfer to be important processes in the degradation of excited triplet ketene.

As shown in Figs. 1 and 2, the lifetime data

[4]Biacetyl should have no major effect on the formation of ethylene from sensitized decomposition of the ketene.

fit a Stern–Volmer mechanism in the form

$$[1] \qquad 1/\tau = 1/\tau_0 + k_q[K]$$

The value of k_q for the HFA–ketene system is normal in the sense that it is about one order of magnitude less than the hard sphere collisional rate constant, and is comparable with values found in similar systems (13, 17). That k_q for the biacetyl–ketene system is over five orders of magnitude smaller still can be understood if the energy transfer from biacetyl to ketene is endothermic (18).[5]

On the basis that the triplet state of ketene lies higher than that of biacetyl by an energy ΔE, the ratio of the energy transfer rate constants k_q^B (from biacetyl to ketene) and k_q^K (from ketene to biacetyl) will be given by

$$[2] \qquad k_q^B/k_q^K = \exp(-\Delta E/RT)$$

This equation implies that the triplet state molecules of both ketene and biacetyl become thermodynamically equilibrated with the medium in every sense except that of electronic excitation. For our analysis it is essential that this be so for the biacetyl triplet state, but it need not be so for ketene. At the pressures used here, the lifetime of the triplet state of biacetyl is of the order of 1 ms, while the collision rate is *ca.* 10 ns. Internal equilibration of the biacetyl triplet state molecules is thus assured.

In order to apply eq. 2, it was necessary to have an estimate of k_q^K, which cannot be measured directly. We have therefore assumed that exothermic energy transfer processes in the gas phase will all have about the same rate constants, somewhat less than the hard sphere constant. We use then the value found here for transfer from HFA to ketene: 8.5×10^9 M^{-1} s^{-1}, for k_q^K. Substitution of the two rate constants in eq. 2 gives for ΔE the value 7 kcal/mol. This places the origin of the ketene triplet state at 61 kcal/mol. The estimate of k_q^K can hardly be in error by more than one order of magnitude, therefore ΔE should be reliable to within one kcal/mol.

[5]It is conceivable that the quenching of biacetyl phosphorescence is caused by an impurity in the ketene of low concentration but high efficiency. However, the pyrolysis of acetic anhydride (12) is so clean a reaction that such an impurity is quite unlikely.

We have not attempted to measure the temperature dependence of k_q^B itself. Direct measurements of this kind were reported recently by Jackson and Yarwood (19) for energy transfer processes with activation energies. Even though their data for the 2,3-pentanedione to acrolein energy transfer cover a 45° temperature range, the pre-exponential factor found exceeds the hard sphere bimolecular rate constant by about 10^3. If this difference does represent experimental error, as seems likely, the compensating error in the activation energy is 4.5 kcal/mol.

That E_T is 61 kcal/mol for ketene is in agreement with the conclusions of Dixon and Kirby (7), but not with those of Laufer and Keller (8). The latter have suggested that the spectrum reported by Dixon and Kirby as two overlapping transitions is in fact only one, the lowest singlet–singlet transition, with its origin at 61 kcal/mol. A spectral assignment of this type is, however, notoriously difficult when only diffuse spectra are available. Our data support the conclusion that the bands at the long wavelength end of the absorption spectrum do indeed represent the lowest singlet–triplet transition. The main absorption bands in the near ultraviolet with maximum intensity near 330 nm must be assigned to the lowest singlet–singlet transition simply on the basis of extinction coefficient and position.

A recent determination of the heat of formation of the methylene radical (20) leads to a bond dissociation energy for ketene: $D(CH_2{=}CO) =$ 80 kcal/mol, with triplet (ground) state methylene as one fragment. According to our assignment, the lowest triplet state of ketene lies 19 kcal/mol below the dissociation limit. With so large an energy barrier, triplet state ketene molecules which have been vibrationally equilibrated cannot be responsible for production of triplet methylene. This dissociation must occur from non-equilibrium vibronic levels of the triplet state formed by energy transfer in sensitization or by intersystem crossing in direct photolysis. Thus we find that neither biacetyl nor HFA can cause photodissociation of ketene by energy transfer, yet benzene, with $E_T = 85$ kcal/mol, and mercury, with $E_T = 113$ kcal/mol, both sensitize the dissociation of ketene (9, 10).

Can. J. Chem. Downloaded from www.nrcresearchpress.com by 210.87.254.40 on 09/05/12
For personal use only.

This work was made possible by the generous support of the National Research Council of Canada.

1. J. W. SIMONS and B. S. RABINOVITCH. J. Phys. Chem. **68**, 1322 (1964).
2. B. A. DEGRAFF and G. B. KISTIAKOWSKY. J. Phys. Chem. **71**, 3984 (1967).
3. G. B. KISTIAKOWSKY and T. A. WALTER. J. Phys. Chem. **72**, 3952 (1968).
4. A. N. STRACHAN and D. E. THORNTON. Can. J. Chem. **46**, 2353 (1968).
5. S.-Y. HO, I. UNGER, and W. A. NOYES, JR. J. Am. Chem. Soc. **87**, 2297 (1965).
6. G. A. TAYLOR and G. B. PORTER. J. Chem. Phys. **36**, 1353 (1962).
7. R. N. DIXON and G. H. KIRBY. Trans. Faraday Soc. **62**, 1406 (1966).
8. A. H. LAUFER and R. A. KELLER. J. Am. Chem. Soc. **93**, 61 (1971).
9. F. J. DUNCAN and R. J. CVETANOVIĆ. J. Am. Chem. Soc. **84**, 3593 (1962).
10. S.-Y. HO and W. A. NOYES, JR. J. Am. Chem. Soc. **89**, 5091 (1967).
11. M. GROSSMAN, G. P. SEMELUK, and I. UNGER. Can. J. Chem. **47**, 3079 (1969).
12. G. J. FISHER, H. F. MACLEAN, and A. W. SCHNIZER. J. Org. Chem. **18**, 1055 (1953).
13. J. S. E. MCINTOSH and G. B. PORTER. J. Chem. Phys. **48**, 5475 (1968).
14. I. L. KNUNYANTS and YU. A. CHEBURKOV. Acad. Sci. USSR, Div. of Chem. Sci. Engl. Trans. 604 (1960).
15. H. OKABE and W. A. NOYES, JR. J. Am. Chem. Soc. **79**, 801 (1957).
16. C. S. PARMENTER and H. M. POLAND. J. Chem. Phys. **51**, 1551 (1969).
17. J. HEICKLEN and W. A. NOYES, JR. J. Am. Chem. Soc. **81**, 3858 (1959).
18. R. E. REBBERT and P. AUSLOOS. J. Am. Chem. Soc. **87**, 5569 (1965).
19. A. W. JACKSON and A. J. YARWOOD. J. Am. Chem. Soc. **93**, 2801 (1971).
20. W. A. CHUPKA and C. LIFSHITZ. J. Chem. Phys. **48**, 1109 (1968).

Can. J. Chem. Downloaded from www.nrcresearchpress.com by 210.87.254.40 on 09/05/12
For personal use only.

Sterically Hindered Aromatic Compounds. IV. Solvolysis of *t*-Butyl-, Phenyl-, and Trialkyl-benzyl Chlorides in Ethanol–Water. Evidence for Steric Acceleration in 2,4,6-Tri-*t*-butylbenzyl Chloride

L. R. C. BARCLAY, H. R. SONAWANE,[1] AND J. C. HUDSON[2]

Department of Chemistry, Mount Allison University, Sackville, New Brunswick

Received March 7, 1972

The effect of *o*-, *m*-, and *p*-*t*-butyl and phenyl groups on solvolysis of the benzyl chlorides in 80% by volume ethanol–water was studied through conductometric rates and activation parameters. The rate constants for para- and meta-substituents were correlated by a Brown σ^+ plot indicative of an S_N1-type mechanism. Variations in ΔS^* can be rationalized in terms of differential solvation effects. Solvolysis data for the trialkylbenzyl chlorides-2,4,6-trimethyl-, 2,4,6-tri-*i*-propyl-, 2,4-di-*t*-butyl-6-methyl-, and 2,4,6-tri-*t*-butylbenzyl chloride indicated an unexpected high reactivity for the latter compound. The abrupt increase in ΔS^* for this compound is attributed to steric hindrance to solvation at the reaction site and steric acceleration is offered as an explanation for the unusual reactivity of this compound.

L'influence des groupes *o*, *m*, et *p*-*t*-butyle et phényle sur la solvolyse des chlorures de benzyle, dans un mélange à 80% en volume d'éthanol et d'eau, a été étudiée par les vitesses conductimétriques et par les paramètres d'activation: les constantes de vitesse pour les substituants para et méta ont été correlées par la courbe σ^+ de Brown indiquant un mécanisme de type S_N1. Les variations dans ΔS^* peuvent être expliquées par les effets différentiels de solvatation. Les données pour la solvolyse des chlorures de benzyles trialkylés; triméthyl-2,4,6, tri-isopropyl-2,4,6, di-*t*-butyl-2,4 méthyl-6 et tri-*t*-butyl-2,4,6 chlorure de benzyl, indiquent une grande réactivité inattendue pour le dernier composé. L'accroissement brusque de ΔS^* pour cette molécule est attribué à l'empêchement stérique à la solvatation du site réactionnel et l'accélération stérique est avancée pour expliquer la réactivité inhabituelle dans ce composé.

Canadian Journal of Chemistry, **50**, 2318 (1972)

Introduction

Two ortho *t*-butyl groups are known to exert remarkable *steric hindrance* to reactions of functional derivatives of benzene. In part III of this series, we reported an unexpected high chemical *reactivity* of 2,4,6-tri-*t*-butylbenzyl compounds (1). This included a facile insertion reaction into an ortho *t*-butyl group under acidic conditions. The present investigation was undertaken to explore quantitatively the effect of substituents on the reactivity of benzyl chlorides through measurements of solvolysis rates and activation parameters. The initial study was made on the effect of single bulky substituents-(phenyl and *t*-butyl) at *o*, *m*, and *p* positions on relative rates and activation parameters in ethanol–water solvolyses.

It was thought that kinetic data might lead to some explanation for the origin of the unusual chemical reactivity of 2,4,6-tri-*t*-butylbenzyl chloride. At the same time solvolysis data on this compound, with two bulky *t*-butyls shielding the benzylic carbon, could provide further insight into the phenomenon of specific solvation or solvent sorting in the region of the solute species (2).

With these objectives in mind, a comparative study was undertaken of the solvolytic behavior, including the activation parameters, of a series of 2,4,6-tri-alkylbenzyl chlorides, including 2,4,6-trimethyl-, 2,4,6-triisopropyl-, 2-methyl-4,6-di-*t*-butyl-, and 2,4,6-tri-*t*-butylbenzyl chloride.

Experimental

(a) General Procedures

Most of the substituted benzyl chlorides used are described in the literature. They were usually prepared from the corresponding benzyl alcohols by chlorination with thionyl chloride; either alone or in carbon tetrachloride solution. The excess reagent was distilled and the benzyl chlorides purified by chromatography in petroleum ether solvent on silica gel columns. The compounds were further purified by vacuum distillation or crystallization and vacuum sublimation. The purity of the chlorides was checked by gas chromatography on a F and M-700

[1]Postdoctorate Fellow, on leave of absence from the National Chemical Laboratory, Poona, India.

[2]Recipient of an NRCC Bursary.

Can. J. Chem. Downloaded from www.nrcresearchpress.com by 210.87.254.42 on 09/05/12
For personal use only.

Can. J. Chem. Downloaded from www.nrcresearchpress.com by 210.87.254.42 on 09/05/12
For personal use only.

programmed-temperature instrument using 20% Apiezon grease on Chromosorb W. The samples were generally at least 99% pure. The n.m.r. spectra were measured on the substituted benzyl chlorides on a Varian A-60 spectrometer using carbon tetrachloride solvent containing tetramethylsilane as internal reference. The compounds showed the expected spectra in all cases and this provided a convenient confirmation of the identity of the chlorides. Melting points were determined by the capillary method on a Thomas Hoover apparatus and are uncorrected. The preparations of the substituted benzyl chlorides are summarized below.

(b) Preparations

Benzyl Chloride

The benzyl chloride used was B.D.H. reagent grade freshly distilled, b.p. 167–168°; n_D^{20} 1.5376.

p-Methylbenzyl Chloride

Methyl *p*-toluate (Eastman Kodak) was reduced with lithium aluminum hydride in ethyl ether to yield *p*-methylbenzyl alcohol (m.p. 56–59°, lit. (3) m.p. 59–60°). The alcohol was chlorinated by treatment with excess thionyl chloride and the *p*-methylbenzyl chloride distilled at 90°/20 mm; n_D^{20} 1.5314 (lit. (4) n_D^{20} 1.5316).

m-t-Butylbenzyl Chloride

m-t-Butylbenzoic acid (K and K Laboratories, New York) was reduced with lithium aluminum hydride in ethyl ether to the corresponding alcohol. The alcohol obtained was chlorinated by treatment with excess thionyl chloride. The *m-t*-butylbenzyl chloride was distilled at 152–153°/7 mm; n_D^{20} 1.5196.

p-t-Butylbenzyl Chloride

p-t-Butylbenzoic acid (K and K Laboratories, New York) was reduced with lithium aluminum hydride to the corresponding benzyl alcohol. The latter was distilled at 132–136°/8 mm; n_D^{25} 1.5135 (lit. (5) n_D^{25} 1.5142). The alcohol was converted to the required chloride by treatment with thionyl chloride. The chloride distilled at 89–90°/3 mm; n_D^{25} 1.5202 (lit. (5) n_D^{25} 1.5196).

2,5-Di-t-butylbenzyl Chloride

The procedure for chloromethylation of *p*-di-*t*-butylbenzene reported by Beets and coworkers (6) yielded the desired chloride, b.p. 120–122°/2 mm; n_D^{20} 1.5195 (lit. (6) n_D^{20} 1.5198).

2,4,6-Trimethylbenzyl Chloride

This chloride was prepared by the method of Vavon and Bolle (7). The compound was distilled at 114–115°/4 mm and crystallized on standing, m.p. 34–36° (lit. (8) m.p. 37°).

2,4,6-Triisopropylbenzyl Chloride

2,4,6-Triisopropylbenzyl chloride was prepared by the method of Beets and coworkers (6). The compound distilled at 129–131°/4 mm and gave n_D^{20} 1.5156 (lit. (6) n_D^{20} 1.5160). Our sample crystallized on standing, m.p. 32–34°.

2-Methyl-4,6-di-t-butylbenzyl and 2,4,6-Tri-t-butylbenzyl Chloride

Syntheses of the above chlorides were given in part III (1).

o-Phenylbenzyl Chloride

o-Phenylbenzoic acid (Aldrich Chemical Co.) was reduced by lithium aluminum hydride to *o*-phenylbenzyl alcohol, b.p. 166–168°/5 mm. The alcohol was reacted with thionyl chloride to yield *o*-phenylbenzyl chloride, b.p. 160–168°/20 mm (lit. (9) b.p. 153–155°/11 mm).

m-Phenylbenzyl Chloride

m-Phenylbenzoic acid was prepared by the Grignard method from 3-bromobiphenyl (K and K Chemicals). The acid (m.p. 159.5–160°) was reduced in ethyl ether solution with lithium aluminum hydride to *m*-phenylbenzyl alcohol. The latter was treated without purification with thionyl chloride to yield *m*-phenylbenzyl chloride, m.p. 41.5–44.5°. Reference to this chloride could not be found in the literature and it appears to be a new compound.

Anal. Calcd. for $C_{13}H_{11}Cl$: C, 77.30; H, 5.48; Cl, 17.52. Found: C, 77.03; H, 5.48; Cl, 17.78.

p-Phenylbenzyl Chloride

p-Phenylbenzyl alcohol (Aldrich Chemical Co., m.p. 102°) was converted by the thionyl chloride method into *p*-phenylbenzyl chloride, m.p. 68–70°. (lit. (10) m.p. 68.4–68.8°).

2,4,6-Triphenylbenzyl Chloride

1,3,5-Triphenylbenzene (Aldrich Chemical Co.) was brominated (11) and the resulting 2,4,6-triphenylbromobenzene (m.p. 130–132°; lit. (12) m.p. 129–130°) converted by means of the Grignard Reaction into 2,4,6-triphenylbenzoic acid, m.p. 252–253° (lit. (12) m.p. 253–255°). The acid was converted by treatment with diazomethane in ethyl ether into its methyl ester, m.p. 88–92° (lit. (12) m.p. 92°) and the latter was reduced by lithium aluminum hydride to yield 2,4,6-triphenylbenzyl alcohol, m.p. 127–129° (lit. (13) m.p. 128°). The latter was chlorinated with thionyl chloride to yield 2,4,6-triphenylbenzyl chloride, m.p. 118–119° (lit. (13) m.p. 118.5–119.5°).

(c) Kinetic Measurements

Kinetic measurements were made on the trialkylbenzyl chlorides using both a titrimetric procedure and a conductance method. In the titrimetric procedure the chloride (1.0 g) was dissolved in 100 ml of 80% ethanol–water, stirred, and thermostated at $25 \pm 0.04°$. At appropriate intervals, 10 ml samples were removed and titrated with 0.025 *N* sodium hydroxide using a methyl red–bromocresol green indicator. The first order rate constants were estimated by the graphical method from the straight line plots of the integrated first order rate equation.

The precision conductance method for temperature dependence studies on solvolyses of trialkylbenzyl chlorides was carried out using the equipment in the laboratory of Dr. R. E. Robertson, National Research Council of Canada, Ottawa, Canada. The procedure has already been published by Robertson and coworkers (14). The other conductivity rate constants were measured by means of a manual conductivity bridge (Tinsley, Type 4896). Four conductivity cells (Queen type, magnetically stirred) were filled with 80% by volume ethanol–water and thermostated in an oil bath at the required temperature, $\pm 0.002°$. Approximately 5 mg of the chloride was dissolved in 10 ml of the same solvent and 0.025 ml of this solution was injected into each cell from a hypodermic syringe.

The Guggenheim method (15) was used to treat the kinetic data. An IBM 1130 computer was used to calculate the rate constants by means of the least squares procedure. The computer program also calculated the ΔE^*, ΔS^* from temperature dependence studies, and estimated the devia-

TABLE 1. Rates and activation parameters of solvolysis of *p*-, *m*-, and *o*-*t*-butyl and phenylbenzyl chlorides in 80% ethanol–water

Substituent	Rate ($k_1 \times 10^5$) (s^{-1})	Temperature (°C)	ΔE^* (*k*cal/mol)	ΔS^* (e.u./mol)
p-*t*-Butyl	0.553	44.89	20.6	−20.1
	2.44	60.09		
m-*t*-Butyl	0.206	44.89	21.9	−17.9
	0.991	60.09		
2,5-Di-*t*-butyl	0.465	44.89	22.4	−14.7
	2.34	60.09		
p-Phenyl	0.375	44.89	21.3	−18.7
	1.74	60.09		
m-Phenyl	0.137	44.89	19.5	−26.3
	0.588	60.09		
o-Phenyl	0.267	44.89	20.7	−21.1
	1.19	60.09		
p-Methyl	0.728	44.89	21.0	−18.2
	3.31	60.09		

tions. The standard deviations in rate constants were generally less than 1%. Deviations in ΔE^* were less than 1 kcal/mol and deviations in ΔS^* less than 1 e.u./mol.

(d) Product Analysis

Larger quantities of each chloride (0.10–0.50 g) were treated with the solvent 80% ethanol–water by stirring at the required temperature. After approximately five half-lives, the reaction was cooled, diluted with ice water, and extracted with ether. The ether extract was washed with water, dried, and the solvent distilled. The crude product was analyzed directly by n.m.r. The ratio of the alkylbenzyl alcohol to corresponding alkylbenzyl ethyl ether product was determined by relative integration of the benzylic protons of the alcohol and ether. In cases where these benzylic proton resonances of alcohol and ether were not well separated at ordinary probe temperature, they were resolved satisfactorily at lower temperature.

Results and Discussion

(a) Effects of o-, m-, and p-t-Butyl and Phenyl Groups on Relative Rates and Activation Parameters of Solvolysis of Benzyl Chlorides

As an introduction to our kinetic study, and preparatory to a kinetic analysis of trialkylbenzyl chlorides, it was desirable to know the relative effects of *o*-, *m*-, and *p*-*t*-butyl and phenyl groups on the solvolysis rates of benzyl chloride in 80% ethanol–water; a solvent system required for solubility reasons. While the effect of ring substituents on solvolyses of benzyl systems has been extensively investigated, the effect of varying the position of a *t*-butyl remained unknown as far as we know. In this preliminary kinetic analysis, we used the readily available 2,5-di-*t*-butylbenzyl chloride as a "model" for *o*-*t*-butylbenzyl chloride. The specific first order rate constants and activation parameters for solvolysis of the above compounds are given in Table 1.

Attempts have often been made in the past to correlate solvolytic reaction rates with structural features of the substrate. In the last decade, more attention has been given to solvation effects on both the reactants and transition states (16). For example, Schubert and coworkers (17) took the view that the effect of para and meta *t*-butyls relative to other alkyls on rates and activation parameters for solvolysis of benzhydryl chlorides can be rationalized in terms of steric hindrance to solvation of electron deficient sites on the benzene ring. A detailed study by Arnett and coworkers (18) draws attention to the importance of solvation of the ground state. Clement and coworkers (5) studied the solvolysis of benzyl-, *p*-methylbenzyl-, and *p*-*t*-butylbenzyl chloride in methanol. They emphasized that differential solvation effects in the ground state as well as the transition state cause ambiguity in the interpretation of relative reactivities in

Can. J. Chem. Downloaded from www.nrcresearchpress.com by 210.87.254.42 on 09/05/12
For personal use only.

Can. J. Chem. Downloaded from www.nrcresearchpress.com by 210.87.254.42 on 09/05/12
For personal use only.

terms of the effect of structure on "intrinsic" rates of reaction. Hyne and coworkers (2, 4, 19) developed a "specific solvation hypothesis" to account for the differences in activation parameters for solvolysis of substituted benzyl chlorides. Differences in entropy of activation with varying position of substituents were rationalized in terms of the relative changes in net dipole vector direction, and concomitant solvent reorganization, in the activation process. They even accommodated the lower than expected $-\Delta S^*$ value for *o*-methylbenzyl chloride in terms of steric hindrance to solvent reorganization (19). The analysis of our own results such as in Table 1, are made with the importance of differential solvation effects in mind. The Hyne "hypothesis" (19) for substituted benzyl chlorides is of particular interest in the rationalization of our results for these compounds.

It was desirable to find if these substituted benzyl chlorides could be discussed in terms of a common mechanism (S_N1 or S_N2) before evaluating the results in terms of solvation effects. Hyne and coworkers (4, 19) discussed solvation effects in ethanol–water for substituted benzyl chlorides having both electron-attracting (nitro) and electron-supplying (methyl) groups in terms of a mechanism involving development of positive charge in the activation process (S_N1). However, our solvent system was higher in ethanol content than that used by them and some criterion of mechanism for our conditions seemed desirable. One possible general criterion is the correlation of the rates for the meta- and para-substituted benzyl chlorides in a linear free energy relationship. Brown and Okamoto (20) were able to correlate a set of σ^+ substituent constants for reactions with electron deficient centers in transition states leading to carbonium ions. Correlations of σ^+ constants for solvolysis of benzyl systems are quite well known (21, 22) as are the attempts to draw conclusions about the nature of transition states from such correlations (23). An attempt was first made to correlate the rates for the meta- and para-substituted benzyl chlorides (Table 1) by a Hammett-type plot using the ordinary σ substituent constants. A wide scatter of points results, with no linear correlation. On the other hand, by using a

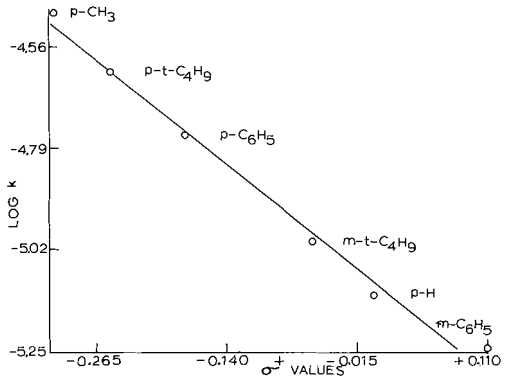

FIG. 1. Brown correlation for solvolysis of substituted benzyl chlorides in 80% ethanol–water at 60°.

Brown correlation of σ^+ substituent constants (21), a good straight line relationship was obtained (Fig. 1) with a $\rho = -1.9$. This may be taken as an indication of a reaction pathway involving a high degree of electron deficiency in the transition state. If this is true, there is some justification in discussing the activation parameters obtained (Table 1) in terms of a common mechanism (S_N1) in this series of compounds.

Similar activation energies were observed for the various *t*-butyl-, phenyl-, and *p*-methylbenzyl chlorides (Table 1). The main notable trend in activation entropy was a decrease in the negative ΔS^* value on going from the meta- to the ortho-substituted derivatives; in both the *t*-butyl- and phenylbenzyl chloride series. This result can be rationalized in terms of steric hindrance to solvent reorganization afforded by the ortho-substituents (19).

It is interesting to note that, while 2,5-di-*t*-butylbenzyl chloride showed a faster solvolysis rate than did *m*-*t*-butylbenzyl chloride, the former compound was actually slower to solvolyze than *p*-*t*-butylbenzyl chloride. That is a single *o*-*t*-butyl group accelerates the rate but comparatively slightly, probably due to the incursion of a steric hindrance factor.

These preliminary results on mono-substituted benzyl chlorides indicated that an S_N1-type mechanism predominated for solvolysis in ethanol–water. Variations in activation entropy (ΔS^*) can be rationalized in terms of solvent reorganization at the transition state or steric hindrance to solvent reorganization, for ortho-

TABLE 2. First order rate constants of solvolysis of trialkylbenzyl chlorides in ethanol–water (80%)

Substituted benzyl chloride	Conductometric $k \times 10^4$ s^{-1} 34.76°	Rates relative to benzyl (34.76°)	Conductometric rates relative to 2,4,6-tri-*i*-propyl (34.76°)	Titrimetric $k \times 10^6$ s^{-1} 25°	Titrimetric rates relative to 2,4,6-tri-*i*-propyl (25°)
Parent	0.0048[a]	1	—	—	—
2,4,6-Trimethyl	1.09	228	3.54	34.1	4.06
2,4,6-Tri-*i*-propyl	0.31	64.6	1	8.40	1
2,4-Di-*t*-butyl-6-methyl	0.405	84.4	1.31	10.6	1.26
2,4,6-Tri-*t*-butyl	7.39	1538	23.8	185	22.0

[a]This value was calculated from rate measurements at higher temperatures.

substituents. Because of such variations in solvation effects it was deemed desirable to obtain data on a series of 2,4,6-trialkylbenzyl chlorides as a preliminary to results for 2,4,6-tri-*t*-butylbenzyl chloride.

(b) Solvolysis of Trialkylbenzyl Chlorides and Related Systems

(1) Initial Results on Relative Rates

Initial data on first order rate constants and relative rates for solvolysis of 2,4,6-trialkylbenzyl chlorides obtained by both conductometric and titrimetric techniques are given in Table 2. The ethanol–water solvolysis of 2,4,6-trimethylbenzyl chloride was studied by Charlton and Hughes (24). Their evidence supported a unimolecular mechanism and the rate acceleration was attributed to a "practically pure polar effect". They discounted the idea of steric acceleration for this compound. Our conductometric and titrimetric relative rates for 2,4,6-triisopropyl- and 2,4-di-*t*-butyl-6-methylbenzyl chloride are somewhat less than for trimethylbenzyl chloride. At this point we cannot say whether this is due to some steric retardation or varying polar influences such as differing hyperconjugative and inductive stabilization of the incipient benzyl cation. There could also be a steric effect due to different degrees of steric hindrance to solvation (or to solvent reorganization) of the reaction site. Of most interest is the fact that two *o*-*t*-butyl groups in 2,4,6-tri-*t*-butylbenzyl chloride *accelerated* the reaction rates quite markedly. This is in contrast to the effect of a single *o*-*t*-butyl group (in 2,5-di-*t*-butylbenzyl chloride, Table 1) and it was desirable to explore the nature of this accelerating effect further by means of temperature dependence studies.

(2) Rates and Activation Parameters. Evidence for Steric Acceleration in the Solvolysis of 2,4,6-Tri-t-butylbenzyl Chloride

It was thought that comparative activation parameters for solvolysis of various trialkylbenzyl chlorides might give some insight into the origin of the interesting reactivity of 2,4,6-tri-*t*-butylbenzyl chloride. The results of this study are given in Table 3. The entropy of activation term shows an interesting variation for these trialkyl compounds. The relatively small decrease in the $-\Delta S^*$ terms for the substituents 2,4,6-trimethyl-, 2,4,6-triisopropyl, and 6-methyl-2,4-di-*t*-butyl- can be accounted for in terms of increased steric hindrance to solvent reorganization in the vicinity of the reaction center as the size of the ortho-substituents increases.[3] There was a very abrupt decrease in the $-\Delta S^*$ term for 2,4,6-tri-*t*-butylbenzyl chloride so that the term became approximately zero or slightly positive. This can be attributed to the very much increased steric hindrance to solvent reorganization at the reaction center due to the *two o*-*t*-butyl groups. The fact that the relative rate shows a sizable increase for this compound could be due to steric congestion in the initial state which is relieved in passing to the S_N1-like transition state; that is, due to some steric acceleration. Steric acceleration has been discussed as a factor influencing the solvolytic reactivity of branched tertiary halides (16). Steric acceleration has also been invoked to explain the

[3]2,4,6-Triphenylbenzyl chloride, under these conditions, gave relative rate = 9.02, $\Delta E^* = 21.1$ kcal/mol, and $\Delta S^* = -17.1$ e.u./mol. This compound does not appear to follow the same trend as the trialkylbenzyl chlorides and is still under investigation.

Can. J. Chem. Downloaded from www.nrcresearchpress.com by 210.87.254.42 on 09/05/12
For personal use only.

TABLE 3. Solvolysis rate constants and activation parameters for trialkylbenzyl chlorides

Substituted benzyl chloride	Conductometric rates, $k \times 10^4$ s^{-1}	Temperature (°C)	Rates relative to benzyl chloride (45.05°)	ΔE^* (kcal/mol)[a]	ΔS^* (e.u./mol)[a]
2,4,6-Trimethyl	1.09	34.76	223	20.8	−11.0
	3.34	45.05			
	8.96	55.01			
2,4,6-Tri-*i*-propyl	0.310	34.76	69.5	21.8	−10.4
	1.04	45.05			
	2.81	55.01			
2,4-Di-*t*-butyl-6-methyl	0.405	34.76	87.3	22.1	−9.0
	1.31	45.05			
	3.77	55.01			
2,4,6-Tri-*t*-butyl	2.14	25.27	1618	23.2	+0.3
	7.39	34.76			
	24.3	45.05			

[a]Activation parameters were calculated using the rate constants at 34.76 and 55.01. In the case of 2,4,6-tri-*t*-butyl chloride rates at 25.27 and 45.05° were used.

solvolytic reactivity of various other systems, including derivatives of highly branched alcohols (25), of certain rigid polycyclic systems (26), as well as of a strained polycyclic system (27).

A more detailed analysis of the effect of ortho alkyls on unimolecular solvolysis of benzyl halides becomes ambiguous because of the complex interplay of the steric and electronic effects in such systems. The effects to be considered include the following:

(i) Polar effects. Alkyl groups are well known to facilitate S_N1 solvolysis of benzyl halides by inductive and/or hyperconjugative stabilization of the incipient carbonium ion. The increased solvolysis rate for 2,4,6-trimethylbenzyl chloride has been accounted for by such effects (24).

(ii) Steric inhibition of resonance. Resonance stabilization of the carbonium ion is at a maximum when the benzene ring and the benzylic carbon are coplanar (**1***a*). As reviewed by Eliel (28), steric hindrance to coplanarity occurs with a bulky group at R_1 or when there is a methyl group at R_1 and R_2. This steric interference may twist the carbonium ion away from the plane of the benzene ring (**1***b*) and thus destabilize the ion. This effect could be important in the case of two *o*-*t*-butyl groups and might account for the observed cyclization into the *o*-*t*-butyl groups in acid-catalyzed reactions of tri-*t*-butylbenzyl compounds (1).

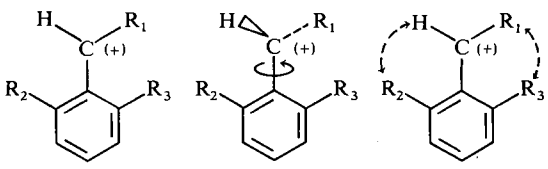

1*a* **1***b* **1***c*

(iii) Steric hindrance to solvation. Hyne and Wills (19) emphasized the role of steric hindrance to solvation of the reaction center in the case of ethanol–water solvolysis of *o*-methylbenzyl chloride. Steric hindrance to solvation is expected to be of importance in the trialkylbenzyl chlorides of Table 3.

(iv) Steric acceleration. There does not appear to be a clear-cut precedent for steric acceleration in solvolysis of a benzylic halide. Kleinfelter and Chen observed an increase in rate of solvolysis in 8-substituted (8-methyl- and 8-methoxy-) 1-chloromethylnaphthalenes (29). Their results could be attributed to steric acceleration caused by strong proximity effects of the *peri*-substituents on the—CH_2Cl group.

Charlton and Hughes reported (24) that the solvolysis rate for the secondary halide 2,4,6-trimethyl-α-phenylethyl chloride was not as fast as might be expected (compared to the 2,4-dimethyl homolog) and they attributed this to *steric retardation* due to development of steric pressure between α- and ortho-methyls in the

Can. J. Chem. Downloaded from www.nrcresearchpress.com by 210.87.254.42 on 09/05/12
For personal use only.

Can. J. Chem. Downloaded from www.nrcresearchpress.com by 210.87.254.42 on 09/05/12
For personal use only.

transition state of ionization. On the other hand, Eliel (28) interpreted the acceleration in rate and high entropy of activation for this compound in terms of *steric strain* in the ground state. Considerations of the possible factors involved in the case of 2,4,6-tri-*t*-butylbenzyl chloride become rather involved. In general congestion at the initial state due to steric compression between the two *o*-*t*-butyls and the benzylic —CH_2Cl group might be expected.[4] But if steric compression is present in the benzylic chloride, it would also be expected in the coplanar carbonium ion (**1***c*) and in the corresponding transition state where the angles tend to open up to approximately 120°.

It is true that such steric compression could be relieved by some rotation of the cation (**1***b*) but only at the expense of loss of some resonance stabilization.[5] We suggest that the interplay of these factors has resulted in an overall net steric acceleration to account for the increased reactivity of 2,4,6-tri-*t*-butylbenzyl chloride over the reactivity of other trialkylbenzyl chlorides (Table 3).

(v) Vertical stabilization of the cation. If the tri-*t*-butylbenzyl cation is forced towards the out-of-plane geometry illustrated in **1***b*, this places the empty "p" orbital of the —CH_2^+ in very close proximity to the —C—H bonds of *o*-*t*-butyl groups. There is the possibility of stabilization of this cation through σ–π interaction in a kind of through space "vertical stabilization" (30) afforded by 18 such interations as illustrated in **2**. There is no experimental evidence as yet to permit any decision

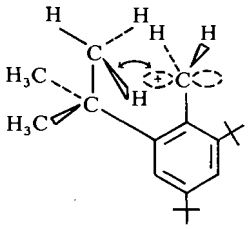

2

[4]Evidence will be presented for this in the succeeding paper from n.m.r. chemical shifts.

[5]It has been suggested (16) that a carbonium ion may be twisted rather severely from the plane of an attached benzene ring and still distribute a considerable amount of charge to the ring.

TABLE 4. Product analyses of the solvolysis of trialkylbenzyl chlorides in 80% ethanol–water at 45 °C

Substituted benzyl chloride	$ArCH_2—O—C_2H_5$ (%)	$ArCH_2—OH$ (%)
2,4,6-Trimethyl	66	34
2,4,6-Triisopropyl	68	32
2-Methyl-4,6-di-*t*-butyl	59	41
2,4,6-Tri-*t*-butyl	58	42

on the importance (if any) of this effect in the solvolysis of 2,4,6-tri-*t*-butylbenzyl chloride.

(3) Product Analyses

It was necessary to analyze the solvolysis products in order to determine if reactions on the trialkylbenzyl chlorides were in fact only with solvent. There was the possibility of *ortho* group participation which, in the case of 2,4,6-tri-*t*-butylbenzyl chloride, could have accounted for the accelerated rate. This might be expected to give products of rearrangement or insertion as were observed earlier (1) under acid-catalyzed conditions. The results of the product analyses are outlined in Table 4. The trialkylbenzyl chlorides all yielded a mixture of the corresponding benzyl ethers and benzyl alcohols. There was no evidence for complications due to the formation of rearrangement or insertion products.

Financial support of this research provided by the National Research Council of Canada is gratefully acknowledged. Some of the conductometric rate measurements were made by H.R.S. in the laboratory of Dr. R. E. Robertson, National Research Council of Canada, Ottawa, Canada. We thank Dr. Robertson and Mr. S. A. Sugamori of that laboratory for their advice and assistance.

1. L. R. C. BARCLAY, H. R. SONAWANE, and C. M. MACDONALD. Can. J. Chem. **50**, 281 (1972).
2. J. B. HYNE. J. Am. Chem. Soc. **82**, 5129 (1960).
3. V. J. SHINER, W. DOWD, R. D. FISHER, S. R. HARTSHORN, M. A. KESSICK, L. MILAKOFSKY, and M. W. RAPP. J. Am. Chem. Soc. **91**, 4838 (1969).
4. J. B. HYNE, R. WILLS, and R. E. WONKKA. J. Am. Chem. Soc. **84**, 2914 (1962).
5. R. A. CLEMENT, J. N. NAGHIZADEH, and M. R. RICE. J. Am. Chem. Soc. **82**, 2449 (1960).
6. M. A. J. BEETS, W. MEERBURG, and H. VAN ESSEN. Rec. trav. chim. **78**, 570 (1959).
7. G. VAVON and J. BOLLE. Compt. rend. **204**, 1826 (1937); Chem. Abstr. **31**, 6626 (1937).
8. W. T. NAUTA and J. W. DIENSKE. Rec. trav. chim. **55**, 1000 (1936).
9. ST. GOLDSCHMIDT and W. L. C. VEER. Rec. trav. chim. **67**, 489 (1948).

10. R. FUCHS and D. M. CARLTON. J. Am. Chem. Soc. **85**, 104 (1963).
11. P. C. MYHRE, G. S. OWEN, and L. L. JAMES. J. Am. Chem. Soc. **90**, 2115 (1968).
12. E. P. KOHLER and L. W. BLANCHARD. J. Am. Chem. Soc. **57**, 367 (1935).
13. G. GREBER and G. EGLE. Makromoleculare Chem. **40**, 1 (1960).
14. L. J. BRUBACHER, L. TREINDL, and R. E. ROBERTSON. J. Am. Chem. Soc. **90**, 4611 (1968).
15. E. A. GUGGENHEIM. Phil. Mag. **75**, 538 (1926).
16. A. STREITWIESER. Solvolytic displacement reactions. McGraw-Hill, 1962.
17. W. M. SCHUBERT, J. M. CRAVEN, R. G. MINTON, and R. B. MURPHY. Tetrahedron, **5**, 194 (1959).
18. E. M. ARNETT, W. G. BENTRUDE, J. J. BURKE, and P. MCC. DUGGLEBY. J. Am. Chem. Soc. **87**, 1541 (1965).
19. J. B. HYNE and R. WILLS. J. Am. Chem. Soc. **85**, 3650 (1963).
20. H. C. BROWN and Y. OKAMOTO. J. Am. Chem. Soc. **79**, 1913 (1957).
21. Y. OKAMOTO and H. C. BROWN. J. Org. Chem. **22**, 485 (1957).
22. G. S. HAMMOND, C. E. REEDER, F. T. FANG, and J. K. KOCHI. J. Am. Chem. Soc. **80**, 568 (1958).
23. C. D. RITCHIE and W. F. SAGER. Progress in physical organic chemistry. Vol. 2. Interscience Publishers, 1964. p. 323.
24. J. C. CHARLTON and E. D. HUGHES. J. Chem. Soc. 850 (1956).
25. P. D. BARTLETT and T. T. TIDWELL. J. Am. Chem. Soc. **90**, 4421 (1968).
26. M. A. BATTISTE, P. F. RANKEN, and R. EDELMAN. J. Am. Chem. Soc. **93**, 6276 (1971).
27. H. C. BROWN and W. C. DICKASON. J. Am. Chem. Soc. **91**, 1226 (1969).
28. E. L. ELIEL. *In* Steric effects in organic chemistry. Chapt. 2. *Edited by* M. S. Newman. John Wiley and Sons Inc., 1956.
29. D. C. KLEINFELTER and P. H. CHEN. J. Org. Chem. **34**, 1741 (1969).
30. T. G. TRAYLOR, W. HANSTEIN, H. J. BERWIN, NYE A. CLINTON, and R. S. BROWN. J. Am. Chem. Soc. **93**, 5715 (1971).

Can. J. Chem. Downloaded from www.nrcresearchpress.com by 210.87.254.42 on 09/05/12
For personal use only.

Thermolysis of Δ^3-1,3,4-Oxadiazolin-2-ones

S. L. LEE, A. M. CAMERON, AND J. WARKENTIN
Department of Chemistry, McMaster University, Hamilton, Ontario
Received January 5, 1972

Δ^3-1,3,4-Oxadiazolin-2-ones are decomposed at moderate temperatures, either neat or in solution, by two parallel, first-order processes. One of these results in the formation of the appropriate diazomethane and carbon dioxide while the other leads to ketone, nitrogen, and carbon monoxide. Rates of these competing processes are reported along with some solvent effects and substituent effects on the product ratios.

Les Δ^3 oxadiazoline-1,3,4 ones-2, soit pures soit en solution sont décomposées à des températures modérées selon deux processus parallèles du premier ordre. L'un deux a pour résultat la formation de diazométhane et du gaz carbonique alors que l'autre conduit à la cétone, l'azote et l'oxyde de carbone. Les vitesses de ces réactions compétitives sont rapportées ainsi que quelques effets de solvants et de substituants sur les rapports des produits.

Canadian Journal of Chemistry, **50**, 2326 (1972)

Can. J. Chem. Downloaded from www.nrcresearchpress.com by 210.87.254.6 on 09/05/12
For personal use only.

Introduction

Lactones of azocarboxylic acids (**1***a*, *b*) were isolated recently and were found to be remarkably reactive (1). For example, **1***a* was found to decompose to acetone azine with a half-life of about 3 weeks at 3° (1). Both **1***a* and *b* reacted in distilled water at room temperature to yield the appropriate ketone as well as the corresponding azine $(R_1R_2C{=}N{-})_2$. In view of the much greater thermal stability of α,β-unsaturated-γ-lactones (**2**), it was of interest to investigate the mechanism of decomposition of the former. In particular it was important to establish whether decomposition of **1** is strictly unimolecular or whether decomposition is also in some way induced by one of the products. Should dissociation turn out to be unimolecular, it would be of interest to determine the timing, stepwise or concerted, of the bond changes involved. This report is concerned with the first question, the kinetics of the reactions. Scheme 1 outlines possible decomposition pathways, including alternative routes to ketazine.

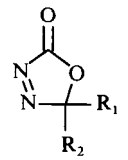

1

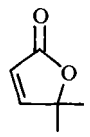

2

a $R_1 = R_2 = CH_3$
b $R_1 = CH_3$; $R_2 = CH_2CH_3$
c $R_1 = CH_3$; $R_2 = C_6H_5$
d $R_1 = R_2 = C_6H_5$

Methods and Results

The two possible mechanisms of ketazine formation should be distinguishable from the kinetics of disappearance of the oxadiazolinone. Reaction of the substrate with one of the products should be detectable in the form of either a deviation from first-order kinetics or a dependence of the apparent first-order rate constant on the substrate concentration. Furthermore the azine:ketone ratio in the product mixture should decrease with time in a given run and its final value should depend on initial oxadiazolinone concentration if induced decomposition of substrate by diazo compound were important. Accordingly, the rate of disappearance of **1***a* and

TABLE 1. Kinetics of thermolysis of 5,5-dimethyl-Δ^3-1,3,4-oxadiazolin-2-one at 84°*

Initial concentration of **1***a* (*M*)	$k_1 \times 10^4$ (s^{-1})	$k_2 \times 10^4$ (s^{-1})	Product ratio, ketone/azine
0.51	1.1	0.27	8.1
0.79	0.90	0.21	8.6
1.03	0.85	0.24	7.1
1.58	0.80	0.21	7.6
2.03	0.84	0.22	7.6
2.30	0.82	0.19	8.6
1.84†	0.88†‡	4.0†‡	0.52†‡

*In CCl_4, unless otherwise indicated. Rate constants are those defined in Scheme 1.
†In CH_3OH.
‡Isopropyl methyl ether, about 13% of the initial 2-propyl groups, was also present. Individual rate constants were calculated from the total first-order rate constant ($k_1 + k_2$) and the product distribution; k_1/k_2 being set equal to the ratio of integrals, ketone/(azine + ether), in which the ether integral was the doublet portion from the isopropyl signal only.

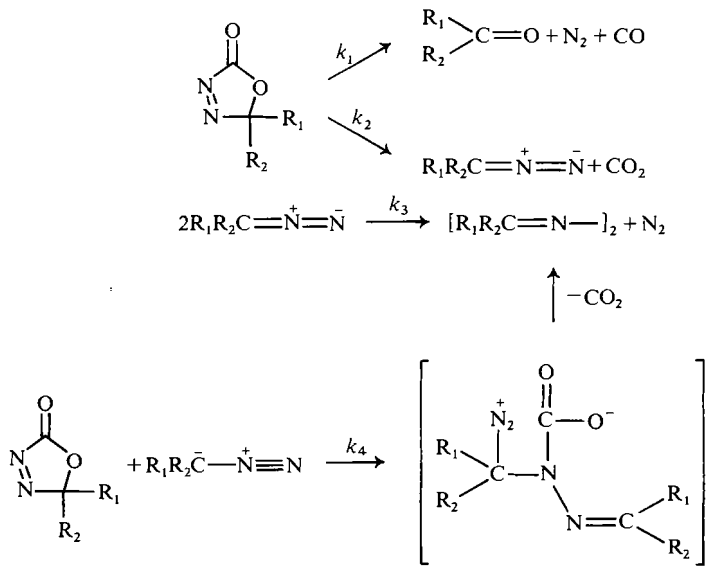

SCHEME 1

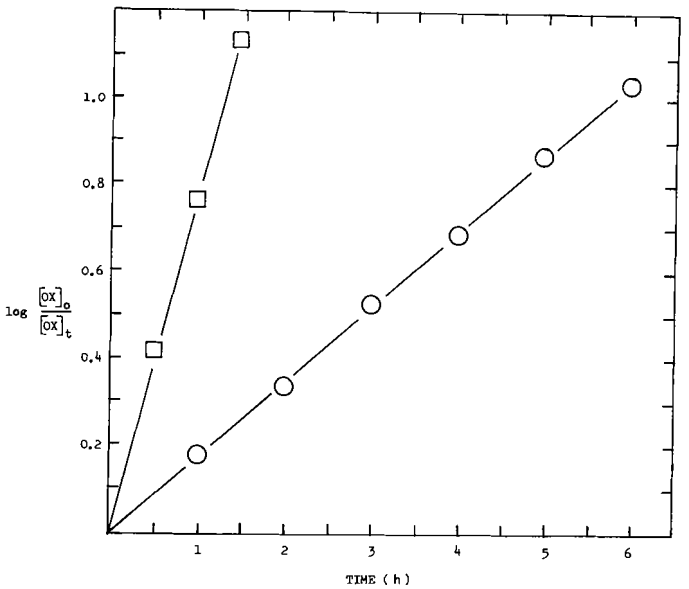

FIG. 1. Decomposition of **1***a* in CCl_4 (circles) and in CH_3OH (squares) at 84°.

the azine:ketone ratio were followed simultaneously by p.m.r. spectroscopy using benzene as internal standard for integration. Results are collected in Table 1 and Fig. 1.

Phenyl-substituted oxadiazolinones **1***c* and *d* are much less stable than **1***a* or *b* and could not be isolated in pure form. Solutions of those compounds in CCl_4 or ether turned red at room temperature and absorbed in the i.r. near 2025 cm^{-1} (2) as a result of decomposition to the appropriate diazo compounds. In CCl_4 at 84°, **1***d* decomposed with a half-life of approximately 30 s, corresponding to an overall rate constant of 2×10^{-2} s^{-1}, assuming first-order decomposition. The major products were diphenyldiazomethane and benzophenone (1653 cm^{-1})

Can. J. Chem. Downloaded from www.nrcresearchpress.com by 210.87.254.6 on 09/05/12
For personal use only.

Can. J. Chem. Downloaded from www.nrcresearchpress.com by 210.87.254.6 on 09/05/12
For personal use only.

with the former predominating. Benzophenone azine (1730 cm^{-1}) was always present in freshly prepared solutions of **1***d* but little, if any, additional azine was formed during the short time required for its decomposition at 84°.

Heating crude **1***c* (neat), at 85° for 25 min, gave acetophenone azine and acetophenone in the ratio 2:1 which corresponds to $k_1/k_2 = 0.25$ (Scheme 1). In solution (CCl_4 or ether) **1***c* also gave much more diazo compound and azine than ketone. Thus phenyl substituents at C-5, relative to methyl groups, enhance the rate of decomposition to CO_2 and diazo compound. Changing the solvent from carbon tetrachloride to methanol also favors decomposition to those products (Table 1).

Discussion

The data of Table 1 and Fig. 1 show that **1***a* decomposed with first-order kinetics in carbon tetrachloride and in methanol. That behavior, together with a concentration–independent product ratio (Table 1), points toward unimolecular first steps. Ketazine must therefore arise by a process other than the last reaction of Scheme 1. Presumably the acetone azine is formed in a bimolecular process from two molecules of dimethyldiazomethane. The latter, which is reported to be quite unstable (3), did not accumulate to a level detectable by p.m.r. Applequist and Babad (4) studied the silver- and zinc-iodide-promoted decomposition of dimethyldiazomethane as well as diphenyldiazomethane and suggested that carbenes are not intermediates in those processes. Ketazines were the main products, with only traces of tetramethylethylene and tetraphenylethylene (4). Our results support their conclusion; propylene, from a 1,2-hydrogen shift in dimethylcarbene, was not detectable in the p.m.r. spectra of our product mixtures although formation of olefins from dialkyl carbenes is a facile process (5). Furthermore, decomposition of **1***a* in styrene gave mainly acetone and acetone azine, plus a small amount (<5%) of phenyl-2,2-dimethylcyclopropane. An upper limit is thus set on the amount of dimethylcarbene that could have been formed, for some of the cyclopropane may have come from decomposition of a pyrazoline intermediate.

During decomposition of **1***d* the concentration of diphenyldiazomethane builds up to substantial levels, for it is relatively stable at about 80°. Thus there is no reason to assign anything other than a unimolecular mechanism to the decomposition of **1***d*. The same probably applies for **1***c*. In what follows we discuss possible mechanisms of unimolecular decomposition of oxadiazolinones and suggest a reason for their instability, relative to lactones **2**.

The weakest bonds in oxadiazolinones (**1**) should be the N—CR_2 and the O—CR_2 bonds of the ring. Homolytic cleavage of the former is well known azo chemistry and stepwise decomposition is possible in view of the fact that some unsymmetric azo compounds may decompose by breaking N—C bonds one at a time (6). A diradical-like, rather than a dipolar transition state for C—N bond-breaking is in keeping with the small solvent polarity effect on k_1 (Table 1). Alternative processes leading to N_2, CO, and ketone by concerted breaking of two or three bonds could also be relatively insensitive to solvent polarity and cannot be excluded at this time.

Decomposition to carbon dioxide and diazo compound probably involves a more polar transition state as depicted by structure **3**. The increase in k_2 on changing the solvent from CCl_4 to CH_3OH (Table 1) is consistent with a polar transition state and the substituent effects (CH_3 *vs.* C_6H_5) are accommodated well in such a mechanism. Moreover, in the series of compounds **5**, which also decompose to di-

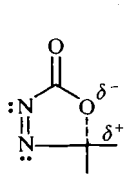

3

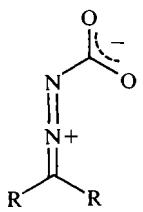

4

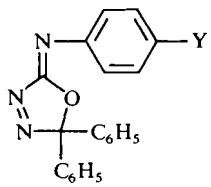

5

Can. J. Chem. Downloaded from www.nrcresearchpress.com by 210.87.254.6 on 09/05/12
For personal use only.

phenyldiazomethane, substituents Y which are electron-withdrawing enhance the rate of that decomposition (7), indicating development of negative change at benzylic nitrogen.

At first sight one might expect **2** to be equally suited to heterolytic C—O bond cleavage, as the negative end of the resulting zwitterionic species is again the carboxylate ion whereas the positive end is an allylic cation. However, the π-electrons of **1** and **2** are in an orbital normal to the C—O single bond and can therefore not provide stabilization until substantial C—O bond breaking, and N—CR_2 (or C—CR_2 in the case of **2**) bond rotation have occurred. Probably the most significant structural feature of **1**, which allows C—O bond-breaking to be relatively facile, is the lone pair of electrons at nitrogen, in an orbital coplanar with the stretching C—O bond. Overlap is thus possible and there may be an intermediate (**4**), at least in polar solvents, which rapidly decarboxylates. However, present data do not require a zwitterionic intermediate nor any other intermediate. Decomposition to diazoalkane and carbon dioxide fits the orbital symmetry requirements for fully-concerted bond changes (8). The solvent effect on k_2 (Table 1) is reasonable for either a stepwise mechanism, with formation of **4** rate-determining, or for a concerted mechanism leading to the polar diazoalkane directly. If the mechanism of the general reverse reaction, 1,3-dipolar cycloaddition of diazoalkanes to dipolarophiles, were firmly established, that knowledge could be used to infer the mechanism of decomposition of **1** to diazocompounds and CO_2, even though the reverse of that particular reaction is unknown. Arguments both for (9) and against (10, 11) concerted 1,3-dipolar cycloadditions have been presented and the matter is still not settled. In fact, it is possible that compounds like **1** will provide a solution, for the CO_2 formed from retrograde cycloaddition should be ideal for measurement of the $^{12}C/^{13}C$ kinetic isotope effect. Concerted decomposition must show an isotope effect whereas stepwise decomposition, through **4** or its diradical analog, with the second step fast, would not involve carbon isotope fractionation in the CO_2. We are currently carrying on such experiments.

Experimental

The u.v. and i.r. spectra were obtained with a Cary, Model 14 and a Perkin–Elmer, Model 521 instrument, respectively. The p.m.r. spectra were recorded with Varian A-60 and T-60 spectrometers and are referred to internal TMS as standard. Mass spectra were obtained with a Hitachi RMU-6A spectrometer. Melting points were determined with a Thomas "Unimelt" capillary melting point apparatus and are uncorrected.

2-Imino-Δ^3-1,3,4-oxadiazolines

A typical procedure is the following for preparation of 5-ethyl-5-methyl-2-methylimino-Δ^3-1,3,4-oxadiazoline by oxidative cyclization of the appropriate semicarbazone (12).

Butanone-4-methyl semicarbazone (13.0 g, 0.09 mol) in methylene chloride (100 ml) was added dropwise to a stirred, ice-cooled solution of lead tetraacetate (53.2 g, 0.12 mol) in methylene chloride (250 ml) under nitrogen. When addition was complete, the ice bath was removed and stirring was continued for 30 min. Ice-cold water (200 ml) was then added and the lead compounds were removed by filtering through a bed of Celite. The organic layer was washed with cold water, cold aqueous bicarbonate solution, and again with cold water. Evaporation of the dried ($MgSO_4$) solution at room temperature *in vacuo* gave an oil which appeared to decompose on chromatographic columns of silica gel, deactivated charcoal, or neutral alumina. Purification by g.l.p.c., on SE 30 at 70°, gave 5-ethyl-5-methyl-2-methylimino-Δ^3-1,3,4-oxadiazoline (3 parts) and 5-ethyl-5-methyl-Δ^3-1,3,4-oxadiazolin-2-one (1 part). The combined yield was 71%. Spectra and analyses of 2-imino-Δ^3-1,3,4-oxadiazolines are in Table 2.

5-Ethyl-5-methyl-Δ^3-1,3,4-oxadiazolin-2-one

The following procedure is typical for the hydrolysis of iminooxadiazolines.

To 5-ethyl-5-methyl-2-methylimino-Δ^3-1,3,4-oxadiazoline (200 mg) in methanol (15 ml) at 0° was added ice-cold, aqueous HCl (1 ml, 2.44 *M*). The mixture was stirred for 5 min before it was diluted with water and extracted with ether. Evaporation of ether from the washed (bicarbonate) and dried ($MgSO_4$) solution at room temperature gave the title compound (140 mg, 77%). Data for other oxadiazolinones are listed in Table 3.

Semicarbazones

Unsubstituted semicarbazones were prepared from ketones and semicarbazide hydrochloride according to the procedure of Cheronis and Entriken (13). 4-Methyl semicarbazones were prepared from 4-methyl semicarbazide, which was made by adding hydrazine to methyl isocyanate (14). 4-(β-Phenylethyl) semicarbazones were made by transamination of the appropriate unsubstituted semicarbazones with β-phenylethyl amine, as described below for one member of the series.

Acetone semicarbazone (57.5 g, 0.5 mol) was added all at once to β-phenylethyl amine (84.7 g, 0.7 mol) at 130–140°. The well-stirred mixture was kept at that temperature until evolution of ammonia ceased. The mixture was then poured into aqueous acetic acid (10%) to precipitate the product which was crystallized from aqueous ethanol (82% yield). Data for new semicarbazones are in Table 4.

Ketazines

The azines of acetone, butanone, acetophenone, and benzophenone were prepared according to a published procedure (15).

TABLE 2. 2-Imino-Δ^3-1,3,4-oxadiazolines, 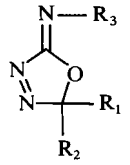

Compound	m.p. (°C)	i.r. (cm^{-1}) (C=N, CCl_4)	p.m.r. (δ, CCl_4)*	Analysis† C	H	N
$R_1 = R_3 = CH_3$ $R_2 = C_2H_5$	oil	1713	0.77, t(7.5), 3 1.57, s, 3 2.02, q(7.5), 2 3.12, s, 3	51.05 51.31	7.85 7.97	29.76 29.53
$R_1 = R_2 = R_3 = CH_3$	oil	1712	1.65, s, 6‡ 3.12, s, 3	§	§	§
$R_1 = R_2 = CH_3$ $R_3 = CH_2CH_2C_6H_5$	oil	1715	1.37, s, 6 2.85, t(7.0), 2 3.55, t(7.0), 2	66.34 66.51	6.96 7.22	19.34 18.98
$R_1 = CH_3$ $R_2 = C_6H_5$ $R_3 = CH_2CH_2C_6H_5$	56–58	1715	1.73, s, 3 3.01, t(7.0), 2 3.81, t(7.0), 2	73.10 73.16	6.13 6.18	15.04 15.18
$R_1 = R_2 = C_6H_5$ $R_3 = CH_2CH_2C_6H_5$	65–66	1715	3.00, t(7.0), 2 3.80, t(7.0), 2	77.40 77.64	5.61 5.82	12.31 12.44

*Signals from aromatic hydrogens are not tabulated. The first entry is the chemical shift, followed by a multiplicity term (with coupling constant in brackets), followed by the relative integral.
†Calculated values in upper rows. Analytical results in lower rows.
‡In $CDCl_3$.
§This compound was not obtained in sufficiently pure form for satisfactory analyses.

TABLE 3. Δ^3-1,3,4-Oxadiazolin-2-ones, 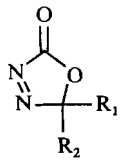

Compound	m.p. (°C)	i.r. (cm^{-1})*	u.v. (hexane)†	p.m.r. (δ, CCl_4)‡	Analysis§ C	H	N
$R_1 = R_2 = CH_3$	36–37	1835	216(3.54); 365(2.51) 373(2.57); 381(2.38)	1.63, s	42.11 41.97	5.30 5.35	24.55 24.81
$R_1 = CH_3$ $R_2 = C_2H_5$	oil	1835	216(3.54); 365(2.51) 373(2.57); 381(2.38)	0.82, t(7.5), 3 2.10, q(7.5), 2	46.87 47.01	6.29 5.99	21.86 21.69
$R_1 = CH_3$ $R_2 = C_6H_5$	oil	1835	‖	1.95, s, 3	‖		

*In CCl_4.
†λ_{max} (nm) followed by log ε in brackets.
‡Aromatic signals not included. The chemical shift is followed by the multiplet symbol, the coupling constant (Hz in brackets), and the relative integral.
§Calculated values in upper rows. Analyses in lower rows.
‖Purity high enough for a reliable u.v. spectrum, or for analysis, was not achieved. The corresponding diphenyl compound ($R_1 = R_2 = C_6H_5$) was obtained only as a solution in CCl_4. That solution also absorbed at 1835 cm^{-1} in the i.r. as well as at 2040 (diphenyldiazomethane), 1730 (benzophenone azine), and 1670 cm^{-1} (benzophenone).

Can. J. Chem. Downloaded from www.nrcresearchpress.com by 210.87.254.6 on 09/05/12
For personal use only.

TABLE 4. 4-Substituted semicarbazones, $R_1R_2C{=}NNHCONHR_3$

Compound	m.p. (°C)	p.m.r. (δ, CCl_4)*				Analysis† C	H	N
$R_1 = R_2 = CH_3$	87–88	1.90	1.94	2.83	3.44	65.75	7.71	19.16
$R_3 = CH_2CH_2C_6H_5$		s, 3	s, 3	t(7), 2	m, 2	65.83	7.84	19.09
$R_1 = CH_3$, $R_2 = C_6H_5$	129–130	2.33	2.87	3.58		72.57	6.81	14.93
$R_3 = CH_2CH_2C_6H_5$		s, 3	t(7), 2	m, 2		72.71	6.82	15.02
$R_1 = R_2 = C_6H_5$	87–88	2.81	3.47			76.94	6.16	12.24
$R_3 = CH_2CH_2C_6H_5$		t(7), 2	m, 2			76.93	6.20	12.34

*Aromatic and N—H signals not included. Upper rows are chemical shifts below which is the multiplicity followed where applicable by the coupling constant (Hz, in brackets) and the relative integral.
†Calculated values in upper rows. Analyses in lower rows.

Thermolysis of 5,5-Dimethyl-Δ^3-1,3,4-oxadiazolinone

Solutions of the oxadiazolinone (concentrations in Table 1) in CCl_4 containing benzene were pumped free of air with several freeze–pump–thaw cycles before they were sealed in n.m.r. tubes. The concentration of benzene was about half that of oxadiazolinone, so that integrals for that reference and the substrate were about equal at 50% reaction of the latter. The p.m.r. spectrum was recorded and integrated before tubes were placed in a bath at 84°, from which they were removed at 1 h intervals for analysis. Reaction was stopped by cooling the tubes quickly in ice water and time outside the bath was not counted. Integrals of p.m.r. signals were normalized with respect to the internal standard. The overall rate constant $(k_1 + k_2)$ for decomposition was obtained from such normalized data from a plot of log $([OX]_0/[OX]_t)$ *vs.* t where [OX] indicates oxadiazoline concentration at the time indicated by the subscript. The slope was set equal to $(k_1 + k_2)/2.303$. Individual rate constants were calculated from the total $(k_1 + k_2)$ and product data; *i.e.* the fraction of oxadiazolinone going to acetone is $k_1/(k_1 + k_2)$.

Product ratios were obtained by comparing averaged integrals, from many sweeps, of the ketazine signals with the ketone signals. In the case of 5,5-diphenyl-Δ^3-1,3,4-oxadiazolinone, where the p.m.r. spectrum is not useful, rate and product data came from measurements of the i.r. absorption bands at 1835 (oxadiazolinone), 2025 (diphenyldiazomethane), and 1730 cm^{-1} (benzophenone azine). Standard solutions of the two latter compounds were used to prepare calibration curves.

Financial support from the National Research Council of Canada, in the form of an Operating Grant and a Scholarship (to A.M.C.), is gratefully acknowledged.

1. S. L. LEE, A. M. CAMERON, and J. WARKENTIN. Chem. Commun. 1074 (1970).
2. P. YATES, B. L. SHAPIRO, N. YODA, and J. FUGGER. J. Am. Chem. Soc. **79**, 5756 (1957).
3. A. C. DAY, P. RAYMOND, R. M. SOUTHAM, and M. C. WHITING. J. Chem. Soc. C, 467 (1966).
4. D. W. APPLEQUIST and H. BABAD. J. Org. Chem. **26**, 288 (1962).
5. W. KIRMSE. Carbene chemistry. Academic Press, Inc., New York, N.Y., 1964. pp. 52–57.
6. (*a*) S. SELTZER and F. T. DUNNE. J. Am. Chem. Soc. **87**, 2628 (1965); (*b*) E. M. KOSOWER. An introduction to physical organic chemistry. John Wiley and Sons, Inc., New York, 1968. pp. 158–160.
7. A. M. CAMERON and J. WARKENTIN. Unpublished work.
8. (*a*) R. B. WOODWARD and R. HOFFMANN. The conservation of orbital symmetry. Verlag Chemie, GmbH, Weinheim, Germany; Academic Press, Inc., New York, N.Y., 1970. (*b*) A. ECKELL, R. HUISGEN, R. SUSTMANN, G. WALLBILLICH, D. GRASHEY, and E. SPINDLER. Chem. Ber. **100**, 2192 (1967).
9. R. HUISGEN. J. Org. Chem. **33**, 2291 (1968).
10. R. A. FIRESTONE. J. Org. Chem. **33**, 2285 (1968).
11. R. A. FIRESTONE. J. Chem. Soc. A, 1570 (1970).
12. A. M. CAMERON, P. R. WEST, and J. WARKENTIN. J. Org. Chem. **34**, 3230 (1969).
13. N. D. CHERONIS and J. B. ENTRIKEN. Semimicro qualitative organic analysis. Interscience Publishers, Inc., New York, N.Y., 1957.
14. C. VOGELSANG. Rec. Trav. Chim. **62**, 5 (1943).
15. E. R. BLOUT, V. W. EAGER, and R. M. GOFSTEIN. J. Am. Chem. Soc. **68**, 1983 (1946).

Can. J. Chem. Downloaded from www.nrcresearchpress.com by 210.87.254.6 on 09/05/12
For personal use only.

Isotope Effect Studies on Elimination Reactions. VIII. The Mechanism of the 1,3-Elimination Reaction of 3-Phenylpropyltrimethylammonium Iodide with Amide Ion in Liquid Ammonia[1]

K. C. WESTAWAY[2] AND A. N. BOURNS

Department of Chemistry, McMaster University, Hamilton, Ontario

Received January 28, 1972

Reaction of 3-phenylpropyltrimethylammonium iodide with potassium amide in liquid ammonia at $-55\,^{\circ}C$ was found to give concurrent 1,3-elimination forming phenylcyclopropane and 1,2-elimination forming 3-phenylpropene and *cis*- and *trans*-1-phenylpropene. Deuterium tracer studies on the salt labelled at C-3 established that neither a carbene nor an ylide are intermediates in the 1,3-elimination process. Isotopic exchange at C-3 was shown to accompany the reaction of the deuterated salt in ordinary ammonia, but it was not detected in the reaction of unlabelled salt in ammonia-d_3. A nitrogen isotope effect, k^{14}/k^{15}, of 1.022 ± 0.001 was found for the 1,3-elimination, while the corresponding hydrogen isotope effect, estimated from the effect of isotopic substitution on the 1,3- and 1,2-elimination ratio, was shown to exceed 20. The hydrogen isotope effect for the disappearance of undeuterated and deuterated salts (elimination and exchange) was approximately 7.4. These observations, as well as the influence of deuterium substitution in both the quaternary salt and the solvent on the relative rates of 1,3- and 1,2-elimination, have been shown to be in accord with an E1cb mechanism in which the rate constants for the conversion of the intermediate 3-carbanion to 1,3-elimination product and for return to reactant by abstraction of a proton from ammonia are of the same order of magnitude.

La réaction de l'amidure de potassium sur l'iodure de phényl-3 propyl triméthylammonium dans l'ammoniac liquide à $-55\,^{\circ}C$ donne lieu à une élimination concurrente de type 1,3 qui conduit au phénylcyclopropane et à une élimination 1,2 conduisant au phényl-3 propène et aux phényl-1 propènes *cis* et *trans*. Les études sur le sel marqué au deutérium au niveau du C-3 montrent que les intermédiaires de l'élimination 1,3 ne sont ni un carbène ni un ylure. Un échange isotopique sur le C-3 accompagne la réaction du sel deutérié dans l'ammoniac ordinaire; cet échange n'a pas été détecté dans la réaction du sel non marqué dans l'ammoniac-d_3. Un effet isotopique sur l'azote $k^{14}/k^{15} = 1.022 \pm 0.001$, a été trouvé pour l'élimination 1,3; l'effet isotopique correspondant sur l'hydrogène, calculé à partir de l'influence de la substitution isotopique sur le rapport de l'élimination 1,3 et 1,2 a été montré supérieur à 20. L'effet isotopique de l'hydrogène sur la disparition des sels non deutériés et deutériés (élimination et échange) est approximativement de 7.4. Ces observations ainsi que l'influence de la substitution par le deutérium (à la fois dans le sel quaternaire et dans le solvant) sur les vitesses relatives de l'élimination 1,3 et 1,2, sont en accord avec un mécanisme de type E1cb dans lequel les constantes de vitesse pour la conversion de l'intermédiaire carbanion-3 en produit d'élimination 1,3 et pour le retour au réactant par arrachement d'un proton de l'ammoniac, sont du même ordre de grandeur.

Canadian Journal of Chemistry, **50**, 2332 (1972)

Introduction

Three-membered ring formation by a 1,3-elimination has been observed with a variety of reactants under widely differing reaction conditions (1). The reaction pathways followed by such reactions have been found to parallel those encountered in 1,2-elimination processes. Thus, the E1 pathway is characteristic of solvolyses involving reactants possessing good leaving groups (2–4), while reaction by either the E2 or E1cb mechanism is favored by the presence of strong base (4–7). A few examples of reaction by way of a carbene intermediate formed in a 1,1-elimination reaction have also been reported (8).

1,3-Elimination competes most effectively with double bond formation in rigid bicyclic systems where the spatial relationship of reacting bonds is favorable for the formation of the three-membered ring (2–6). Base-promoted 1,3-elimination is also found in acyclic systems, but usually, it requires the presence of electron-withdrawing groups (carbonyl (9), sulfonyl (10, 11), nitro (12), cyano (13), and aryl (14–18)) which facilitate the removal of the hydrogen atom. With the more powerful activating groups, there seems little doubt that the reaction proceeds by way of a carbanion intermediate, and

[1]For Part VII in this series, see ref. 39.

[2]Present address: Department of Chemistry, Laurentian University, Sudbury, Ontario.

Can. J. Chem. Downloaded from www.nrcresearchpress.com by 210.87.254.105 on 09/05/12
For personal use only.

this is one of the accepted mechanisms for the 1,3-elimination process involved in the Favorskii rearrangement (7) (carbonyl activation) and the Ramberg-Backlund reaction (11) (sulfonyl activation). Much less certain, however, is the reaction pathway for eliminations in which activation is provided by the more weakly electron-withdrawing aryl group.

Recently, Baker and Spillett (19) have observed rapid deuterium exchange at the 3-position in the reaction of a series of 2-alkyl-1-methylsulfinyl-3-phenylpropanes with dimethylsulfinyl anion in deuterated dimethylsulfoxide, thus demonstrating that the phenyl group provides sufficient activation to sustain the reversible formation of a carbanion under elimination reaction conditions. This observation, however, does not establish that the 1,3-elimination is proceeding by an E1cb mechanism since, as has been pointed out by Breslow (20) with respect to 1,2-elimination reactions, the carbanion may not be on the elimination-reaction coordinate at all but, instead, reversible carbanion formation and E2 elimination may be entirely separate and concurrent processes.

An extensively studied 1,3-elimination involving aryl activation in an acyclic system has been the conversion of 3-arylpropyl- and 3,3-diarylpropyltrialkylammonium salts to aryl-substituted cyclopropanes by reaction with sodium amide in liquid ammonia (15–17). This reaction was first reported by Bumgardner (15) who suggested (16) that it might proceed either by an E1cb mechanism, eq. 1, or by an E2 process, eq. 2, in which the transition state has considerable carbanion character. Banthorpe (21), on the other hand, has suggested the cyclopropane may be formed by the insertion into the C_3—H bond of a carbene formed in a 1,1-elimination process, eq. 3. A less likely pathway, but one which cannot be excluded *a priori*, is a 1′,3-process, eq. 4, involving an ylide intermediate.

The purpose of the present investigation

Elcb Mechanism

[1]

$$C_6H_5CH_2CH_2CH_2\overset{\oplus}{N}(CH_3)_3 + \overset{\ominus}{N}H_2 \underset{k_{-1}}{\overset{k_1}{\rightleftharpoons}} C_6H_5\overset{\ominus}{\ddot{C}}HCH_2CH_2\overset{\oplus}{N}(CH_3)_3 + NH_3$$

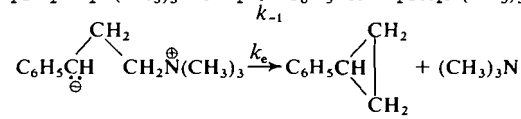

E2 Mechanism

[2]

$$C_6H_5CH_2CH_2CH_2\overset{\oplus}{N}(CH_3)_3 + \overset{\ominus}{N}H_2 \longrightarrow \left[C_6H_5\overset{\delta-}{C}H(CH_2)\cdots CH_2\cdots \overset{\delta+}{N}(CH_3)_3 \;\; H_2\overset{\delta-}{N}\cdots H \right]$$

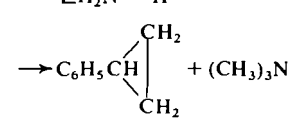

1,1-Elimination Mechanism

[3]

$$C_6H_5CH_2CH_2CH_2\overset{\oplus}{N}(CH_3)_3 + \overset{\ominus}{N}H_2 \longrightarrow C_6H_5CH_2CH_2\underset{\cdot}{C}H\cdot + NH_3 + (CH_3)_3N$$

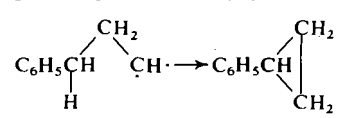

1′,3-Elimination Mechanism

[4]

$$C_6H_5CH_2CH_2CH_2\overset{\oplus}{N}(CH_3)_3 + \overset{\ominus}{N}H_2 \rightleftharpoons C_6H_5CH_2CH_2CH_2\overset{\oplus}{N}(CH_3)_2 + NH_3$$

$$\ominus{:}CH_2$$

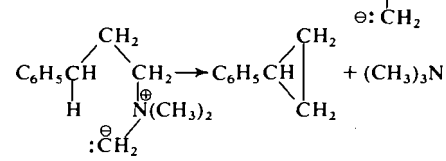

Can. J. Chem. Downloaded from www.nrcresearchpress.com by 210.87.254.105 on 09/05/12
For personal use only.

TABLE 1. Composition of the product formed from undeuterated and deuterated quaternary ammonium salts in light and heavy ammonia at −55 °C

Quaternary salt	Solvent	*cis*-1-Phenylpropene (%)	*trans*-1-Phenylpropene (%)	3-Phenylpropene (%)	Phenylcyclopropane (%)
Undeuterated*	NH_3	—	1.4	2.6	96.0
Deuterated†	NH_3	2.2	21.9	22.2	53.7
Undeuterated‡	ND_3	—	—	—	>99.6
Deuterated	ND_3	—	2.3	—	97.7

*Average of two experiments with agreement to within ±0.5%.
†Average of two experiments with agreement to within ±0.2%; reaction carried to 66% completion based on quaternary salt.
‡Reaction carried to 11% completion.

was to determine the mechanistic details of the 1,3-elimination reaction of 3-phenylpropyltrimethylammonium ion with amide ion in liquid ammonia. In particular, tests were made for the 1,1- and the 1′,3-elimination mechanisms by examining the deuterium content of the products of the reaction of 3,3-dideutero-3-phenylpropyltrimethylammonium ion, a study was made of the extent of isotopic exchange of the deuterated salt with solvent as a means of detecting the presence of carbanionic species under the reaction conditions, and, finally, measurements were made of the hydrogen isotope effects associated with both substrate and solvent and of the nitrogen isotope effect associated with substrate in order to identify the rate-determining step of the reaction.

Results and Discussion

Product Analysis

The 1,3-elimination reaction of 3-phenylpropyltrimethylammonium iodide was studied at −55 °C in liquid ammonia solution using potassium amide as the base.[3] The hydrocarbon product was quantitatively separated by preparative vapor-phase chromatography into three fractions consisting of (*1*) 3-phenylpropene, (*2*) a mixture of phenylcyclopropane and *trans*-1-phenylpropene, and (*3*) *cis*-1-phenylpropene. These were identified by their v.p.c. retention times and i.r. and n.m.r. spectra. The composition of fraction *2* was determined by u.v. spectroscopy and, in the case of the reaction of 3,3-dideutero-3-phenylpropyltrimethylammonium ion in ordinary ammonia, the analysis was confirmed by v.p.c. and by n.m.r. spectroscopy. The results of the product analysis for the reactions of undeuterated and deuterated salts in ammonia and ammonia-d_3 are reported in Table 1.

3-Phenylpropene is the direct product of 1,2-elimination, while the isomeric 1-phenylpropenes are formed by the base-catalyzed isomerization of this product during the reaction (22). The percentage of 1,2-elimination, therefore, is the sum of the percentages of each of the three olefin products. The absence of 3-phenylpropene in the product of reaction of the deuterated salt in deuterated solvent, in contrast to the approximate 1:1 ratio of this olefin to *trans*-1-phenylpropene in the products of the reactions in ammonia, is accounted for by the longer reaction time with the former. This results in a closer approach to an equilibrium composition of the three olefins in which the *trans*-1-phenylpropene predominates (22). No products of 1,2-elimination could be detected in the reaction of the undeuterated salt in deuterated ammonia. Based on the absence of the reddish-brown coloration characteristics of the carbanion $[C_6H_5CH{=}CH{=}CH_2]^{\ominus}$, it is estimated that the total olefin product formed in this reaction is less than 0.4%.

Test for the 1,1-Elimination (Carbene) Mechanism

This test involved a determination of the number and position of the deuterium atoms in the phenylcyclopropane produced from 3,3-dideutero-3-phenylpropyltrimethylammonium iodide. Elimination by way of a carbene intermediate formed by 1,1-elimination will give a product containing two deuterium atoms per molecule, one on the methine and one on a methylene carbon, eq. 5. Any other reasonable

[3]Bumgardner (15, 16) used the less soluble sodamide resulting in a heterogeneous system unsuitable for kinetic isotope effect studies.

Can. J. Chem. Downloaded from www.nrcresearchpress.com by 210.87.254.105 on 09/05/12
For personal use only.

[5] $$C_6H_5CD_2CH_2CH_2\overset{\oplus}{N}(CH_3)_3 + \overset{\ominus}{N}H_2 \longrightarrow C_6H_5CD_2CH_2\dot{C}H\cdot + (CH_3)_3N$$

$$C_6H_5CD_2CH_2\dot{C}H\cdot \longrightarrow C_6H_5CD\begin{cases} CH_2 \\ CHD \end{cases}$$

mechanism for the reaction will result in the loss of one of the deuterium atoms on C-3 and the formation of 1-deutero-1-phenylcyclopropane.

The *trans*-1-phenylpropene – phenylcyclopropane fraction obtained by v.p.c. separation of the product of the reaction of the deuterated salt gave an n.m.r. spectrum in which the broad multiplet associated with the methine proton of phenylcyclopropane (1.55–2.00 p.p.m.) is absent and the complex multiplet associated with the methylene protons (0.45–1.10 p.p.m.) is reduced to two broad lines (23). These changes are consistent with replacing the methine hydrogen of phenylcyclopropane with deuterium. Furthermore, after subtracting the absorption associated with the phenyl protons of *trans*-1-phenylpropene from the total phenyl-proton absorption of the mixture, the ratio of the residual phenyl-proton absorption to that of the methylene protons of the phenylcyclopropane was found to be 5.0:4.0; precisely that expected if deuterium enrichment did not occur in the methylene groups of the cyclopropane ring.

These results were confirmed by mass spectrometry. The *trans*-1-phenylpropene – phenylcyclopropane fraction was found to be 94.4% monodeuterated, 5.5% undeuterated and 0.1% dideuterated. It can be concluded, therefore, that the 1,3-elimination does not proceed by way of a carbene intermediate.

Test for the 1′,3-Elimination (Ylide) Mechanism

The test for the 1′,3-elimination mechanism, eq. 4, was carried out in the conventional way (24) by determining the deuterium content of the trimethylamine formed from 3,3-dideutero-3-phenylpropyltrimethylammonium iodide. The intermediacy of an ylide would require that a deuterium atom be transferred from the 3-position to the *N*-methyl carbon and result in the formation of trimethylamine-d_1.

The trimethylamine formed in the reaction of the dideuterated salt was separated from ammonia and examined mass spectrometrically using the method of Cope and Mehta (25). The mass spectrum of the amine was identical, within the limits of measurement, to that of trimethylamine of natural isotopic abundance from which it was concluded that trimethylamine-d_1 did not exceed 0.5% of the product.

A complication arises in the application of the test because it was observed that exchange of the *N*-methyl hydrogens of the quaternary salt with solvent is quite rapid in comparison with the rate of 1,3-elimination (50% exchange after only 11% reaction). Consequently, if the conversion of the ylide intermediate to phenylcyclopropane were to occur by way of the 3-carbanion, $[C_6H_5\overset{\ominus}{\ddot{C}}DCH_2CH_2\overset{\oplus}{N}(CH_3)_2CH_2D]$, rather than in a one-step process, this carbanion could react with solvent to regenerate quaternary salt which in turn could lose its *N*-methyl deuterium by exchange before undergoing elimination. Analysis of the isotope effect results reported later in this paper, however, show that if the 3-carbanion is an intermediate in the 1,3-elimination, the ratio of the rate it abstracts a proton from solvent to the rate it loses trimethylamine to give phenylcyclopropane cannot exceed fourteen. It follows, then, that *at least* 7.1% of the *N*-methyl deuterium-labelled 3-carbanions, if formed, must react directly to produce trimethylamine-d_1.

A further complication arises because the 1,3-elimination reaction of the dideuterated salt is accompanied by an almost equal amount of 1,2-elimination which, of course, produces only undeuterated trimethylamine. It follows from these considerations that even if the 1,3-elimination were to proceed entirely by the ylide mechanism, only one-half of 7.1% of the trimethylamine would *necessarily* contain a deuterium atom. Since the limit of detection of trimethylamine-d_1 is at least as good as 0.5%, it follows that the 1′,3-elimination mechanism, if involved at all in the formation of phenylcyclopropane, can only be a minor reaction pathway.

Test for Exchange at C-3

With the carbene and ylide mechanisms eliminated as major reaction pathways for the

Can. J. Chem. Downloaded from www.nrcresearchpress.com by 210.87.254.105 on 09/05/12
For personal use only.

Can. J. Chem. Downloaded from www.nrcresearchpress.com by 210.87.254.105 on 09/05/12
For personal use only.

1,3-elimination reaction, there remain the E2 and E1cb processes originally proposed by Bumgardner (16). A deuterium exchange test was performed in an effort to detect the carbanion intermediate involved in the two-step process, eq. 1.

3,3-Dideutero-3-phenylpropyltrimethylammonium iodide containing 9.78 ± 0.01 atom % excess deuterium was allowed to react with potassium amide in liquid ammonia to approximately 66% completion. The unreacted quaternary salt was found to contain only 9.26 ± 0.03 atom % excess deuterium. This corresponds to a replacement of approximately 11% of the dideuterated salt by its monodeuterated analog and establishes that 3-carbanions are present in the reaction mixture. The actual extent of exchange must be considerably greater than these results indicate, however, since the large isotope effect associated with the abstraction of the hydrogen on C-3 (*vide infra*) will result in a more rapid rate of disappearance of the exchanged salt by 1,3-elimination than of the deuterium-labelled reactant.

As was pointed out in the Introduction, the observation that 3-carbanions are present in the reaction solution, although consistent with the E1cb mechanism for 1,3-elimination, does not rule out a concerted reaction pathway. It is entirely possible that reversible formation of the carbanion and elimination are entirely separate but concurrent processes (20). Kinetic nitrogen and hydrogen isotope effect studies were next carried out in an effort to distinguish between the E2 and E1cb reaction pathways.

Nitrogen Isotope Effect

Nitrogen isotope effect measurements were made to determine whether carbon–nitrogen bond rupture is involved in a rate-determining step of the elimination reaction (26, 27). Reactions of 3-phenylpropyltrimethylammonium iodide of natural isotopic abundance were carried to extents of completion varying from 53–94% based on quaternary salt and the nitrogen isotope effect was evaluated from the isotopic composition of the nitrogen in the initial reactant and recovered salt using an expression derived by Bigeleisen and Wolfsberg (28), eq. 6,

$$[6] \quad k^{14}/k^{15} = 1.00 + \frac{\log (R_f/R_0)}{\log [(1-f)(1+R_0)/(1+R_f)]}$$

TABLE 2. Nitrogen isotope effects in the 1,3-elimination reaction of 3-phenylpropyltrimethylammonium iodide with potassium amide in liquid ammonia at -55 °C

Experiment no.	Extent of reaction	$(k^{14}/k^{15} - 1)\,100$
1	53	2.13
2	70	2.15
3	80	2.32
4	82	2.08
5	84	2.21
6	94	2.32
	Mean	2.20 ± 0.09*

*Error limits are given as standard deviation.

where R_f is the N^{14}/N^{15} mass ratio of the nitrogen in the unreacted salt, R_0 is the N^{14}/N^{15} mass ratio of the nitrogen in the starting material, and f is the mole fraction of salt that has reacted. The results of these experiments are shown in Table 2. Since 96% of the reaction leads to phenylcyclopropane, the observed isotope effect of 2.2% is that associated with the 1,3- elimination process.

It is of value to compare this result with the nitrogen isotope effects previously observed in 1,2-elimination reactions of quaternary ammonium salts. Most measurements of the latter have been made at 60° and it is, therefore, necessary to estimate the magnitude of the isotope effect for the 1,3-elimination at this much higher temperature. This was done in two ways, both of which are very approximate. First, it was assumed that the isotope effect at 60° for the 1,3-elimination will be the same fraction of the theoretical maximum, calculated (29) for reaction at this temperature, as the value of 2.2% is of the theoretical maximum at $-55°$. This suggests a value of 1.4% at 60°. Second, the temperature coefficient for the isotope effect (an increase of 0.6% for each decrease of 10°) observed in a previous study in these laboratories for the reaction of *cis*-2-phenylcyclopentyltrimethylammonium ion with ethoxide ion in ethanol (30), was assumed to apply to the present reaction. This method predicts a value of 1.5% at 60°.

The isotope effect of 1.4–1.5% estimated for the 1,3-elimination reaction using amide ion in liquid ammonia may be compared with the results obtained for a number of 1,2-eliminations using ethoxide ion in ethanol: 2-phenylethyltrimethylammonium ion, 0.9% (27); *cis*-2-phenylcyclopentyltrimethylammonium ion, 1.1% (30); *cis*-2-phenylcyclohexyltrimethylammonium ion, 1.2% (30); and ethyltrimethylammonium ion,

TABLE 3. Ratio of 1,3- and 1,2-elimination for reactions of undeuterated and deuterated quaternary salts in ammonia and ammonia-d_3 at -55 °C

Quaternary salt	Base and solvent	% 1,3-Elimination / % 1,2-Elimination	1,3-Elimination / 1,2-Elimination
Undeuterated	KNH_2 in NH_3	96.0: 4.0	24 :1
Deuterated*	KNH_2 in NH_3	53.7:46.3	1.2:1
Undeuterated†	KND_2 in ND_3	>99.6: 0.4	>250 :1
Deuterated	KND_2 in ND_3	97.7: 2.3	43 :1

*Reaction carried 66% to completion based on salt.
†Reaction carried 11% to completion based on salt.

1.7% (27). It can be seen that the isotope effect found in the present study is at least as large as the effects found in 1,2-elimination reactions proceeding by the E2 mechanism with reactants in which there is phenyl activation of the abstracted hydrogen. From this it can be concluded that the 1,3-elimination reaction must be proceeding by a mechanism in which carbon–nitrogen bond rupture is involved in the rate-determining step, that is, either by an E2 process, eq. 2, or an E1cb reaction, eq. 1, in which the rate of return of the carbanion to reactant is at least as large as its rate of decomposition to elimination product (26, 31).

Hydrogen Isotope Effects

If hydrogen exchange with solvent at C-3 does not occur, the isotope effect for 1,3-elimination is given directly by the ratio of 1,3- and 1,2-elimination products from the undeuterated salt divided by this ratio for the products from the 3,3-dideutero-salt, since the rate of 1,2-elimination, except for a small secondary isotope effect, will not be affected by isotopic substitution. The cyclopropane: olefin ratio for the unlabelled reactant was found to be 24 and that for the dideuterated salt 1.2 (see Tables 1 and 3), giving an isotope effect for 1,3-elimination of 20. The elimination reaction, however, is accompanied by exchange resulting in the conversion of a considerable amount of the dideuterated salt to monodeuterated salt which, because of the hydrogen isotope effect, will yield a much higher cyclopropane: olefin ratio than that for the original reactant. This means that the observed value of 20 actually represents a lower limit and that the actual isotope effect for phenylcyclopropane formation must be considerably higher than this. Even for a reaction at $-55°$, this isotope effect is large and suggests the possibility of tunnelling (32).

Of even greater significance with respect to the elucidation of the mechanism of 1,3-elimination is the hydrogen isotope effect associated with the rate of disappearance of the undeuterated and dideuterated quaternary salts. For the undeuterated salt, reaction is by 1,2- and 1,3-elimination only, since isotopic exchange with solvent simply regenerates the original reactant; for the dideuterated salt, reaction involves not only elimination but also exchange giving monodeuterated salt.[4]

This isotope effect was determined by the isotopic competitive method (28). A mixture of undeuterated and dideuterated salts containing 4.75 ± 0.01 atom % excess deuterium was allowed to react until 57.7% of the salt had been converted to elimination products. The recovered quaternary salt was found to contain 8.48 ± 0.02 atom % excess deuterium. The hydrogen isotope effect for the disappearance of dideuterated and undeuterated quaternary salt was then evaluated using eq. 6.

In applying this equation, there is a problem in arriving at an accurate value for R_f, the ratio of undeuterated and dideuterated salt in the recovered reactant, because of the presence of an unknown amount of monodeuterated salt formed by isotopic exchange with solvent. An upper limit to the amount of exchange is the 11% found in the deuterium exchange experiment (*vide ante*) in which 66% of the dideuterated salt had been converted to hydrocarbon compared to the less than 25% conversion of this salt in the present experiment. Assuming this extent of exchange, the composition of the recovered salt is as follows: undeuterated 10.4%, monodeuterated 9.7%, and dideuterated 79.9%.

[4]Further exchange produces undeuterated salt, but this will be small because of the intramolecular isotope effect associated with the abstraction of hydrogen from the monodeuterated compound.

Can. J. Chem. Downloaded from www.nrcresearchpress.com by 210.87.254.105 on 09/05/12
For personal use only.

Can. J. Chem. Downloaded from www.nrcresearchpress.com by 210.87.254.105 on 09/05/12
For personal use only.

The *total* extent of reaction of the undeuterated and dideuterated salts to produce hydrocarbon and monodeuterated salt becomes 61.8%. These data give an isotope effect of 7.3. On the other hand, if it is assumed that the recovered reactant consists only of undeuterated and dideuterated salt (no monodeuterated salt formed by exchange), its composition would be 15.2% undeuterated and 84.8% dideuterated, the extent of reaction 57.7% (*vide ante*) and the isotope effect 7.5. This close correspondence in the calculated isotope effects using the two extreme limits for the extent of exchange may be fortuitous; the significant fact is that there is a large isotope effect associated with the disappearance of the isotopic reactants.

An isotope effect of this magnitude, of course, is consistent with the 1,3-elimination reaction proceeding by the E2 mechanism, eq. 2. It also can be accommodated by an E1cb process, eq. 1, *provided* that the rate of return of the carbanion intermediate to quaternary salt is not *very large* relative to its rate of decomposition to phenylcyclopropane. The reason for this is that carbanion return in the case of the undeuterated salt reaction generates starting compound whereas return in the dideuterated salt reaction produces a reaction product, namely monodeuterated salt. It follows that the greater the extent of carbanion return the faster the rate of disappearance of dideuterated salt relative to that of the undeuterated salt and the smaller the observed isotope effect. At large rates of return, the isotope effect, so defined, would actually favor the deuterated reactant.

In summary, both the nitrogen and hydrogen isotope effect results are in accord with a concerted mechanism for the 1,3-elimination reaction. They may also be accommodated by a two-step process involving a carbanion intermediate provided that certain restrictions are placed on the relative rates with which this intermediate abstracts a proton from solvent to regenerate quaternary salt and loses trimethylamine to form the cyclopropane product. The nitrogen isotope effect of 2.2% would require that this ratio be greater than unity, whereas the hydrogen isotope effect of approximately 7.4 associated with the disappearance of undeuterated and dideuterated salts would require that this ratio not be large. (This will be discussed in more quantitative terms later in this section.)

Studies in Ammonia-d_3

The reactions of both undeuterated and dideuterated quaternary salts were carried out in ammonia-d_3 in an effort to distinguish between the two reaction pathways accommodated by the isotope effect results.

Although the deuterium exchange found in the reaction of deuterated salt in ordinary ammonia demonstrated the presence of 3-carbanions in solution, it was impossible to even estimate the extent of exchange since the resulting monodeuterated salt undergoes 1,3-elimination much faster than the starting compound. It was reasoned that a better estimate of the amount of exchange could be obtained if the exchange test was performed by reacting undeuterated salt in ammonia-d_3 where the monodeuterated salt would react more slowly than the starting compound and would, therefore, accumulate during reaction.

A reaction of the undeuterated salt in ammonia-d_3 was carried to 11% completion and the recovered salt was examined by both i.r. and n.m.r. spectroscopy. It was found that extensive exchange had occurred at the *N*-methyl carbons (50%) and at C-1 (35%), but deuterium was not detected at either C-2 or -3.

The absence of exchange at the 3-position in this reaction compared to the extensive exchange observed in ordinary ammonia cannot be understood in terms of a concerted elimination process which is accompanied by an irrelevant formation of 3-carbanions. This is because the *relative* rate of carbanion formation and E2 elimination should be approximately the same in the two cases, and if the 3-carbanions are *not* intermediates in the elimination reaction, but only react with solvent to produce exchanged salt, the relative rate of exchange and elimination cannot be significantly different whether a hydrogen is being abstracted from ammonia or a deuterium from ammonia-d_3.

On the other hand, the results of the two exchange reactions can be readily understood in terms of an E1cb process, eq. 1, provided there is a large isotope effect associated with the abstraction of a proton from the solvent by the carbanion. If, for the reaction in ordinary ammonia, the rate with which the carbanion abstracts hydrogen from solvent is not much greater than the rate of its decomposition to phenylcyclopropane, then for the reaction in

Can. J. Chem. Downloaded from www.nrcresearchpress.com by 210.87.254.105 on 09/05/12
For personal use only.

deuterated ammonia, a much slower rate of carbanion return will result in an elimination rate which is much greater than the rate of exchange. Since exchange was extensive in ammonia and not within the limits of detection in ammonia-d_3, the isotope effect for proton abstraction from solvent must be extremely large. This is not surprising, however, since, on the basis of zero point energy consideration (29), the isotope effect associated with the rupture of a N—H bond will undoubtedly be larger than that for a C—H bond (33, 34) and it has already been demonstrated that the isotope effect for the abstraction of the hydrogen from C-3 is greater than 20.

The conclusions based on the results of the exchange experiments find confirmation in the relative amounts of 1,3- and 1,2-elimination in the reactions of deuterated and undeuterated salt in ammonia and ammonia-d_3, see Tables 1 and 3. It is seen that the reaction of the undeuterated salt in deuterated solvent gives a very much higher 1,3- to 1,2-elimination ratio than the reaction of this salt in ordinary ammonia. This is difficult to explain if the 1,3- as well as the 1,2-elimination reactions are concerted, since the secondary and solvent isotope effects associated with a change in the isotopic nature of the base and solvent should be approximately the same for the two elimination reactions. The same would apply for the reaction of the deuterated salt in the two base-solvent systems; yet, again, a much higher 1,3- to 1,2- ratio is found in ammonia-d_3. On the other hand, the results are readily understood in terms of an E1cb mechanism, since the large primary isotope effect associated with the return of the carbanion to reactant would result in a much faster overall rate of 1,3-elimination for the reaction in ammonia-d_3.

Similarly, the increase in the 1,3- to 1,2-elimination ratio from 24:1 to 43:1 in going from the reaction of the undeuterated salt in ammonia to that of the deuterated salt in ammonia-d_3 can only be understood in terms of the E1cb mechanism. If the 1,3-elimination is concerted, the primary hydrogen isotope effect associated with the quaternary salt would strongly decrease the rate of 1,3-elimination, while secondary and solvent isotope effects resulting from a change from ammonia to ammonia-d_3 would be approximately the same for the two processes. The result would be a large decrease in the 1,3- to 1,2-elimination ratio, contrary to observation. On the other hand, these results are fully in accord with an E1cb reaction pathway for phenylcyclopropane formation. The decrease in the rate of 1,3-elimination resulting from the substitution of deuterium for hydrogen on C-3 of the quaternary salt will be compensated by an increase in the rate of this elimination as a consequence of a much smaller tendency for carbanion return in the deuterated solvent. In fact, the primary isotope effect associated with solvent is seen to outweigh the effect associated with the substrate, resulting in an overall increase in the 1,3- to 1,2-elimination rate ratio. Other comparisons of the elimination ratios shown in Table 3 are equally in accord with the E1cb mechanism for the 1,3-elimination.

Relative Rates of Carbanion Return and Elimination

Upper and lower limits can be established for the ratio of the rates of carbanion return and conversion to phenylcyclopropane from the hydrogen isotope effects observed for the disappearance and 1,3-elimination of the undeuterated and dideuterated salts in ordinary ammonia.

It may readily be shown that the rate constant, k^H, for the disappearance of the undeuterated salt is given by eq. 7, where $k_{1,2}$ is the rate

$$[7] \qquad k^H = k_{1,2} + \frac{k_1^H k_e}{k_{-1} + k_e}$$

constant for 1,2-elimination, k_1^H is the rate constant for the formation of the 3-carbanion from undeuterated salt, k_{-1} is the rate constant for carbanion return in ordinary ammonia and includes the concentration of the solvent, and k_e is the rate constant for conversion of the carbanion to phenylcyclopropane (see eq. 1). Also, the rate constant, k^D, for the disappearance of the dideuterated salt by elimination and exchange in ordinary ammonia is given by eq. 8,

$$[8] \qquad k^D = k_{1,2} + k_1^D$$

where k_1^D is the rate constant for carbanion formation from the deuterated salt. (In this treatment, secondary isotope effects are neglected as is the formation of undeuterated salt by a double exchange of the dideuterated reactant.)

Combining eqs. 7 and 8 and substituting the

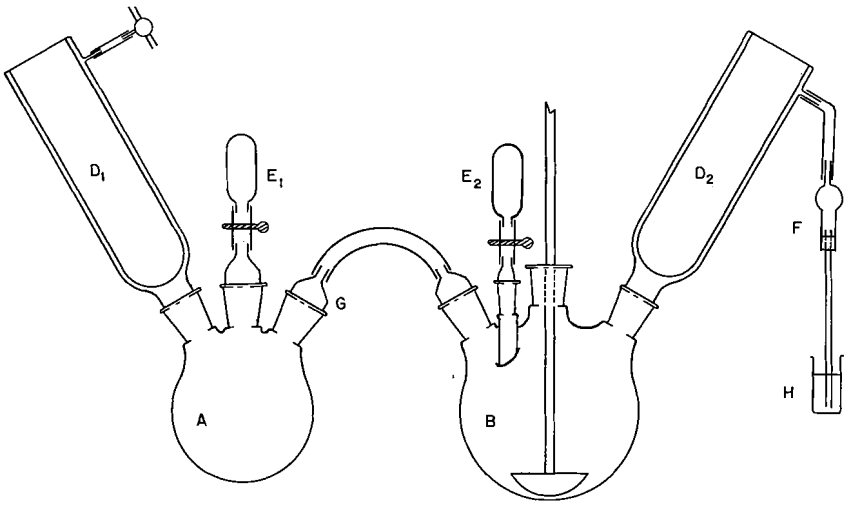

FIG. 1. Apparatus for the reaction of quaternary ammonium salts with potassium amide in liquid ammonia.

observed values of 7.4 for k^H/k^D, the isotope effect for the disappearance of undeuterated and deuterated salts, and 24 for $k_1^H k_e/k_{1,2}(k_{-1} + k_e)$, the ratio of 1,3- and 1,2-elimination from the undeuterated compound (see Table 3), gives eq. 9.

$$[9] \qquad k_{-1}/k_e = 0.099\ k_1^H/k_1^D - 1$$

It has been shown (*vide ante*) that the isotope effect for 1,3-elimination from undeuterated and deuterated quaternary salts is greater than 20. This represents a lower limit for k_1^H/k_1^D, the isotope effect for carbanion formation, and, on substitution into eq. 9, it gives a lower limit of 1.0 for the ratio of k_{-1}/k_e.

An upper limit for this ratio can be established by substituting into eq. 9 the maximum probable value for k_1^H/k_1^D. The largest hydrogen–deuterium isotope effect for a proton transfer reaction has been reported by Lewis and Funderburk (35) who observed a value of 24.8 for the reaction of 2,4,6-trimethylpyridine with 2-nitropropane and 2-nitropropane-2-*d* at 25°. A calculation based on the activation parameters determined by these authors gives a value of approximately 150 for this effect at −55°. Substitution of this value for k_1^H/k_1^D in eq. 9 gives a k_{-1}/k_e ratio of 14.

Neither of these limits represents probable ratios for the rates of carbanion return and elimination. The lower limit of 1.0 has been based on an experimentally observed value for the isotope effect for 1,3-elimination which has not been corrected for the extensive exchange which accompanies the reaction of the deuterated salt; the upper limit of 14 is based on an isotope effect which is undoubtedly much too high for a reaction in which there is relatively little steric hindrance to proton abstraction (35). Although it is not possible to specify narrower limits with any degree of certainty, a range of 3–10 would seem reasonable.

Experimental

Preparation of 3,3-Dideutero-3-phenyltrimethylammonium Iodide

This compound was prepared in four steps from 1,1-dideuterobenzyl chloride (8.6 g, 0.066 mol) which was made by the method of Buncel and Bourns (26). The chloride was converted to the Grignard reagent which was treated with ethylene oxide to give 3,3-dideutero-3-phenylpropanol (36). The alcohol was converted to the tosylate and thence to *N*,*N*-dimethyl-3,3-dideutero-3-phenylpropylamine by reaction with dimethylamine (37). Reaction of the amine with methyl iodide gave the quaternary salt (8.0 g) which was recrystallized from ethanol–ether to a constant m.p. of 178.0–178.5° (uncorrected); lit. m.p. 178.5–180° (37). The product contained 1.96 atoms D/molecule.[5] The undeuterated salt was prepared by the same sequence of reactions.

General Experimental Procedure

The apparatus used for the reaction of the quaternary ammonium salt with potassium amide in liquid ammonia is shown in Fig. 1. Reaction flask A contained a magnetic stirrer and was fitted with a Dry Ice–acetone condenser, D_1, and a vial, E_1, for adding potassium metal. Flask B was

[5]Deuterium analyses were performed by Mr. J. Nemeth, 303 Washington Street, Urbana, Ill.

Can. J. Chem. Downloaded from www.nrcresearchpress.com by 210.87.254.105 on 09/05/12
For personal use only.

Can. J. Chem. Downloaded from www.nrcresearchpress.com by 210.87.254.105 on 09/05/12
For personal use only.

fitted with an air-tight stirrer, a Dry Ice–acetone condenser, D_2, and a vial, E_2, for addition of ammonium chloride. Condenser, D_1, was connected to nitrogen and ammonia purification trains and D_2 to a barium oxide drying tube, F, whose exit tube passed into a bubbler, H, containing oil. Ferric nitrate nonahydrate (10 mg) was placed in flask A and the quaternary salt (usually 2 g) was added to flask B. Following a thorough flaming of the apparatus and flushing with nitrogen, 200 ml of ammonia was condensed into flask B and 100 ml into flask A. Potassium metal (usually 0.57 g) was added slowly with stirring to A. Thirty minutes after the blue color of the potassium had disappeared, D_1 was replaced by an adapter joined to the nitrogen train, both flasks were cooled to $-55 \pm 1°$ in a Dry Ice–diacetone alcohol bath, flask A was inverted, and the amide solution was pushed by nitrogen through a glass wool filter, G, into B.

The reaction was stopped by adding an excess of ammonium chloride. Ether (200 ml) was added to flask B, which was equipped with a water condenser connected to a gas-wash bottle containing ether, and the ammonia was evaporated slowly. Finally, 100 ml of water was added to B to dissolve the residual salts, the ether layer was separated and the aqueous layer extracted with additional ether. The combined ether solutions contained the hydrocarbon products and the aqueous solution the unreacted quaternary salt.

Product Identification and Analysis

The ether solution was concentrated by distillation using a spinning band column and the residue analyzed by gas chromatography using a 3/8 in. × 20 ft column of 30% SE-30 on 45/60 mesh Chromosorb P at 150°. Three components were separated but only component 2 was recovered in sufficient quantity for identification. Both its n.m.r. and i.r. spectra were identical to those reported for phenylcyclopropane (23, 24).

The minor products were present in much larger amounts in the reaction of the deuterated salt. Component 1 was identified as 3-phenylpropene from its retention time on the gas chromatograph and its i.r. spectrum. Component 2 had the same retention time as phenylcyclopropane and *trans*-1-phenylpropene which is known to be formed by isomerization of 3-phenylpropene (component 1) under the reaction conditions (22). Also, its n.m.r. spectrum corresponded to that expected for a mixture of 1-phenylcyclopropane-1-*d* and *trans*-1-phenylpropene-1-*d*. Identification of component 2 as a mixture of these two hydrocarbons was confirmed by the observation that three different methods of quantitative analysis, each assuming this composition, gave identical results: integration of the n.m.r. spectrum, gas chromatographic analysis using temperature programming on a 1/4 in. × 40 ft column of 5% Ucon Polar,[6] and u.v. spectroscopy at 250 mμ, where the molar extinction coefficient for *trans*-1-phenylpropene was found to be 16 000 and for phenylcyclopropane 153. Finally, component 3 had a retention time which was identical to that of *cis*-1-phenylpropene, which is a minor product of the base-catalyzed isomerization of 3-phenylpropene.

Extent of Reaction

The extent of reaction, required for both hydrogen and nitrogen isotope effect measurements, was determined by quantitative recovery of unreacted quaternary ammonium iodide. The water layer from the reaction mixture was taken nearly to dryness to remove ether and ammonia and the concentrated solution was diluted with water and passed through an anion exchange column (Dowex 1-X8, 100/200 mesh) in the chloride form. The eluant was taken to dryness and the residual chloride salts were thoroughly dried. The salts were shaken for several hours with excess anhydrous acetone and the insoluble potassium and ammonium chlorides were separated by filtration. The quaternary chloride, recovered from the filtrate by removal of acetone, was dissolved in water and the solution was treated with silver oxide and filtered. The filtrate was brought to a p*H* of 5.5 with hydriodic acid, filtered and taken to dryness. Control experiments in which the quaternary iodide was recovered by this procedure from a solution of liquid ammonia containing more than twice the amount of potassium and ammonium chloride and iodide salts that would be present in reaction mixtures showed that the error in the extent of reaction would not exceed 3%.

Test for the Carbene Mechanism

Deuterium analyses were done on the phenylcyclopropane–*trans*-1-phenylpropene product (component 2) from the reaction of the deuterated salt using n.m.r. and mass spectroscopy. For the latter, the ionization voltage was 8.5 eV and the relative intensities of the mass peaks were compared with those for a synthetic sample of undeuterated hydrocarbon of the same composition (71% phenylcyclopropane and 29% *trans*-1-phenylpropene). The percentage of undeuterated, monodeuterated, and dideuterated hydrocarbon in the product was calculated by the method described by Biemann (38).

Test for the Ylide Mechanism

To a solution of 3,3-dideutero-3-phenylpropyltrimethylammonium iodide (0.44 g, 0.0014 mol) in 45 ml of ammonia was added a solution of potassium amide prepared by adding potassium (0.30 g, 0.0077 mol) to 65 ml of ammonia. The reaction was quenched with ammonium chloride after 30 min and 100 ml of ether was added. The ammonia and trimethylamine were distilled into 1 l of stirred ice-cold hydrochloric acid. The hydrochloride salts, recovered by removal of excess acid under reduced pressure, were dried and the trimethylammonium chloride was extracted from the large excess of ammonium chloride by stirring successively with 600 ml of ethanol and two 550 ml portions of chloroform. The salt, recovered by evaporation of the combined solutions, was further purified by a second chloroform extraction. It was then dissolved in ethanol, the solution made basic to phenolphthalein with sodium ethoxide and the resulting trimethylamine purified by gas chromatography using a 10 ft × 3/8 in. column of 20% amine 220 on 60/80 mesh, base-washed Chromosorb W[7] at 55°. Its mass spectrum was compared with that obtained from a purified sample of trimethylamine of natural isotopic abundance.

Test for Isotopic Exchange at C-3 of 3,3-Dideutero-3-phenylpropyltrimethylammonium Iodide in Liquid Ammonia

Two deuterium exchange experiments each using 1.1 g (0.0035 mol) of deuterated salt were carried out as described

[6]This analysis was done by Varian Aerograph, Walnut Creek, California.

[7]The column was obtained from Varian Aerograph, Walnut Creek, California.

Can. J. Chem. Downloaded from www.nrcresearchpress.com by 210.87.254.105 on 09/05/12
For personal use only.

under General Experimental Procedure. The reactions were quenched after 9 min, the unreacted salt was recovered, recrystallized from ethanol–diethyl ether, and analyzed for deuterium.[5] The extent of reaction in each case was 66 ± 2%. A control experiment showed that no deuterium is lost in the recovery and purification procedures.

Hydrogen Isotope Effect Determination by the Competitive Method

A mixture of undeuterated and dideuterated quaternary salts (0.395 g, 0.0013 mol and 0.358 g, 0.0012 mol, respectively) in 300 ml of liquid ammonia was treated with base prepared by adding potassium (0.309 g, 0.0075 mol) to 150 ml of liquid ammonia. The reaction was quenched after 92 s by addition of ammonium chloride and the unreacted salt was recovered, purified, and analyzed[5] for deuterium.

Nitrogen Isotope Effect Determination

The nitrogen isotope effect in the elimination reaction was determined by comparing the N^{14}/N^{15} ratios for the quaternary salt recovered from reactions carried to known extents of completion with this ratio in the initial reactant (28). Samples of salt were decomposed in a Kjeldahl digestion to ammonium sulfate which was then oxidized to molecular nitrogen for mass spectrometric analysis (27). A control experiment showed that there is no isotopic fractionation in the recovery and purification procedures.

Studies in Ammonia-d_3

(a) Reaction of Undeuterated Quaternary Salt

3-Phenylpropyltrimethylammonium (1.11 g, 0.0036 mol) in 100 ml of ammonia-d_3 (Merck, Sharpe and Dohme) was treated with base formed by the addition of potassium (0.114 g, 0.0029 mol) to 75 ml of ammonia-d_3. The reaction mixture was colorless rather than the deep reddish-brown of all other reactions. The reaction was quenched after 45 min with ammonium chloride and the unreacted quaternary salt recovered and purified.

The i.r. spectrum of the recovered salt in a potassium bromide disc showed none of the absorptions associated with the C_3—D bonds while the intensities of the C_3—H absorptions were the same as those for the starting compound. On the other hand, the absorptions associated with the *N*-methyl C—H and C_1—H bonds were much less intense and several new absorptions associated with *N*-methyl C—D and C_1—D bonds were observed. Analysis of the 100 MHz n.m.r. spectrum of the recovered salt in deuterium oxide confirmed that there had been no exchange of C-2 and -3 hydrogens but that 50% of the *N*-methyl hydrogens and 35% of the C-1 hydrogens had been replaced by deuterium.

Gas chromatographic analysis of the hydrocarbon product failed to show the presence of any of the isomeric phenylpropenes. An upper limit of 0.4% phenylpropenes was established by showing that the amount of 3-phenylpropene which would have been formed by this percentage of β-elimination produced a distinct coloration whereas the reaction solution was colorless.

(b) Reaction of Deuterated Quaternary Salt

3,3-Dideutero-3-phenylpropyltrimethylammonium iodide (0.97 g, 0.0032 mol) in 100 ml of ammonia-d_3 was treated with base prepared from potassium (0.35 g, 0.009 mol) in 75 ml of ammonia-d_3. The reaction was quenched with ammonium chloride after 90 min. Neither 3-phenylpropene nor *cis*-1-phenylpropene was detected by gas chromatography while only 2.3% of *trans*-1-phenylpropene, the phenylpropene which predominates in basic solution under equilibrium conditions (22), was shown to be present by u.v. spectroscopy. A control experiment showed that the latter olefin does not undergo significant polymerization under the conditions of the experiment.

The authors are greatly indebted to the National Research Council of Canada for the financial support for this investigation and the Department of University Affairs of the Province of Ontario for scholarships (to K.C.W.).

1. A. NICKON and N. H. WERSTIUK. J. Am. Chem. Soc. **89**, 3914 (1967).
2. S. WINSTEIN, E. CLIPPINGER, R. HOWE, and E. VOGELFANGER. J. Am. Chem. Soc. **87**, 376 (1965).
3. B. M. BENJAMIN, B. W. PONDER, and C. J. COLLINS. J. Am. Chem. Soc. **88**, 1558 (1966).
4. A. NICKON and N. H. WERSTIUK. J. Am. Chem. Soc. **89**, 3915 (1967); A. NICKON and N. H. WERSTIUK. J. Am. Chem. Soc. **89**, 3917 (1967).
5. F. M. SONNENBERG and J. K. STILLE. J. Org. Chem. **31**, 3441 (1966); J. K. STILLE and F. M. SONNENBERG. Tetrahedron Lett. 4587 (1966); H. KWART, T. TAKESHITA, and J. L. NYCE. J. Am. Chem. Soc. **86**, 2606 (1964).
6. J. MEINWALD, C. SWITHENBANK, and A. LEWIS. J. Am. Chem. Soc. **85**, 1880 (1963); J. MEINWALD and J. K. CRANDALL. J. Am. Chem. Soc. **88**, 1292 (1966); S. J. CRISTOL and B. B. JARVIS. J. Am. Chem. Soc. **88**, 3095 (1966); S. J. CRISTOL, J. K. HARRINGTON, and M. S. SINGER. J. Am. Chem. Soc. **88**, 1529 (1966); S. J. CRISTOL and B. B. JARVIS. J. Am. Chem. Soc. **89**, 401 (1967).
7. H. O. HOUSE and F. A. RICHEY, JR. J. Org. Chem. **32**, 2151 (1967); H. R. NACE and B. A. OLSEN. J. Org. Chem. **32**, 3438 (1967); F. G. BORDWELL, R. R. FRAME, R. G. SCAMEHORN, J. G. STRONG, and SEYMOUR MEYERSON. J. Am. Chem. Soc. **89**, 6704 (1967); F. G. BORDWELL and M. W. CARLSON. J. Am. Chem. Soc. **92**, 3370 (1970).
8. L. FRIEDMAN and J. G. BERGER. J. Am. Chem. Soc. **83**, 492 (1961); W. KIRMSE and W. VON E. DOERING. Tetrahedron, **11**, 266 (1960).
9. R. A. RAPHAEL. *In* Chemistry of carbon compounds. Vol. IIA. *Edited by* E. H. Rodd. Elsevier Publishing Co., New York, N.Y., 1953. p. 24; J. WEINSTOCK. J. Org. Chem. **21**, 540 (1956).
10. W. E. TRUCE and L. B. LINDY. J. Org. Chem. **26**, 1463 (1961).
11. N. P. NEURIETER and F. G. BORDWELL. J. Am. Chem. Soc. **85**, 1209 (1963).
12. P. G. BAY. Chem. Abstr. **60**, 421 (1964).
13. J. B. CLOKE, E. STEHR, T. R. STEADMAN, and L. C. WESCOTT. J. Am. Chem. Soc. **67**, 1587 (1945); C. GILBERT, M. C. ROUX-SCHMITT, and J. SEYDEN-PENNE. Bull. Soc. Chim. Fr. 2405 (1970).
14. H. M. WALBORSKY and C. G. PITT. J. Am. Chem. Soc. **84**, 4831 (1962).
15. C. L. BUMGARDNER. Chem. Ind., 1555 (1958); C. L. BUMGARDNER. J. Am. Chem. Soc. **83**, 4420 (1961).
16. C. L. BUMGARDNER. J. Am. Chem. Soc. **83**, 4423 (1961).

17. C. L. BUMGARDNER. J. Org. Chem. **29**, 767 (1964); C. L. BUMGARDNER. Chem. Commun. 374 (1965); C. L. BUMGARDNER and H. IWERKS. J. Am. Chem. Soc. **88**, 5518 (1966).
18. R. BAKER and M. J. SPILLETT. J. Chem. Soc. B, 581 (1969).
19. R. BAKER and M. J. SPILLETT. J. Chem. Soc. B, 880 (1969).
20. R. BRESLOW. Tetrahedron Lett. 399 (1964).
21. D. V. BANTHORPE. Elimination reactions. Elsevier Publishing Co., New York, N.Y., 1963. p. 105.
22. T. W. CAMPBELL and W. G. YOUNG. J. Am. Chem. Soc. **69**, 688 (1947); E. A. RABINOVICH, I. V. ASTAF'EV, and A. I. SHATENSHTEIN. Zh. Obshch. Khim. U.S.S.R. **32**, 748 (1962). Chem. Abstr. **58**, 6673*e* (1963).
23. Varian Associates. Varian high resolution N.M.R. spectra catalogue, Vol. 2. Instrument Division, Palo Alto, California. 1963. Spectrum 528.
24. F. WEYGAND, H. DANIEL, and H. SIMON. Chem. Ber. **91**, 1691 (1958); G. AYREY, E. BUNCEL, and A. N. BOURNS. Proc. Chem. Soc. 458 (1961); W. H. SAUNDERS, JR. and D. PAVLOVIĆ. Chem. and Ind., 180 (1962).
25. A. C. COPE and A. S. MEHTA. J. Am. Chem. Soc. **85**, 1949 (1963); A. S. MEHTA. Ph.D. Thesis. Massachusetts Institute of Technology, Cambridge, Mass., 1963.
26. E. BUNCEL and A. N. BOURNS. Can. J. Chem. **38**, 2457 (1960); P. J. SMITH and A. N. BOURNS. Can. J. Chem. **44**, 2553 (1966).
27. G. AYREY, A. N. BOURNS, and V. A. VYAS. Can. J. Chem. **41**, 1759 (1963).
28. J. BIGELEISEN and M. WOLFSBERG. Advances in chemical physics. Vol. 1. Interscience, New York, N.Y., 1958. p. 15.
29. L. MELANDER. Isotope effects on reaction rates. Ronald Press, New York, N.Y., 1960. p. 20.
30. A. C. FROSST. Ph.D. Thesis. McMaster University, Hamilton, Ontario, 1968. pp. 116–118.
31. A. N. BOURNS and P. J. SMITH. Proc. Chem. Soc. 366 (1964); P. J. SMITH and A. N. BOURNS. Can. J. Chem. **48**, 125 (1970).
32. R. P. BELL. The proton in chemistry. Cornell University Press, Ithaca, New York, 1959. p. 211.
33. S. BRATOŽ and M. ALLAVENA. J. Chem. Phys. **37**, 2138 (1962).
34. L. J. BELLAMY. The infra-red spectra of complex molecules. J. Wiley and Sons, New York, N.Y., 1958.
35. E. S. LEWIS and L. H. FUNDERBURK. J. Am. Chem. Soc. **89**, 2322 (1967).
36. R. C. HUSTON and A. H. AGETT. J. Org. Chem. **6**, 123 (1941).
37. A. C. COPE and C. L. BUMGARDNER. J. Am. Chem. Soc. **79**, 960 (1957).
38. K. BIEMANN. Mass spectrometry, organic chemical applications. McGraw–Hill, New York, N.Y., 1962. Chapt. 5.
39. A. N. BOURNS and A. C. FROSST. Can. J. Chem. **48**, 133 (1970).

Can. J. Chem. Downloaded from www.nrcresearchpress.com by 210.87.254.105 on 09/05/12
For personal use only.

Sigma and Pi Electron Contributions to Long-range Spin–Spin Coupling Constants in the Methyl Derivatives of the Fluoropyridines

J. B. ROWBOTHAM[1] AND T. SCHAEFER

Department of Chemistry, University of Manitoba, Winnipeg, Manitoba R3T 2N2

Received February 8, 1972

Seven methyl derivatives of the 3- and 4-fluoropyridines are synthesized and their p.m.r. spectra are analyzed. The nuclear spin–spin coupling constants are compared with previous results for the four methyl derivatives of 2-fluoropyridine. A model in which the nitrogen atom polarizes primarily the σ electron system of the ring, leaving the π electron contribution to the coupling mechanism relatively unaffected, qualitatively accounts for the large majority of the coupling constants. For example, the coupling over six bonds between methyl protons and a fluorine nucleus, J_p^{F,CH_3}, is the same whether the fluorine atom or the methyl group is placed ortho to the nitrogen atom and is little different from its value in *p*-fluorotoluene. The model is consistent with significant σ electron contributions to long-range couplings over four and five bonds from methyl protons to fluorine nuclei or ring protons. Evidence is adduced for resonance structures in which fluorine conjugates with nitrogen or with ring carbon atoms. An earlier suggestion, that hyperconjugation of the methyl group with nitrogen is necessary to the interpretation of the observed couplings, is dropped. Instead, a substantial polarization of the σ electron core near C-2 and -6 is invoked but apparently does not extend appreciably beyond these atoms in the ring.

Sept dérivés méthylés des fluoro-3 et 4 pyridines sont synthétisés et leurs spectres r.m.n. analysés. Les constantes de couplage spin–spin sont comparées aux résultats antérieurs obtenus pour les quatre dérivés méthylés de la fluoro-2 pyridine. Un modèle dans lequel l'atome d'azote polarise principalement le système électronique σ du cycle laissant relativement inchangée la contribution électronique π au mécanisme du couplage, explique qualitativement la grande majorité des constantes de couplage. Par exemple, le couplage à travers six liaisons entre les protons du méthyle et le noyau de fluor, J_p^{F,CH_3}, est le même si le fluor ou le méthyle est placé en ortho par rapport à l'azote et diffère peu de la valeur obtenue dans le *p*-fluorotoluène. Le modèle est compatible avec les contributions importantes des électrons σ aux couplages à longue distance à travers quatre et cinq liaisons, à partir des protons du méthyle au noyau du fluor ou au protons du cycle. Une preuve de structures résonantes dans lesquelles le fluor se conjugue à l'azote ou aux atomes de carbone du cycle est apportée. La suggestion première selon laquelle l'hyperconjugaison du groupe méthyle avec l'azote est nécessaire à l'interprétation des couplages observés, n'est pas retenue. A la place, une polarisation substantielle des électrons σ proches du C-2 et du -6 est avancée mais ne s'étend pas apparemment au-delà de ces derniers de façon notable.

Canadian Journal of Chemistry, **50**, 2344 (1972)

Introduction

A model in which σ and π electron contributions to ring proton and to ring proton – fluorine spin–spin coupling constants are distinguished has been successfully applied to the methyl derivatives, **1**–**4**, of 2-fluoropyridines (1, 2). In these compounds the signs and magnitudes of the long-range coupling constants between the methyl protons and the ring protons or the fluorine nucleus support the assumption (3) that the nitrogen atom primarily polarizes the proximate σ bonds, leaving the π electron contribution to the coupling constants mainly unaffected (2). Certain resonance structures of these molecules were invoked in the interpretation of the coupling data (2) apropos of which a referee pointed out the desirability of the examination of the methyl derivatives of the 3- and

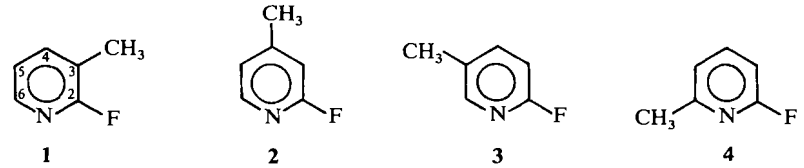

1 **2** **3** **4**

[1]Postdoctoral Fellow, 1970–1972.

Can. J. Chem. Downloaded from www.nrcresearchpress.com by 210.87.254.40 on 09/05/12
For personal use only.

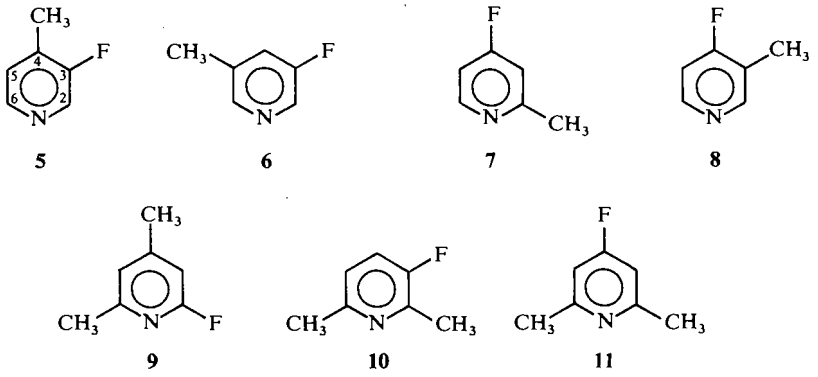

5 6 7 8

9 10 11

4-fluoropyridines. Accordingly the synthesis of a series of these derivatives is reported here, together with the analyses of their p.m.r. spectra. The ensuing spin–spin coupling data are discussed in terms of the earlier model.

Acquaintance with the earlier work (1, 2) is assumed in this final report.

Experimental

(1) Syntheses of Compounds

These were prepared by Schiemann reactions (2) on the respective amines. To prepare **7**, **8**, **9**, and **11** the amine was dissolved in excess 50% aqueous HBF_4 and then treated in the cold with solid $NaNO_2$ over several hours. After heating the solution at 50 °C for 1 h, it was diluted with water, neutralized, and extracted with ether. Distillation of the dried extracts gave poor yields of the methylfluoropyridines.

An improved method (4) was used to prepare **5**, **6** and **10**. The amine was dissolved in the minimum aqueous HBF_4 necessary to maintain fluidity and the cold mixture was treated with excess solid $NaNO_2$ over a period of 0.5 h. The mixture was quickly filtered and the diazonium fluoroborate was covered with pentane (hexane for **5**). The salts decomposed smoothly on heating (**6** and **10** were decomposing on the cool filter but **5** was stable in boiling pentane). A good yield of product was obtained by extraction with dilute HCl, neutralization, steam distillation of the extracts, extraction of the distillate with ether, and distillation under reduced pressure.

Only the amine precursor of **9** was commercially available. The 4-amino-2-picoline, 4-amino-3-picoline, and 4-amino-2,6-lutidine were obtained by nitration and catalytic reduction of the pyridine oxides (5). The 3-amino-2,6-lutidine was prepared via hydrogenation of the commercially available nitro compound in ethanol. 2-Chloro-5-nitro-3-picoline was obtained by nitration, hydrolysis, and treatment with phosphorous oxychloride from 2-amino-3-picoline (6, 7). Hydrogenation over Pd/C in ethanol at 1 atm gave 3-amino-5-picoline. Similarly, 2-amino-4-picoline gave 3-amino-4-picoline. No attempt was made to separate the intermediate isomeric mixtures.

All fluorine compounds had p.m.r. spectra consistent with their structures and all had a mint-like odor. Compounds **5**, **6**, **7**, and **10** have been previously reported (4, 6, 7) while the amine precursors for **8**, **9**, and **11** are known (5, 8).

(2) Proton Magnetic Resonance Measurements

Degassed samples were prepared as 17–30 mol % solutions in carbon disulfide, tetramethylsilane, or benzene-d_6 by the freeze–pump–thaw technique. The choice of solvents, all of low dielectric constant, was dictated by the desire to prevent, as far as possible, the overlap of peaks from different proton groupings.

The peaks belonging to H_2 or H_6 were fairly broad because of incompletely relaxed spin–spin coupling to ^{14}N, but addition of small amounts of trifluoroacetic acid (*1*) did not sharpen these significantly.[2] In consequence the derived coupling constants between fluorine and H_2 or H_6, and between H_2 and H_6, have an uncertainty of about 0.1 Hz.

Proton magnetic resonance spectra were recorded on a Varian DA-60I spectrometer (**10** was measured at 100 MHz on an HA100D spectrometer) in the frequency sweep mode, with internal tetramethylsilane serving as a locking material. The spectra were repeatedly calibrated at intervals of about 5 Hz by reading sweep and manual oscillator frequencies and were measured at a sweep width of 50 Hz at sweep speeds of 0.01 Hz/s. Decoupling as well as weak irradiation experiments (9) employed an HP-4204A audio oscillator and/or a Wavetek 114 sweep generator (10).

For the n.O.e. experiment (11, 12) on **6** in benzene-d_6 solution the spectrometer was locked on internal trifluoroacetic acid. Four scans were made of the H_2 and H_6 regions without strong irradiation of the methyl proton region, followed by four more during which the methyl protons were strongly irradiated. Peak areas were found by weighing and a 10% increase in the area from one set of peaks was taken as indicating that they originated in H_6.

(3) Spectral Analysis

Spectra were analyzed on an IBM 360/65 computer using the program LAME (13) in iterative or noniterative mode; followed by a plotting routine (devised by J.B.R.) which drove a CalComp incremental plotter. The plotting program gave each transition a Lorentzian shape of width $2a$ at half-height, $\Delta\nu_{1/2} = 2a$, retaining this value until the highest point

[2]The splittings of H_6 in **1** were rather larger than those found in the present compounds.

Can. J. Chem. Downloaded from www.nrcresearchpress.com by 210.87.254.40 on 09/05/12
For personal use only.

TABLE 1. Proton chemical shifts* and coupling constants† in some methylfluoropyridines

Parameter	**5**(C_6D_6, 21)‡	**6**(C_6D_6, 24)	7(CS_2, 20)	**8**(TMS, 30)	**9**(CS_2, 17)	**10**(C_6D_6, 24)	**11**(CS_2, 17)
ν_2	8.26	8.20	(2.461)	8.36	—	(2.381)	(2.408)
ν_3	—	—	6.786	(2.162)	6.371	—	6.549
ν_4	(1.899)	6.743	—	—	(2.274)	6.815	—
ν_5	6.626	(1.882)	6.756	6.934	6.725	6.515	6.549
ν_6	8.10	8.08	8.35	8.34	(2.329)	(2.315)	(2.408)
$J_o^{H,H}$	+4.80	—	+5.69	+5.55	—	8.34	—
$J_m^{H,H}$	<0.3	+2.79[2,4]	+2.47	<0.3	1.20	—	—
	—	+1.78[4,6]	—	—	—	—	—
	—	<0.5[2,6]	—	—	—	—	—
$J_p^{H,H}$	+0.51	—	+0.50	+0.43	—	—	—
$J_o^{H,F}$	+1.5	+0.7[2]	9.85[3]	+9.50	−2.24	9.34	9.51
	—	+9.46[4]	+8.57[5]	—	—	—	—
$J_m^{H,F}$	+6.54	—	+8.9	+10.2[2]	—	3.61	—
	—	—	—	+7.8[6]	—	—	—
$J_p^{H,F}$	+1.2	+2.2	—	—	+2.20	—	—
J_o^{H,CH_3}	(−)0.79	−0.75[4]	−0.51	−0.81	(−)0.77[3,4]	(−)0.52	§
	—	−0.70[6]	—	—	(−)0.60[4,5]	—	—
	—	—	—	—	(−)0.60[5,6]	—	—
J_m^{H,CH_3}	+0.34[2]	—	0.27	+0.41	—	0.35[2]	—
	+0.34[6]	—	—	—	—	0.33[6]	—
J_p^{H,CH_3}	—	−0.63	−0.55	−0.62	(−)0.60	(−)0.59	§
J_o^{F,CH_3}	+1.71	—	—	+1.63	—	3.03	—
J_m^{F,CH_3}	—	(−)0.10	−0.27	—	(−)0.17[4]	—	(−)0.25
	—	—	—	—	(−)0.59[6]	—	—
J_p^{F,CH_3}	—	—	—	—	—	1.21	—
$J_m^{CH_3,CH_3}$	—	—	—	—	(−)0.17	(−)0.21	—

*In p.p.m. to low field of internal TMS; parentheses indicate methyl protons.
†In Hz; when the sign is omitted or is given in parentheses it was not determined. Square brackets indicate ring positions.
‡Solvent and concentration (mol %).
§In **11** one can find only $|J_o^{H,CH_3} + J_p^{H,CH_3}| = 1.08$ Hz because of the symmetrical nature of the spectrum.

on the peak was reached, then changing to a Lorentzian shape with $\Delta\nu_{1/2} = 2b$ for the remainder of the peak. Thus the composite computed peak was determined by two parameters: the width, $a + b$, and the asymmetry, $a/(a + b)$. The asymmetry parameter was generally set at 0.6–0.65 to best simulate the experimental effects of finite sweep times. A total width of about 0.15 Hz generally reproduced the experimental linewidth best but a width of up to 0.8 Hz was used to simulate the broad peaks from H_2 or H_6.

Analysis of the spectra was generally straightforward, particularly when decoupling of specific methyl protons was employed in extracting preliminary spectral parameters for ring protons and fluorine. For **9**, **10**, and **11** all transitions were assigned and all parameters (except, of course, the fluorine shift) were allowed to vary in the final iterations. The transitions associated with H_2 and/or H_6 in the other compounds were not assigned and therefore their chemical shifts as well as their couplings to fluorine and to each other could not be allowed to vary. These were determined by trial and error methods employing the noniterative mode of LAME. The r.m.s. deviations between calculated and observed transitions were always less than 0.023 Hz, standard deviations of the spectral parameters were less than 0.01 Hz and correlation coefficients were less than 0.3 except between the chemical shift of H_5 and $^3J_o^{H^5,H^6}$ in 7, which was 0.8; this is a consequence of the incomplete assignment of transitions to observed peak positions in the H_6 region.

In one or two cases the derived spectral parameters were not immediately assignable to specific protons. For instance, in **10** the protons of the two methyl groups differ only in their chemical shifts and in their coupling to fluorine. They were assigned on the basis that $^6J_p^{F,CH_3}$ is smaller than $^4J_o^{F,CH_3}$, and is almost independent of substituent effects, even of the presence of a heteroatom (2, 14, 15). Again, the ring protons in **9** were assigned on the basis of their relative chemical shifts by analogy with **2** and **4**, measured in the same solvent (2) while the methyl protons were assigned so that the couplings to fluorine agreed with those in **2** and **4** (2).

Results and Discussion

The spectral parameters of **5**–**11** are given in Table 1. Tickling experiments provided the relative signs of the couplings in many cases. When

Can. J. Chem. Downloaded from www.nrcresearchpress.com by 210.87.254.40 on 09/05/12
For personal use only.

Can. J. Chem. Downloaded from www.nrcresearchpress.com by 210.87.254.40 on 09/05/12
For personal use only.

the sign is shown in parentheses it was not determined directly but was assigned on the basis of well-documented previous work (1, 2, 15–18). Attempts at confirming the signs of certain couplings failed, usually because the relevant splittings in the spectrum were not sufficiently well resolved. Thus the sign of $^4J_m^{H_2,H_6}$ is not known from this study but is known to be negative in pyridine itself (17); the sign of $^5J_m^{F,CH_3}$ in **6** is also unknown from the present measurements.

For reasons of space the observed and computed spectra are not displayed here, but show excellent agreement with each other and are certainly not inferior to those portrayed in detail for **1** (1).

(1) The Methyl Proton–Ring Proton Coupling Constants

(a) Over Six Bonds, $^6J_p^{H,CH_3}$

In toluene (19) J_p^{H,CH_3} is -0.62 ± 0.02 Hz, the same as in **6**, **8**, **9**, and **10**; confirming the data on **1** and **4** (1, 2) and bearing out the earlier conclusion (2) that, as this coupling constant arises from a π electron mechanism (16, 20, 21), the nitrogen and fluorine atoms are ineffectual in altering the π electron contribution to J_p^{H,CH_3}. The smaller value of -0.55 Hz in **7** is considered as insufficiently different from that in the other compounds to weaken this conclusion.

(b) Over Four Bonds, $^4J_o^{H,CH_3}$

In ref. 2 it was argued that, as the negative π electron contribution to J_o^{H,CH_3} is expected to increase as the mobile bond order of the intervening C=C bond increases, the data for **1**, **2**, and **3** were consistent with a contribution from the resonance structure **12**. Extension of the argument to **5**, **6**, and **8** involves **13**, **14**, and **15**, where on *a priori* grounds **12** and **15** may well be favored over **13** or **14** because the strong nitrogen acceptor is placed ortho or para to the fluorine donor in **12** and **15**. In **2** one has $J_o^{H_3,CH_3}$ equal to 0.81 Hz (2), the same as in **8** and indicating **12** and **15** as equally important structures; in accord with quadrupole resonance data (22) and relevant to a referee's comment on ref. 2 concerning the importance of structures of this type. The somewhat smaller magnitudes of this coupling in **5** and **6** suggest that contributions from **13** and **14** are less important than those of **12** and **15**.

The even smaller magnitudes of -0.5 to -0.6 Hz occurring for J_o^{H,CH_3} when a methyl group is situated ortho to the nitrogen atom, as in **4** (2), **7**, **9**, and **10**, were originally (2) attributed either to a structure of the type **16** which decreases the

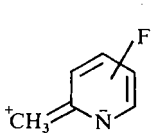

16

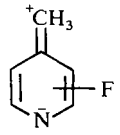

17

mobile bond order between C-5 and -6; or to a decrease in the negative σ electron contribution to J_o^{H,CH_3}, caused by a polarization of the σ core by the nitrogen atom and operating to decrease the σ density near C-6. The former proposal now appears untenable for the following reasons. The methyl group is undoubtedly a weaker π electron donor than a fluorine atom (23). Now because **12** and **15** have here and previously (2) been shown to be fairly important structures in the interpretation of the coupling data, it follows that in **7**, where **15** applies and acts to increase the mobile bond order between C-2 and -3, J_o^{H,CH_3} should have roughly the same magnitude as in **8**. Yet it is 0.3 Hz smaller in magnitude. We think it unlikely that a structure of the type **16** would outweigh one of the type **15**. Again the two different magnitudes of J_o^{H,CH_3} in **2** (2) are in accord with a substantial contribution from **12** but not from **17**.

This conclusion leaves the alternative proposal of σ electron polarization of C-2 or -6 by the nitrogen atom as an explanation of the small magnitude of J_o^{H,CH_3} in those compounds where the methyl group is attached to these carbon atoms. An apparent objection cites the fact that J_o^{H,CH_3} is -0.81 Hz in **8**, involving the ring

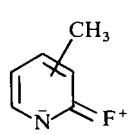

12

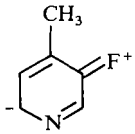

13

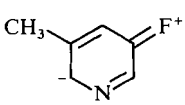

14

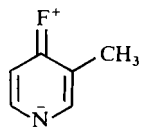

15

Can. J. Chem. Downloaded from www.nrcresearchpress.com by 210.87.254.40 on 09/05/12
For personal use only.

proton at C-2, and asks why the decrease in a σ electron contribution to J_o^{H,CH_3} occurs only when the methyl group is attached at C-2. A probable answer cites the possible coupling pathways recently discussed in detail (24, 25). In brief, the exchange integrals involved in the coupling mechanism in a valence bond formulation may be quite different in the two situations (25). Quantitative calculations by a molecular orbital method (26) on propene derivatives predict a marked positive shift in the *cisoid* allylic coupling when substitution occurs at C-2, in agreement with experiment; while the observed change in this coupling on substitution (by fluorine) at C-1 is zero (27). The situation is analogous to our observations, with nitrogen playing the role of the substituent and J_o^{H,CH_3} the role of the *cisoid* allylic coupling, $^4J_c^{H,CH_3}$, in the propene derivatives.

In terms of our model the positive shift in J_o^{H,CH_3}, occurring when the methyl group is bonded to C-2 or -6, is a σ electron effect. Further evidence that it is not a π electron effect can be adduced from two sources. First, a π electron coupling of this kind is proportional to Q_{CCH}, the hyperfine interaction constant of a methyl proton with the π electron system (28–30). In a series of radical anions of the methylpyridine derivatives no marked dependence of this parameter on the position of the methyl group is found (31). Second, a decrease in the Q_{CCH} value at C-2 and -6, which would account for the small magnitudes of the corresponding J_o^{H,CH_3} values, should then also be reflected in a decrease of J_o^{F,CH_3} in **10** relative to its values in **1**, **5**, and **8**. The opposite occurs.

(c) Over Five Bonds, $^5J_m^{H,CH_3}$

In ref. 2 it was reasoned that, as J_m^{H,CH_3} contains a substantial positive σ electron contribution (16, 21), the values of 0.28 Hz in **2** and **4** (0.1 Hz smaller than the 0.4 Hz observed in **1** and **3**) are in agreement with a σ electron polarization at C-2 or -6 by the nitrogen atom. In **2** and **4** these carbon atoms are involved in the coupling path. The couplings of 0.41 Hz in **8** and of 0.27 Hz in **7** are consistent with this assumption.

However, in **5** and **10** the J_m^{H,CH_3} values lie midway between the above extremes of 0.27 and 0.41 Hz but they are expected to lie near 0.27 Hz on the basis of the σ electron picture. There is the possibility that, because in **5** and **10** the fluorine atom is placed para to C-6 and ortho to C-2, resonance structures of the type **13** will enhance the π electron contribution to J_m^{H,CH_3} and thereby partially compensate for the reduction in the σ electron contribution. This is a reasonable proposal insofar as the fluorine is located meta to the nitrogen in **5** and **10**, disallowing its preferred conjugation with the latter; and a structure of type **13** certainly increases the π electron density at C-6, enlarging the relevant Cp_z orbital and thereby enhancing somewhat the hyperconjugative interaction with the methyl group orbitals. A similar argument would follow for position C-4 in **5**.[3]

In any event the contention that the π electron mechanism is relatively unaffected by the presence of the nitrogen atom is nicely supported by the values of (−) 0.17 and (−) 0.21 Hz for $^6J_m^{CH_3,CH_3}$ in **9** and **10**. They compare with a corresponding value of −0.19 Hz in a *m*-xylene derivative (16). As one or both of the methyl groups in **9** and **10** are bonded to C-2 and/or C-6 and as $^6J_m^{CH_3,CH_3}$ is probably accounted for by a π electron mechanism (21), one may strongly infer that the nitrogen atom acts to polarize the σ electron system without affecting the π electron contribution to J_m^{H,CH_3} and also that structures of type **16** are unnecessary in the explanation of the coupling data. Note that $^4J_m^{H_2,H_6}$ in pyridine is −0.13 Hz (17), in benzene it is 1.37 Hz (33) yet $J_m^{CH_3,CH_3}$ in **10** is the same as in a *m*-xylene derivative, a good example of the application of the present model.

One may also conclude that σ electrons play a substantial part in the transmission of spin information in J_o^{H,CH_3} and J_m^{H,CH_3}, this part being proportionately larger in the latter; in agreement with recent molecular orbital calculations on toluene (21) which imply a preponderant σ electron contribution to J_m^{H,CH_3}. If this implication is indeed valid it helps to account for the present observation of a greater sensitivity of J_m^{H,CH_3} than of J_o^{H,CH_3} to the proposed σ core polarization at the carbon atoms proximate to the nitrogen atom.

(2) The Methyl Proton–Fluorine Couplings

In *p*-fluorotoluene J_p^{F,CH_3} is 1.15 Hz (15) while in **3** it is 1.25 Hz (2), the fluorine atom lying ortho to the nitrogen atom. In **10**, where the positions of the fluorine atom and of the methyl

[3]This argument is perhaps an over-refinement of our model and we recognize that it smacks of "enthusiastic yodelling in the blue distance of ... conjecture"(32).

Can. J. Chem. Downloaded from www.nrcresearchpress.com by 210.87.254.40 on 09/05/12
For personal use only.

group have been interchanged, J_p^{F,CH_3} is 1.21 Hz. As it is unlikely that other than a π mechanism is important for this coupling (14, 21) the heteroatom has very little influence on the π contribution to J_p^{F,CH_3} in **3** and **10**, as predicted by the model. The variation in $J_p^{H,F}$ between 1.2 and 2.5 Hz in **1**–**11** can therefore be attributed mainly to a σ electron effect.

Considering now J_o^{F,CH_3} one has 1.45 Hz in **1** (1), 1.71 Hz in **5**, 1.63 Hz in **8**, and 2.1 Hz in a derivative of *o*-fluorotoluene (14), in line (1) with a dominant π electron contribution to J_o^{F,CH_3}; the variation in magnitude being attributable to a variable σ electron contribution to this coupling over four bonds. When the methyl group is bonded to C-2 as in **10**, J_o^{F,CH_3} is 3.03 Hz, representing a substantial positive shift from the magnitudes in the other compounds, and is at least qualitatively in line with the positive shift of the analogous J_o^{H,CH_3} values. Nevertheless the variations are small compared to the corresponding $J_o^{H,F}$ values which range from -3.12 Hz in **4** (2) to $+9.85$ Hz in **7**.

Finally, although $J_m^{H,F}$ varies between -1.02 Hz in **1** (1) and $+10.2$ Hz in **8**, the range of J_m^{F,CH_3} is only from (−) 0.10 Hz in **6** to -0.60 Hz in **4** (2) and does not deviate greatly from its value of -0.4_3 Hz in a derivative of *m*-fluorotoluene (14). On the basis of the model the large changes in $J_m^{H,F}$ arise mainly via the distortion of the σ core by the nitrogen atom.

(3) Ring Proton and Ring Proton–Fluorine Couplings

The data in Table 1 are in accord with the previous detailed discussion (1, 2) of such parameters in **1**–**4** and will not be fully described here. In brief they are consistent with an alternating (3, 34) electronegativity effect of the substituents, acting primarily through the σ electron system. Unfortunately we were unable to determine the sign of $^4J_m^{H_2,H_6}$ in **5**, **6**, and **8**. This coupling is negative in pyridine (17) but for **8** the additivity scheme (2) predicts $+0.1$ Hz.

The value of 10.2 Hz for $J_m^{H_2,F}$ in **8** is the largest known meta proton-fluorine coupling and is larger than all known $J_o^{H,F}$ values in derivatives of fluorobenzene, except that of 10.4 Hz in *o*-difluorobenzene (35).

Conclusions

The majority of the proton–proton and proton–fluorine spin–spin coupling constants in 11 methyl derivatives of the 2-, 3-, and 4-fluoropyridines can be rationalized in terms of a model in which the nitrogen atom polarizes the σ electron core predominantly at C-2 and -6 but does not strongly alter the π electron contribution to the coupling mechanisms. Thus, in these compounds J_p^{H,CH_3} and J_p^{F,CH_3} are little different from their values in toluene and *p*-fluorotoluene. The results also indicate an appreciable σ electron contribution to long-range couplings over four and five bonds from methyl protons to ring protons or fluorine nuclei.

We are grateful to the National Research Council of Canada for financial support.

1. T. Schaefer, S. S. Danyluk, and C. L. Bell. Can. J. Chem. **47**, 1507 (1969).
2. J. B. Rowbotham, R. Wasylishen, and T. Schaefer. Can. J. Chem. **49**, 1799 (1971).
3. S. Castellano and R. Kostelnik. J. Am. Chem. Soc. **90**, 141 (1968).
4. M. Bellas and H. Suschitzky. J. Chem. Soc. 2096 (1965).
5. R. F. Evans and H. C. Brown. J. Org. Chem. **27**, 1665 (1962).
6. A. Roe and R. B. Seligman. J. Org. Chem. **20**, 1729 (1955).
7. G. F. Hawkins and A. Roe. J. Org. Chem. **14**, 328 (1949).
8. W. Herz and L. Tsai. J. Am. Chem. Soc. **76**, 4184 (1954).
9. R. Freeman and W. A. Anderson. J. Chem. Phys. **37**, 2053 (1962).
10. V. P. Heuring and K. N. Scott. J. Mag. Res. **2**, 302 (1970).
11. F. A. L. Anet and A. J. R. Bourn. J. Am. Chem. Soc. **87**, 5250 (1965).
12. G. E. Bachers and T. Schaefer. Chem. Rev. **71**, 617 (1971).
13. C. W. Haigh and J. M. Williams. J. Mol. Spectrosc. **32**, 398 (1969).
14. D. J. Blears, S. S. Danyluk, and T. Schaefer. J. Chem. Phys. **47**, 5037 (1967).
15. R. Wasylishen and T. Schaefer. Can. J. Chem. **49**, 94 (1971).
16. C. J. Macdonald and W. F. Reynolds. Can. J. Chem. **48**, 1002 (1970).
17. S. Castellano, C. Sun, and R. Kostelnik. J. Chem. Phys. **46**, 327 (1967).
18. P. Diehl and R. J. Chuck. Mol. Phys. **14**, 183 (1968).
19. M. P. Williamson, R. J. Kostelnik, and S. M. Castellano. J. Chem. Phys. **49**, 2218 (1968).
20. M. Barfield and B. Chakrabarti. J. Am. Chem. Soc. **91**, 4346 (1969).
21. R. Wasylishen and T. Schaefer. Can. J. Chem. **50**, 1852 (1972).
22. L. Guibé and E. A. C. Lucken. Mol. Phys. **14**, 79 (1968).
23. C. G. Swain and E. C. Lupton, Jr. J. Am. Chem. Soc. **90**, 4328 (1968).

24. M. BARFIELD and M. KARPLUS. J. Am. Chem. Soc. **91**, 1 (1969).
25. M. BARFIELD and B. CHAKRABARTI. Chem. Rev. **69**, 757 (1969).
26. M. BARFIELD. J. Am. Chem. Soc. **93**, 1066 (1971).
27. M. Y. DEWOLF and J. D. BALDESCHWIELER. J. Mol. Spectrosc. **13**, 344 (1964).
28. H. M. MCCONNELL. J. Mol. Spectrosc. **1**, 11 (1957).
29. M. J. S. DEWAR and R. C. FAHEY. J. Am. Chem. Soc. **85**, 2704 (1963).
30. R. A. HOFFMAN and S. GRONOWITZ. Acta Chem. Scand. **13**, 1477 (1959).
31. C. L. TALCOTT and R. J. MYERS. Mol. Phys. **12**, 549 (1967).
32. Anonymous reviewer. Times Lit. Suppl. No. 3647, 54 (1972).
33. J. M. READ, R. E. MAYO, and J. H. GOLDSTEIN. J. Mol. Spectrosc. **22**, 419 (1967).
34. A. D. COHEN and T. SCHAEFER. Mol. Phys. **10**, 209 (1965).
35. J. E. LOEMKER, J. H. GOLDSTEIN, and J. M. READ, JR. Chem. Commun. 745 (1968).

Can. J. Chem. Downloaded from www.nrcresearchpress.com by 210.87.254.40 on 09/05/12
For personal use only.

Chemical Shift. VII. The Long-range Shielding Effects of the Cyano Group

J. W. ApSimon, H. Beierbeck, and D. K. Todd[1]

Department of Chemistry, Carleton University, Ottawa, Canada K1S 5B6

Received March 6, 1972

Using the methods described in parts I–VI of this series, we have examined the long-range shielding effects of the cyano group upon the C-18 and -19 methyl protons in several cyano-steroids and the ring protons in 2-*endo*- and 2-*exo*-cyanonorbornenes.

It was found that the most important shielding mechanism of the cyano group is its electric field effect, with the magnetic anisotropy effect making at most a minor contribution to the screening. However, only in the cases of the cyano-steroids was good agreement obtained between the calculated and the experimental shifts.

En utilisant les méthodes décrites dans les parties I–VI de cette série, nous avons examiné les effets de blindage à longue distance du groupe cyano sur les protons des méthyles 18 et 19 de plusieurs cyano stéroïdes et sur les protons du cycle des *exo* et *endo* cyano-2 norbornènes. Le mécanisme le plus important de l'effet de blindage du groupe cyano se trouve être son effet de champ électrique, l'anisotropie magnétique apportant une contribution mineure à l'effet d'écran. Cependant, seules dans le cas des cyano stéroïdes, les valeurs calculées et expérimentales pour les déplacements chimiques ont été obtenues avec un bon accord.

Canadian Journal of Chemistry, **50**, 2351 (1972)

Can. J. Chem. Downloaded from www.nrcresearchpress.com by 210.87.254.40 on 09/05/12
For personal use only.

Introduction

The long-range shielding effects of the nitrile group have been investigated by a number of authors (1–5). Zeil and Buchert (1) and Reddy and Goldstein (2) studied proton chemical shifts in aliphatic nitriles and attributed the observed long-range shielding effects of the cyano group to its magnetic anisotropy, $\Delta\chi$(CN). They obtained values of -34×10^{-30} and -27×10^{-30} cm^3/molecule respectively. Cross and Harrison (3) used the second value to calculate the shifts of the C-19 methyl groups in some 5α and 5β cyano-steroids. The predicted shifts were in the wrong direction, a result which was rationalized in terms of conformational changes in the steroidal A-ring caused by substituent dipole–dipole interactions. Jackman and Sarkis (4) suggested that it might have been the neglect of the electrostatic screening effect of the highly polar cyano group that was responsible for the lack of success. Zürcher (5) had found earlier that only an electric field effect had to be invoked in order to predict the methyl shifts in several cyano-steroids and in ethyl cyanide.

Since new chemical shift data for steroidal nitriles have appeared in the literature, it seemed worthwhile to reappraise the relative importance of the magnetic anisotropy effects and of electrostatic shielding with the methods described in parts I–VI of this series (6–11). In addition to studying the shielding effects in cyano-steroids an attempt was made to predict CN induced shift increments in two isomeric cyano-norbornenes.

[1]Taken in part from the M.Sc. thesis of D. K. Todd, Carleton University, Ottawa, Canada, September 1971.

Results and Discussion

The screening contribution at a given proton due to the magnetic anisotropy of axially symmetric groups (δ^M) is given by McConnell's equation (12):

$$[1] \qquad \delta^M = \Delta\chi(1 - 3\cos^2\theta)/3R^3 = \Delta\chi g^M$$

The shift increment caused by the electric field effect of polar groups (δ^E) is given (13) by eq. 2,[2] where

$$[2] \qquad \delta^E = K(2\cos\theta\cos\phi + \sin\theta\cos\psi)/R^3 = Kg^E$$

$\Delta\chi$ is the magnetic anisotropy and K is a parameter descriptive of the electric field effect. The geometric quantities are defined in Fig. 1. If it is assumed that the complete group C—C≡N can be represented by a single point dipole, the change in chemical shift of a proton upon substitution, somewhere in the molecule, of C—H by C—CN is given by eq. 3. Although it had

$$[3] \quad \delta(\text{calc}) = \delta^M(\text{CN}) + \delta^E(\text{CN}) - \delta^M(\text{CH}) = \Delta\chi(\text{CN})g^M(\text{CN}) + K(\text{CN})g^E(\text{CN}) - \Delta\chi(\text{CH})g^M(\text{CH})$$

[2]See ref. 9, Appendix and ref. 10.

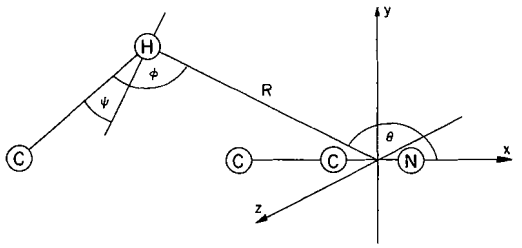

FIG. 1. Definition of geometric quantities. ψ is the angle between the C—H bond and the vector in the plane defined by R and CN and perpendicular to R (see ref. 9, Appendix).

previously been found (10) that the C—H bond anisotropy is small and may safely be neglected, $\Delta\chi$(CH) was included as a variable in one series of calculations to obtain an additional estimate of the magnitude of this parameter. To assess the relative importance of the first two terms was one of the main purposes of this study.

The geometric quantities in eq. 3 for the cyano-steroids were computed from the X-ray data for androsterone (14) (5α,14α-androstane skeleton) and digitoxigenin (15) (15β,14β-androstane ring system). The X-ray data for a *syn*-benzonorbornene derivative (20) were used for the calculations in the cyano-norbornene series. For the derivation of the C—CN (and C—H) bond vectors, tetrahedral valency angles were assumed. The locations of the coincident magnetic and electric point dipoles representing the cyano group, were varied along the bond axes in steps of 0.2 Å. Where the C—H bond anisotropy term was included in the calculations, this dipole was placed 0.8 Å from carbon. In the cyano-steroid series the chemical shifts of the methyl groups were approximated by the averages of the shielding at 72 points around the circle of rotation of the methyl protons, 5° apart (denoted by angle brackets around g^{M}(CN), g^{E}(CN), and g^{M}(CH) in Tables 1 and 2).

In order to assess the relative importance of the magnetic anisotropy effect and the electrostatic shielding of the cyano group, δ(calc) was first equated to δ^{M}(CN), then to δ^{E}(CN), and finally to the sum of the two terms, varying the CN dipole position each time. In addition, as mentioned earlier, the term δ^{M}(CH) was included once.

The results of calculations for both series of compounds, cyano-steroids and cyano-norbornenes, indicate that the electric field effect is the important shielding mechanism of the nitrile group (Table 3), as found by Zürcher (5). The values obtained for K(CN), -13.9 and -13.0×10^{-12} e.s.u. respectively, also agree well with Zürcher's result of -12.2×10^{-12} e.s.u. (5). The standard deviation between experimental and calculated shifts had a minimum near the midpoint of the CN group, 2.1 Å from the ring carbon, and increased only slowly as the dipole location was moved away from this point in either direction. Inclusion of the term δ^{M}(CN) had little effect on the electric field parameter K(CN); $\Delta\chi$(CN) was found to be small and the fit with the experimental shifts did not improve. Inclusion of the anisotropy term for the displaced CH bond, δ^{M}(CH), also had little effect on the other parameters and the calculated shifts. This is further evidence that the CH bond is practically magnetically isotropic.

With a few exceptions the chemical shifts were predicted well in the cyano-steroid series (Table 1). It is somewhat surprising that the predicted shift increment in the case 5β/19 is wrong whereas the calculated shifts in the related cases 2β/19 etc. agree well with experiment. It is likely that the point dipole approximation is inadequate in both situations. Similarly van der Waals interactions might be expected to make comparable contributions in both cases. It is possible that the explanations are in the greater flexibility of the *cis*-fused system which may permit larger conformational changes in the case of the 5β-cyano derivative. It is tempting to ascribe the large error in the case 11β/19 to the fact that the cyano group is virtually sandwiched between the C-18 and -19 methyl groups, although δ(calc) for the case 11β/18 fits rather well. The lack of agreement in the cases 16α/18 and 16β/18 might be due to conformational effects. The nitriles for which shift data were available had an acetyl group in the 17β-position and in some cases a 17α-hydroxyl group as well. As a result of substituent interactions, upon introduction of a nitrile group, either the conformation of the D-ring or the orientation of the highly anisotropic and polar C=O bond of the acetyl group might change. Since calculations with geometric quantities based on X-ray data for steroids with the 16β-bromo, 17α-hydroxy, 17β-acetyl moiety (16, 17) gave essentially the same (incorrect) shifts, the second explanation seems to be more convincing. It is hoped that methyl shifts will

Can. J. Chem. Downloaded from www.nrcresearchpress.com by 210.87.254.40 on 09/05/12
For personal use only.

TABLE 1. Long-range shielding effects of the cyano group in some steroids*

CN/Me†	$\langle g^M(CN)\rangle$‡	$\langle g^E(CN)\rangle$‡	$\langle g^M(CH)\rangle$‡	Δ§	δ(calc)‖	δ(exp)¶	Range of δ(exp)	Number of cases	Reference
9α/18	−183	347	−159	−3	−5	−2		1	25
11α/18	−376	371	−685		−5				
12α/18	−470	895	−931		−12				
14α/18	−456	908	−861		−13				
15α/18	−440	372	−976		−5				
16α/18**	−405	407	−891	10	−6	4	±4	5	26, 34, 35, 36
17α/18	−510	918	−1043		−13				
8β/18	2054	2220	564		−31				
11β/18	1927	2123	663	2	−29	−31		1	25
12β/18	382	1944	1240		−27				
15β/18	1409	1213	1139		−17				
16β/18**	344	711	997	13	−10	−23		2	25, 26
17β/18	768	2355	1596		−33				
1α/19	−483	884	−986	−1	−12	−11	±2	8	21–23
2α/19	−384	336	−704	2	−5	−7		1	24
3α/19	−229	311	−308	−2	−4	−2		1	27
4α/19	−377	341	−701	0	−5	−5	±1	2	24, 28
5α/19	−442	929	−782	1	−13	−14	±4	22	3, 21, 27, 29, 30
6α/19	−380	344	−702		−5				
7α/19	−229	322	−305	−4	−5	−1		1	33
9α/19	−472	873	−953	−1	−12	−11		1	25
11α/19	−69	611	395		−9				
1β/19	330	1861	1251	1	−26	−27	±3	4	22
2β/19	1945	1714	725	0	−24	−24	±3	5	25, 26
3β/19	−143	293	24	1	−4	−5		1	27
4β/19	1861	1834	692	1	−25	−26	±3	4	23, 25, 26
6β/19	2006	1965	653	1	−27	−28	±3	4	21, 29, 32
7β/19	−147	303	18	2	−4	−6		1	33
8β/19	2024	1983	619	−3	−28	−25		1	37
11β/19**	2228	1858	622	12	−26	−38		1	25
14β/18*	500	2000	1231	−1	−28	−27		2	23
5β/19*,**	912	2701	1385	−14	−38	−24	±3	15	3, 23, 25, 26, 31

*Steroid numbering system. 5α,14α-Skeleton except for two last entries.

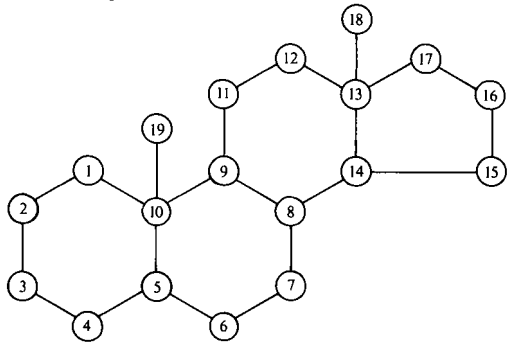

†1α/19: effect of substitution of C—H by C—CN in position 1α on the chemical shift of the C-19 methyl protons, etc.

‡The geometric quantities are quoted in units "$\times 10^{19}$ cm^{-3}". Dipole positions are CN: 2.1, CH: 0.8 Å from the ring carbons. The angle brackets denote averages over the paths of the methyl protons.

§$\Delta = \delta(\text{calc}) - \delta(\text{exp})$.

‖$\delta(\text{calc}) = \delta^E(\text{CN})$.

¶All shifts are converted to Hz at 100 MHz. Solvent $CHCl_3$ in all cases. Negative values are downfield shifts. Where more than one literature value is available δ(exp) is an average. The range of the experimental literature values is given in the next column.

**Omitted from least squares analysis.

Can. J. Chem. Downloaded from www.nrcresearchpress.com by 210.87.254.40 on 09/05/12
For personal use only.

Can. J. Chem. Downloaded from www.nrcresearchpress.com by 210.87.254.40 on 09/05/12
For personal use only.

TABLE 2. Long-range shielding effects of the cyano group in 2-*endo*- and 2-*exo*-cyanonorbornene*

CN/H†	g^M(CN)‡	g^E(CN)‡	g^M(CH)‡	δ(exp)§	δ(calc)‖	Δ¶
2*n*/1	−680	3021	785	−34	−39	−5
2*n*/3*n*	−379	3385	2389	−26	−44	−18
2*n*/3*x*	−804	2613	−1093	−53	−34	19
2*n*/4	−276	1316	−218	−10	−18	−8
2*n*/5	150	1556	511	−22	−20	2
2*n*/6	562	2871	1042	−37	−37	0
2*n*/7*s*	−359	1325	−551	−8	−17	−9
2*n*/7*a*	−665	874	−1744	−13	−11	2
2*x*/1	−599	3157	1425	−35	−41	−6
2*x*/3*n*	−801	2627	−1019	−56	−34	22
2*x*/3*x*	−379	3384	2390	−35	−44	−9
2*x*/4	−267	1374	−182	−19	−18	1
2*x*/5	−310	905	−616	−10	−12	−2
2*x*/6	−388	1144	−707	−27	−15	12
2*x*/7*s*	−157	1743	245	−11	−23	−12
2*x*/7*a*	171	1644	2036	−48	−21	27

*Norbornene numbering system.

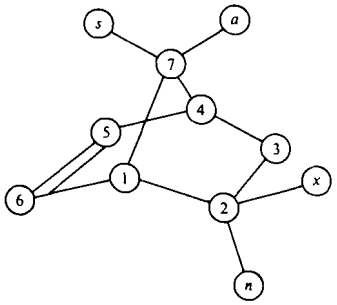

†2*n*/1: effect of substitution of C—H by C—CN in position 2*n* on the chemical shift of proton 1, etc.
‡The geometric quantities are quoted in units "$\times 10^{19}$ cm^{-3}". Dipole positions are CN: 2.1, CH: 0.8 Å from the ring carbon.
§The experimental shifts for the cyano-norbornenes are those of Davis and van Auken (18), the reference shifts for norbornene were taken from ref. 19. Solvent was $CDCl_3$. All shifts were converted to Hz at 100 MHz. Negative values are downfield shifts.
‖δ(calc) = δ^E(CN).
¶$\Delta = \delta$(calc) − δ(exp).

TABLE 3. Shielding parameters for the nitrile group*

	Cyano-steroids				Cyano-norbornenes			
Terms†	1	2	1 + 2	1 + 2 + 3	1	2	1 + 2	1 + 2 + 3
Δχ(CN)	−12.6	—	−0.2	0.5	41.8	—	4.3	−4.8
K(CN)	—	−13.9	−13.7	−13.7	—	−13.0	−12.4	−14.8
Δχ(CH)	—	—	—	0.1	—	—	—	4.5
σ[Hz]	11.8	1.7	1.7	1.7	24.3	12.4	12.3	11.7

*The anisotropy values are quoted in units "$\times 10^{-30}$ cm^3/molecule", the electric field parameter *K*(CN) in units "$\times 10^{-12}$ e.s.u.".
†Terms: 1 = δ^M(CN), 2 = δ^E(CN), 3 = δ^M(CH).

Can. J. Chem. Downloaded from www.nrcresearchpress.com by 210.87.254.40 on 09/05/12
For personal use only.

become available for steroids whose only substituent in the D-ring is a nitrile group.[3]

Although the calculations in the cyano-norbornene series gave essentially the same values for the parameter K(CN), the chemical shifts were not predicted as well as in the cyano-steroid series. The disagreement with experiment is especially serious for the predictions of the chemical shifts of protons α to the CN group, in particular in the cases $2n/3n$ and $2n/3x \simeq 2x/3n$, and in the case $2x/7a$. The problem of the 3-protons was also encountered by Zürcher and is extensively discussed in ref. 5. It is possible that the discrepancy in the case $2x/7a$ is also due to a modification of the solute solvent interaction as suggested by Zürcher for the cases $2n/3x$ and $2x/3n$ (5). Rotation of the CH or C—CN bond vectors in the H—C—H plane by up to $\pm 5°$ had little effect on the geometric factors and chemical shifts. Exclusion of these situations from least squares analysis led to almost the same values for the shielding parameters and did not improve the fit with experiment materially for the remaining cases.

Thus it is concluded that it is mainly the electrostatic shielding, assumed to arise from a point dipole at the CN bond center, that is responsible for the long-range shielding effects of the nitrile group. It is interesting that the calculations both for the steroidal and the bicyclic nitriles led to the same conclusions regarding the shielding mechanism, and gave almost the same value for the electric field parameter K(CN), despite the fact that in the cyano-norbornene series the chemical shifts could not be predicted with any accuracy. The magnetic anisotropy effect of the CN group may make minor contributions to the chemical shifts, but in view of the approximations used and the present results, little appears to be gained by including the anisotropy term.

Experimental

All chemical shift values were taken from the literature and converted to Hz and 100 MHz. Solvent was $CDCl_3$ in the case of the cyano-steroids and CCl_4 for the cyano-norbornenes. The calculations were performed on the SIGMA 6 computer at Carleton University. Programs (in FORTRAN) are available on request.

[3]Prof. D. W. Mathieson, University of Bradford, England is involved in the synthesis of a series of these compounds (private communication).

We thank the National Research Council of Canada for generous financial support.

1. W. Zeil and H. Buchert. Z. Phys. Chem. **38**, 47 (1963).
2. G. S. Reddy and J. H. Goldstein. J. Chem. Phys. **39**, 3509 (1963).
3. A. D. Cross and I. T. Harrison. J. Am. Chem. Soc. **85**, 3223 (1963).
4. L. M. Jackman and G. Y. Sarkis. Bull. Chem. Soc. Japan, **42**, 1179 (1969).
5. R. F. Zürcher. *In* Progress in nuclear magnetic resonance spectroscopy. Vol. 2. *Edited by* J. W. Emsley, J. Feeney, and L. H. Sutcliffe. Pergamon Press, Oxford, 1967. p. 231.
6. J. W. ApSimon, W. G. Craig, P. V. Demarco, D. W. Mathieson, L. Saunders, and W. B. Whalley. Tetrahedron, **23**, 2339 (1967).
7. J. W. ApSimon, W. G. Craig, P. V. Demarco, D. W. Mathieson, L. Saunders, and W. B. Whalley. Tetrahedron, **23**, 2357 (1967).
8. J. W. ApSimon, W. G. Craig, P. V. Demarco, D. W. Mathieson, and W. B. Whalley. Tetrahedron, **23**, 2375 (1967).
9. J. W. ApSimon, P. V. Demarco, D. W. Mathieson, W. G. Craig, A. Karim, L. Saunders, and W. B. Whalley. Tetrahedron, **26**, 119 (1970).
10. J. W. ApSimon and H. Beierbeck. Can. J. Chem. **49**, 1328 (1971).
11. J. W. ApSimon, H. Beierbeck, D. K. Todd, P. V. Demarco, and W. G. Craig. Can. J. Chem. **49**, 1335 (1971).
12. H. M. McConnell. J. Chem. Phys. **27**, 226 (1957).
13. A. D. Buckingham. Can. J. Chem. **38**, 300 (1960).
14. D. F. High and J. Kraut. Acta Cryst. **21**, 88 (1966).
15. I. L. Karle and J. Karle. Acta Cryst. **B25**, 434 (1969).
16. J. M. Ohrt, B. A. Haner, A. Cooper, and D. A. Norton. Acta Cryst. **B24**, 312 (1968).
17. J. M. Ohrt, A. Cooper, and D. A. Norton. Acta Cryst. **B25**, 41 (1969).
18. J. C. Davis, Jr. and T. V. van Auken. J. Am. Chem. Soc. **87**, 3900 (1965).
19. K. Tori, K. Aono, Y. Hata, R. Muneyuki, T. Tsuji, and H. Tanida. Tetrahedron Lett. 9 (1966).
20. T. Sato, M. Shiro, and H. Koyama. J. Chem. Soc. B, 935 (1968).
21. J. C. Jacquesy, R. Jacquesy, J. Levisalles, J. P. Pete, and H. Rudler. Bull. Soc. Chim. Fr. 2224 (1964).
22. A. T. Glen, W. Lawrie, and J. McLean. J. Chem. Soc. C, 661 (1966).
23. A. C. Campbell, W. Lawrie, and J. McLean. J. Chem. Soc. C, 554 (1969).
24. M. E. Kuehne and J. A. Nelson. J. Org. Chem. **35**, 161, 171 (1970).
25. W. Nagata, M. Yoshioka, and T. Okumura. J. Chem. Soc. C, 2365 (1970).
26. R. F. Zürcher. Helv. Chim. Acta, **46**, 2054 (1963).
27. K. Tori and T. Komeno. Tetrahedron, **21**, 309 (1965).

28. P. BEAK and T. L. CHAFFIN. J. Org. Chem. **35**, 2276 (1970).
29. J. C. JACQUESY, J. M. LEHN, and J. LEVISALLES. Bull. Soc. Chim. Fr. 2444 (1961).
30. P. N. RAO and J. E. BURDETT, JR. J. Org. Chem. **34**, 1090 (1969).
31. R. JACQUESY and J. LEVISALLES. Bull. Chim. Soc. Fr. 1642 (1967).
32. H. SUGINONE, T. TSUNENO, and T. MASAMUNE. Tetrahedron Lett. 4605 (1967).
33. O. R. RODIG and N. J. JOHNSTON. J. Org. Chem. **34**, 1942, 1949 (1969).
34. A. D. CROSS and P. CRABBÉ. J. Am. Chem. Soc. **86**, 1221 (1964).
35. G. W. MOERSCH, E. L. WITTLE, and W. A. NEUKLIS. J. Org. Chem. **30**, 1272 (1965); **32**, 1387 (1967).
36. J. ROMO, L. RODRIGUEZ-HAHN, P. JOSEPH-NATHAN, M. MARTINEZ, and P. CRABBÉ. Bull. Soc. Chim. Fr. 1276 (1964).
37. S. W. PELLETIER, C. W. J. CHANG, and K. N. IYER. J. Org. Chem. **34**, 3477 (1969).

Can. J. Chem. Downloaded from www.nrcresearchpress.com by 210.87.254.40 on 09/05/12
For personal use only.

Self Association of Folic Acid in Aqueous Solution by Proton Magnetic Resonance

YUI-FAI LAM AND GEORGE KOTOWYCZ
Department of Chemistry, University of Alberta, Edmonton 7, Alberta

Received January 18, 1972

Proton magnetic resonance experiments on the disodium salt of folic acid in aqueous solutions (p*D* 7.1) indicate that the folate ion exists in an unfolded, extended conformation in solution. However, based on a temperature and concentration dependence of the proton chemical shifts, folate ions are involved in intermolecular association consisting of a vertical stacking interaction. A stacking model is proposed for the association with the hydrophilic ends of the molecule alternating in orientation with respect to the hydrophobic portion of the neighboring molecules.

Les expériences de r.m.n. sur le sel dissodique de l'acide folique en solutions aqueuses (p*D* 7.1) indiquent que l'ion folate existe dans une conformation non plissée et étirée. Cependant, les résultats fondés sur l'influence de la température et de la concentration sur les déplacements chimiques du proton montrent que les ions folates sont impliqués dans une association intermoléculaire régie par une interaction due à un empilement vertical. Un modèle pour cet entassement est proposé où les bouts hydrophiliques de la molécule alternent en orientation avec la portion hydrophobique des molécules voisines.

Canadian Journal of Chemistry, **50**, 2357 (1972)

Introduction

Folic (pteroylglutamic) acid (**1**) has been extensively studied and the properties of this water-soluble vitamin have been well described (1–4). Metabolically, a deficiency of folic acid is observed in the failure to make the purines and thymine required for DNA synthesis (2). A component of the above molecule, 2-amino-4-hydroxy-6-substituted pteridine has been implicated (5) in the primary photochemical reduction in photosynthesis.

Following the observation of a large concentration dependence of the folic acid proton chemical shifts in aqueous solution (Fig. 2), the present study was initiated and is concerned with the further study of the self-association properties of this molecule in aqueous solutions. Pastore (6), on the basis of preliminary p.m.r. experiments, has shown that folic acid and several of its derivatives are involved in the formation of complexes, of unknown conformation in solution. However, the molecule may exist either in an unfolded conformation or in a folded conformation with the two rings superimposed over each other. A folded conformation is observed for many coenzymes, examples being the pyridine dinucleotides (7–15) and flavin adenine dinucleotide (FAD) (16–19). Besides these intramolecular interactions, intermolecular association equilibria must be considered. Nucleosides and nucleotides stack in solution (20, 21) whereas benzylpenicillin ions (22) form micelles. Based on a temperature and concentration dependence of the proton chemical shifts, disodium folate exists in solution in an extended, non-folded conformation. The ions stack in solution and a possible model for this stacking interaction is proposed.

Experimental

Folic acid, obtained from Calbiochem (Lot 321), Los

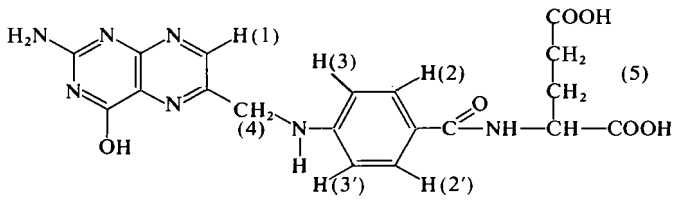

1

Can. J. Chem. Downloaded from www.nrcresearchpress.com by 210.87.254.5 on 09/05/12
For personal use only.

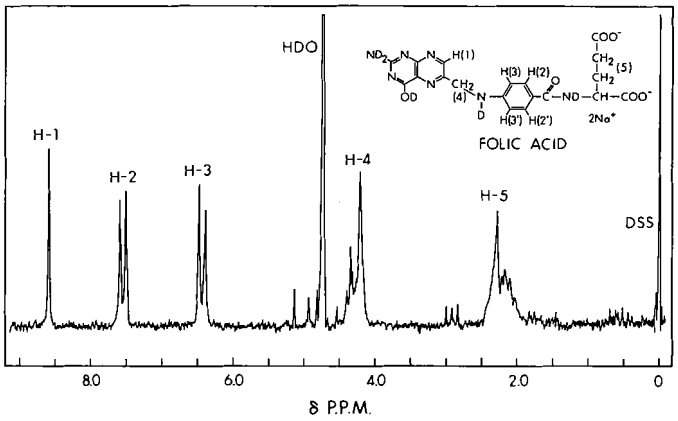

FIG. 1. The 100.0 MHz n.m.r. spectrum of 0.049 *m* disodium folate in D_2O (p*D* 7.1; 30.5 °C). The chemical shifts are with respect to internal DSS.

Angeles, California, was dissolved in a minimal amount of aqueous sodium hydroxide. Further purification was carried out by passing the salt through a cation exchange column and the effluent was freeze-dried. The labile protons were exchanged by dissolving disodium folate in D_2O and freeze-drying the solutions three times. Solutions for the n.m.r. experiments were prepared by weighing out the salt and the internal reference sodium 2,2-dimethyl-2-silapentane-5-sulfonate (DSS) (0.8 mg/g of D_2O) and dissolving them in a weighed amount of D_2O. The p*D* was 7.1 ± 0.1 (meter reading + 0.4) (23). The titration curve for folic acid showed that in solution at a p*D* of 7.1 folic acid exists as the disodium salt. *p*-(Methylamino)benzoic acid, obtained from K & K Laboratories, Inc. and DSS from Merck, Sharp and Dohme of Canada Ltd., were both used without further purification. The solvent D_2O from Columbia Organic Chemical Co. was distilled before use. 2-Amino-4-hydroxy-6-methyl pteridine was a gift from Dr. R. B. Angier of the Lederle Laboratories Division, American Cyanamid Company (24). It only dissolves in an aqueous solution at a p*D* of 12.9.

Instrumentation

The p.m.r. measurements were carried out on the Varian HA-100-15(100.0 MHz) and the Brüker HFX-90(90.0 MHz) NMR spectrometers. For measurements on the Varian spectrometer, tetramethylsilane (TMS) (5%) in deuterated acetone in a co-axial tube was used for the lock signal. The solution temperatures were calibrated within ± 0.5 °C before and after each set of measurements using an ethylene glycol sample obtained from Dr. O. Yamamoto, Government Chemical Industrial Research Laboratories, Tokyo, Japan (25). Measurements on the Bruker spectrometer were carried out using a heteronuclear ^2D lock and the lock signal was derived from the deuterium resonance of the solvent D_2O. The temperature was calibrated using the built-in thermocouple temperature control unit. Several measurements of the chemical shifts were made at various temperatures on both spectrometers and were in agreement within experimental error. All samples remained in the probe for 25 min to reach thermal equilibrium before spectra were obtained. All chemical shifts were calibrated with respect to internal DSS and represent the average of three measurements.

Results

The 100 MHz p.m.r. spectrum of 0.049 *m* disodium folate in D_2O (p*D* 7.1) is shown in Fig. 1 together with the assignment of the resonances. The chemical shifts of protons 1 to 4 were determined using a first order analysis. The singlet at lowest field corresponds to proton H-1 of the pteridine ring. The low-field

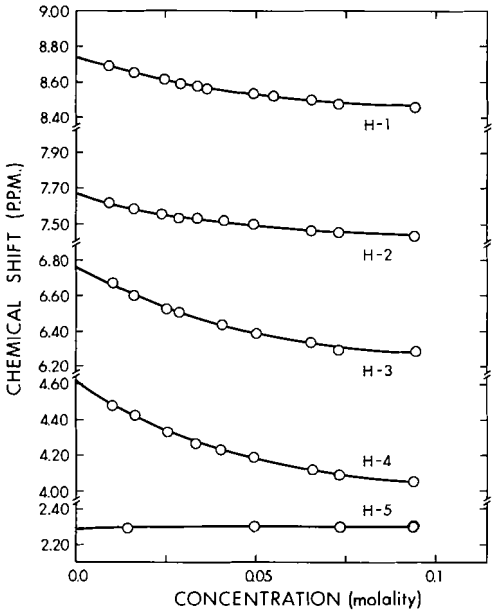

FIG. 2. The concentration dependence of the proton chemical shifts of disodium folate in D_2O (p*D* 7.1; 30.5 °C).

Can. J. Chem. Downloaded from www.nrcresearchpress.com by 210.87.254.5 on 09/05/12
For personal use only.

TABLE 1. The concentration dependence of the proton chemical shifts* of disodium folate and related compounds in D_2O at 30.5 °C

Compound	Concentration (*m*)	Proton chemical shifts (p.p.m.) H-1	H-2	H-3	H-4	H-5
Disodium folate (p*D* 7.1)	0.00†	8.73 ± 0.01	7.66 ± 0.01	6.74 ± 0.01	4.57 ± 0.01	2.29 ± 0.01
	0.094	8.457 ± 0.002	7.438 ± 0.002	6.271 ± 0.002	4.054 ± 0.002	2.308 ± 0.002
	Δ‡(0.00–0.094)	0.27	0.22	0.47	0.52	−0.02
Sodium *p*-(methylamino)-benzoate (p*D* 7.1)	0.228 m§		7.766 ± 0.002	6.768 ± 0.002		
	Δ (Benzoate-folate at infinite dilution)‖		0.11	0.03		
Disodium folate (p*D* 12.9)	0.00¶	8.61 ± 0.02				
2-Amino-4-hydroxy-6-methyl-pteridine (p*D* 12.9)	0.00¶	8.51 ± 0.02				

*The chemical shifts are to low field of internal DSS.
†The infinite dilution chemical shifts are obtained from a least-squares analysis of the data in Fig. 2 using the IBM 360/65 computer. The error limits represent standard deviations.
‡A positive value of Δ represents a net shielding of the folate protons in the 0.094 *m* solution with respect to an infinitely dilute solution.
§The chemical shifts are independent of concentration and temperature.
‖Δ represents the net shielding of protons H-2 and -3 in the folate ion with respect to the *p*-(methylamino)benzoate ion.
¶The infinite dilution chemical shifts are obtained from a least-squares analysis of data obtained at six concentrations using the IBM 360/65 computer.

doublet with a chemical shift of 7.6 p.p.m. and the high-field doublet at 6.4 p.p.m. were assigned to protons H-2 and -3 of the para-disubstituted benzene moiety of the molecule. These two assignments are based on the proton chemical shifts observed in substituted benzene derivatives (26, 27). The singlet at 4.2 p.p.m. corresponds to proton H-4 whereas the multiplet just to low field of this resonance corresponds to the α-CH proton of the glutamic acid residue of the folate ion. The spectrum of the CH_2—CH_2 (H-5) fragment of the glutamic acid residue was very complex yet remained completely unchanged with a change of temperature or concentration. Hence the position of the most intense line of the multiplet was used as a monitor of the chemical shift of these protons. In fact, calibration of the positions of each of the lines in the multiplet showed them to be independent of temperature and concentration.

A pronounced concentration dependence of the chemical shifts of protons H-1 to -4 was observed for the folate ion in the concentration range from 0.0091 *m* up to the solubility limits of the ion. The results of the measurements at 30.5 °C and p*D* 7.1 are summarized in Fig. 2. A least-squares analysis using the IBM-360/65 computer was applied to the data and the chemical shifts of the protons at infinite dilution were thus determined. These are given in Table 1. The resonances corresponding to protons H-1 to -4 shift to higher field with an increase in solute concentration. This diamagnetic shielding effect is largest for protons H-3 and -4, namely 0.5 p.p.m. over the concentration range of 0.0–0.094 *m*. It is much smaller for protons H-1 and -2 (0.25 p.p.m.) whereas the glutamic acid fragment methylene protons (H-5) are concentration independent. Infinite dilution chemical shifts have also been determined for the H-2 and -3 protons of disodium folate at 60 °C and are 7.68 ± 0.02 and 6.83 ± 0.02 p.p.m., respectively.

Proton chemical shifts for the H-1 to -4 folate ion protons were also studied over a 60° temperature range at two concentrations, namely 0.009 and 0.049 *m*. The temperature measurements are summarized in Fig. 3. The proton chemical shifts for the folate ion at infinite dilution (Table 1) (30.5 °C) are within

Can. J. Chem. Downloaded from www.nrcresearchpress.com by 210.87.254.5 on 09/05/12
For personal use only.

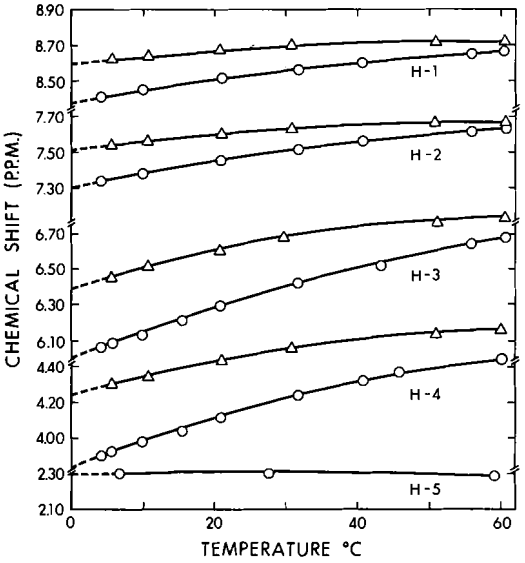

FIG. 3. The temperature dependence of the proton chemical shifts of disodium folate in D_2O (p*D* 7.1). The measurements are carried out at two concentrations, namely: ○ 0.049 *m*; △ 0.009 *m*.

0.05 p.p.m. of the chemical shifts obtained for the 0.009 *m* solution at the highest temperature (Table 2). The H-5 proton chemical shift is completely temperature independent (0.049 *m* solution, Table 2 and Fig. 3) even at the highest concentration (0.094 *m*).

Discussion

Intramolecular interactions of the folate ion may be studied by comparing the chemical shifts of the folate ion protons at infinite dilution, when intermolecular shielding effects are minimized, with the chemical shifts observed for nearly equivalent protons in a model compound. The model compounds chosen were sodium *p*-(methylamino)benzoate and 2-amino-4-hydroxy-6-methyl-pteridine because of their structural similarities with fragments of the folate ion. The proton chemical shifts of sodium *p*-(methylamino)benzoate are concentration and temperature independent and a comparison of the H-2 and -3 proton chemical shifts in the folate ion with those in the model compound at 30.5 °C shows that proton H-3 is shielded by 0.03 p.p.m. whereas proton H-2 is shielded by 0.11 p.p.m. in the folate ion at infinite dilution. These chemical shift differences are much smaller than those arising either from intermolecular or intramolecular diamagnetic ring current shielding in molecules such as flavin adenine dinucleotide (16, 18). Proton H-2 in the folate ion is adjacent to a C(O)—NH-group whereas in *p*-(methylamino)benzoate it is adjacent to a carboxyl group. This will contribute to the 0.11 p.p.m. difference of the H-2 proton chemical shifts. These results indicate that protons H-2 and -3 in the folate ion do not experience a diamagnetic ring-current shielding effect which would arise if the pteridine portion of the molecule was folded over the aromatic benzene ring. Therefore the folate ion exists in an unfolded, extended conformation in solution (Fig. 4).

This result is supported by several other experiments. A similar comparison of the H-2 and -3 proton chemical shifts at infinite dilution at 60 °C, when intramolecular interactions should decrease, again shows small chemical shift differences. Proton H-2 is shielded by 0.09 p.p.m. whereas proton H-3 is deshielded by 0.06 p.p.m. The chemical shift of the H-1 proton of disodium folate can only be compared with the chemical shift of the corresponding proton in the second model compound 2-amino-4-hydroxy-6-methyl-pteridine at a p*D* of 12.9 when the latter compound begins to dissolve. The chemical shifts for this proton at infinite dilution (30.5 °C) are given in Table 1. Proton H-1 experiences a very small deshielding (0.1 p.p.m.) in disodium folate with respect to the model compound. However, the pteridine ring in the two molecules may be ionized to slightly different extents at a p*D* of 12.9 so this comparison should be treated cautiously.

The unfolded, extended conformation for the folate ion in aqueous solution is supported by the temperature studies. From Fig. 3 smooth, monotonic curves are obtained for the temperature dependence of the proton chemical shifts. Sigmoidal curves, characteristic of an equilibrium between folded and unfolded conformers in solution, were not observed. A CPK model of the molecule also indicates that the folded conformation would be highly strained.

In considering intermolecular associations, dilution shifts for aromatic systems are usually of the order of 1 p.p.m. ranging from a pure liquid to the liquid at infinite dilution (28). In organic solvents the dilution shift of azulene in dioxane is 0.1 p.p.m. for the five-membered ring

Can. J. Chem. Downloaded from www.nrcresearchpress.com by 210.87.254.5 on 09/05/12
For personal use only.

TABLE 2. The temperature dependence of the proton chemical shifts* of disodium folate in D_2O

Concentration (m)	T (°C)	Proton chemical shifts (p.p.m.) H-1	H-2	H-3	H-4	H-5
0.009	60.0	8.74	7.67	6.79	4.62	
	5.8	8.62	7.54	6.45	4.30	
	Δ†(60.0–5.8)	0.12	0.13	0.34	0.32	
0.049	60.0	8.66	7.62	6.66	4.42	2.29
	5.8	8.42	7.35	6.08	3.93	2.30
	Δ†(60.0–5.8)	0.24	0.27	0.58	0.49	−0.01

*The chemical shifts are to low field of internal DSS.
†A positive value of Δ indicates a net shielding of the folate protons at 5.8 °C with respect to 60.0 °C.

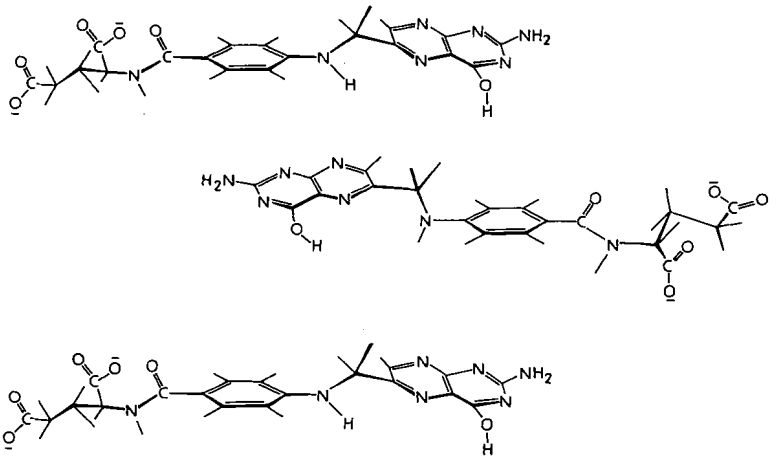

FIG. 4. The proposed, alternating, head-to-tail intermolecular stacking model for folate ions in aqueous solution (pD 7.1).

protons and 0.25 p.p.m. for the seven-membered ring protons in going from a 20 mol % to a 3 mol % solution. However, for aqueous solutions intermolecular association between bases, nucleosides, and nucleotides has been well studied (20). The concentration dependence for protons in purine ranges from 0.69–0.48 p.p.m. over the concentration range 0.0–1.0 m (about 2 mol %) (29). The concentration dependence observed for the folate ion in going from a 0.094 m solution (about 0.2 mol %) to infinite dilution is 0.27, 0.22, 0.47, and 0.52 p.p.m. for protons H-1 to -4 respectively. Hence intermolecular association is proposed for folate ions in aqueous solution.

The large shielding of the aromatic protons with an increase in concentration or a decrease in temperature suggests that intermolecular association consists of a vertical stacking interaction. The data in Table 1 and Fig. 2 indicate that protons H-3 and -4 experience a concentration dependence which is twice as large as that experienced by protons H-1 and -2. The much larger diamagnetic shielding of H-3 and -4 is also observed in the temperature studies. From the data in Table 2 and Fig. 3, for a given temperature interval, the chemical shifts of protons H-3 and -4 vary twice as much as for protons H-1 and -2. This is interesting, especially in view of the fact that both protons H-2 and -3 are part of the same aromatic ring. The glutamic acid fragment methylene protons are temperature and concentration independent.

Intermolecular stacking may occur with the planes of the hydrophobic ends of the molecules stacking one above the other with the hydro-

Can. J. Chem. Downloaded from www.nrcresearchpress.com by 210.87.254.5 on 09/05/12
For personal use only.

Can. J. Chem. Downloaded from www.nrcresearchpress.com by 210.87.254.5 on 09/05/12
For personal use only.

philic groups all next to each other (head-to-head interaction) or in a vertical stack with the hydrophilic ends of the molecule alternating in orientation with respect to the hydrophobic portion of the neighboring molecules (head-to-tail interaction). For head-to-head intermolecular association, proton H-1 of the pteridine ring would be very closely associated with the pteridine ring of the neighboring molecule. Similarly, protons H-2 and -3 of the para-disubstituted benzene fragment of the folic acid molecule will be closely associated with the neighboring molecule aromatic ring. Hence all three protons would be shielded to the same extent by the magnetic anisotropy of the neighboring ring and would exhibit a similar dependence on concentration. However, this is not observed. In fact, the concentration dependence of protons H-3 and -4 is twice as large as that for protons H-1 and -2 (Table 1). This is surprising also since both protons H-2 and -3 are on the same aromatic ring.

Since protons H-3 and -4 experience the largest diamagnetic shielding, they are most closely associated with the shielding region of a neighboring molecule whereas protons H-1 and -2 are further removed. From a study of molecular models, this is possible only for head-to-tail vertical stacking. A possible intermolecular association model is shown in Fig. 4. From this model it is seen that protons H-3 and -4 are associated with the aromatic ring-current shielding cone of the neighboring molecule pteridine base, protons H-1 and -2 are further removed from a ring-current shielding area whereas the protons of the glutamic acid residue are completely concentration independent and hence removed from any ring-current effects.

Finally, the possibility of micelle formation was investigated. If folate ions should form a spherical micelle with all hydrophobic groups associating together and the hydrophilic, carboxyl groups projecting outwards, protons H-1 to -4 would be expected to exhibit a similar dependence on concentration. This was not observed. Secondly, a mathematical treatment (30) in which the proton chemical shifts are plotted *vs.* the reciprocal of the concentration was carried out. Smooth curves were obtained for all protons and the sharp change in the slope of the curves, corresponding to a critical micelle concentration, was not observed. Therefore it is unlikely that folate ions undergo micelle formation as do the benzylpenicillin ions (22).

Conclusions

The p.m.r. experiments on disodium folate in aqueous solution (p*D* 7.1) indicate that the folate ion exists in an unfolded, extended conformation in solution. Folate ions, however, are involved in intermolecular association consisting of a vertical stacking interaction. A head-to-tail vertical stacking model is proposed with the hydrophilic ends of the molecule alternating in orientation with respect to the hydrophobic portion of the neighboring molecules.

We are grateful to Dr. Kikuko Hayamizu for valuable discussions, to Dr. R. B. Angier for the gift of 2-amino-4-hydroxy-6-methyl-pteridine, and to the National Research Council of Canada for financial support.

1. R. E. HANDSCHUMACHER and A. D. WELCH. Agents which influence nucleic acid metabolism. *In* The nucleic acids. Vol. III. *Edited by* E. Chargaff and J. N. Davidson. Academic Press, New York, 1960. p. 453.
2. A. WHITE, P. HANDLER, and E. L. SMITH. Principles of biochemistry. 4th ed. McGraw-Hill Book Co., Inc., New York, 1968. Chapt. 49.
3. G. W. E. PLAUT. Ann. Rev. Biochem. **30**, 409 (1961).
4. J. C. RABINOWITZ. Folic Acid. *In* The enzymes. *Edited by* P. D. Boyer, H. Lardy, and K. Myrback. Vol. II. 2nd ed. Academic Press, New York, 1960. p. 185.
5. R. C. FULLER and N. A. NUGENT. Proc. Natl. Acad. Sci. U.S. **63**, 1311 (1969).
6. E. J. PASTORE. Ann. N.Y. Acad. Sci. **186**, 43 (1971).
7. O. JARDETZKY and N. G. WADE-JARDETZKY. J. Biol. Chem. **241**, 85 (1966).
8. R. H. SARMA, V. ROSS, and N. O. KAPLAN. Biochem. **7**, 3052 (1968).
9. R. H. SARMA and N. O. KAPLAN. J. Biol. Chem. **244**, 771 (1969).
10. D. J. PATEL. Nature, **221**, 1239 (1969).
11. W. A. CATTERALL, D. P. HOLLIS, and C. F. WALTER. Biochem. **8**, 4032 (1969).
12. R. H. SARMA and N. O. KAPLAN. Biochem. **9**, 539 (1970).
13. R. H. SARMA, M. MOORE, and N. O. KAPLAN. Biochem. **9**, 549 (1970).
14. R. H. SARMA and N. O. KAPLAN. Biochem. **9**, 557 (1970).
15. J. JACOBUS. Biochem. **10**, 161 (1971).
16. R. H. SARMA, P. DANNIES, and N. O. KAPLAN. Biochem. **7**, 4359 (1968).
17. D. W. MILES and D. W. URRY. Biochem. **7**, 2791 (1968).
18. G. KOTOWYCZ, N. TENG, M. P. KLEIN, and M. CALVIN. J. Biol. Chem. **244**, 5656 (1969).
19. D. W. URRY. *In* Spectroscopic approaches to bio-

molecular conformation. *Edited by* D. W. Urry. American Medical Association, Chicago, Ill., 1970. Chapt. 3.
20. P. O. P. Ts'O, M. P. SCHWEIZER, and D. P. HOLLIS. Ann. N.Y. Acad. Sci. **158**, 256 (1969).
21. P. O. P. Ts'O. *In* Fine structure of proteins and nucleic acids. *Edited by* G. D. Fasman and S. N. Timasheff. Marcel Dekker, Inc., New York, 1970. p. 49.
22. A. L. THAKKAR and W. L. WILHAM. Chem. Commun. 320 (1971).
23. P. K. GLASOE and F. A. LONG. J. Phys. Chem. **64**, 188 (1960).
24. R. B. ANGIER, J. H. BOOTHE, J. H. MOWAT, C. W. WALLER, and J. SEMB. J. Am. Chem. Soc. **74**, 408 (1952).
25. O. YAMAMOTO and M. YANAGISAWA. Anal. Chem. **42**, 1463 (1970).
26. J. S. MARTIN and B. P. DAILEY. J. Chem. Phys. **39**, 1722 (1963).
27. G. W. SMITH. J. Mol. Spectrosc. **12**, 146 (1964).
28. W. G. SCHNEIDER, H. J. BERNSTEIN, and J. A. POPLE. J. Am. Chem. Soc. **80**, 3497 (1958).
29. S. I. CHAN, M. P. SCHWEIZER, P. O. P. Ts'O, and G. K. HELMKAMP. J. Am. Chem. Soc. **86**, 4182 (1964).
30. N. MULLER and R. H. BIRKHAHN. J. Phys. Chem. **71**, 957 (1967).

Can. J. Chem. Downloaded from www.nrcresearchpress.com by 210.87.254.5 on 09/05/12
For personal use only.

Can. J. Chem. Downloaded from www.nrcresearchpress.com by 210.87.254.42 on 09/05/12
For personal use only.

Concerning the Discrepancies in the Reported Infrared Spectra of Dibenzo[*a*,*e*]cyclooctatetraene[1]

THEODORE W. CUTSHALL AND PETER W. RABIDEAU[2]

Department of Chemistry, Indiana-Purdue University at Indianapolis, Indianapolis, Indiana 46205

Received February 1, 1972

Controversy has existed concerning the several syntheses of dibenzo[*a*,*e*]cyclooctatetraene. This controversy has resulted from a discrepancy with the i.r. spectrum contained in one of the original preparations with subsequent samples. We have prepared this hydrocarbon, together with 7-methylenedibenzo[*a*,*e*]cycloheptatriene, and have concluded that this discrepancy has arisen from a mixup of spectra (or samples) with this latter hydrocarbon.

Il existait une controverse concernant plusieurs synthèses du dibenzo[*a*,*e*]cyclooctatétraène. Cette controverse résultait d'une différence observée dans le spectre i.r. d'une des préparations originales avec les échantillons subséquents. Nous avons préparé cet hydrocarbure ainsi que le méthylène-7 dibenzo[*a*,*e*]cycloheptatriène et avons conclu que la divergence était due au mélange des divers échantillons (ou spectres) avec ce dernier hydrocarbure.

Canadian Journal of Chemistry, **50**, 2364 (1972)

The synthesis of dibenzo[*a*,*e*]cyclooctatetraene (1) was originally reported by Fieser and Pechet (1). In an attempt to provide a more useful preparation of this interesting hydrocarbon, its synthesis was later undertaken by Cope and Fenton (2). These workers prepared samples by a new method and by Fieser's method, and reported them to be identical. In this connection, they published the i.r. spectra of both samples, showing them to be identical. This hydrocarbon has subsequently been prepared by several investigators (3). However, a serious discrepancy exists concerning the integrity of the various preparations. Griffin (3*c*) pointed out that his i.r. spectrum of **1** was identical to the spectrum reported by Wittig (3*a*), but different from that reported by Cope (2). This same observation was later reported by another group of investigators (3*e*, 4). However, Nenitzescu (3*b*) and Schröder (3*d*) have reported their samples of **1** to be identical with that of Fieser (1) (and Cope (2)). We would now like to report our results which provide a solution to this puzzling problem.

[1]This research was supported in part by grants from the Eli Lilly Company, and the Purdue University Cancer Research Committee.

[2]To whom correspondence should be addressed.

In a paper immediately following the report on **1**, Cope and Fenton also reported the synthesis and i.r. spectrum of **2** (5). We have prepared samples of dibenzo[*a*,*e*]cyclooctatetraene (**1**) and 7-methylenedibenzo[*a*,*e*]cycloheptatriene (**2**), made certain of their identities by their n.m.r. spectra, and recorded the i.r. spectra.

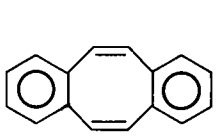

1

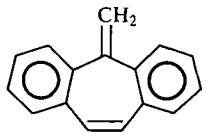

2

We have found that our i.r. spectrum of **1** is superimposable with that *reported by Cope for compound* **2**, *and our spectrum of* **2** *is superimposable with that reported by Cope for* **1**. Hence, it appears that all of the synthetic procedures which have appeared in the last 25 years are correct, and the controversy merely resulted from a mixup of spectra (or samples).

Experimental

Dibenzo[a,e]cyclooctatetraene (1)

This was prepared by the photolysis of dibenzobarrelene (3*e*, 4). The i.r. spectrum was identical with that published by Wittig (3*a*) with major absorptions at 12.9 and 13.4 μ.

The n.m.r. δ 7.0 (m, 8H) aromatic and 6.6 (s, 4) vinyl is consistent with the structure of **1**, and identical with that previously reported (4).

7-Methylenedibenzo[a,e]cycloheptatriene (2)

Samples were prepared by two methods: (*a*) by refluxing **1** with an excess of *p*-toluenesulfonic acid hydrate in benzene followed by refluxing the tosylate with sodium hydroxide–ethanol,[3] and (*b*) by reacting dibenzo[*a*,*e*]cycloheptatrienone with methylmagnesium iodide followed by dehydration (2). After recrystallization from aqueous ethanol, the respective samples proved identical, m.p. 117–118° (lit. (6) 118–119°). The i.r. showed major absorptions at 11.0, 12.3, 12.5, and 12.9 μ, and was identical with that published by Cope (2), incorrectly indicated as **1**. The n.m.r. δ 7.35 (m, 8H) aromatic, 6.82 (s, 2) vinyl, and 5.25 (s, 2) *exo*-vinyl is quite consistent with the structure of **2**.

[3]Essentially the procedure of Bucur *et al.* (6).

1. L. A. F. Fieser and M. Pechet. J. Am. Chem. Soc. **68**, 2577 (1946).
2. A. C. Cope and S. W. Fenton. J. Am. Chem. Soc. **73**, 1668 (1951).
3. (*a*) G. Wittig, G. Koenig, and K. Clauss. Ann. **593**, 127 (1955). (*b*) M. Avram, D. Dinu, G. Mateescu, and C. D. Nenitzescu. Ber. **93**, 1789 (1960). (*c*) C. E. Griffin and J. A. Peters. J. Org. Chem. **28**, 1715 (1963). (*d*) G. Schröder, W. Martin, and J. F. M. Oth. Angew. Chem. Intern. *Ed.* **6**, 870 (1967). (*e*) P. W. Rabideau, J. B. Hamilton, and L. Friedman. J. Am. Chem. Soc. **90**, 4465 (1968).
4. P. W. Rabideau. Ph.D. Thesis. Case Western Reserve University, Cleveland, Ohio, 1968.
5. A. C. Cope and S. W. Fenton. J. Am. Chem. Soc. **68**, 1673 (1951).
6. E. C. A. Bucur, M. Elian, M. Banciu, M. Voicu, and C. D. Nenitzescu. Chem. Abstr. **63**, 11 458 (1965).

Thermal Rearrangement of Acyl Groups in Anhydronucleosides. A Convenient Synthesis of 5′-*O*-Acetylanhydrouridine[1]

K. K. Ogilvie, J. B. Westmore, G. Taylor, D. Lin, D. Iwacha,[2] H. Wayborn, and G. E. Dunn

Department of Chemistry, University of Manitoba, Winnipeg, Manitoba

Received March 8, 1972

The mass spectra of acylanhydronucleosides suggested that the acyl groups undergo a thermal rearrangement. This was confirmed by studying the melting profiles of these compounds in a differential scanning calorimeter. The results have led to a convenient synthesis of 5′-acetylanhydrouridine.

Les spectres de masse des acylanhydronucléosides laissent penser que les groupes acyle subissent un réarrangement thermique. Ceci a été confirmé par l'étude des profils de fusion de ces composés, dans un calorimètre à balayage différentiel. Les résultats ont conduit à une synthèse commode de l'acétyl-5′ anhydrouridine.

Canadian Journal of Chemistry, **50**, 2365 (1972)

We have recently developed a method for incorporating 2′-anhydronucleosides into nucleotide chains (1). To permit maximum flexibility in this approach we needed acid- and base-labile protecting groups for both the 3′- and 5′-positions. Further, these groups should be sufficiently labile to be removed without opening the anhydro-ring, yet stable during phosphorylation procedures. The monomethoxytrityl (MTr—) and the acetyl (—Ac) groups satisfy these requirements for acid- and base-labile protecting groups respectively. Schemes 1 and 2 (to be discussed later) illustrate the methods by which 3′- and 5′-*O*-acetyl derivatives can be prepared. These multistep procedures are required because acetylating reagents generally have little preference for reaction at the 5′-position *vs.* the 3′-position. 5′-Derivatives in particular are not easy to prepare in high overall yield in just a few reaction steps. For example 5′-*O*-acetylanhydrouridine has been prepared by Todd and co-workers (2) and Verheyden and Moffat (3) both using the same five-step synthesis from uridine giving an overall yield of about 25%. We wish to report a simple synthesis of 5′-*O*-acetyl-2,2′-anhydro-1-β-D-arabinofuranosyluracil (5′-AcAU, **6**) by a method suggested from our mass spectral investigations of 3′,5′-di-*O*-acetyl-2,2′-anhydro-1-β-D-arabino-

[1]Part VII in a series on anhydronucleosides.
[2]NRCC Scholarship holder 1968-1972.

Can. J. Chem. Downloaded from www.nrcresearchpress.com by 210.87.254.42 on 09/05/12
For personal use only.

The n.m.r. δ 7.0 (m, 8H) aromatic and 6.6 (s, 4) vinyl is consistent with the structure of **1**, and identical with that previously reported (4).

7-Methylenedibenzo[a,e]cycloheptatriene (2)

Samples were prepared by two methods: (*a*) by refluxing **1** with an excess of *p*-toluenesulfonic acid hydrate in benzene followed by refluxing the tosylate with sodium hydroxide–ethanol,[3] and (*b*) by reacting dibenzo[*a*,*e*]cycloheptatrienone with methylmagnesium iodide followed by dehydration (2). After recrystallization from aqueous ethanol, the respective samples proved identical, m.p. 117–118° (lit. (6) 118–119°). The i.r. showed major absorptions at 11.0, 12.3, 12.5, and 12.9 μ, and was identical with that published by Cope (2), incorrectly indicated as **1**. The n.m.r. δ 7.35 (m, 8H) aromatic, 6.82 (s, 2) vinyl, and 5.25 (s, 2) *exo*-vinyl is quite consistent with the structure of **2**.

[3]Essentially the procedure of Bucur *et al.* (6).

1. L. A. F. Fieser and M. Pechet. J. Am. Chem. Soc. **68**, 2577 (1946).
2. A. C. Cope and S. W. Fenton. J. Am. Chem. Soc. **73**, 1668 (1951).
3. (*a*) G. Wittig, G. Koenig, and K. Clauss. Ann. **593**, 127 (1955). (*b*) M. Avram, D. Dinu, G. Mateescu, and C. D. Nenitzescu. Ber. **93**, 1789 (1960). (*c*) C. E. Griffin and J. A. Peters. J. Org. Chem. **28**, 1715 (1963). (*d*) G. Schröder, W. Martin, and J. F. M. Oth. Angew. Chem. Intern. *Ed.* **6**, 870 (1967). (*e*) P. W. Rabideau, J. B. Hamilton, and L. Friedman. J. Am. Chem. Soc. **90**, 4465 (1968).
4. P. W. Rabideau. Ph.D. Thesis. Case Western Reserve University, Cleveland, Ohio, 1968.
5. A. C. Cope and S. W. Fenton. J. Am. Chem. Soc. **68**, 1673 (1951).
6. E. C. A. Bucur, M. Elian, M. Banciu, M. Voicu, and C. D. Nenitzescu. Chem. Abstr. **63**, 11 458 (1965).

Thermal Rearrangement of Acyl Groups in Anhydronucleosides. A Convenient Synthesis of 5′-*O*-Acetylanhydrouridine[1]

K. K. Ogilvie, J. B. Westmore, G. Taylor, D. Lin, D. Iwacha,[2] H. Wayborn, and G. E. Dunn

Department of Chemistry, University of Manitoba, Winnipeg, Manitoba

Received March 8, 1972

The mass spectra of acylanhydronucleosides suggested that the acyl groups undergo a thermal rearrangement. This was confirmed by studying the melting profiles of these compounds in a differential scanning calorimeter. The results have led to a convenient synthesis of 5′-acetylanhydrouridine.

Les spectres de masse des acylanhydronucléosides laissent penser que les groupes acyle subissent un réarrangement thermique. Ceci a été confirmé par l'étude des profils de fusion de ces composés, dans un calorimètre à balayage différentiel. Les résultats ont conduit à une synthèse commode de l'acétyl-5′ anhydrouridine.

Canadian Journal of Chemistry, **50**, 2365 (1972)

We have recently developed a method for incorporating 2′-anhydronucleosides into nucleotide chains (1). To permit maximum flexibility in this approach we needed acid- and base-labile protecting groups for both the 3′- and 5′-positions. Further, these groups should be sufficiently labile to be removed without opening the anhydro-ring, yet stable during phosphorylation procedures. The monomethoxytrityl (MTr—) and the acetyl (—Ac) groups satisfy these requirements for acid- and base-labile protecting groups respectively. Schemes 1 and 2 (to be discussed later) illustrate the methods by which 3′- and 5′-*O*-acetyl derivatives can be prepared. These multistep procedures are required because acetylating reagents generally have little preference for reaction at the 5′-position *vs.* the 3′-position. 5′-Derivatives in particular are not easy to prepare in high overall yield in just a few reaction steps. For example 5′-*O*-acetylanhydrouridine has been prepared by Todd and co-workers (2) and Verheyden and Moffat (3) both using the same five-step synthesis from uridine giving an overall yield of about 25%. We wish to report a simple synthesis of 5′-*O*-acetyl-2,2′-anhydro-1-β-D-arabinofuranosyluracil (5′-AcAU, **6**) by a method suggested from our mass spectral investigations of 3′,5′-di-*O*-acetyl-2,2′-anhydro-1-β-D-arabino-

[1]Part VII in a series on anhydronucleosides.
[2]NRCC Scholarship holder 1968-1972.

Can. J. Chem. Downloaded from www.nrcresearchpress.com by 210.87.254.6 on 09/05/12
For personal use only.

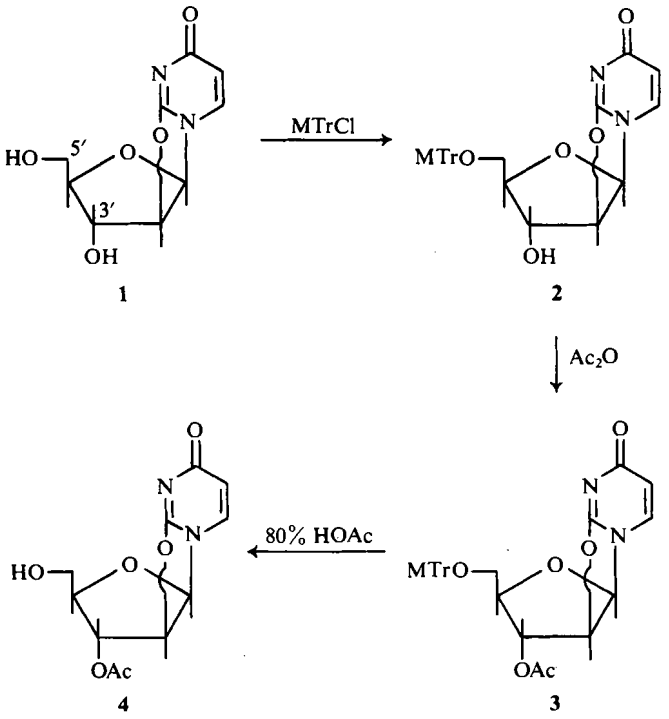

SCHEME 1

furanosyluracil (DiAcAU, **5**) and 3′-*O*-acetyl-2,2′-anhydro-1-β-D-arabinofuranosyluracil (3′-AcAU, **4**).

As part of our investigation of anhydronucleosides we have been carrying out a systematic study of their mass spectra. A sample of 3′-AcAU was prepared by the route shown in Scheme 1. Monomethoxytrityl chloride (MTrCl) reacts with 2,2′-anhydro-1-β-D-arabinofuranosyluracil (AU, **1**) in pyridine to produce 5′-*O*-monomethoxytritylanhydrouridine (**2**) in 60% yield. Acetylation of **2** to produce **3** followed by detritylation using acetic acid at room temperature yields **4**.

In the course of the mass spectral studies we noticed that the mass spectra obtained when **4** and **5** were introduced into the mass spectrometer were similar. In particular, the mass spectrum obtained when **4** had been placed in the mass spectrometer sample probe showed a peak at *m/e* 310 (mw of **5** is 310) as well as at *m/e* 268 (mw of **4**) and at 226 (mw of **1**). Samples of **4** were carefully analyzed by paper chromatography before they were introduced into the mass spectrometer. No diacetylanhydrouridine or anhydrouridine could be detected in these samples under conditions where less than 1% could be detected. However, when the unvaporized residues were removed from the mass spectrometer sample probe (after the spectrum had been recorded) and analyzed by paper chromatography they were always found to contain **1**, **4**, **5**, and a material moving slightly faster (solvent A) than **4**. This unidentified material had an u.v. spectrum characteristic of anhydrouridines and was suspected to be 5′-*O*-acetyl-2,2′-anhydro-1-β-D-arabinofuranosyluracil (**6**).

We synthesized **6** by an alternate route (Scheme 2) for comparison with our unidentified derivative. 5′-Acetyluridine (4) was treated with diphenyl carbonate in dimethylformamide (5) to give **6**. Compounds **1** and **5** were also detected among the products but no **4** was observed. The yield of **6** from this reaction was 45%. We found the synthetic **6** to be identical to our unidentified material from the residue recovered from the mass spectrometer when **4** had been inserted into the sample probe.

The mass spectrum of **6** was similar to that of **4** showing again major peaks at *m/e* 310, 268, and 226. The relative peak heights differed in

Can. J. Chem. Downloaded from www.nrcresearchpress.com by 210.87.254.6 on 09/05/12
For personal use only.

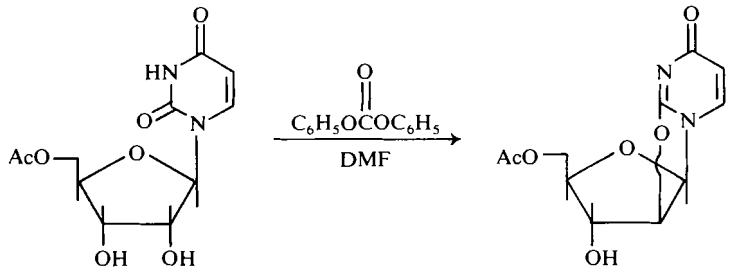

6

SCHEME 2

TABLE 1. Analysis of mass spectral residues and DMF reaction products (%)

Starting material:	3′-AcAU		5′-AcAU	
	Residue from		Residue from	
Product composition	Mass spectroscopy	DMF reaction	Mass spectroscopy	DMF reaction
DiAcAU	6.6	16	14	6
5′-AcAU	2.6	13	58	69
3′-AcAU	84.2	50	5	0
AU	6.6	21	23	25

the two cases. The paper chromatographic analyses of the residues recovered from the sample probe are shown in Table 2. Similar mass spectral results were obtained when samples were studied with a Finnigan 1015 quadrupole mass spectrometer.

The mass spectrometric results are not an artifact of electron impact but are evidently thermal in origin. The thermal rearrangement of the anhydro-derivatives was studied further in a differential scanning calorimeter (Perkin–Elmer DSC-1B). Samples of **4** were heated from room temperature to 260 °C at 10°/min in specially designed glass containers (6) sealed at reduced pressure. The results of paper chromatographic analyses are shown in Table 1. These results clearly show that the rearrangement was affected only slightly by reduction in pressure (at atmospheric pressure a small amount of decomposition to a material having a uracil-like u.v. spectrum occurred). The rearrangement was also independent of whether a glass or aluminum sample holder was used. Subsequent experiments were carried out in aluminum pans at atmospheric pressure.

Tables 1 and 2 show that compound **6** undergoes a thermal rearrangement to produce the same kind of products obtained from **4**. The presence of diacetylanhydrouridine in the products clearly indicated that some intermolecular transesterification had occurred. As

TABLE 2. Thermal rearrangement of acetylated anhydrouridines in the DSC

Sample container	Starting material	Pressure	Temperature reached (°C)	Product composition (%)				
				DiRAU	5′-RAU	3′-RAU	AU	U
GP*	3′-AcAU	10^{-6} mm	260	23	35	20	22	
GP	3′-AcAU	10^{-3} mm	260	22	32	22	24	
AP†	3′-AcAU	1 atm	260	24	24	28	22	2
GP	3′-AcAU	1 atm	260	22	20	34	22	2
AP	5′-AcAU	1 atm	210	12	57	4	27	
AP	DiAcAU + AU (1:1.15)	1 atm	260	19	37	10	25	9
AP	3′-PvAU	1 atm	270	23	51		21	5
AP	DiPvAU + AU (1:1.7)	1 atm	270	14	40		40	6

*GP = glass pan (6).
†AP = aluminum pan.

Can. J. Chem. Downloaded from www.nrcresearchpress.com by 210.87.254.6 on 09/05/12
For personal use only.

Can. J. Chem. Downloaded from www.nrcresearchpress.com by 210.87.254.6 on 09/05/12
For personal use only.

a result a mixture of **5** and **1** was heated to 260 °C under controlled conditions in the DSC. The presence of **6** as the major product (Table 2) was encouraging. There was also a significant amount (9%) of decomposition to material having a uracil-like u.v. spectrum (this could result from cleavage of either the anhydro or both the anhydro and glycosidic bonds to give uracil derivatives).

To test the utility of the method as a source of **6** on a preparative scale, 100 mg of a mixture of **5** and **1** (1:1.15 mol ratio) was placed in a small test tube which was suspended in an oil bath maintained at 260 °C (this temperature would ensure rapid melting of the mixture). Complete melting occurred in 55 s and the sample was cooled rapidly to room temperature. The products, isolated by chromatography, contained **6** and **4** in 51 and 12% yields (crystallized from methanol) respectively. Since the monoacetyl derivatives have very similar properties, a combination of thick-layer and paper chromatography was required to separate them. This difficulty is easily avoided by heating the mixtures in the melt for slightly longer periods of time. This results in exclusive formation of the 5′-isomer **6** which is readily isolated and in higher yields by thick-layer chromatography in tetrahydrofuran. The reaction is easily carried out on larger scales in the same manner. The method of heating is not critical and for our own purposes the sample is kept in the melt for 2–3 min using a gas-burner for heat and in all cases only the 5′-isomer is obtained. This represents an exceedingly simple synthesis of **6** from readily available materials.

In the preparative reaction some decomposition had occurred to yield products having a uracil-like spectrum. These products were very numerous and only uracil was positively identified. Most of the other products were probably acetylated uridines or arabinouridines. Samples maintained at 260 °C for longer periods of time gave greater amounts of decomposition products. Uracil was the only identifiable product from a reaction mixture held at 260 °C for 15 min.

In order to check on the generality of this rearrangement, samples of 3′-*O*-pivaloylanhydrouridine (PvAU) and a mixture of 3′,5′-di-*O*-pivaloylanhydrouridine (DiPvAU) and anhydrouridine were heated in the DSC from room temperature to 270 °C at 10°/min. The results, shown in Table 2, confirm that rearrangement had occurred. We have been unable to separate mixtures of 3′-PvAU and 5′-PvAU and as a result only the sum of the two is shown in Table 2.

A similar thermal transfer of acetyl groups in nucleoside derivatives using a fusion method has been described by Michelson *et al.* (7). In their case acetyl groups migrated among secondary hydroxyl groups in protected adenosine derivatives. In our case the migration occurs between secondary and primary hydroxyls with the product being the more stable primary ester.

We also heated samples of **4** and **6** individually in dimethylformamide solutions held at 150 °C and found that rearrangement also occurred in solution. These results are shown in Table 1.

This study has produced a very useful route to 5′-*O*-acetylanhydrouridine. However, it also points out the necessity of exercising care when interpreting the mass spectra of semiesterified molecules of low volatility.

Experimental

General Methods

Thin-layer chromatography was carried out on Eastman Chromagram Sheets 6060 by the ascending technique. Thick-layer chromatography was carried out on glass plates (20 × 20 cm) coated with a 2 mm thick layer of silica gel DSF-5 (Mondray Chemicals Ltd.). Paper chromatography was carried out on Whatman 3MM paper by the descending technique. The solvent system employed in paper chromatography was solvent A; *n*-butanol:ethanol:water (4:1:5, v/v/v), the organic phase was used. Nucleosides and their derivatives were detected on paper chromatograms, thin- and thick-layer plates, using an u.v. source (Mineralite, output ≃ 254 nm). Nucleosides were eluted from the paper chromatograms, diluted to volume and their absorbances recorded in the u.v. on a Cary 14 spectrophotometer. The term o.d. unit (8) refers to the extinction of a solution of a nucleoside at neutral p*H* in 1 ml of solution using a 1 cm light path quartz cell.

The i.r. spectra were obtained on a Perkin–Elmer 337 recording instrument using KBr disks for sample preparation. Melting points were determined on a Fisher–Johns melting point apparatus and are reported uncorrected. Elemental analyses were performed by Galbraith Labs, Knoxville, Tennessee.

Mass Spectra

Mass spectra were recorded by a Perkin–Elmer Hitachi RMU-6D single-focusing instrument. Samples were introduced to the mass spectrometer in a solid sample probe via a vacuum lock. The electron energy was 50 V. After preliminary experiments the following procedure was used. The

Can. J. Chem. Downloaded from www.nrcresearchpress.com by 210.87.254.6 on 09/05/12
For personal use only.

ionization chamber temperature and sample heater block were each maintained at 135 °C. The sample probe was inserted into the heater block and spectra were recorded as soon as vaporization started to occur. After the spectra were recorded (total time 15 min) the remains of the samples were withdrawn from the instrument and analyzed by paper chromatography. Results of these experiments are shown in Table 1. Clearly **1**, **4**, **5**, and **6** were obtained when starting with pure samples of either **4** or 6.

Calorimetric Studies

Samples were heated through the melting endotherm (6) in a differential scanning calorimeter (Perkin–Elmer DSC-1B). Typical samples of 2–10 mg and a heating rate of 10°/min were used. After melting, the samples were removed, cooled to room temperature, and analyzed by paper chromatography in solvent A. The results are shown in Table 2. In some cases a product moving slightly faster than DiAcAU (solvent A) was observed. The u.v. spectrum (water) of this material was similar in form to that of uracil with λ_{max} at 260 nm (this compound was most likely an acetylated uridine or arabinouridine resulting from some decomposition of the anhydro-structure).

3′-*O*-Pivaloyl-2,2′-anhydrouridine, 5′-*O*-pivaloyl-2,2′-anhydrouridine, and 3′,5′-di-*O*-pivaloyl-2,2′-anhydrouridine were prepared as described by Wayborn (9). 2,2′-Anhydrouridine was prepared by the method of Hampton and Nichol (5).

5′-O-Monomethoxytrityl-2,2′-anhydrouridine (MTrAU, 2)

Anhydrouridine (4.35 g, 19.2 mmol) and monomethoxytrityl chloride (6 g, 19.5 mmol) were stirred in dry pyridine (100 ml) for 4 days. The solvent was removed at reduced pressure and the residue was dissolved in a mixture (300 ml) of chloroform and water (1:1). The chloroform layer was separated and concentrated to a small volume. White crystals of MTrAU separated and were collected by filtration (5.7 g, 60%), m.p. 154–158 °C. Principal bands in the i.r. spectrum occurred at 6.07, 6.13, 8.05, and 14.2 μ.

Anal. Calcd. for $C_{29}H_{26}O_6N_2$: C, 69.87; H, 5.26; N, 5.62. Found: C, 70.23; H, 5.28; N, 5.53.

5′-O-Monomethoxytrityl-3′-O-acetyl-2,2′-anhydrouridine (MTrAU-Ac, 3)

MTrAU (**2**, 2.5 g, 5 mmol) and acetic anhydride (0.8 ml) were stirred in dry pyridine (15 ml) for 12 h. The solution was poured into ice water (500 ml) and the precipitate was collected, dissolved in chloroform, and dried over sodium sulfate. The chloroform solution was concentrated to a small volume and on addition of hexane a white precipitate formed which was collected by filtration and dried to yield 2.6 g (95%) of MTrAU-Ac (**3**, m.p. 100–107 °C). Principal bands in the i.r. spectrum occurred at 5.7, 6.1, 12.1, 13.3, and 14.2 μ. The u.v. spectrum in ethanol showed λ_{max} of 230 (ε 19 000) and λ_{min} of 223 nm (18 300).

Anal. Calcd. for $C_{31}H_{28}N_2O_7$: C, 68.88; H, 5.22; N, 5.18. Found: C, 68.78; H, 5.14; N, 5.08.

3′-O-Acetyl-2,2′-anhydrouridine (3′-AcAU, 4)

MTrAU-Ac (**3**, 2.2 g, 4 mmol) was dissolved in 80% acetic acid (25 ml) and stirred at room temperature for 3 h. The solvents were removed at reduced pressure and the residue was washed with ether and crystallized from ethanol (0.7 g, 66%), m.p. 204–209 °C. The i.r. spectrum showed principal bands at 5.8, 5.99, 8.2, and 13.1 μ. The u.v. spectrum in ethanol showed λ_{max} 249 (ε 8220), 224 (9600), and λ_{min} 237 nm (ε 7330).

Anal. Calcd. for $C_{11}H_{12}N_2O_6$: C, 49.25; H, 4.51; N, 10.44. Found: C, 49.10; H, 4.50; N, 10.26.

TABLE 3. Physical properties of anhydronucleosides

Compound	m.p. (°C)	λ_{max}, (nm)*	R_f(A)†	R_fTHF
AU	244–248	249	0.30	0.05
3′-AcAU	204–209	249	0.46	0.11
5′-AcAU	164–167	249	0.51	0.16
DiAcAU	186–187	249	0.60	0.23
3′-PvAU	240–242	249	0.75	0.23
5′-PvAU	210–215	249	0.75	0.23
DiPvAU	227–231	249	0.87	0.47

*Both water and ethanol used as solvents in all cases.
†Solvent A experimental section.

5′-O-Acetyl-2,2′-anhydro-1-β-D-arabinofuranosyluracil (5′-AcAU, 6)

(*A*) 5′-Acetyluridine ((4), 140 mg, 0.5 mmol), diphenyl carbonate (140 mg), and sodium bicarbonate (12 mg) were added to DMF (0.5 ml) and the mixture was heated at 150 °C for 30 min. The solution was cooled to room temperature and applied to two t.l.c. plates which were developed first in ethyl acetate and then three times in tetrahydrofuran. Three anhydronucleoside bands were apparent including diacetylanhydrouridine, anhydrouridine, and a product moving between these two. This latter product was isolated and identified as 5′-AcAU (60 mg, 45%) with m.p. 164–167 °C (lit. m.p. 166–167 °C (2)). R_f values are shown in Table 3.

(*B*) One hundred milligrams of a mixture of DiAcAU and AU (1:1.15, molar ratio) was placed in a small test tube suspended in an oil bath maintained at 260 °C. As soon as the mixture had completely melted (55 s) the sample was removed, cooled to room temperature, and applied to a thick-layer plate which was developed first in tetrahydrofuran (THF). Two nucleoside bands moved up the plate in THF (R_f 0.5, 0.7) and were eluted. Both of these bands contained numerous products (paper chromatography solvent A) all of which had λ_{max} (H_2O) 260 and λ_{min} (H_2O) 231 nm. The total weight of material from the two bands was 20 mg and the only compound positively identified was uracil (4 mg).

The original thick-layer plate was developed in ethanol and another nucleoside band was obtained. This band was eluted and re-applied to another thick-layer plate which was developed five times in THF. Four bands separated with DiAcAU (8 mg, 0.026 mmol) moving fastest and AU (16 mg, 0.071 mmol) moving slowest. In between these were two bands moving very close together. The fastest band contained only 5′-AcAU while the slower band contained a mixture of 5′-AcAU and 3′-AcAU. This mixture was applied to Whatman 3MM paper developed in solvent A and the two materials separated cleanly. The yield of 3′-AcAU was 11 mg (0.041 mmol, 12%) while the total yield of 5′-AcAU (crystallized from ethanol) was 48 mg (0.18 mmol, 51% based on the total mmoles of acetyl groups in the starting materials, m.p. 165–167 °C).

(*C*) A mixture containing 62 mg of DiAcAU and 51 mg of AU was heated as above at 260 °C for 2.5 min. The product was dissolved in ethanol and applied to a single thick-layer plate which was developed four times in THF. Behind the decomposition products (at the solvent front) were three cleanly separated bands which were eluted with ethanol and identified as DiAcAU (3 mg), 5′-AcAU (75 mg, 70%), and AU (10 mg).

When this experiment was repeated, except that the sample was held at 260 °C for longer periods of time, the amount of decomposition increased markedly. In one reaction held at 260 °C for 15 min the only identifiable u.v. absorbing material was uracil.

(*D*) A mixture containing 620 mg of DiAcAU and 504 mg of AU was heated at 260 °C in a 100 ml round-bottom flask for 3 min and cooled to room temperature. The product was dissolved in ethanol and applied to eight thick-layer plates developed as in section *C* above. The yield of 5′-AcAU from this reaction was 720 mg (67%). The same result was obtained when the mixture was melted using a gas-burner for heat (total time in the melt 2–3 min).

Thermal Rearrangement of Acetyl Groups in Dimethylformamide (DMF)

Samples of **4** and **6** were heated separately in DMF at 150 °C for 30 min. The solutions were cooled to room temperature and applied to Whatman 3MM paper developed in solvent A. The results are shown in Table 1.

We wish to acknowledge financial support from the National Research Council of Canada.

1. K. K. OGILVIE and D. IWACHA. Can. J. Chem. **48**, 862 (1970).
2. D. M. BROWN, D. B. PARIHAR, and SIR A. TODD. J. Chem. Soc. 4242 (1958).
3. J. P. H. VERHEYDEN and J. G. MOFFATT. J. Org. Chem. **35**, 2868 (1970).
4. D. M. BROWN, SIR A. TODD, and S. VARADARAJAN. J. Chem. Soc. 2388 (1958).
5. A. HAMPTON and A. W. NICHOL. Biochem. **5**, 2076 (1966).
6. G. R. TAYLOR, G. E. DUNN, and W. B. EASTERBROOK. Anal. Chim. Acta, **53**, 452 (1971).
7. A. M. MICHELSON, L. SZABO, and SIR A. TODD. J. Chem. Soc. 1546 (1956).
8. S. A. NARANG and H. G. KHORANA. J. Am. Chem. Soc. **87**, 2981 (1965).
9. H. WAYBORN. Masters Thesis. University of Manitoba, Winnipeg, Manitoba, 1971.

A Nuclear Magnetic Resonance Study of the Symmetry of the Proton Spins in Ethylene Sulfite in a Nematic Solvent[1]

M. A. RAZA AND L. W. REEVES

The Chemistry Department, University of Waterloo, Waterloo, Ontario

Received February 10, 1972

The proton magnetic resonance spectrum of ethylene sulfite dissolved in the nematic phase *N*(*p*-methoxybenzylidene)-*p*-*n*-butylaniline has been recorded and analyzed. The dipole–dipole coupling constants derived show that the four protons are arranged in an effective plane with C_{2v} symmetry. The spectrum is deceptively similar to that expected for D_{2h} symmetry but errors between the experimental and the optimized computed spectrum are unacceptably large with this assumption. The two vicinal protons *cis* to the extra ring oxygen are closer together than the two *trans* vicinal protons. A comparison is made with the molecule ethylene carbonate studied previously in the same nematic solvent.

Le spectre de résonance magnétique nucléaire du sulfite d'éthylène dissout en phase nématique *N*(*p*-méthoxybenzylidène) *p*-*n*-butylaniline a été enregistré et analysé. Les constantes de couplage dipôle–dipôle montrent que les quatre protons sont dans un arrangement effectif plan selon la symétrie C_{2v}. Le spectre est d'une similitude "décevante" à celui attendu pour la symétrie D_{2h} mais les écarts entre les spectres expérimental et calculé sont trop grands pour retenir une telle hypothèse. Les deux protons vicinaux en *cis* par rapport à l'oxygène sont plus rapprochés que les deux protons vicinaux *trans*. Une comparaison est faite avec la molécule de carbonate d'éthylène précédemment étudiée, dans le même solvant nématique.

Canadian Journal of Chemistry, **50**, 2370 (1972)

Introduction

We have recently reported comparative studies of the proton magnetic resonance (n.m.r.) spectra of a series of ring compounds with four spins dissolved in both lyotropic and thermotropic nematic phases (1–4). Ethylene carbonate (EC) and ethylene monothiocarbonate (EMTC) do not have the same geometry in the two types of nematic phase. Ring puckering motions which

[1]Research supported by operating grants provided by the Defence Research Board and the National Research Council of Canada.

Can. J. Chem. Downloaded from www.nrcresearchpress.com by 210.87.254.6 on 09/05/12
For personal use only.

(*C*) A mixture containing 62 mg of DiAcAU and 51 mg of AU was heated as above at 260 °C for 2.5 min. The product was dissolved in ethanol and applied to a single thick-layer plate which was developed four times in THF. Behind the decomposition products (at the solvent front) were three cleanly separated bands which were eluted with ethanol and identified as DiAcAU (3 mg), 5′-AcAU (75 mg, 70%), and AU (10 mg).

When this experiment was repeated, except that the sample was held at 260 °C for longer periods of time, the amount of decomposition increased markedly. In one reaction held at 260 °C for 15 min the only identifiable u.v. absorbing material was uracil.

(*D*) A mixture containing 620 mg of DiAcAU and 504 mg of AU was heated at 260 °C in a 100 ml round-bottom flask for 3 min and cooled to room temperature. The product was dissolved in ethanol and applied to eight thick-layer plates developed as in section *C* above. The yield of 5′-AcAU from this reaction was 720 mg (67%). The same result was obtained when the mixture was melted using a gas-burner for heat (total time in the melt 2–3 min).

Thermal Rearrangement of Acetyl Groups in Dimethylformamide (DMF)

Samples of **4** and **6** were heated separately in DMF at 150 °C for 30 min. The solutions were cooled to room temperature and applied to Whatman 3MM paper developed in solvent A. The results are shown in Table 1.

We wish to acknowledge financial support from the National Research Council of Canada.

1. K. K. OGILVIE and D. IWACHA. Can. J. Chem. **48**, 862 (1970).
2. D. M. BROWN, D. B. PARIHAR, and SIR A. TODD. J. Chem. Soc. 4242 (1958).
3. J. P. H. VERHEYDEN and J. G. MOFFATT. J. Org. Chem. **35**, 2868 (1970).
4. D. M. BROWN, SIR A. TODD, and S. VARADARAJAN. J. Chem. Soc. 2388 (1958).
5. A. HAMPTON and A. W. NICHOL. Biochem. **5**, 2076 (1966).
6. G. R. TAYLOR, G. E. DUNN, and W. B. EASTERBROOK. Anal. Chim. Acta, **53**, 452 (1971).
7. A. M. MICHELSON, L. SZABO, and SIR A. TODD. J. Chem. Soc. 1546 (1956).
8. S. A. NARANG and H. G. KHORANA. J. Am. Chem. Soc. **87**, 2981 (1965).
9. H. WAYBORN. Masters Thesis. University of Manitoba, Winnipeg, Manitoba, 1971.

A Nuclear Magnetic Resonance Study of the Symmetry of the Proton Spins in Ethylene Sulfite in a Nematic Solvent[1]

M. A. RAZA AND L. W. REEVES

The Chemistry Department, University of Waterloo, Waterloo, Ontario

Received February 10, 1972

The proton magnetic resonance spectrum of ethylene sulfite dissolved in the nematic phase *N*(*p*-methoxybenzylidene)-*p*-*n*-butylaniline has been recorded and analyzed. The dipole–dipole coupling constants derived show that the four protons are arranged in an effective plane with C_{2v} symmetry. The spectrum is deceptively similar to that expected for D_{2h} symmetry but errors between the experimental and the optimized computed spectrum are unacceptably large with this assumption. The two vicinal protons *cis* to the extra ring oxygen are closer together than the two *trans* vicinal protons. A comparison is made with the molecule ethylene carbonate studied previously in the same nematic solvent.

Le spectre de résonance magnétique nucléaire du sulfite d'éthylène dissout en phase nématique *N*(*p*-méthoxybenzylidène) *p*-*n*-butylaniline a été enregistré et analysé. Les constantes de couplage dipôle–dipôle montrent que les quatre protons sont dans un arrangement effectif plan selon la symétrie C_{2v}. Le spectre est d'une similitude "décevante" à celui attendu pour la symétrie D_{2h} mais les écarts entre les spectres expérimental et calculé sont trop grands pour retenir une telle hypothèse. Les deux protons vicinaux en *cis* par rapport à l'oxygène sont plus rapprochés que les deux protons vicinaux *trans*. Une comparaison est faite avec la molécule de carbonate d'éthylène précédemment étudiée, dans le même solvant nématique.

Canadian Journal of Chemistry, **50**, 2370 (1972)

Introduction

We have recently reported comparative studies of the proton magnetic resonance (n.m.r.) spectra of a series of ring compounds with four spins dissolved in both lyotropic and thermotropic nematic phases (1–4). Ethylene carbonate (EC) and ethylene monothiocarbonate (EMTC) do not have the same geometry in the two types of nematic phase. Ring puckering motions which

[1]Research supported by operating grants provided by the Defence Research Board and the National Research Council of Canada.

Can. J. Chem. Downloaded from www.nrcresearchpress.com by 210.87.254.6 on 09/05/12
For personal use only.

Can. J. Chem. Downloaded from www.nrcresearchpress.com by 210.87.254.6 on 09/05/12
For personal use only.

have been a controversial issue in EC (5–7) are much more pronounced in the lyotropic nematic phase. In the present series of studies we have been able to show that provided the spectral quality in terms of resolution is excellent then extremely small changes in geometry represented by the symmetry change D_{2h} to C_{2v} can be readily detected (1–3). β-Propiolactone has 4 protons arranged in C_{2v} symmetry such that a 1° change in the H—C—H angle adjacent to the carbonyl with respect to the other methylene protons is readily detected (2). The number of transitions increases when the symmetry change occurs, though this is complicated by the chemical shift effect not present in an AA′A″A‴ spectrum but present in an AA′BB′ spectrum (8). It is interesting to note that the C_{2v} symmetry of the 5 spins in parachloro- and parabromo-fluorobenzene is not detected in the AA′BB′ subspectra for the protons probably because of lack of quality in the resolution of the spectrum (9). In the present paper we report a study of ethylene sulfite in a thermotropic nematic phase. The expected C_{2v} symmetry of the four proton spins in this molecule is principally related to *cis* vicinal proton distances rather than geminal as in the molecules reported previously (1–3).

Standard methods based on the general analysis of Snyder (10) are used, with the simplifications appropriate to four spins in a plane in C_{2v} or D_{2h} symmetry (11–14). The interproton distance ratios are obtained directly in terms of the dipole–dipole coupling constants by elimination of the motional constants $C_{3z^2-r^2}$ and $C_{x^2-y^2}$.

Experimental

The nematic compound *N*(*p*-methoxybenzylidene)-*p*-*n*-butylaniline supplied by the Distillation Products Division of Eastman Organic Chemicals was used as the solvent. The nematic range in the pure state is between +18 and 41 °C. The clearing point of 41 °C is depressed on adding solutes, but in our previous experience it is possible to maintain nematic properties with a standard amount of 5 wt % of solute (2–4). If the sample remains in the magnet for some hour or so the line widths for a non-spinning sample can be reduced to 8 Hz and consequently peak positions are measured to ±0.5 Hz maximum error. Side band modulation techniques described previously with cross checks, and at least five averaged spectra are satisfactory in achieving these small error limits (2, 3).

Ethylene sulfite was supplied by Eastman Organic Chemicals Co., and purified by distillation under 10 mm Hg pressure. Proton magnetic resonance spectra were recorded in the H.R. mode of a Varian HA100 at a probe temperature of 30.5 ± 0.1 °C.

Results

The proton spectrum of ethylene sulfite in the neat isotropic state has been analyzed in this laboratory previously (1). It is a tightly coupled AA′BB′ spectrum which analyzes to give the following parameters; $\delta_1 = \delta_2 = +503.81 \pm 0.02$, $\delta_3 = \delta_4 = +474.76 \pm 0.02$, $J_{14} = J_{23} = -8.47 \pm 0.02$, $J_{12} = J_{34} = 6.74 \pm 0.02$, $J_{13} = J_{24} = 6.52 \pm 0.02$. The chemical shifts are measured with respect to an external tetramethylsilane (TMS) lock signal and refer to Hz at 100 MHz. The spin–spin coupling constants are in Hz. The non-equivalent protons are identified in the structure below as being *cis* or *trans* to the extra ring oxygen. H_1, H_2 are *cis* to the extra ring oxygen and H_3, H_4 are *trans*.

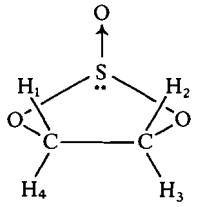

The spectrum of oriented ethylene sulfite is reproduced as Fig. 1. There are twelve observable transitions which could be considered appropriate for the AA′BB′ spectrum with a negligibly small chemical shift δ_{AB} and D_{2h} symmetry. The observed spectrum is very similar in form to that observed for EC (1, 3) and ETTC (4).

The spectrum can be calculated assuming an internal chemical shift $\delta_1 = \delta_2 \neq \delta_3 = \delta_4$ but assuming that the dipolar coupling constants $D_{12} = D_{34}$. Since the cube root of D_{12}/D_{34} is the interproton distance ratio r_{12}/r_{34} then the assumption $D_{12} = D_{34}$ means distances r_{12}, r_{34} are equal. The best fit between the experimental and computed spectrum using the program NMRFIT gives an r.m.s. error for the experimental spectrum for all line positions of 4.9 Hz. This is unacceptably large since the error on the position of proton resonance peaks in this and previous studies is certainly less than 2 Hz even in the thermotropic nematic phase (1, 3). The spectrum was therefore computed on the assumption that $D_{12} \neq D_{34}$. A spectral fit with an r.m.s. error for the difference between frequencies for all computed and experimental lines of 0.8 Hz was achieved. This is in agree-

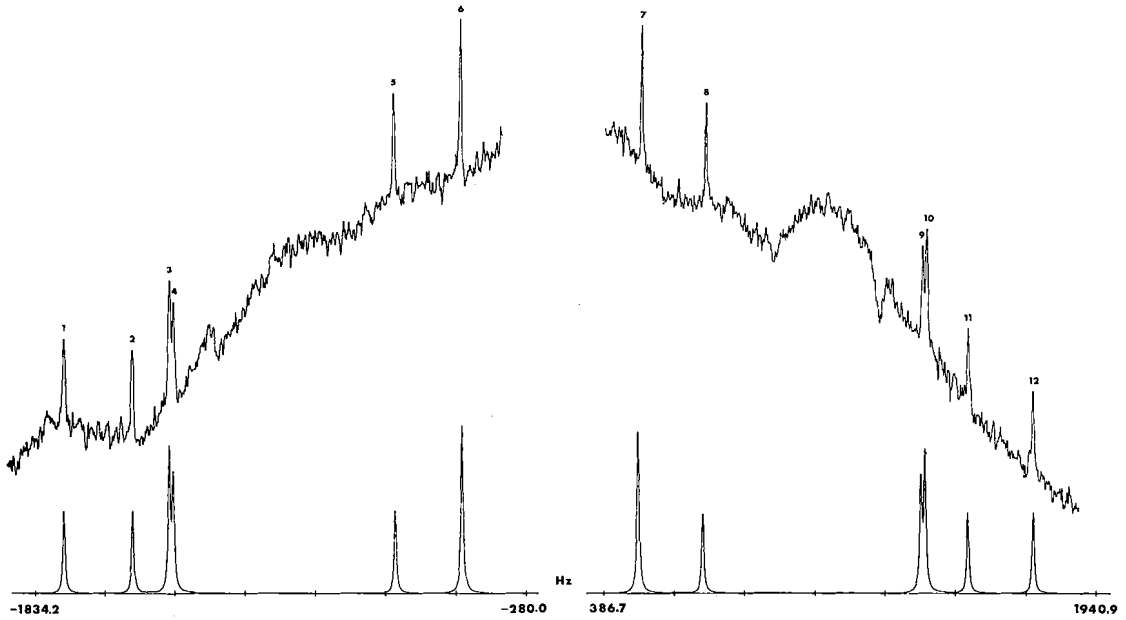

FIG. 1. Spectrum of ethylene sulfite in the nematic phase at 30.5 °C and 5 wt %. Below the experimental spectrum is the simulated spectrum obtained using parameters from Table 1 appropriate to C_{2v} symmetry of the four protons.

TABLE 1. The analyses of the spectrum of ethylene sulphite in the nematic phase assuming C_{2v} and D_{2h} symmetry for the four protons using $\delta_1 = \delta_2$, $\delta_3 = \delta_4$, $\delta_1 - \delta_3 = 68.8$*

Parameter	Value	
	C_{2v} (Assuming $D_{12} \neq D_{34}$)	D_{2h} (Assuming $D_{12} = D_{34}$)
Root-mean-square error	±0.77	±4.90
D_{12}	−763.7	−696.4
$D_{13} = D_{24}$	−140.5	−138.6
$D_{14} = D_{23}$	+1481.7	+1484.1
D_{34}	−630.1	−696.4

*All measurements are quoted in Hz at 100 MHz. Chemical shift convention is that low-field chemical shifts have increasing positive value. The error limits are too large if D_{2h} symmetry is assumed. The dipole–dipole coupling constants are listed for each analysis.

ment with the random error analysis of our experimental peak positions in this paper and is the error we expect from previous and directly comparable studies (2–4). It is extremely important in the present case to use the best resolution and to measure the positions of all peaks as accurately as possible. The parameters for equal and non-equal D_{12}, D_{34} are presented with the r.m.s. errors in Table 1. In β-propiolactone the C_{2v} symmetry of the four proton spins is due to a geminal H—C—H angle change which produces a trapezoidal arrangement where the parallel sides are the shortest ones. Since the dipolar coupling constants depend on r_{ij}^{-3} between protons, this symmetry change has a relatively large effect on the dipolar coupling and the spectrum of β-propiolactone has more transitions (16 peaks observable) with no apparent symmetry in the spectrum (2). In ethylene sulfite, however, the vicinal eclipsed protons are not equidistant along the long parallel sides of trapezoidal arrangement C_{2v}. The relative change in r_{ij}^{-3} is small and hence an extremely careful analysis is required to deter-

Can. J. Chem. Downloaded from www.nrcresearchpress.com by 210.87.254.6 on 09/05/12
For personal use only.

TABLE 2. Interproton distance ratios for the molecule ethylene sulfite derived from the dipole–dipole coupling constants in Table 1 for C_{2v} symmetry are listed. A comparison is made with a previous study of ethylene carbonate

Parameter	Value	
	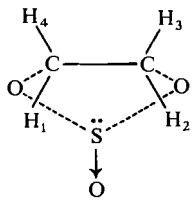	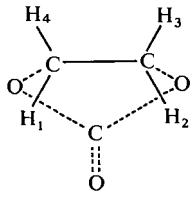
r_{23}/r_{14}	1.000	1.000
r_{34}/r_{14}	1.429 1.384*	1.358
r_{12}/r_{14}	1.340	1.358
r_{13}/r_{14}	1.707	1.686
$\angle H_3CC = \angle H_4CC$	114.6° (assumed)	114.6°
$\angle H_1CC = \angle H_2CC$	110.3°†	114.6°
$\angle H_3CH_2 = \angle H_1CH_4$	103.4°	111.0°

*$\frac{1}{2}(r_{34}/r_{14} + r_{12}/r_{14})$.
†A value of 110° for the angle HCC in ethylene sulfite has been reported by an electron-diffraction study (15).

mine the symmetry. The cases of *p*-chloro- and *p*-bromobenzene are similar, but in these molecules the symmetry C_{2v} has not been detected (9).

Discussion

Interproton distance ratios obtained in this study for ethylene sulfite are given in Table 2. These are compared with interproton distance ratios determined previously in the same nematic solvent for EC (3). In thermotropic solvents EC is assumed to be planar and the interproton distance ratios shown in Table 2 are in agreement with a structure; $\angle H—C—H = 111°$, $\angle HCC = 114.6°$, bond length C—H = 1.08 Å, and bond length C—C = 1.52 Å. An error arising from vibrational motions is expected of up to 3% in these comparisons (8) so that the agreement should not be considered as giving an absolute structure (1–4).

Protons 1 and 2 are *cis* to the extra ring oxygen in ethylene sulfite and are closer together than the *trans* protons 3 and 4. This is reflected in the interproton distance ratios r_{34}/r_{14} and r_{12}/r_{14}. An electron diffraction study of ethylene sulfite (15) gives a bond angle 110° for HCC. The measured interproton distance ratios in ethylene sulfite can be calculated using C—H distance = 1.08 Å, C—C distance = 1.52 Å, and $\angle H_4CC = 114.6°$, $\angle H_1—C—C = 110.3°$, and $\angle H_1CH_4 = 103.4°$.

1. S. A. BARTON, M. A. RAZA, and L. W. REEVES. J. Mag. Res. In press.
2. M. A. RAZA and L. W. REEVES. Mol. Phys. In press.
3. M. A. RAZA and L. W. REEVES. J. Mag. Res. In press.
4. M. A. RAZA and L. W. REEVES. J. Chem. Phys. In press.
5. C. J. BROWN. Acta. Cryst. **7**, 92 (1954).
6. C. L. ANGELL. Trans. Faraday Soc. **52**, 1178 (1956).
7. I. WANG, C. O. BRITT, and J. E. BOGGS. J. Am. Chem. Soc. **87**, 4950 (1965).
8. P. DIEHL and C. L. KHETRAPAL. N.m.r. basic principles and progress. Vol. 1. Springer-Verlag, New York, Heidelberg, Berlin, 1969. p. 1.
9. P. DIEHL, C. L. KHETRAPAL, and U. LIENHARD. Org. Mag. Res. **1**, 93 (1969).
10. L. C. SNYDER. J. Chem. Phys. **43**, 4041 (1965).
11. P. DIEHL, C. L. KHETRAPAL, and U. LIENHARD. Mol. Phys. **14**, 465 (1968).
12. P. DIEHL and C. L. KHETRAPAL. Mol. Phys. **15**, 201 (1968); **14**, 327 (1968).
13. E. E. BURNELL and C. A. DELANG. Mol. Phys. **16**, 95 (1969).
14. P. DIEHL, C. L. KHETRAPAL, and U. LIENHARD. Can. J. Chem. **46**, 2645 (1968).
15. B. A. ARBUZOV, V. A. NAUMOV, N. M. ZARIPOV, and L. D. PRONICHEVA. Dokl. Akad. Nauk. SSR, **195** (6), 1333 (1970); Chem. Abstr. **74**, 92295*d* (1971).

Can. J. Chem. Downloaded from www.nrcresearchpress.com by 210.87.254.6 on 09/05/12
For personal use only.

Can. J. Chem. Downloaded from www.nrcresearchpress.com by 210.87.254.6 on 09/05/12
For personal use only.

The Self-Reaction of *sec*-Alkylperoxy Radicals: A Kinetic Electron Spin Resonance Study

J. A. HOWARD[1] AND J. E. BENNETT

Shell Research Ltd., Thornton Research Centre, P.O. Box 1, Chester CH1 3SH, England

Received May 16, 1972

Absolute rate constants for the self-reaction of cyclopentylperoxy, cyclopentenylperoxy, and *sec*-butylperoxy radicals have been determined over a 125 °C temperature range. Arrhenius plots derived from these rate constants suggest that the mechanism for this reaction is more complex than the currently accepted Russell mechanism.

Les constantes absolues de vitesse pour l'autoréaction des radicaux cyclopentylperoxy, cyclopentènylperoxy et *sec*-butylperoxy, ont été déterminées dans un intervalle de température de 125 °C. Les dérivés des courbes d'Arrhénius, à partir des constantes de vitesse, laissent penser que le mécanisme de la réaction est plus complexe que celui proposé par Russell qui est couramment accepté.

Canadian Journal of Chemistry, **50**, 2374 (1972)

The rate controlling termination reaction for the liquid-phase autoxidation of hydrocarbons with labile primary or secondary hydrogens usually involves the mutual reaction of alkylperoxy

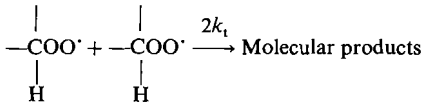

radicals (1) where $2k_t$ is the overall termination rate constant. This reaction is generally believed to proceed through a cyclic transition state (*i.e.*, the Russell mechanism) (2–5)

[1] 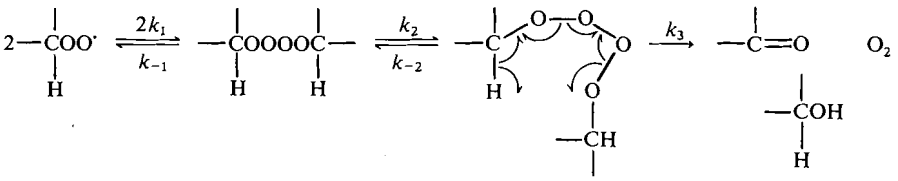

with

$$2k_t = \frac{2k_1k_2k_3}{k_{-1}k_{-2}}$$

The intermediacy of alkoxy radicals and consequently a mechanism analogous to the one generally accepted for the self-reaction of *tert*-alkylperoxy radicals has been discounted (2, 5).

A knowledge of absolute values of $2k_t$ (typically 10^6 to 10^8 M^{-1} s^{-1}) (1) has enabled Ingold and co-workers (6) to conclude from thermochemical calculations that if scheme 1 is the only viable mechanism for the self-reaction of *sec*-alkylperoxy radicals, then the overall activation energy (E_t) should be *negative*. Published values of E_t (1), although they are of low accuracy, are, however, *positive* (0–4 kcal/mol).

We report here accurate measurements of $2k_t$ for cyclopentylperoxy, cyclopentenylperoxy, and *sec*-butylperoxy radicals by kinetic e.s.r. spectroscopy (7) over a temperature range of 125 °C in an attempt to obtain reliable values of E_t. The radicals were generated directly in the cavity of an e.s.r. spectrometer by photolysis of di-*t*-butyl peroxide in the appropriate oxygen saturated hydrocarbon. In the temperature range −16 to −140 °C the peroxy radicals

[1]Visiting scientist, permanent address: Division of Chemistry, National Research Council of Canada, Ottawa K1A OR9, Canada.

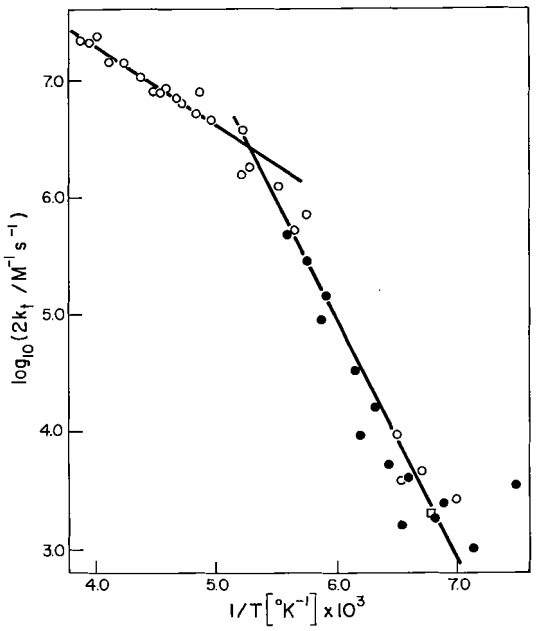

FIG. 1. A plot of log $2k_t$ for the cyclopentylperoxy radical *vs.* the reciprocal of the absolute temperature. Key: ○, 100% cyclopentane; ●, 50% cyclopentane – 50% cyclopropane; □, 25% cyclopentane – 75% cyclopropane.

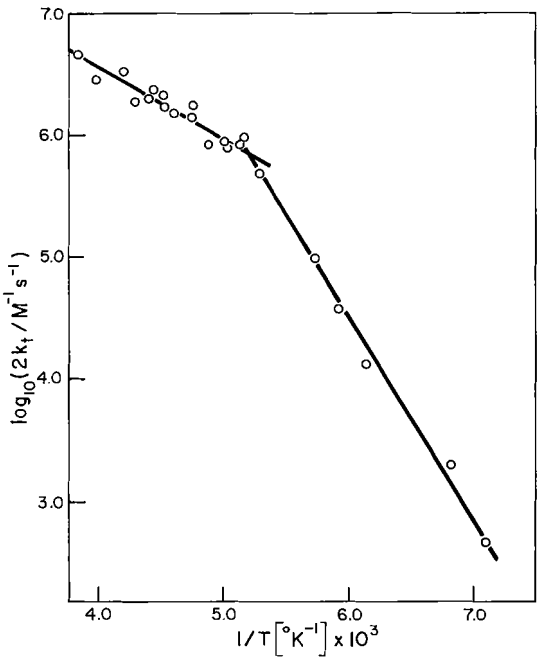

FIG. 2. A plot of log $2k_t$ for the *sec*-butylperoxy radical *vs.* the reciprocal of the absolute temperature.

generally decayed by second order kinetics, *i.e.*, $-d[ROO^{\cdot}]/dt = 2k_t[ROO^{\cdot}]^2$. Figures 1 and 2 show plots of log $2k_t$ against the reciprocal of the absolute temperature for two of the radicals.

Arrhenius parameters for the self-reaction of the *sec*-alkylperoxy radicals above −80 °C are given in Table 1 together with those for *tert*-butylperoxy determined by the same technique. The last two columns in Table 1 compare extrapolated values of $2k_t$ at 30 °C with values determined using either the rotating sector method (1) or the pulse radiolysis technique (8). The rate constants obtained in the present work are slightly larger than those previously reported but these differences are probably caused by the inherent inaccuracies in the various techniques.

Values of A_t for all the radicals listed in Table 1 are similar and consequently the large differences in $2k_t$ between *sec*- and *tert*-alkylperoxy radicals are due primarily to differences in E_t. Thomas and Ingold (9) also came to this conclusion from their kinetic e.s.r. study of the self-reaction of alkylperoxy radicals.

Although the values of E_t for *sec*-alkylperoxy radicals are about 5 kcal/mol lower than the values of E_t for *tert*-alkylperoxy radicals they are still *positive* by several kcal/mol. Thus the present kinetic evidence in conjunction with thermochemical calculations (6) suggests that the self-reaction of *sec*-alkylperoxy radicals (and almost certainly primary alkylperoxy radicals) does not proceed exclusively through a cyclic transition state.

At temperatures below −80 °C values of $2k_t$ for *sec*-butylperoxy and cyclopentylperoxy radicals are described by $2k_t = 10^{15.3} \exp(-8.2/RT)$ M^{-1} s^{-1} and $2k_t = 10^{16.5} \exp(-8.5/RT)$ M^{-1} s^{-1}, respectively, with the activation energies in kcal/mol. Although radical decays below −80 °C were second order, the estimated *A*-factors are much too large for bimolecular reactions. Thus below −80 °C the self-reaction of *sec*-alkylperoxy radicals is not a simple bimolecular reaction but is probably a complex free radical process.

There is e.s.r. evidence from −120 to −160 °C for the formation of a diamagnetic dimer (probably a tetroxide) from two cyclopentylperoxy radicals. Unfortunately the radicals decayed too quickly for reliable estimates to be made for ΔH_1 and ΔS_1 for the equilibrium process.

However, if the values of ΔS_1 and ΔH_1 for *sec*-alkylperoxy radical–tetroxide equilibria are

Can. J. Chem. Downloaded from www.nrcresearchpress.com by 210.87.254.6 on 09/05/12
For personal use only.

TABLE 1. Bimolecular rate constants and Arrhenius parameters* for the self-reaction of some alkylperoxy radicals

Peroxy radical	$\log_{10}(A_t/M^{-1}\,s^{-1})$	E_t (kcal/mol)	$2k_t$ at 30 °C* $(M^{-1}\,s^{-1})$	
Cyclopentyl	10.0	3.1	6×10^7	1.7×10^7†
Cyclopentenyl	7.8	1.0	1.2×10^7	6×10^6‡
sec-Butyl	9.0	2.7	1×10^7	1.5×10^6‡
tert-Butyl	9.2	7.8	4.0×10^3	1.2×10^3‡
tert-Butyl	9.3	7.6	6.6×10^3§	

*Determined from the Arrhenius plot at temperatures above −80 °C.
†Determined by monitoring the radical decay after pulse radiolysis of oxygenated cyclopentane (8).
‡Determined from hydrocarbon autoxidations in conjunction with the rotating sector technique (1).
§Radicals were prepared by photolysis of *t*-butyl hydroperoxide in oxygen free isobutane.

comparable to the values for *tert*-alkylperoxy radical–tetroxide equilibria (10, 11), then only above −80 °C should di-*sec*-alkyl tetroxides be almost completely dissociated. It is therefore tempting to conclude that the dramatic decrease in $2k_t$ for the self-reaction of *sec*-alkylperoxy radicals below −80 °C is associated with the presence of a significant concentration of tetroxide.

The self-reaction of *tert*-alkylperoxy radicals is a complex process that proceeds *via* a tetroxide intermediate (1) with *A*-factors and activation

[2] $\mathrm{ROO^{\cdot} + ROO^{\cdot} \rightleftharpoons RO_4R \rightarrow}$ Molecular products

energies for the overall reaction of about 10^9 $M^{-1}\,s^{-1}$ and 10 kcal/mol (1). This mechanism cannot, however, be invoked to describe the self-reaction of *sec*-alkylperoxy radicals below −80 °C because although the activation energies for the two systems are similar, the *A*-factors differ by about 10^7. It is also improbable that the overall rate of such a process would slow down at −80 °C.

An alternative mechanism is

[3] $\mathrm{RO_4R} \underset{2k_1}{\overset{k_{-1}}{\rightleftharpoons}} \mathrm{2ROO^{\cdot}} \xrightarrow{2k_t}$ Molecular products

and is represented by the potential energy–reaction coordinate curve shown in Fig. 3. The general expression (12) for radical decay by this mechanism is

$$\frac{-\mathrm{d[ROO^{\cdot}]}}{\mathrm{d}t} = \frac{2k_t[\mathrm{ROO^{\cdot}}]^2}{1 + 4k_1[\mathrm{ROO^{\cdot}}]/k_{-1}}$$

At high temperatures (*i.e.*, temperatures at which the tetroxide is completely dissociated)

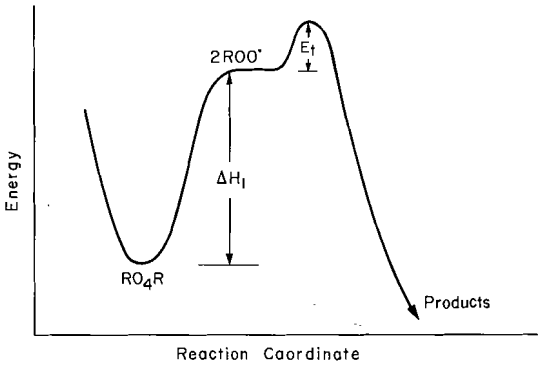

FIG. 3. A possible potential energy curve for the self-reaction of *sec*-alkylperoxy radicals.

$4k_1[\mathrm{ROO^{\cdot}}]/k_{-1} < 1$ and this equation reduces to the usual second order rate expression

$$[4] \qquad \frac{-\mathrm{d[ROO^{\cdot}]}}{\mathrm{d}t} = 2k_t[\mathrm{ROO^{\cdot}}]^2$$

If below −80 °C, $4k_1[\mathrm{ROO^{\cdot}}]/k_{-1} > 1$, then

$$[5] \qquad \frac{-\mathrm{d[ROO^{\cdot}]}}{\mathrm{d}t} = \frac{2k_tk_{-1}[\mathrm{ROO^{\cdot}}]}{4k_1}$$

which could give an overall rate constant $(k_tk_{-1}/2k_1)$ with a higher *A*-factor and activation energy than $2k_t$. However, this expression requires a first-order decay for ROO· at low temperatures whereas our experimental results were generally closer to a second-order process. Further, the equilibrium constant $(2k_1/k_{-1})$ for the tetroxide formation would have to be 10^3 to 10^4 times higher than those for tertiary tetroxides.

Although the present results cannot be described adequately by any of the mechanisms

Can. J. Chem. Downloaded from www.nrcresearchpress.com by 210.87.254.6 on 09/05/12
For personal use only.

considered, they do cast considerable doubt on the general validity of the Russell mechanism.

We thank Mr. R. Summers for performing most of the experimental work.

1. J. A. HOWARD. Adv. Free Radical Chem. **4**, 49 (1972).
2. G. A. RUSSELL. J. Am. Chem. Soc. **79**, 3871 (1957).
3. J. A. HOWARD and K. U. INGOLD. J. Am. Chem. Soc. **90**, 1056 (1968); **90**, 1058 (1968).
4. R. E. KELLOGG. J. Am. Chem. Soc. **91**, 5433 (1969).
5. R. HIATT and L. ZIGMUND. Can. J. Chem. **48**, 3967 (1970).
6. D. F. BOWMAN, T. GILLAN, and K. U. INGOLD. J. Am. Chem. Soc. **93**, 6555 (1971).
7. J. E. BENNETT, D. M. BROWN, and B. MILE. Trans. Faraday Soc. **66**, 386 (1970).
8. B. SMALLER, J. R. REMKO, and E. C. AVERY. J. Chem. Phys. **48**, 5174 (1968).
9. J. R. THOMAS and K. U. INGOLD. Adv. Chem. **75**, 258 (1968).
10. J. E. BENNETT, D. M. BROWN, and B. MILE. Trans Faraday Soc. **66**, 397 (1970).
11. K. ADAMIC, J. A. HOWARD, and K. U. INGOLD. Can. J. Chem. **47**, 3803 (1969).
12. J. BROKENSHIRE, J. R. ROBERTS, and K. U. INGOLD. J. Am. Chem. Soc. In press.

Can. J. Chem. Downloaded from www.nrcresearchpress.com by 210.87.254.6 on 09/05/12
For personal use only.

A Stereospecific Synthesis of Ring A-aromatic Steroids

R. A. DICKINSON, R. KUBELA, G. A. MACALPINE, Z. STOJANAC, AND Z. VALENTA

Department of Chemistry, University of New Brunswick, Fredericton, New Brunswick

Received December 21, 1971[1]

A diene synthesis using 2,6-xyloquinone as dienophile and boron trifluoride as catalyst does not follow the normal orientation rules and leads to a facile synthesis of ring A-aromatic steroids. A tetracyclic adduct prepared by a similar reaction and containing the steroidal C_{19}-methyl group is also reported.

Une synthèse de diène utilisant la 2,6-xyloquinone comme diénophile et le trifluorure de bore comme catalyseur ne suit pas les règles d'orientation normales et nous amène à une synthèse facile de stéroïdes cycliques A-aromatiques. On rapporte aussi la synthèse d'un dérivé tétracyclique préparé à l'aide d'une réaction semblable et contenant le groupe stéroïdal méthyle-C_{19}.

Canadian Journal of Chemistry, **50**, 2377 (1972)

We wish to report a steroid synthesis based on an efficient inversion of the usually observed Diels–Alder reaction orientation (1).

Treatment of diene **1** (2) and 2,6-xyloquinone (**2**) with 1.3 mol equiv of boron trifluoride etherate in ether at room temperature gave the desired tetracyclic enedione **3**,[2] m.p. 194–196°, in a 69% yield.[3] A second compound **4**, m.p. 164–167°, obtained in about 14% yield, proved identical with the only product of a thermal reaction of **1** and **2** in boiling benzene. The relative configuration of *d,l*-**3** follows from the expected *endo-cis* course of the diene synthesis (4) and from subsequent transformations. Compound **3** was converted quantitatively to its *trans*-epimer **5**, m.p. 146–148°, on treatment with sodium bicarbonate in refluxing methanol. Lithium aluminum tri-tert-butoxyhydride in tetrahydrofuran at room temperature then reduced one of the carbonyl groups of **5** selectively to give alcohol **6**, m.p. 211–213°, which was converted to the corresponding mesylate **7**. Reduction with zinc (5) in refluxing methanol–benzene followed by treatment with sodium carbonate gave the desired *d,l*-enone **8**, m.p. 174–176°. Hydrogenation with 10% palladium on calcium carbonate in glacial acetic acid gave, after recrystallization from benzene–hexane,

[1]Resubmitted June 20, 1972.

[2]Adduct **3** crystallized from the ether solution within a few minutes and was recrystallized from ethyl acetate.

[3]To our knowledge, such an orientation inversion has not been reported previously. For selected references on catalyzed diene synthesis, see ref. 3.

considered, they do cast considerable doubt on the general validity of the Russell mechanism.

We thank Mr. R. Summers for performing most of the experimental work.

1. J. A. HOWARD. Adv. Free Radical Chem. **4**, 49 (1972).
2. G. A. RUSSELL. J. Am. Chem. Soc. **79**, 3871 (1957).
3. J. A. HOWARD and K. U. INGOLD. J. Am. Chem. Soc. **90**, 1056 (1968); **90**, 1058 (1968).
4. R. E. KELLOGG. J. Am. Chem. Soc. **91**, 5433 (1969).
5. R. HIATT and L. ZIGMUND. Can. J. Chem. **48**, 3967 (1970).
6. D. F. BOWMAN, T. GILLAN, and K. U. INGOLD. J. Am. Chem. Soc. **93**, 6555 (1971).
7. J. E. BENNETT, D. M. BROWN, and B. MILE. Trans. Faraday Soc. **66**, 386 (1970).
8. B. SMALLER, J. R. REMKO, and E. C. AVERY. J. Chem. Phys. **48**, 5174 (1968).
9. J. R. THOMAS and K. U. INGOLD. Adv. Chem. **75**, 258 (1968).
10. J. E. BENNETT, D. M. BROWN, and B. MILE. Trans Faraday Soc. **66**, 397 (1970).
11. K. ADAMIC, J. A. HOWARD, and K. U. INGOLD. Can. J. Chem. **47**, 3803 (1969).
12. J. BROKENSHIRE, J. R. ROBERTS, and K. U. INGOLD. J. Am. Chem. Soc. In press.

A Stereospecific Synthesis of Ring A-aromatic Steroids

R. A. DICKINSON, R. KUBELA, G. A. MACALPINE, Z. STOJANAC, AND Z. VALENTA

Department of Chemistry, University of New Brunswick, Fredericton, New Brunswick

Received December 21, 1971[1]

A diene synthesis using 2,6-xyloquinone as dienophile and boron trifluoride as catalyst does not follow the normal orientation rules and leads to a facile synthesis of ring A-aromatic steroids. A tetracyclic adduct prepared by a similar reaction and containing the steroidal C_{19}-methyl group is also reported.

Une synthèse de diène utilisant la 2,6-xyloquinone comme diénophile et le trifluorure de bore comme catalyseur ne suit pas les règles d'orientation normales et nous amène à une synthèse facile de stéroïdes cycliques A-aromatiques. On rapporte aussi la synthèse d'un dérivé tétracyclique préparé à l'aide d'une réaction semblable et contenant le groupe stéroïdal méthyle-C_{19}.

Canadian Journal of Chemistry, **50**, 2377 (1972)

We wish to report a steroid synthesis based on an efficient inversion of the usually observed Diels–Alder reaction orientation (1).

Treatment of diene **1** (2) and 2,6-xyloquinone (**2**) with 1.3 mol equiv of boron trifluoride etherate in ether at room temperature gave the desired tetracyclic enedione **3**,[2] m.p. 194–196°, in a 69% yield.[3] A second compound **4**, m.p. 164–167°, obtained in about 14% yield, proved identical with the only product of a thermal reaction of **1** and **2** in boiling benzene. The relative configuration of *d,l*-**3** follows from the expected *endo-cis* course of the diene synthesis (4) and from subsequent transformations. Compound **3** was converted quantitatively to its *trans*-epimer **5**, m.p. 146–148°, on treatment with sodium bicarbonate in refluxing methanol. Lithium aluminum tri-tert-butoxyhydride in tetrahydrofuran at room temperature then reduced one of the carbonyl groups of **5** selectively to give alcohol **6**, m.p. 211–213°, which was converted to the corresponding mesylate **7**. Reduction with zinc (5) in refluxing methanol–benzene followed by treatment with sodium carbonate gave the desired *d,l*-enone **8**, m.p. 174–176°. Hydrogenation with 10% palladium on calcium carbonate in glacial acetic acid gave, after recrystallization from benzene–hexane,

[1]Resubmitted June 20, 1972.

[2]Adduct **3** crystallized from the ether solution within a few minutes and was recrystallized from ethyl acetate.

[3]To our knowledge, such an orientation inversion has not been reported previously. For selected references on catalyzed diene synthesis, see ref. 3.

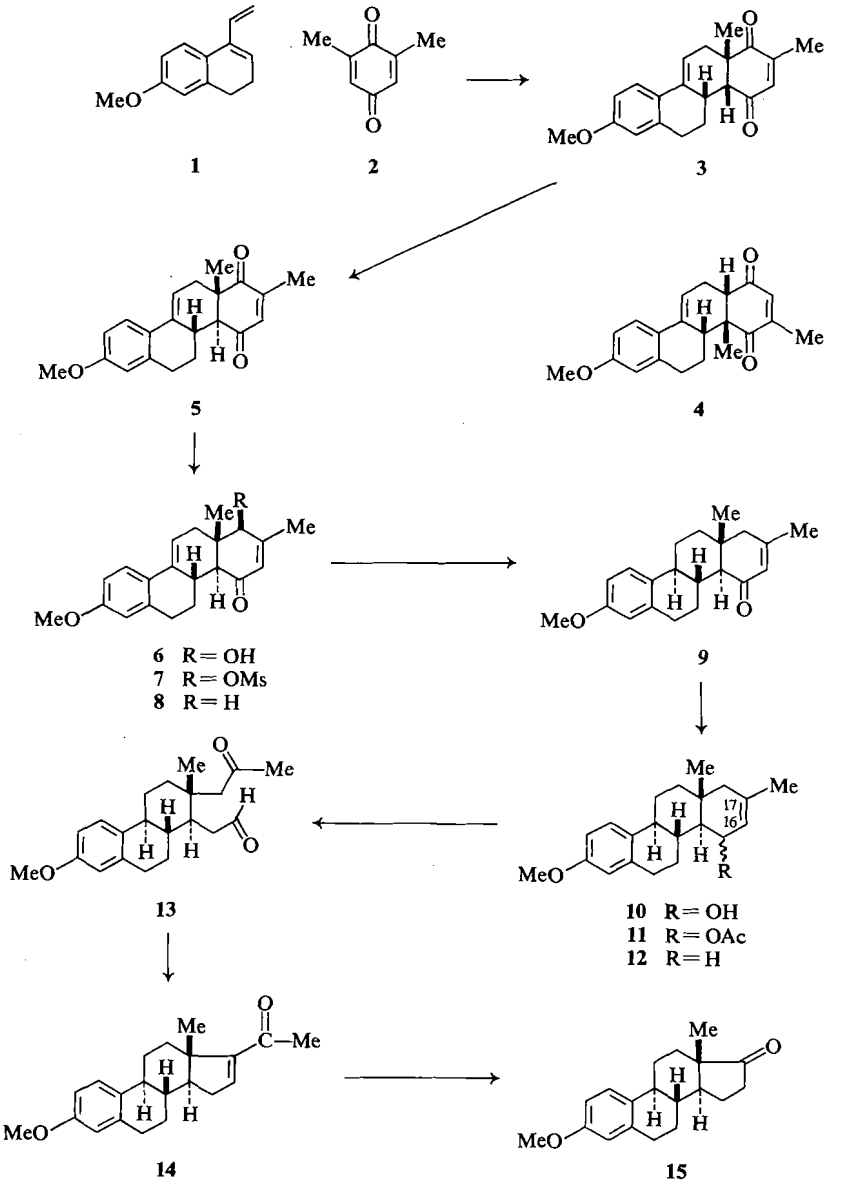

an 85% yield of the desired epimer **9**, m.p. 142–144°. The position of the keto group in **9** follows from the n.m.r. spectrum (C_{16}-H at 4.2 τ, coupled only to the C_{17}-methyl at 8.1 τ).

Reduction of enone **9** with sodium bis(2-methoxyethoxy) aluminum hydride (6) gave a mixture of epimeric alcohols **10**. Conversion of **10** to acetates **11**, followed by reduction of **11** with excess lithium in tetrahydrofuran-refluxing liquid ammonia[4] gave olefin **12** (8) (m.p. 96–97°, 75% yield based on **9** after recrystallization from ether–methanol). Treatment of **12** with osmium tetroxide in pyridine (9) followed by cleavage with lead tetraacetate in tetrahydrofuran at 0° gave oily keto aldehyde

[4]A similar reaction using lithium in ethyl amine has been reported (7).

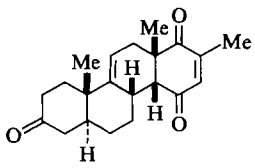

17

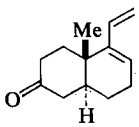

16

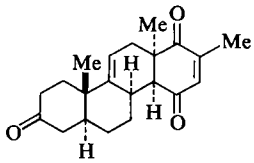

18

13 which after reaction with 5% aqueous hydrochloric acid in tetrahydrofuran at 70° for 40 h and recrystallization from benzene–hexane gave enone **14**, m.p. 159–162°, in a 60% yield based on **12**. The overall yield of the conversion **1** + **2** → **14** is 22%.[5]

Enone **14** was converted to *d,l*-estrone methyl ether **15** (40% yield) by the reported Beckmann rearrangement of the corresponding oxime (10). Compound **15**, m.p. 140–141° (11), was found to be identical with the methyl ether of natural estrone in t.l.c., n.m.r., solution i.r., and m.s.

The present sequence does not as yet match in brevity and overall yield some of the efficient synthetic pathways already reported for ring A-aromatic steroids (12). In addition, its elaboration to optically active compounds without recourse to resolution (13) will require an asymmetric induction in the Diels-Alder step itself.

However, it has important advantages. It automatically generates the 9,11-double bond, as well as the 17-acetyl side chain. Furthermore, it promises to be equally effective in the synthetically more challenging saturated steroid series. We now find that a reaction of diene **16** (14) with quinone **2** in the presence of boron trifluoride etherate gives two compounds, **17**, m.p. 187–189° and **18** in a 2:1 ratio.[6] The non-identity of these two adducts with any of the products obtained in a thermal reaction of **16** with **2**, as well as consideration of the *endo* rule (4) and of steric factors (16), strongly favor structure **17** for the major product. Its elaboration into steroids of the progesterone and cortisone type along the lines reported in this Communication is under active study.

[5]This is a minimum yield since recrystallized material was used at several stages of the sequence **3** → **12**, the quoted yield of the conversion **12** → **14** does not include substantial amounts of **14** present in the semi-crystalline mother liquors (n.m.r., t.l.c.) and since no attempt has been made to optimize all individual yields.

[6]Since the precursor to diene **16** has been synthesized under asymmetric induction (15), the diene and its adducts will be readily available in optically active form.

Support of this work by the National Research Council of Canada is gratefully acknowledged.

1. A. S. ONISHCHENKO. Diene synthesis. Translated by Israel Program for Scientific Translations, Jerusalem, 1964. Oldbourne Press, London. p. 22; YU. A. TITOV. Russ. Chem. Rev. **31**, 267 (1962); J. SAUER. Angew. Chem. Intern. Ed. **6**, 16 (1967).
2. I. N. NAZAROV, I. V. TORGOV, and G. P. VERKHOLETOVA. Doklady Akad. Nauk SSSR **112**, 1067 (1957).
3. A. WASSERMANN. J. Chem. Soc. 618 (1942); P. YATES and P. EATON. J. Am. Chem. Soc. **82**, 4436 (1960); SIR ROBERT ROBINSON and G. I. FRAY. J. Am. Chem. Soc. **83**, 249 (1961); H. WOLLMEHER. Methoden der organischen chemie. Georg Thieme Verlag, Stuttgart, 1970. p. 1092.
4. K. ALDER and G. STEIN. Angew. Chem. **50**, 510 (1937).
5. A. J. SPEZIALE, J. A. STEPHENS, and Q. E. THOMPSON. J. Am. Chem. Soc. **76**, 5011 (1954).
6. M. CAPKA, V. CHVALOVSKY, K. KOCHLOEFL, and M. KRAUS. Coll. Czech. Chem. Commun. **34**, 118 (1969).
7. A. S. HALLSWORTH, H. B. HENBEST, and T. I. WRIGLEY. J. Chem. Soc. 1957 (1969).
8. S. J. DAUM. Dissertation Abstr. **24**, 4992 (1964). Chem. Abstr. **61**, 8357g (1964).
9. J. S. BARAN. J. Org. Chem. **25**, 257 (1960).
10. G. ROSENKRANZ, O. MANCERA, F. SONDHEIMER, and C. DJERASSI. J. Org. Chem. **31**, 520 (1956).
11. G. ANNER and K. MIESCHER. Exp. **4**, 25 (1948); Helv. Chim. Acta, **31**, 2173 (1948); Helv. Chim. Acta, **32**, 1957 (1949); W. S. JOHNSON, D. K. BANERJEE, W. P. SCHNEIDER, C. D. GUTSHE, W. E. SHELBERG, and L. E. CHIN. J. Am. Chem. Soc. **74**, 2882 (1952).
12. I. V. TORGOV. Pure and Appl. Chem. **6**, 525 (1963);

T. B. WINDHOLZ and M. WINDHOLZ. Angew. Chem. Intern. Ed. **3**, 353 (1964); R. PAPPO. Intra-science chemistry reports. **3**, 123 (1969).
13. C. RUFER, H. KOSMOL, E. SCHRODER, K. KIESLICH, and H. GABIAN. Ann. **702**, 141 (1967); R. BUCOURT, L. NEDILEC, J. C. GASC, and J. WEILL-RAYNALL. Bull. Soc. Chim. (Fr.) 561 (1967).
14. I. N. NAZAROV and I. A. GURVICH. Zhur. Obshchei Khim. **25**, 956 (1955).
15. U. EDER, G. SAUER, and R. WIECHERT. Angew. Chem. Intern. Ed. **10**, 496 (1971).
16. I. N. NAZAROV and I. A. GURVICH. Izvest. Akad. Nauk SSSR, Otdel. Khim. Nauk 283 (1959).

Juvenile Hormone Mimics in Conifers. I. Isolation of (−)-*cis*-4-[1′(*R*)-5′-Dimethyl-3′-oxohexyl]-cyclohexane-1-carboxylic Acid from Douglas-fir Wood

I. H. ROGERS AND J. F. MANVILLE

Department of the Environment, Canadian Forestry Service, Western Forest Products Laboratory, Vancouver, British Columbia

Received March 9, 1972

The petroleum ether extract from the whole-wood meal of a British Columbia Interior variety of Douglas-fir has yielded a new and potentially useful juvenile hormone mimic, (−)-*cis*-4-[1′(*R*)-5′-dimethyl-3′-oxohexyl]-cyclohexane-1-carboxylic acid (**3***a*). This compound possesses the opposite steric configuration at C-1′ to that of (+)-juvabione (**1***a*), which has been isolated by others from balsam fir. Also, it occurs exclusively as the free acid. Not all Douglas-firs contain this compound and the biological consequences of its formation are being explored.

Une imitation nouvelle et potentiellement utile de l'hormone juvénile, l'acide (−)-*cis*-4-[1′(*R*)-5′-diméthyl-3′-oxohexyl]-cyclohexane-1-carboxylique (**3***a*), a été obtenue de l'extrait d'éther de pétrole de la poudre de bois entier d'une variété de sapin de Douglas, de l'intérieur de la Colombie britannique. Ce composé possède la configuration stérique opposée en C-1′, à celle du (+)-juvabione (**1***a*), que d'autres chercheurs avaient isolé du sapin baumier. On le retrouve seulement sous forme d'acide libre. Il est à remarquer que les sapins de Douglas, ne contiennent pas tous ce composé; nous étudions présentement les conséquences biologiques de sa formation.

Canadian Journal of Chemistry, **50**, 2380 (1972)

The isolation of (+)-juvabione (**1***a*) from the wood of balsam fir (1) (*Abies balsamea* (L.) Miller) of North American origin and the demonstration of its juvenile hormone activity against the hemipteran bug *Pyrrhocoris apterus* L. (2) has evoked wide interest because of the potential for insecticidal application. Subsequently, a second compound, (+)-dehydrojuvabione (**2**), was isolated from balsam fir grown in Czechoslovakia (3) and this also possessed juvenile hormone activity. (+)-Juvabione is the methyl ester of (+)-todomatuic acid ((+)-4(*R*)-[1′(*S*)-5′-dimethyl-3′-oxohexyl]-cyclohex-1-ene-1-carboxylic acid, **1***b*), isolated (4) in 1940 from bisulfite-treated pulp oil of a Japanese fir (*Abies sachalinensis* Schmidt). There is thus reason to expect that active compounds may be widely distributed in the true firs. We report herein the isolation of (−)-*cis*-4-[1′(*R*)-5′-dimethyl-3′-oxohexyl]-cyclohexane-1-carboxylic acid (**3***a*), from the British Columbia Interior variety of Douglas-fir (*Pseudotsuga menziesii* var. *glauca* (Beissn.) Franco) which is not a true fir (*Abies* sp.). In contrast to the true firs, some of which contain (+)-juvabione (*S* configuration at C-1′), compound **3***a* occurs with the opposite configuration (*R*) at C-1′ and is found exclusively as the free acid in certain Douglas-fir trees.

A bolt was cut from the butt log of a 164-year-old Douglas-fir tree growing near Savona, British Columbia. The air-dry wood was milled and the wood meal extracted with petroleum ether in a soxhlet apparatus. A fraction com-

T. B. WINDHOLZ and M. WINDHOLZ. Angew. Chem. Intern. Ed. **3**, 353 (1964); R. PAPPO. Intra-science chemistry reports. **3**, 123 (1969).
13. C. RUFER, H. KOSMOL, E. SCHRODER, K. KIESLICH, and H. GABIAN. Ann. **702**, 141 (1967); R. BUCOURT, L. NEDILEC, J. C. GASC, and J. WEILL-RAYNALL. Bull. Soc. Chim. (Fr.) 561 (1967).
14. I. N. NAZAROV and I. A. GURVICH. Zhur. Obshchei Khim. **25**, 956 (1955).
15. U. EDER, G. SAUER, and R. WIECHERT. Angew. Chem. Intern. Ed. **10**, 496 (1971).
16. I. N. NAZAROV and I. A. GURVICH. Izvest. Akad. Nauk SSSR, Otdel. Khim. Nauk 283 (1959).

Can. J. Chem. Downloaded from www.nrcresearchpress.com by 210.87.254.5 on 09/05/12
For personal use only.

Juvenile Hormone Mimics in Conifers. I. Isolation of (−)-*cis*-4-[1′(*R*)-5′-Dimethyl-3′-oxohexyl]-cyclohexane-1-carboxylic Acid from Douglas-fir Wood

I. H. ROGERS AND J. F. MANVILLE

Department of the Environment, Canadian Forestry Service, Western Forest Products Laboratory, Vancouver, British Columbia

Received March 9, 1972

The petroleum ether extract from the whole-wood meal of a British Columbia Interior variety of Douglas-fir has yielded a new and potentially useful juvenile hormone mimic, (−)-*cis*-4-[1′(*R*)-5′-dimethyl-3′-oxohexyl]-cyclohexane-1-carboxylic acid (**3***a*). This compound possesses the opposite steric configuration at C-1′ to that of (+)-juvabione (**1***a*), which has been isolated by others from balsam fir. Also, it occurs exclusively as the free acid. Not all Douglas-firs contain this compound and the biological consequences of its formation are being explored.

Une imitation nouvelle et potentiellement utile de l'hormone juvénile, l'acide (−)-*cis*-4-[1′(*R*)-5′-diméthyl-3′-oxohexyl]-cyclohexane-1-carboxylique (**3***a*), a été obtenue de l'extrait d'éther de pétrole de la poudre de bois entier d'une variété de sapin de Douglas, de l'intérieur de la Colombie britannique. Ce composé possède la configuration stérique opposée en C-1′, à celle du (+)-juvabione (**1***a*), que d'autres chercheurs avaient isolé du sapin baumier. On le retrouve seulement sous forme d'acide libre. Il est à remarquer que les sapins de Douglas, ne contiennent pas tous ce composé; nous étudions présentement les conséquences biologiques de sa formation.

Canadian Journal of Chemistry, **50**, 2380 (1972)

The isolation of (+)-juvabione (**1***a*) from the wood of balsam fir (1) (*Abies balsamea* (L.) Miller) of North American origin and the demonstration of its juvenile hormone activity against the hemipteran bug *Pyrrhocoris apterus* L. (2) has evoked wide interest because of the potential for insecticidal application. Subsequently, a second compound, (+)-dehydrojuvabione (**2**), was isolated from balsam fir grown in Czechoslovakia (3) and this also possessed juvenile hormone activity. (+)-Juvabione is the methyl ester of (+)-todomatuic acid ((+)-4(*R*)-[1′(*S*)-5′-dimethyl-3′-oxohexyl]-cyclohex-1-ene-1-carboxylic acid, **1***b*), isolated (4) in 1940 from bisulfite-treated pulp oil of a Japanese fir (*Abies sachalinensis* Schmidt). There is thus reason to expect that active compounds may be widely distributed in the true firs. We report herein the isolation of (−)-*cis*-4-[1′(*R*)-5′-dimethyl-3′-oxohexyl]-cyclohexane-1-carboxylic acid (**3***a*), from the British Columbia Interior variety of Douglas-fir (*Pseudotsuga menziesii* var. *glauca* (Beissn.) Franco) which is not a true fir (*Abies* sp.). In contrast to the true firs, some of which contain (+)-juvabione (*S* configuration at C-1′), compound **3***a* occurs with the opposite configuration (*R*) at C-1′ and is found exclusively as the free acid in certain Douglas-fir trees.

A bolt was cut from the butt log of a 164-year-old Douglas-fir tree growing near Savona, British Columbia. The air-dry wood was milled and the wood meal extracted with petroleum ether in a soxhlet apparatus. A fraction com-

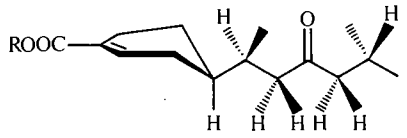

1

a R = CH_3
b R = H

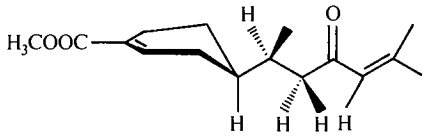

2

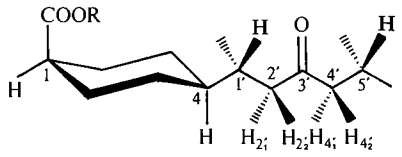

3

a R = H
b R = CH_3

prising a mixture of resin acids and fatty acids was obtained by ion exchange chromatography of the petroleum ether extract on a column of diethylaminoethyl Sephadex (A-25) following the procedure of Zinkel and Rowe (5). The resin acids were removed after selective esterification with sulfuric acid–methanol reagent. Argentative chromatography of the fatty acid ester fraction on a silica column resulted in the isolation of **3***b* and the methyl ester of an unknown acid.[1]

The ester (**3***b*) was a colorless oil $[\alpha]_D^{23}$ 0°, b.p. 150 °C at 0.5 mm, elemental analysis agreed with the empirical formula $C_{16}H_{28}O_3$. The presence of a carbonyl group in a saturated environment was evident from the i.r. spectrum (1710 cm^{-1}). Absence of olefinic double bonds was inferred from the i.r. and n.m.r. spectra and from the behavior of the compound on silver nitrate-impregnated silica thin layers. From the empirical formula, the presence of one degree of unsaturation associated with a ring was evident.

The mass spectral fragmentation pattern of the unknown ester (**3***b*) which contained many metastable ions was most informative. The molecular ion (*m/e* 268) was accompanied by low abundance satellite ions at *m/e* 237 (M − 31) and 209 (M − 59) arising from homolytic cleavages in the carbomethoxy group. Much more significant fragmentations of the molecular ion were associated with cleavage within the side chain giving rise to abundant species at *m/e* 211 (M − 57, *m** 166.1) and 168 (M − 100, *m** 105.4). The latter fragment gave rise to the base peak of the spectrum (*m/e* 108) by elimination of the carbomethoxy function as methyl formate (*m** 69.5). Loss of an eight-carbon side chain containing a carbonyl group from the molecular ion was indicated by the presence of an abundant fragment at *m/e* 127 (*m** 60.3) in which process the charge was carried by the side chain moiety.

Some major species in the fragmentation pattern of juvabione include the molecular ion *m/e* 266 and fragments at *m/e* 207 (M − 59), 177, 167, 166, 127, 85, 79, 59, and 57 as discussed by Sorm and coworkers (3). These were all present in the spectrum of **3***b* with the displacement of the first five species listed by two additional mass units.

The n.m.r. spectrum of **3***b* (Varian HR-220, $CDCl_3$) yielded the following 1st order n.m.r. parameters: τ 6.43 (3 H, singlet, methyl ester), 7.39 (1 H, quintet, $J \simeq 4$ Hz, H_1), 7.59 (1 H, quartet, $J_{2_1,2_2} = 15.8$ Hz, $J_{2_1,1'} = 4.5$ Hz, H_{2_1}), 7.74 (2 H, doublet, $J_{vic} = 6.7$ Hz, H_{4_1} and H_{4_2}), 7.86 (1 H, quartet, $J_{2_2,2_1} = 15.8$, $J_{2_2,1_1} = 9.0$ Hz, H_{2_2}), 7.87 (1 H, multiplet, $H_{5'}$), 8.05 (1 H, multiplet, $H_{1'}$), 8.5 (5 H, broad band, ring protons), 8.8 (4 H, broad band, ring protons), 9.08_6 (3 H, doublet, $J = 6.7$ Hz, $C_{5'}$ methyl), 9.09_1 (3 H, doublet, $J = 6.7$ Hz, $C_{5'}$ methyl), and 9.17 (3 H, doublet, $J = 6.7$ Hz, $C_{1'}$ methyl). The magnitude of the vicinal couplings observed in H_1 indicated that the carboxylic acid methyl ester group was in an axial orientation. It is thus most probable that **3***b* possesses a *cis* configuration with the bulky side chain in the equatorial position.

Gas–liquid chromatographic analysis of hydrogenated (±)-juvabione (3) demonstrated that **3***b* had a retention time identical to that

[1]Structural identification of this related acid is in progress. Initial bioassays, performed at the Pacific Forest Research Centre, Victoria, B.C., against Tenebrio molitor (L.), have shown positive results for both compounds. Further testing is in progress.

Can. J. Chem. Downloaded from www.nrcresearchpress.com by 210.87.254.5 on 09/05/12
For personal use only.

of the more volatile component. Epimerization (6) of **3***b* revealed that the compound with the longer retention time must be the *trans* isomer since it was the major component in the epimerized mixture. Thus the minor component, **3***b*, must possess the *cis* configuration.

The o.r.d. spectrum of **3***b* was (*c* 1.0, methanol, 23°) $[\Phi]_{350}$ −107, $[\Phi]_{308}$ −749, $[\Phi]_{292}$ 0, $[\Phi]_{260}$ +1584, and $[\Phi]_{230}$ +780°. With reference to the work of Pawson and coworkers (7), this result establishes the *R* configuration at C-1′ and also that it is the (−)-isomer. This result should allow assessment of the effect of configuration at C-1′ on the juvenile hormone activity of compounds of this structural type.

We wish to thank B. A. Pawson for a sample of (±)-juvabione and W. S. Bowers for a sample of natural (+)-todomatuic acid.

1. W. S. Bowers, H. M. Fales, M. J. Thompson, and E. C. Uebel. Sci. **154**, 1020 (1966).
2. K. Slama and C. M. Williams. Proc. Nat. Acad. Sci. U.S. **54**, 411 (1965).
3. V. Cerny, L. Dolejs, L. Labler, F. Sorm, and K. Slama. Coll. Czech. Chem. Commun. **32**, 3926 (1967).
4. R. Tutihasi and T. Hanazawa. J. Chem. Soc. Japan, **61**, 1041 (1940); Chem. Abstr. **37**, 258 (1943).
5. D. F. Zinkel and J. W. Rowe. Anal. Chem. **36**, 1160 (1964).
6. K. Mori and M. Matsui. Tetrahedron, **24**, 3127 (1968).
7. B. A. Pawson, H.-C. Cheung, S. Gurbaxani, and G. Saucy. J. Am. Chem. Soc. **92**, 336 (1970).

4,6-*O*-(1-Carboxyethylidene)-D-mannose as a Structural Unit in Capsular Polysaccharide of *Klebsiella* K-type 5[1]

G. G. S. Dutton and M. T. Yang

Department of Chemistry, University of British Columbia, Vancouver 8, British Columbia

Received April 21, 1972

Methylation, periodate oxidation, and partial hydrolysis techniques have each been used to demonstrate the presence of 4,6-*O*-(1-carboxyethylidene)-D-mannopyranosyl units in the capsular polysaccharide of *Klebsiella* K-type 5. The structure of this polysaccharide differs from those known for other *Klebsiella* capsules by the lack of any carbohydrate side chain. A repeating unit of

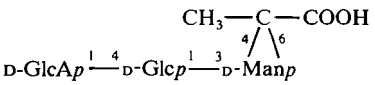

(plus one unassigned *O*-acetyl group) is in accord with the experimental data.

Les méthodes de méthylation, oxydation périodique et hydrolyse partielle ont été utilisées pour démontrer la présence de restes de 4,6-*O*-(1-carboxyethylidene)-D-mannopyranose dans le polyoside capsulaire de *Klebsiella* K-type 5. La structure de ce polysaccharide se distingue de toutes les autres connues pour *Klebsiella* par la manque d'une chaîne latérale de sucre. On propose une structure du type

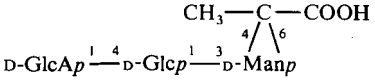

(avec un groupe *O*-acétyle) qui se répète.

Canadian Journal of Chemistry, **50**, 2382 (1972)

The occurrence of pyruvic acid as a covalently linked ketal unit in polysaccharides was first reported by Hirase (1) in a study on agar which contains 4,6-*O*-(1-carboxyethylidene)-D-galactose units. The presence of 4,6-*O*-(1-carboxyethylidene)-D-glucose units was subsequently demonstrated by Sloneker and Orentas (2) in the exocellular polysaccharide from *Xanthomonas campestris*. Since then the presence of this D-galactose ketal has also been shown in the polysaccharides from *Corynebacterium insidiosum* (3), *Klebsiella* K-type 21 (4), and colanic acid (5, 6). Pyruvic acid has been found as well in the M-antigens of *Salmonella* and in *E. coli* linked as 3,4-*O*-(1-carboxyethylidene)-D-galactose (7, 8).

[1]Presented at the 55th Canadian Chemical Conference of the Chemical Institute of Canada, Quebec City, Quebec, June, 1972.

Can. J. Chem. Downloaded from www.nrcresearchpress.com by 210.87.254.5 on 09/05/12
For personal use only.

of the more volatile component. Epimerization (6) of **3***b* revealed that the compound with the longer retention time must be the *trans* isomer since it was the major component in the epimerized mixture. Thus the minor component, **3***b*, must possess the *cis* configuration.

The o.r.d. spectrum of **3***b* was (*c* 1.0, methanol, 23°) $[\Phi]_{350}$ −107, $[\Phi]_{308}$ −749, $[\Phi]_{292}$ 0, $[\Phi]_{260}$ +1584, and $[\Phi]_{230}$ +780°. With reference to the work of Pawson and coworkers (7), this result establishes the *R* configuration at C-1′ and also that it is the (−)-isomer. This result should allow assessment of the effect of configuration at C-1′ on the juvenile hormone activity of compounds of this structural type.

We wish to thank B. A. Pawson for a sample of (±)-juvabione and W. S. Bowers for a sample of natural (+)-todomatuic acid.

1. W. S. Bowers, H. M. Fales, M. J. Thompson, and E. C. Uebel. Sci. **154**, 1020 (1966).
2. K. Slama and C. M. Williams. Proc. Nat. Acad. Sci. U.S. **54**, 411 (1965).
3. V. Cerny, L. Dolejs, L. Labler, F. Sorm, and K. Slama. Coll. Czech. Chem. Commun. **32**, 3926 (1967).
4. R. Tutihasi and T. Hanazawa. J. Chem. Soc. Japan, **61**, 1041 (1940); Chem. Abstr. **37**, 258 (1943).
5. D. F. Zinkel and J. W. Rowe. Anal. Chem. **36**, 1160 (1964).
6. K. Mori and M. Matsui. Tetrahedron, **24**, 3127 (1968).
7. B. A. Pawson, H.-C. Cheung, S. Gurbaxani, and G. Saucy. J. Am. Chem. Soc. **92**, 336 (1970).

4,6-*O*-(1-Carboxyethylidene)-D-mannose as a Structural Unit in Capsular Polysaccharide of *Klebsiella* K-type 5[1]

G. G. S. Dutton and M. T. Yang

Department of Chemistry, University of British Columbia, Vancouver 8, British Columbia

Received April 21, 1972

Methylation, periodate oxidation, and partial hydrolysis techniques have each been used to demonstrate the presence of 4,6-*O*-(1-carboxyethylidene)-D-mannopyranosyl units in the capsular polysaccharide of *Klebsiella* K-type 5. The structure of this polysaccharide differs from those known for other *Klebsiella* capsules by the lack of any carbohydrate side chain. A repeating unit of

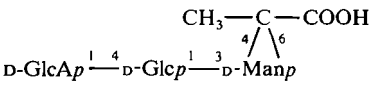

(plus one unassigned *O*-acetyl group) is in accord with the experimental data.

Les méthodes de méthylation, oxydation périodique et hydrolyse partielle ont été utilisées pour démontrer la présence de restes de 4,6-*O*-(1-carboxyethylidene)-D-mannopyranose dans le polyoside capsulaire de *Klebsiella* K-type 5. La structure de ce polysaccharide se distingue de toutes les autres connues pour *Klebsiella* par la manque d'une chaîne latérale de sucre. On propose une structure du type

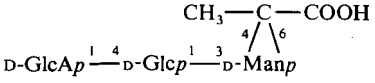

(avec un groupe *O*-acétyle) qui se répète.

Canadian Journal of Chemistry, **50**, 2382 (1972)

The occurrence of pyruvic acid as a covalently linked ketal unit in polysaccharides was first reported by Hirase (1) in a study on agar which contains 4,6-*O*-(1-carboxyethylidene)-D-galactose units. The presence of 4,6-*O*-(1-carboxyethylidene)-D-glucose units was subsequently demonstrated by Sloneker and Orentas (2) in the exocellular polysaccharide from *Xanthomonas campestris*. Since then the presence of this D-galactose ketal has also been shown in the polysaccharides from *Corynebacterium insidiosum* (3), *Klebsiella* K-type 21 (4), and colanic acid (5, 6). Pyruvic acid has been found as well in the M-antigens of *Salmonella* and in *E. coli* linked as 3,4-*O*-(1-carboxyethylidene)-D-galactose (7, 8).

[1]Presented at the 55th Canadian Chemical Conference of the Chemical Institute of Canada, Quebec City, Quebec, June, 1972.

Can. J. Chem. Downloaded from www.nrcresearchpress.com by 210.87.254.42 on 09/05/12
For personal use only.

Can. J. Chem. Downloaded from www.nrcresearchpress.com by 210.87.254.42 on 09/05/12
For personal use only.

In addition to these ketals of known structure the existence of pyruvic acid has also been demonstrated in other bacteria (*e.g.* 9–12) and in certain cases this acid may be an immunodominant group (11). We now report a new ketal of pyruvic acid namely 4,6-*O*-(1-carboxyethylidene)-D-mannose which is a structural unit in the capsular polysaccharide of *Klebsiella* K-type 5.

The capsular polysaccharide of *Klebsiella* K-5 has been qualitatively analyzed by Nimmich (13) and shown to contain glucose, mannose, and glucuronic acid. A culture of K-5 (E 5051) was obtained from Dr. I. Ørskov, Copenhagen, as an agar slant and was grown on sucrose–yeast extract–agar. Cells were harvested after 3 days, diluted with 5 volumes of water containing 1% phenol and centrifuged at 65 000 g for 1 h. Crude polysaccharide was obtained by freeze drying the supernatant. Pure capsular polysaccharide was obtained by treating a solution of this material with Cetavlon and working-up the precipitate thus formed. The freeze-dried product had $[\alpha]_D^{23}$ −45.2° (*c* 0.4, H_2O). Analysis indicated one *O*-acetyl group and two carboxyl units per three sugar residues. The molecular weight by gel-filtration on Sagavac 6F[2] was about 9×10^5. Hydrolysis of the polysaccharide with 0.5 *M* sulfuric acid at 100° for 8 h showed, by paper chromatography, glucose, mannose, glucuronic acid, and an aldobiouronic acid. The ratio of glucose to mannose was approximately 3:5 (g.l.c. of alditol acetates–ECNSS-M). Hydrolysis of the polysaccharide with 1 *M* hydrochloric acid showed the presence of pyruvic acid by the *o*-phenylenediamine spray (14) and by t.l.c. of the 2,4-dinitrophenylhydrazone.

Polysaccharide (400 mg) was methylated by the method of Hakomori (15, 16) followed by three treatments with Purdie's reagents to give a product free of absorption at 3600 cm^{-1} in the i.r. A portion (300 mg) was hydrolyzed with sulfuric acid, neutralized with barium carbonate, and separated by ion-exchange resins into neutral (178 mg) and acidic (60 mg) fractions. Paper chromatography (butanone–water azeotrope) of the neutral fraction showed the presence of only two components with the mobilities expected of a mono- and a trimethylhexose (R_f 0.07 and 0.55). Elution of the appropriate areas of the chromatogram with water and concentration of the extracts gave 2-*O*-methyl-D-mannose (48 mg), m.p. and mixed m.p. 138–140 °C (from ethanol, lit. (17) m.p. 138–139 °C), and 2,3,6-tri-*O*-methyl-D-glucose (32 mg), m.p. and mixed m.p. 116–118 °C (from ethyl ether, lit. (18) m.p. 121–123 °C).

The acidic fraction was treated with methanolic hydrogen chloride, reduced with sodium borohydride, and the product was hydrolyzed with sulfuric acid. Paper chromatography showed, by comparison with authentic samples, the presence of 2,3-di and 2,3,6-tri-*O*-methyl-D-glucose. G.l.c. of the methylated alditol acetates (19) showed the former in greater amount consistent with the acidic fraction being a mixture of methylated D-glucuronic acid and a methylated aldobiouronic acid. The identity of the two methylated glucoses was further confirmed by the mass spectra of their alditol acetates (20).

Isolation of a large amount of 2-*O*-methyl-D-mannose and the absence of a corresponding quantity of end-group means that the mannose cannot represent a branch point. The pyruvic acid cannot be linked as a ketal to the D-glucose or the D-glucuronic acid and must thus be present as 4,6-*O*-(1-carboxyethylidene)-D-mannose. This is confirmed by the following experiment.

A sample of K-5 capsular polysaccharide was autohydrolyzed and the non-dialyzable residue (200 mg) was recovered and methylated. Hydrolysis and examination on paper of the neutral sugars showed a weak response for tetramethylhexose and a strong response for trimethyl hexose with no slower moving compounds. (Butanone-water does not separate 2,3,6-tri-*O*-methyl-D-glucose and 2,4,6-tri-*O*-methyl-D-mannose.) Analysis of the neutral fraction as alditol acetates on 3% ECNSS-M programmed from 170° at 1°/min showed peaks corresponding to 2,3,6-tri-*O*-methyl-D-glucose (21.6 min) and 2,4,6-tri-*O*-methyl-D-mannose (18.0 min). The alditol acetate of the latter crystallized spontaneously (4) and had m.p. and mixed m.p. 64–66 °C. There was in addition a small peak at 9 min corresponding to a tetramethyl sugar.

These results indicate a repeating structure as

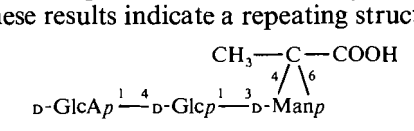

into which one *O*-acetyl group, at present unassigned, must be accommodated. In support of

[2]An agarose-type gel obtained from Seravac Laboratories, Cape Town, South Africa.

this structure the polysaccharide was found to consume 0.7 mol of periodate per sugar residue. Smith degradation of the polyalcohol gave erythritol and a component with the same mobility as erythritol on paper chromatography in 1-butanol–acetic acid–water (2:1:1). The latter compound, 3-*O*-(4,6-*O*-(1-carboxyethylidene)-D-mannopyranosyl)-D-erythronolactone, gave a positive reaction with the ferric hydroxamic acid spray for lactones (21) and the n.m.r. spectrum in D_2O showed a characteristic singlet for CH_3—C at τ 8.53 (6, 22). Total hydrolysis of this lactone and paper chromatography in ethyl acetate–acetic acid–formic acid–water (18:3:1:4) showed mannose, erythronolactone, and pyruvic acid (R_{Man} 1.0, 2.0, and 4.6). G.l.c. analysis of the acetylated reduced hydrolyzate gave erythritol tetraacetate and D-mannitol hexaacetate, m.p. and mixed m.p. 122–123° (ethanol, lit.(23) m.p. 125 °C).

Further details of the proposed structure and the possible presence of 4,6-*O*-(1-carboxyethylidene)-D-mannose units in other Klebsiella polysaccharides are currently under active investigation.

We are indebted to Dr. I. Ørskov, Copenhagen, for a culture (E 5051) of *Klebsiella* K-5, to Dr. P. J. Salisbury of this department for growing the bacteria, and to Dr. E. G. Gros for an authentic sample of 2-*O*-methyl-D-mannose. The financial support of the National Research Council of Canada, Ottawa, is gratefully acknowledged and we thank Dr. S. C. Churms for the molecular weight determination.

1. S. HIRASE. Bull. Chem. Soc. Japan, **30**, 75 (1957).
2. J. H. SLONEKER and D. G. ORENTAS. Can. J. Chem. **40**, 2188 (1962).
3. P. A. J. GORIN and J. F. T. SPENCER. Can. J. Chem. **42**, 1230 (1964).
4. G. G. S. DUTTON and Y. M. CHOY. Carbohydr. Res. **21**, 169 (1972).
5. I. W. SUTHERLAND. Biochem. J. **115**, 935 (1969).
6. C. J. LAWSON, C. W. MCCLEARY, H. I. NAKADA, D. A. REES, I. W. SUTHERLAND, and J. F. WILKINSON. Biochem. J. **115**, 947 (1969).
7. P. J. GAREGG, B. LINDBERG, T. ONN, and T. HOLME. Acta Chem. Scand. **25**, 1185 (1971).
8. P. J. GAREGG, B. LINDBERG, T. ONN, and I. W. SUTHERLAND. Acta Chem. Scand. **25**, 2103 (1971).
9. R. W. WHEAT, C. DORSCH, and G. GODOY. J. Bacteriol. **89**, 539 (1965).
10. B. J. GORMUS, R. W. WHEAT, and J. F. PORTER. J. Bacteriol. **107**, 150 (1971).
11. M. HEIDELBERGER, W. F. DUDMAN, and W. NIMMICH. J. Immunol. **104**, 1321 (1970).
12. W. NIMMICH. Personal communication.
13. W. NIMMICH. Z. med. Mikrobiol. Immunol. **154**, 117 (1968).
14. M. DUCKWORTH and W. YAPHE. Chem. Ind. (London), 747 (1970).
15. S. HAKOMORI. J. Biochem. (Tokyo), **55**, 205 (1964).
16. P. A. SANDFORD and H. E. CONRAD. Biochem. **5**, 1508 (1966).
17. J. O. DEFERRARI, E. G. GROS, and I. O. MASTRONARDI. Carbohydr. Res. **4**, 432 (1967).
18. E. J. BOURNE and S. PEAT. Advan. Carbohydr. Chem. **5**, 145 (1950).
19. H. BJÖRNDAL, B. LINDBERG, and S. SVENSSON. Acta Chem. Scand. **21**, 1801 (1967).
20. H. BJÖRNDAL, B. LINDBERG, and S. SVENSSON. Carbohydr. Res. **5**, 433 (1967).
21. M. ABDEL-AKER and F. SMITH. J. Am. Chem. Soc. **73**, 5859 (1951).
22. P. A. J. GORIN and T. ISHIKAWA. Can. J. Chem. **45**, 521 (1967).
23. L. HOUGH and A. C. RICHARDSON. *In* Rodd's chemistry of carbon compounds. 2nd ed. Vol. IF. Elsevier, Amsterdam. 1967. p. 22.

Can. J. Chem. Downloaded from www.nrcresearchpress.com by 210.87.254.42 on 09/05/12
For personal use only.

Matrix Infrared and Raman Spectroscopic Evidence for $Pd(N_2)_3$ in Solid Nitrogen

G. A. OZIN,[1] M. MOSKOVITS, P. KÜNDIG, AND H. HUBER

Lash Miller Chemistry Department and Erindale College, University of Toronto, Toronto, Ontario

Received April 28, 1972

Cocondensation of palladium atoms with $^{14}N_2$ at 4.2–10 °K leads to the formation of a binary dinitrogen complex. The complex is detected by matrix isolation infrared and Raman spectroscopy. Isotope studies using equimolar $^{14}N_2/^{15}N_2$ mixtures, together with isotope frequency and integrated absorption intensity calculations, suggest that the species is tris-dinitrogen palladium(0), $Pd(N_2)_3$.

La condensation d'atomes de palladium avec $^{14}N_2$ à 4.2–10 °K permet de former un complexe binaire diagoté. On détecte ce complexe par spectroscopie infrarouge d'isolation de matrice et Raman. Les études isotopiques utilisant des mélanges équimolaires $^{14}N_2/^{15}N_2$, de même que les calculs de fréquence d'isotope et d'intensité d'absorption intégrée, désignent le complexe comme étant le palladium(0) tris-dinitré, ou $Pd(N_2)_3$.

Canadian Journal of Chemistry, **50**, 2385 (1972)

Since the preparation of $[Ru(NH_3)_5N_2]^{2+}$ in 1965 which was the first complex of a transition metal that contained the nitrogen molecule as a neutral ligand (1), many exotic transition metal nitrogen complexes have been reported. For example, di- and trinuclear transition metal complexes are known, in $[(NH_3)_5RuN_2Ru(NH_3)_5]^{4+}$ and $[(NH_3)_5RuN_2Os(NH_3)_4N_2Ru(NH_3)_5]^{6+}$ respectively (2, 3), as well as complexes containing two nitrogen molecules coordinated to a single metal atom, for example, $[Os(NH_3)_4(N_2)_2]^{2+}$ (4).

Recently the cocondensation of metal vapors in their monatomic form with a variety of molecules at cryogenic temperatures has been found to produce a number of new and interesting chemical species and has provided a unique route by which to prepare binary transition metal nitrogen complexes (5).

We have combined the techniques of matrix isolation infrared and laser Raman spectroscopy together with $^{15}N_2$ isotope substitution experiments to study the cocondensation reaction of atomic palladium with molecular nitrogen in nitrogen matrices as well as in dilute nitrogen–argon matrices.

In this preliminary communication we are presenting the data for pure nitrogen matrices in which we have spectroscopic evidence for $Pd(N_2)_3$, the first reported example of a transition metal – nitrogen complex containing more than two neutral dinitrogen molecules coordinated to a single transition metal atom.

Using methods similar to those developed by DeKock (6), Timms (7), Andrews and co-worker (8), Ogden and Darling (9) and Burdett and Turner (5), palladium atoms were cocondensed with molecular nitrogen at 4.2–10 °K, using an Air Products liquid helium transfer system for matrix Raman experiments and a Displex closed cycle helium refrigerator for matrix infrared experiments. The furnace and cryotip arrangements are identical to those previously described (10). The rate of deposition of nitrogen gas was controlled by a fine needle valve and the rate of deposition of palladium atoms was continuously monitored using a quartz crystal microbalance incorporated into the furnace (11). The metal atom concentration was arranged so that the probability of forming a palladium aggregate in the matrix was about 0.1%.

In a number of experiments using pure $^{14}N_2$ as the matrix gas, one strong infrared absorption was observed at 2241 cm^{-1} as well as a very weak band at 2273 cm^{-1} (Fig. 1 *A*). In the analogous matrix Raman experiment one strong polarized line was observed at 2273 cm^{-1}. Matrix Raman depolarization measurements have been described previously (12).

When the matrix infrared experiment was repeated using an approximately equimolar mixture of $^{14}N_2$ and $^{15}N_2$ as matrix gas the spectrum shown in Fig. 1 *B* was observed. The single line observed at 2241 cm^{-1} in pure

[1]To whom correspondence should be addressed.

Can. J. Chem. Downloaded from www.nrcresearchpress.com by 210.87.254.40 on 09/05/12
For personal use only.

Can. J. Chem. Downloaded from www.nrcresearchpress.com by 210.87.254.40 on 09/05/12
For personal use only.

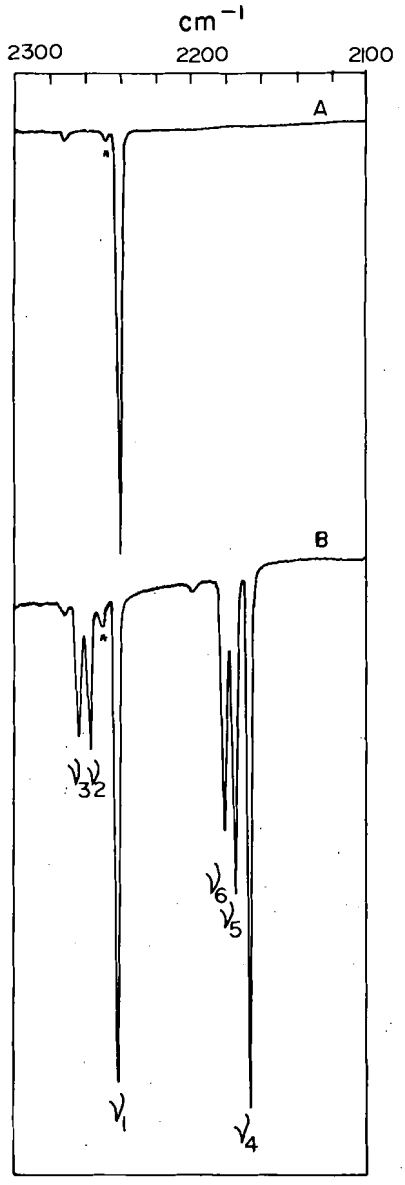

FIG. 1. *A*, the matrix infrared spectrum (2300–2100 cm^{-1}) of the products of the cocondensation reaction of palladium atoms with pure $^{14}N_2$. *B*, the matrix infrared spectrum (2300–2100 cm^{-1}) of the products of the cocondensation reaction of palladium atoms with an approximately equimolar mixture of $^{14}N_2/^{15}N_2$. The asterisks indicate the presence of trace quantities of a palladium species containing more than a single palladium atom.

$^{14}N_2$ was replaced by *two* groups of *three* main lines at 2263.4, 2256.3, 2241.4 cm^{-1} and 2182.5, 2175.6, 2166.9 cm^{-1}, respectively, with two very weak lines observed at 2273 and 2200 cm^{-1}. In a pure $^{15}N_2$ matrix one strong band was observed at 2167 cm^{-1} as well as a very weak band at 2200 cm^{-1}.

TABLE 1. Calculated and observed frequencies for $Pd(^{14}N_2)_n(^{15}N_2)_{3-n}$ where $n = 0$–3

Frequency notation		Calculated	Observed
Infrared	ν_1	2242.8	2241.4
	ν_2	2255.1	2256.3
	ν_3	2264.3	2263.4
	ν_4	2166.8	2166.9
	ν_5	2174.1	2175.6
	ν_6	2182.9	2182.5
Raman	ν_7	2272.0	2273.0

The six line spectrum obtained in the $Pd/^{14}N_2/^{15}N_2$ matrix together with the simplicity of the infrared and Raman spectra for the $Pd/^{14}N_2$ system strongly suggest that the most abundant species in the matrix is $Pd(N_2)_3$, containing three neutral dinitrogen molecules bonded directly to a palladium atom, with either D_{3h} or C_{3v} symmetry.

Following the methods used by Bor (13) and Haas and Sheline (14) for carbonyls we have assigned the six lines in the $Pd/^{14}N_2/^{15}N_2$ spectrum as follows

(E) $Pd(^{14}N_2)_3 + (B_1)Pd(^{14}N_2)_2(^{15}N_2)$	2241.4(ν_1)
(A_1) $Pd(^{14}N_2)_2(^{15}N_2)$	2263.4(ν_3), 2175.6(ν_5)
(A_1) $Pd(^{14}N_2)(^{15}N_2)_2$	2256.3(ν_2), 2182.5(ν_6)
(E) $Pd(^{15}N_2)_3 + (B_2)Pd(^{14}N_2)(^{15}N_2)_2$	2166.9(ν_4)

where the higher of the two A_1 frequencies for the two mixed species are the in-phase modes (13).

A simple calculation assuming the validity of the Cotton–Kraihanzel force field approximation (15) for a D_{3h} molecule indicates that $(\lambda_1\mu_{15}/\lambda_4\mu_{14})$ and $(\lambda_2\lambda_6/\lambda_3\lambda_5)$ should both equal unity, where λ_i is proportional to ν_i^2 and μ_{14} and μ_{15} are, respectively, the inverse reduced masses of $^{14}N_2$ and $^{15}N_2$. Experimentally one finds that $(\lambda_1\mu_{15}/\lambda_4\mu_{14}) = 0.9986$ and $(\lambda_2\lambda_6/\lambda_3\lambda_5) = 1.00004$, in excellent agreement with the predicted values.

A least-squares analysis yielded 20.91 and 0.18 mdyn/Å for the N–N stretch and stretch–stretch interaction force constants, respectively. The calculated frequencies based on these force constants are shown in Table 1.

The integrated absorption intensities of the various bands can also be approximately pre-

dicted using the technique suggested by Haas and Sheline (14). Applying their method one predicts that for an equimolar mixture of $^{14}N_2/^{15}N_2$, $A_3/A_5/A_4$ and $A_2/A_6/A_1$ are in the ratio 1.3:4.6:9.3 and 2.9:3.0:10.0, respectively, where the A_i refer to the absorbances associated with the frequencies ν_i. Experimentally we find that $A_3/A_5/A_4$ is in the ratio 1.85:4.7:8.3 and $A_2/A_6/A_1$ is in the ratio 1.8:3.9:10.

The agreement between the expected and measured band frequencies and integrated absorption intensities provides convincing evidence that the six line spectrum reported in Fig. 1 *B* probably belongs to the pure and mixed species of $Pd(N_2)_3$.

We wish to thank Professor A. D. Allen for helpful discussion and continued interest in this work and also thank the National Research Council of Canada and the Research Corporation for financial support.

1. A. D. Allen and C. V. Senoff. Chem. Commun. 621 (1965).
2. D. E. Harrison, H. Taube, and E. Weissberger. Science, **159**, 320 (1968).
3. A. D. Allen and J. R. Stevens. Can. J. Chem. In press.
4. H. A. Scheidegger, J. M. Armor, and H. Taube. J. Am. Chem. Soc. **90**, 3263 (1968).
5. J. K. Burdett and J. J. Turner. Chem. Commun. 885 (1971).
6. R. L. DeKock. Inorg. Chem. **10**, 1205 (1971).
7. P. L. Timms. Endeavour, **27**, 133 (1969).
8. L. Andrews and G. C. Pimentel. J. Chem. Phys. **44**, 2361 (1966). L. Andrews. J. Chem. Phys. **48**, 973 (1968).
9. J. S. Ogden and J. H. Darling. Inorg. Chem. **11**, 666 (1972).
10. H. Huber, M. Moskovits, and G. A. Ozin. J. Chem. Phys. In press.
11. M. Moskovits and G. A. Ozin. Appl. Spectrosc. In press.
12. H. Huber, A. VanderVoet, and G. A. Ozin. Nature Phys. Sci. **232**, 166 (1972). J. Nibber and D. Coe. J. Chem. Phys. **55**, 5133 (1971).
13. G. Bor. J. Organometal. Chem. **10**, 343 (1967).
14. H. Haas and R. K. Sheline. J. Chem. Phys. **47**, 2996 (1967).
15. F. C. Cotton and C. S. Kraihanzel. J. Am. Chem. Soc. **84**, 4432 (1962).

A Regiospecific Construction of α-Haloketones by the Reaction of Enol Borinates with *N*-Bromo- and *N*-Chlorosuccinimide. A Convenient Method for Converting Olefins into α-Haloketones and Esters

John Hooz and John N. Bridson[1]

Department of Chemistry, University of Alberta, Edmonton, Alberta

Received April 7, 1972

α-Bromo- and α-chloroketones may be synthesized in a regiospecific manner in high yields by treatment of an enol borinate with *N*-bromo- or *N*-chlorosuccinimide. This method preassembles the carbon skeleton of the ketone, and thereby avoids the problems (isomer formation, polyhalogenation) inherent in other methods. α-Haloesters are also easily synthesized by this procedure.

Les α-bromo et α-chlorocétones peuvent être synthétisées de façon régiospécifique, avec de bons rendements, en traitant le borinate d'énol avec le *N*-bromo et *N*-chlorosuccinimide. Cette méthode assemble d'avance le squelette carboné de la cétone et évite de ce fait les problèmes inhérents aux autres méthodes (formation d'isomères, polyhalogénation). Les α-haloesters sont également synthétisés facilement par ce procédé.

Canadian Journal of Chemistry, **50**, 2387 (1972)

α-Haloketones are precursors for several synthetically important processes (such as the Cornforth olefin synthesis (1) Favorskii rearrangement, etc.) yet their preparation is frequently a troublesome operation. According to usual practise an unsymmetrical ketone is halogenated directly; yet, despite the choice of halogenating reagent, or temptation to predict product formation on the basis of kinetic or thermodynamic

[1]University of Alberta, Postdoctoral Research Fellow, 1970–present.

Can. J. Chem. Downloaded from www.nrcresearchpress.com by 210.87.254.40 on 09/05/12
For personal use only.

dicted using the technique suggested by Haas and Sheline (14). Applying their method one predicts that for an equimolar mixture of $^{14}N_2/^{15}N_2$, $A_3/A_5/A_4$ and $A_2/A_6/A_1$ are in the ratio 1.3:4.6:9.3 and 2.9:3.0:10.0, respectively, where the A_i refer to the absorbances associated with the frequencies ν_i. Experimentally we find that $A_3/A_5/A_4$ is in the ratio 1.85:4.7:8.3 and $A_2/A_6/A_1$ is in the ratio 1.8:3.9:10.

The agreement between the expected and measured band frequencies and integrated absorption intensities provides convincing evidence that the six line spectrum reported in Fig. 1 *B* probably belongs to the pure and mixed species of $Pd(N_2)_3$.

We wish to thank Professor A. D. Allen for helpful discussion and continued interest in this work and also thank the National Research Council of Canada and the Research Corporation for financial support.

1. A. D. Allen and C. V. Senoff. Chem. Commun. 621 (1965).
2. D. E. Harrison, H. Taube, and E. Weissberger. Science, **159**, 320 (1968).
3. A. D. Allen and J. R. Stevens. Can. J. Chem. In press.
4. H. A. Scheidegger, J. M. Armor, and H. Taube. J. Am. Chem. Soc. **90**, 3263 (1968).
5. J. K. Burdett and J. J. Turner. Chem. Commun. 885 (1971).
6. R. L. DeKock. Inorg. Chem. **10**, 1205 (1971).
7. P. L. Timms. Endeavour, **27**, 133 (1969).
8. L. Andrews and G. C. Pimentel. J. Chem. Phys. **44**, 2361 (1966). L. Andrews. J. Chem. Phys. **48**, 973 (1968).
9. J. S. Ogden and J. H. Darling. Inorg. Chem. **11**, 666 (1972).
10. H. Huber, M. Moskovits, and G. A. Ozin. J. Chem. Phys. In press.
11. M. Moskovits and G. A. Ozin. Appl. Spectrosc. In press.
12. H. Huber, A. VanderVoet, and G. A. Ozin. Nature Phys. Sci. **232**, 166 (1972). J. Nibber and D. Coe. J. Chem. Phys. **55**, 5133 (1971).
13. G. Bor. J. Organometal. Chem. **10**, 343 (1967).
14. H. Haas and R. K. Sheline. J. Chem. Phys. **47**, 2996 (1967).
15. F. C. Cotton and C. S. Kraihanzel. J. Am. Chem. Soc. **84**, 4432 (1962).

A Regiospecific Construction of α-Haloketones by the Reaction of Enol Borinates with *N*-Bromo- and *N*-Chlorosuccinimide. A Convenient Method for Converting Olefins into α-Haloketones and Esters

John Hooz and John N. Bridson[1]

Department of Chemistry, University of Alberta, Edmonton, Alberta

Received April 7, 1972

α-Bromo- and α-chloroketones may be synthesized in a regiospecific manner in high yields by treatment of an enol borinate with *N*-bromo- or *N*-chlorosuccinimide. This method preassembles the carbon skeleton of the ketone, and thereby avoids the problems (isomer formation, polyhalogenation) inherent in other methods. α-Haloesters are also easily synthesized by this procedure.

Les α-bromo et α-chlorocétones peuvent être synthétisées de façon régiospécifique, avec de bons rendements, en traitant le borinate d'énol avec le *N*-bromo et *N*-chlorosuccinimide. Cette méthode assemble d'avance le squelette carboné de la cétone et évite de ce fait les problèmes inhérents aux autres méthodes (formation d'isomères, polyhalogénation). Les α-haloesters sont également synthétisés facilement par ce procédé.

Canadian Journal of Chemistry, **50**, 2387 (1972)

α-Haloketones are precursors for several synthetically important processes (such as the Cornforth olefin synthesis (1) Favorskii rearrangement, etc.) yet their preparation is frequently a troublesome operation. According to usual practise an unsymmetrical ketone is halogenated directly; yet, despite the choice of halogenating reagent, or temptation to predict product formation on the basis of kinetic or thermodynamic

[1]University of Alberta, Postdoctoral Research Fellow, 1970–present.

Can. J. Chem. Downloaded from www.nrcresearchpress.com by 210.87.254.6 on 09/05/12
For personal use only.

TABLE 1. The formation of α-bromo- and α-chloroketones by reaction of enol borinates with *N*-bromo- and *N*-chlorosuccinimide

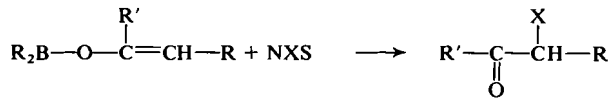

R_3B R	$R'COCHN_2$ R′	NXS X	Product*	Yield (%)†
C_2H_5‡	CH_3	Br	3-Bromo-2-pentanone	83
C_2H_5‡	CH_3	Cl	3-Chloro-2-pentanone	86
C_2H_5‡	C_6H_5	Br	α-Bromobutyrophenone	76
n-C_7H_{15}	$CH(CH_3)_2$	Br	4-Bromo-2-methyl-3-undecanone	84
n-C_7H_{15}	$CH(CH_3)_2$	Cl	4-Chloro-2-methyl-3-undecanone	88
C_2H_5‡	$CH(CH_3)_2$	Cl	4-Chloro-2-methyl-3-hexanone	93
n-C_6H_{13}	$CH(CH_3)_2$	Br	4-Bromo-2-methyl-3-decanone	80
n-C_6H_{13}	C_6H_5	Br	α-Bromooctanophenone	79
n-C_7H_{15}	C_6H_5	Br	α-Bromononanophenone	83

*Structures were corroborated by direct comparison with authentic samples or acceptable (±0.30%) compositional analyses and compatible spectral (i.r., n.m.r., mass spectroscopic) data.

†Yields are based on diazoketone using a 1:1 molar ratio of organoborane:diazoketone, and established by v.p.c. analysis. For the preparation of α-bromoketones, a 20% excess of *N*-bromosuccinimide was used at *ca.* 0°, whereas α-chloroketones were synthesized using a ratio of R_3B:NCS = 1:3, at room temperature for *ca.* 1 h. All organoboranes (except triethylborane‡) were prepared by the hydroboration of the appropriate olefin (9).

‡Commercial (Alfa Inorganics, Inc.) triethylborane was employed.

control, low yields and/or difficultly separable mixtures[2] are not an uncommon experimental outcome (eq. 1).

[1] 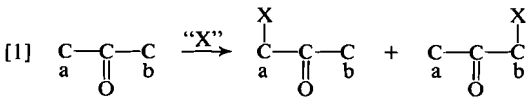

Indirect procedures, halogenation of enol derivatives (acetates, ethers, etc), have also been employed. Nonetheless, since enol derivatives are almost invariably constructed from parent ketone, disadvantages similar to those experienced for direct methods accrue, unless rather special circumstances (thermodynamic, steric factors, etc.) predominate (eq. 2) (5).

[2] 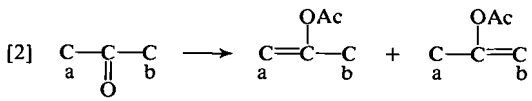

An approach has been developed which obviates these ambiguities: enol borinates react with *N*-bromo- or *N*-chlorosuccinimide[3] to provide the corresponding α-haloketones (eq. 3), *and significantly, in no case was there evidence for formation of the positional isomer.* Since enol borinates are conveniently assembled from readily available materials in an unambiguous fashion, the method allows for the unequivocal synthesis of the more- or less-highly substituted internal α-haloketone.

As a typical example, treatment of the enol borinate (derived from reaction of trihexylborane and diazomethyl isopropyl ketone) with *N*-bromosuccinimide at *ca.* 0° gave (80%) 4-bromo-2-methyl-3-decanone (eq. 4).

This illustrates one general approach in which the requisite intermediate enol borinate is easily generated in high yield upon reaction of an α-diazocarbonyl compound (6) with a trialkylborane (eq. 5). After the evolution of nitrogen is complete, intermediates of this type are employed *in situ*, in accordance with eq. 3, to provide an operationally convenient (one-flask), good yield, regiospecific route to α-haloketones. Bromination is complete in *ca.* 15 min at 0°, whereas chloroketone formation requires ap-

[2]Normally the predominant isomer is the one in which halogen enters the more highly substituted α position (most stable enol). Bromination of 2-pentanone (2), for example, gives a mixture of 3-bromo- (53%) and 1-bromo-2-pentanone (32%). A recent example (which appears somewhat extreme but nonetheless reflects the difficulties) is the chlorination (SO_2Cl_2) of 3-methyl-2-butanone to give (17% yield) 3-chloro-3-methyl-2-butanone (3). Yet chlorination of 2-methylcyclohexanone (SO_2Cl_2) gives an 83–85% yield of 2-chloro-2-methylcyclohexanone (4).

[3]Exploratory experiments by Dr. Hiromichi Kono established that molecular bromine gives a rather complex mixture from which only low yields of α-bromocarbonyl compound can be isolated. Dr. Kono's skillful efforts paved the way for the present developments.

Can. J. Chem. Downloaded from www.nrcresearchpress.com by 210.87.254.6 on 09/05/12
For personal use only.

Can. J. Chem. Downloaded from www.nrcresearchpress.com by 210.87.254.6 on 09/05/12
For personal use only.

[3] 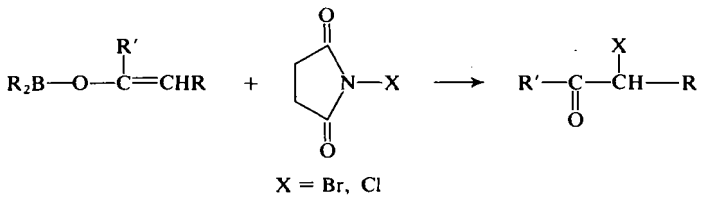

X = Br, Cl

[4] 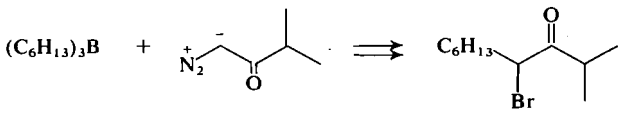

[5] 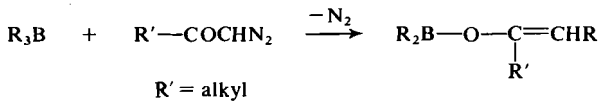

R′ = alkyl
aryl

[6] 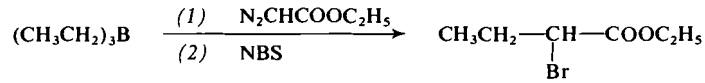

[7] 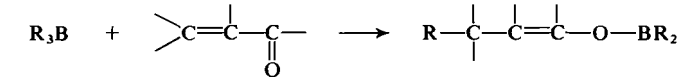

[8] 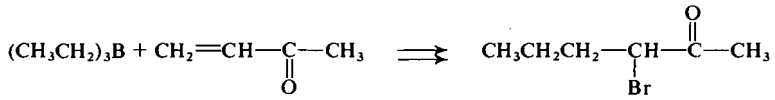

proximately 1 h at room temperature. Due to the hydrolytic sensitivity of enol borinates,[4] anhydrous conditions (nitrogen atmosphere, strictly anhydrous solvent and reagents) are necessary; failure to observe these precautions usually results in *ca.* 10–15% less haloketone with concurrent (and bothersome) formation of ketone by adventitious hydrolysis. Some typical examples are illustrated by the results summarized in Table 1.[5]

α-Haloesters are also easily prepared by this method. For example, treatment of triethylborane with ethyl diazoacetate followed by reaction with *N*-bromosuccinimide gave (85%) ethyl 2-bromobutyrate (eq. 6).

Moreover, that these developments possess potential for considerably broader scope immediately becomes clear upon recognition that enol borinates are implicated as intermediates in a wide variety of organoborane-based synthetic procedures (among others, the reaction of organoboranes with methyl vinyl ketone (8*a*), acrolein (8*b*), 2-bromo- and 2-methylacrolein (8*c*), cyclic α,β-unsaturated ketones (8*d*, *e*), etc.) (eq. 7).

To illustrate the applicability of this route, we investigated the reaction of triethylborane with methyl vinyl ketone, followed by treatment with NBS. A 70% yield of 3-bromo-2-hexanone was realized (eq. 8).

[4]The *in situ* capture of these intermediates by D_2O provides an unambiguous route to α-deuterioketones and esters (7).

[5]An interesting facet of the R_3B-α-diazocarbonyl reaction is the selective migration of the primary alkyl groups. Although the hydroboration of simple terminal olefins produces approximately 94% primary and 6% secondary boron-bound alkyl groups, no 4-bromo-2,5-dimethyl-2-nonanone was detected (from the reaction of the trialkylboranes obtained from 1-hexene with diazomethyl isopropyl ketone). This fortunate circumstance offers considerable synthetic advantage, since, in general, the products of these reactions appear to be free of any potential isomeric contaminants. Also, we should like to remind potential users that the R_3B-diazo reaction is sensitive to steric factors, and although, in general, yields are excellent for terminal olefins, they fall off with increasing steric hindrance in the organoborane (6).

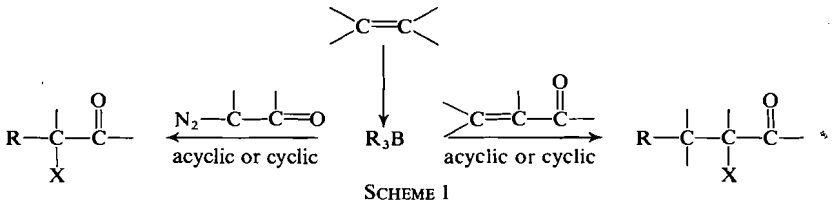

SCHEME 1

Since there is considerable structural flexibility when choosing among appropriate organoborane, α-diazo substrate, and unsaturated carbonyl component, the simplicity and high yields, combined with the unequivocal regiospecificity of this new alkylation–halogenation method, permits the synthesis of a wide array of useful structures difficult to obtain by present methodology (Scheme 1).

The synthesis of 4-bromo-2-methyl-3-decanone is representative of the standard experimental procedure. A solution of trihexylborane (20 mmol) in 40 ml tetrahydrofuran was prepared by the hydroboration (9) of 1-hexene (60 mmol). To the magnetically-stirred solution was added, dropwise, a solution of 2.24 g (20 mmol) of diazomethyl isopropyl ketone in 20 ml tetrahydrofuran while maintaining the temperature below *ca.* 15° (ice-bath cooling). After stirring at *ca.* 25° for an additional hour, nitrogen evolution was quantitative. The solution was cooled to *ca.* 0°, and *N*-bromosuccinimide (22 mmol) was added at once, while nitrogen was passed over the mixture; an exothermic reaction took place. After stirring at *ca.* 0° an additional 15 min, 20 ml of cold 3 *N* NaOH solution was added. The mixture was stirred vigorously (15 min), then poured into cold saturated brine solution (200 ml), and extracted with pentane (three 50-ml portions). The residue remaining after concentration (rotary evaporator) of the dried (Na_2SO_4) extract was distilled to provide 3.14 g (63%) of 4-bromo-2-methyl-3-decanone, b.p. 92.5–94° (1.9 mm), n_D^{20} 1.4583.

Anal. Calcd. for $C_{11}H_{21}BrO$: C, 53.01; H, 8.49; Br, 32.07. Found: C, 53.08; H, 8.21; Br, 32.29.

We wish to thank the National Research Council of Canada for financial support of this work. Dr. Hiromichi Kono contributed significantly and tirelessly to the initial stages of the study.

1. J. W. CORNFORTH, R. H. CORNFORTH, and K. K. MATHEW. J. Chem. Soc. 112 (1959).
2. J. R. CATCH, D. H. HEY, E. R. H. JONES, and W. WILSON. J. Chem. Soc. 276 (1948).
3. C. RAPPE, L. KNUTTSON, N. J. TURRO, and R. B. GAGOSIAN. J. Am. Chem. Soc. **92**, 2032 (1970).
4. E. W. WARNHOFF, D. G. MARTIN, and W. S. JOHNSON. Org. Synth. Coll. Vol. 4, 162 (1963).
5. P. A. HART. *In* Steroid reactions, an outline for organic chemists. *Edited by* C. Djerassi. Holden-Day, Inc., San Francisco. 1963. Chapt. 4.
6. J. HOOZ and S. LINKE. J. Am. Chem. Soc. **90**, 5936 (1968); J. HOOZ and S. LINKE. J. Am. Chem. Soc. **90**, 6891 (1968); J. HOOZ, D. M. GUNN, and H. KONO. Can. J. Chem. **49**, 2371 (1971); J. HOOZ and G. F. MORRISON. Can. J. Chem. **48**, 868 (1970); J. HOOZ and D. M. GUNN. Chem. Comm. 139 (1969).
7. J. HOOZ and D. M. GUNN. J. Am. Chem. Soc. **91**, 6195 (1969).
8. (*a*) A. SUZUKI, A. ARASE, H. MATSUMOTO, M. ITOH, H. C. BROWN, M. M. ROGIĆ, and M. W. RATHKE. J. Am. Chem Soc. **89**, 5708 (1967); (*b*) H. C. BROWN, M. M. ROGIĆ, M. W. RATHKE, and G. W. KABALKA. J. Am. Chem. Soc. **89**, 5709 (1967); (*c*) H. C. BROWN, G. W. KABALKA, M. W. RATHKE, and M. M. ROGIĆ. J. Am. Chem. Soc. **90**, 4165 (1968); (*d*) H. C. BROWN, M. W. RATHKE, G. W. KABALKA, and M. M. ROGIĆ. J. Am. Chem. Soc. **90**, 4166 (1968); (*e*) H. C. BROWN and G. W. KABALKA. J. Am. Chem. Soc. **92**, 714 (1970).
9. H. C. BROWN. Hydroboration. W. A. Benjamin, Inc., New York. 1962; G. ZWEIFEL and H. C. BROWN. Org. React. **13**, 1 (1963).

Can. J. Chem. Downloaded from www.nrcresearchpress.com by 210.87.254.6 on 09/05/12
For personal use only.

Can. J. Chem. Downloaded from www.nrcresearchpress.com by 210.87.254.105 on 09/05/12
For personal use only.

Canadian Journal of Chemistry

Published by THE NATIONAL RESEARCH COUNCIL OF CANADA

VOLUME 50 AUGUST 1, 1972 NUMBER 15

The Far Ultraviolet Photolysis of Alkenes: The Use of Hydrogen Sulfide as a Radical Scavenger

GUY J. COLLIN, PATRICK M. PERRIN, AND CHRISTIAN M. GAUCHER

Département des Sciences Pures et Appliquées, Université du Québec à Chicoutimi, Chicoutimi, Québec

Received January 26, 1972

The far u.v. photolysis of *cis*-2-butene, *n*-1-pentene, and *cis*-2-pentene was carried out in the presence of various quantities of hydrogen sulfide. We showed that in these systems, hydrogen atoms add to the double bond and are not scavenged by 5–10% hydrogen sulfide. On the other hand, alkyl radicals such as methyl, ethyl, *s*-butyl, and *s*-pentyl react with hydrogen sulfide, and the formation of the corresponding alkanes may be used to measure the absolute yields of the radical species. The same holds true for vinyl radicals. We also report some experiments published elsewhere. In particular, in the case of 1,3-butadiene, identification of the principal radicals is possible; however, measurement of absolute yields becomes more difficult.

La photolyse dans l'ultraviolet lointain du *cis*-2-butène, 1-pentène et du *cis*-2-pentène a été faite en présence de diverses quantités d'hydrogène sulfuré. On a montré que dans ces systèmes, les atomes d'hydrogène s'additionnent sur la double liaison et ne sont pratiquement pas interceptés par l'hydrogène sulfuré. Par contre, les radicaux saturés méthyles, éthyles, *s*-butyles et *s*-pentyles réagissent avec l'hydrogène sulfuré et la formation de l'alcane correspondant permet d'obtenir le rendement absolu des espèces radicalaires. Il en est de même des radicaux vinyles. Nous rapportons également des résultats partiels publiés par d'autres auteurs. En particulier, dans le cas du 1,3-butadiène, l'identification des principaux radicaux est possible, bien que la mesure quantitative de leur rendement soit devenue plus difficile.

Canadian Journal of Chemistry, **50**, 2391 (1972)

Introduction

The photo-induced addition of hydrogen sulfide to olefins has been known for many years. In the presence of ultraviolet radiation, it is accepted that this addition occurs via a radical chain mechanism and the products obtained are mercaptan derivatives or disulfides (for a general survey, see for example, ref. 1).

[1] $$H_2S + h\nu \rightarrow HS^{\cdot} + H^{\cdot}$$

[2] $$HS^{\cdot} + RCH{=}CH_2 \rightarrow R\dot{C}H{-}CH_2SH$$

[3] $$R\dot{C}H{-}CH_2SH + H_2S \rightarrow HS^{\cdot} + RCH_2CH_2SH$$

[4] $$2R\dot{C}H{-}CH_2SH \rightarrow HS{-}CH_2{-}\underset{\displaystyle R}{\underset{|}{CH}}{-}\underset{\displaystyle R}{\underset{|}{CH}}{-}CH_2SH$$

In the preceding abstract (1) and in other publications (2–5) high concentrations of hydrogen sulfide were used. In this manner, most of the incident radiation is absorbed by the hydrogen sulfide, thus preventing a photo- or radio-induced decomposition of the olefins. Moreover, high concentrations of hydrogen sulfide increase the importance of reaction 3 compared to reaction 4.

In the u.v. photochemistry of saturated hydrocarbons in the gaseous state, Ausloos and co-workers have shown that hydrogen sulfide in small concentrations (2 to 10%) is an excellent radical scavenger and that it allows one (*a*) to identify the nature of the radicals and (*b*) to measure their absolute yields (6).

In this publication we present the results of our study of olefins in the far u.v. in the presence of low concentrations of hydrogen sulfide and discuss these along with others from the literature (7–8).

Can. J. Chem. Downloaded from www.nrcresearchpress.com by 210.87.254.105 on 09/05/12
For personal use only.

Experimental

cis-2-Butene (99.0%), *trans*-2-butene (99.0%) (Matheson of Canada Limited) were purified by chromatography and degassed. Hydrogen sulfide (99.5%) (Matheson of Canada Limited), and 1-pentene and the *cis*-2-pentene (Chem. Sample Co.) were used after being degassed.

All samples were prepared in a mercury-free vacuum system equipped with Teflon stopcocks which were capable of maintaining a vacuum of about 10^{-5} mm Hg. Pressure measurements of samples were made with two metallic membrane manometers (Wallace and Tiernan).

The gaseous samples were irradiated in a 1 l flask sealed to an electrodeless xenon discharge lamp (9) excited by a 125 W microwave generator (Raytheon 2450 Mc unit). This lamp was equipped with a 1.5 mm thick lithium fluoride window and it produced 8.4 eV photons. Isobutene or 1-butene (10) irradiations were carried out to determine the quantum yields. Generally, the intensity was of the order of 7×10^{13} photons s^{-1}. Although we tried to keep the intensity constant, a sulfur deposit slowly accumulated on the window which became increasingly opaque. After approximately 8 h of irradiation, the window was washed with carbon disulfide; the lamp regained its initial intensity after this treatment.

A fraction of the irradiated sample was introduced in the gaseous state into a gas-chromatograph equipped with either a squalane column (25 ft), operated at room temperature, or with an alumina column (10 ft), temperature programmed between 50 and 150 °C. The detector consisted of a double flame ionization system and the calibrations were made by the introduction of known samples. The accuracy of the method of analysis is very good and the experimental error is probably less than 4%.

Discussion and Results

(A) Hydrogen Atoms

In the radiolysis of propane (6), 4.5% hydrogen sulfide is sufficient to scavenge more than 99.5% of thermal hydrogen atoms. In such a system, the rate of abstraction of a hydrogen atom from propane is much slower than from hydrogen sulfide:

[5] $$H^{\cdot} + H_2S \rightarrow H_2 + HS^{\cdot}$$

[6] $$H^{\cdot} + CH_3CH_2CH_3 \rightarrow H_2 + s\text{-}\dot{C}_3H_7$$

The reaction 6 is much slower than reaction 5. In an unsaturated system, the situation is more complex because the hydrogen atoms also add to the double bond:

[7] $$H^{\cdot} + cis\text{-}2\text{-}C_4H_8 \rightarrow s\text{-}\dot{C}_4H_9$$

[8] $$H^{\cdot} + cis\text{-}2\text{-}C_4H_8 \rightarrow H_2 + \dot{C}_4H_7$$

In the literature (11), it was demonstrated that reaction 8 is much slower than reaction 7: $k_8/k_7 = 6.6 \times 10^{-2}$. In the case of *trans*-2-butene, the same ratio k_8/k_7 is close to 11.7×10^{-2}. Thus more than 90% of the hydrogen atoms add to the double bond. In the presence of hydrogen sulfide, the efficiency of reactions 5 and 7 must be compared. It is known that hydrogen atoms add to ethylene at a rate twice that of reaction 5 (12). Also, the addition of hydrogen atoms to *cis*-2-butene (or *trans*-2-butene) occurs at approximately the same rate as that of the addition to ethylene (0.8 and 1.1 times faster respectively) (11):

[9] $$H^{\cdot} + C_2H_4 \rightarrow \dot{C}_2H_5$$

Thus the ratio k_7/k_5 is of the order of 1.6 and since the concentrations of hydrogen sulfide are less than 20%, more than 87% of the thermal hydrogen atoms react with *cis*-2-butene. In the case of *trans*-2-butene, 1-butene, and isobutene, 20% hydrogen sulfide captures less than 9, 5, and 2% of these atoms, respectively. These conclusions were confirmed by the photolysis of hydrogen sulfide in the presence of various alkenes (13).

If reaction 5 is ignored in unsaturated systems as a first approximation, we can consider that the thermal hydrogen atoms are transformed into alkyl (90%) and alkenyl (10%) radicals. Later, we will demonstrate that these radicals probably react with hydrogen sulfide to give an alkane and an alkene, respectively. To summarize, in an unsaturated system, the hydrogen sulfide does not capture the thermal hydrogen atoms. In the case of compounds containing conjugated double bonds, the hydrogen sulfide has no effect on thermal hydrogen atoms because these atoms add more readily to conjugated double bond systems than to simple olefins (14–15).

(B) Photolysis of cis-2-Butene (see Table 1)

Methyl Radical

Ausloos and Lias (6) have demonstrated that in the photolysis of propane, the thermal methyl radicals react with hydrogen sulfide at a rate 2.5×10^5 times greater than with propane in experiments carried out at room temperature. Under these conditions, 0.5% hydrogen sulfide added to propane captures 99.9% of the methyl radicals

[10] $$CH_3^{\cdot} + H_2S \rightarrow CH_4 + HS^{\cdot}$$

Can. J. Chem. Downloaded from www.nrcresearchpress.com by 210.87.254.105 on 09/05/12
For personal use only.

TABLE 1. Quantum yield in the irradiation of *cis*-2-butene*

cis-2-Butene (Torr)	Additive		Φ								
	Compound	Amount (Torr)	CH_4	C_2H_2	C_2H_4	C_2H_6	C_3H_6	C_3H_8	C_3H_4†	C_3H_4‡	iso-C_4H_{10}
8.00	—	—	0.27_1	0.30_5	0.12_3	0.35_2	0.20	0.20	0.12_1§	0.08_5	0.00
8.00	O_2	0.4	0.10_3	0.30_3	0.09_8	0.000_4	0.20	0.00	0.12_1§	0.08_1	0.00
8.00	H_2S	1.15	1.3_3	0.29_8	0.16_1	0.08_2	n.d.‖	0.00	0.12_1§	n.d.	0.00

*Irradiation time: 15 min; (pressure: 1064 N/m^2); figures are quantum yield values.
†Allene.
‡Propyne.
§Taken as reference.
‖Not determined.

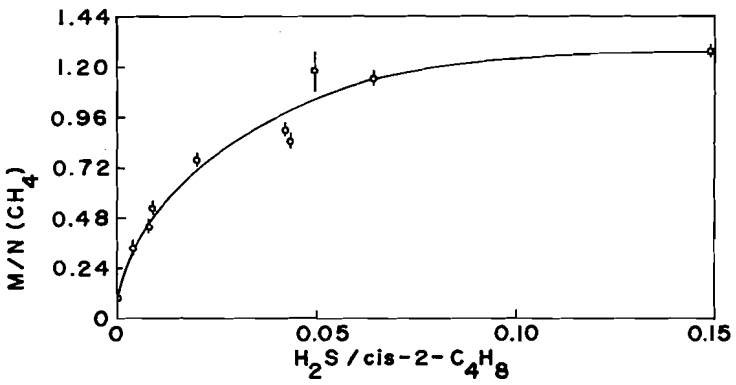

FIG. 1. Yields of methane formed in the photolysis (147.0 nm) of *cis*-2-butene at a pressure of 1.32 Torr and in the presence of varying amounts of hydrogen sulfide: irradiation time 15 min.

The increase in the yields of methane when hydrogen sulfide is added to propane thus allows the determination of the quantum yield of methyl radicals.

In unsaturated systems, the radicals can abstract a hydrogen atom or add to the double bond as in the case of hydrogen atoms

[11] $CH_3^{\cdot} + cis\text{-}2\text{-}C_4H_8 \rightarrow \dot{C}_5H_{11}$

[12] $CH_3^{\cdot} + cis\text{-}2\text{-}C_4H_8 \rightarrow CH_4 + {}^{\cdot}C_4H_7$

The k_{11}/k_{12} ratio is close to unity (14, 16). Moreover, the activation energy of reactions 11 and 12 is of the order of 7.8 ± 0.3 kcal mol^{-1} whereas that of reaction 10 is of the order of 2.6 kcal mol^{-1} (17). From these values, one can estimate that the methyl radicals react about 1000 times faster with hydrogen sulfide than with *cis*-2-butene. Thus in the presence of 5% hydrogen sulfide added to *cis*-2-butene, 99% of the methyl radicals react with the hydrogen sulfide. Therefore, the increase in the yield of methane in the presence of hydrogen sulfide again will permit the evaluation of the quantum yield of methyl radicals. Figure 1 shows that in the presence of 5% hydrogen sulfide, at least $90 \pm 5\%$ of the methyl radicals react according to reaction 10. Reaction between a methylene radical and H_2S produces methane (18). But in the 8.4 eV photolysis, the quantum yield of methylene is 0.02 (19). This yield is negligible and need not be considered here.

Further confirmation that the proposed mechanism is correct is obtained by following the yields of the products that are formed from methyl radicals in the absence of all free radical scavengers. In the case of pure *cis*-2-butene, methyl radicals essentially react with other radicals formed during the photolysis. It is known that in this system the methyl and the *s*-butyl radicals are the most important (8)

[13] $\dot{C}H_3 + \dot{C}H_3 \rightarrow C_2H_6$

[14] $\dot{C}H_3 + s\text{-}\dot{C}_4H_9 \rightarrow (CH_3)_2CHC_2H_5$

Figure 2 shows that the presence of hydrogen sulfide will cause a very rapid decrease in the yields of ethane and isopentane (19). From the increase in methane, the quantum yield of $CH_3^{\cdot}$ is less than or equal to 1.32. In the absence of all radical scavengers, part of the methane is formed by dismutating radical reactions involving the methyl radical and the other part is formed by molecular decomposition of excited *cis*-2-butene molecules. The preceding value must be reduced for the quantity of molecular methane (that is, that formed in the presence of 2% oxygen) which leads to an average value for the quantum yield of $\dot{C}H_3$ of about 1.2 ± 0.1.

In addition, the decrease of the yields of ethane and isopentane allows one to deduce the value of the yield of methyl radicals. Reaction 14 must be corrected for the following dismutation reaction:

[15] $\dot{C}H_3 + s\text{-}\dot{C}_4H_9 \rightarrow CH_4 + C_4H_8$

The ratio k_{15}/k_{14} is not well known: 0.30 or 0.07 (17). If it is assumed that reactions 13–15 are the only reactions involving methyl radicals, then

$$\Phi({}^{\cdot}CH_3) = 2(C_2H_6) + (1 + k_{15}/k_{14})(\text{iso-}C_5H_{12})$$

Can. J. Chem. Downloaded from www.nrcresearchpress.com by 210.87.254.105 on 09/05/12
For personal use only.

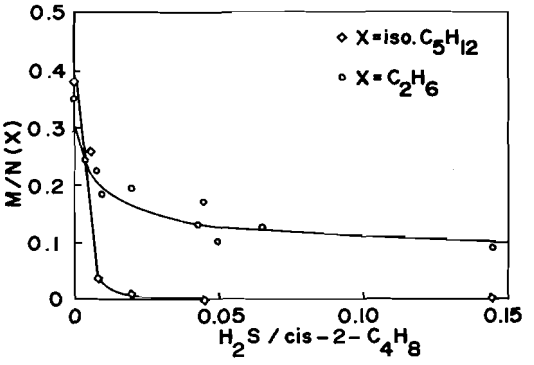

FIG. 2. Yields of ethane and isopentane formed in the photolysis of *cis*-2-butene. The experiments were carried out with conditions similar to those reported in Fig. 1.

These two values lead to quantum yield of $^{\cdot}CH_3$ of about 1.20 or 1.12, respectively. Thus obtained, these two values are minimum values because the methyl radicals also react with other radicals present. However, the methyl and *s*-butyl radicals are really the most important radicals, and if there are any other radicals, they are present in very small quantities. Thus the value of the methyl radical yield is probably close to 1.2.

Of course, the preceding deductions are only valid as long as other reactions do not interfere with the proposed mechanism. In particular, the thiyl radicals ($HS^{\cdot}$) that are formed in reaction 10, as a first approximation, are thought not to interfere with the measurement of methyl radicals, and for various reasons: (*a*) the low intensity used in this work; (*b*) the high degree of reactivity of methyl radicals and other radicals towards hydrogen sulfide; (*c*) the possibility for thiyl radicals to react with themselves or with other radicals that have a high molecular weight; (*d*) finally, in a future publication, we will demonstrate that thiyl radicals react very rapidly with 1,3-butadiene which is formed during the photolytic experiments.

s-Butyl Radicals

As in the case of methyl radicals, one can expect the majority of *s*-butyl radicals to be scavenged by 5% hydrogen sulfide

[16] $$s\text{-}\dot{C}_4H_9 + H_2S \rightarrow n\text{-}C_4H_{10} + HS^{\cdot}$$

In fact, the yield of normal butane was not measured but as was seen before, the variation of the yield of isopentane confirms indirectly this mechanism. The dismutation reactions of *s*-butyl radicals with each other are added to reactions 14 and 15

[17] $$s\text{-}\dot{C}_4H_9 + s\text{-}\dot{C}_4H_9 \rightarrow C_4H_8 + n\text{-}C_4H_{10}$$

[18] $$s\text{-}\dot{C}_4H_9 + s\text{-}\dot{C}_4H_9 \rightarrow C_8H_{18}$$

Even if the yield of normal butane was not measured, the yield of *s*-butyl radicals may be calculated (see note 19, ref. 18) and, depending on the ratio k_{15}/k_{14} (0.07 or 0.30), the value of the yield of $^{\cdot}C_4H_9$ is either 1.1 or 1.3, respectively. The first value seems to be in better agreement with a value obtained by another method in this laboratory (19): $\Phi(s\text{-}C_4H_9) = 1.05 \pm 0.10$. Once again, this calculation disregards other alkyl or thiyl radicals that are present. However, the similarity of the measurements is good and it is probable that the quantum yield of $s\text{-}C_4H_9$ is close to 1.1. Since the *s*-butyl radical is formed by the addition of hydrogen atoms to *cis*-2-butene, the yield of thermal hydrogen atoms is also of the order of 1.15, which is a reasonable value.

Radicals Present in Small Amounts

Ethyl radicals are also present in this system. In the presence of 14.5% hydrogen sulfide, ethane cannot be formed by the addition of two methyl radicals, and since the yield of molecular ethane (that is, the one formed in the presence of oxygen) is 0.004, it is possible to calculate a value of the yield of ethyl radicals. $\Phi(C_2H_5)$ is of the order of 0.08 if we postulate that the ethane in the presence of hydrogen sulfide is formed in the following reaction

[19] $$C_2H_5^{\cdot} + H_2S \rightarrow C_2H_6 + HS^{\cdot}$$

The presence of ethyl radicals in low concentrations is confirmed by the presence of propane that is formed by the addition of methyl and ethyl radicals in the absence of all radical scavengers.

The yield of ethylene also increases in the presence of hydrogen sulfide (Fig. 3). This slight increase can be attributed to the reaction of vinyl radicals with hydrogen sulfide

[20] $$C_2H_3^{\cdot} + H_2S \rightarrow C_2H_4 + HS^{\cdot}$$

This possibility could be questioned because of the manner in which the actinometry is carried out. We have assumed that the yield of allene is constant whatever the operating conditions. In fact it could well be that the yield in allene

Can. J. Chem. Downloaded from www.nrcresearchpress.com by 210.87.254.105 on 09/05/12
For personal use only.

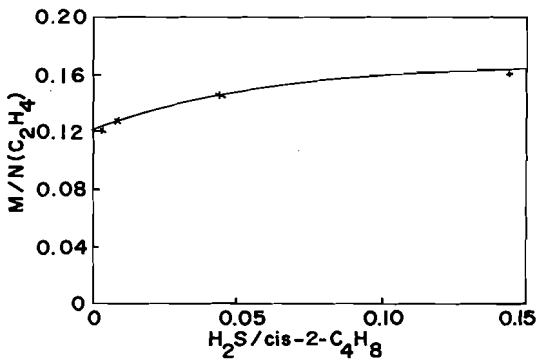

FIG. 3. Variations of the yield of ethylene in the photolysis of *cis*-2-butene (conditions reported under Fig. 1).

decreases slightly in the presence of hydrogen sulfide and is thus responsible for the apparent increase in the yield of ethylene. If the allene is formed by the decomposition of excited *cis*-2-butene molecules, it is improbable that this reaction will be influenced by the presence of hydrogen sulfide. On the other hand, a small part of the allene (30%) may be formed by the decomposition of a C_3H_5 radical. The latter would lead to the formation of propene in the presence of hydrogen sulfide. In the gaseous phase, the C_3H_5 radical, if it is formed, stems from the decomposition of an excited *cis*-2-butene molecule. Considering the energy of the incident photon, the C_3H_5 radical should decompose to allene and to a hydrogen atom well before a molecular collision. Finally, the ratio acetylene/allene is constant whatever the concentration of hydrogen sulfide, showing again that the yield of allene is constant. Thus, the quantum yield of vinyl radicals is of the order of 0.04.

In the irradiation of pure *cis*-2-butene, the absence of isobutane demonstrated without a doubt the absence of *s*-propyl, isobutyl, and *t*-butyl radicals. The absence of these radicals was also confirmed by the absence of propane and isobutane in the experiments that were carried out in the presence of hydrogen sulfide. Nothing can be said about the allyl radicals, if they are present, for the analysis of hydrogen sulfide interferes with the analysis of propene on the chromatographic columns.

(C) Photolysis of 1-Pentene (see Table 2)

In this system, actinometry was not carried out. However, because the yield of allene did not seem to vary, all the given yields are relative to that of allene: $R(C_3H_4) = 100$.

Ethyl Radicals

The most important radicals in the photolysis of 1-pentene are probably ethyl and *s*-pentyl radicals. This assertion is confirmed by the results in Table 2: 7% hydrogen sulfide added to 1-pentene will increase substantially the yields of ethane and normal pentane.

The activation energy of the abstraction of a hydrogen atom by an ethyl radical from olefinic molecules is of the order of 8.0 kcal mol^{-1} and the same reaction with hydrogen sulfide is less than 3 kcal mol^{-1}. Thus the conclusions deduced for the methyl radicals may be applied to the ethyl radicals.

It is rather interesting to attempt to determine the mechanism of formation of these ethyl radicals. *A priori*, two modes of formation can be considered: first of all, by decomposition of excited pent-1-ene molecules

$$[21] \qquad (n\text{-}1\text{-}C_5H_{10})^{**} \rightarrow C_2H_5^{\cdot} + C_3H_4 + H^{\cdot}$$

This decomposition reaction is endothermic by 128 kcal mol^{-1}, which is less than the energy of the incident photons: 194.5 kcal mol^{-1}. Moreover, this reaction is undoubtedly independent of pressure, at least in the region 0.03–100 Torr, and it is similar to the decomposition reactions of excited isobutene (7) and 1-butene (10) molecules. The second possibility for the formation of ethyl radicals stems from the decomposition of excited *s*-pentyl radicals formed by the addition of a hydrogen atom to the 1-pentene molecule

$$[22] \qquad (s\text{-}C_5H_{11})^{*} \rightarrow C_2H_5^{\cdot} + C_3H_6$$

$$[23] \qquad (s\text{-}C_5H_{11})^{*} + M \rightarrow s\text{-}C_5H_{11} + M$$

As shown in reaction 23, the decomposition reaction 22 depends upon the pressure of the system (20). As an example, at 1.32 Torr approximately 75% of the *s*-pentyl radicals are stabilized [23]. Above 100 Torr, reaction 22 does not occur (20). As a result, regardless of the pressure

$$R_1(C_2H_5^{\cdot}) = R(C_2H_6)_{7\%\ H_2S} - R(C_2H_6)_{\text{molecular}}$$

and

$$R_2(C_2H_5^{\cdot}) = R(C_3H_6) - R(C_3H_6)_{\text{molecular}} + R(C_3H_4)$$

Can. J. Chem. Downloaded from www.nrcresearchpress.com by 210.87.254.105 on 09/05/12
For personal use only.

Can. J. Chem. Downloaded from www.nrcresearchpress.com by 210.87.254.105 on 09/05/12
For personal use only.

TABLE 2. Relative yields of products in the photolysis of 1-pentene (147.0 nm)*

Pentene (Torr)	Additive		Relative yield										
	Compound	Amount (Torr)	CH_4	C_2H_2	C_2H_4	C_2H_6	C_3H_6	C_3H_8	C_3H_4†	C_3H_4‡	iso-C_4H_{10}	n-C_4H_{10}	n-C_5H_{12}
1.32	—	—	12.6	41.9	328.4	24.5	142.6	26	100	10.6	trace	13.5	n.d.§
1.32	O_2	0.065	0.0	n.d.	330.0	5.75	142.0	0.0	100	10.4	0.0	0.0	n.d.
1.32	O_2 He	0.065 80	n.d.	39.6	333.2	5.3	37.5	0.0	100	10.6	0.0	0.0	0.0
1.32	H_2S	0.09	n.d.	43.1	331.2	244.4	n.d.	54.9	100	n.d.	0.0	0.0	$\simeq$1000
1.32	H_2S He	0.09 300	55.7	59.4	391.8	n.d.	n.d.	57.2	100	n.d.	0.0	0.0	n.d.
1.32	H_2S He	0.19 300	40.7	58.3	362.6	n.d.	n.d.	59.0	100	n.d.	0.0	n.d.	n.d.

*Irradiation time: 15 minutes; pent-1-ene pressure: 1.32 Torr; (175 N/m^2).
†Allene; all yields are relative to allene yield.
‡Propyne.
§Not determined.

Can. J. Chem. Downloaded from www.nrcresearchpress.com by 210.87.254.105 on 09/05/12
For personal use only.

$R(C_2H_6)_{molecular}$ is the relative yield of ethane produced in the presence of oxygen; $R(C_3H_6)_{molecular}$ is the relative yield of propane produced at high pressure and in the presence of oxygen; finally $R_1(C_2H_5)$ and $R_2(C_2H_5)$ are the relative yields of ethyl radicals. From Table 2 at 1.32 Torr, $R_1(C_2H_5)$ is equal to 237 and $R_2(C_2H_5)$ is equal to 216. These values are in good agreement and are within the limits of error if it is accepted that each independant measurement is given at $\pm 4\%$.

s-Pentyl Radicals

The high yield of normal pentane formed in the presence of 7% hydrogen sulfide confirms first of all the efficiency of the addition of the hydrogen atoms to the double bond and also, the high reactivity of the hydrogen sulfide with *s*-pentyl radicals. However, we must mention that the addition of a thermal hydrogen atom to the double bond of pentene leads to two types of radicals: primary radicals ($\dot{C}H_3(CH_2)_2\dot{C}H_2$) and secondary radicals ($CH_3(CH_2)_2\dot{C}HCH_3$).

The proportion of the primary radical is probably less than 8% of the total as has already been shown in a similar system (10). An independant measurement of this proportion confirms this value (19). In any case, the primary and secondary radicals probably both lead to the normal pentane in the presence of hydrogen sulfide.

Radicals Present in Small Amounts

Since an increase of 7–15% in the quantity of hydrogen sulfide does not modify the yields of methane and propane, once again we must conclude that 7% hydrogen sulfide is sufficient to scavenge the majority of methyl and propyl radicals *n*-propyl; moreover $R(CH_3) = 30 \pm 10$ and $R(C_3H_7) = 57 \pm 3$.

The absence of isobutane and normal butane in the irradiations carried out in the presence of hydrogen sulfide is an indication of the absence of butyl radicals in this system. In the same manner, the yield of ethylene is constant at constant pressure regardless of the quantity of radical scavengers. The relative yield of vinyl radicals is thus within the limits of error of the measurements, that is, $R(C_2H_3) \leqslant 12$.

(D) Photolysis of cis-2-Pentene

Like the yield of allene in the case of pent-1-ene, the yield of ethylene is also constant regardless of the concentration of hydrogen sulfide. Consequently, the yield of vinyl is low and within the limits of error. As a point of reference, we will use the yield of ethylene: $R(C_2H_4) = 100$. This selection of $R(C_2H_4)$ under all conditions can indeed mask the appearance of C_2H_3 radicals. Figure 4 gives the variation in the yields of methane, ethane, and normal pentane. From these curves, we arrive at the following values: $R(C_5H_{11}) = 480$, $R(CH_3) = 680$, and $R(C_2H_5) = 125$. Once again, these curves demonstrate the efficiency of hydrogen sulfide as a radical scavenger of methyl, ethyl, and pentyl radicals (probably $CH_3\dot{C}HCH_2CH_2CH_3$ and $CH_3CH_2\dot{C}HCH_2$-CH_3).

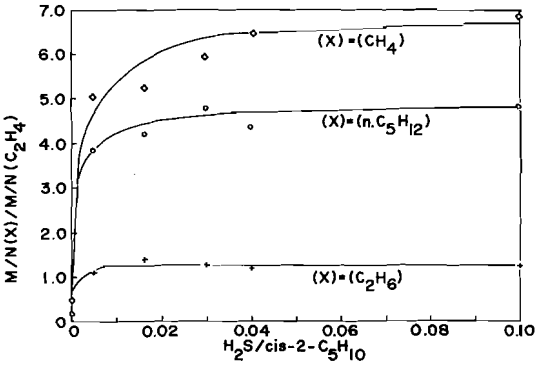

FIG. 4. Relative yields of methane, normal pentane and ethane in the photolysis of *cis*-2-pentene: experimental conditions similar to those reported under Fig. 1.

(E) Other Results Found in the Literature

In the photolysis of isobutene (7) conclusions which are similar to those reported here can be derived. Hydrogen atoms add to the double bond and methyl and butyl radicals (probably for the most part *t*-butyl) react with hydrogen sulfide to give either methane or isobutane. It is interesting to note that in this case, the yield of methyl radicals is close to the yield of C_3 products. In the photolysis of cyclohexane, methyl and cyclohexyl radicals are readily scavenged by 10% hydrogen sulfide (21).

In a more unsaturated system, 1,3-butadiene, hydrogen sulfide was used in order to study the nature of the radicals (8). When 10% hydrogen sulfide was added to 1,3-butadiene, the yield of methane increased by a factor of 10 or more; with higher concentrations of hydrogen sulfide, the yield of methane continued to increase (Fig. 5). The presence of methyl radicals was

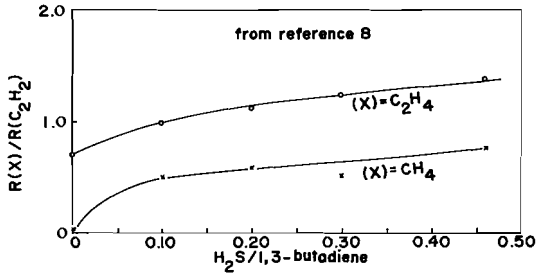

FIG. 5. Variation of relative yield of ethylene and methane (acetylene yield = 100) in the photolysis of 1,3-butadiene: see ref. 8.

proven but it is very difficult to obtain the absolute yield. This is not surprising because it is well known that the addition of methyl radicals to 1,3-butadiene takes place at a speed approximately 300 times faster than to *trans*-2-butene and 75 times faster than to but-1-ene at 65 °C (15). The activation energy of the addition reaction of the methyl radical to 1,3-butadiene is only 4.4 kcal mol^{-1}. This is not much greater than the activation energy of reaction 10. In this system, more than 50% hydrogen sulfide ($H_2S/1,3\text{-}C_4H_6 = 1.0$) is needed to scavenge 95% or more of the methyl radicals.

In the same manner, in the photolysis of 1,3-butadiene at 220.0 nm, the addition of hydrogen sulfide does not increase the yield of ethylene whereas at 147.0 nm, the yield of ethylene increases. The author concludes that at 220.0 nm, there is no formation of vinyl radicals whereas there is formation at 147.0 nm. In Fig. 5, it is possible to see that here again it is difficult to obtain the absolute yield of vinyl radicals.

The high reactivity of 1,3-butadiene toward methyl and vinyl radicals is probably general (15). Consequently, in unsaturated systems with conjugated double bonds, hydrogen sulfide is a poor radical scavenger and it can be used only to indicate the formation of radicals that are formed in appreciable yields, unless very high concentrations of hydrogen sulfide are used at the risk of completely changing the nature of the system studied. Similar observations have been reported in the photochemistry of 1,2-butadiene (22) and of cyclobutene (23).

The authors wish to thank the Université du Québec à Chicoutimi for the subsistence allowance accorded to one of us (P.M.P.), and also the National Research Council of Canada which has partially financed this research.

1. F. W. STACEY and J. F. HARRIS, JR. Organic reactions **13** (4), 191 (1965). J. Wiley and Sons, New York.
2. C. WALLING and W. HELMREICH. J. Am. Chem. Soc. **81**, 1144 (1959).
3. W. E. VAUGHAN and F. F. RUST. J. Org. Chem. **7**, 472 (1942).
4. K. SUGIMOTO, W. ANDO, and S. OAE. Bull. Chem. Soc. Jap. **37**, 365 (1964).
5. O. P. STRAUSZ, T. HIKIDA, and H. E. GUNNING. Can. J. Chem. **43**, 717 (1965).
6. P. AUSLOOS and S. LIAS. J. Chem. Phys. **44**, 521 (1966).
7. J. HERMAN, K. HERMAN, and P. AUSLOOS. J. Chem. Phys. **52**, 28 (1970).
8. R. DOEPKER. J. Phys. Chem. **72**, 4037 (1968).
9. R. GORDEN, JR., R. E. REBBERT, and P. AUSLOOS. NBS. Technical Note 496, 1969.
10. G. J. COLLIN and P. AUSLOOS. Fifth Intern. Conf. Photochem. Yorktown Heights, N.Y. 1969.
11. K. R. JENNINGS and R. J. CVETANOVIĆ. J. Chem. Phys. **35**, 1233 (1961).
12. N. L. ARTHUR and T. N. BELL. J. Chem. Soc. 4866 (1962).
13. G. R. WOOLEY and R. J. CVETANOVIĆ. J. Chem. Phys. **50**, 4697 (1969).
14. R. J. CVETANOVIĆ and R. S. IRWIN. J. Chem. Phys. **46**, 1694 (1967).
15. R. J. CVETANOVIĆ and L. C. DOYLE. J. Chem. Phys. **50**, 4705 (1969).
16. R. P. BUCKLEY and M. SZWARC. Proc. Roy. Soc. (London), **A240**, 396 (1957).
17. A. F. TROTMAN-DICKENSON and G. S. MILE. NSRDS-NBS, **9**, 50 (1967).
18. S. G. LIAS, G. J. COLLIN, R. E. REBBERT, and P. AUSLOOS. J. Chem. Phys. **52**, 1847 (1970).
19. G. J. COLLIN and P. M. PERRIN. Unpublished results.
20. M. J. PEARSON and B. S. RABINOVITCH. J. Chem. Phys. **42**, 1624 (1965).
21. R. LESCLAUX, S. SEARLES, L. W. SIECK, and P. AUSLOOS. J. Chem. Phys. **53**, 3336 (1970).
22. R. D. DOEPKER and K. L. HILL. J. Phys. Chem. **73**, 1313 (1969).
23. A. DELEON and R. D. DOEPKER. J. Phys. Chem. **75**, 3656 (1971).

Can. J. Chem. Downloaded from www.nrcresearchpress.com by 210.87.254.105 on 09/05/12
For personal use only.

Photoisomerization of 2-Alkenes in the Presence of Hydrogen Sulfide

GUY J. COLLIN AND PATRICK M. PERRIN

Département des Sciences Pures et Appliquées, Université du Québec à Chicoutimi, Chicoutimi, Québec

Received January 26, 1972

In far u.v. photochemistry, the radicals formed react with hydrogen sulfide to give, amongst others, thiyl radicals (HS·). These radicals initiate the *cis–trans* isomerization of 2-olefins in a chain mechanism. We have tried to demonstrate that the thiyl radicals are also chain carriers. Quantum yields for the isomerization of *cis* to *trans* compound are probably of the order of $6–7 \times 10^3$ and the length of the chain, of the order of 4.7×10^3. We have also studied the radiolysis of these reactions in the liquid phase. The effect of oxygen and of conjugated di-olefins, such as 1,3-butadiene and 1,3-pentadiene is also discussed.

En photochimie de l'ultraviolet lointain, les radicaux formés réagissent avec l'hydrogène sulfuré pour donner entre autres des radicaux thiyles (HS·). Ces derniers initient l'isomérisation *cis-trans* des 2-oléfines dans un mécanisme en chaîne. Nous avons essayé de montrer que ces radicaux thiyles sont aussi les porteurs de chaîne. Les rendements quantiques pour l'isomérisation *cis* vers *trans* sont probablement de l'ordre de $6–7 \times 10^3$ et la longueur de chaîne de l'ordre de 4.7×10^3. Nous avons également étudié la radiolyse de ces systèmes en phase liquide. L'effet de l'oxygène et des di-oléfines conjuguées telles que 1,3-butadiène et 1,3-pentadiène est aussi discuté.

Canadian Journal of Chemistry, **50**, 2400 (1972)

Introduction

In the preceding paper we have studied the efficiency of hydrogen sulfide as a radical scavenger in the far u.v. photolysis of unsaturated compounds (1).

Hydrogen sulfide is a good radical scavenger and its use permits not only the identification of the nature of the radicals, but also the measurement of their absolute yields.

[1] $$R^{\cdot} + H_2S \rightarrow RH + HS^{\cdot}$$

The increase in the yield of the RH compound in the presence of hydrogen sulfide will permit the identification of the nature of the radical $R^{\cdot}$ and the measurement of its quantum yield. However, the chemical activity of the thiyl radical formed in reaction 1 was not considered earlier (1). We had simply stated that the formation of this radical did not intervene in the measurement of the other radicals. Here, we consider the effect of the presence of hydrogen sulfide in low concentrations on the photochemistry and the radiochemistry of 2-olefins.

Experimental

The photolytic techniques in the gaseous phase for the preparation of samples have already been described (1). Helium (Canadian liquid air: 99.995%) was used as received.

Each liquid sample contained 5.8×10^{-3} moles of unsaturated hydrocarbons. The cell was made of a small Pyrex tube equipped with a Pyrex break seal. Its volume was less than double the liquid volume. In this way more than 99.5% of the hydrocarbon was in the liquid phase.

After irradiation, the cell was sealed at the base of a 1 l flask. The liquid vaporized into the evacuated flask immediately after the breakseal was ruptured. Analysis of the irradiated sample was carried out as already described (1).

Irradiation of liquid samples was accomplished in a Gammacell, 220 type; the rate of energy absorption by 2-butene was 1.9×10^{17} eV/mol s.

Discussion and Results

Mechanism

Initiation Steps

The results show that the presence of low concentrations of hydrogen sulfide in the far u.v. photolysis of *cis*-2-butene, *trans*-2-butene, and *cis*-2-pentene isomerizes these compounds into *trans*-2-butene, *cis*-2-butene, and *trans*-2-pentene, respectively (see Table 1, Figs. 1–3). The question then arises as to whether this isomerization is dependent on the absorption of energy by the olefin or by the hydrogen sulfide. Because the absorption coefficient of hydrogen sulfide is not known at the exciting wavelength, it is assumed as a first approximation that this coefficient is at most equal and probably less than that of the olefin. Since the percentage of hydrogen sulfide is, for the most part, less than 15%, more than 85% of the energy is absorbed by the olefin. Generally this percentage is probably greater than 95%. Moreover, since an increase of 2 to 15% of the concentration of hydrogen

Can. J. Chem. Downloaded from www.nrcresearchpress.com by 210.87.254.105 on 09/05/12
For personal use only.

TABLE 1. Isomerization yields of 2-olefines*

2-Alkene (Torr)	Additives: Compound	Additives: Amount (Torr)	Irradiation time (min)	Final ratio *trans*/*cis*	Quantum yields
cis-2-C_4H_8					
1.32	H_2S	0.03	0.5	0.177	2960
1.32	H_2S	0.09	0.5	0.75	4650
1.32	H_2S	0.26	0.5	0.30	4660
1.32	H_2S	0.09	0.25	0.125	5615
1.32	H_2S	0.09	8	2.84	1095
1.32	H_2S	0.09	20	2.64	580
	He	110			
1.32	H_2S	0.09	30	2.84	345
	He	235			
1.32	H_2S	0.09	60	2.84	195
	He	235			
10	H_2S	0.66	20	1.69	1100
10	H_2S	0.66	40	2.7	910
trans-2-C_4H_8					
1.32	H_2S	0.09	30	4.0	100±20
cis-2-C_5H_{10}					
8.0	H_2S	1.0	90	4.1±0.2	—

*147 nm photolysis.

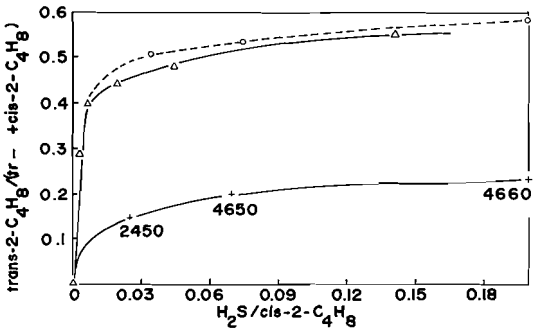

FIG. 1. Photoisomerization of *cis*-2-butene: variation of the *trans*-/(*trans*- + *cis*-2-butene) ratio *vs.* the hydrogen sulfide/*cis*-2-butene ratio: ○, *cis*-2-butene, 1.32 Torr, irradiation time = 2.5 min; △, *cis*-2-butene, 7.92 Torr, irradiation time = 15 min; +, *cis*-2-butene, 1.32 Torr; irradiation time = 0.5 min. Figures are quantum values: Φ (*trans*-2-butene).

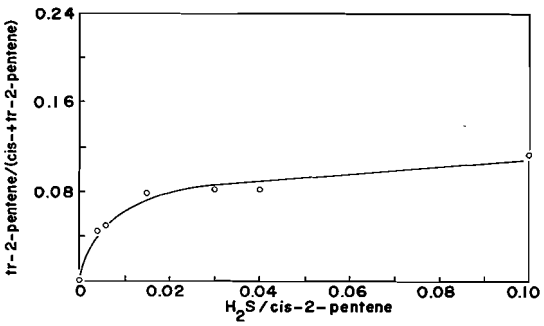

FIG. 2. Photoisomerization of *cis*-2-pentene: variation of the *trans*-/(*trans*- + *cis*-2-pentene) ratio *vs.* the hydrogen sulfide/*cis*-2-pentene ratio: *cis*-2-pentene, 7.92 Torr, irradiation time = 15 min.

sulfide has no, or very little effect on the isomerization yield, the absorption by hydrogen sulfide can be ignored, as far as this last reaction is concerned.

At the wavelength used, the absorption of photons by the olefins does not produce ions. The ionization potential of *cis*-2-butene and *trans*-2-butene is 9.13 eV and that of *cis*-2-pentene is 9.11 eV (2). In fact, absorption of photons leads to the formation of excited neutral molecules that decompose to give hydrogen atoms, radicals, and neutral molecules:

[2] $2\text{-}C_4H_8 + h\nu \rightarrow (C_4H_8)^{**}$

[3] $(C_4H_8)^{**} \rightarrow H^{\cdot}, R^{\cdot}, R_1R_2, \ldots$ etc.

As was recently shown (1), hydrogen atoms react mostly with the double bond by addition; the abstraction reaction of a hydrogen atom is of lesser importance

[4] $H^{\cdot} + 2\text{-}C_4H_8 \xrightarrow{k_4} s\text{-}C_4H_9^{\cdot}$

[5] $H^{\cdot} + 2\text{-}C_2H_8 \xrightarrow{k_5} H_2 + C_4H_7^{\cdot}$

The value of the k_5/k_4 ratio is either 6.6 ×

Can. J. Chem. Downloaded from www.nrcresearchpress.com by 210.87.254.105 on 09/05/12
For personal use only.

Can. J. Chem. Downloaded from www.nrcresearchpress.com by 210.87.254.105 on 09/05/12
For personal use only.

TABLE 2. Effects of additives in the xenon-photolysis of *cis*-2-C_4H_8 or *cis*-2-C_5H_{10}

Olefinic system (Torr)	Additives: Compound	Additives: Amount (Torr)	Irradiation time (min)	CH_4	C_2H_2	C_2H_4	C_2H_6	C_3H_4	iso-C_4H_{10}	1,3-C_4H_6	*trans*-2-olefin	Final ratio *trans*/(*cis* + *trans*)
cis-2-C_4H_8: (8.00)												
	H_2S	1.14	15	1.31*	0.29_8	0.13_9	0.16_7	0.12_5†	0.03_6	<0‡	2350	0.58
	H_2S + O_2	1.14 + 0.08	15	0.401	0.26_4	0.16_1	0.02_3	0.12_5	—	<0‡	518	0.145
	H_2S	0.35	15	0.88	0.31_0	0.14_5	0.18	0.12_5	0.01_1	<0‡	1480	0.48
	H_2S + 1,3-C_5H_8	0.33 + 0.08	15	1.2	0.28_5	0.15_3	0.10_2	0.12_5	0.02_0	<0‡	228	0.005
	H_2S + 1,3-C_5H_8	0.39 + 0.008	15	0.93	0.30_2	0.13_9	0.13_4	0.12_5	0.00_9	≃0.3	22.5	0.036
	O_2	0.07	15	0.08_2	0.26_3	0.10_0	0.00_4	0.12_5	0.00	0.43	<0.1	≃0.00
	—		10§	0.12_7	0.27	0.10	0.37	0.12_5	0.0	0.43	0.14	≃0.00
cis-2-C_5H_{10}: (8.00)												
	H_2S	0.33	15	1.1_2	—	0.17‖	0.18	0.05_3¶	—	—	358	0.13
	H_2S + O_2	0.33 + 0.03	30	0.06	—	0.17	0.02_4	—	—	—	39.2	0.018
	H_2S + 1,3-C_5H_8	0.33 + 0.13	30	0.95	—	0.17	0.19_2	—	—	—	<1.0	~0.00

*Figures are the quantum yield values.
†In the *cis*-2-C_4H_8 system: C_3H_4 = allene; this product was used as reference.
‡Starting material contained about 1000 p.p.m. of 1,3-C_4H_6 and in the presence of H_2S it was consumed during photolytic experiments.
§*cis*-2-C_4H_8 pressure: 1.32 Torr.
‖Ethylene was taken as reference in the *cis*-2-C_5H_{10} system.
¶C_3H_4 = allene + propyne.

Can. J. Chem. Downloaded from www.nrcresearchpress.com by 210.87.254.105 on 09/05/12
For personal use only.

10^{-2} or 11.7×10^{-2} (3) depending on the *cis*- or *trans*- structure of the 2-butene. The *s*-butyl radical reacts with hydrogen sulfide (reaction 1) to produce the normal butane and the thiyl radical (1). In the same manner, it is probable that the alkenyl radical reacts in the same way to produce 2-butene and a thiyl radical, so that all of the hydrogen atoms indirectly produce thiyl radicals. Of course, the same applies for the majority of other alkyl (methyl, ethyl, etc.) radicals.

Walling and Helmreich have reported the isomerization of 2-butene in a different system (4). Some methanethiol (CH_3SH) was added to a mixture of 2-butene and of azoisobutyronitrile at a temperature of 60 °C. At this temperature, the azoisobutyronitrile was decomposed and formed free radicals. These radicals reacted with methanethiol in the same way as in reaction 1, and the thiyl radical formed is the $CH_3S^{\cdot}$ radical

[6] $$R^{\cdot} + CH_3SH \rightarrow RH + CH_3S^{\cdot}$$

The 2-butenes are rapidly isomerized one into the other and the following mechanism is proposed:

[7] $$HS^{\cdot} + \textit{cis}\text{-}CH_3CH{=}CHCH_3 \underset{k_{-7}}{\overset{k_7}{\rightleftharpoons}} HS{-}\overset{CH_3}{\overset{|}{C}}{-}\overset{CH_3}{\overset{|}{C}}{}^{\cdot}\ (H,H)$$

[8] $$HS{-}\overset{CH_3}{\overset{|}{C}}{-}\overset{CH_3}{\overset{|}{C}}{}^{\cdot}\ (H,H) \underset{k_{-8}}{\overset{k_8}{\rightleftharpoons}} HS{-}\overset{CH_3}{\overset{|}{C}}{-}\overset{H}{\overset{|}{C}}{}^{\cdot}\ (H,CH_3)$$

[9] $$HS{-}\overset{CH_3}{\overset{|}{C}}{-}\overset{H}{\overset{|}{C}}{}^{\cdot}\ (H,CH_3) \underset{k_{-9}}{\overset{k_9}{\rightleftharpoons}} HS^{\cdot} + \textit{trans}\text{-}CH_3CH{=}CHCH_3$$

Naturally, if the concentration in hydrogen sulfide is particularly high, the adduct radical could react with it in a reaction similar to reaction 1. This phenomenon does not seem important with the concentrations of hydrogen sulfide used here since the major part of initial 2-butene seems to have been recovered contrary to results already mentioned in the literature (4–7).

In order to demonstrate that the thiyl radicals cause this isomerization, it is interesting to compare the increase in the methane yield, or the decrease in the yields of ethane and isopentane, with the increase in the yield of isomerization as a function of the concentration of

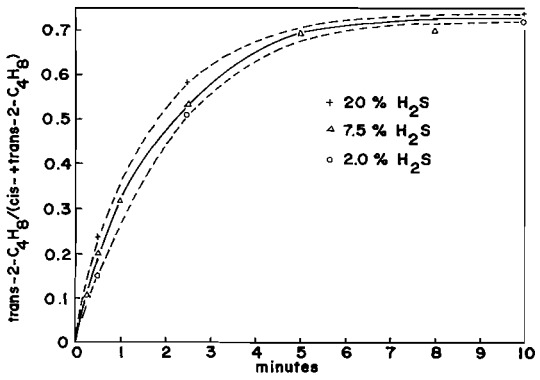

FIG. 3. Influence of irradiation time on the *trans*-/(*trans*- + *cis*-2-butene) ratio in the photoisomerization of *cis*-2-butene: *cis*-2-butene pressure = 1.32 Torr.

hydrogen sulfide between 0.0 and 2%. Moreover, between 2 and 15%, the increase of the hydrogen sulfide concentration has no important effect either on the isomerization yield, or on the methane yield. Therefore there exists a parallel between the effect of the radical scavenger and the isomerization of the olefin.

The relationship that exists between these two phenomena is demonstrated by the effect of the presence of small quantities of oxygen. It is well known that oxygen is an excellent radical scavenger. The activation energy of the reaction between the radicals and oxygen is much lower than that of reaction 1. Thus in the presence of high concentrations of oxygen (5%), the yields of methane, ethane, and isopentane are not affected by the addition of low concentrations of hydrogen sulfide and the quantum yield of isomerization is zero. On the other hand, in the presence of 14% of hydrogen sulfide and of 1% of oxygen some of the radicals react with hydrogen sulfide and the isomerization occurs with a lower yield than in the absence of oxygen. Thus there is no doubt that thiyl radicals are involved in the isomerization(see Table 2).

Despite the above mentioned mechanism, apart from being the initiator of isomerization, the thiyl radical is not demonstrated to be the chain carrier. At this stage, one must report recent work on the photoisomerization of 2-butenes which is initiated by sulfur atoms in the ground state $S(^3P)$ (8). In that study, the isomerization presents approximately the same characteristics as those in the present work. The photostationary ratio *trans*-2-butene/*cis*-2-bu-

TABLE 3. Isomerization of *cis*- or *trans*-2-butene

Systems	Chain propagating species	Photostationary state ratio	Temperature (°C)	Total pressure (Torr)	Reference
Photolytic systems					
$COS + 2\text{-}C_4H_8$ (253.7 nm)	$S(^3P)$	2.83 ± 0.06	23	3.5	8
		2.9 ± 0.1	23	200	8
$2\text{-}C_4H_8$ + trace of H_2S (147.0 nm)	$HS^\cdot$	2.84 ± 0.04	25	1–235	this work
(253.7 nm)	$CH_3S^\cdot$	2.8	20–80	—	16
Radiolytic systems					
H_2S + *trans*-$2\text{-}C_4H_8$ ($\simeq$2:1)	$HS^\cdot$	2.57	23	1810	7
H_2S + *cis*-$2\text{-}C_4H_8$ ($\simeq$2:1)	$HS^\cdot$	2.7	23	1810	7
H_2S + *cis*-$2\text{-}C_4H_8$ / H_2S + *trans*-$2\text{-}C_4H_8$ (0.02:1)	$HS^\cdot$	2.8 ± 0.1	23	liquid	15
Thermolytic system					
$2\text{-}C_4H_8 + CH_3SH$ + Azoisobutyronitrile	$CH_3S^\cdot$	—	60	solution in $n\text{-}C_4H_{10}$	3

tene is the same 2.83 ± 0.06. Oxygen, like 1,3-butadiene, has a very strong negative effect on the yield of isomerization.

A way to reconcile the two mechanisms is to assume that the thiyl radicals react so slowly with either the 2-butene or the hydrogen sulfide that only mutual interactions remain

[10] $$HS^\cdot + HS^\cdot \xrightarrow{k_{10}} H_2S + S^\cdot$$

[11] $$HS^\cdot + HS^\cdot \xrightarrow{k_{11}} H_2 + S_2$$

The k_{11}/k_{10} ratio is either equal to 0.15 (9) or even smaller (10, 11); thus 86% or more of the thiyl radicals are transformed into sulfur atoms. However, this theory can be accepted only with difficulty. First, a reaction (or several) can compete with reaction 10. If the thiyl radicals do not react with 2-butene and hydrogen sulfide, they should at least react with the other radicals. Since this does not seem to be the case, they must react with other species present or formed in the course of irradiation. In particular, thiyl radicals react very readily with conjugated di-olefins. This is well demonstrated by the fact that in the presence of very small amounts of 1,3-pentadiene, the methane yield in the 2-butene/hydrogen sulfide is not greatly affected. The reaction of H_2S or 1,3-butadiene with methyl radicals requires approximately the same activation energy (12, 13). Thus 1,3-pentadiene does not inhibit reaction 1 when the ratio H_2S/1,3-pentadiene is 4. But, on the other hand, the isomerization yield is practically reduced to zero. Other proofs that reaction 10 is not important in this system can be seen from ref. 8. In the photoisomerization of 2-butenes by sulfur atoms, the addition of 12.5% of hydrogen sulfide decreases the isomerization yield by a factor of 2.5, probably because of a reaction between sulfur atoms and hydrogen sulfide. In the present work, an increase of 2 to 15% in the concentration of hydrogen sulfide has no effect.

Alternatively the similarities between the present work and the one involving sulfur atoms (8) could only be accidental. The effect of oxygen leads to a radical mechanism in both systems. The photostationary ratio depends on thermodynamic considerations rather than on the radical involved, and the effect of 1,3-butadiene could be the result of a general reaction between different substituted thiyl radicals ($RS^\cdot$) and conjugated di-olefins.

In these conditions, the reaction mechanism of *cis–trans* isomerization of 2-olefins is a general one that takes place with diverse thiyl substituted radicals ($RS^\cdot$) (see Table 3). In fact, in similar systems, the photo-induced addition of mercaptan alkyls to simple olefins is well known (14*a*, *b*, *c*). It is the case with butyl mercaptan (14*b*), and the $C_4H_9S^\cdot$ radical seems to be the chain carrier although isomerization was not observed.

Termination Steps

Since no study has been undertaken on the effect of the intensity or of the volume of the reactor nothing can be said about the termination reaction(s) of the isomerization mechanism.

Can. J. Chem. Downloaded from www.nrcresearchpress.com by 210.87.254.105 on 09/05/12
For personal use only.

Can. J. Chem. Downloaded from www.nrcresearchpress.com by 210.87.254.105 on 09/05/12
For personal use only.

However, from the results (see Table 2) one can estimate that the thiyl radical is added to 1,3-pentadiene about 500 times faster than to 2-butenes. This is important, because at the present wavelength, 1,3-butadiene is an important product of the photolysis (15). Moreover, in the presence of hydrogen sulfide, the quantum yield of 1,3-butadiene decreases in an important way, which permits one to foresee a reaction that will make this product disappear. It is thus probable that in such a system, the following reaction is important,

[12] $$HS^{\cdot} + 1,3\text{-}C_4H_6 \rightarrow C_4H_6SH$$

and that the preponderant termination reaction occurs in a homogeneous phase. The C_4H_6SH radical is stabilized by resonance (16) and does not itself decompose, thus removing chain carriers from the system.

Concentration Effects

The addition of helium to the mixture of 2-butene:hydrogen sulfide has no major effect even for a total pressure of the order of 300 Torr. This is in accord with irradiations in the gas phase which are described in the literature under a total pressure of 1800 Torr (7). Even in the liquid phase (see results), the radiolysis of the mixture of 2-butene:hydrogen sulfide (100:3.3) leads to an isomerization which has a very high *G*-value, proving that the isomerization reaction is extremely rapid in the liquid phase. Nevertheless, the radiolysis in the liquid phase is a much more complex system than the photolysis in the gas phase at 147.0 nm. Ionic reactions (with positive or negative ions) not only exist, but also effects of energy concentration around trajectories of energetic particles will have important consequences. Consequently, radiolytic experiments should only be taken as an indication and not as an absolute demonstration. Other current studies will permit the elucidation of mechanisms in the liquid phase.

Quantum Yields

It is now interesting to consider the value of the quantum yield of the *cis–trans* isomerization. Table 1 gives apparent quantum yields between 5600 and 1100 depending on the time of irradiation (or percentage of conversion). This quantum yield decreases with the irradiation time, since the reverse reaction competes rapidly after the accumulation of the *trans*-isomer. For a very short irradiation time, the quantum yield is probably around $6–7 \times 10^3$ (Fig. 4). It is difficult to know the exact length of the chain since the yield of the chain initiator ($HS^{\cdot}$) is not exactly known. However, one can admit that the majority, if not all, of the primary radicals produced in the photolysis, form a thiyl radical (1). From the preceding results, the M/N ($HS^{\cdot}$) value is close to 2.0 ± 0.2. In the far u.v. photolysis, decomposition reactions of each excited neutral hydrocarbon molecule will produce a neutral molecule and two radicals. One hydrogen atom is assimilated to a radical since, as already seen, it is added to the double bond to give the corresponding radical (17–20). This leads to an apparent chain length close to 3500. Since this value is measured from the apparent *trans*-2-butene yield (reaction 9), it must be increased with the yield of the *cis*-2-butene (reaction 7). In admitting that the ratio of the rate of formation of *trans*-2-butene and of *cis*-2-butene is equal to the photostationary ratio, 2.84, the real length of the chain is of the order of 4700.

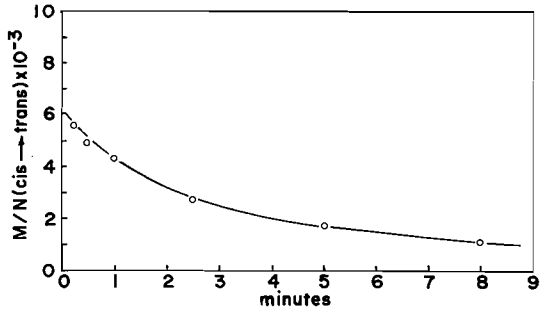

FIG. 4. Variation of M/N (*trans*-2-butene) values *vs.* irradiation time in the photoisomerization of *cis*-2-butene in the presence of hydrogen sulfide: *cis*-2-butene pressure = 1.32 Torr, hydrogen sulfide pressure = 0.09 Torr.

Kinetics and Thermochemistry

Considering only reactions 2 and 1 as initiation steps, reactions 7, −7, 8, −8, 9, and −9 as chain propagating steps and reaction 12 as the only termination step, and admitting that the concentration of the radicals R$^{\cdot}$ and of the *cis* and *trans* forms of the composite radical are constant with irradiation time, the ratio of initial rates of isomerization is (8)

$$\frac{R_{c \rightarrow t}}{R_{t \rightarrow c}} = \frac{k_7 k_8 k_9}{k_{-7} k_{-8} k_{-9}}$$

and this ratio is probably equal to the photo-

stationary state ratio. This does not indicate which is the rate determining step.

It is worthwhile to compare the present results to those obtained from NO_2, NO, and I catalyzed isomerization. With NO_2 the addition step is rate determining (21), and with NO and I (22), bond rotation is rate determining (21). The difference results from the thermochemistry of the addition reaction. With NO_2, the addition reaction is exothermic by 2.8 kcal mol^{-1}, while for NO and I, the addition step is endothermic by 19 and 5 kcal mol^{-1}, respectively. From thermochemical data, the heat of formation of s-C_4H_9S radical was estimated to be 12 ± 3 kcal mol^{-1}, (23), and reaction 7 is exothermic by 10.7 ± 3.0 kcal mol^{-1} and in the $HS^{\cdot}$ catalyzed isomerization, the addition step is probably rate determining.

The authors wish to acknowledge the National Research Council of Canada and l'Université du Québec à Chicoutimi for financial assistance, and le département de Chimie de l'Université Laval for the use of the cobalt bomb.

1. G. J. COLLIN, P. M. PERRIN, and C. M. GAUCHER. Can. J. Chem. In press.
2. J. L. FRANKLIN, J. G. DILLARD, H. M. ROSENSTOCK, J. T. HERRON, K. DRAXL, and F. H. FIELD. NSRDS-NBS, 26 (1969).
3. K. R. JENNINGS, and R. J. CVETANOVIĆ. J. Chem. Phys. **35**, 1233 (1961).
4. C. WALLING, and W. HELMREICH. J. Am. Chem. Soc. **81**, 1144 (1959).
5. F. T. BARR, and D. B. KEYES. Ind. Eng. Chem. **26**, 1111 (1935).
6. W. E. VAUGHAN and F. F. RUST. J. Org. Chem. **7**, 472 (1942).
7. K. SUGIMOTO, W. ANDO, and S. OAE. Bull. Chem. Soc. Jap. **37**, 365 (1964); K. SUGIMOTO and W. ANDO. Ann. Report Radiation Center Osaka Prefect, **4**, 96 (1963); K. SUGIMOTO, W. ANDO, and S. OAE. Bull. Chem. Soc. Jap. **38**, 224 (1965).
8. M. W. SCHMIDT and E. K. C. LEE. J. Chem. Phys. **51**, 2024 (1969).
9. A. R. KNIGHT and H. E. GUNNING. Can. J. Chem. **39**, 2466 (1961).
10. B. DE B. DARWENT, R. L. WALDINGER, and M. J. ALLARD. J. Phys. Chem. **71**, 2346 (1967).
11. G. R. WOOLEY and R. J. CVETANOVIĆ. J. Chem. Phys. **50**, 4697 (1969).
12. R. J. CVETANOVIĆ and R. S. IRWIN. J. Chem. Phys. **46**, 1694 (1967).
13. A. F. TROTMAN-DICKENSON and G. S. MILNE. NSRDS-NBSG, 50 (1967).
14. (*a*) C. SIVERTZ, W. ANDREWS, W. ELDSON, and K. GRAHAM. J. Polym. Sci. **19**, 587 (1956); (*b*) R. BACK, G. TRICK, C. MCDONALD, and C. SIVERTZ. Can. J. Chem. **32**, 1078 (1954): (*c*) C. SIVERTZ. J. Phys. Chem. **63**, 34 (1959).
15. G. J. COLLIN and P. M. PERRIN. Can. J. Chem. In press.
16. D. M. GRAHAM, R. L. MIEVILLE, and C. SIVERTZ. Can. J. Chem. **42**, 2239 (1964).
17. J. HERMAN, K. HERMAN, and P. AUSLOOS. J. Chem. Phys. **52**, 28 (1970).
18. H. OKABE and J. R. MCNESBY. J. Chem. Phys. **36**, 601 (1962).
19. E. TSCHWIKOW-ROUX. J. Phys. Chem. **71**, 2355 (1967).
20. G. J. COLLIN and P. AUSLOOS. Fifth Int. Conf. Photochem. New York, 1969.
21. J. L. SPRUNG, H. AKIMOTO, and J. N. PITTS, JR. J. Am. Chem. Soc. **93**, 4358 (1971).
22. S. W. BENSON, K. W. EGGER, and D. M. GOLDEN. J. Am. Chem. Soc. **87**, 468 (1965).
23. D. H. FINE and J. B. WESTMORE. Can. J. Chem. **48**, 395 (1970).

Can. J. Chem. Downloaded from www.nrcresearchpress.com by 210.87.254.105 on 09/05/12
For personal use only.

The Molecular and Crystal Structure of an Oxindole Alkaloid (6-Hydroxy-2′-(2-methylpropyl)-3,3′-spirotetrahydropyrrolidino-oxindole)

M. N. G. James and G. J. B. Williams

Department of Biochemistry, The University of Alberta, Edmonton 7, Alberta

Received January 21, 1972

A previously unknown alkaloid of molecular formula $C_{15}H_{20}O_2N_2$ was isolated from the dried root bark of *Eleagnus Commutata* (Wolf willow or Silverberry). An X-ray analysis was undertaken to complete the structural characterization of the molecule. Columnar crystals obtained from diethyl ether have the unit cell constants, $a = 13.1949(10)$ Å, $b = 9.4525(6)$ Å, $c = 12.1186(6)$ Å, $\beta = 109° 47(1)'$ and belong to space group $P2_1/c$. The structure was solved using an automated symbolic addition procedure and refined by block-diagonal least-squares to weighted and unweighted R factors of 6.25% and 4.30%, respectively. The previous structural studies were shown to be essentially correct except for the incorrect placement of the phenolic hydroxyl on C(5) of the oxindole nucleus. The correct molecular structure is implied by the systematic name given. The —OH group engages in two intermolecular hydrogen bonds with the two nitrogen atoms, but the carbonyl moiety is not involved in any such interactions.

Un alcaloide, inconnu jusqu'à présent, de formule générale $C_{15}H_{20}O_2N_2$, a été isolé à partir d'écorce de racines desséchées de *Eleagnus Commutata*. Une analyse aux rayons-X a été faite pour compléter la caractérisation structurale de la molécule. Les cristaux en forme de colonne, obtenus dans l'éther, possèdent les paramètres suivants pour la maille élémentaire: $a = 13.1949(10)$ Å, $b = 9.4525(6)$ Å, $c = 12.1186(6)$ Å, $\beta = 109° 47(1)'$ et appartiennent au groupe $P2_1/c$. La structure a été résolue par l'utilisation du procédé d'addition symbolique automatique et perfectionnée par la méthode de la diagonalisation de la matrice des moindres carrés appliqués aux facteurs R, pondérés ou non, respectivement de 6.25% et 4.30%. On a montré que les études des précédentes sur la structure sont essentiellement correctes sauf pour la position de l'hydroxyle phénolique sur le C(5) du noyau oxindole. La structure moléculaire correcte est comprise dans le nom systématique cité. Le groupe OH est engagé dans deux liaisons hydrogènes intermoléculaires avec les deux atomes d'azote mais le groupe carbonyle n'est pas impliqué dans de telles interactions.

Canadian Journal of Chemistry, **50**, 2407 (1972)

Introduction

A previously unknown alkaloid of molecular formula $C_{15}H_{20}O_2N_2$ was isolated from the dried root bark of *Eleagnus Commutata* (Wolf willow or Silverberry) by workers at this University (1) during their work on the phytochemistry of this species. Extensive work on the chemical and physical characterization of the compound resulted in the proposed structure shown in Fig. 1 (2). The major point of uncertainty of this structure was the location of the phenolic oxygen atom, although the bonding pattern of the spiran ring and its associated alkyl chain was in some doubt at the time this study was initiated.

Experimental

Columnar crystals of the alkaloid grown from diethyl ether which proved suitable for X-ray diffraction studies were supplied by Locock and Slywka. Preliminary rotation and Weissenberg photographs of a specimen measuring 0.3 × 0.2 × 0.13 mm and rotated about the needle axis revealed $2/m$ diffraction symmetry and the systematic zonal absences: $h0l$, $l = 2n + 1$; $0k0$, $k = 2n + 1$. The space

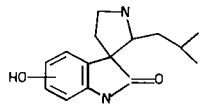

FIG. 1. The proposed molecular structure of the alkaloid.

group was thus uniquely determined as $P2_1/c$ and the c axis shown to be the direction of elongation of the crystals. The unit cell parameters, originally obtained from films, were refined during the initial alignment process on a Picker FACS-1 diffractometer and are $a = 13.1949(10)$ Å, $b = 9.4525(6)$ Å, $c = 12.1186(6)$ Å, $\beta = 109° 47(1)'$. The density calculated for 4 formula units of $C_{15}H_{20}N_2O_2$ (m.w. = 260.34) per unit cell of volume 1422.3 Å^3 is 1.216 g/cm^3. This estimate agrees with that obtained experimentally (1.220(2) g/cm^3) by flotation in a mixture of chlorobenzene and chloroform.

The reflection intensities were collected with Ni filtered CuK_α radiation ($\lambda = 1.54051$ Å) with the diffractometer in the coupled $\theta/2\theta$ scan mode. A total of 2397 unique and space group permissible reflections were collected, within the sphere defined by $2\theta \leqslant 130°$, of these 1915 (80%) had net intensities greater than 3σ and were thus considered observed. Normalized structure factors (E_{hkl}'s) were calculated, and the 221 E's greater than 1.7 were phased using a set of computer programs (3) which automatically select origin defining reflections and apply the symbolic addition

Can. J. Chem. Downloaded from www.nrcresearchpress.com by 210.87.254.40 on 09/05/12
For personal use only.

Can. J. Chem. Downloaded from www.nrcresearchpress.com by 210.87.254.40 on 09/05/12
For personal use only.

procedure as appropriate to centrosymmetric space groups (4). All non-hydrogen atoms of the molecule except the two methyl carbons were found in a map computed using these phased E's. The remaining two atoms were located in a subsequent electron density difference map and the structure refined using a block-diagonal least-squares procedure. The scattering factors used were derived from the analytical coefficients of Cromer and Mann (5), except for the hydrogen curve which was that of Mason and Robertson (6). The difference Fourier technique was used to find the hydrogen atoms. Block-diagonal least-squares refinement of the model assuming anisotropic vibration for the non-hydrogen atoms and allowing the hydrogens variable isotropic thermal parameters has resulted in final weighted and unweighted R factors $((\sum w||F_o| - |F_c||^2)^{\frac{1}{2}}/(\sum w|F_o|^2)^{\frac{1}{2}}$ and $(\sum||F_o| - |F_c||/\sum|F_o|))$, over the included data, of 6.25% and 4.30%, respectively. Observation weights were calculated according to the expression $\sqrt{w} = 2F_o/[T + (kI)^2 + B]^{\frac{1}{2}}$ (7) at the data reduction stage and were applied during the refinement. In the above equation T is the total peak count, I is the net peak count, B is the background, F_o is the derived structure amplitude, and k is a small constant (0.04 in this case) included to allow for minor instrumental errors. A tabulation of the observed structure amplitudes and the structure factors calculated from the final set of atomic parameters has been lodged with the Depository of Unpublished Data.[1]

TABLE 1. "Heavy" atom positional parameters ($\times 10^4$)*

Atom	x/a	y/b	z/c
N(1)	2090(1)	−64(2)	4144(1)
C(2)	1774(2)	1313(2)	3974(2)
C(3)	1593(1)	1705(2)	2699(2)
C(4)	1576(1)	−111(2)	1053(1)
C(5)	1775(2)	−1506(2)	826(1)
C(6)	2135(1)	−2481(2)	1738(2)
C(7)	2277(1)	−2091(2)	2889(2)
C(8)	2052(1)	−701(2)	3083(1)
C(9)	1717(1)	292(2)	2186(1)
O(2)	1671(1)	2100(1)	4724(1)
O(6)	2356(1)	−3820(1)	1469(1)
C(4′)	2437(1)	2826(2)	2642(2)
N(5′)	1999(1)	4193(2)	2847(1)
C(6′)	811(2)	4063(2)	2341(2)
C(7′)	529(2)	2503(2)	2134(2)
C(8′)	3583(2)	2577(2)	3444(2)
C(9′)	4430(2)	3539(3)	3244(2)
C(10)	4591(3)	3284(5)	2087(3)
C(11)	5494(2)	3360(4)	4249(3)

*Estimated standard deviations in parentheses.

Results and Discussion

The atomic parameters, and their associated estimated standard deviations, obtained from the final least-squares cycle are given in Tables 1, 2, and 3. Figure 2, which is a diagram of one molecule viewed parallel to the c axis, shows that the compound is a 6-hydroxy derivative of an oxindole nucleus, with a spiro linked secondary alkylamine moiety attached to C(3). Bond distances and interbond angles involving the non-hydrogen atoms are presented in Figs. 3 and 4. Table 4 is a listing of the molecular parameters involving the hydrogen atoms. The numbering scheme for the hydrogen atoms is derived from that used for the non-hydrogen atoms (refer to Fig. 3), *e.g.* H(81′) and H(82′) are bonded to C(8′) and H(6) is bonded to O(6). Interatomic correlations were not considered in the derivations of the estimated standard deviations in these molecular parameters. The bond distances involving those "terminal" atoms of importance were corrected for the effects of thermal motion according to the riding motion model (8) and are: C(2)—O(2) = 1.248(3) Å, C(6)—O(6) = 1.378(3) Å, C(9′)—C(10) = 1.537(4) Å, and C(9′)—C(11) = 1.582(5) Å.

The benzenoid section of the oxindole system is very closely planar with maximum exoplanar displacement of 0.01 Å from the plane with equation $-0.9603x - 0.2424y - 0.1378z + 1.7190 = 0$ (in this context the x, y, and z axes are parallel to the crystallographic a, b, and c^* axes, respectively, and the unit vectors are 1 Å in length). The phenoxy oxygen atom displacement is only −0.043(2) Å from this plane but the phenolic hydrogen is displaced +0.33(3) Å, thus permitting the O—H bond vector to point towards atom N(5′) of another molecule (see Fig. 5). The O—H ---N bond so formed is 2.659(2) Å long and the relevant inter bond angles are C(6)—O(6)—H(6) = 113.7(1.5)°, O(6)—H(6) ---N(5′) = 171.1 (2.4)°, H(6) ---N(5′)—C(4′) = 110.4(0.9)°, H(6) ---N(5′)—C(6′) = 103.9(0.9)°, and H(6) ---N(5′)—H(5′) = 120.4(1.7)°. The (uncorrected) distances involving the hydrogen atoms of this intermolecular bond are O(6)—H(6) = 0.971(25) Å and H(6) ---N(5′) = 1.695(25) Å.

The weighted average of the bond lengths within the benzenoid ring is 1.388 Å with an associated e.s.d. of 0.006 Å. The 0.006 Å discrepancy between this average bond length and the 1.394 Å found in highly accurate work (ref. 9, p. S21s) is not significant and indicates that

[1]Photocopies may be obtained upon request from the Depository of Unpublished Data, National Science Library, National Research Council of Canada, Ottawa, Canada K1A 0S2.

TABLE 2. Thermal parameters for the non-hydrogen atoms ($\times 10^4$)*

Atom	U_{11}	U_{22}	U_{33}	U_{12}	U_{23}	U_{13}
N(1)	322(5)	152(3)	159(3)	10(3)	4(3)	89(3)
C(2)	269(5)	162(4)	201(4)	−8(4)	−19(3)	93(4)
C(3)	214(5)	146(4)	187(4)	5(3)	−2(3)	65(3)
C(4)	238(5)	171(4)	165(4)	2(4)	20(3)	53(3)
C(5)	267(5)	184(4)	152(4)	−11(4)	−10(3)	69(4)
C(6)	226(5)	135(4)	193(4)	−9(3)	−14(3)	80(4)
C(7)	232(5)	142(4)	176(4)	−2(3)	13(3)	68(3)
C(8)	207(4)	148(4)	158(4)	−10(3)	−4(3)	59(3)
C(9)	199(4)	143(4)	174(4)	−3(3)	2(3)	54(3)
O(2)	467(5)	191(3)	230(4)	26(3)	−34(3)	163(4)
O(6)	395(5)	140(3)	220(3)	8(3)	−19(2)	147(3)
C(4′)	219(5)	141(4)	195(4)	3(3)	3(3)	63(4)
N(5′)	282(5)	146(4)	266(4)	11(3)	4(3)	103(4)
C(6′)	241(6)	184(5)	435(8)	37(4)	50(5)	107(5)
C(7′)	220(5)	185(5)	293(6)	24(4)	8(4)	66(4)
C(8′)	228(5)	228(5)	260(6)	3(4)	12(4)	53(4)
C(9′)	234(6)	316(7)	344(7)	−23(5)	−8(6)	86(5)
C(10)	394(9)	737(16)	405(10)	−118(10)	−17(10)	200(8)
C(11)	266(7)	592(12)	467(11)	−45(8)	−71(9)	42(6)

*Estimated standard deviations in parentheses.

TABLE 3. The hydrogen atom parameters ($\times 10^3$)*

Atom	x/a	y/b	z/c	U_{iso}
H(1)	223(2)	−52(2)	488(2)	65(5)
H(4)	136(2)	59(2)	43(2)	76(6)
H(5)	168(1)	−184(2)	4(2)	53(5)
H(6)	230(2)	−452(3)	202(2)	97(8)
H(7)	257(1)	−280(2)	356(2)	60(5)
H(4′)	238(1)	290(2)	179(2)	56(5)
H(5′)	224(2)	429(3)	373(2)	108(8)
H(61′)	53(2)	458(3)	168(2)	95(8)
H(62′)	45(2)	449(3)	290(2)	105(9)
H(71′)	30(2)	233(2)	131(2)	77(6)
H(72′)	0(2)	225(2)	244(2)	80(7)
H(81′)	357(2)	268(2)	430(2)	73(6)
H(82′)	386(2)	155(2)	335(2)	81(7)
H(9′)	417(2)	455(3)	325(2)	90(8)
H(101)	518(3)	397(4)	201(3)	137(13)
H(102)	476(2)	211(3)	214(3)	121(10)
H(103)	387(3)	337(3)	140(3)	149(11)
H(111)	532(3)	356(3)	503(3)	146(10)
H(112)	568(2)	213(3)	419(3)	132(9)
H(113)	606(3)	404(3)	412(3)	151(12)

*Estimated standard deviations in parentheses.

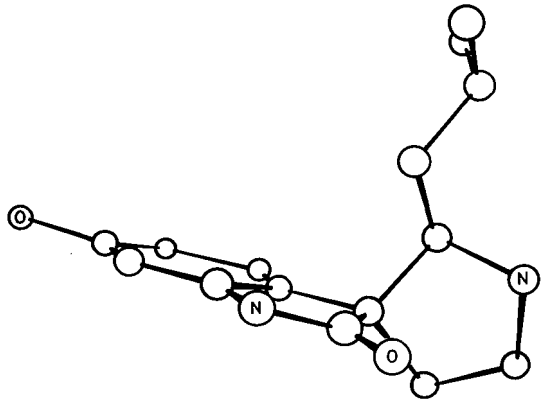

FIG. 2. A perspective view of one molecule as seen parallel to the c axis.

the effects of "rigid body libration" (10) on this molecule in the solid state are small.

The five membered ring of the oxindole nucleus is not planar, the "spiro" atom, C(3), deviates by −0.114(2) Å from the best four-atom least-squares plane which is defined by the four other atoms C(2), N(1), C(8), C(9). This plane has equation $-0.9465x - 0.2723y - 0.1731z + 1.7989 = 0$ and is very nearly parallel to the plane of the benzenoid ring (dihedral angle = 2.8°). None of the four atoms which define the oxindole plane is displaced more than 0.005 Å from it. Interpretation of the geometric details of this ring is complicated by the presence of the delocalized π electrons of the benzenoid system. The —C—NH—CO—C grouping here resembles a *cis* peptide bond and exhibits some of the features associated with this structural unit. All of these 6 atoms are within 0.04 Å from the 5 atom least-squares plane, defined by the non-hydrogen members of this group, with equation $-0.9371x - 0.2572y - 0.2358z +$

Can. J. Chem. Downloaded from www.nrcresearchpress.com by 210.87.254.40 on 09/05/12
For personal use only.

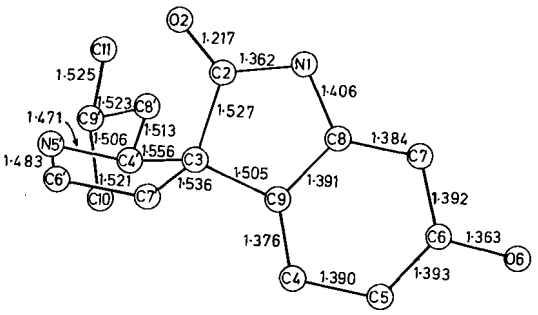

FIG. 3. The intramolecular bond distances in Å. The estimated standard deviations average 0.003 Å overall except for those involving the methyl carbons which are 0.005 Å each. These distances are uncorrected for the effects of thermal motion. Corrected values for the bonds to the four "terminal" atoms may be found in the text.

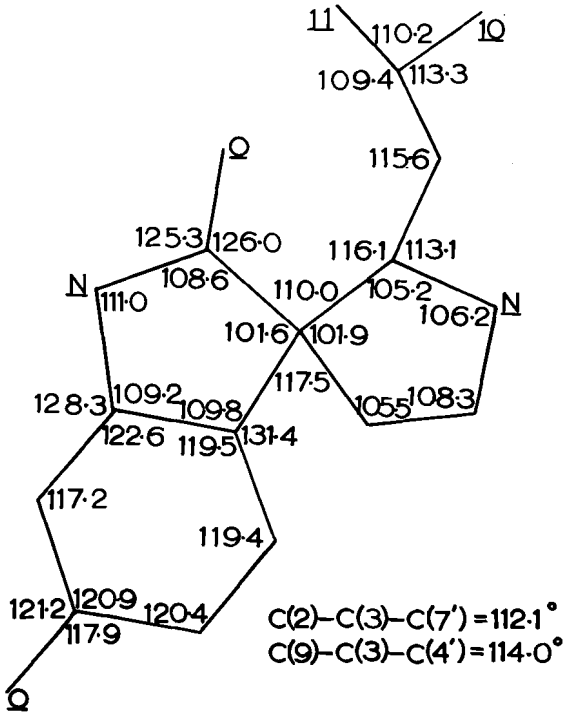

FIG. 4. The interbond angles in deg. The e.s.d.'s average 0.2°.

2.0524 = 0. That the delocalized π electron system of the benzenoid ring extends over the atoms N(1), C(2), and O(2) is indicated by this planarity and also by the lengthening of the C(2)—O(2) bond and the shortening of the N(1)—C(2) linkage. Simple aldehydes and ketones are found to exhibit C=O bond lengths of 1.215(5) Å (ref. 9, p. S21s) the C—N distances for simple tervalent nitrogen compounds are encompassed by 1.472(5) Å (ref. 9, p. S19s). Bond angle distortions forced upon this system by virtue of its cyclic nature probably preclude the most favorable overlap of atomic orbital hybrids and hence the shortening of the OC—N bond here is not as extreme as in more normal peptide bonds where this length is found to be 1.325 Å (11). The nitrogen atom N(1) is engaged in forming the second intermolecular

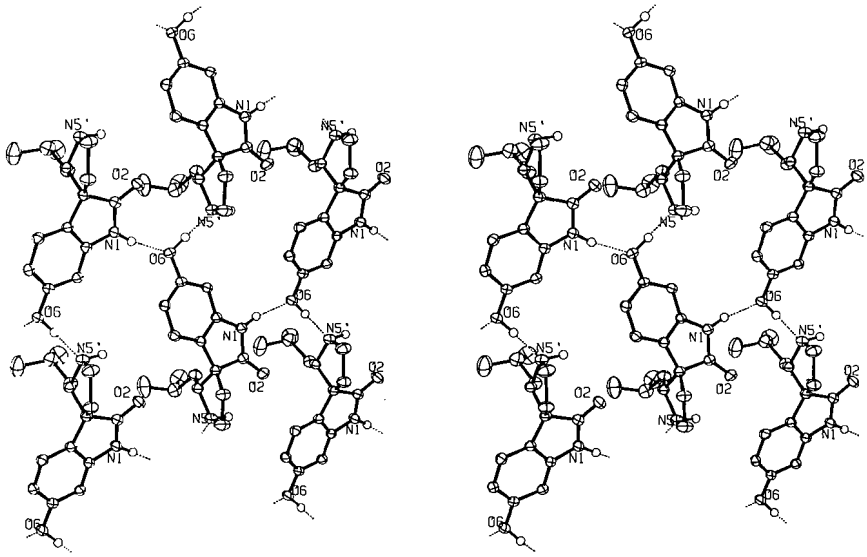

FIG. 5. A stereoscopic pair of several molecules viewed parallel to a^*. Thermal ellipsoids were scaled to include 30% probability. This is a computer drawn diagram using the program ORTEP (13).

Can. J. Chem. Downloaded from www.nrcresearchpress.com by 210.87.254.40 on 09/05/12
For personal use only.

Can. J. Chem. Downloaded from www.nrcresearchpress.com by 210.87.254.40 on 09/05/12
For personal use only.

TABLE 4.
(*a*) The bond distance involving the hydrogen atoms of one molecule

Bond	Distance (Å)	Bond	Distance (Å)
N(1)—H(1)	0.96(2)	C(7′)—H(72′)	0.94(2)
C(4)—H(4)	0.98(2)	C(8′)—H(81′)	1.04(2)
C(5)—H(5)	0.98(2)	C(8′)—H(82′)	1.05(2)
O(6)—H(6)	0.97(3)	C(9′)—H(9′)	1.02(3)
C(7)—H(7)	1.03(2)	C(10)—H(101)	1.04(4)
C(4′)—H(4′)	1.00(2)	C(10)—H(102)	1.13(3)
N(5′)—H(5′)	1.02(2)	C(10)—H(103)	1.03(4)
C(6′)—H(61′)	0.91(2)	C(11)—H(111)	1.07(4)
C(6′)—H(62′)	1.04(3)	C(11)—H(112)	1.20(4)
C(7′)—H(71′)	0.96(2)	C(11)—H(113)	1.03(3)

(*b*) The interbond angles involving the hydrogen atoms of one molecule

Bonds	Angle (deg)	Bonds	Angle (deg)
H(1)—N(1)—C(2)	123(1)	H(72′)—C(7′)—C(3)	114(2)
H(1)—N(1)—C(8)	126(1)	H(72′)—C(7′)—C(6′)	111(2)
H(4)—C(4)—C(5)	121(1)	H(81′)—C(8′)—C(4′)	106(1)
H(4)—C(4)—C(9)	120(1)	H(81′)—C(8′)—C(9′)	111(1)
H(5)—C(5)—C(4)	123(1)	H(81′)—C(8′)—H(82′)	109(2)
H(5)—C(5)—C(6)	117(1)	H(82′)—C(8′)—C(4′)	112(1)
H(6)—O(6)—C(6)	114(2)	H(82′)—C(8′)—C(9′)	103(1)
H(7)—C(7)—C(6)	120(1)	H(9′)—C(9′)—C(8′)	107(1)
H(7)—C(7)—C(8)	123(1)	H(9′)—C(9′)—C(10)	108(1)
H(4′)—C(4′)—C(3)	107(1)	H(9′)—C(9′)—C(11)	109(1)
H(4′)—C(4′)—N(5′)	102(1)	H(101)—C(10)—C(9′)	109(2)
H(4′)—C(4′)—C(8′)	112(1)	H(101)—C(10)—H(102)	119(3)
H(5′)—N(5′)—C(4′)	105(1)	H(101)—C(10)—H(103)	113(3)
H(5′)—N(5′)—C(6′)	111(1)	H(102)—C(10)—C(9′)	101(2)
H(61′)—C(6′)—N(5′)	113(2)	H(102)—C(10)—H(103)	103(3)
H(61′)—C(6′)—C(7′)	112(2)	H(103)—C(10)—C(9′)	111(2)
H(61′)—C(6′)—H(62′)	103(2)	H(111)—C(11)—C(9′)	106(2)
H(62′)—C(6′)—N(5′)	111(2)	H(111)—C(11)—H(112)	110(2)
H(62′)—C(6′)—C(7′)	110(2)	H(111)—C(11)—H(113)	114(3)
H(71′)—C(7′)—C(3)	107(1)	H(112)—C(11)—C(9′)	102(2)
H(71′)—C(7′)—C(6′)	108(1)	H(112)—C(11)—H(113)	115(2)
H(71′)—C(7′)—H(72′)	111(2)	H(113)—C(11)—C(9′)	109(2)

hydrogen bond of this structure to oxygen O(6). This bond is significantly bent, N(1)—H(1)---O(6) = 168.0(1.8)°, and the distance between the donor and acceptor atoms is 2.916(2) Å.

The 1.505 Å bonding distance between atoms C(3) and C(9) appears abnormally short for a C—C single bond length; however, a comparison with documented values (ref. 9, p. S15s) shows that this value is exactly that expected for tetracoordinated carbon bonded to a benzenoid system.

The best 4 atom plane of the saturated spiran ring is that defined by the atoms N(5′), C(6′), C(7′), C(3) and has equation $0.4359x - 0.0076y - 0.9000z + 2.3292 = 0$. The distances of the 5 ring atoms from this plane are: −0.020, 0.527, 0.017, −0.055, and 0.043 Å for C(3), C(4′), N(5′), C(6′), and C(7′), respectively. These distances and the χ^2 value ($\chi^2 = \sum p_i^2/\sigma_{(p_i)}^2$ where p_i is the distance of atom i from the plane and $\sigma_{(p_i)}$ is the e.s.d. in that distance) of 1007.8 imply that this plane has notional existence only and therefore should not be interpreted as an important structural feature.

A more precise description of the conformation of this ring may be given in terms of the relevant torsion angles. If A—B—C—D is a set of atoms connected as shown then the torsion angle about the B—C bond is defined as the dihedral angle between the planes defined by the positions of the atoms A—B—C and B—C—D. A positive angle is one that requires a clockwise

rotation of atom A to achieve superposition of the A—B and C—D bond vectors when viewed in the direction B → C. These angles are: C(7′)—C(3)—C(4′)—N(5′) = −36.2°, C(3)—C(4′)—N(5′)—C(6′) = +32.3°, C(4′)—N(5′)—C(6′)—C(7′) = −15.5°, N(5′)—C(6′)—C(7′)—C(3) = −7.7°, C(6′)—C(7′)—C(3)—C(4′) = +26.1°. An alternative description of this five membered ring, and one that has been proposed for furanose ring forms (12), is in terms of atomic displacements from the plane through those three atoms which are common to both the best and the second best four-atom least-squares plane. In this case these atoms are N(5′), C(6′), and C(7′) and the plane has equation $0.3842x + 0.0724y - 0.9204z + 2.1370 = 0$ and the displacements of C(3) and C(4′) are −0.197 and +0.376 Å, respectively. These two atoms are on opposite sides of the reference plane and so the ring has the "twist" (T) conformation.

The molecular packing is shown in the stereoscopic Fig. 5 which is a projection onto (100). This diagram shows that the molecules form infinite layers with the hydrogen bond network shown being the principal intralayer bonding interactions. Interlayer bonding is the result of nonspecific, nondirectional van der Waals dispersion forces between the isobutyl side chains.

The technique of proton magnetic resonance (p.m.r.) has been developed to the point where it is usually possible to distinguish isomers from one another. The distinction in this case involved deciding whether the phenolic hydroxyl was on C(5) or C(6). A tentative decision in favor of a 5-hydroxy was reached after consideration of the p.m.r. coupling constants between the three benzenoid protons (2). A detailed appraisal of this analysis is out of place here; however, it may be pointed out that the p.m.r. peak assignment, which rests on the supposed shielding and deshielding properties of the phenolic oxygen and the oxindole nitrogen, may be influenced by the possibility of intermolecular hydrogen bonding. Atom N(1) is a donor in its hydrogen bond to O(6) and O(6) is in turn the donor in the intermolecular bond to N(5′). Electronic effects due to this may be lessened in the p.m.r. sample because of the high dielectric constant of the solvent (deuterated DMSO), but this possibility nevertheless exists and its implications may be important.

We thank Drs. Locock and Slywka for the crystalline sample of the alkaloid. Financial support from the Medical Research Council of Canada (grant #MA-3406) is gratefully acknowledged. The set of crystallographic computer programs of F. R. Ahmed *et al.* of N.R.C.C. Ottawa were used throughout this analysis. Miss C. M. Smith and Mr. D. J. Steenkamp were involved in the early stages of this work and we thank them for their help.

1. R. A. Locock and G. W. Slywka. Unpublished results.
2. G. W. Slywka. Doctoral Dissertation, The University of Alberta, Edmonton, Alberta. 1969.
3. F. R. Ahmed and S. R. Hall. Program NRC4 from A set of crystallographic computing programs for the IBM/360. NRCC, Ottawa, 1968.
4. J. Karle, and I. L. Karle. Acta Cryst. **21**, 849 (1966).
5. D. T. Cromer and J. B. Mann. Acta Cryst. A**24**, 321 (1968).
6. R. Mason and G. B. Robertson. Advances in structure research by diffraction methods. Vol. 2. *Edited by* R. Brill and R. Mason. Interscience, New York. 1966. p. 57.
7. S. W. Peterson and H. A. Levy. Acta Cryst. **10**, 70 (1957).
8. W. R. Busing and H. A. Levy. Acta Cryst. **17**, 142 (1964).
9. L. E. Sutton. (*Editor*). Tables of interatomic distances and configuration in molecules and ions. Special Publication No. 18. The Chemical Society London. 1965.
10. D. W. J. Cruickshank. Acta Cryst. **9**, 757 (1956).
11. R. E. Dickerson and I. Geis. The structure and action of proteins. Harper and Row, New York. 1969. p. 12.
12. M. Sundaralingam, S. T. Rao, and J. Abola. Science, **172**, 725 (1971).
13. C. K. Johnson. ORTEP, Report ORNL-3794, Oak Ridge National Laboratory, Oak Ridge, Tennessee. 1965.

Can. J. Chem. Downloaded from www.nrcresearchpress.com by 210.87.254.40 on 09/05/12
For personal use only.

La photo-oxydation du Hg(I) par le Ce (IV) en solution aqueuse d'acide perchlorique

A. NUYT ET M. ZADOR

Département de chimie, Université de Montréal, c.p. 6128, Montréal 101, Québec

Reçu le 21 février 1972

La photo-oxydation du Hg(I) par le Ce(IV) a été étudiée à 366 mμ dans des solutions aqueuses d'acide perchlorique. Le rendement quantique varie avec les concentrations en Hg(I) et en Ce(III) et cette variation est différente lorsque l'absorption est faible ou forte. De plus le rendement quantique augmente sensiblement avec l'acidité du milieu. Il est proposé, que ceci est dû au fait que le Ce^{4+} est l'espèce impliquée dans le processus photochimique primaire.

The photo-oxidation of Hg(I) by Ce(IV) has been studied at 366 mμ in aqueous perchloric acid solutions. The quantum yield depends on the concentrations of both Hg(I) and Ce(III). This dependence is different at high and low absorptions. There is a marked increase of the quantum yield with the acid concentration. It is proposed therefore that Ce^{4+} is the species involved in the primary photochemical process.

Canadian Journal of Chemistry, **50**, 2413 (1972)

Can. J. Chem. Downloaded from www.nrcresearchpress.com by 210.87.254.5 on 09/05/12
For personal use only.

Introduction

La photo-réduction du Ce(IV) a été étudiée par plusieurs auteurs, aussi bien en solution aqueuse d'acides qu'en présence de divers ions ou molécules (1–6). La première étude quantitative est due à Weiss et Porret (1) qui ont proposé la formation d'un radical OH comme intermédiaire:

[1] $$Ce(IV) + H_2O \xrightarrow{h\nu} Ce(III) + H^+ + OH$$

La formation d'oxygène lors de la photo-réduction de l'eau est expliquée en faisant intervenir ce radical. De plus, la diminution du rendement quantique de la réaction avec l'augmentation de la concentration en Ce(III) s'explique bien à l'aide de l'éq. 2.

[2] $$Ce(III) + OH \longrightarrow Ce(IV) + OH^-$$

Finalement l'oxydation de divers substrats (5, 6) et la formation de radicaux NO_3 et HSO_4 lors de la photolyse éclaire (7), seraient dues aux réactions du radical OH avec les solutés. Ce radical est également proposé comme intermédiaire lors de la radiolyse des solutions du Ce(IV) (8). Récemment la formation directe des radicaux NO_3 à partir d'un complexe Ce(IV)—NO_3 a pu être démontrée à haute concentration en nitrate (9). Toutefois, ce mécanisme ne semble être probable que lorsqu'il y a formation appréciable de complexe avec l'ion cérique, ce qui n'est évidemment pas le cas avec les ions métalliques.

Il est bien établi que le Ce(IV) est hydrolysé partiellement en solution aqueuse (10, 11). La question la moins éclaircie dans la photo-réduction concerne justement l'espèce du Ce(IV) impliquée dans l'acte photo-chimique primaire. Dans diverses publications on trouve Ce^{4+}, sans qu'il soit prouvé que ce soit effectivement la forme réactionnelle (1, 3–6) d'autres proposent un dimère, $CeOCe^{6+}$ (2) ou une forme hydrolysée (ou paire d'ion, $Ce^{4+}\cdot OH^-$ (12), comme responsable de l'éq. 1. On trouve aussi Ce(IV), sans autres indications (7).

L'effet de la paroi a été mis en évidence, ce qui implique qu'une des étapes au moins est hétérogène (3).

L'oxydation thermique du Hg(I) par le Ce(IV) a déjà été étudiée (13), et la réaction est très lente à température ambiante.

Dans ce travail nous nous sommes intéressés à chercher si le Hg(I) pouvait être oxydé par le Ce(IV) par voie photochimique, caractériser cette réaction et, par la suite, d'élucider la nature de l'espèce du Ce(IV) impliquée dans le processus primaire. Nous avons choisi de travailler à une longueur d'onde de 366 mμ pour éviter l'effet de filtre interne des réactifs et produits autres que le Ce(IV) ce qui serait très important à des longueurs d'onde plus courtes utilisées dans d'autres études sur le Ce(IV). On évite aussi la photo-oxydation du Ce(III) en Ce(IV) (14).

Partie expérimentale

Réactifs

Tous les réactifs sont de pureté analytique ou ont été préparés à partir de réactifs de cette qualité. Toutes les

TABLEAU 1. Influence de la concentration en Ce(III) et en Hg(I) sur le rendement quantique à absorption faible*

[Hg(I)] (mol l^{-1})	[Ce(III)] (mol l^{-1})	$\Phi_{Ce(IV)}$	$1/\Phi_{Ce(IV)}$	$\frac{[Ce(III)]}{[Hg(I)]}$
1×10^{-3}	8×10^{-2}	0.061	15.7	80
3×10^{-3}	8×10^{-2}	0.102	9.6	26.6
6×10^{-3}	8×10^{-2}	0.133	7.5	3.3
1×10^{-2}	8×10^{-2}	0.164	6.1	8
5×10^{-2}	8×10^{-2}	0.174	5.7	1.6
1×10^{-1}	8×10^{-2}	0.198	5.0	0.8
1×10^{-2}	0.6×10^{-3}	0.212	4.7	0.06
1×10^{-3}	0.6×10^{-3}	0.187	5.3	0.6
1×10^{-2}	0.6×10^{-3}	0.207†	4.8	0.06

*Distance lampe–cellule = 8.7 cm; temps d'irradiation 1 à 6 min; $T = 25 \pm 1$ °C; $[Ce(IV)] = 2\times10^{-3}$ *M*; $[HClO_4] = 0.5$ *M*; force ionique = 2 *M*.
†Force ionique = 0.5 *M*.

solutions ont été préparées avec de l'eau distillée. Le Ce(IV) a été fourni en solution de concentration 0.5 *M* dans l'acide perchlorique 5 *M* par la compagnie G. F. Smith, Ohio, U.S.A. Cette solution contient également une certaine quantité de Ce(III), qui a été déterminée. La solution du Ce(III) a été préparée à partir de perchlorate cereux hydraté et la solution de perchlorate mercureux a été préparée à partir de HgO et Hg en milieu acide perchlorique (15). La solution stock de perchlorate mercureux est maintenue en présence d'un excès de mercure. La solution de $NaClO_4$ a été préparée par neutralisation de $HClO_4$ concentré par la quantité appropriée de NaOH pour éviter les impuretés chlorure présentes dans les sels commerciaux.

Dosages

Les dosages du Ce(IV) et du Ce(III) ont été faits par iodométrie et par gravimétrie (16). Le dosage du $HClO_4$ a été effectué à l'aide d'une solution de NaOH de concentration connue, après précipitation de tout le cérium sous forme d'oxalate cereux. Le dosage de Hg(I) a été effectué suivant une méthode donnée par la littérature (15), par gravimétrie et par spectrophotométrie à 236.5 mμ (17).

En cours de réaction, les dosages ont été effectués par spectrophotométrie du Ce(IV) à 370 mμ en milieu $HClO_4$ 1 *M*. Pour déterminer les rendements quantiques, nous avons mesuré l'intensité lumineuse reçue par la cellule par actinométrie (18). L'actinomètre utilisée est le ferrioxalate de potassium.

Appareillage

Nous avons utilisé une lampe Hanovia medium Pressure Mercury-Vapor 673 A10, ayant une raie intense à 366 mμ, qui a été utilisée pour l'irradiation. Les autres raies ont été éliminées grâces aux filtres Hanovia 6544-001 et 6540-001. Les intensités absorbées étaient de l'ordre de 10^{-5} einstein l^{-1} s^{-1}. Les différents éléments ainsi que la cellule de réaction sont placés sur un banc optique. La cellule est cylindrique avec des parois en quartz optiquement parallèles. Elle est refroidie par circulation forcée d'air. La longueur du chemin optique est de 1 cm.

Procédure

Pour chaque réaction, nous avons préparé 100 ml de mélange réactionnel en prélevant un certain volume des solutions stocks. La force ionique a été maintenue à 2 *M* par du $NaClO_4$. De ce mélange, 20 ml sont placés dans la cellule en quartz et on y fait barboter de l'azote pendant 20 min. Des essais en absence de Ce(IV) ont montré qu'il y a photo-oxydation du Hg(I) en présence d'oxygène. Après un temps d'irradiation donné, on effectue l'analyse. Pour la réaction thermique, une correction est chaque fois effectuée.

Résultats et discussion

La réaction globale est la suivante:

$$[3] \qquad Ce(IV) + Hg(I) \xrightarrow{h\nu} Ce(III) + Hg(II)$$

La stoechiométrie de la réaction est de 1:1, et ceci quelles que soient les conditions expérimentales. Si l'on poursuit la photo-réduction du Ce(IV) après l'oxydation de la totalité du Hg(I), la réaction devient beaucoup plus lente, ce qui implique aussi que la contribution de la photo-oxydation de l'eau par le Ce(IV) est négligeable.

Influence du Hg(I) et du Ce(III)

L'influence de ces ions a été étudiée dans deux conditions expérimentales différentes, soit à absorption faible et à absorption totale.

Absorption faible

A des concentrations en Ce(IV) de l'ordre de 2×10^{-3} *M*, l'absorption, et la réaction, ont lieu dans toute l'épaisseur de la cellule. En effet, à cette concentration la densité optique à 366 mμ est de 0.7. Les rendements quantiques calculés en tenant compte de la fraction de la lumière absorbée par la solution, par la loi de Beer, sont donnés au tableau 1. Ces résultats montrent que le rendement quantique diminue

Can. J. Chem. Downloaded from www.nrcresearchpress.com by 210.87.254.5 on 09/05/12
For personal use only.

TABLEAU 2. Influence de la concentration en Ce(III) et en Hg(I) sur le rendement à absorption forte*

[Hg(I)] (mol l^{-1})	[Ce(III)] (mol l^{-1})	$\Phi_{Ce(IV)}$	$1/\Phi_{Ce(IV)}$	$\frac{[Ce(III)]}{[Hg(I)]}$
1×10^{-2}	0.35×10^{-2}	0.124	8.05	0.35
2×10^{-2}	0.35×10^{-2}	0.127	7.9	0.175
4×10^{-2}	0.35×10^{-2}	0.124	8.05	0.085
8×10^{-2}	0.35×10^{-2}	0.124	8.05	0.042
16×10^{-2}	0.35×10^{-2}	0.122	8.2	0.021
1×10^{-2}	1×10^{-2}	0.117	8.55	1.0
1×10^{-2}	2×10^{-2}	0.108	9.26	2.0
1×10^{-2}	4×10^{-2}	0.099	10.1	4.0
1×10^{-2}	6×10^{-2}	0.092	10.9	6.0
1×10^{-2}	8×10^{-2}	0.082	12.0	8.0
1×10^{-2}	12×10^{-2}	0.077	13.0	12.0
8×10^{-2}	8×10^{-2}	0.092	10.9	1.0
12×10^{-2}	8×10^{-2}	0.077	13.0	0.66
0.5×10^{-2}	8×10^{-2}	0.077	13.0	16.0
0.25×10^{-2}	8×10^{-2}	0.077	13.0	32.0

*Distance lampe–cellule = 8.7 cm; temps d'irradiation = 20 min; $T = 25 \pm 1$ °C; [Ce(IV)] = 2×10^{-2} M; [$HClO_4$] = 0.5 M; force ionique = 2 M.

avec l'augmentation du rapport Ce(III)/Hg(I), comme c'était le cas dans l'étude de photo-oxydation du Tl(I) et de l'acide formique (6, 7). Le mécanisme, proposé par Sworski, permet d'expliquer les résultats

[4] $Ce(IV)\cdot H_2O \xrightarrow{h\nu} Ce(IV)\cdot H_2O^*$

[5] $Ce(IV)\cdot H_2O^* \longrightarrow Ce(III) + H^+ + OH$

[6] $OH + Ce(III) \xrightarrow{k_1} Ce(IV) + OH^-$

[7] $OH + Hg(I) \xrightarrow{k_2} Hg(II) + OH^-$

L'expression pour le rendement quantique est obtenue en exprimant l'état stationnaire pour le radical OH:

$$[8] \qquad \Phi_{Ce(IV)} = \frac{\Phi_{OH}\cdot k_2[Hg(I)]}{k_2[Hg(I)] + k_1[Ce(III)]}$$

L'inverse de cette expression donne

$$[9] \qquad \frac{1}{\Phi_{Ce(IV)}} = \frac{1}{\Phi_{OH}} + \frac{1}{\Phi_{OH}}\cdot\frac{k_1}{k_2}\frac{[Ce(III)]}{[Hg(I)]}$$

La fig. 1 permet de voir que cette expression est vérifiée dans une grande gamme de concentrations et on obtient pour le rapport k_2/k_1 la valeur de 26. Cette valeur est comparable au rapport des constantes d'étapes analogues dans le cas du Tl(I) dans l'acide sulfurique (5), pour lequel on a rapporté la valeur de 42. La valeur de Φ_{OH} est de 0.19, semblable à celui observé dans d'autres systèmes (4–6).

Absorption totale

A forte concentration en Ce(IV), l'absorption est localisée dans une couche mince près de la paroi de la cellule. Dans ces conditions, les rendements quantiques ne dépendent plus de la concentration en Hg(I) (tableau 2), même à

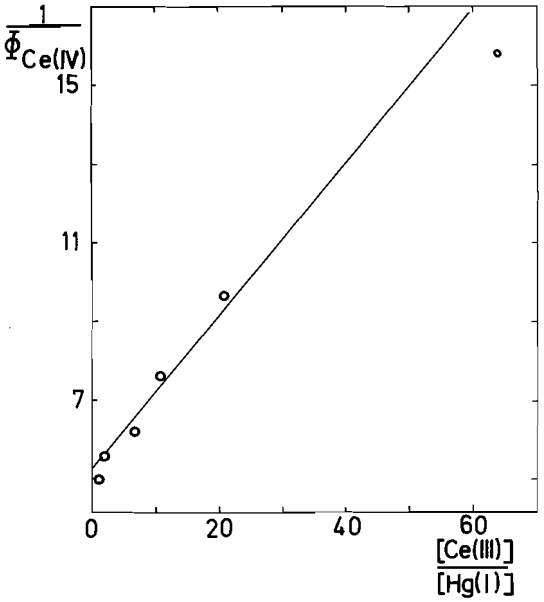

FIG. 1. Graphique de $1/\Phi_{Ce(IV)}$ en fonction du rapport [Ce(III)]/[Hg(I)]. Distance lampe–cellule = 8.7 cm; temps d'irradiation 1 à 6 min; $T = 25 \pm 1$ °C, [Ce(IV)] = 2×10^{-3} M, [$HClO_4$] = 0.5 M; force ionique = 2 M.

Can. J. Chem. Downloaded from www.nrcresearchpress.com by 210.87.254.5 on 09/05/12
For personal use only.

grand excès de ce réactif, ce qui exclut la possibilité d'un appauvrissement local.

Le rendement quantique diminue toutefois avec l'augmentation de la concentration en Ce(III) et on peut obtenir une relation linéaire entre $1/\Phi$ et [Ce(III)].

Ces résultats impliquent qu'il n'y a plus de compétition entre le Hg(I) et le Ce(III) pour l'intermédiaire actif formé dans l'étape primaire (le radical OH).

De plus, le rendement quantique varie de 0.2 à 0.07 avec l'augmentation de la concentration du Ce(IV) de 5×10^{-4} à 5×10^{-2}. Dans la photo-oxydation de l'eau, à forte absorption, l'influence favorable de la paroi a été bien montrée (3).

Une explication plausible dans notre cas serait l'intervention de la paroi comme piège à radicaux, qui serait en compétition pour ceux-ci avec le Ce(III).

[10] $\quad OH + \text{paroi} \rightarrow OH \text{ ads.}$

Toutefois, l'influence de la haute intensité locale est extrêmement difficile à étudier et les conclusions restent fragiles.

Il est à noter que le changement de mécanisme n'influence pas la stoechiométrie qui reste 1:1, ce qui implique que le Hg(I) est finalement oxydé en Hg(II) et que la photo-oxydation de l'eau reste négligeable.

Nous avons voulu vérifier si le même phénomène avait lieu dans le cas de la photo-oxydation du Tl(I), pour lequel on a rapporté, en milieu acide sulfurique, un mécanisme de compétition. A une concentration de 0.02 *M* en Ce(IV) une variation d'un facteur de dix en Tl(I) ne change pas le rendement quantique.

Etant donné que ce mécanisme intervient partiellement à absorption plus faible, la valeur $k_2/k_1 = 26$ doit être considérée comme une valeur limite, la vraie valeur devrait être légèrement supérieure.

Influence de l'acidité

L'influence de l'acidité a été étudiée à basses concentrations en Ce(III) où la réaction 2 peut être négligée.

La nature des espèces en solution aqueuse, ainsi que leur concentration dépend de l'acidité d'après les équations:

[11] $\quad Ce^{4+} + H_2O \underset{}{\overset{K_1}{\rightleftharpoons}} CeOH^{3+} + H^+$

[12] $\quad 2CeOH^{3+} \overset{K_2}{\rightleftharpoons} CeOCe^{6+} + H_2O$

TABLEAU 3. Influence de la concentration en acide perchlorique sur le rendement quantique*

$HClO_4$ (mol l^{-1})	$\frac{1}{[H^+]}$	$\Phi_{Ce(IV)}$	$1/\Phi_{Ce(IV)}$
0.08	12.5	0.042	23.5
0.10	10.0	0.051	19.8
0.125	8.0	0.056	17.7
0.15	6.8	0.073	13.6
0.24	4.2	0.092	10.9
0.50	2.0	0.120	8.3
0.50	2.0	0.121	8.2
0.75	1.33	0.130	7.7
1.00	1.0	0.147	6.8
1.25	0.8	0.138	7.3
1.50	0.68	0.164	6.1
1.50	0.68	0.149	6.7
1.75	0.57	0.157	6.4
2.00	0.5	0.157	6.4
2.00	0.5	0.149	6.7

*Distance lampe–cellule = 8.7 cm; temps d'irradiation = 20 min; $T = 25 \pm 1$ °C; $[Ce(IV)] = 2 \times 10^{-2}$ *M*; $[Ce(III)] = 6 \times 3510^{-3}$ *M*; $[Hg(I)] = 1 \times 10^{-2}$ *M*; force ionique = 2 *M*.

Il est donc évident que l'influence de l'acidité devrait permettre de décider quelle forme du Ce(IV) est impliquée dans l'acte primaire.

L'étude a été effectuée en absorption totale de lumière et en maintenant les concentrations du Ce(IV), du Hg(I) et du Ce(III) constantes.

Les résultats du tableau 3 montrent que le rendement quantique augmente avec l'augmentation de la concentration en acide perchlorique. Ceci est attribué à l'augmentation de la concentration du Ce^{4+} par le déplacement des éqs. 11 et 12 vers la gauche.

L'énergie absorbée sert à l'excitation d'un électron de la liaison de transfert de charge Ce^{4+}—OH_2 (avec une des molécules d'eau de coordination), [4]. Par après il y a rupture de cette liaison, formation d'un radical OH et de H^+, ainsi que réduction du Ce^{4+} (éq. 5).

Ces résultats sont incompatibles avec les hypothèses voulant que $CeOH^{3+}$ ou $CeOCe^{6+}$ soient responsables de l'acte primaire. La concentration de ces deux espèces diminue quand l'acidité augmente.

Etant donné qu'à la longueur d'onde utilisée les autres réactifs et produits ne contribuent pas à l'absorption de la lumière, on peut exprimer la fraction de lumière absorbée par le Ce^{4+} en tenant compte des éqs. 11 et 12 et des coefficients d'absorption des diverses espèces. Le rendement quantique expérimental, $\Phi_{Ce(IV)}$, est alors donné par l'éq. 13:

Can. J. Chem. Downloaded from www.nrcresearchpress.com by 210.87.254.5 on 09/05/12
For personal use only.

$$[13] \qquad \Phi_{Ce(IV)} = \Phi_{Ce^{4+}} \frac{\varepsilon_{Ce^{4+}}[Ce^{4+}]}{\varepsilon_{Ce^{4+}}[Ce^{4+}] + \varepsilon_{CeOH^{3+}}[CeOH^{3+}] + \varepsilon_{CeOCe^{6+}}[CeOCe^{6+}]}$$

où $\Phi_{Ce^{4+}}$ est le rendement quantique pour l'espèce Ce^{4+}.

Cette équation contient trop de paramètres pour être vérifiée expérimentalement de manière significative. Elle se simplifie si on néglige la concentration en dimères, ce qui est plausible, surtout à haute acidité.

En faisant le bilan de matière et en utilisant l'éq. 13 on obtient alors:

$$[14] \qquad \Phi_{Ce(IV)} = \Phi_{Ce^{4+}} \frac{\varepsilon_{Ce^{4+}}}{\varepsilon_{Ce^{4+}} + \varepsilon_{CeOH^{3+}} K_1[H^+]}$$

et

$$[15] \qquad \frac{1}{\Phi_{Ce(IV)}} = \frac{1}{\Phi_{Ce^{4+}}} + \frac{\varepsilon_{CeOH^{3+}} K_1}{\Phi_{Ce^{4+}} \varepsilon_{Ce^{4+}}} \cdot \frac{1}{[H^+]}$$

La fig. 2 montre que l'éq. 15 est vérifiée de manière très satisfaisante. L'ordonnée à l'origine permet d'obtenir la valeur de 0.19 pour $\Phi_{Ce^{4+}}$.

En faisant l'approximation que $\varepsilon_{CeOH^{3+}}$ est à peu près égale à $\varepsilon_{Ce^{4+}}$, ce qui est raisonnable étant la faible variation du coefficient d'extinction du Ce(IV) à cette longueur d'onde avec l'acidité, la pente donne la valeur de 0.27 *M* pour K_1. Cette valeur est du même ordre de grandeur que celle obtenue par d'autres méthodes (11).

L'influence de l'acide sulfurique est négligeable dans la photo-oxydation de l'eau (3), mais ces données ne peuvent être comparées à nos résultats étant donné que le Ce(IV) est complexé par l'ion sulfate et l'augmentation de la concentration en acide sulfurique influence les équilibres de formation de ces complexes.

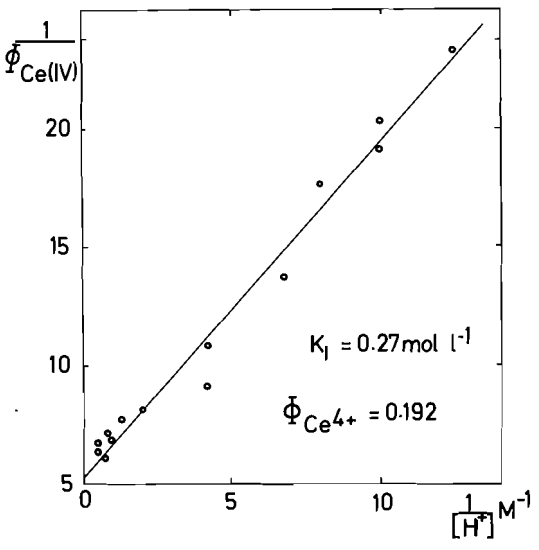

FIG. 2. Variation de $1/\Phi_{Ce(IV)}$ en fonction de $1/[H^+]$ en solution d'acide perchlorique. Distance lampe–cellule = 8.7 cm; temps d'irradiation = 20 min; $T = 25 \pm 1$ °C; [Ce(IV)] = 2×10^{-2} *M*; [Ce(III)] = 6.35×10^{-3} *M*; [Hg(I)] = 1×10^{-2} *M*; force ionique = 2 *M*.

En conclusion, nous proposons que l'espèce responsable de la formation des radicaux OH lors du processus photo-chimique primaire est le Ce^{4+}, non pas $CeOH^{3+}$ ou $CeOCe^{6+}$.

Les réactions ultérieures de ces radicaux dépendent de l'endroit où ils sont formés. Près de la paroi il est probable que la réaction hétérogène, avec adsorption de radicaux soit prépondérante. Par contre, au sein de la solution il y a compétition entre le Ce(III) et le Hg(I) pour ces radicaux de manière analogue aux systèmes étudiés auparavant.

Les auteurs remercient le Conseil National de Recherches du Canada pour l'octroi grâce auquel ce travail a pu être réalisé.

1. J. J. WEISS et D. PORRET. Nature, **139**, 1019 (1937).
2. L. J. HEIDT et M. E. SMITH. J. Am. Chem. Soc. **70**, 2476 (1948).
3. B. YA. DAIN et A. A. KACHAN. Dokl. Akad. Nauk. SSSR, **67**, 85 (1949); A. A. KACHAN et P. P. MAKHOVKA. Russ. J. Phys. Chem. (Eng. Ed.), **36**, 273 (1962).
4. T. J. SWORSKI. J. Am. Chem. Soc. **77**, 1074 (1955).
5. T. J. SWORSKI. J. Am. Chem. Soc. **79**, 3655 (1957).
6. T. J. SWORSKI. J. Phys. Chem. **67**, 2858 (1963).
7. L. DOGLIOTTI et E. HAYON. J. Phys. Chem. **71**, 3802 (1967).
8. T. J. SWORSKI. Radiat. Res. **4**, 483 (1956); R. W. MATTHEWS, H. A. MAHLMAN, et T. J. SWORSKI. J. Phys. Chem. **74**, 3835 (1970).
9. T. W. MARTIN, L. L. SWIFT, et J. H. VENABLE, JR. J. Chem. Phys. **52**, 2138 (1970).
10. R. L. MOORE et R. C. ANDERSON. J. Am. Chem. Soc. **67**, 167 (1945); M. S. SHERRIL, C. G. KING, et R. C. SPOONER. J. Am. Chem. Soc. **65**, 170 (1943); T. J. HARDWICK et E. ROBERTSON. Can. J. Chem. **29**, 818 (1951).

Can. J. Chem. Downloaded from www.nrcresearchpress.com by 210.87.254.5 on 09/05/12
For personal use only.

11. H. G. OFFNER et D. A. SKOOG. Anal. Chem. **38**, 1520 (1966).
12. M. G. EVANS et N. URI. Nature, **166**, 602 (1950).
13. A. M. ARMSTRONG et J. HALPERN. Can. J. Chem. **35**, 1020 (1957).
14. L. J. HEIDT et A. F. MCMILLAN. J. Am. Chem. Soc. **76**, 2135 (1954).
15. A. I. VOGEL. Quantitative inorganic analysis 2nd ed. Longmans, Green and Co. London. 1951. p. 363.
16. H. WILLARD *et al.* Elements of quantitative analysis. D. Van Nostrand Co. Inc., Princeton, N.J. 1956. p. 262.
17. W. C. E. HIGGINSON. J. Chem. Soc. 1438 (1951).
18. J. G. CALVERT et J. N. PITTS. Photochemistry. John Wiley and Sons, N.Y. 1967. p. 783.

Can. J. Chem. Downloaded from www.nrcresearchpress.com by 210.87.254.5 on 09/05/12
For personal use only.

The Relation between Contact Angle and Drop Size for Water at its Boiling Point for a Pressure Range 50–760 Torr

A. B. PONTER
Department of Chemical Engineering, University of New Brunswick, Fredericton, New Brunswick

AND

A. P. BOYES
Department of Chemical Engineering, University of Birmingham, Birmingham, England

Received January 10, 1972

Contact angles have been measured using water drops of specified sizes, and in equilibrium with their vapor only, at their boiling point when residing on a copper surface at pressures ranging from 50–760 Torr.

No appreciable change of contact angle with drop diameter was evident for sizes of 0.5 cm or more, but below this value the angles were dependent on the drop diameter, the effect of reducing pressure being to increase the dependency. The phenomenon is qualitatively explained in terms of gravity and surface roughness influences.

Les angles de contact ont été mesurés en utilisant des gouttes d'eau de dimensions déterminées, en équilibre seulement avec leur vapeur et à leur point d'ébullition, lorsque celles-ci sont placées sur une surface de cuivre sous des pressions allant de 50 à 760 Torr.

On n'a pas mis en évidence de changement appréciable d'angle de contact avec le diamètre des gouttes pour des valeurs supérieure ou égale à 0.5 cm mais au-dessous de cette valeur les angles dépendent du diamètre de la goutte. L'influence d'une baisse de la pression étant d'accroître cette dépendance. Le phénomène est expliqué qualitativement en fonction des influences de la gravité et de la rugosité de la surface.

Canadian Journal of Chemistry, **50**, 2419 (1972)

Introduction

Many considerations have been given to the effect of drop size on surface tension, stemming from the initial theory of Gibbs (1) which was later developed extensively by Tolman (2). For drop diameters less than 10^{-6} cm it was concluded that the surface tension decreased appreciably with decreasing drop sizes. Recently in the study of drop size on the attainment of the advancing contact angle of water on polyethylene, poly(methyl methacrylate), and surfactant coated surfaces Hertzberg and Marian (3) suggested that their results demonstrated that the difference in value between minimum and maximum contact angles was a manifestation of hysteresis. In their investigation the final advancing contact angle was determined for a number of drop volumes and it was reported that there was no obvious and consistent change in the contact angle as the drop volume was altered.

The work now described was carried out to ascertain if the contact angle changed with drop size at conditions where the liquid was at its boiling point and in the presence of its own vapor. These conditions were selected because of the practical implication when studying the process of dropwise condensation.

Experimental

The copper specimen used in the experiments was 99.99% pure and was prepared in the following manner. A flat plate 2.54 cm diameter and 0.7 cm in thickness was polished with numbers 220, 330, 400, and 600 silicon carbide paper and then finally polished on a wheel using "Buehler A B Microcloths" impregnated with 6 μ diamond paste. The specimen was then degreased with a mild soap solution and washed with distilled water, absolute ethyl alcohol and distilled water again. The surface roughness (1.01 μin., center line average) of the specimen was measured using a Talysurf meter employing the standard techniques, the result being an average of at least 15 readings. The specimen was prepared as described, before each run.

The glassware was washed with absolute ethanol to remove excess grease then cleaned with a sodium dichromate–sulfuric acid solution, before finally being irrigated several times with distilled water.

The water was triple distilled, each stage incorporated a surface overflow section which continuously removed surface contaminants. Using a Du Nouy Ring Balance the final product was shown to have a surface tension of 72.8 dyn/cm at 20 °C, which is in excellent agreement with reported values.

As the experiments were carried out over a range of pressures a pressure control was required, a Cartesian manostat being selected above all others since it was suitable for the pressure range investigated.

Can. J. Chem. Downloaded from www.nrcresearchpress.com by 210.87.254.6 on 09/05/12
For personal use only.

Can. J. Chem. Downloaded from www.nrcresearchpress.com by 210.87.254.6 on 09/05/12
For personal use only.

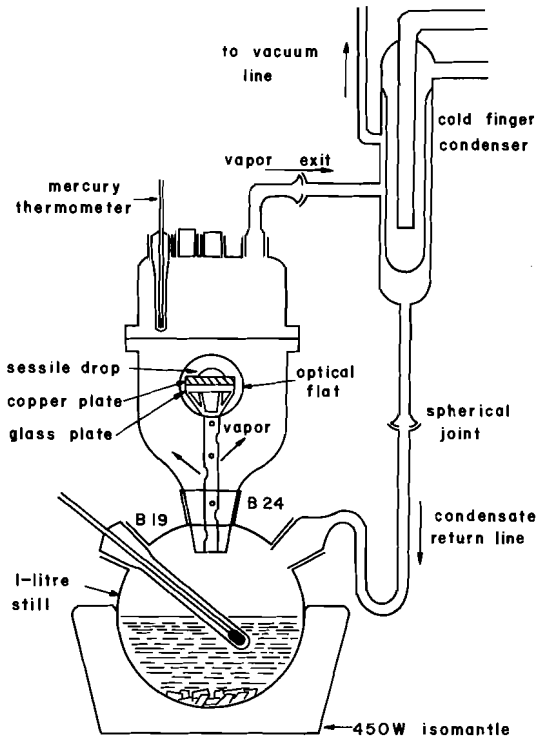

FIG. 1. Equilibrium cell for contact angle measurement.

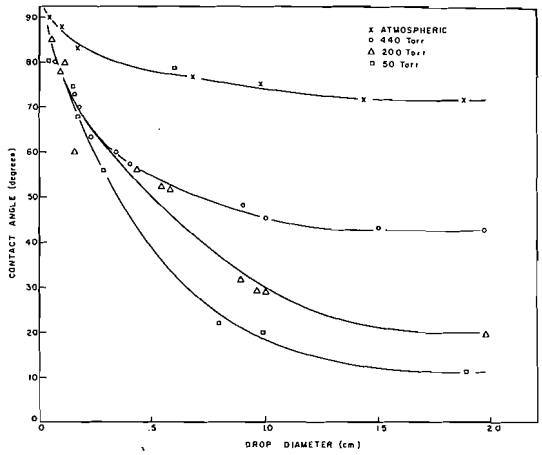

FIG. 2. Contact angle *vs.* drop diameter for the pressure range 50–760 Torr.

All septems used on the apparatus were repeatedly boiled in water which showed no change in surface tension at the end of the operation and all joints on the apparatus were fitted with Tefion sleeves to eliminate contamination from conventional sealants. The "Speedivac" high vacuum oil pump used for the low pressure work was situated some 6 m from the apparatus and had an ice–acetone vapor trap in the glass line between the pump and the apparatus to eliminate any oil contamination in the vapor phase and also to protect the pump.

A diagram of the apparatus used is given in Fig. 1. It consisted of a 1 l flask, a cell in which the contact angles were measured and a cold finger, water-cooled condenser. The 1 l flask was fitted with a thermometer pocket, a condensate return line and was heated by means of a 450 W isomantle fitted with a control. Stainless steel wire guaze was added to the contents of the flask to prevent "bumping". The cylindrical cell (15 cm × 10 cm o.d.), comprised of two sections which were held together with a ring clamp, was fitted with a Teflon gasket. On the bottom section two optical flats were placed on opposite sides of the cell to facilitate readings using transmitted light. A horizontal glass table (3 cm × 3.5 cm) was supported by four legs which were held by a central vapor line. The top section had three B.14 necks, fitted with a thermometer pocket, a vapor exit line to the condenser and a septum to allow the sample to be introduced by means of a syringe fitted with a stainless steel needle. Both sections of the cell were fitted with heaters consisting of coils of resistance wire controlled by a variac. The apparatus was also lagged with asbestos rope to keep heat losses to a minimum.

The glass table was tested to be horizontal by means of a spirit level; once this was achieved the sample plate, prepared and cleaned as described previously, was introduced into the cell and the cell set up as shown in Fig. 1. The copper plate was ensured to be horizontal by aligning one of the cross wires in the microscope with a thin plumb line, then rotating the goniometer eyepiece through 90° and lining up the cross wires with the surface. The contents of the flask were brought to the boil and the heat input to the cell was controlled to keep the temperature of the enclosure slightly above the dew point of the vapor. After equilibrium was reached, which took 2–3 h, a liquid sample was removed from the still, through a side arm fitted with a septum, by means of a syringe fitted with a stainless steel needle. The liquid was then introduced onto the specimen through the central B.14 neck at the top of the cell. The end of the needle was placed just above the plate and the drop was formed slowly. Great care was taken in the removal of the needle from the drop so that no disturbance of the drop ensued. When the sessile drop had come to equilibrium with its vapor the contact angle was measured by direct observation using the travelling microscope fitted with a goniometer eyepiece. The reported values, an average of at least five readings, have standard deviations in the range 0.5–1.0 deg.

Results and Discussion

Plots of contact angle *vs.* drop diameter for pressures ranging from 50–764 Torr for water at its boiling point are given in Fig. 2. Since in practice condensation conditions are usually quoted in terms of the pressure the data have also been presented as contact angle *vs.* pressure curves for given drop diameter in Fig. 3. From Fig. 2 it can be seen that for atmospheric pressure measurements there is a change of less

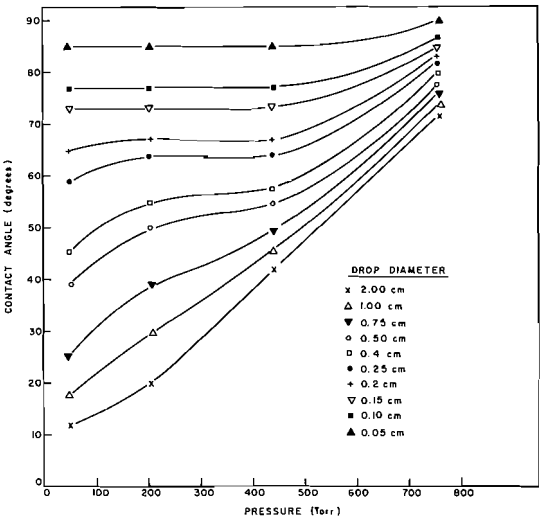

FIG. 3. Contact angle *vs.* pressure for given drop diameters.

than 8% in the contact angle for drop diameters 0.5 cm and upwards which is in agreement with the work of Hertzberg and Marian (3), who showed that there was no appreciable change in contact angle for drop volumes of 5–40 μl which approximate to these drop diameters. However, for drop diameters below 0.5 cm an appreciable increase in contact angle was observed. At the same time for reducing pressures the contact angle becomes more dependent upon drop size. For clarity the effect of pressure and drop diameter on the contact angle is given in Fig. 4.

Considering Young's equation for ideal surfaces

$$[1] \qquad \cos\theta = \frac{\gamma_{SV} - \gamma_{SL}}{\gamma_{LV}}$$

where θ = intrinsic contact angle, γ = interfacial free energy, and S, V, L refer to solid,

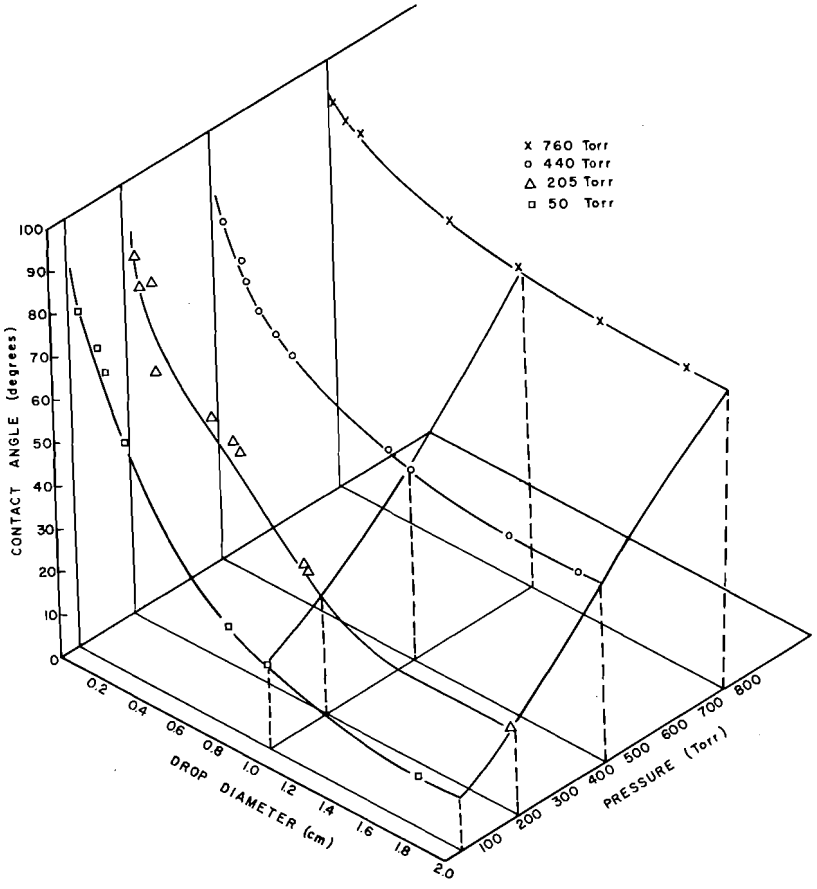

FIG. 4. Contact angle *vs.* drop diameter for a range of pressures.

Can. J. Chem. Downloaded from www.nrcresearchpress.com by 210.87.254.6 on 09/05/12
For personal use only.

vapor, and liquid state, respectively. Then for a given pressure and temperature the contact angle should be independent of drop diameter. The variation of contact angle with drop size for a given pressure cannot be explained in terms of the change in surface tension (1, 2) as this is only significant for drop diameters less than 10^{-6} cm which are several orders of magnitude below our minimum size. It has been discussed in the literature (5, 6) that gravity has a negligible effect on the contact angle, this however was purported for ideal surfaces (*i.e.* uniform, plane, non-deformable). Tovbin and Fal'ko (7) demonstrated that gravity affects the shape of the drop resting on a solid surface and that this distortion could lead to errors in the calculation of θ from drop dimensions. The effect of gravity on the contact angle for non ideal surfaces has however not been clarified.

In these experiments only one surface roughness was considered *i.e.* 1.01 μin. (center line average). It would be expected that for a copper surface exhibiting another roughness that because of Wenzel's (4) relationship

$$\cos \bar{\theta} = r \cos \theta$$

(where $\bar{\theta}$ = observed contact angle and r = surface roughness) for contact angles diverging considerably from 90° the contact angle–drop diameter curve would relocate. At 90°, of course, roughness does not affect the contact angle and hence the pattern of behavior described above will be expected to be similar for a surface of any roughness up to values where air becomes entrapped so producing a composite surface.

1. J. W. GIBBS. Collected works. Vol. 1. Longmans Green and Company, New York. 1928.
2. R. C. TOLMAN. J. Chem. Phys. **17**, 333 (1949).
3. W. J. HERTZBERG and I. E. MARIAN. J. Colloid Int. Sci. **33**, 161 (1970).
4. R. N. WENZEL. Ind. Eng. Chem. **28**, 988 (1936).
5. B. A. PETHICA and T. J. P. PETHICA. Proc. 2nd. Int. Congr. Surf. Act. (London), **3**, 131 (1957).
6. V. R. GRAY. Proc. 2nd Int. Congr. Surf. Act. (London), **3**, 191 (1957).
7. M. V. TOVBIN and I. M. FAL'KO. Visn Kiivs'k Univ. No. 5 Ser. Fiz. Ta Khim No. 2, 86 (1962).

Can. J. Chem. Downloaded from www.nrcresearchpress.com by 210.87.254.6 on 09/05/12
For personal use only.

Thiohydantoins. IX. Tautomerism of some Methylation Products

J. T. EDWARD AND J. K. LIU
Department of Chemistry, McGill University, Montreal, Quebec

Received October 1, 1969[1]

The methylation product of 5,5-pentamethylene-2-thiohydantoin has been shown by u.v. and i.r. spectral studies to exist predominantly as 2-methylthio-4,4-pentamethylene-2-imidazolin-5-one in chloroform or cyclohexane, and as 2-methylthio-5,5-pentamethylene-2-imidazolin-4-one in water. The tautomerism of the methylation product of 5,5-pentamethylene-2,4-dithiohydantoin exhibits a similar sensitivity to solvent.

Des études dans l'u.v. et dans l'i.r. démontrent que le produit fourni par l'action d'iodure de méthyle sur le pentaméthylène-5,5 thio-2 hydantoïne existe comme méthylthio-2 pentaméthylène-4,4 2-imidazoline-5-one en solution de chloroforme ou de cyclohexane, mais comme méthylthio-2 pentaméthylène-5,5 2-imidazoline-4-one en solution aqueuse. Le produit fourni par la méthylation de pentaméthylène-5,5 dithio-2,4 hydantoïne démontre une tautomerie semblable.

Canadian Journal of Chemistry, **50**, 2423 (1972)

Carrington and Waring (1) obtained a product (**1/2**, X = O) from the methylation of 5,5-pentamethylene-2-thiohydantoin (**3**, X = O) to which they assigned the unconjugated structure **1** (X = O) on the basis of analogies which cannot be considered conclusive. Edward and Martlew (2) pointed out that the u.v. spectral characteristics reported for the compound supported rather the conjugated structure **2** (X = O). Recently it has been shown (3) that the related spiroimidazolone **1/2** (X = O; H in place of SMe) exists practically exclusively as the unconjugated tautomer in chloroform solution. However, in aqueous solution it exists as an approximately 70:30 mixture of the unconjugated:conjugated tautomer, and this proportion should be decreased by the presence of the 2-methylthio group.

In the present work we show that **1/2** (X = O) can exist almost entirely in one tautomeric form or the other depending on its solvent. This has been done by u.v. and i.r. studies making use of **4** and **5** (X = O) as models for **1** and **2** (X = O). The compound **4** (X = O) had already been synthesized by Carrington and Waring (1), and **5** (X = O), hitherto unknown, was prepared by treating 1-methyl-5,5-pentamethylene-2-thiohydantoin (**6**; X = O) with methyl iodide in ether (*cf.* ref. 4),[2] and decomposing the hydriodide thus obtained with aqueous bicarbonate. The structure **5** (X = O) was proved by hydrolyzing the compound with dilute acid to methanethiol and 1-methyl-5,5-pentamethylenehydantoin.

The u.v. spectra of these model compounds (Table 1 and Fig. 1) were similar to those of the simpler compounds **4** and **5** (X = O, H in place of SMe) studied earlier (3), the conjugated compound **5** (X = O) absorbing at longer wavelength than the unconjugated **4** (X = O). The

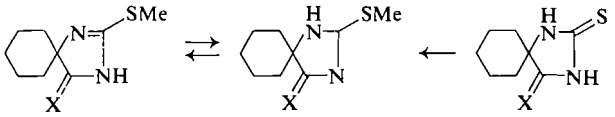

1 2 3

4 5 6

[1]Revision received March 30, 1972.

[2]Carrington and Waring, in exhaustive studies which furnished every other possible methylation product of 5,5-pentamethylene-2-thiohydantoin, failed to obtain this compound because they treated **6** with methyl iodide in alkaline solution. This has the effect of increasing the amount of *N*-methylation and of causing the hydrolysis of any of the *S*-methyl compound which may be formed to 1-methyl-5,5-pentamethylenehydantoin.

Can. J. Chem. Downloaded from www.nrcresearchpress.com by 210.87.254.6 on 09/05/12
For personal use only.

TABLE 1. Ultraviolet peaks (in nm) of ionized (BH^+) and unionized (B) imidazolones in different solvents

	B in EtOH		B in H_2O		BH^+ in H_2O	
Compound	λ_{max}	ε_{max}	λ_{max}	ε_{max}	λ_{max}	ε_{max}
1/2 (X = O)	236.5	11200	252	7200	229	16700
			242	17500		
4 (X = O)	236	6500	240	4000	235	20400
			212	11250		
5 (X = O)	263	7500	262	7400	248	9400
	234	15500	237.5	17500	228	15000

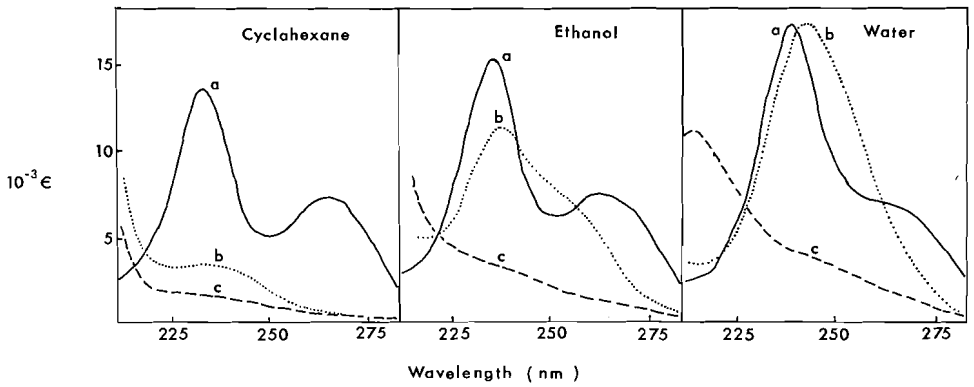

FIG. 1. Ultraviolet absorption spectra in different solvents of **5** (X = O) (*a*), **1/2** (X = O) (*b*), and **4** (X = O) (*c*).

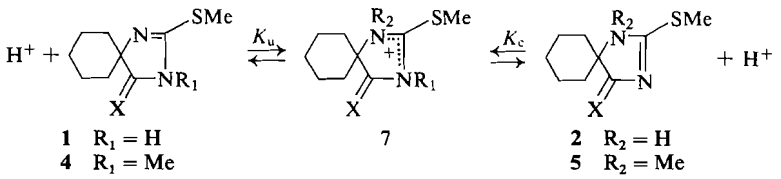

1 R_1 = H
4 R_1 = Me

7

2 R_2 = H
5 R_2 = Me

confusion in the literature over the spectral characteristics of compounds of this class (reviewed in ref. 5), which had prevented a study of their tautomerism, probably arose from a neglect of solvent effects.

The spectra of **4** and **5** (X = O), presented in Fig. 1, show a small dependence on solvent polarity. However, the spectrum of **1/2** (X = O) shows a very large dependence, which is best explained on the assumption that the compound exists predominantly as the tautomer **1** (X = O) in cyclohexane, as **2** (X = O) in water, and as a mixture (very roughly in the proportions 1:2) of **1** and **2** (X = O) in ethanol.

The composition of the tautomeric mixture in water was confirmed by spectrophotometric determination (6) of the ionization constants of **4**, **5**, and **1/2** (X = O). All of these compounds can be expected to be protonated to give an ion of the general structure **7** (7), and it has been shown (8) that the tautomeric constant K_{Tau} (= [**2**, X = O]/[**1**, X = O]) is related to the apparent ionization constant K_{obs} of **1/2** (X = O)[3] and the separate ionization constants K_u of **1** (X = O) and K_c of **2** (X = O) by the relations:

$$[1] \qquad K_{Tau} = K_c/K_u$$

$$[2] \qquad = (K_{obs} - K_u)/K_u$$

$$[3] \qquad = K_c/(K_{obs} - K_c)$$

K_u and K_c are not directly observable, but are approximated by the constants K_u' of **4** (X = O) and K_c' of **5** (X = O), the substitution

[3]This and other ionization constants refer to the ionization of the conjugate acid of the base or bases.

Can. J. Chem. Downloaded from www.nrcresearchpress.com by 210.87.254.6 on 09/05/12
For personal use only.

TABLE 2. Infrared absorption maxima (in cm^{-1}) of imidazolones in different phases

Compound	Phase	ν(C=O)	ε_A	ν(C=N)	ε_A
1/2 (X = O)	DMSO	1698	400	1500	80
		1722	480	1570	260
	$CHCl_3$	1725		1580	
	$CDCl_3$	1725		1583	
	KBr	1682		1505	
		1700	(shoulder)		
4 (X = O)	DMSO	1722	740	1570	700
	$CHCl_3$	1715	550	1580	540
	$CDCl_3$	1720		1580	
	KBr	1730		1585	
5 (X = O)	DMSO	1695	520	1500	260
	$CHCl_3$	1704	560	1494	180
	$CDCl_3$	1704		1495	
	KBr	1705		1505	

of hydrogen by methyl generally having a small effect on the basicity of a compound. The pK values of **1/2**, **4**, and **5** (X = O) are 3.04, 3.78, and 3.00; substituting the appropriate K values into eqs. 1 and 2 gives K_{Tau} of 86:14 and 82:18 respectively. However, it is theoretically impossible for $K_{obs} < K_u$ or K_c, and the fact that $K_{obs} < K_c'$, indicates that the assumption: $K_c = K_c'$, is not strictly valid. For this reason a rational value of K_{Tau} is not obtained by application of eq. 3, but the results would indicate that K_{Tau} is very large. Summing up all the estimates, it would appear the $K_{Tau} \simeq 6:1$, the amount of unconjugated tautomer present in aqueous solution thus being small.

On the other hand, the unconjugated form is the predominant tautomer in chloroform solution, as shown by the i.r. data in Table 2. Comparison of the spectra of **4** and **5** (X = O) shows that the stretching frequencies of C=O and C=N are higher for the former compound, the values for both compounds being close to those for similar compounds already reported (3, 9, 10). In the more polar solvent, dimethyl sulfoxide, peaks indicative of both **1** and **2** (X = O) are present, and examination of the peak intensities (Table 2) indicates that the proportion of **1**:**2** (X = O) is roughly 60:40. The spectrum of the solid in KBr discs indicates that it crystallizes from ethanol mainly in the conjugated form **2** (X = O).

In summary, the proportion of conjugated tautomer present increases with the polarity of the solvent. Peresleni *et al.* (10) observed a similar effect in the tautomerism of 2-acylamino-thiazolines, which also contain the tautomeric system:

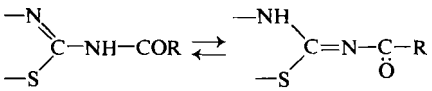

and which exhibit similar u.v. and i.r. changes on tautomerization. It consequently became of interest to observe the effect of replacing the C=O group of **1/2** by C=S. Carrington and Waring (1), by methylating 5,5-pentamethylene-2,4-dithiohydantoin (**3**, X = S), had obtained a compound ($\lambda\lambda_{max}$ 330, 297, and 255 nm in methanol) to which they assigned the structure **1** (X = S). However, the model compound **4** (X = S) showed u.v. peaks only at 295 and 250 nm, and it seemed likely that the peak at 330 nm was due to the presence of the tautomer **2** (X = S). This supposition was shown to be correct by preparing the hitherto unknown model compound **5** (X = S) by treatment of 1-methyl-5,5-pentamethylene-2,4-dithiohydantoin (**6**, X = S) with methyl iodide (*vide supra*). The model compound in ethanol had a strong u.v. peak (probably due to a $\pi \rightarrow \pi^*$ transition) at 340 nm, as well as a weak $n \rightarrow \pi^*$ peak at 404 nm[4] and a strong type of IV peak (5) at 263 nm.

Comparison of the spectra of the compound

[4]The $n \rightarrow \pi$ peaks of **4** and **5** (X = S) show a *red* shift when the compounds are protonated to form the ions **7** (R_1 = Me, R_2 = H, X = S, and R_1 = H, R_2 = Me, X = S) (see Table 3). This shift is reasonable, since there is a net flow of electronic charge inwards from sulfur in an $n \rightarrow \pi^*$ transition, and this should be aided by the positive charge spread over the amidine portion of the ring.

Can. J. Chem. Downloaded from www.nrcresearchpress.com by 210.87.254.6 on 09/05/12
For personal use only.

TABLE 3. Ultraviolet peaks (in nm) of ionized (BH^+) and unionized (B) imidazolthiones in different solvents

Compound	B in cyclohexane		B in EtOH		B in H_2O		BH^+ in H_2O	
	λ_{max}	ε_{max}	λ_{max}	ε_{max}	λ_{max}	ε_{max}	λ_{max}	ε_{max}
1/2 (X = S)	250	8550	252	7890	266	8810	263	11700
	293	11750	295	9750	325	18000	296	16100
			330	5740				
4 (X = S)	245.5	8250	248	8570	256	9420	258	11500
	293	11430	293	11900	293	12100	299	19000
			370	94			402	32.2
5 (X = S)	261	10000	263	10800	270	6100	262.5	13400
	342	18650	340	20100	334	19500	300	12600
			404	70			425	36.4

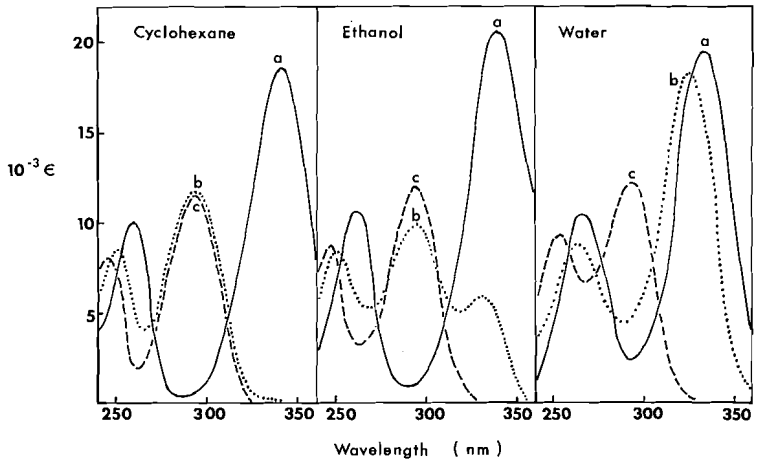

FIG. 2. Ultraviolet absorption spectra in different solvents of **5** (X = S) (*a*), **1/2** (X = S) (*b*), and **4** (X = S) (*c*).

1/2 (X = S) in cyclohexane, ethanol, and water with the spectra of the model compounds **4** and **5** (X = S) (Table 3 and Fig. 2) shows **1/2** (X = S) to be present almost entirely as the unconjugated **1** (X = S) in cyclohexane, as an approximately 4:1 mixture of **1** and **2** (X = S) in ethanol, and as an approximately 1:5 mixture of **1** and **2** (X = S) in water. Application of eqs. 1–3 to the experimental pK values of **1/2**, **4**, and **5** (X = S) (2.40, 3.06, and 2.48 respectively) in water gives K_{Tau} of 79:21, 78:22, and 82:18, which averages to a 1:4 ratio of **1**:**2** (X = S), in fair agreement with the estimate from examination of the u.v. spectra of the aqueous solutions.

In non-polar solvents, **1** (X = S) becomes (like **1** (X = O)) the more stable tautomer. This is shown by the i.r. data in Table 4. The assignments of i.r. spectral bands are based on analogy

TABLE 4. Infrared absorption maxima (in cm^{-1}) of imidazolthiones in different phases

Compound	Phase	ν(C=O)	ε_A	ν(C=N)	ε_A
1/2 (X = S)	DMSO	1270	550	1585	600
		1245	900	1500	300
	$CHCl_3$	1262	500	1592	640
	$CDCl_3$	1258		1595	
	KBr	1225		1525	
		1266			
4 (X = S)	DMSO	1280	1000	1575	750
	$CHCl_3$	1296		1584	
	$CDCl_3$	1298		1585	
	KBr	1300		1592	
		1260			
5 (X = S)	DMSO	1255	1700	1508	400
	$CHCl_3$	1255		1505	
	$CDCl_3$	1257		1495	
	KBr	1248		1525	
		1266			

Can. J. Chem. Downloaded from www.nrcresearchpress.com by 210.87.254.6 on 09/05/12
For personal use only.

Can. J. Chem. Downloaded from www.nrcresearchpress.com by 210.87.254.6 on 09/05/12
For personal use only.

with literature values (11) and on comparison of the spectra with those of **4** and **5** (X = O); the latter resemble closely the spectra of **4** and **5** (X = S) except in the C=O and C=S regions. From the positions and intensities of the peaks, it appears that the ratio of **1** (X = S):**2** (X = S) in dimethyl sulfoxide is about 1:1, but that in chloroform it becomes so large, that no **2** (X = S) is discernible.

Experimental

1-Methyl-2-methylthio-5,5-pentamethylene-2-imidazolin-4-one (5, X = O)

A solution of 1-methyl-5,5-pentamethylene-2-thiohydantoin (1.0 g) (1) and methyl iodide (25 ml) in anhydrous ethyl ether (25 ml) was kept in the dark for 48 h. Colorless needles of the hydriodide (0.63 g), m.p. 155–157°, separated, and were removed by filtration and washed with anhydrous ether.

Anal. Calcd. for $C_{10}H_{17}IN_2OS$: C, 35.3; H, 5.0; N, 8.2; O, 4.2; S, 9.4. Found: C, 35.3; H, 5.0; N, 8.1; O, 4.2; S, 9.6.

The hydriodide (0.5 g) in water (25 ml) was treated with sodium bicarbonate (200 mg). After evolution of carbon dioxide, the mixture was evaporated to dryness at room temperature under reduced pressure, and the residue extracted with chloroform (4 × 10 ml). The chloroform solution was dried (Na_2SO_4) and evaporated to give colorless needles of **5** (X = O), m.p. 83–85° (yield 80%). After one crystallization from ethanol the compound melted at 85–86°.

Anal. Calcd. for $C_{10}H_{16}N_2OS$: C, 56.6; H, 7.6; N, 13.2; O, 7.5; S, 15.1. Found: C, 56.4; H, 7.6; N, 13.0; O, 7.7; S, 14.9.

A solution of the compound **5** (X = O) in hydrochloric acid (20%; 5 ml) was heated under reflux for 30 min. Methanethiol was evolved, and the solution on cooling deposited colorless crystals of 1-methyl-5,5-pentamethylenehydantoin, m.p. 173–174° (lit. m.p. 174° (1)).

1-Methyl-2-methylthio-5,5-pentamethylene-2-imidazolin-4-thione (5, X = S)

1-Methyl-5,5-pentamethylene-2,4-dithiohydantoin (3.0 g) (1) was dissolved in methyl iodide (50 ml). On standing at room temperature in the dark for 24 h the solution deposited a brownish solid (3.2 g) which was dissolved in water. A small residue was removed by filtration, and the filtrate was treated with sodium bicarbonate solution until alkaline to litmus paper. Bright yellow crystals of **5** (X = S) separated which after recrystallization from ethanol were obtained in 22% yield, m.p. 149–150°.

Anal. Calcd. for $C_{10}H_{16}N_2S_2$: C, 52.5; H, 7.0; N, 12.2; S, 28.2. Found: C, 52.6; H, 7.0; N, 12.2; S, 28.0.

A solution of **5** (X = S) (0.2 g) in hydrochloric acid (20%; 5 ml) was heated under reflux for 45 min. Methanethiol was evolved, and on cooling a quantitative yield of 1-methyl-5,5-pentamethylene-4-thiohydantoin separated. It crystallized from ethanol as pale yellow needles, m.p. 187–188° (reported m.p. 188° (1)).

Spectral Measurements

The i.r. spectra were obtained with a Perkin–Elmer 337 infracord spectrophotometer, and u.v. spectra with a Unicam SP 800 spectrophotometer. General procedures have been described previously (12). Ionization constants are averaged from values calculated using data for different wavelengths and p*H* values at 25.0°, and have a precision of about ±0.05 units; they have not been corrected for the ionic strength (0.05–0.1) of the buffer solutions used. The compound **5** (X = S) hydrolyzed slowly in 0.4 *M* hydrochloric acid, and spectral measurements were taken at known time intervals and extrapolated back to zero time.

Grateful acknowledgment is made to the National Research Council of Canada for financial support.

1. H. C. CARRINGTON and W. S. WARING. J. Chem. Soc. 354 (1950).
2. J. T. EDWARD and E. F. MARTLEW. Chem. Ind. (London), 193 (1954).
3. J. T. EDWARD and I. LANTOS. J. Heterocycl. Chem. **9**, 363 (1972).
4. R. HAZARD, J. CHEYMOL, P. CHABRIER, and K. SMARZEWSKA. Bull. Soc. Chim. Fr. 228 (1949).
5. J. T. EDWARD. The chemistry of organic sulfur compounds. Vol. II. *Edited by* C. Y. Meyers and N. Kharasch. Pergamon Press, Oxford, 1966. p. 287.
6. L. A. FLEXSER, L. P. HAMMETT, and A. DINGWALL. J. Am. Chem. Soc. **57**, 2103 (1935).
7. G. K. BRANCH and M. CALVIN. The theory of organic chemistry. Prentice-Hall, New York, 1941. p. 196.
8. S. J. ANGYAL and C. L. ANGYAL. J. Chem. Soc. 1461 (1952). S. F. MASON. J. Chem. Soc. 847 (1958).
9. E. S. SCHIPPER and E. CHINERY. J. Org. Chem. **26**, 4480 (1961).
10. E. M. PERESLENI, Y. N. SHEINKER, N. P. ZOSIMOVA, and Y. I. POMERANSEV. Russ. J. Phys. Chem. **37**, 1469 (1963).
11. D. HADZI. J. Chem. Soc. 847 (1957). R. MECKE and R. MECKE. Ber. **89**, 343 (1956). L. J. BELLAMY. The chemistry of organic sulfur compounds. Vol. I. *Edited by* N. Kharasch. Pergamon Press, Oxford, 1961. p. 51.
12. J. T. EDWARD and J. K. LIU. Can. J. Chem. **47**, 1117 (1969).

Fluorine and Proton Nuclear Magnetic Resonance Spectra of *N*-Dialkylaminosulfur Trifluorides

D. G. IBBOTT AND A. F. JANZEN

Department of Chemistry, University of Manitoba, Winnipeg, Manitoba R3T 2N2

Received March 2, 1972

The fluorine and proton n.m.r. spectra of *N*-dimethylaminosulfur trifluoride and *N*-diethylaminosulfur trifluoride have been recorded under anhydrous conditions at −68 and +22°. Chemical shifts and coupling constants of axial and equatorial fluorines are reported.

Les spectres de r.m.n. du fluor et du proton dans le *N*-diméthylaminosoufre trifluorure et dans le *N*-diéthylaminosoufre trifluorure, ont été enregistrés dans des conditions anhydres à −68 et +22°. Les déplacements chimiques et les constantes de couplage du fluor axial et équatorial sont rapportés.

Canadian Journal of Chemistry, **50**, 2428 (1972)

Can. J. Chem. Downloaded from www.nrcresearchpress.com by 210.87.254.6 on 09/05/12
For personal use only.

The geometry of tetracoordinate group VI compounds is predicted, on the basis of Gillespie's electron-pair repulsion theory (1), to be trigonal bipyramidal with an electron-pair occupying one of the equatorial sites. In the case of *N*-dialkylaminosulfur trifluorides, $(CH_3)_2NSF_3$ and $(CH_3CH_2)_2NSF_3$, Demitras and MacDiarmid (2) and von Halasz and Glemser (3) have postulated a trigonal bipyramidal structure in which the dialkylamino group also occupies an equatorial site.

Fluorine n.m.r. studies of these compounds have been complicated by fluorine exchange effects and thus Demitras and MacDiarmid observed only a broad signal for $(CH_3)_2NSF_3$ at room temperature and two signals at −100°; von Halasz and Glemser observed a broad signal at room temperature and two signals at −84° for $(CH_3CH_2)_2NSF_3$. However, additional fluorine–fluorine or fluorine–hydrogen spin–spin splitting was apparently not observed.

Fluorine exchange in sulfur fluorides has been explained by intra- and intermolecular mechanisms (4); however, it occurred to us, on the basis of our recent n.m.r. study of the hydrolysis of fluorosilanes (5), that hydrolysis may also be responsible for fluorine exchange in R_2NSF_3. If so, recording the spectra under anhydrous conditions might lead to further understanding of structural and exchange properties of sulfur fluorides.

$(CH_3)_2NSF_3$ and $(CH_3CH_2)_2NSF_3$ were prepared from SF_4 and $R_2NSi(CH_3)_3$ (2, 3) at room temperature in standard n.m.r. tubes which had previously been silylated (with $[(CH_3)_3Si]_2NH$), flamed out and evacuated (at 10^{-4} mm). The tubes were sealed under vacuum and kept at −78° while transferring to the n.m.r. spectrometer, equipped with a variable temperature probe cooled to −68°.

The fluorine n.m.r. spectrum of $(CH_3)_2NSF_3$ at −68° (Fig. 1*a*) shows a doublet ($J_{F^a-S-F^e}$ = 58 Hz) of septets ($J_{F^a-S-N-C-H}$ = 5.0 Hz) at −59.4 p.p.m. assigned to the axial fluorines. A triplet ($J_{F^e-S-F^a}$) of septets ($J_{F^e-S-N-C-H}$ = 8.2 Hz) at −20.2 p.p.m. is assigned to the equatorial fluorine. The proton n.m.r. spectrum at −68° (Fig. 1*b*) shows a doublet ($J_{H-C-N-S-F^e}$ = 8.2 Hz) of triplets ($J_{H-C-N-S-F^a}$ = 5.0 Hz) at −3.06 p.p.m. assigned to the dimethylamino group.

The well resolved multiplets at −68° indicate that fluorine exchange has been significantly slowed down under anhydrous conditions. On warming the sample, the multiplets begin to collapse and fine structure is lost; however, even at +22° two peaks remain which can clearly be identified as a doublet and a triplet, assigned to axial and equatorial fluorines, respectively, as shown in Fig. 2.

The fluorine n.m.r. spectrum of $(CH_3CH_2)_2NSF_3$ at −68° (Fig. 3*a*) shows a doublet ($J_{F^a-S-F^e}$ = 62 Hz) at −54.0 p.p.m. assigned to the axial fluorines. Additional fine structure is apparent and an approximate value for the coupling constant is $J_{F^a-S-N-C-H}$ = 3 Hz.

A triplet ($J_{F^e-S-F^a}$ = 62 Hz) of quintuplets ($J_{F^e-S-N-C-H}$ = 6.1 Hz) at −34.4 p.p.m. is assigned to the equatorial fluorine.

The proton n.m.r. spectrum at −68° (Fig. 3*b*)

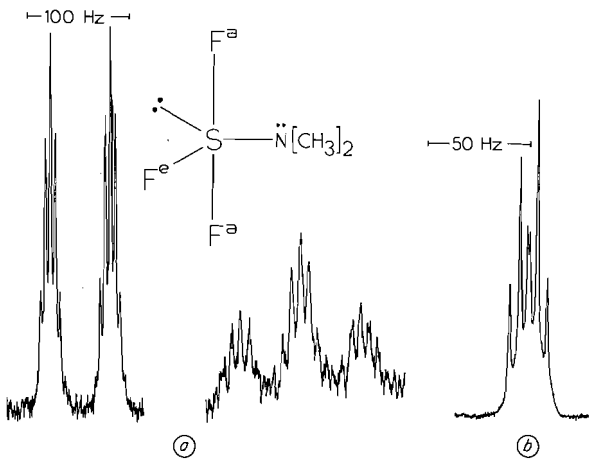

FIG. 1. The n.m.r. spectrum of $(CH_3)_2NSF_3$ at $-68°$ (*a*) fluorine; (*b*) proton.

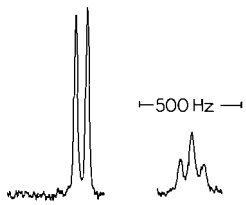

FIG. 2. Fluorine n.m.r. spectrum of $(CH_3)_2NSF_3$ at $+22°$.

shows a multiplet at -3.49 p.p.m. assigned to the CH_2 group. The multiplet may be analyzed as a first order spectrum consisting of a quartet ($J_{H-C-C-H} = 7.0$ Hz) of doublets ($J_{H-C-N-S-F^e} = 6.1$ Hz) of triplets ($J_{H-C-N-S-F^a} = 3$ Hz). The triplet ($J_{H-C-C-H} = 7.0$ Hz) at -1.25 p.p.m., assigned to the CH_3 group, shows no further coupling to fluorines. A summary of chemical shifts and coupling constants is found in Table 1.

During our n.m.r. study of the diethylamine catalyzed hydrolysis of $(CH_3)_3SiF$ (5), it was observed that rapid exchange in a sample containing $(CH_3)_3SiF$, $(C_2H_5)_2NH$, and H_2O could be stopped by adding $(CH_3)_3SiN(C_2H_5)_2$, the latter reagent apparently reacting with HF and H_2O to stop hydrolysis and fluorine exchange. A similar experiment was tried for $(C_2H_5)_2NSF_3$.

Addition of H_2O (5.6×10^{-4} g, 0.031 mmol) to anhydrous $(C_2H_5)_2NSF_3$ (1.0 mmol in 0.5 ml $CFCl_3$) resulted in loss of fine structure and only two broad peaks were observed in the fluorine n.m.r. spectrum. On adding $(CH_3)_3SiN(C_2H_5)_2$ (8.4×10^{-2} g, 0.58 mmol), a well resolved spectrum re-appeared, identical to the anhydrous spectrum of $(C_2H_5)_2NSF_3$ (Fig. 3*a*).

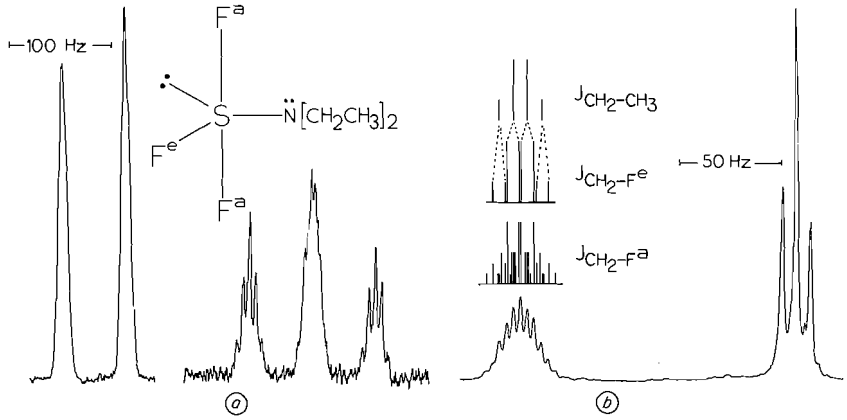

FIG. 3. The n.m.r. spectrum of $(CH_3CH_2)_2NSF_3$ at $-68°$ (*a*) fluorine; (*b*) proton.

Can. J. Chem. Downloaded from www.nrcresearchpress.com by 210.87.254.6 on 09/05/12
For personal use only.

Can. J. Chem. Downloaded from www.nrcresearchpress.com by 210.87.254.6 on 09/05/12
For personal use only.

TABLE 1. Fluorine and proton n.m.r. data for $(CH_3)_2NSF_3$ and $(CH_3CH_2)_2NSF_3$ at $-68°$. Nuclei are labelled as in Figs. 1*a* and 3*a*

	Fluorine							Proton		
	δ (p.p.m.)		J (Hz)					δ (p.p.m.)		J (Hz)
	F^a	F^e	F^a—F^e	F^a—CH_2	F^e—CH_2	F^a—CH_3	F^e—CH_3	CH_2	CH_3	CH_2—CH_3
$(CH_3)_2NSF_3$	−59.4	−20.2	58	—	—	5.0	8.2	—	−3.06	—
$(CH_3CH_2)_2NSF_3$	−54.0	−34.4	62	3	6.1	0.0	0.0	−3.49	−1.25	7.0

In a separate experiment it was shown that $(CH_3)_3SiN(C_2H_5)_2$ did not react with $(C_2H_5)_2NSF_3$ under the same conditions. These experiments support our hypothesis that hydrolysis is the mechanism of fluorine exchange in *N*-dialkylaminosulfur trifluorides.

If hydrolysis provides the lowest energy pathway for fluorine exchange in *N*-dialkylaminosulfur trifluorides, then it is obvious that the absence of significant exchange at $-68°$ (Figs. 1 and 3) and at $+22°$ (Fig. 2) under anhydrous conditions, suggests a much higher energy barrier to fluorine exchange via alternate intra- or intermolecular exchange mechanisms than has previously been suggested.

Experimental

Sulfur tetrafluoride (Matheson Co.) was handled in a metal vacuum system. Reaction of $(CH_3)_2NSi(CH_3)_3$ and $(CH_3CH_2)_2NSi(CH_3)_3$ (Peninsular ChemResearch) with SF_4 was carried out in a U-tube attached directly to a standard n.m.r. tube in a 1:1 molar ratio on a 2 mmol scale, a modification of the method of Demitras and MacDiarmid (2) and von Halasz and Glemser (3). The n.m.r. tubes were silylated with $[(CH_3)_3Si]_2NH$, flamed out, and evacuated at 10^{-4} mm. After reaction of $R_2NSi(CH_3)_3$ with SF_4, trichlorofluoromethane was condensed in and n.m.r. tubes sealed under vacuum and kept at $-78°$ while transferring to the n.m.r. spectrometer equipped with a variable temperature probe cooled to $-68°$. The n.m.r. spectra were recorded on a Varian A-56/60A spectrometer using 56.4 and 60 MHz for fluorine and proton respectively. Spectra are shown in Figs. 1–3 and coupling constants and chemical shifts are summarized in Table 1. Trimethylfluorosilane was used as internal standard for proton n.m.r. spectra, but chemical shifts are reported relative to internal tetramethylsilane (TMS) using the formula δ p.p.m. ($(CH_3)_3SiF$ internal) − 0.179 p.p.m. = δ p.p.m. (TMS internal). Chemical shifts for fluorine spectra are relative to internal trichlorofluoromethane.

The financial assistance of the National Research Council of Canada is gratefully acknowledged.

1. R. J. GILLESPIE. J. Chem. Ed. **40**, 295 (1963); Angew. Chem. Int. Ed. **6**, 819 (1967).
2. G. C. DEMITRAS and A. G. MACDIARMID. Inorg. Chem. **6**, 1903 (1967).
3. S. P. VON HALASZ and O. GLEMSER. Chem. Ber. **103**, 594 (1970).
4. E. L. MUETTERTIES and W. D. PHILLIPS. J. Am. Chem. Soc. **81**, 1084 (1959).
5. J. A. GIBSON and A. F. JANZEN. Can. J. Chem. In press.

Can. J. Chem. Downloaded from www.nrcresearchpress.com by 210.87.254.6 on 09/05/12
For personal use only.

The Barrier to Rotation in Cyclopropylmethyl Cations

ALLISTER BROWN[1] AND GEORGE H. SCHMID
Department of Chemistry, University of Toronto, Toronto 181, Ontario

Received December 16, 1971

The barrier to rotation of a cyclopropyl ring around the planar carbon of a cyclopropylmethyl cation has been estimated from rates of solvolysis to be 14 kcal/mol. This value is obtained by a comparison of the rates of solvolysis of molecules which contain conformationally rigid cyclopropane rings. The results obtained compare favorably with estimates made by other methods.

La barrière de rotation du cycle cyclopropyle autour du carbone plan du cation cyclopropyl méthyle a été évaluée à 14 kcal/mol, à partir des vitesses de solvolyse. Cette valeur a été obtenue en comparant les vitesses de solvolyse des molécules contenant des cycles cyclopropane de conformation rigide. Les résultats obtenus sont tout à fait comparables à ceux calculés à partir des autres méthodes.

Canadian Journal of Chemistry, **50**, 2432 (1972)

Can. J. Chem. Downloaded from www.nrcresearchpress.com by 210.87.254.42 on 09/05/12
For personal use only.

The mechanism of solvolysis of cyclopropylmethyl compounds has been the object of numerous investigations (1). It has been observed that their rates of solvolysis are generally much higher than those of model compounds. The solvolysis products often exhibit a high degree of skeletal rearrangement, as well as a degenerate cyclopropylmethyl–cyclopropylmethyl rearrangement (2, 3).

One of the first definitive pieces of information regarding the structure of cyclopropylmethyl cations was presented simultaneously by Pittman and Olah (4), and Deno *et al.* (5). The n.m.r. spectra observed by these workers, for the 2-cyclopropyl-2-propyl cation in SbF_5–SO_2–SOClF, can be explained by assuming that the cyclopropyl cation exists in the bisected conformation, **1**, $R_1 = R_2 = CH_3$

Support for **1** as the structure of the cyclopropylmethyl cation has been derived from the interpretation of the u.v. spectra of several cyclopropyl ketones and esters (6). Electron diffraction data (7) are also consistent with **1** as the structure of the cyclopropylmethyl cation.

Evidence that **1** is an intermediate formed on solvolysis of substituted cyclopropylmethyl compounds has been presented by several authors (1, 8). Schleyer and van Dine (1) showed that the effects of methyl substituents on the rate of solvolysis were consistent with **1** as an intermediate while both Vogel and Roberts (8) and Richey and Richey (9) showed that ionization of optically active 1-cyclopropyl-1-ethyl compounds led to racemization, an observation consistent only with **1**, $R_1 = CH_3$, $R_2 = H$, as intermediate. Brown and Cleveland (10) showed that the intermediate formed on solvolysis of *p*-cyclopropyl-*t*-cumyl chloride (**3**), $R_1 = R_2 = H$ adopts conformation **1**. Introduction of two methyl groups ortho to the cyclopropyl substituent forces the cyclopropyl group to rotate away from the bisected conformation and a decrease in the rate of solvolysis was observed. In a similar study Sharpe and Martin (11) found that the pK_{R^+} of **4** was similarly affected by

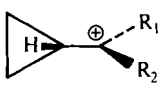

1

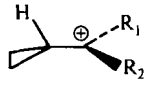

2

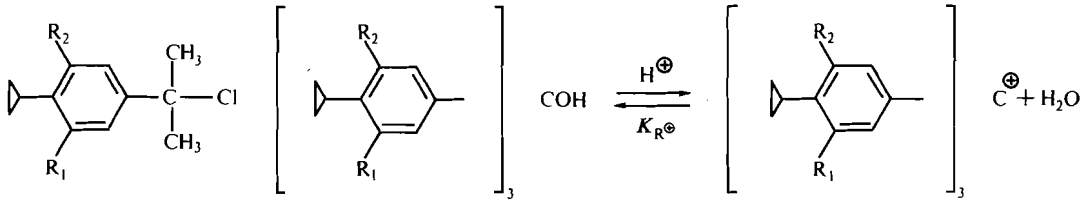

3 **4** **5**

[1]Holder of NRCC Scholarship, 1966–1969.

Can. J. Chem. Downloaded from www.nrcresearchpress.com by 210.87.254.42 on 09/05/12
For personal use only.

ortho methyl groups. However, the chemical shift difference for the cyclopropyl ring protons in **4** and **5**, $R_1 = R_2 = CH_3$, indicates that charge is still delocalized into the cyclopropyl ring, even though the preferred conformation **1** is not accessible. The slower rate of solvolysis of spiro[cyclopropane-1,2-adamantyl] derivatives (12) **6** than model compounds is significant. In

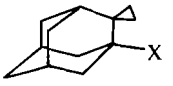

6

X = Cl or CH_3—C$_6$H$_4$—SO_3—

these compounds the solvolysis intermediate is restricted to conformation **2**. Thus, there appears to be a large net destabilization of cyclopropylmethyl cations when the cyclopropyl group is rotated from the bisected conformation of **1** to that in **2**.

We wish to report experimental results which indicate the magnitude of the torsional barrier for rotation of the cyclopropyl group about the plane of the cationic carbon in secondary cyclopropylmethyl cations. We have obtained such data from a measurement of the rates of solvolysis of *N*-methyl-4-(*cis*- and *trans*-2-bicyclo-[3.1.0]hexanoxy)pyridinium iodides (**7***a* and **8***a*) and *N*-methyl-4-(spiro[2.4]heptan-4-oxy) pyridinium iodide (**9***a*) in 80% aqueous ethanol.

Results and Discussion

cis-2-Bicyclo[3.1.0]hexanol (**7***b*) was prepared by the method of Dauben and Berezin (13). *trans*-2-Bicyclo[3.1.0]hexanol (**8***b*), was obtained by the aluminum isopropoxide equilibration of **7***b*. 4-Spiro[2.4]heptanol (**9***b*), was prepared according to the method of Closson and Kwiatkowski (14). The mixture of **7***b* and **8***b* obtained by equilibration with aluminum isopropoxide could not be separated on a preparative scale using various techniques. The mixture of isomeric compounds also proved inseparable at the various stages in the preparation of the *N*-methyl-4-alkoxypyridinium iodides. However, since **7***a* could be obtained as a single isomer, the solvolysis of a mixture of **7***a* and **8***a* of known composition gave the data required for the solvolysis of **8***a*.

TABLE 1. The rates of solvolysis of *N*-methyl-4-alkoxy pyridinium iodides in 80% aqueous ethanol

Substrate	Temperature (°C)	$10^4 k_{obs}$ (s^{-1})
7*a*	86.4	2.20 ±0.05
8*a*	86.4	1.70 ±0.05
9*a*	39.6	0.498±0.003
"	49.3	2.06 ±0.01
"	59.3	6.41 ±0.01
"	86.4	148

The rates of solvolysis of **7***a* and **8***a* were measured in 80% aqueous ethanol at 86.4°. The rate constant for **9***a* at 86.4° was obtained by extrapolation of the values obtained at lower temperatures. The progress of the reaction was monitored by an acidimetric titration using the ampoule technique. The rate of liberation of acid followed first order kinetics for more than three half-lives in all cases.

The rate constants at 86.4° and the relative rates are presented in Table 1. The value listed for **8***a* was calculated using eq. 1, where k_{obs} is the rate constant observed for the solvolysis of a mixture of 49.5% of **7***a* and 50.5% of **8***a*, X_{8a} being the mole fraction of **8***a* and k_{7a} the independently measured rate constant for solvolysis of **7***a*. Equation 1 is only an approximation and

$$[1] \qquad k_{8a} = \frac{k_{obs} - (1 - X_{8a})k_{7a}}{X_{8a}}$$

is strictly obeyed only in the initial stages of the reaction. However, in the case where the rate constants are similar, as with **7***a* and **8***a*, the deviation from first order behavior is much less than the experimental error.

Vogel and Roberts (8) showed that the intermediate cation formed on solvolysis of *N*-methyl-4-(1-cyclopropyl-ethyl)pyridinium iodide in the rate determining step must have a plane of symmetry. They concluded that **1**, $R_1 = H$, $R_2 = CH_3$, is a reasonable representation of the structure of this intermediate. The mechanism of solvolysis of derivatives of **7**, **8**, and **9**, have been discussed previously (14–18). Compounds **7***a*, **8***a*, and **9***a* all undergo solvolysis reactions that involve the formation of a cyclopropylmethyl cation in the rate determining step. The cationic intermediate formed in the

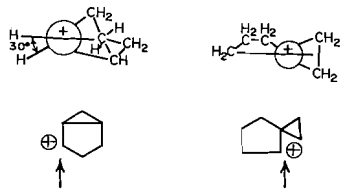

FIG. 1. Structures of the cations obtained by solvolysis of **7***a*, **8***a*, and **9***a*.

rate determining step of the solvolysis of **9***a* has been shown to be symmetrical (15) having the structure shown in Fig. 1. While the solvolysis of **7** and **8** was originally postulated to occur with the homoallylic ions as intermediates (16, 17) it has recently been established (19) that the intermediate formed in the rate determining step in the solvolysis of cyclopropylmethyl compounds retains the structure of the substrate. In the case of **7***a* and **8***a* this intermediate is best represented by a structure which is planar at the cationic carbon, C-2, with the neighboring cyclopropyl group rotated approximately 30° from **1**, as illustrated in Fig. 1. The slight differences in the rates for **7***a* and **8***a* reflect the difference in ground state stabilities, **7***a* being slightly less stable (18). The solvolysis products from either **7***a* or **8***a* consist of the alcohols and corresponding ethyl ethers derived from **7**, **8**, and 3-cyclohexenol (18). The products of the solvolysis of **9***a* were found to be identical to those previously reported (14, 15). These products are consistent with the formation of a cationic intermediate.

Schleyer and van Dine (1) have found that substitution at the α- and β-positions of the cyclopropane ring produces a five-fold and eight- to eleven-fold increase in rate, respectively; over that of the unsubstituted compound. Thus, substitution at the β-position of the cyclopropyl ring is twice as effective as substitution at the α-position. In the absence of any additional gross complications **7***a* and **8***a* would be expected to solvolyze twice as fast as **9***a*. The rate constants in Table 1 reveal that this is not the case.

If it is assumed that the major difference in the rates of solvolysis of **8***a* and **9***a* is caused by the fact that the cyclopropyl ring in **8***a* cannot assume the preferred bisected conformation **1**, an approximation to the torsional barrier for rotation of the cyclopropyl group in **1**, R_1—H, R_2—CH_3, can be calculated. Using eq. 2, the difference in the free energies of activation for **8***a* and **9***a* is found to be approximately 3.5 kcal/mol at 86.4° (3.48 kcal/mol for **7***a* and 3.66 kcal/mol for **8***a*). If it is assumed that the difference in energy between the *cis*- and *trans*-conformers of the 1-cyclopropyl-1-ethyl cation is small compared to the barrier of rotation between the conformers, then the barrier will appear to have two-fold symmetry. The energy, $V(\theta)$, required to rotate a group from the minimum potential energy through an angle, θ, is given by eq. 3 (20), where V_o is the barrier to rotation through $\pi/2$.

[2] $$\Delta\Delta G^{+} = RT \ln (k_{8a}/2k_{9a})$$

[3] $$V(\theta) = V_o/2(1 - \cos 2\theta)$$

The difference in free energy of activation for **8***a* and **9***a* is equal to the energy required to rotate the cyclopropyl group by 30° away from the bisected conformation. In this way the torsional barrier, V_0, can be calculated to be 14 kcal/mol.

There are several assumptions inherent in this calculation. Firstly, the assumption is made that the barrier to rotation of **1**, $R_1 = H$, $R_2 = CH_3$, will have the same angular dependence on energy as the intermediate formed on solvolysis of **7***a* and **8***a*. Secondly, the usual assumption is made that during the rotation of the cyclopropane ring, the entropy changes, as well as $\Delta\Delta S^{+}$, are zero.

Finally it is assumed that rotation of the cyclopropane ring does not alter the α and β substituent effects determined by Schleyer and van Dine (1).

The value of 14 kcal/mol calculated in this study is in good agreement with the value of 13.7 kcal/mol calculated by Kabakoff and Namanworth (22) for **1**, $R_1 = H$, $R_2 = CH_3$, using n.m.r. measurements, as well as other values from *ab initio* calculations (21) (17.5 kcal/mol) and from the solvolysis of **6** (23, 24) (10 kcal/mol).

Our result for the rotational barrier is obtained by using an average value for $\Delta\Delta G^{+}$. If the rotational barrier is calculated from the data of solvolysis of **7***a* and **8***a* values of 13.9 and 14.6 kcal/mol are obtained respectively. This small difference of 0.7 kcal/mol indicates that our third assumption is reasonable.

Can. J. Chem. Downloaded from www.nrcresearchpress.com by 210.87.254.42 on 09/05/12
For personal use only.

Can. J. Chem. Downloaded from www.nrcresearchpress.com by 210.87.254.42 on 09/05/12
For personal use only.

We would like to conclude from these results, that the major factor which causes the barrier to rotation in cyclopropylmethyl ions must also be a major factor contributing to the stability of cyclopropylmethyl cations. This factor may be "vertical" stabilization as defined by Traylor and co-workers (25), but charge delocalization, as in the allyl cations, can not be great. This view is supported by the hundred-fold greater effectiveness of a methyl group at the C-1 position of a cyclopropane ring in stabilizing the transition state than methyl groups at positions C-2 and -3 (2). Further, the products from solvolysis of **7***a* and **8***a* are derived mainly from solvent capture at C-2, even though considerable strain release would be achieved by solvent capture at C-5, giving 3-cyclohexenyl derivatives (26).

Further support of this conclusion is derived from the contrasting effects of methyl groups on the rotational barriers estimated for allylic and cyclopropylmethyl cations described by Schleyer and co-workers (23). These authors also concluded that the cyclopropylmethyl cation is stabilized in a different manner than the allyl cation.

Experimental

Melting and boiling points are uncorrected. Elemental micro-analyses were carried out by A. B. Gygli of Toronto.

cis-2-Bicyclo [3.1.0]hexanol (7b)

Compound **7***b* was prepared by the procedure of Dauben and Berezin (13) in 60% yield; b.p. 62–65° (9 mm); n_D^{25} 1.4790 (lit. b.p. 78–79.5° (20 mm), n_D^{25} 1.4742 (13); b.p. 76° (17 mm), n_D^{25} 1.4788 (26)).

4-(cis-Bicyclo [3.1.0.]hexyl-2-oxy)pyridine

This compound was prepared according to the method of Schmid and Wolkoff (27) in 76.5% yield. The liquid was sublimed onto a cold finger rather than being distilled. I.r. ν_{max} (CCl_4); 3090, 3050, (cyclopropyl C—H stretch); 2950–2980, 1590, 1560, (pyridyl ring vib.) 1495, 1420, 1366, 1330, 1275, 1210, (pyridyl C—O stretch), 1015 cm^{-1}. N.m.r. ($CDCl_3$); 1.6–1.8, quart., $J_1 = 5$, $J_2 = 1$ Hz, (2H), 2,6-pyridyl protons; 3.0–3.2, quart., (2H), $J_1 = 5$, $J_2 = 1$ Hz, 3,5-pyridyl protons; 4.9–5.2, mult., (1H), methine proton; 7.2–8.9, mult., (6H), cycloalkyl protons; 9.2–9.8, mult., (2H), cyclopropyl methylene protons.

N-Methyl-4-(cis-bicyclo[3.1.0]hexyl-2-oxy)pyridinium Iodide (7a)

Iodide **7***a* was prepared from 4-(*cis*-bicyclo[3.1.0]hexyl-2-oxy)pyridine by the method of Schmid and Wolkoff (27) in 96.5% yield. The solid was recrystallized from methylene chloride and ether as white needles, m.p. 118–119.5°. I.r. ν_{max} ($CHCl_3$); 2930, 1645, 1570, (pyridyl ring vib.), 1340, 1295, 975 cm^{-1}. N.m.r. ($CDCl_3$); 0.7–1.0, doub., $J = 7$ Hz, (2H), 2,6-pyridyl protons; 2.4–2.6, doub., $J = 7$ Hz, (2H), 3,5-pyridyl protons; 4.4–4.8, mult., (1H), methine proton; 5.5, sing., (3H), *N*-methyl protons; 7.5–8.8, mult., (6H), cycloalkyl protons; 9.2–9.6, mult., (2H), cyclopropyl methylene protons.

Anal. Calcd. for $C_{12}H_{16}ONI$: C, 45.58; H, 5.16; N, 4.46; I, 40.23. Found: C, 45.49; H, 5.21; N, 4.43; I, 40.03.

trans-2-Bicyclo [3.1.0]hexanol (8b)

Hexanol **8***b* was prepared by isomerizing **7***b* by the method of Eliel and Ro (28). The fractions obtained by distillation, b.p. 61–65° (11.5 mm) varied in ratio of **7***b* to **8***b* and weighed 4.36 g (44% recovery).

2-Carbomethoxycyclopentanone

Following the method of Pinkney (29), 342.1 g of methyl adipate (1.97 mol) gave 212 g (79% yield) of a clear liquid after distillation under vacuum, b.p. 95–96° (11 mm) (lit. (29) b.p. 83–88° (5 mm); yield, 81%).

4-Spiro [2.4]heptanone

The heptanone was prepared by the method of Mayer (30, 31) from 56 g of 2-carbomethoxycyclopentanone (0.394 mol) in an overall yield of 32%; b.p. 44–46° (10 mm) (lit. (30, 31) b.p. 54–55° (14 mm)).

4-Spiro [2.4]heptanol

The heptanol was prepared by lithium aluminum hydride reduction of 4-spiro[2.4]heptanone in 76% yield; b.p. 59.5–60° (9 mm) (lit. b.p. 68–69° (13–14 mm) (32).

4-Spiro [2.4]heptan-4-oxy)pyridine

The compound was prepared according to the method of Schmid and Wolkoff (27) in 81.5% yield, b.p. 80° (0.075 mm). I.r. ν_{max} (neat); 3010, 2955–2860, 1590, 1565, (pyridyl C=C vib.), 1495, 1280, 1210, (pyridyl C—O stretch), 1080, (alkyl C—O stretch) cm^{-1}. N.m.r. (CCl_4); 1.7–1.8, quart., $J_1 = 5$, $J_2 = 2$ Hz, (2H), 2,6-pyridyl protons; 3.3–3.4, quart., $J_1 = 5$, $J_2 = 2$ Hz, 3,5-pyridyl protons; 5.8–5.9, doub., (1H), methine proton; 7.6–8.8, mult., (6H), cycloalkyl protons; 8.9–9.6, mult., (4H), cyclopropyl protons.

Anal. Calcd. for $C_{12}H_{17}ON$: C, 76.15; H, 7.99; N, 7.40. Found: C, 76.32; H, 8.11; N, 7.41.

N-Methyl-4-(spiro[2.4]heptan-4-oxy)pyridinium Iodide

The iodide was prepared by the method of Schmid and Wolkoff (27) from 4-(spiro[2.4]heptan-4-oxy)pyridine in 97% yield, m.p. 86–88.5°. I.r. ν_{max} ($CHCl_3$); 2930, 1645, 1590, 1510, (pyridyl ring vib.), 1485, 1330, 1305, 1290 (pyridyl C—O stretch), 1080 (alkyl C—O stretch), 1015, 945 cm^{-1}. N.m.r. ($CDCl_3$); 0.6–0.9, doublet; $J = 7$ Hz, (2H), 2,6-pyridyl protons; 2.5–2.7, doublet $J = 7$ Hz, (2H), 3,5-pyridyl protons; 5.4–5.6, multiplet, methine proton; 5.5 singlet, *N*-methyl protons (3H); 7.4–8.7; multiplet, (6H), cycloalkyl protons; 9.0–9.5, multiplet (4H), cyclopropyl protons.

Kinetics

All kinetic runs were carried out in thermostated oil baths, with temperature controlled to maximum deviation of ±0.05°. The rate constants were determined using the general procedure of sealing portions of the reacting solutions in glass ampoules, removing ampoules at chosen intervals from the bath, freezing, and titrating. All samples were titrated automatically to a predetermined p*H* using a Coleman Model 31 p*H* meter and Companion Automatic Titrator. The end point for the titration was determined from a titration curve of *N*-methyl-4-pyridone hydroiodide.

The rate constants were calculated from the volume of base required for neutralization, V_t, in the usual manner (33).

Products

The ratios of products obtained by the solvolysis of **7***a*, **8***a*, and **9***a* were determined using several v.p.c. columns. The ethers and alcohols from **7***a* and **8***a* were isolated as two mixtures and examined by n.m.r. spectroscopy. It was possible to determine the ratio of the three products from the integrated ratios of the three methine resonances as well as from the chromatograms. The n.m.r. product ratio agreed well with that determined by v.p.c.

The products of the solvolysis of **9***a* were isolated by v.p.c. and the structure of each was established by comparing its infrared and n.m.r. spectra with published data (14, 15).

Continued financial support by the National Research Council of Canada is gratefully acknowledged.

1. P. VON R. SCHLEYER and G. H. VAN DINE. J. Am. Chem. Soc. **80**, 2321 (1966).
2. K. B. WIBERG and G. SZEIMIES. J. Am. Chem. Soc. **90**, 4195 (1968).
3. L. E. FRIEDRICH and F. R. WIGHT. J. Am. Chem. Soc. **92**, 1808 (1970).
4. C. U. PITTMAN and G. A. OLAH. J. Am. Chem. Soc. **87**, 2998 (1965).
5. N. C. DENO, J. S. LIU, J. O. TURNER, D. N. LINCOLN, and R. E. FRUIT, JR. J. Am. Chem. Soc. **87**, 3000 (1965).
6. E. M. KOSOWER and M. ITO. Pro. Chem. Soc. 25, 1962.
7. L. S. BARTELL, J. P. GUILLORY, and A. J. PARKER. J. Phys. Chem. **69**, 3043 (1965), and previous papers.
8. M. VOGEL and J. D. ROBERTS. J. Am. Chem. Soc. **88**, 2262 (1962).
9. H. G. RICHEY, JR., and J. M. RICHEY. J. Am. Chem. Soc. **88**, 4971 (1966).
10. H. C. BROWN and J. D. CLEVELAND. J. Am. Chem. Soc. **88**, 2051 (1966).
11. T. SHARPE and J. C. MARTIN. J. Am. Chem. Soc. **88**, 1815 (1966).
12. P. VON R. SCHLEYER and V. BUSS. J. Am. Chem. Soc. **91**, 5880 (1969).
13. H. G. DAUBEN and G. H. BEREZIN. J. Am. Chem. Soc. **88**, 3449 (1967).
14. W. D. CLOSSON and G. T. KWIATKOWSKI. Tetrahedron, **21**, 2779 (1965).
15. K. B. WIBERG and J. E. HIATT. Tetrahedron Lett. 3009 (1968).
16. P. R. BROOK, R. M. ELLAM, and A. S. BLOOS. Chem. Commun. 425 (1968).
17. M. HANACK and H. J. SCHNEIDER. Tetrahedron, **20**, 1863 (1964).
18. A. BROWN and G. H. SCHMID. Tetrahedron Lett. 4695 (1968).
19. K. B. WIBERG and J. G. PFEIFFER. J. Am. Chem. Soc. **92**, 553 (1970).
20. H. J. MOORE. Physical chemistry, 3rd ed. Prentice Hall. 1962. p. 634.
21. L. RADOM, J. A. POPLE, V. BUSS, and P. VON R. SCHLEYER. J. Am. Chem. Soc. **92**, 6380 (1970).
22. D. S. KABAKOFF and E. NAMANWORTH. J. Am. Chem. Soc. **92**, 3234 (1970).
23. V. BUSS, R. GLEITER, and P. VON R. SCHLEYER. J. Am. Chem. Soc. **93**, 3927 (1971).
24. B. R. REE and J. C. MARTIN. J. Am. Chem. Soc. **92**, 1660 (1970).
25. H. HANSTEIN, H. J. BERWIN, and T. G. TRAYLOR. J. Am. Chem. Soc. **92**, 829 (1970).
26. M. HANACK and H. ALLMENDINGER. Ber. **97**, 1669 (1964).
27. G. H. SCHMID and A. W. WOLKOFF. Can. J. Chem. **50**, 1181 (1972).
28. E. L. ELIEL and R. S. RO. J. Am. Chem. Soc. **79**, 5992 (1957).
29. P. S. PINKNEY. Organic synthesis. Coll. Vol. II. J. Wiley and Sons, New York. 1943. p. 116–118.
30. R. MAYER and H. H. SCHUBERT. Ber. **91**, 768 (1958).
31. R. MAYER and E. ALDER. Ber. **88**, 1866 (1955).
32. D. E. APPLEQUIST and J. A. LANDGREBE. J. Am. Chem. Soc. **86**, 1543 (1964).
33. A. A. FROST and R. G. PEARSON. Kinetics and mechanism. 2nd ed. John Wiley and Sons, Inc., New York. 1965. p. 99.

Can. J. Chem. Downloaded from www.nrcresearchpress.com by 210.87.254.42 on 09/05/12
For personal use only.

The ^{13}C Fourier Transform Spectrum of Heparin. Evidence for a Biose Repeating Sequence of Residues

A. S. PERLIN, N. M. K. NG YING KIN,[1] AND S. S. BHATTACHARJEE[1]
Department of Chemistry, McGill University, Montreal, Quebec

AND

L. F. JOHNSON[2]
Varian Associates, Palo Alto, California

Received February 15, 1972

Carbon-13 Fourier transform n.m.r. spectra of the biopolymer, heparin, are described. The proton-decoupled spectrum corresponds to that of a molecular structure based on 12 carbon atoms, and the observed chemical shifts are shown to be consistent with a previously-proposed alternating sequence consisting of (1 → 4) linked residues of α-L-idopyranosyluronic acid 2-sulfate and 2-deoxy-2-sulfamino-α-D-glucopyranosyl 6-sulfate. Line-broadening of the C-6 signal of the latter residue indicates that spin–spin relaxation of the ^{13}C nucleus of this sulfated primary carbinol group is more effective than for the ^{13}C nuclei of the sugar rings. Among model compounds utilized for assignment of the signals from heparin is a disaccharide, 4-*O*-(α-L-idopyranosyluronic acid 2-sulfate)-2,5-anhydro-D-mannose 6-sulfate, prepared in 65% yield by deaminative degradation of heparin.

Les spectres carbone 13, transformés de Fourier, du biopolymère héparine sont décrits. Le spectre, avec les protons découplés, correspond à celui d'une structure moléculaire contenant douze atomes de carbone; on a montré que les déplacements chimiques observés sont compatibles avec la séquence alternée que nous avons précédemment proposée, consistant des résidus α-L-iodopyranosyluronique acide sulfate-2 et déoxy-2 sulfamino-2-α-D-glucopyranosyl sulfate-6, liés (1 → 4). La largeur de raie du signal C-6 du dernier residu indique que la relaxation spin–spin du noyau ^{13}C de ce groupe carbinol primaire sulfaté est plus facile que celle des noyaux ^{13}C pour les cycles des sucres. Parmi les composés modèles utilisés pour l'attribution des signaux de l'héparine nous signalons que le disaccharide 4-*O*-(α-L-iodopyranosyl uronique acide sulfate-2) anhydro-2,5-D-mannose sulfate-6 a été préparé avec un rendement de 65% par dégradation déaminative de l'héparine.

Canadian Journal of Chemistry, **50**, 2437 (1972)

In conjunction with studies (1–4) on the structure of heparin it became of interest to examine the ^{13}C n.m.r. spectrum of this polymer. However, attempts to obtain the ^{13}C resonance data by the continuous wave technique were unsuccessful; multiple-scanning even for several days failed to yield satisfactory signals. Similarly the use of this technique with another polysaccharide, low molecular weight cellulose acetate has been reported (5) to give a relatively poor spectrum. The current paper describes a high quality spectrum of heparin obtained by Fourier transform (FT) n.m.r. spectroscopy and hence also demonstrates the superior potential of this method for the measurement of ^{13}C spectra of carbohydrate macromolecules.

The FT spectrum of heparin in deuterium oxide has been recorded both with proton-decoupling (Fig. 1A) and without decoupling (Fig. 1B), using a Varian XL-100-15 spectrometer and spectrum accumulation times of 18 and 50 h, respectively. In Fig. 1A, the relative intensities of signals (moving progressively downfield from 134 to 92 p.p.m. from CS_2) are 1.0, 0.9, 4.0, 3.0, 0.8, and 0.9.[3] Together with the signal of 18 p.p.m.,[4] these data correspond to a repeating formula based on a minimum of

[1]Postdoctoral Fellow, 1970–1971 and 1970–1972, respectively.

[2]Present address: Transform Technology Inc., Palo Alto, California.

[3]For a discussion of the accuracy of FT n.m.r. ^{13}C integrated intensities of smaller molecules see ref. 6. Under the conditions used, the acquisition time was estimated to be at least 4–5 times the relaxation time.

[4]The intensity of this signal (carboxyl ^{13}C) cannot be compared satisfactorily with that of the others because carbonyl ^{13}C generally gives weaker signals than H-bearing carbons. Noteworthy, however, is the relative intensity of this signal in 1A as compared with 1B, which illustrates the large improvement in signal-to-noise due to the nuclear Overhauser effect of proton-decoupling.

Can. J. Chem. Downloaded from www.nrcresearchpress.com by 86.111.144.194 on 09/06/12
For personal use only.

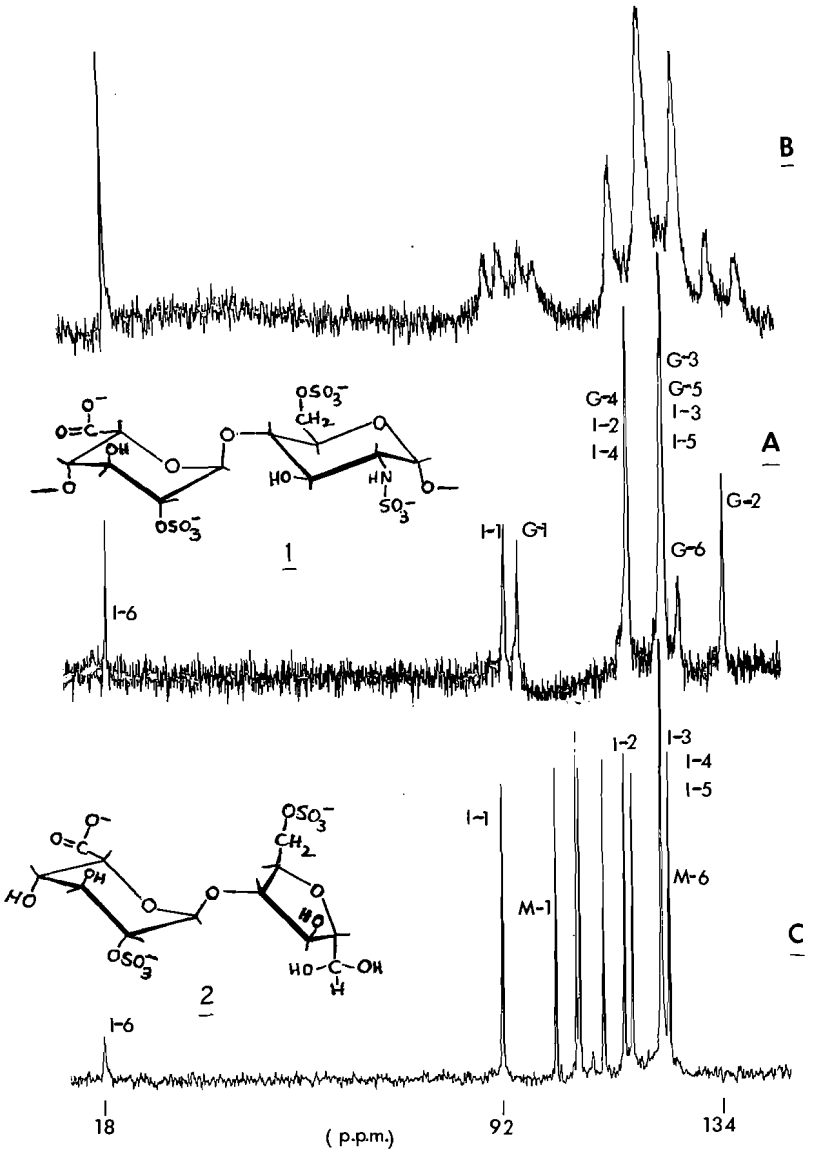

FIG. 1. ^{13}C Fourier transform n.m.r. spectrum of (A) heparin in deuterium oxide, with proton-decoupling (I-signal ascribed to α-L-idosyluronic acid residue, G-signal ascribed to 2-amino-2-deoxy-α-D-glucose residue); (B) heparin in deuterium oxide, without proton-decoupling; (C) disaccharide **2** in deuterium oxide, with proton-decoupling (I-signal ascribed to α-L-idosyluronic acid residue, M-signal ascribed to 2,5-anhydro-D-mannose residue; the unmarked signals also are ascribed to this residue). Chemical shifts (p.p.m.) are relative to downfield carbon disulfide.

12 carbon atoms, such as in the main heparin segment **1** composed of residues of α-L-iduronic acid and 2-amino-2-deoxy-α-D-glucose (2–4, 7–9). The following discussion shows that the observed chemical shifts also are consistent with structure **1**.

The two signals at 92 and 95 p.p.m. are attributable to anomeric carbons, because of their downfield positions (10–13). Also, they show relatively broad C—H coupling: that is, J_{CH} is about 165 Hz in each instance, which is noticeably larger than couplings (130–150 Hz) for the other carbons, as found with α- and β-D-glucose (11). By overlaying traces A and B,

Can. J. Chem. Downloaded from www.nrcresearchpress.com by 86.111.144.194 on 09/06/12
For personal use only.

Can. J. Chem. Downloaded from www.nrcresearchpress.com by 86.111.144.194 on 09/06/12
For personal use only.

the signal at 125 p.p.m. is found to be that of a CH_2 group, *i.e.* it appears as a triplet in contrast to the doublet structures of the other proton-bearing carbons, and hence is ascribed to C-6 of the hexosamine residue. Relative to the chemical shift (131 p.p.m.) of C-6 of 2-amino-2-deoxy-α- or β-D-glucose hydrochloride, its position corresponds to a downfield displacement of 6 p.p.m. by the 6-*O*-sulfate group of the residue. This assignment is consistent also with the fact that the signal has a greater line-width than do individual signals from the other carbon atoms.[5] The heparin macromolecule must have a relatively long correlation time and correspondingly short relaxation times, T_1 and T_2 (14). Now, T_1 of a given carbon is inversely proportional to the number of attached protons (6). Since T_2 cannot be longer than T_1 (14), the ^{13}C nucleus of the CH_2 group should accordingly experience more effective spin–spin relaxation (shorter T_2) than nuclei of the CH groups, and hence give rise to the relatively greater line-broadening observed.

Assignment of the signal furthest upfield to G-2 is based on the analogous location of C-2 in the spectrum of 2-amino-2-deoxy-α-D-glucose hydrochloride (C-2 of the β-anomer is more deshielded by 3 p.p.m.). Continuing with this comparison, C-3, -4, and -5 of the α-hexosamine resonate of 120–122 p.p.m., *i.e.* close to the chemical shift of the largest group of signals at 122 p.p.m., which leads to the G-3 and -5 designations in Fig. 1A. G-4, however, must be much further downfield because of strong deshielding by an adjacent glycosyl residue linked through O-4. Hence, a shift downward of 7–8 p.p.m. as observed with several oligosaccharides (5, 15), would reasonably place G-4 among the signals resonating at 116 p.p.m.

Reference to the ^{13}C spectrum of sodium methyl α-D-idopyranosiduronate (16), as a possible model for the uronic acid moiety of heparin, shows that signals of C-2 to -5 are closely grouped within the range 121.0–122.5 p.p.m. which again coincides with the broad four-carbon signal at 122 p.p.m. However, since C-4 of uronosyl residues in heparin is glycosidically bonded, it should resonate downfield and, like C-4, is probably one of the signals at 116 p.p.m. Similarly, the signal designated I-2 takes account of the presence of a 2-*O*-sulfate group in heparin; as noted above in relation to G-6 (and this is found also for the effect of an *O*-sulfate group introduced at C-2 of methyl α-D-glucopyranoside) the associated deshielding is expected to place I-2 about 8 p.p.m. downfield of the C-2 signal of methyl α-D-idopyranosiduronic acid.

These various assignments also are in close accord with the ^{13}C spectrum of disaccharide **2** (Fig. 1C),[6] the major product obtained by deaminative degradation of heparin (see below). Thus the three-carbon signal at 122 p.p.m. is coincident with I-3 and -5 of the heparin spectrum, and I-4 of **2** should then account for the remaining signal in this upfield region because O-4 is not engaged in inter-residue bonding as when in the parent polymer. Other signals common to both Figs. 1A and C are those at 93 p.p.m. (which specifically suggests the I-1 designation in 1A), at 111 p.p.m., ascribable in each instance to I-2, and those of the carboxyl ^{13}C at 18 p.p.m.

The high degree of consistency found in comparing appropriate chemical shifts within the series heparin, disaccharide **2**, and methyl α-D-idopyranosiduronic acid, indicates that the conformation of L-iduronic acid residues in heparin is close to that in the smaller molecules. Information available about the methyl glycoside (16) favors a predominance of the C1(D) conformation for it and, accordingly, the L-iduronic acid residues of heparin may be depicted most satisfactorily by the 1C(L) conformation.

Quantitative aspects of ^{13}C FT n.m.r. spectra (6) are of particular interest from the general standpoint of polymer characterization (18). In principle, a reliable measure of the proportion of constituent residues in a mucopolysaccharide, or other polysaccharide, should be afforded by the number and relative intensities

[5]An expanded plot of Fig. 1B shows for example that its line-width is 1.6 times that of the adjacent, upfield, signal. It appears most probable that these line-widths are, in reality, natural line-widths.

[6]Signals of the 2,5-anhydro-D-mannose residue in **2** are seen to be markedly downfield relative to those of the hexosamine residue from which it was derived. This effect is consistent with the fact that most ^{13}C signals of furanose derivatives are more deshielded by 5–10 p.p.m. than are their six-membered ring counterparts (17*a* and *b*).

Can. J. Chem. Downloaded from www.nrcresearchpress.com by 86.111.144.194 on 09/06/12
For personal use only.

of the resonance signals in its ^{13}C spectrum. Although many of the signals from heparin coincide in chemical shift, the evidence clearly favors a total of 12 different carbons, and therefore accords with a biose repeating sequence such as represented by **1**. It is noteworthy, nevertheless, that there are no additional, lower intensity signals detected to account for the minor (2, 9) D-glucuronic acid moiety of heparin (7), as found also on examination of its 220 MHz p.m.r. spectrum (3). Presumably, such relatively weak signals in these spectra are obscured through overlap, although insufficient accuracy in the measurement of signal intensities also could be a contributing factor. Despite such limitations, n.m.r. spectroscopy obviously constitutes a valuable adjunct to chemical and enzymic methods for characterizing carbohydrate polymers.

Deaminative Degradation of Heparin[7]

When treated with nitrous acid, heparin is degraded extensively to fragments containing residues of 2,5-anhydro-D-mannose and uronic acid (19, 20). Recent examination of these fragments by Lindahl and Axelsson (9), and now also in this laboratory, shows that the main product is a disaccharide consisting of L-iduronic acid and the anhydromannose. In conformity with sequence **1**, proposed (3, 4) as the major structural feature of the heparin molecule, this disaccharide may be formulated as **2**, *i.e.* 4-*O*-(α-L-idopyranosyluronic acid 2-sulfate)-2,5-anhydro-D-mannose 6-sulfate.

In our study, **2** has been isolated as a chromatographically- and electrophoretically-pure compound[8] in 65% yield by use of column chromatography on Sephadex G-10, and converted to a crystalline brucinium salt. Borohydride-reduced **2** has a specific rotation ($[\alpha]_D$ +2°) of the magnitude expected for a disaccharide composed of 2,5-anhydro-D-mannitol ($[\alpha]_D$ +58° (19)) and α-L-idopyranosyluronic acid (*ca.* $[\alpha]_D$ −70° (16)). As would be expected, acid hydrolysis of the reduced disaccharide yielded 2,5-anhydromannitol and iduronic acid and, following exhaustive borohydride-reduction of the latter, iditol.

As noted above, the ^{13}C spectrum of this disaccharide is commensurate with structure **2**. P.m.r. spectroscopy affords additional supporting evidence. The 100 MHz p.m.r. spectrum of **2** is almost indistinguishable from that of the total deamination product presented in ref. 1, Fig. 1D. At 220 MHz, the superior resolution more clearly shows the doublet (*J* 5.5 Hz) at 5.3 p.p.m. due to H-1 of the hydrated aldehydic group (21) of the anhydromannose residue. Signals ascribable to H-1 and -5 of the L-idosyluronic acid residue, at 4.8 and 5.4 p.p.m., respectively, virtually coincide in shift with the corresponding resonances from heparin (1, 3). Similarly, the narrow spacings (2.0–2.5 Hz) of these signals (which are better resolved as doublets at 220 than at 100 MHz) are consistent with the α-L-*ido* configuration and 1C(L) assignments proposed earlier for the uronic acid residues (3, 4, 16). Aside from a triplet (*J* 5.5 Hz) at 3.9 p.p.m., due to the anhydromannose H-2, all signals of the spectrum appear downfield of 4.0 p.p.m. Since H-2 of methyl α-D-idopyranosyl uronic acid resonates at 3.6 p.p.m., this observation is in accord with the expected strong deshielding of H′-2 of **2** by the *O*-sulfate group. Noteworthy also is the fact that all three signals upfield of 4.0 p.p.m. in the spectrum of heparin (3) have been ascribed to protons of the 2-amino-2-deoxy-D-glucose residues, because corresponding signals are absent from the spectrum from **2**.

The findings of this study based on the isolation of disaccharide **2**, taken in the context of the other evidence available, lead to the conclusion that at least two-thirds to three-quarters (4) of the heparin macromolecule consists of repeating biose residue sequences of structure **1**.

Experimental

Fourier transform ^{13}C n.m.r. spectra of heparin were recorded at 25.2 MHz with a Varian XL-100-15 spectrometer using deuterium oxide as the source of the lock signal. The heparin (sodium salt, Upjohn; *N*-acetyl, trace (2, 3)) (0.23 g in 2.5 ml of D_2O) was contained in a 12 mm tube, the spectrum width was 5000 Hz, acquisition time 0.4 s, and pulse width 75 μs; with concomitant proton-

[7]A preliminary account of this study has been presented by A. S. Perlin and N. M. K. Ng Ying Kin at the ACFAS Conference, Laval University, Quebec, October 17, 1970.

[8]The ^{13}C spectrum of the compound furnishes an additional criterion of its purity: signals from the 12 carbons are clearly accounted for (integration (6) of the expanded spectrum from 90 to 125 p.p.m. confirms that the relative intensities are correct), and the only indication of a possible contaminant is the very weak signal at 115 p.p.m.

Can. J. Chem. Downloaded from www.nrcresearchpress.com by 86.111.144.194 on 09/06/12
For personal use only.

decoupling the total spectrum accumulation time was 18 h, and without decoupling it was extended to 50 h.

Deaminative Degradation of Heparin

To a solution of heparin (sodium salt, Upjohn) (0.63 g) in 1.1 *M* acetic acid (6 ml), sodium nitrite (0.3 g) was added,[9] producing a vigorous effervescence. The solution was stored at 20 °C for 24 h, then concentrated to 1/2 volume, and applied to a column of Sephadex G-10 (2.5 × 105 cm). The column was washed with a buffer consisting of disodium phosphate and citric acid (3.6 and 1.6 g, respectively, per liter), with the eluant being collected at a rate of 30–35 ml/h. Fractions were examined by paper electrophoresis and pooled where appropriate.

Products of the Deamination Reaction

Disaccharide (2)

The major product was recovered by concentrating those eluate fractions comprising 288–310 ml; yield, 0.40 g, $[\alpha]_D$ 0 ± 1° (*c*, 0.5 H_2O). A brucinium salt was prepared, and crystallized from solution in cold aqueous ethanol or aqueous acetone (yield 35%); $[\alpha]_D$ −20° (*c*, 1 H_2O).

Anal. Calcd. for $C_{81}H_{98}O_{29}S_2N_6$: C, 57.8; H, 5.8; S, 3.8; N, 5.0. Found: C, 58.5; H, 5.7; S, 3.9; N, 5.3.

Some preparations of the disaccharide contained sodium sulfate (derived presumably from the original sulfamino group) and, in one experiment, led to co-crystallization of the brucinium salt of **2** with 1 mol of brucinium sulfate.

Anal. Calcd. for $C_{127}H_{152}O_{41}S_3N_{10}$: C, 59.3; H, 5.9; S, 3.7; N, 5.4. Found: C, 59.7; H, 6.3; S, 3.8; N, 5.9.

The product was reduced with sodium borohydride ($[\alpha]_D$ of the neutralized solution, +2° (*c*, 1)), then partially desulfated by treatment with hot methylsulfoxide–pyridine (22), and hydrolyzed with 0.5 *N* sulfuric acid at 95 °C for 3 h. Paper electrophoretic and chromatographic examination of the hydrolysate indicated the presence of iduronic acid and 2,5-anhydromannitol. A second borohydride reduction was carried out, the resulting aldonic acid converted to the methyl ester with diazomethane, and the borohydride reduction repeated. Finally, the products were acetylated with pyridine–acetic anhydride and the acetates examined by g.l.c.: these products corresponded to iditol hexaacetate and 2,5-anhydromannitol tetraacetate in a ratio of about 1:1.

Other Degradation Products

Several minor products that were formed in the deamination reaction emerged from the Sephadex column ahead of disaccharide **2**. Fractions were recovered from eluate volume 80–215 (15 mg), 215–255 (61 mg), and 255–280 ml (81 mg). The latter two fractions gave p.m.r. spectra distinctly different from that of **2**, although each spectrum contained a doublet and triplet (at 4.8 and 3.9 p.p.m., respectively; *J* 5.5 Hz) indicative of the presence of a 2,5-anhydro-D-mannose residue. Presumably, these materials correspond to the higher molecular weight fractions described by Lindahl and Axelsson (9), and have not been further characterized.

[9]The hydrogen-ion concentration of this solution was p*H* 3.5. In other experiments, deaminative degradation was effected with substantially the same results using hydrochloric acid (at this same p*H*) in place of the acetic acid. The latter, however, was more easily removed in the subsequent work-up.

The authors gratefully acknowledge generous support by the National Research Council of Canada and the Pulp and Paper Research Institute of Canada. Heparin was kindly supplied by Dr. E. L. Masson and the Upjohn Company, Don Mills, Ontario.

1. A. S. PERLIN, M. MAZUREK, L. B. JAQUES, and L. W. KAVANAGH. Carbohydr. Res. **7**, 369 (1968).
2. A. S. PERLIN and G. R. SANDERSON. Carbohydr. Res. **12**, 183 (1970).
3. A. S. PERLIN, B. CASU, G. R. SANDERSON, and L. F. JOHNSON. Can. J. Chem. **48**, 2260 (1970).
4. A. S. PERLIN, D. M. MACKIE, and C. P. DIETRICH. Carbohydr. Res. **18**, 185 (1971).
5. D. E. DORMAN and J. D. ROBERTS. J. AM. Chem. Soc. **93**, 4463 (1971).
6. A. ALLERHAND, D. DODDRELL, and R. KOMOROWSKI. J. Chem. Phys. **55**, 189 (1971).
7. M. L. WOLFROM, J. R. VERCELLOTTI, and D. HORTON. J. Org. Chem. **29**, 540 (1964).
8. M. L. WOLFROM, H. TOMOMATSU, and W. A. SZAREK. J. Org. Chem. **31**, 1173 (1966).
9. U. LINDAHL and O. AXELSSON. J. Biol. Chem. **246**, 74 (1971).
10. L. D. HALL and L. F. JOHNSON. Chem. Commun. 509 (1968).
11. A. S. PERLIN and B. CASU. Tetrahedron Lett. 2921 (1969).
12. D. E. DORMAN and J. D. ROBERTS. J. Am. Chem. Soc. **92**, 1355 (1970).
13. A. S. PERLIN, B. CASU, and H. J. KOCH. Can. J. Chem. **48**, 2596 (1970).
14. N. BLOEMBERGEN, E. M. PURCELL, and R. V. POUND. Phys. Rev. **73**, 678 (1948).
15. A. S. PERLIN, B. CASU, and H. J. KOCH. Unpublished data.
16. A. S. PERLIN, B. CASU, G. R. SANDERSON, and J. TSE. Carbohydr. Res. **21**, 123 (1972).
17. (*a*) A. S. PERLIN. Am. Chem. Soc. Abstr. 162nd Meeting, Washington, D.C., September 12–17, 1971. p. 48. (*b*) A. S. PERLIN, H. J. KOCH, and N. CYR. Unpublished data.
18. A. ALLERHAND, D. DODDRELL, V. GLUSHKO, D. W. COCHRAN, E. WENKERT, P. J. LAWSON, and F. R. N. GAUD. J. Am. Chem. Soc. **93**, 544 (1971).
19. A. B. FOSTER, R. HARRISON, T. D. INCH, M. STACEY, and J. M. WEBBER. J. Chem. Soc. 2279 (1963).
20. M. L. WOLFROM and P. Y. WANG. Chem. Commun. 241 (1967).
21. A. S. PERLIN. Can. J. Chem. **42**, 1365 (1964).
22. A. J. USOV, K. S. ADAMYANTS, L. I. MIROSHNIKOVA, A. A. SHAPOSHNIKOVA, and N. K. KOCHETKOV. Carbohydr. Res. **18**, 336 (1971).

Rhodium(I) Complexes of 1,2,5-Triphenylphosphole Oxide

D. G. HOLAH, A. N. HUGHES, AND B. C. HUI
Department of Chemistry, Lakehead University, Thunder Bay, Ontario

Received November 5, 1971

Rhodium trichloride hydrate and rhodium carbonyl chloride react with 1,2,5-triphenylphosphole oxide (TPPO) to produce a rhodium(I) complex $[RhCl(TPPO)]_2$, where the metal is bonded to the ligand through the π system. This complex reacts with $FeCl_3$ to produce $RhCl(TPPO).FeCl_3$ where the iron is bonded through the oxygen of the P=O group. Reactions of $[RhCl(TPPO)]_2$ with other species including nitrogen, phosphorus, and sulfur bases and carbon monoxide are described.

L'hydrate de trichlorure de rhodium et le chlorure de rhodium carbonyle réagissent avec l'oxyde de triphényl-1,2,5 phosphole (OTPP) pour conduire à un complexe de rhodium(I) $[RhCl(OTPP)]_2$, où le métal est lié au ligand par l'intermédiaire du système π. Ce complexe réagit avec $FeCl_3$ et donne $RhCl(OTPP).FeCl_3$ où le fer est lié à l'oxygène du groupe P=O. Les réactions de $[RhCl(OTPP)]_2$ avec d'autres espèces comprenant les bases azotée, phosphorée et sulfurée et l'oxyde de carbone, sont décrites.

Canadian Journal of Chemistry, **50**, 2442 (1972)

Introduction

In a previous paper (1) we reported some transition metal complexes of 1,2,5-triphenylphosphole (TPP) and its oxide (TPPO), sulfide, and selenide. In all cases, coordination of the ligands to the metal ions (in their normal valence states) occurs through the appropriate donor atom (P, O, S, Se) and not through the π system of the ligand. However, in reactions between metal carbonyls and certain phosphole oxides, π bonded systems have been produced. Thus 1,2,3,4,5-pentaphenylphosphole oxide forms (2) an iron carbonyl complex **1**, while TPPO (**2**) also forms with $Fe(CO)_5$ (3) a π complex similar to **1**. Bonding through the oxygen atom is ruled out because no changes are observed in the P=O stretching frequency (3).

Because of the potential use of metal complexes of cyclic unsaturated phosphines and their derivatives as hydrogenation or hydroformylation catalysts (4), we have extended our previous study to include rhodium, and this paper reports our findings regarding a π-bonded complex obtained from reactions between rhodium(III) chloride and TPPO, together with various reactions of this complex.

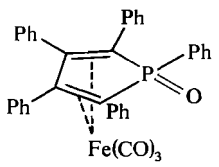

1

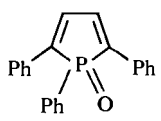

2 (TPPO)

Results and Discussion

When an ethanolic solution of rhodium trichloride hydrate is heated under reflux with an excess of TPPO, an orange solid of composition RhCl(TPPO) slowly separates. No reaction is observed when either methanol or methylene chloride is used as solvent. The complex can also be obtained by the reaction of TPPO with rhodium carbonyl chloride $Rh_2Cl_2(CO)_4$ in methanol or ethanol solutions.

The complex RhCl(TPPO) is extremely stable, diamagnetic, almost insoluble in ethanol, benzene, and acetonitrile, and slightly soluble in chloroform, methylene chloride, and tetrahydrofuran (THF); it can be recrystallized from THF. The limited solubility of the compound precluded n.m.r. and molecular weight measurements, but infrared data (see Table 1) in the 1200 cm^{-1} region of the spectrum clearly indicate that the TPPO is bonded to the metal by the π system. In TPPO, the P=O stretching frequency occurs as a strong band at 1181 cm^{-1}, and in the complex there are two areas of P=O absorption at 1220 and 1180 cm^{-1}: *i.e.* there is no reduction in the energy of this frequency as occurs with complexes having $>$P=O$\rightarrow$M linkages (1). Other evidence (*vide infra*) suggests that the complex should be formulated as the dimer **3** in which case the complexity of the spectrum in the 1200 cm^{-1} region could be due to the presence of different isomers, the non-equivalence of the ligands because of a puckered bridging structure, or possibly to symmetric and

Can. J. Chem. Downloaded from www.nrcresearchpress.com by 210.87.254.40 on 09/05/12
For personal use only.

Can. J. Chem. Downloaded from www.nrcresearchpress.com by 210.87.254.40 on 09/05/12
For personal use only.

TABLE 1. Analytical and spectral data

Compound	Color	Melting point (°C)	Analyses: Found C	Found H	Found Other	Calculated C	Calculated H	Calculated Other	I.R. Spectral Data: νP=O cm^{-1}	νC=O cm^{-1}	νM—Cl cm^{-1}
TPPO	yellow	237–239							1181		
$[RhCl(TPPO)]_2$	orange	>310	56.5	3.8	7.2(Cl)	56.62	3.67	7.6	1220 s, 1200 w 1180 s, 1160 sh		295, 240 m 220 m
RhCl(TPPO)(*o*-phen)	yellow	decomp. ~285	63.1	3.9	4.3(N)	62.93	3.88	4.32(N)	1192 m, 1180 s		280 m
$RhCl(TPPO)py_2$	yellow	decomp. ~175	62.1	4.5	4.4(N) 5.8(Cl)	61.51	4.36	4.48(N) 5.67(Cl)	1220 m, 1200 sh 1185 s, 1160 sh		302 m
$RhCl(TPPO)(CO).(Ph_3P)$	brown	decomp. 148–151	64.6	4.3	4.5(Cl)	65.05	4.26	4.68(Cl)	1220 s, 1200 sh 1185 s, 1160 sh	1970 s	310 m
$RhCl(TPPO)(Ph_3P)$	pink-red	163–165	65.6	4.6	4.5(Cl)	65.90	4.42	4.86(Cl)	1212 m, 1160 sh 1185 s		318 m
$RhCl(TPPO)(Me_2S)$	orange	decomp. 298	54.7	4.0	6.8(Cl)	54.51	4.38	6.70(Cl)	1200 s, 1181 s		300 m
$RhCl(TPPO)(CO)_2$	orange-red	decomp. 305	54.9	3.6	6.9(Cl)	55.15	3.28	6.78(Cl)	1185 s, 1140 m	2090 s 2020 s	300 m
$RhCl(TPPO).FeCl_3$	grey	decomp. 270	42.3	2.9	22.2(Cl)	42.01	2.72	22.55(Cl)	1120 s		385 m (Fe—Cl) 325 m, 312 m (Rh—Cl)
$[Rh(OAc)(TPPO)]_2$	brown	decomp. ~150	58.5	3.8		58.80	4.11		1190 s, 1150 ms 1182 s		1595 s, 1410 w OAc^-

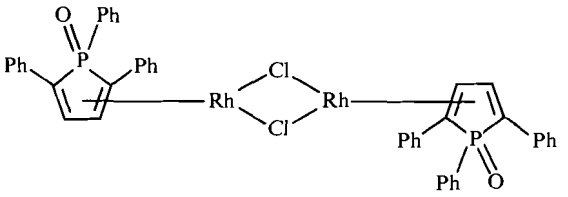

3

antisymmetric vibrations. Other ligands containing P=O groups but no π-diene system, such as triphenylphosphine oxide and 9-phenyl-9-phosphafluorene-9-oxide (a dibenzophosphole derivative designated here as DBPO) reduce rhodium(III) to rhodium metal, presumably because of the absence of a π-system capable of stabilizing the rhodium(I). The rhodium behaves therefore as a typical class (b) acceptor (5) showing a reluctance to coordinate to the oxygen atom of TPPO, while forming (6) a simple $RhCl_3$.TPP adduct, *via* the phosphorus atom, with 1,2,5-triphenylphosphole.

The infrared spectrum of **3** also shows bands at 295, 240, and 220 cm^{-1} assigned to Rh—Cl stretching frequencies and this too is not inconsistent with a bent bridging structure (7). Similar dimeric π-complexed structures have been postulated for rhodium(I) adducts with other ligands having *cis*-diene π-systems such as 2,3,4,5-tetraphenylcyclopentadienone rhodium(I) chloride (8) **4** and duroquinone rhodium(I) (8, 9) **5**.

The π-complex $[RhCl(TPPO)]_2$ undergoes an extremely wide range of reactions which are summarized in Fig. 1. A particularly interesting reaction occurs with iron(III) chloride, producing a dark-colored solid of composition $RhCl(TPPO).FeCl_3$ from methylene chloride

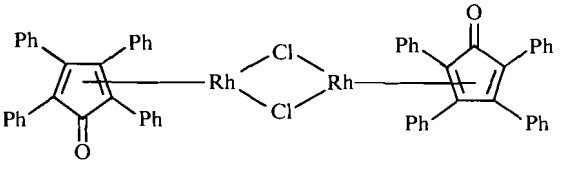

4

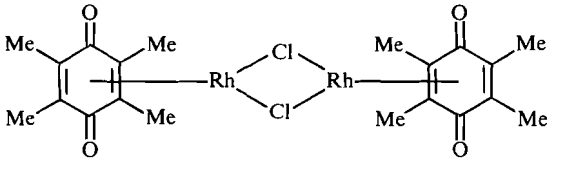

5

solutions. The compound is stable in dry air but decomposes when exposed to moisture or alcohol liberating **3**. Its effective magnetic moment (calculation based upon a monomer) is 5.7 B.M. confirming the presence of five unpaired electrons on the iron atom. The infrared spectrum shows a single sharp absorption at 1120 cm^{-1} associated with the P=O group coordinated to the iron *cf.* $FeCl_3.2TPPO$ (1), 1145 cm^{-1}) together with metal–chloride bands at 385 cm^{-1} (Fe—Cl) and at 325, 312 cm^{-1} (Rh—Cl). The most likely structure appears to be as shown in **6**

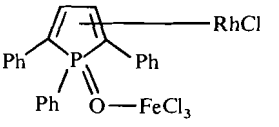

6

with a chlorine atom from $FeCl_3$ possibly occupying the fourth coordination position about the rhodium. No reaction was observed between **3** and the divalent chlorides of manganese, nickel, and copper, while cobalt(II) partially reacts with **3** to give a crude product having a P=O stretch at 1130 cm^{-1} but which proved impossible to purify. The complex **6** is interesting in that it represents an example of a system in which the ligand is both σ and π bonded to different metal atoms in the same molecule.

$[RhCl(TPPO)]_2$ also reacts with nitrogen donor ligands such as *o*-phenanthroline (*o*-phen) and pyridine (py) in THF and ethanol respectively to give RhCl(TPPO)(*o*-phen) and $RhCl(TPPO)(py)_2$. With phosphorus donor ligands, such as 1,2-bis(diphenylphosphino)ethane(diphos), $RhCl(diphos)_2$ (10) is produced. The reaction of **3** with Ph_3P in 1:1 ratios in MeOH gives $RhCl(TPPO)(Ph_3P)$, but reaction in THF followed by addition of ether produces an impure sample of $RhCl(TPPO)(CO)(Ph_3P)$ in which the CO group has been abstracted from ether (11). The latter compound can also be prepared by the addition of formaldehyde (12) to a solution of $RhCl(TPPO)(Ph_3P)$, prepared *in situ*. With a 6-fold excess of Ph_3P in ethanol solution, $RhCl(Ph_3P)_3$ is produced. The adduct **3** also reacts with dimethyl sulfide (Me_2S) in THF solution to give $RhCl(TPPO)(Me_2S)$, although no reaction was observed with diphenyl sulfide. There is little correlation in Table 1 between the infrared spectra of the above com-

Can. J. Chem. Downloaded from www.nrcresearchpress.com by 210.87.254.40 on 09/05/12
For personal use only.

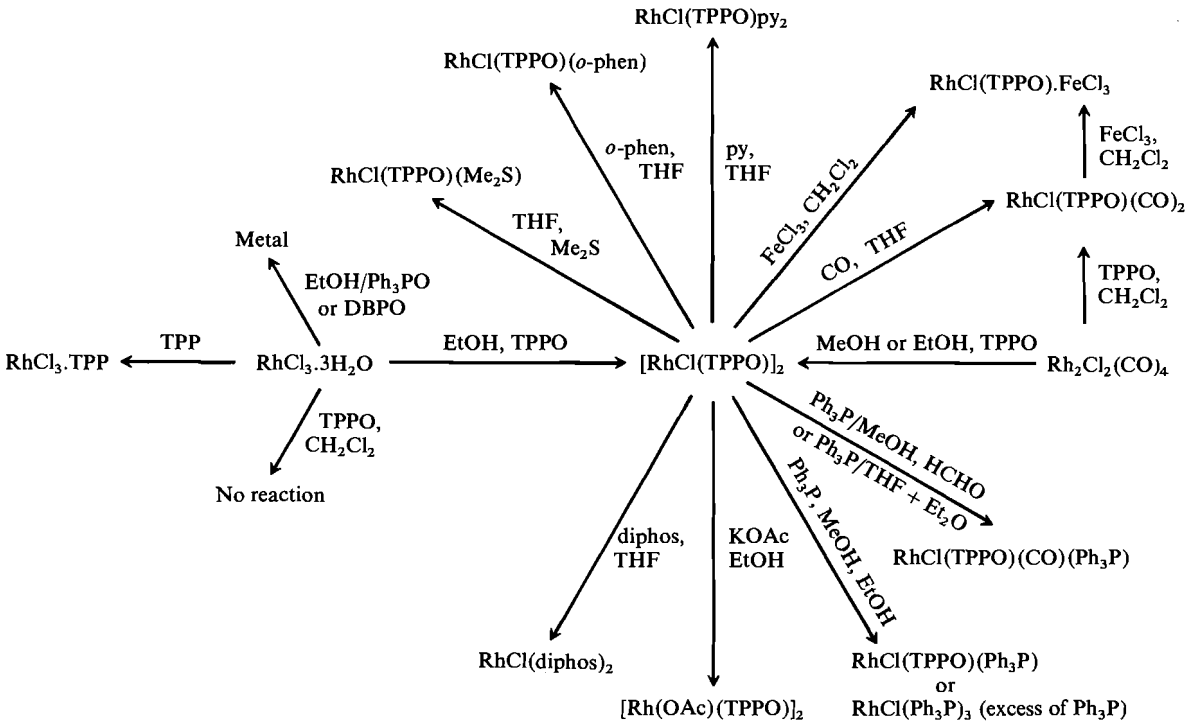

FIG. 1. Summary of some reactions of $[RhCl(TPPO)]_2$.

plexes in either the P=O or the Rh—Cl regions and it is therefore impossible to decide on this basis alone whether the complexes exist as dimers with 6-coordinate rhodium or as monomers with 5-coordinate rhodium (13).

Carbon monoxide reacts with **3** in THF solution under reflux to produce $RhCl(TPPO)(CO)_2$. The same compound is also obtained from the reaction of TPPO with $Rh_2Cl_2(CO)_4$ in methylene chloride at room temperature. The two CO stretching frequencies at 2020 and 2090 cm^{-1} are indicative of *cis* CO groups, possibly with retention of the dimeric structure. The adduct $RhCl(TPPO)(CO)_2$ reacts with $FeCl_3$ in methylene chloride solution to give **6**.

The chloride bridges in **3** can be replaced by acetate groups by treating **3**, in ethanol solution, with an excess of potassium acetate (KOAc). Infrared bands at 1595 and 1410 cm^{-1} in $[Rh(OAc)(TPPO)]_2$ are assigned to the antisymmetric and symmetric stretching frequencies of the $MeCOO^-$ group, indicative of a bridging acetate group (14).

Preliminary results on the catalytic properties of these complexes are encouraging (15).

Thus, in contrast with the other metal systems so far examined (1), the ligand TPPO behaves with rhodium(III) as a reducing diene, forming complexes of comparable stability with other rhodium(I) diene complexes (16).

Experimental

The ligand TPPO was prepared as previously described (17). After isolation, all complexes were dried by pumping under high vacuum (10^{-6} Torr) for prolonged periods at 25–50 °C. Microanalyses and physical measurements were as previously described (1). Chloride was determined potentiometrically (18).

$[RhCl(TPPO)]_2$

$RhCl_3.3H_2O$ (0.52 g) and a 2 molar excess of TPPO (1.4 g) in ethanol (100 ml) were heated under reflux for 12 h producing an orange solid **3** which was recrystallized from THF (yield 70%). An uncharacterized, THF-insoluble, orange phase which could be recrystallized from acetonitrile/ethanol was also obtained.

The same complex was also produced by heating under reflux for 5 h a methanol or ethanol solution of equal molar ratios of $Rh_2Cl_2(CO)_4$ and TPPO (yield 90%).

Subsequent reactions involving the above complex generally involved ~150 mg **3** in 100 ml solvent.

$RhCl(TPPO).FeCl_3$

$FeCl_3.6H_2O$ and either **3** or $RhCl(TPPO)(CO)_2$ in a 1:1 molar ratio were heated under reflux for 12 h in methylene

Can. J. Chem. Downloaded from www.nrcresearchpress.com by 210.87.254.40 on 09/05/12
For personal use only.

chloride after which the initially orange colored solution had become very dark. The solution was cooled, the excess of iron(III) chloride filtered off and the filtrate reduced in volume by 1/5. The solution was allowed to stand at 0° for 3 days after which a grey solid had precipitated; this was washed with cold methylene chloride and dried under vacuum (yield 80%). ($\chi_M = 14\,800 \times 10^{-6}$ at 27 °C, $\chi_M^{corr} = 14\,500 \times 10^{-6}$).

RhCl(TPPO)(o-phen) and RhCl(diphos)$_2$

o-Phen or diphos and **3** in 3:1 and 5:1 mole ratios respectively, were mixed and warmed in THF solution. Yellow precipitates formed immediately, and were washed with THF (90% yields). RhCl(diphos)$_2$ was recrystallized from methanol/benzene and identified from its analysis, infrared spectrum, and melting point (10).

RhCl(TPPO)(py)$_2$ and RhCl(TPPO)(Me_2S)

An excess of pyridine or dimethyl sulfide was added dropwise to warm solutions of **3** in EtOH and THF, respectively. The solutions were concentrated to small volumes and *n*-hexane and ether added to precipitate the respective products (yields 60%).

RhCl(TPPO)(Ph_3P), RhCl(TPPO)(CO)(Ph_3P), and RhCl(Ph_3P)$_3$

Ph_3P and **3** were mixed (1:1 mole ratios) in MeOH and heated under reflux for 1 h during which time the solution became red. The solution was concentrated to ~1/5 volume and RhCl(TPPO)(Ph_3P) separated as brown crystals (yield 80%).

A mixture of formaldehyde (1 ml, 37%) solution and RhCl(TPPO)(Ph_3P) (0.15 g) in MeOH (40 ml) was heated under reflux for $\frac{1}{2}$ h, the solution was reduced to ~1/5 volume and RhCl(TPPO)(CO)(Ph_3P) separated as a pink solid. Reaction with a 6:1 molar ratio of Ph_3P to **3** in ethanol solution produced RhCl(Ph_3P)$_3$ (19).

RhCl(TPPO)(CO)$_2$

CO was passed into a suspension of **3** (0.2 g) in THF (100 ml) under reflux. The solution became clear red in $\frac{1}{2}$ h and the volume was then reduced by ~1/5. The product was precipitated by addition of ether and was recrystallized from benzene in high yield (80%).

The same product was also obtained by the addition of TPPO to a methylene chloride solution of $Rh_2Cl_2(CO)_4$ (1:1 mole ratios). The solution was stirred for 12 h and *n*-hexane added to precipitate the product (yield 90%).

[Rh(OAc)TPPO]$_2$

A mixture of **3** and potassium acetate (5 fold excess) was heated under reflux for ~12 h in ethanol during which time the solution turned dark brown. The reaction mixture was cooled to room temperature and filtered. The dark colored ethanol filtrate was evaporated to dryness and the product recrystallized twice from EtOH as an ethanol adduct from which the ethanol was removed by pumping under high vacuum at ~50 °C. (Yield 50%).

We acknowledge the assistance of the personnel of the Science Instrumentation laboratory in obtaining micro analytical data.

We also thank the Senate Research Committee of Lakehead University and the National Research Council of Canada for generous financial support of this work.

1. D. Budd, R. Chuchman, D. G. Holah, A. N. Hughes, and B. Hui. Can. J. Chem. **50**, 1008 (1972).
2. E. H. Braye, W. Hübel and I. Caplier. J. Am. Chem. Soc. **83**, 4406 (1961).
3. R. C. Cookson, G. W. A. Fowles, and D. K. Jenkins. J. Chem. Soc. 6406 (1965).
4. Shell Internationale Research Maatschappij N. V., Netherlands Patent Application 6516164(1966); Chem. Abstr. **66**, 28392*r* (1967).
5. S. Ahrland, J. Chatt, and N. R. Davies. Quart. Rev. **12**, 265 (1958).
6. R. A. Walton. J. Chem. Soc. A. 365 (1966).
7. D. M. Adams and P. J. Chandler. J. Chem. Soc. A. 588 (1969).
8. S. McVey and P. M. Maitlis. Can. J. Chem. **44**, 2429 (1966).
9. G. N. Schrauzer and K. C. Dewhirst. J. Am. Chem. Soc. **86**, 3265 (1964).
10. A. Sacco and R. Ugo. J. Chem. Soc. 3274 (1964).
11. A. Rusina and A. A. Vlček. Nature, **206**, 295 (1965).
12. D. Evans, J. A. Osborn and G. Wilkinson. Inorg. Synth. **11**, 99 (1968).
13. S. J. LaPlaca and J. A. Ibers. Acta Cryst. **18**, 511 (1965); K. W. Muir and J. A. Ibers. Inorg. Chem. **8**, 1921 (1969).
14. T. A. Stephenson, S. M. Morehouse, A. R. Powell, J. P. Heffer, and G. Wilkinson. J. Chem. Soc. A. 3632 (1965).
15. D. Budd, D. G. Holah, A. N. Hughes, and B. C. Hui. To be published.
16. J. Chatt and L. M. Venanzi. J. Chem. Soc. 4735 (1957).
17. I. G. M. Campbell, R. C. Cookson, M. B. Hocking, and A. N. Hughes. J. Chem. Soc. 2184 (1965).
18. Standard Methods for the Examination of Water and Wastewater, U.S. Public Health Association, 13th ed., 1971, p. 377.
19. J. A. Osborn, F. H. Jardine, J. F. Young, and G. Wilkinson. J. Chem. Soc. A, 1711 (1966).

Can. J. Chem. Downloaded from www.nrcresearchpress.com by 210.87.254.40 on 09/05/12
For personal use only.

Complex Fluorides of Tetravalent Cobalt

J. W. QUAIL AND G. A. RIVETT

Department of Chemistry and Chemical Engineering, University of Saskatchewan, Saskatoon, Saskatchewan S7N 0W0

Received December 8, 1971

A new compound, Rb_2CoF_6 has been prepared. Rb_2CoF_6 and Cs_2CoF_6 both have the cubic K_2PtCl_6 structure with $a = 8.460(3)$ Å and $d(Co—F) = 1.65(5)$ Å for Rb_2CoF_6 and $a = 8.914(2)$ Å and $d(Co—F) = 1.73(5)$ Å for Cs_2CoF_6. The temperature dependent magnetic susceptibilities of Rb_2CoF_6 and Cs_2CoF_6 are reported and interpreted. The data are consistent with the Co^{IV} having a $^2T_2$ ground state and both Rb_2CoF_6 and Cs_2CoF_6 exhibiting complex ferromagnetic behavior with a Curie temperature above ambient.

Un nouveau composé, Rb_2CoF_6, a été préparé. Rb_2CoF_6 et Cs_2CoF_6 ont tous deux la structure cubique de K_2PtCl_6 avec $a = 8.460(3)$ Å et $d(Co—F) = 1.65(5)$ Å pour Rb_2CoF_6 et $a = 8.914(2)$ Å et $d(Co—F) = 1.73(5)$ Å pour Cs_2CoF_6. L'influence de la température sur les susceptibilités magnétiques de Rb_2CoF_6 et Cs_2CoF_6 est rapportée et interprétée. Les données concordent avec le fait que Co^{IV} est dans l'état fondamental $^2T_2$ et que Rb_2CoF_6 et Cs_2CoF_6 exhibent tous deux un état ferromagnétique complexe avec une température de Curie au dessus de la température ambiante.

Canadian Journal of Chemistry, **50**, 2447 (1972)

Introduction

The first known complex fluoride of tetravalent cobalt, Cs_2CoF_6, was prepared by Hoppe through treatment of Cs_2CoCl_4 with elemental fluorine at 300 °C in a flow reactor (1). Klemm *et al.* (2) repeated the preparation and studied the magnetic susceptibility of the compound. They found a magnetic moment of 2.53 B.M. at 90 °K and 3.04 B.M. at 294 °K. Cs_2CoF_6 has recently (3) been shown to have a $^2T_2$ ground state. If the spin–orbit coupling constant is taken to be 650 cm^{-1} (4) the magnetic moments would be expected to be 1.9 B.M. at 90 °K and 2.3 B.M. at 300 °K. No satisfactory explanation of this anomalous magnetic behavior has been advanced to date.

We have prepared Cs_2CoF_6 and the previously unknown Rb_2CoF_6. We have measured the reflectance spectra and magnetic susceptibilities of these compounds and have determined their crystal structures from powder diffraction data.

Experimental

Cs_2CoCl_4 and Rb_2CoCl_4 were prepared by the method of Figgis (5). Cs_2CoF_6 and Rb_2CoF_6 were obtained by fluorinating Cs_2CoCl_4 and Rb_2CoCl_4 with elemental fluorine in a flow reactor at a temperature of 250 °C. To improve crystallinity the products were sealed at the reaction temperature under 1 atm of fluorine for periods of time up to 120 h. Both compounds obtained in this way were light gold in color.

Attempts to prepare K_2CoF_6 by similar methods failed.

Analyses were by the tetraphenylboron method for cesium and rubidium (6, 7), the pyridine–thiocyanate method for cobalt (8) and the lead chlorofluoride method for fluorine (8).

Anal. Calcd. for Cs_2CoF_6: Cs, 60.59; Co, 13.43; F, 25.98. Found: Cs, 60.12; Co, 13.61; F, 25.83.

Anal. Calcd. for Rb_2CoF_6: Rb, 49.71; Co, 17.14; F, 33.15. Found: Rb, 49.26; Co, 17.25; F, 33.14.

Powder photographs of the hexafluorocobaltates were taken with FeK_α radiation. Film densities were measured with a Jarrell-Ash Model JA-203 recording microphotometer. 2θ angles were measured on a film illuminator.

The crystal lattice constants and their probable errors were evaluated with the Gvildys least-squares computer program (9). The expected X-ray diffraction pattern was calculated using Smith's computer program (10).

Cs_2CoF_6 f.w. = 438.73

Cubic, $a = 8.914(2)$ Å, $V = 708.3$ Å^3, $\rho_o = 3.93(3)$ g cm^{-3}, $\rho_c = 4.11$ g cm^{-3}, $z = 4$, space group $Fm3m$ (20 °C, FeK_α, $\lambda = 1.9373$ Å).

Rb_2CoF_6 f.w. = 343.87

Cubic, $a = 8.460(3)$ Å, $V = 605.5$ Å^3, $\rho_o = 3.60(3)$ g cm^{-3}, $\rho_c = 3.83$ g cm^{-3}, $z = 4$, space group $Fm3m$ (20 °C, FeK_α, $\lambda = 1.9373$ Å).

The reflectance spectra were obtained on a Cary Model 14 spectrophotometer using a Cary 1411 diffuse reflectance accessory.

Magnetic susceptibilities were measured on a Faraday balance. The design of this instrument was adapted from Hatfield *et al.* (11), while the constant temperature device was as adapted by Clark and O'Brien (12) from Figgis and Nyholm (13). The accuracy of temperature measurements was estimated to be ±0.2 °K. Magnetic susceptibilities were measured as a function of temperature for both compounds and as a function of field for Cs_2CoF_6. The magnetic field was calibrated using $HgCo(SCN)_4$ as a standard (14).

Results and Discussion

Both Cs_2CoF_6 and Rb_2CoF_6 show the K_2PtCl_6 crystal structure, with cobalt ions in

Can. J. Chem. Downloaded from www.nrcresearchpress.com by 210.87.254.40 on 09/05/12
For personal use only.

TABLE 1. Interatomic distances for Cs_2CoF_6 and Rb_2CoF_6

Cs_2CoF_6		Rb_2CoF_6	
Bond	Distance (Å)	Bond	Distance (Å)
Cs—F	3.18±0.09	Rb—F	3.02±0.09
Co—F	1.73±0.05	Co—F	1.65±0.05
F—F*	2.46±0.07	F—F*	2.33±0.07
F—F†	3.22±0.09	F—F†	3.06±0.09

*Distance between fluorine atoms in the same octahedron.
†Distance between fluorine atoms in adjacent octahedra.

position *a*, alkali metal ions in position *c*, and fluoride ions in position *e* of the O_h^5 (*Fm3m*) space group. The unit cell is tetramolecular. It is composed of a face centered cube of CoF_6^{2-} octahedra with alkali metal cations in all tetrahedral holes.

The cell edge for the cesium salt was determined to be 8.914(2) Å. Klemm *et al.* (2) reported 8.91 Å. The cell edge for the rubidium salt was found to be 8.460(3) Å. These cell edges are distinctly different from those of Cs_3CoF_6 and Rb_3CoF_6 which are 9.22 and 8.86 Å, respectively. These latter salts differ structurally from the former only in that alkali metal cations are also found in all of the octahedral holes between CoF_6^{2-} ions in the unit cell.

For both Cs_2CoF_6 and Rb_2CoF_6 the only structural parameter not fixed by symmetry is the cobalt–fluorine distance. By comparing observed intensities with intensities calculated for different values of this parameter, a value of 0.195 ± 0.005, in units of cell edges, was determined to give the best fit for both compounds. The observed and calculated spacings and intensities for the X-ray powder diffraction patterns for Cs_2CoF_6 and Rb_2CoF_6 have been placed in the Depository of Unpublished Data.[1] Interatomic distances for both compounds are noted in Table 1.

Attempts to prepare K_2CoF_6 by the fluorination of a molar ratio of $2KCl:CoCl_2.6H_2O$ were unsuccessful. The product was a mixture and only KF could be positively identified.

Cs_2CoF_6 is a stable at 335 °C while Rb_2CoF_6 decomposes at this temperature. Both Cs_2CoF_6 and Rb_2CoF_6 are hygroscopic, reacting with moisture to produce O_2 (identified by mass spectrometry) and O_3 (identified by smell).

[1]Complete set of data may be obtained upon request from the Depository of Unpublished Data, National Science Library, National Research Council of Canada, Ottawa K1A 0S2, Canada.

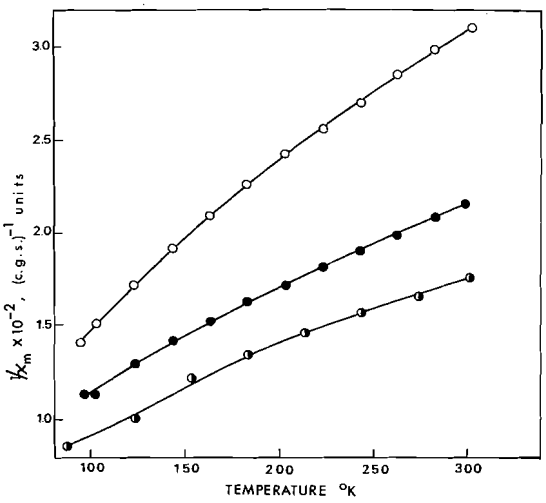

FIG. 1. Variation of the reciprocal of the magnetic susceptibility (corrected for diamagnetism) with temperature: ●, Cs_2CoF_6 for a value of $H \cdot (\delta H/\delta x)$ of 11.26×10^5 G^2 cm^{-1}; ◑, Cs_2CoF_6 for a value of $H \cdot (\delta H/\delta x)$ of 4.37×10^5 G^2 cm^{-1}; ○, Rb_2CoF_6 for a value of $H \cdot (\delta H/\delta x)$ of 11.26×10^5 G^2 cm^{-1}.

The reflectance spectrum for Cs_2CoF_6 has previously been reported by Allen and Warren (3). Our measurements are substantially in agreement with theirs. Our interpretations of the reflectance spectra of Rb_2CoF_6 and Cs_2CoF_6 are both consistent with their interpretation of the reflectance spectrum of Cs_2CoF_6, which indicated that the ground state of Co(IV) in CoF_6^{2-} is the low spin $^2T_2$.

The magnetic susceptibility data have been placed in the Depository of Unpublished Data.[1] A least squares computer program fitted the data for each salt to the Curie–Weiss law. For Cs_2CoF_6 the Weiss constants obtained were -137 and -135 °K for the high and low magnetic field measurements, respectively. The Weiss constant determined for Rb_2CoF_6 was -92 °K. The inverse susceptibilities are plotted *vs.* the absolute temperature in Fig. 1. Magnetic moments were not calculated using the Curie–Weiss law for two reasons. First, the large Weiss constants indicated that application of the Curie–Weiss law might mask temperature dependent behavior of the magnetic properties. Second, the plots of inverse molar susceptibility *vs.* absolute temperature (Fig. 1) are not straight line plots but are curved. Since the value of *H*

Can. J. Chem. Downloaded from www.nrcresearchpress.com by 210.87.254.40 on 09/05/12
For personal use only.

TABLE 2. Effective magnetic moments for Rb_2CoF_6 and Cs_2CoF_6

Rb_2CoF_6		Cs_2CoF_6			
T(°K)	μ_{eff}*	T(°K)	μ_{eff}*	T(°K)	μ_{eff}†
94.9	2.32	96.9	2.63	87.6	2.84
303.1	2.80	298.6	3.32	300.9	3.68

*$H\cdot(\delta H/\delta x)$ was 11.26×10^5 G^2 cm^{-1}.
†$H\cdot(\delta H/\delta x)$ was 4.37×10^5 G^2 cm^{-1}.

increases as $H(\delta H/\delta x)$ increases, the susceptibility of Cs_2CoF_6 was shown to be field dependent.

Magnetic moments calculated on the basis of the Curie law are given in Table 2.

The $^2T_2$ ground state would exhibit both spin and orbital contributions to the magnetic moment. The magnitude of the orbital contribution depends on the absolute temperature and the value of the spin–orbit coupling constant, which was taken to be 650 cm^{-1} (4). Magnetic moments including spin–orbit coupling, calculated by the method of Figgis (4) for both the cesium and rubidium hexafluorocobaltate(IV) salts were 2.3 B.M. at 300 °K and 1.9 B.M. at 95 °K. These values are considerably lower than those obtained experimentally. In addition the magnetic susceptibility of Cs_2CoF_6 is field dependent. Thus, contrary to Allen and Warren (3), the anomalously high magnetic moments cannot be attributed to spin–orbit coupling.

Thermal population of the $^6A_1$ state has been suggested (2, 3) as the reason for the anomalously high magnetic moments. The observed magnetic susceptibility in such a case would be a weighted average of the field independent magnetic susceptibilities of the two species and would be essentially field independent. Although the possibility of thermal population of the $^6A_1$ state cannot be eliminated, the observed field dependence of the magnetic susceptibility of Cs_2CoF_6 is not explained by thermal population of the $^6A_1$ state.

On the basis of our data it appears that Cs_2CoF_6 and Rb_2CoF_6 are ferromagnetic and that spin alignment is occurring between neighboring cobalt ions. These neighboring ions are separated by two fluoride ions. The Co—Co distances in Cs_2CoF_6 and Rb_2CoF_6 are less than 6.5 Å. Interaction over 8.5 Å has been reported for the Mn^{2+}—Cl—Cl—Mn^{2+} system (15) and

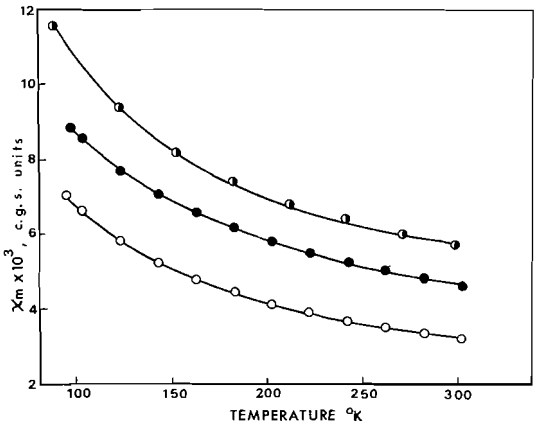

FIG. 2. Variation of magnetic susceptibility (corrected for diamagnetism) with temperature: ●, Cs_2CoF_6 for a value of $H\cdot(\delta H/\delta x)$ of 11.26×10^5 G^2 cm^{-1}; ◑, Cs_2CoF_6 for a value of $H\cdot(\delta H/\delta x)$ of 4.37×10^5 G^2 cm^{-1}; ○, Rb_2CoF_6 for a value of $H\cdot(\delta H/\delta x)$ of 11.26×10^5 G^2 cm^{-1}.

fluorine has been noted as being a powerful agent in providing spin transfer in such superexchange phenomena (16). Ferromagnetism is shown by the susceptibility decrease as magnetic saturation is approached (*i.e.*, as field increases) for Cs_2CoF_6.

Plots of molar susceptibility *vs.* temperature were prepared to determine if the Curie temperature could be ascertained, but no inflection points were noted. The plots of χ_m *vs.* temperature are given in Fig. 2. These plots clearly indicate that Cs_2CoF_6 behaves as a ferromagnetic substance with a Curie temperature above ambient. The Curie temperature for Rb_2CoF_6 is also apparently above ambient.

We wish to thank the National Research Council of Canada for financial support. We also wish to thank Dr. R. G. Cavell of the University of Alberta, Department of Chemistry, for the use of the Faraday balance on which our magnetic susceptibility measurements were made. We wish to express our appreciation to E. D. Day and Dr. R. G. Cavell for guidance and help in the use of the Faraday balance.

1. R. HOPPE. Rec. Trav. Chim. **75**, 569 (1956).
2. W. KLEMM, W. BRANDT, and R. HOPPE. Z. anorg. u. allgem. Chem. **308**, 179 (1961).
3. G. C. ALLEN and K. D. WARREN. Inorg. Chem. **8**, 1902 (1969).
4. B. N. FIGGIS. Introduction to ligand fields. Interscience Publishers, New York. 1966.
5. B. N. FIGGIS. J. Chem. Soc. 3423 (1964).
6. L. ERDEY. Gravimetric analysis. Part II. Pergamon Press, Oxford. 1965.

Can. J. Chem. Downloaded from www.nrcresearchpress.com by 210.87.254.40 on 09/05/12
For personal use only.

7. W. GEILMANN and W. GEBAUHR. Z. Anal. Chem. **139**, 161 (1953).
8. A. VOGEL. A textbook of quantitative inorganic analyses. John Wiley and Sons, Inc., London. 1961.
9. J. GVILDYS. Crystal lattice constant determination. Program Library B106. Argonne National Laboratory, Argonne, Illinois.
10. D. K. SMITH. A revised program for calculating X-ray powder diffraction patterns. Lawrence Radiation Laboratory, Livermore, California.
11. W. E. HATFIELD, R. C. FAY, C. E. PFLUGER, and T. S. PIPER. J. Am. Chem. Soc. **85**, 265 (1963).
12. H. C. CLARK and R. J. O'BRIEN. Can. J. Chem. **39**, 1030 (1961).
13. B. N. FIGGIS and R. S. NYHOLM. J. Chem. Soc. 331 (1959).
14. B. N. FIGGIS and R. S. NYHOLM. J. Chem. Soc. 4190 (1958).
15. T. B. SWANSON and V. W. LAURIE. J. Chem. Phys. **49**, 4407 (1968).
16. B. N. FIGGIS and J. LEWIS. *In* Progress in inorganic chemistry. Vol. 6. Interscience Publishers, New York. 1964. p. 97.

Can. J. Chem. Downloaded from www.nrcresearchpress.com by 210.87.254.40 on 09/05/12
For personal use only.

Heterogeneous Interactions of Methylamines on porous Adsorbents Part II. Interactions on Silica–Alumina and Silica Gel Surfaces of Di- and Tri-methylamine in the Region of their Boiling Points

W. G. Cook and R. A. Ross
Department of Chemistry, Lakehead University, Thunder Bay 'P', Ontario

Received March 17, 1972

The adsorption of di- and tri-methylamine has been studied at 280 and 276 °K, respectively, on a range of silica gels and on silica–alumina. Adsorption–desorption isotherms and isothermal calorimetric heats of adsorption were measured. Heats of adsorption for di-methylamine on silica gel varied from 29.0 kcal/mol at $\theta = 0.05$ to 12.0 kcal/mol at monolayer completion, while for silica–alumina the heats fell from 31.4 to 9.0 kcal/mol between these same values of surface coverage. For tri-methylamine on silica gel, heats fell from 21.0, $\theta = 0.05$, to 10.3 kcal/mol, $\theta = 1.00$, while heats of 21.4 and 9.9 kcal/mol, respectively, were found at these same surface coverages on silica–alumina. The values of the heats of adsorption are discussed in terms of interactions in the adsorbed layer which are believed to be influenced by the pore sizes in the adsorbent and by the basicity of the amine molecules.

L'absorption de la di- et triméthylamine a été étudiée respectivement à 280 et 276 °K, sur une variété de silicagels et de silica-alumines. Les isothermes d'absorption de désorption et les chaleurs d'absorption isothermales calorimétriques ont été mesurées. Les chaleurs d'absorption de la diméthylamine sur le silicagel, varient de 29.0 kcal/mol pour $\theta = 0.05$ à 12.0 kcal/mol pour la saturation monocouche tandis que pour le silica–alumine, les chaleurs chutent de 31.4 à 9.0 kcal/mol entre les mêmes valeurs pour la surface recouverte. Pour la triméthylamine sur les silicagels, les chaleurs tombent de 21.0 pour $\theta = 0.05$ à 10.3 kcal/mol pour $\theta = 1.00$ tandis qu'on trouve respectivement 21.4 et 9.9 kcal/mol pour le silica–alumine dans les mêmes conditions. Les valeurs des chaleurs d'absorption sont discutées en fonction des interactions dans la couche d'absorption qui, on le pense, dépendent des dimensions des pores de l'absorbant et de la basicité de l'amine.

Canadian Journal of Chemistry, **50**, 2451 (1972)

Introduction

In Part I, studies of the interactions of mono-methylamine vapor, near its boiling point, on silica gel and silica–alumina were reported (1). Adsorption–desorption isotherms and isothermal calorimetric heats of adsorption were measured. The data obtained for the variation of the heat of adsorption of the amine with surface coverage on silica gel were particularly striking in that three heat rises were observed in the regions $\theta = 0.15$, 0.28, and 0.40. These phenomena were related to pore interactions of adsorbing amine molecules with preadsorbed ionic-type species formed by a charge-transfer mechanism in the early stages of adsorption on highly active hydroxyl groups.

The work has now been extended to a study of the adsorption of di- and tri-methylamine on siliceous adsorbents in order to obtain comparative and more extensive information on amine interactions with such surfaces. The possible effects of changes in basicity and molecular size of the amines through the series was of particular interest. Experimental data were obtained mainly by measurement of adsorption–desorption isotherms and isothermal calorimetric heats of adsorption.

Experimental

The sorption balance, calorimeter and techniques of measurement have been described previously (2, 3) and the physical and chemical properties of the adsorbents specified (1, 4). Both di- and tri-methylamine (anhydrous grade, Hopkins and Williams Ltd.) were frozen under vacuum and out-gassed thrice before vacuum distillation over three columns of sodium hydroxide. The middle fraction of the distillate was accepted and again out-gassed three times immediately before use. The final purity was 99.80% v/v for di-methylamine and 99.99% v/v for tri-methylamine, determined by gas-liquid chromatography. The principal impurity detected in di-methylamine was water at 0.11% v/v which concentration is of no significance in these experiments considering the volatility of the component at 280 °K, the large volume of the apparatus (~3 l), the sample mass (~0.75 g) and the pressure range studied.

Results

Di-methylamine and Tri-methylamine Adsorption–Desorption Isotherms and Isosteric Heats of Adsorption

The complete adsorption–desorption iso-

Can. J. Chem. Downloaded from www.nrcresearchpress.com by 210.87.254.105 on 09/05/12
For personal use only.

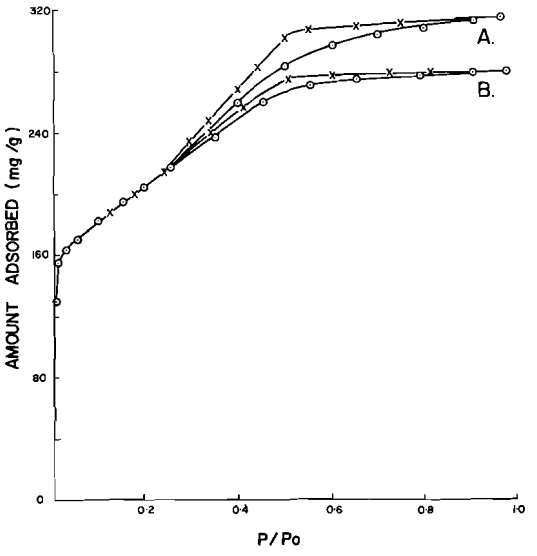

FIG. 1. Adsorption–desorption isotherms for di-methylamine (*A*) at 280 °K and tri-methylamine (*B*) at 276 °K on Davison "923" gel.

therms for di- and tri-methylamine on Davison "923" silica gel at 280 and 276 °K, respectively, are shown in Fig. 1. The gel was activated at 513 °K for 3 h prior to admission of the adsorbates. At low pressures adsorption was very rapid with about 150 to 155 mg/g adsorbed in both cases below $p/p_0 = 0.01$. Equilibrium times were between 5 and 10 min in this pressure region increasing gradually to 60 min above $p/p_0 = 0.90$. At $p/p_0 = 0.97$, 316.0 mg/g dimethylamine was adsorbed and 281.6 mg/g tri-methylamine was adsorbed. Hysteresis was exhibited on desorption of both adsorbates and the monolayer capacities were estimated by the BET method at 164.2 and 165.3 mg/g, respectively, for di- and tri-methylamine. Tests of the reversibility of adsorption (2) were carried out at four points on each isotherm, between 141.0 and 310.0 mg/g adsorbed for di-methylamine and 155.3 and 278.0 mg/g for tri-methylamine. The temperature changes made were between 280 and 360 °K and 276 and 343 °K, respectively, for di- and tri-methylamine. Complete reversibility was found at all points in these temperature cycles.

Isosteric heats of adsorption were determined for the adsorption of both amines on "923" silica gel using the method described previously for mono-methylamine (1). Due to the proximity of the monolayer isotherms, isosteric heats could only be estimated for the surface coverage region $\theta > 0.90$. This fraction of surface coverage lay within the region of proven reversibility. The isosteric heats of adsorption for di-methylamine fell from 10.5 to 9.6 kcal/mol between $\theta = 0.91$ to 1.00 while for tri-methylamine, heats remained constant at 8.6 kcal/mol between these same values of surface coverage.

Adsorption–desorption isotherms for di- and tri-methylamine at 280 and 276 °K, respectively, were also determined on several silica gels with different pore structures and on a silica–alumina, Figs. 2 and 3. Samples were pre-treated in air at 513 °K for 3 h prior to isotherm determination. The principal adsorption characteristics of these adsorbents are summarized in Table 1.

Isothermal Calorimetric Heats of Adsorption

The heat curves for di-methylamine at 280 °K and tri-methylamine at 276 °K were determined on "923" gel and silica–alumina pre-treated as before. Figure 4 shows the di-methylamine heat curves for both adsorbents. The heats for "923" gel decreased from 30.7 kcal/mol at $\theta = 0.04$ to 12.0 kcal/mol at monolayer completion with some intermediate fluctuations. The heat curve for silica-alumina showed no such fluctuations. The main fall in heat, from 33.6 to 14.4 kcal/mol, occurred between $\theta = 0.04$ and 0.20. The heat curves for tri-methylamine adsorption on "923" gel and silica–alumina are shown also in Fig. 4. The general form of the heat curve given by tri-methylamine on "923" gel was similar to that given by di-methylamine. The heat rise of around 1.5 kcal/mol at $\theta = 0.73$ for tri-methylamine on silica–alumina was reproduced with particular care.

Discussion

The very rapid initial adsorption of both amines on Davison "923" silica gel at pressures below those required to complete a monolayer, indicates that adsorption in this region involves forces that are normally associated with chemisorptive interactions. Further, at $p/p_0 = 0.036$ and 0.037 when monolayer completion had been achieved for each of the amines, the gel had adsorbed 164.2 and 165.3 mg/g of di-

Can. J. Chem. Downloaded from www.nrcresearchpress.com by 210.87.254.105 on 09/05/12
For personal use only.

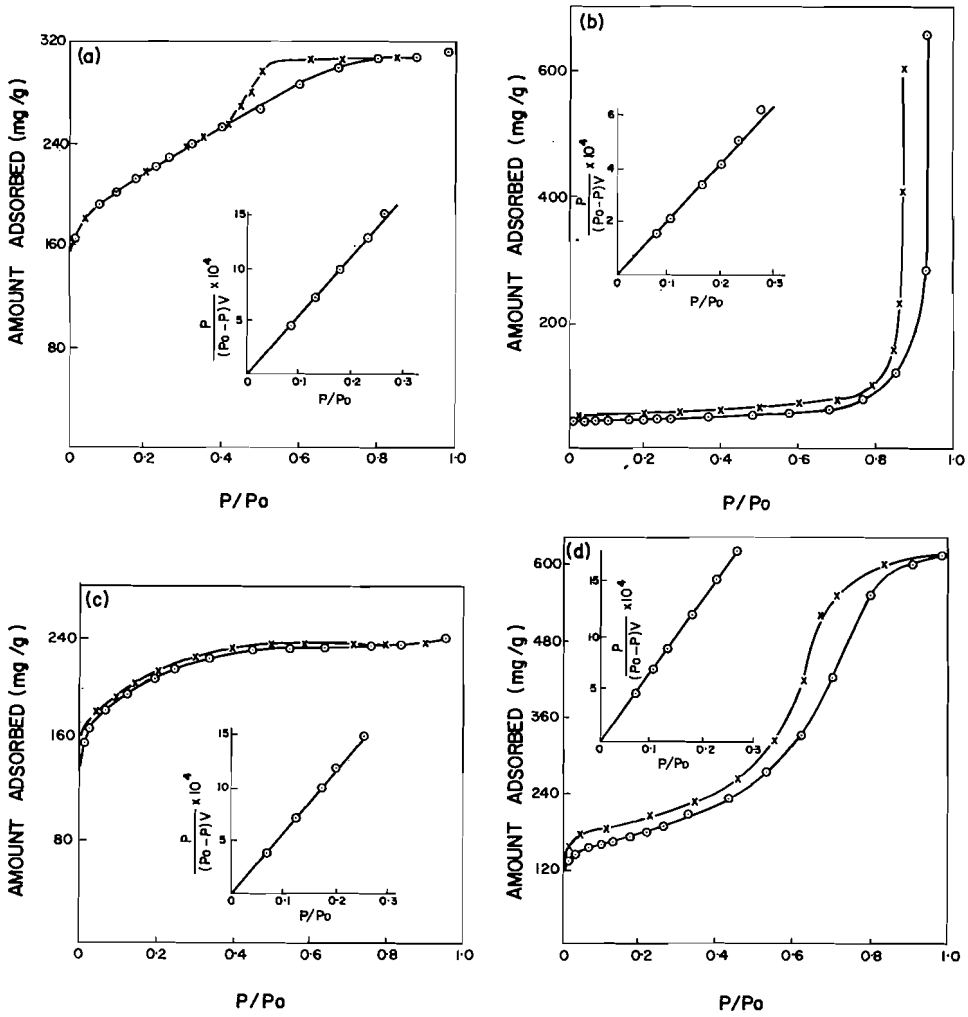

FIG. 2. Adsorption–desorption isotherms for di-methylamine on (*a*), "high surface area" gel; (*b*), "macroporous" gel; (*c*), "microporous" gel; (*d*), silica–alumina. Inset B.E.T. plots.

and tri-methylamine respectively. Both of these adsorbed amounts were over one-half of the total adsorption capacity of the gel for each amine. Then, for example, after pumping gel samples to 10^{-5} mm at 280 °K for 1 h subsequent to monolayer completion, 103.2 mg/g of di-methylamine remained held by the adsorbent while raising this out-gassing temperature to 360 °K still failed to achieve the removal of all the adsorbate. All of these observations are in accord with previous conclusions made from infrared work (5) on the adsorption of di-methylamine on silica when the adsorption interaction was reported as "unusually strong". While hydrogen bonding was believed to be involved, its nature was discussed then in terms of a "special case" of a charge-transfer interaction.

In general, silanol group protons are believed to be more positive than carbinol protons due to π-bonding between one of the unshared electron pairs on the oxygen of the silanol group and a vacant d orbital of the silicon atom (6). Hence interactions of silanol groups with molecules which have lone pair electrons may be expected to involve stronger forces than those normally associated with the formation of hydrogen bonds between such molecules

Can. J. Chem. Downloaded from www.nrcresearchpress.com by 210.87.254.105 on 09/05/12
For personal use only.

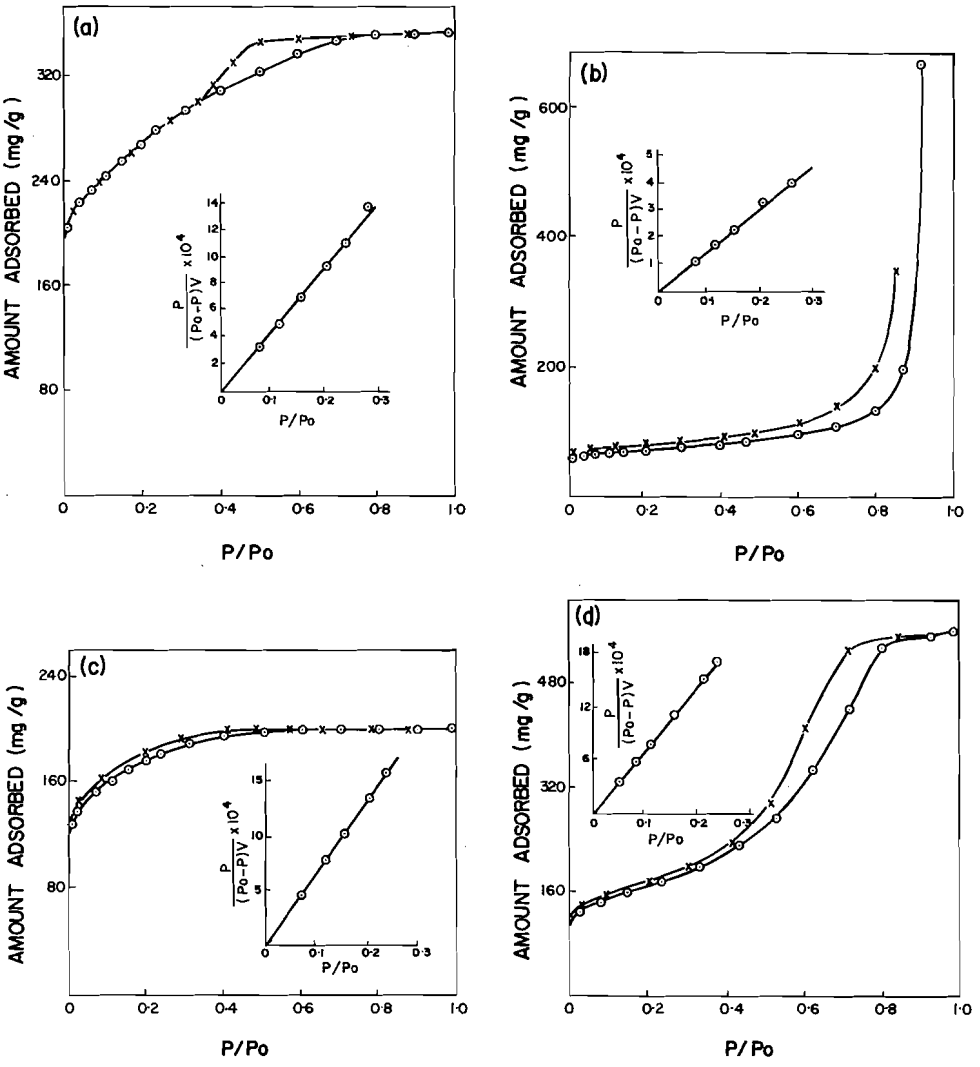

FIG. 3. Adsorption–desorption isotherms for tri-methylamine on (*a*), "high surface area" gel; (*b*), "macroporous" gel; (*c*) "microporous" gel; (*d*) silica–alumina. Inset B.E.T. plots.

and, for example, the carbinol group in alcohols (5). In the particular coverage region $\theta > 0.10$ because of the structural heterogeneity (3) of silica gel the silanol groups involved in the adsorption of the methylamines are those most likely to be capable of taking part in reactions involving proton displacement towards the adsorbed molecule such that charge-transfer adsorbed species could be formed.

The hysteresis loops given by di- and tri-methylamine adsorption of "923" gel are best classified as "type E" (7). The di-methylamine loop is of slightly greater height (8) than for tri-methylamine. This may be explained by the occurrence of a small measure of restricted adsorption of the larger tri-methylamine molecule into the interior pore matrix of the material through narrow pore necks which approach molecular dimensions (4). The molecular cross-sectional area of di-methylamine is slightly smaller at 25 Å^2 than that of tri-methylamine at 30 Å^2. Hence a slightly greater amount of di- than tri-methylamine is likely to be internally adsorbed and subsequently retained longer on

Can. J. Chem. Downloaded from www.nrcresearchpress.com by 210.87.254.105 on 09/05/12
For personal use only.

TABLE 1. Characteristics of di- and tri-methylamine adsorption on silica gels and silica–alumina

Adsorbate	Adsorbent	Monolayer coverage value (mg/g)	Monolayer coverage pressure (p/p_0)	Hysteresis loop properties			Amount adsorbed at $p/p_0 = 0.95$ (mg/g)
				Opened (p/p_0)	Closed (p/p_0)	Max. height of loop (mg/g)	
Di-methylamine (280 °K)	Davison "923"	164.2	0.036	0.91	0.25	19.2	314.5
	"High Surface Area"	172.9	0.030	0.80	0.42	27.5	309.3
	"Microporous"	165.7	0.020	0.95	—	3.9	239.0
	"Macroporous"	42.9	0.010	—	—	—	—
	Silica–alumina	144.7	0.028	0.98	—	120.0	610.0
Tri-methylamine (276 °K)	Davison "923"	165.3	0.037	0.85	0.25	7.6	279.5
	"High Surface Area"	212.4	0.020	0.73	0.36	22.7	349.0
	"Microporous"	143.0	0.036	0.60	—	7.2	202.0
	"Macroporous"	63.5	0.010	—	—	—	—
	Silica–alumina	136.5	0.031	0.93	—	95.0	550.0

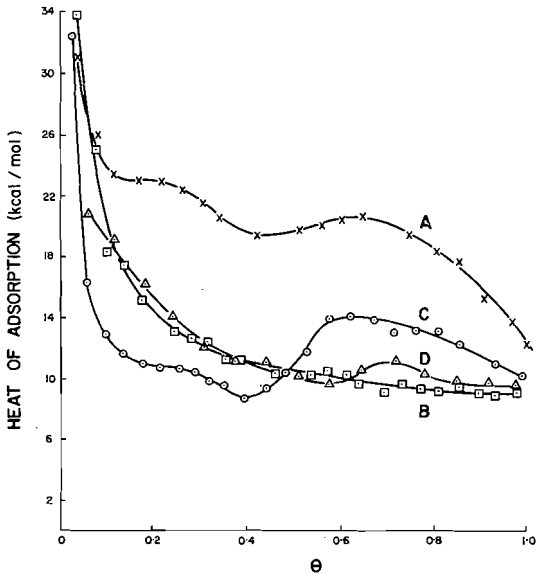

FIG. 4. Variation of isothermal calorimetric heat of adsorption for di-methylamine with surface coverage on (*A*) Davison "923" gel, (*B*) silica–alumina and for tri-methylamine with surface coverage on (*C*) Davison "923" gel, and (*D*) silica–alumina.

desorption. The hysteresis loops determined for di- and tri-methylamine on "high surface area" silica gel and silica–alumina show a similar effect, Figs. 2 and 3.

The adsorption isotherms for di- and tri-methylamine on "microporous" gel, Figs. 2 and 3, are almost Langmuirian in type while both adsorbents exhibit long narrow hysteresis loops. No hysteresis was found for mono-methylamine adsorption on this gel (2) which has a maximum in its pore diameter distribution between 20 and 30 Å. The effects observed for the larger size amines are considered to be brought about possibly by intercalation of small amounts of these adsorbates at high pressures into pores with monomolecular dimensions such that the hysteresis loops open at the saturation pressure in each case and remain open to below $p/p_0 = 0.01$.

The weight of di-methylamine adsorbed at $p/p_0 = 0.95$ on all adsorbents was greater than that of tri-methylamine except for "high surface area" gel. This can be linked simply to the greater total adsorption capacity of the porous materials for the smaller amine molecule. However, the "high surface area" adsorbent gave monolayer coverage values of 172.9 and 212.4 mg/g for di- and tri-methylamine, respectively. This difference of about 40 mg/g was also reflected in the amount adsorbed at $p/p_0 = 0.95$ and can be understood best when the weights adsorbed are expressed in molar quantities. Thus for di- and tri-methylamine the monolayer coverages are equivalent to 4.6 and 4.3 μmol m^{-2}, respectively, so that the difference in weights adsorbed arises from the greater molecular weight of tri-methylamine. Previously it has been shown that mono-methylamine molecules adsorb on a 1:1 basis with hydroxyl groups on silica gel (2) while the mono-methylamine monolayer coverage value of 6.6 μmol m^{-2} for "high surface area" gel indicates an average surface concentration of 4 hydroxyl groups per 100 $Å^2$. Because of steric hindrance effects it is

Can. J. Chem. Downloaded from www.nrcresearchpress.com by 210.87.254.105 on 09/05/12
For personal use only.

unlikely that di- or tri-methylamine can achieve a simple 1:1 ratio with silanol groups on adsorption and hence the number of these amine molecules adsorbed per unit area will be less than that for mono-methylamine.

The tendency for di-methylamine to undergo a reaction of the base–acid type with silanol groups would be expected to be greater than that of tri-methylamine since the respective K_b values are 5.12×10^{-4} and 5.27×10^{-5} (9). These values would be expected to reflect on the magnitude of the heats of adsorption. Thus the heat curve for di-methylamine on "923" silica gel lies above that for tri-methylamine, Fig. 4, implying stronger interactions over the whole range of θ.

The initial heats of adsorption for di- and tri-methylamine on "923" gel, Fig. 4, were 29.0 and 21.0 kcal/mol, respectively, at $\theta = 0.05$. These heats are compatible with the strong adsorbate–adsorbent interactions believed to be involved at low surface coverage, $p/p_0 < 0.04$. The heat curves then fall to 19.4 kcal/mol at $\theta = 0.44$ for di-methylamine and to 8.8 kcal/mol at $\theta = 0.40$ for tri-methylamine. In both curves the fall is interrupted by a short plateau, at 23.0 kcal/mol between $\theta = 0.12$ and 0.21 for di-methylamine and at 11.0 kcal/mol between $\theta = 0.20$ and 0.30 for tri-methylamine. These interruptions which occur immediately after the initially high heats, which are believed to be due to the formation of the charged species, could arise from lateral attractive interactions (10–13) between adsorbed molecules. The possibility would be enhanced if the previously adsorbed amine molecules were sited on those hydroxyl groups which exist in dense clusters (14) or are present on the walls of micropores within the gel, particularly at this surface coverage where pores of < 20 Å diameter are filling. The heat curve for di-methylamine rises from 19.4 kcal/mol at $\theta = 0.44$ to 20.6 kcal/mol at $\theta = 0.65$ and for tri-methylamine from 8.8 kcal/mol at $\theta = 0.40$ to 14.1 kcal/mol at $\theta = 0.60$. In this region of monolayer coverage these heat rises are too large to be explained solely by the occurrence of van der Waals' attractive interactions between adsorbed molecules (15), but are likely to include contributions resulting from surface rearrangements of the adsorbed species such as might be caused by interactions among groups of molecules as clusters spread (11) and infringe on their neighbors. The mono-methylamine heat curve on this gel (2) did not show a heat rise in this region. Thus the extent of the interactions seems to be related to the molecular size of the amines and may be a function of an increase in the steric contribution. Towards monolayer coverage the heat curves fall to values of 12.0 and 10.3 kcal/mol for di- and tri-methylamine, respectively, as might be expected since the adsorbed layer covers about 75% of the surface at this point and repulsive interactions between the adsorbed layer and adsorbing molecules should become increasingly significant.

The heat curve for di-methylamine adsorption on silica–alumina, Fig. 4, falls smoothly from 31.4 to 9.0 kcal/mol between $\theta = 0.05$ and 1.00. Its shape is similar to that previously determined for ammonia adsorption on silica–alumina (16). The corresponding heat curve for tri-methylamine falls from 21.4 to 9.0 kcal/mol between these same θ values but exhibits a heat rise of about 1.5 kcal/mol at $\theta = 0.73$. This was the only heat curve determined for silica–alumina with any of the amines to show such a rise and this may be explained in the same fashion as that earlier for silica gel.

1. W. G. Cook and R. A. Ross. Can. J. Chem. **50**, 1666 (1972).
2. R. A. Ross and A. H. Taylor. Proc. Brit. Ceram. Soc. **5**, 167 (1965).
3. E. Robinson and R. A. Ross. J. Chem. Soc. (A), 2521 (1969).
4. R. A. Ross and A. H. Taylor. J. Catal. **9**, 104 (1967).
5. M. R. Basila. J. Chem. Phys. **35**, (4) 1151 (1961).
6. R. West and R. H. Baney. J. Am. Chem. Soc. **81**, 6145 (1959).
7. J. H. de Boer. Colston papers. Vol. 10. Butterworths Scientific Publications, London. 1958. p. 68.
8. D. H. Everett. The solid–gas interface. 2nd ed. E. A. Flood. Edward Arnold Publishers, London. 1967. p. 1067.
9. N. A. Lange. Handbook of Chemistry. 10th ed. McGraw-Hill Book Company, Inc. 1961.
10. A. V. Kiselev and V. V. Kulichenko. Dokl. Akad. Nauk., S.S.S.R. **93**, 101 (1953).
11. T. Tezuka and T. Takeuchi. Bull. Chem. Soc. Jap. **38**, (3) 485 (1965).
12. P. Hseih. J. Catal. **2**, 211 (1963).
13. V. Kervorkian and R. O. Steiner. J. Phys. Chem. **67**, 545 (1963).
14. A. V. Kiselev. Infrared spectra of adsorbed species. Academic Press, Inc., New York. 1966. p. 276.
15. J. H. de Boer. The dynamical character of adsorption. 2nd ed. Oxford University Press, London. 1968. p. 157.
16. F. S. Stone and L. Whalley. J. Catal. **8**, 173 (1967).

Can. J. Chem. Downloaded from www.nrcresearchpress.com by 210.87.254.105 on 09/05/12
For personal use only.

The Addition of 4-Chloro- and 2,4-Dinitrobenzenesulfenyl Chloride to *cis*- and *trans*-1-Phenylpropene[1]

GEORGE H. SCHMID, VALERIA M. CSIZMADIA, VINCENT J. NOWLAN, AND DENNIS G. GARRATT

Department of Chemistry, University of Toronto, Toronto 181, Ontario

Received January 12, 1972

The *threo-anti*-Markownikoff and *threo*-Markownikoff adducts are the products of addition of 4-chloro- and 2,4-dinitrobenzenesulfenyl chloride to *cis*-1-phenylpropene while only the *erythro* Markownikoff adduct is the product of addition to *trans*-1-phenylpropene. The addition reaction follows second order kinetics, first order in both olefin and arylsulfenyl chloride, with the rate of addition to the *trans*-olefin faster than to the *cis*. These results are consistent with a mechanism involving bridged transition states in both the rate and product determining steps.

Les produits d'addition *thréo-anti*-Markownikoff et *thréo*-Markownikoff sont obtenus par l'action du chlorure de chloro-4 et de dinitro-2,4 benzène sulfènyle sur le phényl-1 propène *cis* tandis que la même réaction sur le composé *trans* conduit uniquement au composé d'addition *erythro*-Markownikoff. La réaction d'addition suit des cinétiques d'ordre deux; l'ordre étant de un à la fois pour l'oléfine et pour le chlorure d'arylsulfènyle, la vitesse de l'addition sur l'oléfine *trans* est plus rapide que pour le *cis*. Ces résultats sont compatibles avec un mécanisme impliquant des états de transition pontés à la fois pour les étapes déterminantes de la cinétique et du produit.

Canadian Journal of Chemistry, **59**, 2457 (1972)

Can. J. Chem. Downloaded from www.nrcresearchpress.com by 210.87.254.42 on 09/05/12
For personal use only.

Introduction

The mechanism of the addition of sulfenyl chlorides to olefins has been postulated to involve an episulfonium ion intermediate whose formation is rate determining (Scheme 1) (2, 3). Attack by chloride ion on the intermediate in the product determining step leads to the adduct. In this mechanism both the rate and product determining steps involve bridged transition states. An alternate mechanism which seems to be consistent with the experimental facts involves a bridged transition state in the first step leading to an episulfonium ion intermediate which then opens to a carbonium ion prior to the product determining step (Scheme 2). The *trans* stereospecificity of the reaction is due to the steric hindrance of the adjacent arylthio group which forces the chloride ion to attack from the opposite side. Such a mechanism might be expected in the addition of sulfenyl halides to olefins such as styrene in which the incipient carbonium ion would be of greater stability. We present experimental evidence which has direct bearing upon this question.

Results

The addition of 4-chlorobenzenesulfenyl chloride to *cis*-1-phenylpropene at 25 °C in

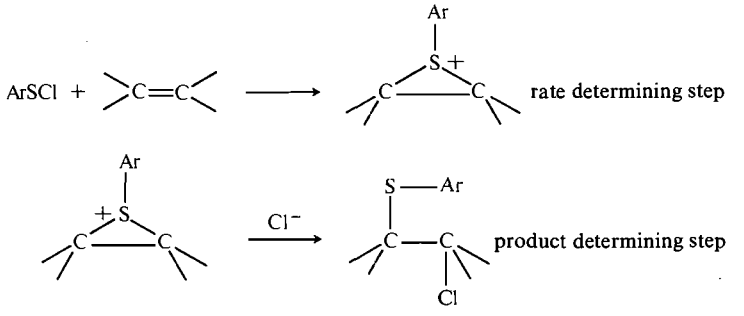

SCHEME 1

[1]Reactions of Sulfenyl Chlorides and their Derivatives. V. For Part IV see ref. 1*a*. For a preliminary communication, see ref. 1*b*.

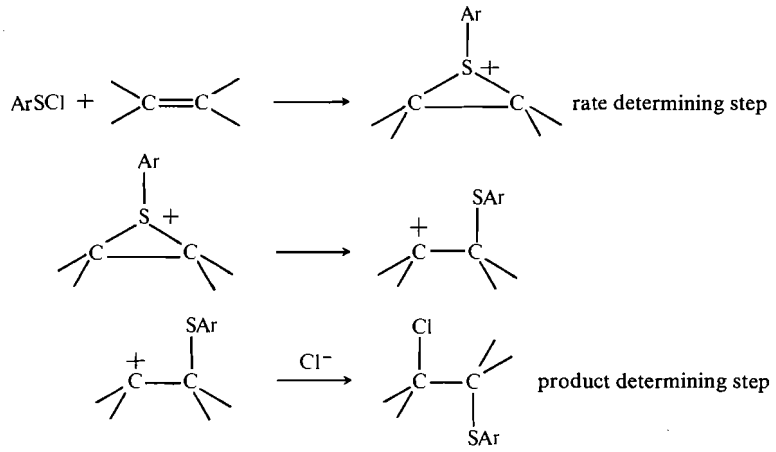

SCHEME 2

1,1,2,2-tetrachloroethane gives two products, **1** and **2** in 34 and 66% yields respectively, while the addition to *trans*-1-phenylpropene gives initially only compound **3**. After standing for several months at room temperature the formation of a second product, **4**, was observed by n.m.r. No difference in products was observed in the presence of added oxygen or in the presence or absence of light.

It proved possible to obtain a pure sample of each of the four isomers. The pure isomers **2** and **4** were obtained by the slow rearrangement of the corresponding isomers **1** and **3** respectively (4) followed by fractional crystallization. Isomer **1** was obtained by carrying out the addition reaction of the *cis*-olefin in dry formic acid and immediately working-up the product while isomer **3** was the sole product of the addition to the *trans*-olefin at room temperature.

Purification or separation of these adducts by vapor phase chromatography, distillation, or column chromatography proved unsuccessful because of the isomerization tendency of the isomers. The structure and stereochemistry of the four adducts (**1**–**4**) were assigned from their n.m.r. spectra and by chemical means.

The two adducts **1** and **3** were reduced with lithium aluminum hydride to give 1-phenyl-2-(4′-chlorophenylthio)-propane **5** which was prepared by the free radical addition of 4-chlorobenzenethiol to 1-phenylpropene (5) in 1,2-dichloroethane at room temperature (eq. 1).

The two isomers **2** and **4** were treated with boiling potassium *t*-butoxide in *t*-butyl alcohol (6), or 1,5-diazabicyclo[4.3.0]nonene in benzene (7) in the cold (eq. 2). The n.m.r. spectra of the products from both **2** and **4** showed two doublets at δ 2.01 and 1.7 and two quartets at δ 6.38 and 6.16 in CCl_4, indicating that the two olefins, **6** and **7** were formed in the ratio of 4:1. These results are not surprising since elimination of HCl from β-chlorosulfides has been shown to occur non-stereospecifically (8).

On the basis of this evidence compounds **1** and **2** resulting from the addition reaction of the *cis*-olefin were tentatively assigned as the *threo*-Markownikoff (M) and *anti*-Markownikoff (aM) isomers[2] whereas compounds **3** and **4** are

[1] **1** or **3** $\xrightarrow[\text{ether}]{LiAlH_4}$ MeCH(SAr)—CHPh(H) $\xleftarrow[DCE(r.t.)]{ArSH}$ MeCH=CHPh

5

[2]The terms *erythro* and *threo* are not strictly applicable where only one group on adjacent carbon atoms are identical. In this work the name *erythro* is given to the isomer formed by the *trans*-addition to the *trans*-olefin. Also in this work, "Markownikoff" orientation indicates adducts with the chlorine on the benzylic (C_α) carbon while "*anti*-Markownikoff" adducts have the chlorine on the β-carbon.

Can. J. Chem. Downloaded from www.nrcresearchpress.com by 210.87.254.42 on 09/05/12
For personal use only.

TABLE 1. The n.m.r. data for the adducts of 4-chlorobenzenesulfenyl chloride and *cis*- and *trans*-1-phenylpropene

	Compound	Proton chemical shift*; coupling constants†					m.p. (°C)
		δ_a	J_{ab}	δ_b	J_{bc}	δ_c	
1	Ph—$CH^aCH^bCH_3^c$ (Cl, SAr) *threo*	4.97 (d, 1H)	5.5	3.66 (q, 1H)	7.0	1.23 (d, 3H)	oil
2	Ph—$CH^aCH^bCH_3^c$ (ArS, Cl) *threo*	4.34 (m)	—	4.34 (m)	6.5	1.44 (d, 3H)	59–60
3	Ph—$CH^aCH^bCH_3^c$ (Cl, SAr) *erythro*	4.82 (d, 1H)	7.0	3.49 (q, 1H)	7.0	1.38 (d, 3H)	oil
4	Ph—$CH^aCH^bCH_3^c$ (ArS, Cl) *erythro*	4.14 (d)	7.0	4.32 (q)	6.5	1.54 (d, 3H)	65–67

*In p.p.m. from internal TMS in CCl_4; d, doublet; q, "quintet"; m, multiplet.
†J in Hz.

[2] **2** or **4** $\xrightarrow[t\text{-BuOH}]{t\text{-BuO}^{\ominus}}$ 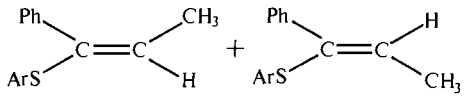 +

6 **7**

the *erythro*-Markownikoff and *anti*-Markownikoff isomers respectively.

The n.m.r. spectra of the isomers, given in Table 1, are in accord with these structural assignments. From an examination of the n.m.r. spectra of a series of racemic *erythro*- and *threo*-isomers of 1,2-disubstituted 1-arylpropanes, it has been found (9) that the methyl protons of the *erythro*-isomer always appear at lower field than those of the *threo*-isomer. On this basis compounds **1** and **3** resulting from *trans*-Markownikoff addition to *cis*- and *trans*-1-phenylpropene are the *threo*- and *erythro*-isomers respectively whereas compounds **2** and **4** are the *threo*- and *erythro*-isomers respectively of the *anti*-Markownikoff addition. In the two Markownikoff adducts **1** and **3** the peaks of the vicinal hydrogens are well separated and they can easily be identified. The benzylic hydrogen on the carbon bearing the chloride appears at lower field as a doublet, while the hydrogen on the β-carbon, 1 p.p.m. upfield, appears as a "quintet".

The crystalline *anti*-Markownikoff adducts have more complex spectra. The vicinal hydrogens overlap and only the spectrum of the *erythro-anti*-Markownikoff product can be resolved into a doublet and "quintet" by the HA-100 n.m.r. spectrometer. This complexity is due to the fact that in the *anti*-Markownikoff adducts the chlorine is now attached to the carbon bearing the methyl group and consequently both the methyl doublet and hydrogen "quintet" are shifted to lower field, while the benzylic hydrogen doublet shifts to higher field because of the presence of the less electronegative sulfur.

The addition of 2,4-dinitrobenzenesulfenyl chloride to *trans*-1-phenylpropene in 1,2-dichloroethane at 25° yields a single yellow crystalline product **8**. The addition to the *cis*-olefin results in a mixture of two products **9** and **10** in a ratio of 60:40, which can be separated by fractional crystallization. The products are stable and they do not rearrange at room temperature. The stereochemistry of the three adducts **8**, **9**, and **10** was assigned from their n.m.r. spectra, based on the knowledge gained in the addition of 4-chlorobenzenesulfenyl chloride. It is thus concluded that the *trans*-olefin gives only Markownikoff oriented addition product **8** while the *cis*-olefin gives both the Markownikoff **9** and the *anti*-Markownikoff addition product **10**. The n.m.r. spectra of the

Can. J. Chem. Downloaded from www.nrcresearchpress.com by 210.87.254.42 on 09/05/12
For personal use only.

TABLE 2. The n.m.r. data* for the adducts of 2,4-dinitrobenzenesulfenyl chloride to *cis*- and *trans*-1-phenylpropene

Compound†	H_a	J_{ab}	H_b	J_{bc}	H_c	m.p. (°C)
Ph—CH^a(Cl)—CH^b(SAr)—CH_3^c *erythro*-M	5.06(d)‡	7.0	3.99(q)‡	7.0	1.66(d)	92–93
Ph—CH^a(Cl)—CH^b(SAr)—CH_3^c *threo*-M	5.12(d)	6.0	4.07(q)	7.0	1.45(d)	75–76
Ph—CH^a(SAr)—CH^b(Cl)—CH_3^c *threo*-aM	4.70(d)	6.0	4.47(q)	6.5	1.56(d)	131–132

*δ (p.p.m.) from TMS, 4.2% (g/v) in CCl_4; J in Hz.
†Ar, 2,4-dinitrophenyl.
‡d, doublet; q, "quintet".

TABLE 3. Specific rate constant for the addition of 4-chlorobenzenesulfenyl chloride to *cis*-1-phenylpropene in tetrachloroethane at 25°

$[ArSCl]_0 \times 10^3$ (mol/l)	$[cis\text{-olefin}]_0 \times 10^2$ (mol/l)	k (M^{-1} s^{-1})	No. of runs
1.017	1.250	42.5±0.2	4
8.136	1.250	43.0±0.3	1
1.017	2.500	43.3±0.3	3
10.170	2.500	43.4±0.6	4
10.170	3.526	40.1±0.2	2
10.170	6.632	39.2±0.3	2
10.170	2.724	45.9±0.3	2
	Weighted mean (10)	43.0±0.2	

TABLE 4. Specific rate constant for the addition of 4-chlorobenzenesulfenyl chloride to *trans*-1-phenylpropene in tetrachloroethane at 25°

$[ArSCl]_0 \times 10^3$ (mol/l)	$[trans\text{-olefin}]_0 \times 10^2$ (mol/l)	k (M^{-1} s^{-1})	No. of runs
10.170	3.870	125.6±0.8	2
10.170	2.322	125.5±0.6	2
10.170	7.544	109.5±0.7	2
7.670	5.066	112.1±0.8	2
7.798	2.724	113.4±0.4	3
1.017	7.544	115.5±0.8	2
	Weighted mean (10)	118.3±0.7	

TABLE 5. Specific rate constants for the addition of 2,4-dinitrobenzenesulfenyl chloride to *cis*- and *trans*-1-phenylpropene in tetrachloroethane at 30°

Olefin	$[olefin]_0 \times 10^2$ (mol/l)	$[ArSCl]_0 \times 10^3$ (mol/l)	$k \times 10^4$ (M^{-1} s^{-1})
trans	6.250	8.468	5.98±.02
cis	5.465	11.40	2.80±.04
cis	7.292	12.70	2.80±.04
			Average 2.84±.05

pure adducts are very straightforward and easy to analyze. Table 2 summarizes the n.m.r. characteristics of the three adducts.

The rate of the addition of 4-chlorobenzenesulfenyl chloride to *cis*- and *trans*-1-phenylpropene in 1,1,2,2-tetrachloroethane at 25° was followed by the stopped-flow technique using a Durrum–Gibson stopped-flow spectrophotometer. The rate of disappearance of 4-chlorobenzenesulfenyl chloride was followed by measuring the decrease in its absorption at 392.5 nm. The addition was found to exhibit normal second order kinetics, first order in olefin and first order in sulfenyl chloride, to 80% completion of the reaction. The results are given in Tables 3 and 4.

The rate of the addition of 2,4-dinitrobenzenesulfenyl chloride to *cis*- and *trans*-1-phenylpropene in 1,1,2,2-tetrachloroethane at 30° was followed by the usual titration technique (14). Again the reaction was found to exhibit normal second order kinetics; first order in olefin and first order in sulfenyl chloride. The results are given in Table 5.

Discussion

From the results presented in this paper, it is clear that the addition of 4-chloro- and 2,4-dinitrobenzenesulfenyl chloride to *cis*- and *trans*-1-phenylpropene is stereospecifically *trans*

Can. J. Chem. Downloaded from www.nrcresearchpress.com by 210.87.254.42 on 09/05/12
For personal use only.

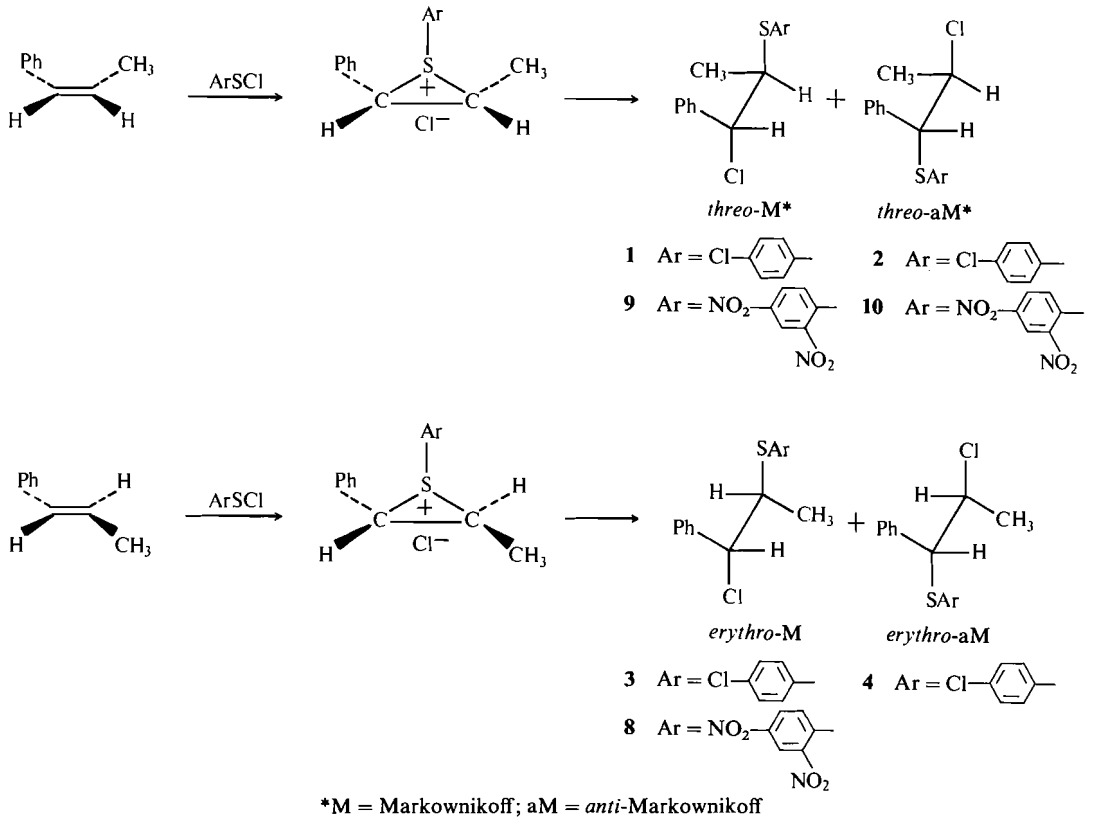

*M = Markownikoff; aM = *anti*-Markownikoff

SCHEME 3

within the limits of our n.m.r. analysis. This result as well as the formation of the *anti*-Markownikoff product in the addition to the *cis*-olefin can best be explained by a mechanism involving transition states that resemble the intermediate episulfonium ion in both the rate and product determining steps. This mechanism is illustrated in Scheme 3. These results can be contrasted with other ionic additions to *cis*- and *trans*-1-phenylpropene. The additions of bromine (11) and chlorine (6) are non-stereospecific and are postulated to involve an open benzylic carbonium ion – ion pair mechanism indicating that the benzyl carbonium ion is more stable than the bridged "halonium" ion. Our results show that the episulfonium ion is more stable than a benzylic carbonium ion as an intermediate in the addition of arylsulfenyl chlorides to *cis*- and *trans*-1-phenylpropene. Such a result is consistent with the relative abilities of sulfur, chlorine, and bromine to act as a neighboring group.

It is interesting that the products are analogous for the addition of either 4-chloro or 2,4-dinitrobenzenesulfenyl chloride. Thus the ortho nitro group does not seem to be involved in the product determining step in contrast to its apparent involvement in other reactions (12).

An interesting finding of the work is that the addition to the *trans*-olefin initially yields only the *erythro*-Markownikoff product while the *cis*-isomer yields both the *threo*-Markownikoff and *anti*-Markownikoff products. These results can be accounted for on the basis of the difference in steric crowding in the two intermediate episulfonium ions (see Scheme 4). The steric crowding is more severe in the case of the episulfonium ion intermediate formed by the addition to the *cis* than the *trans* olefin. As a result, these two intermediates have a small but significant difference. The steric crowding in the *cis* episulfonium ion prevents the phenyl ring from assuming a position where it can assist in stabilizing the positive charge on the adjacent

Can. J. Chem. Downloaded from www.nrcresearchpress.com by 210.87.254.42 on 09/05/12
For personal use only.

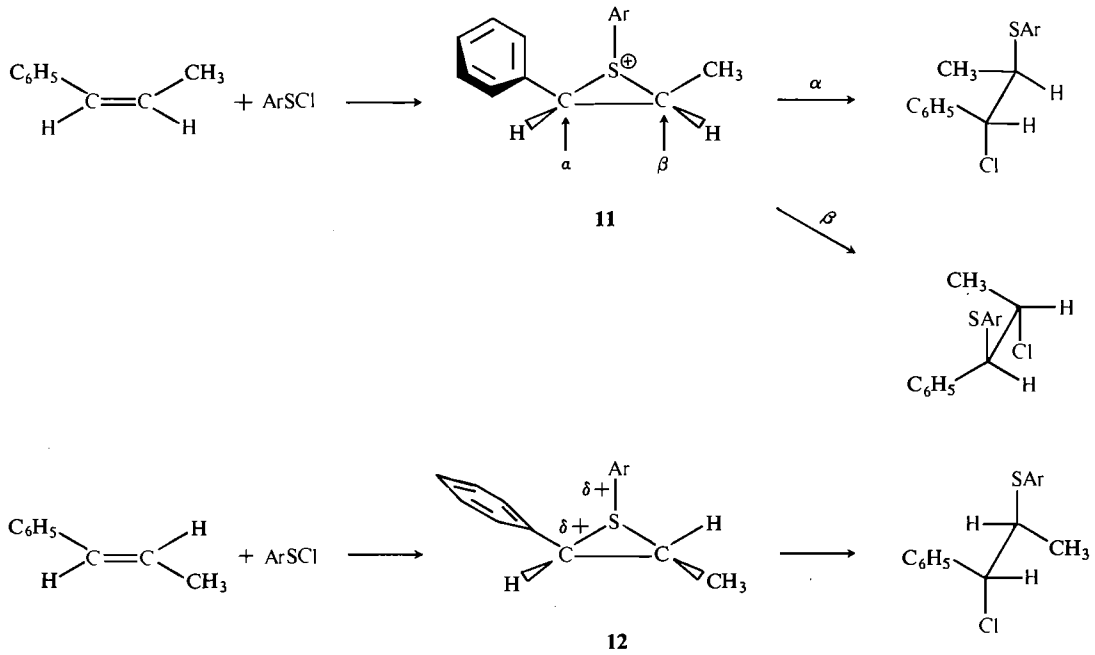

SCHEME 4

benzylic carbon. As a result, it has a more symmetrical electronic structure **11** than the one from the *trans*-olefin **12**. This difference in the structure of the two episulfonium ions is carried into the product determining transition states. Thus the two transition states for attack of chloride ion at the α and β carbons of **11** are of comparable energy resulting in the formation of products with both Markownikoff and *anti*-Markownikoff orientation. In the case of chloride attack on intermediate **12**, the transition state for attack at the benzylic carbon is of lower energy than the one for attack at the β carbon resulting in the formation of only the Markownikoff product.

If steric crowding in the intermediate episulfonium ions affects the relative energy levels of the product determining transition states, such steric crowding should also be present in the rate determining step leading to these intermediates. The kinetic data are consistent with this idea. Thus in the addition of both 4-chloro- and 2,4-dinitrobenzenesulfenyl chloride to 1-phenylpropene, the *trans*-isomer reacts faster than the *cis* even though the ground state energy of the *trans*-isomer is the lower. This is in contrast to the results of chlorination where *cis*-1-phenylpropene reacts faster than the *trans*-isomer (17). The energy of the rate determining transition state for the addition of arylsulfenyl chloride to the *cis*-isomer must therefore be higher than that of the *trans*-isomer. This is consistent with the formation of a bridged rate determining transition state which shows increased steric interaction over that in the ground state. The difference in the energies between the two transition states must be greater than the 2.8 kcal/mol difference in the starting olefins.

Experimental

All melting points and boiling points are uncorrected. Microanalyses were carried out by A. B. Gygli Microanalysis Laboratory, Toronto.

cis- and trans-1-Phenylpropene

These compounds were obtained commercially from Columbia or Aldrich Chemical Company and their purity was verified by v.p.c. and n.m.r. (b.p. *cis* 160 °C/760 mm, *trans* 98 °C/84 mm).

Bis(2,4-Dinitrophenyl)disulfide

This disulfide was obtained commercially from Eastman Organic Chemicals and used without purification (m.p. 240–280 °C (dec.)).

Bis(4-chlorobenzene)disulfide

In a 2 l Erlenmeyer flask equipped with a magnetic stirrer were placed 1000 ml of distilled water, 86.7 g (0.60 mol) of *p*-chlorothiophenol, and 24.0 g (0.60 mol) of sodium hydroxide. The crystalline *p*-chlorothiophenol dissolved as a fluffy

Can. J. Chem. Downloaded from www.nrcresearchpress.com by 210.87.254.42 on 09/05/12
For personal use only.

Can. J. Chem. Downloaded from www.nrcresearchpress.com by 210.87.254.42 on 09/05/12
For personal use only.

precipitate of sodium *p*-chlorothiophenoxide was formed. To the mixture was added 450 ml of 3% hydrogen peroxide at such a rate that the temperature of the reaction mixture did not exceed 30 °C. The light-yellow disulfide precipitated as it was formed. After the addition of the hydrogen peroxide, the reaction mixture was stirred overnight at room temperature. The crystals were filtered and washed with warm tap water and then distilled water until the filtrate was alkaline free. Recrystallization from 95% ethyl alcohol gave a 95% yield of pale-yellow plates, m.p. 73.0–77.5 °C (lit. (2) m.p. 71–71.5 °C).

p-Chlorobenzenesulfenyl Chloride

This compound was prepared by the method of Lawson and Kharasch (13) in 81% yield, b.p. 33–34 °C at 0.22 mm (lit. (13) b.p. 86–90 °C at 5 mm). The purity of the material was determined by the method of Kharasch and Wald (14) and found to be 99.8 ± 1%.

2,4-Dinitrobenzenesulfenyl Chloride

This compound was prepared by the method of Kharasch *et al.* (15) in 85% yield, m.p. 97–98 °C (lit. (15) m.p. 95–95.5 °C).

1,1,2,2-Tetrachloroethane

This compound was purified by washing with concentrated H_2SO_4 until the acid wash remained colorless. The solvent was then washed with water until neutral, dried over K_2CO_3, then distilled from K_2CO_3 through a Vigreux column, b.p. 146° (lit. (16) b.p. 146°).

The Reaction of p-Chlorobenzenesulfenyl Chloride with cis- and trans-1-Phenylpropene

General Procedure

A solution of *p*-chlorobenzenesulfenyl chloride (1.18 g, 0.01 mol) in 20 ml 1,1,2,2-tetrachloroethane (TCE) was added dropwise to a solution containing 1.79 g (0.01 mol) of either *cis*- or *trans*-1-phenylpropene in 20 ml of TCE at room temperature. The reaction mixture was stirred and it immediately became opaque, then a very fine floating precipitate separated. The reaction mixture was allowed to stand in the dark and the precipitate disappeared. After the solvent was evaporated in a stream of nitrogen gas, the residual oil which corresponded to a quantitative yield was analyzed by n.m.r.

I. Preparation of the Pure anti-Markownikoff threo-Adduct (2)

The general procedure given above was followed except that 1,2-dichloroethane was used as solvent and the reaction mixture was refluxed until the n.m.r. spectrum indicated that the equilibrium product ratio was reached. Then the solvent was evaporated and the residual oil was dissolved in *n*-pentane and was allowed to stand in the refrigerator until crystals formed. The solvent was decanted quickly from the crystals, which were then recrystallized repeatedly from *n*-pentane until its n.m.r. indicated that the pure *anti*-Markownikoff product had been obtained. The colorless solid melted at 59–60 °C.

Anal. Calcd. for $C_{15}H_{14}Cl_2S$: C, 60.61; H, 4.74; Cl, 23.85; S, 10.68. Found: C, 60.67; H, 4.68; Cl, 23.88; S, 10.76.

II. Preparation of the Pure threo-Markownikoff Adduct (1)

The *threo*-Markownikoff addition product was prepared by carrying out the addition in dry formic acid, shaking it, then pouring it very quickly into ice water and extracting with chloroform. The chloroform extract was washed with 5% ice-cold $NaHCO_3$ and then dried over $MgSO_4$. After evaporation of the solvent the oily product was found, by n.m.r., to be the Markownikoff product contaminated by disulfide. No purification method was found because of the isomerization tendency of the Markownikoff adduct to the *anti*-Markownikoff adduct. However, the oil was stable for months at −20 °C.

III. Preparation of the Pure erythro-Markownikoff Adduct (3)

The general procedure was followed except that the *trans*-olefin was used and in this case only the *erythro*-Markownikoff addition product was obtained. The n.m.r. was taken directly on the oil because no purification method has been found which did not also cause isomerization.

IV. Preparation of the Pure anti-Markownikoff erythro-Adduct (4)

The *erythro-anti*-Markownikoff product was obtained in low yield by a method analogous to that of the *threo*-isomer except that the *trans*-olefin was used, m.p. 67–68 °C.

Anal. Calcd. for $C_{15}H_{14}Cl_2S$: C, 60.61; H, 4.74; Cl, 23.85; S, 10.78. Found: C, 60.59; H, 4.65; Cl, 23.95; S, 10.69.

Reduction of the threo- and erythro-Markownikoff Addition Products Obtained from cis- and trans-1-Phenylpropene and p-Chlorobenzenesulfenyl Chloride

The addition product, 5.94 g (0.02 mol), was dissolved in 100 ml of dry ether and a solution of $LiAlH_4$ (0.60 g, 0.04 mol) in 100 ml ether was added in small portions while the reaction mixture was stirred with a magnetic stirrer in a three-necked round-bottomed flask, equipped with a reflux condenser. The reaction mixture was left stirring for 1 h at room temperature. The excess $LiAlH_4$ was destroyed by adding ethyl acetate dropwise, followed by aqueous HCl until a clear liquid separated which was decanted. Ether was added, the mixture stirred, and the ether decanted again. The combined ethereal solution was washed three times with aqueous Na_2CO_3 (because of the very strong mercaptan smell it was also washed twice with dilute NaOH solution), then with distilled water, and dried over anhydrous Na_2SO_4. Concentration on the rotary evaporator gave 4.86 g yellowish oil (yield 83%). Chromatography on a 4 × 48 cm silica gel (28–200 mesh) column using petroleum ether, CCl_4, and $CHCl_3$, followed by concentration of appropriate fractions, gave 3.17 (65% yield) of a pale yellow oil.

Anal. Calcd. for $C_{15}H_{15}ClS$: C, 68.55; H, 5.75; Cl, 13.49; S, 12.20. Found: C, 68.26; H, 5.67; Cl, 14.06; S, 12.23.

Addition of p-Chlorothiophenol to trans-1-Phenylpropene

The addition reaction was carried out by the method of Posner (5) affording a yellowish oil which was purified by column chromatography. The purified adduct was characterized by n.m.r. which was identical to that of the $LiAlH_4$ reduced adduct.

Dehydrochlorination of the Markownikoff and anti-Markownikoff Addition Products Obtained from p-Chlorobenzenesulfenyl Chloride and cis- and trans-1-Phenylpropene

Two methods were used: (1) When the reaction was carried out by the technique described by Fahey and Schubert (6) using potassium *t*-butoxide in *t*-butyl alcohol, all four isomers appeared to give the same olefinic product mixture in a ratio of 80:20. (2) When the method of Eiter and Oedinger (7) was used with 1,5-diazabicyclo[4.3.0]nonene

Can. J. Chem. Downloaded from www.nrcresearchpress.com by 210.87.254.42 on 09/05/12
For personal use only.

(DBN) in benzene, the Markownikoff adducts did not react, while the *anti*-Markownikoff adducts gave the same olefinic product mixture as with Fahey's method.

The Reaction of 2,4-Dinitrobenzenesulfenyl Chloride with cis- and trans-1-Phenylpropene

In general the addition reaction was carried out as previously described in dry 1,2-dichloroethane and the reaction mixture was analyzed by n.m.r.

I. Preparation of the Pure erythro-Markownikoff Adduct (8)

To a solution of 2.35 g (0.01 mol) of 2,4-dinitrobenzenesulfenyl chloride in 20 ml 1,2-dichloroethane was added slowly 1.18 g (0.01 mol) of *trans*-1-phenylpropene in 20 ml 1,2-dichloroethane while dry nitrogen gas was bubbled through the reaction mixture. The flask was stoppered and was allowed to stand at room temperature in the dark. The end of the reaction was confirmed by the disappearance of the olefinic methyl peak in the n.m.r. spectrum (~16 h).

The solvent from the yellow reaction mixture was removed on a rotary evaporator and the crude oily residue was analyzed by n.m.r. which indicated a single product. The crude product was recrystallized repeatedly from carbon tetrachloride, m.p. 92–93 °C.

Anal. Calcd. for $C_{15}H_{13}O_4N_2ClS$: C, 51.07; H, 3.71; N, 7.94; Cl, 10.05; S, 9.09. Found: C, 51.06; H, 3.70; N, 7.87; Cl, 10.23; S, 9.14.

II. Preparation of the Pure threo-Markownikoff (9) and threo-anti-Markownikoff (10) Adduct

The addition reaction was carried out by the same technique described in section I. The n.m.r. analysis of the crude reaction product indicated the presence of two addition products. The separation of the two adducts by fractional crystallization proved to be the only method.

The crude reaction mixture was dissolved in a mixture of chloroform and *n*-hexane (9:1) at room temperature and the solution was allowed to stand in the refrigerator until a solid separated. After filtration both the solid and the filtrate were analyzed by n.m.r. The solid, which was enriched in the *threo-anti*-Markownikoff adduct, was dissolved again in a mixture of chloroform and *n*-hexane (9:1) and was kept in the refrigerator for crystallization. The filtrate, which was enriched in the *threo*-Markownikoff adduct, was concentrated to a small volume by means of the rotary evaporator and returned to the refrigerator. The process was repeated until n.m.r. analysis indicated that the pure addition products were obtained.

Kinetic Procedure

(a) Stopped-Flow

All kinetic runs were carried out on a Durrum-Gibson stopped-flow spectrophotometer. Prior to any set of kinetic runs the instrument was allowed to stabilize for at least 2 h. A constant temperature bath was maintained at 25.00 ± 0.03°. The instrument was checked out and calibrated prior to each set of runs. Zero and 100% transmittance lines were determined by running pure solvent *vs.* the olefin solution. The time base was accurate to ±1–2% on any time scale. Kinetic runs with each olefin were carried out until a reproducible trace was stored on the oscilloscope. An infinity line was added after an appropriate time lapse. The single run was then recorded on type 107 B & W Polaroid film. Measurements from the film were treated in the usual manner (10).

(b) Titration

An adaptation of the method of Kharasch and Wald (14) was used to follow the decrease in concentration of the sulfenyl chloride. Rate constants were calculated from the slope of the straight line obtained by a least square fit to the second order rate equation.

Continued financial support by the National Research Council of Canada is gratefully acknowledged.

1. (*a*) G. H. SCHMID and P. H. FITZGERALD. J. Am. Chem. Soc. **93**, 2547 (1971). (*b*) G. H. SCHMID and V. M. CSIZMADIA. Chem. and Ind. 1811 (1968).
2. N. KHARASCH and C. M. BUESS. J. Am. Chem. Soc. **71**, 2724 (1949).
3. (*a*) W. H. MUELLER and P. E. BUTLER. J. Am. Chem. Soc. **88**, 2866 (1966). (*b*) D. R. HOGG. Quart. Reports on Sulfur Chem. **2**, 339 (1967).
4. For details of this rearrangement see G. H. SCHMID and V. M. CSIZMADIA. Can. J. Chem. This issue.
5. T. POSNER. Ber. **38**, 646 (1905).
6. R. C. FAHEY and C. SCHUBERT. J. Am. Chem. Soc. **87**, 5172 (1965).
7. K. EITER and H. OEDINGER. Ann. 682, 62 (1965).
8. N. KHARASCH. Organic sulfur compounds. Vol. 1. N. Kharasch, *editor*. Pergamon Press Inc., London, 1961. p. 259.
9. G. H. SCHMID. Can. J. Chem. **46**, 3415 (1968).
10. S. BENSON. The foundation of chemical kinetics. McGraw-Hill, New York, 1960. p. 86.
11. J. H. ROLSTON and K. YATES. J. Am. Chem. Soc. **91**, 1483 (1969).
12. E. N. GIVENS and H. KWART. J. Am. Chem. Soc. **90**, 378, 386 (1968).
13. D. D. LAWSON and N. KHARASCH. J. Org. Chem. **24**, 858 (1959).
14. N. KHARASCH and M. WALD. Anal. Chem. **27**, 996 (1955).
15. N. KHARASCH, G. I. GLEASON, and C. M. BUESS. J. Am. Chem. Soc. **72**, 1796 (1950).
16. Handbook of chemistry and physics. 47th ed. Chemical Rubber Co. p. C308.
17. K. YATES. University of Toronto, Toronto, Ontario. Private Communication.

The Effect of Temperature and Solvent upon the Addition of 4-Chlorobenzenesulfenyl Chloride to *cis*- and *trans*-1-Phenylpropene[1]

GEORGE H. SCHMID AND VALERIA M. CSIZMADIA
Department of Chemistry, University of Toronto, Toronto 181, Ontario

Received January 12, 1972

The effect of temperature upon the product composition of the addition of 4-chlorobenzenesulfenyl chloride to *cis*- and *trans*-1-phenylpropene in 1,1,2,2-tetrachloroethane has been studied. The kinetically controlled product in both cases is the adduct with Markownikoff orientation while the thermodynamically controlled product is the one with the *anti*-Markownikoff orientation. Kinetic and thermodynamic parameters have been determined for the isomerization of the *threo* as well as the *erythro* adducts. The effect of different solvents on the product composition has been studied at 25°. The regioselectivity towards Markownikoff product parallels the increasing acidity and anion solvating ability of the solvent.

L'influence de la température sur la composition des produits issus de l'addition du chlorure de chloro-4 benzène sulfènyle au phényl-1 propène *cis* et *trans* dans le tétrachloro-1,1,2,2 éthane, a été étudiée. Le produit cinétique dans les deux cas est le produit d'addition selon l'orientation Markownikoff, tandis que le produit thermodynamique est celui qui suit l'orientation *anti*-Markownikoff. Les paramètres cinétique et thermodynamique ont été déterminés pour l'isomérisation des produits d'addition *thréo* et *erythro*. L'influence des divers solvants sur la composition en produit a été étudiée à 25°. La régiosélectivité pour le produit Markownikoff va de pair avec l'acidité croissante et le pouvoir de solvatation de l'anion du solvant.

Canadian Journal of Chemistry, **50**, 2465 (1972)

We have found that the relative amounts of Markownikoff and *anti*-Markownikoff adducts formed in the addition of 4-chlorobenzenesulfenyl chloride to *cis*- and *trans*-1-phenylpropene are strongly dependent upon the solvent used and the temperature at which the reaction is carried out.

Table 1 summarizes the results of the influence of the temperature on the initial product distribution in 1,1,2,2-tetrachloroethane. The proportions of Markownikoff and *anti*-Markownikoff adducts were determined by measuring the area of their characteristic methyl peaks (1) in the n.m.r. spectrum of the mixture at room temperature. The values listed are the averages of at least six consecutive integrations.

From the data, it is clear that the addition to *cis*-1-phenylpropene gives an initial product mixture of *threo*-Markownikoff and *anti*-Markownikoff product in a ratio of 79:21 respectively at −42 °C. As the temperature at which the addition is carried out is increased, the percentage of *threo-anti*-Markownikoff adduct also increases. Thus the addition is stereospecific based on analysis of the product by HA-100 n.m.r. spectra. The addition to *trans*-1-phenylpropene gives an initial product of only *erythro*-Markownikoff adduct up to about 50 °C, and even at 146 °C gives mainly *erythro*-Markownikoff adduct (90:10). Again no evidence of *threo*-products could be detected from the HA-100 n.m.r. spectra indicating that the addition is stereospecific.

With time this initial product composition changes until an equilibrium mixture of both the Markownikoff and *anti*-Markownikoff isomers is obtained. These final product distributions are given in Table 1. These results are consistent with isomerization occurring by means of an episulfonium ion (2).

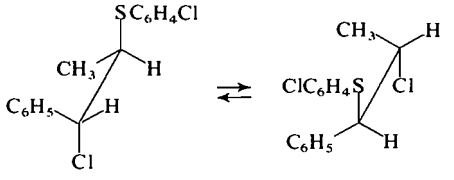

If the final product mixture is allowed to stand for 3 h at 146° leakage between the *threo* and *erythro* adducts occurs. These results are given in Table 2. This leakage can occur by two mechanisms. The first involves the formation of an open carbonium ion which could permit *erythro–threo* isomerization. This means that the activation energy to form the open ion is almost equal to that for formation of the episulfonium

[1]Reactions of Sulfenyl Chlorides and their Derivatives. VI. For Part V see ref. 1.

Can. J. Chem. Downloaded from www.nrcresearchpress.com by 210.87.254.105 on 09/05/12
For personal use only.

TABLE 1. Effect of temperature on product distribution of the addition of 4-chlorobenzenesulfenyl chloride to *cis*- and *trans*-1-phenylpropene in 1,1,2,2-tetrachloroethane

	cis-1-Phenylpropene				*trans*-1-Phenylpropene			
	Initial product distribution (%)		Final product distribution (%)		Initial product distribution (%)		Final product distribution (%)	
T (°C)	M*	aM†	M	aM	M	aM	M	aM
−42	79	21	—	—	—	—	—	—
−20	73	27	—	—	—	—	—	—
0	69	31	—	—	—	—	—	—
25	66	34	—	—	100	0	—	—
50	63	37	18	82	100	0	—	—
70	58	42	20	80	99	1	32	68
100	53	47	23	77	97	3	33	67
146	48	52	24	76	90	10	35	65

*Markownikoff.
†*anti*-Markownikoff.

TABLE 2. Effect of heating for 3 h at 146° on the products of the addition of 4-chlorobenzenesulfenyl chloride to *cis*- and *trans*-1-phenylpropene in 1,1,2,2-tetrachloroethane

Starting olefin	Product	Distribution (%)
cis	*threo*-M*	24
	threo-aM†	68
	erythro-M	3
	erythro-aM	5
trans	*erythro*-M	32
	erythro-aM	54
	threo-M	6
	threo-aM	8

*Markownikoff.
†*anti*-Markownikoff.

ion. The second possible mechanism is one that involves the reverse of the addition, which regenerates the olefin and 4-chlorobenzenesulfenyl chloride (3). Traces of HCl present in the reaction could cause equilibration of the olefins which would result in the eventual presence of adducts from both the *cis*- and *trans*-olefins, making it appear that the rearrangement is not stereospecific. (see Scheme 1). The latter explanation is preferred since all evidence so far points to a substantial difference in activation energy for formation of the open ion compared to the bridged ion in this system.

The rate of the stereospecific isomerization could be followed by measuring the rate of disappearance of the methyl peak in the n.m.r. spectrum of the Markownikoff adduct as well as the appearance of the methyl peak of the *anti*-Markownikoff adduct. Treating the data obtained from the integrated peak areas according to the method of Frost and Pearson (4) the rate constants given in Table 3 were obtained for this conversion.

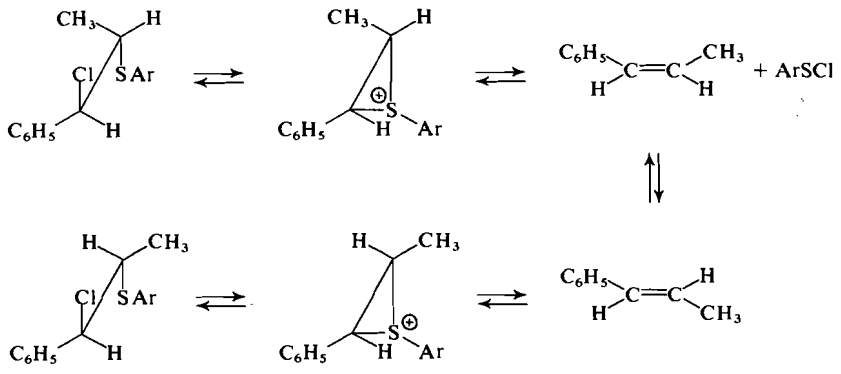

SCHEME 1

Can. J. Chem. Downloaded from www.nrcresearchpress.com by 210.87.254.105 on 09/05/12
For personal use only.

TABLE 3. Rate constants (s^{-1}) of isomerization in 1,1,2,2-tetrachloroethane*

	erythro		*threo*	
T (°C)	M $\xrightarrow{k_f}$ aM	M $\xleftarrow{k_r}$ aM	M $\xrightarrow{k_f}$ aM	M $\xleftarrow{k_r}$ aM
50	—	—	4.10×10^{-5}	0.92×10^{-5}
70	0.97×10^{-5}	0.45×10^{-5}	5.82×10^{-5}	1.44×10^{-5}
100	32.0×10^{-5}	16.0×10^{-5}	28.20×10^{-5}	7.71×10^{-5}
146	333.0×10^{-5}	179.5×10^{-5}	77.70×10^{-5}	24.5×10^{-5}

*k_f, $k_{forward}$; k_r, $k_{reverse}$; M, Markownikoff; aM, *anti*-Markownikoff.

TABLE 4. Relative stability parameters for the isomerization*

A. Product determining step			B. Thermodynamic stability of addition products		
Parameter	*cis*-Olefin	*trans*-Olefin	Parameter	*threo*-Adduct	*erythro*-Adduct
$\Delta\Delta H^{\ddagger}$ (kcal/mol)	1.3	9.0	ΔH° (kcal/mol)	−0.9	−0.6
$\Delta\Delta S^{\ddagger}$ (cal/mol deg)	3.0	17.0	ΔS° (cal/mol deg)	−0.1	−0.1

C. Kinetics of isomerization

	threo-M	aM	*erythro*-M	aM
Parameter	Forward	Reverse	Forward	Reverse
$\Delta H^{\ddagger}$ (kcal/mol)	8.0	8.9	20.4	21.0
$\Delta S^{\ddagger}$ (cal/mol deg)	−53.9	−54.0	−21.1	−19.2
r (correlation coefficient)	0.997	0.997	0.902	0.900

*Measurements were made by n.m.r.-A60.

The thermodynamic parameters for the isomerization were calculated from the data in Table 3 and are listed in Table 4. The quantities ΔH and ΔS are defined as the difference in enthalpy and entropy respectively of the *anti*-Markownikoff and Markownikoff adducts while $\Delta\Delta H^{\ddagger}$ and $\Delta\Delta S^{\ddagger}$ are defined as the difference in $\Delta H^{\ddagger}$ and $\Delta S^{\ddagger}$ respectively for the isomerization of the *anti*-Markownikoff to the Markownikoff adduct.

The data of Table 4 clearly illustrate that the kinetically controlled product is the Markownikoff adduct while the thermodynamically controlled product is the one with the *anti*-Markownikoff orientation.

It should be noted that there is a large difference in $\Delta H^{\ddagger}$ and $\Delta S^{\ddagger}$ for isomerization of the *threo* and *erythro* adducts. The larger negative value of $\Delta S^{\ddagger}$ for isomerization of the *threo* compared to the *erythro* adduct is consistent with a transition state involving considerable steric crowding with a subsequent loss of entropy. The reason for the large difference in the values of $\Delta H^{\ddagger}$ for the two adducts is not readily apparent. We are hampered by the fact that the relative enthalpies of the *erythro* and *threo* adducts are not known. Further discussion on the mechanistic significance of these quantities must await more experimental data.

The product ratio and stereochemistry of the addition of 4-chlorobenzenesulfenyl chloride to *cis*- and *trans*-1-phenylpropene has been studied in solvents of widely different polarity. The instantaneously formed addition products were analyzed by n.m.r. and are summarized in Table 5.

Both olefins show 100% *trans*-stereospecificity at room temperature independent of solvent polarity. The *trans*-olefin gives 100% solvent

Can. J. Chem. Downloaded from www.nrcresearchpress.com by 210.87.254.105 on 09/05/12
For personal use only.

TABLE 5. Solvent dependence of the product ratio of the addition of 4-chlorobenzenesulfenyl chloride to *cis*- and *trans*-1-phenylpropene at 23–25 °C

Solvent	D*	*cis*-Olefin (%)		*trans*-Olefin (%)	
		M†	aM†	M‡	aM‡
CH_3COOH‖	6.15	100	0	100	0
HCOOH‖	58.50	100	0	100	0
$Cl_2C{=}CCl_2$	—	70	30	100	0
$Cl_2CHCHCl_2$	8.20	66	34	100	0
$HCCl_3$	4.80	63	37	100	0
CCl_4	2.20	63	37	100	0
$ClCH_2CH_2Cl$	11.20	58	42	100	0
$PhNO_2$	34.8	52	48	100	0
Benzene	2.28	50	50	100	0

*Dielectric constant (5).
†*threo*-Markownikoff (M); *threo-anti*-Markownikoff (aM).
‡*erythro*-Markownikoff (M); *erythro-anti*-Markownikoff (aM) adducts.
‖Addition reaction was carried out at ~10 °C.

TABLE 6. Addition of *p*-chlorobenzenesulfenyl chloride to *cis*- and *trans*-1-phenylpropene in dry acetic acid

Time (days)	Product composition as the function of time at 25 °C*			
	trans-Olefin		*cis*-Olefin	
	Product	Yield (%)	Product	Yield (%)
0	e-M-Cl	100	t-M-Cl	91
	—	—	t-aM-Cl	9
~0.5	e-M-Cl	78	t-M-Cl	80
	e-aM-Cl	22	t-aM-Cl	20
3	e-M-Cl	39	t-M-Cl	65
	e-aM-Cl	38	t-aM-Cl	35
	e-M-OAc	23	—	—
18	e-M-Cl	26	t-M-Cl	26
	e-aM-Cl	50	t-aM-Cl	72
	e-M-OAc	24	t-M-OAc	trace
21	e-M-Cl	24	t-M-Cl	23
	e-aM-Cl	51	t-aM-Cl	72
	e-M-OAc	25	t-M-OAc	~5

*e-M-Cl, *erythro*-Markownikoff-Cl adduct; e-aM-Cl, *erythro-anti*-Markownikoff-Cl adduct; e-M-OAc, acetate of the *erythro*-M-Cl adduct; t-M-Cl, *threo*-Markownikoff-Cl adduct; t-aM-Cl, *threo-anti*-Markownikoff-Cl adduct; t-M-OAc, acetate of the *threo*-M-Cl adduct.

independent regiospecific Markownikoff addition product. The result for the *cis*-isomer is completely different.

The regioselectivity depends on the nature of the solvent, the products ranging from a mixture of Markownikoff and *anti*-Markownikoff adducts to predominantly Markownikoff adduct. The most striking feature is that the regioselectivity toward Markownikoff product parallels the increasing acidity and anion solvating ability of the solvent.

No products due to rotation of an open carbonium ion or solvent incorporation are observed at room temperature in the initial product composition. When the product ratio is plotted as a function of the solvent dielectric constant it fails to give a linear relationship.

During the study of the solvent effect in formic acid, acetic acid, trifluoroacetic acid, and its anhydride, subsequent solvolysis of the adduct occurs.

The result of addition in acetic acid as a

Can. J. Chem. Downloaded from www.nrcresearchpress.com by 210.87.254.105 on 09/05/12
For personal use only.

function of time is shown in Table 6. No *anti*-Markownikoff acetate was ever detected. This is strange but the possibility exists that the *anti*-Markownikoff-acetate forms but its n.m.r. peaks are underneath those of an *anti*-Markownikoff-chloride and therefore not easily detectable.

The results clearly establish that isomerization of the Markownikoff and *anti*-Markownikoff adducts occurs more rapidly than does their solvolysis to the acetate. This suggests that isomerization of the adducts occurs by means of tight or intimate ion-pairs (6) while solvolysis occurs by means of solvent separated ion pairs or perhaps even completely dissociated ions. This implies that the stability of the episulfonium ion intermediate is at least as great as that of the norbornyl, cholesteryl, and methoxyphenylethyl ions, all of which show this type of behavior (6).

Experimental

Determination of Product Composition

The reaction was carried out in the dark in a 15 ml, three-neck, round-bottom flask equipped with a thermometer, condenser, drying tube, and magnetic stirrer. The flask was immersed in the appropriate bath containing liquid ammonia, water, or oil. Two stock solutions, one of sulfenyl chloride and the other of the olefin were prepared in 1,1,2,2-tetrachloroethane (TCE) as follows:

(1) 4.476 g 4-chlorobenzenesulfenyl chloride in 25 ml TCE (1 mol/l) and a 4 ml (4.16×10^{-3} mol) portion was used for each experiment.

(2) 2.9540 g *cis*- or *trans*-1-phenylpropene in 10 ml TCE (1 mol/l) and a 1.66 ml (4.16×10^{-3} mol) portion was used in each experiment.

Four milliliters of the sulfenyl chloride solution was placed in the flask which was immersed in the bath at the desired temperature. While this flask was in the constant temperature bath it was cooled about 10° below the temperature of the bath by blowing air on the flask and its immediate surroundings. Then 1.66 ml of the solution, containing the olefin, was introduced dropwise or as quickly as possible into the sulfenyl chloride solution, to keep the temperature as near the bath temperature as possible but at the same time to be able to take out the first sample within the first minute of the reaction. This procedure was adopted because the reaction is extremely rapid and exothermic and an initial increase of 20 °C in the temperature of the reaction is not unusual. At the boiling point of the solvent (TCE) the olefin was added in one portion and the first sample was taken out after 0.4 min. At temperatures below 0 °C the first sample was taken 1–3 min after mixing because the rate of isomerization is slow. The samples were placed in n.m.r. tubes by means of a pipette and were kept in a Dry Ice–acetone bath. All the n.m.r. measurements were then recorded at room temperature with the same setting of the instrument. At least six integrations were made for each measurement.

Isomerization Kinetics

The method used for the determination of the product composition was extended by taking samples at specific time intervals. The method of analysis used was identical.

Continued financial support by the National Research Council of Canada is gratefully acknowledged.

1. G. H. SCHMID, V. M. CSIZMADIA, V. NOWLAN, and D. G. GARRATT. Can. J. Chem. This issue.
2. J. F. KING and K. ABIKAR. Can. J. Chem. **46**, 9 (1968).
3. G. H. SCHMID and P. H. FITZGERALD. J. Am. Chem. Soc. **93**, 2547 (1971).
4. A. A. FROST and R. G. PEARSON. Kinetics and mechanism. John Wiley and Sons, Inc., New York. 1953. p. 113.
5. A. WEISSBERGER, E. S. PROSKAMER, J. A. RIDDICK, and E. E. TROOPS, *editors*. Technique of organic chemistry. Vol. VII. 2nd. Ed. Interscience Publishers, New York. 1955.
6. S. WINSTEIN and E. CLIPPINGER. J. Am. Chem. Soc. **78**, 2784 (1956).

Can. J. Chem. Downloaded from www.nrcresearchpress.com by 210.87.254.105 on 09/05/12
For personal use only.

Hindered Rotation in an *o*-Substituted Acetophenone

VINOD DAVE AND E. W. WARNHOFF

Department of Chemistry, University of Western Ontario, London, Ontario

Received February 2, 1972

In the substituted acetophenone **2**, rotation is so restricted that the n.m.r. absorption of the methyl ketone is a broad band in several solvents at room temperature. At 90° this absorption becomes a sharp singlet, while at −60° it separates into two sharp peaks of unequal intensity. At −60° the n.m.r. absorption of the quaternary methyl groups of **2**, **3**, and **11** all show line broadening which is attributed to slowed rotation of these meshed vicinal methyl groups.

Dans l'acétophénone substituée **2**, la rotation est tellement empêchée que l'absorption r.m.n. de la méthylcétone apparaît sous forme d'une bande large dans plusieurs solvants à la température ambiante. A 90° on obtient un singulet fin tandis qu'à −60° ce dernier se sépare en deux pics fins d'intensité inégale. A −60°, l'absorption r.m.n. des groupes méthyles quaternaires de **2**, **3**, et **11**, donne pour tous un signal élargi qui est attribué à une rotation ralentie de ces groupes méthyles vicinaux.

Canadian Journal of Chemistry, **50**, 2470 (1972)

During the study of the rearrangement of the ubiquitous oxidation–dimerization product **1** ($C_{20}H_{22}N_2O_2$) from 2,3-dimethylindole (1), a crystalline compound, $C_{20}H_{20}N_2O_2$, m.p. 217°, was encountered twice. Since its anomalous n.m.r. spectrum, which belied the structure of the compound, has some features of general interest, and since the compound undergoes interesting reactions, further details are reported here and in the accompanying paper. The compound was first obtained on acid treatment of the dimer **1** (Scheme 1), a reaction whose initially obscure nature did not provide enough information for structural assignment, particularly since an oxidation had occurred. The n.m.r. spectrum at both 60 (Fig. 1) and 100 MHz contained eight aromatic protons, one proton exchangeable on addition of D_2O, a two-proton AB pattern, two unsplit quaternary methyl signals, and a broad lump (three protons) centered at δ 2.25. The second appearance of this compound was as the product of the sodium metaperiodate oxidation of both the 1,2-diol **4** and the indole **3** (Scheme 1), reactions which suggested the assignment of structure **2**, at least to the initial product of reaction. Therefore,

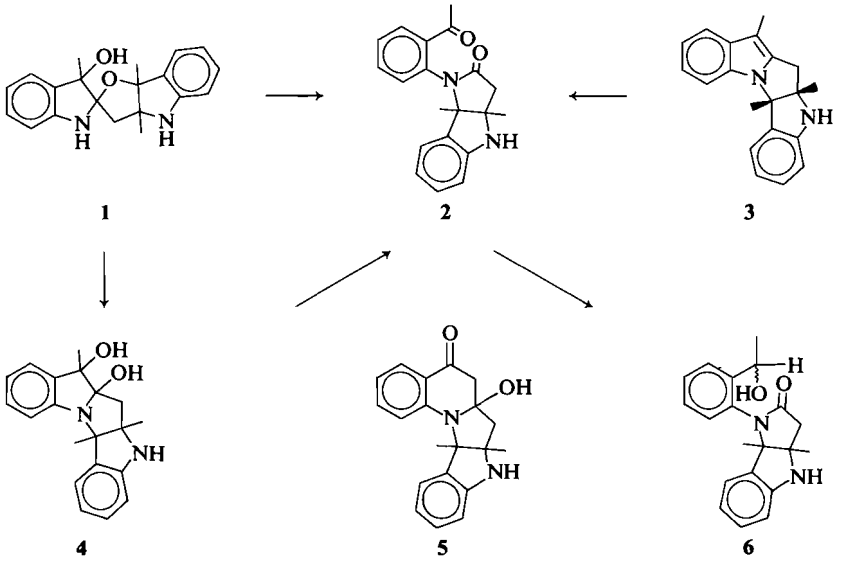

SCHEME 1

Can. J. Chem. Downloaded from www.nrcresearchpress.com by 210.87.254.105 on 09/05/12
For personal use only.

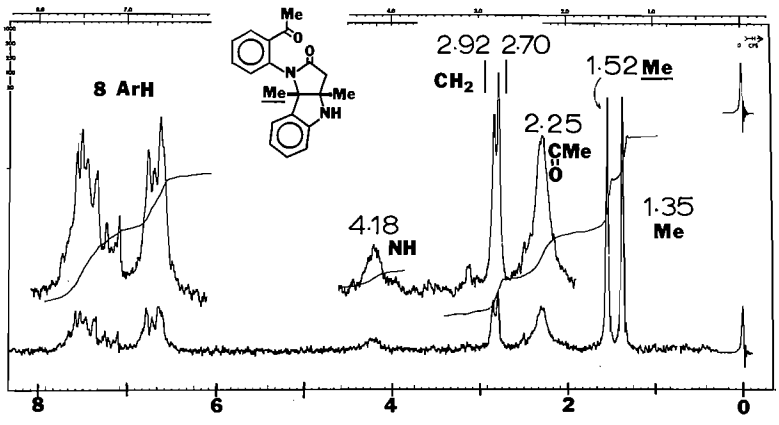

FIG. 1. The n.m.r. spectrum (60 MHz, $CDCl_3$ solution) of keto pyrrolidone **2**.

whatever the structure of the compound, the protons responsible for the broad absorption at δ 2.25 were suspected to be derived from the acetyl methyl group of **2**.

The most obvious structural possibility was the aldol **5** in which the hydroxyl and new methylene absorptions might overlap. Or alternatively, **2** and **5** might have been involved in a sufficiently rapid equilibration to result in the observed pattern. Both of these explanations were excluded in several ways. The first possibility requires that there be two exchangeable protons instead of the one found. It also requires that the compound prepared by periodate oxidation of the d_6-diol **7** (Scheme 2) (1) contain at most five D atoms, whereas in fact it still contained six, and also its n.m.r. spectrum was lacking the δ 1.52 methyl peak and the three-proton lump at δ 2.25. The second possibility of a rapid **2**$\rightleftharpoons$**5** equilibration would require that the three protons of the acetyl group of **2** be exchanged rapidly contrary to the retention of all six deuterium atoms during the periodate cleavage of the d_6-diol **7**. The remaining possibility, that the compound was actually **2** in which the environment of the acetyl methyl group was changing relatively slowly, was implicated.

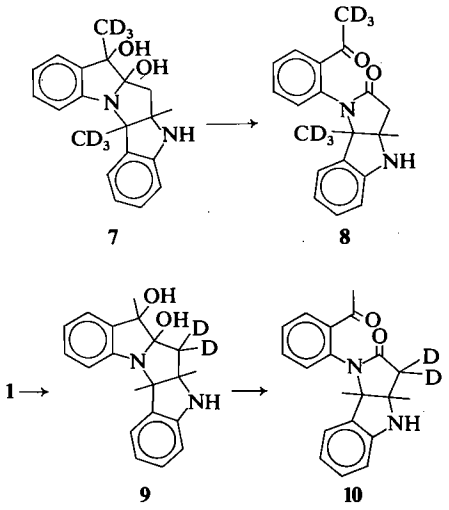

SCHEME 2

Chemical and other spectroscopic evidence was in agreement with this conjecture. In the i.r. spectrum of the compound the NH group was apparent at 3390 cm^{-1} as were the two superimposed carbonyl groups at 1680 cm^{-1} (see footnote 5 in ref. 1*b*). When the oxidative cleavage was carried out on 1,2-diol-d_2 **9**, prepared from dimer **1** in DCl–D_2O–dioxane, the d_2-compound **10** lacked the AB pattern centered at δ 2.81 in its n.m.r. spectrum. An oxime of the methyl ketone of **2** was prepared. Sodium borohydride reduced the methyl ketone to a mixture of stereoisomeric methyl carbinols **6** (Scheme 1) which still retained the 1680 cm^{-1} i.r. absorption of the pyrrolidone carbonyl group.

The n.m.r. spectrum in some other solvents was also consistent with structure **2**. With both pyridine and trifluoroacetic acid solutions the spectrum exhibited *three* singlet methyl peaks. When deuterium oxide was added to the pyridine solution, the low field methyl peak became the familiar broad lump. That no irreversible chem-

Can. J. Chem. Downloaded from www.nrcresearchpress.com by 210.87.254.105 on 09/05/12
For personal use only.

Can. J. Chem. Downloaded from www.nrcresearchpress.com by 210.87.254.105 on 09/05/12
For personal use only.

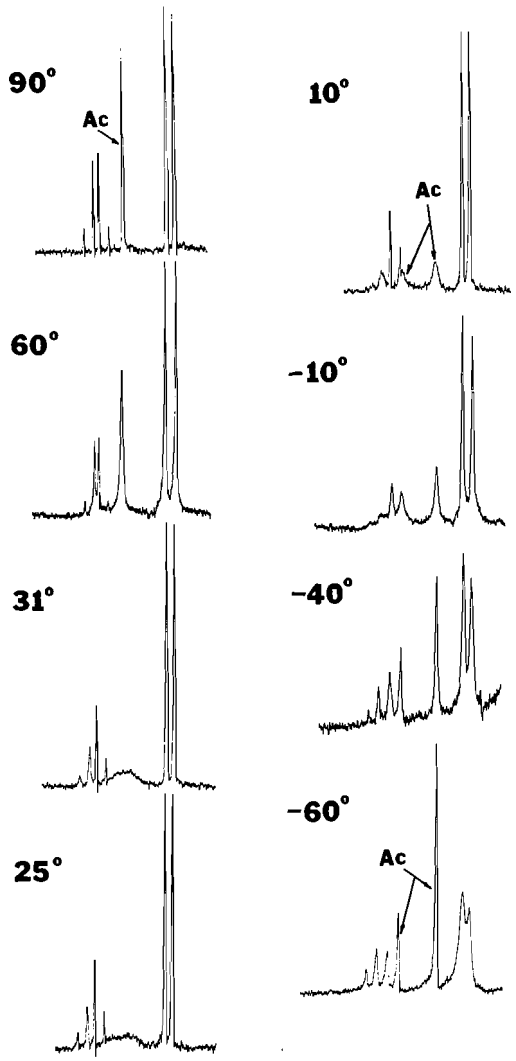

FIG 2. Variable temperature n.m.r. spectra (100 MHz, $CDCl_3$ solution) of the methyl and methylene protons of keto pyrrolidone **2**.

ical change had taken place in trifluoroacetic acid was proved on recovery of the solute; its n.m.r. spectrum in deuteriochloroform was identical with Fig. 1. On the other hand, in perdeuterioacetic acid and acetonitrile there appeared two sharp methyl peaks and the broad lump. To remove any doubts that **2** was indeed the correct structure, a variable temperature study of the spectrum in deuteriochloroform was undertaken.

As the temperature was raised from ambient to 90°, the broad lump gradually became a sharp three-proton singlet at δ 2.28 (Fig. 2) as a well-behaved acetyl methyl group should appear. Moreover, the AB pattern sharpened, and the aromatic pattern was much better resolved (Fig. 3). As the temperature was lowered, the original spectrum reappeared. Below room temperature the broad lump gradually separated at −60° into two sharp signals at δ 2.02 and 2.64 (Fig. 2) in the ratio of 80:20 totalling three protons.[1] These two sharp peaks then corresponded to the acetyl methyl group of two different conformations of the molecule. In deuteriochloroform the coalescence temperature for the acetyl methyl signals of these two conformations is fortuitously near room temperature, more precisely between 25–30° (Fig. 2). Other changes also occurred in the spectrum. At −60° the broad NH signal separated into two sharper peaks at δ 4.20 and 4.48 (Fig. 3) in the ratio of about 20:80, respectively, corresponding to the two "frozen" conformations.

On the other hand, the two narrow high-field peaks from the indolinyl methyl groups gradually *broadened* as the temperature decreased (Fig. 2), and at −60° the broadening was enough to cause the two peaks to merge partially. Although, *a priori*, the line broadening could have been caused by (*a*) lower resolution due to increased viscosity, (*b*) slightly different chemical shifts for the methyl groups in the two conformers, or (*c*) ^{14}N quadrupole-induced relaxation effects, we believe that the line broadening is due instead to slower rotation of these methyl groups, which bear a meshed cogwheel relation to each other, as the temperature is lowered. Decreased resolution is not the explanation since the acetyl methyl signal is relatively narrow ($w_{1/2}$ 3 Hz) at −60°. Moreover, the low temperature spectra of the related compounds **3** and **11** (Fig. 4) show the same broadening of the two indolinyl methyl peaks (albeit to a lesser extent) relative to the indole methyl signal which remains narrow and sharp. If, as seems likely, the broadening has the same cause in all three compounds, then explanation (*b*) is excluded because no conformational changes are possible in the rigid skeletons of **3** and **11**. Explanation (*c*) would have as a corollary that nitrogen quadrupole effects in **11** should be different for the two indolinyl methyl groups. On the contrary, the extent of broad-

[1]After correction is made for the high-field peak of the AB methylene group under the δ 2.64 peak.

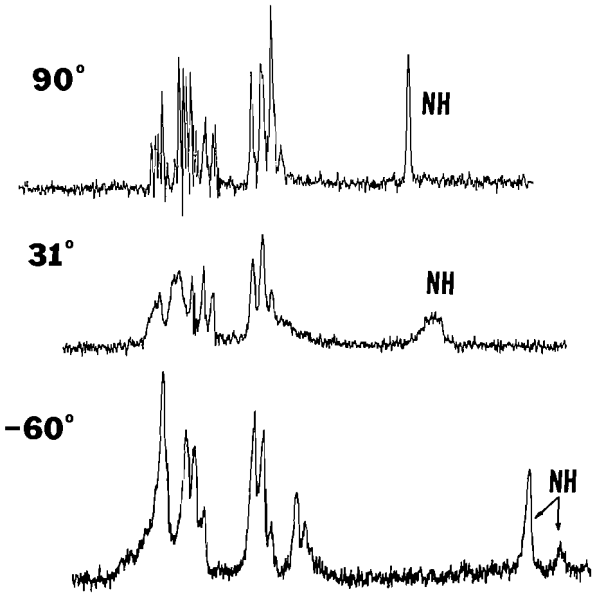

FIG. 3. Variable temperature n.m.r. spectra (100 MHz, $CDCl_3$ solution) of the aromatic and NH protons of keto pyrrolidone **2**.

ening of these two methyl groups is the same (Fig. 4). However, this equal extent of broadening of both indolinyl methyl groups in **3** and **11** is required if slower rotation of the meshed groups is responsible for the broadening.

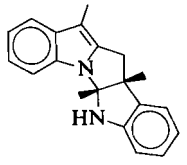

11

From examination of Stuart–Briegleb models the two conformations of **2** which (*a*) maintain the maximum degree of coplanarity of the conjugated ketone and amide with the benzene ring, and yet (*b*) have the fewest repulsive steric interactions are represented in **2***a* and **2***b*. Of the two conformers, **2***a*, in which the oxygen–oxygen dipole repulsion is minimized, should

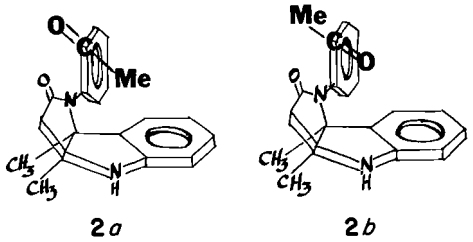

2*a* **2***b*

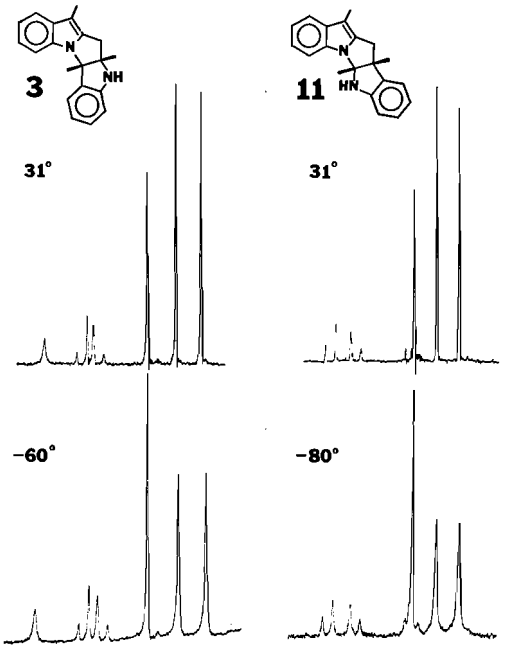

FIG. 4. Variable temperature n.m.r. spectra (100 MHz, CD_2Cl_2 solutions) of the methyl and methylene protons of compounds **3** and **11**.

be of lower energy. Since the acetyl methyl group of **2***a* is directly over the shielding zone of the aromatic ring, this conformer should give rise to the higher field acetyl absorption at δ 2.02

Can. J. Chem. Downloaded from www.nrcresearchpress.com by 210.87.254.105 on 09/05/12
For personal use only.

in the $-60°$ spectrum, and this peak is the larger of the two acetyl peaks. The lower field acetyl peak at δ 2.26 is close to the normal range ($\delta \sim$ 2.33–2.59) for acetophenone and *o*-substituted acetophenones (2). Although there are other instances of hindered rotation about the aromatic–carbonyl bond (3), this is the only example of hindered rotation at room temperature involving a methyl ketone group of which we are aware.

Experimental[2]

Preferred Method of Preparation of Keto Pyrrolidone **2**

The following procedure is somewhat more convenient and gives higher yields than the methods reported previously (1*b*).

To a stirred (magnetic bar) solution of dimer **1** (1.00 g, 3.1 mmol) in acetone (25 ml) was added a solution consisting of $NaIO_4$ (1.32 g, 6.2 mmol) in water (10 ml) plus 0.1 *N* HCl (2 ml). Within a few seconds a solid precipitated. After 1 h at room temperature, the reaction mixture was extracted with chloroform. The organic solution was washed with water, dried, and evaporated to leave a brown solid. Two recrystallizations from chloroform – petroleum ether gave 840 mg (84%) of almost colorless **2**,[3] m.p. 212–216°, identical in all respects with previous samples (1*b*).

The oxime was prepared by refluxing a mixture of **2** (150 mg), NaOAc (150 mg), H_2NOH–HCl (150 mg), water (1 ml), and 95% ethanol (8 ml) for 4 days. The crude product was recrystallized from chloroform – petroleum ether to give colorless crystals, m.p. 249–252°; ν_{max} 3570 (NH and OH) and 1670 cm^{-1} (pyrrolidone C=O); *m/e* 335 (molecular ion).

Anal. Calcd. for $C_{20}H_{21}N_3O_2$ (335.4): C, 71.62; H, 6.31. Found: C, 71.77; H, 6.59.

Reduction of Keto Pyrrolidone **2** *with* $NaBH_4$

To a stirred (magnetic bar) solution of **2** (55 mg) in methanol (2 ml) was added at room temperature $NaBH_4$ (100 mg) during 5 min. After 5 h, the reaction mixture was partitioned between water and chloroform. The organic layer was dried and concentrated to leave 57 mg of colorless solid. Two recrystallizations from chloroform – petroleum ether gave 17 mg of crystalline **6**, m.p. 270° (dec., sealed capillary), ν_{max} 3545 (OH), 3390 (NH), and 1675 cm^{-1} (pyrrolidone C=O); *m/e* 322 (molecular ion). The t.l.c. on alumina (PF_{254}, Merck, Germany) in ethyl acetate:methanol (95:5) revealed two spots, one more polar than **2**, and the other less polar than **2**.

Anal. Calcd. for $C_{20}H_{22}N_2O_2$ (322.4): C, 74.51; H, 6.88; N, 8.69. Found: C, 74.70; H, 6.80; N, 8.58.

Preparative thick layer separation of the recrystallization mother liquors on alumina in the same solvent system gave 8 mg of one stereoisomer of **6**, m.p. 248° (dec.); δ 1.16 (Me, d, $J = 6$ Hz), 1.39, (Me, s), 1.67 (Me, s), 2.74 and 2.86 (AB of CH_2, $J = 17$ Hz), 4.08 (1 H, q, $J = 6$ Hz), 4.2 (OH or NH, b.m.), and 6.35–7.60 (8 ArH, m).

Oxidative Cleavage of Diol-d_2 **9**

A solution of dimer **1** (600 mg) in dioxane (5 ml) and 0.1 *N* DCl in D_2O (1.5 ml) was stirred (magnetic bar) at room temperature for 13 h. The solution was diluted with chloroform, washed with water, dried, and concentrated to leave 584 mg of brown oil which was chromatographed on a column of alumina. After elution of rearrangement products (1*b*) by petroleum ether and benzene, deuterated **2** was eluted with chloroform. The pale yellow solid was recrystallized from chloroform – petroleum ether to give 30 mg of **2**-d_2, m.p. 214–216°, whose n.m.r. spectrum was identical with that of **2** except that the AB pattern at δ 2.70 and 2.92 was missing. Deuterium analysis by mass spectroscopy gave 5% d_0, 28% d_1, and 67% d_2.

We would like to thank Mrs. Heather Schroeder for the variable temperature n.m.r. spectra and the National Research Council of Canada for financial support.

1. (*a*) V. DAVE and E. W. WARNHOFF. Can. J. Chem. **49**, 1911 (1971); (*b*) Can. J. Chem. **49**, 1921 (1971).
2. (*a*) Varian Associates. N.m.r. Spectra Catalog. Vol. 1. (*b*) J. B. STOTHERS and K. S. DHAMI. Unpublished data.
3. (*a*) T. H. SIDDALL and R. H. GARNER. Tetrahedron Lett. 3513 (1966); (*b*) A. MANNSCHRECK. Tetrahedron Lett. 1341 (1965); (*c*) T. H. SIDDALL and W. E. STEWART. Chem. Commun. 393 (1967).

[2]For general experimental methods see ref. 1*a*.

[3]1-(*o*-Acetylphenyl)-3,3*a*,4,8*b*-tetrahydro-3*a*,8*b*-dimethylpyrrolo[3,2-*b*]indol-2(1*H*)-one.

Can. J. Chem. Downloaded from www.nrcresearchpress.com by 210.87.254.105 on 09/05/12
For personal use only.

A New Indoline Rearrangement

VINOD DAVE, J. B. STOTHERS, AND E. W. WARNHOFF
Department of Chemistry, University of Western Ontario, London, Ontario

Received February 2, 1972

The keto pyrrolidone **2** in the presence of acid produces the enamine **3***a* and the rearranged quinolone **4**. Evidence is presented for the mechanism of this new rearrangement, the key step being a remarkably facile opening and reclosure of the indoline ring (**9** ⇌ **10**) which even occurs in acetic acid.

La cétopyrrolidone **2** en présence d'acide donne l'énamine **3***a* et la quinolone réarrangée **4**. Le mécanisme de ce nouveau réarrangement a été mis en évidence; l'étape-clé étant une ouverture et une refermeture, d'une facilité remarquable, du cycle indoline (**9** ⇄ **10**) qui se produit même dans l'acide acétique.

Canadian Journal of Chemistry, **50**, 2475 (1972)

During the structural investigation of the keto pyrrolidone **2** formed from the dimer **1** as described in the preceding paper (1), it was found that in testing the exchangeability of the acetyl protons further reactions occurred. When **2** was refluxed in DOAc-d_3–DCl or HOAc–HCl (or HBr), two isomeric dehydration products were formed. The less polar (t.l.c.) minor compound, m.p. 183°, is assigned the unstrained enamine structure **3***a* formed by addition of the indoline nitrogen atom to the acetyl carbonyl group followed by dehydration. Its n.m.r. spectrum (Fig. 1) contained two 1-H olefinic singlets at δ 5.12 and 5.93 but no NH peak (also absent from its i.r. spectrum). Hydrogenation over palladium (Scheme 1) gave the dihydro deriva-

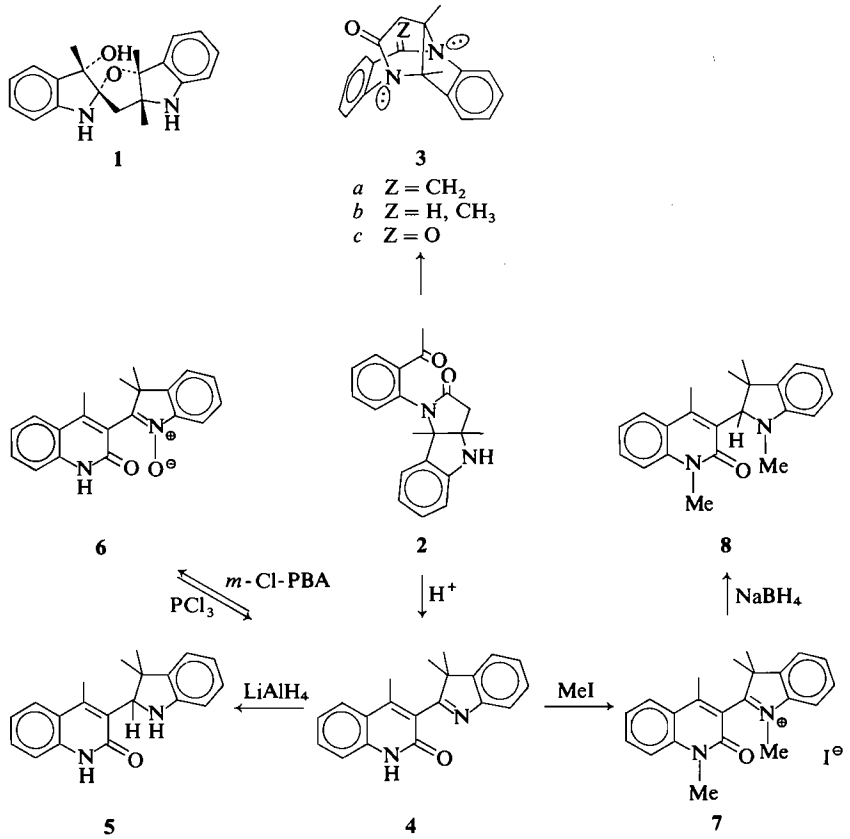

SCHEME 1

Can. J. Chem. Downloaded from www.nrcresearchpress.com by 210.87.254.40 on 09/05/12
For personal use only.

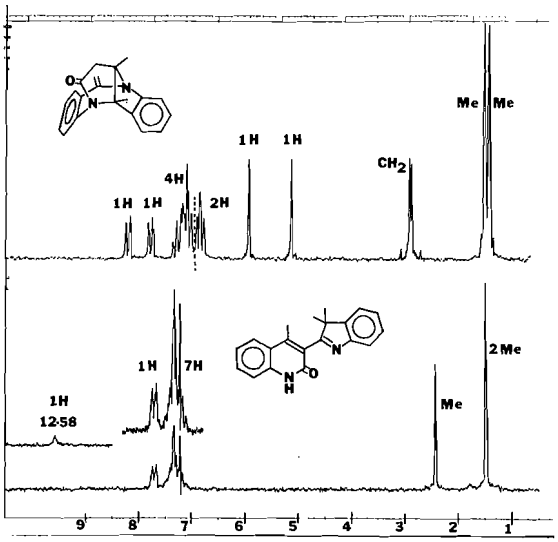

FIG. 1. The n.m.r. spectra (100 MHz, $CDCl_3$ solutions) of the two products, **3***a* and **4**, from treatment of keto pyrrolidone **2** with acid. See Table 1 for peak positions and assignments.

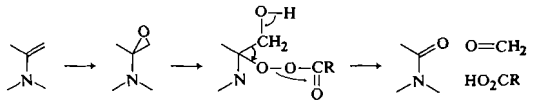

SCHEME 2

tive **3***b* whose n.m.r. spectrum lacked the olefinic protons, but contained a new methyl doublet at δ 1.75 ($J = 7$) and a 1-H quartet from the methine proton at δ 4.67 ($J = 7$). Treatment of the enamine with *m*-chloroperbenzoic acid gave the bis-amide **3***c*, presumably formed by some such process as shown in Scheme 2.

The more polar (t.l.c.) major component, m.p. 321° (dec.), proved to be the product **4** of extensive rearrangement. Its n.m.r. spectrum (Fig. 1) contained a singlet methyl peak, a singlet two-methyl peak and one exchangeable NH peak in addition to the absorption from eight aromatic protons, but lacked the methylene AB pattern of **2**. The u.v. absorption (Fig. 2) contained the readily recognizable 2-quinolone chromophore which must have been formed by condensation of the acetyl carbonyl with the pyrrolidone α-methylene group. Evidence for the presence of the indolenine imine function was provided by several reactions (Scheme 1). Lithium aluminum hydride reduction of **4** furnished the dihydro

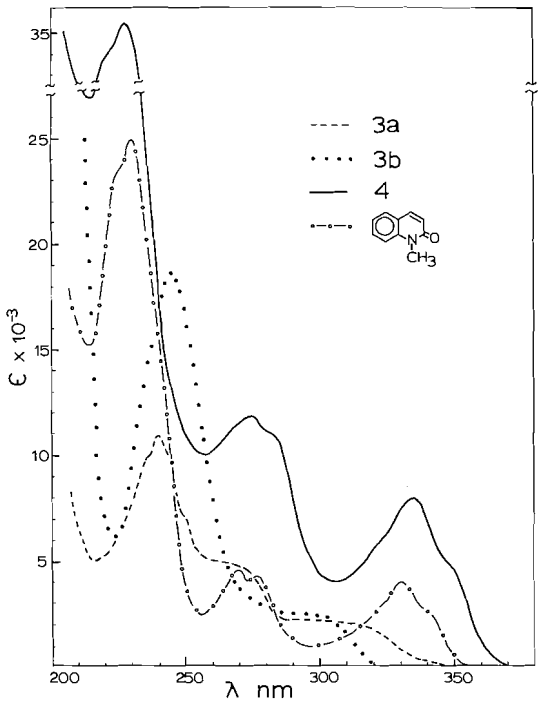

FIG. 2. The u.v. spectra of transformation products of the keto pyrrolidone **2**.

compound **5** whose n.m.r. spectrum contained a singlet at δ 5.58 from the new methine hydrogen. Oxidation of **4** with *m*-chloroperbenzoic acid produced the nitrone **6**[1] from which **4** was regenerated by treatment with phosphorus trichloride (3). Methylation of **4** with methyl iodide gave the *N*,*N*′-dimethyl derivative **7** which was reduced by sodium borohydride to **8** whose n.m.r. spectrum contained a 1-H singlet at δ 4.85 due to the new methine hydrogen in addition to the two *N*-methyl peaks. Of the two possible structures, **4** and **14**, consistent with these structural features, only **4** would have two methyl groups with the same δ 1.47

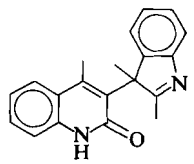

14

[1]Although an oxazirane may have been the initial oxidation product, the treatment during workup and purification should have caused isomerization to the nitrone (2).

Can. J. Chem. Downloaded from www.nrcresearchpress.com by 210.87.254.40 on 09/05/12
For personal use only.

Can. J. Chem. Downloaded from www.nrcresearchpress.com by 210.87.254.40 on 09/05/12
For personal use only.

chemical shift, and would give imine reduction products (**5** and **8**) in which the newly introduced methine hydrogen would appear as a singlet in their n.m.r. spectra.

The condensation of the acetyl carbonyl and pyrrolidone α-methylene groups of **2** to form the 2-quinolone is not sterically possible unless the pyrrolidone ring is broken first. Convincing evidence that this ring *is* very easily opened came unexpectedly from the deuterium exchange of **2** in refluxing DOAc-d_3 without any added stronger acid. In this medium ketone **2** is relatively stable, and the rearrangement to **3***a* and **4** was only detectable after several hours. It was found that recovered ketone **2** had incorporated up to 9 D atoms bound to carbon. The n.m.r. spectrum revealed that the acetyl methyl group and one of the other methyl groups were almost completely deuterated.[2] The missing methyl peaks were the same ones missing from the spectrum of the product **16** of periodate cleavage of the d_6-diol **15** prepared earlier (4). Therefore it is the 3-indolinyl methyl group which has been deuterated! Since D-exchange can only occur by cleavage of the benzylic nitrogen bond (**9** → **10**, Scheme 3) and reclosure, this opening and closure of the pyrrolidone ring must be rapid compared to any other reaction of **2**.

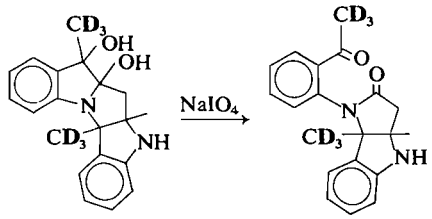

15 **16**

The surprising facility of this cleavage is perhaps best emphasized by the realization that very little (< ~10%) enolization of the pyrrolidone in the direction of its α-methylene group (**2** ⇌ **17**) and no β-elimination of the other nitrogen atom (**2** ⇌ **18**) occurred so far as could be judged by deuterium incorporation into the methylene and third methyl group of **2**. As mentioned previously, some molecules of **2** recovered from DOAc-d_3 did contain up to 9 D

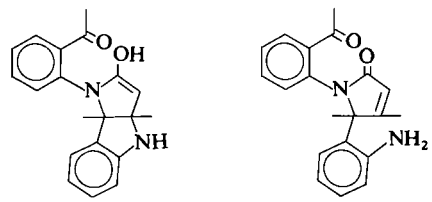

17 **18**

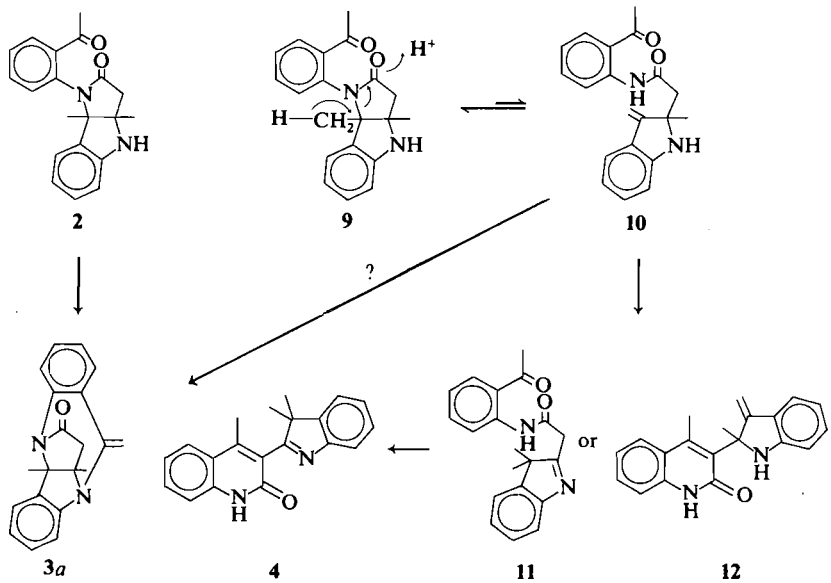

SCHEME 3

[2]The location of the remaining 3 D atoms is discussed further on in this paper.

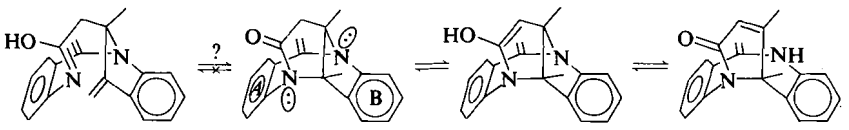

13 3*a* 19 20

SCHEME 4

atoms (33% d_7, 24–33% d_8, and 3–8% d_9). Although the location of the seventh and eighth D atoms in excess of the six shown in **16** was not definite from proton n.m.r. patterns or integration, comparison of the proton-decoupled ^{13}C-n.m.r. spectra of **2** and deuterated **2** (see Experimental) showed clearly that these two D atoms had entered the indolinyl benzene ring, presumably by electrophilic substitution *o* and *p* to the nitrogen atom. The location of the ninth D atom in one configuration adjacent to the pyrrolidone carbonyl group was suggested by the proton n.m.r. pattern and supported by the deuteration result with **3***a* (see below).

If stronger acid catalyst (*e.g.* HX) is present, reaction rates are increased to the point that formation of **3***a* and rearrangement of the indolinyl portion of **10** by methyl migration (**10** → **4**) become important.[3] When the incorporation of deuterium into these products was examined, the results placed strict limitations on the intermediates and the reversibility of steps as described in the sequel.

It might be expected that formation of the enamine **3***a* from **2**[4] would be reversible and that therefore **3***a* could be rearranged to **4** via hydrolysis to **2**. However, a control reaction with **3***a* gave no indication of the formation of **2** or **4** under the HOAc–H_2O–HCl reaction conditions. This negative result was confirmed in a striking way by comparison of two samples of deuterated **3***a*. The **3***a* isolated from the reaction of **2** with DOAc-d_3 – DCl contained up to 9 D atoms per molecule whose location was apparent from its integrated proton n.m.r. spectrum (see Table 1) and is shown in **3***a*-d_9 (Scheme 5).[5] The **3***a* isolated from the control reaction of undeuterated **3***a* with DOAc-d_3 – DCl contained only up to **4** D atoms per molecule located (see Table 1) as depicted in **3***a*-d_4.[5] Therefore, in **3***a*-d_9 the 2 D atoms in the indoline benzene ring and the 3 D atoms in the second methyl group must have been introduced at some stage before **3***a* was formed. Conversely, once **3***a* is formed it is not re-opened to **2** or else it would have exchanged up to 9 D atoms instead of the 4 D found. The only reactions **3***a* does undergo are reversible enolization of the pyrrolidone carbonyl (**3***a* ⇌ **19**, Scheme 4) and reversible β-elimination of the indolinyl nitrogen atom from the enol (**19** ⇌ **20**) which allows deuteration of the 2-indolinyl methyl group via enolization of **20**.[6] Enolization of **3***a* allows only one methylene hydrogen to be exchanged, presumably because proton loss and capture occur only from the unshielded side of the methylene group.

The unusual behavior of **3***a* is understandable when its geometry is taken into accout (see Scheme 4). It is not a normal *N*-arylenamine because overlap of the nitrogen lone pair orbital with the π-systems of both the double bond and the aromatic ring B is minimal. Hence the failure of the aromatic ring B to undergo *o*- and *p*-electrophilic substitution of deuterium for hydrogen

[3]The probable reason that the alternative migration of the methylene group (→ **14**) is not observed is that its ability to bear positive charge during migration is reduced by the inductive effect of the adjacent carbonyl group. Other apparent examples of inductive inhibition of migration have been encountered in this series of indole derivatives (4).

[4]It is also possible that **3***a* might be formed from **10** via **13** provided that the reaction were irreversible. This path would involve less steric repulsion of the methylene group with the developing sp^3 carbinolamine carbon atom than the direct **2** → **3***a* path, but the probability of having the acetyl group and the indoline nitrogen in close proximity would be lower than for the direct **2** → **3***a* route.

[5]In DOAc-d_3 the enamine β-carbon of **3***a* is undoubtedly deuterated, but the β-deuterium atoms are readily exchanged for hydrogen during workup, and the β-carbon atom is present as $=CH_2$ in the deuterated **3***a* samples. The olefinic proton signals in the n.m.r. spectrum of **3***a* even vanish in a few hours after addition of D_2O to the $CDCl_3$ solution.

[6]The assignments of the two indolinyl methyl peaks in the n.m.r. spectrum of **3***a* are unequivocal. When **2**-d_9 (from **2** + DOAc-d_3) lacking completely the 3-indolinyl methyl peak at δ 1.52 is transformed into **3***a* (in DCl – DOAc-d_3), the n.m.r. peak at δ 1.39 is completely gone; hence this peak must be due to the 3-indolinyl methyl group in **3***a*. Of course, the other methyl peak in the spectrum of **3***a* has also been diminished by exchange involving enolization of **20** after **3***a* has been formed from **2**.

Can. J. Chem. Downloaded from www.nrcresearchpress.com by 210.87.254.40 on 09/05/12
For personal use only.

TABLE 1. The n.m.r. data exclusive of most aromatic protons*

Compound	Absorption δ
o-Aminoacetophenone	2.55 (s, Me), 6.30 (s, NH_2)
Keto-pyrrolidone **2**	1.35 (s, Me), 1.52 (s, Me), 2.25 (b.l., COMe), 2.70, and 2.92 (AB of CH_2, $J = 17$), 4.18 (NH), 6.1–7.9 (8 ArH).
" " **2**-d_9	Same as **2** except 1.52 and 2.25 peaks completely missing, ~10% reduction in 2.92 peak, possibly some reduction in intensity of aromatic peaks.
Enamine **3***a*	1.39 (s, 3-indolinyl Me), 1.48 (s, 2-indolinyl Me), 2.77 and 2.97 (AB of CH_2, $J = 16$), 5.12 (s, C=C—H), 5.93 (s, C=C—H), 6.74–6.94 (2 ArH), 6.94–7.42 (4 ArH), 7.79 (dd, 1 ArH, $J = 7, 2$), 8.21 (dd, 1 ArH, $J = 7, 2$).
" **3***a*-d_4	Same as **3***a* except 1.48 peak reduced to ~2H and 2.97 peak missing completely.
" **3***a*-d_9	Same as **3***a* except 1.39 peak missing completely, 1.48 peak reduced to ~2H, 2.97 peak missing, and the 2 ArH absorption at 6.74–6.94 was missing completely.
Dihydroenamine **3***b*	1.35 (s, Me), 1.55 (s, Me), 1.75 (d, Me, $J = 7$), 2.73 and 2.97 (AB of CH_2, $J = 17$), 4.67 (q C*H*—(CH_3), $J = 7$).
Bis-amide **3***c*	1.53 (s, Me), 1.66 (s, Me), 2.83 (s, CH_2).
Quinolone-indolenine **4**	1.47 (s, *gem* di-Me), 2.43 (s, C=C—Me), 7.00–7.58 (7 ArH), 7.71 (b.d., 1 ArH, $J = 7$), and 12.58 (NH).
Quinolone-indolenine **4**-d_5	Same as **4** except that the 2.43 peak was reduced to ~1H intensity, and the 7.00–7.58 ArH absorption was apparently reduced in intensity by ~1H.
" " **4**-d_8	Same as **4** except that the 1.47 peak was reduced to 3H intensity, the 2.43 peak was completely missing, and the 7.00–7.58 ArH absorption was reduced in intensity by ~1H.
Quinolone-indoline **5**	1.14 (s, Me), 1.59 (s, Me), 2.68 (s, C=C—Me), 5.58 (bs, C=C—CH—N), 12.5 (b, NH).
Quinolone-nitrone **6**	1.46 (s, Me), 1.71 (s, Me), 2.41 (s, C=C—Me), 11.7 (b, NH).
N-Methyl methiodide **7**	1.68 (s, Me), 1.80 (s, Me), 2.68 (s, C=C—Me), 3.84 (s, O=C—NMe), 4.20 (s, $^{\oplus}$NMe).
N,*N*′-Dimethyl derivative **8**	1.13 (s, Me), 1.42 (s, Me), 2.59 (s, C=C—Me or NMe), 2.63 (s, N—Me or C=C—Me) 3.59 (O=C—NMe), 4.85 (s, C=C—CH—N).
N-Methylquinolone	3.60 or 3.68 (s, O=C—NMe)†

*Chemical shifts are given in p.p.m. from tetramethylsilane (δ) and coupling constants in Hz for $CDCl_3$ solutions; s = singlet, d = doublet, q = quartet, b = broad, l = lump.
†Values for two different solution concentrations.

is due to the inability to use the nitrogen lone pair to stabilize the required intermediate cation. Also, the exocyclic methylene group should show diminished enamine character and more normal double bond character in addition reactions. Moreover, addition of water to the double bond in the rigid **3***a* skeleton would cause severe steric interactions with the pyrrolidone α-methylene group.[7] Finally, the failure of **3***a* to exhibit the facile 3-indolinyl–*N*-cleavage (**3***a* → **13**), analogous to the reaction of **2** (**9** → **10**), may be ascribed both to the decreased nitrogen–carbonyl overlap in the pyrrolidone ring of **3***a* and to the geometrical inability of the aromatic ring A to help stabilize the incipient C—N bouble bond in the cleavage to **13**.

As would be expected from the extent of deuterium incorporation into **2**, the quinolone rearrangement product **4** isolated from the DOAc-d_3 – DCl medium or from long reflux in DOAc-d_3 alone contained up to 8 D per molecule as shown in **4**-d_8 (Scheme 5).[8] Most of this deuterium incorporation occurred prior to the

[7]Apparently it is possible to add a proton alone to the exo methylene group and leave the adjacent carbon of the π-system still in its sp^2 state because the olefinic protons can be exchanged on standing with D_2O–$CDCl_3$ in the n.m.r. tube.[5]

[8]The location of the 2 D atoms on the aromatic ring of **4**-d_8 is assumed from their location in **2**-d_9. In one deuteration (**2**-d_9 + DCl + DOAc-d_3) some d_9 molecules were formed, probably by exchange with an aromatic ring of **4**-d_8 after it was formed because under the same conditions **4** incorporated up to 2 D atoms more than the 3 D in the quinolone methyl group.

Can. J. Chem. Downloaded from www.nrcresearchpress.com by 210.87.254.40 on 09/05/12
For personal use only.

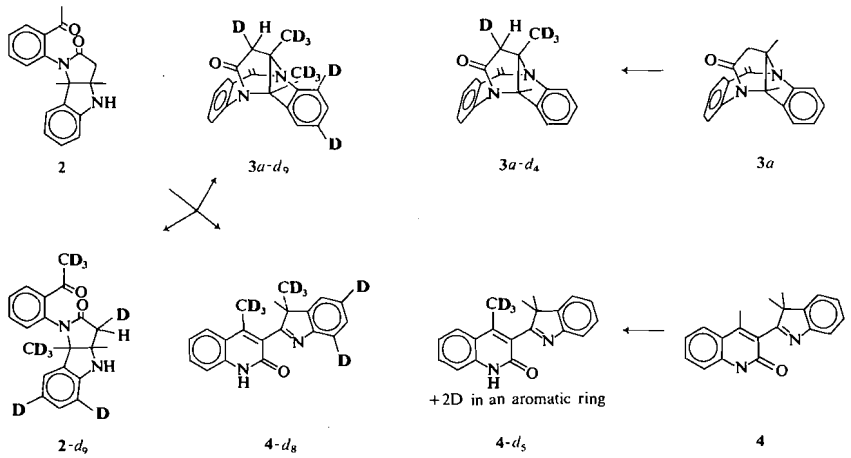

SCHEME 5

formation of **4** because control experiments showed that only 3 D atoms were introduced into the quinolone methyl group (decrease in δ 2.43 n.m.r. peak) when **4** was refluxed with DOAc-d_3, and a maximum of only 5 D atoms were introduced when **4** was refluxed with DCl–DOAc-d_3. In the two possible routes for the formation of **4**, **10** → **11** → **4** and **10** → **12** → **4**, the steps involving methyl migration, **10** → **11** and **12** → **4**, are not reversible under the conditions used; otherwise the third methyl group of **4** would have been deuterated too. Of the two routes for the formation of **4**, the **10** → **11** → **4** path seems more likely since the methylene group of **11** is then doubly activated for the enolization required for aldol closure of the quinolone ring.

In the previous work on the rearrangement of the dimer **1** (4), the fusion of the indolinyl ring to the adjacent five-membered ring was postulated to remain *cis* (and therefore the *vic* methyl groups also remain *cis*) throughout the rearrangement sequence,[9] although the first step in the rearrangement allows stereochemical change, because the *cis*-fusion of two five-membered rings is more stable than the *trans* in spite of the methyl interactions in the *cis*-arrangement.[10] This assignment is supported by two observations in the present work. First, the opportunity for equilibration provided by the opening and reclosure (**9** ⇌ **10**) of the indoline ring of **2** (formed *after* the first step of the rearrangement sequence[9]) in acetic acid reforms the original stereoisomer, thus proving that the ring fusion in **2** and the rearrangement intermediates[9] really is the more stable *cis* configuration. Second, the intramolecular enamine **3***a* can only form without serious strain if the indolinyl ring fusion is *cis*.

Experimental[11]

Rearrangement of Keto Pyrrolidone **2** *in HOAc–HBr*

A solution of **2** (400 mg), glacial acetic acid (4 ml), and hydrobromic acid (0.4 ml of 47% aqueous acid) was refluxed for 6 h. The cooled solution was diluted with chloroform, washed with aqueous $NaHCO_3$, water, and dried. Evaporation of the organic solution left 371 mg of yellowish solid. Two recrystallizations from chloroform–petroleum ether gave 202 mg (53%) of colorless crystals of the **quinolone-indolenine 4**[12], m.p. 317–321° (dec., sealed capillary); ν_{max} 3400–3100 (broad NH) and 1650 cm^{-1} (quinolone C=O); λ_{max} 228 (35 000), 275 (12 000), and 335 nm (8000); *m/e* 302 (molecular ion).

Anal. Calcd. for $C_{20}H_{18}N_2O$ (302.4): C, 79.44; H, 6.00; N, 9.26. Found: C, 79.36; H, 5.96; N, 8.91.

The mother liquors from the above recrystallizations were chromatographed on two thick plates developed in benzene:ether (50:50). Extraction of a band at R_f 0.87 gave 36 mg of pale yellow liquid ***o*-aminoacetophenone** perhaps containing traces of solvent, ν_{max} 3048 and 3033 (NH), and 1635 cm^{-1} (C=O); λ_{max} 227 (16 000), 258 (5200), and 365 nm (2700); *m/e* 135 molecular ion. Acetylation with acetic

[9]See p. 1923 of ref. 4.

[10]*cis*-Bicyclo[3.3.0]octane is about 6 kcal/mol more stable than the *trans* isomer (5) while the energy difference between *cis*- and *trans*-1,2-dimethyl cyclopentane is only about 1.5 kcal/mol in favor of the *trans* isomer at 130° (6).

[11]For general experimental methods see ref. 7. DOAc-d_3 was supplied by Merck, Sharp, and Dohme of Canada, 99.5 atom % D.

[12]3-(3,3-Dimethyl-3*H*-indol-2-yl)-4-methylcarbostyril.

Can. J. Chem. Downloaded from www.nrcresearchpress.com by 210.87.254.40 on 09/05/12
For personal use only.

Can. J. Chem. Downloaded from www.nrcresearchpress.com by 210.87.254.40 on 09/05/12
For personal use only.

anhydride–pyridine gave *o*-acetamidoacetophenone (i.r., t.l.c.) (7).

Extraction of a band at R_f 0.69 on the thick plates gave 118 mg (31%) of pale yellow solid. Two recrystallizations from chloroform–petroleum ether gave 73 mg of small colorless granules of **enamine** **3***a*,[13] m.p. 180–183°; ν_{max} 1670 cm^{-1} (pyrrolidone C=O); λ_{max} 240 (11 000), 265 (5000), and 295 nm (2000); *m/e* 302 (molecular ion).

Anal. Calcd. for $C_{20}H_{18}N_2O$ (302.4): C, 79.44; H, 6.00; N, 9.26. Found: C, 79.24; H, 5.86; N, 9.38.

The mother liquors from recrystallization of **3***a* showed the presence of *o*-acetamidoacetophenone (n.m.r., t.l.c.) (7).

The enamine **3***a* was recovered unchanged from attempts to cause it to hydrolyze to **2** and rearrange to **4** under the following conditions: (*a*) refluxing HOAc–H_2O for 60 h, (*b*) refluxing HOAc–HBr–H_2O for 6 h, and (*c*) refluxing CF_3COOH–H_2O for 10 h.

Deuteration of Keto Pyrrolidone **2**

(a) In DOAc-d_3

A solution of **2** (150 mg) in DOAc-d_3 (2 ml) was refluxed for 14 h. The cooled solution was diluted with chloroform, washed with aqueous $NaHCO_3$ and water, and dried. Concentration gave a brown solid which was chromatographed on a thick plate developed in ether. The band at R_f 0.19 gave colorless oily solid **deuterated 2** whose n.m.r. spectrum completely lacked the broad acetyl methyl peak at δ 2.25 and also the methyl peak at δ 1.52. Four recrystallizations from chloroform–petroleum ether gave 26 mg (17%) of colorless crystals of **2**-d_9, m.p. 213–215°. Deuterium analysis by mass spectroscopy gave 0.8% d_3, 3.2% d_4, 11% d_5, 25% d_6, 33% d_7, 24% d_8, and 3.0% d_9.

A second sample of **deuterated 2** prepared in the same way had 1.4% d_4, 6.1% d_5, 18% d_6, 33% d_7, 33% d_8, and 8% d_9. At room temperature after 37 h **2** had 75% d_0, 22% d_1, and only 3% d_2.

(b) In DOAc-d_3

From another experiment similar to (*a*), compounds **4** and **3***a* were also isolated. A solution of **2** (607 mg) in DOAc-d_3 (3 ml) was refluxed for 15 h. The reaction mixture was worked-up as in (*a*) to yield 629 mg of brown solid which was recrystallized twice from chloroform–petroleum ether to give 370 mg of colorless solid. Although t.l.c. on silica gel (chloroform:methanol, 95:5) showed a single spot, t.l.c. on alumina (PF_{254}, Merck, Germany) in the same solvent system revealed two spots, corresponding in R_f to **2** and **4**. The mixture (370 mg) was separated on four thick layer alumina plates developed in chloroform:methanol (97.5:2.5). Extraction of the band at R_f 0.45 gave 193 mg of colorless **deuterated 2**. Two recrystallizations from chloroform–petroleum ether afforded 164 mg of **2**-d_9, m.p. 212–216°, which was used for determination of the ^{13}C-n.m.r. spectrum. D-Analysis by mass spectroscopy gave 3% d_2, 8.5% d_3, 17.5% d_4, 27% d_5, 25% d_6, 13.5% d_7, 5% d_8, and 0.5% d_9.

The proton decoupled ^{13}C-n.m.r. spectrum of **2** (~150 mg/1.5 ml of $CDCl_3$, Varian XL-100-15 with Fourier transform) exhibited the following peaks (p.p.m. from tetramethylsilane): aliphatic carbons: 18.2 (CH_3C=O), 21.5 (CH_3), 28.9 (CH_3), 43.4 (CH_2), 69.2 (**4** °C), 75.5 (**4** °C); aromatic carbons: 109.7, 118.2, 125.0, 128.0, 128.8, 130.1, 131.1, 131.7 (each of the preceding eight carbons bears H), 133.3, 149.7 (neither of preceding two carbons bears H); and 172.6 (amide C=O). Two other peaks from aromatic carbons without hydrogen are hidden behind peaks mentioned above, probably the ones at 128.0 and 128.8 p.p.m. The spectrum was not scanned at low enough field to observe the acetyl carbonyl carbon. The proton-decoupled ^{13}C-n.m.r. spectrum of **2**-d_9 was missing the two highest field aromatic peaks at 109.7 and 118.2 p.p.m. assigned to the *o* and *p* positions of the indoline aromatic ring. Moreover, the two methyl peaks at 18.2 and 28.9 p.p.m. were almost completely obliterated.

Extraction of the alumina band of R_f 0.13 gave 18 mg of colorless crystalline **4**-d_8. D-Analysis by mass spectroscopy gave 1.3% d_0, 3.6% d_1, 7% d_2, 10% d_3, 15% d_4, 19% d_5, 20% d_6, 15% d_7, 7% d_8, and 2% d_9(?).[14]

The n.m.r. spectrum of the mother liquors from the original recrystallization of the 629 mg of crude product showed the presence of the deuterated **enamine** **3***a*. Chromatography on two thick layer plates in benzene:ether (50:50) gave a band at R_f 0.67 from which 43 mg of pale yellow solid was extracted. Two recrystallizations from chloroform–petroleum ether gave 20 mg of **3***a*-d_{10}, m.p. 173–181°. D-Analysis by mass spectroscopy gave 1% d_2, 3% d_3, 6% d_4, 11% d_5, 17% d_6, 23% d_7, 22% d_8, 13% d_9, and 4% d_{10}.[15]

(c) In DOAc-d_3–DCl

A solution of **2** (100 mg) in a mixture of DOAc-d_3 (1.5 ml), $SOCl_2$ (300 mg), and D_2O (0.5 ml) was refluxed for 10 min. The cooled solution was worked up as described in (*a*) to leave 102 mg of almost colorless oily solid. The t.l.c. on alumina (PF_{254}, Merck, Germany) showed the presence of some **3***a* and **4** in the recovered **2**. Thick layer chromatography on two alumina plates developed in chloroform:methanol (95:5) separated the components. Extraction of the band at R_f 0.73 gave 49 mg of colorless **2**. Two recrystallizations from chloroform–petroleum ether gave 38 mg of **2**-d_9, m.p. 212–217°. Deuterium analysis by mass spectroscopy gave 3% d_3, 10% d_4, 25% d_5, 32% d_6, 21% d_7, 7% d_8, and 2% d_9.

Rearrangement of the Keto Pyrrolidone **2** *in DOAc-d_3–DCl*

A solution of **2** (200 mg) in a mixture of DOAc-d_3 (2 ml), $SOCl_2$ (600 mg, 5.1 mmol), and D_2O (1.0 ml, 55 mmol) was refluxed for 6 h. The cooled solution was diluted with chloroform, washed with aqueous $NaHCO_3$, water, and dried. The pale yellow solid left on evaporation of the organic layer was recrystallized from chloroform–petroleum ether to give 42 mg of colorless crystalline **4**-d_8, m.p. 315–320° (dec.). Deuterium analysis by mass spectroscopy gave 2.7% d_3, 8.3% d_4, 25% d_5, 28% d_6, 25% d_7, 9.3% d_8, and 1.8%(?) d_9.[14]

The mother liquors were chromatographed on a thick plate developed with benzene:ether (50:50). Extraction of the band at R_f 0.78 gave 5 mg of ***o*-aminoacetophenone-d_3** ($COCD_3$).

[13]6,13-Dimethyl-12-methylene-6*H*,12*H*-5,6,11-[1]propanyl[3]ylidenedibenzo[*b*,*f*][1,5]diazocin-15-one.

[14]The small amount of d_9 molecules may not be real because D-analysis of **4** by mass spectroscopy must make allowance for the M – 1 peak of **4** which is not completely suppressed even at low ionization voltage.

[15]The tenth D atom in the small amount of d_{10} compound in this one reaction probably replaced the second hydrogen on the pyrrolidone α-methylene group in **3***a*-d_9 either before or after cyclization of **2**.

Can. J. Chem. Downloaded from www.nrcresearchpress.com by 210.87.254.40 on 09/05/12
For personal use only.

Extraction of the band at R_f 0.66 gave 43 mg (23%) of pale yellow solid. Two recrystallizations from chloroform–methanol–petroleum ether gave 30 mg of pale yellow crystals of **3***a*-d_9, m.p. 175–180°. Deuterium analysis by mass spectroscopy gave 0.4% d_1, 2.8% d_2, 7.5% d_3, 16% d_4, 23% d_5, 25% d_6, 17% d_7, 6.1% d_8, and 1.2% d_9.

Rearrangement of Deuterated Keto Pyrrolidone **2**-d_9 *in DOAc-*d_3*–DCl*

A solution of **2**-d_9 (180 mg from (*b*) above), DOAc-d_3 (2 ml), $SOCl_2$ (300 mg), and D_2O (0.5 ml) was refluxed for 6 h. When the work-up as described for the previous deuterations gave a very low yield, the aqueous washings were further basified with 20% aqueous NaOH and extracted with chloroform. Evaporation of the dried chloroform solution and combination with the original low yield gave 168 mg of brown oily solid. Three recrystallizations from chloroform–petroleum ether gave 50 mg of colorless crystalline quinolone **4**-d_9. D-Analysis by mass spectroscopy gave 4.5% d_5, 14% d_6, 38% d_7, 32% d_8, and 11.5% d_9.[8]

The mother liquors from recrystallization were chromatographed on a thick plate developed in benzene:ether (50:50). Extraction of the band at R_f 0.62 gave 65 mg of pale yellow solid. Recrystallization from chloroform–petroleum ether gave 30 mg of colorless enamine **3***a*-d_{10}. D-Analysis by mass spectroscopy gave 3% d_4, 11.5% d_5, 28% d_6, 33% d_7, 19% d_8, 5% d_9, and 0.5% d_{10}(?).

Reduction of Quinolone-indolenine **4** *with* $LiAlH_4$

To a refluxing solution of **4** (30 mg) in dry tetrahydrofuran (7 ml) was added $LiAlH_4$ (60 mg). After 4 h the cooled reaction mixture was quenched with water and extracted thoroughly with ether. The water-washed and dried ether solution was evaporated, and the residual oily solid was chromatographed on a thick plate developed with chloroform:methanol (97.5:2.5). A band at R_f 0.24 yielded 25 mg (83%) of pale yellow solid. Three recrystallizations from chloroform–petroleum ether gave almost colorless granules of **dihydro compound 5**[16] with a faint yellow tinge, m.p. 240° (dec.); ν_{max} 3400–3000 (broad NH) and 1640 cm^{-1} (quinolone C=O); λ_{max} 230 (28 000), 274 (6300), 283 (6300), and 330 nm (6900); *m/e* 304 (molecular ion).

Anal. Calcd. for $C_{20}H_{20}N_2O$ (304.4): C, 78.92; H, 6.62; N, 9.20. Found: C, 78.04; H, 6.61; N, 8.84.

Methylation and Reduction of Quinolone-indolenine **4**

A solution of **4** (175 mg) and methyl iodide (2.5 ml) in dry tetrahydrofuran–acetonitrile (10 ml of each) was kept in the dark at room temperature for 36 h. The reaction mixture was diluted with chloroform, washed with water, dried, and concentrated to leave an amber oil (**7**), ν_{max} 1765 and 1635 cm^{-1}, λ_{max} 225 (17 000) and 285 nm (4800); λ_{inf} 315 nm (2900). The oil was dissolved in methanol (10 ml) and reduced with $NaBH_4$ (350 mg.) for 3.5 h. The reaction mixture was diluted with chloroform, washed with water, dried, and concentrated to leave 125 mg of pale yellow oil. Chromatography of this oil on a thick plate developed in benzene:ether (37:63) gave a yellow band R_f 0.72 from which was extracted a pale yellow oil which crystallized on trituration with petroleum ether. Three recrystallizations from chloroform–petroleum ether gave pale yellow crystals of **8**,[17] m.p. 138–142°; ν_{max} 1630 cm^{-1} (quinolone C=O); λ_{max} 233 (34 000), 260 (15 000) (broad), and 330 nm^{-1} (7700); *m/e* 332 (molecular ion).

Anal. Calcd. for $C_{22}H_{24}N_2O$ (332.4): C, 79.48; H, 7.28; N, 8.43. Found: C, 79.41; H, 7.43; N, 8.48.

Oxidation of Quinolone-indolenine **4**

To a stirred solution of **4** (50 mg) in chloroform (1 ml) was added a solution of *m*-chloroperbenzoic acid (100 mg) in chloroform (1 ml). After 5 h at room temperature the solution was washed with aqueous Na_2SO_3, aqueous $NaHCO_3$, and water. The dried organic layer was concentrated to leave a white solid. Two recrystallizations from chloroform–methanol–petroleum ether gave 31 mg (59%) of colorless crystalline nitrone **6**,[18] m.p. 337° (dec.) with softening at 275°; ν_{max} 3000–3200 (NH broad) and 1630 cm^{-1} (quinolone C=O); λ_{max} 233 (23 000), 275 (8000), and 340 nm (5000); *m/e* 318 (molecular ion).

Anal. Calcd. for $C_{20}H_{18}N_2O_2$ (318.4): C, 75.45; H, 5.70; N, 8.80. Found: C, 75.52; H, 5.93; N, 8.83.

Reduction of Nitrone **6** *with* PCl_3

The procedure of Sternbach and Reeder (3) was used. A solution of **6** (25 mg) and PCl_3 (0.8 ml) in chloroform (8 ml) was refluxed for 10 h. The cooled solution was washed with aqueous $NaHCO_3$ and water. The dried solution was evaporated to leave 24 mg of colorless solid. Two recrystallizations from chloroform–methanol–petroleum ether gave 14 mg of colorless crystals of **4** identical (m.p., mixed m.p., t.l.c., i.r., n.m.r., mass spectroscopy) with an authentic specimen.

Deuteration of Quinolone-indolenine **4**

(a) In DOAc-d_3

A solution of **4** (25 mg) in DOAc-d_3 (1.0 ml) was refluxed for 9 h. The cooled solution was diluted with chloroform, washed with aqueous $NaHCO_3$ and with water. The dried organic layer was concentrated to leave 25 mg of crystalline solid. Two recrystallizations from chloroform–methanol–petroleum ether gave 12 mg of colorless crystals of **4**-d_3 in whose n.m.r. spectrum the area under the δ 2.43 methyl peak was equivalent to ~1.5H. D-Analysis by mass spectroscopy gave 14% d_0, 42% d_1, 35% d_2, and 9% d_3.

(b) In DOAc-d_3*–DCl*

Part of the partially trideuterated sample from (*a*) (10 mg) was dissolved in DOAc-d_3 (1.0 ml) containing $SOCl_2$ (300 mg) and D_2O (0.5 ml). The mixture was refluxed for 7 h and then worked up as in (*a*). One recrystallization from chloroform–methanol–petroleum ether gave 8 mg of colorless **4**-d_5 whose n.m.r. spectrum did not appear to be different from that in (*a*). D-Analysis by mass spectroscopy gave 8% d_0, 20% d_1, 29% d_2, 22% d_3, 16% d_4, and 5% d_5.

Deuteration of Enamine **3***a in DOAc-*d_3*–DCl*

A solution of **3***a* (30 mg) in a mixture of DOAc-d_3 (1.0 ml), $SOCl_2$ (300 mg), and D_2O (0.5 ml) was refluxed for 6 h. The cooled reaction mixture was partitioned between chloroform and water. The separated organic layer was washed with aqueous $NaHCO_3$ and water, and then dried.

[16]3-(3,3-Dimethyl-2-indolinyl)-4-methylcarbostyril.

[17]1,4-Dimethyl-3-(1,3,3-trimethyl-2-indolinyl)carbostyril.

[18]3-(3,3-Dimethyl-3*H*-indol-2-yl)-4-methylcarbostyril *N*-oxide.

Evaporation of the chloroform left 13 mg of crystalline **3***a*. The original aqueous layer was basified with aqueous NaOH and extracted with chloroform. Evaporation of the dried chloroform layer gave 20 mg more of **3***a*. The combined crude products were recrystallized once from methanol–petroleum ether and once from chloroform–methanol–petroleum ether to afford 20 mg of crystalline **3***a*-d_4, m.p. 175–182°. D-Analysis by mass spectroscopy gave 4% d_0, 21% d_1, 39% d_2, 27% d_3, 8% d_4, and 1% d_5 (?).

Hydrogenation of Enamine 3a

A mixture of **3***a* (60 mg) and 5% Pd/C (45 mg) in methanol (4.5 ml) was stirred under an atmosphere of hydrogen for 1 h. Filtration and evaporation of solvent left a solid which was recrystallized twice from methanol–petroleum ether and twice from chloroform–petroleum ether to give 27 mg (45%) of colorless crystals of **3***b*,[19] m.p. 119–122°. The analytical sample had m.p. 125–129°; ν_{max} 1685 cm^{-1} (pyrrolidone C=O); λ_{max} 243 (18 000) and 295 nm (2400) (broad); *m/e* 304 (molecular ion).

Anal. Calcd. for $C_{20}H_{20}N_2O$ (304.4): C, 78.92; H, 6.62. Found: C, 78.74; H, 6.71.

Peracid Oxidation of Enamine 3a

To a stirred solution of **3***a* (60 mg) in chloroform (2 ml) was added a solution of *m*-chloroperbenzoic acid (120 mg) in chloroform (2 ml). After 12 h at room temperature the solution was washed with aqueous Na_2SO_3, aqueous $NaHCO_3$, and water. The dried organic layer was concentrated to leave an almost colorless solid. Recrystallization from ether–petroleum ether (b.p. 30–60°) gave 21 mg (35%) of colorless crystals of the **bis amide 3***c*,[20] m.p. 147–150°; ν_{max} 1715 and 1650 cm^{-1} (amide C=O); λ_{max} 223 (8000) and 300 nm (3000), λ_{inf} 237 nm (4000); *m/e* 304 (molecular ion).

Anal. Calcd. for $C_{19}H_{16}N_2O_2$ (304.4): C, 74.98; H, 5.30; N, 9.20. Found: C, 75.26; H, 5.59; N, 9.27.

We would like to thank the National Research Council of Canada for financial support.

1. V. DAVE and E. W. WARNHOFF. Can. J. Chem. This issue.
2. W. D. EMMONS. J. Am. Chem. Soc. **78**, 6208 (1956).
3. L. H. STERNBACH and E. REEDER. J. Org. Chem. **26**, 4936 (1961).
4. V. DAVE and E. W. WARNHOFF. Can. J. Chem. **49**, 1921 (1971).
5. S. J. CHANG, D. MCNALLY, S. SHARY-TEHRANY, M. J. HICKEY, and R. H. BOYD. J. Am. Chem. Soc. **92**, 3109 (1970).
6. O. A. AREF'EV, V. A. ZAKHARENKO, and A. A. PETROV. Neftekhimiya, **4**, 854 (1964); CA **62**: 8967f (1965).
7. V. DAVE and E. W. WARNHOFF. Can. J. Chem. **49**, 1911 (1971).

[19] 6,12,13-Trimethyl-6*H*,12*H*-5,6,11-[1]propanyl[3]ylidenedibenzo[*b*,*f*][1,5]diazocin-15-one.

[20] 6,13- Dimethyl- 6*H*,12*H*- 5,6,11-[1]propanyl[3]ylidenedibenzo[*b*,*f*][1,5]diazocin-12,15-dione.

Can. J. Chem. Downloaded from www.nrcresearchpress.com by 210.87.254.40 on 09/05/12
For personal use only.

Preparation, Vibrational Spectra, Normal Coordinate Analysis, and Structures of bis-Pyridine and Orthophenanthroline Complexes of Mixed Halogenosilanes

D. H. BOAL AND G. A. OZIN[1]

Lash Miller Chemistry Laboratory and Erindale College, University of Toronto, Toronto, Ontario

Received February 17, 1972

The compounds py_2SiCl_3X (where X = H, F, or Br), $py_2SiCl_2X_2$ (where X = F or Br) and the corresponding orthophenanthroline complexes are prepared and the vibrational spectra reported for the first time. Using a combination of the vibrational data and normal coordinate calculations, the stereochemistries may be defined for most of the complexes. Preferences for certain configurations in the series are qualitatively discussed in terms of the spatial requirements of the various atoms and groups within each complex.

Les composés py_2SiCl_3X (où X = H, F, ou Br), $py_2SiCl_2X_2$ (où X = F ou Br) et les complexes orthophénantroline correspondants ont été préparés et leurs spectres de vibration rapportés pour la première fois. En utilisant une combinaison des données vibrationnelles et des calculs des coordonnées normales, les stéréochimies ont pu être établies pour la plupart des complexes. Les préférences pour certaines configurations dans la série sont discutées qualitativement en fonction des exigences spatiales des divers atomes et groupes à l'intérieur de chaque complexe.

Canadian Journal of Chemistry, **50**, 2484 (1972)

Can. J. Chem. Downloaded from www.nrcresearchpress.com by 210.87.254.6 on 09/05/12
For personal use only.

Introduction

There has been considerable interest in the molecular structures of pyridine complexes of the main group halides, especially those of group IVB (1). Certain trends have emerged as definitive structural information (usually from X-ray, infrared, and Raman data) has gradually appeared in the literature.

One finds an apparently universal preference for *trans*-octahedral stereochemistries for bis-pyridine adducts; for example, py_2SiF_4 (2), py_2SiCl_4 (3), py_2GeCl_4 (4), py_2SnCl_4, py_2SnBr_4, py_2SeCl_4, and py_2TeCl_4 (5). Monopyridine complexes, such as $pyAlCl_3$ (6) and $pyPCl_5$ (7) have the molecular structures which would be predicted on simple electron-pair repulsion principles. When pyridine is reacted with silicon halides containing SiI bonds, ionization often occurs. This may be illustrated by the unusual compounds py_3SiCl_3I and $py_4SiCl_2I_2$ which were shown to contain the cations $py_3SiCl_3^+$ and $py_4SiCl_2^{2+}$ having C_{2v} and D_{4h} symmetries, respectively (7).

A group of molecules for which stereochemical information has not yet been reported are the bis-pyridine and orthophenanthroline complexes of the mixed halogenosilanes. A combination of infrared and Raman data should allow their stereochemistries to be determined.

As the parent species py_2SiX_4 (where X = F, Cl, or Br) are all *trans*-octahedral, it is reasonable to assume that all combinations of F, Cl, or Br in the *mixed* halide complexes $py_2SiX_nY_{4-n}$ contain *trans*-pyridine ligands.

Results

bis-Pyridine Complexes

(A) Py_2SiCl_3F, py_2SiCl_3Br, and py_2SiCl_3H

Let us consider the complexes py_2SiCl_3X (where X = F, Br, or H) which would be expected to yield very similar infrared and Raman spectra, characteristic of *trans*-pyridine ligands with a *T*-shaped $SiCl_3$ skeleton (**1** to **3**) shown below

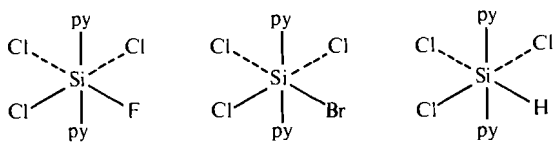

1 (C_{2v}) **2** (C_{2v}) **3** (C_{2v})

The *T*-shaped $SiCl_3$ grouping is easily recognized by a diagnostic pattern of *three* Raman lines, illustrated schematically by their symmetry coordinates below

[1]To whom correspondence should be addressed.

TABLE 1. Vibrational spectra* of py_2SiCl_3X, X = H, F, and Br

Frequency (cm^{-1})						
py_2SiCl_3H		py_2SiCl_3F		py_2SiCl_3Br		Approximate description of mode
Infrared	Raman	Infrared	Raman	Infrared	Raman	
	2085w					νSiH
	2065w					
		855vw	*860vw*			νSiF
482s	*482w*	*486s*	*480vvw*	*489s*	—	$S_3\nu$SiCl (asym)
447vs br	*449mw*	463m	458vw	466s	460vw	pyridine out-of-plane ring mode + $S_2\nu$SiCl (sym)
		425s br	*430vw*			
				410s	*411vvw*	
374vs br	372vw	376ms	371ms	387s br	386vvw	νSiN (asym)
		337vw	332w			δSiF
301w	*305vs*	*306w*	*303s*	—	*312vs*	$S_1\nu$SiCl (sym)
				282w	*285m*	νSiBr (sym)
		252m	252ms		261mw	
	244ms					
		215m	215w	232w	223m	
	203w			202w		
		196m	184w		188ms	
		178w	175vw sh		170vw	
					156vw	
			134s		129s	
		110m	102s	106m		
		73w	65m		83s	

*SiCl and SiBr stretching modes are in italics (see text for description of S_1, S_2, and S_3).

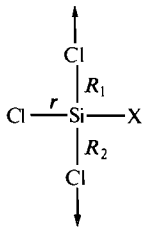

$S_1 = (1/\sqrt{2})(\Delta R_1 + \Delta R_2)$
Very intense (a_1), *low* frequency Raman line (330–270 cm^{-1})

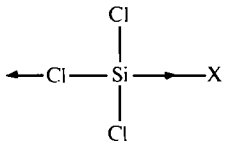

$S_2 = \Delta r$
Medium to low intensity (a_1), *high* frequency Raman line (460–380 cm^{-1})

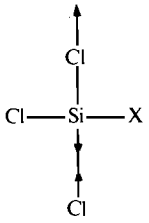

$S_3 = (1/\sqrt{2})(\Delta R_1 - \Delta R_2)$
Low intensity (b_2), *high* frequency Raman line (500–470 cm^{-1}). Very intense in the infrared

Thus, for py_2SiCl_3X we calculate and observe (Tables 1 and 2) a *low* frequency, totally symmetrical SiCl stretching mode S_1 at 303 cm^{-1} (X = H), 304 cm^{-1} (X = F), and 312 cm^{-1} (X = Br) characteristic of *T*-shaped $SiCl_3$. We note that S_1 occurs at low frequency because the central silicon atom remains stationary during the mode and cannot make a contribution to the respective *G* matrix element. This is not so for S_2 which appears at higher frequencies, 448 cm^{-1} (X = H), 427 cm^{-1} (X = F), and 410 cm^{-1} (X = Br). The monotonical drop to lower frequency parallels the increasing mass of the X grouping *trans* to chlorine and the resulting decreasing motion of the central silicon atom. The asymmetrical SiCl stretching mode S_3 is calculated and observed at *high* frequencies in the range 482–489 cm^{-1} for X = F, Br, and H.

The complex $[py_3SiCl_3^+]I^-$ which has also been assigned a *T*-shaped $SiCl_3$ residue (7) displays a *similar* pattern of $SiCl_3$ stretching modes at 315(S_1), 410(S_2), and 482(S_3) cm^{-1}.

Can. J. Chem. Downloaded from www.nrcresearchpress.com by 210.87.254.6 on 09/05/12
For personal use only.

TABLE 2. Calculated vibrational spectra of py_2SiCl_3X*

Frequency (cm^{-1})			Approximate description of mode‡
py_2SiCl_3H	py_2SiCl_3F	py_2SiCl_3Br	
1722			A_1 νSiH
	744		A_1 νSiF
463	479	470	B_1 νSiCl (S_3)
428	385	477†	A_1 νSiCl (S_2)
411	492	462	B_2 νSiN
279	272	322†	A_1 νSiCl (S_1)
		226†	A_1 νSiBr
133	135	131	A_1 νSiN

*Deformational modes are not listed.
†Highly coupled modes.
‡See text for description of S_1, S_2, and S_3.

TABLE 3. Vibrational spectra† of $py_2SiCl_2X_2$*

Frequency (cm^{-1})				
$py_2SiCl_2F_2$		$py_2SiCl_2Br_2$		Approximate description of mode
Infrared	Raman	Infrared	Raman	
489s	*490vw*	*484s*	—	νSiCl (asym)
455s	458w	458s br	—	py out-of-plane ring mode
420s	425w	408m	—	νSiN (asym)
		384s	—	νSiBr (asym)
352m	357w			
340w				δSiF
	279vs		*311m*	νSiCl (sym)
		280m	284ms	
		225m	*225vs*	νSiBr (sym)
230m	222w	207mw	210w	
192w	202w	191w	192w	
175m	174mw		176w	
	140w		153w	
108m	110m	102w		
90w				
	74m			

*SiCl and SiBr stretching modes are in italic.

(B) $py_2SiCl_2F_2$ and $py_2SiCl_2Br_2$

Having established the spectral characteristics of a *T*-shaped $SiCl_3$ grouping we will extend the method to the stereochemical problem presented by the complexes $py_2SiCl_2X_2$ (where X = F or Br). Using the *trans*-pyridine approximation described previously, it remains to distinguish the *cis* and *trans* possibilities (**4** and **5**) shown below

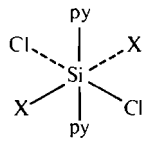

4 (D_{2h})

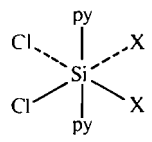

5 (C_{2v})

A mode involving little or no motion of the central silicon atom is expected to appear as an intense, low frequency line in the Raman spectrum of the above complexes.

We find that the Raman spectrum of $py_2SiCl_2Br_2$ displays a *low* frequency SiBr (225 cm^{-1} vs) and *low* frequency SiCl (311 cm^{-1} vs) stretching mode characteristic of *trans*-$SiBr_2$ and *trans*-$SiCl_2$ residues, respectively (configuration **4** and Table 3). Similarly, the Raman spectrum of $py_2SiCl_2F_2$ shows an intense, *low* frequency SiCl stretching mode (279 cm^{-1} vs) which also favors the all *trans* configuration **4**. The characteristic *high* frequency asymmetrical SiCl stretching mode appears in the infrared at 484 and 489 cm^{-1} for $py_2SiCl_2Br_2$ and $py_2SiCl_2F_2$, respectively (Table 3).

Additional evidence for the all *trans* assignment for $py_2SiCl_2F_2$ and $py_2SiCl_2Br_2$ may be obtained by comparing the observed and calculated vibrational spectra for the molecules in the possible conformations, that is, *trans*-pyridines, *trans*-halogens (D_{2h}), and *trans*-pyridines, *cis*-halogens (C_{2v}). The results of the calculations are shown in Table 4 and strongly favor the D_{2h} structure for $py_2SiCl_2X_2$.

Orthophenanthroline Complexes

It is interesting to consider the stereochemical behavior of the silicon–halogen residue when the complexes are locked in a *cis* configuration with the bulky chelate ligand orthophenanthroline. We have prepared the compounds *o*-phen.$SiCl_2X_2$ and *o*-phen.$SiCl_3X$ (where X = F or Br) and will discuss their infrared and Raman spectra using stereochemical arguments similar to those described for the analogous pyridine complexes.

(A) o-phen.$SiCl_2Br_2$ and o-phen.$SiCl_2F_2$

The spectra of the orthophenanthroline adducts are more complex than the corresponding pyridine adducts mainly because of (*a*) the lower molecular symmetries and (*b*) the complexity of the ligand modes in the SiCl stretching region (510–350 cm^{-1}).

Careful examination of the Raman spectrum of *o*-phen.$SiCl_2Br_2$ (Table 5) shows only one intense, *low* frequency SiBr stretching mode

Can. J. Chem. Downloaded from www.nrcresearchpress.com by 210.87.254.6 on 09/05/12
For personal use only.

TABLE 4. Calculated vibrational spectra for $py_2SiCl_2X_2$*

Frequency (cm^{-1}) for D_{2h} model		Approximate description of mode	Frequency (cm^{-1}) for C_{2v} model		Approximate description of mode
$py_2SiCl_2F_2$	$py_2SiCl_2Br_2$		$py_2SiCl_2F_2$	$py_2SiCl_2Br_2$	
836		B_{3u} νSiF			
			758		A_1 νSiF
606		A_g νSiF	739		B_1 νSiF
517	468	B_{1u} νSiCl	517	458	B_2 νSiN
517	458	B_{2u} νSiN			
	440	B_{3u} νSiBr	433	457	A_1 νSiCl
			355	454	B_1 νSiCl†
284	307	A_g νSiCl			
				292	A_1 νSiBr
	174	A_g νSiBr			
				212	B_1 νSiBr†
137	126	A_g νSiN	138	128	A_1 νSiN

*Deformational modes are not listed.
†Highly coupled mode.

TABLE 5. Vibrational spectra of o-phen.$SiCl_2X_2$*

Frequency (cm^{-1})				Approximate description of mode
o-phen.$SiCl_2F_2$		o-phen.$SiCl_2Br_2$		
Infrared	Raman	Infrared	Raman	
	506w	506w	503vw	o-phen ring mode
476s		*464s*		νSiCl (asym)
448w	447ms	449ms		o-phen ring mode
430w	429mw	429s	430m	
418s	414m	406s	405mw	
350vw	346w	360w	359w br	
332w	331vw	332w	333vw	
306vw	*298vs*			νSiCl (sym)
	273s	282m	283m br	
		234m	*237vs*	νSiBr (sym)
		206m	197m	
		172m	168m	
		154w	152m	
		114w	114ms	

*SiCl and SiBr stretching modes are in italic.

($237\ cm^{-1}$) characteristic of *trans*-bromines shown below (**6**)

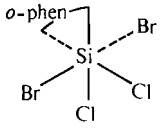

6

The absence of a *low* frequency SiCl stretching mode also supports the *cis*-chlorine assignment for o-phen.$SiCl_2Br_2$. Examination of the corresponding data for o-phen.$SiCl_2F_2$ (Table 5) shows an intense, *low* frequency SiCl stretching mode ($298\ cm^{-1}$) characteristic of *trans*-chlorines shown below (**7**)

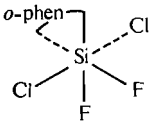

7

The different stereochemical arrangements for o-phen.$SiCl_2F_2$ and o-phen.$SiCl_2Br_2$ may be rationalized by considering the steric properties of the orthophenanthroline ring and the repulsion between *cis*-halogens. For example, it is

Can. J. Chem. Downloaded from www.nrcresearchpress.com by 210.87.254.6 on 09/05/12
For personal use only.

TABLE 6. The infrared and Raman spectra* of *o*-phen.$SiCl_3X$ (where X = F or Br) and bipy.$SiCl_3F$

Frequency (cm^{-1})						
o-phen.$SiCl_3F$		bipy.$SiCl_3F$		*o*-phen.$SiCl_3Br$		Approximate description of mode
Infrared	Raman	Infrared	Raman	Infrared	Raman	
509w	508m				506w	*o*-phen ring mode
477s			*~487w*	*470s*	*478ww*	*ν*SiCl (asym)
467s	*465vw*		*~460w*	488s		*ν*SiCl (sym)
427s br	432s		~420vvw	*430s*	*428vs*	*ν*SiCl and *o*-phen ring mode
	413w		384w	403s	410vwsh	
371w	369w		360ms			
331m	330m		317w	~330vw	343w	
306w	304ms			291w	307vwsh	
					290mw	
278m	*276ms*		*273vs*		276wsh	*ν*SiCl (sym)
247m	242ms		252m		263w	
222m	230msh			233w	244w	
210w	210w		211msh		229mw	
190m	191m		201m	193w	198wsh	
167m				182w	178msh	
122w				153w	159ms	
				124w		

*SiCl stretching modes are in italic.

known (8) that $[(o\text{-phen})_2py_2Ru]^{3+}3Cl^-$ will not adopt conformations in which the orthophenanthroline rings are *trans* to one another (*i.e.* it will only adopt optically active *cis* conformations). This would indicate that the hydrogens H_α shown below can interact sterically with atoms occupying the other two positions in the plane about silicon. With this in mind, the con-

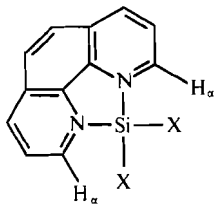

figurations **6** and **7** which we favor for *o*-phen.$SiCl_2Br_2$ and *o*-phen.$SiCl_2F_2$ are those which would have been preferred simply from steric arguments. That is, one would predict that the *larger* halogens would chose positions in the complex such that they were both *out* of the plane of the bulky orthophenanthroline ligand and *as far apart* (*trans*) from each other as possible. In this way the repulsions between (*a*) the hydrogens H_α and the *cis*-halogens in the plane and (*b*) *cis*-halogens are both minimized.

(B) o-phen.$SiCl_3F$ and o-phen.$SiCl_3Br$

In the above complexes containing the $SiCl_3$ residue we do have a stereochemical ambiguity, which was not the case for py_2SiCl_3X. The possible configurations for *o*-phen.$SiCl_3F$ and *o*-phen.$SiCl_3Br$ (**8** and **9**) are shown below

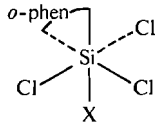

8

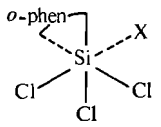

9

o-phen.$SiCl_3Br$ shows an exceptionally intense, *high* frequency Raman line at 428 cm^{-1} (Table 6) (its unusually high intensity makes it unlikely to be an orthophenanthroline mode, by comparison with Raman data for many orthophenanthroline complexes), which favors a pyramidal $SiCl_3$ residue as shown in configuration **9**. However, *o*-phen.$SiCl_3F$ shows a characteristic intense, *low* frequency SiCl stretching mode (276 cm^{-1} and for comparison at 273 cm^{-1} in the analogous bipy.$SiCl_3F$) which strongly favors the *T*-shaped $SiCl_3$ residue of configuration **8** (Table 6).

As with *o*-phen.$SiCl_2X_2$ we find that the configurations favored for *o*-phen.$SiCl_3X$ (where X = F or Br) are those which would have been predicted from simple steric arguments. That is, the larger halogen prefers a molecular site in the

Can. J. Chem. Downloaded from www.nrcresearchpress.com by 210.87.254.6 on 09/05/12
For personal use only.

TABLE 7. Analyses of bispyridine and orthophenanthroline complexes of mixed halogenosilanes

Complex	% halide		Base:metal
	Observed	Calculated	
py_2SiCl_3F	34.4	34.2 (Cl)	1.96:1
py_2SiCl_3Br	28.2 21.3	28.0 (Cl) 21.5 (Br)	2.07:1
$py_2SiCl_2F_2$	18.5	18.0 (Cl)	1.90:1
$py_2SiCl_2Br_2$	16.0 39.0	17.7 (Cl) 38.0 (Br)	2.05:1
o-phen.$SiCl_3F$	31.6	31.8 (Cl)	1.06:1
o-phen.$SiCl_3Br$	23.0 17.9	23.4 (Cl) 17.5 (Br)	1.04:1
o-phen.$SiCl_2F_2$	22.4	22.6 (Cl)	1.03:1
o-phen.$SiCl_2Br_2$	14.5 36.0	16.2 (Cl) 36.4 (Br)	0.94:1

complex, such that it is out of the plane occupied by the bulky orthophenanthroline ligand and minimizes *cis*-halogen repulsions.

Conclusion

We may summarize the data for the pyridine and orthophenanthroline complexes of mixed halogenosilanes by stating that interesting structural trends are observed, which appear to be controlled by the spatial requirements of the respective ligands and halogens in the molecule. It appears that electronegativity and π bonding arguments do not have to be invoked in order to explain the data.

Experimental

Trichlorosilane was purchased from Matheson.

The chlorofluorosilanes were prepared using the method of Booth and Swineheart (9) in which a Swarts type reaction was involved. Here, $SiCl_4$ was partially fluorinated using SbF_3, incorporating $SbCl_5$ as a catalyst. The mixed chlorofluorosilanes were initially passed through cold traps, at ice/salt, CO_2/acetone, and liquid nitrogen temperatures, respectively, which thereby achieved a crude separation. Each crude fraction was introduced in turn into a specially designed, double vacuum jacketed, low temperature fractionation column, with a finely controlled take off head. Yields of $SiCl_3F$ and $SiCl_2F_2$ were collected; their vapor pressure/temperature dependence agreed very closely with those quoted by Schumb and Gamble (10). These were separately stored in 5 l bulbs, each having a finger immersed continuously in liquid nitrogen. The latter precaution was to prevent the disproportionation of the gases to SiF_4 and $SiCl_4$. It was found that after a period of three months, on refractionating the gases, no detectable sign of disproportionation was observable. Infrared spectra of the gases $SiCl_3F$ and $SiCl_2F_2$ were taken and were in agreement with those of Stokr and Schneider (11).

The chlorobromosilanes were initially prepared by refluxing $SiBr_4$ and $SbCl_3$ using phosphorus pentoxide guard tubes. The resulting mixture was then fractionated but yielded mainly $SiCl_3Br$. The preparation was repeated, using the method of Forbes and Anderson (12), where a 1:1 mixture of $SiCl_4$ and $SiBr_4$ was sealed off in a thick walled glass bomb which was then heated at 140 °C for 72 h. Again the resulting mixture was fractionated producing $SiCl_3Br$ and $SiCl_2Br_2$ in reasonable yields, b.p. 78 and 103 °C, respectively. The infrared spectra agreed with those of Mlle. Delwaulle (13) where the presence of one fraction in the other was negligible. Pyridine was dried with $SiCl_4$ and then vacuum distilled. Orthophenanthroline and bipyridyl were dried by slow, repeated vacuum sublimation. All solvents were dried with CaH_2 and vacuum distilled. A typical preparation involved the reaction of the appropriate halogenosilane with a slight excess of the ligand in either the pure state or in chloroform solution. The complexes always formed as white precipitates, which remained as white powders after removal of the excess ligand and solvent. All manipulations where possible were carried out in all glass vacuum systems. Raman spectra were recorded for the powdered solids in glass ampoules which had been sealed off directly from the vacuum line preparation. Samples for infrared mull spectra were handled in glove boxes which were continuously purged with dry air. Nujol was dried over molten sodium for 24 h prior to use.

Infrared spectra were recorded on a Beckmann IR 11 spectrometer and Raman spectra on a Spex 1401 spectrometer using krypton or argon ion laser excitation.

Analyses

Analyses were performed by quantitatively hydrolyzing the product and analyzing for halide and py:Si by using argentometric (14) and p*H* titrations, respectively. The preparation of the known compound py_2SiCl_3H was exactly the same as that reported (1). Results of analyses are shown in Table 7.

Can. J. Chem. Downloaded from www.nrcresearchpress.com by 210.87.254.6 on 09/05/12
For personal use only.

TABLE 8. Force constants used in normal coordinate calculations of py_2SiX_4

Force constant*	Value			
	X = H†	X = F	X = Cl	X = Br
f_R	1.72	3.89	1.57	1.45
f_l	1.00	1.00	1.00	1.00
$f_{RR}^{cis} = f_{Rl}$	0.28	0.28	0.28	0.28
$f_{RR}^{trans} = f_{ll}$	0.14	0.14	0.14	0.14
f_α	0.55	1.18	0.70	0.60
$f_{R\alpha}$	0.18	0.34	0.20	0.17
$f_{\alpha\alpha} = f_{\alpha\beta} = f_{\beta\beta}$	0.10	0.10	0.10	0.10

*Force constants in units of mdyn/Å, mdyn/rad or mdyn Å/rad².
†Force constants for the hypothetical molecule py_2SiH_4.

Normal Coordinate Calculations

Force fields for the parent molecules py_2SiX_4 were derived using methods similar to those described previously for py_2SiCl_4 (1) and $pyPCl_5$ (7). These force constants were transferred directly to the respective mixed halogeno–pyridine complexes. The pyridine ligand was treated as a point mass with a SiN bond stretching constant of about 1.0 mdyn/Å. Force constants not listed in Table 8 for the parent molecules were set equal to zero in the mixed halo species. Table 9 contains the bond lengths used in the calculations.

The calculated spectra for py_2SiCl_3X are shown in Table 2 for a molecular symmetry of C_s. In the case of $py_2SiCl_2X_2$ the spectra were computed for *trans*-pyridines but with both *trans*-halogens (D_{2h}) and *cis*-halogens (C_{2v}). Within the approximations made in the force fields only the D_{2h} $py_2SiCl_2X_2$ calculated frequencies gave a satisfactory fit with the observed spectra.

The computer programs used for the calculation of the vibrational spectra are based on those of Schactschneider's G.MAT, F.MAT, and EIGV. and were run on an IBM 7094 computer system.

We would like to thank the National Research Council of Canada for financial support and an N.R.C.C. scholarship for D.H.B.

TABLE 9

(*a*) Internal coordinates of parent molecules py_2SiX_4

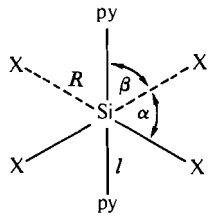

(*b*) Bond distances used in vibrational analysis of py_2SiX_4

Bond	Distance (Å)
Si—H	1.55
Si—F	1.62
Si—Cl	2.13
Si—Br	2.28
Si—py	2.01

1. I. R. BEATTIE. Quart. Rev. **17**, 383 (1963). H. J. CAMPBELL-FERGUSSON and E. A. V. EBSWORTH. J. Chem. Soc. (A), 1508 (1966); 705 (1967). I. R. BEATTIE, T. R. GILSON, and G. A. OZIN. J. Chem. Soc. 2773 (1968).
2. V. BAIN, R. C. G. KILLEAN, and M. WEBSTER. Acta Cryst. **B25**, 156 (1969).
3. R. C. G. KILLEAN. J. Chem. Soc. A, 2772 (1968).
4. R. HULME, G. O. LEIGH, and I. R. BEATTIE. J. Chem. Soc. 366 (1960).
5. I. R. BEATTIE, P. JONES, M. MILNE, and M. WEBSTER. J. Chem. Soc. A, 482 (1969).
6. I. R. BEATTIE, T. R. GILSON, and G. A. OZIN. J. Chem. Soc. A, 2373 (1968).
7. I. R. BEATTIE and G. A. OZIN. J. Chem. Soc. A, 370 (1969).
8. B. BOSNICH and F. P. DWYER. Aust. J. Chem. **19**, 2227 (1969).
9. H. A. BOOTH and C. F. SWINEHEART. J. Am. Chem. Soc. **57**, 1333 (1935).
10. W. C. SCHUMB and E. L. GAMBLE. J. Am. Chem. Soc. **54**, 3943 (1932).
11. JAN STOKR and BOHDAN SCHNEIDER. Chem. listy, **52**, 985 (1958).
12. G. S. FORBES and H. H. ANDERSON. J. Am. Chem. Soc. **66**, 931 (1944).
13. M. L. DELWAULLE. J. Phys. Rad. [8], 7 (1946).
14. V. J. SHINER and M. L. SMITH. Anal. Chem. **28**, 1043 (1956).

Can. J. Chem. Downloaded from www.nrcresearchpress.com by 210.87.254.6 on 09/05/12
For personal use only.

Influence des paramètres géométriques sur la résistance d'une cellule électrolytique

J. C. SISI, C. DUBEAU, ET J. P. PÉLISSIER
Département de Génie Chimique, Ecole Polytechnique, Montréal, Québec
ET
L. MITNYAN
Département de Génie Physique, Ecole Polytechnique, Montréal, Québec

Reçu le 18 janvier 1972

Les valeurs de la résistance d'une solution aqueuse de K_2SO_4 à 25 °C dans une cellule électrolytique ont été calculées théoriquement en fonction des paramètres géométriques de la cellule. Les valeurs calculées ont été vérifiées expérimentalement avec une nouvelle méthode utilisant un courant alternatif de 2000 cycles.

The resistance of an aqueous solution of K_2SO_4 in an electrolytic cell has been calculated theoretically as a function of geometric parameters of the cell. The calculated values have been verified with a new experimental method using an alternating current of 2000 cycles.

Canadian Journal of Chemistry, **50**, 2491 (1972)

Introduction

Depuis plusieurs années déjà, l'électrochimie a quitté le modeste rôle de frontière entre la physique et la chimie. Des résultats importants lui sont dus dans des domaines de plus en plus divers et les applications sont de plus en plus nombreuses. Bien que les recherches de pointe en électrochimie soient abondantes, on doit remarquer que beaucoup de résultats plus classiques ou plus anciens mais aussi des résultats récents se limitent souvent à des cas simples. Ceci est dû, en général, aux difficultés mathématiques rencontrées (13).

Une énorme quantité de recherches et d'applications utilisent au moins deux électrodes plongeant dans des cellules diverses (1, 6, 9–11). Il nous a paru intéressant de montrer avec une bonne précision quelle peut être l'influence des facteurs géométriques sur les autres paramètres de ces cellules.

Il semble que les "facteurs géométriques" englobent des concepts variés conduisant chacun à un point de vue d'étude différent: (*i*) forme des électrodes, (*ii*) forme de la cellule, (*iii*) état de surface des électrodes.

Chacun de ces concepts prend plus ou moins d'importance selon que l'on se place en régime hydrostatique ou hydrodynamique. A ce propos, il est bon de rappeler que le régime statique ne peut être employé que si on est sûr que la convection peut être complètement négligée, sinon la convection naturelle peut entraîner des erreurs.

La forme des électrodes est un facteur très important car dans de multiples applications on étudie le comportement d'une électrode particulière en la plaçant vis-à-vis d'une contre-électrode beaucoup plus grande. Il n'est donc pas inutile de vérifier dans quelles mesures cette disposition si fréquente n'entraîne aucune correction et d'essayer d'établir un moyen de mesure précise des corrections à effectuer lorsque c'est nécessaire.

Partie théorique

Problème général

Nous avons limité la majeure partie de notre travail à l'étude de la partie réelle de l'impédance des solutions, c'est-à-dire à la résistance de la cellule.

Nous avons également limité notre étude, quant à la forme des cellules, à un des cas les plus intéressants: des cellules cylindriques dont les deux électrodes sont circulaires, planes et centrées sur l'axe du cylindre. Les calculs et vérifications que nous avons effectués pour ce type de cellule peuvent cependant dans bien des cas être facilement adaptés à des formes différentes.

Evidemment, lorsque les deux électrodes ont le même diamètre, la loi d'Ohm est immédiatement intégrable sous sa forme simple bien connue:

$$\frac{V}{I} = R = \frac{\rho d}{\pi R_i^2} \qquad [1]$$

V, différence de potentiel entre les deux élec-

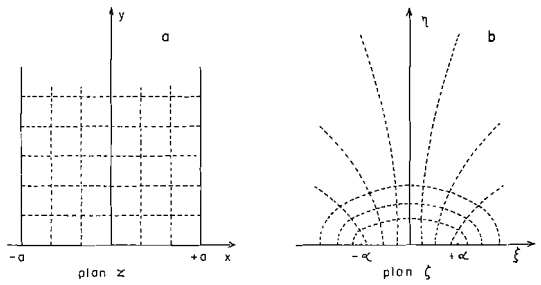

FIG. 1. Transformée de Schwarz simple.

trodes; I, courant passant dans la cellule; R, résistance de la cellule; ρ, résistivité de la solution; d, distance entre les électrodes; R_i, rayon des électrodes.

Par contre, si les rayons des deux électrodes sont différents, la loi d'Ohm n'est plus intégrable directement par une méthode analytique.

C'est essentiellement le problème de cette intégration dont nous allons développer la solution et les vérifications de cette solution.

Etude physique du problème

Les seules transformations mathématiques que l'on puisse faire subir à notre système doivent satisfaire la condition suivante: on doit conserver l'équation fondamentale de Laplace $\nabla^2\varphi = (\partial^2\varphi/\partial x^2) + (\partial^2\varphi/\partial y^2) = 0$, où, dans le cas du potentiel à l'intérieur d'une solution, $\varphi = V = V(\rho, d, R_1, R_2, I)$.

Le groupe des transformations conformes et particulièrement la transformation de Schwarz satisfont cette condition.

D'autre part, on sait que plusieurs auteurs ont appliqué avec succès les transformations de Schwarz à certains problèmes de transport de matière dans les liquides (8, 16).

Transformées de Schwarz simples et doubles

La demi-bande du plan Z (fig. 1*a*) représente le potentiel complexe $\Omega = \varphi + i\varphi$ soumis aux conditions $\varphi(x, 0) = 0$, $-a < x < +a$, $\varphi(-a, y) = -\alpha$, $\varphi(+a, y) = +\alpha$ pour $y > 0$, et $\partial\Omega/\partial Z \to 0$ lorsque $Z \to \infty$.

Cette demi-bande peut être considérée comme étant la surface d'un triangle dégénérée (1) et être transformée dans le demi-plan ξ (fig. 1*b*) par la transformée (1, 3, 16).

$$Z = \frac{2a}{\pi} \arcsin\left(\frac{\zeta}{\alpha}\right)$$

où $\zeta = \xi + i\eta$ et $Z = x + iy$, la transformation inverse étant

$$\zeta = \alpha \sin\left(\frac{\pi Z}{2a}\right)$$

En séparant les parties réelles et imaginaires, on obtient

$$\frac{\xi^2}{\mathrm{ch}^2\left(\frac{\pi y}{2a}\right)} + \frac{\eta^2}{\mathrm{sh}^2\left(\frac{\pi y}{2a}\right)} = \alpha^2$$

qui transforme les ellipses confocales (les foyers aux points $-\alpha$ et $+\alpha$) du plan ζ dans les droites (y = constant) du plan Z, et

$$\frac{\xi^2}{\sin^2\left(\frac{\pi x}{2a}\right)} + \frac{\eta^2}{\cos^2\left(\frac{\pi x}{2a}\right)}$$

qui transforme les hyperboles confocales (les foyers aux points $-\alpha$ et $+\alpha$) du plan ζ dans les droites (x = constant) du plan Z.

D'autre part, l'ensemble géométrique qui représente la distribution des lignes de force à l'intérieur d'une solution comprise entre deux électrodes possède une conformation semblable à celle montrée dans la fig. 2*c*.

Cette conformation peut être obtenue en re-

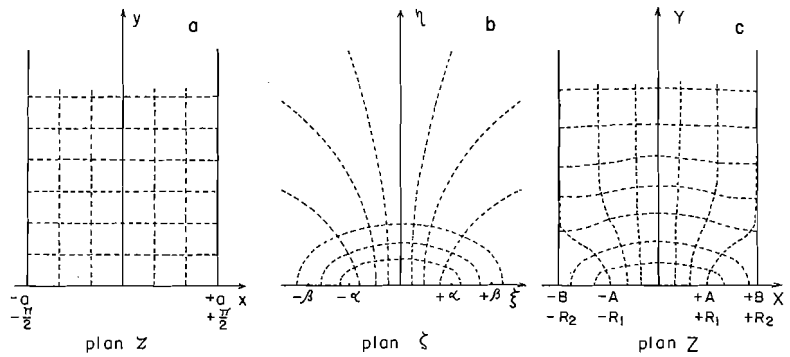

Fig. 2. Transformée de Schwarz double.

pliant de 90° vers le haut l'axe réel du plan ζ aux deux points $-\beta$ et $+\beta$, différents de $-\alpha$ et $+\alpha$ (3, 16).

La série de transformations conformes qui permettent le passage de la fig. 2*a* à la fig. 2*c* à travers la fig. 2*b* sont:

$$Z = \frac{2a}{\pi} \arcsin\left(\frac{\zeta}{\alpha}\right)$$

$$\zeta = \beta \sin\left(\frac{\pi Z}{2B}\right)$$

$$\alpha = \beta \sin\left(\frac{\pi A}{2B}\right)$$

d'où on obtient

$$Z = \frac{2a}{\pi} \arcsin \frac{\sin\left(\frac{\pi Z}{2B}\right)}{\sin\left(\frac{\pi A}{2B}\right)}$$

Si on prend $|a| = \pi/2$, $|B| = R_2$ et $|A| = R_1$

$$Z = \arcsin \frac{\sin\left(\frac{\pi Z}{2R_2}\right)}{\sin\left(\frac{\pi R_1}{2R_2}\right)}$$

Application de la double transformée de Schwarz au calcul de la résistance

Le fait que cette transformation soit conforme nous autorise à calculer la résistance d'une cellule indifféremment dans l'un ou l'autre des espaces associés dans cette transformation.

L'espace Z (fig 2*c*) correspondra à l'espace réel de mesure, l'espace z (fig. 2*a*) sera utilisé pour permettre les calculs.

En coupe, l'électrode de rayon R_1 a pour trace le segment $(-A, +A)$ de l'axe des x, l'électrode de rayon R_2 a pour trace le segment $(-B, +B)$ de la droite $y = d$. La courbe transformée de la 1ère électrode est, comme nous l'avons vu, le segment $(-\pi/2, +\pi/2)$ de l'axe des x. La courbe transformée de la 2ème électrode, est donnée par

$$z_e = \arcsin\left[\frac{\sin\left(\frac{\pi}{2}\frac{X + id}{R_2}\right)}{\sin\left(\frac{\pi R_1}{2R_2}\right)}\right]$$

z_e étant le lieu de la trace de la 2ème électrode dans le plan z, avec X variant entre $-R_2$ et R_2

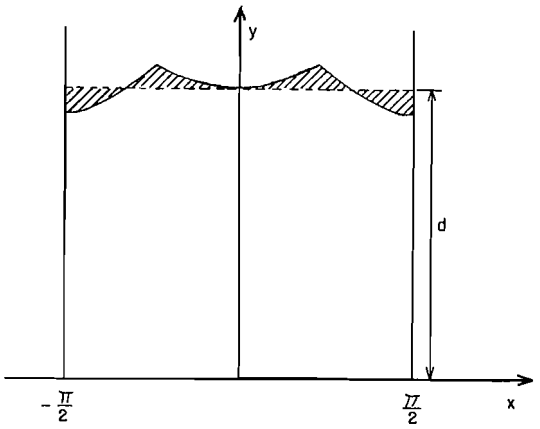

FIG. 3. Tracé de l'électrode no. 1.

$$z_e = \arcsin\,[A + iB]$$

ou en représentation logarithmique

$$z_e = -i \log\,[i(A + iB) \pm \sqrt{1 - (A + iB)^2}]$$

où

$$A = \frac{\operatorname{ch}\left(\frac{\pi d}{2R_2}\right)}{\sin\left(\frac{\pi R_1}{2R_2}\right)} \sin\left(\frac{\pi X}{2R_2}\right)$$

et

$$B = \frac{\operatorname{sh}\left(\frac{\pi d}{2R_2}\right)}{\sin\left(\frac{\pi R_1}{2R_2}\right)} \cos\left(\frac{\pi X}{2R_2}\right)$$

D'où

$$x_e = \arcsin\{\tfrac{1}{2}[(A^2 + B^2 + 1) \pm \sqrt{(A^2 + B^2 + 1)^2 - 4A^2}]\}^{1/2}$$

$$y_e = \operatorname{arg\,sh}\{\tfrac{1}{2}[(A^2 + B^2 - 1) \pm \sqrt{(A^2 + B^2 - 1)^2 + 4B^2}]\}^{1/2}$$

Cette courbe, z_e, a l'allure donnée par la fig. 3. On peut montrer par un calcul simple mais long, qu'en général, la surface de la zone hachurée est négligeable.

Dans ce cas, on voit que la résistance peut être calculée à l'aide de la section de cylindre de hauteur d.

On prendra pour valeur de $d = y_e$

$$y_e = \text{partie imaginaire}\left[\text{arc sin}\left(\frac{\sin\left(\frac{\pi i d}{2R_2}\right)}{\sin\left(\frac{\pi R_1}{2R_2}\right)}\right)\right]$$

$$= \text{arg sh}\frac{\text{sh}\left(\frac{\pi d}{2R_2}\right)}{\sin\left(\frac{\pi R_1}{2R_2}\right)}$$

La surface de section du cylindre est $\pi^3/4$. La résistance de la cellule est donc

$$R = \rho'\frac{4}{\pi^3}\text{arg sh}\frac{\text{sh}\left(\frac{\pi d}{2R_2}\right)}{\sin\left(\frac{\pi R_1}{2R_2}\right)}$$

où ρ' représente la résistivité dans l'espace transformé. Appliquons cette formule au cas où $R_1 = R_2$.

$$R = \rho\frac{d}{\pi R_2^2} \quad \text{d'où} \quad \rho' = \rho\frac{\pi}{2R_2}$$

où ρ représente la résistivité dans l'espace réel. Donc dans le cas général

$$[2] \qquad R = \rho\frac{2}{\pi^2 R_2}\text{arg sh}\frac{\text{sh}\left(\frac{\pi d}{2R_2}\right)}{\sin\left(\frac{\pi R_1}{2R_2}\right)}$$

Pour plus de commodité par la suite, nous utiliserons le rapport Λ définit ainsi

$$\Lambda = \frac{\text{Résistance de la cellule définie par } (d, R_1, R_2)}{\text{Résistance de la cellule définie par } (d, R_2, R_2)}$$

Si $R_2 > R_1$

$$\Lambda = \frac{2R_2}{\pi d}\text{arg sh}\left(\frac{\text{sh}\left(\frac{\pi d}{2R_2}\right)}{\sin\left(\frac{\pi R_1}{2R_2}\right)}\right)$$

et si nous définissons toutes les dimensions géométriques par rapport à R_2 en posant

$$\frac{\pi d}{2R_2} = L$$

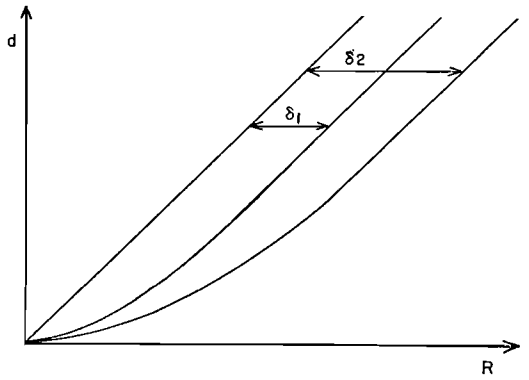

FIG. 4. Résistance *vs.* distance entre les électrodes (relation théorique).

et

$$\frac{\pi R_1}{2R_2} = \Delta$$

$$\Lambda = \frac{1}{L}\text{arg sh}\left(\frac{\text{sh } L}{\sin\Delta}\right)$$

et

$$R = \frac{2\rho}{\pi^2 R_2}\text{arg sh}\left(\frac{\text{sh } L}{\sin\Delta}\right)$$

Quand $L \to \infty$

$$\text{arg sh}\left(\frac{\text{sh } L}{\sin\Delta}\right) \simeq \log\frac{e^L}{\sin\Delta} = L - \log\sin\Delta$$

Donc

$$R_\infty \simeq \frac{2\rho}{\pi^2 R_2}(L - \log\sin\Delta)$$

Or $(2\rho/\pi^2 R_2)\,L$ représente la résistance de la cellule à 2 electrodes de rayons R_2.

Donc la distance δ (fig. 4) est calculée par

$$\delta = \frac{2\rho}{\pi^2 R_2}\log\sin\Delta = K\log\sin\Delta$$

ou

$$[3] \qquad \frac{\delta_1}{\delta_2} = \frac{\log\sin\Delta_1}{\log\sin\Delta_2}$$

Partie expérimentale

Le dispositif de thermostatisation (fig. 5)

L'influence de la température sur la conductivité des cellules électrochimies est grande. De plus les gradients thermiques constituent une source importante de convection naturelle. Pour ces deux raisons il était nécessaire d'effectuer nos mesures à température fixe contrôlée avec une grande précision. Des essais de thermostatisation par immersion de la cellule dans l'eau ont montré que même si la cellule est bien

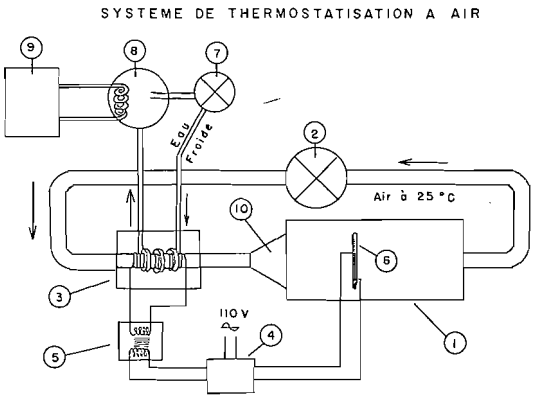

FIG. 5. Système de thermostatisation à air. *1*, Enceinte thermostatisée; *2*, soufflerie; *3*, thermoregulateur; *4*, relais électronique; *5*, autotransfo; *6*, thermomètre à contacts de précision; *7*, pompe de circulation d'eau; *8*, *9*, echangeur de chaleur et système de refroidissement; *10*, diffuseur conique.

isolée, le bain de régulation influence les mesures de façon difficilement contrôlable. C'est pour cette raison que la thermostatisation par air a été choisie en définitive. La température de la salle d'expérience n'ayant aucune fenêtre, il a été facile de régler sa température à 1 °C près.

Le dispositif décrit ci-dessous a permis de fixer la température de la cellule à 25 °C avec une précision supérieure à 1/100° de °C. L'enceinte thermostatisée elle même est en plexiglass à deux épaisseurs séparées par une couche d'air. Des gants permettent d'effectuer des manipulations à l'intérieur mais au cours des mesures les orifices sont fermés par des bouchons en mousse de polystyrène. Outre le thermorégulateur, un thermomètre au 1/100° de degré préalablement étalonné plonge dans cette enceinte.

Les tuyaux de circulation de l'air sont matelassés avec de la laine de verre. Un cône de diffusion percé de trous obturables permet une bonne répartition de la circulation d'air dans l'enceinte.

La cellule de mesure et ses accessoires (fig. 6)

La cellule de mesure elle-même est composée d'un tube de verre cylindrique calibré de 2.992 cm de rayon intérieur et de 8 cm de hauteur, placé verticalement.

Le tube de verre cylindrique s'engage dans la rainure circulaire d'un support en plastique muni d'un trou en son centre. Ce trou est muni d'un tuyau permettant l'arrivée ou le départ du mercure formant l'électrode inférieure (rayon fixe égal au rayon intérieur du tube de verre). Le support en plastique décrit ci-dessus se trouve lui-même monté sur un bâti dont l'horizontalité est contrôlee par deux niveaux à bulle perpendiculaires. La partie supérieure du tube de verre est recouverte par une couronne de plastique munie d'une rainure circulaire, enchassant une électrode plaquée or. Le plastique est percé de deux petits trous permettant l'évacuation de l'électrolyte en cas d'élévation du niveau du mercure. Il existe 6 montures supérieures différentes dont les électrodes mesurent respectivement 1, 3/4, 7/8, 1/2, 1/4, 1/8 de pouce de rayon.

Pour assurer l'étanchéité du système, on a placé sur la monture supérieure une masse assez lourde. Le niveau du

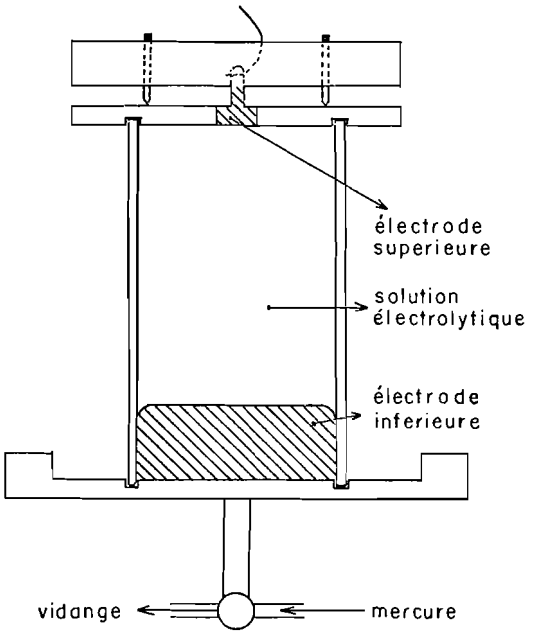

FIG. 6. Schéma de la cellule électrolytique.

mercure dans la cellule est contrôlé par un siphon qui aboutit d'une part à la canalisation sous la cellule et d'autre part à une ampoule à brome fixe sur un support à crémaillère. A la fin de chaque expérience, la cellule est vidée par la canalisation inférieure et le mercure est passé à travers un filtre spécial.

Les appareils de mesure

(a) Mesures géométriques

Le niveau de la surface du mercure (électrode inférieure) et celui de la surface de l'électrode supérieure sont mesurés à l'aide d'un cathétomètre de précision extérieur au montage. Sa verticalité est assurée grâce à des niveaux à bulle.

(b) Mesures électriques

Pour éviter tout phénomène de polarisation, toutes les mesures électriques se font en courant alternatif.

La source de courant est un générateur à fréquence variable utilisant le courant du secteur stabilisé. La tension fournie par ce générateur est appliquée aux bornes d'un point de mesure de type dont tous les éléments de mesures ont été remplacés par des éléments plus précis.

La mesure de l'équilibre du pont s'effectue à l'aide d'un oscilloscope cathodique. On applique respectivement les tensions à mesurer au balayage vertical et horizontal. L'équilibre est obtenu quand l'ellipse correspondant au déséquilibre a pu être réduite à un segment de droite horizontal. Cet équilibre est obtenu en ajustant des résistances et des capacités soigneusement étalonnées au préalable. La mesure de la résistance de la cellule est facilitée par l'existence sur le pont de mesure d'une "terre de Wagner" que l'on ajuste séparément de façon à contrebalancer au mieux la partie capacitive de l'impédance de la cellule.

Choix des conditions expérimentales

Après plusieurs essais, le choix de l'électrolyte a été fixé

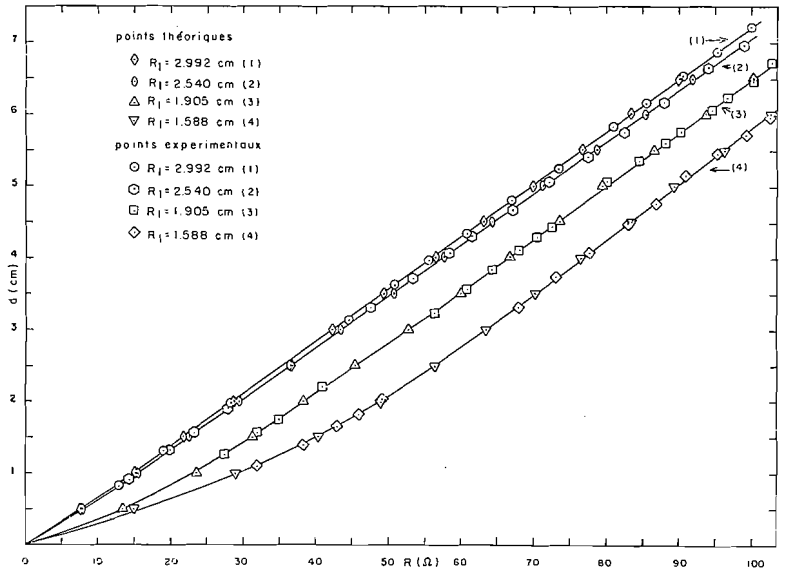

FIG. 7. Résistance *vs.* distance entre les électrodes (relation expérimentale).

sur le sulfate de potassium en solution aqueuse de molalité 10^{-2}, les travaux de Shaw et Remick (15) ayant montré qu'on évite ainsi au maximum les sustensions de toute nature. La fréquence, choisie pour les mêmes raisons entre 500 et 10000 Hz finalement été fixée à 2000 Hz car c'est pour cette valeur que les résultats sont les plus reproductibles.

Résultats expérimentaux

Résultats préliminaires

Un étalonnage minutieux de tous les appareils de mesure (en particulier les résistances d'équilibrage du pont) a permis d'obtenir une précision et une reproductibilité des résultats de $2 \times 10^{-2}\Omega$ pour des résistances comprises entre 1 et 300 Ω.

Résistance de la cellule de mesure (voir fig. 7)

Tous les résultats ont été obtenus à 25 °C ± 0.05 °C avec des solutions de K_2SO_4 de molalité 0.01 ± 0.0001, à une fréquence de 2000 ± 2 Hz.

La distance entre les électrodes est mesurée en centimètres avec une précision de 10^{-3} cm.

Le rayon de l'électrode inférieure (en mercure) est de $R_2 = 2.992$ cm (Tableaux 1, 2).

Etude des écarts

$\delta_1 = 1.80$, $\delta_2 = 10.41$, $\delta_3 = 19.38$ écarts mesurés 1e/2e électrodes, 1e/3e électrodes, 1e/4e électrodes, respectivement.

$\delta_1 = 1.87$, $\delta_2 = 11.31$, $\delta_3 = 19.67$ écarts calculés par la formule $\delta = k \log \sin \Delta$.

Discussion des résultats

On voit que les résultats ci-dessus confirme avec précision l'emploi des formules établies plus haut.

Cependant, des essais avec une électrode de rayon $R_1 = 0.317$ cm ont donné des résultats nettement plus dispersés. Nous avons dû négliger ce résultat car il a été prouvé que l'isolement des flans de cette électrode était défectueux. Cependant, il est certain que pour des distances de moins de 4 cm l'approximation faite sur la fig. 3 ne peut plus être appliquée à une aussi petite électrode.

Extension possible de la recherche

La configuration du système électrolytique étudiée constitue un cas particulier. Nous nous proposons d'étudier d'autres configurations et de vérifier les résultats obtenus par la même méthode expérimentale au moyen de la théorie de la distribution du courant de convection dans une cellule électrolytique.

Le courant d'une cellule électrolytique, comparé au courant limite de diffusion, sera analysé en fonction des paramètres physico-chimiques, tels que la conductivité spécifique de la solution, la forme géométrique des électrodes, l'état de la surface des électrodes, etc.

En appliquant la théorie des distributions nous pouvons considérer le courant électrique, à un instant donné, comme une masse ponctuelle animée d'une vitesse représentée par son vecteur

TABLEAU 1. Résistances mesurées

d (cm)	R (Ω)	d (cm)	R (Ω)
(a) 1ère électrode, $R_1 = 2.992$ cm			
7.218	100.00	4.336	60.92
6.886	95.22	3.946	55.75
6.544	90.65	3.600	50.82
6.152	85.44	3.120	44.07
5.824	81.04	1.972	28.14
5.246	73.41	1.294	19.10
4.794	67.03	0.812	12.90
(b) 2ème électrode, $R_1 = 2.54$ cm			
6.976	98.89	4.096	58.46
6.682	94.06	3.690	53.52
6.192	88.17	3.312	47.75
5.764	82.31	1.910	28.18
5.402	77.52	1.536	23.24
5.050	72.00	1.356	19.80
4.682	67.27	0.906	14.37
4.334	61.43		
(c) 3ème électrode, $R_1 = 1.905$ cm			
6.716	103.11	4.278	70.64
6.484	100.29	4.106	67.92
6.244	96.76	3.824	64.36
6.056	94.55	3.574	70.87
5.758	90.28	3.244	56.49
5.614	88.27	2.218	40.83
5.362	84.69	1.738	35.16
5.062	80.21	1.562	32.13
4.416	72.62	1.246	27.47
(d) 4ème électrode, $R_1 = 1.588$ cm			
7.170	118.50	4.088	77.61
6.642	111.04	3.746	72.95
6.386	108.18	3.314	67.85
5.982	102.40	2.004	49.10
5.734	99.27	1.808	46.13
5.462	95.90	1.644	43.01
5.156	90.79	1.398	38.30
4.732	86.95	1.074	32.10
4.472	82.91		

TABLEAU 2. Résistances calculées

	Résistances			
d (cm)	1ère el.	2ème el.	3ème el.	4ème el.
6.5	90.07	91.87	100.48	109.45
6.0	83.40	85.54	93.75	102.66
5.5	76.76	78.82	86.65	96.37
5.0	69.94	71.36	79.48	89.38
4.5	63.11	64.21	73.61	83.35
4.0	56.47	57.29	66.58	76.41
3.5	49.41	50.62	59.88	70.05
3.0	42.40	43.39	52.77	63.36
2.5	36.74	36.42	45.13	56.20
2.0	28.53	29.43	38.25	49.04
1.5	21.85	22.55	31.22	40.25
1.0	15.32	15.50	23.54	29.89
0.5	7.66	7.93	13.30	14.94
0.0	0.0	0.0	0.0	0.0

tangent au point donné. En déterminant le champ des vecteurs-distributions nous obtenons l'intensité du courant de convection comme étant définie par une charge en mouvement. Lorsque l'espace de la cellule électrolytique est orienté, il existe un isomorphisme canonique et les distributions sur l'espace généraliseront les fonctions.

Les distributions se transforment, par changement des variables, comme les fonctions correspondantes et l'intégrale partielle d'une forme différentielle sur la section de l'espace fibré conduira à l'image directe d'un courant de la base.

Cette application de la théorie des distributions, par une transformation de Fourier des courants tempérés sur un espace vectoriel de dimension finie (14), permettra de déterminer les paramètres géométriques de la surface des électrodes.

En expliquant les résultats obtenus avec la théorie des distributions par la géométrie différentielle nous nous proposons d'établir une équation intégrale générale du courant électrolytique dont les constantes pourront être évaluées par l'analyse des courbes expérimentales.

Enfin cette recherche devrait nous conduire à l'établissement d'une relation directe entre le courant électrolytique et les paramètres géométriques moyens de la cellule.

Ce travail a pu être réalisé grâce aux subventions du Conseil National de Recherches du Canada et du Centre de Recherche de l'Hydro-Québec.

1. J. N. AGAR et T. P. HOAR. Discuss. Faraday Soc. **1**, 158 (1947).
2. G. F. CARRIER, M. KROOK, et C. E. PEARSON. Function of a complex variable. McGraw-Hill. 1966. p. 142.
3. E. DURAND. Electrostatique. Masson. 1964.
4. I. EPELBOIN et M. KEDDAM. J. Electrochem. Soc. **117**, 8, 1052 (1970).
5. M. GUILLOU. Thèse de doctorat, Masson. 1963.
6. T. P. HOAR et J. N. AGAR. Discuss. Faraday Soc. **1**, 162 (1947).
7. L. HSUEH et J. NEWMAN. J. Electrochem. Soc. **117**, 10, 1242 (1970).
8. V. G. LEVICH. Physicochemical hydrodynamics, Prentice Hall. 1962.
9. V. P. MASHOVETS et G. V. FORSBLOM. Zhur. Fiz. Khim. **26**, 10, 1389 (1952).
10. V. P. MASHOVETS et G. V. FORSBLOM. Zhur. Priklad. Khim. **27**, 3, 280 (1954).

11. V. P. MASHOVETS et V. G. FOMICHEV. Zhur. Fiz. Khim. **34**, 11, 2587 (1960).
12. J. NEWMAN. J. Electrochem. Soc. 501 (1966).
13. B. B. OWEN et H. S. HARNED. The physical chemistry of electrolytic solutions. Reinhold. 1943.
14. R. SCARFIELLO. Nuovo Cimento, **12**, 471 (1954).
15. M. SHAW et E. REMICK. J. Electrochem. Soc. **97**, 10, 324 (1950); **102**, 9, 534 (1955); **109**, 7, 628 (1962): III, 8, 981 (1964).
16. W. R. SMYTHE. Static and Dynamic Electricity. McGraw-Hill. 1960.
17. A. M. WEINBERG. Bull. Math. Biophys. **3**, 39 (1941).

The Photolysis of 4-Hydroxybenzil and the Effect of Triethylamine on the Photolysis of Benzil and 4-Hydroxybenzil

DAVID L. BUNBURY[1] AND THERESA MAK CHAN[2]

Department of Chemistry, St. Francis Xavier University, Antigonish, Nova Scotia

Received January 18, 1972

Benzil is photoreduced in neat triethylamine and mixtures of triethylamine and 2-propanol. In neat 2-propanol the principal products are; benzil pinacol, 20%; benzoin benzoate, 19%; benzoin, 18%; and benzoic acid, 12%. When the amine concentration is as low as 0.2 m*M* the benzil pinacol formation is almost completely suppressed. At amine concentrations higher than 0.36 m*M* the principal product is benzoin, 80%. At intermediate amine concentrations benzoin benzoate is important. The rate of benzil disappearance reaches a maximum and then declines as either the benzil concentration in triethylamine is increased or the amine concentration in 2-propanol is increased.

4-Hydroxybenzil is not photoreduced by 2-propanol. It is reduced by triethylamine. The quantum yield of disappearance is 0.04 at a concentration of 47.8 m*M* and in solutions containing at least 0.36 *M* of amine. 4-Hydroxybenzoin is the principal product but at low starting 4-hydroxybenzil concentrations 4,4′-dihydroxybenzil is important. A rate maximum is also observed in this case.

4,4′-Dihydroxybenzil is not photoreduced by 2-propanol. It does undergo photoreaction in neat triethylamine but no products were isolated.

Triethylamine also appears to suppress biacetyl pinacol formation in the photoreaction of biacetyl with 2-propanol.

Le benzile a été photoréduit dans la triéthylamine pure et dans des mélanges de triéthylamine et de propanol-2. Dans le propanol-2 pur les principaux produits sont le benzile pinacol 20%, le benzoate de benzoïne 19%, la benzoïne 18%, et l'acide benzoïque 12%. Pour une concentration en amine aussi basse que 0.2 m*M*, la formation du benzile pinacol est presque complètement supprimée. Pour des concentrations en amine supérieures à 0.36 m*M*, le produit principal est la benzoïne 80%. Pour des concentrations intermédiaires en amine, le benzoate de benzoïne devient important. La vitesse de la disparition du benzile atteint un maximum puis décroît soit par augmentation de la concentration du benzile dans la triéthylamine soit par accroissement de la concentration en amine dans le propanol-2.

L'hydroxy-4 benzile n'est pas photoréduit par le propanol-2, il est réduit par la triéthylamine. Le rendement quantique de la disparition est de 0.04 pour une concentration de 47.8 m*M* et dans des solutions contenant au moins 0.36 *M* d'amine. On obtient principalement l'hydroxy-4 benzoïne mais pour de faibles concentrations initiales en hydroxy-4 benzile, le dihydroxy-4,4′ benzile devient important. Un maximum dans la vitesse a été également observé dans ce cas.

Le dihydroxy-4,4′benzile n'est pas photoréduit par le propanol-2. Il subit une réaction photochimique dans la triéthylamine pure mais on n'a pas isolé de produits. Il apparaît également que la triéthylamine supprime la formation du biacétyle pinacol dans la réaction photochimique du biacétyle sur le propanol-2.

Canadian Journal of Chemistry, **50**, 2499 (1972)

Introduction

There has been much recent work on the photolysis of various benzophenones and of fluorenone using tertiary amines as solvents and hydrogen donors (1–12). This work has shown that those ketones which do not undergo photoreduction in 2-propanol because the lowest lying excited state is unreactive toward hydrogen abstraction, are photoreduced in triethylamine and other tertiary amines. It was thought interesting to see if *p*-hydroxybenzil would show the same behavior relative to benzil that *p*-hydroxybenzophenone shows relative to benzophenone. Since benzil has two carbonyl groups it is conceivable that in *p*-hydroxybenzil the CT state might not necessarily be lowest in energy and that the usual photoreduction takes place. Alternatively the second carbonyl group might perturb the excited carbonyl enough so that intersystem crossing is a facile process even in polar solvents. Cohen *et al.* (10) have shown that *p*-aminobenzophenone is not reduced in 2-propanol due to lack of intersystem crossing.

Experimental

Benzil and benzoin were from Eastman and twice recrys-

[1]Address until August 1972: Chemistry Department, University of Western Ontario; after, St. Francis Xavier University.

[2]Taken from the M.Sc. thesis of Theresa Mak Chan. Present address: Department of Physiology, Medical School, University of Massachusetts, Worcester, Mass.

Can. J. Chem. Downloaded from www.nrcresearchpress.com by 210.87.254.42 on 09/05/12
For personal use only.

Can. J. Chem. Downloaded from www.nrcresearchpress.com by 210.87.254.42 on 09/05/12
For personal use only.

tallized from methanol. 4-Hydroxybenzil[3] and 4,4′-dihydroxybenzil were prepared from their corresponding benzoins (Aldrich) by oxidation with cupric sulfate, pyridine, and water (13), then cleaving the methoxy group with pyridine hydrochloride at 190–200° (14). Triethylamine and tri-*n*-butyl amine were from Eastman and distilled immediately before use. 2-Propanol, benzene, and pyridine were Fisher certified reagents and were freshly distilled. Quinuclidine was obtained by dissolving 6.5 g quinuclidine hydrochloride in 4 ml water and adding an excess of potassium hydroxide flakes to the solution. The solution was extracted with petroleum ether which was then evaporated. Pyrene was Aldrich reagent grade. *p*-Hydroxybenzophenone was from Aldrich and recrystallized before use. Biacetyl from Eastman was freshly distilled. Silica gel used in column chromatography was Fisher Certified grade 100–200 mesh. It was dried at 150° for 1 h, then cooled in a desiccator.

All melting points were taken either on a Fisher–Johns or Mel–Temp melting point apparatus. Elemental analyses were done by Organic Microanalyses, Dr. C. Daesslé, 5757 Decelles Ave., Montreal, Quebec. Molecular weights were determined on a Hitachi Perkin–Elmer Model 115 Molecular Weight Apparatus. Gas chromatography was performed on a Burrell Model K-1 with thermal conductivity detector. The column was 1/4 in. i.d. 250 cm long and filled with 20% Dow Corning high vacuum silicone grease on 80–100 mesh chromosorb W. The lights used in irradiation and actinometry have already been described (15). Quantitative t.l.c. was made using a Photovolt Densicord Model 542 Densitometer with a light source of 254 nm. T.l.c. was performed using Eastman Chromagram Sheet 6060 (silica gel with fluorescent indicator). A planimeter was used to measure the areas (because of the drifting baseline the planimeter was found to give better results than the automatic integrator). The R_f for 4-hydroxybenzil, when a solution containing triethyl amine was directly applied to the t.l.c. sheet, was considerably lower (0.25, developing solvent, hexane:ether, 1:1) than when solvents such as 2-propanol THF or chloroform were used to apply the solid (R_f 0.48). The usual R_f was obtained by removing the Et_3N by evaporation and dissolving the residue in some other solvent.

Column chromatography was used to separate the products. The solvent was removed under reduced pressure and the residue redissolved in 50 ml of chloroform. This was shaken with 15 ml saturated sodium bisulfite and after separation washed twice with saturated sodium bicarbonate, twice with 50 ml portions of distilled water, then dried over sodium sulfate. The chloroform was removed under vacuum and the residue redissolved in ether then adsorbed onto silica gel. The silica gel with adsorbed products was placed on top of 300 g silica gel in a previously packed column. The column was eluted with about 6 l of ether–hexane, which varied in concentration from 0–60% ether in the case of benzil and 0–80% in the case of 4-hydroxybenzil. Finally the column was washed with 2.5 l of acetone. Each fraction was examined by t.l.c. Five percent ether brought out benzil, 15% benzoin benzoate, 25% benzoin, 40% 4-hydroxybenzil, 55% 4-hydroxybenzoin, and 75% 4,4′-dihydroxybenzil. The material eluted by acetone could not be separated further and was brownish. There was also a very little material which could not be removed from the column.

Three vessels were used for irradiations. The 70 ml vessel was made of Vycor and used in those runs degassed by the freeze–pump–thaw technique. The 400 ml vessel was Pyrex and the 600 ml vessel Vycor. The volumes of the reaction mixture were 50, 250, and 500 ml respectively. The reaction mixture in the two larger sizes was flushed with nitrogen or helium for 30 min prior to irradiation and during the irradiation.

The products of the reaction were identified and measured as follows. Benzaldehyde: the irradiated solution was directly injected onto the gas chromatograph, and a peak was obtained with the same retention time as authentic benzaldehyde. The solvent was distilled off under reduced pressure and the peak was in the distillate. Benzaldehyde was confirmed by precipitating its 2,4-dinitrophenylhydrazone. It was measured quantitatively by comparing its area on the g.c. with that of a standard solution. Unreacted benzil: after column chromatography it was identified by its i.r. spectrum and melting point. It was measured quantitatively by t.l.c. Benzoic acid: was recovered by acidification of the bicarbonate extract followed by ether extraction. After evaporation of the ether, the residue was identified by its m.p. and i.r. spectrum. It was weighed. Benzoin: was obtained by column chromatography and identified by its i.r. spectrum and m.p. It was measured quantitatively by t.l.c. Benzoin benzoate: was identified by its i.r. spectrum and m.p. It was measured quantitatively by t.l.c. Benzil pinacol: when obtained, was separated from the reaction mixture by filtration and identified by its m.p. and i.r. spectrum. It was measured quantitatively by weighing. Unreacted 4-hydroxybenzil: was obtained by column chromatography and identified by its m.p. and i.r. spectrum. It was measured quantitatively by t.l.c. 4-Hydroxybenzoin: was obtained by column chromatography and after recrystallization had a melting point of 172–175° with some decomposition. Its i.r. and n.m.r. spectra were identical with an authentic sample prepared by sodium borohydride reduction of the 4-hydroxybenzil. The same compound was also prepared by reduction of 4-hydroxybenzil by benzpinacol according to Rubin and Ben Bass (16*a*). The i.r. has a carbonyl band at 1660 cm^{-1}. The n.m.r. spectrum is also consistent with 4-hydroxybenzoin. In DMSO a broad peak at δ 6.06 (2H CH and OH); doublet at 6.85 (2H); multiplet at 7.40 (5H); doublet at 7.98 (2H); broad peak at 9.82 (1H); J for the doublets 8.5 Hz.

Anal. Calcd. for $C_{14}H_{12}O_3$ (mol. wt. 228): C, 73.66; H, 5.30. Found (223): C, 73.89; H, 5.48. 4′-Hydroxybenzoin is reported to melt at 187–189° (16*b*). It was measured quantitatively by t.l.c. 4,4′-Dihydroxybenzil: was obtained by column chromatography and had a melting point and i.r. spectrum identical with an authentic sample. It was measured quantitatively by t.l.c. Polymer: was obtained from triethylamine solutions of benzil in the form of a brown precipitate during irradiation. It was separated by filtration but when it came in contact with air it became oily and very dark colored. Addition of a small amount of water to this oily compound led to the formation of a brown precipitate.

Anal. Found for the last precipitate (mol. wt. >1000): C, 68.69; H, 7.74; N, 2.88.

[3]Both refs. 29 and 30 give the m.p. of 4-hydroxybenzil as 175° based on a report by Weisl (31). Gorvin (32) showed that the true m.p. is 129–130°. Reference 14 also obtains this m.p. as does Friedman *et al.* (33).

TABLE 1. Benzil photolysis in triethylamine: reaction conditions, products, and rates

Run	Conditions*	Concentration (m*M*)†	Time (min)	Benzil destroyed (mmol)	Rate (mmol/h)	Products as % benzil lost: Benzoin	Benzaldehyde	Benzoic acid	High mol. wt. compounds‡
1	N_2-flushed	10.7	9.0	0.735	4.9	80	2.0	10.2	7.8
2	N_2-flushed	52.8	20.4	4.02	11.8	78.5	0.5	15.2	5.8
3	N_2-flushed	122.1	33.0	5.35	9.7	75	0.4	19.0	5.6
4*a*	Degassed (stopcock)	53.0	11.7	0.67	3.5	79	2.0	10.5	8.5
4*b*	Degassed (sealed tube)	48.5	20.0	0.875	2.6	84	—§	2.5	—

*Temperature 25–30°.
†The volume of the reaction mixture was 250 ml except for run 4 which was 50 ml.
‡High mol. wt. compounds obtained by difference.
§—Not measured.

Quantum yields: the quantum yield for the disappearance of 4-hydroxybenzil in triethylamine was measured using the actinometer of Hatchard and Parker (17). The light from the medium pressure mercury arc was filtered by a Corning No. 7-39 filter with a peak between 340–380 nm. Both the actinometer solution and the hydroxybenzil solution were stirred by a current of nitrogen during irradiation. The quantum yield for the disappearance of benzil in triethylamine was estimated by comparing it with the rate of disappearance of benzil in 2-propanol (Table 2).

Results and Discussion

Table 1 shows the products of irradiation of benzil in neat triethylamine and the effect of the concentration of benzil on the rate of the reaction. The amount of benzoic acid is much less in the sealed tube run than others, but some was still formed. In a small series of runs where just the acid was measured it was found that if the time between opening the sealed tube and work-up was increased the amount of benzoic acid increased. In comparison with 2-propanol as the solvent it is seen that benzoin is now the major product and no benzil pinacol, benzoin benzoate, or its dimer (15) are produced. These results are somewhat different from those of Gream *et al.* (18) who on an 18 h irradiation of benzil in triethylamine found *N,N*-diethylbenzamide (19%) and a mixture of the two hydrobenzoins (7%). The percentage of the benzil reacting is not mentioned. The hydrobenzoins could arise from photoreduction of first-formed benzoin but explanation of the *N,N*-diethylbenzamide is not immediately apparent.

After formation of the ketyl radical $C_6H_5\dot{C}OHCOC_6H_5$ (**2***a*) Bunbury and Chaung (15) postulated a complex between the ketyl radical and an unexcited benzil molecule leading to the formation of benzil pinacol ($C_6H_5\overset{|}{C}OHCOC_6H_5)_2$ (**6***a*). Based on e.s.r. evidence Schenck *et al.* (19) have proposed that the ketyl radical of benzophenone forms a complex with benzophenone which leads to benzpinacol. If triethylamine is able to coordinate to radicals much better than is benzil or 2-propanol this would explain the lack of benzil pinacol and benzoin benzoate in the products when triethylamine is the solvent. By coordinating more firmly with the ketyl radical, no complex with unreacted benzil can form, and pinacol formation is suppressed. By providing a more easily abstractable hydrogen or by stabilizing the radical against decomposition into benzaldehyde and benzoyl radical, benzoin benzoate is suppressed. Such a stabilized radical would then end up as benzoin, the major product. This is outlined in Scheme 1.

There is another reason possible for benzoin being the principal product. Cohen and Sherman (20) proposed a path, in the photoreduction of aromatic carbonyl compounds in basic solution, that leads to secondary alcohols rather than pinacols. Davidson and coworkers (21) suggested that triethylamine could act the same way in the photoreduction of fluorenone. The same path shown in Scheme 2 for benzil would lead to benzoin.

Stapelfelt and Perone (22), in a study of the photoelectrochemical behavior of benzil, have suggested that in the p*H* range 6.5–10 in aqueous methanol the reaction between the ketyl radical

Can. J. Chem. Downloaded from www.nrcresearchpress.com by 210.87.254.42 on 09/05/12
For personal use only.

Can. J. Chem. Downloaded from www.nrcresearchpress.com by 210.87.254.42 on 09/05/12
For personal use only.

TABLE 2. Effect of triethylamine on the benzil 2-propanol reaction*

Run	2-Propanol (M)	Et_3N (M)	Et_3N mol fraction	Benzil (mM)	Time (min)	Benzil lost (mmol)	Rate (mmol/h)	Products as % benzil lost				
								Benzil pinacol	Benzoin benzoate	Benzoin	Benzal-dehyde	Benzoic acid
5	13.01	0	0	50.0	50	10.7	12.8	20.4	19.5	18.3	5.3	12.0
6	13.0	0.0002	1.54×10^{-5}	62.6	19	4.9	15.0	0.2	24.0	28.8	2.0	9.7
7	13.0	0.002	1.54×10^{-4}	60.0	21	5.6	15.2	0.0	21.2	37.5	—†	11.2
8	13.0	0.0036	2.8×10^{-4}	46.2	13	3.2	15.3	0.0	15.0	51.0	2.0	10.0
9	12.35	0.36	2.8×10^{-2}	50.5	23.5	10.1	25.8	0.0	6.0	79.0	1.5	8.0
10	10.4	1.44	0.122	50.5	12	4.3	13.4	0.0	0.0	84.0	2.3	11.0
11	6.5	3.6	0.356	49.5	9	1.9	12.7	0.0	0.0	75.0	2.0	16.0
12	3.24	5.44	0.625	50.8	10.2	2.0	11.7	0.0	0.0	65.0	1.0	21.2
13	0.0	7.22	1.0	49.5	11	2.1	11.8	0.0	0.0	72.5	0.6	23.5

*The volume of the reaction mixture was 250 ml except for run 5 in which it was 500 ml. All runs were helium flushed.
†—Not measured.

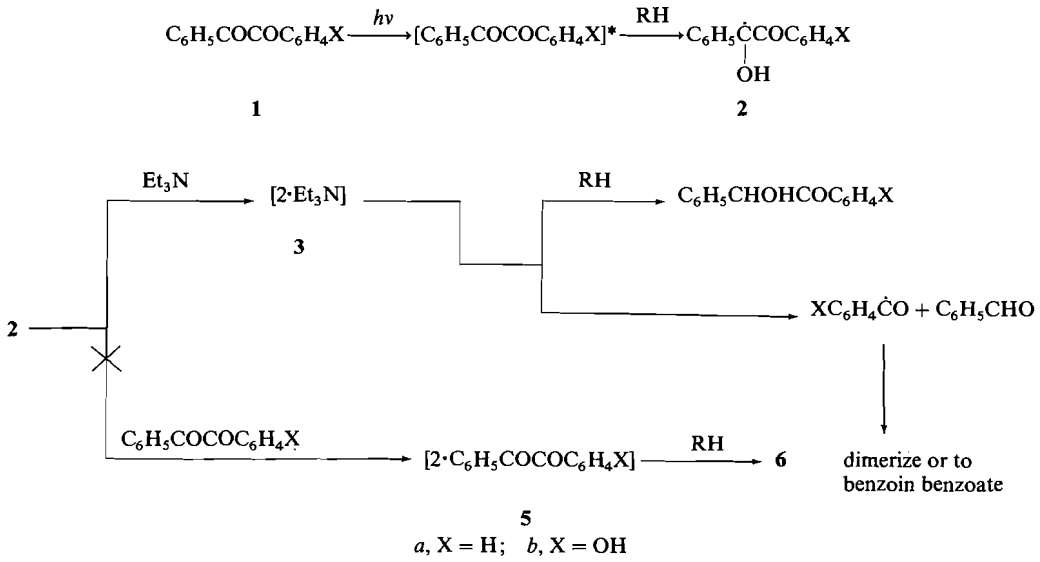

SCHEME 1

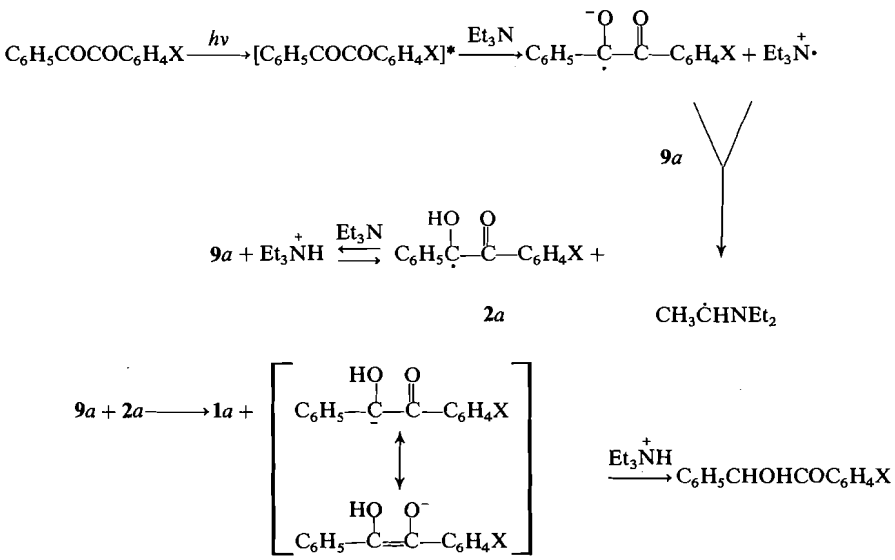

SCHEME 2

and radical anion leading to benzoin is the most important.

To see if it was possibly the geminate amine radical rather then triethylamine itself which was complexing the ketyl radical a series of runs was carried out in which an increasing amount of triethylamine was added to 2-propanol. These results are shown in Table 2.

First, it is seen in run 6 that when the concentration of triethylamine is only 0.2 m*M* that the benzil pinacol is almost completely suppressed. Since 4.9 mmol of benzil were lost, the 2-propanol must have provided the bulk of the hydrogen for the reduction. The conclusion is then that the amine is the species complexing with the ketyl radical **2** and thus preventing benzil pinacol formation. The alternative idea that **2** is being rapidly removed by triethylamine,

Can. J. Chem. Downloaded from www.nrcresearchpress.com by 210.87.254.42 on 09/05/12
For personal use only.

TABLE 3. Effect of tri-*n*-butyl amine on the benzil 2-propanol reaction*

Run	2-Propanol (*M*)	Tri-*n*-butyl amine (*M*)	Benzil (m*M*)	Time (min)	Benzil lost (mmol)	Rate (mmol/h)	Products as % of benzil lost†			
							Benzil pinacol	Benzoin benzoate	Benzoin	Benzoic acid
14	13.0	1.7×10^{-4}	57.4	17.0	3.7	13.4	2.65	20.3	30.4	15.2
15	13.0	1.7×10^{-3}	58.8	17.0	4.2	15.2	0.24	11.2	33.6	—‡
16	13.0	3.4×10^{-3}	59.8	22.5	5.9	15.7	0.0	14.0	34.0	5.2
17	12.9	1.7×10^{-2}	59.0	17.0	5.8	20.8	0.0	—	71.0	9.7
18	12.6	0.17	58.6	17.0	6.3	22.6	0.0	0.0	81.5	—‡

*All runs were 250 ml in volume and helium flushed.
†Benzaldehyde and dimer were not measured.
‡—Not measured.

TABLE 4. Effect of pyridine on the benzil 2-propanol reaction*

Run	2-Propanol (*M*)	Pyridine (*M*)	Benzil (m*M*)	Time (min)	Benzil lost (mmol)	Rate (mmol/h)	Products as % of benzil lost†			
							Benzil pinacol	Benzoin benzoate	Benzoin	Benzoic acid
19	12.95	2.5×10^{-2}	57.2	17.0	4.7	16.8	5.35	21.0	18.9	—‡
20	12.9	0.100	59.6	17.0	4.7	16.8	2.16	21.5	19.0	14.3
21	12.5	0.424	57.4	17.0	5.1	18.2	0.47	32.5	21.0	—
22	12.2	0.75	57.2	17.0	5.0	18.0	0.24	26.0	21.0	—
23	11.9	1.00	57.8	17.0	5.4	19.5	0.0	24.0	16.0	15.0
24	11.6	1.24	57.7	17.0	5.8	20.8	0.0	28.5	16.2	—

*All runs were 250 ml in volume and helium flushed.
†Benzaldehyde and dimer were not measured.
‡— Not measured.

as in Scheme 2, thus preventing complex formation with benzil does not seem as likely. The benzil pinacol is almost completely gone but the benzoin yield has not picked up half of the difference. If Scheme 2 were followed the benzoin yield should have gone up more.

Second, as the triethylamine concentration rises, benzoin benzoate is no longer formed. This would appear to be because triethylamine, as suggested by Davidson and Lambeth (4) and Cohen and Baumgarten (23), is a much better hydrogen donor than 2-propanol and the ketyl radicals are removed by their abstracting a hydrogen from the solvent before the dissociation reaction can take place. Also as suggested earlier the triethylamine coordinated radical might have a smaller tendency to dissociate.

Third, there is a marked maximum in the rate of the reaction (quantum yield also since light conditions are constant) with the changing triethylamine concentration. This parallels the results of Cohen and Chao (24) who found that the rate of photoreduction of benzophenone by tertiary amines increased on dilution of the amine with benzene.[4] These authors ascribed the increase to the formation of light absorbing transients in the more concentrated solutions of the amine. It should be noted that there is also a maximum in the rate as the benzil concentration is varied, Table 1.

Three other amines were tried to see if they also caused suppression of benzil pinacol production. The results are shown in Tables 3–5. All three suppress benzil pinacol formation at low concentrations but pyridine requires a concentration of 200–300 times greater than triethylamine, tri-*n*-butyl amine, or quinuclidine. This agrees with the work of Davidson and Wilson (25) who suggest that amines solvate the $Ph_2\dot{C}OH$, and 9-hydroxyfluorenyl radicals. They further suggest that the amount of solvation depends on the basicity of the amine. Triethylamine (p*K* 10.7) is a much stronger base than is pyridine (p*K* 5.2). The tri-*n*-butyl amine and the

[4]The same effect has been noted for fluorenone (8–10).

Can. J. Chem. Downloaded from www.nrcresearchpress.com by 210.87.254.42 on 09/05/12
For personal use only.

TABLE 5. Effect of quinuclidine on the benzil 2-propanol reaction*

Run	2-Propanol	Quinuclidine (M)	Benzil (mM)	Time (min)	Benzil lost (mmol)	Rate (mmol/h)	Products as % of benzil lost†			
							Benzil pinacol	Benzoin benzoate	Benzoin	Benzoic acid
25	13.0	2.0×10^{-4}	47.6	8.7	0.72	4.9	6.7	23.1	26.2	14.0
26	13.0	6.0×10^{-4}	55.3	8.7	0.74	5.6	0.0	22.4	28.8	20.3
27	13.0	2.0×10^{-3}	48.5	10.0	0.7	4.4	0.0	13.5	40.0	21.3
28	13.0	1.8×10^{-2}	53.5	8.5	0.8	5.4	0.0	11.9	47.0	23.8
29	12.9	7.6×10^{-2}	56.2	8.5	1.1	7.7	0.0	11.0	46.3	18.5

*All runs were 50 ml in volume and helium flushed.
†Benzaldehyde and dimer were not measured.

TABLE 6. Effect of pyrene on the photoreduction of benzil in triethylamine and 2-propanol*

Run	Solvent	Pyrene (mM)	Benzil (mM)	Time (min)	Benzil lost (mmol)	Rate (mmol/h)	Products as % of benzil lost†		
							Benzil pinacol	Benzoin benzoate	Benzoin
30	Et_3N	4.9	80.0	37.5	5.3	8.2	0.0	0.0	63.0
31	0.386 M Et_3N in benzene	4.6	79.3	41.7	8.0	11.4	0.0	0.0	65.0
32	0.0036 M Et_3N in 2-propanol	4.6	80.0	116.6	5.3	2.7	0.0	17.0	36.0
33	2-propanol	4.6	80.2	111.2	5.1	2.7	31.0	21.2	18.7

*All runs were 250 ml and helium flushed.
†Benzaldehyde, benzoic acid, and dimer were not measured.

quinuclidine also cause a rise in the benzoin and a fall off in the benzoin benzoate similar to that caused by triethylamine. The pyridine however, shows no increase in the benzoin nor any fall in the benzoin benzoate. This is exactly what would be expected if the last two changes were due to easier abstraction of hydrogens from tertiary amines, pyridine having no hydrogens that may be easily removed.

If the suppression of benzil pinacol formation was due to Scheme 2 being in operation, even in the case of pyridine a corresponding rise in benzoin should have been noted. (Pyridine would enter at the reaction $\mathbf{2}a + C_5H_5N \rightleftarrows \mathbf{9}a + C_5H_5N^+$ after $\mathbf{2}a$ is formed by reaction with 2-propanol.) Since this was not observed, radical complexing by amines again seems more probable. Further evidence that the amines suppressed benzil pinacol formation by associating with the ketyl radicals was obtained in the following way. It is known that hydrocarbon quenchers are much less efficient in the photoreduction of benzophenone in amines than in alcohols (24, 26).

This lack of efficiency has been attributed (6) to a very fast electron transfer from the amine to the excited ketone as the first step in the photoreduction. The same lack of efficiency appears in benzil photolysis in triethylamine; the results of which are shown in Table 6. If the rate of reaction in run 30, Table 6, is compared with the interpolated value (11.0) between runs 2 and 3, Table 1, it is seen that the reduction caused by the pyrene is not very great. This is also shown if the rate of 31 is compared with the interpolated value (16.8) between runs 35 and 36, Table 7. On the other hand the rate reduction in run 32, where the triethylamine concentration is 0.0036 M in 2-propanol, is the same as the rate reduction in neat 2-propanol: compare run 33, Table 6, with run 5, Table 2.

Since the quenching in run 32 is the same as in neat 2-propanol we can conclude that at this amine concentration the initial chemical step

Can. J. Chem. Downloaded from www.nrcresearchpress.com by 210.87.254.42 on 09/05/12
For personal use only.

TABLE 7. Effect on the photoreaction by dilution with benzene*

Run	Solvent	Benzil (m*M*)	Time (min)	Benzil lost (mmol)	Rate (mmol/h)	Products as % of benzil lost†		
						Benzil pinacol	Benzoin benzoate	Benzoin
34	0.384 *M* Et_3N in benzene	11.1	5.1	0.7	8.6	0.0	0.0	83.5
35	0.384 *M* Et_3N in benzene	48.3	10.1	2.5	14.7	0.0	0.0	81.0
36	0.384 *M* Et_3N in benzene	122.2	25.4	8.2	19.2	0.0	0.0	64.0
37	Et_3N	47.6	43.7	11.8	16.4	0.0	0.0	74.7
38	0.386 *M* Et_3N in benzene	50.5	44.1	15.3	20.7	0.0	0.0	83.0
39	2-propanol	50.5	51.2	15.7	18.3	18.5	18.0	18.1
40	0.52 *M* 2-propanol in benzene	47.6	44.4	2.8	3.8	0.0	17.0	25.0

*For runs 34–36, the volume was 250 ml; 37–40, volume was 500 ml. All runs helium flushed.
†Benzaldehyde, benzoic acid, and dimer were not measured.

in the photoreduction is a hydrogen transfer to the excited benzil from the 2-propanol. But the benzil pinacol formation is completely suppressed by that small amount of amine. The amine must then be intervening at the reactions of the ketyl radical.

It was also thought possible that salt formation between the ground state benzil and the triethylamine might be contributing to the fall in rate observed when both the amine concentration and benzil concentration were increased past the value where the maximum occurred. Attempts to obtain u.v. spectra were thwarted by the intense absorption of benzil in the concentration ranges at which the photolyses were carried out. Using *t*-butyl alcohol as a cryoscopic solvent (23) the following results were obtained. Benzil (7.55 mmol) was dissolved in 100 ml of *t*-butyl alcohol and a depression of 0.88° was observed. The calculated value then is 8.38 mmol. Similarly 28.8 mmol of triethylamine gave a depression of 3.00° which solution was calculated to contain 28.5 mmol. The same amounts of benzil and triethylamine were then dissolved together in 100 ml of *t*-butyl alcohol and a depression of 3.20° was observed. This depression corresponds to 30.4 mmol, which is less than 36.9, the sum of the two individual calculations. The conclusion is that there is a fairly strong interaction between benzil and triethylamine at these concentrations.

To see if there is a different effect of varying the benzil concentration when a more dilute amine is used as solvent, three runs were made with benzene diluted triethylamine. These results are shown in Table 7. There is now no decrease in rate with increasing benzil concentration but the effect of transients and/or salt formation are not easily separable.

Comparing runs 5 and 13 in Table 2, it is seen that the quantum yield of disappearance of benzil is almost the same in neat triethylamine as it is in neat 2-propanol. Taking ϕ_{dis} in 2-propanol as 0.11 (15) leads to ϕ_{dis} of 0.10 in triethylamine.

4-Hydroxybenzil Irradiations

4-Hydroxybenzil showed no appreciable photoreduction in 2-propanol, 50% cyclohexane–50% 2-propanol, or in *N*,*N*-dimethylformamide. It was photoreduced in triethylamine and the results are shown in Table 8. As with benzil the quantum yield of photoreduction depends on the initial concentration of 4-hydroxybenzil and shows a maximum around 0.06 *M*. At a concentration of 0.0478 mol in triethylamine and with Corning filter 7-39 the quantum yield of disappearance is 0.04. The principal product is again the corresponding benzoin. As the initial concentration of 4-hydroxybenzil is increased there is a decrease in 4,4′-dihydroxybenzil and benzaldehyde. Both of these products

Can. J. Chem. Downloaded from www.nrcresearchpress.com by 210.87.254.42 on 09/05/12
For personal use only.

Can. J. Chem. Downloaded from www.nrcresearchpress.com by 210.87.254.42 on 09/05/12
For personal use only.

would have to be formed via dissociation of the ketyl radical, Scheme 1, X = OH. Presumably 4-hydroxybenzoin is the major product for the same reason that benzoin is the major product of benzil photolysis in triethylamine. The decrease in the dissociation of the ketyl radical of 4-hydroxybenzil at higher initial concentrations suggests that the ground state molecule is involved somehow but no dimeric products were isolated.

Since the benzoin isolated is the 4-hydroxy (nearer the carbonyl group) rather than the 4′- it could be argued that reduction takes place on the carbonyl not conjugated with the 4-hydroxy group. However since both thermal reductions also give the 4-hydroxybenzoin it may just be the more stable isomer.

Since there is not enough benzaldehyde corresponding to the 4,4′-dihydroxybenzil there must be another product derived from benzaldehyde but we were unable to find it. Possibly some appears as benzoic acid although this product is formed under all conditions.

When the triethylamine was diluted with 2-propanol the rate increased and passed through a maximum as seen in Table 9. This is qualitatively similar to what is seen with benzil but the concentration of amine at which the maximum occurs is ten times as high. This again could be due to a combination of solvent effects and/or different concentrations of light absorbing transients at different initial concentrations. It is interesting that in run 51 where the molar ratio of 2-propanol to triethylamine was as high as 34, that the reduction proceeded at a rate greater than half that in neat triethylamine. Presumably the polarity of the solvent is about that of neat 2-propanol and that reduction still takes place argues for close association between the amine and the 2-hydroxybenzil. The effect of triethylamine on the photoreduction of 4-hydroxybenzil cannot then be just due to the changing polarity of the solvent. Using the same cryoscopic method as with benzil, 10.03 mmol of 4-hydroxybenzil gave a depression corresponding to 9.98 mmol. 4-Hydroxybenzil (10.03 mmol) and triethylamine (28.8 mmol) were dissolved together and the depression corresponded to 25.7 mmol. There is obviously a great degree of association.

Because such small amounts of triethylamine had such a marked effect on the photoreaction of 4-hydroxybenzil a few runs were made with 4-hydroxybenzophenone to see if the same effect could be observed. *p*-Hydroxybenzophenone in a solution of neat 2-propanol gave a rate of disappearance of 2.88 mmol/h for a 250 ml solution. Comparing this with run 5, Table 2, where the rate of disappearance of benzil is 12.8 mmol/h and the quantum yield of benzil disappearance is 0.11 (15), the calculated quantum yield of 4-hydroxybenzophenone is 0.013. This is fairly close to the 0.02 reported by Beckett and Porter (27) considering all the uncertainties in the present calculation.

It was found that as little as 0.1% triethylamine in the 2-propanol (mole ratio $1:1.82 \times 10^{-3}$) increased the rate of disappearance to 3.8 mmol/h, a 30% increase. Five percent added triethylamine increased the rate to 5.78 mmol/h. In neat 2-propanol there are two products as shown by t.l.c. The principal one is the corresponding pinacol. Enough of the minor could not be isolated for identification. Whenever there is triethylamine present there are three products besides the pinacol, one of them being the coupling product between the amine derived radical and the ketyl radical of the *p*-hydroxybenzophenone. Coupling in the presence of amines has been pointed out by Cohen *et al.* (5).

4,4′-Dihydroxybenzil Irradiations

Solutions of 4,4′-dihydroxybenzil in 2-propanol, 1:1 (v/v) cyclohexane:2-propanol, cyclohexane, and dimethylformamide were irradiated for 3 h. No significant changes were observed by the use of t.l.c. No reaction was found after a 2 h irradiation in a 1:1 (v/v) 2-propanol:triethylamine solution. Reaction occurred in a mixed solvent of cyclohexane:2-propanol, 5:1, and in neat triethylamine. In both of these solvents, however, the solubility was so low (approximately 2 m*M*) that product isolation was not attempted.

In two benzils studied, small amounts of triethylamine have a marked effect on the kinds of products and their relative amounts. Association between the amine and benzil seems to play an important but not well defined role. In the case of benzil itself the amine definitely complexes the intermediate ketyl radical.

To see if the same effect could be observed

Can. J. Chem. Downloaded from www.nrcresearchpress.com by 210.87.254.42 on 09/05/12
For personal use only.

TABLE 8. 4-Hydroxybenzil photolysis in triethylamine: reaction conditions,* products, and rates

Run	Concentration (m*M*)	Time (min)	Lost (mmol)	Rate (mmol/h)	Products as % of 4-hydroxybenzil lost				
					4-OH-Benzoin	4,4′-Di-OH-benzil	Benzaldehyde	Benzoic acid	High mol. wt. compounds†
44	8.0	16.5	0.22	0.8	58.5	11.3	5.6	5.6	19
45	22.0	28.5	0.71	1.5	72.0	8.0	1.6	4.6	14
46	49.5	36.0	1.65	2.8	77.2	7.0	1.7	3.8	12
47	70.8	52.0	2.50	2.9	75.5	2.4	0.4	3.8	18
48	93.2	75.0	3.00	2.4	70.5	2.0	0.2	12.7	15
49	50.0	25.0	0.60	1.5	70.0	8.5	2.1	4.0	15

*Volume was 250 ml except for run 49 which was 50 ml. All runs were nitrogen flushed except 49, which was degassed using a stopcock. The temperature was 25–30°.
†Obtained by difference.

TABLE 9. Effect of varying the triethylamine/2-propanol ratio on the photoreaction of 4-hydroxybenzil*

Run	2-Propanol (*M*)	Et_3N (*M*)	Sample (m*M*)	Time (min)	Lost (mmol)	Rate (mmol/h)	Products as % of 4-hydroxybenzil lost†		
							4-Hydroxybenzoin	4,4′-Di-OH-benzil	Benzoic acid
50	12.90	0.07	47.0	26.0	0.0	0.0	0.0	0.0	0.0
51	12.35	0.36	48.8	25.5	0.27	0.62	61.5	—‡	6.0
52	10.00	1.80	49.5	26.0	0.49	1.13	77.2	7.0	—
53	6.50	3.60	49.5	25.0	0.75	1.70	80.0	5.0	—
54	0.0	7.22	51.2	26.3	0.43	1.00	76.0	8	3.5

*The volume was 50 ml for all runs. All runs were helium flushed.
†Benzaldehyde was not measured.
‡— Not measured.

TABLE 10. Effect of triethylamine on biacetyl photoreduction in 2-propanol*

Run	Volume % Et_3N	Et_3N added (mol)	Biacetyl (mol)	Biacetyl / Et_3N	% Converted to biacetyl pinacol
55	0.0	0.0	0.250	—	100.0
56	0.1	2.15×10	0.150	69.6	15.8
57	0.5	1.08×10	0.150	13.9	7.9
58	1.0	2.15×10	0.150	7.0	1.4
59	10.0	2.15×10	0.150	0.7	0.0

*The volume was 500 ml 2-propanol in 55 and 300 in the rest. All solutions were 0.5 *M* biacetyl in 2-propanol with the amine added after. All runs were inert gas flushed. Temperature was 34–36°.

in a non-benzil system a few runs were carried out using biacetyl. These results are shown in Table 10.[5] All measurements were made by visual comparison of the intensity of the t.l.c. spots with those of standard solutions of biacetyl-pinacol at different concentrations and are therefore very approximate.[6] It appears that small amounts of triethylamine also cause a marked suppression of the production of biacetyl pinacol. This result is apparently opposite to that of Turro and Engel (28) who isolated biacetyl pinacol as a major product in the photolysis of biacetyl in tri-*n*-propyl amine. These results would indicate that the ketyl radical from biacetyl is also being complexed by triethylamine, preventing formation of the pinacol. This would be true whether the biacetyl pinacol is formed from dimerization of two ketyl radicals or some other mechanism involving the ketyl radicals. The reaction was carried to disappearance of the yellow color of biacetyl and therefore was not simply quenching of the reaction by the triethylamine.

Possible association in the ground state was checked in the same way as with the benzils. Triethylamine (0.359 mmol) was added to *t*-butyl alcohol and 0.332 mmol calculated from the freezing point depression. Biacetyl added: 0.575. Calculated: 0.725 mmol. Amine (0.359 mmol) and biacetyl (0.575 mmol) were added together for a total of 0.934 mmol. A value of 1.09 mmol was calculated from the freezing point depression which is very close to the sum of the individual calculated values. It was concluded that unlike the benzils there is no association in the ground state. Davidson and Wilson (25) suggest that the association of triethylamine with the ketyl radical of benzophenone and of fluorenone involves the hydroxy group of the radical so the apparent association with the radical but not biacetyl itself is consistent with this.

[5]These runs were made by Miss Mary Carol Losier.

[6]The spots were visualized with a diphenylpicrylhydrazyl spray and the densitometer could not be used.

The authors are pleased to acknowledge support by the National Research Council of Canada for this work and by the St. Francis Xavier University Council for Research for partial summer support of Miss Losier.

1. S. G. COHEN and R. J. BAUMGARTEN. J. Am. Chem. Soc. **87**, 2996 (1965).
2. R. S. DAVIDSON. Chem. Commun. 575 (1966).
3. S. G. COHEN and JACOB I. COHEN. J. Am. Chem. Soc. **89**, 164 (1967).
4. R. S. DAVIDSON and P. F. LAMBETH. Chem. Commun. 1265 (1967).
5. S. G. COHEN, N. STIEN, and HELEN M. CHAO. J. Am. Chem. Soc. **90**, 521 (1968).
6. S. G. COHEN and J. I. COHEN. J. Phys. Chem. **72**, 3782 (1968).
7. S. G. COHEN and J. B. GUTTENPLAN. Tetrahedron Lett. 5353 (1968).
8. R. A. CALDWELL. Tetrahedron Lett. 2121 (1969).
9. J. B. GUTTENPLAN and S. G. COHEN. Tetrahedron Lett. 2125 (1969).
10. S. G. COHEN, M. D. SALTZMAN, and J. B. GUTTENPLAN. Tetrahedron Lett. 4321 (1969).
11. S. G. COHEN, and A. D. LITT. Tetrahedron Lett. 837 (1970).
12. I. H. LEAVER. Tetrahedron Lett. 2333 (1971).
13. A. H. BLATT. Organic syntheses, Coll. Vol. 1. John Wiley and Sons. 1947. p. 87.
14. J. N. SOMIN and S. G. KUZNETZOV. Khim. Nauka i Prom. **4**, 801 (1959). Chem. Abstr. **54**, 10950*h* (1960).
15. D. L. BUNBURY and TZE TANG CHAUNG. Can. J. Chem. **47**, 2045 (1969).
16. (*a*) M. B. RUBIN and J. M. BEN BASS. Tetrahedron Lett. 3403 (1971). (*b*) D. J. COOPER and L. N. OWEN. J. Chem. Soc. C, 533 (1966).
17. C. G. HATCHARD and C. A. PARKER. Proc. Roy. Soc. A-235, 578 (1956).
18. G. E. GREAM, J. C. PAICE, and B. S. J. USZYNSKI. Chem. Commun. 895 (1970).

Can. J. Chem. Downloaded from www.nrcresearchpress.com by 210.87.254.42 on 09/05/12
For personal use only.

19. G. O. SCHENCK, G. BEHRENS, and E. ROSELIUS. Tetrahedron Lett. 5185 (1970).
20. S. G. COHEN and W. V. SHERMAN. J. Am. Chem. Soc. **85**, 1642 (1963).
21. R. S. DAVIDSON, P. F. LAMBETH, F. A. YOUNIS, and R. WILSON. J. Chem. Soc. C, 2203 (1969).
22. H. E. STAPELFELT and S. P. PERONE. Anal. Chem. **41**, 628 (1969).
23. S. G. COHEN and R. J. BAUMGARTEN. J. Am. Chem. Soc. **89**, 3471 (1967).
24. S. G. COHEN and H. M. CHAO. J. Am. Chem. Soc. **90**, 165 (1968).
25. R. S. DAVIDSON and R. WILSON. J. Chem. Soc. B, 71 (1970).
26. R. S. DAVIDSON and P. F. LAMBETH. Chem. Commun. 511 (1968).
27. A. BECKETT and G. PORTER. Trans. Faraday Soc. **59**, 2051 (1963).
28. N. J. TURRO and R. ENGEL. J. Am. Chem. Soc. **91**, 7113 (1969).
29. Deutschen Chemischen Gesellschaft. Beilstein. 1st. ed. Vol. 8. Julius Springer, Berlin. p. 329.
30. J. R. A. POLLOCK and R. STEVENS. Dictionary of organic compounds. 4th ed. Eyre and Spottiswoode Ltd. 1965. p. 1789.
31. S. WEISL. Monatsh Chem. **26**, 992 (1905).
32. J. H. GORVIN. Nature, **161**, 208 (1948).
33. A. FRIEDMAN *et al.* J. Org. Chem. **24**, 516 (1959).

Can. J. Chem. Downloaded from www.nrcresearchpress.com by 210.87.254.42 on 09/05/12
For personal use only.

Can. J. Chem. Downloaded from www.nrcresearchpress.com by 210.87.254.105 on 09/05/12
For personal use only.

Reaction of *N*-Methyl-4-(2′-octoxy)pyridinium Iodide with Silver Oxide. Evidence for a Mechanism Involving a Pseudobase Intermediate

G. H. SCHMID AND A. W. WOLKOFF[1]

Department of Chemistry, University of Toronto, Toronto 181, Ontario

Received March 9, 1972

The reaction of optically active *N*-methyl-4-(2′-octoxy)pyridinium iodide with silver oxide results in the formation of optically active 2-octanol with 91% retention of configuration. A mechanism involving a pseudobase intermediate is consistent with this result.

La réaction de l'iodure de *N*-méthyl (octoxy-2′)-4-pyridinium optiquement actif avec l'oxyde d'argent a pour résultat la formation d'octanol-2 optiquement actif avec 91% de rétention de configuration. Un mécanisme faisant intervenir un intermédiaire pseudo-base est compatible avec ce résultat.

Canadian Journal of Chemistry, **50**, 2511 (1972)

In connection with a study of the mechanism of the thermal elimination reaction of *N*-methyl 4-alkoxypyridinium iodides (1, 2), we wanted to prepare the corresponding hydroxides. An attempt was made to prepare *N*-methyl-4-(2′-octoxy)pyridinium hydroxide (**1***b*) by treatment of the methiodide (**1***a*) with silver oxide in water, in much the same manner (3) that alkyltrimethylammonium iodides are converted to quaternary alkyltrimethylammonium hydroxides. This procedure did not yield the expected hydroxide but instead gave 2-octanol, indicating cleavage of the heteroaromatic ether.

This alcohol can arise by any (or a combination) of the three mechanisms shown in Scheme 1. Pathway 1 involves solvolysis of the substrate via a carbonium ion (S_N1), a route that was proposed by Vogel and Roberts (4) for the solvolysis of cyclopropylcarbinyl derivatives in ethanol. Nucleophilic attack by hydroxide ion (S_N2) at the secondary carbon (pathway 2) leads directly to 2-octanol. A third possibility involves attack of hydroxide ion on the pyridine ring (S_NAr) leading to intermediate **2**, which can then subsequently decompose to give 2-octanol. A mechanism involving nucleophilic displacement by iodide ion on the alkyl group is ruled out by the results of pyrolysis of *N*-methyl-4-alkoxypyridinium iodides (1, 2).

In order to determine which route was operative, the *N*-methyl-4-alkoxypyridinium iodide derived from optically active 2-octanol was synthesized. In Scheme 1, pathway 1 should lead to largely racemized alcohol. Pathway 2 should result in 2-octanol of inverted configuration, while pathway 3 should lead to an alcohol with retained configuration.

We wish to report that treatment of optically active methiodide (**1***a*) with silver oxide in cold water gave a 17% yield of optically active 2-octanol with 91% retention of configuration. Since the reaction proceeds with a high reten-

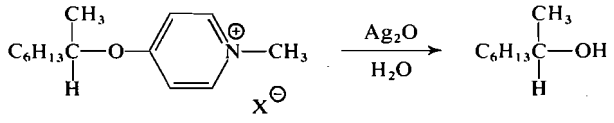

1

a X = I
b X = OH

[1]Holder of an NRCC Scholarship, 1968–1971.

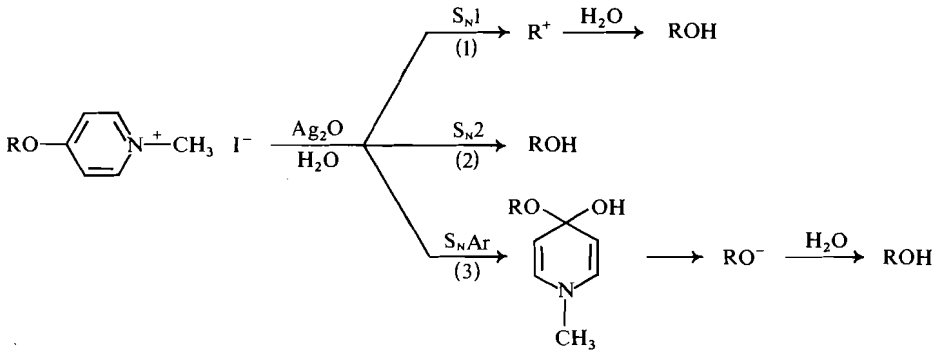

2

SCHEME 1. Possible mechanisms for cleavage of *N*-methyl-4-(2′-octoxy)pyridinium iodide.

tion of configuration, it may be concluded that little or no C_α—O bond breaking occurs, implying that pathway 3 is the major route for the formation of alcohol.

The reactions of aromatic nitro compounds with base have been shown (5) to involve Meisenheimer complexes. *N*-Alkyl derivatives would be expected to form similar complexes since the *N*-alkyl aza group and a nitro substituent both withdraw electrons from the ring by an inductive and conjugative mechanism. Evidence in support of such intermediates has been summarized by Illuminati (6). Recently Bunting and Meathrel (7) have presented evidence of the formation of pseudobases by the *N*-methyl cations of diazanaphthalenes. Our results are in accord with such a mechanism and indicate that this is the major route to the formation of 2-octanol in the hydroxide ion cleavage of *N*-methyl-4-(2′-octoxy)pyridinium iodide.

Experimental

Optical rotations were determined by means of a Perkin–Elmer 141 Polarimeter. Optically active 2-octanol was prepared by the method of Vogel (8). Elemental analyses were carried out by M. B. Gygli of Toronto, Ontario.

4-(d-2′-Octoxy)pyridine

This compound was prepared by a slight modification (2) of the method of Vogel and Roberts (4) to give 0.72 (76% yield) of the 4-alkoxypyridine, b.p. 98° (0.140 mm).

Anal. Calcd. for $C_{13}H_{21}ON$: C, 75.32; H, 10.21; N, 6.76. Found: C, 75.39; H, 10.29; N, 6.92.

Reaction of N-Methyl-4-(d-2′-octoxy)pyridinium Iodide with Ag_2O

To 0.72 g (3.48 mmol) of 4-(*d*-2′-octoxy)pyridine was added excess methyl iodide (3 ml; 48.1 mmol). After standing overnight, the excess methyl iodide was removed under vacuum to give 1.40 g of an orange oil. Previous work (2) with this material showed that the oil could not be induced to crystallize and so the material was used without further purification. To this oil was added 10 ml of water and 1.86 g (8.05 mmol) of silver oxide. The solution was allowed to stir for 4 h in an ice bath and then filtered. Distillation of the filtrate gave two layers. The distillate was extracted with ether, and the combined ether extracts dried over anhydrous magnesium sulfate. The ether was removed under vacuum to give 79 mg of 2-octanol, $[\alpha]_D^{23}$ 7.94 (*c* 4.0, EtOH), corresponding to 91% retention of configuration. No further purification of the material was attempted, meaning that 91% is a lower limit on the percent retention of configuration.

Continued support by the National Research Council of Canada is gratefully acknowledged.

1. A. W. WOLKOFF. Ph.D. Thesis. University of Toronto, Toronto, Ontario, 1971.
2. A. W. WOLKOFF and G. H. SCHMID. Can. J. Chem. **50**, 1191 (1972).
3. A. C. COPE, R. A. PIKE, and C. F. SPENCER. J. Am. Chem. Soc. **75**, 3213 (1953).
4. M. VOGEL and J. D. ROBERTS. J. Am. Chem. Soc. **88**, 2262 (1966).
5. M. J. STRAUSS. Chem. Rev. **70**, 667 (1970).
6. G. ILLUMINATI. *In* Advances in heterocyclic chemistry. Vol. 3. *Edited by* A. R. Katritzky. Academic Press, New York. 1964. p. 360.
7. J. W. BUNTING and W. G. MEATHREL. Can. J. Chem. **50**, 917 (1972).
8. A. I. VOGEL. Practical organic chemistry. 3rd ed. Longmans, London. 1961. p. 505.

Can. J. Chem. Downloaded from www.nrcresearchpress.com by 210.87.254.105 on 09/05/12
For personal use only.

The Thermolytic Generation of Benzofuran from *o*-Hydroxyacetophenone

O. A. MAMER

The Mass Spectrometry Unit, Royal Victoria Hospital, Department of Experimental Medicine, McGill University, Montreal, Quebec

Received April 4, 1972

The flash thermolysis of *o*-hydroxyacetophenone in a low pressure inert carrier occurs with an apparent rearrangement and subsequent elimination of water to yield benzofuran. A competing minor thermolytic pathway involves the elimination of the elements of acetaldehyde to yield cyclopentadienylidenecarbonyl. There appears to be little similarity between the mechanisms of the thermal and electron impact fragmentations.

La thermolyse flash de l'*o*-hydroxyacétophénone, dans un gaz vecteur inerte à basse pression, se produit avec un réarrangement apparent et une élimination subséquente d'eau pour conduire au benzofurane. Une voie thermolytique mineure et compétitive fait intervenir l'élimination de la portion acétaldéhyde avec obtention du cyclopentadiénylidéne carbonyle. De petites similitudes apparaissent entre les mécanismes de fragmentation thermique et ceux issus de l'impact électronique.

Canadian Journal of Chemistry, **50**, 2513 (1972)

Cyclopentadienylidenecarbonyl (**1**) has been shown (1) to be the major thermolytic fragment of salicylaldehyde (Scheme 1). It was therefore anticipated that *o*-hydroxyacetophenone (**2**) might thermally fragment by a route analogous to Scheme 1.

An unexpected rearrangement and subsequent elimination of water represent the major pathway for the thermolysis of **2** in the interval 400–1100° and form the substance of this brief report.

Thermolyses of **2** were conducted in two modes, both previously described in detail (1). The first was in a low pressure helium flow in a quartz reactor attached through a helium separator to the ion source of a mass spectrometer. Slow scans at low ionizing energy (12 eV) of the furnace effluent permitted the detection of molecular ions of thermal fragments. Figure 1 shows the variation of the intensities of significant masses with furnace temperature.

The second thermolytic mode was semi-preparative in nature and involved the thermolysis of **2** in a low pressure argon carrier in a hot filament reactor. The reactor effluent was rapidly quenched by bubbling through methanol at −78°. The methanol solution was then analyzed by coupled gas chromatography–mass spectrometry (Fig. 2). Individual thermolytic runs were conducted over a series of filament temperatures from 600° (onset of incandescence) to the filament limit of approximately 1100°. Figure 2 represents the product analysis for a filament temperature of approximately 800°. With increasing wire temperature, the ratio of **3** to **2** and the proportion of hydrocarbon products both increase.

The consistently reproducible initial increase in the apparent intensity of *m/e* 136 (Fig. 1) with increasing furnace temperature suggests that **2** begins to rearrange above 400° to an intermediate having an increased ionization efficiency at 12 eV that subsequently decomposes above 700°. The rearrangement may involve acetyl group enolization and cyclization prior to the elimination of water. As *m/e* 136 decomposes, a fragment with *m/e* 118 is produced corresponding to the molecular ion of benzofuran (**3**) detected in the semi-preparative experiment. Relatively smaller increases in *m/e* 92

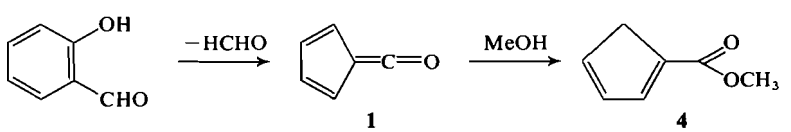

1 **4**

SCHEME 1

Can. J. Chem. Downloaded from www.nrcresearchpress.com by 210.87.254.40 on 09/05/12
For personal use only.

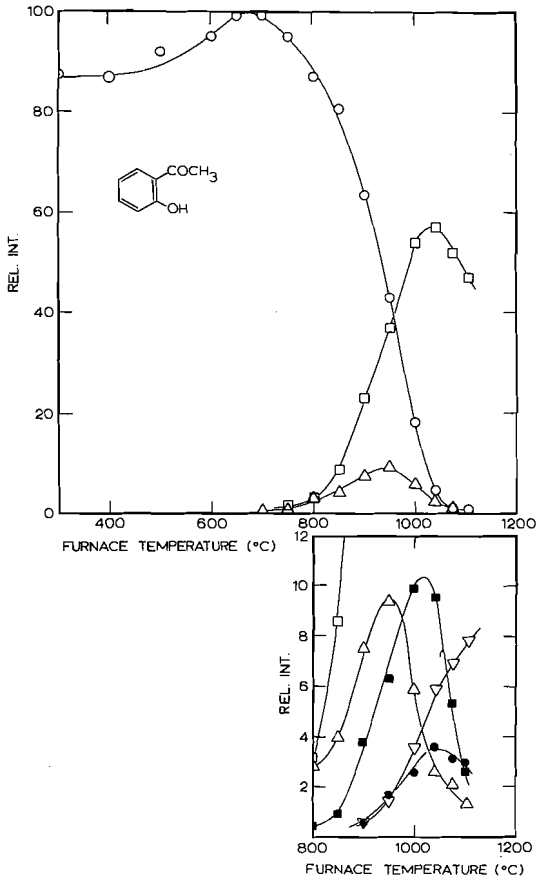

FIG. 1. Relative intensity of apparent molecular ions at 12 eV in furnace effluent *vs.* furnace temperature: ○, *m/e* 136, **2**; □, *m/e* 118, **3**; △, *m/e* 92, **1**; ■, *m/e* 130, $C_{10}H_{10}$; ●, *m/e* 64, **5**; ▽, *m/e* 66 and 128 coinciding, cyclopentadiene and naphthalene, respectively.

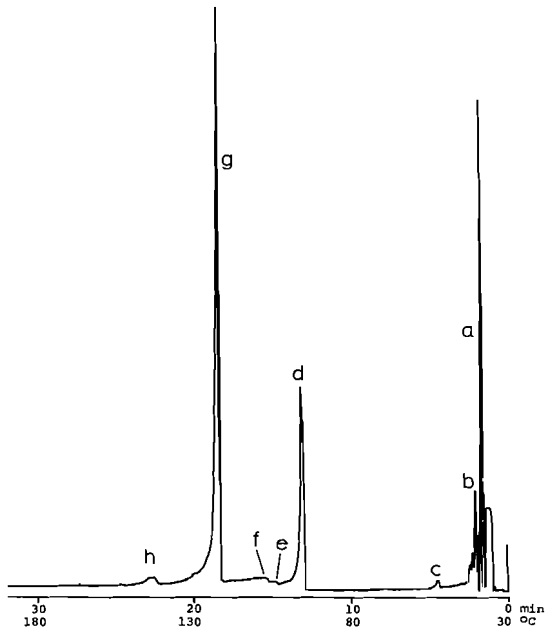

FIG. 2. Gas chromatographic record of the analysis by coupled g.c.–m.s. (LKB 9000) of the preparative scale methanol-trapped thermolysate of **2**. Analytical conditions: column, 72 × 0.25 in. glass, 3% OV-1 on chromosorb W, temperature programmed from 30 + 5°/min; injector and separator 280°; helium flow 35 ml/min; ion source, 290°, 70 eV at 60 μA. Peak assignments, confirmed by direct comparisons with authentic compounds: *a*, methanol tail; *b*, benzene; *c*, toluene; *d*, benzofuran (**3**); *e*, phenol; *f*, carboxymethylcyclopentadiene (**4**); *g*, *o*-hydroxyacetophenone (**2**); *h*, 1- and 2-methylnaphthalene. Peak *d* accounts for 73% of the integrated voltatile components in the preparative thermolysate (methanol and **2** excluded).

and the detection of a small yield of carboxymethylcyclopentadiene (**4**, the methanol adduct of **1**) confirm a minor thermolytic pathway of **2** via **1** and probably acetaldehyde.

In a manner similar to that reported in the thermolysis of salicylaldehyde (1), an increase in *m/e* 64 at the expense of *m/e* 92 supports the proposal of DeJongh and Brent (2) that at elevated temperatures **1** decarbonylates to yield cyclopentadienylidene (**5**). This same decarbonylation reaction has been noted in the electron-impact fragmentation of *o*-nitrobenzamide and *o*-nitroanisole (3).

Coincident with the rise of *m/e* 66, an ion at *m/e* 128 is probably naphthalene produced by the rearrangement of fulvalene (**6**), the dimer of **5**. In addition, the rise and fall of *m/e* 130 ($C_{10}H_{10}$ by % M + 1 and % M + 2 measurements) suggests that **6** may suffer addition of 1 mol of hydrogen and further thermolyze. At the upper limit of the furnace *m/e* 132 and 136 corresponding to $C_{10}H_{12}$ and $C_{10}H_{16}$ also show increases, further providing for the removal of *m/e* 130 by further hydrogenation.

Scheme 2, consistent with the experimental data, is proposed to account for the thermolysis of **2**. 2,3-Dihydrobenzofuran-3-ol (**7**) may be a transient species formed by a thermally induced intra-molecular addition of the phenolic hydroxyl moiety to the enolic unsaturation. If **7** plays an intermediate role in the formation of **3** from **2**, it probably would not survive the high

Can. J. Chem. Downloaded from www.nrcresearchpress.com by 210.87.254.40 on 09/05/12
For personal use only.

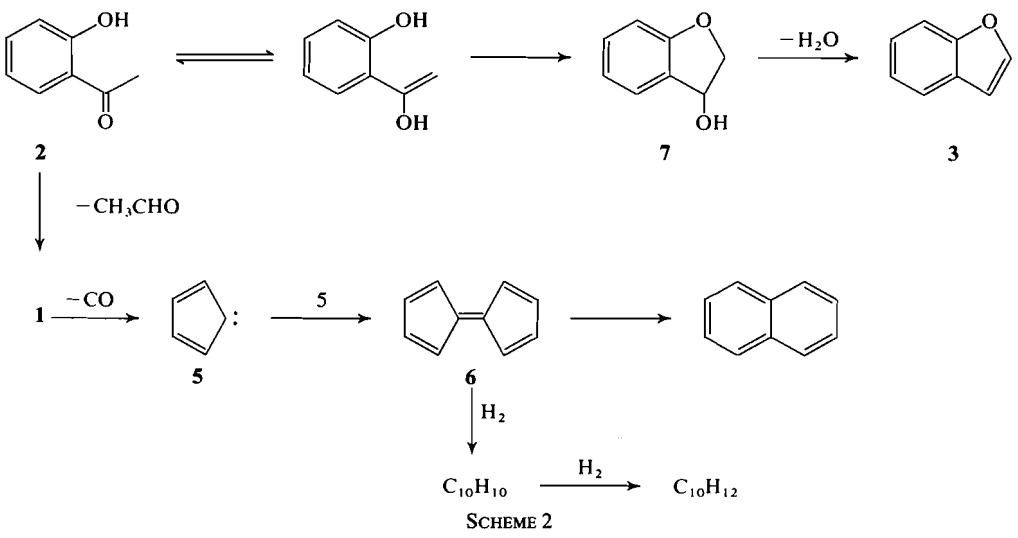

SCHEME 2

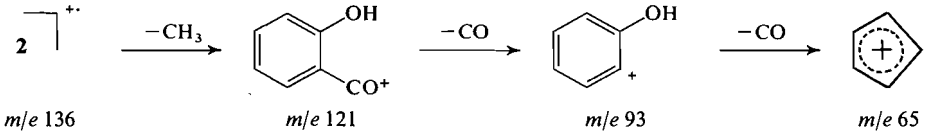

SCHEME 3

temperatures of the gas chromatographic inlet system in the analysis of the preparative thermolysate. Attempted distillation of **7** is reported (4) to result in the formation of **3** via water loss.

Scheme 3 outlines the metastable confirmed principal fragmentation route for radical cation **2** (mass spectrum, Fig. 3) and bears relatively little similarity to the thermal route for neutral **2**, particularly in the major initial processes.

There is an interesting parallel, however, between the neutral sequence:

$$136 \rightarrow 92 + CH_3CHO$$
$$92 \rightarrow 64 + CO$$

and the cationic sequence:

$$136^+ \rightarrow 121^+ + CH_3$$
$$121^+ \rightarrow 93^+ + CO$$
$$93^+ \rightarrow 65^+ + CO$$

Masses 93 and 65 might be considered to be protonated (and therefore cationic) 92 and 64, respectively. In the neutral fragmentation, however, there is no corresponding apparent accumulation of mass 120 (*i.e.* the deprotonated *m/e* 121 which is the 70 eV base peak of **2**). On the other hand there appears to be no cationic analogy to the thermal rearrangement and elimination of water. This fragmentation reac-

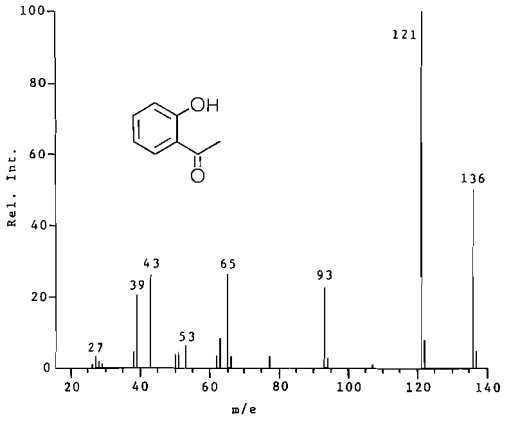

FIG. 3. Mass spectrum of *o*-hydroxyacetophenone at 70 eV. Relative intensities are insensitive to ion source temperature in the interval 150–310°.

Can. J. Chem. Downloaded from www.nrcresearchpress.com by 210.87.254.40 on 09/05/12
For personal use only.

tion of the neutral species appears to be the major thermolytic route for **2** while there is only a very weak *m/e* 118 (0.47% at 70 eV and 0.24% at 15 eV) for this same elimination for the radical cation of **2**.

The LKB 9000 GC mass-spectrometer used in this work was granted by the Medical Research Council of Canada (grant no. ME 3720) to the Faculty of Medicine of McGill University. Several helpful suggestions made by Dr. E. Hedaya in the course of this work are gratefully acknowledged.

1. O. A. MAMER. Can. J. Chem. **49**, 3602 (1971).
2. D. C. DEJONGH and D. A. BRENT. J. Org. Chem. **35**, 4204 (1970).
3. F. BENOIT and J. L. HOLMES. Org. Mass Spectrom. **3**, 993 (1970).
4. B. HOLT and P. A. LOWER. Tetrahedron Lett. **7**, 683 (1966).

Can. J. Chem. Downloaded from www.nrcresearchpress.com by 210.87.254.40 on 09/05/12
For personal use only.

Collisional Deactivation Rates of Electronically Excited Molecular Ions. III. O_2^+ ($b^4\Sigma_g^-$)

G. I. MACKAY, J. P. ANGLESEY, AND R. E. MARCH
Department of Chemistry, Trent University, Peterborough, Ontario

Received March 21, 1972

Electron beam excitation of oxygen was utilized to produce ions in the $b^4\Sigma_g^-$ state. Rate constants for the deactivation of $O_2^+(b^4\Sigma_g^-)$ for each of O_2 and N_2 were determined. Charge transfer is a possible mode of deactivation.

L'excitation de l'oxygène par un faisceau d'électrons a été utilisé pour produire des ions dans l'état $b^4\Sigma_g^-$. Les constantes de vitesse pour la désactivation de $O_2^+(b^4\Sigma_g^-)$ pour chaque O_2 et N_2 ont été déterminées. Le transfert de charge est un mode de désactivation possible.

Canadian Journal of Chemistry, **50**, 2516 (1972)

Thermal energy positive ion–neutral deactivation rate constants have been determined for electronically excited molecular oxygen ions, produced in a high energy electron beam. The apparatus has been described previously (1). Deactivation rate constants are presented for the O_2^+ ($b^4\Sigma_g^-$) ion deactivated by oxygen and nitrogen.

There are three known excited state transitions of O_2^+. The Hopfield system ($c^4\Sigma_u^- \rightarrow b^4\Sigma_g^-$) was not observed in our apparatus above 2000 Å. The first negative (1N) system ($b^4\Sigma_g^- \rightarrow a^4\Pi_u$) occurred strongly and the second negative (2N) system ($A^2\Pi_u \rightarrow X^2\Pi_g$) was observed also. It has been shown previously (2) that deactivation of some diatomic molecular ions possessing a single vibrational quantum appears to proceed at a rate which is slower by a factor of 2–3 in comparison to the respective rates for ions possessing zero or two such quanta. In order to avoid this effect with O_2^+, should it exist, the $\Delta v = -2$ band of the 1N system was selected for deactivation studies. The data, which are shown in Fig. 1, were treated as before, but were obtained with a slight modification. Whereas the signal intensity was previously taken as the integrated areas as recorded, in these experiments the signal was fed to a counter and the time to attain a given total count was recorded. This time is inversely proportional to the intensity.

The deactivation rate constant for parent molecules is obtained as a product with the radiative lifetime of the excited ion. Early determinations (3) of the lifetimes of the $v' = 0$, 1, and 2 levels were quite long and of the order of 1.2 μs. More recent work (4) suggests that these were lifetimes of cascade components and that the true lifetime of the $b^4\Sigma_g^-$ state is 170 ± 20 ns for $0 \leqslant v \leqslant 7$, while that of the $c^4\Sigma_u^-$ state is inferred to be 1.2 ± 0.2 μs.

On the basis of this latter value for the lifetime of the $b^4\Sigma_g^-$ state, the deactivation rate constant for parent molecules, k_1 was found to

tion of the neutral species appears to be the major thermolytic route for **2** while there is only a very weak *m/e* 118 (0.47% at 70 eV and 0.24% at 15 eV) for this same elimination for the radical cation of **2**.

The LKB 9000 GC mass-spectrometer used in this work was granted by the Medical Research Council of Canada (grant no. ME 3720) to the Faculty of Medicine of McGill University. Several helpful suggestions made by Dr. E. Hedaya in the course of this work are gratefully acknowledged.

1. O. A. MAMER. Can. J. Chem. **49**, 3602 (1971).
2. D. C. DEJONGH and D. A. BRENT. J. Org. Chem. **35**, 4204 (1970).
3. F. BENOIT and J. L. HOLMES. Org. Mass Spectrom. **3**, 993 (1970).
4. B. HOLT and P. A. LOWER. Tetrahedron Lett. **7**, 683 (1966).

Can. J. Chem. Downloaded from www.nrcresearchpress.com by 210.87.254.105 on 09/05/12
For personal use only.

Collisional Deactivation Rates of Electronically Excited Molecular Ions. III. O_2^+ ($b^4\Sigma_g^-$)

G. I. MACKAY, J. P. ANGLESEY, AND R. E. MARCH
Department of Chemistry, Trent University, Peterborough, Ontario

Received March 21, 1972

Electron beam excitation of oxygen was utilized to produce ions in the $b^4\Sigma_g^-$ state. Rate constants for the deactivation of $O_2^+(b^4\Sigma_g^-)$ for each of O_2 and N_2 were determined. Charge transfer is a possible mode of deactivation.

L'excitation de l'oxygène par un faisceau d'électrons a été utilisé pour produire des ions dans l'état $b^4\Sigma_g^-$. Les constantes de vitesse pour la désactivation de $O_2^+(b^4\Sigma_g^-)$ pour chaque O_2 et N_2 ont été déterminées. Le transfert de charge est un mode de désactivation possible.

Canadian Journal of Chemistry, **50**, 2516 (1972)

Thermal energy positive ion–neutral deactivation rate constants have been determined for electronically excited molecular oxygen ions, produced in a high energy electron beam. The apparatus has been described previously (1). Deactivation rate constants are presented for the O_2^+ ($b^4\Sigma_g^-$) ion deactivated by oxygen and nitrogen.

There are three known excited state transitions of O_2^+. The Hopfield system ($c^4\Sigma_u^- \rightarrow b^4\Sigma_g^-$) was not observed in our apparatus above 2000 Å. The first negative (1N) system ($b^4\Sigma_g^- \rightarrow a^4\Pi_u$) occurred strongly and the second negative (2N) system ($A^2\Pi_u \rightarrow X^2\Pi_g$) was observed also. It has been shown previously (2) that deactivation of some diatomic molecular ions possessing a single vibrational quantum appears to proceed at a rate which is slower by a factor of 2–3 in comparison to the respective rates for ions possessing zero or two such quanta. In order to avoid this effect with O_2^+, should it exist, the $\Delta v = -2$ band of the 1N system was selected for deactivation studies. The data, which are shown in Fig. 1, were treated as before, but were obtained with a slight modification. Whereas the signal intensity was previously taken as the integrated areas as recorded, in these experiments the signal was fed to a counter and the time to attain a given total count was recorded. This time is inversely proportional to the intensity.

The deactivation rate constant for parent molecules is obtained as a product with the radiative lifetime of the excited ion. Early determinations (3) of the lifetimes of the $v' = 0$, 1, and 2 levels were quite long and of the order of 1.2 μs. More recent work (4) suggests that these were lifetimes of cascade components and that the true lifetime of the $b^4\Sigma_g^-$ state is 170 ± 20 ns for $0 \leqslant v \leqslant 7$, while that of the $c^4\Sigma_u^-$ state is inferred to be 1.2 ± 0.2 μs.

On the basis of this latter value for the lifetime of the $b^4\Sigma_g^-$ state, the deactivation rate constant for parent molecules, k_1 was found to

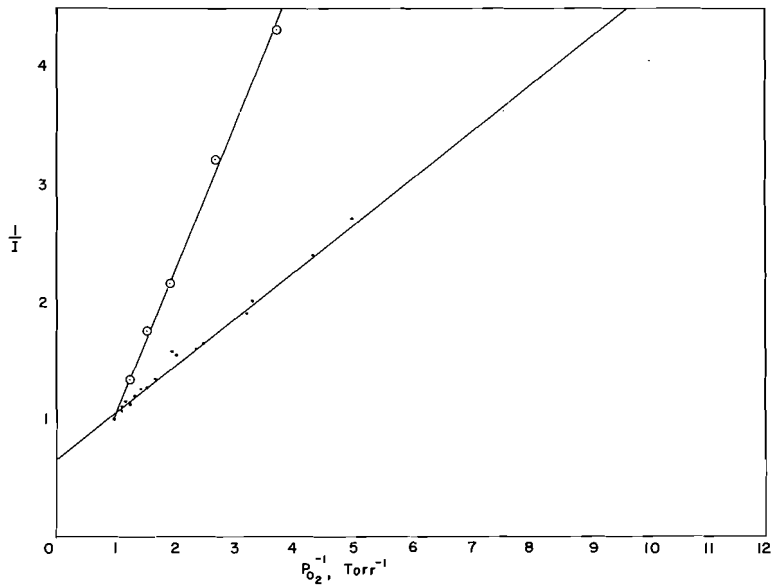

FIG. 1. Plot of the reciprocal intensity (arbitrary units) of the $\Delta v = -2$ band of the O_2 1N system *vs.* reciprocal oxygen pressure: dots, pure oxygen; circled dots, oxygen plus nitrogen, total pressure = 1 Torr.

be $18 \pm 6 \times 10^{10}$ l mol^{-1} s^{-1}. However, no attempt was made to determine the nature of the products. Therefore on the basis of the evidence available it was not possible to distinguish between various plausible contributing modes of deactivation, for example charge transfer.

$$[1a] \qquad O_2^+(b^4\Sigma_g^-)_{v' \geq 2} + O_2 \rightarrow O_2 + O_2^+(X) \qquad k_{1a}$$

or collision induced radiationless transitions, such as

$$[1b] \qquad O_2^+(b^4\Sigma_g^-) + O_2 \rightarrow O_2^+ A^2\Pi_u + O_2 \qquad k_{1b}$$

$$[1c] \qquad \rightarrow O_2^+ a^4\Pi_u + O_2 \qquad k_{1c}$$

Similarly for deactivation of the $b^4\Sigma_g^-$ state with nitrogen, it was not possible to distinguish between charge transfer,

$$[2a] \qquad O_2^+(b^4\Sigma_g^-) + N_2 \rightarrow N_2^+(X) + O_2 \qquad k_{2a}$$

collision induced radiationless transitions, such as

$$[2b] \qquad O_2^+(b^4\Sigma_g^-) + N_2 \rightarrow O_2^+ A^2\Pi_u + N_2 \qquad k_{2b}$$

$$[2c] \qquad \rightarrow O_2^+ a^4\Pi_u + N_2 \qquad k_{2c}$$

or atom exchange

$$[2d] \qquad O_2^+(b^4\Sigma_g^-) + N_2 \rightarrow NO^+(X) + NO \qquad k_{2d}$$

Reactions 2*a* and 2*d* are both exoergic to the extent of some 2.8 and 2.4 eV, respectively, for $b^4\Sigma_g^-$ state ion in the $v' = 2$ vibrational level. The total deactivation rate constant, k_2, was found to be $24 \pm 8 \times 10^{10}$ l mol^{-1} s^{-1}.

The total deactivation rate constants obtained are in fair numerical agreement with the theoretical values of the collision rate constant $k_c = 2\pi e(\alpha/\mu)^{1/2}$ where α is the polarizability of the neutral molecule and μ is the reactant reduced mass. For reaction 1, $k_c = 44 \times 10^{10}$ l mol^{-1} s^{-1} while for reaction 2, $k_c = 47 \times 10^{10}$ l mol^{-1} s^{-1}. It should be emphasized that although there is no clear reason for assuming that either rate constant should be equal to k_c, it is gratifying to note that k_c is not substantially exceeded.

The authors gratefully acknowledge the financial support of the National Research Council of Canada, Trent University (J.P.A.) and the Province of Ontario for a Graduate Fellowship (G.I.M.).

1. G. I. MACKAY and R. E. MARCH. Can. J. Chem. **49**, 1268 (1971).
2. G. I. MACKAY and R. E. MARCH. Can. J. Chem. **50**, 1 (1972).
3. M. JEUNEHOMME. J. Chem. Phys. **44**, 4253 (1966); E. H. FINK and K. H. WELGE. Z. Naturforsch. **23***a*, 358 (1968).
4. G. E. COPELAND. J. Chem. Phys. **54**, 3482 (1971).

Can. J. Chem. Downloaded from www.nrcresearchpress.com by 210.87.254.105 on 09/05/12
For personal use only.

Can. J. Chem. Downloaded from www.nrcresearchpress.com by 210.87.254.42 on 09/05/12
For personal use only.

Canadian Journal of Chemistry

Published by THE NATIONAL RESEARCH COUNCIL OF CANADA

VOLUME 50 AUGUST 15, 1972 NUMBER 16

The Structure of $Na_4P_2O_7$ at 22 °C

K. Y. LEUNG AND C. CALVO

Department of Physics, McMaster University, Hamilton, Ontario

Received January 5, 1972

At room temperature $Na_4P_2O_7$ crystallizes in the orthorhombic space group $P2_12_12_1$ with $a = 9.367(5)$, $b = 5.390(2)$, $c = 13.480(8)$ Å, and $z = 4$. The structure was refined by full-matrix least-squares using 1337 reflections measured with a Syntex Automatic diffractometer. The final R value is 0.022. The anion has nearly an eclipsed configuration with a P—O—P angle of 127.5(1)°. The two bridging P—O bond lengths are 1.631(2) and 1.642(2) Å with terminal P—O bond lengths averages of 1.512 and 1.514 Å on either side of the anion. Two of the four Na^+ ions are coordinated to five oxygen atoms while the remainder are coordinated to six oxygen atoms. The structure contains chains of cations with four nearly collinear Na^+ per cell paralleling the c axis. These are surrounded by six anions with the bridging oxygen atoms lying approximately at the corners of an octahedron with the P—P vector of the anion also paralleling the c axis. Adjacent anions along the c axis are separated by a pair of Na^+ ions.

A la température de la pièce, $Na_4P_2O_7$ cristallise sous la forme du groupe spatial $P2_12_12_1$ orthorhombique, où $a = 9.367(5)$, $b = 5.390(2)$, $c = 13.480(8)$ Å et $z = 4$. Nous avons raffiné la structure par la méthode de la matrice pleine par moindres carrés, au moyen de 1337 réflexions mesurées par un diffractomètre syntex automatique. La valeur finale de R est 0.022. L'anion possède une configuration quasi-éclipsée, l'angle P—O—P étant de 127.5(1)°. La longueur des deux liaisons P—O pontées est de 1.631(2) et 1.642(2) Å et la moyenne des liaisons P—O terminales est de 1.512 et 1.514 Å, d'un côté ou l'autre de l'anion. Deux parmi les quatre ions Na^+ sont coordonnés à cinq atomes d'oxygène tandis que les autres sont coordonnés à six atomes d'oxygène. La structure contient des chaînes de cations où quatre Na^+ par maille sont presque colinéaires et parallèles à l'axe c. Ils sont entourés de six anions et les atomes d'oxygène servant de pont sont situés approximativement aux coins d'un octaèdre, où le vecteur P—P de l'anion est aussi parallèle à l'axe c. Les anions adjacents le long de l'axe c sont séparés par des paires d'ions Na^+.

Canadian Journal of Chemistry, **50**, 2519 (1972)

Introduction

Although a large number of crystallographic studies have been devoted toward elucidating the phases and phase transformations of $M_2X_2O_7$ and MX_2O_7 systems, where X ions are tetrahedrally coordinated, the $M_4X_2O_7$ system has largely been ignored. Various members of this series show phase transformations, for example $Li_4P_2O_7$ (1), $Li_4As_2O_7$ (2), and $Na_4As_2O_7$ (3). However, $Na_4P_2O_7$ with four transformations, as determined by differential thermal analysis (4), thermal expansion (5) and recent crystallographic studies (6) seem to be the most complex.

Crystal Data for $Na_4P_2O_7$ at 22 °C:

$Na_4P_2O_7$ molecular weight = 265.91

Space group, $P2_12_12_1$; orthorhombic, $a = 9.367(5)$, $b = 5.390(2)$, $c = 13.480(8)$ Å;[1] $V = 680.58$ Å^3, $z = 4$, $\rho_c = 2.595$ g/cm^3, $\rho_m = 2.53$ g/cm^3.

Experiments

Crystals of $Na_4P_2O_7$ were grown from a melt prepared from $Na_4P_2O_7 \cdot 10H_2O$. The crystals varied from colorless to pale blue-green depending upon the run, and often occurred in the form of flakes.

The structure was determined with 493 unique data points obtained from integrated precession photographs taken with MoKα radiation. The trial structure was determined by direct methods using the procedures of Karle and Hauptman (7). This model was refined by weighted full-

[1]Determined from a least-squares fit of fifteen 2θ values measured with the Syntex Automatic diffractometer using MoKα radiation ($\lambda = 0.71069$ Å).

Can. J. Chem. Downloaded from www.nrcresearchpress.com by 210.87.254.42 on 09/05/12
For personal use only.

TABLE 1. Atomic parameters for $Na_4P_2O_7$ with estimated standard deviations in parentheses*

Atom	x	y	z	U_{11}	U_{22}	U_{33}	U_{12}	U_{13}	U_{23}
Na(1)	0.4725(1)	0.4992(2)	−0.01678(7)	0.0146(4)	0.0144(4)	0.01591(4)	0.0009(5)	−0.0006(3)	0.0008(4)
Na(2)	0.4919(1)	0.4848(2)	0.23603(7)	0.0197(5)	0.0193(5)	0.0180(4)	−0.0034(5)	0.0059(4)	−0.0019(5)
Na(3)	0.1221(1)	0.4961(2)	0.15454(7)	0.0165(5)	0.0198(5)	0.0179(4)	0.0006(5)	0.0023(3)	−0.0020(5)
Na(4)	0.6654(1)	−0.0368(2)	0.16744(8)	0.0161(5)	0.0161(5)	0.0210(4)	−0.0013(4)	0.0008(4)	−0.0006(4)
P(A)	0.30704(6)	0.0113(1)	−0.10609(4)	0.0088(2)	0.0091(2)	0.0082(2)	−0.0001(2)	−0.0001(2)	0.0001(2)
P(B)	0.31380(6)	−0.0223(1)	0.11128(4)	0.0090(2)	0.0100(2)	0.0083(2)	−0.0006(2)	0.0006(2)	0.0000(2)
O(CE)	0.3602(2)	0.0971(3)	0.0040(1)	0.0152(8)	0.0140(7)	0.0081(6)	−0.0051(6)	0.0002(5)	0.0000(6)
O(A1)	0.3444(2)	0.2338(3)	−0.1693(1)	0.025(6)	0.0119(7)	0.0132(7)	0.0005(6)	0.0004(6)	0.0052(6)
O(A2)	0.3953(2)	−0.2131(3)	−0.1339(1)	0.0179(9)	0.0119(7)	0.0140(7)	0.0055(7)	0.0019(6)	−0.0018(6)
O(A3)	0.1490(2)	−0.0447(4)	−0.1019(1)	0.0087(8)	0.0275(10)	0.0152(7)	−0.0019(7)	−0.0006(5)	−0.0043(8)
O(B1)	0.4264(2)	0.0803(4)	0.1805(1)	0.0122(8)	0.0241(9)	0.0115(7)	−0.0027(7)	−0.0035(5)	−0.0028(7)
O(B2)	0.3205(2)	−0.3017(3)	0.1009(4)	0.0205(9)	0.0093(7)	0.0206(8)	−0.0009(7)	0.0063(7)	0.0001(6)
O(B3)	0.1654(2)	0.0744(4)	0.1333(1)	0.0110(8)	0.0191(8)	0.0149(7)	0.0018(6)	0.0032(5)	−0.0023(6)

*U_{ij}'s in Å^2 are computed from $\beta_{ij} = 2\pi^2 b_i b_j U_{ij}$ where $T = \exp\{-[\beta_{11}h^2 + 2\beta_{12}hk + \ldots]\}$ appears in the structure factor expression and b_j are reciprocal lattice cell vectors.

Can. J. Chem. Downloaded from www.nrcresearchpress.com by 210.87.254.42 on 09/05/12
For personal use only.

matrix least-squares to a final R value of 0.109 with individual isotropic temperature factors.

A second data set, consisting of 1337 symmetry independent reflections, was recorded utilizing a Syntex automatic diffractometer and graphite monochromatized MoKα radiation. The crystal used was ground to a sphere of radius 0.25 mm. The peaks were scanned in a θ–2θ mode at a variable rate, from 2 to 24° per min depending upon the peak intensity. Data were recorded up to a sin θ/λ of 0.77 $Å^{-1}$. Backgrounds were measured at either side of the peak for the same period of time as the peak scan. Reflections whose intensity, corrected for background, exceeded 3σ were considered observed. The remaining reflections were assigned a maximum possible value of 3σ, with those whose apparent intensity was negative inserted only in the very last few cycles. The data were corrected for absorption, Lorentz and polorization effects. The final coordinates obtained with the film data were used as initial parameters and were refined by full matrix least-squares using a program written by Stephens for the CDC 6400. Atomic scattering factors curves for Na^+, P^{3+}, and O^- were taken from the International Tables for Crystallography (8). Unit weights were chosen since there seemed to be no systematic variation in $|F_o - F_c|$ with F_o. When a minimum had been obtained with isotropic temperature factors the refinement was completed with individual anisotropic thermal parameters. The final R value, determined when the maximum shift was less then 0.2σ, was 0.022 ($R\omega = \{\Sigma\,\omega(|F_o|-|F_c|)^2/\Sigma\,\omega F_o^2\}^{1/2} = 0.027$). The final atomic parameters are found in Table 1. Table 2 contains the calculated and observed structure factors.[2] Sixteen reflections too strong to be measured with the diffractometer are included in Table 2, but excluded from the refinement, with their film measured values. A final difference electron density map showed no residual peaks larger than 0.1 of an oxygen atom peak.

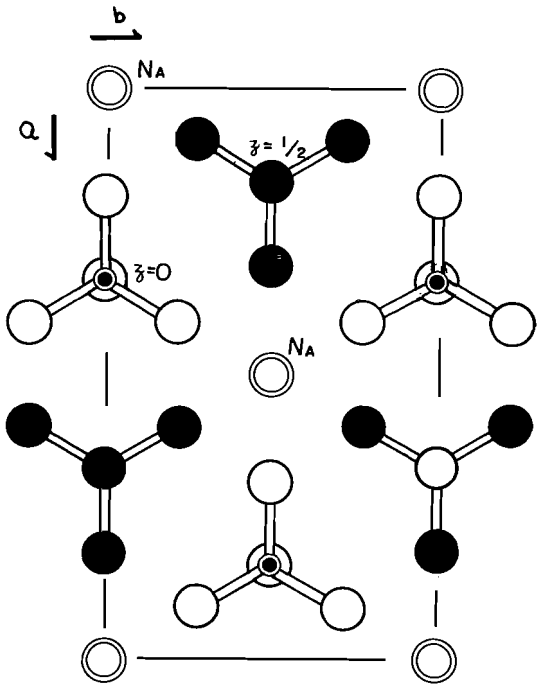

FIG. 1. The idealized structure of $Na_4P_2O_7$ projected onto the *ab* plane. The large circles represent oxygen atoms with the pyrophosphate anion in an eclipsed configuration. The large circles are oxygen atoms. Those bonded to the anion with the bridging oxygen atom at $z = 1/2$ are indicated by filled circles while those attached to the pyrogroup at $z = 0$ are shown as open circles. The small filled circles represent two superimposed phosphorus atoms. The Na ions collinear with these pyrogroups are not indicated.

Description of the Structure

The structure of anhydrous sodium pyrophosphate can be described as a deviant from a simple idealized structure shown in Fig. 1. This ideal structure consists of diphosphate ions formed by a pair of PO_4^{3-} groups sharing a bridging oxygen atom with a P—O—P angle of 180°. The oxygen atoms of the anion are in an eclipsed configuration as viewed down the P—P vector, with this vector paralleling the c axis. These anions lie in layers such that the bridging oxygen atoms lie at the corners of an octahedron elongated parallel to the c axis with adjacent layers related by a 6_3 axis. Chains of Na^+ ions coincide with the 6_3 axis with Na(1) coplanar with the bridging oxygen atoms and Na(2) lying in an octahedral site between layers formed by the terminal oxygen atoms of six separate anions. The terminal oxygen atoms are coplanar with the plane containing the anion and the chain of cations. Two additional Na^+ ions per formula units, Na(3) and Na(4), are collinear with the P—P vectors separating pyrogroups in adjacent cells along the c axis.

Na(1) in this idealized structure has a coordination number of nine as a result of sharing the bridging oxygen atom and one terminal oxygen atom from each end of three pyrogroups. This configuration, with the bridging oxygen atom lying $b/\sqrt{3}$ Å from three Na(1) ions, is unstable towards a bent anion where the Na(1) ion forms a strong bond with only one bridging oxygen atom. It is of interest that an infinite number of configurations are possible for an infinite layer where the only constraint is that each Na(1) is bonded to one and only one bridging oxygen atom, and visa versa. If

[2]Photocopies of Table 2 may be obtained upon request from the Depository of Unpublished Data, National Science Library, National Research Council of Canada, Ottawa, Canada. K1A 0S2.

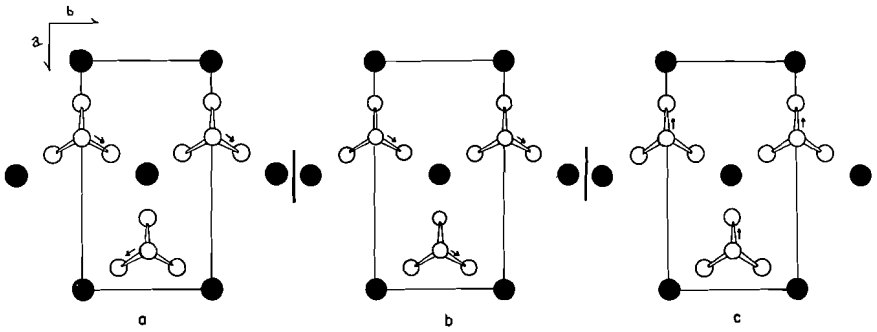

FIG. 2. *(a)* Schematic representation of a possible arrangement of bent anions. Only half a layer is shown. The large filled circles represent Na(1), the open circles are oxygen atoms. The arrows indicate the direction of the displacements of the bridging oxygen atoms when the structure has a 2_1 axis at the level of the central oxygen atoms relating adjacent rows. *(b)* Same as *(a)* except that adjacent rows in the layer are related by a centering operation. *(c)* Same as *(a)* except that adjacent rows in the layer are related by both a 2_1 axis and the centering operation.

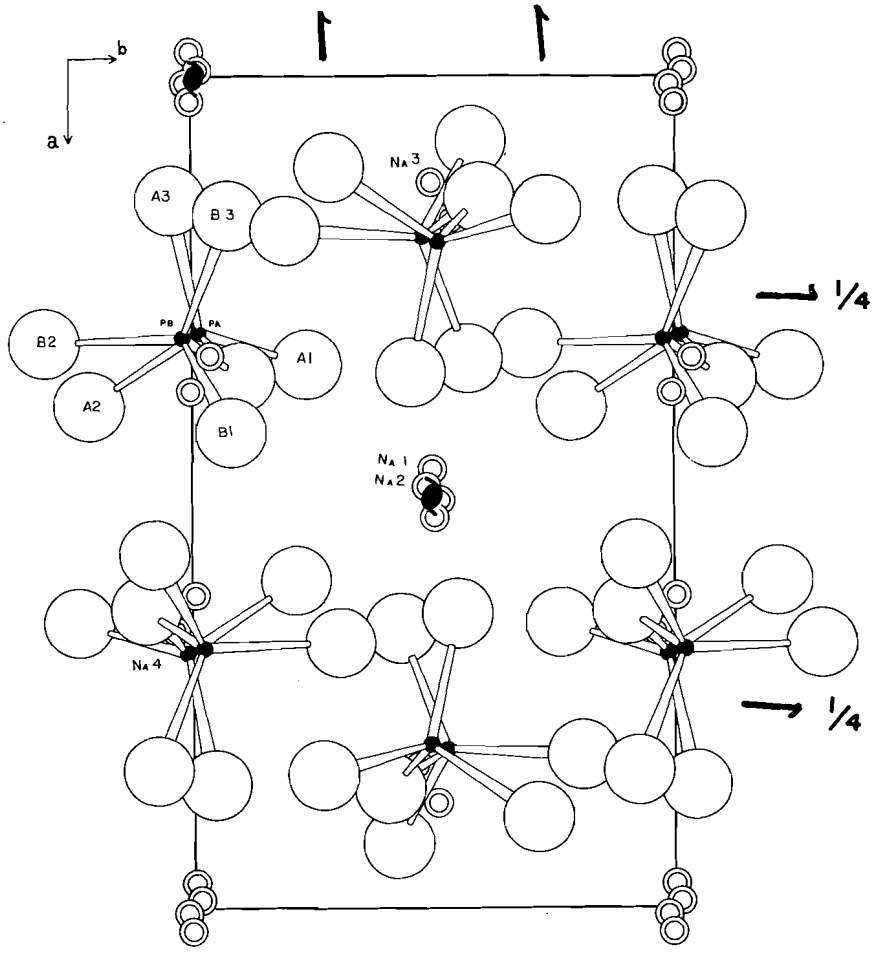

FIG. 3. The structure of $Na_4P_2O_7$ projected onto the *ab* plane. The large open circles represent oxygen atoms, the smaller double open circles are sodium ions while the smaller filled circles are phosphorus atoms.

Can. J. Chem. Downloaded from www.nrcresearchpress.com by 210.87.254.42 on 09/05/12
For personal use only.

Can. J. Chem. Downloaded from www.nrcresearchpress.com by 210.87.254.42 on 09/05/12
For personal use only.

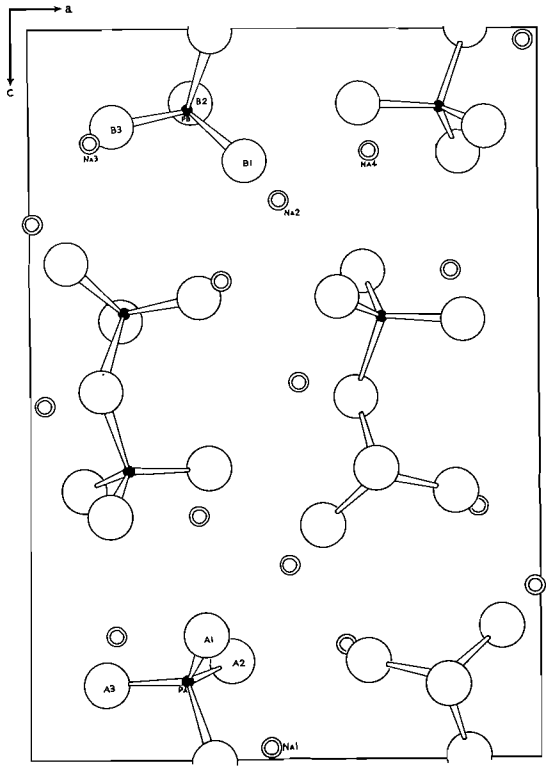

FIG. 4. The structure of $Na_4P_2O_7$ projected onto the *ac* plane. The details are the same as for Fig. 3.

the further constraints of translational periodicity corresponding to the determined *a* and *b* axes are imposed three configurations are possible. The arrangement shown in Fig. 2(*a*) is found in the present structure while that in Fig. 2(*b*) is found in the structure at 400 °C. The configuration seen in Fig. 2(*c*) consistent with either a 2_1 axis or a centering in the layer has not been found as yet.

Since the diphosphate ion bends at the bridging oxygen atom the plane of the terminal oxygen atoms no longer coincides with the *ab* plane. In addition, the two ends of the anion twist slightly destroying the eclipsed configuration and the anion rotates as a whole so that the P—P vector is no longer collinear with the *c* axis. However, as can be seen in Fig. 3, the gross features of the idealized model remain in the present structure. These distortions lead to coordination numbers of five for Na(3) and Na(4) rather than three as expected from the idealized model. See Fig. 4.

Na(1) shares two oxygen atoms with three pyrophosphate ions and shows bond lengths ranging from 2.313(2) to 2.777(2) Å. See Table 3. As predicted this ion shares oxygen atoms from either end of two anions and shares an edge with one of the tetrahedra of a third anion. One of the oxygen atoms in this edge is a bridging oxygen atom. The second cation, Na(2), lies at the center of a distorted octahedron formed by six oxygen atoms arising from six separate anions. The bond lengths range from 2.347(2) to 2.687(2) Å. The environment of Na(3) consists of a very irregular arrangement of five oxygen atoms contributed by four separate anions. Here the bond lengths range from 2.272(2) to 2.441(2) Å for the four shorter Na—O bonds and 2.888(2) Å for Na(3)–O(A1*b*). The five neighbouring oxygen atoms to Na(4) also arise from four separate anions but with the tighter range 2.333(2) to 2.580(2) Å.

The P—O bridging bond lengths at 1.631(2) Å for side A and 1.642(2) Å for side B are significantly longer than the terminal P—O bond lengths which all lie between 1.512 and 1.514 Å. The individual terminal P—O bond lengths are insignificantly different. The P—O—P bond angle, at 127.5(1)°, is the smallest reported for a diphosphate ion. As commonly found for this anion the O—P—O bond angles involving the bridging oxygen atom are less than the ideal tetrahedral value in every case while those involving only terminal oxygen atoms are all larger than the ideal.

Discussion

It is of some interest to compare the geometries of the $P_2O_7^{4-}$ ion in the three sodium pyrophosphates studied to date. In $Na_4P_2O_7 \cdot 10H_2O$(9) the anion has a nearly staggered configuration with crystallographic two-fold axis through the bridging oxygen atom. The P—O—P bond angle is 130.2° while the O—P—O angles involving the bridging oxygen atom range from 101.8 to 108.9° The O—P—O angles among only terminal oxygen atoms range from 111.1 to 115.0°. The average terminal P—O bond length is 1.513 Å while the P—O(—P) bond is 1.612(5) Å long. The two unique Na^+ ions are coordinated to six oxygen atoms but only one is bonded directly to the anion; involving O(2) and O(4). These

TABLE 3. Bond lengths and angles in $Na_4P_2O_7$ with estimated standard deviations in parentheses*

Bond	Distance (Å)	Bonds	Angle (deg)	Bonds	Angle (deg)
P_2O_7 group					
P(A)—O(CE)	1.631(2)	O(CE)—P(A)—O(A3*a*)	108.8(1)	O(A3*a*)—P(A)—O(A2*a*)	112.6(1)
—O(A3*a*)	1.512(2)	—O(A2*a*)	106.6(1)	—O(A1*a*)	113.9(1)
—O(A2*a*)	1.512(2)	—O(A1*a*)	102.5(1)	O(A2*a*)—P(A)—O(A1*a*)	111.6(1)
—O(A1*a*)	1.512(2)				
P(B)—O(CE)	1.642(2)	O(CE)—P(B)—O(B2*a*)	107.3(1)	O(B2*a*)—P(B)—O(B1*a*)	113.1(1)
—O(B2*a*)	1.514(2)	—O(B1*a*)	102.4(1)	—O(B3*a*)	113.5(1)
—O(B1*a*)	1.513(2)	—O(B3*a*)	106.4(1)	O(B1*a*)—P(B)—O(B3*a*)	113.2(1)
—O(B3*a*)	1.514(2)				
P(A)—P(B)	2.936(1)	P(A)—O—P(B)	127.5(1)		
Na(1)–O_6 group†					
Na(1)—O(CE)	2.426(2)	O(CE)—Na(1)—O(A1*a*)	55.78(5)	O(A1*a*)—Na(1)—O(A2*a*)	72.95(6)
—O(A1*a*)	2.777(2)	—O(A2*a*)	122.57(7)	—O(B2*a*)	117.77(7)
—O(A2*a*)	2.329(2)	—O(B2*a*)	93.79(6)	—O(B3*b*)	76.02(6)
—O(B2*a*)	2.387(2)	—O(B3*b*)	104.59(7)	—O(A3*b*)	151.08(7)
—O(B3*b*)	2.427(2)	—O(A3*b*)	108.98(7)	O(A2*a*)—Na(1)—O(B2*a*)	88.04(7)
—O(A3*b*)	2.313(2)	O(B2*a*)—Na(1)—O(B3*b*)	161.42(8)	—O(B3*b*)	84.33(7)
		—O(A3*b*)	85.36(7)	—O(A3*b*)	128.34(8)
		O(B3*b*)—Na(1)—O(A3*b*)	86.15(6)		
Na(2)–O_6 group†					
Na(2)—O(B1*a*)	2.386(2)	O(B1*a*)—Na(2)—O(B2*a*)	91.43(6)	O(B2*a*)—Na(2)—O(B3*a*)	92.60(7)
—O(B2*a*)	2.687(2)	—O(B3*a*)	105.19(7)	—O(A2*c*)	166.47(7)
—O(B3*a*)	2.347(2)	—O(A2*c*)	78.17(6)	—O(A3*b*)	78.12(6)
—O(A2*c*)	2.517(2)	—O(A3*b*)	92.59(7)	—O(A1*c*)	116.83(7)
—O(A3*b*)	2.353(2)	—O(A1*c*)	150.52(8)	O(B3*a*)—Na(2)—O(A2*c*)	81.99(6)
—O(A1*c*)	2.506(2)	O(A2*c*)—Na(2)—O(A3*b*)	110.63(7)	—O(A3*b*)	160.22(9)
		—O(A1*c*)	74.97(6)	—O(A1*c*)	82.96(7)
		O(A3*b*)—Na(2)—O(A3*c*)	85.73(7)		
Na(3)–O_5 group†					
Na(3)—O(A1*b*)	2.888(2)	O(A1*b*)—Na(3)—O(B3*a*)	75.30(6)	O(B3*a*)—Na(3)—O(A2*b*)	127.29(7)
—O(B3*a*)	2.327(2)	—O(A2*b*)	55.23(6)	—(B2*a*)	106.67(7)
—O(A2*b*)	2.441(2)	—O(B2*a*)	164.63(7)	—O(B1*d*)	110.11(7)
—O(B2*a*)	2.272(2)	—O(B1*d*)	80.86(6)	O(A2*b*)—Na(3)—O(B2*a*)	116.47(7)
—O(B1*d*)	2.315(2)	O(B2*a*)—Na(3)—O(B1*d*)	111.84(7)	—O(B1*d*)	81.08(6)
Na(4)–O_5 group†					
Na(4)—O(B1*a*)	2.333(2)	O(B1*a*)—Na(4)—O(A3*b*)	102.60(7)	O(A3*b*)—Na(4)—O(A2*b*)	60.23(6)
—O(A3*b*)	2.428(2)	—O(A2*b*)	162.83(8)	—O(A1*b*)	134.22(7)
—O(A2*b*)	2.580(2)	—O(A1*b*)	119.87(8)	—O(A1*c*)	85.50(6)
—O(A1*b*)	2.341(2)	—O(A1*c*)	90.78(7)	O(A2*b*)—Na(4)—O(A1*b*)	76.61(6)
—O(A1*c*)	2.445(2)	O(A1*b*)—Na(4)—O(A1*c*)	108.67(7)	—O(A1*c*)	87.82(6)

*Transformations: $a = x, y, z$; $b = 1/2 + x, 1/2 - y, -z$; $c = x, -y, 1/2 + z$; $d = 1/2 - x, 1/2 + y, 1/2 - z$. Calculated from diagonal elements of least squares matrix and including e.s.d.'s in unit cell parameters.
†Includes all interactions less than 3.0 Å except a PA—Na(4) interaction of 2.998 Å.

P—O bonds are the longer of the three at 1.510 and 1.526 Å, respectively, although they do not differ significantly from the remaining terminal P—O bond length of 1.503 Å.

In $Na_2H_2P_2O_7 \cdot 6H_2O$(10) the anion again contains a crystallographic two-fold axis and has a nearly staggered configuration. The P—O—P bond angle is 136.1° with O(bridge)—P—O angles ranging from 103.4 to 108.8°. The remaining O—P—O angles of the PO_4 group range from 109.9 to 117.7°. The terminal P—O(—H) bond is 1.569(2) Å long while the remaining terminal P—O bond lengths are within 0.002 of 1.493 Å. These two oxygen atoms are bonded to the sodium ion which is coordinated to a total of six oxygen atoms. In this case the P—O(—P) bond is shortened to 1.598(1) Å.

Can. J. Chem. Downloaded from www.nrcresearchpress.com by 210.87.254.42 on 09/05/12
For personal use only.

Can. J. Chem. Downloaded from www.nrcresearchpress.com by 210.87.254.42 on 09/05/12
For personal use only.

TABLE 4. Correlation between predicted and experimental P—O bond lengths in sodium pyrophosphate systems

Bond	Bond length (Å) Observed	Predicted
$Na_4P_2O_7$		
P—O	1.631, 1.642	1.62
P—O(AB)	1.512	1.49
P—O(A2)	1.512	1.54
P—O(A1)	1.512	1.56
P—O(B2)	1.514	1.52
P—O(B1)	1.513	1.52
P—O(B3)	1.514	1.52
*$Na_4P_2O_7 \cdot 10H_2O$**		
P—O(1)	1.612	1.60
—O(2)	1.510	1.47
—O(3)	1.503	1.47
—O(4)	1.526	1.47
$Na_2H_2P_2O_7 \cdot 6H_2O$†		
P—O(1)	1.598	1.60
—O(2)	1.492	1.47
—O(3)	1.495	1.47
—O(4)	1.569	1.57

*Reference 9.
†Reference 10.

In Table 4 the results for these two structures and $Na_4P_2O_7$ are compared with the predictions of Baur (11). In no case have thermal corrections been made. It is clear that these predictions are, except with a few glaring exceptions, not far off the mark. In particular, the predicted value for the P—O(A1) bond length in $Na_4P_2O_7$ results from including the two rather long Na—O bonds in the counting. It is clear that weighting the contribution to the electrostatic bond strength by some function inversely related to the atomic separation would improve the agreement. The P—O—P bond angle is small in $Na_4P_2O_7$ probably because the bridging oxygen atom is coordinated to Na^+. A similar effect has been noted in comparing the $Zn_2V_2O_7$ structure (12) to those of $Mg_2V_2O_7$(12) and $Co_2V_2O_7$(13). This effect can be rationalized in the sense that Baur's (11) relationship would predict a lengthened P—O(—P) bond while Cruickshank's considerations (14) suggest that as the ratio of P—O(—P) to P—O increases, the P—O—P angle must contract.

In Table 5 are found data on the principle axes of vibration of the atoms in the $Na_4P_2O_7$ structure. The major components of vibration for P(A), P(B), and O(CE) are in the *ab* plane as would be expected either from the nature of the bonding or if some errors occur in the directions of the bending of the anion relative to the idealized structure. The fact that Na(1) vibrates nearly isotropically and with an

TABLE 5
(*a*) Principal axes of the thermal ellipsoids in $Na_4P_2O_7$

Root-mean-square amplitude	Direction cosines to *a*	*b*	*c*
Atom Na(1)			
0.128	0.1319	−0.3911	−0.9108
0.124	−0.8110	−0.5709	0.1276
0.115	−0.5699	0.7219	−0.3925
Atom Na(2)			
0.163	−0.6922	0.4588	−0.5572
0.133	0.2296	0.8718	0.4327
0.114	−0.6843	−0.1716	0.7088
Atom Na(3)			
0.146	−0.2088	0.7625	−0.6124
0.137	0.6405	0.5798	0.5036
0.119	0.7390	−0.2871	−0.6094
Atom Na(4)			
0.146	−0.2286	0.1787	−0.9570
0.131	0.6757	−0.6786	−0.2881
0.122	−0.7009	−0.7125	0.0344
Atom O(CE)			
0.140	−0.7277	0.6856	−0.0198
0.097	0.6805	0.7253	0.1041
0.089	−0.0857	−0.0623	0.9944
Atom O(A3)			
0.170	−0.0812	0.9555	−0.2837
0.118	0.1861	−0.2651	−0.9461
0.094	0.9792	0.1297	0.1563
Atom O(A2)			
0.147	0.8762	0.4738	0.0877
0.123	−0.0998	0.3566	−0.9289
0.088	0.4714	−0.8052	−0.3597
Atom O(A1)			
0.158	0.9959	0.0639	0.0646
0.134	0.0907	−0.6508	−0.7538
0.085	−0.0061	0.7565	−0.6539
Atom O(B2)			
0.164	−0.7158	0.0399	−0.6971
0.122	0.6899	−0.1141	−0.7149
0.096	−0.1080	−0.9927	0.0541
Atom O(B1)			
0.158	−0.1701	0.9735	−0.1530
0.126	−0.7274	−0.0193	0.6859
0.086	0.6648	0.2279	0.7114
Atom O(B3)			
0.142	−0.0468	−0.9305	0.3633
0.129	0.5528	0.2788	0.7853
0.092	0.8320	−0.2376	−0.5014

TABLE 5 (*Concluded*).

(*b*) Angle between principal component of the thermal ellipsoid of X and P—X bond vector

X	Angle (deg)
OCE(—PA)	7.5
OCE(—PB)	5.3
O(A3)	8.5
O(A2)	9.8
O(A1)	1.4
O(B2)	5.6
O(B2)	2.2
O(B3)	20.0

amplitude comparable to the remaining cations suggests that the structure has very little residual configurational disorder at room temperature. The thermal motions of the oxygen atoms are significantly anisotropic with the largest component nearly perpendicular to the P—O bond.

A plurality of phases can be generated by the manner in which bent pyrophosphate ions correlate in a layer and how adjacent layers correlate along the *c* axis. A number of these phases have been identified and the one found at the highest temperature is a disordered structure with an average structure corresponding to that of the "ideal" $Na_4P_2O_7$ (6). Details concerning these phases and phase transformations will be treated elsewhere.

This research was supported by a grant from the Defence Research Board of Canada.

1. T. Y. TIEN and F. A. HUMMEL. J. Am. Ceram. Soc. **44**, 206 (1961).
2. F. REMY. Bull. Soc. Chim. **10**, 3380 (1969).
3. K. Y. LEUNG and C. CALVO. To be published.
4. E. P. PARTRIDGE, V. HICKS, and G. V. SMITH. J. Am. Chem. Soc. **63**, 454 (1941).
5. R. VON SAHNEN and G. TAMMANN. Ann. Phys. **10**, 879 (1903).
6. D. DELAMATTER. Masters Thesis, McMaster University. Hamilton, Ontario, 1972.
7. J. KARLE and H. HAUPTMAN. Acta Cryst. **9**, 635 (1956).
8. International Tables for X-Ray Crystallography. Vol. III. Kynoch Press, Birmingham. 1963.
9. W. S. MCDONALD and D. W. J. CRUICKSHANK. Acta Cryst. **22**, 43 (1967).
10. R. L. COLLINS and M. WILLIS. Acta Cryst. **27B**, 291 (1971).
11. W. H. BAUR. Trans. Am. Cryst. Assoc. **6**, 129 (1970).
12. R. GOPAL. Ph.D. Thesis, McMaster University, Hamilton, Ontario. 1972.
13. E. SAUERBREI. M.Sc. Thesis, McMaster University, Hamilton, Ontario. 1972.

Can. J. Chem. Downloaded from www.nrcresearchpress.com by 210.87.254.42 on 09/05/12
For personal use only.

CN Emission in Active Nitrogen. II. The Role of Energy Transfer and Atom Transfer Reactions in $CN(X^2\Sigma^+)$ Excitation

G. M. PROVENCHER AND D. J. MCKENNEY

Department of Chemistry, University of Windsor, Windsor, Ontario

Received July 27, 1971[1]

A simplified mechanism is presented for excitation of ground state $CN(X^2\Sigma^+)$ formed from carbonaceous impurity in flowing N_2 subjected to a microwave discharge.

Analysis of absolute intensity data from spectrometer recordings of $CN(B^2\Sigma^+ \rightarrow X^2\Sigma^+)$ violet band emission enabled order of magnitude estimates of rate constants for $CN(X^2\Sigma^+)$ excitation by energy transfer from vibrationally excited ground state nitrogen, N_2^*

[5] $$N_2^* + CN(X^2\Sigma^+) \rightarrow CN^*(B^2\Sigma^+) + N_2 \qquad k_5 = 10^{13}\ \text{cm}^3/\text{mol s}$$

and formation of electronically excited NCN* in a three body reaction

[8] $$N + CN + M \rightarrow NCN^* + M \qquad k_8 = 10^{16}\ \text{cm}^6/\text{mol}^2\ \text{s}$$

Energy transfer from $N_2(A^3\Sigma_u^+)$ is shown to be a minor source of excitation of CN to radiative levels. $N_2(A)$ is a source of vibrationally excited ground state nitrogen, N_2^*, which in turn excites CN. Vibrational population profiles under all conditions in this work are shown to be primarily a function of $[N_2^*]$. Evidence for the participation of the $A^2\Pi$ state of CN is shown in the population maxima at $v = 4$ and 10 of the $B^2\Sigma^+$ state.

Un mécanisme simplifié est donné pour l'excitation de l'état fondamental $CN(X^2\Sigma^+)$ formé à partir d'impureté carbonée dans un flux d'azote, soumis à une décharge microonde.

L'analyse des données sur l'intensité absolue à partir des enregistrements du spectromètre de la bande d'émission violette de $CN(B^2\Sigma^+ \rightarrow X^2\Sigma^+)$, rend possible des estimations sur l'ordre de grandeur des constantes de vitesse pour l'excitation de $CN(X^2\Sigma^+)$ par une énergie de transfert de l'état fondamental de l'azote, vibrationnellement excité N_2^*

[5] $$N_2^* + CN(X^2\Sigma^+) \rightarrow CN^*(B^2\Sigma^+) + N_2 \qquad k_5 = 10^{13}\ \text{cm}^3/\text{mol s}$$

et la formation de NCN* électroniquement excité, dans une réaction à trois constituents

[8] $$N + CN + M \rightarrow NCN^* + M \qquad k_8 = 10^{16}\ \text{cm}^6/\text{mol}^2\ \text{s}$$

On montre que l'énergie de transfert à partir de $N_2(A^3\Sigma_u^+)$ est une source mineure dans l'excitation de CN aux niveaux radiatifs. $N_2(A)$ est une source pour l'état fondamental de l'azote, vibrationnellement excité, N_2^* qui à son tour excite CN. On montre que les profils de population vibrationnelle, dans toutes les conditions de ce travail, sont principalement une fonction de $[N_2^*]$. La preuve d'une participation de l'état $A^2\Pi$ du CN est montrée par le maximum de population à $v = 4$ et 10 dans l'état $B^2\Sigma^+$.

Canadian Journal of Chemistry, **50**, 2527 (1972)

Introduction

In the past decade several investigators (1–5) have advanced a variety of explanations to account for CN radical emission generated in "active" nitrogen systems. The mechanism is known to be complex and appears to be a function of "fuel", pressure, and relative concentration of reactants (5). These parameters can be characterized by specific vibrational population profiles in the upper states of the two observed band systems. Bayes (4) labeled the distributions P_1 and P_2 for the CN red $(A^2\Pi \rightarrow X^2\Sigma^+)$ system and subsequently Setser and Thrush (1) used designations P_1' and P_2' to identify the corresponding profiles in the violet $(B^2\Sigma^+ \rightarrow X^2\Sigma^+)$ bands. More recently Iwai *et al.* (5) found still a third distribution which they called P_3 and P_3' for the red and violet

[1]Revision received May 5, 1972.

Can. J. Chem. Downloaded from www.nrcresearchpress.com by 210.87.254.5 on 09/05/12
For personal use only.

Can. J. Chem. Downloaded from www.nrcresearchpress.com by 210.87.254.5 on 09/05/12
For personal use only.

systems, respectively. This latter profile known as the "blue flame" distribution does not depend on the nature of the fuel but occurs at low fuel concentrations (less than 0.05%) and higher (above 1 Torr) pressures.

The blue flame features enhanced intensity of the violet emission relative to the red, maxima in vibrational populations of the A state at $v = 7$, for the B state of CN at $v = 7$ and the appearance of a well developed tail band system ($5 \leqslant v \leqslant 15$) in the ($B^2\Sigma^+ \rightarrow X^2\Sigma^+$) emission. Evidence collected by all groups indicates the involvement of at least two distinct processes responsible for excitation of CN to appropriate radiative levels. Boden and Thrush (2) postulated excitation of ground state CN by a combination of steps involving the metastable $N_2(A^3\Sigma_u^+)$ and ground state $N_2(X^1\Sigma_g^+)$ in high vibrational levels. Meyer and Setser (6) have proposed, however, that A state nitrogen is not a major energy transfer agent in CN excitation. Our earlier results (7) and evidence presented in this paper suggest blue flame emission arises as a result of energy transfer to $CN(X)$ by vibrationally excited ground state nitrogen, $N_2^{\neq}$, and through a transfer reaction involving the free radical NCN. Vibrational population profiles obtained suggest that excitation of $CN(B^2\Sigma^+)$ levels is significantly dependent on transfer from the $CN(A^2\Pi)$ state in agreement with Radford and Broida (8) and Brown and Broida (9).

Experimental

The flow system consisted of a reactor, illustrated previously (7), attached to an ancillary glass system evacuable to 1 μTorr pressure. Flow was maintained by a fast (425 l/min) mechanical pump and controlled with a large stopcock. Inlet flows were adjusted and monitored by means of calibrated, capillary flow meters and Matheson needle valves. Pressure measurement was accomplished with an H_2SO_4 manometer. Total pressures were typically 1.5 Torr for "low pressure" work and 5.0–10 Torr for data referred to as "high pressure". Nitrogen flow rate through the discharge was 110 μmol s^{-1} for all experiments while added gases were admixed at 0–10 μmol s^{-1}. Linear flow rates ranged from 3 to 19 cm s^{-1} in the large reactor. Both linear and bulk flow rates were calculated assuming ideal gas conditions.

The spectrometer system was a 0.3 m McPherson scanning monochromator positioned to observe the afterglow emission down the long axis of the reactor. The monochromator exit slit was covered by an RCA 1 P28 photomultiplier tube mounted in a Pacific Photometric housing. The signal from the tube was fed to a Keithley model 417 picoammeter for amplification and subsequent display on a Keithley model 370 strip chart recorder. Survey spectra were frequently recorded over the interval 2000 Å $\leqslant \lambda \leqslant$ 6500 Å to insure detection of pertinent features and possible impurity (*e.g.* NO emission). All kinetic data presented were obtained by scanning the $\Delta v = 0$ sequence of the CN violet bands and then switching rapidly to the region 5000–5900 Å for the signal intensity at 5074 Å ($Hg(6^3P_0 \rightarrow 6^1S_0)$ second order) and/or that at 5804 Å (N_2, $B^3\Pi_g \rightarrow A^3\Sigma_u^+$ (11, 7) transition). For all but high resolution studies a 100 μ entrance and exit slit width was employed. High resolution spectra were taken with the slits adjusted to 10 μ. Matheson "certified" (g.c. analysis furnished) nitrogen was passed over 450 °C copper turnings, through a column packed with P_2O_5 and then through two successive refrigerated (77 °K) traps, the first packed with glass wool covered with apiezon grease – silica gel, the second filled with glass wool. The absence of detectable NO emission under all kinetic conditions indicated an estimated upper limit of $\sim 10^{11}$ atoms/cm^3 for O atoms. NO and CH_4 added to the afterglow were first passed through a P_2O_5 column and then subjected to several freeze, thaw, pump cycles at reduced pressure. Nitrogen (Matheson "high purity") added at the inlet jet was used without further purification. (In experiments using mercury the nitrogen carrier was first saturated with mercury at ambient temperature before admixture.)

The discharge–afterglow was established using a "Microtron 200" (Electro Medical Supplies) microwave generator which coupled 2450 MHz power to the flowing gas by means of a foreshortened quarter-wave coaxial cavity. This type of cavity is known (10) to show less than 1% reflected power over the full range of experimental parameters encountered in this work.

Conversion of raw intensity data to rate constants or concentrations was accomplished by comparison with NO emission developed in this reactor of appropriate wavelength regions of the spectra of interest according to an extension of the method of Fontijn *et al.* (11) by Gross and Cohen (12). The CN violet $\Delta v = +1$ sequence and the NO β (0,10) band were compared over the interval 3570 Å $\leqslant \lambda \leqslant$ 3600 Å. The partial rate constant for the chosen NO band as reported in ref. 12 was adjusted to account for the fact that only 80% of the total emission intensity of this band was used in the comparison.

Intensity maxima of selected bands were monitored as a function of various parameters. Bands were chosen so as to minimize the effect of overlap and while it is recognized that changes in rotational temperature due to rotational perturbations and relaxation could lead to some error in the calculation of relative population of vibrational levels from band head intensities, it is felt that the magnitude of such error would be small at the pressures used in this work.[2]

Intensities were converted to relative populations through the use of the expression derived from Nicholls (14).

$$\frac{N_{v'}}{N_0} = \frac{I_{(v',v'')}}{I_{(0,0)}} \frac{\nu^4_{(0,0)}}{\nu^4_{(v',v'')}} \frac{q_{(0,0)}}{q_{(v',v'')}}$$

where N_i are populations (relative to $N_0 = 10$); I_i are intensities; ν_i are frequencies of spectral lines; q_i are the

[2]Comparison of our high resolution spectra with those of Evenson and Broida (13) at lower pressure shows that at the relatively high pressures employed in this work, significant rotational relaxation has occurred.

Can. J. Chem. Downloaded from www.nrcresearchpress.com by 210.87.254.5 on 09/05/12
For personal use only.

Franck Condon factors for $v' \rightarrow v''$ transitions, taken from ref. 15.

To avoid calibration of spectrometer response, relative populations were calculated using the above equation and the bands of the $\Delta v = 0$ sequence whenever possible. In those cases where sequences other than $\Delta v = 0$ were used, population was normalized by assigning the value calculated for a given level from the $\Delta v = 0$ sequences to that same upper level for bands in the $\Delta v \neq 0$ sequence.

Results and Discussion

In this system $CN(B^2\Sigma^+ \rightarrow X^2\Sigma^+)$ violet band emission appeared to be a function of $[N]^2$ at low (1.0–5.0 Torr) pressures. Work above 5.0 Torr discussed in ref. 7, showed the CN violet emission intensity, Φ_{CN}, to be a complex function of experimental variables related to the concentration of vibrationally excited ground state nitrogen, N_2^*. Two band heads of the $\Delta v = 0$ sequence were chosen as observables in kinetic experiments because of their relatively high intensities and freedom from overlap. These were the strong (0,0) head at 3883 Å and the (4,4) head at 3850 Å. The 3850 Å head was chosen with the further consideration that it could possibly reflect the behavior of the (5,5) emission in this same system, the upper level of which is in near resonance to $v = 17$ of the $CN(A^2\Pi)$ state. Hereinafter Φ_{CN} will refer to the total relative emission intensity of the violet system while Φ_λ indicates maximum intensity in arbitrary units for emission at wavelength λ.

It is convenient to discuss the experimental data in terms of the following simplified mechanism,

[1] $2N + M \longrightarrow N_2^* + M$

[2] $2N + M \longrightarrow N_2^{\ddagger} + M$

[3] $N_2^{\ddagger} \xrightarrow{\text{wall}} N_2$

[4] $N_2^{*} \xrightarrow{\text{wall}} N_2$

[5] $N_2^{\ddagger} + CN \longrightarrow CN^* + N_2$

[6] $N_2^{\ddagger} + M \longrightarrow N_2 + M$

[7] $CN^* \longrightarrow CN + h\nu$

[8] $N + CN + M \longrightarrow NCN + M$

[9] $N + NCN \longrightarrow N_2 + CN^*$

[10] $N + N_2^{*} \longrightarrow N_2^{\ddagger} + N$

where $N_2^{\ddagger}$ indicates vibrationally excited ground state nitrogen, N_2^* designates $N_2(A^3\Sigma_u^+)$ and CN* refers to $CN(B^2\Sigma^+)$.

This scheme does not preclude excitation through the $CN(A^2\Pi)$ state, as will be discussed below.

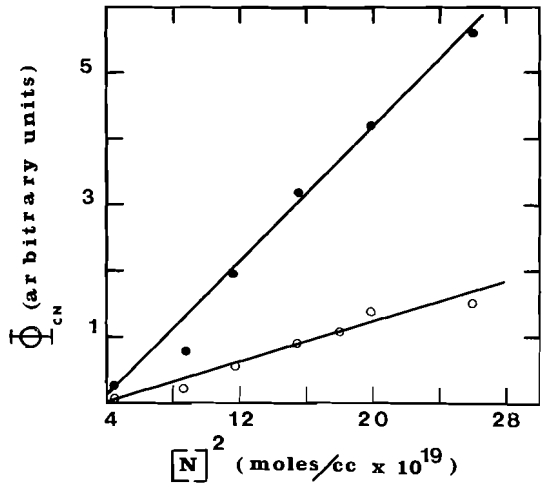

FIG. 1. CN violet band head intensities (●, (0,0) head at 3883 Å; ○, (4,4) head at 3850 Å) as a function of $[N]^2$. Pressure 1.5 Torr at 298 °K.

Application of the usual steady state assumptions yields

[11] $$\Phi_{CN} = k_5[CN]\left[\frac{k_1[N]^2[M] + \dfrac{k_{10}k_2[N]^3[M]}{k_4 + k_{10}[N]}}{k_3 + k_5[CN] + k_6[M]}\right] + k_8[N][CN][M]$$

and at suitably high [N] and [M]

[12] $$\frac{\Phi_{CN}}{[N]^2} = \frac{k_5}{k_6}(k_1 + k_2)[CN] + \frac{k_8[CN][M]}{[N]}$$

Figure 1 illustrates the predicted second order dependence of Φ_{3883} and Φ_{3850} on N atoms. Figure 1 is typical of the results obtained under all conditions, *i.e.*, total pressures ranging from 1.5 to 5.0 Torr and [N] ranging from 10^{-10} to 10^{-9} mol/cm^3. It may be noted that the rates of population of two levels $v = 4$ and $v = 0$ of the B state of CN are different at these lower pressures, perhaps indicative of a lower concentration of suitable activators for level $v = 4$ or alternately reflective of relatively inefficient deactivation from $v = 5$, should resonance crossing at this latter level be the predominant mode of population for $v = 5$ of the $B^2\Sigma^+$ state.

Figure 2 is a representation of $\Phi_{CN}/[N]^2$ plotted against pressure with constant but

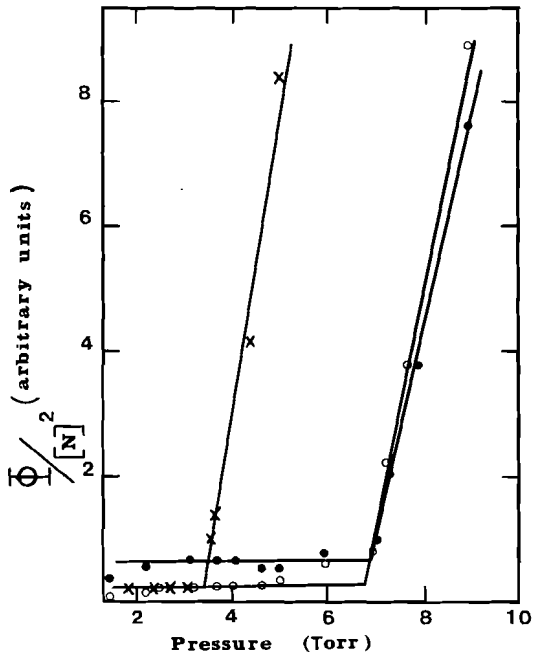

FIG. 2. $\Phi_{CN}/[N]^2$ *vs.* pressure. ●, (0,0) transition; ○, (4,4) transition of CN($B^2\Sigma^+ \rightarrow X^2\Sigma^+$), $[N] = 6 \times 10^{-9}$ mol/cc, $\Phi_{CN}/[N]^2 = 10^8$ cm^3/mol s at 7 Torr. ×, (0,0) transition of CN violet, $[N] = 2 \times 10^{-10}$ mol/cc, $\Phi_{CN}/[N]^2 = 10^7$ cm^3/mol s at 3.5 Torr. Temperature 298 °K.

varied [N]. The data demonstrate the pressure dependence predicted in eq. 12 when the second term on the right of that expression becomes dominant. It may also be noted from the same data that the indicated inverse dependence of the function $\Phi_{CN}/[N]^2$ on [N] is also substantiated. The break in these plots should occur when

$$[13] \quad \frac{k_8[CN][M]}{[N]} = \frac{k_5}{k_6}(k_1 + k_2)[CN] = \tfrac{1}{2}\frac{\Phi_{CN}}{[N]^2}$$

Campbell and Thrush (16) estimated $[CN]/[N] \simeq 10^{-2}$ in reasonable agreement with a value calculated from the data of Iwai *et al.* (3) for $[CN]/[M] \simeq 10^{-6}$ since the Campbell and Thrush work was done at $[N]/[M] \simeq 10^{-3}$. The larger reactor used in this work and the similar atom to molecule ratio for nitrogen suggested use of $[CN]/[N] \simeq 10^{-3}$.

Use of this estimate and conversion to absolute intensity values by the method of Fontijn *et al.* (11) enabled calculation of order of magnitude estimates of $k_8 \simeq 10^{16}$ cm^6/mol^2 s or the ratio $k_5/k_6 \simeq 10^5$, $k_1 \simeq k_2 \simeq 10^{14}$ cm^6/mol^2 s (16).

It is possible to roughly estimate k_6 from data tabulated by Stevens (17), restricting evaluation of that constant to those vibrational levels of ground state N_2 sufficiently highly excited to participate in reaction 5, *i.e.* $N_2^{\ddagger}$ ($v > 15$). It may be shown from Stevens (17) that

$$[14] \quad k_6 = \sum_{i>15}^{v} v_i/15\tau n$$

where v_i denotes the vibrational level of $N_2(X^1\Sigma_g^+)$, τ represents the relaxation time for vibrators in level $v = 1$ to level $v = 0$ and n is the concentration of ground state molecules. The vibrational levels selected were so chosen as to insure a minimum energy of ~4.0 eV (sufficient to excite ground state CN to $B^2\Sigma^+_{v=0}$ or $A^2\Pi_{v=10}$). In addition, that relatively low portion of the $N_2(X^1\Sigma_g^+)$ potential well is still a reasonable approximation of harmonic oscillator form.

Taking $\Sigma \simeq 100$, $\tau \simeq 1$ s at 300 °K (17) and $n \simeq 10^{-7}$ mol/cm^3, $k_6 \simeq 10^8$ cm^3/mol s was calculated leading to an estimate of $k_5 \simeq 10^{13}$ cm^3/mol s.

Boden and Thrush (2) found third order dependence of Φ_{CN} on [N] at concentrations nearly identical to those used in this study. These authors also report a change to second order dependence on [N] in "narrow" tubing in their system.

Expression 11 predicts such behavior. When $k_4 \gg k_{10}[N]$ third order dependence on [N] should dominate. The polymer film and intensity gradient reported in ref. 2 suggest the above inequality holds in the large (i.d.) portion of the reactor. In the narrow tubing

$$k_1[N]^2[M] \gg \frac{k_{10}k_2[N]^3[M]}{k_4}$$

if wall deactivation of $N_2(A^3\Sigma_u^+)$ is efficient. The apparent discrepancy between data presented in this paper and those in ref. 2 may be resolved by noting that neither the polymer nor intensity gradient was observed in this reactor (larger i.d.) and additionally data accumulated near 5.0 Torr have shown Φ_{CN} to be a complex function of power input (7). This is consistent with the mechanism [1]–[10] if wall deactivation of $N_2^{\ddagger}$ is assumed to be negligible and if it is further

Can. J. Chem. Downloaded from www.nrcresearchpress.com by 210.87.254.5 on 09/05/12
For personal use only.

Can. J. Chem. Downloaded from www.nrcresearchpress.com by 210.87.254.5 on 09/05/12
For personal use only.

assumed that the experimental system is a source of relatively high concentrations of N_2^+ at low power and high pressure. That N_2^+ is present in relatively high concentration in microwave discharged nitrogen under these conditions has been demonstrated in many studies (ref. 7 cites some examples) and at high pressures wall deactivation is minimal. Investigations are presently in progress which should further elucidate the behavior of N_2^+ in this system. Evidence cited earlier from the Meyer and Setser work (6) and observations from this work indicate that $N_2(A)$ must play a minor role in excitation of CN by direct energy transfer. Figure 3 shows the behavior of $N_2(A)$ in our system as indicated by the mercury (5074 Å) signal due to the rapid reaction

$$N_2(A^3\Sigma_u^+) + Hg(^1S_0) \rightarrow Hg(^3P_1) + N_2(X^1\Sigma_g^+)$$

Additionally, a hypothetical "rate constant" for direct excitation of CN by $N_2(A)$ using absolute intensity data can be calculated. It is first necessary to estimate the concentration of $N_2(A)$ using an expression and rate constants from Thrush (18). Accordingly, $[N_2(A)] \simeq 10^{-15}$ mol/cm^3 and with $[CN]/[N] = 10^{-3}$, again using the method presented in ref. 11 for the reaction

$$[15] \qquad N_2(A^3\Sigma_u^+) + CN \rightarrow N_2(X^1\Sigma_g^+) + CN^*$$

$k_{15} \simeq 10^{16}$ cm^3/mol s. This is clearly an unacceptable value since it is orders of magnitude greater than the collisional frequency. The validity of the above results rests on the assumption concerning [CN] (*i.e.* $[CN]/[N] \simeq 10^{-3}$). To test this premise methane was added to the flowing gas, both before the discharge and in the afterglow region. In all cases the additive gas quenched the emission. The lowest concentration of added CH_4 was 10^{-11} mol/cm^3 and since this gas is known to serve as a quenching agent above optimum ratios of $[CH_4]/[N_2] \simeq 10^{-3}$ (19), the results are indicative of the fact that the concentration of CN produced from impurity in the N_2 is less than the additive methane concentration.

It may be shown

$$[16] \qquad \frac{\Phi_{CN}}{\Phi_{NO_2}} = \frac{G(\lambda)}{G'(\lambda)} \frac{\tau_{CN}}{\tau_{NO_2}} \frac{[CN^*]}{[NO_2^*]}$$

where Φ_i represents the absolute intensity of

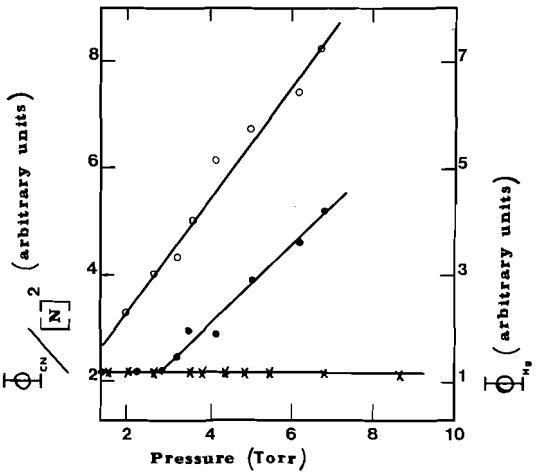

FIG. 3. $\Phi_{CN}/[N]^2$ (left hand ordinate) and mercury 5074 Å emission intensity (right ordinate) as a function of pressure. ○, 5074 Å Hg line intensity, ●, (0,0) head of $CN(B^2\Sigma^+ \rightarrow X^2\Sigma^+)$, $[N] = 1 \times 10^{-10}$ mol/cc. ×, (0,0) CN violet band head intensity, $[N] = 4 \times 10^{-9}$ mol/cc. Flow rate of inletted Hg = 3×10^{-10} mol/s. All data at 298 °K.

emission by molecule i over a given wavelength interval, $G(\lambda)$ and $G'(\lambda)$ are combined geometric and instrument functions over the appropriate spectral intervals. τ_i represents the radiative lifetime of molecule i and the asterisks denote molecules undergoing radiative transitions. Using $\tau_{CN} \simeq 10^{-8}$ s (20), $\tau_{NO_2} \simeq 10^{-6}$ s (21), a rate constant for formation of NO_2^* of $\sim 10^7$ cm^3/mol s and a quantum efficiency (defined as the fraction of NO_2^* formed which undergoes radiation) of 10^{-9} (21) and a ratio of $\Phi_{CN}/\Phi_{NO_2} \simeq 10^{-1}$, it is possible to calculate a value of $[CN^*] \simeq 10^{-19}$ mol/cm^3 from eq. 16. This result is in reasonable accord with a value of $[CN^*] = 5 \times 10^{-19}$ mol/cm^3 computed by Iwai *et al.* (3) for the $v = 0$ level of the $CN(B)$ state.

The ratio $\Phi_{CN}/\Phi_{NO_2} \simeq 10^{-1}$ is an experimentally determined value which reflects the different efficiencies of the spectrometer for detection of 3600 and 7800 Å photons. Calibration of the spectrometer system was effected by comparing a photon density value determined by using spectral data accumulated in this work and rate constants from ref. 12 to determine Φ_{CN} in the region 3570–3600 Å. This value was then compared with a similar computation for determination of Φ_{NO_2} from experimental data according to the method described in ref. 11.

Figures 2 and 3 suggest participation of a

Can. J. Chem. Downloaded from www.nrcresearchpress.com by 210.87.254.5 on 09/05/12
For personal use only.

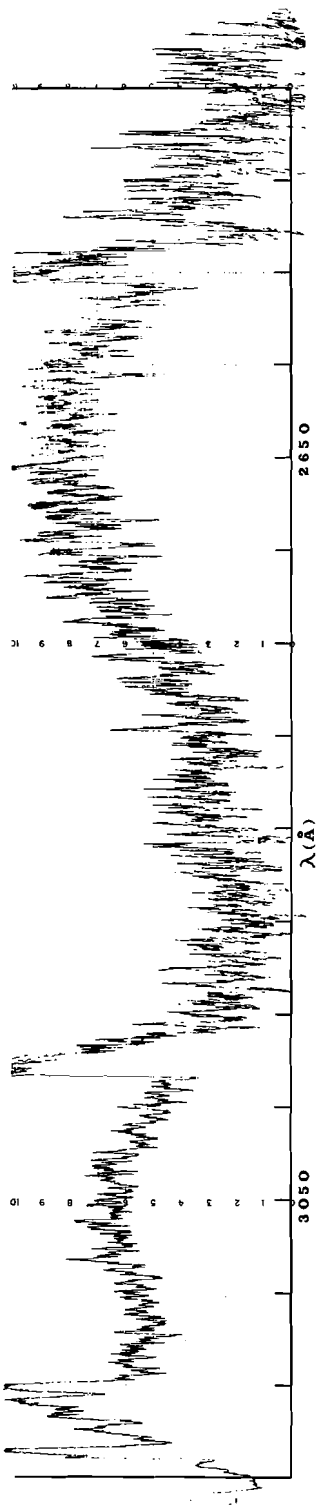

FIG. 4. Spectrometer record of low wavelength continuum of NCN(?) radical. Intensity (arbitrary units) *vs.* wavelength. Note changes in scale at 2535 Å (× 3) and 2985 Å (× 10) relative to base line of 1 at 2450 Å. [N] = 1×10^{-10} mol/cc, pressure = 10 Torr, temperature = 298 °K. Structure near 3150 Å is part of CN violet tail band system.

Can. J. Chem. Downloaded from www.nrcresearchpress.com by 210.87.254.5 on 09/05/12
For personal use only.

species in the excitation of CN which must be produced independently of the N atom recombination steps [1] and [2]. The data can be explained by including [8] and [9] in the mechanism. Inclusion of these reactions produces a term in [12] with the needed pressure dependence to account for the data in Figs. 2 and 3. NCN has been previously detected in active nitrogen (22) and some spectroscopic work has been carried out on this radical (23, 24). Setser and Thrush (1) note that production of NCN should be favored in systems where [N]/[N_2] is low. A careful search of the u.v. near the quartz cutoff under such conditions resulted in observation of a weak "continuum" with maxima at 3050 and 2650 Å (see Fig. 4). The most prominent feature of the "usual" NCN spectrum at 3290 Å was not detected but may have been obscured by strong CN violet tail band emission. Milligan *et al.* (24) refer to an allowed transition in absorption which terminates on a non-linear excited state configuration of NCN, one possible source of the observed feature in this system. As noted in ref. 1 a second possibility for formation of such a non-linear configuration would be excitation of ground state NCN by collision rather than direct formation as in reaction 8. It is not possible to choose between these two explanations on the basis of the present experimental evidence.

Excitation of CN by reactions 8 and 9 has been suggested earlier (4) but Setser and Thrush (1) have argued against reaction 9 on the basis of accumulated evidence which indicates that excitation of products of transfer reactions usually occurs in the newly formed bond. Reaction 9 involving ground state NCN is suggested to be $\sim$125 kcal/mol exothermic (1) and thus provides sufficient energy for excitation of CN to electronically excited radiative states. Excitation to levels requiring more than 125 kcal could be explained if NCN was itself vibrationally or electronically excited. Arrington *et al.* (25) suggest reaction 9 produces $N_2(A^3\Sigma_u^+)$, requiring that NCN is in fact vibrationally hot, since formation of $N_2(A^3\Sigma_u^+)$ requires 149 kcal/mol. If reaction 9 produces $N_2(A^3\Sigma_u^+)$ the simultaneous excitation of CN to the B state would be precluded on energetic grounds. It is possible, however, that a significant fraction of reaction 9 leads to CN excitation since such an event is not spin forbidden and others (1) have noted that such excitation is probable should NCN be non-linear. Reactions 8 and 9 are included in the mechanism largely on the basis of the pressure and atom dependence and behavior of the observed continuum. The calculated rate constant k_8 also appears to be reasonable by comparison with a value of formation of ground state NCN from Arrington *et al.* ($1 \times 10^{18} < k_{NCN} < 8 \times 10^{18}$).

Excitation of CN(X) through energy transfer by collision with other metastable states of nitrogen cannot be definitely excluded. The $N_2(W^3\Delta_u)_{v=0}$ state is probably long-lived in active nitrogen (26) and could be involved. It is not known, however, how this state behaves with respect to pressure and atom concentration changes. The $N_2(a'^1\Sigma_u^-)$ and the $N_2(a^1\Pi_g)$ states have been reported (27) to show dependence on pressure and [N] which would not be compatible with our observations. This is also the case with the N(^2P) atomic state which has been detected in flowing discharged nitrogen (28, 29) through observation of the 3466 Å "line" of the N($^2P \rightarrow {}^4S$) transition. A moderately high concentration of N(^2P) atoms is therefore indicated because of the long ($\tau = 12$ s) radiative lifetime (29) of the transition. The N(^2D) state ($\tau = 26$ h) (30) has not been detected.

The vibrational profile of the $B^2\Sigma^+$ state of CN appears to be sensitive to several factors over a comparatively narrow range of parametric variation. As illustrated in Fig. 5, low pressure (1.5 Torr) limits the emission to those levels in the B state below $v = 6$. A fourfold increase in pressure results in a change to emission from levels in this state up to $v = 15$. The population maxima at $v = 0$, 4, 10, evident at 6 Torr pressure provides strong evidence for the involvement of the CN($A^2\Pi$) state in the overall mechanism of CN excitation–emission since the above levels are quite likely populated through resonance transfer from levels $v = 10$, 17, and 24 of the CN(A) state. In this connection, high resolution spectra of the rotational structure of the (0,0) band (3883 Å), CN($B^2\Sigma^+$) $\rightarrow$ CN($X^2\Sigma^+$), taken at 7 Torr, show perturbations at $K' = 4$, 7, 11, and the "extra" lines reported by Radford and Broida (8). Figure 5 also illustrates the effect of N atom concentration on the profiles. Increase in [N] at low pressure produced a monotonic increase in population of all observed levels while a similar

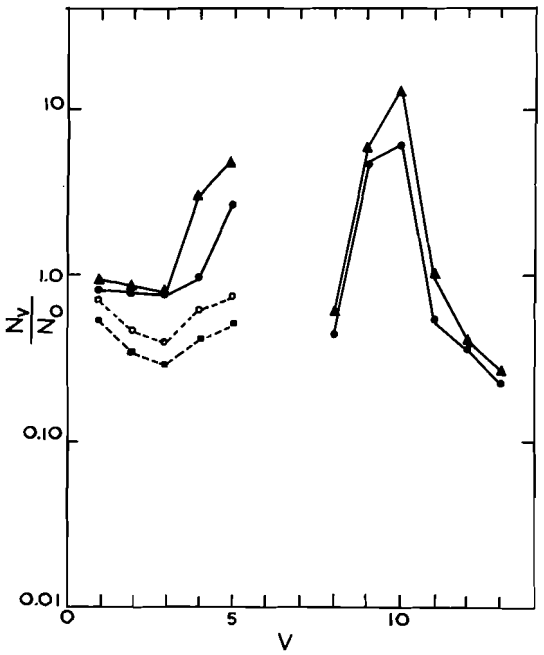

FIG. 5. Relative populations of vibrational levels in the $CN(B^2\Sigma^+)$ state: ■, Pressure = 1.5 Torr, [N] = 6.2×10^{-10} mol/cc; ○, Pressure = 1.5 Torr, [N] = 1.5×10^{-9} mol/cc; ▲, Pressure = 6.0 Torr, [N] = 3.0×10^{-10} mol/cc; ●, Pressure = 6.0 Torr, [N] = 2.3×10^{-9} mol/cc. All data collected at 298 °K. Missing levels (6 and 7) were not listed because of severe overlap. Emission to $v = 15$ was detected.

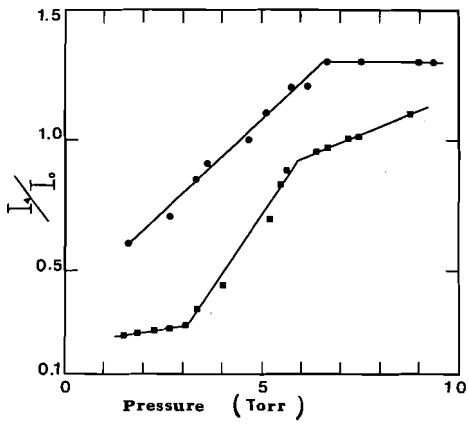

FIG. 6. Relative intensity of the (4,4) band of $CN(B_2\Sigma^+ \rightarrow X^2\Sigma^+)$ to that of the (0,0)-band of the same transition as a function of pressure: ■, [N] = 3.0×10^{-9} mol/cc; ●, [N] = 2.2×10^{-10} mol/cc.

atom concentration increase at higher pressures (>6 Torr) produced the reverse effect. These observations are consistent with the mechanism presented above.

The essential feature of the mechanism is that CN excitation occurs predominantly through energy transfer from vibrationally excited nitrogen. This conclusion is supported by Taieb and Legay (31) who explained excitation of CN to emitting levels in the $CO–N_2$ laser by energy transfer from vibrationally excited nitrogen. At relatively high microwave power the concentration of N_2^* is governed by homogeneous recombination of N atoms and by deactivation of $N_2(A)$ by N atoms. Deactivation by ground state nitrogen is very slow (17). Consequently, the concentration of $N_2(A)$ increases with pressure and decreases with increasing [N].

Equation 11 predicts the observed increase in intensity with [N] at low pressure ($k_3 + k_5[CN] \gg k_6[M]$) and the decrease of $N_2(A)$ by increasing [N] at high pressure (second term in the numerator). The removal of $N_2(A)$ by ground state atoms can produce either ^2P atoms or vibrationally hot ground state N_2. The latter will be formed in levels near $v = 25$ of $X^1\Sigma_g^+$ state of N_2 unless the product atom $N(^4S)$ carries off a large quantity of translational energy. Formation of these hot vibrators, favored at high pressure and high [N], would be expected to change the vibrational profile of the excited CN and produce the higher vibrational level populations responsible for tail band emission.

Figure 6 offers evidence for the participation of two processes in population of the B state. The ratio I_4/I_0 (proportional to N_4/N_0), where I_i stands for the intensity of a transition originating in level i of the B state of CN and N_i represents the population of that same vibrational level, is observed to increase sharply over a small threefold change in pressure. Because of the short radiative lifetime of the B state ($\tau \sim 10^{-8}$ s) (20) vibrational relaxation cannot be important and the effect must be on the precursor. Since the process populating the level $v = 4$ is seen to be favored by pressure increase and retarded by increasing atom concentration, it would appear to be a process involving $N_2(A^3\Sigma_u^+)$. To further test the premise concerning $N_2(A)$, mercury was added to the reactor in the afterglow region. Mercury is known to react rapidly with $N_2(A)$ (32–34).

Can. J. Chem. Downloaded from www.nrcresearchpress.com by 210.87.254.5 on 09/05/12
For personal use only.

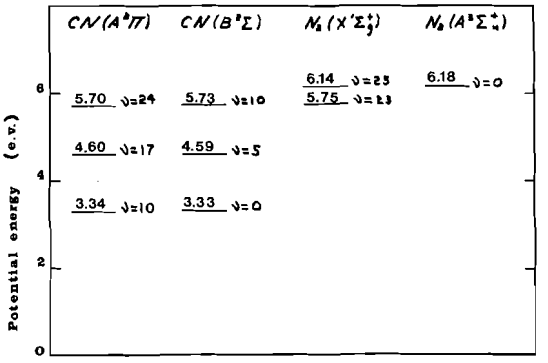

FIG. 7. Partial potential energy scheme for pertinent vibrational levels of molecules discussed in this paper. Energies and levels are indicated under appropriate electronic states. Data for $N_2(X'\Sigma_g^+)$ and $N_2(A^3\Sigma_u^+)$ from Gilmore (35). Energies for $CN(A^2\Pi)$ and $CN(B^2\Sigma^+)$ calculated from data tabulated by Herzberg (36).

The effect of mercury addition was discussed in ref. 7 and provided strong evidence that $N_2(A)$ is not responsible for direct excitation of $CN(B^2\Sigma^+)$ in agreement with Meyer and Setser (6). All of these observations are consistent with the postulated mechanism. The excitation of $CN(B^2\Sigma^+)$ to levels as high as $v = 15$ requires a minimum of 6.49 eV. Excitation to $CN(B)_{v=10}$ requires 5.73 eV. Figure 7 shows the pertinent energies for the species involved. The reaction of $N(^4S)$ with $N_2(A)_{v=1,0}$ will produce either

$$N(^4S) + N_2(A^3\Sigma_u^+) \rightarrow N_2(X^1\Sigma_g^+)_{v<10} + N(^2P)$$

(both products are incapable of exciting CN to $v = 10$ of the B state from $v = 0$ of $CN(X^2\Sigma^+)$), or

$$N(^4S) + N_2(A^3\Sigma_u^+) \rightarrow N_2(X^1\Sigma_g^+)_{v=25} + N(^4S)$$

A large fraction of the $N_2^\ddagger$ produced in this case will be formed at 6.2 eV of the $X^1\Sigma_g^+$ state unless the atom carries off some of the energy in translation, or the $N_2(A^3\Sigma_u^+)$ is itself vibrationally excited. Thus, when the concentration of $N_2(A^3\Sigma_u^+)$ is sufficiently large, it could become a significant source of $N_2^\ddagger$ which could account for the enhancement of tail band emission at high pressures.

Under conditions where NCN is thought to be involved the vibrational profiles were similar to "high pressure" profiles in Fig. 5. Increasing pressure increases intensities from all levels. A decision regarding the relative importance of direct and/or indirect population of CN(B) via the NCN reaction is not possible at this time.

The authors are grateful to the National Research Council of Canada for financial support.

1. D. W. SETSER and B. A. THRUSH. Proc. Roy. Soc. A, **288**, 256 (1965).
2. J. C. BODEN and B. A. THRUSH. Proc. Roy. Soc. A, **305**, 107 (1968).
3. T. IWAI, D. W. PRATT, and H. P. BROIDA. J. Chem. Phys. **49**, 919 (1968).
4. K. D. BAYES. Can. J. Chem. **39**, 1074 (1961).
5. T. IWAI, M. I. SAVADATTI, and H. P. BROIDA. J. Chem. Phys. **47**, 3861 (1967).
6. J. A. MEYER and D. W. SETSER. J. Phys. Chem. **74**, 3452 (1970).
7. G. M. PROVENCHER and D. J. MCKENNEY. Chem. Phys. Lett. **10**, 365 (1971).
8. H. E. RADFORD and H. P. BROIDA. J. Chem. Phys. **38**, 644 (1963).
9. R. L. BROWN and H. P. BROIDA. J. Chem. Phys. **41**, 2053 (1964).
10. F. K. MCTAGGART. Plasma chemistry in electrical discharges. Elsevier, Amsterdam. 1967. p. 65.
11. A. FONTIJN, C. B. MEYER, and H. I. SCHIFF. J. Chem. Phys. **40**, 64 (1964).
12. R. W. F. GROSS and N. COHEN. J. Chem. Phys. **48**, 2582 (1968).
13. K. M. EVENSON and H. P. BROIDA. J. Chem. Phys. **44**, 1637 (1966).
14. R. W. NICHOLLS. Can. J. Chem. **47**, 1847 (1969).
15. R.W. NICHOLLS. J. Res. N.B.S. **68A**, 75 (1964).
16. I. M. CAMPBELL and B. A. THRUSH. Proc. Roy. Soc. A, **296**, 201 (1967).
17. B. STEVENS. Collisional activation in gases. Pergamon Press, Oxford. 1967. pp. 134, 202.
18. B. A. THRUSH. J. Chem. Phys. **47**, 3691 (1967).
19. F. J. LEBLANC. J. Chem. Phys. **48**, 1980 (1968).
20. T. WENTINK, JR., L. ISAACSON, and J. MORREAL. J. Chem. Phys. **41**, 278 (1964).
21. F. KAUFMAN. Progress in reaction kinetics Vol. I. Pergamon Press, New York. 1961.
22. K. R. JENNINGS and J. W. LINNETT. Trans. Faraday Soc. **56**, 1737 (1960).
23. G. HERZBERG and D. N. TRAVIS. Can. J. Phys. **42**, 1658 (1964).
24. D. E. MILLIGAN, M. E. JACOX, and A. M. BASS. J. Chem. Phys. **43**, 3149 (1965).
25. C. A. ARRINGTON, JR., O. O. BERNARDINI, and G. B. KISTIAKOWSKI. Proc. Roy. Soc. A, **310**, 161 (1969).
26. W. M. BENESCH and K. A. SAUM. J. Phys. B, Atom. Molec. Phys. **4**, 732 (1971).
27. I. M. CAMPBELL and B. A. THRUSH. Trans. Faraday Soc. **65**, 32 (1969).
28. G. M. PROVENCHER and D. J. MCKENNEY. Chem. Phys. Lett. **5**, 26 (1970).
29. R. N. GARSTANG. Aurora and airglow. Pergamon Press, New York, N.Y. 1956. p. 324.
30. C. W. UFFORD and R. M. GILMOUR. Astrophys. J. **111**, 580 (1950).

Can. J. Chem. Downloaded from www.nrcresearchpress.com by 210.87.254.5 on 09/05/12
For personal use only.

31. G. TAIEB and F. LEGAY. Can. J. Phys. **48**, 1956 (1970).
32. D. H. STEDMAN, J. A. MEYER, and D. W. SETSER. J. Chem. Phys. **48**, 278 (1968).
33. A. B. CALLEAR and P. M. WOOD. Trans. Faraday Soc. **67**, 272 (1971).
34. R. A. YOUNG and G. A. ST. JOHN. J. Chem. Phys. **48**, 895 (1968).
35. F. R. GILMORE. Potential energy curves for N_2, NO, O_2 and corresponding ions. Memorandum RM-4034-PR Rand Corp., Santa Monica, California. 1964.
36. G. HERZBERG. Spectra of diatomic molecules. D. Van Nostrand Co., Princeton. 1950. p. 520.

Can. J. Chem. Downloaded from www.nrcresearchpress.com by 210.87.254.5 on 09/05/12
For personal use only.

Surface Studies of Heat-treated γ-Aluminas in the Adsorption of Sulfur Dioxide below Monolayer Coverage

R. W. GLASS AND R. A. ROSS

Department of Chemistry, Lakehead University, Thunder Bay, Ontario

Received February 10, 1972

Calorimetric heats of adsorption of sulfur dioxide at surface coverages from 0.1 to 3.5 μmol m^{-2} have been measured on a series of γ-aluminas heat-treated at 500, 700, and 900 °C. Essential features of the structures of the adsorbents have been characterized by analysis of nitrogen adsorption/desorption isotherms and by both direct and indirect electron microscopy.

Heats of adsorption of 423 °K for adsorbed amounts of 0.1 μmol m^{-2} were 48.0, 59.0, and 85.0 kcal mol^{-1} for the 500, 700 and 900 °C samples, respectively. The values for the 500 and 700 °C samples fell rapidly with increasing coverage to around 19.0 kcal mol^{-1} at 3.2 to 3.3 μmol m^{-2}, while the values for the 900 °C sample decreased slowly to 15.0 kcal mol^{-1} at the same coverage.

The pores had circular cross sections and mean diameters of 25, 35, and 40 Å were observed for the 500, 700, and 900 °C samples, respectively. Examination of carbon/platinum replicas of the surface showed the presence of agglomerates of spherical particles approximately 400 Å in diameter.

It is proposed that the high initial heats on the 500 and 700 °C samples are due to the formation of a sulfate-like species on the surface and at higher coverage extensive hydrogen bonding is present. The very high heats obtained on the 900 °C sample are believed to be due to interactions with high-energy defect centers in the oxide which were created by heat treatment.

Les chaleurs calorimétriques de l'adsorption de l'anhydride sulfureux sur des surfaces recouvertes de 0.1 à 3.5 μmol m^{-2}, ont été mesurées pour une série d'alumine γ traitées par la chaleur à 500, 700, et 900 °C. Les caractéristiques essentielles sur les structures des adsorbants ont été obtenues par l'analyse des isothermes d'adsorption et de désorption de l'azote et par la microscopie électronique directe et indirecte.

Les chaleurs d'adsorption à 423 °K pour des quantités adsorbées de 0.1 μmol m^{-2} sont respectivement de 48.0, 59.0, et 85.0 kcal mol^{-1} pour les échantillons à 500, 700, et 900 °C. Les valeurs à 500 et 700 °C chutent rapidement jusqu'à 19.0 kcal mol^{-1} pour 3.2 à 3.3 μmol m^{-2} lorsque la surface d'adsorption croît, tandis que les valeurs à 900 °C décroissent lentement jusqu'à 15.0 kcal mol^{-1} pour la même surface.

Les pores sont de 25, 35, et 40 Å respectivement pour les échantillons à 500, 700, et 900 °C. L'examen des reproductions en carbone–platine de la surface montre la présence d'agglomérats de particules sphériques dans les diamètres qui sont de l'ordre de 400 Å.

On a suggéré que les hautes chaleurs initiales pour les échantillons à 500 et 700 °C sont dues à la formation sur la surface d'espèce de type sulfate, pour des surfaces d'adsorption plus grande, il y a présence très forte de liaison hydrogène. On pense que les très hautes chaleurs obtenues sur l'échantillon à 900 °C sont dues aux interactions entre les défauts de haute énergie dans l'oxyde, créés par la chaleur.

Canadian Journal of Chemistry, **50**, 2537 (1972)

Introduction

Studies have been reported recently of the adsorption of sulfur dioxide up to one-twentieth monolayer coverage on silica gels (1) and on transition metal oxides supported on silica gel (2). Calorimetric heats of adsorption and adsorption isotherms were determined at 423 °K and the adsorbents characterized by measurement of surface areas, pore size distributions, and hydroxyl group concentrations. These data were used to interpret the nature of the adsorbate–adsorbent interactions (1, 2) and now the work has been extended to include a systematic study of the adsorption of sulfur dioxide on heat-treated γ-aluminas.

Although there have been several studies of the adsorption of sulfur dioxide on doped aluminas (3, 4), little work has been reported on pure alumina and little or no heat of adsorption data are available for the sulfur dioxide/alumina system. However, it has been suggested (5) from infrared studies of the adsorption of sulfur dioxide on γ-alumina that both chemisorption and hydrogen-bonding between the oxygen of the sulfur dioxide molecule and hydroxyl groups on the oxide surface takes place.

Experimental

Materials

γ-Alumina was prepared by heating boehmite in air at 500 °C or above for 20 h. The boehmite was prepared by an

Can. J. Chem. Downloaded from www.nrcresearchpress.com by 210.87.254.6 on 09/05/12
For personal use only.

Can. J. Chem. Downloaded from www.nrcresearchpress.com by 210.87.254.6 on 09/05/12
For personal use only.

adaptation of a previous method (6) as follows. A 4.5 *M* aluminum sulfate solution was prepared at 60–65 °C and maintained at this temperature. Ammonium hydroxide (4.5 *M*) was then run in slowly, with vigorous stirring over a period of about 1 h. Throughout this period a continuous stream of ammonia vapor was bubbled into the solution to maintain p*H* 9. The precipitate was allowed to stand for 20 h. After washing the gel with ammoniated water until free of sulfate ions it was dried at 150 °C for 20 h. "AnalaR" grade reagents were used throughout.

X-Ray powder diffraction photographs showed that the product was boehmite (7). Samples of this material were heat-treated in air at 500, 700, and 900 °C for 20 h and X-ray powder diffraction photographs showed that γ-alumina had been formed at all three temperatures although the diffraction lines obtained for the 900 °C sample were much sharper than those for the others.

Immediately after heat-treatment, samples were cooled over phosphorous pentoxide, transferred to the appropriate apparatus and then out-gassed at 150 °C overnight at $< 10^{-4}$ mm.

High-purity nitrogen (>99.99%; Canadian Liquid Air Ltd.) was used in the determination of the low-temperature nitrogen adsorption isotherms. Sulfur dioxide (Matheson Co.) was anhydrous quality and was drawn directly from the cylinder after line-flushing to a tray attached to the apparatus. It was then out-gassed at 10^{-4} mm and vacuum distilled over trays of phosphorous pentoxide. Middle portions only were used and g.l.c. analysis showed these to be >99.99% pure.

Apparatus

Heats of adsorption were determined calorimetrically in a similar apparatus to that described earlier (2). Nitrogen adsorption–desorption isotherms (77 °K) were measured in a standard apparatus (8) and pore size distributions (9) calculated with the aid of an IBM 360/50 computer. Mercury "lump" densities were measured as described previously (10).

Hydroxyl group/water "concentrations" were determined gravimetrically (11) to constant weight at 1200 °C in a static air atmosphere using a recording thermobalance (Stanton–Redcroft Model HT5A).

Electron micrographs were taken with a Philips EM 300G instrument operated at 100 kV. Pore structures were examined by the technique of direct transmission electron microscopy since replica techniques (12) have poor replicating resolution (>50 Å). Specimens were crushed in an agate mortar and suspended in *n*-butyl alcohol. Drops of the suspension were placed on the carbon support film on the microscope grids and the alcohol subsequently removed by evaporation at $< 10^{-5}$ mm. Samples were examined also by the single-stage replication technique (13). The oxides were crushed and suspended as before and drops of the suspension placed on a glass coverslip prior to removal of the alcohol by evacuation. A carbon film was deposited onto the slowly rotating sample in a vacuum evaporator. The entire coverslip fragment was floated on 24% v/v HF for 3 h to dissolve the coverslip and the alumina sample. The replica was then transferred to distilled water and a portion picked up on 200 mesh copper grids before shadowing with platinum at an angle of 35°. The specimen was examined at an accelerating voltage of 80 kV. Instrumental magnification errors were ±2%.

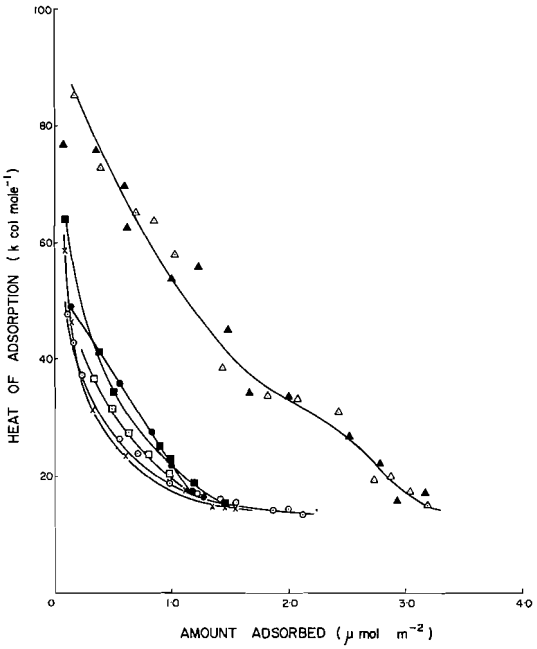

FIG. 1. Heat curves for the adsorption of sulfur dioxide at 423 °K on various heat-treated aluminas. Heat treatment at ○, 500 °C; ×, 700 °C; and △ (run 1), ■ (run 2), ● (run 3), □ (run 4), 900 °C; ▲, 900 °C duplicate sample freshly prepared from boehmite.

Results

Heats of Adsorption and Adsorption Isotherms for Sulfur Dioxide on γ-Alumina

Heats were determined at 423 °K for surface coverages from 0.1 to 2.0 μmol m^{-2} for the 500 and 700 °C samples and between 0.1 and 3.2 μmol m^{-2} for the 900 °C sample. At 423 °K, 7.0 μmol m^{-2} is approximately equivalent to monolayer coverage (2).

All adsorbents exhibited high heats at the lowest coverage, Fig. 1. The heat curves obtained for the 500 and 700 °C samples were almost identical, but differed significantly from that for the 900 °C sample. After a rapid fall between 0.1 and 1.3 μmol m^{-2} the heat curves of the 500 and 700 °C samples levelled out between 13 and 14 kcal mol^{-1} at a surface coverage of 1.5 to 2.0 μmol m^{-2}. In contrast, the curve for the 900 °C sample showed an almost linear decrease in the heat values from 85.0 kcal mol^{-1} at 0.1 μmol m^{-2} to 15.0 kcal mol^{-1} at 3.2 μmol m^{-2}.

The adsorption isotherms for sulfur dioxide at 423 °K are shown in Fig. 2. The shape of the

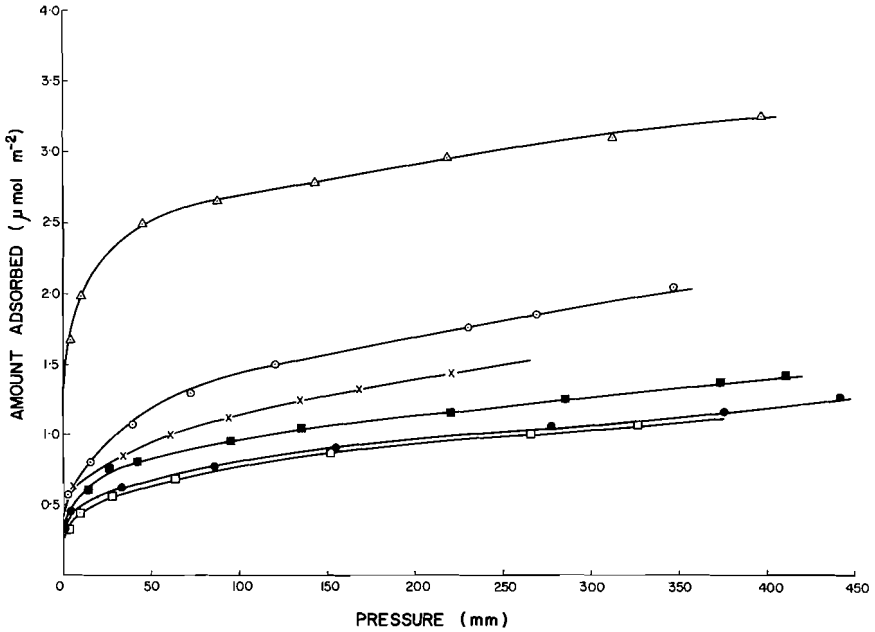

FIG. 2. Adsorption isotherms for sulfur dioxide at 423 °K on heat-treated aluminas. Heat treatment at ○, 500 °C; ×, 700 °C; and △ (run 1), ■ (run 2), ● (run 3), □ (run 4), 900 °C.

isotherms is similar for all samples. A large amount of sulfur dioxide was adsorbed at pressures up to 50 mm followed by a much smaller amount at pressures up to 400 mm. It should be observed that while the amount adsorbed on the 700 °C sample was smaller than that on the 500 °C sample, as might be expected, the amount adsorbed on the 900 °C sample was considerably more than that on the 500 °C sample over the whole pressure range examined.

Additional experiments were carried out with the 900 °C sample to test the possibility of regenerating the "original" surface. The heat curve was measured up to a coverage of 3.2 μmol m^{-2}, the maximum that could be obtained experimentally, corresponding to a maximum pressure of 400 mm. The alumina was then out-gassed overnight at 423 °K at $< 10^{-4}$ mm and samples of the desorbed gas analyzed with a Beckman IR-12 infrared spectrophotometer. No water or any other impurity could be detected. After this procedure, sulfur dioxide was readmitted to the sample and the heat curve determined. The entire experiment was repeated thrice. The heat curves are shown in Fig. 1. No change in the surface area of the alumina was observed after measurement at the end of the fourth run.

The heat curves for the second, third, and fourth runs are close together but at any given coverage, the heat value is only around half of that determined in the first run. The curves for the second, third, and fourth runs appear to begin to level out at about 1.2 μmol m^{-2} to a value approaching 15.0 kcal mol^{-1}, (*cf.* 500 and 700 °C samples, Fig. 1). The amount of sulfur dioxide adsorbed at a given pressure in the second, third, and fourth runs was considerably reduced when compared with that adsorbed during the first run, Fig. 2, and with each succeeding run the adsorption isotherms came closer together.

Nitrogen Adsorption/Desorption Measurements

The nitrogen adsorption/desorption isotherms have the same general shape (Type II) while the amount of nitrogen adsorbed decreases with increase in temperature of heat treatment of the alumina, Fig. 3.

Some differences in the pattern of the desorption isotherms are apparent. The hysteresis loop for the 500 °C sample extended from $p/p_0 = 0.90$ to $p/p_0 = 0.45$, with the loop closing almost vertically. The 700 °C sample had a hysteresis loop extending from $p/p_0 = 0.93$ to 0.58; again the loop closed almost vertically

Can. J. Chem. Downloaded from www.nrcresearchpress.com by 210.87.254.6 on 09/05/12
For personal use only.

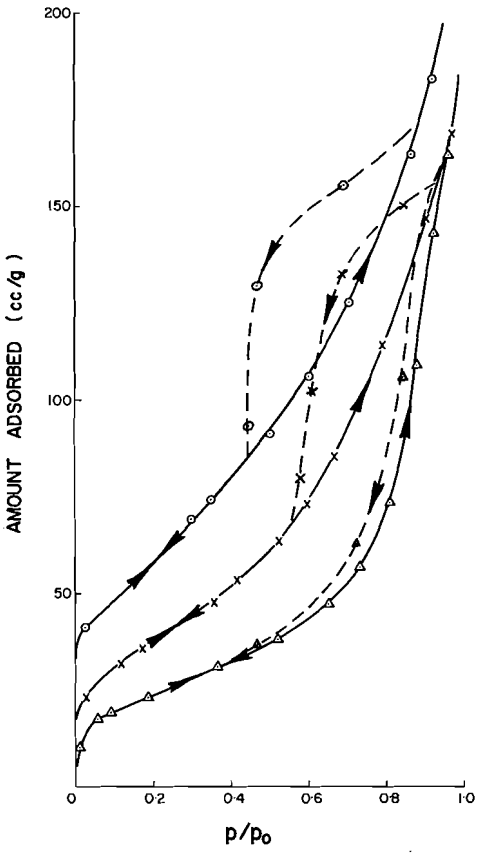

FIG. 3. Nitrogen adsorption/desorption isotherms at 77 °K on heat-treated aluminas. Heat treatment at ○, 500 °C; ×, 700 °C; △, 900 °C.

with its width smaller than that for the 500 °C sample. The 900 °C sample exhibited a hysteresis loop of completely different shape. It was very narrow, extended from $p/p_0 = 0.95$ to 0.50 and closed slowly and smoothly into the path followed by the adsorption isotherm.

The pore size distributions, calculated from the desorption leg of the isotherm on a differential basis, are shown in Fig. 4. The 500 °C sample exhibited two maxima, one at 38 Å and a smaller one at 55 Å. The pore diameter range extended from 28 to 130 Å. The 700 °C sample also showed two maxima, the principal one at 55 Å and the other at 38 Å. The pore diameter range for this sample extended from 23 to 155 Å. The 900 °C sample exhibited at least four maxima at 55, 70, 100, and 145 Å with a pore diameter range from 48 to 220 Å. Figure 4 shows that the percentage of pores larger than 60 Å was greatest for the 900 °C sample.

Table 1 summarizes the data obtained for surface areas (B.E.T. plots), water "concentrations", mercury densities, and the mean pore diameter for each alumina.

Electron Microscope Examinations

The direct transmission micrographs of the three samples (total magnification × 825 000; microscope magnification × 125 000) were very similar. The mean pore diameters of the samples determined from these micrographs are given in Table 1.

A reproduction of the negative of a single-stage replica (total magnification × 125 000; microscope magnification × 25 000) of a 500 °C alumina sample is shown in Fig. 5. The alumina particles consist of globules which appear to have coalesced, each globule being approximately 400 Å diameter. The fine structure which can be observed in the globules is due to the replicating procedure and should not be interpreted as indicating the presence of fine pores. The large white areas are simply due to shadowing effects.

Discussion

The heat curves for the 500 and 700 °C samples are identical, apart from the values measured at the lowest coverage (0.1 μmol m^{-2}), 48.0 and 58.0 kcal mol^{-1} for the 500 and 700 °C samples, respectively. Heats of this order of magnitude clearly indicate that chemisorption has occurred (14). This conclusion is supported by infrared data (5) which suggest that a chemisorbed sulfur dioxide species is present on γ-alumina at 473 °K. One interpretation (5) of the infrared results is that a "sulfate-like" structure may be formed:

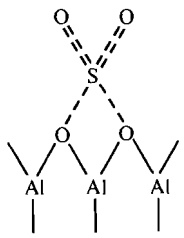

Chemical analysis of the residues in the present experiments did not show the presence of sulfate ions.

Can. J. Chem. Downloaded from www.nrcresearchpress.com by 210.87.254.6 on 09/05/12
For personal use only.

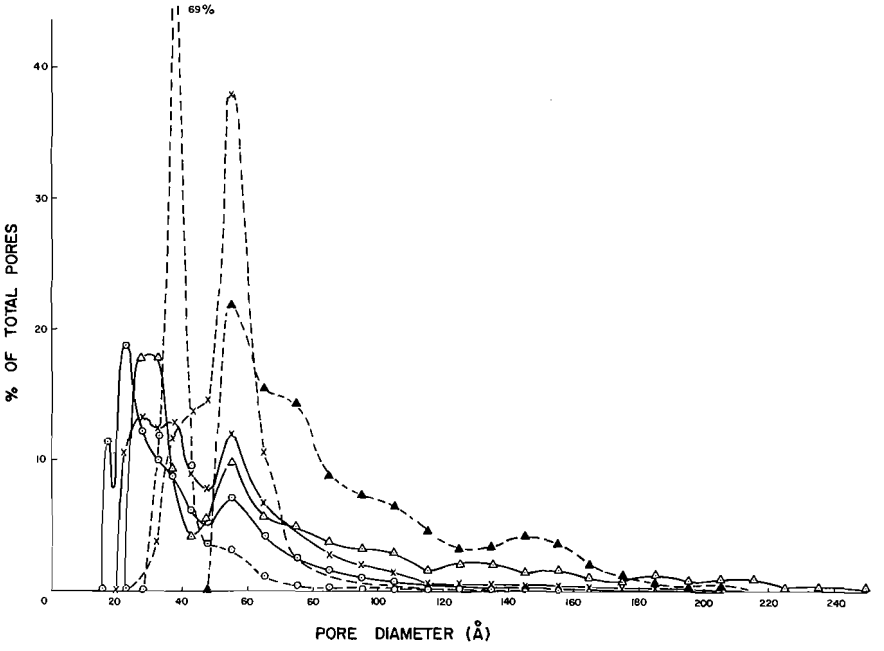

FIG. 4. Pore size distributions based on nitrogen adsorption (—) and desorption (---) isotherms. Alumina heat-treated at ○, 500 °C; ×, 700 °C; △, 900 °C.

TABLE 1. Surface areas, water "concentrations", mercury densities, and mean pore diameters for the heat-treated aluminas

Temperature of heat-treatment (°C)	Surface area ($m^2\ g^{-1}$)	Water "concentration" ($\mu mol\ m^{-2}$)	Mercury density ($g\ cc^{-1}$)	Mean pore diameter (Å)
500	230	19.8	0.6812	25
700	160	18.6	0.6864	35
900	90	7.3	0.6915	40

An approximate value of 10.4 $\mu mol\ m^{-2}$ for a monolayer coverage of water molecules on γ-alumina can be calculated assuming one water molecule is adsorbed (as two OH^- ions) on 16 $Å^2$ in the (100) plane of the oxide (15). Although the present samples are unlikely to be preferentially oriented, this coverage value does give an indication that bulk water is most probably present in the 500 and 700 °C samples. The high concentration of hydroxyl groups and/or water likely to be present on the surface (Table 1), together with the magnitude of the heat of adsorption (16) above a sulfur dioxide coverage of 1.0 $\mu mol\ m^{-2}$, strongly supports the suggestion (5) that bridge-type hydrogen bonds may be formed between the hydroxyl hydrogens and the oxygen atoms of the sulfur dioxide molecule. This is a similar complex to that proposed for the adsorption of sulfur dioxide on silica gel (2).

Peri (15) has made a computerized simulation of the dehydration of spinel-type aluminas and although valid criticisms of his assumptions have been stated (7), the model is still useful. For example, if a spinel-type alumina exposes only (100) planes on the surface then below a surface hydroxyl ion coverage of about 10%, no more adjacent hydroxyl ion pairs are present; and it can be shown (15) that further dehydration is only possible through migration of surface ions. The 900 °C sample has apparently a much higher total hydroxyl group content than 10% (Table 1) but no distinction can be made between surface and bulk water

Can. J. Chem. Downloaded from www.nrcresearchpress.com by 210.87.254.6 on 09/05/12
For personal use only.

FIG. 5. Single stage carbon/platinum replica of alumina after heat-treatment at 500 °C (total magnification × 125 000; microscope magnification × 25 000).

molecules with the present gravimetric method; hence these results are inconclusive in this context.

Above 800 °C protons migrate readily on the surface of alumina (7) while the gradual loss of surface area and slow formation of high temperature forms indicate that both oxide and aluminum ion migration occur (7). Thus the number of surface defects and active acidic sites (17) is likely to increase considerably with the 900 °C sample. The presence of these centers and sites will considerably increase the heterogeneous nature of the 900 °C sample surface when compared with those surfaces prepared at lower temperatures. Normally, it is to be expected that heats of adsorption increase with increase in surface heterogeneity (7) and the results of Fig. 1 are clearly in accord with this concept.

Earlier (1) it was shown that the total amount of sulfur dioxide adsorbed on heat-treated silica gels at 423 °K was closely related to the surface hydroxyl group concentration. Although precise data concerning the surface hydroxyl group concentration cannot be obtained for γ-alumina samples for the reasons outlined, it is likely that the adsorption of sulfur dioxide on the 500 and 700 °C samples follows a similar trend. However, the trend is unlikely to be followed by the 900 °C sample when the interaction between sulfur dioxide molecules and defect centers may be expected to be stronger than that for a bridge-type hydrogen bond interaction.

The data in Figs. 1 and 2 are not in conflict with the concept of the presence of these highly active adsorption centers on the 900 °C sample. In Fig. 1, the heats observed on the second run are only about half the magnitude of those of the first at a given coverage and in each succeeding run the heats become lower still. This pattern would be expected with a heterogeneous surface if after the first run most high energy centers were "neutralized" with fewer high energy sites remaining available for adsorption in succeeding runs. Evidence in favor of this view is found in the observation that 1.05 μmol m^{-2} of sulfur dioxide remained adsorbed following desorption after the first run and this value increased only marginally to 1.10 μmol m^{-2} after the fourth run. Further, if adsorption proceeds principally by interactions with high energy centers and these centers are not regenerated on evacuation, then the amount of sulfur dioxide adsorbed at a given equilibrium pressure should be reduced with each succeeding run as is clearly shown in Fig. 2.

The shapes of the nitrogen adsorption/desorption isotherms are very similar to those found previously (18) for samples of heat-treated boehmite. The hysteresis loops are best described as type "E" for the 500 and 700 °C aluminas and approximately type "A" for the 900 °C sample. Type "E" hysteresis loops can be attributed to tubular pores of some effective diameter which have widened parts of varying diameter (18). This feature is clearly shown in the pore size distributions of the 500 and 700 °C samples in which the effective diameters lie at 30 and 55 Å, respectively. Type "A" hysteresis loops can be related to (*i*) open-ended tubular pores with various forms of cross section with only slightly or no widened parts or to (*ii*) "ink bottle" types of pores with wide or very short necks (18). Either of these possibilities suggests that a wider range of diameters would be observed from the pore size distribution data.

Can. J. Chem. Downloaded from www.nrcresearchpress.com by 210.87.254.6 on 09/05/12
For personal use only.

These data show that with increase in the temperature of heat treatment the maximum in the distribution shifts to pores of wider diameters. At 900 °C sintering of the small pores has probably occurred thus creating an almost random distribution of pores larger than the parents.

The transmission electron micrographs show that the average pore diameter increased with increase in the temperature of heat treatment (Table 1), which supports the trend shown by the pore size distribution data, Fig. 4. However, the average pore diameter for a given sample does not coincide with the pore diameter corresponding to the maximum in the pore size distribution although the average diameter of the pores in the 500 °C sample compares well with other electron micrograph results (19) on γ-alumina.

The apparent discrepancy between the values obtained by the two methods could possibly be explained by the use of the Cranston and Inkley (20) method to determine the pore size distribution. This method was computed for cylindrically-shaped pores closed at one end, whereas the pores of alumina are expected to be slit-shaped (21). However, neither the shapes of the nitrogen adsorption/desorption isotherms nor the electron micrographs confirm the presence of slit-shaped pores and if the pore size distribution is determined from the adsorption leg of the nitrogen isotherm then the maxima correspond more closely with the electron microscope results (Fig. 5).

Various structures have been described (22, 23) for γ-alumina which depend on the conditions of its preparation. For example, agglomerates of (*i*) spherical particles, (*ii*) fibrils, and (*iii*) plate-like layers have all been reported. Clearly, the present preparative method yields agglomerates of spherical particles.

1. R. W. Glass and R. A. Ross. Can. J. Chem. **50**, 124 (1972).
2. R. W. Glass and R. A. Ross. Can. J. Chem. **49**, 2832 (1971).
3. J. I. Paige, J. W. Town, J. H. Russell, and H. I. Kelly. U.S. Govt. Res. Develop. Rep. 70 (21), 55 (1970).
4. J. G. Myers and J. H. Field. (United States Dept. of the Interior) U.S. 3, 551, 093 (Cl. 23-2; B 01j), 1970.
5. A. V. Deo, I. G. Dalla Lana, and H. W. Habgood. J. Catal. **21**, 270 (1971).
6. R. Bennett. Ph.D. Thesis. The Queen's University of Belfast, Belfast, N. Ireland. 1966.
7. B. C. Lippens and J. J. Steggerda. Physical and chemical aspects of adsorbents and catalysts. *Edited by* B. G. Linsen. Academic Press, New York. 1970.
8. L. G. Joyner. Scientific and industrial glass blowing and laboratory techniques. *Edited by* W. E. Barr and V. J. Anhorn. Instruments Publishing Company. Pittsburgh. 1949.
9. A. H. Taylor and R. A. Ross. J. Chem. Eng. Data, **14** (3), 347 (1969).
10. W. B. Jepson. J. Sci. Inst. **36**, 319 (1959).
11. A. V. Kiselev. *In* Colston papers. Vol. 10. Butterworths, London. 1958.
12. D. E. Bradley. Techniques for electron microscopy. *Edited by* D. Kay. Blackwell Scientific Publications, Oxford. 1967.
13. I. Korpenko. J. Am. Ceram. Soc. **51**, (7), 408 (1968).
14. S. J. Gregg. Surface chemistry of solids. Chapman and Hall, London. 1961.
15. J. B. Peri. J. Phys. Chem. **69**, 211 (1965).
16. A. V. Kiselev and V. I. Lygin. Infrared spectra of adsorbed species. *Edited by* L. H. Little. Academic Press, New York. 1966.
17. D. H. McIver, W. H. Wilmot, and J. M. Bridges. J. Catal. **3**, 502 (1964).
18. B. C. Lippens, B. G. Linsen, and J. H. de Boer. J. Catal. **3**, 32 (1964).
19. J. H. Bowen, R. Bowrey, and A. S. Malin. J. Catal. **7**, 209 (1967).
20. R. W. Cranston and F. A. Inkley. Adv. Catal. **9**, 143 (1957).
21. J. H. de Boer, J. J. Steggerda, and P. Zwietering. Konikl. Ned. Akad. Wetenschap., Proc. **B59**, 435 (1956).
22. P. Souza Santos, A. Vallejo-Freire, and H. L. Souza Santos. Kolloid-Z. **133**, 101 (1953).
23. L. Moscou and G. Van der Vlies. Kolloid-Z. **163**, 35 (1959).

Can. J. Chem. Downloaded from www.nrcresearchpress.com by 210.87.254.6 on 09/05/12
For personal use only.

Synthesis and Reactions of 1-Alkyl-3-(*o*-carbalkoxyphenyl)-triazenes

RAYMOND J. LEBLANC AND KEITH VAUGHAN[1]

Department of Chemistry, St. Mary's University, Halifax, Nova Scotia

Received December 23, 1971

The reaction of diazotized anthranilate esters with primary aliphatic amines has been reinvestigated, giving rise to a new series of comparatively unstable 1-alkyl-3-(*o*-carbalkoxyphenyl)-triazenes (**3**). The structures of the products have been confirmed by spectroscopic analysis, molecular ion mass measurements, and from the results of chemical degradation. The spectroscopic properties indicate a preference for the tautomer in which the azo-group is non-conjugated with the benzene ring, Ar·NH·N=N·R; this hypothesis is partly supported by the chemical degradation. In general, the triazenes (**3**) break down by fragmentation of the triazene moiety to give anthranilic acid derivatives, or undergo cyclization to 3-alkyltriazinones (**1**). The alkyltriazinones are also obtained directly in the coupling reaction of the diazonium salt with the amine in the presence of a sodium acetate buffer. The cyclization is quantitative when catalyzed by activity V alumina; a wide variation in the product distribution obtained by reaction with different types of alumina has been observed, and the correlation of these results with the known surface structure of alumina is discussed. Finally, an explanation is offered for the difference between the results of the present work and previous reports.

La réaction des esters anthraniliques diazotés sur les amines primaires aliphatiques a été réexaminée, donnant lieu à une nouvelle série d'alkyl-1 (*o*-carbalkoxyphenyl)-3 triazènes (**3**) relativement instables. Les structures des produits ont été confirmées par analyse spectroscopique, mesure de masse des ions moléculaires et à partir des résultats de la dégradation chimique. Les propriétés spectroscopiques indiquent une préférence pour le tantomère dans lequel le groupe azo n'est pas conjugué au cycle benzènique ArNH·N=N·R; cette hypothèse est en partie confirmée par dégradation chimique. En général les triazènes (**3**) se décomposent par fragmentation du reste triazène qui conduit aux dérivés de l'acide anthranilique, ou subissent une cyclisation en alkyl-3 triazinones (**1**). Les alkyltriazinones sont également obtenues par couplage direct du sel de diazonium avec l'amine en présence du tampon acétate de sodium. La cyclisation est quantitative par catalyse sur alumine d'activité V; une grande variété dans la distribution du produit obtenue par réaction avec divers types d'alumine, a été observée; une corrélation de ces résultats avec la surface d'une structure connue d'alumine est discutée. Finalement, une explication est donnée pour la différence entre les résultats de ce travail et ceux rapportés jusqu'ici.

Canadian Journal of Chemistry, **50**, 2544 (1972)

Generally, the reaction of a diazonium salt with a primary aliphatic amine results in substitution of both amino hydrogen atoms, yielding a 3-alkylpentaz-1,4-diene, Ar·N=N·NR·N=N·Ar, and the intermediate diazoamino compound, Ar·N=N·NHR, is not usually isolated (1). In contrast, 1,3-diaryltriazenes, Ar·N=N·NH·Ar, are readily obtained in high yield from the coupling reaction of the diazonium salt with a primary aromatic amine (2). A much used method of synthesis of 3-aryl-1,2,3-benzotriazin-4-ones (**1**, R = aryl) involves diazotization of an alkyl anthranilate (**2**, R′ = Me or Et), coupling of the diazonium salt solution with a primary aromatic amine, $ArNH_2$, and cyclization of the resulting *o*-carbalkoxyphenyltriazene (**3**, R = aryl, R′ = alkyl) in boiling aqueous ethanol (3). On the other hand, the reaction of diazotized anthranilate esters with primary aliphatic amines has been reported (4–6) to afford directly the 3-alkyl-1,2,3-benzotriazinone (**1**, R = alkyl), although often in low yield. 1-Alkyl-3-(*o*-carbalkoxyphenyl)-triazenes (**3**, R and R′ = alkyl) have been postulated (4, 6) as intermediates in the latter reaction, but in no previously reported case has the intermediate been isolated.

We report a reinvestigation of the reaction of diazotized anthranilate esters with primary aliphatic amines, affording a series of 1-alkyl-3-(*o*-carbalkoxyphenyl)-triazenes (**3**) in good to excellent yields, and an extensive study of the properties and reactions of these compounds.

For example, treatment of a solution of *o*-carbethoxybenzene diazonium salt with excess of methylamine affords an 84% yield of 1-methyl-3-(*o*-carbethoxyphenyl)-triazene (**3***a*); the product must be isolated from the reaction

[1]To whom all correspondence should be addressed.

Can. J. Chem. Downloaded from www.nrcresearchpress.com by 210.87.254.40 on 09/05/12
For personal use only.

Can. J. Chem. Downloaded from www.nrcresearchpress.com by 210.87.254.40 on 09/05/12
For personal use only.

mixture immediately after addition of the amine. 3-Methyl-1,2,3-benzotriazin-4-one (**1***a*) is obtained in excellent yield if the reaction mixture is stirred for a while after the addition of methylamine. Evidently, under the strongly basic conditions employed, the intermediate triazene (**3***a*) is sufficiently stable to be isolated, but undergoes a slow cyclization when left in the reaction mixture. The cyclization is apparently acid-catalyzed since the methyltriazinone (**1***a*) is formed rapidly, when the coupling reaction of the diazonium salt with methylamine is carried out in the presence of a sodium acetate buffer (weak acid). In fact, as described later, the methyltriazinone (**1***a*) is one of the products of acid hydrolysis of the triazene (**3***a*).

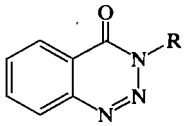

1

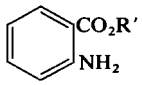

2

a R = Me
b R = Et
c R = *n*-Pr
d R = *i*-Pr
e R = $PhCH_2$

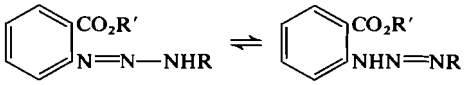

i *ii*

3

a R = Me; R′ = Et
b R = R′ = Et
c R = *n*-Pr; R′ = Et
d R = cyclohexyl; R′ = Et
e R = $PhCH_2$; R′ = Et
f R = Et; R′ = Me
g R = R′ = Me

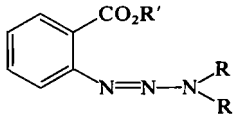

4

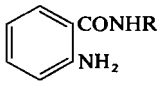

5

The reaction of diazotized anthranilate esters with primary aliphatic amines to give triazenes is not entirely general. 1-Alkyl-3-(*o*-carbalkoxyphenyl)-triazenes (**3***a*–*g*) were obtained in 40–100% yields by diazotization of the alkyl anthranilate (**2**), followed by rapid treatment of the cold diazonium salt solution with an excess of the amine, RNH_2. In the case of reaction of ethylamine with diazotized ethyl anthranilate, a minor yield of the ethyltriazinone (**1***b*) was also obtained. In one reaction, that of *iso*-propylamine with the diazonium salt, the intermediate triazene was not isolated, but in that instance an 80% yield of the *iso*-propyltriazinone (**1***d*) was obtained. This anomaly does not seem to be a function of the nature of the alkyl group, since reaction of the closely similar cyclohexylamine proceeds normally. In two instances, the reactions of *n*- and *iso*-butylamine, neither the expected triazenes nor the cyclization products were isolated; in both cases a quantitative recovery of the anthranilate ester results.

The triazenes (**3***a*–*g*) were frequently obtained contaminated with anthranilate ester if, in the coupling reaction, the amine was added slowly to the diazonium salt solution or if the temperature of the reaction mixture was not maintained at or close to 0°. van Heyningen (4) also observed anthranilate ester regeneration in these reactions. Since it is unlikely that the amine could be formed directly from the diazonium salt (1), it appears that triazene formation does take place in these reactions and that the regeneration of anthranilate ester arises from a fragmentation of the triazene (see later discussion).

The 1-alkyl-3-(*o*-carbalkoxyphenyl)-triazenes (**3**) (Table 1) are unstable, low melting solids or viscous oils, which decompose on standing, in some instances completely within 48 h, affording the corresponding 3-alkyltriazinone (**1**). The solid triazenes are also prone to decomposition when recrystallization is attempted, in some cases precluding further purification. Attempted distillation of the oils resulted in decomposition at approximately 130°. Attempted purification by column chromatography (alumina or silica) results in rapid decomposition on the column with gas evolution. All efforts to separate mixtures of triazene and anthranilate, obtained in the coupling reactions described above, failed due to decomposition of the triazene. Consequently, some of the physical and spectroscopic data in Table 1 relate to unpurified products, but these data show that the triazenes are obtained quite pure directly from the reaction mixture.

Can. J. Chem. Downloaded from www.nrcresearchpress.com by 210.87.254.40 on 09/05/12
For personal use only.

TABLE 1. 1-Alkyl-3-(*o*-carbalkoxyphenyl)-triazenes*

Compound	R	R′	Yield (%)	m.p. (°C)	b.p. (°C)	Molecular formula	Molecular ion (mass spectrum) Found	Calcd.	N.m.r. ($CDCl_3$) δ(p.p.m.)	Protons	ν_{max} (cm^{-1})
a	Me	Et	84	35–36†	—	$C_{10}H_{13}N_3O_2$	207.1010	207.1008	11.93(1H, s) 6.75–8.09(4H, m) 4.33(2H, q) 3.57(3H, s) 1.37(3H, t)	NH aromatic O—CH_2 N—Me C—Me	3300 (NH) 1690 (CO) 1495 (N=N)
b	Et	Et	75	—	dec. 132	$C_{11}H_{15}N_3O_2$	221.1166	221.1164	11.90(1H, s) 6.70–8.05(4H, m) 4.30(2H, q) 3.71(2H, q) 1.30(3H, t) 1.23(3H, t)	NH aromatic O—CH_2 N—CH_2 O·C·Me N·C·Me	"
c	*n*-Pr	Et	100	—	dec. 130	$C_{12}H_{17}N_3O_2$	235.1320	235.1321	11.95(1H, s) 6.67–8.10(4H, m) 4.33(2H, q) 3.70(2H, t) 1.55–1.99(2H, m) 1.35(3H, t) 0.99(3H, t)	NH aromatic O—CH_2 N—CH_2 C·CH_2·C O·C·Me C·Me	"
d	Cyclohexyl	Et	86	35–36‡	—	$C_{15}H_{21}N_3O_2$	275.1633	275.1634	11.87(1H, s) 6.70–8.06(4H, m) 4.30(2H, q) 3.5(1H, m, broad) 1.0–2.1(10H, m) 1.30(3H, t)	NH aromatic O—CH_2 N—CH methylenes O·C·Me	"
e	$PhCH_2$	Et	80	28–29‡	—	$C_{16}H_{17}N_3O_2$	283.1319	283.1321	12.02(1H, s) 6.67–8.00(9H, m) 4.83(2H, s) 4.25(2H, q) 1.25(3H, t)	NH aromatic N—CH_2 O—CH_2 O·C·Me	"
f	Et	Me	40	26–27§	—	$C_{10}H_{13}N_3O_2$	207.1002	207.1008	11.88(1H, s) 6.72–8.05(4H, m) 3.83(3H, s) 3.70(2H, q) 1.28(3H, t)	NH aromatic O—Me N—CH_2 O·C·Me	"
g	Me	Me	67	33–34§	—	$C_9H_{11}N_3O_2$	193.0849	193.0851			"

*Due to the unstable nature of these compounds, satisfactory elemental analyses could not be obtained.
†From aqueous ethanol.
‡From ethanol.
§Decompose upon recrystallization.
‖A satisfactory n.m.r. spectrum could not be obtained due to rapid decomposition in solution.

[1] 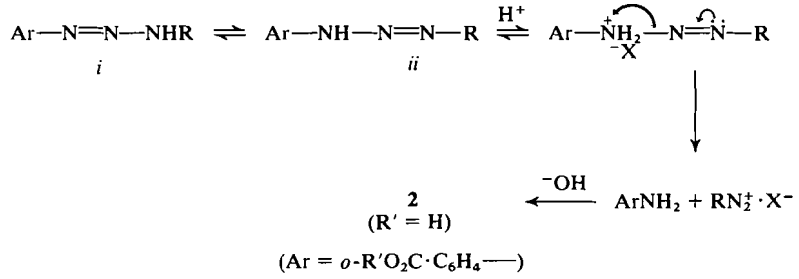

The i.r. spectra of all the triazenes (**3***a–g*) display N—H absorption at 3300 cm^{-1}, carbonyl absorption at 1690 cm^{-1}, and a strong band at 1495 cm^{-1}, assigned to the azo group, N=N, stretching vibration. The N=N stretching frequency of 1-aryl-3,3-dialkyl triazenes (**4**) has been identified with absorption at 1410–1415 cm^{-1} in the i.r. (7); absorption in the region 1400–1420 cm^{-1} is either very weak or non-existent in the i.r. spectra of the triazenes (**3**). The high frequency of N=N absorption in the triazenes (**3**) suggests non-conjugation of the azo and phenyl groups, indicating a preference for tautomer **3***ii* over **3***i*. The n.m.r. chemical shifts and splitting patterns are consistent with the assigned structures (**3**), and also favor tautomer *ii*. The amino (NH) proton signal is broad in the range 11.87–12.02 p.p.m., compared with 10.95 p.p.m. for compounds of the type ArNH·N=C< (8). Molecular formulae are supported by high resolution molecular ion mass measurement.

The chemical properties of the triazenes (**3**) are also in accord with the assigned structures. Thus, refluxing the triazenes (**3***a*, *e* and *g*) in aqueous ethanol gave the corresponding 3-alkyltriazinones (**1***a* or *e*) in 65–92% yields. Similar treatment of the *n*-propyltriazene (**3***c*) gave a mixture of the *n*-propyltriazinone (**1***c*) and ethyl anthranilate, and of triazenes (**3***b* and *d*) gave only ethyl anthranilate. The formation of the triazines in these reactions compares with analogous cyclizations of 1-aryl-3-(*o*-carbalkoxyphenyl)-triazenes (**3**, R = aryl, R′ = alkyl) (3), but the formation of ethyl anthranilate has not been observed in the reactions of the aryl series. The overall yield of alkyltriazinone (**1**) in these reactions, based on alkyl anthranilate as starting material, is as high as 60%, and is raised to over 80% when the alumina-catalyzed method of cyclization, described below, is employed, representing a substantial improvement over the 20–30% yields reported previously (4). Alkaline hydrolysis of the methyltriazene (**3***a*) gave a high yield of anthranilic acid (**2**, R′ = H), whereas the major product of acid hydrolysis is ethyl anthranilate, with a minor yield of the methyltriazinone (**1***a*).

The formation of anthranilate esters in the degradation reactions of the triazenes (**3**) is best described as an example of general acid–base catalysis. In the case of acid catalysis, either mineral or very weak acid such as water or ethanol, the reaction probably proceeds by protonation of tautomer *ii*, followed by a fragmentation similar to that observed in the diazoamino → aminoazobenzene rearrangement (7) eq. 1.

In the case of alkaline hydrolysis, the equilibrium *i* ⇌ *ii* may be facilitated to the right, leading eventually to exclusive formation of anthranilic acid (**2**, R′ = H), after hydrolysis of the ester group. An alternative route to anthranilic acid in an alkaline medium involves nucleophilic displacement at the azo-nitrogen atom in tautomer *ii*, resulting in replacement of the arylamino group by hydroxide ion eq. 2. There is no evidence in the literature to support

[2] 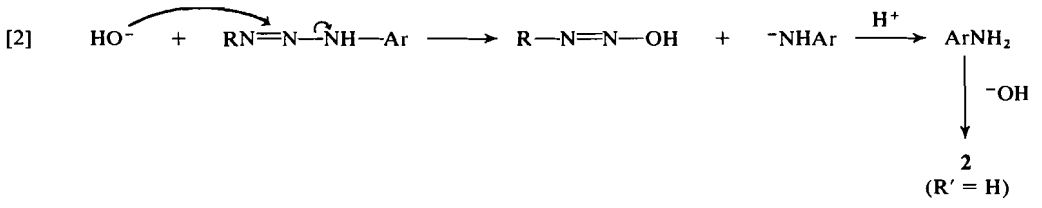

Can. J. Chem. Downloaded from www.nrcresearchpress.com by 210.87.254.40 on 09/05/12
For personal use only.

TABLE 2. Product distribution in the alumina-catalyzed decomposition of 1-methyl-3-(*o*-carbethoxyphenyl)-triazene (**3***a*)

Type of alumina	Activity	Bake-out temperature* (°C)	Reaction time (min)	Yield (%)	
				Ethyl anthranilate	Triazine (**1***a*)
Basic	I	—	35	41	38
Neutral	I	—	35	54	24
Acid	I	—	35	62	8
Basic	I	120	35	—	100
Neutral	I	120	35	23	73
Acid	I	120	35	64	36
Basic	I	300	35	11	81
Neutral	I	300	35	51	36
Acid	I	300	35	61	16
Basic	I	600	35	33	64
Acid	I	600	35	79	10
Basic	II†	—	35	—	91
Basic	V†	—	12 (h)	—	100
Neutral	V†	—	12 (h)	—	100
Acid	V†	—	12 (h)	—	100

*Activity I alumina was baked out at the given temperature for an overnight period immediately prior to use.
†Activity II and V alumina were obtained from the commercial activity I alumina by addition of the quantity of water specified by the manufacturer.

this latter postulation, although van Heyningen (4) made a similar proposal to account for reformation of anthranilate ester in the coupling reaction described previously.

The observation that the triazenes (**3**) undergo cyclization to the triazinones (**1**) under acidic conditions, frequently accompanied by fragmentation to anthranilate ester, suggests that protonation at the carbonyl-oxygen competes successfully with protonation at the amino-nitrogen, catalyzing the cyclization reaction, thus [3].

The alumina-catalyzed decomposition of 1-methyl-3-(*o*-carbethoxyphenyl)-triazene (**3***a*) in anhydrous benzene has been extensively studied. Two modes of reaction are evident: (*a*) cyclization to the methyltriazinone (**1***a*); (*b*) triazene cleavage to ethyl anthranilate, with concomitant evolution of nitrogen gas. The proportion of the two products varies a great deal with the nature of the alumina, and the product distributions obtained with various types of alumina are shown in Table 2.

The compositions of mixtures of ester and triazinone obtained in these reactions, and also in the acid hydrolysis of **3***a*, have been determined by a quantitative i.r. method, which permits rapid analysis and does not require separation of the components. The method thus eliminates any inaccuracies that might be introduced if the mixtures were separated by distillation or chromatography. The method derives from the fact that ethyl anthranilate absorbs strongly at 3500 cm^{-1} (NH stretch) in the i.r., whereas the triazinone (**1***a*) is essentially transparent above 3000 cm^{-1}, but absorbs strongly at 960 cm^{-1} (assigned to N—N stretch). Ethyl anthranilate is almost transparent between 900 and 1000 cm^{-1}. Measurement of the relative intensities of the 3500 and

[3]

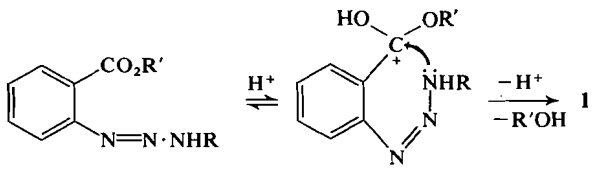

Can. J. Chem. Downloaded from www.nrcresearchpress.com by 210.87.254.40 on 09/05/12
For personal use only.

960 cm^{-1} peaks in the i.r. spectrum of an unknown mixture, and comparison with a series of mixtures of known composition, allowed determination of the composition of the unknown without separation.

Several general trends are evident from the data in Table 2. The yield of triazinone increases as the activity of the alumina is lowered, and is quantitative for activity V alumina, whether acid, neutral, or basic. (This reaction represents the most efficient way of synthesizing the methyltriazinone (**1***a*) from the triazene.) For a particular activity, the ratio of the yields, triazinone:ester, is greatest for basic alumina, least for acid alumina, and intermediate for neutral alumina. The yield of triazinone is also increased markedly by baking out the alumina at 120° prior to reaction, but this effect is lessened somewhat by baking out at higher temperatures.

The product distributions in the acid alumina-catalyzed reactions are almost identical to the distribution of products obtained in the reaction of the triazene (**3***a*) with mineral acid. The acidic sites on the surface of alumina can be either Bronsted or Lewis acid sites, the latter probably being due to the exposure of Al^{3+} ions at the surface (9, 10), so it seems likely that the acid alumina-catalyzed reaction proceeds according to eqs. 1 and 3, or by similar routes involving Al^{3+} ion instead of H^+. The action of acid alumina is completely changed by addition of a small amount of water (activity V), triazinone formation taking over completely, suggesting that adsorbed water molecules cover the previously exposed Lewis acid sites.

The reaction of the triazene (**3***a*) with basic alumina, giving triazinone formation almost exclusively, is very different from the reaction with aqueous alkali. The mechanisms represented by eqs. 1 and 2 are seemingly not applicable in this instance. An alternative course for triazinone formation, involving base catalysis, is proton abstraction from the amino nitrogen, followed by nucleophilic addition at the ester carbonyl group (eq. 4). There does not appear to be a reasonable explanation for the fact that cyclization does not take place in aqueous alkali.

The effect of baking out the alumina before use is more pronounced for basic than for acid alumina, resulting in preference for triazinone formation. de Boer (11) has shown that surface water in alumina is removed easily at 120°, exposing a greater number of active sites. In the case of basic alumina, this might result in a greater facility to catalyze the cyclization by a mechanism such as [4]. At higher temperatures, adjacent ^-OH groups are expelled as water molecules, leaving behind exposed Al^{3+} ions and thus increasing the proportion of acid sites on the surface (10). The observation that the triazinone yield drops in favor of anthranilate formation if the alumina is baked out at a higher temperature, 300 or 600°, is in accordance with these postulations.

Conclusion

The results presented in this paper provide an explanation for the fact that previous workers did not isolate the intermediate triazenes (**3**). The use of a sodium acetate buffer in the coupling reaction is very common, but the present work shows that the 1-alkyl-3-aryltriazenes cannot be isolated when the coupling reaction is buffered. This is in contrast to the reaction of diazonium salts with aromatic primary amines, in which case the yield of diazoamino compound is increased by the use of a buffer (2, 3). van Heyningen (4) used a direct coupling reaction with the aliphatic amine without a buffer, but yet did not isolate the intermediates. Indeed, the conditions of reaction in the present work are virtually identical with those employed by van Heyningen; the difference must be in the method of work-up.

van Heyningen purified his products by distillation under reduced pressure, obtaining low yields of triazinone (**1**) and a high recovery of the starting material, alkyl anthranilate. We have shown here that the coupling reaction of diazonium salts with aliphatic primary amines

[4] 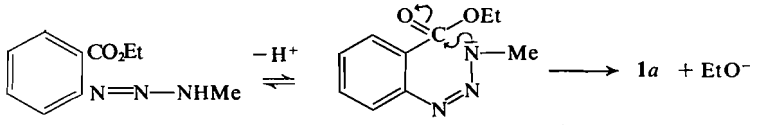

Can. J. Chem. Downloaded from www.nrcresearchpress.com by 210.87.254.40 on 09/05/12
For personal use only.

Can. J. Chem. Downloaded from www.nrcresearchpress.com by 210.87.254.40 on 09/05/12
For personal use only.

sometimes affords a mixture of the intermediate triazene and *regenerated* alkyl anthranilate, that the intermediates are extremely unstable, resisting all attempts at separation from mixtures, and further that the decomposition of the triazenes (**3**) frequently gives rise to a mixture of triazinone and alkyl anthranilate. Thus, it seems very likely that van Heyningen did in fact isolate the triazenes, either pure or as mixtures with anthranilate, but also equally likely that they decomposed on distillation. Therefore, there is little contradiction between the present work and previously reported results; simply a slight modification of conditions and work-up that results in the isolation of previously unobserved reaction intermediates.

Experimental

Melting points were obtained on a Fisher–Johns apparatus and are corrected. The i.r. spectra were recorded with liquid paraffin mulls on a Perkin–Elmer Infracord spectrophotometer. N.m.r. spectra were obtained with a Varian A-60A spectrometer using tetramethylsilane as the internal standard, and mass spectra with a Dupont/C.E.C. model 21-110B high resolution spectrometer. Molecular ion mass measurements were done by the peak-matching method using electrical detection. Merck grade alumina was obtained from Brinkmann Instruments (Canada) Limited.

*1-Alkyl-3-(o-carbalkoxyphenyl)-triazenes (**3***a–g*)*

Methyl or ethyl anthranilate (0.006 mol) was added to 2 *M* hydrochloric acid (9.0 ml) and diluted with water (20 ml) to dissolve the precipitated salt. The resulting solution was cooled to 0°, diazotized with sodium nitrite (0.45 g) in a minimum volume of water, and stirred at 0° until a clear solution was obtained (up to 1 h). An aqueous solution of the appropriate amine (0.036 mol) was added to the cold diazonium salt solution in one portion, and the solid which separated was isolated immediately by filtration and crystallized from ethanol or aqueous ethanol to afford the *1-alkyl-3-(o-carbalkoxyphenyl)-triazenes* (**3**) as colorless or pale yellow prisms (Table 1). Some of the products separated from the reaction mixture as oils; these were isolated by extraction with ether and evaporation of the washed and dried (Na_2SO_4) ether extract. Attempted purification of the oils by distillation or chromatography resulted in decomposition.

In the reaction of diazotized ethyl anthranilate with ethylamine, affording the triazene (**3***b*), the aqueous mother liquor gave a precipitate on standing, identified as 3-ethyl-1,2,3-benzotriazin-4-one (**1***b*) (11%), m.p. 68.5–70° (lit. (4) 70–71°), ν_{max} 1675 cm^{-1}.

The reaction of diazotized methyl anthranilate with *n*-butylamine or *iso*-butylamine resulted in quantitative recovery of methyl anthranilate.

*3-Methyl-1,2,3-benzotriazin-4-one (**1a**)*

(*a*) 1-Methyl-3-(*o*-carbethoxyphenyl)-triazene (**3***a*) (1.0 g) was refluxed in 70% aqueous ethanol (30 ml) for 4 h. The solution was concentrated *in vacuo* and the precipitated solid was filtered to yield 3-methyl-1,2,3-benzotriazin-4-one (**1***a*) (0.5 g, 65%), m.p. 121–122 °C (ethanol), ν_{max} 1670 cm^{-1} (C=O), which was identical with an authentic sample (i.r. spectrum and mixed m.p. 122–122.5 °C) prepared by diazotization of *N*-methylanthranilamide (**5**, R = Me) (12).

Similar treatment of 1-methyl-3-(*o*-carbomethoxyphenyl)-triazene (**3***g*) gave an identical product (yield 92%).

(*b*) A cold solution of ethyl anthranilate (1.0 g) in concentrated hydrochloric acid (1.75 ml) and water (30 ml) was diazotized with aqueous sodium nitrite (0.45 g in a minimum volume of water). The resulting diazonium salt solution was treated with 40% aqueous methylamine dropwise with constant agitation, at such a rate that the temperature did not rise above 0 °C, until the solution was strongly alkaline ($pH > 11$). A precipitate appeared at this stage, but was not separated. The mixture was allowed to warm to room temperature slowly with stirring, and after stirring overnight the precipitate was collected to yield the methyltriazinone (**1***a*) (0.8 g, 82%), m.p. 120 °C, identical with a sample prepared above.

(*c*) Ethyl anthranilate (1.0 g) was dissolved in 2 *M* hydrochloric acid (9 ml) and water (20 ml) and the solution cooled to 0 °C. The cold solution was diazotized with sodium nitrite to starch–iodide end-point and then made neutral by the addition of a solution of sodium acetate (17.2 g) in water. 40% aqueous methylamine (3.5 ml) was added quickly in one portion, forming a yellow precipitate which was filtered immediately to yield the methyltriazinone (**1***a*) (0.8 g, 82%), identical with a sample prepared above.

(*d*) 1-Methyl-3-(*o*-carbethoxyphenyl)-triazene (**3***a*) (0.5 g) was dissolved in anhydrous benzene (50 ml) and activity V alumina (6.0 g) was added. The resulting slurry was stirred for 12 h at room temperature and filtered. The residual alumina was washed several times with aliquots (10 ml) of anhydrous benzene and the combined filtrate and washings evaporated to dryness *in vacuo* to yield the methyltriazinone (**1***a*) (yield quantitative) identical with a sample prepared above.

*3-Benzyl-1,2,3-benzotriazin-4-one (**1e**)*

Refluxing 1-benzyl-3-(*o*-carbethoxyphenyl)-triazene (**3***e*) in aqueous ethanol, as under procedure *a* above, gave the benzyltriazinone (**1***e*), in 70% yield, m.p. 120–121.5 °C (lit. (5) 122–123 °C), ν_{max} 1670 cm^{-1}.

*3-(n-Propyl)-1,2,3-benzotriazin-4 one (**1c**)*

1-(*n*-Propyl)-3-(*o*-carbethoxyphenyl)-triazene (**3***c*) (0.5 g) was refluxed in 70% aqueous ethanol (15 ml) for 2 h. The solution was concentrated *in vacuo* to remove ethanol and the aqueous residue was extracted with chloroform. Evaporation of the dried (Na_2SO_4) extract yielded a yellow oil which partly solidified on standing. Filtration of the mixture yielded, from the solid phase, the *n*-propyltriazinone (**1***c*) (0.11 g, 27.5%), m.p. 56–56.5 °C (aqueous ethanol) (lit. (13) 61–62°), ν_{max} 1675 cm^{-1}. The oily filtrate was identified as ethyl anthranilate (0.23 g, 66%) by comparison with an authentic sample (Eastman).

Similar treatment of 1-ethyl-3-(*o*-carbethoxyphenyl)-triazene (**3***b*) or of 1-cyclohexyl-3-(*o*-carbethoxyphenyl)-triazene (**3***d*) gave only ethyl anthranilate (yields 78 and 67% respectively).

*3-(i-Propyl)-1,2,3-benzotriazin-4-one (**1d**)*

A solution of methyl anthranilate (1.0 g) in 2 *M* hydro-

Can. J. Chem. Downloaded from www.nrcresearchpress.com by 210.87.254.40 on 09/05/12
For personal use only.

chloric acid (9.9 ml) and water (20 ml) was cooled below 5 °C and diazotized with sodium nitrite (0.45 g) in water. 40% aqueous *iso*-propylamine (6.4 ml) was added slowly, giving a strongly alkaline solution (no precipitate was evident at this stage), which was stirred at room temperature for 5 days. The precipitated solid was filtered to afford the *iso*-propyltriazinone (**1***d*) (1.0 g, 80%), m.p. 55.5–56.0° (lit. (5) 60–61°), ν_{max} 1680 cm^{-1}.

*Alkaline Hydrolysis of 1-Methyl-3-(o-carbethoxyphenyl)-triazene (**3***a*)

1-Methyl-3-(*o*-carbethoxyphenyl)-triazene (0.75 g) was refluxed in 2 *M* sodium hydroxide (25 ml) for 1 h. The resulting yellow solution was cooled, acidified to p*H* 5.5 by the addition of glacial acetic acid (6.8 ml) and extracted with chloroform. Evaporation of the dried (Na_2SO_4) chloroform extracts afforded anthranilic acid (0.45 g, 90%), identical (m.p. and mixed m.p. 143–144°, i.r. spectrum) with an authentic sample (Eastman).

*Acidic Hydrolysis of 1-Methyl-3-(o-carbethoxyphenyl)-triazene (**3***a*)

The triazene (**3***a*) (0.5 g) was added to cold 1 *M* sulfuric acid (10 ml), whereupon a vigorous effervescence took place and a clear pink solution resulted immediately. The solution was basified at once with concentrated ammonia (2.0 ml) and extracted with chloroform, yielding an orange oil (0.35 g). Analysis of the residue by quantitative i.r. measurements showed that it was a mixture of ethyl anthranilate (75% yield) and 3-methyl-1,2,3-benzotriazin-4-one (**1***a*) (14% yield).

*Alumina-catalyzed Decomposition of 1-Methyl-3-(o-carbethoxyphenyl)-triazene (**3***a*)

General Procedure

The triazene (**3***a*) (1.0 g) was dissolved in anhydrous benzene (100 ml) and alumina (12 g) was added in one portion. The slurry was stirred at room temperature for 35 min or 12 h, dependent on the activity of the alumina (see Table 1). The alumina was removed by filtration and washed with 5 × 10 ml aliquots of anhydrous benzene; in some cases Soxhlet extraction was necessary to desorb all organic material from the catalyst. The combined benzene washings and extracts were evaporated to dryness *in vacuo*. At this stage, the residue was either a solid or an oil. In the former case, the solid was invariably identified as 3-methyl-1,2,3-benzotriazin-4-one (**1***a*) by comparison (m.p., mixed m.p., and i.r. spectrum) with an authentic sample (12). The oils were shown to be mixtures of the triazine (**1***a*) and ethyl anthranilate, and the composition was determined by quantitative i.r. measurements of the relative intensities of the absorption peaks at 3500 (NH stretch, anthranilate) and 960 cm^{-1} (N—N stretch, triazine) (see Discussion). The results of this analysis for reactions with various types of alumina are shown in Table 2.

The financial support of the National Research Council of Canada is gratefully acknowledged. We are also grateful to Drs. W. D. Jamieson and A. W. McCulloch of the Atlantic Regional Laboratory, NRCC, Halifax, N.S., for mass spectral and n.m.r. data respectively.

1. H. ZOLLINGER. Azo and diazo chemistry. Interscience Publishers Inc., New York. 1961. p. 179.
2. B. F. DAY, T. W. CAMPBELL, and G. M. COPPINGER. J. Am. Chem. Soc. **73**, 4687 (1951); J. C. EARL. Chem. and Ind. **55**, 192 (1936); P. GRIESS. Ann. **121**, 258 (1862).
3. H. MEHNER. J. prakt. Chem. **63**, 241 (1901 [2]); F. D. CHATTAWAY and A. J. WALKER. J. Chem. Soc. 329 (1927); P. GRAMMATICAKIS. Compt. Rend. **243**, 2094 (1956); P. GRAMMATICAKIS. Bull. Soc. Chim. Fr. **26**, 480 (1959).
4. E. VAN HEYNINGEN. J. Am. Chem. Soc. **77**, 6562 (1955).
5. K. HASSPACKER and G. OHNAKER. U.S. Pat. 3 316 262; Chem. Abstr. **67**, 64445*q* (1967).
6. A. C. MAIR and M. F. G. STEVENS. J. Chem. Soc. C, 2317 (1971).
7. P. A. S. SMITH. Open-chain nitrogen compounds. Vol. II. Benjamin, New York. 1966. p. 336 *ff*.
8. L. M. JACKMAN and S. STERNHELL. Applications of nuclear magnetic resonance spectroscopy in organic chemistry. 2nd Ed. Pergamon. 1969. p. 217.
9. B. G. LINSEN, *editor*. Physical and chemical aspects of adsorbents and catalysts. Academic Press, London and New York. 1970. pp. 203–208.
10. J. B. PERI and R. B. HANNAN. J. Phys. Chem. **64**, 1526 (1960); J. B. PERI. J. Phys. Chem. **69**, 211 (1965); **69**, 220 (1965); **69**, 231 (1965); **70**, 3168 (1966).
11. J. H. DE BOER. J. Catal. **2**, 1 (1963).
12. A. WEDDIGE and H. FINGER. J. prakt. Chem. **35**, 263 (1887 [2]).
13. K. THOMAE. Ger. Pat. 1 223 846: Chem. Abstr. **65**, 18602*d* (1966).

Etude des oxyphosphoranes en tant qu'intermédiaires lors de la réduction de l'ozonide du styrène par les phosphites

J. CARLES ET S. FLISZÁR

Département de chimie, Université de Montréal, Montréal, Québec

Reçu le 17 février 1972

L'étude cinétique de la réduction de l'ozonide du styrène par une série de phosphites suggère la formation d'un intermédiaire oxyphosphorane. Une réévaluation du mécanisme d'ozonolyse des oxyphosphoranes comportant une double liaison C—C est présentée.

The kinetic study of the reduction of styrene ozonide by various phosphites suggests the formation of an oxyphosphorane intermediate. A reevaluation of the mechanism of ozonolysis of selected oxyphosphoranes having a C—C double bond is presented.

Canadian Journal of Chemistry, **50**, 2552 (1972)

Can. J. Chem. Downloaded from www.nrcresearchpress.com by 210.87.254.105 on 09/05/12
For personal use only.

Depuis leurs premières synthèses par Kukhtin (1) en 1958, les oxyphosphoranes ont fait l'objet de nombreuses études tant du point de vue de leurs propriétés que de leur structure (2). Ces composés sont normalement produits par condensation de composés α-dicarbonylés avec des phosphites trisubstitués (3). De plus, Denney et Jones (4) ont trouvé que les phosphites peuvent réagir avec certains composés peroxydiques pour engendrer des oxyphosphoranes. Parallèlement il est également apparu récemment que des oxyphosphoranes instables à six chaînons peuvent être des intermédiaires se décomposant selon des processus bien définis, lors de réactions entre les composés phosphorés trivalents et des peroxydes présentant une autre fonction oxygénée, tels que les β-peroxylactones (5) et les ozonides (6, 7).

Des études antérieures (6, 7) sur la réduction des ozonides par la triphénylphosphine ont permis de déterminer l'influence des substituants du cycle ozonidique et de conclure au caractère nucléophile de l'attaque de la triphénylphosphine.

Le présent travail a pour objet l'étude de l'influence de la nature du composé phosphoré trivalent sur la cinétique de la réduction d'un ozonide donné. Une telle étude permettra, d'une part, de corroborer les résultats antérieurs (6) concernant le rôle des substituants du cycle ozonidique et, d'autre part, de détecter l'intervention éventuelle d'un composé intermédiaire instable du type oxyphosphorane pour divers composés phosphorés trivalents. Ces derniers forment une série de phosphites $P(RO)_3$ avec $R = CH_3$, C_2H_5, $i\text{-}C_3H_7$, $t\text{-}C_4H_9$, C_6H_5. L'ozonide utilisé est le phényl-2 trioxa-1,3,4 cyclopentane (ozonide du styrène).

Partie expérimentale

La réduction de l'ozonide du styrène a été étudiée à température contrôlée, en solution dans le chloroforme, en déterminant la formation du benzaldéhyde en fonction du temps. Celle-ci a été suivie en spectroscopie i.r. par l'évolution de la bande d'absorption à 1710.4 cm^{-1} due à la vibration du groupement carbonylé.

La stoechiométrie de la réaction a été vérifiée par des analyses des mélanges réactionnels. Après un temps de réaction de 7 jours, à 25 °C, la réduction de l'ozonide du styrène (0.1 *M*) par un phosphite $(RO)_3P$ (0.1 *M*) est pratiquement quantitative (>99%) d'après l'analyse du benzaldéhyde et du phosphate formés. Ainsi, par exemple, lors de quatre expériences indépendantes de réduction de 1 mmol d'ozonide par 1 mmol de triméthylphosphite, il a été obtenu après 7 jours à 25°: 0.995, 0.999, 0.998, 0.996 mmol d'aldéhyde benzoïque et 0.997, 0.995, 1.00, et 0.995 mmol de $(CH_3O)_3PO$. Le formaldéhyde qui est également produit lors de la réaction n'a pas pu être dosé en raison de sa volatilité.

Il a été montré antérieurement (6) que si la réduction de l'ozonide est du deuxième ordre, soit du premier ordre par rapport à chacun des réactifs, la constante de vitesse k peut être déterminée d'après l'éq. 1, où D représente la densité

$$[1] \qquad 1/D = 1/D_\infty + (1/akD_\infty)(1/t)$$

optique du benzaldéhyde au temps t, D_∞ est la valeur de D pour $t = t_\infty$, et a = concentration initiale en ozonide = concentration initiale en phosphite.

Les résultats obtenus permettent de tracer la droite $1/D$ en fonction de $1/t$. Dans tous les cas il a été obtenu une droite satisfaisant l'éq. 1, dont la pente permet le calcul de la constante de vitesse k. L'ordonnée à l'origine ($1/t \to 0$) permet le calcul de D_∞. La valeur de D_∞ calculée à partir des données cinétiques peut être facilement contrôlée par la mesure directe de D_∞ obtenue soit par sa détermination après un temps de réaction suffisamment long, soit par la comparaison avec une solution d'aldéhyde de concentration

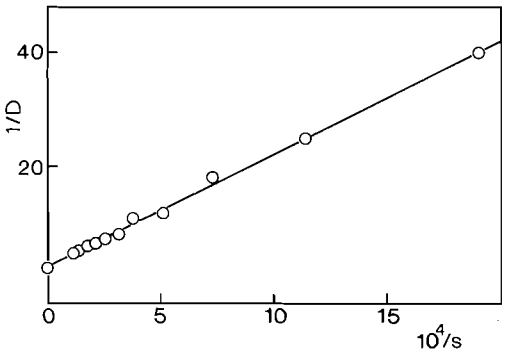

FIG. 1. Vérification de l'éq. 1 pour la réduction de l'ozonide du styrène par le triméthylphosphite dans le méthanol à 25°.

TABLEAU 1. Réduction de l'ozonide du styrène par le triméthylphosphite, dans le chloroforme à 25 °C

a (M)*	$t_{1/2}$ (s)	$10^3\,k$ (1 mol^{-1} s^{-1})
0.1	9250	1.06
0.2	4640	1.08
0.4	2270	1.10
1.0	924	1.06

*a = concentration initiale en ozonide et en phosphite.

égale à a. La méthode est illustrée par la fig. 1, pour la réduction par le triméthylphosphite dans le méthanol absolu à 25°.

La constante de vitesse peut être également calculée directement à partir de l'éq. 1, en y insérant les valeurs de D observées pour différents t. Les équations cinétiques utilisées ont été également vérifiées dans le cas de la réduction de l'ozonide du styrène par le triméthylphosphite, à 25° dans le chloroforme, par des mesures des temps de demi-réaction $t_{1/2}$ effectuées au moyen de solutions de différentes concentrations initiales (a) en ozonide et en phosphite. Les résultats rapportés au tableau 1 montrent bien la constance des valeurs de k ainsi calculées ($k = 1/at_{1/2}$).

D'ultérieures précisions expérimentales sont indiquées dans la réf. 6.

Résultats et discussion

Les constantes de vitesse de réduction, à 25°, de l'ozonide du styrène dans le chloroforme par divers phosphites sont indiquées dans le tableau 2.

Afin d'étudier l'ordre de grandeur des énergies d'activation de la réduction par les phosphites, la dépendance de k en fonction de la température a été étudiée pour le triméthylphosphite. Dans le chloroforme, les valeurs de k (1 mol^{-1} s^{-1}) suivantes ont été obtenues: 1.06×10^{-3} (25°), 2.25×10^{-3} (35°), 4.51×10^{-3} (45°). La loi d'Arrhenius est bien suivie et conduit à une énergie d'activation de 13.6 kcal/mol. Cette valeur est donc assez semblable à celle obtenue précédemment (6) (12.7 kcal/mol) pour la réduction de l'ozonide du styrène par la triphénylphosphine.

TABLEAU 2. Constantes de vitesse de réduction de l'ozonide du styrène par les phosphites $(RO)_3P$, dans le chloroforme, à 25 ± 0.1 °C

R	k (1 mol^{-1} s^{-1})
CH_3	1.06×10^{-3}
C_2H_5	2.15×10^{-3}
i-C_3H_7	2.71×10^{-3}
t-C_4H_9	2.80×10^{-3}
C_6H_5	4.33×10^{-5}

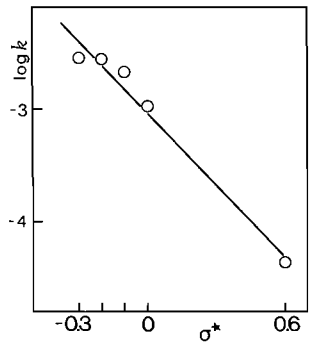

FIG. 2. Vérification de l'éq. de Taft [2] par les résultats du tableau 2.

L'examen des résultats du tableau 2 permet l'étude de l'influence du substituant R de l'agent réducteur sur la constante de vitesse. Il ressort notamment que l'équation de Taft (éq. 2) est

$$[2] \qquad \log k/k_0 = \rho^*\sigma^*$$

bien vérifiée, ainsi que l'illustre la fig. 2.

La pente négative de la droite de Taft indique que les phosphites possédant un substituant donneur d'électrons réduisent plus rapidement l'ozonide du styrène que ceux possédant un substituant attracteur d'électrons. Les phosphites sont donc des agents nucléophiles lors de la réduction des ozonides. Ces résultats sont à rapprocher des études précédentes (6, 7) avec la

Can. J. Chem. Downloaded from www.nrcresearchpress.com by 210.87.254.105 on 09/05/12
For personal use only.

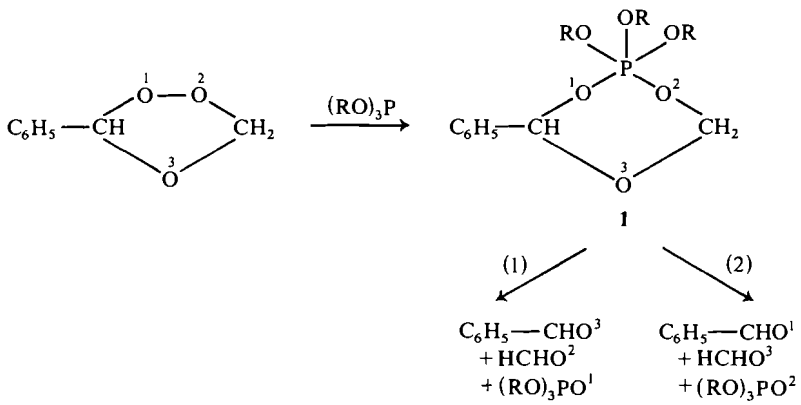

SCHÉMA 1

triphénylphosphine montrant que cette dernière agit en tant qu'agent nucléophile vis-à-vis des ozonides. Le caractère nucléophile des composés phosphorés trivalents est clairement illustré par la comparaison des constantes de vitesse pour la réduction de l'ozonide du styrène par la triphénylphosphine (6.64×10^{-2}) et par le triphénylphosphite (4.33×10^{-5} l mol^{-1} s^{-1}) à 25°.

Comme cela avait été considéré dans le cas de la réduction des ozonides par la triphénylphosphine, il y a lieu d'envisager deux modes d'attaque (schémas 1 et 2).

L'attaque du phosphite pourrait s'effectuer par un processus unique, par une étape où les deux atomes d'oxygène peroxydiques sont simultanément mis en jeu, cette étape contrôlant la cinétique (schéma 1).

Le processus impliqué pourrait alors correspondre à la formation d'un produit d'addition intermédiaire instable, semblable à l'oxyphosphorane suggéré par Adam *et al.* (5) pour la réduction des β-peroxylactones par les composés phosphorés trivalents.

L'intermédiaire (**1**) se décomposerait ensuite très rapidement selon les deux voies possibles: la voie *1* conduisant à l'incorporation de l'oxygène O-3 dans le benzaldéhyde et la voie *2* où l'oxygène O-3 est incorporé dans l'aldéhyde formique. Un tel mécanisme est en accord avec les équations cinétiques utilisées et vérifiées expérimentalement.

Une autre hypothèse consiste à envisager que la réduction des ozonides peut avoir lieu par le truchement de deux mécanismes parallèles (schéma 2), l'un d'entre eux s'effectuant par une attaque sur l'oxygène O-1 et l'autre ayant lieu par une attaque sur l'oxygène O-2.

La comparaison des étapes cinétiques proposées pour les mécanismes 1 et 2 indique que l'intermédiaire intervenant dans le mécanisme 2 possède un caractère nettement plus polaire que celui postulé pour le mécanisme 1. Dès lors, l'étude de l'effet de solvant sur les constantes de

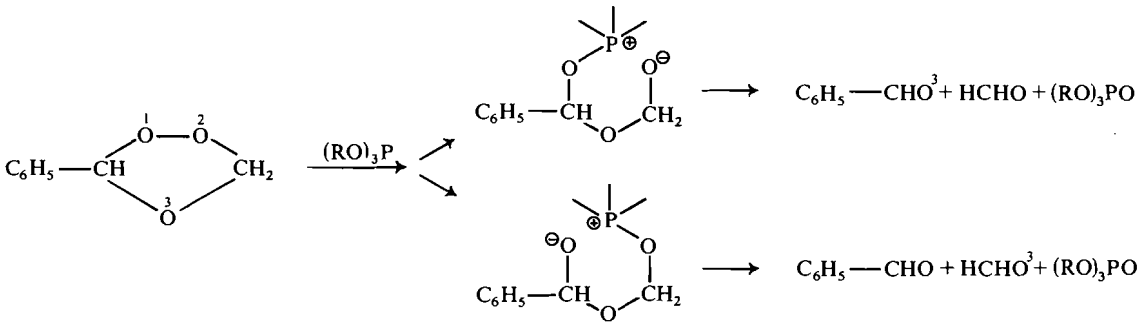

SCHÉMA 2

Can. J. Chem. Downloaded from www.nrcresearchpress.com by 210.87.254.105 on 09/05/12
For personal use only.

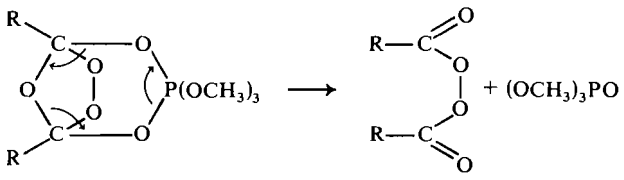

4 3

TABLEAU 3. Effet du solvant sur la réduction de l'ozonide du styrène par le triméthylphosphite à 25 °C

Solvant	Constante diélectrique	$10^3 k$ ($l\ mol^{-1}\ s^{-1}$)
CCl_4	2.228	1.20
$CHCl_3$	4.718	1.06
$C_2H_4Cl_2$	10.36	1.23
CH_3OH	32.63	1.26

vitesse peut permettre une distinction entre les deux mécanismes. Les résultats du tableau 3 indiquent que les constantes de vitesse de réaction dépendent très peu des solvants utilisés, ce qui semble être en faveur du mécanisme 1 qui implique un oxyphosphorane **1**.

L'intervention d'un intermédiaire oxyphosphorane *instable* du type **1** permet d'expliquer de nombreux résultats ayant trait à l'ozonation d'oxyphosphoranes stables **2** comportant une double liaison.

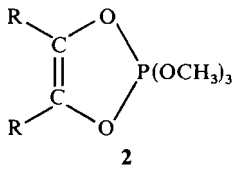

2

Ramirez *et al.* (8) ont notamment trouvé que l'ozonation d'oxyphosphoranes du type **2** engendre, outre le diacétyle et l'anhydride acétique, le peroxyde d'acétyle **3**. L'explication suggérée par Ramirez *et al.* postule la formation de l'ozonide primaire (1,2,3-trioxolane) de **2** qui, lors de son clivage, conduit à une attaque de l'atome de phosphore par l'oxygène terminal zwittérionique (8).

La grande facilité avec laquelle se forment, en général (9), les ozonides à partir de doubles liaisons C—C comprises dans un anneau à cinq atomes suggère qu'il semble raisonable de considérer la formation d'une proportion importante d'ozonide **4**, dérivé de **2**.

De par sa structure, l'ozonide **4** est voisin à l'intermédiaire **1** postulé précédemment. La décomposition de l'ozonide intermédiaire **4**, en suivant la même voie de décomposition que l'intermédiaire **1**, conduirait alors au peroxyde d'acétyle **3**.

L'éventuelle participation de l'ozonide intermédiaire **4** peut également rendre compte de la formation des autres produits observés lors de l'ozonolyse de **2**. Ainsi, une élimination d'oxygène moléculaire via une rupture hétérolytique du pont peroxyde, semblable à celle rencontrée en spectrométrie de masse des ozonides (10), pourrait rendre compte de la formation de dicétone. Une telle élimination d'oxygène moléculaire est en accord avec les observations de Ramirez *et al.* (8) et s'explique ainsi sans l'intervention d'un hypothétique perozonide, postulé par ces auteurs.

Il est entendu qu'à ce stade toute interprétation des résultats d'ozonolyse des oxyphosphoranes **2**, tant par les mécanismes suggérés par Ramirez *et al.* que par la voie esquisée ci-haut, ne saurait être que spéculative. Cependant, la vraisemblance de la participation d'oxyphosphoranes **1** très instables lors de la réduction des ozonides par les phosphites suggère une instabilité comparable pour les

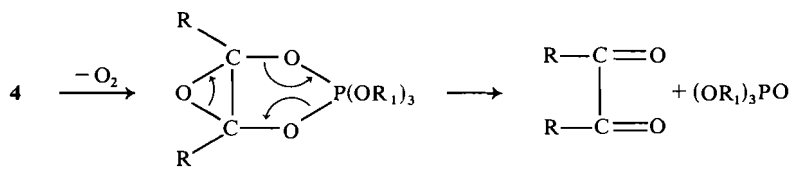

Can. J. Chem. Downloaded from www.nrcresearchpress.com by 210.87.254.105 on 09/05/12
For personal use only.

ozonides **4** pouvant être attendus lors de l'ozonolyse d'oxyphosphoranes du type **2**. Dès lors, la *possibilité* d'une interprétation des résultats d'ozonolyse des oxyphosphoranes **2** via **4** semble pouvoir être temporairement retenue, dans l'attente de résultats pouvant trancher définitivement entre les mécanismes 1 et 2.

Nous remercions le Conseil National de Recherches du Canada pour un octroi qui a permis le présent travail, et une bourse d'études à J. C.

1. V. A. KUKHTIN. Dokl. Akad. Nauk SSSR, **121**, 466 (1958); Chem. Abstr. **53**, 1105*b* (1959).
2. (*a*) F. RAMIREZ. Acc. Chem. Res. **1**, 168 (1968). (*b*) E. L. MUETTERTIES et R. A. SCHUNN. Quart. Rev. (London), **20**, 245 (1966). (*c*) R. J. GILLESPIE. Angew. Chem. Intern. Ed. **6**, 819 (1967). (*d*) F. H. WESTHEIMER. Acc. Chem. Res. **1**, 70 (1968).
3. F. RAMIREZ et N. B. DESAI. J. Am. Chem. Soc. **82**, 2652 (1960); F. RAMIREZ. Organophosphorus compounds. Int. Symp., Heidelberg, 1964. IUPAC. Butterworth and Co. Ltd., London, **9**, 1964. p. 337–369.
4. D. B. DENNEY et D. M. JONES. J. Am. Chem. Soc. **91**, 5821 (1969).
5. W. ADAM, R. J. RAMIREZ, et SHIH-CHUAN TSAI. J. Am. Chem. Soc. **91**, 1254 (1969).
6. J. CARLES et S. FLISZÁR. Can. J. Chem. **48**, 1309 (1970).
7. J. CARLES et S. FLISZÁR. Can. J. Chem. **47**, 1113 (1969).
8. F. RAMIREZ, S. B. BHATIA, R. B. MITRA, Z. HAMLET, and N. B. DESAI. J. Am. Chem. Soc. **86**, 4394 (1964).
9. R. CRIEGEE et G. LOHAUS. Chem. Ber. **86**, 1 (1953).
10. J. CASTONGUAY, M. BERTRAND, J. CARLES, S. FLISZÁR, et Y. ROUSSEAU. Can. J. Chem. **47**, 919 (1969).

Can. J. Chem. Downloaded from www.nrcresearchpress.com by 210.87.254.105 on 09/05/12
For personal use only.

Adducts of Piperidine, Piperazine, Methylpiperazine, and Morpholine with Bis(β-Ketoenolates) of Nickel(II)

G. MARCOTRIGIANO,[1] R. BATTISTUZZI, AND G. C. PELLACANI

Istituto di Chimica Generale, Università di Modena, Via G. Campi 183, 41100 Modena, Italy

Received January 4, 1972

The bis(β-ketoenolates)nickel(II) adducts of piperidine, piperazine, methylpiperazine, and morpholine are isolated in the solid state and investigated by magnetic measurements and electronic and i.r. spectra. Magnetic measurements and electronic spectra give evidence of *trans*-octahedral configuration while i.r. spectra show that the amines are coordinated to the nickel atom towards the nitrogen atom. The new band found in the range 385–300 cm^{-1} for all complexes can be assigned to Ni—N vibration. In the $Ni(DBM)_2 \cdot 4B$ (B = methylpiperazine and morpholine) the two additional bases are not coordinated to the metal atom.

Les composés d'addition du nickel(II) bis(β-cétoénolates) avec la pipéridine, pipérazine, méthylpipérazine, et morpholine, ont isolés à l'état solide et étudiés par des mesures magnétiques et des spectres i.r. et électroniques. Les mesures magnétiques et les spectres électroniques prouvent la configuration *trans*-octaédrale tandis que les spectres i.r. indiquent que les amines sont coordinées à l'atome de nickel par l'intermédiaire de l'atome d'azote. La bande nouvelle, située dans la région 385–300 cm^{-1}, trouvée pour tous ces complexes peut être assignée à la vibration Ni—N. Dans $Ni(DBM)_2 \cdot 4B$ (B = méthylpipérazine et morpholine) les deux bases supplémentaires ne sont pas coordinées à l'atome de métal.

Canadian Journal of Chemistry, **50**, 2557 (1972)

Can. J. Chem. Downloaded from www.nrcresearchpress.com by 210.87.254.6 on 09/05/12
For personal use only.

It is known that, on account of the tendency of bis(β-ketoenolates)nickel(II) to be six-coordinate, it easily gives adducts of the type NiL_2B_2 (B = monodentate ligand, L = β-ketoenolate) together with monodentate ligands.

A wide variety of base-adducts of the type NiL_2B_2 have been reported with B as nitrogen-donor ligands (1–6).

X-Ray and spectrophotometric measurements (3, 5) have established, for several of these base-adducts, a *trans*-octahedral configuration, while i.r. measurements show a marked shift to lower frequencies of ν(C—O), ν(C—C), and ν(M—O) of the bis(acetylacetonate)nickel(II) on coordination (4, 6).

Since bis(β-ketoenolate)nickel(II) adducts with aliphatic etherocyclic amines having one or two donor sites (nitrogen for piperidine, nitrogen–nitrogen for piperazine and methylpiperazine, and nitrogen–oxygen for morpholine) are not known, except for the adducts of piperidine with nickel(II)dipivaloylmethanate (7), we have investigated the coordination ability of these amines.

In this work, we have prepared some new adducts of $Ni(AcAc)_2$, $Ni(BA)_2$, and $Ni(DBM)_2$ (AcAc = acetylacetonate; BA = benzoylacetonate; DBM = dibenzoylmethanate) with piperidine, piperazine, methylpiperazine, and morpholine characterized by i.r., near-i.r., visible spectroscopy, and magnetic measurements.

[1] To whom correspondence should be addressed.

Experimental

Preparations

Bis(β-ketoenolates)nickel(II) was prepared by adding a stoichiometric amount of the corresponding β-diketone in methanolic solution (4×10^{-2} mol in 10–80 ml) to aqueous solutions of the $NiCl_2 \cdot 6H_2O$ (2×10^{-2} mol in 20 ml of water) while stirring at 50–60 °C.

The crystalline products were filtered, washed with water, methanol, and ether, and vacuum-dried.

The adducts with piperidine, methylpiperazine, and morpholine were prepared by crystallization of the bis(β-ketoenolates)nickel(II) from these amines. The adduct $Ni(AcAc)_2 \cdot$piperazine was obtained by mixing a methanolic solution of $Ni(AcAc)_2 \cdot 2H_2O$ with an excess of piperazine in the same solvent at 40–50 °C.

The adducts of the $Ni(AcAc)_2$ and $Ni(BA)_2$ were collected by filtration, washed with benzene or ether, and dried at atmospheric pressure, while $Ni(DBM)_2 \cdot 4$(morpholine) and $Ni(DBM)_2 \cdot 4$(methylpiperazine) were dried in the folds of a filter paper. The latter complexes lose the amines and $Ni(DBM)_2 \cdot 2$(methylpiperazine) was obtained by crystallization of $Ni(DBM)_2 \cdot 4$(methylpiperazine) from benzene.

The analytical data and physical properties for the crystalline solids are given in Table 1.

Analyses

Nickel was determined by complexometric titration with EDTA and nitrogen by the Kjeldhal method.

Physical Measurements

The i.r. spectra were recorded in potassium bromide

TABLE 1. Physical properties and analytical data*

Compound	Color	Melting point (°C)	% metal		% nitrogen	
			Calcd.	Found	Calcd.	Found
$Ni(AcAc)_2 \cdot (Pipd)_2$	sky-blue	137–140	13.74	13.78	6.55	6.55
$Ni(AcAc)_2 \cdot Pipz$	sky-blue	230 (d)	17.13	16.98	8.17	7.99
$Ni(AcAc)_2 \cdot (CH_3\text{-pipz})_2$	sky-blue	105–107 (d)	12.84	12.87	12.26	12.21
$Ni(AcAc)_2 \cdot (Morph)_2$	sky-blue	114–116 (d)	13.62	13.62	6.49	6.29
$Ni(BA)_2 \cdot (Pipd)_2$	green-yellow	118–120	10.64	10.67	5.07	5.11
$Ni(BA)_2 \cdot (CH_3\text{-pipz})_2$	green-yellow	142–143	10.09	10.13	9.63	9.58
$Ni(BA)_2 \cdot (Morph)_2$	green-yellow	136–138	10.57	10.63	5.04	5.01
$Ni(DBM)_2 \cdot (Pipd)_2$	yellow-green	145–148	8.69	8.59	4.14	4.18
$Ni(DBM)_2 \cdot (CH_3\text{-pipz})_2$	yellow-green	156–158 (d)	8.32	8.34	7.94	7.92
$Ni(DBM)_2 \cdot (CH_3\text{-pipz})_4$	yellow-green	156–158 (d)	6.48	6.51	12.37	12.15
$Ni(DBM)_2 \cdot (Morph)_4$	green-yellow	95–97 (d)	6.87	6.91	6.55	6.48

*Abbreviations: AcAc, acetylacetonate; BA, benzoylacetonate; DBM, dibenzoylmethanate; Pipd, piperidine; Pipz, piperazine; CH_3-pipz, methylpiperazine; Morph, morpholine.

TABLE 2. More important i.r. bands (cm^{-1})*

Compound	ν(N—H)	ν(C—O)	ν(C—C)	ν(Ni—O)	ν(Ni—N)
$Ni(AcAc)_2 \cdot (Pipd)_2$	3265m	1595vs	1510vs	570s 412s	312ms
$Ni(AcAc)_2 \cdot Pipz$	3272w	1590vs	1515vs	575s 416s	382s
$Ni(AcAc)_2 \cdot (CH_3\text{-pipz})_2$	3255w	1593vs	1515vs	574s 412s	371s
$Ni(AcAc)_2 \cdot (Morph)_2$	3272w	1590vs	1513vs	568s 414s	334s
$Ni(BA)_2 \cdot (Pipd)_2$	3265w	1562vs	1505vs	422s	310m
$Ni(BA)_2 \cdot (CH_3\text{-pipz})_2$	3270w	1571vs	1510vs	444s	373s
$Ni(BA)_2 \cdot (Morph)_2$	3263w	1565vs	1508vs	433s	343vs
$Ni(DBM)_2 \cdot (Pipd)_2$	3270m	1549vs	1508vs	391ms	300m
$Ni(DBM)_2 \cdot (CH_3\text{-pipz})_4$	3275w	1547vs	1515vs	402ms	374s
$Ni(DBM)_2 \cdot (Morph)_4$	3240w	1548vs	1513vs	405ms	330s

*For piperidine ν(N—H) = 3290 cm^{-1} (11); for piperazine ν(N—H) = 3328 cm^{-1} (21, 22): for morpholine ν(N—H) = 3340 cm^{-1} (17).

discs over the 4000–500 cm^{-1} region and in Nujol mulls supported between thin polyethylene sheets over the range 600–250 cm^{-1} using a Perkin–Elmer 521 spectrophotometer.

Solid-state electronic spectra were recorded in Nujol mulls on filter paper as support using a Beckman DK2 spectrophotometer (1500–500 mμ).

Magnetic susceptibilities were taken on the solid complexes at room temperature by the Gouy method, using $Nien_3S_2O_3$ as calibrant (8).

Results and Discussion

Infrared Spectra

The more important i.r. bands are reported in Table 2. The formation of coordinate bonds in the bis(β-ketoenolates)nickel(II) adducts is immediately apparent from the considerable shifts to lower frequencies (200–100 cm^{-1}) of ν(N—H) that occur in the case of coordinated but not of uncoordinated ligands. These shifts show that piperazine, methylpiperazine, and morpholine are coordinated to metal by means of the nitrogen atom of their N—H group (9, 10). In the morpholine adducts, the positive shift of C—O—C stretching vibration at 1109 cm^{-1} in acetylacetonate, 1105 cm^{-1} in benzoylacetonate, and 1100 cm^{-1} in dibenzoylmethanate adducts, with respect to free morpholine (1095 cm^{-1}), excludes a possible oxygen-to-metal coordination (10). Although for piperidine adducts we have found a small shift to lower frequencies (25–20 cm^{-1}) of ν(NH), nevertheless the great change in the H—N—C deformation region (870–860 cm^{-1}) (11) affords evidence of the coordination of the N-atom of piperidine.

The coordination of the amines also results in corresponding shifts of the C=O, C=C, and Ni—O absorption bands (4, 6).

The assignments of ν(C—O) and ν(C—C) in the range of 1600–1500 cm^{-1} are made on the

Can. J. Chem. Downloaded from www.nrcresearchpress.com by 210.87.254.6 on 09/05/12
For personal use only.

Can. J. Chem. Downloaded from www.nrcresearchpress.com by 210.87.254.6 on 09/05/12
For personal use only.

basis of previously suggested assignments for acetylacetonates (14, 15) and for phenyl substituted β-ketoenolate nickel complexes (13).

The bands in the region 600–400 cm^{-1} assigned to Ni—O modes (6, 12, 13, 16) shift to lower frequencies by 10–60 cm^{-1} in the adducts, while the bands assigned to ν(C—O) and ν(C—C) shift only slightly in comparison with the corresponding bis(β-ketoenolates)nickel(II) (4, 6).

Moreover, the absence of coordinated water bands in the spectra suggests that the compounds are hexa-coordinated. In addition, in the far i.r., strong bands are observed in the range 390–300 cm^{-1} for all complexes. This band is most probably the (Ni—N) mode due to coordinated amines because such a band is not observed in the spectra of ligands and of bis(β-ketoenolates)nickel(II) and it is in good agreement with the values reported for Ni—N modes by Ahuja (9) for the nickel morpholine sulfate complexes.

The assignment of these bands to metal–nitrogen modes seems reasonable as absorptions in this region have been allocated to M—N modes in most other metal ammonia complexes (500–420 cm^{-1}) and metal–aniline complexes (430–350 cm^{-1}) (17). The set of bands in the range 600–400 cm^{-1}, assignable to coupled metal–oxygen stretching modes (6) (two bands well localized for our acetylacetonate and only one for our phenyl-substituted acetylacetonate adducts), are shifted to lower frequencies in our adducts than in the pyridine adducts. This shift affords evidence that the heterocyclic saturated amines are stronger ligands than pyridine (6, 12). Therefore we could suggest that the third Ni—O absorption band found at 270 cm^{-1} for $Ni(AcAc)_2 \cdot (pyridine)_2$ (12) in our adducts falls at lower energy and within the range of the instrument (250 cm^{-1}).

The nickel–nitrogen stretching frequencies provide a measure of the relative metal–ligand bond strengths in piperazine, methylpiperazine, morpholine, and piperidine, in that order.

Magnetism and Electronic Spectra

The electronic spectra and magnetic moments at room temperature of our adducts have been measured using solid samples. μ_{eff} is calculated from the expression

$$\mu_{eff} = 2.83(\chi_M^C T)^{1/2}$$

where χ_M^C is the molar susceptibility corrected by diamagnetic contribution, using Pascal's constants (18) and by TIP contribution (19).

TABLE 3. Magnetic moments and solid-state electronic spectra

Compound	μ_{eff} (BM)	Absorption maxima (cm^{-1})	
$Ni(AcAc)_2 \cdot (Pipd)_2$	3.16	10400	17000
$Ni(AcAc)_2 \cdot Pipz$	3.23	10200	17240
$Ni(AcAc)_2 \cdot (CH_3\text{-pipz})_2$	3.16	10150	16530
$Ni(AcAc)_2 \cdot (Morph)_2$	3.16	10200	16530
$Ni(BA)_2 \cdot (Pipd)_2$	3.10	10250	17090
$Ni(BA)_2 \cdot (CH_3\text{-pipz})_2$	3.07	10000	17090
$Ni(BA)_2 \cdot (Morph)_2$	3.12	10150	16950
$Ni(DBM)_2 \cdot (Pipd)_2$	3.17	10000	17180
$Ni(DBM)_2 \cdot (CH_3\text{-pipz})_2$	3.12	10000	17390
$Ni(DBM)_2 \cdot (CH_3\text{-pipz})_4$	3.30	10000	17390
$Ni(DBM)_2 \cdot (Morph)_4$*	3.01	10200	17240

*Loses morpholine.

The obtained magnetic moments (Table 3) agree well with the spin-free experimental moments for octahedral nickel complexes (2.90–3.30 BM) (20) with a triplet ground-state, $^3A_{2g}$.

The electronic spectra (Table 3) of all adducts show two d–d bands in the explored range 6 000–20 000 cm^{-1}, at 10 000 and 17 000 cm^{-1}, which may be assigned to the $^3A_{2g} \rightarrow {}^3T_{2g}$ ($= 10\,Dq$) and $\rightarrow {}^3T_{1g}(F)$ transitions, respectively, in O_h symmetry.

In the complex $(Ni(AcAc)_2 \cdot piperazine)_n$ the *trans*-octahedral arrangement could have arisen owing to the formation of linear polymeric chains with piperazine "bridging" two metal atoms.

The i.r. spectra of this complex, in which only one N—H band is found, and its insolubility in methanol (unlike all the other complexes) are in agreement with the above assignment. The tendency of piperazine to give "bridge-complexes" is not unusual as it has been found for $CdCl_2 \cdot C_4H_{10}N_2$ (21). This complex and also our adduct, contain long chains of piperazine molecules in the "chair" configuration, "bridging" metal ions (21).

$Ni(DBM)_2 \cdot 2H_2O$ and methylpiperazine in benzene solution give the $Ni(DBM)_2 \cdot (methylpiperazine)_2$ adduct, while $Ni(DBM)_2 \cdot 4B$ (B =

methylpiperazine, morpholine) is prepared by dissolving $Ni(DBM)_2 \cdot 2H_2O$ in the respective base. The identical magnetic and spectral properties of $Ni(DBM)_2 \cdot (methylpiperazine)_2$ and $Ni(DBM)_2 \cdot 4B$ support the hypothesis that the additional base in $Ni(DBM)_2 \cdot 4B$ is accommodated in the crystal lattice, and not coordinated to the metal atom (5).

1. F. P. DWYER and A. M. SARGESON. J. Proc. Roy. Soc. N.S.W. **90**, 29 (1956).
2. E. J. OLSZEWSKI and D. F. MARTIN. J. Inorg. Nucl. Chem. **27**, 1043 (1965).
3. J. T. HASHAGEN and J. P. FACKLER, JR. J. Am. Chem. Soc. **87**, 2821 (1965).
4. M. K. MISRA and D. V. RAMANA RAO. J. Inorg. Nucl. Chem. **31**, 3875 (1969).
5. D. P. GRADDON. Coord. Chem. Rev. **4**, 1 (1969).
6. J. N. HAIGH, N. P. SLABBERT, and D. A. THORNTON. J. Inorg. Nucl. Chem. **32**, 3635 (1970): J. Mol. Struct. **7**, 199 (1971).
7. P. E. RAKITA, S. J. KOPPERL, and J. P. FACKLER. J. Inorg. Nucl. Chem. **30**, 2139 (1968).
8. N. F. CURTIS. J. Chem. Soc. 3147 (1961).
9. I. S. Ahuja. Inorg. Chim. Acta, **3**, 110 (1969).
10. I. S. AHUJA and A. GARG. Inorg. Nucl. Chem. Lett. **7**, 937 (1971).
11. R. SARIEGO and J. A. COSTAMAGNA. J. Inorg. Nucl. Chem. **33**, 1528 (1971).
12. K. NAKAMOTO, C. UDOVICH, and J. TAKEMOTO. J. Am. Chem. Soc. **92**, 3973 (1970).
13. R. D. HANCOCK and D. A. THORNTON. J. Mol. Struct. **4**, 361 (1969).
14. G. T. BEHNKE and K. NAKAMOTO. Inorg. Chem. **6**, 433 (1967).
15. S. PINCHAS, BRIAN L. SILVER, and I. LAULICHT. J. Chem. Phys. **46**, 1506 (1967).
16. D. M. ADAMS. Metal–Ligand and related vibrations. E. Arnold Publ. Ltd., London. 1967. p. 260.
17. I. S. AHUJA. J. Inorg. Nucl. Chem. **29**, 2091 (1967).
18. B. N. FIGGIS and J. LEWIS. Technique of inorganic chemistry — magnetochemistry. Vol. IV. J. Wiley and Sons, New York, N.Y. 1965. p. 142.
19. B. N. FIGGIS and J. LEWIS. Progr. Inorg. Chem. **6**, 72 (1964).
20. B. N. FIGGIS and J. LEWIS. Progr. Inorg. Chem. **6**, 197 (1964).
21. P. J. HENDRA and D. B. POWELL. J. Chem. Soc. **350**, 5105 (1960).
22. P. J. HENDRA and D. B. POWELL. Spectrochim. Acta **18**, 229 (1962).

Can. J. Chem. Downloaded from www.nrcresearchpress.com by 210.87.254.6 on 09/05/12
For personal use only.

Novel Rearrangement During Alkaline Hydrolysis of 1,1,1-Trichloro-2-alken-4-ones

EBERHARD KIEHLMANN, B. C. MENON, AND J. I. WELLS

Department of Chemistry, Simon Fraser University, Burnaby 2, British Columbia

Received October 25, 1971

The action of a five-fold excess of potassium hydroxide in methanol on 1,1,1-trichloro-2-penten-4-one (**1**), 1,1,1-trichloro-6-methyl-2-hepten-4-one (**5**), and 1,1,1-trichloro-6,6-dimethyl-2-hepten-4-one (**9**) gives rise to the potassium salt of 5-chloro-2,4-pentadienoic acid (**2**), the potassium salt and methyl ester of 5-chloro-6-methyl-2,4-heptadienoic acid (**7**), and the methyl ester of 5-chloro-6,6-dimethyl-2,4-heptadienoic acid (**10**), respectively.

When the same reaction is performed with an equimolar amount of base, **1** is converted into methyl 5-chloro-2,4-pentadienoate (**3**) as well as 1,1,1-trichloro-2-methoxy-4-pentanone (**4**); the latter compound (**4**) is shown to be a true intermediate in the formation of **3**.

Neither 1,1,1-trichloro-5-methyl-2-hexen-4-one (**11**) nor 1,1,1-trichloro-5-ethyl-2-hepten-4-one (**14**) yields the expected dienoic acid or ester when treated with an equimolar amount of potassium hydroxide. Instead, alkaline methanolysis of **11** leads to the formation of a mixture of 1,1,1-trichloro-2-methoxy-5-methyl-4-hexanone (**12**) and 1,1-dichloro-2,5-dimethoxy-5-methyl-4-hexanone (**13**), whereas **14** gives predominantly 1,1,1-trichloro-2-methoxy-5-ethyl-4-heptanone (**15**) and traces of 1,1-dichloro-2,5-dimethoxy-5-ethyl-4-heptanone (**16**).

On the basis of these observations, a mechanism is proposed for the formation of **2**, **7**, and **10** which requires the presence of two geminal α-hydrogen atoms in the olefinic starting material.

L'action de la potasse dans le méthanol, en excès de cinq fois sur la trichloro-1,1,1 pentène-2 one-4 (**1**), la trichloro-1,1,1 méthyl-6 heptène-2 one-4 (**5**), et la trichloro-1,1,1 diméthyl-6,6 heptène-2 one-4 (**9**) conduit respectivement au sel de potassium de l'acide chloro-5 pentadiène-2,4 oïque (**2**), au sel de potassium et à l'ester méthylique de l'acide chloro-5 méthyl-6 heptadiène-2,4 oïque (**7**) et à l'ester méthylique de l'acide chloro-5 diméthyl-6,6 heptadiène-2,4 oïque.

Quand la même réaction est effectuée avec une quantité équimolaire de base, **1** est converti en chloro-5 pentadiène-2,4 date de méthyle (**3**) ainsi qu'en trichloro-1,1,1 méthoxy-2 pentanone-4 (**4**); le dernier composé (**4**) étant le véritable intermédiaire dans la formation de (**3**).

Le traitement par une quantité équimolaire de potasse de la trichloro-1,1,1 méthyl-5 hexène-2 one-4 (**11**) et de la trichloro-1,1,1 éthyl-5 heptène-2 one-4 (**14**) ne conduit ni à l'acide diénoïque attendu, ni à l'ester. A la place, la méthanolyse alcaline de **11** conduit à un mélange de trichloro-1,1,1 méthoxy-2 méthyl-5 hexanone-4 (**12**) et de dichloro-1,1 diméthoxy-2,5 méthyl-5 hexanone-4 (**13**) tandis que **14** donne de façon prédominante la trichloro-1,1,1 méthoxy-2 éthyl-5 heptanone-4 (**15**) accompagnée de traces de dichloro-1,1 diméthoxy-2,5 éthyl-5 heptanone-4 (**16**).

Sur la base de ces observations, un mécanisme est proposé pour la formation de **2**, **7** et **10** qui nécessite la présence de deux atomes d'hydrogène géminal en α dans l'oléfine de départ.

Canadian Journal of Chemistry, **50**, 2561 (1972)

Introduction

The acetate-catalyzed reaction of chloral with alkyl methyl ketones in glacial acetic acid leads to the formation of 1,1,1-trichloro-2-hydroxy-4-alkanones by a crossed aldol condensation (1, 2). Although these β-ketols resist dehydration under the preparative reaction conditions, they are quite reactive when heated in the presence of acidic or basic catalysts. Thus, treatment with silica or strong mineral acid at elevated temperatures leads to dehydration and rearrangement (3).

The literature on the base-catalyzed reactions of these compounds is confusing. Uschakov (4) and Salkind (5) obtained a carboxylic acid, $C_5H_5ClO_2$, by treatment of 1,1,1-trichloro-2-hydroxy-4-pentanone with cold aqueous or alcoholic potassium hydroxide. Caujolle and coworkers (6) found that certain 1,1,1-trichloro-2-hydroxy-4-alkanones react with 4 equiv of sodium hydroxide per mole of starting material to form 3 mol of sodium chloride, and postulated β-ketoaldehydes and sodium formates as the major organic reaction products. However, they were not successful in isolating and identifying these compounds. Kiehlmann (7), on the other hand, reported that the reaction of 1,1,1-trichloro-2-hydroxy-6-methyl-4-heptanone with

Can. J. Chem. Downloaded from www.nrcresearchpress.com by 210.87.254.105 on 09/05/12
For personal use only.

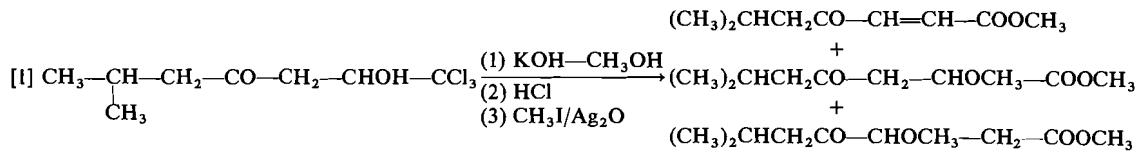

methanolic potassium hydroxide at 50° gives a mixture of three esters (eq. 1).

In view of the diverse nature of the literature on this subject we decided to investigate this reaction by subjecting the dehydration products $RCOCH{=}CHCCl_3$ (assumed to be the first intermediates in the reaction of the corresponding β-ketols with base) of several 1,1,1-trichloro-2-hydroxy-4-alkanones to the action of methanolic bases and by examining the resulting reaction products.

Results and Discussion

Slow addition of a five-fold excess of methanolic potassium hydroxide to a stirred solution of 1,1,1-trichloro-2-penten-4-one (**1**) in methanol at low temperature followed by acidification of the reaction mixture and standard work-up gave a white, crystalline acid $C_5H_5ClO_2$ which was identified as 5-chloro-2,4-pentadienoic acid (**2**) (eq. 2). Compound **2** was found to be identical to the acid $C_5H_5ClO_2$ obtained by Uschakov (4) and Salkind (5) in low yield by treatment of 1,1,1-trichloro-2-hydroxy-4-pentanone with cold aqueous or alcoholic potassium hydroxide. Uschakov and Salkind had proposed $CH_3{-}CCl{=}C{=}CH{-}COOH$ or $CH_2{=}CCl{-}CH{=}CH{-}COOH$ as the most probable structural formula for this compound.

Primarily on the basis of spectral data we have now been able to rule out both of these structures in favor of **2**. Acid **2** exhibits typical olefinic and carbonyl stretching bands (1626 and 1675 cm^{-1}, respectively) in its i.r. spectrum. The high-intensity u.v. absorption maximum (in EtOH) at 255 nm (ε 27 700) is characteristic of highly conjugated carbonyl compounds (8–10). The n.m.r. spectrum (Fig. 1) clearly reveals the compound to be 5-chloro-2,4-pentadienoic acid. Esterification of **2** with diazomethane shifts the carbonyl band to 1720 cm^{-1} in the methyl ester (**3**).

Since reaction 2 was accompanied by the formation of appreciable quantities of unidentified byproducts when a large excess of potassium hydroxide was used as hydrolyzing agent, we carried out a systematic study of the reaction of **1** with several bases in methanolic solution under less severe conditions in order to improve the yield of **2** and to isolate any intermediate that might be present in the reaction mixture. Thus, when equimolar quantities of **1** and sodium carbonate in methanol were heated at 50° for 15 h, the resulting product mixture was found to consist of 25% methyl 5-chloro-2,4-pentadienoate (**3**) and 75% 1,1,1-trichloro-2-methoxy-4-pentanone (**4**) with only trace amounts of other components present, while an identical reactant mixture kept at 100° for 8 h gave a product mixture containing approximately 55% of **3** and 45% of **4** (eq. 3).

Equimolar quantities of **1** and potassium hydroxide in methanol at 0–25° ($2\frac{1}{2}$ h) gave a product mixture which was estimated to contain 24% of ester **3** and 76% of the addition product **4** with traces of **2** also present. That **4** is a true intermediate in these reactions was revealed when equimolar quantities of this compound and potassium hydroxide in methanol at 0–25° ($2\frac{1}{2}$ h) were found to give 38% of ester **3** and 62% of unreacted starting material (eq. 3); neither

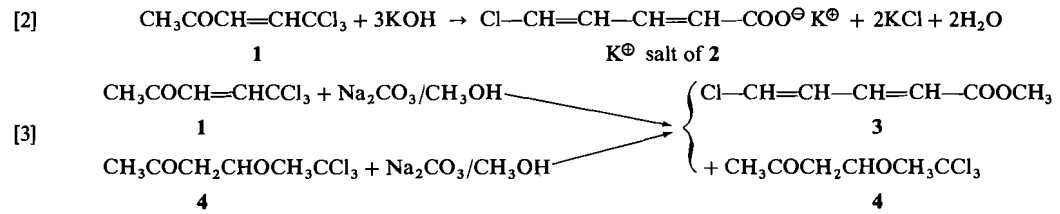

Can. J. Chem. Downloaded from www.nrcresearchpress.com by 210.87.254.105 on 09/05/12
For personal use only.

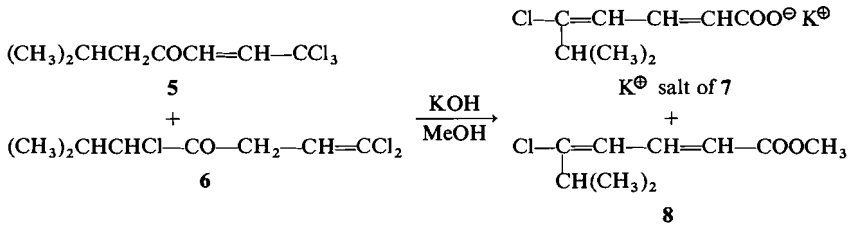

[4] $(CH_3)_2CHCH_2COCH{=}CH{-}CCl_3$ (**5**) + $(CH_3)_2CHCHCl{-}CO{-}CH_2{-}CH{=}CCl_2$ (**6**) $\xrightarrow[MeOH]{KOH}$ $Cl{-}C(CH(CH_3)_2){=}CH{-}CH{=}CHCOO^{\ominus}\,K^{\oplus}$ ($K^{\oplus}$ salt of **7**) + $Cl{-}C(CH(CH_3)_2){=}CH{-}CH{=}CH{-}COOCH_3$ (**8**)

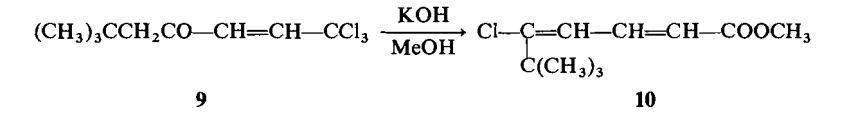

[5] $(CH_3)_3CCH_2CO{-}CH{=}CH{-}CCl_3$ (**9**) $\xrightarrow[MeOH]{KOH}$ $Cl{-}C(C(CH_3)_3){=}CH{-}CH{=}CH{-}COOCH_3$ (**10**)

1 nor **2** was detected in the crude product mixture, suggesting that the base-catalyzed addition of methanol to **1** (eq. 3) is irreversible.

The formation of homologous dienoic acids and/or their methyl esters has also been observed in the cases of other 1,1,1-trichloro-2-alken-4-ones which contain a minimum of two geminal α-hydrogen atoms. Thus, treatment of a mixture[1] containing 52% 1,1,1-trichloro-6-methyl-2-hepten-4-one (**5**) and 42% 1,1,5-trichloro-6-methyl-1-hepten-4-one (**6**) with a solution of potassium hydroxide in methanol gave 5-chloro-6-methyl-2,4-heptadienoic acid (**7**) and its methyl ester (**8**) which were identified by molecular weight determination, i.r. and n.m.r. spectroscopy (eq. 4).

The 100 MHz n.m.r. spectrum of **7** in C_6D_6 exhibited absorption peaks at τ 4.13 (α-H, unsymmetrical doublet, $J_{\alpha\beta} = 13.0$ Hz), 3.45 (β-H, quartet, $J_{\alpha\beta} = 13.0$, $J_{\beta\gamma} = 12.0$ Hz), 3.06 (γ-H, unsymmetrical doublet, $J_{\beta\gamma} = 12.0$ Hz), 7.35 ($(CH_3)_2CH$—, multiplet), 8.88 (6 protons, CH_3—, doublet, $J = 6.8$ Hz), and −2.45 (—COOH, singlet) which are consistent only with a 5,5-disubstituted 2,4-pentadienoic acid. Under similar reaction conditions 1,1,1-trichloro-6,6-dimethyl-2-hepten-4-one (**9**) formed the methyl ester of 5-chloro-6,6-dimethyl-2,4-heptadienoic acid (**10**) (eq. 5).

When the methanolysis reaction was extended to 1,1,1-trichloro-2-alken-4-ones containing less than two geminal α-hydrogen atoms, neither the expected dienoic acid nor its methyl ester was formed. Thus, when 1,1,1-trichloro-5-methyl-2-hexen-4-one (**11**) was treated with methanolic potassium hydroxide, v.p.c., i.r., and n.m.r. analysis of the product mixture revealed the presence of 1,1,1-trichloro-2-methoxy-5-methyl-4-hexanone (**12**) and 1,1-dichloro-2,5-dimethoxy-5-methyl-4-hexanone (**13**) in the approximate molar ratio 3:2 and the complete absence of pentadienoic acid derivatives similar to **2** or **5**; and 1,1,1-trichloro-5-ethyl-2-hexen-4-one (**14**) was converted into a mixture containing predominantly 1,1,1-trichloro-2-methoxy-5-ethyl-4-heptanone (**15**) and traces of 1,1-dichloro-2,5-dimethoxy-5-ethyl-4-heptanone (**16**) (eq. 6).

We conclude from this difference in the behavior of **1**, **5**, and **9**, on the one hand, and **11** and **14**, on the other, towards methanolic potassium hydroxide that a minimum of two geminal α-hydrogens are necessary for the formation of the dienoic acid/ester. On the basis of these

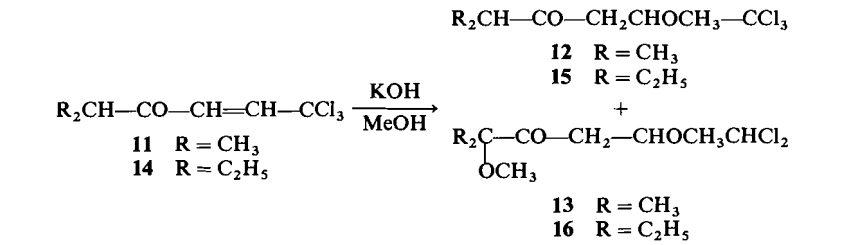

[6] $R_2CH{-}CO{-}CH{=}CH{-}CCl_3$ (**11** R = CH_3; **14** R = C_2H_5) $\xrightarrow[MeOH]{KOH}$ $R_2CH{-}CO{-}CH_2CHOCH_3{-}CCl_3$ (**12** R = CH_3; **15** R = C_2H_5) + $R_2C(OCH_3){-}CO{-}CH_2{-}CHOCH_3CHCl_2$ (**13** R = CH_3; **16** R = C_2H_5)

[1]Component 6 was subsequently shown to be an intermediate in reaction 4 (see Scheme 1). For details, see Experimental.

Can. J. Chem. Downloaded from www.nrcresearchpress.com by 210.87.254.105 on 09/05/12
For personal use only.

Can. J. Chem. Downloaded from www.nrcresearchpress.com by 210.87.254.105 on 09/05/12
For personal use only.

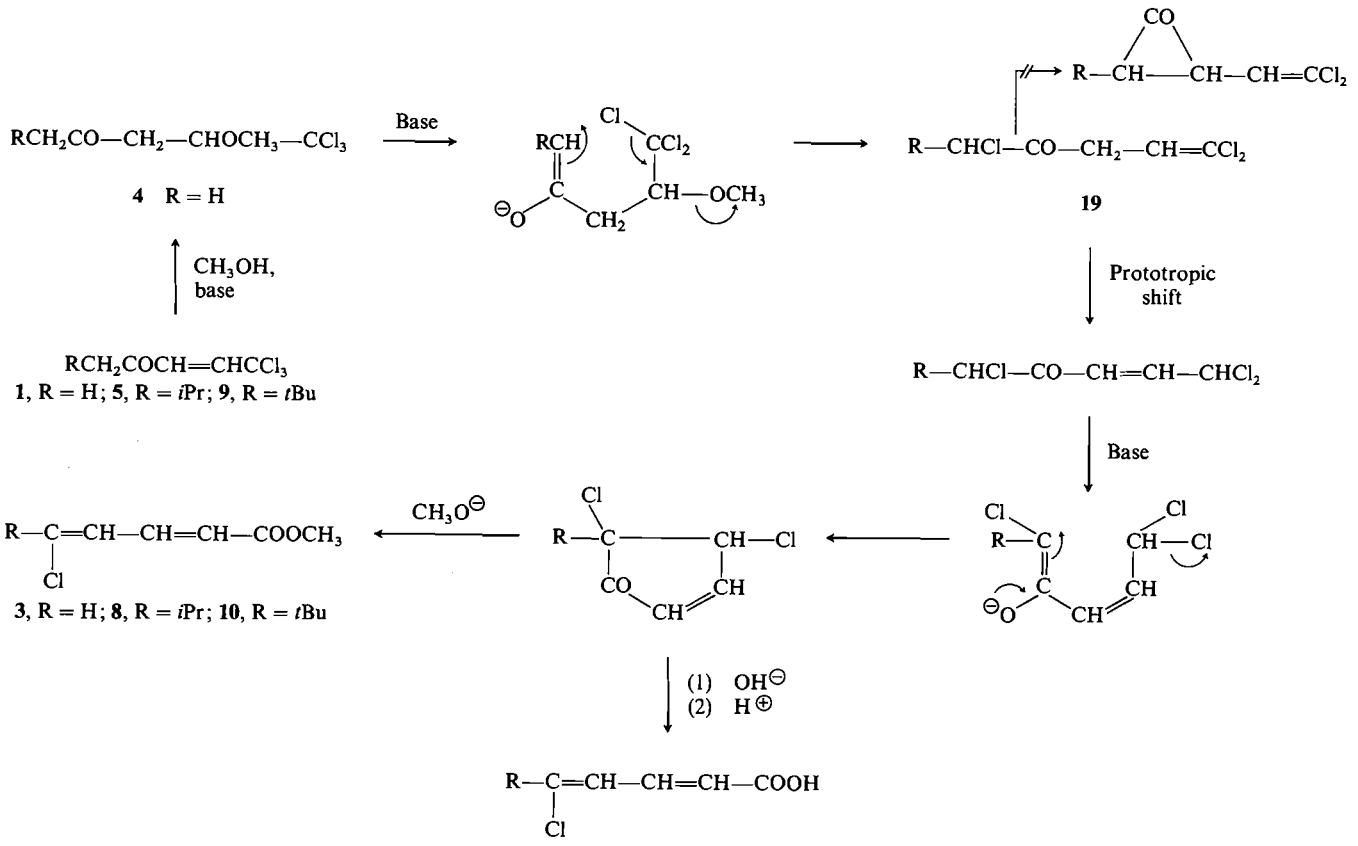

SCHEME 1

Can. J. Chem. Downloaded from www.nrcresearchpress.com by 210.87.254.105 on 09/05/12
For personal use only.

observations, the mechanism shown in Scheme 1 is proposed for reactions 3, 4, and 5.

Base-catalyzed enolization of the enone–methanol addition product (**9**, R = H) is followed by migration of chlorine to form a 1,1,5-trichloro-1-alken-4-one (**3**). A prototropic shift leads to the formation of the more stable enolate ion of an α,β-unsaturated ketone and is similar to the proton migration reported by Takeda and Tsuboi (11) for the reaction of 1,1,3-trichloro-1-penten-4-one with triethylamine. Subsequent ring closure is postulated to give a substituted 2-cyclopentenone intermediate[2] which is cleaved by the nucleophilic attack of methoxide or hydroxide ion at the carbonyl carbon and elimination of chloride ion. Relief of angle strain and resonance stabilization of the highly conjugated product (**2**, **3**, **7**, **8**, and **10**) are believed to be the major driving forces for this final step which is completely identical to the previously reported (12) ring opening of perchloro-2-cyclopentenone by methoxide ion to form methyl pentachloropentadienoate.

The mechanism postulated in Scheme 1 also explains suitably the formation of 1,1-dichloro-2,5-dimethoxy-5-methyl-4-hexanone (**13**) from 1,1,1-trichloro-5-methyl-2-hexen-4-one (**11**), and 1,1-dichloro-2,5-dimethoxy-5-ethyl-4-heptanone (**16**) from 1,1,1-trichloro-5-ethyl-2-hepten-4-one (**14**) with methanolic potassium hydroxide. Due to the lack of a second α-hydrogen, the formation of a cyclopentenone derivative is prevented in this case and, consequently, the intermediates (**17** and **18**) undergo methanolysis (13) and methoxide addition to the double bond to form **13** and **16**, respectively (eq. 7).

Finally, it is noteworthy that although an α-chloroketone is shown to be an intermediate in the mechanistic pathway (Scheme 1), no Favorskii reaction products have been detected in any of the above reactions. A likely explanation is that the developing negative charge on the unsubstituted α-carbon of intermediate **19** is part of an allylic system and hence is not available for the formation of the cyclopropanone intermediate of the Favorskii reaction (14).

Experimental

Elemental analyses were performed by A. Bernhardt, Microanalytical Laboratory, Elbach, Germany. The n.m.r. spectra were recorded on Varian A 56/60 and HA-100 instruments with TMS as internal standard. The u.v. spectra were run on a Unicam SP-200 and the i.r. spectra on a Perkin–Elmer 457 spectrometer. The v.p.c. analyses were carried out on a Varian Aerograph Model 1200-1 HY-F1 111 gas chromatograph using 5 ft × 1/8 in. columns, nitrogen as carrier gas and the specified stationary phases on Aeropak 30. All quantitative estimates of the composition of product mixtures by v.p.c. analysis were obtained by integration of the peak areas of the components using a disc chart integrator.

5-Chloro-2,4-pentadienoic Acid (2)

A solution of 56.0 g (1.0 mol) of potassium hydroxide in 240 ml of methanol was added dropwise (75 min) and with cooling (0–15°) into a solution of 37.5 g (0.2 mol) of **1** (3) in 60 ml of methanol. The mixture was stirred for another 30 min and the potassium chloride (27.14 g) was filtered off. Filtrate and washings were concentrated to 150 ml, extracted with ether to remove neutral products, acidified (concentrated HCl), and again extracted with ether. The ether layer was dried ($MgSO_4$) and evaporated to give 20.6 g (76% crude yield) of a brown solid. Recrystallization from carbon tetrachloride followed by sublimation gave white **2**, m.p. 168–169° (lit. (4, 5) 171–172°).

Anal. Calcd. for $C_5H_5ClO_2$: C, 45.30; H, 3.80; Cl, 26.74. Found: C, 45.16; H, 3.98; Cl, 26.61.

N.m.r. (CD_3COCD_3, 100 MHz) τ 4.98 (2d, α-H, $J_{\alpha\beta}$ = 15.2, $J_{\alpha\gamma}$ = 0.9 Hz), 3.72 (4d, β-H, $J_{\alpha\beta}$ = 15.2, $J_{\beta\gamma}$ = 11.3, $J_{\beta\delta}$ = 0.8 Hz), 4.25 (q, γ-H, $J_{\beta\gamma}$ = 11.3, $J_{\gamma\delta}$ = 13.1 Hz), and 4.08 (2d, δ-H, $J_{\beta\delta}$ = 0.8, $J_{\gamma\delta}$ = 13.1 Hz); n.m.r. (CF_3COOD, 100 MHz, Fig. 1) τ 4.01 (d, α-H, $J_{\alpha\beta}$ = 15.1 Hz), 2.52 (4d, β-H, $J_{\alpha\beta}$ = 15.1, $J_{\beta\gamma}$ = 11.4, $J_{\beta\delta}$ = 0.9 Hz), 3.33 (q, γ-H, $J_{\beta\gamma}$ = 11.4, $J_{\gamma\delta}$ = 13.2 Hz), and 3.20 (d, δ-H, $J_{\gamma\delta}$ = 13.2 Hz); i.r. and u.v.: see Results and Discussion.

Methyl 5-Chloro-2,4-pentadienoate (3)

Esterification of **2** with diazomethane was carried out by the standard procedure (15).

Anal. Calcd. for $C_6H_7ClO_2$: C, 49.17; H, 4.81; Cl, 24.19. Found: C, 49.37; H, 4.92; Cl, 24.09.

N.m.r. ($CDCl_3$, 60 MHz) τ 4.16 (d, α-H, $J_{\alpha\beta}$ = 14.8 Hz), 2.84 (4d, β-H, $J_{\alpha\beta}$ = 14.8, $J_{\beta\gamma}$ = 7.4, $J_{\beta\delta}$ = 3.5 Hz), 3.47 (m, γ-H and δ-H), and 6.32 (s, 3H, OCH_3). Mass spectrum (80 eV): *m/e* 146 (M) and 148 (M+2), ratio 100:35.

Reaction of 1 with Base (Molar Ratio 1:1)

(*a*) A solution of 5.0 g (0.027 mol) of **1** and 2.86 g (0.027

[7] $R_2C(Cl)—CO—CH=CH—CHCl_2 \xrightarrow[-Cl^{\ominus}]{CH_3OH/CH_3O^{\ominus}} R_2C(OCH_3)—CO—CH_2—CH(OCH_3)—CHCl_2$

17 R = CH_3; **18** R = C_2H_5 — **13** R = CH_3; **16** R = C_2H_5

[2]We were not successful in isolating or trapping cyclopentenone intermediates.

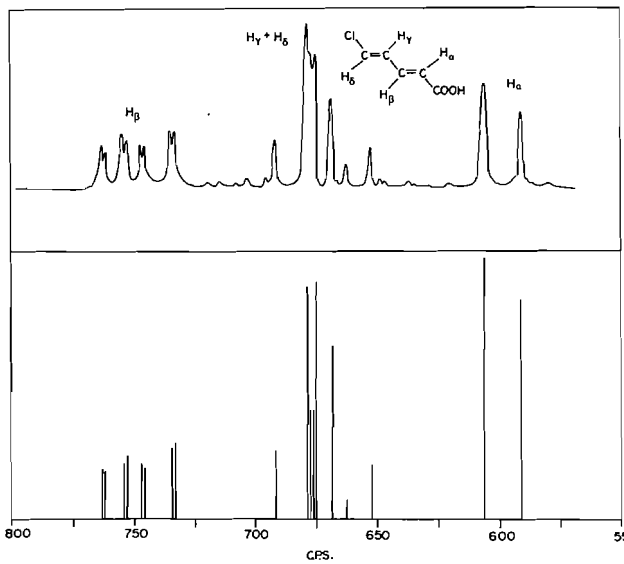

FIG. 1. Experimental n.m.r. spectrum (100 MHz, CF_3COOD as solvent) of 5-chloro-2,4-pentadienoic acid (**2**) (top) as compared to the computer-generated line spectrum (bottom) using LAOCOON (17) program.

mol) of sodium carbonate in 40 ml of methanol was heated at 50° for 15 h and worked-up as described above for the preparation of **2**. The neutral fraction (4.6 g) was shown by v.p.c. (SE-52, 120°) and n.m.r. analysis to contain only **3** (25%) and **4** (75%), the acid fraction (<0.1 g) contained mainly **2**.

(*b*) Heating an identical reactant mixture (see section *a*) at 100° for 8 h gave 4.4 g of neutral fraction (55% of **3** and 45% of **4**) and less than 0.1 g of acid fraction.

(*c*) A solution of 5.0 g (0.027 mol) of **1** in 20 ml of methanol and 1.58 g (0.027 mol) of potassium hydroxide in 20 ml of methanol, obtained by the dropwise addition of the latter to the former, was kept at 0–25° for $2\frac{1}{2}$ h (work-up as described before) to yield 4.3 g of neutral fraction (24% of **3** and 76% of **4**) and 0.1 g of **2** (acid fraction).

1,1,1-Trichloro-2-methoxy-4-pentanone (4)

This compound was separated from **3** (see above) by partition chromatography on silicic acid (Mallinckrodt AR 100 Mesh) using hexane–chloroform (1:1 by volume) as eluent; n.m.r. ($CDCl_3$, 60 MHz) τ 7.89 (s, 3H, CH_3CO), 7.05 (m, 2H, CH_2CO), 6.31 (s, 3H, OCH_3), 5.67 (m, 1H, $CHOCH_3$); i.r. (neat) 1720 (CO), and 1100 cm^{-1} (C—O—C); mass spectrum (80 eV): *m/e* 182 and 184 (ratio 100:65, 2 Cl, probably M-HCl), 101 (100%, $CH_3COCH_2^{\oplus}$ $CHOCH_3$), M not observable.

Reaction of 4 with KOH

A solution of 0.35 g (5.0 mmol) of potassium hydroxide in 5.0 ml of methanol was added dropwise to 1.0 g (5.0 mmol) of **4** in 5.0 ml of methanol and stirred at 25° for 2 h. Evaporation of methanol, addition of 10 ml of water, extraction with ether, drying ($MgSO_4$), and removal of solvent gave 0.63 g of a mixture of 38% **3** and 62% **4**. The aqueous layer contained traces of **2**.

5-Chloro-6-methyl-2,4-heptadienoic Acid (7) and its Methyl Ester (8)

1,1,1-Trichloro-6-methyl-2-hepten-4-one (**5**) was prepared by acid-catalyzed dehydration of 1,1,1-trichloro-2-hydroxy-6-methyl-4-heptanone (3). Since this reaction was accompanied by rearrangement of **5** to 1,1,5-trichloro-6-methyl-1-hepten-4-one (**6**), and large-scale separation of these two isomers to obtain pure **5** proved to be difficult, a mixture of **5** and **6** (10.0 g, 0.043 mol) was treated with potassium hydroxide (11.2 g, 0.2 mol) and methanol (65 ml) as described above for the preparation of **2**. The aqueous layer, on acidification, gave 3.5 g (46%) of a brown solid which was sublimed and recrystallized from carbon tetrachloride to give pale yellow **7**, m.p. 112–113°.

Anal. Calcd. for $C_8H_{11}ClO_2$: C, 55.02; H, 6.35; Cl, 20.30. Found: C, 54.85; H, 6.22; Cl, 20.37.

Mol. wt. calcd. for $C_8H_{11}{}^{37}ClO_2$: 176.0418. Found (mass spectrum): 176.0424.

U.v. (EtOH) max 260 nm (23 900); i.r. and n.m.r.: see Results and Discussion. The ether layer was dried ($MgSO_4$) and evaporated to give 7.3 g of a brown liquid. From this a sample of pure **8** was obtained by column chromatography on silicic acid using hexane–chloroform (1:1) as eluent; n.m.r. ($CDCl_3$, 60 MHz) τ 3.0–3.8 (m, 3H, olefinic), 6.29 (s, 3H, $COOCH_3$), 7.0 (septet, 1H, $(CH_3)_2CH$), and 8.80 (d, 6H, $(CH_3)_2CH$).

Repetition of the above experiment with pure **6** (1.2 g, 5.2 mmol) and KOH (1.45 g, 26 mmol) also gave **8** (see footnote 1) as identified by n.m.r.

Methyl 5-Chloro-6,6-dimethyl-2,4-heptadienoate (10)

The reaction of 10.0 g (0.041 mol) of **9** (3) with 11.2 g (0.20 mol) of potassium hydroxide in 65 ml of methanol and usual work-up yielded a brown oil (6.0 g) which was chromatographed on silicic acid (using hexane–chloroform as

Can. J. Chem. Downloaded from www.nrcresearchpress.com by 210.87.254.105 on 09/05/12
For personal use only.

Can. J. Chem. Downloaded from www.nrcresearchpress.com by 210.87.254.105 on 09/05/12
For personal use only.

eluent) to give pure **10**: n.m.r. ($CDCl_3$, 60 MHz) τ 3.2–4.1 (m, 3H, olefinic), 6.22 (s, 3H, $COOCH_3$), and 8.87 (s, 9H, $(CH_3)_3C$); mass spectrum (80 eV): *m/e* 202 (M), 143 (M-$COOCH_3$); u.v. (EtOH) max 242 nm (20 000). No carboxylic acid (corresponding to **10**) was detected in the aqueous layer.

1,1,1-Trichloro-5-methyl-2-hexen-4-one (11)

Following a previously reported procedure (3), 40.5 g (0.172 mol) of 1,1,1-trichloro-2-hydroxy-5-methyl-4-hexanone, 70.2 g (0.69 mol) of acetic anhydride and 3.0 g of anhydrous sodium acetate were heated at 100° for 90 min. Standard work-up and vacuum distillation of the crude product gave 22.4 g (60% yield) of **11** (90% pure), b.p. 67°/0.5 mm: i.r. (neat) 1700 (CO) and 1650 cm^{-1} (C=C); n.m.r. ($CDCl_3$, 60 MHz) τ 2.87 (d, 1H, C=CHCCl$_3$, J = 15.0 Hz), 3.27 (d, 1H, CO—CH=C, J = 15.0 Hz), 7.14 (septet, 1H, $(CH_3)_2CH$, J = 7.0 Hz), and 8.82 (d, 6H, CH_3, J = 7.0 Hz).

Reaction of 11 with KOH

Treatment of **11** (5.0 g, 2.3 mmol) with 2.4 mmol potassium hydroxide (see reaction of **1** with base, section *c*) yielded 4.95 g of a neutral fraction which was found by n.m.r. and v.p.c. (SE-52, 120°) analysis to contain only 1,1,1-trichloro-2-methoxy-5-methyl-4-hexanone (**12**) (60%) and 1,1-dichloro-2,5-dimethoxy-4-hexanone (**13**) (40%). Pure samples of **12** and **13** were obtained by chromatography on silicic acid using hexane–chloroform as eluent.

Anal. Calcd. for $C_8H_{13}Cl_3O_2$ (**12**): C, 38.82; H, 5.29; Cl, 42.96. Found: C, 39.00; H, 5.17; Cl, 43.12.

I.r. (neat) 1720 cm^{-1} (CO); n.m.r. ($CDCl_3$, 60 MHz) τ 8.87 (d, 6H, $(CH_3)_2C$), 7.40 (septet, 1H, $CH(CH_3)_2$), 7.0 (m, 2H, $COCH_2$), 6.34 (s, 3H, OCH_3), and 5.65 (m, 1H, $CHOCH_3$).

Anal. Calcd. for $C_9H_{16}Cl_2O_3$ (**13**): C, 44.46; H, 6.63; Cl, 29.16. Found: C, 44.66; H, 6.51; Cl, 29.31.

N.m.r. ($CDCl_3$, 60 MHz) τ 8.70 (s, 6H, $(CH_3)_2C$), 6.77 (s, 3H, $(CH_3)_2C$—OCH_3), 6.97 (m, 2H, $COCH_2$), 6.50 (s, 3H, $CHOCH_3$), 5.88 (m, 1H, $CHOCH_3$), and 4.10 (d, 1H, $CHCl_2$, J = 3.7 Hz); mass spectrum (80 eV): *m/e* 73 (100%, $(CH_3)_2C^{\oplus}$—OCH_3) and other fragments characteristic of keto ethers (16).

1,1,1-Trichloro-5-ethyl-2-hepten-4-one (14)

According to a previously reported procedure (3), 17.0 g (0.0654 mol) of 1,1,1-trichloro-2-hydroxy-5-ethyl-4-heptanone, 26.5 g (0.26 mol) of acetic anhydride, and 2.0 g of anhydrous sodium acetate were heated at 100° for 90 min. Work-up and vacuum distillation of the crude product gave 8.1 g (51%) of **14** (99% pure), b.p. 83–87°/0.5 mm; i.r. (neat) 1700 (C=O) and 1660 cm^{-1} (C=C); n.m.r. ($CDCl_3$, 60 MHz) τ 2.88 (d, 1H, $CHCCl_3$, J = 15.0 Hz), 3.35 (d, 1H, CO—CH=C<, J = 15.0 Hz), 7.45 (quintet, 1H, Et_2CH, J = 7.0 Hz), 8.34 (m, 4H, $(CH_3CH_2)_2CH$), and 9.15 (t, 6H, $(CH_3CH_2)_2CH$, J = 7.0 Hz).

Reaction of 14 with KOH

Treatment of 2.0 g (8.2 mmol) of **14** with 0.46 g (8.2 mmol) of potassium hydroxide in 20.0 ml of methanol and work-up (procedure as before) yielded 1.72 g of an oil which was shown by v.p.c. to contain 95% of **15** and a small amount of **16**. N.m.r. of **15** ($CDCl_3$, 60 MHz) τ 5.6 (m, 1H, $CHOCH_3$), 6.28 (s, 3H, OCH_3), 7.0 (m, 2H, CH_2CO), 7.65 (quintet, 1H, $(CH_3CH_2)_2CH$), 8.35 (m, 4H, $(CH_3CH_2)_2C$), 9.1 (t, 6H, $(CH_3CH_2)_2C$). Spectral identification of **16**: n.m.r. ($CDCl_3$, 60 MHz) τ 4.05 (d, 1H, $CHCl_2$, J = 3.5 Hz), 5.87 (m, 1H, $CHOCH_3$), 6.48 (s, 3H, CH_3OCH), 6.8 (s, 3H, $(CH_3CH_2)_2C$—OCH_3), 7.0 (m, 2H, CH_2CO), 7.65 (q, 4H, $(CH_3CH_2)_2C$, J = 6.0 Hz), 9.12 (t, 6H, $(CH_3CH_2)_2C$, J = 6.0 Hz); mass spectrum (80 eV): *m/e* 101 (100%, $(CH_3CH_2)_2C^{\oplus}$—OCH_3).

The authors wish to express their sincere thanks to Miss E. G. Kayser of the Advanced Chemistry Division, U.S. Naval Ordinance Laboratory, White Oak, Maryland for running the 100 MHz n.m.r. spectra, to Dr. W. Reeve of the Chemistry Department, University of Maryland, College Park, Maryland, for many helpful comments on the interpretation of these spectra, to Morris Pudek for technical assistance, and to the National Research Council of Canada, Ottawa, Canada, for financial support.

1. E. KIEHLMANN and P. W. LOO. Can. J. Chem. **49**, 1588 (1971).
2. B. C. MENON and E. KIEHLMANN. Can. J. Chem. **49**, 3648 (1971).
3. E. KIEHLMANN, P. W. LOO, B. C. MENON, and N. McGILLIVRAY. Can. J. Chem. **49**, 2964 (1971).
4. P. Uschakov. Zh. Russ. Fiz.-Khim. Obshchest. **29**, 113 (1897).
5. J. SALKIND. Zh. Russ. Fiz.-Khim. Obshchest. **30**, 906 (1898).
6. F. CAUJOLLE, P. COUTURIER, and C. DULAURANS. Bull. Soc. Chim. Fr. 19 (1950).
7. E. KIEHLMANN. Dissertation. University of Maryland College Park, Maryland, 1964.
8. F. F. ULLMAN and W. J. FANSHAWE. J. Am. Chem. Soc. **83**, 2379 (1961).
9. G. VOGEL. J. Org. Chem. **30**, 203 (1965).
10. R. R. SHAGIDULLIN, A. V. CHERNOVA, E. A. ISHMAEVA, and A. N. PUDOVIK. Dokl. Akad. Nauk SSSR, **173**, 135 (1967).
11. A. TAKEDA and S. TSUBOI. J. Org. Chem. **35**, 2690 (1970).
12. E. D. WEIL and J. LINDER. J. Org. Chem. **28**, 2218 (1963).
13. F. G. BORDWELL and R. G. SCAMEHORN. J. Am. Chem. Soc. **93**, 3410 (1971).
14. A. A. AKHREM, T. K. USTYNYUK, and Y. A. TITOV. Russ. Chem. Rev. **39**, 732 (1970).
15. H. VON PECHMANN. Ber. Deut. Chem. Ges. **27**, 1888 (1894); **28**, 855 (1895).
16. P. E. BUTLER. J. Org. Chem. **29**, 3024 (1964).
17. S. CASTELLANO and A. A. BOTHNER-BY. J. Chem. Phys. **41**, 3863 (1964).

The Reaction of some Isothiazolium Salts with Sulfur in Pyridine

G. E. BACHERS, D. M. MCKINNON, AND J. M. BUCHSHRIBER
Chemistry Department, University of Manitoba, Winnipeg, Manitoba

Received March 21, 1972

A variety of *N*-methyl and *N*-phenylisothiazolium salts has been synthesized and treated with sulfur in boiling pyridine. The products have been examined by chromatography and their structures determined. While 5-unsubstituted isothiazolium salts appear to give the corresponding isothiazoline-5-thiones, 3-unsubstituted salts give either the corresponding isothiazoline-3-thiones if the nitrogen is alkyl substituted, or 1,2-dithiole-3-imines if the nitrogen is aryl substituted. *N*-Alkyl compounds also give dealkylated products, and dithiolethiones are also found. The initial stages in the reaction appear to involve deprotonation of the isothiazolium salt.

Une série de sels de *N*-méthyl et *N*-phénylisothiazolium ont été synthétisés et traités par du soufre dans la pyridine à ébullition. Les produits ont été examinés en chromatographie et leurs structures déterminées. Tandis que les sels d'isothiazolium non substitués en 5 donnent des isothiazolinethiones-5 correspondantes, les sels non substitués en 3 donnent soit des isothiazolinethiones-3 si l'azote est substitué par un alkyle, ou des dithiole-1,2 imines-3 si l'azote est substitué par un aryle. Les composés *N*-alkyles donnent également des produits déalkylés et des dithiolethiones. Les étapes initiales dans la réaction semblent faire intervenir la déprotonation du sel isothiazolium.

Canadian Journal of Chemistry, **50**, 2568 (1972)

In a previous paper the reaction of two isothiazolium salts, 2-methyl-5-phenylisothiazolium perchlorate (**1***a*) and 2,5-diphenylisothiazolium perchlorate (**1***b*) with sulfur in boiling pyridine was examined (1). It was suggested that the products of the reactions were the corresponding isothiazoline-3-thiones, **2***a* and *b* respectively. The structure of one of these was later confirmed by an alternate synthesis and by ^{15}N n.m.r. and by chemical tests (2, 3). Later work, however, (4) indicated that the product of the other of these reactions was not 2,5-diphenylisothiazoline-3-thione (**2***b*) but was in fact the isomeric 5-phenyl-3-phenylimino-1,2-

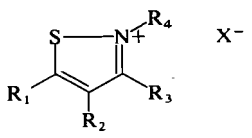

1

a $R_1 = Ph, R_2 = R_3 = H, R_4 = Me, X = ClO_4$
b $R_1 = Ph, R_2 = R_3 = H, R_4 = Ph, X = ClO_4$
c $R_1 = R_2 = Ph, R_3 = H, R_4 = Me, X = ClO_4$
d $R_1 = R_2 = Ph, R_3 = H, R_4 = Ph, X = ClO_4$
e $R_1 = Ph, R_2 = H, R_3 = Ph, R_4 = Me, X = ClO_4$
f $R_1 = Ph, R_2 = H, R_3 = R_4 = Ph, X = ClO_4$
g $R_1 = H, R_2 = Ph, R_3 = H, R_4 = Me, X = ClO_4$
h $R_1 = H, R_2 = Ph, R_3 = H, R_4 = Ph, X = ClO_4$
i $R_1 = R_2 = H, R_3 = R_4 = Ph, X = ClO_4$
j $R_1 = SMe, R_2 = Ph, R_3 = H, R_4 = Ph, X = I$
k $R_1 = SEt, R_2 = H, R_3 = Ph, R_4 = Ph, X = I$

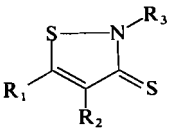

2

a $R_1 = Ph, R_2 = H, R_3 = Me$
b $R_1 = Ph, R_2 = H, R_3 = Ph$
c $R_1 = R_2 = Ph, R_3 = Me$

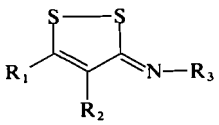

3

a $R_1 = Ph, R_2 = H, R_3 = Ph$
b $R_1 = R_2 = R_3 = Ph$

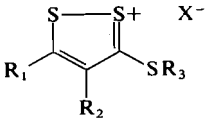

4

a $R_1 = H, R_2 = Ph, R_3 = Me, X = I$
b $R_1 = H, R_2 = Ph, R_3 = Br, X = Br$
c $R_1 = Ph, R_2 = H, R_3 = Et, X = I$
d $R_1 = Ph, R_2 = H, R_3 = Br, X = Br$

Can. J. Chem. Downloaded from www.nrcresearchpress.com by 210.87.254.6 on 09/05/12
For personal use only.

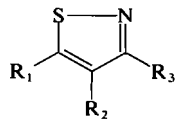

5

a $R_1 = R_2 = Ph, R_3 = H$
b $R_1 = Ph, R_2 = H, R_3 = Ph$
c $R_1 = Ph, R_2 = R_3 = H$
d $R_1 = H, R_2 = Ph, R_3 = H$

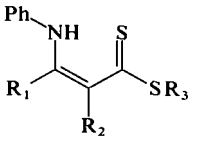

6

a $R_1 = H, R_2 = Ph, R_3 = Me$
b $R_1 = Ph, R_2 = H, R_3 = Et$

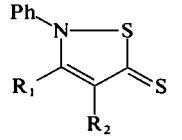

7

a $R_1 = H, R_2 = Ph$
b $R_1 = Ph, R_2 = H$

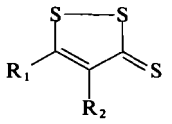

8

a $R_1 = H, R_2 = Ph$
b $R_1 = Ph, R_2 = H$
c $R_1 = R_2 = Ph$

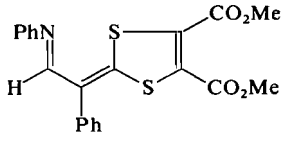

9

dithiole (**3***a*), arising from a molecular rearrangement. It therefore seemed desirable to investigate such reactions further to determine the products and the reactions leading to them.

A representative variety of isothiazolium salts was chosen for this investigation, containing *N*-phenyl-, **1***b*, *d*, *f*, *h*, and *i*, and *N*-methyl, **1***a*, *c*, *e*, and *g* substituents. The latter were available by methylation of isothiazoles, formed by treatment of suitable 1,2-dithiolium salts with ammonia (5). One of these isothiazoles **5***a* is previously unreported, although an attempted synthesis (6) appears to have met with failure. The former salts, **1***b*, *d*, and *f*, were prepared according to established methods (1) by oxidative cyclization of 3-anilinopropenethiones, which are available by treatment of certain 1,2-dithiolium salts with aniline (1, 7).

The synthesis of the two other compounds **1***h* and *i* presented more difficulty, since the methods used for the others are inapplicable to the direct synthesis of these. A modified approach was successful. The 3-alkylthio-1,2-dithiolium salt **4***a* treated with aniline gave the acyclic methyl 2-phenyl-3-anilinopropenedithioate (**6***a*) (8) which oxidized by iodine to form the isothiazolium salt **1***j* as its triiodide. Conversion of this to the perchlorate and demethylation by pyridine gave the thione **7***a* which was converted by hydrogen peroxide in acetic acid to the isothiazolium salt **1***h*. This method appears to represent a new synthesis of isothiazolium salts. Similar oxidations are reported for 1,2- and 1,3-dithiolethiones, (9–12) and for thiopyran-2-thiones (13). The thione **7***a* was more conveniently prepared by treatment of 4-phenyl-1,2-dithiole-3-thione (**8***a*) with bromine, followed by aniline. This reaction of 5-unsubstituted-4-aryl-1,2-dithiole-3-thiones, **8**, had been previously reported (14) to give 1,2-dithiole-3-imines, **3**, by nucleophilic attack of aniline at the 3-position of the initially formed 3-bromothiodithiolium bromide, **4***b*, but it now appears more likely that the products formed are in fact the isomeric isothiazoline-5-thiones, **7**, arising by nucleophilic attack at the unsubstituted 5-position. This is what would have been expected on steric grounds and in accordance with the position of nucleophilic attack on 5-unsubstituted-3-alkylthiodithiolium salts (**8**). Similar considerations may be used to explain the nucleophilic ring-opening of cyclopentenodithiolium salts (15). The structure of the isothiazoline-5-thione was further confirmed by its reaction with dimethyl acety-

Can. J. Chem. Downloaded from www.nrcresearchpress.com by 210.87.254.6 on 09/05/12
For personal use only.

Can. J. Chem. Downloaded from www.nrcresearchpress.com by 210.87.254.6 on 09/05/12
For personal use only.

lenedicarboxylate. The adduct **9** was formed. Had the compound been the isomeric 1,2-dithiole-3-imine, a thioacylmethylenethiazole would have been obtained (16). This, being a thial, would have been unstable and rapidly reacted further in a fashion similar to related thioacylmethylene-1,3-dithioles (17).

However, when 5-phenyl-1,2-dithiole-3-thione (**8***b*) was treated with bromine, followed by aniline, the product obtained was the imine, **3***a*, with greater or lesser amounts of the thione **8***b*, *vide infra*. In this case the steric bulk of the phenyl group blocks attack at the 5-position, and attack at the less hindered 3-position provides imine or thione.

A similar scheme via an aminodithioenoate was used to prepare **7***b*. 3-Ethylthio-5-phenyl-1,2-dithiolium iodide (**4***c*) reacted with aniline in acetic acid to provide as a main product the imine, **3***a* (8, 18). A minor product was the dithioester **6***b*, which was readily separated from the imine. Similar results have been obtained in the reaction of alkylthio-1,2-dithiolium salts with aliphatic amines (19). The dithioester oxidized satisfactorily to the isothiazolium salt **1***k*, and dealkylation of this with pyridine afforded the thione **7***b*. This was oxidized by hydrogen peroxide in acetic acid to the isothiazolium salt **1***i*. Attempted conversion of the 5-alkylthioisothiazolium salts **1***j* and *k* to the thiones **7***a* and *b*, respectively, by treatment with sodium hydrosulfide failed. Instead the dithioesters, **6***a* and *b*, were obtained. It appears that in this case ring cleavage is the dominant reaction, possibly by initial nucleophilic attack at ring nitrogen or sulfur. Traces of the corresponding 1,2-dithiole-3-thiones **8***a* and *b* were also found.

An attempted preparation of the thione **2***b* by treatment of thione **8***b* with bromine, followed by aniline gave only thione **8***b* and imine **3***a*. These are both formed by nucleophilic attack on the initially formed dithiolium salt **4***d* since this salt can be isolated satisfactorily from the reaction. Treatment of the salt **1***b* with sulfur in boiling pyridine afforded the imine **3***a* and traces of thione **8***b*, and treatment of the salt **1***d* afforded the imine **3***b* only. These results indicate that the reaction is proceeding in these cases by ring opening and recyclization. The most likely scheme would involve deprotonation by base to form a carbene or zwitterionic species which would undergo ring fission to a thioketimine, similarly to known reactions of isoxazolium salts (20). This intermediate could then react with a polysulfide or chain (21, 22) formed by reaction of pyridine with sulfur to form the imine (Scheme 1*a*). Direct attack by polysulfide ion on the salt is considered unlikely since the salt **1***f*, which has no reactive hydrogens at 3- or 5-position, was completely unaffected by treatment with sulfur in pyridine. Despite the steric bulk of the phenyl groups, ring opening would have been likely had polysulfide attack been the initial stage.

The thione **8***b* detected in the first of these reactions was not formed from the imine **3***a* since prolonged treatment of the imine under the reaction conditions did not produce any thione. Only prolonged fusion of the imine at 180° gave some thione, along with numerous other products. It thus appears that thione is formed from an acyclic precursor. No thione **8***c* was detected in the reaction of the salt **1***d* with sulfur. Possibly conjugative or steric effects are important, although some thione was detected in the reaction of **1***c*.

Compounds **1***h* and *i* gave thiones **7***a* and *b* respectively on reaction. While **1***i* has only one reactive hydrogen (the 5-position) available and can only give the 5-thione, compound **1***h* has two available, one adjacent to nitrogen and one adjacent to sulfur. That only the product derived from the abstraction of a proton adjacent to sulfur is found, is likely a consequence of the greater ability of sulfur over nitrogen to stabilize an adjacent carbanion by d-orbital participation. Supporting data are available from other isothiazolium salt reactions (23). Since nucleophilic attack at the 3-position is favored by inductive and coulombic considerations, the isolation of products derived from attack at the 5-position is further evidence for deprotonation as the first stage in the reaction. Small amounts of the corresponding dithiolethiones **8***a* and *b* were also obtained in these reactions.

Of course, the detection of isothiazoline-5-thione products rather than dithioleimines does not allow differentiation between a mechanism involving ring opening comparable to Scheme 1 or one involving direct sulfurization of initially formed carbene or zwitterion, as was earlier suggested (1), but the detection of dithiolethione products suggests that there is ring fission to an acyclic precursor of both types of thiones **7** and **8**.

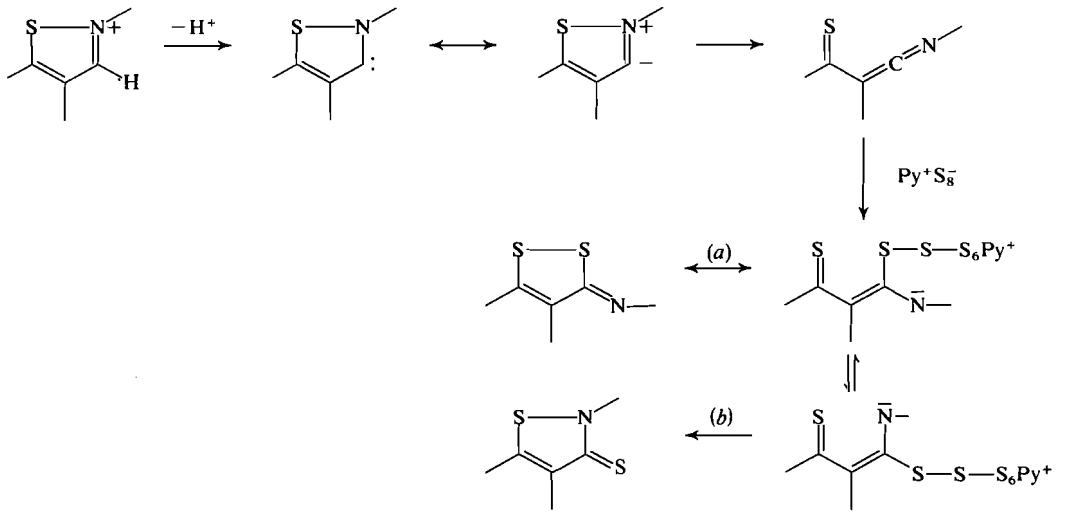

SCHEME 1

When the *N*-alkyl compound **1***e* was treated under these conditions, only the isothiazole **5***b* was obtained, corresponding to a simple demethylation reaction. Treatment of **1***a* under these conditions had been reported (1) to give the isothiazoline-3-thione, **2***a*, but chromatography of the product indicated three fractions, 5-phenylisothiazole **8***c*, the thione **8***b*, and the isothiazoline-3-thione **2***a*, whose structure has been conclusively demonstrated (2). Similarly the salt **1***c* gave the isothiazole **5***d*, the isothiazoline-3-thione **2***c*, and a trace of the dithiolethione **8***c*.

Reaction of the salt **1***g* gave only two products, the isothiazole **5***d* and the thione **8***a*. The lack of any isothiazolinethione or dithioleimine product obtained is probably a consequence of the instability of intermediates. Deprotonation of salt adjacent to sulfur would provide an iminothione. Lacking an aromatic substituent on nitrogen this would be expected to decompose more readily than the intermediate from the reaction of **1***h* with sulfur in pyridine. Deprotonation adjacent to nitrogen, although more unlikely, would give a ketiminothial, which would likewise be unstable.

That the *N*-aryl compounds, **1***b* and *d*, give dithioleimines, and the *N*-alkyl compounds, **1***a* and *c*, give isothiazoline-3-thiones by such treatment may be explained by alternate modes of cyclization of the intermediate in the reaction (Scheme 1*a* or 1*b*), with Scheme 1*a* being favored when the substituent on nitrogen is aryl, and Scheme 1*b* being favored when the substituent is alkyl. Inductive effects appear to be important. Similar differences in products obtained by reaction of 3-alkylthio-1,2-dithiolium salts with aromatic and aliphatic amines have been noted (2) and are probably due to similar causes.

Experimental

The n.m.r. spectra were obtained on a Varian model 56/60A spectrometer in deuterochloroform using tetramethylsilane as an internal standard. Mass spectra were obtained on a Finnegan 1015 quadrupole mass spectrometer. Chromatography (t.l.c.) was performed on "Camag" silica gel type D.S.F.5 supplied by Mondray Ltd. and column chromatography on alumina 504-c, also supplied by Mondray. Elution of both, unless otherwise stated, was by benzene. Melting points (m.p.) were obtained on a precalibrated Fisher–Johns apparatus.

4,5-Diphenylisothiazole (5a)

3,4-Diphenyl-1,2-dithiolium perchlorate (3.55 g, 10 mmol) (1) was slowly added to a boiling solution of ammonium acetate (20 g) in acetic acid (30 ml). The mixture became brown and was boiled 10 min. Dilution with water and extraction with benzene gave a brown solution which was washed once with saturated sodium bicarbonate and once with water. Evaporation gave a brown oil which was extracted with petroleum ether b.p. 60–80° to give a reddish oil. Column chromatography gave three bands. The first (yellow) gave ~0.5 g of an oil which could not be crystallized. The second (red) gave 4,5-diphenyl-1,2-dithiole-3-thione (0.3 g). The third (yellow) gave 4,5-diphenyliso-

Can. J. Chem. Downloaded from www.nrcresearchpress.com by 210.87.254.6 on 09/05/12
For personal use only.

Can. J. Chem. Downloaded from www.nrcresearchpress.com by 210.87.254.6 on 09/05/12
For personal use only.

thiazole. The product was further recrystallized from ethanol. Pale yellow needles, m.p. 92°, were obtained (23%).

Anal. Calcd. for $C_{15}H_{11}NS$: C, 75.94; H, 4.64; N, 5.92; S, 13.51. Found: C, 76.11; H, 4.72; N, 5.92; S, 13.39.

The n.m.r. spectrum: τ 2.83–2.76 (10H, two closely spaced singlets, the aromatic protons), 1.71 (1H singlet, the heterocyclic proton). The mass spectrum: M^+ 237; calcd. 237.

2-Methyl-4,5-diphenylisothiazolium Perchlorate (1c)

4,5-Diphenylisothiazole (1 g) was heated with an excess of dimethyl sulfate at 100° for 1 h. Dilution with ether precipitated a salt which was converted to the perchlorate in acetic acid containing perchloric acid, and recrystallized from the same solvent as yellow needles, m.p. 99° (80%).

Anal. Calcd. for $C_{16}H_{14}NSClO_4$: C, 54.70; H, 3.99; N, 3.99; S, 9.12; Cl, 9.97. Found: C, 54.62; H, 3.80; N, 3.98; S, 9.00; Cl, 9.95.

2-Methyl-4-phenylisothiazolium Perchlorate (1g)

4-Phenylisothiazole (7) was heated with excess dimethyl sulfate and worked-up as in the previous preparation. Pale brown needles, m.p. 102°, were obtained (85%).

Anal. Calcd. for $C_{10}H_{10}NSClO_4$: C, 43.45; H, 3.64; N, 5.09; S, 11.64; Cl, 12.91. Found: C, 43.15; H, 3.99; N, 5.25; S, 11.51; Cl, 12.70.

2,4-Diphenyl-5-methylthioisothiazolium Perchlorate (1i)

Methyl 2-phenyl-3-anilinopropenedithioate (1 g) (8) was dissolved in the minimum quantity of ethanol, and slowly titrated with a saturated ethanolic iodine solution until precipitation was complete. The buff precipitate of triiodide was converted to the perchlorate in acetone, and precipitated by dilution with ether. Recrystallization from acetic acid containing perchloric acid gave the perchlorate as yellow needles, m.p. 158° (34%).

Anal. Calcd. for $C_{16}H_{15}NS_2ClO_4$: C, 49.10; H, 3.81; N, 3.65; S, 16.62; Cl, 9.26. Found: C, 50.10; H, 3.76; N, 3.72; S, 16.57; Cl, 9.33.

2,4-Diphenylisothiazoline-5-thione (7a)

(*a*) 2,4-Diphenyl-5-methylthioisothiazolium perchlorate (384 mg, 1 mmol), pyridine (1 ml), and benzene (20 ml) were refluxed for 16 h. The mixture was diluted with water and extracted with ether. The ether extract was washed with dilute hydrochloric acid, dried, and evaporated to give a yellow oil which was examined by t.l.c. Three bands were obtained, but only the third eluted gave other than traces of product. The compound was recrystallized from petroleum ether, b.p. 60–80°, as orange prisms, m.p. 168°, (9%).

Anal. Calcd. for $C_{15}H_{11}NS_2$: C, 67.01; H, 4.09; N, 5.20; S, 23.78. Found: C, 66.91; H, 3.94; N, 3.56; S, 23.82.

The i.r. spectrum: 1146 cm^{-1} (tentatively C=S str.). The mass spectrum: M^+ 269, calcd. 269.

(*b*) 4-Phenyl-1,2-dithiole-3-thione (2.10 g, 10 mmol) (24), in carbon tetrachloride (50 ml) was slowly treated with a solution of bromine (1.76 g, 11 mmol) in carbon tetrachloride (20 ml) with stirring. A tan solid formed and was collected and washed with carbon tetrachloride. The solid was added portionwise to aniline (10 ml) with stirring, and the mixture stirred 1 h. Dilution with ether gave a solid which was heated with water (20 ml) for 10 min. The mixture was extracted with benzene. The benzene solution was treated with decolorizing charcoal and evaporated to a small volume. Dilution with petroleum ether gave the product as orange prisms, m.p. 168° (82%). These were identical with that obtained above.

Reaction of 5-Phenyl-1,2-dithiole-3-thione with Bromine, followed by Aniline

5-Phenyl-1,2-dithiole-3-thione (2.10 g, 10 mmol) (10) in carbon tetrachloride (50 ml) was treated with bromine as above. A tan solid was obtained which was added to aniline (10 ml) with stirring. Addition of ether precipitated a solid which was found to be aniline salts. The ether solution was washed with water and shaken with dilute hydrochloric acid (25%). A yellow solid which separated was filtered off. Evaporation of the ether solution gave the thione **8***b* (19%). Treatment of the yellow solid with dilute sodium hydroxide gave the imine (**3***a*) (40%).

Reaction of 3-Ethylthio-5-phenyl-1,2-dithiolium Iodide with Aniline, Ethyl 3-Anilinodithiocinnamate (6b)

The iodide (14.6 g, 0.04 mol) (25) in acetic acid (100 ml) was heated to boiling and aniline (10 ml) added. The mixture was heated until homogeneous (~5 min) then diluted with water, and extracted with a chloroform:carbon tetrachloride 1:1 mixture (200 ml). The extract was shaken with 25% hydrochloric acid (100 ml) and filtered. The yellow precipitate gave the imine (**3***a*) on basification. The filtrate was separated and on evaporation gave a red oil which was examined by column chromatography. The first red band eluted gave a dark red oil which crystallized on trituration under ethanol. The product was recrystallized from ethanol as orange-red needles, m.p. 91° (14%).

Anal. Calcd. for $C_{17}H_{17}NS_2$: C, 68.20; H, 5.68; N, 4.68; S, 21.40. Found: C, 68.12; H, 5.75; N, 4.51; S, 21.37.

The mass spectrum: M^+ 299, calcd. 299. The n.m.r. spectrum: τ 8.69 (3H triplet, $J = 3.6$ Hz, CH_3 group) 6.33 (2H quartet, $J = 3.6$ Hz, CH_2), 3.81 (1H singlet, vinyl proton), 3.40–2.85 (5H multiplet, anilino protons), 2.74 (5H singlet, protons on other phenyl group), −3.09 (1H singlet, proton on nitrogen, hydrogen bonded to sulfur).

2,3-Diphenyl-3-ethylthioisothiazolium Perchlorate (1k)

Ethyl 3-anilinodithiocinnamate (1.50 g, 0.05 mol) in ethanol (20 ml) was slowly titrated with a saturated ethanolic solution until separation of buff-colored needles was complete. The product was filtered off and recrystallized from acetone as dark red needles, m.p. 139°. The triiodide was dissolved in acetone (10 ml) and 70% perchloric acid (1 ml) added. The mixture was carefully refluxed 10 min, then cooled, and diluted with ether. The product was filtered off and recrystallized from acetic acid containing perchloric acid as yellow needles, m.p. 142–144° (70%).

Anal. Calcd. for $C_{17}H_{16}NS_2ClO_4$: C, 51.41; H, 4.03; N, 3.53; S, 16.14; Cl, 8.94. Found: C, 51.25; H, 4.18; N, 3.45; S, 16.24; Cl, 8.88.

2,3-Diphenylisothiazoline-5-thione (7b)

2,3-Diphenyl-3-ethylthioisothiazolium perchlorate (408 mg, 1 mmol) in pyridine (10 ml) was refluxed for 5 min. The orange solution was poured into water, and ether extracted. The extract was washed with dilute hydrochloric acid, dried, and evaporated to give an orange oil which crystallized on standing. The product was recrystallized from ethanol as orange needles, m.p. 117° (28%).

Anal. Calcd. for $C_{15}H_{11}NS_2$: C, 67.01; H, 4.09; N, 5.20; S, 23.78. Found: C, 67.83; H, 4.12; N, 5.31; S, 23.98.

The mass spectrum: M^+ 269, calcd. 269.

TABLE 1. Reactions of isothiazolium salts with sulfur in pyridine

Isothiazolium salt **1**	Source	Reaction time (min)	Products in order of elution (yields %), t = trace
a	*	30	**8***b* (2), **5***c* (26), **2***a* (1)
b	*	30	**8***b* (2), **3***a* (17)
c	This work	30	**8***c* (t), **5***a* (29), **2***c* (6)†
d	*	30	**3***b* (24)‡
e	*	30	**5***b* (63)
f	*	30	Only traces of ether soluble products obtained
g	This work	30	**8***a* (5), **5***d* (36)
h	This work	10	**8***a* (5), **7***a* (11)
i	This work	5	**8***b* (t), **7***b* (21)

*Reference 1.
†M.p. 133°, lit. (2, 3) 133°.
‡M.p. 173°, lit. (8) 173°.

2,3-Diphenylisothiazolium Perchlorate (1i)

2,3-Diphenylisothiazoline-5-thione (108 mg, 0.4 mmol) in acetic acid (5 ml) was treated with 30% hydrogen peroxide solution (0.13 g), and the solution allowed to stand 1 h. To the mixture was added 70% perchloric acid (0.2 ml), and the whole diluted with ether. Yellow needles separated. These were collected and recrystallized from acetone containing perchloric acid as yellow needles, m.p. 188–189° (67%).

Anal. Calcd. for $C_{15}H_{12}NSClO_4$: C, 53.28; H, 3.56; N, 4.15; S, 9.48; Cl, 10.51. Found: C, 53.14; H, 3.52; N, 4.05; S, 9.53; Cl, 10.56.

2,4-Diphenylisothiazolium Perchlorate (1h)

To 2,4-diphenylisothiazoline-5-thione (1.08 g, 0.04 mol) in acetic acid (20 ml) was added hydrogen peroxide (1.36 g, 25 mmol). The mixture became warmer as the thione dissolved. Temperature was maintained at 30° for 1 h, then the solution was filtered, 70% perchloric acid (1 ml) added, and the mixture diluted with ether. The precipitated solid was recrystallized from acetic acid containing perchloric acid as yellow needles, m.p. 198–199° (72%).

Anal. Calcd. for $C_{15}H_{12}NSClO_4$: C, 53.28; H, 3.56; N, 4.15; S, 9.48; Cl, 10.51. Found: C, 53.23; H, 3.60; N, 4.11; S, 9.28; Cl, 10.45.

Reactions of Isothiazolium Salts with Sulfur in Pyridine

General Method

The isothiazolium salts were added portionwise to saturated solutions of sulfur in refluxing pyridine, and the mixtures refluxed for 30 min. Lesser times were used for **1***h* and *i* since products from these appeared to be rather less stable in boiling pyridine. The mixtures were diluted with water and ether extracted. The ether extracts were washed with dilute hydrochloric acid (5%) dried, and on evaporation gave pasty solids which were examined by t.l.c. using benzene with increasing proportions of chloroform as an eluant.

The types and yields of the various products are summarized in Table 1.

Reaction of 2,4-Diphenyl-5-methylthioisothiazolium Perchlorate (1j) with Sodium Hydrosulfide

To the salt (0.5 g) in ethanol (3 ml) was added saturated ethanolic sodium hydrosulfide solution. The mixture became red and was warmed until homogeneous. The mixture was poured into water, ether extracted and evaporated. The red oil obtained was identified by its i.r. spectrum as methyl 2-phenyl-3-anilinopropenedithioate (**6***a*) (8).

Reaction of 2,5-Diphenyl-3-ethylthioisothiazolium Perchlorate (1k) with Sodium Hydrosulfide

This experiment was carried out as above. The oil obtained was chromatographed on alumina in benzene. Three bands were obtained. The first eluted was ethyl 3-anilinodithiocinnamate (**6***b*) (75%). The second was the thione **8***b* (7%) and the third was the imine **3***a* (9%).

Reaction of 2,4-Diphenylisothiazoline-5-thione with Dimethyl Acetylenedicarboxylate

The thione (0.538 g, 2 mmol) and the ester (0.284 g, 2 mmol) in benzene (30 ml) were refluxed 4 h. Evaporation gave a red oil which crystallized on trituration under methanol. The product was recrystallized from methanol as yellow prisms, m.p. 117° (91%).

Anal. Calcd. for $C_{21}H_{17}NS_2O_4$: C, 61.31; H, 4.13; N, 3.41; S, 15.59. Found: C, 61.47; H, 3.95; N, 3.28; S, 15.77.

The n.m.r. spectrum: τ 7.19, 7.10 (two 3H singlets, methyl protons), 3.92–3.56 (5H bands, phenyliminoprotons), 3.54 (5H singlet, phenyl protons), 1.80 (1H singlet, aldimine proton).

The i.r. spectrum: 1712, 1732 (C=O str.); 1588 cm^{-1} (C=N str.). The mass spectrum: M^+ 411, calcd. 411.

The authors wish to thank the National Research Council of Canada for financial support of this research. We also wish to thank Mr. M. Arneson for preparation of mass spectra and Mr. R. Dickinson for the preparation of n.m.r. spectra.

1. D. M. McKINNON and E. A. ROBAK. Can. J. Chem. **46**, 1855 (1968).
2. G. LE COUSTUMER and Y. MOLLIER. C.R. Acad. Sci. Paris Ser. C, **270**, 433 (1970).
3. G. LE COUSTUMER and Y. MOLLIER. Bull. Soc. chim. Fr. 3076 (1970).
4. J. M. BUCHSHRIBER. Ph.D. Thesis. University of Manitoba, Winnipeg, Manitoba, 1971.
5. R. A. OLOFSON, J. M. LANDESBERG, R. O. BERRY, D. LEAVER, W. A. H. ROBERTSON, and D. M. MCKINNON. Tetrahedron, **22**, 2119 (1966).
6. H. PRINZBACH and E. FUTTERER. The 1,2- and 1,3-dithiolium salts. *In* Adv. Heterocycl. Chem. **7**, 39 (1966).
7. D. LEAVER, D. M. MCKINNON, and W. A. H. ROBERTSON. J. Chem. Soc. 32 (1965).

Can. J. Chem. Downloaded from www.nrcresearchpress.com by 210.87.254.6 on 09/05/12
For personal use only.

8. C. PAULMIER, Y. MOLLIER, and N. LOZAC'H. Bull. Soc. chim. Fr. 2463 (1965).
9. E. KLINGSBERG. Chem. and Ind. 1568 (1960).
10. E. KLINGSBERG and A. SCHREIBER. J. Am. Chem. Soc. **83**, 2934 (1961).
11. D. LEAVER, W. A. H. ROBERTSON, and D. M. MCKINNON. J. Chem. Soc. 5104 (1962).
12. E. KLINGSBERG. J. Am. Chem. Soc. **84**, 3410 (1962).
13. D. M. MCKINNON. Can. J. Chem. **48**, 3388 (1970).
14. J. L. ADELFANG. J. Org. Chem. **31**, 2388 (1966).
15. R. MAYER and H. HARTMANN. Chem. Ber. **97**, 1886 (1964).
16. J. M. BUCHSHRIBER, D. M. MCKINNON, and M. AHMED. Can. J. Chem. **47**, 2039 (1969).
17. J. M. BUCHSHRIBER and D. M. MCKINNON. Can. J. Chem. **49**, 3299 (1971).
18. Y. MOLLIER and N. LOZAC'H. Bull. Soc. chim. Fr. 614 (1961).
19. G. LE COUSTUMER and Y. MOLLIER. C. R. Acad. Sci. Paris, Ser. C, **267**, 1423 (1968).
20. R. A. OLOFSON and R. B. WOODWARD. J. Am. Chem. Soc. **83**, 1007 (1961).
21. R. E. DAVIS and H. F. NAKSHBENDI. J. Am. Chem. Soc. **84**, 2085 (1962).
22. W. G. HODGSON, S. A. BUCKLER, and G. PETERS. J. Am. Chem. Soc. **85**, 543 (1963).
23. R. A. OLOFSON and J. M. LANDESBERG. J. Am. Chem. Soc. **88**, 4263 (1966).
24. E. K. FIELDS. J. Am. Chem. Soc. **77**, 4255 (1955).
25. C. BOUILLON and J. VIALLE. Bull. Soc. chim. Fr. 4560 (1968).

Can. J. Chem. Downloaded from www.nrcresearchpress.com by 210.87.254.6 on 09/05/12
For personal use only.

Long-range Spin–Spin Coupling Constants from Amino Protons and ^{15}N to Ring Protons in Aniline-^{15}N and Some Derivatives. INDO Molecular Orbital Calculations

R. WASYLISHEN,[1] J. B. ROWBOTHAM,[2] L. ERNST,[2] AND T. SCHAEFER
Department of Chemistry, University of Manitoba, Winnipeg, Manitoba R3T 2N2

Received March 1, 1972

A complete analysis (8-spins) is given of the p.m.r. spectrum of aniline-^{15}N, of the spectra of some haloanilines-^{15}N and of 2-aminoacetophenone-^{15}N. Intermolecular exchange of the amino protons is slow enough for observation of their spin–spin coupling to the ring protons. The magnitudes of the coupling constants between amino protons and ^{15}N or ring protons are a measure of the geometry of the amino group. This is not true of the couplings between ^{15}N and the ring protons. Long-range couplings computed in the CNDO/2 and INDO approximations of molecular orbital theory show points of agreement with experiment. For example, their signs and magnitudes are consistent with a nonplanar but not with a planar conformation of aniline. Couplings from ^{15}N to ring protons are also computed for nitrobenzene.

L'analyse complète (8 spins) du spectre de r.m.n. est donnée pour l'aniline ^{15}N, quelques haloanilines ^{15}N et pour l'amino-2 acétophénone ^{15}N. L'échange intermoléculaire des protons de l'amino est suffisamment lente pour pouvoir observer leur couplage spin–spin avec les protons du cycle. Les amplitudes des constantes de couplage entre les protons de l'amino et ^{15}N ou les protons du cycle donnent une mesure de la géométrie du groupe amino. Cela n'est plus vrai pour les couplages entre ^{15}N et les protons du cycle. Les couplages à longue distance calculés avec les approximations du CNDO/2 et INDO de la théorie des orbitales moléculaires sont en accord avec les valeurs expérimentales. Par exemple, les signes et les amplitudes des couplages ne sont compatibles qu'avec la conformation non plane de l'aniline. Les couplages entre ^{15}N et les protons du cycle ont été également calculés pour le nitrobenzène.

Canadian Journal of Chemistry, **50**, 2575 (1972)

Can. J. Chem. Downloaded from www.nrcresearchpress.com by 210.87.254.5 on 09/05/12
For personal use only.

Introduction

The one-bond ^{15}N—H spin–spin coupling constants in aniline-^{15}N and many of its derivatives have been discussed in detail (1–4). Ring substituents which diminish electron density on the nitrogen atom cause an increase in the magnitude of these coupling constants, apparently implying an alteration in the geometry of the amino group and describable as a change in hybridization of the nitrogen atom. The chemical shifts of the amino protons (5–8) and of ^{15}N are interpreted in a similar manner (1).

Long-range coupling constants between ring protons and protons of sidechain functions such as methyl (9–13), formyl (14–17), hydroxyl (18, 19), and amino (20, 21) groups are stereospecific. Such couplings for the amino protons therefore offer another approach to the study of the geometry of this moiety. The couplings are less than 1 Hz in magnitude and this approach has until recently (22–24) been hampered by the facile intermolecular exchange of the amino protons in solutions of aniline and its derivatives. The mean lifetime before exchange must be increased to the order of seconds before these long-range couplings become observable in a slow-passage experiment. In this paper these parameters are described for aniline-^{15}N itself and also for some of its derivatives.

The spin–spin interactions between ^{15}N and the ring protons are also measured. Other workers have observed their magnitudes only for protons situated ortho to the amino group (1).

In addition, the long-range coupling constants involving the $^{15}NH_2$ fragment are calculated by the finite perturbation technique (25) in the INDO molecular orbital approximation (26). A comparison of calculated with observed couplings leads to inferences about the conformation of the amino group in aniline.

Experimental

(1) Preparation of Compounds

Acetanilide-^{15}N was prepared by the addition of 5.3 ml of acetic anhydride to a solution of 4.2 g of aniline-^{15}N (96.5 at. % ^{15}N from Azote et Produits Chimiques, Toulouse,

[1]NRCC Scholarship, 1971–72.
[2]Postdoctoral Fellow, 1971–72.

Can. J. Chem. Downloaded from www.nrcresearchpress.com by 210.87.254.5 on 09/05/12
For personal use only.

France) in 2.4 ml of acetic acid. After the mixture solidified, 50 ml of water were added and the product was filtered off and dried at 60 °C/0.01 Torr for 3 h, m.p. 114–116 °C. The mass spectrum was consistent with that expected on the basis of the mass spectrum from a commercial sample of acetanilide.

To prepare 2-aminoacetophenone-^{15}N, a solution of 5.00 g of acetanilide-^{15}N in 120 ml of absolute ethanol was irradiated for 18 h at 254 nm while bubbling dry nitrogen through the solution. Steam distillation and extraction of the distillate gave 0.12 g of a mixture of 2-aminoacetophenone-^{15}N and acetanilide-^{15}N. This mixture was submitted to dry column chromatography: silica gel, column length 80 cm, diameter 2.5 cm, eluant ethyl acetate/cyclohexane 95:5, v:v. The yield[3] of pure 2-aminoacetophenone-^{15}N was 0.10 g, 2%. Extraction of the residue from the steam distillation yielded 4.4 g (88%) of starting material.

A 3:2 mixture of 4-bromo-2-chloroaniline-^{15}N and 2-chloro-4,6-dibromoaniline-^{15}N was obtained by the addition of bromine to 0.2 g of 2-chloroaniline-^{15}N (96.47 at. % ^{15}N from Merck, Sharp, and Dohme of Canada) in 5 ml of acetic acid. When a slight color remained, 10 ml of water were added and the precipitate was collected. An analogous bromination of aniline-^{15}N yielded a 2:1 mixture of 2,4-dibromoaniline-^{15}N and 2,4,6-tribromoaniline-^{15}N.

(2) Preparation of Samples for Spectral Work

All samples (solvents and concentrations given in Table 1) were degassed by the freeze–pump–thaw technique. Internal tetramethylsilane was added as reference material. Intermolecular exchange of the amino protons was retarded by adding basic alumina to the sample tubes before sealing and some of the solutions were stored over NaOH pellets for several hours.

The reaction of equimolar quantities of aniline-^{15}N and D_2O yielded a mixture containing the ^{15}NHD group among others. The mixture was dried over NaOH pellets and was transferred to a sample tube containing basic alumina and sufficient toluene-d_8 to yield a 15 mol % solution of nonexchanging amine. The sample was degassed and the p.m.r. spectrum indicated equimolar amounts of the $^{15}NH_2$ and ^{15}NHD moieties.

(3) Proton Magnetic Resonance Spectra

Spectra were recorded in the frequency sweep mode on an HA100-D spectrometer at sweep rates of 0.01 and 0.02 Hz/s at sweep widths of 1 Hz/cm. They were calibrated by reading sweep and manual oscillator frequencies at intervals of a few Hz, and double and triple resonance experiments (28) yielded the signs of the coupling constants.

Results and Discussion

(1) Spectral Analysis

(a) Aniline-^{15}N

Two samples were subjected to spectral analysis. In one (17% in benzene-d_6) the rate of intermolecular proton exchange was low enough to allow the observation of the long-range coupling constants between ring and amino protons. In the other (30 mol % in benzene-d_6) the rate of proton exchange was high enough to eliminate the effects of these coupling constants from the observed high resolution spectrum.

Each of the 165 peaks observed in the nonexchanging solution was calibrated at 0.01 Hz/s. The spectrum was analyzed as an 8-spin system by means of the computer program LACX (29). Because so many of the 640 calculated transitions were nearly degenerate it was not sensible to assign more than 380 to observed peaks (348 of the 512 calculated ring proton transitions were assigned). The results given in Tables 1 and 2 were obtained when all parameters were allowed to vary in the final iterative stages. The r.m.s. error was 0.015 Hz and the probable error of all parameters was equal to or less than 0.003 Hz, except that the probable error in $^1J(^{15}N,H)$ was 0.006 Hz. The observed ring proton spectrum, together with the calculated spectrum, is shown in Fig. 1. The widths at half-height of nondegenerate peaks in the experimental spectrum are less than 0.11 Hz.

In the spectrum for the exchanging solution, 127 of the 130 transitions of significant intensity calculated by the computer program LAME (30) were assigned to observed peaks. The r.m.s. error was 0.021 Hz in the final iteration and the probable error was less than or equal to 0.008 Hz. Agreement between observed and calculated spectra was excellent. Because all of the coupling constants obtained in this analysis are the same to within 0.01 Hz as those obtained for the nonexchanging sample, the spectra are not reproduced here and the spectral parameters are omitted from the tables.

Only the amino proton resonance peaks were studied for the sample containing $^{15}ND_2$, ^{15}NHD, and $^{15}NH_2$ groups. At 31 °C the (isotope) shift in the ^{15}NHD group was 0.0235 ± 0.0020 p.p.m. to high field of the $^{15}NH_2$ proton shift, compared to 0.0255 ± 0.0020 p.p.m. in 2-chloroaniline-^{15}N (23). At this temperature the line-widths of the ^{15}NHD and $^{15}NH_2$ proton resonance peaks were 1.35 and 0.85 Hz, respectively. In line with the experiments described for 2-chloroaniline-^{15}N (23), we esti-

[3]Elad (27) obtained a 20% yield of 2-aminoacetophenone by using a high pressure mercury vapor lamp.

Can. J. Chem. Downloaded from www.nrcresearchpress.com by 210.87.254.5 on 09/05/12
For personal use only.

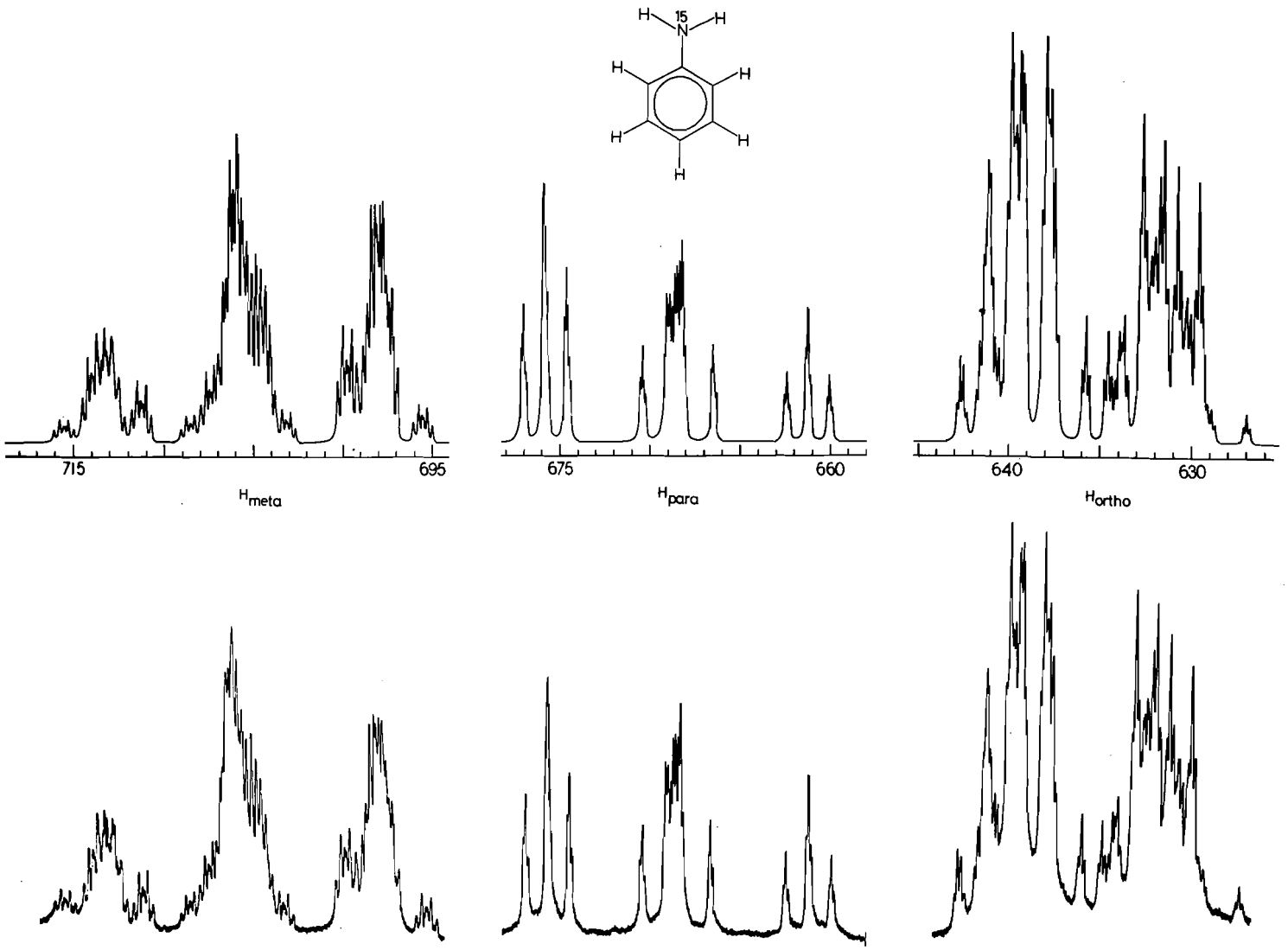

FIG. 1. The lower part shows the ring proton magnetic resonance spectrum of aniline-^{15}N as a 17 mol % solution in benzene-d_6 under conditions where long-range coupling between amino and ring protons is clearly observable. In the upper part of the figure the calculated spectrum employs the parameters given in Tables 1 and 2. In the observed spectrum linewidths at half-height of nondegenerate peaks were less than 0.11 Hz.

Can. J. Chem. Downloaded from www.nrcresearchpress.com by 210.87.254.5 on 09/05/12
For personal use only.

TABLE 1. Observed coupling constants in Hz between ^{15}N and protons and between amino and ring protons in aniline and some derivatives*

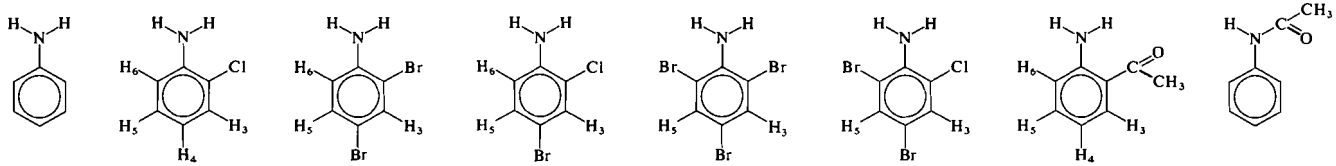

Solvents	C_6D_6	C_6D_6	C_6D_6	C_6D_6	C_6D_6	C_6D_6	Toluene-d_8	Acetone-d_6
Concentration (mol %)	17	10	2	3	1	2	15	11
$^1J(^{15}N,H)$	−78.875	−82.3	−83.115	−83.148	−85.465	−85.596	−88.6	−91.3†
$^3J(^{15}N,H_o)$	−1.935	−1.984	−1.873	−1.938	—	—	−2.456	−1.85
$^4J(^{15}N,H_m)$: H_3	−0.476	−0.787	−0.671	−0.706	−0.608	−0.613	−0.834	−0.50
: H_5	−0.476	−0.362	−0.300	−0.308	−0.608	−0.561	−0.305	−0.50
$^5J(^{15}N,H_p)$	0.009	0.166	—	—	—	—	$<\pm0.10$	±0.21
$^4J_o^{H,NH}$	−0.189	−0.122	−0.099	−0.099	—	—	$<\pm0.06$	—
$^5J_m^{H,NH}$: H_3	0.296	0.351	0.283	0.346	0.324	0.356	0.403	—
: H_5	0.296	0.306	0.290	0.324	0.324	0.342	0.305	—
$^6J_p^{H,NH}$	−0.137	−0.108	—	—	—	—	$<\pm0.06$	—

*See text for probable errors of the coupling parameters: they are generally well below 0.01 Hz except for acetanilide-^{15}N where they lie near 0.04 Hz.
†In a 9 mol % solution in DMSO.

Can. J. Chem. Downloaded from www.nrcresearchpress.com by 210.87.254.5 on 09/05/12
For personal use only.

TABLE 2. Observed proton chemical shifts* and coupling constants† between ring protons in aniline-^{15}N and some derivatives

	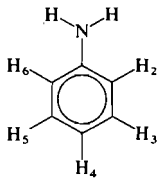	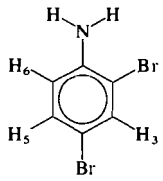	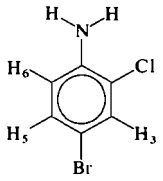	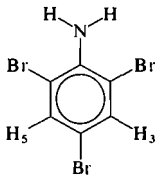	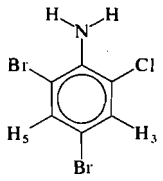	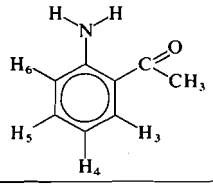	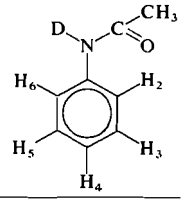
ν_{NH_2}	293.969	323.829	318.240	388.475	381.285	609.0	—
ν_2	635.634	—	—	—	—	215.74 (CH_3)	764.41
ν_3	705.018	737.368	720.853	719.413	702.542	732.223	723.72
ν_4	669.189	—	—	—	—	639.008	699.91
ν_5	705.018	689.039	686.455	719.413	716.357	697.127	723.72
ν_6	635.634	584.620	585.411	—	—	621.654	764.41
$^3J_o^{H,H}$	8.034 (2,3)‡ 7.369 (3,4)	8.561 —	8.575 —	— —	— —	8.092 (3,4) 7.048 (4,5) 8.357 (5,6)	8.19 (2,3) 7.42 (3,4)
$^4J_m^{H,H}$	1.102 (2,4) 2.496 (2,6) 1.619 (3,5)	2.243 — —	2.242 — —	— — —	2.145 — —	1.557 (3,5) 1.197 (4,6)	1.17 (2,4) 2.42 (2,6) 1.49 (3,5)
$^5J_p^{H,H}$	0.496	0.238	0.264	—	—	0.427	0.50

*In Hz at 100 MHz to low field of internal tetramethylsilane; solvent and concentration as in Table 1.
†In Hz, errors as in Table 1.
‡Numbers in brackets refer to ring positions.

Can. J. Chem. Downloaded from www.nrcresearchpress.com by 210.87.254.5 on 09/05/12
For personal use only.

mate the magnitude of the geminal proton coupling in the amino group, $^2J_g^{HNH}$, as 1.6 ± 0.6 Hz.

(b) 2-Aminoacetophenone-^{14}N and -^{15}N

The derived coupling parameters for the two isotopomers are in close agreement and only those for the sample containing the nonexchanging ^{15}N compound are given in the tables. The methyl protons are coupled to H_6 (ortho to the acetyl group) by ± 0.187 Hz.[4] On assigning all of the 264 calculated ring proton transitions to observed peaks the results given in Tables 1 and 2 are obtained. The r.m.s. error was 0.024 Hz and all probable errors were less than or equal to 0.006 Hz.

(c) Acetanilide-^{15}ND

Because of its low solubility in benzene, the p.m.r. spectrum of an 11 mol % solution in acetone-d_6 was calibrated and analyzed using the program LACX. When freshly prepared, the amino proton resonance was observable as a doublet. Its disappearance after several weeks is attributed to slow exchange of the amino protons with deuterium in the solvent molecules. The rough analysis gave the results in Tables 1 and 2 and the probable errors were less than or equal to 0.021 Hz but a reasonable error estimate probably lies near 0.04 Hz.

(d) Halogenated Derivatives of Aniline-^{15}N

These were studied as dilute solutions in benzene-d_6. The two bromine derivatives were present as a mixture, as were the two bromochloro derivatives. The peaks originating in each compound in the two mixtures were readily distinguishable. All observed peaks, including those of the amino protons, were assigned in the analysis by LAME. The derived parameters, given in Tables 1 and 2, had probable errors of less than 0.013 Hz and the r.m.s. error varied between 0.015 and 0.023 Hz. The amino proton – ring proton couplings had probable errors lying between 0.003 and 0.006 Hz (one value).

(2) Molecular Orbital Calculations

The coupling constants appearing in Tables 3 and 4 were calculated by the finite perturbation technique (25) in the INDO approximation (26) on an IBM 360/65 computer. Our convergence criteria have been previously described (17, 31). As many as 100 cycles in the SCF procedure were necessary to obtain convergence to 0.01 Hz. The parameterization is available only for first-row elements. Therefore computations were done only for aniline, 2-aminoacetophenone, acetanilide, and nitrobenzene. Standard geometries (26, 32) were employed to calculate the atomic coordinates in the benzene ring.

For aniline the geometry of the amino group was taken from the microwave results of Lister and Tyler (33). Another calculation on aniline assumed complete planarity of the molecule with C—N and N—H bond lengths equal to those given (33) for the nonplanar molecule. Standard geometries were used in a planar (apart from the methyl protons) model of 2-aminoacetophenone and also for nitrobenzene. The geometry of the sidechain in acetanilide was found in the literature (34–36).

According to INDO the nonplanar form of aniline is 11.3 kcal/mol more stable than the planar form. Lister and Tyler (33) suggest an inversion barrier of less than 0.3 kcal/mol. An optimization of the geometry of the amino group at each successive stage of its inversion might well improve the computed value.

The calculated (observed) dipole moments in Debyes are: aniline 1.46 (1.56); planar aniline 1.105; acetanilide 4.10 (3.88 to 4.02); nitrobenzene 5.22 (3.93); 2-aminoacetophenone 1.85 (2.05). Experimental dipole moments are cited from the compilation of McClellan (37).

(3) The Coupling between ^{15}N and Amino Protons

(a) Experimental Data

Three different linear relationships between the one-bond ^{15}N—H coupling and the percent s character of the nitrogen bond orbitals have been proposed (2, 3, 23). Two (2, 3) are based mainly on the observation for $^1J(^{15}N,H)$ of about -75 Hz in ammonium ion (sp^3 hybridization), -90 Hz in amides (sp^2), and about -136 Hz in protonated nitriles (sp). The third (23) uses anilinium ion and the geometry of aniline in the gas phase as calibration points. The latter writes $\%\,s = -0.59\,^1J(^{15}N,H) - 17.5$ and yields 29% s character in aniline and 52% in sp systems. The former two give 46 and 52% for sp hybridization and 27 and 28% s character for aniline. Clearly, only semiquantitative predic-

[4]The value of ± 0.187 Hz is obtained by a complete analysis of the spectrum using LAME and does not represent the observed splitting in the methyl proton resonance.

TABLE 3. Computed long-range proton—proton coupling constants in Hz in aniline and 2-aminoacetophenone

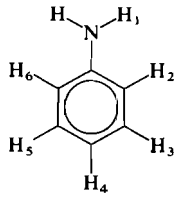

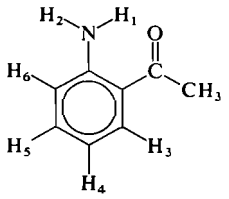

Coupling constant	Nonplanar CNDO/2	Nonplanar INDO	Planar INDO	Coupling constant	Planar* INDO
$^4J_o^{H_2,NH_1}$	0.353	0.088	0.686	$^4J_o^{H_6,NH_2}$	0.702
$^4J_o^{H_6,NH_1}$	0.010	−0.727	−0.166	$^4J_o^{H_6,NH_1}$	−0.143
$\langle {}^4J_o^{H,NH}\rangle$	0.181	−0.319	0.260	$\langle {}^4J_o^{H,NH}\rangle$	0.279
$^5J_m^{H_3,NH_1}$	0.065	0.080	−0.148	$^5J_m^{H_3,NH_1(H_2)}$	−0.211 (0.972)
$^5J_m^{H_5,NH_1}$	0.513	0.983	0.799	$^5J_m^{H_5,NH_1(H_2)}$	0.826 (−0.183)
$\langle {}^5J_m^{H,NH}\rangle$	0.289	0.532	0.325	$\langle {}^5J_m^{H,NH}\rangle$	0.380(H_3) 0.321(H_5)
$^6J_p^{H,NH}$	0.010	−0.203	0.127	$^6J_p^{H_4,NH_1(H_2)}$	0.187 (0.119)
$^2J_\theta^{HNH}$	5.704	−0.041	8.231	$^2J_\theta^{HNH}$	7.61

*$\langle {}^5J^{H_3,CH_3}\rangle$ = 0.20 Hz when one C—H bond of the methyl group eclipses the C=O bond and the other two are staggered with respect to the C—H_3 bond of the ring.

TABLE 4. Computed coupling constants in Hz between ^{15}N and protons in some aniline derivatives* and in nitrobenzene

Coupling constants	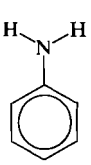	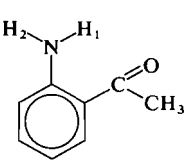	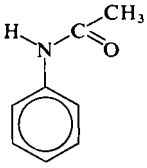	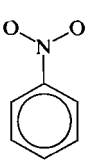
$^1J(^{15}N,H)$: H_1	−59.53†‡	−99.25	−73.48	—
: H_2	−59.53	−87.76	—	—
$^3J(^{15}N,H_o)$	−2.52	−3.90	−3.86§	−3.75
$^4J(^{15}N,H_m)$: H_3	−1.06	−1.10	−1.12	−0.63
: H_5	−1.06	−0.94	−0.77	−0.63
$^5J(^{15}N,H_p)$	0.18	−0.33	−0.62	−0.82

*The nonplanar geometry for aniline and planar geometries for the other compounds were employed as described in the text. Planar geometries assume an HNH angle of 120°.
†For an amino group coplanar with the aromatic ring one finds $^1J(^{15}N,H)$ = −92.20 Hz.
‡CNDO/2 finds −43.0 Hz.
§This is the average of $^3J(^{15}N,H_2)$ = −3.461 and $^3J(^{15}N,H_6)$ = −4.267.

tions of the geometry of the amino group in aniline derivatives are possible by these methods. Furthermore, the coupling is solvent dependent (1, 4, 38) and the effective nuclear charge (39) is probably rather different in some of the compounds used for calibration, adding to the uncertainty in the reference points.

Nevertheless, in aniline derivatives containing meta and para substituents (1, 4), electron withdrawing substituents cause an increase in the magnitude of $^1J(^{15}N—H)$: interpretable as a decrease in π electron density, a flattening of the pyramid and therefore as a change in hybridization, at nitrogen. In Table 1, the ring-substituted anilines all contain one or two groups ortho to the amino group. The observed magnitudes of $^1J(^{15}N,H)$ in these compounds are compatible with such an interpretation.

Can. J. Chem. Downloaded from www.nrcresearchpress.com by 210.87.254.5 on 09/05/12
For personal use only.

Can. J. Chem. Downloaded from www.nrcresearchpress.com by 210.87.254.5 on 09/05/12
For personal use only.

However, in the presence of ortho substituents intramolecular hydrogen bonding is an additional factor which may lead to a flattening of the nitrogen pyramid. Evidence for such bonds comes from X-ray diffraction data (40), the amino proton chemical shifts (5–8), as well as from N—H stretching frequencies (41, 42). The relatively large magnitude of 88.6 Hz for $^1J(^{15}N,H)$ in 2-aminoacetophenone in toluene solution, compared to 86.4 Hz for 4-nitroaniline in chloroform solution (1), can therefore be regarded as arising from a composite effect: electron withdrawal by the acetyl group, described by **1**, together with hydrogen bonding between the N—H and C=O bonds as in **2**.

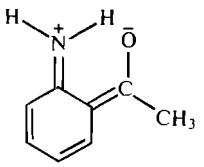

1

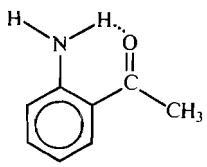

2

Both structures favor an HNH angle larger than the 114° in aniline (33). The linear relationship above yields 35% s character at nitrogen and an HNH angle of 122° in 2-aminoacetophenone (using $\cos\theta/\cos\theta - 1 =$ fractional s character), perhaps somewhat large[5] but rather smaller than the 133° deduced from i.r. data (41).

In an attempt to provide another measure of the degree of intramolecular hydrogen bonding in aniline derivatives Axenrod and Wieder (43) argue that the difference between the magnitudes of $^1J(^{15}N,H)$ in dimethylsulfoxide solution, where a strong tendency to intermolecular N—H hydrogen bonds to solvent molecules exists, and in chloroform solution, where intramolecular hydrogen bonds are preferred, is a measure of the hydrogen bonding abilities of the ortho substituent. These are deduced as $NO_2 > C{=}O > Br$, in reasonable agreement with *a priori* expectations. The data in Table 1 imply similar hydrogen bonding tendencies for Cl and Br substituents if due allowance is made for their electron withdrawing abilities, also indicated (1) as nearly the same by the $^1J(^{15}N,H)$ magnitudes in the meta and para haloanilines.

(b) Computed Data

For ammonia the computed $^1J(^{15}N,H)$ is −42.6 Hz (26, 44) while the experimental value is ±65.1 Hz (45). A similar ratio of the two quantities, −59.5 and −78.9 Hz, is found for aniline in Tables 1 and 4. However, when a planar form is assumed for aniline the computed is larger than the observed magnitude. In this sense the INDO results are in qualitative agreement with the nonplanar geometry of aniline.

For 2-aminoacetophenone one observes −88.6 Hz for $^1J(^{15}N,H)$ whereas the average computed value for a planar 2-aminoacetophenone is −93.5 Hz, not strikingly different from the −92.2 Hz calculated for a planar aniline. The relatively good agreement between observed and calculated values is consistent with an almost planar 2-aminoacetophenone but unfortunately cannot be treated as confirmation of this conformation.[6]

Qualitatively the calculated one-bond ^{15}N—H couplings are in accord with the observed trend towards larger magnitudes as the nitrogen pyramid becomes more shallow in ring-substituted anilines.

(4) Long-range Couplings from Amino to Ring Protons

(a) Experimental Data

By means of our earlier calibration procedure (22) $^6J_p^{H,NH}$ was estimated (22) as −0.14 Hz in aniline. Because of problems with intermolecular proton exchange, this parameter was not observable at that time (22) but the prediction is now borne out by the observed value of −0.137 Hz (Table 1). The prediction assumes the geometry of the aniline molecule in the gas phase (33), having an angle ϕ of 20° between the ring plane and the plane defined by the nuclei in the C—N—H fragment (see

[5]For acetanilide, $^1J(^{15}N,H)$ attains −91.3 Hz in DMSO solution (Table 1) but in view of the known solvent effects (1, 38) it could well be equal to $^1J(^{15}N,H)$ in 2-aminoacetophenone if both compounds were measurable in toluene solution. Planarity of the geometry about the nitrogen atom in 2-aminoacetophenone is therefore not ruled out by this difference in $^1J(^{15}N,H)$.

[6]There is a much larger difference between calculated and observed values when the acetyl group is bonded directly to the nitrogen atom, as in acetanilide (Tables 1 and 4). However, it should be noted that in the latter case the calculations were carried out assuming that the planar acetamido group was twisted 38° out of the benzene ring plane (36).

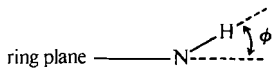

3

3). From the value of -0.108 Hz for $^6J_p^{H,NH}$ in 2-chloroaniline an average ϕ of 17.5° follows. $J_p^{H,NH}$ is not observable in 2-aminoacetophenone (Table 1) but an upper limit of 0.06 Hz for this coupling then yields a maximum angle ϕ of 12°. The observed coupling in 2-aminoacetophenone is of course also compatible with $\phi = 0°$ and is an illustration of the unfortunate insensitivity of $J_p^{H,NH}$ to small angles ϕ, a consequence of its proportionality to $\sin^2 \phi$ in the assumed coupling mechanism (22).

Our assumption (22) that $J_p^{H,NH}$ originates in a hyperconjugative overlap between the N—H bonds and the π electron system of the ring, analogous to the mechanism described for methyl proton interactions in toluene (31, 46), is consistent with its observed values in Table 1. Alternatively, it might have been argued that a decrease in ϕ implies an increase in the conjugation of the nitrogen atom with the π system of the ring. A π electron mechanism operating via the nitrogen atom, *i.e.*, via the partially double C⋯N bond, would then serve to enhance the magnitude of $J_p^{H,NH}$ in 2-aminoacetophenone relative to aniline. In fact the opposite occurs, in agreement with the hyperconjugative model. The application of the model to the conformational problem also assumed the absence of an intrinsic, as distinct from a steric, effect on $J_p^{H,NH}$; in line with similar assumptions for other sidechains (17, 31, 46).[7]

Such an effect is harder to exclude for $^4J_o^{H,NH}$, other four-bond couplings in unsaturated systems being subject to intrinsic substituent effects, (17, 47), but its behavior in Table 1 is roughly parallel to that of $J_p^{H,NH}$. An intrinsic effect on $^5J_m^{H,NH}$ is found for the aniline derivatives in Table 1. For example, $J_m^{H_5,NH}$ is 0.1 Hz smaller than $J_m^{H_3,NH}$ in 2-aminoacetophenone. This behavior is reproduced by the molecular orbital calculations.

(b) Computed Data

In Table 3 the computed couplings between the amino and ring protons are given for the nonplanar conformation of aniline as well as for the planar forms of aniline and of 2-aminoacetophenone. Their high stereospecificity is of conformational interest. As the experimental values in Table 1 are measured for molecules in which rapid rotation occurs about the C—N bond, they should be compared with the average calculated couplings (indicated by angular brackets) in Table 3.

Inasmuch as INDO considers one-center exchange integrals it includes the π electron contribution to the coupling constants (26). Thus, INDO finds their correct signs for the nonplanar form of aniline, whereas CNDO/2 calculates positive values for $^4J_o^{H,NH}$ and $^6J_p^{H,NH}$. On the other hand, INDO tends to overestimate the negative π electron contribution to these two couplings as well as the positive π contribution to $^6J_m^{H,NH}$ (reminiscent of a similar situation in benzaldehyde derivatives (17)). CNDO/2 agrees quantitatively with experiment for $^5J_m^{H,NH}$, suggesting a dominance of the σ electron contribution to this coupling; and furthermore finds $^6J_p^{H,NH} = 0.01$ Hz, thereby supporting our assumption that this parameter originates in π electron effects.

The signs of $^4J_o^{H,NH}$ and $^6J_p^{H,NH}$ calculated by INDO for the planar form of aniline are opposite to the observed sign. Although their magnitudes are probably again exaggerated, the implied conformational dependence qualitatively confirms the empirical use of the observed couplings in conformational deductions.

For a planar 2-aminoacetophenone the INDO results reproduce the substituent dependence of the two $^5J_m^{H,NH}$ values but again appear to overestimate the magnitudes of $^4J_o^{H,NH}$ and $^6J_p^{H,NH}$. The average coupling between the methyl protons and ring proton H_3 (configuration of the methyl group as given in Table 3) is computed as 0.20 Hz, compared to the observed value of ± 0.19 Hz. Couplings of this kind occur when the protons are in close proximity (often called "through-space" couplings) and the comparison indicates that INDO can cope with such interactions (49, 50).

(5) Coupling of ^{15}N to Ring Protons

The observed couplings in Table 1 are apparently not closely related to the geometry of the amino group although substituent effects on their magnitudes are present, particularly

[7]Even when the "substituent" atom forms part of the aromatic ring, as in pyridine, its intrinsic effect on couplings over six bonds is relatively minor (48).

Can. J. Chem. Downloaded from www.nrcresearchpress.com by 210.87.254.5 on 09/05/12
For personal use only.

for $^4J(^{15}N,H_m)$. In Table 4 the computed couplings are rather larger than, but roughly in the proportion of, the measured parameters. The computed couplings in nitrobenzene are not strikingly different from those in aniline derivatives. In nitrobenzene, $^3J(^{15}N,H_o)$ is calculated as -3.75 Hz, which may be compared to an observed value of ± 2.5 Hz in 1-nitronaphthalene (51).

(6) Coupling between Amino Protons

CNDO/2 finds $^2J_g^{HNH}$ equal to 1.60 Hz in ammonia and INDO finds -6.37 Hz (26). Similar behavior is found for aniline in Table 3, CNDO/2 computing 5.70 Hz for this coupling whereas INDO calculates -0.04 Hz. For a planar aniline model the INDO estimate rises to 8.23 Hz. The INDO results are consistent with a nonplanar aniline form because the observed value is ± 1 to ± 2 Hz.

INDO computes 7.61 Hz in a planar 2-aminoacetophenone. In this respect and also from the viewpoint of the other computed couplings in Table 3, it would be of interest to analyze the spectrum of this compound under conditions where rapid rotation about C—N bond does not occur.

Conclusions

The magnitudes of the coupling constants between amino protons and ^{15}N or ring protons in aniline and some of its derivatives constitute a measure of the degree of flattening at the nitrogen pyramid. In contrast, the coupling constants between ^{15}N and the ring protons are sensitive to the presence of substituents but are not simply related to the geometry of the amino group. The long-range coupling constants computed by molecular orbital theory in the CNDO/2 and INDO approximations are sensitive to the stereochemistry and are in agreement with a nonplanar conformation of aniline.

We are grateful to the National Research Council of Canada for financial support.

1. T. Axenrod, P. S. Pregosin, M. J. Wieder, E. D. Becker, R. B. Bradley, and G. W. A. Milne. J. Am. Chem. Soc. **93**, 6536 (1971).
2. G. Binsch, J. B. Lambert, B. W. Roberts, and J. D. Roberts. J. Am. Chem. Soc. **86**, 5564 (1964).
3. A. J. R. Bourn and E. W. Randall. Mol. Phys. **8**, 567 (1964).
4. M. R. Bramwell and E. W. Randall. Chem. Commun. 250 (1969).
5. H. Suhr. Z. Elektrochem. **66**, 466 (1962).
6. L. K. Dyall. Austral. J. Chem. **17**, 419 (1964).
7. T. Yonemoto, W. F. Reynolds, H. M. Hutton, and T. Schaefer. Can. J. Chem. **43**, 2668 (1965).
8. B. M. Lynch, B. C. Macdonald, and J. K. G. Webb. Tetrahedron, **24**, 3595 (1968); B. M. Lynch. Tetrahedron Lett. 1357 (1969).
9. H. Rottendorf and S. Sternhell. Austral. J. Chem. **17**, 1315 (1964).
10. A. D. Cohen and K. A. McLauchlan. Mol. Phys. **9**, 49 (1965).
11. G. Kotowycz and T. Schaefer. Can. J. Chem. **44**, 2743 (1966).
12. M. P. Williamson, R. J. Kostelnik, and S. M. Castellano. J. Chem. Phys. **49**, 2218 (1968).
13. A. F. Janzen and T. Schaefer. Can. J. Chem. **49**, 1818 (1971).
14. G. J. Karabatsos and F. M. Vane. J. Am. Chem. Soc. **85**, 3886 (1963).
15. S. Forsén, B. Akermark, and T. Alm. Acta Chem. Scand. **18**, 2313 (1964).
16. D. G. DeKowalewski and S. Castellano. Mol. Phys. **16**, 567 (1969).
17. R. Wasylishen and T. Schaefer. Can. J. Chem. **49**, 3216 (1971).
18. S. Forsén and R. A. Hoffman. J. Mol. Spectrosc. **20**, 168 (1966).
19. R. Freeman. Mol. Phys. **6**, 535 (1963).
20. J. A. Weil, A. Blum, A. H. Heiss, and J. K. Kinnaird. J. Chem. Phys. **46**, 3132 (1967).
21. T. Schaefer and R. Wasylishen. Can. J. Chem. **48**, 1343 (1970).
22. R. Wasylishen and T. Schaefer. Can. J. Chem. **48**, 1263 (1970).
23. R. Wasylishen and T. Schaefer. Can. J. Chem. **49**, 3627 (1971).
24. W. B. Smith, A. M. Ihrig, and J. L. Roark. J. Phys. Chem. **74**, 812 (1970).
25. J. A. Pople, J. W. McIver, and N. S. Ostlund. Chem. Phys. Lett. **1**, 465 (1967).
26. J. A. Pople and D. L. Beveridge. Approximate molecular orbital theory. McGraw-Hill Book Co., New York. 1970.
27. D. Elad. Tetrahedron Lett. 873 (1963).
28. R. Freeman and W. A. Anderson. J. Chem. Phys. **37**, 2053 (1962).
29. C. W. Haigh. Private communication.
30. C. W. Haigh and J. M. Williams. J. Mol. Spectrosc. **32**, 398 (1969).
31. R. Wasylishen and T. Schaefer. Can. J. Chem. **50**, 1852 (1972).
32. J. A. Pople and M. S. Gordon. J. Am. Chem. Soc. **89**, 4253 (1967).
33. D. G. Lister and J. K. Tyler. Chem. Commun. 152 (1966).
34. J. K. Olsen and S. Kang. Theoret. Chim. Acta (Berl.), **17**, 329 (1970).
35. R. Carter. Acta Chem. Scand. **21**, 75 (1967).
36. L. E. Sutton. *Ed.* Chem. Soc. Spec. Publ. No. 11, M1-M19 (1958); No. 18, S1-S23 (1965).
37. A. L. McClellan. Tables of experimental dipole

Can. J. Chem. Downloaded from www.nrcresearchpress.com by 210.87.254.5 on 09/05/12
For personal use only.

moments. W. H. Freeman and Company, San Francisco, California. 1963.
38. L. PAOLILLO and E. D. BECKER. J. Magn. Resonance, **2**, 168 (1970).
39. D. M. GRANT and W. M. LITCHMAN. J. Am. Chem. Soc. **87**, 3995 (1965).
40. D. L. HUGHES and J. TROTTER. J. Chem. Soc. A, 2181 (1971).
41. P. J. KRUEGER. Can. J. Chem. **40**, 2300 (1962).
42. L. K. DYALL. Austral. J. Chem. **23**, 947 (1970).
43. T. AXENROD and M. J. WIEDER. J. Am. Chem. Soc. **93**, 3541 (1971).
44. J. A. POPLE, J. W. MCIVER, and N. S. OSTLUND. J. Chem. Phys. **49**, 2965 (1968).
45. R. A. BERNHEIM and H. BATIZ-HERNANDEZ. J. Chem. Phys. **40**, 3446 (1964).
46. C. J. MACDONALD and W. F. REYNOLDS. Can. J. Chem. **48**, 1002 (1970).
47. M. BARFIELD. J. Am. Chem. Soc. **93**, 1066 (1971).
48. J. B. ROWBOTHAM, R. WASYLISHEN, and T. SCHAEFER. Can. J. Chem. **49**, 1799 (1971).
49. P. C. MYHRE, J. W. EDMONDS, and J. D. KRUGER. J. Am. Chem. Soc. **88**, 2459 (1966).
50. M. BARFIELD and M. KARPLUS. J. Am. Chem. Soc. **91**, 1 (1969).
51. Y. KAWAZOE, M. ARAKI, S. SAWAKI, and M. OHNISHI. Chem. Pharm. Bull. (Tokyo), **18**, 381 (1970).

Can. J. Chem. Downloaded from www.nrcresearchpress.com by 210.87.254.5 on 09/05/12
For personal use only.

Temperature and Pressure Dependence of ^{209}Bi Nuclear Quadrupole Resonance in $BiCl_3$

G. C. GILLIES AND R. J. C. BROWN

Department of Chemistry, Queen's University, Kingston, Ontario

Received February 24, 1972

The temperature and pressure dependence of the ^{209}Bi nuclear quadrupole coupling constant and asymmetry parameter in solid $BiCl_3$ have been measured near room temperature. It is not possible to account for the results on the basis of the conventional theory in which the field gradient parameters depend only on the crystal volume.

L'influence de la température et de la pression sur la constante de couplage nucléaire quadrupole du ^{209}Bi et sur le paramètre d'asymétrie du $BiCl_3$ solide, a été mesurée à une température proche de la température ambiante. Il n'a pas été possible d'expliquer les résultats à partir de la théorie classique dans laquelle les paramètres du gradient de champ dépendent seulement du volume du cristal.

Canadian Journal of Chemistry, **50**, 2586 (1972)

Can. J. Chem. Downloaded from www.nrcresearchpress.com by 210.87.254.105 on 09/05/12
For personal use only.

Introduction

Nuclear quadrupole resonance frequencies are dependent upon both volume and temperature, and in order to compare theory with experiment properly it is necessary to separate the explicit volume effects from the frequency measurements made at atmospheric pressure (1). A number of studies of the shift of n.q.r. frequencies under hydrostatic compression have been reported which allows this separation to be made; in addition to the temperature and pressure coefficients of the n.q.r. frequency, the thermal expansion and compressibility coefficients must be known, and in many cases the latter information is not available.

The observed n.q.r. frequencies are determined by two parameters of the effective Hamiltonian, the quadrupole coupling constant (eqQ) and the asymmetry parameter (η). For the common case of a nuclear spin of 3/2, η cannot be determined reliably without measurements of the Zeeman splitting of the resonance in a single crystal which can be re-oriented readily, and so in most high pressure n.q.r. experiments on nuclei of spin 3/2, the asymmetry parameter has been ignored; this assumption is logically consistent since the resonant frequency is almost independent of η except for very large values:

$$\nu_Q = \tfrac{1}{2}eqQ(1 + \eta^2/3)^{1/2}$$

Hence in order to obtain information on the temperature and pressure dependence of the asymmetry parameter, it is advantageous to deal with spins other than 3/2. The temperature dependence of the asymmetry parameter has not been measured for many crystals, even though in suitable cases it provides information which is complementary to that obtained from the coupling constant itself.

Bismuth trichloride provides an interesting case for study. The ^{209}Bi resonances have been measured at 299 and 83 K (2), and fall in a convenient frequency range; there are four resonances and η is large enough that two of the resonances lie close together, so the same high pressure bomb may be used to measure both resonance frequencies. Measurement of two of the four resonances suffices to determine the values of eqQ and η using the analysis of the spin 9/2 quadrupolar Hamiltonian given by Cohen (3). The crystal structure (4) and Raman spectrum (5) of solid $BiCl_3$ have been reported. The thermal expansion coefficient has been reported (6) but not the compressibility, and as a result the analysis of the quadrupole spectrum is limited.

The Pure Quadrupole Spectrum for Spin 9/2

There are five energy levels, whose energies may be written in the form (3)

$$[1] \qquad E = x(\eta)(eqQ)/24$$

where $x(\eta)$ are the roots of the equation $f(x, \eta) = 0$.

$$[2] \quad f(x,\eta) = x^5 - 11(3+\eta^2)x^3 - 44(1-\eta^2)x^2 + \tfrac{44}{3}(3+\eta^2)^2x + 48(3+\eta^2)(1-\eta^2)$$

Can. J. Chem. Downloaded from www.nrcresearchpress.com by 210.87.254.105 on 09/05/12
For personal use only.

The frequencies of the transitions between adjacent energy levels can therefore be written

$$[3] \qquad \nu_i = r_i(\eta)(eqQ)/24h$$

where $r_i(\eta)$ is the difference between two adjacent roots of eq. 2. In the following, $i = 1$ refers to the $\pm 1/2 \leftrightarrow \pm 3/2$ transition and $i = 2$ refers to the $\pm 3/2 \leftrightarrow \pm 5/2$ transition; in $BiCl_3$ these transitions occur near 31.8 and 25.1 MHz, respectively (2), and are the transitions which were measured as a function of temperature and pressure. The frequencies were found to be linear functions of the temperature and pressure over the ranges investigated, and the subsequent analysis was therefore carried out in terms of the derivatives $(\partial\nu_i/\partial T)_P$ and $(\partial\nu_i/\partial P)_T$. Using eq. 3 these derivatives can be written

$$[4] \qquad \left(\frac{\partial \nu_i}{\partial T}\right)_P = \frac{r_i(\eta)}{24h}\left(\frac{\partial eqQ}{\partial T}\right)_P + \frac{dr_i}{d\eta}\left(\frac{\partial \eta}{\partial T}\right)_P \frac{eqQ}{24h}$$

$$[5] \qquad \left(\frac{\partial \nu_i}{\partial P}\right)_T = \frac{r_i(\eta)}{24h}\left(\frac{\partial eqQ}{\partial P}\right)_T + \frac{dr_i}{d\eta}\left(\frac{\partial \eta}{\partial P}\right)_T \frac{eqQ}{24h}$$

The derivatives $dr_i/d\eta$ are calculated from differences of the derivatives $dx/d\eta$, which are obtained from setting the total derivative of $f(x, \eta)$ equal to zero.

$$[6] \qquad \frac{dx}{d\eta} = -\left(\frac{\partial f}{\partial \eta}\right)\Big/\left(\frac{\partial f}{\partial x}\right)$$

In evaluating r_i and its derivatives, the value of η at room temperature was used. When $(\partial\nu_i/\partial T)_P$ is known for two resonances, eq. 4 may be solved simultaneously for $(\partial eqQ/\partial T)_P$ and $(\partial\eta/\partial T)_P$, and similarly for the pressure derivatives. It is advantageous to measure the $\pm 1/2 \rightarrow \pm 3/2$ transition no matter which of the other three transitions is measured, for the frequency of this transition varies strongly with the value of η; the frequencies of the other transitions are less sensitive to the value of η and reflect changes in the coupling constant more directly.

Experimental

Spectra were recorded with a self-quenched superregenerative spectrometer similar to that described by Dean (7); for frequency measurements it was found advantageous to remove the coherence feedback control function in order to allow quick manual change in the quench conditions. Frequency modulation and lock-in detection were used to record the resonances on a chart recorder; the shape of the resonances recorded was complex but was not affected by changes of temperature or pressure so that shifts in the resonance frequency could be measured consistently.

Frequency measurement was performed as follows. The unquenched, unmodulated oscillator was driven slowly in frequency by a synchronous motor, and its frequency as measured by a frequency counter was recorded regularly on the chart record; as the frequency of the oscillator approached the resonance the quench and modulation were switched on, and the resonance was recorded. After the resonance had been passed, further frequency measurements on the unquenched, unmodulated oscillator were recorded. The recorded frequency was fitted to a least squares parabolic function of displacement along the record, and the resonance frequency calculated from this function. A correction for the shift in oscillator frequency with grid time constant was applied by also recording the zero beat of the quenched modulated oscillator with an appropriate harmonic of 100 kHz derived from the frequency counter, either before or after the resonance was recorded; the correction was generally less than 10 kHz. Individual frequency measurements made by this technique appear to be repeatable to within several kHz.

The bomb used for the high pressure measurements was of conventional design, with an O-ring seal which was satisfactory up to a pressure of about 275 MNm^{-2}. The coned electrical seal was insulated with epoxy resin. The pressure coefficients of the resonances were large enough that it was not necessary to carry the measurements to very high pressures, the highest pressure used being about 140 MNm^{-2}; vacuum pump oil was used as a hydraulic medium. The powdered sample was mixed with oil and placed inside a short section of drinking straw with the ends sealed with wax, in order to prevent contact with the stainless steel bomb. The coil of the oscillator was a close fit around the sample. The bomb was thermally insulated, and its temperature was recorded; some temperature drift occurred during the measurements and the frequencies were corrected to 25.0 °C later using the measured temperature dependence.

The temperature dependence was measured using a sample sealed under vacuum. The temperature was varied between 0 and 50 °C using a refrigerated thermostat; the temperature was measured with a mercury thermometer which was compared with a calibrated thermometer in a separate experiment.

Bismuth trichloride from the Matheson, Coleman and Bell Company was dried *in vacuo* at 100 °C over phosphorus pentoxide, before being sealed in an evacuated sample tube, or mixed with oil in a dry atmosphere.

Results and Discussion

The frequencies of both resonances varied linearly with both pressure and temperature over the restricted ranges investigated, with the following coefficients. For the 31.8 MHz resonance,

$$\left(\frac{\partial \nu_1}{\partial T}\right)_P = -10.42 \pm 0.06 \text{ kHz K}^{-1}$$

$$\left(\frac{\partial \nu_1}{\partial P}\right)_T = +1.36 \pm 0.02 \text{ kHz (MN m}^{-2})^{-1}$$

Can. J. Chem. Downloaded from www.nrcresearchpress.com by 210.87.254.105 on 09/05/12
For personal use only.

and for the 25.1 MHz resonance

$$\left(\frac{\partial \nu_2}{\partial T}\right)_P = -4.46 \pm 0.03 \text{ kHz K}^{-1}$$

$$\left(\frac{\partial \nu_2}{\partial P}\right)_T = -1.720 \pm 0.008 \text{ kHz (MN m}^{-2})^{-1}$$

The pressure coefficients refer to a temperature of 25 °C. The extrapolated zero pressure frequencies measured for the sample in the high pressure bomb were 31 878.3 ± 1.1 and 25 137.3 ± 0.7 kHz, respectively, while the measurements on the larger sample *in vacuo* at the same temperature (25 °C) were 31 893.8 ± 2.0 and 25 136.6 ± 0.9 kHz, respectively; the value of η derived from these measurements is 0.5544 ± 0.0002, and the quadrupole coupling constant is 318.70 ± 0.15 MHz. The two measurements of the lower frequency resonance are in good agreement, but there is a discrepancy of about 15 kHz in the results for the higher frequency; the latter line was weaker than the former, and the assignment of the central point of the resonance pattern for the sample in the bomb may have been in error, without affecting the value of the derivatives. Substituting these values into eqs. 4 and 5 and solving, the temperature and pressure derivatives of the coupling constant and asymmetry parameter are found to be

$$\frac{1}{h}\left(\frac{\partial eqQ}{\partial T}\right)_P = -40.6 \pm 0.7 \text{ kHz K}^{-1}$$

$$\frac{1}{h}\left(\frac{\partial eqQ}{\partial P}\right)_T = -33.6 \pm 0.2 \text{ kHz (MN m}^{-2})^{-1}$$

$$\left(\frac{\partial \eta}{\partial T}\right)_P = -(1.54 \pm 0.03) \times 10^{-4} \text{ K}^{-1}$$

$$\left(\frac{\partial \eta}{\partial P}\right)_T = +(1.15 \pm 0.07) \times 10^{-4} \text{ (MN m}^{-2})^{-1}$$

These results may be combined in an analysis following the method of Kushida *et al.* (1); the parameters q and η of the electric field gradient tensor are assumed to depend explicitly upon the volume V of a fixed amount of solid, as well as the temperature:

$$[7] \qquad q = q(T, V)$$

$$\eta = \eta(T, V)$$

These are fairly drastic assumptions, for it is implied that the effects of thermal expansion and hydrostatic pressure upon the electric field gradient tensor are functions of a single variable, the volume; in a rigorous analysis of a complex crystal, changes of shape and atomic positions within the unit cell must be included as well as the volume, but it is not practical to carry out such an analysis at present. Within the approximations implied by eq. 7, it is found that

$$[8] \qquad \left(\frac{\partial q}{\partial T}\right)_P = -\frac{\alpha}{\beta}\left(\frac{\partial q}{\partial P}\right)_T + \left(\frac{\partial q}{\partial T}\right)_V$$

$$[9] \qquad \left(\frac{\partial \eta}{\partial T}\right)_P = -\frac{\alpha}{\beta}\left(\frac{\partial \eta}{\partial P}\right)_T + \left(\frac{\partial \eta}{\partial T}\right)_V$$

where $\alpha = (1/V)(\partial V/\partial T)_P$ is the coefficient of bulk thermal expansion, and $\beta = -(1/V)(\partial V/\partial P)_T$ is the isothermal compressibility. The value of α has been reported (6) as 2.8×10^{-4} K^{-1}, but the compressibility does not appear to have been measured, and so an approximate value of α/β based upon the Gruneisen–Mie equation of state for solids (8) will be used

$$[10] \qquad \alpha/\beta = \gamma \bar{C}_V/\bar{V}$$

where γ is the Gruneisen constant, generally between 1 and 2, $\bar{C}_V$ is the molar specific heat at constant volume, and $\bar{V}$ is the molar volume. Since $\bar{C}_V$ is not available experimentally, $\bar{C}_p$ may be used together with $\gamma = 2$ to calculate an estimated upper limit for α/β. For $BiCl_3$, $\bar{C}_p = 109$ J K^{-1} mol^{-1} (9) and $\bar{V} = 66 \times 10^{-6}$ m^3 (4), yielding a value $\alpha/\beta \lesssim 3.3$ MNm^{-2} K^{-1}. The compressibility derived from this estimate and the measured value of the thermal expansion coefficient is $\beta \gtrsim 0.8 \times 10^{-4}$ (MNm^{-2})$^{-1}$.

The temperature derivatives of the electric field gradient parameters at constant volume can now be estimated from eqs. 8 and 9

$$\frac{1}{h}\left(\frac{\partial eqQ}{\partial T}\right)_V \cong -150 \text{ kHz K}^{-1}$$

$$\left(\frac{\partial \eta}{\partial T}\right)_V \cong +2 \times 10^{-4} \text{ K}^{-1}$$

The value of $(\partial \eta/\partial T)_V$ is very uncertain, since two terms of opposite sign and comparable magnitude are added together and the uncertainty in the value of α/β is consequently magnified; no further quantitative analysis of the data on the asymmetry parameter is justified.

Can. J. Chem. Downloaded from www.nrcresearchpress.com by 210.87.254.105 on 09/05/12
For personal use only.

The large value of η is probably due to the chlorine atoms in the face-bridging positions, and is likely to be very sensitive to the bismuth—chlorine distance, leading to a positive value of $(\partial\eta/\partial P)_T$, as observed. Chihara and co-workers (10) reported the temperature dependence of η for the Sb nucleus in $SbCl_3$ at constant pressure, obtaining a value $(\partial\eta/\partial T)_P$ of about $-1.1 \times 10^{-4}\,K^{-1}$ near 120°K, which is comparable with the value observed for $BiCl_3$; the attempt to interpret the temperature dependence of η and eqQ/h was not successful, and the present results suggest that the effects of thermal expansion should have been taken into account.

The analysis of the coupling constant data is consistent with these conclusions; the contribution of thermal expansion to the temperature dependence of eqQ/h at constant pressure is considerable, for it cancels out about two-thirds of the Bayer term $(\partial eqQ/\partial T)_V$. It may be concluded that the bridging chlorine atoms reduce the bismuth quadrupole coupling constant appreciably, and are the cause of the negative value of $(\partial eqQ/\partial P)_T$; in other words, the coupling constant is reduced when the intermolecular distances are reduced by hydrostatic pressure.

The interpretation of $(\partial eqQ/\partial T)_V$ in terms of the theory of torsional oscillations (11) is not very satisfactory. If θ_x and θ_y are the angles of rotation about the x and y principal axes of the electric field gradient tensor, q_0 is the coupling constant and η_0 the asymmetry parameter for the solid in the absence of torsional oscillations, then the averaged value of the major component of the electric field gradient tensor is given by eq. 11

$$[11]\quad q = q_0[1 - \tfrac{3}{2}(\langle\theta_x^2\rangle + \langle\theta_y^2\rangle) - \tfrac{1}{2}\eta_0(\langle\theta_x^2\rangle - \langle\theta_y^2\rangle)]$$

The quantities q_0 and η_0 are not accessible experimentally because of zero point vibrations; but for the present purposes, sufficiently accurate values may be obtained by extrapolating q and η measured at room temperature to absolute zero using the measured temperature derivatives

$$(eq_0Q)/h \cong 331\ \text{MHz}$$

$$\eta_0 \cong 0.60$$

Equation 11 may be differentiated at constant volume, treating q_0 and η_0 as constants:

$$[12]\quad \frac{1}{q_0}\left(\frac{\partial q}{\partial T}\right)_V = -1.80\left(\frac{\partial\langle\theta_x^2\rangle}{\partial T}\right)_V - 1.20\left(\frac{\partial\langle\theta_y^2\rangle}{\partial T}\right)_V$$

The left hand side of this equation has the approximate value $-4.5 \times 10^{-4}\,K^{-1}$. In the limit of high temperatures, the temperature coefficient of the mean square amplitude of a torsional oscillator is

$$[13]\quad \left(\frac{\partial\langle\theta^2\rangle}{\partial T}\right)_V = k/4\pi^2\nu^2 I$$

where k is Boltzmann's constant, ν is the frequency of the oscillator and I is the moment of inertia associated with the oscillator. Bismuth trichloride in the solid state contains well-defined $BiCl_3$ groups in a distorted trigonal pyramid; if the distortion is ignored, bond angles taken as 90° and the bond lengths as 0.25 nm, the moment of inertia of this group about an axis perpendicular to the trigonal axis is calculated to be approximately 6×10^{-45} kg m^2. For the lowest frequency line reported in the Raman spectrum of solid $BiCl_3$ (5), namely 37 cm^{-1}, eq. 13 yields

$$\left(\frac{\partial\langle\theta^2\rangle}{\partial T}\right)_V = 0.47 \times 10^{-4}\,K^{-1}$$

and for other, higher frequency, vibrations a smaller value will be obtained. It is therefore not possible to fit the observed value of $(1/q_0)(\partial q/\partial T)_V$ using the Raman spectrum data and eqs. 12 and 13. Although the oscillation which is primarily responsible for the temperature dependence of q may lie at a lower frequency than any reported, a more likely reason for the discrepancy is the restriction placed upon the analysis by the assumptions involved in eq. 7.

This work was supported by the National Research Council of Canada and the Advisory Research Committee of Queen's University.

1. T. Kushida, G. B. Benedek, and N. Bloembergen. Phys. Rev. **104**, 1364 (1956).
2. H. G. Robinson. Phys. Rev. **100**, 1731 (1955).
3. M. H. Cohen. Phys. Rev. **96**, 1278 (1954).
4. S. C. Nyberg, G. A. Ozin, and J. T. Szymanski. Acta Cryst. **B27**, 2298 (1971).

5. E. DENCHIK, S. C. NYBERG, G. A. OZIN, and J. T. SZYMANSKI. J. Chem. Soc. (A), 3157 (1971).
6. V. KURBATOV. Z. Obsc. Chim. **20**, 958 (1950).
7. C. DEAN. Rev. Sci. Inst. **29**, 1047 (1958).
8. M. BORN and K. HUANG. Dynamical theory of crystal lattices. Oxford. 1954.
9. L. E. TOPOL, S. W. MAYER, and L. D. RANSOM. J. Phys. Chem. **64**, 862 (1960).
10. H. CHIHARA, N. NAKAMURA, and H. OKUMA. J. Phys. Soc. Jap. **24**, 306 (1968).
11. T. C. WANG. Phys. Rev. **99**, 566 (1955).

Can. J. Chem. Downloaded from www.nrcresearchpress.com by 210.87.254.105 on 09/05/12
For personal use only.

Biosynthesis of Lycopodine. Pelletierine as an Obligatory Intermediate

J.-C. BRAEKMAN,[1] R. N. GUPTA, D. B. MACLEAN, AND I. D. SPENSER
Department of Chemistry, McMaster University, Hamilton, Ontario

Received March 23, 1972

The distribution of ^{14}C within lycopodine derived from [1,5-^{14}C]-cadaverine and from [2-^{14}C]-Δ^1-piperideine is profoundly affected by the addition of inactive pelletierine. This finding is interpreted as showing that pelletierine is an obligatory intermediate on the pathway from cadaverine and Δ^1-piperideine into lycopodine.

La distribution du ^{14}C dans la lycopodine dérivée de la cadavérine [^{14}C-1,5] et de la Δ^1-pipéridéine [^{14}C-2] est profondément affectée par l'addition de la pelletiérine inactive. Ce résultat est interprété comme suit: le passage de la cadavérine et de la Δ^1-pipéridéine à la lycopodine se fait obligatoirement par l'intermédiaire pelletiérine.

Canadian Journal of Chemistry, **50**, 2591 (1972)

Can. J. Chem. Downloaded from www.nrcresearchpress.com by 210.87.254.42 on 09/05/12
For personal use only.

The structural features of pelletierine (**2**) can be discerned within the skeletons of a variety of alkaloids (Schemes 1–3) of which *N*-methylpelletierine (**3**), sedridine (**1**), ψ-pelletierine (**5**), and anaferine (**4**) are the simplest. Attention has been drawn to the possible biogenetic relationship of pelletierine with these and with more complex structures such as the Lythraceae alkaloids (*e.g.*, decodine (**6**)) (1, 2), and the Lycopodium alkaloids of the luciduline (**8**) (3), the cernuine (**9**) (4), the lycodine-obscurine (**10**) (4), and the lycopodine (**11**) (4) type. The structural relationship of the alkaloid dioscorine (**7**) to pelletierine (Scheme 4) has not hitherto been pointed out.

The biosynthesis of several of these alkaloids has been investigated by tracer methods. Activity from labelled pelletierine (**2**) was incorporated non-randomly into anaferine (**4**) (5), cernuine (**9**) (6, 7), and lycopodine (**11**) (8, 9); and activity from *N*-methylpelletierine (**3**) entered ψ-pelletierine (**5**) in a non-random manner (5).

If pelletierine is indeed a normal intermediate in the biosynthesis of these alkaloids, then precursors of pelletierine must also be incorporated in a predictable manner. It is therefore relevant to summarize current knowledge of the origin of pelletierine.

The biosynthesis of *N*-methylpelletierine (**3**) has been studied in *Sedum sarmentosum* (10, 11) and in *Punica granatum* (5, 12, 13). Methionine supplies the *N*-methyl group (12). The sidechain of *N*-methylpelletierine (5, 11–13) as well as that of pelletierine (5) has been shown to arise from acetate. The piperidine nucleus of *N*-methylpelletierine is generated from a C_5N unit which is derived from L-lysine (but not from D-lysine (14)) by loss of the carboxyl and the α-amino group (5, 10, 11), with retention of the hydrogen atoms at C-2 and -6 (14). The same C_5N unit is derived also from cadaverine in a stereospecific manner, with retention of the pro-R and loss of the pro-s hydrogen[2] at C-1 (14).

It is likely that enzyme-bound cadaverine, formed by decarboxylation of lysine, serves as an intermediate in the biosynthesis of the piperidine nucleus of *N*-methylpelletierine and related alkaloids, and that it is the magnitude of the dissociation constant of this cadaverine-enzyme complex which determines whether incorporation of label from lysine into the nucleus of these alkaloids takes place in a non-symmetrical or a symmetrical manner (14). Oxidation of the enzyme-bound cadaverine yields Δ^1-piperideine, the immediate precursor of the piperidine nucleus, which reacts with the acetate-derived precursor of the sidechain. This pathway is summarized in Scheme 5.

The entry of pelletierine-precursors into some of the alkaloids which bear a structural relationship to pelletierine has been examined. The mode of incorporation of label from acetate into anaferine (**4**) (5), ψ-pelletierine (**5**) (5), dioscorine (**7**) (16), and lycopodine (**11**) (4); from lysine into anaferine (**4**) (5) (non-symmetrical incorporation) and into decodine (**6**)

[1]Chargé de Recherche du Fonds National de la Recherche Scientifique de Belgique.

[2]These assignments are based on the assumption that the enzyme-catalyzed decarboxylation of L-lysine by the L-lysine decarboxylase of *Bacillus subtilis* takes place with retention of configuration (*c.f.* ref. 15).

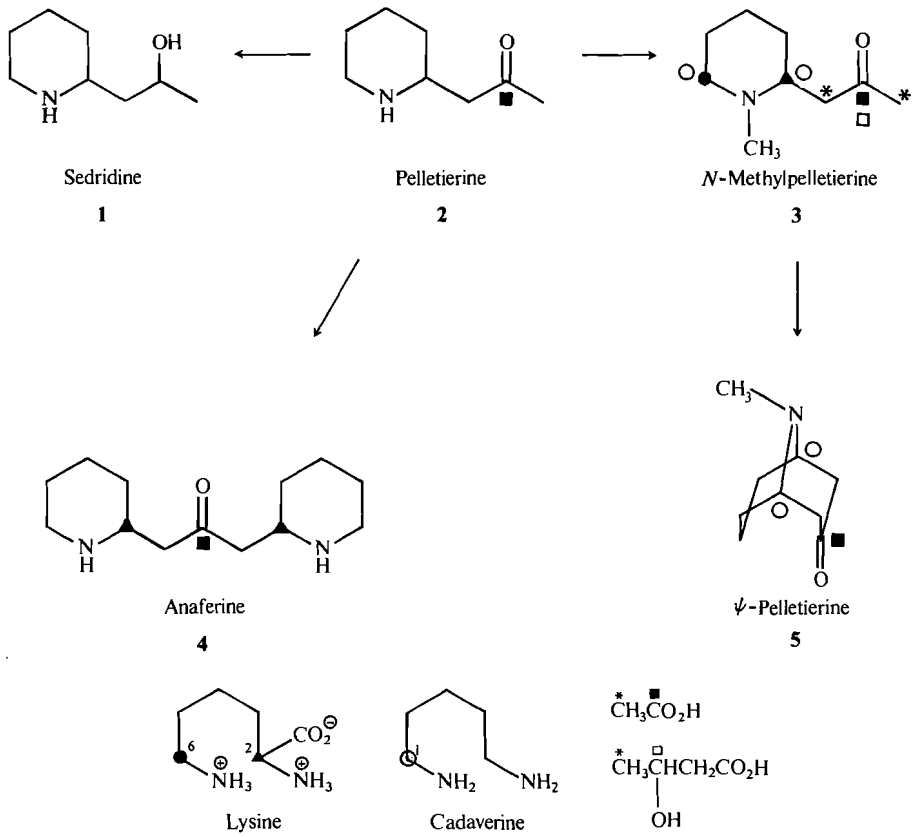

SCHEME 1. Simple alkaloids related to pelletierine. Incorporation of label from lysine, cadaverine, acetate, and β-hydroxybutyrate.

(2), cernuine (**9**) (6, 7), and lycopodine (**11**) (4, 17) (symmetrical incorporation); from cadaverine into ψ-pelletierine (**5**) (12), decodine (**6**) (18), cernuine (**9**) (7), and lycopodine (**11**) (4); and from Δ^1-piperideine into decodine (**6**) (18), cernuine (**9**) (7), and lycopodine (**11**) (9), is consistent in every case with the pelletierine hypothesis of the origin of these alkaloids.

However, none of these experiments establishes pelletierine as an obligatory intermediate.

We now present evidence which confirms that pelletierine is indeed an obligatory intermediate in the biosynthesis of lycopodine.

In earlier papers (4, 9, 17) we described tracer experiments which supported the view that the $C_{16}N_2$ and the $C_{16}N$ Lycopodium alkaloids, and lycopodine in particular, are modified dimers of a C_8N precursor. Radioactivity from each of six different ^{14}C-labelled substrates entered lycopodine in such a manner that the two C_8 units, C-1 to -8 and C-9 to -16, which constitute the two "halves" of the lycopodine skeleton, each contained one half of the activity of the intact alkaloid. Such a distribution of label is obligatory in a biosynthetic product derived from a dimeric intermediate, *i.e.*, one which originates by combination of two identical monomer units. Since the compounds which exhibited this mode of incorporation into lycopodine had been shown to be specific precursors of the pelletierine skeleton (*vide supra*) or were closely related to these precursors (lysine, cadaverine, Δ^1-piperideine, acetate, acetoacetate, β-hydroxybutyrate) we suggested that pelletierine was the monomeric C_8N precursor which was implicated in lycopodine biosynthesis (4, 17).

This hypothesis did not stand up to direct experimental test (9). Pelletierine was indeed found to enter lycopodine, but only one intact

Can. J. Chem. Downloaded from www.nrcresearchpress.com by 210.87.254.42 on 09/05/12
For personal use only.

Can. J. Chem. Downloaded from www.nrcresearchpress.com by 210.87.254.42 on 09/05/12
For personal use only.

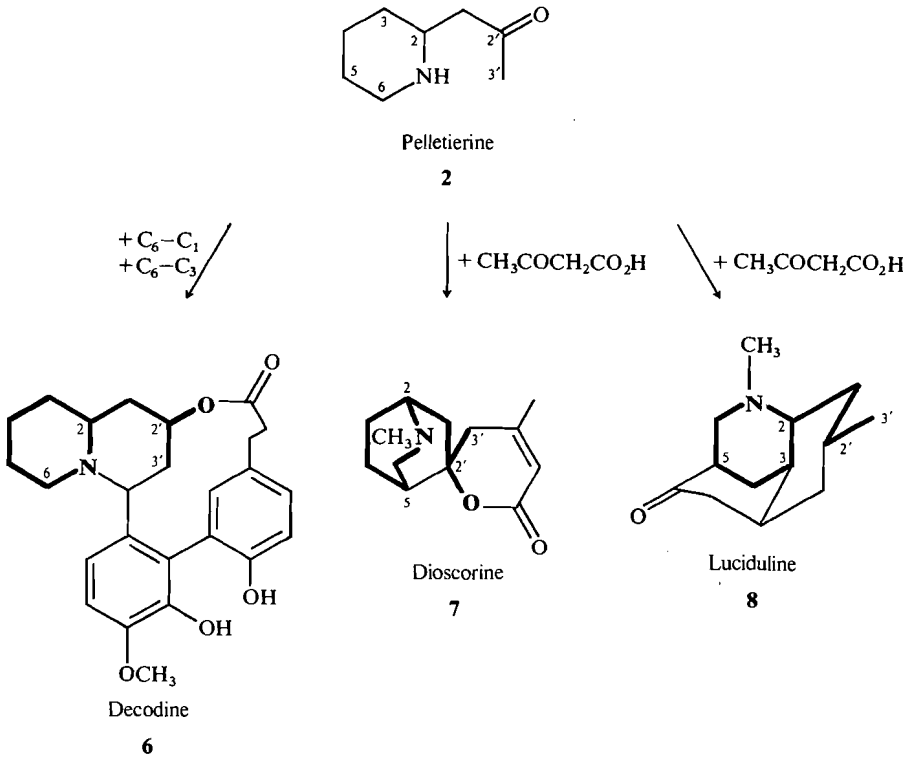

SCHEME 2. Structural relationship of some complex alkaloids to pelletierine.

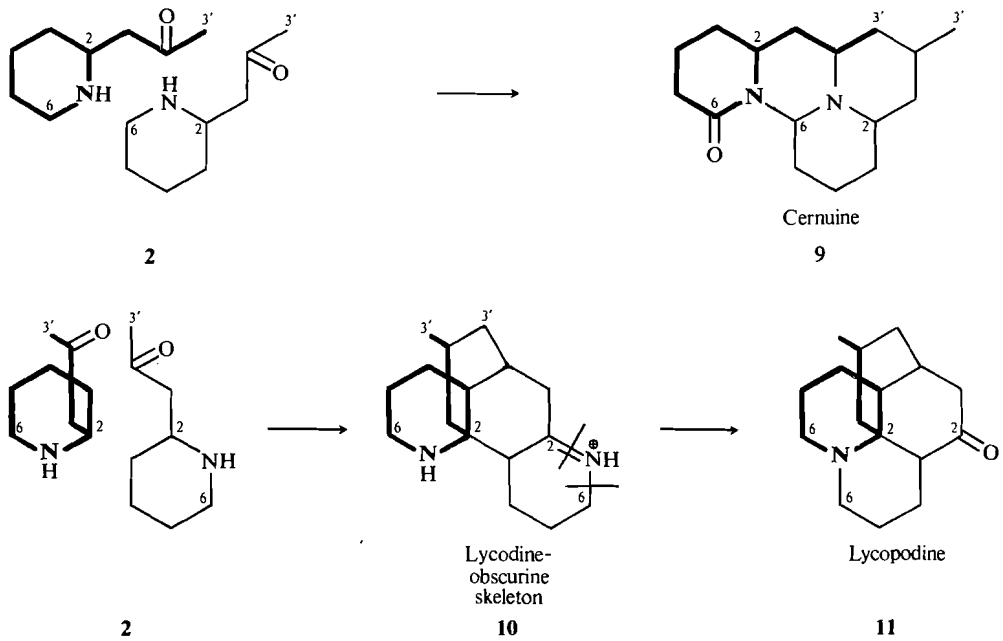

SCHEME 3. Structural relationship of Lycopodium alkaloids to pelletierine.

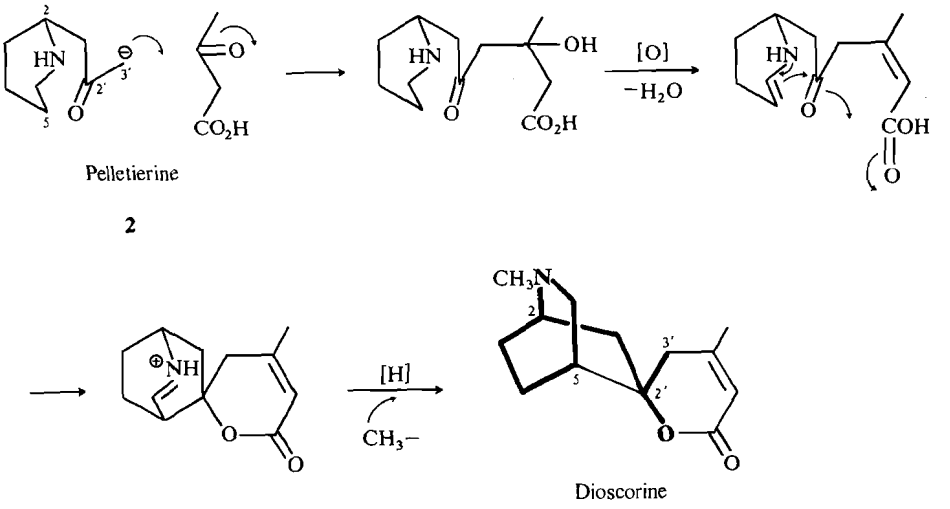

SCHEME 4. The biogenesis of dioscorine from pelletierine and acetoacetate.

pelletierine unit was incorporated, serving as the specific precursor of the C_8 unit, C-9 to -16. The C_8 unit, C-1 to -8, of lycopodine did not originate from pelletierine. Evidently lycopodine was not a modified dimer of pelletierine.

One of two conclusions became unavoidable:

Either (*a*) pelletierine was an obligatory precursor of lycopodine, in which case the alkaloid cannot be derived from a dimeric intermediate. This inference was difficult to reconcile with the finding that the two "halves" of lycopodine were equally labelled in 11 separate experiments with six different substrates. A model consistent with this alternative (ref. 9, Scheme 8) involved intermediacy of 4-(2-piperidyl)acetoacetate (**14**), which not only served as the precursor of the C_8 unit, C-1 to -8, of lycopodine, but which, by irreversible decarboxylation, gave rise to pelletierine, the precursor of the other C_8 unit, C-9 to -16.

Or (*b*) lycopodine was indeed generated from a dimeric intermediate such as (**10**), in which case pelletierine could not be a normal precursor. This conclusion raised the question of the identity of the C_8N monomer, and gave rise to the apparent paradox that pelletierine replaced one but not the other of two identical monomer units. A model capable of rationalizing this alternative (ref. 9, Scheme 9) involved 2-allylpiperidine (3-(2-piperidyl)-prop-1-ene) as the monomeric C_8N unit. This model demands that activity from ^{14}C-labelled 2-allylpiperidine should enter equally into the two "halves" of lycopodine, C-1 to -8, and C-9 to -16. Thus [2-^{14}C]-2-allylpiperidine should yield lycopodine labelled exclusively and equally at C-5 and C-13.

One of the experiments here reported was designed to test this model. The result which was obtained eliminates the allylpiperidine hypothesis from contention. *Lycopodium tristachyum* was kept in contact with a sample of [2-^{14}C]-2-allylpiperidine, prepared by reaction of [2-^{14}C]-Δ^1-piperideine with allyl magnesium chloride (19). The radioactive lycopodine which was isolated from these plants (Table 1, experiment 15) was converted into the phenyldihydro-derivative, which on oxidation yielded benzoic acid (4). Since the benzoic acid, representing C-5 of the allylpiperidine-derived lycopodine, was essentially free of radioactivity (Table 2), allylpiperidine had not served as a specific precursor of the C_8 unit, C-1 to -8, of lycopodine, and cannot be the C_8N monomer unit demanded by model (*b*). The allylpiperidine hypothesis is thus clearly untenable, regardless of whether a 2-allylpiperidine unit is incorporated intact into lycopodine or not,[3] since

[3]The degradation result does not distinguish between these alternatives. It is shown merely that activity from [2-^{14}C]-2-allylpiperidine enters lycopodine non-randomly, since little of this activity was present at C-5 of the alkaloid.

Can. J. Chem. Downloaded from www.nrcresearchpress.com by 210.87.254.42 on 09/05/12
For personal use only.

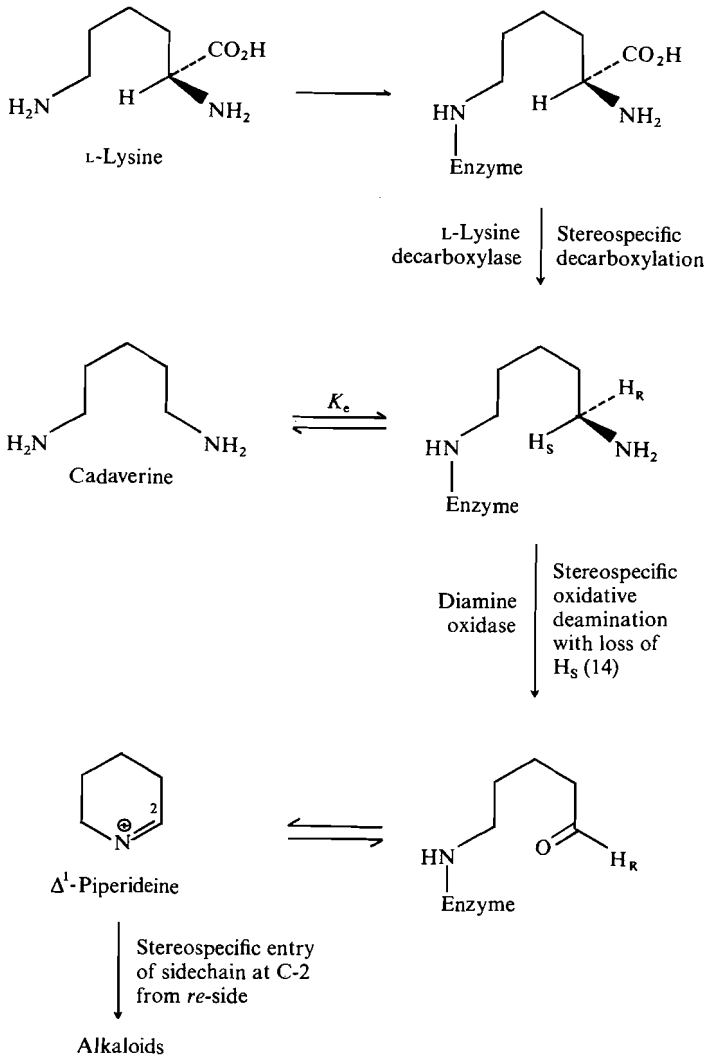

SCHEME 5. The biosynthesis of the lysine-derived piperidine alkaloids (14). If $K_e \leqslant 1$, incorporation of label from [2-^{14}C]- or [6-^{14}C]-lysine into the alkaloids is symmetrical. If $K_e \gg 1$, incorporation of label from [2-^{14}C]- or [6-^{14}C]-lysine into the alkaloids is nonsymmetrical.

even if intact incorporation of such a unit had occurred, it could have served only as the precursor of the C_8 moiety, C-9 to -16, *i.e.*, the same C_8 moiety which is derived from pelletierine, and not of both C_8 moieties. Further examination of the distribution of activity within the sample of lycopodine derived from [2-^{14}C]-2-allylpiperidine was thus unnecessary and was not pursued.

Instead, we directed our attention towards the experimental examination of model (*a*). Since the key intermediate envisaged by this model, 4-(2-piperidyl)-acetoacetate (**14**), has not been described, and since our attempts to prepare this compound have so far been unsuccessful, we focussed our efforts on marshalling evidence that pelletierine is an obligatory intermediate in the biosynthesis of lycopodine, as required by the model.

Absolute proof of an obligatory precursor–product relationship cannot be obtained from experiments with intact organisms. Even in

Can. J. Chem. Downloaded from www.nrcresearchpress.com by 210.87.254.42 on 09/05/12
For personal use only.

TABLE 1. Incorporation of precursors into lycopodine

	Chemical and radiochemical yields		
Experiment no.	15	16	17
Compound administered	[2-^{14}C]-2-Allylpiperidine	[2-^{14}C]-Δ^1-Piperideine plus inactive pelletierine hydrochloride (200 mg)	[1,5-^{14}C]-Cadaverine plus inactive pelletierine hydrochloride (400 mg)
Nominal total activity (mCi)	0.04	0.1	0.1
Nominal specific activity (mCi per mmol)	0.5	1.0	3.2
Date	July 1970	July 1970	May 1971
Weight of dry plant (g)	80	95	54
Lycopodine			
Yield (mg)	42	58	133
Specific activity $\times 10^{-4}$ (counts min^{-1} $mmol^{-1}$)	1.5	75	5.5
Pelletierine hydrochloride			
Yield (mg)	—	5	300
Specific activity $\times 10^{-4}$ (counts min^{-1} $mmol^{-1}$)	—	9.0	0.8

TABLE 2. Distribution of label within lycopodine derived from various precursors

Experiment no.	Precursor	Product: Lycopodine* SA†	Lycopodine* RSA‡	Benzoic acid (C-5) SA†	Benzoic acid (C-5) RSA‡	7-Methyl-5,6,7,8-tetrahydroquinoline (C-7 to -16) SA†	7-Methyl-5,6,7,8-tetrahydroquinoline (C-7 to -16) RSA‡
15	[2-^{14}C]-2-Allylpiperidine	0.523 ± 0.02*	100 ± 3	0.016 ± 0.003	3 ± 1	—	
16	[2-^{14}C]-Δ^1-Piperideine plus inactive pelletierine	3.21 ± 0.05* 6.90 ± 0.16*	100 ± 1 100 ± 2	2.82 ± 0.06 —	88 ± 2	— 0.62 ± 0.02	9 ± 0.3
17	[1,5-^{14}C]-Cadaverine plus inactive pelletierine	2.75 ± 0.07*	100 ± 2	1.20 ± 0.02	44 ± 1	—	

*Obtained from the original samples of lycopodine (Table 1) by dilution with inactive lycopodine, followed by crystallization to constant activity.
†Specific activity (counts min^{-1} $mmol^{-1}$) $\times 10^{-4}$.
‡Relative specific activity: percent (lycopodine = 100).

fragmented systems the experimental difficulties of obtaining conclusive evidence are, for all practical purposes, regarded as insuperable (20). Two criteria which are conditions for a precursor–product relationship, but do not prove the obligatory nature of the relationship between substrate and product, are (*i*) the entry of tracer from specifically labelled samples of substrate into predictable sites within the product, and (*ii*) the formation of the substrate within the system in which the product is formed. Reliable kinetic data which might show the flow of tracer from precursor via intermediates to product in a sequence of successive steps are not readily obtained from experiments with labelled multicarbon substrates in intact plant systems (*e.g.*, 21). Other parameters, *e.g.*, efficiency of incorporation of label from substrate into product, and the sparing of incorporation of label from a general carbon source by the substrate (isotope dilution) are unsatisfactory as criteria for a precursor–product relationship in intact systems (*e.g.*, 22), since they may be controlled by extraneous factors such as permeability and are subject to the variability of the biological material.

Can. J. Chem. Downloaded from www.nrcresearchpress.com by 210.87.254.42 on 09/05/12
For personal use only.

Can. J. Chem. Downloaded from www.nrcresearchpress.com by 210.87.254.42 on 09/05/12
For personal use only.

One of the essential conditions for a precursor–product relationship of pelletierine to lycopodine, specific incorporation of substrate, ((*i*) above), has already been fully documented (9). We now present evidence for the other ((*ii*), above), formation of pelletierine in *Lycopodium tristachyum* at a time when lycopodine is being formed.

Radioactive pelletierine hydrochloride was isolated from *Lycopodium* plants which had been kept in contact with [2-^{14}C]-Δ^1-piperideine (experiment 16) and with [1,5-^{14}C]-cadaverine (experiment 17) (Table 1) by "metabolite swamping" (*i.e.*, by administration of an inactive sample of pelletierine in admixture with the labelled substrate). Non-random incorporation of precursor into the pelletierine isolated in the latter experiment was demonstrated by partial degradation (Table 3). All activity was present in the degradation fragment containing the piperidine nucleus, none in the terminal carbons of the sidechain.

Thus, not only is pelletierine shown to be incorporated into lycopodine in *L. tristachyum* (9), but it is now also shown to be present in the plant, formed from compounds which are known to serve as precursors of lycopodine.

These findings show that a precursor–product relationship exists between pelletierine and lycopodine but they cannot serve as evidence that this relationship represents a normal, obligatory biosynthetic sequence and not merely a minor pathway. Under normal circumstances no further conclusions could have been drawn.

The present instance represents an exceptional case, however.

If pelletierine served as an obligatory intermediate between cadaverine or Δ^1-piperideine and lycopodine, then, in short term experiments under ideal conditions, the efficiency of incorporation of tracer from [^{14}C]-cadaverine and from [^{14}C]-Δ^1-piperideine into lycopodine must be lower in experiments in which inactive pelletierine is administered along with the tracer than in experiments in which tracer alone is fed to the plant. Such ideal conditions obtain only if, in the two experiments which are to be compared, all other variables can be controlled.

Such control cannot be achieved in experiments with intact plants. Thus, since only a small number of plants is used in each of the experiments, it is not possible to eliminate the possible effect of individual biological variation. This factor can be eliminated only by using a very large population of individuals (such as is found in a microbiological culture). Nor is it possible to ensure that the rate of uptake of pelletierine into the cells where biosynthesis occurs is at least as high as the rate of uptake of labelled substrate.

TABLE 3. Distribution of label within pelletierine isolated from *L. tristachyum* grown in contact with [1,5-^{14}C]-cadaverine (experiment 17)

	SA (counts min^{-1} mmol^{-1}) $\times 10^{-4}$	RSA (%)
Pelletierine	0.82 ± 0.02	100 ± 3
Pipecolic acid by oxidation of pelletierine	0.82 ± 0.02	100 ± 4

Thus the apparent lowering of the efficiency of incorporation of [^{14}C] from [^{14}C]-cadaverine and [^{14}C]-Δ^1-piperideine into lycopodine in the presence of added pelletierine (Tables 4 and 5) is, at best, no more than indicative, unless some additional parameter can be used as an independent internal standard, and as a basis for the comparison.

Such an internal standard is not normally available in experiments with intact plants. In the present instance, however, an important additional criterion exists.

It is established that activity from each of [^{14}C]-cadaverine and [^{14}C]-Δ^1-piperideine enters both C_8 units, C-1 to -8 and C-9 to -16, of lycopodine with equal efficiency, whereas pelletierine serves as a precursor of the C_8 unit, C-9 to -16, but not of the C_8 unit, C-1 to -8 (4, 9). Pelletierine cannot therefore lie on the pathway between cadaverine or Δ^1-piperideine and the C_8 unit, C-1 to -8, of lycopodine, but it could be (but need not be) an obligatory intermediate on the route from cadaverine and Δ^1-piperideine into the C_8 unit, C-9 to -16, of lycopodine.

If pelletierine were not an obligatory intermediate, addition of unlabelled pelletierine would not affect the entry of ^{14}C from cadaverine or from Δ^1-piperideine into either of the two C_8 units of lycopodine. Each of these two units would thus contain one half of the label of the intact lycopodine derived from [^{14}C]-

TABLE 4. Incorporation of [1,5-^{14}C]-cadaverine into lycopodine

	Experiment 11 (ref. 4)	Experiment 17
Substrate	[1,5-^{14}C]-Cadaverine	Pelletierine hydrochloride (400 mg) plus [1,5-^{14}C]-Cadaverine
Nominal specific activity (mCi/mmol)	3.2	3.2
Nominal total activity (mCi)	0.1	0.1
Plant Material		
Dried (g)	36	54
Lycopodine		
Yield (mg)	100	133
Specific activity (c.p.m./mmol)	73×10^4	5.5×10^4

TABLE 5. Incorporation of [^{14}C]-Δ^1-piperideine into lycopodine

	Experiment 13 (ref. 9)	Experiment 14 (ref. 9)	Experiment 16
Substrate	[2-^{14}C]-Δ^1-Piperideine	[6-^{14}C]-Δ^1-Piperideine	Pelletierine hydrochloride (200 mg) plus [2-^{14}C]-Δ^1-Piperideine
Nominal specific activity (mCi/mmol)	0.4	0.8	1
Nominal total activity (mCi)	0.1	0.1	0.1
Plant Material			
Dried (g)	35	38	95
Lycopodine			
Yield (mg)	88	104	58
Specific activity (c.p.m./mmol)	104×10^4	190×10^4	75×10^4

cadaverine or [^{14}C]-Δ^1-piperideine, regardless of whether inactive pelletierine were added to the system or not.

If pelletierine were a normal intermediate on the route from cadaverine and Δ^1-piperideine into the C_8 unit, C-9 to -16, of lycopodine, addition of inactive pelletierine to the system would suppress entry of label from [^{14}C]-cadaverine or from [^{14}C]-Δ^1-piperideine into the C_8 unit, C-8 to -16, but not into the C_8 unit, C-1 to -8, of lycopodine. It follows that under these conditions, the two C_8 units of lycopodine derived from [^{14}C]-cadaverine or [^{14}C]-Δ^1-piperideine would no longer be equally labelled. The C_8 unit, C-9 to -16, should contain less activity than the C_8 unit, C-1 to -8. In the limit, suppression of incorporation of label into the C_8 unit, C-9 to -16, by carrier pelletierine would be complete, so that all activity from [^{14}C]-cadaverine or [^{14}C]-Δ^1-piperideine would enter the C_8 unit, C-1 to -8. Since only one carbon, C-5, within this unit is labelled when [2-^{14}C]-Δ^1-piperideine serves as the substrate, all, or most of the activity from this precursor should be located at this carbon atom of the lycopodine obtained when [2-^{14}C]-Δ^1-piperideine is administered in the presence of inactive pelletierine (experiment 16), if pelletierine were an obligatory intermediate, whereas if it were not, only one half of the activity of the intact lycopodine would be located at this site, as found in the absence of added pelletierine (experiment 13, ref. 9). In fact about 90% of the total activity of the lycopodine from experiment 16 was found at C-5 (benzoic acid) (Table 2) (Scheme 6).

Can. J. Chem. Downloaded from www.nrcresearchpress.com by 210.87.254.42 on 09/05/12
For personal use only.

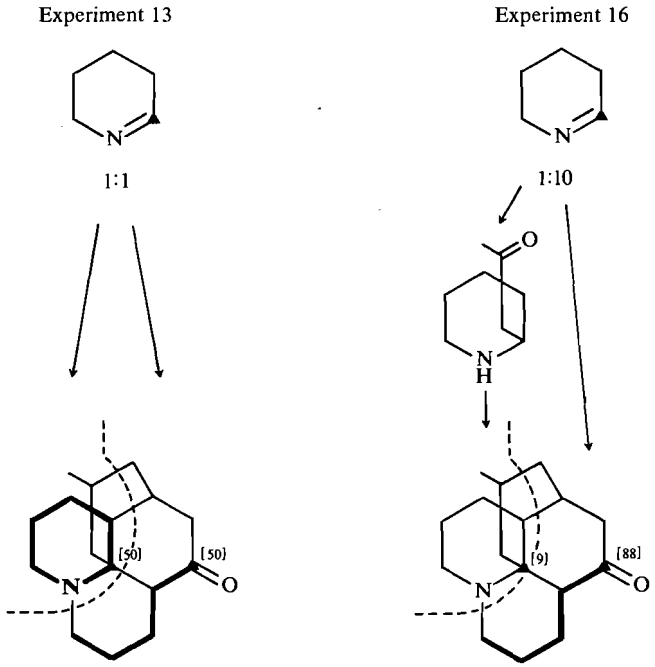

SCHEME 6. The mode of incorporation of activity from [2-^{14}C]-Δ^1-piperideine into lycopodine in the absence (experiment 13) and in the presence (experiment 16) of added inactive pelletierine. (Numbers in square brackets are percent of total specific activity of lycopodine, located at the indicated carbon atom.)

Similarly, two carbon atoms, C-5 and C-1, within the C_8 unit, C-1 to -8, become labelled when [1,5-^{14}C]-cadaverine serves as the substrate. In the presence of inactive pelletierine (experiment 17), all or most of the activity of lycopodine derived from this substrate should be divided equally among these two carbon atoms, so that C-5 should contain 50% of the activity of this lycopodine sample, if pelletierine were an obligatory intermediate between cadaverine and lycopodine and suppression of incorporation of the earlier percursor were complete. If pelletierine were not an obligatory intermediate only one quarter of the activity of the intact lycopodine would reside at this site, a distribution identical with that found in the absence of added pelletierine (experiment 11, ref. 4). In fact 44% of the total activity of the lycopodine from experiment 17 was recovered from C-5 (benzoic acid) (Table 2) (Scheme 7).

Thus, pelletierine is indeed an obligatory intermediate on the route from cadaverine and Δ^1-piperideine into the C_8 unit, C-9 to -16, of lycopodine. Therefore lycopodine cannot be derived from a true dimer. A hypothetical model which reconciles this inference with the observation that activity from six different substrates enters the two halves of lycopodine with equal efficiency is shown in Scheme 8. Provided the steady state concentration of pelletierine (**2**) is small compared to that of its postulated precursor, the coenzyme A derivative of 4-(2-piperidyl)acetoacetic acid (**13**), and the conversion of (**13**) into pelletierine is irreversible, all observations are accounted for. A novel route to **13** and **14**, via the coenzyme A derivative of piperidyl-2-acetic acid (**12**), is now suggested. This route is consistent with the observation that acetoacetate and β-hydroxybutyrate are not incorporated intact into lycopodine (4) or into *N*-methylpelletierine (11). Further experimental support for this hypothesis is being sought.

Experimental

Labelled Compounds

[2-^{14}C]-Δ^1-Piperideine (9) (experiment 16) and [2-^{14}C]-2-allylpiperidine (19) (experiment 15) were prepared from [2-^{14}C]-DL-lysine monohydrochloride (New England Nuclear). [1,5-^{14}C]-Cadaverine hydrochloride (experiment 17) was a commercial sample (New England Nuclear).

Tracer Experiments

In each of the three experiments, excised shoots of *Lycopodium tristachyum* Pursh were packed, cut surfaces

Can. J. Chem. Downloaded from www.nrcresearchpress.com by 210.87.254.42 on 09/05/12
For personal use only.

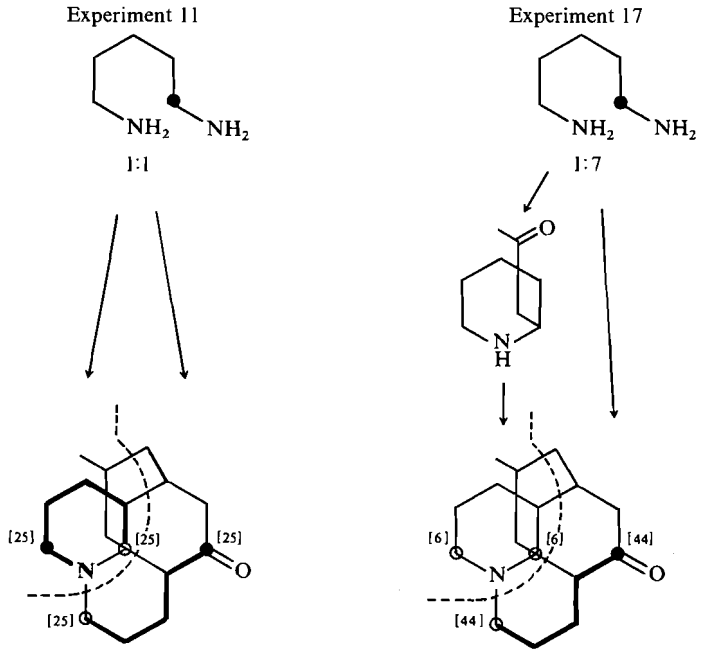

SCHEME 7. The mode of incorporation of activity from [1,5-^{14}C]-cadaverine into lycopodine in the absence (experiment 11) and in the presence (experiment 17) of added inactive pelletierine. (Numbers in square brackets are percent of total specific activity of lycopodine, demonstrated (full circles) or inferred (hollow circles) to reside at the indicated carbon atoms.)

downward, into two 100 ml beakers. The feeding solution was divided among the beakers.

In experiments 16 and 17, unlabelled pelletierine hydrochloride (23) (200 and 400 mg, respectively, in 10 ml glass-distilled water) was administered. When most of this solution had been absorbed by the cuttings, a solution of [2-^{14}C]-Δ^1-piperideine (nominal specific activity, 1.0 mCi per mmol, nominal total activity, 0.1 mCi) (experiment 16) or a solution of [1,5-^{14}C]-cadaverine hydrochloride (nominal specific activity, 3.2 mCi per mmol, nominal total activity, 0.1 mCi) (experiment 17), respectively, in 10 ml glass-distilled water, was added. In experiment 15, [2-^{14}C]-2-allylpiperidine (nominal specific activity, 0.5 mCi per mmol, nominal total activity, 0.04 mCi) in 10 ml glass-distilled water, was administered. In each experiment the cuttings were kept in contact with the tracer solution for 48 h.

Isolation of Lycopodine and of Pelletierine Hydrochloride

Radioactive lycopodine was isolated from each of the three feeding experiments. The method of isolation described in an earlier paper (4) was employed in experiment 15. In experiments 16 and 17, radioactive pelletierine hydrochloride as well as lycopodine was isolated.

The method for the isolation of lycopodine and pelletierine from experiment 16 gave a very poor yield of pelletierine and needs to be recorded in outline only: lycopodine (58 mg) was isolated by fractional crystallization from a hexane solution of the basic fraction of the plant extract, and was further purified by crystallization from hexane, followed by sublimation at 80–100° and 3×10^{-3} mm. Inactive lycopodine (100 mg) was then added to the hexane mother liquor and reisolated, to remove residual activity associated with this alkaloid. The hexane mother liquor was then evaporated, the residue dissolved in dry methanol (0.5 ml), the solution saturated with hydrogen chloride, solvent evaporated, and the residue applied to a plate of silica gel which was developed with chloroform/methanol (9:1). The zone corresponding in R_f value to that of an authentic sample of pelletierine hydrochloride was eluted with chloroform/methanol (1:1), and the product (5 mg) isolated by column chromatography on alumina, followed by sublimation in high vacuum.

An improved procedure was used to isolate the products from experiment 17.

The shoots of *L. tristachyum* were dried and ground to a fine powder in a blender (Osterizer Galaxie 10). The powder was continuously extracted with methanol for 24 h. The extract was evaporated *in vacuo* and the solid residue was repeatedly extracted with hydrochloric acid (5%, 3×100 ml). The mixture was filtered through Celite, and the filtrate was basified with ammonia and extracted with chloroform (3×150 ml). The chloroform extract was dried and evaporated, and the oily residue applied to a column of basic alumina. Elution with benzene afforded lycopodine which was further purified by crystallization from hexane, followed by sublimation at 5×10^{-3} mm. Elution with chloroform gave pelletierine: the chloroform was evaporated at room temperature and the residue dissolved in dry ether. When dry hydrogen chloride was passed through the ether solution pelletierine hydrochloride crystallized (300 mg). Paper chromatography (Whatman No. 1,

Can. J. Chem. Downloaded from www.nrcresearchpress.com by 210.87.254.42 on 09/05/12
For personal use only.

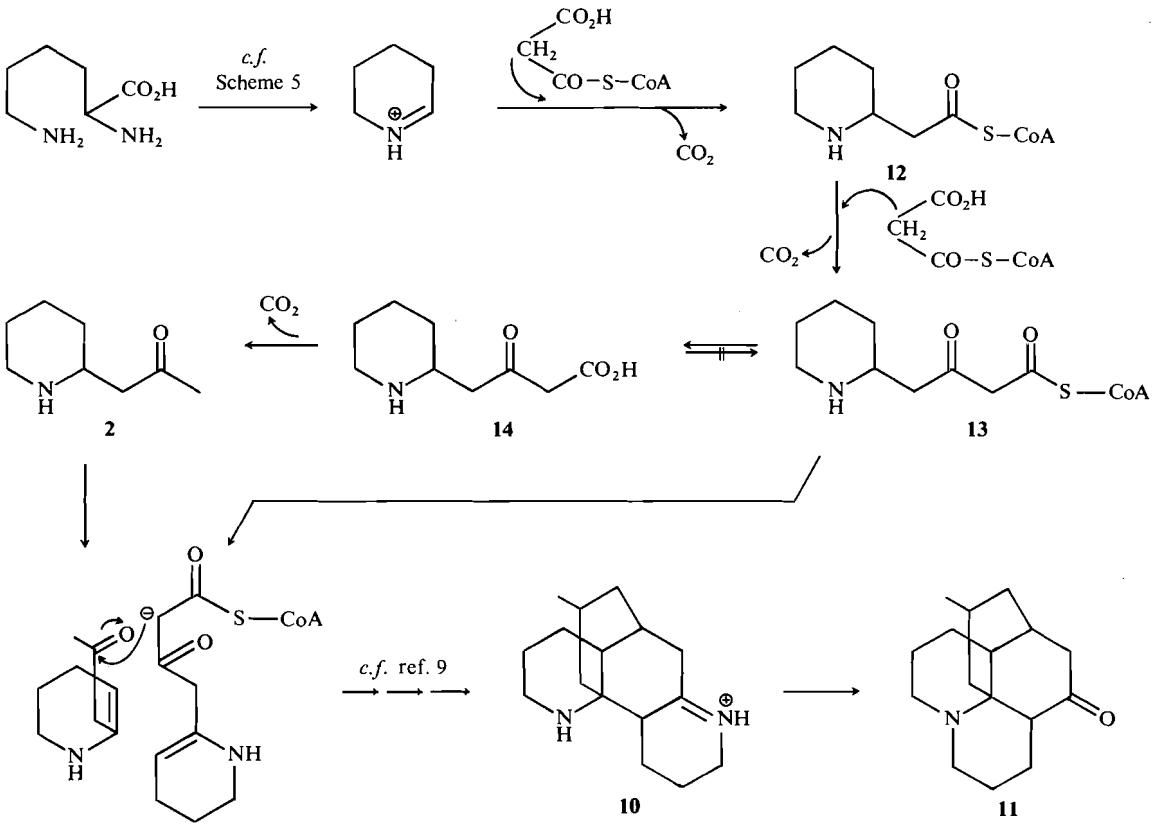

SCHEME 8. The biosynthesis of lycopodine. A hypothetical pathway consistent with the experimental evidence.

n-butanol/acetic acid/water, 2:1:1) of a sample of the crude product from this experiment with [1,5-^{14}C]-cadaverine (experiment 17) revealed the presence of a highly radioactive contaminant whose R_f value was identical with that of cadaverine hydrochloride. A portion of the crude pelletierine hydrochloride (10 mg) was therefore purified by paper chromatography on a preparative scale, using the same solvent system. The pelletierine zone was eluted with methanol, and the product purified to constant radioactivity by recrystallization from ethanol/ether, followed by high vacuum sublimation at 110–120° and 3×10^{-3} mm.

Degradation of Labelled Samples

The labelled samples of lycopodine and of pelletierine were partially degraded. Carbon-5 of lycopodine was separated as benzoic acid (4), and carbons-7 to -16 were recovered as 7-methyl-5,6,7,8-tetrahydroquinoline (4). The labelled pelletierine hydrochloride was oxidized to pipecolic acid (9) which was purified by paper chromatography (*n*-butanol/acetic acid/water, 2:1:1), followed by sublimation at 5×10^{-3} mm.

Determination of Radioactivity

Radioactivity was assayed on samples of finite thickness on aluminum planchettes with a gas-flow system (Model 4342 Nuclear Chicago). The usual corrections for background and self-absorption were applied. For plating, a 1% solution of collodion in dimethylformamide was used as the solvent. In the case of benzoic acid, a drop of a 1% solution of sodium hydroxide in 50% aqueous methanol was added to prevent loss by evaporation.

Confidence limits given in the tables are standard deviation of the mean.

This work was supported by the National Research Council of Canada. One of us (J.-C.B.) thanks the scientific committee of NATO for the award of a fellowship.

1. J. P. FERRIS, C. B. BOYCE, and R. C. BRINER. Tetrahedron Lett. 5129 (1966).
2. S. H. KOO, R. N. GUPTA, I. D. SPENSER, and J. T. WROBEL. Chem. Commun. 396 (1970).
3. W. A. AYER, N. MASAKI, and D. S. NKUNIKA. Can. J. Chem. **46**, 3631 (1968).
4. M. CASTILLO, R. N. GUPTA, D. B. MACLEAN, and I. D. SPENSER. Can. J. Chem. **48**, 1893 (1970).
5. M. F. KEOGH and D. G. O'DONOVAN. J. Chem. Soc. 1792 (1970).
6. R. N. GUPTA, Y. K. HO, D. B. MACLEAN, and I. D. SPENSER. Chem. Commun. 409 (1970).
7. Y. K. HO, R. N. GUPTA, D. B. MACLEAN, and I. D. SPENSER. Can. J. Chem. **49**, 3352 (1971).
8. M. CASTILLO, R. N. GUPTA, Y. K. HO, D. B. MACLEAN, and I. D. SPENSER. J. Am. Chem. Soc. **92**, 1074 (1970).

Can. J. Chem. Downloaded from www.nrcresearchpress.com by 210.87.254.42 on 09/05/12
For personal use only.

9. M. CASTILLO, R. N. GUPTA, Y. K. HO, D. B. MACLEAN, and I. D. SPENSER. Can. J. Chem. **48**, 2911 (1970).
10. R. N. GUPTA and I. D. SPENSER. Chem. Commun. 85 (1968).
11. R. N. GUPTA and I. D. SPENSER. Phytochem. **8**, 1937 (1969).
12. H. W. LIEBISCH, N. MAREKOV, and H. R. SCHÜTTE. Z. Naturforsch. **23B**, 1116 (1968).
13. M. F. KEOGH and D. G. O'DONOVAN. Tetrahedron Lett. 265 (1968).
14. I. D. SPENSER. 23rd Int. Congr. of Pure and Appl. Chem. Boston, July 1971. Symposium 0-13, Abstr. No. 91, p. 36, based on unpublished results of E. W. Leistner and I. D. Spenser.
15. S. MANDELES, R. KOPPELMAN, and M. E. HANKE. J. Biol. Chem. **209**, 327 (1954); B. BELLEAU and J. BURBA. J. Am. Chem. Soc. **82**, 5751 (1960).
16. E. LEETE and A. R. PINDER. Chem. Commun. 1499 (1971).
17. R. N. GUPTA, M. CASTILLO, D. B. MACLEAN, I. D. SPENSER, and J. T. WROBEL. J. Am. Chem. Soc. **90**, 1360 (1968).
18. S. H. KOO and I. D. SPENSER. Unpublished results, 1970.
19. M. PREISS and I. D. SPENSER. Chem. Ber. **104**, 1967 (1971).
20. E. A. ADELBERG. Bacteriol. Rev. **17**, 253 (1953).
21. A. R. BATTERSBY and B. J. T. HARPER. Tetrahedron Lett. No. 27, 21 (1960).
22. D. H. R. BARTON, G. W. KIRBY, J. B. TAYLOR, and G. M. Thomas. J. Chem. Soc. 4545 (1963).
23. R. N. GUPTA and I. D. SPENSER. Can. J. Chem. **47**, 445 (1969).

Can. J. Chem. Downloaded from www.nrcresearchpress.com by 210.87.254.42 on 09/05/12
For personal use only.

Infrared and Electronic Spectral Studies of Cobalt(II) and Nickel(II) Complexes of *N*-Allyl Urea and *N*-Allyl Thiourea

P. P. SINGH AND I. M. PANDE

Chemistry Department, M.L.K. College, Balrampur, U.P., India

Received December 23, 1971

Complexes of *N*-allyl urea (NAU) and *N*-allyl thiourea (NATU) with cobalt(II) and nickel(II) halides and perchlorates have been prepared and characterized by electrical conductance, magnetic susceptibility, infrared and electronic spectra. Infrared spectra suggest coordination in NAU through oxygen and in NATU through nitrogen. The electronic spectra and magnetic susceptibility data indicate tetrahedral and octahedral stereochemistry for cobalt(II) and nickel(II) halide complexes, respectively. The various ligand field parameters Dq, B', and β calculated for these complexes show about 25 and 11% covalency for Co(II) and Ni(II), respectively, and suggest a weak ligand field.

Les complexes de la *N*-allylurée (NAU) et *N*-allyl thiourée (NATU) avec les halogénures et perchlorates de cobalt(II) et nickel(II), ont été préparés et caractérisés par conductance électrique, susceptibilité magnétique, spectres infrarouge et électronique. Les spectres infrarouge suggèrent une coordination dans la NAU à travers l'oxygène et dans la NATU, à travers l'azote. Les spectres électroniques et les données sur la susceptibilité magnétique, indiquent une stéréochimie tétraédrale et octaédrale respectivement pour les complexes avec les halogénures de cobalt(II) et nickel(II). Les divers paramètres du champ de ligand Dq, B', et β, calculés pour ces complexes, donnent environ 25 et 11% de covalence pour le Co(II) et Ni(II) respectivement et laisse penser à un champ de ligand faible.

Canadian Journal of Chemistry, **50**, 2603 (1972)

Introduction

In view of the great variations in structure (1–13) of cobalt(II) and nickel(II) complexes, we have prepared a series of complexes of these ions with *N*-allyl urea and *N*-allyl thiourea, and have carried out conductance, magnetic, infrared and electronic spectral measurements to characterize them. Also we have tried from Dq and B' values to draw some conclusions regarding the site of bonding in ligands and to correlate these with the infrared spectral results.

Experimental

Materials

Reagent grade cobalt(II) and nickel(II) halides and perchlorate (Alfa Inorganics) were used without further purification. *N*-Allyl urea (NAU) and *N*-allyl thiourea (NATU) were of reagent grade and were used as such. Solvents were dried before use, and the water sensitive compounds were handled in dry box flushed with nitrogen.

Physical Measurements

The electrolytic conductance measurements were carried out at 25 °C in nitromethane with a Philips Conductivity measuring bridge Model PR 9500/90 and Conductivity cell Model PV 9055. Magnetic measurements were carried out at room temperature by the Gouy method (14) and the diamagnetic corrections were estimated by the procedure of Figgis and Lewis (15). Infrared spectra of the complexes were obtained on a Perkin–Elmer Model 7I, using KBr pellets. Electronic spectra were obtained using Cary 14 spectrophotometer in nitromethane and a single band for the broad or scattered peaks, was selected by the method of Cotton *et al.* (16). The various spectral parameters Dq, B', and β were calculated by using the secular equation of Tanabe and Sugano (17).

Preparation of the Complexes

Complexes were prepared by refluxing and stirring the anhydrous metal salt and ligand, in suitable molar ratios, in $CHCl_3$ for 24 h. The perchlorate complexes were, however, prepared by first stirring the salts with 6 ml of 2,2-dimethoxypropane before adding a chloroform solution of the ligand (1:4 or 1:6 ratio) and continuing the stirring for 24 h. In each case, except for NATU complexes, insoluble precipitates were obtained which were filtered, washed with the solvent, dried in vacuum, and recrystallized either from ethanol or *n*-butanol.

In the case of NATU complexes, the precipitates frequently appeared as an oil, whose consistency was increased by repeatedly shaking with ether. The viscous mass thus obtained was spread in a thin layer on the surface of a porcelain dish and kept for several weeks over P_4O_{10}; a solid mass was then obtained.

Analysis of the Complexes

Cobalt(II) and nickel(II) complexes were analyzed for halogen and nitrogen as described earlier (18). Cobalt and nickel were determined gravimetrically as anthranilate and dimethylglyoximate, respectively. The analytical results are presented in Table 1.

Results and Discussion

Electrolytic Conductance and Magnetic Study

Reference to Table 1 shows that all the complexes are non-electrolytes except the perchlo-

Can. J. Chem. Downloaded from www.nrcresearchpress.com by 210.87.254.5 on 09/05/12
For personal use only.

Can. J. Chem. Downloaded from www.nrcresearchpress.com by 210.87.254.5 on 09/05/12
For personal use only.

TABLE 1. Analytical results

Complexes	Color	Melting point (°C)	Metal (%)		Halogen (%)		Nitrogen (%)		Molecular conductivity (M/256)	μ_{eff} (B.M.)
			Calcd.	Obs.	Calcd.	Obs.	Calcd.	Obs.		
$[Co(NAU)_2Cl_2]$	Dark blue	106	17.9	17.6	21.5	21.2	16.9	16.6	11.6	4.44
$[Co(NAU)_2Br_2]$	Bluish green	146	14.1	13.8	38.2	37.8	13.4	13.2	14.5	4.50
$[Co(NAU)_2I_2]$	Dark green	110	11.5	11.6	49.5	49.2	10.9	10.5	15.7	4.55
$[Co(NATU)_2Cl_2]$	Dark green	118	16.3	16.0	19.6	19.1	15.5	15.2	—	—
$[Co(NATU)_2Br_2]$	Bluish green	130	13.1	13.2	35.5	35.6	12.4	12.2	—	—
$[Co(NATU)_2I_2]$	Dark green	136	10.8	10.7	46.6	46.5	10.4	10.1	—	—
$[Ni(NAU)_4Cl_2]$	Yellowish green	159–160	11.1	10.9	13.4	13.4	21.1	20.9	15.9	3.18
$[Ni(NAU)_4Br_2]$	Green	164	9.5	9.1	25.8	25.7	18.1	17.9	17.1	3.20
$[Ni(NAU)_4](ClO_4)_2$	Pale yellow	120	9.0	8.8	10.8	10.5	17.0	17.2	152.6	diamagnetic
$[Ni(NAU)_6](ClO_4)_2$	Yellowish green	142	6.9	6.5	8.3	8.1	18.9	18.2	164.3	3.01

TABLE 2. Spectral bands, assignments, and spectral parameters of Co(II) complexes

Complexes	Band positions (cm^{-1})*	Band assignments (cm^{-1})		Dq (cm^{-1})	B' (cm^{-1})	β_{obs}	λ' (cm^{-1})
		$^4A_{2g} \xrightarrow{(\nu_2)} {}^4T_{1g}(F)$	$^4A_{2g} \xrightarrow{(\nu_3)} {}^4T_{1g}(P)$				
$[Co(NAU)_2Cl_2]$	16 800, 16 000, 15 300(332), 6 000	6 000	15 500	356	721	0.74	126
$[Co(NAU)_2Br_2]$	16 800, 15 600(440), 14 900(520), 5 900	5 900	15 100	344	712	0.73	135
$[Co(NAU)_2I_2]$	16 400, 15 200(560), 14 100(640), 5 800	5 800	14 500	334	685	0.70	142
$[Co(NATU)_2Cl_2]$	16 900(152), 15 600, 14 800(170), 6 000	6 000	15 300	350	720	0.74	—
$[Co(NATU)_2Br_2]$	16 300, 15 300(240), 14 100, 5 900	5 900	14 800	340	700	0.72	—
$[Co(NATU)_2I_2]$	16 000, 15 000(276), 13 800, 5 800	5 800	14 600	334	692	0.71	—

*Molar extinction coefficient values are given in parentheses.

Can. J. Chem. Downloaded from www.nrcresearchpress.com by 210.87.254.5 on 09/05/12
For personal use only.

rates which have the high conductance values expected of 1:2 electrolytes (5). The magnetic susceptibility data are in the expected range of tetrahedral and octahedral complexes of cobalt(II) and nickel(II), respectively. The observed regular increase in moments on proceeding from chloro to iodo complexes is in accord with ligand field theory (19, 20).

Electronic Absorption Spectral Study

Cobalt(II) Halide Complexes

The electronic spectral data and the values chosen for the energies ν_2 and ν_3 together with the values of spectral parameters Dq, B', and β derived therefrom are given in Table 2. The ε_{max} values, color of the complexes, and the magnetic susceptibility data indicate that the complexes have tetrahedral configuration (5, 16). So we have made our assignments and calculations on this basis.

The complexes show the characteristic absorption (ν_3), in the 18 000 – 13 500 cm^{-1} range, assigned to $^4A_{2g} \rightarrow {}^4T_{1g}(P)$ transition; this absorption moves towards lower energy from chloro to iodo complexes. They also exhibit the multicomponent absorption in the 6500–5500 cm^{-1} range assigned to $^4A_{2g} \rightarrow {}^4T_{1g}(F)$ transition. The splittings of the components of ν_2 and ν_3 frequencies are presumably due to distortion from tetrahedral symmetry. The values of the spectral parameters Dq, B', and β are in the expected range for tetrahedral cobalt(II) complexes.

The Dq and B' values of ethylene urea and ethylene thiourea complexes can be compared with the previously known tetrahedral complexes of cobalt(II) from Table 3 and the position of the ligand in the spectrochemical and nephelauxetic series can be suggested.

It is interesting to note that the Dq and B' values of NAU and NATU are similar, suggesting that both have similar donor atoms. Thus the donor site in NAU and NATU may be nitrogen, or in the case of NAU it could be oxygen, because there is very little difference (0.5 unit) in the electronegativity of nitrogen (3.0) and oxygen (3.5) and in their π-bonding character. There are no chances of bonding through sulfur in NATU, as it would have caused considerable difference in the values of Dq and B' because it has the possibility of extensive π-bonding through the vacant d-orbital.

Nickel(II) Halide Complexes

The electronic spectral data and crystal field parameters Dq, B', and β calculated from the positions of ν_1 and ν_3 bands, are shown in Table 4. These assignments are well supported by the excellent agreement between the calculated and experimental values of the ν_2 band, obtained for the transition $^3A_{2g} \rightarrow {}^3T_{1g}(F)$ and also by the constancy of the ratio (3.0) of the values of ν_3 and ν_1. In all our nickel(II) complexes, the band assigned to ν_2 around 14 000 cm^{-1} has a double peak, characteristic of weak field complexes (21–25).

The spectrochemical and nephelauxetic series for the nickel(II) complexes can be represented by a reference to Table 3. The energy of $^3T_{1g}(P)$, as calculated from the positions of the bands for different complexes comes to 14 000 – 15 600 cm^{-1}, whereas the gaseous ion energy of $^3T_{1g}(P)$ for nickel(II) complexes is 15 840 cm^{-1}. From these two values, the nephelauxetic parameter β is calculated and found to be of the same order as other oxygen donors (26, 27).

Nickel(II) Perchlorate Complexes

The electronic spectra of the $[Ni(NAU)_4](ClO_4)_2$ complex (Table 4) exhibits an intense band ν_3 at 24 700 cm^{-1} ($\varepsilon_{max} \approx 7.0$), and a much weaker band of ν_2 at 14 200 cm^{-1} ($\varepsilon_{max} \approx 2.5$) and ν_1 at 8600 cm^{-1} ($\varepsilon_{max} \approx 2.0$). Such a spectrum is indicative of a square-planar complex (9). Thus, the complex possibly has D_{4h} symmetry. Donoghue and Drago (12) have suggested a T_d symmetry for the $[Ni(HMPA)_4](ClO_4)_2$ complex on the basis of its great similarity with the spectrum of $[NiCl_4]^{2-}$. As our spectrum of $[Ni(NAU)_4](ClO_4)_2$ is very much different from the spectrum of $[NiCl_4]^{2-}$, we conclude that tetrahedral symmetry in our case is not likely. This further supports D_{4h} symmetry for the complex.

The perchlorate also forms $[Ni(NAU)_6](ClO_4)_2$ which gives a typical spectrum of octahedral nickel(II) complex (10, 26). Thus, NAU, like ethylene thiourea (13), forms two types of perchlorate complex, one having D_{4h} symmetry, the other O_h.

Spin–Orbit Coupling Constants

An important correlation between spectral and magnetic studies has been obtained by calculating the effective values of the spin–orbit coupling constants (λ') for the cobalt(II) and

Can. J. Chem. Downloaded from www.nrcresearchpress.com by 210.87.254.5 on 09/05/12
For personal use only.

TABLE 3. Spectral parameters of substituted amide and thioamide complexes of Co(II) and Ni(II)

	Cobalt(II) complexes						Nickel(II) complexes						
	$CoCl_2.2L$		$CoBr_2.2L$		$CoI_2.2L$		$NiCl_2.4L$		$NiBr_2.4L$		$Ni(ClO_4)_2.6L$		
Ligands	*Dq*	*B'*	*Dq*	*B'*	*Dq*	*B'*	*Dq*	*β*	*Dq*	*β*	*Dq*	*β*	Reference
ε-Thiocaprolactam	387	651	366	656	340	640	—	—	—	—	—	—	5
Ethylene thiourea	366	717	360	676	347	629	782	0.66	760	0.60	800	0.56	2, 9
2-Thiazolidinethione	364	838	362	815	344	712	—	—	—	—	—	—	3
N-Allyl urea	356	721	344	712	334	685	950	0.89	940	0.88	880	0.81	
N-Allyl thiourea	350	720	340	700	334	692	—	—	—	—	—	—	
γ-Thiobutyrolactam	345	718	345	697	338	631	—	—	—	—	—	—	4
N,N'-Dimethylacetamide	322	797	303	788	307	745	—	—	—	—	769	—	6, 7
Diacetamide	—	—	—	—	—	—	—	—	—	—	900	0.86	8
N-Methyl thiourea	—	—	—	—	—	—	770	0.67	—	—	880	0.38	10
N,N'-Diethylthiourea	—	—	—	—	—	—	870	0.40	870	—	800	0.54	10

TABLE 4. Spectral bands, assignments, and spectral parameters of Ni(II) complexes

		Band assignments (cm^{-1})								
Complexes	Band positions (cm^{-1})*	$^3A_{2g} \xrightarrow{(\nu_1)} {}^3T_{2g}(F)$	$^3A_{2g} \xrightarrow{(\nu_2)} {}^3T_{1g}(F)$ (Obs.)	$^3A_{2g} \xrightarrow{(\nu_2)} {}^3T_{1g}(F)$ (Calcd.)	$^3A_{2g} \xrightarrow{(\nu_3)} {}^3T_{1g}(P)$	$E(P) - E(F)$ (cm^{-1})	*Dq* (cm^{-1})	*B'* (cm^{-1})	*β* (%)	*λ'* (cm^{-1})
$[Ni(NAU)_4Cl_2]$	9 500(2.0), 15 700(2.5), 14 800(4.0), 27 000(6.5)	9 500	15 700	15 709	27 000	15 600	950	936	11.3	298
$[Ni(NAU)_4Br_2]$	9 400(3.5), 15 500(3.8), 14 300, 26 700(9.4)	9 400	15 500	15 530	26 700	15 420	940	932	11.8	307
$[Ni(NAU)_4](ClO_4)_2$	8 600(2.0), 14 800, 14 200(2.5), 24 700(7.0)	—	—	—	—	—	—	—	—	—
$[Ni(NAU)_6](ClO_4)_2$	8 500(3.0), 14 700(3.5), 14 000(4.0), 27 300(4.5)	8 500	14 000	14 051	24 300	14 100	850	854	19.1	210

*Molar extinction coefficient values are given in parentheses.

Can. J. Chem. Downloaded from www.nrcresearchpress.com by 210.87.254.5 on 09/05/12
For personal use only.

TABLE 5. Assignments of infrared bands in NAU and NATU and their complexes (cm^{-1})

Compounds	Medium	N—H st.	Amide I/ thioamide I	Double bond	Amide II/ thioamide II	Amide III/ thioamide III	ν(C=S) + δ(NCS)
NAU	$CHCl_3$	3465(sh)*	1670(s)	1610(m)	1575(m,b)	1330(s)	—
	KBr	3360(m)	1650(s)	1600(m)	1555(s)	1318(s)	—
$[Co(NAU)_2Cl_2]$	KBr	3390(s)	1625(s)	1605(m)	1555(s)	1335(m)	—
$[Co(NAU)_2Br_2]$	KBr	3398(s)	1630(s)	1600(m)	1558(m)	1340(m)	—
$[Co(NAU)_2I_2]$	KBr	3400(sh)	1635(s)	1600(m)	1570(s,b)	1345(m)	—
$[Ni(NAU)_4Cl_2]$	KBr	3300(s)	1622(s)	1605(m)	1560(s)	1338(s)	—
$[Ni(NAU)_4Br_2]$	KBr	3370(s)	1625(s)	1600(m)	1570(s)	1342(s)	—
$[Ni(NAU)_4](ClO_4)_2$	KBr	3340(s)	1618(s)	1600(m)	1560(s)	1340(s)	—
$[Ni(NAU)_6](ClO_4)_2$	KBr	3360(s)	1635(s)	1602(m)	1555(s)	1335(sh)	—
NATU	$CHCl_3$	3530(s)	1642(s)	1660(s)	1300(s)	935(s)	1230(s)
	KBr	3430(s)	1440(m)	1650(s)	1300(s)	928(s)	1228(s)
$[Co(NATU)_2Cl_2]$	KBr	3325(s)	1445(m,b)	1650(s)	1328(w)	935(w,b)	1245(w)
$[Co(NATU)_2Br_2]$	KBr	3328(s)	1448(m,b)	1610(sh,w)	1335(w)	932(w,b)	1248(sh)
$[Co(NATU)_2I_2]$	KBr	3330(s)	1450(m)	1654(s,b)	1340(sh)	930(w,b)	1250(m)

*s = strong; m = medium; w = weak; b = broad; sh = shoulder; st = stretching.

Can. J. Chem. Downloaded from www.nrcresearchpress.com by 210.87.254.5 on 09/05/12
For personal use only.

nickel(II) complexes (10, 12). As shown in Tables 2 and 4, the λ' values for Co(II) complexes are about 70–80% of the free ion value (178 cm^{-1}) and Ni(II) complexes about 70–90% of the free ion value (315 cm^{-1}). The λ' values in complexes appear generally lower than the λ values in the free ions. It is due to orbital overlap, resulting in delocalization of the d-electrons. The position of NAU in the nephelauxetic series also suggests a reasonable degree of delocalization.

Infrared Spectral Study

N-Allyl Urea Complexes

The assignments of various bands of NAU and its complexes are presented in Table 5. Considerable difference in the positions of N—H and C=O stretching frequencies in the solid and solution phase of the spectrum of NAU indicates the presence of intermolecular hydrogen bonding (28). We have, therefore, chosen the spectrum of the ligand in solution for the comparison purpose.

A negative shift of the order of 48 and 20 cm^{-1} in amide I (ν(C=O)) and amide II ($\delta(NH_2)$) bands, respectively, and a positive shift of 15 cm^{-1} in amide III (ν(C—N)) band, suggest that carbonyl oxygen is the donor site, but a negative shift of the order of 165 cm^{-1} in the N—H stretching frequency supports linkage through nitrogen. Similar observations by previous workers in many amine (29) and amide (8) complexes have been interpreted as due to hydrogen bonding between N—H and halogen (29, 30) and not to coordination. A small negative shift of the order of 10 cm^{-1} in the double bond on coordination is probably due to drain of electrons towards oxygen.

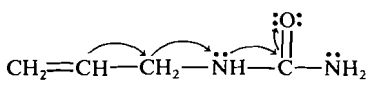

(*N*-allyl urea)

The magnitude of the shift in carbonyl stretching frequency on complex formation is consistent with the order Cl > Br > I for acceptor strength. The magnitude of the shift is higher with Ni(II) complexes, suggesting that the metal–ligand bonding is stronger than that of the Co(II) complexes.

N-Allyl Thiourea Complexes

Comparison of the various assignments of the ligand with those of the complexes (Table 5) shows negative shift of the order of 200 cm^{-1} in N—H stretching frequency, indicating either coordination through nitrogen (3) or hydrogen bonding between the hydrogen of the N—H and halogen of the metal halide (29, 30). However, the bands assigned to thioamide I [ν(C=S) + ν(C—N)] and thioamide II [δ(CH) + δ(NH) + ν(CN)] at 1442 cm^{-1}, respectively, show a positive shift, suggesting coordination through nitrogen. Also, the positive shifts observed in thioamide III [ν(CS) + ν(C'N)] and [ν(C=S) + δ(NCS)] indirectly support our assumption of linkage through nitrogen. This had been well supported from electronic spectral study as well.

The authors wish to express their sincere thanks to the C.S.I.R., New Delhi, for providing financial assistance and to the College authorities for providing research facilities.

1. J. T. Donoghue and R. S. Drago. Inorg. Chem. **2**, 572 (1963).
2. R. L. Carlin and S. L. Holt, Jr. Inorg. Chem. **2**, 849 (1963).
3. P. P. Singh and R. Rivest. Can. J. Chem. **46**, 2361 (1968).
4. S. K. Madan and M. Sulich. Inorg. Chem. **5**, 1662 (1966).
5. S. K. Madan and C. Goldstein. Inorg. Chem. **28**, 1251 (1966).
6. S. K. Madan and A. M. Donohoue. J. Inorg. Nucl. Chem. **28**, 1617 (1966).
7. R. S. Drago, D. W. Meek, M. D. Joesten, and L. Laroche. Inorg. Chem. **2**, 124 (1963).
8. C. S. Kraihanzel and S. C. Grenda. Inorg. Chem. **4**, 1037 (1965).
9. S. L. Holt, Jr. and R. L. Carlin. J. Am. Chem. Soc. **86**, 3017 (1964).
10. R. A. Bailey and T. R. Peterson. Can. J. Chem. **46**, 3119 (1968).
11. J. A. Costamagava and R. Levitus. J. Inorg. Nucl. Chem. **28**, 2685 (1966).
12. J. T. Donoghue and R. S. Drago. Inorg. Chem. **1**, 866 (1962).
13. S. L. Holt, Jr., R. J. Bouchard, and R. L. Carlin. J. Am. Chem. Soc. **86**, 519 (1964).
14. B. N. Figgis and R. S. Nyholm. J. Chem. Soc. 4190 (1958).
15. B. N. Figgis and J. Lewis. Modern coordination chemistry. *Edited by* J. Lewis and R. C. Wilkins. Interscience Publishers, Inc., New York. 1966. p. 403.
16. F. A. Cotton, D. M. L. Goodgame, and M. Goodgame. J. Am. Chem. Soc. **83**, 4690 (1961).
17. Y. Tanabe and S. Sugano. J. Phys. Soc. Jap. **9**, 753 (1954).
18. P. P. Singh and I. M. Pande. J. Inorg. Nucl. Chem. **19**, 591 (1972).
19. F. A. Cotton, O. D. Faut, D. M. L. Goodgame, and R. H. Holm. J. Am. Chem. Soc. **93**, 1780 (1961).

20. R. H. HOLM and F. A. COTTON. J. Am. Chem. Soc. **82**, 2983 (1960).
21. C. K. JØRGENSEN. Acta Chem. Scand. **9**, 1362 (1955).
22. A. RAVI, J. GOPALKRISHNAN, and C. C. PATEL. Ind. J. Chem. **5**, 356 (1967).
23. M. A. ROBINSON, J. D. CURRY, and D. H. BUSCH. Inorg. Chem. **2**, 1178 (1963).
24. A. D. LIEHR and C. J. BALLHAUSEN. Ann. Phys. New York. **6**, 134 (1954).
25. C. J. BALLHAUSEN and A. D. LIEHR. Mol. Phys. **2**, 123 (1959).
26. D. W. MEEK, R. S. DRAGO, and T. S. PIPER. Inorg. Chem. **1**, 285 (1962).
27. H. L. SCHLÄFER and H. P. OPITZ. Electrochem. **65**, 372 (1961).
28. M. DAVIES and H. E. HALLAM. Trans. Faraday Soc. **47**, 1170 (1950).
29. J. CHATT, L. A. DUNCANSON, and L. M. VENANZI. J. Chem. Soc. 2712 (1956).
30. A. NAKAHARA, Y. SAITO, and H. KUROYA. Bull. Chem. Soc. Jap. **25**, 331 (1952).

Can. J. Chem. Downloaded from www.nrcresearchpress.com by 210.87.254.5 on 09/05/12
For personal use only.

Examination of Two Theories for Absorption of Microwave and Far Infrared Radiation by Polar Liquids

M. BENSON, G. D. MARTIN, S. WALKER, J. WARREN, AND R. WILSON

Department of Chemistry and Department of Physics, Lakehead University, Thunder Bay, Ontario

Received September 1, 1971

The far infrared spectra of twenty polar organic liquids have been obtained using a cube interferometer spectrometer. Some new liquids have been examined and some of the previously studied liquids have been re-examined over a wider frequency range and the integrated absorption of the broad band with its peak absorption frequency below about 100 cm^{-1} evaluated, while any contribution from any overlapping higher frequency band has been subtracted. In general, this has not been taken into account in previous such work. Two approaches which have been previously examined to account for the far infrared absorption of such liquids have been tested for a wider variety of liquids and neither mechanism appears to explain quantitatively the observed absorption intensities. Thus the absorption cannot be accounted for by a simple rotational type of mechanism based on Gordon's equation, plus a contribution similar to that which is found in a non polar liquid as has been suggested earlier. In addition, the parameters of the continuous distribution function approach do not match up to those determined experimentally.

Nous avons obtenu le spectre infrarouge lointain de vingt liquides organiques polaires en utilisant un spectromètre à interféromètre cubique. Nous avons examiné quelques nouveaux liquides et quelques liquides déjà étudiés ont été réexaminés sur un plus grand domaine de fréquence; nous avons évalué l'absorption intégrée de la bande large avec la fréquence de son pic d'absorption au-dessous de 100 cm^{-1}, tout en soustrayant la contribution de la bande de fréquence supérieure qui pourrait chevaucher la bande qui nous intéresse. En général, on ne tenait pas compte d'une telle opération dans des travaux précédents. Deux approches qui ont été préalablement étudiées pour tenir compte de l'absorption dans l'infrarouge lointain de tels liquides ont été essayées pour une plus grande variété de liquides et aucun mécanisme ne semble expliquer quantitativement les intensités d'absorption observées. On ne peut donc pas tenir compte de l'absorption par un type simple de mécanisme rotationnel basé sur l'équation de Gordon, plus une contribution semblable à celle qu'on trouve dans un liquide non-polaire, tel qu'il avait été suggéré précédemment. De plus, les paramètres de l'approche à la fonction de distribution continue ne s'accordent pas avec ceux déterminés expérimentalement.

Canadian Journal of Chemistry, **50**, 2610 (1972)

Introduction

Each polar liquid whose far infrared spectrum is reported in the literature has exhibited a band with a maximum somewhere in the 10–100 cm^{-1} region. This type of band which is broad and has a half band width ranging between about 45–90 cm^{-1}, a typical value being about 75 cm^{-1}, has met various interpretations. Some workers have sought to explain it in terms of rotation-like transitions (1, 2), whereas other workers have felt that this absorption may have a translational component (3, 4). A process which involves a collision-induced dipole moment (5) has been identified for non polar liquids which leads to a generally weaker absorption. Hill has examined a model to explain the absorption based on a continuous distribution of resonance frequencies (6); this approach has, however, been tested by only three polar liquids. Rocard (7), Powles (8), and Leroy *et al.* (9) have taken into account the contribution of the inertial term to the Debye absorption. In order to evaluate the full Debye absorption dielectric data are required (*e.g.* see Table 1).

An integrated absorption approach studied by Kroon and van der Elsken (4) and by Davies *et al.* (14) has been tested by only a limited number of polar liquids. Our major aim was to re-examine their approaches (which appeared adequate for their data) with a wider number of polar liquids. Other interesting approaches such as that by Rothschild (15) based on large-size rotational and translational diffusion steps of the polar molecule will not be examined here.

In the approach of Davies *et al.* (14) and also that of Mansingh (16) a band area has been employed to assess a particular theory. We also sought to obtain more accurate band areas and, consequently, where appropriate, corrections have been made for a contribution from an overlapping band due to an intramolecular vibration. In several cases we have re-examined

Can. J. Chem. Downloaded from www.nrcresearchpress.com by 210.87.254.105 on 09/05/12
For personal use only.

Can. J. Chem. Downloaded from www.nrcresearchpress.com by 210.87.254.105 on 09/05/12
For personal use only.

TABLE 1. Observed relaxation time (in ps), static dielectric constant (ε_0), dielectric constant at very high frequency (ε_∞) and average moment of inertia (I_{av} g cm^2 × 10^{40}) for a number of polar liquids

Compound (ref.)	τ	ε_0	ε_∞	I_{ave}
C_6H_5CN (10)	38.5	25.57	3.85	619
$C_6H_5NO_2$ (10)	45.6	35.7	4.07	785
$C_6H_5CH_3$ (11)	5.5	2.3837	2.26_7	404
C_6H_5F (12)	5.4	5.42	2.33_7	404
C_6H_5Cl (12)	11.8	5.56	2.55	616
C_6H_5Br (12)	16.8	5.308	2.62_7	931
C_6H_5I (12)	27.2	4.64	2.76	1155
CH_3CCl_3 (12)	5.8	7.11	2.06	345
$(CH_3)_3CBr$ (13)	6.3	10.41	2.21	412
$(CH_3)_3CCl$ (13)	5.6	10.45	1.95	279
1-$ClC_{10}H_7$ (12)	52.4	5.30	2.67	956

systems reported in the literature where such band overlap occurs where this had not been taken into account in the reported values. Further, the highest frequency employed in the study of Davies *et al.* (14) was 120 cm^{-1}, and since there is often the tail-end of the broad band in this region we have extended the high frequency side to greater than 200 cm^{-1}.

Experimental

The interferograms were recorded on an NPL modular cube interferometer manufactured by Grubb–Parsons. The detector was a Golay pneumatic cell with diamond windows which allow the spectral region from 10–450 cm^{-1} to be investigated. The radiation source was a mercury lamp. Melinex beam-splitters of 25 μ thickness and 6.25 μ thickness provided transparent regions of 10–130 and 130–450 cm^{-1}, respectively. An optical path difference of ±2 mm for both the background and sample interferograms gave a resolution of 5 cm^{-1}. An increased resolution was not deemed necessary because of the broad nature of the absorption. The analog interferograms were converted to digital ones in the form of punched tapes. The spectra were then constructed from the digital interferograms utilizing an IBM 360/50 computer.

All compounds were studied at room temperature (~22 °C) in a variable path cell. The cell windows were polyethylene with a Teflon spacer. A continuously variable path cell with polyethylene windows was used to check the effects of reflections. Quartz windows were used in yet another liquid cell to detect any absorption of the liquid into the polyethylene.

The absorption coefficient (α) was obtained from the intensity against wave number graphs for the background and sample spectra, where α is defined by the equation:

$$[1] \qquad \alpha = \frac{1}{l} \ln \frac{I_0}{I_s}$$

where l is the path length in cm, and I_0 and I_s are the intensities at the particular wave number for the background and sample, respectively.

TABLE 2. The peak absorption (α_{max}), the center (ν_0) and the half width ($\Delta\nu_{1/2}$) of the broad band absorption of the polar liquids at ~22 °C

Molecule	α_{max} (nepers cm^{-1})	ν_0 (cm^{-1})	$\Delta\nu_{1/2}$ (cm^{-1})
C_6H_5F	24	35	80
C_6H_5Cl	17	43	78
C_6H_5Br	13	35	65
C_6H_5I	12	33	64
$C_6H_5NO_2$	77	43	84
C_6H_5CN	93	57	85
$C_6H_5CH_3$	5.6	76	99
o-FC_6H_4F	47	33	72
o-ClC_6H_4Cl	21	45	71
o-BrC_6H_4Br	15	44	56
m-FC_6H_4F	21	51	89
m-ClC_6H_4Cl	12	60	74
CH_3I	101	62	88
$CHCl_3$	18	32	66
$CHBr_3$	8	37	49
CH_3CCl_3	31	27	55
$(CH_3)_3CBr$	48	23	45
$(CH_3)_3CCl$	60	23	45
1-$ClC_{10}H_7$	8.5	50	75

In Table 2 the peak absorption (α_{max} in neper cm^{-1}), the center (ν_0 in cm^{-1}), and half-width ($\Delta\nu_{1/2}$ in cm^{-1}) are listed for the broad band absorption of the polar liquids where any contribution from an intramolecular band has been first subtracted.

For fluoro-, chloro-, and bromobenzene and 1-chloronaphthalene we also measured the absorption at 4.6 cm^{-1} and for chlorobenzene at 2.3 cm^{-1} as well. At both these frequencies a Michelson interferometer technique was employed (17, 18).

The compounds were commercially available and the reagent grade liquids were dried before use.

The moments of inertia for the symmetric top molecules were obtained from microwave spectra. The remaining moments were calculated using appropriate interatomic distances taken mainly from the data compiled by Sutton (19).

Discussion

Two examples of the far infrared spectra of the pure liquids are illustrated in Figs. 1 and 2. The chlorobenzene, as other halobenzenes, has an intramolecular band in the 200 cm^{-1} region.

The integrated absorption (A) was determined for all of the pure liquids by integration of the absorption coefficient (α). The experimental area is given by

$$[2] \qquad A = \frac{1}{N} \int_0^\infty \alpha \, d\nu$$

where N is the number of molecules per cc. The reproducibility of α is about ±5%. In line with

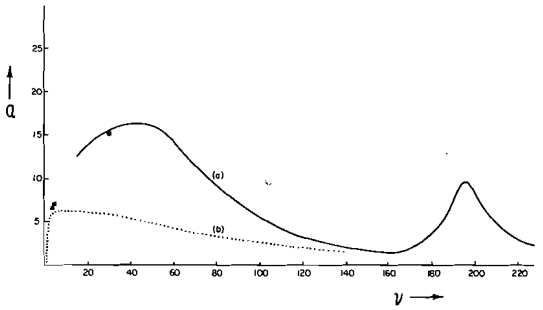

FIG. 1. Far infrared spectrum of chlorobenzene at room temperature (~22 °C): (*a*) observed curve; (*b*) Powles curve: ●, maser point (21) at 29.6 cm^{-1}, ■, microwave points at 2.3 and 4.6 cm^{-1}.

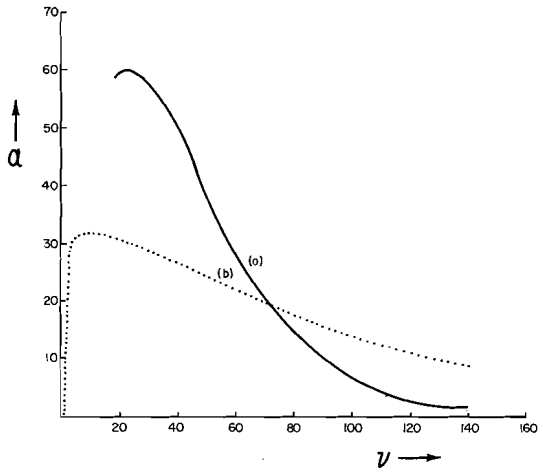

FIG. 2. Far infrared spectrum of *t*-butylchloride at room temperature (~22 °C); (*a*) observed curve, (*b*) Powles curve.

previous workers (10, 14) we have extrapolated α to zero at the low frequency end of the absorption band.

The correction for an overlapping band contribution was obtained by fitting to this band a Lorentz type of function of the form (20):

$$[3] \qquad \ln\left[\frac{I_0}{I_s}\right]_\nu = \frac{a}{(\nu - \nu_{max})^2 + b^2}$$

where

$$\ln\left[\frac{I_0}{I_s}\right]_{\nu_{max}} = \frac{a}{b^2}$$

when

$$[4] \qquad \nu = \nu_{max}$$

and half-band-width $= \Delta\nu_{1/2} = 2b$.

Thus, if we divide eq. 3 by *l*, the cell path length, we obtain from these equations and eq. 1

$$[6] \qquad \alpha = \frac{\alpha_{max}(\Delta\nu_{1/2}/2)^2}{(\nu - \nu_{max})^2 + (\Delta\nu_{1/2}/2)^2}$$

This gave α values for the various ν of the overlapping band. The absorption contribution of this band was then subtracted from the low frequency band, and the remaining area under the lower frequency band was then termed A_{obs} in Table 3.

Of the A_{obs} values in Table 3 seven have been reported also by Mansingh (16), and, on the whole, the agreement between the two sets of values (see Table 3) is reasonable. In the case of toluene Davies *et al.* (14) obtained an A_{obs} of 9.6×10^{-20} cm as opposed to our value of 7×10^{-20} cm. The difference between the two values may be explained by a small contribution from the tail end of an overlapping band, which was not taken account of in their investigation, and of which the highest wave number examined was 120 cm^{-1}. However, in general, comparison of our band data, for cases where there was no appreciable band overlap, yielded similar data (10). Our band center, peak absorption, and half-band-width data are listed in Table 2.

In order to determine how nearly the Debye approach could explain the A_{obs} values for a variety of compounds the *A* values (A_p) have been evaluated from this theory where the contribution to the absorption from the inertial term has been included.

The Rocard and also the Powles treatment, which take this term into account, enable the corresponding Debye type of absorption to be calculated for the far infrared region and lead to an expression from which the loss factor (ε″) may be obtained as a function of frequency. Davies *et al.* (10) showed that for benzonitrile the Rocard and also the Powles treatment led to an almost identical absorption contribution.

The appropriate Powles equation is

$$[7] \qquad \varepsilon'' = \frac{(\varepsilon_0 - \varepsilon_\infty)\omega\tau}{[1 - x(\omega\tau)^2]^2 + (\omega\tau)^2}$$

with

$$[8] \qquad x = \frac{I}{2kT\tau^2}$$

where ε_0, ε_∞ are the static and very high frequency dielectric constants, ω the angular frequency, τ the observed relaxation time, and *I*

Can. J. Chem. Downloaded from www.nrcresearchpress.com by 210.87.254.105 on 09/05/12
For personal use only.

TABLE 3. Integrated absorption data for some polar liquids*

Compound	A_p	A_{obs}	A_g	A_l'	A_l''	ΔA_{PW}	ΔA_0
C_6H_5F	13	32	12	15	12	17	20
C_6H_5Cl	7	21,23†	10	13,14†	10	8,9†	11
C_6H_5Br	5	17,15†	6	9,9†	6	8,6†	11
C_6H_5I	3	19	4	6	4	13	15
$C_6H_5NO_2$	29	114	48	66	47	48	67
C_6H_5CN	24	131	60	82	60	49	71
$C_6H_5CH_3$	0.6	7	1	1	1	6	6
o-FC_6H_4F		55,51†	28	36,36†	29	19,15†	26
o-ClC_6H_4Cl		33,28†	16	22,22†	16	11,6†	17
o-BrC_6H_4Br		18,18†	7	11,17†	7	7,1†	11
m-FC_6H_4F		32,29†	22	29,28†	23	3,1†	9
m-ClC_6H_4Cl		16	11	15,15†	11	1,4†	5
m-BrC_6H_4Br		13,14†	8	11,12†	7	2,2†	6
CH_3I		91	58	79	58	12	33
$CHCl_3$		17	11	15	11	2	6
$CHBr_3$		6	4	5	4	1	2
CH_3CCl_3	19	35	19	24	19	11	16
$(CH_3)_3CBr$	27	47	28	36	29	11	18
$(CH_3)_3CCl$	35	64	38	47	39	17	25
1-$ClC_{10}H_7$	3	16	7	10	6	6	10

*A_{obs} is the experimental value, A_g is the calculated value for the gas phase based on Gordon's equation while A_l' and A_l'' are the values for the corresponding liquid based on the Polo–Wilson and Mecke treatments, respectively. $\Delta A_{PW} = A_{obs} - A_l'$ and $\Delta A_0 = A_{obs} - A_l''$. All the values have been multiplied by 10^{20} and are in cm units.

†Reference 16.

the moment of inertia. From the following equation

$$[9] \qquad \alpha = 2\pi\varepsilon''\nu/n$$

where the corresponding Powles absorption coefficient (termed α_p) may be calculated either by measuring the real part of the refractive index (n) at the wave number (ν) or by assuming it to be 1.6. Davies *et al.* (10) have indicated that n will normally change only some few % between 10 and 100 cm^{-1}. With the exception of the data used for chlorobenzene in Fig. 1 (where the n against frequency data (10) were available), the conversion of ε'' to α values was carried out using a constant value of 1.6 for n. For chlorobenzene the maser point (21) at 29.7 cm^{-1} lies on the experimental curve (Fig. 1) whereas for fluoro- and bromobenzene the maser point (21) lies slightly below. For the maser point to lie on the α against frequency curve for the fluoro- and bromobenzene compounds, the n values would have to be 1.43 and 1.50, respectively. The microwave points at 4.6 cm^{-1} for fluoro-, chloro-, bromo-, and 1-chloronaphthalene appear to lie on the extrapolated far infrared low frequency spectrum and lie either on or very close to the Powles curve which itself passes through the origin. This is illustrated in Fig. 1 for the case of chlorobenzene and the 2.3 cm^{-1} result is also plotted and bears this out.

The data employed in the Powles calculations are given in Table 1. In Figs. 1 and 2 plots of α against frequency (in cm^{-1}) are given for the experimental results and also for the Powles treatment.

For the small fairly spherical molecules with a low moment of inertia such as t-butylchloride (see Fig. 2), the Powles contribution at the very high frequency end of the spectrum lies above the experimental curve and clearly indicates the inadequacy of this treatment for such molecules. The molecules examined here which fall into this category are 1,1,1-trichloroethane, t-butylchloride and bromide.

The approach by Leroy *et al.* (9) using autocorrelation functions leads to similar absorption curves to those by the Powles treatment, the two treatments, of course, being merely different mathematical procedures to calculate the same classical dynamic problem.

It is readily apparent from Figs. 1 and 2 that the Powles treatment cannot account for the total absorption by the liquids at these far infrared frequencies, and as the moment of inertia increases (see Table 1), the discrepancy

Can. J. Chem. Downloaded from www.nrcresearchpress.com by 210.87.254.105 on 09/05/12
For personal use only.

Can. J. Chem. Downloaded from www.nrcresearchpress.com by 210.87.254.105 on 09/05/12
For personal use only.

between the A_{obs} and the A_p values (see Table 3) becomes, in general, more appreciable. In fact, when the compounds are arranged in the sequence of increasing moment of inertia, the ratio of A_{obs}/A_p tends to increase, being 1.8 for *t*-butylchloride and 6.3 for iodobenzene. Benzonitrile and toluene are noticeable exceptions to this sequence, and both have high A_{obs}/A_p ratios for their particular moment of inertia values. Clearly, the Powles type of treatment could in no way account for the A_{obs} values.

Hill (6) and also Davies *et al.* (14) have recently examined two different models by which to interpret the absorption intensity of the broad band. Davies *et al.* (14) and Kroon and van der Elsken (4) have employed integrated absorption approaches to determine the mechanism of the broad band absorption. They treated the molecules in the liquid phase as capable of undergoing rotation and proceeded to compare the integrated absorption with that estimated from Gordon's equation (22) which gives the integrated absorption (A_g) for a molecule undergoing pure rotation in the gaseous phase. This value is then converted into A_l, the corresponding absorption for the liquid phase. For a molecule where the molecular dipole moment (μ_z) lies along a principal axis Gordon's appropriate equation is

$$[10] \quad A_g = \frac{1}{N}\int_0^\infty \alpha \, dv = \frac{\pi}{3c^2}\mu_z^2\left[\frac{1}{I_x}+\frac{1}{I_y}\right]$$

where I_x, I_y are the moments of inertia along the x and y axes which are perpendicular to the z-axis.

Before comparing this calculated value with the observed intensity, one must correct the calculated area for the change in field intensity brought about by the dielectric environment in changing from the gaseous to the liquid state. Three equations have been evolved which enable the calculation of A_l from A_g

$$[11] \quad \frac{A_l'}{A_g} = \frac{1}{n}\left(\frac{n^2+2}{3}\right)^2$$

$$[12] \quad \frac{A_l''}{A_g} = \frac{1}{n}\left(\frac{3n^2}{2n^2+1}\right)^2$$

$$[13] \quad \frac{A_l'''}{A_g} = \frac{(n^2+2)^2(2\varepsilon+1)^2}{9(2\varepsilon+n^2)^2}$$

where n is the refractive index of the liquid and ε its static dielectric constant.

Equation 11 was derived by Polo and Wilson (23) and is the one which, so far, has found the most frequent use in determining A_l. Some workers have felt that it is more generally consistent with experimental observations, and also that the assumptions upon which it is based are more clearly recognized (24). Equation 12 was derived by Mecke (25) and is based upon Onsager's theory. Equation 13 was derived by Hirota (26) and seems to give nearly the same A_l value as the Polo–Wilson equation.

In Table 3 the A_l values are given as calculated from the Polo–Wilson and Mecke equations. The value used for n was n_D where n_D is the refractive index for the sodium-D lines. The n_D values for the organic liquids examined here lie in the 1.4 to 1.6 range, and this is of the same order as the refractive index (n) of the infrared region.

Davies *et al.* (14) examined ΔA values for the broad band absorption of the type

$$[14] \quad \Delta A = A_{obs} - A_l$$

where A_l becomes the A_l' for the Polo–Wilson and A_l'' for the Mecke values respectively. When ΔA is derived from A_l' it will be designated ΔA_{PW} while for the A_l'' case ΔA_0. Davies *et al.* (14) indicated that this absorption can be mainly accounted for by means of the A_l' derived from the value of A_g as deduced from eq. 11 and that the excess absorption ΔA_{PW} for polar liquids is of the same order as the non polar liquid benzene which has a value of 6×10^{-20} cm. This was based on results for only five polar liquids, and of these two had higher ΔA_{PW} values than this. It was suggested that the higher ΔA_{PW} values than that for benzene could be accounted for by a dipole – polarizable molecule interaction. However, the ΔA_{PW} values for fluoro-, chloro-, bromo-, and iodobenzene clearly indicate that a polar effect alone could not explain their values of 17, 8, 8, and 13×10^{-20} cm, respectively, since their dipole moments (27) are all of the same magnitude (1.5 ± 0.1 D) and the polarizability of the fluorobenzene would be least and the iodobenzene the greatest. In fact, of the compounds listed in Table 3 about half of them have ΔA_{PW} values of $\geqslant 11 \times 10^{20}$ cm; that is nearly double or greater than the value of the nonpolar benzene.

The Onsager theory leads to much greater ΔA values. They follow much the same order as

TABLE 4

(*a*) r_+ and r_- values from Hill (6)

g	W	r_+	r_-
1.0	0	1.62	0.62
1.0	0.2	1.64	0.58
1.0	0.4	1.72	0.51
1.0	0.6	1.87	0.44
1.0	0.8	2.09	0.40
0.5	0.6	1.74	0.52
2.0	0.6	2.20	0.32

(*b*) r_+ and r_- values by subtracting the Powles curve from observed curve; r'_+, r'_- from experimental curve

Compound	r_+	r'_+	r_-	r'_-	Compound	r_+	r'_+	r_-	r'_-
C_6H_5F	1.9	2.3	0.35	0.22	$C_6H_5CH_3$	1.7	1.7	0.46	0.34
C_6H_5Cl	1.8	2.0	0.27	0.21	CH_3CCl_3	2.0	2.5	0.38	0.44
C_6H_5I	2.2	2.2	0.32	0.26	$(CH_3)_3CCl$	1.9	2.5	0.41	0.31
C_6H_5Br	2.0	2.0	0.31	0.22					
$C_6H_5NO_2$	2.0	2.3	0.38	0.33	$(CH_3)_3CBr$	2.0	2.3	0.48	0.35
C_6H_5CN	1.6	1.7	0.27	0.23	1-$ClC_{10}H_7$	1.9	1.7	0.28	0.22

ΔA_{PW} but are larger in some cases by a factor of about 1.5. The A''_1/A_g ratio is approximately one for the Mecke equation. Perhaps the main factor from our point of view is that these ΔA_0 values do not offer any more obvious pattern for interpretation than do the ΔA_{PW}.

It is quite apparent from both the ΔA_{PW} and ΔA_0 values in Table 3 that broad band absorption cannot, in general, be accounted for in terms of a simple rotational type of mechanism based on the Gordon equation plus an additional contribution of the type exhibited by nonpolar liquids.

Hill has made a few approaches to account for the far infrared absorption of polar liquids (6, 28, 29). In a recent approach she chose a model based on a continuous distribution of resonance absorptions (6). Two types of distribution functions were examined, a Debye and a Gaussian distribution. The Debye had one adjustable parameter, g (a damping constant), while the Gaussian distribution had two adjustable parameters, g and the width parameter (W). She evaluated integrals involving the two distribution functions for different values of g and W and found that the two types of distributions lead to essentially similar absorption curves. She concluded that the damping parameter of the individual resonances was of the order of unity and characterized her theoretical curves by the following parameters: x_{max} is the frequency at which the absorption is a maximum, x_+ the frequency at which the absorption falls to half its maximum value on the high frequency side and x_- the corresponding frequency on the low frequency side. Further parameters were defined as $r_+ = x_+/x_{max}$, $r_- = x_-/x_{max}$ and the relative frequency of the refractive index minimum $r_{min} = x_{min}/x_{max}$. She then calculated these parameters for the two distribution functions mentioned and compared them with the r_+, r_-, and r_{min} values from the experimental data of the observed minus Powles absorption curves for three polar and two non-polar liquids. The success of the model was assessed in matching up a particular set of the theoretical and experimental values. Unfortunately, we were not in a position to determine r_{min} values.

Our r_+ and r_- values obtained from the observed minus Powles absorption curve are listed in Table 4 as are also the corresponding r'_+ and r'_-, the analogous values which were obtained from the experimental curve itself, since the most recent work of Hill (30) indicates that "no advantage is to be gained by subtracting a Debye tail from the experimentally observed absorption".

We found good agreement for our values of r_+ and r_- with those quoted by Hill for chlorobenzene (1.75 and 0.25) and moderate agreement with her values for toluene (1.5 and 0.42) and 1,1,1-trichloroethane (1.8 and 0.44).

Can. J. Chem. Downloaded from www.nrcresearchpress.com by 210.87.254.105 on 09/05/12
For personal use only.

In the Gaussian distribution for $g = 1.0$ and varying value of W, it can be seen that with increases in the latter r_+ increases while r_- decreases. The width parameter then affects the distribution curve so as to widen it on both sides as W increases in value. What the present data appear to indicate is that the values of "r_+" and "r_-" from the observed spectra vary independently of one another. For example, the experimentally obtained r_+ values of *t*-butylbromide, 1,1,1-trichlorethane, bromobenzene, and nitrobenzene are identical whereas the corresponding r_- values are 0.48, 0.38, 0.31, and 0.38, respectively. The r'_+ values for these compounds are 2.3 ± 0.3 while the r'_- values range between 0.44 and 0.22. For chlorobenzene, benzonitrile, and 1-chloronaphthalene in particular, it appears that the experimentally determined "r" values do not come close to matching up with the theoretical "r" values of either the Debye or Gaussian type of distribution.

It would seem that neither of these two distribution functions can satisfactorily account for the broad band absorption.

1. P. DATTA and G. M. BARROW. J. Chem. Phys. **43**, 2137 (1965).
2. P. DATTA and G. M. BARROW. J. Chem. Phys. **48**, 4662 (1968).
3. M. DAVIES, G. W. F. PARDOE, J. CHAMBERLAIN, and H. A. GEBBIE. Chem. Phys. Lett. **2**, 411 (1968).
4. S. G. KROON and J. VAN DER ELSKEN. Chem. Phys. Lett. **1**, 285 (1967).
5. H. S. GABELNICK and H. L. STRAUSS. J. Chem. Phys. **46**, 396 (1961).
6. N. E. HILL. J. Phys. A. **2**, 398 (1969).
7. Y. ROCARD. J. Phys. Rad. **4**, 277 (1933).
8. J. G. POWLES. Trans. Faraday Soc. **44**, 802 (1948).
9. Y. LEROY, E. CONSTANT, C. ABBAR, and P. DESPLANQUES. Adv. Mol. Relax. Processes. **1**, 273 (1967–68).
10. M. DAVIES, G. W. F. PARDOE, J. E. CHAMBERLAIN, and H. A. GEBBIE. Trans. Faraday Soc. **64**, 847 (1968).
11. A. J. PETRO and C. P. SMYTH. J. Am. Chem. Soc. **79**, 6142 (1957).
12. S. K. GARG and C. P. SMYTH. J. Chem. Phys. **42**, 1397 (1965).
13. Tables of Dielectric Dispersion NBS. 589, No. 1, (1958).
14. M. DAVIES, G. W. F. PARDOE, J. CHAMBERLAIN, and H. A. GEBBIE. Trans. Faraday Soc. **66**, 273 (1970).
15. W. G. ROTHSCHILD. J. Chem. Phys. **53**, 3265 (1970).
16. A. MANSINGH. J. Chem. Phys. **52**, 5896 (1970).
17. W. E. VAUGHAN, W. S. LOVELL, and C. P. SMYTH. J. Chem. Phys. **36**, 535 (1962).
18. S. K. GARG, H. KILP, and C. P. SMYTH. J. Chem. Phys. **43**, 2341 (1965).
19. L. E. SUTTON (*Editor*). Tables of interatomic distances. Chemical Society, London. Spec. Publ. No. 11, (1958).
20. D. A. RAMSAY. J. Am. Chem. Soc. **74**, 72 (1952).
21. J. CHAMBERLAIN, E. WERNER, H. A. GEBBIE, and W. SLOUGH. Trans. Faraday Soc. **63**, 2605 (1967).
22. R. G. GORDON. J. Chem. Phys. **38**, 1725 (1963).
23. S. R. POLO and M. K. WILSON. J. Chem. Phys. **23**, 2376 (1955).
24. A. J. ZELANO and W. T. KING. J. Chem. Phys. **53**, 4444 (1970).
25. R. MECKE. Disc. Faraday Soc. **9**, 1961 (1951).
26. E. HIROTA. Bull. Chem. Soc. Jap. **27**, 295 (1954).
27. A. L. MCLELLAN. Tables of experimental dipole moments. W. H. Freeman and Co., San Francisco. 1963.
28. N. E. HILL. Proc. Phys. Soc. **82**, 723 (1963).
29. N. E. HILL. Chem. Phys. Lett. **2**, 5 (1968).
30. N. E. HILL. J. Phys. C.: Solid St. Phys. **4**, 2322 (1971).

Can. J. Chem. Downloaded from www.nrcresearchpress.com by 210.87.254.105 on 09/05/12
For personal use only.

High Stereoselectivity in the Deuteration of a Primary Carbon L-Threose-4-*d* (4*S*)

A. MARADUFU,[1] D. M. MACKIE,[2] AND A. S. PERLIN
Department of Chemistry, McGill University, Montreal, Quebec

Received March 20, 1972

Chemical synthesis of a deuterated primary carbinol, L-threose-4-*d* (4*S*), has been effected with virtually complete stereoselectivity. It involves deuteride reduction of 2,3,4,6-tetra-*O*-acetyl-α-D-glucopyranosyl bromide, conversion of the resulting 1,5-anhydride-1-*d* into the corresponding 4-deoxy-6-*aldehydo*-hex-4-ene derivative, and then ozonolysis, without deuterium scrambling. In this way, C-4 and stereoselectively-deuterated C-1 of the hexose have been interconverted to become, respectively, C-1 and stereoselectively-deuterated C-4 of the L-threose molecule. This study also furnishes support for previous evidence that D-galactose oxidase catalyzes removal of the *pro-S* 6-hydrogen atom of D-galactose.

La synthèse chimique du carbinol deutérié primaire L-thréose-4-*d* (4*S*), a été réalisée avec une stéréosélectivité pratiquement totale. Cette synthèse comprend: la réduction par le deutérure du bromure de tétra-*O*-acétyl-2,3,4,6-α-D-glucopyranosyle, la conversion de l'anhydride-1,5-1-*d* résultant en dérivé déoxy-4 *aldéhydo*-6 hexène-4 correspondant et enfin l'ozonolyse sans modification sur le deutérium. Ainsi, le C-4 et le C-1, deutérié de façon stéréosélective de l'hexose, ont été interconvertis pour donner respectivement C-1 et C-4 deutérié sélectivement, dans la molécule de L-thréose. Cette étude vient à l'appui de la preuve précédente pour laquelle le D-galactose oxydase catalyse l'enlèvement de l'atome d'hydrogène-6 *pro-S* du D-galactose.

Canadian Journal of Chemistry, **50**, 2617 (1972)

Deuterated (or tritiated) compounds are used widely for the investigation of biological reaction mechanisms (1–6). Usually, highly stereoselective[3] deuteration may be achieved at a secondary position by the use of well-established chemical procedures (5, 6). At a primary position, however, the degree of selectivity is invariably much lower (5, 6), although the enzymatic reduction of aldehydes has been utilized for the preparation of a number of specifically[3] deuterated carbinols (8). The current paper reports *chemical* synthesis of a deuterated primary carbinol of virtually complete optical purity. This compound is L-threose-4-*d* (4*S*) (**1**), its synthesis having been carried out as part of a recent study (9) on the stereochemistry of H-6 abstraction from the homomorphous D-hexose, D-galactose, by D-galactose oxidase.

Scheme 1 shows the reaction sequence utilized in the synthesis of **1**. In the first step, 2,3,4,6-tetra-*O*-acetyl-α-D-glucopyranosyl bromide was reduced (10) with lithium aluminum deuteride with concomitant de-*O*-acylation to 1,5-anhydro-D-glucitol-1-*d* (**2**). In accord with the known characteristics of nucleophilic displacement reactions at C-1 of glycosyl halides (*e.g.* refs. 11–13), as well as of the deuteride reduction of 1,2-*cis*-tri-*O*-acetyl-pentopyranosyl bromides (14), it was to be expected that the deuterium atom would be incorporated with inversion,[4] *i.e.*, equatorially in this instance. The stereochemistry of the reaction was confirmed by the fact that **2** produced only one H-1 resonance signal (Fig. 1; **2** tetraacetate) and that this signal appeared as a doublet of 9.8 Hz consistent with the axial coplanar disposition of H-1 with respect to axial H-2 (16).

Compound **2** was converted into the 6-*O*-trityl ether, then acetylated and de-tritylated, affording triacetate **3** in which the primary carbinol group is unsubstituted. As shown previously (17, 18), **3** should undergo oxidation and elimination when treated with methyl sulfoxide in the presence of triethylamine and sulfur trioxide (19). Accordingly in the current instance it gave the deuterated α,β-unsaturated aldehyde **4**. Ozonolysis of **4** then effected ring cleavage and led to generation of the desired tetrose-4-*d* (**1**), which was converted into its crystalline α-triacetate (**6**).

Although ozonolysis was expected to yield an *O*-glyoxalyl ester (**5**) as an intermediate, the

[1]C. B. Purves Scholarship Holder, 1970–1972.

[2]NRCC Scholarship Holder, 1969–1971.

[3]The terms "stereoselective" and "stereospecific" are used here in the sense defined by Mislow (7).

[4]Stereoselective deuteration in this manner by reduction of alkyl halides is well known (5, 6, 15).

Can. J. Chem. Downloaded from www.nrcresearchpress.com by 210.87.254.40 on 09/05/12
For personal use only.

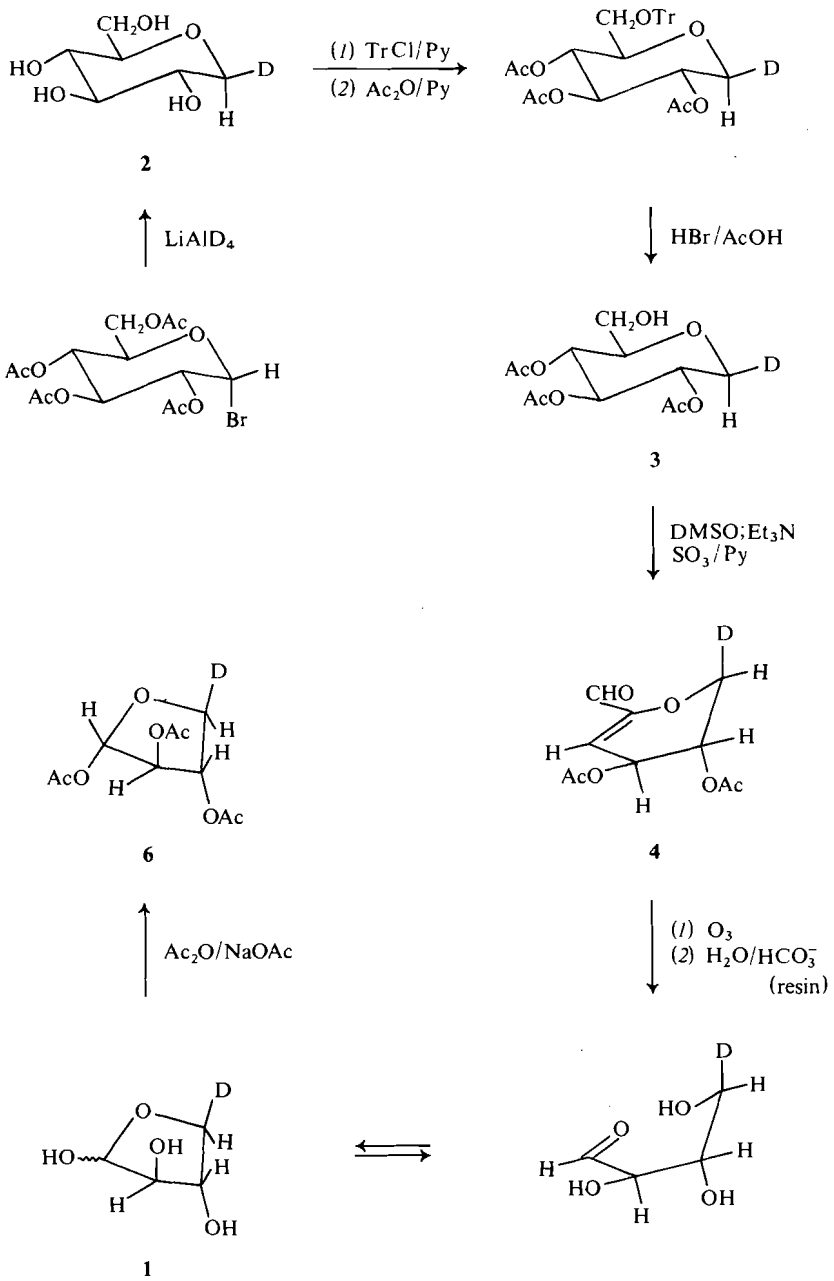

2 3 4 6 1

SCHEME 1

only product isolated was **1** itself, *i.e.*, complete de-esterification took place. *O*-Acetyl groups are stable towards ozone (see *e.g.* ref. 20), but it is possible that the *O*-glyoxalate moiety suffered oxidation, because the reaction mixture invariably became strongly acidic; presumably, this acidity accounted for hydrolysis of the ester groups during subsequent work-up. It may be noted also that attempts to obtain **1** via cleavage of the double bond of **4** with osmate–periodate (21) were unsuccessful.

A comparison of the p.m.r. spectrum of 1,2,3-tri-*O*-acetyl-α-L-threofuranose-4-*d* (4*S*) (**6**) with that of the unlabelled compound shows that

Can. J. Chem. Downloaded from www.nrcresearchpress.com by 210.87.254.40 on 09/05/12
For personal use only.

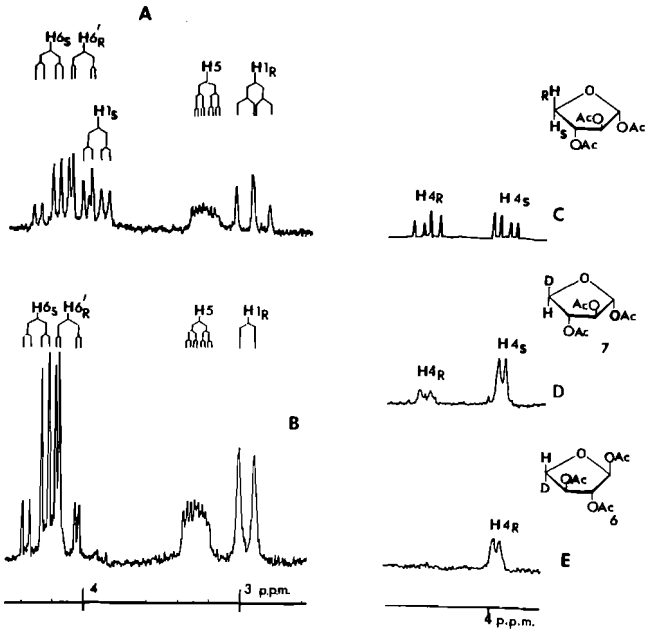

FIG. 1. Partial p.m.r. spectra of (A) 2,3,4,6-tetra-*O*-acetyl-1,5-anhydro-D-glucitol (24) and (B) 2,3,4,6-tetra-*O*-acetyl-1,5-anhydro-D-glucitol-1-*d* (1*S*) (**8**) in benzene-d_6; (C) 1,2,3-tri-*O*-acetyl-α-D-threose, (D) 1,2,3-tri-*O*-acetyl-α-D-threose-4-*d* (4*R*, 4*S*), and 1,2,3-tri-*O*-acetyl-α-L-threose-4-*d* (4*S*), in chloroform-*d*.

one of the H-4 signals is completely (within the limits of detection) eliminated by deuteration (Fig. 1). Accordingly the H-4 signal at 4.0 p.p.m. appears in the spectrum of **6** as a doublet slightly broadened by deuterium coupling. This shows that the high degree of stereoselectivity effected in the initial, deuteride reduction step, is retained during the succeeding transformations. Furthermore, the assignment of an *S*-configuration at C-4 is in harmony with the stereochemistry of 1,2,3-tri-*O*-acetyl-α-D-threofuranose-4-*d* synthesized previously as unequal mixtures of 4 *R* and 4 *S* isomers (9). That is, the p.m.r. spectrum (Fig. 1) of the predominantly *R* isomer (**7**) much more closely resembles that of **6**, with which it should be enantiomeric, than does the spectrum of the predominantly *S* isomer (9). Hence the synthesis of **6**, by providing an independent proof of the configuration at C-4 of **7**, also serves to support previous conclusions about the stereochemistry of the dehydrogenation of D-galactose by D-galactose oxidase.

Experimental

P.m.r. spectra were recorded with a Varian HA-100 spectrometer, using tetramethylsilane as an internal reference. T.l.c. was carried out with silica gel (Macherey Nagel) as adsorbent and with the solvents indicated below. Solvents were dried over sodium. Melting points are uncorrected.

*1,5-Anhydro-*D*-glucitol-1-d (1S) (***2***)*

The procedure of Ness *et al.* (10) was used. 2,3,4,6-Tetra-*O*-acetyl-α-D-glucopyranosyl bromide (34.0 g) in benzene (5 ml) and ether (400 ml) was added to a stirred suspension of lithium aluminum deuteride (10 g; 99% deuterium) in ether (100 ml) maintained under gentle reflux. When the reaction had been completed (t.l.c., benzene : ether (1 : 1)), the excess deuteride was decomposed with ethyl acetate, followed by water, and then more water (300 ml) was added. The ether layer was decanted off, and the aqueous layer was clarified by centrifugation, de-ionized with Amberlite-IR-120 (H^+) and Dowex-(HCO_3^-) exchange resins, and concentrated. A thick syrup was obtained; when dried through azeotrope-formation with benzene : ethanol, it solidified (yield, 11.2 g); after recrystallization from methanol : ether, m.p. 145–147°, $[\alpha]_D$ +43° (*c*, 2 water), (lit. (10), non-deuterated, m.p. 141–142°, $[\alpha]_D$ +42.5°).

*2,3,4-Tri-O-acetyl-6-O-trityl-1,5-anhydro-*D*-glucitol-1-d (1S)*

To a solution of the deuterated anhydride (2) (7.0 g) in pyridine (25 ml), triphenylchloromethane (13.0 g) was added and the solution was heated with stirring at 45–50° for 12 h (reaction complete according to t.l.c.; *n*-propanol : ethyl acetate : water (3 : 2 : 1)). Pyridine (20 ml) and acetic anhydride (30 ml) were introduced to the cooled solution, and after 48 h at room temperature the solution was poured onto ice, diluted with chloroform, and the chloroform layer washed successively with 2 *N* hydrochloric acid, saturated sodium bicarbonate, and water. The dried chloroform extract afforded a syrup which was purified by

Can. J. Chem. Downloaded from www.nrcresearchpress.com by 210.87.254.40 on 09/05/12
For personal use only.

chromatography on a column of silica gel (benzene:ether: petroleum ether 65–110° (1:3:5) as eluent), and crystallized from ethanol; m.p. 93–95 °C, $[\alpha]_D$ +69° (*c*, 3 chloroform) (lit. (18), non-deuterated, m.p. 92–93°, $[\alpha]_D$ +82° (*c*, 3 pyridine).

*2,3,4-Tri-O-acetyl-1,5-anhydro-*D*-glucitol-1-d (1S) (**3**)*

De-*O*-tritylation of the preceding compound (7.0 g) was effected by brief treatment with cold hydrobromic acid (32% in acetic acid), which yielded **3** (3.2 g), m.p. 113–114 °C, $[\alpha]_D$ +37° (*c*, 4 chloroform), (lit. (18), non-deuterated, m.p. 111–113°, $[\alpha]_D$ 49° (*c*, 3 chloroform).

*4,5-di-O-acetyl-2,6-anhydro-3-deoxy-aldehydo-*L*-threo-hex-2-enose-6-d (**4**)*

The triacetate (**3**) (0.6 g) was dissolved in methyl sulfoxide (8 ml), triethylamine (2.6 ml) was added followed by a solution of sulfur trioxide–pyridine (2.6 g) in methyl sulfoxide (8 ml). The mixture was shaken for 10 min, cooled in an acetone–CO_2 bath, diluted with chloroform, and the chloroform solution was washed successively with cold 2 *N* hydrochloric acid, saturated sodium bicarbonate, and water. Evaporation of the solvent afforded an oil (0.30 g) which was purified by chromatography on silica gel (eluent, benzene:ether (9:1); $[\alpha]_D$ +189° (*c*, 0.4 chloroform); 2,4-dinitrophenylhydrazone, m.p. 177–179°, undepressed by admixture with a non-deuterated specimen (18). (A higher melting form (m.p. 185–186°) of the hydrazone has also been prepared in this laboratory (18), and it is indistinguishable from the lower melting material by i.r. and p.m.r. spectroscopy.)

*Ozonolysis of **4**. Preparation of **6***

Ozone (Welsback generator) was bubbled into a solution of **4** (0.13 g) in cold (acetone–CO_2) ethyl acetate at an oxygen rate of 0.5 l/min for 15–20 min (t.l.c., benzene:ether (1:1)) at which time **4** was absent. Evaporation of the solvent left an acidic syrup (0.15 g) (sparingly soluble in chloroform) which was triturated in water (2 ml) and then left with stirring for 10 h. After neutralization with Dowex-1 (HCO_3^-) ion exchange resin, the solution was shown chromatographically to contain a major product, travelling at the rate of D-threose (solvent, *n*-propanol:ethyl acetate: water (3:2:1)); minor components, presumably partially acetylated derivatives of threose, were also detected. The solution was lyophilized, benzoyl chloride and pyridine at 0° were added to the residue, and the benzoylation product was purified by chromatography on silica gel (eluent, benzene:ether (9:1)),(yield, 30 mg) and then by crystallization from ethanol; m.p. 175–178°; (1,2,3-tri-*O*-benzoyl-α-D-threofuranose has m.p. 178–180°, $[\alpha]_D$ 0° (*c*, 5 chloroform)).

In another ozonolysis experiment, carried out for 10 min, a lower proportion of free tetrose was obtained (yield 48 mg from 150 mg of **4**). The crude product was acetylated with acetic anhydride/sodium acetate affording, after purification by chromatography on silica gel as above and crystallization from ethanol, 1,2,3-tri-*O*-acetyl-α-L-threofuranose-4-*d* (**6**) m.p. 121–122°, $[\alpha]_D$ −26° (*c*, 0.4 chloroform); (1,2,3-tri-*O*-acetyl-α-D-threofuranose has m.p. 120–122°, $[\alpha]_D$ +34° (22)). Benzoylation of the crude ozonolysis product afforded material which, according to p.m.r. spectroscopy, appeared to be mono-*O*-benzoyl-di-*O*-acetyl-α,β-L-threose.

*Oxidation of **4** with Osmium Tetroxide–Periodate*

Attempts were made to obtain **6** via cleavage of the double bond of **4** with osmium tetroxide–sodium periodate (21). Two sets of conditions were examined: *i.e.*, according to ref. 21 using ether as the solvent, and to ref. 23 using dioxane:*t*-butanol:water as solvent. In each instance, the reaction was very slow (48–72 h, as shown by t.l.c. examination) and a dark syrupy product, possibly containing osmate ester, was isolated. The p.m.r. spectrum of the product was poorly resolved and suggestive of a mixture of components.

*2,3,4,6-Tetra-O-acetyl-1,5-anhydro-*D*-glucitol-1-d (1S) (**8**)*

Compound 2 was acetylated in acetic anhydride–pyridine. Evaporation of excess acetic anhydride and pyridine gave a syrup which crystallized in ether–petroleum ether (b.p. 30–60°). Recrystallization in the same solvent afforded crystals m.p. 73–75°, $[\alpha]_D$ +40.2° (*c*, 2 chloroform), (lit. (25), non-deuterated), m.p. 73–74° $[\alpha]_D$ +38.9° (c, 2 chloroform).

The authors express their gratitude to the Pulp and Paper Research Institute of Canada and to the National Research Council of Canada for generous support. Sincere thanks are due also to Dr. H. J. Koch and R. Simoneau for recording the p.m.r. spectra, and to G. Suranyi for kindly providing facilities for the generation of ozone.

1. H. R. Levy, P. Talalay, and B. Vennesland. *In* Progress in stereochemistry. Vol. 3. *Edited by* P. B. D. de la Mare and W. Klyne. Butterworth, Washington, D.C. 1962. p. 299.
2. S. Englard and K. R. Hanson. *In* Methods in enzymology. Vol. 13. S. P. Colowick and N. O. Kaplan, Editors. Academic Press, New York, N.Y. 1969. p. 567.
3. I. A. Rose. Ann. Rev. Biochem. **35**, 23 (1966).
4. J. W. Cornforth and G. Ryback. Ann. Repts. (Progr. Chem.) **62**, 428 (1965).
5. D. Arigoni and E. L. Eliel. *In* Topics in stereochemistry. Vol. 4. *Edited by* N. L. Allinger and E. L. Eliel. Interscience, New York, N.Y. 1969. p. 127.
6. L. Verbit. Prog. Phys. Org. Chem. **7**, 51 (1970).
7. K. Mislow. *In* Introduction to stereochemistry. Benjamin, New York, N.Y. 1966. p. 128, 137.
8. V. E. Althouse, K. Ueda, and H. S. Mosher. J. Am. Chem. Soc. **82**, 5938 (1960).
9. A. Maradufu, G. M. Cree, and A. S. Perlin. Can. J. Chem. **49**, 3429 (1971).
10. R. K. Ness, H. G. Fletcher, Jr., and C. S. Hudson. J. Am. Chem. Soc. **72**, 4547 (1950).
11. R. U. Lemieux. Adv. Carbohydr. Chem. **9**, 1 (1954).
12. L. J. Haynes and F. H. Newth. Adv. Carbohydr. Chem. **10**, 207 (1955).
13. F. Micheel and A. Klemer. Adv. Carbohydr. Chem. **16**, 85 (1961).
14. H. R. Greenberg and A. S. Perlin. Unpublished results.
15. G. K. Helmkamp and B. F. Rickborn. J. Org. Chem. **22**, 479 (1957).
16. R. U. Lemieux, R. K. Kullnig, H. J. Bernstein, and W. G. Schneider. J. Am. Chem. Soc. **80**, 6098 (1958).
17. G. M. Cree, D. M. Mackie, and A. S. Perlin. Can. J. Chem. **47**, 511 (1969).
18. D. M. Mackie and A. S. Perlin. Carbohydr. Res. In press.

Can. J. Chem. Downloaded from www.nrcresearchpress.com by 210.87.254.40 on 09/05/12
For personal use only.

19. J. R. PARIKH and W. DOERING. J. Am. Chem. Soc. **89**, 5505 (1967).
20. P. DESLONGCHAMPS and C. MOREAU. Can. J. Chem. **49**, 2465 (1971).
21. R. PAPPO, D. S. ALLEN, R. U. LEMIEUX, and W. S. JOHNSON. J. Org. Chem. **21**, 478 (1956).
22. A. S. PERLIN and C. BRICE. Can. J. Chem. **34**, 541 (1956).
23. B. RADATUS, M. YUNKER, and B. FRASER-REID. J. Am. Chem. Soc. **93**, 3086 (1971).
24. A. G. PERKIN and Y. UYEDA. J. Chem. Soc. **121**, 66 (1922).
25. N. K. RICHTMYER and C. S. HUDSON. J. Am. Chem. Soc. **65**, 64 (1943).

Can. J. Chem. Downloaded from www.nrcresearchpress.com by 210.87.254.40 on 09/05/12
For personal use only.

Coordination Compounds of Indium. Part XV.[1] The Stability Constants of some Trifluoromethyl-β-diketonate Complexes of Indium (III)

KEITH BOWDEN,[2] (MRS.) G. M. TANNER, AND D. G. TUCK
Department of Chemistry, Simon Fraser University, Burnaby 2, British Columbia

Received March 7, 1972

The stability constants K_1 and K_2 have been measured for the interaction of indium(III) with the ligands $R{\cdot}CO{\cdot}CH_2{\cdot}CO{\cdot}CF_3$ (R = 2-furyl, 2-thienyl, phenyl, 2-naphthyl, *i*-butyl, and *t*-butyl). The pK_a values for these compounds, and for R = 3-pyridyl and methyl, are also reported. A conventional potentiometric technique was used; the results refer to 46% aqueous acetone, at an ionic strength of approximately 0.1 *M*. The results are compared with published values for complexes of these ligands with divalent cations in other solvent systems.

Les constantes de stabilité K_1 et K_2 ont été mesurées pour l'interaction de l'indium(III) avec les ligands $R{\cdot}CO{\cdot}CH_2{\cdot}CO{\cdot}CF_3$ (R = furyl-2, thienyl-2, phenyl, naphthyl-2, isobutyl, et *t*-butyl). Les valeurs des pK_a de ces composés et pour R = pyridyl-3 et méthyle, ont été rapportées. La technique potentiométrique courante a été utilisée, les résultats ayant pour référence l'acétone aqueuse à 46%, à une force ionique de 0.1 *M* approximativement. Les résultats sont comparés aux valeurs publiées pour les complexes de ces ligands avec des cations divalents dans d'autres systèmes de solvants.

Canadian Journal of Chemistry, **50**, 2622 (1972)

The mechanism of the ligand exchange reaction

$$[1] \qquad In(L^-)_3 + L \rightarrow In(L^-)_3 + L$$

in a series of organic solvents has recently been investigated in this laboratory by n.m.r. techniques (1), using a number of 1,1,1-trifluoromethyl-β-diketonate ligands, **1**, $(CF_3{\cdot}CO{\cdot}CH{\cdot}CO{\cdot}R)^-$. The free energy of activation for the exchange, and hence the rate of exchange, depends both on the particular solvent chosen and on the nature of the terminal group R (= methyl, *i*-butyl, phenyl, 2-naphthyl, 2-furyl, or 2-thienyl).

One possible mechanism for the exchange process [1] would involve dissociation of the complex into free ligand (or ligand anion) and a residue of lower coordination number. In order to investigate the significance of such processes, we have now measured the stability constants of a series of these chelate complexes. Results have been obtained for the pK_a of the diketones themselves, and for the first and second stability constants using a simple potentiometric titration method; it proved impossible to obtain reproducible values for K_3 due to the chemical instability of the parent diketones in strongly alkaline solution (see below). Measurements have been carried out for the ligands listed above, and for R = 3-pyridyl and *t*-butyl. A number of solvents and solvent mixtures were examined in preliminary experiments, with approximately 50% aqueous acetone proving the most satisfactory in terms of solubility for both ligands and indium complexes.

There are relatively few references in the literature to stability constant measurements with these ligands, and none referring to complexes of Group IIIA cations. The ligand most widely studied has been 1,1,1-trifluoro-4(2-thienyl)-2,4-butanedione (TTA; **1**, R = 2-thienyl), presumably because of the well established use of this compound in solvent extraction. Of special interest, however, are the studies of Van Uitert *et al.* (2) on the stability constants for the reaction of Ba^{2+}, Cu^{2+}, and Ni^{2+} with four of the ligands studied by us (**1**; R = methyl, naphthyl, thienyl, and furyl). Their results show many of the same general features found in the present work.

Experimental

Materials

All the trifluoromethyl-β-diketonates were obtained from Eastman Organic Chemicals and were used as supplied. Acetone was Analytical Grade material.

Tetraethylammonium perchlorate was prepared by mixing hot aqueous solutions of tetraethylammonium bromide and sodium perchlorate, and recrystallized from water.

A weighed amount of indium metal (~1 mmol) was dissolved in concentrated aqueous hydrochloric acid, and the resultant solution evaporated to yield $InCl_3 \cdot \sim 3H_2O$. This material was dissolved in 10 ml of 0.1 *M* perchloric acid in the preparation of the titration solution.

[1]For Part XIV, see ref. 11.

[2]Permanent address: Department of Chemistry, University of Essex, Colchester, England.

Can. J. Chem. Downloaded from www.nrcresearchpress.com by 210.87.254.42 on 09/05/12
For personal use only.

TABLE 1. pK_a values for some 1,1,1-trifluoromethyl-β-diketones in aqueous acetone

R	pK_a	Literature values	pK_a for $CH_3 \cdot CO \cdot CH_2 \cdot CO \cdot R$[a]	pK_a for RCOOH in water[b]	pK_a for RCOOH in 80% methyl cellosolve[c]
3-Pyridyl	4.81	—	—	(4.82)	5.56
Methyl	5.81	6.7[d] 8.7[e]	12.70	4.75	6.84
2-Furyl	5.82	5.40[f] 8.5[e]	—	3.13	5.53
2-Thienyl	5.90	5.70[g] 6.18[h] 9.1[e]	12.35	3.53	5.97
Phenyl	6.17	9.2[i]	12.85	4.20	6.65
2-Naphthyl	6.24	6.35[g] 9.3[g]	—	4.16	6.54
i-Butyl	6.65	—	—	4.79	7.33
t-Butyl	7.65	—	14.20	5.05	7.76

[a]Reference 3: 75% dioxan, 30°.
[b]Reference 4.
[c]Reference 5.
[d]Reference 6: 50% dioxan, 20°.
[e]Reference 2: 75% dioxan, 30°.
[f]Reference 7: 75% dioxan, 20°, ionic strength ~0.1; ref. 7*b* is also quoted in ref. 8, p. 577.
[g]Reference 7*a*: 75% dioxan (corr. to H_2O), 20°, ionic strength ~0.1.
[h]Reference 9: 25°, ionic strength → 0; also quoted in ref. 8, p. 590.
[i]Reference 10: 75% dioxan, 30°.

Apparatus and Procedures

For measurements of pK_a, pH changes were recorded with a Corning Model 10 pH meter and a glass electrode, calibrated for work in aqueous acetone. Solutions were thermostated to 25 ± 0.2°. The results so obtained (Table 1) refer to ~0.1 *M* ionic strength tetraethylammonium perchlorate in 46% aqueous acetone (by volume) at a diketone concentration of 0.02 *M*.

The bulk phase in the stability constant measurements was 90 ml acetone, 100 ml aqueous (0.2 *M*) tetraethylammonium perchlorate solution, and 10 ml 0.1 *M* aqueous perchloric acid containing 1 mmol In(III) as the hydrated chloride. This mixture was titrated with an acetone solution of the ligand, previously neutralized with concentrated aqueous tetraethylammonium hydroxide solution and made up to 10 ml with acetone. The mid-point of the titration curve therefore refers to a solution of approximately 0.1 *M* total ionic strength, in 46% aqueous acetone (by volume).

Van Uitert *et al.* (2) have commented on the low chemical stability of 1,1,1-trifluoromethyl-β-diketones, and the experimental problems resulting from this instability, which they ascribe to hydrolysis. While this fission reaction is likely to be of general importance for the diketones, we observed that in the case of the methyl compound, the addition of excess tetraethylammonium hydroxide to an acetone solution of the diketone produced a red oil, and we were therefore unable to carry out any stability constant measurements with this ligand. This red product probably arises from an intermolecular base-catalyzed condensation between the acidic methyl group and the highly electrophilic carbonyl group α to the trifluoromethyl group. Following Van Uitert *et al.*, all measurements were carried out as rapidly as possible but despite this, results at high pH were irreproducible and no K_3 values could be obtained in highly alkaline solution.

Calculation of Results

In the first series of experiments, pK_a values were obtained graphically; duplicate experiments agreed to ±0.02 pK units.

The potentiometric results in the stability constant experiments were treated by a least-squares computer program (IBM 360/50) to give values of $\bar{n}$, the average ligand number, and hence β_1 and β_2. No significant changes were found when values of β_1 and β_2 were computed after removing those experimental values, showing high deviations in the least-squares analysis. The values in Table 2 are the mean of at least two determinations, and are assigned a probable error of ±0.05 units.

TABLE 2. Stability constants for indium(III) complexes of some 1,1,1-trifluoromethyl-β-diketonates

R	log K_1	log K_2
2-Furyl	5.93	5.45
2-Thienyl	5.97	5.76
Phenyl	5.85	5.95
2-Naphthyl	6.93	6.65
i-Butyl	6.78	6.40
t-Butyl	6.85	6.56

Can. J. Chem. Downloaded from www.nrcresearchpress.com by 210.87.254.42 on 09/05/12
For personal use only.

Can. J. Chem. Downloaded from www.nrcresearchpress.com by 210.87.254.42 on 09/05/12
For personal use only.

Results and Discussion

pK_a Measurements

The pK_a values for the trifluoromethyl diketones studied are given in the Table 1, together with earlier results in the literature, and relevant data for other acidic compounds containing the same substituent groups.

We note first that the pK_a values of β-diketones are strongly dependent on the solvent involved; Van Uitert *et al.* (10) have published graphs showing the changes in the measured pK_a with composition in water:dioxane mixtures. In view of this, a detailed comparison of our results with those of other workers is not productive, but we note that the order of pK_a values is the same in both columns 2 and 3 of Table 1, with the sole exception of the methyl/furyl pair. The differences here are however small, and this apparent anomaly may well arise from errors in the measurements for $CF_3 \cdot CO \cdot CH_2 \cdot CO \cdot CH_3$ due to the instability of this compound in alkaline solution (see Experimental section). Similar comments apply to the comparison of the present pK_a results with the values for the $CH_3 \cdot CO \cdot CH_2 \cdot CO \cdot R$ diketones (column 4, Table 1).

Table 1 also shows that the various substituent groups investigated have substantially parallel effects on the pK_a's of $CF_3 \cdot CO \cdot CH_2 \cdot CO \cdot R$, $CH_3 \cdot CO \cdot CH_2 \cdot CO \cdot R$, and $R \cdot COOH$ over the relatively small range of values involved. Such linear correlations are to be expected, provided that there are no other compensating effects. The results in Table 1 refer to a range of aliphatic, aromatic, and heterocyclic substituents, so that a strictly linear relationship between the present results and the values in columns 5 and 6 of Table 1 would be unlikely. It is, however, of interest to note that the pK_a values of the $CF_3 \cdot CO \cdot CH_2 \cdot CO \cdot R$ compounds do in fact depend significantly on the nature of R. This suggests that the structure of the anion involves considerable distribution of the negative charge onto all three possible sites (*i.e.*, the central carbon atom and both oxygens), despite the presence of the very strongly electron-withdrawing trifluoromethyl group, which might have been expected to localize the anionic charge on sites proximate to this group.

Stability Constant Measurements

The stability constants K_1 and K_2 obtained in the present experiments are shown in Table 2. It is clear that all the complexes are thermodynamically very stable; the log β_2 values are in the range 11–13, from which one may reasonably deduce that log $\beta_3 > 15$. The implications of this finding for the kinetic studies are discussed elsewhere (1). As in other studies with these trifluoromethyl-β-diketones (2), the K_2 values are only slightly smaller than those for K_1. The experimental errors for K_2 are greater than for K_1, since the former arise from experimental results in alkaline conditions, where ligand decomposition is an important consideration. For the phenyl compound, we find K_2 slightly larger than K_1; this is almost certainly an artefact arising from the reasons just outlined.

It is instructive to compare the results in Table 2 with those reported for the interaction of some of these ligands with Ba^{2+}, Ni^{2+}, and Cu^{2+} (2) (see Table 2). A dependence of, for example, pK_1 on pK_a is generally found in such studies; in particular, the stability constants of β-diketonate complexes show a monotonic increase with pK_a for a variety of alkyl and aromatic terminal groups, over a pK_a range of 6–14 (and a corresponding pK_1 range, for Ni^{2+}, of 4–12). Within this wide range however some non-linear relationships appear, and it is interesting to note that this is the case for complexes of certain of the present ligands with the three M^{2+} ions studied by Van Uitert *et al.* (2). A graph of the pK_a values against pK_1 (Tables 1 and 2) demonstrates that there are also significant deviations from a linear relationship for the indium(III) complexes. The results may of course have been affected by the instability of the ligands in alkaline solution. Alternatively, this non-linearity may be evidence of some unusual thermodynamic factors in these systems; in particular, steric interactions between CF_3 and R groups in a constrained conformation around the metal could lead to destabilization relative to the free ligand anion.

We note finally that the failure in earlier work (1) to obtain the $In(py \cdot CO \cdot CH \cdot CO \cdot CF_3)_3$ complex was presumably due to the choice of inappropriate experimental conditions; the extrapolated values for pK_1, etc.,

which can be obtained from a comparison of Tables 1 and 2 show that this compound should be thermodynamically stable.

This work was supported in part by an Operating Grant (to D.G.T.) from the National Research Council of Canada. We wish to thank Mr. R. C. Ferguson for advice on computer programs.

1. (MRS.) G. T. TANNER, D. G. TUCK, and E. J. WELLS. Unpublished results.
2. L. G. VAN UITERT, W. C. FERNELIUS, and B. E. DOUGLAS. J. Am. Chem. Soc. **75**, 457 (1953).
3. L. G. VAN UITERT, W. C. FERNELIUS, and B. E. DOUGLAS. J. Am. Chem. Soc. **75**, 2736 (1953); **75**, 2739 (1953).
4. *(a)* G. KORTUM, W. VOGEL, and K. ANDRUSSOW. Pure Appl. Chem. **1**, 163 (1960). *(b)* A. ALBERT and E. P. SERJEANT. Ionization constants of acids and bases. Methuen and Co. Ltd., London. 1962.
5. W. SIMON *et al.* Zusammenstellung von scheinbaren dissoziation-konstanten in losungmittelsystem methyl-cellosolve–wasser. Vols. I, II, and III. Juris–Verlag, Zurich. 1959, 1962, 1963.
6. M. CALVIN and K. W. WILSON. J. Am. Chem. Soc. **67**, 2003 (1945).
7. (*a*) L. G. VAN UITERT, W. C. FERNELIUS, and B. E. DOUGLAS. AEC Report NYD-626. 1951. *(b)* L. G. VAN UITERT. Ph.D. Thesis. Pennsylvania State University, 1951.
8. Stability constants. Chemical Society Special Publication No. 17, London. 1964.
9. M. CALVIN. Unpublished result.
10. L. G. VAN UITERT, C. G. HAAS, W. C. FERNELIUS, and B. E. DOUGLAS. J. Am. Chem. Soc. **75**, 455 (1953).
11. J. S. POLAND and D. G. TUCK. J. Organometal. Chem. In press.

Can. J. Chem. Downloaded from www.nrcresearchpress.com by 210.87.254.42 on 09/05/12
For personal use only.

INDO–MO Calculations and Proton Isotropic Shifts of Methyl-Substituted Pyridine Ligands in Ni(II) Complexes

M. S. SUN, F. GREIN, AND D. G. BREWER

Department of Chemistry, University of New Brunswick, Fredericton, New Brunswick

Received March 7, 1972

Relative p.m.r. isotropic shifts for the ligands in the complexes $NiL_4(NO_3)_2$ (L = 4-picoline and 3,5-lutidine), $NiL_3(NO_3)_2$ (L = 3-picoline and 3,4-lutidine), and $NiL_2(NO_3)_2$ (L = 2-picoline, 2,3-lutidine, 2,4-lutidine, and 2,5-lutidine) were determined in $CDCl_3$. Proton hyperfine coupling constants for corresponding pyridine cations and analogous phenyl radicals were calculated by the INDO–MO method. Analysis of the p.m.r. shifts and subsequent correlation with the INDO data revealed that the spin transfer process between metal and ligand was dominated by a σ-mechanism, as indicated by ring protons at the α- and β-positions. The γ-ring proton and methyl protons at all positions indicated a π-mechanism was also operative through σ–π spin polarization at the nitrogen atom. The INDO calculations based on spin densities of the hydrogen 1s orbitals, however, predicted that all ring protons would be dominated by a σ-mechanism, and that methyl protons at the α- and γ-positions should manifest a π-mechanism. Both mechanisms should be operative for the β-CH_3 protons, with 50–60% σ-contribution in the pyridine cations and 30–50% σ-contribution in the phenyl radicals. The pattern of spin polarization (*i.e.*, negative at α-C and γ-C, positive at β-C) is not altered by a small excess of α or β spin in the π-system. However, the π-spin density ratios, especially at the α- and γ-positions, are affected, as is the magnitude of the π-spin densities on each carbon. A comparison of the observed isotropic shifts for the methyl protons and for the γ-ring proton with the INDO calculated π-spin densities allows a determination of the spin delocalization in the ligand π-system.

Les déplacements isotropiques relatifs p.m.r. pour les ligands dans les complexes $NiL_4(NO_3)_2$ (L = picoline-4 et lutidine-3,5), $NiL_3(NO_3)_2$ (L = picoline-3 et lutidine-3,4), et $NiL_2(NO_3)_2$ (L = picoline-2, lutidine-2,3, lutidine-2,4 et lutidine-2,5), ont été déterminés dans le $CDCl_3$. Les constantes de couplage hyperfin du proton pour les cations pyridine correspondants et les radicaux analogues du phényle, ont été calculées par la méthode INDO–MO. L'analyse des déplacements p.m.r. et la corrélation subséquente avec les données INDO, révèlent que le processus de transfert de spin entre le métal et le ligand est surtout un mécanisme-σ, comme le montrent les protons du cycle en position α et β. Le proton γ du cycle et les protons du méthyle dans toutes les positions indiquent qu'un mécanisme-π est aussi effectif, par l'intermédiaire d'une polarisation de spin σ–π sur l'atome d'azote. Les calculs INDO, fondés sur les densités de spin dans les orbitales ls de l'hydrogène, laissent prévoir cependant que tous les protons du cycle seraient dominés par un mécanisme-σ et que les protons du méthyle sur les positions α et γ manifesteraient un mécanisme de type π. Ces deux mécanismes seraient effectifs pour les protons du CH_3-β, avec une contribution σ de 50–60% dans les cations pyridine et 30–50% dans les radicaux phényles. Le modèle de la polarisation de spin (c'est-à-dire négative sur C-α et C-γ, positive sur C-β) n'est pas effecté par un léger excès de spin en α ou β dans le système π. Cependant, les rapports de densité de spin π, surtout en position α et γ, sont modifiés de même que l'amplitude des densités de spin π sur chaque carbone. En comparant les déplacements isotropiques observés pour les protons du méthyle et pour le proton en γ du cycle, avec les densités de spin π calculées par la méthode INDO, il a été possible de déterminer la délocalisation de spin dans le système π du ligand.

Canadian Journal of Chemistry, **50**, 2626 (1972)

Introduction

Nuclear magnetic resonance isotropic shifts arising from electron–nuclear hyperfine contact interactions have been employed to study paramagnetic Ni(II) complexes with considerable success in recent years (1–6). A typical example is the spin delocalization in the π-electron system of Ni(II) complexes with aminotroponeimines (1–3), where the observations agreed very well with valence bond (VB) calculations. Other examples, such as the Ni(II)–pyrromethene (4) and the Ni(II)–salicylaldimine (6) systems gave results which correlated well with molecular orbital (MO) calculations. Thus, spin delocalization in a π-fragment of an aromatic molecule is predicted to exhibit shifts alternating in sign at adjacent positions, and substitution of a methyl group for a proton should give a shift opposite in sign to that of the replaced proton (7). In 1963, Happe and Ward (8) first reported the isotropic shifts of pyridine type ligands coordinated to Ni(II) acetylacetonate. They concluded that spin delocalization in pyridines was dominated

Can. J. Chem. Downloaded from www.nrcresearchpress.com by 210.87.254.40 on 09/05/12
For personal use only.

Can. J. Chem. Downloaded from www.nrcresearchpress.com by 210.87.254.40 on 09/05/12
For personal use only.

by a σ-mechanism, as the ring protons demonstrated decreasing downfield shifts (*viz.* $\alpha:\beta:\gamma = 1.00:0.294:0.077$ for pyridine) in contrast to the alternating sign characteristic of a π-mechanism. They also indicated that a small π-mechanism might be operative because of upfield shifts of the methyl protons at the α- and γ-positions.

Molecular orbital calculations appear to be essential in interpreting observed shifts in terms of some spin transfer mechanism. MO calculations involving only π-electrons[1] cannot account for the proton shifts, including methyl protons, of a pyridine type molecule. Although the extended Hückel theory (E.H.T.) is applicable to large molecules involving all valence electrons (10), calculations on pyridine carried out by Holm *et al.* (11) correlated poorly with the experimental data, particularly for the γ-proton where too large a contact shift ($\alpha:\beta:\gamma = 1.00:0.291:1.97$) was predicted. Cramer and Drago (12) did more refined E.H.T. calculations on pyridine and some methyl-substituted pyridines. They claimed that the β-spin was also delocalized in the Ni(II)–pyridine π-system via a $d-p_\pi$ or $d-p_{\pi^*}$ interaction. In their calculations (*viz.* $\alpha:\beta:\gamma = 1.00:0.382:1.01$ for pyridine), little improvement was obtained for the γ-proton. Furthermore, the E.H.T. was unable to handle negative spin densities.

Very recently, a more sophisticated "approximate molecular orbital theory" has been developed by Pople *et al.* (13) to handle large molecules. Scarlett *et al.* (14) have used the "intermediate neglect of differential overlap" (INDO) method to perform open-shell calculations on pyridine and some monosubstituted pyridine cations. Their results correlated fairly well with the p.m.r. data. Substantial improvement was obtained for the γ-proton ($\alpha:\beta:\gamma = 1.00:0.28:0.58$ for the pyridine cation) though it was still too large in comparison with the experimental data. Signs of the methyl proton shifts at different positions were correctly predicted by the INDO method. Horrocks and Johnston (15) performed similar calculations on analogous monomethyl phenyl radicals isoelectronic with the corresponding pyridine cations. The results ($\alpha:\beta:\gamma = 1.00:0.326:0.208$ for the phenyl radical) compared even better with p.m.r. data of the Ni(II)–pyridine complexes and they concluded that the observed isotropic shifts, including those of the methyl protons, in Ni(II)–pyridine complexes can be attributed to a σ-mechanism only.

In this paper, p.m.r. data are presented for some dimethyl pyridines coordinated to Ni(II) nitrate. INDO open-shell calculations are carried out on dimethyl pyridine cations and their analogous isoelectronic radicals. Two CH_3 groups on each ring, in the case of dimethyl pyridines, provide a better basis for the study of CH_3 proton shifts. An analysis of the CH_3 proton data should show if there is any correlation between the CH_3 proton shifts and a purely π-spin delocalization in pyridine ligands. Furthermore, in view of the good agreement between the calculated hyperfine coupling constants for the phenyl radical and its e.s.r. data (*viz.* $\alpha:\beta:\gamma = 1.00:0.34:0.11$ observed) (16), the INDO method should do equally well with the pyridine cation radical.

Experimental

Complex compounds $NiL_4(NO_3)_2$ (where L = 4-picoline and 3,5-lutidine), $NiL_3(NO_3)_2$ (where L = 3-picoline and 3,4-lutidine), and $NiL_2(NO_3)_2$ (where L = 2-picoline, 2,3-lutidine, 2,4-lutidine, and 2,5-lutidine) were prepared according to published procedures (17–19).[2] Compounds were checked via electronic spectroscopy confirming an octahedral configuration in chloroform solutions in agreement with those reported in the literature (17–19).

P.m.r. spectra of the complexes were obtained in $CDCl_3$ with TMS as internal standard at 29 ± 1 °C. A Varian 4300B high resolution n.m.r. spectrometer of 56.4 Mc/s was used for the measurement. The isotropic shifts were determined by subtracting the diamagnetic ligand shifts from the paramagnetic complexed ligand shifts. All complexes were very soluble in chloroform. The solutions of the complexes with 2,3-lutidine and 2,4-lutidine were clouded, and yellowish green precipitates settled upon standing. This was probably caused by moisture from both solvent and air. Fortunately however, p.m.r. spectra were not appreciably affected by such precipitation. The concentration of the samples was about 50 mg/ml or less giving sufficiently strong peaks of good resolution. The assignment of peaks was based on an analysis of the intensity ratios and line widths. The line widths should be greatest for protons closest to the paramagnetic ion (20, 21). However, the peaks of non-equivalent β-protons in 2-picoline and 2,4-lutidine

[1]Recent detailed treatment on pyridine π-electrons is given by Zeiss (9).

[2]We obtained, however, $NiL_3(NO_3)_2$ instead of $NiL_4(NO_3)_2$ with L = 3,4-lutidine.

Anal. Calcd. for $NiL_3(NO_3)_2$: C, 50.02; H, 5.40; O, 19.04; N, 13.89; Ni, 11.64. Found: C, 49.98; H, 5.45; O, 18.95; N, 14.09; Ni, 11.76.

Can. J. Chem. Downloaded from www.nrcresearchpress.com by 210.87.254.40 on 09/05/12
For personal use only.

could not be distinguished (J–J coupling was not observed) on such a basis. They were assigned from the results of MO calculations. There is fast ligand exchange in solution with excess ligand. No attempt was made to obtain the "absolute shifts".

INDO open-shell calculations were performed on an IBM System/360 Model 50I computer using CNINDO program written by P. A. Dobosh, obtained from the Quantum Chemistry Program Exchange at Indiana University. Geometrical parameters for the pyridine molecule were chosen according to the summary by Wong and Brewer (22). Additional bond lengths and bond angles for the methyl group were taken as follows: C—H 1.09 Å; C—CH_3 1.53 Å; ⟨HCH and ⟨HCC 109.467°. Of the three methyl protons, one was placed above the plane of the ring and the other two symmetrically below. The methyl proton hyperfine coupling constants were obtained by averaging over the three individual values assuming free rotation of the methyl group. The standard geometry of benzene was used for the phenyl radicals (C—H 1.08 Å; C—C 1.40 Å; ⟨CCC and ⟨HCC 120°).

Results and Discussion

Isotropic shifts may arise from either a hyperfine contact interaction between the unpaired electrons and the nucleus or a pseudo-contact (dipolar) interaction owing to electronic g-factor anisotropy of the transition metal (23). The latter is absent in the case of purely octahedral Ni(II) complexes because of magnetical isotropy of the $^3A_{2g}$ ground state.

The isotropic hyperfine coupling constant A_n (G) is related to the contact shift $\Delta\nu_n$ (c.p.s.) according to the equation

$$[1] \qquad A_n = -\left(\frac{3kT}{g\beta S(S+1)H}\cdot\frac{\gamma_n}{\gamma_e}\right)\Delta\nu_n$$

where g is the electronic g factor; β is the Bohr magneton; γ_e and γ_n are the gyromagnetic ratios for electron and nucleus, respectively; H is the probe frequency and S is the total spin (23). For a particular system involving similar nuclei, the quantity in brackets is a constant and A_n is directly proportional to $\Delta\nu_n$. Theoretically, A_n is directly related to the spin density at the magnetic nucleus n by the equation

$$[2] \qquad A_n = K\langle\psi|\rho(\hat{r}_n)|\psi\rangle$$

where $K = (4\pi/3)\, g\beta\gamma_n\hbar\langle S_z\rangle^{-1}$; $\rho(\hat{r}_n)$ is the spin density operator at the nucleus n; ψ is the electronic molecular wavefunction, and $\langle S_z\rangle$ is the average spin (13). If ψ is a MO wavefunction containing only valence orbitals (as in the INDO method) and if contributions to the spin density at the nucleus n from neighboring atomic orbitals are neglected, eq. 2 reduces to

$$[3] \qquad A_n = [K|\phi_{sn}(\hat{r}_n)|^2]\rho_{sn}$$

where ρ_{sn} is the spin density of the valence s orbital ϕ_{sn} of atom n, and $|\phi_{sn}(\hat{r}_n)|^2$ is the density at the nucleus n. For a particular atom, the quantity in brackets is constant and can be evaluated by a least-squares fit between the observed A_n and the calculated ρ_{sn}. In the case of hydrogen atoms, this quantity was found to be 539.86 G (13).

Relative hyperfine coupling constants from p.m.r. data for pyridine ligands in Ni(II) complexes and those obtained from INDO calculations according to eq. 3 for pyridine cations and analogous phenyl radicals are listed in Table 1. The results of our calculations on the pyridine and the picolines are almost identical to those reported by Scarlett *et al.* (14). The INDO data for the monomethylphenyl radicals were taken from ref. 15. More elaborate calculations based on eq. 2, taking account of neighboring atomic orbitals, show only slight improvement as far as the γ-H is concerned (*e.g.*, for pyridine cation, $\alpha:\beta:\gamma = 19.47:5.96:10.07 = 1.00:0.306:0.517$). The assumptions of eq. 3 are apparently justified in this case.

P.m.r. data for pyridine ligands in various types of Ni(II) complexes obtained by different investigators are listed for comparison. The results are very similar, indicating that the relative isotropic shifts are independent of the geometry of the complex. This means that the dipolar shift which depends on geometry and magnetic anisotropy of the molecule is not important in these complexes, and the isotropic shift is dominated by the contact term. It has been found, however, that some magnetic anisotropy does exist in pseudo-tetrahedral Ni(II) complexes (24, 25). In Table 1, the p.m.r. data of NiL_2I_2 which is pseudo-tetrahedral show no appreciable difference from the corresponding distorted octahedral case, in which the magnetic anisotropy was estimated to be less than 5% (26); apparently the dipolar shift in NiL_2I_2 is also very small. The relative shifts of β- and γ-protons in the octahedral $NiL_6(ClO_4)_2$ are substantially larger than those in the complexes of other geometries. This should not be considered as the result of complete removal of

Can. J. Chem. Downloaded from www.nrcresearchpress.com by 210.87.254.40 on 09/05/12
For personal use only.

TABLE 1. Comparison of relative isotropic shifts of pyridine ligands in Ni(II) complexes with calculated relative hyperfine coupling constants of pyridine cations and analogous phenyl radicals

Ligand	Proton position	Experimental (relative $-\Delta\nu_H$)					Calculated (relative A_H)‖		
		$NiL_4(NO_3)_2$*	$NiL_3(NO_2)_2$*	$NiL_2(NO_3)_2$*	$NiL_2(aa)_2$†	$NiL_6(ClO_4)_2$‡	NiL_2I_2§	Pyr cations	Phenyls
Pyridine	2-H				1.000	1.000	1.000	1.000(19.04)	1.000(18.74)
	3-H				0.294	0.385	0.297	0.265(5.04)	0.326(6.11)
	4-H				0.077	0.116	0.066	0.546(10.41)	0.210(3.94)
2-Picoline	6-H			1.000(−8350)	1.000			1.000(17.56)	1.000(17.4)¶
	3-H			0.199(−1663)	0.212			0.235(4.12)	0.305(5.3)¶
	4-H			0.094(−786)	0.068			0.614(10.78)	0.241(4.2)¶
	5-H			0.365(−3046)	0.415			0.323(5.68)	0.379(6.6)¶
	2-CH_3			−0.097(+812)	−0.147			−0.077(−1.35)	−0.109(−1.9)¶
3-Picoline**	2-H		1.000(−6173)		1.000	1.000	1.000	1.000(17.77)	1.000(17.4)¶
	4-H		0.081(−502)		0.063	0.104	0.060	0.585(10.95)	0.234(4.3)¶
	5-H		0.279(−1725)		0.296	0.365	0.303	0.250(4.69)	0.310(5.7)¶
	6-H		1.000(−6173)		1.000	1.000	1.000	1.000(19.69)	1.000(19.3)¶
	3-CH_3		0.053(−330)		0.055	0.072	0.043	0.104(1.94)	0.087(1.6)¶
4-Picoline	2-H	1.000(−5873)			1.000	1.000	1.000	1.000(19.45)	1.000(19.2)¶
	3-H	0.235(−1380)			0.278	0.328	0.287	0.288(5.60)	0.338(6.5)¶
	4-CH_3	−0.072(+420)			−0.090	−0.092	−0.063	−0.069(−1.35)	−0.063(−1.2)¶
2,3-Lutidine	6-H			1.000(−6930)				1.000(18.05)	1.000(17.91)
	4-H			0.075(−517)				0.624(11.25)	0.251(4.49)
	5-H			0.219(−1515)				0.296(5.35)	0.347(6.22)
	2-CH_3			−0.098(+681)				−0.078(−1.41)	−0.097(−1.74)
	3-CH_3			0.070(−482)				0.107(1.93)	0.081(1.45)
2,4-Lutidine	6-H			1.000(−7839)				1.000(17.95)	1.000(17.89)
	3-H			0.170(−1331)				0.260(4.66)	0.321(5.75)
	5-H			0.322(−2522)				0.349(6.27)	0.387(6.93)
	2-CH_3			−0.093(+727)				−0.069(−1.24)	−0.097(−1.73)
	4-CH_3			−0.071(+555)				−0.070(−1.25)	−0.062(−1.11)
2,5-Lutidine	6-H			1.000(−7837)				1.000(16.28)	1.000(16.44)
	3-H			0.352(−2757)				0.231(3.76)	0.309(5.08)
	4-H			0.077(−605)				0.695(11.31)	0.275(4.52)
	2-CH_3			−0.096(+755)				−0.091(−1.47)	−0.106(−1.74)
	5-CH_3			0.046(−358)				0.112(1.83)	0.087(1.43)
3,4-Lutidine**	2-H		1.000(−6806)					1.000(18.05)	1.000(17.92)
	5-H		0.275(−1872)					0.272(5.21)	0.329(6.16)
	6-H		1.000(−6806)					1.000(20.25)	1.000(19.57)
	3-CH_3		0.058(−395)					0.100(1.92)	0.077(1.45)
	4-CH_3		−0.080(+542)					−0.074(−1.41)	−0.059(−1.10)
3,5-Lutidine	2-H	1.000(−5433)						1.000(18.41)	1.000(18.02)
	4-H	0.068(−371)						0.622(11.46)	0.251(4.52)
	3-CH_3	0.052(−284)						0.107(1.96)	0.080(1.44)

*This work, one and two nitrato group as bidentate ligand in $NiL_3(NO_3)_2$ and $NiL_2(NO_3)_2$, respectively. See refs. 18 and 19. Numbers in parentheses are isotropic shifts $\Delta\nu_H$ in c.p.s. with no additional ligand.

†Data from ref. 8 (aa = acetylacetonate).

‡Data from ref. 12.

§Data from ref. 11.

‖Numbers in parentheses are calculated hyperfine coupling constants in G.

¶Data from ref. 15.

**Average value of 2-H and 6-H is used for normalization.

TABLE 2. Average ratio of calculated relative A_H to experimental relative $-\Delta\nu_H$ of the nitrato complexes

Proton	Average ratio	
	Pyr cations	Phenyls
α-H	1.00	1.00
β-H	1.09	1.33
γ-H	8.05	3.21
α-CH_3	0.82	1.06
β-CH_3	1.92	1.49
γ-CH_3	0.98	0.84

the dipolar contribution in $NiL_6(ClO_4)_2$. According to the geometrical positions suggested by Happe and Ward (8) for the ligand protons in $NiL_2(aa)_2$, it is impossible to obtain a pure contact case similar to that of $NiL_6(ClO_4)_2$ by subtracting any reasonable amount of dipolar contribution from the data of $NiL_2(aa)_2$. Therefore, the discrepancies among p.m.r. data for the complexes of different geometries listed in Table 1 may be attributed to different experimental conditions (27)[3] and to experimental errors. Our experience indicates that the accuracy of locating very broad peaks is questionable and that the nonlinear sweeping of the magnetic field over a large range of chemical shifts may be the greatest source of error, and could have been ignored by some investigators.

INDO calculations on the corresponding radicals (pyridine cations and phenyls) assumed to be in doublet states show that the unpaired electron is delocalized in the highest bonding MO of σ-symmetry (σ_b). The average ratios of calculated A_H to experimental $-\Delta\nu_H$ (both normalized) are summarized in Table 2. The ratio should be equal to 1.0 if experiment and calculations agree perfectly. The data of the distorted octahedral nitrato complexes, $NiL_4(NO_3)_2$, $NiL_3(NO_3)_2$, and $NiL_2(NO_3)_2$, were used for such comparisons. The results in Table 2 indicate that our p.m.r. data compare favorably with the INDO calculations for the pyridine cations at the positions α-H, β-H, α-CH_3, and γ-CH_3, but poorly at the γ-H and β-CH_3 positions. The calculations for phenyl radicals, on the other hand, show substantial improvement at the γ-H and β-CH_3 positions, but the agreement is still far from satisfactory. Furthermore, the discrepancy for the β-H is large. Overall, the phenyl radical model cannot be judged superior to the pyridine cation model.

[3]Some of the results in ref. 27 are quite different from those in ref. 8.

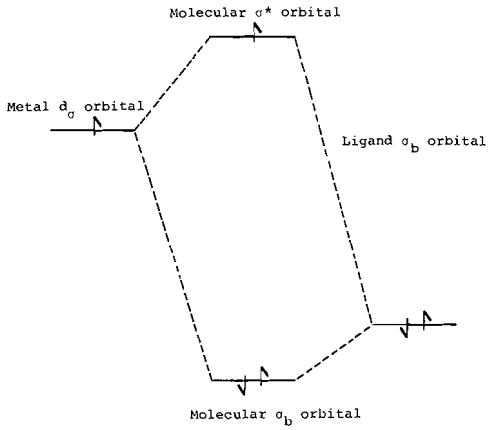

FIG. 1. Spin delocalization in molecular σ* orbital of metal–ligand system.

Spin delocalization in the σ-system of Ni(II)–pyridine complexes can be explained as being due to the interaction between the ligand σ_b (bonding) orbital containing the lone pair and the metal d_σ orbital containing the unpaired electron; this would place some α-spin in the pyridine ring. The discrepancies, especially at γ-H, between observation and theory might be the result of neglecting the metal–ligand interactions in the INDO calculations. Such weak interactions, of course, would not appreciably affect the parameters for the nitrogen atom, but would place the unpaired electron in a σ*-orbital (anti-bonding) of the metal–ligand system, contrary to the case of pyridine cations where the unpaired electron is placed in a σ_b orbital. This is illustrated in Fig. 1. Since only a small fraction of spin is transferred from metal to ligand, the σ* orbital would be mainly localized on the metal, and the σ_b orbital, on the other hand, would be filled and mainly localized on the ligand. The pattern of spin distribution, as far as the pyridine ring is concerned, in a σ* orbital of the complexes may be very different from that in a σ_b orbital of the cations.

Since the CNINDO program is, however, not capable of handling the transition metals, we have performed calculations where the hydrogen atom and selected first row atoms take the place of the Ni metal atom. Some of the

Can. J. Chem. Downloaded from www.nrcresearchpress.com by 210.87.254.40 on 09/05/12
For personal use only.

Can. J. Chem. Downloaded from www.nrcresearchpress.com by 210.87.254.40 on 09/05/12
For personal use only.

TABLE 3. Calculated relative A_H

Model	X–N (Å)	A_H α-H	A_H β-H	A_H γ-H
H–Pyr doublet*	2.00	1.00	−0.70	−0.24
O–Pyr triplet	2.50	1.00	0.05	1.37
F–Pyr doublet	2.00	1.00	1.68	0.96
F–Pyr$^+$ triplet	1.60	1.00	0.41	0.35

*Spin densities multiplied by −1.

results are summarized in Table 3. All these models, at the X–N distances indicated, demonstrate spin delocalization in the σ^* orbitals. The X–N distances were adjusted so that the interactions were sufficiently weak and the energy levels of the σ^* orbitals were below the π^* orbitals. A strong X–L interaction would bring the unpaired electron into a π^* orbital. These calculations show that the coefficients of the σ^* orbital depend heavily on the nature of the elements perturbing the lone pair. None of the results agree with the p.m.r. data. The closest is the F–Pyr$^+$ triplet case; however, more than 80% of an unpaired electron is delocalized in the ligand in this case.

The p.m.r. data for the methyl protons exhibit alternation of signs at different positions, in agreement with the INDO prediction. This may be an indication of spin delocalization in the π-system. However, the relative magnitudes of shifts do not agree with the relative spin densities predicted for any π-type orbitals of the pyridine molecule. Happe and Ward (8) and other investigators (21, 28) have already proposed that such a phenomenon was probably due to σ–π spin polarization mechanisms induced by the excessive α-spin in the lone pair of a σ-type orbital. The pattern of such spin polarization in a pyridine framework could never be checked by theory until the INDO method became available. The INDO spin densities in the π-system resulting from σ–π spin polarization mechanism for the pyridine cations are listed in Table 4. The total spin density, ρ_π^t, for the non-substituted pyridine cation is zero, as no spin transfer takes place from any source. In the case of methyl substituted pyridine cations, some spins could be delocalized in the π-systems via a hyperconjugation mechanism with the methyl protons. The data in Table 4 indicate that α-spins are delocalized in the π-systems of α- and γ-substituted cations whereas β-spins are found in the β-substituted cases. Note that there is no appreciable change in the pattern of spin polarization with a small amount of excessive spin in the π-system. There is, however, a trend which indicates that the ratio $\rho_\pi^\gamma/\rho_\pi^\alpha$ is dependent upon ρ_π^t. Thus, the ratio tends to go down when ρ_π^t is positive such as in the case of 2,4-lutidine; and to go up if ρ_π^t is negative, such as in the case of 3,5-lutidine. In the case of phenyl radicals, however, no such trend is found.

The total spin density ρ_π^t should equal in magnitude the spin density (opposite in sign) in the methyl protons, ρ_s', assuming a complete hyperconjugation mechanism. Hence, ρ_s' can be recalculated based on a hyperconjugation model, and then both p.m.r. and INDO data can be checked. For the picolines, ρ_s' is readily obtained from Table 4 by reversing the sign of ρ_π^t. As to the lutidines, a set of simultaneous equations has to be solved in order to obtain the values for each methyl group. According to Levy's equation (29),

$$[4] \qquad A_H = Q'_{CH_3}(\rho_s' + \rho_\pi' + \rho_\pi)$$

where ρ_π' is the π-spin density on the methyl carbon and ρ_π on the ring carbon next to the methyl group. Since $A_H = (539.86/3)\rho_s'$, the unknowns Q'_{CH_3}, ρ'_{sx}, and ρ'_{sy} can be obtained by solving

$$(\rho'_{sx} + \rho'_{\pi x} + \rho_{\pi x})Q'_{CH_3} = 180\rho'_{sx}$$

$$(\rho'_{sy} + \rho'_{\pi y} + \rho_{\pi y})Q'_{CH_3} = 180\rho'_{sy}$$

$$\rho'_{sx} + \rho'_{sy} = -\rho_\pi^t$$

The recalculated spin densities for the methyl protons are summarized in Table 5. The average value of Q'_{CH_3} is 27.6 G comparing favorably with 25.7 G reported by Talcott and Myers (30) on methyl substituted pyridine anions. Almost identical spin densities were obtained using McLachlan's relation (7), $A_H = Q_{CH_3}\rho_\pi$. The average Q_{CH_3} value is 30.7 G.

The INDO predicted spin densities ρ_s for α-CH_3 and γ-CH_3 agree well with the recalculated values. However, the INDO ρ_s for β-CH_3 is about 100–200% greater than the ρ_s'. We may conclude that the INDO predicted hyperfine coupling constants for the methyl groups in pyridine cations are dominated by a π-mechanism at the α- and γ-positions, resulting

Can. J. Chem. Downloaded from www.nrcresearchpress.com by 210.87.254.40 on 09/05/12
For personal use only.

TABLE 4. INDO spin densities in π-system of pyridine cations*

Cation	Spin density									Total (ρ_π^1)
	N	2-C	3-C	4-C	5-C	6-C	α-CH_3	β-CH_3	γ-CH_3	
Pyridine	0.0717 (1.70)	−0.0422 (−1.00)	0.0259 (0.61)	−0.0391 (−0.93)	0.0259 (0.61)	−0.0422 (−1.00)	—	—	—	0.0
2-Picoline	0.0690 (1.73)	−0.0399 (−1.00)	0.0260 (0.65)	−0.0363 (−0.91)	0.0239 (0.60)	−0.0389 (−0.97)	0.0024	—	—	0.0062
3-Picoline	0.0737 (1.71)	−0.0430 (−1.00)	0.0266 (0.62)	−0.0418 (−0.97)	0.0274 (0.64)	−0.0452 (−1.05)	—	−0.0014	—	−0.0037
4-Picoline	0.0700 (1.78)	−0.0392 (−1.00)	0.0238 (0.61)	−0.0352 (−0.90)	0.0238 (0.61)	−0.392 (−1.00)	—	—	0.0019	0.0059
2,3-Lutidine	0.0709 (1.74)	−0.0408 (−1.00)	0.0265 (0.65)	−0.0386 (−0.95)	0.0253 (0.62)	−0.0415 (−1.02)	0.0024	−0.0014	—	0.0028
2,4-Lutidine	0.0671 (1.82)	−0.0369 (−1.00)	0.0242 (0.66)	−0.0326 (−0.88)	0.0216 (0.58)	−0.0360 (−0.98)	0.0024	—	0.0019	0.0117
2,5-Lutidine	0.0715 (1.66)	−0.0430 (−1.00)	0.0276 (0.64)	−0.0392 (−0.91)	0.0249 (0.58)	−0.0396 (−0.92)	0.0026	−0.0013	—	0.0035
3,4-Lutidine	0.0723 (1.79)	−0.0403 (−1.00)	0.0248 (0.61)	−0.0380 (−0.94)	0.0256 (0.63)	−0.0423 (−1.05)	—	−0.0013	0.0020	0.0028
3,5-Lutidine	0.0756 (1.65)	−0.0459 (−1.00)	0.0280 (0.61)	−0.0444 (−0.97)	0.0280 (0.61)	−0.0459 (−1.00)	—	−0.0030†	—	−0.0076

*Numbers in parentheses are relative spin densities based on the value of 2-C.
†2(−0.0015).

Can. J. Chem. Downloaded from www.nrcresearchpress.com by 210.87.254.40 on 09/05/12
For personal use only.

TABLE 5. Recalculated spin densities for the methyl hydrogens using the hyperconjugation model*

	α-CH_3			β-CH_3			γ-CH_3		
Cation	INDOρ_s	ρ'_s	A'_H	INDOρ_s	ρ'_s	A'_H	INDOρ_s	ρ'_s	A'_H
α-Picoline	−0.0075	−0.0062	−0.064						
β-Picoline				0.0108	0.0037	0.036			
γ-Picoline							−0.0075	−0.0059	−0.055
2,3-Lutidine	−0.0078	−0.0081	−0.081	0.0107	0.0053	0.053			
2,4-Lutidine	−0.0069	−0.0062	−0.062				−0.0069	−0.0055	−0.055
2,5-Lutidine	−0.0082	−0.0084	−0.093	0.0102	0.0049	0.054			
3,4-Lutidine				0.0107	0.0053	0.050	−0.0078	−0.0081	−0.076
3,5-Lutidine				0.0109	0.0038	0.037			

*ρ'_s = recalculated spin density; A'_H = relative A_H calculated with ρ'_s.

TABLE 6. Ratios of relative methyl proton with relative α-CH_3 contact shifts in pyridine ligands (normalized to -1 for α-CH_3)

Ligands	Experimental ($-\Delta\nu_H$)			Recalculated (A'_H)		
	α-CH_3	β-CH_3	γ-CH_3	α-CH_3	β-CH_3	γ-CH_3
Picolines and 3,5-Lutidine	−1.00	0.54	−0.74	−1.00	0.57	−0.86
2,3-Lutidine	−1.00	0.71		−1.00	0.65 0.68*	
2,4-Lutidine	−1.00		−0.76	−1.00		−0.89 −0.87*
2,5-Lutidine	−1.00	0.48		−1.00	0.58 0.70*	
3,4-Lutidine		0.58†	−0.80		0.60† 0.69*†	−0.91 −0.85*
Average	−1.00	0.58	−0.77	−1.00	0.60 0.69*	−0.89 −0.86*

*Data for phenyl radicals.
†Based on the average value of β-CH_3.

from σ–π spin polarization, whereas both σ- and π-mechanisms are operative at the β-position with 50–60% σ-participation. A similar conclusion can be drawn from the data for the phenyl radicals with 30–50% σ-mechanism at the β-position. Good agreement between p.m.r. data and the recalculated values taking the ratio of the relative contact shift of the methyl proton to that of the α-CH_3 proton (with the value of α-CH_3 normalized to -1.00) is illustrated in Table 6. Thus, another conclusion is that the p.m.r. isotropic shifts of the methyl protons at all positions of the pyridine type ligands coordinated to Ni(II) are caused by a π-mechanism through hyperconjugation with the ρ_π electrons whose spins are polarized by the unpaired electron in a σ-type metal–ligand bond.

As far as the pyridine ligands are concerned, the σ-contributions to β-CH_3 and γ-H are overemphasized by the INDO theory. In view of the observed small shifts of γ-H in the ligands, we may assume that the σ-mechanism is also absent at this position and the shift is dominated by a π-mechanism. Then with spin densities presented in Table 4 and a Q_H value of 24.5 G reported by Talcott and Myers (30), A_H for γ-H can be recalculated using McConnell's relation (31), $A_H = Q_H\rho_\pi$. An overall comparison between p.m.r. and the recalculated data is presented in Table 7. The data in Table 7 reveal that the recalculated values for methyl groups and γ-H are lower than those from p.m.r. data. This is expected since the spin polarization in a π-system is not linearly correlated to the amount of spin density in the σ-system of a pyridine framework and the σ-spin in a pyridine ligand is far less than that in a pyridine cation. This is clearly illustrated in Table 8. Assuming that, in Table 8, ρ^t_σ is linearly related to the spin density in α-H, the ratio ρ_π/ρ^t_σ should be a measure of the relative A_H (or $-\Delta\nu_H$) for the methyl protons and γ-H, as A_H is almost directly proportional to $\rho\pi$. It is clear that ρ_π/ρ^t_σ increases readily with decreasing ρ^t_σ. In a pyridine ligand coordinated to Ni(II), ρ^t_σ should be far less than unity and, therefore, a larger relative $-\Delta\nu_H$ for protons dominated by a π-mechanism would be expected. It can be concluded that the relative proton hyperfine coupling constants at γ-H, α-CH_3, β-CH_3, and γ-CH_3 positions dominated

TABLE 7. Revised average ratios of calculated relative A_H to experimental relative $-\Delta\nu_H$ of nitrato complexes

Proton	Revised average ratio	
	Pyr cations	Phenyls
α-H	1.00	1.00
β-H	1.09	1.33
γ-H	0.71	0.72*
α-CH_3	0.78	0.79*
β-CH_3	0.83	0.82*
γ-CH_3	0.84	0.80*

*Data based on dimethyl phenyls.

Can. J. Chem. Downloaded from www.nrcresearchpress.com by 210.87.254.40 on 09/05/12
For personal use only.

Can. J. Chem. Downloaded from www.nrcresearchpress.com by 210.87.254.40 on 09/05/12
For personal use only.

TABLE 8. Effect of total σ-spin density upon spin polarization in pyridine π-system*

Proton	H–N (Å)	ρ_σ^l	ρ_π				ρ_π/ρ_σ^l			
			N	α-C	β-C	γ-C	N	α-C	β-C	γ-C
H–Pyridine, doublet	1.59	0.1601	0.0269	−0.0151	0.0081	−0.0128	0.168	−0.094	0.051	−0.080
H–Pyridine, doublet	1.70	0.1202	0.0210	−0.0120	0.0066	−0.0102	0.175	−0.100	0.055	−0.085
H–Pyridine, doublet	1.80	0.0896	0.0164	−0.0097	0.0057	−0.0083	0.183	−0.108	0.064	−0.093
H–Pyridine, doublet	1.90	0.0649	0.0124	−0.0075	0.0045	−0.0064	0.191	−0.115	0.069	−0.099
H–Pyridine, doublet	2.00	0.0460	0.0093	−0.0057	0.0035	−0.0049	0.202	−0.124	0.076	−0.106
H–Pyridine, doublet	2.10	0.0320	0.0069	−0.0043	0.0028	−0.0038	0.216	−0.134	0.087	−0.119
H–Pyridine, doublet	2.20	0.0220	0.0052	−0.0034	0.0022	−0.0030	0.236	−0.154	0.100	−0.136
H–Pyridine, doublet	3.00	0.0009	0.0018	−0.0015	0.0012	−0.0014	2.0	−1.7	1.3	−1.6

*ρ_σ^l = total spin density delocalized in pyridine σ-system.

Can. J. Chem. Downloaded from www.nrcresearchpress.com by 210.87.254.40 on 09/05/12
For personal use only.

TABLE 9. Correlation between total π-spin density and spin polarization in pyridine π-system*

Model	O–N (Å)	ρ_σ^t	ρ_π^t	ρ_π N	ρ_π α-C	ρ_π β-C	ρ_π γ-C	ρ_π/ρ_σ^t N	ρ_π/ρ_σ^t α-C	ρ_π/ρ_σ^t β-C	ρ_π/ρ_σ^t γ-C
O–Pyridine$^+$, quartet	1.60	0.7474	0.0293	0.0491 (4.27)	−0.0115 (−1.00)	0.0053 (0.46)	−0.0074 (−0.64)	0.066	−0.015	0.007	−0.010
O–Pyridine$^+$, quartet	1.80	0.8297	0.0069	0.0610 (2.01)	−0.0304 (−1.00)	0.0171 (0.56)	−0.0275 (−0.90)	0.073	−0.037	0.021	−0.033
Pyridine$^+$, doublet		1.0	0.0	0.0717 (1.70)	−0.0422 (−1.00)	0.0259 (0.61)	−0.0391 (−0.93)	0.072	−0.042	0.026	−0.039
O–Pyridine$^+$, doublet†	2.00	0.8995	−0.0015	0.0673 (1.69)	−0.0399 (−1.00)	0.0241 (0.60)	−0.0372 (−0.93)	0.075	−0.044	0.027	−0.041
O–Pyridine$^+$, doublet†	1.80	0.7413	−0.0053	0.0587 (1.63)	−0.0361 (−1.00)	0.0211 (0.58)	−0.0340 (−0.94)	0.079	−0.049	0.028	−0.046
O–Pyridine$^+$, doublet†	1.60	0.2590	−0.0179	0.0345 (1.22)	−0.0283 (−1.00)	0.0162 (0.57)	−0.0282 (−1.00)	0.133	−0.109	0.062	−0.109

*Numbers in parentheses are relative spin densities based on the value of α-C.
†All spin densities are multiplied by −1 in order to compare.

Can. J. Chem. Downloaded from www.nrcresearchpress.com by 210.87.254.40 on 09/05/12
For personal use only.

by a π-mechanism are influenced by the amount of σ-spins delocalized in the pyridine molecules. Comparing the recalculated data of pyridine cations, the larger relative values at those positions in the pyridine ligands may be attributed to the smaller amounts of σ-spins delocalized in the ligands.

As discussed before, some excessive spin in the π-system would affect the ratio $\rho_\pi^\gamma/\rho_\pi^\alpha$. This is better demonstrated in Table 9. It shows that 2.93% of an α-spin in the π-system brings the ratio down to 0.64, whereas the ratio is 1.00 with 1.79% of a β-spin delocalization, and 0.93 with little or no spin delocalization. Thus in Table 6, the shift ratio of methyl protons, $\Delta\nu_H^\gamma/\Delta\nu_H^\alpha = 0.77$, smaller than the cation case, 0.89, may be an indication of α-spin delocalization in the ligand π-system, though this is not favored by the symmetry of the distorted octahedral Ni(II) complexes. Both Tables 4 and 9 reveal that the excess α-spin in the π-system tends to depress spin polarization; *i.e.*, reduce ρ_π at each ring atom, while the β-spin tends to enhance it. Hence the magnitude of ρ_π/ρ_σ^l is influenced by both ρ_σ^l and ρ_π^l. According to the results in Table 7, one may infer that the trend shown by ρ_π/ρ_σ^l is dominated by ρ_σ^l in the complexed ligands but its magnitude has been reduced by the influence of ρ_π^l (α-spin). Nevertheless, in view of the smaller relative shifts of γ-H, β-CH_3, and γ-CH_3 in NiL_2I_2 complexes (Table 1), more α-spin may have been delocalized in the π-system of the ligands, and this is allowed by symmetry.

From the results and discussions presented above, the importance of σ–π spin polarization in pyridine complex systems is obvious. Neglect of this has led to incorrect conclusions by some investigators (12, 15). The simultaneous equations set up by Cramer and Drago (12) in an attempt to separate σ and π contributions to the observed contact shifts indicate that no π-shifts should be observed for the methyl proton if the *net* spin density in the π-system is zero. This is not correct when σ–π spin polarization arises. In fact, σ–π spin polarization in the pyridine framework would have overrun any spin polarization pattern characteristic of a particular π-orbital, if there is any spin in that orbital. Therefore, it is inadequate to compare the observed π-shifts with the spin densities in a particular π-orbital of the pyridine ligands.

The conclusion drawn by Horrocks and Johnston (15) on the methyl proton shifts implies that the unpaired electrons in the methyl hydrogen atoms giving rise to contact shifts have been directly transferred from a σ-network. Our results show that these spins resulted from hyperconjugation between the methyl hydrogen 1s orbitals and the filled π-orbitals of the pyridine ring, and the unpaired electrons in the π-system are generated via σ–π spin polarization mechanism.

Conclusions

(*1*) The spin transfer process between Ni(II) and pyridine type ligands is dominated by a σ-mechanism. However, only ring protons at α- and β-positions manifested such a mechanism via proton isotropic shifts.

(*2*) The unpaired electron is delocalized in a σ^* orbital of the metal–ligand system while for the corresponding cation radicals spin delocalization takes place in a bonding σ orbital. Such a difference may be the cause of discrepancies between observation and theory.

(*3*) The σ–π spin polarization mechanism is very important in the metal–ligand system. The isotropic shifts of all methyl protons and γ-H are dominated by this mechanism which becomes more significant as the amount of σ-spin decreases (*i.e.*, ρ_π/ρ_σ^l increases). Thus zero spin density in the π-system, $\rho_\pi^l = 0$, would not zero the π-contact shifts of these protons.

(*4*) The spin density ratio $\rho_\pi^\gamma/\rho_\pi^\alpha$ will remain constant if the net spin in the π-system, $\rho_\pi^l = 0$. However, the ratio will increase if $\rho_\pi^l < 0$ and decrease if $\rho_\pi^l > 0$. The ratio is manifested by the isotropic shifts of the methyl protons at α- and γ-positions.

(*5*) The magnitudes of π-spin densities on the ring carbons are affected by ρ_π^l. They will decrease if $\rho_\pi^l > 0$, and increase if $\rho_\pi^l < 0$. The magnitudes are manifested by the isotropic shifts of methyl protons and γ-H.

We thank the National Research Council of Canada for financial support. A University of New Brunswick Graduate Research Assistantship to M. S. Sun is gratefully acknowledged.

1. W. D. PHILLIPS and R. E. BENSON. J. Chem. Phys. 33, 607 (1960).
2. D. R. EATON, A. D. JOSEY, W. D. PHILLIPS, and R. E. BENSON. J. Chem. Phys. 37, 347 (1962).

3. D. R. EATON, W. D. PHILLIPS, and D. J. CALDWELL. J. Am. Chem. Soc. **85**, 397 (1963).
4. D. R. EATON and E. A. LALANCETTE. J. Chem. Phys. **41**, 3534 (1964).
5. R. H. HOLM, A. CHAKRAVORTY, and G. O. DUDEK. J. Am. Chem. Soc. **86**, 379 (1964).
6. G. N. LA MAR. Mol. Phys. **12**, 427 (1967).
7. A. D. MCLACHLAN. Mol. Phys. **1**, 233 (1958).
8. J. A. HAPPE and R. L. WARD. J. Chem. Phys. **39**, 1211 (1963).
9. G. D. ZEISS. Private communication.
10. R. HOFFMANN. J. Chem. Phys. **39**, 1397 (1963).
11. R. H. HOLM, G. W. EVERETT, JR., and W. DEW. HORROCKS, JR. J. Am. Chem. Soc. **88**, 1071 (1966).
12. R. E. CRAMER and R. S. DRAGO. J. Am. Chem. Soc. **92**, 66 (1970).
13. J. A. POPLE, D. L. BEVERIDGE, and P. A. DOBOSH. J. Am. Chem. Soc. **90**, 4201 (1968).
14. M. J. SCARLETT, A. T. CASEY, and R. A. CRAIG. Aust. J. Chem. **23**, 1333 (1970).
15. W. DEW. HORROCKS, JR. and D. L. JOHNSTON. Inorg. Chem. **10**, 1835 (1971).
16. P. H. KASAI, E. HEDAYA, and E. B. WHIPPLE. J. Am. Chem. Soc. **91**, 4364 (1969).
17. S. BUFFAGNI, L. M. VALLARINO, and J. V. QUAGLIANO. Inorg. Chem. **3**, 671 (1964).
18. S. BUFFAGNI, L. M. VALLARINO, and J. V. QUAGLIANO. Inorg. Chem. **3**, 480 (1964).
19. L. M. VALLARINO, W. E. HILL, and J. V. QUAGLIANO. Inorg. Chem. **4**, 1598 (1965).
20. G. N. LA MAR and G. R. VAN HECKE. J. Am. Chem. Soc. **91**, 3442 (1969).
21. G. N. LA MAR and G. R. VAN HECKE. Inorg. Chem. **9**, 1546 (1970).
22. P. T. T. WONG and D. G. BREWER. Can. J. Chem. **46**, 139 (1968).
23. H. M. MCCONNELL and R. E. ROBERTSON. J. Chem. Phys. **29**, 1361 (1959).
24. G. N. LA MAR. J. Chem. Phys. **41**, 2992 (1964).
25. W. DEW. HORROCKS, JR. and E. S. GREENBERG. Inorg. Chem. **10**, 2190 (1971).
26. D. FORSTER. Inorg. Chim. Acta, **5**, 465 (1971).
27. D. DODDRELL and J. D. ROBERTS. J. Am. Chem. Soc. **92**, 6839 (1970).
28. A. F. GARITO and B. B. WAYLAND. J. Am. Chem. Soc. **91**, 866 (1969).
29. D. H. LEVY. Mol. Phys. **10**, 233 (1966).
30. C. L. TALCOTT and R. J. MYERS. Mol. Phys. **12**, 549 (1967).
31. H. M. MCCONNELL and D. CHESTNUT. J. Chem. Phys. **28**, 107 (1958).

Can. J. Chem. Downloaded from www.nrcresearchpress.com by 210.87.254.40 on 09/05/12
For personal use only.

Determination of $D[(CH_3)_3Pb—CH_3]$ by the Toluene Carrier Method

K. M. GILROY, S. J. PRICE, AND N. J. WEBSTER
Chemistry Department, University of Windsor, Windsor 11, Ontario

Received March 10, 1972

The pyrolysis of tetramethyl lead has been studied in a toluene carrier flow system over the temperature range 671–753 °K (contact times 0.72–1.67 s, 3–77% decomposition). The reaction was followed by measuring the amount of methane, ethane, and ethylbenzene formed. Comparison of the extent of reaction based on product analysis and on alkyl recovery indicates that approximately four methyl radicals are released for each molecule undergoing reaction 1.

[1] $$Pb(CH_3)_4 \rightarrow Pb(CH_3)_3 + CH_3$$

The method of least squares gives $k_1 = 5.0 \times 10^{14} \exp(-49\,400/RT)\ sB^1$ with an estimated uncertainty of $\pm$ 1 000 cal mol^{-1} in E_1. Under the conditions used E_1 should be a reasonable measure of $D[(CH_3)_3Pb—CH_3]$.

La pyrolyse du Plomb tétraméthyle a été étudiée dans un système continu avec le toluène pour gaz vecteur, dans l'intervalle de température 671–753 °K (durées de contact 0.72–1.67 sec, décomposition 3–77%). La réaction a été suivie en mesurant la quantité de méthane, d'éthane et d'éthylbenzène formée. La comparaison de l'étendue de la réaction fondée sur l'analyse du produit et l'alkyle retrouvé, indique que quatre radicaux méthyles approximativement sont libérés par chaque molécule subissant la réaction (1)

[1] $$Pb(CH_3)_4 \rightarrow Pb(CH_3)_3 + CH_3$$

La méthode des moindres carrés permet d'avoir $k_1 = 5.0 \times 10^{14} \exp(-49400/RT)\ s^{-1}$ avec une incertitude sur E_1 estimée à $\pm$ 1 000 cal mol^{-1}. Dans les conditions utilisées E_1 serait une mesure raisonnable de $D[(CH_3)_3Pb—CH_3]$.

Canadian Journal of Chemistry, **50**, 2639 (1972)

Introduction

The kinetics of the pyrolysis of $Pb(CH_3)_4$ has been previously studied by Eltenton (1). With a very dilute stream of $Pb(CH_3)_4$ in He at a total pressure of 0.4 mm he obtained $k_1 = 1.5 \times 10^{10} \exp(-28\,200/RT)\ s^{-1}$ (400–700 °C, decomposition essentially complete above 600 °C).

[1] $$Pb(CH_3)_4 \rightleftharpoons Pb(CH_3)_3 + CH_3$$

Both the A factor and activation energy are unreasonably low. A recent investigation (2) combined mass spectrometric data (A.P. and I.P.) with pertinent thermochemistry to give $D[(CH_3)_3Pb—CH_3] = 48.8$ kcal mol^{-1}, based on $\Delta H^0_{f0}(CH_3,g) = 34.8$ kcal mol^{-1} (3). The present work was designed to obtain a revaluation of both A_1 and D_1

Experimental

Materials

(*a*) Toluene from sulfonic acid (Eastman organic X 325) was refluxed over sodium under vacuum and then degassed by bulb-to-bulb distillation.

(*b*) Tetramethyl lead was obtained from the Ethyl Corporation as a blend containing 68% $Pb(CH_3)_4$ and 32% toluene. The $Pb(CH_3)_4$ was separated by a series of four successive fractional crystallizations in each stage of which approximately 50% of the solution was allowed to solidify and the remaining liquid was discarded. The resulting product had a refractive index of 1.5120 at 20 °C in agreement with the literature value (4). A small quantity of residual toluene (approx. 0.3%) was found by gas chromatographic analysis. Apart from necessitating a small correction in the weight of alkyl used in a run, the residual toluene was of no significance as all experiments were carried out in a toluene carrier system.

Apparatus and Procedure

Except for the substitution of an electron capture detector for the hydrogen flame detector when tests were made for possible lead containing products, all apparatus and procedures were identical to those used previously for $Sn(CH_3)_4$ (5).

Results and Discussion

Selected experimental results are given in Tables 1–4. They may be discussed in terms of the following mechanism

[1] $$Pb(CH_3)_4 \rightleftharpoons Pb(CH_3)_3 + CH_3$$

[2] $$Pb(CH_3)_3 \rightleftharpoons Pb(CH_3)_2 + CH_3$$

[3] $$Pb(CH_3)_2 \rightleftharpoons PbCH_3 + CH_3$$

[4] $$PbCH_3 \rightleftharpoons Pb + CH_3$$

Can. J. Chem. Downloaded from www.nrcresearchpress.com by 210.87.254.5 on 09/05/12
For personal use only.

TABLE 1. Selected results for the pyrolysis of tetramethyl lead

T (°K)	P (mm)	t_c (s)	Alkyl used (mol × 10^4)	Products (mol × 10^4) CH_4	C_2H_6	$C_6H_5C_2H_5$	k_1 (s^{-1})
743	12.0	0.81	7.37	5.50	5.50	3.47	1.39
734*	14.4	1.00	5.83	5.86	4.24	2.70	1.30
725	13.4	0.82	6.10	3.24	2.59	1.96	0.68
715	15.5	1.37	3.72	2.87	1.23	0.91	0.39
711*	14.1	1.08	6.23	2.76	2.05	1.57	0.38
708	13.5	0.85	5.17	1.61	1.03	1.22	0.32
700	14.7	0.83	8.22	1.90	0.97	1.22	0.20
693	15.2	0.80	16.70	3.00	1.01	1.89	0.14
692*	14.7	1.02	6.06	1.44	0.66	0.75	0.15
683	13.7	0.88	7.56	0.87	0.33	0.39	0.074
671	14.1	0.96	9.40	0.63	0.23	0.29	0.038

*Runs in packed reaction vessel, surface-to-volume ratio 17 times that in unpacked vessel.

TABLE 2. Comparison of percent decomposition based on product analysis with that determined by residual alkyl analysis

T (°K)	% decomposition Product analysis	Alkyl recovery	CH_3 per $Pb(CH_3)_4$ undergoing reaction*
734†	73.7	76.5	3.86
728	63.6	64.7	3.93
724	63.6	63.7	3.99
714	46.2	45.7	4.04
712	44.5	43.7	4.06
711	41.6	44.0	3.80
711†	34.4	35.7	3.86
692†	15.4	15.7	3.92

*Assuming residual alkyl analysis is exact.
†Runs in packed reaction vessel. If no allowance is made for the toluene in the alkyl or for the traces of C_2H_4 and xylenes then the average CH_3 per $Pb(CH_3)_4$ undergoing reaction has an apparent average value of 3.80 *cf.* 3.93 obtained above.

TABLE 3. Effect of alkyl concentration

T (°K)	Initial $Pb(CH_3)_4$ [(mol/cc) × 10^9]	k_1 (s^{-1})
720	0.76	0.53
	1.04	0.55
	2.58	0.54
714	2.17	0.38
	4.03	0.39
	4.25	0.39

TABLE 4. Effect of total pressure on k_1

T (°K)	Pressure (cm)	k_1 (s^{-1})
714	2.79	0.39
	1.62	0.40
	0.53	0.38

[5] $$CH_3 + C_6H_5CH_3 \rightleftharpoons CH_4 + C_6H_5CH_2$$

[6] $$2CH_3 + M \rightleftharpoons C_2H_6 + M$$

[7] $$CH_3 + C_6H_5CH_2 \rightleftharpoons C_6H_5C_2H_5$$

plus the formation of dibenzyl and minor ring hydrogen abstraction by CH_3 that leads to the formation of small yields of xylenes.

As shown by the product distribution in Table 1, reactions 5–7 are all major processes under the experimental conditions used (toluene/ alkyl molar ratios 50 to 300 with the bulk of these between 65 and 100).

In Table 2 a comparison is made between the % decomposition based on product analysis

[8] $$\%\ \text{decomp.} = 100\left(\frac{\text{moles}\ (CH_4 + C_6H_5C_2H_5) + 2(\text{moles}\ C_2H_6)}{4(\text{moles}\ Pb(CH_3)_4\ \text{used})}\right)$$

and

[9] $$\%\ \text{decomp.} = 100\left(\frac{\text{moles alkyl used} - \text{moles alkyl recovered}}{\text{moles alkyl used}}\right)$$

Can. J. Chem. Downloaded from www.nrcresearchpress.com by 210.87.254.5 on 09/05/12
For personal use only.

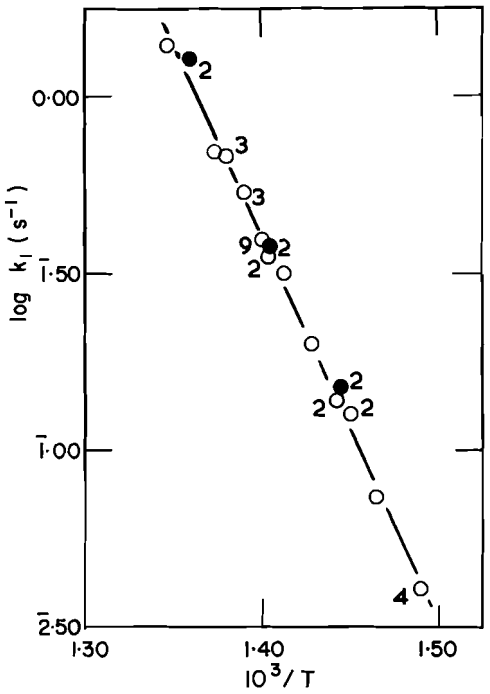

FIG. 1. Arrhenius plot of k_1. Full circles, runs in packed reaction vessel. Numbers indicate number of runs averaged to obtain the given point.

The agreement between these methods shows that essentially four methyl radicals are released for each molecule undergoing reaction 1 and indicates that no undetected major products were produced. Acid digestion of the deposit formed outside the reactor did indicate the formation of about 0.1% $(Pb—CH_3)_n$ or some similar compound. Early results also seemed to indicate the formation of a very small amount of a volatile lead containing product but this could not be confirmed.

The values of k_1 shown in Tables 1, 3, and 4 and used to obtain the Arrhenius plot shown in Fig. 1 have all been calculated from the usual first order equation,

$$k_1 = \frac{2.3}{t_c} \log \frac{100}{100 - x}$$

where x, the percent decomposed, has been calculated from eq. 8. The results in Table 3 support the assumption of first order behavior and Table 4 shows that as expected no significant unimolecular pressure effects are observed.

Least-squares analysis of the points in Fig. 1 gives $k_1 = 5.0 \times 10^{14} \exp(-49\,400/RT)$ s^{-1} with an estimated uncertainty of $\pm 1\,000$ cal mol^{-1} in E_1. This result has been obtained at the high pressure limit and using flow conditions selected to minimize errors due to thermal equilibrium or diffusion problems (6, 7). The observed activation energy should therefore be a reasonable measure of $D[(CH_3)_3Pb—CH_3]$. Comparison with the value of Lappert *et al.* (2), 48.8 kcal mol^{-1} indicates good agreement.

With $\Delta H^0_{f298}(CH_3,g) = 33.2$ kcal mol^{-1} (8), $\Delta H^0_{f298}(Pb,g) = 46.6$ kcal mol^{-1} (8), and $\Delta H^0_{f298}(Pb(CH_3)_4,g) = 32.5$ kcal mol^{-1} (8), $(D_1 + D_2 + D_3 + D_4)$ 298 °K = 146.9 kcal mol^{-1} or at 0 °K approx. 142.9 kcal mol^{-1}. This leads to an average bond dissociation energy for the four Pb—CH_3 bonds of $\bar{D} = 35.7$ kcal mol^{-1} compared to the value of 38.4 kcal mol^{-1} used by Lappert *et al.* (2). 0.8 kcal mol^{-1} of the difference is due to different values accepted for $\Delta H^0_{f0}(CH_3,g)$, 34.0 kcal mol^{-1} in the present work (8) and 34.8 by Lappert (3). The bulk of the remaining 1.9 kcal mol^{-1} difference is due to an error in Lappert's work caused by using $\Delta H^0_{f0}(CH_3,g)$, and $\Delta H^0_{f0}(Pb,g)$ in conjunction with $\Delta H^0_{f298}(Pb(CH_3)_4,g)$. Therefore accepting E_1 as a reasonable measure of D_1 gives $D_2 + D_3 + D_7 = 93.5$–96.7 kcal mol^{-1} (depending on the value chosen for $\Delta H^0_{f0}(CH_3,g)$). An estimated correction for the effect of pressure thus gives $E_2 + E_3 + E_4 =$ approximately 85–88 kcal mol^{-1}. With any reasonable choice of A_2, A_3, and A_4 (5) it is obvious that values of E_2, E_3, and E_4 can be assigned which satisfy the relationship $k_1 \gg k_2, k_3, k_4$. Decomposition by reactions 1–4 with reaction 1 rate controlling is therefore plausible.

1. G. C. ELTENTON. J. Chem. Phys. **15**, 455 (1947).
2. M. F. LAPPERT, J. B. PEDLEY, J. SIMPSON, and T. R. SPALDING. J. Organometal. Chem. **29**, 195 (1971).
3. W. A. CHUPKA. J. Chem. Phys. **48**, 2337 (1968).
4. Handbook of chemistry and physics. 50th edition. Chem. Rubber Co., Cleveland, Ohio. 1969–70.
5. R. P. JOHNSON and S. J. W. PRICE. Can. J. Chem. **50**, 50 (1972).
6. J. J. BATTEN. Aust. J. Appl. Sci. **12**, 11 (1961).
7. M. F. R. MULCAHY and M. R. PETHARD. Aust. J. Chem. **16**, 527 (1963).
8. Selected values of chemical thermodynamic properties. Natl. Bur. Std. U.S. Tech. Notes, No. 270–3. 1968.

Can. J. Chem. Downloaded from www.nrcresearchpress.com by 210.87.254.5 on 09/05/12
For personal use only.

Photoelectron Spectra of Some Bromoethylenes and 2-Bromopropene

D. CHADWICK,[1] D. C. FROST, A. KATRIB, C. A. MCDOWELL AND R. A. N. MCLEAN[2]

Department of Chemistry, University of British Columbia, Vancouver 8, British Columbia

Received April 10, 1972

The photoelectron spectra of vinyl bromide, *cis*- and *trans*-1,2-dibromoethylene and 2-bromopropene have been obtained. Interaction of the bromine "lone pair" electrons with those in the C=C π bond is discussed. The assignments are considered in relation to the chloroethylenes. The spectra provide experimental evidence for a proposal by Klasson and Manne that previous studies have reported too many I.P.'s for some of the chloroethylenes.

Les spectres photoélectroniques du bromure de vinyle, du dibromo-1,2 éthylène *cis* et *trans* et du bromo-2 propène ont été obtenus. L'interaction du doublet électronique libre du Brome avec les électrons de la liaison π est discutée. Les attributions ont été faites en relation avec les chloroéthylènes. Les spectres apportent une preuve expérimentale à la suggestion de Klasson et Manne selon laquelle les études précédentes avaient exagéré le rôle des doublets libres dans certains chloroéthylènes.

Canadian Journal of Chemistry, **50**, 2642 (1972)

Introduction

The electronic structure of ethylene and its derivatives is a problem of great chemical interest (1). Photoelectron spectroscopy (p.e.s.) offers the possibility of evaluating the orbital structures of these molecules, and ethylene itself has been the subject of several investigations (2–5). In the case of the haloethylenes one can use p.e.s. to study the inductive and resonance effects (6). More specifically, the latter effect is the interaction between the halogen "lone pair" electrons and those in the C=C π bond. Evidence for this may be obtained from many physical and chemical properties, but not all of these clearly distinguish between the two effects. For example, the C—Cl bond length in vinyl chloride (1.726 Å) (7) is much shorter than the C—Cl bond length (8) in ethyl chloride (1.788 Å), but this cannot be attributed wholly to π-bonding because of the different carbon hybridization in the two molecules. On the other hand, chlorine nuclear quadrupole coupling constants measured for several chloroethylenes (7, 9, 10) do indicate directly that the C—Cl bonds have considerable "π character". Any "π" interaction, by its very nature, must be reflected in the molecular energy levels and thus in the photoelectron spectrum. Since only one of the possible "lone pair" orbitals in each haloethylene has the correct symmetry to interact with the C=C π orbital, the resonance effect is to be observed as a stabilization of one "lone pair" orbital relative to the other(s).

In view of the recent work on the p.e. spectra of chloro- (6, 11) and fluoroethylenes (6, 12) it is of interest to examine the "π" interaction in some bromoethylenes. In this paper, we present the HeI photoelectron spectra of vinyl bromide, *cis*- and *trans*-1,2-dibromoethylene and 2-bromopropene.

There remains considerable uncertainty over the correct assignment of the p.e. spectra of the chloroethylenes with the exception of the first i.p.'s. On the basis of a comparison with Cl K_β X-ray emission spectra, extended Hückel calculations, and a consideration of the total number of states which should be observed up to 21.2 eV, Klasson and Manne (13) have suggested that too many i.p.'s have been reported by previous workers (6, 11) in some cases. The p.e. spectra of the bromoethylenes, reported here, are found to provide experimental support for this proposal of Klasson and Manne.

Experimental

The p.e. spectra were obtained using the 584 Å HeI resonance line excited by a 2450 MHz microwave discharge. The spectrometer employs a hemispherical electrostatic analyzer with a 4 in. radius. The resolution (f.w.h.m.) of the instrument as measured by the argon doublet was 15 mV. The spectra were calibrated by flowing a small amount of argon through the spectrometer simultaneously with the sample gas.

[1]Present address: Central Electricity Research Laboratories, Kelvin Avenue, Leatherhead, Surrey, U.K.

[2]Present address: Department of Chemistry, University of Ife, Ile-Ife, Nigeria.

Can. J. Chem. Downloaded from www.nrcresearchpress.com by 210.87.254.105 on 09/05/12
For personal use only.

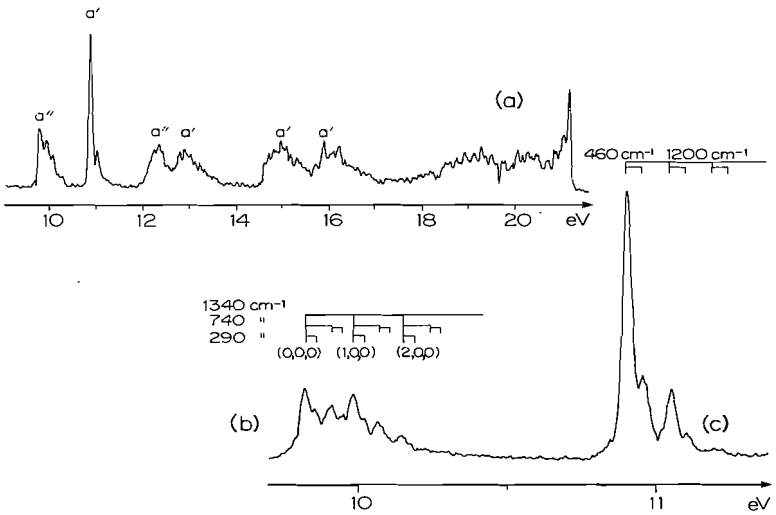

FIG. 1. The 584 Å p.e. spectrum of vinyl bromide: (*a*) shows the complete spectrum, and (*b*), the first, and (*c*), the second bands in more detail.

The samples of bromoethylenes and 2-bromopropene were obtained from commercial sources. The *cis* and *trans* isomers of 1,2-dibromoethylene were separated using preparative vapor phase chromatography.

Results and Discussion

The photoelectron spectra of the four molecules studied are reproduced in Figs. 1–4. Measured ionization potentials are given in Table 1. For each molecule, many of the observed p.e. bands exhibit resolvable fine structure due to vibrational excitation of the corresponding ion. The measured vibrational spacings are given in Table 1 where appropriate. These vibrational frequencies of the ions may

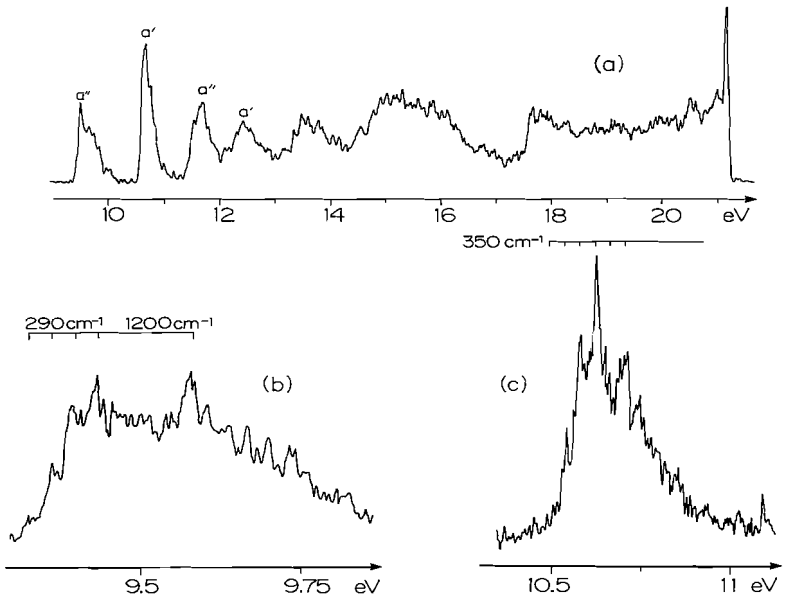

FIG. 2. The 584 Å p.e. spectrum of 2-bromopropene: (*a*) shows the complete spectrum, and (*b*), the first, and (*c*), the second bands in more detail.

Can. J. Chem. Downloaded from www.nrcresearchpress.com by 210.87.254.105 on 09/05/12
For personal use only.

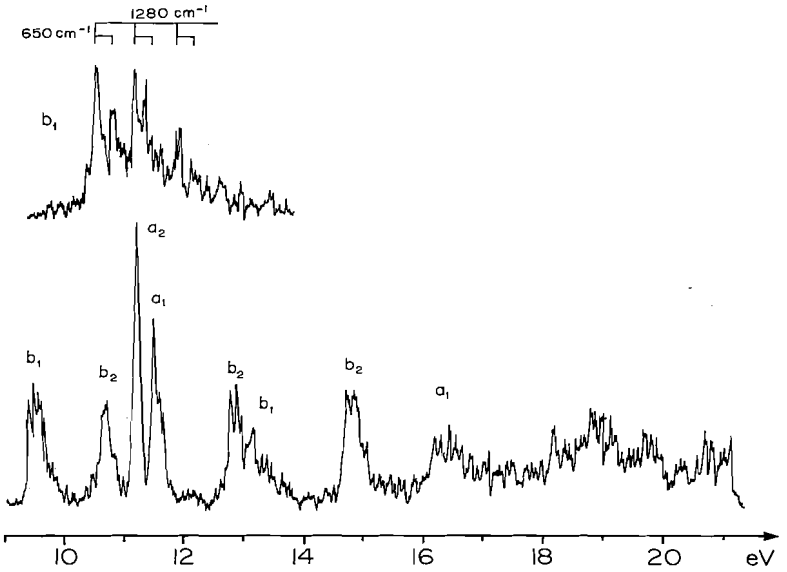

FIG. 3. The 584 Å p.e. spectrum of *cis*-1,2-dibromoethylene: (*a*) shows the complete spectrum, and (*b*), the first band in more detail.

be compared with the known frequencies of the ground state molecule. Such a comparison often indicates the bonding characteristics of the molecular orbital associated with a particular i.p.

It is worthwhile to consider briefly the features which can be expected to occur in the p.e. spectra of these four molecules. Ionizations arising from the C=C π orbital should all lie in the lower binding energy region of the spectra. In each molecule, one of the possible "lone pair" orbitals has the correct symmetry to interact with the π orbital. In the monobromo species this will simply be the out-of-plane "lone pair", while in *cis*- and *trans*-1,2-dibromoethylene it will be the b_1 and a_u combinations,

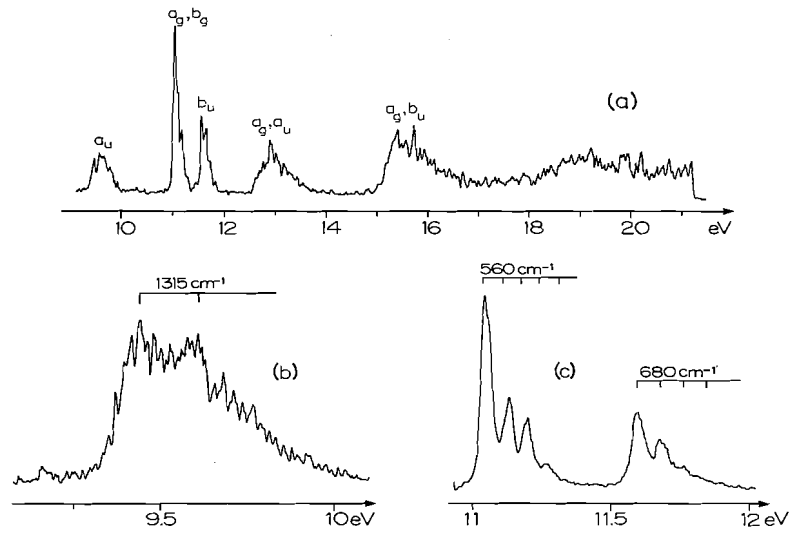

FIG. 4. The 584 Å p.e. spectrum of *trans*-1,2-dibromoethylene: (*a*) shows the complete spectrum, and (*b*) shows the first and (*c*), the second and third bands in more detail.

Can. J. Chem. Downloaded from www.nrcresearchpress.com by 210.87.254.105 on 09/05/12
For personal use only.

TABLE 1. Vertical ionization potentials of bromoalkenes (eV)*

Vinyl bromide	*cis*-1,2-Dibromoethylene	*trans*-1,2-Dibromoethylene	2-Bromopropene
9.80 (1340, 740, 290)	9.44 (1280, 650)	9.44 (1315)	9.58 (1200, 290)
10.90 (1200, 460)	10.74	11.05† (560)	10.63 (~350)
12.28	11.24		11.62
12.94	11.56	11.60 (680)	12.40
15.02	12.85	*ca.* 13.00†	13.53
16.21	13.27		15.15
19.20	14.80	*ca.* 15.90†	15.84
	16.49	19.14	

*Values are ±0.02 eV except where indicated; vibrational frequencies (cm^{-1}), where resolved, are given in parentheses and are ±40 cm^{-1}.
†Two i.p.'s.

respectively. A value of 10.5 eV for the unperturbed π orbital in these molecules can be taken from ethylene itself (3). Comparison with bromine (14) and the bromomethanes (15) places the binding energies of the bromine "lone pair" orbitals in the range 10.5–13 eV. Hence, any "π" interaction must result in a destabilization of the C=C π orbital and a stabilization of the appropriate "lone pair" orbital. In this event, the perturbed C=C π orbital would possess C—Br antibonding character. The inductive effect of bromine should stabilize the π orbital. Thus, with respect to the C=C π orbital, the inductive and resonance effects work in opposite directions. In the fluoroethylenes they apparently balance, resulting in the π orbital binding energies remaining unmodified relative to ethylene (6, 12). This has been established for other fluorinated planar molecules which contain π orbitals (12). In the chloroethylenes (6, 11) the resonance effect dominates, resulting in an overall destabilization of the C=C π orbital relative to ethylene. We would expect this to be true also for the bromoethylenes. For 2-bromopropene we must consider the addition effect of the methyl group.

Vinyl Bromide

At least seven bands can be seen in the p.e. spectrum of vinyl bromide (Fig. 1*a*). A low resolution p.e. spectrum of this molecule, reported previously by Turner *et al.* (16), did not reveal any vibrational structure. The low symmetry of CH_2=CHBr (C_s) gives rise to two irreducible representations, a' and a''. Only two valence molecular orbitals possess a'' symmetry, the C=C π orbital and the out-of-plane bromine "lone pair".

The first band, shown in Fig. 1*b*, exhibits extensive vibrational structure. This is interpreted in terms of the excitation of three ionic vibrational modes at 1340, 740, and 290 cm^{-1}. The adiabatic i.p. of 9.80 eV is in good agreement with the previously reported photoionization value (17). In view of the above discussion, this first band can be assigned with certainty to the removal of an electron from the C=C π orbital (a''). It may be noted that in the first bands of ethylene (3) and vinyl bromide the 0–0 component is the strongest. The 1340 cm^{-1} vibration is assigned to the C=C stretching frequency which occurs at 1595 cm^{-1} in the ground state of the neutral molecule (18, 19). The reduction in frequency upon ionization (255 cm^{-1}) is similar to that observed in ethylene (273 cm^{-1}) (3) and vinyl chloride (208 cm^{-1}) (6) and is strong evidence for the assignment. At the same time this substantiates our original assignment of the observed vibrational frequency for the ethylene ion and refutes the recent contrary, and in our view, erroneous contentions made by Brundle and Brown (5). The 740 cm^{-1} vibration corresponds to the C—Br stretch which is slightly increased in frequency from its ground state value of 598 cm^{-1}. The same effect is observed in vinyl fluoride and chloride (6). The 290 cm^{-1} vibration is assigned to the in-plane C—C—Br bending mode which occurs at 345 cm^{-1} in the neutral molecule (18). This vibrational mode was excited also in the first band of vinyl chloride. The observed increase in the C—Br

Can. J. Chem. Downloaded from www.nrcresearchpress.com by 210.87.254.105 on 09/05/12
For personal use only.

Can. J. Chem. Downloaded from www.nrcresearchpress.com by 210.87.254.105 on 09/05/12
For personal use only.

stretching mode on ionization may be taken as an indication of the C—Br antibonding character of the C=C π orbital and, hence, some degree of "π" interaction with the bromine a'' "lone pair". Since the binding energy of the C=C π orbital is lower than that of the corresponding orbital in ethylene, we conclude that the resonance effect dominates over the inductive effect by approximately 0.7 eV. This will be discussed further below.

The second p.e. band has an adiabatic i.p. of 10.90 eV and is shown in Fig. 1*c*. The observed structure corresponds to two ionic vibrational modes at 1200 and 460 cm^{-1}. It may be concluded from the strength of the 0–0 component that the parent orbital for this ionization is relatively non-bonding. Since the resonance effect is significantly larger than the inductive effect (*vide supra*), we expect the bromine a'' "lone pair" to be stabilized relative to the a'. Also, any interaction of the a' "lone pair" with higher σ bonding orbitals would enhance this effect. On this basis we assign this second band to the in-plane (a') "lone pair". From the p.e. spectrum of vinyl chloride, Lake and Thompson (6) conclude that the two chlorine "lone pair" orbitals are almost degenerate at 11.72 and 11.87 eV. Klasson and Manne (13) and Turner *et al.* (16) do not agree with this interpretation on the grounds that one of the chlorine "lone pair" orbitals is demonstrably interacting with the C=C π orbital, because of the observed destabilization of the latter orbital relative to ethylene. Extended Hückel calculations on the chloroethylenes (13) predict strong mixing of the a'' orbitals. Similar large mixing of π orbitals has been concluded for $Cl_2C{=}O$ and $Cl_2C{=}S$ (20). Klasson and Manne (13) have suggested that there is only one i.p. at 11.72 eV in $CH_2{=}CHCl$ and that the 11.87 eV peak is due to vibrational structure. Returning to the second band of $CH_2{=}CHBr$, it can be inferred that there is no coincidence of ionization potentials at 10.90 eV. The C=C π orbital binding energies do not vary greatly over the four molecules studied here (*vide infra*). Thus, if the two bromine "lone pair" orbitals in vinyl bromide are degenerate, a similar situation must exist in the remaining three molecules in order to explain the p.e. spectra in the range 10.5–12.0 eV. This is very unlikely and no evidence in favor of it was obtained from any of the spectra (Figs. 1–4). The 460 cm^{-1} vibration probably corresponds to the C—Br stretch compared to 598 cm^{-1} in the neutral molecule, which would indicate some C—Br bonding character. The 1200 cm^{-1} vibration may be the CH_2 deformation which occurs at 1260 cm^{-1} in the molecular ground state (18). It is interesting to note that the difference between the 11.72 and 11.87 eV peaks in the spectrum of vinyl chloride is 1200 cm^{-1}.

The third and fourth bands occur at vertical i.p.'s of 12.28 and 12.94 eV, respectively. Both bands are broad which indicates the bonding nature of the molecular orbitals involved. In view of the above assignments, one of these i.p.'s must correspond to the second a'' orbital. The remaining i.p. must arise from a σ bonding orbital (a') which may be essentially either C—H or C—Br bonding. Ionization from the $1b_{3g}$ C—H bonding orbital in ethylene occurs at a vertical i.p. of 12.85 eV (12). It is expected that this orbital will be stabilized to some extent in the vinyl halides with the highest binding energy occurring in vinyl fluoride. The corresponding i.p. in $CH_2{=}CHF$ is at 13.79 eV and 13.14 or 13.6 eV in $CH_2{=}CHCl$ (6). Ionization from an essentially C—Br orbital occurs at 13.49 eV in methyl bromide (15) and should shift to higher binding energy in vinyl bromide due to the increased carbon s orbital participation. Thus, we can confidently assign the fourth band in $CH_2{=}CHBr$ at 12.94 eV as arising from an a' orbital which correlates with the $1b_{3g}$ orbital in ethylene. Therefore, the third band at 12.28 eV must correspond to the second a'' orbital. If we take the separation of the bromine "lone pair" orbitals as an approximate measure of the extent of the "π" interaction, then we obtain values of 1.4 and 0.7 eV for the resonance and inductive effects, respectively.

The broad fifth and sixth bands at 15.02 and 16.21 eV, respectively, must arise from σ bonding orbitals (a'). A recently reported p.e. spectrum of Br_2CO (21) shows that the highest energy σ orbitals are overlapping in the range 15.5–16.5 eV. A σ orbital with significant C—Br character should occur at lower binding energy in $CH_2{=}CHBr$, but higher than in CH_3Br (*vide supra*). On this basis, we assign the fifth band in vinyl bromide as corresponding to an

Can. J. Chem. Downloaded from www.nrcresearchpress.com by 210.87.254.105 on 09/05/12
For personal use only.

essentially C—Br σ bonding orbital and the sixth band to a C—C and C—H bonding orbital, as far as such divisions are possible.

Summarizing, the orbital structure of vinyl bromide is concluded to be $....(a')^2(a'')^2(a')^2(a'')^2$. These assignments are shown in Fig. 1*a*.

2-Bromopropene

In 2-bromopropene we have the additional complication of a methyl group. It has been assumed in the following discussion that $CH_2{=}CBr.CH_3$ possesses C_s symmetry, so that $a'(\sigma)$ and $a''(\pi)$ are still valid orbital descriptions. The p.e. spectra of the methyl halides (15), methyl cyanide, and methyl acetylene (22) indicate that the methyl group in 2-bromopropene should provide two i.p.'s in the 14–16 eV region, arising from a' and a'' orbitals. Thus, the spectrum below 14 eV should be similar to that of vinyl bromide.

The p.e. spectrum of 2-bromopropene, shown in Fig. 2*a*, reveals at least eight bands below 21.2 eV and, indeed, the region below 14 eV is almost identical in appearance to $CH_2{=}CHBr$. The apparent effect of the methyl group has been to destabilize the four highest energy orbitals relative to vinyl bromide and it is tempting to assign the p.e. bands by a straightforward comparison of the two spectra. The vibrational structure of the first band at 9.58 eV (Fig. 2*b*) is complex and appears to contain two ionic modes at 1200 and 290 cm^{-1}. The former may be assigned to the C=C stretch reduced in frequency from the neutral molecule (1636 cm^{-1}) (18), or a CH_2 or CH_3 deformation. The 290 cm^{-1} vibration must correspond to the C—C—Br bending mode, which was also excited in the first band of vinyl bromide. There can be no doubt that this first band in 2-bromopropene arises from the C=C π orbital (a''). As in vinyl bromide, this orbital has been destabilized relative to ethylene. If we assume a similar interaction with the a'' bromine "lone pair", then the overall effect of the methyl group has been to destabilize the C=C π orbital by *ca.* 0.2 eV.

The second band has an adiabatic i.p. at 10.51 eV and is rather sharp (Fig. 2*c*) indicating that the parent orbital is relatively non-bonding. There is also an indication of vibrational structure of *ca.* 350 cm^{-1} which would probably correspond to the in-plane C—C—Br bending mode (345 cm^{-1} in the ground state of vinyl bromide). We assign this band to the bromine a' "lone pair", for reasons discussed previously in relation to the second band of vinyl bromide.

Direct comparison with the p.e. spectrum of vinyl bromide would lead us to assign the third band in 2-bromopropene at 11.62 eV to the a'' bromine "lone pair", and the fourth at 12.40 eV to an a' orbital. However, it is possible that introduction of the methyl group would reverse this ordering. The third i.p. of vinyl bromide is 12.28 eV which is slightly lower than the fourth i.p. of 2-bromopropene. Were we to assign this latter i.p. as arising from the a'' bromine orbital, the apparent stabilization relative to the corresponding orbital in $CH_2{=}CHBr$ may be attributed to a slight increase in the mixing with the C=C π orbital (*cf.* the 0.2 eV destabilization of this orbital with respect to $CH_2{=}CHBr$), or to the presence of the methyl group. This assignment would imply, therefore, that the methyl group leads to a destabilization of the lower binding energy a' orbitals only. This is unlikely, since the methyl group introduces both a' and a'' orbitals in the 15 eV region, and so we prefer to assign the third and fourth bands in $CH_2{=}CBr{-}CH_3$ to a'' and a' orbitals, respectively, as is the case for vinyl bromide. The order of the outer orbitals in 2-bromopropene is therefore $.....(a')^2(a'')^2(a')^2(a'')^2$.

Definite assignment of the higher i.p.'s, which must arise from σ bonding orbitals, is difficult, because of the low molecular symmetry. The broad band between 14–17 eV is, however, similar in appearance to ionizations from the methyl group orbitals in other low symmetry compounds such as CH_3SH (23).

cis-1,2-Dibromoethylene

The p.e. spectrum of *cis*-1,2-dibromoethylene shows eight distinct bands below 21.2 eV (Fig. 3). The first band has an adiabatic i.p. of 9.32 eV and two vibrational modes of the ion are observed at 1280 and 650 cm^{-1}. The vertical i.p. of 9.44 eV is in good agreement with the photoionization value of 9.45 eV (17). By analogy with the p.e. spectra of the dichloroethylenes (6, 11), vinyl bromide, and 2-bromopropene (*vide supra*), we attribute this first band to ionization from the C=C π orbital (b_1). The

Can. J. Chem. Downloaded from www.nrcresearchpress.com by 210.87.254.105 on 09/05/12
For personal use only.

1280 cm^{-1} vibration is assigned to the C=C stretching mode which is reduced from the molecular ground state value of 1584 cm^{-1}. The 650 cm^{-1} vibration corresponds to the C—Br stretching mode, showing a slight increase over the 580 cm^{-1} for the neutral molecule (18). This indicates that the C=C π orbital possesses some C—Br antibonding character and, therefore, that some mixing with the b_1 bromine "lone pair" orbital has occurred. A similar conclusion was reached for vinyl bromide (*vide supra*). The same vibrational modes were observed in the first band of *cis*-1,2-dichloroethylene (6). The binding energy of the C=C π orbital is less than the corresponding orbital in ethylene, and even in vinyl bromide. Again, we interpret this in terms of the resonance effect being larger than the inductive effect by approximately 1.07 eV.

The 10–12 eV region contains three bands at vertical i.p.'s of 10.74, 11.24, and 11.56 eV (Fig. 3). No vibrational structure was resolved on any of these bands which may indicate the short lifetime of the ion in the corresponding states. The sharpness of the 11.24 and 11.56 eV bands compared to the remainder of the spectrum clearly suggests that they arise from bromine "non-bonding" orbitals. In *cis*-1,2-dibromoethylene there will be four orbitals derived from the 4p "lone pair" atomic orbitals of the bromine atoms namely, b_2, b_1, a_2, and a_1. The order is that expected on the basis of bromine–bromine overlap only, with the a_1 combination occurring at the highest binding energy. The importance of the interaction of these "lone pair" orbitals with other molecular orbitals in modifying the above ordering has been pointed out for dichloro- and dibromomethane (24), dichlorosilane (25), and other dichloro compounds (20, 26). The a_2 orbital is symmetry determined and cannot interact with any other valence molecular orbital. Therefore, one might expect ionization from this orbital to result in a narrow p.e. band. We anticipate ionizations from bromine non-bonding orbitals to occur in the 10.5–13 eV region. Since we have demonstrated that the resonance effect is at least 1.07 eV, the b_1 bromine orbital must be at higher binding energy than the b_2, a_2, and a_1 non-bonding combinations. As there is no b_2 orbital at lower binding energy than the bromine "lone pair" orbitals, the order b_2 lower than a_2 should remain unaltered. Therefore, we assign the 10.74, 11.24, and 11.56 eV bands as arising from the b_2, a_2, and a_1 bromine orbitals, respectively. The fact that the 11.24 eV band is the sharpest of these three is consistent with its assignment to the a_2 orbital.

The fifth band contains two i.p.'s at 12.85 and 13.27 eV. One of these must arise from the inner b_1 orbital and comparison with the third (a'') and fourth (a') bands in the p.e. spectrum of vinyl bromide suggests that the other may be due to a C—H σ bonding orbital of b_2 symmetry. b_2 and a_1 C—Br σ bonding orbitals in CH_2Br_2 (15) give rise to ionizations in the 14–15 eV range. It is expected that these orbitals will be more stable in dibromoethylene. Therefore, it is the essentially C—H σ bonding orbital (b_2) which is responsible for either the 12.85 or the 13.27 eV i.p. Both i.p.'s are lower than those corresponding to the highest energy σ bonding orbitals in *cis*-1,2-difluoroethylene (12) and *cis*-1,2-dichloroethylene (6, 11), and are greater or equal to the $1b_{3g}$ ionization in ethylene (3) so that no assignment is forthcoming from such a comparison. Since the two b_2 orbitals are at similar energies the higher energy b_2 may be above the inner b_1 orbital. However, comparison with CH_2=CHBr indicates the reverse, namely b_1 above b_2. The problem may be resolved in the following way. If we assume that the unperturbed b_1 bromine "lone pair" ionization would occur between the assigned a_2 and a_1 bands at $\sim$11.4 eV, then assignment of the 12.85 eV ionization to the inner b_1 orbital leads to a resonance stabilization of 1.45 eV. Furthermore, the inductive effect of the two bromines on the C=C π orbital would be $1.45 - 1.07 \approx 0.4$ eV, whereas in vinyl bromide it is 0.7 eV. That is, this assignment would imply that the inductive effect of two bromines is less than one. Alternatively, if the 13.27 eV band is the b_1, then the resonance effect becomes *ca.* 1.9 eV and the inductive effect *ca.* 0.8 eV. Although the reliability of such calculations is probably limited, we prefer this latter interpretation.

In the light of the above discussion the seventh and eighth i.p.'s at 14.80 and 16.49 eV are assigned to ionization from b_2 and a_1 orbitals, respectively, which are essentially C—Br in character, the former being the anti-

Can. J. Chem. Downloaded from www.nrcresearchpress.com by 210.87.254.105 on 09/05/12
For personal use only.

bonding combination. The orbital structure of *cis*-1,2-dibromoethylene is concluded to be

$$\ldots.(a_1)^2(b_2)^2(b_1)^2(b_2)^2(a_1)^2(a_2)^2(b_2)^2(b_1)^2$$

These assignments are shown in Fig. 3.

trans-1,2-dibromoethylene

Only six distinct bands are observed in the p.e. spectrum of *trans*-1,2-dibromoethylene (Fig. 4*a*). Clearly, some overlapping of bands has occurred. A straightforward comparison of the spectra of *cis*- and *trans*-dibromoethylene suggests that the second (11.05 eV), fourth (*ca.* 13 eV), and fifth (15.9 eV) bands each contain two i.p.'s.

The first p.e. band, shown in Fig. 4*b*, has an adiabatic i.p. of 9.30 eV and a vertical i.p. of 9.44 eV which agrees well with the photoionization value of 9.46 eV (27). There is an indication of a vibrational spacing of 1315 cm^{-1}, which is assigned to the C=C stretching frequency, reduced from its value of 1578 cm^{-1} in the neutral molecule (18). The broad nature of the peaks may be due to the short lifetime of the ion in this state or to the presence of a low frequency ionic vibrational mode which is unresolved. The band is assigned to ionization from the C=C π orbital which in *trans*-CHBr=CHBr possesses a_u symmetry. The vertical i.p. is identical to that of *cis*-1,2-dibromoethylene and so we again conclude that the resonance effect dominates over the inductive effect by *ca.* 1.07 eV.

Figure 4*c* shows the 11–12 eV region, which appears to contain only two p.e. bands, at high resolution. The cross-section of the band with adiabatic i.p. at 11.05 eV is twice that of the band at 11.60 eV, indicating that two i.p.'s may be superimposed in the former. Clearly, there can be no more than three i.p.'s in this range, which supports the assignment of only one i.p. at 10.90 eV in vinyl bromide and three i.p.'s in the range 10–12 eV in *cis*-1,2-dibromoethylene (*vide supra*). One component of the second band must have a vertical i.p. at 11.05 eV. However, it is difficult to assess the true adiabatic or vertical i.p. of the second component. It may be at 11.05 eV also, or at 11.13 eV (the second peak). Neither is an interpretation of the vibrational structure any easier since the spacing is not quite regular and more than one vibrational mode may be involved. The 680 cm^{-1} spacing observed on the third band probably corresponds to the C—Br stretching frequency which is only slightly reduced from its ground-state value of 748 cm^{-1} (18). All three ionizations are sharp and there can be no doubt that they arise from bromine "lone pair" orbitals. The b_2, a_2, b_1, and a_1 combinations in *cis*-CHBr=CHBr become a_g, b_g, a_u, and b_u, respectively, in the *trans* isomer. The a_u ionization must be at higher binding energy than the other three due to the conjugative interaction with the a_u C=C π orbital (*vide supra*). The strong peak at 11.05 eV must correspond to the b_g "pure" bromine orbital. Since the a_g orbital should be at higher energy than the b_g, we assign both to be degenerate at 11.05 eV. Thus, the 11.60 eV band is due to ionization from the b_u orbital. As the two bromine atoms are further apart in the *trans* compound than in the *cis*, their mutual interaction is smaller, resulting in the "lone pair" orbitals being more nearly degenerate.

The fourth and fifth bands at 13 and 15.9 eV, respectively, are both the result of two ionizations. We assign a_g and a_u ionizations to the 13 eV band and a_g and b_u ionizations to the 15.9 eV band by direct comparison with our assignments for the p.e. spectrum of *cis*-CHBr=CHBr. It may be noted that this coalescence of higher i.p.'s in the *trans* isomer is also observed in *trans*-1,2-dichloroethylene (6). The orbital structure of *trans*-CHBr=CHBr is therefore

$$\ldots\ldots.(b_u)^2(a_g)^2(a_u)^2(a_g)^2(b_u)^2(b_g)^2(a_g)^2(a_u)^2$$

where the ordering of the seemingly degenerate orbitals has been made with reference to *cis*-1,2-dibromoethylene.

General Comments

The results derived from the p.e. spectra of the bromoethylenes, 2-bromopropene, chloroethylenes, and ethylene are reproduced in the form of an orbital correlation diagram, Fig. 5. The i.p.'s of the chloroethylenes were taken from ref. 6 and those of ethylene from ref. 12. The assignments of the chloroethylenes below 15 eV are those suggested by Klasson and Manne (13).

It is important to consider the number of states which should be observed below 21.2 eV

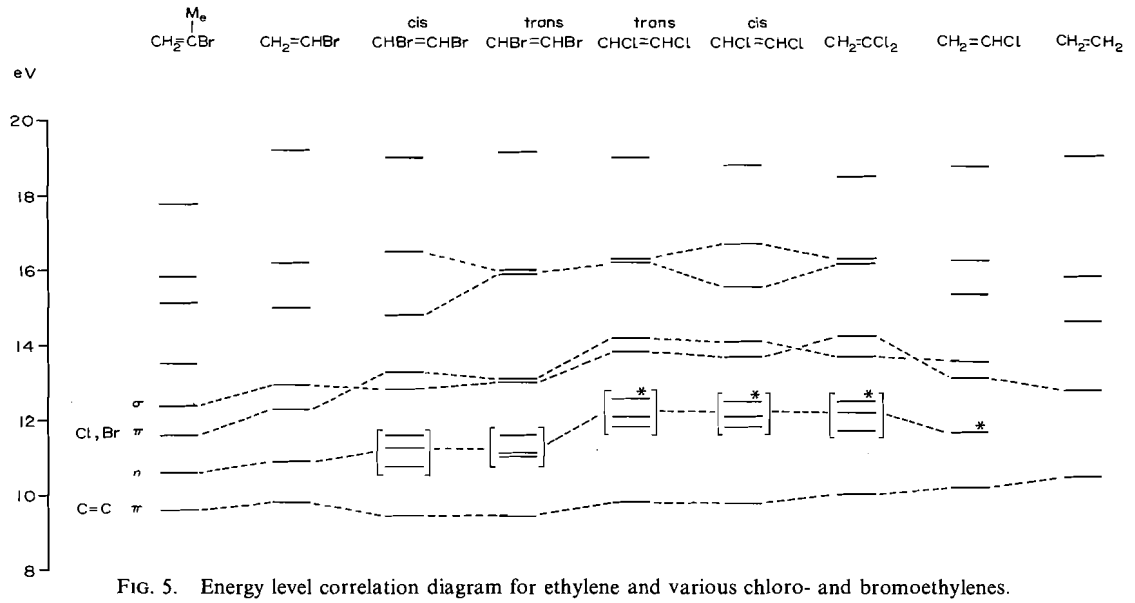

FIG. 5. Energy level correlation diagram for ethylene and various chloro- and bromoethylenes.

in the chloro- and bromoethylenes. Klasson and Manne have pointed out that one i.p. for each chlorine atom and one i.p. for the two carbon atoms should be above 21.2 eV in the chloroethylenes (13). We can expect the same in the bromoethylenes, although these high i.p.'s may be lower than in the chloroethylenes, and and it is possible that one may fall at or just below 21.2 eV. With this provision, we should observe seven states in the HeI p.e. spectra of vinyl bromide and chloride, and nine states for the dichloro- and dibromoethylenes. Reference to Fig. 5 shows that the correct number of states has been observed in the bromoethylenes, though there is some overlapping in *trans*-CHBr=CHBr. However, on the basis of the above argument, Klasson and Manne (13) suggested that previous workers reported too many states for *cis*-1,2-dichloroethylene and too few for 1,1-dichloroethylene (6, 11). We consider first the region above 15 eV. Three states are observed between 15 and 20 eV for the bromoethylenes, so that the same should be true of corresponding chloroethylenes. Simple comparison assigns two states to the 16.2 eV bands in *trans*-CHCl=CHCl and CH_2=CCl_2. This conclusion was reached also by Klasson and Manne (13). Although there are apparent accidental degeneracies in these molecules, the actual p.e. bands involved are very broad and the true vertical i.p.'s may be 0.5–1.0 eV apart.

In each chloroethylene there are indisputably two states between 13–15 eV (6, 11) which are consistent with the two states in the 12–14 eV range in the bromoethylenes. Thus, adjustment to the correct number of states in the chloroethylenes must be made in the 11–13 eV region which contains the ionizations from chlorine "lone pair" orbitals. Klasson and Manne (13) suggested that one too many i.p.'s were reported in this region for *cis*- and *trans*-dichloroethylene and vinyl chloride. A comparison with the corresponding bromoethylenes supports this interpretation and in Fig. 5 we have eliminated one i.p. for each of these three molecules.

Let us consider the alternative. If the number of i.p.'s reported (6, 11) for vinyl chloride and the dichloroethylenes in the 11–13 eV range is correct then the chlorine "lone pair" orbitals which are interacting with the C=C π orbital are assigned (6) to the levels marked with asterisks in Fig. 5. In this event there will be two bands at *ca.* 11.7 eV in vinyl chloride. Comparing these assignments to our interpretation of the p.e. spectra of the bromoethylenes, we would conclude that (*i*) the resonance effects are smaller in the chloroethylenes than in the bromoethylenes, (*ii*) the

Can. J. Chem. Downloaded from www.nrcresearchpress.com by 210.87.254.105 on 09/05/12
For personal use only.

Can. J. Chem. Downloaded from www.nrcresearchpress.com by 210.87.254.105 on 09/05/12
For personal use only.

inductive effect of chlorine on the C=C π orbital is less than bromine, and (*iii*) the mutual overlap of chlorine 3p orbitals in the dichloroethylenes is less than that of the bromine 4p orbitals in the corresponding bromo compounds. None of these three items is likely. However, for the chloroethylene assignments shown in Fig. 5, irrespective of the order of the states in the 13–15 eV range, we conclude that (*i*) the resonance effects in the bromo- and chloroethylenes are approximately the same, (*ii*) the inductive effect of chlorine on the C=C π orbital is greater than that of bromine, and (*iii*) the mutual overlap of the chlorine 3p orbitals and the bromine 4p orbitals in these molecules is approximately the same. These conclusions are more reasonable and argue strongly for the interpretation presented in Fig. 5.

Klasson and Manne assign the two bands in the 13–15 eV region in the chloroethylenes by reference to extended Hückel calculations (13), with the exception of $CH_2{=}CCl_2$ which they assign on the basis of the observed excitation of a C—H vibration on the higher of the two i.p.'s (6). Recently reported HeII spectra of vinyl chloride and C_2Cl_4 (12) may be important in this respect. The reduced cross-section for HeII compared to HeI of all the bands in the 11–14 eV region in C_2Cl_4 demonstrates that they arise from chlorine 3p orbitals. Of the two bands at 15 eV, the lower binding energy component has a much lower cross-section for HeII, but the higher component does not. It would appear that the lower component is a chlorine 3p ionization, whereas the higher i.p. probably arises from a σ orbital. The results for vinyl chloride are less clear, although the 11.72 eV band is shown to be a chlorine "lone pair" ionization by its reduced cross-section for HeII. If anything, the HeII spectra of $CH_2{=}$CHCl indicates that it is the 13.6 eV band which is the other chlorine 3p ionization rather than the one at 13.1 eV, which agrees with the assignment of Klasson and Manne (13).

This work was supported by generous financial grants from the National Research Council of Canada. D.C. thanks the Science Research Council of Great Britain for the award of a N.A.T.O. Fellowship. R.A.N.M. acknowledges the receipt of a Killam Fellowship from The University of British Columbia. We thank Dr. F. G. Herring for his interest.

1. A. J. Merer and R. S. Mulliken. Chem. Rev. **69**, 639 (1969).
2. A. D. Baker, C. Baker, C. R. Brundle, and D. W. Turner. Int. J. Mass Spectrom. Ion Phys. **1**, 285 (1968).
3. G. R. Branton, D. C. Frost, T. Makita, C. A. McDowell, and I. A. Stenhouse. J. Chem. Phys. **52**, 802 (1970).
4. C. R. Brundle, M. B. Robin, H. Basch, M. Pinsky, and A. Bond. J. Am. Chem. Soc. **92**, 3863 (1970).
5. C. R. Brundle and D. B. Brown. Spectrochim. Acta, **27A**, 2491 (1971).
6. R. F. Lake and H. Thompson. Proc. Roy. Soc., London, **A315**, 323 (1970).
7. D. Kivelson, E. B. Wilson, Jr., and D. R. Lide. J. Chem. Phys. **32**, 205 (1960).
8. R. H. Schwendeman and G. D. Jacobs. J. Chem. Phys. **36**, 1245 (1962).
9. S. Sekino and T. Nishikawa. J. Phys. Soc. Jap. **12**, 43 (1957).
10. W. H. Flygare and J. A. Howe. J. Chem. Phys. **36**, 440 (1962).
11. N. Jonathan, K. Ross, and V. Tomlinson. Int. J. Mass Spectrom. Ion Phys. **1**, 111 (1968).
12. M. B. Robin, N. A. Kuebler, and C. R. Brundle. International Conference on Electron Spectroscopy. Asilomar, U.S.A. 1971.
13. M. Klasson and R. Manne. International Conference on Electron Spectroscopy. Asilomar, U.S.A. 1971.
14. A. B. Cornford, D. C. Frost, C. A. McDowell, J. L. Ragle, and I. A. Stenhouse. J. Chem. Phys. **54**, 2651 (1971).
15. A. W. Potts, H. J. Lempka, D. G. Streets, and W. C. Price. Phil. Trans. Roy. Soc., London, **A268**, 59 (1970).
16. D. W. Turner, C. Baker, A. D. Baker, and C. R. Brundle. Molecular photoelectron spectroscopy. Wiley–Interscience, London. 1970.
17. R. Bralsford, P. V. Harris, and W. C. Price. Proc. Roy. Soc., London, **A258**, 459 (1960).
18. P. Torkington. J. Chem. Phys. **17**, 1279 (1949).
19. G. J. Martin and M. L. Martin. J. Chim. Phys. **61**, 1222 (1964).
20. D. Chadwick. Can. J. Chem. **50**, 737 (1972).
21. R. K. Thomas and H. Thompson. Proc. Roy. Soc. London, **A327**, 13 (1972).
22. D. C. Frost, F. G. Herring, C. A. McDowell, and I. A. Stenhouse. Chem. Phys. Lett. **4**, 533 (1970).
23. D. C. Frost, F. G. Herring, A. Katrib, C. A. McDowell, and R. A. N. McLean. J. Phys. Chem. **76**, 1030 (1972).
24. R. N. Dixon, J. N. Murrell, and B. Narayan. Mol. Phys. **20**, 611 (1971).
25. D. C. Frost, F. G. Herring, A. Katrib, R. A. N. McLean, J. E. Drake, and N. P. C. Westwood. Chem. Phys. Lett. **10**, 347 (1971); Can. J. Chem. **49**, 4033 (1971).
26. D. Chadwick, A. B. Cornford, D. C. Frost, F. G. Herring, A. Katrib, C. A. McDowell, and R. A. N. McLean. International Conference on Electron Spectroscopy. Asilomar, U.S.A. 1971.
27. J. Momigny. Bull. Sci. Acad. Roy. Belg. **46**, 686 (1960).

Possible Intermediates in the Biosynthesis of Porphyrins[1]

J. M. OSGERBY,[2] J. PLUSCEC,[3] Y. C. KIM,[4] F. BOYER,[5] N. STOJANAC,[6] H. D. MAH,[7] AND S. F. MACDONALD

Division of Biological Sciences, National Research Council of Canada, Ottawa, Canada K1A 0R6

Received April 5, 1972

Details of our synthesis of 5-aminomethyl-4,3′-dicarboxymethyl-3,4′-di-(2-carboxyethyl)-dipyrrylmethane (**1***b*), as a stable potassium salt are now reported. This synthetic product had been shown to be an intermediate in the biosynthesis of uroporphinogen 1. The analogous tripyrrane, **15**, should be available from the lactam of 2-(2-methoxycarbonylethyl)-3-methoxycarbonylmethyl-4,6-di-(2-ethoxycarbonylethyl)-5-ethoxycarbonylmethyl-7-carboxymethyl-8-aminomethyl-tripyrrane (**22**) which has also been synthesized.

5-Formyl-4,3′-di-ethoxycarbonylmethyl-3,4′-di-(2-ethoxycarbonylethyl)-5′-benzyloxycarbonyldipyrrylmethane (**24**), was obtained through the condensation of the bromomethyl pyrrole **2***b* with the hydrazone, **23**, from a 2-formyl-5-free pyrrole and Girard's "T" reagent. This depends on the supression of the deactivating effect of the aldehyde group in a hydrazone from which the aldehyde is easily regenerated.

Notre synthèse de l'aminométhyl-5 dicarboxyméthyl-4,3′ di(carboxy-2 éthyl)-3,4′ dipyrrylméthane (**1***b*), comme sel de potassium stable est maintenant rapportée de façon détaillée. On a montré que ce produit synthétique est un intermédiaire dans la biosynthèse de l'uroporphinogène 1. L'analogue tripyrrane **15** pourrait être disponible à partir de la lactame de la (méthoxycarbonyl-2 éthyl)-2 méthoxycarbonyl méthyl-3 di(éthoxycarbonyl-2 éthyl)-4,6 éthoxy carbonylméthyl-5 carboxyméthyl-7 aminométhyl-8 tripyrrane (**22**), qui a été également synthétisée. Le formyl-5 diéthoxycarbonylméthyl-4,3′ di(éthoxycarbonyl-2 éthyl)-3,4′ benzyloxycarbonyl-5′ dipyrridylméthane (**24**), a été obtenu par condensation du bromométhylpyrrole **2***b* avec l'hydrazone **23** du formyl-2 pyrrole libre en -5 et le réactif "T" de Girard. Cela dépend de la suppression de l'effet désactivant du groupe aldéhyde dans une hydrazone à partir de laquelle l'aldéhyde est facile à regénérer.

Canadian Journal of Chemistry, **50**, 2652 (1972)

Introduction

Some time ago we undertook the synthesis of compounds which might be intermediates between porphobilinogen and the uroporphinogens in the biosynthesis of the porphyrins. Although there was no evidence at the time that such intermediates existed, they would be identified if the synthetic materials were substrates for the enzymes involved. Another incentive arose because the value of labelling is minimized when four identical units of porphobilinogen condense to the uroporhinogen; a second substrate, not equivalent to porphobilinogen, would provide one solution to this difficulty.

After it was shown (1) that neither opsopyrrole-dicarboxylic acid (2) nor *iso*-porphobilinogen (3) were intermediates, we turned to dipyrrylmethanes. Neither **1***a* nor its symmetrical isomers were intermediates (1, 4). However, their synthesis (5, 6) showed that unsymmetrical 5,5′-dicarbethoxydipyrrylmethanes, free of symmetrical isomers, could be obtained by condensing 2-free and 2-bromomethyl pyrroles[9] in hot AcOH–NaOAc. More important, unstabilized dipyrrylmethanes such as **1***a* were easily obtained from their carboxylated derivatives, and their quite unexpected stability (*cf.* 7, 8) was a prerequisite for further work in this direction.

Attention was then directed to aminomethyl dipyrrylmethanes, first to methylene-bis-porphobilinogen (3) which was not an intermediate (1, 4), and then to **1***b*. A synthesis of **1***b* based on that of **1***a* would involve the condensation of **2***b*, presumably available by known general methods, with a 5-free pyrrole bearing a potential 2-aminomethyl group. Such groups, like

[1]Issued as NRCC No. 12693.
[2]NRCC Postdoctorate Fellow, 1960–1962.
[3]NRCC Postdoctorate Fellow, 1962–1964.
[4]NRCC Postdoctorate Fellow, 1965–1967.
[5]NRCC Postdoctorate Fellow, 1967–1968.
[6]NRCC Postdoctorate Fellow, 1968–1969.
[7]NRCC Postdoctorate Fellow, 1971–present.
[8]To whom enquiries should be addressed.

[9]In hot AcOH–NaOAc, bromomethyl pyrroles are equivalent to acetoxymethylpyrroles into which they are rapidly converted.

Can. J. Chem. Downloaded from www.nrcresearchpress.com by 210.87.254.6 on 09/05/12
For personal use only.

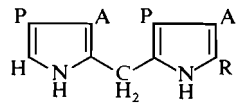

1

$A = CH_2COOH$ $P = CH_2CH_2COOH$
$A^{Me} = CH_2COOMe$ $P^{Me} = CH_2CH_2COOMe$
$A^{Et} = CH_2COOEt$ $P^{Et} = CH_2CH_2COOEt$
$A^{Bz} = CH_2COOCH_2Ph$ $P^{Bz} = CH_2CH_2COOCH_2Ph$

a R = H
b R = CH_2NH_2

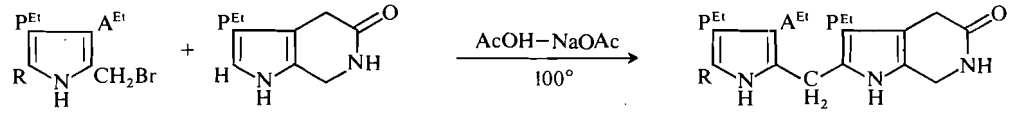

2 3 4

(*a*) R = COOEt; (*b*) R = $COOCH_2Ph$; (*c*) R = COOH; (*d*) R = I; (*e*) R = H

CN, frequently deactivate the 5-position, but a suitable component was found in the ethyl ester of porphobilinogen lactam, **3**, which condensed with **2***a* to **4***a* (3).

We have indicated the later steps in the synthesis of **1***b* (9), and the product, used as its potassium salt, was shown to be an intermediate in the biosynthesis of uroporphyrin 1, into which up to *ca.* 50% of **1***b* was incorporated by the enzyme system (22, 10). We have been reluctant to publish the synthetic work in detail because the product **1***b* has not been characterized in a way which would distinguish it from its isomers, and because it contained about 10% of an impurity. This limits the usefulness of **1***b*: its 10% incorporation would be ambiguous, and a natural intermediate could not be positively identified merely by comparison with it. In its critical steps, our synthesis does not differ in principle from those that have been described (11) or outlined (12).

In order to obtain the bromomethylpyrrole **2***b*, we first converted **5** to **8** by methods which were also applicable to the conversion of **9** into **12**; the latter would be required for isomers of **1***b*. We failed to obtain **8** from the diethyl ester

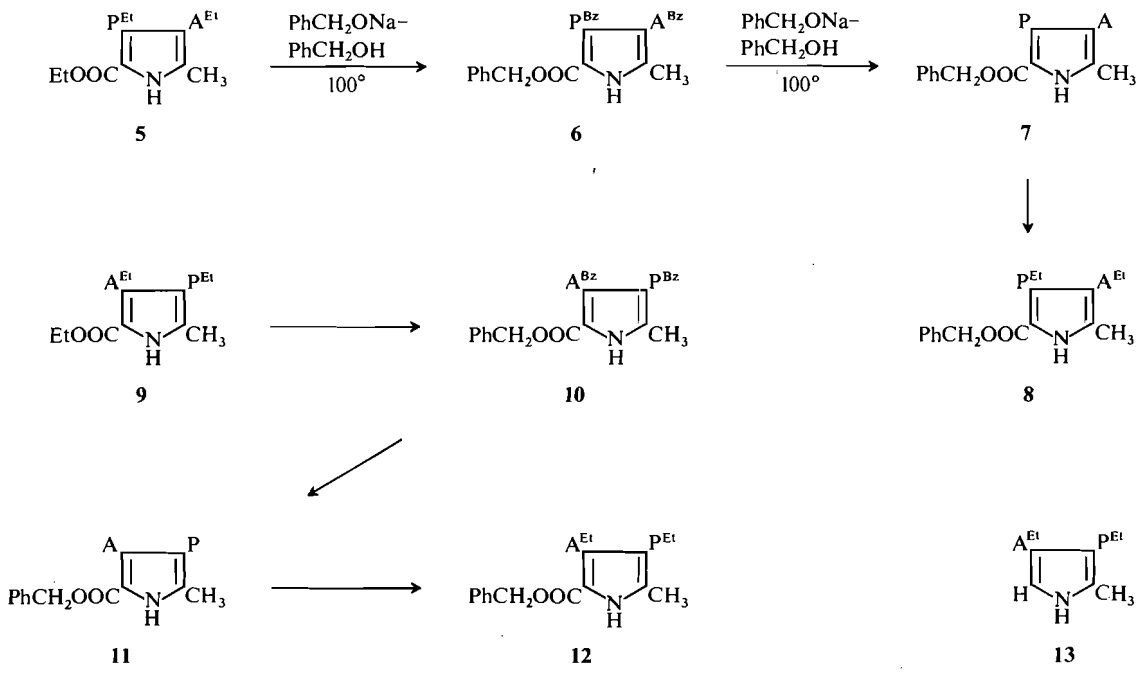

5 6 7 9 10 8 11 12 13

Can. J. Chem. Downloaded from www.nrcresearchpress.com by 210.87.254.6 on 09/05/12
For personal use only.

Can. J. Chem. Downloaded from www.nrcresearchpress.com by 210.87.254.6 on 09/05/12
For personal use only.

of hemopyrrole-dicarboxylic acid with phosgene, dimethylaniline, and benzyl alcohol, *cf.* (13). Although this method converted the diethyl ester of cryptopyrrole-dicarboxylic acid, **13**, into **12**, the overall yield from **9** was only 15%. Another general method involving successive transesterifications, *cf.* (14), also failed, but a modification in its first step was useful. When **5** or **9** were heated with sodium benzylate in benzyl alcohol, the tribenzyl esters **6** and **10** first formed were converted to **7** and **11**. These conversions occurred directly rather than during the work-up, *cf.* (14), and the formation of acids here was not unprecedented (15). Under modified conditions, **7** and **11** became the chief products, and these were esterified to **8** and **12**. The hydrogenation of **6**, **7**, or **8** removed the benzyl groups to yield the expected acids. Neither the partial hydrolysis of **6** to **7** nor the partial transesterification of **10** to **12** was promising.

The 2-methylpyrroles **6** and **8** were brominated to the corresponding 2-bromomethylpyrroles one of which, **2***b* from **8**, was condensed with **3** to **4***b*, *cf.* (3). The latter was hydrogenated to **4***c* which gave **4***d* with iodine in bicarbonate, and thence **4***e* by hydrogenation. It was later found that this last could be obtained by decarboxylating **4***c* directly in water at 100°, but the product then contained impurities which were only evident through t.l.c. and were difficult to remove.

It was essential to obtain the dipyrrylmethane **1***b*, an acid-labile acid, in a stable form. Further, a product containing excess salts could not be subjected to thin-layer electrophoresis. Many pyrrole-polycarboxylic acids are precipitated as their potassium salts when the corresponding esters are heated in ethanolic KOH, and **4***e* was thus converted into the tetrapotassium salt of **1***b*. Sodium and barium salts were obtained likewise but to no advantage.

The potassium salt was stable when dry and, in the absence of porphobilinogen, gave no uroporphinogen under the conditions of incubation (10), *cf.* however (11). The analysis of the first specimen obtained was satisfactory, but those of later specimens were less so, and their n.m.r. spectra showed that ethoxy was present. This was not due to ester groups for, after the products had been dissolved in water and freeze-dried, ethoxy was absent and the analyses were satisfactory. It was also evident that the lactam ring, in which the CH_2CO protons are easily exchanged, was not present in the product, *cf.* (9). Thus, when **4***e* was hydrolyzed in NaOH–EtOH or in NaOD–EtOD, the sodium salt isolated showed *ca.* 4 or 2 protons respectively at τ 6.7, before or after subsequent treatment with $NaOD–D_2O$ or $NaOH–H_2O$. Evidently the hydrolyses were complete and ethoxy in the products was due to ethanol. Thin-layer electrophoresis of the potassium salt revealed the more troublesome faster running impurity mentioned above; subject to the uncertainty of the Ehrlich color, the amount of this was roughly 10%.[10]

When **4***a* was heated in ethanolic KOH a potassium salt again separated. The free acid, **14**, obtained from it, analyzed badly and

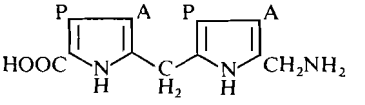

14

attempts to decarboxylate it were, as expected, unpromising.

When **1***b* proved to be an intermediate in the biosynthesis of uroporphyrin 1, we undertook the synthesis of the corresponding tripyrrane **15**. This has been carried to the lactam ester **22** analogous to **4***e*. However, in view of the impurity found in **1***b*, the hydrolysis of **22** as well as the biochemical work on the product, are being studied in cooperation with Bogorad, so the hydrolysis of **22** can be monitored by thin-layer electrophoresis.

The synthesis of **22** by a repetition of the reactions which had converted **3** into **4***e* would probably involve more labile intermediates. In particular, the tripyrrane from **2***b* and **4***e* might not be stable in the acid medium in which it was formed, and some preliminary experiments were unpromising. We turned to the condensation of 2-formylpyrroles with **4***e* because the resulting tripyrrenes should be more stable than tripyrranes in acid, and because pyrrole-2-aldehydes, unlike 2-bromomethylpyrroles, could be obtained without blocking groups (benzyloxycarbonyl) in the 5-position. In preliminary experiments, the aldehydes **16***a* and *b* were condensed with **4***e* to give **17***a* and *b*; the latter was hydrogenated to **18**. When the aldehydes **19***a* or *b* were used, the products were not

[10]L. Bogorad. Private communication.

Can. J. Chem. Downloaded from www.nrcresearchpress.com by 210.87.254.6 on 09/05/12
For personal use only.

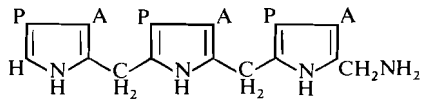

15

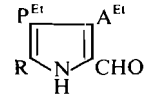

16

a R = COOEt
b R = $COOCH_2Ph$
c R = H

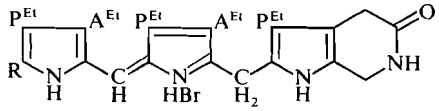

17

a R = COOEt
b R = $COOCH_2Ph$

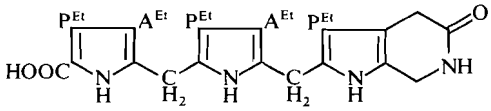

18

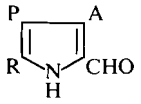

19

a R = H
b R = I
c R = COOH

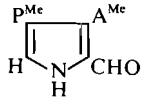

20

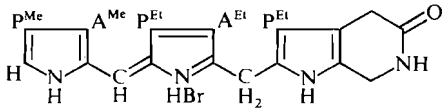

21

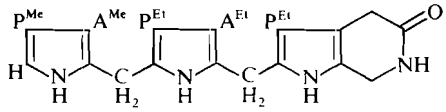

22

crystalline; the aldehyde **16***c*, which we have not obtained pure, also failed to give a crystalline product. However, **20** condensed with **4***e* to give the beautifully crystalline tripyrrene **21**, and this was hydrogenated with **22**.

We had explored other approaches to aminomethyl derivatives of dipyrrylmethanes, tripyrranes, and tetrapyrranes. One such, which we have not followed up, might depend on the interconversion (19) of 5-chloro- and 5-hydroxydipyrrylmethenes, and the latter (unlike the former) undergoing typical pyrrole reactions. Another might have been based on the conversion of 5-methyl- to 5-formyl-dipyrrylmethenes (20) had this been sufficiently general. A third approach, now attractive in connection with tetrapyrranes, was to condense **2***b* with pyrroles other than **3**, avoiding the limitations imposed by the use of the latter. 2-Formyl pyrroles, and to a lesser extent their condensation products with malondinitrile, etc., are strongly deactivated at the 5-position. The corresponding oximes, however, condensed with bromomethyl pyrroles to oximes of 5-formyl-dipyrrylmethanes. These condensations are not reported here because the results were erratic, but they did suggest the use of **23**, for Girard hydrazones are stable in AcOH but are easily split by dilute HCl. The condensation of **2***b* with **23** in hot AcOH–NaOAc gave the water-soluble hydrazone from which the aldehyde **24** was obtained with dilute HCl. Other 5-formyl-5′-benzyloxy-

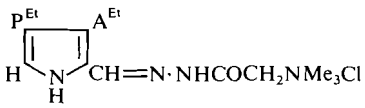

23

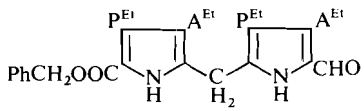

24

Can. J. Chem. Downloaded from www.nrcresearchpress.com by 210.87.254.6 on 09/05/12
For personal use only.

carbonyl-dipyrrylmethanes, with difierent β-substituents, have been obtained from the corresponding 5-*t*-butoxycarbonyl-dipyrrylmethanes (21), a route which would involve more intermediates in the present case. The benzyl ester **24** was hydrogenated to the corresponding acid, to which we referred some time ago (20); but we have recently had difficulty in repeating this hydrogenation.

Experimental

2-Methyl-3-carboxymethyl-4-β-carboxyethyl-5-benzyloxycarbonylpyrrole (7), and 2-Methyl-3-benzyloxycarbonylmethyl-4-β-benzyloxycarbonylethyl-5-benzyloxycarbonylpyrrole (6)

2-Methyl-3-ethoxycarbonylmethyl-4-β-ethoxycarbonylethyl-5-carbethoxypyrrole (**5** (16), 10.8 g) was added to a warm solution of 2.2 g of sodium in 260 ml of pure benzyl alcohol. The mixture was heated for 1 h on the steam bath with frequent swirling while a gel formed, then for 3 h under water-pump vacuum. Benzyl alcohol was then removed (rotary, 0.05 mm, bath 100°). The solution of the residue in 150 ml of water was extracted with ether (2 × 100 ml), then slowly acidified to congo red with 10% HCl. The precipitate was recrystallized from acetone (thimble) as colorless needles of the monobenzyl ester (7.2 g, 65%), m.p. 244°. Ehrlich's reaction, weakly positive on warming.

Anal. Calcd. for $C_{18}H_{19}O_6N$: C, 62.60; H, 5.55; N, 4.06; OEt, 0.00. Found: C, 62.81; H, 5.82; N, 3.47; OEt, 0.00.

Ether and benzyl alcohol were removed from the ether washings, finally at 100° and 0.1 mm, and the residue was crystallized from hexane (thimble) as colorless hairs of the tribenzyl ester (0.4 g), m.p. 108°. The yield of this is increased by using less sodium.

Anal. Calcd. for $C_{32}H_{31}O_6N$: C, 73.12; H, 5.95; N, 2.67. Found: C, 72.91; H, 5.91; N, 3.08.

Both the monobenzyl ester and the tribenzyl ester were converted into the corresponding tricarboxylic acid, m.p. 151–152° dec. (lit. (16), 155–156° dec.), by hydrogenation in ethanol over palladium black.

When the tribenzyl ester (400 mg) was refluxed for 1.5 h in 65 ml of tetrahydrofuran and 15 ml of *N*/10 NaOH, the unchanged tribenzyl ester (147 mg) and the monobenzyl ester (76 mg) were recovered.

2-Methyl-3-ethoxycarbonylmethyl-4-β-ethoxycarbonylethyl-5-benzyloxycarbonylpyrrole (8)

The monobenzyl ester (**7**, 2.8 g) was left in the dark overnight in 80 ml of 5% absolute ethanolic HCl at 20°. Ethanol was evaporated at $<50°$, more ethanol was added and evaporated, and the residue was recrystallized from hexane (thimble) as colorless needles (2.6 g, 79%), m.p. 97–98°.

Anal. Calcd. for $C_{22}H_{27}NO_6$: C, 65.82; H, 6.78; N, 3.49. Found: C, 65.89; H, 6.83; N, 3.67.

2-Methyl-3-ethoxycarbonylmethyl-4-β-ethoxycarbonylethyl-5-carboxypyrrole

The corresponding 5-carbobenzoxypyrrole, **8**, was hydrogenated in ethanol over palladium black. The catalyst and solvent were removed, and the residue was crystallized from cold acetone–hexane as colorless plates, m.p. 126–127°, Ehrlich's reaction, strongly positive cold.

Anal. Calcd. for $C_{15}H_{21}O_6N$: C, 57.85; H, 6.80; N, 4.50. Found: C, 58.01; H, 6.84; N, 4.63.

2-Bromomethyl-3-ethoxycarbonylmethyl-4-β-ethoxycarbonylethyl-5-benzyloxycarbonylpyrrole (2b)

Method a; Using Bromine

The corresponding 2-methylpyrrole (**8**, 204 mg) in 5 ml of carbon tetrachloride, was treated with a solution of bromine (0.025 ml) in carbon tetrachloride (2 ml), and the solution was irradiated for 20 min under a u.v. lamp. The solvent was removed *in vacuo* at 20°, more was added and removed in the same way, and the residue was crystallized from *n*-hexane (thimble) as colorless needles (45–55%), m.p. 119–120°.

Anal. Calcd. for $C_{22}H_{26}NO_6Br$: C, 55.00; H, 5.46; N, 2.92; Br, 16.64. Found: C, 54.78; H, 5.39; N, 3.04; Br, 16.49.

To scale up this preparation, the crude products from small runs were crystallized together.

Method b; Using N-Bromosuccinimide

The 2-methylpyrrole (**8**, 4 g) in 105 ml of CCl_4 under dry N_2 was heated (bath 89–90°) and stirred for 20 min under reflux with 1.78 g of NBS and a trace of benzoylperoxide. The filtrate and washings from the cooled mixture were evaporated and the crystalline residue was crystallized from 45 ml of benzene–*n*-hexane (1:2) using Darco, then recrystallized twice from the same solvents; yield 40–50%.

2-Acetoxymethyl-3-ethoxycarbonylmethyl-4-β-ethoxycarbonylethyl-5-benzyloxycarbonylpyrrole

The bromomethylpyrrole **2***b* (500 mg) in 15 ml of acetic acid containing 50 mg of anhydrous sodium acetate, was warmed for 10 min at 70°. Water was then added and the turbid solution was left at 10°. The colorless product was separated and recrystallized from aqueous ethanol as needles, m.p. 105–106°.

Anal. Calcd. for $C_{24}H_{29}NO_8$: C, 62.73; H, 6.36; N, 3.05. Found: C, 62.55; H, 6.51; N, 2.89.

2-Bromomethyl-3-benzyloxycarbonylmethyl-4-β-benzyloxycarbonylethyl-5-benzyloxycarbonylpyrrole

The corresponding 2-methyl pyrrole (**6**, 988 mg) was dissolved in 10 ml CCl_4, 0.1 ml of bromine was added, and the solution was irradiated by a u.v. lamp for 20 min. The solution, from which some of the product had precipitated, was evaporated below 50°; more solvent was added and removed in the same way. The residue was crystallized from ether–hexane (thimble), dissolved in ether, and the ether solution was filtered through Darco. When the solution was concentrated, the product separated. It was recrystallized twice from ether–hexane as colorless hairs, m.p. 140–141°.

Anal. Calcd. for $C_{32}H_{30}NO_6Br$: C, 63.57; H, 5.01; N, 2.32; Br, 13.23. Found: C, 63.43; H, 5.00; N, 2.40; Br, 13.02.

2-Methyl-3-β-carboxyethyl-4-carboxymethyl-5-benzyloxycarbonyl-pyrrole (11)

Sodium (0.52 g) was warmed to solution in 35 ml of pure benzyl alcohol and 2-methyl-3-β-ethoxycarbonylethyl-4-ethoxycarbonylmethyl-5-carbethoxypyrrole (**9** (17), 2.59 g) in 40 ml of benzyl alcohol was added. The solution was heated on the steam bath for 5 1/4 h, cooled, poured into 400 ml of ether, and the whole was extracted with water.

Can. J. Chem. Downloaded from www.nrcresearchpress.com by 210.87.254.6 on 09/05/12
For personal use only.

The product (68%), m.p. 211–215°, was precipitated when the aqueous layer was acidified. It was recrystallized from acetone–hexane then from acetone as colorless prisms, m.p. 217–218°.

Anal. Calcd. for $C_{18}H_{19}NO_6$: C, 62.60; H, 5.55; N, 4.06. Found: C, 63.20; H, 5.87; N, 3.86.

The ether layer was evaporated and the residue was crystallized from hexane to give the tribenzyl ester (see below) as colorless needles (67 mg), m.p. 89–92°.

*2-Methyl-3-β-benzyloxycarbonylethyl-4-benzyloxycarbonylmethyl-5-benzyloxycarbonylpyrrole (**10**)*

2-Methyl-3-β-ethoxycarbonylethyl-4-ethoxycarbonylmethyl-5-carbethoxypyrrole (**9**, 4.99 g) was dissolved in 25 ml of pure benzyl alcohol, 0.105 g of sodium were added, and the mixture was heated in the steam bath first for 1 h excluding moisture, then for 2 h at 12 mm. The solvent was removed *in vacuo* at 100°, water was added to the residue, and the mixture was extracted with ether. The product which crystallized from the ether at 0° was recrystallized from *n*-hexane as colorless needles (31%), m.p. 92–93°.

Anal. Calcd. for $C_{32}H_{31}NO_6$: C, 73.12; H, 5.95; N, 2.67. Found: C, 72.84; H, 5.88; N, 2.96.

When the tribenzyl ester was refluxed with sodium (1.5 atoms) in ethanol for 20 min, it was reconverted into the triethyl ester (50%), m.p. and mixed m.p. 63°.

*2-Methyl-3-β-ethoxycarbonylethyl-4-ethoxycarbonylmethyl-5-benzyloxycarbonylpyrrole (**12**)*

2-Methyl-3-β-carboxyethyl-4-carboxymethyl-5-benzyloxycarbonylpyrrole, **11**, was left overnight in 30 parts of 5% ethanolic HCl in the dark. The solvent was removed at 50°, more ethanol was added and removed in the same way, and the residue (98%) was recrystallized from *n*-pentane as colorless needles, m.p. 88–89°.

Anal. Calcd. for $C_{22}H_{27}NO_6$: C, 65.82; H, 6.78; N, 3.49. Found: C, 65.74; H, 6.72; N, 3.46.

*Lactam of 5-Aminomethyl-4-carboxymethyl-3,4′-di-(β-ethoxycarbonylethyl)-3′-ethoxycarbonylmethyl-5′-benzyloxycarbonyldipyrrylmethane (**4b**)*

The ethyl ester of porphobilinogen lactam (**3** (3), 118 mg) and the 2-bromomethylpyrrole (**2***b*, 240 mg) in 5 ml of acetic acid containing 50 mg of anhydrous sodium acetate were heated for 40 min on the steam bath. Water (9 ml) was then slowly added, and the mixture was heated until clear. When crystals appeared in the cooled solution, 50 ml of hot water were added, and the mixture was allowed to cool, finally at 10°. The product was separated and recrystallized from 35% ethanol (60 ml) as pale yellow micro-crystals (55–75%), m.p. 142–142.5°; other forms melting up to 180° may appear directly or from the melt. T.l.c.[11] in $CHCl_3$–MeOH (9:1): R_f 0.60 and usually a small spot on the start line. Larger runs are equally satisfactory. The analogous trimethyl-benzyl ester has been described (11).

Anal. Calcd. for $C_{34}H_{41}N_3O_9$: C, 64.24; H, 6.50; N, 6.62. Found: C, 64.11; H, 6.60; N, 6.49.

*Lactam of 5-Aminomethyl-4-carboxymethyl-3,4′-di-(β-ethoxycarbonylethyl)-3′-ethoxycarbonylmethyl-5′-carboxydipyrrylmethane (**4c**)*

The corresponding 5′-carbobenzoxydipyrrylmethane (**4***b*, 1.91 g) in 1 l of 95% ethanol was shaken with 400 mg of palladium black for 24 h under hydrogen. The mixture was then warmed to dissolve the product and filtered. The filtrate was concentrated and then cooled. The product which separated was recrystallized from 250 ml of 95% ethanol as a gray micro-crystalline powder (60–75%), m.p. 192.5–193.5 (dec.). T.l.c. in $CHCl_3$–MeOH (1:1): R_f 0.6 only.

Anal. Calcd. for $C_{27}H_{35}N_3O_7$: C, 59.43; H, 6.46; N, 7.70. Found: C, 59.29; H, 6.39; N, 7.66.

*Lactam of 5-Aminomethyl-4-carboxymethyl-3,4′-di-(β-ethoxycarbonylethyl)-3′-ethoxycarbonylmethyl-5′-iododipyrrylmethane (**4d**)*

The corresponding 5′-carboxy-dipyrrylmethane (**4***c*, 347 mg) was warmed to solution in 17.5 ml of 95% ethanol and 7 ml of water containing 165 mg of sodium bicarbonate. Iodine (164 mg) in ethanol (7 ml) was added to the cooled solution, which was heated briefly then refrigerated overnight. The product (55–70%) was washed with water then with ethanol. For analysis, it was recrystallized from ethanol–acetone (1:2) as small light yellow crystals, m.p. 149–150° (dec.). T.l.c. in $CHCl_3$–MeOH (1:1): R_f 0.8 only.

Anal. Calcd. for $C_{26}H_{34}N_3O_7I$: C, 49.76; H, 5.57; N, 6.70; I, 20.23. Found: C, 49.98; H, 5.50; N, 6.81; I. 19.99.

*Lactam of 5-Aminomethyl-4-carboxymethyl-3,4′-di-(β-ethoxycarbonylethyl)-3′-ethoxycarbonylmethyldipyrrylmethane (**4e**) (J. M. Osgerby)*

A suspension of the 5′-iodo-dipyrrylmethane (**4***d*, 232 mg) in 500 ml of ethanol, to which had been added 35 mg of anhydrous sodium acetate in 3 ml of water, was shaken in the dark overnight with palladium black under hydrogen. The colorless solution was filtered and the solvent removed below 50°. The residue was recrystallized from aqueous ethanol as small grey prismatic rods (70–80%), m.p. 180°; Ehrlich's reaction, strongly positive cold. For analysis, it was recrystallized from ether (thimble). N.m.r. ($CDCl_3$) τ 8.78 (m, 9.4, OCH_2CH_3), 7.38 (sym. m, 7.9, CH_2CH_2CO), 6.68, 6.50, 6.21, 5.92, and 5.66 (poorly resolved t, J = 2.5–3.0 Hz, s, s, m, broad s, 13.6, CH_2CONH, CH_2COO, bridge CH_2, OCH_2CH_3, CH_2NHCO), 3.58 and 3.19 (d, J = 2.5 Hz, broad s, 2.4, pyrrole C*H*, CON*H*), 0.94 and 0.64 (poorly resolved d, J = 2.0–2.5 Hz, s, 1.7, two pyrrole N*H*). T.l.c. ($CHCl_3$–MeOH, 4:1): R_f 0.74 only. The analogous trimethyl ester has been described (11).

Anal. Calcd. for $C_{26}H_{35}N_3O_7$: C, 62.26; H, 7.04; N, 8.38. Found: C, 62.20; H, 7.07; N, 8.44.

*Tetrapotassium Salt of 5-Aminomethyl-4,3′-di-carboxymethyl-3,4′-di-β-carboxyethyldipyrrylmethane (**1b**), cf. (11) (J. Pluscec)*

The lactam ester (**4***e*, 113 mg) in 5 ml of absolute ethanol containing 560 mg of KOH was refluxed on the steam bath for 80 min; the product began to separate after 5 min. The product was washed by decantation with absolute ethanol, with ether, then with acetone. It was transferred to a tube using acetone, then dried for 15 h in the dark (1×10^{-4} mm, 20°). The product was a light brown powder (75%), very hygroscopic before it was dried; Ehrlich's reaction, strongly positive cold. For the second analysis and for the n.m.r. spectrum, a specimen was dissolved in water and then freeze-dried; n.m.r. (D_2O) τ 7.48 (m, 8, CH_2CH_2CO), 6.68 (s, 3.9, CH_2COO), 6.27 (s, 1.9, bridge CH_2), 5.92 (s, 1.7, CH_2NH_2), 3.50 (s, 0.8, pyrrole C*H*); u.v. no strong absorption 650–300 mμ.

[11]All t.l.c. on silica gel H coated plates.

Can. J. Chem. Downloaded from www.nrcresearchpress.com by 210.87.254.6 on 09/05/12
For personal use only.

Anal. Calcd. for $C_{20}H_{21}N_3O_8K_4$: C, 40.87; H, 3.60; N, 7.15; K, 26.61. Found: C, 40.52, 40.48; H, 3.97, 3.97; N, 7.32, 6.92; K, 26.23, 26.39.

A sample was heated for 20 min at 100° in 0.5 *N* HCl. The product was a mixture of isomeric uroporphyrins (40%), methyl ester m.p. 250°.

*5-Aminomethyl-4,3′-di-carboxymethyl-3,4′-di-(β-carboxyethyl)-5′-carboxydipyrrylmethane (**14**), cf. (11)*

The tetra-ethyl ester of the corresponding lactam (**4***a* (3), 460 mg) was refluxed for 1 3/4 h in 22 ml of absolute ethanol containing 2.25 g of KOH. The light-brown precipitate was washed by decantation, first with ethanol then with ether. It was dissolved in 4 ml of water and the product (90%) was precipitated by dilute HCl. It was obtained as a pinkish amorphous powder, m.p. 193–195° (reddening at 125°) by precipitating three times from 0.5 *N* ammonia with *N*-acetic acid, using de-aerated water; Ehrlich's reaction, positive after standing in the cold.

Anal. Calcd. for $C_{21}H_{25}N_3O_{10}$: C, 52.61; H, 5.26; N, 8.77. Found: C, 52.64; H, 6.51; N, 9.72.

In an attempt to decarboxylate the product, it was heated with water for 2 h at 100° in a tube which had been sealed under vacuum. From the dark red product, only uroporphyrin (2%) was isolated. This contained some uroporphyrin 2 for the m.p. of its methyl ester was raised from 265–275° to 295–305° by recrystallizing it from chloroform–acetone, *cf.* (18).

*2-Formyl-3-ethoxycarbonylmethyl-4-β-ethoxycarbonylethyl-5-benzyloxycarbonylpyrrole (**16***b*)

Sulfuryl chloride (0.43 ml) was slowly added to a stirred solution of the 2-methyl pyrrole (**8**, 1g) in 15 ml of absolute ether at 0–4°. After 5 min, the ice bath was removed and stirring was continued for 30 min. The ether was removed *in vacuo* below 20°, and 3 × 10 ml of ether were added and removed in the same way. The oily residue was boiled for 3 min with 40 ml of water containing 2.5 g of sodium acetate. The mixture was quickly cooled to 0°. The product which separated was crystallized from 40 ml of ethanol and 190 ml of water, then recrystallized from hexane (thimble) as colorless needles (80%), m.p. 89–91°. For analysis it was twice recrystallized from hexane, m.p. then 90–92°.

Anal. Calcd. for $C_{22}H_{25}NO_7$: C, 63.60; H, 6.07; N, 3.37. Found: C, 63.38; H, 6.24; N, 3.56.

2-Formyl-3-β-ethoxycarbonylethyl-4-ethoxycarbonylmethyl-5-benzyloxycarbonylpyrrole

The preparation of this from the 2-methyl pyrrole **12** and sulfuryl chloride followed that of its isomer with the 3- and 4-substituents interchanged. The colorless needles of the product (80%), m.p. 98–100°, were recrystallized twice from hexane for analysis, m.p. then 99–101°.

Anal. Calcd. for $C_{22}H_{25}NO_7$: C, 63.60; H, 6.07; N, 3.37. Found: C, 63.43; H, 6.00; N, 3.51.

*Lactam of 1-Ethoxycarbonyl-2,4,6-tri-β-ethoxycarbonylethyl-3,5-di-ethoxycarbonylmethyl-7-carboxymethyl-8-aminomethyltripyrrene-12-hydrobromide (**17***a*)

The 5-carbethoxypyrrole aldehyde (**16***a* (2), 35 mg) and the dipyrrylmethane (**4***e*, 50 mg, prepared by decarboxylating its 5′-carboxylic acid directly in water at 100°) in 5 ml of ethanol were treated with 2 drops of 48% HBr, cooling, and scratching. After the product began to separate, the mixture stood at 10° overnight. The solvent was evaporated and the crystalline residue was washed with ethanol then recrystallized from the same solvent (3 ml) as small red crystals (31%), m.p. 130–132°. For analysis, it was recrystallized again as small red rods, m.p. unchanged; t.l.c. in $CHCl_3$–MeOH (9:1): R_f 0.74 only; u.v. in ethanol λ_{max} (ε): 493 (32 000), 277 mμ (17 400).

Anal. Calcd. for $C_{43}H_{57}N_4O_{13}Br$: C, 56.27; H, 6.21; N, 6.11; Br, 8.72. Found: C, 55.99; H, 6.17; N, 6.21; Br, 8.79.

*Lactam of 1-Benzyloxycarbonyl-2,4,6-tri-β-ethoxycarbonylethyl-3,5-di-ethoxycarbonylmethyl-7-carboxymethyl-8-aminomethyltripyrrene-12-hydrobromide (**17***b*)

This was obtained like the 1-ethoxycarbonyl derivative as small red rods (45%), m.p. 137–139° (dec.), from the 5-benzyloxycarbonylpyrrole aldehyde **16***b* and the dipyrrylmethane **4***e*. Here the mixture was not left overnight, nor was the residue washed before being recrystallized. U.v. in ethanol λ_{max}(ε): 493 (29 800), 277 mμ (17 300).

Anal. Calcd. for $C_{48}H_{59}N_4O_{13}Br$: C, 58.90; H, 6.03; N, 5.72; Br, 8.18. Found: C, 58.76; H, 6.13; N, 5.67; Br, 8.24.

*Lactam of 1-Carboxy-2,4,6-tri-β-ethoxycarbonylethyl-3,5-di-ethoxycarbonylmethyl-7-carboxymethyl-8-aminomethyltripyrrane (**18**) (F. Boyer)*

The 1-benzyloxycarbonyl derivative (**17***b*, 100 mg) in 40 ml of absolute ethanol was converted into the yellow base with ammonia vapor then shaken with 100 mg of palladium black under hydrogen. The absorption was theoretical in about 1 h. The catalyst was separated and the solvent was removed. The residue was crystallized from 10 ml of ethanol as tiny colorless crystals (48 mg), m.p. 194–196° (dec.), unchanged on recrystallization.

Anal. Calcd. for $C_{41}H_{54}N_4O_{13}$: C, 60.74; H, 6.66; N, 6.91. Found: C, 60.58; H, 6.70; N, 6.85.

Lactam of 2-β-Carboxyethyl-3,7-di-carboxymethyl-4,6-di-β-ethoxycarbonylethyl-5-ethoxycarbonylmethyl-8-aminomethyltripyrrene-12-hydrobromide

3-Carboxymethyl-4-β-carboxyethylpyrrole-2-aldehyde (**19***a*) (3) and the dipyrrylmethane **4***e* were condensed as above. After the solvent was removed, ethanol was twice added to the residue and evaporated. The residue was dissolved in hot absolute ethanol, the solution was cooled and dry ether was added to turbidity. The dark red partially crystalline product, m.p. 140° (dec.), was re-precipitated for analysis.

Anal. Calcd. for $C_{36}H_{45}N_4O_{11}Br$: C, 54.76; H, 5.73; N, 7.10; Br, 10.26. Found: C, 54.71; H, 5.64; N, 7.19; Br, 10.30.

*2-Formyl-3-methoxycarbonylmethyl-4-β-methoxycarbonylethylpyrrole (**20**), cf. (11)*

To the corresponding pure decarboxylic acid (**19***a* (3), 128 mg) in 2 ml of absolute ethanol and 5 ml of dry ether, ethereal diazomethane (from 3 g of nitrosomethylurea) was slowly added. When the solvent was evaporated below 20°, the residue crystallized at once. It was recrystallized from 85% ethanol as flattened rods (70%), m.p. 99–100°; t.l.c. in chloroform–methanol (9:1): R_f 0.70 only (iodine or Ehrlich's). This had not been obtained crystalline (11).

Anal. Calcd. for $C_{12}H_{15}NO_5$: C, 56.91; H, 5.97; N, 5.53. Found: C, 56.81; H, 6.10; N, 5.69.

Can. J. Chem. Downloaded from www.nrcresearchpress.com by 210.87.254.6 on 09/05/12
For personal use only.

*Lactam of 2-β-Methoxycarbonylethyl-3-methoxycarbonylmethyl-4,6-di-(β-ethoxycarbonylethyl)-5-ethoxycarbonylmethyl-7-carboxymethyl-8-aminomethyltripyrrene-12-hydrobromide (**21**)*

The aldehyde **20** (32 mg) and the dipyrrylmethane **4e** (55 mg, obtained from its 5′-iodo derivative) were gently warmed to solution in 3 ml of absolute ethanol. To the cooled solution, two drops of 48% HBr were added, and crystallization was induced in the deep red solution by scratching, first in the ice-bath then at room temperature (*ca.* 1/2 h). After the mixture had stood 2 h in the cold, the product was separated on a sintered glass funnel and washed with 2 ml of ether. It formed small red rods (64%), m.p. 117–119°. For analysis, it was recrystallized from ethanol as red rods, m.p. 119–120°, t.l.c. in acetone–methanol (2:1): R_f 0.70 only, a yellow spot turned brown by iodine, or light grey with Ehrlich's reagent and HCl vapor; u.v. in ethanol λ_{max} 482 mμ (26 400).

Anal. Calcd. for $C_{38}H_{49}N_4O_{11}Br$: C, 55.81; H, 6.04; N, 6.85; Br, 9.77. Found: C, 55.83; H, 6.19; N, 6.80; Br, 9.59.

*Lactam of 2-β-Methoxycarbonylethyl-3-methoxycarbonylmethyl-4,6-di-(β-ethoxycarbonylethyl)-5-ethoxycarbonylmethyl-7-carboxymethyl-8-aminomethyltripyrrane (**22**) (N. Stojanac)*

The tripyrrene hydrobromide **21** (126 mg) was dissolved in 100 ml of 95% ethanol and converted to the yellow base by adding 3 drops of NH_4OH. Palladium black (80 mg) was added, and the solution was shaken for 2 h under hydrogen (1 atm, 21°); the uptake ceased at the theoretical amount in 15 min. The catalyst was separated and washed with hot ethanol. Ethanol was evaporated (rotary, bath 35°) and the residue was crystallized from 12 ml of ethanol as a grey micro-crystalline powder (68%), m.p. 169–171° (dec.); Beilstein test for halogen negative, Ehrlich's reaction, positive cold. For analysis, it was recrystallized from ether (thimble, 7 h) as a light grey powder, m.p. 171–173° (dec.); t.l.c. (crude product or pure) in acetone–methanol (2:1): R_f 0.69 only; n.m.r. ($CDCl_3$, TMS) τ 8.83 (m, 13.1, OCH_2CH_3), 7.40 (sym. m, 12.3 CH_2CH_2CO), 6.66 and 6.57 (singlets, 5.2, CH_2CONH and CH_2COOR), 6.35 and 6.27 (singlets, 8.4, OCH_3 and bridge CH_2), 5.94 (m, 4.7, OCH_2CH_3), 5.65 (broad s, 1.2, CH_2NH), 3.73 and 3.61 (singlets, 2.7, pyrrole CH and CH_2NH), 1.40 (s, 0.9, pyrrole NH), 0.83 (s, 1.40, pyrrole NH).

Anal. Calcd. for $C_{38}H_{50}N_4O_{11}$: C, 61.75; H, 6.82; N, 7.58. Found: C, 61.81; H, 6.67; N, 7.40.

*Hydrazone (**23**) from 2-Formyl-3-ethoxycarbonylmethyl-4-(2-ethoxycarbonylethyl)-pyrrole and Girard's "T" Reagent*

A solution of the aldehyde (**16c**, 0.8 g) and Girard's "T" reagent (0.55 g) in 10 ml of 95% ethanol and 0.9 ml of AcOH was refluxed on the steam-bath for 30 min. The solvents were removed from the cooled solution (rotary, finally at 0.1 mm). The residue was dissolved in *n*-propanol, ether was added to turbidity, and some Girard's reagent which separated at once was removed. When more ether was added to the solution, the product crystallized. It was recrystallized until t.l.c. showed it to be pure (about four times) by dissolving it in a little *n*-propanol, filtering from some undissolved Girard's reagent, and adding ether to turbidity. It formed colorless plates (50%), m.p. 212–214°; t.l.c. (ethanol–ammonia–water, 7:1:2) R_f 0.3 only.

Anal. Calcd. for $C_{19}H_{31}N_4O_5Cl$: C, 52.95; H, 7.25; N, 13.00; Cl, 8.23. Found: C, 52.81; H, 7.08; N, 13.09; Cl, 8.14.

*5-Formyl-4,3′-di-ethoxycarbonylmethyl-3,4′-di-(2-ethoxycarbonylethyl)-5′-benzyloxycarbonyl-dipyrrylmethane (**24**)*

A solution of **2b** (165 mg), **23** (150 mg), and anhydrous NaOAc (34 mg) in 3.4 ml of acetic acid was heated 30 min on the steam-bath. The solvent was then removed, finally at 1×10^{-4} mm. The residual hydrazone was dissolved in 7.5 ml of water by gentle warming and concentrated HCl (1.6 ml) was added to the filtered solution. After 10 min, the precipitated oily aldehyde was washed with water by decantation until it was neutral. Its dried (Na_2SO_4) solution in benzene was poured onto a column of alumina (grade 3, made up in benzene), from which the product was eluted with ether. The eluate was evaporated and the residue was crystallized from aqueous ethanol to give the product (35%), m.p. 94–97°. For analysis it was recrystallized twice as colorless needles, m.p. 102.5–104°; Ehrlich's reaction, negative cold; t.l.c. (chloroform–ether, 3:1) R_f 0.2 only; n.m.r. ($CDCl_3$) 8.82 (m, 11, OCH_2CH_3), 7.32 (m, 7.1, CH_2CH_2COO), 6.52 and 6.38 (singlets, 3.7, CH_2COO), 6.06 and 5.96 (m and s, 9, bridge CH_2 and OCH_2CH_3), 4.86 (s, 1.7, Ph CH_2), 2.86 (s, 4.5, C_6H_5), 0.64 (s, 0.9, CHO), 0.06 (broad s, 0.7, NH), −0.4 (broad s, 0.8, NH).

Anal. Calcd. for $C_{36}H_{44}N_2O_{11}$ (mol. wt. 680.7): C, 63.53; H, 6.52; N, 4.12. Found (681 (mass spectrum)): C, 63.35; H, 6.64; N, 4.30.

2-Formyl-4,3′-di-ethoxycarbonylmethyl-3,4′-di-(2-ethoxycarbonylethyl)-5′-carboxydipyrrylmethane (J. Pluscec)

The corresponding 5′-benzyloxycarbonyl derivative (**24**, 485 mg) was hydrogenated in 10 ml of 95% ethanol over palladium black (150 mg). After the theoretical uptake of hydrogen, the catalyst was separated and the solution was concentrated to 2 ml. The product (56%), m.p. 154–156° (dec.) separated at 10°.

For analysis, it was recrystallized twice as colorless prisms turning red in air, m.p. 156–158° (dec.), Ehrlich's reaction, positive cold.

Anal. Calcd. for $C_{29}H_{38}N_2O_{11}$ (neut. equiv. 591): C, 58.96; H, 6.49; N, 4.74. Found (589): C, 59.13; H, 6.66; N, 4.88.

1. A. T. CARPENTER and J. J. SCOTT. Biochem. J. **71**, 325 (1959); Biochim. Biophys. Acta, **52**, 195 (1961).
2. D. M. MACDONALD and S. F. MACDONALD. Can. J. Chem. **33**, 573 (1955).
3. G. P. ARSENAULT and S. F. MACDONALD. Can. J. Chem. **39**, 2043 (1961).
4. D. S. HOARE and H. HEATH. Biochim. Biophys. Acta, **39**, 167 (1960).
5. G. P. ARSENAULT, E. BULLOCK, and S. F. MACDONALD. J. Am. Chem. Soc. **82**, 4384 (1960).
6. E. J. TARLTON, S. F. MACDONALD, and E. BALTAZZI. J. Am. Chem. Soc. **82**, 4389 (1960).
7. H. FISCHER and H. ORTH. Die chemie des pyrrols. Leipzig, 1934 and 1937. Vol. I, p. 334; II/1, p. 4.
8. R. B. WOODWARD. Pure Appl. Chem. **2**, 383 (1961).
9. Y. C. KIM. Can. J. Chem. **47**, 3259 (1969).
10. J. PLUSCEC and L. BOGORAD. Biochem. **9**, 4736 (1970).

11. B. FRYDMAN, S. REIL, A. VALASINAS, R. B. FRYDMAN, and H. RAPOPORT. J. Am. Chem. Soc. **93**, 2738 (1971).
12. A. R. BATTERSBY. I.U.P.A.C. Meeting, Boston. July 25–30, 1971.
13. A. TREIBS and W. OTT. Ann. Chem. **615**, 137 (1958).
14. A. HAYES, G. W. KENNER, and N. R. WILLIAMS. J. Chem. Soc. 3779 (1958).
15. R. F. BACON. Am. Chem. J. **33**, 94 (1905).
16. S. F. MACDONALD and R. J. STEDMAN. Can. J. Chem. **33**, 458 (1955).
17. S. F. MACDONALD. J. Chem. Soc. 4184 (1952).
18. S. F. MACDONALD and K. H. MICHL. Can. J. Chem. **34**, 1768 (1956).
19. A. MARKOVAC, B. K. KULKARNI, K. B. SHAW, and S. F. MACDONALD. Can. J. Chem. **44**, 2329 (1966).
20. A. MARKOVAC and S. F. MACDONALD. Can. J. Chem. **43**, 3364 (1965).
21. A. H. JACKSON, G. W. KENNER, and K. M. SMITH. J. Chem. Soc. C, 502 (1971).
22. L. BOGORAD. *In* The chlorophylls. *Edited by* L. P. Vernon and G. R. Seely. Academic Press, New York. 1966. p. 481.

Can. J. Chem. Downloaded from www.nrcresearchpress.com by 210.87.254.6 on 09/05/12
For personal use only.

Hydrazine Derivatives. I. Transcarbamylation Reaction

JACQUES A. LENOIR AND (in part) LAWRENCE D. COLEBROOK AND DONALD F. WILLIAMS
Department of Chemistry, Sir George Williams University, Montreal 107, Quebec

Received April 4, 1972

Improvements in the synthesis of urazoles via a proposed transcarbamylation reaction are reported. Some experimental evidence for a transcarbamylation mechanism as indicated by the formation of identified intermediate products is shown. ^{13}C n.m.r. studies on 1-phenyl-4-anilinourazole have settled the controversy on the structure of Pinner's compounds by establishing that they are 1,2,4-triazoles rather than *sym*-tetrazines.

Amélioration des synthèses des urazoles au moyen de conditions favorables aux réactions de transcarbamylation. L'identification de quelques produits intermédiaires favorise le postulat d'un mécanisme de transcarbamylation. La controverse sur la structure des tétrazines symmétriques et triazoles-1,2,4 est définitivement réglée. Les études de r.m.n. basées sur le C^{13} établissent clairement la nature des produits de Pinner.

Canadian Journal of Chemistry, **50**, 2661 (1972)

It has long been known that upon prolonged boiling, aqueous solutions of semicarbazide give rise to biurea and hydrazine (1). Scheme 1 can be postulated.

From a comprehensive study of the work of Thiele and Stange (1) and of Pellizzari and Roncagliolo (2) it may be concluded that, in reactions of this type carried out under similar conditions, a transcarbamylation mechanism is predominant (3). In 1864, von Baeyer (4) recognized the nature of the reaction and proposed that it involved a *Umamidierung* between urea and primary amines at temperatures between 150 and 170° (molten state). A study of the literature on reactions of this type suggested a few innovations capable of providing further information on the nature and utility of such transcarbamylation reactions and resulting in improved methods of synthesis. Some of these reactions are summarized below.

The results in Table 1 indicate that the transcarbamylation reaction in the hydrazine series occurs within the temperature range 160–210 °C with a reaction time never less than 3–4 h. The synthesis of 4-aminourazole is the most convenient until now (experiments nos. 3 and 4, Table 1). The reaction pattern is in accord with the fact that the cyclization of carbohydrazide-*N*-carboxamide gives rise to 4-aminourazole by heating with hydrochloric acid (5) (see Scheme 2).

Further, for an efficient transcarbamylation reaction to take place the amine function of the reagent must be present specifically as the hydrochloride salt as shown in Table 2. Contrary to some opinions, carbanilide is a superior transcarbamylation reagent as compared to biurea. Also, Table 2 shows the best and most convenient methods for the preparation of 4-phenylurazole, 4-aminourazole, and guanazoguanazole.

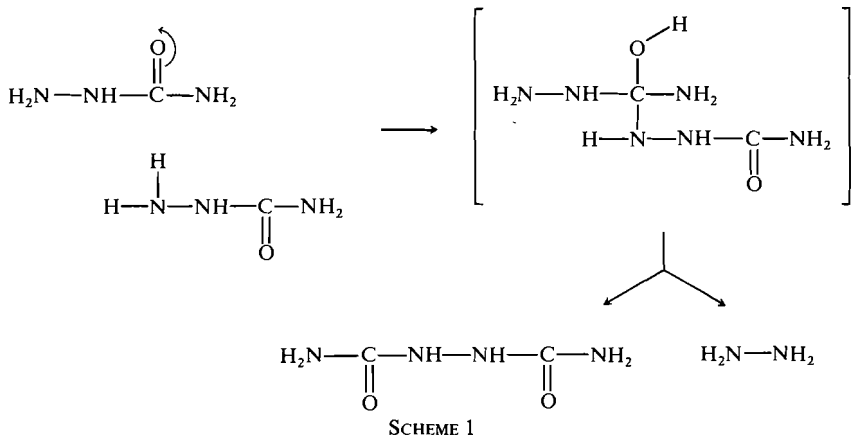

SCHEME 1

Can. J. Chem. Downloaded from www.nrcresearchpress.com by 210.87.254.5 on 09/05/12
For personal use only.

TABLE 1. Influence of temperature and of time

Experiment no.	Starting material	Medium	Temperature (°C)	Period (h)	Products (yield, %)
1	Semicarbazide·HCl	*n*-Hexanol	155–157	4	Biurea and hydrazine·HCl
2	"	*n*-Octanol	195–197	0.5	Biurea (some), 4-aminourazole (20)
3	"	*n*-Octanol	195–197	4	4-Aminourazole (62)
4	"	Kerosene	211	4	4-Aminourazole (62), a small amount of hydrazine (isolated as benzalazine)
5	Semicarbazide·HCl: aniline (2:1)	*n*-Octanol	195–197	4	4-Aminourazole (**1**) (38), *n*-octyl *N*-phenylcarbamate (**2**) (32), and 4-phenylurazole (**3**) (10)

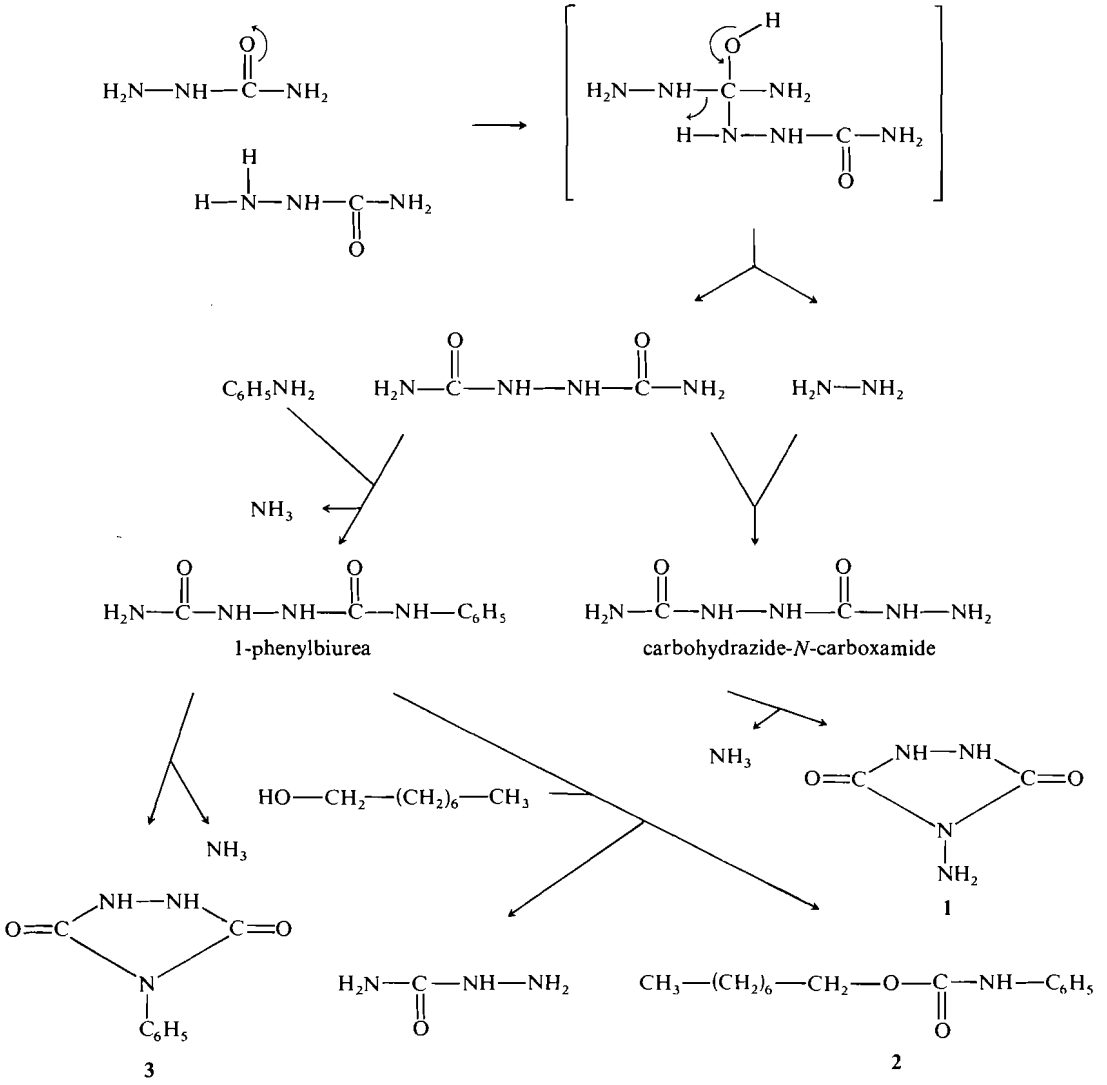

SCHEME 2

Can. J. Chem. Downloaded from www.nrcresearchpress.com by 210.87.254.5 on 09/05/12
For personal use only.

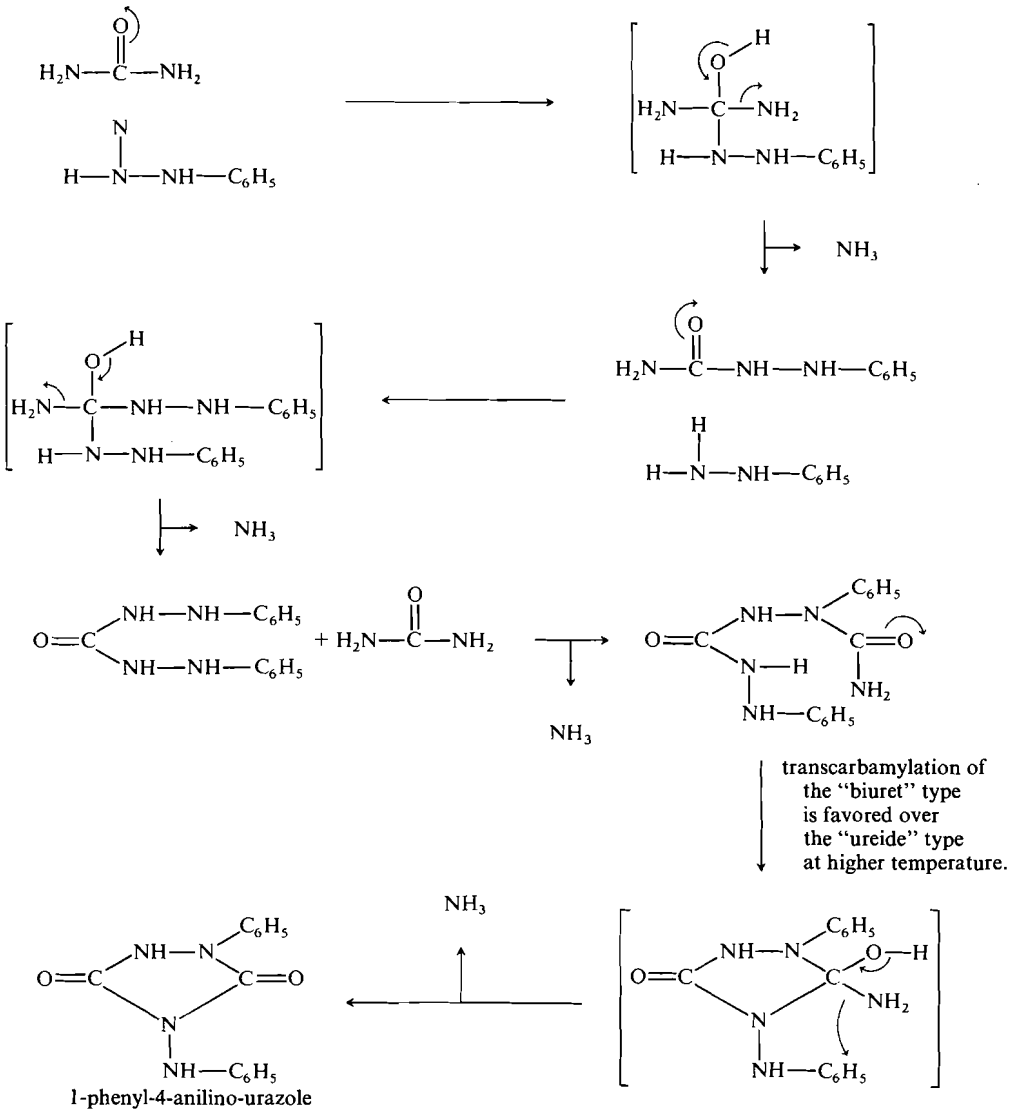

SCHEME 3

According to Pinner (6), Skinner and Ruhemann (7) phenylhydrazine hydrochloride and urea (or biuret) (1:4) give 1-phenylurazole. This conclusion is based on erroneous analysis. Later, Pinner (8) proposed the structure of a tetrazine for his diphenylurazine favoring the formula 1,2-diphenyl-tetrahydro-1,2,3,5-tetrazine-4,6-dione over that of a 1,4-diphenyl-tetrahydro-1,2,4,5-tetrazine-3,6-dione by reasoning from the structure of his 1-phenylurazole. Also, Pinner (8) as well as many other authors retained the 1-phenylurazole structure for the product formed from 1-phenylsemicarbazide and urea. The 1-phenylsemicarbazide was obtained from the reaction between phenylhydrazine hydrochloride and urea (1:1). Various authors (9) accepted Pinner's views although these were challenged by Busch (10). The latter's argument was not rigorous enough to solve the problem of Pinner's "phenylurazole" structure. There is also some doubt about the structure of the "phenylurazole" of Dains and coworkers

Can. J. Chem. Downloaded from www.nrcresearchpress.com by 210.87.254.5 on 09/05/12
For personal use only.

TABLE 2. Influence of hydrochloride salt, time, and temperature

Experiment no.	Starting material	Medium	Temperature (°C)	Period (h)	Products (yield, %)
1	Biurea	*n*-Octanol	195–197	4	Biurea (100)
2	Biurea:aniline (1:1)	*n*-Octanol	195–197	4	*n*-Octyl *N*-phenylcarbamate (26)
3	Carbanilide	*n*-Octanol	195–197	4	*n*-Octyl *N*-phenylcarbamate (40)
4	Biurea	Kerosene	211	18	Biurea (98), urazole (2)
5	Biurea:aniline (1:3)	Kerosene	211	12	Biurea (almost 100% recovery)
6	Biurea:NH_4Cl (1:1)	Kerosene	211	11	Urazole (only)
7	"	Petroleum	157–160	11	Biurea (90) and a very small amount of impure cyanuric acid
8	Biurea:aniline·HCl (1:1)	Kerosene	211	1	1-Phenylbiurea (almost 100%)
9	"	Kerosene	211	7	1-Phenylbiurea (10), 4-Phenylurazole (62)
10	Biurea:hydrazine dihydrochloride (1:1)	Kerosene	211	4	4-Aminourazole (65)
11	Hydrazine·2HCl: cyanoguanidine (1:2)	Petroleum	157–160	2–3	Guanazoguanazole (83)

(11). The controversy on whether Pinner's "phenylurazole" and "diphenylurazine" are *sym*-tetrazines or 1,2,4-triazoles has now been settled in this laboratory by ^{13}C n.m.r. The product formed by the action of phenylhydrazine hydrochloride and urea (1:4) using the procedure described by Pinner (6, 8) is identical with the product obtained by the method described in this paper (see Scheme 3).

The reactants were heated in petroleum ether (b.p. 155–160°) for 5 h under reflux to give 1-phenyl-4-anilino-urazole in almost quantitative yield. The products of both of these reactions have identical melting points and i.r. spectra. Numerous 4-alkylurazoles were prepared and compared with those reported by Tsuji (12). His results and other inherent difficulties and contradictions are too involved to be published at this time (3).

Discussion

The proton n.m.r. spectrum does not provide information useful in enabling a distinction to be made between the two possible structures, **1** and **2**, because of the very broad nature of the N—H signals (DMSO-d_6 solution). A distinction between these structures may be made on the basis of the number of lines appearing in the ^{13}C n.m.r. spectrum.

In the noise decoupled spectra of **1** and **2**, all magnetically distinct carbon atoms must give rise to individual single lines. However, in the coupled spectra only the carbonyl and the aryl carbon atoms at the point of attachment should give rise to single lines, the other aryl carbon lines being split by coupling to hydrogen to give doublets with separation J, considering only single bond ^{13}C–H coupling. In the case of off-resonance decoupling this separation will be reduced to J_r, but can be used to identify carbons directly bound to hydrogen (13). Under the conditions of partial decoupling employed, only the direct ^{13}C–H couplings are detectable, so that the smaller couplings involving more than one bond do not complicate the spectra.

In structure **1**, both carbonyl groups and both aryl groups are equivalent since the molecule has a center of symmetry. Providing that accidental overlap is absent, five lines (one carbonyl and four aryl) are predicted in the noise decoupled ^{13}C spectrum. Two of these should remain unsplit in the off-resonance decoupled spectrum, for which eight lines are predicted.

Ten lines are predicted for the noise decoupled spectrum of the less symmetrical structure, **2**. Of these, four should remain unsplit in the off-resonance decoupled spectrum, for which a maximum of 16 lines is predicted. The experimental data are summarized in Table 3. Seven lines are observed in the noise decoupled spectrum. Of these, four remain unsplit in the off-resonance decoupled spectrum, which shows ten resolved lines. These data are consistent only with structure **2**. Fewer lines are observed

Can. J. Chem. Downloaded from www.nrcresearchpress.com by 210.87.254.5 on 09/05/12
For personal use only.

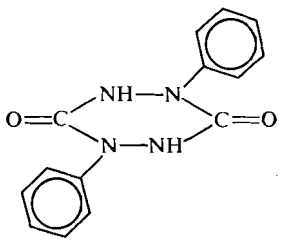

1

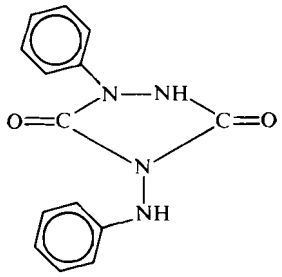

2

TABLE 3. Carbon[13] chemical shifts*

Peak	Noise decoupling	Off-resonance decoupling
1	153.5	153.7
2	150.9	150.9
3	149.2	149.4
4	136.4	136.5
5	128.3	128.5†, $J_r = 47$ Hz
6	124.1	124.2†, $J_r = 46$ Hz
7	117.9	117.8†, $J_r = 49$ Hz

*p.p.m. downfield from TMS.
†Center of doublet.

than are predicted for this structure because of overlap between lines from corresponding carbons of the non-equivalent aryl groups, only the carbon atoms at the points of attachment being fully resolved. Incomplete resolution of the other aryl carbons is evident from their line widths. Structure **1** must be excluded because both the fully decoupled spectrum and the off-resonance decoupled spectrum show more than the predicted maximum numbers of lines. The chemical shifts in Table 3 agree well with those of some 3-aryl substituted hydantoins and arylureas under investigation in this laboratory.

Conclusion

Of the two possible structures, **1** is quite inconsistent whereas the five-membered ring structure **2** is fully consistent with the experimental spectra.

Experimental

Melting points were taken on a Mettler melting point apparatus.

The ^{13}C n.m.r. spectra were obtained from a 32% solution of 1-phenyl-4-anilinourazole in DMSO in an 8 mm spinning sample tube. Spectra were recorded in the frequency sweep mode using a Varian HA-100 spectrometer operating at 25.15 MHz and equipped with a V-3530 wide sweep accessory and a V-4335-1 probe. A V-3512-1 heteronuclear decoupler provided irradiation centered on the DMSO protons, with a noise bandwidth of 1.8 kHz for complete proton decoupling, and in the coherent mode for single frequency off-resonance decoupling. One hundred scans of 1.2 kHz width were accumulated in a C-1024 time averaging computer, using scan times of 50 s. The instrument was locked to the natural abundance ^{13}C signal of the proton decoupled solvent, which was also used as the internal reference. The chemical shifts relative to TMS were calculated by taking the chemical shift of DMSO to be 39.9 p.p.m. downfield from TMS, and are estimated to be internally accurate to ± 0.2 p.p.m.

Authentic samples of the following compounds were prepared: urazole (Moeller) (14), also purchased from the Aldrich Chemical Company: 4-aminourazole (*p*-urazine) (Bailar) (5); 4-phenylurazole (Zinner and Deucker) (15); *n*-octyl *N*-phenylcarbamate (Cheronis and Entrikin) (16); guanazoguanazole (Kaiser, Peters and Wystrach) (17); 1-phenyl-4-anilinourazole (Pinner) (6, 8) and (Skinner and Ruhemann) (7); biurea, very conveniently, according to Müller (18) (from hydrazine sulfate and urea), to Thiele (19) (from hydrazine sulfate and potassium cyanate), and to Leboucq (20) (from semicarbazide hydrochloride and potassium cyanate). All the above compounds gave identical i.r. with the compounds prepared as described in this paper.

General Procedure

As a typical example, the preparation of 1-phenyl-4-anilinourazole is given.

A suspension of 14.5 g (0.1 mol) of phenylhydrazine hydrochloride and 24–25 g (0.4 mol) of urea was heated under reflux in 100 ml of petroleum ether (b.p. 155–160°) with magnetic stirring. Within 15 min the solid mixture melted and shortly after copious fumes of ammonia were evolved. After 5 h the reaction mixture was cooled with the stirring maintained. The crude product was filtered off and washed with petroleum ether (b.p. 35–60°). After having been dried the product was extracted with water to remove water soluble impurities and was purified by recrystallization from aqueous ethanol. The yield of 1-phenyl-4-anilinourazole, m.p. 264.2°, (lit. 262–263 (6); 260 (7); 264° (8)) was almost quantitative. This product was subjected to ^{13}C n.m.r. studies.

4-Aminourazole (p-Urazine)

The synthesis of this compound did not follow the general procedure as described above. The method used is much more accessible, the yields are higher, and the procedure is very simple compared to previously described methods (5).

Can. J. Chem. Downloaded from www.nrcresearchpress.com by 210.87.254.5 on 09/05/12
For personal use only.

A suspension of 11.2 g (0.1 mol) of semicarbazide hydrochloride and 10 ml (0.2 mol) of hydrazine hydrate (99–100%) was heated under reflux in 50 ml of 95% ethanol for 3 h. Vacuum distillation of the reaction mixture yielded a thick syrup.

A thermometer was arranged to dip into the syrup in such a way that its tip did not come in contact with a teflon coated magnetic stirring bar. After the addition of 12 ml of concentrated hydrochloric acid heat was slowly applied. Foaming occurred but later subsided. The temperature was controlled between 210–215°, the total heating time being about 2 h. When the material had cooled, 50 ml of water was added, and the mixture heated to 90° in order to dissolve the solid. After a few hours in a refrigerator at -5°C the solution deposited crystals of 4-aminourazole. These were filtered off, washed with a little ice cold water, then ice cold 95% ethanol, and finally with diethyl ether. This sequence quickly yielded a dry product. The yield of 4-aminourazole, m.p. 276 °C (dec.) (lit. 276° (5)) was 3.8 g (65%). The product was characterized as its benzaldehyde derivative, m.p. 254 °C (lit. 253 °C (5)). Both 4-aminourazole and its benzal derivative gave i.r. spectra identical with those of control preparations as given in ref. 5.

1. J. THIELE and O. STANGE. Ann. **283**, 1 (1894).
2. G. PELLIZZARI and C. RONCAGLIOLO. Gazz. chim. ital. **31**, I, 477 (1901).
3. J. A. LENOIR. Can. J. Chem. To be published.
4. A. VON BAEYER. Ann. **131**, 252 (1864).
5. J. BAILAR. Inorganic synthesis. Vol. IV, McGraw-Hill Book Co. Inc., New York. 1953. p. 31.
6. A. PINNER. Ber. **20**, 2358 (1887); Ber. **21**, 1219 (1888).
7. S. SKINNER and S. RUHEMANN. Ber. **20**, 3372 (1887).
8. A. PINNER. Ber. **21**, 2329 (1888).
9. S. F. ACREE. Ber. **35**, 553 (1902); M. BUSCH and A. STERN. J. Prakt. Chem. (2) **60**, 235 (1899); G. HELLER. Ann. **263**, 269 (1891); H. RUPE. Ber. **29**, 829 (1896); H. RUPE and H. GEBHARDT. Ber. **32**, 10 (1899).
10. M. BUSCH. Ber. **34**, 2311 (1901).
11. F. B. DAINS and E. WERTHEIM. J. Am. Chem. Soc. **42**, 2303 (1920); J. A. MURRAY, F. B. DAINS. J. Am. Chem. Soc. **56**, 144 (1934).
12. T. TSUJI. Pharm. Bull. Japan, **2**, 403 (1954); Chem. Abstr. **50**, 12 033 (1956).
13. R. A. ARCHER, R. D. G. COOPER, P. V. DEMARCO, and L. F. JOHNSON. Chem. Commun. 1291 (1970).
14. T. MOELLER. Inorganic synthesis. Vol. V. McGraw-Hill Book Co. Inc., New York. 1957. p. 52.
15. G. ZINNER and W. DEUCKER. Arch. Pharm. **294**, 370 (1961).
16. N. D. CHERONIS and J. B. ENTRIKIN. Semimicro qualitative organic analysis. 2nd Ed. Interscience Publ. Inc., New York. 1957. p. 377 and 572.
17. D. W. KAISER, G. A. PETERS, and V. P. WYSTRACH. J. Org. Chem. **18**, 1610 (1953).
18. E. MÜLLER. Houben-Weyl Methoden der organischen Chemie. Vol. 10. Part 2. Georg Thieme Verlag, Stuttgart. 1967. p. 140.
19. J. THIELE. Ann. **271**, 128 (1892).
20. J. LEBOUCQ. J. pharm. chim. (8) **5**, 531 (1927).

Can. J. Chem. Downloaded from www.nrcresearchpress.com by 210.87.254.5 on 09/05/12
For personal use only.

Mobilities and Ranges of Electrons in Liquids: Effect of Molecular Structure in C_5–C_{12} Alkanes

JEAN-POL DODELET AND GORDON R. FREEMAN
Chemistry Department, University of Alberta, Edmonton 7, Alberta

Received January 26, 1972

X-radiolysis free ion yields and electron mobilities were measured in a series of branched chain hydrocarbons at several temperatures. The numbers listed after the following compounds are the temperature (K), G_{fi}, most probable penetration range of the secondary electrons (Å) and thermal electron mobility ($cm^2/V\ s$): 2,2-dimethylpropane (neopentane), 294, 1.09, 213, 50; 2,2,3,3-tetramethylbutane, 379, 0.80, 130, –; 2,2,4,4-tetramethylpentane, 295, 0.83, 158, 24; 2,2,5,5-tetramethylhexane, 293, 0.67, 138, 12; 2,2,6,6-tetramethylheptane, 293, 0.47, 113, —; 2,2,7,7-tetramethyloctane, 383, 0.58, 100, —; 2,2,3,3-tetramethylpentane, 295, 0.42, 102, 5.2; cyclohexane, 294, 0.16, 67, 0.45. The difference between the activation energies of the reactions

[14] $$[M^+ + e^-] \rightarrow \text{geminate neutralization}$$

and

[15] $$[M^+ + e^-] \rightarrow \text{free ions}$$

is $(E_{15} - E_{14}) \approx (2 \text{ to } 3)RT$ for twenty two different hydrocarbons, including olefins and benzene. The rate of energy loss by epithermal electrons in liquid hydrocarbons increases with increasing anisotropy of polarizability of the molecules or groups; the range of the electron interaction in a given molecule appears to be about two C—C bonds in series (groups up to neopentyl in size). There is a correlation between the mobilities of thermal electrons in liquids and the penetration ranges of the secondary electrons in the liquids. The electron mobility in a liquid alkane appears to be limited by inelastic scattering. The inelastic scattering cross sections for both thermal (<0.1 eV) and epithermal (~1 eV) electrons in liquid alkanes are affected in similar ways by the anisotropy of polarizability of the molecules. In both instances the scattering apparently involves rotational (librational) excitation of the medium.

Les rendements en ions libres et les mobilités électroniques ont été mesurés, sous irradiation X, à plusieurs températures, pour un certain nombre d'hydrocarbures à chaîne ramifiée. En utilisant le symbolisme suivant: liquide, température (K), rendement en ions libres, valeur la plus probable de pénétration pour les électrons secondaires (Å) et mobilité de l'électron thermique ($cm^2/V\ s$), il est possible de donner une idée rapide des résultats obtenus: 2,2-diméthylpropane (néopentane), 294, 1.09, 213, 50; 2,2,3,3-tétraméthylbutane, 379, 0.80, 130, —; 2,2,4,4-tétraméthylpentane, 295, 0.83, 158, 24; 2,2,5,5-tétraméthylhexane, 293, 0.67, 138, 12; 2,2,6,6-tétraméthylheptane, 293, 0.47, 113, —; 2,2,7,7-tétraméthyloctane, 383, 0.58, 100, —; 2,2,3,3-tétraméthylpentane, 295, 0.42, 102, 5.2; cyclohexane, 294, 0.16, 67, 0.45. La différence entre les énergies d'activation des réactions

[14] $$[M^+ + e^-] \rightarrow \text{neutralisation dans les grappes}$$

et

[15] $$[M^+ + e^-] \rightarrow \text{ions libres}$$

est $(E_{15} - E_{14}) \approx (2 \text{ à } 3)RT$; cette valeur est obtenue pour vingt-deux hydrocarbures y compris des oléfines et le benzène. Les électrons épithermiques perdent d'autant plus rapidement leur énergie, dans les hydrocarbures liquides, que l'anisotropie de polarisabilité de ces molécules (ou groupements) est importante; il semble qu'un électron puisse perturber une molécule donnée sur une distance équivalant à 2 liens C—C consécutifs, c'est à dire, un domaine couvrant l'ensemble d'un groupement néopentyle. Il y a, en phase liquide, une corrélation entre les mobilités des électrons thermiques et les distances de pénétration des électrons secondaires produits lors de l'irradiation. Les mobilités électroniques, dans un alcane liquide, semblent être limitées par la diffusion inélastique dont les sections efficaces, pour les électrons épithermiques (~1 eV) et thermiques (<0.1 eV), sont influencées d'une manière similaire par l'anisotropie de polarisabilité des molécules. Dans les deux cas, la diffusion impliquerait l'excitation de la rotation (libration) dans le milieu.

Can. J. Chem. Downloaded from www.nrcresearchpress.com by 210.87.254.40 on 09/05/12
For personal use only.

Can. J. Chem. Downloaded from www.nrcresearchpress.com by 210.87.254.40 on 09/05/12
For personal use only.

Introduction

The radiolytic free ion yields G_{fi} (1–6) and the mobilities of electrons u_e (6–11) in liquid alkanes increase with increasing sphericity of the hydrocarbon molecules (1, 3, 6). The values of G_{fi} and u_e do not correlate with the dipole moments of the molecules, all of which are $\mu \leqslant 0.1$ D (12). The significant property of the molecules studied thus far seems to be the degree of anisotropy of polarizability (1, 6). The anisotropy of polarizability varies inversely with the degree of sphericity of the molecules.

It had previously been noted that *t*-butyl groups augment the radiation induced electrical conductance C of hydrocarbons (13). This is consistent with the above correlation because *t*-butyl groups are globular and

$$[1] \qquad C = \mathrm{fn}(G_{fi}, u_e, u_p)$$

where u_p is the mobility of the positive ions. In an attempt to learn more about the electron molecule interactions in hydrocarbon liquids the free ion yields and electron mobilities have been measured in a series of compounds $(CH_3)_3C(CH_2)_nC(CH_3)_3$ with $n = 0$, 1, 2, 3, and 4. By progressively separating the *t*-butyl groups from each other it has been possible to estimate the effective range of the electron–molecule interaction.

Experimental

Materials

The cyclohexane and neopentane were Phillips Research Grade. The 2,2,3,3-tetramethylbutane (2233TMB), 2,2,4,4-tetramethylpentane (2244TMP), 2,2,3,3-tetramethylpentane (2233TMP), 2,2,5,5-tetramethylhexane (2255TMH), 2,2,6,6-tetramethylheptane (2266TMHp), and 2,2,7,7-tetramethyloctane (2277TMO) were obtained from Chemical Samples Co. All these compounds were $\geqslant 99\%$ pure. The 2233TMB (m.p. 374 K) and 2277TMO (m.p. 315 K) are solid at room temperature, while the other compounds are liquid.

The liquids were purified by shaking with concentrated sulfuric acid to remove olefins. They were then washed several times with a dilute solution of sodium carbonate, then repeatedly with triply distilled water, then dried over lithium aluminum hydride. They were then distilled under vacuum onto sodium mirrors to remove the last traces of water and to react with traces of halides that might be present.

The 2233TMB and 2277TMO were purified by degassing above the melting point and treatment of the melt for at least 10 h with a sodium mirror.

All the compounds were thoroughly degassed before being sealed into the conductance cell under a remaining pressure of $< 7 \times 10^{-4}$ N/m^2 (5×10^{-6} Torr). The final criterion of purity was the observation of an electron conductance transient (ECT). In most of the liquids at 293 K the ECT had a half-life of 2–3 μs after a 1 μs pulse of X-rays. In order to achieve the maximum half-life and intensity of the ECT it was usually necessary to irradiate the filled conductance cell with γ rays to a dose of 10^{18}–10^{19} eV/g. Irradiation converted the remaining traces of oxygen and carbon dioxide into less efficient electron scavengers.

Although an ECT was obtained in each of the liquids studied, those observed in 2233TMB, 2266TMH$_p$, and 2277TMO had decay times equal to that of the measuring circuit, $t_{1/2} = 0.5$ μs. These liquids apparently contained small amounts of electron scavengers that were not removed by the purification treatment. However, the fact that an ECT was observed indicates that the scavenger concentration was low enough that the free ion yield would be decreased only slightly.

Equipment and Technique

(a) Conductance Cell

The plain, parallel, stainless steel electrodes were 30 mm in diameter and 3 mm apart, sealed in a 32 mm i.d. Pyrex envelope. The liquid entered the cell from side-arms joined to the flat ends, so that the cylindrical space between the electrodes was completely confined by a proximate glass wall. The cell constant (L/A cm^{-1}) was measured conductiometrically using standard KCl solutions.

The high voltage and charge-collection leads were shielded from the cooling or heating bath by glass tubes sealed to the cell and emerging out of the bath.

(b) Constant-Temperature Baths

Solid-liquid slushes of the following compounds were used to obtain refrigerant baths: chloroform (212 K), chlorobenzene (229 K), bromobenzene (254 K), water (273 K). A thermostated silicone oil bath was used for temperatures 293–473 K.

(c) Determination of the Free Ion Yields

The charge clearing technique (2, 3) was used. The irradiation dose per pulse (1 μs, 1.7 MeV X-rays) was 2–3 $\times 10^{10}$ eV/cm^3. The electric field (0.5–15 kV/cm) was applied across the cell throughout each experiment. The charge collected after a radiation pulse was fed into a low drift, high sensitivity integrator for 0.5–5 s to allow maximal collection of the ions; the signal was then put into half of the memory of a Fabritek 1062 Signal Averager. After each signal a blank (no pulse from the van de Graaff) was measured by the integrator for 0.5–5 s and put into the other half of the 1062 memory. In a typical run four alternate signals and blanks were fed into the 1062; the signals and blanks were then averaged separately and subtracted. The net signal was displayed on an oscilloscope. Larger numbers of signals and blanks were used for smaller collected charges. The signals and blanks were also monitored with a Tektronix 549B oscilloscope with a type 1A7 plug-in.

The circuit used was similar to that reported elsewhere (5), with a sensitivity up to 2 pcoul/cm.

(d) Measurement of the Electron Conductance Transient (ECT)

The circuit used is shown in Fig. 1. The greatest useful current sensitivity was 20 nA/cm. The response time of earlier circuits (6) increased with increasing capacitance of the conductance cell. The present circuit decay half-time is

Can. J. Chem. Downloaded from www.nrcresearchpress.com by 210.87.254.40 on 09/05/12
For personal use only.

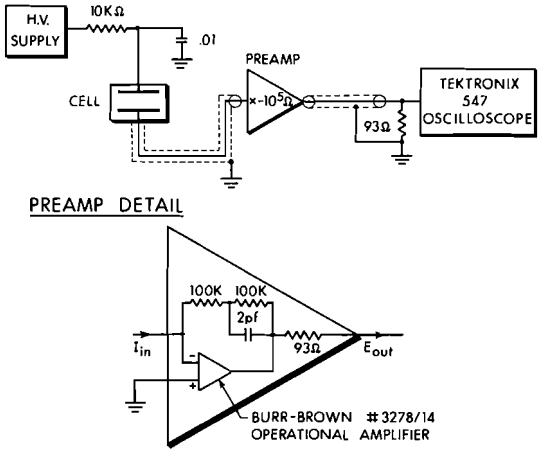

FIG. 1. Circuit for measuring the electron conductance transient.

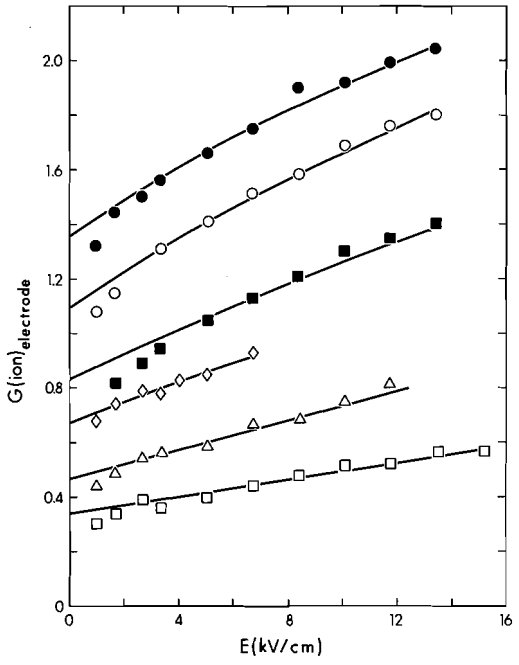

FIG. 2. Yield of ions collected at each electrode as a function of applied field strength E. Neopentane 293 K ○; 333 K ●; 2244TMP, 295 K ■; 2255TMH, 293 K ◇; 2266TMHp, 293 K △; 2277TMO, 316 K □. The curves were calculated by the method in refs. 17 and 18.

0.5 μs, independent of the cell capacitance; the noise level rather than the response time increases with increasing capacitance.

The 1 μs irradiation pulse dose used was $3–6 \times 10^{10}$ eV/cm^3.

(e) Dosimetry

The method used was the same as that described elsewhere (5, 6).

(f) Physical Properties of the Liquids

The densities d (14, 15) and dielectric constants ε (15) of the compounds were obtained by extrapolation or calculation from data in the references indicated. When necessary the value of the dielectric constant at one temperature was obtained from the relation $\varepsilon = n_D^2$, and values at other temperatures were calculated from the Clausius Mosotti equation (16); n_D is the refractive index. By comparison with values for other hydrocarbons (12), the dipole moments of all of the present alkanes are probably $\leqslant 0.1$ D and would contribute $<1\%$ to the dielectric constant of the liquid.

Results

Free Ion Yields and Secondary Electron Ranges

The free ion yields increase with increasing applied electric field strength and with increasing temperature. Typical results are shown in Fig. 2. For a given temperature the 100 eV yields of free ions at field strengths E, G_{fi}^E, were extrapolated to the value at zero field strength, G_{fi}^0, using eq. 2 (17, 18).

$$[2]\quad G_{fi}^E/G_{fi}^0 = 1 + \frac{9.69E}{\varepsilon T^2} + \frac{35.2E^2}{\varepsilon^2 T^4} - \frac{4.21 \times 10^4 E^2}{\varepsilon T^3} \frac{\int_0^\infty F(y)\, e^{-r/y} y\, dy}{\int_0^\infty F(y)\, e^{-r/y}\, dy} + \ldots$$

where ε is the dielectric constant of the liquid, T is the absolute temperature, $F(y)$ is the fraction of electron–ion pairs that have an initial separation distance y between the thermalized electron and its parent ion, $r = \xi^2/\varepsilon kT$, ξ is the electronic charge and k is Boltzmann's constant. Furthermore,

$$G_{fi}^0 = G_{tot} \int_0^\infty F(y)\, e^{-r/y}\, dy$$

where G_{tot} is the total ionization yield.

It was assumed that $F(y)$ had a Gaussian form

$$[3]\quad F(y) = (4y^2/\pi^{1/2}b^3) \exp(-y^2/b^2)$$

where b is the dispersion parameter; b is also the most probable value of y. The use of Gaussian distributions for liquids that give $G_{fi}^0 > 0.2$ was justified earlier (18). It was also assumed that in all of the liquids $G_{tot} = 4.3$, which equals the gas phase ionization yield in many alkanes (19, 20).

TABLE 1. G_{fi}^0 and most probable electron range b

Liquid	T (K)	G_{fi}^0	ε	b (Å)	bd (10^{-8} g/cm^2)	bd_{av} (10^{-8} g/cm^2)
Neopentane	273	1.02	1.84	214	131	128
CMe_4	294	1.09	1.80	215	127	
	302	1.13	1.78	219	127	
	312	1.18	1.76	222	126	
	322	1.27	1.74	229	128	
	333	1.35	1.71	239	130	
2233TMB	379	0.80	1.84	130	85	85
Me_3CCMe_3						
2244TMP	212	0.59	2.12	164	130	117
$Me_3CCH_2CMe_3$	229	0.59	2.09	154	120	
	254	0.64	2.05	149	113	
	295	0.83	1.98	158	114	
	324	0.96	1.92	166	114	
	385	1.19	1.80	174	108	
2255TMH	293	0.67	1.97	138	99	102
$Me_3CCH_2CH_2CMe_3$	319	0.79	1.93	145	101	
	353	0.96	1.89	154	103	
	383	1.08	1.85	160	104	
2266TMHp	293	0.47	1.97	113	81	81
$Me_3C(CH_2)_3CMe_3$	330	0.59	1.92	117	81	
	358	0.70	1.88	123	82	
	383	0.78	1.84	126	81	
	428	0.92	1.78	131	80	
	465	1.12	1.74	143	83	
2277TMO	316	0.34	2.13	83	66	70
$Me_3C(CH_2)_4CMe_3$	348	0.50	2.02	96	71	
	383	0.58	1.94	100	70	
	423	0.75	1.84	111	71	
2233TMP	273	0.38	2.08	103	80	74
$Me_3CCMe_2CH_2CH_3$	295	0.42	2.05	102	77	
	318	0.46	2.01	101	75	
	346	0.52	1.97	100	71	
	375	0.60	1.93	103	71	
	402	0.70	1.89	108	72	
	431	0.81	1.84	114	73	
Cyclohexane	293	0.16	2.03	67	52	53
	306	0.18	2.01	69	52	
	315	0.20	2.00	71	53	
	325	0.23	1.98	73	54	
	340	0.26	1.96	74	54	
	360	0.30	1.92	77	54	
	380	0.34	1.89	78	54	
	395	0.37	1.86	79	53	

The yields of ions collected at the electrodes with a field strength of 1 kV/cm were slightly below the calculated $G_{fi}^{1\ kV}$ values because some of the ions and electrons were lost by mutual neutralization before they could be collected at this field strength.

The values of G_{fi}^0 and b for all the compounds at the various temperatures are listed in Table 1.

Thermal Electron Mobilities

The mobility of thermal electrons in a liquid was calculated from C_0, which was obtained from the initial magnitude of the ECT (6, 8).

$$[4] \qquad C_0 = \frac{6.24 \times 10^{20}\ i_0}{\text{dose}\ AE} = G_{fi}^E u$$

where i_0 is the peak current (A), the pulse dose

Can. J. Chem. Downloaded from www.nrcresearchpress.com by 210.87.254.40 on 09/05/12
For personal use only.

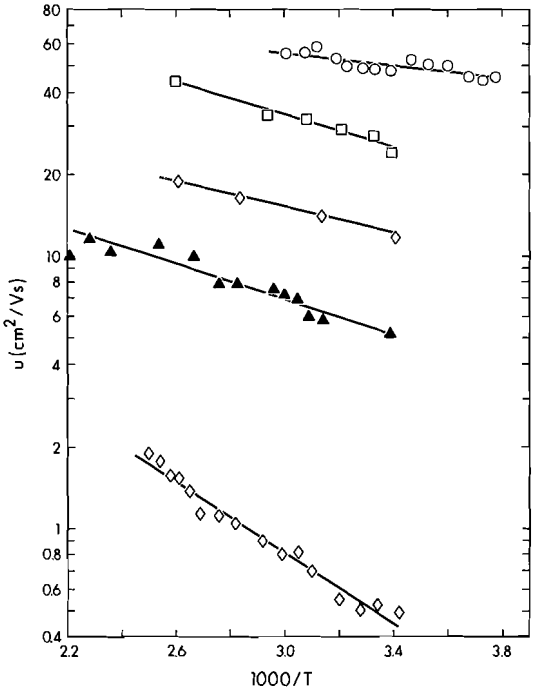

FIG. 3. Arrhenius plots of electron mobilities in liquid hydrocarbons. The electric field strengths used in the various hydrocarbons are listed in Table 2. ○, neopentane; ■, 2244TMP; ◇, 2255TMH; ▲, 2233TMP; ◆, cyclohexane. Many of the points are averages of two sets of values.

is expressed in eV/cm^3, A is the area of the collecting electrode (cm^2), E is the applied field strength (V/cm), G_{fi}^E is the free ion yield at field strength E, and u is the electron mobility. It was assumed that the positive ion mobility was negligible, which would be true in the absence of an electronic mechanism for positive hole migration in these liquids.

To obtain the value of C_0 the observed ECT was corrected for decay that occurred during the measurement. This was necessary because neither the pulse duration ($t_p = 1.0$ μs) nor the circuit response time ($t_{cr} = 0.5$ μs) was negligible by comparison with the ECT decay half-life (1–2 μs). The ECT decay was first order. To minimize the error in C_0 the magnitude of the ECT was read at a time $t \geqslant (t_p + 2t_{cr})$, measured from the beginning of the radiation pulse as $t = 0$. For an ECT with a first order decay half-life $t_{1/2}$ and a magnitude C_t at $t \geqslant (t_p + 2t_{cr})$, the value of C_0 for use in eq. 4 is given by eq. 5.

$$[5]\quad C_0 = C_t\left\{\frac{t_{1/2}}{0.69t_p}[1 - \exp(-0.69t_p/t_{1/2})] \times \exp(-0.69[t - t_p]/t_{1/2})\right\}^{-1}$$

Representative values of u and G_{fi}^E are given in Table 2. More complete mobility data are shown in Fig. 3. Values of the activation energies E_u for the electron mobilities were derived from Fig. 3 and are listed in Table 2.

Values of C_0 and hence of u could not be determined in 2233TMB, 2266TMHp, or 2277-TMO because the observed ECT decay times in these liquids equaled that of the measuring circuit.

Discussion

Free Ion Yields and Secondary Electron Ranges

The relationship between the radiolytic free ion yields and the secondary electron ranges has been extensively discussed (1–4, 17, 18, 21, 22) and does not require repetition here.

In each of the liquids the range b increases somewhat with increasing temperature (Table 1). However, the product of b and the liquid density d is constant for a given compound; the small increases or decreases in bd with increasing temperature recorded for some of the compounds in Table 1 do not seem to form a pattern and may be within the experimental error.

It was noted earlier that the electron ranges (1) and values of bd (2, 4) increase with increasing degree of sphericity of small molecules (3, 5). The values of bd in Table 1 indicate that for larger molecules the situation is more complex. The molecules of 2244TMP are much less sphere-like than are those of neopentane, yet the values of bd for the two liquids are similar, being 117 and 127, respectively (10^{-8} g/cm^2).

Consider for a moment the results of Schmidt and Allen (4) listed in Table 3. Methyl substitution on either n-butane or n-pentane has little effect on the value of bd as long as no carbon becomes completely substituted. However, formation of a t-butyl group (complete substitution of a carbon) on either butane or pentane increases the value of bd by about 30%. The last compound in the first column of Table 3 is denoted by A and that in the second column by B. Addition of one methyl group to A, to

Can. J. Chem. Downloaded from www.nrcresearchpress.com by 210.87.254.40 on 09/05/12
For personal use only.

Can. J. Chem. Downloaded from www.nrcresearchpress.com by 210.87.254.40 on 09/05/12
For personal use only.

TABLE 2. Values of G_{fi}^{E}, electron mobilities (u) and activation energies (E_u)

Liquid	T (K)	G_{fi}^{E}	u (cm^2/Vs)	E (V/cm)	E_u (kcal/mol)	Literature u	Literature E	Literature E_u	Literature Reference	η_{293} (mP)	E_η (kcal/mol)
Neopentane	273	1.03	48	100	0.6						
	294	1.10	50	100		55	⩾1000		9	2.5†	2.3†
	302	1.14	51	100		40	10		6		
	312	1.19	53	100							
	322	1.28	54	100							
2244TMP	295	0.86	24	590	1.4						
	324	0.99	32	590							
	385	1.22	44	590							
2255TMH	293	0.68	12	340	1.1						
	319	0.81	14	340							
	353	0.98	16	340							
	383	1.09	19	340							
2233TMP	295	0.44	5.2	1000	1.5						
	318	0.48	5.9	1000							
	346	0.54	7.5	1000							
	375	0.62	9	1000							
	431	0.83	11	1000							
Cyclohexane	294	0.25	0.45	6700	2.9	0.35	⩾5000		9	9.7‡	3.0‡
	315	0.29	0.62	6700							
	340	0.35	0.89	6700							
	380	0.44	1.4	6700							
	395	0.48	1.7	6700							
n-Hexane	296					0.09	⩾7000	5.5	9	3.2‡	1.9‡
	300					0.07	1000	4.3	11		

*G_{fi} obtained at the field strength E listed.
†Reference 42.
‡Reference 14.

TABLE 3. Values of *bd* for methyl-substituted *n*-butanes and *n*-pentanes at 295 K (4)*

Substituted *n*-butanes		Substituted *n*-pentanes	
Structure	bd (10^{-8} g/cm^2)	Structure	bd (10^{-8} g/cm^2)
C—C—C—C	48	C—C—C—C—C	45
C—C(C)—C—C	47	C—C(C)—C—C—C	46
C—C(C)—C(C)—C	49	C—C—C(C)—C—C	46
C—C(C)(C)—C—C	60	C—C—C(C)—C(C)—C	50
C—C(C)(C)—C(C)—C (A)	63	C—C(C)(C)—C—C(C)—C (B)	65

*For neopentane the value $bd = 105 \times 10^{-8}$ g/cm^2 was reported (4).

complete a second *t*-butyl group in the molecule, increased *bd* by 35% from 63 to 85 units (see 2233TMB in Table 1). Addition of one methyl group to B, to complete a second *t*-butyl group in the molecule, increased *bd* by 80% from 65 to 117 units (see 2244TMP in Table 1); *bd* is 38% larger in 2244TMP than in 2233TMB. A 2244TMP molecule is comprised of two neopentyl groups overlapping at the central CH_2. Neopentyl groups are more sphere-like than are the two *t*-butyl groups that comprise 2233-TMB. It appears that a large molecule that is not sphere-like but that contains sphere-like groups is characterized by a large value of *bd*. The value of *bd* in 2244TMP is only slightly smaller than that in neopentane (Table 1).

Increasing the length of the central—$(CH_2)_n$—chain, where $n = 1, 2, \ldots$, between the globular end groups progressively decreases the value of *bd* (see 2244TMP to 2277TMO in Table 1). Straight chain hydrocarbons have $bd \approx 48 \times 10^{-8}$ g/cm^2 (Table 1 and ref. 4), so this value would presumably be asymptotically approached with increasing n if the present series were extended.

It now remains to discuss possible reasons for the effect of hydrocarbon molecular structure on the ranges of the secondary electrons in the liquids.

Correlation Between Electron Energy Loss Efficiency and Taft's σ^*

The Taft coefficient σ^* (23) indicates the relative inductive effect of a functional group. The electron-accepting powers of three hydrocarbon groups of interest here decrease in the order $CH{=}CH_2 > C_2H_5 > C(CH_3)_3$ ($\sigma^* = +0.7, -0.1$, and -0.3, respectively).

The value of the density-normalized range of the secondary electrons *bd* is inversely related to the efficiency of the electron energy loss processes. From the relative values of *bd* (1, 4, 5) one may conclude that the efficiencies of the electron energy loss processes in the liquids also decrease in the order $RCH{=}CH_2 > RC_2H_5 > RC(CH_3)_3$, where R is an alkyl group ($bd = 35$, 45, and 60, respectively, when R is C_2H_5 or n-C_4H_9 (4)). Thus there is a correlation between the electron accepting power of the groups and the efficiency of the electron energy loss interactions with the molecules.

Although the correlation is only crude it might indicate that one of the electron energy loss processes involves the approach to a transient negative ion state of the molecules (24), resulting in vibrational excitations of the molecule.

Inductive effects have short ranges, being negligible after two consecutive C—C bonds

Can. J. Chem. Downloaded from www.nrcresearchpress.com by 210.87.254.40 on 09/05/12
For personal use only.

TABLE 4. Inverse correlation between *bd* and the anisotropy of Polarizability

Compound	Polarizability components (Å^3)*					*bd* (10^{-8} g/cm^2)
	α_1	α_2	α_3	$\bar{\alpha}$	α^a	
CH_4	2.6	2.6	2.6	2.6	0.0	210†
CMe_4	9.8	9.8	9.8	9.8	0.0	128‡ (105§)
$Me_3CCH_2CMe_3$	17.0	17.0	17.0	17.0	0.0	117‡
C_2H_6	4.9	4.2	4.2	4.4	0.7	65†
$Me_3CCH_2CH_3$	12.1‖	11.4‖	11.4‖	11.6	0.7	(60§)
Me_3CCMe_3	14.7	15.4	15.4	15.2	0.7	85‡
$Me_3CCH_2CH_2CMe_3$	19.3‖	18.6‖	18.6‖	18.8	0.7	102‡
C_3H_8	6.2	6.7	5.7	6.2	0.9	59†
C_2H_4	5.4	3.4	3.3	4.0	2.1	39†
C_3H_6	7.2‖	5.4‖	4.9‖	5.8	2.1	41†
$Me_3CCH{=}CH_2$	12.6‖	10.6‖	10.5‖	11.2	2.1	(48§)

*α_1, α_2, and α_3 are the principal components of the molecular polarizability. The mean value is $\bar{\alpha} = (1/3)(\alpha_1 + \alpha_2 + \alpha_3)$ and the anisotropy α^a is given by $(\alpha^a)^2 = (1/2)[(\alpha_1 - \alpha_2)^2 + (\alpha_2 - \alpha_3)^2 + (\alpha_3 - \alpha_1)^2]$. The values were calculated from information in ref. 27. The values of α_1, α_2, and α_3 reported for ethane and propane in ref. 43 lead to $\alpha^a = 1.5$ Å^3 for ethane and 1.9 Å^3 for propane. They should be rejected because they were taken from data (44) that indicate $\alpha^a = 0.9$ Å^3 for methane. Landolt–Börnstein report $\alpha^a = 0.0$ Å^3 for methane, on the basis of symmetry. If one subtracts the methane error of 0.9 from the ethane and propane values one obtains 0.6 and 1.0 Å^3, respectively, in reasonable agreement with the values in the above table. The Le Fèvre work (27) is also preferred because it is two decades more recent than that of Stuart. The depolarization of 90° scattered light is nearly an order of magnitude greater from a liquid compound than from its vapor (45), but the trends are similar from compound to compound. The phase effect is discussed by Bhagavantam in ref. 46.

†Reference 5.

‡Present work.

§Reference 4. These values should be increased somewhat for comparison with the present work because our value of *bd* in neopentane is 21% greater than that reported in ref. 4.

‖Using the CH_2—CH_3, CH_2—CH_2, or CH=CH_2 axis as the direction of α_1.

(25). Thus larger molecules would be sensed by the electrons as collections of groups rather than as whole molecules.

Taft reactivity coefficients are determined empirically. They are rationalized in terms of group electronegativities, but are not basically understood (23). The correlation between the Taft coefficients and the epithermal electron energy loss efficiencies might have an indirect cause. Fundamental interpretations of the effects of molecular structure on these phenomena are needed.

Correlation Between Electron Energy Loss Efficiency and Anisotropy of Polarizability of the Molecules

From studies of C_1–C_6 hydrocarbons it has been found that there is a qualitative correlation between the degree of sphericity of the molecules and the value of *bd* for the secondary electrons in the liquid (1, 5, 6). This has been attributed to a correlation, not yet understood, between the anisotropy of polarizability of the molecules and the efficiency of the electron energy loss (and perhaps localization) processes in the liquid (1, 5, 6).

The polarizability α of a molecule can be divided into three principal components α_1, α_2, and α_3 at right angles to each other (26, 27). The mean value $\bar{\alpha}$ is given by eq. 6 and the magnitude of the anisotropy of the polarizability of α^a is governed by eq. 7.

$$[6] \qquad \bar{\alpha} = 1/3(\alpha_1 + \alpha_2 + \alpha_3)$$

$$[7] \qquad (\alpha^a)^2 = 1/2[(\alpha_1 - \alpha_2)^2 + (\alpha_2 - \alpha_3)^2 + (\alpha_3 - \alpha_1)^2]$$

Values of α_1, α_2, α_3, $\bar{\alpha}$, and α^a have been calculated for a number of hydrocarbon molecules from information in ref. 27. It was assumed that the molecules were rigid, *i.e.*, not vibrating. The results are listed along with the values of *bd* in Table 4.

Consider first the series of isotropically polarizable molecules ($\alpha^a = 0.0$). The value of *bd* decreases with increasing molecular complexity (Table 4). The decrease in *bd* might be partly

Can. J. Chem. Downloaded from www.nrcresearchpress.com by 210.87.254.40 on 09/05/12
For personal use only.

Can. J. Chem. Downloaded from www.nrcresearchpress.com by 210.87.254.40 on 09/05/12
For personal use only.

due to anisotropy introduced by antisymmetric vibrations in the molecule, and partly due to the short range of the electron induced-dipole interaction. The net coulombic interaction energy between a particle of charge ξ and a nonpolar molecule at distance r from it in a medium of dielectric constant ε is given approximately by eq. 8.

$$[8] \qquad E_{coul} = \frac{-\xi^2\alpha}{\varepsilon^2 r^4}$$

In the simplest case r is large compared with the molecular diameter and ε is a constant. However, the coulombic interaction between an electron and a nearest neighbor molecule in a liquid varies across the molecule, mainly due to variation in r^{-4} but partly also due to the change in ε^{-2}. The variation is greater the larger the molecule. Thus a methane molecule, with its isotropically polarizable C—H bonds (27), will appear more isotropic to a colliding electron than will a neopentane molecule with its outer C—H bonds and anisotropically polarizable inner C—C bonds (27). For electron approach to most of the surface of Me_3CCH_2-CMe_3 the molecule will interact like neopentane (CMe_4), but for approach to the CH_2 group the interaction will be more like that with propane, which has an anisotropic polarizability.

Now consider the series of molecules with $\alpha^a = 0.7$ (Table 4). The value of *bd* is much smaller in ethane than it is in methane, but increases with increasing molecular complexity in the $\alpha^a = 0.7$ series. This can also be attributed to the short range of the electron–molecule interactions. The anisotropy of $Me_3CCH_2CH_2$-CMe_3 is due to the central —CH_2CH_2— group, but the two ends of the molecule are neopentane-like. Thus the average appearance of the large molecule to the myopic electron is more like neopentane than ethane.

The value of α^a is greater in ethylene than in ethane, and the value of *bd* is smaller in the former than in the latter. This confirms the inverse correlation between *bd* and α^a and supports the suggestion that there is a connection between the value of α^a and the efficiency of electron energy loss processes in the liquid. The fact that *bd* is greater in $Me_3CCH{=}CH_2$ than in C_2H_4 also supports the suggestion that the effective interactions are short range; an electron directly approaching the Me_3 end is largely shielded from the double bond. From space-filling molecular models one can determine that about 20% of the surface of $Me_3CCH{=}CH_2$ would look like that of neopentane to a myopic electron, while the olefin group would dominate the interaction for approach to the other 80% of the surface. Thus the value of *bd* in $Me_3CCH{=}CH_2$ is much closer to that in C_2H_4 than to that in neopentane.

Having demonstrated the correlation between the anisotropy of polarizability of the molecules and the electron energy loss efficiencies in the liquids, one still has not arrived at an explanation. It should be stated, however, that the short range of the energy loss interactions is not compatible with any previous concept that used the de Broglie wavelength for the interaction distance; $\lambda = 12$ Å for a 1.0 eV electron.

The anisotropies of the molecules reflect the anisotropic fields encountered by the electrons in the liquids.

Raman-Type Rotational Excitation

The only well known type of molecular excitation process that depends upon the anisotropy of polarizability is Raman rotational excitation (refs. 26, 28; in particular chapter 6 of ref. 28).

Raman excitational processes require a periodic variation in polarizability,

$$[9] \qquad \frac{d\alpha}{dt} = f(\omega t)$$

where $\omega/2\pi$ is the periodic frequency and t is the time. When the polarizability changes with internuclear distance R, *i.e.* for $d\alpha/dR \neq 0$, the molecule is susceptible to Raman vibrational excitation because for a vibration $dR/dt = f'(\omega t)$. Hence,

$$[10] \qquad \frac{d\alpha}{dR}\cdot\frac{dR}{dt} = f_v(\omega t)$$

When the polarizability in a given direction changes during the rotation of a molecule, *i.e.* $d\alpha/d\theta \neq 0$, the molecule is susceptible to Raman rotational excitation because for a rotation

TABLE 5. Temperature coefficients $E_{G_{f1}}$ and E_{esc}

Liquid	$E_{G_{f1}}$*	E_{esc}*	RT_m*	E_{esc}/RT_m
CMe_4	0.9	1.4	0.61	2.3
$Me_3CCH_2CMe_3$	0.8	1.1	0.60	1.8
$Me_3CCH_2CH_2CMe_3$	1.2	1.5	0.68	2.2
$Me_3C(CH_2)_3CMe_3$	1.3	1.6	0.76	2.1
$Me_3C(CH_2)_4CMe_3$	1.8	2.1	0.74	2.8
$Me_3CCMe_2CH_2CH_3$	1.2	1.3	0.70	1.9
c-C_6H_{12}	2.0	2.1	0.69	3.0

*Averaged over the temperature range studied; kcal/mol. T_m is the mean temperature.

$d\theta/dt = f''(\omega t)$ and so

$$[11] \qquad \frac{d\alpha}{d\theta}\cdot\frac{d\theta}{dt} = f_r(\omega t)$$

The condition $d\alpha/d\theta \neq 0$ is fulfilled when $\alpha^a \neq 0$.

In normal Raman spectroscopy the symmetric stretching vibrations of a molecule often have the largest values of $d\alpha/dR$ and hence the largest Raman intensities. This is true, for example, in methane (ref. 26, p. 306). If Raman-type intramolecular vibrational excitation were the main energy sink for the epithermal electrons, *bd* should have been nearly the same in methane and in ethane, because $d\alpha/dR = 1.0 \times 10^{-16}$ cm^2 for both C—H and C—C bonds (29). The present results (Table 5) imply that for molecules with $\alpha^a \neq 0$ Raman-type vibrational excitation is not the predominant process by which the electrons lose their energy. Raman-type rotational excitation would be consistent with the observations; rotational motion is greatly hindered in the liquid, but excitation of the hindred rotations (librations) would also fulfill the present requirements.

Normal Raman processes involve interactions between molecules and photons that have energies less than the lowest electronic excitation energy of the molecules (ref. 26, p. 261). In the present discussion the major concern is with interactions between molecules and electrons that have energies less than the lowest electronic excitation energy of the molecules ($T_{e^-} \approx 10^{0\pm1}$ eV).

An energetic electron passing near to a molecule is felt by the molecule as an impulsive electric field. The force exerted on the molecule varies in direction with time, but can be resolved into two normal components, one parallel to the electron path (longitudinal component) and the other perpendicular to it (transverse component) (30). Each component of the impulsive electric field can be decomposed by Fourier transformation into a series of waves of different frequencies ν_i. Thus the effect on a molecule of an electron passing close to or colliding with it is analogous to that of a beam of photons with frequencies ν_i traversing it. The transverse component is much more intense than is the longitudinal component (30). The energies $h\nu_i$ of the virtual photons vary from that of the electron down to zero, and the effective number of photons at each frequency increases approximately as ν_i^{-1} (30). Perhaps the relatively large number of low energy virtual photons associated with the subelectronic-excitation-energy electrons explains why it is the rotational modes rather than the vibrational modes of the molecules that serve as the principal energy sink in liquid hydrocarbons. The energy spacings of C—H stretching vibrations are 0.4 eV (ref. 26, p. 306), while those of intermolecular motions such as librations are ~0.01 eV in many liquids (31, 32).

The electric field at a distance of 3 Å from an electron is 10^8 V/cm, and it varies as $1/r^2$. At such high field strengths the induced dipole moment μ_{ind} does not vary linearly with electric field strength (33), but is given by

$$[12] \qquad \mu_{ind} = \alpha E + \tfrac{1}{2}\beta E^2 + \tfrac{1}{6}\gamma E^3 + \ldots$$

where β and γ are the first and second hyperpolarizabilities, respectively. The hyperpolarizabilities do not have the same symmetry properties as does α, and β is often negative whereas α is always positive (33). An electron is always surrounded by its intense, inhomogeneous field, so the hyperpolarizabilities might influence the electron energy loss processes.

Molecules with isotropic polarizabilities are less efficient in taking energy from the electrons,

Can. J. Chem. Downloaded from www.nrcresearchpress.com by 210.87.254.40 on 09/05/12
For personal use only.

Can. J. Chem. Downloaded from www.nrcresearchpress.com by 210.87.254.40 on 09/05/12
For personal use only.

so the density normalized electron penetration distances *bd* are greater in such liquids (Table 4). If Raman-type processes are important in liquid hydrocarbons, direct excitations of librations should be important in liquids that contain permanent dipoles. Interactions between ions and permanent dipoles are usually stronger than those between ions and induced dipoles. Thus the value of *bd* should be smaller in polar liquids than in *n*-hexane or cyclohexane. This will be shown to be true in a subsequent publication (34).

Temperature Dependence of G^0_{fi}

The variation of the free ion yields with temperature in the present liquids is adequately described by eq. 3. The behavior is not of the simple Arrhenius type because the exponential factor $\exp(-\xi^2/\varepsilon kTy)$ must be integrated over the distribution $F(y)$. Furthermore, ε decreases and y increases with increasing temperature. The net effect is found empirically to be a tendency for the temperature coefficient to increase with increasing temperature.

Plots of $\ln G_{fi}$ against T^{-1} were made to obtain estimates of the exponential temperature coefficient $E_{G_{fi}}$. Values of $E_{G_{fi}}$ averaged over the temperature range studied are listed in Table 5; they are in the region of 1–2 kcal/mol.

From the point of view of competition between reactions 14 and 15

[13] $\quad M \rightsquigarrow [M^+ + e^-]$

[14] $\quad [M^+ + e^-] \rightarrow$ geminate neutralization

[15] $\quad [M^+ + e^-] \rightarrow M^+ + e^-$ (free ions)

one may write

$$[16] \quad E_{esc} = E_{15} - E_{14} = -R[\partial \ln (G_{fi}/G_{gn})/\partial T]$$

where G_{gn} is the geminate neutralization yield, taken as $(4.3 - G_{fi})$ in the present liquids. The rates of both reactions 14 and 15 increase with temperature through the increases in the diffusion coefficients of M^+ and e^-. The net exponential temperature coefficient of escape from geminate neutralization is E_{esc}.

It was reported earlier (5) that the value of E_{esc} was 2–3 times the mean value of RT in the low temperature studies of C_2 and C_3 hydrocarbons. The same is true in the present high temperature studies (Table 5). Analysis of the data from earlier temperature studies of free ion yields in hydrocarbons (2, 4–6, 35) shows that in every case, including olefins and benzene, $E_{esc}/RT_m = 2$–3, where T_m is the mean temperature. The average of the twenty two values obtained to date is 2.4 ± 0.3. In terms of the present model, the temperature sensitivity of the free ion yields in hydrocarbons arises mainly from the pairs that have y values between about 80 and 300 Å.

Thermal Electron Mobilities

The mobility of thermal electrons in a liquid hydrocarbon is affected by the structure of the molecules (Table 2 and refs. 3, 6, 9–11). The activation energy of the electron mobilities tends to be smaller in the alkanes in which the mobilities are larger (Table 2 and refs. 6, 9); extrapolation to "infinite temperature" gives $u_\infty \approx 10^2$ cm^2/V s in each alkane, which is the normally accepted region of mobilities of quasi-free electrons (36). The enormous range of mobilities observed in liquid hydrocarbons indicates that a continuous variation in the "degree of freeness" of electrons is possible. It is not sufficient to distinguish simply between quasifree and localized states of electrons in these liquids. The degree of freeness is characterized by the mobility.

There is no correlation between the electron mobility and the viscosity of the liquid, nor between the activation energy of electron mobility and that of the liquid viscosity (Table 2). The electron mobility is governed by the electron scattering property of the liquid. The electron scattering property and the viscosity both depend upon the molecular properties and the liquid density, but in different ways.

There is, however, a correlation between the mobilities of thermal electrons in liquids and the penetration ranges b of the secondary electrons in the irradiated liquids. Values of u from Table 2 are plotted against those of b from Table 1, along with other data from the literature (4–6, 8–10, 34, 37–39) in Fig. 4. Although most of the compounds in Fig. 4 are alkanes, tetramethylsilane (4, 9), argon (6, 38), water (34, 37), and two alcohols (34) are included.[1] The correlaton is striking.

The continuous nature of the degree of freeness of electrons in liquids is evident from Fig. 4. The mobility of electrons in liquid argon may be

[1]Values of u_{e^-} in methanol and ethanol were calculated from data of ref. 39*a*, using u_{H^+} and u_{RO^-} from ref. 39*b*.

Can. J. Chem. Downloaded from www.nrcresearchpress.com by 210.87.254.40 on 09/05/12
For personal use only.

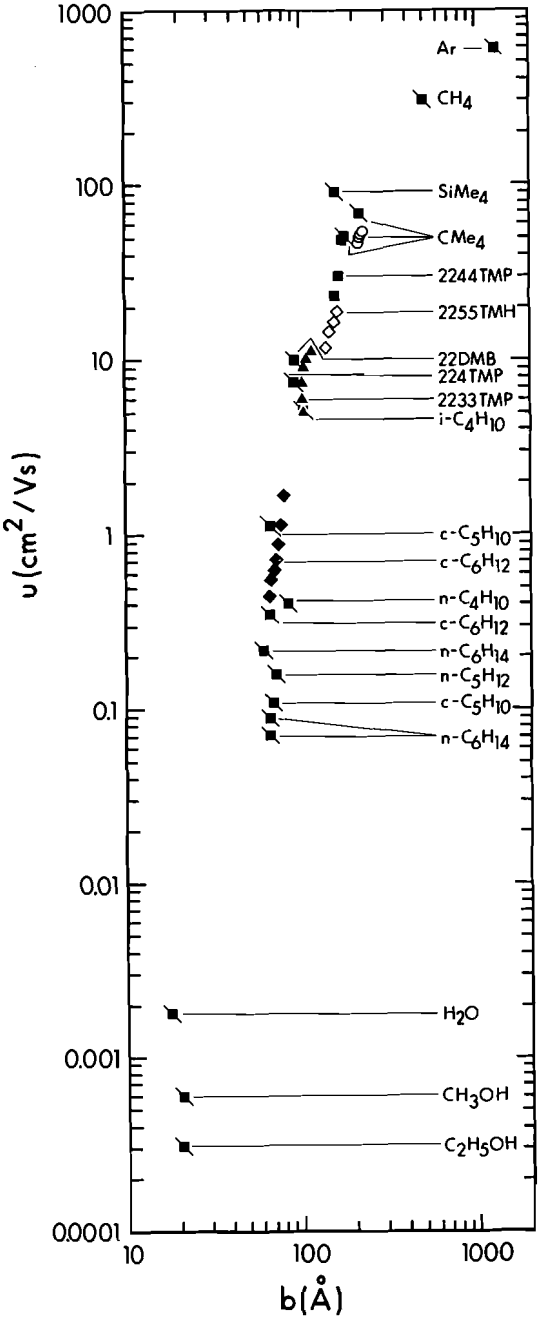

FIG. 4. Correlation between thermal electron mobility (u) and the most probable range (b) of the secondary electrons in irradiated liquid saturated compounds. The symbols ○, ◇, △, ◆, ▲, ■ represent the present results. Each type of symbol represents the compound indicated. The values from the literature (4–6, 8–10, 34, 37, 38) are designated by the symbol ■ and each point is labelled.

explained by assuming that an electron is scattered by only one atom at a time (single-body scattering approximation), because the electron scattering cross section of argon is small (40, 41). As one considers molecules that have larger and larger electron scattering cross sections it becomes necessary to consider interactions of the electron with more than one molecule at a time in the liquids (multi-body scattering). Electron localization may be considered as an extreme case of multi-body scattering, including both elastic and inelastic modes. Relaxation of the initial localized state to the solvated state involves inelastic scattering and solvent rearrangement; maintenance of the localized state, including the solvated state, involves elastic scattering. The short range interactions that must be considered in theoretical treatments of the solvated state may be considered to be scattering interactions.

It appears that the inelastic (incoherent) scattering cross sections of alkanes for thermal electrons are affected by the same things as are those for epithermal electrons. The dominant molecular property in alkanes appears to be the anisotropy of polarizability of groups containing up to two C—C bonds in series (up to neopentyl in size). In polar liquids the permanent dipole moment probably predominates.

The density of the liquid is important in the above processes because it affects the mean free path of the electrons.

We are grateful to the staff of the Radiation Research Center for help with the electronics. The financial support of the National Research Council of Canada is much appreciated.

1. P. H. TEWARI and G. R. FREEMAN. J. Chem. Phys. **49**, 4394 (1968).
2. W. F. SCHMIDT and A. O. ALLEN. J. Phys. Chem. **72**, 3730 (1968).
3. P. H. TEWARI and G. R. FREEMAN. J. Chem. Phys. **51**, 1276 (1969).
4. W. F. SCHMIDT and A. O. ALLEN. J. Chem. Phys. **52**, 2345 (1970).
5. M. G. ROBINSON, P. G. FUOCHI, and G. R. FREEMAN. Can. J. Chem. **49**, 3657 (1971).
6. P. G. FUOCHI and G. R. FREEMAN. J. Chem. Phys. **56**, 2333 (1972).
7. R. M. MINDAY, L. D. SCHMIDT, and H. T. DAVIS. J. Chem. Phys. **50**, 1473 (1969).
8. E. E. CONRAD and J. SILVERMAN. J. Chem. Phys. **51**, 450 (1969).

9. W. F. SCHMIDT and A. O. ALLEN. J. Chem. Phys. **52**, 4788 (1970).
10. R. M. MINDAY, L. D. SCHMIDT, and H. T. DAVIS. Phys. Rev. Lett. **26**, 360 (1971).
11. R. M. MINDAY, L. D. SCHMIDT, and H. T. DAVIS. J. Chem. Phys. **54**, 3112 (1971).
12. R. D. NELSON, JR., D. R. LIDE, JR., and A. A. MARYOTT. Selected values of electric dipole moments for molecules in the gas phase. NSRDS-NBS 10 (1967).
13. R. GIBAUD. J. Chim. phys. **64**, 521 (1967).
14. R. W. GALLANT. Physical properties of hydrocarbons. Vol. 1. Gulf Publishing Co., Houston, Texas. 1968.
15. R. R. DREISBACH. Adv. Chem. Ser. **22** (1959). Physical properties of chemical compounds.
16. A. H. PRICE. *In* Dielectric properties and molecular behavior. *Edited by* N. E. Hill, W. Vaughan, A. H. Price, and M. Davies. Van Nostrand Reinhold Co., London. 1969. p. 235.
17. G. R. FREEMAN. J. Chem. Phys. **39**, 1580 (1963).
18. J.-P. DODELET, P. G. FUOCHI, and G. R. FREEMAN. Can. J. Chem. **50**, 1617 (1972).
19. G. R. FREEMAN and E. D. STOVER. Can. J. Chem. **46**, 3235 (1968).
20. T. A. STONEHAM, D. R. ETHRIDGE, and G. G. MEISELS. J. Chem. Phys. **54**, 4054 (1971).
21. L. ONSAGER. Phys. Rev. **54**, 554 (1938).
22. G. R. FREEMAN and J. M. FAYADH. J. Chem. Phys. **43**, 86 (1965).
23. J. TAFT. *In* Steric effects in organic chemistry. *Edited by* M. S. Newman. Wiley, New York. 1956. pp. 586–629.
24. M. J. W. BONESS, I. W. LARKAN, J. B. HASTED, and L. MOORE. Chem. Phys. Lett. **1**, 292 (1967).
25. I. MOCHIDA and Y. YONEDA. Bull. Chem. Soc. Jap. **41**, 1479 (1968).
26. G. HERZBERG. Molecular spectra and molecular structure. II. Infrared and Raman spectra of polyatomic molecules. Van Nostrand, Toronto. 1945. Chap. 3.
27. R. J. W. LE FÈVRE. Adv. Phys. Org. Chem. **3**, 1 (1965).
28. M. DAVIES (*Editor*). Infrared spectroscopy and molecular structure. Elsevier, Amsterdam. 1963.
29. Y. YOSHINO and H. J. BERNSTEIN. Spectrochem. Acta, **14**, 127 (1959).
30. R. L. PLATZMAN. Vortex, **23**, 372 (1962).
31. C. C. BRADLEY, H. A. GEBBIE, A. C. GILBY, V. V. KECHIN, and J. H. KING. Nature, **211**, 839 (1966).
32. S. K. GARG, J. E. BERTIE, H. KILP, and C. P. SMYTH. J. Chem. Phys. **49**, 2551 (1968), and their refs. 15, 22, 26–28.
33. A. D. BUCKINGHAM and B. J. ORR. Quart. Rev. Chem. Soc. London, **21**, 195 (1967).
34. J.-P. DODELET and G. R. FREEMAN. Can. J. Chem. In press.
35. A. HUMMEL, A. O. ALLEN, and F. H. WATSON, JR. J. Chem. Phys. **44**, 3431 (1966).
36. J. JORTNER. Actions Chim. Biol. Radiat. **14**, 1 (1970); Ber. Bunsenges. Phys. Chem. **75**, 696 (1971).
37. K. SCHMIDT and W. BUCK. Science, **151**, 70 (1966).
38. H. SCHNYDERS, S. A. RICE, and L. MEYER. Phys. Rev. **150**, 127 (1966).
39. (*a*) P. FOWLES. Trans. Faraday Soc. **67**, 428 (1971). (*b*) B. CONWAY. Electrochemical data. Elsevier Publishing Co., Amsterdam. 1952. p. 162.
40. J. LEKNER. Phys. Rev. **158**, 130 (1967).
41. M. H. COHEN and J. LEKNER. Phys. Rev. **158**, 305 (1967).
42. J. TIMMERANS. Physico-chemical constants of pure organic compounds. Vol. 2. Elsevier, Amsterdam. 1965.
43. LANDOLT-BÖRNSTEIN. Zahlenwerte und funktionen. IBd., 3 Tiel. 1951. p. 511.
44. H. A. STUART and S. VON SCHLIESZL. Ann. Phys., 6 Folge, **2**, 321 (1948).
45. LANDOLT-BÖRNSTEIN. Zahlenwerte und functionen. II. 8, 1962. p. 817.
46. S. BHAGAVANTAM. *In* Scattering of light and the Raman effect. Chemical Publications Co., Brooklyn, N.Y. 1942.

Can. J. Chem. Downloaded from www.nrcresearchpress.com by 210.87.254.40 on 09/05/12
For personal use only.

Potentiometric Titration of Fulvic Acid: Equivalence Point Calculations and Acidic Functional Groups[1]

DONALD S. GAMBLE

Soil Research Institute, Canada Department of Agriculture, Ottawa, Canada K1A 0C6

Received February 25, 1972

Gran's functions corrected for buffering and H_2O dissociation have been incorporated into the iterative calculation for the two equivalence points and the acid dissociation equilibria. The experimental and mathematical conditions required for accurate, dependable operation of the method have been examined. The resulting equivalence point calculations are based directly on a chemical interpretation of the system, without approximations. The first equivalence point is higher than previously reported, and is displaced upward by KCl. Detailed chemical information has been obtained for some of the acidic functional groups, from plots of $K_A = (m_H \delta m_A / \delta m_{AH})$ *vs.* mequiv./g. Carboxyl groups at the chelating sites are essentially all ionized for H^+ concentrations less than 1×10^{-5} *m*.

Les fonctions de Gran corrigées pour le tampon et la dissociation de H_2O ont été introduites dans le calcul itératif des deux points d'équivalence et d'équilibre de dissociation acide. Les conditions expérimentales et mathématiques requises pour une opération sûre et précise de la méthode ont été examinées. Les calculs du point d'équivalence qui en résultent, sont fondés directement sur une interprétation chimique du système sans approximations. Le premier point d'équivalence est plus élevé que celui précedemment rapporté et se trouve déplacé par KCl. Une information chimique détaillée a été obtenue pour certains des groupes fonctionnels acides, à partir des courbes de $K_A = m_H \delta m_A / \delta m_{AH}$ en mequiv./g. Les groupes carboxyles sur les sites de chélation sont essentiellement et entièrement ionisés pour des concentrations en H^+ inférieures à 1×10^{-5} *m*.

Canadian Journal of Chemistry, 50, 2680 (1972)

Introduction

The characterization of fulvic acid is prerequisite to studies of such phenomena as its metal ion chelation and sorption by clays. The complex nature of fulvic acid requires that it be characterized by a number of experimental techniques. Potentiometric titration with standard base is one of the more important of these methods. It requires, however, some adaptation to this kind of polyelectrolyte system. The two particular problems that must be solved for this purpose are the evaluation of titration equivalence points, and the calculation of acid dissociation equilibrium functions as functions of their corresponding degrees of ionization.

Even for monomeric, monobasic weak acids, Meites and Goldman (1) found that the first of the two inflection points generally differs from 1/2 the equivalence point except for the special case in which $K_a = \sqrt{K_w}$. The second one occurs before the equivalence point, although the discrepancy is small for $K_a \geqslant 10^{-8}$. These effects increase with increasing dilution. Polyelectrolytes are rather less tractable, and van Dijk (2) and Posner (3) have both pointed out the difficulty of determining equivalence points from potentiometric titrations of humic materials. A number of authors have simply chosen arbitrary pH values as the "end points" for such titrations (4–6). Speiser *et al.* (7) assumed the inflection point at p$H = 7.5$ to be the equivalence point for pectin titrations.

Pommer and Breger took a more promising direction (8) by applying Gran's calculation method (9, 10) to humic acid titration curves for which they had observed only one equivalence point. They assumed the equivalence point to be at the point of intersection of a pair of Gran's functions uncorrected for buffering and H_2O dissociation. Because their Gran's functions were linear and because they obtained agreement between two calculation methods, they believed their equivalence point values to be correct. In a similar way, uncorrected Gran's functions were used in the previously reported part of this work (11) for the two fulvic acid equivalence points. Like those of Pommer and Breger, these Gran's functions did not vanish

[1]Presented in preliminary form at the 54th Annual Conference of the Chemical Institute of Canada, Halifax, May 30 – June 2, 1971. Contribution No. 409.

Can. J. Chem. Downloaded from www.nrcresearchpress.com by 210.87.254.42 on 09/05/12
For personal use only.

Can. J. Chem. Downloaded from www.nrcresearchpress.com by 210.87.254.42 on 09/05/12
For personal use only.

at the points of intersection, which were taken to be the equivalence points. Unlike those of Pommer and Breger, however, the Gran's functions of this fulvic acid were not linear. Because the Gran's functions were non-ideal in these two respects, conductivity titrations were used as an independent experimental check on the equivalence point values. The two methods were apparently in agreement for that particular case. This implied that the calculation errors caused by the neglect of buffering and H_2O dissociation were either small, largely cancelled, or both. Subsequent examination has not only revealed that correction terms for buffering and H_2O dissociation can be comparable in size to Gran's original functions, but also has indicated that the first equivalence point values could be low. Another difficulty is the doubtful chemical authenticity of equivalence points calculated directly from voltage readings as Gran originally recommended.

The determination of potentiometric titration equivalence points for fulvic acid therefore required re-examination. In addition to the buffering effects which Rossotti and Rossotti (12) have shown to be the causes of non-linear, non-vanishing Gran's functions for monomeric weak acids, the previously reported dependence of $\bar{K}$ on the degree of ionization of fulvic acid (11) contributes further to such non-ideal behavior. Liteanu and Cőrmős (13) have investigated potentiometric titrations for which the Gran's functions are linear but do not vanish at the equivalence point. They first fitted each of the pair of Gran's functions to a straight line by the method of least squares. The solution to this pair of simultaneous equations was not generally at the equivalence point. They then calculated the equivalence point by applying an algebraic correction for the asymmetry of the titration curve. Apart from its not being applicable to non-linear fulvic acid results, the Liteanu–Cőrmős calculation techniques has two possible disadvantages. Firstly, the correction calculation is based on a symmetry argument rather than on direct chemical reasoning. Secondly, Gran's functions that do not vanish at the equivalence point lack the insensitivity to experimental and calculation errors which Lanza and Mazzei (14) have demonstrated for those that do vanish.

The first objectives of this work are to obtain characteristic, reproducible equivalence point values, and to establish that they correspond to chemical reality rather than being merely mathematical or experimental artifacts. Another objective is to characterize the Type I carboxyl groups, that is, those ortho to phenolic-OH groups (11). The best experimental method for this purpose is to "map out" detailed H^+ concentrations *vs.* mls titration curves with large numbers of H^+ concentration standards. This may be done by adapting the previously reported procedure (11) for extension into the basic region of the titration curve. Other authors have fully discussed the reasons for doing this rather than using the more usual pH measurements (15–18). The method adopted here for basing the equivalence point calculations directly on chemical reasoning is to use Gran's functions corrected for buffering, H_2O dissociation, and the dependence of the two $\bar{K}$ functions on their respective degrees of ionization. Such corrected Gran's functions will vanish at the equivalence points. Each of the two equivalence points may therefore be calculated with just one corrected Gran's function. Those used are the one before the first equivalence point and the one after the second equivalence point.

Theory

(a) Weak Acid Properties

The concepts developed in the previously reported part of the work (11) must now be adapted to cases for which the first titration equivalence point extends beyond the Type I carboxyl groups, which are defined as those on aromatic rings ortho to phenolic OH groups. Let C be the total molality of acidic functional groups, both ionized and unionized, accumulated in the order of decreasing acid strengths up to some point in the titration. If Type A functional groups are all of those up to the first equivalence point, then for Type I and Type A functional groups respectively, C becomes

$$C_L = m_L + m_{LH} \quad [1]$$

$$C_A = m_A + m_{AH} \quad [2]$$

Ionized and unionized functional groups are indicated by the subscripts. Generally, $C_L \leqslant C_A$.

Can. J. Chem. Downloaded from www.nrcresearchpress.com by 210.87.254.42 on 09/05/12
For personal use only.

Accordingly for Type B acidic functional groups between the two equivalence points,

$$[3] \qquad C_B = m_B + m_{BH} = C_{MAX} - C_A$$

In terms of the A and B types of acidic functional groups, the total titratable acid remaining at any point in the titration becomes

$$[4] \quad C_H = \frac{C_A}{\left(\frac{\bar{K}_A}{m_H} + 1\right)} + \frac{C_B}{\left(\frac{\bar{K}_B}{m_H} + 1\right)} + m_H - \frac{K_w}{m_H}$$

$\bar{K}_A$ and $\bar{K}_B$ are the previously defined type of weighted average H^+ dissociation equilibrium function (11), and m_H is the H^+ molality.

The Type A functional groups are of the greatest chemical interest because they are strongly acidic, and because they include the Type I carboxyl groups located at bidentate chelating sites (19, 20). Detailed chemical information about these functional groups is not provided by $\bar{K}_A = \bar{f}_A(\alpha_A)$, since it is an average. Such information should be available, however, from K_A which has been defined according to eq. 5 for an infinitesimal increment of functional groups.

$$[5] \quad K_A = \frac{m_H \delta m_A}{\delta m_{AH}} = K_A^0 \Gamma_A \, e^{-\Delta G_A^e/RT} = f_A(\alpha_A)$$

Γ_A is a ratio of activity coefficient products, and ΔG_A^e is the electrostatic free energy. The K_A calculation described earlier is simplified by means of the familiar relationship $\bar{K}_A = \alpha_A m_H/(1 - \alpha_A)$. The result is eq. 6.

$$[6] \qquad K_A = -\frac{d(\alpha_A m_H)}{d\alpha_A}$$

For cases in which $C_L < C_A$, the degree of ionization of the Type I carboxyl groups, α_1, is not identical to α_A. The method of calculating α_1 is developed from eq. 7, the material balance equation for ionized Type A functional groups.

$$[7] \qquad m_A = \sum_{i=0}^{k} m_{A_i}$$

The index "i" denotes the ith small increment of Type A functional groups, $c_i = m_{A_i} + m_{A_iH}$. The degree of ionization of this ith increment is

$$[8] \qquad \beta_i = \frac{m_{A_i}}{c_i}$$

With substitution into eq. 7 from eq. 8 and division by C_A, α_A is found to be a weighted average of the β_i values.

$$[9] \qquad \alpha_A = \frac{1}{C_A} \sum_{i=0}^{k} \beta_i c_i$$

Assume that the increments become very small, so that

$$\lim_{c_i \to 0} c_i = \delta C = (\delta m_A + \delta m_{AH})$$

The β_i values may then be replaced by a continuous function,

$$[10] \quad \beta_A = \frac{\delta m_A}{\delta C} = \frac{K_A}{K_A + m_H} = \beta_A(C, m_H)$$

β_A is a function of two variables, since its value depends not only on the H^+ molality, but also on the particular infinitesimal increment of Type A functional groups being considered. This is characterized by C, its position in the "inventory" of acidic functional groups accumulated in the order of decreasing acid strength. Therefore, the summation of eq. 9 may be replaced by an integration at a constant H^+ molality.

$$[11] \quad \alpha_A = \frac{1}{C_A} \int_0^{C_A} \beta_A \, dC = \alpha_A(m_H) = \alpha(C_A, m_H)$$

Differentiating eq. 11 at this same H^+ molality gives

$$\left(\frac{\partial \alpha_A}{\partial C}\right)_{m_H} = \frac{\beta_A}{C_A}$$

$$\partial m_A = \beta_A(C, m_H) \partial C$$

For the carboxyl groups in the region $C \leqslant C_L$, that is, the Type I carboxyl groups,

$$\partial m_A = \partial m_L = C_L \partial \alpha_1$$

$$[12] \qquad \left(\frac{\partial \alpha_1}{\partial C}\right)_{m_H} = \frac{\beta_A}{C_L}$$

The degree of ionization of the Type I carboxyl groups as a function of H^+ molality is therefore calculated by integrating between the limits 0 and C_L.

$$[13] \quad \alpha_1 = \frac{1}{C_L} \int_0^{C_L} \beta_A(C, m_H) dC = \alpha_1(m_H)$$
$$= \alpha(C_L, m_H)$$

Can. J. Chem. Downloaded from www.nrcresearchpress.com by 210.87.254.42 on 09/05/12
For personal use only.

This calculation requires an experimental measurement of C_L, the total molality of Type I carboxyl groups.

(b) Corrected Gran's Functions

The molality of total base added by titration is given by eq. 14:

$$[14] \qquad C_{OH} = m_{OH} + m_A + m_B - m_H = \left(\frac{N_B}{W_0 + R_w R_v V}\right) V$$

N_B is the normality of standard base used for the titration, W_0 is the initial weight of water in the sample solution, V is the volume of standard base added by titration, and R_w and R_v are constants for converting volume of standard base to weight of water. This and similar equations for C_B and C_H are combined with the expression for $\bar{K}_A$ to give the First Gran's Function, eq. 15.

$$[15] \qquad Y_1 \equiv (Vm_H - Q_1) = \bar{K}_A(V_{e1} - V)$$
$$Q_1 = \left(\frac{W_0 + R_w R_v V}{N_B}\right)\left(m_B - m_H + \frac{K_w}{m_H}\right) \times (\bar{K}_A + m_H)$$

This is applicable before the first equivalence point, V_{e1}. In a similar way, eq. 14 and the equations for C_A, C_B, and K_w are used to derive Y_4, the Fourth Gran's Function. It is applicable after V_{e2}, the second equivalence point.

$$[16] \qquad Y_4 \equiv \left(\frac{W_0 + R_w R_v V}{m_H} - Q_4\right) = \frac{N_B}{K_w}(V - V_{e2})$$
$$Q_4 = \left(\frac{W_0 + R_w R_v V}{K_W}\right)(m_{AH} + m_{BH} + m_H)$$

Equations 15 and 16 are simple extensions of Gran's original work, and differ from his equations essentially only by the inclusion of the correction terms Q_1 and Q_4.

The numerical values of Q_1 and Q_4 depend quite directly on the current values of V_{e1} and V_{e2}, while Gran's original terms are independent of them. The ease with which iterative calculations using Y_1 and Y_4 converge should therefore depend on the sizes of the ratios $|Q_1/Y_1|$ and $|Q_4/Y_4|$. The effects on Y_1 and Y_4 of errors in $\bar{K}_A$ and $\bar{K}_B$ should likewise depend on the sizes of these ratios.

Calculation Techniques for V_{e1}, $\bar{K}_A$, V_{e2}, and $\bar{K}_B$

The evaluation of Q_1 and Q_4 requires estimates of the functions

$$\bar{K}_A \equiv \bar{f}_A(\alpha_A)$$
$$\bar{K}_B \equiv \bar{f}_B(\alpha_B)$$

The corrected Gran's functions have therefore been incorporated into the iterative calculation for V_{e1}, $\bar{K}_A$, V_{e2}, and $\bar{K}_B$. The steps for each iteration are as follows:

1. $\bar{K}_A$ is calculated for each titration data point from eq. 4, over the range $0.000 \leqslant V < V_{e1}$. The current values of V_{e1}, V_{e2}, $\bar{K}_B$, and K_w are used, with K_w being evaluated from the KCl solution data of Harned and Hamer (21). For the first iteration, $\bar{K}_B = 0$ is used. Beyond the V range used, $\bar{K}_A$ is set equal to the average of the last six values.

2. $\bar{K}_B$ is calculated in a similar way from eq. 4, over the range $V_{e1} \leqslant V \leqslant V_{e2}$. Before and after this range $\bar{K}_B$ is set equal respectively to the average of the first six and to the average of the last six $\bar{K}_B$ values.

3. α_A and α_B are calculated for each titration data point.

4. Y_1 is calculated for each titration data point from the start of the titration up to the point at which negative Y_1 values occur. Y_1 calculation then ceases, and values for which $|Q_1/Y_1| > 0.500$ are discarded.

5. The remaining Y_1 values are fitted to a polynomial by the method of least squares, and V_{e1} is calculated by the Newton–Raphson method (22) at the point $Y_1(V_{e1}) = 0$.

6. Y_4 is calculated for each titration data point from $V > V_{e1}$ to the end of the titration. Values for which $|Q_4/Y_4| > 0.500$ are rejected.

7. Except that a linear least squares fit is used, V_{e2} is calculated as is V_{e1}.

The mathematical requirements for proper convergence of this calculation are:

1. The least squares fitting requires a sufficient density of titration data points without excessive scatter.

2. $\bar{K}$ values strongly affected by experimental errors in the high error regions where α approaches 0 or 1 must be rejected.

3. Data points for which the ratios $|Q_1/Y_1|$ and $|Q_4/Y_4|$ are too high must be rejected from the sets of Gran's function values.

4. The zero order approximations for V_{e1} and V_{e2} must be within certain limits of the final values. For V_{e2} this might typically be $\pm 10\%$, but V_{e1} usually has wider limits.

5. The Y_1 *vs.* V curve must not approach the $Y_1 = 0$ line at too small an angle.

6. All negative values of $\bar{K}_A$, $\bar{K}_B$, α_A, α_B, Y_1, and Y_4 must be rejected from the calculation.

These calculations were programmed in Fortran V for the Univac 1108.

Experimental

(a) Chemicals

Fulvic Acid Batch FA1 was prepared essentially as previously described, from a soil sample collected at the same geographical location (23, 24). Freeze drying was substituted for flash evaporation in the last step, to minimize exposure to higher temperatures. The ash content was 1.1%. Analysis by atomic absorption spectrophotometry indicated less than 0.1 p.p.m. each, of Ca^{2+}, K^+, Na^+, Fe^{3+}, Cu^{2+}, Al^{3+}, Zn^{2+}, and Mg^{2+}. Final drying to constant weight before use was as previously reported (11).

H_2O, redistilled under N_2.

KCl, Anachemia A.C.S. Reagent grade crystals. Lot No. 86B920. Dried to constant weight at 110 °C.

HCl Standard (0.1 *N*), Fisher reagent, Lot No. 784176.

KOH Standard (0.1 *N* at 25.0 °C), Lot No. 782654.

KOH Standard (0.01 *N* at 25.0 °C); prepared gravimetrically from 0.1 *N* standard KOH.

(b) Apparatus

The potentiometric titration apparatus was the same as previously described (11).

(c) H^+ Molality Standards

These were all prepared under N_2 with redistilled H_2O. For the acid range of the titration, 23 to 29 H^+ standards were prepared gravimetrically over the range 3×10^{-3} to 1×10^{-6} *m* H^+. Their KCl concentrations were adjusted to compensate for KCl dilution during titration. The base range of the titration was covered by 38 to 43 standards from about 10^{-8} *m* to 1×10^{-11} *m* H^+. These were prepared by titrating 100 g of solvent with either 0.01 or 0.1 *N* standard KOH. Literature activity coefficient data (21) were used in correcting the H^+ concentrations for H_2O dissociation.

(d) Potentiometric Titration Procedure

Sample preparations and potentiometric measurements were done under N_2. The measurements were carried out at 25.00 ± 0.05 °C in a room maintained at 23.2 ± 2 °C.

Sample solutions were prepared gravimetrically with either 0.01 or 0.1 g of fulvic acid per 100 g of solution, and with various KCl concentrations from 0 to 0.2 *m*. Some were prepared directly from solvent and fulvic acid powder. Dry fulvic acid powder rapidly takes up electrostatic charge and atmospheric moisture. To avoid consequent weighing errors in the samples used for measuring the milliequivalents of acidic groups per g of dry fulvic acid, they were prepared with particular care from gravimetric stock solutions.

Each sample solution and its acid range standards were thermostated overnight at 25.00 ± 0.05 °C. Voltage readings were first taken for the acid range standards, and then the titration was carried out. The base range standard H^+ measurements were finally done by titration of solvent. Each set of measurements always proceeded in the direction of decreasing H^+ concentrations. Stirring was required for proper electrode response and steady readings with H^+ concentrations less than 1×10^{-5} *m*, but had no effect above that. Gregor and Frederick for example (28) have also noted the importance of proper stirring procedures. Voltage readings were more difficult to obtain in the absence of background KCl.

When not in use the combination microelectrode was stored in saturated KCl solution, and during an experiment it was kept in dilute KCl between sets of readings. The electrode system including cables was found to be free from field effects. The p*H* meter was kept carefully grounded.

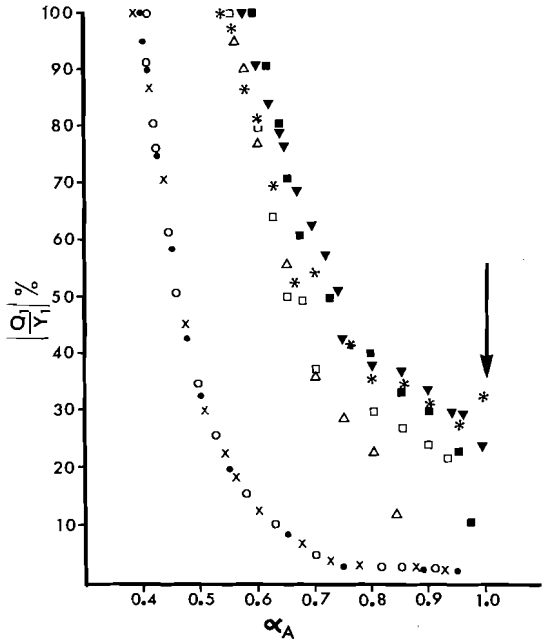

FIG. 1. First equivalence point in 0.1 *M* KCl. $|Q_1/Y_1|$, the relative size of the correction term, as a function of α_A. Each symbol represents a separate titration, and the arrow gives the equivalence point location. Upper set of curves, 0.01 g fulvic acid/100 g of solution. Lower set of curves, 0.1 g fulvic acid/100 g of solution.

Results

Both the natures of the correction terms and the effects of concentrations on them are observed in Figs. 1 and 2. The points to note are:

1. The relative size of Q_1, $|Q_1/Y_1|$, decreases as the equivalence point is approached. In contrast, $|Q_4/Y_4|$ increases as the equivalence point is approached.

Can. J. Chem. Downloaded from www.nrcresearchpress.com by 210.87.254.42 on 09/05/12
For personal use only.

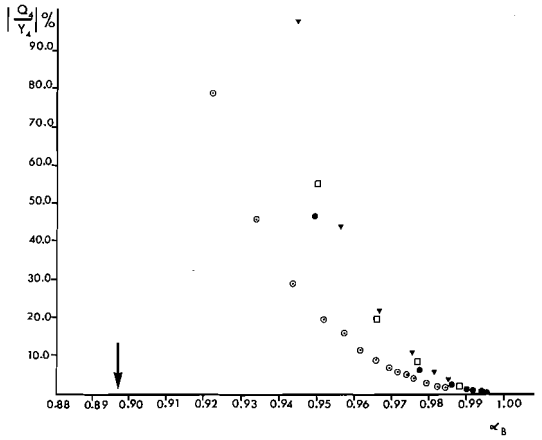

FIG. 2. Second equivalence point in 0.1 *m* KCl. Relative size of the correction term, as a function of α_B. Each symbol represents a different titration with (0.1 g fulvic acid/100 g of solution). The arrow shows the equivalence point location.

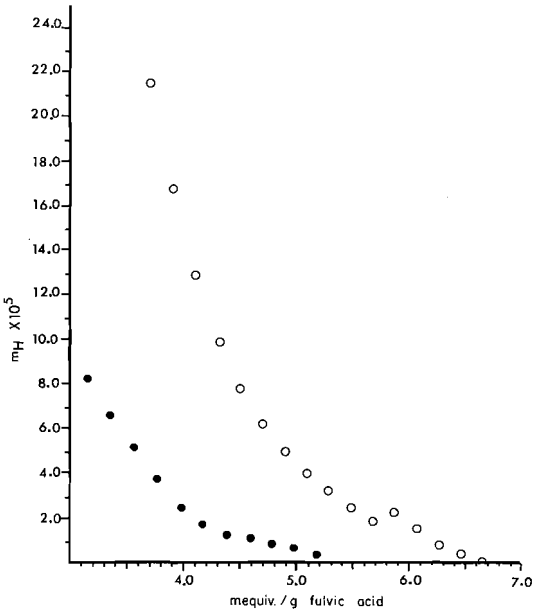

FIG. 3. Effect of KCl on fulvic acid titration at 25.0 °C. m_H as a function of the amount of standard base added. Typical examples with (0.1 g fulvic acid/100 g of solution): ○, 0.1 *m* KCl. ●, no KCl.

2. For titrations of 0.1 g of fulvic acid per 100 g of solution, $|Q_1 Y_1|$ falls sharply with little scatter in the data. The results for 0.01 g of fulvic acid per 100 g solution are somewhat less favorable to the iterative calculations.

3. Experimental error has a much more serious effect on $|Q_4/Y_4|$ than on $|Q_1/Y_1|$, even at the higher concentration of fulvic acid.

4. A curve not shown in Fig. 1 indicates that at 0.1 g fulvic acid per 100 g of solution, KCl has little effect if any on these curves. The V_{e1} calculation is consequently expected to converge well and give reproducible values, for the higher fulvic acid concentration. Poorer calculation results are expected for V_{e2}, and for V_{e1} with titrations of 0.01 g fulvic acid per 100 g of solution.

An approximately thousand-fold drop in H^+ molality occurs at the first equivalence point, when 0.1 g of fulvic acid in 100 g of sample solution is titrated. The anticipated release of H^+ by KCl added to the sample solution is so great that the location of this thousand-fold drop, and therefore the first equivalence point, is shifted to a higher titration value. The points at which typical curves drop off, and the effect of KCl are illustrated in Fig. 3.

As is illustrated in Fig. 3, KCl increases the angle of approach of the m_H curve to the $m_H = 0$ line. These curves reflect the shapes of the corresponding Gran's functions, especially near the equivalence point. Since the V_{e1} calculation consists of solving the simultaneous equations

$$Y_1 = Y_1(V)$$

$$Y_1 = 0$$

KCl is therefore expected to improve the performance of the Newton–Raphson calculation.

The data presented in Tables 1 and 2 verify these predictions about the effects of fulvic acid and KCl concentrations on the calculations.

Another conclusion drawn from Table 2 is

TABLE 1. Effect of sample solution composition on the iterative Gran's calculation

Nominal concentrations		Number of iterations for convergence to 5 significant figures	
g fulvic acid / 100 g solution	KCl (*m*)	First equivalence point	Second equivalence point
0.01	0.2	7 to 8	10
0.01	0.1	>10	>10
0.10	0.1	3 to 5	6
0.10	0.0	7 to >10	6 to >10

Can. J. Chem. Downloaded from www.nrcresearchpress.com by 210.87.254.42 on 09/05/12
For personal use only.

TABLE 2. Fulvic acid equivalence point values calculated with corrected Gran's functions (25 °C)

Titration no.	KCl concentration	mequiv. acid groups/g fulvic acid: First equivalence point	Second equivalence point	Type B acid groups
E-18	0.1 *m*	6.520	7.75	1.23
E-19		6.598	7.73	1.13
E-20		6.505	8.11	1.60
		Average 6.54±0.06	7.86±0.35	1.32±0.28
E-24	0.0 *m*	4.91	6.91	2.00
E-25		5.28	7.62	2.34
E-26		5.43	8.00	2.57
E-27		4.96	8.09	3.13
E-28		4.72	7.59	2.86
E-29		4.62	7.58	2.96
		Average 4.99±0.25	7.63±0.28*	2.64±0.34

*Average of all 9 values for the second equivalence point is 7.71 ± 0.25.

that KCl had no effect on the second equivalence point that is observable outside the experimental errors.

$\bar{K}_A$ as a function of α_A is given in Table 3. The two 0.1 *m* KCl equations covering the ranges $0.38 \leqslant \alpha_A < 0.50$ and $0.50 \leqslant \alpha_A < 0.70$ were obtained directly by least squares fitting of the computer printout. The 0.1 *m* KCl result for the range $0.70 \leqslant \alpha_A \leqslant 0.90$ was produced by recalculating $\bar{K}_A$ with the average V_{e1} value of 6.54 (mequiv./g) from Table 2, and then averaging the computer output. For comparison, the 0.1 *m* KCl titration curves with 0.1 g fulvic acid/100 g of solution gave $\bar{K}_A = 0.15 \times 10^{-3}$ with $\sigma = \pm 0.03 \times 10^{-3}$ over this same α_A range. The two cases without KCl were obtained by recalculation with the V_{e1} average of 4.99 (mequiv./g) and least squares fitting. These $\bar{K}_A$ *vs.* α_A curves show a distinct and reproducible change of slope in the region $0.5 < \alpha_A < 0.6$.

The $\bar{K}_B$ calculations summarized in Table 4 show no dependance on α_B outisde the experimental errors. It should be noted that the 0.0 *m* KCl value belongs to acid functional groups including the 1.5 mequiv./g of functional groups strongly affected by KCl, while the 0.1 *m* KCl value does not (see Fig. 3 and Table 2). Considering the sizes of the experimental errors, these two $\bar{K}_B$ values cannot be assumed to be different.

K_A, calculated according to eq. 6 and plotted in Fig. 4, gives a useful picture of the acidic functional groups up to the first equivalence point. The 0.1 and 0 *m* KCl curves in Fig. 4 were calculated with data from six and five titration curves, respectively. In the former curve, the horizontal region above 5 mequiv./g is equal to $\bar{K}_A = (0.170 \pm 0.006) \times 10^{-3}$, since for the constant $\bar{K}_A$,

$$K_A = -\frac{d[(1-\alpha_A)\bar{K}_A]}{d\alpha_A} = \bar{K}_A$$

The very distinct break at 3 ± 0.1 mequiv./g corresponds to the above mentioned sudden

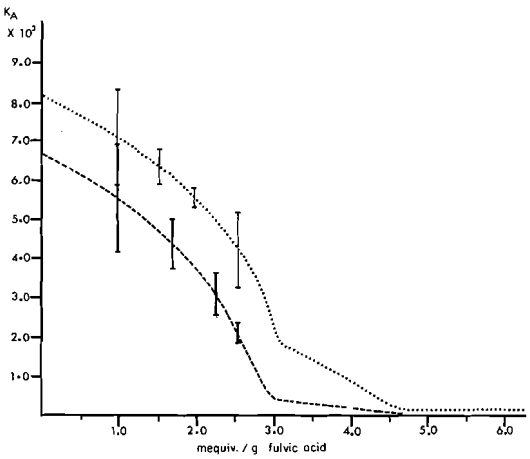

FIG. 4. Acid dissociation equilibrium function for an infinitesimal increment of functional groups at 25.0 °C as a function of its location in the titration curve. Dots, 0.1 *m* KCl, calculated from six titrations; dashes, no KCl, calculated from five titrations.

Can. J. Chem. Downloaded from www.nrcresearchpress.com by 210.87.254.42 on 09/05/12
For personal use only.

Can. J. Chem. Downloaded from www.nrcresearchpress.com by 210.87.254.42 on 09/05/12
For personal use only.

TABLE 3. Weak acid dissociation equilibrium of Type A functional groups at 25.0 °C

$$\bar{K}_A \times 10^3 = \sum_{i=0}^{m} C_i \alpha_A^i$$

Nominal concentrations												
g fulvic acid / 100 g solution	KCl (m)	Number of titrations	Number of data points	Range of α_A values	C_0	C_1	C_2	C_3	C_4	C_5	Standard deviation	Standard error
0.1	0.1	6	85	$0.38 \leqslant \alpha_A < 0.50$	5.508	−9.757					±0.16	±0.017
0.1*	0.1	6	58	$0.50 \leqslant \alpha_A < 0.70$	1.40794×10^3	-1.15687×10^4	3.79769×10^4	-6.22090×10^4	5.08299×10^4	-1.65700×10^4	±0.060	±0.0078
0.01	0.1	2	19	$0.70 \leqslant \alpha_A \leqslant 0.90$	0.170						±0.006	±0.0014
0.1	0.0	5	73	$0.40 \leqslant \alpha_A \leqslant 0.60$	9.009	−26.79	20.21				±0.22	±0.026
0.1	0.0	5	35	$0.60 \leqslant \alpha_A \leqslant 0.84$	1.398	−2.866	1.556				±0.039	±0.007

*Extra significant figures are carried to avoid rounding off errors. Answers should be rounded off to two decimal places.

TABLE 4. Acid dissociation equilibrium of Type B functional groups at 25.0 °C

KCl (m)	Region of the titration curve mequiv. / g fulvic acid	Number of titrations	Number of data points	$\bar{K}_B \times 10^{10}$ (average)	Standard deviation $\times 10^{10}$	Standard error $\times 10^{10}$
0.1	6.6 to 7.7	3	23	5.8	±0.9	±0.2
0	5.6 to 7.7	6	64	6.6	±2.1	±0.3
0.05 to 0.2	6.6 to 7.7	9	136	*7	±3	

*Rough results from preliminary work.

TABLE 5. Ionization of fulvic acid in 0.1 m KCl at 25.0 °C*

H^+ (m)	α_A ±2%	α_1 ±2%
2.60×10^{-3}	0.392	0.72
2.21×10^{-3}	0.406	0.72
1.50×10^{-3}	0.442	0.77
1.30×10^{-3}	0.454	0.82
1.00×10^{-3}	0.472	0.85
5.08×10^{-4}	0.52	0.92
1.97×10^{-4}	0.61	0.97
1.00×10^{-4}	0.68	0.98
1.00×10^{-5}	0.94	1.00
1.00×10^{-6}	0.99	

*Type 1 carboxyl groups, 3.0 ± 0.1 mequiv./g fulvic acid; Type A acid groups, 6.54 ± 0.06 mequiv./g fulvic acid.

TABLE 6. Ionization of fulvic acid in aqueous solution at 25.0 °C*

H^+ (m)	α_A ±4.0%	α_1 ±4.0%
2.00×10^{-3}	0.41	0.66
1.80×10^{-3}	0.42	0.67
1.60×10^{-3}	0.43	0.69
1.40×10^{-3}	0.44	0.71
1.20×10^{-3}	0.46	0.74
1.00×10^{-3}	0.47	0.78
8.00×10^{-4}	0.49	0.81
6.00×10^{-4}	0.51	0.85
4.00×10^{-4}	0.53	0.88
2.00×10^{-4}	0.58	0.92
1.00×10^{-4}	0.66	0.96
6.00×10^{-5}	0.71	0.99
2.00×10^{-5}	0.83	1.00
5.00×10^{-6}	0.92	

*Type 1 carboxyl groups, 3.0 ± 0.1 mequiv./g fulvic acid; Type A acid groups, 4.99 ± 0.25 mequiv./g fulvic acid.

slope change of the $\bar{K}_A$ *vs.* α_A equations in Table 3. These first 3 mequiv./g of acidic functional groups are evidently the Type 1 carboxyl groups originally identified by Schnitzer and co-workers (11, 23–27). There are two other distinct types of functional groups, occupying the regions $3 \leqslant$ mequiv./g $\lesssim 5$ and $5 \leqslant$ mequiv./g $\lesssim 6.54$, respectively. Not only do they respond very differently to the presence of KCl, but also one is a constant at constant KCl concentration while the other is a decreasing function of α_A.

The degree of ionization of Type I carboxyl groups, α_1, has been calculated according to eqs. 10 and 13 for fulvic acid solutions both with and without KCl. These are given in Tables 5 and 6, together with corresponding α_A values for comparison.

Experimental Errors

As in the previous work (11), the most important source of experimental error was the potentiometric measurements. In addition to the experimental scatter expected from the earlier work, the H^+ molality *vs.* mls titrations were found to have biases of comparable sizes, as shown in Fig. 5. This curve shows the anticipated rapid rise near neutrality. Examination of sets of titrations, however, indicates that these biases occur randomly. Because K_A is calculated by differentiation, it is especially sensitive to errors in the shape of the titration curve. It is therefore necessary to average out the random errors of a number of titration curves, in order to obtain chemical information from K_A. The standard errors indicated in Fig. 4 for the K_A curves were conservatively estimated from the number of biased titration curves used for each, rather than from the total numbers of titration data points used.

$\bar{K}_B$ is necessarily measured in the high error

Can. J. Chem. Downloaded from www.nrcresearchpress.com by 210.87.254.42 on 09/05/12
For personal use only.

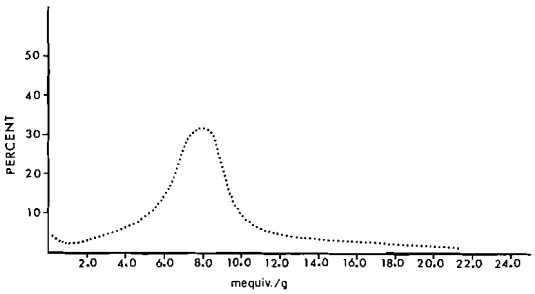

FIG. 5. Average H^+ molality error for titration curves at 25.0 °C, 0.1 *m* KCl, 0.1 g fulvic acid/100 g of solution.

region of Fig. 5. This requires that a large number of values be averaged, and limits the chemical conclusions that may be drawn about the acidic functional groups in this region. $\bar{K}_B$ values outside the approximate range 5.4 to 7.6 mequiv./g must be discarded because of the exaggeration of experimental errors at high and low α_B values.

Discussion

(a) Analytical Chemistry Aspects

Ratios such as $Z_1 = |Q_1/Y_1|$ and $Z_4 = |Q_4/Y_4|$ prove useful in various ways.

1. They measure the applicability and inherent limitations of corrected Gran's functions for particular equivalence points.

2. They facilitate judgements about the effects of experimental error on the equivalence point calculations.

3. Optimum experimental conditions for equivalence point determinations may be found using them.

4. These ratios are essential for establishing the ranges of Gran's function values for which the iterative calculation will converge.

Because Z_1, for example, is found to decrease as the equivalence point is approached, the First Corrected Gran's Function is an excellent technique for the first equivalence point. In contrast to this, the use of the Second and Third Corrected Gran's Functions was found from Fig. 5 and their correction terms to be unwise.

The first equivalence point could be estimated directly from the sudden drop in H^+ concentration in the region $6.5 <$ mequiv./g < 6.8. An important virtue of Gran's method, however, is that it employs data from a relatively extensive section of the titration curve rather than poorer quality data just at the equivalence point.

(b) Fulvic Acid Chemistry

The differences between the two curves of Fig. 4 are in the direction expected for the effect of salt, and above 3 mequiv./g are well outside the estimated standard errors. Below this point the difference is probably also real, but should be checked by further experiment. The existence of the 3 mequiv./g break in Fig. 4 is further verified by the shape of the $\bar{K}_A$ *vs.* α_A curves found in Table 3, since the decisive slope change of the $\bar{K}_A$ curves occurs in the neighborhood of this 3 mequiv./g break.

The acidic functional groups in the $3 \leqslant$ mequiv./g $\lesssim 5$ region of Fig. 4 are likely carboxyl groups. The relatively small effect of KCl on their acid strength suggests that some or all of them might represent monomeric acids. Schnitzer and co-workers (29, 30) have separated and identified a number of monomeric acids from fulvic acid, by methylating the sample. The amounts of these which they report indicate an upper limit of 0.07 mequiv./g for monomeric acids in fulvic acid. Monomeric acids therefore cannot account for any sizeable portion of the carboxyl groups in this region of Fig. 4. Because of the strong effect of KCl on their acid strength, the functional groups in the region $5 \lesssim$ mequiv./g $\leqslant 6.54$ of Fig. 4 must certainly represent polymeric functions of the fulvic acid. What is not clear, however, is whether all or only some of these acidic groups are carboxyl groups. The differences in chemical structure between these two types of functional groups beyond 3 mequiv./g are also unknown. The benzene carboxylic acids whose structures and acid constants were discussed by Maxwell and Partington (31) may serve as useful models, since some of them were among the monomeric acids isolated from fulvic acid by Schnitzer and co-workers.

The H^+ displacement effects of salt reported by Posner (3) for humic acids may be the same phenomena that are described here. In addition to the expected increase in acid strength, he found a slight increase in the "exchange capacities of the acid region", with increasing KCl concentration.

Posner (3) has also recognized that $\bar{K}$ is an average, by postulating a Gaussian distribution of acid strengths for humic acids. If this postulate is valid for fulvic acid, then it applies to $\mathscr{K}_A^0 = K_A^0 \gamma_H^0 \gamma_A^0 / \gamma_{AH}^0$ rather than to K_A, in eq. 5.

Can. J. Chem. Downloaded from www.nrcresearchpress.com by 210.87.254.42 on 09/05/12
For personal use only.

A direct, rigorous test of Posner's postulate would require that the electrostatic and activity coefficient terms of eq. 5 be evaluated. This would need to be done separately for each of the three types of functional groups shown in Fig. 4.

Soil solutions and surface waters are typically found with pH values of 5 to 6. Tables 5 and 6 indicate that at such pH's the Type I carboxyl groups are essentially all ionized, and the Type A functional groups are more than 80% ionized. This must favor metal ion chelation under natural conditions. It also implies that fulvic acid and similar humic materials sorbed onto or into clay particles must exist as metal complexes or chelates. The chelation or complexing of divalent and trivalent metal ions may sorb fulvic acid onto undissolved humic materials, by bridging between polymer molecules. The carboxyl groups remaining free on such sorbed fulvic acid would then become ion exchange sites. In addition to these reactions, fulvic acid in a soil system might decompose clay crystals through a combination of acid attack and chelation of cations from the crystal lattice. The elucidation of such soil chemistry will require equilibrium measurements of the chelation and electrostatic binding of cations by fulvic acid. The degrees of ionization of acidic functional groups as a function of H^+ concentration or activity, as presented in Tables 5 and 6, are prerequisite to the calculation of such equilibria. The application of weighted average and differential functions comparable to the $\bar{K}_A$ and K_A already described (11, 20) will be useful and perhaps necessary for dealing with such fulvic acid problems in soils.

Mr. D. A. Hindle and Mr. H. T. Lie carried out the careful experimental work, including a large number of very exacting measurements.

1. Louis Meites and James A. Goldman. Anal. Chim. Acta, **29**, 472 (1963).
2. H. van Dijk. Sci. Proc. Royal Dublin Soc. Ser. A, **1**, 163 (1960).
3. A. M. Posner. 8th Int. Congr. of Soil Sci. Bucharest, Romania. 1964. page 161. Publishing House of the Academy of the Socialist Republic of Romania.
4. A. E. Martin and R. Reeve. J. Soil Sci. **9**, 89 (1958).
5. A. M. Posner. J. Soil Sci. **17**, 65 (1966).
6. H. R. Geering and J. F. Hodgson. Soil. Sci. Soc. Am. Proc. **33**, 54 (1969).
7. R. Speiser, C. H. Hills, and C. R. Eddy. J. Phys. Chem. **49**, 328 (1945).
8. A. M. Pommer and I. A. Breger. Geochim. et Cosmochim. Acta, **20**, 30 (1960).
9. Gunnar Gran. Analyst, **77**, 661 (1952).
10. Gunnar Gran. Acta Chem. Scand. **4**, 559 (1950).
11. Donald S. Gamble. Can. J. Chem. **48**, 2662 (1970).
12. F. J. C. Rossotti and Hazel Rossotti. J. Chem. Ed. **42**, 275 (1965).
13. Candin Liteanu and Dumitru Cŏrmŏs. Talanta, **7**, 32 (1960).
14. Pietro Lanza and Ileana Mazzei. J. Electroanal. Chem. **7**, 320 (1964).
15. Samuel B. Ellis and Samuel J. Kiehl. J. Am. Chem. Soc. **57**, 2139 (1935).
16. H. M. Irving, M. G. Miles, and L. D. Pettit. Anal. Chim. Acta, **38**, 475 (1967).
17. W. A. E. McBryde. Analyst, **94**, 337 (1969).
18. G. R. Hedwig and H. K. J. Powell. Anal. Chem. **43**, 1206 (1971).
19. M. Schnitzer and J. G. Desjardins. Can. J. Soil Sci. **49**, 151 (1969).
20. Donald S. Gamble, M. Schnitzer, and I. Hoffman. Can. J. Chem. **48**, 3197 (1970).
21. Herbert S. Harned and Walter J. Hamer. J. Am. Chem. Soc. **55**, 2194 (1933).
22. Daniel D. McCracken and William S. Dorn. Numerical methods and fortran programming; with applications in engineering and science. John Wiley, New York. 1964.
23. M. Schnitzer and J. G. Desjardins. Soil Sci. Soc. Am. Proc. **26**, 362 (1962).
24. M. Schnitzer and S. I. M. Skinner. Soil Sci. **96**, 86 (1963).
25. M. Schnitzer and S. I. M. Skinner. Soil Sci. **99**, 278 (1965).
26. M. Schnitzer and J. R. Wright. Trans. 9th Int. Congr. Soil Sci. **11**, 112 (1960).
27. M. Schnitzer and I. Hoffman. Geochim. Cosmochim. Acta, **29**, 859 (1965).
28. Harry P. Gregor and Michael Frederick. J. Polym. Sci. **23**, 451 (1957).
29. S. U. Khan and M. Schnitzer. Can. J. Chem. **49**, 2302 (1971).
30. G. Ogner and M. Schnitzer. Can. J. Chem. **49**, 1053 (1971).
31. W. R. Maxwell and J. R. Partington. Trans. Faraday Soc. **33**, 670 (1937).

Can. J. Chem. Downloaded from www.nrcresearchpress.com by 210.87.254.42 on 09/05/12
For personal use only.

The Infrared and Raman Spectra of Dimethyliodoarsine

H. F. SHURVELL, M. R. GOLD, AND A. R. NORRIS
Department of Chemistry, Queen's University, Kingston, Ontario

Received February 22, 1972

The infrared and laser–Raman spectra of liquid dimethyliodoarsine, $(CH_3)_2AsI$, have been recorded. Assignments of the observed frequencies have been made to the 24 normal modes of vibration of the molecule. A normal coordinate calculation has been carried out in support of the assignment.

Les spectres infrarouge et Raman laser de la diméthyliodoarsine liquide $(CH_3)_2$ AsI ont été enregistrés. Les attributions des fréquences observées ont été faites pour les 24 modes de vibration normaux de la molécule. Le calcul dans les coordonnées normales a été effectué pour appuyer cette assignation.

Canadian Journal of Chemistry, **50**, 2691 (1972)

Can. J. Chem. Downloaded from www.nrcresearchpress.com by 210.87.254.6 on 09/05/12
For personal use only.

Introduction

The compound $(CH_3)_2AsI$ is an important reagent in the synthesis of a number of organo–arsenic compounds, including *cis*- and *trans*-1,2-bis(dimethylarsino)ethylene (**1** and **2**) and 1,2-bis(dimethylarsine)acetylene (**3**), which serve as very powerful ligands. As part of a general study of the complexes of **1**, **2**, and **3** with Pt(II), Pd(II), Au(III), and Au(I), we require detailed i.r. and Raman spectra of the ligands and in order to interpret the spectra of **1**, **2**, and **3**, it is essential to have the complete i.r. and Raman spectra of $(CH_3)_2AsI$, together with a reliable assignment of the fundamentals.

Some information is available in the literature on the vibrational spectra of organoarsenic halides. The methylhaloarsines were examined by Raman spectroscopy using mercury arc excitation (1). More recently, i.r. and Raman spectra and tentative assignments have been published for $(CH_3)_2AsCl$ and CH_3AsCl_2 (2). Infrared and Raman spectra of CH_3AsCl_2, $(CH_3)_2AsCl$ and $(CH_3)_2AsCl_3$ and some phenylarsenic halides have been reported (3), and very recently, spectra of CH_3AsCl_2, CH_3AsBr_2, CH_3AsI_2, and CD_3AsI_2 have been studied in another laboratory (4).

It appears that the only spectroscopic datum available for $(CH_3)_2AsI$ is the partial Raman spectrum published by Van der Kelen and Herman in 1956 (1). We have therefore recorded i.r. and laser Raman spectra for this molecule and attempted to make assignments of the observed frequencies to the 24 normal modes. Since 24 separate i.r. bands or Raman lines were not observed, it was decided to carry out a normal coordinate calculation to predict the frequencies of the fundamentals. For the skeletal vibrations of the C_2AsI group and the vibrations involving bending of the As—C—H angles, the calculation proved to be useful in deciding among possible assignments. A band contour resolution technique was applied to two of the bands as a further aid in assigning frequencies to the fundamentals.

Experimental

Dimethyliodoarsine was prepared by the method described by Burrows and Turner (5). The oily layer containing $(CH_3)_2AsI$ was dried over molecular sieves, then distilled under nitrogen at 1 atm pressure (b.p. 157 °C; lit. 154–157 °C (5)). The proton magnetic resonance spectrum of the sample in CCl_4 solution showed a single peak at 2.04 p.p.m. (TMS, internal standard). The mass spectrum of the compound was recorded on a JEOL model JMS 01SC mass spectrometer. The main peak at mass 232 and all other strong peaks due to fragmentation were consistent with the compound $(CH_3)_2AsI$.

Infrared survey spectra were recorded on a Beckman IR 10 spectrometer. High resolution spectra were recorded using Perkin–Elmer Ebert single beam and Perkin–Elmer model 180 instruments. The Raman spectrum was recorded on a Perkin–Elmer LR 1 laser Raman spectrometer, using He/Ne laser excitation. A 2.5 ml multiple reflection cell was used and the laser power at the sample was about 25 mW. The Raman instrument was calibrated using known frequencies of $CHCl_3$, benzene, etc., and neon emission lines. The Raman frequencies are only accurate to ± 5 cm^{-1}, whereas the infrared frequencies are believed to be correct to within ± 1 cm^{-1}. This may explain some apparent differences between our reported i.r. and Raman frequencies.

Normal Coordinate and Band Contour Calculations

A calculation of vibrational frequencies and force constants for the skeletal modes of $(CH_3)_2AsCl$ and $(CH_3)_2AsBr$ has been reported previously (6). Trimethylarsine has also been the subject of similar calculations (7, 8), so that initial values for the force constants of the C_2AsI skeleton are

TABLE 1. Frequencies and assignments in the infrared and Raman spectra of $(CH_3)_2AsI$

Infrared*		Raman*			Approximate description and assignment†
cm^{-1}	Intensity	cm^{-1}	Intensity	Depolarization	
2998	s	2995	w	0.75 dp	CH_3 antisym. str. ($2A''$)
2976	s	2978			CH_3 antisym. str. ($2A'$)
2910	vs	2905	s	0.05 p	CH_3 sym. str. (A' and A'')
2785	m	—	—	—	c
2470	w	—	—	—	c
2045	w	—	—	—	c
1815	w	—	—	—	c
1570	vw	—	—	—	c
1430	sh	1430	sh	0.74 dp	CH_3 antisym. def. ($2A''$)
1415	vs	1420	m		CH_3 antisym. def. ($2A'$)
1255	vs	1262	m	0.20 p	CH_3 sym. def. (A' and A'')
1135	w	—	—	—	c
900	vs	906	m	0.23 p	As—C—H def. (A' and A'')
830	vs	836	s	0.60 p	As—C—H def. (A' and A'')
576	vs	—	—	—	As—C antisym. str. (A'')
567	vs	564	vs	0.16 p	As—C sym. str. (A')
450	w	—	—	—	c
365	w	365	w	—	c
237	wsh	—	—	—	c
229.5	vs	228	vs	0.23 p	AsI str. (A')
225	wsh	—	—	—	c
177	m	176	m	0.31 p	C—As—C def. (A')
—	—	ca. 95	sh	—	C—As—I def. (A' and A'')
—	—	ca. 70	sh	—	CH_3 torsions (A' and A'')

*w = weak, m = medium, s = strong, v = very, sh = shoulder, p = polarized, dp = depolarized.
†antisym. = antisymmetric, sym. = symmetric, str. = stretch, def. = deformation, c = combination or overtone.

available. Cossee and Schachtschneider (9) performed a vibrational analysis for acetone, from which force constants for the methyl groups can be taken. Force constant calculations for AsI_3 (10, 11) provided a starting value for the As—I stretching constant.

The Wilson **FG** matrix method (12) was used for the normal coordinate calculations which were carried out using a computer program originally written by Schachtschneider (13) and modified by Brooks (14) for the IBM 360/50 computer. It is assumed that the molecule has a plane of symmetry containing the As and I atoms. Bond lengths and angles used in the calculation were (15): As—C = 1.98 Å; As—I = 2.52 Å; C—H = 1.09 Å; ∠CAsC = 96°; ∠CAsI = 98°; ∠HCH and ∠AsCH = 109.5°. It is assumed that the methyl groups are tetrahedral. Internal coordinates were chosen as changes in bond lengths and angles and the two torsions about the As—C bonds. A detailed list of internal coordinates is given in Table A1 of the Appendix, which is available from the Depository of Unpublished Data.[1] A valence force field containing 8 diagonal and 22 interaction constants was used. Descriptions of these 30 force constants are given in Table A2 of the Appendix. A set of symmetry coordinates was chosen to factor the **F** and **G** matrices into A' and A'' blocks. Details of these symmetry coordinates are given in Table A3 of the Appendix.

[1]Complete set of tables in Appendix is available, at a nominal charge, from the Depository of Unpublished Data, National Science Library, National Research Council of Canada, Ottawa, Canada, K1A 0S2.

All interactions were initially set equal to zero and the initial set of diagonal force constants was varied, with the addition of interactions, until a satisfactory fit was obtained between observed and calculated frequencies. Several assignments of the low frequency vibrations were tried. The results of these calculations will be introduced where pertinent in the discussion part of this paper.

For cases where overlapping infrared or Raman bands cannot be resolved, a method of band resolution by the computer has been devised by Jones and co-workers (16). The method involves digitizing the spectrum. This can be done mechanically, producing a punched paper tape, or manually from a band that has been spread out by an abscissa expansion device. Manual digitization may be accomplished fairly quickly with the aid of a computer program devised by Bulmer and Shurvell (17), which minimizes the actual labor involved. The digitized spectrum is fitted by a synthetic spectrum containing two or more bands calculated by the computer. A Gaussian–Lorentzian product function was used to study two bands in the present work and the results will be used later in the discussion.

Results and Discussion

The observed i.r. and Raman frequencies are listed in Table 1. The Raman spectrum is shown in Fig. 1 and an i.r. spectrum in Fig. 2. In Fig. 3 one of the far i.r. bands is shown under high resolution, together with the computed

Can. J. Chem. Downloaded from www.nrcresearchpress.com by 210.87.254.6 on 09/05/12
For personal use only.

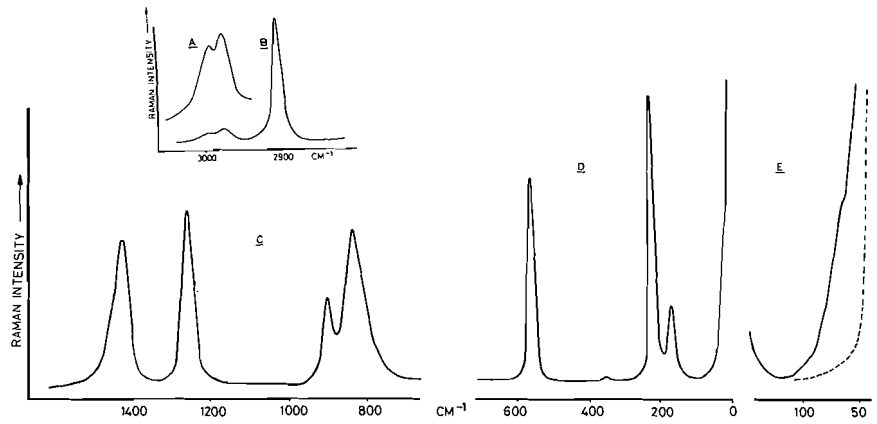

FIG. 1. The Raman spectrum of dimethyliodoarsine from a 2.5 ml multiple reflection cell. Spectral slit widths for spectra *A*, *B*, *C*, *D*, and *E* were: 12, 8, 5, 7, and 20 cm^{-1}, respectively. A higher amplifier gain was used for *A* than for *B*. High gain was also used for regions *C* and *E*. Medium and low gains were used for regions *B* and *D*, respectively. The dashed line in region *E* was obtained with pure CCl_4 in the cell under similar instrumental conditions.

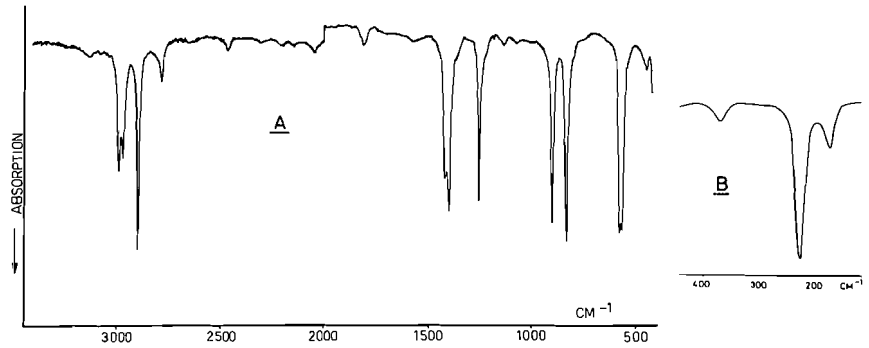

FIG. 2. The i.r. spectrum of dimethyliodoarsine. For region *A*, a liquid film between two KBr plates was used. For region *B*, a disposable polyethylene cell of path length 0.5 mm was used.

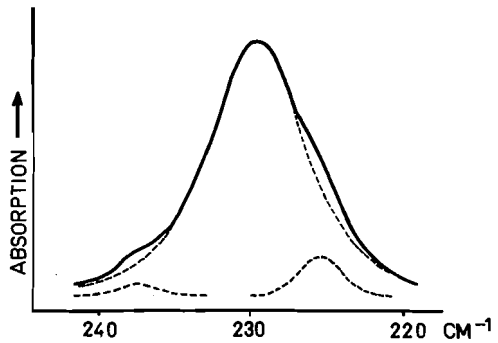

FIG. 3. The components of the 230 cm^{-1} infrared band of $(CH_3)_2AsI$ resolved by computer. The solid line is the observed band and the dotted curves are the computed components.

components from the band resolution program mentioned earlier.

Relatively simple i.r. and Raman spectra are expected for $(CH_3)_2AsI$. The spectra should consist basically of four main features due to methyl group stretching and bending modes plus the vibrations of the C_2AsI skeleton. All combinations and overtones are allowed, so that some additional weak bands are also expected. However, only a few overtones and combinations were observed and these have been included in Table 1.

Assignments

CH Stretching

A high resolution i.r. spectrum of the CH stretching region shows a doublet at 2998 and 2976 cm^{-1}. This is assigned to the in-phase (*A'*) and out-of-phase (A'') components of the antisymmetric CH_3 stretching mode. The assignment is confirmed by the Raman spectrum in which these lines are weak and depolar-

Can. J. Chem. Downloaded from www.nrcresearchpress.com by 210.87.254.6 on 09/05/12
For personal use only.

Can. J. Chem. Downloaded from www.nrcresearchpress.com by 210.87.254.6 on 09/05/12
For personal use only.

ized. It is assumed that the local C_{3v} symmetry determines the depolarization, so that, while the in-phase combination is A' with respect to the C_s symmetry of the molecule, the actual vibrations are of E species with respect to the C_{3v} symmetry of the methyl groups and are therefore depolarized. The 2910 cm^{-1} band on the other hand is strong and polarized in the Raman spectrum, as expected for the symmetric CH_3 stretching mode.

CH_3 Deformation

Again, the antisymmetric mode is split into a doublet in the i.r. spectrum at 1415 and 1430 cm^{-1}. A line with a shoulder is observed in the Raman spectrum and this was depolarized, consistent with the assigment to the antisymmetric CH_3 deformation.

The symmetric CH_3 deformations were observed as a single peak in both i.r. and Raman. The Raman line was polarized, although not as strongly as the line due to the symmetric stretching vibration.

C—As Stretching

It is generally agreed that compounds containing C—As bonds give rise to i.r. absorption bands and Raman lines in the range 560–590 cm^{-1} (3, 4, 6, 7). In $(CH_3)_2AsI$, there should be two features attributable to C—As stretching. A very strong polarized Raman line at 564 cm^{-1} corresponds with the lower frequency component of a strong doublet in the i.r. at 567/576 cm^{-1}. These two frequencies are assigned to the symmetric and antisymmetric C—As stretching modes, respectively.

As-I Stretching

The very strong polarized Raman line at 228 cm^{-1} and the corresponding very strong i.r. band centered at 230 cm^{-1} are assigned to the As—I stretching mode in agreement with frequencies reported for CH_3AsI_2 (4) and AsI_3 (11).

As—C—H Deformations (CH_3 Rocking)

For the dimethylhaloarsines there should be four normal modes involving As—C—H deformations. Normal coordinate calculations indicate that all four vibrations have frequencies in the 900–800 cm^{-1} region. Frequencies near 830 cm^{-1} were reported for the three methyldihaloarsines, CH_3AsX_2 (X = Cl, Br, and I) (4). We assume that the 900 and 830 cm^{-1} bands in the i.r. and Raman spectra of dimethyliodoarsine are both due to two fundamentals and in fact resolution of the 830 cm^{-1} band was achieved using the contour resolution program.

CH_3 Torsions

Torsional vibrations of methyl groups have been observed over a wide range of frequencies (270 to 100 cm^{-1}) in a variety of compounds (18, 19). For the CH_3AsX_2 molecules (4) it was concluded that the torsions should lie in the range 185–135 cm^{-1}, but a definite assignment was only made in one case, namely 134 cm^{-1} for CH_3AsBr_2.

In the present work, the normal coordinate calculation predicts two almost degenerate frequencies for the torsions, but the calculated values can vary over a wide range depending on the choice of torsional force constant. For example, using a force constant of 0.05 mdyn Å/sq. radian, the calculated frequencies are 168 cm^{-1} for the A' mode and 170 cm^{-1} for the A'' vibration. These are close to observed i.r. and Raman frequencies, but alternative assignments are preferable and will be discussed below. Torsional force constants of 0.007 and 0.009 mdyn Å/sq. radian were used for acetone (9). A value near 0.01 mdyn Å/sq. radian would seem to be reasonable for $(CH_3)_2AsI$ and this leads to calculated frequencies of 70 and 71 cm^{-1}.

Methyl torsions are often very weak in both i.r. and Raman spectra and it is possible that in the present case they lie near 70 cm^{-1}, where a weak shoulder is observed in the Raman spectrum.

Other Skeletal Vibrations

Three skeletal vibrations remain to be assigned: the C—As—C deformation and two C—As—I deformation modes. In related molecules, C—As—C deformation modes were assigned to frequencies in the 240–220 cm^{-1} region (7, 8). The possibility of finding more than one component in the 230 cm^{-1} band previously assigned to the As—I stretch leads us to carry out a contour resolution calculation, with the result shown in Fig. 3. The observed band is composed of two weak absorptions at 225 and 237 cm^{-1}, in addition to the strong peak at 229.5 cm^{-1}. The 237 cm^{-1} band can be explained as a combination of the 177 cm^{-1} fundamental with the lowest frequency fundamental believed to be observed as a

Can. J. Chem. Downloaded from www.nrcresearchpress.com by 210.87.254.6 on 09/05/12
For personal use only.

TABLE 2. Calculated force constants, frequencies and major contributions to the P.E.D. for $(CH_3)_2AsI$

Force constants			A' frequencies (cm^{-1})			A'' frequencies (cm^{-1})		
	Values*	Descriptions	Observed	Calculated	Major contributions to P.E.D.†	Observed	Calculated	Major contributions to P.E.D.†
f_1	4.750	C—H stretch	2998	3010	$f_1 = 0.970$	2998	3013	$f_1 = 0.966$
f_2	0.4733	H—C—H bend	2976	2959	$f_1 = 1.008$	2976	2959	$f_1 = 1.008$
f_3	0.5407	As—C—H bend	2910	2905	$f_1 = 0.975$	2910	2906	$f_1 = 0.974$
f_4	2.505	As—C stretch	1430	1425	$f_2 = 0.868$	1430	1424	$f_2 = 0.869$
f_5	1.400	As—I stretch	1415	1420	$f_2 = 0.855$	1415	1420	$f_2 = 0.859$
f_6	0.5128	C—As—C bend	1255	1255	$f_2 = 0.512, f_3 = 0.583$	1255	1256	$f_2 = 0.511, f_3 = 0.582$
f_7	0.2566	C—As—I bend	900	887	$f_3 = 0.923$	900	882	$f_3 = 0.927$
f_8	0.009865	Torsion	830	850	$f_3 = 0.962$	830	838	$f_3 = 0.986$
f_{18}	0.05835	C—H, C—H interaction	567	564	$f_4 = 0.932$	576	572	$f_4 = 0.933$
f_{19}	−0.07502	C—H, H—C—H interaction (common bond)	229.5	228	$f_5 = 0.938$	95	94	$f_7 = 0.896$
f_{20}	0.05695	C—H, H—C—H interaction (no common bond)	177	176	$f_6 = 0.975$	70	71	$f_8 = 0.892$
f_{23}	−0.03000	H—C—H, H—C—H interaction	95	97	$f_7 = 0.802$			
f_{24}	0.1783	C—H, As—C—H interaction (no common bond)	70	70	$f_8 = 0.841$			
f_{25}	−0.4632	C—H, As—C—H interaction (common bond)						
f_{26}	0.1500	H—C—H, As—C—H interaction (adjacent angles)						
f_{27}	−0.2500	H—C—H, As—C—H interaction (opposite angles)						
f_{28}	−0.03669	As—C—H, As—C—H interaction						

*Units of stretching constants are mdyn/Å, bending, torsion, and bend–bend interactions are in mdyn/Å/sq. radian, and bend–stretch interactions are in mdyn/radian.
‡Certain entries or sums of entries in the P.E.D. are greater than 1.0, because of the contributions from negative interaction constants.

Can. J. Chem. Downloaded from www.nrcresearchpress.com by 210.87.254.6 on 09/05/12
For personal use only.

shoulder on the Rayleigh line in the Raman spectrum. The 225 cm^{-1} feature could be assigned as the C—As—C deformation. In this case, the 177 cm^{-1} frequency would be assigned as the A'' C—As—C deformation, and the shoulder near 95 cm^{-1} in the Raman spectrum as the A' mode. This assignment follows that of Van der Kelen and Herman (1), but there is a serious objection to it, since a large difference in frequency (80 cm^{-1}) between A' and A'' C—As—I deformation modes is unlikely. It is possible of course that the 177 cm^{-1} frequency is due to both A' and A'' modes, but this is definitely not in agreement with the normal coordinate calculation.

We believe that the following assignment of the low frequency modes is the correct one. The 177 cm^{-1} frequency is the C—As—C bending mode and the shoulder near 95 cm^{-1} in the Raman spectrum is due to both C—As—I deformations. The 225 cm^{-1} component of the band centered at 230 cm^{-1} is most likely a hot band, $(\nu_{As-I} + \nu_i - \nu_i)$, where ν_i is one of the lowest frequency fundamentals. The normal coordinate calculation definitely supports this assignment, since in each of the A' and A'' blocks, a frequency is predicted near 100 cm^{-1}. The potential energy distribution indicates that these modes are between 80–90% CAsI deformations. Only for the A' block is there a calculated frequency near 177 cm^{-1}. The P.E.D. for this frequency indicates nearly 100% C—As—C deformation.

The calculated force constants seem to be very reasonable for this assignment and only a few small interactions are necessary to produce a satisfactory fit between observed and calculated frequencies. The results of the calculation including the major contributions to the P.E.D.'s are listed in Table 2. The P.E.D.'s are in complete agreement with the descriptions given in Table 1. The 1255 cm^{-1} frequency is correctly assigned to HCH bending, but because in this mode the AsCH angles bend simultaneously, the AsCH and HCH bending force constants contribute almost equally to the P.E.D. The CAsI bends are coupled to a small extent to the torsions and as discussed above, a change in the torsional force constant can change the assignment of the low frequency modes. However, it is felt that the present assignment is the correct one.

Conclusions

The i.r. and Raman spectra of dimethyliodoarsine have been interpreted in terms of methyl group vibrations and vibrations of the C_2AsI skeleton. Band contour resolution techniques and normal coordinate calculations have been useful in locating some of the fundamentals and making assignments.

The present assignment should prove to be useful in future studies on dimethylarsine-containing ligands and their complexes.

The authors are grateful to Dr. W. V. F. Brooks of the University of New Brunswick for the use of his programs for the normal coordinate calculations and to Dr. R. N. Jones of the National Research Council of Canada, Ottawa, for the band contour resolution programs. The financial assistance of the National Research Council of Canada is also gratefully acknowledged.

1. G. P. Van der Kelen and M. A. Herman. Bull. Soc. Chim. Belg. **65**, 350 (1956).
2. J. H. S. Green, W. Kynaston, and G. A. Rodley. Spectrochim. Acta, **24A**, 853 (1968).
3. D. M. Revitt and D. B. Sowerby. Spectrochim. Acta, **26A**, 1581 (1970).
4. J. R. Durig, C. F. Jumper, and J. N. Willis, Jr. Appl. Spectrosc. **25**, 218 (1971).
5. G. J. Burrows and E. E. Turner. J. Chem. Soc. 1370 (1920).
6. E. G. Claeys and G. P. Van der Kelen. Spectrochim. Acta, **22**, 2103 (1966).
7. H. Siebert. Z. Anorg. Allgem. Chem. **273**, 161 (1953).
8. G. Bouquet et M. Bigorgne. Spectrochim. Acta, **23A**, 1231 (1967).
9. P. Cossee and J. H. Schachtschneider. J. Chem. Phys. **44**, 97 (1966).
10. H. Stammreich, R. Forneris, and Y. Tavares. J. Chem. Phys. **25**, 580 (1956).
11. T. R. Manley and D. A. Williams. Spectrochim. Acta, **21**, 1773 (1965).
12. E. B. Wilson, Jr., J. C. Decius, and P. C. Cross. Molecular vibrations. McGraw–Hill, New York. 1956.
13. J. H. Schachtschneider. Tech. Rept. 57–65. Shell Development Co. 1965.
14. W. V. F. Brooks. Private communication.
15. Interatomic distances. Special Publication No. 11, The Chemical Society, London. 1958.
16. R. N. Jones, T. E. Bach, H. Fuhrer, V. B. Kartha, J. Pitha, K. S. Seshadri, R. Venkataraghavan, and R. P. Young. Computer programmes for absorption spectrophotometry. N.R.C. Bulletin No. 11, National Research Council of Canada, Ottawa. 1968.
17. T. Bulmer and H. F. Shurvell. Can. Spectrosc. **16**, 94 (1971).
18. F. A. Miller. Molecular spectroscopy. Institute of Petroleum, London. 1968. p. 10.
19. J. R. Durig, S. M. Craven, and J. Bragin. J. Chem. Phys. **53**, 38 (1970).

Can. J. Chem. Downloaded from www.nrcresearchpress.com by 210.87.254.40 on 09/05/12
For personal use only.

Comparison between Molecular Structure Effects in Triplet Positronium Annihilation Rates and Radiolysis Free Ion Yields in Liquid Hydrocarbons

G. R. FREEMAN AND J.-P. DODELET
Chemistry Department, University of Alberta, Edmonton, Alberta T6G 2G2

Received January 26, 1972

Two seemingly unrelated phenomena in liquid hydrocarbons have similar trends in their dependences upon the molecular structure of the hydrocarbon. The phenomena are the annihilation half-life of triplet positronium and the radiolysis free ion yield. In *n*-alkanes the effect of increasing the molecular chain length, upon both phenomena, appears to be simply to increase the density of interacting sites. Branching the alkane chain decreases the strength of molecular interaction with both electrons and positronium, although the relative decrease is much greater for the former than for the latter. The effects of double bonds on the phenomena, after separating out the density effect, are different from each other.

Le rendement en ions libres obtenus dans les hydrocarbures liquides sous radiolyse gamma et le temps de demi vie, lors de l'annihilation du positronium à l'état triplet dans ces liquides, sont deux phénomènes en apparence indépendants. Toutefois il semble que leur dépendance vis-à-vis de la structure moléculaire des hydrocarbures soit semblable: dans les alcanes normaux l'alongement de la chaîne carbonée agirait en changeant la densité des sites d'interaction; les alcanes à chaîne ramifiée seraient responsables d'une diminution de l'interaction de la molécule avec l'électron ou le positronium. Cet effet est cependant beaucoup plus marqué pour les électrons. D'autre part, après avoir tenu compte de l'effet dû à la densité, il semble que les deux phénomènes soient différents pour les molécules contenant des double liaisons.

Canadian Journal of Chemistry, **50**, 2697 (1972)

The annihilation half-life τ_2 of triplet positronium in a liquid hydrocarbon is influenced by the molecular structure of the hydrocarbon (1, 2). The yield of free ions generated during the radiolysis of a liquid hydrocarbon is also affected by molecular structure (3–6). The trends in the two phenomena are similar and it is informative to compare them.

Values of τ_2 and G_{fi} (number of pairs of free ions formed per 100 eV of energy absorbed) for a number of liquids are listed in Table 1. Both τ_2 and G_{fi} decrease with increasing chain length in the *n*-alkanes.

The effect of chain length on G_{fi} in the *n*-alkanes is due simply to the change in liquid density (5). The free ion yield is related exponentially to the penetration range b of the secondary electrons in the liquid (7, 8).

$$[1] \qquad G_{fi} \propto \exp(-1/b)$$

The value of b decreases with increasing density d of the liquid (9). The product bd has a constant value for all *n*-alkanes from *n*-butane to *n*-tetradecane (5); examples are given in Table 1. This means that the density-normalized rate of energy loss of the electrons, which is proportional to $(bd)^{-1}$, is constant. The electron–molecule energy transfer interactions are short range (6), so changing the *n*-alkane chain length from C_4 to C_{14} does not increase the strength of the interactions but merely decreases the electron mean free path by increasing the density of scattering centers.

The product of τ_2 and the liquid density is also constant for the *n*-alkanes (Table 1); $\tau_2 d$ is inversely proportional to the density-normalized rate of annihilation. The annihilation rate has been empirically related to the molar polarization of the liquids (1), but the correlation is not exact and is not fundamentally understood (2). In *n*-alkanes the effect of chain length is probably simply to increase the density of interacting sites.

Branching the alkane chain increases both bd and $\tau_2 d$, but the effect is greater on the former than on the latter (Table 1). The polarizability of neopentane is nearly isotropic, which greatly reduces the inelastic scattering

TABLE 1. Variation of the annihilation half-lives τ_2 of triplet positronium and of the X-radiolysis free ion yields in liquid hydrocarbons

Liquid	τ_2 (ns)*	G_{fi}†	b(Å)†	bd (10^{-8} g/cm^2)†	$\tau_2 d$ (ns g/cm^3)
		Effect of Chain Length			
n-C_4H_{10}	4.6	0.19	83	48	2.6
n-C_5H_{12}	4.1	0.15	72	45	2.5
n-C_6H_{14}	3.9	0.13	67	44	2.5
n-C_7H_{16}	3.7	0.13	66	45	2.5
n-C_8H_{18}	3.6	0.12	64	45	2.5
n-C_9H_{20}	3.5	0.12	62	45	2.5
n-$C_{10}H_{22}$	3.4	0.12	62	45	2.5
		Effect of Chain Branching			
C_5: n-C_5H_{12}	4.1	0.15	72	45	2.5
C_5: $C_2H_5CH(CH_3)_2$	4.5	0.17	76	47	2.8
C_5: $C(CH_3)_4$	5.0	0.86	178	105	2.9
		1.09‡	213‡	126‡	
C_8: n-C_8H_{18}	3.6	0.12	64	45	2.5
C_8: 2,3,4-TMP	3.7	0.17	72	51	2.6
C_8: 2,2,4-TMP	4.0	0.33	95	65	2.8
		Effect of Double Bonds			
n-C_6H_{14}	3.9	0.13	67	44	2.5
C_6H_{12}-2	3.7	0.08	55	37	2.5
C_6H_{12}-1	3.7	0.06	49	33	2.5
C_6H_6	3.1	0.05	42	37	2.7

*At 299 K, ref. 1.
†At 296 K, ref. 5: b is the most probable penetration range of the secondary electrons and d is the liquid density.
‡At 294 K, ref. 6.

cross section of the molecules for epithermal electrons (6). Anisotropy of polarizability appears to be less important in the positronium annihilation process. Although the structure effect on τ_2 is small, it is believed to be real (1, 2). The smaller effect on τ_2 might be related to the fact that positronium is neutral, whereas the electron is not.

The value of bd in a straight chain olefin is smaller than that in an n-alkane, whereas the value of $\tau_2 d$ is the same in the two types of liquid (Table 1). In benzene bd is smaller than in n-hexane, whereas the $\tau_2 d$ is larger in benzene than in hexane. The double bond effects are different in the two processes.

The structure effects on bd were greatest in the series of simple molecules CH_4, C_2H_6, and C_2H_4, with $bd = 210$, 81, and 54×10^{-8} g/cm^2, respectively (10). It would be useful to determine $\tau_2 d$ in these liquids to confirm the partial annihilation rates that have been assigned to bonds (1, 2). The partial rate assigned to a given type of bond depends on the position of the bond in the molecule (1, 2), which makes it doubtful that the effect can accurately be attributed to individual bonds.

We are grateful to the National Research Council of Canada for financial assistance.

1. P. R. GRAY, G. P. STURM, JR., and C. F. COOK. J. Chem. Phys. **46**, 1145 (1968).
2. M. B. PERKAL and W. B. WALTERS. J. Chem. Phys. **54**, 3750 (1971).
3. W. F. SCHMIDT and A. O. ALLEN. J. Phys. Chem. **72**, 3730 (1968).
4. P. H. TEWARI and G. R. FREEMAN. J. Chem. Phys. **49**, 4394 (1968).
5. W. F. SCHMIDT and A. O. ALLEN. J. Chem. Phys. **52**, 2345 (1970).
6. J.-P. DODELET and G. R. FREEMAN. Can. J. Chem. This issue.
7. L. ONSAGER. Phys. Rev. **54**, 554 (1938).
8. G. R. FREEMAN and J. M. FAYADH. J. Chem. Phys. **43**, 86 (1965).
9. D. E. LEA. Actions of radiations on living cells. University Press, Cambridge. 1955. Chap. 1.
10. M. G. ROBINSON, P. G. FUOCHI, and G. R. FREEMAN. Can. J. Chem. **49**, 3657 (1971).

Can. J. Chem. Downloaded from www.nrcresearchpress.com by 210.87.254.40 on 09/05/12
For personal use only.

Optical and Thermal Bleaching of Trapped Electrons in Aliphatic Amine Glasses

SHOJI NODA, KENJI FUEKI, AND ZEN-ICHIRO KURI

Department of Synthetic Chemistry, Faculty of Engineering, Nagoya University, Chikusa-ku, Nagoya, Japan

Received April 4, 1972

An optical bleaching study has been made of trapped electrons in γ-irradiated aliphatic amines at -196 °C. The results indicate that the optical absorption of the trapped electrons in the amines is attributed to optical transitions to both bound excited states and a continuum state. The thermal decay of the trapped electrons has been studied by the e.s.r. technique at temperatures above -196 °C. It has been found that the line width of the e.s.r. spectra of the trapped electrons in some of the amines changes on warming.

Nous avons effectué une étude thermique de décoloration d'électrons piégés dans des amines irradiées par des rayons-γ à -196 °C. Les résultats indiquent que l'absorption optique des électrons jugés dans les amines est attribuable à des transitions optiques entre les deux niveaux liants excités et un niveau continu. Nous avons aussi étudié par r.p.c. la désintégration thermique à des températures au-dessus de -196 °C. Nous trouvons que la largeur des raies du spectre r.p.c. des électrons piégés dans quelques amines change au cours du chauffage.

Canadian Journal of Chemistry, **50**, 2699 (1972)

Introduction

In the previous communication (1) we have reported optical and e.s.r. observations on trapped electrons produced in γ-irradiated aliphatic amine glasses at -196 °C, giving the optical and e.s.r. parameters as well as yields of the trapped electrons.

In this work, we have made an optical bleaching study of the trapped electrons in aliphatic amine glasses at -196 °C to get a better understanding of the nature of the excited states to which optical transitions occur. Using the e.s.r. technique we have also made a thermal bleaching study of the trapped electrons at temperatures above -196 °C to demonstrate the temperature at which the trapped electrons decay rapidly in these matrices and to obtain some information about the effect of matrix relaxation on the e.s.r. spectra of the trapped electrons.

Experimental

Aliphatic amines (*s*-butylamine, diisopropylamine, triethylamine, 2-methyl-*n*-amylamine, *N*-methyl-*n*-butylamine, and 3-methylpiperidine) were purified by refluxing over potassium hydroxide pellets followed by repeated middle-cut distillation under nitrogen atmosphere. The middle portion from distillation was treated with sodium blocks and distilled under vacuum on a freshly prepared sodium mirror. The purified amines were transferred to e.s.r. tubes or optical absorption cells and were sealed under vacuum.

Samples were irradiated by ^{60}Co γ-rays at -196 °C in the dark. The dose rate was 1.2×10^{18} eV min^{-1} g^{-1} and the total dose was 3.6×10^{19} eV g^{-1}. Optical bleaching experiments were performed with a monochromatic light which was obtained from a 45-W tungsten (quartz–iodine) lamp combined with a high intensity Shimazu–Bausch and Lomb monochromator. The full width at half height of the light band emitted from the monochromator was 38 nm when entrance and exit widths of the monochromator were 3.0 and 1.5 mm, respectively.

E.s.r. measurements were carried out with a conventional X-band spectrometer using 100 kc.p.s. magnetic field modulation. Optical absorption spectra were taken on a Hitachi EPU-2A spectrophotometer. Both the e.s.r. and optical absorption measurements were carried out at -196 °C. A variable-temperature e.s.r. Dewar was employed for annealing the samples at temperatures above -196 °C. Any desired temperature was obtained by controlling the flow rate of cold nitrogen gas and the temperature of the samples was measured with a copper–constantan thermocouple.

Results and Discussion

Optical Bleaching

Relative quantum efficiencies for photobleaching were obtained for trapped electrons produced in γ-irradiated *s*-butylamine, diisopropylamine, and triethylamine at -196 °C, which are the primary, the secondary, and the tertiary amine, respectively. In Figs. 1–3 are shown the initial relative quantum efficiencies for photobleaching *vs.* the energy of photon used for the photobleaching together with their optical absorption spectra. It can be seen in Figs. 1–3 that the threshold energies for photobleaching are around the energies at which the optical absorption maxima are located, *i.e.*, 1.1 eV (1170 nm) for the *s*-butylamine, 0.87 eV

Can. J. Chem. Downloaded from www.nrcresearchpress.com by 210.87.254.40 on 09/05/12
For personal use only.

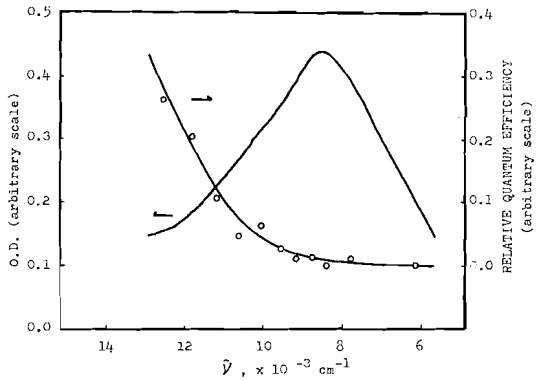

FIG. 1. Relative quantum efficiency for photobleaching of the trapped electrons in *s*-butylamine at −196 °C versus the wavenumber of the bleaching light. The optical absorption spectrum of the trapped electrons is shown on the same wavenumber scale.

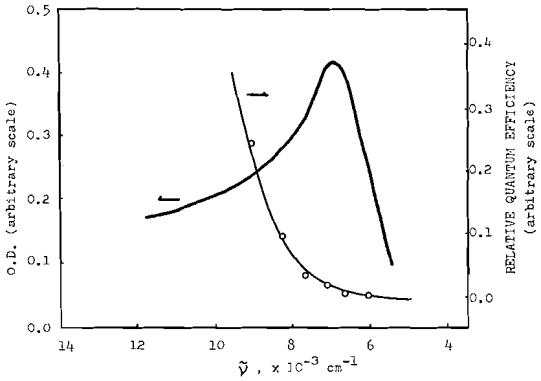

FIG. 2. Relative quantum efficiency for photobleaching of the trapped electrons in diisopropylamine at −196 °C *vs.* the wavenumber of the bleaching light. The optical absorption spectrum of the trapped electrons is shown on the same wavenumber scale.

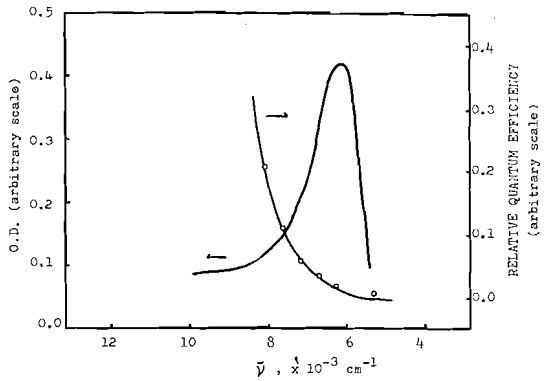

FIG. 3. Relative quantum efficiency for photobleaching of the trapped electrons in triethylamine at −196 °C *vs.* the wavenumber of the bleaching light. The optical absorption spectrum of the trapped electrons is shown on the same wavenumber scale.

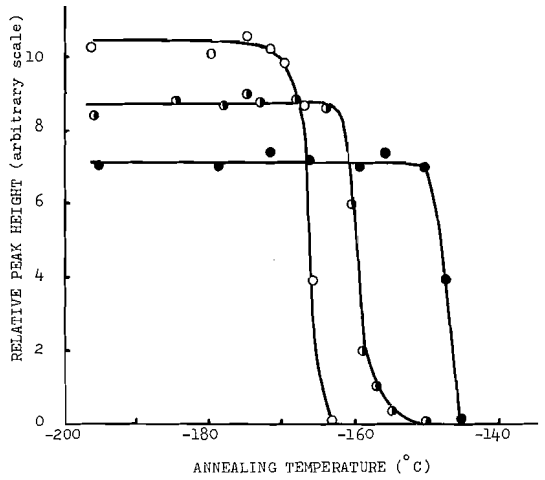

FIG. 4. The effect of thermal annealing at temperatures above −196 °C on the concentration of the trapped electrons in aliphatic amines: ○, *s*-butylamine; ◑, diisopropylamine; ●, 2-methyl-*n*-amylamine.

(1430 nm) for the diisopropylamine, and 0.75 eV (1650 nm) for the triethylamine.

These results indicate that the optical absorption of the trapped electrons in aliphatic amine glasses corresponds to optical transitions to both bound excited states and a continuum state, and the probabilities of these transitions depend on the photon energy. Similar observations on photobleaching behavior were previously reported on trapped electrons in glassy methyltetrahydrofuran (2, 3) and alcohols (4, 5), and in the single crystal of ice doped with impurities (6) at −196 °C. It is noted here that alkaline ice (7, 8) is one exception, where no bound excited state exists for trapped electrons in this matrix.

Thermal Bleaching

Thermal decay experiments were carried out to demonstrate the temperature at which the trapped electrons disappeared rapidly. Small temperature increments were used and in each run the sample was kept for about 5 min at each temperature.

Figure 4 shows plots of the intensity of the singlet e.s.r. spectra of the trapped electrons against the temperature for γ-irradiated *s*-butylamine, diisopropylamine, and 2-methyl-*n*-amylamine. As can be seen in Fig. 4, the trapped electrons decayed rapidly in a temperature region of −170 to −163 °C for the *s*-butyla-

Can. J. Chem. Downloaded from www.nrcresearchpress.com by 210.87.254.40 on 09/05/12
For personal use only.

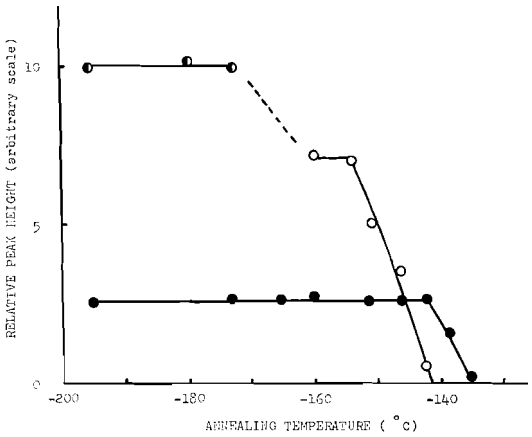

FIG. 5. The effect of thermal annealing at temperatures above −196 °C on the concentrations of the trapped electrons and radicals in *N*-methyl-*n*-butylamine: ◐, trapped electrons; ○, trapped electrons in the sample annealed at −161 °C for 2 h after γ-irradiation at −196 °C; ●, trapped radicals responsible for the underlying spectrum.

mine, −164 to −155 °C for the diisopropylamine, and −153 to −148 °C for the 2-methyl-*n*-amylamine.

A thermal annealing profile for trapped electrons in *N*-methyl-*n*-butylamine is displayed in Fig. 5. It is noted that when the temperature of the sample was kept at −161 °C for 2 h after γ-irradiation at −196 °C, the line width between derivative maxima, ΔH_{ms}, increased from 12 to 17 G accompanied by a decrease in the peak height. Both ΔH_{ms} and the peak height remained constant from −161 to −154 °C. A broad underlying e.s.r. spectrum decayed at a temperature higher than the temperature at which the trapped electron spectrum decayed. Since our primary interest was in the trapped electron, we did not try to identify the trapped radicals responsible for the underlying spectrum. An e.s.r. study of the trapped radicals in γ-irradiated aliphatic amines at −196 °C was recently made by Wardman and Smith (9). In the e.s.r. spectrum of trapped electrons in 3-methylpiperidine an increase in ΔH_{ms} from 14 to 17 G was observed when the sample was annealed in a temperature region of −173 to −148 °C.

Such a change in the e.s.r. spectra of the trapped electrons at an annealing temperature higher than −196 °C may be attributed to relaxation of electron trapping sites which is presumably due to re-orientation of the solvent dipoles around the trapped electrons. Similar phenomena were previously observed for trapped electrons in glassy ethanol and methyltetrahydrofuran upon warming from 4 to 77 °K after γ-irradiation at 4 °K (10, 11). Optical studies of trapped electrons in alcohol glasses also revealed the effect of such matrix relaxation on the optical absorption spectra of the trapped electrons (12–14).

1. S. NODA, K. FUEKI, and Z. KURI. Chem. Phys. Lett. **8**, 407 (1971).
2. P. J. DYNE and O. A. MILLER. Can. J. Chem. **43**, 2696 (1965).
3. T. HUANG, I. EISELE, D. P. LIN, and L. KEVAN. J. Chem. Phys. **56**, 4702 (1972).
4. A. HABERSBERGEROVÁ, L. JOSIMOVIĆ, and J. TEPLÝ. Trans. Faraday Soc. **66**, 656 (1970); **66**, 669 (1970).
5. A. BERNAS, D. GRAND, and C. CHACHATY. Chem. Commun. 1667 (1970).
6. K. KAWABATA. J. Chem. Phys. **55**, 3672 (1971).
7. P. HAMLET and L. KEVAN. J. Am. Chem. Soc. **93**, 1102 (1971).
8. H. HASE and L. KEVAN. J. Chem. Phys. **54**, 908 (1971).
9. P. WARDMAN and D. R. SMITH. Can. J. Chem. **49**, 1869 (1971).
10. D. R. SMITH and J. J. PIERONI. Can. J. Chem. **45**, 2723 (1967).
11. H. YOSHIDA and T. HIGASHIMURA. Can. J. Chem. **48**, 504 (1970).
12. H. HASE, M. NODA, and T. HIGASHIMURA. J. Chem. Phys. **54**, 2975 (1971).
13. J. T. RICHARDS and J. K. THOMAS. J. Chem. Phys. **53**, 218 (1970).
14. L. KEVAN. J. Chem. Phys. **56**, 838 (1972).

Can. J. Chem. Downloaded from www.nrcresearchpress.com by 210.87.254.40 on 09/05/12
For personal use only.

Reactivity of Organic Halides toward the Mobile Electron in Methyltetrahydrofuran Glass

NORIYUKI KATO, KENJI FUEKI, AND ZEN-ICHIRO KURI

Department of Synthetic Chemistry, Faculty of Engineering, Nagoya University, Chikusa-ku, Nagoya, Japan

Received March 28, 1972

The relative reactivity of a number of organic halides with the mobile electron produced in γ-irradiated methyltetrahydrofuran glass at 77 °K has been studied by a scavenger competition kinetics. It has been found that for the organic halides there exists a correlation between the relative electron capture cross section in the glassy matrix and the heat of reaction for dissociative electron capture estimated from gas phase data.

Nous avons étudié la réactivité relative de certains halogénures organiques vis-à-vis l'électron mobile produit en irradiant par des rayons-γ le méthyltétrahydrofuranne vitreux à 77 °K, au moyen d'une cinétique de compétition de piège. Nous avons trouvé qu'il existe, pour les halogénures organiques, une corrélation entre la surface relative de capture d'électron dans la matrice vitreuse et la chaleur de réaction dans le cas de la capture dissociative d'électron, estimée à partir des résultats en phase gazeuse.

Canadian Journal of Chemistry, **50**, 2702 (1972)

Can. J. Chem. Downloaded from www.nrcresearchpress.com by 210.87.254.6 on 09/05/12
For personal use only.

The effect of a number of different electron scavengers have been studied on both the optical and e.s.r. absorption of trapped electrons in polar glasses, such as alkaline ice (1–3), alcohols (4–12), water–alcohol mixtures (13–15), and methyltetrahydrofuran (16–25). One objective of scavenger studies has been to produce new anions from the reaction of the mobile electron with the scavenger molecule. The second objective has been to study the relative reactivity of the radiation produced mobile electron with various scavenger solutes.

In this note we report the relative cross sections of various organic halides for capturing mobile electrons (e_m^-) produced in γ-irradiated methyltetrahydrofuran (MTHF) glass at 77 °K. We also show that for the organic halides there exists a correlation between the electron capture cross section in the glassy matrix and the heat of reaction for dissociative electron capture estimated from gas phase data.

MTHF was purified by passage through a column of activated alumina, and was degassed by the freeze–pump–thaw technique and dried over calcium hydride under vacuum. MTHF was further dried with a sodium mirror prior to use. Biphenyl was purified by recrystallization from *n*-hexane. Organic halides as solutes were the purest grade commercially available. They were alkyl iodides (CH_3I, C_2H_5I, *n*-C_3H_7I, *i*-C_3H_7I, *n*-C_4H_9I), alkyl bromides (C_2H_5Br, *i*-C_3H_7Br, *n*-C_4H_9Br, *t*-C_4H_9Br), alkyl chlorides (*n*-C_3H_7Cl, *i*-C_3H_7Cl, *n*-C_4H_9Cl, *i*-C_4H_9Cl, *t*-C_4H_9Cl), and benzyl bromide and chloride.

γ-Irradiations of samples containing 0.13 mol% biphenyl and the halides at various concentrations were carried out at 77 °K in the dark to a dose of 1.04×10^4 rad. The optical absorption band of biphenyl anion with a peak at 408 nm was measured on the γ-irradiated samples at 77 °K in the dark.

The efficiencies of electron capture by the halides were determined by making use of competitive reactions between biphenyl (ϕ_2) as the reference substance and the halides (RX) as second solutes (reactions 1 and 2).

$$[1] \qquad \phi_2 + e_m^- \rightarrow \phi_2^-$$

$$[2] \qquad RX + e_m^- \rightarrow R + X^-$$

A simple competition kinetics based on reactions 1 and 2 leads to eq. 3 (16):

$$[3] \qquad \frac{1}{G_{\phi_2^-}} = \frac{1}{G^0_{\phi_2^-}} + \frac{1}{G^0_{\phi_2^-}} \frac{\sigma_{RX}[RX]}{\sigma_{\phi_2}[\phi_2]}$$

where $G_{\phi_2^-}$ and $G^0_{\phi_2^-}$ are the G-values of biphenyl anion in the presence and absence of a halide, [RX] and $[\phi_2]$ are the concentrations of the halide and the biphenyl, respectively, and σ_{RX} and σ_{ϕ_2} are the cross sections for electron capture by the halide and the biphenyl respectively. Equation 3 indicates that $1/G_{\phi_2^-}$ be linear to [RX]. It was found that several data points for each halide fit a straight line as expected from eq. 3. Figure 1 illustrates such plots for the iodides. The relative electron capture cross section, σ_{RX}, was determined from the slope of the straight line, and $G^0_{\phi_2^-}$ was obtained from

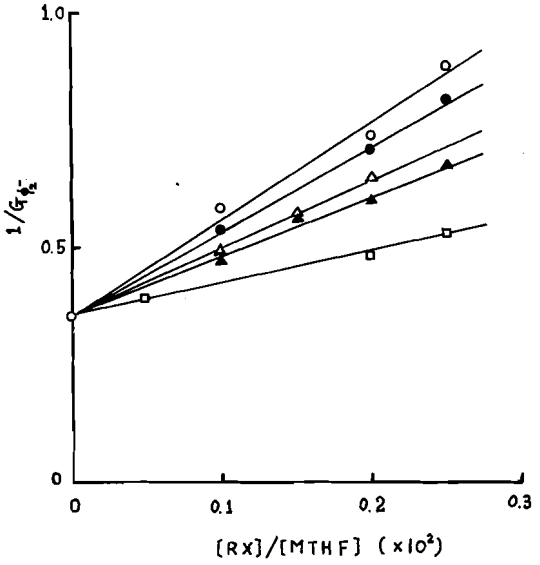

FIG. 1. Plot of $1/G_{\phi_2^-}$ *vs.* [RX]/[MTHF]: ○, *i*-C_3H_7I; ●, *n*-C_4H_9I; △, C_2H_5I; ▲, *n*-C_3H_7I; □, CH_3I. Concentration of biphenyl = 0.13 mol %.

the intercept on the ordinate by extrapolating the straight line to [RX] = 0. $G^0_{\phi_2^-}$ was 2.8 assuming that the extinction coefficient of biphenyl anion at 408 nm is 3.7×10^4 mol^{-1} cm^{-1} (17). It should be noted here that the relative electron capture cross sections of the halides are independent of the absolute *G*-value of biphenyl anion.

The values of σ_{RX} are listed in Table 1, where σ_{RX} of benzyl bromide is taken to be 1.0. In Table 1, the heats of reaction, ΔH, for dissociative electron capture by the halides in the gas phase are also given, and the rate constants for reaction of the halides with the hydrated electron (e^-_{aq}) are shown for comparison.

It can be seen in Table 1 that σ_{RX} is in decreasing order for the iodide, the bromide, and the chloride when the same type of RX is compared. A similar trend is seen for the hydrated electron rate constants, although the difference in rate constant between the iodide and the bromide is rather small and the rate constants for the chlorides are much smaller than those of the iodides and the bromides. However, within each series of the iodides, the bromides, and the chlorides, the individual values of σ_{RX} do not correspond to those of $k(e^-_{aq} + RX)$. It appears that the smaller halides have the higher rate constants for reaction with the hydrated electron. For the reaction of the halides with mobile electrons in MTHF glass, there exists a

TABLE 1. Relative electron capture cross section of organic halides in MTHF glass at 77 °K

Compound	$-\Delta H^*$ (kcal mol^{-1})	σ_{RX}	$k(e^-_{aq} + RX)$† (mol^{-1} s^{-1})
CH_3I	17	0.18	1.7×10^{10}
C_2H_5I	20	0.36	1.5×10^{10}
n-C_3H_7I	19	0.33	1.3×10^{10}
i-C_3H_7I	20	0.52	
n-C_4H_9I	20	0.45	1.2×10^{10}
C_2H_5Br	12	0.10	1.2×10^{10}
i-C_3H_7Br	13	0.13	
n-C_4H_9Br	13‡	0.12	1.0×10^{10}
t-C_4H_9Br	18	0.21	
$C_6H_5CH_2Br$	30	1.0	
n-C_3H_7Cl	5	0.03	6.9×10^8
i-C_3H_7Cl	6	0.04	
n-C_4H_9Cl	6‡	0.07	3.2×10^8
i-C_4H_9Cl	7	0.07	
t-C_4H_9Cl	8	0.08	
$C_6H_5CH_2Cl$	19	0.28	5.3×10^9

*Reference 26.
†Reference 27.
‡The values of ΔH of *n*-butyl bromide and chloride are assumed to be the same as those of *i*-propyl bromide and chloride respectively.

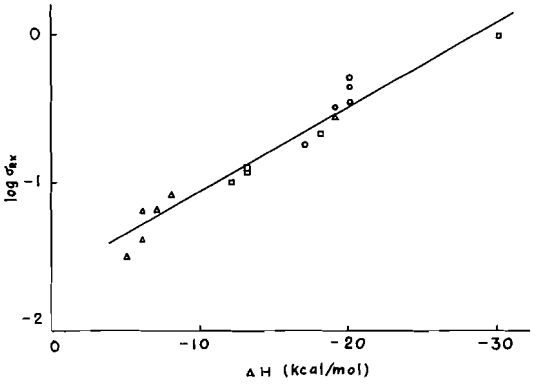

FIG. 2. Plot of $\log \sigma_{RX}$ *vs.* ΔH: ○, iodides; □, bromides; △, chlorides.

correlation between σ_{RX} and ΔH, *i.e.*, the larger the magnitude of ΔH, the higher is σ_{RX}. Figure 2 shows a plot of $\log \sigma_{RX}$ *vs.* ΔH. It is seen in Fig. 2 that there is approximately a linear relationship between these quantities.

1. K. EIBEN and D. SCHULTE-FROHLINDE. Z. Phys. Chem. **45**, 20 (1965).
2. W. A. SEDDON and D. R. SMITH. Can. J. Chem. **45**, 3083 (1967).
3. L. KEVAN. J. Am. Chem. Soc. **89**, 4238 (1967).
4. C. CHACHATY and E. HAYON. J. Chim. Phys. **61**, 1115 (1964).
5. C. CHACHATY. J. Chim. Phys. **64**, 614 (1967).
6. J. A. WARD and W. H. HAMILL. J. Am. Chem. Soc. **87**, 1853 (1965).

Can. J. Chem. Downloaded from www.nrcresearchpress.com by 210.87.254.6 on 09/05/12
For personal use only.

7. F. S. DAINTON, G. A. SALMON, and J. TEPLÝ. Proc. Roy. Soc. A**286**, 27 (1965).
8. F. S. DAINTON, G. A. SALMON, and P. WARDMAN. Proc. Roy. Soc. A**313**, 1 (1969).
9. F. S. DAINTON, G. A. SALMON, and U. F. ZUCKER. Proc. Roy. Soc. A**320**, 1 (1970).
10. F. S. DAINTON, G. A. SALMON, and U. F. ZUCKER. Proc. Roy. Soc. A**325**, 23 (1971).
11. A. HABERSBERGEROVÁ, L. JOSIMOVIĆ, and J. TEPLÝ. Trans. Faraday Soc. **66**, 656 (1970).
12. S. FUJII and J. E. WILLARD. J. Phys. Chem. **74**, 4313 (1970).
13. T. SAWAI and W. H. HAMILL. J. Phys. Chem. **73**, 2750 (1969).
14. H. B. STEEN. J. Phys. Chem. **74**, 4059 (1970).
15. H. B. STEEN, O. KAALHUS, and M. KONGSHAUG. J. Phys. Chem. **75**, 1941 (1971).
16. J. P. GUARINO, M. R. RONAYNE, and W. H. HAMILL. Radiat. Res. **17**, 379 (1962).
17. M. R. RONAYNE, J. P. GUARINO, and W. H. HAMILL. J. Am. Chem. Soc. **84**, 4230 (1962).
18. W. H. HAMILL, J. P. GUARINO, M. R. RONAYNE, and J. A. WARD. Disc. Faraday Soc. **36**, 169 (1963).
19. N. CHRISTODOULEAS and W. H. HAMILL. J. Am. Chem. Soc. **88**, 5413 (1964).
20. F. S. DAINTON and G. A. SALMON. Proc. Roy. Soc. A**285**, 319 (1965).
21. P. J. DYNE and O. A. MILLER. Can. J. Chem. **43**, 2696 (1965).
22. M. SHIROM and J. E. WILLARD. J. Phys. Chem. **72**, 1702 (1968).
23. S. NODA, K. FUEKI, and Z. KURI. Bull. Chem. Soc. Jap. **41**, 2882 (1968).
24. T. WAKAYAMA, T. KIMURA, T. MIYAZAKI, K. FUEKI, and Z. KURI. Bull. Chem. Soc. Jap. **42**, 266 (1969).
25. T. SHIDA. J. Phys. Chem. **73**, 4311 (1969).
26. V. I. VEDENEYEV, L. V. GURVICH, V. N. KONDRAT'YEV, V. A. MEDVEDEV, and YE. L. FRANKEVICH. Bond energies, ionization potentials and electron affinities. Edward Arnold Publishers, Ltd., London. 1966. J. A. KERR. Chem. Rev. **66**, 465 (1966).
27. E. J. HART and M. ANBAR. The hydrated electron. Wiley–Interscience, New York. 1970.

Hypersonic Velocities in Molten Salts by Brillouin Spectroscopy

V. C. REINSBOROUGH[1] AND J. P. VALLEAU
Lash Miller Chemical Laboratories, University of Toronto, Toronto 5, Ontario

Received April 17, 1972

Hypersonic velocities in three molten nitrates have been obtained by Brillouin spectroscopy. Velocity dispersions in molten $AgNO_3$ and $Ca(NO_3)_2 \cdot 4H_2O$ suggest that these two melts are more complex structurally than molten $NaNO_3$.

Les vitesses supersoniques dans trois nitrates fondus ont été obtenues par la spectroscopie Brillouin. Les vitesses de dispersion dans $AgNO_3$ fondu et $Ca(NO_3)_2 \cdot 4H_2O$ laissent penser que ces deux masses fondues sont plus complexes dans leurs structures que $NaNO_3$ fondu.

Canadian Journal of Chemistry, **50**, 2704 (1972)

Introduction

Frequency dispersion in sound velocity occurs in liquids when structural relaxations or other rapid processes are encountered in the frequency range under investigation. This note reports on velocity dispersion in three molten nitrates as revealed by the hypersonic velocities in these melts measured through Brillouin spectroscopy. This technique has not, as far as is known, been applied previously to molten salts.

The three melts were chosen because they are generally assumed to exhibit a wide range of structural complexity and yet do not show velocity dispersion in the ultrasonic range. Sodium nitrate is a simple ionic liquid. Physicochemical measurements in molten silver nitrate differ in many respects from such simple melts. This has been explained in terms of covalent bonding in molten silver nitrate (1–3). Molten calcium nitrate tetrahydrate is a viscous glass-former that is more complex than both of the two anhydrous nitrates.

Experimental

The Brillouin spectrometer was modelled on that of Chiao and Stoicheff (4) with modifications to be described elsewhere.[2] In short, the spectra were detected photo-

[1]Present address: Chemistry Department, Mount Allison University, Sackville, New Brunswick.

[2]R. S. Mitchell, J. P. Valleau, and J. E. Guillet. To be published.

Can. J. Chem. Downloaded from www.nrcresearchpress.com by 210.87.254.6 on 09/05/12
For personal use only.

7. F. S. DAINTON, G. A. SALMON, and J. TEPLÝ. Proc. Roy. Soc. A**286**, 27 (1965).
8. F. S. DAINTON, G. A. SALMON, and P. WARDMAN. Proc. Roy. Soc. A**313**, 1 (1969).
9. F. S. DAINTON, G. A. SALMON, and U. F. ZUCKER. Proc. Roy. Soc. A**320**, 1 (1970).
10. F. S. DAINTON, G. A. SALMON, and U. F. ZUCKER. Proc. Roy. Soc. A**325**, 23 (1971).
11. A. HABERSBERGEROVÁ, L. JOSIMOVIĆ, and J. TEPLÝ. Trans. Faraday Soc. **66**, 656 (1970).
12. S. FUJII and J. E. WILLARD. J. Phys. Chem. **74**, 4313 (1970).
13. T. SAWAI and W. H. HAMILL. J. Phys. Chem. **73**, 2750 (1969).
14. H. B. STEEN. J. Phys. Chem. **74**, 4059 (1970).
15. H. B. STEEN, O. KAALHUS, and M. KONGSHAUG. J. Phys. Chem. **75**, 1941 (1971).
16. J. P. GUARINO, M. R. RONAYNE, and W. H. HAMILL. Radiat. Res. **17**, 379 (1962).
17. M. R. RONAYNE, J. P. GUARINO, and W. H. HAMILL. J. Am. Chem. Soc. **84**, 4230 (1962).
18. W. H. HAMILL, J. P. GUARINO, M. R. RONAYNE, and J. A. WARD. Disc. Faraday Soc. **36**, 169 (1963).
19. N. CHRISTODOULEAS and W. H. HAMILL. J. Am. Chem. Soc. **88**, 5413 (1964).
20. F. S. DAINTON and G. A. SALMON. Proc. Roy. Soc. A**285**, 319 (1965).
21. P. J. DYNE and O. A. MILLER. Can. J. Chem. **43**, 2696 (1965).
22. M. SHIROM and J. E. WILLARD. J. Phys. Chem. **72**, 1702 (1968).
23. S. NODA, K. FUEKI, and Z. KURI. Bull. Chem. Soc. Jap. **41**, 2882 (1968).
24. T. WAKAYAMA, T. KIMURA, T. MIYAZAKI, K. FUEKI, and Z. KURI. Bull. Chem. Soc. Jap. **42**, 266 (1969).
25. T. SHIDA. J. Phys. Chem. **73**, 4311 (1969).
26. V. I. VEDENEYEV, L. V. GURVICH, V. N. KONDRAT'YEV, V. A. MEDVEDEV, and YE. L. FRANKEVICH. Bond energies, ionization potentials and electron affinities. Edward Arnold Publishers, Ltd., London. 1966. J. A. KERR. Chem. Rev. **66**, 465 (1966).
27. E. J. HART and M. ANBAR. The hydrated electron. Wiley–Interscience, New York. 1970.

Hypersonic Velocities in Molten Salts by Brillouin Spectroscopy

V. C. REINSBOROUGH[1] AND J. P. VALLEAU
Lash Miller Chemical Laboratories, University of Toronto, Toronto 5, Ontario

Received April 17, 1972

Hypersonic velocities in three molten nitrates have been obtained by Brillouin spectroscopy. Velocity dispersions in molten $AgNO_3$ and $Ca(NO_3)_2 \cdot 4H_2O$ suggest that these two melts are more complex structurally than molten $NaNO_3$.

Les vitesses supersoniques dans trois nitrates fondus ont été obtenues par la spectroscopie Brillouin. Les vitesses de dispersion dans $AgNO_3$ fondu et $Ca(NO_3)_2 \cdot 4H_2O$ laissent penser que ces deux masses fondues sont plus complexes dans leurs structures que $NaNO_3$ fondu.

Canadian Journal of Chemistry, **50**, 2704 (1972)

Introduction

Frequency dispersion in sound velocity occurs in liquids when structural relaxations or other rapid processes are encountered in the frequency range under investigation. This note reports on velocity dispersion in three molten nitrates as revealed by the hypersonic velocities in these melts measured through Brillouin spectroscopy. This technique has not, as far as is known, been applied previously to molten salts.

The three melts were chosen because they are generally assumed to exhibit a wide range of structural complexity and yet do not show velocity dispersion in the ultrasonic range. Sodium nitrate is a simple ionic liquid. Physicochemical measurements in molten silver nitrate differ in many respects from such simple melts. This has been explained in terms of covalent bonding in molten silver nitrate (1–3). Molten calcium nitrate tetrahydrate is a viscous glass-former that is more complex than both of the two anhydrous nitrates.

Experimental

The Brillouin spectrometer was modelled on that of Chiao and Stoicheff (4) with modifications to be described elsewhere.[2] In short, the spectra were detected photo-

[1]Present address: Chemistry Department, Mount Allison University, Sackville, New Brunswick.

[2]R. S. Mitchell, J. P. Valleau, and J. E. Guillet. To be published.

Can. J. Chem. Downloaded from www.nrcresearchpress.com by 210.87.254.6 on 09/05/12
For personal use only.

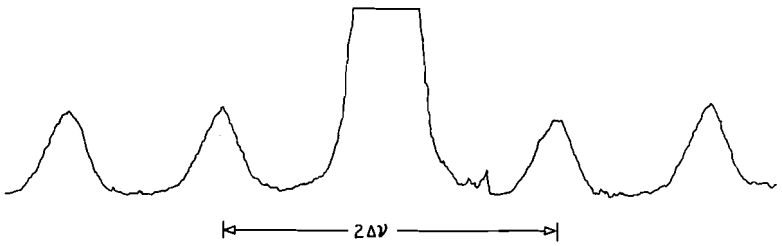

FIG. 1. Brillouin spectrum for molten $AgNO_3$ at 260° showing the truncated Rayleigh peak with its two Brillouin peaks separated by a distance $2\Delta\nu$. The Brillouin peaks of the preceding and following interferometric orders are included as well.

electrically with a high resolution Fabray–Perot interferometer that pressure-scanned light scattered from the 6328 Å laser beam as it was transmitted through the molten salt.

A thermally insulated optical cell contained the molten salt at the high temperatures employed. It consisted of a vertically mounted Pyrex cylinder 22 mm in diameter with two diametrically opposed side-arms, one serving as the light inlet and the other as a back-reflection trap (Wood's horn). Four heater coils encircled the horizontal and vertical sections of the cell. Scattered light in the range 45° to 135° could be observed by means of a horizontal viewing slit in the furnace. Temperature was noted to the nearest degree by an iron–constantan thermocouple situated in the melt, just above the slit.

Analytical grade reagents were used without purification. Considerable care was taken in filtering the melts prior to use, to minimize "dust" scattering. Calcium nitrate tetrahydrate was melted slowly in a sealed Seitz filtration vessel and then filtered by positive pressure through a 0.1 μ asbestos filter. Molten $AgNO_3$ and $NaNO_3$ were filtered by vacuum at 50° above their melting points through an ultrafine fritted disc (porosity 1 μ).

Results

The scattering consists of a triplet of a central line at the same frequency as the incident light (the Rayleigh peak) and two symmetrically located lines of changed frequency (the Brillouin peaks). Figure 1 depicts the Rayleigh and Brillouin spectra for molten $AgNO_3$ at 260°. The frequency separation of the Brillouin lines from the Rayleigh component is

$$\Delta\nu = \pm 2\nu_0\eta(V/c)\sin(\theta/2)$$

where ν_0 is the frequency of the incident light travelling at velocity c, θ is the scattering angle, and V is the hypersonic velocity in the medium of refractive index η. Precise measurements of V are made simply by measuring $\Delta\nu$ from spectra such as Fig. 1.

The scattering angle was chosen so that the Brillouin lines were midway between the Rayleigh line and the Brillouin line of the next interferometric order. This minimizes the "shrinkage effect" caused by the pulling of the spectral components towards one another (5).

TABLE 1. Hypersonic velocities in molten $NaNO_3$, $AgNO_3$, and $Ca(NO_3)_2.4H_2O$

T(°C)	Frequency (GHz)	Hypersonic velocity* ($m\,s^{-1}$)	Ultrasonic velocity ($m\,s^{-1}$)
$NaNO_3$, scattering angle: 60°			
396	4.78	1750	1720†
399	4.74	1740	1715†
419	4.65	1700	1690†
$AgNO_3$, scattering angle: 75°			
245	5.37	1752	1580‡
262	5.27	1722	1560‡
266	5.25	1720	1560‡
270	5.23	1712	1555‡
282	5.21	1706	1545‡
295	5.17	1697	1535‡
313	5.08	1671	1520‡
323	5.03	1653	1510‡
$Ca(NO_3)_2.4H_2O$, scattering angle: 60°			
29	5.84	2510	1925‡
37.5	5.41	2330	1890‡
45	5.20	2200	1870‡
61	4.72	2045	1820‡
78	4.38	1900	1800‡

*Present work.
†Reference 8.
‡Reference 9, 10.

Table 1 lists the hypersonic velocities and the frequency at which they were determined for molten $NaNO_3$ (395–400°), $AgNO_3$ (240–325°), and $Ca(NO_3)_2.4H_2O$ (25–80°). Literature values of the ultrasonic velocity are included for comparison. The refractive indices required in the calculations were taken from Rao and Angell,[3] Bloom and Rhodes (6) and Janz (7). The scattering angles were 60° for the molten hydrate and 75° for the anhydrous melts. Each

[3]K. J. Rao and C. A. Angell. Unpublished data.

Can. J. Chem. Downloaded from www.nrcresearchpress.com by 210.87.254.6 on 09/05/12
For personal use only.

velocity in Table 1 was obtained by averaging the Brillouin shifts of at least five interferometric orders. The random error was $\pm 0.5\%$ with the absolute error estimated at $\pm 1\%$ in the hypersonic velocities for the first two melts. With molten $NaNO_3$, the error was more likely $\pm 2\%$ because of the higher temperature and the more pronounced "dust" scattering. Exact centering of the cell was crucial for a 1% difference in the velocity was registered when the sample vessel was shifted a few mm off-center.

Discussion

The velocity in both the ultrasonic and hypersonic regions was the same within experimental error for molten sodium nitrate. On the other hand, for molten silver nitrate melts the hypersonic velocities were consistently 10% greater than the ultrasonic velocities from the literature. This means that a relaxation process occurs in the range 100 MHz to 5 GHz for molten silver nitrate. This difference in behavior presumably results from the occurrence of covalent bonding in the silver nitrate case. This relaxation could result from the formation of complexes, for example; or could, on the other hand, be structural relaxation due to the formation of covalent networks in the melt. The present results do not allow one to specify the details of the mechanism.

The velocity dispersion was much more temperature dependent in molten $Ca(NO_3)_2 \cdot 4H_2O$ (m.p. 42°). At 29°, the dispersion was 30% while at 70° it was only 5%. These large dispersions with large negative temperature variations are of the type observed in other highly viscous liquids such as glycerol (5). From their work with molten $Ca(NO_3)_2 \cdot 3.2H_2O$, Darbari and co-workers (11) have predicted a viscoelastic relaxation for the molten tetrahydrate in the several hundred MHz region for low temperatures where the high viscosity causes an increase in the relaxation time. Presumably, the marked velocity dispersion in the GHz region at low temperatures reflects this relaxation.

Acknowledgement is made to D. Lane and R. S. Mitchell for technical assistance and to the National Research Council of Canada for financial support.

1. V. C. Reinsborough. Aust. J. Chem. **20**, 1037 (1967).
2. B. Cleaver and B. C. J. Neil. Trans. Faraday Soc. **65**, 2860 (1969).
3. D. W. James and W. H. Leong. Trans. Faraday Soc. **66**, 1948 (1970).
4. R. Y. Chiao and B. P. Stoicheff. J. Opt. Soc. Am. **54**, 1286 (1964).
5. D. P. Eastman, A. Hollinger, J. Kennemuth, and D. H. Rank. J. Chem. Phys. **50**, 1567 (1969).
6. H. Bloom and D. C. Rhodes. J. Phys. Chem. **60**, 791 (1956).
7. G. J. Janz. Molten salts handbook. Academic Press, New York, N.Y. 1967. p. 89.
8. R. W. Higgs and T. A. Litowitz. J. Acoust. Soc. Am. **32**, 1108 (1960).
9. S. Petrucci and F. Fittipaldi. J. Acoust. Soc. Am. **42**, 517 (1967).
10. G. S. Darbari and S. Petrucci. J. Phys. Chem. **73**, 921 (1969).
11. G. S. Darbari, M. R. Richelson, and S. Petrucci. J. Chem. Phys. **55**, 4351 (1971).

Can. J. Chem. Downloaded from www.nrcresearchpress.com by 210.87.254.6 on 09/05/12
For personal use only.

Mass Spectra of β-Keto Esters

LARRY WEILER
Department of Chemistry, University of British Columbia, Vancouver 8, British Columbia

Received April 6, 1972

The mass spectra of several γ-substituted β-keto esters have been recorded and interpreted. The fragmentation patterns are compared to those of α-substituted β-keto esters and are found to be very useful in differentiating the α- and γ-substituted isomers. The mass spectral fragmentation schemes are dominated by cleavages α to the carbonyl groups and by McLafferty rearrangements.

Les spectres de masse de plusieurs β-cétoesters γ-substitués ont été enregistrés et interprétés. La comparaison des spectres de fragmentation avec ceux des β-cétoesters α-substitués a été très utile pour différencier les isomères α et γ. Les schémas de fragmentation sont dominés par les clivages en α des groupes carbonyles et par les réarrangements de McLafferty.

Canadian Journal of Chemistry, **50**, 2707 (1972)

Can. J. Chem. Downloaded from www.nrcresearchpress.com by 210.87.254.6 on 09/05/12
For personal use only.

Recently we developed a useful synthetic route to a variety of γ-substituted β-keto esters (**1**). In the course of this study it was imperative to demonstrate that we had obtained the γ-substituted isomer (**1**) and not the α-substituted isomer (**2**). We have found that mass spectrometry can be very useful in distinguishing the two isomers. A comparison of the mass spectra of **1** (R = R′ = Me) and **2** (R = R′ = Me) reveals that there are gross differences in the two spectra which should aid the structural assignments. Bowie *et al.* (2) measured the mass spectra of a small number of α-substituted β-keto esters **2** (R = alkyl, R′ = Et). They found that the major fragmentation pathways follow two different McLafferty rearrangements and simple α-cleavage to give a base peak at *m/e* 43 (CH_3CO). Later Reed and Takhistov extended this study to a larger number of esters **2** (R = alkyl, R′ = Et, Me) (3). These later workers arrived at essentially the same fragmentation pathway.

The mass spectra of several γ-substituted β-keto esters (**1**) which we have prepared are given in Table 1. Schemes 1 and 2 account for

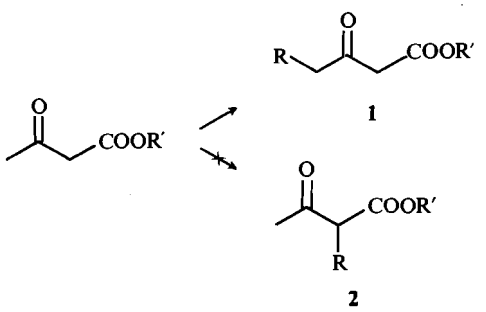

1

2

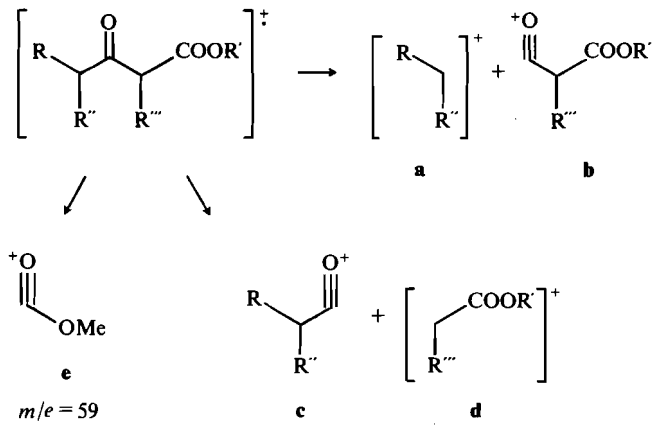

SCHEME 1. α-Cleavage of β-keto esters.

Can. J. Chem. Downloaded from www.nrcresearchpress.com by 210.87.254.6 on 09/05/12
For personal use only.

TABLE 1. Mass spectra of $RCH(R'')-CO-CH(R''')-CO_2R'$ at 70 eV

R	R′	R″	R‴																									
Me	Me	H	H	*m/e*	41	42	43	45	57	59	69	74	78	99	101	130												
				%	6	15	28	11	100	35	16	6	7	7	22	12												
Et	Me	H	H	*m/e*	41	42	43	57	59	69	71	74	84	85	101	113	116	129	144									
				%	28	22	100	12	32	20	90	8	8	6	40	6	11	2	12									
i-Pr	Me	H	H	*m/e*	41	42	43	57	59	69	74	84	85	101	116	127	143	158										
				%	48	20	53	100	34	33	23	26	98	57	50	7	14	16										
n-Bu	Me	H	H	*m/e*	41	42	43	55	56	57	59	69	71	74	84	85	99	101	116	117	129	130	141	143	154	172		
				%	32	23	100	23	16	13	36	25	35	37	27	15	55	39	82	14	19	6	4	2	3	5		
Allyl	Me	H	H	*m/e*	41	42	43	54	55	57	59	69	74	82	83	85	96	101	124	125	138	156						
				%	25	23	74	48	100	18	51	33	7	58	39	6	8	46	17	5	2	11						
Benzyl	Me	H	H	*m/e*	41	43	51	55	59	63	65	74	77	78	79	85	91	92	101	103	104	105	106	117	133	148	159	182	206
				%	15	20	24	11	6	10	18	3	25	18	15	24	100	10	10	11	17	98	11	24	17	67	2	1	1
Allyl	Et	H	H	*m/e*	41	42	43	53	54	55	60	68	69	79	81	82	83	87	96	101	115	124	125	130	142	152	156	170	
				%	46	39	83	21	62	100	10	13	59	6	11	56	43	39	16	4	19	14	6	1	2	1	1	11	
Et	Et	H	Me	*m/e*	43	47	48	49	57	71	83	84	85	87	102	115	118	120	130	172									
				%	12	24	11	9	8	7	100	7	66	11	3	2	3	3	2	1									
H	Me	H	Me	*m/e*	41	43	56	57	59	70	83	87	88	98	99	130												
				%	5	100	6	23	10	3	3	7	36	3	9	5												
Benzyl	Me	Me	H	*m/e*	42	51	59	65	69	74	77	78	91	92	101	103	104	105	118	119	128	131	132	142	146	147	163	175	
				%	12	6	11	11	9	3	6	4	100	9	18	3	4	3	19	11	3	4	6	4	11	14	1	1	
				m/e	188	189	202	205	220																			
				%	2	1	1	1	12																			
Benzyl	Me	*n*-Bu	H	*m/e*	41	43	55	59	65	69	74	91	92	101	104	105	117	128	130	131	132	145	153	160	161	173	188	189	205
				%	11	6	7	11	8	11	2	100	10	21	12	7	10	5	6	21	6	4	15	4	2	3	4	8	32
				m/e	206	219	220	244	262																			
				%	9	1	1	2	9																			
Allyl	Me	*n*-Bu	H	*m/e*	41	42	43	54	55	56	57	59	67	69	71	74	81	82	83	84	85	91	95	96	97	98	99	101	
				%	87	25	86	18	66	19	23	55	14	80	30	41	20	48	12	39	10	10	12	11	22	20	52	94	
				m/e	110	111	116	117	124	129	130	138	139	141	155	156	169	172	181	212									
				%	6	9	100	12	14	26	14	13	11	8	13	34	11	9	2	7									

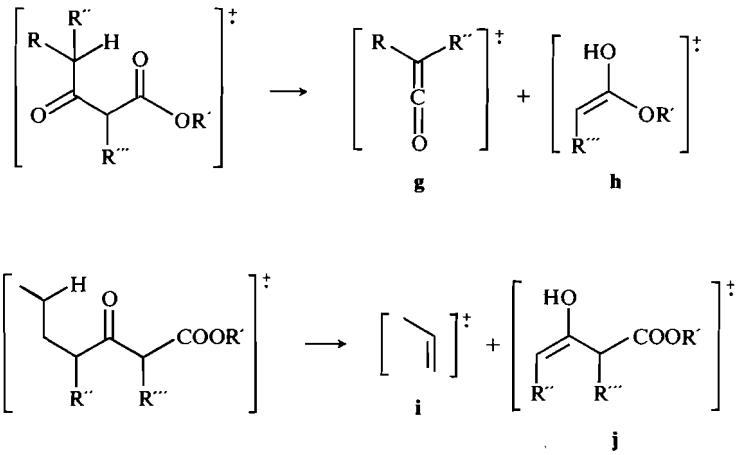

SCHEME 2. McLafferty rearrangements of β-keto esters.

most of the significant ions observed. There is α-cleavage to the keto group to give ion **a** which is always significant and ion **b** (R‴ = H, R′ = Me; *m/e* = 101) which is a major ion in the case of the methyl esters. Ion **c** also is a significant fragment in each spectra, but ion **d** is not usually significant. The compounds which do not contain a phenyl group have peaks at *m/e* = M − OR′ and, in addition, the methyl esters which lack a phenyl group have significant peaks at *m/e* 59. This corresponds to ion **e**. The dominant peaks in the spectra of the compounds containing the phenyl group are ions with this moiety, for example, ion **f** (R″ = H, Me, *n*-Bu). The alkyl and allyl compounds also have relatively abundant ions arising from either of the McLafferty cleavages shown in Scheme 2. Ions **g**–**j** usually appear in the mass spectra of the

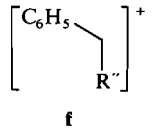

f

compounds which do not contain a phenyl group. Most of the remaining peaks in the spectra of these compounds arise from fragmentations of ions **a**–**j**. For example, the large peak at *m/e* 43 is due to ion **k**.

A few of the molecular ions lose water to give weak (M − 18) peaks and fragment ions from this. Not surprisingly we could not correlate the intensity of the (M − 18) peak with the enol content of the neutral molecule in solution from

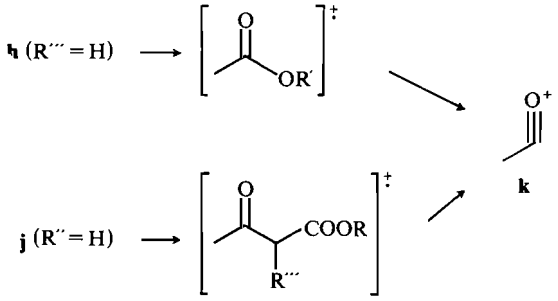

n.m.r. data. Only the esters with an allyl group had peaks due to ion **m** (M − R′OH) and in each case ion **m** readily lost CO. Although we have written **m** as an open-chain ion it may in fact be cyclic. This might explain why only the allyl derivatives have this mode of fragmentation. It is also noteworthy that the α-substituted allyl derivative **2** (R = allyl, R′ = Et) did not readily lose EtOH and then CO (3). In most

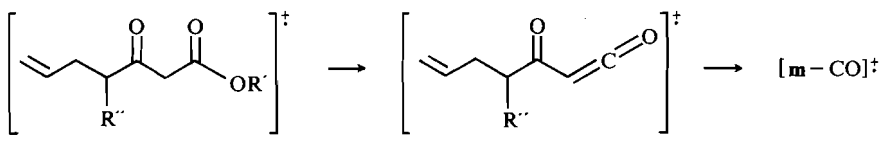

m

Can. J. Chem. Downloaded from www.nrcresearchpress.com by 210.87.254.6 on 09/05/12
For personal use only.

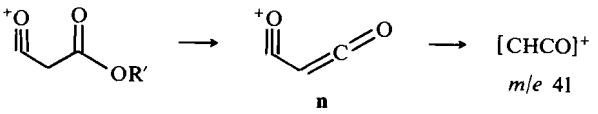

n

compounds the peak at *m/e* 69 is due to ion **n**. High resolution measurements showed that the peak at 69 often was a doublet with composition C_3HO_2 and C_5H_9. Ion **n** readily loses CO to give a fragment at *m/e* 41.

In most cases the composition of the ions discussed was verified by high resolution measurements and in some cases the fragmentation paths were corroborated by a metastable analysis. Thus we can say that the mass spectra of a large number of β-keto esters fit the fragmentation pathways shown, and we can utilize the mass spectral data to determine the substitution pattern in β-keto esters.

Experimental

All of the mass spectral data were recorded on an AEI-MS 9 operating with a source temperature of 200° and an ionizing voltage of 70 eV.

The preparation and analytical data for the β-keto esters have been reported (1).

I am grateful to the Research Corporation and the National Research Council of Canada for financial support.

1. L. WEILER. J. Am. Chem. Soc. **92**, 6702 (1970).
2. J. H. BOWIE, S.-O. LAWESSON, G. SCHROLL, and D. H. WILLIAMS. J. Am. Chem. Soc. **87**, 5742 (1965).
3. R. I. REED and V. V. TAKHISTOV. Tetrahedron, **23**, 2807, 4425 (1967).

INDO MO Calculations of the Conformational Dependence of the vicinal $^{13}C,H$ Spin–Spin Coupling Constant in Propane

R. WASYLISHEN AND T. SCHAEFER

Department of Chemistry, University of Manitoba, Winnipeg, Manitoba R3T 2N2

Received March 21, 1972

Molecular orbital theory at the INDO level of approximation is used to calculate the Fermi contact contribution to three-bond carbon–proton coupling constants in propane. The calculations predict a dihedral angle dependence of $^3J(^{13}C,H)$ in the $^{13}C—C—C—H$ fragment similar to that observed for $^3J(,H,H)$, $^3J(^{19}F,H)$, and for $^3J(^{31}P,H)$ in the saturated X—C—C—H fragments.

La théorie des orbitales moléculaires au niveau des approximations INDO, est utilisée pour calculer la contribution du "Fermi-contact" aux constantes de couplage des trois liaisons carbone–hydrogène, dans le propane. Les calculs laissent prévoir une dépendance diédrale angulaire de $^3J(^{13}C,H)$ dans le fragment $^{13}C—C—C—H$ semblable à celle observée pour $^3J(H,H)$, $^3J(^{19}F,H)$, et pour $^3J(^{31}P,H)$ dans les fragments saturés X—C—C—H.

Canadian Journal of Chemistry, **50**, 2710 (1972)

The famous Karplus relationship (1), relating the proton–proton spin–spin coupling constant in the fragment H—C—C—H to the dihedral angle, has been extensively applied to the study of molecular conformations. Its applicability has recently been reviewed by Thomas (2) and by Booth (3). Similar relationships have been explored experimentally and sometimes theoretically in the fragments $^{19}F—C—C—H$ (4–6), $^{31}P—C—C—H$ (7, 8), $H—C—N^+—H$ (9), $^{15}N—C—C—H$ (8), and H—C—O—H (10–12). The finite perturbation technique in the INDO formulation of molecular orbital theory has been successful in at least qualitatively reproducing the known behavior of the coupling constants in the fragments H—C—C—H (13), $^{19}F—C—C—H$ (5, 6), and $^{15}N—C—C—H$ (6).

In view of the recent interest in organic ^{13}C magnetic resonance spectroscopy we have calculated the conformational dependence of the vicinal $^{13}C,H$ coupling in propane using the INDO formulation (14–16) in the manner we

Can. J. Chem. Downloaded from www.nrcresearchpress.com by 210.87.254.6 on 09/05/12
For personal use only.

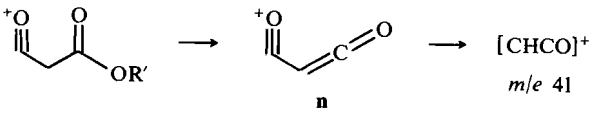

n

compounds the peak at *m/e* 69 is due to ion **n**. High resolution measurements showed that the peak at 69 often was a doublet with composition C_3HO_2 and C_5H_9. Ion **n** readily loses CO to give a fragment at *m/e* 41.

In most cases the composition of the ions discussed was verified by high resolution measurements and in some cases the fragmentation paths were corroborated by a metastable analysis. Thus we can say that the mass spectra of a large number of β-keto esters fit the fragmentation pathways shown, and we can utilize the mass spectral data to determine the substitution pattern in β-keto esters.

Experimental

All of the mass spectral data were recorded on an AEI-MS 9 operating with a source temperature of 200° and an ionizing voltage of 70 eV.

The preparation and analytical data for the β-keto esters have been reported (1).

I am grateful to the Research Corporation and the National Research Council of Canada for financial support.

1. L. WEILER. J. Am. Chem. Soc. **92**, 6702 (1970).
2. J. H. BOWIE, S.-O. LAWESSON, G. SCHROLL, and D. H. WILLIAMS. J. Am. Chem. Soc. **87**, 5742 (1965).
3. R. I. REED and V. V. TAKHISTOV. Tetrahedron, **23**, 2807, 4425 (1967).

INDO MO Calculations of the Conformational Dependence of the vicinal $^{13}C,H$ Spin–Spin Coupling Constant in Propane

R. WASYLISHEN AND T. SCHAEFER

Department of Chemistry, University of Manitoba, Winnipeg, Manitoba R3T 2N2

Received March 21, 1972

Molecular orbital theory at the INDO level of approximation is used to calculate the Fermi contact contribution to three-bond carbon–proton coupling constants in propane. The calculations predict a dihedral angle dependence of $^3J(^{13}C,H)$ in the $^{13}C—C—C—H$ fragment similar to that observed for $^3J(,H,H)$, $^3J(^{19}F,H)$, and for $^3J(^{31}P,H)$ in the saturated X—C—C—H fragments.

La théorie des orbitales moléculaires au niveau des approximations INDO, est utilisée pour calculer la contribution du "Fermi-contact" aux constantes de couplage des trois liaisons carbone–hydrogène, dans le propane. Les calculs laissent prévoir une dépendance diédrale angulaire de $^3J(^{13}C,H)$ dans le fragment $^{13}C—C—C—H$ semblable à celle observée pour $^3J(H,H)$, $^3J(^{19}F,H)$, et pour $^3J(^{31}P,H)$ dans les fragments saturés X—C—C—H.

Canadian Journal of Chemistry, **50**, 2710 (1972)

The famous Karplus relationship (1), relating the proton–proton spin–spin coupling constant in the fragment H—C—C—H to the dihedral angle, has been extensively applied to the study of molecular conformations. Its applicability has recently been reviewed by Thomas (2) and by Booth (3). Similar relationships have been explored experimentally and sometimes theoretically in the fragments $^{19}F—C—C—H$ (4–6), $^{31}P—C—C—H$ (7, 8), $H—C—N^+—H$ (9), $^{15}N—C—C—H$ (8), and H—C—O—H (10–12). The finite perturbation technique in the INDO formulation of molecular orbital theory has been successful in at least qualitatively reproducing the known behavior of the coupling constants in the fragments H—C—C—H (13), $^{19}F—C—C—H$ (5, 6), and $^{15}N—C—C—H$ (6).

In view of the recent interest in organic ^{13}C magnetic resonance spectroscopy we have calculated the conformational dependence of the vicinal $^{13}C,H$ coupling in propane using the INDO formulation (14–16) in the manner we

Can. J. Chem. Downloaded from www.nrcresearchpress.com by 210.87.254.40 on 09/05/12
For personal use only.

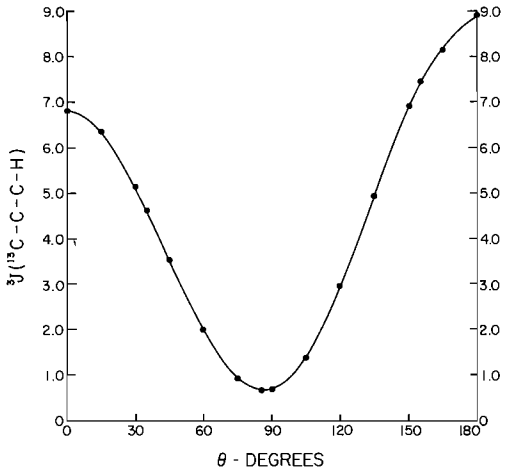

FIG. 1. The calculated vicinal coupling constant in Hz between the carbon-13 nucleus and the proton in propane is plotted *vs.* the dihedral angle in the fragment $^{13}C—C—C—H$. A staggered conformation is assumed for the $^{13}CH_3$ group.

have previously described (17, 18) for other molecules. Atomic coordinates were calculated using the standard geometrical model of Pople and Gordon (19).

In Fig. 1 the computed coupling is plotted *vs.* the dihedral angle in the fragment $^{13}C—C—C—H$. In Table 1 the computed values are given at intervals of 15° or less of the dihedral angle. The curve in Fig. 1 can be reproduced to within 0.03 Hz by the equation:

$$^3J(^{13}C,H) = 4.26 - 1.00 \cos\theta + 3.56 \cos 2\theta$$

where θ is the dihedral angle. As pointed out by a referee, this formula is easy to use in that 4.26 Hz corresponds to the average coupling constant for free rotation, while 2×1.00 Hz is the difference between the couplings at $\theta = 0$ and 180°.

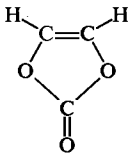

1

The close resemblance of the computed curve to those known for analogous vicinal couplings (minimum at approximately 90°, maxima at 0 and 180°) implies its potentially wide applicability in structural studies. At present almost no relevant experimental data, for example, for cyclohexane derivatives, is available. However, the temperature dependence of the proton spectra of propionaldehyde-3-^{13}C and its oxime indicates that *trans* $J(^{13}C—C—C—H)$ is greater than the *gauche* coupling (20), corresponding to $\theta = 180$ and 60°, respectively. The vicinal $^{13}C,H$ coupling in benzene is 7.4 Hz (21) where $\theta = 180°$ and INDO finds 9.4 Hz (15). In vinylene carbonate, **1**, we calculate[1] (6) the vicinal coupling $^3J(^{13}C—O—C—H)$ as 8.35 Hz, whereas the observed value is ± 9.26 Hz (23) and θ is again 180°.

Comparison of the last two examples with the computed data in Table 1 and Fig. 1 suggests a degree of insensitivity of the vicinal $^{13}C,H$ coupling to the hybridization state of the carbon atoms as well as to substituent effects. Further experimental and computational investigation of these effects is clearly in order.

TABLE 1. The calculated $^{13}C,H$ coupling in Hz over three bonds in propane as a function of the dihedral angle, θ

Angle (deg)	$^3J(^{13}C—C—C—H)$	Angle (deg)	$^3J(^{13}C—C—C—H)$
0	6.82	105	1.41
15	6.36	120	2.95
30	5.15	135	4.96
35	4.63	150	6.91
45	3.54	155	7.46
60	2.00	165	8.31
75	0.94	180	8.81
85	0.68		
90	0.70		

We are grateful to a referee for the proper formulation of the above equation and to the National Research Council of Canada for financial assistance.

1. M. KARPLUS. J. Chem. Phys. **30**, 11 (1959); J. Am. Chem. Soc. **85**, 2870 (1965).
2. W. A. THOMAS. Ann. Rep. NMR Spectrosc. **1**, 44 (1968); **3**, 1 (1970).
3. H. BOOTH. Prog. NMR Spectrosc. **5**, 149 (1969).
4. K. L. WILLIAMSON, Y.-F. LI HSU, F. H. HALL, S. SWAGER, and M. S. COULTER. J. Am. Chem. Soc. **90**, 6717 (1968).

[1]The geometry is taken from recent microwave data (22). The other computed values are $^1J(^{13}C,H) = 202.90$ (220.15), $^2J(^{13}C,H) = 4.36$ (17.45), $^3J(H,H) = 1.60$ (1.47) Hz, $\mu = 4.35$ (4.51) D, where the observed (23) quantities are given in brackets.

Can. J. Chem. Downloaded from www.nrcresearchpress.com by 210.87.254.40 on 09/05/12
For personal use only.

5. M. S. GOPINATHAN and P. T. NARASIMHAN. Mol. Phys. **21**, 1141 (1971).
6. R. WASYLISHEN. Unpublished calculations.
7. L. EVELYN, L. D. HALL, P. R. STEINER, and D. H. STOKES. Chem. Commun. 576 (1969).
8. A. A. BOTHNER-BY and R. H. COX. J. Phys. Chem. **73**, 1830 (1969).
9. W. F. REYNOLDS and T. SCHAEFER. Can. J. Chem. **42**, 2119 (1964).
10. N. L. BAULD and Y. S. RIM. J. Org. Chem. **33**, 1303 (1968).
11. R. D. STORVLOW and A. A. GALLO. Tetrahedron Lett. 3331 (1968).
12. E. F. KIEFER, W. GERICKE, and S. T. AMIMOTO. J. Am. Chem. Soc. **90**, 6246 (1968).
13. G. E. MACIEL, J. W. MCIVER, JR., N. S. OSTLUND, and J. A. POPLE. J. Am. Chem. Soc. **92**, 4151, 4497 (1970).
14. J. A. POPLE, J. W. MCIVER, JR., and N. S. OSTLUND. Chem. Phys. Lett. **1**, 465 (1967).
15. J. A. POPLE and D. L. BEVERIDGE. Approximate molecular orbital theory. McGraw-Hill Book Co., New York. 1970.
16. P. A. DOBOSH. Program No. 141 QCPE. Indiana University, Bloomington, Ind. 47401.
17. R. WASYLISHEN and T. SCHAEFER. Can. J. Chem. **49**, 3216 (1971).
18. R. WASYLISHEN and T. SCHAEFER. Can J. Chem. **50**, 1852 (1972).
19. J. A. POPLE and M. GORDON. J. Am. Chem. Soc. **89**, 4253 (1967).
20. G. J. KARABATSOS, C. E. ORZECH, and N. HSI. J. Am. Chem. Soc. **88**, 1817 (1966).
21. F. J. WEIGERT and J. D. ROBERTS. J. Am. Chem. Soc. **89**, 2967 (1967).
22. W. F. WHITE and J. E. BOGGS. J. Chem. Phys. **54**, 4714 (1971).
23. K. A. MCLAUCHLAN and T. SCHAEFER. Can. J. Chem. **44**, 321 (1966).

Steroids and Steroidases. XVI.[1] An Evaluation of Synthetic Routes to Variously C-17-Substituted Δ^5-3-Ketosteroids

J. BRYAN JONES AND KEITH D. GORDON

Lash Miller Chemical Laboratories, Department of Chemistry, University of Toronto, Toronto 181, Ontario

Received April 24, 1972

Several routes to variously C-17-substituted Δ^5-3-ketosteroids have been surveyed. The most convenient method was found to be oxidation of Δ^5-3β-alcohol precursors with the Collins reagent, dipyridine chromium trioxide in methylene chloride. The purities of the desired acid- and base-labile compounds obtained were $\geqslant$99% in each case.

Plusieurs voies d'accès aux divers Δ^5 céto-3 stéroides C-17 substitués ont été examinées. La méthode la plus commode est l'oxydation de précurseurs Δ^5 alcool-3β avec le réactif de Collins, le trioxyde de chrome dipyridine dans le chlorure de méthylène. Les puretés des composés obtenus labiles en milieu acide et basique sont supérieures à 99% dans tout les cas.

Canadian Journal of Chemistry, **50**, 2712 (1972)

Our previous studies (1) on the influence of the C-17 group on micelle formation of Δ^5-3-ketosteroids in aqueous solutions, and on the consequences of such aggregation with respect to the specificity of a Δ^5-3-ketosteroid isomerase, prompted us to undertake a more systematic investigation of such C-17-substituent effects. For the aggregation and enzymic studies projected, steroid-5-en-3-ones possessing C-17 groups intermediate in polarity and steric bulk between the oxo function of the standard substrate androst-5-ene-3,17-dione (**3***a*) and the C_8H_{17} group of cholest-5-en-3-one (**3***h*) were desired and the range of substitution patterns considered is recorded in Scheme 1.

At the time this investigation was begun the most convenient general approaches to the extremely labile Δ^5-3-keto steroid structures were by Pfitzner–Moffatt oxidation (1–3) of the corresponding Δ^5-3β-alcohols (**1**) or by deconjugation (1, 4) of the isomeric Δ^4-3-ketones (**2**). Of the precursor compounds **1** and/or **2** required, those needed for the preparation of all the desired Δ^5-3-ketones except **3***c*, *f*, and *g* were

[1]For part XV, see ref. 26. Abstracted from the theses submitted by K. D. G. in partial fulfillment of the requirements for the degrees of M.Sc. (University of Toronto, 1968) and Ph.D. (University of Toronto, 1971). Presented in part in the Enzyme Action session of the 54th Canadian Chemical Conference of the Chemical Institute of Canada, Halifax, May 31, 1970.

Can. J. Chem. Downloaded from www.nrcresearchpress.com by 210.87.254.40 on 09/05/12
For personal use only.

5. M. S. GOPINATHAN and P. T. NARASIMHAN. Mol. Phys. **21**, 1141 (1971).
6. R. WASYLISHEN. Unpublished calculations.
7. L. EVELYN, L. D. HALL, P. R. STEINER, and D. H. STOKES. Chem. Commun. 576 (1969).
8. A. A. BOTHNER-BY and R. H. COX. J. Phys. Chem. **73**, 1830 (1969).
9. W. F. REYNOLDS and T. SCHAEFER. Can. J. Chem. **42**, 2119 (1964).
10. N. L. BAULD and Y. S. RIM. J. Org. Chem. **33**, 1303 (1968).
11. R. D. STORVLOW and A. A. GALLO. Tetrahedron Lett. 3331 (1968).
12. E. F. KIEFER, W. GERICKE, and S. T. AMIMOTO. J. Am. Chem. Soc. **90**, 6246 (1968).
13. G. E. MACIEL, J. W. MCIVER, JR., N. S. OSTLUND, and J. A. POPLE. J. Am. Chem. Soc. **92**, 4151, 4497 (1970).
14. J. A. POPLE, J. W. MCIVER, JR., and N. S. OSTLUND. Chem. Phys. Lett. **1**, 465 (1967).
15. J. A. POPLE and D. L. BEVERIDGE. Approximate molecular orbital theory. McGraw-Hill Book Co., New York. 1970.
16. P. A. DOBOSH. Program No. 141 QCPE. Indiana University, Bloomington, Ind. 47401.
17. R. WASYLISHEN and T. SCHAEFER. Can. J. Chem. **49**, 3216 (1971).
18. R. WASYLISHEN and T. SCHAEFER. Can J. Chem. **50**, 1852 (1972).
19. J. A. POPLE and M. GORDON. J. Am. Chem. Soc. **89**, 4253 (1967).
20. G. J. KARABATSOS, C. E. ORZECH, and N. HSI. J. Am. Chem. Soc. **88**, 1817 (1966).
21. F. J. WEIGERT and J. D. ROBERTS. J. Am. Chem. Soc. **89**, 2967 (1967).
22. W. F. WHITE and J. E. BOGGS. J. Chem. Phys. **54**, 4714 (1971).
23. K. A. MCLAUCHLAN and T. SCHAEFER. Can. J. Chem. **44**, 321 (1966).

Steroids and Steroidases. XVI.[1] An Evaluation of Synthetic Routes to Variously C-17-Substituted Δ^5-3-Ketosteroids

J. BRYAN JONES AND KEITH D. GORDON

Lash Miller Chemical Laboratories, Department of Chemistry, University of Toronto, Toronto 181, Ontario

Received April 24, 1972

Several routes to variously C-17-substituted Δ^5-3-ketosteroids have been surveyed. The most convenient method was found to be oxidation of Δ^5-3β-alcohol precursors with the Collins reagent, dipyridine chromium trioxide in methylene chloride. The purities of the desired acid- and base-labile compounds obtained were $\geqslant 99\%$ in each case.

Plusieurs voies d'accès aux divers Δ^5 céto-3 stéroides C-17 substitués ont été examinées. La méthode la plus commode est l'oxydation de précurseurs Δ^5 alcool-3β avec le réactif de Collins, le trioxyde de chrome dipyridine dans le chlorure de méthylène. Les puretés des composés obtenus labiles en milieu acide et basique sont supérieures à 99% dans tout les cas.

Canadian Journal of Chemistry, **50**, 2712 (1972)

Our previous studies (1) on the influence of the C-17 group on micelle formation of Δ^5-3-ketosteroids in aqueous solutions, and on the consequences of such aggregation with respect to the specificity of a Δ^5-3-ketosteroid isomerase, prompted us to undertake a more systematic investigation of such C-17-substituent effects. For the aggregation and enzymic studies projected, steroid-5-en-3-ones possessing C-17 groups intermediate in polarity and steric bulk between the oxo function of the standard substrate androst-5-ene-3,17-dione (**3***a*) and the C_8H_{17} group of cholest-5-en-3-one (**3***h*) were desired and the range of substitution patterns considered is recorded in Scheme 1.

At the time this investigation was begun the most convenient general approaches to the extremely labile Δ^5-3-keto steroid structures were by Pfitzner–Moffatt oxidation (1–3) of the corresponding Δ^5-3β-alcohols (**1**) or by deconjugation (1, 4) of the isomeric Δ^4-3-ketones (**2**). Of the precursor compounds **1** and/or **2** required, those needed for the preparation of all the desired Δ^5-3-ketones except **3***c*, *f*, and *g* were

[1]For part XV, see ref. 26. Abstracted from the theses submitted by K. D. G. in partial fulfillment of the requirements for the degrees of M.Sc. (University of Toronto, 1968) and Ph.D. (University of Toronto, 1971). Presented in part in the Enzyme Action session of the 54th Canadian Chemical Conference of the Chemical Institute of Canada, Halifax, May 31, 1970.

Can. J. Chem. Downloaded from www.nrcresearchpress.com by 210.87.254.105 on 09/05/12
For personal use only.

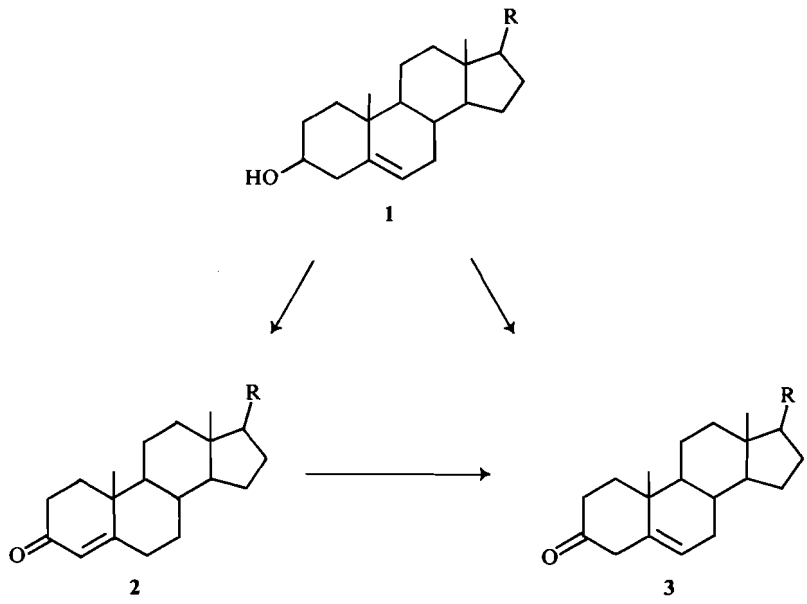

a R = O
b R = H
c R = CH_3
d R = $COCH_3$
e R = CH_2CH_3
f R = $CH(CH_3)_2$
g R = $CH(CH_3)CH_2CH_3$
h R = C_8H_{17}

SCHEME 1

readily available (see Experimental). Attention was thus concentrated initially on the preparation of the C-17β-methyl, -isopropyl, and -isobutyl Δ^5-3β-ol-intermediates, **1***c*, *f*, and *g*.

17β-Methylandrost-5-en-3β-ol (**1***c*) was obtained as outlined in Scheme 2. Conversion of 3β-hydroxyandrost-5-en-17-one (**1***a*) to the 17-methylene derivative **4***a* was effected smoothly by the standard Wittig procedure and following acetylation of the reaction mixture, the 3β-acetate **4***a* was obtained in 67% yield (5). Hydrolysis of **4***a* with methanolic potassium hydroxide afforded **4***b* in 90% yield. In view of the literature data on the less-substituted double bond reduction preference of tris(triphenylphosphine)rhodium catalysts (6–9) and the α-face addition of hydrogen to be anticipated for steroid olefins (7, 8), selective and stereospecific reduction of **4***b* to the 17β-methyl compound **1***c* was expected using the above catalyst. However, although reduction of the C-17,20 double bond occurred exclusively, a mixture of the C-17 methyl epimers was formed as evidenced by the two C-20 doublets at δ 0.78 and 0.83 p.p.m. in the n.m.r. spectrum of the product. Selective hydrogenation of **4***b* with a 5% palladium – calcium carbonate catalyst (10) also gave a thin-layer chromatographically inseparable mixture

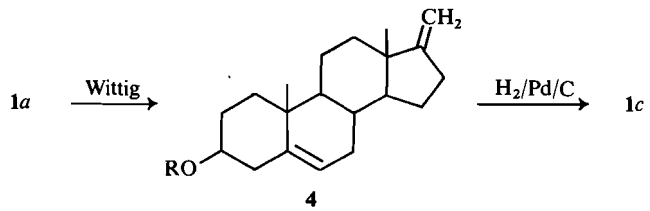

a R = Ac
b R = H

SCHEME 2

Can. J. Chem. Downloaded from www.nrcresearchpress.com by 210.87.254.105 on 09/05/12
For personal use only.

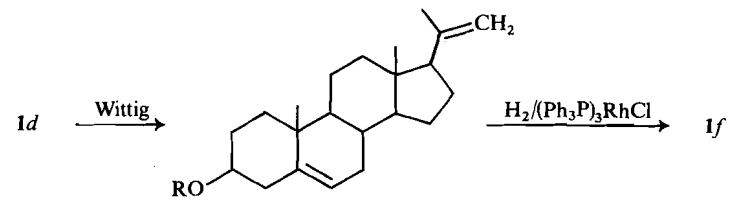

5

a R = Ac
b R = H

SCHEME 3

of the two epimers in which the 17β-methyl isomer (δ 0.83 p.p.m.) predominated.[2] Selective and stereospecific α-face hydrogenation of **4***b* to give **1***c* in 84% yield was finally effected using 10% palladium–charcoal as the catalyst. 20-Methylpregn-5-en-3β-ol (**1***f*) was prepared similarly (Scheme 3) from **1***d* with the acetylated Wittig reaction product **5***a* being obtained in 62% yield. Following its hydrolysis to **5***b* (86% yield) selective hydrogenation of the Δ^{20}-double bond to give **1***f* was achieved almost quantitatively with the tris(triphenylphosphine)rhodium chloride catalyst.

An attempt was also made to introduce a C-17 sec-butyl substituent by a route analogous to that outlined in Scheme 3. Pregnenolone (**1***d*) was reacted with the Wittig reagent derived from ethyltriphenylphosphonium bromide to give a mixture containing the Z- and E-isomers of 20-ethylpregna-5,20-dien-3β-ol which could not be separated by a variety of chromatographic methods. Neither of the trisubstituted double bonds of the latter was reducible using the rhodium catalyst and hydrogenation in the presence of palladium–calcium carbonate resulted in saturation of both the Δ^5 and Δ^{20} bonds. Although application of 5% palladium–charcoal as a catalyst did afford some selectivity of reduction, the results generally were discouraging and in view of the further difficulties anticipated in separating the C-20,22 diastereomers of the desired product, attempts to prepare **1***g* were discontinued.

In previous applications of the Pfitzner–Moffatt oxidation procedure to the Δ^5-3β-ols **1***a*, *b*, and *h*, good yields of the corresponding βγ-unsaturated ketones had been obtained (3). However, on treatment of the 17-alkyl analogues **1***c*, *e*, and *f* under the same conditions the reactions were incomplete. When the slightly more vigorous conditions required to achieve oxidation of the majority of the starting alcohols were applied, extensive contamination of the desired Δ^5-3-keto products by the conjugated isomers was observed. Accordingly, the alternative deconjugation route (1, 4) to **3***c*, *e*, and *f* was explored.

The starting Δ^4-3-ketosteroids **2***c*, *e*, and *f* required were obtained in 75–90% yields by Oppenauer oxidation of **1***c*, *e*, and *f* respectively. Our experience (1) with the potassium *t*-butoxide-mediated deconjugation of several steroid-Δ^4-3-ketones had shown that the reactions could be carried out in air to give the corresponding βγ-unsaturated ketones uncontaminated by their conjugated isomers or by C-4 or -6 oxygenated by-products (11, 12). In contrast, when similar conditions were applied to the C-17-isopropyl Δ^4-3-ketone **2***f*, none of the expected unconjugated isomer **3***f* was formed. Instead, a 30% yield of 4-hydroxy-20-methylpregn-4,6-dien-3-one (**6**) was obtained. Although prior deoxygenation of the solutions and carrying out the deconjugation in an oxygen-free nitrogen atmosphere suppressed the formation of the 4-hydroxylated derivative to a large extent, the Δ^5-3-keto product **3***f* obtained was always contaminated with small but significant amounts of **6**. The latter impurity could be removed by preparative layer chromatography but owing to the progressive isomerization of **3***f* to **2***f* which occurred during the separation process pure samples of the 17β-isopropyl-Δ^5-3-ketone could not be obtained in this way.

Base-catalyzed oxygenation of steroid-Δ^5-3-ketones is known to be a very facile process and

[2]Sondheimer and his co-workers (10) reported a double m.p., 133–135° and 157–159°, for a sample of **1***c* prepared in this way and it now seems probable this earlier material also contained the 17α-epimer.

Can. J. Chem. Downloaded from www.nrcresearchpress.com by 210.87.254.105 on 09/05/12
For personal use only.

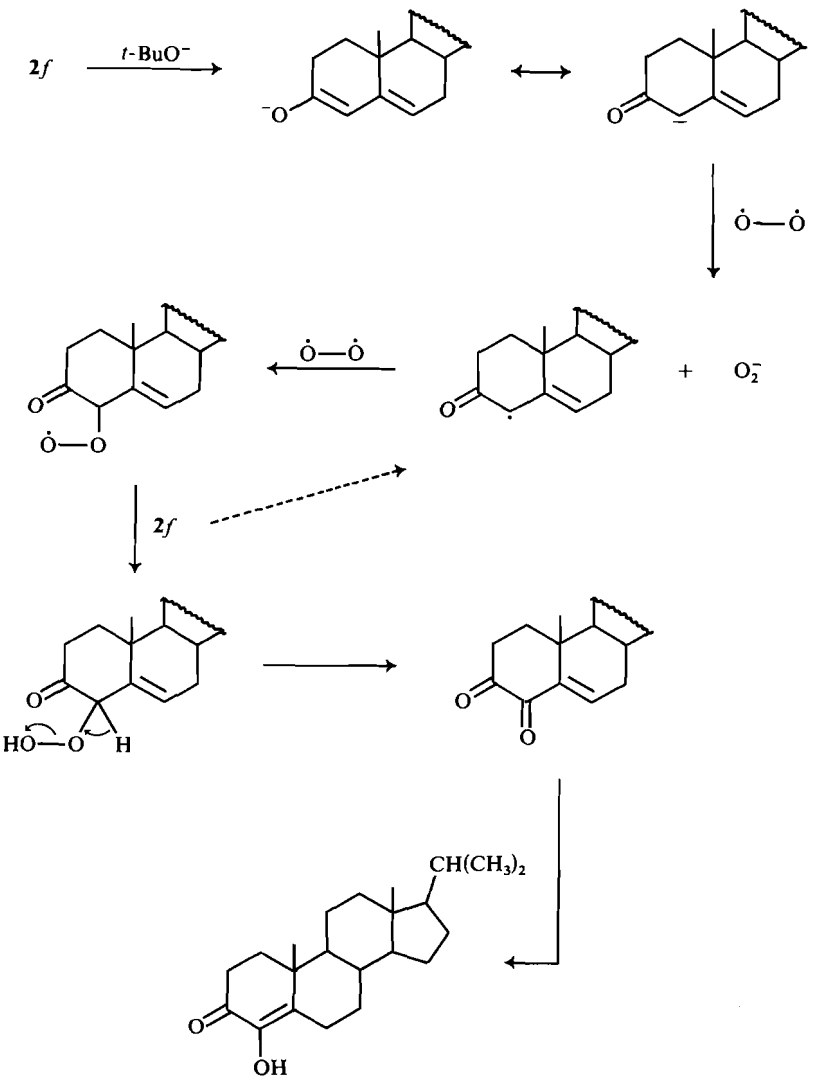

6

SCHEME 4

is considered to involve radical intermediates (13, 14). A mechanism for oxygenation at C-4 involving singlet oxygen has been proposed (14); however, participation of the latter species under the reaction conditions employed is questionable and the mechanism outlined in Scheme 4 incorporating a radical-chain process (15) to a hydroperoxide intermediate (13) is preferred. At present it is not understood why the dienolate anion of **2***f* should be so much more sensitive to attack by oxygen than the Δ^4-3-ketones examined earlier (1) nor why Pfitzner–Moffatt oxidations of **1***c*, *e*, and *f* should not have been facile.

As a result of the above difficulties, attention was turned to some of the alternative routes to Δ^5-3-ketones which had subsequently become available. One attractive possibility appeared to be the method developed by Mazur and his coworkers (16) in which deconjugation of $\alpha\beta$-unsaturated ketones had been effected by controlled methanolysis of dienoltrichloroacetate

Can. J. Chem. Downloaded from www.nrcresearchpress.com by 210.87.254.105 on 09/05/12
For personal use only.

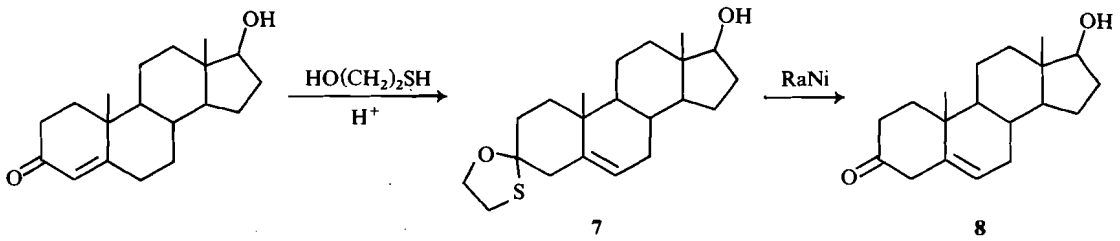

7 8

SCHEME 5

derivatives. Evaluation of this procedure for the conversion of **2***f* into **3***f* indicated that it was not without its disadvantages since isomerization of the initially formed Δ^5-3-ketone was difficult to prevent unless ketonization of the intermediate trichloracetate with the recommended (16) methanol solutions was very carefully regulated. Another potential route which was considered is exemplified in Scheme 5. In contrast to thioketal formation, formation of an oxythioketal such as **7** from a Δ^4-3-ketone is accompanied by migration of the double bond to the Δ^5 position (17, 18). It was felt that since ketonization of such derivatives can be effected with Raney nickel under essentially neutral conditions (17), little or no isomerization should occur of a Δ^5-3-one prepared in this way. The validity of the method was demonstrated by the conversion of the oxythioketal **7** into **8**, but although relatively pure samples of the $\beta\gamma$-unsaturated ketone were produced, the low yields ($\sim$10%) obtained precluded any serious consideration of this approach.

The method finally adopted as providing the most satisfactory route to the variously C-17 substituted Δ^5-3-ketones desired was oxidation of the appropriate Δ^5-3β-ol precursor with the mild, neutral, dipyridine chromium trioxide in dichloromethane reagent developed by Collins and his collaborators (19). Oxidation of each of **1***a–f, h* was complete within 10 min at 0° and 40–50% yields of the corresponding Δ^5-3-ketones **3***a–f, h* were obtained. In each case the degree of purity of the desired product was found to be higher than that attainable by any of the previous methods and analyses of each sample by i.r. and u.v. spectroscopy showed less than 1% of the conjugated Δ^4-3-keto isomer to be present.

The influence of the C-17 substituents on the aggregation properties and Δ^5-3-ketoisomerase specificity of **3***a–f, h* will be reported shortly.

Experimental

The dimethylsulfoxide used in the Wittig reactions was distilled from calcium hydride and stored over molecular sieves. All other solvent purifications, criteria of purity, instrumentation used, etc. were as described previously (3). Spectral data for all compounds were as expected and selected distinguishing features only are cited. Any steroid for which a preparative procedure is not detailed below was purchased from Aldrich, Searle, Sigma, or Nutritional Biochemical Corporation.

17β-Methylandrost-5-en-3β-ol (1c)

3β-Acetoxy-17-methyleneandrost-5-ene (**4***a*), m.p. 103–104° (lit. (5) m.p. 103–105°), was obtained in 67% yield from 3β-hydroxyandrost-5-en-17-one (**1***a*) as described by Drefahl *et al.* (5). Hydrolysis of **4***a* with 3% methanolic potassium hydroxide (5) gave 3β-hydroxy-17-methyleneandrost-5-ene (**4***b*, 90%), m.p. 132–133.5° (lit. (5) m.p. 133–134°). Hydrogenation of **4***b* (200 mg) was carried out at 21° in methanol (50 ml) containing 10% palladium–charcoal (50 mg). Following the uptake of 1 equiv of hydrogen (4 h), the catalyst was filtered off and the filtrate evaporated. Recrystallization of the residue from methanol gave 17β-methylandrost-5-en-3β-ol (**1***c*, 170 mg) m.p. 160–163°;[2] i.r. ($CHCl_3$) 3571 cm^{-1}; n.m.r. ($CDCl_3$) δ 0.83 (3, d, $J = 6$ Hz, C-17 —CH_3), and 5.38 p.p.m. (1, broad s, C-6 H).

Anal. Calcd. for $C_{20}H_{32}O$: C, 83.27; H, 11.18. Found: C, 83.15; H, 11.35.

Pregn-5-en-3β-ol (1e)

This compound, m.p. 131–134° (lit. (20) m.p. 132–133°), was obtained in 80% yield following prolonged ($\sim$2 days) Wolff–Kishner reduction (20) of 3β-hydroxypregn-5-en-20-one (**1***d*).

20-Methylpregn-5-en-3β-ol (1f)

Treatment of 3β-hydroxypregn-5-en-20-one (**1***d*) with methylenetriphenylphosphorane in dimethylsulfoxide (21), followed by acetylation of the reaction mixture, chromatography on alumina (CCl_4 elution), and recrystallization from methanol yielded 3β-acetoxy-20-methylpregna-5,20-diene (**5***a*, 62%), m.p. 133–135° (lit. (21) m.p. 128.5–129°). Hydrolysis of **5***a* with 3% methanolic potassium hydroxide for 2 h at 21° gave 20-methylpregna-5,20-dien-3β-ol (**5***b*, 86%) which after recrystallization from aqueous methanol had m.p. 133–135° (lit. (21) m.p. 133.5–134°). Selective hydrogenation of **5***b* (600 mg) was effected in benzene (50 ml) containing 60 mg of tris(triphenylphosphine)rhodium chloride (7) at 21° in a hydrogen atmosphere. After the uptake of 1 equiv of hydrogen (3 h), the benzene solution

Can. J. Chem. Downloaded from www.nrcresearchpress.com by 210.87.254.105 on 09/05/12
For personal use only.

Can. J. Chem. Downloaded from www.nrcresearchpress.com by 210.87.254.105 on 09/05/12
For personal use only.

was filtered through a Florisil (50 g) column and the elution was completed with ether. Evaporation of the steroid containing fractions (first 75 ml of eluents) followed by recrystallization from methanol gave 20-methylpregn-5-en-3β-ol (**1***f*, 560 mg) m.p. 140–141°, (lit. (21) m.p. 136–137°), i.r. ($CHCl_3$), 3584 cm^{-1}; n.m.r. ($CDCl_3$) δ 0.83 (3, d, $J = 7$ Hz, C-20 or -21 CH_3), 0.89 (3, d, $J = 7$ Hz, C-20 or -21 CH_3); and 5.36 p.p.m. (1, broad s, C-6 H).

Δ^4-3-Ketosteroids **2***b, c, e, and f*

Oppenauer oxidation of the precursor Δ^5-3β-alcohols **1***b*, *c*, *e*, and *f* with cyclohexanone and aluminum isopropoxide in toluene (22) gave 75–90% yields of the corresponding Δ^4-3-ketones. Recrystallization from methanol or aqueous methanol gave samples with the following properties: *androst-4-en-3-one (2b)* m.p. 98–100° (lit. (23) m.p. 105–106°); *17β-methylandrost-4-en-3-one (2c)* m.p. 109–110° (lit. (10) m.p. 109–110°), n.m.r. ($CDCl_3$) δ 0.82 p.p.m. (3, d, $J = 6$ Hz, C-17β CH_3); *pregn-4-en-3-one (2e)* m.p. 99–101° (lit. (20) m.p. 102–104°); and *20-methylpregn-4-en-3-one (2f)* m.p. 143–145° (lit. (21) m.p. 143–144°), n.m.r. ($CDCl_3$) δ 0.85 (3, d, $J = 6$ Hz, C-20 or -21 CH_3) and 0.92 p.p.m. (3, d, $J = 6$ Hz, C-20 or -21 CH_3).

*Formation of 4-Hydroxy-20-methylpregn-4,6-dien-3-one (**6**) During Attempted Deconjugation of 20-Methylpregn-4-en-3-one (2f)*

Potassium *t*-butoxide (375 mg, 3.5 mmol) was added to a solution of 20-methylpregn-4-en-3-one (100 mg, 0.32 mmol) in *t*-butanol (10 ml) and the mixture was stirred in air for 90 min at 21°. Ten percent aqueous acetic acid (10 ml) followed immediately by saturated aqueous sodium bicarbonate solution (15 ml) was then added and the mixture was then extracted with ether (4 × 20 ml), dried ($MgSO_4$), and evaporated. Recrystallization of the residue from methanol yielded 4-hydroxy-20-methylpregn-4,6-dien-3-one (**6**, 30 mg) m.p. 198–199°; i.r. (KBr) 3390, 1667, and 1618 cm^{-1}; u.v. λ_{max} (CH_3OH) 318 nm (ε 7500); n.m.r. ($CDCl_3$) δ 6.05 (1, d of d, $J = 9$ and 2 Hz, C-7 H), 6.2 (1, s, partially exchangeable with D_2O, C-4 OH), and 6.65 p.p.m. (1, d of d, $J = 9$ and 2 Hz, C-6 H); mass spectrum (70 eV) *m/e* 328 (parent ion).

Anal. Calcd. for $C_{22}H_{32}O_2$: C, 80.44; H, 9.82. Found: C, 80.68; H, 9.73.

Preparation of 17β-Hydroxyandrost-5-en-3-one via the Oxythioketal 7

17β-Hydroxyandrost-5-en-3-one 3-ethyleneoxythioketal (**7**), m.p. 188–190° (lit. (17) m.p. 192–194°) was obtained in 50% yield from 17β-hydroxyandrost-4-en-3-one and 2-mercaptoethanol as described by Djerassi and Gorman (17). Treatment of **7** with acetone-deactivated Raney nickel W-2 in refluxing acetone for 4 h gave 17β-hydroxyandrost-5-en-3-one, m.p. 158–160° (lit. (1) m.p. 162–164°), in 10% yield following purification by t.l.c.

Preparation of the Δ^5-3-Ketosteroids 3a–f, h using the Dipyridine Chromium Trioxide Reagent

The same general procedure was used for each $\beta\gamma$-unsaturated ketone.[3] Dipyridine chromium trioxide (1.0 g, 3.87 mmol), freshly prepared according to the procedure of Collins *et al.* (19*a*), was dissolved at 0° in dichloromethane (40 ml) and the dark red solution stirred for 10 min. The appropriate Δ^5-3β-alcohol (200 mg, ~0.5–0.75 mmol) in dichloromethane (5 ml) was then added dropwise with stirring at 0°. The mixture turned dark grey almost immediately following the addition of all the alcohol and after stirring for a further 10 min at 0°, it was filtered. The cold filtrate was washed with water (3 × 10 ml), and then *rapidly* with 3% aqueous hydrochloric acid (3 × 10 ml) followed by water (3 × 10 ml). Evaporation of the dried ($MgSO_4$) solution and recrystallization of the residual solid from *warm*[3] methanol yielded the desired Δ^5-3-ketone which i.r. and u.v. analysis showed to be ≥99% pure. Application of the above procedure proceeded without complication in each of the following preparations.

Androst-5-ene-3,17-dione (3a). From **1***a*, 74 mg, m.p. 146–150°[4] (lit. (3) m.p. 150–155°); i.r. ($CHCl_3$) 1730 and 1709 cm^{-1}.

Androst-5-en-3-one (3b). From **1***b*, 60 mg, m.p. 114–117°[4] (lit. (3) m.p. 129–131°); i.r. ($CHCl_3$) 1709 cm^{-1}.

17β-Methylandrost-5-en-3-one (3c). From **3***b*, 40 mg, m.p. 115–118°; i.r. ($CHCl_3$) 1706 cm^{-1}.

Anal. Calcd. for $C_{20}H_{30}O$: C, 83.86; H, 10.56. Found: C, 83.67; H, 10.71.

Pregn-5-ene-3,20-dione (3d). From **1***d*, 110 mg, m.p. 156–159° (lit. (24) m.p. 139–148°); i.r. ($CHCl_3$) 1701 and 1698 cm^{-1}.

Pregn-5-en-3-one (3e). From **1***e*, 69 mg, m.p. 123–126° (lit. (25) m.p. 129–133°); i.r. ($CHCl_3$) 1706 cm^{-1}.

20-Methylpregn-5-en-3-one (3f). From **1***f*, 67 mg, m.p. 136–139°; i.r. ($CHCl_3$) 1706 cm^{-1}.

Anal. Calcd. for $C_{22}H_{34}O$: C, 84.02; H, 10.90. Found: C, 84.10; H, 11.00.

Cholest-5-en-3-one (3h). From **1***h*, 80 mg, m.p. 116–120° (lit. (3) m.p. 120–122°); i.r. ($CHCl_3$) 1709 cm^{-1}.

This work was supported by the National Research Council of Canada and was carried out during the tenure of awards (to K.D.G.) of L.V. Redman and NRCC Scholarships.

1. J. B. Jones and D. C. Wigfield. Can. J. Chem. **46**, 1459 (1968).
2. K. E. Pfitzner and J. G. Moffatt. J. Am. Chem. Soc. **85**, 3027 (1963); J. Am. Chem. Soc. **87**, 5670 (1965).
3. J. B. Jones and D. C. Wigfield. Can. J. Chem. **44**, 2517 (1966).
4. H. J. Ringold and S. K. Malhotra. Tetrahedron Lett. 669 (1962).
5. G. Drefah, K. Ponsold, and H. Schick. Chem. Ber. **98**, 604 (1965).
6. F. H. Jardine, J. A. Osborn, and G. Wilkinson. J. Chem. Soc. A, 1574 (1967) and references therein.
7. A. J. Birch and K. A. M. Walker. J. Chem. Soc. C, 1894 (1966); Tetrahedron Lett. 4939 (1966).
8. C. Djerassi and J. Gutzwiller. J. Am. Chem. Soc. **88**, 4537 (1966).

[3]All the precautions found necessary (3) to prevent isomerization of Δ^5-3-ketosteroids by the glassware used, or by application of excessive heating during recrystallization, were applied throughout.

[4]Melting points of many Δ^5-3-ketones are not easily reproduced owing to the facility with which isomerization occurs on heating (3). Melting point determinations were carried out with the temperature increasing at 8°/min.

9. J.-F. BIELLMAN and H. LIESENFELT. Bull. Soc. Chim. Fr. 4029 (1966).
10. O. MANCERA, G. ROSENKRANZ, and F. SONDHEIMER. Naturwiss. **43**, 17 (1956).
11. B. CAMERINO, B. PATELLI, and R. SCIAKY. Tetrahedron Lett. 554 (1961).
12. J.-F. BIELLMAN and M. RAJIC. Bull. Soc. Chim. Fr. 1945 (1961).
13. L. L. CHINN. Selection of oxidants in synthesis. Marcel Dekker Inc., New York, N.Y. 1971. pp. 34–35.
14. D. N. KIRK and M. P. HARTSHORN. Steroid reaction mechanisms. Elsevier, New York, N.Y. 1968. p. 178.
15. J. O. HAWTHORNE, K. A. SCHOWALTER, A. W. SIMON, M. H. WILT, and M. S. MORGAN. Oxidation of organic compounds. Vol. 1. *Edited by* R. F. Gould. American Chemical Society Publications, Washington, D.C. 1967. p. 203.
16. D. AMAR, V. PERMUTTI, and Y. MAZUR. Tetrahedron, **25**, 1717 (1969).
17. C. DJERASSI and M. GORMAN. J. Am. Chem. Soc. **75**, 3704 (1953).
18. H. HAUPTMANN. J. Am. Chem. Soc. **69**, 562 (1947).
19. (*a*) J. C. COLLINS, W. W. HESS and F. J. FRANK. Tetrahedron Lett. 3363 (1968); (*b*) *cf.* R. RATCLIFFE and R. RODEBORST. J. Org. Chem. **35**, 4000 (1970).
20. C. W. SHOPPEE, R. E. LACK, and B. C. NEWMAN. J. Chem. Soc. 3388 (1964).
21. J. P. DUSZA and W. BERGMANN. J. Org. Chem. **25**, 79 (1960).
22. J. F. EASTHAM and R. TERANISHI. Org. Synth. Coll. Vol. IV, 192 (1963).
23. M. FETIZON and M. GOLFIER. Bull. Soc. Chim. Fr. 167 (1963).
24. C. DJERASSI, R. R. ENGLE, and A. BOWERS. J. Org. Chem. **21**, 1547 (1956).
25. H. WERBIN, W. EWALD, and I. L. CHAIKOFF. Biochim. Biophys. Acta, **130**, 556 (1966).
26. J. B. JONES and R. GRAYSHAN. Can. J. Chem. **50**, 1414 (1972).

Synthesis of *cis*-Jasmone and Dihydrojasmone

HONOR C. HO, TSE-LOK HO, and C. M. WONG
Department of Chemistry, University of Manitoba, Winnipeg, Manitoba R3T 2N2

Received February 15, 1972

cis-Jasmone and dihydrojasmone have been synthesized from levulonitrile by a four-step reaction sequence. Application of ceric ammonium nitrate for dethioketalization is described.

La Jasmone *cis* et la dihydrojasmone ont été synthétisées à partir du levulonitrile selon une séquence réactionnelle en quatre étapes. L'application du nitrate d'ammonium cérique pour la déthiocétalisation est décrite.

Canadian Journal of Chemistry, **50**, 2718 (1972)

cis-Jasmone (**1***a*) and dihydrojasmone (**1***b*) have commanded undiminished endeavors in their syntheses (1, 2) over the past three decades, owing to their importance in the perfume industry and because they often serve as testing targets pertinent to development of γ-diketone and cyclopentenone syntheses. We wish to report a simple synthesis of both of these natural products which may have certain merits since the starting materials are relatively inexpensive and easily accessible.

It appeared to us that a levulinic acid derivative would be an attractive starting point in view of the presence of differential bifunctionality in the correct positions of the carbon skeleton, amenable to the elaboration of *cis*-jasmone and dihydrojasmone precursors. In this context, levulonitrile was selected because its ketone function can be masked temporarily, while the cyano group is being transformed into another carbonyl by the action of an organometallic reagent.

Thus, levulonitrile (3) was converted to the ethylenethioketal **2** in good yield. Reaction of **2** with appropriate Grignard reagents followed by acid hydrolysis of the resulting imine complexes on work-up furnished **3***a* and *b* respectively.[1] To facilitate isolation of the products in

[1]The use of the ethyleneketal protecting group for levulonitrile was found to be unsuitable.

Can. J. Chem. Downloaded from www.nrcresearchpress.com by 210.87.254.105 on 09/05/12
For personal use only.

9. J.-F. BIELLMAN and H. LIESENFELT. Bull. Soc. Chim. Fr. 4029 (1966).
10. O. MANCERA, G. ROSENKRANZ, and F. SONDHEIMER. Naturwiss. **43**, 17 (1956).
11. B. CAMERINO, B. PATELLI, and R. SCIAKY. Tetrahedron Lett. 554 (1961).
12. J.-F. BIELLMAN and M. RAJIC. Bull. Soc. Chim. Fr. 1945 (1961).
13. L. L. CHINN. Selection of oxidants in synthesis. Marcel Dekker Inc., New York, N.Y. 1971. pp. 34–35.
14. D. N. KIRK and M. P. HARTSHORN. Steroid reaction mechanisms. Elsevier, New York, N.Y. 1968. p. 178.
15. J. O. HAWTHORNE, K. A. SCHOWALTER, A. W. SIMON, M. H. WILT, and M. S. MORGAN. Oxidation of organic compounds. Vol. 1. *Edited by* R. F. Gould. American Chemical Society Publications, Washington, D.C. 1967. p. 203.
16. D. AMAR, V. PERMUTTI, and Y. MAZUR. Tetrahedron, **25**, 1717 (1969).
17. C. DJERASSI and M. GORMAN. J. Am. Chem. Soc. **75**, 3704 (1953).
18. H. HAUPTMANN. J. Am. Chem. Soc. **69**, 562 (1947).
19. (*a*) J. C. COLLINS, W. W. HESS and F. J. FRANK. Tetrahedron Lett. 3363 (1968); (*b*) *cf.* R. RATCLIFFE and R. RODEBORST. J. Org. Chem. **35**, 4000 (1970).
20. C. W. SHOPPEE, R. E. LACK, and B. C. NEWMAN. J. Chem. Soc. 3388 (1964).
21. J. P. DUSZA and W. BERGMANN. J. Org. Chem. **25**, 79 (1960).
22. J. F. EASTHAM and R. TERANISHI. Org. Synth. Coll. Vol. IV, 192 (1963).
23. M. FETIZON and M. GOLFIER. Bull. Soc. Chim. Fr. 167 (1963).
24. C. DJERASSI, R. R. ENGLE, and A. BOWERS. J. Org. Chem. **21**, 1547 (1956).
25. H. WERBIN, W. EWALD, and I. L. CHAIKOFF. Biochim. Biophys. Acta, **130**, 556 (1966).
26. J. B. JONES and R. GRAYSHAN. Can. J. Chem. **50**, 1414 (1972).

Synthesis of *cis*-Jasmone and Dihydrojasmone

HONOR C. HO, TSE-LOK HO, and C. M. WONG
Department of Chemistry, University of Manitoba, Winnipeg, Manitoba R3T 2N2

Received February 15, 1972

cis-Jasmone and dihydrojasmone have been synthesized from levulonitrile by a four-step reaction sequence. Application of ceric ammonium nitrate for dethioketalization is described.

La Jasmone *cis* et la dihydrojasmone ont été synthétisées à partir du levulonitrile selon une séquence réactionnelle en quatre étapes. L'application du nitrate d'ammonium cérique pour la déthiocétalisation est décrite.

Canadian Journal of Chemistry, **50**, 2718 (1972)

cis-Jasmone (**1***a*) and dihydrojasmone (**1***b*) have commanded undiminished endeavors in their syntheses (1, 2) over the past three decades, owing to their importance in the perfume industry and because they often serve as testing targets pertinent to development of γ-diketone and cyclopentenone syntheses. We wish to report a simple synthesis of both of these natural products which may have certain merits since the starting materials are relatively inexpensive and easily accessible.

It appeared to us that a levulinic acid derivative would be an attractive starting point in view of the presence of differential bifunctionality in the correct positions of the carbon skeleton, amenable to the elaboration of *cis*-jasmone and dihydrojasmone precursors. In this context, levulonitrile was selected because its ketone function can be masked temporarily, while the cyano group is being transformed into another carbonyl by the action of an organometallic reagent.

Thus, levulonitrile (3) was converted to the ethylenethioketal **2** in good yield. Reaction of **2** with appropriate Grignard reagents followed by acid hydrolysis of the resulting imine complexes on work-up furnished **3***a* and *b* respectively.[1] To facilitate isolation of the products in

[1]The use of the ethyleneketal protecting group for levulonitrile was found to be unsuitable.

Can. J. Chem. Downloaded from www.nrcresearchpress.com by 210.87.254.40 on 09/05/12
For personal use only.

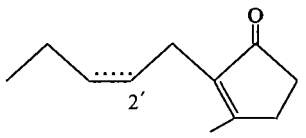

1

a $\Delta^{2'}$
b saturated

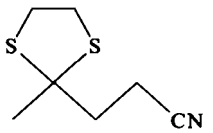

2

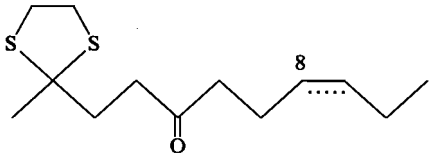

3

a Δ^{8}
b saturated

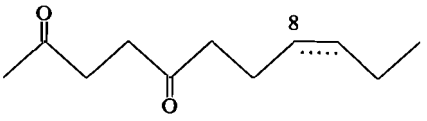

4

a Δ^{8}
b saturated

the scale we used, Girard T derivatives were prepared; however, this technique would not be required in larger preparations where fractional distillation would be expedient and sufficient.

The next task called for removal of the dithioketal group, and this was performed either by utilizing the elegant procedure recently disclosed by Wynberg and his collaborators (4), or by ceric ammonium nitrate oxidation (5) in aqueous acetonitrile, a novel and efficacious method which could be of wide applicability to regenerate carbonyl compounds from the corresponding 2-substituted 1,3-dithiolanes and 1,3-dithianes under very mild conditions. In our hands, this latter convenient process was found to be superior to Wynberg's method for dithioketal cleavage involved in the synthesis reported herein. Cyclization of **4***a*, *b* to *cis*-jasmone and dihydrojasmone was effected by alkali according to the literature (1*k*). These synthetic compounds were shown to be identical with authentic specimens of the natural products by spectroscopy (i.r., n.m.r.) and chromatography (t.l.c.).

The approach described in this paper defines a potentially useful general fabrication of the γ-diketone synthon, since homologues of levulonitrile can be prepared readily by the cyanoethylation of nitroalkanes followed by the Nef reaction (3).

Experimental

I.r. spectra were recorded on a Perkin-Elmer 710 Spectrophotometer using methylene chloride as solvent. N.m.r. spectra were taken on a Varian A56/60A spectrometer in the solvent indicated and with tetramethylsilane as internal standard. Mass spectra were obtained from a Finnigan 1015 mass spectrometer and high resolution mass spectra were measured with an AEI MS9 Spectrometer (University of Alberta) operating at 70 eV. Solutions were dried over anhydrous magnesium sulfate.

Levulonitrile Ethylenethioketal

A mixture of levulonitrile (4.20 g), ethanedithiol (4.0 ml), and boron trifluoride etherate (1.0 ml) and anhydrous magnesium sulfate (5 g) in benzene (40 ml) was allowed to stand at ambient temperature for 2 days. It was then diluted with benzene (100 ml), washed with 2% potassium hydroxide, dried, and evaporated *in vacuo*. Levulonitrile ethylenethioketal (6.53 g, 88.2%) was obtained as a clear oil, b.p. 78–80° (0.6 Torr). I.r. ν 2240 cm^{-1}; n.m.r. (CCl_4) τ 6.68 (4H, s), 7.56 (4H, sym. m), 8.22 (3H, s); mass (M^+): calcd. for $C_7H_{11}N^{32}S$, 173.0334; found, 173.0330.

Anal. Calcd. for $C_7H_{11}NS$: C, 48.5; H, 6.4; N, 8.1; S, 37.0. Found: C, 48.7; H, 6.2; N, 8.2; S, 36.8.

cis-Undec-8-ene-2,5-dione Monoethylenethioketal (**3***a*)

To a Grignard reagent prepared from *cis*-1-bromohex-3-ene (1.62 g) and magnesium turnings (240 mg) in dry ether (20 ml) was introduced a solution of levulonitrile ethylenethioketal (173 mg) in ether (5 ml). After stirring at room temperature for 18 h, the reaction mixture was run into dilute hydrochloric acid and extracted with ether. The crude product was treated directly with Girard T reagent (200 mg) in methanol (10 ml) containing glacial acetic acid (0.2 ml) for 3 h under reflux. T.l.c. homogeneous *cis*-undec-8-ene-2,5-dione monoethylenethioketal (**3***a*) (156 mg, 60.5%) was obtained from the Girard derivative. An analytical sample was prepared by evaporative distillation in high vacuum

Can. J. Chem. Downloaded from www.nrcresearchpress.com by 210.87.254.40 on 09/05/12
For personal use only.

Can. J. Chem. Downloaded from www.nrcresearchpress.com by 210.87.254.40 on 09/05/12
For personal use only.

(bath temperature 100–110°). I.r. ν 1710 cm^{-1}; n.m.r. ($CDCl_3$)τ4.65 (2H, m), 6.79 (4H, s), 8.25 (3H, s), 9.05 (3H, t, J=7.5 Hz); mass (M^+): calcd. for $C_{13}H_{22}O^{32}S_2$, 258.1113; found, 258.1107.

Anal. Calcd. for $C_{13}H_{22}OS_2$: C, 60.5; H, 8.5; S, 24.8. Found: C, 60.8; H, 8.6; S, 24.2.

cis-Undec-8-ene-2,5-dione (4a)

(*a*) Following the procedure of Wynberg and coworkers (4), a solution of chloramine T (570 mg) in 80% methanol (2.5 ml) was added to **3***a* (150 mg) in methanol (2 ml) and ethanol (1 ml). After stirring at room temperature for 2 min, water was added and it was extracted with ether (80 ml). The ether solution was washed with 10% sodium hydroxide, water, and dried. The crude diketone **4***a* (102 mg) secured by evaporation of solvent was purified by preparative t.l.c. on silica gel (benzene; R_f 0.2); yield 80 mg (70%). I.r. ν 1710 cm^{-1}; n.m.r. ($CDCl_3$) τ 4.65 (2H, m), 7.32 (4H, s), 7.83 (3H, s), 9.05 (3H, t, J = 7 Hz); mass spectrum m/e 182 (M^+).

(*b*) Ceric ammonium nitrate (550 mg) was added to a stirred solution of **3***a* (62 mg) in 75% aqueous acetonitrile (4 ml) at ambient temperature. At the end of 5 min the reaction was quenched with water and extracted with ether (50 ml). The ether extract was then washed with water to remove coloring material, dried, evaporated, and the resulting product was subjected to preparative t.l.c. to give **4***a* (34 mg, 77.8%).

cis-Jasmone

A mixture of *cis*-undec-8-ene-2,5-dione (80 mg), 0.5 *N* sodium hydroxide (1.0 ml), and ethanol (2.0 ml) was refluxed under nitrogen for 5 h. On cooling, the mixture was acidified with dilute hydrochloric acid and extracted with ether. The crude product was purified by preparative t.l.c. on silica gel (benzene:ether, 85:15; R_f 0.6) to give *cis*-jasmone (55 mg, 76.4%). I.r. ν 1690, 1640 cm^{-1}; n.m.r. ($CDCl_3$) τ 4.64 (2H, m), 7.02 (2H, d, J = 5 Hz), 7.92 (3H, s), 9.00 (3H, t, J = 7 Hz); mass spectrum m/e 164 (M^+). 2,4-DNP, m.p. 115–116° (lit. (*lb*) m.p. 116°).

Undecan-2,5-dione Monoethylenethioketal (3b)

A solution of levulonitrile ethylenethioketal (1.00 g) in dry ether (10 ml) was added to a stirred Grignard reagent prepared from 1-bromohexane (10.00 g) and magnesium turnings (1.44 g) in ether (80 ml). The reaction mixture was stirred at room temperature for 20 h and added dropwise to a stirred mixture of dilute hydrochloric acid and chloroform. After separation into layers, the aqueous phase was extracted with chloroform (2 × 60 ml). The combined extracts were dried and evaporated to given an oil. The diketone monoethylenethioketal **3***b* (1.035 g, 65.5%) was isolated by treatment of the crude oil with Girard T reagent (1.20 g) in refluxing methanol (40 ml, containing 1.0 ml glacial acetic acid) for **3 h**. I.r. ν 1710 cm^{-1}; n.m.r. ($CDCl_3$) τ 6.68 (4H, s), 7.1–**8.0** (**6**H, m), 8.25 (3H, s), 8.5–8.9 (8H, m), 9.11 (3H, t, J=5 Hz); mass (M^+): calcd. for $C_{13}H_{24}O^{32}S_2$, 260.1269; found, 260.1263.

Anal. Calcd. for $C_{13}H_{24}OS_2$: C, 60.0; H, 9.3; Found: C, 59.8; H, 9.4.

Undecan-2,5-dione

(*a*) A solution of **3***b* (460 mg) in methanol–ethanol (2:1, 3 ml) was treated with a solution of chloramine T (1.128 g) in 80% methanol (5 ml) at room temperature for 2 min. Water was added and the resulting mixture was extracted with ether (80 ml). The extract was washed with 10% potassium hydroxide, water, and dried. Evaporation of the organic solution yielded undecan-2,5-dione (226 mg, 67.3%) which was homogeneous on t.l.c. I.r. ν 1710 cm^{-1}; n.m.r. (CCl_4) τ 7.43 (4H, s), 7.62 (2H, t, J = 6.5 Hz), 7.90 (3H, s), 9.10 (3H, t, J = 5 Hz); mass spectrum m/e 184 (M^+).

(*b*) To a solution of **3***b* (130 mg) in 75% aqueous acetonitrile (8 ml) was added ceric ammonium nitrate (1.10 g) in portions. After swirling at room temperature for 5 min, the reaction mixture was poured into water and extracted with ether (80 ml). The ethereal solution was washed thrice with water (until colorless), dried, and evaporated. The crude product, virtually homogeneous on t.l.c., was filtered through a short column of alumina (1.5 g) with benzene as eluent to give pure undecan-2,5-dione (73 mg, 80%).

Dihydrojasmone

A mixture of undecan-2,5-dione (210 mg), 0.5 *N* sodium hydroxide (2.0 ml), and ethanol (1.0 ml) was refluxed under nitrogen for 5 h. The cooled mixture was acidified with dilute hydrochloric acid and extracted with ether. The crude product was eluted through a short column of neutral alumina with ether–benzene mixture (1:9) to furnish pure dihydrojasmone (158 mg, 83%). I.r. ν 1705, 1650 cm^{-1}; n.m.r. ($CDCl_3$) τ 7.96 (3H, s), 9.13 (3H, t, J=5 Hz); mass spectrum m/e 166 (M^+). Semicarbazone m.p. 174–175° (lit. (*2a*) m.p. 173–175°).

We thank Dr. W. I. Taylor (International Flavors & Fragrances) and Prof. E. Wenkert (Indiana University) for the most generous gifts of *cis*-jasmone and dihydrojasmone respectively. Support from the National Research Council of Canada is gratefully acknowledged.

1. (*a*) S. M. Weinreb and R. J. Cvetovich. Tetrahedron Lett. 1233 (1972); (*b*) W. F. Berkowitz. J. Org. Chem. **37**, 341 (1972); (*c*) J. E. McMurry and J. Melton. J. Am. Chem. Soc. **93**, 5309 (1971); (*d*) G. Stork, G. L. Nelson, F. Rouessac, and O. Gringore. J. Am. Chem. Soc. **93**, 3091 (1971); (*e*) G. Büchi and B. Egger. J. Org. Chem. **36**, 2021 (1971); (*f*) J. E. McMurry and T. E. Glass. Tetrahedron Lett. 2575 (1971); (*g*) J. Ficini, J. d'Angelo, J. P. Genêt, and J. Noiré. Tetrahedron Lett. 1569 (1971): (*h*) M. Fétizon and J. Schalbar. La France et ses parfums. **12**, 330 (1969); (*i*) K. Shishido and Y. Kawashima. Japan 7014779 (Patent); Chem. Abstr. **73**, 120 181*p* (1970); (*j*) L. Crombie, P. Hemesley, and G. Pattenden. J. Chem. Soc. C, 1024 (1969); (*k*) G. Büchi and H. Wüest. J. Org. Chem. **31**, 977 (1966); (*l*) T. Yoshida, A. Yamaguchi, and A. Komatsu. Agri. Biol. Chem. **30**, 370 (1966); (*m*) K. Shishido, Y. Kawashima, and T. Ishida. Perfum. Essent. Oil Rec. **57**, 364 (1966); (*n*) G. Stork and R. Borch. J. Am. Chem. Soc. **86**, 936 (1964); (*o*) J. H. Amin, R. K. Razdan, and S. C. Bhattacharyya. Perfum. Essent. Oil Rec. **49**, 502 (1958); (*p*) S. H. Harper and R. J. D. Smith. J. Chem. Soc. 1512 (1955); (*q*) L. Crombie and S. H. Harper. J. Chem. Soc. 869 (1952); (*r*) H. Hunsdiecker. Ber. **75**, 460 (1942).

2. (*a*) E. WENKERT, A. MUELLER, E. J. REARDON, JR., S. S. SATHE, D. J. SCHARF, and G. TOSI. J. Am. Chem. Soc. **92**, 7428 (1970); (*b*) J. KATSUBE and M. MATSUI. Agri. Biol. Chem. **33**, 1078 (1969); (*c*) R. T. DAHILL. J. Org. Chem. **31**, 2694 (1966); (*d*) A. TAKEDA, H. HOSISIMA, and S. TORII. Bull. Chem. Soc. Japan, **39**, 1354 (1966); (*e*) E. THIELE. Ger. (East) Pat. 30 727; Chem. Abstr. **65**, 8789*h* (1966); (*f*) J. L. ERICKSON and F. E. COLLINS. J. Org. Chem. **30**, 1050 (1965); (*g*) M. ELLIOTT. J. Chem. Soc. 2231 (1956); (*h*) R. L. FRANK, P. G. ARVAN, J. W. RICHTER, and C. R. VANNEMAN. J. Am. Chem. Soc. **66**, 4 (1944); (*i*) H. HUNSDIECKER. Ber. **75**, 455 (1942); (*j*) H. STAUDINGER and L. RUZICKA. Helv. Chim. Acta, **7**, 245 (1924); (*k*) T. L. Ho. J. Chinese Chem. Soc. (II) **18**, 153 (1971).
3. G. D. BUCKLEY, T. J. ELLIOTT, F. G. HUNT, and A. LOWE. J. Chem. Soc. 1505 (1947).
4. W. F. J. HUURDEMAN, H. WYNBERG, and D. W. EMERSON. Tetrahedron Lett. 3449 (1971).
5. T. L. Ho, H. C. Ho, and C. M. WONG. Chem. Commun. In press.

The Photolysis of Tetra(trifluoromethyl)thiophene Vapor[1]

H. A. WIEBE,[2] SILVIA BRASLAVSKY, AND JULIAN HEICKLEN

Department of Chemistry and Center for Air Environment Studies, The Pennsylvania State University, University Park, Pa. 16802

Received March 20, 1972

The photolysis of tetra(trifluoromethyl)thiophene (TTFT) at 2139 Å or by mercury sensitization at 2537Å yields hexafluorobutyne-2 and 1,2,3,4-tetra(trifluoromethyl)5-thiabicyclo[2,1,0]pentene-2 (also called tetra(trifluoromethyl)cyclobutadiene episulfide) as the principal gas phase products. The latter is colored a pale yellow and is stable at room temperature. These results suggest that a possible mechanism for the reaction of photoexcited thiophenes is via the formation of valence bond isomers as intermediates.

La photolyse du tétra(trifluorométhyl)thiophène (TTFT) à 2139 Å ou par sensibilisation par le mercure à 2537 Å, donne l'hexafluorobutyne-2 et le tétra(trifluorométhyl)-1,2,3,4 thia 5 bicyclo[2,1,0] penetène-2 (appelé aussi tétra(trifluorométhyl)cyclobutadiène épisulfure) comme produits principaux de la phase gazeuse. Ce dernier, de couleur jaune pâle, est stable à la température ambiante. Ces résultats laissent penser qu'un mécanisme possible dans la réaction des thiophènes photoexcités, est le passage par les isomères de liaison de valence au stade intermédiaire.

Canadian Journal of Chemistry, **50**, 2721 (1972)

Introduction

The photolysis of a number of five-membered heterocyclic compounds proceeds through the intermediate **1**, (1–8), the reaction being

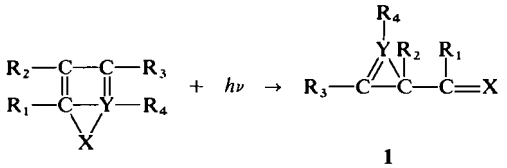

1

where X is a heteroatom and Y is either carbon or a heteroatom.

Wynberg and his coworkers (9–12) have studied the photolysis of substituted thiophenes in solution and have observed that the substituted groups shift. Labelling experiments have shown that ring carbons move, carrying the substituent groups with them. Such an isomerization could proceed through a ring contracted intermediate or "benzenoid" type valence bond isomer, but Wynberg *et al.* (12) preferred a species involving valence shell expansion of the sulfur atom.

Recent studies (13–15) have shown that the irradiation of solutions of thiophenes or furans in amines leads to the formation of pyrroles. The same pyrroles are formed from furans as from the corresponding thiophenes. This was taken to imply that cyclopropenyl intermediates (ketones or aldehydes for the furan systems, thioketones or thioaldehydes for the thiophene systems) are involved in the reaction.

In an earlier report from our laboratory (16), the photolysis of thiophene was reported. The mechanistic details required that the initially formed electronically excited thiophene pass

[1]CAES Report No. 164–70.

[2]Present address: Division of Chemistry, National Research Council of Canada, Ottawa, Canada.

Can. J. Chem. Downloaded from www.nrcresearchpress.com by 210.87.254.40 on 09/05/12
For personal use only.

2. (*a*) E. WENKERT, A. MUELLER, E. J. REARDON, JR., S. S. SATHE, D. J. SCHARF, and G. TOSI. J. Am. Chem. Soc. **92**, 7428 (1970); (*b*) J. KATSUBE and M. MATSUI. Agri. Biol. Chem. **33**, 1078 (1969); (*c*) R. T. DAHILL. J. Org. Chem. **31**, 2694 (1966); (*d*) A. TAKEDA, H. HOSISIMA, and S. TORII. Bull. Chem. Soc. Japan, **39**, 1354 (1966); (*e*) E. THIELE. Ger. (East) Pat. 30 727; Chem. Abstr. **65**, 8789*h* (1966); (*f*) J. L. ERICKSON and F. E. COLLINS. J. Org. Chem. **30**, 1050 (1965); (*g*) M. ELLIOTT. J. Chem. Soc. 2231 (1956); (*h*) R. L. FRANK, P. G. ARVAN, J. W. RICHTER, and C. R. VANNEMAN. J. Am. Chem. Soc. **66**, 4 (1944); (*i*) H. HUNSDIECKER. Ber. **75**, 455 (1942); (*j*) H. STAUDINGER and L. RUZICKA. Helv. Chim. Acta, **7**, 245 (1924); (*k*) T. L. Ho. J. Chinese Chem. Soc. (II) **18**, 153 (1971).
3. G. D. BUCKLEY, T. J. ELLIOTT, F. G. HUNT, and A. LOWE. J. Chem. Soc. 1505 (1947).
4. W. F. J. HUURDEMAN, H. WYNBERG, and D. W. EMERSON. Tetrahedron Lett. 3449 (1971).
5. T. L. Ho, H. C. Ho, and C. M. WONG. Chem. Commun. In press.

The Photolysis of Tetra(trifluoromethyl)thiophene Vapor[1]

H. A. WIEBE,[2] SILVIA BRASLAVSKY, AND JULIAN HEICKLEN

Department of Chemistry and Center for Air Environment Studies, The Pennsylvania State University, University Park, Pa. 16802

Received March 20, 1972

The photolysis of tetra(trifluoromethyl)thiophene (TTFT) at 2139 Å or by mercury sensitization at 2537Å yields hexafluorobutyne-2 and 1,2,3,4-tetra(trifluoromethyl)5-thiabicyclo[2,1,0]pentene-2 (also called tetra(trifluoromethyl)cyclobutadiene episulfide) as the principal gas phase products. The latter is colored a pale yellow and is stable at room temperature. These results suggest that a possible mechanism for the reaction of photoexcited thiophenes is via the formation of valence bond isomers as intermediates.

La photolyse du tétra(trifluorométhyl)thiophène (TTFT) à 2139 Å ou par sensibilisation par le mercure à 2537 Å, donne l'hexafluorobutyne-2 et le tétra(trifluorométhyl)-1,2,3,4 thia 5 bicyclo[2,1,0] penetène-2 (appelé aussi tétra(trifluorométhyl)cyclobutadiène épisulfure) comme produits principaux de la phase gazeuse. Ce dernier, de couleur jaune pâle, est stable à la température ambiante. Ces résultats laissent penser qu'un mécanisme possible dans la réaction des thiophènes photoexcités, est le passage par les isomères de liaison de valence au stade intermédiaire.

Canadian Journal of Chemistry, **50**, 2721 (1972)

Introduction

The photolysis of a number of five-membered heterocyclic compounds proceeds through the intermediate **1**, (1–8), the reaction being

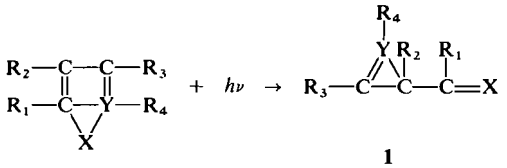

1

where X is a heteroatom and Y is either carbon or a heteroatom.

Wynberg and his coworkers (9–12) have studied the photolysis of substituted thiophenes in solution and have observed that the substituted groups shift. Labelling experiments have shown that ring carbons move, carrying the substituent groups with them. Such an isomerization could proceed through a ring contracted intermediate or "benzenoid" type valence bond isomer, but Wynberg *et al.* (12) preferred a species involving valence shell expansion of the sulfur atom.

Recent studies (13–15) have shown that the irradiation of solutions of thiophenes or furans in amines leads to the formation of pyrroles. The same pyrroles are formed from furans as from the corresponding thiophenes. This was taken to imply that cyclopropenyl intermediates (ketones or aldehydes for the furan systems, thioketones or thioaldehydes for the thiophene systems) are involved in the reaction.

In an earlier report from our laboratory (16), the photolysis of thiophene was reported. The mechanistic details required that the initially formed electronically excited thiophene pass

[1]CAES Report No. 164–70.

[2]Present address: Division of Chemistry, National Research Council of Canada, Ottawa, Canada.

Can. J. Chem. Downloaded from www.nrcresearchpress.com by 210.87.254.40 on 09/05/12
For personal use only.

over to some other intermediate as a precursor to allene formation. At that time we preferred the valene intermediate to the ring-contracted cyclopropene carbonyl compound, because cyclopropene was not found as a product.

In order to investigate the nature of the intermediate in thiophene photolysis, we have studied the photolysis of tetra(trifluoromethyl)-thiophene (TTFT), and those results are

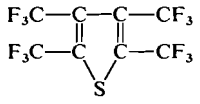

TTFT

reported here. This compound was chosen since the migration of either CF_3 groups or fluorine atoms is not likely in gas phase kinetic studies. The formation of the products resulting from H-atom migration in thiophene photolysis should be inhibited.

Results and Discussion

TTFT has a strong absorption starting at about 2550 Å. We have decomposed the vapor with 2139 Å radiation and by mercury sensitization at 2537 Å at room temperature (25 ± 2 °C). A pressure equal to the vapor pressure at that temperature (~ 5.5 Torr) was used. The main gas-phase products were hexafluorobutyne-2 and 1,2,3,4-tetra(trifluoromethyl)5-thiabicyclo[2,1,0]pentene-2 (**2**) (tetra-(trifluoromethyl)cyclobutadiene episulfide).

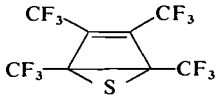

2

Originally we though the product **2** was tetra-(trifluoromethyl)cyclopropene-3-thioketone

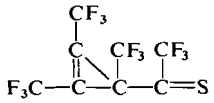

as stated in a previous publication (17) from our laboratory based on the work here. The evidence now suggests that this is not so.

Two minor products (<1% of the total gaseous products) and a white polymer were also produced. The mass spectra of the minor products indicated molecular weights of 164 and 214. The product with mass 214 is probably

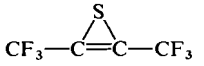

but the product with mass 164 is difficult to identify. The polymer was removed from the cell by heating after each run with an oxygen torch to about 500 °C.

The compound **2** had a gas chromatographic retention time of 14 min compared to 26 min for TTFT. It was stable at room temperature, even to prolonged irradiation (2 h) with 2139 Å light, pale yellow in color, and could be passed through the gas chromatograph without any appreciable loss.

The mass spectrum of product **2** was obtained on an AEI MS-9 mass spectrometer operating at 70 eV. The spectrum is reported in Table 1

TABLE 1. Mass spectra at 70 eV

		Relative intensity	
m/e	Ion	**2***	TTFT
31	CF^+	6.5	7.0
69	CF_3^+	*100*	53.4
87	C_3FS^+	8.2	8.0
93	$C_3F_3^+$	21.0	11.4
111	C_5FS^+	7.4	3.3
113	$C_2F_3S^+$	10.0	2.0
117	$C_5F_3^+$	16.3	10.0
130	$C_5F_2S^+$	15.1	16.0
143	$C_4F_5^+$	7.9	6.0
149	$C_5F_3S^+$	10.4	26.0
199	$C_6F_5S^+$	24.4	20.0
200	$C_4F_8^+$	16.3	2.0
201	$C_3F_7S^+$	10.5	1.0
237	$C_6F_7S^+$	37.2	21.4
238	" †	0.3	0.3
239	" †	0.1	0.1
287	$C_7F_9S^+$	97.5	80.0
288	" †	9.3	8.7
289	" †	4.9	5.3
306	$C_7F_{10}S^+$	29.0	21.4
307	" †	0.3	0.3
308	" †	0.1	0.1
337	$C_8F_{11}S^+$	97.5	*100*
338	" †	12.1	13.3
339	" †	6.3	6.7
356	$C_8F_{12}S^+$	99.0	80.0
357	" †	10.0	6.0
358	" †	5.1	3.5

*1,2,3,4-Tetra(trifluoromethyl)5-thiabicyclo[2,1,0]pentene-2.
†Isotopically shifted because of ^{13}C or ^{34}S.

Can. J. Chem. Downloaded from www.nrcresearchpress.com by 210.87.254.40 on 09/05/12
For personal use only.

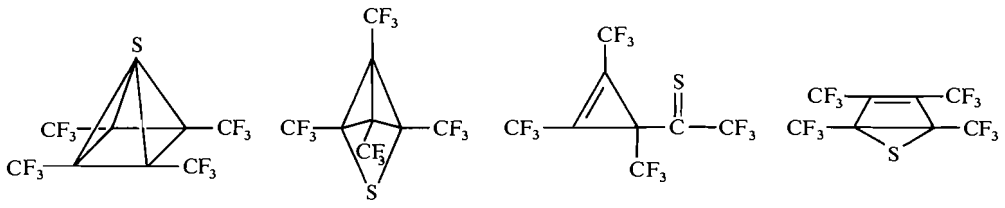

along with that of TTFT. The similarity of the two spectra indicates that the two molecules are isomers.

If the CF_3 groups have not migrated, which seems likely, then the photo product **2** could be one of four valence bond isomers of TTFT (*a–d*). Further structural identification was obtained from i.r., u.v., and n.m.r. spectra.

The i.r. spectrum of **2** was obtained on a Beckman IR-10.[3] The product has bands at 1698, 1428, 1400, 1340, 1320, 1275, 1238, 1218, 1195, 1175, 1145, 1090, 1050, 1025, 985, 883, 805, 780, 749, 713, 647, 633, and 607 cm^{-1}. The band at 1698 cm^{-1} in **2**, which is absent in TTFT, is identified as the carbon–carbon double-bond stretch. This wavelength is in the region for a non-conjugated C=C stretching vibration (18). The intense absorptions in the remainder of the spectrum are characteristic of molecules containing a large proportion of fluorine (18). The presence of a C=C rules out isomers *a* and *b* as possible structures for product **2**.

The F^{19} n.m.r. spectrum of **2** revealed two CF_3 peaks of equal intensity at -1310 and -1047 Hz. For TTFT two n.m.r. bands of equal intensity are observed at -2040 and -1880 Hz. These results in conjunction with mass spectral and i.r. absorption data definitely establish product **2** to have the Dewar thiophene structure *d*, since product *c* would have three peaks of intensities 2/1/1.

The u.v. absorption spectrum of **2** was taken on a Cary 15 spectrophotometer. Peak absorptions occurred at 2475 Å ($\varepsilon = 1.3 \times 10^{-2}$ $Torr^{-1}$ cm^{-1} to base 10) and 3365 Å ($\varepsilon = 2.7 \times 10^{-3}$ $Torr^{-1}$ cm^{-1} to base 10).

[3]These spectra may be obtained, upon request, from the Depository of Unpublished Data, National Science Library, National Research Council of Canada, Ottawa, Canada K1A 0S2. These spectra also are contained in Report No. 164-70 of the Center for Air Environment Studies, Pennsylvania State University, University Park, Pa. 16802.

The present isolation and characterization of 1,2,3,4-tetra(trifluoromethyl)5-thiabicyclo-[2,1,0]pentene-2 in the photolysis of tetra(trifluoromethyl)thiophene establishes the importance of valance bond isomers (other than the ring-contracted intermediate found in the photolysis of other five-membered heterocyclic molecules) as intermediates in the photochemistry of thiophenes.

Experimental

Tetra(trifluoromethyl)thiophene (TTFT) was prepared by heating hexafluorobutyne-2 (Pierce Chemical Co.) with an equivalent of sulfur and one-half equivalent of iodine at 180 °C for 48 h in a stainless steel container (19). It was purified by g.l.c. on a 1/4-in. diameter by 10 ft long column packed with 30% dinonylphthalate on chromosorb W(AW) operated at 80 °C with a helium flow rate of 50 cc/min. Photolysis was done in a cylindrical (50 mm diameter by 100 mm long) quartz reaction vessel attached to a grease-free high-vacuum system. The radiation sources were a Phillips type 93106E, 25 Watt zinc resonance lamp for direct irradiation at 2139 Å and a Hanovia flat spiral low-pressure mercury-arc for the mercury-photosensitized reactions. After irradiation, the products were separated and analyzed on the same gas chromatographic column operating at 30 °C with a helium flow rate of 50 cc/min.

The n.m.r. spectra were obtained on a Varian Associates spectrometer operating at 94.1 mHz and approximately 14 000 Gauss. Calibration of the spectra was in terms of displacements in c.p.s. from the ^{19}F spectrum of trifluoroacetic acid. The negative frequency displacements indicate resonances occurring at lower field than the reference.

This work was supported by the U.S. Public Health Service, National Air Pollution Control Administration under Grant No. AP00718, for which we are grateful.

1. E. F. Ullman and B. Singh. J. Am. Chem. Soc. **88**, 1844 (1966).
2. R. Srinivasan. J. Am. Chem. Soc. **89**, 4812 (1967).
3. H. Hiraoka and R. Srinivasan. J. Am. Chem. Soc. **90**, 2720 (1968).
4. R. Srinivasan. Pure Appl. Chem. **16**, 65 (1968).
5. H. Hiraoka. J. Phys. Chem. **74**, 574 (1970).
6. S. Boué and R. Srinivasan. J. Am. Chem. Soc. **92**, 1824 (1970).
7. R. Srinivasan. As reported in ref. 6.

Can. J. Chem. Downloaded from www.nrcresearchpress.com by 210.87.254.40 on 09/05/12
For personal use only.

8. E. E. VAN TAMELEN and T. H. WHITESIDES. J. Am. Chem. Soc. **90**, 3894 (1968).
9. H. WYNBERG, H. VAN DRIEL, R. M. KELLOGG, and J. BUTER. J. Am. Chem. Soc. **89**, 3487 (1967).
10. R. M. KELLOGG and H. WYNBERG. J. Am. Chem. Soc. **89**, 3495 (1967).
11. H. WYNBERG, G. E. BEEKHUIS, H. VAN DRIEL, and R. M. KELLOGG. J. Am. Chem. Soc. **89**, 3498 (1967).
12. H. WYNBERG, R. M. KELLOGG, H. VAN DRIEL, and G. E. BEEKHUIS. J. Am. Chem. Soc. **89**, 3501 (1967).
13. A. COUTURE and A. LABLACHE-COMBIER. Chem. Commun. 524 (1969).
14. A. COUTURE and A. LABLACHE-COMBIER. Tetrahedron **27**, 1059 (1971).
15. A. COUTURE and A. LABLACHE-COMBIER. Chem. Commun. **891**, (1971).
16. H. A. WIEBE and J. HEICKLEN. Can. J. Chem. **47**, 2965 (1969).
17. E. C. WU and J. HEICKLEN. J. Am. Chem. Soc. **93**, 3432 (1971).
18. L. J. BELLAMY. The infrared spectra of complex molecules. John Wiley and Sons, New York. 1958.
19. C. G. KRESPAN. J. Am. Chem. Soc. **83**, 3434 (1961).

Can. J. Chem. Downloaded from www.nrcresearchpress.com by 210.87.254.40 on 09/05/12
For personal use only.

Can. J. Chem. Downloaded from www.nrcresearchpress.com by 210.87.254.40 on 09/05/12
For personal use only.

Conversion of Nonlinear Shift Reagent Plots to Linear Plots

J. W. ApSimon,[1] H. Beierbeck, and A. Fruchier
Department of Chemistry, Carleton University, Ottawa, Canada

Received May 4, 1972

A method is presented for converting partially or completely nonlinear shift reagent plots to perfectly linear plots, from which highly accurate intercepts and slope ratios can be obtained even for nuclei, whose signals can only be observed in the nonlinear region of the original plots.

On présente une méthode permettant de transformer en droites les courbes obtenues dans l'étude des substrats organiques en présence de chélates de lanthanides. A partir de ces droites on peut calculer avec précision les ordonnées à l'origine (déplacements chimiques en l'absence de chélate) et les rapports des pentes, même pour les noyaux dont les signaux ne peuvent être observés que dans la région non linéaire des courbes initiales.

Canadian Journal of Chemistry, **50**, 2725 (1972)

It is known (1, 2) that plots of chemical shifts *vs.* amount of added shift reagent are only linear for small [L]/[S] ratios ([L] and [S] are the total concentrations of shift reagent and substrate respectively). We have shown (3) that in the linear region accurate slope ratios and intercepts can be obtained, even with inaccurate shift reagent concentrations, because the chemical shifts are very accurate and because the [L]/[S] ratios must be exactly the same for all protons in a given sample. Instead of plotting the chemical shifts against the experimental [L]/[S] ratios, they are plotted against "corrected" values which are proportional to the sums of the shifts in each spectrum (3).

As the [L]/[S] ratios increase the plots of chemical shifts *vs.* [L]/[S] become nonlinear. However, since the lanthanide induced shifts are equal to the product of the fractions [LS]/[S] of the complexed substrate and the induced chemical shifts Δ in the complexed state

$$[1] \qquad \delta = \frac{[LS]}{[S]}\Delta$$

([LS] is the concentration of complexed substrate), there exists another variable, [LS]/[S], such that the chemical shifts are a linear function of this variable for any value of [L]/[S]. Since the [LS]/[S] are also the same for all nuclei in any given sample, regardless of the amount of added shift reagent, it is again possible to obtain accurate slope ratios and intercepts without any knowledge of the values of [LS]/[S]. As before the chemical shifts are simply plotted against coordinates c_j which are proportional to the sums of the shifts in each spectrum (3). If the limiting shifts (the shifts in the complexed substrate) are known these values can be normalized to the actual values for the fractions [LS]/[S] of complexed substrate. The slope ratios are equal to the ratios of the limiting shifts and the same values must be obtained from the linear part of the δ *vs.* [L]/[S] plot and from the linear δ *vs.* [LS]/[L] plot.

$$[2] \quad c_j = (c_n - c_1)(\sum \delta_{ij} - \sum \delta_{i1})/(\sum \delta_{in} - \sum \delta_{i1}) + c_1$$

Figures 1 and 2 illustrate this conversion for the methyl group signals of β-amyrin in the presence of $Pr(fod)_3$ (the assumption that the shifts in the last spectrum represent the limiting shifts is certainly incorrect in this case; however, this does not affect the following results). Table 1 shows that, within experimental error, the slope ratios are the same whether the range of [L]/[S] ratios is 0.5, 1.0, or 1.5. Similarly the intercepts vary little and are in good agreement with the experimental shifts in the spectrum of β-amyrin alone (Table 2).

[1]To whom correspondence should be addressed.

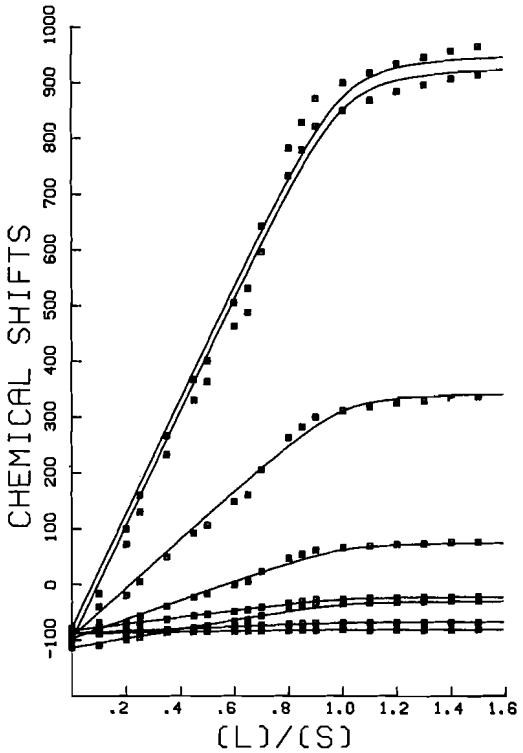

FIG. 1. Plot of chemical shifts *vs.* [L]/[S] for the methyl groups of β-amyrin in the presence of $Pr(fod)_3$.

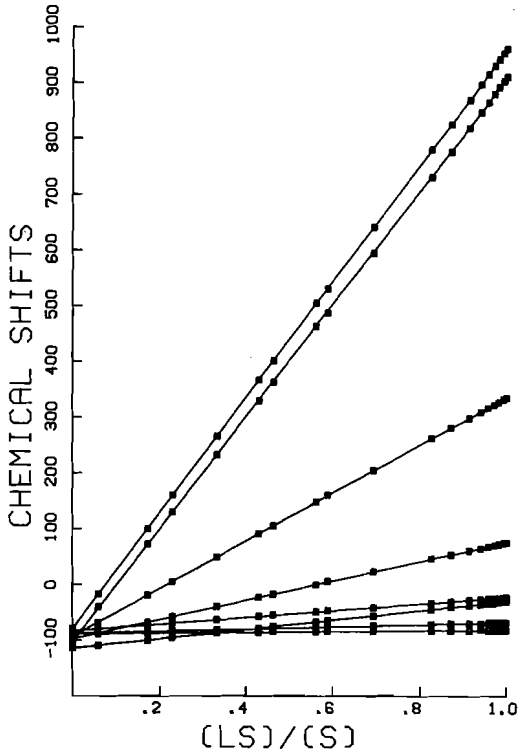

FIG. 2. Plot of chemical shifts *vs.* [LS]/[S] for the methyl groups of β-amyrin in the presence of $Pr(fod)_3$. It is assumed that the last points represent limiting shifts.

TABLE 1. Slope ratios for the methyl group signals of β-amyrin* in the presence of $Pr(fod)_3$

Range of [L]/[S]:	0–0.5	0–1.0	0–1.5	0.5–1.0†
Me	Slope ratios‡			
30	8.6	7.0	6.4	6.4
29	23.2	20.4	19.8	18.1
28	63.7	59.4	59.0	57.1
27	81.2	81.7	81.4	80.0
26	169.4	167.7	166.9	167.2
25	415.9	414.4	413.0	412.2
24	964.1	970.4	973.5	970.4
23	1000.0	1000.0	1000.0	1000.0

*β-Amyrin

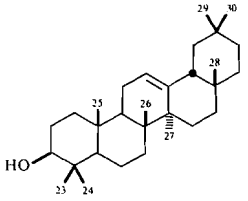

†Only the chemical shifts for methyl groups 23 and 24 were used to derive relative [LS]/[S] values.

‡All slopes are normalized to a slope of 1000.0 for methyl group 23.

Can. J. Chem. Downloaded from www.nrcresearchpress.com by 210.87.254.40 on 09/05/12
For personal use only.

TABLE 2. Intercepts for the methyl group signals of β-amyrin in the presence of $Pr(fod)_3$

Range of [L]/[S]:		0–0.5	0–1.0	0–1.5	0.5–1.0*
Me	exp†	Intercepts			
30	87.5	87.8	87.4	87.2	87.0
29	87.5	88.3	87.5	87.2	85.6
28	83.0	84.0	82.8	82.7	81.0
27	113.5	113.6	113.6	113.5	112.2
26	97.0	97.3	97.0	96.7	96.6
25	94.0	93.3	93.0	92.5	91.2
24	100.0	99.1	101.6	102.9	101.6
23	79.0	78.1	78.6	78.7	78.6

*Only the chemical shifts for methyl groups 23 and 24 were used to derive relative [LS]/[S] values.
†Chemical shifts in the spectrum of β-amyrin without $Pr(fod)_3$.

This extension of the linearity of the shift reagent plots should be useful for working with ring protons, since their signals are usually hidden in the methylene envelope for small values of [L]/[S]. In order to obtain the intercepts in this case it is necessary to "calibrate" the plots with signals, such as methyl group shifts, which can be seen in the spectrum of the pure substrate. That in this case accurate intercepts can still be obtained can be demonstrated with the methyl group signals of β-amyrin. Thus, it was assumed that the signals for the methyl groups 23 and 24 were observed in every spectrum including the "zero" spectrum, but that for the remaining six methyl groups only the signals in the range $0.5 < [L]/[S] < 1.0$ were available. First the shifts for methyls 23 and 24 were used to obtain corrected shift reagent coordinates in the usual way (3). Then the remaining signals were plotted against these corrected values. As Tables 1 and 2 show, slope ratios and intercepts for methyl groups 25–30 agree well with the values obtained previously.

To conclude we have shown that the excellent correlation between the chemical shifts for the different nuclei in the substrate molecule makes it possible to convert partially or completely nonlinear plots to perfectly linear plots, from which highly accurate intercepts and slope ratios can be obtained even for nuclei whose signals can only be observed in the non-linear region of the original plots.

We thank the National Research Council of Canada for generous financial support. (Grant in Aid, J.W.A.: Post Doctoral Fellowship, A. F.)

1. C. C. HINCKLEY. J. Am. Chem. Soc. **91**, 5160 (1969).
2. See for example W. DE W. HORROCKS, JR., J. P. SIPE, III, and J. R. LUBER. J. Am. Chem. Soc. **93**, 5258 (1971) and references therein.
3. J. W. APSIMON and H. BEIERBECK. Chem. Commun. 172 (1972).

Can. J. Chem. Downloaded from www.nrcresearchpress.com by 210.87.254.40 on 09/05/12
For personal use only.

Can. J. Chem. Downloaded from www.nrcresearchpress.com by 210.87.254.5 on 09/05/12
For personal use only.

Canadian Journal of Chemistry

Published by THE NATIONAL RESEARCH COUNCIL OF CANADA

VOLUME 50 SEPTEMBER 1, 1972 NUMBER 17

Kinetics of Charge Scavenging in γ Irradiated Liquids with Large Free Ion Yields[1]

JEAN-POL DODELET AND GORDON R. FREEMAN

Chemistry Department, University of Alberta, Edmonton 7, Alberta

Received February 11, 1972

The extent to which the calculated scavenging yields are affected by the form of the ion–electron spacial distribution decreases as the free ion yield increases. The increasing free ion yield may be due to larger electron ranges or to a larger dielectric constant. The free ion yields in neopentane and water are respectively 1.0 (due to large electron ranges) and 2.7 (due to large dielectric constant). The scavenging yields in neopentane calculated with three different forms of spacial distribution, using the forced diffusion (FD) approximation, are significantly affected by the form of the spacial distribution. The scavenging yields in water calculated with four different forms of spacial distribution, using the FD approximation, are all within the experimental error of the measured yields. Use of the prescribed diffusion (PD) approximation permits satisfactory yields to be calculated for neopentane, but leads to the unsatisfactory result that all of the secondary electrons in the liquid have the same range (delta function distribution YD). The scavenging yield curves obtained using the PD approximation for water did not have a steep enough slope even when the distribution YD was used; YD leads to a steeper slope than any other form of distribution. The PD approximation gives an overestimate of the breadth of the geminate neutralization time distribution. The calculated time required for half of the geminate neutralization reaction to occur is similar whether the FD or PD approximation is used, but the spread of the neutralization times is an order of magnitude greater from the latter than from the former. Calculations were also done for electron scavenging in methylcyclopentane and in methanol. Methylcyclopentane behaves like cyclohexane and methanol behaves much like water with regard to the kinetics of ion–electron reactions in the spurs.

Les courbes de capture calculées réagissent d'autant moins au changement de la distribution des interdistances initiales ion–électron que le rendement en ions libres augmente. De grandes distances de pénétration électronique ou une constante diélectrique importante peuvent, entre autres, être responsables de l'accroissement de ce dernier. Le rendement en ions libres vaut 1.0 pour le néopentane (grande distance de pénétration) et 2.7 pour l'eau (constante diélectrique importante). Les rendements de capture calculés pour le néopentane, dans l'approximation de la diffusion forcée, FD, au moyen de trois distributions spatiales, réagissent à la forme de ces distributions. Dans le cas de l'eau, quatre distributions furent utilisées pour l'approximation FD. Les différences dans les résultats sont de l'ordre de grandeur des erreurs expérimentales. L'approximation de la diffusion prescrite, PD, donne des rendements calculés en bon accord pour le néopentane mais aboutit à la conclusion gênante que les distances de pénétration attribuées aux électrons secondaires sont identiques (fonction de distribution delta: YD). Les courbes de capture obtenues avec l'approximation PD, pour l'eau, n'ont pas une pente assez raide même pour une distribution YD; cette dernière donne pourtant la pente la plus raide. L'approximation PD conduit à une surestimation de la dispersion des temps de neutralisation dans les grappes. Le temps de demi-vie des ions dans ces grappes est semblable pour les deux approximations alors que la dispersion des temps de neutralisation est environ un ordre de grandeur plus grande pour l'approximation PD. Des courbes de capture furent également calculées pour le méthylcyclopentane et le méthanol. La cinétique des réactions ion–électron dans les grappes est similaire pour le méthylcyclopentane et le cyclohexane; c'est également le cas pour le méthanol et l'eau.

Canadian Journal of Chemistry, **50**, 2729 (1972)

Introduction

In a recent article, a stochastic model of charge scavenging in γ irradiated liquids was examined to determine to what extent the calculated scavenging yields were affected by the initial shape of the ion–electron spacial distribution and by the temporal form of the drift and diffusion that was assumed for the

[1]Supported by the National Research Council of Canada.

Can. J. Chem. Downloaded from www.nrcresearchpress.com by 210.87.254.5 on 09/05/12
For personal use only.

charges in an ion–electron pair (1). The examination was made for a typical saturated hydrocarbon that has often been studied, namely, cyclohexane. It was found that in the original model (2), the calculated yields at low and high scavenging concentrations were affected by the form of spacial distribution that was assumed. The yields in the middle of the scavenging range are not affected by the assumed form of the spacial distribution because the scavenging efficiency parameter is always adjusted to make the model fit in this region. It is necessary to focus one's attention on the ends of the scavenging curves. The low-concentration end is to be preferred for experimental and theoretical reasons.

It was also found (1) that use of the prescribed diffusion approximation in the model reduced the sensitivity of the model to the initial form of the ion–electron distribution. However, there was an indication that the prescribed diffusion approximation led to an exaggerated spread of neutralization times in the liquid.

The radiolyses of most liquid hydrocarbons are characterized by low free ion yields, $G_{fi} = 0.1–0.2$ (3–6), as is cyclohexane. The stochastic model has also been applied to charge scavenging in the γ radiolysis of liquids that have large free ion yields, such as neopentane (7) and water (8), which have $G_{fi} = 1.0 \pm 0.1$ (4, 7, 9) and 2.7 ± 0.1 (8, 10), respectively.[2] The free ion yield in neopentane is large because the ranges of the secondary electrons in that liquid are unusually long; the yield in water is large because of the high dielectric constant of that liquid. The magnitudes of the electron range and dielectric constant are also important in the scavenging kinetics. It is, therefore, desirable to extend the earlier examination of the kinetics model (1) to the neopentane and water systems. The purpose of this article is to report the results of the extended examination. Calculations have also been done on the methanol and methylcyclopentane systems and are briefly mentioned.

Theory

The model concerns the competition between geminate neutralization of the ions and electrons in radiolytic spurs and reaction of the ions or electrons with solute molecules.

Diffusion Approximations and Geminate Neutralization Times

The model involves the time required for geminate neutralization to occur. Two different diffusion approximations have been used (1, 2, 12, 13). In much of the earlier work (2, 8, 12, and others) a "forced diffusion" (FD) approximation was used in which only the drift of the ion and electron in their mutual electric field was considered; the "spreading" effect of Brownian motion on the geminate neutralization time was neglected. In the FD approximation, the time $t_{gn}(y)$ required for the geminate neutralization of a thermalized electron–ion pair that has an initial separation distance y is given by eq. 1 (12).

$$[1] \quad t_{gn}(y) = 2.3 \times 10^6 \, \varepsilon y^3 (u_+ + u_-)^{-1} \text{ s}$$

where ε is the dielectric constant of the liquid and u_+ and u_- are the mobilities of the ion and electron, respectively. In this approximation, for a given value of y, the probability that neutralization has occurred at time t is zero for $t < t_{gn}$ and unity for $t \geqslant t_{gn}$. A distribution of neutralization times is generated by a distribution of y values.

The second treatment of the neutralization time (13) was based on the prescribed diffusion (PD) approximation in which Brownian motion in a coulomb field was considered; it was assumed that the spacial distribution of the ions and electrons, averaged over all the spurs, remained in the Gaussian form at all times. Associated with each initial separation distance y for an assembly of pairs there is a distribution of neutralization times that is assumed to be described by eq. 2 (13).

$$[2] \quad -dF_y(t) = \frac{\xi^2 F_y(t)}{\varepsilon k T (4\pi D)^{1/2} t^{3/2}} \exp(-y^2/4Dt)\, dt$$

where $-dF_y(t)$ is the fraction of ion pairs that begin at $t = 0$ with intradistance y and undergo neutralization during the interval between the times t and $t + dt$, $F_y(t)$ is the probability that a pair beginning at y remains unneutralized at time t, ξ is the electronic charge, k is Boltzmann's constant, T is the absolute temperature, and D

[2]See also Table III of ref. 11 and references therein to the work of Allen, Hochanadel, Matheson, Gordon, Hart, and others.

Can. J. Chem. Downloaded from www.nrcresearchpress.com by 210.87.254.5 on 09/05/12
For personal use only.

is the sum of the diffusion coefficients of the ion and electron ($D = kT(u_+ + u_-)/c$, where c is the unit electronic charge).

Scavenging Equations

Introduction of an electron scavenger into the liquid puts the electron neutralization reaction into competition with scavenging. The time limit during which scavenging can occur is the normal neutralization time of the electron. The free ions have relatively long lifetimes under normal radiolysis conditions and are much more readily scavenged than are those that undergo geminate neutralization. The probability ϕ_y^{fi} that an ion–electron pair will become free ions is

$$[3] \qquad \phi_y^{fi} = \exp\ (-\xi^2/\varepsilon kTy)$$

and the probability of their being scavenged is usually taken as unity at all scavenger concentrations greater than zero (2).

Using the FD approximation, the total probability Φ_y^{FD} that an electron in a pair with an initial separation distance y will be scavenged is given by eq. 4 (1, 2).

$$[4] \quad \Phi_y^{FD} = \phi_y^{fi} + (1 - \phi_y^{fi})[1 - (1 - fN_s)^{1.4 \times 10^7\, \varepsilon y^3 \beta}]$$

where $(1 - \phi_y^{fi})$ is the fraction of the ions that undergo geminate neutralization, f is the encounter efficiency of the scavenging reaction, N_s is the mole fraction of scavenger in the solution, and β is an adjustable parameter that relates to the relative motions of the electron, its parent positive ion and the scavenger molecules. For the sake of simplicity, the value of f is taken as unity in the present work.

Alternatively, if the PD approximation is used, the total probability Φ_y^{PD} that an electron in a pair with an initial separation distance y will be scavenged is described by eq. 5 (1).

$$[5] \qquad \Phi_y^{DP} = 1 + \int_{t=0}^{\infty} (1 - fN_s)^{\alpha t}\, dF_y(t)$$

where α is the number of new molecules that an electron meets per unit time.

In any given system, there is a distribution of y values. One may represent by $F(y)dy$ as the fraction of thermalized pairs that have initial intradistances between y and $y + dy$. The final expression for the total scavenging efficiency to be used with either eq. 4 or eq. 5 is

$$[6] \qquad \Phi = \int_{y=0}^{\infty} F(y)\Phi_y\, dy$$

Nitrogen yields from nitrous oxide solutions are calculated from eq. 7. The small g is used to signify a scavenging yield (1).

$$[7] \qquad g(N_2) = \Phi g(N_2)_{max}$$

Distribution Functions F(y)

Different forms of the pair intradistance function $F(y)$ have been used by various authors; a summary is given in ref. 1. The present work includes four forms:

(*a*) YP, a power function (1, 14)

$$[8] \quad \begin{cases} F(y) = x y_{min}^{x} y^{-(x+1)} & y \geqslant y_{min} \\ F(y) = 0 & y \leqslant y_{min} \end{cases}$$

(*b*)YD, a delta function, which is the particular case of YP with $x = \infty$ and $y = y_{min} = y_d$ for all pairs;

(*c*) YG, a single parameter, 3-dimensional Gaussian function

$$[9] \qquad F(y) = (4y^2/\pi^{1/2}b^3) \exp\ (-y^2/b^2)$$

where b is the dispersion parameter.

(*d*) YSE, a semi-empirical function used in the original work (2, 3).

Calculations of Scavenging Yields

Nitrogen yields were calculated with eq. 7 for solutions of nitrous oxide in neopentane and in water. Calculations were first done using the FD approximation (eq. 4), then repeated using the PD approximation (eq. 5). In each set of calculations, all of the above mentioned forms of $F(y)$ function were tried, with the exception of YSE in neopentane because YSE is not suitable for the large y values in that liquid (7). The values of the parameters y_d and b in YD and YG, respectively, were determined with the aid of the general plots in Fig. 1.

The experimental quantities needed for the calculations are listed in Table 1.

Details of the computer calculation method were reported in ref. 1. Theoretical yields $g(N_2)_{calc}$ were calculated as functions of the mole fraction of nitrous oxide in solution. Depending upon the neutralization time approximation used, the value of the parameter α or β

TABLE 1. Experimental data used in the calculations

Parameter	Value			
	$C(CH_3)_4$ [a]	H_2O [b]	c-$C_5H_9CH_3$ [c]	CH_3OH [d]
T (K)	295	296	298	298
ε	1.82	79	1.98	33
d(g/cm^3)	0.590	0.997	0.745	0.788
$g(N_2)_{fi}$	0.95	2.7	0.13	2.0
$g(N_2)_{max}$	4.7	4.0	4.9	4.6
D_{e^-}(cm^2/s) [e]	1.4 [f]	4.6×10^{-5} [g]	9×10^{-3} [h]	1.6×10^{-5} [i]
D_+(cm^2/s) [e]	[j]	9.2×10^{-5} [k]	[j]	3.8×10^{-5} [k]
D(cm^2/s) [e]	1.4	1.38×10^{-4}	9×10^{-3}	5.4×10^{-5} [b]

[a] Reference 7.
[b] Reference 8.
[c] Reference 24.
[d] Reference 25.
[e] At 296 K, $D = 0.0255$ u is where u is in units of cm^2/V s.
[f] Reference 26.
[g] Reference 27.
[h] Assumed equal to that for cyclohexane reported in ref. 26.
[i] Estimated from data in ref. 28 and 29.
[j] Assumed $D_+ \ll D_{e^-}$.
[k] Reference 28.
[l] Reference 29.

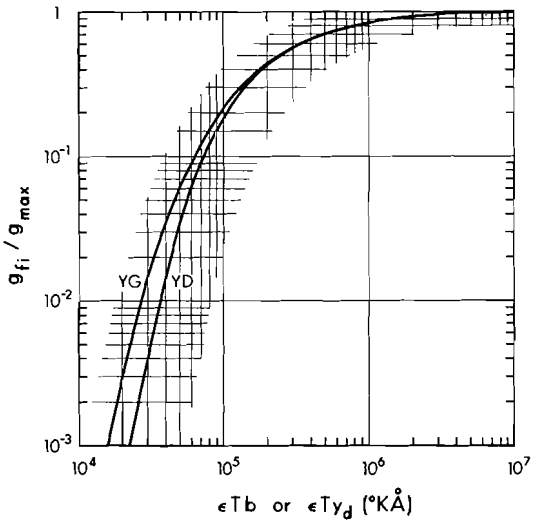

FIG. 1. General plots of g_{fi}/g_{max} against εTb and εTy_d to facilitate the determination of the values of the Gaussian parameter b and the YD range y_d. ε is the dielectric constant and T the absolute temperature of the medium.

was adjusted to give the best agreement with the experimental points (7, 8, 15, 16). The best agreement was chosen to give the minimum $\overline{\Delta g}$

$$[10] \qquad \overline{\Delta g} = \frac{1}{n}\sum_{i=1}^{n} |g(N_2)_{calc} - g(N_2)_{exp}|$$

where n is the number of experimental points.

It should be mentioned that the static dielectric constant was used for all the calculations in both liquids. The average value of the dielectric constant ε_{av} of the medium with respect to the pair of charges during the geminate neutralization time may be taken as (17)

$$[11] \qquad \varepsilon_{av} = \varepsilon_\infty + \frac{\varepsilon_0\tau}{t_{gn}} \times \ln\left\{\frac{1+[(\varepsilon_\infty-\varepsilon_0)/\varepsilon_0]\exp(-\varepsilon_\infty t_{gn}/\varepsilon_0\tau)}{1+[(\varepsilon_\infty-\varepsilon_0)/\varepsilon_0]}\right\}$$

where ε_∞ and ε_0 are the static and high frequency values of ε and τ is the dielectric relaxation time. Charge–dipole interactions probably reduce τ below the normal value that is measured with weak fields such as those in microwave beams (18). In neopentane $\varepsilon_{av} = \varepsilon_\infty$ because $\varepsilon_\infty = \varepsilon_0$. In water at 296 K one has $\varepsilon_0\tau/\varepsilon_\infty \leqslant 5.7\times10^{-13}$ s (19), so $\varepsilon_{av} \simeq \varepsilon_\infty$ at all times used in the present work.

The results obtained for the different $F(y)$ distributions in neopentane and in water are presented in Table 2 for the forced diffusion (FD) approximation and in Table 3 for the prescribed diffusion (PD) approximation. The findings are discussed below under several headings.

Electron Ranges

It had been found that the calculated median range y_{med} of the electrons in cyclohexane

Can. J. Chem. Downloaded from www.nrcresearchpress.com by 210.87.254.5 on 09/05/12
For personal use only.

TABLE 2. Summary of the best scavenging calculations using the FD approximation with several $F(y)$ distributions

Liquid	$F(y)$	$F(y)$ parameters	y_{med} (Å) [a]	$\beta(10^{13}\text{V/cm}^2)$	$\overline{\Delta g}$
Neopentane	YP	$x = 1.4$, $y_{min} = 89$ Å	146	0.084	0.07
	YD	$y_d = 195$ Å	195	0.035	0.19
	YG	$b = 176$ Å	190	0.050	0.12
Water	YSE		16	27	0.05
	YP	$x = 2.0$, $y_{min} = 12$ Å	16	31	0.05
	YD	$y_d = 18$ Å	18	22	0.06
	YG	$b = 18$ Å	20	31	0.07
Methylcyclopentane	YSE		20	61	0.16
	YP	$x = 1.5$, $y_{min} = 21$ Å	33	19	0.13
	YD	$y_d = 78$ Å	78	1.3	0.27
	YG	$b = 61$ Å	66	3.7	0.24
Methanol	YSE [b]		19	2.4	0.14
	YP	$x = 1.5$, $y_{min} = 12$ Å	18	3.8	0.13
	YD [b]	$y_d = 22$ Å	22	1.6	0.18
	YG	$b = 20$ Å	22	3.7	0.14

[a] y_{med} is the median value of y.
[b] The time dependent dielectric constant was averaged using eq. 11 and $\varepsilon_\infty = 33$, $\varepsilon_0 = 5.6$, and $\tau = 4.7 \times 10^{-11}$ s (19). The static dielectric constant was used with the other functions because the calculations would have consumed excessive amounts of computer time.

TABLE 3. Summary of the best scavenging calculations using the PD approximation with several $F(y)$ distributions

Liquid	$F(y)$	$F(y)$ parameters	y_{med} (Å) [a]	$\alpha(10^{12}\text{ s}^{-1})$	$\overline{\Delta g}$
Neopentane	YP	$x = \infty$ (becomes YD)			
	YD	$y_d = 195$ Å	195	40	0.07
	YG	$b = 176$ Å	190	58	0.14
Water	YSE		16	5.3	0.11
	YP	$x = \infty$ (becomes YD)			
	YD	$y_d = 18$ Å	18	4.2	0.11
	YG	$b = 18$ Å	20	6.5	0.11
Methanol	YSE		19	0.26	0.19
	YP	$x = \infty$ (becomes YD)			
	YD	$y_d = 20$ Å [b]	20	0.32	0.13
	YG	$b = 20$ Å	22	0.45	0.18

[a] y_{med} is the median value of y.
[b] This value is slightly smaller than that in Table 2 because the static dielectric constant was used in the present calculation.

depended greatly on the form of $F(y)$ distribution used, varying from 19 to 76 Å (1). It can be seen from Tables 2 and 3 that the calculated values of the median range in neopentane and in water are much less dependent on the form assumed for $F(y)$. The electron ranges in neopentane are an order of magnitude greater than those in water.

Profiles of the different $F(y)$ distributions for neopentane and water are shown in Figs. 2 and 3, along with the escape probabilities ϕ_y^{fi}. The curves for cyclohexane are included in Fig. 2 for comparison. The total area under each distribution curve is $\int_0^\infty F(y)dy = 1$. The greater dependence of y_{med} on $F(y)$ in cyclohexane is due to the small free ion yield and the different lengths of the tails of the distributions at high y values. In these calculations, the y distributions are adjusted to fit the free ion yields (1): $g_{fi} = g_{max} \int_0^\infty F(y)\phi_y^{fi}dy$. This means that when g_{fi} is small, the entire distribution is adjusted to suit a minor portion of it, and a serious error can result if the correct form of the function is not used. When g_{fi} is large, as it is in neopentane

Can. J. Chem. Downloaded from www.nrcresearchpress.com by 210.87.254.5 on 09/05/12
For personal use only.

Can. J. Chem. Downloaded from www.nrcresearchpress.com by 210.87.254.5 on 09/05/12
For personal use only.

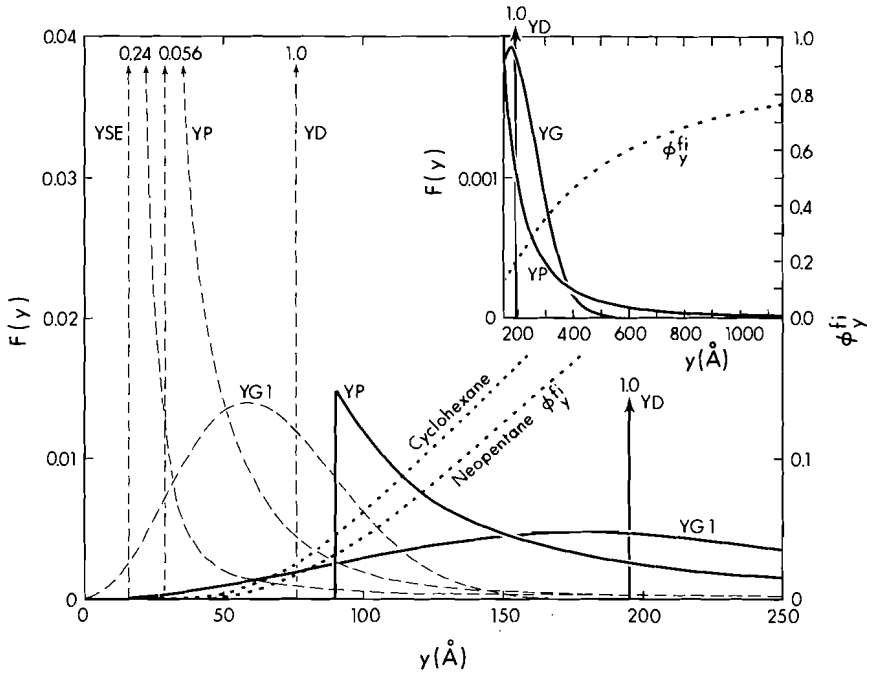

FIG. 2. Electron range distributions $F(y)$ and free ion formation probability ϕ_y^{fi} plotted against electron range for neopentane and cyclohexane. $F(y)$: —, neopentane; ---, cyclohexane; ..., ϕ_y^{fi}. The $F(y)$ distributions are the best of each type for use with the FD approximation (Table 2).

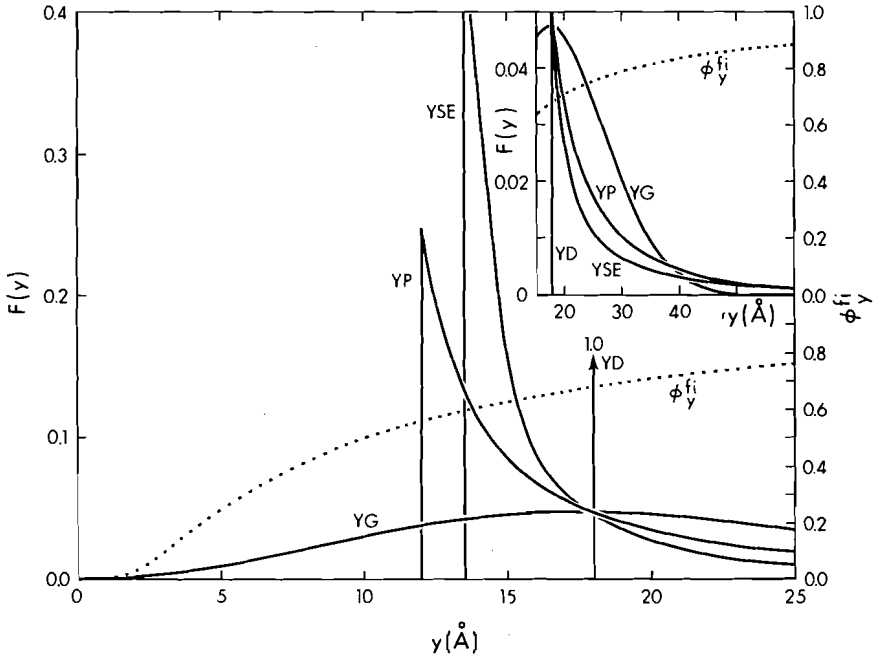

FIG. 3. Electron range distributions $F(y)$ and free ion formation probability ϕ_y^{fi} plotted against electron range for water: —, $F(y)$; ..., ϕ_y^{fi}. The $F(y)$ distributions are the best of each type for use with the FD approximation (Table 2).

Can. J. Chem. Downloaded from www.nrcresearchpress.com by 210.87.254.5 on 09/05/12
For personal use only.

and water, the function is adjusted to fit a large fraction of the y distribution. In this case, a smaller error results from the use of an inexact form of the distribution function.

Comparison of Results from the FD and PD Approximations

The best yield curves calculable using the FD and PD approximations for neopentane and water are shown with the experimental points in Fig. 4. The plots for the two systems are made on the same size of scale to facilitate comparison.

Concerning the choice of $F(y)$ distribution, all four of the "best" curves are obtainable using the YP function. This is not surprising because YP contains two adjustable parameters, namely, x and y_{min}, whereas YD and YG each contain one, y_d and b, respectively, and YSE contains none (1).

The best YP distribution for use with the FD approximation has $x = 1.4$ for neopentane and $x = 2.0$ for water (Table 2 and Figs. 2 and 3). Both of these distributions have a spread of y values that does not seem unreasonable. By contrast, the best YP distribution for use with the PD approximation has $x = \infty$ in both solvents (Table 3). YP with $x = \infty$ is YD, which would imply that all of the electrons in a given liquid have the same penetration range, which cannot be true. As the value of x in YP is increased, the calculated yield curve becomes steeper in slope in its central portion. With the PD approximation, a steep enough slope could be obtained for neopentane by using $x = \infty$ (Fig. 3), but for water even $x = \infty$ did not provide a steep enough slope in the calculated yield curve (Fig. 3). The value $G_{fi} = 2.7$ in water seems to be well established (8, 10, 11), but that of G(total ionization) is not. Better results could be obtained with the PD approximation by using a larger value of $g(N_2)_{max}$ and smaller values of y_{med} (hence of y_d or b) and α. However, the difficulty of providing a steep enough scavenging curve with the PD approximation indicates that the latter leads to an overestimate of the breadth of the distribution of neutralization times.

Neutralization time distributions that were calculated using the FD approximation are shown for the best y distribution of each form in Fig. 5. All the curves begin at the total ionization yield and decrease to the free ion yield in the time range displayed. Neutralization times calculated from the PD approximation are shown in Fig. 6. To facilitate comparison of the dispersions of the ion lifetimes obtained from the two diffusion approximations, the YG curves from Fig. 6 are included in Fig. 5. The exaggeration of the dispersion of lifetimes due to the PD approximation is especially serious in water, which supports the conclusion drawn from Fig. 4.

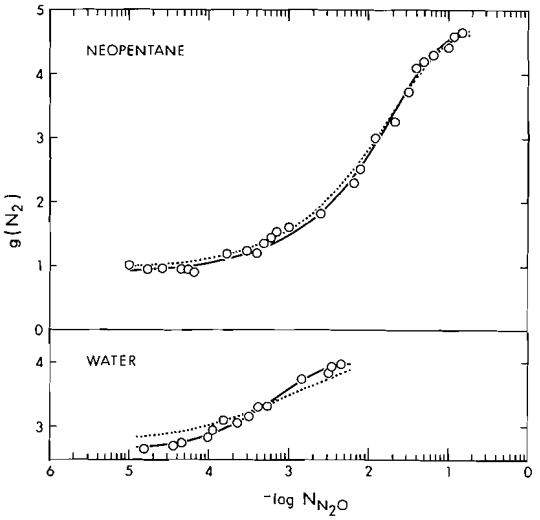

FIG. 4. Best scavenging yield curves for neopentane and water calculable using the FD (—) and PD (...) approximations. All four curves were obtainable using the YP distribution functions (Tables 2 and 3). The experimental points (○) represent nitrogen yields from nitrous oxide solutions in neopentane (7) and water (8, 15, 16). N_{N_2O} is the mole fraction of nitrous oxide.

Information derived from Figs. 5 and 6 is summarized in Table 4. It appears that geminate neutralization in neopentane is two orders of magnitude more rapid than that in water. The calculated time required for half of the geminate neutralization to occur is only slightly dependent on the diffusion approximation used. However, the dispersion of the neutralization times, represented by the spread between the times when 10% and 90% of the geminate neutralization have occurred, is an order of magnitude greater with the PD than with the FD approximation.

One should remember that all these calculations have been done with a single-pair-spur model. Introduction of a distribution of spur populations into the model would significantly reduce the calculated geminate neutralization

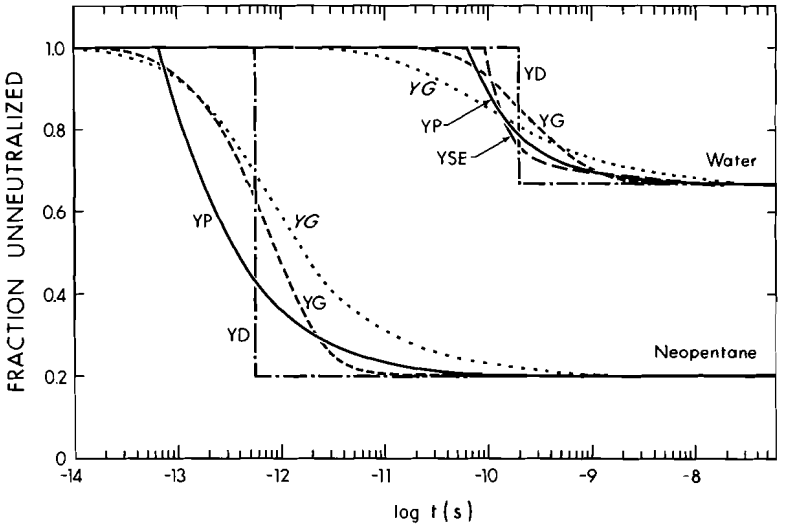

FIG. 5. Ion–electron neutralization time distributions calculated for neopentane and water, using the FD approximation and the $F(y)$ functions indicated. The ... curves were obtained using the PD approximation and YG and are included for comparison.

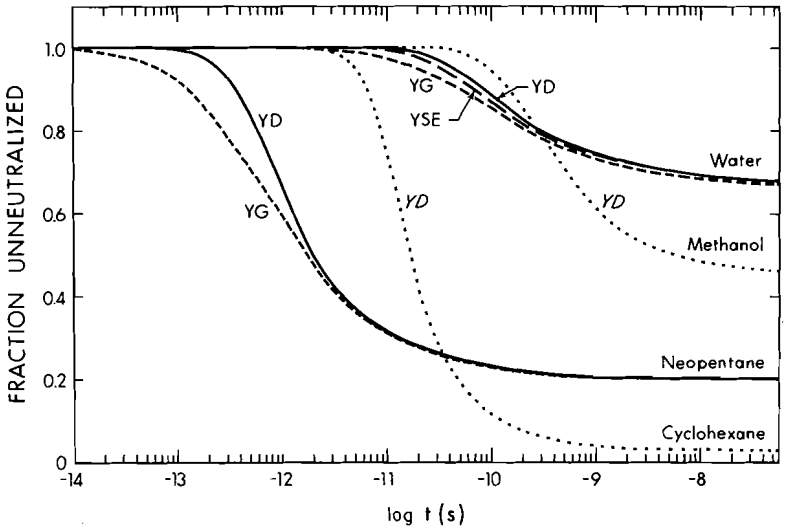

FIG. 6. Ion–electron neutralization time distributions calculated for neopentane and water, using the PD approximation and the $F(y)$ functions indicated. The ... curves were calculated for cyclohexane and methanol using the PD approximation and YD, and are included for comparison.

times, especially in water. Results of Hunt and co-workers (20, 21) seem to require shorter neutralization times than those calculated here for water. It might also be necessary to use a larger diffusion coefficient for the electrons that undergo geminate neutralization in water than that measured for the free ion-solvated electrons, as has been suggested by Hamill and co-worker (22, 23) and Mozunder (13).

Influence of Changing the Form of $F(y)$

The PD approximation does not allow satisfactory results to be obtained with reasonable forms of the $F(y)$ distribution, so the remaining discussion concerns only the model containing the FD approximation.

Values of $[g(N_2) - g(N_2)_{fi}]$ are plotted against the square root of the nitrous oxide concentration in neopentane (7) and water (8, 15, 16) in

Can. J. Chem. Downloaded from www.nrcresearchpress.com by 210.87.254.5 on 09/05/12
For personal use only.

TABLE 4. Ion–electron neutralization time distributions: summary[a]

Liquid	$F(y)$ [b]	FD approximation		PD approximation	
		$t_{gn1/2}$ [c]	$(10\% \rightarrow 90\%)t_{gn}$ [d]	$t_{gn1/2}$ [c]	$(10\% \rightarrow 90\%)t_{gn}$ [d]
Neopentane	YP	0.23	2.7	(Becomes YD)	
	YD	0.56	0.0	1.30	20
	YG	0.63	2.4	0.98	18
Water	YSE	150	790	180	6500
	YP	150	830	(Becomes YD)	
	YD	198	0	140	6500
	YG	230	950	150	3000

[a]All times are given in ps.
[b]See Tables 2 and 3 for the values of the parameters.
[c]Time required for the fraction unneutralized to reach $(1.0–0.5\phi_{gn})$, where ϕ_{gn} is the fraction of electrons that undergo geminate neutralization.
[d]Time required for the fraction unneutralized to pass from $(1.0–0.1\phi_{gn})$ to $(1.0–0.9\phi_{gn})$.

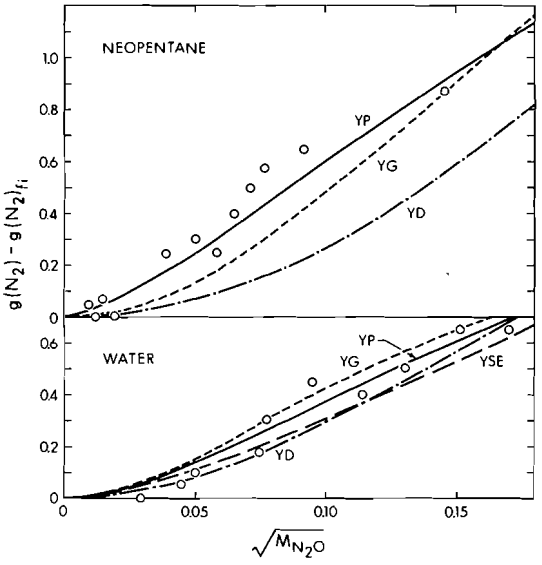

FIG. 7. Best scavenging yield curves for neopentane and water calculable using the FD approximation and the $F(y)$ distributions indicated. The experimental points (○) represent yields of nitrogen formed in spur reactions in nitrous oxide solutions in neopentane (7) and water (8, 15, 16); $g(N_2)_{fi} = 0.95$ in the former and 2.7 in the latter were used. M_{N_2O} is the molarity of nitrous oxide.

Fig. 7. The best curves calculable with the various forms of $F(y)$ distribution are also shown. Each curve was calculated for the total set of experimental results from a given solvent, shown in Fig. 4. Only the low concentration ends of the curves are displayed in Fig. 7 because only the ends of the curves can be affected by the form of the $F(y)$ distribution in the model calculations.

Calculated yields for neopentane solutions are affected by the form of $F(y)$, as shown in Fig. 7 and Table 2, but less so than were the yields in cyclohexane (1). The distribution YP gives the best agreement with experiment in both systems. The calculated yields for aqueous solutions are less affected by the form of $F(y)$; all the scavenging curves are within the uncertainty of the experimental points (Fig. 7). The influence of the form of $F(y)$ is greater when the geminate neutralization yield is greater.

Calculations for Methylcyclopentane and Methanol Systems

Electron neutralization times and scavenging probabilities were also calculated for methylcyclopentane and methanol solvents. Experimental scavenging yields were taken from refs. 24 and 25 for comparison. Other data necessary for the calculations are given in Table 1.

Calculations using the FD approximation were done for both systems and the results are summarized in Table 2. Methylcyclopentane behaves essentially the same as cyclohexane (1) and methanol behaves much like water.

The PD approximation was also used with the methanol system and it was found that a steep enough scavenging curve could not be obtained even with YP. This substantiates the conclusion that the prescribed diffusion approximation overestimates the breadth of the distribution of neutralization times.

Neutralization time distributions calculated using the PD approximation and YD for methanol and cyclohexane are shown in Fig. 6 for comparison with those obtained for neopentane and water. The cyclohexane curve falls between those of neopentane and water, while the methanol curve is near to that of water.

Can. J. Chem. Downloaded from www.nrcresearchpress.com by 210.87.254.5 on 09/05/12
For personal use only.

Curves calculated using the FD approximation are similarly situated relative to each other, but to prevent congestion the cyclohexane and methanol curves are not given in Fig. 5.

1. J.-P. DODELET and G. R. FREEMAN. Can. J. Chem. **49**, 2643 (1971).
2. G. R. FREEMAN. J. Chem. Phys. **46**, 2822 (1967).
3. G. R. FREEMAN and J. M. FAYADH. J. Chem. Phys. **43**, 86 (1965).
4. W. F. SCHMIDT and A. O. ALLEN. J. Phys. Chem. **72**, 3730 (1968).
5. W. F. SCHMIDT and A. O. ALLEN. J. Chem. Phys. **52**, 2345 (1970).
6. M. G. ROBINSON, P. G. FUOCHI, and G. R. FREEMAN. Can. J. Chem. **49**, 3657 (1971).
7. K. HORACEK and G. R. FREEMAN. J. Chem. Phys. **53**, 4486 (1970).
8. J. C. RUSSELL and G. R. FREEMAN. J. Chem. Phys. **48**, 90 (1968).
9. P. G. FUOCHI and G. R. FREEMAN. J. Chem. Phys. **56**, 2333 (1972).
10. M. HAISSINSKI. J. Chim. phys. **62**, 1149 (1965).
11. J. K. THOMAS. Adv. Radiat. Chem. **1**, 103 (1969).
12. J. W. BUCHANAN and F. WILLIAMS. J. Chem. Phys. **44**, 4377 (1966).
13. A. MOZUNDER. J. Chem. Phys. **50**, 3153, 3162 (1969).
14. J.-P. DODELET, P. G. FUOCHI, and G. R. FREEMAN. Can. J. Chem. **50**, 1617 (1972).
15. F. S. DAINTON and S. R. LOGAN. Trans. Faraday Soc. **61**, 715 (1965).
16. D. HEAD and D. C. WALKER. Nature, **207**, 517 (1965).
17. K. N. JHA and G. R. FREEMAN. J. Chem. Phys. **51**, 2839 (1969), following a suggestion of R. Schiller at the 2nd L. H. Gray Conference, Cambridge, England, April 1969.
18. G. R. FREEMAN. Adv. Chem. Ser. **82**, 339 (1968).
19. Calculated from data *In* F. BUCKLEY and A. A. MARYOTT. Tables of dielectric dispersion data. Natl. Bur. Std. (US) Circ. no. 589, 1958.
20. M. J. BRONSKILL, R. K. WOLFF, and J. W. HUNT. J. Chem. Phys. **53**, 4201 (1970).
21. J. E. ALDRICH, M. J. BRONSKILL, R. K. WOLFF, and J. W. HUNT. J. Chem. Phys. **55**, 530 (1971).
22. W. H. HAMILL. J. Phys. Chem. **73**, 1341 (1969).
23. T. SAWAI and W. H. HAMILL. J. Chem. Phys. **52**, 3843 (1970).
24. E. D. STOVER and G. R. FREEMAN. J. Chem. Phys. **48**, 3902 (1968).
25. K. N. JHA and G. R. FREEMAN. J. Chem. Phys. **48**, 5480 (1968).
26. W. F. SCHMIDT and A. O. ALLEN. J. Chem. Phys. **52**, 4788 (1970).
27. K. SCHMIDT and W. BUCK. Science, **151**, 70 (1966).
28. B. E. CONWAY. Electrochemical data. Elsevier Publishing Co., Amsterdam. 1952. pp. 145 and 162.
29. P. FOWLES. Trans. Faraday Soc. **67**, 428 (1971).

Can. J. Chem. Downloaded from www.nrcresearchpress.com by 210.87.254.5 on 09/05/12
For personal use only.

Mechanistic Information on the Aquations of Complexes of the Pentaamminecobalt(III) Series from Kinetic Studies at High Pressures

W. E. JONES, L. R. CAREY, AND T. W. SWADDLE[1]

Department of Chemistry, The University of Calgary, Calgary 44, Alberta

Received March 22, 1972

The logarithm of the pseudo-first-order rate coefficient k for the aquation of $Co(NH_3)_5X^{(3-n)+}$ can be represented by a quadratic equation in the pressure P, or, better, by

$$\ln k = \ln k_0 - P\Delta V_0^*/RT - (30.17x/T)[(P + 3.06)\ln(1 + P/3.06) - P]$$

where P is in kbar, ΔV_0^* is the volume of activation at $P = 0$, and x is the increase in the number of water molecules solvating the complex as it goes to the transition state. For $X^{n-} = SO_4^{2-}$, Cl^-, Br^-, NO_3^-, and N_3^- at 25° (75° for N_3^-) and ionic strength $I = 0.1$ M $LiClO_4/HClO_4$, $\Delta V_0^* = -18.5$, -10.6, -9.2, -6.3, and $+16.8$ cm^3 mol^{-1}, and $x = 8.0$, 4.1, 3.9, 1.9, and -4.2; for $X^{n-} = NCS^-$, the mean ΔV^* from $P = 0.001$ to 2.5 kbar at 88° is -4 cm^3 mol^{-1}. Detailed consideration of these data, especially their correlation with the molar volume of reaction by a straight line of unit slope for $X^{n-} = SO_4^{2-}$, Cl^-, Br^-, NO_3^-, and H_2O, provides strong evidence for a dissociative interchange mechanism. For $X^{n-} = N_3^-$, the separating entity is probably HN_3 rather than N_3^-. For $X^{n-} = NCS^-$, aquation is incomplete, at practical complex concentrations; at 88.0°, 1 bar, and $I = 0.1$ M $LiClO_4/HClO_4$, $k = 3.3 \times 10^{-6}$ s^{-1} and the stability constant of $Co(NH_3)_5NCS^{2+}$ is 490 M^{-1}.

Le logarithme du coefficient de vitesse d'ordre pseudo-un, k, pour l'hydratation de la molécule $Co(NH_3)_5X^{(3-n)+}$, peut être représenté au moyen d'une équation quadratique impliquant la pression P, soit

$$\ln k = \ln k_0 - P\Delta V_0^*/RT - (30.17x/T)[(P + 3.06)\ln(1 + P/3.06) - P]$$

où P est en kbar, ΔV_0^* est le volume d'activation à $P = 0$ et X est l'augmentation du nombre de molécules d'eau solvatant le complexe lorsqu'il passe vers l'état de transition. Dans le cas de $X^{n-} = SO_4^{2-}$, Cl^-, Br^-, NO_3^- et N_3^- à 25° (75° pour N_3^-), une force ionique $I = 0.1$ M $LiClO_4/HClO_4$, $\Delta V_0^* = -18.5$, -10.6, -9.2, -6.3 et $+16.8$ cm^3 mol^{-1}, $x = 8.0$, 4.1, 3.9, 1.9, et -4.2; pour $X^{n-} = NCS^-$, la valeur moyenne de ΔV^* à $P = 0.001$ à 2.5 kbar à 88° est de -4 cm^3 mol^{-1}. L'étude détaillée de ces résultats, spécialement leur relation avec le volume molaire de réaction par une ligne droite de pente unitaire pour $X^{n-} = SO_4^{2-}$, Cl^-, Br^-, NO_3^-, et H_2O, fournit la preuve d'un mécanisme d'échange dissociatif. Pour $X^{n-} = N_3^-$, l'entité de séparation est probablement HN_3 plutôt que N_3^-. Pour $X^n = NCS^-$ l'hydratation est incomplète, à des concentrations habituelles de complexe; à 88.0°, 1 bar et $I = 0.1$ M $LiClO_4/HClO_4$, $k = 3.3 \times 10^{-6}$ s^{-1} et la constante de stabilité de $Co(NH_3)_5NCS^{2+}$ est 490 M^{-1}.

Canadian Journal of Chemistry, **50**, 2739 (1972)

Introduction

Of the various activation parameters that characterize the kinetics of a chemical reaction in terms of transition-state theory, the volume of activation ΔV^* is potentially the most useful criterion of reaction mechanism, because the spatial requirements of the various alternative models can be visualized relatively easily. We have therefore measured the pressure dependence of the pseudo-first-order rate coefficients k of reactions of the type

$$[1]\quad Co(NH_3)_5X^{(3-n)+} + H_2O \xrightarrow{k} Co(NH_3)_5OH_2^{3+} + X^{n-}$$

In a preliminary note (1), it was remarked that ΔV^* for reaction 1 is in general pressure-dependent, but that ΔV_0^* ($= \Delta V^*$ at zero pressure) was almost equal to the molar volume of reaction ΔV for $X^{n-} = Cl^-$, Br^-, NO_3^-, and SO_4^{2-}, which suggested a dissociative mechanism (I_d or D, in the nomenclature of Langford and Gray (2)). We now present a full account of that work, together with new data for $X^{n-} = N_3^-$ and NCS^- and an analysis of the pressure dependence of ΔV^*.

[1]To whom correspondence should be addressed.

Experimental

Materials

Baker Analysed perchloric acid was used without further purification. Lithium perchlorate trihydrate was made from Baker Analysed $HClO_4$ and Li_2CO_3 and recrystallized twice from water before use.

Can. J. Chem. Downloaded from www.nrcresearchpress.com by 210.87.254.5 on 09/05/12
For personal use only.

Can. J. Chem. Downloaded from www.nrcresearchpress.com by 210.87.254.5 on 09/05/12
For personal use only.

Perchlorate salts of the ions $Co(NH_3)_5X^{(3-n)+}$ were used for all the kinetic measurements, and were made by precipitation of the cation from aqueous solution with 72% perchloric acid or sodium or ammonium perchlorate. Salts of the ions for which $X^{n-} = Cl^-$, Br^-, NO_3^-, and N_3^- were made by published methods (3–7). The purity of the products was checked by microanalysis and by comparing the ultraviolet–visible solution spectra with published data where available.

For $X^{n-} = SO_4^{2-}$, carbonatopentaamminecobalt(III) nitrate (11.5 g) was dissolved in 6 *M* H_2SO_4 (50 ml) and kept at 75° for 1.5 h; on adding 50 ml water and 20 g NH_4ClO_4 (not all of which dissolved) and cooling to 0° for 2 h, a red impurity was precipitated first and was rejected.[2] Further cooling yielded red crystals which, after recrystallization from 2 *M* aqueous $NaClO_4$, washing with alcohol and ether and drying *in vacuo*, were shown spectroscopically (8) to be $[(NH_3)_5CoSO_4]ClO_4$.

Anal. Calcd. for $[(NH_3)_5CoSO_4]ClO_4$: N, 20.63; H, 4.6. Found: N, 20.98; H, 4.8.

For $X^{n-} = NCS^-$, aquopentaamminecobalt(III) perchlorate (15 g) was heated in 400 ml water containing 1 ml glacial acetic acid and 15 g NaNCS for 1.5 h at 80–90°, then filtered hot into a hot solution of 30 g NH_4ClO_4 in water (total volume 80 ml). On cooling the solution in ice, red crystals of $[(NH_3)_5CoNCS](ClO_4)_2$ separated; recrystallization was found to be unnecessary.

Anal. Calcd. for $[Co(NH_3)_5NCS](ClO_4)_2$: N, 20.95; C, 2.99; H, 3.77. Found: N, 20.89; C, 3.00; H, 3.90.

At the 306 nm absorption maximum, $\varepsilon = 1500\ M^{-1}\ cm^{-1}$.

Kinetic Measurements

For the aquations of the chloro-, bromo-, nitrato-, and sulfato-complexes, the reaction mixtures were prepared by dissolving a known weight of the perchlorate salt in 100 ml 0.1 *M* $LiClO_4$ which was 5.0×10^{-5} *M* in $HClO_4$. The solution was placed in a 100 ml commercial glass syringe, and this was enclosed in a thermostated (25.00 ± 0.01°) pressure vessel as previously described (9). The assembly was left for about 1 h after initial pressurization, in every case, to attain full thermal equilibrium; this time was short relative to the half-lives of the reactions under investigation.

At selected intervals, samples were withdrawn from the syringe through a tantalum capillary tube, and were chilled at once to 0°; experiments using a Hastelloy B capillary failed because this alloy slowly reduced the cobalt complex, especially at high acidities. The optical absorbances of the samples were determined (at 20°) at 280 ($X^{n-} = SO_4^{2-}$), 282 (Cl^-), 300 (NO_3^-), and 310 nm (Br^-), using a Cary 15 spectrophotometer. Absorbances at "infinite time" were very small, and were obtained either by direct measurement after 10 half-lives of the aquation reaction, or by calculation from known molar absorbancy indices. Some runs at atmospheric pressure were made in darkened, stoppered Pyrex vessels instead of the pressure assembly, to check for possible catalysis by the components of the assembly.

The aquation of the azido-complex was studied similarly, but at 75.00 ± 0.05° and with $[HClO_4] = 1.0 \times 10^{-3}$ *M* and $[LiClO_4] = 0.10$ *M*; it was shown that, under these conditions, contributions to the aquation rate by hydrogen-ion-dependent pathways were negligible.

The aquation of the *N*-thiocyanato-complex was studied at 88.00 ± 0.05°, with $[HClO_4] = 0.10$ *M or* with $[HClO_4] = 0.01$ *M* and $[LiClO_4] = 0.09$ *M*. Runs at atmospheric pressure were carried out in sealed Pyrex tubes which were wrapped in aluminum foil to exclude light. Optical measurements were made at 306 nm.

Molar Volumes of Reaction

All attempts to measure the molar volume change ΔV for the aquation of $Co(NH_3)_5N_3^{2+}$ by Spiro's dilatometric method (10) failed because of the precipitation of hydrous cobalt oxides under the conditions of alkalinity and temperature needed to obtain sufficiently rapid hydrolysis. Trial experiments with bromopentaamminecobalt(III) perchlorate, on the other hand, confirmed the results of Spiro *et al.* (10). No attempt was made to measure ΔV for the poorly soluble and kinetically inert thiocyanato-complex.

Spectroscopic Studies at High Pressures

The apparatus previously described (11) was used to study the effects of pressure on the visible spectrum of aqueous $[(NH_3)_5CoOH_2](ClO_4)_3$.

Results

The aquations of $Co(NH_3)_5X^{(3-n)+}$ were accurately first-order in complex ion to at least 80% completion of reaction, except for $X^{n-} = NCS^-$, for which the rate of decay of optical density at 88° in 0.01 or 0.10 *M* $HClO_4$ was in accordance with incomplete aquation:

$$[2]\quad (NH_3)_5CoNCS^{2+} + H_2O \rightleftharpoons (NH_3)_5CoOH_2^{3+} + NCS^-$$

The corresponding rate law is

$$[3]\qquad kt = \frac{(c_0 - c_\infty)}{(c_0 + c_\infty)} \ln \frac{(c_0^2 - c_t c_\infty)}{c_0(c_t - c_\infty)}$$

where c represents the concentration of the thiocyanato-complex at times 0, t, and ∞. Since the dimensions cancel, and since the combined molar optical absorbances of the products were 1% of that of $Co(NH_3)_5NCS^{2+}$, absorbance readings were substituted directly into eq. 3. In practice, c_∞ could not be measured directly because of the slow decomposition of the reaction products at 88°. Thus, we have found spectrophotometrically that $Co(NH_3)_5OH_2^{3+}$ (6.0×10^{-3} *M*) in 0.1 *M* $HClO_4$ decomposes to Co^{2+} with a half-period of about 60 h at 102°. Furthermore, it is known (12, 13) that thiocyanate ion, though kinetically stable in neutral aqueous solution up to 180–200°, is hydrolyzed to H_2S, CO_2, and NH_4^+ in acidic solutions at relatively low temperatures, and indeed we have observed that 0.05 *M* NCS^- in 0.10 *M* $HClO_4$

[2]Throughout this article, *M* signifies mol l^{-1} of solution as measured at 25.0° and 1.0 bar pressure.

TABLE 1. First-order rate coefficients k for the aquation of $Co(NH_3)_5X^{(3-n)+}$ at 25.00° (except where stated) and 0.1 M $HClO_4/LiClO_4$ (see text)

X^{n-}	P, kbar	Mean 10^6k, s^{-1}	X^{n-}	P, kbar	Mean 10^6k, s^{-1}
NO_3^-	0.001	23.8	Cl^-	0.001	1.44
	0.010	23.7		0.010	1.45
	0.491	27.1		0.517	1.84
	0.507	27.4		0.998	2.13
	0.517	26.4		1.500	2.40
	0.760	27.9		2.03	2.73
	0.983	28.9		3.09	3.32
	1.013 (2)*	30.3		4.05	3.71
	1.256	31.1			
	1.520	32.0	SO_4^{2-}	0.010	1.05
	1.824	35.1		0.456	1.39
	2.03	35.5		0.998	1.91
	2.23 (2)	36.6		2.03	3.06
	2.63	38.2		3.09	3.85
	3.03	39.4		4.05	4.43
	3.09	43.1			
	3.19	42.1	NCS^-†	0.001 (6)	3.3
	4.05	44.7		2.03	4.2
				2.55	4.8
Br^-	0.001	5.67			
	0.010	5.72	N_3^-‡	0.001 (4)	7.70
	0.507	6.76		0.051 (2)	7.60
	1.013 (2)	7.82		0.127	7.36
	1.479	8.60		0.203 (3)	7.06
	2.03	9.83		0.507	5.78
	4.05	12.0		1.013	4.63
				2.03	2.84
				2.74 (2)	2.31
				3.04	2.03
				4.05	1.50

*Figures in parentheses indicate number of independent measurements of k.
†88.0°.
‡75.0°.

developed a slight but unmistakable odor of H_2S in less than 0.4 h in a sealed vessel at 90°.

Accordingly, in the analysis of rate data for experiments at 1 bar pressure, c_∞ was treated as a variable, along with k, in a least-squares fit of the data to eq. 3 using an IBM 360/50 computer. Thus, both k and (from c_∞) the stability constant K of the thiocyanato complex could be obtained; at 88.0°, $[H^+] = 0.01$ M, ionic strength $I = 0.1$ M and c ranging from 2.5×10^{-4} to 1.0×10^{-3} M, $K = (4.9 \pm 0.4) \times 10^2$ M^{-1}. In general, however, more accurate values of k (especially at high pressures) could be obtained by graphical treatment of the first 10–15% of the aquation reaction as first-order in thiocyanato-complex, assuming 100% aquation at infinite time; this procedure does not yield K values, but these were in any event neither very accurate nor germane to the purpose of this study. The k values so obtained were reliable to $\pm 0.2 \times 10^{-6}$ s^{-1} and were the same (within this uncertainty) for both 0.10 M $HClO_4$ and 0.01 M $HClO_4$/0.09 M $LiClO_4$; the value for 1 bar (Table 1) agrees satisfactorily with that interpolated from the measurements of Gay and Lalor (14), although these authors do not report the reversibility of eq. 2.

For all the other $Co(NH_3)_5X^{(3-n)+}$, the rate coefficients k were evaluated by the method of least squares and could be reproduced to within 2% at worst. Rate coefficients obtained at atmospheric pressure using conventional darkened Pyrex reaction vessels agreed within these limits with the k values obtained at atmospheric pressure in the pressure assembly, except where a Hastelloy "B" capillary was used (see under

Can. J. Chem. Downloaded from www.nrcresearchpress.com by 210.87.254.5 on 09/05/12
For personal use only.

TABLE 2. Analysis of the data of Table 1 on the basis of equation 5 (25°, $I = 0.1$ M, except as stated)

X^{n-}	ΔV_0^* (cm^3 mol^{-1})	ΔV (cm^3 mol^{-1})†	$10^3(\partial\Delta V^*/\partial P)_T$ (cm^3 bar^{-1} mol^{-1})	$10^4\kappa^*$ (bar^{-1})
SO_4^{2-}	-17.0 ± 0.6	-19.2	$+4.1\pm0.5$	2.2
Cl^-	-9.9 ± 0.5	-11.6	$+2.1\pm0.2$	1.9
Br^-	-8.7 ± 0.2	-10.8	$+2.0\pm0.2$	2.0
NO_3^-	-5.9 ± 0.4	-7.2	$+1.0\pm0.2$	1.4
NCS^-‡	-4.0 ± 1.0	—	—	—
H_2O§	$+1.2\pm0.1$	0.0	0.0 ± 0.1	—
N_3^-‖	$+16.0\pm0.4$	—	-2.1 ± 0.3	1.4

†Estimated for ionic strength $I = 0.1$ M from the data for $I = 1.0$ M (30°) given in ref. 10 (see text).
‡88.0°; $(\partial\Delta V^*/\partial P)_T$ taken as zero because of experimental uncertainty.
§Reference 15.
‖75.0°.

Experimental). The results are summarized in Table 1.

Discussion

The volume of activation ΔV^* is defined by the equation

$$[4] \qquad (\partial \ln k/\partial P)_T = -\Delta V^*/RT$$

so that a plot of $\ln k$ *vs.* P is linear if ΔV^* is independent of pressure to within the experimental uncertainty. This is true (15) for the case $X^{n-} = H_2O$ in eq. 1, but not for any of the data listed in Table 1 (with the possible exception of $X^{n-} = NCS^-$, for which the experimental uncertainty is about four times that of the other cases). Thus, the problem is to choose an appropriate analytical function to give the best fit of the data with the minimum number of parameters, and so to extract the mechanistically-useful quantity ΔV_0^*. Golinkin *et al.* (16) favor an empirical quadratic in the pressure P

$$[5] \qquad \ln k = \ln k_0 + BP + CP^2$$

which yields $\Delta V_0^* = -RTB$, but which implies that $(\partial\Delta V^*/\partial P)_T$ is independent of pressure and equal to $-2RTC$. In fact, eq. 5 represents the data of Table 1 quite satisfactorily, and the corresponding values of ΔV_0^* and $(\partial\Delta V^*/\partial P)_T$ obtained in a least-squares fit are listed in Table 2.

Table 2 also lists values of ΔV, the molar volume change associated with the completed reaction 1, at 1 bar and 30.0°, corrected approximately to ionic strength $I = 0.1$ M from the data of Spiro *et al.* (10) for $I = 1.0$ M. For the aquation of $Co(NH_3)_5X^{2+}$, ΔV need only be made 1.2 cm^3 mol^{-1} more negative to accommodate this change in I; this correction originates entirely in the corresponding increase in ΔV for reaction 6, upon which the dilatometric method of Spiro *et al.* relies.

$$[6] \quad Co(NH_3)_5OH_2^{3+} + OH^- \rightarrow Co(NH_3)_5OH^{2+} + H_2O$$

We have taken the values of ΔV at $I = 0.1$ M for reaction 6, and for the aquation of $Co(NH_3)_5SO_4^+$, to be equal to those obtained by Spiro *et al.* (10) without added $NaClO_4$, as I was then not greatly different from 0.1 M.

An important deduction from the data of Table 2 is that ΔV_0^* is a linear function of ΔV for $X^{n-} = SO_4^{2-}$, Cl^-, Br^-, NO_3^-, and H_2O at least; ΔV values could not be obtained for $X^{n-} = N_3^-$ or NCS^-. Furthermore, the slope of the line is about 0.97, *i.e.*, close to unity, and this constitutes compelling evidence for a dissociative mechanism, since it indicates that the departing ion X^{n-} must be essentially as fully formed in the transition state as in the ultimate products. The straight line clearly includes the aquo-complex, and so confirms Hunt and Taube's conclusion (15) that the aquo-exchange reaction of $Co(NH_3)_5OH_2^{3+}$ is dissociatively activated.

There is substantial evidence (17–20) that the transition-state of reaction 1 may *not* be the same for all X^{n-}, and almost certainly does *not* comprise an independent $Co(NH_3)_5^{3+}$ species. Thus, the transition state probably has the structure $\{Co(NH_3)_5^{3+}, X^{n-}, y\,H_2O\}$, where X^{n-} remains within the bounds of the second

Can. J. Chem. Downloaded from www.nrcresearchpress.com by 210.87.254.5 on 09/05/12
For personal use only.

Can. J. Chem. Downloaded from www.nrcresearchpress.com by 210.87.254.5 on 09/05/12
For personal use only.

coordination sphere and y is large enough to permit full solvation of both $Co(NH_3)_5^{3+}$ and X^{n-}.

Our earlier remark (1) that ΔV_0^* was apparently *equal* to ΔV is perhaps misleading, as the near-equality resulted accidentally from the use of ΔV values for $I = 1.0$ M instead of 0.1 M. It is now clear that the ΔV_0^* values are, on the average, about 1 cm^3 mol^{-1} more negative than ΔV, *i.e.*, the intercept of the ΔV_0^* *vs.* ΔV plot is $\sim +1$ cm^3 mol^{-1} on the ΔV_0^* axis. We take this to mean that the bond-breaking component ΔV_b^* of ΔV_0^* is approximately constant for all X^{n-}, and could be conveniently set equal to ΔV^* for $X^{n-} = H_2O$, for which there is no electrostrictive component, ΔV_{el}^*. Writing ΔV_{el}^{0*} for ΔV_{el}^* at zero pressure, we have

$$[7] \qquad \Delta V_0^* = \Delta V_b^* + \Delta V_{el}^{0*}$$

This permits an approximate calculation of ΔV_{el}^{0*} for the complexes of anionic X, and, because ΔV^* (and hence ΔV_b^*) is independent of P for $X^{n-} = H_2O$ (15), the pressure dependence of ΔV^* for anionic X can be ascribed entirely to ΔV_{el}^*. The last column of Table 2 lists "electrostrictive compressibilities of activation", κ^*, defined as $-(\partial \Delta V^*/\partial P)_T/\Delta V_{el}^{0*}$; these values are not greatly different for the various X (mean value $(1.8 \pm 0.3) \times 10^{-4}$ bar^{-1}), which supports the notion that the pressure dependence of ΔV^* has in all these cases a common origin, *viz.*, increases in the degree of solvation of the complexes (or decrease, in the case of $X^{n-} = N_3^-$) as they go to the transition state of aquation.

These deductions suggest that the pressure dependence of ΔV^* might be better represented as arising entirely from the loss of compressibility of bulk water molecules when they enter the solvation sheath of an ion. The compressions $(V_0 - V_P)/V_0$ of aqueous solutions can be represented empirically by the modified Tait equation,

$$[8] \qquad (V_0 - V_P)/V_0 = \rho \log_{10} (1 + P/\Pi)$$

where ρ and Π are constants. We have

$$[9] \qquad \Delta V^* = \Delta V_b^* + x(V_{el} - V_{H_2O}) = \Delta V_0^* + 18.0x\rho \log_{10} (1 + P/\Pi)$$

where V_{H_2O} and V_{el} are respectively the molar volumes of bulk water and electrostricted water ($V_{H_2O} = 18.0$ cm^3 mol^{-1} at 1 bar and 25°), and x is the increase in the number of water molecules solvating the complex as it goes from the initial state to the transition state. V_{el} may be taken to be independent of pressure, since it is known that aqueous ions are intrinsically less compressible than bulk water. On integrating eq. 4 over the pressure range zero to P, we have

$$[10] \qquad \ln k_p = \ln k_0 - P\Delta V_0^*/RT - (18.0x\rho/2.303RT)[(\Pi + P) \ln (1 + P/\Pi) - P]$$

TABLE 3. Analysis of the data of Table 1 on the basis of eq. 10 (25°, $I = 0.1$ M, except as stated)

X^{n-}	ΔV_0^*, cm^3 mol^{-1}	x	$\bar{V}^0$†
SO_4^{2-}	-18.5 ± 0.7	8.0 ± 0.6	14.0
Cl^-	-10.6 ± 0.4	4.1 ± 0.4	17.8
Br^-	-9.2 ± 0.2	3.9 ± 0.2	24.7
NO_3^-	-6.3 ± 0.4	1.9 ± 0.4	29.0
NCS^-‡	-4.0 ± 1.0	—	35.7
H_2O§	$+1.2 \pm 0.1$	0.0 ± 0.1	—
N_3^-‖	$+16.8 \pm 0.5$	-4.2 ± 0.5	24.9

†Partial molal volumes of X^{n-} relative to H^+ at 25° (except N_3^-, 20°) and $I = 0$; from ref. 24.
‡88.0°; x taken as zero because of large experimental uncertainty.
§Reference 15.
‖75.0°.

Table 3 lists values of ΔV_0^* and x obtained using $\Pi = 3.06$ kbar and $\rho = 0.321$, which apply for pure water at 25° over the pressure range used in these experiments (11); the data of Table 1 are significantly better represented by eq. 10 than by eq. 5 (the mean square error being 15% greater, on the average, for eq. 5). The use of Π and ρ values for 0.1 M aqueous perchlorate solutions (11) rather than pure water gave a slightly poorer fit of the experimental data; this is because the solvation of the complex ion involves bulk water *per se*, and should not be sensitive to the presence of moderate concentrations of other electrolytes in the solution.

The values of ΔV_0^* obtained from eq. 10 are only slightly numerically greater than those obtained from eq. 5, and are preferred because compression of the solvent is realistically (albeit empirically) represented by eq. 8, whereas eq. 5 has no basis in high-pressure physics. Hamann (21) has criticized Benson and Berson's (22) somewhat different application of the Tait equation in the interpretation of the pressure-dependence of ΔV^* in non-polar reactions, largely on the grounds that the Tait equation has no theoretical foundation (it is actually unrealistic,

Can. J. Chem. Downloaded from www.nrcresearchpress.com by 210.87.254.5 on 09/05/12
For personal use only.

in that it predicts negative volumes at very high pressures, *e.g.* above 4.0×10^6 bars for water) and that the Benson–Berson equation represents experimental data rather poorly. Hamann's theoretical objections obviously apply to eq. 10 also, but we have sought merely to allow for the compressibility of water as it applies to our model, without introducing an excessive number of parameters, and the quality of the fit of the data of Table 1 justifies our procedure.

Values of ΔV_0^* from Table 3 again give an excellent linear plot *vs.* ΔV (from Table 2), with a slope of 0.98 ± 0.01 and an intercept (identifiable with the mean value of ΔV_b^*) of $+1.3 \pm 0.1$ cm^3 mol^{-1}. A plot of x against ΔV_0^* is a smooth, gentle curve, rather than the straight line that would be anticipated if V_{el} were the same for all $Co(NH_3)_5X^{(3-n)+}$ aquations. Thus, it seems that V_{el} becomes somewhat greater when large numbers of water molecules are added to the complex as it goes to the transition state; this is perhaps to be expected, since, the larger the solvation sheath becomes, the less will be the central electrostatic field acting to compress the outer solvating water molecules. The slope of the curve at $x = 0$ is about -3.1 cm^3 mol^{-1}, so that $V_{el} \sim (18.0 - 3.1) = 14.9$ cm^3 mol^{-1} for the case $X^{n-} = H_2O$; thus the molar volume of water is about 1 cm^3 mol^{-1} larger in the second coordination sphere than in the first, according to Biltz's (23) estimate for the latter (14.0 ± 0.3 cm^3 mol^{-1}, mean of three different salts of $Co(NH_3)_5OH_2^{3+}$). The difference is thus comparable with ΔV_0^* ($= 1.2$ cm^3 mol^{-1}) for the aquo-exchange reaction, in accordance with the proposed I_d mechanism in which the Co—OH_2 bond is completely broken, and H_2O has a molar volume characteristic of the second coordination sphere, in the transition state.

Table 3 shows that ΔV_0^* increases monotonically as the conventional partial molal volume $\bar{V}^0$ of X^{n-}(aq) increases; an exact linear relationship would exist between $\bar{V}^0$ and the partial molal volume of the transition state, if the proposed I_d mechanism is correct, but the latter quantity is the sum of ΔV_0^* and the partial molal volume of $Co(NH_3)_5X^{(3-n)+}$(aq), which last is not known but can be expected to vary appreciably with X. Thus, ΔV_0^* is not expected to be a linear function of $\bar{V}^0$. Nevertheless, the relatively positive value of ΔV^* recorded for $X^{n-} = NCS^-$ is entirely consistent with the high $\bar{V}^0$ value of the aqueous thiocyanate ion; the discrepancy between the temperatures at which these parameters were measured is not important, since Millero's review (24) shows that $\bar{V}^0$ is not in general very sensitive to temperature over the range 0–90°.

On the other hand, the ΔV_0^* value for $X^{n-} = N_3^-$ is about 25 cm^3 mol^{-1} larger than predicted on the basis of $\bar{V}^0$. This striking aberration can be attributed to an anomalous mechanism in which HN_3 separates from a dipositive moiety, rather than N_3^- from $Co(NH_3)_5^{3+}$, so that some of the water solvating the ground state may actually be released, rather than further water electrostricted, on going to the transition state (7). The observed value of x supports this view. Alternatively, it may be that the *initial* state is unusually heavily solvated, because of hydrogen-bonding between the basic azide ligand and solvent water; probably, *both* of these factors contribute to the overall aquation mechanism, leading to extensive desolvation on going to the transition state. The nature of the dipositive moiety is an open question; the proton abstracted by the departing azide ion could come directly from the rather feebly-acidic ammine ligands, but a more likely source would be the water molecules of the solvation sheath of the cobalt complex, as these would be significantly more acidic than bulk water by virtue of the proximity of the metal ion. It should be noted that the solvation sheath can be regarded as a permanent integral part of the complex ion, for the short time needed to proceed from the ground state to the transition state.

It may be noted that ΔV_0^* tends in general to increase as the entropy of activation ΔS^* increases (for ΔS^* data, see refs. 25 and 26). However, the correlation is a rough one and does not appear to be linear (*cf.* Laidler and Chen (27)).

An intriguing feature of eq. 10 is that it purports to give the mean number x of molecules of water which are added to the complex (here considered as comprising both the first and second coordination spheres) in order to reach the transition state of aquation. As noted above, we should regard the second coordination sphere

Can. J. Chem. Downloaded from www.nrcresearchpress.com by 210.87.254.5 on 09/05/12
For personal use only.

as permanent for the duration of the single molecular vibration which takes the complex to the transition state and on toward the products. However, the number of water molecules in the second coordination sphere will fluctuate considerably about a statistical average; presumably, when an average of x additional waters happen to be present at a given time in the second coordination sphere, a wide excursion of a Co—X vibration can result in the transient formation of X^{n-} which, in these circumstances, can be "trapped" by solvation. On the other hand, if there are insufficient water molecules present to solvate X^{n-}, then X^{n-} will recombine with $Co(NH_3)_5^{3+}$ within the timespan of a molecular vibration.

The electrostrictive power of an ion is expected to be directly proportional to the square of its charge and inversely proportional to its effective radius (24). Indeed, we see from Table 3 that x increases ($NO_3^- < Br^- < Cl^-$) with the decreasing ionic size of X^{n-} and, for ions of comparable size, x increases sharply ($NO_3^- \ll SO_4^{2-}$) with increasing n in X^{n-}. For the anomalous case of $X^{n-} = N_3^-$, the x value indicates extensive *de*solvation on going to the transition state, in accordance with the HN_3 separation mechanism proposed above.

The slowness of substitution at cobalt(III) centers has been attributed (28, 29) to the loss of 4 Dq in ligand field stabilization energy (LFSE) on going from $Co(NH_3)_5X^{(3-n)+}$ to a $Co(NH_3)_5^{3+}$ ion of C_{4v} symmetry which, in the light of the above discussion and the fact that the aquation of *trans*-$Co(NH_3)_4(ND_3)Br^{2+}$ is stereoretentive (20), is a fairly accurate representation of the reaction mechanism as it involves the cobalt(III) center. A correlation may therefore be sought between the pressure dependence of the energy ($= 10\,Dq - C'$) of the first ligand field band ($^1T_{1g} \leftarrow {}^1A_{1g}$) of a cobalt(III) complex, and ΔV_b^*. For $Co(NH_3)_5OH_2^{3+}$, we have observed that the position of the maximum of the $^1T_{1g} \leftarrow {}^1A_{1g}$ band changes from 20 410 to 20 530 cm^{-1} ($\pm 0.2\%$), and that of the $^1T_{2g} \leftarrow {}^1A_{1g}$ band from 28 990 to 29 150 cm^{-1}, when the pressure is raised from 1 bar to 3.55 kbars. If we assume that the pressure dependences of the Racah parameter C', of ΔS^* and of ΔV_b^* can all be neglected, then we have, for aquo-exchange, $\Delta\Delta H^* = \Delta(4\ Dq) \sim 0.1_4$ kcal mol^{-1}, whence $\Delta V_b^* = \Delta\Delta H^*/\Delta P = +1._6\ cm^3\ mol^{-1}$. This is close to the experimental value of $+1.2\ cm^3\ mol^{-1}$, suggesting that LFSE loss may well be a dominant factor in determining the magnitude of ΔV_b^* for the substitution reactions of pentaamminecobalt(III) complexes at least.

We thank the International Nickel Company of Canada for a Fellowship (to W.E.J.), the National Research Council of Canada for an operating grant, and Drs. E. Whalley and J. B. Hyne for advice and assistance in the construction of the high pressure apparatus.

1. W. E. Jones and T. W. Swaddle. Chem. Commun. 998 (1969).
2. C. H. Langford and H. B. Gray. Ligand substitution processes. W. A. Benjamin, Inc., New York. 1966.
3. W. A. Hynes, L. K. Yanowski, and M. Shiller. J. Am. Chem. Soc. **60**, 3053 (1938).
4. H. Diehl, H. Clark, and H. H. Willard. Inorg. Synth. **1**, 186 (1939).
5. W. E. Jones, R. B. Jordan, and T. W. Swaddle. Inorg. Chem. **8**, 2504 (1969).
6. M. Linhard and H. Flygare. Z. anorg. allgem. Chem. **262**, 328 (1950).
7. T. W. Swaddle and G. Guastalla. Inorg. Chem. **8**, 1604 (1969).
8. L. L. Po and R. B. Jordan. Inorg. Chem. **7**, 526 (1968).
9. L. R. Carey, W. E. Jones, and T. W. Swaddle. Inorg. Chem. **10**, 1566 (1971).
10. T. G. Spiro, A. Revesz, and J. Lee. J. Am. Chem. Soc. **90**, 4000 (1968).
11. T. W. Swaddle and P.-C. Kong. Can. J. Chem. **48**, 3223 (1970).
12. J. Milbauer. Z. anorg. Chem. **49**, 53 (1906).
13. C. J. Hansen. French Patent 661,508. October 5, 1928; Fr. 674,187. April 27, 1929; U.S. 1,853,679. April 12, 1932; Ger. 576,158. May 10, 1933; U.S. 1,932, 819. October 31, 1934.
14. D. L. Gay and G. C. Lalor. J. Chem. Soc. (A), 1179 (1966).
15. H. R. Hunt and H. Taube. J. Am. Chem. Soc. **80**, 2642 (1958).
16. H. S. Golinkin, W. G. Laidlaw, and J. B. Hyne. Can. J. Chem. **44**, 2193 (1966).
17. R. G. Pearson and J. W. Moore. Inorg. Chem. **3**, 1334 (1964).
18. D. A. Loeliger and H. Taube. Inorg. Chem. **5**, 1376 (1966).
19. D. A. Buckingham, I. I. Olsen, and A. M. Sargeson. Inorg. Chem. **6**, 1807 (1967).
20. D. A. Buckingham, I. I. Olsen, and A. M. Sargeson. Aust. J. Chem. **20**, 597 (1967).
21. S. D. Hamann. High pressure physics and chemistry. *Edited by* R. S. Bradley. Academic Press, New York. 1963. Vol. 2. p. 181.
22. S. W. Benson and J. A. Berson. J. Am. Chem. Soc. **84**, 152 (1962).

23. W. BILTZ. Z. anorg. Chem. **164**, 245 (1927).
24. F. J. MILLERO. Structure and transport processes in water and aqueous solutions. *Edited by* R. A. Horne. J. Wiley and Sons, Inc., New York. 1970. Chap. 15.
25. T. W. SWADDLE and W. E. JONES. Can. J. Chem. **48**, 1054 (1970).
26. H. TAUBE and F. A. POSEY. J. Am. Chem. Soc. **75**, 1463 (1953).
27. K. J. LAIDLER and D. T. Y. CHEN. Can. J. Chem. **37**, 599 (1959).
28. F. BASOLO and R. G. PEARSON. Mechanisms of inorganic reactions. 2nd ed. J. Wiley and Sons, Inc., New York. 1967. p. 145.
29. S. T. SPEES, J. R. PERUMAREDDI, and A. W. ADAMSON. J. Am. Chem. Soc. **90**, 6626 (1968).

Can. J. Chem. Downloaded from www.nrcresearchpress.com by 210.87.254.5 on 09/05/12
For personal use only.

The Ultraviolet Flash Photolysis of Ozone and the Reaction of $O(^1D)$ with H_2O

C. J. FORTIN,[1] D. R. SNELLING,[2] AND A. TARDIF

Defence Research Establishment Valcartier and Centre de Recherches sur les Atomes et les Molecules
P.O. Box 880, Courcelette, Québec

Received March 21, 1972

The decomposition of gas mixtures containing ozone has been studied following a short duration u.v. light pulse. From an analysis of the O_3 decomposition curves for $O_3:N_2$ and $O_3:H_2O$ mixtures, it is shown that the relative rate of $O(^1D)$ reaction with H_2O and N_2 is $k_{H_2O}/k_{N_2} = 3.5 \pm 1.5$. It is also shown that less than 6% of the O_2, formed directly by photolysis, is in the $^1\Sigma_g^+$ state. The water catalyzed decomposition of ozone is also discussed.

Nous avons étudié la décomposition de mélanges de gaz contenant de l'ozone, au moyen d'une pulsation de courte durée de lumière ultraviolette. Nous montrons qu'à partir d'une analyse des courbes de décomposition des mélanges $O_3:N_2$ et $O_3:H_2O$, la vitesse relative de la réaction d'$O(^1D)$ avec H_2O et N_2 est $k_{H_2O}/k_{N_2} = 3.5 \pm 1.5$. Nous montrons aussi que moins de 6% de l'oxygène, formé directement par photolyse, est dans l'état $^1\Sigma_g^+$. Nous discutons également de la décomposition de l'ozone catalysée par l'eau.

Canadian Journal of Chemistry, **50**, 2747 (1972)

Can. J. Chem. Downloaded from www.nrcresearchpress.com by 210.87.254.40 on 09/05/12
For personal use only.

Introduction

An understanding of the processes occurring in the u.v. photolysis of ozone in the Hartley continuum is of fundamental importance to the problem of ozone balance in the atmosphere. Ozone photolysis at wavelengths $\leqslant 3100$ Å produces $O(^1D)$ atoms (7), and the reaction of these excited oxygen atoms with H_2O is thought to be one of the principal mechanisms for producing OH and thus initiating the water-catalyzed decomposition of ozone. This indirect photodissociation of H_2O in the stratosphere is a critical process in the photochemical models of stratospheric ozone balance. Since the reactions of $O(^1D)$ with O_2 and N_2 are almost collision limited this species is always in photomechanical equilibrium in the stratosphere. Thus relative rates of $O(^1D)$ reactions with H_2O, N_2 and O_2 are sufficient to estimate the indirect H_2O photodissociation. Until recently (8–10), no information was available on the rate of the reaction of $O(^1D)$ with H_2O.

An apparatus has been built to study the time history of ozone decomposition following a short duration, ultraviolet light pulse. The ozone was monitored continuously, and the experimental ozone decay curves were fitted to a proposed mechanism by integrating the appropriate rate equations. This technique has been developed as part of a laboratory investigation (1–6) of aeronomic chemical processes.

In this paper we report a determination of the relative rates of reaction of $O(^1D)$ with N_2 and H_2O. The water catalyzed decomposition of ozone is also discussed. This apparatus will be used in the future to study a wide range of ozone photochemical processes.

Experimental

A. Apparatus

A schematic diagram of the apparatus is shown in Fig. 1. Both the cylindrical photolysis cell (53 cm long and 18 cm in diameter), and the end plates were made of stainless steel. The two quartz flash tubes (57 cm long and 1.4 cm diameter) were positioned with their axes 4.2 cm from the center of the cell. The cell contained a set of 3 multiple reflection mirrors and two quartz windows. The end plates, flash tubes, and mirror adjustment screws were all vacuum

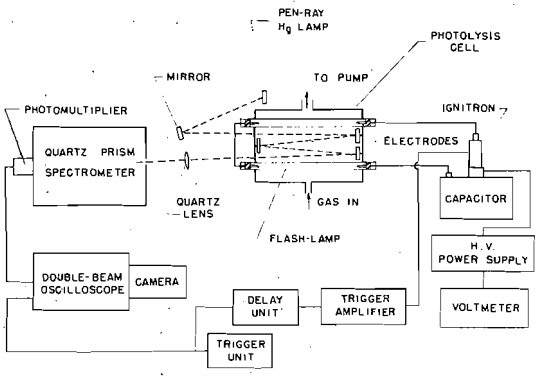

FIG. 1. Schematic diagram of apparatus.

[1]Present address: Département de Chimie, Université de Montréal, Montréal, Québec.

[2]To whom all correspondence should be addressed.

Can. J. Chem. Downloaded from www.nrcresearchpress.com by 210.87.254.40 on 09/05/12
For personal use only.

sealed with neoprene O-rings. The tantalum electrodes were press-fitted into a brass electrode assembly which was vacuum fitted in the quartz tubing by means of O-ring seals. The flash tubes were filled with xenon through two of the brass electrode assemblies. The two split mirrors were 6.3 cm square, and the single mirror which was 6.2 cm by 7.5 cm, was notched in the upper corners to allow passage of the entrance and exit beams to the cell.

The ozone concentration was monitored by following its absorption of 2537 Å light from a low pressure mercury lamp. The optical arrangement is shown in Fig. 1. The signal from the Pen Ray lamp was detected by a Medium Quartz Hilger spectrometer fitted with a 1P28 Photomultiplier. The spectrometer was set at 2537 Å, with a band pass of approximately 2 Å, in order to reduce the scattered light from the flash. Typically, the scattered light signal had decayed sufficiently for measurements to begin in the interval 100 to 200 μs after the flash. The flash lamps were triggered after the oscilloscope to provide a short segment of oscilloscope trace showing the initial ozone absorption. The multiple-reflection mirrors provided the long, adjustable path length necessary in order to measure low ozone pressures. With this optical arrangement absorption measurements were confined to the center of the photolysis cell.

The observed region consisted of a set of cones of base 5 cm × 5 cm at the split mirrors. Thus the maximum observed cross section was a rectangle extending 10 cm horizontally and 5 cm vertically. The two flash lamps were positioned inside the cell with their axes 4.2 cm above and below the observed region, respectively. This geometry was chosen to provide uniform illumination of the observed region.

The low inductance capacitors used were either 4.88 or 14.2 μF with a maximum voltage rating of 20 kV. The voltage was controlled by a General Electric 7703 Ignitron which was fired by discharging a 0.2 μF capacitor charged to 3000 V into the firing pin. The cell was pumped by means of a 4 in. diffusion pump backed by a rotary vacuum pump.

B. Reagents and Sample Preparation

Ozone was produced by a Welsback "Ozonator" and condensed in a liquid nitrogen cooled trap. Approximately half the ozone sample was then distilled to a second liquid-nitrogen cooled trap while pumping to remove any traces of oxygen. The ozone was then evaporated into a 22 l bulb and diluent gases were added. The mixtures were stirred by a glass-enclosed magnetic stirrer. The O_2 and N_2 were Matheson "Gold Label" and "Prepurified" grades, respectively, and they were used without further purification. The CO_2 and SF_6 were purified by condensing them at liquid nitrogen temperatures to remove any air present. Water samples were degassed repeatedly to remove air. Pressures in the bulbs and in the cell were measured using a quartz Bourdon gauge supplied and calibrated by Texas Instruments.

C. Experimental Procedure

The photomultiplier signal with the cell empty (V_0) was displayed on a chart recorder. The cell was filled with a sample until a predetermined transmission was attained (usually 5 or 10%); the total pressure in the cell was recorded, and the signal leads were transferred to the dual-beam, dual-time-base oscilloscope. This procedure ensured that a constant ozone pressure was used for each experiment. With the two beams operated on separately adjustable time bases, the photolysis flash was delayed after triggering the oscilloscope to provide a short record of the initial signal (V_i) on the most sensitive time scale. This arrangement was found to be necessary since a slow decomposition (typically 20% decomposition in 5 min) of the ozone occurred after the sample was admitted to the cell. The signal voltages as a function of time (V_t) were photographed and recorded on Polaroid prints. Typically, measurements were taken in the time interval 200 μs to 0.5 s after the flash using oscilloscope time base settings of 200 μs cm^{-1}, 1 ms cm^{-1}, and 50 ms cm^{-1}. This required only two fillings of the cell since two independent time base settings were available. Finally, the photomultiplier signal was recorded approximately 10 s after the flash (V_∞) and the cell was pumped. The photomultiplier signal with the cell empty (V_0) was found to be constant to within 1% during the course of an experiment. The cell was pumped to less than 10^{-5} Torr between experiments.

The signal height of each polaroid trace was read and processed automatically and measurements were taken every 0.25 mm across the 80 mm trace. For each measurement from the polaroid trace the fraction of ozone decomposed was calculated, and all values falling within selected time intervals were averaged. Finally, the results from all the polaroid traces were averaged to provide graphs of fraction of ozone decomposed *vs.* time. The precision of these results as judged from the standard deviation of a set of measurements (5 to 10 measurements were taken at each oscilloscope time base setting) depended on the initial transmission (V_i/V_0) and the fraction of ozone decomposed. For an initial transmission of 5% and fractional O_3 decomposition (f_t) of 0.20 to 0.60 the single standard deviation was $\sim$1–2% of f_t. Thus the plotting symbols in Figs. 7 to 9 represent $\sim$3 standard deviations in the ordinate.

Initially, some measurements were made of the flash intensity as a function of time and wavelength. The latter measurements were made by replacing the 1P28 photomultiplier with Kodak 103a0 plates and recording spectra of the flash-lamp output reflected off magnesium oxide coated blocks. The plates were calibrated using an NBS calibrated quartz–iodine lamp and neutral density filters. Measurements of the flash intensity distribution with time at various wavelengths were made photometrically using the Medium Quartz Hilger spectrometer and the 1P28 photomultiplier. For these experiments the oscilloscope was triggered with a signal obtained by wrapping 3 turns of copper wire around one of the quartz flash tubes. A complete description of the apparatus, experimental technique, data reduction and some initial results has been presented previously (11).

Results

A. Characteristics of the Flash

The dashed curve in Fig. 2 shows the wavelength distribution of the photolysis flash output for an input energy of 2800 J. The solid curve, which is the product of the relative flash

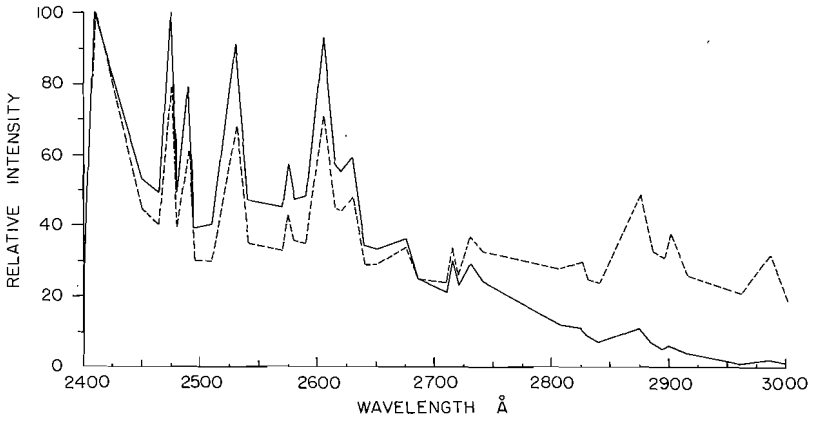

FIG. 2. Wavelength distribution of photolysis radiation. Broken curve incident radiation, solid curve radiation absorbed by ozone.

intensity and the ozone absorption coefficient, represent the wavelength distribution of the radiation absorbed by ozone. Because of the difficulties of calibrating the photographic plates, these distribution curves should be regarded as semi-quantitative, but they do show that almost all the ozone absorption occurs at $\lambda \leqslant 2950$ Å (well below the threshold for $O(^1D)$ formation). The distribution of photons absorbed by ozone in the wavelength intervals: 2400–2450, 2450–2500, 2500–2575, 2575–2625, 2625–2725, 2725–2825, and 2825–2925 Å is 0.18, 0.15, 0.21, 0.16, 0.16, 0.09, and 0.04, respectively. The corresponding photon distribution for a flash energy of 1000 J was 0.18, 0.21, 0.19, 0.18, 0.15, 0.06, and 0.03; thus there appears to be no marked change of energy distribution with flash energies in the range 1000–2800 J. The data in Fig. 2 were obtained with a pressure of 25 Torr of xenon in the flash tubes although both the total intensity and the energy distribution were independent of xenon pressure in the range 6–25 Torr.

Although the time distribution of the photolysis flash energy is only of secondary importance to the results presented in this paper, an extensive series of measurements has been made at various flash energies and xenon pressures. Some typical results, presented in Fig. 3, show that the time distribution is essentially independent of wavelength in the region where absorption by ozone occurs. Somewhat larger differences are observed in the time

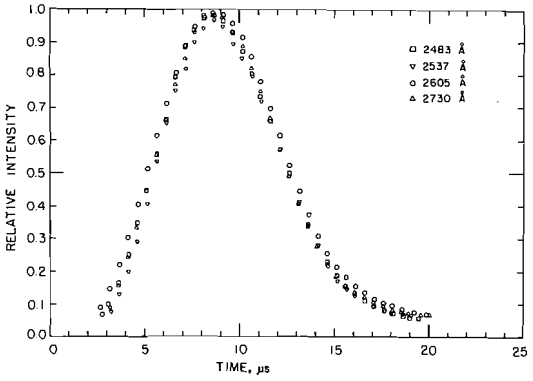

FIG. 3. Time distribution of photolysis radiations at various wavelengths for a flash energy of 2800 J.

interval 50 to 100 μs, but typically only 4% of the total flash energy occurs after 50 μs.

To take account of the small changes with wavelength, the overall time distribution was obtained using a photometer equipped with a 2550 Å interference filter and a 1P28 photomultiplier whose combined response approximated that of the ozone absorption curve.

The flash lamps were regularly refilled with xenon after 3 flashes, although experiments showed that a filling could be used at least 30 times with no significant loss of light output.

B. Photolysis of Ozone

The ozone absorption coefficient at 2537 Å (close to the ozone absorption maximum) is (12) 306 cm^{-1}. The absorption of radiation is

Can. J. Chem. Downloaded from www.nrcresearchpress.com by 210.87.254.40 on 09/05/12
For personal use only.

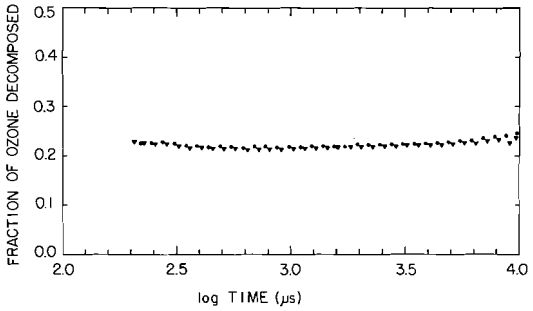

FIG. 4. Ozone decomposition: solid circles are experimental data of an $O_3/O_2/N_2/SF_6$ mixture, pressures 0.0144:0.0048:8.20:8.20 Torr, respectively; $f_\infty = 0.778$. The solid triangles are experimental data for an $O_3/O_2/N_2/CO_2$ mixture pressures 0.0144:0.0049:8.20:8.20 Torr, respectively; $f_\infty = 0.832$; flash energy 1000 J. See text for description of computed curves.

given by:

$$[1] \qquad I/I_0 = \exp\left(-306 \times \frac{P}{760} \times \frac{273}{T} \times L\right)$$

where I and I_0 are the transmitted and incident intensities, P is the ozone pressure in Torr, L is the path length in cm, and T is the absolute temperature (295 °K). For a typical ozone pressure of 0.01 Torr and an average path length of 9 cm for flash radiation in the observation region, the term in parentheses in eq. 1 above is 0.033. Thus, the linear absorption approximation holds, and the radiation absorbed $(I_0 - I)$ is proportional to ozone pressure. This point can be checked experimentally, since if the absorption is linear in ozone, the fraction of ozone decomposed is independent of ozone pressure. It will be shown later, that for O_3/N_2 mixtures in the time region 200–800 μs after the flash, the ozone decomposition is due to photolysis only. The fraction of ozone decomposed in this time interval was measured for a mixture of O_3 and N_2 in the ratio 1:1000. For ozone pressures of 0.014, 0.028, and 0.042 Torr the fraction decomposed was found to be 0.185, 0.182, and 0.185, respectively. Thus, experimentally, the linear absorption approximation holds for O_3 pressures $\leqslant 0.042$ Torr. For the data reported in this paper maximum ozone pressures between 0.01 and 0.015 Torr were used.

C. Ozone Decomposition Curves

Ozone decomposition as a function of time has been measured for various ozone added gas mixtures, and the results are shown in Figs. 4–10. The ordinate of these graphs shows the fraction of ozone decomposed (f_t) which, using Beer's law, was calculated from the formula

$$[2] \qquad f_t = \log(V_t/V_i)/\log(V_0/V_i)$$

The fractional ozone decomposition (f_∞) measured 10 s after the flash is also given. All experiments were conducted at 295 ± 2 °K. The initial ozone pressure $[O_3]_i$ was calculated from the initial transmission (V_i/V_0) using eq. 1. In all experiments there was some oxygen present due to decomposition of the ozone. When the gas mixtures were prepared the pressures of the freshly evaporated ozone and added gases were recorded, and the fractional ozone content of the mixture (F_{O_3}) was calculated. The oxygen present in the photolysis cell was then calculated from the formula $[O_2] = \frac{3}{2}(F_{O_3} \times P_T - [O_3]_i)$ where P_T is the total pressure of mixture in the cell. In deriving this equation

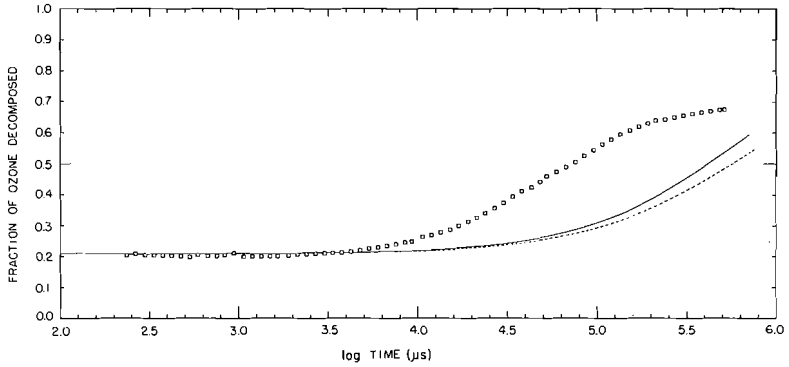

FIG. 5. Ozone decomposition: the open squares are experimental data for an $O_3/O_2/N_2$ mixture, pressures 0.0142:0.0038:5.2 Torr, respectively; $f_p = 0.200$, $f_\infty = 0.798$; flash energy 620 J.

Can. J. Chem. Downloaded from www.nrcresearchpress.com by 210.87.254.40 on 09/05/12
For personal use only.

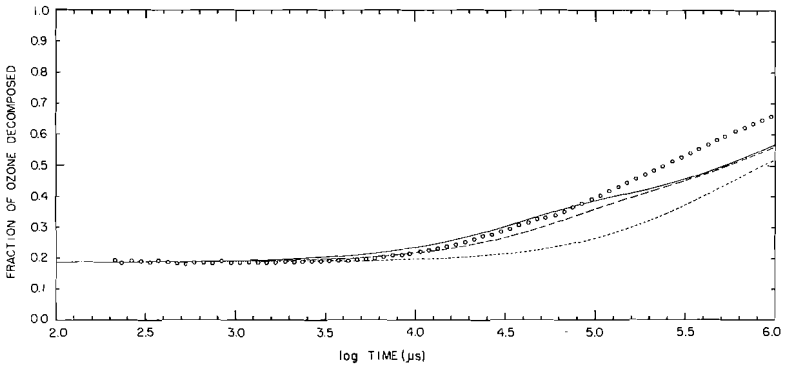

FIG. 6. Ozone decomposition: the open circles are experimental data for an $O_3/O_2/N_2/SF_6$ mixture, pressures 0.0144: 0.011:6.36:6.36 Torr, respectively; $f_p = 0.185$, $f_\infty = 0.750$; flash energy 615 J. See text for description of solid dotted and dashed computed curves.

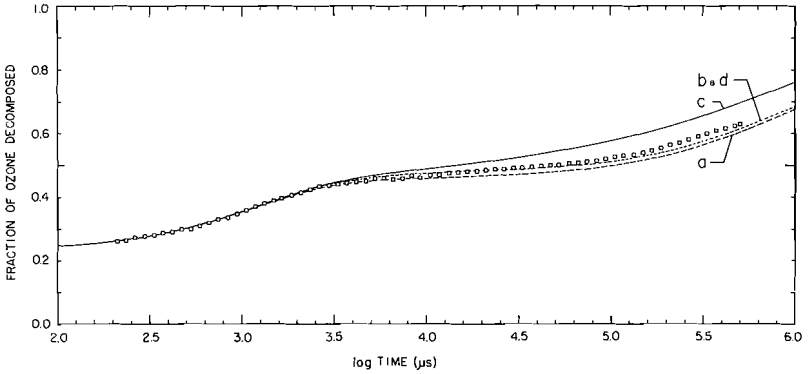

FIG. 7. Ozone decomposition: the open squares are experimental data for an $O_3/O_2N_2/H_2O$ mixture pressures 0.0141: 0.0382:18.4:0.79 Torr, $f_p = 0.243$, $f_\infty = 0.718$; flash energy 1000 J. The labelled computed curves correspond to mechanisms (*a*), (*b*), (*c*), and (*d*) discussed in text.

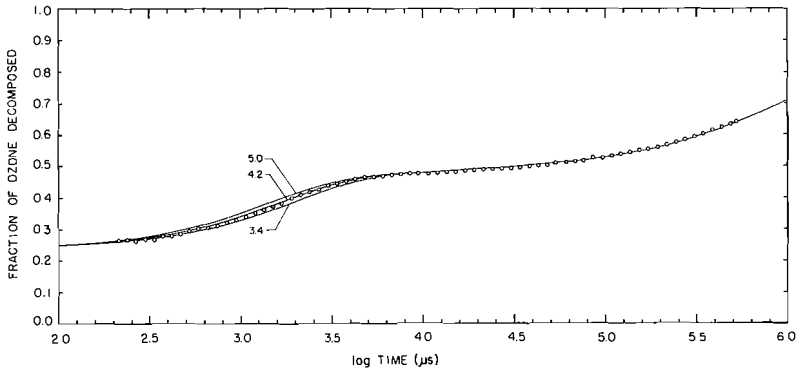

FIG. 8. Ozone decomposition: the open circles are experimental data for an $O_3/O_2/N_2/H_2O$ mixture; pressures 0.0142: 0.0185:24.7:0.529 Torr, respectively; $f_p = 0.248$, $f_\infty = 0.758$; flash energy 1000 J. The number associated with each calculated curve represents the value of k_5 assumed (see text).

Can. J. Chem. Downloaded from www.nrcresearchpress.com by 210.87.254.40 on 09/05/12
For personal use only.

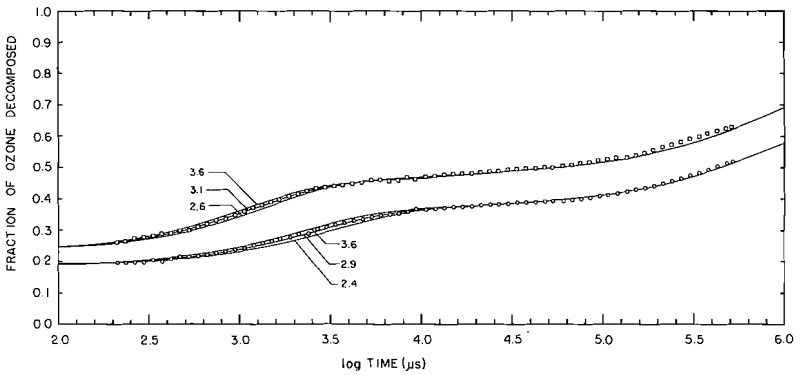

FIG. 9. Ozone decomposition: the open squares are experimental data for an $O_3/O_2/N_2/H_2O$ mixture pressures 0.0141 : 0.0382:18.4:0.79 Torr, respectively; $f_p = 0.243$, $f_\infty = 0.718$; flash energy 1000 J. The open circles are experimental data for an $O_3/O_2/N_2/H_2O$ mixture pressures 0.0144:0.014:22.04:0.475 Torr, respectively; $f_p = 0.187$, $f_\infty = 0.633$; flash energy 625 J. The number associated with each calculated curve represents the value of k_5 assumed (see text).

it is implicity assumed that the ozone decomposition occurred subsequently to the initial evaporation. If the decomposition occurred during evaporation then the oxygen present would only be 2/3 of that given by the above formula. Thus the calculated oxygen pressure is an upper limit. O_3/N_2 or $O_3/N_2/SF_6$ mixtures were studied at regular intervals throughout these experiments in order to determine the fraction of O_3 photolyzed. This proved necessary since a slow decrease in flash lamp intensity, and hence O_3 photolysis, occurred throughout these experiments. This loss of intensity could be regained by cleaning the flash lamps with HF and was probably caused by deposits forming in the flash-tubes.

Discussion

A. Reaction Scheme and Integration of Rate Equations

The relevant reactions and their rate constants are listed in Tables 1 and 2, respectively. All rate constants are given in molecular units (cm^3 $molecule^{-1}$ s^{-1} or cm^6 $molecule^{-2}$ s^{-1}). The reactions have been arbitrarily divided into two groups: principal reactions and reactions which are of secondary importance because of their slow rates or because of the presence of competing reaction.

Much of the available information on O(D) reactions has been reviewed recently (13), and additional information has appeared subsequently (3, 4, 9, 10, 14, 15). The available evidence indicates that the reactions of O(D) with N_2 and O_2 are almost collision limited $(2–20) \times 10^{-11}$, and that the rates of these reactions are approximately equal. The reaction of O(D) with O_3 is some 10 times faster. The efficiency of reaction 13 in producing $O_2(\Sigma)$ is between 0.3 and 1.0. Only relative O(D) reaction rates have been used in our calculations, and the values assumed are listed in Table 2 based on $k_4 = 1.0$. An efficiency of 0.8 for $O_2(\Sigma)$ formation in reaction 13 has been adopted. Any error in these assumed rates is not important since a large excess of H_2O and/or N_2 was present in all the gas mixtures studied.

The calculated ozone decay curves were obtained by a numerical integration of the appropriate rate expressions using a Runge–Kutta integration routine. It proved difficult to integrate the rate expression directly, since the very large O(D) reaction rates necessitated too small a time step for the integration to be practical. Since $k_4 \geqslant 2 \times 10^{-11}$ (13), and the minimum N_2 pressure used in any of our experiments was 5 Torr; then the time constant for O(D) disappearance was always less than 0.3 μs. Since this time constant was short compared to the flash duration, the O(D) was taken to be in photochemical equilibrium. The steady state O(D) concentration is then given by $[O(D)] = k_1 I_t[O_3]/(k_4[N_2] + k_5[H_2O] + k_{13}[O_2] + k_{14}[O_3])$. The rate of any individual O(D) reaction, *e.g.*, deactivation by N_2, is then given by $k_4[N_2][O(D)]$, and hence only relative O(D) reaction rates are required to

Can. J. Chem. Downloaded from www.nrcresearchpress.com by 210.87.254.40 on 09/05/12
For personal use only.

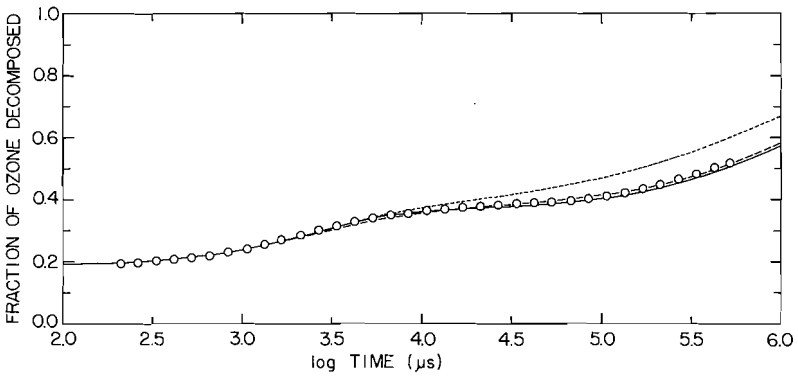

FIG. 10. Ozone decomposition: the open circles are experimental data for an $O_3/O_2/N_2/H_2O$ mixture, pressures 0.0144: 0.014:22.04:0.475 Torr, respectively; $f_p = 0.187$, $f_\infty = 0.633$; flash energy 625 J. The dotted, dashed, and solid curves are computed; see text for discussion.

TABLE 1. Reaction scheme*

	Principal reactions
[3]	$O_3 + h\nu \rightarrow O_2(\Delta) + O(D)$
[4]	$O(D) + N_2 \rightarrow O + N_2$
[5]	$O(D) + H_2O \rightarrow 2OH$
[6]	$O_2(\Delta) + O_3 \rightarrow 2O_2 + O$
[7]	$O_2(\Delta) + H_2O \rightarrow O_2 + H_2O$
[8]	$O + O_3 \rightarrow 2O_2$
[9]	$O + OH \rightarrow O_2 + H$
[10]	$H + O_3 \rightarrow OH + O_2$
[11]	$OH + OH \rightarrow H_2O + O$
[12]	$OH + OH + M \rightarrow H_2O_2 + M$
	Secondary reactions
[13]	$O(D) + O_2 \rightarrow O + O_2(\Sigma)$ $\rightarrow O + O_2$
[14]	$O(D) + O_3 \rightarrow 2O_2$
[15]	$O_2(\Sigma) + O_3 \rightarrow 2O_2 + O$
[16]	$O + O_2 + M \rightarrow O_3 + M$
[17]	$\dagger OH + O_3 \rightarrow HO_2 + O_2$
[18]	$\dagger HO_2 + O_3 \rightarrow OH + 2O_2$
[19]	$H + O_2 + M \rightarrow HO_2 + M$
[20]	$O + HO_2 \rightarrow OH + O_2$
[21]	$OH + HO_2 \rightarrow H_2O + O_2$
[22]	$HO_2 + HO_2 \rightarrow H_2O_2 + O_2$
[23]	$O + H_2O_2 \rightarrow OH + HO_2$
[24]	$OH + H_2O_2 \rightarrow HO_2 + H_2O$

*The excited states of atomic and molecular oxygen, $O(^1D)$, $O_2(^1\Delta g)$ and $O_2(^1\Sigma_g^+)$ are abbreviated to O(D), $O_2(\Delta)$, and $O_2(\Sigma)$, respectively.

†Reactions 17 and 18 have been invoked to explain the chain decomposition of O_3 in the presence of H_2O although no direct proof is available for the occurrence (17). Extrapolation of recent measurements (29) of k_{17} for vibrational excited OH ($v = 2$ to 9) indicate that the upper limit given for k_{17} is approximately correct for OH ($v = 0$).

compute the fraction of O(D) participating in the various reactions.

The rate of ozone photolysis has been shown to be proportional to ozone concentration and can be represented by $k_1 I_t[O_3]$ where I_t is the time-dependent relative flash intensity and k_1 is an empirically determined constant which depends on flash lamp intensity, cell geometry, etc. For O_3/N_2 mixtures in the period 200–800 μs following the flash no further O_3 decomposition occurs. Thus the O_3 decomposition at 200 μs results from O_3 photolysis with an additional small contribution from the reaction of O(D) with O_3[14]. k_1 was determined by integrating the rate equations with photolysis and the O(D) reactions 4 and 14 included and varying k_1 in order to obtain the observed amount of O_3 decomposition in these mixtures.

B. Mixtures Containing no Added H_2O

For O_3/N_2, $O_3/N_2/CO_2$, and $O_3/N_2/SF_6$ mixtures (Figs. 4–6), there is no O_3 decomposition in the period 200–800 μs following the flash. This is to be expected, since in the presence of excess N_2 the bulk of the O(D) is deactivated to O, and the subsequent reactions of O and $O_2(\Delta)$ with O_3 are too slow to occur in this time interval. Thus it appears that O_3 decomposition at 200 μs results from photolysis and reaction 14, only. A possible exception could arise if $O_2(\Sigma)$ were formed directed by photolysis (reaction 3) since the $O_2(\Sigma)$ would then react rapidly with O_3 (reaction 15). However, it has been shown that for O_3 photolysis at 2537 Å, less than 5% of the O_2 is in the $O_2(\Sigma)$ state (4) and that the quantum yield of $O_2(\Delta)$ production is between 0.7 and 1.0 (24). The absence of $O_2(\Sigma)$ as a product of reaction 3 can be verified by the data shown in Fig. 4 which shows that the O_3 decomposition is

Can. J. Chem. Downloaded from www.nrcresearchpress.com by 210.87.254.40 on 09/05/12
For personal use only.

TABLE 2. Values used in calculating the efficiency of reaction in producing $O_2(\Sigma)$

Reaction	Rate constants used*	Comments†	Reference
[3]	$k_1 I_t$ (see text)		4, 24
[4]	1.0	†	
[5]	See text		
[6]	3.5×10^{-15} (298 °K)	$E = 5600$¶	5
[7]	$(0.4\text{–}1.4) \times 10^{-17}$		6, 20
[8]	1×10^{-14}	$E = 4000$	16, 19
[9]	$(5 \pm 2) \times 10^{-11}$		17
[10]	$(2.6 \pm 0.5) \times 10^{-11}$		17
[11]	$(2.0 \pm 0.6) \times 10^{-12}$		17
[12]	$M = N_2$ 3.3×10^{-30}		
	$M = O_2$ 5.1×10^{-30}	‖	18, 21*a*
	$M = SF_6$ 1.0×10^{-29}		
	$M = H_2O$ 1.8×10^{-29}	§	
[13]	1.4	‡	4
[14]	13.5	‡	4
[15]	2.5×10^{-11}		22
[16]	$M = O_2$ 7.4×10^{-34}		16, 18
[17]	$\leqslant 5 \times 10^{-13}$	**	17
[18]	$\leqslant 5 \times 10^{-13}$	**	18
[19]	$M = N_2$ 4.5×10^{-32}		17
	$M = O_2$ 3.0×10^{-32}		
	$M = H_2O$ 6.0×10^{-31}		
	$M = SF_6$ 1.5×10^{-31}	§	
[20]	$\geqslant 10^{-11}$		17
[21]	$\geqslant 10^{-11}$		17
[22]	$\geqslant 1.5 \times 10^{-12}$		17
[23]	$\geqslant 4.0 \times 10^{-15}$		21*b*
[24]	9.0×10^{-13}		23

*Wherever possible, rate constants have been taken from recent review articles (16–20). When this was not possible, a publication which summarizes the information available has been chosen.

†Where applicable energy of activation given in cal/mol.

‡Relative rates only with $k_4 = 1.0$; see text for discussion.

§Estimates from relative rates of SF_6 in other three body reactions.

‖These rate constants are based on a single measurement of k_{A_r}, and dependence on M was obtained from an earlier study. The value of k_{A_r} found in this earlier study was approximately 100 times less but is probably less reliable; see reference (21(*a*)) for a discussion.

¶Other results, discussed in ref. 5, indicate a lower value of E of 3100 cal/mol.

**k_{17} and k_{18} are estimated rate constants; see footnote Table 1.

identical with and without addition of CO_2 to O_3/N_2 mixtures. In the absence of CO_2 the $O_2(\Sigma)$ would react with O_3 [15] rather than be deactivated by $N_2(k(N_2) = 2 \times 10^{-15}$ (20)), but with the addition of CO_2, deactivation by CO_2 ($k(CO_2) = 3 \times 10^{-13}$ (20)) predominates. Since the O_3 decomposition is identical for both mixtures we conclude that $O_2(\Sigma)$ is not a product of reaction 3. From a detailed analysis of the data in Fig. 4 the fraction of O_3 decomposed in the time interval 200–1000 μs is 0.211 ± 0.003 ($O_3/N_2/SF_6$) and 0.217 ± 0.003 ($O_3/N_2/CO_2$). (The errors given are twice the standard deviation.) Thus the maximum difference between these two values of the fraction of O_3 decomposed, which can be attributed to $O_2(\Sigma)$ production in reaction 3, is 0.012 or 6% of the ozone photolyzed.

Nearly all the difference between the two results given above can be attributed to reaction 3. For the $O_3/N_2/SF_6$ mixture ~2.5% of the O(D) reacts with O_3 [14], while for the $O_3/N_2/CO_2$ mixture this figure is only 0.5% (a relative rate of O(D) quenching by CO_2 of 3.0 was taken (13)). Thus both of the above results are consistent with a fraction of O_3 photolyzed (f_p) of 0.210. In calculating the values of f_p used in this work the small correction for reaction 14 was always made.

A comparison of the O_3 decomposition curves

Can. J. Chem. Downloaded from www.nrcresearchpress.com by 210.87.254.40 on 09/05/12
For personal use only.

Can. J. Chem. Downloaded from www.nrcresearchpress.com by 210.87.254.40 on 09/05/12
For personal use only.

in Figs. 5 and 6 shows that addition of SF_6 reduces the rate of O_3 decomposition. Since, for these mixtures, the O_3 decomposition should only involve reactions 3, 4, 6, and 8 (which do not directly involve SF_6) the effect of SF_6 must be to remove energy from the system. This conclusion was supported by an attempt to fit the experimental O_3 decay curves by the simple mechanism outlined above. A reaction scheme involving reactions 3, 4, 6, 8, 13, 14, 15, and 16 was integrated numerically. Although reactions 13 to 16 were included they had a very minor influence on the O_3 decomposition. The results of these calculations are shown by the dotted lines in Figs. 5 and 6. It can be seen that the measured O_3 decomposition is consistently greater than the computed curves in the region 10^4 to 10^6 μs after the flash, particularly in the absence of added SF_6.

For the O_3/N_2 data the effect of gas heating was also examined. For this calculation (solid curve in Fig. 5) it was assumed that both the excess energy available in the photolysis reaction and the heat liberated by O_3 decomposition were rapidly equilibrated. The consequent temperature rise was then calculated from the known heat capacity of the mixture. Using the temperature dependence for reactions 6 and 8 given in Table 2 the observed O_3 decomposition is still much faster than the computed value.

It should be noted that for the data in Figs. 5 and 6 the final quantum yield of O_3 destruction (Φ) is 3.99 and 4.05, respectively (where $\Phi = f_\infty/f_p$). A quantum yield of 4.0 is expected for the mechanism discussed above and no energy-chain mechanism is required to explain the observations. It is only the approach to this final quantum yield which is anomalously fast.

A possible explanation of these results lies in the vibrationally excited O_2 formed in reaction 8. It is known (25) that vibrational energy released in this reaction readily transfers to O_3 and leads to enhanced O_3 reaction rates. For the O_3/N_2 mixtures used in this work, it appears unlikely that the vibrationally excited $O_2(O_2\dagger)$ will be removed sufficiently fast by vibrational–vibrational (V–V) energy transfer to N_2 (26), or by vibrational–translational (V–T) energy transfer with O (27). The $O_2\dagger$ may decay by V–V transfer to O_3 followed by V–T deactivation of the $O_3\dagger$. Deactivation may also occur through traces of water vapor since this mechanism is very rapid (28). It is difficult to model this mechanism since the energy transfer mechanism is not well defined, and the effect of O_3 vibrational energy in overcoming the energy barrier to reactions 6 and 8 is not known. However, qualitatively, if the energy released in reaction 8 were rapidly equilibrated between the vibrational degrees of freedom of O_2 and O_3 then vibrational temperatures of several thousand degrees would be anticipated. If degradation of this vibrational energy to kinetic energy is sufficiently slow, this mechanism may explain the observed results. For the purposes of further discussion the important point to be noted is the almost complete absence of O_3 reaction in the period 10^2 to 10^4 μs following the flash for these mixtures.

Anticipating later discussion, the effect of traces of water vapor in promoting the O_3 decomposition has been examined. In Fig. 6 the dashed and solid curves represent the computed O_3 decay curves for H_2O pressure of 3×10^{-3} and 6×10^{-3} Torr, respectively. A value of k_5 of 3 and a mechanism involving reactions 3 to 16 were used for these calculations. Reactions 9 and 10 together are equivalent to reaction 8 and, in effect, lead to the catalyzed reaction of O with O_3. (The mixtures containing SF_6 could possibly have contained traces of water vapor, since the SF_6 used was of lower purity than the other gases, and was simply purified by trap-to-trap distillation.) Although traces of water vapor have a profound effect on the O_3 decomposition it appears that the vibrational energy exchange mechanism must be invoked in order to explain the $O_3/N_2/SF_6$ results in Fig. 6.

C. Mixtures Containing Added H_2O

Ozone decomposition curves for various $O_3/N_2/H_2O$ mixtures are shown in Figs. 7–10. The most obvious difference between these results and those in Figs. 5 and 6 is that O_3 decomposition is now occurring in the 10^2 to 10^4 μs time interval. This decomposition can be understood in terms of the mechanism outlined at the end of the previous section where there is now considerably greater production of OH in reaction 5 because of the added water vapor. This larger OH concentration leads to very much more rapid decomposition of O_3 by reactions 9 and 10. This data will be interpre-

Can. J. Chem. Downloaded from www.nrcresearchpress.com by 210.87.254.40 on 09/05/12
For personal use only.

ted initially by fitting the experimental data in the 10^2 to 10^4 μs interval. Interpreting the data in the 10^4 to 10^6 μs time range is more uncertain, both because of the larger number of reactions involved, and also because of the problems encountered in this time interval with mixtures not containing water vapor. However, anomalous effects due to vibrationally excited O_2 are not likely with these mixtures, since first, reaction of O and O_3 occurs through reactions 9 and 10 rather than reaction 8, and secondly, water vapor is an excellent deactivator of vibrationally excited species, particularly O_2† (28).

f_p, the fraction of O_3 photolyzed (and hence k_1), was obtained as discussed earlier from $O_3/N_2/SF_6$ experiments performed both before and after each of the $O_3/N_2/H_2O$ experiments shown in Figs. 8 and 9.

The experimental data shown in Fig. 7 (and repeated in Fig. 9) were chosen to study the effects of different assumed mechanisms on the calculated ozone decay curves. For the higher $[H_2O]/[N_2]$ ratio of this experiment the production of OH in reaction 5 was correspondingly greater. With this larger OH production, the calculated O_3 decay curves were more sensitive to changes in the assumed mechanism. In particular we wish to investigate the possible effects of reactions 17 and 18 which have frequently been proposed to explain the chain decomposition observed in wet ozone mixtures (see footnotes in Tables 1 and 2).

In Fig. 7 three computed decay curves are shown. To calculate these curves the rate constants given in Table 2 were used (exceptions are noted below) with $k_5 = 3.0$ (chosen to give a close fit to the experimental data) and $k_7 = 6 \times 10^{-18}$. The following mechanisms were assumed: (*a*) For the dashed curve (Fig. 7) reactions 17 and 18 were excluded; (*b*) for the dotted curve reaction 17, but not 18, was included; (*c*) for the solid curve both reactions 17 and 18 were included; (*d*) same as (*a*) above with k_{12} reduced to 1/3 of the value shown in Table 2 (see footnote in Table 2). This latter decay curve was almost indistinguishable from (*b*), being only slightly lower (~ 0.005) in the region $\log t = (\mu s) = 3.6$ to 4.0.

The detailed computer output, which listed both the concentration of all the species, and the contribution of specific terms to the rate equations, was examined to determine the effects of specific reactions. For all the mechanisms and for $t \leqslant 10^4$ μs the reactions of $O_2(\Delta)$ were negligible ($\leqslant 1\%$ of the $O_2(\Delta)$ reacted) as were any uncertainties in the rates of reactions 13–16. Reactions 19 and 22–24 had a total negligible effect. The small differences in computed O_3 decomposition at $t \leqslant 10^4$ μs for the various mechanisms were due to different OH decay mechanisms (reactions 11, 12, and 17). (For this experiment approximately 10% of the O(D) formed in reaction 3 reacts with H_2O[5] for $k_5 = 3.0$). Both reactions 11 and 17 lead to loss of O_3, the latter directly and the former by the subsequent reactions of the O atom produced. Reaction 12 does not lead to O_3 decomposition. For mechanism (*a*) the rates of reactions 11 and 12 are approximately equal; thus the reduction of k_{12} in (*d*) leads to increased O_3 decomposition. Including reaction 17, (*b*) led to a similar small increase in O_3 decomposition. Including both reactions 17 and 18, (*c*) produced greater increases in O_3 decomposition than mechanisms (*a*) or (*b*). However, a tenfold increase in k_{20} and k_{21} above the lower limits given in Table 2 produced a curve which was almost indistinguishable from that for mechanism (*b*). Mechanisms (*a*), (*b*), and (*d*), were not sensitive to increases in k_{20} and k_{21}.

Thus, with the possible exception of (*c*), the various mechanisms assumed have a negligible effect on O_3 decomposition for $t \leqslant 10^4$ μs. Furthermore, these mechanisms are not sensitive to variations in k_{19} to k_{24}. Mechanism (*c*) (with lower limits for k_{20} and k_{21}) appears to be ruled out by the large deviations from the experimental data in the 10^4 to 10^6 μs range; this point will be discussed further in a later section. Mechanism (*d*) was arbitrarily selected to fit the remainder of the data on $O_3/N_2/H_2O$ mixtures shown in Figs. 8 and 9.

Using mechanism (*d*) the value of k_5 was varied in order to obtain the best fit to the experimental data shown in Figs. 8 and 9. The number associated with each curve in Figs. 8 and 9 represents the value of k_5 assumed. From a visual inspection of the curves in Figs. 8 and 9 it was concluded that the best fit value of k_5 was 3.5 ± 0.5.

Because of the uncertainty in k_9 and k_{10} (see Table 2), the effect of varying these reaction

Can. J. Chem. Downloaded from www.nrcresearchpress.com by 210.87.254.40 on 09/05/12
For personal use only.

rates on the best fit value of k_5 was examined. For the data in Fig. 9 (upper curve) the best fit k_5 was 2.0 and 5.0 for limiting values of k_9 of 7×10^{-11} and 3×10^{-11} (*cf.* $k_5 = 3.1$ for $k_9 = 5 \times 10^{-11}$), respectively. For $k_9 = 3 \times 10^{-11}$ no entirely satisfactory fit was obtained; the computed curves were 0.015 too low in the region log t (μs) = 3.4 to 3.7. This arose because the consequent increase in k_5 leads to higher OH concentrations, and reaction 11 then produced significant reduction in OH before all the O atoms reacted through reactions 9 and 10. The smaller uncertainty in k_{10} produced correspondingly smaller changes in the best fit k_5 (2.7 and 3.5). Taking into account these additional systematic errors $k_5 = 3.5 \pm 1.5$ was adopted.

D. Possible Ozone Chain Decomposition Mechanisms

If reaction 18 is neglected the slopes of the ozone decomposition curves for $t = 10^4$ to 10^6 μs are not affected by changes in the rates of reactions involving OH, H, and HO_2. (Small differences in the absolute O_3 decomposition are produced, as discussed earlier, by the varying effects of the OH decay reactions 11, 12, and 17 in leading to O_3 destruction.) This arises since the rate controlling step is the release of O atoms in reaction 6 rather than the subsequent reaction of O atoms in reaction 8 or reactions 9 and 10. However, the computed curves are sensitive to k_7. $k_7 = 6 \times 10^{-18}$ (towards the low end of the range given in Table 2) was found to give the best fit to the data, and with this value approximately 10% of the $O_2(\Delta)$ is deactivated and 90% reacts with O_3.

The effect of including reaction 18, which leads to the chain decomposition of O_3, was indicated earlier. In Fig. 10 a set of computed O_3 decay curves are shown. The rate constants given in Table 2 were used with $k_5 = 3.2$ and $k_7 = 6 \times 10^{-18}$. For the solid curve reaction 18 was neglected, but for the dotted and dashed curves $k_{18} = 5 \times 10^{-13}$ was adopted. For the dotted curve the lower limit to k_{21} (1×10^{-11}) was assumed, and for the dashed curve this rate was increased to 1×10^{-10}. The results show that including reaction 18 leads to a much higher O_3 decomposition which is not consistent with the experimental data. However, a tenfold increase in k_{21} produces a satisfactory fit to the data. This is to be expected since reaction 21 along with reactions 11, 12, and 22 produce a net loss of hydrogen containing free radicals. We conclude that a chain mechanism involving reactions 17 and 18 is not consistent with our results unless $k_{21} \approx 1 \times 10^{-10}$.

Two mechanisms for the chain decomposition of ozone involving vibrationally excited OH (OH†) have been proposed (30, 31). These mechanisms have not been included in our model. Kaufman (30) proposed the following mechanism

[10] $$H + O_3 \rightarrow OH\ (v \leqslant 9) + O_2$$

[17*a*] $$OH\ (v \geqslant 3) + O_3 \rightarrow OH + O + O_2$$

[9] $$O + OH \rightarrow O_2 + H$$

and De More (31) modified this mechanism as follows:

[5] $$O\ (D) + H_2O \rightarrow OH\ (v \leqslant 2) + OH$$

[17*b*] $$OH\ (v \geqslant 1) + O_3 \rightarrow 2O_2 + H$$

[10] $$H + O_3 \rightarrow OH\ (v \leqslant 9) + O_2$$

Reaction 10 is sufficiently exothermic to form OH in vibrational levels $v \leqslant 9$, and recent measurements (32) have shown that OH† is preferentially formed in $v = 9$ with monotonically decreasing amounts into lower vibrational levels. Reaction 5 has been observed (33) to form OH ($v = 2$, 1, 0) with the excitation in the newly formed bond.

Very recently information on the rate of reaction of vibrationally excited OH ($v = 2$ to 9) with O_3 has become available (29). The products were not identified, so the observed k_{17} represents the sum of the rates of reactions 17, 17*a*, and 17*b*. For OH ($v = 9$) k_{17} was 7.7×10^{-12}. The rate constants decreased monotonically with vibrational level to 1.9×10^{-12} for OH ($v = 2$).

Although reaction 10 is undoubtedly occurring in our experiments we have not detected any effect which can be attributed to these chain mechanisms. As discussed earlier the ozone decomposition at $t = 10^4$ μs is entirely consistent with production of O atoms by reactions 3 and 4 followed by reactions 9 and 10. The fraction of O(D) atoms reacting with H_2O (reaction 5) is small (5 to 10%). Thus our mechanism leads to a quantum yield for ozone destruction of ~ 2.0 at $t = 10^4$ μs. Although the OH† formed in reaction 10 does not appear

Can. J. Chem. Downloaded from www.nrcresearchpress.com by 210.87.254.40 on 09/05/12
For personal use only.

to be involved in a chain reaction with O_3, there is a possibility of enhanced reactivity in reaction 9. In order to present a semi-quantitative description of the fate of OH† we adopt an average value of k_{17} of 5×10^{-12}.

For the data in Fig. 8, immediately following the flash, the ratio $[O_3]/[0]$ is ~ 3. Then, since $k_9 = 5 \times 10^{-11}$ (*i.e.* 10 times faster than the reaction of OH† with O_3), the OH^- lifetime is controlled by reaction 9. Once an appreciable fraction of the O atoms have reacted the lifetime of OH† becomes longer, and reactions 17, 17*a*, and 17*b* become more likely. However, adopting an average O_3 pressure of 0.01 Torr the lifetime of OH† is $1/k_{17}[O_3]$ or ~ 700 μs. In this time OH† will undergo 3×10^3 and 1.5×10^5 collisions with H_2O and N_2, respectively. With the well known efficiency of water vapor in V–V transfer processes it seems likely that the OH† would be relaxed. A recent measurement (34) showed that V–V transfer from HCl† to H_2O required ~ 10 collisions. In fact the absence of any effect of OH† in reactions 17*a* or 17*b*, can be adduced as evidence for relaxation of OH†.

Returning to the possibility of enhanced reactivity of OH† in reaction 9 we note that the lifetime of OH† is $\leqslant 1/k_9[O]$. Immediately following the flash the O atom concentration is typically 0.003 Torr corresponding to an OH† lifetime of $\leqslant 200$ μs. If the reaction of OH† with O atoms were collision limited (2×10^{-10}) the OH† lifetime could be as short as 50 μs, corresponding to ~ 250 collisions with H_2O. However, no satisfactory fit to the experimental data could be found for $k_9 = (1 \text{ to } 2) \times 10^{-10}$. The best fit computed curves were too low for $\log t$ (μs) = 2.9 and markedly too high for $\log t$ (μs) = 3.5. Furthermore, the experimental data is not consistent with an initially enhanced rate for reaction 9 followed by a slower rate when the OH† lifetime becomes longer as the O atoms are consumed and the OH† is preferentially deactivated. We conclude therefore from the evidence of very fast V–V transfer rates to H_2O, and from the absence of any evidence for OH† reactions in our experiments, that enhanced reactivity of OH† is unimportant.

E. Comparison of Various k_5 Determinations

The object of this study is to provide information on the relative rates of O(D) reactions with H_2O and the major atmospheric constituents, O_2 and N_2. Accordingly, the available evidence on k_5 will be discussed in these terms. In order to refer the values to k_{air} (where $k_{air} = 0.21\,k_{13} + 0.78\,k_4$) the rate constant ratio k_4/k_{13} must be known. Most of the available evidence (4, 13, 15, 36, 37) is consistent with $k_4/k_{13} = 1.0 \pm 0.4$.

Two recent measurements (8, 9) have given $k_5/k_{14} \simeq 0.5$. Both experiments used flash photolysis techniques and involved ozone decomposition measurements on O_3/M and $O_3/M/H_2O$ mixtures where M was Ar (9) or He (8). Ar and He are gases which do not deactivate O(D). In both experiments k_5/k_{14} was obtained from an analysis of the effect of H_2O in reducing the O_3 decomposition due to reaction 14.

The recent flash photolysis measurements of Bair and co-workers (8) were interpreted to give $k_5/k_{14} = 0.45 \pm 0.2$. Using a value of k_{14}/k_4 of 15 previously determined by this group[3] (this ratio is consistent with that reported in ref. 4, namely, $k_{14}/k_4 = 13.5$) gives k_5/k_4 6.8 ± 3.0, where the uncertainty given does not include any possible error in k_{14}/k_4.

In a somewhat similar study (9) using O_3/Ar and $O_3/Ar/H_2O$ mixtures O_3 concentrations were obtained in the time period beginning 1 ms after the flash. The O_3 concentration immediately after the flash was obtained by extrapolation of these measurements. $k_5/k_{14} = 0.5$ was then obtained from these extrapolated measurements on four $O_3/Ar/H_2O$ mixtures in the ratio $1:100:M$ (where $M = 0$, 1, 5, and 10) with an O_3 pressure of 1 Torr. The details of the analysis have not been given, but only reactions

[3]Some confusion exists in the literature concerning the work of Bair and co-workers (38). The value of k_{13} deduced in ref. 35 and used subsequently (41) represents a composite rate constant for all forms of O_2 present (*i.e.*, $O_2(\Delta)$, vibrationally excited ground state O_2, and any O_2 which is present as an impurity in the O_3) and should not be compared with determinations of k_{13} for ground state O_2 only (see discussion ref. 35 p. 6124). Thus k_{13} should not be used in comparing relative rate constants obtained by this group with those of other workers. Furthermore, due to misprint in ref. 8, 35, 39, and 41 k_{14} is given, incorrectly, as 4×10^9 rather than 4×10^{11} (units l mol^{-1} s^{-1}). With this correct k_{14} the value of k_{14}/k_4 obtained from the rate constants given in ref. 8 is 20. However, because of rounding-off in the reported rate constants the "best estimate" of k_{14}/k_4 is 15 rather than 20. The authors are indebted to Dr. E. J. Bair for clarification of these points.

Can. J. Chem. Downloaded from www.nrcresearchpress.com by 210.87.254.40 on 09/05/12
For personal use only.

3, 5, 6, 8, and 14 appear to have been considered. We have calculated the O_3 decomposition for an $O_3/Ar/H_2O$ mixture (1:100:10) with $k_5/k_{14} = 0.5$ (*i.e.*, $k_5 = 7$ in terms of the relative O(D) rates of Table 2), $k_{12}(Ar) = 10^{-30}$ (19), and $k_{17} = k_{18} = 0$. Other rate constants were taken from Table 2 and k_1 was chosen to give the observed fraction of O_3 photolyzed (0.16). The results indicate that at $t = 1$ ms, approximately 15% of the total O_3 decomposition arises from reactions 9 and 10 where the O atoms are produced in reactions 6 and 11. Furthermore, the analysis predicts temperature increases of $\sim 30°$ which lead to increases in the rates of reactions 6 and 8. The final observed O_3 decomposition was 0.29 (9), which corresponds to a quantum yield for O_3 destruction of 1.8. This is hard to explain in terms of the mechanism used (9), since reactions 3, 6, and 8 (or the equivalent reactions 9 and 10) should lead to a minimum quantum yield of 3.0. (The computed final O_3 decomposition was ~ 0.50 corresponding to a quantum yield of ~ 3.0.) Because of the higher O_3 pressure (1 Torr) used in this study (9) compared to the 0.01 to 0.02 Torr used by Bair *et al.* and the present authors, it becomes much more difficult to isolate the slower processes 6 and 8 from the faster reactions 3, 5, 13, and 14. Because the complete mechanism has not been considered the extrapolation procedure used (9) is somewhat uncertain.

The authors further claim (9) that since the quantum yield for O_3 destruction is small (~ 1.8) then $k_{17} \leqslant 10^{-16}$ cm^3 molecule^{-1} s^{-1}. In the absence of detailed modelling of the full mechanisms such a conclusion is unwarranted since the OH can be preferentially removed by reactions 11, 12, 24, and 21 with reaction 17 being of only minor importance. A much more detailed analysis of these results is required in order to justify the conclusion drawn.

There are further problems associated with flash photolysis experiments performed in the absence of an excess of an O(D) deactivant. These problems have been encountered, refs. 11 and 35, in interpreting the results of O_3/Ar and O_3/He mixtures containing small quantities of O_2. If the initial O_3 decomposition ($t \leqslant 1$ ms for O_3 pressures of 0.01 to 0.02 Torr) is interpreted in terms of the fast reactions 3, 13, 14, and 15 then a large $O_2(\Sigma)$ production is required at relatively low $[O_2]/[O_3]$. This interpretation (11, 35) leads to a large value of k_{13} (or k_{13}/k_{14}) which is not consistent with the existing information in this rate constant. It has been suggested (4, 35) that the reaction

$$O(D) + O_2(\Delta) \rightarrow O_2(\Sigma) + O$$

may be responsible for part of the $O_2(\Sigma)$ production. The $O_2(\Sigma)$ may also arise from enhanced reactivity of O(D) with the vibrationally excited O_2 produced in reaction 14. The product formed is not necessarily $O_2(\Sigma)$; any species which would react with O_3 with a rate constant of $\sim 10^{-11}$ cm^3 molecule^{-1} s^{-1} could explain the results. Thus it is possible that the products of reaction 14 could also lead to further O_3 decomposition. It has been suggested that these products include O atoms (40, 41) or $O_2(^3\Sigma_u^+)$ (42) (but not $O_2(\Sigma)$ or $O_2(\Delta)$ (4)) as well as vibrationally excited ground state O_2. However, O atoms would not react sufficiently fast to effect the initial O_3 decomposition unless the rate of reaction 8 was enhanced by vibrational excitation of the O_3. Evidence for excited product formation in reaction 14 is also discussed in ref. 4.

Because of the obvious complexity of the reaction mechanism involving reactions 13 and 14 the value of k_5/k_{14} of ~ 0.5 should be adopted with some caution. However, using $k_{14}/k_4 \simeq 14$ (see above discussion) the ratio k_5/k_{air} obtained from this result is ~ 7. (It is because of the problems discussed above that we have made all our measurements in mixtures containing an excess of an O(D) deactivant (H_2O and/or N_2) when reactions 13 and 14 are unimportant.)

Cvetanović *et al.* have recently determined the rate of reaction 5 relative to nitrous oxide (10) ($k_5/k_{N_2O} = 1.50$) and neopentane (15) ($k_5/k_{neop} = 0.376$). They converted the neopentane rate to $k_5/k_{13} = 10.7$ and $k_5/k_4 = 9.6$ using the previously determined ratios k_{13}/k_{neop} and k_4/k_{neop}. The k_5/k_{N_2O} value was converted to $k_5/k_{13} = 4.2$ using the k_{13}/k_{N_2O} ratio determined in the same experiment (10). Because of the unknown cumulative errors in such conversions it is difficult to assess the accuracy of the final results. However, a value of k_5/k_{air} of 4 to 11 is indicated.

Recent experiments conducted in our laboratories[4] using the technique described in ref. 4

[4]M. Gauthier and D. R. Snelling, private communication.

have given $k_5/k_{13} = 6.0 \pm 2.0$. For consistency we use the value of $k_4/k_{13} = 0.72 \pm 0.08$ previously determined (4) by this technique to give $k_5/k_{air} = 8 \pm 3$.

The value of k_5/k_{air} obtained in the present study (3.5 ± 1.5) is somewhat lower than the values discussed above. Therefore, we have investigated the possible effect of water absorption in our experiments which could lead to a lower k_5/k_{air}. Direct analyses of the gas mixtures used for fractional water content indicated that less than 15% of the water vapor was lost by absorption. Thus applying this maximum correction for loss of water vapor would only increase k_5/k_{air} from 3.5 to 4.0.

The consistency of the various determinations of k_5/k_{air} discussed above is not very satisfactory but a value of k_5/k_{air} of 7.5 ± 4.0 includes all the measurements.

In applying these values of k_5/k_{air} to atmospheric calculations our determination has the following advantages. The rate of k_5 was determined relative to the major atmospheric constituent, N_2. Furthermore, k_5 was calculated from the effects of reactions 9 and 10 which are responsible for the mesospheric control of ozone. Thus any errors in k_9 or k_{10} are partially compensated for in the final k_5/k_{air} value.

The authors are indebted to J. Oman for his pains-taking help in performing these experiments.

1. F. D. Findlay, C. J. Fortin, and D. R. Snelling. Chem. Phys. Lett. **3**, 204 (1969).
2. M. Gauthier and D. R. Snelling. Chem. Phys. Lett. **5**, 93 (1970).
3. D. R. Snelling and M. Gauthier. Chem. Phys. Lett. **9**, 254 (1971).
4. M. Gauthier and D. R. Snelling. J. Chem. Phys. **54**, 4317 (1971).
5. F. D. Findlay and D. R. Snelling. J. Chem. Phys. **54**, 2750 (1971).
6. F. D. Findlay and D. R. Snelling. J. Chem. Phys. **55**, 545 (1971).
7. W. B. DeMore and O. F. Raper. J. Chem. Phys. **44**, 1780 (1966).
8. D. Biedenkapp, L. G. Hartshorn, and E. J. Bair. Chem. Phys. Lett. **5**, 379 (1970).
9. K. F. Langley, and W. D. McGrath. Planet. Space Sci. **19**, 413 (1971).
10. P. Scott, and R. J. Cvetanović. J. Chem. Phys. **54**, 1440 (1970).
11. C. Fortin, and D. R. Snelling. DREV Technical Note, 1943/71 and C. Fortin, M.Sc. Thesis, University of Montreal.
12. E. C. Y. Inn and Y. Tanaka. J. Opt. Soc. Am. **43**, 870 (1954).
13. R. J. Donovan and D. Husain. Chem. Rev. **70**, 489 (1970).
14. K. F. Langley and W. D. McGrath. Planet. Space Sci. **19**, 416 (1971).
15. G. Paraskevopoulos and R. J. Cvetanović. Chem. Phys. Lett. **9**, 603 (1971).
16. H. I. Schiff. Can. J. Chem. **47**, 1903 (1969).
17. F. Kaufman. Can. J. Chem. **47**, 1917 (1969).
18. K. Schofield. Planet. Space Sci. **15**, 643 (1967).
19. H. S. Johnston. Gas phase reaction kinetics of neutral oxygen species. U.S. Dept. of Commerce NSRDS-NBS20. 1968.
20. K. H. Becker, W. Groth, and U. Schurath. Chem. Phys. Lett. **8**, 259 (1971).
21. M. Venugopalan and R. S. Jones. Chemistry of dissociated water vapor and related systems. Interscience. 1968. (*a*) p. 290; (*b*) p. 400.
22. R. Gilpin, H. I. Schiff and K. Welge. J. Chem. Phys. **55**, 1087 (1971).
23. N. R. Greiner. J. Phys. Chem. **72**, 406 (1968).
24. I. T. N. Jones and R. P. Wayne. Proc. Roy. Soc. London, A**321**, 409 (1971).
25. V. D. Baiamonte, D. R. Snelling, and E. J. Bair. J. Chem. Phys. **44**, 673 (1966).
26. R. L. Taylor and S. Bitterman. Rev. Mod. Phys. **41**, 26 (1969).
27. J. H. Kiefer and R. W. Lutz. J. Chem. Phys. **44**, 658 (1966).
28. M. C. Henderson, A. V. Clark, and P. R. Lintz. J. Acous. Soc. Am. **37**, 457 (1965).
29. R. N. Coltharp, S. D. Worley, and A. E. Potter. Appl. Opt. **10**, 1786 (1971).
30. F. Kaufman. Ann. Geophys. **20**, 106 (1964).
31. W. B. DeMore. J. Chem. Phys. **46**, 813 (1967).
32. P. E. Charters, R. G. Macdonald, and J. C. Polanyi. Appl. Opt. **10**, 1747 (1971).
33. R. Engleman, Jr. J. Am. Chem. Soc. **87**, 4193 (1965).
34. H. L. Chen and C. B. Moore. J. Chem. Phys. **54**, 4072 (1971).
35. D. Biedenkapp and E. J. Bair. J. Chem. Phys. **52**, 6119 (1970).
36. M. Lowenstein. J. Chem. Phys. **54**, 2282 (1971).
37. W. B. DeMore. J. Chem. Phys. **52**, 4309 (1970).
38. E. J. Bair. Private Communication.
39. H. Webster III and E. J. Bair. J. Chem. Phys. **53**, 4532 (1970).
40. E. Castellano and H. J. Schumacher. Z. Physik. Chem. **65**, 62 (1969). G. V. Ellenrieder, E. Castellano, and H. J. Schumacher. Chem. Phys. Lett. **9**, 152 (1971).
41. V. D. Baiamonte, L. G. Hartshorn, and E. J. Bair. J. Chem. Phys. **55**, 3617 (1971).
42. W. D. McGrath and J. J. McGarvey. Planet. Space Sci. **15**, 427 (1967).

Can. J. Chem. Downloaded from www.nrcresearchpress.com by 210.87.254.40 on 09/05/12
For personal use only.

Infrared Band Progressions in the CH_2 Scissoring Region and the Ring Puckering Vibration of Trimethylene Oxide and some Deuterated Analogs[1]

H. WIESER AND M. DANYLUK

Department of Chemistry, University of Calgary, Calgary, Alberta T2N 1N4

Received February 28, 1972

Band progressions have been observed in the CH_2 scissoring region of the i.r. spectra of trimethylene oxide (C_3H_6O) and three of its deuterated analogs (α-d_2, β-d_2, and α,α'-d_4). With the aid of the pure ring puckering transitions (published previously) and a simple theoretical model of puckering–vibrational interactions the absorptions have been assigned to combination tones of CH_2 scissoring vibrations with the ring puckering mode and its overtones. The scissoring fundamentals of the α- and β-methylene groups have been identified and assigned. Of all the vibrations for which combination progressions are observed, only the β-CH_2 scissoring mode of the normal compound exhibits significant differences between the ring puckering transitions in the ground state and the vibrational excited state.

Nous avons observé les progressions de bande dans la région de cisaillement du CH_2 du spectre i.r. de l'oxyde de triméthylène (C_3H_6O) et trois de ses analogues deutériés (α-d_2, β-d_2 et α,α'-d_4). A l'aide des transitions de pulsation cycliques pures (publié précédemment) et d'un modèle théorique simple d'intéractions de pulsation vibrationnelles, nous avons assigné les absorptions comme étant dues aux tons de combinaison des vibrations de cisaillement du CH_2, avec le mode cyclique de pulsation et ses harmoniques. Les fondamentales de cisaillement des groupes méthylène en α et en β ont été identifiées et assignées. De toutes les vibrations pour lesquelles on observe des progressions de combinaison, seul le mode de cisaillement du CH_2 en β du composé non-deutérié montre des différences marquées entre les transitions de pulsation cycliques dans l'état fondamental et dans l'état vibrationnel excité.

[Traduit par le journal]

Canadian Journal of Chemistry, **50**, 2761 (1972)

Introduction

In connection with some other work in this laboratory we have recently undertaken a comprehensive vibrational analysis of trimethylene oxide, C_3H_6O (TMO), and four of its deuterated analogs, *viz.* α-d_2, β-d_2, α,α'-d_4, and d_6 TMO. In particular, it was of interest to study the band sequences occurring in the CH_2 scissoring regions resulting from the combination of the scissoring fundamentals with the low-frequency, out-of-plane torsional vibration (the ring puckering mode) of the four-membered ring. The only previous work in this regard is that of Green (1) who has reported ring puckering transitions determined from "combination" and "difference" i.r. bands observed in the CH_2 scissoring region of normal trimethylene oxide. Since there are three CH_2 scissoring modes in TMO, the study of the partially deuterated compounds should reveal which of the three modes is responsible for the sequence observed by Green, and further, whether or not the other two modes also combine with the puckering vibration in a similar fashion.

This communication summarizes the analysis of our i.r. spectra of normal, α-d_2, β-d_2, and α,α'-d_4 TMO in the CH_2 scissoring region, while the following paper describes the corresponding Raman results (2).

Theoretical Considerations

It is customary to separate the low frequency, large amplitude puckering motion from the remaining $3N-7$ vibrational degrees of freedom (3). Solution of the separate wave equations will define puckering potential functions which may be different for various vibrational states. As a first approximation one can assume that this potential does not alter significantly with vibrational excitation. For normal trimethylene oxide, Chan *et al.* (4) have been able to fit their far-infrared data to a double minimum function of the type $A(Z^4 - BZ^2)$, Z the puckering coordinate; accordingly, TMO appears to have only a small barrier to inversion (15.3 cm^{-1}) whereby the lowest energy level still lies 12 cm^{-1} above the barrier top. The spacing between two consecutive puckering levels in the ground state increases with increasing puckering quantum numbers for all molecules investigated here (4, 5). We may therefore expect to find

[1]Based on the M.Sc. Thesis of M. Danyluk, University of Calgary, 1971.

Can. J. Chem. Downloaded from www.nrcresearchpress.com by 210.87.254.105 on 09/05/12
For personal use only.

Can. J. Chem. Downloaded from www.nrcresearchpress.com by 210.87.254.105 on 09/05/12
For personal use only.

combination band sequences in various fundamental regions corresponding to simultaneous changes in the vibrational quantum number of $\Delta v = +1$, and in the puckering quantum number of $\Delta v_p = 0$ or $\Delta v_p = \pm 1$, selection rules permitting.

As a result of the low inversion barrier, TMO can be considered to be essentially planar. Hence, the normal and the symmetrically deuterated molecules have C_{2v} symmetry, whereas α-d_2 TMO belongs to C_s point group. The out-of-plane puckering vibration is, respectively, B_1 and A''. The selection rules may be established in a fashion similar to that outlined in detail recently by Stone and Mills (3) for cyclobutane. The dipole moments are expanded as a function of the $3N-7$ vibrational coordinates Q_r and the puckering coordinate Z in the usual manner. In this expansion, all first derivatives and, due to the large displacements in Z, only the second derivatives in Q_r and Z, (*i.e.* $\partial^2\mu/\partial Q_r \partial Z$) are retained, all other higher order terms neglected. Considering only the symmetry allowed components in this expansion, the puckering–vibrational matrix element of, for example, the μ_x component[2] is:

$$|\mu_x|_{nm} = \sum_{B_1} \left(\frac{\partial \mu_x}{\partial Q_{B_1}}\right)_0 \langle \Psi_n | Q_{B_1} | \Psi_m \rangle \langle \phi_n | \phi_m \rangle + \sum_{A_1} \left(\frac{\partial^2 \mu_x}{\partial Q_{A_1} \partial Z}\right)_0 \langle \Psi_n | Q_{A_1} | \Psi_m \rangle \langle \phi_n | Z | \phi_m \rangle$$

where the Ψ's and ϕ's are the wavefunctions for the vibrational and puckering levels, respectively, and n and m refer to the vibrational excited and ground states. The first term in this expression gives the μ_x component of the B_1 modes, the intensities of which are modified by the overlap integral $\langle \phi_n | \phi_m \rangle$.[3] This integral limits the transitions to those for which the puckering quantum number does not change; *i.e.*, it results in the fundamental and higher $\Delta v_p = 0$ transitions. The second term gives rise to the μ_x component of A_1 vibrations which, however, are modified by the factor $\langle \phi_n | Z | \phi_m \rangle$.[3] This restriction clearly allows only transitions for which $\Delta v_p = \pm 1$ (or 3, 5, etc.).

Assuming that the geometry of the deuterated compounds is the same as that of normal TMO, we can use the geometrical parameters determined by Chan *et al.* (6) to estimate the principal moments of inertia. We find that all molecules are near oblate symmetric tops with the axis of the greatest moment of inertia, the C axis, being perpendicular to the molecular plane. Accordingly, we expect to find the vapor phase band contours resembling those compiled in Table 1 corresponding to the dipole moment changes in the specified directions.

TABLE 1. Vapor phase band contours for trimethylene oxide and some deuterated analogs

Compound	Band contour		
	$\mu_x^*(B_1,A'')$	$\mu_y^*(B_2,A')$	$\mu_z^*(A_1,A')$
Normal	*C*	*B*	*A*
α-d_2	*C*	*A*–*B* hybrid	
β-d_2	*C*	*B*	*A*
α,α'-d_4	*C*	*A*	*B*

*The *x*-axis is defined as being perpendicular to the molecular plane and the *z*-axis as lying along the C—O diagonal.

For the analysis of the spectra it is of particular importance to note, for example, the following. For some A_1 vibration of the normal compound which by chance has a small dipole moment derivative, we would expect weak *A*-type i.r. bands for the $\Delta v_p = 0$ transitions (and probably quite strong Raman bands, see following paper (2)), but relatively stronger *C*-type $\Delta v_p = \pm 1$ combinations.

Experimental

The synthesis of the deuterated compounds has been described previously (5). The i.r. spectra were obtained on a Perkin–Elmer Model 621 spectrophotometer purged with dry air. A Perkin–Elmer variable path length gas cell, with a range from 1.25–10 m in 1.25 m intervals, was used with sample pressures ranging from 10–40 Torr at room temperature. The calculated spectral slit width was better than 0.8 cm^{-1} in all cases. The instrument was calibrated against water vapor absorptions in the 1600–1400 cm^{-1} region. The reported frequencies constitute averages of several measurements and are believed to be accurate to within ± 0.5 cm^{-1}. Traces of water vapor were often difficult to eliminate, particularly at long path lengths. Residual water bands have been marked with an asterisk in the spectra.

Results and Discussion

The spectra of the four trimethylene oxide molecules between 1650 and 1300 cm^{-1} are shown in Figs. 1–4. In order to make the assignments we proceeded as follows. The difference between $\Delta v_p = +1$ and $\Delta v_p = -1$ transi-

[2]The *x*-axis is defined as being perpendicular to the molecular plane and the *z*-axis as lying along the C—O diagonal.

[3]The significance of these factors has been discussed by Stone and Mills in some detail (3).

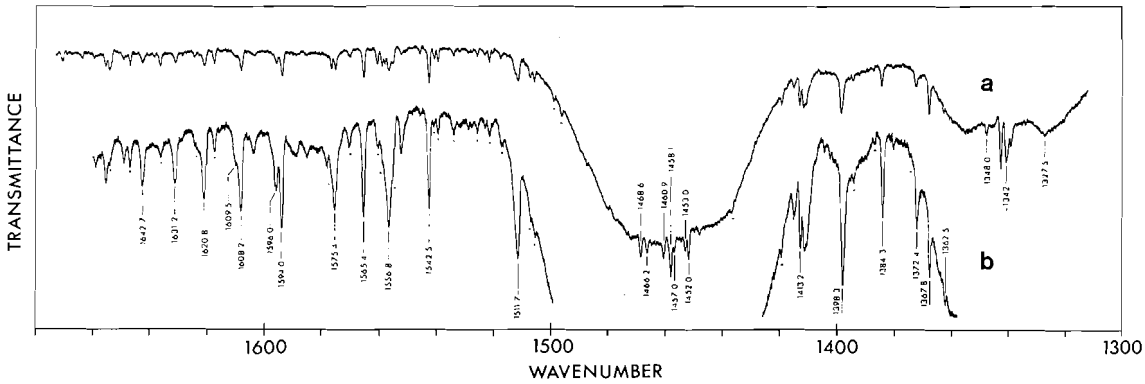

FIG. 1. Infrared spectrum in the CH_2 scissoring region of normal trimethylene oxide vapor: 0.8 cm^{-1} spectral slit width; (*a*) 20 Torr pressure and 1.25 m path length; (*b*) 40 Torr pressure and 5.0 m path length.

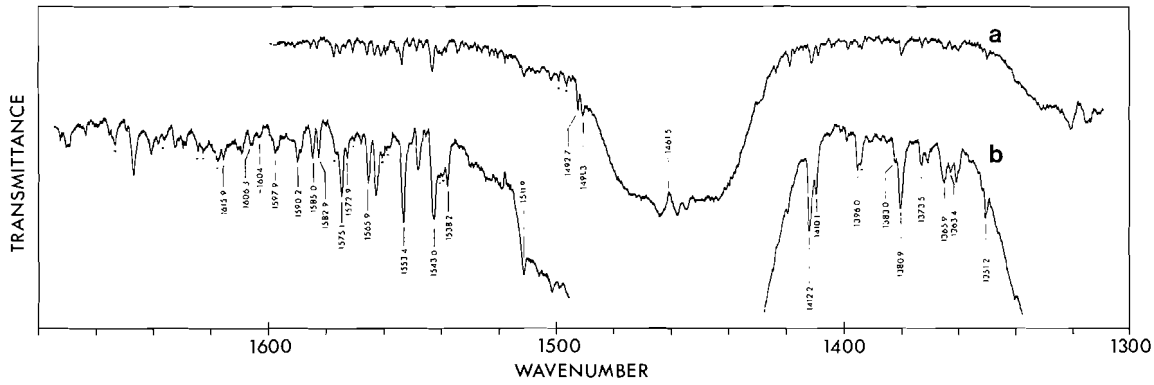

FIG. 2. Infrared spectrum in the CH_2 scissoring region of α-d_2 trimethylene oxide vapor; 0.8 cm^{-1} spectral slit width, 40 Torr pressure; (*a*) 1.25 m path length; (*b*) 10.0 m path length.

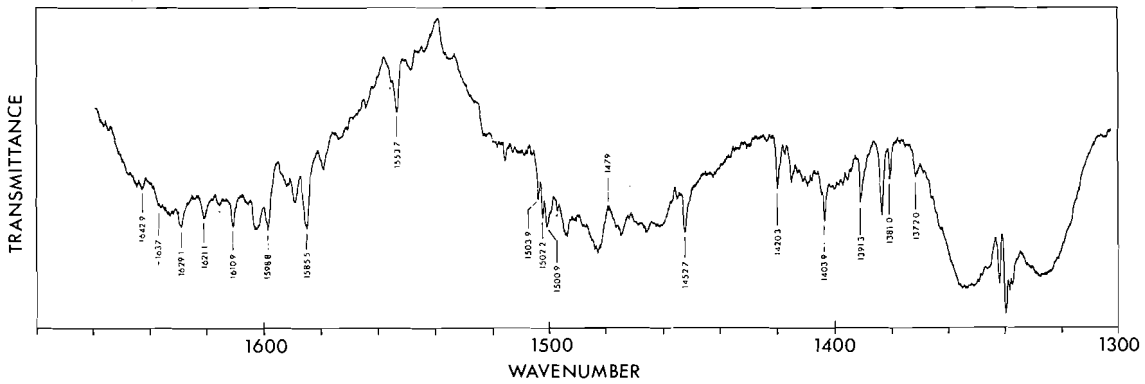

FIG. 3. Infrared spectrum in the CH_2 scissoring region of β-d_2 trimethylene oxide vapor; 0.8 cm^{-1} spectral slit width, 40 Torr pressure and 10.0 m path length.

tions which have a common puckering level in the vibrational excited state corresponds to the sum of two consecutive puckering transitions in the vibrational ground state. If such combination bands can be observed, and since the values for the pure puckering transitions are known (5), it is possible to identify the various absorptions. In Table 2 we summarize the assignments that we were able to make in this manner. If the position of the fundamental is known, the

Can. J. Chem. Downloaded from www.nrcresearchpress.com by 210.87.254.105 on 09/05/12
For personal use only.

Can. J. Chem. Downloaded from www.nrcresearchpress.com by 210.87.254.105 on 09/05/12
For personal use only.

TABLE 2. Sum and difference i.r. combinations centered on CH_2 scissoring vibrations of trimethylene oxide and some deuterated analogs

Compound	Pure puckering differences*		α-CH_2 (cm^{-1})			β-CH_2 (cm^{-1})		
	Assignment†	Values (cm^{-1})	$\Delta v_p = +1$ bands	$\Delta v_p = -1$ bands	Δ§	$\Delta v_p = +1$ bands	$\Delta v_p = -1$ bands	Δ§
Normal	0→2	(53.5 + 90.0) = 143.5	1556.8	1413.2	143.6	1511.7	1367.8	143.9
	1→3	(90.0 + 105.0) = 195.0	1594.0	1398.3	195.7	1542.5	1348.0	194.5
	2→4	(105.0 + 118.2) = 223.2	1608.2	1384.3	223.9	1565.4	~1342	~223
	3→5	(118.2 + 129.2) = 247.4	1620.8	1372.4	248.4	1575.4	1327.5	247.9
	4→6	(129.2 + 138.6) = 267.8	1631.2	1362.5	268.7			
α-d_2	0→2	(48.7 + 81.7) = 130.4	1538.2	1410.1	128.1	1511.9	1380.9	131.0
	1→3	(81.7 + 95.1) = 176.8	1572.9	1396.0	176.9	1543.0	1365.9	177.1
	2→4	(95.1 + 107.2) = 202.3	1585.0	1383.0	202.0	1553.4	1351.2	202.2
	3→5	(107.2 + 117.0) = 224.2	1597.9	1373.5	224.4			
	4→6	(117.0 + 125.5) = 242.5	1606.3	1363.4	242.9			
β-d_2	0→2	(49.6 + 83.5) = 133.1	1553.7	1420.3	133.4			
	1→3	(83.5 + 97.2) = 180.7	1585.5	1403.9	181.6			
	2→4	(97.2 + 109.6) = 206.8	1598.8	1391.3	207.5			
	3→5	(109.6 + 119.7) = 229.3	1610.9	1381.0	229.9			
	4→6	(119.7 + 128.5) = 248.2	1621.1	1372.0	249.1			
α,α'-d_4	0→2	(43.7 + 73.4) = 117.1				1507.5	1391.1	116.4
	1→3	(73.4 + 85.3) = 158.7				1537.5	1378.9	158.6
	2→4	(85.3 + 96.1) = 181.4				1550.4	—	—
	3→5	(96.1 + 104.9) = 201.0				1559.6	1358.3	201.3
	4→6	(104.9 + 112.6) = 217.5				1567.9	1349.7	218.2

*Far-infrared values reported elsewhere (5); the difference values are accurate to ±0.6 cm^{-1}.
†The numbers refer to the puckering quantum numbers, v_p.
‡Accurate to ±0.5 cm^{-1} in nearly all cases.
§Difference between the $\Delta v = +1$ and -1 band values; accurate to ±1.0 cm^{-1}.

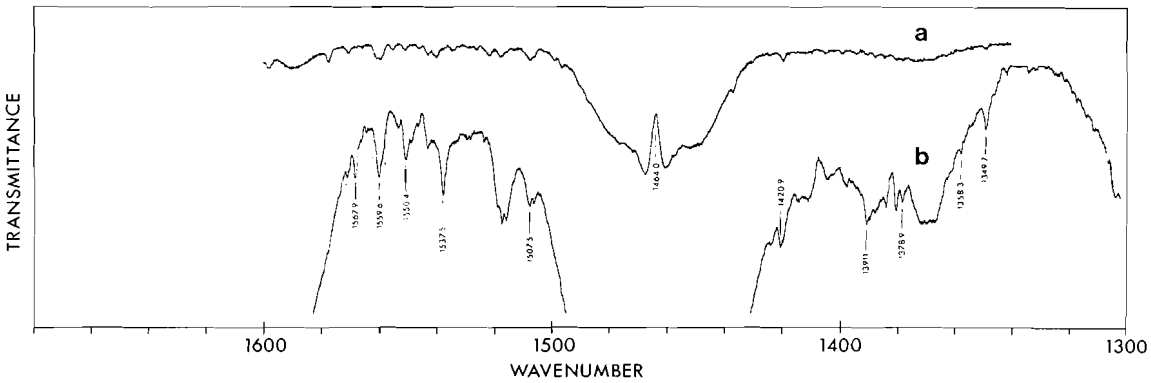

FIG. 4. Infrared spectrum in the CH_2 scissoring region of α,α'-d_4 trimethylene oxide vapor; 0.8 cm^{-1} spectral slit width; (*a*) 10 Torr pressure and 1.25 m path length; (*b*) 40 Torr pressure and 5.0 m path length.

first $\Delta v_p = -1$ band can be located readily. Conversely, if it is possible to identify the first $\Delta v_p = -1$ band one can deduce a value for the fundamental. In either case, these transitions must be consistent with the first $\Delta v_p = +1$ band and the first two $\Delta v_p = 0$ bands (if observed). In a similar manner, all transition energies must be internally consistent whichever way they are deduced. The assignments so derived are tabulated in Tables 3–5. Finally, once we have values assigned to the various transitions we may estimate the energy differences between the puckering levels in the vibrationally excited states. This we have done in Table 6, which also shows estimated differences between the corresponding puckering transitions in the ground and excited states. The accuracy of these differences is of the order of ± 1.6 cm^{-1}.

α-CH_2 Scissoring Vibrations

Normal and *β*-d_2 TMO are expected to show an in-phase (A_1) and out-of-phase (B_2) combination of the α-CH_2 scissoring vibration. These should be most easily detected in the *β*-d_2 compound. As Fig. 3 shows, there is no prominent absorption in the entire region that could be readily assigned to either of these fundamental modes, even though they are i.r. active. This is not entirely unexpected as experience has shown that scissoring vibrations of methylene groups adjacent to an oxygen atom are relatively weak (7). However, we do find a sequence of absorptions which shows an excellent correlation with the pure ring puckering transitions (Table 2). Since the first $\Delta v_p = -1$ band is clearly visible at 1452.7 cm^{-1}, the fundamental can be placed near 1502.3 ± 0.8 cm^{-1} (Table 5). There is indeed a weak absorption at 1502.2 cm^{-1} (Fig. 3) which, moreover, corresponds to a Raman line at 1502.4 cm^{-1} (2). Correlation with the $\Delta v_p = +1$ and $\Delta v_p = -1$ bands of the same series allows us to assign the neighboring weak absorptions (*i.e.* 1503.9 and 1500.9 cm^{-1}) to $\Delta v_p = 0$ transitions (Table 5). The preceding simple theoretical analysis suggests that an A_1 fundamental mode may give rise to puckering combination tones whereas they are symmetry forbidden for B_2 vibrations. We can therefore assign the band at 1502.2 cm^{-1} to the in-phase combination of the α-CH_2 scissoring vibration. The apparent *C*-type contours of the accompanying $\Delta v_p = \pm 1$ bands seem to corroborate this, since these combination transitions have B_1 symmetry for which *C* bands are expected (Table 1).

For normal TMO we expect to find corresponding band progressions. Figure 1 and Table 2 confirm this. Unfortunately, the first $\Delta v_p = -1$ band is masked so that the fundamental cannot be located. There is, however, a distinct Raman line at 1505.0 cm^{-1} (2) which we assign to the vibration in question. This is consistent with its absence in the i.r. spectrum. It is this band sequence which Green had reported earlier and for which he was able to deduce correctly the same band origin (1).

For the out-of-phase combination (B_2 symmetry) of the α-CH_2 scissoring in both compounds we expect to find *B*-type contours. Moreover, as stated above, the puckering com-

Can. J. Chem. Downloaded from www.nrcresearchpress.com by 210.87.254.105 on 09/05/12
For personal use only.

Can. J. Chem. Downloaded from www.nrcresearchpress.com by 210.87.254.105 on 09/05/12
For personal use only.

TABLE 3. Infrared band assignments for normal trimethylene oxide

$\Delta v_p = +1$ bands			$\Delta v_p = 0$ bands*			$\Delta v_p = -1$ bands		
	Band position (cm^{-1})‡			Band position (cm^{-1})‡			Band position (cm^{-1})‡	
Assignment†	α-CH_2	β-CH_2	Assignment†	α-CH_2	β-CH_2	Assignment†	α-CH_2	β-CH_2
0,0 → 1,1	1556.8	1511.7	0,0 → 1,0	(1505.0§)	1452.0			
0,1 → 1,2	1594.0	1542.5	0,1 → 1,1		1458.1	0,1 → 1,0		~1398
0,2 → 1,3	1608.2	1565.4	0,2 → 1,2		1453.0	0,2 → 1,1	1413.2	1367.8
0,3 → 1,4	1620.8	1575.4	0,3 → 1,3		1460.9	0,3 → 1,2	1398.3	1348.0
0,4 → 1,5	1631.2	1596.0	0,4 → 1,4		1457.0	0,4 → 1,3	1384.3	~1342
0,5 → 1,6	1642.7	1609.5	0,5 → 1,5		1466.2	0,5 → 1,4	1372.4	1327.5
			0,6 → 1,6		1468.6	0,6 → 1,5	1362.5	

*A_1 symmetry CH_2 scissoring vibrations.
†The designations stand for (v,v_p), where v is the vibrational and v_p the puckering quantum number.
‡Accurate to ± 0.5 cm^{-1} in nearly all cases.
§Observed in the Raman only (2).

TABLE 4. Infrared band assignments for α-d_2 trimethylene oxide

$\Delta v_p = +1$ bands			$\Delta v_p = 0$ bands*			$\Delta v_p = -1$ bands		
	Band position (cm^{-1})‡			Band position (cm^{-1})‡			Band position (cm^{-1})‡	
Assignment†	α-CH_2	β-CH_2	Assignment†	α-CH_2	β-CH_2	Assignment†	α-CH_2	β-CH_2
0,0 → 1,1	1538.2	1511.9	0,0 → 1,0	1492.7	1461.5			
0,1 → 1,2	1572.9	1543.0	0,1 → 1,1			0,1 → 1,0		1412.2
0,2 → 1,3	1585.0	1553.4	0,2 → 1,2	1491.3		0,2 → 1,1	1410.1	1380.9
0,3 → 1,4	1597.9	1565.9	0,3 → 1,3			0,3 → 1,2	1396.0	1365.9
0,4 → 1,5	1606.3	1575.1	0,4 → 1,4			0,4 → 1,3	1383.0	1351.2
0,5 → 1,6	1615.9	1582.9				0,5 → 1,4	1373.5	
0,6 → 1,7		1590.2				0,6 → 1,5	1363.4	
0,7 → 1,8		~1604						

*A' symmetry CH_2 scissoring vibrations.
†Designations as in Table 3.
‡Accurate to ± 0.5 cm^{-1} in nearly all cases.

Can. J. Chem. Downloaded from www.nrcresearchpress.com by 210.87.254.105 on 09/05/12
For personal use only.

TABLE 5. Infrared band assignments for β-d_2 and α,α'-d_4 trimethylene oxide

$\Delta v_p = +1$ bands			$\Delta v_p = 0$ bands*			$\Delta v_p = -1$ bands		
	Band position (cm^{-1})‡			Band position (cm^{-1})‡			Band position (cm^{-1})‡	
Assignment†	α-CH_2§	β-CH_2‖	Assignment†	α-CH_2§	β-CH_2‖	Assignment†	α-CH_2§	β-CH_2‖
0,0 → 1,1	1553.7	1507.5	0,0 → 1,0	1502.2	1464.0			
0,1 → 1,2	1585.5	1537.5	0,1 → 1,1	1503.9		0,1 → 1,0	1452.7	1420.9
0,2 → 1,3	1598.8	1550.4	0,2 → 1,2	1500.9		0,2 → 1,1	1420.3	1391.1
0,3 → 1,4	1610.9	1559.6	0,3 → 1,3			0,3 → 1,2	1403.9	1378.9
0,4 → 1,5	1621.1	1567.9	0,4 → 1,4			0,4 → 1,3	1391.3	
0,5 → 1,6	1629.1		0,5 → 1,5			0,5 → 1,4	1381.0	1358.3
0,6 → 1,7	~1637					0,6 → 1,5	1372.0	1349.7
0,7 → 1,8	1642.9							

*A_1 symmetry CH_2 scissoring vibrations.
†Designations as in Table 3.
‡Accurate to ± 0.5 cm^{-1} in most cases.
§Observed in the spectrum of β-d_2 TMO.
‖Observed in the spectrum of α,α'-d_4 TMO.

Can. J. Chem. Downloaded from www.nrcresearchpress.com by 210.87.254.105 on 09/05/12
For personal use only.

TABLE 6. Estimated puckering transitions in the excited state of the CH_2 scissoring vibrations of trimethylene oxide and some deuterated analogs

Compound	Puckering transitions	Observed ground state transitions* (cm^{-1})	Estimated excited state transitions (cm^{-1})									
			α-CH_2 Scissoring					β-CH_2 Scissoring				
			$\Delta v_p = +1$ bands	$\Delta v_p = 0$ bands	$\Delta v_p = -1$ bands	Average	Difference†	$\Delta v_p = +1$ bands	$\Delta v_p = 0$ bands	$\Delta v_p = -1$ bands	Average	Difference†
Normal	0→1	53.5	51.8	—	51.7	51.8	−1.7	59.7	59.6	~59.5	59.6	+6.1
	1→2	90.0	90.7	—	90.1	90.4	+0.4	84.3	84.9	85.2	84.8	−5.2
	2→3	105.0	104.2	—	104.2	104.2	−0.8	112.9	112.9	~112	112.9	+7.9
	3→4	118.2	117.6	—	116.9	117.3	−0.9	115.0	114.3	~115	114.7	−3.5
	4→5	129.2	128.6	—	128.7	128.7	−0.5	138.8	138.4	—	138.6	+9.4
	5→6	138.6	140.7	—	—	140.7	+2.1	142.7	141.0	—	141.9	+3.3
α-d_2	0→1	48.7	45.5	—	—	45.5	−3.2	50.4	—	50.4	50.4	+1.7
	1→2	81.7	83.4	—	81.0	82.2	+0.5	79.8	—	80.1	80.0	−1.7
	2→3	95.1	93.8	—	94.2	94.0	−1.1	92.1	—	92.5	92.3	−2.8
	3→4	107.2	108.0	—	107.5	107.8	+0.6	107.6	—	—	107.6	+0.4
	4→5	117.0	115.6	—	115.4	115.5	−1.5	116.4	—	—	116.4	−0.6
	5→6	125.5	126.6	—	—	126.6	+1.1	124.8	—	—	124.8	−0.7
	6→7	133.0	—	—	—	—	—	132.8	—	—	132.8	−0.2
	7→8	146.3	—	—	—	—	—	~147	—	—	~147	—
β-d_2	0→1	49.6	51.4	51.3	51.1	51.3	+1.7					
	1→2	83.5	81.4	~81	80.8	81.1	−2.4					
	2→3	97.2	96.8	~97	97.0	96.9	−0.3					
	3→4	109.6	109.3	—	109.4	109.4	−0.2					
	4→5	119.7	119.8	—	119.5	119.7	0					
	5→6	128.5	127.7	—	—	127.7	−0.8					
	6→7	136.3	~136	—	—	~136	—					
	7→8	143.4	~142	—	—	~142	—					
α,α'-d_4	0→1	43.7						43.5	—	43.6	43.6	−0.1
	1→2	73.4						73.7	—	73.1	73.4	0
	2→3	85.3						86.3	—	—	86.3	+1.0
	3→4	96.1						94.5	—	—	94.5	−1.6
	4→5	104.9						104.4	—	104.0	104.2	−0.7

*Far-infrared values reported elsewhere (5).
†Estimated differences between the puckering transitions in the ground and excited states of the scissoring vibrations.

Can. J. Chem. Downloaded from www.nrcresearchpress.com by 210.87.254.105 on 09/05/12
For personal use only.

bination tones should be absent since they are not allowed by symmetry. Indeed, no corresponding absorptions in the spectrum of normal TMO can be found. The spectrum of β-d_2 TMO, on the other hand, shows an apparent *B* band with its central gap at 1479 cm^{-1}. We tentatively assign this position to the vibration in question.

Finally, the single α-CH_2 group of α-d_2 TMO is also seen to give rise to band progressions (Fig. 2 and Table 2). Again, it is not possible from the i.r. spectrum to infer the band origin. We are, however, able to place the fundamental transition at 1492.7 cm^{-1} from a Raman line at 1492.4 cm^{-1} (2).

β-CH_2 Scissoring Vibration

The β-CH_2 scissoring vibration should appear most distinctly in the spectrum of α,α'-d_4 TMO. In fact, Fig. 4 exhibits the anticipated *B* band, centered at 1464.0 cm^{-1}. It is interesting to note that deuteration in the α positions reverses the values of the moments of inertia in the *y* (parallel to the C—C diagonal) and *z* (along the C—O diagonal) directions. Thus *A*-type contours are expected for the same vibration in normal and β-d_2 TMO (Table 1). On either side of the main absorption, weak $\Delta v_p = \pm 1$ bands can be identified (Table 2) which we have assigned as indicated in Table 5. Again, these combination bands have *C*-type contours as expected. It is also noteworthy that, in contrast to the α-CH_2 scissoring mode, the fundamental transition is more intense than its combination tones.

With the aid of Table 2 we were able to identify the corresponding band progressions in normal TMO (Fig. 1). The first $\Delta v_p = -1$ band in this progression at $\sim$1398 cm^{-1} apparently coincides with the $0,3 \rightarrow 1,2$ transition of the α-CH_2 scissoring mode, explaining the anomalous intensity of that band. This places the fundamental absorption at $\sim$1452 cm^{-1}. With the aid of the $\Delta v_p = \pm 1$ progressions the sequence of peaks between 1450–1470 cm^{-1} can then be assigned to $\Delta v_p = 0$ transitions. The fact that these bands are spread over such a wide region must indicate that the puckering energy levels in the excited state of the β-CH_2 scissoring mode are significantly altered from those in the ground state. As was observed for α,α'-d_4 TMO, the fundamental and apparently also the other $\Delta v_p = 0$ transitions are again considerably more intense than the corresponding $\Delta v_p = \pm 1$ bands.

Finally, the β-CH_2 scissoring vibration is seen to give rise to $\Delta v_p = \pm 1$ sequences also in α-d_2 TMO (Tables 2 and 4, Fig. 2). The first $\Delta v_p = -1$ band at 1412.2 cm^{-1} allows one to locate the fundamental near 1460.9 $\pm$ 0.8 cm^{-1}. The spectrum exhibits an apparent *B*-type contour with its central gap at 1461.5 cm^{-1}, so that we may consider this to be the origin for the band progressions of the mode in question.

Puckering Potentials

As has been pointed out in a preceding section, it may be assumed in some cases that the puckering potential essentially has the same form in the vibrational ground state and various vibrationally excited states. Ample verifications of this assumption have been reported in literature (see for example refs. 1 and 3 and refs. cited therein). It appears that also for the scissoring vibrations of trimethylene oxide and its deuterated analogs the puckering potentials in the vibrationally excited states are the same, or nearly so, as the potential in the ground state. As Table 6 shows, the differences between the puckering transitions observed in the ground state (5) and those estimated for the first excited states of the various scissoring modes are well within the experimental uncertainties in most cases. It should be noted that the average excited state transitions have been estimated invariably from at least two independent sources, *i.e.* $\Delta v_p = +1$ and -1 bands, and in a few instances additionally also from $\Delta v_p = 0$ transitions.

There is one notable exception to the overall trend exhibited in Table 6. Namely, for the β-CH_2 scissoring vibration of normal TMO we find significantly large differences that are well beyond the experimental uncertainties. Moreover, these differences appear to alternate in sign for the first five transitions. Although it is difficult to see explicitly how the form of the potential may vary, it seems peculiar that this phenomenon occurs only when the β-methylene group is flanked by two α-CH_2 groups. We are presently engaged in investigating whether or not a suitable potential function can be found to explain these differences. Stone and Mills (3) have recently also suggested other mechanisms that may alter the puckering potential function upon excitation of a vibra-

TABLE 7. Assignment of methylene scissoring vibrations of trimethylene oxide and some deuterated analogs

Compound		α-CH_2	β-CH_2
Normal	A_1	1505.0	1452.0
	B_2	not resolved	
α-d_2		1492.7	1461.5
β-d_2	A_1	1502.2	—
	B_2	1479	
α,α'-d_4		—	1464.0

tional mode. In any event, this interesting variation in the excited state transitions must remain unexplained at this time.

Conclusions

A series of combination transitions arising from an interaction between the ring puckering vibration and several CH_2 scissoring modes have been observed in the i.r. spectra of trimethylene oxide and some of its deuterated analogs. By means of a simple theoretical model for the puckering–vibrational interactions (3) and with the help of the pure puckering transitions (5) the observed absorptions can be explained and assigned. In particular this sort of analysis of the spectra enables us to locate accurately the scissoring vibrations of the CH_2 groups in trimethylene oxide for the first time. The corresponding assignments, summarized in Table 7, are fundamentally different from the only other previous assignments for normal TMO which have been made by Zürcher and Günthard (8) some time ago.

It was also possible to estimate the puckering transitions in the first excited states of some of the CH_2 scissoring vibrations. In all cases except one the form of the puckering potential in the vibrationally excited states appears to be similar to that in the ground state, at least within the experimental accuracies. The β-CH_2 scissoring mode of the normal compound constitutes the only exception, where the differences between the ground state and excited state transitions are significantly large and alternate in sign.

M.D. acknowledges the financial support received from the National Research Council of Canada in the form of an NRCC Scholarship. This research was supported by the National Research Council of Canada.

1. W. H. GREEN. J. Chem. Phys. **52**, 2156 (1970).
2. H. WIESER, M. DANYLUK, W. KIEFER, and H. J. BERNSTEIN. Can. J. Chem. This issue.
3. J. M. R. STONE and I. M. MILLS. Mol. Phys. **18**, 631 (1970).
4. S. I. CHAN, T. R. BORGERS, J. W. RUSSELL, H. L. STRAUSS, and W. D. GWINN. J. Chem. Phys. **44**, 1103 (1966).
5. H. WIESER, M. DANYLUK, and R. A. KYDD. J. Mol. Spectrosc. In Press.
6. S. I. CHAN, J. ZINN, and W. D. GWINN. J. Chem. Phys. **34**, 1319 (1961).
7. See for example, H. WIESER, W. G. LAIDLAW, P. J. KRUEGER, and H. FUHRER. Spectrochim. Acta, **24A**, 1055 (1968).
8. R. F. ZÜRCHER and H. H. GÜNTHARD. Helv. Chim. Acta, **38**, 851 (1955); **40**, 89 (1957).

Can. J. Chem. Downloaded from www.nrcresearchpress.com by 210.87.254.105 on 09/05/12
For personal use only.

Vapor Phase Raman Transitions in the CH_2 Scissoring Region and the Ring Puckering Vibration of Trimethylene Oxide and some Deuterated Analogs[1]

H. WIESER AND M. DANYLUK

Department of Chemistry, University of Calgary, Calgary, Alberta T2N 1N4

AND

W. KIEFER AND H. J. BERNSTEIN

Division of Chemistry, National Research Council of Canada, Ottawa, Canada K1A 0R6

Received February 28, 1972

The vapor phase Raman spectra of trimethylene oxide (TMO) and two of its deuterated analogs (α-d_2 and β-d_2) each show one sharp line on a weak, broad, and unresolved band in the CH_2 scissoring region. Under high resolution these lines are resolved into several components. They are assigned to the fundamentals of the scissoring mode of α-CH_2 (in-phase, A_1 symmetry, in the case of the normal and β-d_2 compound) and overlapping bands resulting from interaction with the low frequency puckering vibration. The agreement between Raman and i.r. data is excellent and the assignments are entirely consistent. Raman lines corresponding to the out-of-phase combination (B_2 symmetry) of the α-CH_2 scissoring vibration and the scissoring mode of the β-CH_2 group (in normal, α-d_2 and α,α'-d_4 TMO) cannot be resolved.

Les spectres Raman en phase gazeuse de l'oxide de triméthylène (OTM) et de ses deux homologues deuteriés (α-d_2 et β-d_2) résultent en une raie prononcée incluse dans une bande faible, large et non-résolue, dans la région du cisaillement des CH_2. Ces raies se séparent en plusieurs composantes dans le spectre à haute résolution. Nous avons assigné celles-ci aux fondamentales du mode de cisaillement du CH_2 en α (en phase, symétrie A_1; cas des composés normal et β-d_2) et à les bandes chevauchantes que résultent de l'interaction avec la vibration de pulsation à basse fréquence. Les résultats des spectres i.r. et Raman concordent très bien et l'assignation des bandes se fait facilement. Les raies Raman correspondant à la combinaison hors-phase (symétrie B_2) de la vibration de cisaillement du CH_2 en α et du mode de cisaillement du groupe CH_2 en β (dans l'OTM normal, α-d_2 et α,α'-d_4) n'ont pas être résolues.

[Traduit par le journal]

Canadian Journal of Chemistry, **50**, 2771 (1972)

Introduction

During the past few years a number of investigators have reported observing combination band progressions in the mid- and near-infrared regions of four- and five-membered ring compounds resulting from the interaction between the low-frequency out-of-plane ring vibration (ring puckering motion) and some other suitable vibrational mode (1–3). Observation of the same phenomenon by means of vapor phase Raman spectroscopy has so far been rare. Recently we have reported combination progressions in the C—H stretching region observed in the Raman spectrum of normal trimethylene oxide (4). It appears that for some normal modes at least, the i.r. and Raman spectra are complementary in nature and thus facilitate the assignment of the fundamental and combination transitions. As part of a vibrational analysis of trimethylene oxide and several of its deuterated analogs (α-d_2, β-d_2 and α,α'-d_4) it was therefore of considerable interest to obtain the Raman data corresponding to the i.r. band sequences found in the CH_2 scissoring region of these compounds (5).

[1]NRCC No. 12659.

Theoretical Considerations

In a manner similar to the dipole moments, the polarizabilities may be expanded as a function of the $3N-7$ vibrational coordinates, Q_r, and the puckering coordinate, Z (5). Considering only the symmetry-allowed components of this expansion the puckering–vibrational matrix element of, for example, the α_{x^2} component is

$$|\alpha_{x^2}|_{nm} = \sum_{A_1}\left(\frac{\partial\alpha_{x^2}}{\partial Q_{A_1}}\right)_0 \langle\Psi_n|Q_{A_1}|\Psi_m\rangle\langle\phi_n|\phi_m\rangle + \sum_{B_1}\left(\frac{\partial^2\alpha_{x^2}}{\partial Q_{B_1}\partial Z}\right)_0 \langle\Psi_n|Q_{B_1}|\Psi_m\rangle\langle\phi_n|Z|\phi_m\rangle$$

where the Ψ's and ϕ's are the eigenfunctions for the vibrational and puckering levels, respec-

Can. J. Chem. Downloaded from www.nrcresearchpress.com by 210.87.254.42 on 09/05/12
For personal use only.

Can. J. Chem. Downloaded from www.nrcresearchpress.com by 210.87.254.42 on 09/05/12
For personal use only.

TABLE 1. Raman band assignments for α-CH_2 scissoring modes of trimethylene oxide and some deuterated analogs

	Normal (cm^{-1})			α-d_2 (cm^{-1})			β-d_2 (cm^{-1})		
	Observed			Observed			Observed		
	Raman	Infrared*	Calculated†	Raman	Infrared*	Calculated†	Raman	Infrared*	Calculated†
0,0 → 1,0	1505.0	—	—	1492.4	1492.7	—	1502.4	1502.2	—
0,1 → 1,1			1503.3			1490.7	1503.8	1503.9	1504.0
0,2 → 1,2	1502.8	—	1503.7	1491.0	1491.3	1491.2			1501.6
0,3 → 1,3			1502.9			1490.0	1501.1	1500.9	1501.3
0,4 → 1,4			1502.1			1490.6			1501.0

*Reference 5.
†Calculated from $\Delta v_p = \pm 1$ bands observed in the i.r. (5).

Can. J. Chem. Downloaded from www.nrcresearchpress.com by 210.87.254.42 on 09/05/12
For personal use only.

tively, and n and m refer to the vibrational excited and ground states. The factor $\langle \phi_n | \phi_m \rangle$ in the first term gives rise to transitions for which the puckering quantum number, v_p, does not change (*i.e.* $\Delta v_p = 0$), while the factor $\langle \phi_n | Z | \phi_m \rangle$ in the second term will permit only $\Delta v_p = \pm 1$ bands (the vibrational quantum number changing by $+1$ in both cases) (5). It follows that, for example for an A_1 mode, the fundamental and higher $\Delta v_p = 0$ bands should show measurable intensity only by virtue of their α_{x^2}, α_{y^2}, and α_{z^2} components, whereas the α_{xz} component should give rise only to $\Delta v_p = \pm 1$ bands. B_1 vibrations follow the reverse order. For A_2 and B_2 modes only α_{yz} and α_{xy} are permissible, again in the similar complementary fashion as A_1 and B_1. Clearly, whatever is observed in the Raman spectra depends very much on the relative magnitudes of the polarizability derivatives. It should be noted that this analysis is valid for the symmetric molecules (C_{2v} symmetry) as well as the α-d_2 compound (C_s symmetry) since isotopic substitution should change primarily the moments of inertia and leave the electronic distribution essentially unchanged.

Referring specifically to the scissoring vibrations, we note that the α-CH_2 groups of the symmetrically substituted TMO molecules give rise to an in-phase (A_1) and an out-of-phase (B_2) combination of the bending mode. The analogous β-CH_2 scissoring vibrations also belong to the A_1 symmetry species. It is generally accepted that totally symmetric vibrations normally exhibit higher Raman intensities than non-totally symmetric ones. Moreover, as a result of rotation–vibration interactions, totally symmetric Raman bands (*i.e.* the α_{x^2}, α_{y^2}, and α_{z^2} polarizability components) are characterized by a strong central line-like Q branch, whereas non-totally symmetric Raman bands may resemble type C, B or A infrared contours when α_{xy}, α_{xz} or α_{yz}, respectively, are non-zero depending on the asymmetry of the molecules (6).[2] In the CH_2 scissoring region of the symmetric molecules of the TMO series we may therefore expect to find the fundamentals and the higher $\Delta v_p = 0$ bands of the A_1 vibrations as the most prominent features. The $\Delta v_p = \pm 1$ bands of A_1 modes and all transitions corresponding to the B_2 modes should give rise only to diffuse bands. For α-d_2 TMO one would again expect to see predominantly the $\Delta v_p = 0$ transitions of the single α-CH_2 and the β-CH_2 group.

[2]Normal TMO and all its deuterated modifications considered here are near oblate symmetric top molecules; one could therefore also say that totally symmetric Raman bands resemble parallel i.r. contours, and non-totally symmetric Raman bands resemble perpendicular i.r. contours (6).

Experimental

The synthesis of these compounds (7) and the experimental method used for obtaining the vapor phase Raman spectra (8) were described on previous occasions. The line positions reported in this communication have been measured several times, using superimposed discharge lines from neon and argon lamps for calibration. The accuracy is therefore believed to be $\pm 0.5\ cm^{-1}$. As the Raman signals were very weak especially with the high resolution desired, it was not possible to get polarization data. Gas pressures were about 250–280 Torr (saturated vapor pressure at room temperature).

Results and Discussion

The low-resolution vapor phase Raman spectra of normal trimethylene oxide and its three deuterated modifications (α-d_2, β-d_2, and α,α'-d_4) in general show a weak unresolved band around $1500\ cm^{-1}$ extending over a region of about $50\ cm^{-1}$. In addition, they all exhibit one relatively more intense and sharp line in the same area. For α,α'-d_4 TMO this line (at $1441\ cm^{-1}$) does not correspond to a CH_2 scissoring vibration; the single β-CH_2 group gives rise to an A_1 scissoring vibration which has been clearly assigned to a distinct B-type i.r. band centered at $1464.0\ cm^{-1}$ (5). For the other three compounds we were able to examine the sharp lines under high resolution. The corresponding spectra are reproduced in Figs. 1 to 3. The lines shown in these spectra are all clearly resolved and entirely reproducible.

The line positions are summarized in Table 1. In the same table we also compare these positions with observed infrared bands and values for $\Delta v_p = 0$ transitions derived from infrared $\Delta v_p = \pm 1$ bands (5). The agreement is seen to be excellent and well within the experimental uncertainties. Moreover, the assignment of these Raman lines to $\Delta v_p = 0$ transitions of the α-CH_2 (A_1 in the case of normal and β-d_2 TMO) scissoring mode is confirmed by the internal consistency among the complete infrared and Raman data.

As suggested in the preceding theoretical

Can. J. Chem. Downloaded from www.nrcresearchpress.com by 210.87.254.42 on 09/05/12
For personal use only.

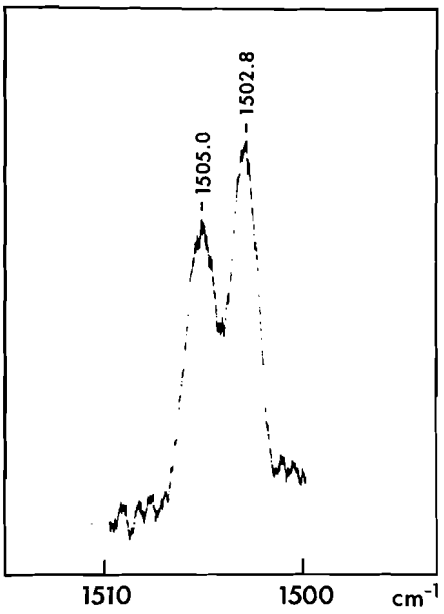

FIG. 1. Vapor phase Raman spectrum in the CH_2 scissoring region of normal trimethylene oxide: 1 W at 4880 Å excitation; slits 1.5 cm^{-1}.

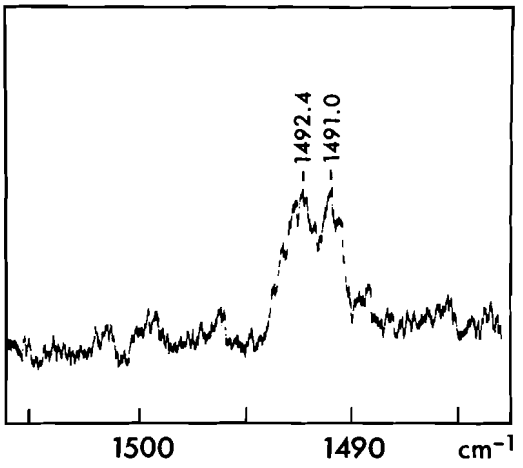

FIG. 2. Vapor phase Raman spectrum in the CH_2 scissoring region of α-d_2 trimethylene oxide: 1 W at 4880 Å excitation; slits 1.5 cm^{-1}.

section, the A_1 $\Delta v_p = 0$ transitions are indeed the most prominent feature at least for the α-CH_2 vibrations of normal and β-d_2 TMO. The corresponding out-of-phase combinations (B_2 symmetry) do not appear to give rise to Raman bands with measurable intensities. In

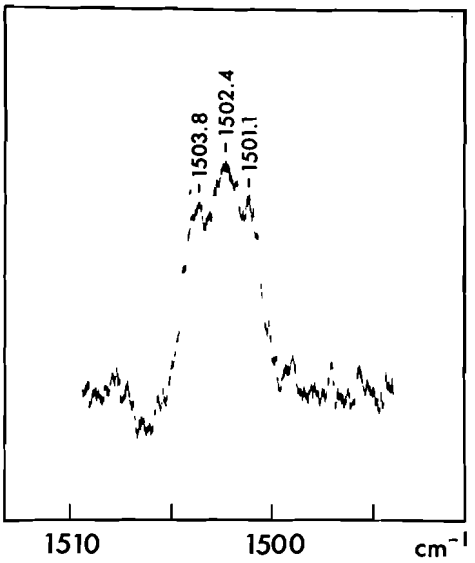

FIG. 3. Vapor phase Raman spectrum in the CH_2 scissoring region of β-d_2 trimethylene oxide: 1 W at 4880 Å excitation; slits 1.0 cm^{-1}.

α-d_2 TMO the most intense Raman lines originate from the $\Delta v_p = 0$ transitions of the single α-CH_2 scissoring mode. It is of particular interest to note that corresponding infrared absorptions for all three compounds are observed either only very weakly or not at all (5). Indeed, it is the $\Delta v_p = \pm 1$ bands of these modes which constitute the prominent features in the infrared spectra of these compounds.

The β-CH_2 scissoring mode does not exhibit the same pattern, even though the vibration has A_1 symmetry (in normal, β-d_2, and α,α'-d_4 TMO). There are no distinct Raman lines in the spectra of any of the compounds which may be assigned to the vibration in question. One can only conclude that these Raman intensities are intrinsically low by virtue of a small polarizability change during the vibration. It is of interest to note that in the i.r. spectrum, especially in the case of α,α'-d_4 TMO, the fundamental transition of β-CH_2 scissoring was found to be significantly more intense than its $\Delta v_p = \pm 1$ bands (5).

This research was supported by the National Research Council of Canada.

1. J. M. R. STONE and I. M. MILLS. Mol. Phys. **18**, 631 (1970).

2. T. UEDA and T. SHIMANOUCHI. J. Chem. Phys. **49**, 470 (1968).
3. T. B. MALLOY, JR., F. FISHER, and R. M. HEDGES. J. Chem. Phys. **52**, 5325 (1970).
4. W. KIEFER, H. J. BERNSTEIN, M. DANYLUK, and H. WIESER. Chem. Phys. Lett. **12**, 605 (1972).
5. H. WIESER and M. DANYLUK. Can. J. Chem. This issue.
6. G. HERZBERG. Molecular spectra and molecular structure. Vol. II. Infrared and raman spectra of polyatomic molecules. Van Nostrand Inc., Princeton, N.J. 1945.
7. H. WIESER, M. DANYLUK, and R. A. KYDD. J. Mol. Spectrosc. In press.
8. W. KIEFER, H. J. BERNSTEIN, H. WIESER, and M. DANYLUK. J. Mol. Spectrosc. In press.

Can. J. Chem. Downloaded from www.nrcresearchpress.com by 210.87.254.42 on 09/05/12
For personal use only.

Mass Spectrometry in Structural and Stereochemical Problems. CCXVII.[1] Electron Impact Promoted Fragmentation of *O*-Methyl Oximes of some α,β-Unsaturated Ketones and Methyl Substituted Cyclohexanones

YOUNUS M. SHEIKH, RAYMOND J. LIEDTKE, A. M. DUFFIELD, AND CARL DJERASSI

Departments of Chemistry and Genetics, Stanford University, Stanford, California 94305

Received February 15, 1972

Deuterium labeling and high resolution mass spectrometry have been utilized to delineate the modes of mass spectrometric fragmentation of *O*-methyl oximes of α,β-unsaturated ketones and methyl substituted cyclohexanones. α,β-Unsaturated ketone and 2- and 4-methylcyclohexanone *O*-methyl oxime ether derivatives fragment upon electron impact in a manner reminiscent of the carbonyl derivatives from which they were prepared. However, several fragmentation sequences characteristic of the *O*-methyl oxime ether group were observed.

Le marquage au deutérium et la spectrométrie de masse à haute résolution ont été utilisés pour décrire le spectre de fragmentation des oximes *O*-méthylés de cétones α,β insaturées et de cyclohexanones substituées par le méthyle. La cétone α,β insaturée et les dérivés de la méthyl-2 et -4 cyclogexanone oxime *O*-méthyle éther se fragmentent lors de l'impact électronique, de façon semblable aux dérivés carbonylés à partir desquels ils ont été préparés. Cependant, plusieurs séquences de fragmentation caractéristiques du groupe oxime *O*-méthyl éther ont été observées. [Traduit par le journal]

Canadian Journal of Chemistry, **50**, 2776 (1972)

Can. J. Chem. Downloaded from www.nrcresearchpress.com by 210.87.254.42 on 09/05/12
For personal use only.

O-Methyl oxime ether derivatives have found extensive use in g.c. and g.c./m.s. studies of relatively complex molecules (1). Recent publications (2) described for the first time the electron impact sponsored fragmentation processes of *O*-methyl oxime ethers. The present paper extends the knowledge of the mass spectral fragmentation behavior of this class of compound to α,β-unsaturated ketones and methyl substituted cyclohexanone derivatives and defines, using deuterium labeling, some of the rearrangement processes accompanying their fragmentation.

O-Methyl Oxime Ethers of Aliphatic α,β-Unsaturated Ketones

Prominent molecular ions are an important and useful feature of the mass spectra (see for example Figs. 1–4) of the *O*-methyl ether oxime derivatives of the α,β-unsaturated ketones

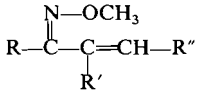

1 R = R′ = R″ = CH_3
2 R = C_2H_5; R′ = H; R″ = CH_3
3 R = CH_3; R′ = H; R″ = *n*-C_3H_7
4 R = CH_3; R′ = H; R″ = *n*-C_4H_9
5 R = CH_3; R′ = H; R″ = *n*-C_5H_{11}
6 R = CH_3; R′ = H; R″ = *n*-C_6H_{13}

[1]For part CCXVI, see ref. 5.

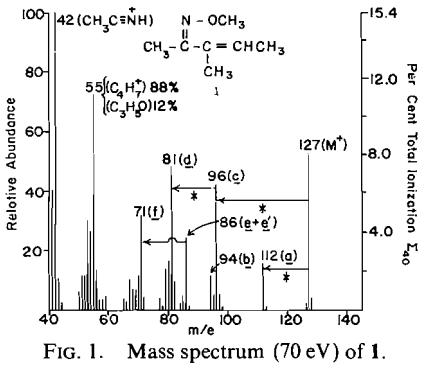

FIG. 1. Mass spectrum (70 eV) of **1**.

examined. Loss of a methyl radical from the molecular ion of **1** could involve either the two alkyl branches or the methyl group of the oxime ether function. Deuterium labeling (**1**, R = CD_3) established that 10% of the methyl lost in this fragmentation arose from C-1. Since ions due to M − CH_3 occur in the spectra of compounds **1–6** the most likely position for the remaining loss of CH_3 in **1** is the *O*-methyl oxime ether group (formation of **a**) but other sources not completely eliminated include the alkyl chains of **1–6**. The facile expulsion of the methyl ether entity in aliphatic α,β-unsaturated ketone *O*-methyl ether oxime derivatives (see Figs. 1–4) should be contrasted to the behavior observed (2) with the same derivative of aromatic aldehydes and ketones in which this process was not observed.

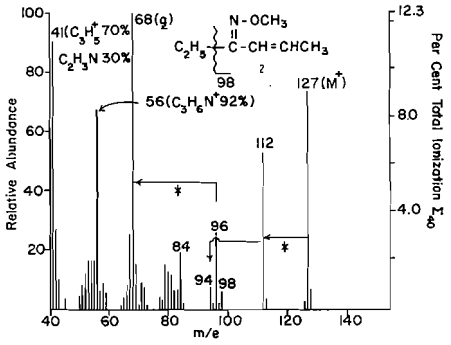

FIG. 2. Mass spectrum (70 eV) of **2**.

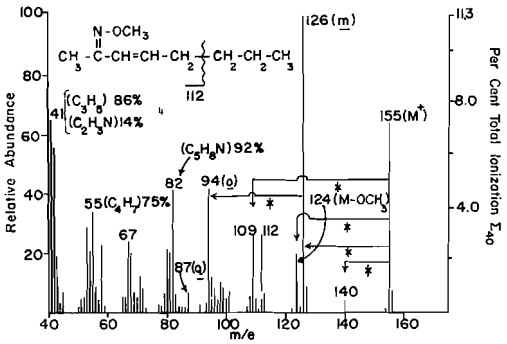

FIG. 3. Mass spectrum (70 eV) of **4**.

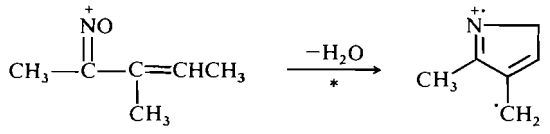

a, *m/e* 112 **b**, *m/e* 94

SCHEME 1

A characteristic fragmentation of the species **a** occurs by the elimination of water (metastable ion observed in all instances) and one representation for the product ion, using **1** as an example, is **b**, *m/e* 94 (Scheme 1). In the trideuterio derivative (**1**, R = CD_3) most (80%) of the label was retained.

The ion of mass 96 (M − OCH_3) in the mass spectrum (Fig. 1) of **1** is moved predominantly to *m/e* 99 in the corresponding trideuterated analog (**1**, R = CD_3). This ion, assigned structure **c**, *m/e* 96, is envisaged as arising from a four-centered reaction in which the methoxyl radical attached to nitrogen is expelled. The species **c** decomposes by the elimination of a methyl radical (metastable ion observed) and the product is rationalized in terms of **d**, *m/e* 81. Only 60% of the ion yield at *m/e* 81 in Fig. 1 was located at *m/e* 84 in the spectrum of the tri-

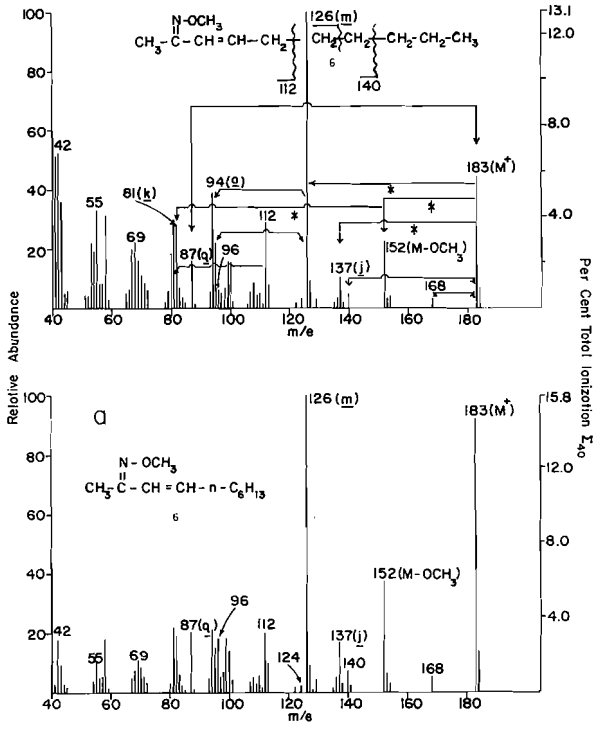

FIG. 4. Mass spectrum (70 eV) of **6**. (*a*) Mass spectrum (15 eV) of **6**.

Can. J. Chem. Downloaded from www.nrcresearchpress.com by 210.87.254.42 on 09/05/12
For personal use only.

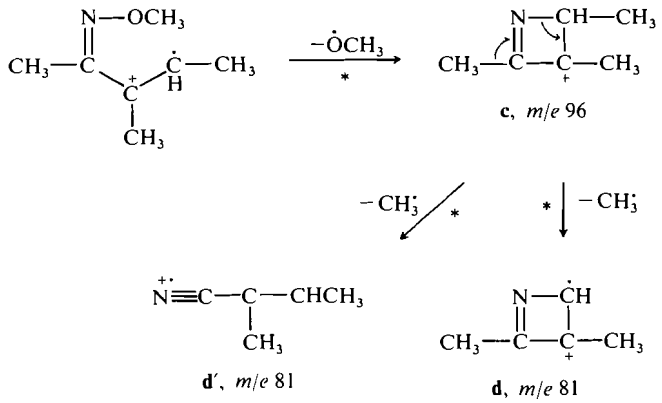

SCHEME 2

deuterated compound **1** ($R = CD_3$) indicating that other modes of formation of *m/e* 81 exist. One possibility, which accounts for 25% of the ion yield, is depicted by **1** → **d′**, *m/e* 81 (Scheme 2).

The ion of mass 86 ($M - CH_3CN$) in the spectrum (Fig. 1) of **1** is analogous to the low abundance ion of mass 72 ($M - C_2H_5CN$) observed in the mass spectrum (Fig. 2) of the ethyl analog **2**. These processes presumably occur by a four-centered transition state (for instance **1** → **e**, *m/e* 86) (see Scheme 3). The CD_3 analog of **1** ($R = CD_3$) surprisingly indicated that 70% of the trideuteriomethyl label was eliminated while loss of CHD_2CN (15%), CH_2DCN (40%), and CH_3CN (11%) contributed to the overall process. Clearly some hydrogen–deuterium exchange must precede the formation of **e**. One rationalization for H–D scrambling is depicted by **1** → **1***a*.

Further loss of a methyl radical from **e** serves as the origin for the ion (97% $C_4H_7O^+$) of mass 71 in Fig. 1. In the CD_3 analog of **1** ($R = CD_3$) the peak in question is distributed between *m/e* 71, 72, and 73. This indicates that further randomization of the label occurs prior to the formation of a species which we represent as **f**, *m/e* 71.

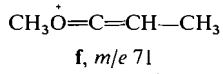

f, *m/e* 71

High resolution mass spectrometry established the composition of *m/e* 55 in the mass spectrum (Fig. 1) of **1** as 88% $C_4H_7^+$; 10% $C_3H_5N^+$, and 2% $C_3H_3O^+$ while the corresponding ion in the ethyl analog (**2**, Fig. 2) at *m/e* 41 consisted of $C_3H_5^+$ (70%) and $C_2H_3N^+$ (30%). The hydrocarbon ions can be interpreted as arising from the alkenyl portions of **1** and **2** respectively.

The abundant ion of mass 68 in the spectrum

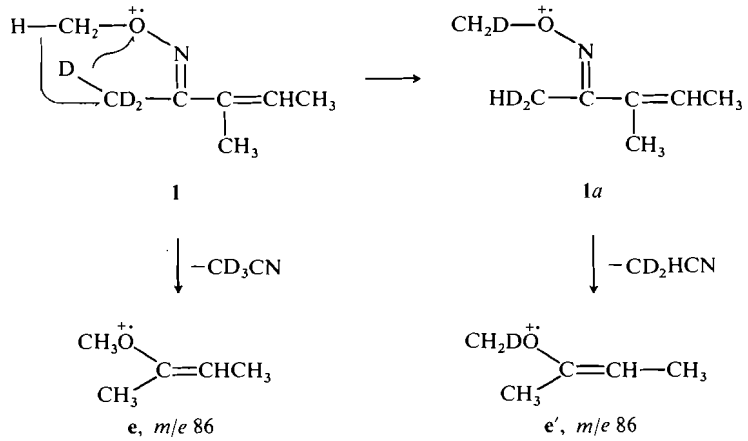

SCHEME 3

Can. J. Chem. Downloaded from www.nrcresearchpress.com by 210.87.254.42 on 09/05/12
For personal use only.

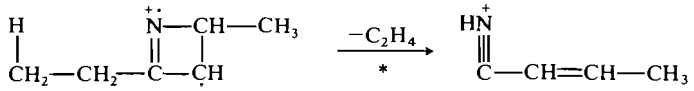

c′, *m/e* 96 **g**, *m/e* 68

SCHEME 4

(Fig. 2) of **2** owes its genesis (mestastable ion recognized) to the loss of ethylene (high resolution) from the ion **c′**, *m/e* 96 ($M - OCH_3$). This process could be rationalized in terms of a five-membered transfer of hydrogen to nitrogen (**c′** → **g**) (Scheme 4). Protonated acetonitrile (**h**, $R = CH_3$) and propionitrile (**h**, $R = C_2H_5$) ions respectively account for the appearance of charged fragments of mass 42 and 56 in the mass spectra (Figs. 1 and 2) of **1** and **2**. These conclusions are in agreement with the results from high resolution mass spectrometry.

$$R{-}C{\equiv}\overset{+}{N}H$$

h; **1**, $R = CH_3$, *m/e* 42
2, $R = C_2H_5$, *m/e* 56

The effect of substituting an alkyl chain for the methyl group (R″) can be gauged from the mass spectra (Figs. 3 and 4) of compounds **4** and **6** which contain an *n*-butyl and *n*-hexyl chain respectively. In the case of the *n*-hexyl derivative (**6**) extensive deuterium labeling has made possible the presentation of plausible fragmentation pathways.

The molecular ions of compounds (**3**–**6**) are abundant (see for instance Figs. 3 and 4) while the M − 15 species is of reduced ion yield. The expulsion of a methyl radical from the parent species of these compounds is ascribed in 50% yield to a process analogous to that postulated for the formation of **a** since equal losses of CD_3 and CH_3 were observed in the spectrum of **6***a*. On lowering the ionizing voltage to 15 eV loss of CH_3 was twice as frequent in **6***a* as loss of CD_3. The low ion yield resulting from the elimination of CD_3 in **6***a* should be contrasted to the situation observed (3) for the parent α,β-saturated ketone (**7**) where expulsion of C-1 accounted for the origin of the base peak at 12 eV.

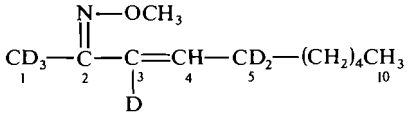

6*a*

The loss of a methoxyl radical from the molecular ions of the alkyl substituted derivatives (**3**–**6**) is explicable by a process analogous to that suggested for the formation of ion **c**. The ion of mass 137 ($M - CH_4NO$ by high resolution) in the mass spectrum (Fig. 4) of **6** is accompanied by metastable ion formation, indicating the molecular ion to be its precursor, and similar expulsions are observed in the mass spectra of **3**, **4**, and **5**. Deuterium labeling in the *n*-hexyl derivative indicated that hydrogen was eliminated from C-6 (0.55), C-7 (0.20), and a combined total of 0.25 from C-1 and -3. This process, using the *n*-hexyl analog **6** as example, would yield **j**, *m/e* 137 (see Scheme 5). A metastable ion established a parent–daughter relationship between **j** and the species of mass 81 which we designate as **k**. High resolution mass spectrometry confirmed the loss of C_4H_8 in this process since the ion of mass 81 was composed of $C_6H_9^+$ (60%), $C_5H_7N^+$ (33%), and $C_5H_5O^+$ (7%).

The peak at *m/e* 126 is the base peak in the spectra (see for instance Figs. 3 and 4) of the C-4 alkyl substituted methoxy oximes (**3**–**6**) studied. The results obtained from deuterated analogs of **6** are consistent with the assignment of structure **m**, *m/e* 126 to this ion. At low ionizing voltages (15 eV) the ion **m** remains the base peak (see Fig. 4*a*) and it should be noted that a similar process (γ-cleavage) generated an abundant ion in the mass spectra of the α,β-unsaturated ketones (3) from which the methoxy oximes were prepared. Loss of methanol from **m** (verified by a metastable ion) affords the fragment **o**, *m/e* 94 and high resolution mass spectrometry established this ion's composition as 97% $C_6H_8N^+$ and 3% $C_7H_{10}^+$. Deuterium labeling indicated that only 0.30 of one hydrogen atom (see Scheme 6, **m** → **o**) originated from

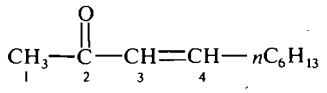

7

Can. J. Chem. Downloaded from www.nrcresearchpress.com by 210.87.254.42 on 09/05/12
For personal use only.

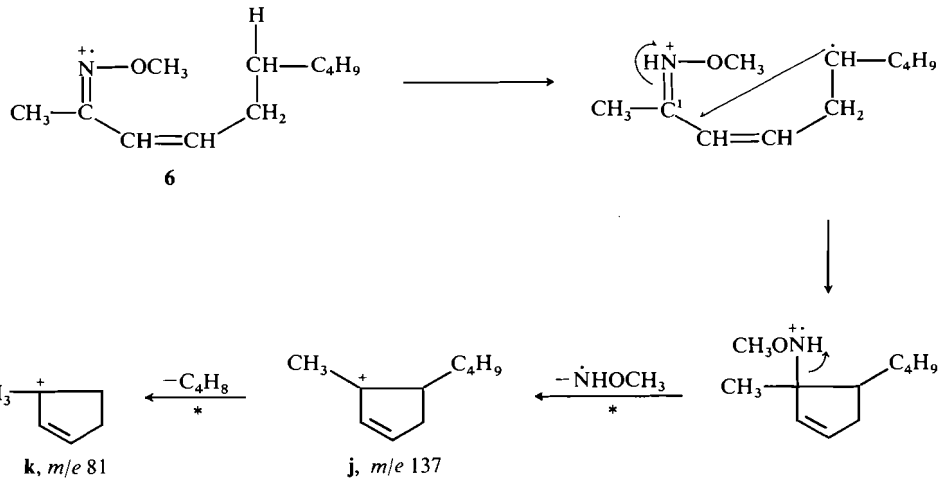

SCHEME 5

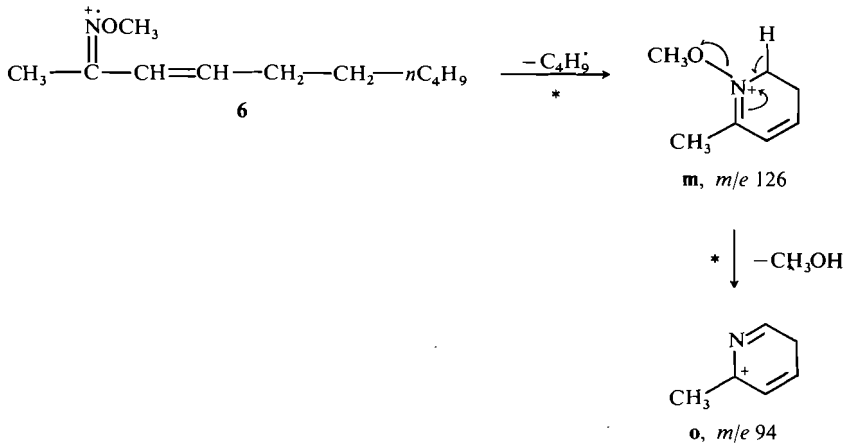

SCHEME 6

C-6 together with a total of 0.25 from C-1 plus C-3. This result indicates essentially a random loss of hydrogen in the formation of the species of mass 94 from that of mass 126.

In a previous publication (3) concerned with the mass spectral fragmentation of α,β-unsaturated ketones we observed the expulsion of acetone from the molecular ion of **7** to be a significant process at 70 eV and the second most intense fragmentation (86% relative abundance) at 12 eV. The analogous fragmentation in the case of the *O*-methyl oxime ether (**6**) would generate the species **p**, *m/e* 96 and **q** would be the neutral molecule (*O*-methyloxime of acetone) eliminated (see Scheme 7). High resolution mass spectrometry confirmed the composition of **q**, *m/e* 87 but no ion corresponding to **p** was observed.[2] The appearance of **q** in the *O*-methyl ether oxime derivatives can be attributed to charge localization on the nitrogen atom. The sources of hydrogen in this double hydrogen rearrangement (formation of **q**) were determined (from the mass spectra of **6***b*, **6***c*, and **6***d*) to be: C-5 (0.35), C-6 (0.40), and C-7 (0.55). In the case of the ketone **7** the values for hydrogen transfer leading to acetone elimination and the formation of a hydrocarbon ion

[2]The composition of the ion of mass 96 in Fig. 4 was determined to be 84% $C_6H_{10}N^+$ and 16% $C_6H_8O^+$. The nitrogen-containing component at this ion yield could arise from the loss of formaldehyde (CH_2O) from the species **m** but no metastable ion was found to support this contention.

Can. J. Chem. Downloaded from www.nrcresearchpress.com by 210.87.254.42 on 09/05/12
For personal use only.

Can. J. Chem. Downloaded from www.nrcresearchpress.com by 210.87.254.42 on 09/05/12
For personal use only.

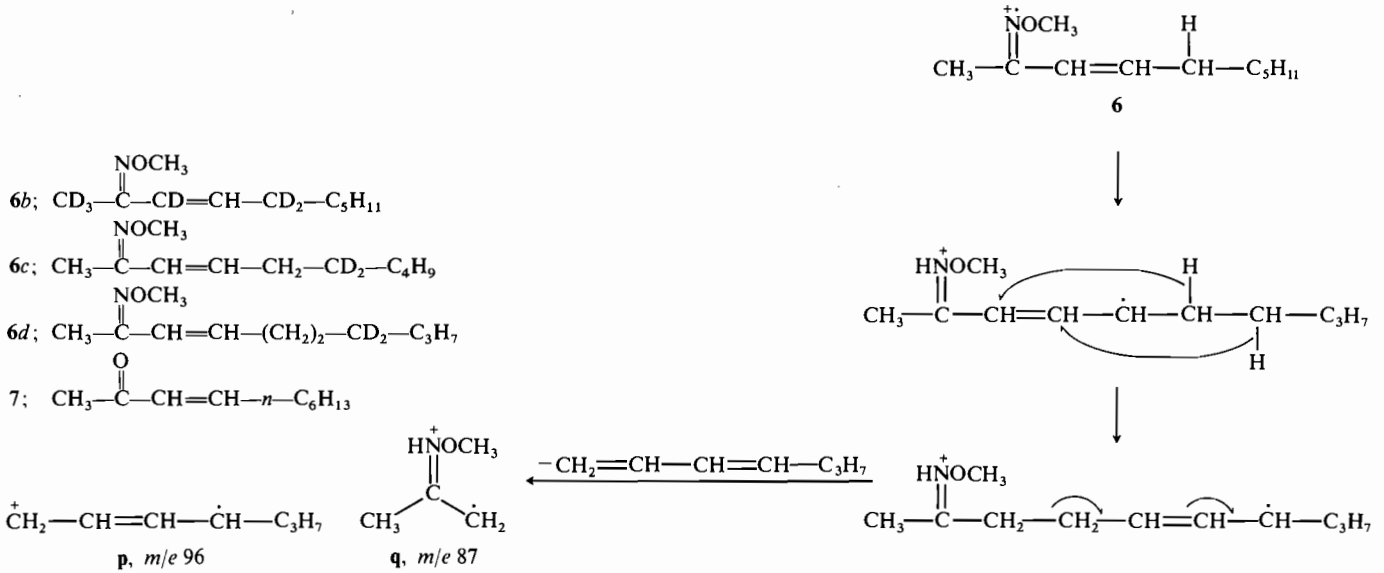

SCHEME 7

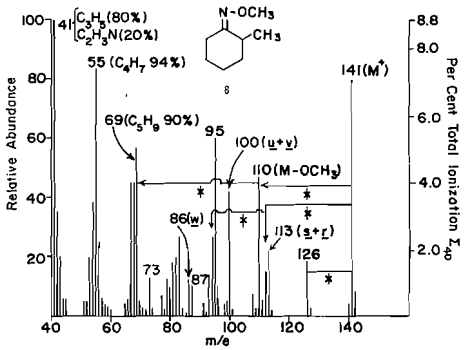

FIG. 5. Mass spectrum (70 eV) of **8**.

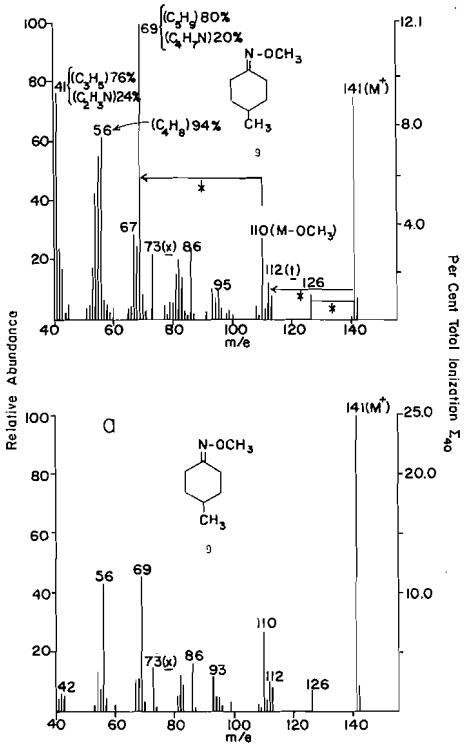

FIG. 6. Mass spectrum (70 eV) of **9**. (*a*) Mass spectrum (15 eV) of **9**.

species were C-5 (0.50), C-6 (0.80), and C-7 (0.30) (3).

The ions below mass 80 in the four alkyl *O*-methyl ether oximes investigated (**3**–**6**) do not appear to contain any ions of appreciable diagnostic utility and no discussion of their possible geneses will be presented.

Except for the presence of an abundant molecular ion, the mass spectra of *O*-methyl oxime ethers of α,β-unsaturated ketones offer no diagnostic advantages, as compared to the ketones from which they are derived, in interpretation because of the large number of fragment ions observed.

O-Methyl Oximes of 2- and 4-Methylcyclohexanone

The base peak in the mass spectra (Figs. 5 and 6) of 2-methyl and 4-methylcyclohexanone *O*-methyl oxime (**8** and **9**) and of cyclohexanone *O*-methyl oxime (2*a*) corresponds to their respective molecular ions. This behavior is in contrast to cyclohexanone oxime where the parent ion attains only 20% relative abundance (4). Loss of a methyl radical from the parent ions of **8** and **9** yields low abundance ions which are rationalized as arising from loss of the *O*-methyl group.

Loss of 28 a.m.u. (ethylene) from the molecular ion of **8** and **9** yields the peak at *m/e* 113 in Figs. 5 and 6. Deuterium labeling (**8***a*) indicated that for the 2-methyl isomer 50% of the ethylene expropriated originated from C-5 and -6 allowing the rationalization **8** → **r**, *m/e* 113 to be presented (Scheme 8). The remaining source of extruded ethylene could be explained by β-fission of the molecular ion (see **8** → **s**, *m/e* 113) followed by homolytic fission of the C_3—C_4 bond. This process has analogy with that found to operate in the extrusion of ethylene from cyclohexanone oxime (4).

In contrast the 4-methyl derivative (**9**) expelled ethylene by a more complex route since 40% of this species' yield involved the loss of a single deuterium atom from the parent ion of **9***a*. The remaining 60% of this ion contribution could arise by a process similar to that depicted

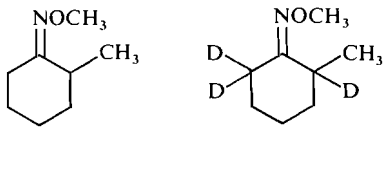

8 **8***a*

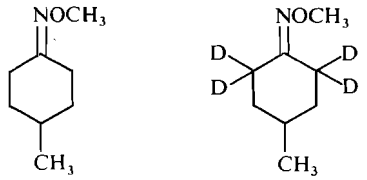

9 **9***a*

Can. J. Chem. Downloaded from www.nrcresearchpress.com by 210.87.254.42 on 09/05/12
For personal use only.

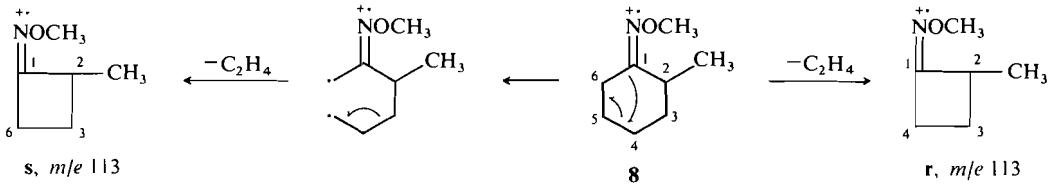

SCHEME 8

by **8** → **r** but the presence of an M − 29 ion in the unlabeled compound ruled against a quantitative answer being presented. In contrast to the process **8** → **s**, suggested for the loss of ethylene from 2-methylcyclohexanone *O*-methyl oxime, the elimination of propene from the parent ion of **9** yielded only a low (3% relative abundance, see Fig. 6) intensity ion of mass 99.

The ion of mass 110 (M − OCH_3) in the mass spectra of **8** and **9** (Figs. 5 and 6) requires no discussion. However, both of these compounds, as did the *O*-methyl ether oxime of cyclohexanone (2*a*), eliminate 41 a.m.u. (C_3H_5) from their respective molecular ions. In the case of the 2-methyl derivative (**8**) 55% of the ion in question arose from loss of C-6, -5, and -4 (less one hydrogen atom) while the remainder (45%) could be explained by loss of C-5, -4, and -3 (less one hydrogen atom). These results are explicable by invoking an initial α-cleavage (path A) or β-cleavage (path B) of the molecular ion relative to the imine bond (Scheme 9).

If the rationalization depicted as path A occurred by fission of the C_1—C_2, bond of **8** the peak at *m/e* 86 (M − C_4H_7) in Fig. 5 would result (Scheme 10). However, no more than 50%

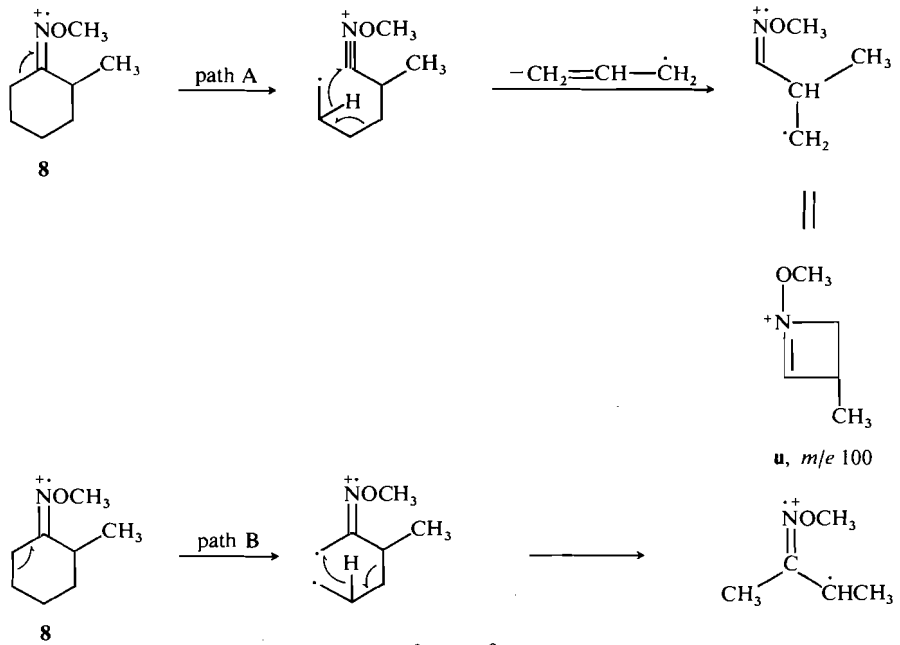

SCHEME 9

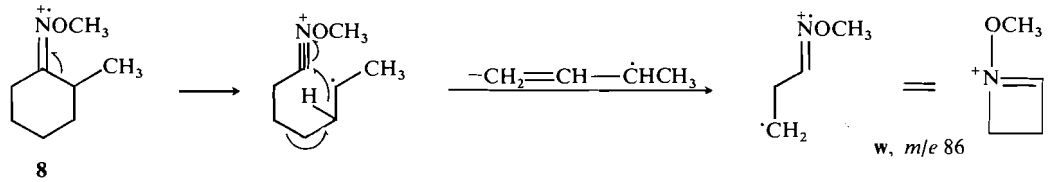

SCHEME 10

Can. J. Chem. Downloaded from www.nrcresearchpress.com by 210.87.254.42 on 09/05/12
For personal use only.

Can. J. Chem. Downloaded from www.nrcresearchpress.com by 210.87.254.42 on 09/05/12
For personal use only.

of this ion's (**w**) yield can arise from this process since only this portion was displaced to *m/e* 88 in the spectrum of **8***a*. The proximity of other ions did not allow an indication of the remaining disposition of this peak in the spectrum of **8***a*.

The loss of 55 a.m.u. (C_4H_7) in the mass spectrum (Fig. 6) of **9** occurred by the following two fragmentations as shown from the mass spectrum of **9***a* where this ion was located at *m/e* 90 (55%, β-cleavage) and *m/e* 88 (45%, α-cleavage).

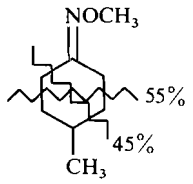

9

Loss of C_5H_8 (high resolution) from the molecular ion of **9** generates (Fig. 6) a fragment of mass 73 and this species remains prominent at low ionizing (15 eV) voltages (see for instance Fig. 6*a*). This ion was located at mass 75 (60%) and mass 76 (40%) in the tetradeuterio derivative **9***a*. The rationalizations (**9** → **x**, *m/e* 73 by paths A and B) explain the distribution of the fragment **x** at *m/e* 75 (path A) and *m/e* 76 (paths A and B) in the spectrum of the labeled analog **9***a* (Scheme 11).

Analogous rationalizations to **9** → **x**, *m/e* 73 (paths A and B) can be applied to the formation of the ions of mass 73 and 87 in the mass spectrum (Fig. 5) of **8**. The former was shifted to *m/e* 76 in 70% yield in the trideuterio analog (**8***a*) while *m/e* 87 was located at *m/e* 89 (70%) in the spectrum of this labeled derivative.

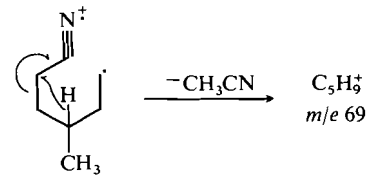

y, *m/e* 110

SCHEME 12

The prominent ions of mass 69 in Figs. 5 and 6 were shown to consist of (for **8**) $C_5H_9^+$ (92%), $C_4H_7N^+$ (5%), and $C_4H_5O^+$ (3%) and (for **9**) $C_5H_9^+$ (80%) and $C_4H_7N^+$ (20%). The hydrocarbon contribution in each instance could arise (metastable ions observed) from the M − OCH_3 species (**y**, *m/e* 110) by the elimination of CH_3CN and formation of $C_5H_9^+$ (Scheme 12). As suggested previously (2*a*), and confirmed from this investigation of labeled methyl cyclohexanone *O*-methyl oxime ethers, their electron impact fragmentation processes are relatively complex with the formation of many ions which serve to complicate interpretation of these mass spectra.

Experimental

Mass spectra were obtained by Mr. R. G. Ross with an

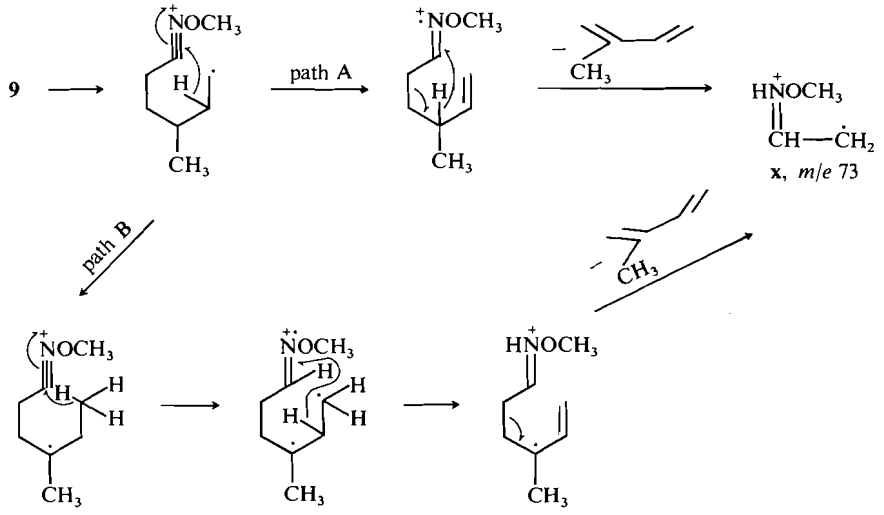

SCHEME 11

MS-9 mass spectrometer operating at 70 eV, 100 μA trap current and an ion source temperature of 180°. Samples were introduced by the heated inlet system (150°) and low voltage measurements refer to nominal values only. High resolution mass measurements were obtained using the MS-9 mass spectrometer interfaced to the ACME computer system of the Stanford University Medical School. The hydrogen transfer processes determined by deuterium labeling are considered accurate to $\pm 5\%$.

Deuterated and non-deuterated α,β-unsaturated ketones were either obtained commercially or prepared according to previously reported procedures (3).

Preparation of O-Methyloximes

The appropriate α,β-unsaturated ketone or cyclic ketone (100 mg) in pyridine (0.2–0.3 ml) was warmed with methoxyamine hydrochloride (100 mg) to 80° for 15 min and then allowed to stand overnight. The reaction was worked up with ether in the usual way and a final purification was achieved by preparative gas chromatography over a 10% SE 30 on Gas Chrom W (60–80) column (1/4 in. × 10 ft).

Preparation of 8a and 9a

The appropriate cyclohexanone was exchanged twice in an excess of D_2O/NaOD for 2 days under reflux. The ketone was isolated by ether extraction and the exchange procedure repeated for an additional 2 days. The deuterated cyclohexanones were then converted to their *O*-methyl oxime derivatives as described above.

The following isotopic purities were obtained: **8***a*, 92% d_3, 5% d_2, 3% d_1; **9***a*, 94% d_4, 4% d_3, 2% d_2.

Financial support from the National Institutes of Health of the U.S. Public Health Service (Grant No. AM 04257 and GM 06840) and the National Aeronautics and Space Administration (NGR 05-020-004) is gratefully acknowledged.

1. See for instance: H. M. FALES and T. LUUKKAINEN. Anal. Chem. **37**, 955 (1965); M. G. HORNING, A. M. MOSS, and E. C. HORNING. Anal. Biochem. **22**, 284 (1968); K. GREEN. Chem. Phys. Lipids, **3**, 254 (1969); F. DRAY and I. WELIKY. Anal. Biochem. **34**, 387 (1970); L. L. ENGEL, A. MUNTO NEVEILLE, J. C. ORR, and P. R. RAGGATT. Steroids, **16**, 377 (1970); C. J. W. BROOKS and D. J. HARVEY. Steroids, **14**, 283 (1970).
2. (*a*) R. G. COOKS and A. G. VARVOGLIS. Org. Mass Spectrom. **5**, 687 (1971); (*b*) B. S. MIDDLEDITCH and B. A. KNIGHTS. Org. Mass Spectrom. **6**, 179 (1972).
3. Y. M. SHEIKH, A. M. DUFFIELD, and C. DJERASSI. Org. Mass Spectrom. **4**, 273 (1970).
4. D. GOLDSMITH, D. BECHER, S. SAMPLE, and C. DJERASSI. Tetrahedron, Suppl. 7, 1945 (1966).
5. J. R. DIAS and C. DJERASSI. Org. Mass Spectrom. In press.

Can. J. Chem. Downloaded from www.nrcresearchpress.com by 210.87.254.42 on 09/05/12
For personal use only.

A New Preparative Method of 1,6-Diketones from Fatty Acids and Vinylmagnesium Chloride

SHOJI WATANABE, KYOICHI SUGA, TSUTOMU FUJITA, AND YUKIO TAKAHASHI

Department of Applied Chemistry, Faculty of Engineering, Chiba University, Yayoicho, Chiba, Japan 280

Received April 11, 1972

The reaction of vinylmagnesium chloride with a fatty acid or its ester in the presence of cuprous chloride gives a 1,6-diketone. From *n*-valeric acid, *n*-tetradecane-5,10-dione is obtained in 53% yield. From methyl *n*-valerate, a mixture of *n*-tetradecane-5,10-dione (33%) and 5-oxo-1-nonene (34%) is obtained.

La réaction du chlorure de vinyle magnésium avec les acides gras et leurs esters, en présence de chlorure cuivreux, donne une dicétone-1,6. A partir de l'acide *n*-valérique, on obtient la *n*-tétradécanedione-5,10 avec un rendement de 53%. A partir du *n*-valérate de méthyle, on obtient un mélange de *n*-tétradécanedione-5,10 (33%) et d'oxo-5 nonène-1. [Traduit par le journal]

Canadian Journal of Chemistry, **50**, 2786 (1972)

Various preparative methods of diketones are known (1). However, a direct synthesis of 1,6-diketones from a fatty acid or its ester has not been known. These authors reported that the reaction of vinylmagnesium chloride with benzoic acid gave 5-oxo-5-phenyl-1-pentene (2). We have found that such a reaction in the presence of cuprous chloride with fatty acids gives 1,6-diketones, and that with methyl esters leads to a mixture of 1,6-diketones and vinyl ketones.

Thus, vinylmagnesium chloride (0.2 mol) in tetrahydrofuran was added to a mixture of *n*-valeric acid (**1**) (0.05 mol) and cuprous chloride (0.05 mol), the reaction mixture was agitated for 8 h, and allowed to stand overnight. Decomposition of excess Grignard reagent with saturated ammonium chloride solution, and work-up gave *n*-tetradecane-5,10-dione (**2**) in 53% yield. Various 1,6-diketones were prepared

$$\underset{\mathbf{1}}{CH_3CH_2CH_2CH_2COOH} \xrightarrow[CuCl]{CH_2=CHMgCl} CH_3CH_2CH_2CH_2\overset{\overset{O}{\|}}{C}CH_2CH_2CH_2CH_2\overset{\overset{O}{\|}}{C}CH_2CH_2CH_2CH_3$$

2

from fatty acids and the results are listed in Table 1.

From the reaction of methyl *n*-valerate with vinylmagnesium chloride in the presence of cuprous chloride, a mixture of compound **2** (yield, 33%) and 5-oxo-1-nonene (**3**) (yield, 34%) was obtained. From the reaction of other esters of fatty acids, similar mixtures were obtained (Table 1). However, the reaction of benzoic acid gave 1,6-diphenyl-1,6-hexanedione in poor yield.

$$CH_3CH_2CH_2CH_2COOCH_3 \xrightarrow[CuCl]{CH_2=CHMgCl} CH_3CH_2CH_2CH_2\overset{\overset{O}{\|}}{C}CH_2CH_2CH_2CH_2\overset{\overset{O}{\|}}{C}CH_2CH_2CH_2CH_3$$

2

$$CH_3CH_2CH_2CH_2\overset{\overset{O}{\|}}{C}CH_2CH_2CH{=}CH_2$$

3

This procedure for the synthesis of 1,6-diketones from fatty acids or their esters and vinylmagnesium chloride is a new useful method.

Experimental

Reaction of Vinylmagnesium Chloride with n-Valeric Acid (1)

A solution of vinylmagnesium chloride (0.2 mol) in tetrahydrofuran was prepared from magnesium and gaseous vinylchloride as reported previously (3, 4). The solution was then added to a mixture of *n*-valeric acid (5.1 g, 0.05 mol) and cuprous chloride (4.95 g, 0.05 mol) at room temperature. The reaction mixture was agitated for 10 h at room temperature and worked-up with aqueous ammonium chloride. The mixture was repeatedly extracted with isopropylether, the extract dried, solvent removed, and the residue distilled *in vacuo* to give 3.0 g of compound **2**; b.p. 120°/5 Torr; m.p. 57°; i.r. (cm^{-1}): 1700 (>C=O); n.m.r. (δ, p.p.m.): 1.4 (6H, triplet, CH_3—), 1.9 (12H, multiplet, —CH_2—), 2.3 (8H, triplet, —CH_2—CO—CH_2—).

Anal. Calcd. for $C_{14}H_{26}O_2$: C, 74.30; H, 11.58. Found: C, 74.29; H, 11.53.

The same technique was used on the reaction of vinylmagnesium chloride with other carboxylic acids. These products are listed in Table 1. The physical constants of these compounds are as follows.

Can. J. Chem. Downloaded from www.nrcresearchpress.com by 210.87.254.6 on 09/05/12
For personal use only.

TABLE 1. Reaction of fatty acids or their esters with vinylmagnesium chloride

Acid or Ester	Product	Yield (%)
Propionic acid	3,8-Decadione (1)*	1
n-Butyric acid	4,9-Dodecadione (2)*	2
iso-Butyric acid	2,9-Dimethyl-3,8-decadione (3)*	24
n-Valeric acid	5,10-*n*-Tetradecadione (4)*	53
n-Caproic acid	6,11-*n*-Hexadecadione (5)*	20
Methyl propionate	3,8-Decanedione (1)*	5
	5-Oxo-1-heptene (6)†	17
Methyl *n*-butyrate	4,9-Dodecadione (2)*	19
	5-Oxo-1-octene (7)†	47
Methyl *iso*-butyrate	2,9-Dimethyl-3,8-decadione (3)*	22
	6-Methyl-5-oxo-1-heptene (8)†	31
Methyl *n*-valerate	5,10-*n*-Tetradecadione (4)*	33
	5-Oxo-1-nonene (9)†	34
Methyl *n*-caproate	6,11-*n*-Hexadecadione (5)*	6
	5-Oxo-1-decene (10)†	40
Methyl enanthate	7,12-Octadecanedione (12)*	5
	5-Oxo-1-undecene (11)†	22
Methyl *n*-caprylate	8,13-Eicosanedione (14)*	7
	5,Oxo-1-dodecene (13)†	28
Methyl pelargonate	9,14-*n*-Docosanedione (16)*	11
	5-Oxo-1-tridecene (15)†	17
Methyl *n*-caprate	10,15-*n*-Tetracosanedione (18)*	6
	5-Oxo-1-tetradecene (17)†	24
Methyl benzoate	1,6-Diphenyl-1,6-hexanedione (20)*	5
	5-Phenyl-5-oxo-1-pentene (19)†	6

*Elementary analyses (carbon and hydrogen) agreed with the calculated data.
†Identified by comparison of i.r., n.m.r., and gas chromatography with those of authentic samples (5).

4,9-Dodecanedione: m.p. 57°, b.p. 87°/10 Torr; 2,9-dimethyl-3,8-decanedione: b.p. 80°/5 Torr; n_D^{27} 1.4425; 6,11-*n*-hexadecanedione: m.p. 71°, b.p. 160°/5 Torr; 7,12-octadecanedione: m.p. 80°; 8,13-eicosanedione: m.p. 83°; 9,14-docosanedione: m.p. 88°; 10,15-*n*-tetracosanedione: m.p. 92°; 1,6-diphenyl-1,6-hexanedione: m.p. 105°; u.v. (MeOH) λ_{max} 243 (ε 25 800), 279 mμ (ε 8650).

Reaction of Vinylmagnesium Chloride with Methyl n-Valerate

Vinylmagnesium chloride (0.4 mol) in tetrahydrofuran was added to a mixture of methyl *n*-valerate (11.6 g, 0.1 mol) and cuprous chloride (9.9 g, 0.1 mol) in tetrahydrofuran (50 ml) at 0° under nitrogen. The reaction mixture was agitated for 7 h at room temperature and worked-up in the usual manner to give 3.7 g (yield 33%) of compound **3** (b.p. 86°/7 Torr) and 4.8 g (yield 34%) of the compound **2** (b.p. 138°/7 Torr). The same technique was used on the other esters. The products are listed in Table 1.

1. R. B. WAGNER and H. D. ZOOK. Synthetic organic chemistry. John Wiley & Sons, Inc. 1953.
2. K. SUGA, S. WATANABE, Y. YAMAGUCHI, and M. TOHYAMA. Syn. 189 (1970).
3. S. WATANABE, K. SUGA, Y. SUEMATSU, and T. SUZUKI. Aust. J. Chem. **21**, 531 (1968).
4. H. NORMANT. J. Org. Chem. **22**, 1602 (1957).
5. S. WATANABE, K. SUGA, and Y. YAMAGUCHI. J. Appl. Chem. Biotechnol. **22**, 43 (1972).

Can. J. Chem. Downloaded from www.nrcresearchpress.com by 210.87.254.6 on 09/05/12
For personal use only.

Doubling Proton Magnetic Resonance Signals by Use of Tris(dipivalomethanato)europium(III)

P. JOSEPH-NATHAN, J. E. HERZ, AND V. M. RODRÍGUEZ[1]

Departamento de Química del Centro de Investigación y de Estudios Avanzados, Instituto Politécnico Nacional, P.O. Box 14-740, México 14, D.F., México

Received January 18, 1972

Doubling of some p.m.r. signals from some steroidal diastereoisomers following treatment with the shift reagent, $(DPM)_3Eu(III)$, is reported for the first time. Similar examination of the hemithioethyleneketal of methyl isopropyl ketone provided the first evidence for the diastereotopic nature of the methyl groups of the isopropyl moiety of this compound. The resolution of signals from diastereoisomers and the failure to detect the diastereotopic nature of the methylene protons of different hemithioethyleneketals is discussed briefly in terms of inhibition of free rotation in pseudocontact association.

Le dédoublement de certains signaux p.m.r. à la suite du traitement par le $(DPM)_3Eu(III)$ de certains stéroïdes diastéréoisomères, est rapporté pour la première fois. De même, l'examen de l'hémithioéthylénecétal de la méthyl isopropyl cétone fournit la première preuve de la nature diastéréotopique des groupes méthyles de la partie isopropyle dans ce composé. La résolution des signaux à partir des diastéréoisomères et l'échec dans la détection de la nature diastéréotopique des protons du méthylène de divers hémithioethylènecétals sont discutés brièvement en fonction de la rotation libre inhibée dans l'association par pseudo contact.

[Traduit par le journal]

Canadian Journal of Chemistry, **50**, 2788 (1972)

The determination of the optical purity of enantiomeric mixtures by n.m.r. has been approached in several ways (1, 2). The magnetic non-equivalence of diastereotopic nuclei is detected either by suitable derivation (2–5) or by the use of chiral solvents (6).

Nuclei which are diastereotopic[2] must have different chemical shifts in both achiral and chiral solvents. However, in many cases the non-equivalence is not large enough to be observed even with superconducting magnets and therefore the nuclei show apparent accidental coincidence of n.m.r. signals. In extreme cases, it has been found that while the p.m.r. spectra gave only one doublet for two methyl groups of an isopropyl moiety, the carbon-13 magnetic resonance spectra (7, 8) showed a signal for each methyl.

Achiral solvent-induced changes in the magnitude of the chemical shift non-equivalence for diastereotopic nuclei are well known (*i.e.* the use of benzene). Because this method is limited in application by the nature of solvent–substrate interaction, the use of shift reagent was investigated to determine the utility of these agents in pseudocontact interaction with diastereotopic substrates. Recently the use of optically active shift reagents has been reported for the determination of enantiomeric purity (9–11).

In the present communication we describe the use of tris(dipivalomethanato)europium(III) in carbon tetrachloride solutions for both the resolution of the p.m.r. signals of diastereoisomeric mixtures and for the detection of the diastereotopic nature of the methyl groups of an isopropyl moiety. In both cases, doubling of the p.m.r. signals was caused by the shift reagent.

The formation of tetrahydropyranyl ethers from steroidal alcohols and dihydropyran results in the creation (12) of a new chiral center. The product is a mixture of diastereoisomers and we know of no case where the presence of both constituents has been visualized unequivocally.

When 3β-tetrahydropyranyloxy-5α-cholestane (**1**) (13), 3β-tetrahydropyranyloxy-cholest-5-ene (**2**) (14), 3β-(1′-methoxyethoxy)-5α-cholestane (**3**), and 3β-(1′-methoxyethoxy)-cholest-5-ene (**4**) were subjected to p.m.r. analysis in the

[1]Present address: Escuela de Ciencias Químicas, Universidad Michoacana de San Nicolás de Hidalgo, Morelia, Mich., México.

[2]This description was introduced by Kessler (19) in reference to "degenerate isomers" for which he proposed the term "topomers"; thus magnetically non-equivalent groups are also termed "diastereotopic groups"; see also Ref. 20.

Can. J. Chem. Downloaded from www.nrcresearchpress.com by 210.87.254.40 on 09/05/12
For personal use only.

Can. J. Chem. Downloaded from www.nrcresearchpress.com by 210.87.254.40 on 09/05/12
For personal use only.

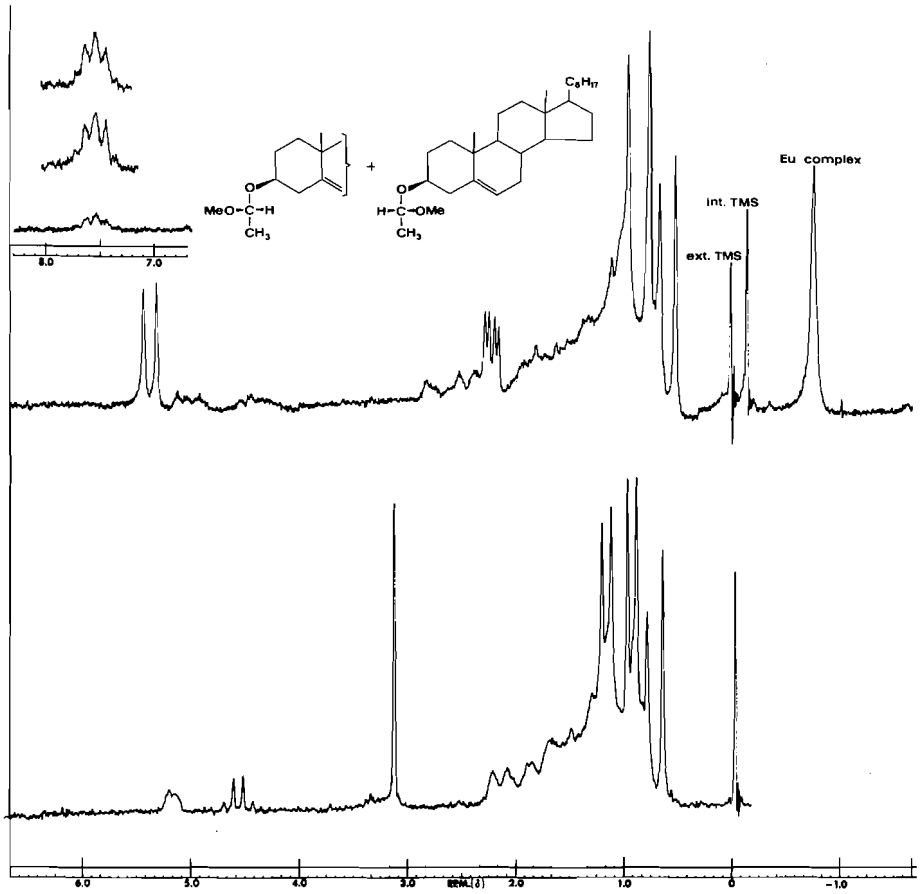

FIG. 1. P.m.r. spectra of 0.1 mmol of 3β-(1′-methoxyethoxy)-cholest-5-ene before and after the addition of 0.014 mmol of $(DPM)_3Eu(III)$ in 0.3 ml of CCl_4.

presence of $(DPM)_3$(III), various signals showed duplicity. This is attributable to the two diastereoisomeric constituents of these ketals. The results obtained with 3β-(1′-methoxyethoxy)-cholest-5-ene (**4**) are shown in Fig. 1.

It can be seen that the doublet ($J = 5.2$ Hz) centered at 1.20 p.p.m., which corresponds to the methyl group of the acetaldehyde moiety, is resolved into two partially superimposed doublets ($J = 5.2$ Hz each) centered at 2.18 and 2.22 p.p.m. (from external TMS (15)). The singlet at 3.15 p.p.m., corresponding to the methoxyl group, is resolved into two singlets at 5.32 and 5.43 p.p.m. respectively, which can be integrated for diastereoisomeric ratio estimations. The signal of the proton attached to the carbon bearing both oxygens of the ketal is originally found as a quartet ($J = 5.2$ Hz) centered at 4.58 p.p.m. After the addition of the shift reagent (Fig. 1) the signal appears as a quintet ($J = 5.2$ Hz) of relative intensities 1:4:6:4:1 centered at 7.55 p.p.m. which results from a partial overlap of two quartets of relative intensities 1:3:3:1 arising from a first order spin–spin coupling with the protons of the 2′-methyl group. In this experiment the C-19 methyl group shifts from 1.00 to 0.95 p.p.m. while the C-18 angular methyl shifts from 0.67 to 0.50 p.p.m. The C-21 protons are obscured by the rest of the signals and could not be assigned but the isopropyl methyl groups of the side chain shift from 0.87 to 0.72 p.p.m.

Straight lines are obtained when the shifts of the various protons (abscissa) are plotted (15)

TABLE 1. Induced chemical shifts in p.p.m.*

Observed signal	Compound 1	2	3	4
H-3	10.0	11.0	8.0	9.0
OCH	26.7	26.0–24.5	23.4–23.0	24.5–21.0
OCH_2	23.0–19.0	26.0–24.0	—	—
OCH_3	—	—	19.5	18.5–17.0
CH—CH_3	—	—	8.7– 8.6	10.0– 7.0
H-6	—	2.5– 1.5	—	2.5– 1.5

*Determined for 0.1 mmol substrate plus 0.1 mmol shift reagent in 0.3 ml of CCl_4.

against increasing quantities of europium complex (ordinate). The inverse of the slopes of these lines, which represent the shift in p.p.m. when 1 mol of $(DPM)_3Eu(III)$ per mol of the substrate is present, are listed in Table 1.

The first entries in Table 1 correspond to the signal which is shifted most and the second one to the same proton of the other diastereoisomer. Some multiplets became broader due to partial resolution of the signals of the diastereoisomers but it is very difficult to assign chemical shifts to each constituent of such signals. In these cases Table 1 shows the overall center of the multiplets.

Although it is very difficult to determine which of the two diastereoisomers shifts more, the difference in chemical shifts is in some cases sufficient to observe two separated resonances for the protons of the C-19 angular methyl group when an adequate amount of the shift reagent is added to the diastereoisomeric mixture.

Although the ketals (**1**–**4**) are mixtures of two diastereoisomers, in the absence of shift reagents they display p.m.r. spectra of a single compound. There should be a fast (on the n.m.r. time scale) free rotation of the steroidal 3β-substituents and the chemical shifts of the various protons will therefore correspond to averages of conformers. Since europium complexes interact with 3-substituted steroids in a stereospecific way (15), upon addition of the bulky shift reagent, the association will decrease the conformational liberty of the 3β-substituent, which will now have different chemical environment, thus permitting the observation of both constituents of the mixture.

In order to obtain additional evidence for the free rotation inhibition process, a series of simple pure molecules (no stereoisomeric mixtures), which should fulfill the sterical requirements for the duplication of p.m.r. signals, were prepared and analyzed.

The most striking results were obtained with the hemithioethyleneketal of methyl isopropyl ketone (**5**). Its n.m.r. spectrum showed the presence of the methyl group as a singlet at 1.45 p.p.m., the isopropyl moiety as a heptet ($J = 7$ Hz) centered at 2.00 p.p.m. and a doublet ($J = 7$ Hz) centered at 0.96 p.p.m. The ethylene protons appeared as two complex signals at 4.05 and 2.95 p.p.m. The chemical shifts of all signals were measured from the TMS signal of a capillary tube containing also carbon tetrachloride (*vide infra*). In the absence of shift reagents this external TMS signal is coincident with the internal TMS resonance frequency. It is important to mention that the line widths at half height of the signals of the doublet at 0.96 p.p.m. were similar to the line width of the TMS signals. Upon addition of the $(DPM)_3Eu(III)$ complex only small shifts of several signals to lower fields occur, since the ketal does not associate well with the europium reagent. However the isopropyl methyl groups now appear as two partially superimposed doublets ($J = 7$ Hz each) at 0.93 and 0.87 p.p.m. from external TMS.

The doubling of the signals of the isopropyl group of compound **5** indicates the diastereotopic nature of the methyl groups. The association process inhibits the free rotation of the group and therefore the methyl groups are now found in different chemical environments. When the isopropyl group is separated by an additional carbon atom from the association site, as in the hemithioethyleneketal of methyl isobutyl ketone (**6**) (16), the doubling of signals is no longer observed, nor is it observed to

Can. J. Chem. Downloaded from www.nrcresearchpress.com by 210.87.254.40 on 09/05/12
For personal use only.

Can. J. Chem. Downloaded from www.nrcresearchpress.com by 210.87.254.40 on 09/05/12
For personal use only.

reveal the diastereotopic nature of the methylene protons of the hemithioethyleneketals derived from methyl ethyl ketone (**7**) (16), methyl propyl ketone (**8**) or diethyl ketone (**9**). This suggests that the process of inhibition of rotation must fill some strict steric requirements to be observable. The only other cases in which similar observations are reported correspond to some sulfoxides (17).

Experimental

Melting points are uncorrected. Optical rotations were measured in chloroform solution using a Perkin–Elmer 141M polarimeter. N.m.r. measurements were performed on a Varian Associates A-60 spectrometer operated at normal probe temperature in carbon tetrachloride solutions with internal TMS and a capillary containing TMS in carbon tetrachloride. Solutions of 0.1 mmol of the compounds in 0.3 ml solvent were utilized. Microanalytical determinations were carried out by Mr. Joseph F. Alicino, New Hope, Pa.

The hemithioethylene ketals derived from methyl isopropyl ketone, from methyl propyl ketone, and from diethyl ketone were prepared using the method of Djerassi and Gorman (16). N.m.r. spectra confirmed their structures and purity.

The steroidal ketals were prepared according to the procedure of Herz *et al.* (18). 3β-(1′-Methoxyethoxy)-5α-cholestane (**3**) showed m.p. 62–63°, $[\alpha]_D$ +15°.

Anal. Calcd. for $C_{30}H_{54}O_2$: C, 80.65; H, 12.18. Found: C, 80.50; H, 12.21.

3β-(1′-Methoxyethoxy)-cholest-5-ene (**4**) showed m.p. 91–92°, $[\alpha]_D$ −55°.

Anal. Calcd. for $C_{30}H_{52}O_2$: C, 81.02; H, 11.79. Found: C, 80.85; H, 11.54.

Proton Magnetic Resonance Measurements

Solutions of 0.1 mmol of the substrate were weighed directly in an n.m.r. tube to which 0.3 ml of CCl_4 were added. The capillary was inserted and the spectrum recorded. Successive additions of 5 mg of $(DPM)_3Eu(III)$ and spectra determination were carried out until no more shift reagent could be dissolved. The shifts of the various protons and the corresponding substrate shift reagent ratios were graphed as previously shown (15).

1. P. Joseph-Nathan and E. Díaz. Introducción a la resonancia magnética nuclear. Limusa–Wiley, Mexico City, 1970. p. 131.
2. M. Raban and K. Mislow. Top. Stereochem. **2**, 199–230 (1967).
3. J. A. Dale and H. S. Mosher. J. Am. Chem. Soc. **90**, 3732 (1968).
4. D. R. Galpin and A. C. Huitric. J. Org. Chem. **33**, 921 (1968).
5. J. P. Casey, R. L. Lewis, and K. Mislow. J. Am. Chem. Soc. **91**, 2789 (1969).
6. W. H. Pirkle and S. D. Beare. Tetrahedron Lett. 4039 (1967); J. Am. Chem. Soc. **89**, 5487 (1967); **91**, 5150 (1969).
7. J. I. Kroschwitz, M. Winokur, H. J. Reich, and J. D. Roberts. J. Am. Chem. Soc. **91**, 5927 (1969).
8. P. Joseph-Nathan, Ma. P. González, L. F. Johnson, and J. N. Shoolery. Org. Magn. Res. **3**, 23 (1971).
9. G. M. Whitesides and D. W. Lewis. J. Am. Chem. Soc. **92**, 6997 (1970); **93**, 5914 (1971).
10. H. L. Goering, J. N. Eikenberry, and G. S. Koermer. J. Am. Chem. Soc. **93**, 5913 (1971).
11. R. R. Fraser, M. A. Petit, and J. K. Saunders. Chem. Commun. 1450 (1971).
12. C. Djerassi. Steroid reactions. Holden–Day, San Francisco. 1963. p. 76.
13. M. Kielczewski and Z. Parysek. Chem. Abstr. **69**, 87305 (1968).
14. A. C. Ott, M. F. Murray, and R. L. Peduson. J. Am. Chem. Soc. **74**, 1239 (1952).
15. J. E. Herz, V. M. Rodríguez, and P. Joseph-Nathan. Tetrahedron Lett. 2949 (1971).
16. C. Djerassi and M. Gorman. J. Am. Chem. Soc. **75**, 3704 (1953).
17. K. K. Andersen and J. J. Uebel. Tetrahedron Lett. 5253 (1970).
18. J. E. Herz, J. Lucero, Y. Santoyo, and E. S. Waight. Can. J. Chem. **49**, 2418 (1971).
19. H. Kessler. Angew. Chem. Int. Ed. **9**, 219 (1970).
20. G. Binsch, E. L. Eliel, and H. Kessler. Angew. Chem. Int. Ed. **10**, 570 (1971).

A Curious Synthesis of some μ_4-Oxo-hexa-μ-halotetracopper(II) Complexes

B. CARR AND J. F. HARROD

Department of Chemistry, McGill University, Montreal, Quebec

Received March 29, 1972

The thermal decomposition of a series of phenoxo complexes of copper(II), in solution, containing either trichlorophenoxo or tribromophenoxo ligands and a variety of neutral ligands, has led to a rather unique method for the synthesis of μ_4-oxo-hexa-μ-halotetracopper(II) complexes. The yield of this complex was found to increase considerably with the ability of the solvent to autoxidize, and also with the addition of hydroperoxides.

La décomposition thermique d'une série de complexes phenoxo cuivre(II), en solution, contenant des ligands soit de trichlorophenoxo ou de tribromophenoxo et une variété de ligands neutres, a conduit à une méthode de synthèse plutôt unique de complexes de μ_4-oxo-hexa-μ-halotétra-cuivre(II). On constate que le rendement en complexe croît considérablement avec le pouvoir d'autoxydation du solvant ainsi que par addition d'hydroperoxydes.

Canadian Journal of Chemistry, **50**, 2792 (1972)

Introduction

For several years the mechanism of the reactions in [1] has been investigated in our laboratory. These reactions may be carried out in solution in organic solvents, or in the solid state (1, 2).

It has long been recognized that reaction 1 is an idealized equation since the polymers **3** are well known to be branched (1). Even more important, it is also known that these polymers have only modest number average molecular weights ($10^4 - 10^5$), not essentially infinite molecular weights as required by the exact stoichiometry of reaction 1.

In the course of a spectrophotometric study of reaction 1 in benzene, or toluene as solvent and with the complex bis(2,4,6-trichlorophenoxy)bis(pyridine)copper(II), **1***a*, as reactant, it was noted that the absorbance of the solutions did not go to negligibly small levels at 22 500 cm^{-1} on completion of reaction, as expected. The dichloro complex, **2***a*, is completely insoluble, and even on removal of **3***a* from solution, the anomalous absorption remained. This result suggested the presence of a hitherto unidentified reaction product.

A careful workup of reaction products yielded a small amount of golden crystals which proved to be the complex μ_4-oxo-μ-hexahalotetrakis(pyridine copper(II)), previously prepared and characterized by Kilbourn and Dunitz (3). The structure of the complex was confirmed by X-ray crystallography.[1] Further work described in the present paper revealed that formation of μ_4-oxo-copper(II) complexes is a common feature of the decomposition of phenoxocopper(II) complexes in the presence of oxygen, or hydrocarbon hydroperoxides.

[1] 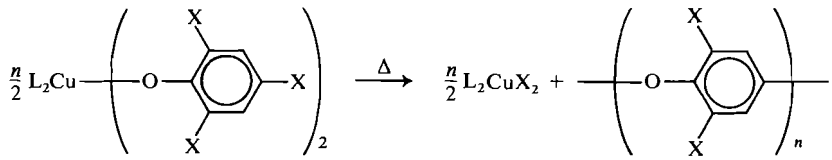

1 **2** **3**

$L = C_5H_5N$;	$X = Cl$: *a*
C_5H_5N;	Br: *b*
$C_2H_5NH_2$;	Cl: *c*
$(C_6H_6)_3PO$;	Cl: *d*
NH_3;	Cl: *e*
$(CH_3)_2NCHO$;	Cl: *f*
$(CH_3)_2SO$;	Cl: *g*

[1]Data obtained for us by Dr. P. Bird of Sir George Williams University, Montreal, Quebec.

Can. J. Chem. Downloaded from www.nrcresearchpress.com by 210.87.254.5 on 09/05/12
For personal use only.

Can. J. Chem. Downloaded from www.nrcresearchpress.com by 210.87.254.5 on 09/05/12
For personal use only.

Several μ_4-oxo-hexa-μ-halotetracopper(II) complexes have been prepared by other workers, where X is bromine or chlorine, and L is a variety of neutral and anionic ligands (4–8). These complexes were usually prepared in a straightforward manner by refluxing $CuCl_2$ and CuO in various reaction media, and collecting the desired crystals after a few days. Because of the importance of these complexes in understanding the mechanism of reaction 1, we decided to investigate the generality of our own observations.

Results

Decomposition of Bis(2,4,6-trichlorophenoxy) bis(pyridine)copper(II)

The decomposition of **1***a* in benzene in air produced a coarse crystalline precipitate of **2***a* in almost quantitative yield. After filtration and drying, the latter precipitate, under microscopic examination, was found to be contaminated by a small amount of crystalline **4***a* which could be removed by extraction with methylene chloride or acetone. The amount of **4***a* in the precipitate was usually about 3% by weight, and a trace amount was in solution in the reaction solvent.

Repetition of the above procedures in toluene and in cumene as reaction solvents gave **4***a* in *ca.* 15 and 100% yields, respectively. Repetition of the reaction in benzene in the presence of a five-to-one molar ratio of cumylhydroperoxide to **1***a* gave a near quantitative yield of **4***a*.

A series of decomposition of **1***a* in benzene in the presence of some common free radical initiators was followed spectrophotometrically. The results are shown in Fig. 1. Although all of the initiators caused a diminution of the normally observed induction period, the behavior of hydroperoxides was distinctly different from that of peroxide and azo initiators. It is evident that hydroperoxides undergo a very rapid reaction with the starting complex that is qualitatively different from that occurring with other initiators. This difference is also reflected in the difference in the reaction products, as listed in Table 1.

Synthesis of Other μ_4-Oxo-copper(II) Complexes

The synthesis of a number of other μ_4-oxo-copper(II) complexes was attempted by first preparing the starting complex **1** and then decomposing in the same manner as with the formation of **4***a*.

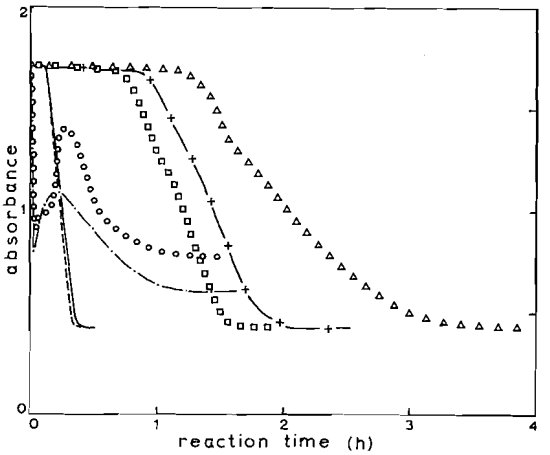

FIG. 1. Decomposition of bis(pyridine)bis(2,4,6-trichlorophenolato)copper(II) at 72 °C in benzene in the presence of a 10:1 molar ratio (I/Cu) of various initiators; absorbance at 22.5 kK: △, no initiator; -+-, *t*-butyl peroxide; □, dicumyl peroxide; —, benzoyl peroxide; ---, 2,2′-azobis[propionitrile]; ·-·, *t*-butyl hydroperoxide; ○, cumene hydroperoxide.

TABLE 1. Effect of various initiators on the reaction products in the decomposition of bis(pyridine)bis(2,4,6-trichlorophenolato) copper(II) in benzene at 72 °C; molar ratio 5:1 I/Cu

Initiator	Wt. % μ_4-oxo*
No initiator	4
Benzoyl peroxide	3
t-Butyl peroxide	4
Dicumyl peroxide	3
t-Butyl hydroperoxide	100
Cumene hydroperoxide	100

*Precipitated reaction product is a mixture of Py_2CuCl_2 and $Py_4Cu_4Cl_6O$.

μ_4-Oxo-hexa-μ-bromotetrakis(pyridine copper(II))

Decomposition of bis(2,4,6-tribromophenoxy)bis(pyridine)copper(II), compound **1***b*, in benzene or toluene produced a green crystalline precipitate which was shown to be Py_2CuBr_2 (**2***b*), by infrared and far-infrared spectroscopy, in quantitative yield. Further extraction with benzene and methylene chloride showed no additional complexes.

Decomposition of **1***b* in cumene gave a dark green precipitate which was found to be a mix-

Can. J. Chem. Downloaded from www.nrcresearchpress.com by 210.87.254.5 on 09/05/12
For personal use only.

TABLE 2. Infrared data for various dihalo- and μ_4-oxo-copper(II) complexes*

Complex	Absorption frequency (cm^{-1})																
$(C_5H_5N)_2CuCl_2$†	1605 1599	1572	1490	1449	1366	1242	1220	1154	1080 1065	1044	1020 1011	951	876	762	690	648	
$(C_5H_5N)_4Cu_4Cl_6\cdot O$	1605 1599	1572	1488	1449	1362	1242	1219	1158 1148	1070	1050	1020 1010	960	890	772 768 762	705 700	665	576‡
$(C_5H_5N)_2CuBr_2$†	1605 1598	1572	1490	1449	1366	1240	1220	1161 1156	1082 1075	1049	1021 1015	950	875	762	692	650	
$(C_5H_5N)_4Cu_4Br_6\cdot O$	1605 1598	1570	1486	1444	1368	1239	1219	1156 1150	1072	1049	1021 1015	955	890	772 770 764	702 698	650	535‡
$[(C_6H_5)_3PO]_2CuCl_2$	1590 1575		1485	1436 1397	1332 1313	1277	1190 1185 1170	1155 1140§ 1115	1090 1084 1070	1029	1000 984 975	931	869 864 854	760 754	728 700		
$[(C_6H_5)_3PO]_4Cu_4Cl_6\cdot O$	1590 1575		1484	1433 1396	1340 1318	1262	1194‖ 1180	1120‖ 1100	1070	1035	1001 975	935	860	768 760 753	730 700		535
$(C_2H_5NH_2)_4Cu_4Cl_6\cdot O$		1572	1468	1450 1395 1880	1360		1198		1068	1045			892 805			650	582
$[(CH_3)_2N\cdot CHO]_4Cu_4Cl_6\cdot O$	1635		1492	1430	1366	1250		1115		1059	1009				710		580‡

*Data cited for spectra in KBr pellets.
†Agrees with ref. 15.
‡Agrees with ref. 5; data cited for Nujol mull on KBr plates.
§Agrees with ref. 16 for P=O stretch at 1142 cm^{-1}.
‖Agrees with ref. 17 for P=O stretch.

TABLE 3. Far-infrared data for various dihalo- and μ_4-oxo-copper(II)*

Complex	Absorption frequency (cm^{-1})									
$(C_5H_5N)_2CuCl_2$§			291	268		235	202		178	
$(C_5H_5N)_4Cu_4Cl_6\cdot O$					247†		202			
$(C_5H_5N)_2CuBr_2$§				267	255		205	194‡		128
$(C_5H_5N)_4Cu_4Br_6\cdot O$						220,	200		166,	135
$[(C_6H_5)_3PO]_2CuCl_2$	330	300	289	267				189	168	
$[(C_6H_5)_3PO]_4Cu_4Cl_6\cdot O$			293		257,	234		195,	170	
$(C_2H_5NH_2)_2CuCl_2$‖		313		263	250‡			186		
$(C_2H_5NH_2)_4Cu_4Cl_6\cdot O$				270			209			
$[(CH_3)_2N\cdot CHO]_4Cu_4Cl_6\cdot O$					240			194		
$[(CH_3)_2SO]_4Cu_4Cl_6\cdot O$					240			186		

*Data cited for Nujol mull on polyethylene plates.
†For all μ_4-oxo complexes, bracket under absorption indicates broad band.
‡Shoulder.
§Agrees with ref. 15.
‖Reproduced from ref. 11.

ture of approximately 60% **2***b* and a dark brown complex which on extraction with THF and recrystallization by evaporation was shown to be $Py_4Cu_4Br_6\cdot O$ (**4***b*), by infrared spectroscopy and elemental analysis. Repetition of the decomposition in benzene, in the presence of a one-to-one molar ratio of cumene hydroperoxide to **1***b* gave only a small trace of the μ_4-oxo complex.

μ_4-Oxo-hexa-μ-chlorotetrakis ((ethylamine)copper(II))

Thermal decomposition of **1***c* in benzene, toluene, or cumene, or in benzene in the presence of a hydroperoxide yielded only intractable products, possibly due to autoxidation of the ethylamine ligand. However, catalyzed decomposition in the presence of traces of carbon tetrachloride[2] yielded a precipitate which contained 75% of a lime-green methylene chloride – soluble complex and an intractable gold colored residue. Spectra and elemental analyses of the methylene chloride soluble complex were in accord with those expected for the complex $(C_2H_5NH_2)_4Cu_4Cl_6O$ (**4***c*).

μ_4-Oxo-hexa-μ-chlorotetrakis ((triphenylphosphine oxide)copper(II))

We have thus far been unable to prepare and characterize a stable bis(trichlorophenoxo)bis(triphenylphosphine oxide)copper(II) (**1***d*), because of the extreme ease with which this complex loses neutral ligand. However, a mixture of copper(II) trichlorophenolate and triphenylphosphine oxide (both individually completely insoluble in cumene) in cumene gave a dark brown solution which on thermal decomposition precipitated a large amount of orange-yellow powder, admixed with a small amount of green material. Extraction of this mixture with methylene chloride, followed by evaporation, produced a large yield of beautiful well-formed orange crystals. All physical measurements agreed with the formulation of this complex as $(Ph_3PO)_4Cu_4Cl_6O$ (**4***d*), previously synthesized by Bertrand and Kelley by a different method (7).

Other Attempted Syntheses

Attempts have been made to synthesize μ_4-oxo complexes with dimethylformamide, dimethylsulfoxide, or hexamethylphosphoramide as ligand. Although strong evidence for the formation of the desired products in the former two cases was obtained, the extreme facility with which these ligands dissociate has thus far frustrated complete isolation and characterization.

Bis(trichlorophenoxo)diammine copper(II) (**1***e*) was decomposed under all of the various conditions described above. In all cases the complexes produced were intractable and could not be satisfactorily characterized.

Spectra of μ_4-Oxo Complexes

Tables 2 and 3 list the principal infrared and far-infrared absorptions, respectively, of the

[2]Reaction 1 is powerfully catalyzed by traces of carbon tetrahalides. Full details of this phenomenon will be published elsewhere.

Can. J. Chem. Downloaded from www.nrcresearchpress.com by 210.87.254.5 on 09/05/12
For personal use only.

[2] 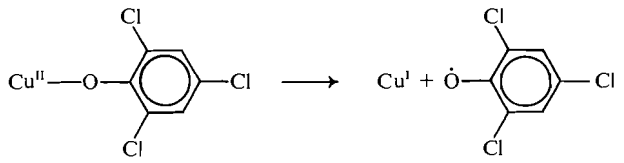

[3] 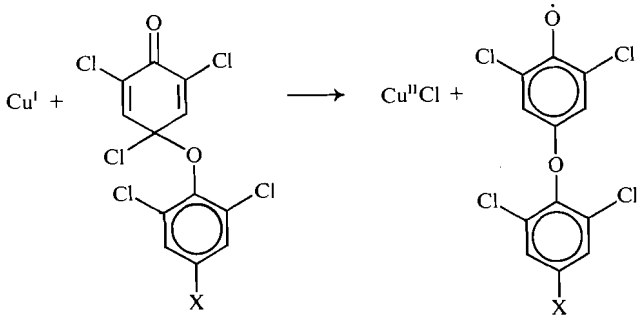

dihalo and μ_4-oxo complexes. tom Dieck and Brehm (5) have reported that a band at 588–515 cm^{-1} assigned to an asymmetric group vibration of the Cu_4O tetrahedron is a facile method of identifying the μ_4-oxo-copper complexes. These reported values in this region, along with values reported by other authors (3, 7) provide substantial support for identification of the μ_4-oxo complexes reported in the present work.

Discussion

The present study indicates that reaction 1 is only a rather poor first approximation to the actual reactants and products involved in the thermal decomposition of **1**. In fact, under the best conditions of purity we have been able to achieve, the decomposition of complex **1***a* exhibits an exceedingly long, perhaps infinite, induction period, suggesting the need for an initiator. There is no doubt that oxygen can function as an initiator and reactions in air exhibit quite reproducible behavior, unlike those carried out under vacuum.

The trends observed for the dependence of yield of **4** on solvent strongly indicated that **4** was a product associated with solvent autoxidation. In the case of reactions in benzene, the small amount of **4** produced possibly results from direct reaction of a copper(I) species with molecular oxygen. The most likely first step in reaction 1 is a homolytic dissociation as shown in reaction 2. Apparently reaction 2 does not occur spontaneously, but may be induced by such species as oxygen, radical initiators, and carbon tetrahalides. If Cu(I) is produced it will be subject to competitive oxidation either by phenol-derived oxidants, as in reaction 3 (9), or by added initiator species.

Oxidation as in reaction 3 will eventually produce the complexes **2**, but introduction of an oxide, or hydroxide, ligand during oxidation by O_2, or ROOH, will produce **4**.

The facts that the effectiveness of non-hydroperoxide initiators follows their ease of decomposition, *cf.* Fig. 1, and that no initiator fragments appeared in product copper complexes with such initiators favor the hypothesis that these initiators function by rapid radical attack on coordinated phenoxide, as in reaction 4, rather than by attack at copper.[3] The extremely rapid reactions of hydroperoxides, as manifest by the very rapid fall in absorbance in Fig. 1, are out of line with their ease of homolytic dissociation relative to the other initiators examined (10). The initial rapid reaction is possibly a simple solvolysis of the phenoxo-copper(II) complex by the moderately acidic hydroperoxide.

Since the μ_4-oxo-μ-hexahalotetracopper(II) nucleus has the stoichiometry $3CuCl_2 \cdot CuO$, the

[3]A study of the decomposition of **1***a* in solution by e.p.r. has shown that no detectable concentrations of free radicals build up in the presence of phenoxo-copper complexes. However, phenoxy radicals do appear *after* the phenoxo-copper complex has largely decomposed, due to the slow dissociation of quinol ethers. Details of this study will be reported elsewhere.

Can. J. Chem. Downloaded from www.nrcresearchpress.com by 210.87.254.5 on 09/05/12
For personal use only.

[4] 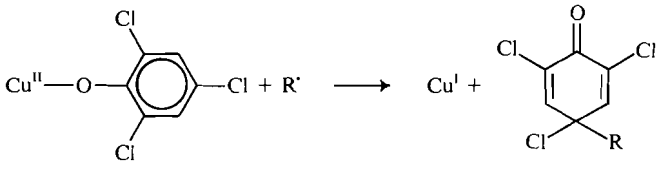

reaction of **1** with hydroperoxides cannot be occurring to the exclusion of reaction 3 and it is clear that a great deal of additional information is required before a definitive understanding of these reactions is achieved.

The much greater reluctance of **1***b* to yield a μ_4-oxo complex is presumably due to a lower reactivity of bromocopper(I) species towards oxidation and a greater selectivity with respect to the appropriate analog of reaction 3. Bromophenoxocopper(II) complexes decompose much more readily than their chloro-analogs and this presumably reflects a greater facility for reaction 2.

Both **1***c* and **1***e* are difficult to decompose in solution and in the presence of oxygen, or hydroperoxides, yield intractable products. It seems very likely that the neutral ligands become involved in an autoxidation sequence in these cases to give polymerized complexes as products. The decomposition of **1***c* in the presence of CCl_4, although probably still a radical chain process, does not involve oxygen and side reactions of the ligand are less serious. Ethylamine complexes of Cu(II) are often oxidatively unstable (11).

The complexes **4***a*, **4***b*, **4***d*, **4***f*, and **4***g* have been reported previously, and their structures have been established either crystallographically or by infrared spectroscopy in the region of 588–515 cm^{-1}. In addition, a number of other $Cu_4OX_6L_4$ complexes have been prepared and their structures determined. The structural features of these complexes have been discussed in some detail by Bertrand and Kelley (7).

The present study indicates that decomposition of halophenoxocopper(II) complexes may provide a fairly general route to the preparation of μ_4-oxo-copper(II) derivatives. However, their appearance as products in reaction 1 is a complicating and avoidable feature, specifically related to the involvement of oxygen in the initiation process. Our continuing studies of the mechanism of reaction 1 are being carried out under conditions where autoxidation does not occur. Unfortunately, the autoxidation feature is unavoidable in the commercially important catalytic oxidative coupling of phenols, but its influence on the reaction is unknown (13, 14).

Experimental

Materials

For the preparation and isolation of the stable L_2Cu(trihalophenolate)$_2$ complexes, all chemicals, including solvents, were of reagent-grade quality and were used without further purification. For the thermal decomposition of these complexes, all solvents were refluxed over CaH_2 and distilled.

Preparation of Phenoxo-Cu(II) Complexes

Copper(II) Trichlorophenolate

Copper(II) trichlorophenolate was prepared by dissolving sodium hydroxide (0.04 mol) in 150 ml of water, adding 2,4,6-trichlorophenol (0.04 mol), and stirring for about 1 h. A solution of $CuSO_4 \cdot 5H_2O$ (0.02 mol) in 150 ml of water was then added. The resulting dark purple-brown precipitate was then washed with methanol to remove any excess phenol. A near quantitative yield of product was obtained.

Pyridine, Ammonia, or Ethylamine as Neutral Ligand

The complexes L_2Cu(trihalophenolate)$_2$, where the halogen is Cl or Br and L is pyridine, ammonia, or ethylamine, were prepared as described previously (2).

Dimethylformamide or Dimethylsulfoxide as Neutral Ligand

Complexes containing dimethylformamide or dimethylsulfoxide as neutral ligand were prepared by dissolving copper(II) trichlorophenolate (0.02 mol) in an excess (100 ml) of either dimethylformamide or dimethylsulfoxide and stirring for 1 h. The solutions were then added to water, with stirring.

In the case of dimethylformamide a dark brown precipitate was obtained which was recrystallized by dissolution in benzene and addition of hexane. The resulting product had the empirical formula $[(CH_3)_2N \cdot CHO] \cdot Cu \cdot [C_6H_2Cl_3O]_2$ and was presumably a formamide bridged dimer analogous to the hexamethylphosphoramide-bridged dimer described by Tsuruya *et al.* (12).

Anal. Calcd. for $[(CH_3)_2N \cdot CHO] \cdot Cu \cdot [C_6H_2Cl_3O]_2$: C, 33.99; H, 2.07; N, 2.64. Found: C, 34.40; H, 2.11; N, 2.53.

In the case of dimethylsulfoxide, deep purple crystals were obtained which decomposed readily in solution precluding purification of the product. Infrared spectroscopy indicated the presence of both trichlorophenolate and dimethylsulfoxide in the complex.

Decomposition of Phenoxo-Cu(II) Complexes

Spectrophotometric Study

Spectrophotometric studies were carried out with a Perkin–Elmer 124 ultraviolet–visible spectrophotometer. Since $(C_5H_5N)_2Cu$(trichlorophenolate)$_2$, **1***a*, shows a maxi-

Can. J. Chem. Downloaded from www.nrcresearchpress.com by 210.87.254.5 on 09/05/12
For personal use only.

Can. J. Chem. Downloaded from www.nrcresearchpress.com by 210.87.254.5 on 09/05/12
For personal use only.

mum absorption at 22 500 cm^{-1}, this is a convenient region for following the decomposition of this complex. The temperature used in all cases was 72 °C.

Preparation of μ_4-Oxo-Copper(II) Complexes

μ_4-Oxo-hexa-μ-chlorotetrakis[pyridine copper(II)]

$(C_5H_5N)_2Cu(trichlorophenolate)_2$ (5 g) was dissolved in cumene (100 ml) and heated in air at 72 °C for 24 h. The resulting precipitate was filtered and extracted with methylene chloride to give gold needle-shaped crystals of $(C_5H_5N)_4Cu_4Cl_6{\cdot}O$ (1.6 g, 97% yield).

Anal. Calcd. for $C_{20}H_{20}N_4Cl_6Cu_4{\cdot}O$: C, 30.03; H, 2.50; N, 7.01; Cl, 26.65; Cu, 31.78; O, 2.00. Found: C, 30.48; H, 2.50; N, 7.04; Cl, 27.06; Cu, 32.29; O, <0.5%.

Molecular weight in methylene chloride, 797. Melted with decomposition at 251 °C.

μ_4-Oxo-hexa-μ-bromotetrakis[pyridine copper(II)]

$(C_5H_5N)_2Cu(tribromophenolate)_2$ (5 g) was dissolved in cumene (100 ml) and heated in air at 50 °C for 24 h. The resulting dark green precipitate was extracted with tetrahydrofuran and recrystallized by evaporation, giving dark brown crystals of $(C_5H_5N)_4Cu_4Br_6{\cdot}O$ (0.6 g, 40% yield).

Anal. Calcd. for $C_{20}H_{20}N_4Br_6Cu_4{\cdot}O$: C, 22.51; H, 1.88; Br, 23.80; Cu, 45.30. Found: C, 23.70; H, 2.01; Br, 23.71; Cu, 45.30.

Melted with decomposition at 217 °C.

μ_4-Oxo-hexa-μ-chlorotetrakis(ethylamine copper(II))

$(Ethylamine)_2Cu(trichlorophenolate)_2$ (2 g) was dissolved in toluene (75 ml) containing carbon tetrachloride (5 ml) and heated at 72 °C for 4 h. The resulting olive-green precipitate (0.7 g), upon extraction with methylene chloride and recrystallization with hexanes, gave a lime-green complex (0.5 g, 82% yield).

Anal. Calcd. for $C_8H_{28}N_4Cl_6Cu_4{\cdot}O$: C, 14.48; H, 4.22; N, 8.45; Cl, 32.31. Found: C, 15.51; H, 4.77; N, 8.91; Cl, 31.44.

Melted with decomposition at 162 °C.

The poor analysis for this compound is probably due to the fact that it decomposes slowly in air.

μ_4-Oxo-hexa-μ-chlorotetrakis(triphenylphosphine oxide copper(II))

The phenoxo-copper(II) complex containing triphenylphosphine oxide as neutral ligand could not be isolated in the solid state, but appeared to be readily obtained in solution by the addition of copper(II) trichlorophenolate (0.01 mol) to triphenylphosphine oxide (0.02 mol) in cumene (125 ml), resulting in a brown solution which was filtered to remove any unreacted materials. This solution was then reacted in air at 72 °C for 24 h. Extraction of the precipitate with methylene chloride and recrystallization gave orange crystals of **4***d*.

Anal. Calcd. for $C_{72}H_{60}P_4Cl_6Cu_4{\cdot}O_5$: C, 54.17; H, 3.76; Cu, 15.92. Found: C, 53.53; H, 3.79; Cu, 15.72.

Melted with decomposition at 239 °C.

μ_4-Oxo-hexa-μ-chlorotetrakis(dimethylformamide copper(II))

(Dimethylformamide)Cu(trichlorophenolate)$_2$ (2 g) was dissolved in cumene (100 ml) and heated in air at 50 °C for 24 h. The resulting yellow-brown precipitate was extracted with methylene chloride. Evaporation gave a yellow crystalline product with an infrared spectrum corresponding to that reported for compound **4***f*.

μ_4-Oxo-hexa-μ-chlorotetrakis(dimethylsulfoxide copper(II))

(Dimethylsulfoxide)Cu(trichlorophenolate)$_2$ (2 g) was dissolved in cumene (100 ml) and heated in air at 50 °C for 24 h resulting in a yellow-brown precipitate containing a mixture of copper complexes. Isolation by extraction with methylene chloride led to further decomposition. However, an infrared spectrum of the unextracted yellow-brown precipitate gave an absorption at 583 cm^{-1}, suggesting the presence of $[(CH_3)_2SO]_4Cu_4Cl_6{\cdot}O$ (5).

Infrared Spectroscopy

Infrared spectra in the range 4000–625 cm^{-1} were measured with a Perkin–Elmer Model 257 Grating Spectrophotometer. Samples were dispersed in potassium bromide pellets.

Infrared spectra in the range 625–470 cm^{-1} were measured with a Perkin–Elmer Model 521 Spectrophotometer. Samples were measured in a Nujol mull on potassium bromide plates.

Far-infrared spectra were measured in a Nujol mull using a Perkin–Elmer Model FIS-3 Spectrophotometer.

The authors would like to thank Dr. P. Bird of Sir George Williams University, Montreal, Quebec, for the X-ray analysis of μ_4-oxo-hexa-μ-chlorotetrakis(pyridine copper (II)) complex. Financial support for this work from the National Research Council of Canada is gratefully acknowledged.

1. H. S. Blanchard, H. L. Finkbeiner, and G. A. Russell. J. Polym. Sci. **58**, 469 (1962).
2. J. F. Harrod. Can. J. Chem. **47**, 637 (1969).
3. B. T. Kilbourn and J. D. Dunitz. Inorg. Chim. Acta, **1**, 209 (1967).
4. Von H. Bock, H. tom Dieck, H. Pyttlik, and M. Schnoller. Z. Anorg. Allg. Chem. **357**, 54 (1968).
5. H. tom Dieck and H-P. Brehm. Chem. Ber. **102**, 3577 (1969).
6. N. S. Gill and M. Sterns. Inorg. Chem. **9**, 1619 (1970).
7. J. A. Bertrand and J. A. Kelley. J. Am. Chem. Soc. **88**, 4746 (1966).
8. J. A. Bertrand and J. A. Kelley. Inorg. Chem. **8**, 1982 (1969).
9. J. K. Kochi. Science, **155**, 415 (1967).
10. J. Brandrup and E. H. Immergut. Polymer handbook. John Wiley and Sons, Inc., New York. 1966. Ch. 2.
11. J. R. Clifton and J. T. Yoke, III. Inorg. Chem. **7**, 39 (1968).
12. S. Tsuruya, T. Kawamura, and T. Yonezawa. J. Polym. Sci. Part A, **9**, 1659 (1971).
13. A. S. Hay. Adv. Polym. Sci. **4**, 496 (1967).
14. H. Finkbeiner, A. S. Hay, H. S. Blanchard, and G. F. Endres. J. Org. Chem. **28**, 1300 (1962).
15. M. Goldstein, E. F. Mooney, A. Anderson, and H. A. Gebbie. Spectrochim. Acta, **21**, 105 (1965).
16. D. M. L. Goodgame and F. A. Cotton. J. Chem. Soc. 2298 (1961).
17. J. A. Bertrand. Inorg. Chem. **6**, 495 (1967).

Dielectric Studies. Part XXXIV. Relaxation Evidence for Complex Formation of 1,4-Dioxan with Chelated Ring Systems

M. D. MAGEE AND S. WALKER

Department of Chemistry, Lakehead University, Thunder Bay, Ontario

Received January 31, 1972

The dielectric constant (ε') and loss factor (ε'') of solutions of (*i*) 8-hydroxyquinoline in cyclohexane, carbon tetrachloride, *p*-xylene and 1,4-dioxan, (*ii*) *o*-nitrophenol in *n*-heptane, cyclohexane, carbon tetrachloride, and 1,4-dioxan, (*iii*) 2,4-dinitrophenol in 1,4-dioxan, and (*iv*) 2,6-dinitrophenol also in 1,4-dioxan have been recorded at four microwave frequencies and at 25 °C. A comparison of the relaxation time data of 1-nitronaphthalene with that of 8-hydroxyquinoline in a number of solvents indicates that a strong specific interaction occurs between the latter solute and the solvent 1,4-dioxan which leads to the formation of a complex. In addition, a comparative study of nitrobenzene and *o*-nitrophenol indicates a similar phenomenon. Strong interaction of the 1,4-dioxan with an atom or atoms in the chelated ring system appears to take place which produces a larger reorienting species than the solute molecule itself and appreciably lengthens the relaxation time, although the data do not establish the point of attachment of the 1,4-dioxan to the chelated ring. The complex formation is accompanied by an additional component to the dipole moment. For the dinitrophenols significant interaction with the solvent *p*-xylene complicates the interpretation of the relaxation time data, although in the 2,4-dinitrophenol the formation of a complex is indicated in 1,4-dioxan.

Nous avons enregistré la constante diélectrique (ε') et le facteur de perte (ε'') de solutions de (*i*) 8-hydroxyquinoline dans le cyclohexane, le tétrachlorure de carbone, le *p*-xylène et le 1,4-dioxanne, (*ii*) de l'*o*-nitrophénol dans le *n*-heptane, le cyclohexane, le tétrachlorure de carbone et le 1,4-dioxanne, (*iii*) du 2,4-dinitrophénol dans le 1,4-dioxanne et (*iv*) du 2,6-dinitrophénol dans le 1,4-dioxanne, à quatre fréquences microondes, à une température de 25 °C. La comparaison des résultats de temps de relaxation du 1-intronaphtalène avec ceux du 8-hydroxyquinoline dans plusieurs solvants indique qu'il existe une forte interaction spécifique entre ce soluté et le solvant 1,4-dioxanne, ce qui conduit à la formation d'un complexe. De plus, une étude comparative du nitrobenzène et de *o*-nitrophénol révèle un phénomène semblable. Il semble se produire une forte interaction entre le 1,4-dioxanne et l'atome ou les atomes dans le système cyclique chelaté, ce qui a pour effet de produire une plus grande réorientation que dans le cas de la molécule de soluté même et d'allonger considérablement le temps de relaxation, quoiqu'on ne puisse pas tirer des résultats le site d'attachement du 1,4-dioxanne à l'anneau chelaté. La formation de complexe est accompagnée d'une composante additionnelle au moment dipolaire.

Dans le cas des dinitrophénols, une interaction importante avec le *p*-xylène complique l'interprétation des résultats de temps de relaxation, quoique pour le 2,4-dinitrophénol, on peut remarquer la formation d'un complexe avec le 1,4-dioxanne. [Traduit par le journal]

Canadian Journal of Chemistry, **50**, 2799 (1972)

The free phenolic hydroxyl group is well known to form an intermolecular hydrogen bond with suitable electron donor molecules (1). Mecke's (2) early near infrared work was followed by extensive investigations in the infrared region by, for example, Bellamy (3) and Hallam (3, 4), and Josien (5). The considerable frequency shifts which occur can be related to specific solute–solvent effects, principally hydrogen bonding, rather than to bulk effects (4). These interactions are also effective in enhancing dipole moments (6) and altering the n.m.r. chemical shift to high or low field strengths (7).

Part of the work of the present series of papers has been devoted to a comprehensive investigation of hydroxyl group relaxation, more specially in phenols. In previous papers (8, 9) the influence of self-association of phenols has been considered. Strong concentration dependence of relaxation times, distribution coefficients and dipole moments has been noted and also the apparent concentration dependence of the weight factor C_2 for hydroxyl relaxation under certain conditions of analysis (9). However, hydroxyl group relaxation, with possibly one exception (10), has usually been considered to be absent (11, 12) in phenols possessing an intramolecular hydrogen bond strong enough to shift the hydroxyl stretching frequency by more than about 150 cm^{-1}, although hydroxyl group relaxation has been detected in phenols with weaker hydrogen bonds (13).

In a recent study Magee and Walker (14)

Can. J. Chem. Downloaded from www.nrcresearchpress.com by 210.87.254.6 on 09/05/12
For personal use only.

Can. J. Chem. Downloaded from www.nrcresearchpress.com by 210.87.254.6 on 09/05/12
For personal use only.

showed that the *trans* forms of *o*-nitrophenol and *o*-chlorophenol hydrogen bonded with 1,4-diazabicyclo-2,2,2-octane (DBO) in non polar solution in such a way that the *trans/cis* ratio increased in the presence of DBO. The net effect was that the DBO complexes with the *trans* form of phenols via the hydrogen bond involving the hydroxyl hydrogen and competes with the intramolecular hydrogen bonded system causing rupture of a proportion of the latter. The effect was more appreciable in the *o*-chlorophenol than in the *o*-nitrophenol, and the increase in moment in the latter ranged between $0.2_7 - 0.5_8$ D while in the former $0.3_6 - 0.7_2$ D the increment increases with increased DBO concentration. With 1,4-dioxan as solvent polarization studies have previously shown that the dipole moments of *o*-nitrophenol and 2,6-dinitrophenol significantly decrease compared with the values in the more inert solvent benzene, whereas that of 2,4-dinitrophenol increases. The magnitude of the change in moment is too appreciable to be ascribed to a normal solvent effect. Both dipole moment and infrared evidence favor a strong interaction of the chelated ring system with 1,4-dioxan in which, somehow, an additional moment component is brought about from the attachment of the 1,4-dioxan (6). This moment appears to lie approximately along or parallel to the direction of the N—O bond in the chelated ring, and could be attributed to dipolar attachment of the 1,4-dioxan along the N—O bond in the chelated ring (6) or even a bifurcated hydrogen bond involving an oxygen atom from the nitro group of the chelated ring and one from an interacting oxygen atom of a 1,4-dioxan molecule. The work reported here is not aimed at deciding between these two possibilities.

The dipole moment evidence for the chelated nitrophenols rules out a switch from a *cis* O—H to a *trans* on passing from an inert solvent to 1,4-dioxan, since if this occurred for *o*-nitrophenol the moment would increase and not decrease (~0.15 D) as, in fact, is observed, while for 2,6-dinitrophenol no change in moment would be anticipated from the switching of the O—H from one planar position to the other, whereas ~0.2 D decrease in moment is observed. The dipole moment change for 8-hydroxyquinoline on passing from cyclohexane to 1,4-dioxan is ~0.3 D decrease while the O—H stretching frequency (3) exhibits only an 18 cm^{-1} change on passing from *n*-hexane to 1,4-dioxan, whereas for phenol it is 307 cm^{-1}.

It seemed of interest to explore the interaction of 1,4-dioxan with these chelated ring systems by the dielectric absorption technique since this method yields information on both shift of charge and size of species. For all these chelated ring systems where interaction with 1,4-dioxan may be inferred from the dipole moment or infrared evidence it would be a more convincing indication of complex formation if it could be shown that the size of the reorienting species had increased.

Experimental

The apparatus and procedure for determining the dielectric constant (ε') and loss factor (ε'') have been described previously (15). Assessments of the accuracy of the method (16) and validity of the procedure (17) have also been given. Measurements were made at 25 ± 0.01 °C at all the following frequencies 34.86, 23.98, 16.20, and 9.313 GHz, known as Q, K, P, and X-bands, respectively. The static dielectric constant (ε_0) was measured at 2 MHz for all the solutions.

Evaluation of α, τ_0, *and* ε_∞

The procedure for the determination of the dielectric constant at very high frequency (ε_∞), the distribution parameter (α) and the mean relaxation time (τ_0) is to fit the experimental data to the equations:

$$[1] \qquad \frac{\varepsilon' - \varepsilon_\infty}{\varepsilon_0 - \varepsilon_\infty} = \frac{1 + \omega\tau_0^{(1-\alpha)} \cos(1-\alpha)(\tfrac{1}{2}\pi)}{1 + 2\omega\tau_0^{(1-\alpha)} \cos(1-\alpha)(\tfrac{1}{2}\pi) + (\omega\tau_0)^{2(1-\alpha)}}$$

$$[2] \qquad \frac{\varepsilon''}{\varepsilon_0 - \varepsilon_\infty} = \frac{\omega\tau_0^{(1-\alpha)} \sin(1-\alpha)(\tfrac{1}{2}\pi)}{1 + 2\omega\tau_0^{(1-\alpha)} \cos(1-\alpha)(\tfrac{1}{2}\pi) + (\omega\tau_0)^{2(1-\alpha)}}$$

The input data to a computer program include the following (*a*) the measured values of ε'_{obs} and ε''_{obs} at the appropriate angular frequencies, (*b*) guesses for the variables *e.g.* an initial estimate of τ_0 can often be made from an ε' *vs.* $\varepsilon''\omega$ plot and initial estimates of α and ε_∞ from the Cole–Cole plot, (*c*) ε_0. The dielectric constant value of the solvent provides a restraint (a lower limit) for ε_∞, and the computer program turns out a value for ε_∞ which best fits. In the sequence of operations the ε'_{calc} and ε''_{calc} values obtained from eqs. 1 and 2 are compared with the observed values by the use of a function A where

$$[3] \qquad A = \sum (\varepsilon''_{obs} - \varepsilon''_{calc})^2 + \sum \left\{ \frac{\varepsilon'_{obs} - \varepsilon'_{calc}}{n} \right\}^2$$

where n is a scaling factor chosen to reduce the errors in ε' to about the same magnitude as those in ε'' and the sum is taken over the number of frequencies employed. A value of 2 to 4 is appropriate for n, although its value is not critical providing that it is sufficient to prevent ε' from dominating the function. For the wavebands reported here n was taken to be 4.

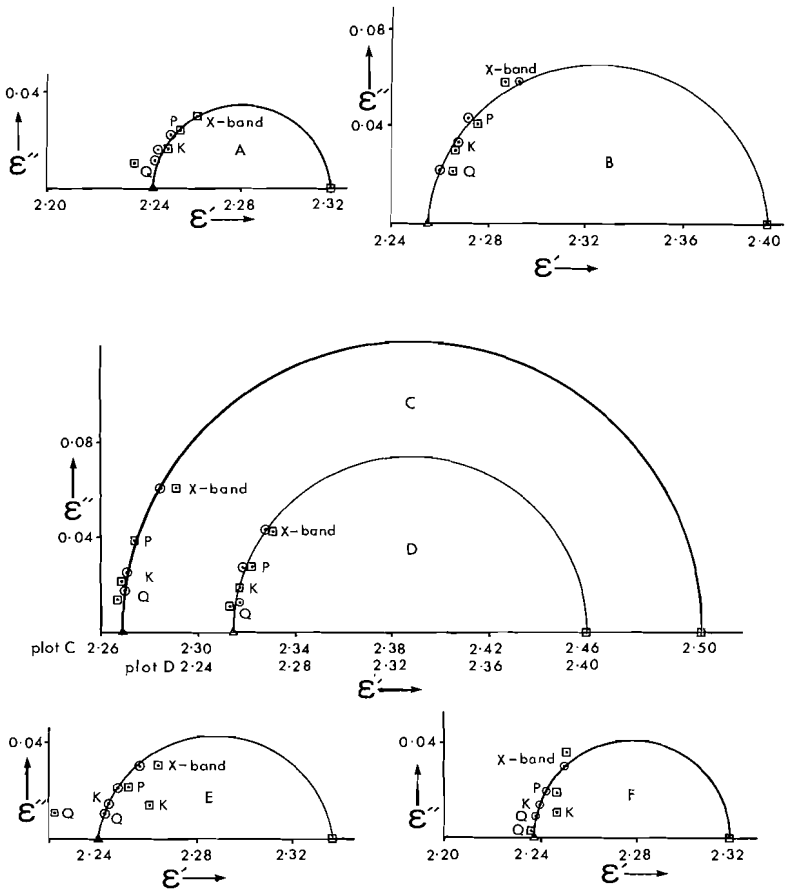

FIG. 1. Cole–Cole plots of the nitrophenols and 8-hydroxyquinoline in 1,4-dioxan solution at 25 °C. Plots are: (*A*) *o*-nitrophenol ($f_2 = 0.0063$); (*B*) *o*-nitrophenol ($f_2 = 0.012$); (*C*) 2,4-dinitrophenol ($f_2 = 0.0158$); (*D*) 2,4-dinitrophenol ($f_2 = 0.099$); (*E*) 2,6-dinitrophenol ($f_2 = 0.0058$); (*F*) 8-hydroxyquinoline ($f_2 = 0.010$). The points designated by □ are experimental ones; ○ are those calculated from τ_0, α, and ε_∞ while ε_∞ is represented by △.

The computer takes each variable of eqs. 1 and 2 in turn and augments it by given step sizes so that A is reduced. The variables have upper and lower limits within which the computer works, and the step sizes are reduced until two complete cycles fail to improve A. At this stage the final value of the variables and the dielectric constant and loss at each frequency are recorded together with the current step sizes, the final function value and the number of evaluations of A performed during the program. The size of A indicates how well the final analysis fits the experimental points.

Materials

8-Hydroxyquinoline was recrystallized from light petroleum spirit (b.p. 60–80 °C). The purification of *o*-nitrophenol, 2,4-dinitrophenol, and 2,6-dinitrophenol has been given elsewhere (6). Cyclohexane, *n*-heptane, *p*-xylene, and 1,4-dioxan were dried, then distilled from sodium and stored over sodium in dark, stoppered bottles. Carbon tetrachloride was distilled from phosphorus pentoxide. The solutes were kept in spring stoppered bottles and stored in dark cupboards. When not in use solutions were also kept in tightly stoppered bottles.

Results and Discussion

Experimental dielectric constant and loss data have been placed in the Depository of Unpublished Data.[1] Corrections for the slight solvent losses were made where appropriate (18).

For the systems described here the lowest loss points are the least accurate and are mostly found in the 1,4-dioxan solutions. To gain some appreciation of the accuracy for these cases the Cole–Cole plots are given in Fig. 1 for the 1,4-

[1]Complete set of tabular data is available, at a nominal charge, from the Depository of Unpublished Data, National Science Library, National Research Council of Canada, Ottawa, Canada K1A 0S2.

Can. J. Chem. Downloaded from www.nrcresearchpress.com by 210.87.254.6 on 09/05/12
For personal use only.

TABLE 1. Values of parameters*

Solute	Solvent	Concentration (mole fraction)	α	τ_0	ε_∞	ε_0	μ
8-Hydroxyquinoline	C_6H_{12}	0.0049	0.04	11.4	2.01_8	2.051_9	2.6_1
8-Hydroxyquinoline	CCl_4	0.0111	0.05	17.5	2.23_3	2.330_8	2.6_9
8-Hydroxyquinoline	CCl_4	0.0216	0.05	18.6	2.23_8	2.423_2	2.6_5
8-Hydroxyquinoline	*p*-Xylene	0.0180	0.02	14.7	2.27_9	2.390_3	2.4_8
8-Hydroxyquinoline	1,4-Dioxan	0.0113	~0	39	2.23_7	2.318_2	2.3_1
o-Nitrophenol	*n*-Heptane	0.0066	0.03	6.4	1.90_9	1.960_6	3.4_0
o-Nitrophenol	*n*-Heptane	0.0119	0.03	6.8	1.91_2	2.003_4	3.3_6
o-Nitrophenol	C_6H_{12}	0.0051	~0.0	8.4	2.02_3	2.070_4	3.1_0
o-Nitrophenol	C_6H_{12}	0.0071	~0.0	8.9	2.02_4	2.091_2	3.1_0
o-Nitrophenol	C_6H_{12}	0.0079	0.02	8.5	2.02_4	2.100_0	3.0_8
o-Nitrophenol	CCl_4	0.0202	0.04	14.4	2.23_9	2.480_0	3.1_2
o-Nitrophenol	CCl_4	0.0250	0.04	14.5	2.24_9	2.539_2	3.0_8
o-Nitrophenol	*p*-Xylene	0.0069	0.02	13.3	2.26_7	2.329_8	3.0_4
o-Nitrophenol	1,4-Dioxan	0.0063	0.02	30	2.24_3	2.317_5	2.9_6
o-Nitrophenol	1,4-Dioxan	0.0120	0.04	30	2.25_5	2.396_1	2.9_5
2,4-Dinitrophenol	*p*-Xylene	0.0278	0.1	34	2.29_4	2.520_4	2.8_6
2,4-Dinitrophenol	1,4-Dioxan	0.0099	~0	53	2.25_5	2.398_6	3.2_8
2,4-Dinitrophenol	1,4-Dioxan	0.0158	~0	64	2.26_8	2.509	3.3_6
2,6-Dinitrophenol	*p*-Xylene	0.0077	0.03	29	2.26_3	2.371_6	3.7_5
2,6-Dinitrophenol	1,4-Dioxan	0.0058	0.05	47	2.24_0	2.337_4	3.5_2

*The distribution parameter α, the relaxation time (τ_0) in picoseconds evaluated from the experimental data, the high frequency dielectric constant (ε_∞) the static dielectric constant (ε_0) and dipole moment (μ) in Debye units for some intramolecularly hydrogen bonded aromatic molecules in various solvents at 25 °C. Values for nitrophenols in *p*-xylene are from ref. 14.

dioxan solutions. The experimental points are compared with the ones calculated from the τ_0, α, and ε_∞ values.

The calculated dipole moments for the *cis* and *trans* isomers of *o*-nitrophenol are 2.6 and 5.2 D, respectively (6), while the measured value in cyclohexane at 25 °C is 3.1 D (see Table 1). The difference in calculated and observed moments may be attributed to (*a*) a predominance of *cis* form with the presence of a small amount of *trans* or (*b*) redistribution of charge in the chelated ring (this would include inductive effects) or (*c*) contributions from (*a*) and (*b*). Thus, it is not possible to establish from the measured dipole moment whether any significant amount of *trans* form is present. Further, although the dielectric data can be analyzed into contributions from two relaxation times (τ_1 and τ_2) where the weight factor of the shorter relaxation time (τ_2) is only ~0.2 or less, the interpretation of τ_2 in terms of a meaningful molecular or intramolecular motion is uncertain and in the light of recent studies on, for example, the microwave and far-infrared absorption of chlorobenzene in *p*-xylene (19) may be attributed to a process other than that of (hydroxyl) group relaxation. Fortunately, however, for the four chelated ring systems considered, since the C_2 value (10) if meaningful is less than 0.2, then this results in the τ_1 value being within the normal error of the order of the mean relaxation time value (τ_0); for example, the τ_1 value for *o*-nitrophenol in *p*-xylene at 25 °C is 15×10^{-12} s, and the τ_0 is 13.3×10^{-12} s, while for 8-hydroxyquinoline the τ_1 and τ_0 values are 16×10^{-12} and 15×10^{-12} s. For our purposes we shall take the τ_0 value as being equal to the relaxation time of the reorienting species (molecule or complex) which would correspond with the case where $\alpha = 0$. This could result in our underestimating but not overestimating the size of a reorienting species.

The relaxation time of 8-hydroxyquinoline in cyclohexane at 15 °C of 11.4×10^{-12} s is slightly longer than the value for isoquinoline (20) in cyclohexane at 20 °C of 10.5×10^{-12} s as would be expected from molecular volume considerations. The relaxation time of 8-hydroxyquinoline in carbon tetrachloride (18.6×10^{-12} s) is similar to that of isoquinoline (21) in the same solvent at 20 °C and a little shorter than the relaxation time of 1-nitronaphthalene in carbon tetra-

Can. J. Chem. Downloaded from www.nrcresearchpress.com by 210.87.254.6 on 09/05/12
For personal use only.

TABLE 2. Relaxation times of *o*-nitrophenol and nitrobenzene at ambient temperatures in different solvents expressed relative to the value in *n*-heptane*

Solvent	Relative solvent viscosities	Relative relaxation times	
		o-Nitrophenol	Nitrobenzene (21)
n-Heptane	1	1	1
Cyclohexane	2.3	1.3	1.3
Carbon tetrachloride	2.3	2.2	2.3
p-Xylene	1.5	2.0	2.1
1,4-Dioxan	2.8	4.5	2.3 (24)

*The behavior of *o*-nitrophenol parallels that of nitrobenzene in each solvent except 1,4-dioxan in which the relaxation time of *o*-nitrophenol is considerably enhanced. Viscosities of the solvents relative to that of *n*-heptane are given for purposes of comparison.

chloride (21) at 20 °C. Again this is in agreement with the relative volumes of the two molecules.

The hydroxyl is smaller than the nitro group, and it would be reasonable to expect that the molecular relaxation time of *o*-nitrophenol would be only slightly longer than that of nitrobenzene. In fact, the τ_0 of *o*-nitrophenol in *n*-heptane at 25 °C is within experimental error, the same as that of nitrobenzene (22) (6.8×10^{-12} s) in the same solvent at 20 °C as is expected from the volumes of the molecules, and this is true also for *o*-nitrophenol in cyclohexane ($\sim 8.5 \times 10^{-12}$ s) since the nitrobenzene value at 20 °C is 8.8×10^{-12} s in the same solvent (21). Whiffen (22) gives 15.2×10^{-12} s for the relaxation time of nitrobenzene in carbon tetrachloride at 20 °C, and this is to be compared with the value in Table 1 for *o*-nitrophenol of 14.5×10^{-12} s at 25 °C in the same solvent. In *p*-xylene at 25 °C the τ_0 of *o*-nitrophenol was found to be 13.3×10^{-12} s which again is similar to the relaxation time of nitrobenzene under the same conditions (13.1×10^{-12} s) (14). Thus, in each case, the relaxation times of nitrobenzene and *o*-nitrophenol in a common solvent are either the molecular relaxation time or a value close to it.

8-Hydroxyquinoline in Flett's classification (23) is in the category of hydrogen bonds of medium strength, but the shift of the OH stretching frequency due to intramolecular hydrogen bonding is smaller (180 cm^{-1}) than that of typical compounds in this category, such as *o*-nitrophenol, for which the shift is 368 cm^{-1} (23).

Direct comparison amongst the observed relaxation times for a particular solute in different solvents is open to the objection that the observed relaxation time in 1,4-dioxan is expected to be longer than that in the other solvents in Table 1 because 1,4-dioxan has the greatest viscosity. To make some allowance for this the relaxation times in Table 2 are expressed relative to the value in *n*-heptane, together with the viscosities of the solvents relative to that of *n*-heptane and the relaxation times of nitrobenzene also relative to the value in *n*-heptane. Nitrobenzene is a very similar molecule to *o*-nitrophenol, being very slightly smaller, incapable of relaxation by an intramolecular process and having a rather larger dipole moment (which, in the absence of hydrogen bonding, should make it more likely to interact). Viscosity and non-specific environment effects should be similar for *o*-nitrophenol and nitrobenzene so that differences in relaxation behavior are attributable to specific interaction.

From Table 2 it can be seen that the relaxation times of *o*-nitrophenol have a closely similar dependence on the solvent to those of nitrobenzene in the solvents, *n*-heptane, cyclohexane, carbon tetrachloride, and *p*-xylene. However, in 1,4-dioxan solution a striking deviation occurs between the behavior of the two solutes where for *o*-nitrophenol the relative observed relaxation time value is almost double that of the nitrobenzene value. It seems that the difference in behavior can be accounted for by a specific interaction between *o*-nitrophenol and 1,4-dioxan which increases the size of the reorienting species so that it is appreciably greater than that of the nitrobenzene in 1,4-dioxan system.

In Table 3 the data for 8-hydroxyquinoline are treated similarly, the relaxation times being

Can. J. Chem. Downloaded from www.nrcresearchpress.com by 210.87.254.6 on 09/05/12
For personal use only.

TABLE 3. Relaxation times of 8-hydroxyquinoline and 1-nitronaphthalene at ambient temperatures and in different solvents expressed relative to the value in carbon tetrachloride*

Solvent	Relative solvent viscosities	Relative relaxation times	
		8-Hydroxyquinoline	1-Nitronaphthalene (21)
Cyclohexane	2.3	1.4	1.5
Carbon tetrachloride	2.3	2.3	2.3
p-Xylene	1.5	1.9	1.9
1,4-Dioxan	2.8	5.0	2.1

*Values are scaled by the factor of 2.3 to permit comparison with the previous table. Solvent viscosities relative to that of *n*-heptane are also given.

expressed relative to carbon tetrachloride as 2.3 so that direct comparison can be made with the previous table.

1-Nitronaphthalene is a slightly larger molecule than 8-hydroxyquinoline but of similar shape and, in the absence of special interactions with the chelated ring, should be more capable of interacting than 8-hydroxyquinoline by virtue of its much larger dipole moment. Yet Table 3 indicates a pronounced interaction between 8-hydroxyquinoline and 1,4-dioxan relative to the 1-nitronaphthalene and 1,4-dioxan system, even though the behavior of the two solutes is similar in the more inert solvents. In fact, the relative relaxation time for the 8-hydroxyquinoline–1,4-dioxan system is $\sim 2\frac{1}{2}$ times that for the 1-nitronaphthalene–1,4-dioxan one. Thus a significantly larger reorienting species is to be inferred in the former system.

It is revealing to compare the ratio of the relaxation time values for the two chelated ring systems, *o*-nitrophenol and 8-hydroxyquinoline, in 1,4-dioxan and cyclohexane which are 3.5 and 3.6, respectively, with the value for *o*-hydroxyacetophenone (12) which is 1.9. *o*-Hydroxyacetophenone is classified by Flett (23) as a strongly intramolecularly hydrogen bonded compound and behaves as a rigid molecule (12). Thus the two types of chelated ring system exhibit quite different behavior. The ratio obtained for *o*-hydroxyacetophenone may be compared with that of 1.8 for nitrobenzene in the two solvents (see Table 3) and is a fairly typical ratio for a non-interacting solute in the two solvents. Similarly, the data of Chitoku and Higasi (24) for nitrobenzene, *m*-dinitrobenzene, *p*-nitrotoluene, and 4-nitrodiphenyl in the solvents 1,4-dioxan and *n*-hexane give ratios of the same order, that is 1.8, 2.0, 2.0, and 2.2, respectively. *n*-Hexane is a very similar solvent to *n*-heptane both in viscosity and inertness. Altogether from the relaxation data it may be inferred that the chelated ring system of *o*-hydroxyacetophenone exhibits no appreciable interaction with 1,4-dioxan whereas for those of *o*-nitrophenol and 8-hydroxyquinoline the size of the reorienting species is significantly greater in 1,4-dioxan than in cyclohexane as solvent. Altogether, there is good evidence for strong complex formation in the former solvent.

The dinitrophenols were insufficiently soluble in the inert solvents to permit dielectric measurements of the necessary accuracy so only *p*-xylene and 1,4-dioxan were used. Their relaxation times in 1,4-dioxan were almost twice as long as in *p*-xylene, a ratio which is similar to the solvent viscosity ratio. However, 2,4- and 2,6-dinitrophenols, like picric acid, are likely to interact appreciably (25) with *p*-xylene as we have already noted (14). The relaxation times in *p*-xylene are therefore probably enhanced, and any further increase in 1,4-dioxan would not appear so pronounced. A comparison can be made, however, with the relaxation times of *m*-dinitrobenzene in benzene (24) and in 1,4-dioxan. The ratio of these is only 1.5, significantly less than the predicted ratio of almost 2 from the ratio of viscosities and only slightly less than the observed ratio of relaxation times for the 2,4-dinitrophenol in Table 1. 2,6-Dinitrophenol apparently behaves in a similar fashion to *m*-dinitrobenzene, $\tau_0(\text{diox})/\tau_0(p\text{-xylene})$ being 1.6. The low frequency measurements indicate a similar behavior for picric acid in xylene and 1,4-dioxan (26). There can be no doubt that the relaxation times for 2,4- and 2,6-dinitro-

Can. J. Chem. Downloaded from www.nrcresearchpress.com by 210.87.254.6 on 09/05/12
For personal use only.

Can. J. Chem. Downloaded from www.nrcresearchpress.com by 210.87.254.6 on 09/05/12
For personal use only.

phenol in *p*-xylene at 25 °C, which are 34×10^{-12} and 29×10^{-12} s, are anomalously long; this follows from comparisons of their values with *m*-iodobenzene in *p*-xylene (27) at 15 °C which has a value of 23×10^{-12} s and is a larger solute molecule with a similar shape.

For the dinitrophenols it is clear that the relaxation time ratios do not unequivocably demonstrate interaction with 1,4-dioxan but are not incompatible with such an interaction, and, in fact, the relaxation time for 2,4-dinitrophenol in this solvent must be more than $2\frac{1}{2}$ times the value for *m*-iodobenzene at the same temperature in *p*-xylene. This is a similar ratio obtained for 8-hydroxyquinoline and *o*-nitrophenol in these two solvents. In addition, the dipole moment evidence shows interaction of the 1,4-dioxan with both the 2,4-dinitrophenol and 2,6-dinitrophenol since in the former the moment is increased by ~ 0.4 D while in the latter there is a decrease of ~ 0.2 D from *p*-xylene to 1,4-dioxan. These results bear out those of the polarization (6) method and establish their values since they do not suffer from having to equate n_D to the refractive index for infrared radiation which is implicit in the latter method. Further, the difference in dipole moment for 8-hydroxyquinoline in 1,4-dioxan and cyclohexane is -0.3 D while for *o*-nitrophenol it is -0.15 D. All these dipole moment changes are well beyond experimental errors and simple solvent effects. The changes in moment and their signs between 1,4-dioxan and the less interacting solvent can be explained by invoking an additional moment arising from the attachment of the 1,4-dioxan molecule to an atom or atoms of the chelated ring.

Conclusions

Both the dipole moment and dielectric data favor strong attachment of the 1,4-dioxan to *o*-nitrophenol, 8-hydroxyquinoline and 2,4-dinitrophenol. The attachment is such that the observed relaxation time lengthens (compared with the value in an inert solvent) far beyond that which could be expected for a non-complexed molecule in such a solvent, and an increase in size of the reorienting species may be inferred. In fact, interaction of 1,4-dioxan with an atom or atoms of the chelated ring system seems likely for all four solute molecules. For *o*-nitrophenol and 2,4-dinitrophenol the infrared (6), dipole moment, and relaxation data favor this conclusion, while for 8-hydroxyquinoline (6) the key evidence is from the latter two approaches.

1. G. C. Pimentel and A. L. McClellan. The hydrogen bond. W. H. Freeman and Co., San Francisco. 1960.
2. R. Mecke. Disc. Faraday Soc. **9**, 161 (1950).
3. L. J. Bellamy and H. E. Hallam. Trans. Faraday Soc. **55**, 220 (1959).
4. H. E. Hallam. Infrared spectra and molecule structure. *Edited by* M. Davies. Elsevier, Amsterdam and London. 1963.
5. M. L. Josien. Molecular spectroscopy. Proc. Fifth Eur. Congr., Amsterdam, 1961. Butterworth, London. 1962.
6. J. H. Richards and S. Walker. Trans. Faraday Soc. **57**, 399 (1961); **57**, 406 (1961).
7. J. A. Pople, W. G. Schneider, and H. J. Bernstein. High resolution nuclear magnetic resonance. McGraw-Hill, New York. 1959.
8. M. D. Magee and S. Walker. Can. J. Chem. **49**, 1106 (1971).
9. M. D. Magee and S. Walker. J. Phys. Chem. **74**, 2378 (1970).
10. M. D. Magee and S. Walker. Chem. Soc. Spec. Publ. No. 20. Molecular relaxation processes. Academic Press, London and New York. 1966.
11. A. Aihara and Mansel Davies. J. Colloid Sci. **11**, 671 (1956).
12. A. A. Antony and C. P. Smyth. J. Am. Chem. Soc. **86**, 156 (1964).
13. M. D. Magee and S. Walker. Trans. Faraday Soc. **62**, 1748 (1966).
14. M. D. Magee and S. Walker. J. Chem. Phys. **55**, 3068 (1971).
15. W. F. Hassell, M. D. Magee, S. W. Tucker, and S. Walker. Tetrahedron, **20**, 2137 (1964).
16. M. D. Magee and S. Walker. Trans. Faraday Soc. **62**, 3093 (1966).
17. M. D. Magee and S. Walker. J. Chem. Phys. **50**, 2580 (1969).
18. J. Crossley. Ph.D. Thesis. University of Aston in Birmingham, England, 1967.
19. M. Davies, G. W. F. Pardoe, J. E. Chamberlain, and H. A. Gebbie. Trans. Faraday Soc. **64**, 847 (1968).
20. F. Hufnagel and H. Kilp. Z. Naturforsch. **18***a*, 769 (1963).
21. J. Y. H. Chau, R. J. W. Le Fèvre, and J. Tardif. J. Chem. Soc. 2293 (1957).
22. D. H. Whiffen. Trans. Faraday Soc. **46**, 150 (1950).
23. M. St. C. Flett. Spectrochim. Acta, **10**, 21 (1957).
24. K. Chitoku and K. Higasi. Bull. Chem. Soc. Jap. **36**, 1064 (1963).
25. J. A. A. Ketelaar. Chemical constitution. Elsevier, Amsterdam and London. 1958.
26. A. H. Price. J. Phys. Chem. **64**, 1442 (1960).
27. P. F. Mountain. Ph.D. Thesis. University of Aston in Birmingham, England, 1969.

Kinetics of Pentadienyl Cation Cyclizations

R. BLADEK AND T. S. SORENSEN

The Department of Chemistry, University of Calgary, Calgary, Alberta

Received February 22, 1972

A series of methyl-substituted pentadienyl cations has been prepared and characterized. A careful study was then made of the rate at which these cations cyclize to give cyclopentenyl cation products. Rate constants and activation parameters have been determined for this rearrangement in several different solvents and at several different cation concentrations. There is an unexpectedly large factor of 10^8 difference in rate between the extremes of the cations studied and a rationalization of this is presented.

The cyclopentenyl cation products themselves undergo numerous rearrangements involving methyl or hydride shifts and a detailed discussion of the tetramethyl case is given. It is shown that a 3-cyclopenten-1-yl cation intermediate is involved in these rearrangements.

Une série de pentadiènylcations substitués par le méthyle a été préparée et caractérisée. Une étude soignée est faite sur la vitesse à laquelle ces cations se cyclisent pour donner les produits du cyclopenténylcation. Les constantes de vitesse et les paramètres d'activation ont été déterminés pour ce réarrangement dans une grande variété de solvants et pour diverses concentrations en cation. Un facteur inattendu de 10^8 a été trouvé dans la différence de vitesse entre les cations extrêmes étudiés; une rationalisation de ce fait est présentée.

Les produits du cyclopentènylcation subissent eux-mêmes de nombreux réarrangements impliquant des déplacements du méthyle ou d'hydrure et une discussion détaillée du composé tétramethylé est donnée. On a montré que l'intermédiaire cyclopentène-3 yl-1 cation est concerné dans ces réarrangements.

[Traduit par le journal]

Canadian Journal of Chemistry, **50**, 2806 (1972)

Introduction

The cyclization of pentadienyl cations **1** to cyclopentenyl cations **2** is an electrocyclic reaction proceeding in a conrotatory manner (1). The product ions from various methyl-substituted pentadienyl cation cyclizations have previously been characterized (2) but no systematic study of the rates of these reactions has been published. The electrocyclic ring closure

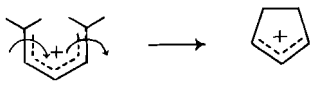

1 **2**

of an ionic molecule has an added feature over and above those of most hydrocarbons, namely, a large change in the charge density of various atoms in the course of proceeding over the transition state barrier to products. Since methyl groups stabilize a positively charged carbon atom, it is possible to use these as probes, *i.e.*, if a methyl-substituted carbon atom experiences a large increase in charge density in going to the transition state, then the reaction will be facilitated compared to that of a hydrogen substituent. The replacement of hydrogen by methyl will result however in sizable non-bonded interactions (2, 3*a* and *b*) which may become severe in certain cases and therefore tend to mask the charge stabilizing effects.

Nine methyl-substituted pentadienyl cations (**3**–**11**) were studied. Of these, **3**, **4**, **8**, and **10**

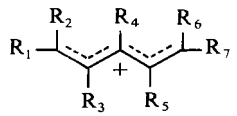

3 $R_1 = R_7 = CH_3$
4 $R_1 = R_2 = R_7 = CH_3$
5 $R_1 = R_2 = R_4 = R_7 = CH_3$
6 $R_1 = R_2 = R_5 = R_7 = CH_3$
7 $R_1 = R_2 = R_3 = R_7 = CH_3$
8 $R_1 = R_2 = R_6 = R_7 = CH_3$
9 $R_1 = R_2 = R_3 = R_6 = R_7 = CH_3$
10 $R_1 = R_2 = R_4 = R_6 = R_7 = CH_3$
11 $R_1 = R_2 = R_3 = R_4 = R_5 = R_6 = R_7 = CH_3$

have previously been reported and some crude rate data were available (2–7).

In each case, except **11**, the dienylic cation was initially observed (*in situ*) and the cyclization kinetics measured. Activation parameters were obtained for each system except for ions **5** and **11**. Ions **4** and **8** were each studied in two and three different acid solvents respectively, sulfuric acid, chlorosulfonic acid, and also for **4**, 1:1 fluorosulfonic acid–antimony pentafluoride.

Can. J. Chem. Downloaded from www.nrcresearchpress.com by 210.87.254.42 on 09/05/12
For personal use only.

TABLE 1. The n.m.r. spectra of the dienylic cations

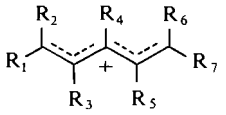

R = CH_3 or H

Ion	Chemical Shift[a]						
	R_1	R_2	R_3	R_4	R_5	R_6	R_7
3	7.288[b,r]	[c]	2.600[d]	[c]	2.600[d]	[c]	7.288[b,r]
4	7.200[r]	7.200[r]	2.730[e]	1.100[f]	2.775[g]	1.660[h]	7.430[i]
5	7.13 or 7.20	7.13 or 7.20	2.68[r]	7.13 or 7.20	2.87[e,r]	1.54[q]	7.51[b]
6	7.200	7.200	2.630[j,r]	1.240[j,r]	7.830	1.800[k]	7.475[i]
7	7.240[l] or 7.120	7.240[l] or 7.120	7.790	1.060[m,r]	2.655[n]	1.735[h]	7.430[b]
8	7.350[l] or 7.310	7.350[l] or 7.310	2.845[p,r]	0.920[f]	2.845[p,r]	7.350[l] or 7.310	7.350[l] or 7.310
9	7.340[l] or 7.210	7.340[l] or 7.210	7.810	0.820[p]	2.740[p,r]	7.340[l] or 7.210	7.340[l] or 7.210
10	7.420[l] or 7.460	7.420[l] or 7.460	2.79[r]	7.150	2.79[r]	7.420[l] or 7.460	7.420[l] or 7.460

[a] In τ p.p.m. relative to internal tetramethylammonium cation = 6.900 (8). The error is estimated as ±0.005 p.p.m. Only centers of coupled patterns are given.
[b] d, J = 6.5, abbreviations used, d = doublet, t = triplet, qt = quartet, all coupling constants are in Hz.
[c] Complex multiplet with peaks at 1.41, 1.37, 1.34, 1.25, and 1.12.
[d] t, J = *ca.* 13.5.
[e] d, J = *ca.* 14.
[f] t, J = 13.
[g] t, J = 13.5.
[h] Center of two overlapping quartets, $J_{5,6}$ = 14, $J_{6,7}$ = 7.
[i] d, J = 7.
[j] d, J = 14.
[k] qt, J = 7.
[l] Unambiguous assignment not possible.
[m] d, J = 12.
[n] t, J = 12.
[p] d, J = 13.
[q] Complex multiplet.
[r] This peak used in the area analysis.

Results

Characterization of the Dienylic Cations

The dienylic ions were prepared by adding either a conjugated triene or a dienol to the strong acid solvents following published procedures appropriate for the particular solvent (1). The dienols were prepared mainly by the reaction of a substituted vinyl lithium and an α,β-unsaturated carbonyl compound (see Experimental). Most of the dienylic cation solutions exhibited exceedingly clean and clear-cut n.m.r. spectra, summarized in Table 1.

The Rate Measurements

Preliminary rate measurements in sulfuric acid using ion **8** in concentrations of 2.7, 5.0, and 10.0% w/v solutions showed that the rate and activation parameters did not vary significantly with ion concentration. A 10% w/v cation concentration was subsequently used in all cases. The kinetic procedures were unexceptional. In all cases, simple (singlet or doublet), mutually non-interfering n.m.r. peaks could be found for both the dienylic cation and the cyclopentenyl cation product and these were used for area measurements. The temperature range used for the activation energies was not large since fast or slow rates are not conveniently measured in an n.m.r. probe. This meant that the temperature had to be very carefully controlled and measured and this was accomplished by inserting a thermocouple directly into the n.m.r. tube for the duration of the run and monitoring the temperature frequently. The

Can. J. Chem. Downloaded from www.nrcresearchpress.com by 210.87.254.42 on 09/05/12
For personal use only.

TABLE 2. Rate parameters

Ion	Solvent	Temperature[a]	$k_{obs} \times 10^4$ (s^{-1})	$\sigma \times 10^4$	ΔH^+	ΔF^+	ΔS^+
3	$ClSO_3H$	−30.0	2.02	0.07	17.3[b]	18.5[b]	−4[c]
4	$ClSO_3H$	−21.4	0.55	0.01	18.8	19.6	−3
	H_2SO_4	−18.2	0.53	0.02	20.0	19.9	0
	FSO_3H–SbF_5 (1:1)	−18.1	0.66	0.008	—	—	—
5	FSO_3H–SO_2ClF (1:4)	−100.0	1.3	—	—	13.1	—
6	$ClSO_3H$	−21.8	0.99	0.03	23.9	18.3	+19
7	$ClSO_3H$	−26.6	1.09	0.02	19.5	18.6	+3
8	$ClSO_3H$	+40.0	0.20	0.005	19.9	24.6	−16
	H_2SO_4	+40.0	0.33	0.01	19.2	24.5	−18
9	$ClSO_3H$	−5.6	1.62	0.04	21.5	20.1	+5
10	$ClSO_3H$	−57.0	3.0	0.27	12.7	17.2	−15
11	$ClSO_3H$	−80.0	fast	—	—	—	—

[a]Within ±0.1°. In most cases, the range of temperatures used was about 15° and this results in considerable uncertainty in ΔH^* and especially ΔS^*. However, several completely independent runs, using a different solvent, gave reasonably similar ΔS^* values. It is, nevertheless, difficult to account for the apparent variation in ΔS^* (37 e.u.). The measured activation entropy, like the other thermodynamic parameters, is a complex term involving ΔS changes in the equilibria processes together with a true entropy of activation. We concede that the error in ΔS^+ could be of a magnitude so that the quoted values are meaningless.

The particular values quoted for the rate constants in this Table are in general those for temperatures nearer the lower end of the temperature range covered and have lower than average standard deviations. The rate constants are for the disappearance of the dienylic cations.

[b]In kcal/mol.

[c]In e.u.

data obtained analyzed well for a first order reaction, as expected, and the rate constants and activation parameters are given in Table 2.

Product Ions

The cyclization reactions are characteristically extremely clean with no extraneous base-line absorptions present even at high gain. The cyclopentenyl cations themselves show rather simple spectra with several sharp peaks present in most cases. Even with a multi-component product, *e.g.* from ion **6**, sharp peaks characteristic of each of the four product ions can easily be located. Table 3 lists the product ions formed and in Table 4, the n.m.r. spectra of some of these ions are tabulated. Only ions **17** and **26** were new and these could be unambiguously characterized. For ion **26**, there is no alternative structure; for ion **17**, the n.m.r. spectrum is broadly consistent with either structure **17** or **27**. However, ion **27** would rearrange to ion **18** much more rapidly than observed; the formation of **27** is mechanistically improbable and on closer consideration, does not fit the n.m.r. spectra (in particular, the C-1 methyl group is a triplet and this has been shown in other cases (9) to be the result of coupling with a methylene group at C-4).

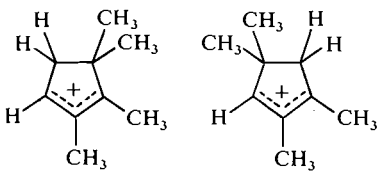

17 **27**

The products from dienylic ion **10** are **23** and **25**. This result has also been found by Brouwer and Van Doorn (7) using the FSO_3H–SbF_5 solvent system and, as reported by these authors, the products reported (5) in an earlier study of this system are not those first formed.

In the last column of Table 3 are listed the cyclopentenyl cation products eventually formed and in Table 5 the rate constants for several of these processes are given. The last measurements show, for example, that the dienylic ion **6** produces the 50% of cyclopentenyl cation **18** from some intermediate ion and that this ion is not produced from **17**, **19**, or **20** since these reactions occur at much higher temperatures. By contrast, in the case of the dienylic ion **9**, the cyclopentenyl ion product **23** is quite possibly the primary product with the others, **21**, **22**, and **24**, being formed at a rate comparable with the rate of disappearance of the dienylic cation. The further rearrangement of the cyclopentenyl cations derived from the

Can. J. Chem. Downloaded from www.nrcresearchpress.com by 210.87.254.42 on 09/05/12
For personal use only.

TABLE 3. Product ions observed

Dienylic ion	Solvent	First observed product[a]	Final observed product[a]
3	$ClSO_3H$	**12**	**13**
4	$ClSO_3H$, H_2SO_4, or FSO_3H–SbF_5 (1:1)	**14**	**15**
5	SO_2ClF–FSO_3H (4:1)	**16**	**16**
6	$ClSO_3H$	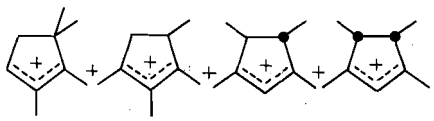 **17** (25%) **18** (50%) **19** (7%) **20** (18%)	**18**
7	$ClSO_3H$	**17**	**18**
8	$ClSO_3H$ or H_2SO_4	**18**	**18**
9	$ClSO_3H$	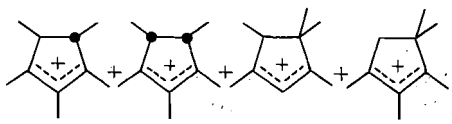 **21** **22** **23** (major) **24**	**21, 22, 24**
10	$ClSO_3H$	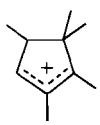 +**23** (38%) **25** (62%)	**21, 22, 24**
11	$ClSO_3H$	**26**	**26**

[a]Previous reports, **12** and **13** (4, 5); **14** (3*a*); **15**, prepared by an unambiguous synthesis; **16** (3*a*); **18** (3*a*, 6); **19** and **20**, prepared by an unambiguous synthesis; **21** and **22** (1); **23** (3–5, 7, 10); **24** (3–7, 10); **25** (7).
[b]The lines indicate methyl groups, with protons occupying the remaining positions.

Can. J. Chem. Downloaded from www.nrcresearchpress.com by 210.87.254.42 on 09/05/12
For personal use only.

TABLE 4. The n.m.r. spectra of cyclopentenyl cations[a]

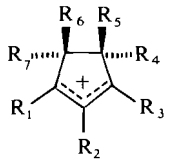

R = CH_3 or H

Ion	Chemical shift[b] R_1	R_2	R_3	R_4	R_5	R_6	R_7
12	6.80	2.12[c]	[j]	←6.85→		8.42[d,e]	6.25
13	6.90	7.72[c]	0.25	←6.23 and		6.50→	
14	6.85[f]	2.16[g]	−0.01[g]	←6.44→		←8.46[e]→	
15	7.08[h]	7.81[e]	7.08[h]	←6.50→			
17	7.055[i]	7.68	0.33	←6.60→		←8.50→	
26	7.23	7.85	7.23	←8.67→			

[a]Only those unreported or in cases where the spectra observed in this work are a considerable improvement over previous results. Most assignments of J (Hz) were confirmed by double irradiation.
[b]See footnote *a* of Table 1.
[c]d, $J = 4$.
[d]d, $J = 8$.
[e]This peak used for the area analysis.
[f]t, $J = 2$.
[g]d, $J = 3.7$.
[h]Complex peak due to coupling with methylene protons.
[i]t, $J = 2.5$.
[j]Too close to the acid lock signal to observe.

cyclization of cations **9** or **10** is quite dependent on the solvent. In H_2SO_4, only **24** is formed (3*a*), while in 1:1 FSO_3H–SbF_5, **24**, **21**, and **22** are formed (7). In $ClSO_3H$, an intermediate situation is realized with only small amounts of **21** and **22** present. In addition, the rate constant for this process (Table 4), for the $ClSO_3H$ solvent, is intermediate between the other two.

The ion **26** was heated to 100° and showed no indication of a line-broadening at this temperature from a degenerate methyl migration.

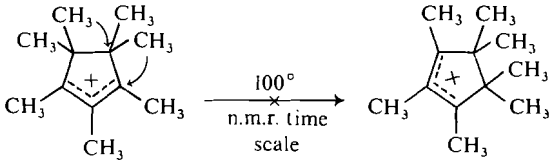

26

Discussion

Nomenclature of Dienylic Cations

Linear dienylic cations should, in our opinion, be named as derivatives of the basic pentadienyl unit,[1] numbering from 1 to 5. This procedure conveys a clearer mental picture of the structures under consideration than use of the "longest chain" criterion. A further drawback of the "longest chain" criterion occurs because one names these "by the rules" as undelocalized

TABLE 5. Rates of rearrangement of some cyclopentenyl cations[a]

Reaction	Solvent	$k_{obs} \times 10^4$ (s^{-1})	Temperature (°C)
12 → **13**	$ClSO_3H$	0.99	−10.4
14 → **15**	$ClSO_3H$	0.625	+25.0
17 → **18**	$ClSO_3H$	0.93	+25.0
23 → **24** + **21** + **22**	$ClSO_3H$	0.98[b]	+25.0

[a]The rates for **19** → **18** and **20** → **18** will be reported separately. The reactions are slow at 25°.
[b]Rate for the disappearance of cation **23**. Cations **21** and **22** are formed only in small amounts.

[1]The penta prefix might be considered redundant. It would in theory be possible however to have a butadienyl or a hexadienyl cation, *i.e.* C=C=C—$\dot{C}$ or C=C—C—C=C—$\dot{C}$. The penta therefore denotes a chain of five consecutive sp^2 centers.

Can. J. Chem. Downloaded from www.nrcresearchpress.com by 210.87.254.42 on 09/05/12
For personal use only.

Can. J. Chem. Downloaded from www.nrcresearchpress.com by 210.87.254.42 on 09/05/12
For personal use only.

structures; thus, the following resonance structures are penta-2,4-dien-1-yl and penta-1,4-dien-3-yl cation respectively.

A dienylic cation is a delocalized system and the dotted line formulation commonly used conveys this. A disadvantage of the dotted line formulation is the implication (false) that each bond order is the same in a completely charge delocalized structure. The dotted lines should therefore be taken only as an indication of charge delocalization with the bond orders generally alternating along the chain. In all finite-length chains, Hückel calculations will give each bond at least some π-bond order. In the case of pentadienyl cations, both theory and experiment (1) show that the 1–2 "bond" is stronger than the 2–3 "bond".

Two further nomenclature problems arise. (*1*) Theoretically, there are three possible planar structures for a pentadienyl cation, the so-called W, sickle and U forms (1). These designations

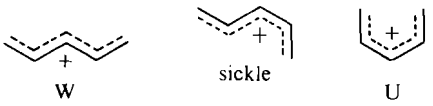

are apt in describing a pentadienyl cation but are not applicable to the higher polyenylic systems. (*2*) Substituents at the 1 or 5 positions can occupy two geometrically different positions and this needs to be designated in a complete description of the ion. We suggest that the E,Z nomenclature system (11) be used to designate both the shape of the pentadienyl cation and the position of terminal substituents. Thus, the following ions would be named:

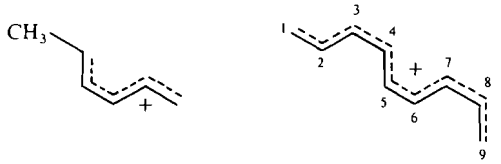

1E-Methyl-(2Z,3E)-pentadienyl cation

(2E,3Z,4E,5Z,6E,7Z)-Nonatetraenyl cation

For cyclic ions, where in general there are few, if any, geometrical isomers possible, it is probably more useful to employ the ring size criterion in naming the ion.

TABLE 6. Relative cyclization rates

Ion	Relative rate (25°)
8	1.0
9	2.4×10^3
4	5.4×10^3
7	3.1×10^4
3	3.7×10^4
6	5.2×10^4
10	3.2×10^5
5[a]	*ca.* 2×10^8

[a]Activation energy not measured. The extrapolation to 25° was made assuming $\Delta F^* \sim \Delta H^*$.

Structure of the Pentadienyl Cations in this Work

The coupling constants observed between vicinal protons of the chain are usually in the region 13–14 Hz, characteristic of a *trans* configuration. As previously postulated (2, 3*a*), the ground-state shape of the dienylic cations is very probably (2E,3E). Attempts in this laboratory to prepare a (2E,3Z) cation have so far failed, only the (2E,3E) isomer being observed.

Molecular model studies indicate that ions such as **10** would likely be non-planar (2, 3*a*) but

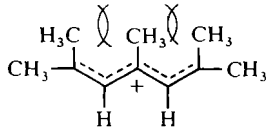

10

this does not appear to affect the chemical shift positions noticeably (Table 1).

The Cyclization Reaction

The cyclizations have very nearly the same rate in solvents of very different acid strength, adding to the previously observed stereospecificity (1) in showing that the reaction is in fact an electrocyclic one (12). This is also, of course, consistent with the observed invariance of the rates to concentration changes.

Taking the rate of the slowest member of the series, cation **8**, as unity, the relative cyclization rates at 25° are given in Table 6. The extreme values occur between two isomeric systems involving simply the placement of a methyl group at either C-1 or -3. These rate constants are not identical to the rate constants for the actual electrocyclic process since two equilibria are probably involved before the rate-determining

step. These equilibria are between the observed (2E,3E) ion and the less stable (2E,3Z or 2Z,3E) and (2Z,3Z) isomers.

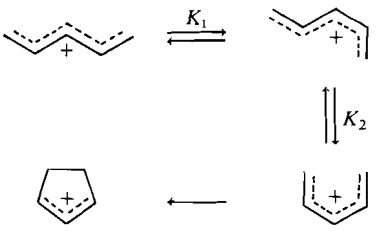

The first process is almost certainly an equilibrium situation since attempted preparation of the (2E,3Z) ion leads not to product but to the (2E,3E) ion. No experiments aimed at generating the (2Z,3Z) ion have been performed so that a rate-determining k_2 step is not precluded. However, analogy to the K_1 process makes this seem unlikely and if both equilibria are involved, $k_{obs} = K_1 K_2 k_{cyclization}$. Since a factor of 10^8 in cyclization rate between ions **8** and **5** seems inexplicable for $k_{cyclization}$, it is tempting to ascribe most of this difference to K_1 and K_2. There is, however, no steric or electronic reason why K_1 should be very different for these two ions and while K_2 might be larger because of the less serious 1,5-interaction in **5**, this particular effect cannot be very important since both cations **10** and **11** (like **5**) cyclize very rapidly.

From Table 2, one observes that all ions with a C-3 methyl-substituent cyclize very rapidly; other published (1) and unpublished examples confirm this. Conceivably a C-3 methyl group might radically change K_1, K_2, or $k_{cyclization}$. Once again, however, molecular model studies indicate that K_1 should not be radically changed. The effect on K_2 is less certain. In a non-planar (2Z,3Z) ion, one might preserve a planar allyl resonance by having the remaining double bond twisted out of the plane. In these circumstances, a C-3 substituent would certainly act to stabilize the ion. In a completely orthogonal system,[2] *i.e.* a purely allyl cation, one can estimate that a methyl *vs.* H at C-3 will be worth at least 5 kcal/mol (7, 13) energy difference. In a symmetrical dienylic cation, there are two equivalent structures but in an unsymmetrical case, it is possible that one form would be preferred.

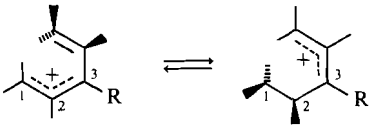

R = H or CH_3

An additional factor may be involved if one compares a non-planar (2E,3E) ion equilibrated with the corresponding, also non-planar (2Z,3Z) ion and a planar (2E,3E) ion equilibrated with the corresponding non-planar (2Z,3Z) ion. Then, if the (2Z,3Z) ions are of similar energy, there is clearly less energy difference in the former case (K larger).

Before culminating this discussion, it is worth examining the possible effects of methyl substituents on $k_{cyclization}$. The model reaction is the electrocyclic conversion of a (2Z,3Z)-pentadienyl cation to a cyclopentenyl cation. In this reaction, charge density is transferred from carbon atoms 1, 3, and 5 to atoms 2 and 4.

If this charge migration has partially occurred at the transition state, then methyl substitution at C-2 and -4 should aid the reaction. This is found experimentally but it is difficult to rule out a steric explanation for this.

In summary, we believe that the origin of the "C-3 methyl effect" lies mainly in the stabilizing effect of this group on a non-planar (2Z,3Z) intermediate ion, further increased in certain cases, by the destabilizing effect this group has on the ground state planarity of the (2E,3E) ion.

Rearrangements Within the Product Ions

At this point it should be made clear that the structure of the primary cyclopentenyl cation product produced in an electrocyclic reaction is known if one knows the structure of the dienylic cation. In our present examples, only cyclopentenyl cation **26** is a primary product. In the other cases, a rearranged cyclopentenyl cation (often of intermediate stability) is initially observed. This then rearranges to the final room temperature stable product ion in an observable reaction (Table 5). For this to happen, the rate

[2]In this extreme case, the distinction between a (2E,3Z) and a (2Z,3Z) ion disappears since the rotation occurs about an essentially single bond.

Can. J. Chem. Downloaded from www.nrcresearchpress.com by 210.87.254.42 on 09/05/12
For personal use only.

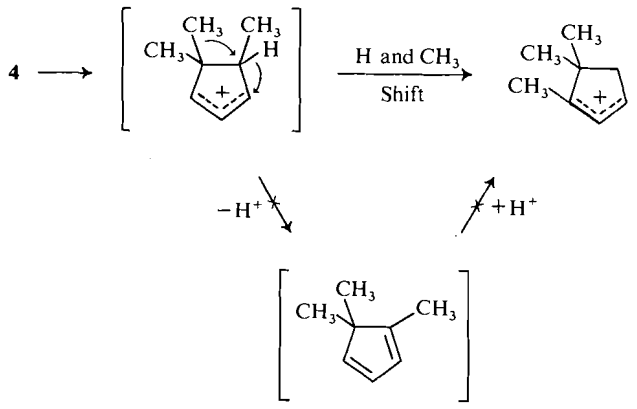

SCHEME I

of this latter process is comparable with or slower than the cyclization rate of the dienylic cation. One will therefore *observe* the least stable product ions in those cases where the dienylic cation cyclizations are fastest.

Several of the rearranged ions contain the same methyl substitution pattern as the primary product ions (**12**, **14**, and **16**). These ions could have been formed by way of methyl and/or hydride shifts or by a deprotonation–protonation mechanism (10, 14) (see Scheme 1). However, in cases where these reactions have been carried out in D_2SO_4 solvent (9), no deuterium atoms were initially observed in the product and it seems very likely that only methyl and/or hydride shifts are involved in the reactions of the very unstable, primary, cyclopentenyl ions. Some of the subsequent, much slower, observable rearrangements occur however by the deprotonation–protonation mechanism (10, 14).

The product ions observed from the cyclization of pentadienyl cations **6**, **7**, **9**, and **10**, although more complex, offer in many ways a better insight into the mechanism of the reactions than do the simpler cases. Since the cyclization of **9** has been discussed in considerable detail (7), we will concentrate mainly on the others.

The Tetramethyl Case

The four isomeric dienylic cations **5**, **6**, **7**, and **8** each gives its own characteristic product mixture (Table 3). At this juncture, we shall assume that these rearrangements involve only methyl and/or hydride shifts and, like Brouwer and Van Doorn (7), that the intermediate obtained by these shifts be a tertiary cation. For a tetramethyl system, there are only six possible non-conjugated cation structures, labelled **A**–**F**.

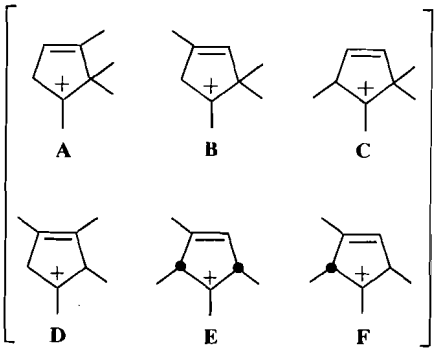

In the conjugated cyclopentenyl cations, there are twelve isomers possible; those observed in this work (Table 3) are **16**, **17**, **18**, **19**, and **20**. The remainder, **27**–**33**, are shown below:

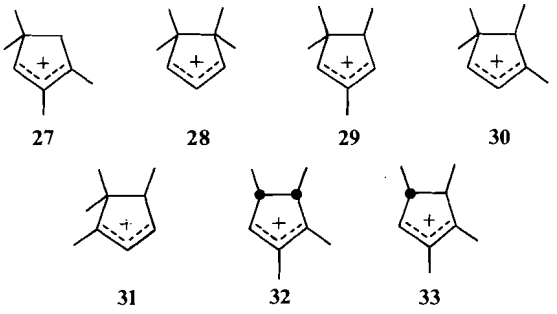

Can. J. Chem. Downloaded from www.nrcresearchpress.com by 210.87.254.42 on 09/05/12
For personal use only.

Can. J. Chem. Downloaded from www.nrcresearchpress.com by 210.87.254.42 on 09/05/12
For personal use only.

The cyclization reactions of ions **5**, **6**, **7**, and **8** can now be written:

$$\mathbf{5} \rightarrow [\mathbf{29}] \rightarrow [\mathbf{B}] + [\mathbf{E}] + [\mathbf{F}]$$

$$\mathbf{6} \rightarrow [\mathbf{30}] \rightarrow [\mathbf{C}] + [\mathbf{E}] + [\mathbf{F}]$$

$$\mathbf{7} \rightarrow [\mathbf{31}] \rightarrow [\mathbf{C}] + [\mathbf{A}]$$

$$\mathbf{8} \rightarrow [\mathbf{28}] \rightarrow [\mathbf{C}]$$

When the intermediates **A**–**F** rearrange back to the conjugated compounds we will assume that this process will occur preferentially so as to leave a tertiary center on what now will become part of the developing allyl cation. This then results in the following:

$$[\mathbf{A}] \rightarrow \mathbf{17}$$

$$[\mathbf{B}] \rightarrow \mathbf{16}$$

$$[\mathbf{C}] \rightarrow [\mathbf{30}] + [\mathbf{31}]$$

$$[\mathbf{D}] \rightarrow \mathbf{18}$$

$$[\mathbf{E}] \rightarrow \mathbf{20} + [\mathbf{32}]$$

$$[\mathbf{F}] \rightarrow \mathbf{19} + [\mathbf{33}]$$

Each of the bracketed ions is still an unobservable intermediate under the conditions of these experiments. The ions **30** and **31** can re-enter the previous reaction scheme. The ions **32** and **33** give the following:

$$[\mathbf{32}] \rightarrow [\mathbf{E}] + [\mathbf{D}]$$

$$[\mathbf{33}] \rightarrow [\mathbf{F}] + [\mathbf{D}]$$

Exit via intermediate [**D**] should then give ion **18** as the ultimate product. Putting all these predictions together, one gets the following:

$$\mathbf{5} \rightarrow \mathbf{16} + \mathbf{18} + \mathbf{19} + \mathbf{20}$$

$$\mathbf{6} \rightarrow \mathbf{17} + \mathbf{18} + \mathbf{19} + \mathbf{20}$$

$$\mathbf{7} \rightarrow \mathbf{17} + \mathbf{18} + \mathbf{19} + \mathbf{20}$$

$$\mathbf{8} \rightarrow \mathbf{17} + \mathbf{18} + \mathbf{19} + \mathbf{20}$$

The predictions work in the case of **6** and probably also for **8** since it can be shown that **17**, **19**, and **20** all yield **18** in reactions which are considerably faster than the initial cyclization reaction of **8**. However, the dienylic cation **5** forms only **16** and **7** forms only **17**. This suggests that cyclopentenyl cation **29** does not give the intermediate **E** and that **31** does not give the intermediate **C**. Both these processes are methyl migrations and it appears that hydride shifts may involve a slightly lower activation energy in most cases.

Further Rearrangements within This Series

The observable cations **17**, **19**, and **20** eventually rearrange to **18** (see Tables 3 and 5). Based on our previous rules, cation **17** is in a blind maze and cannot exit to a more stable product, *i.e.*, $\mathbf{17} \rightarrow [\mathbf{A}] \rightarrow \mathbf{17} \rightarrow [\mathbf{A}]$, etc. This process could for example be followed with an isotopic label. One could relax the game rules in any one of three ways: (*1*) one could allow secondary cation intermediates; (*2*) one could allow migration back from the intermediate in which a secondary allyl cation center was generated; or (*3*) one could change the mechanism to a deprotonation–protonation process. Only the first process can explain the reaction of $\mathbf{17} \rightarrow \mathbf{18}$ and the high energy of the secondary intermediate accounts for the fact that **17** can even be observed. The mechanism of the rearrangement of **19** and **20** to **18** will be published separately.

Proof of the Existence of Intermediates (i.e. **A**–**F**)

The methyl and hydride migrations could plausibly have occurred via a direct 1,3-shift (although this is not allowed as a thermal, suprafacial, sigmatropic reaction (12)) or by two concerted 1,2-shifts (*3a*). The present results can be added to those of Brouwer and Van Doorn (7) in showing that an actual intermediate must be involved. The dienylic cation **6** gives both the *trans* and *cis* ions **19** and **20**. These could only have been formed by conducting both migrations between the *same* two carbon atoms, an obviously non-concerted process (see Scheme 2). The formation of more of the *cis* ion **20** than of the *trans* ion **19** indicates that the more sterically hindered methyl group in **30** preferentially migrates. Little can be said about the charge delocalization in these "unconjugated intermediates" beyond the observation that considerable charge must be situated at the formal cation center since there appears to be a large difference in energy between secondary and tertiary structures.

The general principles discussed in this paper can be used to rationalize the formation of the rearrangement products in the cyclization of the dienylic cations **3**, **4**, **9**, and **10**.

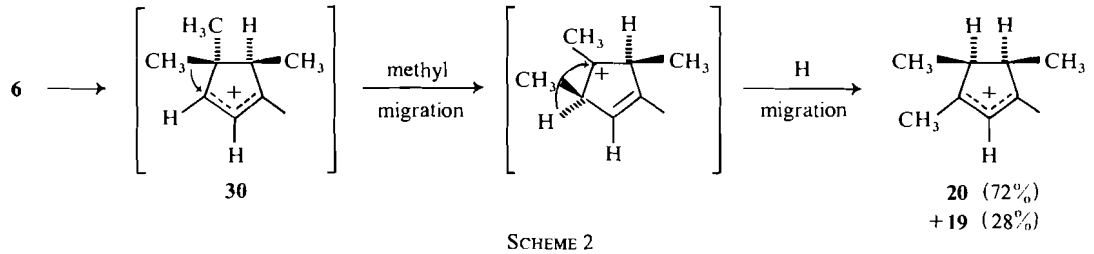

SCHEME 2

Experimental

Preparation of the Cations

The cations **8** and **9** were prepared by the gas phase addition of the corresponding trienes, to the acids, as described previously (*3a*). In all other cases, the alcohols were added directly to the acids using a microlitre syringe to reduce the drop size. The sulfuric acid solutions were supercooled to *ca.* $-30°$ during the addition. The chlorosulfonic acid was BDH reagent grade and was cooled in a Dry-Ice bath during the alcohol addition operation. A magnetic stirring bar was used to stir both solutions. In the chlorosulfonic acid case, care is needed to ensure that the addition is carried out slowly since the alcohol droplets mostly solidify on contact with the cold acid. Under these conditions, cation formation is relatively slow and in some cases this necessitates a slight warming of the acid solution. The alcohol addition to 1:1 FSO_3H–SbF_5 was carried out at about $-30°$ since this mixture becomes very viscous at lower temperatures. The very low temperature preparations were accomplished by adding the dienol to 4:1 SO_2ClF–FSO_3H, contained in an n.m.r. tube at $-130°$. The dienol was frozen in small amounts onto the end of a cold, coiled platinum wire and this was then introduced into the n.m.r. tube and vigorously moved up and down in the acid. The cation concentrations, unless specified, were *ca.* 10% weight of alcohol per volume of acid. The n.m.r. spectra of the cations are reported in Tables 1 and 4.

Kinetic Procedures

Initially, the methanol calibration method was used to obtain the temperatures of the solutions in the n.m.r. probe, but this proved hopeless, partly because of the large temperature uncertainty ($\pm 1°$) and partly the unknown temperature change which may have accompanied the switch of n.m.r. tubes for the calibration. Temperatures were therefore monitored using a 40 gauge copper–constantin thermocouple in a sealed glass capilliary immersed directly into the acid solution. The n.m.r. tubes spun around the stationary thermocouple and the lower level of this was adjusted to be just outside the cavity region, since no appreciable temperature gradient was observed. Placing the thermocouple directly into the cavity region was possible but this tended to upset the leakage and therefore gave erratic peak sizes. A Honeywell model 2781 potentiometer combined with a model 3131 millivolt galvanometer was used for the e.m.f. measurement. It was usually necessary, to counter gradual temperature drifts within the samples, to maintain a constant liquid nitrogen level and to periodically adjust the nitrogen gas flow level. It is difficult to put an error value on the temperatures quoted for the kinetics. Runs in which the temperature range of recorded values exceeded 0.1° were discontinued so an outside error range of $\pm 0.05°$ seems reasonable. The cyclization rates for cation **8** were obtained using a constant temperature bath, periodically quenching the solutions in Dry-Ice, and then recording the spectra at a temperature where the reaction rate is very slow. The first order rate constants for each reaction, using the integrated rate law form, were obtained from an unweighted least squares fit, the computer input being the peak height and peak width at half peak height or the planimeter area, together with the number of protons that the peak represents. The actual dienylic cation peaks used in each case are denoted in Table 1. In Table 4, some of the cyclopentenyl cation peaks used are also noted. Where several products result, the area of the product peak followed was corrected for the percentage of the total that this particular product represented. The errors were calculated in two ways: (*1*) The standard deviations were obtained by least squares analysis, having first rejected points $> 1.7\,\sigma$ from the mean in an iterative process. Relatively few points were actually rejected. (*2*) The regression equation of $\ln(a/a - x)$ on t (*s*) had the analytical error applied to the ln term as a plus and minus quantity at the start and finish respectively. The analytical error was based on the reproducibility of peak heights, areas, etc. and temperature variations, although the latter do not contribute much. These data can be found in ref. 15. Repeat runs are difficult to do because the temperature cannot be exactly matched. All runs were therefore single determinations. The thermodynamic parameters were calculated using a simple least squares fit of the rate data. Rate constant values were not used if $\sigma/k \times 100$ was greater than 7%. The error in E_a was estimated using the analytical errors estimated for the rate constants using the vector sum method (16). These ranged from ± 1.5 to $\pm 7.7\%$ ($\Delta E_a/E_a \times 100$).

Preparation of the Dienols

The n.m.r. spectra of the dienols (10% solutions in CCl_4 or $CDCl_3$) were recorded on a Varian Assoc. A-60 n.m.r. spectrometer and are reported in the τ scale relative to internal TMS. All compounds were checked for purity using g.l.c. (5% SE-30 on Chromosorb), but most of the dienols dehydrate under these conditions. The dienols were therefore carefully fractionated using an 18 in. spinning band column, employing a high reflux ratio, and purity judgements were based on the n.m.r. spectra observed. All boiling points are uncorrected. The n.m.r. spectra are reported in the text using the following abbreviations, s = shoulder, d = doublet, t = triplet, (3H) = integrates approximately for three protons, all coupling constants are in Hz units, and each peak of the presumed multiplet is listed. No

Can. J. Chem. Downloaded from www.nrcresearchpress.com by 210.87.254.42 on 09/05/12
For personal use only.

attempt was made to completely analyze complex multiplets beyond ascertaining that this complexity was expected.

(3E,5E)-3,5-Heptadien-2-ol

This alcohol was prepared by the addition of methyl lithium to sorbaldehyde (3*a*).

(5E)-2-Methyl-2,5-heptadien-4-ol, (5E)-2,3-Dimethyl-2,5-heptadien-4-ol, and (5E)-2,4-Dimethyl-2,5-heptadien-4-ol

These alcohols were prepared as described by Braude and co-workers (18, 19, 20).

2,4,6-Trimethyl-2,5-heptadien-4-ol

This alcohol and the dehydration products were prepared as described in the literature (17).

(5E)-2,5-Dimethyl-2,5-heptadien-4-ol

To 3.7 g (0.50 mol) of lithium metal (1% Na) in 500 ml of dry ether, under an argon atmosphere, and contained in a 2 l three-necked flask fitted with a condenser, gas inlet tube, and mercury vent and stirred with a magnetic stirring bar, at 0°, was added, over a 1 h period, 33.5 g (0.25 mol) of 1-bromo-2-methyl-1-propene in 200 ml of ether. The reaction started immediately. After standing for an additional hour, 21 g (0.25 mol) of (2E)-2-methylbut-2-enal in 100 ml of ether was slowly added. The excess lithium was filtered off and water added cautiously. The aqueous layer was separated and extracted with a further 200 ml of ether and the combined ether layer washed three times with water (3 × 100 ml). The solution was dried over anhydrous $MgSO_4$ and, after removal of the ether, distilled through an 18 in. spinning band column to give 19.6 g (56%) of the title alcohol, b.p. 82° (8.5 mm).

Anal. Calcd. for $C_9H_{16}O$: C, 77.09; H, 11.50. Found: C, 77.44; H, 11.34.

The n.m.r. spectrum showed: 8.46 (3H); 8.35, 8.33, 8.30, and 8.28 (9H); 7.40 (1H) OH peak; 5.51 and 5.37, d, $J = 8$, (1H); multiplets centered at 4.91 and 4.77, (1H), with a primary coupling constant of *ca.* 8; a series of peaks from 4.4–5.1 (1H).

2,3,6-Trimethyl-2,5-heptadien-4-ol

The title alcohol, b.p. 57.5° (0.85 mm), was prepared in 59% yield from 2-bromo-3-methyl-2-butene (21) and 3-methyl-2-butenal (22), 0.13 *M* scale, using the above procedure.

Anal. Calcd. for $C_{10}H_{18}O$: C, 77.87; H, 11.76. Found: C, 77.82; H, 11.73.

The n.m.r. spectrum showed: 8.20, 8.10, and 8.03, complex multiplets, *ca.* (13H); 5.05 and 4.93, broad, d, $J = 7$ (1H); 3.78 and 3.65, d, $J = 7$, both halves further split by methyl groups (1H).

3,4-Dimethyl-1-pentyne-3-ol

This alcohol was prepared by the procedure of Naves and Ardizio (23), except that the 3-methyl-2-butanone was added after the acetylene addition to the sodium amide–liquid ammonia.

3,4-Dimethyl-3-penten-2-one

This ketone was prepared from 3,4-dimethyl-1-pentyne-3-ol using the procedure of Takeshima *et al.* (24). The crude compound was purified from what appeared to be an aldehydic impurity by column chromatography on basic alumina.

2,3,4,5,6-Pentamethyl-2,5-heptadien-4-ol

The title alcohol, b.p. 43.5° (0.01 mm), was prepared from 2-bromo-3-methyl-2-butene and 3,4-dimethyl-3-penten-2-one using the standard procedure (0.4 *M* scale). The yield of pure alcohol obtained was 0.5 g (7%) but there is further impure material in the forerun and residue fractions.

Anal. Calcd. for $C_{12}H_{22}O$: C, 79.06; H, 12.16. Found: C, 79.29; H, 12.25.

The n.m.r. spectrum showed: 8.68 (3H); 8.41, 8.34, and 8.25, a complex series of peaks, *ca.* (19H).

The authors wish to thank the National Research Council of Canada for financial support.

1. P. H. Campbell, N. W. K. Chui, K. Deugau, I. J. Miller, and T. S. Sorensen. J. Am. Chem. Soc. **91**, 6404 (1969).
2. T. S. Sorensen. *In* Carbonium ions. *Edited by* G. A. Olah and P. v. R. Schleyer. Volume II. Wiley–Interscience Publishers, New York. 1970. Chapt. 19.
3. (*a*) T. S. Sorenson. Can. J. Chem. **42**, 2768 (1964). (*b*) N. C. Deno, R. C. Haddon, and E. N. Nowak. J. Am. Chem. Soc. **92**, 6691 (1970).
4. T. S. Sorensen. Can. J. Chem. **43**, 2745 (1965).
5. G. A. Olah, C. U. Pittman, Jr., and T. S. Sorensen. J. Am. Chem. Soc. **88**, 2331 (1966).
6. N. C. Deno, and C. U. Pittman, Jr. J. Am. Chem. Soc. **86**, 1871 (1964).
7. D. M. Brouwer and J. A. Van Doorn. Rec. Trav. Chim. **89**, 333 (1970).
8. N. C. Deno, H. G. Richey, Jr., N. Friedman, J. D. Hodge, J. J. Houser, and C. U. Pittman, Jr. J. Am. Chem. Soc. **85**, 2991 (1963).
9. T. S. Sorensen. J. Am. Chem. Soc. **89**, 3782 (1967).
10. N. C. Deno. Progr. in Phys. Org. Chem. **2**, 129 (1964).
11. IUPAC tentative rules for the nomenclature of organic chemistry. Section E. Fundamental stereochemistry. J. Org. Chem. **35**, 2849 (1970).
12. R. B. Woodward and R. Hoffman. The conservation of orbital symmetry. Verlag Chemie, Weinheim. 1970.
13. T. S. Sorensen and K. Ranganayakulu. Can. J. Chem. In press.
14. T. S. Sorensen, I. J. Miller, and C. M. Urness. Can. J. Chem. **48**, 3374 (1970).
15. R. Bladek. M.Sc. Thesis. University of Calgary, Calgary, Alberta. 1971.
16. S. W. Benson. The foundations of chemical kinetics. McGraw–Hill Co. Inc., New York. 1960. p. 86.
17. T. S. Sorensen. Can. J. Chem. **42**, 2781 (1964).
18. E. A. Braude and C. J. Timmons. J. Chem. Soc. 2007 (1950).
19. E. A. Braude and J. A. Coles. J. Chem. Soc. 1425 (1952).
20. E. A. Braude and E. A. Evans. J. Chem. Soc. 3331 (1955).
21. J. K. Farrell and C. B. Bachman. J. Am. Chem. Soc. **57**, 1281 (1935).
22. N. L. Wendler and H. L. Slater. J. Am. Chem. Soc. **72**, 5341 (1950).
23. Y. R. Naves and P. Ardizio. Helv. Chim. Acta **31**, 2252 (1948).
24. T. Takeshima, N. Nagaoka, M. Yokoyama, and S. Morita. Bull. Chem. Soc. Jap. **32**, 548 (1959).

Can. J. Chem. Downloaded from www.nrcresearchpress.com by 210.87.254.42 on 09/05/12
For personal use only.

Adiabatic Calorimetric Studies of the Adsorption of Sulfur Dioxide at 423 °K on Heat-treated Magnesias Characterized by Electron Microscopy

R. W. GLASS AND R. A. ROSS

Department of Chemistry, Lakehead University, Thunder Bay, Ontario

Received April 4, 1972

Calorimetric heats of adsorption of sulfur dioxide at surface coverages from 0.2 to 7.7 μmol m^{-2} have been measured on a series of magnesias heat-treated at 600, 700, and 800 °C. Structural features of the adsorbents have been characterized by analysis of nitrogen adsorption–desorption isotherms and by transmission electron microscopy.

Heats of adsorption at 423 °K for adsorbed amounts of 0.3 μmol m^{-2} were respectively, 86.0, 87.0, and 77.0 kcal mol^{-1} for the 600, 700, and 800 °C samples. The values for the 600 and 700 °C samples fell rapidly above a coverage of 2.0 μmol m^{-2} to around 44.0 kcal mol^{-1} at 5.0 to 7.0 μmol m^{-2}, while the values for the 800 °C sample decreased continuously to 39.0 kcal mol^{-1} at the same coverage.

Crystallite shapes tended increasingly towards the cubic form as the temperature of heat-treatment was increased and average particle sizes were 80, 240, and 320 Å for the 600, 700, and 800 °C samples, respectively.

It is proposed that the very high heats obtained on all the samples are due to interactions with high-energy defect centers in the oxide and with the formation of magnesium sulfite initially, and magnesium sulfate towards monolayer completion.

Les chaleurs calorimétriques d'adsorption du dioxyde de soufre pour des recouvrements de surface de 0.2 à 7.7 μmol m^{-2}, ont été mesurées sur une série de magnésies, traitées à 600, 700 et 800 °C. Les caractéristiques structurales des adsorbants ont été identifiées par analyse des isothermes d'adsorption et de désorption de l'azote et par microscopie électronique par transmission.

Les chaleurs d'adsorption à 423 °K pour des quantités adsorbées de 0.3 μmol m^{-2} sont respectivement de 86.0, 87.0, et 77.0 kcal mol^{-1}, pour les échantillons à 600, 700, et 800 °C. Les valeurs pour les échantillons à 600 et 700 °C tombent rapidement pour un recouvrement supérieur à 2.0 μmol m^{-2}; environ 44.0 kcal mol^{-1} pour 5.0 à 7.0 μmol m^{-2}; tandis que les valeurs pour l'échantillon à 800 °C décroissent de façon continue jusqu'à 39.0 kcal mol^{-1} pour le même recouvrement. Les formes cristallines tendent de façon croissante vers la forme cubique, au fur et à mesure que la température du traitement augmente; les dimensions moyennes des particules sont de 80, 240, et 320 Å respectivement pour les échantillons pris à 600, 700, et 800 °C.

Il a été proposé que les très fortes chaleurs obtenues sur tous les échantillons sont dues aux interactions entre les centres de défaut de haute énergie dans l'oxyde et la formation initiale du sulfite de magnésium et de sulfate de magnésium avec la monocouche de saturation.

[Traduit par le journal]

Canadian Journal of Chemistry, **50**, 2817 (1972)

Introduction

Studies have been reported recently of the adsorption of sulfur dioxide on transition metal oxides supported on silica gel (1), on silica gels (2), and on γ-aluminas (3). Calorimetric heats of adsorption and adsorption isotherms were determined at 423 °K. The adsorbents were characterized by measurement of surface area, pore size distributions, and hydroxyl group concentrations. These data were used to interpret the nature of the adsorbate–adsorbent interactions (1–3).

The results obtained for the sorption of sulfur dioxide on silica gels (2), largely covalent solids, and γ-aluminas (3), covalent solids with some ionic sites, indicated that a study of the sorption of sulfur dioxide on an oxide adsorbent in which ionic bonds predominate would help to elucidate any general features regarding the rôle of the solids in the surface reactions. Magnesia was chosen for this purpose with the added incentive that little or no work has been reported on the sorption of sulfur dioxide on this material.

Useful previous studies of the sorption of gases on magnesia of some relevance to this work include those on water vapor (4) and carbon dioxide (5, 6). Results from the latter have been used to estimate the number (5) and type (6) of basic sites present on the surface of the oxide.

Experimental

Materials

Magnesia was prepared by decomposing "Baker An-

Can. J. Chem. Downloaded from www.nrcresearchpress.com by 210.87.254.5 on 09/05/12
For personal use only.

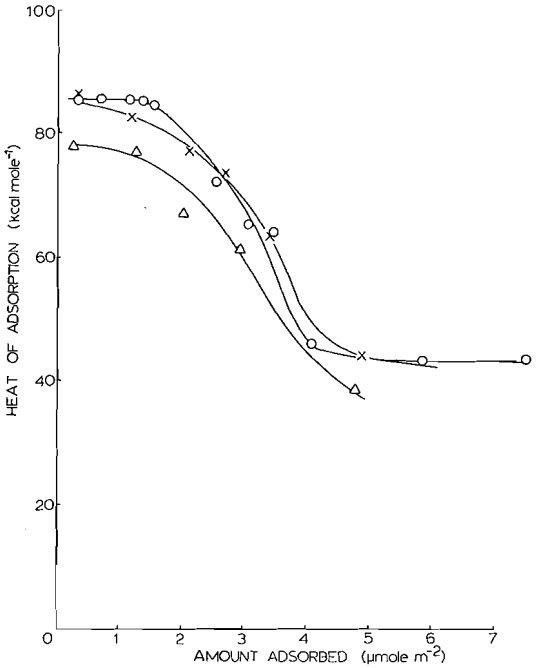

FIG. 1. Heat curves for the adsorption of sulfur dioxide at 423 °K on heat-treated magnesias. Heat treatment at ○, 600 °C; ×, 700 °C; △, 800 °C.

alyzed" basic magnesium carbonate in air at 550 °C for 1 h. Samples of this material were then heat-treated in air at 600, 700, and 800 °C for 24 h. X-Ray powder diffraction photographs showed the characteristic lines of magnesium oxide (7) for all the samples. However, the lines for the 600 °C sample were more diffuse than for the others.

Immediately after heat-treatment, samples were cooled over phosphoric anhydride, transferred to the appropriate apparatus and then outgassed at 150 °C overnight at $<10^{-4}$ mm.

The quality of the nitrogen and sulfur dioxide has been described (1).

Apparatus

Heats of adsorption were determined calorimetrically in a similar apparatus to that described earlier (1). Nitrogen adsorption–desorption isotherms (77 °K) were measured in a standard apparatus (8) and pore size distributions (9) calculated with the aid of an IBM 360/50 computer. Mercury "lump" densities were measured as described previously (10).

The "water content" of the magnesias was determined gravimetrically (8) to constant weight at 1200 °C in a static air atmosphere using a recording thermobalance (Stanton–Redcroft Model HT5A). This method gives the total amount of water released by the sample at 1200 °C and was not used to distinguish among the various states of water or its dissociated forms that may be present in the bulk or surface of the magnesias.

Electron micrographs were taken with a Philips EM 300G instrument and crystallite structures examined by the direct transmission technique described earlier (3).

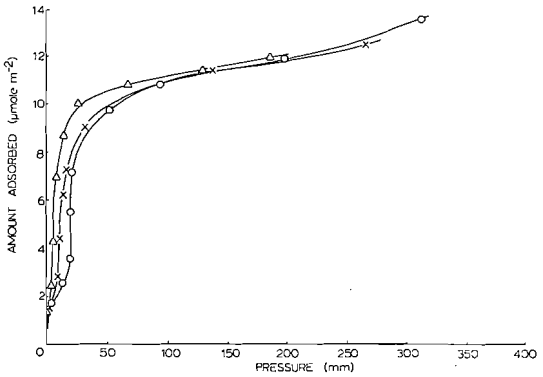

FIG. 2. Adsorption isotherms for sulfur dioxide at 423 °K on heat-treated magnesias. Heat treatment at ○, 600 °C; ×, 700 °C; △, 800 °C.

Results

Heats of Adsorption and Adsorption Isotherms for Sulfur Dioxide

Heats were determined at 423 °K for surface coverages from 0.2 to 7.7 μmol m^{-2} for the 600 °C sample, and between 0.2 and 4.9 μmol m^{-2} for the 700 and 800 °C samples.

High heats of adsorption were observed on all the adsorbents even at coverages approaching a monolayer (7.0 μmol m^{-2} (1)), Fig. 1. The heat curves are of similar general shape although the curve for the 600 °C sample exhibits a sharper heat drop than the others at a coverage of about 2.0 μmol m^{-2}. In addition, although the heats evolved could be measured up to coverages of 11.4 μmol m^{-2} for all the samples, the volume of gas adsorbed was too small (<0.1 cc) to be measured accurately. A minimum estimate of these heats could be made by taking the volume of gas adsorbed as 0.1 cc for heats at coverages greater than a monolayer. On this basis these heats are of the order of 45 ± 10 kcal mol^{-1}.

Figure 2 shows the adsorption isotherms for sulfur dioxide at 423 °K. With the 600 °C sample a definite change in the shape of the isotherm occurs at a coverage of approximately 2.0 μmol m^{-2}. Adsorption equilibrium times for all the adsorbents were of the order of 15 to 45 min for coverages up to 2.0 to 5.0 μmol m^{-2}, respectively, and up to 24 h for coverages greater than 7.0 μmol m^{-2}.

Analysis

Samples of the desorbed gas from all surfaces were analyzed using a Beckman IR-12 infrared

Can. J. Chem. Downloaded from www.nrcresearchpress.com by 210.87.254.5 on 09/05/12
For personal use only.

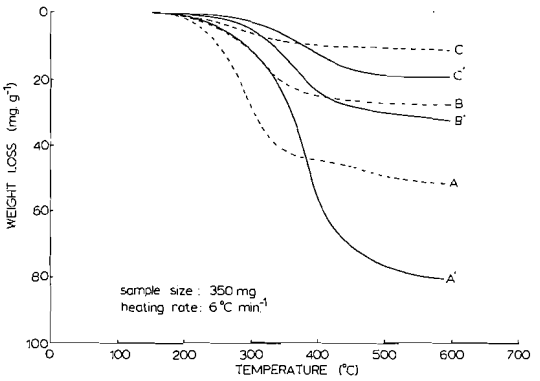

FIG. 3. Thermograms of MgO and MgO residues after adsorption of sulfur dioxide at 423 °K. Samples pre-heated to constant weight at 423 °K. *A*, MgO_{600}; *B*, MgO_{700}; *C*, MgO_{800}; the primes refer to MgO residues. Sample size, 350 mg; heating rate, 6 °C min^{-1}.

spectrophotometer. Neither water nor any other impurity was detected in any of these samples.

The residues were pumped at 150 °C at $< 10^{-4}$ mm for 30 min and then subjected to qualitative chemical analysis (11). The presence of magnesium sulfite and a very small amount of magnesium sulfate was detected on all samples. Tests for the presence of magnesium sulfide and elementary sulfur were inconclusive.

Samples of the residues were analyzed thermogravimetrically in a static air atmosphere. The samples were heated until constant weight at 150 °C and then programed at a uniform rate of 6 °C min^{-1}, Fig. 3. All three residues exhibited a maximum rate of weight loss at about 375 °C. Although some water had been adsorbed onto the samples in the act of transfer prior to thermogravimetric analysis, approximately 90% of this water was removed at 350 °C, Fig. 3. Taking this factor into account, the weight losses observed for the 600, 700, and 800 °C residues correspond to adsorbed amounts of sulfur dioxide at 423 °K of 7.5, 5.5, and 6.0 μmol m^{-2}, respectively.

Nitrogen Adsorption–Desorption Measurements

The nitrogen adsorption–desorption isotherm for the 600 °C sample has a different shape from those of the 700 and 800 °C samples, Fig. 4. A relatively large amount of nitrogen is adsorbed below $p/p_0 = 0.03$ while above this value the amount adsorbed increased rapidly as $p/p_0 \rightarrow 1$. The desorption isotherm formed a very narrow hysteresis loop which extended

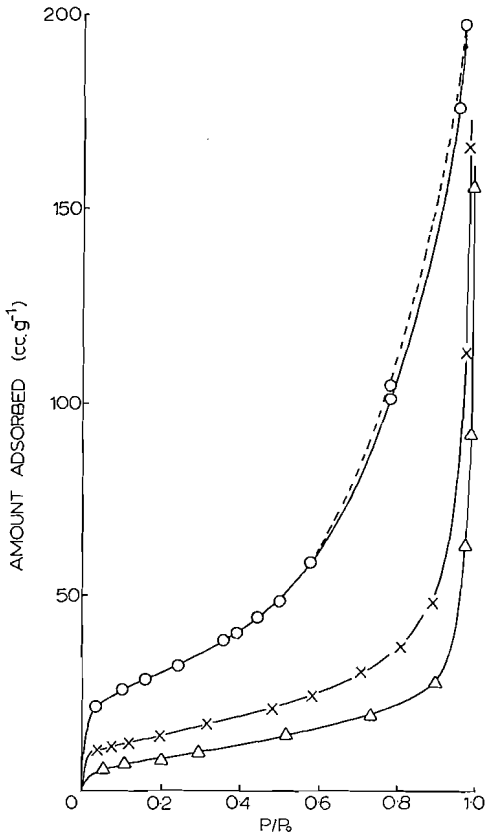

FIG. 4. Nitrogen adsorption–desorption isotherms at 77 °K on heat-treated magnesias. Heat treatment at ○, 600 °C; ×, 700 °C; △, 800 °C.

from $p/p_0 \sim 1$ to $p/p_0 = 0.6$ and closed smoothly with the adsorption leg.

The isotherms of the 700 and 800 °C samples were very similar in shape. Above $p/p_0 = 0.03$ the isotherms were linear up to $p/p_0 = 0.7$. Above $p/p_0 = 0.9$ the amount of nitrogen adsorbed increased very rapidly as $p/p_0 \rightarrow 1$. The isotherms of the 700 and 800 °C samples were completely reversible and no hysteresis was observed.

The pore size distributions, calculated from the desorption leg of the isotherm on a differential basis, are shown in Fig. 5. The 600 °C sample exhibited two maxima, one at 55 Å and a smaller one at 38 Å. The pore diameter range extended from 22 to 180 Å. The distributions for the 700 and 800 °C samples were very similar: both samples showed principal maxima at 22 and 35 Å. The pore diameter range extended from 19 to 200 Å for both samples.

Can. J. Chem. Downloaded from www.nrcresearchpress.com by 210.87.254.5 on 09/05/12
For personal use only.

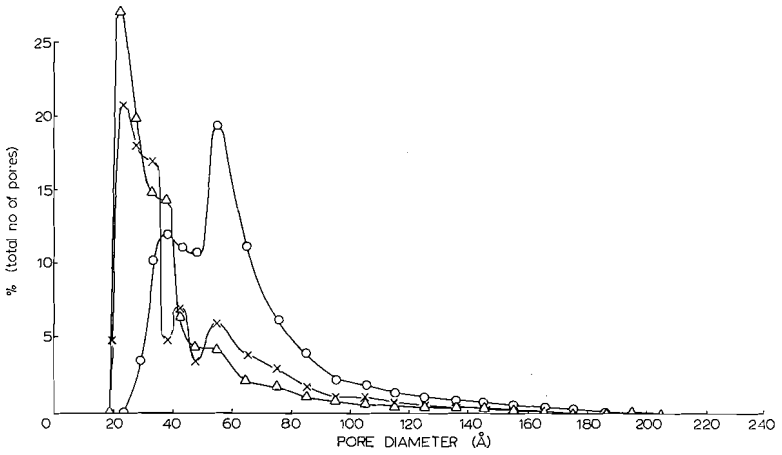

FIG. 5. Pore size distributions based on nitrogen desorption isotherms. Magnesia heat-treated at ○, 600 °C; ×, 700 °C; △, 800 °C.

TABLE 1. Surface area, "water contents", and mercury densities for the heat-treated magnesias

Temperature of heat-treatment (°C)	Surface area ($m^2 g^{-1}$)	"Water content" ($\mu mol\ H_2O\ m^{-2}$)	Mercury density ($g\ cc^{-1}$)
600	110	7.1	0.3656
700	50	5.0	0.4166
800	30	3.0	0.4982

Table 1 summarizes the data obtained for surface areas (BET plots), "water contents", and mercury densities for each magnesia sample.

Electron Microscope Examinations

The direct transmission micrographs of the three samples (total magnification × 250 000; microscope magnification × 125 000) are shown in Fig. 6. The 600 °C sample has a porous structure, in which the majority of pores have diameters of about 60 Å. The 700 °C sample has an irregular array of crystallites of average size about 240 Å. A small number of pores about 20 to 25 Å diameter can be observed in the crystallites. The 800 °C sample has crystallites of a more regular shape with an average size of 320 Å. Again, a small number of pores about 20 to 25 Å diameter can be observed in the crystallites. In general, an increase in the size and regularity of the crystallites occurs with increase in the temperature of heat-treatment.

Figure 6 also shows typical electron micrographs of the residues. The straight edges observed with the "fresh" 700 and 800 °C samples have a much rougher appearance after sulfur dioxide adsorption. In addition, small, dark areas approximately 50 Å diameter can be seen clearly in both the 700 and 800 °C residues.

Discussion

The heat values for all the samples are similar in magnitude at all points on the curves, Fig. 1. Heats greater than 35.0 kcal mol^{-1} were exhibited over the entire range of surface coverage studied and values of this order of magnitude clearly indicate that chemical adsorption and/or reaction of the sulfur dioxide has occurred (12).

The principal sulfur compound detected in the residues was magnesium sulfite which has a heat of formation (13) of −27.7 kcal mol^{-1} at 423 °K according to the reaction

[1] $$MgO_{(s)} + SO_{2(g)} \rightarrow MgSO_{3(s)}$$

Thus, in the absence of any significant quantities of other residues, substantial surface phenomena other than purely chemical combination have taken place.

Studies of the effect of small water vapor pressures (<5mm) on the sintering of MgO (4) suggest that the presence of H_2O provides a mode of surface transport for the O^{2-} ion and possibly, also, for electrostatic reasons, induces cation migration. The postulated mechanism involves dissociative chemisorption of H_2O on

Can. J. Chem. Downloaded from www.nrcresearchpress.com by 210.87.254.5 on 09/05/12
For personal use only.

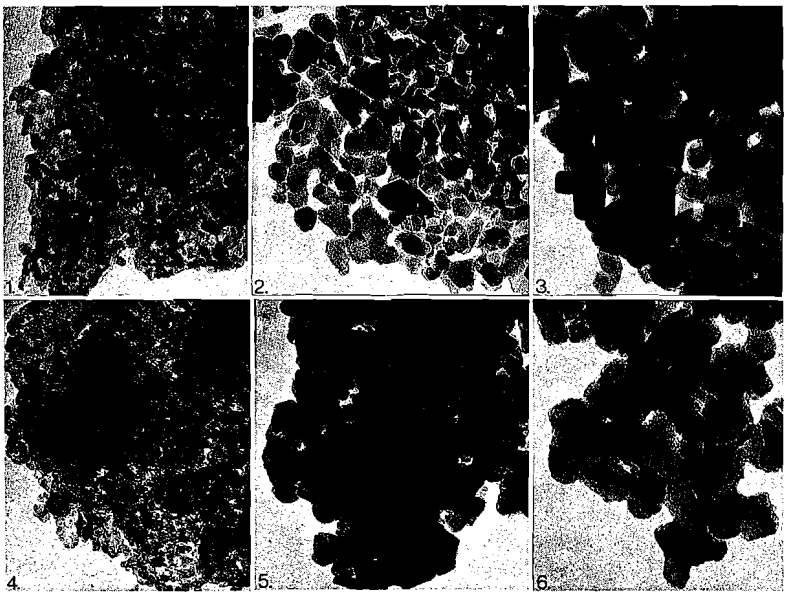

FIG. 6. Transmission electron micrographs (total magnification × 250 000; microscope magnification × 125 000) of (*a*) MgO heat-treated at 600 (*1*), 700 (*2*), and 800 °C (*3*); and (*b*) MgO heat-treated at 600 (*4*), 700 (*5*), and 800 °C (*6*) after adsorption of sulfur dioxide at 423 °K.

the Mg^{2+} and O^{2-} ions, and desorption of water from adjacent hydroxyl groups. Since water vapor pressures of this order of magnitude are present on calcining in air at temperatures up to 800 °C, similar active centers are probably generated on the surfaces of the heat-treated magnesias used in the present study. In addition such active anion sites may be created purely by the calcination process which involves a dehydration mechanism among adjacent hydroxyl groups. Figure 1 shows that the fairly steady high heats for the 800 °C sample do not occur at higher coverages than those obtained with the 600 and 700 °C samples. This may be explained by the greater degree of agglomeration of the 800 °C material with the formation of larger crystallites which act to reduce the number of active sites and lattice defects (14).

The heat values of around 75 and 80 kcal mol^{-1} for the 800 °C sample at coverages up to 2 μmol m^{-2} indicate the possibility of the sulfur dioxide reacting directly with the active anion centers. Similar observations can be made for the 600 and 700 °C samples. Thus sulfite formation probably occurs at these centers with a consequent readjustment of the position of lattice ions in the magnesia matrix.

Above a surface coverage of 4.0 μmol m^{-2} the levelling off of the heat values, particularly noticeable with the 600 °C sample, is paralleled by a large increase in the amount of sulfur dioxide adsorbed, Fig. 2. The major weight loss observed on heating the residues above 350 °C, the decomposition temperature of magnesium sulfite (15), together with the observation that the amounts of gas lost are approximately equivalent to one monolayer coverage of sulfur dioxide, strongly suggest that predominantly magnesium sulfite is formed in this region of the heat curves. However, the possibility of some reaction of sulfur dioxide with the magnesium sulfite has to be considered. Thus the difference between the theoretical heat of formation of magnesium sulfite and the observed heat, around 40 kcal mol^{-1}, could be explained if some sulfur dioxide was preferentially adsorbed on the magnesium sulfite prior to the apparent completion of the monolayer

[2] $$2MgSO_{3(s)} + SO_{2(g)} \rightarrow 2MgSO_{4(s)} + \tfrac{1}{2}S_{2(s)}$$

$$\Delta H_f(423\ °K) = -58.8\ \text{kcal mol}^{-1}\ (14)$$

The rapid fall in the heats for all samples between 2.0 and 4.0 μmol m^{-2} can be explained by a gradual increase in the contribution of reaction 2 to the overall process. Above mono-

Can. J. Chem. Downloaded from www.nrcresearchpress.com by 210.87.254.5 on 09/05/12
For personal use only.

layer coverage, the estimated heats of 45 ± 10 kcal mol^{-1} suggest that reaction 2 may predominate. These suggestions are supported by the presence of small amounts of sulfate ions detected on all the residues.

Although disproportionation of magnesium sulfite is thermodynamically possible at 423 °K (15)

[3] $$4MgSO_3 \rightarrow 3MgSO_4 + MgS$$

only about 5% of the change would occur (15). It would not account for the very slow, but significant, adsorption of sulfur dioxide on the samples. Further, no magnesium sulfide could be detected in the residues.

It is expected that some interaction of the sulfur dioxide with hydroxyl groups on the magnesia surfaces occurs but it is difficult to ascertain the influence of such interactions on the measured heats since the numbers of surface hydroxyl groups are unknown. However, infrared evidence (5) suggests that these numbers are relatively small at the temperatures of heat treatment used, and thus the "water content" must largely consist of bulk water/hydroxyl groups.

The nitrogen adsorption–desorption isotherms are similar to those observed earlier (16), although no hysteresis loops were formed with the 700 and 800 °C samples. However, this is not unexpected (17) since the present 700 and 800 °C samples are essentially nonporous, having only a few pores in the region of 20 to 25 Å diameter. The difference between these observations and those made earlier (16) is explained simply by differences in the methods of preparation.

The electron micrographs, Fig. 6, support the surface area and mercury density results of Table 1. At 600 °C, significant sintering has not occurred which agrees with earlier postulates that sintering is not expected below 640 °C (14). At 700 and 800 °C, particles have clearly agglomerated with cubic crystallites formed in the 800 °C sample. This sintering has clearly occurred within rather than between the aggregates of magnesia crystals in accord with earlier observations (4).

It is particularly significant that the electron micrographs of the 700 and 800 °C residues, Fig. 6, indicate that the edges of the magnesia crystallites have been attacked by the sulfur dioxide as indicated by the irregularity and smoothness of the edges. The presence of the small dark areas in the large, sintered crystallites may suggest that small crystallites of some other material, probably magnesium salts, may be present.

When these heat curves of sulfur dioxide on magnesias at 423 °K are compared with those determined earlier on heat-treated silica gels (2) and γ-aluminas (3), a general trend is apparent. The heats of adsorption at a given coverage increase with an increase in the degree of ionicity of the solid, thus: magnesia > γ-alumina > silica. A feature which is clearly related to the known ability of these materials to form compounds with sulfur dioxide.

1. R. W. GLASS and R. A. ROSS. Can. J. Chem. **49**, 2832 (1971).
2. R. W. GLASS and R. A. ROSS. Can. J. Chem. **50**, 1241 (1972).
3. R. W. GLASS and R. A. ROSS. Can. J. Chem. In press.
4. P. J. ANDERSON and P. L. MORGAN. Trans. Faraday Soc. **60**, 930 (1964).
5. ST. MALINOWSKI, S. SZCZEPANSKA, and J. SLOCZYNSKI. J. Catal. **7**, 67 (1967).
6. O. V. KRYLOV, Z. A. MARKOVA, I. I. TRETIAKOV, and E. A. FOKINA. Kinetika i Kataliz. **6**, 128 (1965).
7. X-Ray powder data file. Inorganic volume PDIS 5iRB, 4-0829. A.S.T.M. Philadelphia, Pa. 1966.
8. L. G. JOYNER. Scientific and industrial glass blowing and laboratory techniques. *Edited by* W. E. Barr and V. J. Anhorn. Instruments Publishing Company, Pittsburg. 1949.
9. A. H. TAYLOR and R. A. ROSS. J. Chem. Eng. Data, **14** (3), 347 (1969).
10. W. B. JEPSON. J. Sci. Inst. **36**, 319 (1959).
11. F. FEIGL. Spot tests in inorganic analysis. Elsevier, New York. 1958.
12. S. J. GREGG. Surface chemistry of solids. Chapman and Hall, London. 1961.
13. Handbook of chemistry and physics. Chemical Rubber Publishing Co., Cleveland. 1970.
14. R. M. DELL and S. W. WELLER. Trans. Faraday. Soc. **55**, 2203 (1959).
15. P. S. LOWELL, K. SCHWIZGEBEL, T. B. PARSONS, and K. J. SLADEK. Ind. Eng. Chem. Proc. Res. Develop. **10**, 384 (1971).
16. W. F. N. M. DE VLEESSCHAUWER. Physical and chemical aspects of adsorption and catalysis. *Edited by* B. G. Linsen. Academic Press, London. 1970.
17. D. H. EVERETT. The solid–gas interface. Vol. 2. *Edited by* E. A. Flood. Marcel Dekker, Inc., New York. 1967.

Can. J. Chem. Downloaded from www.nrcresearchpress.com by 210.87.254.5 on 09/05/12
For personal use only.

Photolyse dans l'ultraviolet à vide du *Cis*- et du *trans*-butène-2

GUY J. COLLIN ET PATRICK M. PERRIN

Département des sciences pures et appliquées, Université du Québec à Chicoutimi, Chicoutimi, Québec

Reçu le 14 mars 1972

Lors de la photolyse en phase gazeuse du *cis*- et du *trans*-butène-2 avec les raies de résonnance du xénon et du krypton (8.4 et 10.0 eV), on a mis en évidence les principales réactions de décomposition de la molécule butène-2 excitée. Les produits principaux formés dans ces décompositions sont le butadiène-1,3 (0.4), l'acétylène (0.3), l'allène + le propyne (0.2), et l'éthylène (0.1) à 8.4 eV. Nous avons également suivi la décomposition du radical butyle secondaire chimiquement activé en fonction de la pression. De ces études il ressort qu'aumoins à 10.0 eV, certains atomes d'hydrogène ne peuvent plus être considérés comme thermiques, bien que leur énergie cinétique ne soit probablement pas considérable. Finalement la molécule butène-2 excitée à 8.4 eV se décompose en donnant un atome d'hydrogène et un radical libre.

In the far u.v. photolysis of *cis*- and *trans*-2-butene in the gas phase with the xenon and krypton resonance lines (8.4 and 10.0 eV), we show the main decomposition reactions of the excited 2-butene molecules. Main products from these reactions are 1,3-butadiene (0.4), acetylene (0.3), propadiene + propyne (0.2), and ethylene (0.1) at 8.4 eV. The pressure effect on the decomposition reaction of the chemically activated *s*-butyl radical was also examined. From these studies, it appears that some of the hydrogen atoms are not "thermal", but carry kinetic energy, although this amount is probably not very large. Decomposition reactions of excited 2-butene molecules (8.4 eV) give one hydrogen atom plus a free radical.

Canadian Journal of Chemistry, **50**, 2823 (1972)

Can. J. Chem. Downloaded from www.nrcresearchpress.com by 210.87.254.105 on 09/05/12
For personal use only.

Introduction

La photolyse des alcènes est déjà bien connue en ce qui concerne la région de l'ultraviolet comprise entre 185 et 203 nm (1). Dans la région de l'ultraviolet à vide (région de 145 à 105 nm) les résultats sont eux aussi nombreux en ce qui concerne les oléfines simples (2–5). L'irradiation de l'isobutène a été rapportée (6), et un rapport préliminaire sur le butène-1 a aussi été présenté (7). Le présent travail est une suite logique des travaux déjà entrepris.

Procédure expérimentale

Les techniques expérimentales ont déjà fait l'objet d'une description dans la littérature (8). Les lampes d'irradiation ont été elles aussi décrites (9). La lampe au krypton est équipée d'une fenêtre en LiF de 1.0 mm d'épaisseur. Placée dans la cavité d'un générateur microonde, Unité Raytheon 2450 Mc, son spectre d'émission entre 100 et 200 nm comprend essentiellement deux raies, plus de 99% du total, l'une située vers 124 nm (89%) et l'autre située vers 116 nm (11%). Ce spectre a été enregistré sur un appareil McPherson, modèle 235, et il correspond aux deux raies de résonnance émises par le krypton, c'est-à-dire à 123.58 et à 116.49 nm (9). En ce qui concerne la lampe au xénon, la préparation et l'irradiation des échantillons, la dosimétrie, le lecteur trouvera toutes les indications dans une autre publication (8).

Le butène-2-d_8 (mélange *cis–trans*, 50/50) provient de Merck, Sharp and Dohme of Canada et contient 9.0% de butène-2-d_7. Toutes les analyses isotopiques ont été faites sur un spectromètre de masse CEC 21-104 et ont été corrigées pour la présence de l'impureté isotopique.

Résultats

Les résultats obtenus sont donnés dans les différents tableaux et figures de ce texte. Il faut essentiellement retenir pour le moment la linéarité des rendements relativement à celui de l'allène en fonction du temps d'irradiation (voir figs. 1–4). Ainsi, sans plus entrer dans le détail, les réactions faisant intervenir comme réactif l'un quelconque des produits de l'irradiation sont à ignorer. Les analyses des produits principaux formés dans l'irradiation des mélanges isotopiques C_4H_8:C_4D_8-2:O_2 (50:50:5) dans différentes conditions sont rapportées ci-après: (*a*) irradiation xénon; pression totale 1.3 Torr: C_3D_6:C_3D_5H:C_3H_5D:C_3H_6 = 14.1:12.7:34.8:38.4; (*b*) irradiation krypton: pression totale 10.0 Torr: C_3D_6:C_3D_5H:C_3H_5D:C_3H_6 = 15.3:12.7:32.4:39.8.

Les irradiations des mélanges butène-2:oxygène (100:5) ne donnent pas lieu à la formation d'hydrocarbures en C_6, C_7, et C_8.

Caractéristiques générales

Le potentiel d'ionisation de la molécule butène-2, qu'elle soit de configuration *cis*- ou *trans*-, est de 9.13 eV (10). Avec la lampe au

Can. J. Chem. Downloaded from www.nrcresearchpress.com by 210.87.254.105 on 09/05/12
For personal use only.

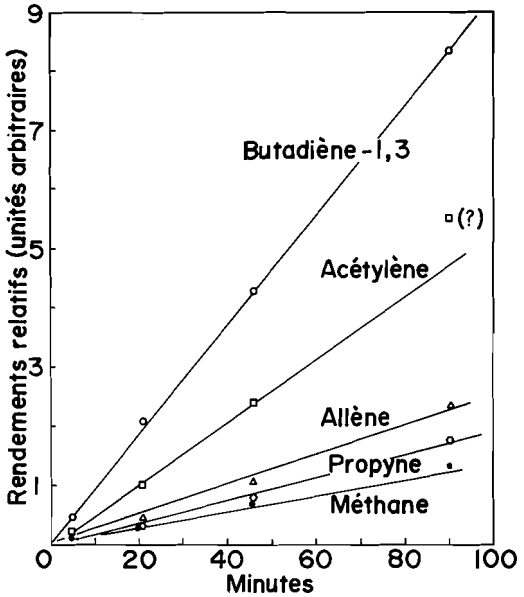

FIG. 1. Photolyse xénon du *cis*-butène-2 (1.32 Torr – 175 N m^{-2}) en présence d'hélium (147 Torr – 19 500 N m^{-2}) et d'oxygène (0.07 Torr – 9.3 N m^{-2}).

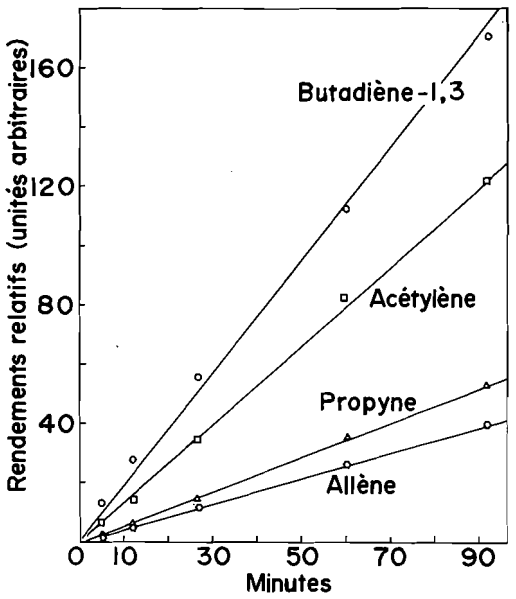

FIG. 3. Photolyse xénon du *trans*-butène-2 (1.32 Torr – 175 N m^{-2}) en présence d'hélium (129 Torr – 17 150 N m^{-2}) et d'oxygène (0.24 Torr – 32 N m^{-2}).

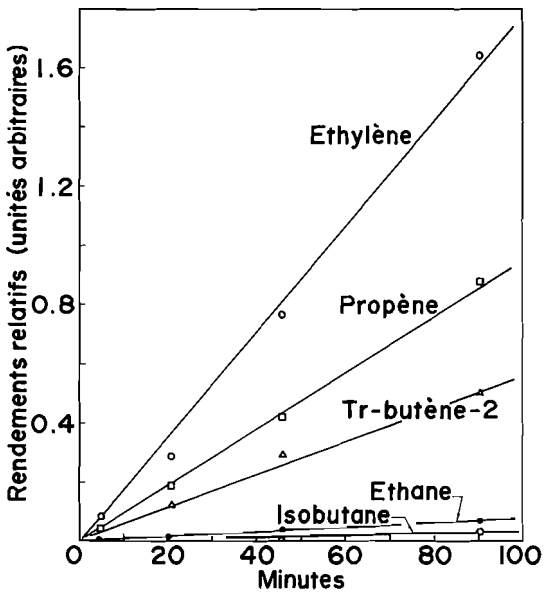

FIG. 2. Photolyse xénon du *cis*-butène-2 (1.32 Torr – 175 N m^{-2}) en présence d'hélium (147 Torr – 19 500 N m^{-2}) et d'oxygène (0.07 Torr – 9.3 N m^{-2}).

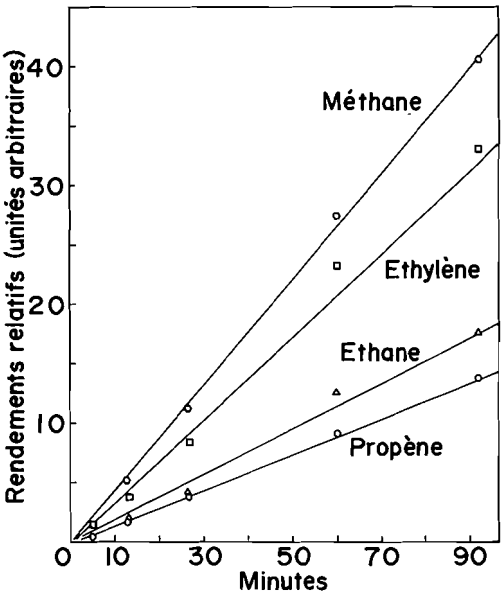

FIG. 4. Photolyse xénon du *trans*-butène-2 (1.32 Torr – 175 N m^{-2}) en présence d'hélium (129 Torr – 17 150 N m^{-2}) et d'oxygène (0.24 Torr – 32 N m^{-2}).

xénon, l'énergie des photons (8.44 eV) n'est pas suffisante pour ioniser les molécules. Cependant avec la lampe de krypton, l'énergie des deux raies de résonnance est supérieure au potentiel d'ionisation. A 123.6 nm le rendement quantique d'ionisation est de 0.25_5 (9), par conséquent une molécule sur quatre ayant absorbé un photon est ionisée. L'énergie de la raie à

Can. J. Chem. Downloaded from www.nrcresearchpress.com by 210.87.254.105 on 09/05/12
For personal use only.

116.5 nm est inférieure au potentiel d'apparition de la première fragmentation de l'ion $(C_4H_8\text{-}2)^+$ excité; aucun des ions formés n'est donc fragmenté (10). Comme nous ne dirons rien des réactions ioniques, toutes les considérations qui suivent se rapportent aux molécules neutres excitées et les rendements mesurés seront indiqués comme M/N_{Exc} où M est le nombre de molécules formées pour le nombre total de molécules butène-2 excitées.

La première constatation qui se dégage des résultats (voir tableau 1) est la similitude de la répartition des produits de décomposition dans la photolyse du *cis*- et du *trans*-butène-2. Ce résultat est en fait prévisible car la différence de structure des deux composés est négligeable, et d'autre part la hauteur de la barrière de potentiel qu'il faut franchir pour isomériser une structure dans l'autre est de 62.8 kcal mol^{-1} (*11a*) ce qui est, somme toute, peu devant l'énergie minimum des photons utilisés ici, soit 194.5 kcal mol^{-1}. Ainsi donc, le fait d'augmenter l'énergie d'excitation initiale ne modifie pas beaucoup la distribution des produits de décomposition, si ce n'est pour l'apparition des ions $(C_4H_8\text{-}2)^+$. Cette observation a déjà été faite dans le cas de l'isobutène (6) et de celui du butène-1 (7).

Il faut enfin noter la faible part des rendements d'isomérisation des butènes-2 en butène-1, isobutène, ou même cyclobutane (voir les tableaux 1 et 2). Ceci est également le fait de la grande quantité d'énergie disponible dans la molécule excitée vis-à-vis de l'énergie requise pour briser l'une quelconque des liaisons. Même si le rendement en *trans*-butène-2 est élevé ($M/N = 0.14$) dans la photolyse du *cis*-butène-2 (tableau 1), celui-ci vient essentiellement des réactions radicalaires de dismutation mettant en cause le radical butyle secondaire (voir plus loin).

Décomposition du monomère excité

L'absorption d'un photon par une molécule butène-2 entraîne la formation d'une molécule très excitée qui se décompose rapidement.

[1] $C_4H_8\text{-}2 + h\nu \rightarrow (C_4H_8\text{-}2)^{**}$

[2] $(C_4H_8\text{-}2)^{**} \rightarrow H\cdot, R_1R_2\cdot, R_3 \ldots$ etc.

R_1R_2 représente un produit moléculaire stable et $R_3\cdot$ un radical lui aussi stable, c'est-à-dire ayant une énergie interne insuffisante pour donner lieu à d'autres fragmentations. En présence de quelques pourcents d'oxygène, hormis les atomes d'hydrogène, ou quelques radicaux excités, ou "chauds", tous les radicaux réagissent avec l'oxygène pour donner des composés peroxygénés non analysés. Par conséquent la majorité des produits moléculaires formés en présence d'oxygène peuvent être formés dans la réaction 2. Puisque la molécule butène-2 excitée contient une énergie de beaucoup supérieure à l'énergie requise pour briser l'une quelconque ses liaisons, elle se décompose bien avant la première collision. Par conséquent, aux pressions relativement basses de ce présent travail, la réaction 2 n'est pas sensible à la variation de pression et les rendements des produits moléculaires R_1R_2 de cette réaction sont indépendants de la variation de pression. C'est en effet le cas de la plupart des produits formés en présence d'oxygène, sauf pour le propène. Le rendement de ce produit subit une décroissance très importante lorsque la pression de l'échantillon passe de 0.05–300 Torr (tableau 1, figs. 5 et 6). Il est donc formé dans une ou plusieurs réactions différentes de la réaction 2. Une première possibilité de décomposition de l'espèce butène-2 excitée est donnée dans les réactions 3 et 4.

[3] $(C_4H_8\text{-}2)^{**} \rightarrow C_3H_4 + CH_4 \qquad \Delta H = 30$ kcal mol^{-1}

[4] $(C_4H_8\text{-}2)^{**} \rightarrow C_3H_4 + \cdot CH_3 + H\cdot \qquad \Delta H = 126$ kcal mol^{-1}

L'énergie requise pour ces deux réactions est inférieure à l'énergie déposée dans chaque molécule par les photons les moins énergétiques utilisés dans ce travail: 194.5 kcal mol^{-1}. Le produit moléculaire C_3H_4 est soit l'allène, soit le propyne. Puisque le rendement du méthane "moléculaire", c'est-à-dire celui formé en présence d'oxygène, est plus faible que celui de l'allène et du propyne, le rapport $k_3/(k_3 + k_4)$ est inférieur ou égal à 0.5. Ceci est normal, car les deux produits de la réaction 3 ont plus de 160 kcal mol^{-1} d'énergie à se partager. Il en résulte une grande probabilité que l'une ou l'autre des deux molécules produites dans cette réaction se décompose avant une collision moléculaire (6, 12). Il est enfin fort possible que le méthane soit formé dans une ou plusieurs autres réactions.

Un autre type de réactions de décomposition

Can. J. Chem. Downloaded from www.nrcresearchpress.com by 210.87.254.105 on 09/05/12
For personal use only.

TABLEAU 1. Rendements M/N_{Exc} dans la photolyse des butènes-2

	trans-C_4H_8-2 (8.4 eV)				*cis*-C_4H_8-2 (8.4 eV)			*cis*-C_4H_8-2 (10.0 eV)			
C_4H_8	0.018*	1.3	1.3	1.3	0.018	1.3	1.3	0.015	1.3	1.03	1.3
O_2	—	0.07	—	0.06	—	—	0.06	—	0.06	—	0.06
H_c	—	—	—	234	—	—	310	—	—	—	300
Temps d'irradiation	16†	20	17	20	10	10	60	60	60	60	60
CH_4	n.d.‡	0.11_3	0.10	0.10	0.12_5	0.12_7	0.08_3	0.19	0.09	0.23	0.11
C_2H_2	0.25	0.27	0.28	0.31	0.24	0.24	0.32_6	0.30	0.30	0.30	0.34
C_2H_4	0.15	0.11_5	0.11	0.10_5	0.12_5	0.10	0.09_4	0.24_6	0.12	0.16	0.11
C_2H_6	0.84	0.01_4	n.d.	0.00_4	0.89	0.37	0.00_3	1.07	0.00	0.46	0.00_5
C_3H_6	0.96	0.37_5	n.d.	0.02_7	1.00	0.39	0.02_1	1.28	n.d.	0.66	0.03_5
C_3H_8	0.15_2	0.00	0.13_7	0.158	0.06	0.08_7	0.00	0.12_7	0.09_2	0.14_3	0.11
C_3H_4§		0.11_1					0.10				
C_3H_4‖	0.125	0.125	0.125	0.125	0.125	0.125	0.125	0.107	0.107	0.107	0.107
iso-C_4H_{10}	0.00_4	0.00	0.00_5	0.00	0.00	n.d.	0.00	0.00	0.00	0.00	0.00
C_4H_8-1-*iso*-C_4H_8	n.d.	0.00	n.d.	n.d.	n.d.	n.d.	0.00	n.d.	n.d.	n.d.	n.d.
C_4H_6-1,3	0.40	0.39	0.40	0.46	0.40	0.43	0.42	0.37	n.d.	n.d.	n.d.
trans-C_4H_8-2	—	—	—	—	n.d.	0.14	n.d.	n.d.	n.d.	n.d.	n.d.
cis-C_4H_8-2	n.d.	n.d.	n.d.	n.d.	—	—	—	—	—	—	—
iso-C_5H_{12}	0.00	0.00	n.d.	0.00	0.00	0.38	0.00	0.00	0.00	0.4	0.0
Taux en conversion (%)¶	4.5	0.3	0.3	0.18	2.5	0.24	1.1	6.9	0.3	0.2	0.3

*En Torr.
†En min.
‡Non déterminé.
§Propyne.
‖Allène; pris comme référence pour la dosimétrie.
¶Le taux de conversion est calculé de la façon suivante: taux = (propène + propyne + allène + butadiène) × 100/pentène.

Can. J. Chem. Downloaded from www.nrcresearchpress.com by 210.87.254.105 on 09/05/12
For personal use only.

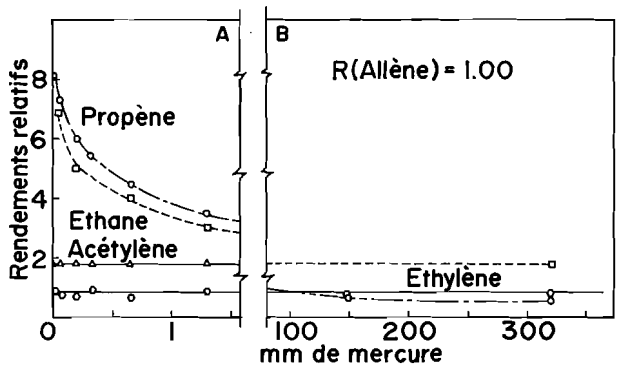

FIG. 5. Photolyse xénon du *cis*-butène-2. (A) Temps d'irradiation: 10 min; (B) Temps d'irradiation: 60 min; *cis*-butène-2 (1.32 Torr – 175 N m^{-2}); additif: hélium.

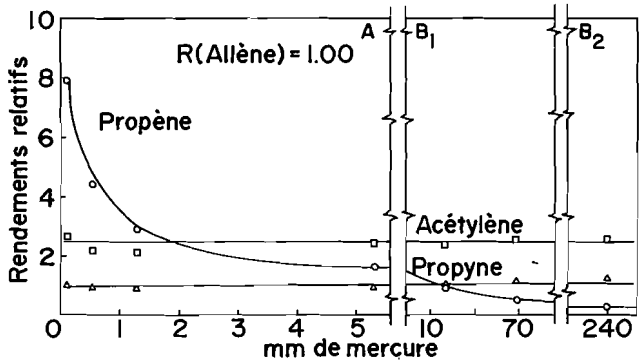

FIG. 6. Photolyse xénon du *trans*-butène-2. Temps d'irradiation: 20 min; (A) *trans*-butène-2 pur; (B_1) et (B_2) *trans*-butène-2 (1.32 Torr – 175 N m^{-2}); additif: hélium.

TABLEAU 2. Photolyse du *cis*-butène-2 à 8.4 eV*

Additif		Hélium: 300 Torr (4000 N m^{-2})
Méthyle-3-butène-1	0.03_3†	0.04_3
Cyclobutane	0.00_1	0.00_5
Isopentane	0.37	0.51
n-Pentane	0.04_0	0.05_6
Pentène-2	0.04_0	0.04_3
Méthyle-2-butène-2	0.00	0.00
cis-Diméthyle-1,2-cyclopropane	0.00	0.00

*1.32 Torr (175 N m^{-2}); temps d'irradiation : 100 min.
†Valeurs M/N_{Exc}.

du butène-2 excité permet d'expliquer la formation du butadiène.

[5] $(C_4H_8\text{-}2)^{**} \rightarrow C_4H_6\text{-}1,3 + H_2$ (ou -1,2)

$\Delta H = 28$ kcal mol^{-1}

[6] $(C_4H_8\text{-}2)^{**} \rightarrow C_4H_6\text{-}1,3 + 2H\cdot$ (ou -1,2)

$\Delta H = 132$ kcal mol^{-1}

Pour les mêmes raisons que celles précédemment émises pour les réactions 3 et 4, la réaction 6 est *a priori* plus probable que la réaction 5. Comme l'hydrogène n'a pas été mesuré, rien ne peut être dit de l'importance relative de ces deux réactions. Une autre série de produits est également formée dans l'une ou l'autre des réactions de décomposition du butène-2.

[7] $(C_4H_8\text{-}2)^{**} \rightarrow C_2H_6 + C_2H_2$

$\Delta H = 36$ kcal mol^{-1}

[8] $(C_4H_8\text{-}2)^{**} \rightarrow 2\cdot CH_3 + C_2H_2$

$\Delta H = 112$ kcal mol^{-1}

[9] $(C_4H_8\text{-}2)^{**} \rightarrow \cdot C_2H_5 + C_2H_2 + H\cdot$

[10] $(C_4H_8\text{-}2)^{**} \rightarrow \cdot C_2H_3 + C_2H_4 + H\cdot$

Avec des considérations similaires à celles déjà rapportées, la réaction 7 a peu d'importance, et d'après le rendement en éthane moléculaire, celui formé en présence d'oxygène, la réaction 7 compte pour moins de 1% dans la formation de l'acétylène. Quant à la réaction 8, elle est observée dans la photolyse du butène-2

Can. J. Chem. Downloaded from www.nrcresearchpress.com by 210.87.254.105 on 09/05/12
For personal use only.

à 185 nm (1). Le rendement élevé en radicaux méthyles (voir plus loin) est de plus en faveur de cette réaction. Les réactions 9 et 10 sont semblables. Dans la première rupture de la molécule excitée, il se forme les radicaux éthyles et vinyles. L'un des deux radicaux contient encore suffisamment d'énergie pour se décomposer à nouveau en un atome d'hydrogène et en acétylène ou éthylène selon le cas. Les rendements en radicaux éthyles et vinyles ont déjà été estimés être de l'ordre de 0.08 et 0.04. Aux très faibles pressions, le seul radical important, est donc le radical méthyle. Par conséquent, les radicaux éthyles doivent se retrouver sous forme de propane. Aux erreurs expérimentales près, le rendement en propane est inférieur à 0.03, confirmant ainsi la faible valeur du rendement en radicaux éthyles.

D'autres réactions, thermiquement acceptables, peuvent rendre compte de la formation d'éthylène (13, 14). Il est cependant, dans l'état actuel des présentes mesures, spéculatif d'entrer plus avant dans la discussion de ce sujet. Une autre réaction mineure de décomposition du monomère excité est clairement démontrée par les résultats.

[11] $(C_4H_8\text{-}2)^{**} \rightarrow C_3H_6 + :CH_2$

[12] $:CH_2 + cis\text{-}C_4H_8\text{-}2 \rightarrow cis\text{-diméthyle-1,2-cyclopropane}$

A haute pression, en présence de 300 Torr d'hélium, le rendement en propylène est de l'ordre de 0.03, et il est probablement formé par réaction 11. Cette réaction est mise en évidence par la formation relativement plus importante du propène-d_0 et -d_6 que de propène-d_1 et -d_5 dans l'irradiation du mélange butène-2-d_0: butène-2-d_8: oxygène (50:50:5). D'après ces résultats le rendement de la réaction 11 est de 0.04 dans la photolyse à 10.0 eV, alors qu'il est de 0.02 à 8.4 eV (voir résultats des analyses isotopiques).

Les radicaux méthylènes réagissent avec le *cis*-butène-2 qu'ils soient dans leur état fondamental triplet ($^3\Sigma_g$) ou dans leur premier état excité singulet ($^1A_1$). Dans les deux cas le produit d'insertion est en majorité le *cis*-diméthyle-1,2-cyclopropane (15, 16), composé qui n'est pas détecté par chromatographie (voir tableau 2). Par conséquent les radicaux méthylènes, s'ils sont formés, le sont avec un rendement relativement faible. En admettant une limite supérieure compatible avec le pouvoir de détection de l'appareillage analytique, la valeur $M/N(CH_2)$ est inférieure ou égale à 0.03 à 8.4 eV en accord avec les deux valeurs rapportées plus haut.

Réactions des atomes d'hydrogène

L'analyse des fragments radicalaires démontre essentiellement la présence d'atomes d'hydrogène et de radicaux méthyles et butyles (8). Les atomes d'hydrogène thermiques réagissent avec le butène-2, soit par abstraction d'un atome d'hydrogène, soit par addition sur la double liaison.

[13] $H\cdot + C_4H_8\text{-}2 \rightarrow H_2 + C_4H_7\cdot$

[14] $H\cdot + C_4H_8\text{-}2 \rightarrow (s\text{-}C_4H_9)^*$ $\quad \Delta H = -39$ kcal mol^{-1}

Ces deux réactions ne sont pas affectées par la présence d'hydrogène sulfuré (8), ou d'oxygène (voir plus loin) en accord avec les constantes de vitesse publiées dans la littérature (17*a*–*c*). Le rapport des constantes de vitesse k_{13}/k_{14} est de l'ordre de 0.07 (18) et la réaction 13 est peu importante. Le radical butyle secondaire formé dans la réaction 14 contient plus d'énergie qu'il ne lui en faut pour se décomposer (19).

[15] $(s\text{-}C_4H_9)^* \rightarrow CH_3\cdot + C_3H_6$ $\quad \Delta H = 25$ kcal mol^{-1}

[16] $(s\text{-}C_4H_9)^* + M \rightarrow s\text{-}C_4H_9\cdot + M$

Cependant, comme l'indique la réaction précédente, si la pression est suffisante, le radical butyle secondaire est stabilisé par collision et à haute pression la réaction 15 est à ignorer. La variation du rendement en propène démontre l'activité d'un tel processus (figs. 5 et 6). Tout comme le rendement en propène, le rendement en éthylène décroît légèrement lorsque la pression de l'échantillon passe de 0.02–300 Torr. A 8.4 eV, la décroissance du rendement en éthylène relativement à celui du propène est de 3.5%. A 10.0 eV, ce pourcentage est de 11% (tableau 3). Or l'éthylène dans ce cas est formé par décomposition du radical butyle primaire lui-même formé par isomérisation du radical butyle secondaire (11*b*):

[17] $(s\text{-}C_4H_9)^* \rightarrow (n\text{-}C_4H_9)^*$

[18] $(n\text{-}C_4H_9)^* \rightarrow C_2H_5\cdot + C_2H_4$

Puisqu'à 10.0 eV, les réactions 17 et 18 sont favorisées par rapport à la réaction 15, cela entraîne que certains atomes d'hydrogène, au

Can. J. Chem. Downloaded from www.nrcresearchpress.com by 210.87.254.105 on 09/05/12
For personal use only.

TABLEAU 3. Photolyse des butènes-2

	trans-C_4H_8-2 (8.4 eV)	*cis*-C_4H_8-2 (8.4 eV)	*cis*-C_4H_8-2 (10.0 eV)
(C_2H_4)*	0.04_5	0.03_1	0.13_6
(C_3H_6)†	0.94	0.98	1.22_5
$\frac{(C_2H_4)\times 100}{(C_3H_6)}$	4.8	3.1	11.1

*Décroissance du rendement en éthylène $= \underset{P\to 0}{M/N(C_2H_4)} - \underset{P\to\infty}{M/N(C_2H_4)}$

†Décroissance du rendement en propène $= \underset{P\to 0}{M/N(C_3H_6)} - \underset{P\to\infty}{M/N(C_3H_6)}$

TABLEAU 4. Rendements radicalaires primaires: photolyse des butènes-2*

$M/N(R\cdot)_1$	*trans*-Butène-2 (8.4 eV)	*cis*-Butène-2 (8.4 eV)	*cis*-Butène-2 (10.0 eV)
$M/N(\cdot CH_3)_1$	0.75	0.80	0.89
$M/N(\cdot C_2H_5)_1$	0.08†	0.08†	0.08‡
$M/N(:CH_2)_1$	0.02	0.02	0.04
$M/N(\cdot C_2H_3)_1$	0.04†	0.04†	0.04‡
$M/N(H\cdot)_1$	1.09	1.11	1.47
Total	1.98	2.05	2.52

*Pour le calcul de chaque valeur $M/N(R\cdot)_1$, voir les explications dans le texte.

†Voir réf. 8; Valeurs déterminées par l'usage d'H_2S comme intercepteur radicalaire.

‡Valeurs estimées indépendantes de l'énergie incidente.

moins à 10.0 eV, transportent une quantité d'énergie cinétique non nulle. Les radicaux butènyles formés dans la réaction 13 peuvent avoir initialement la structure $\cdot CH_2—CH{=}CH—CH_3$ ou $CH_3—\dot{C}{=}CH—CH_3$. La première structure est bien entendu en résonnance avec la forme $CH_2{=}CH—\dot{C}H—CH_3$. Ces radicaux réagissent en particulier avec les radicaux méthyles présents:

[19] $CH_3\cdot + \cdot CH_2—CH{=}CH—CH_3 \rightarrow C_2H_5—CH{=}CH—CH_3$

[20] $CH_3\cdot + CH_2{=}CH—\dot{C}H—CH_3 \rightarrow CH_2{=}CH—CH—(CH_3)_2$

[21] $CH_3\cdot + CH_3—\dot{C}{=}CH—CH_3 \rightarrow (CH_3)_2—C{=}CH—CH_3$

L'absence de méthyle-2-butène-2 (tableau 2) indique que s'il est formé, le radical $CH_3—\dot{C}{=}CH—CH_2$ a disparu avant de réagir avec le radical méthyle. Cela est l'indication que l'abstraction d'un atome d'hydrogène de deux groupements méthyles est plus favorable et il est donc probable que le radical butènyle $CH_3—\dot{C}{=}CH—CH_3$ n'est pas formé dans la réaction 13. Les rendements similaires en pentène-2 et en méthyle-3-butène-1 indiquent que la réaction d'isomérisation du radical $\cdot CH_2CH{=}CH—CH_3$ est importante. D'après l'importance du rendement en radicaux méthyles (voir plus loin), et en supposant que ceux-ci réagissent avec les radicaux butènyles par addition, on peut estimer à 0.12 ± 0.03 le rendement de ces derniers. En retenant la valeur du rapport k_{13}/k_{14} égale à 0.066 (18) et en connaissant le rendement de la réaction 14, ce rendement devrait être de 0.07. Les deux valeurs sont assez éloignées l'une de l'autre et la différence peut indiquer la participation non encore discutée de la réaction de décomposition du monomère excité suivante:

[22] $(C_4H_8\text{-}2)^{**} \rightarrow C_4H_7\cdot + H\cdot$

Mesure des rendements radicalaires

Avant d'entrer plus avant dans ce sujet, il faut distinguer deux sortes de radicaux: ceux directement formés lors de la décomposition du monomère excité (réactions 2 à 11 et 22) et ceux provenant d'un tout autre processus. Puisque les réactions de décomposition du monomère excité sont en principe indépendantes de la pression, il en est de même des radicaux primaires, mais cela n'est pas nécessairement la même chose pour les autres radicaux formés dans les réactions 13 à 21. Les rendements en radicaux primaires seront notés $M/N(R\cdot)_1$ (tableau 4).

En plus des atomes d'hydrogène, qui conduisent soit aux radicaux méthyles à très basses pressions, soit aux radicaux butyles à hautes pressions, il existe d'autres sources de radicaux méthyles, et en particulier dans les réactions de décomposition du monomère excité (réactions 4 et 8). A pression "nulle", c'est-à-dire aux plus basses pressions présentées dans ce travail, les radicaux méthyles sont les plus importants, car tous les radicaux butyles secondaires se décomposent en radicaux méthyles et en propène. Ils constituent plus de 90% du total. Par conséquent, la mesure du rendement en éthane est la meilleure indication du rendement en radicaux méthyles:

[23] $\cdot CH_3 + \cdot CH_3 \rightarrow C_2H_6$

A pression "infinie", aux environs de 300

TABLEAU 5. Photolyse du *cis*-butène-2: réactions du radical butyle secondaire

Lampe	Pression (Torr)	$M/N(C_2H_6)$	$M/N(iso\text{-}C_5H_{12})$	$2M/N([26]+[27])$	$M/N(s\text{-}C_4H_9\cdot)$	$M/N(H\cdot)_i$*
Kr†	0.066	1.12	0.08	0.01	0.095	1.64
Kr	0.132	0.98	0.18	0.03	0.22	1.71
Kr	0.26	0.89	0.29	0.07	0.38	1.76
Kr	0.52	0.72	0.40	0.16	0.59	1.70
Kr	1.05	0.50	0.39	0.22	0.64	1.49
Kr	2.1	0.37	0.395	0.30	0.72	1.39
Kr	5.0	0.35	0.40	0.33	0.76	1.29
						1.57 ± 0.15
Xe‡	0.06	0.89	0.05	$\simeq 0$	0.06	1.04
Xe	0.20	0.68	0.15_3	0.03	0.21	1.04
Xe	0.33	0.57_5	0.17	0.04	0.24	0.99
Xe	0.66	0.50_5	0.24	0.08	0.37	1.00
Xe	1.32	0.37_4	0.38	0.28	0.73	1.21
						1.05 ± 0.06

*Rendement en atomes d'hydrogène primaires; voir les explications dans le texte.
†Temps d'irradiation, 60 min.
‡Temps d'irradiation, 10 min.

TABLEAU 6. Décomposition de la molécule 2-butène excitée

				M/N_{Exc}		
	Réactions			λ(nm) 185*	147	123.6
4†	$(C_4H_8\text{-}2)$**	→	$C_3H_4 + \cdot CH_3 + H\cdot(CH_4)$	(0.07)‡	0.23	0.20
6		→	$C_4H_6 + 2H\cdot(H_2)$	(0.11)§	0.42	0.37
8		→	$C_2H_2 + 2\cdot CH_3$	0.23	0.25	0.27
9		→	$C_2H_5\cdot + C_2H_2 + H\cdot$	—	0.08	0.08
10		→	$C_2H_3\cdot + C_2H_4 + H\cdot$	—	0.04	0.04
13		→	$C_3H_6 + :CH_2$	—	0.02	0.04
—		→	C_4H_8(isomérisation)	0.1	0.02	0.02
22		→	$C_4H_7\cdot + H\cdot$	0.6	0.05	ind.‖
			Total	1.11	1.11	1.02

*Référence 21.
†Numéro de la réaction dans le texte.
‡Rendement en méthane moléculaire.
§Rendement en hydrogène moléculaire.
‖Indéterminé.

Torr, la réaction 15 est inactive, puisque les radicaux butyles secondaires sont en majorité stabilisés. Le rendement en radicaux méthyles à pression infinie, est donc égal au précédent diminué de la décroissance du rendement en propène, et il est probablement alors égal au rendement en radicaux méthyles primaires.

Le rendement en atomes d'hydrogène primaires est égal aux rendements des réactions 15, 18, et 22 à basses pressions, augmentés du rendement de la réaction 13. Les rendements en radicaux éthyles et vinyles ont été obtenus ailleurs (8) et celui des radicaux méthylènes a déjà été discuté. Le rendement total en radicaux primaires est ainsi calculé en faisant la somme des rendements en atomes d'hydrogène, des radicaux vinyles et méthylènes et des radicaux méthyles et éthyles à haute pression. Il est enfin intéressant de remarquer que l'absorption d'un photon de 8.4 eV conduit à la formation de deux fragments radicalaires: un atome d'hydrogène et un radical libre (tableaux 4–6).

Il existe d'autres possibilités de mesurer les rendements des radicaux, comme par exemple

Can. J. Chem. Downloaded from www.nrcresearchpress.com by 210.87.254.105 on 09/05/12
For personal use only.

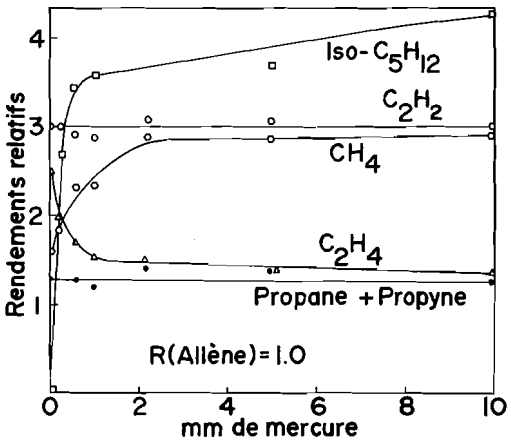

FIG. 7. Photolyse krypton du *cis*-butène-2 pur; temps d'irradiation 60 min.

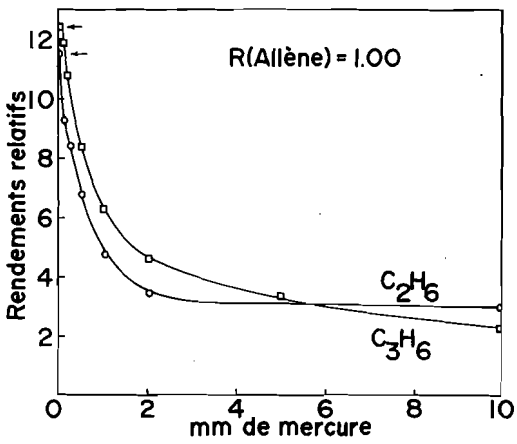

FIG. 8. Photolyse krypton du *cis*-butène-2 pur; temps d'irradiation 60 min.

l'usage de l'hydrogène sulfuré (8). En outre la mesure des radicaux butyles à hautes pressions permet d'estimer le rendement en atomes d'hydrogène. Lorsque les réactions de stabilisation des radicaux butyles jouent complètement leur rôle, ces radicaux ne peuvent réagir qu'avec eux-mêmes ou avec les radicaux méthyles dans le système réactionnel suivant auquel il faut adjoindre la réaction 23 (figs. 7 et 8):

[24] $CH_3\cdot + s\text{-}C_4H_9\cdot \rightarrow CH_4 + C_4H_8$

[25] $CH_3\cdot + s\text{-}C_4H_9\cdot \rightarrow iso\text{-}C_5H_{12}$

[26] $2\ s\text{-}C_4H_9\cdot \rightarrow n\text{-}C_4H_{10} + C_4H_8$

[27] $2\ s\text{-}C_4H_9\cdot \rightarrow C_2H_5CH(CH_3)CH(CH_3)C_2H_5$

La somme $M/N([24] \text{ et } [25])$ peut être estimée en connaissant le rapport des constantes de vitesse k_{24}/k_{25}. Celui-ci est égal à 0.3 ou à 0.07 (17*d*). La mesure du rendement en isopentane permet donc d'évaluer le rendement des réactions 24 et 25. En admettant que l'éthane radicalaire n'est formé que dans la réaction 23, il est alors possible d'estimer le rendement des réactions 26 et 27 à travers la relation suivante (20):

$$\frac{M/N([24]+[25])}{M/N([23])^{\frac{1}{2}}\cdot M/N([26]+[27])^{\frac{1}{2}}} = 2$$

Ces calculs sont résumés dans le tableau 5, ainsi que le rendement en atomes d'hydrogène primaires. Celui-ci est bien entendu, obtenu en faisant la somme des rendements du radical butyle secondaire, de celui du propène (réaction 15), de la réaction d'isomérisation 17 et enfin de la réaction 13. Les résultats sont en bon accord avec ceux déjà calculés étant donné la précision de chaque mesure et l'hypothèse qui est faite: à savoir que dans le présent système, les réactions radical–radical suivent une loi statistique simple.

Conclusions

Le tableau 6 indique l'importance relative de chacun des processus de décomposition du monomère excité en même temps que ceux obtenus à 184.9 nm (21). A 147 et à 123.6 nm, il manque probablement un certain nombre de processus non mis en évidence comme par exemple le montre l'insuffisance du rendement en atomes d'hydrogène à 10.0 eV. Alors qu'à 184.9 nm, la réaction essentielle est celle de la rupture d'une seule liaison C—H; à plus courtes longueurs d'onde, il y a rupture de deux liaisons, soit C—H, soit C—C ou les deux simultanément.

Nous remercions l'Université du Québec à Chicoutimi pour le salaire qu'elle a fourni à l'un de nous (P.M.P.) et le Conseil National de Recherches du Canada qui nous a assisté financièrement. Nous voulons également exprimer notre gratitude au groupe Propulsion du Centre de Recherches de la Défense de Valcartier qui a mis son spectromètre de masse à notre disposition, et le Docteur J. A. Herman, de l'Université Laval qui a enregistré le spectre de la lampe au krypton.

1. P. BORELL, P. CASHMORE, A. CERVENKA, et F. C. JAMES. J. Chim. Phys. 229 (1970); J. P. CHESICK. J. Chem. Phys. **45**, 3934 (1966).
2. J. R. MCNESBY et H. OKABE. Adv. Photochem. **3**, 157 (1964).

Can. J. Chem. Downloaded from www.nrcresearchpress.com by 210.87.254.105 on 09/05/12
For personal use only.

3. D. A. BECKER, H. OKABE, et J. R. MCNESBY. J. Phys. Chem. **69**, 538 (1965).
4. E. TSCHUIKOW-ROUX. J. Phys. Chem. **71**, 2355 (1967).
5. R. GORDEN, JR., R. DOEPKER, et P. AUSLOOS. J. Chem. Phys. **44**, 3733 (1966).
6. J. HERMAN, K. HERMAN, et P. AUSLOOS. J. Chem. Phys. **52**, 28 (1970).
7. G. J. COLLIN et P. AUSLOOS. Présenté à la 5ième Conférence Internationale de Photochimie. Yorktown Heights, N.Y. 1969.
8. G. J. COLLIN, P. M. PERRIN, et C. M. GAUCHER. Can. J. Chem. **50**, 2391 (1972).
9. R. GORDEN, JR., R. E. REBBERT, et P. AUSLOOS. NBS-Tech. Note 496 (1969).
10. J. L. FRANKLIN, J. G. DILLARD, H. M. ROSENSTOCK, J. T. HERRON, et K. DRAXL. NSRDS-NBS 26 (1969).
11. S. W. BENSON et H. E. O'NEAL. NSRDS-NBS 21 (1970). (*a*) p. 21; (*b*) p. 576.
12. G. J. COLLIN et J. A. HERMAN. Can. J. Chem. **47**, 3097 (1967).
13. R. D. DOEPKER et P. AUSLOOS. J. Chem. Phys. **43**, 3814 (1965).
14. R. D. DOEPKER. J. Phys. Chem. **73**, 3219 (1969).
15. S. KRZYSANOWSKI et R. J. CVETANOVIĆ. Can. J. Chem. **45**, 665 (1967).
16. T. W. EDER et R. W. CARR, JR. J. Phys. Chem. **73**, 2074 (1969).
17. A. F. TROTMAN-DICKENSON et G. S. MILNE. NSRDS-NBS, **9** (1967). (*a*) p. 6; (*b*) p. 9; (*c*) p. 10 et 11; (*d*) p. 110. p. 110.
18. K. R. JENNINGS et R. J. CVETANOVIĆ. J. Chem. Phys. **35**, 1233 (1961).
19. Voir par exemple: B. S. RABINOVITCH, R. F. KUBIN, et R. E. HARRINGTON. J. Chem. Phys. **38**, 405 (1963).
20. Voir note 19 dans: S. G. LIAS, G. J. COLLIN, R. E. REBBERT, et P. AUSLOOS. J. Chem. Phys. **52**, 1841 (1970).
21. P. BORELL et F. C. JAMES. Trans. Faraday Soc. **62**, 2452 (1966).

Can. J. Chem. Downloaded from www.nrcresearchpress.com by 210.87.254.105 on 09/05/12
For personal use only.

Pulse Radiolysis of Aqueous Papain

J. R. CLEMENT AND D. A. ARMSTRONG

Department of Chemistry, University of Calgary, Calgary, Alberta T2N 1N4

AND

N. V. KLASSEN AND H. A. GILLIS

Division of Physics, National Research Council of Canada, Ottawa, Canada K1A 0R6

The pulse radiolysis of the proteolytic enzyme papain has been studied in nitrogen-purged and N_2O-purged aqueous solutions at p*H* 6.4. The rate constant for reaction of OH with papain is $4.7 \times 10^{10}\ M^{-1}\ s^{-1}$. The initial spectrum of the intermediate formed by this radical is consistent with a major fraction of attack at tyrosine residues with smaller proportions reacting at tryptophan and other sites. Subsequent spectral changes are also consistent with the preferential attack of OH on tyrosine. The overall rate constant for reaction of e^-_{aq} with papain is $4.1 \times 10^{10}\ M^{-1}\ s^{-1}$ and the spectrum of the electron adduct closely resembles that of the disulfide anion —SS$\dot{-}$. However, there is evidence that not all reactions of e^-_{aq} with papain lead to the formation of this species. The results are discussed in the light of deactivation yields for $Co^{60}\gamma$ radiolysis measured by biochemical techniques.

Nous avons étudié la radiolyse par pulsation de l'enzyme protéolytique papain dans des solutions aqueuses purgées à l'azote et au N_2O, à un p*H* de 6.4. La constante de vitesse pour la réaction de OH avec le papain est de $4.7 \times 10^{10}\ M^{-1}\ s^{-1}$. Le spectre initial de l'intermédiaire formé par ce radical suggère qu'une fraction importante de l'attaque s'effectue sur les résidus de tyrosine, une autre fraction se produisant, de façon moins importante, sur le tryptophane et d'autres sites. Les changements apportés aux spectres subséquents suggèrent aussi une attaque préférentielle des résidus OH sur la tyrosine. La constante de vitesse globale pour la réaction de e^-_{aq} avec le papain est de $4.1 \times 10^{10}\ M^{-1}\ s^{-1}$ et le spectre de l'espèce électronique ressemble fortement à celui de l'anion disulfure —SS$\dot{-}$. Il semble toutefois que ce ne sont pas toutes les réactions de e^-_{aq} avec le papain qui donnent naissance à ces espèces. Nous discutons de ces résultats à la lumière des rendements de désactivation, dans le cas de la radiolyse par rayons-γ du ^{60}Co, mesurée par des techniques biochimiques.

[Traduit par le journal]

Canadian Journal of Chemistry, **50**, 2833 (1972)

Can. J. Chem. Downloaded from www.nrcresearchpress.com by 210.87.254.40 on 09/05/12
For personal use only.

Introduction

Damage to DNA molecules is now generally accepted as the main cause for the radiation-induced death of living cells (1, 2). However, most cells contain "repair enzymes", which can restore damaged DNA molecules to their normal structure during or after the period of exposure to radiation. The radiation-resistance of these is also crucial for the survival of the cell (3) and studies of the radiolysis of enzyme molecules in aqueous systems are therefore germane to an understanding of radiobiology at the molecular level. We have chosen papain as a model enzyme for studying radiation effects, because the amino acid sequence, three-dimensional structure and components of the active site are all well known (4). Also papain contains the biologically important CysSSCys and CysSH residues, the radiation chemistry of which has interested us for some time (5, 6).

In an earlier paper (7) we reported the results of a ^{60}Co γ-radiolysis of papain. The enzyme exhibited a high sensitivity to inactivation by e^-_{aq}, a large part of which could be repaired by postirradiation treatment with cysteine. The sensitivity to OH was less, but in this instance the damage was largely irrepairable. The purpose of the present pulse radiolysis study was to determine the rate constants for the reactions of e^-_{aq} and OH with papain and to examine the absorption spectra of the transients formed. The rate constants are of interest in assessing the sensitivity of the enzyme to radiation damage and the concentrations of radical scavengers which would be required to protect it. The absorption spectra of the transients are a potentially valuable source of information concerning the structures of the intermediates formed by e^-_{aq} and OH (8, 9). Also the lifetimes and decay kinetics of these intermediates are of interest since they can lead to information concerning the mechanism of deactivation of the molecule by e^-_{aq} and OH.

Experimental

Papain in the crude powder form as obtained from

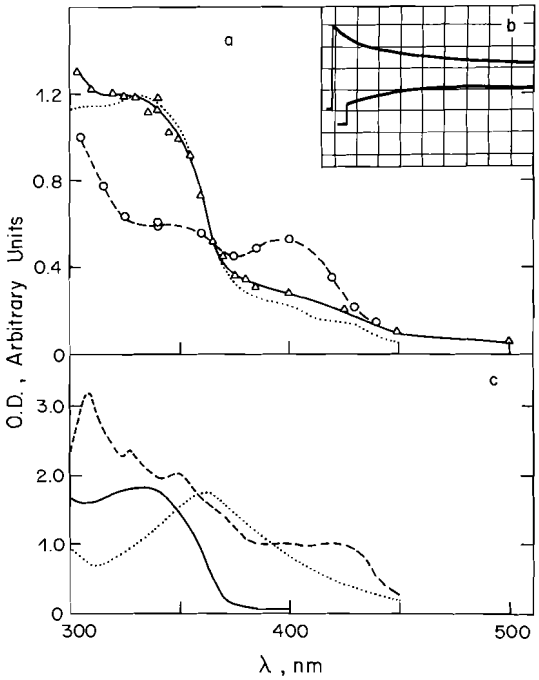

FIG. 1. (*a*) Absorption spectra in N_2O saturated papain solution: △, after 5 μs; ○, after 800 μs. Dotted line, a calculated composite spectrum (see text). (*b*) Oscillogram showing time dependence of the OH adduct of papain. Lower trace (indented), 400 nm; upper trace, 340 nm. Time base: 100 μs/division. (*c*) Initial spectra of: solid line, OH adduct of tyrosine (25, and Lynn *et al.*);[1] dashed line, OH adduct of tryptophan (26); (dotted line) —NHCHCO— (27).

Sigma Chemical Company was purified by the affinity chromatography method of Blumberg (10). All irradiations were carried out using unbuffered solutions of papain in triply distilled water at the elution p*H* of 6.4. This p*H* remained unchanged with doses of up to 20 krad. Solutions were irradiated with 0.04–0.5 μs pulses of 35 MeV electrons with doses of 0.8–2.4 krad per pulse. Spectra were measured in the range 300–600 nm, the lower limit resulting from the strong absorption and photosensitivity of papain below this wavelength (11).

Absorbance measurements were made with a split light beam system which included Bauch and Lomb high intensity monochromators, Philips XP1003 photomultipliers and suitable filters to reduce scattered light. N_2O-saturated aqueous potassium thiocyanate solutions were used for dosimetry with $G\varepsilon$ taken as 4.22×10^4 (12).

Results

The Reaction of Papain with OH Radicals

The solid line in Fig. 1*a* shows the absorption spectrum taken 5 μs after the pulse for N_2O-saturated papain solutions at p$H = 6.4$. This was independent of papain concentration in the range $2.3–7.5 \times 10^{-5}$ *M*. From additional experiments outlined below the contribution of H atoms is relatively small and the spectrum in Fig. 1*a* is attributed mainly to the products of OH radical reactions. The absorption in the wavelength range 310–350 nm was found to build up in a first order manner during the first 3 μs after the pulse, at a rate which was within experimental error proportional to the papain concentration. Typical plots of this behavior are

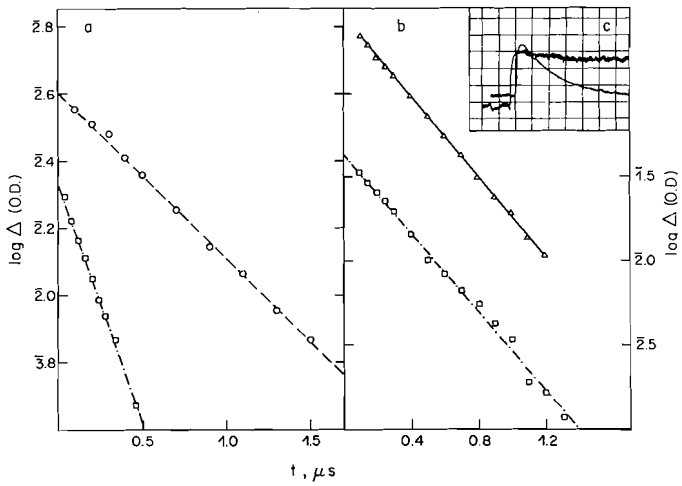

FIG. 2. (*a*) First order plots for the growth of the OH adduct of papain in N_2O saturated solutions: ○, 23×10^{-5} *M* papain, 325 nm; □ 7.3×10^{-5} *M* papain, 310 nm. (*b*) 6.8×10^{-5} *M* papain with 100 m*M* isobutanol: △, decay of e^-_{aq} at 700 nm; □ growth of e^-_{aq} adduct of papain at 425 nm. (*c*) Oscillogram corresponding to Fig. 2*b*. Time base: 0.2 μs/division. Indented trace, 700 nm; other trace, 425 nm.

Can. J. Chem. Downloaded from www.nrcresearchpress.com by 210.87.254.40 on 09/05/12
For personal use only.

Can. J. Chem. Downloaded from www.nrcresearchpress.com by 210.87.254.40 on 09/05/12
For personal use only.

shown in Fig. 2*a*. From the mean of several experiments the rate constant for the reaction of OH with papain was found to be 4.7×10^{10} M^{-1} s^{-1}.

On longer time scales the time dependence of the absorption spectrum in N_2O-saturated solutions is complex. During the first millisecond there is decay of the absorption below 360 nm and a growth above this wavelength. The behavior is illustrated by the traces of oscilloscope photographs in Fig. 1*b*. The dashed line in Fig. 1*a* shows the absorption spectrum taken 800 μs after the pulse.

The Reaction of Papain with e^-_{aq} and H

The absorption spectrum of the H atom adduct was observed by pulsing 6.5×10^{-5} M papain solutions which had been purged with N_2O and contained 0.5 M *t*-butanol. At these concentrations *t*-butanol scavenges 98% of OH (13) but not more than 10% of H (14) if $k_{H + papain} > 5 \times 10^9$ M^{-1} s^{-1}. The transients produced from *t*-butanol do not absorb above 300 nm (15). As shown by the square points in Fig. 3*a*, the absorption of the H adduct is small and no attempt was made to measure its build up. A similar spectrum was obtained when the *t*-butanol was replaced with 20 mM isobutanol, which will scavenge over 90% of the OH radicals (13). At low wavelengths (~305 nm) in these solutions a small component of decay, attributable to isobutanol radicals (15), was observed during the first 10 μs after the pulse. There was, however, no growth of the absorption at wavelengths above 310 nm during this period. Thus there is no reason to suppose that attack of isobutanol radicals on papain contributes to the absorption above this wavelength.

The absorption spectrum observed in Ar-purged 6.5×10^{-5} M papain solutions containing 20 mM isobutanol is shown by the solid line in Fig. 3*a*. This was taken 5 μs after the pulse, when the e^-_{aq} absorption had become negligible. The spectrum at 0.3 μs, when approximately half of e^-_{aq} had reacted, was determined by subtracting the contribution of e^-_{aq} and found to be essentially the same. The strong resemblance to the spectrum of the disulfide anion of cystamine (16), which is shown by the dashed line, confirms an earlier observation (17) that e^-_{aq} reacts with the —S—S— bonds in papain.

The rate constant for the reaction of e^-_{aq} with

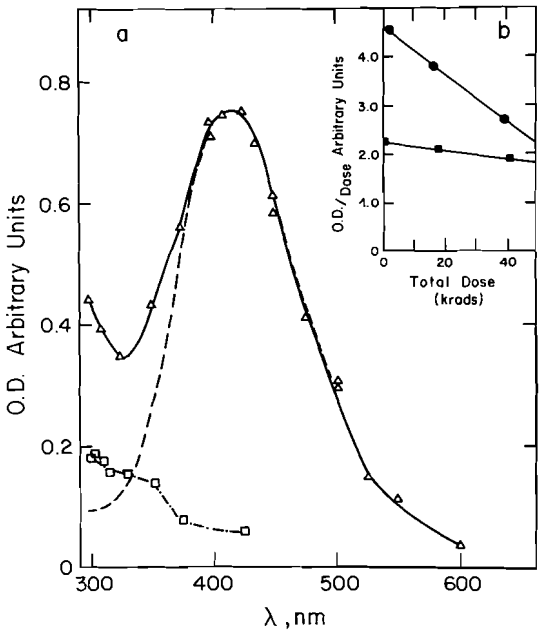

FIG. 3. (*a*) Solid line, absorption spectrum in Ar-purged, 6.5×10^{-5} M papain solutions containing 20 mM isobutanol, 5 μs after the pulse. Dash–dot line, absorption spectrum in N_2O-purged 6.5×10^{-5} M papain solutions containing 0.5 M *t*-butanol, 3 μs after the pulse. Dashed line, disulfide anion of cystamine (16). (*b*) Effect of large doses on spectrum of e^-_{aq} adduct in 2.3×10^{-5} M papain solutions containing 100 mM isobutanol. ●, 415 nm; ■, 310 nm.

papain in previously unirradiated solutions was determined by following the first order decay of the e^-_{aq} absorption at 700 nm. An example of this is given in Fig. 2*b*. From several experiments the mean rate constant for the reaction of e^-_{aq} with papain was found to be 4.1×10^{10} M^{-1} s^{-1}, independent of papain concentration in the range $2–7 \times 10^{-5}$ M.

The indented oscillograph trace in Fig. 2*c* shows an example of the absorption due to e^-_{aq} at 700 nm in the presence of 6.8×10^{-5} M papain. The second trace shows the behavior of the optical density at 425 nm, which is close to the isobestic point in the absorption spectra of e^-_{aq} and the —SS⁻ anion. The contribution of the latter species to the optical density at this wavelength was calculated at various times after the pulse by subtracting the e^-_{aq} absorption, taking for e^-_{aq} $\varepsilon_{425/700} = 0.178$ (18). The difference between the optical density due to —SS⁻ at "infinite time" and time "t" was then plotted in a first order fashion as shown by the square

Can. J. Chem. Downloaded from www.nrcresearchpress.com by 210.87.254.40 on 09/05/12
For personal use only.

points in Fig. 2*b*. The slope of this line gives a rate constant which agrees within 3% with that calculated from the e^-_{aq} decay (see Discussion section). The same correspondence between the growth of —SS⁻— and decay of e^-_{aq} was observed with a 1.37×10^{-5} *M* papain solution, for which the lifetimes of e^-_{aq} decay and —SS⁻— growth are five times longer than in the 6.8×10^{-5} *M* solution.

Papain solutions which had been subjected to sequences of pulses giving total doses of 10 krad or more showed enhanced rate constants for reaction with e^-_{aq} as calculated from the decay of its absorption at 700 nm. At 100 krad, when each papain molecule would on the average have reacted with ten e^-_{aq}, the rate constant had increased to 6.7×10^{10} M^{-1} s^{-1} and was still rising. It is known that the denaturation of enzymes leads to enhanced rate constants for reaction with e^-_{aq} (19) and it seems probable that the increasing value of $k_{e_{aq}+\text{papain}}$ with dose is caused by denaturation due to radiation damage. Cleavage of the S—S bonds and formation of SH has already been demonstrated in the ^{60}Co γ-radiolysis (7), and further evidence for loss of —S—S— groups was obtained in this study in the following way. The spectrum of the e^-_{aq} adduct in Fig. 3*a* was taken with papain solutions which had received doses of 0–3.5 krad and was independent of dose in this range. After very high doses (~15 krad) delivered in a sequence of pulses the spectrum changed appreciably. As shown in Fig. 3*b* the intensity per unit dose in the region of the —SS⁻— peak at 415 nm fell markedly. The drop in the 310 nm absorption is much less.

Discussion

Reactions of OH

The magnitudes of the rate constants for the reactions of OH radicals with the individual amino acid constituents of papain can provide valuable information concerning the relative sensitivities of various side groups and the probable sites of the enzyme at which this free radical will react. The rate constants for the nine most reactive amino acids which occur in papain have been measured by competition kinetics using CNS^- and thymine as primary standards (13). Their values, corrected for new determinations (20) of k_{OH+CNS^-} and $k_{OH+\text{thymine}}$ are listed in Table 1 with other data. The remaining amino acid residues have been assigned an average rate constant of 3×10^8 M^{-1} s^{-1}. This is larger than the weighted mean rate constant for the free acids because of the activating effect of peptide bond formation on the α-hydrogens (21). Thus for the remaining amino acids, attack at the α-hydrogens is considered to be the dominant effect for the purpose of these calculations.

We have calculated the value of $n_{exp}k_{OH+A}$ for each amino acid (A), or peptide unit and expressed it as a fraction of the sum $\sum_{i=1}^{212} n_{exp}k_{OH+A}$. The sources of information concerning n_{exp}, the number of residues of each type considered to be exposed, are presented in footnotes in Table 1.

It is evident from column 5 that the residue of highest $n_{exp}k_{OH+A}$ is tyrosine, with significant reaction of OH also expected at the α-hydrogens of the peptide backbone and the tryptophans. If the fractional values of $n_{exp}k_{OH+A}$ are used as a measure of the fraction of OH radicals attacking each type of group, it is found that the above three sites should account for approximately 70% of all OH radical reactions. The remaining 30% are expected to be spread over all other amino acids.

The absorption spectra of the transients produced by reaction of OH with free tyrosine (25) (also Lynn *et al.*[1]) and free tryptophan (26) and

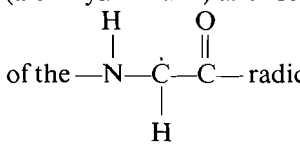

of the —N—C—C— radical observed by Hayon and Simic (27) in the pulse radiolysis of cyclic dipeptides are shown in Fig. 1*c*. All these are initial spectra obtained in aqueous solutions of p*H* 5 to 7. A composite spectrum was constructed assuming that the spectra produced by OH attack on these residues when incorporated in papain were the same. The contribution of each residue to the total absorption at each wavelength was calculated from the known dose per pulse, $G(OH) = 5.9$ molecules per 100 eV in N_2O-saturated solutions (12) and the fractional values of $n_{exp}k_{OH+A}$. This calculated spectrum is compared with the observed spectrum on an absolute basis in Fig. 1*a* (see dotted line).

[1]K. R. Lynn, H. A. Gillis, and N. V. Klassen. Unpublished data.

TABLE 1. Data for reactivity toward OH and accessibility of constituent amino acids in papain

A	n_{total}	n_{exp}*	k_{OH+A} (M^{-1} s^{-1} ($\times 10^{-9}$))	$n_{exp}k_{OH+A}$ (M^{-1} s^{-1} ($\times 10^{-9}$))	$\frac{n_{exp}k_{OH+A}}{\sum n_{exp}k_{OH+A}}$
Cysteine	1	1†	12.3	12.3	0.04
Histidine	2	2	4.7	9.4	0.03
Cystine	3	2	5.6	11.2	0.04
Phenylalanine	4	2	5.5	11.0	0.04
Tryptophan	5	2.2‡§	13.3	29.3	0.10
Leucine	11	5	1.7	8.5	0.03
Isoleucine	12	6	1.7	10.2	0.03
Arginine	12	8	3.3	26.4	0.09
Tyrosine	19	13‡	10.1	131.3	0.47
Peptide Units		106	0.3	31.8	0.11

*n_{exp} is the number of amino acid residues of each type considered to be exposed. In the case of amino acids for which experimental values of n_{exp} were not available these were estimated on the basis of static accessibility probabilities for amino acids in proteins (24) and the known main chain configuration of papain (4).
†X-ray crystallography (4).
‡Perturbation difference spectroscopy (22).
§Selective photo-oxidation (23).

Although there are some unexplained absorptions, the agreement with the observed spectrum in terms of both shape and intensity of absorption is good, implying that in general terms the conclusions derived from the fractional values of $n_{exp}k_{OH+A}$ are borne out for the OH radical. Thus tyrosine appears to be the amino acid residue most frequently hit, reacting with about 47% of the OH radicals.

More direct evidence for reaction with tyrosine is seen in the decay of the transient absorption below 370 nm and the growth above this wavelength in the 0–800 μs period after its formation. This behavior is similar to that observed by Land and Ebert (25) with free tyrosine at low doses per pulse. As in their work the build up at 400 nm and the decay at 340 nm are both approximately first order with the same rate constant. For the case of papain solutions at pH 6.4 the value of the rate constant calculated for the first two half-lives is 4.5×10^3 s^{-1}, which is comparable to 1×10^3 s^{-1} for the decay of the OH adduct of free tyrosine in neutral solution (25). The spectral change was attributed to the elimination of H_2O:

[1] 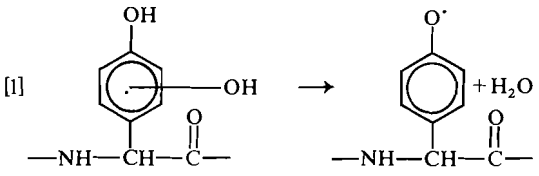

and formation of the phenoxyl radical. This has a maximum in its absorption at ~400 nm, a feature which is also exhibited by the 800 μs spectrum in Fig. 1*a*.

Of the thirteen exposed tyrosines in papain only two are located in the active center (Tyr-61 and Tyr-67), and, although these are believed to play a role in determining the specificity of papain toward peptide substrates,[2] they are not directly involved in the catalytic activity.

Thus our conclusion that approximately 47% of the OH radicals attack tyrosine is consistent with the inefficient (less than one in five) nonrepairable inactivation by OH (7). In fact a large portion of this small yield may be the result of the 10% of OH radicals which attack the highly reactive indole groups of the tryptophan residues. Trp-69 is very accessible, while Trp-177 is largely buried. Both lie in the region of the active center but only loss of Trp-177 affects the esterase activity of papain (23). Of the three other tryptophans, Trp-26 and Trp-181 are deeply buried and nonreactive, while Trp-7 is exposed but not near the active site. Abstraction of hydrogen from the active site sulfydryl

[2] $$OH + Cys—SH \rightarrow Cys—S\cdot + H_2O$$

may also contribute to inactivation, since this reaction is well known for free cysteine (5) and its smaller peptides (6). The absorption of Cys—S· above 300 nm is small and could not make an appreciable contribution to the observed spectrum (28, 29). Reaction with the

[2]A. Berger, I. Schechter, H. Benderli, and N. Kurn. To be published.

Can. J. Chem. Downloaded from www.nrcresearchpress.com by 210.87.254.40 on 09/05/12
For personal use only.

Can. J. Chem. Downloaded from www.nrcresearchpress.com by 210.87.254.40 on 09/05/12
For personal use only.

catalytically important His-159 may also be involved in the inactivation of papain by OH radicals. The attacks of OH radicals on other residues such as cystine, arginine, etc., should be widely spread over the enzyme and should only contribute to inactivation if they caused significant conformational changes.

For purposes of comparison it may be noted that Adams *et al.* (8) have investigated the radiolysis of chicken egg white lysozyme. Their G values in N_2O saturated solutions suggest that about one in three OH radicals causes inactivation and from kinetic and other evidence they conclude that this occurs through attack of OH on Trp-108, which is one of three tryptophans lying in the region of the active center. This enzyme contains a total of six tryptophans and only three tyrosines. Therefore a greater proportion of OH attack on tryptophans is expected than occurs in papain. In fact calculations[3] similar to those above predict 40% of OH reactions at tryptophan and only ~13% at tyrosine residues. The spectrum of the OH adduct of chicken egg white lysozyme (8) bears this out, for it strongly resembles that of the OH adduct of free tryptophan shown in Fig. 1*c*.

Reactions of e^-_{aq}

Evidence from radiation chemistry and other sources (30, 31) suggests that electrons may be conducted quite efficiently through large areas of protein molecules. Therefore the products of reaction of e^-_{aq} with a protein are likely to be determined on energetic rather than kinetic grounds, and we have made no attempt here to calculate fractional values of $n_{exp}\, k_{e^-_{aq}+A}$ as was done for the OH radical. Nonetheless by virtue of their appreciable electron affinities the disulfide bridges are recognized as likely targets. Thus it is not surprising that the absorption spectrum of the solvated electron adduct of papain resembles that of the —SS⁼— anion of cystamine very closely in the region of the 415 nm peak and at higher wavelengths (see Fig. 3*a*). This peak was found to be extremely long lived. About 20% of the absorption disappeared within 100 μs after the pulse with $t_{1/2} \approx 30$ μs. The remainder had a half-life longer than 0.05 s, which is beyond the range of observation of our present equipment. This indicates that the observable —SS⁼— ions in papain are highly stable. In this respect they resemble —SS⁼— ions in organic glasses (32).

In discussing the reactions of e^-_{aq} with a molecule of the complexity of papain it is necessary to consider the possibility that intermediates of significant lifetime may be formed prior to migration of electrons through the enzyme to —S—S— bonds. If —SS⁼— is formed without the involvement of an intermediate of measurable lifetime the instantaneous concentrations of —SS⁼— and e^-_{aq} will be related by expression 3

$$[3] \qquad (\text{—SS}^{=}\text{—})_t = \frac{k'}{k_T}\left[(e^-_{aq})_0 - (e^-_{aq})_t\right]$$

where k' is the rate constant for the reaction giving —SS⁼— and the overall rate constant k_T is the sum of this and the rate constants for all other reaction paths between e^-_{aq} and papain (see below). From this expression the first order integrated rate expression

$$[4] \quad \ln\left[(O.D.\text{—SS}^{=}\text{—})_\infty - (O.D.\text{—SS}^{=}\text{—})_t\right] = \ln\left[(O.D.\text{—SS}^{=}\text{—})_\infty\right] - k_T(\text{papain}) \times t$$

can be derived, so that k_T can be evaluated from the growth of the disulfide absorption as well as from the disappearance of e^-_{aq}. The plot of our results in Fig. 2*b* conforms to eq. 4 and gives the same value of $k_T(= 4.0 \pm 0.2 \times 10^{10})$ as the first order plot for the e^-_{aq} disappearance ($4.1 \pm 0.1 \times 10^{10}$). From the error limits on these rate constants it can be shown that any intermediate involved in the production of —SS⁼— must be short lived ($t_{1/2} \lesssim 0.03$ μs).

The highly stable nature of the observed disulfide anions and the rapidity of their formation would imply that each e^-_{aq} which encounters a papain molecule should form —SS⁼—. However, there are several features of the present results which indicate that this is not so. In the first place there is excess absorption on the low wavelength side of the 415 nm peak, leading to a rising absorption below 320 nm. This cannot be accounted for entirely by the H atom adduct and the 8% of unscavenged OH radicals which still react with papain in the presence of 20 mM isobutanol. Furthermore, as shown in Fig. 3*b* the intensity per unit dose of the absorption in the region of the peak at 415 nm falls with

[3] G. M. Gaucher and F. E. Robertson. Unpublished data.

Can. J. Chem. Downloaded from www.nrcresearchpress.com by 210.87.254.40 on 09/05/12
For personal use only.

increasing dose. This can be attributed to the destruction of one or more of the three disulfide bridges of papain, evidence for which has already been obtained in the ^{60}Co γ-radiolysis of the enzyme (7). The fact that the absorption at 310 nm changes less with increasing dose suggests that much of the intensity at the lower wavelengths is due to different species. In the second place, if the extinction coefficient at 410 nm for —SS^{-}— in papain is similar to that in cystamine (9.4×10^3 (16)) and other —SS^{-}— ions ($\varepsilon_{(PenS)_2} = 7.5 \times 10^3$ (29), $\varepsilon_{(HOC_2H_4S)_2} = 8.3 \times 10^3$ (33)), one would have expected an approximately four fold greater absorption at this wavelength than was observed. The discrepancy implies that only a small fraction (about 25%) of e^-_{aq} produces —SS^{-}— which are detected 5 μs after the pulse.[4] Since we have seen that the observable disulfide ions are long lived it appears probable that there are competing reactions of e^-_{aq} which do not yield *stable* disulfide anions.

A more complete picture of the reactions of e^-_{aq} with papain cannot be given at this time. However, it should be noted that the different environments (4) of the disulfide bridges between $\frac{1}{2}$ cystine residues 22–63, 56–95, and 153–200 may not all give stable disulfide anions. For example, the proximity of amino acid residues with aromatic sidechains might provide reaction pathways which could reduce the lifetime of —SS^{-}— ions below the limit of observation and give products that do not absorb strongly in the 340–600 nm range. Another possibility is that e^-_{aq} reacts with peptide units

to produce the radical anion —Ċ—N—C— (27). This has been shown to react with disulfides at an appreciable rate, although the products are as yet unknown. While highly speculative, it is evident that reactions of the kinds mentioned above may have important implications for the high efficiency of e^-_{aq} in deactivating papain and the fact that this deactivation is largely repairable by CysSH and certain other nucleophiles (7) (also footnote 5).

[4]It may be noted that similar observations in the pulse radiolysis of trypsin indicate that only 60% of e^-_{aq} form stable —SS^{-}— ions on attacking this enzyme (9).

[5]G. M. Gaucher, B. Mainman, and D. A. Armstrong. To be published.

We wish to thank Professor G. M. Gaucher for many valuable comments during the course of this work. We also acknowledge the help of Miss B. Mainman who prepared the papain solutions and Mr. G. G. Teather who assisted in the operation of the lineac.

Financial assistance from the Defence Research Board of Canada, the National Research Council of Canada, and the University of Calgary is gratefully acknowledged.

1. P. ALEXANDER. Ann. New York Acad. Sci. **163**, 652 (1969).
2. H. DERTINGER and H. JUNG. Molecular radiation biology. Springer–Verlag, New York. 1970.
3. A. K. BRUCE, P. A. SANSONE, and T. J. MACVITTIE. Rad. Res. **38**, 95 (1969).
4. B. G. WOLTHERS, J. DRENTH, J. N. JANSONIUS, R. KOEKOEK, and H. M. SWEN. *In* Structure–function relationships of proteolytic enzymes. *Edited by* P. Desnuelle, H. Neurath, and M. Ottesen. Munksgaard, Copenhagen. 1970. p. 272.
5. V. G. WILKENING, M. LAL, M. ARENDS, and D. A. ARMSTRONG. J. Phys. Chem. **72**, 185 (1969).
6. M. LAL, D. A. ARMSTRONG, and M. WIESER. Rad. Res. **37**, 246 (1969).
7. G. M. GAUCHER, B. MAINMAN, G. P. THOMPSON, and D. A. ARMSTRONG. Rad. Res. **46**, 457 (1971).
8. G. E. ADAMS, R. L. WILLSON, J. E. ALDRICH, and R. B. CUNDALL. Int. J. Radiat. Biol. **16**, 333 (1969).
9. T. MASUDA, J. OVADIA, and L. I. GROSSWEINER. Int. J. Radiat. Biol. **20**, 447 (1971).
10. S. BLUMBERG, I. SCHECHTER, and A. BERGER. Eur. J. Biochem. **15**, 97 (1970).
11. K. DOSE and S. RISI. Photochem. Photobiol. **15**, 43 (1972).
12. G. E. ADAMS, J. W. BOAG, J. CURRANT, and B. D. MICHAEL. *In* Pulse radiolysis. *Edited by* M. Ebert, J. P. Keene, A. J. Swallow, and J. H. Baxendale. Academic Press, London. 1965. p. 117.
13. M. ANBAR and P. NETA. Int. J. Appl. Radiat. Isotope, **18**, 493 (1967).
14. P. NETA, R. W. FESSENDEN, and R. H. SCHULER. J. Phys. Chem. **75**, 1654 (1971).
15. M. SIMIC, P. NETA, and E. HAYON. J. Phys. Chem. **73**, 3794 (1969).
16. G. E. ADAMS, G. S. MCNAUGHTON, and B. D. MICHAEL. *In* Excitation and ionization. *Edited by* G. Scholes and G. R. A. Johnson. Taylor and Francis, London. 1967. p. 281.
17. G. E. ADAMS, R. B. CUNDALL, and R. L. WILLSON. *In* Chemical reactivity and biological role of functional groups in enzymes. *Edited by* R. M. S. Smellie. Academic Press, London. 1970. p. 171.
18. J. P. KEENE. Rad. Res. **22**, 1 (1964).
19. R. BRAAMS and M. EBERT. Int. J. Radiat. Biol. **13**, 195 (1967).
20. R. L. WILLSON, C. L. GREENSTOCK, G. E. ADAMS, R. WAGEMAN, and L. M. DORFMAN. Int. J. Radiat. Phys. Chem. **3**, 211 (1971).
21. M. SIMIC, P. NETA, and E. HAYON. J. Am. Chem. Soc. **92**, 4763 (1970).
22. I. WEINRYB and R. F. STEINER. Biochem. **9**, 135 (1970).

23. G. JORI and G. GALIAZZO. Photochem. Photobiol. **14**, 607 (1971).
24. B. LEE and F. M. RICHARDS. J. Mol. Biol. **55**, 379 (1971).
25. E. J. LAND and M. EBERT. Trans. Faraday Soc. **63**, 1181 (1967).
26. R. C. ARMSTRONG and J. SWALLOW. Rad. Res. **40**, 563 (1969).
27. E. HAYON and M. SIMIC. J. Am. Chem. Soc. **93**, 6781 (1971).
28. M. SIMIC and M. Z. HOFFMANN. J. Am. Chem. Soc. **92**, 6096 (1970).
29. J. W. PURDIE, H. A. GILLIS, and N. V. KLASSEN. Chem. Commun. **19**, 1163 (1971).
30. L. AUGENSTEIN, T. BRUSTAD, and R. MASON. Adv. Radiat. Biol. **1**, 227 (1964).
31. Y. VLADIMIROV, D. ROSHCHUPKIN, and E. FESENKO. Photochem. Photobiol. **11**, 227 (1970).
32. T. SHIDA. J. Phys. Chem. **72**, 2597 (1968).
33. W. KARMANN, A. GRANZOW, G. W. MEISSNER, and A. HENGLEIN. Int. J. Rad. Phys. Chem. **1**, 395 (1969).

Can. J. Chem. Downloaded from www.nrcresearchpress.com by 210.87.254.40 on 09/05/12
For personal use only.

Quantitative Investigation of the Ozonolysis Reaction. XVII. Relative Reaction Rates for the Ozone Attack on Phenylethylenes[1]

G. KLUTSCH AND S. FLISZÁR

Department of Chemistry, Université de Montréal, Montréal, Québec

Received March 14, 1972

The relative rate constants for the reaction of ozone with a variety of ring-substituted phenylethylenes in CCl_4 solution obey Hammett's equation $\log k_{rel} = \log k^0_{rel} + \rho\sigma$, with $\sigma \approx -0.9$. Non-conjugating β-substituents affect the rate constants in Taft's σ^* order $k^0_{rel}(CH_3) > (H) > k^0_{rel}(COOCH_3)$. These results illustrate the electrophilic mode of attack of ozone.

Les constantes de vitesse relatives pour l'ozonolyse de phényléthylènes substitués dans le noyau, en solution dans le CCl_4, obéissent à l'équation de Hammett $\log k_{rel} = \log k^0_{rel} + \rho\sigma$, avec $\sigma \approx -0.9$. Les substituants β ne conjugant pas avec la double liaison éthylénique affectent k^0_{rel} dans l'ordre polaire de Taft $k^0_{rel}(CH_3) > (H) > k^0_{rel}(COOCH_3)$. Ces résultats illustrent le mode d'attaque électrophile de l'ozone.

Canadian Journal of Chemistry, **50**, 2841 (1972)

Can. J. Chem. Downloaded from www.nrcresearchpress.com by 210.87.254.40 on 09/05/12
For personal use only.

The dipolar character of ozone has been stressed by Huisgen (1), who advocated that the reaction between ozone and olefin is in general a 1,3-dipolar cycloaddition. This is confirmed by recent kinetic studies (2) which demonstrated the electrophilic nature of the ozone attack. Cvetanović's results (2*a*) illustrate this point clearly: the rate of ozone attack on chloroethylenes (in CCl_4 solution) decreases strongly as the number of chlorine atoms in the olefin molecules is increased. In terms of the 1,3-cycloaddition model for the reaction it would, thus, appear that, although the two new σ bonds are formed quasi-simultaneously, their rates of formation seem to differ because the ozone appears to attack by its positive pole.

Earlier kinetic studies (2*b*, *c*) indicated, however, that the observed trends in reactivity cannot be explained only in terms of an electrophilic attack by ozone, although this appeared to be the predominant factor in many cases. The possible participation of an alternative reaction path via a π or a σ complex has been considered by several authors (2–5). The kinetic results were interpreted in terms of the mechanisms represented in Scheme 1 (2, 5).[2]

The study of the relative reaction rates for the ozone attack on alkyl-substituted ethylenes in inert solvents (5) also contributes in supporting the participation of a reaction path implying a reversible intermediate complex formation. Contrasting with the situation in which the overall electrophilic character of the ozone attack is preserved, the relative reaction rates for the ozone attack on alkyl-substituted ethylenes follow an overall nucleophilic trend. In CCl_4 solution, the kinetics are described adequately by Taft's equation

$$[1] \qquad \log k = \log k^0 + \rho^* \sum \sigma^*$$

where $\sum\sigma^*$ is the sum of Taft's polar constants for the two substituents, and $\rho^* = 7.58$ (*trans*) and $\rho^* = 5.37$ (*cis*) are the polar reaction constants (5). These positive ρ^* values suggest, within the mechanism outlined in Scheme 1, that electron-releasing alkyl groups delay the oxygen O^- attack on the corresponding carbon atom to give the primary ozonide (1,2,3-trioxolane). Hence, the global process appears to be nucleophilic in nature when the final step is the ring-closure, implying, thus, that the determining step is not the formation of the initial olefin–ozone complex but its conversion to give the primary ozonide.[3]

[1]Extracted from the Ph.D. Thesis of G. Klutsch, Université de Montréal, Montréal, Québec, 1971.

[2]The following structures were suggested for the intermediary complex (3–5).

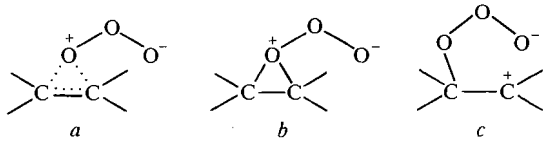

a *b* *c*

The contribution of c is not considered likely; the possible rotation about the C—C σ bond would result in a non-stereospecific ozone addition on the olefin, in violation with Greenwood's observations (6) that a *trans* (or *cis*) olefin yields only *trans* (or *cis*) primary ozonide.

[3]The results in ref. 5 indicated only a minor, if any, steric effect to be attributed to the alkyl groups.

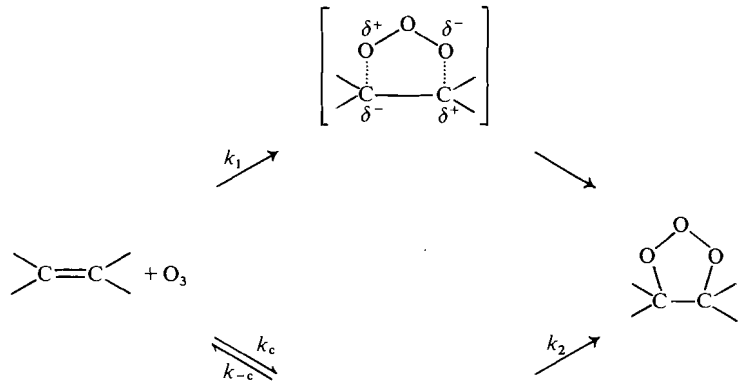

SCHEME 1

As pointed out by Huisgen (1), the exaltation of the polarizability of the olefinic carbon–carbon double bond is expected to favor the concerted 1,3-cycloaddition. This should namely occur in the ozonolysis of phenylethylenes, where the important conjugation increases significantly the polarizability of the reacting ethylenic π bond. For phenylethylenes it is hence expected that the ring-closure is not the rate determining step. Consequently, an overall electrophilic character should prevail for the ozone attack on phenylethylenes, which reflects the initial ozone–olefin complex formation. This aspect is investigated in the present paper, by the study of the substituent effects on the relative rates of ozonolysis of selected ring-substituted phenylethylenes.

Experimental

On the basis of the evidence (2*a*) that, in solution, the ozone–olefin reaction takes place with a 1 : 1 stoichiometry, the consumption of olefin i may be written

$$-\mathrm{d}x_i/\mathrm{d}t = k_i[O_3]x_i$$

where x_i = concentration of olefin i at time = t. Hence, in the conventional ozonolysis of a mixture of two olefins which are identified by the subscripts 1 and 2, it is

$$\log (x_1/x_{1,0}) = -k_1[O_3]t/2.3$$

$$\log (x_2/x_{2,0}) = -k_2[O_3]t/2.3$$

and, consequently,

$$[2] \qquad k_1/k_2 = \log (x_1/x_{1,0})/\log (x_2/x_{2,0})$$

where $x_{1,0}$ and $x_{2,0}$ are the concentrations of the olefins at time $t = 0$. Equation 2 enables the relative rate constants $k_{rel} = k_1/k_2$ (with respect to olefin 2) to be measured in a simple way, from the analyses of the unreacted olefins.

TABLE 1. Relative rate constants for the ozonolysis of *trans* 1-phenylpropene (1) with respect to styrene (2), in CCl_4 at 0°, calculated by means of eq. 2

% ozonolysis*	x_1 (*M*)	x_2 (*M*)	k_{rel}
0	0.0630	0.1110	
5	0.0596	0.1098	5.14
17	0.0522	0.1072	5.40
38	0.0391	0.1012	5.16
47	0.0332	0.0979	5.10
57	0.0270	0.0934	4.91
64	0.0224	0.0901	4.96
72	0.0177	0.0864	5.07
			Average 5.11 ± 0.15

*With respect to olefin 1.

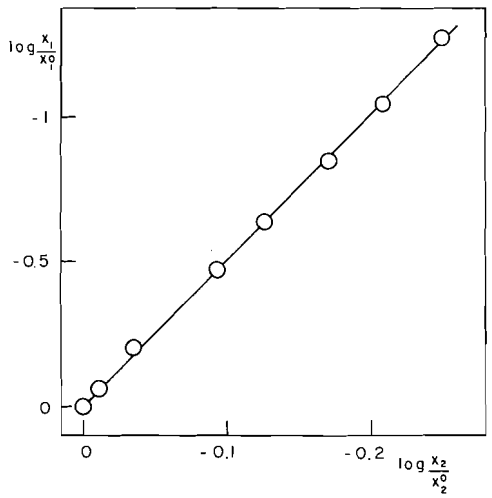

FIG. 1. Verification of eq. 2, for the ozonolysis of *trans* β-methylstyrene, with respect to styrene, in CCl_4 solution at 0°.

Can. J. Chem. Downloaded from www.nrcresearchpress.com by 210.87.254.40 on 09/05/12
For personal use only.

Can. J. Chem. Downloaded from www.nrcresearchpress.com by 210.87.254.40 on 09/05/12
For personal use only.

TABLE 2. Effect of the initial olefin concentration on k_{rel}, with respect to styrene (2)

Olefin 1	x_1^0 (M)	x_2^0 (M)	k_{rel}*	n
β-Methylstyrene	0.106	0.100	5.2	7
	0.063	0.111	5.1	7
Isosafrole	0.110	0.118	8.9	3
	0.037	0.103	8.9	7

*Calculated from n determinations.

The fact that k_{rel} is independent of the ozone concentration and of reaction time considerably facilitates the measurements of k_{rel}. The example given in Table 1 indicates that k_{rel} does not depend on the progress of the reaction, *i.e.*, on the time of reaction.

The values of k_{rel} were obtained by a least-square analysis of the lines constructed from the plots of log $(x_1/x_{1,0})$ *vs.* log $(x_2/x_{2,0})$ (Fig. 1), using data such as those given in the example (Table 1).

The examples given in Table 2 confirm that k_{rel} is independent of the initial olefin concentrations.

In the present work, k_{rel} is always expressed with reference to styrene (subscript 2), and the results are indicated with a 95% confidence limit, from 6–8 individual experiments. Carbon tetrachloride was used as solvent. Most of the experiments were carried out at 0 °C, but it has been verified that k_{rel} does not depend on the temperature, at least not in the temperature interval from 0 to 25 °C.

Most of the olefins are commercial products. Some β-substituted phenylethylenes with a substituent on the phenyl ring were prepared by Granger (7). The purity of the olefins was controlled by g.l.c. and by the standard KI test. The ozonolyses were carried out on 5–10 ml of the olefin solutions. Immediately after completion of the ozonolysis, the solutions were analyzed for unreacted olefins by g.l.c., using a Hewlett–Packard F&M 5750 gas chromatograph with flame detector and a 6 ft UCW-98 column. The intensities of the g.l.c. peaks were measured by planimetry and compared to the appropriate references. Control experiments were also made using internal standards.

Results and Discussion

The relative rate constants with respect to styrene, as determined at 0° in CCl_4 solution, for a series of *trans* substituted phenylethylenes are reported in Table 3.

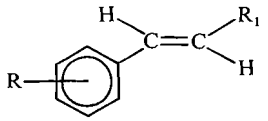

As indicated by Fig. 2, the relative rate constants for any series with an invariant R_1 substituent obey satisfactorily Hammet's equation

$$[3] \qquad \log k_{rel} = \log k_{rel}^0 + \rho\sigma$$

where k_{rel}^0 represent the relative rate constants for the compounds having no substituent in the aromatic ring, *i.e.*, R = H. The reaction constants ρ which are calculated by means of eq. 3 from the results reported in Table 3 are given in Table 4.

These results indicate that, within experimental error, the slopes ρ are similar for the different series of phenylethylenes which were examined, irrespective of the nature of R_1. The negative ρ value which is observed in each case clearly indicates that the overall character of the ozone attack on phenylethylenes is electrophilic in nature. The process of cycloaddition, favored by the exaltation of the polarizability of the ethylenic π bond due to its conjugation with the aromatic ring, implies postulates similar to those discussed by Huisgen (1) in terms of a 1,3-dipolar cycloaddition. Although the extent of simultaneity in the formation of the two carbon–oxygen bonds is an open question, it may be assumed that the transition state resembles closely the final state, *i.e.*, the 1,2,3-trioxolane, and that its

TABLE 3. Relative rate constants for the ozonolysis of *trans* β- and ring-substituted styrenes, in CCl_4 solution

	R_1				
R	$COOCH_3$	H*	C_6H_5	CH_3	$COCH_3$
p-NO_2			0.77 ± 0.03		
m-NO_2	0.0034 ± 0.0001	0.24			
m-Cl		0.48			
p-Cl	0.0079 ± 0.0002	0.625	2.23 ± 0.07	3.12 ± 0.06	
H	0.0120 ± 0.0003	1.000	3.48 ± 0.07	5.11 ± 0.15	0.43 ± 0.01
p-CH_3	0.0150 ± 0.0003	1.50	5.15 ± 0.09		
3,4-CH_2O_2				8.9 ± 0.3	
p-OCH_3	0.0238 ± 0.0005			9.4 ± 0.3	

*The values for R_1 = H are extracted from ref. 8.

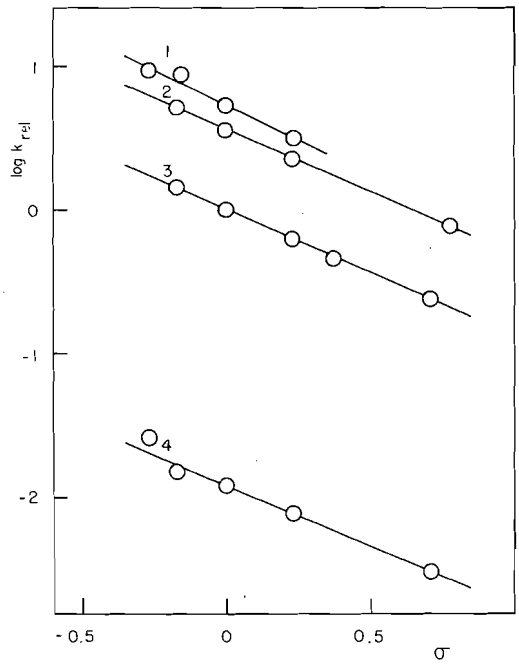

FIG. 2. Hammett plots (eq. 3), from the results of Table 3. $R_1 = CH_3$ (1), C_6H_5 (2), H (3), $COOCH_3$ (4).

final conversion to give the primary ozonide occurs most rapidly. The rate determining step is, hence, the addition of ozone on the olefin. The dual role, *i.e.*, a dipolar character of ozone, exhibiting both an electrophilic and a nucleophilic tendency in the cycloaddition to give the primary ozonide has been discussed earlier by Williamson and Cvetanović (2*a*). The present results suggest that in its reaction with phenylethylenes the ozone molecule prefers an attack by its positive pole.

This aspect is confirmed by the effects exhibited by the β-substituents R_1. These can be evaluated from a comparison of their corresponding k^0_{rel} values which, as indicated by eq. 3 with $\sigma = 0$ (*i.e.*, R = H) depend solely on the nature of R_1.

The behavior exhibited by the CH_3, H, and $COOCH_3$ groups indicates that k^0_{rel} decreases markedly as the polar electron-releasing ability of R_1 is decreased. This confirms the electrophilic trend of the ozone attack on the olefinic double bond revealed by the negative slopes ρ describing the effects of ring substitution.

With $R_1 = C_6H_5$ and $COCH_3$ the relative rate constants are significantly higher than those expected from a consideration of the polar effects of these groups alone. This exaltation of the reaction rates can be attributed to their conjugation with the ethylenic carbon–carbon double bond. In the case of the *trans* methyl cinnamate, such a resonance would be negligible because of the resonating structure $-C(O^-) = O^+ - CH_3$ of the ester group, which appears, hence, to contribute only by its polar effect.

Finally, the similarity in the ρ slopes (Table 4) suggests that the substituents in position 2 influence the kinetics always in the same manner, irrespective of the substituent in position 1. This may suggest an additivity rule for the substituent effects, similar to that observed for the 1,2-dialkyl substituted ethylenes (5). This conclusion, however, can at present only be drawn for ethylenes with a phenyl group in position 1, and should, therefore, not be generalized.

TABLE 4. Hammett's reaction constants ρ (eq. 3) for the ozonolysis of ring- and β-substituted styrenes

Substituent R_1	ρ	Correlation coefficient
$COOCH_3$	−0.87	0.9903
CH_3	−1.03	0.9847
C_6H_5	−0.87	0.9995
H	−0.89	0.9994

The financial aid given by the National Research Council of Canada is gratefully acknowledged.

1. R. HUISGEN. Angew. Chem. **75**, 604, 742 (1963); Eng. Ed. **2**, 565, 633.
2. (*a*) D. G. WILLIAMSON and R. J. CVETANOVIĆ. J. Am. Chem. Soc. **90**, 4248 (1968); (*b*) T. VRBASKI and R. J. CVETANOVIĆ. Can. J. Chem. **38**, 1053 (1960); (*c*) Y. K. WEI and R. J. CVETANOVIĆ. Can. J. Chem. **41**, 913 (1963); (*d*) D. G. WILLIAMSON and R. J. CVETANOVIĆ. J. Am. Chem. Soc. **90**, 3668 (1968).
3. P. S. BAILEY. Chem. Ind. 1148 (1957). P. S. BAILEY. Chem. Rev. **58**, 925 (1958). P. S. BAILEY and A. G. LANE. J. Am. Chem. Soc. **89**, 4473 (1967).
4. R. W. MURRAY, R. D. YOUSSEFYEH, and P. R. STORY. J. Am. Chem. Soc. **89**, 2429 (1967).
5. J. CARLES and S. FLISZÁR. Adv. Chem. Ser. In press. Preprints, Ozone Symposium. Division of Petroleum Chemistry. American Chemical Society. Los Angeles, March 1971. p. A 38.
6. L. J. DURHAM and F. L. GREENWOOD. Chem. Commun. 843 (1967); L. J. DURHAM and F. L. GREENWOOD. J. Org. Chem. **33**, 1629 (1968).
7. M. GRANGER. Ph.D. Thesis. Université de Montréal, Montréal, Québec, 1970.
8. J. CARLES. Ph.D. Thesis. Université de Montréal, Montréal, Québec, 1970.

Can. J. Chem. Downloaded from www.nrcresearchpress.com by 210.87.254.40 on 09/05/12
For personal use only.

Conductances, Densities, and Viscosities of Solutions of Sodium Nitrate in Water and in Dioxane–Water, at 25 °C

ELINOR M. KARTZMARK

Department of Chemistry, University of Manitoba, Winnipeg, Manitoba R3T 2N2

Received March 14, 1972

The conductances, densities, and viscosities of solutions of sodium nitrate in water and in 20, 40, 60, 70, and 80 wt. % dioxane–water have been measured at 25 °C, from $C \simeq 5 \times 10^{-4}$ *M* to saturation. The data have been fitted to the Fuoss–Onsager equation, yielding values of Λ_0, $\mathring{a}$, and K_A; and in concentrated solutions to the equations of Wishaw–Stokes and Gellings. Apparent molar volumes have been calculated.

No appreciable ion association is apparent in solutions whose dioxane content is less than 60% by weight. Passing from water to 80% dioxane, the values of $\mathring{a}$ obtained from the Fuoss–Onsager equation increased from 2.74 to 7.60 Å, a sharp increase occurring beyond 60%.

Les conductances, densités et viscosités des solutions de nitrate de sodium dans l'eau et dans des mélanges à 20, 40, 50, 70, et 80% en poids de dioxane et d'eau; ont été mesurées à 25° pour $C \simeq 5 \times 10^{-4}$ *M* jusqu'à saturation. Les données ont été rajustées à l'équation de Fuoss-Onsager donnant ainsi les valeurs de Λ_0, $\mathring{a}$, et K_A; et pour les solutions concentrées, aux équations de Wishaw–Stokes et Gellings. Les volumes molaires apparents ont été calculés.

Il n'y a pas d'association ionique appréciable dans les solutions dont la teneur en dioxane est inférieure à 60% en poids. En passant de l'eau au dioxane à 80%, les valeurs de å obtenues à partir de l'équation de Fuoss–Onsager augmentent de 2.74 à 7.60 Å, avec un accroissement marqué au-delà de 60%.

[Traduit par le journal]

Canadian Journal of Chemistry, **50**, 2845 (1972)

Previously in this laboratory, the conductances of solutions of lithium and of sodium chlorates in water and in water–dioxane have been measured, and the degrees of association calculated (1). The present paper is a report on a similar study, using sodium nitrate. The only previous work on the conductance of sodium nitrate in aqueous solution, at 25 °C, in the dilute region, is that due to Jones (2). The concentrated region has been investigated by Gellings (3), up to 4.84 *M*. No previous studies have been made on sodium nitrate in water–dioxane mixed solvents.

Conductance measurements in the dilute region yield Λ_0 as a function of dielectric constant and values of $\mathring{a}$ and K_A can be calculated using the Fuoss–Onsager equation. The concentrated region is of great interest, compounding as it does the problems of viscosity, association, and solvation. For some salts, the Wishaw–Stokes equation gives a relatively good quantitative representation of the concentrated region but it has been found to be quite inadequate for others (1). This paper reports measurements of density, viscosity, and conductance over the complete concentration range, that is, from 5×10^{-4} *M* to saturation in water and in 20, 40, 60, 70, and 80 wt.% dioxane–water.

Experimental

Purity of Materials

Sodium Nitrate

Fisher "Certified" sodium nitrate was recrystallized twice from conductance water, dried in an oven at 120 °C with periodic grinding.

Conductance Water

This was prepared by distillation of water which had passed through a mixed resin demineralization column, using a silica still and collecting flasks. Dissolved carbon dioxide was removed by purging with purified nitrogen.

Dioxane

Fisher "Certified" dioxane was further purified by the method of Hess and Frahm (4). The purified dioxane had a density of 1.0278 g/ml and refractive index of $n_{25}^{D} = 1.4202$. Lind and Fuoss (5) report a density of 1.02794 after a week's refluxing over sodium. Frey and Gilbert (6) report a refractive index of 1.42025.

Potassium Chloride

This was recrystallized from conductance water, dried and fused in air.

Procedure

The experimental procedures have been recorded in ref. 1; only minor changes have been made. A Beckmann conductance bridge, Model RC-18 A, was used. All weighings were reduced to vacuum. The temperature was controlled at 25.00 ± 0.005 °C. The dielectric constants of pure dioxane and 60 and 80 wt. % dioxane were measured with a Sargent Model 5 Oscillometer, thermostated to 25.00 °C. It was calibrated using spectroscopically pure benzene, nitrobenzene, and ethylene dichloride. The dielectric constants of 20 and 40% dioxane were taken from Harned and Owen (7). Viscosities were measured with a Cannon and Fenske

Can. J. Chem. Downloaded from www.nrcresearchpress.com by 210.87.254.6 on 09/05/12
For personal use only.

Can. J. Chem. Downloaded from www.nrcresearchpress.com by 210.87.254.6 on 09/05/12
For personal use only.

TABLE 1. Densities, viscosities, and conductances of sodium nitrate at 25 °C in water and water–dioxane mixtures; $\Delta\Lambda_{calcd}$ using Wishaw–Stokes' equation and Gellings' equation

(*a*) Aqueous solution*

c	d (g/ml)	η_{rel}	Λ	$\Delta\Lambda_1$	$\Delta\Lambda_2$
0.01029	—	—	113.34	+0.17	+0.17
0.01798	—	—	111.00	+0.25	+0.25
0.02650	—	—	109.14	+0.24	+0.24
0.03371	—	—	107.92	+0.17	+0.16
0.07171	1.0008	—	103.26	+0.04	+0.02
0.09617	1.0025	1.0040	101.15	−0.41	−0.07
0.3315	1.0155	1.0269	90.10	−2.13	−0.41
0.9782	1.0508	1.0642	76.21	−1.73	+0.04
1.9511	1.1024	1.1695	63.39	−1.93	+1.40
2.8509	1.1490	1.3006	54.43	−2.30	+2.32
3.7502	1.1939	1.4695	46.98	−2.87	+2.81
5.1299	1.2625	1.8432	37.83	−4.53	+2.34
6.0413	1.3064	2.1558	32.79	−5.16	+1.45
6.9868	1.3513	2.5844	28.31	−5.90	+0.04
7.79	1.3864	2.9849	25.02	−6.04	−1.55

*$\Delta\Lambda_1$, W–S equation: $\Lambda_0 = 121.55$; $\mathring{a} = 3.00$. $\Delta\Lambda_2$, Gellings' equation: $\Lambda_0 = 121.55$; $\mathring{a} = 2.74$; $z = 0.0842$.

(*b*) 20 wt.% dioxane ($d = 1.0139$ g/ml)*

c	d (g/ml)	η_{rel}	Λ	$\Delta\Lambda_1$	$\Delta\Lambda_2$
0.009706	—	—	79.89	+0.47	+0.60
0.01449	1.0145	—	78.72	+0.32	+0.40
0.01891	1.0149	—	77.88	+0.17	+0.39
0.02089	—	—	77.47	+0.19	+0.43
0.03066	1.0155	—	75.82	+0.18	+0.49
0.04080	1.0161	—	74.40	+0.22	+0.60
0.05095	1.0166	1.003	73.91	−0.67	0
0.09924	1.0192	1.009	70.45	−1.53	−0.25
0.1984	1.0245	1.020	66.29	−2.78	−0.63
0.5414	1.0426	1.034	58.89	−3.77	−1.18
0.8602	1.0591	1.075	54.00	−4.54	−0.70
1.754	1.1051	1.168	45.08	−4.71	−0.20
2.306	1.1331	1.269	40.57	−5.27	+0.25
3.637	1.1992	1.550	31.82	−5.48	+0.58
4.425	1.2379	1.793	27.58	−5.89	+0.23
4.742	1.2533	—	26.15	—	+0.01
6.259	1.3219	2.536	20.18	−6.05	−2.02

*$\Delta\Lambda_1$, W–S equation: $\Lambda_0 = 87.20$; $\mathring{a} = 2.93$. $\Delta\Lambda_2$, Gellings' equation: $\Lambda_0 = 87.20$; $\mathring{a} = 3.06$; $z = 0.1004$.

(*c*) 40 wt.% dioxane ($d = 1.0280$ g/ml)*

c	d (g/ml)	η_{rel}	Λ	$\Delta\Lambda_1$	$\Delta\Lambda_2$
0.006038	—	—	58.27	−0.13	−0.15
0.02043	1.0294	—	54.49	+0.13	+0.05
0.03811	1.0303	—	52.22	+0.03	−0.09
0.05969	1.0314	—	50.35	−0.03	−0.21
0.07955	1.0325	—	49.09	−0.10	−0.33

TABLE 1(*c*) (*Concluded*).

c	*d* (g/ml)	η_{rel}	Λ	$\Delta\Lambda_1$	$\Delta\Lambda_2$
0.1049	1.0338	1.004	47.83	−0.38	−0.47
0.4489	1.0517	1.066	40.02	−2.69	−1.14
0.9499	1.0771	1.134	34.51	−3.33	−0.94
1.4284	1.1011	1.226	30.70	−1.79	−0.54
1.9832	1.1285	1.341	26.96	−4.17	0
2.4220	1.1500	1.474	24.48	−4.73	+0.26
3.0848	1.1823	1.673	21.20	−4.92	+0.49
3.987	1.2229	1.982	17.54	−4.92	+0.35

*$\Delta\Lambda_1$, W–S equation: $\Lambda_0 = 63.50$; $\mathring{a} = 4.0$. $\Delta\Lambda_2$, Gellings' equation: $\Lambda_0 = 63.50$; $\mathring{a} = 3.06$; $z = 0.1123$.

(*d*) 60 wt.% dioxane ($d = 1.0360$ g/ml)

c	*d* (g/ml)	η_{rel}	Λ
0.0102	1.0365	—	39.28
0.0205	1.0372	—	36.28
0.0407	1.0374	—	33.64
0.0548	1.0389	—	32.34
0.1040	1.0416	—	29.72
0.5075	1.0623	1.132	22.95
1.0360	1.0889	1.295	18.98
1.4825	1.1112	1.451	16.49
1.9549	1.1343	1.655	14.40
2.642	1.1669	1.988	12.02

(*e*) 80 wt.% dioxane ($d = 1.0353$ g/ml)

c	*d* (g/ml)	Λ
0.003651	—	16.17
0.004265	—	15.46
0.009432	1.0359	12.70
0.01973	1.0366	10.84
0.03979	1.0374	9.58
0.05405	1.0381	9.09

(8) type viscometer, with a run-time with water of 340.4 s. The viscosity values for dioxane–water mixtures compared very well with the data of Lind and Fuoss (5). A silica cell of the Shedlovsky type was used for the conductance measurements of the dilute solutions. At the end of each series of measurements with the Shedlovsky cell, the density of the solution was determined; no detectable change was observable from the density of the solvent (*i.e.* within 0.0001).

Results

The equivalent conductances in the dilute region are to be found in Table A in the Depository of Unpublished Data, together with calculations from the Fuoss–Onsager equation.[1] The data of Jones which extend from $c = 5 \times 10^{-4}$ to 0.5 *M*, range from 3 to 6 mhos lower than the present data and do not fit the Debye–Hückel slope in the limiting region.

In the concentrated region, densities, viscosities, and equivalent conductances were measured and are shown in Table 1, together with the deviation in Λ calculated using the

[1]Tables A and B are available, at a nominal charge, from the Depository of Unpublished Data, National Science Library, National Research Council of Canada, Ottawa, Canada, K1A 0S2.

Can. J. Chem. Downloaded from www.nrcresearchpress.com by 210.87.254.6 on 09/05/12
For personal use only.

Can. J. Chem. Downloaded from www.nrcresearchpress.com by 210.87.254.6 on 09/05/12
For personal use only.

equations of Wishaw–Stokes and of Gellings. An extended form of this table, including calculations of the apparent molar volume, is given as Table B in the Depository of Unpublished Data.

Discussion

Dilute Region

Λ_0 was determined in all solvents, either by extrapolation of the Λ *vs.* $\sqrt{c}$ plot (for water, 20, and 40% dioxane), or by the best fit of the data with the Fuoss–Onsager equation:

$$[1] \qquad \Lambda = \Lambda_0 - Sc^{1/2} + Ec \log c + Jc$$

$$[2] \quad \Lambda = \Lambda_0 - Sc_i^{1/2} + Ec_i \log c_i + Jc_i - K_A c_i f^2 \Lambda$$

where $c_i = c\gamma$, concentration of free ions, and $K_A = (1-\gamma)/(c\gamma^2 f^2)$, the association constant. The activity coefficient, f, was calculated from the Debye–Hückel equation

$$-\log f = \frac{\beta'' C^{1/2}\gamma^{1/2}}{1 + K\mathring{a}C^{1/2}\gamma^{1/2}}$$

For solvents containing 0, 20, and 40% dioxane, no ionic association was found; eq. 1 was thus used. Following the procedure of Fuoss and Accascina (9), a preliminary graphical determination of Λ_0 allowed calculation of S and E, from which $\Lambda' = \Lambda + Sc^{1/2} - Ec \log c$ was calculated. Λ' was plotted *vs.* c, yielding a straight line whose slope is J. From the value for J, the parameter $\mathring{a}$ was determined. The limit $K\mathring{a} < 0.2$ was adhered to. Finally $\delta = \Lambda'_{obs} - (\Lambda'_0 + Jc)$ was calculated for each concentration. Solutions containing 60, 70, and 80% dioxane showed ion association and were treated using eq. 2. Again the method outlined in Fuoss and Accascina was followed. Here the graphical method of finding Λ_0 was not as clear-cut and necessitated several trials until a straight line y *vs.* x was obtained. J, the intercept, was used to calculate $\mathring{a}$, the new value was introduced in the expression for f^2 and the procedure repeated. K_A is obtained as the slope of the y *vs.* x line. The whole procedure was tested for consistency by substituting S, E, J, K_A, f^2, and γ back into eq. 2 and obtaining the difference from Λ exp.

Λ_0 decreases from 121.55 in aqueous solution to 41.00 in 80% dioxane–water. The values of $\mathring{a}$ increase from 2.74 in water to 7.60 in 80% dioxane. These results are shown in Fig. 1. The viscosity of dioxane–water mixtures passes through a sharp maximum at 60% dioxane. This seems to have no marked effect on Λ_0, because the Λ_0 *vs.* D plot shows no change in curvature in this range. The $\mathring{a}$ values begin to increase steeply at around 60% dioxane, suggesting that the solvation sheath may be predominantly dioxane. Indeed, the change in Λ_0 with dioxane content can only be explained in terms of solvation. A plot $\Lambda_0\eta_0$ *vs.* dioxane content shows a marked decrease beyond 40% dioxane, even though the viscosity increases by 17% in the range 40 → 60% dioxane.

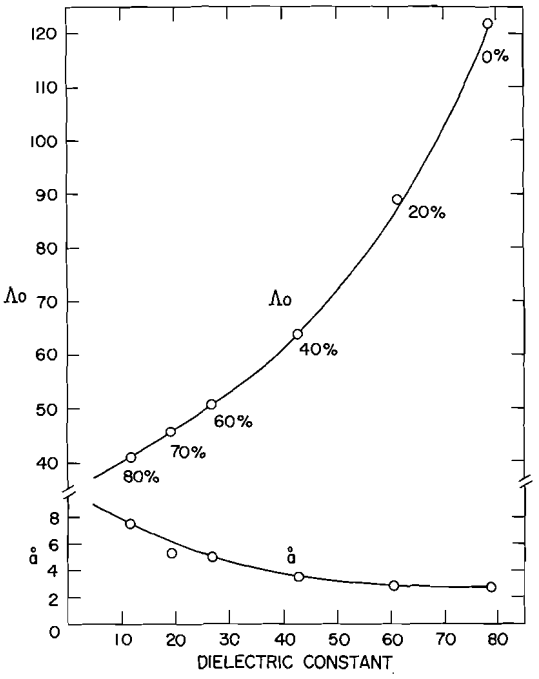

FIG. 1. Λ_0, $\mathring{a}$ *vs.* dielectric constant.

Ion association as determined by K_A does not become marked until a dioxane content of approximately 60% has been attained. The data of Table A may be summarized in Table 2. The $\mathring{a}$ and K_A are very similar to those of Lind and Fuoss for potassium chloride.

The Concentrated Region

The conductance–viscosity data in the concentrated region were fitted to the Wishaw–Stokes equation (10)

$$\Lambda = \left(\Lambda_0 - \frac{B_2\sqrt{c}}{1 + B\mathring{a}\sqrt{c}}\right)\left(1 - \frac{B_1\sqrt{c}}{1 + B\mathring{a}\sqrt{c}}F\right)\frac{\eta_0}{\eta}$$

Generally, the $\mathring{a}$ obtained from the Fuoss–

TABLE 2. Summary of Table A in the Depository of Unpublished Data

Wt.% Dioxane	D	η (P)	Λ_0 (mho)	J	$\mathring{a}$	K_A
0	78.54	0.008903	121.55	143	2.74	—
20	60.79	0.01262	87.20	197	2.93	—
40	42.98	0.01673	63.50	418	3.70	—
60	26.80	0.01929	50.75	1 270	5.00	12.5
70	19.40	0.01897	46.00	3 580	5.25	107.0
80	11.90	0.01703	41.00	16 600	7.60	1 980.0

Onsager equation gave the best results. Where the dilute region showed marked association, *i.e.*, in dioxane > 40%, the Wishaw–Stokes equation failed completely. Taking a 3% error as maximum, the data for aqueous solutions fitted the equation up to $c \simeq 1.95\ M$; the range was very much reduced in solutions containing dioxane ($c \simeq 0.15\ M$). The failure of the equation in aqueous solution at higher concentrations may be attributed to inadequacy of the viscosity correction but is probably due also to association. The viscosity factor is more pronounced in 20 and 40% dioxane.

Table B gives calculations of Λ, using Gellings' equation

$$\frac{\Lambda}{\Lambda_0} = (1 - zc) \exp - \frac{\left(\alpha + \frac{\beta}{\Lambda_0}\right)\sqrt{c}}{1 + B\mathring{a}\sqrt{c}}$$

where a, β, B, $\mathring{a}$ have the same significance as in Debye–Hückel theory and z is an empirical constant. For $\mathring{a}$, Gellings used the effective radii of the ions in the solution as calculated by Böttcher (11) from refractive index and density of electrolytic solutions. Z is evaluated from the conductance data by the method of least squares. No correction is made for the viscosity of the solution. The data of Gellings for sodium nitrate in water plot on the same Λ *vs.* $\sqrt{c}$ curve but do not extend to saturation nor to the very dilute region. The present paper extends Gellings' data to $c = 7.79\ M$ in aqueous solution. With $\mathring{a} = 2.74$ (the value obtained from the dilute region) and $z = 0.0842$, the equation fits the data over the entire concentration range, within about 5%. The 20 and 40% dioxane solutions are equally well handled but, at higher dioxane concentrations, no constancy in z was found for reasonable $\mathring{a}$ values. Admittedly, while Gellings' equation fits the experimental data over a much wider range than Wishaw–Stokes', it contains an empirical constant, which has no obvious theoretical basis and it ignores the viscosity correction entirely.

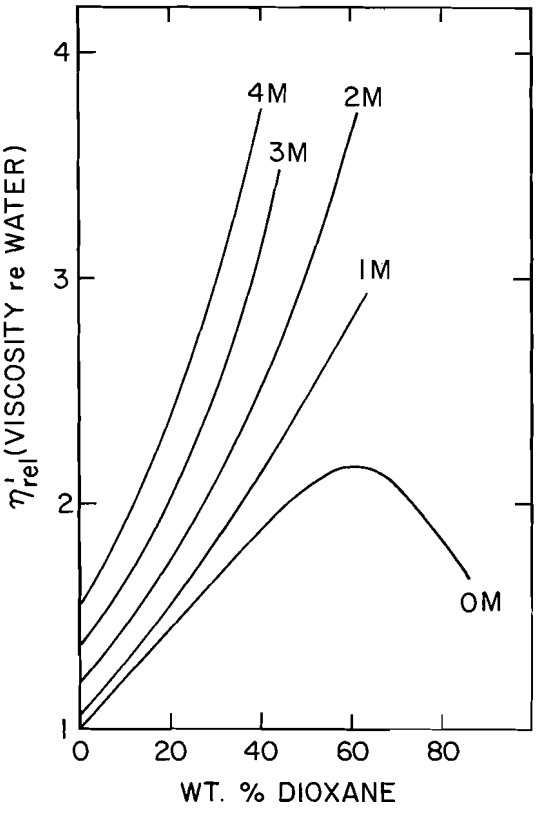

FIG. 2. η'_{rel} *vs.* wt. % dioxane.

Viscosities and Associated Properties

The relative viscosities (solvent = 1) of sodium nitrate solutions increase with concentration (to 2.98 in saturated aqueous solution) and also with increase in dioxane content in the mixed solvents. When the viscosities relative to water (η'_{rel}) are plotted against % dioxane, for 1, 2, 3, and 4 M solutions of sodium nitrate, Fig. 2

Can. J. Chem. Downloaded from www.nrcresearchpress.com by 210.87.254.6 on 09/05/12
For personal use only.

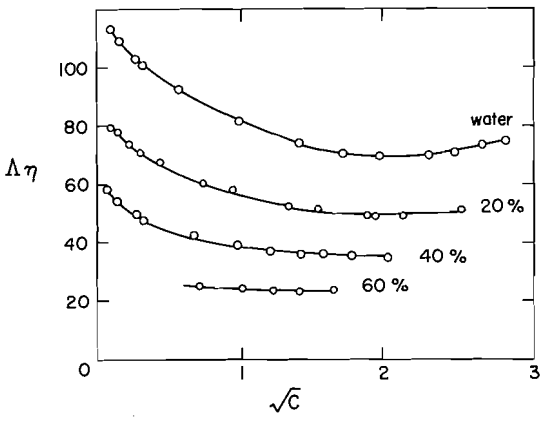

FIG. 3. $\Lambda\eta$ *vs.* $\sqrt{c}$.

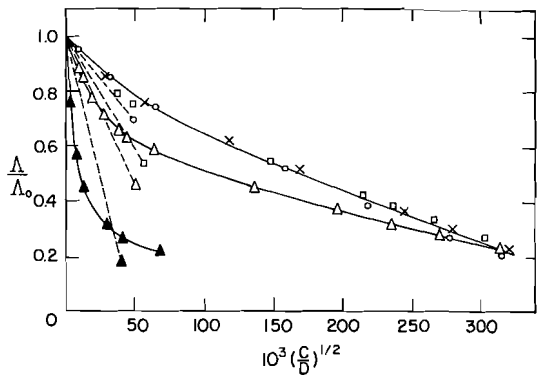

FIG. 4. Λ/Λ_0 *vs.* $(c/D)^{1/2}$.

is obtained. The ratios of η'_{rel}/η_{rel} increase with dioxane content and this indicates that the same concentration of salt increases the viscosity of solvent to a greater extent, the greater the dioxane content. The viscosity of dioxane–water solutions (0.0 *M* curve) passes through a maximum at 60% and falls off rapidly. The limited solubility of sodium nitrate does not allow investigation beyond the solvent maximum; from 1 to 4 *M* there is no suggestion of a maximum. In 80% dioxane–water two liquid layers are produced shortly after 0.054 *M* sodium nitrate.

The apparent molar volumes ϕ_v (Table B) increase with concentration of sodium nitrate and also with dioxane content to an apparent maximum between 40 and 60% dioxane. This was also found to be true of sodium chlorate (12), which approached a maximum at 64.5% dioxane. The difference ϕ_v $(ClO_3^- - NO_3^-)$ remains roughly constant between 1 and 6 *M*, in water, and in 40% dioxane, the values being around 1.3 ml/mol greater in the latter.

A plot of $\Lambda\eta$ *vs.* $\sqrt{c}$ (Fig. 3) shows a minimum around 4 *M* in aqueous and 20% dioxane solutions; the minimum is not observable in solutions of higher dioxane content, which have limited solubility of sodium nitrate.

Figure 4, a plot of Λ/Λ_0 *vs.* $(c/D)^{1/2}$, shows an interesting regularity in solutions in 0, 20, and 40% dioxane. All data points fall on the same curve, to within about 5%, a type of reduced conductance. In the very dilute region, solutions with dioxane content less than 60% show the well known "anabatic phoreogram" typical of complete dissociation, *i.e.*, the limiting slope lies below the Λ *vs.* $\sqrt{c}$ plot. For 60 and 80% dioxane, the limiting slope lies above the Λ *vs.* $\sqrt{c}$ plot, "catabatic phoreogram", a sign of association.

1. A. N. CAMPBELL, E. M. KARTZMARK, and B. G. OLIVER. Can. J. Chem. **44**, 925 (1966).
2. H. C. JONES. Carn. Inst. Wash. Pub. No. 170, 11 (1912).
3. P. J. GELLINGS. Rec. Trav. Chim. **75**, 209 (1956).
4. K. HESS and H. FRAHM. Ber. **71**, 2627 (1938).
5. J. E. LIND and R. M. FUOSS. J. Am. Chem. Soc. **65**, 999 (1960).
6. P. R. FREY and E. C. GILBERT. J. Am. Chem. Soc. **59**, 1344 (1937).
7. H. S. HARNED and B. B. OWEN. The physical chemistry of electrolytic solutions. 3rd ed. Rheinholdt Publishers, New York. 1958. p. 713.
8. M. J. CANNON and M. R. FENSKE. Ind. Eng. Chem. Anal. Edit. **10**, 299 (1938).
9. R. M. FUOSS and F. ACCASCINA. Electrolytic conductance. Interscience Publ. New York. 1959.
10. B. F. WISHAW and R. H. STOKES. J. Am. Chem. Soc. **76**, 2065 (1954).
11. C. J. F. BÖTTCHER. Rec. Trav. Chim. **65**, 14 (1946).
12. B. G. OLIVER and A. N. CAMPBELL. Can. J. Chem. **47**, 4207 (1969).

Can. J. Chem. Downloaded from www.nrcresearchpress.com by 210.87.254.6 on 09/05/12
For personal use only.

The Oxygenation of 2-Oxazolin-5-ones: A New Synthesis of Imides[1]

R. BISSON, R. B. YEATS,[2] AND E. W. WARNHOFF
Department of Chemistry, University of Western Ontario, London, Ontario

Received February 21, 1972

In the presence of mild base such as triethylamine, the two 4-alkylidene-2-phenyl-2-oxazolin-5-ones, **1** and **8**, rapidly absorb oxygen at room temperature with the loss of carbon dioxide and the formation of the imides **4** and **10**. The imide probably arises by decomposition of a hydroperoxide resulting from the reaction of oxygen and the anion of the oxazolinone. A hydroperoxide intermediate will also account for the origin of the acidic by-products **6***a* and **11***a*. The 2-methyl-2-oxazolin-5-one **14** did not react with oxygen at room temperature; at 60° some reaction occurred but no imide was formed.

Lorsque mis en présence d'une base faible comme la triéthylamine, les deux alkylidène-4 phenyl-2 oxazolin-5-ones, **1** et **8** absorbent rapidement de l'oxygène à la température ambiante pour ensuite libérer du gaz carbonique et conduire aux imides **4** et **10**. La formation d'un imide peut être attribuée à la décomposition d'un hydroperoxyde issu de la réaction entre l'oxygène et l'anion de l'oxazolinone. L'intermédiaire hydroperoxyde peut aussi expliquer l'origine des produits secondaires acidiques **6***a* et **11***a*. La méthyl-2-oxazolin-5-one **14** ne réagit pas avec l'oxygène à la température ambiante: toutefois à 60° une transformation fut observée mais non la formation d'un imide.

Canadian Journal of Chemistry, **50**, 2851 (1972)

Can. J. Chem. Downloaded from www.nrcresearchpress.com by 210.87.254.5 on 09/05/12
For personal use only.

In the course of synthetic approaches to peptide alkaloid derivatives (1), a conjugate addition of a phenol to the isobutylidene-2-oxazolin-5-one (isobutylidene azlactone) **1** was attempted (2). When *N*-(*N'*-carbobenzoxyphenylalanyl)-tyramine and **1** were allowed to react in acetonitrile solution containing some triethylamine, instead of the desired addition product there was isolated a colorless solid, $C_{12}H_{13}NO_2$, m.p. 113°, which contained no feature of the protected phenylalanyltyramine group. It was established that the product, whose formula was that of the azlactone minus one carbon atom, arose from the azlactone when it was found that **1** alone in acetonitrile–triethylamine became bright yellow at room temperature and rapidly gave the same compound in up to 58% yield. The suspicion that oxygen was also involved was confirmed when the product was not formed in an attempted reaction in CH_3CN–Et_3N solution under a nitrogen atmosphere. Moreover, oxygen was presumably reacting with the anion **2** of the azlactone since no reaction occurred when an acetonitrile solution of **1** was exposed to oxygen in the absence of base. The choice of solvent was not critical since the same product was formed in acetone and dimethylformamide solutions.

The oxidation product absorbed 1 mol of hydrogen to form the dihydro derivative, m.p. 83°. Comparison of the n.m.r. spectra of these two compounds uniquely defined the dihydro derivative to be benzoyl isovaleryl imide **5**, and the oxidation product itself to be benzoyl β,β-dimethylacrylyl imide **4** with which structure the u.v. and i.r. spectra were in agreement. Final proof of identity was obtained by comparison with an authentic specimen of **4** prepared by reaction of the *N*-lithio salt of benzamide with β,β-dimethylacrylyl chloride.

The reaction probably occurs (Scheme 1) through electron transfer (3) from the resonance stabilized anion **2** of the oxazolinone to oxygen and either recombination of the resulting radical and radical anion, or else reaction of the radical with oxygen and **2**, to produce a peroxide which could have a number of formulations, **3***a*, *b*, or *c*.[3,4] Involvement of the

[1]Presented in part at the 54th Canadian Chemical Conference of the Chemical Institute of Canada, Halifax, Nova Scotia, June 1, 1971.

[2]Department of Chemistry, Bishop's University, Lennoxville, Québec.

[3]It is recognized that in principle oxygen could become attached at three other positions to produce hydroperoxides **i**, **ii**, and **iii** or their cyclic peroxide addition products, two of which can readily explain the carboxylic acid by-products. However, since a peroxide of type **3** most readily explains the formation of imide, and since the carboxylic

Can. J. Chem. Downloaded from www.nrcresearchpress.com by 210.87.254.5 on 09/05/12
For personal use only.

anion **2** is supported not only by the failure of **1** to react in the absence of base, but also by the ready exchange of the allylic methine hydrogen of **1** when D_2O was added to the CH_3CN–Et_3N solution in the absence of oxygen. The oxazolinone **1** also exchanges this tertiary hydrogen slowly at room temperature in acetone-d_6–Et_3N solution. Breakdown of the peroxide (Scheme 1) with loss of carbon dioxide would yield the imide **4** directly, and in fact carbon dioxide was isolated as $BaCO_3$ in a yield almost equal to that of the imide **4**.

A peroxide intermediate can also explain the formation of a major carboxylic acid by-product. The bicarbonate soluble portion of the oxygenation reaction was esterified with diazomethane, and the predominant one of seven compounds isolated by t.l.c. Since this product was clearly a dienoic ester from its u.v. absorption, the structure **6***b* follows and is in agreement with the n.m.r. spectrum. Hydrogenation of the ester gave racemic *N*-benzoylleucine methyl ester **7** whose i.r. and n.m.r. spectra were identical with those of authentic *N*-benzoyl-L-leucine methyl ester. The possible origin of the dienoic acid **6***a* by an elimination reaction of the peroxide[5] followed by acylimine ⇌ enamide tautomerism is depicted for **3***b* in Scheme 2.[5]

To test the generality of this new oxidation, two other oxazolinones were treated with oxygen in CH_3CN–Et_3N solution. The azlactone **8** from hippuric acid and phenylacetone also rapidly absorbed oxygen with the formation of the imide **10** in 43% yield (Scheme 3). In fact the uptake of oxygen was faster than with **1** as would be expected from the greater acidity of the methylene hydrogens in **8** which are both allylic and benzylic. The product was identical with an authentic specimen made by the reaction of the *N*-lithio salt of benzamide and the acid chloride of (*E*)-α-methylcinnamoyl chloride. Also in this oxygenation there was a carboxylic acid by-product formed in 36% yield. The n.m.r. and u.v. spectra identified the methyl ester of the acid to be methyl 3-benzylidene-2-oxobutyrate **11***b*. Oxidative degradation of the α-keto acid **11***a* gave (*E*)-α-methylcinnamic acid. The α-keto acid **11***a* could also have arisen from the hydroperoxide, *e.g.* **9**, which could not in this case give a dienoic acid of the **6***a* type because of the absence of a δ-hydrogen atom. However, the hydroperoxide (*e.g.* **9**) could undergo ring opening[5] and hydrolysis of the benzoylimine **9** → **12** → **11***a*.

The final azlactone tested was the 4-isobutylidene-2-methyl derivative **14**. At room temperature under the same conditions resulting in rapid oxygen absorption by both 2-phenyloxazolinones **1** and **8**, the 2-methyl compound did not react. At 60° over a period of 3 days the azlactone was consumed but no imide **15** was produced. Apparently additional stabilization such as provided by a 2-phenyl substituent is required for facile oxygenation, and the reaction may not be as general as first thought.[6]

acid by-products can be rationalized on the basis of **3***a*–*c*, there is no need to invoke the alternative peroxide formulations in the absence of evidence for them.

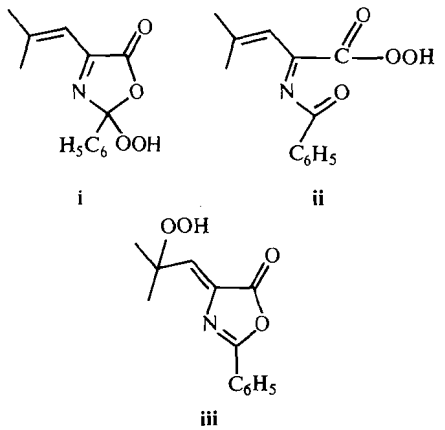

[4]The oxygenation of Schiff base anions (4*a*) and 3,7-dihydroimidazo[1,2-*a*]pyrazin-3-ones (4*b*) follows a similar path. In these cases the breakdown of cyclic four-membered peroxides often radiates visible light, but the absence of observable visible *luminescence* in the present oxygenations (the reactions did become bright yellow) does not necessarily exclude a structure such as **3***b*.

[5]The peracid so formed would break down to the carboxylic acid either by exchange or oxygen loss. Although the formation of the carboxylic acid by-products is shown for one of the possible peroxide structures, similar mechanisms can be written for the other peroxide formulations, and no preference is intended. Some of the other compounds present in the acid fraction may result from attack of the peracid on double bonds.

[6]The apparent failure to form any hydroperoxide which would lead to **15** is probably not due to the acidity of the 2-methyl group. Although in 2-alkyloxazolin-5-ones the α-hydrogens of the 2-alkyl group are acidic enough to be removed to some extent by triethylamine, the pK_a's of the

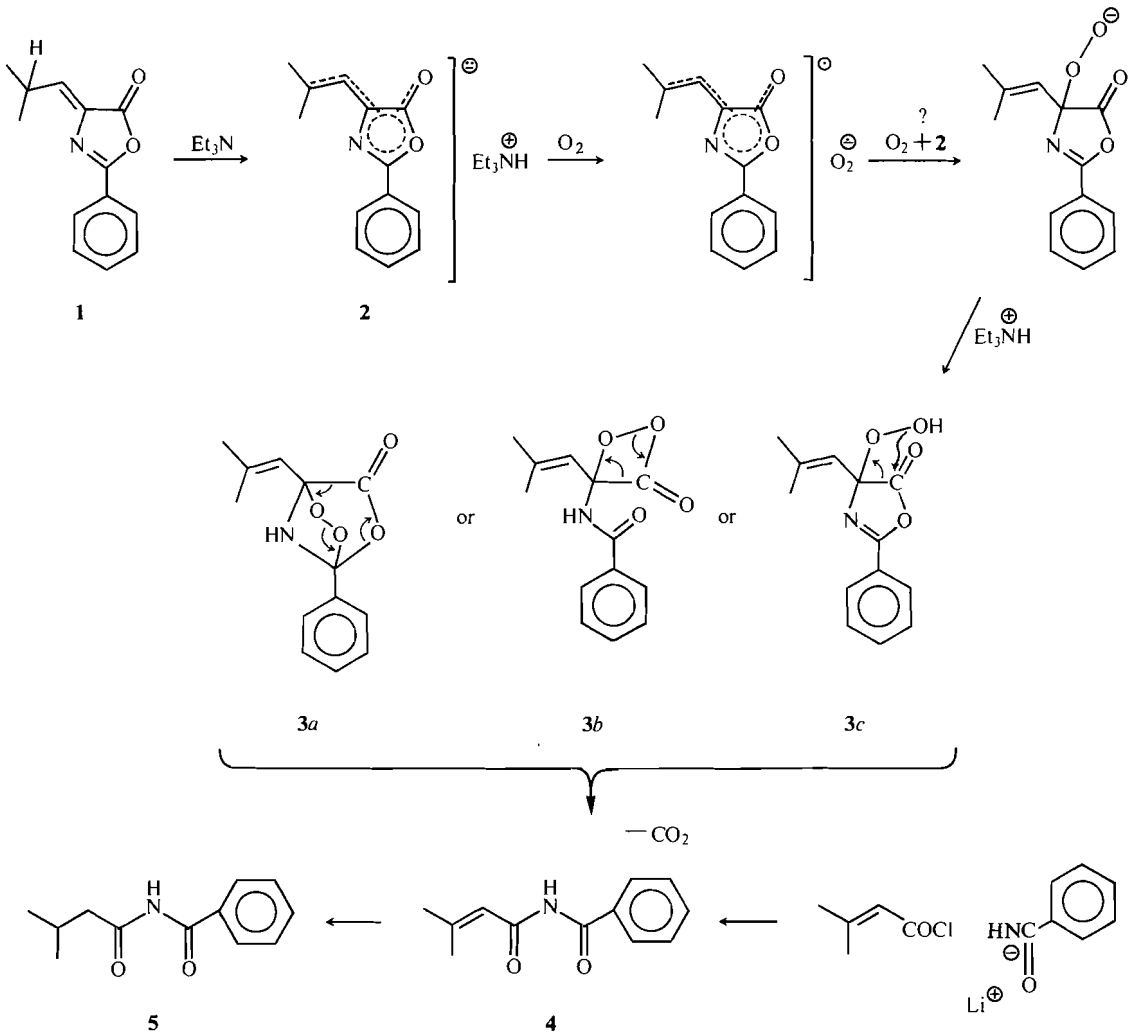

SCHEME 1

Experimental

General

Melting points were determined on a Reichert–Kofler microscope hot stage and are corrected.

I.r. spectra were recorded on a Beckman IR-10 instrument with chloroform solutions. N.m.r. spectra were recorded on Varian A-60 and T-60 spectrometers with deuteriochloroform solutions. Peak positions are given in p.p.m. from internal tetramethylsilane = 0(δ); s = singlet, d = doublet, m = multiplet, b = broad. Aromatic peaks are not reported for most spectra. U.v. spectra were recorded on a Cary 14 spectrometer with methanol solutions.

Silica gel GF_{254} (Merck, Germany) was used for thin and thick layer (20 g/20 × 20 cm plate) chromatography. Thin layer plates were visualized by u.v. and/or by charring (H_2SO_4:HNO_3, 4:1). B.D.H. silica gel was used for column chromatography.

Organic solutions from work-up of reactions were washed to neutrality with aqueous $NaHCO_3$ and water, dried over anhydrous $MgSO_4$ and then evaporated to dryness under reduced pressure on a rotary evaporator. Petroleum ether refers to the fraction boiling at 60–80°.

allylic and 2-methyl hydrogens of **14** are probably close enough to allow formation of both monoanions in which case the allylic anion could lead to some imide **15**. However, the ability of oxygen to abstract an electron from the allylic anion will depend on the energy difference between the anion and its corresponding radical. Provided that phenyl stabilizes the radical more than the anion, a 2-phenyl group may serve to lower the activation energy enough for electron abstraction to occur, while the effect of the 2-alkyl group may not be sufficient to make electron abstraction by oxygen facile.

Can. J. Chem. Downloaded from www.nrcresearchpress.com by 210.87.254.5 on 09/05/12
For personal use only.

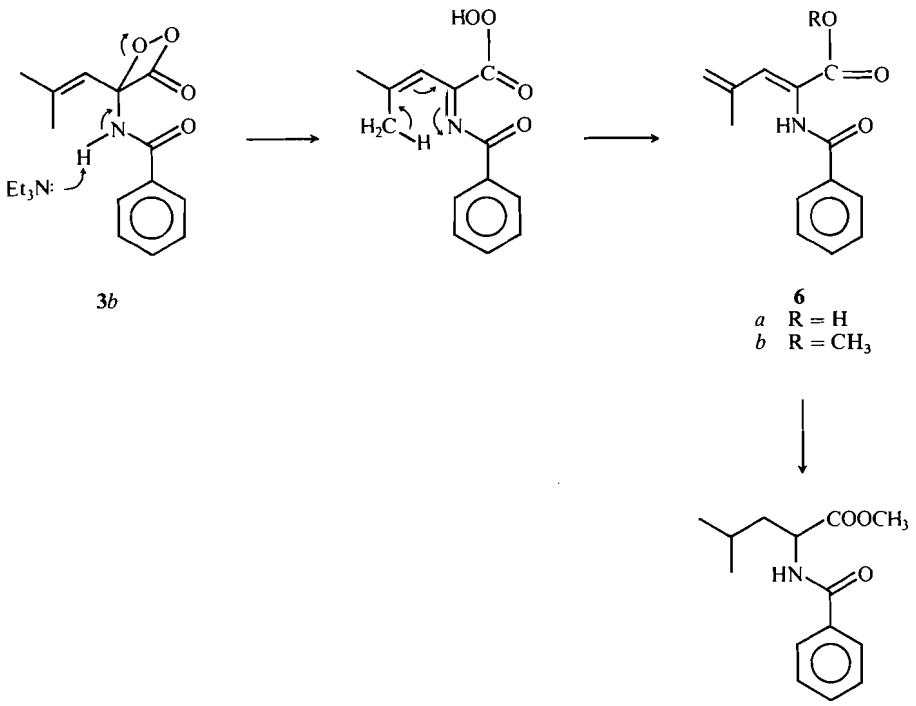

3*b*

6
a R = H
b R = CH_3

7

SCHEME 2

*(Z?)-4-Isobutylidene-2-phenyl-2-oxazolin-5-one (**1**)*

The procedure of Galantay *et al.* (5) was used. A mixture of hippuric acid (17.9 g, 0.10 mol), $Pb(OAc)_2 \cdot 3H_2O$ (16.0 g, 0.04 mol), acetic anhydride (30 g, 0.30 mol), isobutyraldehyde (7.7 g, 0.12 mol), and tetrahydrofuran (230 ml) was stirred magnetically at reflux temperature for 5 h. After cooling, the mixture was filtered and concentrated under vacuum. The residue was diluted with 350 ml of benzene and treated with an excess of H_2S. The filtered solution was evaporated to leave an orange oil that crystallized at room temperature. Recrystallization from petroleum ether to constant melting point gave 5.75 (26%) of pure oxazolinone **1**, m.p. 86–87° (lit. (6) 87°); ν_{max} 1800 (C=O) and 1675 cm^{-1} (C=N); δ 1.19 (Me_2CH, d, $J = 7$ Hz), 3.30 (Me_2CH, m), and 6.51 p.p.m. (=CH—, d, $J = 10$ Hz).

(E) or *(Z)-4-(2'-Phenylisopropylidene)-2-phenyl-2-oxazolin-5-one (**8**)*

A mixture of hippuric acid (18.6 g, 0.10 mol), $Pb(OAc)_2 \cdot 3H_2O$ (16 g, 0.04 mol), acetic anhydride (40 g, 0.40 mol), phenylacetone (16.6 g, 0.12 mol), and tetrahydrofuran (240 ml) was stirred magnetically during 8 h at reflux temperature and then left overnight. The ether soluble material after concentration under vacuum was distilled under reduced pressure to allow the recovery of 11.7 g (70%) of phenylacetone. Column chromatography of the distillation residue on silica gel gave 1.4 g (14%) of crude oxazolone **8** (mixture of stereoisomers) in the petroleum ether:ether (97:3) eluate. Recrystallization from petroleum ether afforded 536 mg (5%) of silky needles of pure (*E*)- or (*Z*)-oxazolinone **8**, m.p. 88–89°, ν_{max} 1790, 1760 shoulder (C=O), and 1665 cm^{-1} (C=N); δ 2.28 (CH_3, s) and 4.00 ($—CH_2—$, s).

Anal. Calcd. for $C_{18}H_{15}NO_2$ (277.3): C, 77.96; H, 5.45. Found: C, 77.97; H, 5.47.

*(Z?)-4-Isobutylidene-2-methyl-2-oxazolin-5-one (**14**)*

The experimental procedure followed was patterned closely on that of Herbst and Shemin (7). A mixture of *N*-acetylglycine (14.6 g, 0.12 mol), anhydrous NaOAc (7.5 g, 0.09 mol), isobutyraldehyde (13.0 g, 0.18 mol), and acetic anhydride (31 g, 0.45 mol) was stirred magnetically at 105° for 2 h. The mixture was stirred at room temperature for 2 h more, then diluted with water and extracted with ether. After washing and drying, the combined ether layers were concentrated under vacuum to leave 20.3 g of reddish brown oil (acetic anhydride still present). Fractional distillation through an 8-cm Vigreux column under reduced pressure gave the following four fractions: (*i*) b.p. 30–47° (0.9 Torr), 3.8 g, Ac_2O and *i*-$PrCH(OAc)_2$; (*ii*) b.p. 47–48° (0.9 Torr), 3.8 g, *i*-$PrCH(OAc)_2$ (mostly) and **14**; (*iii*) b.p. 50–75° (0.9 Torr), 3.7 g, mostly **14**; and (*iv*) b.p. 78–80° (0.9 Torr), 3.8 g, unknown mixture. The oxazolinone **14** was not readily purified in quantity and decomposed on standing in a sealed tube. However, successive preparative layer chromatography in petroleum ether:ether (85:15) afforded enough **14** (mixture of *cis* and *trans* isomers) for spectroscopic characterization, b.p. ~48° (0.8 Torr) (lit.

Can. J. Chem. Downloaded from www.nrcresearchpress.com by 210.87.254.5 on 09/05/12
For personal use only.

Can. J. Chem. Downloaded from www.nrcresearchpress.com by 210.87.254.5 on 09/05/12
For personal use only.

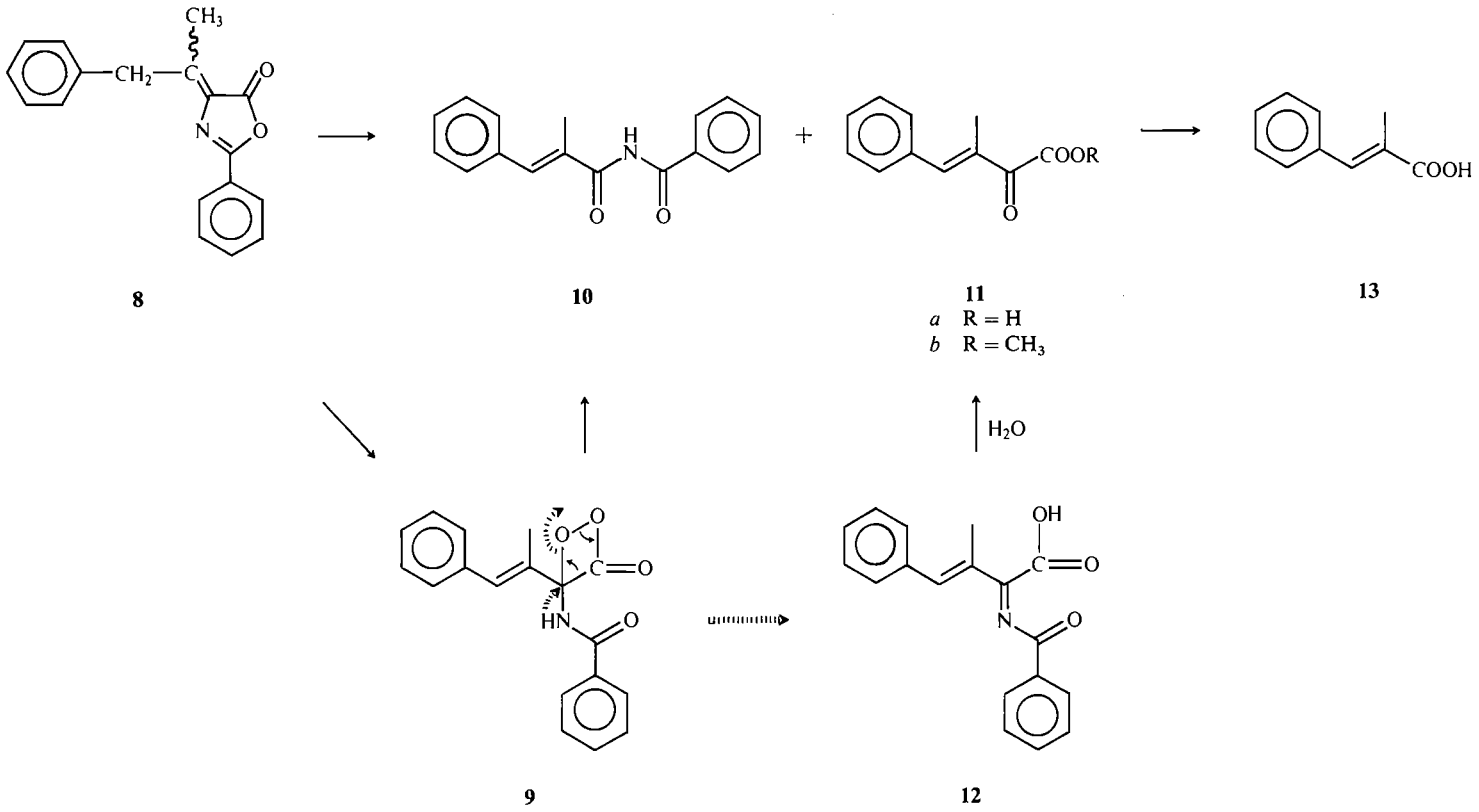

8 **10** **11** **13**

a R = H
b R = CH_3

9 **12**

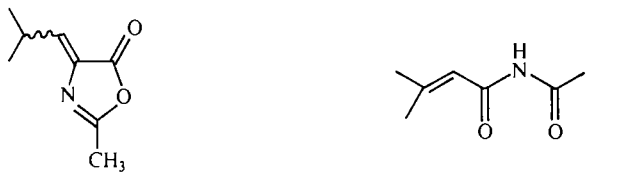

14 **15**

SCHEME 3

Can. J. Chem. Downloaded from www.nrcresearchpress.com by 210.87.254.5 on 09/05/12
For personal use only.

(8) 68–69° (0.15 Torr)), ν_{max} 1800 (C=O) and 1675 cm^{-1} (C=N); δ 1.09 and 1.11 (Me_2CH, d, $J \sim 6$ Hz), 2.23 and 2.28 (Me—C=, s), 2.9–3.8 (Me_2CH), b.m.), and 6.32 and 6.40 p.p.m. (—CH=, d, $J \sim 10$ Hz); *m/e* 153 (molecular ion).

Oxygenation of Oxazolinone ***1***

Oxygen was bubbled through a solution of oxazolinone **1** (538 mg, 2.5 mmol) and triethylamine (513 mg, 6.3 mmol) in acetonitrile (30 ml) at room temperature for 4 h at which point t.l.c. showed the absence of **1**. The yellow reaction mixture was evaporated to dryness to leave 683 mg of brownish solid whose t.l.c. (petroleum ether:ether, 70:30) gave a spot corresponding to the imide **4** and a spot near the application point. The crude product was partitioned between ether and 10% aqueous $NaHCO_3$. From the ether layer was recovered 295 mg (58%) of brownish solid which after recrystallization from cyclohexane gave colorless flat prisms of ***N*-benzoyl-β,β-dimethylacrylamide (4)**, m.p. 112.5–113°, λ_{max} 246 nm (36 000), found to be identical with the authentic sample whose preparation is described below.

Anal. Calcd. for $C_{12}H_{13}NO_2$ (203.2): C, 70.92; H, 6.45; N, 6.89; O, 15.74. Found: C, 70.82; H, 6.37; N, 6.88; O, 15.86.

Acidification of the $NaHCO_3$ solutions and extraction with ether gave 230 mg of yellowish solid amorphous carboxylic acids which were esterified with ethereal diazomethane. The 270 mg of methyl esters gave seven spots on t.l.c. (petroleum ether:ether, 70:30). The major compound (R_f 0.13) was separated by preparative t.l.c. in the same solvent system, and after two recrystallizations from ether–petroleum ether there was obtained 37 mg (6%) of colorless crystals of **2-benzamido-4-methyl-2,4-pentadienoic acid methyl ester (6*b*)**, m.p. 123–124°; λ_{max} 235 (10 400) and 260 nm (11 500); ν_{max} 3400 (NH), 1710 (ester C=O), and 1675 cm^{-1} (amide C=O; δ 1.97 (CH_3, s), 3.80 (CH_3O, s), 5.30 (=CH_2, b.s), and 7.10 p.p.m. (=CH—, s) (NH not apparent).

The ratio of the imide **4** to the acid **6*a*** in the crude oxygenation mixture was about 3:1 from n.m.r. integration.

In an experiment to measure the volume of oxygen absorbed, a solution of **1** (107 mg, 0.50 mmol) and triethylamine (102 mg, 1.0 mmol) in 6 ml of acetonitrile gently shaken under an atmosphere of oxygen at 25° absorbed 11.8 ml (theor. 12.5 ml) in 27 h at 745 Torr. Most of this absorption occurred during the first 9 h. From the 127 mg of crude oxygenation product there was obtained 50 mg (50%) of **imide 4** by preparative layer chromatography.

Trapping of the Carbon Atom Lost from ***1***

Oxygen freed from carbon dioxide by passage through Ascarite was bubbled through a solution of oxazolinone **1** (215 mg, 1.00 mmol) and triethylamine (205 mg, 2.5 mmol) in acetonitrile (12 ml), and the exiting gas was passed through a clear saturated aqueous solution of $Ba(OH)_2$. At the end of the reaction 93 mg (47%) of precipitated $BaCO_3$ was collected by filtration. Preparative t.l.c. (petroleum ether:ether, 70:30) of the crude product and recrystallization from cyclohexane gave 93 mg (45%) of **imide 4**.

Hydrogenation of Oxygenation Product from ***1***

A solution of 36 mg of the oxygenation product from **1** in 5 ml of ethanol absorbed 4.28 ml (1.0 mol) of hydrogen in the presence of 8 mg of 10% Pd/C catalyst at 29° and 743 Torr. Filtration, evaporation, and recrystallization from ether–petroleum ether gave colorless crystals of **benzoyl isovaleryl imide 5**, m.p. 82–83°; ν_{max} 3400 (NH), 1715 (imide C=O), and 1690 cm^{-1} (imide C=O); δ 1.03 (Me_2CH, d, $J \sim 6$ Hz), 1.8–2.7 (Me_2CH, m), 2.92 (CH—CH_2, d, $J \sim 6$ Hz), and 9.07 p.p.m. (NH, b.s.).

Anal. Calcd. for $C_{12}H_{15}NO_2$ (205.3): C, 70.22; H, 7.37; N, 6.82. Found: C, 69.93; H, 7.15; N, 6.80.

Hydrogenation of Methyl Ester ***6b***

A solution of ester **6*b*** (37 mg) in methanol (6 ml) was shaken for 1.5 h under a hydrogen atmosphere in the presence of 5% Pd/C (10 mg). Filtration and concentration left 29 mg (78%) of **(±)-*N*-benzoylleucine methyl ester (7)**, m.p. 94–95° (lit. (9) 95–95.5°) after recrystallization from petroleum ether, whose i.r. and n.m.r. spectra were identical with an authentic specimen of *N*-benzoyl-L-leucine methyl ester, m.p. 102–102.5° (lit. (10) 102°); ν_{max} 3440 (NH), 1740 (ester C=O), and 1660 cm^{-1} (amide C=O); δ 0.99 (Me_2CH, d, $J \sim 5$ Hz), 1.5–2.1 (3H, m), 3.78 (CH_3O, s), 4.93 (O=C—N—CH—C=O, m) and 6.66 p.p.m. (NH, b.d., $J \sim 8$ Hz).

*N-Benzoyl-β,β-dimethylacrylamide (****4****)*

β,β-Dimethylacrylic acid, prepared from mesityl oxide as reported by Smith *et al.* (11), was converted into the acyl chloride by treatment with PCl_5 according to the procedure of Feuer and Pier (12).

A solution of benzamide (500 mg, 4.1 mmol) in tetrahydrofuran (20 ml) was placed in a septum-sealed flask into which was injected a solution of *n*-butyllithium in hexane (2 ml, 4 mmol). The precipitated *N*-lithio salt was washed with three portions (10 ml) of tetrahydrofuran and then suspended in the same solvent (10 ml). A solution of β,β-dimethylacrylyl chloride (450 mg, 3.8 mmol) in tetrahydrofuran (4 ml) was injected into the *N*-lithio salt suspension. The reaction mixture was diluted with ether, washed with saturated aqueous NaCl, dried, and evaporated at reduced pressure to leave 700 mg of yellow solid. Recrystallization from cyclohexane gave 117 mg (15%) of colorless crystals, m.p. 110–111.5°, ν_{max} 3430 (NH), 1705 (imide C=O), 1675 (imide C=O), and 1630 cm^{-1} (C=C); δ 2.02 (CH_3, d, $J \sim 1$ Hz), 2.22 (CH_3, b.s.), 6.97 (C=CH, b.s.), and 9.53 (NH, b.m.).

Oxygenation of Oxazolinone ***8***

Oxygen was bubbled through a mixture of **8** (348 mg, 1.26 mmol) and triethylamine (260 mg, 2.5 mmol) in acetonitrile (16 ml) during 0.5 h at which point t.l.c. showed the absence of starting material **8**. The reaction mixture was concentrated under reduced pressure to leave 540 mg of dark yellow oil whose t.l.c. (petroleum ether:ether, 70:30) gave two spots, one corresponding to the imide **10** and the other at the point of application. The product was partitioned between ether containing a little chloroform and 10% aqueous $NaHCO_3$ solution. Evaporation of the dried ethereal layer left 148 mg (43%) of crude yellow imide. Preparative layer chromatography and recrystallization from petroleum ether–chloroform gave 60 mg of pure **(*E*)-*N*-benzoyl-2-methylcinnamamide (10)**, identical (mixed m.p., t.l.c., i.r., and n.m.r.) with the authentic sample prepared as described below.

Acidification of the $NaHCO_3$ solution and ether extraction gave 239 mg of greenish oily carboxylic acid mixture. Esterification with ethereal diazomethane and preparative

Can. J. Chem. Downloaded from www.nrcresearchpress.com by 210.87.254.5 on 09/05/12
For personal use only.

t.l.c. of the methyl esters (petroleum ether–ether, 80:20) yielded 97 mg (36%) of yellow liquid **methyl (*E*)-3-benzylidene-2-oxobutyrate (11*b*)**, λ_{max} 222 (4200) and 292 nm (19 400); ν_{max} 1735 (ester C=O), 1665 (ketone C=O), and 1615 cm^{-1} (C=C); δ 2.13 (CH_3, b.s.), 3.97 (CH_3O, s), 7.28 (=CH—, b.s.), and 7.43 p.p.m. (5 phenyl H, s). Some **benzamide** was also isolated from the crude methyl ester.

In another oxygenation the crude acidic fraction (263 mg) was esterified with diazomethane and the crude methyl ester mixture was recrystallized from chloroform–petroleum ether to give 25 mg of **benzamide**, m.p. 125–126°, identical (i.r. and n.m.r.) with an authentic specimen.

Trapping of the Carbon Atom Lost from 8

With the same procedure for trapping CO_2 used for oxazolinone **1**, the oxygenation of a solution of oxazolinone **8** (277 mg, 1.00 mmol) and triethylamine (205 mg, 2.0 mmol) in acetonitrile (12 ml) gave 47 mg (24%) of $BaCO_3$ and 80 mg (30%) of **imide 10**.

(E)-N-Benzoyl-2-methylcinnamamide (10)

The procedure of Perkin (13) was used to prepare (*E*)-2-methylcinnamic acid from benzaldehyde and propionic acid. The acid was converted into its acid chloride by treatment with PCl_5 according to the procedure of Feuer and Pier (12).

Into a suspension of the *N*-lithio salt of benzamide, prepared from benzamide (500 mg, 4.1 mmol) in the same manner described for the preparation of **4**, in tetrahydrofuran (4 ml) was injected a solution of (*E*)-2-methylcinnamoyl chloride (508 mg, 2.8 mmol). The reaction mixture was diluted with ether, washed with three portions of water, dried, and evaporated at reduced pressure to leave an orange residue. Recrystallization of the ether soluble material from chloroform–ether yielded 28 mg (4%) of long feathery needles, m.p. 128.5–129.5°; ν_{max} 3390 (NH), 1740 (imide C=O), 1675 (imide C=O), and 1625 cm^{-1} (C=C); δ 2.14 (CH_3, d, $J \sim 1.5$ Hz) and 9.20 (NH, b.s.) (the olefinic H was hidden in the aromatic proton absorption).

Anal. Calcd. for $C_{17}H_{15}NO_2$ (265.7): C, 76.96; H, 5.70; N, 5.28. Found: C, 76.45; H, 5.69; N, 5.31.

Oxidative Cleavage of α-Keto Acid 11a

In a procedure similar to the one outlined by Stecher and Gelblum (14), crude α-keto acid **11*a*** (130 mg, 0.68 mmol) was dissolved in dioxane (6 ml) and treated at room temperature alternately with small portions (magnetic bar stirring) of 1% aqueous Na_2CO_3 solution and a total of 8 ml of 30% aqueous H_2O_2. Care was taken to maintain a p*H* of ~8 in the reaction mixture which was stirred for 4 h. Acidification and ether extraction yielded an oily residue after removal of ether. The residue was further purified by solution in petroleum ether. Evaporation of the petroleum ether soluble portion left 80 mg of yellowish oil whose t.l.c. (petroleum ether:ether:acetic acid, 86:10:4) revealed the presence of *(E)*-α-methylcinnamic acid. Preparative t.l.c. in the same solvent system yielded 31 mg (28%) of **(*E*)-α-methylcinnamic acid**, m.p. 79.5–80.5° (lit. (13) 81°) after recrystallization from petroleum ether; λ_{max} 207 (14 300) and 267 nm (17 400); ν_{max} 1685 (C=O) and 1630 cm^{-1} (conj. C=C); δ 2.12 (CH_3, d, $J \sim 1.5$ Hz), 7.30 (5 phenyl H, s), 7.73 (=CH—, b.s.), and 11.63 (—COOH, b.s.).

Oxygenation of Oxazolinone 14

When a solution of oxazolinone **14** (153 mg, contaminated with *i*-PrCH$(OAc)_2$) and triethylamine (225 mg) in acetonitrile (25 ml) was shaken under an oxygen atmosphere in a mercury sealed burette system for 3 h no uptake of oxygen occurred. However, after oxygen was bubbled through the same solution at 60° with stirring for 3 days, the reaction mixture no longer contained **13**. T.l.c. comparison of the crude product with authentic ***N*-acetyl-β,β-dimethylacrylamide (15)** prepared as described below, showed the absence of this imide. When this oxygenation was carried out at room temperature to check the evolution of any CO_2 in an experiment similar to the ones with **4** and **8**, no $BaCO_3$ precipitated.

N-Acetyl-β,β-dimethylacrylamide (15)

A mixture of sublimed acetamide (540 mg, 9.1 mmol), sodium hydride (430 mg, 56% oil suspension, ~9 mmol), and dioxane (20 ml) was stirred magnetically for 30 min and then treated with a solution of β,β-dimethylacrylyl chloride (1.18 g, 10 mmol) in dioxane (10 ml). The resulting mixture was stirred magnetically at reflux temperature for 30 min. The cooled reaction mixture was diluted with chloroform, filtered, and evaporated to leave 1.07 g of brownish solid. Several recrystallizations from ether–petroleum ether afforded 173 mg (13%) of white needles, m.p. 92–93°; ν_{max} 3400 (NH), 1720 (imide C=O), 1680 (imide C=O), and 1640 cm^{-1} (C=C); δ 1.95 (CH_3, d, $J \sim 1.5$ Hz), 2.21 (CH_3, d, $J \sim 1.5$ Hz), 2.41 (CH_3, s), 6.10 (=CH—, b.s.), and 9.43 p.p.m. (NH, b.s.).

Anal. Calcd. for $C_7H_{11}NO_2$ (141.2): C, 59.56; H, 7.85; N, 9.92. Found: C, 59.83; H, 7.87; N, 10.16.

Hydrogen Exchange of Oxazolinone 1

(a) In CD_3CN–D_2O

To a solution of **1** in CD_3CN used for recording of the n.m.r. spectrum was added a drop of Et_3N and a drop of D_2O. The 1-H multiplet near δ 3.3 decreased rapidly and a sharp singlet from DOH appeared at δ 3.6 before much of the **1** had been changed by the D_2O.

(b) In Acetone-d_6

A solution of 50 mg of **1** in 0.25 ml of acetone-d_6 gave an n.m.r. spectrum unchanged by time. One drop of Et_3N was added (solution became yellow) and the n.m.r. spectrum was recorded periodically during 2 days. The methine hydrogen gradually disappeared, and the expected simplification of the methyl (d → b.s.) and olefinic (d → b.s.) signals slowly occurred at room temperature.

We thank the National Research Council of Canada for financial support of this work.

1. E. W. WARNHOFF. Fortschr. der Chemie Organ. Naturstof. **28**, 162 (1970).
2. W. STEGLICH. Fortschr. der Chem. Forschung, **12**, 77 (1969).
3. G. A. RUSSELL and A. G. BEMIS. J. Am. Chem. Soc. **88**, 5491 (1966).
4. (*a*) F. MCCAPRA and R. WRIGGLESWORTH. Chem. Commun. 91 (1969). (*b*) T. GOTO. Pure Appl. Chem. **17**, 421 (1968).
5. E. GALANTAY, A. SZABO, and J. FRIED. J. Org. Chem. **28**, 98 (1963).
6. E. ERLENMEYER and J. KUNLIN. Ann. **316**, 151 (1901).

7. R. M. HERBST and D. SHEMIN. Org. Syn. Coll. Vol. **2**, 1 (1943).
8. D. G. DOHERTY, J. E. TIETZMAN, and M. BERGMAN. J. Biol. Chem. **147**, 617 (1943).
9. M. JUTISZ, D. M. MEYER, and L. PENASSE. Bull. Soc. chim. Fr. 1087 (1954).
10. P. KARRER and W. KEHL. Helv. Chim. Acta, **13**, 50 (1930).
11. L. I. SMITH, W. W. PRICHARD, and L. J. SPILLANE. Org. Syn. Coll. Vol. **3**, 302 (1955).
12. H. FEUER and S. M. PIER. Org. Syn. Coll. Vol. **4**, 554 (1963).
13. W. H. PERKIN. J. Chem. Soc. **31**, 388 (1877).
14. E. D. STECHER and E. GELBLUM. J. Org. Chem. **26**, 2693 (1961).

Can. J. Chem. Downloaded from www.nrcresearchpress.com by 210.87.254.5 on 09/05/12
For personal use only.

Studies on Nucleation from Solution of some Nickel Dioximates

J. D. HANNA AND O. E. HILEMAN, JR.[1]
Department of Chemistry, McMaster University, Hamilton, Ontario
Received September 23, 1971[2]

Nucleation studies on two nickel dioximates have been carried out by using a direct mixing technique coupled with rapid particle counting. It is concluded that homogeneous nucleation was being observed. The Volmer–Weber, Becker–Doring model of the nucleation process was used to correlate the data.

Nous avons effectué des études de nucléation sur deux différents dioximates de nickel au moyen d'une technique de mélange directe associée à un comptage rapide des particules. On en conclut qu'une nucléation homogène se produit. Pour faire une corrélation entre les résultats, nous avons utilisé le modèle Volmer–Weber, Becker–Doring du processus de nucléation.

[Traduit par le journal]

Canadian Journal of Chemistry, **50**, 2859 (1972)

Can. J. Chem. Downloaded from www.nrcresearchpress.com by 210.87.254.40 on 09/05/12
For personal use only.

It was recognized long ago that the phenomenon of supersaturation observed in nucleation from solution implies the existence of an energy barrier which opposes the initiation of crystallization. The objective of any experimental study or theory concerned with nucleation from solution is to account for this barrier and, further, to suggest a mathematical model which permits calculation of various nucleation parameters. Much of the literature reporting on nucleation from solution, however, presents conflicting and inconsistent evidence about the process. In addition, the Volmer–Weber, Becker–Doring model of the nucleation process, the one used most often to help interpret nucleation data, has recently been criticized by several authors when applied to liquid nucleation from the vapor phase. Apparently then, its adequacy as a model for the more complex process of nucleation from solution is somewhat limited. Thus, any advancement in the understanding of the initial formation of crystals from solution seems to await new or improved experimental techniques for its study. Recently, in our laboratories, we have been developing such techniques. This communication reports and discusses some experimental results obtained by one of them during studies on two nickel oximates.

Experimental

Apparatus

Mixing System: Two 10-ml syringes were separately connected to the input ports of a Roughton Cell (1). The plungers of the syringes were interlocked so that they operated simultaneously. The appropriate metal ion buffer solution was placed in one of the syringes and a solution of the chelating agent was placed in the second. After mixing, the resulting solution was led through the outlet port of the cell to a third syringe.

Particle Counting System: The particle counting system was a component system made up of a "Coulter Counter" (Industrial Model B, Coulter Electronics Industrial Division), a multichannel analyzer (Model ND 161F, Nuclear Data Inc.), and a magnetic tape recording unit (Model MT36, Potter Instrument Co. Inc.). Part of the signal appearing in the line connecting the main amplifier to the oscilloscope of the "Coulter Counter" was fed to the input of the multichannel analyzer. The data collected during each step of the particle size analysis by the analyzer were dumped onto magnetic tape, thus freeing the analyzer for a subsequent step. The data on the tapes were processed and recovered by computer.

Reagents and Solutions

Calibration Dispersions for the Particle Counting System: 1.099, 3.49, 11.7, and 18.8 μ diameter particles (polystyrene spheres (Dow Chemical Co.) or rag weed pollen (Coulter Electronics, Industrial Division)) were separately dispersed in 1% (w/v) NH_4Cl solutions. Triton X-100 was added to the dispersion containing the smallest particles to prevent agglomeration. Each dispersion contained approximately 10^5 particles/ml. Mixtures of these were used to determine the resolution of the system.

Nucleation Studies: Stock solutions of Ni^{2+} (0.1 *M*), from nickel chloride, nioxime (1.0×10^{-2} *M*) and heptoxime (1.0×10^{-2} *M*) were each prepared in aqueous 1% (w/v) NH_4Cl. All other concentrations of these reagents were prepared by dilution with 1% (w/v) NH_4Cl solution. p*H* adjustments were made with NH_3 or HCl solutions. Before use, each solution was filtered at least twice through 0.1 μ PVC membrane filters.

Procedures

Calibration of the Particle Counting System: The particle counter probe (30 μ aperture) was inserted into 100 ml of a calibration dispersion. The number and size distribution of the standard-sized particles in this dispersion were deter-

[1]To whom correspondence to be addressed.
[2]Revision received May 10, 1972.

TABLE 1. Experimental conditions for nucleation studies

Dioxime	Electrolyte	Supersaturation	Diluent	Dilution factor	Typical final counts/ml
Heptoxime	NH_3/NH_4Cl	3.12×10^2	NH_3/NH_4Cl	4×10^3	3.48×10^7
	1% w/v	2.50×10^2	1% w/v	2×10^3	1.42×10^7
	$pH = 3.40$	1.87×10^2	$pH = 3.40$	2.22×10^2	1.77×10^6
		1.25×10^2		2.00×10^1	3.35×10^5
		9.33×10^1		2.00×10^1	7.7×10^4
		6.16×10^1			
Nioxime	NH_3/NH_4Cl	3.33×10^2	NH_3/NH_4Cl	2×10^3	23.3×10^6
	1% w/v	2.49×10^2	1% w/v	2.22×10^2	14.2×10^6
	$pH = 2.80$	1.66×10^2	$pH = 2.80$	2.22×10^2	4.92×10^6
		1.33×10^2		2.00×10^1	3.88×10^5
		8.32×10^1			

mined for each of the ten amplification settings of the instrument using 0.5 ml for each measurement.

The data from each setting were dumped onto magnetic tape and stored for later processing and recovery. This procedure was followed for each calibration dispersion and also for mixtures of standard-sized particles.

Nucleation Studies: Appropriate Ni^{2+} and dioxime solutions were added respectively to each of the 10-ml syringes connected to the input ports of a Roughton Cell. These solutions were mixed and led to the third syringe. After a certain time, part of the contents of the latter syringe were transferred to a beaker containing enough 1% (w/v) NH_4Cl solution to yield 200.0 ml of a dispersion containing about 10^5 countable particles/ml. Then the same counting procedure was carried out as described above for the calibration of the system. The specific data for each set of experiments are shown in Table 1.

Data Handling: To produce composite size distribution curves the data from each of the ten amplification settings were correlated by averaging the overlapping portions. These data along with the total area under the size distribution curves were recovered in tabular form.

Results and Discussion

Particle Counting System

Part of the electronic signal appearing at various points in the particle counter circuit were fed to an oscilloscope. Photographs of the pulse shapes appearing on the screen were taken and the results compared with the pulse shapes required by the multichannel analyzer. Figure 1 shows typical pulse shapes and sizes for standard particles when the signal was interrupted in the line between the main amplifier and the oscilloscope of the particle counter. The characteristics of most of the pulses fall within those recommended for best resolution and linearity of the analyzer. Similar results were found when the spherical particles were replaced by an actual precipitating system.

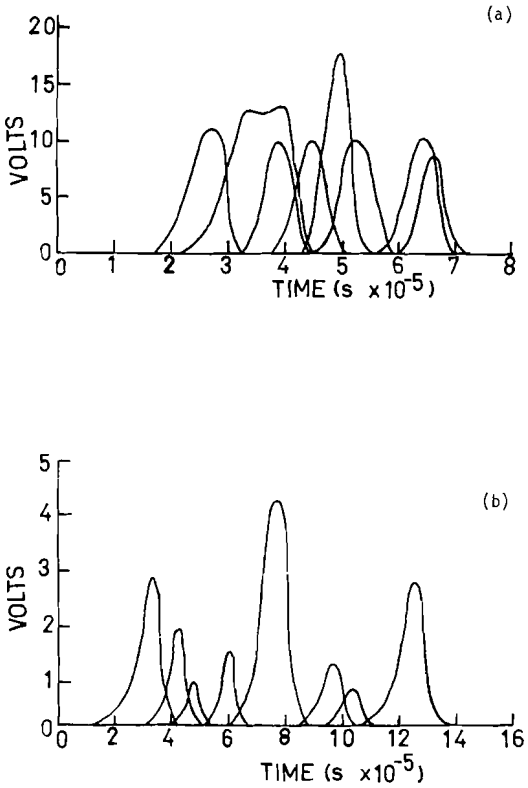

FIG. 1. (*a*) Pulse shapes for 3.49 μ diameter spheres. (*b*) Pulse shapes for nickel dimethylglyoximate crystals.

Figure 2 shows the results of an analysis of a mixture of 1.099 and 3.49 μ standard-sized particles. From such data, the standard deviation for each of the standard-sized particles was calculated and compared with the manufacturers' specifications where available (see Table 2). The ten calibration curves, one for each

Can. J. Chem. Downloaded from www.nrcresearchpress.com by 210.87.254.40 on 09/05/12
For personal use only.

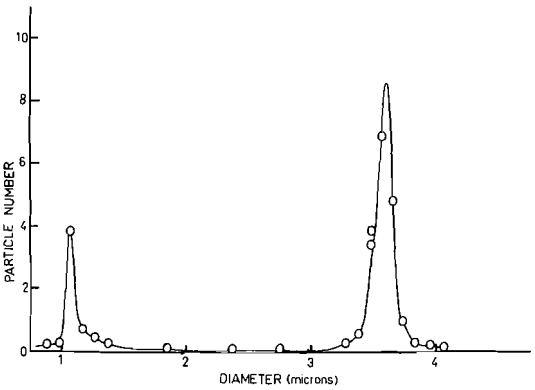

FIG. 2. Size distribution of a suspension of 1.099 and 3.49 μ diameter spheres.

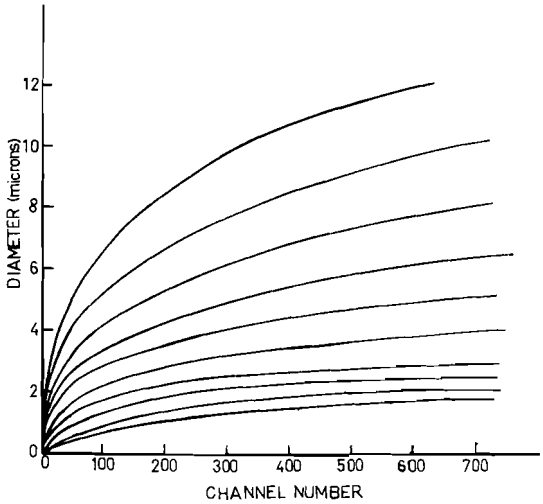

FIG. 3. Calibration curves for the 30 μ aperture. (Each curve represents the data for a separate amplification setting.)

amplification setting on the particle counter, shown in Fig. 3 were also calculated from these data by using eq. 1. This equation accurately describes the functional relationship between channel number of the multichannel analyzer, p, and particle size, d, over a range of 4 to 5 μ.

$$[1] \qquad p = \frac{\pi d^3}{6IBK}$$

where I = the current in the detector system; B = the amplification setting; and K = a collection of instrumental constants.

The results of the experiments described above led to the conclusion that our combination of a particle counter–multichannel analyzer–magnetic tape unit could be used to measure the total number of particles above 1 μ in size, the particle size distribution, and the variation of the particle size distribution with time during a nucleation and growth experiment.

Nucleation Studies

For each initial concentration of the metal chelate being studied several sets of size distri-

TABLE 2. Standard deviations found for standard-sized particles

Aperture diameter (μ)	Particle size (μ)	Amplification setting	σ Found (μ)	σ Quoted (μ)
30	1.099	1/4	0.060	0.0059
		1/2	0.047	
		1	0.036	
	3.49	2	0.068	Not available
		4	0.065	
		8	0.097	
	11.7	64	0.47	Not available
70	1.099	1/8	0.39	0.0059
	11.7	64	0.66	Not available
		32	0.72	
		16	0.79	
		8	0.89	
	18.8	32	0.67	Not available
		64	0.64	Not available

Can. J. Chem. Downloaded from www.nrcresearchpress.com by 210.87.254.40 on 09/05/12
For personal use only.

Can. J. Chem. Downloaded from www.nrcresearchpress.com by 210.87.254.40 on 09/05/12
For personal use only.

bution curves, determined at specific reaction times, were measured using the particle counter – multichannel analyzer – magnetic recording tape combination. Typical results for a single set, shown as size distribution curves for various reaction times for each of three different initial concentrations of nickel hepoximate are illustrated in Fig. 4. Similar results were observed for nickel nioximate. To increase the mass available for crystal growth the intrinsic solubility of each was increased by decreasing the pH of the reaction mixture. Consequently, there was an increase in the number of particles which surpassed the sensitivity limit of the particle counter.

Study of about 300 such size distribution curves has led to three general observations. Firstly, in all but the very early size distributions in any one set a large maximum with a small shoulder on the larger particle side in the curve is observed. Secondly, for increasing initial supersaturations there was a marked increase in the total number of particles formed. Thirdly, as the mass of material available for nucleation and growth increased, the average size of the particles formed decreased. Taken together these observations indicate that homogeneous nucleation is the primary type of initial transformation taking place in these experiments. Therefore, nucleation rates derived from the data are rates of homogeneous nucleation.

The rate of nucleation for a set of size distribution curves is defined by eq. 2.

$$[2] \qquad J = \frac{\partial N(t)}{\partial t}$$

where J = the rate of nucleation; N = the total number of particles formed with diameter "d" > $2r^*$ cm; t = the time after mixing the reactants; and r^* = the radius of the nucleus (critical). The total number of particles with a diameter greater than $2r^*$ formed in an experiment up to time "t" is given by eq. 3.

$$[3] \qquad N(2r^*,t) = \int_{2r^*}^{\infty} \frac{\partial N(d,t)}{\partial d}$$

The slope of a plot of $N(2r^*,t)$ *vs.* time, then, is the rate of nucleation for any particular initial supersaturation. Because the particle counter had a lower sensitivity limit of about 1 μ $N(2r^*,t)$ was replaced by $N(1\ \mu,t)$ in all of the data analyses. Plots of $N(1\ \mu,t)$ *vs.* time constructed from the data of Fig. 4 are shown in Fig. 5. The slope of each of these curves measures the rate of appearance of particles to the sensor of the particle counter. Over the initial linear portion of these curves this slope was equated with the rate of nucleation. The change in sign of the slope at later times in each set is probably due to agglomeration (see Figs. 4 and 5).

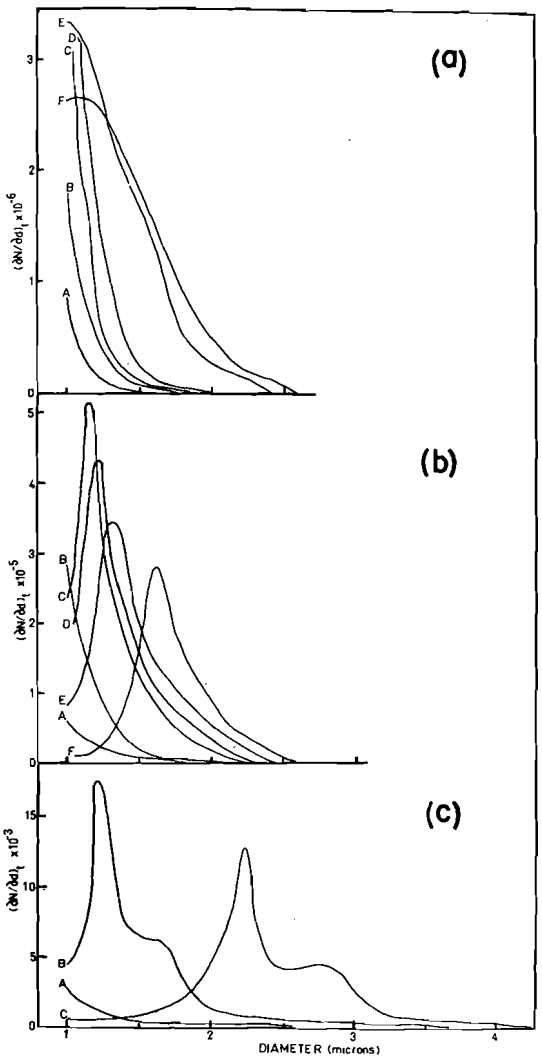

FIG. 4. Nickel heptoximate size distributions: (*a*) size distributions A, B, C, D, E, and F taken after 23, 41, 80, 100, 180, 300 s, respectively ($c_0 = 1.25 \times 10^{-3}$ M); (*b*) size distributions A, B, C, D, E, and F taken after 100, 160, 251, 313, 600, and 1260 s, respectively ($c_0 = 0.75 \times 10^{-3}$ M): and (*c*) size distributions A, B, and C taken after 7, 26, and 45 min, respectively ($c_0 = 3.75 \times 10^{-4}$ M).

Can. J. Chem. Downloaded from www.nrcresearchpress.com by 210.87.254.40 on 09/05/12
For personal use only.

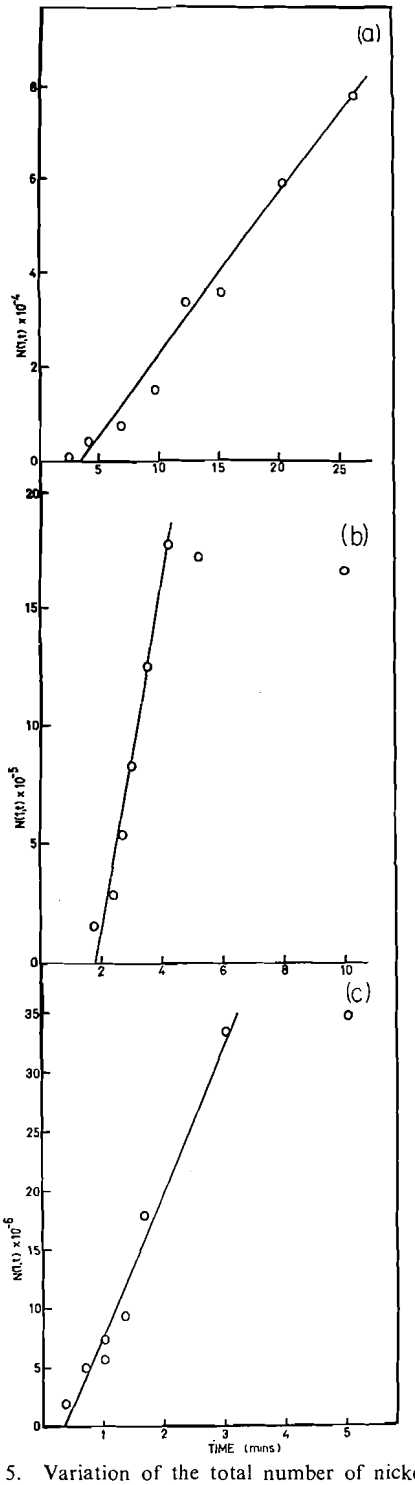

FIG. 5. Variation of the total number of nickel heptoximate crystals formed (above 1 μ) *vs.* time: (*a*) $c_0 = 1.25 \times 10^{-3}\ M$; (*b*) $c_0 = 0.75 \times 10^{-3}\ M$; and (*c*) $c_0 = 3.75 \times 10^{-4}\ M$.

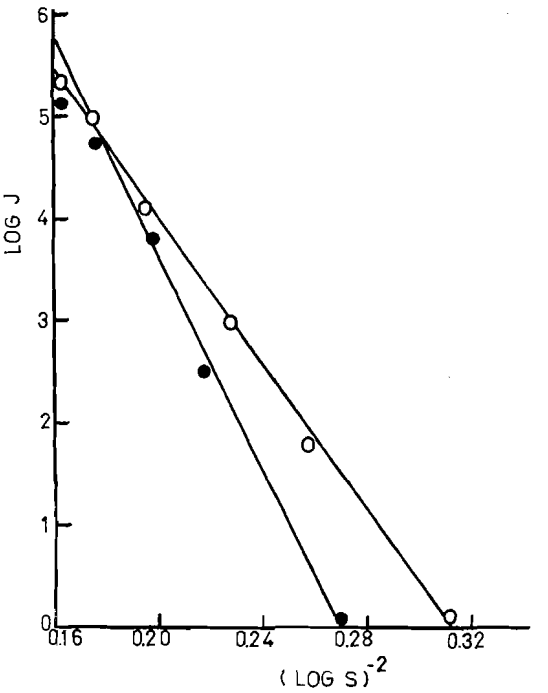

FIG. 6. Variation of log J with (log S)$^{-2}$ for nickel heptoximate and nickel nioximate (filled circles).

Plots of the functional relationship between J and S, the supersaturation within the system, predicted by the Volmer–Weber, Becker–Doring (V–W, B–D) model of the nucleation process are shown for each of the chelates in Fig. 6. In light of the recent criticism of the model, the linearity of this plot may be somewhat surprising (2–4). We have found, however, linear V–W, B–D plots in all of our studies on both molecular and ionic substances and find them to be useful for correlating and comparing rate-supersaturation data even though they may be fortuitous.

Using the slopes and intercepts of the plots of Fig. 6 along with eqs. 4 and 5 various parameters important in the V–W, B–D model were calculated.

$$[4] \qquad J = A \exp\left[-\frac{\beta\sigma^3 v^2}{(kT)^3\ (\ln S)^2}\right]$$

$$[5] \qquad r\dagger = \frac{2\sigma v}{kT \ln S}$$

where A = an empirical constant theoretically identified with $(2D/d_0^5 n^*)\,(4\Delta G^*/3\pi kT)^{1/2}$; β = a shape factor; σ = the surface tension; v = the

TABLE 3. Values of various parameters for the Ni(II) chelates

Compound	μ (cm^3)	log A^a	$S\dagger^b$	β	σ (ergs cm^{-2})	$\gamma\dagger$ (nm)	$n\dagger$
Nickel nioxymate	3.31×10^{-22}	14, 8.0[c]	96, 8.8[d]	109	13		14, 17[d]
				$16\pi/3$	25, 15[d]	0.47, 0.11[d]	
Nickel heptoxymate	3.5×10^{-22}	11, 7.3[c]	65, 7.5[d]	109	13		13, 17[d]
				$16\pi/3$	25, 13[d]	0.48, 0.11[d]	

[a]log A calculated theoretically = 27.
[b]$S\dagger$ = the value of S when $J = 1$.
[c]Taken from ref. 4.
[d]Calculated from the data of ref. 4.

molecular volume in the solid phase; D = the diffusion coefficient of the molecules in solution; d_0 = the molecular diameter; ΔG^* = the critical free energy change; and $n\dagger$ and $r\dagger$ = the number of molecules in and the radius of the nucleus when $J = 1$, respectively.

The results are shown in Table 3.

Parameter values, calculated from data obtained by using Vonnegut's droplet technique in combination with precipitation from homogeneous solution and previously reported by one of us (5), are shown in Table 3 for comparison. The rather close agreement between the two sets of parameters derived from two entirely different experimental approaches tends to confirm our earlier conclusion that the rates observed are rates of homogeneous nucleation. Values of "A" many orders of magnitude lower than the calculated value have been reported before for these metal chelates (5), for other molecular compounds (6, 7), and for ionic salts (8). Some possible reasons for this discrepancy have been discussed in other publications (5–8).

1. F. J. ROUGHTON and B. CHANCE. *In* Techniques of organic chemistry. *Edited by* A. Weissberger. Interscience, New York, **8** (2), 704 (1963).
2. FARID F. ABRAHAM. J. Chem. Phys. **50**, 3977 (1969).
3. E. R. BUCKLE. Trans. Faraday Soc. **65**, 1267 (1969).
4. F. L. BINSBERGEN. Koll-Zeit. Zeit. fur Polymere, **237**, 289 (1970).
5. J. A. VELAZQUEZ and O. E. HILEMAN, JR. Talanta, **17**, 623 (1970).
6. W. J. DUNNING and N. T. NOTLEY. Z. Electrochem. **61**, 55 (1957).
7. W. J. DUNNING and A. J. SHIPMAN. Proc. Agr. Ind. Tenth Int. Congr. Madrid. 1954.
8. J. A. VELAZQUEZ and O. E. HILEMAN, JR. Can. J. Chem. **48**, 2896 (1970).

Can. J. Chem. Downloaded from www.nrcresearchpress.com by 210.87.254.40 on 09/05/12
For personal use only.

Electrical Conduction Properties of Liquid Vanadates. I. Vanadium Pentoxide

R. C. KERBY

Extraction Metallurgy Research Section, Mines Branch, Department of Energy, Mines and Resources, Ottawa, Canada

AND

J. R. WILSON

Department of Metallurgical Engineering, Queen's University, Kingston, Ontario

Received April 11, 1972

The electrical conductivity of liquid vanadium pentoxide was measured as a function of temperature and oxygen partial pressure. A positive temperature coefficient and a negative oxygen partial pressure coefficient of conduction were found for the temperature range 670 to 1000 °C and oxygen partial pressures from 0.1 to 1.0 atm. The activation energy of conduction was 0.77 eV and the oxygen partial pressure coefficient was −0.16. At oxygen partial pressures less than 0.1 atm, for the same temperature range, a negative temperature coefficient and a negative oxygen partial pressure coefficient of conduction were found.

An n-type semiconduction model was used to explain the electrical conduction properties of liquid vanadium pentoxide at oxygen partial pressures greater than 0.1 atm. At lower oxygen partial pressures, electrical conduction was considered to occur by collective-electron conduction in partially filled 3d bands, due to an overlapping of the diffuse valence and conduction bands. The overlapping could result from a decrease in the cation separation distance in the melt due to the removal of oxygen ions from the melt.

Nous avons mesuré la conductivité électrique du pentoxyde de vanadium liquide en fonction de la température et de la pression partielle d'oxygène. Nous trouvons un coëfficient de température positif et un coëfficient de pression partielle de conduction négatif, sur une gamme de température allant de 670 à 1000 °C et de pressions partielles d'oxygène de 0.1 à 1.0 atm. L'énergie d'activation de conduction est 0.77 eV et le coëfficient de pression partielle de l'oxygène −0.16. A des pressions partielles d'oxygène plus faibles que 0.1 atm, pour une même gamme température, nous trouvons un coëfficient de température négatif et un coëfficient de pression partielle de conduction négatif.

Nous avons utilisé un modèle de semi-conduction de type n afin d'expliquer les propriétés de conduction électrique du pentoxyde de vanadium liquide à des pressions partielles d'oxygène plus grandes que 0.1 atm. A des pressions partielles d'oxygène plus faibles, nous considérons que la conduction électrique se produit au moyen de sauts d'électrons dans les orbitales 3d partiellement remplies, causés par le recouvrement des couches de valence et de conduction diffuses. Le recouvrement proviendrait d'une diminution de la distance de séparation des cations dans la fondue, à cause du départ des ions oxygène de la fondue.

[Traduit par le journal]

Canadian Journal of Chemistry, **50**, 2865 (1972)

Introduction

A number of alloys which normally show excellent high-temperature oxidation resistance are known to undergo accelerated corrosion in the presence of vanadium-containing fly-ash deposits or slags at temperatures greater than 500 °C (1). This accelerated corrosion, which is commonly called "catastrophic" vanadate corrosion, is thought to occur because of the presence of liquid vanadates in the fly-ash deposits (2). Liquid vanadates have been shown to increase the corrosion rate of metals by fluxing or altering the normally protective oxide layers present on the surface of the alloys and by providing a source of oxide ion for the corrosion reaction (3).

Only limited information is available on the physical and chemical properties of such liquid vanadates as iron, nickel, cobalt, chromium, sodium, and magnesium, which are commonly found in fly-ash deposits. In order to gain a better understanding of the mechanism of liquid vanadate corrosion, a program was initiated to characterize more fully the physical properties of the liquid vanadates, in particular their phase relationships and electrical conduction properties (4). The electrical conduction properties are reported in this series of articles.

The electrical conduction properties of solid (5–22) and liquid (18–25) vanadium pentoxide have been reported previously. There are a number of discrepancies in the reported data,

Can. J. Chem. Downloaded from www.nrcresearchpress.com by 210.87.254.40 on 09/05/12
For personal use only.

Can. J. Chem. Downloaded from www.nrcresearchpress.com by 210.87.254.40 on 09/05/12
For personal use only.

due in part to the presence of impurities. Vanadium pentoxide was found to show predominantly n-type semiconduction in both the solid and liquid states. Several mechanisms have been proposed to account for the semiconduction properties of solid vanadium pentoxide. A number of authors (13, 15, 22) consider the semi-conduction to occur via the hopping of electrons (small polarons) between V^{4+} and V^{5+} centers in the vanadium pentoxide lattice. The relationship between V^{4+} ion concentration and magnitude of electrical conduction has been confirmed by electron spin resonance (e.s.r.) and nuclear magnetic resonance (n.m.r.) measurements (26). Perlstein (17) considered the electronic conductivity above 170 °K to result from thermal excitation of electrons from vanadium-pair traps with an activation energy of 0.15 eV and electron hopping from one vanadium site to another with an activation energy of 0.05 eV. McCulloch (14) proposed a two-step process in which the electron was ionized from a V^{4+} – oxygen vacancy center and then moved through the lattice via polaron movement.

Allersma *et al.* (22), Pantony and Vasu (24), and Pastukhov *et al.* (25) have recently reported studies of the electrical conduction properties of liquid vanadium pentoxide. The electrical conductivity increased with temperature and with decreasing oxygen partial pressure. The activation energy of conduction was reported as 0.73 (22), 0.75 to 1.13 (24), and 2.2 eV (25). Allersma *et al.* found that the activation energy decreased with decreasing oxygen partial pressure, while the other workers reported no effect. The conductivity was reported to vary with oxygen partial pressure by a power of −0.167 (22), −0.240 at oxygen partial pressures greater than 0.033 atm and −0.580 at lower oxygen partial pressures (24), and −0.17 at temperatures between 660–770 °C and −0.27 at temperatures between 830–1500 °C (25). The magnitude of the specific electric conductance in oxygen at 1 atm at 900 °C was reported as 0.2 (22), 0.47 (24), and 0.35 $ohm^{-1}\ cm^{-1}$ (25). Because of the significant discrepancies between the reported electrical conduction properties of liquid vanadium pentoxide, these properties were re-examined as part of a study of the electrical conduction properties of the liquid vanadates.

Experimental

The electrical conductivity was measured using a dipping electrode cell, which has been found to be satisfactory for use with many molten oxides (27). The corrosiveness of liquid vanadates towards many oxides and metals limited the choice of construction materials. A gold (80 at.%) – palladium (20 at.%) alloy was found to show good corrosion resistance and was used in the apparatus.

Two gold–palladium electrodes, 2 mm in diameter and mounted in a pyrophyllite block, were dipped into a gold–palladium cylindrical crucible contained in an Inconel 600 crucible. The depth of the electrodes in the melt (0.500 in.) was accurately controlled by a threaded rod mechanism. A chromel–alumel thermocouple was positioned within 1 mm of the bottom of the crucible in order to estimate the temperature of the melt. The conductivity cell was contained in a vacuum-tight, grounded Inconel 600 tube fitted with flanges, which allowed the oxygen and argon gas mixtures over the melt to be accurately controlled. Operating temperatures, in the super Kanthal wound tube furnace, were maintained to better than ±1 °C.

Electrical conductivity measurements were made using a General Radio 1608-A Impedance Bridge with an auxiliary audio oscillator and a tuned amplifier and null detector. An oscilloscope was used as an auxiliary null detector. The conductivity cell was calibrated with 1.0 and 0.1 Demal KCl solution at 25.00 ± 0.01 °C (28). The resistance change with temperature of the shielded leads from the conductivity cell was accounted for. Negligible frequency dependence from 10^3 to 10^4 Hz was found for the molten vanadium pentoxide. An analysis of the experimental errors involved indicated the measurements were accurate to within ±2%.

Two grades of vanadium pentoxide were used. Fisher A.R. grade vanadium pentoxide had the following major impurities (in p.p.m.): Fe(150), Si(75), Co(75), Ni(75), Ca(30), Mn(20), Mg(20), Mo(15). Johnson and Matthey "specpure" vanadium pentoxide had the following impurities: Ti(20), Si(5). The two grades are identified in this paper as 99.9% and 99.997% vanadium pentoxide, respectively. These numbers do not refer to the stoichiometric composition of the oxides. Ultrahigh purity gases (O_2 = 99.9%, Ar = 99.999%) were used to give controlled atmospheres above the melt. The flow rates were controlled using calibrated rotometers.

Results

The temperature dependence of the electrical conduction of molten vanadium pentoxide under pure oxygen at a pressure of 1 atm is shown in Fig. 1. The data can be represented by the equations

$$\log K = 2.480 - \frac{3864}{T} \quad [1]$$

for the "specpure" vanadium pentoxide and

$$\log K = 2.412 - \frac{3669}{T} \quad [2]$$

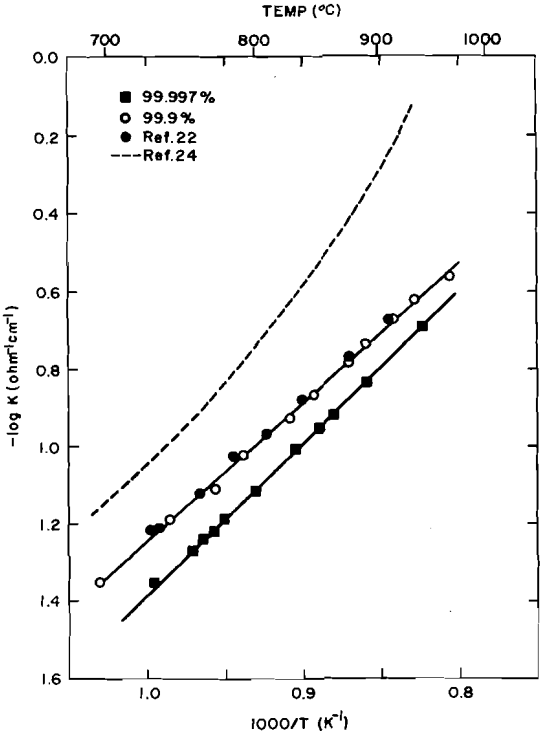

FIG. 1. Temperature dependence of the electrical conductivity of liquid V_2O_5.

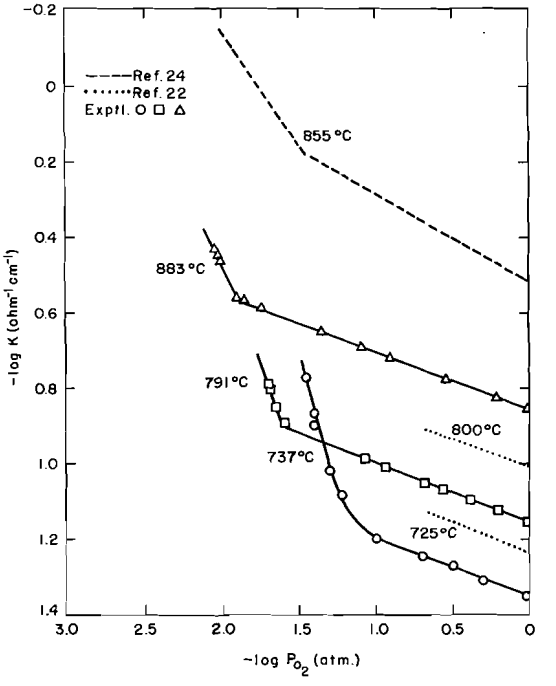

FIG. 2. Oxygen partial pressure dependence of the electrical conductivity of liquid V_2O_5.

for the A.R. grade vanadium pentoxide, where K is the specific conductance in ohm^{-1} cm^{-1} and T is the temperature in deg. Kelvin. The results for the A.R. grade of vanadium pentoxide compare favorably with those reported by Allersma *et al.* (22) for the same grade of material. Several hours were required for the electrical conductivity to reach a steady value between various temperature or oxygen partial pressure settings for the "specpure" vanadium pentoxide, but the A.R. grade vanadium pentoxide required only about an hour between settings.

The temperature dependence of the specific conductance can be represented by an equation of the type

$$[3] \qquad K = A \exp(-E/RT)$$

where E is the activation energy for conduction and A is a constant. The "specpure" V_2O_5 had an activation energy of conduction of 17.8 kcal/mol or 0.77 eV and the A.R. grade V_2O_5 had an activation energy of 16.7 kcal/mol or 0.73 eV under oxygen at 1 atm pressure.

The variation of the electrical conduction with oxygen partial pressure for "specpure" molten vanadium pentoxide is shown in Fig. 2. The oxygen partial pressure dependence of electrical conduction can be expressed by the equation:

$$[4] \qquad K = cP_{O_2}^{1/x}$$

where c is a constant and $1/x$ is the power of the oxygen partial pressure dependence. The present results indicate that the power of the oxygen partial pressure dependence is -0.16 at oxygen partial pressures greater than 0.1 atm in the temperature range 700 to 900 °C. A large increase in the power of the oxygen partial pressure dependence of electrical conduction was found below a specific oxygen partial pressure, depending on the temperature. When the data from Fig. 2 is replotted on the Arrhenius diagram of Fig. 3, the temperature dependence of the electrical conductivity of liquid vanadium pentoxide is found to change from positive to negative as the oxygen partial pressure decreases. The point at which the change in temperature dependence is found to occur takes

Can. J. Chem. Downloaded from www.nrcresearchpress.com by 210.87.254.40 on 09/05/12
For personal use only.

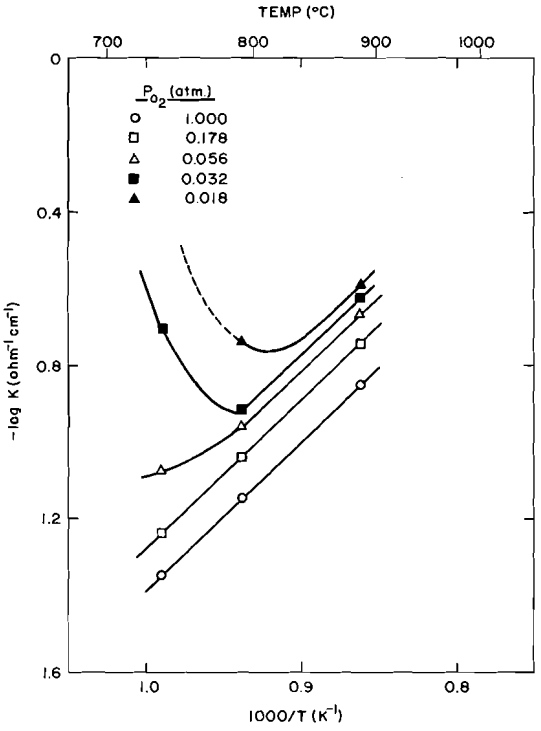

FIG. 3. Temperature dependence of the electrical conductivity of liquid V_2O_5 under various oxygen partial pressures.

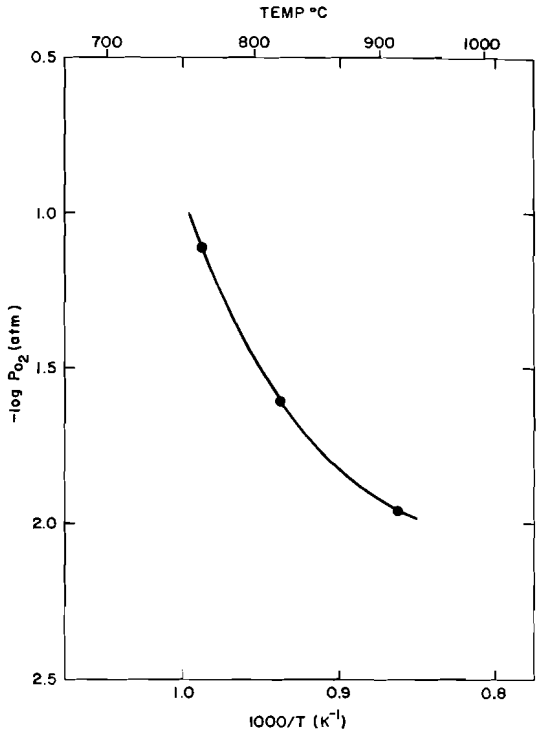

FIG. 4. Temperature–oxygen partial pressure dependence of the semiconduction–metallic conduction transition of liquid V_2O_5.

place at lower oxygen partial pressures as the temperature increases, as shown in Fig. 4.

Discussion

Liquid vanadium pentoxide exhibits several n-type semiconduction characteristics, such as a positive temperature coefficient and a negative oxygen partial pressure coefficient at oxygen partial pressures greater than 0.1 atm. The presence of impurities in vanadium pentoxide has a large effect on the magnitude of electrical conduction, as indicated by the different conductivities of the two grades used. The effect of impurities could account for some of the discrepancies in the reported electrical conduction properties of liquid vanadium pentoxide. As has been shown elsewhere (4), the addition of impurities to the melt has the effect of increasing the magnitude of electrical conduction and decreasing the oxygen partial pressure dependence.

The mechanism of n-type semiconduction in liquid vanadium pentoxide at higher oxygen partial pressures likely occurs via the hopping or the small-polaron model (29), in which electrons travel from V^{4+} ions to V^{5+} ions by a thermally activated diffusion mechanism. The dislocation model proposed by Perlstein (17) for electronic conduction in solid V_2O_5 would probably not apply as such to liquid V_2O_5.

The concentration of V^{4+} ions in the liquid state is dependent on the oxygen partial pressure above the melt, as shown below

$$[5] \qquad 2V^{5+} + O^{2-} \rightleftharpoons 2V^{4+} + \tfrac{1}{2}O_{2(g)}$$

Decreasing oxygen partial pressure will lead to an increased V^{4+} ion concentration, with a corresponding increase in electrical conduction. The existence of a relationship between an increase in V^{4+} ion concentration and an increase in electrical conduction was indicated by e.s.r. measurements on vanadium pentoxide samples quenched under various oxygen partial pressures.

Can. J. Chem. Downloaded from www.nrcresearchpress.com by 210.87.254.40 on 09/05/12
For personal use only.

Can. J. Chem. Downloaded from www.nrcresearchpress.com by 210.87.254.40 on 09/05/12
For personal use only.

Several authors (22, 24, 25) have analyzed the oxygen partial pressure dependence of electrical conduction of liquid vanadium pentoxide by means of an oxygen-deficient semiconducting oxide model. It was assumed that sufficient short-range order existed in the melt to allow transfer of charge between V^{5+} and V^{4+} ions. The power of the oxygen partial pressure dependence was predicted to be -0.167 if the conducting electrons, which were derived from fully ionized anion vacancies, associated with the cations to form V^{4+} ions. The value of -0.16 found for the power of the oxygen partial dependence in the present study would indicate that electrical conduction in liquid vanadium pentoxide at oxygen partial pressures greater than 0.1 atm occurred predominately by thermally activated polaron conduction between the vanadium cations, which is in agreement with two previous studies (22, 25).

At low oxygen partial pressures (<0.1 atm), liquid vanadium pentoxide shows a negative temperature dependence of electrical conduction (Fig. 4). Mott (30) has predicted that semiconductors should show a transition to metallic conduction if the distance between lattice points is reduced enough to allow overlapping of valence and conduction bands. Rogers *et al.* (31) and Goodenough (32) have proposed that localized-electron conduction will switch to collective-electron conduction when the cation separation becomes less than a critical separation defined as

$$[6] \quad R_c(\text{Å}) = 3.20 - 0.05m - 0.03(Z - Z_{T_1}) - 0.04S(S+1)$$

where m is the cation charge, Z is the cation atomic number, and S is the cationic spin. A study of several vanadium spinels indicated that the critical separation between vanadium ions was close to 2.972 Å.

Semiconduction to metallic conduction transitions have been observed for the lower solid oxides of vanadium. This was indicated by the conductivity increasing sharply by a factor of four to six times as the temperature was increased (33). The oxides VO, V_2O_3, and VO_2 undergo these temperature induced transitions near 120, 160, and 340 °K, respectively. The transitions were considered to be due, at least partially, to phase transitions involving a shortening of the distance between vanadium ions (32–34). The oxide V_2O_3 has also been found to switch to metallic conduction when put under pressure (30). The semiconductor to metallic conduction transition has not yet been observed with solid V_2O_5, however.

In the present case, it is possible that the vanadium ions in the liquid vanadium pentoxide were brought closer together than some critical separation distance when the oxygen ions were removed from the melt by the reduction in oxygen partial pressure. This could result in an overlapping of the diffuse valence and conduction bands, allowing collective-electron conduction in partially filled 3d bands to predominate over thermally activated polaron conduction between vanadium ions. No data is at present available on what effect the oxygen partial pressure has on the cation–cation separation distance in liquid vanadium pentoxide. An increase in temperature would be expected to increase the separation between the cations, so that the switching effect would be observed at lower oxygen partial pressures as the temperature was increased. This effect was observed experimentally (Fig. 3).

Conclusions

(*1*) Liquid vanadium pentoxide is an n-type semiconducting oxide in the temperature range 670 to 1000 °C and at oxygen partial pressures greater than 0.1 atm, as indicated by a positive temperature coefficient of conduction and a negative dependence of electrical conduction on oxygen partial pressure. Liquid vanadium pentoxide can have a negative temperature coefficient of conduction at oxygen partial pressures less than 0.1 atm.

(*2*) Electrical conduction in liquid vanadium pentoxide was considered to occur via the small polaron model, with electrons "hopping" from V^{4+} to V^{5+} centers, at oxygen partial pressures greater than 0.1 atm. At oxygen partial pressures less than 0.1 atm, conduction was thought to occur by collective-electron conduction in partially filled 3d bands, provided the diffuse valence and conduction bands overlapped due to the cation separation in the melt becoming less than some critical distance.

This work was supported by grants from the Defence Research Board of Canada. The authors are grateful to

Dr. M. Sayer of the Dept. of Physics, Queen's University, for several e.s.r. measurements and for helpful discussions.

1. H. R. JOHNSON and D. J. LITTLER (*Editors*). Mechanism of corrosion by fuel impurities. Butterworths, London. 1963.
2. K. SACHS. Metallurgia, **57**, 123 (1958); **57**, 167 (1958); **57**, 224 (1958).
3. R. C. KERBY and J. R. WILSON. Trans. ASME. To be published.
4. R. C. KERBY. Ph.D. Thesis. Queen's University, Kingston, Ontario. 1971.
5. A. N. ARSEN'EVA and B. V. KURCHATOV. Zh. Eksp. Teor. Fiz. **4**, 576 (1934).
6. B. M. HOKHBERG. Zh. Eksp. Teor. Fiz. **4**, 1090 (1937).
7. J. BOROS. Z. Phys. **126**, 721 (1949).
8. G. L. SIMARD, J. F. STEGER, R. J. ARNOTT, and L. A. SIEGEL. Ind. Eng. Chem. **47**, 1424 (1955).
9. J. D. BUTLER. Trans. Faraday Soc. **56**, 1842 (1960).
10. T. KAWAGUCHI. Paper presented at 18th Intern itional Congress of Pure and Applied Chemistry, Montreal, Canada, August 6–12, 1961.
11. S. KACHI, T. TAKADA, and K. KOSUGE. J. Phys. Soc. Jap. **18**, 1839 (1963).
12. J. HAEMERS. C.R. **259**, 3740 (1964).
13. I. B. PATRINA and V. A. IOFFE. Sov. Phys. Solid State, **6**, 2581 (1965).
14. J. C. MCCULLOCH. Report TR-3 (AD-670560), Oregon State Univ., Corvallis, U.S.A. May 27, 1968. p. 53.
15. D. S. VOLZHENSKII and M. V. PASHKOVSKII. Sov. Phys. Solid State, **11**, 950 (1969).
16. A. R, TOURKEY, Z. HANAFI, and K. AL. SEWEL. Z. Phys. Chem. **242**, 298, 305 (1969).
17. J. H. PERLSTEIN. J. Solid State Chem. **3**, 217 (1971).
18. V. A. YURKHOV. Zh. Eskp. Teor. Fiz. **22**, 223 (1952).
19. O. A. ESIN and V. L. ZYOSEV. Zh. Neorgan. Khim. **2**, 1998 (1957).
20. A. I. MANADOV, O. A. ESIN, and B. M. LEPINSKIKH. Russ. J. Phys. Chem. **36**, 1481 (1962); Russ. J. Inorg. Chem. 7, 1149 (1964).
21. T. S. ZOLYAN and A. R. REGEL. Sov. Phys. Solid State, **6**, 1189 (1964).
22. T. ALLERSMA, R. HAKIM, T. N. KENNEDY, and J. D. MACKENZIE. J. Chem. Phys. **46**, 154 (1967).
23. (*a*) A. E. VAN ARKAL, E. A. FLOOD, and N. F. H. BRIGHT. Can. J. Chem. **31**, 1009 (1953). (*b*) R. RENAUD, G. ODENT, and F. A. JOSIEN. Rev. Chim. Miner. **6**, 557 (1969).
24. D. A. PANTONY and K. I. VASU. J. Inorg. Nucl. Chem. **30**, 433 (1968).
25. (*a*) E. A. PASTUKHOV, O. A. ESIN, and N. A. VATOLIN. Izv. Akad. Nauk. SSSR, Neorg. Mater. **4**, 1960 (1968). (*b*) V. I. MUSIKHIN, E. A. PASTUKHOV, N. A. VATOLIN, and B. M. LEPINSKIKH. Isv. Akad. Nauk SSSR, Neorg. Mater. **7**, 99 (1971).
26. L. V. DMITRIEVA, V. A. IOFFE, and I. B. PATRINA. Sov. Phys. Solid State, **7**, 228 (1966); **10**, 639 (1968).
27. E. F. RIEBLING and P. C. LOGEL. Rev. Sci. Instrum. **36**, 425 (1965).
28. G. JONES and B. C. BRADSHAW. J. Am. Chem. Soc. **55**, 1780 (1933).
29. I. G. AUSTIN and N. F. MOTT. Adv. Phys. **18**, 41 (1969).
30. N. F. MOTT. Can. J. Phys. **34**, 1356 (1956); Phil Mag. **20**, 1 (1970).
31. D. B. ROGERS, R. J. ARNOTT, A. WOLD, and J. B. GOODENOUGH. J. Phys. Chem. Solids, **24**, 347 (1963).
32. J. B. GOODENOUGH. Czech. J. Phys. **4**, 304 (1967); Annu. Rev. Mater. Sci. **1**, 101 (1971).
33. (*a*) I. G. AUSTIN and C. E. TURNER. Phil. Mag. **19**, 939 (1969). (*b*) G. J. HYLAND. J. Solid State Chem. **2**, 318 (1970).
34. K. VAN STEENSEL, F. VAN DE BURG, and C. KOOY. Philips Res. Repts. **22**, 170 (1967).

Can. J. Chem. Downloaded from www.nrcresearchpress.com by 210.87.254.40 on 09/05/12
For personal use only.

Electrical Conduction Properties of Liquid Vanadates. II. The Sodium Vanadates

R. C. KERBY

Extraction Metallurgy Research Section, Mines Branch, Department of Energy, Mines and Resources, Ottawa, Canada

AND

J. R. WILSON

Department of Metallurgical Engineering, Queen's University, Kingston, Ontario

Received April 20, 1972

The liquid sodium vanadates exhibited n-type semiconduction properties at sodium oxide concentrations less than 10 mol% and ionic conduction properties at concentrations greater than 25 mol%. The transition from semiconduction to ionic conduction occurred gradually as the sodium oxide concentration increased. The activation energy of conduction decreased with increasing sodium oxide concentration and increasing temperature. Negative oxygen partial pressure coefficients of conduction were found for sodium oxide concentrations less than 25 mol%. The oxygen partial pressure coefficient decreased with increasing temperature and sodium oxide concentration. The electrical conduction mechanism was considered to change from delocalized electron or polaron movement between V^{4+} and V^{5+} centers for the semiconducting liquid sodium vanadates to the probable movement of sodium and oxygen ions as the charge-carrying species for the ionic liquid sodium vanadates.

Les vandanates de sodium liquides manifestent des propriétés de semiconduction de type n, à des concentrations d'oxyde de sodium plus faibles que 10 mol% et des propriétés de conduction ionique à des concentrations plus grandes que 25 mol%. La transition de la semiconduction à la conduction ionique se produit graduellement, au fur et à mesure que diminue la concentration d'oxyde de sodium. L'énergie d'activation de conduction diminue si on augmente la concentration d'oxyde de sodium et la température. Nous trouvons des coëfficients de conduction de pression partielle d'oxygène négatifs pour des concentrations d'oxyde de sodium plus faibles que 25 mol%. Le coëfficient de pression partielle d'oxygène diminue avec la température et la concentration d'oxyde de sodium croissantes. Nous considérons que le mécanisme de conduction électrique change d'un mouvement d'électron délocalisé ou polaron entre les centres V^{4+} et V^{5+} pour les vandanates de sodium liquides semiconducteurs à un mouvement probable des ions sodium et oxygène, comme les espèces porteuses de charges dans les vandanates de sodium liquides ioniques.

[Traduit par le journal]

Canadian Journal of Chemistry, **50**, 2871 (1972)

Can. J. Chem. Downloaded from www.nrcresearchpress.com by 210.87.254.5 on 09/05/12
For personal use only.

Introduction

The electrical conduction properties of the solid sodium vanadates, in particular the sodium–vanadium "bronzes", have been well characterized (1–5). The sodium–vanadium "bronzes" are oxygen-deficient solid sodium vanadates of several compositional ranges, of which the following are representative: $Na_xV_2O_5$, where $[0.1 < x < 0.67]$ and $Na_{(1+y)}V_3O_8$, where $[0.0 < y < 0.8]$ (6–8). These compounds generally exhibit n-type semiconduction properties, although p-type semiconduction properties have also been reported (4). Incorporation of sodium into the V_2O_5 lattice structure causes a reduction in valence of the vanadium atoms from V^{5+} to V^{4+}, due to donation of the alkali metal valence electron to a vanadium atom. The reduced valence states of the vanadium atoms are not localized, but can move from one site to another, giving rise to semiconduction via the hopping of electrons or small polarons from one vanadium atom to the next (2).

Only two limited studies have been reported on the measurement of the electrical conductivities of the liquid sodium vanadates (9). Increasing conductance and decreasing activation energies were reported for increasing sodium oxide concentrations. In the present study, the electrical conductivities of several liquid sodium vanadates and the viscosity of one liquid sodium vanadate were measured as part of a program to characterize more fully the physical properties of the liquid vanadates (10).

Experimental

The apparatus used to measure the electrical conductivity of the liquid vanadates has been described in detail elsewhere (10). The electrical conductivity was measured in a dipping electrode cell constructed from an 80/20 gold/palladium alloy. Electrical conductivity measurements were made

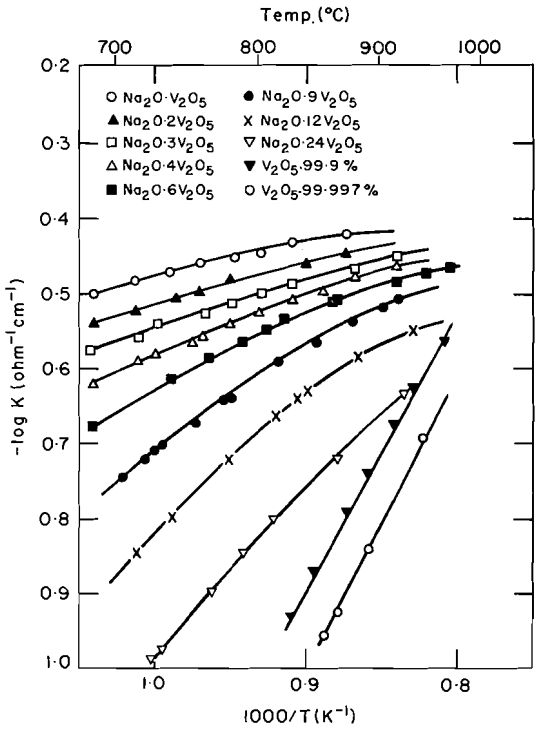

FIG. 1. Arrhenius plot of the electrical conductivities of the molten sodium vanadates.

using a General Radio 1608-A Impedance Bridge with an auxiliary audio oscillator and tuned amplifier and null detector. A.C. frequencies up to 10^4 Hz were used. Oxygen partial pressures over the melt were controlled by the use of regulated, high-purity oxygen–argon mixtures.

The sodium vanadates were prepared by thoroughly mixing the required amounts of sodium carbonate and vanadium pentoxide and then fusing the mixtures. On fusion, carbon dioxide was evolved for several minutes and then evolution ceased. No evidence was found for any carbonate remaining in the melt. Reagent grade sodium carbonate and Johnson and Matthey "specpure" vanadium pentoxide, containing 20 p.p.m. titanium and 5 p.p.m. silicon, were used.

Viscosity measurements were made by the rotating crucible method, in which the outer crucible is rotated and the torque is measured on an inner concentric crucible (18, 19). Platinum crucibles and cylinders were used in these measurements.

Results

The temperature dependence of the electrical conductivities of the liquid sodium vanadates, in the presence of oxygen at a pressure of 1 atm, is shown in the Arrhenius plot of Fig. 1. The data for vanadium pentoxide, which are also shown in the diagram, have been taken from previously published data (10). The data have been fitted to an equation of the form

TABLE 1. Compiled coefficients of electrical conductivities of liquid sodium vanadates at 1 atm oxygen pressure*

Composition	a	$b(10^3)$	$c(10^6)$
V_2O_5 (99.997%)†	2.1466	−4.4408	2.3386
V_2O_5 (99.9%)†	1.6210	−3.5739	2.0075
$24V_2O_5 \cdot Na_2O$	−0.1664	−0.0504	0.3199
$12V_2O_5 \cdot Na_2O$	−1.7689	2.9785	−1.0608
$9V_2O_5 \cdot Na_2O$	−1.2720	2.1876	−0.7232
$6V_2O_5 \cdot Na_2O$	−1.3068	2.4324	−0.8907
$4V_2O_5 \cdot Na_2O$	−0.7480	1.5022	−0.4927
$3V_2O_5 \cdot Na_2O$	−0.7219	1.5509	−0.5451
$2V_2O_5 \cdot Na_2O$	−0.8910	1.9400	−0.7422
$V_2O_5 \cdot Na_2O$	−0.8388	1.9324	−0.7597

*Specific conductance: $K(\text{ohm}^{-1}\,\text{cm}^{-1}) = a + bT + cT^2$ (T in °K); temperature range: melting point to 1000 °C.
†Reference 10.

[1] $$K = a + bT + cT^2$$

where K is the specific conductance in $\text{ohm}^{-1}\,\text{cm}^{-1}$, T is the temperature in Kelvin and a, b, and c are constants. The calculated coefficients for each composition, as determined by a least squares polynomial analysis of the data, are listed in Table 1. Isotherms of the electrical conductivities of the liquid sodium vanadates were determined from the data listed in Table 1. They are plotted as a function of sodium oxide concentration in Fig. 2. From this diagram, it can be seen that the conductivity increases with increasing temperature and sodium oxide concentration.

Activation energies of conduction were calculated from the data shown in the Arrhenius plots of Fig. 1 and are illustrated in Fig. 3. The activation energy decreases with increasing sodium concentration. The activation energies of conduction of the liquid sodium vanadates decrease with increasing temperature, although no effect of temperature was observed for the activation energy of conduction of liquid vanadium pentoxide (10).

The variation of the electrical conductivity with oxygen partial pressure for the molten sodium vanadates is shown in Fig. 4. The oxygen partial pressure dependence of electrical conduction can be expressed by the equation

[2] $$K = cP_{O_2}^{1/x}$$

where c is a constant and $1/x$ is the power of the oxygen partial pressure dependence. The power

Can. J. Chem. Downloaded from www.nrcresearchpress.com by 210.87.254.5 on 09/05/12
For personal use only.

Can. J. Chem. Downloaded from www.nrcresearchpress.com by 210.87.254.5 on 09/05/12
For personal use only.

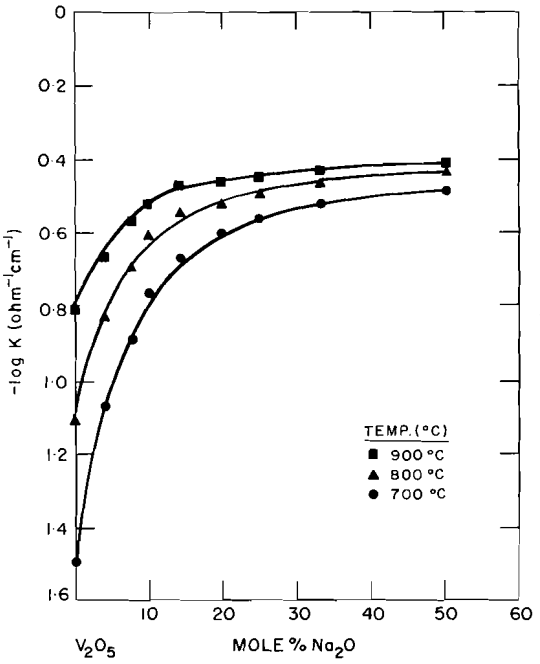

FIG. 2. Electrical conductivity isotherms of the molten sodium vanadates.

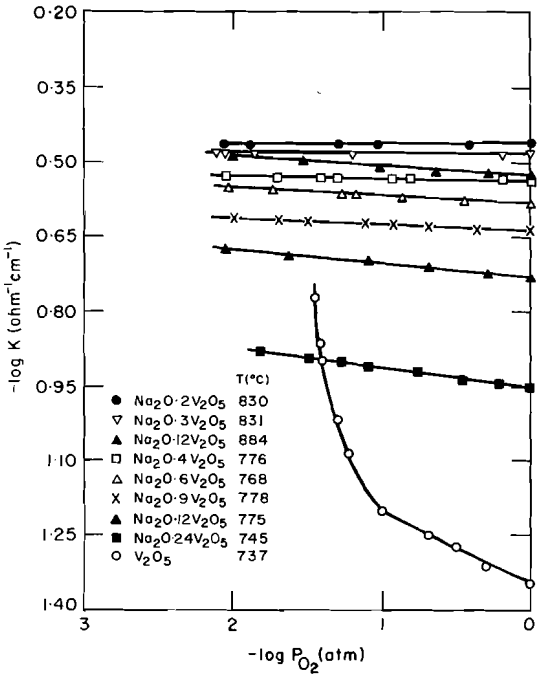

FIG. 4. Oxygen partial pressure dependence of the electrical conductivity of the molten sodium vanadates.

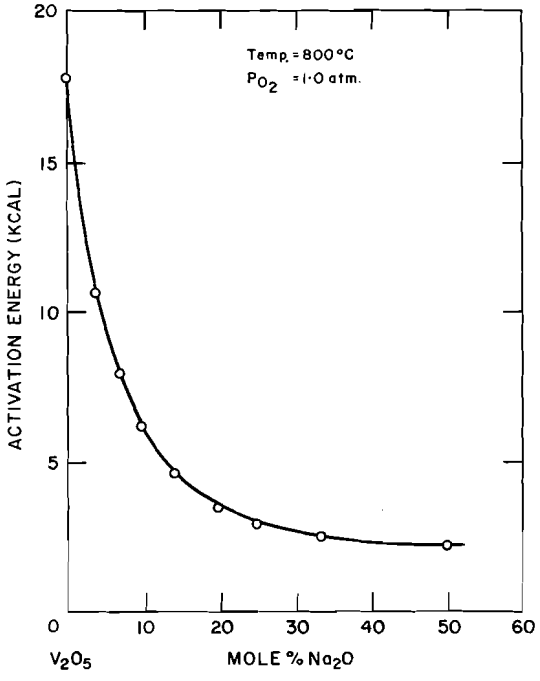

FIG. 3. Activation energies of conduction of the molten sodium vanadates.

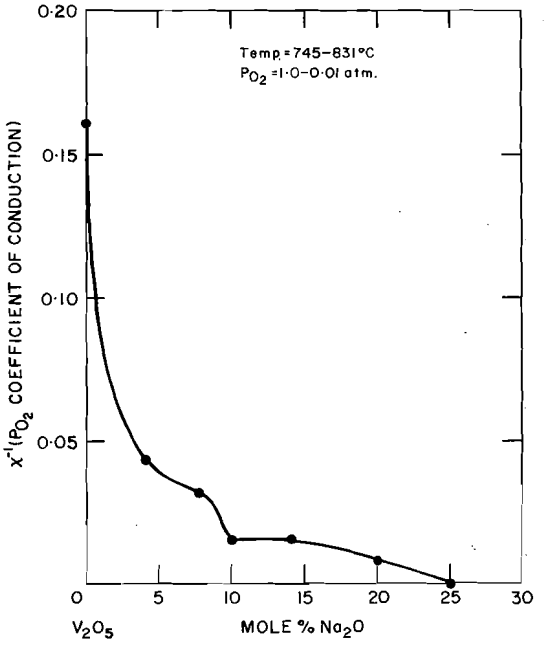

FIG. 5. Variation of the oxygen partial pressure dependence of conduction with Na_2O concentration for the molten sodium vanadates at 800 °C.

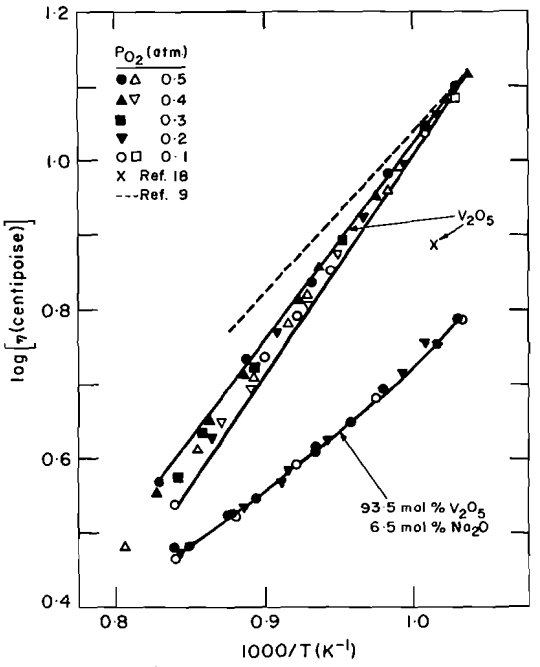

FIG. 6. Viscosity of liquid V_2O_5 and a liquid sodium vanadate.

of the oxygen partial pressure dependence decreases as the sodium oxide concentration increases, as shown in Fig. 5. No oxygen partial pressure dependence is observed at sodium oxide concentrations greater than 25 mol%, *i.e.*, for sodium oxide concentrations greater than the liquid sodium vanadate $Na_2O{\cdot}3V_2O_5$.

The viscosities of liquid vanadium pentoxide and a liquid mixture of 93.5 mol% vanadium pentoxide and 6.5 mol% sodium oxide were measured and are shown in Fig. 6. There is an appreciable decrease in viscosity with the addition of sodium oxide. Oxygen partial pressures did not greatly affect the viscosity. An increase in temperature had a larger effect in decreasing the viscosity of liquid vanadium pentoxide than in decreasing the viscosity of the liquid sodium vanadate.

Discussion

The liquid sodium vanadates of low sodium oxide concentration (< 20 mol%) were found to exhibit some n-type semiconduction properties, such as a negative oxygen partial pressure coefficient and a positive temperature coefficient of conduction. However, the n-type semiconduction properties differed significantly from those found for liquid vanadium pentoxide (10). No sharp increases in the oxygen partial pressure coefficients, at lower oxygen partial pressures, were observed for the sodium vanadates. The activation energies of these melts were found to decrease with increasing temperature and increasing sodium oxide concentration.

The mechanism of semiconduction probably involves the movement of delocalized electrons or polarons between V^{4+} and V^{5+} centers in these liquid sodium vanadates, similar to that proposed for the sodium vanadium "bronzes" (2) and liquid vanadium pentoxide (10). However, the presence of mobile sodium ions in the liquid should also give rise to some ionic conduction via sodium and oxygen ions.

When the sodium oxide concentration is increased above 25 mol%, ionic conduction becomes the predominant conduction mechanism. The evidence for ionic conduction predominating at higher sodium concentrations includes the lower activation energies of conduction (2 to 5 kcal/mol), the absence of an oxygen partial pressure effect on the conductance, and an increased tendency to show polarization effects at low frequencies during resistance measurements. The decrease in the activation energy of conduction with temperature which was detected for the sodium vanadates is commonly observed with many ionic liquids. This phenomenon is considered to be due to the expansion of the melt with a consequent decrease in the coulombic forces associated with the movement of ions through the melt (11).

The change in the conduction mechanism from semiconduction to ionic conduction as the sodium oxide content of the melt increases probably results from a breakdown of the short-range order about the complex vanadium ions in the melt. Solid vanadium pentoxide is considered to consist of layers of VO_4 tetrahedra (12). Since liquid V_2O_5 shows considerable viscosity (Fig. 6), it is likely that there is considerable short-range order in the liquid state, with oxygen ions closely associated about the vanadium ions and possibly some V—V homopolar bonding (13). Other amorphous vanadium-containing oxygen compounds, such as a number of glasses, also show semiconduction properties and considerable short-range order (14, 15). Long chains of VO_4 tetrahedra are

Can. J. Chem. Downloaded from www.nrcresearchpress.com by 210.87.254.5 on 09/05/12
For personal use only.

Can. J. Chem. Downloaded from www.nrcresearchpress.com by 210.87.254.5 on 09/05/12
For personal use only.

believed to be present in these glasses. The solid sodium vanadates of the sodium–vanadium "bronze" composition range consist of sodium ions located between layers of VO_4 tetrahedra (10). In the liquid state, the oxygen ions from the added sodium oxide would tend to associate with the complex vanadate ions to form simpler vanadate ions such as the metavanadate ion $[VO_3]^-$. Much the same process has been shown to occur in the case of silicate melts, where the network structure breaks down and the polyanions reduce in size with the addition of sodium oxide until they are reduced to the simplest silicate anions (16). An indication of the breakdown of the complex vanadate ions is shown by the decrease in viscosity of liquid vanadium pentoxide as sodium oxide is added (Fig. 6).

The semiconduction process involving electron or polaron transfer between V^{4+} and V^{5+} centers requires some association between vanadium atoms to assure an overlapping of conduction bands; therefore, the breakup of the complex vanadate ions due to the addition of sodium oxide to liquid vanadium pentoxide is associated with a decrease in semiconduction and an increase in the ionic conduction. The ionic conduction mechanism probably involves the transport of sodium and oxygen ions, as in the case of sodium silicate melts (16), and possibly vanadate ions.

The oxygen partial pressure dependence of conduction decreased with increasing temperature (Fig. 4). This could result from the increased dissociation of the complex vanadate ions with temperature, resulting in a decrease in semiconduction and an increase in ionic conduction. The oxygen partial pressure dependence remained at a steady value (0.016 at 775 °C) in the concentration range 10 to 15 mol% sodium oxide (Fig. 5). This compositional range corresponds approximately to the solid sodium vanadium bronze, $Na_2O \cdot xV_2O_4 \cdot (6-x)V_2O_5$, which has been shown to exist as a stable compound (17). Therefore, it is possible that a stable, complex vanadate ion may exist in the liquid sodium vanadate over this compositional range.

Conclusions

(*1*) The liquid sodium vanadates of low sodium oxide concentration are n-type semiconduction compounds in the temperature range 670 to 1000 °C. As the sodium oxide concentration is increased, the electrical conduction mechanism becomes progressively more ionic; for solutions contaning more than 25 mol% sodium oxide, electrical conduction is primarily ionic. The activation energy of conduction decreases and the specific conductivity increases with increasing sodium oxide concentration. Negative oxygen partial pressure coefficients of conduction which decrease with increasing sodium oxide concentration and temperature are found for sodium oxide concentrations less than 25 mol%.

(*2*) The mechanism of electrical conduction of the semiconducting liquid sodium vanadates is considered to involve the movement of delocalized electrons or polarons between V^{4+} and V^{5+} centers in the liquid. When sodium oxide is added to the liquid, the additional oxygen ions associate with the complex vanadate ions to form simpler vanadate ions such as the metavanadates $[VO_3]^-$. The reduction in association between vanadium atoms is associated with a reduction in semiconduction, but the increased concentration of mobile sodium ions results in an increase in ionic conduction involving sodium and oxygen ions.

This work was supported by grants from the Defence Research Board of Canada. The authors are indebted to B. M. Watts of the Department of Physical Metallurgy, Birmingham University, for the viscosity measurements.

1. M. J. Sienko and J. B. Sohn. J. Chem. Phys. **44**, 1369 (1966).
2. J. H. Perlstein and M. J. Sienko. J. Chem. Phys. **44**, 174 (1968).
3. S. Grocan, C. Liteanu, I. Lukacs, and C. Strusievici. Rev. Roum. Chim. **2**, 151 (1966).
4. I. Lukacs, C. Strusievici, E. Weissman, and C. Liteanu. Rev. Roum. Chim. **3**, 993 (1967).
5. B. G. Golovkin, A. A. Fotiev, and A. D. Neuimin. Zh. Fiz. Khim. **45**, 2247 (1971).
6. A. D. Wadsley. Acta Cryst. **8**, 695 (1955); **10**, 261 (1957).
7. R. P. Ozerov, G. A. Gol'der, and G. S. Zhdanov. Soc. Phys.-Crystallogr. **2**, 211 (1957).
8. J. Galy, J. Darriet, A. Casalot, and J. B. Goodenough. J. Solid State Chem. **1**, 339 (1970).
9. (*a*) D. A. Pantony and K. I. Vasu. J. Inorg. Nucl. Chem. **30**, 433 (1968). (*b*) J. Dubois, J. Richard, and J. Millet. C. R. Acad. Sci., Ser. C, **271**, 1452 (1970).
10. R. C. Kerby and J. R. Wilson. Can. J. Chem. This issue.
11. I. S. Yaffe and E. R. van Artsdalen. J. Phys. Chem. **60**, 1125 (1956).

12. H. G. BACHMAN, F. R. AHMED, and W. H. BARNES. Z. Krist. **115**, 110 (1961).
13. J. D. MACKENZIE. Modern aspects of the vitreous state. Vol. 1. Butterworths, London. 1960, p. 188.
14. E. P. DENTON, H. RAWSON, and J. E. STANWORTH. Nature, **173**, 1030 (1954).
15. T. N. KENNEDY and J. D. MACKENZIE. Phys. Chem. Glasses, **8**, 169 (1967).
16. J. O'M. BOCKRIS, J. A. KITCHENER, S. IGNATOWICZ, and J. W. TOMLINSON. Trans. Faraday Soc. **48**, 75 (1952).
17. R. C. KERBY and J. R. WILSON. Can. J. Chem. To be published.
18. H. R. THRESH. Trans. Am. Soc. Met. **55**, 790 (1962).
19. M. W. OZELTON and J. R. WILSON. J. Sci. Instrum. **43**, 359 (1966).

Can. J. Chem. Downloaded from www.nrcresearchpress.com by 210.87.254.5 on 09/05/12
For personal use only.

Electrical Conduction Properties of Liquid Vanadates. III. The System V_2O_5–Na_2O–Fe_2O_3

R. C. KERBY

Extraction Metallurgy Research Section, Mines Branch, Department of Energy, Mines and Resources, Ottawa, Canada

AND

J. R. WILSON

Department of Metallurgical Engineering, Queen's University, Kingston, Ontario

Received April 20, 1972

The liquid ferric vanadates exhibited n-type semiconduction properties at oxygen partial pressures greater than 0.1 atm. For ferric oxide concentrations less than 16 mol%, the activation energy of conduction was less than the activation energy associated with liquid vanadium pentoxide, but at greater ferric oxide concentrations, the activation energy increased to values greater than that associated with liquid vanadium pentoxide. The negative oxygen partial pressure coefficients of conduction were found to decrease with increasing ferric oxide concentration. The addition of sodium oxide to the liquid ferric vanadates decreased the activation energies of conduction. The electrical conductivities of these sodium ferric vanadates were found to be independent of oxygen partial pressure.

The electrical conduction mechanism of the ferric vanadates was considered to involve the movement of delocalized electrons or polarons between V^{4+} and V^{5+} centers at low ferric oxide concentrations and the additional movement of delocalized electrons between Fe^{2+} and Fe^{3+} centers for ferric oxide concentrations greater than 16 mol%. The addition of sodium oxide to the liquid ferric vanadates apparently changed the electrical conduction mechanism from semiconduction to ionic conduction. Sodium and oxygen ions are probably the charge-carrying species in these ionic melts.

Les vanadates ferriques liquides présentent des propriétés de semi-conduction du type n pour des pressions partielles en oxygène supérieures à 0.1 atm. Pour des concentrations en oxyde ferrique inférieures à 16 mol%, l'énergie d'activation de conduction est inférieure à l'énergie d'activation associée au pentoxyde de vanadium liquide; mais pour des concentrations plus élevées en oxyde ferrique, l'énergie d'activation croît jusqu'à des valeurs supérieures à celles associées au pentoxyde de vanadium liquide. Les coefficients négatifs de pression partielle d'oxygène dans la conduction ont été trouvés décroissants lorsque les concentrations en oxyde ferrique augmentaient. L'addition d'oxyde de sodium aux vanadates ferriques liquides fait décroître les énergies d'activation de conduction. Les conductivités électriques des vanadates ferriques de sodium sont alors indépendantes de la pression partielle en oxygène. Le mécanisme de conduction électrique dans les vanadates ferriques est considéré comme impliquant le mouvement des électrons délocalisés ou polarons entre les centres V^{4+} et V^{5+} pour de faibles concentrations en oxyde ferrique; et le mouvement supplémentaire des électrons délocalisés entre les centres Fe^{2+} et Fe^{3+} lorsque les concentrations en oxyde ferrique sont supérieures à 16 mol%. L'addition d'oxyde de sodium aux vanadates ferriques liquides change apparemment le mécanisme de la conduction électrique, on passe alors de la semi-conduction à la conduction ionique. Les ions sodium et oxygène sont les espèces chargées probables dans ces masses fondues ioniques.

[Traduit par le journal]

Canadian Journal of Chemistry, **50**, 2877 (1972)

Introduction

The electrical conduction properties of liquid vanadium pentoxide and the sodium vanadates have been reported previously (Parts I and II, see refs. 1 and 2). Liquid vanadium pentoxide was found to exhibit n-type semiconduction properties at oxygen partial pressures above 0.1 atm in the temperature range 670° to 1000 °C, but, at oxygen partial pressures less than 0.1 atm, a positive temperature coefficient of resistance was found. The liquid sodium vanadates exhibited n-type semiconduction properties at low sodium oxide concentrations. As the sodium oxide concentration was increased, ionic conduction became the principal electrical conduction mechanism. The electrical conduction properties of the ferric vanadates and the sodium ferric vanadates are reported in this paper.

Esin and Zyazev (3) and Pantony and Vasu (4) have measured the electrical conductivities of several liquid ferric vanadates. They were

Can. J. Chem. Downloaded from www.nrcresearchpress.com by 210.87.254.105 on 09/05/12
For personal use only.

Can. J. Chem. Downloaded from www.nrcresearchpress.com by 210.87.254.105 on 09/05/12
For personal use only.

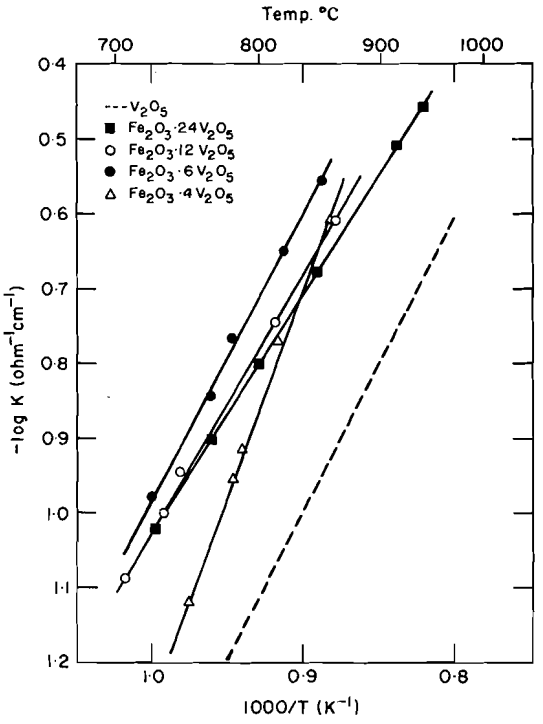

FIG. 1. Temperature dependence of the electrical conductivity of the molten ferric vanadates.

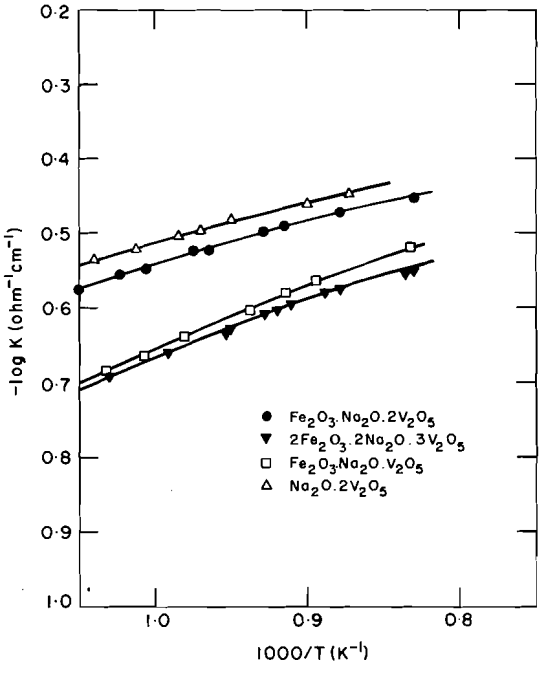

FIG. 2. Temperature dependence of the electrical conductivity of the molten ferric sodium vanadates.

reported to be semiconducting liquids. The specific conductance was found to increase as the ferric oxide concentration increased. The electrical conductivity of solid vanadium pentoxide has been found to increase with increasing ferric oxide concentration (5). The Fe^{3+} ions replaced the V^{5+} ions isomorphically in the lattice. This had the effect of introducing more oxygen vacancies into the lattice. The excess electrons collected at vanadium centers and increased the electrical conduction.

Experimental

The apparatus used to measure the electrical conduction of the liquid vanadates has been previously described in detail (1). The electrical conductivity cell was of the dipping electrode design and was constructed from a 80/20 gold/palladium alloy. A General Radio 1608-A Impedance Bridge with an auxiliary audio oscillator and a tuned amplifier and null detector was used for electrical conductivity measurements. A.C. frequencies up to 10^4 Hz were used. Oxygen partial pressures over the melt were controlled by the use of regulated, high-purity oxygen–argon mixtures.

The ferric vanadates and the sodium ferric vanadates were prepared by thoroughly mixing the required amounts of powdered ferric oxide, sodium carbonate, and vanadium pentoxide together and then fusing the mixture. Reagent grade ferric oxide and sodium carbonate and "specpure" vanadium pentoxide (Johnson and Matthey), containing 20 p.p.m. titanium and 5 p.p.m. silicon, were used.

Results

The temperature dependence of the electrical conductivities of the liquid ferric vanadates and the ferric sodium vanadates, in the presence of oxygen at a pressure of 1 atm, is shown in Figs. 1 and 2, respectively. The data for vanadium pentoxide, also shown in Fig. 1, are taken from previously published data (1).

The data have been fitted to an equation of the form

$$[1] \qquad K = a + bT + cT^2$$

where K is the specific conductance in ohm^{-1} cm^{-1}, T is the temperature in Kelvin, and a, b, and c are constants. The calculated coefficients for each composition, as determined by a least squares polynomial analysis of the data, are listed in Table 1. Isotherms for the liquid ferric vanadate conductivities, as illustrated in Fig. 3, were determined from the data listed in Table 1. The electrical conductivity increases with ferric oxide additions up to 16 mol%, but at greater concentrations, the conductivity decreases. The

Can. J. Chem. Downloaded from www.nrcresearchpress.com by 210.87.254.105 on 09/05/12
For personal use only.

TABLE 1. Compiled coefficients of electrical conductivities of liquid ferric vanadates and ferric sodium vanadates at 1 atm oxygen pressure*

Composition	a	$b(10^3)$	$c(10^6)$
$Fe_2O_3 \cdot 24V_2O_5$	1.2045	−3.0141	1.8984
$Fe_2O_3 \cdot 12V_2O_5$	1.7623	−4.0898	2.4226
$Fe_2O_3 \cdot 6V_2O_5$	2.1760	−5.1402	3.0680
$Fe_2O_3 \cdot 4V_2O_5$	5.2505	−11.0036	5.8113
$Fe_2O_3 \cdot Na_2O \cdot 2V_2O_5$	−0.6755	1.4906	−0.5272
$2Fe_2O_3 \cdot 2Na_2O \cdot 3V_2O_5$	−0.7447	1.4892	−0.5286
$Fe_2O_3 \cdot Na_2O \cdot V_2O_5$	−0.3868	0.7757	−0.1660

*Specific conductance: $K(\text{ohm}^{-1}\,\text{cm}^{-1}) = a + bT + cT^2$ (T in °K); temperature range: melting point to 1000 °C.

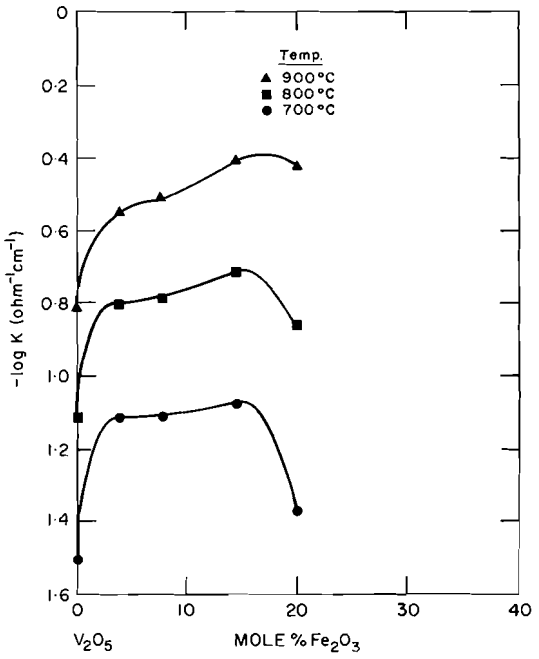

FIG. 3. Isotherms of the electrical conductivity of the molten ferric vanadates.

activation energy of conduction for the ferric vanadates containing less than 16 mol% ferric oxide is less than that associated with liquid vanadium pentoxide (Table 2), but at larger concentrations of ferric oxide, the activation energy increases above that for liquid vanadium pentoxide. All of the activation energies of conduction for the liquid ferric sodium vanadates were found to be below 4.0 kcal/mol (Table 3).

The oxygen partial pressure dependence of the electrical conductivity of the liquid ferric vanadates is shown in Fig. 4. The oxygen partial

TABLE 2. Oxygen partial pressure dependence of electrical conduction*

Composition	P_{O_2} (atm)	$1/x$
V_2O_5†	0.1–1.0	−0.150
$Fe_2O_3 \cdot 24V_2O_5$	0.1–1.0	−0.112
$Fe_2O_3 \cdot 12V_2O_5$	0.1–1.0	−0.090
$Fe_2O_3 \cdot 6V_2O_5$	0.1–1.0	−0.067
$Fe_2O_3 \cdot 4V_2O_5$	0.1–1.0	−0.030
$Fe_2O_3 \cdot Na_2O \cdot 2V_2O_5$	0.03–1.0	0.0

*Specific conductance: $K = cP_{O_2}^{1/x}$.
†Reference 1.

TABLE 3. Activation energies of electrical conduction at 1 atm oxygen pressure*

Composition	E (kcal/mol) (±0.1) (at 800 °C)
V_2O_5†	17.8
$Fe_2O_3 \cdot 24V_2O_5$	14.7
$Fe_2O_3 \cdot 12V_2O_5$	15.2
$Fe_2O_3 \cdot 6V_2O_5$	16.8
$Fe_2O_3 \cdot 4V_2O_5$	25.0
$Fe_2O_3 \cdot Na_2O \cdot 2V_2O_5$	2.8
$2Fe_2O_3 \cdot 2Na_2O \cdot 3V_2O_5$	3.3
$Fe_2O_3 \cdot Na_2O \cdot V_2O_5$	3.7

*Specific conductance: $K = A \exp(-E/RT)$.
†Reference 1.

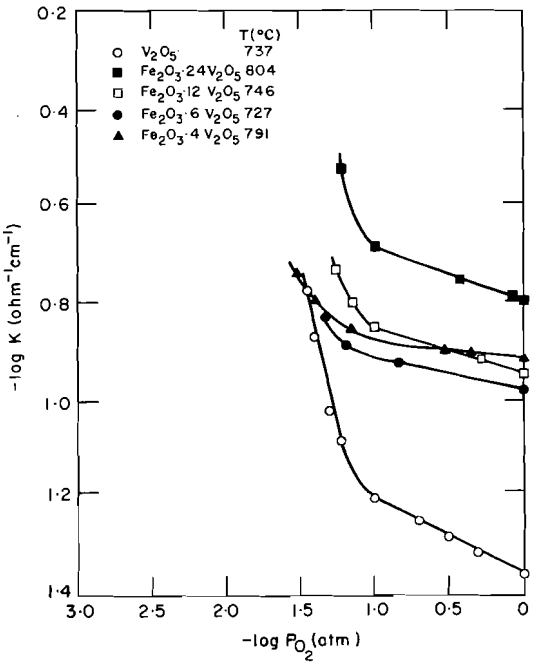

FIG. 4. Oxygen partial pressure dependence of the electrical conductivity of the molten ferric vanadates.

Can. J. Chem. Downloaded from www.nrcresearchpress.com by 210.87.254.105 on 09/05/12
For personal use only.

pressure dependence of electrical conduction can be expressed by the equation

$$[2] \qquad K = cP_{O_2}^{1/x}$$

where c is a constant and $1/x$ is the power of the oxygen partial pressure dependence. For the liquid ferric vanadates, the power of the oxygen partial pressure dependence decreases as the ferric oxide concentration increases for oxygen partial pressures greater than 0.1 atm (Table 2). At oxygen partial pressures less than 0.1 atm, a large increase in the oxygen partial pressure dependence of conduction is observed. A similar observation was previously reported for liquid vanadium pentoxide (1). No oxygen partial pressure dependence of electrical conduction is observed for the ferric sodium vanadates (Table 2).

Discussion

The addition of ferric oxide to liquid vanadium pentoxide did not cause any large change in the semiconduction behavior of these melts, although the oxygen dependence of conduction at oxygen partial pressures greater than 0.1 atm decreased with increasing concentrations of ferric oxide. At ferric oxide concentrations less than 16 mol%, the semiconduction mechanism probably involves the movement of delocalized electrons or polarons between V^{4+} and V^{5+} centers, similar to that reported for liquid vanadium pentoxide (1). The increase in electrical conduction and decrease in the activation energy of conduction with increasing ferric oxide concentration could be explained by assuming that the ferric ions replace the vanadium ions in the structured melt, in much the same manner as when ferric ion impurities are introduced into solid vanadium pentoxide (5). The ferric ions would have the effect of decreasing the oxygen stoichiometry present in the melt and allowing the excess electrons, resulting from the loss of oxygen, to collect at vanadium centers. The resultant increase in V^{4+} concentration would then lead to increased electrical conduction, in the same manner as a decrease in oxygen partial pressure results in an increase in V^{4+} concentration and hence an increase in the electrical conductivity.

The decrease in electrical conduction and increase in the activation energy of conduction at ferric oxide concentrations greater than 16 mol% could be due to dissociation of the complex vanadate ions which allowed semiconduction to occur in liquid vanadium pentoxide (1). Phase diagram studies (6) have indicated that the iron vanadate $FeVO_4$ will precipitate from solution at concentrations greater than 20 mol%. Thus, there is a marked tendency for the vanadate ion $[VO_4]^{3-}$ to exist in the solution in these concentration ranges. As electronic conduction via polaron hopping between V^{4+} and V^{5+} centers in the melt becomes less important with increasing ferric oxide concentration, electronic conduction via polaron hopping between Fe^{2+} and Fe^{3+} centers would tend to become more important. If ferric oxide concentrations are greatly increased, ionic conduction via ferric and oxide ions could predominate, although this was not shown in the results presented here.

At oxygen partial pressures less than 0.1 atm, the conductivity of the liquid ferric vanadates showed a sharp increase with respect to the oxygen partial pressure dependence. A similar effect was found for liquid vanadium pentoxide and was considered to be due to a transition from semiconduction to metallic behavior (1). A similar transition may be occurring in the case of the liquid ferric vanadates, although insufficient data is available from the present study to verify this.

The addition of sodium oxide to the liquid ferric vanadates tended to make the melts more ionic, as indicated by the absence of a dependence of the electrical conduction properties on oxygen partial pressure and by the low activation energy of conduction. As was postulated in the case of the sodium vanadates (2), the addition of sodium oxide tends to break down the complex vanadate ions which are likely present in those melts containing predominately vanadium pentoxide. Simpler vanadate ions such as the metavanadate ion $[VO_3]^-$ will then be present in the melts. The decrease in association between vanadium atoms, and between iron and vanadium atoms, results in a decrease in semiconduction, allowing ionic conduction via sodium and oxygen ions, and possibly vanadate ions, to predominate.

Conclusions

(*1*) The liquid ferric vanadates exhibit n-type semiconduction properties, such as a negative

oxygen partial pressure coefficient and a positive temperature coefficient of conduction, at oxygen partial pressures greater than 0.1 atm. At ferric oxide concentrations less than 16 mol%, the activation energy of the liquid ferric vanadates was less than that observed for liquid vanadium pentoxide. The oxygen partial pressure coefficient decreases and the conductivity increases with increasing ferric oxide concentration. For ferric oxide concentrations greater than 16 mol%, the activation energy increases to above the value observed for liquid vanadium pentoxide.

(*2*) The addition of sodium oxide to the liquid ferric vanadates results in ionic conduction predominating in the melts. The activation energies of conduction are all less than 4.0 kcal/mol. The oxygen partial pressure has no effect on the conduction.

(*3*) The mechanism of electrical conduction of the liquid ferric vanadates is considered to primarily involve the movement of delocalized electrons or polarons between V^{4+} and V^{5+} centers in the liquid at low ferric oxide concentrations. Electron movement involving Fe^{2+} and Fe^{3+} centers is probably also important for ferric oxide concentrations greater than 16 mol%. When sodium ions are present at concentrations greater than 10 mol% in the liquid, electrical conduction is considered to primarily involve the movement of sodium and oxygen ions in the liquid.

1. R. C. KERBY and J. R. WILSON. Can. J. Chem. This issue.
2. R. C. KERBY and J. R. WILSON. Can. J. Chem. This issue.
3. O. A. ESIN and V. L. ZYAZEV. Izvest. Akad. Nauk SSSR, Otdel. Takh. Nauk. 6, 7 (1958).
4. D. A. PANTONY and K. I. VASU. J. Inorg. Nucl. Chem. **30**, 433 (1968).
5. V. A. IOFFE and I. B. PATRINA. Sov. Phys.—Solid State, **6**, (10), 2425 (1965).
6. R. C. KERBY and J. R. WILSON. Can. J. Chem. To be published.

Can. J. Chem. Downloaded from www.nrcresearchpress.com by 210.87.254.105 on 09/05/12
For personal use only.

Etude de la réaction gaz–solide organique entre l'isobutène et le paraphénylphénol

R. LAMARTINE ET R. PERRIN

Groupe de Recherches sur les Phénols, Université Claude Bernard-Lyon I, Unité de Chimie et de Biochimie, 43, Bd du 11 Novembre 1918, 69, Villeurbanne, France

Reçu le 7 mars 1972

Dans le cadre de l'étude des réactions gaz–solide organique, nous avons considéré la réaction de l'isobutène gazeux avec le paraphénylphénol solide dopé à l'acide sulfurique. Parallèlement à la réaction de polymérisation de l'isobutène conduisant aux hydrocarbures en C_8 et C_{12}, le ditertiobutyl-2,6 phényl- 4 phénol est produit avec un très bon rendement par rapport au phénol de départ. La réaction d'alcoylation correspondante a pour ordre apparent 1 par rapport au paraphénylphénol; l'énergie d'activation est égale à 21 kcal/mol.

La réaction s'effectue à partir de centres actifs et se transmet à la presque totalité de la substance solide, le proton étant probablement l'entité migrante.

Within the scope of the study of organic gas–solid reactions, we considered the reaction of gaseous isobutene with solid paraphenylphenol doped with sulfuric acid. Parallel to the polymerization of isobutene leading to C_8 and C_{12} hydrocarbons, there is a very good yield of 2,6-di-*t*-butyl-4-phenylphenol production as compared to initial phenol. The corresponding alkylation reaction is apparently of the order 1 as compared to paraphenylphenol; the activation energy of the reaction is equal to 21 kcal/mol.

The reaction spreads out from active centers and is transmitted to almost the entirety of the solid substance; the proton is probably the migrating entity.

Canadian Journal of Chemistry, **50**, 2882 (1972)

Le comportement des réactifs organiques est principalement étudié lorsque ceux-ci sont à l'état liquide, à l'état gazeux ou en solution. Peu de travaux concernent l'étude de la réactivité de l'état solide organique et ce n'est que récemment que certains auteurs (1–4) s'y sont intéressés. La première question qui se pose est de savoir si l'on a affaire à une véritable réaction de l'état solide organique. Morawetz (2) a indiqué des critères qui apparaissent comme indiscutables; il s'agit essentiellement de montrer que l'on a des produits de réaction différents ou des vitesses de transformation différentes suivant la modification cristalline considérée ou suivant l'état dans lequel se trouve la substance étudiée. Il n'est pas toujours facile de mettre en évidence de tels phénomènes; aussi peut-on d'une manière plus générale considérer que des réactions concernent l'état solide organique lorsque l'un au moins des réactifs est solide à la température de la réaction.

Exception faite pour les réactions de décomposition thermiques unimoléculaires, les réactions propres à l'état solide font intervenir comme facteur important le phénomène de diffusion des entités réactives. En chimie minérale, ces entités réactives sont généralement des atomes métalliques ou de petits ions qui se déplacent dans les positions interstitielles ou dans les lacunes du réseau. En chimie organique, on peut considérer de la même façon que les réactions de l'état solide nécessitent pour avoir lieu l'existence d'entités réactives de petite taille. La diffusion de ces entités permet l'avancement de la réaction. Enfin, il est important d'avoir présent à l'esprit le rôle que peuvent jouer dans les réactions de l'état solide organique, l'état de division de la substance et les défauts que présentent ses cristaux.

L'étude de la réaction entre l'isobutène et le paraphénylphénol contenant des traces d'acide sulfurique a été entreprise pour plusieurs raisons. Tout d'abord, le phénol retenu présente un point de fusion relativement élevé pour une substance organique (165 °C) (5) et peut, de ce fait, constituer facilement un réactif solide à différentes températures; de plus, son insolubilité dans les solvants d'alcoylation habituels justifie l'étude de la réaction à l'état solide; enfin, le produit de réaction, le ditertiobutyl-2,6 phényl-4 phénol pourrait constituer un excellent antioxydant. Parallèlement à cette réaction, l'isobutène se condense sur lui-même et conduit à des hydrocarbures en C_8 et C_{12}. L'étude

Can. J. Chem. Downloaded from www.nrcresearchpress.com by 210.87.254.40 on 09/05/12
For personal use only.

Can. J. Chem. Downloaded from www.nrcresearchpress.com by 210.87.254.40 on 09/05/12
For personal use only.

suivante consiste à déterminer les conditions précises de la réaction, son aspect quantitatif et sa cinétique.

Partie expérimentale

Nous avons utilisé du paraphénylphénol pur (Eastman Kodak), de l'isobutène très pur et de l'acide sulfurique R.P. (Prolabo) de densité 1.83.

L'introduction d'acide sulfurique dans le paraphénylphénol a été réalisée de la manière suivante: au paraphénylphénol fondu, on ajoute 1.1% en poids d'acide sulfurique, on agite puis on laisse recristalliser. Le phénol ainsi dopé est réduit en grains qui sont calibrés par tamisage.

Pour l'étude cinétique, nous avons employé des grains de tailles comprises entre 200 et 315 μ. La réaction a lieu à pression constante. Le degré d'avancement de la réaction est déterminé par mesure du volume d'isobutène absorbé.

L'appareil permettant de mesurer l'isobutène consommé comporte essentiellement: (*a*) une burette à gaz de 100 cm^3 reliée par l'intermédiaire d'un tube flexible à un réservoir à mercure permettant ainsi de compenser la diminution de pression résultant de la consommation d'isobutène; (*b*) un système de pompage constitué par une pompe à palettes conduisant à une pression limite inférieure à la tension de vapeur du phénol aux températures étudiées; (*c*) une chambre à réaction thermorégularisée permettant d'opérer en couche mince et d'éliminer à chaque instant les énergies qui pourraient être mises en jeu.

Les analyses chromatographiques ont été réalisées à l'aide d'un appareil Intersmat modèle I.G.C. 12M équipé d'un catharomètre. La colonne est remplie de chromosorb W 60/80 imprégné de silicone SE 30. L'aire des pics a été déterminée grâce à un intégrateur numérique LTT M 924 couplé avec le chromatographe. Tous les échantillons analysés ont été traités au préalable par l'eau carbonatée car en présence d'acide et dans les conditions d'analyse choisies, le ditertiobutyl-2,6 phényl-4 phénol perd des groupes tertiobutyle.

Les spectres de r.m.n. ont été effectués avec un appareil Varian A 60.

Les spectres de masse ont été enregistrés dans les laboratoires Firmenich à Genève sur un appareil M.A.T. CH_4.

Les solubilités des phénols étudiés ont été déterminées dans le mélange d'hydrocarbures en C_8 et C_{12}. Les tertiobutyl-2 et ditertiobutyl-2,6 phényl-4 phénols sont solubles. Le paraphénylphénol est pratiquement insoluble. Ses solubilités limites ont été déterminées par évaporation du mélange d'hydrocarbures et dosage par spectrophotométrie u.v. du mélange restant repris dans l'alcool. Ces solubilités sont à 60 °C: 5/1000 et à 50 °C: 3.5/1000.

Caractérisation du ditertiobutyl-2,6 phényl-4 phénol: p. de f.: 104–106 °C; spectre de masse: pic moléculaire $M = 282$; spectre r.m.n. δ ($(CD_3)_2C{=}O$): 1.45 (s, $(CH_3)_3C$), 6(s, O*H*), 7.2–7.6 (m, *H* aromatiques).

Anal. calc. pour $C_{20}H_{26}O$: C, 85.10; H, 9.21; O, 5.67. Trouvée: C, 85.20; H, 9.18; O, 5.78.

Les hydrocarbures en C_8 et C_{12}, dimère et trimère de l'isobutène ont été mis en évidence par chromatographie et caractérisés par cryométrie dans le benzène.

Le tertiobutyl-2 phényl-4 phénol a été obtenu en appliquant le mode opératoire décrit dans le brevet de Preston (10).

Caractérisation du tertiobutyl-2 phényl-4 phénol: p. de f.: 42 °C; spectre r.m.n. δ ($(CD_3)_2C{=}O$): 1.45 (s, $(CH_3)_3C$), 8.45 (s, O*H*), 6.9–7.6 (m, *H* aromatiques).

Anal. calc. pour $C_{16}H_{18}O$: C, 84.97; H, 7.96; O, 7.07. Trouvée: C, 85.22; H, 8.01; O, 7.02.

Résultats et discussion

(1) Bilan réactionnel

La détermination volumétrique des quantités d'isobutène entré en réaction au cours du temps et l'analyse chromatographique des mélanges réactionnels obtenus pour différents degrés d'avancement de la réaction mettent en évidence qu'une certaine quantité d'isobutène consommée ne sert pas à former des tertiobutylphénols. Pour différentes températures et différents degrés d'avancement de la réaction, pour le paraphénylphénol et le tertiobutyl-2 phényl-4 phénol, le rapport d'isobutène absorbé à la quantité d'isobutène fixé sur le phénol est voisin de 2. Dans ces conditions, la transformation chimique étudiée peut être traduite par les réactions concurrentes, [1] et [2].

[1] 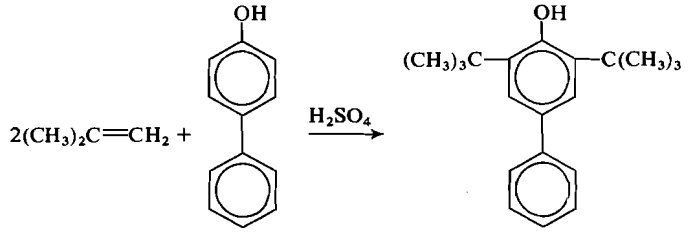

[2] $$\begin{cases} 2(CH_3)_2C{=}CH_2 \xrightarrow{H_2SO_4} \text{Diisobutène} \\ (CH_3)_2C{=}CH_2 + \text{Diisobutène} \xrightarrow{H_2SO_4} \text{Triisobutène} \end{cases}$$

Can. J. Chem. Downloaded from www.nrcresearchpress.com by 210.87.254.40 on 09/05/12
For personal use only.

Les réactions de formation du dimère et du trimère de l'isobutène s'effectuent bien dans les conditions expérimentales adoptées comme le montrent différents auteurs (6–8). Il est à noter que les réactions [2] n'ont jamais été prises en considération à notre connaissance, lors de l'étude de la tertiobutylation des phénols.

(2) Etude de la réaction

La réaction entre l'isobutène et les phénols a été réalisée en solution dans le benzène par Stillson *et al.* (9). Malheureusement, dans le cas du paraphénylphénol, ces auteurs ne précisent ni la proportion de benzène, ni la température de la réaction, ni le rendement en produits formés. Aussi, avons-nous effectué la même expérience dans les conditions suivantes (5 g de paraphénylphénol à 1.1% d'acide sulfurique à 94% dissous dans 200 ml de benzène, 50 °C, temps de réaction 5 h). Dans ces conditions, le taux de transformation est très faible, de l'ordre de quelques pour cent. A l'état solide, un échantillon de la même préparation conduit à un taux de transformation beaucoup plus élevé (70%). D'autre part, la même réaction effectuée dans le diméthyl-3,5 phénol conduit aux tertiobutyl-2, ditertiobutyl-2,4′, et tritertiobutyl-2,6, 4′ phényl-4 phénols suivant les conditions adoptées (10).

Ainsi, il apparaît que la différence de réactivité observée en solution d'une part et à l'état solide d'autre part, laisse supposer que l'on a affaire à une réaction de l'état solide organique conformément au critère retenu par Morawetz. De plus, l'écart important entre la température de fusion de la substance étudiée et la température de la réaction fait que celle-ci doit bien concerner l'état solide organique, tout au moins dans sa première étape. Naturellement, la présence de traces d'acide sulfurique peut toujours amener à penser qu'à l'échelle microscopique, l'isobutène réagit avec un liquide.

L'examen photographique d'une préparation permet de préciser le phénomène. Celle-ci correspond à un échantillon de paraphénylphénol à 1.1% d'acide sulfurique placé à 55 °C, au bout d'une demi-heure de réaction avec l'isobutène. On observe à l'échelle macroscopique que la réaction s'effectue en des points déterminés, se propage à partir de ces centres actifs et conduit à des monocristaux du produit de transformation que l'on distingue très nettement. Il n'est cependant pas possible de conclure à une transformation solide–solide. En effet, la formation simultanée de di et triisobutène conduit à une phase liquide dans laquelle peuvent se dissoudre les tertiobutylphénylphénols. On notera cependant que le paraphénylphénol est pratiquement insoluble dans le mélange de di et triisobutène et de ce fait, doit bien réagir à l'état solide. Là encore, il est possible de dire que ce corps ne réagit pas à l'état solide parce qu'il serait soluble dans un mélange de di et triisobutène et de ditertiobutyl-2,6 paraphénylphénol formé au cours de la réaction. Il apparaît ainsi difficile de montrer d'une façon absolue que l'on a affaire à une réaction de l'état solide organique. Aussi considérons-nous la réaction étudiée comme une réaction gaz–solide organique au sens large, c'est-à-dire lorsque l'un des réactifs est solide, à l'échelle macroscopique, à la température de la réaction.

(3) Etude de l'influence de différents facteurs

Influence de la taille des grains

Il a été observé que lorsque le diamètre des grains de phényl-4 phénol augmente de 63–315 μ par exemple, la quantité d'isobutène absorbée augmente. Toutefois, lorsque le diamètre des grains augmente considérablement, cette vitesse diminue. De plus, on constate que lorsque les grains deviennent très fins, ils s'agglomèrent entre eux; ils ne sont plus individualisés. On peut penser que la diminution de la quantité d'isobutène absorbé lorsque les grains deviennent très gros, semble pouvoir s'expliquer par la diminution de la surface réactive et des possibilités de diffusion. Lorsque les grains deviennent petits et s'agglomèrent, les possibilités de diffusion doivent être réduites.

Influence du dégazage

A une poudre non soumise à un dégazage préalable, correspond une vitesse d'absorption d'isobutène très faible. De plus, la vitesse d'absorption trouvée varie d'une expérience à l'autre. Le chauffage préalable de l'échantillon accélère la réaction d'autant plus que le temps de chauffage est long et la température élevée. Cependant, la technique la meilleure pour obtenir des résultats reproductibles, consiste à placer la substance sous vide à la température ambiante pendant au moins une heure. Des temps de dégazage supérieurs ne modifient pas les résultats obtenus.

Can. J. Chem. Downloaded from www.nrcresearchpress.com by 210.87.254.40 on 09/05/12
For personal use only.

L'influence du dégazage sur la vitesse d'évolution de la réaction étudiée nous apparaît comme un argument supplémentaire en faveur d'une véritable réaction à l'état solide. Il est rare en effet que le dégazage d'un liquide modifie sensiblement la vitesse de réaction.

Influence de la concentration en acide sulfurique et de la pression d'isobutène

De faibles concentrations en acide sulfurique, de l'ordre de 0.4% conduisent à de très faibles vitesses de transformation. Lorsque les concentrations sont beaucoup plus élevées, 5% par exemple, la réaction étudiée n'est pas sélective; au moins cinq substances sont produites et l'on peut penser que les deux noyaux aromatiques sont alcoylés. La concentration de 1.1% a été retenue parce qu'elle correspond à une réaction sélective et de vitesse aisément mesurable dans le domaine de températures choisi.

En ce qui concerne l'influence de la pression d'isobutène, on observe que la marche globale de la réaction n'est pas modifiée pour des pressions comprises entre 400 et 760 Torr. On note seulement une augmentation de la vitesse de réaction lorsque la pression s'élève.

(4) Etude cinétique de la réaction d'alcoylation du paraphénylphénol

Soit x le volume d'isobutène fixé sur le noyau phénolique au temps t et a le volume correspondant à la réaction totale. La vitesse s'écrit $dx/dt = k\,(a-x)$; ce qui donne après intégration $\log\,(a/(a-x)) = kt$, expression générale pour des réactions du premier ordre. En portant $\log\,(a/(a-x))$ en fonction du temps et à différentes températures, nous avons obtenu le faisceau de droites de la fig. 1 qui sont les transformées logarithmiques des courbes donnant la marche globale de la réaction en fonction du temps. Les constantes de vitesse trouvées à différentes températures sont les suivantes:

T (°C)	$k \times 10^{-4}$ (s^{-1})
60	0.388
55	0.253
50	0.144
45	0.088
40	0.047

Elles vérifient d'une façon remarquable (fig. 2) la relation d'Arrhénius

$$k = k_0\, e^{-E/RT}$$

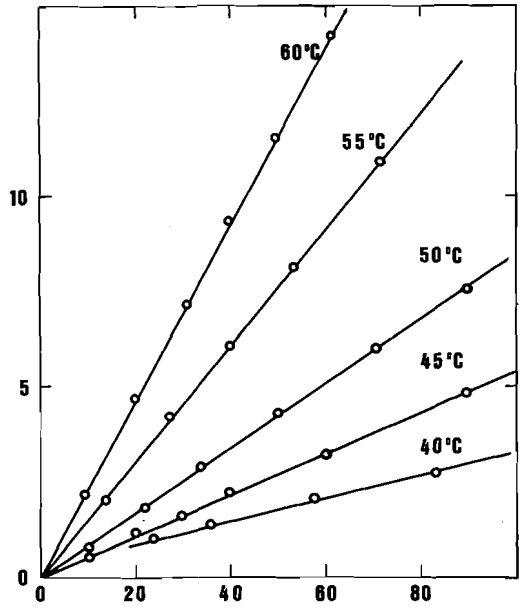

FIG. 1. Variation de la fonction $\log\,(a/(a-x)) \times 10^2$ en fonction du temps (min) pour la réaction de tertiobutylation du paraphénylphénol à différentes températures.

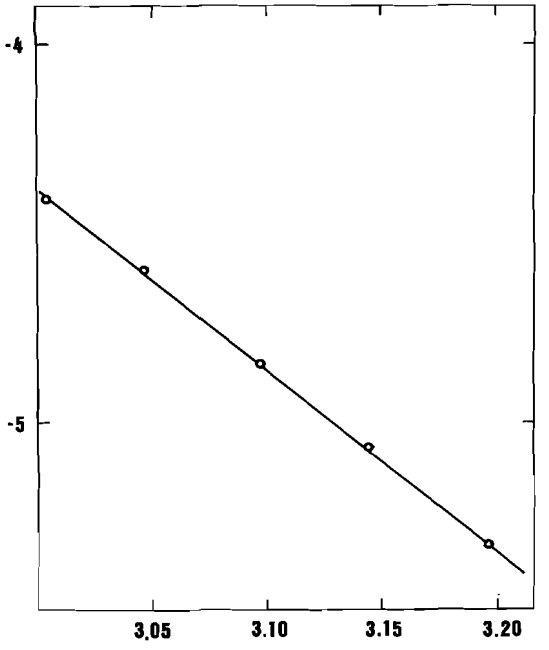

FIG. 2. Variation de la fonction $\log k$ en fonction de $10^3/T$ (°K).

on trouve ainsi pour énergie d'activation de la réaction étudiée 21 ± 1 kcal/mol^{-1}.

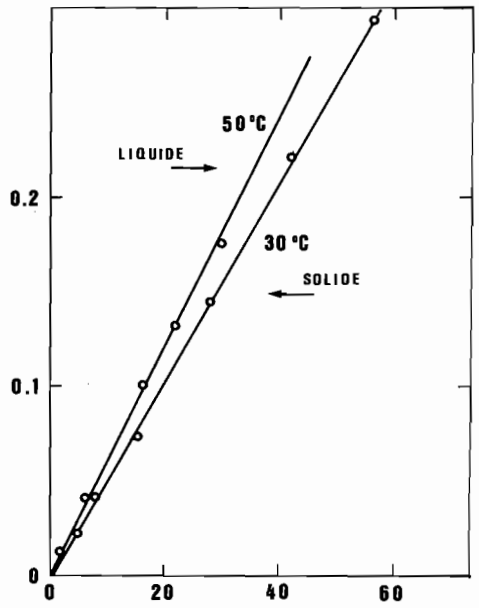

FIG. 3. Variation de la fonction log $(a/(a-x))$ en fonction du temps (min) pour la réaction de tertiobutylation du tertiobutyl-2 phényl-4 phénol.

(5) Etude cinétique de la réaction d'alcoylation du tertiobutyl-2 phényl-4 phénol

La fig. 3 met en évidence que la réaction de tertiobutylation du tertiobutyl-2 phényl-4 phénol contenant 1.1% d'acide sulfurique est une réaction d'ordre 1, que le phénol soit à l'état solide ou à l'état liquide. La différence de vitesse aux deux températures choisies est de faible importance (50 °C: $k = 1 \times 10^{-4}\ s^{-1}$; 30 °C: $k = 0.84 \times 10^{-4}\ s^{-1}$). On note par contre la très grande différence de vitesse de cette réaction, à la température de 50 °C, avec celle correspondant à la tertiobutylation du paraphénylphénol ($k = 0.144 \times 10^{-4}\ s^{-1}$).

(6) Conclusions

De l'ensemble des résultats ainsi obtenus, il apparaît que l'une des réactions étudiées, la réaction d'alcoylation du paraphénylphénol, pourrait être une réaction de l'état solide organique tout au moins dans sa première étape. Il est surprenant de constater que pour des degrés variés d'avancement de la réaction, le produit principal formé est le dérivé dialcoylé. L'étude cinétique explique aisément ce résultat puisqu'elle montre que la vitesse d'alcoylation du phénol monoalcoylé est environ sept fois la vitesse d'alcoylation du phénol de départ. Une molécule de monoalcoylphénol est transformée en dialcoylphénol dès qu'elle est formée; l'étape limitante correspond ainsi à la monoalcoylation.

D'autre part, les réactions de polymérisation de l'isobutène et d'alcoylation du phénol choisi s'effectuant dans les mêmes conditions, on peut penser que les entités réactives sont les mêmes dans les deux cas. Etant donné que les mécanismes proposés pour la réaction de polymérisation font intervenir comme entité migrante le proton (11, 12, 8), il est fort probable que celui-ci est l'entité migrante de petites dimensions, permettant à la réaction d'alcoylation de se propager.

1. H. MORAWETZ. Physics and chemistry of organic solid state. Vol. I D. Fox, M. M. Labes, et A. Weissberger, Editeurs. Interscience, New York, N.Y. 1963. p. 287.
2. H. MORAWETZ. Science, **152**, 705 (1966).
3. G. ADLER, Editeur. Organic solid state chemistry. Gordon and Breach Science Publishers, New York, N.Y. 1969.
4. R. S. MILLER, D. Y. CURTIN, et I. C. PAUL. J. Am. Chem. Soc. **93**, 2784 (1971).
5. D. AMEROS. Chem. Ber. **89**, 463 (1956).
6. H. STAUDINGER et M. BRUNNER. Helv. Chem. Acta, **13**, 1375 (1930).
7. V. N. IPATIEFF et H. PINES. J. Org. Chem. **1**, 467 (1936).
8. M. KATSUNO. J. Soc. Chem. Ind. Japan, **44**, 831 (1941); **45**, 523 (1942).
9. G. H. STILLSON, D. W. SAWYER, et C. K. HUNT. J. Am. Chem. Soc. **67**, 303 (1945).
10. R. W. G. PRESTON. Brevet anglais, 833 022 (1960).
11. F. C. WHITMORE. J. Am. Chem. Soc. **54**, 3274 (1932).
12. M. ST. C. FLETT et P. M. PLESCH. J. Chem. Soc. 3355 (1952).

Can. J. Chem. Downloaded from www.nrcresearchpress.com by 210.87.254.40 on 09/05/12
For personal use only.

Can. J. Chem. Downloaded from www.nrcresearchpress.com by 210.87.254.42 on 09/05/12
For personal use only.

Application of Cusp-Satisfying Orbitals to Some Two-Electron Systems

J. E. BROWN[1] AND D. P. CHONG

Department of Chemistry, University of British Columbia, Vancouver 8, British Columbia

Received April 5, 1972

The kind of cusp-satisfying orbitals used earlier for the lithium atom is tested on the helium isoelectronic series and the hydrogen molecule. Excellent values are obtained for the electron density at the nucleus, $Q^e(0)$, for the atoms. The results for various wavefunctions for the hydrogen molecule are not as systematic, but are still quite reasonable.

Nous appliquons le type d'orbitales (cusp-satisfying), utilisées précédemment pour l'atome de lithium, aux séries isoélectroniques de l'hélium et à la molécule d'hydrogène. Nous obtenons ainsi d'excellentes valeurs pour la densité électronique au noyau $Q^e(0)$ des atomes. Les résultats concernant les différentes fonctions d'onde de la molécule d'hydrogène ne sont pas aussi systématiques, mais sont toutefois raisonnables.

[Traduit par le journal]

Canadian Journal of Chemistry, **50**, 2887 (1972)

Introduction

In a recent paper, Chapman and Chong (1) defined a cusp remainder operator for the coalescence of the ith electron with nucleus A as

$$[1] \quad R_A(i) = \lim_{r_{iA}\to 0} (Z_A + \partial/\partial r_{iA})(4\pi)^{-1} \int d\Omega_{iA}$$

Among the hierarchy of cusp conditions, they decided to impose the cusp constraint

$$[2] \quad R_A\varphi_j = 0$$

on the one-electron basis orbitals $\{\varphi\}$. If each φ_j is expanded as a linear combination of Slater-type orbitals (S.t.o.)

$$[3] \quad \varphi_j = \sum_k a_{jk}\chi_k$$

then, eqs. 2 and 3 can be expressed alternatively as

$$[4] \quad \varphi_j = \sum_{k\neq l} a_{jk}\xi_k$$

$$[5] \quad \xi_k = \chi_k - (R_A\chi_k)(R\chi_l)^{-1}\,\chi_l$$

where χ_l is any S.t.o. for which $R_A\chi_l$ is not zero.

In the calculation of the electron and spin densities at the nucleus of the ground-state lithium atom, Chapman and Chong (1) found that very simple wavefunctions[2] constructed from cusp-satisfying orbitals give excellent results. On the other hand, Poling and co-workers (2) did not find cusp satisfaction as useful.

The purpose of this work is to test the effect of similar cusp-satisfying orbitals on the calculated electron densities at the nucleus, $Q^e(0)$, for some two electron systems.

He Isoelectronic Series

In this study, we follow the procedure of Chapman and Chong (1): (*a*) simple wavefunctions Φ are chosen from the literature; (*b*) each 1s S.t.o. is augmented[3] with a "spike" function δ (*i.e.*, a 1s orbital with an unusually large exponent)

$$[6] \quad \xi_{1s} = 1s - (R_A 1s)(R_A\delta)^{-1}\,\delta$$

(*c*) the expansion in eq. 4 is limited to a single term, so that $\varphi_j = \xi_j$; (*d*) cusp-satisfying wavefunctions Ψ are constructed by replacing each 1s orbital in the original wavefunction Φ with φ_{1s}; (*e*) the orbital exponent of each spike function ζ_δ is optimized; (*f*) the resulting wavefunctions are then scaled with a uniform scale

[1]Present address: Department of Chemistry, College of the Holy Cross, Worcester, Mass., 01610 U.S.A.

[2]The expansion in eq. 4 is limited to a single term.

[3]For comparison, Bishop (3) augmented one-center orbitals with a special cusp-satisfying function ψ: χ = (one-center orbital) + $a\psi$, where a is determined variationally and $R_A\chi \neq 0$.

Can. J. Chem. Downloaded from www.nrcresearchpress.com by 210.87.254.42 on 09/05/12
For personal use only.

TABLE 1. Properties of various wavefunctions Ψ_i for ground-state helium isoelectronic series*

i	Z	k	k'	η	$E(\Psi_i)$	$E(\Phi_i)$
1	1	3.118	—	0.872382	−0.48325674	−0.47265625
	2	2.967	—	0.960612	−2.8569855	−2.8476562
	3	2.935	—	0.976387	−7.2317451	−7.222656
	4	2.918	—	0.983071	−13.606653	−13.597656
	5	2.910	—	0.986826	−21.981593	−21.972656
	6	2.918		0.989324	−32.356505	−32.347656
2	1	5.269	12.037	0.994789	−0.51351509	−0.51330289
	2	8.979	7.906	0.995460	−2.8761300	−2.8756614
	3	8.032	7.145	0.996601	−7.2493184	−7.2487480
	4	6.942	6.571	0.997111	−13.623596	−13.622965
	5	5.521	5.850	0.997286	−21.998193	−21.997539
	6	4.226	5.093	0.997504	−32.372851	−32.372271
3	1	13.202	12.076	0.995080	−0.52474909	−0.52457420
	2	9.659	7.874	0.995483	−2.8956805	−2.8952278
	3	8.447	7.244	0.996739	−7.2703100	−7.2697602
	4	8.078	7.081	0.997450	−13.645183	−13.644592
	5	7.908	6.990	0.998063	−22.020121	−22.019506
	6	7.855	6.953	0.998427	−32.395088	−32.394456

*The energies for Φ_i are also listed for comparison. The exact energies for $Z = 1$ to 6 are (ref. 5): −0.52775102, −2.9037244, −7.2799134, −13.655566, −22.030972 and −32.406247, respectively.

TABLE 2. % errors* in $Q^e(0)$ for the helium isoelectronic series

	% error in $Q^e(0)$					
Z	Φ_1	Ψ_1	Φ_2	Ψ_2	Φ_3	Ψ_3
1	−37.1	−20.0	−2.0	−0.12	−4.3	−1.3
2	−15.5	−6.8	−3.3	−0.19	−3.7	−0.53
3	−9.8	−4.1	−2.4	−0.07	−2.6	−0.22
4	−7.2	−3.0	−1.9	−0.05	−1.9	−0.12
5	−5.7	−2.3	−1.5	−0.10	−1.6	−0.07
6	−4.7	−1.9	−1.3	−0.23	−1.4	−0.04

*See text.

factor η to minimize the energy; (g) finally, we calculate the electron densities at the nucleus, $Q^e(0)$.

For the helium isoelectronic series, with $Z_A = 1$ through 6, the simple wavefunctions chosen are

$$\Phi_1 = 1s^2 \quad [7]$$

$$\Phi_2 = 1s1s' + 1s'1s \quad [8]$$

$$\Phi_3 = 1s1s' + 1s'1s + c2p^2 \quad [9]$$

taken from Silverman *et al.* (4). All computations were performed in double precision on an IBM 360/67 computer. The cusp-satisfying wavefunctions Ψ_1, Ψ_2, and Ψ_3 are presented in Table 1. The ratio of δ and 1s orbital exponents is given by k; that of δ' and 1s' exponents, by k'. When a 1s' orbital is present, we choose $\zeta_{1s} > \zeta_{1s'}$. It is interesting to note that the "spike" function for Ψ_1 is not as sharply peaked as those in Ψ_2 and Ψ_3. On the other hand, the energy improvements are about 0.01 atomic units in going from Φ_1 to Ψ_1, but are less than 0.001 for the other two functions. We are inclined to conclude that δ in Ψ_1 acts partly as an additional basis orbital while it is making Ψ_1 satisfy the cusp condition.

Finally, the calculated $Q^e(0)$ are summarized in Table 2. For the purpose of comparison, we have made use of the accurate values obtained by Pekeris (6–9) and listed the percentage errors[4] only. It is gratifying to see that our procedure of satisfying the cusp condition has led to improvements in the calculated $Q^e(0)$ in

[4]% error in $Q^e(0) = 100 \times$ (calculated − Pekeris)/(Pekeris).

TABLE 3. Properties of various wavefunctions Ψ_i for ground-state H_2*

i	R	k	k'	η	$E(\Psi_i)$	$E(\Phi_i)$
4	1.3856	4.160	—	1.000207	−1.1282301	−1.1282296
5	1.4142	1.754	—	1.026404	−1.1475445	−1.1390813
6	1.4303	2.957	—	1.002528	−1.1482577	−1.1479359
II	1.40	12.998	2.866	1.004923	−1.1320421	−1.1314919
IV	1.40	9.832	3.027	1.013174	−1.1510632	−1.1501573
VII	1.40	14.065	2.896	1.004478	−1.1427662	−1.1421476
VIII	1.40	10.433	2.956	1.013329	−1.1606712	−1.1597294

*The energies for Φ_i are also listed for comparison. The exact energy at $R = 1.4011$ a.u. is −1.1744746 a.u. (ref. 14).

all eighteen cases considered. The improvements of Ψ_1 over Φ_1 are the least drastic and may be associated with the low values of ζ_δ already discussed. On the other hand, the % errors in $Q^e(0)$ for the other two wavefunctions are reduced by an order of magnitude! For comparison, the % error in $Q^e(0)$ calculated from Clementi's 5-term self-consistent field wavefunction for helium (10) is −0.69% (11).

Hydrogen Molecule

A slight modification was made in our procedure for H_2. Instead of eq. 6, we write

$$[10] \qquad \varphi_A = 1s_A + \lambda\delta_A + \mu\delta_B$$

$$[11] \qquad \varphi_B = 1s_B + \lambda\delta_B + \mu\delta_A$$

where λ and μ are determined from

$$[12] \qquad R_A\varphi_A = 0 = R_B\varphi_A$$

Among the numerous wavefunctions for the hydrogen molecule available in the literature, we have chosen two sets. The first set, Φ_4, Φ_5, and Φ_6, includes the usual minimal-basis Coulson molecular-orbital (m.o.), Wang valence-bond (v.b.), and Weinbaum configuration-interaction (c.i.) wavefunctions, respectively. However, we use the parameters obtained by Benston and Kirtman (12). The second set, Φ_{II}, Φ_{IV}, Φ_{VII}, and Φ_{VIII}, were taken from the c.i. study of McLean *et al.* (13), with the same Roman designation.[5] The presence of 2s orbitals would complicate our procedure and therefore those wavefunctions containing them were omitted. Otherwise, the parameters of McLean *et al.* at $R = 1.40$ a.u. were used.

TABLE 4. % errors* in $Q^e(0)$ and in $\langle\delta(r_{1A})\delta(r_{2B})\rangle$ for ground-state H_2

	$Q^e(0)$		$\langle\delta(r_{1A})\delta(r_{2B})\rangle$	
i	Φ_i	Ψ_i	Φ_i	Ψ_i
4	−0.72	−0.84	−18.4	−18.4
5	−2.76	−1.11	+46.5	+10.2
6	+0.54	−0.65	+30.1	+15.8
II	+5.67	−1.58	−20.0	−27.2
IV	+7.40	+2.58	+26.7	+15.2
VII	+5.15	−2.17	−20.4	−27.8
VIII	+6.84	+1.73	+24.6	+12.8

*See text.

The cusp-satisfying wavefunctions are presented in Table 3. The calculated $Q^e(0)$ are listed in Table 4 again as percentage errors, based on the accurate value of 0.22990 obtained at $R = 1.4011$ a.u. by Kolos and Wolniewicz (14). Although these results are not as systematic as those for the atoms, they are still fairly reasonable. Except when the percentage error in $Q^e(0)$ is less than 1% in magnitude, the introduction of cusp-satisfying orbitals improves the calculated $Q^e(0)$.

Finally, the expectation values $\langle\delta(r_{1A})\delta(r_{2B})\rangle$ were also calculated for these wavefunctions. The percentage errors based on the accurate value of 0.0637 are also listed in Table 4.[6] These disappointing results are somewhat surprising. The only trend seems to be a decrease of $\langle\delta(r_{1A})\delta(r_{2B})\rangle$ in going from Φ_i to Ψ_i.

The authors are grateful to the National Research Council of Canada for financial support.

1. J. A. CHAPMAN and D. P. CHONG. Can. J. Chem. **48**, 2722 (1970).

[5] $\Phi_{II} = (\sigma_g1s, \sigma_g1s')$; $\Phi_{IV} = (\sigma_g1s, \sigma_g1s') + a(\sigma_u1s, \sigma_u1s')$; $\Phi_{VII} = (\sigma_g1s, \sigma_g1s') + b(\pi_u2p)^2$; $\Phi_{VIII} = (\sigma_g1s, \sigma_g1s') + c_1(\sigma_u1s, \sigma_u1s') + c_2(\pi_u2p)^2$.

[6] This value was obtained from the 50-term Kolos–Roothaan wavefunction (see ref. 15) as well as from the 50-term James–Coolidge function (16).

Can. J. Chem. Downloaded from www.nrcresearchpress.com by 210.87.254.42 on 09/05/12
For personal use only.

2. S. M. POLING, E. R. DAVIDSON, and G. VINCOW. J. Chem. Phys. **54**, 3005 (1971).
3. D. M. BISHOP. J. Chem. Phys. **40**, 1322 (1964).
4. J. N. SILVERMAN, O. PLATAS, and F. A. MATSEN. J. Chem. Phys. **32**, 1402 (1960).
5. K. FRANKOWSKI and C. L. PEKERIS. Phys. Rev. **146**, 46 (1966).
6. C. L. PEKERIS. Phys. Rev. **112**, 1649 (1958).
7. C. L. PEKERIS. Phys. Rev. **115**, 1216 (1959).
8. C. L. PEKERIS. Phys. Rev. **126**, 143 (1962).
9. C. L. PEKERIS. Phys. Rev. **126**, 1470 (1962).
10. E. CLEMENTI. IBM J. Res. Dev. Suppl. **9**, 2 (1965).
11. D. P. CHONG and D. M. SCHRADER. Mol. Phys. **16**, 137 (1969).
12. M. L. BENSTON and B. KIRTMAN. J. Chem. Phys. **44**, 119 (1966).
13. A. D. MCLEAN, A. WEISS, and M. YOSHIMINE. Rev. Mod. Phys. **32**, 211 (1960).
14. W. KOLOS and L. WOLNIEWICZ. J. Chem. Phys. **41**, 3663 (1964).
15. M. BARFIELD and D. M. GRANT. Adv. Mag. Res. **1**, 149 (1965).
16. D. E. O'REILLY. J. Chem. Phys. **36**, 274 (1962); **38**, 2582 (1963).

Electric Moments and Conformations of ortho-, meta-, and para-Fluorobenzaldehyde

E. BOCK

Parker Chemistry Laboratory, University of Manitoba, Winnipeg, Manitoba

AND

E. TOMCHUK

Department of Physics, University of Winnipeg, Winnipeg, Manitoba

Received April 27, 1972

The dipole moments of ortho-, meta-, and para-fluorobenzaldehyde were determined in dilute benzene solutions at 25 °C. The experimental data are in complete agreement with the conclusions reached by Wasylishen and Schaefer (1), *viz.* the *O-trans* conformer is the more stable conformer for ortho- and meta-fluorobenzaldehyde.

Les moments dipolaires de l'ortho-, méta-, et para-fluorobenzaldéhyde ont été déterminés en solution benzénique diluée à 25 °C. Les données expérimentales sont en accord total avec les conclusions de Wasylishen et Schaefer (1) à savoir que le conformère *O-trans* est le plus stable pour l'ortho- et méta-fluorobenzaldéhyde. [Traduit par le journal]

Canadian Journal of Chemistry, **50**, 2890 (1972)

Introduction

In a recent paper, Wasylishen and Schaefer (1) concluded on the basis of n.m.r. data and INDO calculations that the *O-trans* conformer was the more stable conformer for ortho- and meta-fluorobenzaldehyde (see Fig. 1). In their paper, Wasylishen and Schaefer suggested that electric moment measurements would provide conclusive evidence for the correct conformation of the fluorobenzaldehyde molecules. In this work we report on the electric moments of *o*-, *m*-, and *p*-fluorobenzaldehyde.

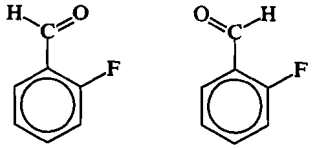

O-cis *O-trans*

FIG. 1. *o*-Fluorobenzaldehyde.

Experimental

Solvent

Fisher certified reagent benzene was used as solvent. The benzene was dried by repeated shaking with Linde molecular sieve 4A. The purity of the solvent was checked by gas chromatography as well as by determining the usual physical constants, *i.e.* the boiling point, density, and refractive index, and comparing the latter with the appropriate literature values.

Solute

The solute molecules were obtained from Pierce Chemical Co. of Rockford, Ill., and were used without further purification. The solutes used were the same solutes used

Can. J. Chem. Downloaded from www.nrcresearchpress.com by 210.87.254.42 on 09/05/12
For personal use only.

2. S. M. POLING, E. R. DAVIDSON, and G. VINCOW. J. Chem. Phys. **54**, 3005 (1971).
3. D. M. BISHOP. J. Chem. Phys. **40**, 1322 (1964).
4. J. N. SILVERMAN, O. PLATAS, and F. A. MATSEN. J. Chem. Phys. **32**, 1402 (1960).
5. K. FRANKOWSKI and C. L. PEKERIS. Phys. Rev. **146**, 46 (1966).
6. C. L. PEKERIS. Phys. Rev. **112**, 1649 (1958).
7. C. L. PEKERIS. Phys. Rev. **115**, 1216 (1959).
8. C. L. PEKERIS. Phys. Rev. **126**, 143 (1962).
9. C. L. PEKERIS. Phys. Rev. **126**, 1470 (1962).
10. E. CLEMENTI. IBM J. Res. Dev. Suppl. **9**, 2 (1965).
11. D. P. CHONG and D. M. SCHRADER. Mol. Phys. **16**, 137 (1969).
12. M. L. BENSTON and B. KIRTMAN. J. Chem. Phys. **44**, 119 (1966).
13. A. D. MCLEAN, A. WEISS, and M. YOSHIMINE. Rev. Mod. Phys. **32**, 211 (1960).
14. W. KOLOS and L. WOLNIEWICZ. J. Chem. Phys. **41**, 3663 (1964).
15. M. BARFIELD and D. M. GRANT. Adv. Mag. Res. **1**, 149 (1965).
16. D. E. O'REILLY. J. Chem. Phys. **36**, 274 (1962); **38**, 2582 (1963).

Electric Moments and Conformations of ortho-, meta-, and para-Fluorobenzaldehyde

E. BOCK

Parker Chemistry Laboratory, University of Manitoba, Winnipeg, Manitoba

AND

E. TOMCHUK

Department of Physics, University of Winnipeg, Winnipeg, Manitoba

Received April 27, 1972

The dipole moments of ortho-, meta-, and para-fluorobenzaldehyde were determined in dilute benzene solutions at 25 °C. The experimental data are in complete agreement with the conclusions reached by Wasylishen and Schaefer (1), *viz.* the *O-trans* conformer is the more stable conformer for ortho- and meta-fluorobenzaldehyde.

Les moments dipolaires de l'ortho-, méta-, et para-fluorobenzaldéhyde ont été déterminés en solution benzénique diluée à 25 °C. Les données expérimentales sont en accord total avec les conclusions de Wasylishen et Schaefer (1) à savoir que le conformère *O-trans* est le plus stable pour l'ortho- et méta-fluorobenzaldéhyde. [Traduit par le journal]

Canadian Journal of Chemistry, **50**, 2890 (1972)

Introduction

In a recent paper, Wasylishen and Schaefer (1) concluded on the basis of n.m.r. data and INDO calculations that the *O-trans* conformer was the more stable conformer for ortho- and meta-fluorobenzaldehyde (see Fig. 1). In their paper, Wasylishen and Schaefer suggested that electric moment measurements would provide conclusive evidence for the correct conformation of the fluorobenzaldehyde molecules. In this work we report on the electric moments of *o*-, *m*-, and *p*-fluorobenzaldehyde.

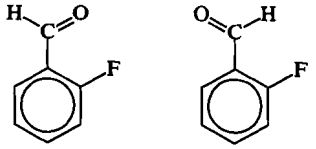

O-cis *O-trans*

FIG. 1. *o*-Fluorobenzaldehyde.

Experimental

Solvent

Fisher certified reagent benzene was used as solvent. The benzene was dried by repeated shaking with Linde molecular sieve 4A. The purity of the solvent was checked by gas chromatography as well as by determining the usual physical constants, *i.e.* the boiling point, density, and refractive index, and comparing the latter with the appropriate literature values.

Solute

The solute molecules were obtained from Pierce Chemical Co. of Rockford, Ill., and were used without further purification. The solutes used were the same solutes used

Can. J. Chem. Downloaded from www.nrcresearchpress.com by 210.87.254.6 on 09/05/12
For personal use only.

Can. J. Chem. Downloaded from www.nrcresearchpress.com by 210.87.254.6 on 09/05/12
For personal use only.

TABLE 1. Weight fraction, w, dielectric constant, ε, and refractive index, n, of benzene solutions at 25 °C

$w \times 10^{-3}$	ε	n
o-Fluorobenzaldehyde		
1.005	2.2823	1.4979
2.069	2.2908	1.4979
4.650	2.3123	1.4979
6.949	2.3310	1.4979
10.601	2.3611	1.4979
m-Fluorobenzaldehyde		
0.936	2.2798	1.4979
2.838	2.2912	1.4979
5.403	2.3072	1.4979
7.597	2.3202	1.4979
10.304	2.3365	1.4979
p-Fluorobenzaldehyde		
1.309	2.2783	1.4979
3.461	2.2862	1.4979
6.677	2.2978	1.4979
7.235	2.3003	1.4979
10.374	2.3116	1.4979

by Wasylishen and Schaefer (1). Their n.m.r. analyses showed that the impurities amounted to less than 1%. In particular no presence of water or alcohol in the solutes was detected (see Fig. 2 of ref. 1).

Experimental Procedure

The dipole moment apparatus and experimental procedure have been described elsewhere (2). The experimental error in the dipole moment values is estimated to be ±0.05 D.

Results and Discussion

The experimental results are shown in Table 1. The dipole moments derived from these data by the method of Smith (3) are summarized in Table 2. Included in Table 2 are the moment values calculated from group moments (4) and using the INDO calculation as well as experimental literature values. From a perusal of Table 2 it is evident that for *o*-fluorobenzaldehyde the *O-trans* conformation is the most stable conformation and that *m*-fluorobenzaldehyde exists in benzene (a nonpolar solvent) in roughly equal proportions of *O-trans* and *O-cis* conformations. Wasylishen and Schaefer (1) found that at 31 °C in acetone solution the mole fraction of *O-cis* and *O-trans* conformer of *o*-fluorobenzaldehyde was 0.14 and 0.86, respectively. And that for *m*-fluorobenzaldehyde under similar conditions the mole fraction of the *O-cis* and *O-trans* conformer was 0.43 and 0.57, respectively. Using our experimental value for *o*-fluorobenzaldehyde at 25 °C in benzene solution and the estimated dipole moments of the *O-trans* and *O-cis* conformer for *o*-fluorobenzaldehyde derived from group moment calculations, we calculate the mole fraction of the *O-cis* conformer as 0.27 and that of the *O-trans* conformer as 0.73. A similar calculation for *m*-fluorobenzaldehyde yielded a mole fraction of 0.34 and 0.66 for the *O-cis* and *O-trans* conformer, respectively. Bearing in mind that group moment calculations are accurate to only 0.2–0.3 D at best, our experimental results may be said to be in complete agreement with the conclusions reached by Wasylishen and Schaefer (1) based on n.m.r. data.

TABLE 2. Experimental and calculated dipole moments in debye units, D

	Calculated				
	INDO		Group moments		
	O-cis	*O-trans*	*O-cis*	*O-trans*	Experimental
o-Fluorobenzaldehyde	4.32	2.95	4.22	2.52	3.07
m-Fluorobenzaldehyde	3.47	1.13	4.14	1.32	2.63
p-Fluorobenzaldehyde	—	—	2.27		2.03 1.98(5)

The financial assistance of the National Research Council of Canada is very much appreciated.

1. R. WASYLISHEN and T. SCHAEFER. Can. J. Chem. **49**, 3216 (1971).
2. E. BOCK and E. F. DOJACK. Can. J. Chem. **45**, 1097 (1967).
3. J. W. SMITH. Trans. Faraday Soc. **46**, 394 (1950).
4. C. P. SMYTH. Dielectric behavior and structure. McGraw-Hill Book Co., Inc., New York. 1955. p. 253.
5. A. L. MCCLELLAN. Tables of experimental dipole moments. W. H. Freeman and Co., San Francisco and London. 1963.

Can. J. Chem. Downloaded from www.nrcresearchpress.com by 210.87.254.6 on 09/05/12
For personal use only.

The Use of Polymer Supports in Organic Synthesis. The Synthesis of Monotrityl Ethers of Symmetrical Diols

CLIFFORD C. LEZNOFF AND JACK Y. WONG
Department of Chemistry, York University, Downsview, Ontario

Received May 15, 1972

A modified Merrifield polymer containing acid chloride groups was used in the selective synthesis of the monotrityl ethers of the symmetrical diols, HO—$(CH_2)_n$—OH, where $n = 2, 4, 6, 8$, and 10. This procedure constitutes a unique method of blocking one functional group of a completely symmetrical difunctional compound.

Une résine modifiée du type Merrifield comprenant des groupes chlorure d'acide, a été utilisée dans la synthèse sélective d'éthers monotritylés de diols symétriques HO—$(CH_2)_n$—OH avec $n = 2, 4, 6, 8$, et 10. Ce procédé constitue une méthode unique pour bloquer un groupe fonctionnel dans un composé bifonctionnel complètement symétrique. [Traduit par le journal]

Canadian Journal of Chemistry, **50**, 2892 (1972)

The use of insoluble polymer supports in the synthesis of polypeptides (1), polynucleotides (2), and even polysaccharides (3) has been well documented. The unique potential of solid phase synthesis, however, has not generally been applied to organic synthetic problems. The synthesis of a threaded carbocycle by Harrison and Harrison (4), hydrogenation on polymer supported catalysts (5), polymer supported Wittig reagents (6), and the base condensation of mixed esters (7, 8), are, however, some of the few attempts to use insoluble polymer supports to solve specific synthetic problems.

The concept of using blocking groups in organic synthesis is well established. For example, the use of trityl chloride in specifically blocking only the 5′-hydroxyl group of deoxyribonucleosides is well known (9), but this procedure depends on the fact that the 5′-hydroxyl group is a primary alcohol and hence reacts much faster than the 3′-hydroxy group which is a secondary alcohol. It is this difference in the nature of the alcohol groups that allows selective blocking to occur. In this communication, we propose a general method whereby one can selectively block one alcohol group of a completely symmetrical diol.

The selective blocking of one functional group of a completely symmetrical difunctional compound can be accomplished using functionalized insoluble polymer containing acid chloride available Merrifield resin (2% cross-linked polystyrene beads with 1.7 mmol of —CH_2Cl groups per gram of resin, obtained from Schwarz/Mann) was modified, according to the procedure of Kusama and Hayatsu (10), to an insoluble polymer containing acid chloride groups, Ⓟ—C_6H_4—CH_2COCl (**1**). The acid chloride **1** contained 0.8 mequiv Cl^1/g of polymer as determined by the modified Vollhard procedure (11). Polymer **1** contains only one in six functionalized phenyl groups along the polymer chain and hence the acid chloride polymer **1** acts as a dilute reagent.

In a typical experiment, 4.2 g of resin **1** and 4.0 g of 1,4-butanediol (**2***b*) in 40 ml of pyridine were stirred for 48 h at room temperature and for 24 h at 105 °C, to yield a resin ester (**3***b*) in which the diol is attached to the polymer by only one of the alcohol moieties.[1] The use of the insoluble polymer support allows one to use a large excess of diol, the excess of which can be recovered, after reaction has occurred, by simple filtration of the polymer. The quantity

[1]The possibility exists that two adjacent phenyl rings are functionalized and hence both ends of the symmetrical diol (**2***b*) could attach themselves to the polymer. Although Kraus and Patchornik have demonstrated that this in fact can happen (7), the use of a large excess of diol greatly diminishes the chance of this occurring.

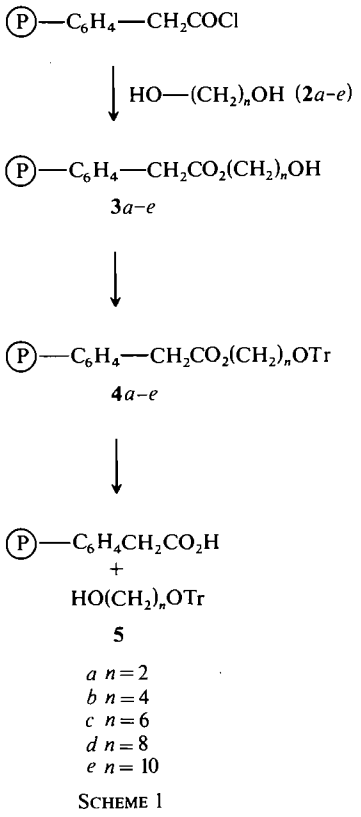

SCHEME 1

of diol **2***b* attached to the polymer was determined by hydrolysis of 4.7 g of resin **3***b* with 20 ml of a 1:1 mixture of dioxane and concentrated ammonia for 94 h. The recovery of 78.5 mg of diol **2***b* showed that the polymer **1** has a capacity of being charged with 0.20 mmol of **2***b* per gram.

Reaction of resin ester **3***b* with trityl chloride in pyridine (9, 12) gave the resin trityl ether (**4***b*). Hydrolysis of 3.71 g of **4***b* as described above and purification on t.l.c. gave 90 mg of 1-*O*-trityl-1,4-butanediol (**5***b*) in 37% yield based on amount of diol charged on the polymer. The properties and yields of a series of 1-*O*-trityl-1,*n*-alkanediols, synthesized by the polymer support method are listed in Table 1. Hydrolysis of **5***a–e* with 80% acetic acid led to quantitative recovery of trityl alcohol and starting diols **2***a–e* (9).

As shown in Table 1, only the monotrityl ether of ethylene glycol (**2***a*) had been previously prepared by classical methods (12). It is interesting to note that the yield of compound **2***a* was not recorded (12). Our own attempts to prepare the monotrityl ether of 1,10-decanediol (**5***e*) by classical methods (12) gave a mixture of four compounds, **2***e*, **5***e*, di-*O*-trityl-1,10-decanediol, and trityl alcohol, which proved difficult to separate even by preparative t.l.c.

TABLE 1. Physical data of 1-*O*-trityl-1,*n*-alkanediols

Compound*	M.p. (°C)	Yield (mmol/g polymer)	Yield† (%)
TrO(CH2)2OH	95–96‡	0.087	44
TrO(CH2)4OH	65–67	0.074	37
TrO(CH2)6OH	68–69	0.085	47
TrO(CH2)8OH	oil	0.072	51
TrO(CH2)10OH	oil	0.048	51

*All compounds showed satisfactory elemental analyses.
†Based on amount of diol released from the polymer on base hydrolysis.
‡Literature 98–100° (12).

The modification of one functional group of symmetrical difunctional compounds by the use of insoluble polymer supports will be further explored.

We thank the National Research Council of Canada for a grant in aid of this research.

1. R. B. MERRIFIELD. J. Am. Chem. Soc. **85**, 2149 (1963); R. B. MERRIFIELD. Sci. **150**, 178 (1965).
2. R. L. LETSINGER and V. MAHADEVAN. J. Am. Chem. Soc. **88**, 5319 (1966).
3. J. M. FRECHET and C. SCHUERCH. J. Am. Chem. Soc. **93**, 492 (1971).
4. I. T. HARRISON and S. HARRISON. J. Am. Chem. Soc. **89**, 5724 (1967).
5. R. H. GRUBBS and LEROY C. KROLL. J. Am. Chem. Soc. **93**, 3063 (1971); R. L. LAZCANOT and J. E. GERMAIN. Bull. Chim. Soc. Fr. 1869 (1971).
6. F. CAMPS, J. CASTELLS, J. FONT, and F. VELA. Tetrahedron Lett. 1715 (1971); S. V. MCKINLEY and J. W. RAKSHYS Jr. Chem. Commun. 134 (1972).
7. M. A. KRAUS and A. PATCHORNIK. J. Am. Chem. Soc. **93**, 7325 (1971).
8. J. I. CROWLEY and H. RAPOPORT. J. Am. Chem. Soc. **92**, 6363 (1970).
9. A. M. MICHELSON and A. R. TODD. J. Chem. Soc. 951 (1953); G. WEIMANN and H. G. KHORANA. J. Am. Chem. Soc. **84**, 419 (1962).
10. T. KUSAMA and H. HAYATSU. Chem. Pharm. Bull. **18**, 319 (1970).
11. J. M. STEWART and J. D. YOUNG. Solid phase peptide synthesis. W. H. Freeman, San Francisco. 1969. p. 27; P. B. HAWK, B. L. OSER, and W. H. SUMMERSON. Practical physiological chemistry. 13th ed. Blakiston, 1954. p. 955.
12. B. HELFERICH, P. E. SPEIDEL, and W. TOELDTE. Chem. Ber. **56**, 769 (1923).

Can. J. Chem. Downloaded from www.nrcresearchpress.com by 210.87.254.6 on 09/05/12
For personal use only.

Sulfur-free Penicillin Derivatives. I. Functionalization at C-5

SAUL WOLFE,[1] WHA SUK LEE, GÉRARD KANNENGIESSER, AND JEAN-BERNARD DUCEP
Department of Chemistry, Queen's University, Kingston, Ontario

Received May 17, 1972

Direct chlorination of an anhydropenicillin produces a sulfur-free dichloride in which the two C—S bonds are replaced by two C—Cl bonds. The reaction is general for anhydropenicillins and proceeds with predominant retention of configuration at C-5 except in the case of anhydro-6-phthalimidopenicillin, which gives variable stereochemical results.

Hydrolysis of the COCl function to COOH, conversion of the acids or acid chlorides to methyl, *t*-butyl, and benzhydryl esters, and regeneration of the acids from the latter two esters are described.

Nucleophilic substitution at C-5 of these compounds proceeds smoothly and with inversion of configuration. The rate of the reaction depends on the C-6 substituent in the direction H_2N > acylamino > phthalimido.

La chloration directe de l'anhydropénicilline conduit à un dérivé dichloré avec absence de soufre, dans lequel les deux liaisons C—S sont remplacées par deux liaisons C—Cl. Cette réaction est générale pour les anhydropénicillines et se fait avec prédominance de rétention de configuration sur le C-5, sauf dans le cas de l'anhydro phtalimido-6 pénicilline qui donne des résultats variables concernant la stéréochimie.

L'hydrolyse de la fonction COCl en COOH, la conversion des acides ou chlorures d'acides en esters méthylique, t-butylique et diphenyl méthylique et la regénération des acides à partir de ces deux derniers esters, sont décrites.

La substitution nucléophile au niveau du C-5 de ces composés se fait de façon douce, avec inversion de configuration. La vitesse de la réaction dépend du substituant sur le C-6, avec dans l'ordre NH_2 > acylamino > phtalimido. [Traduit par le journal]

Canadian Journal of Chemistry, **50**, 2894 (1972)

There is much current interest in chemical modifications of the penicillin nucleus which retain the β-lactam ring (1). Most of these transformations produce compounds which also retain the sulfur atom, but there are three exceptions (2–4) which are relevant to the work reported here and in the accompanying communications (5). In the work of Kukolja (4), shown in eq. 1, both C5-epimers[2] of **2** were obtained in crystalline form, but the epimers of **3** were not,[3] and the reaction conditions indicate that fission of the *thiazolidine* ring requires careful attention to experimental detail.

We report here a *general* reaction of *anhydro*-penicillins which, like that shown in eq. 1, involves a chlorinolysis. In the present reaction, quantitative conversion to sulfur-free compounds is achieved and, with the exception

[1]

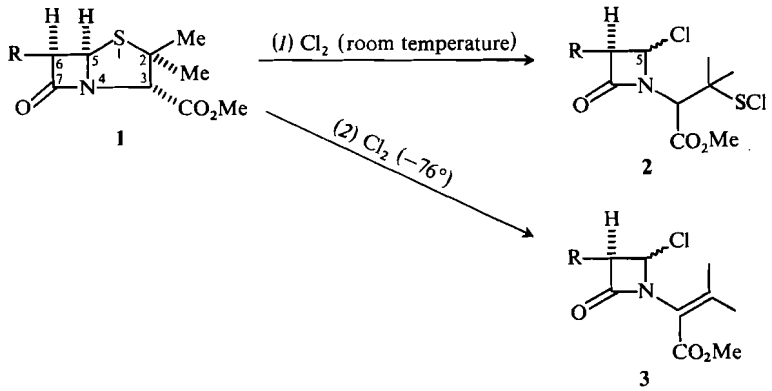

[1]This work was presented in the Merck, Sharp and Dohme Award Lecture, Quebec City, Quebec, June, 1972.
[2]The penicillin numbering system is employed here (*cf.* **1**).
[3]A 4:1 mixture of 5S:5R epimers was obtained "in high yield".

Can. J. Chem. Downloaded from www.nrcresearchpress.com by 210.87.254.40 on 09/05/12
For personal use only.

Can. J. Chem. Downloaded from www.nrcresearchpress.com by 210.87.254.40 on 09/05/12
For personal use only.

of anhydro-6-phthalimidopenicillin[4] (**4***a*; see below), the opposite stereoselectivity is observed, *i.e.*, the **R** configuration predominates at C-5. In addition, careful control of solvent composition, temperature, and chlorine concentration is not necessary. Thus, direct chlorination (excess chlorine, CH_2Cl_2, 20°, 3 min) of **4***a*, followed by removal of the solvent under reduced pressure, afforded a quantitative yield (by n.m.r.) of a 3:2 mixture of two isomeric compounds (**5***a* and **6***a*). The major isomer **5***a*, m.p. 210° (dec.), was crystallized from $CHCl_3$–petroleum ether, λ_{max} ($CHCl_3$) 242 (10 000).

Anal. Calcd. for $C_{16}H_{12}N_2O_4Cl_2$: C, 52.3; H, 3.31; N, 7.69; Cl, 19.4. Found: C, 52.03; H, 2.96; N, 7.76; Cl, 19.53.

The i.r. spectrum (KBr) of **5***a* (and of the mixture of **5***a* and **6***a*) shows peaks at 5.48 (COCl), 5.55 (β-lactam), 5.62, 5.79 μ (phthalimido). The n.m.r. spectrum[5] has peaks at 2.13 (4H, d), 3.78 (1H, d, 4.2 Hz), 4.75 (1H, d, 4.2 Hz), 7.57 (3H, s), 7.65 (3H, s).

The relative amounts of **5***a* and **6***a* were not significantly affected by chlorination in the presence of excess $Et_4N^+Cl^-$ or by a change in the temperature of the reaction; other chlorinating agents (SO_2Cl_2, pyridinium trichloride, pyrrolidone hydrotrichloride) gave more complex mixtures.

Interestingly, in some reactions, under otherwise identical experimental conditions, the opposite stereoselectivity[4] was obtained. The difference appears to be related to the origin and purity of the starting material **4***a*. The R stereoselectivity described above was achieved from **4***a* prepared by rearrangement (1*a*) of the penicillanic acid, and containing trace amounts (*ca.* 1%) of *N*-carboethoxyphthalimide (7). In contrast a 3:1 5S:5R ratio of epimers was obtained following chlorination of rigorously purified **4***a* or **4***a* prepared from anhydrotritylaminopenicillin (1*b*). The pure dichloride **6***a* could be isolated from such mixtures.

Hydrolysis of **5***a* (boric acid – borax buffer

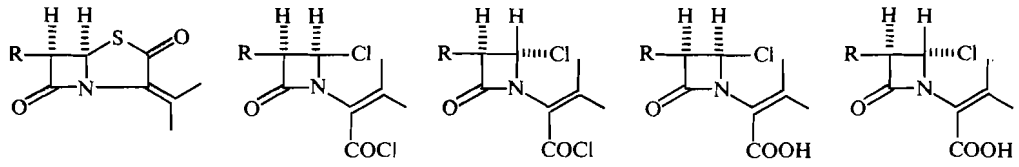

4 **5** **6** **7** **9**

4–9: *a*, R = $C_6H_4(CO)_2N$; *b*, R = $TsOH{\cdot}H_2N$; *c*, R = $C_6H_5CH_2CONH$; *d*, R = $C_6H_5CH_2OCONH$; *e*, R = CCl_3CH_2OCONH

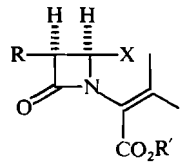

8

a R = $C_6H_4(CO)_2N$; R′ = CH_3; X = Cl
b R = $C_6H_4(CO)_2N$; R′ = *t*-C_4H_9; X = Cl
c R = $C_6H_5CH_2CONH$; R′ = CH_3; X = Cl
d R = $TsOH{\cdot}H_2N$; R′ = CH_3; X = Cl
e R = H_2N; R′ = CH_3; X = Cl
f R = $C_6H_4(CO)_2N$; R′ = CH_3; X = N_3
g R = $C_6H_4(CO)_2N$; R′ = CH_3; X = OAc
h R = H_2N; R′ = CH_3; X = N_3
i R = $C_6H_5CH_2CONH$; R′ = CH_3; X = N_3

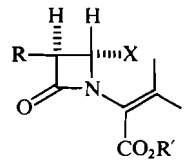

10

a R = $C_6H_5(CO)_2N$; R′ = CH_3; X = Cl
b R = $C_6H_5(CO)_2N$; R′ = $CH(C_6H_5)_2$; X = Cl
c R = $C_6H_5(CO)_2N$; R′ = *t*-C_4H_9; X = Cl
d R = $C_6H_5(CO)_2N$; R′ = CH_3; X = N_3
e R = H_2N; R′ = CH_3; X = Cl
f R = H_2N; R′ = CH_3; X = N_3
g R = $C_6H_5CH_2CONH$; R′ = CH_3; X = N_3

[4]Phthalimidopenicillanic acid and its derivatives often display different chemical properties from the (biologically more significant) 6-acylaminopenicillanic acids (2*b*, *c*, 6).

[5]Unless otherwise mentioned, all n.m.r. spectra were recorded in $CDCl_3$ at 60 MHz. Chemical shifts are given in τ values relative to internal TMS. Although, to conserve space, spectroscopic data are not quoted in detail for all new compounds, all of these gave i.r., n.m.r., and high resolution mass spectra in full accord with the assigned structures and stereochemistry. In addition, all crystalline compounds gave satisfactory elemental analyses (C, H, N, Cl).

Can. J. Chem. Downloaded from www.nrcresearchpress.com by 210.87.254.40 on 09/05/12
For personal use only.

(8), aqueous acetone, or aqueous THF) gave the acid **7***a*, m.p. 168–174° (dec.) in 73–90% yield. Methylation of **7***a* (CH_2N_2, Et_2O–CH_2Cl_2) produced the ester **8***a*, m.p. 178–180° (dec.), $[\alpha]_D^{20}$ −8.9° ($CHCl_3$) in 97% yield. The same compound was obtained from **5***a* in 93% yield upon treatment with absolute methanol (30 min, 20°). Similarly, hydrolysis of **6***a* afforded the acid **9***a*, m.p. 164–166° (dec.), which was converted to the corresponding methyl ester **10***a*, m.p. 192–194°, $[\alpha]_D^{20}$ −144° ($CHCl_3$).

The *t*-butyl ester **8***b* was obtained in 33% yield by *refluxing* **5***a* in anhydrous *t*-BuOH for 21 h. The C5-epimer **10***c*, prepared similarly, melted at 170–172°. Dissolution of **8***b* in trifluoroacetic acid (TFA), and evaporation of the solvent after 3 min, gave **7***a* in quantitative yield. The benzhydryl ester **10***b*, prepared (Ph_2CN_2) in 99% yield from **9***a*, also underwent ready reconversion to **9***a* upon treatment with TFA.

Anhydrotritylaminopenicillin (1*b*) decomposed during chlorination. However the derived (1*b*) *p*-toluenesulfonic acid salt **4***b* reacted smoothly to give a 4:1 5R:5S mixture of **5***b* and **6***b* as a stable (below 20°) white powder, m.p. 148–149° (dec.). Hydrolysis of this powder afforded a 4:1 mixture of the acids **7***b* and **9***b*. Phenylacetylation of this mixture ($NaHCO_3$, $PhCH_2COCl$, H_2O–CH_3COCH_3) gave the penicillin G analog **7***c*, whose methyl ester **8***c* was crystallized in 51% yield (from **4***b*), m.p. 111–115° (dec.). Alternatively, methanol treatment of the mixture of **5***b* and **6***b*, and crystallization from chloroform–hexane, produced the pure 5R ester **8***d*, m.p. 125–130° (dec.), in 67% yield (from **4***b*).

Neutralization of **8***d* and reaction of the free base **8***e*, m.p. 67–70° (dec.), with Nefkens' reagent (7) yielded **8***a*, confirming that chlorinolysis proceeds in the same manner with both side chains. Phenylacetylation of **8***e* gave **8***c* in 82% yield. This provides an alternative to the sequence **5***b* → **7***b* → **7***c* → **8***c*, and indicates that **7***b* can serve as a general intermediate for acylamino members of this class of compounds.

The anhydro derivatives (**4***c*–*e*) of benzyl, benzyloxycarbonyl,[6] and trichloroethoxycarbonylpenicillin[7] underwent ready chlorination–hydrolysis to give quantitative yields of the acids **7***c* + **9***c*, **7***d* + **9***d*, and **7***e* + **9***e*. In each case a 3–4:1 mixture of 5R (**7**): 5S (**9**) epimers was obtained and the proportion of epimers was not significantly affected by changes in the experimental conditions. Methylation of the mixture of **7***c* + **9***c* afforded **8***c*, completing the interrelation of the phthalimido, amino and acylamino series of derivatives.[8]

Equilibration of **8***a* and **10***a* proceeded smoothly, upon refluxing (acetone, 12 h; 2-butanone, 4 h) in the presence of tetraethylammonium chloride. The same equilibrium mixture, containing in all cases an excess (1.5–2.5:1) of the *trans*-isomer **10***a* was obtained starting with either pure epimer, the position of equilibrium depending upon solvent, temperature, and concentration of tetraethylammonium chloride. The compounds recovered from equilibrium mixtures were identical in all respects to those prepared directly from **4***a*.

Reaction of **8***a* with sodium azide (DMF, 90°, 3 h) afforded the 5S azide **10***d*, m.p. 144–145°, in 67% yield, uncontaminated by the 5**R** isomer **8***f*. Under the same conditions **10***a* yielded **8***f*, m.p. 183–187° in 52% yield, uncontaminated by **10***d*. With tetraethylammonium acetate ($CHCl_3$, reflux, 17 h) **10***a* gave **8***g* in 62% yield. These various observations demonstrate that nucleophilic displacement on a β-lactam ring proceeds with inversion of configuration (9).

Equilibration of **8***e* and **10***e* was best achieved (**10***e*:**8***e* = 6:1) with tetramethylguanidinium chloride (CH_2Cl_2, reflux, 12 h). Reaction of **8***e* with tetramethylguanidinium azide (10) (2 equiv, $CHCl_3$, reflux) yielded **10***f* (90%); the epimer **8***h*, m.p. 116–117°, was obtained similarly from **10***e* in 85% yield. Phenylacetylation of **8***h* ($C_6H_5CH_2COOH$, DCC, CH_2Cl_2) afforded the 5-azidopenicillin G analog **8***i*, m.p. 102–103° (97%); the C5-epimer **10***g* was obtained similarly from **10***f* or by reaction of **8***c* with tetramethylguanidinium azide (2 equiv, $CHCl_3$, reflux).

Each of the reactions **8***a* → **10***d*, **8***e* → **10***f*, **8***c* → **10***g* represents the conversion of a 5R-chloro into a 5S-azido compound. Reaction

[6]Prepared in 90% yield from **4***b*.

[7]Prepared in 85% yield from **4***b*.

[8]Structure proofs of the benzyloxycarbonyl and trichloroethoxycarbonyl acids are based on their subsequent reactions (2).

8*e* → **10***f* was complete in 0.5 h; under the same conditions **8***c* → **10***g* was complete in 2 h and **8***a* was recovered unchanged. Consequently the effect of the C6-substituent on the rate of nucleophilic displacement from C-5 is H_2N > acylamino > phthalimido.

The sequences established here provide general routes to carboxyl-protected sulfur-free penicillin derivatives, with control over the substituent at C-6 and the functionality and stereochemistry at C-5.

We thank Bristol Laboratories for financial support of this work.

1. See *inter alia* (*a*) S. WOLFE, J. C. GODFREY, C. T. HOLDREGE, and Y. G. PERRON. Can. J. Chem. **46**, 2549 (1968); (*b*) S. WOLFE. Can. J. Chem. **46**, 459 (1968); (*c*) S. WOLFE and W. S. LEE. Chem. Commun. 262 (1968); (*d*) Y. G. PERRON, L. B. CRAST, J. M. ESSERY, R. R. FRASER, J. C. GODFREY, C. T. HOLDREGE, W. F. MINOR, M. E. NEUBERT, R. A. PARTYKA, and L. C. CHENEY. J. Med. Chem. **7**, 483 (1964); (*e*) J. C. SHEEHAN and K. G. BRANDT. J. Am. Chem. Soc. **87**, 5468 (1965); (*f*) R. B. WOODWARD and K. HEUSLER. Chem. Abstr. **72**, 100689*m* (1970); (*g*) J. A. WEBBER, E. M. VAN HEYNINGEN, and R. T. VASILEFF. J. Am. Chem. Soc. **91**, 5674 (1969); (*h*) R. B. MORIN, B. G. JACKSON, R. A. MUELLER, E. R. LAVAGNINO, W. B. SCANLON, and S. L. ANDREWS. J. Am. Chem. Soc. **91**, 1401 (1969); (*i*) R. D. G. COOPER and F. L. JOSÉ. J. Am. Chem. Soc. **92**, 2575 (1970); (*j*) D. O. SPRY. J. Am. Chem. Soc. **93**, 5008 (1970); (*k*) G. V. KAISER, C. W. ASHBROOK, and J. E. BALDWIN. J. Am. Chem. Soc. **93**, 2344 (1971); (*l*) D. H. R. BARTON, D. G. T. GREIG, G. LUCENTE, P. G. SAMMES, M. V. TAYLOR, C. M. COOPER, G. HEWITT, and W. G. E. UNDERWOOD. Chem. Commun. 1683 (1970); (*m*) D. H. R. BARTON, D. G. T. GREIG, P. G. SAMMES, and M. V. TAYLOR. Chem. Commun. 845 (1971); (*n*) R. D. G. COOPER. J. Am. Chem. Soc. **94**, 1018 (1972); (*o*) R. D. G. COOPER and F. L. JOSÉ. J. Am. Chem. Soc. **94**, 1021 (1972); (*p*) L. D. CAMA, W. J. LEANZA, T. R. BEATTIE, and B. G. CHRISTENSEN. J. Am. Chem. Soc. **94**, 1408 (1972); (*q*) R. A. FIRESTONE, N. SCHELECHOW, D. B. R. JOHNSTON, and B. G. CHRISTENSEN. Tetrahedron Lett. 375 (1972).
2. (*a*) J. C. SHEEHAN. Molecular modification in drug design. Adv. in Chem. Series, No. 45. American Chemical Society, Washington, D.C., 1964. p. 15; (*b*) D. H. R. BARTON, F. COMER, and P. G. SAMMES. J. Am. Chem. Soc. **91**, 1529 (1969); (*c*) D. H. R. BARTON, F. COMER, D. G. T. GREIG, P. G. SAMMES, C. M. COOPER, G. HEWITT, and W. G. E. UNDERWOOD. J. Chem. Soc. C, 3540 (1971).
3. E. G. BRAIN, A. J. EGLINGTON, J. H. C. NAYLER, M. J. PEARSON, and R. SOUTHGATE. Chem. Commun. 229 (1972).
4. S. KUKOLJA. J. Am. Chem. Soc. **93**, 6267 (1971).
5. S. WOLFE, W. S. LEE, G. KANNENGIESSER, and J. B. DUCEP. This issue.
6. S. WOLFE, W. S. LEE, and R. MISRA. Chem. Commun. 1067 (1970).
7. G. H. L. NEFKENS. Nature, **185**, 309 (1960).
8. S. WOLFE, R. N. BASSETT, S. M. CALDWELL, and F. I. WASSON. J. Am. Chem. Soc. **91**, 7205 (1969).
9. M. D. BACHI and O. GOLDBERG. Chem. Commun. 319 (1972).
10. A. J. PAPA. J. Org. Chem. **31**, 1426 (1966).

Can. J. Chem. Downloaded from www.nrcresearchpress.com by 210.87.254.40 on 09/05/12
For personal use only.

Sulfur-free Penicillin Derivatives. II. Functionalization of the Methyl Groups

SAUL WOLFE,[1] WHA SUK LEE, JEAN-BERNARD DUCEP, AND GÉRARD KANNENGIESSER
Department of Chemistry, Queen's University, Kingston, Ontario

Received May 17, 1972

Allylic bromination of anhydropenicillin chlorination products by *N*-bromosuccinimide (NBS) is described. With two molar-equivalents of NBS both methyl groups are functionalized; with one molar-equivalent of NBS a mixture of Z and E monobrominated isomers is obtained.

Nitrogen and oxygen nucleophiles attack the dibrominated derivatives at the β-lactam carbonyl group, with concomitant ring-opening. However, the mono-brominated derivatives undergo ready displacement by azide and formate ions. The mechanism of these reactions, leading to preferred formation of Z-isomer, is discussed.

Cyclization of the allylic formates yields sulfur-free derivatives corresponding to the cephalosporin C_c class of compounds.

La bromation allylique des produits de chloration de l'anhydropénicilline par la *N*-bromosuccinimide (NBS) est décrite. Avec deux équivalents molaires de NBS les deux groupes méthyles sont fonctionnalisés en même temps; avec un seul équivalent de NBS, un mélange d'isomères Z et E de monobromation est obtenu.

Les nucléophiles azote et oxygène attaquent les dérivés dibromés au niveau du carbonyle du β-lactame, avec ouverture simultanée du cycle. Les dérivés monobromés subissent cependant un déplacement facile par les ions azoture et formiate. Le mécanisme de ces réactions, qui conduisent préférentiellement à l'isomère Z, est discuté.

La cyclisation des formiates allyliques conduisent aux dérivés, avec absence de soufre, de la classe des composés de la céphalosporine C_c. [Traduit par le journal]

Canadian Journal of Chemistry, **50**, 2898 (1972)

Anhydropenicillins (**1**) are stable to the action of lead tetraacetate and selenium dioxide (1). Reactions are observed with chlorine, *N*-bromoacetamide (2), *N*-bromosuccinimide (NBS), palladium acetate (3), and mercuric acetate (4), but in each case the products are formed by attack on nitrogen (1) or sulfur (5) rather than the double bond.

The stability of **1** towards allylic oxidation has been rationalized (1, 6, 7) in terms of enamine-type character of the carbon–carbon double bond, causing functionalization of the methyl groups to correspond to attack at the β-position of a masked carbonyl. The effect of opening of the five-membered ring (*e.g.*, **1** → **2**) on the properties of the double bond could not have been predicted *a priore*, but this question was answered by the demonstration (7) that the anhydropenicillin rearrangement can be reversed. The Michael addition **2** → **3** which must have occurred during the latter process is possible only if **2** reacts as an α,β-unsaturated acid rather than an enamine. It follows that functionalization of the methyl groups of an anhydropenicillin ought to become feasible following lysis of the five-membered ring.

In agreement with this conclusion, and in direct contrast to the recent work of Nayler and coworkers (8),[2] anhydropenicillin chlorination products (5) undergo rapid allylic bromination by NBS.[3] The reaction of **4***a* with two molar-equivalents of NBS[2] was complete within 5 min. The product **5***a* crystallized from CCl_4 – petroleum ether in 81% yield, m.p. 70–72° (dec.).[4] Under identical conditions the C_5-epimer **4***b* afforded **5***b* in 70% yield. The extraordinary facility of this oxidation is seen in the successful functionalization, under the same conditions, of **4***c*.

The methyl groups of **4***a* showed no difference

[1]This work was presented in the Merck, Sharp and Dohme Award Lecture, Quebec City, Quebec, June, 1972.

[2]These workers reported that 1,2-secopenicillins (9) do not undergo allylic oxidation with NBS or lead tetraacetate.

[3]For general reaction conditions, see ref. 2.

[4]The compositions of **5***a*, **5***b*, **6***a* + **6***b* and **7***a* + **7***b* were confirmed by elemental analysis. Other compounds were obtained in chromatographically pure form and their constitutions confirmed by high resolution mass spectrometry, in addition to their n.m.r. spectra, summarized in Table 1.

Can. J. Chem. Downloaded from www.nrcresearchpress.com by 210.87.254.6 on 09/05/12
For personal use only.

TABLE 1. Nuclear magnetic resonance spectra*

Compound	C-5 and/or C-6 Substituent	β-Lactam protons	Methylene protons	Methyl groups
5*a*	2.13	3.80, 4.21 (two doublets, 4.2 Hz)	5.07, 5.27 (10.2 Hz)† 5.23, 5.33 (10.9 Hz)	6.11
5*b*	2.08	3.62, 4.27 (two doublets, 1.7 Hz)	5.05, 5.36 (10.0 Hz)† 5.38, 5.57 (11.0 Hz)	6.04
5*c*	2.67 (5H), 3.33 (1H), 6.28 (2H)	4.32, 4.50 (two doublets, 4.0 Hz)	5.38 (2H, sl. br) 5.63 (2H, sl. br)	6.17
6*a* + **6***b*	2.20	3.83, 3.87, 4.28, 4.32 (four doublets, 4.2 Hz)	5.10–5.88 (2H) (overlapping AB quartets)	6.15, 6.17, 7.55
6*c* + **6***d*	2.17	3.78, 4.22 (two doublets, 4.0 Hz)	5.12–5.87 (2H) (overlapping quartets)	6.12, 7.58
6*e*	1.82 (1H), 2.18 (4H)	3.81, 4.28 (two doublets, 4.0 Hz)	4.64 (2H, br)	6.15, 7.67
6*f*	1.87 (1H), 2.18 (4H)	3.81, 4.28 (two doublets, 4.0 Hz)	4.64 (2H, br)	6.15, 7.70
6*g*‡	2.10	3.28, 4.03 (two doublets, 4.0 Hz)	5.03 (quartet, 0.9 Hz)	7.62 (triplet, 0.9 Hz)
7*a* + **7***b*	2.17	3.73, 4.37 (two doublets, 2 Hz)	5.27–5.67 (2H) (overlapping quartets)	6.15 (3H) 7.59 (1.2H) 7.82 (1.8H)
7*c* + **7***d*	2.17	3.76 (1H, m, overlapping doublets), 4.40 (1H, d, 2.0 Hz)	5.52, 5.58 (0.8H, quartet of one isomer), 5.87 (1.2H, br)	6.15 (3H), 7.67 (1.2H), 7.87 (1.8H)
7*e* + **7***f*	1.87, 2.19	3.73, 3.76 (two doublets, 1.9 Hz), 4.40 (d, 1.9 Hz)	4.75 (sl. br., one isomer), 4.95 5.09 (q, 13.5 Hz, other isomer)	6.12 (3H), 7.70 (1.5H), 7.88 (1.5H)
7*g*§	2.17	3.29, 4.37 (two doublets, 1.9 Hz)	5.10 (2H, q, 0.9 Hz)	7.70 (3H, t, 0.9 Hz)

*Spectra were recorded at 60 MHz, in $CDCl_3$, except where noted. Chemical shifts are given in τ values relative to internal TMS.
†Two pairs of diastereotopic protons.
‡Spectrum recorded in deuteroacetone.
§Spectrum recorded in deuteroacetone–$CDCl_3$.

in reactivity. Oxidation of this compound with one molar-equivalent of NBS afforded a crystalline 1:1 mixture of **6***a* + **6***b*. The methyl groups of **4***b* showed a slight difference in reactivity, and a 3:2 mixture of **7***a* + **7***b* was obtained from this compound.

The brominated substances described above contain the functionality found in C3-substituted cephalosporins (**8**) (10). Nucleophilic displacement at the C3-methylene group of these compounds proceeds (10) by one of two paths, shown in eqs. 1 and 2. In the present work the dibrominated derivatives **5** apparently reacted with nucleophiles (N_3^-, $OCHO^-$,[5] OH^-) via path [2], since rapid incorporation of the nucleophile was observed together with concomitant loss of the β-lactam. However, the monobrominated derivatives **6***a* + **6***b* and **7***a* + **7***b* underwent ready displacement of bromine without loss of the β-lactam, presumably via path [1].

Treatment of the mixture **6***a* + **6***b* with tetramethylguanidinium azide (**11**) (1 equiv, $CHCl_3$, 3 h, 20°) afforded a mixture of **6***c* + **6***d* (λ_{max} ($CHCl_3$) 4.7, 5.55, 5.62, 5.78, 5.79 μ). The mixture of **7***a* + **7***b* similarly afforded **7***c* + **7***d*. Alternatively the 1:1 mixture of **6***a* + **6***b* reacted with tetramethylguanidinium formate (**12**) (5 molar equivalents, $CHCl_3$, 9 h, 20°) to give, in 53% yield, a 2:1 mixture of **6***e* + **6***f*,[4] containing an excess of the Z-isomer **6***f* (λ_{max} ($CHCl_3$) 5.52, 5.58, 5.79 μ). The assignment of configurations

[5]Displacement of the C_3-acetate of cephalosporins by oxygen nucleophiles has not been observed (10).

Can. J. Chem. Downloaded from www.nrcresearchpress.com by 210.87.254.6 on 09/05/12
For personal use only.

Can. J. Chem. Downloaded from www.nrcresearchpress.com by 210.87.254.6 on 09/05/12
For personal use only.

[1]

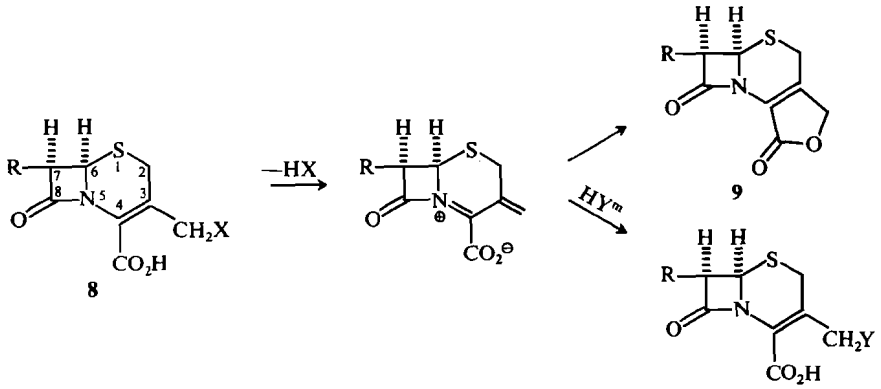

[2]

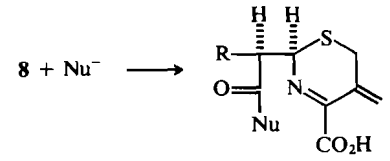

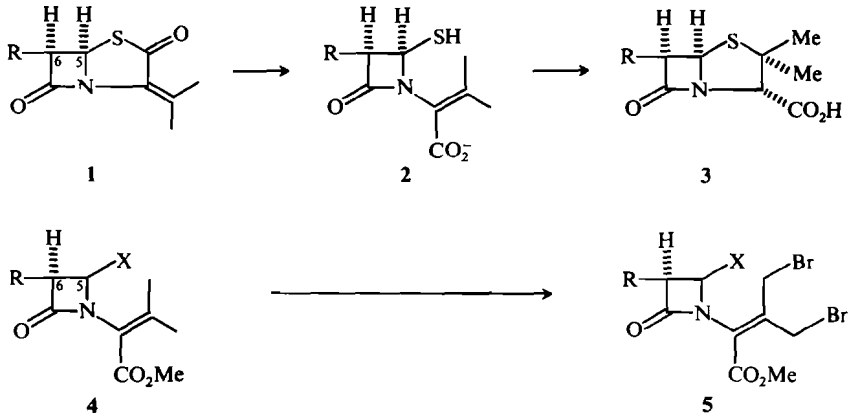

a R = $C_6H_4(CO)_2N$; X = 5R-Cl (*cis*)
b R = $C_6H_4(CO)_2N$; X = 5S-Cl (*trans*)
c R = $C_6H_5CH_2CONH$; X = 5R-N_3 (*cis*)

to **6***e* + **6***f* is based on the finding that chromatography (alkaline alumina, ethyl acetate) of the mixture gave, in 67% yield, the crystalline lactone **6***g*, m.p. 124–128° (dec.) (λ_{max} (KBr) 5.54, 5.62, 5.69, 5.79 μ). An analogous sequence on **7***a* + **7***b* afforded **7***e* + **7***f* in 70% yield as a 1:1 mixture of Z- and E-isomers; this mixture produced the lactone **7***g* in 50% yield upon treatment with alumina.

The lactones **6***g* and **7***g* are sulfur-free analogs of the cephalosporin C_c class of compounds (**9**). If displacement of bromine from the mixtures **6***a* + **6***b* or **7***a* + **7***b* does proceed via path [1], the same intermediate (**10**) will be generated from the Z- and E-isomers. This intermediate can exist in *s-trans* (**10***a*) or *s-cis* (**10***b*) conformations. In general the *s-trans* conformation is more stable (13) and inspection of molecular models suggests that the steric interaction between the methyl and carbomethoxy groups will enhance this tendency. Completion of the reaction by S_N2' attack of nucleophile on **10** should therefore lead to preferred formation of Z-isomer and, subsequently, lactone.

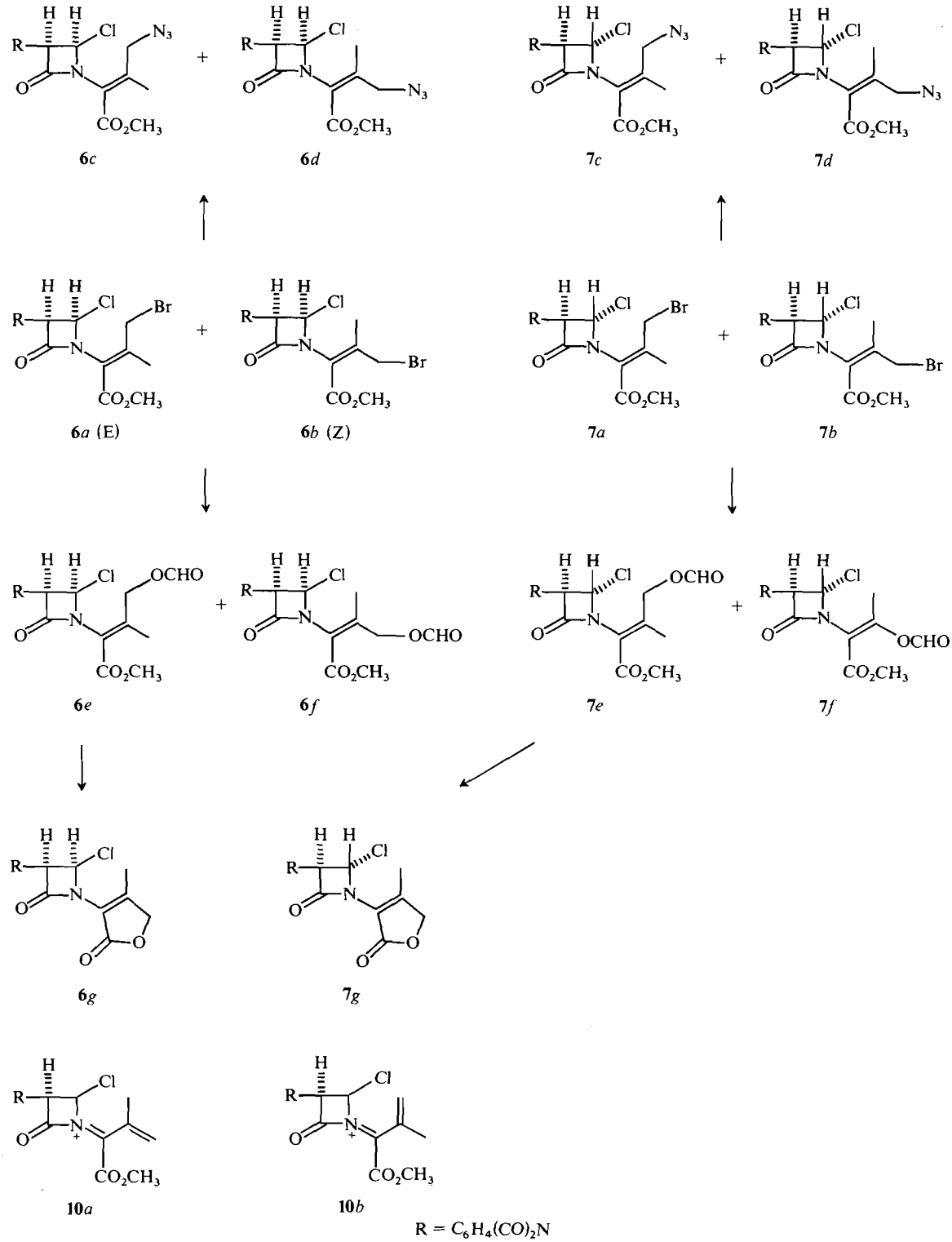

Can. J. Chem. Downloaded from www.nrcresearchpress.com by 210.87.254.6 on 09/05/12
For personal use only.

We thank Bristol Laboratories for financial support of this work.

1. S. WOLFE, C. FERRARI, and W. S. LEE. Tetrahedron Lett. 3385 (1969).
2. S. WOLFE and D. V. C. AWANG. Can. J. Chem. **49**, 1384 (1971).
3. S. WOLFE and P. G. C. CAMPBELL. J. Am. Chem. Soc. **93**, 1497 (1971).
4. S. WOLFE, P. G. C. CAMPBELL, and G. E. PALMER. Tetrahedron Lett. 4203 (1966); Z. RAPPOPORT, S. WINSTEIN, and W. G. YOUNG. J. Am. Chem. Soc. **94**, 2320 (1972).
5. S. WOLFE, W. S. LEE, G. KANNENGIESSER, and J. B. DUCEP. This issue.
6. S. WOLFE, J. C. GODFREY, C. T. HOLDREGE, and Y. G. PERRON. Can. J. Chem. **46**, 2549 (1968).
7. S. WOLFE, R. N. BASSETT, S. M. CALDWELL, and F. I. WASSON. J. Am. Chem. Soc. **91**, 7205 (1969).
8. E. G. BRAIN, A. J. EGLINGTON, J. H. C. NAYLER, M. J. PEARSON, and R. SOUTHGATE. Chem. Commun. 229 (1972).
9. J. P. CLAYTON, J. H. C. NAYLER, R. SOUTHGATE, and P. TOLLIDAY. Chem. Commun. 590 (1971).
10. R. B. MORIN and B. G. JACKSON. Progress in the chemistry of organic natural products. **29**, 343 (1971).
11. A. J. PAPA. J. Org. Chem. **31**, 1426 (1966).
12. S. WOLFE and J. B. DUCEP. To be published.
13. E. L. ELIEL, N. L. ALLINGER, S. J. ANGYAL, and G. A. MORRISON. Conformational analysis. Interscience Publishers, 1965.

Can. J. Chem. Downloaded from www.nrcresearchpress.com by 210.87.254.6 on 09/05/12
For personal use only.

Sulfur-free Penicillin Derivatives. III. Regeneration of Fused β-Lactams via Intramolecular Displacement

SAUL WOLFE,[1] JEAN-BERNARD DUCEP, GÉRARD KANNENGIESSER, AND WHA SUK LEE

Department of Chemistry, Queen's University, Kingston, Ontario

Received May 17, 1972

Recyclization of a variety of sulfur-free penicillin derivatives is described. Fused oxazoline-azetidinones, a fused oxazolidone-azetidinone, an *oxa*anhydropenicillin and an *aza*cephem have been prepared.

La recyclisation d'une variété de dérivés de la pénicilline avec absence de soufre, est décrite. Des oxazoline-azétidinones et oxazolidone-azétidinones fusionnées, une *oxa*anhydropenicilline et un *aza*céphem ont été préparés. [Traduit par le journal]

Canadian Journal of Chemistry, **50**, 2902 (1972)

Sheehan (1) and Barton *et al.* (2, 3) have reported the conversion of **1**, the methyl ester of penicillin G, into the fused β-lactam-oxazoline **2***a* upon treatment with *t*-butyl hypochlorite–triethylamine (1) or iodobenzene dichloride (2). Low yields of **2***a* were obtained in each case and it was not possible to define the mechanism of the reaction. A thiazoline analog (**3**) of **2***a* has also been prepared (4) and converted (5) to an array of penam and cephem derivatives. These latter observations have led to the interesting speculation (5) that **4** could represent a common intermediate for the biosynthesis of both penicillins and cephalosporins.

We report here rational syntheses of **2***a*, **2***b*, a trichloroethoxy analog of **2***a*, and **2***c*, an oxygen analog of **4**, via intramolecular recyclization of appropriate anhydropenicillin chlorination products (6). Various other fused β-lactam systems are also described, including the oxazolidone **5**, the 1-oxa-5-epianhydropenicillin **6** and the 1-aza-6-epicephem **7**.

Phenylacetylation of **8***a* afforded **9***a* (82%).[2] This compound cyclized in over 70% yield, upon refluxing or bicarbonate washing of a CH_2Cl_2 solution, to give **2***a*, m.p. 126.5–127° (1, 3).[2,3] The cyclization presumably proceeds by anti-displacement of chlorine by the amide oxygen (7) since, under the same conditions, the C5-epimer **9***b* is recovered unchanged.

[1]This work was presented in the Merck, Sharp and Dohme Award Lecture, Quebec City, Quebec, June, 1972.

[2]I.r. and n.m.r. spectra are in full accord with the proposed structure.

[3]Satisfactory elemental analyses or high resolution mass spectra were secured.

We thank Bristol Laboratories for financial support of this work.

1. S. WOLFE, C. FERRARI, and W. S. LEE. Tetrahedron Lett. 3385 (1969).
2. S. WOLFE and D. V. C. AWANG. Can. J. Chem. **49**, 1384 (1971).
3. S. WOLFE and P. G. C. CAMPBELL. J. Am. Chem. Soc. **93**, 1497 (1971).
4. S. WOLFE, P. G. C. CAMPBELL, and G. E. PALMER. Tetrahedron Lett. 4203 (1966); Z. RAPPOPORT, S. WINSTEIN, and W. G. YOUNG. J. Am. Chem. Soc. **94**, 2320 (1972).
5. S. WOLFE, W. S. LEE, G. KANNENGIESSER, and J. B. DUCEP. This issue.
6. S. WOLFE, J. C. GODFREY, C. T. HOLDREGE, and Y. G. PERRON. Can. J. Chem. **46**, 2549 (1968).
7. S. WOLFE, R. N. BASSETT, S. M. CALDWELL, and F. I. WASSON. J. Am. Chem. Soc. **91**, 7205 (1969).
8. E. G. BRAIN, A. J. EGLINGTON, J. H. C. NAYLER, M. J. PEARSON, and R. SOUTHGATE. Chem. Commun. 229 (1972).
9. J. P. CLAYTON, J. H. C. NAYLER, R. SOUTHGATE, and P. TOLLIDAY. Chem. Commun. 590 (1971).
10. R. B. MORIN and B. G. JACKSON. Progress in the chemistry of organic natural products. **29**, 343 (1971).
11. A. J. PAPA. J. Org. Chem. **31**, 1426 (1966).
12. S. WOLFE and J. B. DUCEP. To be published.
13. E. L. ELIEL, N. L. ALLINGER, S. J. ANGYAL, and G. A. MORRISON. Conformational analysis. Interscience Publishers, 1965.

Sulfur-free Penicillin Derivatives. III. Regeneration of Fused β-Lactams via Intramolecular Displacement

SAUL WOLFE,[1] JEAN-BERNARD DUCEP, GÉRARD KANNENGIESSER, AND WHA SUK LEE

Department of Chemistry, Queen's University, Kingston, Ontario

Received May 17, 1972

Recyclization of a variety of sulfur-free penicillin derivatives is described. Fused oxazoline-azetidinones, a fused oxazolidone-azetidinone, an *oxa*anhydropenicillin and an *aza*cephem have been prepared.

La recyclisation d'une variété de dérivés de la pénicilline avec absence de soufre, est décrite. Des oxazoline-azétidinones et oxazolidone-azétidinones fusionnées, une *oxa*anhydropenicilline et un *aza*céphem ont été préparés. [Traduit par le journal]

Canadian Journal of Chemistry, **50**, 2902 (1972)

Sheehan (1) and Barton *et al.* (2, 3) have reported the conversion of **1**, the methyl ester of penicillin G, into the fused β-lactam-oxazoline **2***a* upon treatment with *t*-butyl hypochlorite–triethylamine (1) or iodobenzene dichloride (2). Low yields of **2***a* were obtained in each case and it was not possible to define the mechanism of the reaction. A thiazoline analog (**3**) of **2***a* has also been prepared (4) and converted (5) to an array of penam and cephem derivatives. These latter observations have led to the interesting speculation (5) that **4** could represent a common intermediate for the biosynthesis of both penicillins and cephalosporins.

We report here rational syntheses of **2***a*, **2***b*, a trichloroethoxy analog of **2***a*, and **2***c*, an oxygen analog of **4**, via intramolecular recyclization of appropriate anhydropenicillin chlorination products (6). Various other fused β-lactam systems are also described, including the oxazolidone **5**, the 1-oxa-5-epianhydropenicillin **6** and the 1-aza-6-epicephem **7**.

Phenylacetylation of **8***a* afforded **9***a* (82%).[2] This compound cyclized in over 70% yield, upon refluxing or bicarbonate washing of a CH_2Cl_2 solution, to give **2***a*, m.p. 126.5–127° (1, 3).[2,3] The cyclization presumably proceeds by anti-displacement of chlorine by the amide oxygen (7) since, under the same conditions, the C5-epimer **9***b* is recovered unchanged.

[1]This work was presented in the Merck, Sharp and Dohme Award Lecture, Quebec City, Quebec, June, 1972.

[2]I.r. and n.m.r. spectra are in full accord with the proposed structure.

[3]Satisfactory elemental analyses or high resolution mass spectra were secured.

Can. J. Chem. Downloaded from www.nrcresearchpress.com by 210.87.254.5 on 09/05/12
For personal use only.

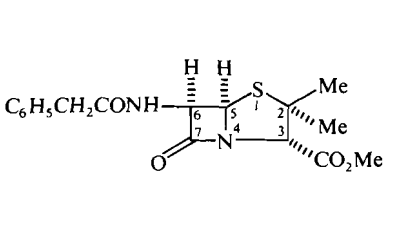

1

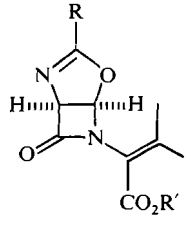

2

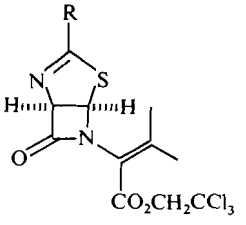

3

a R = $C_6H_5CH_2$; R′ = CH_3
b R = Cl_3CCH_2O; R′ = $(C_6H_5)_2CH$
c R = $C_6H_5CH_2$; R′ = H

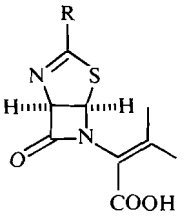

4

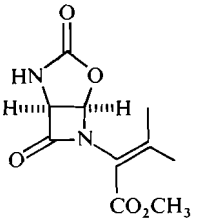

5

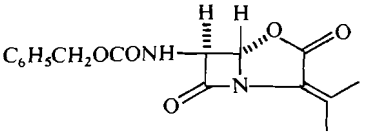

6

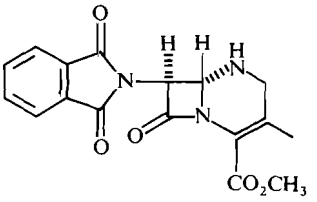

7

However, the latter could also be converted to **2***a*, upon silica gel or (neutral) alumina chromatography; we suggest that **10***a* is an intermediate in this case. Bicarbonate treatment and reacidification of the acid **9***c* (6) afforded **2***c* in 53% yield, m.p. 119–122° (dec.)[3] $[\alpha]_D^{20}$ +13.2° (H_2O–$NaHCO_3$); λ_{max} (KBr) 4.0 (br), 5.64, 5.92, 6.1 μ (zwitterionic structure); n.m.r. (D_2O): τ 2.67 (5H), 3.88 (1H, d, 3.8 Hz), 4.75 (1H, d, 3.8 Hz), 6.25 (2H), 8.09 (3H), 8.69 (3H).[4] The cyclization with apparent retention of configuration at C-5 may proceed via the intermediate **10***b*.[5]

The benzhydryl ester **11***b*[2,3] was obtained in 70% yield from anhydrotrichloroethoxycarbonyl penicillin (**11***a*) by the sequence shown. Epimerization at C-5 (tetramethylguanidinium chloride) afforded a 2:1 mixture of **11***c*[2] and **11***b*, from which **2***b* was obtained in 24% yield upon refluxing with tetramethylguanidinium formate (8);[6] M^+ 522; i.r. 5.61, 5.76, 5.81, 6.07 μ; n.m.r. ($CDCl_3$): τ 2.68 (10H), 3.08 (1H), 3.99 (1H, d, 3.5 Hz), 4.86 (1H, d, 3.5 Hz), 5.15 (1H, d, 12 Hz), 5.27 (1H, d, 12 Hz; the methylene protons of the trichloroethyl group are non-equivalent), 7.73 (3H), 8.06 (3H).

Reaction of **8***a* with benzyl chloroformate and triethylamine afforded **9***d* (24%)[2,3] together with the fused oxazolidone-azetidinone **5** (12%); M^+ 240; i.r. 3.0, 5.56, 5.62, 5.78, 6.10 μ; n.m.r. ($CDCl_3$): τ 2.87 (1H, br), 3.92 (1H, d, 4.0 Hz), 5.08 (1H, d, 4.0 Hz), 6.20 (3H), 7.70 (3H), 8.02 (3H). In this case cyclization of **9***d* seems to be followed by loss of benzyl alcohol.

[4]This acid has no antibacterial activity at concentrations up to 250 γ/ml.

[5]A referee has suggested that **9***b* is epimerized to **9***a* during chromatography and that **2***c* is formed (by a double inversion) via the phenylacetamido analog of **6**. We have been unable to obtain experimental support for either of these suggestions.

[6]This is a necessary reagent for the cyclization.

Can. J. Chem. Downloaded from www.nrcresearchpress.com by 210.87.254.5 on 09/05/12
For personal use only.

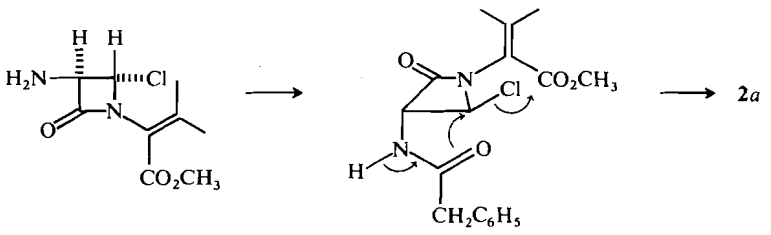

8a **9a** **2a**

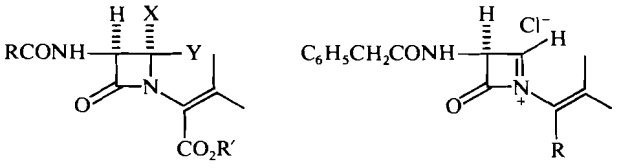

9 **10**

a R = $C_6H_5CH_2$; X = Cl; Y = H; R′ = CH_3
b R = $C_6H_5CH_2$; X = H; Y = Cl; R′ = CH_3
c R = $C_6H_5CH_2$; X = H; Y = Cl; R′ = H
d R = $C_6H_5CH_2O$; X = Cl; Y = H; R′ = CH_3
e R = $C_6H_5CH_2O$; X = H; Y = Cl; R′ = H

a R = CO_2CH_3
b R = CO_2^-

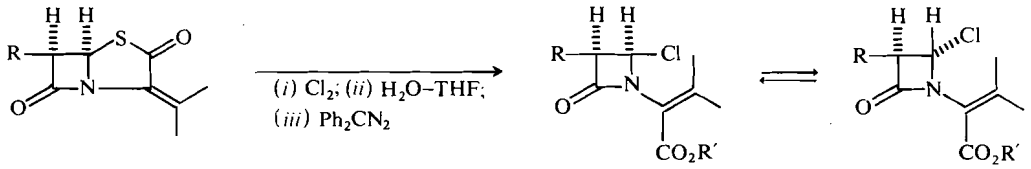

11a **11b** **11c**

R = $C_6H_5CH_2OCO$; R′ = $(C_6H_5)_2CH$

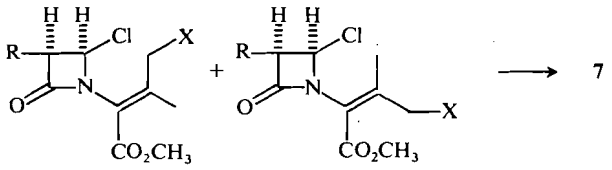

12a **12b**

R = $C_6H_4(CO)_2N$

The relative ease of intramolecular substitution by amide oxygen and carboxylate is seen in the behavior of the *acid* **9e** (6). Within 1 min after addition of $NaHCO_3$ to an aqueous acetone solution of **9e** a crystalline precipitate was formed. This compound, isolated in 40% yield,[3] was assigned the *oxa*anhydropenicillin structure **6** (*cf.* ref. 9); m.p. 170–172° (dec.); $[\alpha]_D^{25}$ −64.5° ($CHCl_3$) (anhydrocarbobenzoxypenicillin has $[\alpha]_D^{25}$ +259° ($CHCl_3$)); M^+ 316; λ_{max} (KBr) 2.98, 5.55, 5.65, 5.88, 6.51 μ; τ ($CDCl_3$): 2.44 (6H), 4.14 (1H, d, 1.8 Hz), 4.82 (2H), 4.98 (1H, q, 1.8, 8 Hz), 7.82 (3H), 7.88 (3H).

Finally, hydrogenation (PtO_2, benzene, 45 psi, 6 h) of the mixture **12a** + **12b** (X = N_3) (6) afforded the mixture **12a** + **12b** (X = NH_2).[2] This mixture was recovered unchanged following refluxing in chloroform. Treatment with *t*-BuOK–*t*-BuOH (20°, 1 h), followed by careful chromatography (neutral alumina, activity II, elution with graded mixtures of benzene–methylene chloride) afforded **7** in 12% yield, m.p.

Can. J. Chem. Downloaded from www.nrcresearchpress.com by 210.87.254.5 on 09/05/12
For personal use only.

121–122°;[3] λ_{max} (KBr): 2.92, 5.56, 5.62, 5.79, 5.82, 6.03 μ; τ ($CDCl_3$): 2.25 (4H), 3.87 (1H, d, 2.0 Hz), 4.30 (1H, d, 2.0 Hz), 6.23 (3H), 7.70 (2H), 7.88 (3H).

We thank Bristol Laboratories for financial support of this work, and Dr. C. T. Claridge for biological evaluation of **2***c*.

1. J. C. SHEEHAN. Molecular modification in drug design. Adv. in Chem. Series No. 45. American Chemical Society, Washington, 1964. p. 15.
2. D. H. R. BARTON, F. COMER, and P. G. SAMMES. J. Am. Chem. Soc. **91**, 1529 (1969).
3. D. H. R. BARTON, F. COMER, D. G. T. GREIG, P. G. SAMMES, C. M. COOPER, G. HEWITT, and W. G. E. UNDERWOOD. J. Chem. Soc. C, 3540 (1971).
4. R. D. G. COOPER and F. L. JOSÉ. J. Am. Chem. Soc. **92**, 2575 (1970).
5. R. D. G. COOPER. J. Am. Chem. Soc. **94**, 1018 (1972).
6. S. WOLFE, W. S. LEE, G. KANNENGIESSER, and J. B. DUCEP. This issue.
7. G. E. MCCASLAND, R. K. CLARK, and H. E. CARTER. J. Am. Chem. Soc. **71**, 637 (1949); G. E. MCCASLAND and D. A. SMITH. J. Am. Chem. Soc. **72**, 2190 (1950); S. WINSTEIN, L. GOODMAN, and R. BOSCHAN. J. Am. Chem. Soc. **72**, 2311 (1950).
8. S. WOLFE and J. B. DUCEP. To be published.
9. S. KUKOLJA. J. Am. Chem. Soc. **93**, 6269 (1971).

Automatic Sorting of Signals in Shift Reagent Spectra

J. W. APSIMON,[1] H. BEIERBECK, AND A. FRUCHIER
Department of Chemistry, Carleton University, Ottawa, Canada K1S 5B6

Received June 15, 1972

This communication shows a simple algorithm for the automatic sorting of signals in shift reagent spectra with an implicit plot of chemical shifts *vs.* improved shift reagent coordinates.

Un algorithme simple est décrit permettant un triage automatique des signaux dans les spectres r.m.n. de substrats organiques étudiés en présence de chélates de lanthanide. La méthode utilise implicitement un graphe des déplacements chimiques en fonction de coordonnées indépendantes de la concentration en chélate.

Canadian Journal of Chemistry, **50**, 2905 (1972)

Lanthanide induced chemical shifts are a linear function of the fraction [LS]/[S] of complexed substrate and, for low shift reagent concentrations, of the molar ratio [L]/[S] of shift reagent and substrate (1, 2) ([L], [S], and [LS] are the total concentrations of shift reagent and substrate and the concentration of bound substrate respectively). It has been demonstrated (2) that accurate slope ratios and intercepts can be obtained without a knowledge of the ratios [LS]/[S] or [L]/[S] by plotting the chemical shifts against coordinates which are proportional to the sum of the shifts in each spectrum. Sometimes, it can be difficult to trace the signal of a given nucleus through a series of spectra, especially if the number of signals is great and if the lines cross in the studied range of molar ratios, as in noise decoupled ^{13}C spectra of a substrate with a large number of carbon atoms. The correlation between the chemical shifts and the improved shift reagent coordinates has been found to be good enough to permit automatic sorting of the signals, and this communication describes a simple algorithm.[2]

Suppose the chemical shifts of m nuclei or groups of magnetically equivalent nuclei are measured in the absence of shift reagent and for n different concentrations of shift reagent. Let the chemical shifts in the shift reagent spectra be arranged as a matrix Δ of dimensions $m \times n$ in which the signals in the i'th spectrum are found in the i'th column. This matrix has

[1]Author to whom correspondence should be addressed.

[2]This method has been found to work well in cases where LS_2 species are formed. In these cases the ratios of the induced shifts were independent of the shift reagent concentrations, suggesting that either LS_2 adducts were exclusively formed or that the limiting shifts were the same in the LS and LS_2 complexes.

Can. J. Chem. Downloaded from www.nrcresearchpress.com by 210.87.254.5 on 09/05/12
For personal use only.

121–122°;[3] λ_{max} (KBr): 2.92, 5.56, 5.62, 5.79, 5.82, 6.03 μ; τ ($CDCl_3$): 2.25 (4H), 3.87 (1H, d, 2.0 Hz), 4.30 (1H, d, 2.0 Hz), 6.23 (3H), 7.70 (2H), 7.88 (3H).

We thank Bristol Laboratories for financial support of this work, and Dr. C. T. Claridge for biological evaluation of **2***c*.

1. J. C. SHEEHAN. Molecular modification in drug design. Adv. in Chem. Series No. 45. American Chemical Society, Washington, 1964. p. 15.
2. D. H. R. BARTON, F. COMER, and P. G. SAMMES. J. Am. Chem. Soc. **91**, 1529 (1969).
3. D. H. R. BARTON, F. COMER, D. G. T. GREIG, P. G. SAMMES, C. M. COOPER, G. HEWITT, and W. G. E. UNDERWOOD. J. Chem. Soc. C, 3540 (1971).
4. R. D. G. COOPER and F. L. JOSÉ. J. Am. Chem. Soc. **92**, 2575 (1970).
5. R. D. G. COOPER. J. Am. Chem. Soc. **94**, 1018 (1972).
6. S. WOLFE, W. S. LEE, G. KANNENGIESSER, and J. B. DUCEP. This issue.
7. G. E. MCCASLAND, R. K. CLARK, and H. E. CARTER. J. Am. Chem. Soc. **71**, 637 (1949); G. E. MCCASLAND and D. A. SMITH. J. Am. Chem. Soc. **72**, 2190 (1950); S. WINSTEIN, L. GOODMAN, and R. BOSCHAN. J. Am. Chem. Soc. **72**, 2311 (1950).
8. S. WOLFE and J. B. DUCEP. To be published.
9. S. KUKOLJA. J. Am. Chem. Soc. **93**, 6269 (1971).

Automatic Sorting of Signals in Shift Reagent Spectra

J. W. APSIMON,[1] H. BEIERBECK, AND A. FRUCHIER
Department of Chemistry, Carleton University, Ottawa, Canada K1S 5B6

Received June 15, 1972

This communication shows a simple algorithm for the automatic sorting of signals in shift reagent spectra with an implicit plot of chemical shifts *vs.* improved shift reagent coordinates.

Un algorithme simple est décrit permettant un triage automatique des signaux dans les spectres r.m.n. de substrats organiques étudiés en présence de chélates de lanthanide. La méthode utilise implicitement un graphe des déplacements chimiques en fonction de coordonnées indépendantes de la concentration en chélate.

Canadian Journal of Chemistry, **50**, 2905 (1972)

Lanthanide induced chemical shifts are a linear function of the fraction [LS]/[S] of complexed substrate and, for low shift reagent concentrations, of the molar ratio [L]/[S] of shift reagent and substrate (1, 2) ([L], [S], and [LS] are the total concentrations of shift reagent and substrate and the concentration of bound substrate respectively). It has been demonstrated (2) that accurate slope ratios and intercepts can be obtained without a knowledge of the ratios [LS]/[S] or [L]/[S] by plotting the chemical shifts against coordinates which are proportional to the sum of the shifts in each spectrum. Sometimes, it can be difficult to trace the signal of a given nucleus through a series of spectra, especially if the number of signals is great and if the lines cross in the studied range of molar ratios, as in noise decoupled ^{13}C spectra of a substrate with a large number of carbon atoms. The correlation between the chemical shifts and the improved shift reagent coordinates has been found to be good enough to permit automatic sorting of the signals, and this communication describes a simple algorithm.[2]

Suppose the chemical shifts of m nuclei or groups of magnetically equivalent nuclei are measured in the absence of shift reagent and for n different concentrations of shift reagent. Let the chemical shifts in the shift reagent spectra be arranged as a matrix Δ of dimensions $m \times n$ in which the signals in the i'th spectrum are found in the i'th column. This matrix has

[1]Author to whom correspondence should be addressed.

[2]This method has been found to work well in cases where LS_2 species are formed. In these cases the ratios of the induced shifts were independent of the shift reagent concentrations, suggesting that either LS_2 adducts were exclusively formed or that the limiting shifts were the same in the LS and LS_2 complexes.

Can. J. Chem. Downloaded from www.nrcresearchpress.com by 210.87.254.5 on 09/05/12
For personal use only.

TABLE 1. Standard deviations for the lines calculated in step 2. The indices i and k are those for the signals in the first (row) and last (column) spectrum, from low to high field

k \ i	1	2	3	4	5	6	7	8
1	6.3	5.6	0.3					
2	0.2							
3	0.6	0.6						
4	1.9	2.7	6.7	1.1	0.7			
5	2.8	3.5	6.0	0.5				
6	5.3	5.8	7.1	9.0	15.3	0.4		
7	13.2	13.8	14.5	16.2	24.7	26.5	0.5	
8	14.5	16.0	18.0	21.1	30.5	34.2	9.5	0.6

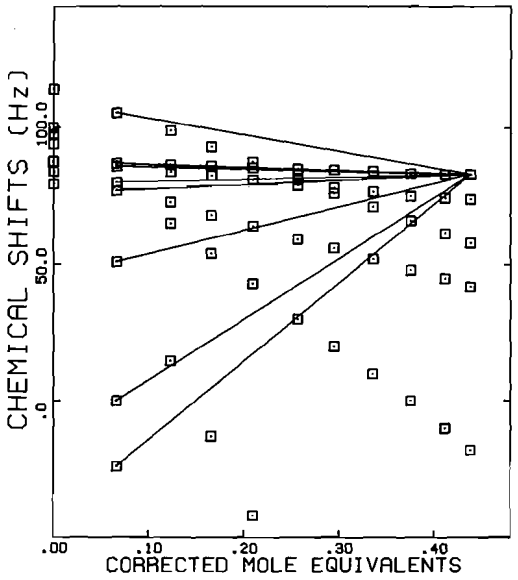

FIG. 1. Illustration of step 2 with the methyl group shifts of β-amyrin in the presence of $Pr(fod)_3$ (shifts upfield from TMS are negative).

to be rearranged so that all signals for any given nucleus are in one row. The chemical shifts in the spectrum without shift reagent then have to be matched with the data in the shift reagent matrix.

Step 1. Corrected shift reagent coordinates are derived in the usual way (2).

Step 2. The signals in the shift reagent spectra are sorted out. Lines are drawn from δ_{1n} (the first signal in the n'th spectrum) to each of the m points δ_{i1} from the first spectrum (see Fig. 1) and the m slopes are calculated. For each of the m lines every column of points is searched for that signal which is closest to the line and the standard deviation of these points is calculated for each line (see Table 1). That combination $(\delta_{i1}, \delta_{1n})$ is taken to be the correct one for which the standard deviation is a minimum. The slope is recalculated using all n points which are then removed from the matrix Δ and form a row in the new matrix Δ'.

This procedure is repeated with the reduced matrix Δ until all signals are sorted out and the new matrix Δ' is completed in which all signals for any nucleus are in one row. If it is not already the case, the rows are ordered according to increasing slopes.

Step 3. The m chemical shifts in the spectrum before addition of shift reagent are matched with the m slopes. First the correction procedure for the shift reagent coordinates is applied to the zero position. In general, the best zero position after correction will not be exactly at the coordinate origin, and it is brought back to zero by displacing the whole plot. Then the intercepts are calculated and the experimental shifts are ordered accordingly.

Spectra in which not all signals can be observed are excluded and the slopes of the best lines are calculated with the shifts in the remaining spectra. If the experimental shift reagent coordinates are accurate enough to permit the assignment of some of the signals, these signals can be used to obtain improved shift reagent coordinates. The remaining signals can then be sorted out as in step 3.

The method is illustrated with the shifts for the eight ($m = 8$) methyl groups of β-amyrin (**1**). 100 MHz spectra for 10 different concentrations ($n = 10$) of $Pr(fod)_3$ in $CDCl_3$ were

Can. J. Chem. Downloaded from www.nrcresearchpress.com by 210.87.254.5 on 09/05/12
For personal use only.

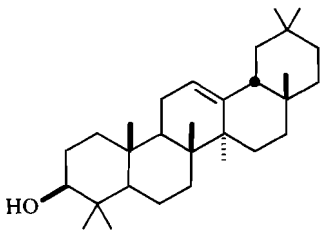

I

obtained at ambient temperature. The signals above -50 Hz are plotted in Fig. 1 (shifts upfield from TMS are negative) which illustrates the first stage in step 2, the combination of δ_{1n} with each of the eight δ_{i1}. The standard deviations for each of the eight combinations are found in column 1 of Table 1. Both the table and the figure indicate that the match $\delta_{21}-\delta_{1n}$ is the correct one. Since δ_{21} is now removed from Δ, there are no further entries in row 2.

The adjustment of the shift reagent coordinates may be unnecessary if the molar ratios of shift reagent and substrate are determined very accurately. However, we prefer to apply these corrections as they guarantee accurate results from routine measurements.

A sorting routine based on the described algorithm is a part of the program that we use for all calculations of slopes, slope-ratios, and intercepts in shift reagent plots for proton and ^{13}C n.m.r. spectra. As part of a program to fit the pseudo contact equation of McConnell–Robertson (3) to the shift reagent data, it is the first stage in the automatic assignment of chemical shifts and structure elucidation with the help of shift reagents.

We thank the National Research Council of Canada for generous financial support (Grant in Aid, J.W.A.; Postdoctoral Fellowship, Canada-France, A.F.).

1. See *e.g.* W. De W. Horrocks, Jr., J. P. Sipe, III, and J. R. Luber. J. Am. Chem. Soc. **93**, 5258 (1971) and refs. therein.
2. J. W. ApSimon and H. Beierbeck. Chem. Commun. 172 (1972); and J. W. ApSimon, H. Beierbeck, and A. Fruchier. Can. J. Chem. **50**, 2725 (1972).
3. H. M. McConnell and R. E. Robertson. J. Chem. Phys. **29**, 1361 (1958).

Can. J. Chem. Downloaded from www.nrcresearchpress.com by 210.87.254.5 on 09/05/12
For personal use only.

Can. J. Chem. Downloaded from www.nrcresearchpress.com by 210.87.254.105 on 09/05/12
For personal use only.

Canadian Journal of Chemistry

Published by THE NATIONAL RESEARCH COUNCIL OF CANADA

VOLUME 50 SEPTEMBER 15, 1972 NUMBER 18

Cyclopropylcarbinyl-oxo-carbonium Ions. Part V.[1] Synthesis and Chemistry of some Cyclopropyl Glycopyranosides[2]

BRUNO RADATUS AND BERT FRASER-REID

Department of Chemistry, University of Waterloo, Waterloo, Ontario

Received March 7, 1972

The synthesis of five cyclopropanated glycopyranosides, **6**α, **6**β, **7**α, **7**β, and **11** capable of providing access to the title ions has been examined. Simmons–Smith methylenation of methyl 4,6-*O*-benzylidene-2,3-dideoxy-α-D-*erythro*-hex-2-enopyranoside (**8**α) under carefully controlled conditions gives an excellent yield of the α-D-*allo* adduct (**6**α). A homoallyl iodide, 4,6-*O*-benzylidene-1,2,3-trideoxy-3-*C*-iodomethyl-D-*ribo*-hex-1-enopyranose, (**9**), is also produced and upon methanolysis undergoes ring closure to an equal mixture of α-D and β-D anomers of **6**. Methylene insertion into the aglycon of the starting olefin **8**α occurs giving small amounts of the ethyl hex-2-enopyranoside (**10**), the cyclopropanated glycoside derived therefrom, **11**, being also obtained. Methylenation of the β-D-hex-2-enopyranoside, **8**β, gives a complex mixture containing at least eight substances, although the expected β-D-*manno* adduct, **7**β, is the major product. There is considerable anomerization of **8**β and of the primary product, **7**β; thus the anomer **7**α is also produced. The 3-epimer (**14**) of the above-mentioned homoallyl iodide (**9**) is obtained in small yield.

The cyclopronated glycosides are very susceptible to prolonged exposure to the Simmons–Smith medium. Particularly in the case of **8**β the yields of the various products can be optimized by judicious choice of the duration of the reaction.

Proton magnetic resonance data for the adducts are presented. The value of the spacing J_{34} provides a clear basis for determining the configuration of the ring. However anisotropy due to the cyclopropane ring-current causes the equatorial H-1 in the β-D-*manno*-anomer (**7**β) to resonate at higher field than H-1 in the α-D anomer **7**α.

On a étudié la synthèse de cinq glycopyranosides cyclopropyles **6**α, **6**β, **7**α, **7**β, et **11** capables de donner accès aux ions du titre annoncé. La méthylénation selon Simmons–Smith du méthyl-*O*-benzylidène-4,6 didéoxy-2,3-α-D-*érythro*-hexeno-2 pyranoside (**8**α) dans des conditions soigneusement contrôlées conduit au composé d'addition α-D-*allo* (**6**α) avec un rendement excellent. Un iodure homoallyle, *O*-benzylidène-4,6 tridéoxy-1,2,3 iodométhyl-3-*C*-D-*ribo*-hexeno-1 pyranose (**9**) est également obtenu, qui subit une fermeture de cycle dans la méthanolyse en un mélange égal d'anomères α-D et β-D de **6**. L'insertion de méthylène dans l'aglycone de l'oléfine de départ **8**α se produit et conduit à de petites quantités d'éthylhexèno-2 pyranoside (**10**), le glycoside cyclopropyle qui en dérive **11**, étant obtenu également. La méthylénation du β-D-hexeno-2 pyranoside **8**β conduit à un mélange complexe de huit composés au moins, bien que le composé d'addition attendu, β-D-manno **7**β, soit le produit majeur. Une anomérisation considérable se produit sur **8**β et sur le produit primaire **7**β, expliquant ainsi l'obtention de l'anomère **7**α. L'épimère-3 (**14**) de l'iodure homoallyle mentionné ci-dessus (**9**) est obtenu avec un rendement faible.

Les glycosides cyclopropylés sont très sensibles à une exposition prolongée dans le milieu du Simmons–Smith. Dans le cas de **8**β en particulier, les rendements des divers produits peuvent être rendus optima selon un choix judicieux de durée de réaction.

Les données de la r.m.n. du proton pour les composés d'addition, sont présentées. La valeur de l'écart J_{34} permet de déterminer de façon claire, la configuration du cycle. Toutefois, l'anisotropie due au courant de cycle du cyclopropane provoque une résonance à des champs plus élevés pour H-1 équatorial de l'anomère β-D-*manno* (**7**β) que pour H-1 dans l'anomère α-D de **7**α. [Traduit par le journal]

Canadian Journal of Chemistry, **50**, 2909 (1972)

[1]For Part IV, see ref. 14. For Parts I, II, and III, see refs. 5, 9, and 17 respectively, which have appeared as preliminary communications.

[2]Taken from the Ph.D. Thesis of B. Radatus, University of Waterloo, 1971.

Can. J. Chem. Downloaded from www.nrcresearchpress.com by 210.87.254.105 on 09/05/12
For personal use only.

The interconversion of cyclopropylmethyl, cyclobutyl, and homoallyl compounds, discovered by Demjanov in 1907 (1) was given its first interpretation in terms of modern carbonium ion theory by Roberts and Mazur (2). Since then, under the name of the cyclopropylcarbinyl or homoallyl rearrangement (3),[3] the interconversion has been utilized in several synthetic sequences (4). Our interest in this system was aroused by the possible inter-

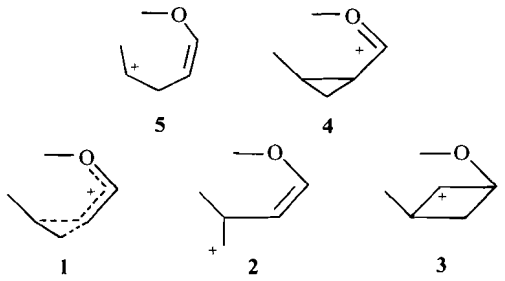

conversion of ions **2**–**5** which are some of the individual species contributing to the highly delocalized ion **1** named a *cyclopropylcarbinyl-oxo-carbonium ion* for reasons described previously (5). Compounds cognate with ions **2**–**5** would be of potential utility in synthetic carbohydrate chemistry, and as a first step towards their obtainment, we have been concerned with the preparation of molecules which upon solvolysis would generate ion **1**.

Cyclopropanated glycosides capable of filling this need were unknown at the inception of this work although in the interim one such member, **6**α, has been obtained by Horton and coworkers (6). We describe herein the syntheses of these four possible glycosides **6**α, **6**β, **7**α, **7**β and report on certain aspects of their chemistry.

*Simmons–Smith Reaction of Methyl 4,6-O-Benzylidene-2,3-dideoxy-*α*-*D*-erythro-hex-2-enopyranoside,* **8**α *(Scheme 1)*

Simmons–Smith cyclopropanation (7) of olefin **8**α (8) gave a complex mixture from which the four products shown in Scheme 1 were obtainable by chromatography on silica. The starting olefin comprised 24% of the mixture under the conditions of optimum product formation. The desired compound, **6**α, was obtained in 82% based on reacted olefin. The material was identical in all respects with a sample kindly supplied by Professor Horton (6).

The second major product, **9**, is configurationally related to **6**α, because silver-ion induced methanolysis converts **9** to an equal mixture of **6**α and **6**β (9). This reaction was particularly significant from the synthetic standpoint, since it proved to be the best route to the latter glycoside, **6**β. The mechanism of these interconversions and the mechanism of the formation of **9** are discussed in the following and adjoining paper in this series (10).

Two minor products from the reaction were **10** and **11**. The n.m.r. parameters for **10** (see Experimental) and the elemental analysis were indicative of an ethyl hex-2-enopyranoside (11–13) which implied that methylene had inserted into the aglycon of the starting olefin **8**α. However, assignment of the anomeric configuration was difficult because (*i*) the identical material was obtained when the anomeric olefin **8**β was cyclopropanated (Scheme 3), and (*ii*) its specific rotation (91.3°) lay nearly midway between the values for the methyl α-D (**8**α) and β-D (**8**β) analogues (129 and 45°, respectively) (12). For this reason

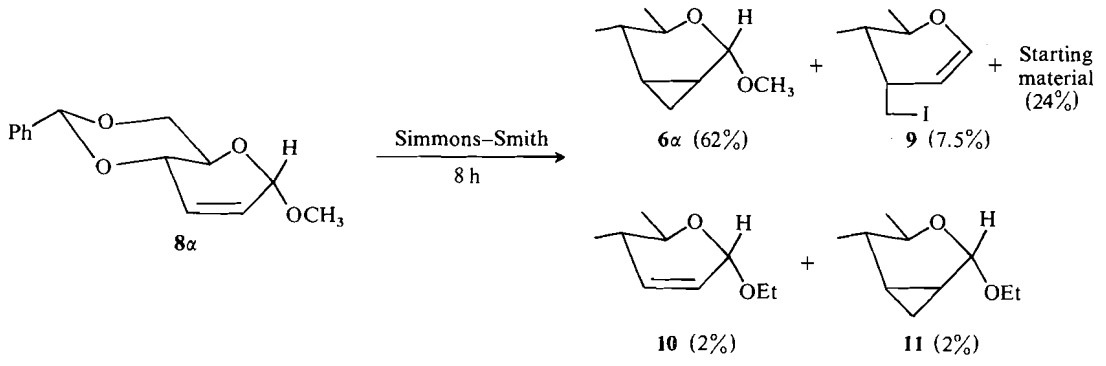

SCHEME 1

[3]We are indebted to Professor H. G. Richey (3*c*) for a photocopy of his review article prior to publication.

TABLE 1. 220 MHz n.m.r. parameters for some alkyl 4,6-*O*-benzylidene-2,3-dideoxy-2,3-*C*-methylene-hexopyranosides in $CDCl_3$*

	Chemical shifts (τ) from TMS									
Compound	Aglycon	H-1	H-2	H-3	H-4	H-5	H-6a	H-6e	H-7$_{exo}$	H-7$_{endo}$
6α	6.63	5.00	8.35	8.49	5.92	6.53	6.32	5.78	9.25	8.74
6β†	6.53	5.23	9.00	8.88	5.70	6.71	6.29	5.78	9.14	8.93
7α	6.60	5.19	8.85	8.59	6.57	6.29	6.36	5.78	9.28	9.68
7β	6.46	4.93	8.74	8.54	6.52	6.75	6.30	5.76	9.10	9.31
11	‡	4.86	8.36	8.50	5.93	6.51	6.34	5.80	9.24	8.62

	Couplings constants (Hz)§			
Compound	J_{12}	$J_{27_{exo}} = J_{37_{exo}}$	J_{34}	In all cases
6α	6.0	8.0	5.0	For benzylidene: ~τ 2.60 (m, 5, Ph); ~τ 4.40 (s, 1, Ph C*H*)
6β	1.0	8.0	5.0	
7α	0.0	9.0	2.0	$J_{23} = 9.0$ $J_{45} = 9.5$
7β	3.5	9.0	2.0	$J_{27_{endo}} = 5.5$ $J_{56_a} = 10.0$
11	6.0	8.0	5.0	$J_{37_{endo}} = 5.5$ $J_{56_e} = 4.5$
				$J_{77} = -5.5$ $J_{66} = -10.5$

*See also individual sections in the Experimental.
†For details of preparation of **6β** see ref. 10.
‡The ethoxy group in **11** is an ABX system (*cf.* ref. 33). The diastereotopic methylene protons occur as octets at τ 6.28 and 6.48: $J_{AB} = 10.0$; $J_{AX} = J_{BX} = 7.0$. The methyl group is a triplet at τ 8.80.
§Read directly from the spectra run at 500 Hz sweep width.

justification of the configuration of **10** is deferred until after the anomerization phenomena shown in Scheme 4 have been discussed. The elemental analysis for compound **11** and the similarity of its n.m.r. parameters and optical rotation to those of **6α** (Tables 1 and 2) pointed to the assigned structure.

In order to determine the effects of prolonged exposure to the reaction medium, the cyclopropyl glycoside **6α** was placed in the Simmons–Smith conditions for 8 h (Scheme 2). In addition to the already encountered homoallyl iodide **9** and methylene insertion product **11**, three new compounds were obtained. Two of these emerged an an inseparable mixture in 13% from a silica column chromatogram. They were judged to be the diastereomers implied in structure **12** because of the mass ion, *m/e* 372.

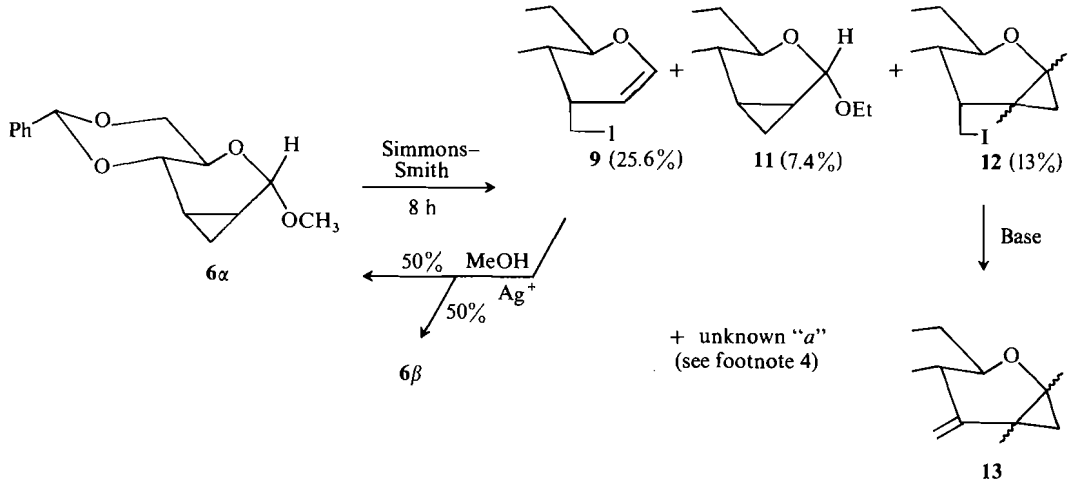

SCHEME 2

Can. J. Chem. Downloaded from www.nrcresearchpress.com by 210.87.254.105 on 09/05/12
For personal use only.

Can. J. Chem. Downloaded from www.nrcresearchpress.com by 210.87.254.105 on 09/05/12
For personal use only.

Broken arrows indicate a possible chronology

SCHEME 3

TABLE 2. Specific rotations of some cyclopropanated glycopyranosides in chloroform

Compound	$[\alpha]_D^{23°}$	Concentration (g/100 ml)
6α	+115.2	2.86
6β	−8.0	3.06
7α	+104.7	4.75
7β	−40.0	5.40
11	+137.5	2.82

This was substantiated by showing that cyclopropanation of **9** produced an identical mixture. The n.m.r. spectrum of the mixture, **12**, showed two complex signals integrating for one proton at τ 7.0 and 7.2, ascribed to H-3 of the assigned structures by analogy with the H-3 resonance of **9** (14). Furthermore dehydroiodination of the mixture leads to inseparable olefins, **13** (M^+, *m/e* 244). The terminal methylene group was apparent from i.r. signals at 3012, 978, and 894 cm^{-1} (15); absorption for four protons τ 8.33–9.63 indicated that the cyclopropane ring had been preserved.

A third new substance was obtained as a syrupy material whose structure is currently being determined and therefore labelled *unknown* "*a*".[4]

*Simmons–Smith Reaction of Methyl 4,6-O-Benzylidene-2,3-dideoxy-β-D-erythro-hex-2-enopyranoside, **8**β (Scheme 3)*

As may be gathered from Scheme 3, Simmons–Smith reaction of **8**β gave a very complex mixture, and the yields of the components varied markedly with the duration of the reaction (Table 3). However, advantage was taken of this feature when it was deemed desirable to accumulate a given product at the expense of the others.

Products listed in Scheme 3 previously encountered are **6**α, **8**α, **8**β, **9**, **10**, and **11**, and a substance with the same R_f as *unknown* "*a*", Scheme 2, was obtained and is designated *unknown* "*b*".[4]

The α-D-*manno* skeleton ascribed to **7**α followed from the n.m.r. parameters listed in Table 1. The value $J_{34} = 2.0$ Hz was different to those listed for *allo*-derivatives (**6** and **11**) and therefore implied different configuration. Furthermore the coupling $J_{12} = 0.0$ Hz agrees precisely with the value found in the analogous α-D-*manno*-epimino, epoxy, and epithio compounds (16). Following this reasoning, the expected reaction product (**7**β), was recognized as *manno* by (*i*) a value of $J_{34} = 2.0$ Hz, and (*ii*) the coupling $J_{12} = 3.5$ Hz which is consistent with β-D orientation.

TABLE 3. Results of Simmons–Smith reaction on compound **8**β* for different reaction times

		1.5 h		4 h		8 h	
Compound	R_f†	Yield (g)	%	Yield (g)	%	Yield (g)	%
9	0.77	0.422	3.0	0.520	3.6	0.400	2.8
14	0.77	0.105	0.74	0.130	0.9	0.100	0.6
10	0.59	0.207	2.0	0.298	2.8	0.198	1.9
7α	0.56	—		0.222	2.1	0.675	6.4
8α	0.51	0.565	5.7	0.481	4.8	0.896	8.9
8β	0.47	3.431	34.3	2.083	20.8	2.070	20.7
Unknown "*b*"	0.46	—		1.275	12.8	1.196	11.2
7β	0.42	2.401	27.5	2.334	22.1	2.690	24.8
6α	0.38	—		0.516	4.9	0.485	4.6
Material recovered‡			73.2		70.3		81.9

*Using 10.0 g of **8**β.
†In petroleum ether (35–60 °C)–ethyl acetate (4:1).
‡Expressed as % of total material placed on the column.

[4]*Unknown* "*a*" and *unknown* "*b*" were obtained as by-products when the *allo*-(**6**) and *manno*-(**7**) cyclopropyl glycosides were exposed to the Simmons–Smith reaction medium for lengthy periods of time. Both unknowns are syrupy, isomeric with **6** and **7**, homogeneous on t.l.c., and have identical R_f values. Nevertheless, their n.m.r. spectra, which are also similar (!), reveal that each is in fact a mixture, because there are two benzylidene–methine spikes whose relative intensity varies (within each unknown) from one preparation to the next. The structure of the unknowns is currently being investigated and will be published in due course.

Can. J. Chem. Downloaded from www.nrcresearchpress.com by 210.87.254.105 on 09/05/12
For personal use only.

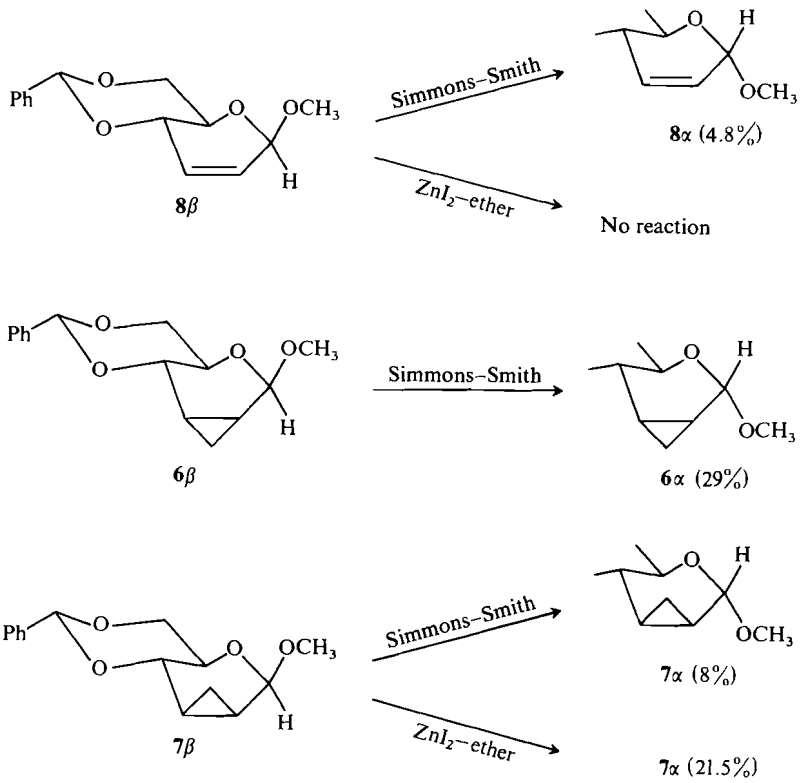

SCHEME 4

The structure of the iodoglycal **14** was determined by an independent synthesis (17) originating with the epimer **9** described in detail in the adjoining paper (10). Interestingly, attempts to convert **7β** to **14** by means of the Simmons–Smith reagents (*cf.* **6α** → **9** Scheme 2) were unsuccessful. The only products obtained were **7α** (Scheme 4) and *unknown* "*b*".[4]

The formation of α-D-cyclopropyl glycosides **6α** and **7α** from the β-D olefin **8β** in Scheme 3 needed explanation because methylene addition to 2-cyclohexenols and their ethers usually occurs *syn* to the oxygen function (18). The ICH_2ZnI complex (19) coordinates through a zinc atom to the allylic oxygen and is thereby constrained to deliver the methylene group on the same side.[5] The formation of **6α** would therefore require that the starting olefin must be anomerized to **8α** prior to reaction with methylene. Compound **7α** however would most likely arise by anomerization of the principal reaction product, **7β**. Both of these anomerizations seemed plausible in view of the Edward–Lemieux effect (21, 22) which stabilizes most α-D-hexopyranosides *vis à vis* their β-D anomers. Acid catalysis required for the anomerization (23), could be provided by ZnI_2 or ICH_2ZnI present in the reaction medium. Already from Scheme 3 it is apparent that **8β** can be anomerized to **8α**, and experiments summarized in Scheme 4 revealed that β-D cyclopropyl glycosides are partially anomerized under the Simmons–Smith conditions. However, as expected, the α-D anomers were not converted to their β-D analogues. Zinc–iodide in ether anomerized the cyclopropyl glycoside **7β** → **7α** in even higher yield, but interestingly the latter conditions were without effect on the *olefinic* glycoside, **8β**. This result reflects the superiority of a suitably-disposed cyclopropyl group over an olefinic group, to stabilize an α-carbonium ion (24).[6]

[5]This does not necessarily hold for rings of larger size (20).

[6]For further evidence, compare the rates of aqueous-dioxan hydrolysis of structures **6** and **10** in ref. 25.

Can. J. Chem. Downloaded from www.nrcresearchpress.com by 210.87.254.105 on 09/05/12
For personal use only.

Can. J. Chem. Downloaded from www.nrcresearchpress.com by 210.87.254.105 on 09/05/12
For personal use only.

The α-D configuration assigned to the ethyl hex-2-enopyranoside occurring in Schemes 1 and 3 (*vide supra*) can now be justified. Theoretically the material could have *either* anomeric configuration arising by methylene insertion into the methoxyl group of **8**α or **8**β and yielding, respectively, **10** or its β-D anomer. However, the ethyl hex-2-enopyranoside produced in Scheme 1 *cannot* have β-D configuration since that would require either (*a*) anomerization of **8**α → **8**β followed by methylene insertion, or (*b*) **8**α → insertion product followed by anomerization to a β-D olefin. In either case α → β anomerization is required and as was shown in the preceding paragraph this does not occur in the reaction medium. The α-D configuration for **10** is therefore indicated, and independent proof comes from the fact that the H-1 resonance at τ 5.00 is closer to that for **8**α (τ 5.05) than for **8**β (τ 4.68) (12).

Nuclear Magnetic Resonance Spectra of the Cyclopropanated Glycosides (Table 1)

Nuclear magnetic resonance parameters obtained from 200 MHz spectra of the cyclopropanated glycosides are shown in Table 1. Perusal of the data shows that the value of J_{34} provides a clear basis for deciding the orientation of the cyclopropyl group in these derivatives. The value $J_{34} = 2.0$ Hz for **7** seems unduly small for two formally *trans*-diaxial protons; it undoubtedly reflects the distortion of six-membered ring and electronic effects associated with the cyclopropyl ring (26).

The chemical shifts of H-1 within each anomeric pair present an interesting contrast. The equatorial proton in **6**α occurs 0.23 p.p.m. to lower field than the axial proton in **6**β in accordance with the situation in saturated hexopyranosides (27). However, the equatorial proton in **7**α occurs 0.36 p.p.m. to *higher* field than the axial proton in the related anomer, **7**β. This result must be due to abnormal shielding effects, due to the anisotropy of the cyclopropane ring. It has been suggested that the cyclopropane ring may have a ring current such that protons near to the equatorial plane are deshielded while those above and below the plane and near to the three-fold axis of the ring would be shielded (26). If this is correct, H-4 in the *manno*-(**7**) derivatives being nearer to the center of the cyclopropane ring, should be more shielded than H-4 in the corresponding *allo*-(**6**) derivatives. In fact the data in Table 1 shows this to be the case. With regard to H-1 in the β-anomers, models show that as one goes from **6**β to **7**β, the axial H-1 moves away from the ring center, and should therefore be less shielded. This is observed. *The overall effect in the cases studied appears to be for the cyclopropane ring to shield vicinal cis-oriented protons located on the pyran ring.*

The assignment of *endo* and *exo* orientation to the geminal cyclopropyl protons rested upon their couplings to H-2 and -3, because *cis*-couplings on a cyclopropane ring are much larger than *trans*-couplings (28). Accordingly the large couplings (Table 1) were assigned as $J_{2\,7_{exo}}$ and $J_{3\,7_{exo}}$. Thus H-7_{exo} and by corollary H-7_{endo} were readily identifiable.

The remaining parameters in Table 1 are in good accord with the trends recognized previously in relation to the relative chemical shifts H-2 (27, 29), the methoxyl protons (30), and the chemical shifts and couplings of the H-6 protons for such benzylidene compounds (12).

Experimental

General

Melting points were determined on a Fischer–Johns heating stage and are uncorrected. The n.m.r. spectra whose analyses are given in Table 1 were recorded using either a Varian T-60, a Varian HA 100, or a Varian HR 220 spectrometer, and unless otherwise specified, the solvent was deuteriochloroform containing 1% tetramethylsilane as internal standard. Coupling constants were obtained by measuring spacings of spectra judged to be first-order. All geminal and allylic (through four bonds) couplings were assigned negative signs as predicted for these systems (31).

I.r. spectra were determined on a Beckman model I.R. 5 spectrometer using 0.1 mm sodium chloride solution cells (chloroform as solvent) and silver chloride plates for smears. Mass spectra were determined on a Hitachi Mass Spectrometer model RMU-6E.

T.l.c. was performed on glass plates coated with silica gel (HF-254, E. Merck) to a thickness of 0.3 mm. The most useful developing phase was petroleum ether (35/60 °C)–ethyl acetate (4:1) and the chromatograms were first viewed under u.v. light, then exposed to iodine vapor, and finally sprayed with concentrated sulfuric acid. For column chromatography E. Merck Silica Gel (0.05–0.20 mm, 70–325 mesh A.S.T.M.) was used.

Simmons–Smith Reaction of Methyl 4,6-O-Benzylidene-2,3-dideoxy-α-D-erythro-hex-2-enopyranoside, 8α (see Scheme 1)

A well-stirred mixture of methylene iodide (1.44 ml; 0.0179 mol), zinc–copper couple (32) (1.0 g; 0.0153 mol),

Can. J. Chem. Downloaded from www.nrcresearchpress.com by 210.87.254.105 on 09/05/12
For personal use only.

TABLE 4. Fractions obtained from column chromatography of the mixture (2.45 g) from Simmons–Smith reaction on compound **8α**

Fraction	R_f	Compound	Weight of material in g (%)
a	0.77	**9**	0.217 (7.5)
b	0.59	**10**	0.050 (2)
c	0.51	**8α**	0.480 (24)
d	0.45	**11**	0.045 (2)
e	0.38	**6α**	1.3093 (62)

diethyl ether (6 ml; 0.0576 mol), and a small crystal of iodine was refluxed for 1 h.[7] The title compound **8α** (8) (2.0 g; 0.008 mol) was added as a solid, and also more diethyl ether (4 ml; 0.0384 mol) and reflux was continued for a further 8 h. *However it was found essential to add dimethoxyethane (7) (0.8 ml; 0.0072 mol) in 0.16 ml portions at times 0.0, 0.5, 1, 3, and 5 h after the addition of compound* **8α** *to the reaction mixture.* After the 8 h reflux period the reaction mixture was poured into a separatory funnel, washed with saturated aqueous ammonium chloride solution, and then with saturated bicarbonate solution. The ether layer was dried and evaporated under reduced pressure, whereby 2.45 g of white crystalline material was obtained. T.l.c. indicated five components with R_f values of 0.77, 0.59, 0.51, 0.45, and 0.38 using 4:1 petroleum ether–ethyl acetate as developing solvent. The mixture was put on a column (100 cm × 1.8 cm) prepared from 200 g Silica Gel and eluted with the same solvent mixture. The results are shown in Table 4.

Fraction a was identified as *4,6-O-benzylidene-1,2,3-trideoxy-3-C-iodomethyl-*D*-ribo-hex-1-enopyranose,* ***9*** *(5, 10).*

Fraction b, obtained from cyclopropanation of both **8α** and **8β** (Schemes 1 and 3), was identified as *ethyl 4,6-O-benzylidene-2,3-dideoxy-α-*D*-erythro-hex-2-enopyranoside,* ***10***, by the following definitive n.m.r. features: ~τ 2.5 (m, 5, Ph), 4.7 (s, 1, PhC*H*), 5.0 (bs, 1, H-1), 3.90 (d, J_{23} = 10 Hz, H-2), 4.30 (dt (partly obscured by benzylidene proton) 1, H-3), 5.57–6.70 (m, 6, H-4, -5, -6a, -6e, —O*H*CH′CH_3, and —OHC*H*′CH_3), $[\alpha]_D^{23}$ +91.3 (*c*, 1.9 in $CHCl_3$). Assignment of the anomeric configuration as α-D was justified in the Discussion.

Fraction c was the starting olefin **8α**.

Fraction d was identified as *ethyl 4,6-O-benzylidene-2,3-dideoxy-2,3-C-methylene-α-*D*-allopyranoside,* ***11***. The material crystallized spontaneously and recrystallization from ethanol afforded an analytical sample, m.p. 156–158°; $[\alpha]_D^{23}$ +137.5° (*c*, 2.82 in $CHCl_3$).

Anal. Calcd. for $C_{16}H_{20}O_4$: C, 69.54; H, 7.30. Found: C, 69.39; H, 7.37.

N.m.r. parameters for **11** are given in Table 1. The appearance of the ring protons was as follows: H-1 (d), -2 (m), -3 (m), -4 (q), -5 (td), -6a (t), -6e (q), -7_{exo} (td), -7_{endo} (q). The optical rotation is reported in Table 2.

[7]It should be noted that the methylene iodide was in excess of the zinc–copper couple (0.0153 mol), the reverse of the usual practice (7, 32). It was found that if the molar amount of methylene iodide was equal to or less than the molar amount of zinc–copper couple, the yields were low and variable or the reaction did not proceed at all.

Fraction e which was crystallized from methanol was identified as *methyl 4,6-O-benzylidene-2,3-dideoxy-2,3-C-methylene-α-*D*-allopyranoside,* **6α**, by spectral comparisons and mixed melting point with a sample of the authentic material kindly supplied by Professor Horton (6).

*Prolonged Exposure of Methyl 4,6-O-Benzylidene-2,3-dideoxy-2,3-C-methylene-α-*D*-allopyranoside,* **6α**, *to the Simmons–Smith Medium (Scheme 2)*

Compound **6α**, (2.0 g, 7.6 mmol) was treated for 8 h with the Simmons–Smith reagents as described above for **8α**, the relative ratio of the reactants being maintained, excepting dimethoxyethane which was not needed. The reaction product (see Scheme 2) on t.l.c. showed starting material (R_f 0.38), the homoallyl iodide **9** (R_f 0.77), the ethyl glycoside **11** (R_f 0.45), *unknown "a"*[4] (R_f 0.62) and a new substance R_f 0.66. Silica column chromatography afforded the components as follows, the percentages being referred to the amount of starting material: 39.4, 25.6, 7.3, 15, and 13% respectively.

The substance of R_f 0.66 gave a positive iodine test with ethanolic silver nitrate and its mass spectrum gave M^+ *m/e* 372. The n.m.r. spectrum showed in addition to benzylidene resonances (see Table 1) τ 8.33–9.63 (m, 4, H-1, -2, -7_{endo}, -7_{exo}), 5.50–7.33 (m, 7, H-3, -4, -5, -6a, -6e, -8, -8′), and two complex patterns at 7.0 and 7.2 amounting to one proton, ascribed to H-3 of the mixture of *4,6-O-benzylidene-1,2,3-trideoxy-3-C-iodomethyl-1,2-C-methylene-α,*D*-allo- and β,*D*-altro-pyranose,* ***12***. Treatment of the material (50 mg) with a refluxing solution of sodium hydroxide in aqueous dioxan afforded a new substance M^+ *m/e* 244. This material did not crystallize but showed i.r. absorptions at 3012, 978, 894 cm^{-1} for terminal methylene (15). Assuming **12** to be correct, this olefin is therefore **13**.

*Methyl 4,6-O-Benzylidene-2,3-dideoxy-β-*D*-erythro-hex-2-enopyranoside,* **8β**

Methyl β-D-glucopyranoside was converted to the 4,6-*O*-benzylidene derivative (33) in the usual way (34), and the resulting substance was treated with excess methanesulfonyl chloride and pyridine. The 4,6-*O*-benzylidene-2,3-di-*O*-methanesulfonyl-β-D-glucopyranoside, **8β**, so obtained (9.0 g, 0.02 mol) was added to an efficiently-stirred mixture of potassium iodide (17 g, 0.1 mol) and zinc–copper couple (32) (6.5 g, 0.1 g atom) in 50 ml of dry dimethyl formamide. The solution was refluxed until t.l.c. indicated completion (~3 h) and then the hot solution was poured into ice-water (~100 ml). Chloroform (50 ml) was added and the mixture was stirred for *ca.* 15 min. The insoluble material was removed by filtration through Celite and the filter cake was stirred with an equal mixture of chloroform and water. After repeating the latter process twice, the washings were combined and the chloroform phase separated. After washing with sodium thiosulfate solution and water, the organic layer was dried ($CaCl_2$) and evaporated to a residue which crystallized (4.52 g, 90% yield). The melting point 95–96° and n.m.r. data were in excellent agreement with those reported for the title compound by Lemieux and coworkers (12).

*Simmons–Smith Reaction of Methyl 4,6-O-Benzylidene-2,3-dideoxy-β-*D*-erythro-hex-2-enopyranoside,* **8β** *(Scheme 3)*

Compound **8β** (10.0 g; 0.0403 mol) was subjected to the Simmons–Smith reaction as described above for **8α**, using

Can. J. Chem. Downloaded from www.nrcresearchpress.com by 210.87.254.105 on 09/05/12
For personal use only.

proportionate amounts of the reagents. However dimethoxyethane was *not* required here, and an olefin (21%) was still present after 4 h. The product was isolated in the usual way, and afforded a complex mixture weighing 11.4 g, which was chromatographed on a silica column (75 cm × 5 cm) using petroleum ether (35–60 °C)–ethyl acetate (4:1) as eluant. Each fraction was rechromatographed on a 100 cm × 1.8 cm column which afforded the pure compounds listed in column four of Table 3 with the exception of compounds **9** and **14** which could not be separated.

Of the compounds listed in Table 3 compounds **8**α and **8**β are starting olefins, while **6**α, **9**, and **10** were encountered in Scheme 1 and **14** has been described previously (17, 10). Structure proof of **7**β and **7**α is offered below.

*Methyl 4,6-O-Benzylidene-2,3-dideoxy-2,3-C-methylene-β-*D*-manno-pyranoside, 7β*

When compound **7**β was the main product required from the preparation, the Simmons–Smith reaction of **8**β was allowed to go for 1.5 h only (Table 3). The material isolated by chromatography as described immediately above, was crystallized from ethyl acetate; m.p. 133–134.5 °C; $[\alpha]_D^{23}$ −40.2° (*c*, 5.4 in $CHCl_3$).

Anal. Calcd. for $C_{15}H_{18}O_4$: C, 68.68; H, 6.92. Found: C, 68.60; H, 7.15.

N.m.r. parameters for **7**β are given in Table 1. The appearance of the ring protons was as follows: H-1 (d), -2 (m), -3 (m), -4 (q), -5 (td), -6a (t), -6e (q), -7_{exo} (td), -7_{endo} (q).

The optical rotation of **7**β is reported in Table 2.

*Methyl 4,6-O-Benzylidene-2,3-dideoxy-2,3-C-methylene-α-*D*-manno-pyranoside, 7α*

(*i*) When compound **7**α was the main product desired from the preparation, the Simmons–Smith reaction of **8**β was allowed to go for 8 h (Table 3). The material was obtained by silica column chromatography as detailed two sections above and was recrystallized from ethyl acetate; m.p. 106–108 °C, $[\alpha]_D^{23}$ +104.7 (*c*, 4.75 in $CHCl_3$).

Anal. Calcd. for $C_{15}H_{18}O_4$: C, 68.68; H, 6.92. Found: C, 68.82; H, 7.18.

(*ii*) The title compound could be obtained by anomerization of compound **7**β. The latter substance (0.1 g) was dissolved in ether (10 ml) containing zinc iodide (0.1 g) and the mixture was refluxed for 14 h. After cooling the solution was washed with dilute sodium thiosulfate and then water. The dried ether layer gave a product which by n.m.r. analysis contained starting material (46%), the desired substance, **7**α (22%) and *unknown "b"*[4] (32%).

N.m.r. parameters for **7**α are given in Table 1. The appearance of the ring protons was as follows: H-1 (s), -2 (m), -3 (m), -4 (q), -5 (td), -6a (t), -6e (q), -7_{exo} (td), -7_{endo} (td).

The optical rotation is given in Table 2.

Financial assistance from the National Research Council of Canada and Bristol Laboratories of Syracuse is gratefully acknowledged. We express our gratitude to the staff of the Canadian 220 MHz NMR Centre for their assistance.

1. N. J. DEMJANOV. Chem. Ber. **40**, 4393, 4961 (1907).
2. J. D. ROBERTS and R. H. MAZUR. J. Am. Chem. Soc. **73**, 2509 (1951).
3. (*a*) N. L. WENDLER. *In* Molecular rearrangements. Part 2. P. de Mayo, Editor. Interscience Publishers, New York. 1964. (*b*) M. HANACK and H.-J. SCHNEIDER. Angew. Chem. Int. Ed. Engl. **6**, 666 (1967). (*c*) H. G. RICHEY, JR.[3] *In* Carbonium ions. Vol. 3. G. Olah and P. V. R. Schleyer, Editors. Interscience Publishers, New York. 1969.
4. E. S. FERNANDI and G. JUST. Can. J. Chem. **49**, 1070 (1971); W. P. SCHNEIDER, U. AXEN, F. H. LINCOLN, J. E. PIKE, and J. L. THOMPSON. J. Am. Chem. Soc. **90**, 5895 (1968); W. P. SCHNEIDER. Chem. Commun. 304 (1969); M. MONGRAIN, J. LAFONTAINE, A. BELANGER, and P. DESLONGCHAMPS. Can. J. Chem. **48**, 3273 (1970); G. STORK and M. GREGSON. J. Am. Chem. Soc., **91**, 2373 (1969); M. JULIA and C. DESCORNS. Bull. Soc. Chem. Fr. 1805, 1822 (1970). J. TADAMIER. J. Org. Chem. **31**, 2124 (1966); K. SYHORA, J. A. EDWARDS, and A. D. CROSS. J. Org. Chem. **31**, 3411 (1966).
5. B. FRASER-REID and B. RADATUS. Can. J. Chem. **47**, 4095 (1969).
6. E. L. ALBANO, D. HORTON, and J. H. LAUTERBACH. Carbohydr. Res. **9**, 149 (1969).
7. E. P. BLANCHARD and H. E. SIMMONS. J. Am. Chem. Soc. **86**, 1337 (1964); H. E. SIMMONS, E. P. BLANCHARD, and R. D. SMITH. J. Am. Chem. Soc. **86**, 1347 (1964).
8. R. D. GUTHRIE, R. D. WELLS, and G. J. WILLIAMS. Carbohydr. Res. **10**, 172 (1969).
9. B. FRASER-REID and B. RADATUS. Can. J. Chem. **48**, 2146 (1970).
10. B. FRASER-REID and B. RADATUS. Can. J. Chem. This issue.
11. B. FRASER-REID and B. BOCTOR. Can. J. Chem. **47**, 393 (1968).
12. R. U. LEMIEUX, E. FRAGA, and K. A. WATANABE. Can. J. Chem. **46**, 61 (1968).
13. R. J. FERRIER and N. PRASAD. J. Chem. Soc. C, 570, 575, 581 (1969).
14. B. FRASER-REID, B. J. CARTHY, and B. RADATUS. Tetrahedron, **28**, 2741 (1972).
15. K. NAKANISHI. Infrared absorption spectroscopy. Holden-Day, Inc., San Francisco. 1964; Figs. 28 and 38.
16. D. H. BUSS, L. HOUGH, L. D. HALL, and J. F. MANVILLE. Tetrahedron, **21**, 69 (1965).
17. B. FRASER-REID and B. RADATUS. Chem. Commun. 779 (1970).
18. H. E. SIMMONS and R. D. SMITH. J. Am. Chem. Soc. **80**, 5323 (1958); W. G. DAUBEN and G. H. BEREZIN. J. Am. Chem. Soc. **85**, 468 (1963); S. WINSTEIN and J. SONNERBERG. J. Am. Chem. Soc. **83**, 3235 (1961).
19. J. H.-H. CHAN and B. RICKBORN. J. Am. Chem. Soc. **90**, 6406 (1968); C. W. BLEWETT. Massachusetts Institute of Technology. Seminar in Organic Chemistry. Dec. 1, 1964. p. 214.
20. A. C. COPE, C. H. PARK, and P. SCHERER. J. Am. Chem. Soc. **84**, 4862 (1962); C. D. POULTER, E. C. FRIEDRICH, and S. WINSTEIN. J. Am. Chem. Soc. **91**, 6892 (1969).
21. S. WOLFE, A. RAUK, L. M. TEL, and I. G. CSIZMADIA. J. Chem. Soc. B, 136 (1971).
22. J. T. EDWARD, P. R. MORANDE, and I. PUSKAS. Can. J. Chem. **39**, 2069 (1961); R. U. LEMIEUX. *In* Molecular rearrangements. P. de Mayo, Editor. Interscience, New York. 1964. p. 709.

23. R. U. LEMIEUX. Advan. Carbohydr. Chem. **9**, 1 (1954); J. N. BEMILLER. Advan. Carbohydr. Chem. **22**, 25 (1967).
24. B. R. REE and J. C. MARTIN. J. Am. Chem. Soc. **92**, 1660 (1970); J. C. MARTIN and B. R. REE. J. Am. Chem. Soc. **91**, 5882 (1969), and ref. cited therein.
25. B. FRASER-REID and B. RADATUS. J. Am. Chem. Soc. **92**, 5288 (1970).
26. D. J. PATEL, M. E. H. HOWDEN, and J. D. ROBERTS. J. Am. Chem. Soc. **85**, 3218 (1963) and ref. cited therein.
27. R. U. LEMIEUX, R. K. KULLNIG, H. J. BERNSTEIN, and W. G. SCHNEIDER. J. Am. Chem. Soc. **80**, 6098 (1958).
28. K. B. WIBERG and B. J. NIST. J. Am. Chem. Soc. **85**, 2788 (1963); J. D. GRAHAM and M. T. ROGERS. J. Am. Chem. Soc. **84**, 2249 (1962).
29. L. D. HALL and J. F. MANVILLE. *In* Deoxy sugars. *Edited by* S. Hanessian. American Chemical Society Publications. 1966.
30. R. U. LEMIEUX and B. FRASER-REID. Can. J. Chem. **42**, 532 (1964).
31. F. A. BOVEY. Nuclear magnetic resonance spectroscopy. Academic Press, New York. 1969. p. 129. E. W. GARBISCH. J. Am. Chem. Soc. **86**, 5561 (1964).
32. J. D. ROBERTS, Editor. Organic synthesis. Vol. 41. John Wiley and Sons, Inc., New York. 1961. p. 72.
33. K. FREUDENBERG. Ber. **61**, 1743 (1928).
34. N. K. RICHTMYER. Meth. Carbohydr. Chem. **1**, 108 (1962).

Can. J. Chem. Downloaded from www.nrcresearchpress.com by 210.87.254.105 on 09/05/12
For personal use only.

Cyclopropylcarbinyl-oxo-carbonium Ions. Part VI.[1] Synthesis and Chemistry of an Epimeric Pair of Homoallyl Iodides (3-Iodomethyl Glycals)[2,3]

BERT FRASER-REID AND BRUNO RADATUS

Department of Chemistry, University of Waterloo, Waterloo, Ontario

Received March 7, 1972

The homoallyl iodide 4,6-*O*-benzylidene-1,2,3-trideoxy-D-*ribo*-hex-1-enopyranose, **4**, is the second major product from Simmons–Smith reaction of methyl 4,6-*O*-benzylidene-2,3-dideoxy-α-D-*erythro*-hex-2-enopyranoside, **6α**. The major product is the cyclopropyl glycoside **7α**, which when treated separately with the Simmons–Smith reagents furnishes an 85% yield of **4**. The mechanism of this transformation is investigated. It is not simply a Lewis-catalyzed iodinolysis since zinc iodide in a variety of solvents does not convert **7α** to **4**. Methylene iodide is essential, as is the organo-zincate complex, operative in Simmons–Smith reactions.

The 3-epimer of the homoallyl iodide **4**, *i.e.* 4,6-*O*-benzylidene-1,2,3-trideoxy-D-*arabino*-hex-1-enopyranose, **5**, is produced in only 0.9% yield in the methylenation of the anomeric olefinic glycoside, **6β**. The low yield is attributable to the extensive anomerization experienced by **6β** itself, and by the primary reaction products. This leads to a plethora of compounds including *both* epimeric homoallyl iodides **4** and **5**.

In order to get it all together, the homoallyl iodide **4** is transformed into its epimer **5** by an unambiguous synthetic sequence. Some of the intermediates in this sequence are polyfunctional molecules of considerable synthetic potential.

The possibility of an alternative route to compound **4** directly from the olefinic glycoside **6α** is discussed. Coordination of the methoxyl oxygen of **6α** to the organo-zincate complex could achieve an ideal S_Ni transition state in which ICH_2^- is delivered at C-3 with synchronous departure of the methoxyl group. This mechanism, called the "reverse" allylic rearrangement for reasons outlined in the text, is discussed.

L'iodure homoallyle *O*-benzylidène-4,6 tridéoxy-1,2,3 D-*ribo* hexeno-1 pyranose **4**, est le second produit majeur de la réaction de Simmons–Smith sur le méthyl *O*-benzylidène-4,6 didéoxy-2,3-α-D-*erythro* hexeno-2 pyranoside, **6α**. Le produit majeur est le cyclopropylglycoside **7α** qui, traité séparément avec les réactifs de Simmons–Smith, conduit à **4** avec un rendement de 85%. Le mécanisme de cette transformation est examinée. Il ne s'agit pas d'une simple iodinolyse catalysée par un acide de Lewis car l'iodure de zinc dans divers solvants, ne transforme pas **7α** en **4**. L'iodure de méthylène est essentiellement, comme l'organozincate, le complexe agissant dans les réactions de Simmons–Smith.

L'épimère-3 de l'iodure homoallyle **4**, à savoir l'*O*-benzylidène-4,6 tridéoxy-1,2,3-D-*arabino* hexeno-1 pyranose **5**, est obtenu avec un rendement de 0.9% seulement lors de la méthylénation de l'anomère glycoside oléfinique, **6β**. Le faible rendement est attribué à l'anomérisation extensive subie par **6β** et par les produits de la réaction primaire. Une pléthore de composés est obtenue incluant à la fois les iodures homoallyliques épimères **4** et **5**.

En vue de les obtenir tous ensembles, l'iodure homoallyle **4** est transformé en son épimère **5** selon une séquence réactionnelle connue. Quelques intermédiaires de cette séquence sont des molécules polyfonctionnelles d'un potentiel synthétique considérable.

La possibilité d'obtenir **4**, par une autre voie d'accès directement à partir du glycoside oléfinique **6α**, est discutée. La coordination de l'oxygène méthoxyle de **6α** au complexe organozincate, permettrait de réaliser un état de transition idéal S_Ni dans lequel $^-CH_2I$ attaque le C-3 avec départ synchronisé du groupe méthoxyle. Ce mécanisme, appelé, "réarrangement allylique inverse" pour les raisons soulignées dans le texte, est discuté.

[Traduit par le journal]

Canadian Journal of Chemistry, **50**, 2919 (1972)

In the preceding paper (1) we discussed the promise held by the *cyclopropylcarbinyl-oxo-carbonium ion*, **1**, (2) for fundamental structure modification of the carbohydrate skeleton, and outlined the syntheses of some cyclopropanated glycosides (**2**) from which **1** might be generated by loss of alkoxyl. The homoallyl system **3** being formally related to **2** by virtue of the cyclopropylcarbinyl rearrangement (3), represents a potential alternative source of ion **1** and for this reason we describe herein two homoallyl iodides **4** and **5** which complement the cyclopropyl derivatives described previously (1).

[1]For Part V see ref. 1.

[2]Portions of this work have appeared as preliminary communications in refs. 2, 8, and 9.

[3]Taken from the Ph.D. Thesis of Bruno Radatus, University of Waterloo, 1971.

Can. J. Chem. Downloaded from www.nrcresearchpress.com by 210.87.254.105 on 09/05/12
For personal use only.

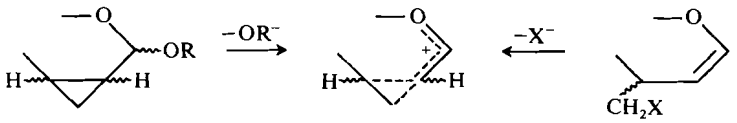

2 1 3

Compound **4** was obtained in 7.5% yield from Simmons–Smith reaction of olefin **6α** (see (Scheme 1). The n.m.r. spectrum[4] indicated the absence of a methoxyl group but the preservation of the benzylidene group. There were quartets at τ 3.66 and 5.00 reminiscent of carbohydrate glycals (5), and this was supported by i.r. absorptions at 1645, 1235, and 1081 cm^{-1} indicative of a vinyl ether (6). The principal product of the Simmons–Smith reaction, the cyclopropanated glycoside **7α**, when subjected independently to the Simmons–Smith conditions afforded the iodoglycal, **4**. Proof for the latter structure was readily supplied by lithium aluminum hydride reduction whereby a substance displaying a methyl doublet at τ 8.86 ($J = 7.5$ Hz) was obtained. The latter was therefore **8**.

The foregoing discussion in fact indicates the presence but not the orientation of the iodomethyl group in **4**. The material underwent "instantaneous" silver-ion assisted methanolysis which afforded a 96% yield of crystalline material whose n.m.r. spectrum showed two methoxyl resonances of equal intensity at τ 6.61 and 6.53. The substances responsible were separated and identified as the cyclopropyl glycosides **7α** and **7β** respectively by comparison with the authentic substances (1, 7).[5] In view of the *allo* configuration of **7**, the iodomethyl group in **4** must be axial.

Further proof of structure **4** was obtained by transformation into the 3-epimer **5** as summarized in Scheme 2 (9).

Dehydroiodination of the iodoglycal **4** gave a diene **9** whose structure was upheld by absorptions in the i.r. at 3012, 1645, and 1600 cm^{-1}, (6) and in the u.v. at 243 nm, ε 4600 (*cf.* ref. 10). Methoxybromination of **9** (11) gave a single substance judged to be the α-D-1,4-addition product **10**, the anomeric configuration being indicated by the fact that the n.m.r. resonance

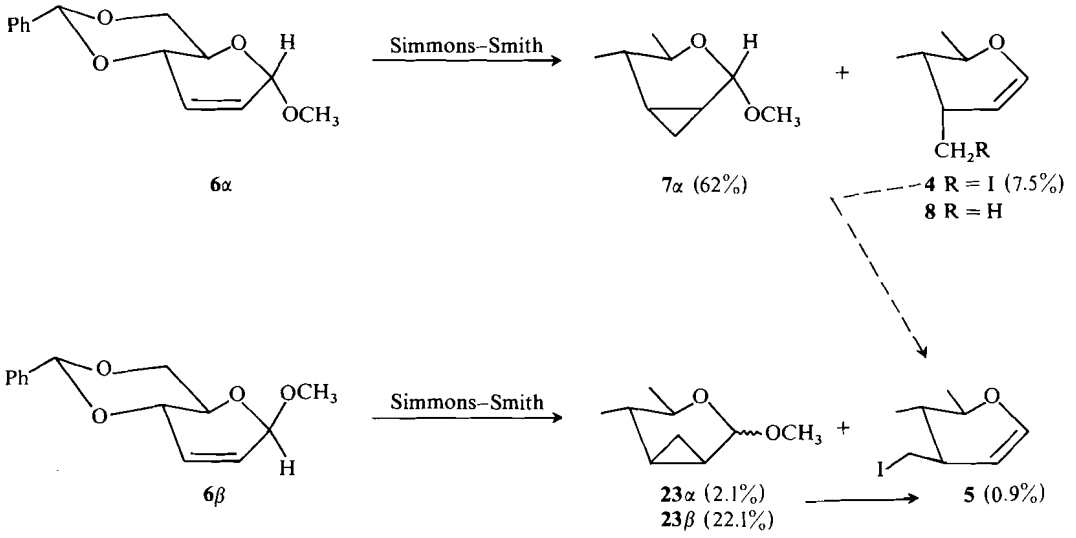

SCHEME I

[4]A detailed computer-assisted analysis of the 220 MHz n.m.r. spectra of the epimeric iodides **4** and **5** has been presented in Part IV of this series (4).

[5]The formation of the anomers **7α** and **7β** in equal amounts implies that there is no bicyclobutonium ion contribution to the intervening cyclopropylcarbinyl-oxo-carbonium ion, **1**, (8). The geometry of these ions will be discussed fully in a forthcoming publication.

Can. J. Chem. Downloaded from www.nrcresearchpress.com by 210.87.254.105 on 09/05/12
For personal use only.

Can. J. Chem. Downloaded from www.nrcresearchpress.com by 210.87.254.105 on 09/05/12
For personal use only.

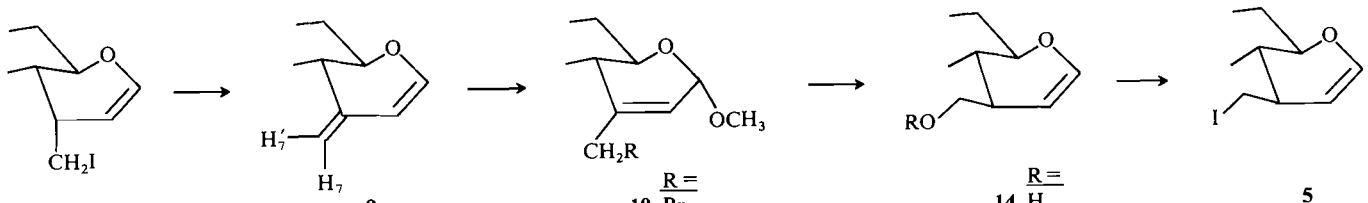

4 **9**

R =
10 Br
11 H
12 OH
13 ONO_2

R =
14 H
15 Ts

5

SCHEME 2

Can. J. Chem. Downloaded from www.nrcresearchpress.com by 210.87.254.105 on 09/05/12
For personal use only.

for H-1 at τ 5.12 was closer to that for α-D-hex-2-enopyranosides (τ 5.0) than for the α-D-analogues (τ 4.6)(4*b*). Treatment of **10** with lithium aluminum hydride gave **11** whose allylic methyl group at τ 8.18 was weakly coupled to H-2 and -4.

The allylic bromide **10** reacted readily with silver nitrate solution to give a mixture of **12** and **13** and spectral comparison of each (see Experimental) with the parent bromide indicated that there had not been any gross structural changes. Each substance on reaction with lithium aluminum hydride gave the 3-deoxy glycal **14**. Thus when compound **14** was the desired material, it was superfluous to separate **12** from **13**.

The structure of **14** rests upon the presence of a vinyl ether (μ_{max} 1645 cm^{-1}) (6) and the n.m.r. quartets at τ 3.73 (H-1) and 5.37 (H-2) (5, 12). The configuration at C-3 follows from the values for J_{13} and J_{23} (−2.5 and 2.0 Hz respectively) which are different from those (−1.3 and ~5.5) for allal derivatives **4** and **8** (4).[4] Chemical proof follows from the stereochemical course of lithium aluminum hydride reductive rearrangement of 2,3-unsaturated glycosides (*e.g.* **12** and **13**) since the hydride adds *syn* to the departing aglycon (13).

p-Toluenesulfonylation of **14** proceeded smoothly to give **15** which underwent iodinolysis in methylisobutyl ketone to the iodide **5**. This substance was identical in all respects to the material produced in 0.9% yield by Simmons–Smith reaction of compound **6**β (Scheme 1) (1). The overall yield in Scheme 2 was 20–25%. That **4** and **5** were indeed epimers was substantiated by treating the latter with methanolic silver nitrate, whereupon the diene **9** previously produced from **4** was also obtained.

Mechanistic Aspects of the Formation of Homoallyl Iodides in Simmons–Smith Reactions

Having established the stereochemistry of the original homoallyl iodide **4**, a question arose as to the mechanism of its formation during the Simmons–Smith reaction of **6**α (Scheme 1). The transformation depicted in its essence in **16** is the addition of the iodomethyl anion with synchronous expulsion of the allylic methoxyl substituent. This mechanism is attractive since it provides for the usually observed *cis* relationship between entering and departing nucleophiles (14). An additionally attractive feature is the fact that the reactive complex depicted in **16** is geometrically closely allied with that in **17** through which the major reaction (*i.e.* cyclopropanation) leading to the cyclopropyl glycoside 7α is thought to proceed (1, 15). Hence the organometallic agent, represented for simplicity as a monomer, (*cf.* ref. 16), approaches the double bond of **6**α and becomes ligated to the oxygen. Subsequent collapse of the complex can then lead either (*a*) to a cyclopropyl or (*b*) to a homoallyl compound. The latter eventuality requires that considerable *nucleophilic* character reside on the methylene group of the complex producing virtually ICH_2^-. The former eventuality suggests that the complex possesses electrophilic character more fully developed in $:CH_2$. The concept of nucleophilic character of the Simmons–Smith complex has been raised before (17), but was shown *not* to be operative in *cyclopropanation* reactions (18). However, the reaction under discussion here is not a cyclopropanation but a nucleophilic (S_Ni) displacement. The process does not appear to depend upon any special activation supplied by the lactol oxygen of **6**, for methylenation of 5,5-dimethylcyclohex-2-enol was found to be accompanied by small amounts of 3-(iodomethyl)-5,5-dimethylcyclohexene (19).

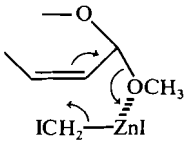

16

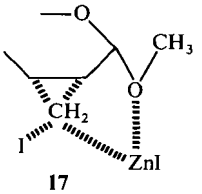

17

"Forward" allylic rearrangements whereby certain acetylated glycals (**18**, Y = OAc) are converted to hex-2-enopyranose derivatives (**19**) are well known in carbohydrate chemistry (20). However the "reverse" process had not been reported prior to the preliminary account (2) in which it was raised as a possibility. Since then there have been a number of interesting reports (13, 21) which may be generalized as "reverse" allylic rearrangements **19** → **18**. These reports support the possibility that such a rearrangement might be occurring in the present case. If a substantial O—Zn bond exists in the complex **16**, then the rearrangement may be appreciated as a simple [3:3] sigmatropic rearrangement

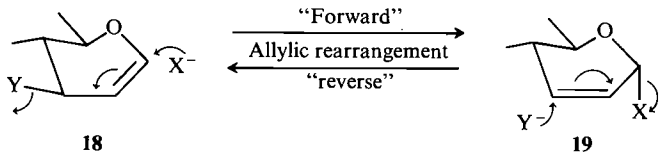

18 19

(22). The possibility that the "forward" allylic rearrangements (*vide supra*) may also fall into this mechanistic category has been discussed by Ferrier and Vethaviyaser (23).

The formation of iodide **4** from the cyclopropyl glycoside **7α** under the Simmons–Smith conditions suggests that some (if not all!) of compound **4** is formed by a mechanism different from the allylic rearrangement depicted in **16**. Four pathways shown in Scheme 3 may be envisaged starting with **7α**. The major difference between mechanisms 1 and 2 is the intermediacy in the latter of the cyclopropylcarbinyl-oxocarbonium ion **20** which might react under thermodynamic control (3*a*, 24) to give **4** directly, or under kinetic control to give the glycosyl iodide **21**. The latter would subsequently rearrange to the homoallyl iodide, **4**. The major difference between mechanisms 3 and 4 is the involvement in the former of 1 mol of methylene iodide. Some experiments were done to differentiate between these four mechanisms.

The conversion **7α** → **4** could not be accomplished by using sodium iodide in diethyl ether,

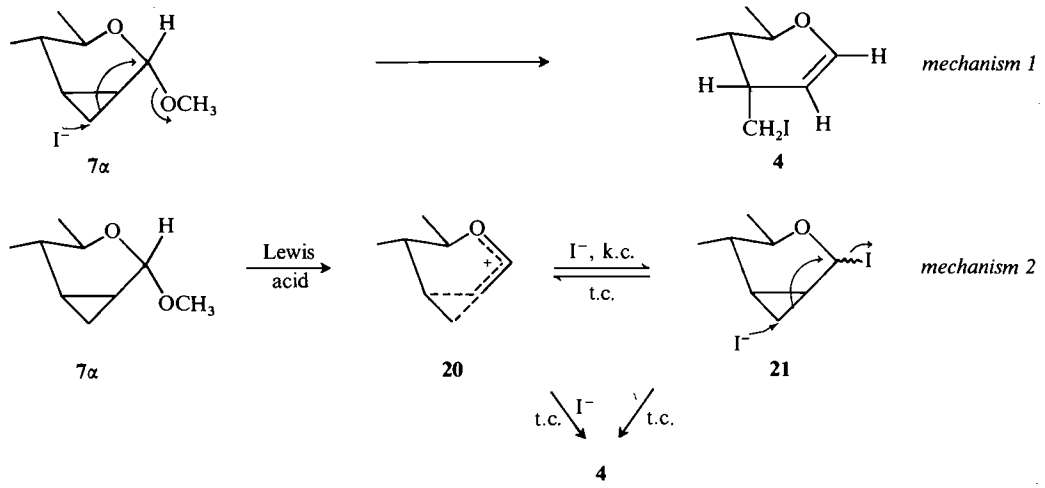

k.c., kinetic control; t.c., thermodynamic control

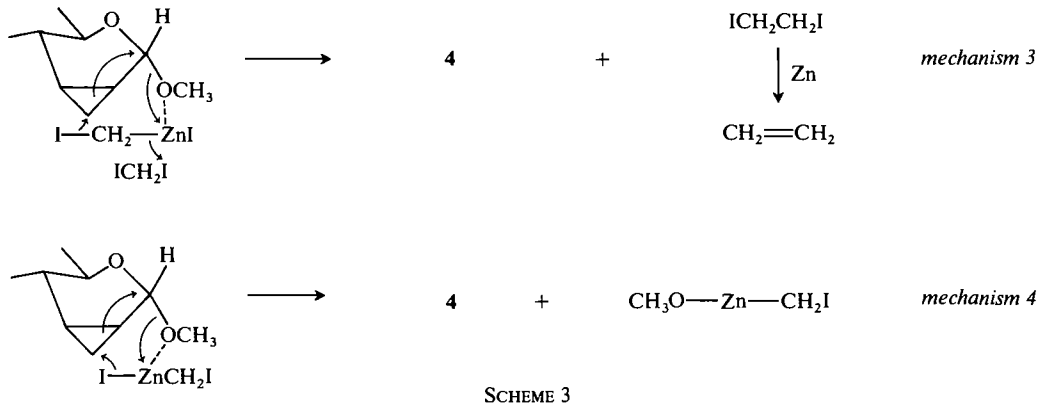

SCHEME 3

Can. J. Chem. Downloaded from www.nrcresearchpress.com by 210.87.254.105 on 09/05/12
For personal use only.

TABLE 1. Simmons–Smith reaction on compounds 7α and 7β under various conditions

Experiment	Initial period of reflux (h)*	Compounds added†	Products (% composition)‡			
			7α	7β	4	Unknown "a"§
1	1.0	7α	46	—	46	8
2	1.0	7β	50	12	30	8
3	1.0	7α, CH_2I_2	36	—	47	17
4	2.5	7α	57	—	28	15
5	2.5	7α, CH_2I_2	23	—	50	27
6	8.5	7α	69	—	—	31

*Zinc (0.1 g), methylene iodide (0.15 ml), a crystal of iodine, and 0.6 ml of ether were refluxed for the time shown in column.

†The substrate (0.1 g), 0.4 ml ether, and 0.15 ml of methylene iodide (as indicated) were added after the period of initial reflux, and reflux was then continued for a further 2 h.

‡Determined from the n.m.r. spectrum of the crude reaction product.

§For information on this substance see footnote 4 in ref. 1.

acetone, methylethyl ketone, or methylisobutylketone which indicates that *mechanism 1* cannot be operative. *Mechanism 2* may also be rejected since zinc iodide in a variety of solvents was also ineffective.

Evaluation of *mechanism 3* required the series of experiments summarized in Table 1. The initial reflux period of 1 h was selected because after this time an appreciable amount of ICH_2ZnI, the functioning agent in *mechanism 3*, has formed (25); the period of 2.5 h, because ICH_2ZnI has then just begun to react appreciably with methylene iodide to form, eventually, ethylene (25); and the period of 8.5 h, because at this time the ICH_2ZnI has virtually all decomposed (25). It can be seen from experiment 6 that the iodomethyl zinc complex is required for the formation of compound **4**. Experiments 1, 3, and 5 show that in order to obtain a 45–50% yield of compound **4** an appreciable amount of methylene iodide is required. Experiments 4 and 5 show dramatically the importance of methylene iodide. Thus the stature of mechanism 3 is enhanced and, by corollary, mechanism 4 is rendered unlikely.

An added requirement of *mechanism 3* is that there be *cis*-relationship between the anomeric methoxy group and the cyclopropane ring. This is indicated by comparison of experiments 1 and 2 (Table 1). Applying corrections for unrecovered starting material, iodide **4** is formed in 85% in experiment 1 but only 34% in experiment 2. In the latter, the principal reaction is anomerization of $7\beta \rightarrow 7\alpha$; it is therefore reasonable to conclude that the 34% of **4** in experiment 2 arose from 7α formed *in situ*. The formation of the D-*arabino* iodide **5** in 0.9% yield during the Simmons–Smith reaction of **6** (Scheme 1) may be envisaged as proceeding from **23**β via *mechanism 3*. Whether a "reverse" allylic rearrangement, such as **19**, is operative to any appreciable extent in the methylenation of **6**α or **6**β (Scheme 1) cannot be answered by means of the present data. Certainly *mechanism 3* would seem quite adequate to explain the formation of **4** and **5**. However, the recently reported "reverse" allylic rearrangements (21) suggest that this option should be kept open.

Experimental

For general experimental conditions see ref. 1. Unless otherwise stated, the n.m.r. spectra in this paper were taken on a Varian T-60 instrument and *J*-values are in Hz.

*4,6-O-Benzylidene-1,2,3-trideoxy-3-C-iodomethyl-*D*-ribo-hex-1-enopyranose (4)*

*(a) From Simmons–Smith Reaction of 6*α

Methyl 4,6-*O*-benzylidene-2,3-dideoxy-α-D-*erythro*-hex-2-enopyranoside, **6**α, was subjected to the Simmons–Smith reaction as described in the accompanying paper (1) and silica column chromatography (1) afforded the title compound in 7.5% yield based on the starting olefin. The substance crystallized after evaporation of the eluant, and recrystallization from methanol afforded the pure sample, m.p. 130–132° $[\alpha]_D^{23}$ +129.0° (*c*, 2.8 in $CHCl_3$).

*(b) From Iodinolysis of Methyl 4,6-O-Benzylidene-2,3-dideoxy-2,3-C-methylene-*α*-*D*-allopyranoside, 7*α

The addition of the reactants was done as indicated in Table 1. At the end of the reaction period the mixture was poured into a separatory funnel and washed with aqueous saturated ammonium chloride then sodium bicarbonate solution. The ether layer was dried and evaporated and the residue examined by n.m.r. The composition of the mixtures given in Table 1 was determined from the integrated in-

Can. J. Chem. Downloaded from www.nrcresearchpress.com by 210.87.254.105 on 09/05/12
For personal use only.

Can. J. Chem. Downloaded from www.nrcresearchpress.com by 210.87.254.105 on 09/05/12
For personal use only.

tensities in the spectra. The conditions in experiment 1 are optimum for the formation of the title compound **4**. The latter was recovered by silica column chromatography as used for the Simmons–Smith reaction product (1).

Anal. Calcd. for $C_{14}H_{15}IO_3$: C, 46.92; H, 4.22; I, 35.47. Found: C, 46.87; H, 4.22; I, 34.67.

The n.m.r. spectrum for **4** shows: τ 2.62 (m, 5, Ph), 4.43 (s, 1, PhC*H*), 3.66 (q, 1, $J_{12} = 6.2$, $J_{13} = -1.3$, H-1), 5.00 (q, 1, $J_{23} = 5.2$, H-2), 7.24 (m, 1, $J_{34} = 6.0$, $J_{37} = 11.0$, $J_{37'} = 4.0$, H-3), 6.00 (q, 1, $J_{45} = 9.5$, H-4), 6.21 (td, 1, $J_{56_a} = 10.0$, $J_{56_e} = 4.5$, H-5), 6.24 (t, 1, $J_{6_a6_e} = -10.5$, H-6a), 5.58 (q, 1, H-6e), 7.01 (q, 1, $J_{77'} = -9.5$, H-7), 6.37 (q, 1, H-7′). I.r. shows: μ_{max} 1645, 1235, and 1081 cm^{-1} associated with a vinyl ether (6).

*4,6-O-Benzylidene-1,2,3-trideoxy-3-C-methyl-*D*-ribo-hex-1-enopyranose, **8***

Compound 4 (0.1 g, 0.28 mmol) was treated with lithium aluminum hydride (0.1 g, 2.6 mmol) in refluxing diethyl ether (10 ml) for 18 h when t.l.c. indicated complete disappearance of the starting material. Customary work-up (1) gave a crystalline residue (0.05 g, 75% yield) which was recrystallized from methanol, m.p. 85–86° $[\alpha]_D^{23}$ +158.4 (*c*, 4.95 in $CHCl_3$).

Anal. Calcd. for $C_{14}H_{16}O_3$: C, 72.39; H, 6.94. Found: C, 72.36; H, 6.88.

The n.m.r. spectrum of compound **8** shows: τ 2.60 (m, 5, Ph), 4.42 (s, 1, PhC*H*), 3.73 (q, 1, $J_{12} = 6.0$, $J_{13} = -1.3$, H-1), 5.22 (t, 1, $J_{23} = 6.0$, H-2), 7.43 (m, 1, $J_{34} = 6.0$, $J_{3CH_3} = 7.5$, H-3), 6.02 (q, 1, $J_{45} = 9.5$, H-4), 6.08 (td, 1, $J_{56_a} = 10.0$, $J_{56_e} = 4.5$, H-5), 6.23 (t, 1, $J_{6_a6_e} = -10.5$), 5.59 (q, 1, H-6e), and 8.86 (d, 3, CH_3).

Irradiation of the proton at τ 7.3 simplified the doublet at τ 8.86 to a singlet. The i.r. spectrum shows a strong absorption at 1645 cm^{-1} for a vinyl ether (6).

*4,6-O-Benzylidene-2,3-dideoxy-2,3-C-methylene-α and β-*D*-allopyranoside, **7α and 7β**.*

Compound **6**, (0.9793 g; 2.74 mmol), was dissolved in 75 ml of dry methanol; then 0.5 g of silver carbonate and 10 ml of saturated methanolic silver nitrate were added. Judging from the precipitated silver iodide, the reaction was complete in seconds but water (75 ml) was not added until 1 min later. The reaction product was recovered by extraction into chloroform which afforded 0.6851 g (0.00261 mol; 96%) of crystalline material. The n.m.r. spectrum of the substance showed two methoxyl absorptions at τ 6.61 and 6.53 of equal area. The two components were separated on a silica column (100 cm × 1.8 cm) eluted with petroleum ether (35–60°)–ethyl acetate (4:1). The slower running substance, **7α**, (0.2632 g) was identified by mixed m.p. (126–128 °C) and spectral comparison (1, 7).

The faster running component **7β**, (0.2135 g) was recrystallized from methanol, m.p. 92–93 °C $[\alpha]_D^{23}$ −8.0° (*c*, 3.06 in $CHCl_3$)

Anal. Calcd. for $C_{15}H_{18}O_4$: C, 68.68; H, 6.92. Found: C, 68.73; H, 7.03.

The n.m.r. spectrum shows: τ 2.60 (m, 5, Ph), 4.37 (s, 1, PhC*H*), 6.53 (s, 3, OCH_3), 5.23 (bs, 1, $J_{12} = 1.0$) obtained from 220 MHz spectrum of H-2), H-1, 9.00 (m, 1, $J_{23} = 9.0$, $J_{27_{exo}} = 8.0$, $J_{27_{endo}} = 5.5$, H-2), 8.88 (m, 1, $J_{34} = 5.0$, $J_{37_{exo}} = 8.0$, $J_{37_{endo}} = 5.5$, H-3), 9.14 (td, 1, $J_{7_{exo}7_{endo}} = -5.5$, H-7*exo*), 8.93 (q, 1, H-7*endo*), 5.70 (q, 1, $J_{45} = 9.5$, H-4), 6.71 (td, 1, $J_{56_a} = 10.0$, $J_{56_e} = 4.5$, H-5), 6.29 (t, 1, $J_{6_a6_e} = -10.5$, H-6a), 5.78 (q, 1, H-6e).

*4,6-O-Benzylidene-1,2,3-trideoxy-3-C-methylene-*D*-erythro-hex-1-enopyranose, **9** (Scheme 2)*

(*a*) 4,6-*O*-Benzylidene-1,2,3-trideoxy-3-*C*-iodomethyl-D-*ribo*-hex-1-enopyranose, **4** (1.374 g; 0.00384 mol) was dissolved in 50 ml of dioxan, *N* sodium hydroxide solution (50 ml) was added; and the solution refluxed for 5 min. The solution was cooled then extracted with chloroform, which afforded 0.862 g (0.00374 mol; 97.4%) of crystalline compound **10**. The compound was recrystallized from ethanol: m.p. 98–100 °C; $[\alpha]_D^{23}$ +98.4° (*c*, 3.6 in $CHCl_3$).

(*b*) Methyl 4,6-*O*-benzylidene-1,2,3-trideoxy-3-*C*-iodomethyl-D-*arabino*-hex-1-enopyranose, **5**, (*vide infra*) (0.02 g) was treated with saturated methanolic silver nitrate (10 ml) for 1 h at room temperature. Precipitate formation was much slower than in the case of compound **6**. Water was added and the mixture was extracted with chloroform. The chloroform layer was washed with saturated sodium bicarbonate, dried, and evaporated under reduced pressure to give a crystalline material whose n.m.r. spectrum was identical to that given by the substance obtained in part *a*.

Anal. Calcd. for $C_{14}H_{14}O_3$: C, 73.02; H, 6.13. Found: C, 72.90; H, 6.38.

The n.m.r. spectrum of **9** shows τ 2.53 (m, 5, Ph), 4.30 (s, 1, PhC*H*), 3.60 (d, 1, $J_{12} = 6.0$, $J_{17} \leqslant 0.5$, $J_{17'} = 1.0$, H-1)[6] 4.53 (d, 1, H-2), 5.11 (bs, 1, H-7),[6] 4.91 (bs, 1, H′-7),[6] 5.67 (q, 1, J_{47} or $J_{47'} = 2.0$, $J_{45} = 8.0$, H-4), 6.06–6.21 (m, 2, $J_{56_a} = 10.0$, $J_{56_e} = 4.5$, H-5, H-6a), 5.60 (q distorted, 1, $J_{6_a6_e} = -10.5$, H-6e).

The i.r. spectrum shows: μ_{max} 3012 cm^{-1} (terminal = CH_2), 2849, 1645 (vinyl ether), 1600 (terminal = CH_2), 978, and 894 (terminal = CH_2) (6). The u.v. spectrum shows: λ_{max} (ethanol) 243 nm (ε 4600) (*cf.* 10).

*Methyl 4,6-O-Benzylidene-2,3-dideoxy-3-C-bromomethyl-α-*D*-erythro-hex-2-enopyranoside, **10***

Diene **10** (0.862 g; 3.74 mmol) was dissolved in a mixture of dry methanol (100 ml) and silver acetate (0.5 g). Bromine (0.3 ml) was diluted to 10 ml with dry methanol, and added slowly with stirring until the solution had a persistent yellow color (8 ml) (11). The solution was poured into water (100 ml), filtered, and the filtrate extracted with chloroform. The chloroform layer was washed with saturated sodium bicarbonate solution, dried, and evaporated under reduced pressure to give the title compound. The material was recrystallized from ethanol, m.p. 119–122 °C with decomposition; $[\alpha]_D^{23}$ −7.35° (*c*, 16.32 in $CHCl_3$).

Anal. Calcd. for $C_{15}H_{17}BrO_4$: C, 52.80; H, 5.02; Br, 23.42. Found: C, 52.68; H, 4.81; Br, 23.21.

The n.m.r. spectrum of compound **10** shows: τ 2.63 (m, 5, Ph), 4.38 (s, 1, PhC*H*), 6.58 (s, 3, OCH_3), 5.12 (bd, 1, $J_{12} = 2.5$, H-1), 4.22 (bs, 1, H-2), 5.53–6.33 (m, 6, H-7, -7′, -4, -5, -6a, -6e).

Compound **10** decomposes readily at room temperature but may be stored in the freezing compartment of a refrigerator.

[6]The assignment of the exocyclic methylene protons as *trans* (H′-7, τ 4.91) and *cis* (H-7, τ 5.11) rests on the precedent that the five-bond coupling is larger for *trans* than for *cis* protons (26). Thus the couplings of 1.0 and ~0.5 Hz are assigned as *trans* ($J_{17'}$) and *cis* (J_{17}) respectively.

Can. J. Chem. Downloaded from www.nrcresearchpress.com by 210.87.254.105 on 09/05/12
For personal use only.

Methyl 4,6-O-Benzylidene-2,3-dideoxy-3-C-methyl-α-D-erythro-hex-2-enopyranoside, 11

Compound **10** (0.2 g; 0.59 mmol) was dissolved in a mixture of diethyl ether (25 ml) and LAH (0.1 g) and refluxed for 15 h. The excess LAH was destroyed by the dropwise addition of water and then the aluminum hydroxide was filtered. The ether solution was dried and evaporated under reduced pressure and resulted in 0.1408 g of crystalline material. T.l.c. in petroleum ether (35–60 °C)–ethyl acetate (4:1) indicated the presence of several components. The mixture was put on a silica column (100 cm × 1.8 cm) and eluted with 4:1 petroleum ether (35–60 °C)–ethyl acetate. The first fraction (R_f 0.64) was starting compound **10** (0.02 g) and the second fraction (R_f 0.47) was compound **11** (0.097 g; 0.00037 mol; 63%). The other fractions contained impurities and were rejected.

Compound **11** was recrystallized from ethanol, m.p. 139–140 °C; $[\alpha]_D^{23}$ +60.6° (*c*, 4.15 in $CHCl_3$).

Anal. Calcd. for $C_{15}H_{18}O_4$: C, 68.68; H, 6.92. Found: C, 68.56; H, 6.77.

The n.m.r. spectrum of compound **11** shows: τ 2.58 (m, 5, Ph), 4.40 (s, 1, PhC*H*), 6.57 (s, 3, OCH_3), 8.18 (s, 3, $J_{2CH_3} <$ 0.5 Hz, CH_3), 5.14 (bs, 1, $J_{12} = 2.5$, H-1), 4.57 (bs, 1, H-2), 5.96 (d, 1, $J_{4CH_3} < 0.5$, $J_{45} = 8.0$, H-4), 6.11 (m, 1, $J_{56_a} =$ 10.0, $J_{56_e} = 4.5$ (assumed), H-5), 6.20 (t, 1, $J_{6_a6_e} = -10.5$, H-6a), 5.70 (q distorted, 1, H-6e). Double irradiation experiments showed that the methyl group was coupled to both H-2 and -4 with coupling less than 0.5 Hz.

Methyl 4,6-O-Benzylidene-2,3-dideoxy-3-C-(hydroxymethyl and O-nitromethyl)-α-D-erythro-hex-2-enopyranosides, 12 and 13 respectively

Compound **10** (1.0 g; 2.94 mmol) was dissolved in dioxane (50 ml) containing suspended silver acetate (1.0 g), and a solution of silver nitrate (5 g) in water (50 ml) was then added. The mixture was stirred for 6 h in the dark at room temperature and then filtered to remove silver salts. The filtrate was extracted with chloroform and the chloroform layers washed with saturated aqueous sodium bicarbonate solution and distilled water. The chloroform layer was dried and evaporated under reduced pressure and resulted in a syrup weighing 0.935 g. T.l.c. using petroleum ether (35–60 °C)–ethyl acetate (7:3) indicated two main components, R_f 0.43 and 0.09 which were separated on a silica column (10 cm × 1.8 cm) eluted with the same solvent mixture. The faster-running component (compound **13** 0.3397 g, 37%) came off first, and then the irrigant was changed to pure ethyl acetate to afford the second component (compound **12**, 0.4487 g; 55%).

The ratio of compound **12** to compound **13** could be varied by changing the reaction conditions. When compound **10** (1.05 g, 3.08 mmol) was treated with 50 ml dioxane, 25 ml water, 1 g silver acetate, and 5 g silver nitrate, the result was 0.279 g (32.5%) of compound **12** and 0.571 g (58%) of compound **13**.

Compound **12** was recrystallized from ethyl acetate, m.p. 120–122 °C; $[\alpha]_D^{23}$ +45.4° (*c*, 4.20 in $CHCl_3$).

Anal. Calcd. for $C_{15}H_{18}O_5$: C, 64.73; H, 6.52. Found: C, 64.44; H, 6.32.

The n.m.r. spectrum of compound **12** shows: τ 2.60 (m, 5, Ph), 4.42 (s, 1, PhC*H*), 6.55 (s, 3, OCH_3), 7.97 (bs, 1, exchangeable, OH), 5.02 (bs, 1, $J_{12} = 2.5$, H-1), 4.27 (bs, 1, H-2), 5.53–6.30 (m, 6, CH_2—OH, H-4, -5, -6a, -6e). Double irradiation at τ 5.89 (—CH_2—OH) caused H-1 and -2 to become doublets with $J_{12} = 2.5$. The chemical shifts for H-1 and -2 are characteristic of 2,3-unsaturated sugars (5, 7).

Compound **13** was recrystallized from ethanol, m.p. 130–132 °C; $[\alpha]_D^{23}$ +35.7° (*c*, 6.0 in $CHCl_3$).

Anal. Calcd. for $C_{15}H_{17}NO_7$: C, 55.72; H, 5.30; N, 4.33. Found: C, 56.41; H, 5.13; N, 4.32.

A satisfactory elemental analysis for this reactive allylic nitrate, **13**, could not be obtained, but (*i*) the manner of its obtainment, (*ii*) the spectral similarities to **12**, and (*iii*) its subsequent reaction with LAH to give alcohol **14**, all indicate that the assigned structure is correct.

The n.m.r. spectrum of compound **13** shows: τ 2.58 (m, 5, Ph), 4.38 (s, 1, PhC*H*), 6.55 (s, 3, OCH_3), 5.06 (bs, 1, H-1), 4.13 (bs, 1, H-2), 5.05 (bd, 1, $J_{77'} = -13.0$, H-7), 4.84 (bd, 1, H-7′), 5.79 (bd, 1, H-3′), 5.79 (bd, 1, $J_{45} = 8.0$, H-4), 6.10 (td, 1, $J_{56_a} = 10.0$, H-5), 6.18 (t, 1, $J_{6_a6_e} = -10.5$, H-6a), 9.68 (m distorted, 1, H-6e).

4,6-O-Benzylidene-1,2,3-trideoxy-3-C-hydroxymethyl-D-arabino-hex-1-enopyranose 14, its p-Toluenesulfonate 15

(*a*) Compound **12** (0.262 g; 0.94 mmol) or compound **13** (0.340 g; 1.05 mmol) was dissolved in 60 ml of dry diethyl ether, lithium aluminum hydride (0.1 g) added, and the mixture was refluxed with stirring for 1 h. The excess LAH was destroyed with water and the mixture was filtered to remove the aluminum hydroxide. The ether layer was dried and evaporated under reduced pressure. Compound **12** yielded 0.204 g (87%) of compound **14** while compound **13** yielded 0.241g (92%) of compound **14**.

(*b*) Alternative to the foregoing, the mixture of compounds **12** and **13** obtained from solvolysis of **10** was purified by passage through a silica column (10 cm × 1.8 cm) using ethyl acetate as eluant and making no attempts at fractionation. LAH reduction of the eluted mixture (as described for the individual components) afforded compound **14** in ~90% yield.

The n.m.r. spectrum of compound **14** shows: τ 2.60 (m, 5, Ph), 4.68 (s, 1, PhC*H*), 8.02 (bs, 1, exchangeable, OH), 3.73 (q, 1, $J_{12} = 7.0$, $J_{13} = -2.5$, H-1), 5.37 (q, 1, $J_{23} = 2.0$ H-2), 7.35 (m, 1, $J_{37} = J_{37'} = 5.5$, H-3), 6.03–6.23 (m, 3, H-4, -5, -6a), 5.58 (q, 1, $J_{6_a6_e} = -10.5$, H-6e), 6.26 (m, 2, H-7, -7′). The i.r. spectrum shows: μ_{max} 1645 cm^{-1} (vinyl ether) (6).

Compound **14** was recrystallized from carbon tetrachloride, m.p. 138–140 °C; $[\alpha]_D^{23}$ −57.2 (*c*, 8.6 in $CHCl_3$). The material was converted to the *p*-toluenesulfonate for characterization by treatment with pyridine and excess tosyl chloride.

Compound **15** so obtained was recrystallized from methanol, m.p. 121.5–123 °C; $[\alpha]_D^{23}$ −50.5° (*c*, 5.20 in $CHCl_3$).

Anal. Calcd. for $C_{21}H_{22}O_6S$: C, 67.72; H, 5.51; S, 7.97. Found: C, 67.68; H, 5.54; S, 8.17.

The n.m.r. spectrum of compound **15** shows: τ 2.60 (m, 5, Ph), 4.50 (s, 1, PhC*H*), 7.62, 2.67, 2.17 (s, d, d, 3, 2, 2, *p*-tolyl), 3.62 (q, 1, $J_{12} = 7.0$, $J_{13} = -2.5$, H-1), 5.37 (q, 1, $J_{23} = 2.0$, H-2), 7.27 (m, 1, $J_{37} = J_{37'} = 5.0$, H-3), 6.07–6.57 (m, 3, H-4, -5, -6a), 5.82 (q, 1, H-6e), 5.82 (d, 2, H-7, -7′).

4,6-O-Benzylidene-1,2,3-trideoxy-3-C-iodomethyl-D-arabino-hex-1-enopyranose, 5

(*a*) Compound **15** (0.085 g); was dissolved in a solution of acetone (25 ml) and sodium iodide (1 g) and refluxed for 20 h. The reaction was followed by t.l.c. using 4:1 petroleum ether–ethyl acetate in which the R_f values of **15**

and **5** are 0.55 and 0.73 respectively. If the reaction was carried beyond 20 h there was considerable decomposition. Decomposition also occurred if compound **15** was not recrystallized at least once after its preparation.

The acetone was evaporated under reduced pressure, 10 ml of water was added, and the solution extracted with chloroform. The chloroform layer was dried and evaporated under reduced pressure. T.l.c. of the crystalline residue showed that there were traces of starting material and other impurities. The material was put on a silica column (10 cm × 1.8 cm) and eluted with 4:1 petroleum ether (35–60 °C)–ethyl acetate. The result was 0.050 g (67%) of the title compound.

Compound **5** was recrystallized from methanol, m.p. 100–102 °C; $[\alpha]_D^{23}$ −125.9° (*c*, 4.76 in $CHCl_3$).

Anal. Calcd. for $C_{14}H_{15}IO_3$: C, 46.94; H, 4.22; I, 35.43. Found: C, 46.84; H, 4.18; I, 35.10.

The n.m.r. spectrum of compound **5**[4] shows: τ 2.57 (m, 5, Ph), 4.38 (s, 1, PhC*H*), 3.55 (q, 1, $J_{12} = 7.0$, $J_{13} = -2.7$, H-1), 5.73 (q, 1, $J_{23} = 2.0$, H-2), 7.48 (m, 1, $J_{34} = 9.0$, $J_{37} = 6.2$, $J_{37'} = 3.5$, H-3), 6.20 (t, 1, $J_{45} = 9.0$, H-4), 6.10 (td, 1, $J_{56_a} = 10.0$, $J_{56_e} = 4.5$, H-5), 6.32 (t, 1, $J_{6_a6_e} = -10.5$, H-6a), 5.54 (q, 1, H-6e), 6.66 (q, 1, $J_{77'} = -10.0$, H-7), 6.56 (q, 1, H-7′).

The overall yield of compound **5** and **4** using the tosylate **15** for the last step was about 20–25%. The overall yield using compound **16** for the last step was 50–60%.

Financial assistance from the National Research Council of Canada and Bristol Laboratories of Syracuse is gratefully acknowledged. We express our gratitude to the staff of the Canadian 220 MHz NMR Centre for their assistance.

1. B. FRASER-REID and B. RADATUS. Can. J. Chem. This issue
2. B. FRASER-REID and B. RADATUS. Can. J. Chem. **47**, 4095 (1969).
3. (*a*) J. D. ROBERTS and R. H. MAZUR. J. Am. Chem. Soc. **73**, 2509 (1951). (*b*) N. L. WENDLER. *In* Molecular rearrangements. Part 2. P. de Mayo, Editor. Interscience Publishers, New York. 1964.
4. B. FRASER-REID, B. J. CARTHY, and B. RADATUS. Tetrahedron. **28**, 2741 (1972).
5. (*a*) L. D. HALL and L. F. JOHNSON. Tetrahedron, **20**, 883 (1964); (*b*) R. U. LEMIEUX, E. FRAGA, and K. A. WATANABE. Can. J. Chem. **46**, 61 (1969).
6. K. NAKANISHI. Infrared absorption spectroscopy. Holden-Day, Inc., San Francisco. 1964.
7. E. L. ALBANO, D. HORTON, and J. H. LAUTERBACH. Carbohydr. Res. **9**, 149 (1969).
8. B. FRASER-REID and B. RADATUS. Can. J. Chem. **48**, 2146 (1970).
9. B. FRASER-REID and B. RADATUS. Chem. Commun. 779 (1970).
10. G. JUST and C. LEZNOFF. Can. J. Chem. **42**, 79 (1964).
11. R. U. LEMIEUX and B. FRASER-REID. Can. J. Chem. **42**, 532 (1964).
12. M. SHARMA and R. K. BROWN. Can. J. Chem. **44**, 2825 (1966).
13. B. FRASER-REID and B. RADATUS. J. Am. Chem. Soc. **92**, 6661 (1970).
14. G. N. STORK and W. N. WHITE. J. Am. Chem. Soc. **78**, 4609 (1956); H. L. GOERING, G. S. KOERMER, and E. C. LINSAY. J. Am. Chem. Soc. **93**, 1230 (1971), and previous papers by H. L. Goering.
15. H. E. SIMMONS and R. D. SMITH. J. Am. Chem. Soc. **80**, 5323 (1958); G. WITTIG and K. SCHWARZENBACH. Angew. Chem. **73**, 27 (1959); G. L. CLOSS and L. E. CLOSS. Angew. Chem. **74**, 431 (1962).
16. J. H.-H. CHAN and B. RICKBORN. J. Am. Chem. Soc. **90**, 6406, (1968).
17. H. HOBERG. Ann. **656**, 1, 15 (1962); Ann. **695**, 1 (1966).
18. S. SAWADA, K. TAKEHANA, and Y. INOUYE. J. Org. Chem. **33**, 1767 (1968).
19. S. W. STANELY and F. L. WISEMAN. J. Org. Chem. **35**, 3868, (1970).
20. R. J. FERRIER. Advan. Carbohydr. Chem. **20**, 67 (1965); **24**, 199 (1969).
21. R. J. FERRIER and M. PONPIPOM. J. Chem. Soc. C, 553 (1971); A. JORDAAN and G. J. LAURENS. Chem. Commun. 581 (1971); E. LEUTZINGER, R. K. ROBINS, and L. B. TOWNSEND. Tetrahedron Lett. 3751, (1970).
22. R. B. WOODWARD and R. HOFFMANN. J. Am. Chem. Soc. **87**, 2511 (1965). R. B. WOODWARD and R. HOFFMANN. The conservation of orbital symmetry. Verlag Chemie GmbH. Academic Press Inc. 1970.
23. R. J. FERRIER and N. VETHAVIYASER. J. Chem. Soc. C, 1907 (1971).
24. M. HANACK and H.-J. Schneider. Angew. Chem. **6**, 666 (1967).
25. E. P. BLANCHARD and H. E. SIMMONS. J. Am. Chem. Soc. **86**, 1337 (1964).
26. L. M. JACKMAN and S. STERNHELL. Applications of nuclear magnetic resonance spectroscopy in organic chemistry. 2nd Ed. Pergamon Press, Oxford. 1969. p. 342.

Can. J. Chem. Downloaded from www.nrcresearchpress.com by 210.87.254.105 on 09/05/12
For personal use only.

The Synthesis of some α-Cyclopropylcarbonyl Glycopyranosides[1]

BERT FRASER-REID AND BERNARD J. CARTHY[2]

Department of Chemistry, University of Waterloo, Waterloo, Ontario

Received May 1, 1972

The syntheses of three α-cyclopropylcarbonyl compounds of carbohydrate origin, **1**, **2**, **3**, are described. The cyclopropyl carboxaldehyde **1** was obtained from the corresponding carbinol by manganese dioxide oxidation of the primary alcohol. However, the secondary cyclopropyl alcohol in **8** did not respond to manganese dioxide and its oxidation (in the tritylated derivative (**14**), to the cyclopropyl ketone, **2**, had to be achieved by ruthenium tetroxide. The sequence leading to **2** (via **8**) began with ethyl 4,6-di-*O*-acetyl-2,3-dideoxy-α-D-*erythro*-hex-2-enopyranoside **11**, which added methylene to give the α-D-*allo* configuration with the cyclopropane ring *syn* to the glycosidic ethoxy group. The diastereomeric tritylated cyclopropyl ketone **3**, possessing the cyclopropyl ring *anti* to the ethoxy group, resulted from cyclopropanation of the αβ-unsaturated ketone, **15**. In the latter case, the acetoxy group apparently provides greater directing influence to the incoming methylene than does the allylic ethoxy group.

Les synthèses de trois composés α-cyclopropylcarbonyles d'origine carbohydrate, **1**, **2**, **3** sont décrites. Le cyclopropyl carboxaldéhyde **1** a été obtenu à partir du carbinol correspondant, par oxydation au dioxyde de manganèse de l'alcool primaire. Cependant, le cyclopropylalcool secondaire dans **8** ne réagit pas sur le dioxyde de manganèse et son oxydation (dans le dérivé tritylé **14**) en cyclopropylcétone **2** a dû être effectuée par le tétroxyde de ruthénium. La séquence conduisant à **2** (via **8**) commence avec l'éthyl di-*O*-acétyl-4,6 didéoxy-2,3-α-D-*érythro* hexeno-2 pyranoside **11**, qui par addition de méthylène conduit à la configuration α-D-*allo* avec le cycle cyclopropane en *syn* par rapport au groupe éthoxy glycosidique. La cyclopropylcétone tritylée diastéréoisomère **3**, avec le cyclopropyl en *anti* par rapport au groupe éthoxy, résulte de la cyclopropanation de la cétone αβ insaturée **15**. Dans ce dernier cas, le groupe acétoxy oriente apparemment de façon plus grande le méthylène qui entre, que ne le fait le groupe éthoxy allylique.

[Traduit par le journal]

Canadian Journal of Chemistry, **50**, 2928 (1972)

α-Cyclopropylcarbonyl compounds undergo several unique rearrangements upon reaction in the ground (2) or excited (3) states, which make them very intriguing synthetic intermediates (4). These compounds caught our attention because of our interest in structural modification of the carbohydrate nucleus, and because they present a logical extension of our studies on cyclopropanated (5) and α,β-unsaturated carbonyl (6, 7) monosaccharides. We have therefore been concerned with some representative cases **1**, **2**, **3**, whose syntheses from readily available precursors we describe herein.

The cyclopropyl carboxaldehyde **1** was chosen as our initial objective since it ought to be readily available from the ester **5** via the alcohol **6**. Meyer zu Reckendorf and Kamprath-Scholtz reported the reaction of methyl 2,3-anhydro-4,6-*O*-benzylidene-α-D-allopyranoside, **4**, with ethyl diethoxyphosphonylacetate (8) (Scheme 1).[3] The authors experienced some difficulty in isolating the expected product (methyl 2,3-

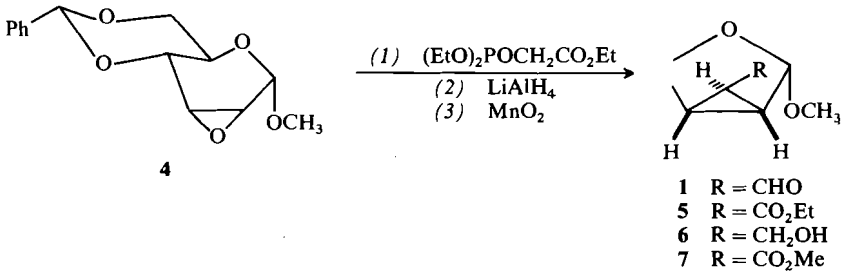

4

1 R = CHO
5 R = CO_2Et
6 R = CH_2OH
7 R = CO_2Me

SCHEME 1

[1]Pyranosiduloses, Part IV. For Part III, see ref. 1.

[2]Taken from the M.Sc. Thesis of B. J. Carthy, University of Waterloo, 1971.

[3]We are grateful to Professor Meyer zu Reckendorf for kindly providing us with details of this reaction prior to publication.

Can. J. Chem. Downloaded from www.nrcresearchpress.com by 210.87.254.40 on 09/05/12
For personal use only.

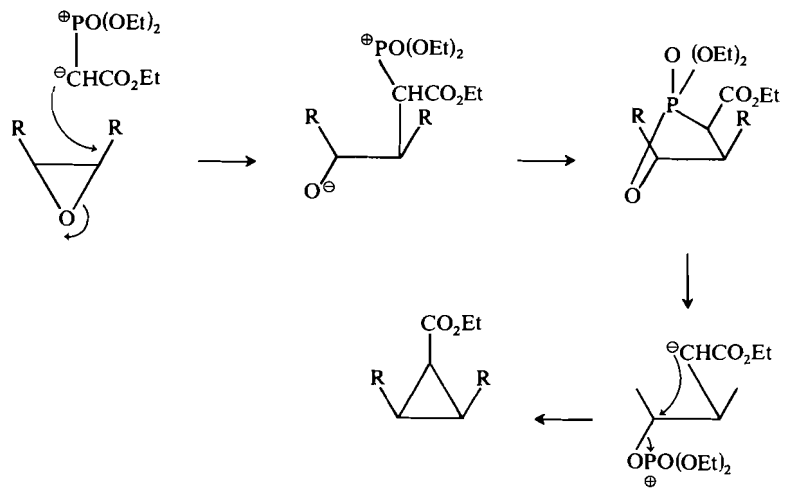

SCHEME 2

dideoxy-2,3-*C*-(*exo*-carbethoxy-*C*-methylene)-α-D-mannopyranoside, **5**) and because of this, the crude reaction product was saponified. The resulting acid was isolated and esterified with diazomethane to give the methyl ester **7**. In the present work the difficulty with isolation of the reaction product has been overcome and the ethyl ester **5** was obtained directly in crystalline condition from the product mixture in 54% yield.

The α-D-*manno* configuration of **7** had been assigned on the basis of the coupling constant, $J_{12} = 0$ Hz; and the *exo* orientation of the carboxy group, on the basis of the coupling constants ($J_{37} = 4.6$; $J_{27} = 5.0$ Hz) indicative of *trans* protons on the cyclopropyl ring (8). We assign the 7-carbethoxy substituent as *exo* on the basis of the proposed mechanism of Wittig cyclopropanation of epoxides (9) (Scheme 2). The α-carbethoxy carbanion intermediate would undoubtedly assume the least hindered orientation prior to the final ring closure leading to the cyclopropyl ring. Certainly the alternative addition leading to the 7-epimer of **5** would possess more severe non-bonded interactions for the *endo*-carbethoxy group. Lithium aluminum hydride reduction of **5** in ether for 15 min gave the known (8) alcohol **6** in quantitative yield.

We were interested to test the response of compound **6** to manganese dioxide oxidation in the hope of providing a model route from α-cyclopropyl alcohols to their carbonyl counterparts. This reaction is not without precedent (10) although it is rarely applied. In the event, treatment of the alcohol **6** in chloroform with manganese dioxide (11) afforded 23% conversion to the desired carboxaldehyde, **1**, recognized by its i.r. (1916 cm^{-1}) and n.m.r. (τ 0.83) data. That there had been no skeletal changes in going from **6** to **1** followed from the preserved n.m.r. parameters for H-1 (see Experimental).

In view of the success of the foregoing, an attempt was made to extend the oxidation to the secondary alcohol in **8** in the hope of obtaining ketol **9**. The cyclopropanated diacetate **10** needed to furnish the desired substrate **8**, was itself obtained *via* cyclopropanation (12) of the olefinic diacetate **11** (13). The conversion was only 27% effective judging from the n.m.r. spectrum of the crude product. Chromatography or recrystallization before or after deesterification gave, at best, a heavily contaminated sample of **8**. However, this was used for preliminary testing and it was found that **8** was in fact inert to manganese dioxide.

This failure could now be used to advantage. The entire reaction product from the incomplete cyclopropanation of **11** was deacetylated and the mixture now containing **8** and **12** was oxidized with manganese dioxide. The olefinic diol **12** went to ketone **13** (6) while **8** remained unchanged. Silica column chromatography now readily separated **8** from **13**.

Prior to attempting more vigorous oxidations, compound **8** was protected as the trityl ether **14**.

Can. J. Chem. Downloaded from www.nrcresearchpress.com by 210.87.254.40 on 09/05/12
For personal use only.

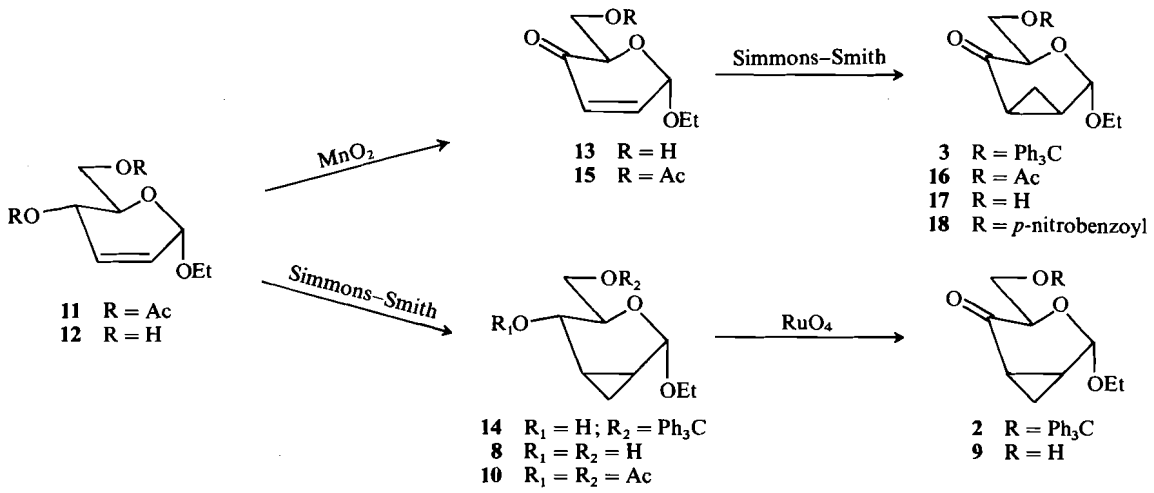

SCHEME 3

Dimethyl sulfoxide/acetic anhydride oxidation (14) proved too messy to be pursued. However, ruthenium tetroxide oxidation of **14** according to the procedure of Lawton *et al.* (15) proceeded smoothly to give ketone **2** in 80% yield based on unrecovered **14** (Scheme 3).

The assignment of *ribo*-configuration to the skeleton of **2** follows from its geneology. Judging from experience in this (16) and Horton's (17) laboratories, the addition of methylene during the Simmons–Smith reaction of **11** is expected to occur *syn* to the glycosidic alkoxyl, giving diacetate **10**. That this had been fulfilled was indicated by n.m.r. examination of the derived diol **8** in deuteriochloroform. The anomeric proton is a doublet whose spacing ($J_{12} = 5.0$ Hz) is exactly that observed in the analogous α-D-*allo*-cyclopropanated glycopyranosides reported previously (16). (Opposite orientation of the cyclopropane ring (*i.e.* the *manno*-configuration) causes a much smaller spacing ($J_{12} \simeq 0$) (16).) Tritylation (to **14**) and oxidation would not be expected to affect the configuration of the ring in the final product, **2**.

In the conversion of **14** to **2**, there is a substantial change in the spacing, J_{12}, for H-1 from 6.0 to 0 Hz. This reflects the extreme distortion of a pyranoside ring forced to accommodate an α-cyclopropyl ketone. Although the Karplus relationship might not apply to a system as strained as this (18), it may be noted that the conformation predicted by the value $J_{12} = 0$ Hz is that shown in **2***a* in which the dihedral angle between H-1 and -2 is 90°. Interestingly, in this arrangement the stabilizing conjugative p–π overlap between the C_2—C_3 bond and the carbonyl group (19) is a maximum. In an alternative conformation **2***b*, preserving the dihedral angle of 90° between H-1 and -2, the conjugative overlap would be between the C_3—C_7 bond and the carbonyl group. However, this conformation (**2***b*) is less favorable than **2***a* because it requires the bulky C-6 substituent to be axial.

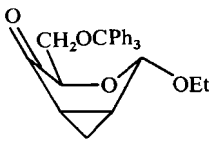

2*a*

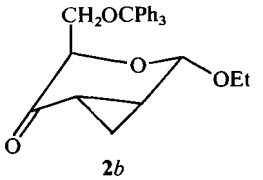

2*b*

In the hope of finding a more economical route to these cyclopropyl ketones, the ketone **15** described in an earlier report from this laboratory (6) was examined (see Scheme 3). Simmons–Smith (12) reaction was allowed to proceed for 2 h at which time a new substance formed in the reaction was present in optimum amount. Silica column chromatography afforded this substance as a syrup which showed cyclopropyl protons (τ 8.00–8.83) in the n.m.r. spectrum and carbonyl (1705 cm^{-1}) and acetate (1735 cm^{-1}) absorptions in the i.r. spectrum. The cyclopropane ring in the product could have either *ribo*-orientation (as in com-

Can. J. Chem. Downloaded from www.nrcresearchpress.com by 210.87.254.40 on 09/05/12
For personal use only.

Can. J. Chem. Downloaded from www.nrcresearchpress.com by 210.87.254.40 on 09/05/12
For personal use only.

pound **2** described above), or *lyxo*-orientation. In order to determine which, the syrupy product (**16**) was de-esterified to give a non-crystalline ketol (**17**) which was immediately converted to a tritylate (**3**) so as to effect direct comparison with the other trityl ketone **2**. Neither **16** nor **3** crystallized, and so the material was characterized as the *p*-nitrobenzoate, **18**.

The two trityl ketones **2** and **3** gave different n.m.r. spectra. Although H-1 in both appeared as a singlet, it occurred at τ 4.45 in the former and τ 4.83 in the latter. In a recent publication from this laboratory (16) it was shown that a cyclopropyl group shields vicinal *cis*-oriented protons. This effect is again apparent here in the higher frequency of H-1 in **3**. On the assumption that the structure assigned above for **2** is secure, the new trityl ketone must have either (*i*) the β-D-anomeric arrangement of **2**, *i.e.* **19**; (*ii*) the α-D-*lyxo* structure already suggested in **3**; or (*iii*) the anomeric β-D-*lyxo*

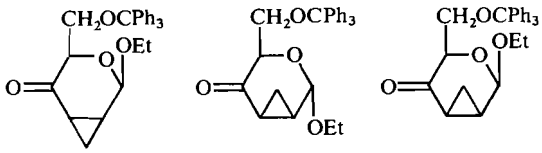

19 **3** **20**

configuration of **20**. The β-D structures **19** and **20** would require, among other things, that the glycosidic ethoxy group of **15** be anomerized from $\alpha \rightarrow \beta$ orientation during the Simmons–Smith reaction. This would be highly unlikely, for although $\beta \rightarrow \alpha$ anomerization has been observed during the cyclopropanation of β-D-hex-2-enopyranosides, it was found that the converse process did not occur during cyclopropanations of the corresponding α-D olefins (16).

The difference in the stereochemical outcome of Simmons–Smith cyclopropanation of **11** and **15** is interesting. In the former, the incoming methylene adds *syn* to the ethoxy group as expected for cyclic six-membered allyl ethers (20). However, with **15** the directing influence apparently comes from the acetoxy group. Conceivably the ester-carbonyl group coordinates with the organo-zinc reagent causing addition *syn* to the C-5 acetoxymethyl group.

The study of access to and transformations of these and other cyclopropyl ketones is continuing and will be reported in due course.

Experimental

General

Melting points were determined on a Fischer–Johns heating stage and are uncorrected. The n.m.r. spectra were recorded using either a Varian T-60, a Varian HA 100, or a Varian HR 220 spectrometer, and unless otherwise specified, the solvent was deuteriochloroform containing 1% tetramethylsilane as internal standard. Coupling constants were obtained by measuring spacings of spectra judged to be first-order. The following abbreviations are used in describing the spectra: s, singlet; m, multiplet; d, doublet; t, triplet; q, quartet; td, triplet of doublets, etc. I.r. spectra were determined on a Beckman model I.R. 5 spectrometer using 0.1 mm sodium chloride solution cells (chloroform as solvent) and silver chloride plates for smears. Optical rotations were determined on a Carl Zeiss model LEP nur 370740 Lichtelektusches Prazisionpolarimeter at 546 and 578 nm at 23 °C, the two values obtained being used to calculate the optical rotation at the sodium D (589 nm) line.

T.l.c. was performed on glass plates coated with silica gel (HF-254, E. Merck) to a thickness of 0.3 mm. The chromatograms were first viewed under u.v. light, then exposed to iodine vapor, and finally sprayed with concentrated sulfuric acid. For column chromatography E. Merck Silica Gel (0.05–0.20 mm, 70–325 mesh A.S.T.M.) was used.

Methyl 4,6-O-Benzylidene-2,3-dideoxy-2,3-C-(exo-carbethoxy-C-methylene)-α-D-mannopyranoside (5)[3]

A 50% oil dispersion of sodium hydride (11 g; 0.46 mol) was washed three times with petroleum ether (30–60°) to remove the oil, and was placed in a flask under dry nitrogen with 225 ml of dry dioxane. Ethyl diethoxyphosphoryl acetate (49.3 g; 0.22 mol) was added dropwise over a period of 1 h, after which time methyl 2,3-anhydro-4,6-*O*-benzylidene-α-D-allopyranoside, **4**, (21) (50 g; 0.22 mol) and a further 225 ml of dry dioxane were added. The whole was refluxed and stirred for 90 h, after which time the reaction was worked-up as follows. The reaction mixture was cooled to room temperature and poured into 500 ml of water. This aqueous solution was extracted twice with 500 and 300 ml portions of chloroform; the chloroform extracts were combined and were extracted with small volumes of water until the aqueous extract was no longer colored. The organic layer was dried (Na_2SO_4), filtered, and the solvent removed under reduced pressure. The crude reaction product was taken up in a small volume of diethyl ether and filtered to remove unreacted epoxide, yielding crude **5** (39.7 g; 54%). Recrystallization from absolute ethanol gave the pure material, m.p. 140–141 °C and optical rotation $[\alpha]_D^{23}$ +26.86° (*c*, 4.2 in chloroform).

Anal. Calcd. for $C_{18}H_{22}O_6$: C, 64.66; H, 6.63. Found: C, 64.63; H, 6.89.

The n.m.r. spectrum of compound **5** showed the following features: τ 5.13 (s, 1, $J_{12} = 0$ Hz, H-1), 7.77–8.45 (complex multiplet, 3H, H-2, -3, -8), ~6.3 (complex multiplet, 3H, H-4, -5, -6a), 5.68 (m, 1, H-6e), 4.43 (s, 1H, PhC*H*), 2.58 (m, 5, Ph), 8.73 (t, 3H, $J = 7.0$ Hz, $-OCH_2-CH_3$), 5.85 (q, 2H, $J = 7.0$ Hz; $O-CH_2-CH_3$), 6.60 (s, 3H, $-OCH_3$).

The i.r. spectrum shows μ_{max} 1720 cm^{-1}.

Methyl 4,6-O-Benzylidene-2,3-dideoxy-2,3-(exo-hydroxymethyl-C-methylene)-α-D-mannopyranoside, 6

Compound **5** (1.002 g; 0.003 mol) was dissolved in 50 ml

Can. J. Chem. Downloaded from www.nrcresearchpress.com by 210.87.254.40 on 09/05/12
For personal use only.

of dry diethyl ether, and lithium aluminum hydride (1.0 g) was added. The reaction mixture was stirred and refluxed for 15 min, after which time the reaction was judged to be complete by t.l.c. The excess lithium aluminum hydride was destroyed by careful addition of water, and the inorganic salts were filtered. The solution was dried (Na_2SO_4), filtered, and the solvent removed to yield the title compound, **6**, (0.8665 g; 98.3%), m.p. 140–143 °C, (lit. 140–142 °C (8)) used without further purification.

*Methyl 4,6-O-Benzylidene-2,3-dideoxy-2,3-(exo-formyl-C-methylene)-α-D-mannopyranoside, **1***

Compound **6** (0.4108 g; 0.0014 mol) was dissolved in 250 ml of chloroform. Active manganese dioxide (11), 2.0 g, was added and the suspension was stirred at room temperature for 27 h, after which time the reaction was worked-up by removal of the manganese dioxide by filtration over Celite filter aid. The solvent was removed under reduced pressure to yield a product which was judged by i.r. spectroscopy to be a mixture of starting material and aldehyde **1**. Consequently, the mixture was chromatographed using 1:1 ethyl acetate–petroleum ether (30–60°) as eluent. This yielded 0.0931 g (23%) of compound **1** which was recrystallized from absolute ethanol to give a m.p. of 188.5–189.5 °C and optical rotation $[\alpha]_D^{23}$ +48.9° (*c*, 3.96 in chloroform).

Anal. Calcd. for $C_{16}H_{18}O_5$: C, 66.20; H, 6.25. Found: C, 66.06; H, 6.47.

The n.m.r. spectrum of compound **1** showed the following features: τ 5.10 (s, 1H, $J_{12} = 0$ Hz, H-1), 7.87–8.23 (complex multiplet, 3H, H-2, -3, -7), 6.37 (complex multiplet, 3H, H-4, -5, -6a), 5.73 (*q*, 1H, $J_{56e} = 4.0$, $J_{6a,6e} = -7.0$ Hz, H-6e), 4.48 (s, 1H, PhC*H*), 0.83 (t, 1H, $J = 2.0$ Hz, —C*H*O), 6.58 (s, 3H, OCH_3), 2.57 (complex multiplet, 5H, Ph).

The i.r. spectrum shows μ_{max} 1716 cm^{-1}.

*Ethyl 2,3-Dideoxy-2,3-C-methylene-α-D-allopyranoside, **8***

*(a) Cyclopropanation of Ethyl 4,6-di-O-acetyl-2,3-dideoxy-α-D-erythro-hex-2-enopyranoside, **11** (13)*

Zinc/copper couple (22) (5.0 g; 0.256 mol), methylene iodide (7.2 ml; 0.0896 mol), dry diethyl ether (30 ml; 0.288 mol), and a single crystal of iodine were stirred and refluxed under anhydrous conditions for 75 min. Compound **11** (10 g; 0.0388 mol) and a further 20 ml (0.192 mol) of dry diethyl ether were then added, and the reaction continued for 48 h, at which point the reaction was worked up, since n.m.r. spectroscopy indicated 50% conversion to the cyclopropanated compound. The cooled reaction mixture was washed twice with 50 ml of saturated aqueous ammonium chloride and once with 50 ml of saturated aqueous sodium bicarbonate. Both aqueous layers were washed once with water, dried (Na_2SO_4), filtered, and the solvent removed. The product, a mixture of starting material, **11**, and ethyl 4,6-di-*O*-acetyl-2,3-dideoxy-2,3-*C*-methylene-α-D-allopyranoside, **10**, weighing 12.2 g, could not be separated by recrystallization or conventional chromatographic techniques. Hence chemical separation was effected via steps *b* and *c* which follow.

(b) De-esterification of the Partially Cyclopropanated Product

The product (12.2 g) was dissolved in a mixture of methanol (71.0 ml), water (31.5 ml), and triethylamine (15.7 ml), and was allowed to stand for 8 h. At this point, t.l.c. indicated that deacetylation was complete, and the solvent was removed under reduced pressure to yield 7.42 g of a syrupy residue. Again, this mixture could not be separated by the usual techniques.

(c) Manganese Dioxide Oxidation

The de-esterified mixture (7.42 g) was dissolved in 4 l of chloroform and active manganese dioxide (11) (40 g) was added. The whole was stirred at room temperature, and after 12 h a further 40 g of manganese dioxide was added. The stirring was continued for a further 24 h, after which time n.m.r. spectroscopy indicated no further increase in the concentration of ketone **13**. The reaction was thus worked-up by filtration of the manganese dioxide and evaporation of the solvent. T.l.c. showed the product to be a complex mixture, partial separation of which was achieved by column chromatography. Ethyl acetate–petroleum ether (30–60°) 1:1 mixture, was used as eluent to remove the faster running fractions, followed by elution with ethyl acetate to recover pure compound **8** (0.9895 g; 27%) as an oil.

The n.m.r. spectrum of the title compound (**8**) showed the following features: τ 4.85 (d, 1H, $J_{12} = 5.0$ Hz, H-1), 8.53 (complex multiplet, 2H, H-2, -3), 6.20 (d, 2H, H-6, -6′), 9.32 (complex multiplet, 2H, H-7, -7′), 6.55 (s, 1H, O*H*), 8.78 (t, 3H, $J = 7$ Hz, —OCH_2CH_3), 6.60 (m, 2H, —OCH_2 —CH_3).

*Attempted Synthesis of Ethyl 2,3-Dideoxy-2,3-C-methylene-α-D-ribohexopyranosid-4-ulose (**9**) by Manganese Dioxide Oxidation of Ethyl 2,3-Dideoxy-2,3-C-methylene-α-D-allopyranoside (**8**)*

Compound **8** (0.453 g; 0.0024 mol) was dissolved in 250 ml of chloroform and active manganese dioxide (10 g) was added. The mixture was stirred at room temperature for 7 days, during which time a further 10 g of manganese dioxide was added periodically in small portions. After this time, the reaction was worked-up by removal of the manganese dioxide by filtration, followed by removal of the solvent. The n.m.r. spectrum of the product showed this to be unchanged **8**, whilst t.l.c. showed no high-running component which might correspond to the ulose **9**. I.r. spectroscopy showed no absorption in the carbonyl region.

*Preparation of Ethyl 2,3-Dideoxy-2,3-C-methylene-6-O-triphenylmethyl-α-D-allopyranoside, **14***

Compound **8** (0.8015 g; 0.0043 mol) was dissolved in 10 ml of dry pyridine, together with triphenylmethyl chloride (2.0 g, 0.0072 mol). After 17 h, crystalline material had deposited on the bottom of the flask and t.l.c. showed two spots, neither of which corresponded to the starting material **8**. The reaction mixture was dropped slowly into 25 ml of iced water, with constant stirring. A white amorphous solid formed during the addition. The supernatant liquid was decanted, and the solid triturated with saturated aqueous sodium bicarbonate. The aqueous solution was again decanted and the solid residue finally washed with a little water. Most of the triphenylcarbinol was crystallized out from diethyl ether–ethanol mixture. The mother liquors were evaporated to dryness and the residue was separated by column chromatography, eluting the column first with methylene chloride to remove the triphenylcarbinol, then with 1:1 ethyl acetate–petroleum ether (30–60°) mixture to recover the desired product (**14**). This

Can. J. Chem. Downloaded from www.nrcresearchpress.com by 210.87.254.40 on 09/05/12
For personal use only.

was an amorphous solid, 1.81 g (79.5%), optical rotation $[\alpha]_D^{23}$ +27.9° (*c*, 4.1 in chloroform), *m/e* 430.

The n.m.r. spectrum showed the following: τ 4.88 (d, 1H, J_{12} = 6.0 Hz, H-1), 9.02 (complex multiplet, 2H, H-2, -3), 9.38 (complex multiplet, 2H, H-7, -7'), 8.10 (s, 1H, —O*H*), 8.77 (t, 3H, *J* = 7.0 Hz, —OCH_2—CH_3), 2.98 (complex multiplet, 15H, Ph).

Satisfactory elemental analysis could not be obtained for this substance, but the assigned structure is correct in view of the subsequent transformation described immediately below.

*Ethyl 2,3-Dideoxy-2,3-C-methylene-6-O-trityl-α-*D*-ribo-hexopyranosid-4-ulose*, **2**

(a) Attempted Manganese Dioxide Oxidation

Compound **14** (0.200 g; 0.465 mmol) was dissolved in 100 ml of chloroform, active manganese dioxide (2 g) was added, and the whole stirred for 48 h, during which time two additional amounts of 1 g each of manganese dioxide were added. After this time, the reaction was worked-up by filtration of the solution, and removal of the solvent. Both i.r. and n.m.r. spectroscopy showed the product to be starting material **14**, with no trace of the desired 4-ulose **2**.

(b) Ruthenium Tetroxide Oxidation

Compound **14** (0.169 g; 0.393 mmol) in 2 ml of freshly prepared ethanol–free chloroform, 2 ml of water, potassium periodate (0.117 g; 0.510 mmol), and potassium carbonate (0.0226 g; 0.164 mmol) were stirred together with catalytic amount of ruthenium dioxide for 9½ h. At this time the reaction was worked-up by the addition of 5 ml of isopropyl alcohol, filtered to remove the ruthenium dioxide, and the organic layer separated. The aqueous layer was washed with a small amount of chloroform and the chloroform layers were combined, dried (Na_2SO_4), filtered, and the solvent was removed. T.l.c. showed the product to be comprised of two components, one being the starting material. These were separated by chromatography on a short column to yield pure ethyl 2,3-dideoxy-2,3-*C*-methylene-6-*O*-trityl-α-D-ribohexopyranosid-4-ulose, **2** (0.0807 g; 48%), which was recrystallized from ethyl acetate, m.p. 169–170.5 °C, $[\alpha]_D^{23}$ +33.20° (*c*, 2.36 in chloroform).

Anal. Calcd. for $C_{28}H_{28}O_4$: C, 78.48; H, 6.59. Found: C, 78.30; H, 6.38.

The n.m.r. spectrum of compound **2** showed the following features: τ 4.45 (s, 1H, J_{12} = 0 Hz, H-1), 8.03 (complex multiplet, 3H, H-2, -3, -7_{endo}), 5.85 (q, 1H, J_{56} = 2.0, $J_{56'}$ = 5 Hz, H-5), 6.73 (q, 1H, $J_{66'}$ = 10.0 Hz, H-6), 6.27 (q, 1H, H-6'), 8.73 (m, 1H, H-7_{exo}), 8.80, (t, 3H, *J* = 7.0 Hz, —OCH_2CH_3), 6.27 (complex multiplet, 2H, —OCH_2CH_3), 2.65 (m, 15H, Ph).

The i.r. spectrum shows μ_{max} 1703 cm^{-1}.

*Ethyl 2,3-Dideoxy-2,3-C-methylene-6-O-p-nitrobenzoyl-α-*D*-lyxo-hex-2-enopyranoside-4-ulose*, ***18***

Compound **16** (0.1911 g; 0.84 mmol) was dissolved in 10 ml of a 5:4:1 methanol–water–triethylamine mixture, and allowed to stand for 2¼ h. After this time, the liquids were removed by evaporation under reduced pressure to yield ethyl 2,3-dideoxy-2,3-*C*-methylene-α-D-*lyxo*-hexopyranosid-4-ulose, **17** (0.1451 g; 93%), which was taken immediately and treated with *p*-nitrobenzoyl chloride (0.300 g; 0.0016 mol) in dry pyridine. Subsequent work-up of this reaction yielded the title material, **18**, which was recrystallized from absolute ethanol, 128.5–129.5 °C, $[\alpha]_D^{23}$ +29.5° (*c*, 1.7 in chloroform).

Anal. Calcd. for $C_{16}H_{17}NO_7$: C, 57.31; H, 5.11; N, 4.18. Found: C, 57.29; H, 5.07; N, 4.16.

*Ethyl 2,3-Dideoxy-2,3-C-methylene-6-O-triphenylmethyl-α-*D*-lyxo-hexopyranosid-4-ulose*, **3**

The acetate **16** (0.0793 g; 0.35 mmol) was deacetylated as in the preceding section, and the resulting sample of **17** (0.0615 g) was dissolved in 5 ml of dry pyridine and treated with triphenylmethyl chloride (0.300 g; 1.08 mmol). After 2 days at room temperature, the reaction was driven to completion by heating on the steam bath for several minutes, after which t.l.c. showed no trace of compound **17** in the reaction mixture. Dropwise addition of 50 ml of ice-water caused a solid to form, which was removed by filtration and washed with saturated aqueous sodium bicarbonate, water, and then dried. Triphenylcarbinol in the product was removed by chromatography on a short column, eluting first with methylene chloride to remove the triphenylcarbinol and finally with ethyl acetate–petroleum ether (30–60°), 1:1 to obtain pure ethyl 2,3-dideoxy-2,3-*C*-methylene-6-*O*-triphenylmethyl-α-D-*lyxo*-hexopyranosid-4-ulose, **3**, (0.0446 g; 22%), a syrup, showing only one spot on t.l.c.

The n.m.r. spectrum of the title compound, **3**, showed the following features: τ 4.83, (s, 1H, H-1), 8.07 (m, 2H, H-2, -3), 5.97 (t, 1H, *J* = 4.5 Hz, H-5) 6.60 (m, 2H, H-6, -6'), 8.73 (m, 2H, H-7, -7'), 8.80 (t, 3H, *J* = 7.0 Hz, —OCH_2—CH_3), 6.37 (m, 2H, —OCH_2CH_3), 2.67 (m, 15H, Ph).

*Ethyl 6-O-Acetyl-2,3-Dideoxy-2,3-C-methylene-α-*D*-lyxo-hexopyranosid-4-ulose*, ***16***

Zinc/copper couple (22) (0.375 g; 0.0192 mol), dry diethyl ether (2.25 ml; 0.0216 mol), methylene iodide (0.537 ml; 0.0067 mol), and a single crystal of iodine were stirred and refluxed for 1 h. After this time, ethyl 6-*O*-acetyl-α-D-*glycero*-hex-2-enopyranosid-4-ulose, **15** (6) (0.642 g, 0.003 mol) was added, along with 1.5 ml (0.014 mol) of diethyl ether and the whole stirred and refluxed under anhydrous conditions for 2 h. After this period, n.m.r. analysis of an aliquot of the reaction mixture showed the reaction to be 70% complete. Preliminary experiments had shown that a signal at τ 4.88 (H-1 of the adduct) reached an optimum intensity at this time and depreciated thereafter. Hence ammonium chloride solution (5 ml) was added to the reaction mixture. The organic layer was separated, the aqueous layer washed with a small portion of ether and the combined ethereal solutions treated with saturated aqueous sodium bicarbonate. After separation and washing the aqueous layer with ether, the organic layer was finally washed with water, dried (Na_2SO_4), filtered, and the solvent removed. T.l.c. of this material indicated at least three components, one of which was the starting olefin, hence this material was chromatographed using 1:1 ethyl acetate–petroleum ether (30–60°) as eluent. This afforded 0.1321 g (22.4%) of pure **16** as a syrup $[\alpha]_D^{23}$ +74.3° (*c*, 5.16 in chloroform).

The n.m.r. spectrum of compound **16** showed the following features: τ 4.88 (s, 1H, H-1), 8.05 (m, 2H, H-2, -3), 5.87 (t, 1H, *J* = 5 Hz, H-5), 5.67 (d, 2H, H-6a, -6e), 8.37 (q, 1H, $J_{7endo} = J_{3endo} = 5.5$, $J_{7endo\ 7exo} = -5.5$ Hz, H-7_{endo})

8.88 (m, 1H, H-7$_{exo}$), 8.77, (t, 3H, $J = 7.0$ Hz, —OCH$_2$CH_3), 6.30 (m, 2H, —OCH_2CH$_3$), 7.95 (s, 3H, —O—CH$_2$—CH_3). The i.r. spectrum shows μ_{max} 1735 and 1705 cm^{-1}.

We are indebted to the National Research Council of Canada and to Bristol Laboratories for financial support for this study.

1. B. FRASER-REID and N. L. HOLDER. Chem. Commun. 31 (1972).
2. W. D. EMNONS and G. B. LUCAS. J. Am. Chem. Soc. **77**, 2287 (1955); C. U. PITMAN and S. P. MCMANUS. J. Am. Chem. Soc. **91**, 5915 (1969). G. CUEILLE and R. FRAISSE-JULLIEN. Tetrahedron Lett. 749 (1969).
3. W. G. DAUBEN and G. W. SHAFFER. Tetrahedron Lett. 4415 (1967); A. Padwa. *In* Organic photochemistry. Vol. 1. *Edited by* O. L. Chapman. Marcel Dekker, Inc., New York. 1967.
4. See for example, W. G. DAUBEN and J. T. DEVINY. J. Org. Chem. **31**, 3794 (1966); E. PIERS, R. W. BRITTON, and W. D. WALL. Can. J. Chem. **47**, 4307 (1969).
5. (*a*) B. FRASER-REID and B. RADATUS. Can. J. Chem. **47**, 4095 (1969); (*b*) Chem. Commun. 779 (1970).
6. (*a*) B. FRASER-REID, A. MCLEAN, and E. W. USHERWOOD. J. Am. Chem. Soc. **91**, 5392 (1969); (*b*) B. FRASER-REID, A. MCLEAN, E. W. USHERWOOD, and M. YUNKER. Can. J. Chem. **48**, 2877 (1970).
7. (*a*) B. FRASER-REID, B. J. CARTHY, N. L. HOLDER, and M. YUNKER. Can. J. Chem. **49**, 3038 (1971); (*b*) B. FRASER-REID and B. RADATUS. J. Am. Chem. Soc. **92**, 5288 (1970).
8. W. MEYER ZU RECKENDORF and U. KAMPRATH-SCHOLTZ. Angew. Chem. Int. Ed. Engl. **7**, 142 (1968).
9. I. TOMOSKOZI. Tetrahedron, **19**, 1969 (1963).
10. R. M. EVANS. Quart. Rev. (London), **13**, 64 (1959).
11. H. B. HENBEST, E. R. H. JONES, and T. C. OWEN. J. Chem. Soc. 4909 (1957).
12. E. P. BLANCHARD and H. E. SIMMONS. J. Am. Chem. Soc. **86**, 1337 (1964); H. E. SIMMONS, E. P. BLANCHARD, and R. D. SMITH. J. Am. Chem. Soc. **86**, 1347 (1964).
13. R. J. FERRIER and N. PRASAD. J. Chem. Soc. C, 570, 575 (1969).
14. F. A. CAREY and K. O. HODGSON. Carbohydr. Res. **12**, 463 (1970).
15. B. T. LAWTON, W. A. SZAREK, and J. K. N. JONES. Carbohydr. Res. **10**, 456 (1969).
16. B. RADATUS and B. FRASER-REID. Can. J. Chem. This issue.
17. E. L. ALBANO, D. HORTON, and J. H. LAUTERBACH. Carbohydr. Res. **9**, 149 (1969).
18. M. KARPLUS. J. Am. Chem. Soc. **85**, 2870 (1963).
19. W. G. DAUBEN and G. H. BEREZIN. J. Am. Chem. Soc. **89**, 3449 (1969).
20. C. D. POULTER, E. C. FRIEDRICH, and S. WINSTEIN. J. Am. Chem. Soc. **91**, 6892 (1969).
21. N. K. RICHTMYER. Meth. Carbohydr. Chem. **1**, 106 (1962).
22. J. D. ROBERTS, *editor*. Org. Synth. **41**, 72 (1961).

Can. J. Chem. Downloaded from www.nrcresearchpress.com by 210.87.254.40 on 09/05/12
For personal use only.

Determination of the Heat of Formation of Hexafluorobenzene

M. KRECH
Chemistry Department, Waterloo Lutheran University, Waterloo, Ontario

AND

S. J. W. PRICE AND W. F. YARED
Chemistry Department, University of Windsor, Windsor, Ontario

Received March 10, 1972

A new method has been developed for determining the heat of combustion of perfluoro aromatic compounds. The basic differences from previous methods are that no auxiliary substance is used and no water is present in the bomb. The combustion of hexafluorobenzene in a platinum lined bomb yields CO_2, CF_4, and F_2. Visual inspection and the material balance indicate that complete combustion is obtained. The value of $\Delta H^0_{f\,298}(C_6F_6,g)$ obtained by this method is -224.0 ± 2.0 kcal/mol. Recalculation of the result of Cox *et al.* (1, 2) obtained from combustion of C_6F_6 in mylar bags in the presence of hydrocarbon oil and water leads to $\Delta H^0_{f\,298}(C_6F_6,g) = -224.3$ kcal/mol.

Une nouvelle méthode a été développée pour déterminer la chaleur de combustion des composés aromatiques perfluorés. Les différences de base par rapport aux méthodes précédentes, sont l'absence de toute substance auxiliaire et d'eau dans la bombe. La combustion de l'hexafluorobenzène dans une bombe à revêtement de platine, conduit au CO_2, CF_4, et F_2. L'examen visuel et la balance pondérale indiquent une combustion complète. La valeur de $\Delta H^0_{f\,298}(C_6F_6,g)$ obtenue par cette méthode est -224.0 ± 2.0 kcal/mol. Le résultat de Cox *et al.* (1, 2) recalculé, donne $\Delta H^0_{f\,298}(C_6F_6,g) = -224.3$ kcal/mol, à partir de la combustion de C_6F_6 dans une enceinte étanche en présence d'huile d'hydrocarbure et d'eau.

[Traduit par le journal]

Canadian Journal of Chemistry, **50**, 2935 (1972)

Introduction

The determination of the heats of combustion of perfluoro aromatic compounds has received relatively little attention. Cox and co-workers (1) determined the heat of combustion of hexafluorobenzene in a platinum lined rotating bomb calorimeter using hydrogen-containing organic auxiliary substances. The value determined by Cox and co-workers for the heat of combustion of hexafluorobenzene in the ideal gas state was -220.4 kcal/mol. Based on a new value for $\Delta H_{f\,298}(HF.2OH_2O)$, this value was later revised to -228.4 kcal/mol (2).

The present paper describes the measurement of the heat of combustion of hexafluorobenzene in a platinum lined rotating bomb calorimeter without the use of any auxiliary substances. This work determines that complete combustion, substantiated by a product mass balance, makes it unnecessary to use any auxiliary substance and that the liquid hexafluorobenzene need not be contained in any manner but simply weighed into the platinum crucible.

Experimental

Hexafluorobenzene

The hexafluorobenzene used was obtained from Imperial Smelting Corporation and was analyzed by means of a thermal conductivity gas chromatograph using 6 ft × 1/4 in. o.d., polypropylene glycol column (110 °C, 60 cc/min He). The only detectable impurity was approximately 0.02% pentafluorobenzene.

Index of refraction at 25 °C, 1.3762 ($n_D^{25} = 1.3761$ (3)). Boiling point, 80.1 °C; freezing point, 5.2 °C (published values, 80 °C and 5.2 °C, respectively (3)).

A modified Ramsay–Young system was used to measure the vapor pressure of C_6F_6 over the range 8 to 62 °C. Approximately 80 vapor pressure measurements were made in four separate runs. The conventional plot of log p *vs.* $10^3/T$ was very slightly curved. The data are adequately represented by

$$[1] \quad \log P\,(\text{cm}) = 27.498 - 2{,}797.2/T - 6.945 \log_{10} T$$

The resulting heat of vaporization and average heat capacity difference (vapor − liquid) are $\Delta H^0_{298} = 8.69 \pm 0.02$ kcal/mol and $\langle \Delta C_p \rangle_{8-62\,°C} = -13.8 \pm 2.0$ cal deg^{-1} mol^{-1}. The error limits on ΔH are representative of the uncertainty in the precision only. The value of ΔH^0_{298} is in good agreement with the previously reported value (1), 8.65 kcal/mol. It is interesting to note that the boiling point of C_6F_6 is virtually identical to that of C_6H_6 and that the $\langle \Delta C_p \rangle$ value

Can. J. Chem. Downloaded from www.nrcresearchpress.com by 210.87.254.105 on 09/05/12
For personal use only.

over 8–62 °C is close to $\langle \Delta C_p \rangle_{25\,°C}$ for benzene, −13.0 cal deg^{-1} mol^{-1} (4).

Apparatus and Calorimetric Procedure

The rotating bomb calorimeter used was similar to that used in the Bureau of Mines Laboratory, Bartlesville (5). The combustion bomb was a platinum lined Parr Model 1004C bomb, 320 cc in volume. It was equipped with a geared rotating mechanism which rotated the bomb axially and end-over-end beneath the water in the calorimeter bucket.

The calorimetric jacket was maintained at 25.000 °C by using a Thermotrol Proportional Temperature Controller Model 1053 to balance the output of small heaters against cooling by a cooling coil supplied from a bath regulated to 16 ± 0.01 °C.

The rotating bomb calorimeter was used only as a matter of convenience. A static system of the same precision would have worked equally well provided it was equipped with a platinum lined bomb. A limited number of combustions was done in a static steel bomb but these combustions produced a green coloration on the inside of the bomb which was visual indication of the formation of compounds presumed to be iron fluorides.

The temperature of the water in the bucket was monitored by a 2000 ohm thermistor in conjunction with a Honeywell Wheatstone Bridge Model 1081 and a Leeds and Northrup D.C. Null Detector with variable sensitivity. The thermistor was calibrated against a Parr certified thermometer capable of being read to 0.001 °C. The resistance of the thermistor could be estimated to 0.01 ohm (about 0.0001 °C) with the null detector at low to moderate sensitivity. Time was measured and recorded on a Simplex timer capable of recording time to 0.01 min.

In a determination of the heat of combustion of hexafluorobenzene only the compound and oxygen were used in the bomb. Care was taken to insure that the interior of the bomb and the inner portion of the bomb lid were clean and moisture free. The sample of hexafluorobenzene to be combusted was weighed in a platinum crucible which was then placed in the gimbal which had previously been fitted with a weighed platinum fuse wire (12 cm long, 36 gauge) fixed to the terminals of the ignition circuit. The lid containing the crucible, compound, and fuse wire was then fitted into the bomb which was in an inverted position and the bomb was sealed by means of the screw cap and sealing bolts.

The length of time from taking the weight of the crucible and hexafluorobenzene to the insertion of the lid into the bomb was measured by means of a stopwatch to the nearest 0.1 s. The amount of hexafluorobenzene lost by evaporation could then be calculated from the rate of evaporation which was determined prior to each experiment. The time between weighing the crucible and compound and the closing of the bomb was such that evaporation of the compound was 0.5% of the total sample weight or less. The correction for evaporation is estimated to be accurate to within at least ±3%. The error in weight generated by the correction procedure therefore should be less than ±0.02% of the sample weight.

After a 15 min period during which the bomb achieved thermal equilibrium with the water in the calorimeter bucket, time and temperature readings were taken every 10–15 s for about 10 min. After this pre-run period, ignition was affected by discharging a pair of 250 mF capacitors charged to a measured voltage (approximately 140 V) and time and temperature readings were taken as often as every 0.05 min for the ensuing 25 min. Rotation of the bomb was started 3 min after ignition and was continued throughout the remainder of the calorimetric experiment.

A computer program was used to calculate the corrected temperature rise (6). The procedure used was based essentially on Dickinson's method (7, 8). The correction to standard states followed the method of Good and Scott (9). The energy equivalent of the calorimeter as determined using standard benzoic acid was 4250.9 ± 0.2 cal/deg.

Analysis of Reaction Products

Before analysis the lid of the bomb was thoroughly dried with special attention being given to the inlet and outlet valves so that no moisture was present. The bomb was then connected by means of Tygon tubing to an analysis train consisting of a Teflon bubbler, a drying tube containing magnesium perchlorate, a gas sample collection tube and a carbon dioxide collection vessel. The bomb outlet valve was opened and the gases were allowed to pass through the analysis train until all the gases had been emptied from the bomb. Analytical grade oxygen was then passed through the inlet valve of the bomb and into the analysis train for about 1½ h to flush the bomb of any remaining combustion products. The entire process of emptying the bomb and flushing with oxygen lasted approximately 16 h.

The solution from the bubbler was analyzed for F^- using a fluoride specific ion electrode in conjunction with an Orion Model 701 digital p*H* meter capable of reading relative millivolts to the nearest 0.1 mV. The 4 cc gas collection tube was removed periodically for analysis on a Perkin–Elmer 154D thermal conductivity gas chromatograph (6 ft × 1/4 in. o.d., silical gel column, 25 °C, He carrier 15 cc/min). When the gas collection tube was removed from the analysis train it was replaced with a short length of Tygon tubing. The chromatographic conditions used gave separation of the tetrafluoromethane peak from the massive oxygen peak and thus permitted a determination of the ratio of carbon dioxide to tetrafluoromethane. The carbon dioxide collection tube contained Lithasorb and magnesium perchlorate. It was evacuated to a constant weight prior to use in the analysis train and was again evacuated to a constant weight subsequent to the flushing procedure (through the magnesium perchlorate end to prevent loss of liberated water). Allowance was made for the small amount of carbon dioxide removed in the gas chromatography samples. Analysis of the gases at the exit of the carbon dioxide collection tube by gas chromatography did not show any carbon dioxide.

Results and Discussion

Gas chromatographic analysis of the gases contained in the gas collection tube gave peaks for CO_2, CF_4, and O_2. Both gas chromatographic and mass spectromatic tests failed to show even traces of F_2O. From Table 1 the average molar ratio of CO_2 to CF_4 is 4.54 ± 0.05 (omitting runs 1 and 3, ±0.02). It should be noted that a change of 0.01 in this ratio leads

Can. J. Chem. Downloaded from www.nrcresearchpress.com by 210.87.254.105 on 09/05/12
For personal use only.

TABLE 1. Combustion data and calculated heat of formation for hexafluorobenzene

Run	Mass C_6F_6 (g)	ΔT corr. (°C)	CO_2/CF_4* (by g.c.)	CO_2 collected (g)	F_2 collected (g)	$\Delta H^0_{f\,298}(C_6F_6,g)$ (kcal/mol)
1	1.437	0.8772	4.48	1.663	0.236	−222.3
2	1.465	0.8890	4.52	1.679	0.248	−224.6
3	1.404	0.8508	4.59	1.608	0.249	−225.7
4	1.427	0.8720	4.56	1.646	0.248	−222.0
5	1.467	0.8883	4.54	1.688	0.243	−226.0
6	1.418	0.8641	4.52	1.619	0.247	−222.9
7	1.432	0.8685	4.55			−225.4
8	1.401	0.8489	4.54	1.612		−225.7
9	1.418	0.8637	4.54	1.656		−223.2
10	1.406	0.8570	4.56		0.226	−222.8
11	1.373	0.8368	4.54	1.594		−223.2

*Molar ratio. Additional typical data (see ref. 7 for notation): ΔE, ign/cal = 2.41, ε(cal)$(-\Delta t_c)$/cal = −3706.79, $\Delta E^0_c/M$ (compound)/cal g^{-1} = −2628.36.

to a change in $\Delta H^0_{f\,298}(C_6F_6,g)$ of about 0.25 kcal/mol. Since only the relative amounts of CO_2 and CF_4 are important many of the possible errors normally associated with absolute gas chromatographic calibration are unimportant. However, in establishing the relative response of CF_4 it is important to use a CF_4–O_2 mixture whose composition is similar to that of the samples from the combustion experiment. Use of pure CF_4 leads to a response factor that is lower by 4.6%. The CO_2 calibration is unaffected. The net result is that if relative response factors determined with pure CF_4 and CO_2 are used a value for $\Delta H^0_{f\,298}(C_6F_6,g)$ is obtained that is about 5 kcal/mol too high.

Based on the observed products and the CO_2/CF_4 ratio the combustion reaction may be written

[2] $C_6F_6 + 4.917O_2 \rightarrow 4.917\ CO_2 + 1.083\ CF_4 + 0.834\ F_2$

The F_2 data in Table 1 average out to within 0.4% of the value predicted from this equation (if $CO_2/CF_4 = 4.53$ rather than 4.54, then exact agreement is obtained). In three of the nine runs in which CO_2 analyses were done the CO_2 yield is also in good agreement. In the other six runs the CO_2 yield was 0.8 to 1.6% low indicating a small loss of CO_2, possibly due to surges in flow which sometimes occurred when the bomb valve was opened too quickly.

In applying eq. 2 to the experimental combustion process it must be remembered that the C_6F_6 sample is not contained in any way and that combustion occurs in a 320 cc bomb with an initial temperature of 23.5 °C and an initial pressure of 450 p.s.i. The experimental procedure therefore involves the combustion of 0.30 g C_6F_6 vapor and $(W - 0.30)$ g C_6F_6 liquid where W = weight C_6F_6 sample in grams. This presence of just over 20% of the samples in the vapor state undoubtedly aids combustion and in fact is probably responsible for the fact that complete combustion is obtained in the absence of any auxiliary compound.

For calculation of $\Delta H^0_{f\,298}(C_6F_6,g)$ the standard heat of formation of the combustion products were taken as (10)

$$\Delta H^0_{f\,298}(CO_2,g) = -94.0517 \text{ kcal/mol}$$

$$\Delta H^0_{f\,298}(CF_4,g) = -221.0 \text{ kcal/mol}$$

and the required correction for the C_6F_6 in the liquid state, $[(W - 0.30)/W]\Delta H^0_{f\,298}(vap)$ was based on a heat of vaporization of 8.7 kcal/mol.

The average value of $\Delta H^0_{f\,298}(C_6F_6,g)$ obtained is -224.0 ± 2.0 kcal/mol. The previously reported values −220.4 (1) and −228.7 kcal/mol (2) were based on $\Delta H^0_{f\,298}(HF.2OH_2O) = -75.63$ and −76.96 kcal/mol, respectively. The NBS selected value (10) is −76.28 kcal/mol. A recent determination of the heat of solution of HF (11) lends strong support to this value. If the NBS value is used to recalculate the result of Cox *et al.* (1, 2) then a value of $\Delta H^0_{f\,298}(C_6F_6, g) = -224.3$ kcal/mol is obtained, a result in excellent agreement with the present work.

Although for the present, the NBS values for the heat of formation of CF_4 and HF are preferred, if for no other reason than the check for internal consistency made on all NBS data, both the present result and that of Cox *et al.* can also

Can. J. Chem. Downloaded from www.nrcresearchpress.com by 210.87.254.105 on 09/05/12
For personal use only.

be calculated using the slightly more recent value $\Delta H^0_{f\,298}(CF_4,g) = -223$ kcal mol^{-1} (12). This result leads to a value of about -76.35 kcal mol^{-1} for $\Delta H^0_{f\,298}(HF.2OH_2O)$. Based on these values the present value for $\Delta H^0_{f\,298}(C_6F_6$, g) becomes -226.0 kcal mol^{-1} and that of Cox *et al.* -225.1 kcal mol^{-1}.

In conclusion the present experimental method seems to provide a simpler and more direct method for determining the heat of formation of perfluoroaromatic compounds. Complete combustion is easily obtained without the aid of heat shields, auxiliary oils, etc. and a simple static bomb calorimeter should produce just as good a result as a rotating bomb system. With slight modification the procedure should be suitable for compounds of the type C_6F_5X where X is another halogen and also possibly for other related compounds.

The authors would like to acknowledge the assistance given by Dr. W. D. Clark and Mr. J. P. Richard in writing computer programs used in this work. Financial assistance from the National Research Council of Canada is also acknowledged.

1. J. D. Cox, H. A. Gundry, and A. J. Head. Trans. Faraday Soc. **60**, 653 (1964).
2. J. D. Cox, H. A. Gundry, D. Harrop, and A. J. Head. J. Chem. Thermodyn. **1**, 77 (1969).
3. Highly fluorinated aromatic and alicyclic compounds. Imperial Smelting Company, St. Andrews Road, Avonmouth, Bristol BS11 9HP, England.
4. Handbook of Chemistry and Physics. 50th ed. The Chemical Rubber Co., Cleveland, Ohio. 1969–1970.
5. W. Good, D. Scott, and G. Waddington. J. Phys. Chem. **60**, 1080 (1956).
6. W. D. K. Clark. Ph.D. Thesis. Windsor, Ontario. 1968.
7. J. Coops, R. S. Jessup, and K. Van Nes. *In* Experimental thermochemistry. Vol. 1. *Edited by* F. D. Rossini, Interscience, New York. 1956.
8. Technical Manual No. 130. Parr Instrument Co. 1960.
9. W. D. Good and D. W. Scott. Combustion in a bomb of organic fluorine compounds. Ch. 2. *In* Experimental thermochemistry. Vol. II. *Edited by* H. A. Skinner. Interscience, London. 1962. p. 15.
10. Selected values of chemical thermodynamic properties. National Bureau of Standards. U.S. Tech. Notes No. 270–3 (1968).
11. C. E. Vanderzee and W. W. Rodenburg. J. Chem. Thermodyn. **3**, 267 (1971).
12. E. Greenberg and W. N. Hubbard. J. Phys. Chem. **72** (1), 222 (1968).

Can. J. Chem. Downloaded from www.nrcresearchpress.com by 210.87.254.105 on 09/05/12
For personal use only.

Alkyl Shifts in Cyclohexenyl Cations

K. RAJESWARI AND T. S. SORENSEN
The Department of Chemistry, University of Calgary, Calgary, Alberta

Received February 22, 1972

The possible ways in which alkyl rearrangements can occur in cycloalkenyl cations are described. With cyclohexenyl cations, two rearrangements unique to this system are discussed and experimental evidence for both of these is presented. Use is made of the n.m.r. spin saturation transfer technique in one case.

In the final part of the paper, we show how, by repeatedly using both rearrangements, it is possible in theory to scramble the relative positions of all of the carbon atoms with respect to both the different positions within a cyclohexenyl cation framework and with respect to the bonding order of consecutive atoms within the framework. In the unsubstituted case, this corresponds to a 360-fold degenerate rearrangement.

Les voies possibles de réarrangements d'alkyle dans les cations cycloalkényles sont décrites. Avec les cations cyclohexènyles, deux réarrangements uniques à ce système sont discutés et une preuve expérimentale pour chacun d'eux est présentée. Dans un cas, la technique de transfert de la saturation de spin en r.m.n. a été utilisée.

Dans la dernière partie du mémoire, nous montrons comment, par l'usage répété de ces deux réarrangements, il est possible en théorie de bouleverser les positions relatives de tous les atomes de carbone par rapport à ces deux positions différentes à l'intérieur du squelette cyclohexènyle cation et par rapport à l'ordre de liaison des atomes consécutifs du squelette. Dans le cas du squellette non-substitué, cela donne un réarrangement dégénéré d'ordre 360. [Traduit par le journal]

Canadian Journal of Chemistry, **50**, 2939 (1972)

In cycloalkenyl cations in general, the highest positive charge density is located at the C-1 and -3 positions, a lesser amount at C-2, and even less on the remaining saturated carbon atoms (n) of the ring.

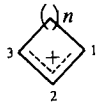

Since alkyl groups stabilize a positive charge, it follows that the most stable alkyl-substituted cations will be those in which the alkyl groups occupy the C-1, -2, and -3 positions. In other words, the most stable monoalkyl cation will be the C-1 or -3 alkyl derivative; for a dialkyl, the C-1,3 derivative, and for a trialkyl, the C-1,2,3 derivative. In those cases where sufficient alkyl groups are present within the ring system but are not located at these centers, the molecules are presented with a tantalizing problem in somehow "moving" the substituents. In a case where $n = 1$, such an operation can be accomplished directly by well-known 1,2-alkyl or hydride shifts,[1] for example, reaction Scheme 1 would be expected. Even in the $n = 2$ case, the process is reasonably efficient and the intermediacy of the 3-cyclopenten-1-yl cation **1** is involved (1–3).

1

The symmetry of this cation (in an unsubstituted case) is an important feature here since one can return to the conjugated cycloalkenyl cation by a different pathway. For example, the rearrangements shown in Scheme 2 are probable. In both the cyclopentenyl and cyclohexenyl cations (but not likely in the cyclobutenyl for obvious reasons) one can sometimes have effective alkyl rearrangements which operate via a base-catalyzed proton loss to give an intermediate diene which can then reprotonate at the opposite end (4–7). However, if one uses a strong enough acid system, it is generally possible to damp this process and in the present experiments, strong acid conditions apply.

When one comes to consider the $n = 3$ (cyclohexenyl) case, the situation becomes more involved. A normal 1,2-substituent shift produces an intermediate which may be considered as a homoallylic cation **2** or as a 2-bicyclo[3.1.0]hexyl cation **3** (a cyclopropylcarbinyl system) (8) (see

[1]The discussion here centers on thermodynamics. In some cases, the rates of these shifts may be quite different because of favorable or unfavorable steric or electronic factors.

Can. J. Chem. Downloaded from www.nrcresearchpress.com by 210.87.254.40 on 09/05/12
For personal use only.

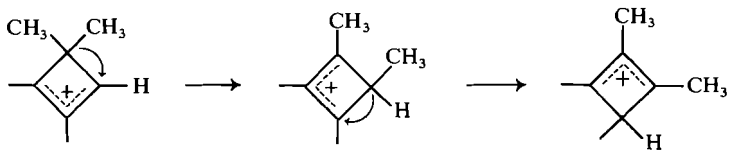

SCHEME 1

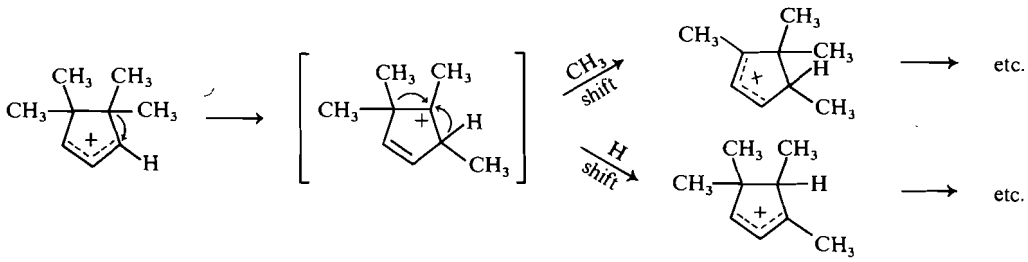

SCHEME 2

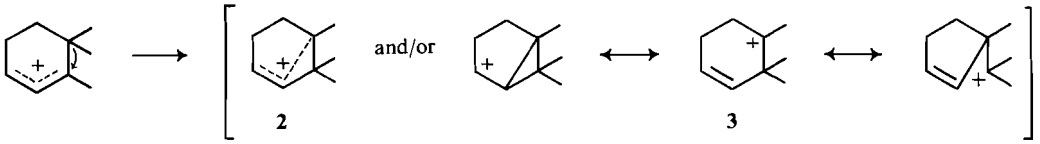

SCHEME 3

Process 1: Degenerate Cyclopropylcarbinyl Rearrangement[2]

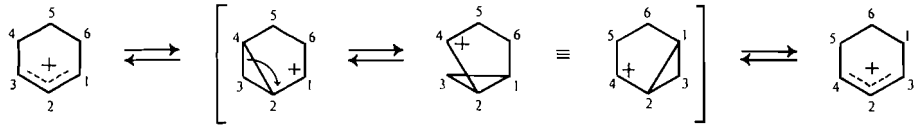

Process 2: Degenerate C-5,4(6) Substituent Shift[3]

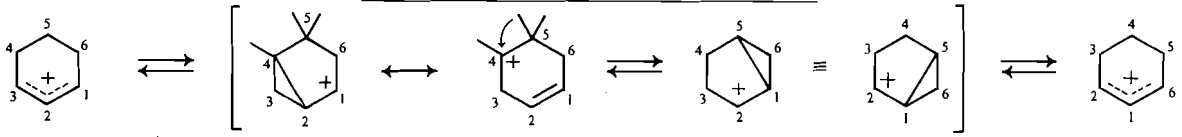

SCHEME 4

Scheme 3). One might get rearrangements in a quite analogous way to that shown for the cyclopentenyl cation case (H shift pathway). In addition to this however, we have recently suggested (9) that intermediates **2** and/or **3** can undergo two kinds of degenerate rearrangements (in the absence of substituents) and that where substituents are present to lift this degeneracy, effective alkyl rearrangements take place. The two processes are shown in Scheme 4, with the atoms keeping their original numbers to indicate what happens in the degenerate rearrangement. Simply for brevity of presentation, the intermediate is pictured as a cyclopropylcarbinyl cation system in both cases. The unique differ-

[2]Only one of two possibilities is shown, *i.e.* migration of either the C-4 or -6 substituent produces the intermediate. No mechanistic details are implied by the formulations. There are in fact some grounds for believing that the process may be a "two-step shuffle".

[3]A resonance formulation of the cyclopropylcarbinyl cation system is employed here to make the electron "bookkeeping" during the rearrangement more obvious.

Can. J. Chem. Downloaded from www.nrcresearchpress.com by 210.87.254.40 on 09/05/12
For personal use only.

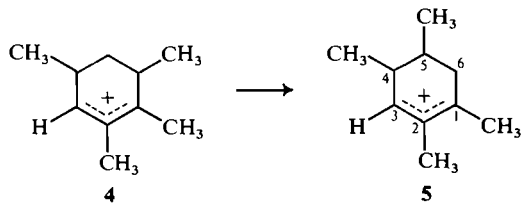

4 5

SCHEME 5

entiating feature of the first rearrangement is that consecutive atoms in the ring become interchanged.

These mechanisms were postulated in earlier work (9) to explain several puzzling methyl group arrangements which were found in the product cyclohexenyl cations derived from some cyclopropylallyl cation rearrangements. The evidence was indirect since we were never able to observe directly a methyl-substituted cyclohexenyl cation actually rearranging by either of these processes.

In the present paper, we describe cation rearrangements which we believe are due to these two processes. The rearrangements are inferred by the very specific way in which alkyl groups are "moved" in the directly observable cyclohexenyl–cyclohexenyl cation rearrangements. In the present examples, the extent of the alkylation at the C-1, -2, and -3 positions of the cyclohexenyl cations is not changed but the validity of the postulates is in no way negated by this fact. Actually, this may be the reason that these rearrangements could be observed at all (*i.e.* otherwise too fast to measure) in our systems since an added driving force may exist when, because of increased alkyl substitution at the active centers, a more stable cation is being formed.

Process 1, Scheme 4

At low temperatures (*ca.* $-90°$), cation **4** can be directly observed by n.m.r. spectroscopy, but on warming to $-50°$, is converted to the isomeric species **5** (Scheme 5). This rearrangement is readily observed because the C-5 methyl peak in **5** is at a characteristically high field.[4] The geometry of the C-4 and -6 methyl groups in **4** is not known with certainty but an unequal doubling of some n.m.r. peaks was observed. This doubling could be due to the presence of both the *cis* and *trans* isomers of **4** or by the "freezing out" of non-equivalent axial–equatorial pairs of a predominantly *trans* form (12). The former situation seems more likely (with the *cis* isomer probably predominant). In the formation of **5**, a similar doubling was fleetingly observed but the spectrum rapidly reduced to one interpretable in terms of a single isomer, presumably that with the *trans* geometry. The rearrangement **4** → **5** is explicable in terms of Process 1 although one is not certain why cation **5** should be more stable.

Process 2, Scheme 4

As the cation **5** solution is further warmed, an n.m.r. line broadening just becomes observable ($-10°$) before a further irreversible rearrangement occurs to give cations **6** and **7**. In these

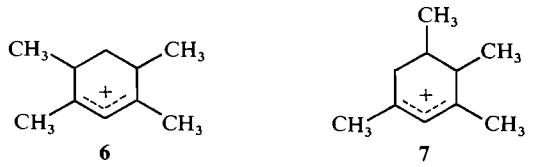

6 7

circumstances, the n.m.r. spin label method of Forsén and Hoffman (13, 14) is invaluable in deciding what n.m.r. exchange processes are actually occurring. The spectrum of cation **5** is described in Fig. 1. At $-10°$, irradiation of the

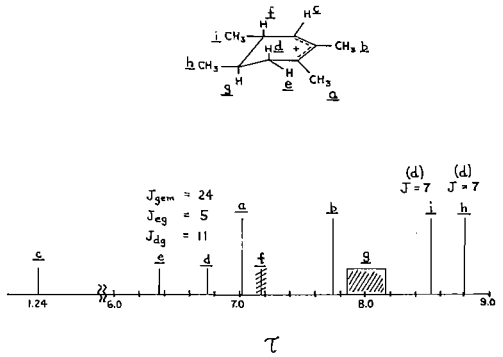

FIG. 1. Schematic n.m.r. spectrum of cation **5**.

Comments: The positions of the *f* and *g* protons were located by noting where the maximum decoupling occurred in the *h* and *i* methyl doublets. Both *f* and *g* give complex peaks which could not be interpreted in detail. The protons *d* and *e* are assigned the above positions and coupling constants. The J_{gem} value seems rather high and one cannot be very certain of this particular assignment except to say that this region in general is certainly due to *d* and *e*. The specific assignment of *d* and *e* is made on the basis of the magnitude of the vicinal coupling constants apparently observed.

[4]The chemical shifts of these alkyl groups are generally a function of their bonded distance from the cation centers (10, 11).

Can. J. Chem. Downloaded from www.nrcresearchpress.com by 210.87.254.40 on 09/05/12
For personal use only.

Can. J. Chem. Downloaded from www.nrcresearchpress.com by 210.87.254.40 on 09/05/12
For personal use only.

d and *e* protons region causes a marked decrease in the *c* proton peak area and irradiation at the *a* methyl causes a marked decrease in the *b* methyl peak area and vice-versa. Other exchanges could not be studied because the presumed exchanging groups are located too close together for this technique to be workable. The *d* and *e* protons peak area covers a wide frequency range and the maximum decrease in the *c* proton area appeared to occur when the lower field portion (assigned the equatorial position *e*) was irradiated.[5] It therefore appears that the *c* and *e* protons are actually involved in this exchange. This degenerate rearrangement is ascribed to Process 2 and the complete group exchange expected is shown below:

$$\left[\begin{array}{c|c} a & b \\ c & e \\ d & f \\ h & i \\ & g \end{array}\right]$$

The proton *g*, although migrating in each sequence, treadmill-like stays the same.

If protons *c* and *e* are exchanging then the process is rather stereospecific. The following structure (see footnote 3) shows the step in which *c* and *e* become equivalent. This then requires that the original migrating proton *f* stay on the top side of the molecule ($f = d$).

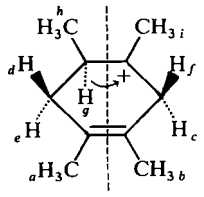

The results and discussion to this point have been concerned primarily with the experimental evidence that Processes 1 and 2, Scheme 4, can occur, at least in the specific cases discussed here, and on the way in which these rearrangements (singly) can then produce "effective" alkyl shifts within the cations. The overall sequence shown in this work can be written:

$$\mathbf{4} \xrightarrow{\text{Process 1}} \mathbf{5} \xrightarrow{\text{Process 2}} \mathbf{5'}$$

[5]The irradiating frequency is quite wide so that the effect of small changes in the center of the irradiating frequency is not large.

Although the previous discussion has emphasized the individual nature of each process it is of interest to examine theoretically the intriguing possibility that multiple rearrangements may occur in some cases (although not in the examples studied here; see later). For this theoretical discussion we will use the unsubstituted cyclohexenyl cation and one is therefore describing degenerate rearrangements.

Theoretical Consequences of Multiple Rearrangements

Each single rearrangement process involves a minimum of three distinct steps with the first and last probably symmetrical. The way in which multiple rearrangements might occur is critically dependent on the rate constants k_1, k_2, k_{-1}, and k_{-3}, the latter two being assumed to be very similar (see Scheme 6). Two limiting situations might arise:

(1) k_2 *and* $k_{-2} \gg k_{-1}$ *or* k_{-3}. In this case, the intermediate would undergo multiple rearrangements before returning to the cyclohexenyl cation. If one alternates the Processes 1 and 2, a 12-fold degenerate rearrangement of the intermediate can be predicted to occur in an unsubstituted case (shown in Fig. 2). Each intermediate could exit to a "different" cyclohexenyl cation and then begin a "different" cycle.

(2) k_{-1} *or* $k_{-3} \gg k_2$ *and* k_{-2}. This is perhaps more likely and in this case, only one intermediate rearrangement, at best, would occur for each k_1 step. However, in an unsubstituted cyclohexenyl cation, one might still get degenerate rearrangement cycles because of the symmetry of this cation. A sequence of Process 1 steps gives five degenerate cyclohexenyl cation structures while a sequence of Process 2 steps gives six degenerate structures (Fig. 3). A combination of the two would allow the formation of all 360 possible degenerate "structures" for the parent cyclohexenyl cation. Whether these reactions occur in the unsubstituted cyclohexenyl cation will have to await labelling experiments.

With alkyl substituents certain "structures" will represent energy minima and effectively quench a multiple process regardless of the actual kinetics of the individual steps (*i.e.* either limiting situation could apply). We believe the results of this paper nicely illustrate this principle. In the situation shown in Scheme 7, cations **4** and **5** can only break out of the box by

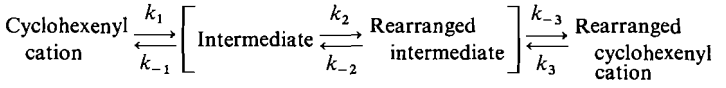

SCHEME 6

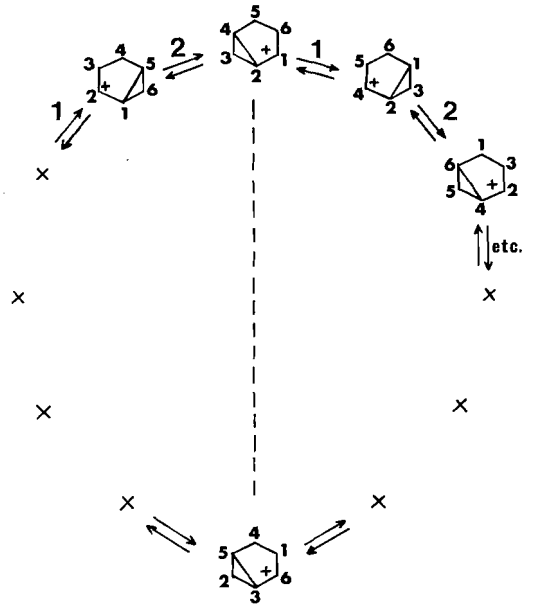

FIG. 2. Degenerate rearrangement cycle of a 2-bicyclo-[3.1.0]hexyl cation. The diagonal structures correspond to the complete reversion of the carbons 1–6, 2–3, and 4–5 diatomic fragments. The cyclopropane ring is "up" in all cases.

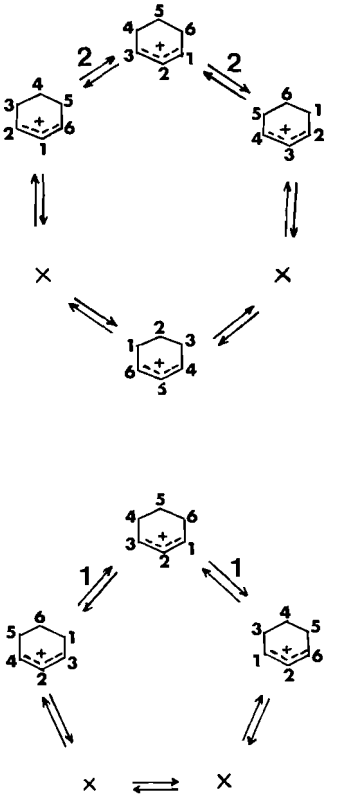

FIG. 3. *Lower:* Degenerate rearrangement cycle of a cyclohexenyl cation using Process 1, Scheme 4. The cycles require the hydride migration, *i.e.* from equivalent C-4 or -6 sites in the upper structure, to alternate in order to produce the cycle.

Upper: Degenerate rearrangement cycle of a cyclohexenyl cation using Process 2, Scheme 4. The same comments as in Process I apply.

forming the intermediates **10** and **11** and then having these rearrange by either Process 1 or 2. These intermediates would be of higher energy than **8** or **9** because of less substitution at the charged centers. We would predict that this sort of behavior would be typical of alkylsubstituted cyclohexenyl cations in general.

Experimental

Preparation of the Cations

Cation **4** was generated by the addition of 2-(α-methylcyclopropyl)-3-methyl-3-*cis*-penten-2-ol to fluorosulfonic acid–sulfuryl chlorofluoride (1:4) at −130° and then allowing the solution to warm to −90°.[6] The n.m.r. peaks of ions **4**, **6**, and **7** are reported in Table 1. Although these cations are unreported, the spectra of a number of similar cyclohexenyl cations have been (9, 11, 12), making the assignments relatively straightforward.

[6]To be published separately. Similar cyclopropylallyl cation rearrangements have previously been reported in ref. 9.

Spin Saturation Transfer Experiments

All n.m.r. spectra were recorded using a Varian Associates HA-100 spectrometer equipped with standard decoupling equipment and a variable temperature probe. Speed of operation was essential in the spin saturation experiments since the cation **5** was disappearing rapidly (to **6** and **7**) at the temperatures used for the experiments (from −10 to −30°). The formation of **6** and **7** made a quantitative measure of the rate difficult and necessitated using fresh solutions frequently. The usual precautions in the spin saturation procedure were used (14). It was not possible to irradiate proton *c* and monitor the proton *e* region since *c* is too close to the acid proton internal lock. Several different tempera-

Can. J. Chem. Downloaded from www.nrcresearchpress.com by 210.87.254.40 on 09/05/12
For personal use only.

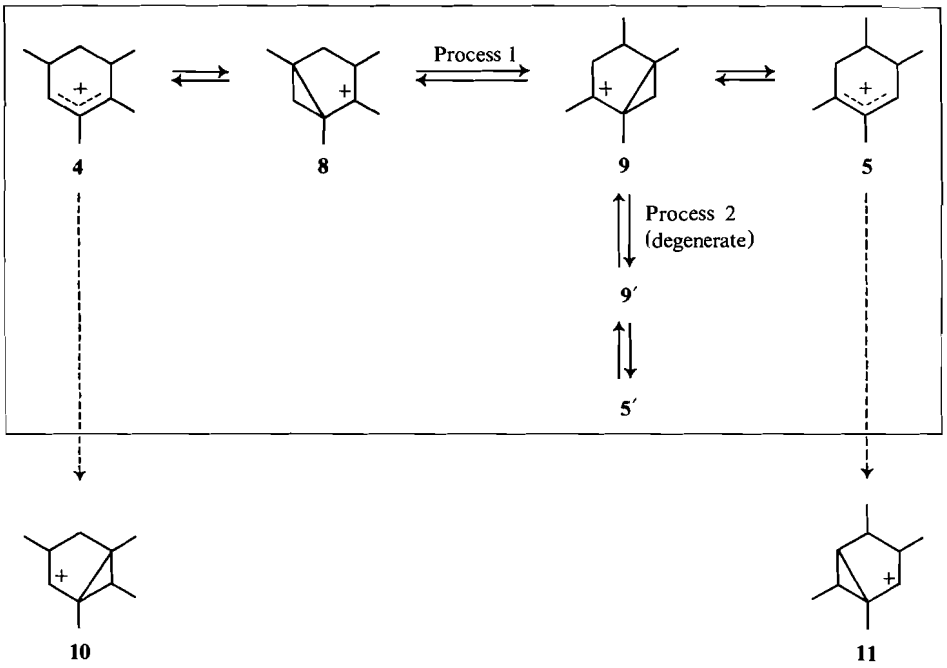

SCHEME 7

TABLE 1. The n.m.r. spectra of the cyclohexenyl cations

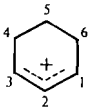

Ion	C-1	C-2	C-3	C-4	C-5	C-6
4	7.01[a]	7.74[b] 7.77	1.24	8.41[b-d] 8.47 (s) 8.50 8.53 8.57 8.60 (s)	7.99 (b)	[d]
6	7.16[e]	2.42[f] 2.49	7.16[e]	8.52 (d); $J = 7$[d] 8.545 (d); $J = 7$ 8.705 (d); $J = 7$	—	[d]
7	7.16[e]	2.42[f] 2.49	7.16[e]	[d]	8.555 (d); $J = 7$ 8.82 (d); $J = 7$	[d]

[a]In τ p.p.m. relative to internal tetramethylammonium cation = 6.90; s = shoulder, d = doublet; center of multiplet is quoted unless specified; coupling constants are in Hz.
[b]Part of the doubling referred to in the text.
[c]These are the actual peak positions.
[d]The specific assignment of C-4 and -6 methyl groups was not possible. The C-4 and -6 protons were likewise unassignable.
[e]This broad peak is typical of methyl groups on allylic centers and overlaps extensively in different compounds.
[f]These peaks are very characteristic of this position but are not assignable to one particular isomer.

Can. J. Chem. Downloaded from www.nrcresearchpress.com by 210.87.254.40 on 09/05/12
For personal use only.

tures were used, to verify the lower expected area decreases at the lower temperatures.

The authors wish to thank the National Research Council of Canada for generous financial support, and the University of Calgary for Intersession Bursaries to K.R.

1. T. S. SORENSEN. Can. J. Chem. **42**, 2768 (1964).
2. D. M. BROUWER and J. A. VAN DOORN. Rec. Trav. Chim. **89**, 333 (1970).
3. R. BLADEK. M.Sc. Thesis. University of Calgary, Calgary, Alberta, 1971.
4. N. C. DENO, H. G. RICHEY, JR., N. FRIEDMAN, J. D. HODGE, J. J. HOUSER, and C. U. PITTMAN, JR. J. Am. Chem. Soc. **85**, 2991 (1963).
5. T. S. SORENSEN. J. Am. Chem. Soc. **89**, 3782, 3794 (1967).
6. T. S. SORENSEN, I. J. MILLER, and C. M. URNESS. Can. J. Chem. **48**, 3374 (1970).
7. N. C. DENO and R. R. LASTOMIRSKY. J. Am. Chem. Soc. **90**, 4085 (1968).
8. T. S. SORENSEN and K. RANGANAYAKULU. J. Am. Chem. Soc. **92**, 6539 (1970).
9. T. S. SORENSEN and K. RAJESWARI. J. Am. Chem. Soc. **93**, 4222 (1971).
10. T. S. SORENSEN. *In* Carbonium ions. *Edited by* G. A. Olah and P. v. R. Schleyer. Vol. II. Wiley-Interscience Publishers, New York. 1970. Chapt. 19.
11. N. C. DENO. Prog. Phys. Org. Chem. **2**, 129 (1964).
12. H. HOGEVEEN and H. C. VOLGER. Rec. Trav. Chim. **88**, 379 (1969).
13. S. FORSÉN and R. A. HOFFMAN. J. Chem. Phys. **39**, 2892 (1963).
14. F. A. L. ANET and A. J. R. BOURNS. J. Am. Chem. Soc. **89**, 760 (1967).

Can. J. Chem. Downloaded from www.nrcresearchpress.com by 210.87.254.40 on 09/05/12
For personal use only.

Electronic Spectrum of Cobalt(II) in Sulfates. Part III. Equilibrium Studies in Li_2SO_4–DMSO Solution and in $NaHSO_4$–$KHSO_4$ Melt

J. R. DICKINSON[1]

Department of Inorganic and Structural Chemistry, University of Leeds, Leeds, England

AND

M. E. STONE

Ladies' College, Cheltenham, England

Received February 17, 1972

The results of a study of the electronic absorption spectrum of cobalt(II) in Li_2SO_4–DMSO solution, an equimolar $NaHSO_4$–$KHSO_4$ melt, a eutectic melt of Li_2SO_4–Na_2SO_4–K_2SO_4, single salt melts of Li_2SO_4 and Na_2SO_4 and a doped single crystal of $K_2Zn_2(SO_4)_3$ have been combined with previous results in sulfate media; all the results can be explained in terms of a blue dodecahedral $[Co(O_2SO_2)_4]^{6-}$ species, a pink octahedral $[Co(OSO_3)_6]^{10-}$ species or an equilibrium mixture of the two.

Nous avons combiné les résultats d'une étude par spectroscopie d'absorption électronique du cobalt(II) en solution dans une solution Li_2SO_4–DMSO, un mélange équimolaire de $NaHSO_4$–$KHSO_4$ fondu, un mélange eutectique de Li_2SO_4–Na_2SO_4–K_2SO_4 fondu, des sels fondus tels Li_2SO_4 et Na_2SO_4 et un cristal contaminé de $K_2Zn_2(SO_4)_3$, avec des résultats ultérieurs en milieu sulfate; les résultats s'expliquent tous en termes de spécimens dodécaédriques bleus $[Co(O_2SO_4)_4]^{6-}$ octaédriques roses $[Co(OSO_3)_6]^{10-}$ ou d'un mélange des deux à l'équilibre. [Traduit par le journal]

Canadian Journal of Chemistry, **50**, 2946 (1972)

Introduction

Previous investigations of the electronic absorption spectrum of cobalt(II) in sulfuric acid solutions (1–3), a sodium hydrogen sulfate–potassium hydrogen sulfate glass and melt (2), a potassium sulfate–zinc sulfate glass (2, 4, 5), and several sulfate melts (4, 6) have led to the conclusion that several distinct sulfato complexes of cobalt(II) exist. In concentrated sulfuric acid and the hydrogen sulfate glass at room temperature Duffy and co-workers (1, 2, 7) characterized a low-temperature, pink, octahedral species which, they suggested, contained monodentate ligands. The same workers have argued that on heating the sulfuric acid solution and the hydrogen sulfate glass the sulfate groups changed from unidentate to bidentate behavior, thus forming the high-temperature, violet, octahedral species $[Co(O_2SO_2)_3]^{4-}$; this has also been claimed to exist in the potassium sulfate–zinc sulfate glass at room temperature (5). In the sulfate melts we have characterized a blue species which we believe to be a tetra-sulfato complex involving bidentate sulfate ligands producing an essentially dodecahedral complex (4). A distorted octahedral species has also been postulated to exist in sulfuric acid solutions (3). None of the postulated structures of these four species have been confirmed by independent means. In this paper, we present the results of further work on cobalt(II) complexes in sulfate environments which provides a complete characterization of the low-temperature pink species. Furthermore, we have discovered the existence of several equilibria which, we believe, allow all the results available at present to be explained in terms of an equilibrium mixture of only two species.

[1]Present address: Centre for Materials Science, University of Birmingham, Birmingham, B15 2TT, England.

Experimental

Absorption spectra were recorded with a Cary 14H spectrophotometer having the furnace assembly and temperature control system described by Griffiths and Scarrow (8).

Anhydrous lithium sulfate was prepared by heating Analar $Li_2SO_4 \cdot H_2O$ at 200 °C for 24 h. Analar grade sodium sulfate and potassium sulfate were also dried in this manner and used without further purification. The ternary alkali sulfate eutectic melt was prepared as previously described (6). The equimolar sodium hydrogen sulfate–potassium hydrogen sulfate melt was prepared by the method used by Duffy *et al.* (2). We were unable to

Can. J. Chem. Downloaded from www.nrcresearchpress.com by 210.87.254.40 on 09/05/12
For personal use only.

Can. J. Chem. Downloaded from www.nrcresearchpress.com by 210.87.254.40 on 09/05/12
For personal use only.

obtain hydrogen sulfate glasses of sufficiently high quality to make accurate spectral measurements worthwhile.

The dimethylsulfoxide–lithium sulfate solution, approximately 0.4 *M* in sulfate, was prepared from reagent grade dimethylsulfoxide and anhydrous lithium sulfate. Cobalt(II) was added as the anhydrous sulfate, the concentrations being such that the $Co:SO_4^{2-}$ ratio was 1:20. Similar solutions containing sodium and potassium sulfates were also examined but did not show the same spectral changes as the lithium sulfate system. This difference was almost certainly due to the much lower solubilities of the sodium and potassium sulfates in dimethylsulfoxide.

A single crystal of cobalt-doped $K_2Zn_2(SO_4)_3$ was grown from the melt by the Stockbarger technique.

Results and Discussion

In the present study the visible region electronic absorption spectrum of cobalt(II) in molten lithium sulfate, molten sodium sulfate, an equimolar melt of sodium hydrogen sulfate and potassium hydrogen sulfate, a eutectic melt of lithium sulfate–sodium sulfate–potassium sulfate, a dimethylsulfoxide solution in which a large excess of anhydrous lithium sulfate had been dissolved, and a doped single crystal of $K_2Zn_2(SO_4)_3$ have been examined. The results, together with all the previously published spectra of cobalt(II) in sulfate media, are collected in Table 1. A close examination of the table shows that the results can be divided into four classes as indicated in the last column of the table.

Comparison of the spectrum of the cobalt-doped single crystal of $K_2Zn_2(SO_4)_3$ to the room-temperature spectra of cobalt(II) in the hydrogen sulfate glass, 98% sulfuric acid and the lithium sulfate–dimethylsulfoxide solution shows that in all four environments the cobalt species are identical. These systems give rise to a Class 1 spectrum which consists of a broad, relatively weak, band centered at 18.4 kK with a shoulder at higher energy (20.5–20.8 kK) and a very much weaker band at lower energies (12.0–13.3 kK); it is often difficult to determine the position of the last band precisely, as it is usually overlapped by the main band. Now, a crystal-structure determination of langbeinite, $K_2Mg_2(SO_4)_3$ (10), has shown that in this compound each sulfate group is bonded to three different magnesium atoms and each magnesium is octahedrally surrounded by six sulfate groups. Since both the zinc and cobalt analogs of langbeinite are known to be isomorphous with the parent compound, our single crystal spectrum can be confidently assigned to an octahedral $[Co(OSO_3)_6]^{10-}$ species in which the sulfate ligands are unidentate with respect to the cobalt. In the protonic media it is unlikely that all the ligating groups would be sulfate. We should certainly expect that in the hydrogen sulfate glass the ligating group would be HSO_4^-, whilst in concentrated sulfuric acid solutions SO_4^{2-}, HSO_4^- and, perhaps, H_2SO_4 may act as unidentate ligands. Although the available results do not permit the exact degree of protonation of the cobalt species to be specified, any protonation that does occur must be concentrated on the outer oxygen atoms, rather than the ligating atoms, such that $[Co(OSO_3H)_6]^{4-}$ is present in the hydrogen sulfate glass and $[Co(OSO_3)_x(OSO_3H)_y(OSO_3H_2)_z]^{(2x+y-2)-}$ $(x + y + z = 6)$ in sulfuric acid. This follows from the fact that inner oxygen protonation in such complexes would, as pointed out by Duffy *et al.* (2), be expected to lead to differences in ligand field parameters, and thus in absorption band maxima, between those complexes in which it is possible and those in which it is not.

The second type of spectrum, consisting of a moderately strong band peaking at 16.6–17.3 kK with shoulders to lower (15.4–15.9 kK) and higher (18.5–18.9 kK) energies, is typified by that found in the ternary alkali sulfate melt at 550 °C; we have previously assigned this to the blue, dodecahedral, bidentate species $[Co(O_2SO_2)_4]^{6-}$. We believe that this species also occurs in the hydrogen sulfate melt, since our spectrum in the melt at 237 °C clearly shows the presence of a shoulder at 15.9 kK, which is typical for this class of spectra. Because of the intermediate values of the spectral parameters, in particular the "low" molar absorptivity values, there have been attempts to assign the spectrum in the $Li_2SO_4–Na_2SO_4–K_2SO_4$ eutectic melt at 550 °C to a distorted octahedral species (11) or to an equilibrium mixture of octahedral and tetrahedral complexes (2). Both these possibilities can now be firmly ruled out by the present results. If an octahedral–tetrahedral equilibrium were present, an increase in temperature would lead to a substantial increase in optical density as some of the octahedral complex was converted into the tetra-

Can. J. Chem. Downloaded from www.nrcresearchpress.com by 210.87.254.40 on 09/05/12
For personal use only.

TABLE 1. Spectra of cobalt(II) in sulfate media

Medium	Temperature (°C)	Reference	Band maxima in kK (ε_{max})*							Class
$K_2Zn_2(SO_4)_3$	20	This work	12.0				18.4		20.5(sh)	1
98% H_2SO_4	12	3, 9		13.3(.25)			18.35(10.8)		20.5(sh)	1
	25	1, 2		13.0(.5)			18.4(11)		20.5(sh)	1
	190	2				17.4(21)			20.5(sh)	4
	199	3, 9	11.7(.55)			17.6(14.9)			20.2(sh)	4
$(Na-K)HSO_4$	25	2		13.1(.4)			18.4(13)		20.5(sh)	1
	131	This work					18.1(21)		20.1(sh)	
	230	2				17.3(31)		18.6(sh)		3
	237	This work			15.9(sh)	17.3(38)		18.53(sh)		2
$(K_2-Zn)SO_4$	14	4, 9				17.54(45)		18.74(sh)	20.7(sh)	3
	25	2		13.0(.9)		17.5(30)		18.6(sh)		3
	191	4, 9				17.2(47)		18.7(sh)	20.5(sh)	3
	580	4, 9			15.6(sh)	16.8(92)		18.65		2
$(Li-Na-K)_2SO_4$	550	4, 9			15.8(sh)	17.0(76)		18.8		2
	770	This work			15.6(sh)	16.78		18.87		2
$(Na_2-K_2-Zn)SO_4$	417	4, 9			15.7(sh)	17.1		18.65		2
Li_2SO_4	878	This work			15.4(sh)	16.72		18.87		2
Na_2SO_4	900	This work			15.6(sh)	16.67		18.87		2
$DMSO/Li_2SO_4$	21	This work					18.38(15.6)		20.8(sh)	1
	179	This work				17.4(50)		18.6		3

*sh = shoulder.

Can. J. Chem. Downloaded from www.nrcresearchpress.com by 210.87.254.40 on 09/05/12
For personal use only.

hedral form, which would have absorption bands of far greater intensity. The distorted octahedral model also leads to the prediction that an increase in optical density, although a smaller increase than for the equilibrium case. However, the results for the ternary alkali metal eutectic melt showed that as the temperature was increased from 550 to 770 °C the optical density decreased. Although we have not measured the density of the melt over this temperature range and so cannot calculate accurate values for the molar absorptivity, it seems likely that, even after correction for the change in density, the molar absorptivity would be lower than that obtained at 550 °C. A decrease in molar absorptivity with increasing temperature has been previously observed for $[CoCl_4]^{2-}$ (12) and $[Co(NCS)_4]^{2-}$ and we suggest that this behavior is typical of tetrahedral cobalt(II) complexes.[2] A similar result has been obtained for $[Co(CH_3CO_2)_4]^{2-}$ but in this case the structure is not strictly tetrahedral, being rather dodecahedral.[2] This has been shown by Duffy and Ingram (13) who compared the spectra of $[Co(CH_3CO_2)_4]^{2-}$ and $[Co(CF_3CO_2)_4]^{2-}$. The trifluoroacetate complex was known to be 8-coordinate dodecahedral involving two sets of Co—O bonds with lengths of 2.00 and 3.11 Å (14). As Lippard (15) points out, a dodecahedron can be regarded as two interpenetrating tetrahedra, one elongated and one flattened. It is possible to visualize the long Co—O bond breaking and a conversion to a tetrahedral complex taking place; the greater the disparity between the long and the short bonds the closer the geometry approaches tetrahedral. Consequently, one would expect dodecahedral complexes to behave in a similar fashion to tetrahedral ones, to a first approximation at least. The temperature dependence observed in the ternary alkali sulfate melt is, therefore, compatible with a description of the melt species as a dodecahedral tetrasulfato complex, as suggested earlier (4).

The third class of spectra, characterized by a strong band at 17.3–17.5 kK with a shoulder at 18.6–18.7 kK, was first identified in the potassium sulfate–zinc sulfate glass and ascribed to a violet, octahedral, bidentate species (2). As Table 1 shows, a similar spectrum was also found for the lithium sulfate–dimethylsulfoxide solution at 179 °C. Although it has been suggested that the same species is present in the $NaHSO_4-KHSO_4$ melt at 230 °C (2), evidence has been presented earlier to suggest that this assignment is incorrect. The structure of the violet species is unknown, although a trisulfato structure $[Co(O_2SO_2)_3]^{4-}$ has been suggested (5). We shall return to discussion of this species.

The only example of the fourth class of spectra found so far is obtained in the 98% sulfuric acid solution at temperatures of ~190 °C. It has the strongest band at 17.4–17.6 kK with a shoulder at 20.2–20.5 kK. The species responsible for this spectrum has been assigned a distorted octahedral structure, primarily on the basis of the molar absorptivity value (3).

Equilibrium Studies

We have discussed in some detail the four types of cobalt(II) spectra that are found in sulfate media. The characterization of two of these, namely those due to the pink, octahedral, monodentate species and the blue, dodecahedral, tetra-sulfato complex, must be regarded as fairly complete. It may be argued, however, that both types 3 and 4 represent equilibrium mixtures of the pink and blue forms. In order to test this proposition, detailed investigations of the Li_2SO_4–DMSO solution and the $NaHSO_4-KHSO_4$ melt over the entire temperature range were undertaken.

The peak positions and intensities in the $NaHSO_4-KHSO_4$ melt spectra, at temperatures between 131 and 237 °C, are shown in Table 2. Over this temperature range, the spectra were found to be internally linear with respect to temperature (16). They were tested by two methods (17): firstly, a plot of the absorbance at 18.2 kK *vs.* that at 16.4 kK showed a good linear relationship over the entire temperature range. Secondly, the more rigorous residual method (17) was applied and it was found that the residual (δ) between calculated and experimental absorbances was very close to zero over the temperature and wavelength range of interest. In spite of our failure to obtain glass spectra of reasonable quality, we were able to show that the region of internal linearity extended down to room temperature by using the data published by Duffy

[2]Unpublished results of J. R. Dickinson and T. R. Griffiths.

TABLE 2. Spectra of cobalt(II) in an equimolar $NaHSO_4$–$KHSO_4$ melt

Temperature (°C)	Band maxima in kK (ε_{max})*		
131	18.1(18)		20.1(sh)
145	18.0(20)		20.1(sh)
160	17.9(22)		20.0(sh)
176	17.7(25)		20.0(sh)
187	17.6(27)		20.0(sh)
198	17.5(29)	18.9(sh)	20.0(sh)
220	17.4(34)	18.9(sh)	
230	16.0(sh) 17.4(37)	18.7(sh)	
237	15.9(sh) 17.3(38)	18.5(sh)	

*sh = shoulder.

et al. (2). We can, therefore, conclude that the complete set of spectra are internally linear. By a similar method, internal linearity was also found in the following systems: Li_2SO_4–DMSO solution at 21–179 °C and 98% H_2SO_4 at 12–199 °C (data from previous work (3, 9) were used). The significance of the internal linearity relationship is that it could have occurred only for an equilibrium mixture.

In all three systems above, the room-temperature component of the equilibrium mixture has been identified as the pink, octahedral $[Co(OSO_3)_6]^{10-}$ species. The results for the $NaHSO_4$–$KHSO_4$ system (Table 2) indicate that, in this case, the high-temperature component is the blue dodecahedral complex $[Co(O_2SO_2)_4]^{6-}$. It is likely that the spectrum of the hydrogen sulfate system at 237 °C represents an equilibrium mixture of the octahedral and dodecahedral forms, its classification as Class 2 arising because the dodecahedral spectrum is much more intense than the octahedral spectrum. Examination of the spectra at intermediate temperatures shows clearly that spectra of Class 4 (187 °C) and of Class 3 (220 °C) occur as Class 1 changes to Class 2. We believe that the high-temperature components in the DMSO–Li_2SO_4 and 98% H_2SO_4 systems can also be identified as the dodecahedral species, so that spectra of Classes 3 and 4 are, in fact, due to equilibrium mixtures of the octahedral and dodecahedral forms.

Our present results show that there are two distinct cobalt(II) sulfato complexes: namely pink, octahedral, monodentate $[Co(OSO_3)_6]^{10-}$ (suitably protonated in protonic media) and blue, dodecahedral, bidentate $[Co(O_2SO_2)]^{6-}$. In general, the former occurs at low temperatures and the latter at high temperatures; if the former is heated, it is converted to the latter, an equilibrium mixture being formed at intermediate temperatures.

This work was supported by the Science Research Council. We should like to thank Dr. T. R. Griffiths for the use of the Cary 14H spectrophotometer.

1. J. ARRIS and J. A. DUFFY. J. Chem. Soc. 5850 (1964).
2. J. A. DUFFY, F. P. GLASSER, and M. D. INGRAM. J. Chem. Soc. (A), 551 (1968).
3. J. R. DICKINSON and K. E. JOHNSON. J. Mol. Spectrosc. **33**, 414 (1970).
4. J. R. DICKINSON and K. E. JOHNSON. J. Mol. Spectrosc. **36**, 1 (1970).
5. M. D. INGRAM and J. A. DUFFY. J. Chem. Soc. (A), 2575 (1968).
6. K. E. JOHNSON and T. S. PIPER. Disc. Faraday Soc. No. 32, 32 (1962).
7. J. A. DUFFY and W. J. D. MACDONALD. J. Chem. Soc. 977 (1970).
8. T. R. GRIFFITHS and R. K. SCARROW. Trans. Faraday Soc. **65**, 1727 (1969).
9. J. R. DICKINSON. Ph.D. Thesis, University of Saskatchewan Regina Campus, Regina, Saskatchewan, 1969.
10. G. GATTOW and J. ZEMANN. Z. Anorg. Allg. Chem. **293**, 233 (1958).
11. D. M. GRUEN. Fused salts. *Edited by* B. R. Sundheim. McGraw–Hill, New York. 1964.
12. D. M. GRUEN and R. L. MCBETH. Pure Appl. Chem. **6**, 23 (1963).
13. J. A. DUFFY and M. D. INGRAM. J. Chem. Soc. (A), 2398 (1969).
14. J. G. BERGMANN and F. A. COTTON. Inorg. Chem. **5**, 1420 (1966).
15. S. J. LIPPARD. Prog. Inorg. Chem. **8**, 109 (1967).
16. J. BRYNESTAD and G. P. SMITH. J. Phys. Chem. **72**, 296 (1968).
17. J. BRYNESTAD, C. R. BOSTON, and G. P. SMITH. J. Chem. Phys. **47**, 3179 (1967).

Can. J. Chem. Downloaded from www.nrcresearchpress.com by 210.87.254.40 on 09/05/12
For personal use only.

Ion Pair Formation in $NaNO_3/D_2O$ Solutions: Raman and Infrared Spectra, Partial Molal Volumes, Conductance, and Viscosity[1]

J. D. RIDDELL, D. J. LOCKWOOD,[2] AND D. E. IRISH[3]

Department of Chemistry, University of Waterloo, Waterloo, Ontario

Received February 2, 1972

Laser Raman and infrared vibrational spectra of solutions of $NaNO_3$ in deuterium oxide reveal the presence of both $Na^+NO_3^-$ ion pairs and solvated nitrate ions. The degree of association has been measured. The concentration quotients are remarkably independent of concentration and almost equal to the thermodynamic association constant, 0.060 ± 0.006 kg mol^{-1} at 25.0 °C. The latter quantity was obtained by an extrapolation procedure, taking account of the activity coefficients. Values are reported for the activity coefficient of the ion pair. Interpretation is also considered in terms of a place-exchange equilibrium involving the solvent. Vibrational assignments are made to the two forms of nitrate ion present. Density, partial molal volume, conductance, and viscosity data are also presented and discussed in terms of the reported constitution.

Les spectres vibrationnels infrarouge et Raman au laser de solutions de $NaNO_3$ dans l'oxyde de deutérium révèlent la présence de paires d'ions $Na^+NO_3^-$ et d'ions nitrate solvatés. Nous avons mesuré le degré d'association. Les quotients de concentration sont indépendants de façon remarquable de la concentration et presqu'égaux à la constante d'association thermodynamique, 0.060 ± 0.006 kg mol^{-1} à 25.0 °C. Nous obtenons cette dernière quantité par extrapolation, en tenant compte des coëfficients d'activité. Nous rapportons des valeurs pour le coëfficient d'activité de la paire d'ions. L'interprétation est faite en termes d'un équilibre d'échange impliquant le solvant. Les assignations vibrationnelles sont faites pour les deux formes d'ions nitrate présentes. Nous présentons aussi la densité, le volume molal partiel, la conductance et la viscosité et en discutons en termes de la structure proposée. [Traduit par le journal]

Canadian Journal of Chemistry, **50**, 2951 (1972)

Can. J. Chem. Downloaded from www.nrcresearchpress.com by 210.87.254.6 on 09/05/12
For personal use only.

An extensive study of the vibrational frequencies, half-widths, intensities, and line shapes of aqueous solutions of lithium, sodium, potassium, and cesium nitrate was previously reported (1). Solutions of $LiNO_3$ received the greatest attention and studies were possible over the greatest concentration range at 25 °C. It was shown that, for solutions more concentrated than 7 *M*, nitrate ion exists in two types of environment. In one environment vibrational lines are generated which resemble crystal frequencies and nitrate can be considered to be bound directly to lithium. In the other environment nitrate is free of such a direct linkage to the cation. The comparisons were later extended and interpreted in terms of a quasi-lattice model (2). A place-exchange equilibrium constant was tentatively estimated as 0.24 at 25 °C for the process

$$Li^+(H_2O)_3 + NO_3^- \rightleftarrows Li^+(H_2O)_2NO_3^- + H_2O$$

The early study suggested that $NaNO_3$ solutions were similar to $LiNO_3$ solutions; however, the spectral features of the ion pair were more difficult to detect. In particular an infrared line at about 740 cm^{-1} was detected, as for $LiNO_3$, and it was believed that the lower solubility was the chief factor preventing detection of the Raman counterpart (1). Subsequently Raman experiments were carried out at elevated temperatures on liquids with as little as two moles water per mole salt but, using 435.8 nm mercury excitation, no asymmetry in the shape of the 718 cm^{-1} Raman line could be detected (3). This observation was apparently at variance with the earlier work and thus an extensive study was in order.

D_2O was chosen as solvent because the 700–800 cm^{-1} infrared region is less obscured than with H_2O. Also the 689 cm^{-1} feature (1) is not present in the Raman spectrum of the D_2O solutions and thus it becomes easier to detect asymmetry on the high frequency side of the 718 cm^{-1} line. Furthermore, knowledge of the infrared and Raman frequencies for the same solvent, D_2O, is desirable in case the extent of interaction is different in H_2O and

[1]Presented in part at the 54th Canadian Chemical Conference of the Chemical Institute of Canada, Halifax, Nova Scotia, May 31 – June 2, 1971.

[2]Present address: Department of Physics, The University, Edinburgh, Scotland.

[3]To whom correspondence should be addressed.

Can. J. Chem. Downloaded from www.nrcresearchpress.com by 210.87.254.6 on 09/05/12
For personal use only.

D_2O. (In previous work i.r. spectra were obtained with D_2O solvent and Raman spectra with H_2O in the 700 cm^{-1} region (1).) Using the 488.0 nm line of an argon ion laser it has been possible to detect the high frequency Raman component. As noted previously (1), the 740 cm^{-1} i.r. component is inherently more intense and thus can be detected when the Raman counterpart is virtually absent. A quantitative Raman intensity study has been made and the results of this study and the implications concerning the constitution of concentrated aqueous $NaNO_3$ solutions are described below. Conductance, viscosity, and density have also been measured to ascertain to what extent the existence of ion pairs is revealed by these macroscopic properties.

Experimental

Thirty solutions were prepared in a nitrogen-purged dry box from dried $NaNO_3$ (Fisher certified reagent) and D_2O. Solutions were filtered through a 0.45 μ Millipore filter prior to spectral measurements. Raman spectra were recorded on a Cary 81 spectrophotometer specially adapted for the use of a Coherent Radiation Model 54 Argon ion laser. The laser beam was directed down the length of a cylindrical glass cell 5 mm in diameter which terminated in a blackened horn to reduce stray light. The cell was positioned parallel to the horizontal slit of the Cary 81 monochromator by means of a specially built adjustable platform. The Raman radiation was focused onto the slit by a cylindrical lens. Thus all of the fore optics of the Cary 81 were bypassed. The gain, slit width, scan speed, and time constant were varied in preliminary studies to determine the combination which would insure no introduction of band distortion. The laser was operated at 488.0 nm and 250 mW. After a 1 h warm up excellent laser power stability was achieved and a yellowish-green fluorescence seen on first introducing the sample had disappeared.

No carbon tetrachloride external standard was used in this laser work because of the difficulty in reproducing the sample cell position relative to the laser beam. Instead, an internal standard was used; namely, the integrated intensity of the 1050 cm^{-1} band of the aqueous $NaNO_3$ solutions. We have assumed a direct proportionality between the integrated intensity of this band and the stoichiometric concentration of the $NaNO_3/D_2O$ solution, based on the work of Davis (4) and Sze (5). Both of these workers employed carbon tetrachloride as an external standard for intensity measurements in their studies. Relative integrated intensities were effectively obtained in this work by dividing the integrated intensity of a given band by that of the 1050 cm^{-1} line of a 1 mol l^{-1} solution of $NaNO_3/D_2O$.

Infrared spectra were obtained on a Beckman IR-9 spectrophotometer operated with the slit program at three times standard and the gain control at 0.8%. In order to eliminate water vapor interference, the instrument was continuously purged by a stream of dry nitrogen. The solutions were contained in a thermostated (25 ± 0.05 °C) R.I.I.C. cell fitted with silver bromide windows that were separated by a 0.012 mm Teflon spacer. Band areas, designated as "integrated absorbances" were measured with a polar planimeter. Since the cell was dismantled and cleaned between solutions, band areas are relative only within a given spectrum, and the infrared spectra are generally of qualitative value. The infrared spectra were run concurrently with the laser Raman spectra of the $NaNO_3/D_2O$ solutions.

The curve resolving of spectral envelopes into component bands was accomplished by means of the CURVER program of the 360/44 IBM computer. This facility is given a more detailed description elsewhere (6), but in essence the program employs one of three distribution functions to fit the Raman bands by an operator-controlled, visual procedure. These model band shapes come from the Lorentzian, Gaussian, and the Lorentz–Gaussian product function. The program provides a measure of the goodness-of-fit.

Soon after the first laser Raman spectra were analyzed, however, it became clear that none of these mathematical functions satisfactorily fitted a single, symmetrical band shape excited by the 488.0 nm laser line. A new model band shape was developed, therefore, specifically for the laser Raman spectra of the $NaNO_3/D_2O$ system. This band shape is a mathematical copy of the 1050 cm^{-1} symmetric stretch of nitrate ion obtained from a spectrum of 4.2 M $NaNO_3/D_2O$. Frequencies and half-widths of band components were maintained at approximately constant values for all spectra of a series of solutions.

Viscosity measurements were taken for a series of $NaNO_3/D_2O$ solutions at 25 ± 0.05 °C using a Cannon–Ubbelohde viscometer. All viscosity efflux times were greater than 100 s and within 0.1 s for at least three repetitions for a given solution. Conductance measurements were performed concurrently with the viscosity measurements at the same temperature using a 1 kHz Industrial Instruments Inc. conductivity bridge with the cell and variable decade resistance in adjacent arms of the Wheatstone bridge arrangement. The cell electrodes were separated by about 15.0 cm of 3 mm i.d. capillary tubing. After a thorough cleaning with dilute HCl and a fresh electrode coating of platinum black, the conductance cell had a cell constant of 319.7 cm^{-1}. This constant was checked periodically using a 0.1000 and a 1.000 mol l^{-1} aqueous solution of KCl. All solutions were allowed at least 20 min to come to temperature equilibrium before measurements were made. Densities were measured at 25 ± 0.05 °C, either with a calibrated pycnometer or in volumetric flasks. The accuracy of the latter method was sufficient for concentrative properties and agreed well with the more accurate measurements.

Results and Discussion

The Degree of Dissociation

The measurement of α, the degree of dissociation of $NaNO_3$, is possible because two Raman lines are observed in the ν_4 region of the Raman spectrum; one at 718 cm^{-1} assignable to the solvated nitrate ion and a second at 728 cm^{-1}

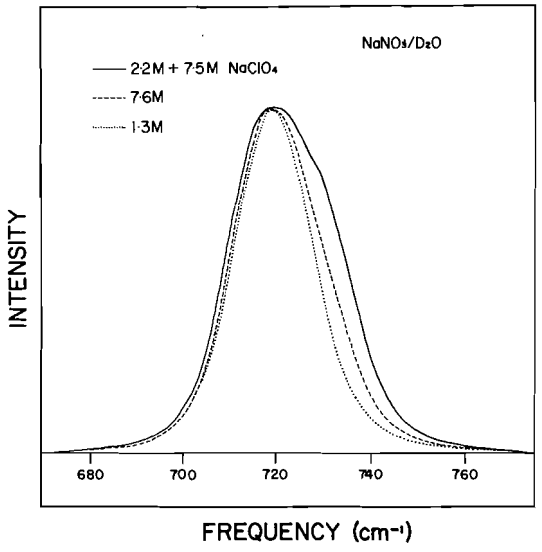

FIG. 1. Comparison of the Raman 720 cm^{-1} regions of ···, 1.3 *M* $NaNO_3/D_2O$; ---, 7.6 *M* $NaNO_3/D_2O$; —, 7.5 *M* $NaClO_4$ + 2.2 *M* $NaNO_3/D_2O$.

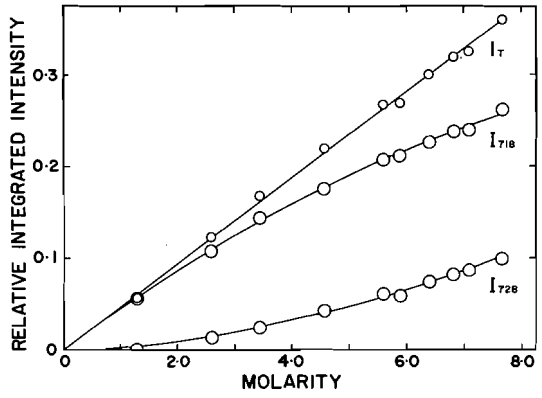

FIG. 2. Relative integrated intensity *vs.* molarity for the 720 cm^{-1} region of the Raman spectrum of $NaNO_3/D_2O$.

assignable to an ion pair (7). The latter frequency is close to that observed for anhydrous sodium nitrate crystal (8). In dilute solution ($C < 1$ mol l^{-1}) the 718 cm^{-1} band is a single symmetrical line. At a concentration of 7.67 mol l^{-1} a small but significant amount of intensity distorts the high frequency side of this band. Increasing the sodium:nitrate concentration ratio to 4.48:1 (a "common ion" effect obtained by mixing $NaClO_4$ and $NaNO_3$) increases the intensity of the 728 cm^{-1} shoulder as expected if an equilibrium was displaced

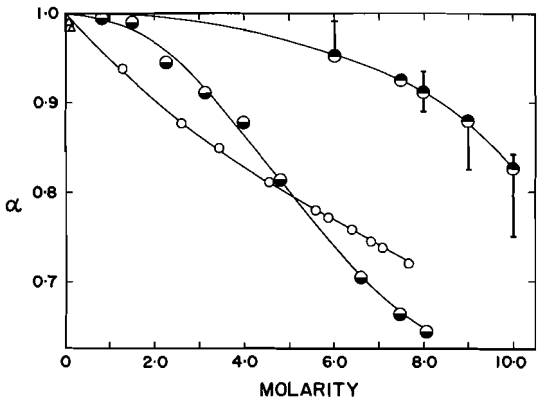

FIG. 3. The degree of ionization, α, *vs.* molarity of nitrate at 25 °C: ◓, $LiNO_3/H_2O$; ◒, HNO_3/H_2O; ○, $NaNO_3/D_2O$; △, Davies' values for $NaNO_3/H_2O$.

to favor a higher concentration of ion-pair (728 cm^{-1}) and a lower concentration of free ion (718 cm^{-1}) (Fig. 1). Using the computer procedure it was possible to fit two bands to the intensity envelope in this spectral region, each with constant half-width and frequency. The relative integrated intensities of the total contour and the components are plotted against concentration in Fig. 2.

The total integrated intensity (I_T) is directly proportional to the stoichiometric concentration. Dividing this concentration into that of ion pairs C_B and that of free ions C_F, one has

$$[1] \qquad I_T = I_{718} + I_{728} = J_B C_B + J_F C_F$$

where J is the molar intensity of the bound (B) or the free (F) forms of nitrate ion. If $J_B = J_F$, eq. 1 will reduce to

$$I_T = J_B(C_B + C_F) = J_B C_T$$

a linear equation with zero intercept consistent with experiment. Thus J_B can be obtained from the slope of I_T *vs.* C_T in Fig. 2. The implication is that although ion association changes the force constant and hence frequency associated with the deformation mode of the nitrate ion, it does not change the molar intensity of the mode. It now follows that

$$[2] \quad C_B = I_{728}/J_B \quad \text{and} \quad \alpha = 1 - C_B/C = C_F/C$$

α is plotted against molarity in Fig. 3. Two data obtained from conductance studies of dilute solutions by Davies (9) are also shown. For comparison the more scattered data (2)

Can. J. Chem. Downloaded from www.nrcresearchpress.com by 210.87.254.6 on 09/05/12
For personal use only.

TABLE 1. Data for the calculation of the thermodynamic association constant

m (mol kg^{-1})	$(1-\alpha)$ Expt.	$(1-\alpha)$ Smoothed	$(\gamma_\pm)^2_{ST}$	${}^TK_A\cdot\gamma_u^{-1}$	$Q_C = m_B\cdot m_F^{-2}$	γ_u
9.35	0.279	0.279	0.110	0.271	0.057	0.222
8.43	0.262	0.262	0.114	0.274	0.057	0.220
8.01	0.255	0.254	0.116	0.274	0.057	0.219
7.37	0.242	0.242	0.120	0.274	0.057	0.219
6.63	0.228	0.228	0.125	0.274	0.058	0.219
6.24	0.220	0.220	0.128	0.275	0.058	0.218
4.88	0.188	0.189	0.143	0.271	0.059	0.221
3.52	0.151	0.152	0.167	0.258	0.060	0.232
2.58	0.123	0.120	0.194	0.239	0.060	0.251
2.00*		0.098	0.218	0.224		0.268
1.23	0.062	0.064	0.268	0.194	0.059	0.311
0.50*		0.028	0.367	0.153		0.393
0.25*		0.014	0.454	0.123		0.487
0.10*		0.0057	0.568	0.100		0.600
0.07*		0.0040	0.612	0.093		0.643
0.05*		0.0029	0.648	0.090		0.668
0.02*		0.0012	0.746	0.080		0.747
0.01*		0.00058	0.796	0.073		0.822
0.0	0.0	0.0	1.000	0.060		1.000

*Interpolated values.

for $LiNO_3/H_2O$ and the values for HNO_3/H_2O obtained by Krawetz from Raman intensity measurements (10) are shown.

The equilibrium process is formulated as

$$Na^+_{(aq)} + NO^-_{3(aq)} \rightleftarrows Na^+\cdot NO^-_{3(aq)}$$

The thermodynamic equilibrium constant for the association can be written as the product of a concentration quotient Q_C and an activity coefficient quotient Q_γ

$$[3]\quad {}^TK_A = \frac{a_u}{a_{Na^+}\cdot a_{NO_3^-}} = \frac{m_u}{m_{Na^+}\cdot m_{NO_3^-}}\cdot\frac{\gamma_u}{\gamma_{Na^+}\cdot\gamma_{NO_3^-}} = Q_C\cdot Q_\gamma$$

where a, m, and γ refer to activity, molality, and activity coefficient, respectively. Solution concentrations are converted from molarity to molality units, through the measured densities, for convenience when using activity coefficients described below.

Considering first $Q_C = (1-\alpha)/\alpha^2 m$ we find that the concentration quotient is remarkably constant, changing from 0.057 to 0.059 kg mol^{-1} for a concentration change from 9.35 to 1.23 m (Table 1). The system's behavior is surprisingly ideal. Such constant Q_C's obtained for salt solutions by Raman spectroscopy have been noted before (11, 12). The same is not true for acid solutions however (13).

It is possible to incorporate values for $\gamma_{Na^+}\cdot\gamma_{NO_3^-}$ and thus explore the concentration dependence of ${}^TK_A\gamma_u^{-1}$. In terms of the mean ionic activity coefficients, $\gamma_{Na^+}\cdot\gamma_{NO_3^-}$ equals $\gamma^2_\pm$ for the free ions. Following the treatment given by Robinson and Stokes (ref. 14, pp. 37, 38)

$$\gamma^2_\pm = (\gamma^2_\pm)_{ST}\alpha^{-2}$$

$(\gamma^2_\pm)_{ST}$, the mean stoichiometric activity coefficients, are reported by Robinson and Stokes (ref. 14, p. 492) for the $NaNO_3/H_2O$ system. In order to use these values a correction has been applied for the fact that the D_2O solutions contain fewer moles of solvent than the H_2O solutions of the same molality. Values of $\gamma_\pm$ were chosen corresponding to the molality of the D_2O solution multiplied by the factor 55.51/49.93. These values are consistent with the trends presented by Bonner (15) for activity coefficients of other salts dissolved in D_2O.

Thus ${}^TK_A\gamma_u^{-1}$ equals $[(1-\alpha)/m]\cdot(1/(\gamma_\pm)^2_{ST})$. Figure 4 is a plot of both ${}^TK_A\gamma_u^{-1}$ and Q_C *vs.* molality. Data are presented in Table 1. $(1-\alpha)$ is zero at zero concentration and thus the experimental values of $(1-\alpha)$ can be expressed

Can. J. Chem. Downloaded from www.nrcresearchpress.com by 210.87.254.6 on 09/05/12
For personal use only.

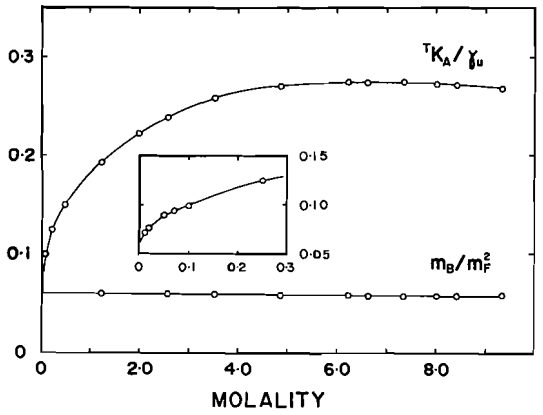

FIG. 4. $^TK_A/\gamma_u$ and m_B/m_F^2 *vs.* molality for $NaNO_3/D_2O$ at 25 °C. The inset shows the horizontal scale expanded and the extrapolation of $^TK_A/\gamma_u$ to zero concentration.

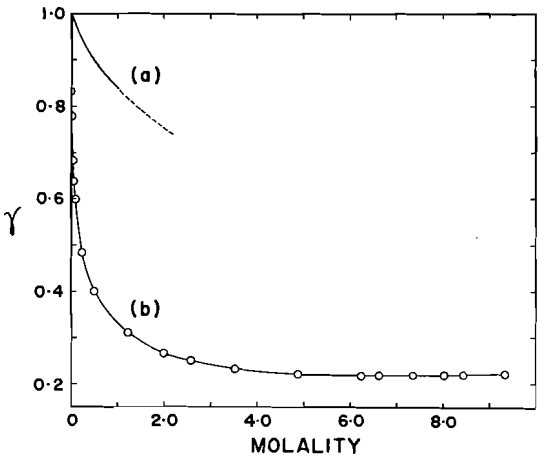

FIG. 5. (*a*) Activity coefficient of glycine (dipolar ion) *vs.* molality of KCl at 25 °C; (*b*) activity coefficient of the $Na^+ \cdot NO_3^-$ ion-pair *vs.* molality of $NaNO_3/D_2O$ at 25 °C.

as a polynomial in m with a required zero intercept:

$$(1-\alpha) = 0.05762_6 m - 0.004827 m^2 + 0.0001989_4 m^3$$

The plot of $^TK_A\gamma_u^{-1}$ has been extrapolated by interpolations using the above polynomial. In the limit of infinite dilution, γ_u is unity and ^TK_A is 0.060 ± 0.006 kg mol^{-1}. As the concentration increases, $^TK_A\gamma_u^{-1}$ rises smoothly and then levels off (Fig. 4). This can be attributed to a decrease of γ_u, as shown in Fig. 5. There are few examples where γ_u is known for an ion pair over such a wide concentration range. Roberts and Kirkwood measured the activity coefficient of glycine in aqueous solutions of KCl (16). Glycine forms a dipolar ion of large electric moment in solvents with a high dielectric constant. Figure 5 shows γ_u for glycine plotted against molality of KCl. The trend is similar to that of γ_u for $NaNO_3$. On the other hand, for HNO_3, γ_u calculated from the data of Krawetz rises continuously from unity.

Davies (9) obtained a value of 0.26 for the association constant of $NaNO_3$ in water at 18 °C. His approach, $\alpha = \Lambda/\Lambda_x$, necessitates questionable assumptions about the form of Λ_x. It is worth noting, however, that Davies' value of α for 0.1 M is 0.985 and ours is 0.995 while at 0.05 M Davies' value is 0.991 and ours is 0.997. The value of $^TK_A\gamma_u^{-1}$ changes by a factor of about four when α changes by only 6 parts in 1000. This comparison serves to point out the extreme sensitivity of $^TK_A\gamma_u^{-1}$ to small differences in α in dilute solutions for an electrolyte as strong as $NaNO_3$. Robinson (17) combined Davies' conductance data and activity coefficient data to obtain a value of 0.38 for K_A.

The near constancy of Q_C implies that Q_γ is almost constant over most of the concentration range. To a good approximation $\gamma_u\gamma_\pm^{-2}$ equals 1.04 when $0.01 < m < 9.35$ but γ_u approaches unity faster than $\gamma_\pm^2$, accounting for the sharp change of slope in Fig. 4 as m approaches zero.

With reference to Fig. 4, the strength of the electrolytes decreases in the order $LiNO_3 > HNO_3 > NaNO_3$ for $C < 5$ M. In keeping with this trend Krawetz reports ^TK_A of HNO_3 equal to 0.042 kg mol^{-1} (10), smaller than our value of 0.060 kg mol^{-1} for $NaNO_3$. The trend of increasing values of ^TK_A with increasing alkali metal radius seems probable (18).

Reliability

In the above analysis an uncertainty of 10% in the value of K has been implied. This is a realistic estimate. When D_2O is used as solvent the spectral base lines are straight. The noise level was less than 1% of the maximum peak height except for the most dilute solutions for which it did not exceed 1.5%. The 1050 cm^{-1} line is an ideal internal standard because it is intense and isolated. Its use also circumvents intensity corrections which may arise because of a changing refractive index.

Can. J. Chem. Downloaded from www.nrcresearchpress.com by 210.87.254.6 on 09/05/12
For personal use only.

Can. J. Chem. Downloaded from www.nrcresearchpress.com by 210.87.254.6 on 09/05/12
For personal use only.

The principle source of uncertainty is the partition of the signal into two components. This problem is common to many types of experimentation and is often more severe than that encountered here. The precision obtainable in this work is a consequence of the singular features of the computer procedure *viz.* an exactly reproduceable, defined line shape and a criterion for the goodness-of-fit (6). Because of this severe overlap, however, an estimated 10% uncertainty may exist in each ratio I_{728}/I_{718}, which leads to an uncertainty of about 8% in individual values of $(1-\alpha)$. Once the equality of J_F and J_B is established or assumed the results are independent of the intensity of the 1050 cm^{-1} line because $(1-\alpha)$ can be expressed as $(I_{728}/I_{718})(1+I_{728}/I_{718})^{-1}$, from which the 8% estimate is derived. To some extent this uncertainty is reduced by the averaging procedure which was used to fit all the points to a smooth curve. Thus 10% reliability is believed to be a reasonable upper limit. The values in Table 1 imply greater precision; the three significant figures quoted there are in fact an indication of our internal consistency. The trends and conclusions are not changed by rounding off.

The Place-Exchange Equilibrium Constant

An alternative way of considering the association process is in terms of a competition between water molecules and nitrate ions for sites in the first coordination sphere of the cation. A place-exchange equilibrium constant for this quasi-lattice model (19) can be expressed in terms of the process

$$Na^+(D_2O)_x + NO_3^- \rightleftarrows Na^+ \cdot NO_3^-(D_2O)_{x-1} + D_2O.$$

The constant (a concentration quotient) is defined as

$$^cK_A = \frac{C_B C_W}{(C - C_B)^2}$$

where C_B is the concentration of bound nitrate and C_W the concentration of free solvent molecules. C_W is calculated from density and weight percent data such that $C_W = [D_2O]_T - x(C - C_B) - (x-1)C_B$. The constant has been evaluated for $1 \leqslant x \leqslant 6$ (Fig. 6). At infinite dilution ^cK_A has a value of 2.98_3, independent of x. With increasing concentration the values decrease.

The less certain data for $LiNO_3/H_2O$ were consistent with the almost constant value for ^cK_A of 0.24 when x is 3. The smaller value is consistent with the view that Li^+ binds waters more strongly than Na^+ and thus nitrate ion competes less successfully with the solvent molecules for a position in the primary solvation sphere of the smaller cation. The sodium ion appears to display little or no preference for a fixed value of x, unlike lithium, magnesium, or zinc for example. The value probably decreases as concentration increases.

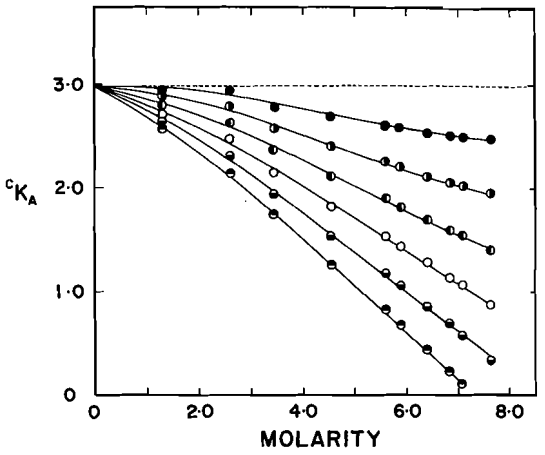

FIG. 6. ^cK_A *vs.* molarity of $NaNO_3/D_2O$ at 25 °C: ●, $x=1$; ◑, $x=2$; ◐, $x=3$; ○, $x=4$; ◒, $x=5$; ◓, $x=6$.

Spectral Properties of the Ion-Pair

The normal modes of vibration of an isolated nitrate ion with D_{3h} symmetry and their approximate frequencies are: $\nu_1(A_1')$ 1050 cm^{-1}; $\nu_2(A_2'')$ 825 cm^{-1}; $\nu_3(E')$ 1385 cm^{-1}; and $\nu_4(E')$ 720 cm^{-1}. Solvation in water causes the $\nu_3(E')$ mode to split into a doublet with maxima about 1356 and 1410 cm^{-1}, the separation also depending on the concentration and cation (12). Attachment of a cation subjects nitrate ion to a larger perturbation and the symmetry is lowered to C_{2v}, C_s or C_1. It is probable that the cation and anion will be oriented in a number of different ways to each other such that no single symmetry designation will be applicable to all ion pairs. This will cause the vibrational lines to broaden. But, for all symmetries above, the effect is to remove the degeneracy of the E' modes. For simplicity we will describe the vibrations of the ion pair in terms of C_{2v} symmetry. Thus the correlations will be: $A_1' \rightarrow A_1$;

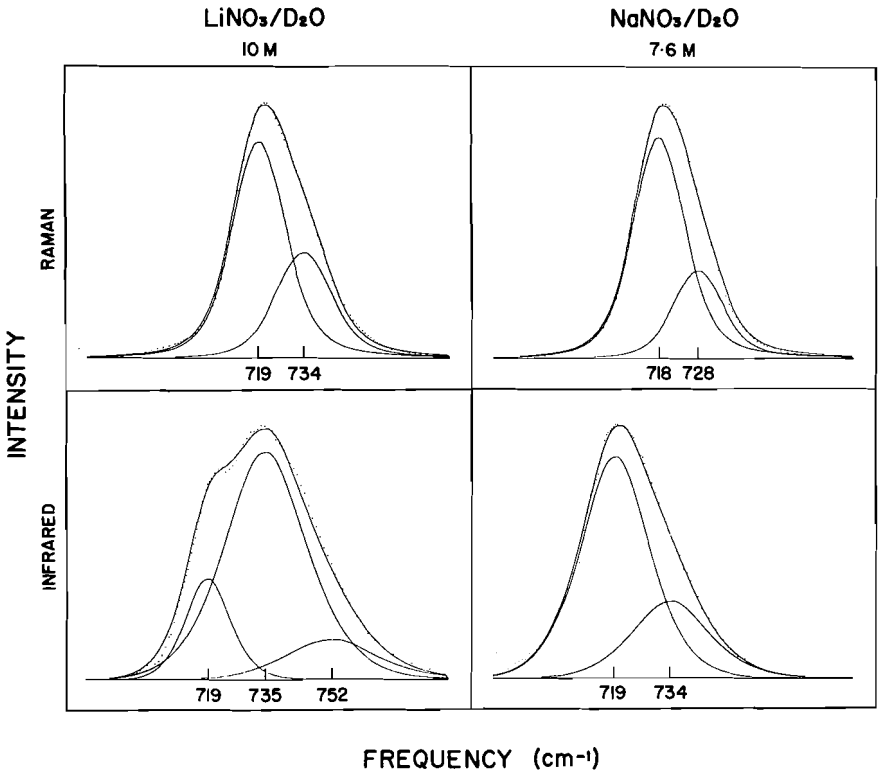

FIG. 7. Comparison of the computer-analyzed Raman and infrared 720 cm^{-1} regions of saturated solutions of $LiNO_3/D_2O$ and $NaNO_3/D_2O$. The 752 cm^{-1} infrared band is due to water in the $LiNO_3$ salt.

$E' \rightarrow A_1 + B_2$ and $A_2'' \rightarrow B_1$. All six modes are allowed in both infrared and Raman.

No lines were detected which could be attributed to a Na^+–nitrate vibration. This suggests that the interaction is largely electrostatic. The ion pair exhibits a Raman line at 728 cm^{-1} as already discussed which is assigned to an A_1 mode; the observed polarization of this line is weak but probably genuine. The infrared contour has two components, the 719 cm^{-1} line of free nitrate and an intense line at about 734 cm^{-1}. This line is ascribed to the B_2 mode of the ion pair. It is assumed that the Raman counterpart is of inherently low intensity. (The observations contrast sharply with those for $LiNO_3$ where infrared and Raman lines are almost identical in frequency at 734 cm^{-1} (see Fig. 7).)

A low intensity band at 831 cm^{-1} is detectable in Raman spectra of solutions more concentrated than 2 mol l^{-1}. The integrated intensity of this band appears to vary directly with the integrated intensity of the 1050 cm^{-1} band which is proportional to total nitrate concentration. It was not detected in the spectrum of the mixture containing $NaNO_3$ and $NaClO_4$ in D_2O where ion–ion contact is forced. This band is therefore assigned to solvated nitrate, perturbed by the solvent such that the normally Raman inactive $\nu_2(A_2'')$ vibration is allowed. The overtone was a single, somewhat more intense symmetric band at 1660 cm^{-1}. The greater intensity is consistent with the fact that it is Raman allowed under D_{3h} selection rules. The 831 cm^{-1} vibration is a single intense line in the infrared spectrum and is assigned to both bound and free nitrate ions.

The line shape of the intense Raman line at 1050 cm^{-1} was studied carefully with 1 cm^{-1} slit width. It is symmetrical. This does not entirely preclude the possibility that more than one band is present under the contour, however. There is a small increase of frequency with increasing concentration and a slight broad-

Can. J. Chem. Downloaded from www.nrcresearchpress.com by 210.87.254.6 on 09/05/12
For personal use only.

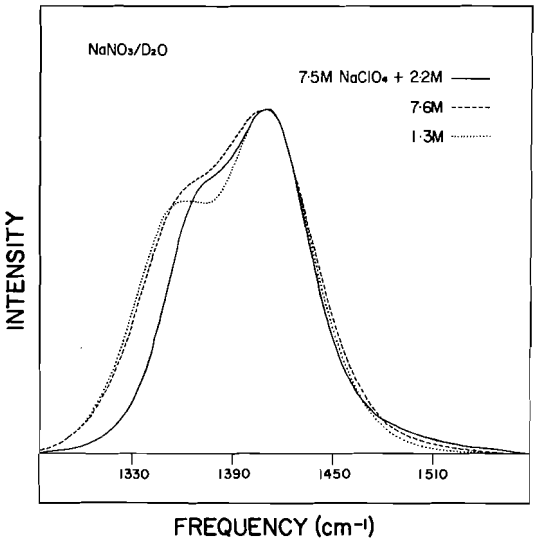

FIG. 8. Comparison of the Raman 1400 cm^{-1} regions of ···, 1.3 *M* $NaNO_3/D_2O$; ---, 7.6 *M* $NaNO_3/D_2O$; —, 7.5 *M* $NaClO_4$ + 2.2 *M* $NaNO_3/D_2O$.

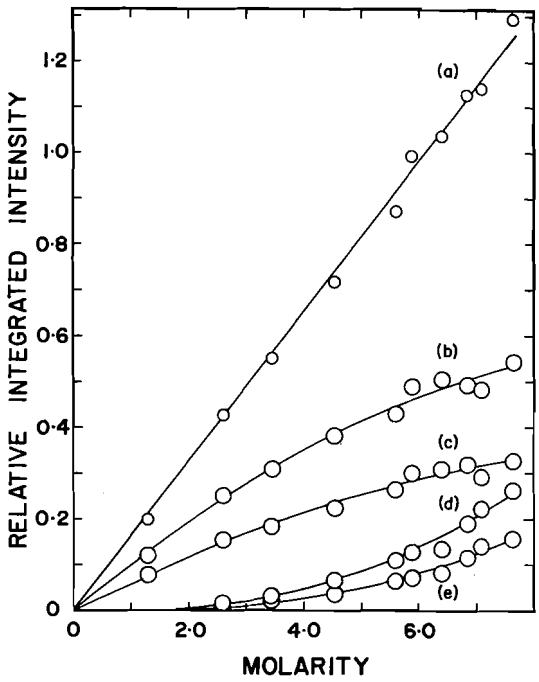

FIG. 9. Relative integrated intensity *vs.* molarity for the 1400 cm^{-1} region of the Raman spectrum of $NaNO_3/D_2O$: (*a*) I_T; (*b*) I_{1415}; (*c*) I_{1355}; (*d*) I_{1417}; (*e*) I_{1368}.

ening. A weak infrared counterpart is observed about 2 cm^{-1} lower in frequency. We believe the ion pair and solvated nitrate ion both contribute to this line (*cf.* ref. 12).

A broad envelope extends from approximately 1300 to 1500 cm^{-1} in the Raman spectrum. For dilute solutions ($C < 1$ mol l^{-1}) this region can be resolved into two components by computer techniques, *viz.* 1355 and 1415 cm^{-1}. At higher concentrations subtle changes in the contour of the band envelope become apparent. As ion pairing is enhanced the intensity *between* the two maxima is enhanced and the overall width of the envelope decreases (Fig. 8). Attempts were made to fit the envelope with two, three, and four bands. Although a two and three band fit can be achieved, it is obtained only by allowing the positions and half-widths to continually change in an inconsistent manner. A four band fit which allows the retention of the frequencies, half-widths, and intensity ratio of the 1355 and 1415 cm^{-1} bands over the entire concentration range is most acceptable. Two new bands, located at 1368 and 1417 cm^{-1}, and assigned to the A_1 and B_2 modes of the ion-pair, respectively, have almost constant line parameters over the concentration range and account for the overall narrowing of the contour. The concentration dependence of the intensities is similar to that observed for the 719–740 cm^{-1} region (Fig. 9). The infrared contours in this region have very high absorbance and are not amenable to study. The assignments are summarized in Table 2.

Density and Partial Molal Volumes

The concentrative properties of the $NaNO_3/D_2O$ system are given in Table 3. The density of D_2O at 25 °C has been taken from Millero *et al.* (20). Smooth values of the density are given by the polynomial, obtained from a least-squares analysis of the data,

$$D = 1.1043_5 + 0.0523_9C - 0.0007_0C^2$$

where C is measured in mol l^{-1}. Similarly, weight percent is given by

$$\text{Wt. percent} = 7.6778C - 0.3574C^2 + 0.02031C^3 - 0.000743C^4$$

The values in Table 3 are for the unsmoothed experimental data.

To a good approximation direct proportionality exists between density and molarity, specific volume and weight percent, and mean molal volume and mole fraction over the con-

Can. J. Chem. Downloaded from www.nrcresearchpress.com by 210.87.254.6 on 09/05/12
For personal use only.

TABLE 2. Vibrational assignments*

	Solvated nitrate ion					$Na^+NO_3^-$ ion pair			
	Raman			Infrared		Raman			Infrared
D_{3h}	$\bar{\nu}$ (cm^{-1})	W (cm^{-1})†	I_R‡	$\bar{\nu}$ (cm^{-1})	C_{2v}	$\bar{\nu}$ (cm^{-1})	W (cm^{-1})	I_R	$\bar{\nu}$ (cm^{-1})
$\nu_1(A_1')$	1051	13.9	100	1050	$\nu_2(A_1)$	1051	13.9	100	1050
$\nu_2(A_2'')$	831	14	0.1	831	$\nu_4(B_1)$	831	14	0.1	831
$\nu_3(E')$	1355	61	4.1	§	$\nu_1(A_1)$	1368	51	2.0	§
	1417	62	6.8	§	$\nu_5(B_2)$	1415	66	3.2	§
$\nu_4(E')$	718	18	3.4	719	$\nu_3(A_1)$	728	17	1.2	‖
					$\nu_6(B_2)$	‖			734
$2\nu_2(A_1')$	1660	16	1.3	§	$2\nu_4(A_1)$	1660	16	1.3	§

*Data are taken for 7.09 M $NaNO_3$ in D_2O. There are small changes with concentration.
†Full width at half-height; for cases of double assignment the value of W does not indicate the value of the component. Spectral slit width ~8 cm^{-1}.
‡Integrated intensity relative to that of the 1052 cm^{-1} line.
§Region not studied because of the high infrared absorbance.
‖Line required by selection rules but obscured or weak.

centration range studied. Similar linearities also exist for comparable plots of the $LiNO_3/H_2O$ data (21).

The partial molal volumes were obtained from apparent molal volumes by an analytical procedure (22). Values of ϕV_2, the apparent molal volume, were computed from the smoothed density, concentration data and fitted to a polynomial in molality, m

$$\phi V_2 = 29.538 + 0.69772m - 0.01975m^2 - 0.00149m^3 + 0.00049m^4$$

The expression for $\bar{V}_2$ is then obtained by differentiation. The partial molal volume of the solvent, $\bar{V}_1$, was obtained from

$$\bar{V}_1 = \frac{20.028}{1000}\left[\frac{1000 + mM_2}{D} - m\bar{V}_2\right]$$

where 20.028 is the molecular weight of the solvent, M_2 is the molecular weight of the solute, m is the concentration in mol kg^{-1}, and D is the density. The linearity of the mean molal volume against mole fraction plot arises because the partial molal volumes balance each other, superficially indicating ideal behavior. This feature can be compared with the ideality revealed by the constancy of Q_C in the previous section.

Conductance and Viscosity

It has long been recognized that the degree of dissociation, α, should be obtainable from conductance measurements. One approach is to adopt the relation $\Lambda/\Lambda_x = \alpha$ where Λ is the observed equivalent conductance and Λ_x is the hypothetical conductance the electrolyte would have if it were completely dissociated into ions and at a concentration αC (23, 24). Much uncertainty exists concerning the appropriate expression for Λ_x which in general is a function of Λ_0, viscosity, concentration, charge type, temperature, and solvent. Considerable effort has been expended on this problem (23) since the interpretation of Davies (9), referred to in the first section of this discussion, was advanced. It is of interest to be able to correlate constitution, a microscopic property measured by Raman spectroscopy, and conductance, a macroscopic property, for this 1:1 electrolyte with a relatively small degree of ion association. The experiments were conducted with this objective in mind.

The Λ_0 value for the $NaNO_3/D_2O$ system is obtainable from Walden's Rule, using the known values for the $NaNO_3/H_2O$ system, because the solvents are comparable (25). Thus

$$\Lambda_0 = \frac{(\eta_0\Lambda_0)_{H_2O}}{(\eta_0)_{D_2O}} = \frac{0.8903 \times 121.56}{1.096_6} = 98.69 \text{ ohm}^{-1} \text{ cm}^2 \text{ equiv}^{-1}$$

The experimental data for specific conductance, κ, equivalent conductance, Λ, and viscosity, η, are presented in Table 4. The viscosity and specific conductance data have also been smoothed by means of a least squares computer

Can. J. Chem. Downloaded from www.nrcresearchpress.com by 210.87.254.6 on 09/05/12
For personal use only.

Can. J. Chem. Downloaded from www.nrcresearchpress.com by 210.87.254.6 on 09/05/12
For personal use only.

TABLE 3. Concentrative properties of $NaNO_3/D_2O$ at 25 °C

Wt. %	D_{25} (g ml^{-1})	C (mol l^{-1})	m (mol kg^{-1})	C_{D_2O} (mol l^{-1})	Sp. Vol (ml g^{-1})	$\bar{V}_2$(cm^3)	$\bar{V}_1$ (cm^3)
0.000	1.1044	0.000	0.000	55.14	0.9055	29.54	18.14
1.010	1.110	0.132	0.120	54.89	0.9005	29.70	18.14
1.652	1.112	0.216	0.198	54.58	0.8996	29.81	18.14
7.410	1.158	1.01	0.941	53.52	0.8637	30.80	18.12
9.312	1.174	1.29	1.21	52.91	0.8518	31.15	18.12
12.31	1.196	1.73	1.65	52.36	0.8361	31.68	18.10
14.11	1.206	2.00	1.93	51.70	0.8295	32.01	18.09
20.36	1.2568	3.01	3.01	49.98	0.7957	33.20	18.03
20.50	1.257	3.03	3.03	49.91	0.7954	33.23	18.03
25.38	1.295	3.87	4.00	48.24	0.7723	34.17	17.96
26.94	1.309	4.15	4.34	47.74	0.7641	34.48	17.94
31.54	1.349	5.01	5.42	46.10	0.7414	35.36	17.85
34.52	1.379	5.60	6.20	45.09	0.7252	35.93	17.78
36.04	1.388	5.88	6.63	44.28	0.7206	36.18	17.75
36.52	1.385	5.95	6.77	43.90	0.7221	36.24	17.74
39.00	1.4146	6.49	7.52	43.08	0.7069	36.68	17.68
40.56	1.430	6.83	8.03	42.53	0.6990	36.93	17.64
41.94	1.437	7.09	8.50	42.06	0.6959	37.10	17.62
42.83	1.455	7.33	8.81	41.53	0.6873	37.25	17.59
44.48	1.466	7.67	9.42	40.94	0.6821	37.43	17.56

TABLE 4. Viscosity and conductivity data for $NaNO_3/D_2O$ at 25.0 °C

C (mol l^{-1})	η (cP)	κ (Ω^{-1} cm^{-1})	Λ(Ω^{-1} cm^2 equiv^{-1})	
			Observed	Calculated
0.0	1.100	0.001	98.69*	98.66†
0.132		0.01083	82.38	80.87
0.216	1.108	0.01703	78.95	77.59
1.009	1.162	0.06383	63.26	64.17
2.002	1.266	0.1059	52.93	54.81
3.033	1.429	0.1357	44.75	46.49
3.866	1.602	0.1520	39.32	40.23
5.006	1.912	0.1654	33.03	32.42
5.951	2.246	0.1706	28.68	26.78
7.332	2.914	0.1704	23.23	20.02

*From Walden's Rule (see text).
†From equation with $C = 10^{-6}$ mol l^{-1} and $\mathring{a} = 4.10$ Å.

program and the smoothed data are given by the polynomials in C (mol l^{-1}):

$$\eta = 1.096_2 + 0.05671C + 0.01077C^2 + 0.00208C^3$$

$$\kappa = 0.00209 + 0.06899C - 0.00941C^2 + 0.00043C^3$$

We anticipate that the ion pairing in $NaNO_3/D_2O$ will be similar to that in $NaNO_3/H_2O$ although some Raman evidence has been accumulated which suggests that the degree of association may be somewhat larger in D_2O. A plot of $\kappa\eta$ against concentration was compared for the two systems. For $NaNO_3/H_2O$ the conductance data of Nelson were used (3) and the viscosity data were measured in our laboratory by Walker (*cf.* Janz *et al.* (26)). The polynomials for these quantities are:

$$\kappa = 0.00062 + 0.09245C - 0.02120C^2 + 0.00332C^3$$

$$\eta = 0.8904 + 0.05234C + 0.009883C^2 + 0.00166C^3$$

The two $\kappa\eta$ curves exhibit the same trends and inflections. Since $\kappa\eta$ is sensitive to solution constitution, such as ion-pair formation, differences are probably not large.

An empirical expression for Λ_x was obtained by dividing the observed conductance by the observed α. The expression

$$\Lambda_x = \Lambda_0 - 50.146C^{1/2} + 30.781C - 14.476C^{3/2} + 3.059C^2 - 0.226C^{5/2}$$

fits the data to within 0.1%. The two conductance curves are shown in Fig. 10. Efforts to develop an equation for Λ_x whose coefficients have real physical meaning for the system at moderate to high concentrations have so far been unsuccessful. Such a theoretical equation, together with measured values of Λ, would allow the computation of α for any concentration.

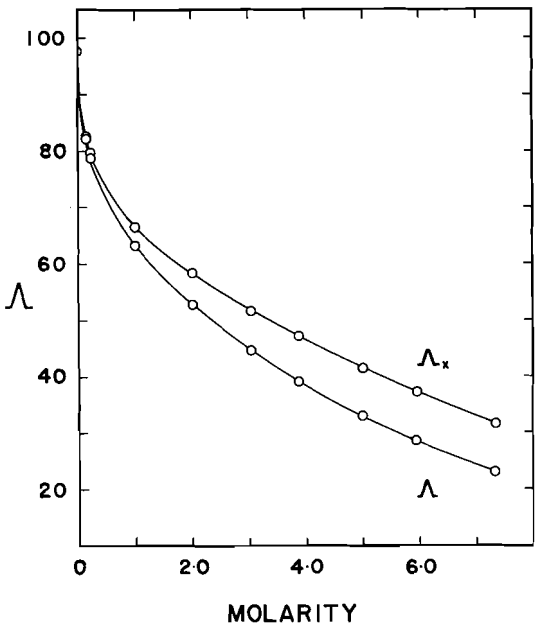

FIG. 10. Λ and Λ_x *vs.* molarity of $NaNO_3/D_2O$ at 25 °C.

Can. J. Chem. Downloaded from www.nrcresearchpress.com by 210.87.254.6 on 09/05/12
For personal use only.

Wishaw and Stokes (27) obtained satisfactory agreement between experimental data and conductance calculated from the equation

$$\Lambda = \left(\Lambda_0 - \frac{B_2\sqrt{C}}{1 + B\mathring{a}\sqrt{C}}\right)\left(1 - \frac{B_1\sqrt{C}}{1 + B\mathring{a}\sqrt{C}}F\right)\frac{\eta_0}{\eta}$$

for NH_4Cl/H_2O when $\mathring{a} = 4.35$ Å. This equation also fits the $NaNO_3$ data fairly well when $\mathring{a}$ is given the reasonable value 4.10 Å (Table 4). The constants used are: $B = 0.32999$; $B_1 = 0.23167$; $B_2 = 49.366$; $F = (e^x - 1)x^{-1}$ where $x = 0.09667\sqrt{c}\,\mathring{a}$ (*cf.* 28). There is no reason to believe that the difference between measured and calculated values should be attributed to ion association; rather it reflects the limitations of the equation; *i.e.*, the equation, with no allowance for ion association, does not give values which differ from the experimental values in any systematic way attributable to the known ion-pair formation.

Aspects of this work were supported by the Department of the Environment, the National Research Council of Canada, and the University of Waterloo Research Grant Programme. We are also grateful to Atomic Energy of Canada, Ltd., for deuterium oxide. Particular appreciation is extended to Dr. W. L. Elsdon for many helpful discussions. D.E.I. also expresses his thanks to Professor R. A. Robinson for his suggestions. J.D.R. acknowledges with thanks an Ontario Graduate Fellowship (1970–1971). We also thank Mr. John Walker for measuring the viscosity of the $NaNO_3/H_2O$ system.

1. D. E. Irish and A. R. Davis. Can. J. Chem. **46**, 943 (1968).
2. D. E. Irish, D. L. Nelson, and M. H. Brooker. J. Chem. Phys. **54**, 654 (1971).
3. D. L. Nelson. Ph.D. Thesis. University of Waterloo, Waterloo, Ontario, 1969.
4. A. R. Davis. Ph.D. Thesis. University of Waterloo, Waterloo, Ontario, 1967.
5. Y.-K. Sze. M.Sc. Thesis. University of Waterloo, Waterloo, Ontario, 1970.
6. A. R. Davis, D. E. Irish, R. B. Roden, and A. J. Weerheim. Appl. Spectrosc. In press.
7. D. E. Irish, G. Chang, and D. L. Nelson. Inorg. Chem. **9**, 425 (1970).
8. M. H. Brooker and D. E. Irish. Can. J. Chem. **48**, 1183 (1970).
9. C. W. Davies. Discuss. Faraday Soc. **23**, 351 (1927).
10. A. A. Krawetz. Ph.D. Thesis, University of Chicago, Chicago, Illinois, 1955. *Summarized by* T. F. Young, L. F. Maranville, and H. M. Smith. *In* The structure of electrolytic solutions. *Edited by* W. J. Hamer. John Wiley and Sons Inc., New York. 1959. p. 35.
11. J. Nixon and R. A. Plane. J. Am. Chem. Soc. **84**, 4445 (1962).
12. D. L. Nelson and D. E. Irish. J. Chem. Phys. **54**, 4479 (1971).
13. H. Chen and D. E. Irish. J. Phys. Chem. **75**, 2672 (1971).
14. R. A. Robinson and R. H. Stokes. Electrolyte solutions. 2nd ed. Butterworths, London. 1968.
15. O. D. Bonner. J. Chem. Thermodyn. **3**, 837 (1971).
16. R. M. Roberts and J. G. Kirkwood. J. Am. Chem. Soc. **63**, 1373 (1941).
17. R. A. Robinson. J. Am. Chem. Soc. **59**, 84 (1937).
18. C. W. Davies. Ion association. Butterworths, London. 1962. p. 77.
19. J. Braunstein. *In* Ionic interactions. Vol. 2. *Edited by* S. Petrucci. Academic Press, N.Y. 1971. p. 243.
20. F. J. Millero, R. Dexter, and E. Hoff. J. Chem. Eng. Data, **16**, 85 (1971).
21. A. N. Campbell, G. H. Debus, and E. M. Kartzmark. Can. J. Chem. **33**, 1508 (1955).
22. I. M. Klotz. Chemical thermodynamics. Prentice-Hall, Inc., Englewood Cliffs, N.J. 1957. p. 200.
23. E. M. Hanna, A. D. Pethybridge, and J. E. Prue. Electrochim. Acta, **16**, 677 (1971).
24. E. M. Hanna, A. D. Pethybridge, and J. E. Prue. J. Phys. Chem. **75**, 291 (1971).
25. R. L. Kay and D. F. Evans. J. Phys. Chem. **69**, 4216 (1965).
26. G. J. Janz, B. G. Oliver, G. R. Lakshminarayanan, and G. E. Mayer. J. Phys. Chem. **74**, 1285 (1970).
27. B. F. Wishaw and R. H. Stokes. J. Am. Chem. Soc. **76**, 2065 (1954).
28. R. A. Robinson and R. H. Stokes. J. Am. Chem. Soc. **76**, 1991 (1954).

Can. J. Chem. Downloaded from www.nrcresearchpress.com by 210.87.254.6 on 09/05/12
For personal use only.

Conformations of Bridged Diphenyls. I. Crystal Structure of 2-(3′-Methyl-4′-nitrophenoxy)-1,3-diisopropylbenzene

E. A. H. GRIFFITH, W. D. CHANDLER, AND B. E. ROBERTSON[1]

Division of Natural Sciences and Mathematics, University of Saskatchewan, Regina, Saskatchewan

Received May 1, 1972

The structure of 2-(3′-methyl-4′-nitrophenoxy)-1,3-diisopropylbenzene, $C_{19}H_{23}NO_3$, has been determined by X-ray diffraction. The crystals are triclinic, $a = 12.422(24)$, $b = 13.180(25)$, $c = 11.241(30)$ Å, $\alpha = 89.99(20)$, $\beta = 95.81(15)$, $\gamma = 105.46(12)°$, $P\bar{1}$ with $Z = 4$. The intensities of 8153 independent reflections were measured on a four circle diffractometer, of which 3701 were used in the refinement of the structure to give a final least-squares weighted residue of 0.053.

The ether oxygen bond angle in each of the two independent molecules is 120°. The two phenyl rings are nearly orthogonal in each case, while the ring containing the electron withdrawing nitro group is conjugated with the ether oxygen atom. The rings show significant deviations from hexagonal symmetry and the nitro-substituted ring is bent away from the other ring.

Nous avons déterminé la structure du 2-(3′-méthyl-4′-nitrophenoxy)-1,3-diisopropylbenzène, $C_{19}H_{23}NO_3$ par diffraction de rayons-X. Les cristaux sont tricliniques avec $a = 12.422(24)$, $b = 13.180(25)$, $c = 11.241(30)$ Å, $\alpha = 89.99(20)$, $\beta = 95.81(15)$, $\gamma = 105.46(12)°$, $P\bar{1}$ avec $Z = 4$. Nous avons mesuré les intensités de 8153 réflexions indépendantes au moyen d'un diffractomètre à quatre cercles; 3701 réflexions ont été utilisées pour le raffinement de la structure pour obtenir une moyenne pondérée par moindres carrés de résidu de 0.053.

L'angle impliquant l'oxygène de la liaison éther dans chacune des deux molécules indépendantes est de 120°. Les deux cycles phényl sont presque orthogonaux dans chaque cas, tandis que le cycle contenant un groupe nitro attracteur d'électrons, est conjugué avec l'atome d'oxygène de l'éther. Les cycles dévient de façon importante de la symétrie hexagonale et le cycle nitro-substitué est éloigné de l'autre cycle.

[Traduit par le journal]

Canadian Journal of Chemistry, **50**, 2963 (1972)

This is the first in a series of reports which will describe studies of substituted, bridged diphenyl compounds using X-ray diffraction. In addition, the results obtained by this technique will be compared with n.m.r. data for the same systems in solution. We intend to examine the effects of several variables, such as the steric and electronic character of the substituents and the nature of the bridging group, on the relative orientations of the phenyl rings and the central plane containing the bridging group.

The bridging groups which have received some attention in the past are O, S, SO, SO_2, CH_2, and CO, with diphenyl ethers having been studied most extensively: (*i*) Infrared and Raman spectroscopy have been employed to a limited extent in the study of diphenyl ether (1, 2). (*ii*) The modes of internal rotation of these compounds have been studied by dielectric relaxation methods (3–7). (*iii*) Comparisons of the sums of the group moments with the measured dipole moment of the molecule have been of some value in predicting the preferred orientations of phenyl rings (8–12). (*iv*) More recently, magnetic shielding of the aromatic hydrogen atoms by currents in the adjacent ring, as measured by n.m.r. (13–19), has proven to be a valuable technique for the study of aromatic molecules. However, the scarcity of more direct observations and verification of the conformation of these molecules by diffraction techniques has hindered the development of the dipole moment and n.m.r. methods as quantitative tools for the study of conformations.

The information obtained by gas phase electron diffraction experiments (20, 21) is of limited value because of the relative complexity of this system. Hamilton and Steinrauf (22) have recently reported the crystal structure of the alkaloid vertaline which contains oxygen bridged phenyl rings and provides information on the geometry in the vicinity of the bridging atom. The freedom of the rings to adopt an optimum conformation is restricted, however, by their being linked through a quinolizidine ring and a lactone group. Camerman and Camerman have recently reported the structure of the thyroid hormone 3,5,3′-triiodo-L-thyro-

[1]To whom correspondence should be addressed.

Can. J. Chem. Downloaded from www.nrcresearchpress.com by 210.87.254.6 on 09/05/12
For personal use only.

Can. J. Chem. Downloaded from www.nrcresearchpress.com by 210.87.254.6 on 09/05/12
For personal use only.

nine (35). They found an ether oxygen bond angle of 125.6° with the phenolic ring nearly coplanar with the central C—O—C plane. The angle between the diiodotyrosine ring and the phenolic ring is 82°. Toussaint has studied diphenyl ether and 4,4′-dibromodiphenyl ether by X-ray diffraction (23, 24). The structural parameters given for these two ethers have been used to some extent for the calculation of n.m.r. shielding parameters (17–19) but the relatively low accuracy of these structural determinations, together with the serious discrepancies between the C—O bond lengths and the C—O—C angles in the two similar molecules suggest that further studies are required.

The use of solid phase structural data for the calculation of n.m.r. shielding parameters has the obvious limitation that the internal rotations of the molecule in the liquid phase are frozen out. The observed n.m.r. data may represent an averaging over a range of conformations associated with the internal motion. Nevertheless, the use of accurate structural parameters in these calculations can be of considerable value in correlating changes in ring current shielding with conformational changes.

The present diphenyl ether has bulky isopropyl groups in the ortho positions of one ring and an electron withdrawing nitro group on the other ring. Montaudo and co-workers (18, 19) have suggested that electron withdrawing groups may enhance conjugation between unshared electrons on the bridging atoms and π electrons in the phenyl ring, although in the liquid phase at least two electron withdrawing substituents are necessary to produce a significant conjugation effect. Variable temperature n.m.r. studies (34) have indicated that the net result of the steric effect of the isopropyl groups and the conjugative effect of the nitro group in solution is an equilibrium of the two conformations **1**, and **2**.[2] This study was undertaken partly to see if the same two conformations (with rings nearly perpendicular) were present in the solid phase.

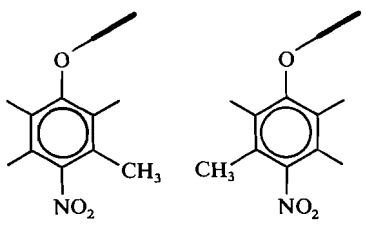

1 **2**

Experimental

Data Collection

2-(3′-Methyl-4′-nitrophenoxy)-1,3-diisopropylbenzene was synthesized by the method of Wright and Jorgensen (25) and recrystallized from 95% ethanol. The melting point was determined to be 90–91°.

A sample was selected with near orthogonal faces and dimensions 0.92 × 0.20 × 0.76 mm. The crystalline quality, symmetry, approximate cell constants and orientation of the crystal were examined by film techniques and it was then mounted on a Picker FACS-I four circle diffractometer. Accurate cell constants were determined by least-squares from the centered positions of 12 reflections with 2θ values between 28 and 42°, where the $K\alpha_1$ and $K\alpha_2$ diffraction maxima were resolved. The cell constants are given below with estimated errors which are three times the estimated standard deviations calculated from the least-squares procedure. Comparison between cell constants determined from different sets of reflections and from different samples suggest that this is a realistic estimate of error. Crystal data are as follows:

2-(3′-Methyl-4′-nitrophenoxy)-1,3-diisopropylbenzene
f.w. = 313

Triclinic $P\bar{1}$, $a = 12.422(24)$, $b = 13.180(25)$, $c = 11.241(30)$ Å, $V = 1764$ Å^3, $\alpha = 89.99(20)$, $\beta = 95.81(15)$, $\gamma = 105.46(12)$°, $\rho_0 = 1.15$ g cm^{-3} (flotation), $Z = 4$, $\rho_c = 1.18$ g cm^{-3}, $F(000) = 672$ e (22 °C, $\mu(\text{MoK}\bar{\alpha}) = 0.85$ cm^{-1}, $\lambda(\text{MoK}\alpha_1) = 0.70926$ Å).

Data were collected with MoKα radiation and a "highly oriented graphite" monochromator. The integrated intensities of 8153 reflections were measured between the 2θ values of 3.5 and 55°. The θ–2θ scan mode was used with a scan rate of 2° min^{-1} and a base width of 3.2°. Background counts (10 s) were made at each end of the scan. The intensities of three standard reflections were collected after every 100 reflections and showed no significant variations. However a machine malfunction, resulting in a collision when the data had been collected out to *ca.* 34° in 2θ, necessitated realignment of the crystal, and the standards showed a small change in intensity after realignment. Two scale constants were used in the subsequent analysis of the data.

The data were reduced to observed structure factors by standard calculations. The polarization factor used was

$$(\cos^2 2\theta_m + \cos^2 2\theta_s)/2 \sin 2\theta_s$$

where θ_m and θ_s are the Bragg angles of the monochromator and sample, respectively. $\sigma(F)$ was calculated from

$$\sigma(F) = A\{NS + (T(NS)/T(BG))^2 BG\}^{1/2}/2\text{Lp}|F|$$

where A is the attenuator constant, NS the number of scan counts, BG the total background count, and $T(NS)$ and

[2]The conformation found for 3,5,3′-triiodo-L-thyronine corresponds to **1**, and may account for the larger ether oxygen bond angle.

Can. J. Chem. Downloaded from www.nrcresearchpress.com by 210.87.254.6 on 09/05/12
For personal use only.

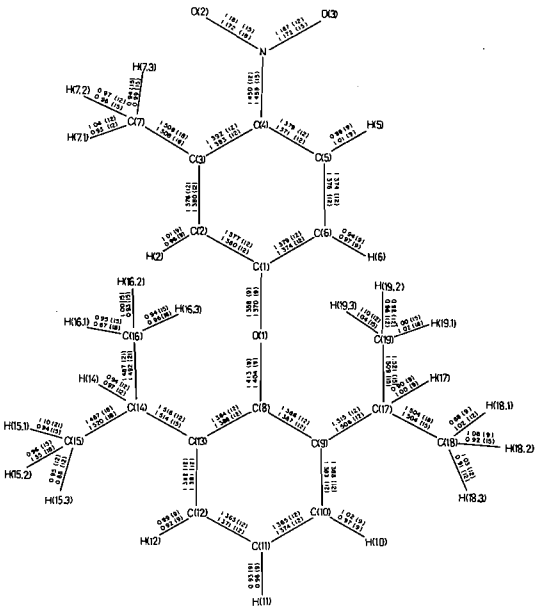

FIG. 1. Bond lengths and atom sequence. The numbers nearest the line refer to molecule 1. The numbers in parentheses are estimated errors based on the errors in Table 2.

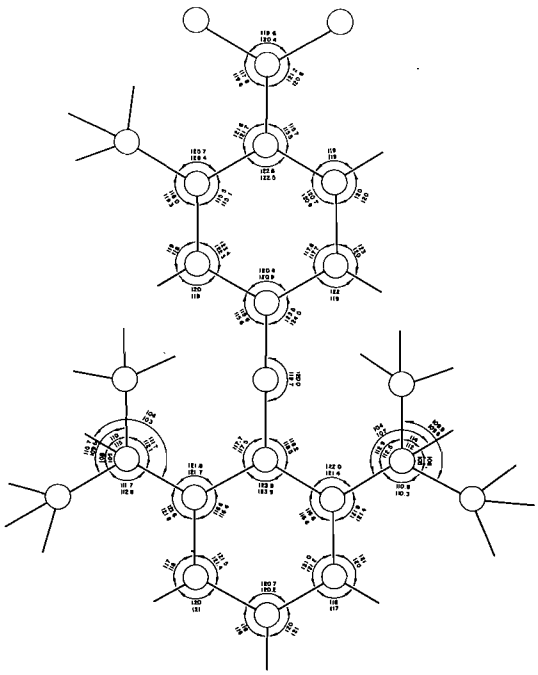

FIG. 2. Bond angles. The number nearest the atom refers to molecule 1. The estimated errors in the angles not involving a hydrogen atom are *ca.* 1.4°. The estimated errors in the angles involving hydrogen atoms are *ca.* 10°.

$T(BG)$ are the scan times and total background count times. No corrections were made for extinction or absorption. The scattering factors of the carbon, nitrogen, and oxygen atoms were taken from Cromer and Mann (26). The scattering factors of the hydrogen atoms were taken from Stewart *et al.* (27).

Determination and Refinement of the Structure

The observed density and cell volume correspond to four molecules in the unit cell. A Wilson statistical calculation gave an overall temperature factor of 4.3 Å^2. Normalized structure factors, E, were calculated and the average values of $|E|$ and $|E^2 - 1|$ were 0.757 and 1.021, indicating the centrosymmetric space group $P\bar{1}$. The 418 reflections with $|E| > 2.0$ were selected and used in the multiple solution, logical symbolic addition method programs of Germain and Woolfson (28). An E map calculated from the solution with highest figures of merit, not associated with a trivial solution, yielded 42 of the 46 non-hydrogen atoms of the two molecules. One cycle of full matrix least-squares refinement, using 2400 low angle reflections reduced the residual R_w, defined as

$$R_w = \{\sum w||F_o| - |F_c||^2 / \sum w|F_o|^2\}^{1/2} \quad \text{with} \quad w = \sigma^{-2}$$

from 0.41 to 0.34. A modified version of the Busing *et al.* program ORFLS (29) was used for least-squares refinement. The program FORDAP, written by Zalkin (30) was used for all Fourier calculations. An electron density Fourier calculation revealed the remaining non-hydrogen atoms and the residual was lowered to 0.18 using individual isotropic temperature factors.

Refinement of anisotropic temperature factors reduced R_w to 0.15. A difference Fourier map revealed 24 hydrogen atoms of a total of 46. Further refinement and difference Fourier calculations revealed the remaining hydrogen atoms. The weighting scheme was changed to $w^{-1/2} = 1.0177 - 0.0887|F_o| + 0.0027|F_o|^2$. The coefficients were determined by fitting the average value of $\Delta = ||F_o| - |F_c||$ to $|F_o|$. 3701 reflections for which $|F_o| > 1.43\,\sigma(F)$ were used in the final cycles of full matrix least-squares refinement. The final values of R_w and the conventional R factor were 0.053 and 0.060, respectively.

The observed and calculated structure factors have been placed in the Depository for Unpublished Data.[3] The final positional and thermal parameters are listed in Table 1. The estimated errors are given as three times the estimated standard deviations calculated from the diagonal components of the inverse least-squares matrix. The U_{ij} in Table 1 are the coefficients in the expression

$$\exp\{-2\pi^2(h^2b_1^2U_{11} + \ldots + 2hkb_1b_2U_{12} + \ldots)\}$$

where the b_i represents the reciprocal lattice constants. The bond lengths and the atom numbering sequence are given in Fig. 1 and the bond angles are given in Fig. 2.

[3]Complete set of tabular data is available, at a nominal charge, from the Depository of Unpublished Data, National Science Library, National Research Council of Canada, Ottawa, Canada K1A 0S2.

Discussion

The bond lengths to hydrogen atoms range from 0.87 to 1.10 Å, except for H(15,2) on molecule 1 which has a least-square minimum 1.35 Å from the C(15) atom. The angles subtended at the C(15) atom by this hydrogen atom are reasonable, however, and it has been included in the calculation of R_w.

TABLE 1. Structural parameters of 2-(3′-methyl-4′-nitrophenoxy)-1,3-diisopropylbenzene (see text for description of errors)

(*a*) Fractional atomic coordinates ($\times 10^4$)

Atom	*x*	*y*	*z*
Molecule 1			
C(1)	2475(7)	6560(6)	1761(7)
C(2)	3133(7)	5914(7)	1493(9)
C(3)	3428(7)	5222(6)	2303(8)
C(4)	3007(7)	5209(6)	3397(8)
C(5)	2351(8)	5845(7)	3676(8)
C(6)	2073(7)	6534(7)	2858(7)
C(7)	4168(14)	4566(12)	1926(14)
C(8)	1707(7)	7979(6)	1106(7)
C(9)	2302(7)	8900(6)	1725(7)
C(10)	1727(8)	9651(7)	1867(8)
C(11)	629(8)	9492(8)	1396(8)
C(12)	77(8)	8575(8)	777(8)
C(13)	596(7)	7786(6)	625(7)
C(14)	−22(9)	6755(8)	−19(10)
C(15)	−665(14)	6930(13)	−1190(11)
C(16)	−807(22)	6050(14)	739(16)
C(17)	3533(7)	9089(8)	2176(8)
C(18)	4267(11)	9679(15)	1279(12)
C(19)	3831(13)	9675(18)	3367(12)
N	3250(8)	4520(8)	4343(10)
O(1)	2278(5)	7224(4)	879(5)
O(2)	3636(16)	3839(14)	4085(12)
O(3)	2955(8)	4564(6)	5294(8)
Molecule 2			
C(1)	2498(6)	9677(6)	6749(7)
C(2)	3093(7)	666(6)	6451(8)
C(3)	3384(7)	1520(6)	7234(8)
C(4)	3029(7)	1318(6)	8367(8)
C(5)	2418(7)	337(7)	8676(8)
C(6)	2141(7)	9501(7)	7871(7)
C(7)	4033(12)	2573(8)	6819(12)
C(8)	1734(7)	7870(6)	6105(7)
C(9)	2331(7)	7236(6)	6702(7)
C(10)	1745(8)	6197(7)	6851(8)
C(11)	645(9)	5826(8)	6406(8)
C(12)	97(8)	6468(7)	5797(8)
C(13)	621(1)	7516(6)	5638(7)
C(14)	7(9)	8242(8)	4994(9)
C(15)	−625(16)	7776(17)	3842(11)
C(16)	−743(20)	8581(19)	5768(14)
C(17)	3569(8)	7640(8)	7130(8)
C(18)	4267(10)	7385(12)	6213(12)
C(19)	3883(14)	7212(16)	8335(12)
N	3288(8)	2130(7)	9302(9)
O(1)	2316(5)	8916(4)	5880(5)
O(2)	3863(14)	2975(8)	9126(10)
O(3)	2969(7)	1943(6)	259(8)

(*b*) Fractional atomic coordinates ($\times 10^3$)

Atom	*x*	*y*	*z*	*B* (Å²)
Molecule 1				
H(2)	344(6)	597(6)	74(7)	4(2)
H(5)	209(8)	582(7)	451(9)	6(2)
H(6)	163(6)	699(6)	307(6)	4(2)
H(7,1)	377(9)	389(9)	208(10)	9(4)
H(7,2)	445(10)	483(9)	119(12)	9(4)
H(7,3)	480(12)	466(10)	257(12)	11(4)
H(10)	210(8)	32(7)	227(8)	5(2)
H(11)	24(7)	1(7)	151(8)	5(2)
H(12)	−67(7)	845(6)	50(7)	3(2)
H(14)	58(10)	648(6)	−25(10)	9(3)
H(15,1)	−31(12)	744(12)	−171(14)	11(5)
H(15,2)	−152(15)	721(13)	−79(16)	16(5)
H(15,3)	−93(11)	630(10)	−153(10)	8(4)
H(16,1)	−40(13)	591(10)	137(15)	11(5)
H(16,2)	−111(10)	539(10)	38(12)	9(4)
H(16,3)	−135(14)	641(13)	91(15)	12(7)
H(17)	370(8)	839(7)	222(8)	6(2)
H(18,1)	404(10)	36(9)	118(10)	8(3)
H(18,2)	406(10)	929(10)	57(12)	9(4)
H(18,3)	502(10)	985(8)	148(9)	6(3)
H(19,1)	327(13)	927(10)	394(14)	12(5)
H(19,2)	457(11)	979(8)	366(10)	7(3)
H(19,3)	364(17)	37(15)	319(17)	14(8)
Molecule 2				
H(2)	332(7)	76(6)	561(8)	5(2)
H(5)	217(7)	25(6)	948(8)	5(2)
H(6)	171(6)	883(6)	804(7)	4(2)
H(7,1)	487(12)	277(9)	719(10)	10(4)
H(7,2)	359(9)	304(8)	702(9)	7(3)
H(7,3)	414(10)	247(9)	602(11)	8(4)
H(10)	213(7)	568(6)	726(8)	5(2)
H(11)	26(7)	513(6)	650(7)	4(2)
H(12)	−69(7)	620(6)	544(7)	4(2)
H(14)	58(9)	883(8)	482(10)	7(3)
H(15,1)	−133(17)	713(14)	409(18)	17(10)
H(15,2)	−24(12)	743(11)	335(13)	11(4)
H(15,3)	−96(9)	828(8)	348(10)	8(3)
H(16,1)	−130(11)	801(10)	605(12)	8(5)
H(16,2)	−111(12)	911(11)	540(13)	11(4)
H(16,3)	−39(12)	889(10)	651(14)	11(4)
H(17)	369(7)	835(6)	713(7)	4(2)
H(18,1)	499(9)	764(7)	642(8)	5(2)
H(18,2)	408(8)	654(8)	612(9)	7(3)
H(18,3)	418(8)	780(8)	544(10)	7(3)
H(19,1)	348(10)	754(10)	888(12)	10(3)
H(19,2)	460(11)	748(9)	858(11)	8(3)
H(19,3)	374(10)	635(10)	823(10)	9(3)

Can. J. Chem. Downloaded from www.nrcresearchpress.com by 210.87.254.6 on 09/05/12
For personal use only.

TABLE 1 (*Concluded*)

(*c*) Thermal parameters $U_{ij} \times 10^3$

Atom	U_{11}	U_{22}	U_{33}	U_{12}	U_{13}	U_{23}
Molecule 1						
C(1)	42(5)	45(2)	39(3)	14(3)	1(3)	2(2)
C(2)	47(5)	53(3)	47(4)	21(3)	7(3)	−3(2)
C(3)	48(5)	44(2)	62(3)	20(3)	1(3)	0(2)
C(4)	52(5)	42(2)	56(4)	19(3)	−1(3)	11(2)
C(5)	57(5)	51(3)	49(4)	18(3)	11(4)	12(2)
C(6)	50(5)	51(2)	47(3)	24(3)	13(3)	6(2)
C(7)	96(10)	78(5)	93(7)	57(5)	21(7)	10(5)
C(8)	50(5)	50(2)	35(3)	25(3)	10(3)	9(2)
C(9)	47(5)	53(2)	36(3)	16(3)	9(3)	10(2)
C(10)	52(6)	45(2)	52(3)	10(3)	7(3)	1(2)
C(11)	62(6)	53(3)	61(4)	31(4)	13(4)	6(3)
C(12)	48(5)	61(3)	58(4)	26(3)	2(4)	6(3)
C(13)	47(5)	52(2)	45(3)	18(3)	3(3)	3(2)
C(14)	61(7)	67(3)	76(5)	20(4)	−6(5)	−14(3)
C(15)	123(12)	110(6)	53(5)	−14(7)	−7(6)	−12(4)
C(16)	173(20)	67(5)	83(7)	−27(8)	−24(10)	9(5)
C(17)	44(5)	62(3)	48(3)	12(3)	5(3)	6(2)
C(18)	45(7)	142(7)	64(5)	18(5)	16(5)	26(5)
C(19)	59(9)	192(9)	52(5)	14(7)	−5(5)	−16(5)
N	104(8)	86(3)	98(5)	66(4)	32(5)	44(3)
O(1)	62(4)	64(2)	37(2)	36(2)	10(2)	9(1)
O(2)	441(24)	322(9)	178(7)	332(14)	171(12)	169(8)
O(3)	146(9)	106(3)	76(4)	61(4)	24(5)	39(2)
Molecule 2						
C(1)	37(5)	42(2)	38(3)	11(2)	2(3)	1(2)
C(2)	45(5)	46(2)	42(3)	10(3)	4(3)	9(2)
C(3)	45(5)	40(2)	50(3)	10(3)	−4(3)	6(2)
C(4)	49(5)	41(2)	53(4)	16(3)	−2(3)	−7(2)
C(5)	48(5)	55(3)	42(3)	15(3)	6(3)	−2(2)
C(6)	44(5)	41(2)	45(3)	7(3)	9(3)	4(2)
C(7)	84(9)	49(3)	77(6)	−3(4)	6(6)	9(3)
C(8)	50(5)	40(2)	36(3)	11(3)	8(3)	−1(2)
C(9)	47(5)	52(2)	38(3)	17(3)	4(3)	−2(2)
C(10)	66(6)	49(2)	53(3)	23(3)	8(3)	4(2)
C(11)	66(7)	36(2)	65(4)	5(3)	12(4)	5(2)
C(12)	49(6)	50(3)	56(4)	3(3)	0(4)	1(2)
C(13)	50(5)	47(2)	42(3)	13(3)	1(3)	2(2)
C(14)	56(6)	64(3)	72(5)	15(4)	−4(4)	16(3)
C(15)	119(13)	172(8)	49(5)	88(10)	−3(6)	19(5)
C(16)	166(18)	141(8)	75(6)	114(11)	−9(9)	−7(6)
C(17)	50(5)	57(3)	62(4)	18(3)	−1(4)	−3(3)
C(18)	47(7)	98(5)	87(6)	14(5)	13(5)	−3(4)
C(19)	79(10)	140(7)	67(5)	39(7)	−16(6)	6(5)
N	81(6)	54(3)	71(4)	3(3)	−2(4)	−17(3)
O(1)	58(4)	42(2)	40(2)	5(2)	12(2)	1(2)
O(2)	376(20)	84(3)	113(5)	−62(7)	81(8)	−47(3)
O(3)	111(7)	99(3)	68(3)	15(3)	16(4)	−29(2)

A stereoscopic view of the packing of the two independent molecules in the unit cell is shown in Fig. 3. Stereoscopic figures were prepared using the program ORTEP (31). Figures 4 and 5 show stereograms of the individual molecules. Molecule 1 is involved in 18 H–H intermolecular contacts less than 2.8 Å in length and 7 contacts involving one non-hydrogen atom which are less than 2.8 Å in length. Molecule 2 is involved in 10 H–H contacts and 7 contacts involving one non-hydrogen atom which are shorter than 2.8 Å. All but one of the non-

Can. J. Chem. Downloaded from www.nrcresearchpress.com by 210.87.254.6 on 09/05/12
For personal use only.

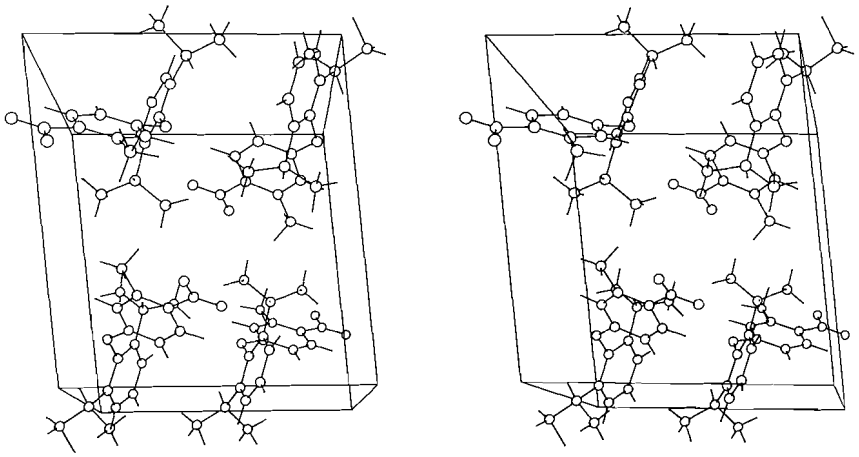

FIG. 3. Stereoscopic view of the packing of the four molecules in the unit cell. The origin is in the upper left forward corner. The ***a*** axis points down, the ***b*** axis points back, and the ***c*** axis points to the left. Stereograms may be viewed with the naked eye or with the aid of a simple lens system available from W. A. Benjamin Inc., 2465 Broadway, New York 25, N.Y.

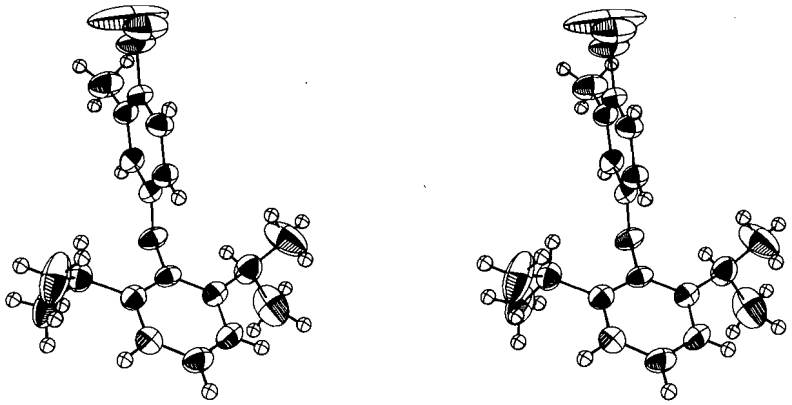

FIG. 4. Stereogram of molecule 1. The thermal ellipsoids are scaled to include 50% probability.

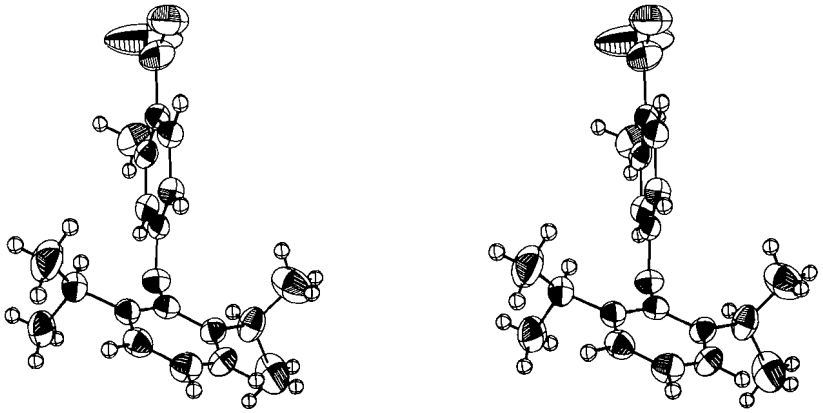

FIG. 5. Stereogram of molecule 2. The thermal ellipsoids are scaled to include 50% probability.

Can. J. Chem. Downloaded from www.nrcresearchpress.com by 210.87.254.6 on 09/05/12
For personal use only.

TABLE 2. Least-square planes

(*a*) Coefficients of planes $Ax + By + Cz = D$*

Plane	*A*	*B*	*C*	*D*
Molecule 1				
1	−0.8819	−0.3288	−0.3375	−6.2269
2	−0.7863	−0.5083	−0.3510	−6.8381
3	−0.8438	−0.4404	−0.3064	−6.3780
4	0.3947	0.3398	−0.8536	3.0839
5	0.2355	−0.8806	−0.4109	−7.8447
6	−0.6493	0.7158	−0.2569	−4.5349
Molecule 2				
1	−0.7871	0.5427	−0.2929	2.8063
2	−0.8235	0.4715	−0.3153	1.4449
3	−0.8363	0.4399	−0.3270	0.9444
4	0.3757	−0.3399	−0.8621	−8.6992
5	0.8938	−0.2932	−0.3392	−5.5963
6	−0.6730	−0.7025	−0.2311	−10.4019

*Coordinates refer to the directions of the a, $c^* \times a$, and c^* axes.

(*b*) Angles between normals to planes

	Angle (deg)	
Planes	Molecule 1	Molecule 2
1,2	11.7	4.8
2,3	5.7	2.1
3,4	77.2	79.5
2,4	79.4	78.6
4,5	56.1	43.3
4.6	78.1	79.3

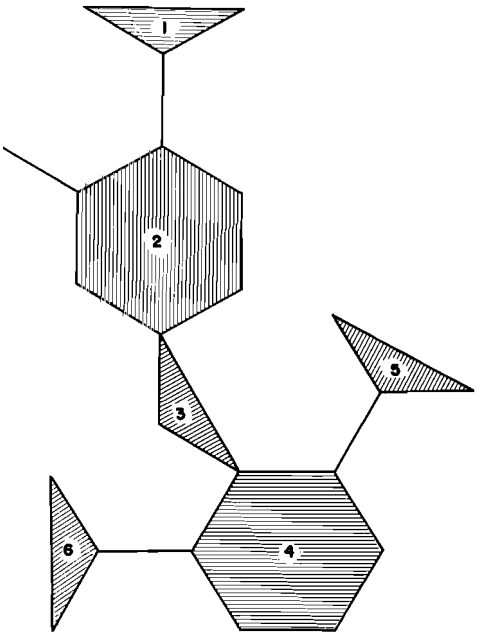

FIG. 6. Labelling nomenclature of the planes of both molecules.

hydrogen atoms mentioned above are oxygen atoms. The shortest contact involves the hydrogen atom H(15,2) on molecule 1. If this atom is removed to a more realistic distance from C(15), the contact length becomes approximately 2.85 Å. This leaves the 2.57 Å distance between O(1) on molecule 2 and H(19,3) on molecule 1 as the shortest contact distance.

The interplanar angles are given in Table 2. The labelling of the planes of the molecules is shown in Fig. 6. The rotation of the plane of the nitro group from the plane of the phenyl ring in the case of both molecules is within the range of such rotations as observed for para-substituted nitrobenzenes (32). Although the N—C(4) distances are similar to those in nitrobenzenes, substituted in the para position with electron donating groups, there is no evidence for the existence of the "edge shortening effect" that has been observed in some of them. The ellipsoid representing the nitro oxygen atom O(2) nearest the methyl group shows large thermal motion perpendicular to the plane of the nitro group. This is unexpected because the methyl hydrogen atom nearest to the plane of the phenyl ring is pointed away from the nitro group, leaving the O(2) atom between the other two methyl hydrogen atoms on either side of the phenyl ring. The N—C(4)—C(3) angles are *ca.* 6° larger than the N—C(4)—C(5) angles and the CH_3—C(3)—C(4) angles are 8.4 and 6.4° larger than the CH_3—C(3)—C(2) angles in molecules 1 and 2, respectively, showing the steric repulsion between the methyl and the nitro groups.

The nitro-substituted phenyl ring is nearly coplanar with plane 3, formed by the ether oxygen atoms and the two ring carbon atoms bonded to it, *i.e.* C(1) and C(8). Also, the length of the C(1)—O(1) bonds are 0.034(14) and 0.055(14) Å shorter than the O(1)—C(8) bonds in the two molecules. It appears that, in the solid state as well as in solution (34), one electron withdrawing substituent such as a nitro group is sufficient to cause significant enhancement of conjugative effects between the phenyl ring and the unshared electrons in the ether oxygen atom.

The angles subtended at the ether oxygen

Can. J. Chem. Downloaded from www.nrcresearchpress.com by 210.87.254.6 on 09/05/12
For personal use only.

TABLE 3. Riding motion corrections to terminal C—C bonds

Bond	Bond length (Å)			
	Molecule 1		Molecule 2	
	Uncorrected	Corrected	Uncorrected	Corrected
C(3) —C(7)	1.508	1.539	1.508	1.535
C(13)—C(14)	1.514	1.534	1.516	1.532
C(14)—C(15)	1.520	1.552	1.487	1.521
C(14)—C(16)	1.492	1.541	1.487	1.537
C(9) —C(17)	1.506	1.524	1.515	1.525
C(17)—C(18)	1.504	1.535	1.504	1.524
C(17)—C(19)	1.509	1.558	1.521	1.559

atom by C(1) and C(8) do not differ significantly from 120°. The diisopropyl substituted ring is within 13° of being perpendicular to plane 3. The range in the orientation of this plane is limited by the contacts between the isopropyl substituents and the nitro-substituted ring. One of these isopropyls is brought closer than the other by the deviation from the perpendicular conformation. Both isopropyl groups on each of the two molecules are oriented with the methine hydrogen atom pointing approximately in the direction of the ether oxygen atom. The isopropyl groups, which are brought closer to the nitro-substituted ring by the twist of the diisopropyl-substituted ring from orthogonality with plane 3, are tilted slightly away from the nitro-substituted ring. They are oriented such that the angle between the planes of the three carbon atoms in the groups and the planes of the phenyl rings to which they are bonded is approximately 80°. The contact distances between the other isopropyl groups and the nitro-substituted ring are increased by the twist of the diisopropyl-substituted ring and they are tilted in the opposite direction. The orientation of these substituents appears to be determined in part by steric hindrances imposed by neighboring molecules, resulting in a 13° difference in the angle between the normals to the planes of the three carbon atoms and the normals to the planes of the diisopropyl-substituted phenyl rings in the two molecules.

The bond lengths within the phenyl rings fall within expected values. The terminal bonds to oxygen and carbon atoms are affected by thermal motion. If "riding motion corrections" as proposed by Busing and Levy (33) are applied, the length of the N—O(3) bonds are increased to 1.195 and 1.218 Å in molecules 1 and 2, respectively. The N—O(2) bonds are increased to 1.376 and 1.347 Å. However, this type of bond length correction is not meaningful when applied to an atom such as O(2), showing anomalous thermal behavior or positional disorder. Riding motion corrections to the terminal C—C bond lengths are given in Table 3.

In the solid state both molecules have the conformation II as discussed earlier (34) in contrast to 3,5,3′-triiodo-L-thyronine (35). The conformation of the latter may be driven by the interaction between the 3′-iodine atom and the π electrons of the thyronine ring, but the ether oxygen angle is increased by *ca.* 6° over the values found here for conformation II.

The geometry of the phenyl rings of 2-(3′-methyl-4′-nitrophenoxy)-1,3-diisopropylbenzene shows a number of significant deviations from the full symmetry assumed in previous calculations of magnetic shielding parameters. The inner ring angles subtended at the atoms C(9) and C(13) which are bonded to the isopropyl groups are decreased to *ca.* 116.5°. This serves to lengthen the distance between the atoms in the isopropyl groups and the rest of the molecules. The deviations from hexagonal symmetry of the internal angles of the nitro-substituted phenyl ring cause the C(3)—C(6) distances to be approximately 0.010 Å longer than the C(2)—C(5) and C(1)—C(4) distances. This distortion removes H(5), but not H(6), further from the diisopropyl-substituted ring.

In each molecule the angle C(6)—C(1)—O(1) is greater than the angle C(2)—C(1)—O(1), indicating a bending of the nitro-substituted ring away from the other ring. A measure of this bending is the difference in these angles, divided

Can. J. Chem. Downloaded from www.nrcresearchpress.com by 210.87.254.6 on 09/05/12
For personal use only.

by 2, giving 4.0° for molecule 1 and 4.2° for molecule 2. This distortion should decrease the expected effect of magnetic shielding at both H(5) and H(6).

Although the bond lengths to the ether oxygen atom are similar to the values 1.395 and 1.410 Å reported for vertaline (22), the bond angle at the ether oxygen atom is larger than the value 116.1 Å for vertaline. Other reports of structural data (20, 23, 24) are of low accuracy, and most comparisons with our results are of little value. However, the short bond (1.28 Å) between the phenyl carbon atoms and the bridging oxygen atom in 4,4′-dibromodiphenyl ether is clearly inconsistent with our data. The crystal structure of a halogen-substituted diphenyl ether will be reported in the near future.

The authors thank Mr. Simon van der Heijden for the preparation of the stereoscopic drawings and the National Research Council of Canada for financial support.

1. A. FRÜHLING. J. Chim. Phys. **46**, 35 (1949); Ann. Physik, **6**, 401 (1951).
2. J. E. KATON, W. FEAIRHELLER, and E. R. LIPPINCOTT. J. Mol. Spectrosc. **13**, 72 (1964).
3. E. FISCHER. Z. Electrochem. **53**, 16 (1949).
4. D. M. ROBERTI, O. F. KALMAN, and C. P. SMYTH. J. Am. Chem. Soc. **82**, 3523 (1960).
5. K. HIGASI and C. P. SMYTH. J. Am. Chem. Soc. **82**, 4759 (1960).
6. K. BERGMANN, D. M. ROBERTI, and C. P. SMYTH. J. Phys. Chem. **64**, 665 (1960).
7. J. E. ANDERSON and C. P. SMYTH. J. Chem. Phys. **42**, 473 (1965).
8. G. C. HAMPSON and L. E. SUTTON. Proc. Roy. Soc. **A140**, 562 (1933).
9. K. HIGASI and S. UYEO. Bull. Chem. Soc. Jap. **14**, 87 (1939).
10. N. J. LEONARD and L. E. SUTTON. J. Am. Chem. Soc. **70**, 1564 (1948).
11. M. GOMEL, H. LUMBROSO, N. MARZIANO, and R. PASSERINI. Bull. Soc. Chim. Fr. 1908 (1959).
12. P. A. LEHMANN and D. M. MCEACHERN. J. Mol. Struct. **7**, 253, 267, 277 (1971).
13. W. D. CHANDLER, W. MACF. SMITH, and R. Y. MOIR. Can. J. Chem. **42**, 2549 (1964).
14. P. A. LEHMANN and E. C. JORGENSEN. Tetrahedron, **21**, 363 (1965).
15. P. A. LEHMANN. Rev. Soc. Quím. Méx. **14**, 122 (1970).
16. P. A. LEHMANN. Org. Mag. Res. **2**, 467 (1970).
17. J. J. BERGMAN, W. D. CHANDLER, and R. Y. MOIR. Can. J. Chem. **49**, 225 (1971).
18. G. MONTAUDO, P. FINOCCHIARO, E. TRIVELLONE, F. BOTTINO, and P. MARAVIGNA. Tetrahedron, **27**, 2125 (1971).
19. G. MONTAUDO, P. FINOCCHIARO, F. BOTTINO, S. CACCAMESE, P. MARVIGNA, and E. TRIVELLONE. Proc. XXIII Int. Cong. Pure and Appl. Chem. Boston, 1971.
20. L. R. MAXWELL, S. B. HENDRICKS and V. M. MOSLEY. J. Chem. Phys. **3**, 699 (1935).
21. K. HIGASI, S. UYEO, and N. YAMAGUCHI. Bull. Inst. Phys. Chem. Res. Tokyo, Chem. Ed. **23**, 506 (1947).
22. J. A. HAMILTON and L. K. STEINRAUF. J. Am. Chem. Soc. **93**, 2939 (1971).
23. J. TOUSSAINT. Bull. Soc. Roy. Sci. Liège, **15**, 86 (1944).
24. J. TOUSSAINT. Mem. Soc. Roy. Sci. Liège. Vol. Hors. Ser. **12**, 1 (1952).
25. J. WRIGHT and E. C. JORGENSEN. J. Org. Chem. **33**, 1245 (1968).
26. D. T. CROMER and J. B. MANN. Acta Cryst. **A24**, 321 (1968).
27. R. F. STEWART, E. R. DAVIDSON, and W. T. SIMPSON. J. Chem. Phys. **42**, 3175 (1965).
28. G. GERMAIN and M. M. WOOLFSON. Acta Cryst. **B24**, 31 (1968).
29. W. R. BUSING, K. O. MARTIN, and H. A. LEVY. ORFLS, Report ORNL-TM-305. Oak Ridge National Laboratory, Oak Ridge Tennessee. 1962.
30. A. ZALKIN. FORDAP, A Fortran program for Fourier calculations. Univ. of California, Berkeley. 1965.
31. C. K. JOHNSON. ORTEP, Report ORNL-3794. Oak Ridge National Laboratory, Oak Ridge, Tennessee. 1965.
32. R. GUTTORMSON and B. E. ROBERTSON. Acta Cryst. In Press.
33. W. R. BUSING and H. A. LEVY. Acta Cryst. **17**, 142 (1964).
34. J. J. BERGMAN and W. D. CHANDLER. Can. J. Chem. **50**, 353 (1972).
35. N. CAMERMAN and A. CAMERMAN. Science, **175**, 764 (1972).

Can. J. Chem. Downloaded from www.nrcresearchpress.com by 210.87.254.6 on 09/05/12
For personal use only.

Conformations of Bridged Diphenyls. II.[1] Crystal Structure of 2-(2′,4′-Dinitrophenoxy)-1,3,5-tri-*t*-butylbenzene

E. A. H. GRIFFITH, W. D. CHANDLER, AND B. E. ROBERTSON[2]

Division of Natural Sciences and Mathematics, University of Saskatchewan, Regina, Saskatchewan

Received May 10, 1972

The structure of 2-(2′,4′-dinitrophenoxy)-1,3,5-tri-*t*-butylbenzene, $C_{24}H_{32}N_2O_5$, has been determined by X-ray diffraction. The crystals are triclinic, $a = 12.160(30)$, $b = 10.564(17)$, $c = 10.684(16)$ Å, $\alpha = 119.23(10)$, $\beta = 96.06(15)$, $\gamma = 96.55(15)°$, $P\bar{1}$ with $Z = 2$. The intensities of 5359 independent reflections were measured on a four circle diffractometer of which 2471 were used in the refinement to give a final least-squares weighted residue of 0.063. The presence of two electron withdrawing groups on one of the phenyl rings increases the conjugation between the ring and the ether oxygen atom to a greater degree than was found in the previous work. The tri-*t*-butyl-substituted ring is nearly orthogonal to the other ring. The bond angle at the ether oxygen atom is less than the value found earlier but ring distortions are similar.

Nous avons déterminé la structure du 2-(2′,4′-dinitrophénoxy)-1,3,5-tri-*t*-butylbenzène, $C_{24}H_{32}N_2O_5$ par diffraction de rayons-X. Les cristaux sont tricliniques: $a = 12.160(30)$, $b = 10.564(17)$, $c = 10.684(16)$ Å, $\alpha = 119.23(10)$, $\beta = 96.06(15)$, $\gamma = 96.55(15)°$, $P\bar{1}$ avec $Z = 2$. Les intensités de 5359 réflexions indépendantes ont été mesurées sur un diffractomètre à quatre cercles; 2471 de ces réflexions ont été utilisées dans le raffinement, ce qui donne un poids moyen de résidu final par moindres carrés de 0.063. La présence de deux groupements attracteurs d'électrons sur un des noyaux phényl augmente la conjugaison entre le cycle et l'atome d'oxygène de type éther de façon plus importante que ce qu'on avait pu croire à la suite des travaux ultérieurs. Le cycle substitué de groupements *t*-butyl est presqu'orthogonal à l'autre cycle. L'angle de liaison à l'atome d'oxygène du groupe éther est moindre que la valeur trouvée précédement, mais les distortions de cycle sont semblables. [Traduit par le journal]

Canadian Journal of Chemistry, **50**, 2972 (1972)

Can. J. Chem. Downloaded from www.nrcresearchpress.com by 210.87.254.42 on 09/05/12
For personal use only.

This is the second in a series of reports which describes n.m.r. and X-ray diffraction studies of bridged diphenyl compounds. A previous paper (1) reported the structure of 2-(3′-methyl-4′-nitrophenoxy)-1,3-diisopropylbenzene, which showed conjugation effects relating to the electron withdrawing character of the ring substituents and steric effects relating to the size of ortho-substituents. The phenyl rings were distorted from hexagonal symmetry and the nitro-substituted ring, which was very nearly coplanar with the central plane containing the ether oxygen atom, was bent away from the other ring. The compound which will be discussed here has even larger ortho substituents which further limit the orientation of the alkyl-substituted ring. In addition, the other ring has two electron withdrawing substituents which should enhance some of the features observed in the previous work as being due to conjugation effects. The substitution of one of the nitro groups in the ortho position could influence the relative orientation of the two aromatic rings.

[1]For Part I, see ref. 1.

[2]To whom correspondence should be addressed.

Experimental

The synthesis of 2-(2′,4′-dinitrophenoxy)-1,3,5-tri-*t*-butylbenzene, $C_{24}H_{32}N_2O_5$, has been reported earlier (2). It was recrystallized from absolute ethanol, m.p. 147–148°.

A sample with well defined faces and approximate dimensions of 0.4 mm on an edge was examined by film techniques. The cell constants and the orientation of the crystal were determined on a Picker FACS-I four circle diffractometer by a least-square fit to the observed settings of 12 reflections with 2θ values between 25 and 30°. The $K\alpha_1$ and $K\alpha_2$ peaks of the Mo radiation were not resolved at these angles. The cell constants are given below with estimated errors calculated as three times the estimated standard deviations obtained from the least-squares analysis. Crystal data are as follows:

$C_{24}H_{32}N_2O_5$ f.w. = 428

Triclinic $P\bar{1}$, $a = 12.160(30)$, $b = 10.564(17)$, $c = 10.684(16)$ Å, $V = 1162$ Å^3, $\alpha = 119.23(10)$, $\beta = 96.06(15)$, $\gamma = 96.55(15)°$, $\rho_o = 1.1$ g cm^{-3} (flotation), $Z = 2$, $\rho_c = 1.2$ g cm^{-3}, $F(000) = 460$ e (21 °C, $\mu(MoK\bar{\alpha}) = 0.91$ cm^{-1}, $\lambda(MoK\bar{\alpha}) = 0.71069$ Å).

The integrated intensities of 5359 independent reflections with 2θ values between 3.5 and 55° were collected with MoKα radiation using a graphite monochromator. The θ, 2θ scan mode was used with a 2° min^{-1} scan rate, a base width of 3.0° and 20 s background counts at each limit of the scan. Although only a small fraction of the reflections collected at 2θ angles greater than 45° were significantly above the background rate of *ca.* 3 counts/s, data were collected to 55° in 2θ in order to obtain adequate accuracy

Can. J. Chem. Downloaded from www.nrcresearchpress.com by 210.87.254.42 on 09/05/12
For personal use only.

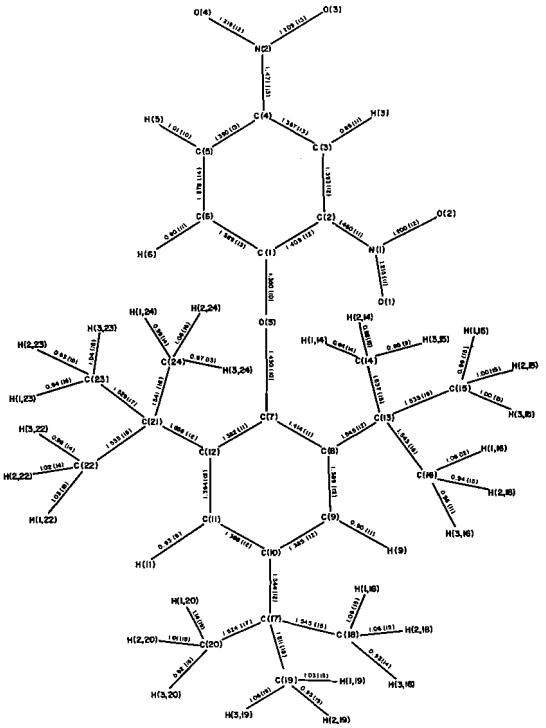

FIG. 1. Bond lengths and atom labelling sequence. Numbers in parentheses are estimated errors.

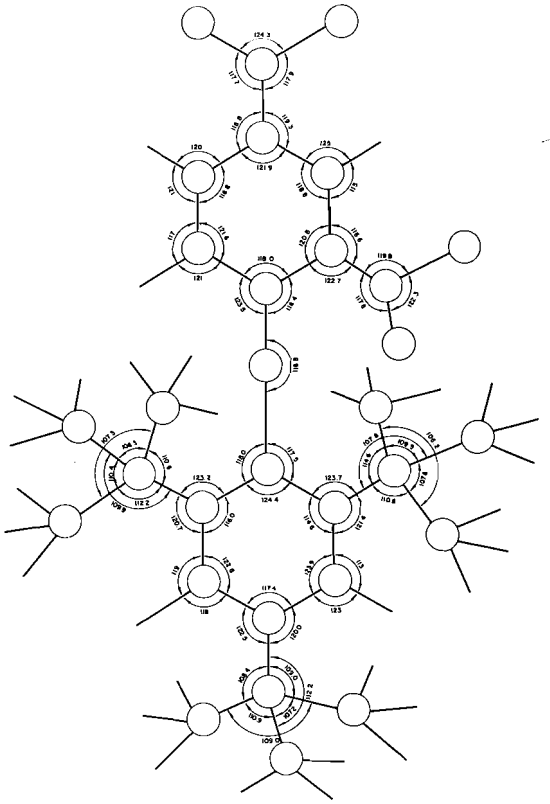

FIG. 2. Bond angles. The estimated errors of the angles not involving hydrogen atoms are *ca.* 1.2°. The estimated errors of the angles involving hydrogen atoms are *ca.* 10°.

in the molecular parameters for comparison of the geometry of this compound with that of related compounds. The intensities of three standard reflections were measured after every 100 reflections and were not found to vary significantly. The data were reduced to observed structure factors using standard procedures. The standard deviation $\sigma(F)$ was calculated as $1.0 + 0.10\,|F| + \sigma'$ where σ' is the error associated with the statistics of the integrated peak counts and the background counts. A Wilson statistical calculation gave an overall temperature factor of 3.6 Å^2. No corrections were made for absorption or extinction effects. The scattering factors for the carbon, oxygen, and nitrogen atoms were taken from those given by Cromer and Mann (3). The scattering factors for the hydrogen atoms were taken from Stewart *et al.* (4). The average values of $|E|$ and $|E^2 - 1|$ were 0.756 and 1.021 indicating the centrosymmetric space group $P\bar{1}$. The 397 reflections with $|E| > 1.8$ were used in the multiple solution, logical symbolic addition method programs of Germain and Woolfson (5). The E map calculated with the solution with the second highest figure of merit yielded 29 of the 31 non-hydrogen atoms. The program FORDAP written by Zalkin (6) was used for all Fourier calculations. Subsequent isotropic least-squares and Fourier calculations using 1623 low angle reflections revealed all non-hydrogen atoms and reduced the least-squares residue, R_w to 0.156, assuming unit weights. The full-matrix Busing *et al.* program ORFLS (7) was used for least-squares calculations. Refinement using anisotropic temperature factors lowered R_w to 0.120. The hydrogen atoms were found by different Fourier calculations and R_w was lowered to 0.070. The 2471 reflections for which $|F_o|/\sigma > 1.0$ were used in the final cycles of refinement with the least-square weights now calculated from

$$w^{-1/2} = 0.47597 - 0.01746|F_o| + 0.00124|F_o|^2$$

The final values of R_w and the conventional R factor were 0.063 and 0.053, respectively.

The observed and calculated structure factors have been placed in the Depository for Unpublished Data.[3] The final positional and thermal parameters are listed in Table 1. The estimated errors are calculated as three times the estimated standard deviations from the least-squares analysis. The U_{ij} in Table 1 are the coefficients in the expression

$$\exp[-2\pi^2(h^2a^{*2}U_{11} + \ldots + 2hka^*b^*U_{12} + \ldots)]$$

The bond lengths and angles and the atom numbering sequence are given in Figs. 1 and 2.

[3]Complete set of tabular data is available, at a nominal charge, from the Depository of Unpublished Data, National Science Library, National Research Council of Canada, Ottawa, Canada K1A 0S2.

Can. J. Chem. Downloaded from www.nrcresearchpress.com by 210.87.254.42 on 09/05/12
For personal use only.

TABLE 1. Structural parameters of 2-(2′,4′-dinitrophenoxy)-1,3,5-tri-*t*-butylbenzene (see text for description of errors)

(*a*) Fractional atomic coordinates ($\times 10^4$)

Atom	*x*	*y*	*z*
C(1)	2236(7)	2840(8)	5149(8)
C(2)	2353(7)	2007(8)	3680(8)
C(3)	1506(8)	1757(9)	2555(9)
C(4)	565(7)	2353(9)	2900(9)
C(5)	405(8)	3136(9)	4334(9)
C(6)	1241(8)	3364(9)	5437(9)
C(7)	2939(7)	3919(8)	7676(7)
C(8)	3248(7)	5475(8)	8402(8)
C(9)	2962(8)	6213(9)	9773(7)
C(10)	2454(7)	5509(8)	427(8)
C(11)	2291(7)	3978(9)	9700(8)
C(12)	2547(7)	3139(8)	8318(8)
C(13)	3958(7)	6309(9)	7818(9)
C(14)	3391(11)	6121(13)	6366(11)
C(15)	5079(10)	5763(14)	7637(16)
C(16)	4226(11)	7986(10)	8920(12)
C(17)	2136(8)	6428(9)	1938(8)
C(18)	3201(12)	7510(14)	3031(11)
C(19)	1690(18)	5474(16)	2531(14)
C(20)	1272(14)	7313(18)	1803(14)
C(21)	2456(8)	1440(8)	7616(9)
C(22)	1485(12)	572(12)	6300(13)
C(23)	3572(11)	1013(14)	7172(14)
C(24)	2242(14)	957(12)	8731(13)
N(1)	3346(7)	1363(8)	3250(7)
N(2)	−301(7)	2177(9)	1727(9)
O(1)	3285(7)	437(9)	1976(7)
O(2)	4197(7)	1792(11)	4136(8)
O(3)	−1117(7)	2734(11)	2065(9)
O(4)	−131(7)	1519(9)	481(8)
O(5)	3099(5)	3099(6)	6200(5)

(*b*) Fractional atomic coordinates ($\times 10^3$)

Atom	*x*	*y*	*z*	*B*(Å^2)
H(3)	164(8)	122(10)	167(11)	4(2)
H(5)	−32(8)	351(9)	456(9)	4(2)
H(6)	111(7)	384(9)	635(10)	4(2)
H(9)	316(8)	720(11)	21(11)	4(2)
H(11)	195(6)	349(7)	13(7)	2(1)
H(1,14)	264(10)	622(13)	637(13)	7(3)
H(2,14)	340(10)	514(15)	554(14)	7(3)
H(3,14)	385(9)	678(9)	618(8)	3(2)
H(1,15)	490(10)	469(15)	693(14)	7(3)
H(2,15)	547(11)	595(13)	860(14)	7(3)
H(3,15)	563(10)	633(13)	737(12)	6(3)
H(1,16)	348(10)	842(12)	908(11)	6(3)
H(2,16)	458(10)	819(13)	984(13)	7(3)
H(3,16)	474(8)	844(11)	857(10)	5(2)
H(1,18)	356(11)	822(14)	268(14)	8(3)
H(2,18)	384(12)	695(16)	315(14)	9(4)
H(3,18)	302(10)	803(13)	395(13)	7(3)
H(1,19)	227(12)	485(16)	259(14)	9(4)
H(2,19)	150(10)	605(14)	345(14)	7(3)
H(3,19)	88(14)	493(18)	187(17)	10(5)

TABLE 1 (*Concluded*)

(*b*) Fractional atomic coordinates ($\times 10^3$)

Atom	*x*	*y*	*z*	B(Å^2)
H(1,20)	56(14)	631(19)	129(17)	11(5)
H(2,20)	164(11)	799(14)	149(14)	8(4)
H(3,20)	107(11)	787(15)	269(15)	8(3)
H(1,22)	73(11)	83(14)	663(14)	8(3)
H(2,22)	166(9)	73(12)	547(13)	6(3)
H(3,22)	136(10)	−47(15)	603(13)	7(3)
H(1,23)	358(11)	2(7)	689(15)	9(4)
H(2,23)	328(10)	119(13)	647(14)	7(3)
H(3,23)	425(11)	168(14)	801(14)	8(3)
H(1,24)	146(11)	103(13)	890(13)	7(3)
H(2,24)	288(11)	157(14)	968(15)	7(3)
H(3,24)	229(9)	−7(13)	831(12)	6(3)

(*c*) Thermal parameters U_{ij} ($\times 10^3$)

Atom	U_{11}	U_{22}	U_{33}	U_{12}	U_{13}	U_{23}
C(1)	46(5)	32(4)	26(4)	8(3)	6(3)	11(3)
C(2)	49(5)	34(4)	29(4)	10(4)	9(3)	13(3)
C(3)	59(6)	36(4)	27(4)	8(4)	7(4)	12(3)
C(4)	50(5)	38(4)	39(4)	4(4)	−2(4)	20(4)
C(5)	44(5)	48(5)	47(5)	10(4)	8(4)	21(4)
C(6)	52(5)	45(5)	31(4)	12(4)	12(4)	11(4)
C(7)	48(5)	37(4)	21(3)	14(4)	5(4)	9(2)
C(8)	46(5)	35(4)	30(4)	12(3)	4(3)	15(3)
C(9)	56(5)	32(4)	31(4)	13(4)	6(4)	10(3)
C(10)	57(5)	36(4)	29(4)	15(4)	6(3)	12(3)
C(11)	55(5)	37(4)	31(4)	8(4)	9(4)	16(3)
C(12)	48(5)	33(4)	28(4)	10(3)	3(3)	12(3)
C(13)	48(5)	38(4)	41(4)	9(4)	8(4)	19(3)
C(14)	72(8)	59(6)	46(5)	1(6)	8(5)	32(5)
C(15)	58(7)	59(7)	84(8)	16(5)	20(6)	36(6)
C(16)	71(7)	39(5)	52(6)	3(5)	12(5)	19(4)
C(17)	76(7)	42(5)	29(4)	21(4)	17(4)	12(4)
C(18)	98(10)	68(7)	35(5)	25(7)	8(5)	6(5)
C(19)	165(17)	76(8)	50(7)	34(10)	60(9)	29(6)
C(20)	104(11)	88(9)	60(7)	52(9)	37(7)	30(7)
C(21)	64(6)	29(4)	36(4)	9(4)	7(4)	12(3)
C(22)	86(9)	38(6)	57(6)	−4(5)	−4(6)	14(5)
C(23)	88(9)	52(6)	65(7)	36(6)	26(7)	29(6)
C(24)	108(11)	40(6)	62(7)	18(6)	26(7)	28(5)
N(1)	58(5)	48(4)	35(4)	19(4)	16(4)	17(3)
N(2)	62(6)	56(5)	49(5)	8(5)	−5(4)	24(4)
O(1)	93(6)	87(5)	45(4)	41(5)	22(4)	2(4)
O(2)	67(5)	140(4)	49(4)	51(5)	13(4)	22(5)
O(3)	69(5)	123(7)	80(6)	39(5)	2(4)	52(5)
O(4)	102(6)	98(6)	42(4)	32(5)	−7(4)	28(4)
O(5)	49(3)	39(3)	25(2)	15(2)	7(2)	9(2)

Discussion

All of the hydrogen atoms appear to be in reasonable positions. The bonds to hydrogen atoms range in length from 0.88(11) to 1.14(18) Å and the isotropic hydrogen temperature factors, B range from 2 to 11 Å^2. A stereoscopic view of the packing of the molecules is shown in Fig. 3. This drawing was prepared with the program ORTEP, written by Johnson (8). Each molecule is involved in 20 intermolecular contacts less than 2.8 Å in length. Of these, 16 are between hydrogen atoms, and the other four are

Can. J. Chem. Downloaded from www.nrcresearchpress.com by 210.87.254.42 on 09/05/12
For personal use only.

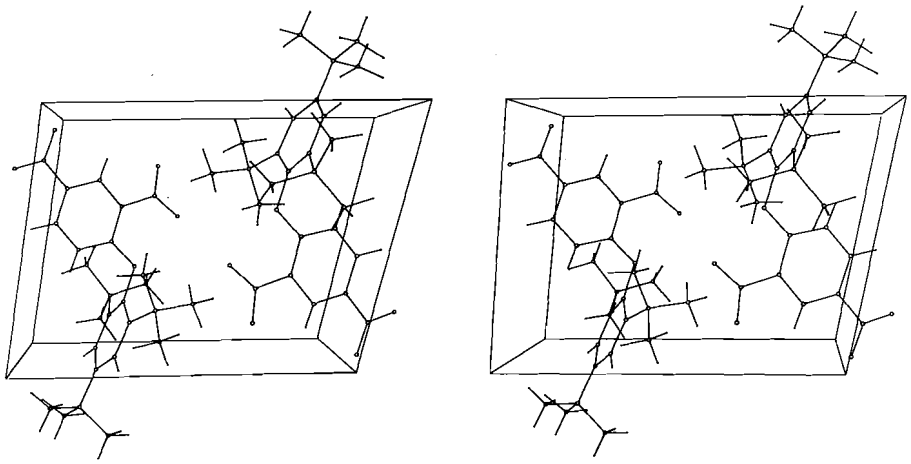

FIG. 3. Sterescopic view of the molecular packing. The origin of the unit cell is in the upper left rear corner. The ***a*** axis points to the left, the ***b*** axis points forward, and the ***c*** axis points down.

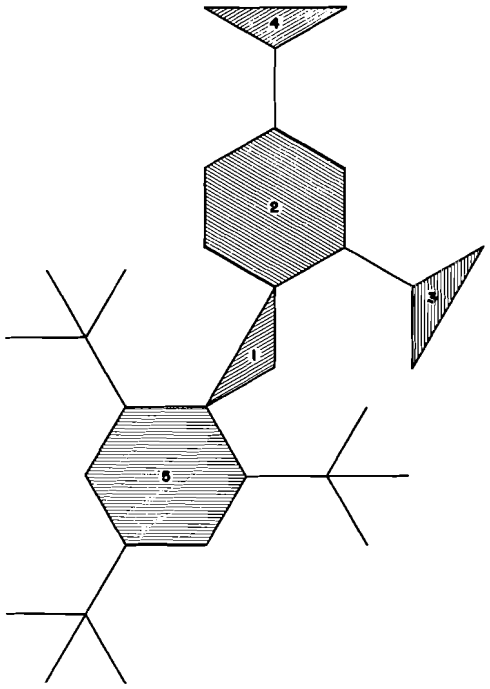

FIG. 4. Labelling sequence of the least-square planes.

between hydrogen atoms and nitro oxygen atoms. The shortest H—H contact is the 2.42 Å distance between H(15,2) and H(18,2). The shortest H—O contact is the 2.60 Å distance between H(14,1) and O(3).

The interplanar angles as labelled in Fig. 4 are given in Table 2. The plane of the para-substituted nitro group is rotated 5.2° from that of the ring to which it is bonded. This rotation is within the range observed for nitrobenzenes substituted in the para position (9). The ortho-substituted nitro group is rotated by 15.8° which is slightly outside the range. A comparison may be made with the ortho nitro group of picric acid which is not hydrogen bonded to the adjacent hydroxy group. The plane of this nitro group has been observed to be rotated 16.5° from the plane of the phenyl ring (14). The twist

TABLE 2. Least-squares planes

(*a*) Coefficients of planes $Ax + By + Cz = D^*$

Plane	*A*	*B*	*C*	*D*
1	−0.3750	−0.9260	−0.0432	0.8857
2	−0.4247	−0.9037	−0.0537	1.0052
3	−0.3213	0.9254	−0.2009	0.1468
4	−0.4746	−0.8716	−0.1228	1.1325
5	−0.8551	0.3192	−0.4087	4.9081

*Coordinates refer to the directions of the ***a***, $c^* \times a$, and c^* axes.

(*b*) Dihedral angles between planes

Planes	Angle (deg)
1,2	3.2
2,3	15.8
2,4	5.2
1,5	87.5
2,5	84.4

Can. J. Chem. Downloaded from www.nrcresearchpress.com by 210.87.254.42 on 09/05/12
For personal use only.

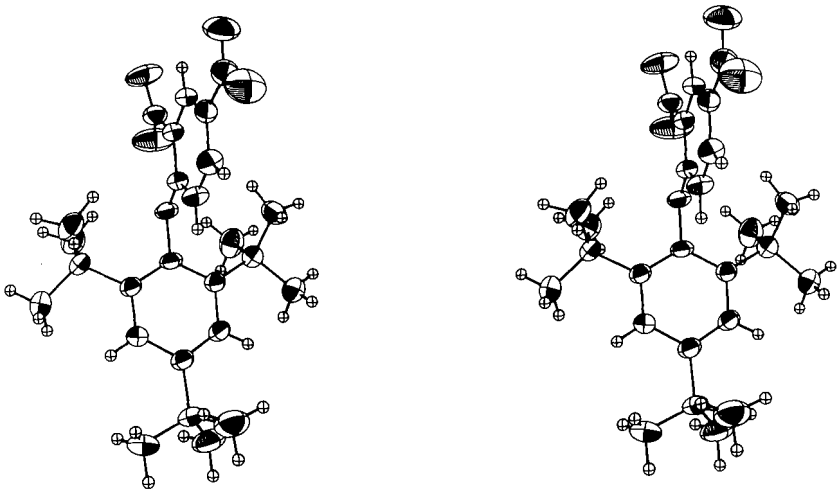

FIG. 5. Sterescopic view of the molecule. The thermal ellipsoids are scaled to include 50% probability.

observed here allows the nitro oxygen atom nearest the ether oxygen atom to be rotated away from the latter. The ortho nitro group is also bent slightly away from the ether oxygen atom at the ring carbon atom C(2) to which it is bonded. The angle between the dinitro-substituted phenyl ring and the plane formed by the ether oxygen atom and the two aromatic carbon atoms bonded to it is 3.2°. Also the C(1)—O(5) bond length is 0.080(18) Å shorter than the O(5)—C(7) bond length. This difference is approximately twice the value found for 2-(3′-methyl-4′-nitrophenoxy)-1,3-diisopropylbenzene (1), reflecting the presence of two electron withdrawing nitro groups on the phenyl ring. This indicates enhancement of the conjugation effect between the π electrons on the ring and the unshared electrons on the ether oxygen atoms, beyond the degree of conjugation which occurs in the presence of one electron withdrawing group. The plane of the tri-*t*-butyl-substituted ring is within 3° of being perpendicular to plane 1, as opposed to *ca.* 12° in the previous study (1). The twist of this ring from orthogonality with plane 1 and the dinitro-substituted ring is limited by the greater bulkiness of the *t*-butyl groups over the isopropyl groups.

The internal ring angles of the tri-*t*-butyl-substituted ring at the three carbon atoms bonded to the *t*-butyl groups are decreased by 2.6 to 5.4° from the 120° expected in a hexagonal ring. This effect was also observed in 2-(3′-methyl-4′-nitrophenoxy)-1,3-diisopropylbenzene and serves to increase the distance between the substituents and the rest of the molecule. The entire dinitro-substituted ring is bent away from the tri-*t*-butyl-substituted ring by a 2.5° twist at atom C(1), similar to the result found in the previous study. However, the bond angle subtended at the ether oxygen atom is smaller than the value found previously. The net result is to bring H(6) closer to the π-electron cloud of the other ring than was the case for the ether of the previous paper. This partly explains the as-yet-unpublished result that the n.m.r. chemical shift of H(6) is far *smaller* than expected. A stereoscopic view of the molecule is shown in Fig. 5.

The bond lengths C(2)—N(1) and C(4)—N(2) to the nitro groups are consistent with the value found earlier and the values reported for nitrobenzenes substituted at the para position with electron donating groups. The terminal bonds to oxygen and carbon atoms are significantly affected by thermal motion. Corrections to these bond lengths assuming "riding motion" (10) are given in Table 3. If these corrections are assumed, all bond lengths in the molecule fall within the range of accepted values. The general conformation of the molecule is essentially the same as that of 2-(3′-methyl-4′-nitrophenoxy)-1,3-diisopropylbenzene, and is the H-inside conformation inferred from solution n.m.r. spectra for similar, triply ortho-substituted diphenyl

Can. J. Chem. Downloaded from www.nrcresearchpress.com by 210.87.254.42 on 09/05/12
For personal use only.

TABLE 3. Thermal corrections to terminal bond lengths

Bond	Bond length (Å)	
	Uncorrected	Corrected
N(1)—O(1)	1.215	1.262
N(1)—O(2)	1.200	1.257
N(2)—O(3)	1.209	1.251
N(2)—O(4)	1.218	1.252
C(13)—C(14)	1.537	1.550
C(13)—C(15)	1.535	1.555
C(13)—C(16)	1.543	1.556
C(16)—C(18)	1.545	1.567
C(17)—C(19)	1.511	1.551
C(17)—C(20)	1.524	1.551
C(21)—C(22)	1.535	1.555
C(21)—C(23)	1.529	1.547
C(21)—C(24)	1.541	1.561

ethers (11–13). The combined steric and electronic factors force the small H(6) atom into the "inside-position" in both the crystal and liquid phases.

The authors gratefully acknowledge the support of the National Research Council of Canada in the form of research grants.

1. E. A. H. GRIFFITH, W. D. CHANDLER, and B. E. ROBERTSON. Can. J. Chem. This issue.
2. W. D. CHANDLER, J. J. BERGMAN, and G. H. HASS. Can. J. Chem. **49**, 583 (1971).
3. D. T. CROMER and J. B. MANN. Acta Cryst. **A24**, 321 (1968).
4. R. F. STEWART, E. R. DAVIDSON, and W. T. SIMPSON. J. Chem. Phys. **42**, 3175 (1965).
5. G. GERMAIN and M. M. WOOLFSON. Acta Cryst. **B24**, 91 (1968).
6. A. ZALKIN. FORDAP, A Fortran program for Fourier calculations. University of California, Berkeley. 1965.
7. W. R. BUSING, K. O. MARTIN, and H. A. LEVY. ORFLS, Report ORNL-TM-305. Oak Ridge National Laboratory, Oak Ridge, Tennessee. 1962.
8. C. K. JOHNSON. ORTEP, Report ORNL-3794. Oak Ridge National Laboratory, Oak Ridge, Tennessee. 1965.
9. R. GUTTORMSON and B. E. ROBERTSON. Acta Cryst. In Press.
10. W. R. BUSING and H. A. LEVY. Acta Cryst. **17**, 142 (1964).
11. W. D. CHANDLER, W. MAE, F. SMITH, and R. Y. MOIR. Can. J. Chem. **42**, 2549 (1964).
12. J. J. BERGMAN, W. D. CHANDLER, and R. Y. MOIR. Can. J. Chem. **49**, 225 (1971).
13. J. J. BERGMAN and W. D. CHANDLER. Can. J. Chem. **50**, 353 (1972).
14. E. CARSTENSEN-OESER, S. GÖTTLICHER, and G. HABERMEHL. Chem. Ber. **101**, 1648 (1968).

Can. J. Chem. Downloaded from www.nrcresearchpress.com by 210.87.254.42 on 09/05/12
For personal use only.

Conformations of Bridged Diphenyls. III.[1] Crystal Structure of 2-(2′-Carbomethoxy-4′-nitrophenoxy)-1,3,5-trichlorobenzene

E. A. H. GRIFFITH, W. D. CHANDLER, AND B. E. ROBERTSON[2]

Division of Natural Sciences and Mathematics, University of Saskatchewan, Regina, Saskatchewan

Received May 24, 1972

The structure of 2-(2′-carbomethoxy-4′-nitrophenoxy)-1,3,5-trichlorobenzene, $C_{14}H_8NO_5Cl_3$, has been determined by X-ray diffraction. The crystals are triclinic, $a = 8.862(10)$, $b = 15.164(10)$, $c = 13.028(14)$ Å, $\alpha = 90.35(8)$, $\beta = 116.28(8)$, $\gamma = 97.54(8)°$, $P\bar{1}$ with $Z = 4$. The intensities of 6417 independent reflections were measured on a four circle diffractometer of which 4526 were used in the refinement to give a final least-squares residue of 0.047. The two independent molecules in the unit cell show a similar conformation to that found in earlier studies of diphenyl ethers, and the conformation appears to be determined partly by steric effects, since conjugation between the nitro-substituted ring and the ether oxygen atoms is less pronounced than found previously.

Nous avons déterminé la structure du 2-(2′-carbométhoxy-4′-nitrophénoxy)-1,3,5-trichlorobenzène, $C_{14}H_8NO_5Cl_3$ par diffraction de rayons-X. Les cristaux sont tricliniques: $a = 8.862(10)$, $b = 15.164(10)$, $c = 13.028(14)$ Å, $\alpha = 90.35(8)$, $\beta = 116.28(8)$, $\gamma = 97.54(8)°$, $P\bar{1}$ avec $Z = 4$. Les intensités de 6417 réflexions indépendantes ont été mesurées sur un diffractomètre à quatre cercles; 4526 de ces réflexions ont été utilisées dans le raffinement pour donner un résidu final par moindres carrés de 0.047. Les deux molécules indépendantes dans la maille possèdent des conformations semblables à celles trouvées au cours d'études ultérieures de diphényl éthers et la conformation semble partiellement déterminée par des effets stériques, puisque la conjugaison entre le cycle substitué par un groupe nitro et l'atome d'oxygène du groupe éther est moins prononcée que ce qu'on avait découvert précédemment. [Traduit par le journal]

Canadian Journal of Chemistry, **50**, 2979 (1972)

Previous reports in this series have described the structures and conformations of doubly and triply ortho-substituted diphenyl ethers with electron withdrawing substituents on one aromatic ring and large electron donating alkyl groups on the other (1, 2). The compound whose structure is reported here differs from the former in that the ortho alkyl groups of one ring have been replaced by halogen atoms which are both smaller and electron withdrawing. The conformation of the trichloro-substituted ring might be expected to be less sterically restricted than was found in the previous work because the substituents in the ortho position are less bulky.

The lengths of the bonds to the ether oxygen atom and the bond angle at that atom might also differ from the previous results because of the presence of electron withdrawing groups on both rings. Toussaint (3) has reported unusually short C—O bond lengths in 4,4-dibromodiphenyl ether. Compounds similar to 2-(2′-carbomethoxy-4′-nitrophenoxy)-1,3,5-trichlorobenzene have been used extensively in previous studies of the effects of ring currents on aromatic hydrogen atoms using n.m.r. techniques (4).

[1]For Parts I and II, see refs. 1 and 2.

[2]To whom correspondence should be addressed.

Experimental

The synthesis of 2-(2′-carbomethoxy-4′-nitrophenoxy)-1,3,5-trichlorobenzene, $C_{14}H_8NO_5Cl_3$, has been reported earlier (5). It was recrystallized from 95% ethanol, m.p. 137–138°. A sample with length 0.8 mm and nearly rectangular cross section 0.5 × 0.6 mm was used for data collection. The cell constants and the orientation of the crystal were determined on a Picker FACS-I four circle diffractometer by a least-squares fit to the observed settings of 12 reflections with 2θ values between 38 and 41°, where the Mo $K\alpha_1$ and $K\alpha_2$ diffraction peaks were well resolved. The cell constants are given below with estimated errors calculated as three times the estimated standard deviations obtained from the least-squares analysis. The crystal was oriented with the $(\bar{1}10)$ diffraction vector nearly colinear with the *phi* rotation axis of the diffractometer. Crystal data are as follows:

$C_{14}H_8NO_5Cl_3$ f.w. = 376.5

Triclinic $P\bar{1}$, $a = 8.862(10)$, $b = 15.164(10)$, $c = 13.028(14)$ Å, $V = 1552$ Å^3, $\alpha = 90.35(8)$, $\beta = 116.28(8)$, $\gamma = 97.54(8)°$, $\rho_o = 1.58$ g cm^{-3} (flotation), $Z = 4$, $\rho_c = 1.61$ g cm^{-3}, $F(000) = 760$ e (20 °C, $\mu(\text{MoK}\bar{\alpha}) = 6.27$ cm^{-1}, $\lambda(\text{MoK}\bar{\alpha}_1) = 0.70926$ Å).

The integrated intensities of 6417 independent reflections with 2θ values between 3.5 and 55° were collected with MoKα radiation using a graphite monochromator. The θ–2θ scan mode was used with a 2° min^{-1} scan rate, a base width of 3.4° and 20 s background counts at each limit of the scan. The intensities of three standard reflections were checked after each group of 100 reflections had been measured. The average intensity of the standards increased to approximately 103% of their initial values over the period

Can. J. Chem. Downloaded from www.nrcresearchpress.com by 210.87.254.6 on 09/05/12
For personal use only.

Can. J. Chem. Downloaded from www.nrcresearchpress.com by 210.87.254.6 on 09/05/12
For personal use only.

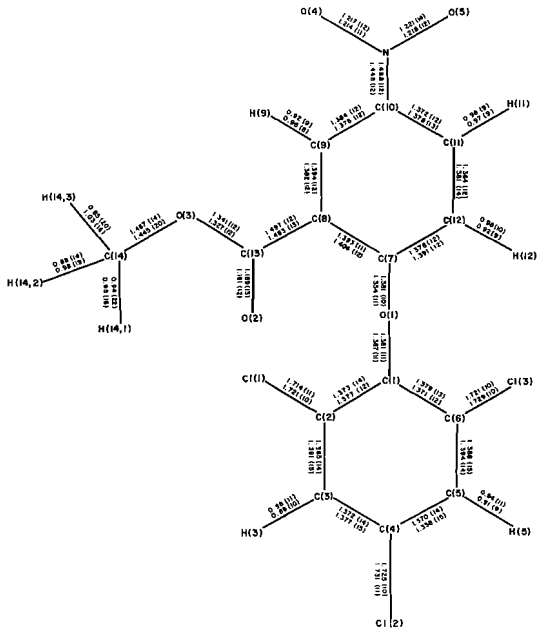

FIG. 1. Bond lengths and atom sequence. The bond length nearest the line refers to molecule 2. The numbers in parentheses are estimated errors.

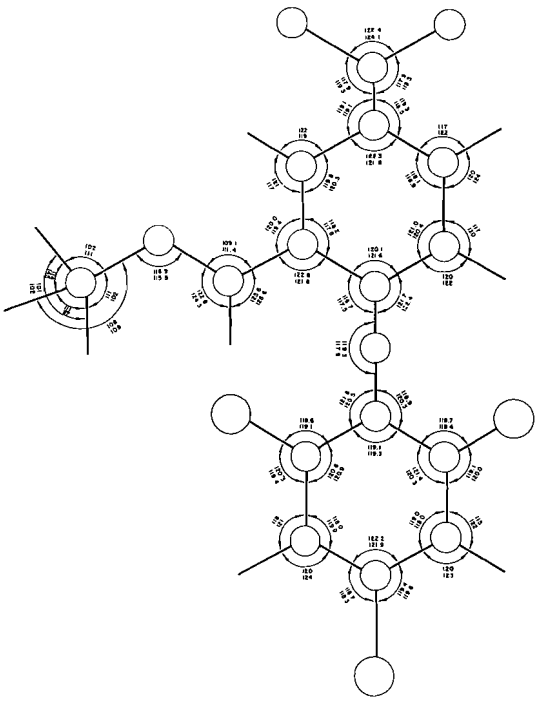

FIG. 2. Bond angles. The angle nearest the atom refers to molecule 2. The estimated errors in the angles not involving hydrogen atoms are *ca.* 1.3° and the estimated errors in the angles involving hydrogen atoms are *ca.* 10°.

in which the data were collected. The data were scaled to the initial intensities using linear interpolations between each set of standards.

The data were reduced to observed structure factors using standard procedures. The standard deviation $\sigma(F)$ was calculated as $1.0 + 0.10|F| + \sigma'$ where σ' is based on counting statistics. A Wilson statistical calculation gave an overall temperature factor of 4.5 Å^2. No corrections were made for absorption or extinction effects. The scattering factors for the carbon, oxygen, nitrogen, and chlorine atoms were taken from the series coefficients given by Cromer and Mann (6). The scattering factors for the hydrogen atoms were taken from Stewart *et al.* (7). The average values of $|E|$ and $|E^2 - 1|$ were determined to be 0.767 and 1.025 indicating the centrosymmetric space group $P\bar{1}$. The 463 reflections with $|E| > 1.85$ were used in the multiple solution, logical symbolic addition method programs of Germain and Woolfson (8). The solution with the third highest figure of merit gave the first non-trivial E map, showing the positions of 42 of the 46 non-hydrogen atoms. The E map and all other Fourier maps were prepared with the program FORDAP, written by Zalkin (9). An electron density Fourier map using phases calculated with the 42 atoms revealed the positions of the remaining 4 non-hydrogen atoms. Full matrix least-squares refinement with unit weights and individual isotropic temperature factors reduced the weighted residue R_w to 0.169. The program ORFLS (10) was used for least-squares refinement. A difference map calculated at this point revealed 7 of the 16 hydrogen atoms. The temperature factors of the non-hydrogen atoms were then refined anisotropically, lowering R_w to 0.106. Further cycles of difference Fourier and least-squares calculations revealed the remaining hydrogen atoms. Only 2270 low angle reflections were used up to this point and now all 4526 reflections for which $|F|/\sigma > 1.03$ were used in the refinement. The least-squares weights, w, were calculated from

$$w^{-1/2} = 1.0948 - 0.07368|F| + 0.00173|F|^2$$

The final values of R_w and the conventional R factor were 0.047 and 0.052, respectively.

The observed and calculated structure factors have been placed in the Depository for Unpublished Data.[3] The final positional and thermal parameters are listed in Table 1. The estimated errors are calculated as three times the estimated standard deviations from the least-squares analysis. The U_{ij} in Table 1 are the coefficients in the expression

$$\exp[-2\pi^2(h^2a^{*2}U_{11} + \ldots + 2hka^*b^*U_{12} + \ldots)]$$

The bond lengths, bond angles, and the atom numbering sequence used for both of the independent molecules in the asymmetric unit of the structure are given in Figs. 1 and 2.

Discussion

All of the hydrogen atoms appear to be well behaved with the bond lengths to hydrogen

[3]Complete set of tabular data is available, at a nominal charge, from the Depository of Unpublished Data, National Science Library, National Research Council of Canada, Ottawa, Canada K1A 0S2.

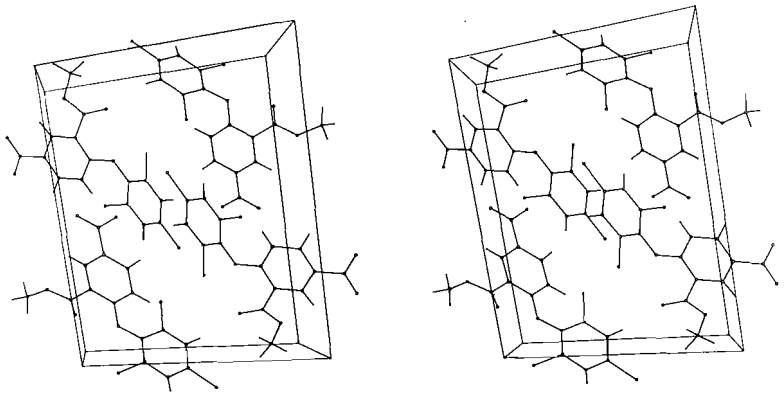

FIG. 3. Stereoscopic view of the molecular packing. The origin is in the lower left front corner. The ***a*** axis points back into the page, the ***b*** axis points up, and the ***c*** axis points to the right. Molecule 1 is nearer the origin.

atoms ranging from 0.85(20) to 1.03(16) Å, and the hydrogen atom temperature factors, B, ranging from 3 to 15 Å^2. A stereoscopic view of the packing of the molecules is shown in Fig. 3. Stereoscopic drawings were prepared with the aid of the program ORTEP (11). Molecule 1 is involved in a total of 6 intermolecular contacts less than 2.8 Å in length, and molecule 2 is involved in 10 such contacts. For each molecule, three of the contacts shorter than 2.8 Å involve

TABLE 1. Structural parameters of 2-(2′-carbomethoxy-4′-nitrophenoxy)-1,3,5-trichlorobenzene (see text for description of errors)

(*a*) Fractional atomic coordinates ($\times 10^4$)

Atom	x	y	z
Molecule 1			
C(1)	851(12)	822(5)	2794(7)
C(2)	2361(12)	1022(6)	3773(8)
C(3)	2801(14)	464(7)	4672(8)
C(4)	1664(13)	−285(6)	4561(8)
C(5)	135(15)	−480(6)	3620(9)
C(6)	−291(12)	89(6)	2736(7)
C(7)	−13(11)	2110(5)	1809(7)
C(8)	−158(10)	2623(5)	884(6)
C(9)	−698(10)	3442(5)	841(7)
C(10)	−1083(10)	3740(5)	1691(7)
C(11)	−967(11)	3233(6)	2585(7)
C(12)	−451(11)	2419(5)	2634(7)
C(13)	247(11)	2302(5)	−42(7)
C(14)	−229(19)	2510(9)	−1962(9)
Cl(1)	3753(4)	1955(2)	3872(3)
Cl(2)	2243(4)	−1007(2)	5649(3)
Cl(3)	−2234(4)	−132(2)	1546(2)
O(1)	495(9)	1303(4)	1832(5)
O(2)	1107(11)	1752(5)	22(6)
O(3)	−558(9)	2728(4)	−988(5)
O(4)	−1748(11)	5051(5)	833(6)
O(5)	−1913(14)	4869(6)	2407(8)
N	−1600(11)	4612(5)	1642(7)
Molecule 2			
C(1)	4424(11)	3813(5)	6721(7)
C(2)	5536(9)	4593(6)	6927(7)
C(3)	4982(13)	5338(6)	6346(8)

Can. J. Chem. Downloaded from www.nrcresearchpress.com by 210.87.254.6 on 09/05/12
For personal use only.

Can. J. Chem. Downloaded from www.nrcresearchpress.com by 210.87.254.6 on 09/05/12
For personal use only.

TABLE 1 (*Continued*)

(*a*) Fractional atomic coordinates ($\times 10^4$)

Atom	x	y	z
C(4)	3309(13)	5287(6)	5554(7)
C(5)	2174(13)	4520(6)	5321(8)
C(6)	2764(11)	3779(5)	5916(7)
C(7)	4902(10)	2928(5)	8295(6)
C(8)	5382(10)	2139(5)	8799(6)
C(9)	5375(10)	2006(5)	9855(7)
C(10)	4879(10)	2640(5)	353(7)
C(11)	4371(12)	3412(6)	9842(8)
C(12)	4397(9)	3552(6)	8803(7)
C(13)	5845(11)	1435(5)	8245(8)
C(14)	7240(24)	165(9)	8568(14)
Cl(1)	7615(3)	4639(2)	7948(2)
Cl(2)	2617(4)	6228(2)	4865(3)
Cl(3)	1344(3)	2814(2)	5682(2)
O(1)	4989(8)	3062(4)	7273(5)
O(2)	5502(6)	1354(5)	7254(6)
O(3)	6743(8)	896(4)	9003(5)
O(4)	5407(10)	1828(5)	1932(6)
O(5)	4514(13)	3082(5)	1914(7)
N	4934(10)	2505(5)	1483(6)

(*b*) Fractional atomic coordinates ($\times 10^3$)

Atom	x	y	z	B (Å^2)
Molecule 1				
H(3)	393(13)	62(6)	534(9)	4(2)
H(5)	−79(13)	−88(7)	361(9)	5(3)
H(9)	−79(10)	377(5)	23(7)	3(2)
H(11)	−140(11)	346(5)	310(7)	4(2)
H(12)	−37(12)	207(6)	328(8)	5(2)
H(14,1)	−137(19)	246(16)	261(9)	9(4)
H(14,2)	−33(16)	193(8)	−207(11)	9(3)
H(14,3)	25(22)	301(12)	−204(15)	15(5)
Molecule 2				
H(3)	570(10)	583(6)	646(8)	5(2)
H(5)	108(11)	450(6)	477(7)	4(2)
H(9)	580(9)	150(5)	27(6)	3(2)
H(11)	406(10)	386(5)	21(7)	3(2)
H(12)	405(11)	406(6)	843(7)	3(2)
H(14,1)	783(25)	37(12)	815(17)	14(6)
H(14,2)	793(21)	−16(11)	922(14)	11(6)
H(14,3)	619(18)	−22(9)	794(12)	8(4)

(*c*) Thermal parameters U_{ij} ($\times 10^3$)

Atom	U_{11}	U_{22}	U_{33}	U_{12}	U_{13}	U_{23}
Molecule 1						
C(1)	67(6)	34(4)	39(5)	18(4)	31(5)	10(4)
C(2)	53(6)	42(5)	54(6)	13(4)	32(5)	8(4)
C(3)	60(7)	58(6)	44(5)	17(5)	23(5)	13(4)
C(4)	68(7)	48(5)	52(5)	27(5)	34(5)	21(4)
C(5)	74(8)	37(5)	59(6)	8(5)	36(6)	12(4)
C(6)	63(6)	38(5)	42(5)	14(4)	23(5)	3(4)
C(7)	43(5)	34(4)	36(4)	9(4)	16(4)	3(3)
C(8)	34(4)	35(4)	32(4)	5(3)	14(3)	3(3)
C(9)	36(4)	38(4)	40(4)	9(3)	15(4)	8(3)

TABLE 1 (*Concluded*)
(*c*) Thermal parameters U_{ij} ($\times 10^3$)

Atom	U_{11}	U_{22}	U_{33}	U_{12}	U_{13}	U_{23}
C(10)	38(5)	35(4)	44(5)	11(4)	12(4)	−1(4)
C(11)	53(5)	46(5)	40(5)	12(4)	22(4)	0(4)
C(12)	52(5)	47(5)	40(5)	16(4)	26(4)	9(4)
C(13)	44(5)	39(5)	37(5)	10(4)	18(4)	6(4)
C(14)	113(4)	81(8)	43(6)	21(8)	44(6)	10(6)
Cl(1)	63(2)	67(2)	97(2)	−2(1)	40(2)	21(2)
Cl(2)	106(2)	76(2)	73(2)	40(2)	46(2)	48(2)
Cl(3)	80(2)	71(2)	59(2)	−2(2)	6(2)	−1(2)
O(1)	90(5)	39(3)	41(3)	28(3)	38(3)	15(2)
O(2)	90(5)	76(5)	57(5)	47(5)	46(4)	20(3)
O(3)	88(5)	68(5)	38(3)	37(4)	35(3)	19(3)
O(4)	108(6)	52(4)	71(5)	41(4)	38(4)	21(4)
O(5)	184(10)	82(6)	102(6)	79(6)	93(7)	24(5)
N	65(5)	49(5)	60(5)	24(4)	24(4)	5(4)
Molecule 2						
C(1)	55(5)	38(4)	34(4)	14(4)	21(4)	7(3)
C(2)	54(5)	51(5)	35(5)	10(4)	19(4)	5(4)
C(3)	58(6)	42(5)	47(5)	5(5)	29(5)	4(4)
C(4)	70(7)	42(5)	41(5)	19(5)	28(5)	11(4)
C(5)	52(6)	56(5)	37(5)	17(5)	15(5)	7(4)
C(6)	50(6)	45(5)	38(5)	5(4)	19(4)	4(4)
C(7)	37(4)	41(4)	33(4)	7(4)	14(3)	5(3)
C(8)	31(4)	38(4)	36(4)	7(3)	11(3)	3(3)
C(9)	41(5)	38(4)	36(4)	6(4)	14(4)	7(3)
C(10)	37(5)	44(5)	35(4)	7(4)	16(4)	7(3)
C(11)	56(6)	48(5)	45(5)	15(4)	26(4)	2(4)
C(12)	57(6)	43(5)	45(5)	21(4)	26(4)	14(4)
C(13)	50(5)	38(5)	43(5)	7(4)	19(4)	0(4)
C(14)	122(13)	59(7)	90(10)	50(8)	56(10)	8(7)
Cl(1)	49(2)	86(2)	65(2)	2(1)	7(1)	17(1)
Cl(2)	103(2)	57(2)	75(2)	35(2)	35(2)	30(1)
Cl(3)	67(2)	56(1)	61(2)	−8(1)	19(1)	6(1)
O(1)	64(4)	46(3)	41(3)	24(3)	28(3)	15(3)
O(2)	145(8)	64(4)	46(4)	44(5)	36(5)	−1(3)
O(3)	80(5)	53(4)	54(4)	39(3)	29(3)	9(3)
O(4)	95(6)	78(5)	58(4)	31(4)	42(4)	32(4)
O(5)	171(9)	70(5)	70(5)	30(5)	82(6)	8(4)
N	62(5)	58(5)	47(4)	10(4)	32(4)	8(4)

a non-hydrogen atom. The shortest contact is between the atom O(2) of molecule 2 and H(3) of molecule 1 and has the length 2.43 Å.

The dihedral angles between the molecular planes which are labelled in Fig. 4 are given in Table 2. In both molecules the nitro group is nearly coplanar with the nitro-substituted ring. Lehmann and Shefter (12) have recently determined the structures of 1-(2′,4′-dinitro-6′-bromophenoxy)-naphthalene and 2-(2′,4′-dinitrophenoxy)-1,3-diiodo-5-methylbenzene. The nitro-inside conformation of the former forces the ortho-nitro substituent near the naphthyl moiety, causing it to rotate so that its plane makes an angle of 25° with the dinitro-substituted ring. The latter compound has the "H-inside" conformation which allows the ortho-nitro substituent to point away from the diiodo-substituted ring and yet this nitro group is rotated 40° from the plane of the dinitro-substituted ring, increasing the contact distance between the ether oxygen atom and the nearest oxygen atom on the ortho nitro group to 2.70 Å. The equivalent rotation found previously for 2-(2′,4′-dinitrophenoxy)-1,3,5-tri-*t*-butylbenzene (2) was 15.8° which gave a nitro oxygen atom to ether oxygen atom intramolecular contact of 2.570 Å. In the present study, the carbomethoxy substituents occupy the equivalent position and are rotated by 23.1 and 20.1° from the plane of the nitro-

Can. J. Chem. Downloaded from www.nrcresearchpress.com by 210.87.254.6 on 09/05/12
For personal use only.

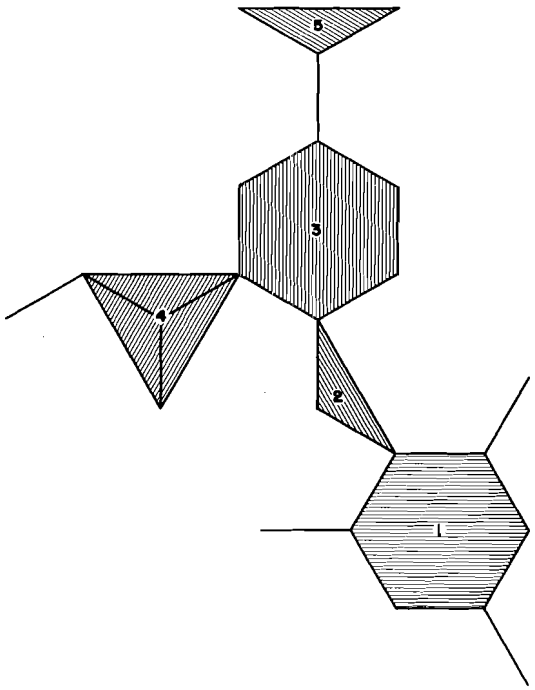

FIG. 4. Labelling sequence of the least-square planes in the two molecules.

substituted ring, giving carbonyl oxygen to ether oxygen distances of 2.715 and 2.690 Å, respectively, in the case of molecule 1 and molecule 2.

The nitro substituted rings are 8.8 and 4.6° from being coplanar with the central plane formed by the ether oxygen atom and the two carbon atoms bonded to it. The former value, relating to molecule 1, is somewhat larger than the values found previously; but the general conformation of both molecules is similar to that found for both 2-(3′-methyl-4′-nitrophenoxy)-1,3-diisopropylbenzene and 2(2′,4′-dinitrophenoxy)-1,3,5-tri-*t*-butylbenzene (1, 2). However, the differences between the two C—O bond lengths, which are 0.033(24) and 0.000(21) Å, are on the average less than the values found previously. This change is related to the presence of the mildly electron withdrawing chlorine substituents rather than electron donating alkyl groups. The results for 1-(2′,4′-dinitro-6′-bromophenoxy)naphthalene indicate a slight difference in C—O bond lengths and those for 2(2′,4′-dinitrophenoxy)-1,3-diiodo-5-methylbenzene do not (12), which is consistent with our results. However, the accuracy with which these structures have been determined is low.

In molecule 2, the plane of the trichloro-substituted ring is perpendicular to the central plane, but in molecule 1, the trichloro-substituted ring is turned 14° from the perpendicular position. Presumably, this difference in the two molecules is imposed by the molecular packing and shows the greater freedom of orientation of the doubly ortho-substituted ring associated with the less bulky character of the chlorine atoms. Stereoscopic views of the molecules are given in Figs. 5 and 6. The thermal ellipsoids of all the non-hydrogen atoms of both molecules show an elongation in the ***a*** direction. This effect may be related to the increased absorption in these crystals over that occurring in the previous studies of this series because of the presence of the chlorine atoms. However, the maximum possible variation in $|F_o|$ resulting from absorption is only 4% for the crystal used for data collection. An alternative explanation is that the long range order of the sample is greater in the plane perpendicular to the ***a*** axis than in the direction parallel to the ***a*** axis. An examination of the packing diagram shows that the crystal is constructed of layers perpendicular to the ***a*** axis and containing the aromatic parts of the molecules, which are interposed by regions containing the polar substituents. The degree of ordering of these layers may be less than the order within the individual layers.

The nitro-substituted ring is bent away from the trichloro-substituted ring by a 2.4° twist at the atom C(7), a value similar to those found earlier (1, 2). The internal ring angles at the carbon atoms bonded to the chlorine atoms are increased from the 120° expected for a hexagonally symmetric ring by an average of 1.2° for the two molecules. This deviation is in the opposite sign to that found for the alkyl groups and may manifest either the smaller size of the chlorine atoms or their electron withdrawing character.

The terminal bonds to the chlorine substituents, the nitro oxygen atoms, the carbonyl oxygen atom, and the methyl carbon atom are significantly affected by thermal motion. Table 3 shows the corrections to those bond lengths assuming *riding motion* as discussed by Busing and Levy (13). The average C—Cl bond length is increased from 1.724 to 1.749 Å. The correc-

Can. J. Chem. Downloaded from www.nrcresearchpress.com by 210.87.254.6 on 09/05/12
For personal use only.

TABLE 2. Least-square planes

(*a*) Coefficients of planes $Ax + By + Cz = D$*

Plane	*A*	*B*	*C*	*D*
Molecule 1				
1	0.6805	−0.5992	−0.4218	−2.6725
2	−0.8662	−0.3003	−0.3994	−0.8956
3	−0.7928	−0.2924	−0.5348	−1.2021
4	−0.7364	−0.6010	−0.3106	−2.2367
5	−0.8061	−0.2993	−0.5105	−1.2171
Molecule 2				
1	0.6170	−0.3299	−0.7145	−7.3275
2	−0.7768	−0.3795	−0.5026	−5.8905
3	−0.8197	−0.3180	−0.4764	−5.3741
4	−0.8640	−0.4746	−0.1681	−2.5852
5	−0.8391	−0.3287	−0.4335	−4.8503

*Coordinates refer to the direct ions of the a, $c^* \times a$, and the c^* axes.

(*b*) Dihedral angles between planes

	Dihedral angle (deg)	
Planes	Molecule 1	Molecule 2
1,2	76.0	89.7
2,3	8.8	4.6
1,3	82.0	86.5
3,4	23.0	20.1
3,5	1.6	2.8

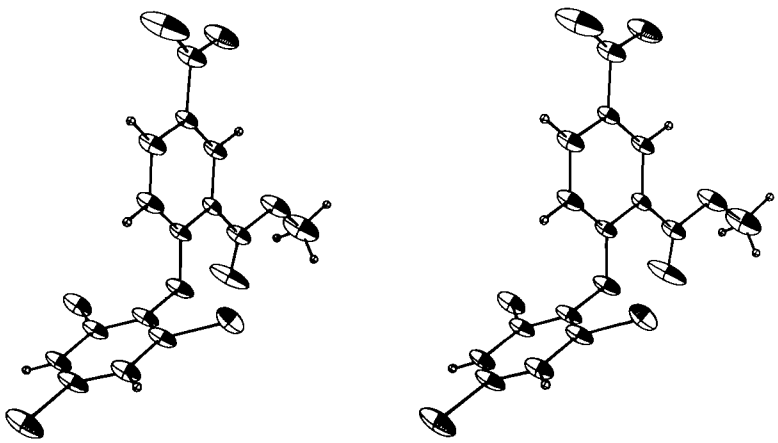

FIG. 5. Stereoscopic view of molecule 1. The thermal ellipsoids are scaled to include 75% probability.

tions for some of the other bond lengths do not appear to be realistic, reflecting the limitations of the *riding motion* model.

The average bond length to the ether oxygen atoms, 1.376(7) Å, is slightly less than the average values of 1.386(6) Å in 2-(3′-methyl-4′-nitrophenoxy)-1,3-diisopropylbenzene and 1.387(7) Å in 2-(2′,4′-dinitrophenoxy)-1,3,5-tri-*t*-butylbenzene, but much larger than the value given by Toussaint for 4,4′-dibromodiphenyl ether (3), and the C—O bond length of 1.28 Å for that compound appears to be inaccurate.

Table 4 shows the ether oxygen atom bond angles of the diphenyl ethers whose structures

Can. J. Chem. Downloaded from www.nrcresearchpress.com by 210.87.254.6 on 09/05/12
For personal use only.

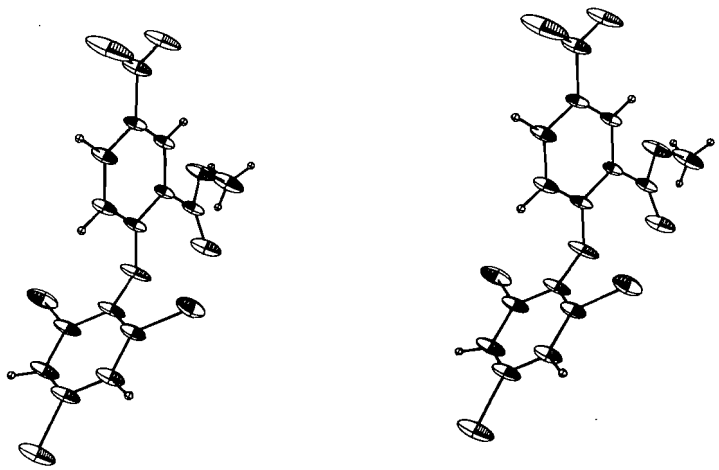

FIG. 6. Stereoscopic view of molecule 2. The thermal ellipsoids are scaled to include 75% probability.

TABLE 3. Thermal corrections to terminal bond lengths

	Bond lengths (Å)			
	Molecule 1		Molecule 2	
Bond	Uncorrected	Corrected	Uncorrected	Corrected
C(2)—Cl(1)	1.714	1.740	1.721	1.747
C(4)—Cl(2)	1.731	1.756	1.725	1.750
C(6)—Cl(3)	1.721	1.750	1.729	1.748
N—O(4)	1.217	1.240	1.214	1.239
N—O(5)	1.221	1.282	1.281	1.266
C(13)—O(2)	1.181	1.214	1.189	1.240
O(3)—C(14)	1.467	1.480	1.445	1.469

TABLE 4. Ether oxygen atom bond angles

	Angle (deg)	References
Diphenyl ether	116	14
4,4′-Dibromodiphenyl ether	123	3
Vertaline	116.1	15
3,5,3′-Triiodo-L-thyronine	125.6	16
3,5-Diiodo-L-thyronine	118	17
2-(2′,4′-Dinitrophenoxy)-1,3-diiodo-5-methylbenzene	119	12
1-(2′,4′-Dinitro-6′-bromophenoxy)naphthalene	121	12
2-(3′-Methyl-4′-nitrophenoxy)-1,3-diisopropylbenzene	119.7, 120.0 (1.4)	1
2-(2′,4′-Dinitrophenoxy)-1,3,5-tri-*t*-butylbenzene	116.8 (1.2)	2
2-(2′-Carbomethoxy)-4′-nitrophenoxy)-1,3,5-trichlorbenzene	119.3, 117.9 (1.3)	

have been determined by X-ray diffraction methods. The values given for diphenyl ether and 4,4′-dibromodiphenyl ether are assumed to be inaccurate and are only shown for comparison. The two aromatic rings of the alkaloid vertaline are joined by bridging groups and this appears to cause a small increase in the bending at the ether oxygen atom. The thyroid hormone 3,5,3′-triiodo-L-thyronine has the conformation with the 3′ iodine substituent inside, toward the diiodo-substituted ring, which causes an increase in the ether bond angle. All of the other examples with a meta or ortho substituent adopt the "substituent outside" conformation and the ether bond angle for these samples and those with no meta or ortho substituents on the equivalent ring, is between 116.8 and 121°.

The results which have been obtained to date

Can. J. Chem. Downloaded from www.nrcresearchpress.com by 210.87.254.6 on 09/05/12
For personal use only.

Can. J. Chem. Downloaded from www.nrcresearchpress.com by 210.87.254.6 on 09/05/12
For personal use only.

allow some observations regarding the conformational tendencies of diphenyl ethers with one diortho-substituted ring. The structure of 3,5-diiodo-L-thyronine, as reported recently by Cody *et al.* (17), shows the diiodo-substituted ring to be approximately perpendicular to the central C—O—C plane. The diortho substituted ring of 1-(2′,4′-dinitro-6′-bromophenoxy)naphthalene has a similar orientation although it is rotated 22° from the position perpendicular to the central plane. This indicates that the steric effects of the two ortho substituents cause the ring to which they are bonded to be approximately perpendicular to the central C—O—C plane. Further, this effect takes precedence over the tendency for the aromatic ring with the electron withdrawing groups to be coplanar with the central plane in order to allow conjugation between the π electrons of the ring and the unshared electrons of the ether oxygen atom. The diphenyl ethers with one meta or ortho substituent on the other ring adopt a similar conformation.

The other ring adopts an orientation nearly perpendicular to the diortho-substituted ring. This applies to rings with only a para substituent or with one ortho or meta substituent. All examples with one ortho-substituent adopt the substituent outside conformation. 2-(3′-Methyl-4′-nitrophenoxy)-1,3-diisopropylbenzene, with one meta substituent, adopts the substituent outside conformation, but 3,5,3′-triiodo-L-thyronine adopts a substituent inside conformation. Camerman and Camerman have attempted to rationalize this conformation using extended Hückel molecular orbital calculations which show the substituent inside conformation to be marginally favorable. This conformation might also be favored on the basis of the relative steric effects of the packing of the molecules for each of the two possible conformations.

Within the limits imposed by the bulkiness of the ortho substituents on the diortho-substituted ring, the planes of the two rings may be rotated from the perpendicular position to accommodate steric interactions with other molecules determined by the molecular packing in the crystal. A rotation about the C—O bond to the diortho-substituted ring brings one ortho substituent near the other ring and tends to *open up* the space between the second ortho substituent and the other ring to utilization by another molecule, thus allowing efficient use of space in the packing of the molecules. Rotation about the C—O bond to the ring which is not diortho-substituted closes up both spaces between the ortho substituents on the diortho-substituted ring and the other ring, which may in some cases allow more efficient packing than that resulting from the previous type of rotation. However, rotation about this bond may be restricted by a strong conjugation effect. 2-(2′,4′-Dinitrophenoxy)-1,3-diiodo-5-methylbenzene shows a rotation of the latter type (12). 1-(2′-4′-Dinitro-6′-bromophenoxy)-naphthalene shows some of each type of rotation (12). 2-(2′,4′-Dinitrophenoxy)-1,3,5-tri-*t*-butylbenzene has large ortho substituents and exhibits very small rotations (2). 2-(3′-Methyl-4′-nitrophenoxy-1,3-diisopropylbenzene shows a rotation of the former type. One molecule of 2-(2′-carbomethoxy-4′-nitrophenoxy-1,3,5-trichlorobenzene exhibits rotations of both types and the other remains nearly unrotated from the position with one plane perpendicular to the central plane and the other coplanar with the central plane.

Lehmann (19) has postulated the existence of intramolecular π complexes with the iodine and bromine atoms substituted on the opposite ring in order to explain the conformations of 2-(2′,4′-dinitrophenoxy-1,3-diiodo-5-methylbenzene and 1-(2′,4′-dinitro-6′-bromophenoxy)-naphthalene. This would seem improbable because in each case the halogen atom is not directly above the opposing ring but rather is slightly outside and above it.

The crystal structure of 2-(2′,4′-dinitrophenoxy)-1,3-diiodo-5-methylbenzene does, in fact, contain an intermolecular O---I charge transfer complex which has not been noted by the original investigators. One of oxygen atoms of the para nitro substituent is 3.11 Å from an iodine atom on an adjacent molecule. This distance is 0.44 Å shorter than the sum of van der Waals radii. The O---I—C angle is 161° which is only slightly smaller than the range of values reported elsewhere (18). The N—O(I) distance, at 1.24 Å, is 0.14 Å longer than the N—O distance to the other oxygen atom of the para nitro substituent, and the O—N—O angle for this group is opened to 139°. This interaction may be partly responsible for the large rotation (26°) of the dinitro substituted ring from the position coplanar with the central C—O—C plane.

The authors thank the National Research Council of Canada for financial support. We also thank Dr. John Rutherford and Dr. R. Guttormson for helpful discussions.

1. E. A. H. GRIFFITH, W. D. CHANDLER, and B. E. ROBERTSON. Can. J. Chem. This issue.
2. E. A. H. GRIFFITH, W. D. CHANDLER, and B. E. ROBERTSON. Can. J. Chem. This issue.
3. J. TOUSSAINT. Mem. Soc. Roy. Sci. Liège. Vol. Hors. Ser. **12**, 1 (1952).
4. J. J. BERGMAN, W. D. CHANDLER, and R. Y. MOIR. Can. J. Chem. **49**, 225 (1971).
5. W. D. CHANDLER, J. J. BERGMAN, and C. H. HAAS. Can. J. Chem. **49**, 583 (1971).
6. D. T. CROMER and J. B. MANN. Acta Cryst. **A24**, 321 (1968).
7. R. F. STEWART, E. R. DAVIDSON, and W. T. SIMPSON. J. Chem. Phys. **42**, 3175 (1965).
8. G. GERMAIN and M. M. WOOLFSON. Acta Cryst. **B24**, 91 (1968).
9. A. ZALKIN. FORDAP, A Fortran program for Fourier calculations. University of California, Berkeley. 1965.
10. W. R. BUSING, K. O. MARTIN, and H. A. LEVY. ORFLS, Report ORNL-TM-305. Oak Ridge National Laboratory, Oak Ridge, Tennessee. 1962.
11. C. K. JOHNSON. ORTEP, Report ORNL-3794. Oak Ridge National Laboratory, Oak Ridge, Tennessee. 1965.
12. P. A. LEHMANN and E. SHEFTER. Rev. Latinoamer Quim. In press.
13. W. R. BUSING and H. A. LEVY. Acta Cryst. **17**, 142 (1964).
14. J. TOUSSAINT. Bull. Soc. Roy. Sci. Liège, **15**, 86 (1944).
15. J. A. HAMILTON and L. K. STEINRAUF. J. Am. Chem. Soc. **93**, 2939 (1971).
16. N. CAMERMAN and A. CAMERMAN. Science, **175**, 764 (1972).
17. V. CODY, W. L. DUAX, and D. A. NORTON. Chem. Commun. 683 (1971).
18. R. FOSTER. Organic charge transfer complexes. Academic Press, N.Y. 1969.
19. P. A. LEHMANN. J. Med. Chem. **15**, 404 (1972).

Can. J. Chem. Downloaded from www.nrcresearchpress.com by 210.87.254.6 on 09/05/12
For personal use only.

INDO Molecular Orbital Calculations of Nitrogen–Proton Spin–Spin Coupling Constants Over Two and Three Bonds. Effects of Lone-pair Orientation, of Dihedral Angles, and of Protonation

R. WASYLISHEN[1] AND T. SCHAEFER

Department of Chemistry, University of Manitoba, Winnipeg, Manitoba R3T 2N2

Received April 12, 1972

Molecular orbital theory at the INDO level of approximation is used to calculate the Fermi contact contribution to two-bond and three-bond nitrogen–proton coupling constants for a wide variety of compounds. The dependence of calculated N,H coupling constants upon the spatial orientation of the nitrogen lone-pair is examined for selected molecules. For both saturated and unsaturated compounds the calculated $^2J(^{15}N,H)$ is large and negative when the lone-pair is oriented *cis* to the proton, and is small and of either sign when the lone-pair lies *trans* to the proton. Calculated $^3J(N,H)$ depends both on the orientation of the nitrogen lone-pair and on the *HCCN* dihedral angle. Computed $^2J(N,H)$ and $^3J(N,H)$ generally follow the experimentally known substituent and structural effects. It is suggested that observed phosphorus–proton coupling constants in tervalent phosphorus compounds are dependent on lone-pair orientation in a manner analogous to the corresponding nitrogen–proton coupling constants. The influence of the nitrogen lone-pair orientation on geminal proton–proton coupling constants in methylamine is computed and compared with experiment. Calculated barriers to pyramidal inversion and methyl group rotation are in reasonable agreement with available experimental data.

Nous utilisons la théorie des orbitales moléculaires associée à l'approximation INDO pour calculer la contribution du contact de Fermi aux constantes de couplage à deux et à trois liaisons entre l'azote et le proton pour une grande variété de composés. Nous examinons la dépendance des constantes de couplage N,H calculées sur l'orientation spatiale de la paire d'électrons libres de l'azote, dans le cas de certaines molécules. Pour les composés saturés ou insaturés, le $^2J(^{15}N,H)$ calculé est grand et négatif si la paire d'électrons libres est *cis* par rapport au proton; il est petit et positif ou négatif si la paire est *trans* par rapport au proton. Le $^3J(N,H)$ calculé dépend à la fois de l'orientation de la paire d'électrons libres de l'azote et de l'angle dièdre *HCCN*. Les $^2J(N,H)$ et $^3J(N,H)$ compilés obéissent généralement aux effets connus expérimentalement de structure et de substituant. Nous suggérons que les constantes de couplage phosphore–proton observées dans les composés de phosphore trivalent dépendent de l'orientation de la paire d'électrons libres, d'une façon semblable aux constantes de couplage correspondantes azote–proton. Nous étudions l'influence de l'orientation du doublet libre de l'azote sur les constantes de couplage géminé proton–proton du méthylamine et comparons avec l'expérience. Les barrières à l'inversion pyramidale calculées et la rotation des groupes méthyle concordent avec les résultats expérimentaux disponibles. [Traduit par le journal]

Canadian Journal of Chemistry, **50**, 2989 (1972)

Introduction

There exists considerable experimental and theoretical interest in the correlation of the signs and magnitudes of nuclear spin–spin coupling constants with molecular structure (1–5). Attention has been focussed on the derivation of empirical relationships between coupling constants and parameters such as the electronegativity and spatial orientation of substituents, the direction of lone-pair electrons,[2] as well as bond angles and bond orders. These relationships have proved useful in conformational studies (5). Recently (2, 3) the success of the INDO molecular orbital approximation in the calculation of geminal and vicinal proton–proton coupling constants has been demonstrated (6–9).

Detailed mapping of structural and substituent effects on two- and three-bond nitrogen–proton coupling constants has been hampered by experimental difficulties arising from the electric quadrupole moment of ^{14}N (natural abundance of 99.635%). Consequently $J(^{14}N,H)$ is only observable in molecules where the fluctuating electric field gradients at the nitrogen atom are small. The other isotope of nitrogen, ^{15}N, has spin 1/2 but its low natural abundance (0.365%) makes the measurement of $J(^{15}N,H)$ values difficult in unenriched samples. Nevertheless, a considerable body of data is now available (10, 11) for comparison with theory.

[1]Holder of an NRCC scholarship, 1971–1972.

[2]In this paper the lone-pair is treated as having directional character, in line with a simple hybridization model.

Can. J. Chem. Downloaded from www.nrcresearchpress.com by 210.87.254.105 on 09/05/12
For personal use only.

Can. J. Chem. Downloaded from www.nrcresearchpress.com by 210.87.254.105 on 09/05/12
For personal use only.

In the present paper, the technique of Pople *et al.* (6–8) is employed in the study of structural and substituent effects on two- and three-bond nitrogen–proton coupling constants. In particular, the dependence of the calculated N,H coupling constants on the orientation of the nitrogen lone-pair, on the *NCCH* dihedral angle, and on the substituent electronegativity is examined. Computed N,H coupling constants are compared with experimental values when these are available. An attempt is made to compare the angular dependence of the calculated N,H coupling constants with that observed for phosphorus–proton coupling constants in certain molecules. The change in N,H couplings caused by protonation at nitrogen is also calculated and is compared to experiment.

Computational Method

In the finite perturbation formalism, the Fermi contact contribution to nuclear spin–spin coupling between two nuclei A and B is given by eq. 1 (6–8).

$$[1]\quad J_{AB} = \frac{\hbar}{2\pi}[(8\pi/3)\beta]^2\gamma_A\gamma_B S_A^2(0)S_B^2(0) \times [(\partial/\partial h_B)\rho^{spin}_{S_AS_A}(h_B)]h_B = 0$$

h_B is the perturbation due to the nuclear moment μ_B and has the form

$$h_B = \frac{8}{3}\pi\,\beta\mu_B S_B^2(0)$$

$\rho^{spin}_{S_AS_A}(h_B)$ is the diagonal element of the spin density matrix (in the presence of the contact perturbation h_B) corresponding to the valence s orbital of atom A, γ_A and γ_B are the magnetogyric ratios of nuclei A and B, β is the Bohr magneton, and $S_A^2(0)$ and $S_B^2(0)$ are the valence s-orbital electron densities of atom A and atom B at their respective nuclei. Using the method of finite differences Pople *et al.* (7) have shown that the derivative in eq. 1 can be approximated by $\rho^{spin}_{S_AS_A}(h_B)/h_B$. Thus the coupling constant (in Hz) is approximated by the expression

$$[2]\quad J_{AB} = \frac{\hbar}{2\pi}[(8\pi/3)\beta]^2\gamma_A\gamma_B S_A^2(0)S_B^2(0) \times [\rho^{spin}_{S_AS_A}(h_B)/h_B]$$

The error in the approximation has a minimum when h_B is approximately 10^{-3} hartrees and $\rho^{spin}_{S_AS_A}(h_B)$ is calculated using open-shell semi-empirical molecular orbitals at the INDO level of approximation (8, 12).

All coupling constants were calculated using eq. 2 with the same parameterization as used previously by Pople *et al.* (7, 8). Because all other terms in eq. 2 are taken as constant, it is the sensitivity of the spin density in the orbital S_A to the presence of the perturbation h_B which determines the spin–spin coupling constants. Because h_B is small, the spin densities are extremely small and therefore the spin density matrix must be known very accurately in the calculation of coupling constants. For nitrogen–proton coupling constants, $J(^{14}N,H) = 141174.7016\ \rho^{spin}_{H_sH_s}$ Hz when $h_N = 10^{-3}$ hartrees. In order to obtain reasonably accurate coupling constants the usual energy criterion for convergence of the SCF iteration was changed to the requirement that

$$[3]\quad 10^{-4} \leqslant \frac{\rho_{ii}^{old} - \rho_{ii}^{new}}{\rho_{ii}^{old}}$$

for all i. By this criterion one can estimate the accuracy of the calculated coupling constants since J_{AB} is directly proportional to ρ^{spin}_{AA}/h or ρ^{spin}_{BB}/h depending on whether A or B is perturbed. For example, consider the accuracy of a calculated $J(^{14}N,H)$ with a magnitude of 14.12 Hz. If the convergence criterion given by eq. 3 is satisfied then the change in $J(^{14}N,H)$ in one SCF cycle is less than 0.00141 Hz. When coupling constants did not converge in 90 SCF cycles using the criterion given by eq. 3, 100 SCF cycles were carried out. An attempt was made to calculate the N,H coupling constants in nitromethane, methylnitrate, and *N*,*N*-dimethylnitrosoamine, but even after 100 SCF cycles the energy and the coupling constants did not converge. Therefore the results of these calculations are not given.

The input data for a calculation required the cartesian coordinates of all atoms, the total charge, and the multiplicity of the molecule. Since the calculated coupling constants were often very sensitive to the molecular geometry, an attempt was made to use the best available structural parameters. The atomic coordinates were usually calculated from these structural parameters with the aid of the "Model-Builder"

Can. J. Chem. Downloaded from www.nrcresearchpress.com by 210.87.254.105 on 09/05/12
For personal use only.

program MBLD (13). The sources of the structural parameters or atomic coordinates are given in the appropriate tables and are discussed in the text.

All calculations were carried out on an IBM 360/65 computer.

Results and Discussion

(1) Two-bond Nitrogen–Proton Coupling Constants

In Table 1 calculated two-bond ^{15}N,H coupling constants in the ^{15}N—C—H fragment are given for 31 compounds. Available experimental data are presented for comparison. In a few cases, where couplings have been observed for large molecules (greater than 40 valence electrons), comparison is made with values calculated for closely related smaller molecules. To simplify the discussion, the compounds in Table 1 are divided into three groups. The compounds in the first group (1–9) contain the

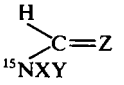

fragment. In the second group (10–15) the carbon atom of the ^{15}N—C—H fragment is bound to four atoms (approximately sp^3 hybridized) or to two atoms (approximately sp hybridized). The compounds in the third group (16–31) are either molecules with which one may associate a "localized nitrogen lone-pair" or are their protonated derivatives.

(a) Compounds 1–9, Table 1

The observed values of $^2J(^{15}N,H)$ in the

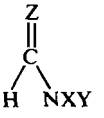

fragment range from −19.0 Hz in formamide (Z = O) through (−)8.3 Hz in *N,N*-dimethyl-^{15}*N*-phenyl-formamidine (Z = NC_6H_5) to ±0.2 Hz in diethylanilinomethylene malonate (Z = CR'_2). The calculated values are in fair agreement with experiment: −17.23 Hz in formamide, −6.65 Hz in formamidine (Z = N—H), and 0.23 Hz in vinylamine (Z = 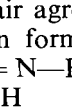). This large range of $^2J(^{15}N,H)$ values is analogous to the range of $^2J(H,H)$ values observed and calculated in the C=Z fragment (2, 18).

The observed decrease in $^2J(^{15}N,H)$ between Z = and Z = O has been attributed to the higher electronegativity of the oxygen atom as well as to the increase in the π-bond order of the C—N bond (10, 11, 23). In Table 2 calculated values of $^2J(^{15}N,H)$ are compared with calculated C—N bond orders and with calculated charge densities at the carbon atom of the *NCH* fragment. As the electronegativity of Z decreases, the C—N bond orders decrease and the positive charge on the carbon atom of the NCH fragment also decreases, confirming the qualitative arguments (10, 11, 23).

The effect of an electronegative substituent placed β to the carbon atom of the N—C—H fragment was also investigated. In Table 3 the calculated values of $^2J(^{15}NCH)$ for three *trans*-X-vinylamines are compared with the calculated and observed $^2J(HCH)$ values in the corresponding substituted ethylenes (2). From Tables 2 and 3, it is apparent that the calculated reduced coupling constants $^2K(NCH)$ show the same trends as the $^2K(HCH)$ values (2, 38).[3]

(b) Compounds 10–15, Table 1

In molecules where the carbon atom of the N—C—H fragment is bound to four atoms (compounds 10–13 and 16–21) the known two-bond ^{15}N,H coupling constants are usually less than 3.5 Hz in magnitude (10). Exceptions have been observed in cyclic molecules where the relevant dihedral angle[4] is fixed on the n.m.r. time scale (see compounds 19–21). In the next section it is shown that when the carbon atom is bound to four groups, one of them being a nitrogen atom with a "localized lone-pair", $^2J(^{15}N,H)$ is predicted to vary over a wide range. However, internal rotation has the consequence that the observed values of these coupling con-

[3]The reduced coupling constant is defined as $K_{AB} = 2\pi J_{AB}/\hbar\gamma_A\gamma_B$. Since $\gamma(^1H)$ and $\gamma(^{15}N)$ are of opposite sign, $K(^{15}N,H)$ and $J(^{15}N,H)$ are also of opposite sign.

[4]In the simple hybridization picture the nitrogen lone-pair has directional character; therefore it is reasonable to define a dihedral angle between the plane containing the NCH fragment and the plane containing the lone-pair, NC fragment.

Can. J. Chem. Downloaded from www.nrcresearchpress.com by 210.87.254.105 on 09/05/12
For personal use only.

TABLE 1. Observed experimental and calculated two-bond $^{15}N,H$ coupling constants*

	Experimental results			Calculated results		
	Compound	$^2J(^{15}N,H)$ observed	Reference	Compound	$^2J(^{15}N,H)$ calculated	Reference†
1	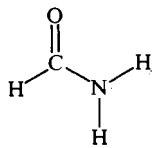	−19.0 (neat liquid) −16.4 (in acetone) −14.47 (in water, 15 mol%)	14 15 16	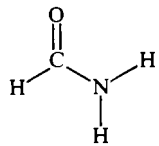	−17.23 −15.62	*a* *b*
2	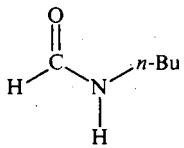	−15.6 (neat liquid)	17	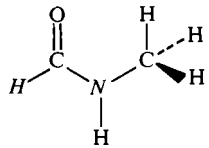	−16.85	*c*
3	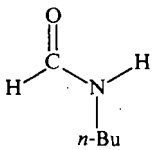	−14.3 (neat liquid)	17	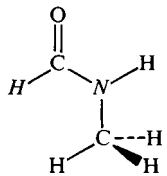	−19.21	*c*
4	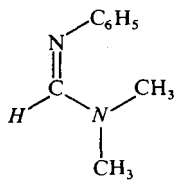	(−) 8.3	18	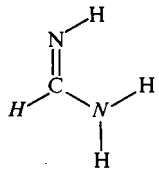	−6.65	*b*
5	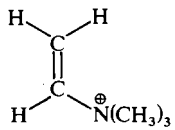	−4.9	19	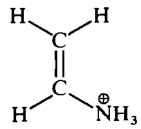	−2.83	*d*

Can. J. Chem. Downloaded from www.nrcresearchpress.com by 210.87.254.105 on 09/05/12
For personal use only.

TABLE 1 (*Continued*).

	Experimental results			Calculated results		
	Compound	$^2J(^{15}N,H)$ observed	Reference	Compound	$^2J(^{15}N,H)$ calculated	Reference†
6	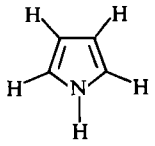	−4.52	20	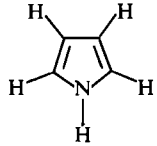	−1.82	*e*
7	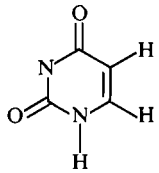	(−) 3.50	21	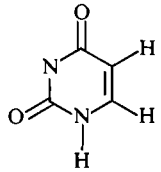	0.67	*f*
8	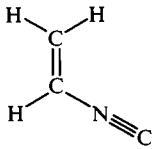	−3.16	19, 22	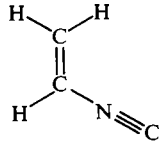	0.52	*g*
9	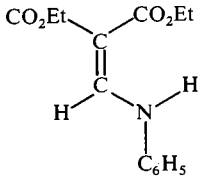	±0.2	18	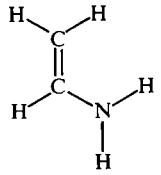	+0.23	*b*
10	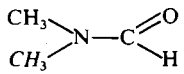	1.10	23	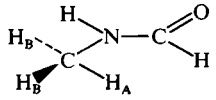	H_A 2.85 H_B 1.49	*b*

Can. J. Chem. Downloaded from www.nrcresearchpress.com by 210.87.254.105 on 09/05/12
For personal use only.

TABLE 1 (*Continued*).

	Experimental results			Calculated results		
	Compound	$^2J(^{15}N,H)$ observed	Reference	Compound	$^2J(^{15}N,H)$ calculated	Reference†
11	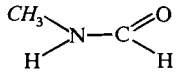	1.20	15	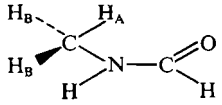	H_A 2.85 H_B 1.49	*b*
12	$CH_3CH_2N{\equiv}C$	2.67	24, 25	$CH_3CH_2N{\equiv}C$ (staggered)	+3.90	*h*
13	$CH_3N{\equiv}C$	3.23	24	$CH_3N{\equiv}C$	+4.29	*i*
14	$H{-}C{\equiv}N$	8.7	26	$H{-}C{\equiv}N$	+5.11	*j*
15	$H{-}C{\equiv}\overset{\oplus}{N}{-}H$	19.0	27	$H{-}C{\equiv}\overset{\oplus}{N}{-}H$	+11.39	*k*
16	CH_3NH_2	−1.0	28	CH_3NH_2	−2.70 (average for staggered conformation)	*l*
17	$CH_3\overset{\oplus}{N}H_3$	±0.8	29	$CH_3\overset{\oplus}{N}H_3$	+2.41 (average for staggered conformation)	*l*
18	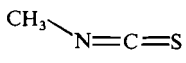	±3.3	29	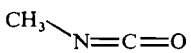	+0.89 (average over all angles)	*m*
19	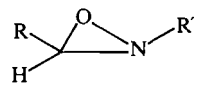	−4.8 to −5.4	30, 31	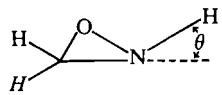 $\theta = 64°$	−5.78	*n*
20	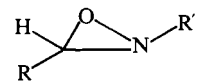	~0.0	30, 31	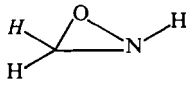 $\theta = 64°$	0.95	*n*
21	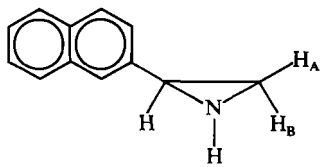	H_A (−) 4.9 H_B (−) 0.3	32	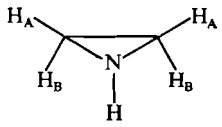 $\theta = 68°$	H_A −9.14 H_B 0.62	*n*

Can. J. Chem. Downloaded from www.nrcresearchpress.com by 210.87.254.105 on 09/05/12
For personal use only.

TABLE 1 (*Continued*).

	Experimental results			Calculated results		
	Compound	$^2J(^{15}N,H)$ observed	Reference	Compound	$^2J(^{15}N,H)$ calculated	Reference†
22	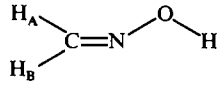	H_A 2.68 H_B −13.88	33	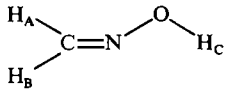	H_A −0.77 H_B −10.90 H_C −5.50	*o*
				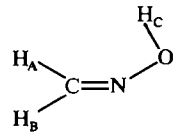	H_A −1.33 H_B −8.53 H_C +6.38	*p*
23	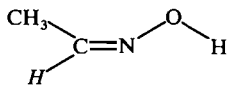	−15.93	33	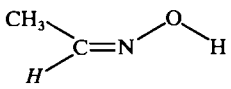	−15.40	*q*
24	—			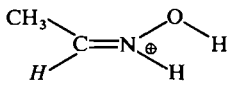	4.66	*q*
25	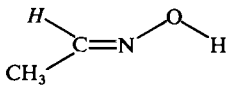	2.93	33	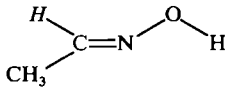	−0.59	*q*
26	—			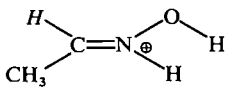	4.43	*q*
27		−10.76	34		−16.98	*r*
28		−3.01	34	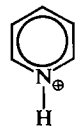	0.48	*s*

TABLE 1 (*Concluded*).

	Experimental results			Calculated results		
	Compound	$^2J(^{15}N,H)$ observed	Reference	Compound	$^2J(^{15}N,H)$ calculated	Reference†
29		−15.0	35		−11.19	*t*
30	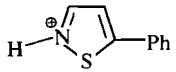	−4.2	35	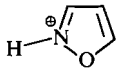	+0.39	*t*
31	—	—	—		−6.58	*u*

*All the coupling constants are $J(^{15}N,H)$ values in Hz; $J(^{14}N,H)$ values have been converted to $J(^{15}N,H)$ values by multiplying by −1.402757 (36).

†The geometries used for the INDO calculations were taken from the following references: (*a*) C. C. Costain and J. M. Dowling. J. Chem. Phys. **32**, 158 (1960). (*b*) Standard geometries were used. J. A. Pople and D. L. Beveridge. Approximate molecular orbital theory. McGraw Book Company. New York, N.Y. 1970. (*c*) Standard bond lengths and bond angles (ref. *b*) were used for the $NHCH_3$ fragment, while the NCOH fragment was assumed to have the same geometry as that given in ref. *a*. (*d*) Standard bond lengths and bond angles were used for the vinyl fragment (see ref. *b*). The C—N and N—H bond lengths were taken as 1.45 and 1.03 Å, respectively. (*e*) L. Nygaard, J. T. Nielsen, J. Kirchheiner, G. Maltesen, J. Rastrup-Andersen, and G. O. Sørensen. J. Mol. Struct. **3**, 491 (1971). (*f*) Same as that given for thymine by L. C. Snyder, R. G. Shulman, and D. B. Neuman. J. Chem. Phys. **53**, 256 (1970) except the methyl group was replaced by a proton with a bond length of 1.086 A. (*g*) The atomic coordinates of the vinyl group were taken from S. Meza and U. Wahlgren. Theoret. Chim. Acta, **21**, 323 (1971). The C—N and N≡C bond lengths were assumed to be 1.424 and 1.166 Å respectively (see ref. *i*). (*h*) The atomic coordinates of the CH_3CH_2 group were taken from W. J. Jorgensen and L. C. Allen. J. Am. Chem. Soc. **93**, 567 (1971). The C—C≡N fragment was assumed to have the same bond lengths and angles as those given in ref. *i*. (*i*) C. C. Costain. J. Chem. Phys. **29**, 864 (1958). (*j*) V. W. Laurie and D. R. Herschback. J. Chem. Phys. **37**, 1687 (1962). (*k*) This molecule was assumed linear with the following bond lengths: 1.12 (H—C), 1.32 (C≡N), and 1.04 Å (N—H). (*l*) W. H. Fink and L. C. Allen. J. Chem. Phys. **46**, 2276 (1967). For protonated methylamine the following geometry was assumed: N—C bond length = 1.50 Å, C—H bond length = 1.09 Å, N—H bond length = 1.03 Å. All angles were assumed tetrahedral. (*m*) R. G. Lett and W. G. Flygare. J. Chem. Phys. **47**, 4730 (1967). (*n*) J. M. Lehn, B. Munsch, P. Millié, and A. Veillard. Theoret. Chim. Acta, **13**, 313 (1969). (*o*) I. N. Levine. J. Chem. Phys. **38**, 2326 (1963). (*p*) Same as ref. *o*, except that the dihedral angle CNOH was taken as zero degrees. (*q*) R. S. Rogowski and R. H. Schwendeman. J. Chem. Phys. **50**, 397 (1969). The protonated oximes were assumed to have the same geometry as the unprotonated species. The angle CNH^+ was assumed to be 120° and the N—H bond length was taken as 1.03 Å. (*r*) B. Bak, L. Hansen-Hygaard, and J. Rastrup-Andersen. J. Mol. Spectrosc. **2**, 361 (1958). (*s*) Same as ref. *r*, except for the additional hydrogen atom which was assumed to be 1.03 Å from the pyridine nitrogen atom. (*t*) M. Cannas, and G. Marongui. Z. Kristallogr. **127**, 388 (1968) and S. Biagini, M. Cannas, and G. Marongui. J. Heterocycl. Chem. **6**, 901 (1969). The protonated isoxazole was assumed to have the same geometry as the unprotonated species. Angle ONH was assumed to be 127.3° and the N—H bond length was taken as 1.03 Å. (*u*) E. Saegebarth and A. P. Cox. J. Chem. Phys. **43**, 166 (1965).

Can. J. Chem. Downloaded from www.nrcresearchpress.com by 210.87.254.105 on 09/05/12
For personal use only.

TABLE 2. A comparison of calculated $^2J(^{15}NCH)$ values with N—C bond orders and carbon charge densities for compounds 1, 4, and 9 of Table 1*

Compound	$^2J(^{15}N,H)$	Bond orders		Total charge at carbon ($\times 10^{+4}$ electrons)
		$N(p_\pi)C(p_\pi)$	N(s)C(s)	
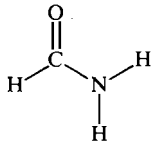	−15.62	0.4412	0.2999	+4382
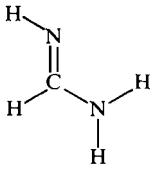	−6.57	0.4043	0.2975	+3018
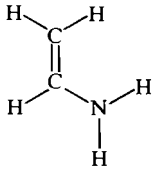	0.23	0.3373	0.2833	+1674

*Standard geometries (8, 37) were used for all calculations.

TABLE 3. Effect of substituent electronegativity on $^2J(^{15}N,H)$ and $^2J(H,H)$*

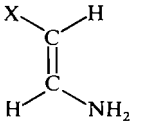
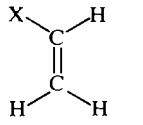

X	$^2J(^{15}N,H)$ calc.	$^2J(H,H)$ calc.	$^2J(H,H)$ obs.
Li	−6.01	13.80	7.1
H	0.23	3.24	2.3
F	1.66	−0.18	−3.2

*Standard geometries (8, 37) were used for all calculations. The C—Li bond length was taken as 2.1 Å (3). Computed and observed values of $^2J(H,H)$ are cited from ref. 2.

stants are small (see compounds 16 and 18, for example).

Calculated values for compounds 10–15 agree fairly well with experiment. Both the calculated and observed $^2J(^{15}N,H)$ increase on going from ethylisocyanide to methylisocyanide. The calculated $^2J(^{15}N,H)$ in protonated hydrogen cyanide is 11.39 Hz, significantly lower than the observed value of 19.0 Hz (27). This discrepancy is probably due in part to the choice of geometry for the protonated species.

(c) Compounds 16–31, Table 1

It is known that the observed two-bond $^{15}N,H$ coupling constants in compounds 19–23, 25, 27, and 29 are stereospecific, depending on the orientation of the nitrogen lone-pair (10, 11, 33). Specifically, if the lone-pair is directed *cis* to the C—H bond then $^2J(^{15}N,H)$ is observed and calculated (see Table 1) to be large and negative; if the nitrogen lone-pair and C—H bond lie *trans* to one another then the absolute value of $^2J(^{15}N,H)$ is small. To test the generality of this rule, the angular dependence of $^2J(^{15}N,H)$ was calculated for methylamine, methylisocyanate, methylenimine, and aziridine. The results of these calculations are presented in Figs. 1, 2, 3, and 4. In each calculation bond lengths were taken to be the same as those in the ground state conformation (see geometry references in Table 1).

(i) Methylamine

In Fig. 1, $^2J(^{15}N,H)$ is plotted as a function of the angle, θ, defined in **I** and **II**. This angle can also be described as the dihedral angle defined by the lone-pair, NC fragment and the NCH fragment.

Can. J. Chem. Downloaded from www.nrcresearchpress.com by 210.87.254.105 on 09/05/12
For personal use only.

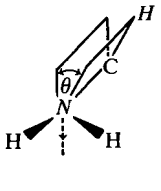

I

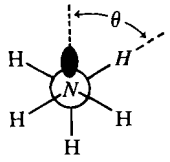

II

For $\theta = \theta^\circ$ one of the C—H bonds eclipses the lone-pair and $^2J(^{15}N,H)$ for the proton in that bond is calculated as large and negative, -14.90 Hz. For $\theta = 180^\circ$, one of the C—H bonds sits *trans* to the lone-pair and $^2J(^{15}N,H)$ is -0.40 Hz. Notice that $^2J(^{15}N,H)_{cis}$ and $^2J(^{15}N,H)_{trans}$ predicted for methylamine are similar to those observed for unsaturated compounds such as formaldoxime (compound 22).

To compare experimental and calculated couplings in methylamine, one need only consider the staggered conformation because the barrier to rotation about the C—N bond is 1.98 kcal/mol (39). For the staggered conformation one calculates an average of -2.70 Hz while the observed value is -1.0 Hz (28) (INDO calculates the barrier to rotation of the methyl group as 1.74 kcal/mol).

Few observations are available for two-bond $^{15}N,H$ coupling constants in saturated systems of fixed geometry. However, it is of some interest to compare calculations for methylamine with those observed for the saturated 1,3-oxazine (**III**). Riddel and Lehn (40) measured $^2(J^{15}N, H_{2a})$ and $^2J(^{15}N,H_{4a})$ as approximately zero, while $^2J(^{15}N,H_{4e})$ was about 1.5 Hz. The sign of the latter coupling is almost certainly negative since on protonation of the nitrogen atom these couplings are no longer resolved.[5] Notice that the relevant angle is approximately 180° for H_{2a} and H_{4a} while for H_{4e} it is approximately 60°. For $\theta = 180 \pm 5^\circ$ and $\theta = 60 \pm 5^\circ$, INDO calculates $^2J(^{15}N,H)$ as -0.4 ± 0.1 and -3.8 ± 1.3 Hz, respectively, for methylamine.

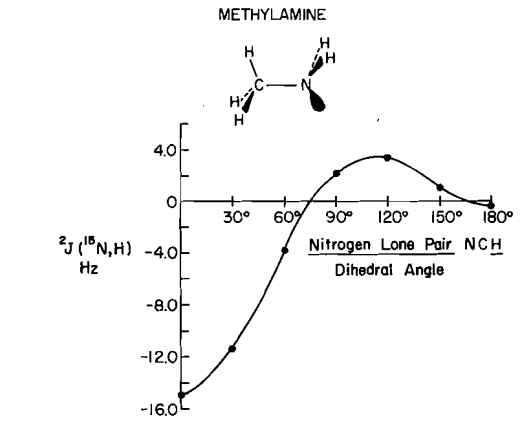

FIG. 1. A plot of the calculated $^2J(^{15}N,H)$ *vs.* the dihedral angle defined by the lone-pair—N—C—H fragment in methylamine.

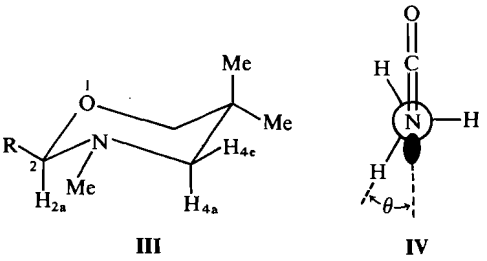

III IV

(ii) Methylisocyanate

In Fig. 2 the calculated $^2J(^{15}N,H)$ in methylisocyanate is plotted as a function of the angle θ, defined in **IV**. The plot closely resembles that calculated for methylamine. For a given θ, this

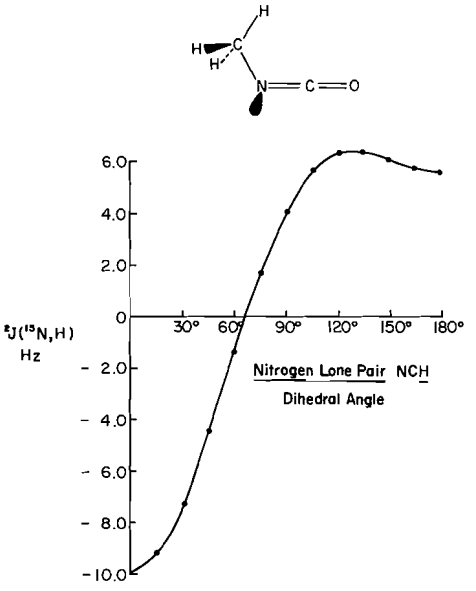

FIG. 2. A plot of the calculated $^2J(^{15}N,H)$ *vs.* the dihedral angle defined by the lone-pair—N—C—H fragment in methylisocyanate.

[5]The choice of sign is based on the observation that $^2J(^{15}N,H)$ usually increases on protonation (33). This observation is supported by the MO calculations. For example, in protonated methylamine INDO calculates $^2J(^{15}N,H) = 2.43 \pm 0.05$ Hz, independent of the HNCH dihedral angle.

Can. J. Chem. Downloaded from www.nrcresearchpress.com by 210.87.254.105 on 09/05/12
For personal use only.

Can. J. Chem. Downloaded from www.nrcresearchpress.com by 210.87.254.105 on 09/05/12
For personal use only.

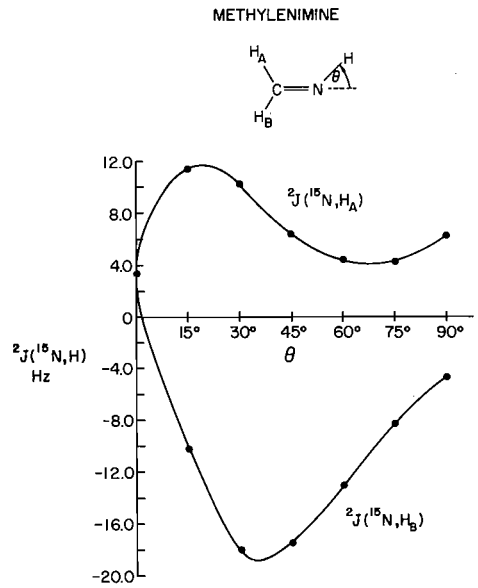

FIG. 3. A plot of the calculated $^2J(^{15}N,H)$ *vs.* the indicated angle θ in methylenimine.

coupling in methylisocyanate is calculated to be larger than in methylamine. $^2J(^{15}N,H)$ is 5.52 Hz when the C—H bond lies *trans* to the lone-pair ($\theta = 180°$); when the C—H bond lies *cis* to the lone-pair ($\theta = 0°$), $^2J(^{15}N,H)$ is -9.93 Hz.

The conformation of lowest energy is calculated as one in which a C—H bond eclipses the nitrogen lone-pair ($\theta = 0°$). The barrier to rotation of the methyl group is calculated as 102 cal/mol, in good agreement with the experimental barrier of 83 ± 15 cal/mol (41). Because the barrier is so small, comparison of calculated with experimental coupling constants entails an average over all angles and one finds $^2J(^{15}N,H) = 0.88$ Hz. This coupling constant has not been measured in methylisocyanate; in the related compound, methylisothiocyanate, $^2J(^{15}N,H) = \pm 3.3$ Hz (29).

TABLE 4. Calculated values of $^2J(^{15}N,H)$ for some substituted methylenimines*

X	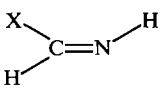 $^2J(^{15}N,H)$	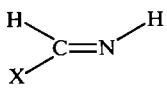 $^2J(^{15}N,H)$
Li†	−17.82	−18.54
H	−9.64	4.27
F	−6.48	10.04

*Standard geometries (8, 37) were used for all calculations.
†The C—Li bond length was taken as 2.1 Å.

(iii) Methylenimine

For methylenimine (**V**), $^2J(^{15}N,H)$ is plotted against θ in Fig. 3. INDO finds the lowest energy when $\theta \simeq 65°$. At this angle $^2J(^{15}N,H_A) = 4.18$ and $^2J(^{15}N,H_B) = -11.41$ Hz.

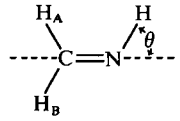

V

The barrier to pyramidal inversion is calculated to be 25.5 kcal/mol, in good agreement with the values of 27.9 and 26.2 kcal/mol found by *ab initio* SCF–LCAO–MO methods (42, 43).

The INDO method was employed to examine substituent effects on $^2J(^{15}N,H)$ values in three hypothetical *syn*- and *anti*-substituted methylenimines (Table 4). As the electronegativity of X increases, $^2J(^{15}N,H)$ increases for both the *syn* and *anti* isomers. Notice that the change in $^2J(^{15}N,H)$ is opposite to the trend observed and calculated in the

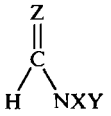

fragment.

(iv) Aziridine

In Fig. 4 the calculated values of $^2J(^{15}N,H)$ in aziridine (**VI**) are plotted as a function of the angle θ between the bisector of the CNC angle and the N—H bond. INDO finds a minimum energy when $\theta \simeq 68°$, and then $^2J(^{15}N,H_A) = -0.62$ and $^2J(^{15}N,H_B) = -9.14$ Hz. The barrier to pyramidal inversion is calculated as 24.5 kcal/mol, somewhat larger than the values of 16–19 kcal/mol observed for aziridine derivatives (44).

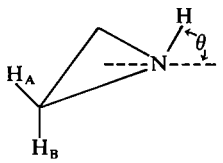

VI

For oxaziridine (see compounds 19 and 20 in Table 1), $^2J(^{15}N,H)$ was also calculated as a

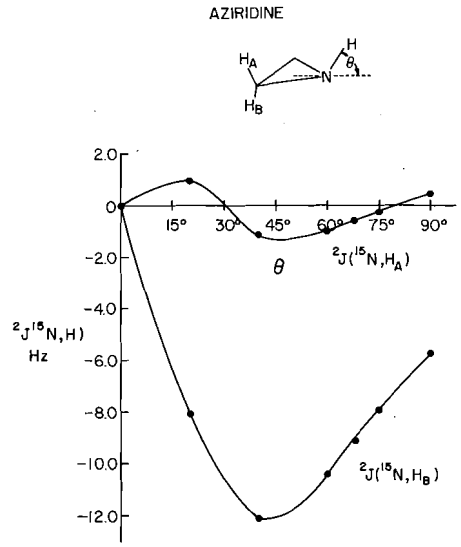

FIG. 4. A plot of the calculated $^2J(^{15}N,H)$ in aziridine *vs.* the angle θ between the N—H bond and the extension of the bisector of the CNC angle.

function of θ. Its angular dependence was very similar to that obtained for aziridine although $^2J(^{15}N,H)$ in oxaziridine was more positive than in aziridine. When $\theta = 64°$, $^2J(^{15}N,H_A) = 0.95$ and $^2J(^{15}N,H_B) = -5.78$ Hz, in excellent agreement with the measurements of Becker (30, 31) on some substituted oxaziridines. INDO calculates the barrier to pyramidal inversion to be approximately 10 kcal/mol larger than the 32 kcal/mol (44, 45) observed for oxaziridine derivatives.

From Figs. 3 and 4 the very similar calculated angular dependence of $^2J(^{15}N,H)$ in methylenimine and aziridine is apparent. In methylenimine and aziridine the hybridization of the nitrogen atom changes with variations in θ. This is not so for methylamine and methylisocyanate in which the hybridization of the nitrogen atom remains essentially unchanged for all values of θ. Because of this difference one does not expect the same angular dependence of $^2J(^{15}N,H)$ in methylamine and methylisocyanate as in methylenimine and aziridine.

In summary, the overall agreement between observed and calculated $^2J(^{15}N,H)$ values in Table 1 is good. Many experimental trends are reproduced by the calculations. For all compounds (with the exception of vinylamine) nitrogen protonation increases $^2J(^{15}N,H)$, in agreement with the experiment. The calculated substituent effects on $^2J(^{15}N,H)$ in the

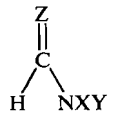

fragment also agree with experiment. The calculated angular dependence of $^2J(^{15}N,H)$ in the methylamine and methylisocyanate seems reasonable in view of the values observed in aziridine and oxaziridine derivatives.

(2) The Influence of the Phosphorus Lone-pair on $^2J(^{31}P,H)$

The effect of the phosphorus lone-pair on two-bond $^{31}P,H$ coupling constants in tervalent phosphorus compounds has been investigated (46–48). For a series of cyclic phosphines, Albrand *et al.* (46, 47) plotted the observed $^2J(^{31}P,H)$ against the dihedral angle involving the phosphorus lone-pair and the PCH fragment. These data are replotted in Fig. 5 along with a plot of $^2J(^{15}N,H)$ as calculated[6] for methylamine in Fig. 1. The similar shape of these two curves suggests a similar mechanism by which spin information is transferred between the nuclei.

(3) The Influence of the Nitrogen Lone-pair on $^2J(H,H)$ in an Adjacent Methylene Group

The effect of lone-pairs on geminal proton–proton coupling constants has been calculated for several conformations of methylamine, two of which are shown in **VII** and **VIII**. $^2J(H_A,H_B)$ is plotted as a function of θ in Fig. 6. According to an earlier MO theory (38) back-donation from the lone-pair into antisymmetrical CH_2 orbitals leads to an increase in $^2J(H,H)$: the present calculations indicate maximum donation for $\theta = 30°$ (**VII**) and minimum donation for $\theta = 120$ and $300°$ (**VIII**).

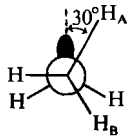

$\theta = 30°$, $^2J(H_A,H_B) = -0.85$ Hz

VII

[6]In comparing the angular dependence of $^2J(^{15}N,H)$ and $^2J(^{31}P,H)$ it is convenient to multiply either parameter by -1 because the magnetogyric ratios of ^{15}N and ^{31}P have opposite sign.

Can. J. Chem. Downloaded from www.nrcresearchpress.com by 210.87.254.105 on 09/05/12
For personal use only.

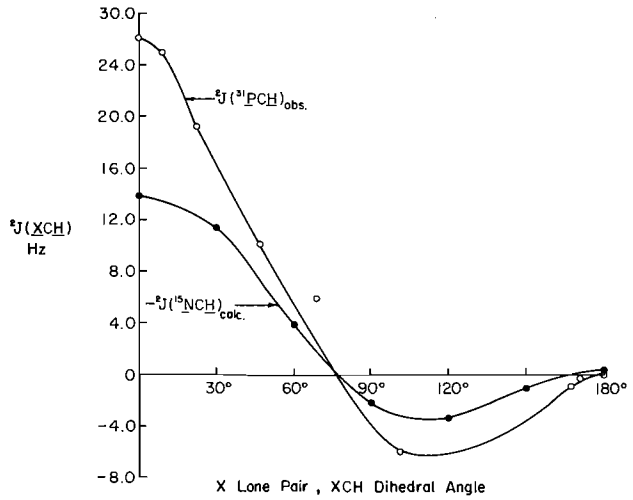

FIG. 5. A plot of the observed $^2J(^{31}P,H)$ in some tervalent phosphorus compounds (46, 47) and of the calculated $-^2J(^{15}N,H)$ in methylamine *vs.* the dihedral angle defined by the lone-pair—X—C—H fragment. See section 2 of the text.

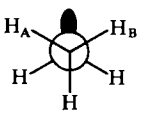

$\theta = 300°$, $^2J(H_A,H_B) = -4.79$ Hz

VIII

In Table 5 the calculated angular dependence of $^2J(H,H)$ is compared with the experimental values for a series of compounds with bridgehead nitrogen atoms (49). The calculated values of $^2J(H,H)$ are obviously too large (2), although the relative values are in fair agreement with experiment. Chivers and Crabb (49) predict $^2J(H,H)$ as most positive when $\theta = 0°$ but INDO calculates $^2J(H,H)_{\theta=30°} > {}^2J(H,H)_{\theta=0°}$. To show that the observed variations in $^2J(HCH)$ are due to lone-pair effects, $^2J(HNH)$ was calculated for the staggered conformation, $^2J(HNH) = -6.57$ Hz, and for the eclipsed conformation, $^2J(HNH) = -7.10$ Hz. The difference was only 0.53 Hz.

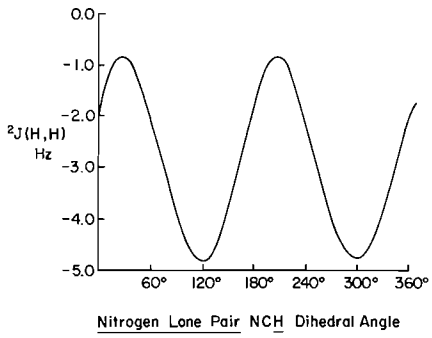

FIG. 6. A plot of the calculated $^2J(HCH)$ in methylamine *vs.* the lone-pair—N—C—H dihedral angle.

TABLE 5. Calculated and observed (49) influence of nitrogen lone-pair orientation on $^2J(HCH)$ values in an adjacent methylene group

$\theta°$	^2J obs.	Δ^* obs.	^2J calc.	Δ^* calc.
30	−8.5	4.9	−0.85	4.0
60	−11.0	2.5	−1.92	2.9
300	−13.6	0.0	−4.79	0.0

$^*\Delta \equiv J_\theta - J_{300°}$.

(4) Three-bond Nitrogen–Proton Coupling Constants, $^3J(N,H)$

In Table 6 the calculated $^3J(^{15}N,H)$ are presented for 15 compounds with rigid geometries. The paucity of experimental data makes a critical evaluation of the calculated $^3J(^{15}N,H)$ values difficult. However, several experimental trends appear to be reproduced by the calculations. On protonation of the nitrogen atom, $^3J(^{15}N,H)$ is predicted to decrease, (see compounds 1 and 2, 3 and 4, 7 and 8, and 11 and 12, Table 6) in line with an experimental rule (33): on quaternization of the nitrogen atom, $^3J(^{15}N,H)$ decreases. In vinyl isocyanide $^3J(^{15}N, H_{trans})$ is calculated as approximately twice

Can. J. Chem. Downloaded from www.nrcresearchpress.com by 210.87.254.105 on 09/05/12
For personal use only.

Can. J. Chem. Downloaded from www.nrcresearchpress.com by 210.87.254.105 on 09/05/12
For personal use only.

TABLE 6. Calculated and observed three-bond $^{15}N,H$ coupling constants*

	Compound		$^3J(^{15}N,H)$ calc.	$^3J(^{15}N,H)$ obs.
1			−0.59	−1.53
2	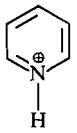		−7.51	−3.98
3	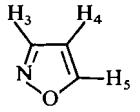	H_4 H_5	−0.74 2.14	— —
4	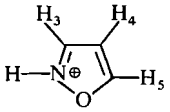	H_4 H_5	−5.45 −17.27	— —
5			−3.19	—
6	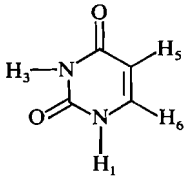	N_1H_3 N_1H_5 N_3H_1 N_3H_5	−7.30 −8.10 −7.01 −7.73	— — — —
7	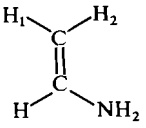	H_1 H_2	−11.17 −4.56	— —
8	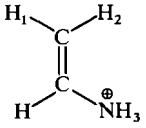	H_1 H_2	−13.56 −6.76	— —
9	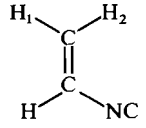	H_1 H_2	−11.96 −5.19	−8.68 −4.26
10	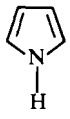		−10.93	−5.40

TABLE 6 (*Concluded*).

	Compound	$^3J(^{15}N,H)$ calc.	$^3J(^{15}N,H)$ obs.
11	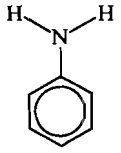	−2.52	−1.94
12	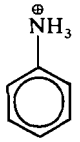	−5.00	—
13	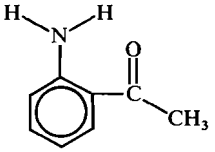	−3.90	−2.46
14	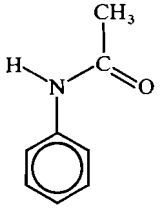	−3.86	−1.85
15	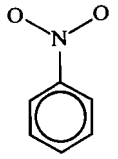	−3.75	2.5†

*References to the geometries and observed coupling constants for the first ten molecules are given in Table 1. The geometries used, and the experimental values observed, for compounds 11, 13, 14 and 15 are given in ref. 50. For the anilinium ion, standard geometries (8, 37) were used to calculate the atomic coordinates of the atoms in the benzene ring fragment. The C—N and N—H bond lengths were taken as 1.431 and 1.03 Å, respectively (5). All CNH and HNH angles were taken as 109.47°.

†This is the experimental value of $^3J(^{15}N,H)$ in α-nitronaphthalene, see Y. Kawazoe, M. Araki, S. Sawaki, and M. Ohnishi. Chem. Pharm. Bull. (Tokyo), **18**, 381 (1970).

$^3J(^{15}N,H_{cis})$, in good agreement with experiment. For aniline, 2-aminoacetophenone, acetanilide, and nitrobenzene, the calculated $^3J(^{15}N,H)$ values range from −2.52 to −3.90 Hz. If $^3J(^{15}N,H)$ in nitrobenzene is negative the observed $^3J(^{15}N,H)$ values fall between −1.85 and −2.5 Hz, in fair agreement with the calcu-

Can. J. Chem. Downloaded from www.nrcresearchpress.com by 210.87.254.105 on 09/05/12
For personal use only.

TABLE 7. Effect of substituent electronegativity on $^3J(^{15}N,H)$ and $^3J(H,H)$*

X	$^3J(^{15}N,H_{cis})$ calc.	$^3J(H_1,H_2)$ calc.	$^3J(H_1,H_2)$ obs.
Li	−13.04	23.03	19.3
H	−6.76	9.31	11.5
F	−1.99	4.74	4.65

*Standard geometries (8, 37) were used for all calculations. The C—Li bond length was taken as 2.1 Å. Computed and observed values of $^3J(H_1,H_2)$ are cited from ref. 3.

lated values. With the exception of $^3J(^{15}N,H_5)$ in isoxazole, all $^3J(^{15}N,H)$ coupling constants are correctly calculated as negative.

In Table 7 the $^3J(^{15}N,H)$ values calculated for three vinylamines are compared with $^3J(H,H)$ calculated in three ethylene derivatives (3). As the electronegativity of X increases, $^3J(^{15}N,H)$ increases while $^3J(H,H)$ decreases. Thus, for the vinyl fragment the reduced coupling constants, $^3K(N,H)_{cis}$ and $^3K(H,H)_{cis}$, show similar substituent effects.

To anticipate future experiments, the angular dependence of $^3J(^{15}N,H)$ was evaluated for ethylamine, protonated ethylamine, ethylisocyanide, *cis*- and *trans*-acetaldoxime, and protonated *cis*- and *trans*-acetaldoxime. Since the

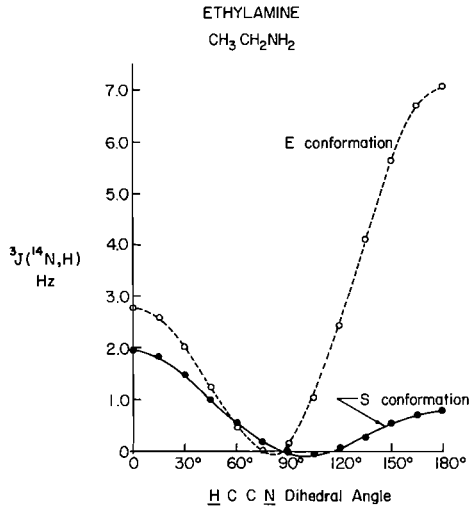

FIG. 7. A plot of the calculated $^3J(^{14}N,H)$ *vs.* the NCCH dihedral angle for the E and S conformations of ethylamine. The E and S conformations are depicted in **IX** and **X** of the text.

experimental plots (52) present $^3J(^{14}N,H)$ *vs.* the *NCCH* dihedral angle, the same convention will be followed here. This facilitates a comparison between $^3J(^{14}N,H)$ and the analogous couplings $^3J(H,H)$, $^3J(F,H)$, and $^3J(P,H)$; all these nuclei having positive gyromagnetic ratios.

(a) The Angular Dependence of $^3J(^{14}N,H)$ in the 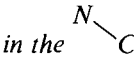 *Fragment*

(i) Ethylamine

In Fig. 7 the NCCH dihedral angle, θ, in ethylamine is plotted against calculated $^{14}N,H$ coupling constants. Two conformations of the amino group are considered: in the E conformation (**IX**) the N—H bonds and the C—H bonds of the adjacent methylene group are eclipsed,

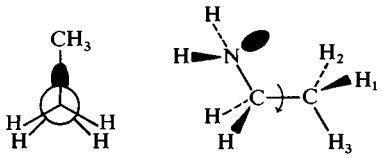

E conformation
$\theta = 180°$ (H_3); $60°$ (H_1 and H_2)

IX

while in the S conformation (**X**) they are staggered. Note that in the E conformation the nitrogen lone-pair lies *cis* to the methyl group while in the S conformation it lies *trans* to the methyl group. The E conformation is calculated to be more stable than the S conformation for all angles θ.

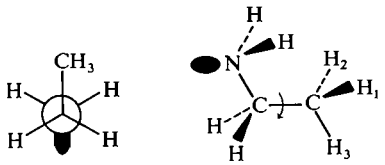

S conformation
$\theta = 180°$ (H_3); $60°$ (H_1 and H_2)

X

From Fig. 7 it is apparent that $^3J(^{14}N,H)$ is dependent both on the orientation of the nitrogen lone-pair and on the NCCH dihedral angle. Both the E and S conformations of ethylamine are most stable when the C—H bonds of the methyl and methylene groups are staggered, *i.e.* for $\theta = 60$ (H_1 and H_2) and $180°$ (H_3). Then $^3J(^{14}N,H)_{ave}$ is 2.65 Hz for the E conformation, and is 0.61 Hz for S. In rigid compounds a similar dependence of $^3J(N,H)$ on lone-pair

Can. J. Chem. Downloaded from www.nrcresearchpress.com by 210.87.254.105 on 09/05/12
For personal use only.

orientation is observed (53–56). For example, in *N,N*-dimethylnitrosamine (**XI**), $^3J(^{15}N,H) = \pm 2.2$ Hz when the methyl group lies *cis* to the lone-pair while $^3J(^{15}N,H) = \pm 0.8$ Hz when the methyl group lies *trans* to the lone-pair (53).

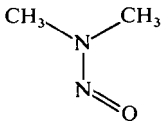

XI

The coordinates of the amino group nuclei were calculated assuming equal C—N and N—H bond lengths in ethylamine and methylamine (ref. *l* in Table 1). In addition, the following bond angles were assumed: angle HNC = 109.47° and dihedral angles HNCC = ±120 (E conformation) and ±60° (S conformation). The atomic coordinates of the ethyl group were taken from the literature (57).

$^3J(^{31}P,H)$ in aminophosphines depends on the orientation of the phosphorus lone-pair (58–60). Below −120 °C the p.m.r. spectrum of methylaminobis(trifluoromethyl)phosphine, $CH_3NH{\cdot}P(CF_3)_2$, indicates the presence of two rotational isomers (**XII***a*) and (**XII***b*). The most abundant isomer is assigned to **XII***a* where $^3J(^{31}P,H) = 13.9$ Hz while in **XII***b*, $^3J(^{31}P,H) \simeq$

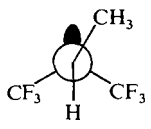

XIIa

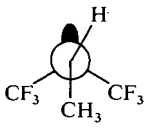

XIIb

4 Hz (58). In phosphines and in nitrogen compounds containing a lone-pair, $^3J(^{31}P,H)$ and $^3J(^{14}N,H)$ apparently display a similar dependence on the orientation of the lone-pair.

(ii) Protonated Ethylamine

In Fig. 8, $^3J(^{14}N,H)$ in protonated ethylamine is plotted against the dihedral angle in the fragment $^+$NCCH. Both the E (**XIII**) and S (**XIV**) conformations of the amino group are considered. The atomic coordinates for protonated ethylamine were essentially the same as those used for the unprotonated species. All H—N—X angles were taken as 109.47° and the N—H bond length was assumed to be 1.03 Å. For every angle θ the S conformation (**XIV**) was more stable than the E conformation (**XIII**).

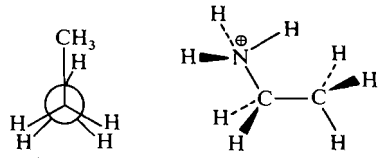

XIII

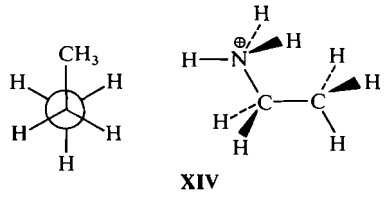

XIV

The curves of $^3J(^+NCCH)$ *vs.* θ in Fig. 8 are very similar, in contrast to those of the unprotonated molecules (Fig. 7). Note the increase in $^3J(^{14}N,H)$ over its values in the unprotonated species.

(iii) Ethylisocyanide

In Fig. 9 the curve depicting the calculated angular dependence of $^3J(^{14}N,H)$ closely resembles the rough experimental curves assembled by Bothner-By and Cox (52). INDO finds 2.345 kcal/mol as the barrier to rotation about C—C bond. Therefore it is best to use the cal-

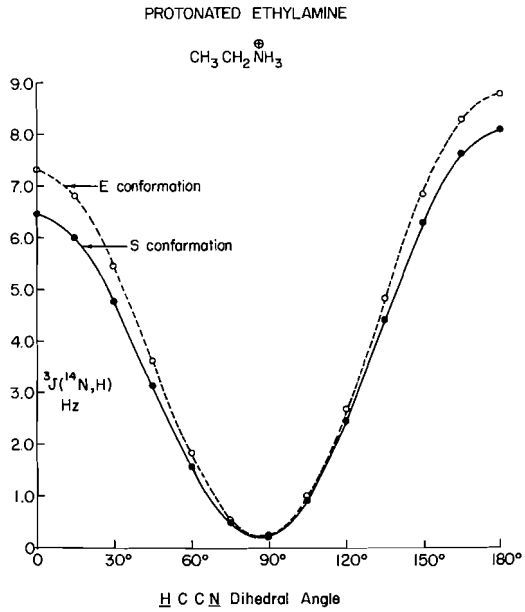

FIG. 8. A plot of the calculated $^3J(^{14}N,H)$ *vs.* the dihedral angle of the NCCH fragment in the E and S conformations of protonated ethylamine.

Can. J. Chem. Downloaded from www.nrcresearchpress.com by 210.87.254.105 on 09/05/12
For personal use only.

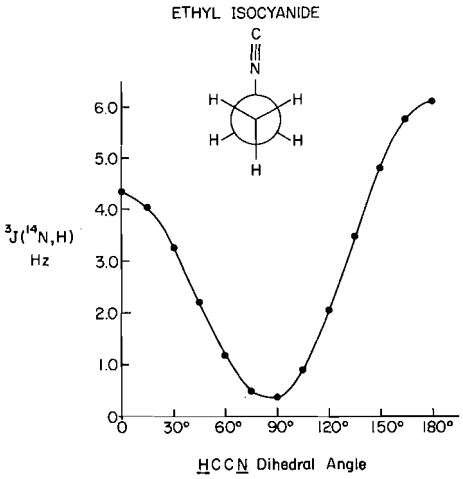

FIG. 9. A plot of the calculated $^3J(^{14}N,H)$ *vs.* the NCCH dihedral angle in ethylisocyanide.

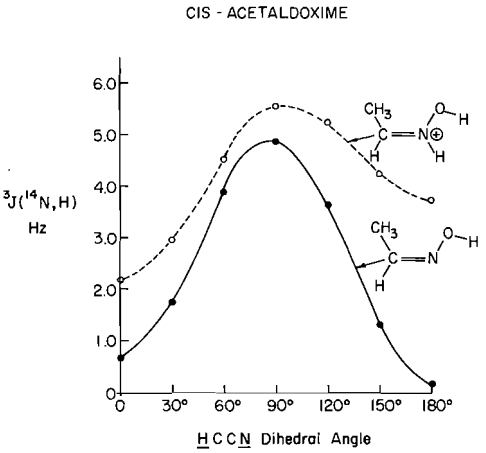

FIG. 10. A plot of the calculated $^3J(^{14}N,H)$ *vs.* the NCCH dihedral angle in *cis*-acetaldoxime and in protonated *cis*-acetaldoxime.

culated average $^{14}N,H$ couplings in the staggered conformation. One has $^3J(^{14}N,H)_{ave} = 2.81$ and $^2J(^{14}N,H)_{ave} = -2.78$ Hz. Maher (25) and MacFarlane (24) observe $^3J(^{14}N,H) = 2.5$ and $^2J(^{14}N,H) = -2.0$ Hz.

The bond lengths and angles in the C—N≡C and the ethyl fragments were taken as those in methylisocyanide and ethane, respectively (refs. *i* and *h* in Table 1).

(b) The Angular Dependence of $^3J(^{14}N,H)$ *in the* $N\equiv C-C^{H}$ *Fragment*

(i) cis-Acetaldoxime and Protonated cis-Acetaldoxime

In Fig. 10 the calculated $^3J(^{14}N,H)$ in **XV** and **XVI** is plotted *vs.* the N=C—C—H dihedral angle. The maximum occurs at an angle of 90° indicating the importance of the π orbitals of the C=N bond in the transmission of the spin information.

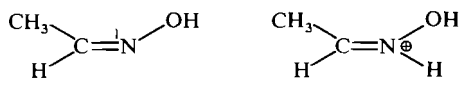

XV **XVI**

The structure used to calculate the atomic coordinates in **XV** was that of Rogowski and Schwendeman (61). With the exception of the methyl group, the protonated species was assumed planar, with all bond angles and bond lengths the same as those used for the unprotonated species; the N—H bond length was taken as 1.03 Å and the CNH angle as 120°. INDO calculates the barrier to rotation of the methyl group to be 208 cal/mol while the observed barrier is 373 cal/mol (61). The barrier in the protonated species is calculated to be slightly larger, 363 cal/mol.

Averaging over all angles yields $^3J(^{14}N,H)$ as 2.65 and 4.22 Hz, respectively, for *cis*-acetaldoxime and protonated *cis*-acetaldoxime.

(ii) trans-Acetaldoxime and Protonated trans-Acetaldoxime

In Fig. 11 the H—C—C=N dihedral angle in **XVII** and **XVIII** is plotted against the calculated $^3J(^{14}N,H)$.

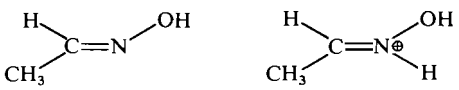

XVII **XVIII**

The structural parameters for *trans*-acetaldoxime were obtained from Rogowski and Schwendeman (61). Except for the additional proton, the protonated species was assumed to have the same structure as the unprotonated species: the N—H bond length was taken as 1.03 Å, the CNH bond angle as 120° and the CCNO dihedral angle as 180°.

INDO finds the barrier to rotation of the methyl group to be 1080 cal/mol while the experimental barrier is 1835 cal/mol (61). The barrier in the protonated species was calculated as 1185 cal/mol. Since the observed barrier is

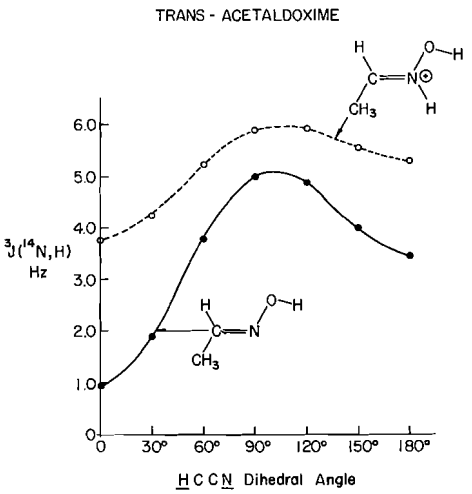

FIG. 11. A plot of the calculated $^3J(^{14}N,H)$ *vs.* the NCCH dihedral angle in *trans*-acetaldoxime and in protonated *trans*-acetaldoxime.

greater than $3kT$ one can compare the calculated and observed coupling constants by considering only the most stable conformation. The average values of $^3J(^{14}N,H)$ for the most stable conformations are 3.57 and 5.25 Hz for *trans*-acetaldoxime and protonated *trans*-acetaldoxime, respectively.

Notice that in the *trans* isomer (**XVII**), the nitrogen lone-pair is *cis* to the methyl group and $^3J(^{14}N,H)$ is calculated to be larger than in the case where the methyl group is *trans* (**XV**) to the lone-pair. This is in good agreement with experiment. For the oxime (**XIX**) $^3J[^{14}N,CH_3(A)]$ is 1.57 and $^3J[^{14}N,CH_3(B)]$ is 2.86 Hz (33). When **XIX** is studied in trifluoroacetic acid, each of

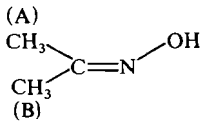

XIX

the $^{14}N,H$ coupling constants becomes larger: $^3J[^{14}N,CH_3(A)]$ is 2.36 and $^3J[^{14}N,CH_3(B)]$ is 3.27 Hz (33). Although all the calculated coupling constants are a little too large, their relative values agree with experiment.

In summary, SCF calculations at the INDO level predict a dihedral angle dependence of $^3J(^{14}N,H)$ in the N—C—C—H fragment similar to that observed for $^3J(H,H)$ (1, 3, 5), for $^3J(^{19}F,H)$ (62, 63), and for $^3J(^{31}P,H)$ (52, 64) in the saturated X—C—C—H fragments. The angular dependence of $^3J(^{14}N,H)$ in the N=C—C—H fragment is computed as different from that in the saturated fragment.

TABLE 8. Calculated and observed $^{15}N,H$ coupling constants for pyridine and the pyridinium ion*

			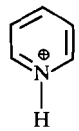	
	J calc.	*J* obs. (34)	*J* calc.	*J* obs. (34)
$^2J(^{15}N,H)$	−16.98	−10.76	0.47	−3.01
$^3J(^{15}N,H)$	−0.59	−1.53	−7.51	−3.98
$^4J(^{15}N,H)$	0.54	±0.21	1.73	±0.69

*The geometries used for these calculations are given in Table 1.

TABLE 9. Calculated and observed $^{15}N,H$ coupling constants for aniline and the anilinium ion*

	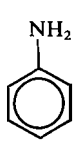		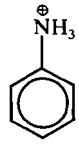	
	J calc.	*J* obs. (50)	*J* calc.	*J* obs. (65)
$^1J(^{15}N,H)$	−59.53	−78.875	−72.36	−76.0±0.5
$^3J(^{15}N,H)$	−2.52	−1.935	−5.00	—
$^4J(^{15}N,H)$	−1.06	−0.476	−1.04	—
$^5J(^{15}N,H)$	+0.18	0.009	−1.34	—

*The geometries used for these calculations are given in Table 6.

(5) The Effect of Protonation on J(N,H) in Pyridine, Aniline, Ammonia, and Methylamine

In Tables 8 and 9 the calculated and observed $^{15}N,H$ couplings are given for pyridine and the pyridinium ion, and for aniline and the anilinium ion. In Table 10, $^1J(^{15}N,H)$ is presented for ammonia, the ammonium ion, methylamine, and protonated methylamine.

INDO predicts a decrease in $^1J(^{15}N,H)$ on protonation, in agreement with experiment for ammonia and methylamine but not for aniline, where uncertainty about the geometry of the amino group may be the cause of the disagreement. Thus, a planar amino group entails a calculated $^1J(^{15}N,H)$ of −92.5 Hz (50).

Can. J. Chem. Downloaded from www.nrcresearchpress.com by 210.87.254.105 on 09/05/12
For personal use only.

TABLE 10. Calculated and observed $^1J(^{15}N,H)$ in ammonia and methylamine*

Compound	$^1J(^{15}N,H)$ calc.	$^1J(^{15}N,H)$ obs.	Reference
NH_3	−42.64	−61.2	66
$^{\oplus}NH_4$	−73.52	−73.2	29
CH_3NH_2	−34.78	−65.0	28
$CH_3\overset{\oplus}{N}H_3$	−75.38	−75.6	29

*Standard geometries (8, 37) were used to calculate the atomic coordinates of ammonia. The N—H bond length was taken as 1.03 Å for ammonia. The geometries used for methylamine and protonated methylamine are given in Table 1.

On protonation, the calculations predict an increase in $^2J(^{15}N,H)$ in pyridine, a decrease in $^3J(^{15}N,H)$ in aniline and pyridine, an increase in $^4J(^{15}N,H)$ in pyridine, and a decrease in $^5J(^{15}N,H)$ in aniline. Such an alternating effect due to protonation has been observed by Crépaux *et al.* (33).

Conclusions

A comparison of theoretical with the available experimental two- and three-bond nitrogen–proton spin–spin coupling constants encourages their combined use in conformational and structural work.[7]

The cooperation of the staff at the University of Manitoba Computer Centre is gratefully acknowledged. We thank the National Research Council of Canada for financial support.

1. (*a*) A. A. BOTHNER-BY. Advan. Magn. Res. **1**, 195 (1965). (*b*) T. YONEZAWA, I. MOROSHIMA, K. FUKUTA, and Y. OHMORI. J. Mol. Spectrosc. **31**, 341 (1969).
2. G. E. MACIEL, J. W. MCIVER, JR., N. S. OSTLUND, and J. A. POPLE. J. Am. Chem. Soc. **92**, 4151 (1970).
3. G. E. MACIEL, J. W. MCIVER, JR., N. S. OSTLUND, and J. A. POPLE. J. Am. Chem. Soc. **92**, 4497 (1970).
4. G. E. MACIEL, J. W. MCIVER, JR., N. S. OSTLUND, and J. A. POPLE. J. Am. Chem. Soc. **92**, 4506 (1970).
5. L. M. JACKMAN and S. STERNHELL. Applications of nuclear magnetic resonance spectroscopy in organic chemistry. Pergamon Press, Oxford. 1969.
6. J. A. POPLE, J. W. MCIVER, JR., and N. S. OSTLUND. Chem. Phys. Lett. **1**, 465 (1967).

[7]After completion of this work, a paper (69) appeared giving the results of CNDO/2 and INDO calculations on N,H; C,H; and H,H coupling constants in several of the molecules discussed above. There are some large discrepancies in the two sets of N,H couplings. Our calculations are in exact agreement with previous data for $^1J(^{14}N,H)$ in ammonia (7, 8), $^1J(^{15}N,^{13}C)$ in methyl cyanide (70), and $^1J(^{13}C,H)$ in methylenimine (71).

7. J. A. POPLE, J. W. MCIVER, JR., and N. S. OSTLUND. J. Chem. Phys. **49**, 2960, 2965 (1968).
8. J. A. POPLE and D. L. BEVERIDGE. Approximate molecular orbital theory. McGraw-Hill Book Company, New York, N.Y. 1970.
9. J. A. POPLE, D. L. BEVERIDGE, and P. A. DOBOSH. J. Chem. Phys. **47**, 2026 (1967).
10. E. W. RANDALL and D. G. GILLIES. *In* Progress in nuclear magnetic resonance spectroscopy. Vol. 6. J. W. Emsley, J. Feeney, and L. H. Sutcliffe, editors. Pergamon Press, Oxford. 1971. p. 119.
11. R. L. LICHTER. *In* Determination of organic structures by physical methods. Vol. 4. F. C. Nachod and J. J. Zuckerman, editors. Academic Press. 1971. p. 195.
12. Program 141. Quantum chemistry program exchange. Indiana University, Bloomington, Indiana.
13. Program 135. Quantum chemistry program exchange. Indiana University, Bloomington, Indiana.
14. B. SUNNERS, L. H. PIETTE, and W. G. SCHNEIDER. Can. J. Chem. **38**, 681 (1960).
15. A. J. R. BOURN and E. W. RANDALL. Mol. Phys. **8**, 568 (1964).
16. R. J. CHUCK, D. G. GILLIES, and E. W. RANDALL. Mol. Phys. **16**, 121 (1969).
17. M. T. ROGERS and L. A. LAPLANCHE. J. Phys. Chem. **69**, 3648 (1965).
18. A. K. BOSE and I. KUGAJEVSKY. Tetrahedron, **23**, 1489 (1967).
19. M. OHTSURU, K. TORI, J. M. LEHN, and R. SEHER. J. Am. Chem. Soc. **91**, 1187 (1969).
20. E. RAHKAMAA. Mol. Phys. **19**, 727 (1970).
21. B. W. ROBERTS, J. B. LAMBERT, and J. D. ROBERTS. J. Am. Chem. Soc. **87**, 5439 (1965).
22. D. S. MATTESON and R. A. BAILEY. J. Am. Chem. Soc. **90**, 3761 (1968).
23. A. J. R. BOURN and E. W. RANDALL. J. Mol. Spectrosc. **13**, 29 (1964).
24. W. MCFARLANE. J. Chem. Soc. A, 1660 (1967).
25. J. P. MAHER. J. Chem. Soc. A, 1855 (1966).
26. G. BINSCH and J. D. ROBERTS. J. Phys. Chem. **72**, 4310 (1968).
27. G. A. OLAH and T. E. KIOVSKY. J. Am. Chem. Soc. **90**, 4666 (1968).
28. L. PAOLILLO and E. D. BECKER. J. Mag. Res. **3**, 200 (1970).
29. G. BINSCH, J. B. LAMBERT, B. W. ROBERTS, and J. D. ROBERTS. J. Am. Chem. Soc. **86**, 5564 (1964).
30. D. M. JERINA, D. R. BOYD, L. PAOLILLO, and E. D. BECKER. Tetrahedron Lett. **18**, 1483 (1970).
31. E. D. BECKER. Private communication.
32. M. OHTSURU and K. TORI. Tetrahedron Lett. **47**, 4043 (1970).
33. D. CRÉPAUX, J. M. LEHN, and R. R. DEAN. Mol. Phys. **16**, 225 (1969).
34. R. L. LICHTER and J. D. ROBERTS. J. Am. Chem. Soc. **93**, 5218 (1971).
35. J. P. KINTZINGER and J. M. LEHN. Chem. Commun. 660 (1967).
36. E. D. BECKER, R. B. BRADLEY, and T. AXENROD. J. Mag. Res. **4**, 136 (1971).
37. J. A. POPLE and M. GORDON. J. Am. Chem. Soc. **89**, 4254 (1967).

Can. J. Chem. Downloaded from www.nrcresearchpress.com by 210.87.254.105 on 09/05/12
For personal use only.

38. J. A. POPLE and A. A. BOTHNER-BY. J. Chem. Phys. **42**, 1339 (1965).
39. T. NISHIKAWA, T. ITOH, and K. SHIMODA. J. Chem. Phys. **23**, 1735 (1955).
40. F. B. RIDDELL and J. M. LEHN. J. Chem. Soc. B, 1224 (1968).
41. R. G. LETT and W. H. FLYGARE. J. Chem. Phys. **47**, 4730 (1967).
42. J. M. LEHN and B. MUNSCH. Theor. Chim. Acta, **12**, 91 (1968).
43. J. M. LEHN, B. MUNSCH, and P. MILLIÉ. Theor. Chim. Acta. **16**, 351 (1970).
44. J. M. LEHN, B. MUNSCH, P. MILLIÉ and A. VEILLARD. Theor. Chem. Acta, **13**, 313 (1969).
45. F. A. L. ANET, J. C. JOCHIMS, and C. H. BRADLEY. J. Am. Chem. Soc. **92**, 2557 (1970).
46. J. P. ALBRAND, D. GAGNAIRE, and J. B. ROBERT. Chem. Commun. 1469 (1968).
47. J. P. ALBRAND, D. GAGNAIRE, J. MARTIN, and J. B. Robert. Bull. Soc. Chim. Fr. 40 (1969).
48. H. GOLDWHITE and D. G. ROWSELL. Chem. Commun. 1665 (1968).
49. P. J. CHIVERS and T. A. CRABB. Tetrahedron, **26**, 3389 (1970).
50. R. WASYLISHEN, J. B. ROWBOTHAM, L. ERNST, and T. SCHAEFER. Can. J. Chem. In press.
51. D. G. LISTER and J. K. TYLER. Chem. Commun. 152 (1966).
52. A. A. BOTHNER-BY and R. H. COX. J. Phys. Chem. **73**, 1830 (1969).
53. W. J. JORGENSEN and L. C. ALLEN. J. Am. Chem. Soc. **93**, 567 (1971).
54. T. AXENROD, P. S. PREGOSIN, and G. W. A. MILNE. Chem. Commun. 702 (1968).
55. T. AXENROD, M. J. WIEDER, and G. W. A. MILNE. Tetrahedron Lett. **6**, 401 (1969).
56. T. AXENROD, M. J. WIEDER, and G. W. A. MILNE. Tetrahedron Lett. **18**, 1397 (1969).
57. T. AXENROD. Spectrosc. Lett. **3**, 263 (1970).
58. A. H. COWLEY, M. J. S. DEWAR, W. R. JACKSON, and W. B. JENNINGS. J. Am. Chem. Soc. **92**, 1085 (1970).
59. A. H. COWLEY, M. J. S. DEWAR, W. R. JACKSON, and W. B. JENNINGS. J. Am. Chem. Soc. **92**, 5206 (1970).
60. J. NELSON, R. SPRATT, and B. J. WALKER. Chem. Commun. 1509 (1970).
61. R. S. ROGOWSKI and R. H. SCHWENDEMAN. J. Chem. Phys. **50**, 397 (1969).
62. K. L. WILLIAMSON, Y. L. HSU, F. H. HALL, S. SWAGER, and M. S. COULTER. J. Am. Chem. Soc. **90**, 6717 (1968).
63. M. S. GOPINATHAN and P. T. NARASIMHAM. Mol. Phys. **21**, 1141 (1971).
64. D. W. WHITE and J. G. VERKADE. J. Mag. Res. **3**, 111 (1970).
65. T. AXENROD, M. J. WIEDER, G. BERTI, and P. L. BARILI. J. Am. Chem. Soc. **92**, 6066 (1970).
66. R. A. BERNHEIM and H. BATIZ-HERNANDEZ. J. Chem. Phys. **40**, 3446 (1964).
67. W. A. ANDERSON and R. FREEMAN. J. Chem. Phys. **39**, 1518 (1963).
68. J. E. LANCASTER. Spectrochim. Acta, **23A**, 1449 (1967).
69. M. S. GOPINATHAN and P. T. NARASIMHAM. Mol. Phys. **22**, 473 (1971).
70. G. E. MACIEL, J. W. MCIVER, JR., N. S. OSTLUND, and J. A. POPLE. J. Am. Chem. Soc. **92**, 11 (1970).
71. G. E. MACIEL, J. W. MCIVER, JR., N. S. OSTLUND, and J. A. POPLE. J. Am. Chem. Soc. **92**, 1 (1970).

Can. J. Chem. Downloaded from www.nrcresearchpress.com by 210.87.254.105 on 09/05/12
For personal use only.

Pyrolysis of 3-Chloro-3-aryldiazirines, Kinetics and Mechanism

MICHAEL T. H. LIU AND K. TORIYAMA

Department of Chemistry, University of Prince Edward Island, Charlottetown, Prince Edward Island

Received April 26, 1972

The thermal decomposition of 3-chloro-3-aryldiazirines in various solvents has been investigated over the temperature range 60–100 °C. The intermediate carbenes have been isolated as norcaranes by the use of cyclohexene. Substituent effects on rates of reaction are small and a Hammett correlation was unsuccessful with either σ or σ^+ constants. Possible mechanisms for the decompositions are discussed.

La décomposition thermique des chloro-3 aryl-3 diazirines dans divers solvants, a été examinée dans un domaine de température de 60 à 100 °C. Les carbènes intermédiaires ont été isolés sous forme de norcaranes en présence de cyclohexène. Les effets des substituants sur les vitesses de réaction sont faibles et une corrélation de Hammett est appliquée sans succès que ce soit avec les constantes σ ou σ^+. Les mécanismes possibles pour ces décompositions sont discutés. [Traduit par le journal]

Canadian Journal of Chemistry, **50**, 3009 (1972)

Can. J. Chem. Downloaded from www.nrcresearchpress.com by 210.87.254.105 on 09/05/12
For personal use only.

Introduction

The nature of the pathway of ring rupture in diazirine is not well understood. In the thermal decomposition of 3-chloro-3-alkyldiazirines (1, 2) Frey *et al.* proposed transition state I as the simplest representation for a diazirine decomposition, where the two carbon—nitrogen bonds are broken simultaneously. Schmitz (3) has postulated an ionic mechanism, II, as the most probable pathway on the grounds of the relative instability of α-ketopentamethylenediazirine as compared with pentamethylenediazirine. Mitsch and co-workers (4, 5) prefer a mechanism involving the transient existence of a diazomethane intermediate prior to the loss of nitrogen. It is likely that such a mechanism would require transition state III. Bottomly and

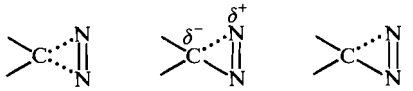

I II III

Nyberg (6) have studied the thermal decomposition of 3,3-dimethyldiazirine at relatively low temperature and suggested that the transition state was non-cyclic and probably radical in nature.

In our recent work (7, 8), we observed that the rate of diazirine decomposition shows very little solvent effect and we concluded that the transition state of the rate determining step is likely to be more radical than ionic. The present work was undertaken to examine the effect of para-substituents on the rates and activation parameters in the thermal decompositions of a series of 3-chloro-3-aryldiazirines, in the hope that a further elucidation of the transition state would be provided.

Experimental

I.r. and n.m.r. spectra were obtained with Perkin–Elmer Model 257 and Varian Associates, T 60 instruments respectively. The chemical shifts are given in τ scale together with splitting patterns, assignments, and relative integrated areas. The u.v. spectra were measured with a Unicam sp. 800 spectrophotometer. V.p.c. analyses were carried out using a Perkin–Elmer model F 11 equipped with a hydrogen flame detector; the peak areas were integrated by a ball and disc integrator. Elemental analyses were by Franz Pascher, Bonn, Germany.

Solvents

Cyclohexene was passed through alumina column to remove impurities and was fractionally distilled. Diethyleneglycol monoethyl ether (DEGME) and dimethyl sulfoxide (DMSO) were stirred with calcium hydride for 1 day and fractionally distilled under anhydrous conditions.

3-Chloro-3-aryldiazirines

These compounds were prepared from the corresponding amidine hydrochlorides by oxidation with aqueous sodium hypochlorite in DMSO according to the method of Graham (9). The phenyl, *p*-tolyl and *p*-chlorophenyl compounds were purified by column chromatography (silica gel – pentane or pentane and dichloromethane). The *p*-methoxyphenyl and *p*-nitrophenyl compounds were recrystallized from pentane (Norite). Yields and physical properties are listed in Table 1.

Kinetics Procedure

(a) By Vapor Phase Chromatography

The rates of reaction were measured by following the disappearance of diazirine, as described previously (8).

(b) By Nitrogen Evolution Method

The reaction was carried out by mixing a specific amount

TABLE 1. Yields and physical properties of 3-chloro-3-aryldiazirines

Aryl	Yield* (%)	I.r.† (N=N, cm^{-1})	U.v. λ max (ε)‡ (nm in cyclohexane)
p-Methoxyphenyl	57	1565	412 (416), 391 (492), 372 (307), 354 (164), 337 (93)
p-Tolyl	58	1566	400 (314), 396 (305), 390 (285), 379 (346), 361 (220), 343 (130)
Phenyl	54	1570	395 (213), 389 (210), 384 (194), 374 (229), 370 (204), 355 (125), 339 (53)
p-Chlorophenyl	59	1570	396 (304), 391 (308), 386 (324), 375 (345), 357 (276), 340 (132)
p-Nitrophenyl	23	1579	385 (395), 380 (492), 366 (624), 348 (490), 330 (407)

*Based on amidine hydrochlorides.
†Neat except *p*-nitrophenyl in carbon tetrachloride.
‡λ_{max} or shoulders of complicated characteristic absorption of diazirines.

TABLE 2. Observed wavelengths (nm) of 3-chloro-3-aryldiazirines

Solvent	*p*-Methoxyphenyl	*p*-Tolyl	Phenyl	*p*-Chlorophenyl	*p*-Nitrophenyl
Cyclohexene	395	412	403	396	384
DMSO	394	410	400	392	—
DEGME	390	414	400	390	380

of diazirine with appropriate thermo-equilibrated solvent in the reaction vessel, which was immersed in the oil bath and connected to a gas burette. The first order rate coefficients were determined graphically from the plot of log $(V_\infty - V_t)$ against time where V_∞ is the volume of nitrogen measured at infinite time and V_t is that at time t.

(c) By Ultraviolet Spectrophotometry

The detailed experimental procedure was as described in our earlier work (8). The first order rate coefficients were determined graphically from the plot of log $(D_t - D_\infty)$ against time, where D_t is the optical density at the wavelength of observation and D_∞ corresponds to that of the complete reaction. The wavelengths of observation are given in Table 2.

Product Analyses

(a) Decompositions in Cyclohexene

(a-1) 7-Chloro-7-p-nitrophenylnorcarane

One gram of 3-chloro-3-*p*-nitrophenyldiazirine in 50 ml of cyclohexene was heated at 80° for 7 h. The solvent was removed under reduced pressure, leaving 1.3 g of yellow oil whose t.l.c. had one main spot with trace amount of other compounds. The n.m.r. of this material showed major peaks at 1.6 ~ 2.7 (m, aromatic-H, 4) and at 7.8 ~ 8.8 (m, cyclohexane ring-H, 10). Other minor absorptions showed two small sharp doublets of equal intensity at 5.27 and 5.40, and a small detectable multiplet at 4.1 ~ 4.8; these absorptions were probably due to the products (~15% estimated from peak area ratio in n.m.r. spectra) resulting from the insertion of carbene into the saturated C—H bonds of the cyclohexene ring. After leaving the oil at room temperature to air for several weeks, the major part crystallized. Repeated crystallization from petroleum ether (b.p. 30–80°) gave pale yellow crystals, m.p. 73.5–74.5: n.m.r. (in $CDCl_3$), 1.6–2.7 (m, aromatic H, 4); 7.7–9.0 (m, $-CH_2-$ and $-\underset{|}{C}H-$, 10).

Anal. Calcd. for $C_{13}H_{14}ClNO_2$: C, 62.03; H, 5.61; N, 5.56; Cl, 14.09. Found: C, 61.75; H, 5.43; N, 5.47; Cl, 14.04.

(a-2) 7-Chloro-7-p-methoxyphenylnorcarane

The decomposition of 3-chloro-3-*p*-methoxyphenyl diazirine was carried out essentially as described in section *a-1*. A yellow oil (2.59 g) was obtained after removal of the solvent from a reaction mixture initially containing 2.0 g of diazirine. The n.m.r. spectrum (CCl_4) of the crude oil showed signals from aromatic protons at 2.5 ~ 3.5, cyclohexane ring protons at 7.8 ~ 9.3, two small sharp doublets at 5.4 and 5.5, and small multiplets at 4 ~ 5; the methyl protons of the methoxy groups showed a triplet centered at 6.30. Unsuccessful attempts were made to separate the mixture by means of column chromatography. After the mixture was left to the atmosphere at room temperature for several weeks, crystals appeared which were extracted with petroleum ether yielding 0.65 g of crude

Can. J. Chem. Downloaded from www.nrcresearchpress.com by 210.87.254.105 on 09/05/12
For personal use only.

crystal. After two recrystallizations from methanol, 7-chloro-7-*p*-methoxyphenylnorcarane (0.4 g) was obtained, m.p. 45.0–45.5: n.m.r. (CCl_4) 2.5 ~ 3.3 (m, aromatic H, 4); 6.30 (s, OCH_3, 3); 7.7–9.0 (m, $—CH_2—$ and $—\underset{|}{C}H—$, 10).

Anal. Calcd. for $C_{14}H_{17}ClO$: C, 71.03; H, 7.24; Cl, 14.98. Found: C, 70.81; H, 7.29; Cl. 14.88.

(a-3) Decomposition of 3-chloro-3-phenyl, 3-chloro-3-p-chlorophenyl and 3-chloro-3-p-tolyldiazirine in cyclohexene

In the decomposition of the above diazirines, the same method was employed as described in the previous section, *a-1*. After the removal of solvent, the oils gave similar n.m.r. spectra as in sections *a-1* and *a-2*, showing the aromatic and cyclohexane ring protons (and methyl protons in the case of *p*-tolyl) as the major, and two small sharp doublets at 5.1 ~ 5.5 together with a multiplet at 4 ~ 5 as the minor. Distillation and column chromatography were ineffective in separating the mixture and no further attempts were made to isolate the products.

(b) Decomposition in DEGME

(b-1) Isolation of p-nitrobenzaldehyde ethylene acetal

3-Chloro-3-*p*-nitrophenyldiazirine (1.8 g) in 80 ml of DEGME was heated at 80–90° for 7 h. On dilution with water, a precipitate was obtained which was dissolved in hot cyclohexane and refluxed with Norite for 5 min. After filtering the warm solution, the collected crystals were recrystallized from ethanol, yielding 0.6 g, m.p. 89.5–90.0°, lit. m.p. 90.59° (10); n.m.r. ($CDCl_3$), 1.6 ~ 2.5 (m, aromatic -H, 4); 4.10 (s, 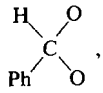 , 1); 5.90 (s, $—CH_2—O—$, 4).

From the extraction of the filtrate with chloroform, an additional 0.6 g of crude acetal was obtained. The acetal was decomposed in 2,4-dinitrophenylhydrazine–sulfuric acid–ethanol solution to give *p*-nitrobenzaldehyde-2,4-dinitrophenylhydrazone; m.p. 317–319° (dec.), lit. m.p. 320° (dec.) (11).

(b-2) Decomposition of other diazirines in DEGME

The procedures are similar to those described in section *b-1*. In the case of the *p*-methoxyphenyl derivative, the crude reaction mixture contained ~95% anisaldehyde and a trace amount of impurity. The n.m.r. spectrum in CCl_4 showed absorptions at 0.20 (s, CHO, 1); 2.1–2.8 (m, aromatic-H, 4) and 4.17 (s, $O—CH_3$, 3) and the i.r. compared well with the authentic sample. In the decompositions of 3-chloro-3-*p*-tolyl, 3-chloro-3-phenyl, 3-chloro-3-*p*-chlorophenyl diazirines, mixtures of aldehydes and acetals were obtained.

(c) Decomposition in DMSO

3-Chloro-3-phenyldiazirine (1 g) in 50 ml DMSO was heated at 80–85° for 3 h. The resulting mixture was diluted with water and extracted with ether. The extract was identified with authentic samples as a mixture of benzoic acid and benzaldehyde, which was left in air and oxidized to benzoic acid, 0.35 g. Similar results were obtained with other diazirines: 0.46 g of *p*-nitrobenzoic acid from 1 g of 3-chloro-3-*p*-nitro-phenyldiazirine and 0.42 g of *p*-toluic acid from 1 g of 3-chloro-3-*p*-tolyldiazirine.

Results

All the compounds were unstable at room temperature; however, except for the *p*-methoxyphenyl derivative, they can be kept in Dry Ice for several weeks without significant decomposition. Owing to the instability of these diazirines, the elemental analyses were not possible. All the diazirines obtained gave the following characteristics: one clear spot on t.l.c. with various solvents, sharp i.r. spectra, complicated u.v. absorption between 420 and 320 nm (in cyclohexane), quantitative nitrogen evolution when heated in diethyleneglycol monoethyl ether (DEGME), crystallization at low temperature, and symmetrical v.p.c. peaks for *p*-tolyl, phenyl, and *p*-chlorophenyl derivatives. Three representative solvents were chosen for the decompositions: cyclohexene for non-polar; DMSO for polar aprotic, and DEGME for polar protic solvent. The concentrations of diazirine in various solvents were adjusted in such a way as to suppress the formation of azine (8). The reactions obeyed first order

TABLE 3. Rate constants for the thermal decomposition of 3-chloro-3-aryldiazirines in cyclohexene

		$10^4 k_1$ (s^{-1})					
3-Aryl	Method	60.0°	70.0°	75.0°	80.0°	90.0°	95.0°
p-Methoxyphenyl	u.v.	1.10	3.2	6.2	10.6	29	—
p-Tolyl	v.p.c.	0.45	1.51	2.91*	4.8	15.3*	24
Phenyl‡	v.p.c.	—	1.06	1.95*	3.6	9.95*	—
p-Chlorophenyl	v.p.c.	0.43	1.42	2.48*	5.0	13.2*	23
p-Nitrophenyl	u.v.	0.34	1.16	2.04	3.64†	10.9	18.7

*Average value of k_1 measured by v.p.c. and u.v.
†Sample not degassed, $k_1 = 3.70 \times 10^{-4}$ s^{-1}.
‡$10^4 k_1$ (s^{-1}), 28.9 at 100°; 79 at 110°.

Can. J. Chem. Downloaded from www.nrcresearchpress.com by 210.87.254.105 on 09/05/12
For personal use only.

TABLE 4. Rate constants for the thermal decomposition of 3-chloro-3-aryldiazirines in various solvents at 75°

Solvent	$10^4 k_1$* (s^{-1})				
	p-Methoxyphenyl	*p*-Tolyl	Phenyl	*p*-Chlorophenyl	*p*-Nitrophenyl
Cyclohexene	6.2	2.91†	1.95†	2.48†	2.04
DEGME	8.4	3.59	2.30	2.84	2.19‡
DMSO	10.1	4.44	3.04	3.46	2.82

*Measured by u.v. spectrophotometer.
†Average value of k_1 measured by v.p.c. and u.v.
‡Measured by nitrogen evolution.

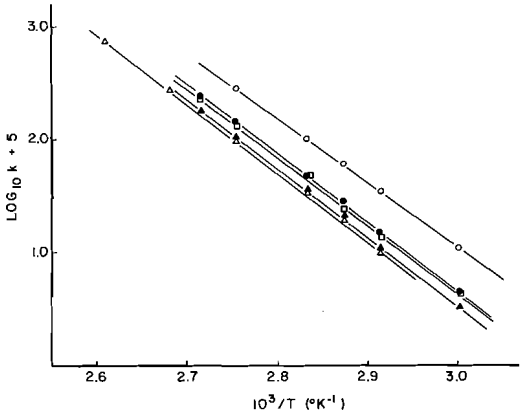

FIG. 1. Arrhenius plots for thermal decompositions of 3-chloro-3-aryldiazirines in cyclohexene:

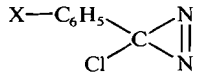

○, X = MeO; ●, X = Me; □, X = Cl; ▲, X = NO_2; △, X = H.

kinetics up to 90% completion (the first order rate constants were determined graphically from a minimum of eight runs). Rate constants for the thermal decompositions of the 3-chloro-3-aryldiazirines in cyclohexene are given in Table 3. The reproducibilities of the rate constants were ±2–6% by v.p.c. and ±1–3% by u.v. spectrophotometry. The Arrhenius plots of the rate data are shown in Fig. 1 and the least-squares treatment of the data gave the following expressions with the errors quoted in standard deviation: k_1 (*p*-methoxyphenyl) = $10^{13.41\pm0.35}$ exp $(-26{,}490 \pm 560/RT)$ s^{-1}; k_1 (*p*-tolyl) = $10^{13.94\pm0.20}$ exp $(-27{,}870 \pm 310/RT)$ s^{-1}; k_1 (phenyl) = $10^{13.87\pm0.13}$ exp $(-28{,}000 \pm 215/RT)$ s^{-1}; k_1 (*p*-chlorophenyl) = $10^{13.81\pm0.24}$ exp $(-27{,}720 \pm 390/RT)$ s^{-1}; k_1 (*p*-nitrophenyl) = $10^{13.80\pm0.07}$ exp $(-27{,}850 \pm 100/RT)$ s^{-1}. Table 4 gives the rate constants for the thermal decomposition of 3-chloro-3-aryldiazirines in various solvents at 75°.

Nature of Products

In the thermal decompositions of diazirines in cyclohexene, the major products were 7-chloro-7-aryl norcaranes, addition products of arylchlorocarbene to the double bond of cyclohexene (see Scheme 1). As the melting points for the isolated norcaranes were sharp, it was assumed that the products consisted of only one of the two isomers whose conformation was not identified. The minor products are probably mixtures of isomers formed from the insertions of carbene to the saturated C—H bonds at the 3- and 4-positions in cyclohexene.

In the decomposition of 3-chloro-3-*p*-nitrophenyl diazirine in DEGME, the major product was benzaldehyde ethylene acetal. On the other hand, anisylaldehyde was isolated as the major product from the decomposition of 3-chloro-3-*p*-methoxyphenyldiazirine. For the decomposition of the *p*-tolyl, phenyl, and *p*-chlorophenyl

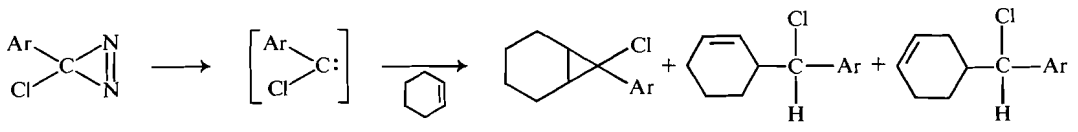

SCHEME 1

Can. J. Chem. Downloaded from www.nrcresearchpress.com by 210.87.254.105 on 09/05/12
For personal use only.

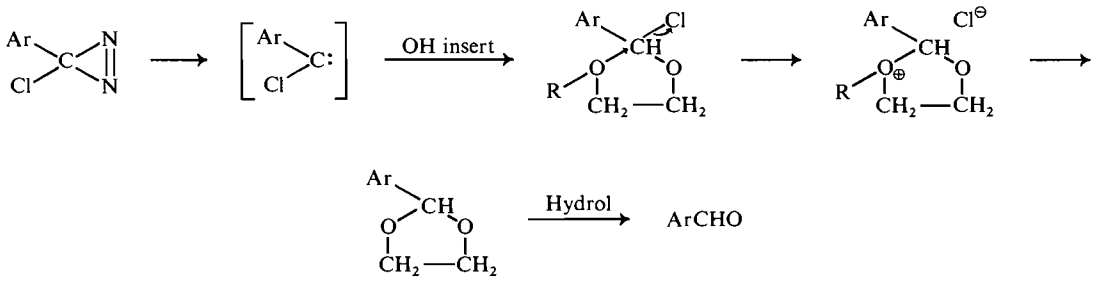

SCHEME 2

derivatives, mixtures of aldehyde and acetals were obtained. The above products were presumably formed via the mechanism shown in Scheme 2. The minor products are probably a mixture of isomers resulting from the insertion of arylchlorocarbene into the C—H bond neighbored to an oxygen atom (12, 13). From the n.m.r. peak area ratio of aldehyde (—CHO), aromatic protons, ethylene acetal (—CH_2—O—), and the methyl proton of —O—CH_2—CH_3 group, the yields of O—H insertion products (aldehydes and acetals) were estimated to be 95, 71, 88, 86, and 80% for the decomposition of *p*-methoxyphenyl, *p*-tolyl, phenyl, *p*-chlorophenyl, and *p*-nitrophenyl derivatives respectively. Since the rates of hydrolysis of benzaldehyde ethylene acetals have a negative ρ value in the Hammett equation (14), the different ratios of acetal/aldehyde are reasonable.

From the thermolysis of 3-chloro-3-aryldiazirines in DMSO, mixtures of substituted benzaldehydes and benzoic acids were isolated. No further attempts were made to study the mechanism of these reactions.

Discussion

For the purpose of comparison, pertinent data from previous workers are summarized in Table 5. The present results confirm the conclusions of the earlier workers. The thermal decomposition of diazirines both in gas phase and in solution are typically unimolecular reactions with A factor equal to $10^{13.7\pm0.5}$. The minor solvent effects from Table 4 also agree with data reported in earlier studies. The decomposition of 3-chloro-3-aryldiazirines in each of the three solvents gave similar organic products and all the free energies of activation

TABLE 5. Activation parameters for the thermal decomposition of diazirines

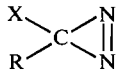

X	R	Condition	log A	E (kcal/mol)	$\Delta S^{\ddagger}$ (e.u.)	Reference
Fluoro	Fluoro	Vapor	13.40	32.5	0.5	4
Ethyl	Ethyl	"	13.73	31.89	2.0	15
Chloro	Methyl	"	14.14	31.07	3.9	1
"	Ethyl	"	13.99	30.45	3.2	2
"	*n*-Propyl	"	13.98	30.98	3.2	2
"	*i*-Propyl	"	14.01	30.59	3.3	2
"	*t*-Butyl	"	13.36	29.50	0.3	2
"	Trichloromethyl	CCl_4	13.80	29.20	2.3	7
"	Phenyl	Cyclohexene	13.87	28.00	2.6	8
"	*p*-Methoxyphenyl	"	13.41	26.49	0.5	This work
"	*p*-Tolyl	"	13.94	27.87	2.9	" "
"	*p*-Chlorophenyl	"	13.81	27.72	2.3	" "
"	*p*-Nitrophenyl	"	13.80	27.85	2.3	" "
Bromo	Phenyl	"	13.75	27.36	2.1	8

Can. J. Chem. Downloaded from www.nrcresearchpress.com by 210.87.254.105 on 09/05/12
For personal use only.

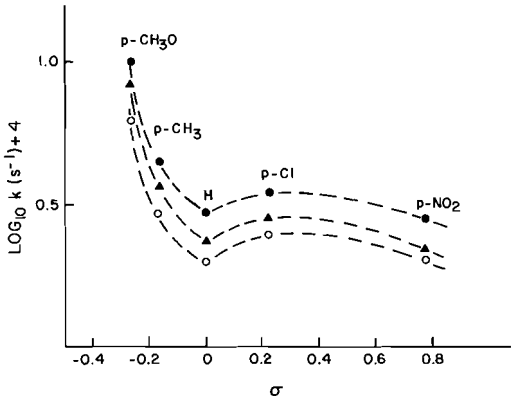

FIG. 2. Plots of $\log_{10} k$ *vs.* σ for 3-chloro-3-aryldiazirine in various solvents; ○, cyclohexene; ▲, DEGME; ●, DMSO.

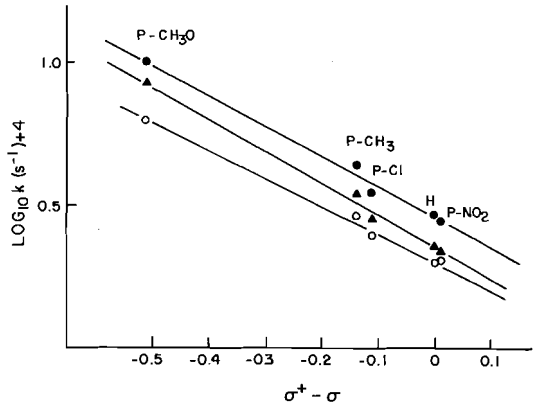

FIG. 3. Plots of $\log_{10} k$ *vs.* $\sigma^+ - \sigma$ for 3-chloro-3-aryldiazirine in various solvents; ○, cyclohexene; ▲, DEGME; ●, DMSO.

are in the range of 26.0 ± 0.3 kcal/mol. The differences in the activation energy between 3-chloro-3-aryldiazirines and 3-chloro-3-alkyldiazirines are reasonably explained by resonance stabilization effects by the aryl group in terms of either mechanism I, II, or III.

The observed substituent effects on reaction rates are not explicable either by the charge separated transition state II or by the simultaneous bond breaking process as proposed by Frey *et al.* in I. If the reaction proceeds by mechanism II, the rate for the following substituents would be in the order of p-NO_2 > p-Cl > H > p-CH_3 > p-CH_3O, which is almost opposite to the observed order: p-CH_3O > p-CH_3 > p-Cl > $H \simeq p$-NO_2. Thus, from the observed effects of substituents and the lack of solvent effects, the contribution of the ionic transition state II is not likely to be important in the thermal decomposition of diazirines. Schmitz (3) suggested that if mechanism I were to take place, the electron distribution on the carbon atom in the transition state must tend towards a sextet and such a transition cannot be stabilized by withdrawal of electrons. Taking the above into consideration, one would expect the rates to be p-CH_3O > p-CH_3 > H > p-Cl > p-NO_2, but these do not agree with the observed results.

Several examples of abnormal Hammett relation have been reported (16), but their explanations could not be applied to our present results. It is seen in Fig. 2 that plots of log k against σ (or σ^+) do not yield straight lines. However, a smooth curve (concave upward) may be drawn through all the points except that for the unsubstituted compound. Further, that the shape of the curves in each solvent is identical and increase in polarity of the solvent only displaces the curve upward. The curvature observed in each solvent is ascribed to varying resonance interactions in the transition state of the para-substituted compounds. Although the Hammett correlation was unsuccessful with our present results, a linear plot was obtained by plotting log k *vs.* $\sigma^+ - \sigma$ as shown in Fig. 3. The differences between σ^+ and σ are p-CH_3O, -0.510; p-CH_3, -0.141; p-Cl, -0.113; H, 0; p-NO_2, $+0.012$, and fall in the order of the kinetic data. These differences may be taken as a measure of the strength of conjugation of the substituents.

The possible structures of the transition state could be drawn as III*a*, *b*, and *c*. However, III*c* contributes little or nothing, as the nitrogen atom is more electronegative than the carbon atom. The free radical form III*a* may

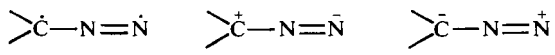

III*a* III*b* III*c*

be classified as an S radical in Walter's concept (17) in which the observed properties are shifted in the same direction with donor and acceptor substituents. On the other hand, the degree of contribution of different substituents to structure III*b* is likely to produce results such as these; p-CH_3O at best; p-CH_3 next in order; p-Cl very

Can. J. Chem. Downloaded from www.nrcresearchpress.com by 210.87.254.105 on 09/05/12
For personal use only.

TABLE 6. Relative rate for the thermal decomposition of 3-chloro-3-aryldiazirines at 75°

	p-Methoxyphenyl	*p*-Tolyl	Phenyl	*p*-Chlorophenyl	*p*-Nitrophenyl
	$k_{solvent}/k_{cyclohexene}$				
Cyclohexene	1	1	1	1	1
DEGME	1.35	1.23	1.18	1.15	1.07
DMSO	1.63	1.53	1.56	1.41	1.38
	k_{Ar}/k_{ph}				
Cyclohexene	3.18	1.49	1	1.26	1.05
DEGME	3.65	1.56	1	1.23	0.95
DMSO	3.32	1.46	1	1.14	0.93

little; and a negative effect by the *p*-NO_2 substituent as compared with the unsubstituted compound. Hence, the fastest rate of decomposition is expected for 3-chloro-3-*p*-methoxyphenyl diazirine because its transition state is stabilized through both structures III*a* and *b*. The transition state of the 3-chloro-3-*p*-tolyldiazirine is also stabilized by both III*a* and *b* to a lesser extent owing to its smaller resonance ability. In the case of 3-chloro-3-*p*-chlorophenyldiazirine, the transition state is stabilized by structure III*a*, but the contribution resulting from III*b* may be little or nothing due to its inductive effect, which is opposite to that of the resonance effect. The contribution of *p*-NO_2 substituent to structure III*a* is likely to be of the same order as the *p*-CH_3O substituent; however, its strong electronegative nature does not favor the resonance structure III*b* and tends to cancel out the stabilization effect resulting from III*a*. Therefore, the observed rate appears to be similar to that of the unsubstituted compound.

The fate of the diazirine after the achievement of the transition state is as interesting as the decomposition mechanism itself. Frey and Liu (2) have confirmed the formation of carbene in the thermal decomposition of 3-chloro-3-*t*-butyldiazirine by observing the formation of 1-chloro-2,2-dimethylcyclopropane. Evidence for carbene formation was also reported in the photolysis of 3-halo-3-phenyldiazirine (18). In our present work, the formation of 7-chloro-7-arylnorcaranes from the reactions in cyclohexene is good evidence for the carbene intermediate. In addition, the formation of the insertion isomers (1:1) into the 3- and 4-positions of cyclohexene was detected. The carbene generated from the thermal decomposition of 3-chloro-3-aryldiazirine is probably in its singlet state which is in agreement with the results from the selectivity studies of halophenyl carbenes (19, 20). Furthermore, if the carbene were singlet and collapsed to a sextet, there could be strong interaction between the empty orbital and an electron-donor species like the methoxy. Thus, the energy of the carbene might be lowered.

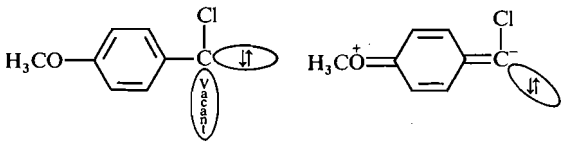

The relative rates for the thermal decomposition of 3-chloro-3-aryldiazirines at 75° are given in Table 6. For each of the compounds studied it is observed that the rate acceleration effect given by $k_{solvent}/k_{cyclohexene}$ shows an increase in going from a non-polar to a polar solvent. The relative magnitude of this effect is in the order of *p*-NO_2 < *p*-Cl < H < *p*-CH_3 < *p*-CH_3O. Although all compounds show an increase in rate constant with polar solvents, the comparison of substituted compounds with the unsubstituted compound shows that k_{Ar}/k_{Ph} increases for *p*-CH_3O and *p*-CH_3 and decreases for *p*-Cl and *p*-NO_2 compounds as the polarity of the solvent is increased. The magnitude of the solvent effect is not large, with a factor of two being the largest increase in going from nonpolar to polar solvents. A much larger effect would be expected if the transition state polarization was a dominant factor in determining the rate of decomposition of diazirines. If a radical

Can. J. Chem. Downloaded from www.nrcresearchpress.com by 210.87.254.105 on 09/05/12
For personal use only.

mechanism were operative, very little solvent effect would be expected. A rather small contribution from a mechanism involving the structure III*b* could account for the observed results. In the photolysis of diazirine, Amrich and Bell (21) have reported that 20% of the primary decomposition of diazirine is an isomerization to diazomethane. There is evidence that substituted diazirines can isomerize to diazo compounds (14, 22). However, most of the available data can also be interpreted by means of the homolytic process. As an example, the instability of α-ketodiazirine (3) could be attributed to the strong resonance effects of the α-carbonyl group. The decomposable nature of 3-chloro-3-methoxydiazirine (9) and the isomerization of 3-methyl-3-vinyldiazirine to 3-methyl-pyrazole (23) could be explained in a similar manner.

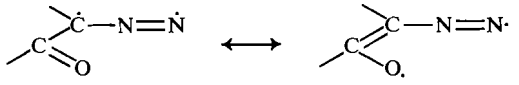

In conclusion, we suggest a mechanism involving the breaking of one of the C—N bonds. This leads to a diradical (III*a*) and a diazomethane (III*b*) intermediate of which the latter contribution is probably small due to the lack of solvent effects. It is likely that the transition states have more radical character. Recently nonempirical self-consistent field and configuration–interaction studies of aziridine and oxazirane have been reported by Hayes and Siu (24). They have concluded that the electronic structure of open forms of these species is essentially a linear combination of the resonance system $B{=}A{-}\overset{+}{C}{\leftrightarrow}\overset{-}{B}{-}\overset{+}{A}{=}C$, and a diradical $\cdot B{-}A{-}C\cdot$ where A, B, and C are CH_2 NH, or O. These studies lend support to the possibility of homolytic and heterolytic dissociation.

Grateful acknowledgement is made by one of us, M.T.H.L., for a grant-in-aid of research from the National Research Council of Canada and the Senate Research Committee of U.P.E.I. The authors wish to thank Drs. B. M. Lynch, L. F. Loucks, and C. Schmidt for their valuable comments.

1. M. R. Bridge, H. M. Frey, and M. T. H. Liu. J. Chem. Soc. A, 91, (1969).
2. H. M. Frey and M. T. H. Liu. J. Chem. Soc. A, 1916, (1970).
3. E. Schmitz. Angew. Chem. Int. Ed. **3**, 333, (1964).
4. E. W. Neuvar and R. A. Mitsch. J. Phys. Chem. **71**, 1229 (1967).
5. P. H. Ogden and R. A. Mitsch. J. Heterocycl. Chem. **5**, 41 (1968).
6. G. A. Bottomly and G. L. Nyberg. Aust. J. Chem. **17**, 406, (1964).
7. M. T. H. Liu and K. Toriyama. Int. J. Chem. Kin. **4**, 229 (1972).
8. M. T. H. Liu and K. Toriyama. J. Phys. Chem. **76**, 797 (1972).
9. W. H. Graham. J. Am. Chem. Soc. **87**, 4396, (1965).
10. G. M. Wright. J. Am. Chem. Soc. **50**, 3357, (1928).
11. R. L. Shrine, R. C. Fuson, and D. Y. Curtin. The systematic identification of organic compounds. John Wiley and Sons Inc. 1965. p. 320.
12. R. A. Moss. Carbene chemistry. Part II. C and EN. 1969. p. 50.
13. W. Kirmse. Carbene chemistry. 2nd ed. Academic Press, New York. 1971.
14. T. H. Fife and I. K. Jao. J. Org. Chem. **30**, 1492 (1965).
15. H. M. Frey and A. W. Scaplehorn. J. Chem. Soc. A, 968 (1966).
16. (*a*) I. R. L. Baker and R. H. Dahm. J. Chem. Soc. B, 650, (1970); (*b*) O. Rogne. J. Chem. Soc. B, 1294, (1968); (*c*) D. F. Bender, T. Thippeswamy, and W. L. Rellahan. J. Org. Chem. **35**, 939, (1970).
17. R. I. Walter. J. Am. Chem. Soc. **88**, 1923, (1966).
18. R. A. Moss, J. R. Whittle, and P. Freidenreich. J. Org. Chem. **34**, 2220 (1969).
19. R. A. Moss and J. R. Prazybyla. Tetrahedron, **25**, 647 (1969).
20. R. A. Moss and A. Mamantov. J. Am. Chem. Soc. **92**, 6951, (1970).
21. M. J. Amrich and J. A. Bell. J. Am. Chem. Soc. **86**, 292 (1964).
22. C. G. Overberger and J-P. Anselme. Tetrahedron Lett. 1405 (1963).
23. E. Schmitz, C. Horig, and C. Grundemann. Chem. Ber. **100**, 2093 (1967).
24. E. F. Hayes and A. K. Q. Siu. J. Am. Chem. Soc. **93**, 2090 (1971).

Can. J. Chem. Downloaded from www.nrcresearchpress.com by 210.87.254.105 on 09/05/12
For personal use only.

Kinetics and Mechanism of Decarboxylation of some Pyridinecarboxylic Acids in Aqueous Solution[1]

G. E. DUNN, GORDON K. J. LEE,[2] AND HAROLD THIMM

Department of Chemistry, University of Manitoba, Winnipeg, Manitoba R3T 2N2

Received April 24, 1972

The first-order rate constants for decarboxylation of picolinic and five substituted picolinic acids in buffered aqueous solution at 150° and ionic strength 1.0 increase as p*H* increases above 0, go through a maximum at p*H* near 1, then level off at about half the maximum. For quinolinic acid at 95° the rate maximum occurs at the isoelectric p*H*. It is therefore concluded that the anion decarboxylates about half as fast as the isoelectric species. Anion and isoelectric species show similar carboxyl-carbon kinetic isotope and substituent effects, so they probably decarboxylate by similar mechanisms. The methyl betaine of picolinic acid decarboxylates about 200 times faster than the anion. From these facts it is concluded that the isoelectric species which decarboxylates is probably zwitterion rather than neutral acid, and that anion and zwitterion decarboxylate by loss of carbon dioxide to form 2-pyridyl carbanion and ylid, respectively. The slower decarboxylation of isoelectric species compared to betaine suggests that only a small fraction of the isoelectric species is zwitterion. However, qualitative estimates from spectra of the fraction of zwitterion present in the isoelectric species at 150° suggest that this cannot be the whole explanation. The relative reactivities of the 2- and 4-positions are similar for decarboxylation and hydrogen exchange in pyridinium ions, but not in the unprotonated species.

Les constantes de vitesse du premier ordre pour la décarboxylation de l'acide picolinique et cinq de ses dérivés substitués, en solution aqueuse tamponnée à 150° et de pouvoir ionique 1.0 augmentent avec un p*H* au-dessus de 0, passent par un maximum pour un p*H* proche de 1, et se stabilisent ensuite à environ la moitié de ce maximum. Pour l'acide quinolinique à 95°, le maximum de vitesse se produit au p*H* isoélectrique. On a conclu par conséquent que l'anion se décarboxyle à une vitesse qui est de moitié celle de l'espèce isoélectrique. L'anion et l'espèce isoélectrique montrent des effets similaires de substituants et de cinétique isotopique carboxyle-carbone, aussi les mécanismes de décarboxylation sont probablement voisins. La bétaine méthylée de l'acide picolinique a une vitesse de décarboxylation de 200 fois supérieure à celle de l'anion. Ces faits ont amenés à conclure que l'espèce isoélectrique qui subit la décarboxylation est probablement le zwitterion plutôt que l'acide neutre et que la décarboxylation de l'anion et du zwitterion se fait par perte de gaz carbonique pour donner respectivement le pyridyl-2 carbanion et l'ylure. La décarboxylation plus lente de l'espèce isoélectrique comparée à la bétaine, laisse penser que seule une petite fraction de l'espèce isoélectrique est à l'état de zwitterion. Toutefois, les estimations qualitatives à partir des spectres de la fraction de zwitterion présente dans l'espèce isoélectrique à 150°, suggère que cette explication ne puisse pas être la seule. Les réactivités relatives des positions -2 et -4 sont semblables pour la décarboxylation et l'échange d'hydrogène dans les ions pyridiniums mais pas dans les espèces non-protonées.

[Traduit par le journal]

Canadian Journal of Chemistry, **50**, 3017 (1972)

Introduction

The mechanism of decarboxylation of pyridinecarboxylic acids was first examined by Hammick, who found that when the 2-, but not the 3- or 4-, pyridine and quinoline carboxylic acids are heated in high-boiling aldehyde or ketone solvents they give α-pyridyl carbinols (1, 2). He postulated that the reaction is a decarboxylation of the zwitterionic form of the amino acid to give a nitrogen ylid which acts as a nucleophile toward the carbonyl solvent as illustrated in eq. 1. All the evidence produced since Hammick's original work can be accommodated by the ylid mechanism. For example, the reaction has a large carboxyl-carbon kinetic isotope effect (3, 4), and is faster

[1] 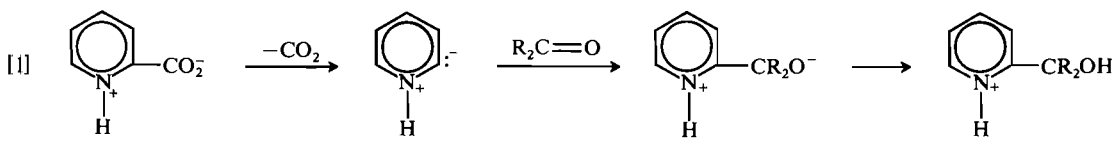

[1]Presented at the 54th Conference of the Chemical Institute of Canada, Halifax, June 1, 1971.
[2]Holder of a Manitoba Fellowship, 1969–1970.

Can. J. Chem. Downloaded from www.nrcresearchpress.com by 210.87.254.5 on 09/05/12
For personal use only.

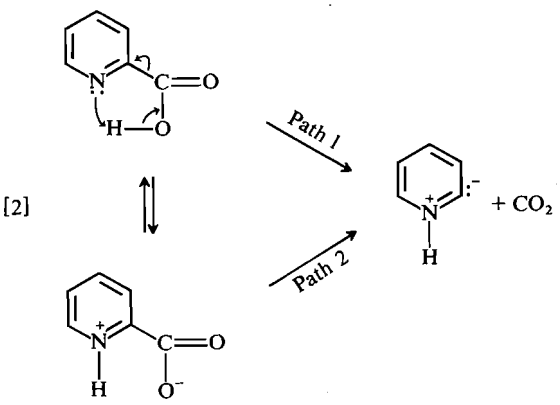

[2]

for the methylbetaine than for the acid itself (5, 6).

Much of the work since Hammick's first paper has concerned the timing of the proton transfer from oxygen to nitrogen in the decarboxylation reaction. Solvent and substituent effects have been used to argue that proton transfer and decarboxylation occur in sequence (*i.e.*, zwitterion decarboxylates, as in path 2, eq. 2) (5, 7) or in concert (*i.e.*, neutral acid decarboxylates as in path 1, eq. 2) (8, 9).

No one has ever suggested that either the cation or anion decarboxylates, or that decarboxylation is preceded or accompanied by electrophilic attack at the ring carbon. Perhaps these possibilities have not been considered because all the work up to now has been done in non-aqueous solvents, where ionic species are not favored. In fact, the decarboxylation of a pyridine or quinoline monocarboxylic acid in aqueous solution has not been reported, although quinolinic acid (2,3-pyridinecarboxylic acid) is known to decarboxylate in water at 120° (10). Obviously, water would have many advantages as a solvent for studying this reaction: it favors ionic intermediates such as zwitterion or ylid, and makes possible through pK data a precise knowledge of the state of protonation of the acid. With these considerations in mind, we undertook a study of the decarboxylation of pyridinecarboxylic acids in aqueous solution.

Results and Discussion

Pyridinemonocarboxylic Acids

It was found that to obtain convenient rates of decarboxylation of picolinic acid in aqueous solution it was necessary to use a temperature as high as 150°. In attempts to find suitable acids which would decarboxylate at lower temperatures, 6-methyl- and 5-nitro-picolinic acids were tried. The data for these acids are shown in Fig. 1.

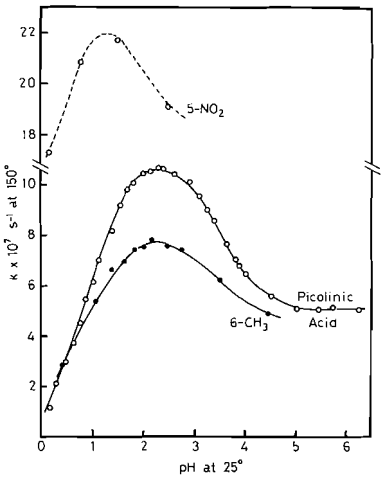

FIG. 1. First-order rate constants for the decarboxylation of substituted picolinic acids at 150° and ionic strength 1.0.

There are several interesting features of the data in Fig. 1. First, the rates of decarboxylation of all three acids are a maximum at an intermediate pH, and decrease at both higher and lower acidities. This is what is predicted by the ylid mechanism or any other in which the species decarboxylating is the isoelectric species, whether neutral acid or zwitterion. More specifically, such a mechanism predicts that the rate maximum should occur at the isoelectric pH. Unfortunately, neither pH's nor pK's are known at 150°, so this prediction cannot be tested.

Second, the rate constant *vs.* pH profile is not symmetrical. At low pH the rate constants decrease sharply, showing that the cation does not decarboxylate. This resembles the behavior of other aromatic acids, where the unionized carboxyl group decarboxylates with great difficulty or not at all (11–13). On the other hand, as pH increases beyond that at the rate maximum, the rate constants at first decrease but then level off, so that at $pH > 5$ the rate is independent of pH. This shows that not only the isoelectric species decarboxylates, as re-

Can. J. Chem. Downloaded from www.nrcresearchpress.com by 210.87.254.5 on 09/05/12
For personal use only.

Can. J. Chem. Downloaded from www.nrcresearchpress.com by 210.87.254.5 on 09/05/12
For personal use only.

quired by the ylid mechanism, but so does the picolinate anion. Furthermore, the anion decarboxylates at as much as half the maximum rate. Anion decarboxylation has not previously been reported and, in terms of the generally accepted mechanism, is unexpected. It has been supposed that picolinic acid decarboxylates more readily than benzoic or nicotinic acids because protonation of the ring nitrogen, either prior to or in concert with, carbon–carbon bond breaking provides a strongly electronegative center to stabilize developing negative charge on the adjacent carbon. But, since the anion is now found to decarboxylate almost as easily without the aid of nitrogen protonation, it must be concluded either that protonation is not very important or that the isoelectric species contains very little zwitterion. Attempts to distinguish between these two interpretations will be described below.

Third, substituent effects are unusual. The 5-nitro- group accelerates and the 6-methyl-group retards decarboxylation, as would be expected for the ylid or any other mechanism in which negative charge develops at the reaction site. However, the effect is much smaller than those shown by most other ionic aromatic substitutions. (Hammett's ρ-constant is less than -4 for most electrophilic, and greater than +4 for most nucleophilic aromatic substitutions.) Furthermore, it is surprising that 6-methyl retards the decarboxylation about as much as 5-nitro accelerates it. (Hammett's $\sigma^- = +1.27$ for *p*-nitro- and $\sigma = -0.069$ for *m*-methyl.) Clearly, substituent effects are very different from those found in the benzene series.

A fourth striking feature of the data in Fig. 1 is that the rate in water is distinctly slower than in non-aqueous solvents. The maximum value of the rate constant for decarboxylation of picolinic acid in water at 150° is 1×10^{-6} s^{-1}. In phenetole at 150.7° it is 4×10^{-5} s^{-1}, and it does not vary by more than a factor of 2 for a wide variety of other non-aqueous solvents (8). This leads to the conclusion that, if the same mechanism applies in aqueous and non-aqueous solvents, the transition state is less polar than the initial state, which would be a fairly strong argument for zwitterion as the isoelectric species undergoing decarboxylation. On this interpretation the solvent effect is even more striking, because the percentage of zwitterion in the isoelectric species should be much less in non-aqueous solvents than in water.

TABLE 1. First-order rate constants for decarboxylation of pyridinedicarboxylic acids in aqueous HCl at 150° and ionic strength 1.0

Acid	λ^* (nm)	p*H* at 25°	k (s^{-1})
2,3-	278	0.37	0.98×10^{-3}
		1.22	1.25×10^{-3}
		2.19†	1.05×10^{-3}
2,4-	294	1.52	1.51×10^{-6}
2,5-	282	1.52	1.79×10^{-6}
2,6-	280	1.52	1.28×10^{-6}

*Wavelength at which concentration of starting material was followed.
†HCl–NaH_2PO_4.

Pyridinedicarboxylic Acids

An attempt was next made to find a pyridinecarboxylic acid which would decarboxylate in water at temperatures below 100° so that its p*K*'s, isoelectric p*H*, and possibly the percent zwitterion in its isoelectric species, could be determined under decarboxylation conditions. Since pyridine-2,3-dicarboxylic (quinolinic) acid is reported to decarboxylate in water at 120° (10), the pyridinedicarboxylic acids were examined. The rate data are shown in Table 1. It is seen that quinolinic acid decarboxylates more than 500 times faster than picolinic or any of the other pyridinedicarboxylic acids. This very large ortho-substituent effect contrasts strongly with the small meta- and para-substituent effects previously noted for methyl and nitro groups.

Quinolinic acid decarboxylates readily enough so that rates can be measured at temperatures below 100°. The product of decarboxylation in water at 120° has been reported to be exclusively nicotinic acid (10) and at 95° the u.v. spectrum of the decarboxylation product coincides precisely with that of nicotinic acid. Table 2 shows the first-order rate constants for decarboxylation of quinolinic acid in water at 95° and ionic strength 1.0. It is seen that the rate profile closely resembles that for picolinic acid.

The ionization equilibria for quinolinic acid are shown in eq. 4. At 25°, pK_2 and pK_3 are reported to be 2.43 and 5.06, respectively (14). No value for pK_1 of quinolinic acid is available, but the value for pyridine-2,5-dicarboxylic acid

Can. J. Chem. Downloaded from www.nrcresearchpress.com by 210.87.254.5 on 09/05/12
For personal use only.

TABLE 2. First-order constants for decarboxylation of quinolinic acid in aqueous HCl at 95° and ionic strength 1.0

	$k \times 10^6$ (s^{-1})	
pH at 95°	Observed	Calculated from eq. 5
0.079	1.69	1.73
0.189	1.92	1.93
0.373	2.24	2.23
0.418	2.26	2.29
0.464	2.34	2.35
0.570	2.50	2.48
0.702	2.57	2.61
0.781	2.66	2.66
0.907	2.71	2.72
0.971	2.76	2.74
1.11	2.76	2.75
1.35	2.67	2.66
1.52	2.56	2.54
1.61	2.42	2.45
1.90	2.14	2.12
2.19*	1.84	1.77
2.87*	1.25	1.24
3.41*	1.08	1.07
3.98*	1.06	1.04

*HCl–NaH_2PO_4.

is 0.5 (10). Since the data of Table 2 were all obtained at pH's less than 4, pK_3 is not important for their interpretation. At 95° and ionic strength 1.0, pK_2 was found to be 1.90 ± 0.03 using a spectrophotometric method described elsewhere (15). The data for this determination are given in Table 3. Attempts to apply the same method to the determination of pK_1 failed because the absorbance change corresponding to this protonation falls in the pH range -1 to 1 where it is impossible to maintain ionic strength 1.0. It appears that pK_1 would be approximately 0. The lack of an accurate value for pK_1 makes it impossible to determine precisely the isoelectric pH under decarboxylation conditions. However, a reasonable estimate would be $pK_2/2 = 0.95$, and this is in good agreement with the pH of about 1.0 at which the rate of decarboxylation is a maximum.

TABLE 3. Data for the calculation of pK_2 of quinolinic acid at 95° and ionic strength 1.0

pH at 95°*	Absorbance at 262 nm of 1.5×10^{-4} M solution
0.301	0.335
0.840	0.331
1.29	0.322
1.68	0.298
2.15	0.273
2.42	0.257
2.70	0.245
2.99	0.239
3.18	0.237
3.65	0.237
4.09	0.237

*Buffers were HCl–KCl at pH < 2, and HCl–NaH_2PO_4–KCl at pH > 2.

Carbon Isotope Effects

A rate maximum at the isoelectric pH can be explained either by a rate-controlling decarboxylation of the isoelectric species, as postulated by Hammick, or by a rate-controlling protonation of the monoanion, such as that found at low acidities for salicylic (11), anthranilic (13), azulene-2-carboxylic (12), and pyrrole-2-carboxylic acids (16) and shown in eq. 3. In the former case carbon–carbon bond breaking is the rate-controlling process, so there should be a carboxyl–carbon kinetic isotope effect on the rate; in the latter case there should not.

Table 4 records the ^{13}C-carboxyl kinetic isotope effects for quinolinic acid at 95° and for picolinic acid at 150°. It is seen that there is a fairly large carbon isotope effect both at the isoelectric point and at higher pH. Evidently carbon–carbon bond breaking is rate determining for decarboxylation of both the isoelectric species and the monoanion. The isotope effect is slightly less in the anion than in the isoelectric species for both picolinic and quinolinic acids, presumably because the zero-point energy difference in the starting material is a smaller fraction of the activation energy for the slower reaction. The size of the isotope

[3] 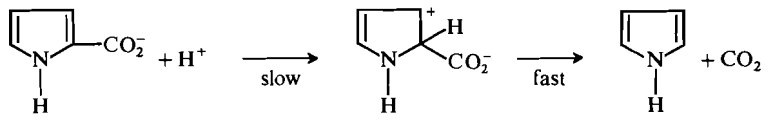

TABLE 4. ^{13}C kinetic isotope effects in the decarboxylation of pyridinecarboxylic acids in aqueous solution at ionic strength 1.0

Acid	pH*	% reaction	$^{13}CO_2/^{12}CO_2$	$100\left(\frac{k_{12}}{k_{13}}-1\right)$
Quinolinic at 95°	1.04	100.0	0.010424	
	1.04	100.0	0.010419	
	1.04	100.0	0.010420	
	0	38.31	0.010197	2.82
	0	6.686	0.010144	2.84
	0	6.919	0.010140	2.87
	2.63	6.422	0.010152	2.74
	2.63	6.757	0.010154	2.74
	2.63	6.420	0.010157	2.70
	3.95	9.445	0.010163	2.67
	3.95	9.075	0.010165	2.66
	3.95	6.764	0.010161	2.67
Picolinic at 150°	2.41	100.0	0.010362	
	2.41	100.0	0.010357	
	2.41	100.0	0.010356	
	1.13	15.61	0.010148	2.25
	1.13	15.61	0.010149	2.23
	1.13	15.61	0.010147	2.26
	3.95	14.76	0.010165	2.06
	3.95	14.76	0.010162	2.09
	3.95	14.76	0.010164	2.08

*The pH of quinolinic acid solutions were measured at 95°, those of picolinic acid at 25°. Buffers were $HClO_4$–$NaClO_4$ at pH < 2; $HClO_4$–NaH_2PO_4–$NaClO_4$ at pH > 2.

effect suggests that carbon–carbon bond breaking is well advanced in the transition states derived from both anion and isoelectric species; that is, the transition states resemble carbanion and ylid, respectively.

Kinetics

Since neither the rate profiles nor the isotope effects require protonation at the α-carbon prior to decarboxylation, the reaction is formulated in eq. 4 as unimolecular decompositions of the isoelectric species, as postulated by Hammick, and of the monoanion. Of course, HA and A^- can each exist in three isoprotonic forms, and any or all of them may decarboxylate without changing the pH profile. As was pointed out

[4]

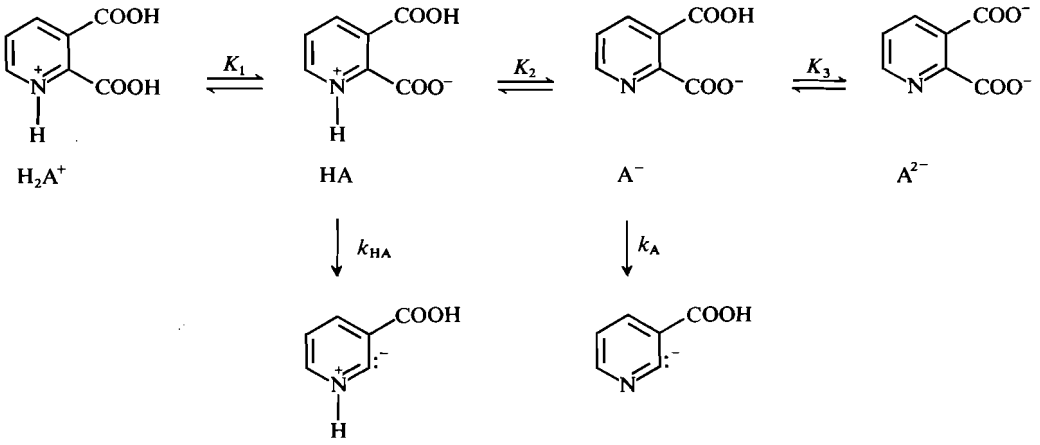

Can. J. Chem. Downloaded from www.nrcresearchpress.com by 210.87.254.5 on 09/05/12
For personal use only.

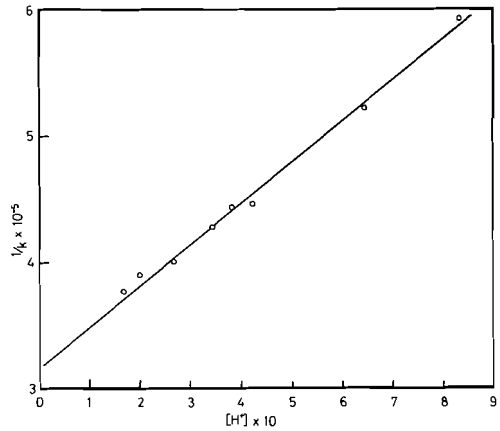

FIG. 2. Rate data at $pH < 0.9$ for the decarboxylation of quinolinic acid at 95° and ionic strength 1.0 plotted according to eq. 6.

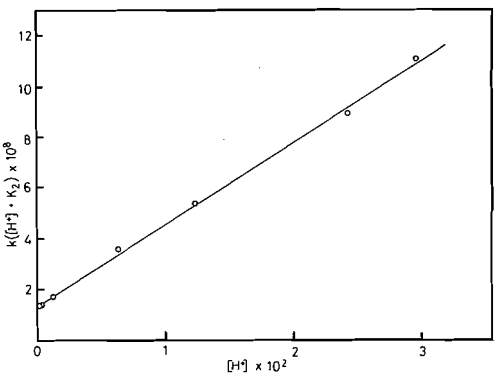

FIG. 3. Rate data at $1 < pH < 4$ for the decarboxylation of quinolinic acid at 95° and ionic strength 1.0 plotted according to eq. 7.

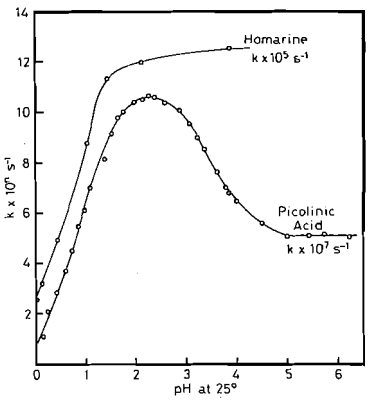

FIG. 4. First-order rate constants for the decarboxylation of picolinic acid and homarine at 150° and ionic strength 1.0.

earlier, the concentration of dianion is so small at the pH's where rates were measured that K_3 and $[A^{2-}]$ can be omitted from the rate expression. Equation 4 will then apply to picolinic as well as to quinolinic acid.

The rate expression is given by eq. 5 in which $[C] = [H_2A^+] + [HA] + [A^-]$ = the stoichiometric concentration of pyridinecarboxylic acid.

$$[5] \quad \frac{d[CO_2]}{dt} = k_{HA}[HA] + k_A[A^-] = \frac{k_{HA} + \dfrac{k_A K_2}{[H^+]}}{\dfrac{[H^+]}{K_1} + 1 + \dfrac{K_2}{[H^+]}}[C] = k_{obs}[C]$$

Because pK_2 for quinolinic acid was found to be 1.90 under the reaction conditions, and because $k_A < k_{HA}$, the terms in K_2 can be neglected at $pH < 0.9$. This produces the approximate eq. 6.

$$[6] \quad \frac{1}{k_{obs}} = \frac{[H^+]}{k_{HA}K_1} + \frac{1}{k_{HA}}$$

Figure 2 shows a plot of eq. 6 for quinolinic acid, from which it is calculated that $k_{HA} = 3.2 \times 10^{-6}$ s^{-1} and $K_1 = 0.96$ at 95° and ionic strength 1.0. This value of K_1 agrees well with the estimate from spectra that $pK_1 \simeq 0$. Accepting this value leads to the conclusion that at $pH > 1$ eq. 5 reduces to eq. 7.

$$[7] \quad k_{obs}([H^+] + K_2) = k_{HA}[H^+] + k_A K_2$$

Figure 3 shows a plot of eq. 7 for quinolinic acid using the experimental value $K_2 = 1.26 \times 10^{-2}$. This plot gives $k_{HA} = 3.3 \times 10^{-6}$ s^{-1} and $k_A = 1.0 \times 10^{-6}$ s^{-1}. The rate constants for decarboxylation of the isoelectric species (k_{HA}) obtained from eqs. 6 and 7 agree very well and are about three times larger than that for decarboxylation of the monoanion (k_A). Insertion of these values into eq. 5 produces the calculated rate constants of Table 2.

Equations 6 and 7 can also be used to fit the rate data for picolinic and 6-methylpicolinic acids to eq. 5. Since K_1 and K_2 are not known at 150° and ionic strength 1.0, values for these constants were chosen to fit the data. The results are given in Table 5, where it is seen that

Can. J. Chem. Downloaded from www.nrcresearchpress.com by 210.87.254.5 on 09/05/12
For personal use only.

TABLE 5. Constants for eq. 2 at ionic strength 1.0

Acid	pK_1*	pK_2*	k_{HA} (s^{-1})	k_A (s^{-1})
Quinolinic at 95°	0.02	1.90(2.43)	3.3×10^{-6}	1.0×10^{-6}
Picolinic at 150°	1.09(1.08)	3.70(5.32)	1.1×10^{-6}	5.0×10^{-7}
6-Methylpicolinic at 150°	0.89(0.90)	3.95(5.83)	7.7×10^{-7}	3.9×10^{-7}

*The numbers in parentheses are pK values at 25° for quinolinic (14), picolinic (18), and 6-methylpicolinic acids (19).

it is necessary to assume a much larger temperature effect on K_2 than on K_1. This is, in fact, what is observed for other amino acids such as glycine (17). The values shown for k_{HA} and k_A will, except in the case of quinolinic acid, contain the errors introduced by using pH's measured at 25° instead of 150°. Since the pH of the buffers used increased by only about 0.06 units from 25 to 95°, the error at 150° is probably not large and is the same for k_{HA} and k_A. The data from Table 5 were used with eq. 5 to generate the solid lines in Figs. 1 and 4.

Homarine

It is surprising to see in Table 5 that the three pyridinecarboxylic acids decarboxylate only two to three times faster in the isoelectric form than as anions. Since neither 3- nor 4-pyridinecarboxylic acids decarboxylate detectably at 150°, it is evident that nitrogen adjacent to the carboxyl group has a profound influence on the decarboxylations. The obvious explanation is that the inductive or field effect of electronegative nitrogen facilitates development of negative charge on the 2-position (1, 2). The fact that other electron-attracting substituents (*e.g.*, 5-nitro-) increase and electron-releasing substituents (*e.g.*, 6-methyl-) decrease the rate of decarboxylation supports this interpretation. It would be expected, then, that the introduction of a positive charge on nitrogen would produce a further large increase in the rate of decarboxylation. To test this hypothesis homarine, the *N*-methyl betaine of picolinic acid, was decarboxylated. Haake and Mantecón showed that homarine hydrochloride decarboxylates 720 times faster than picolinic acid in a mixture of ethylene glycol and quinoline (6), but it is uncertain what species are present in such a solution, and it was not then known that picolinate anion also decarboxylates.

Figure 4 shows that homarine, like the other pyridine-carboxylic acids, does not decarboxylate when the carboxyl group is un-ionized but does readily when the carboxyl group ionizes. The pH *vs.* rate profile can be interpreted in terms of eq. 8. The rate data give $k = 1.3 \times 10^{-4}\ s^{-1}$ and $pK = 0.67$ at 150° and ionic strength 1.0. When this rate constant is compared with that for the unmethylated anion from Table 5, $k_A = 5.0 \times 10^{-7}$, it is seen that quaternization of the picolinate nitrogen does indeed produce a large increase in rate constant, as expected.

Zwitterion

If *N*-methylation of the picolinate anion increases its rate of decarboxylation by a factor of about 250, why does protonation only double it? The most obvious explanation would be that protonation of the anion occurs not on the nitrogen where methylation does, but on the carboxylate group; that is, that picolinic acid in water at 150° and ionic strength 1.0 is mostly neutral acid, not zwitterion.

The protonation equilibria for picolinic acid are shown in eq. 9. The experimental ionization

[8] 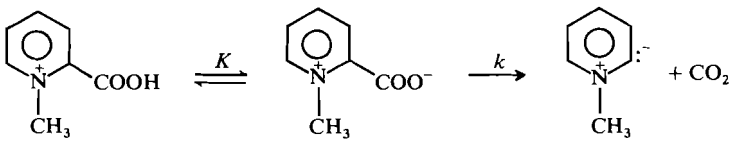

Can. J. Chem. Downloaded from www.nrcresearchpress.com by 210.87.254.5 on 09/05/12
For personal use only.

[9]

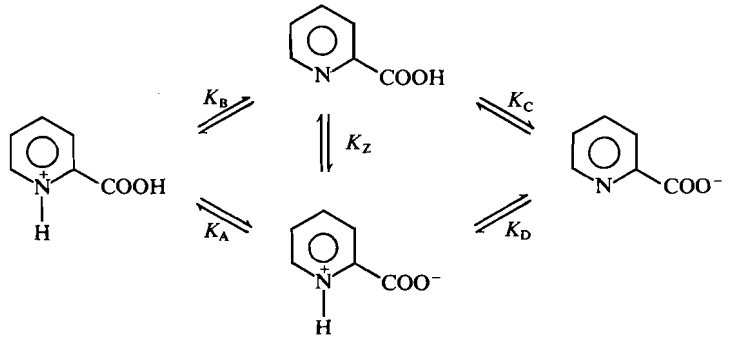

constants, K_1 and K_2, are related to those of eq. 9 as follows:

$$K_1 = K_A + K_B$$

$$\frac{1}{K_2} = \frac{1}{K_C} + \frac{1}{K_D}$$

$$K_Z = \frac{K_A}{K_B} = \frac{K_D}{K_C}$$

Green and Tong, by assuming that K_B is the same as that of the methyl ester, calculated that $K_Z = 15$ for picolinic acid at 25° and ionic strength 0 (20). This corresponds to 94% zwitterion. However, the decarboxylation conditions are distinctly different from these. Increasing the ionic strength to 1.0 would certainly increase the percentage of zwitterion, but increasing the temperature to 150° might well diminish it. Edsall and Blanchard have estimated that K_Z for glycine is exothermic by 11.5 kcal/mol (21). A similar enthalpy for picolinic acid ionization, if it were independent of temperature, would reduce K_Z to 0.05 at 150°. This would reduce the percentage of zwitterion in the isoelectric species from 94% at 25° to 5% at 150° which, if zwitterion were the only species to decarboxylate, would at least partly explain the difference in decarboxylation rates between isoelectric species and betaine.

In an attempt to test this hypothesis, the u.v. spectra of picolinic acid at 25 and 150° were compared. Green and Tong observed that at 25° the spectra of picolinic acid closely resemble those of its methyl ester in both acidic and basic media (20). From this fact they concluded that protonation or alkylation of the picolinate anion has little effect on its u.v. spectrum, whereas protonation of the ring nitrogen has a pronounced effect. In Fig. 5 the spectrum of the isoelectric form of picolinic acid is compared with those of the cation and anion. At 25° the close resemblance of the curves for isoelectric species and cation suggested to Green and Tong that the nitrogen of the isoelectric species is protonated, which agrees well with their conclusion from pK measurements that the isoelectric species is mainly zwitterion at that temperature. Figure 5 also shows the spectra of the same species at 150°. It is seen that the spectra of the isoelectric species is less like cation than at 25°, but is still far from resembling anion. It seems probable, therefore, that the percentage of zwitterion in the isoelectric species decreases at high temperatures, but we estimate that it is still greater than 40% at 150° and ionic strength 1.0.

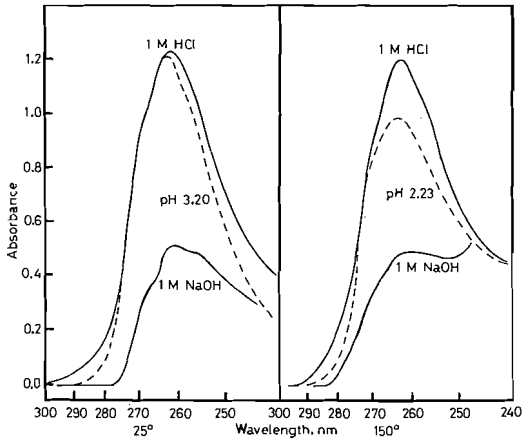

FIG. 5. Ultraviolet spectra of picolinic acid cation, anion, and isoelectric species at ionic strength 1.0. The isoelectric pH at 25° is calculated from K_1 and K_2; at 150° it is obtained from the rate maximum in Fig. 1.

Can. J. Chem. Downloaded from www.nrcresearchpress.com by 210.87.254.5 on 09/05/12
For personal use only.

Can. J. Chem. Downloaded from www.nrcresearchpress.com by 210.87.254.5 on 09/05/12
For personal use only.

Conclusions

The decarboxylation of any acid involves three processes: O—H bond breaking, C—C bond breaking, and C—H bond making. In all the decarboxylations which have been examined mechanistically, O—H breaking precedes or coincides with C—C breaking. C—C breaking and C—H making have been found to occur in three sequences. First, C—H making may precede C—C breaking, as in the aromatic hydroxy and amino acids where, at low acidity C—H making is rate determining. Second, C—H making and C—C breaking may be concerted, as in the β-keto acids where a cyclic intramolecular proton transfer can produce a tautomer of the final decarboxylation product. Third, C—H making may follow C—C breaking in those acids which yield a stable carbanion on loss of carbon dioxide, such as trihalocarbanions from trihaloacetate salts, or enolate anions from β-ketocarboxylate and malonate salts.

For pyridine-2-carboxylic acids in aqueous solution decarboxylation of the isoelectric species, the anion, and the methyl betaine are observed. Neither the anion nor the betaine have a proton for intramolecular transfer, so they cannot belong to the second mechanistic type of the preceding paragraph. Both decarboxylate at rates which are independent of hydrogen ion concentration, so they are not of the first mechanistic type. Hence, the anion and betaine probably fall into the third type: rate-determining loss of the ionized carboxylate group to form a reactive carbanion.

Classification of the decarboxylation of isoelectric species is not so obvious. However, there is much evidence to suggest that the isoelectric species decarboxylates by the same mechanism as the anion and the betaine. First, the rate of decarboxylation of the isoelectric species is intermediate between those of the anion and betaine. Second, the anion and the isoelectric species have almost the same kinetic carbon isotope effect, showing that C—C breaking is well advanced in the transition states of both. Third, substituent effects are almost the same for anion and isoelectric species, with 6-methyl- retarding and 5-nitro- accelerating the rates of both species by nearly the same amount. This means that the 2-position of the pyridine ring is more negative in the transition state than in the ground state by about the same amount for both species. We therefore conclude that the isoelectric species, like the anion, decarboxylates by rate-controlling loss of the ionized carboxyl group.

It is important to note that this conclusion applies only to decarboxylation in aqueous solution. In *m*-nitrotoluene solution, substituent effects vary, but many are in the opposite direction to those in water (9) and it is not unreasonable to expect that zwitterion would have less advantage as an intermediate in organic solvents than in water.

Finally, there remain the questions why the isoelectric species decarboxylates so much slower than the betaine, and why it decarboxylates slower in water than in organic solvents. No doubt part of the answer to the first question lies in the fact that the isoelectric species is only partly zwitterion at 150°, but this cannot be the whole answer. Possibly stabilization of the transition state is less for *N*-protonation than for *N*-methylation because the positive charge on the protonated species is dissipated by solvation of the proton.[3] The answer to the second question would be easy if the isoelectric species decarboxylated by the same mechanism in aqueous and non-aqueous solvents; water stabilizes the zwitterionic ground state more than organic solvents can. However, it seems probable, as mentioned above, that the mechanisms are different in aqueous and non-aqueous solvents, so the question has no simple answer.

Comparison with Proton Exchange

The hydrogens of pyridine exchange with D_2O or DCl only in the 2- and 6-positions (22), but in $NaND_2$–ND_3 (23) and in NaOD–D_2O (22) the order of ease of exchange is $4 > 3,5 > 2,6$. This has been interpreted by Zoltewicz and Smith (22) as meaning that *N*-protonated pyridine exchanges fastest in the 2,6-positions whereas pyridine itself exchanges fastest in the 4-position. They suggest that both exchanges involve proton abstraction by base and that the 4-carbanion of pyridine is more stable than the 2-carbanion, but that the 4-ylid derived from pyridinium ion is less stable than the

[3]The authors are indebted to Dr. R. Breslow for this suggestion.

Can. J. Chem. Downloaded from www.nrcresearchpress.com by 210.87.254.5 on 09/05/12
For personal use only.

2-ylid because of coulombic stabilization of the latter.

Since we have proposed, largely on the basis of carbon isotope effects, that the transition state for decarboxylation of pyridine-2-carboxylic acids resembles carbanion or ylid, it might be expected that the rates of decarboxylation would parallel those of hydrogen exchange. That is, that the zwitterion would decarboxylate fastest in the 2-position while the anion would decarboxylate fastest in the 4-position. To test this hypothesis, 3×10^{-4} *M* solutions of picolinic and isonicotinic acids in 1 *M* NaOH were thermostatted at 150°. The rate constant for decarboxylation of picolinic acid was 5×10^{-7} s^{-1}, but the isonicotinate salt showed no decarboxylation after 20 days ($k < 10^{-9}$ s^{-1}). Evidently the 2-acid decarboxylates faster than the 4-acid both as isoelectric species and as anion. Consequently, we must conclude that, although the relative reactivities of the 2- and 4-positions in both decarboxylation and hydrogen exchange of pyridinium ions may be governed by the stabilities of transition states which resemble ylides, the same cannot be true for the corresponding reactions of unprotonated pyridines. In the latter case, either one or both transition states do not resemble anions, or else other factors, such as ground state stabilities, are of increased importance. This question is being investigated.

Experimental

Materials

5-Nitropicolinic acid (m.p. 210–212°) was synthesized from 2-bromo-5-nitropyridine in 34% yield by the method of Thome and Goebel (24).

Homarine bisulfate was prepared, according to the method of Nienburg (25), by methylating ethyl picolinate using dimethyl sulfate, and hydrolyzing the *N*-methyl ester with HCl. The very hygroscopic product, after crystallization from isopropyl alcohol (90% yield, m.p. 113–125°), neutralized 93.3% of the theoretical amount of base. Further recrystallization from isopropyl alcohol did not improve the titer, perhaps because of decarboxylation.

All other reagents were commercial products. Pyridines were distilled before use and pyridinecarboxylic acids were recrystallized to constant melting point from benzene.

Buffers

Two criteria were used in the choice of buffers: they must not absorb in the u.v. where substrate absorbance was used to follow the rate of reaction, and their p*H* at 25° must not have changed after they have been heated to 150° for 500 h. The organic acids commonly used in buffers failed one or both of these requirements, so the buffering agents used were hydrochloric acid, sodium dihydrogen phosphate, and disodium hydrogen phosphate. Perchloric acid replaced hydrochloric when carbon dioxide was to be recovered for isotopic analysis. Buffers were adjusted to constant ionic strength with potassium chloride. p*H* measurements were made with a Radiometer Model 4C meter, using the electrodes specified by the manufacturer at 25 and 95° respectively, and were reproducible to ±0.005 units.

Spectra

Ultraviolet absorption spectra were obtained with a Perkin–Elmer Model 450 spectrophotometer. At 150 ± 0.5° an electrically heated aluminum block was used as cuvette holder. The temperature of the block was measured by a copper–constantan thermocouple and adjusted by a variable transformers in the heating circuit. The sample was sealed in a cuvette made from 1-cm square quartz tubing (Vitro Dynamics QS110), scanned at 25°, then placed in the pre-heated block. After about 20 min, block and cuvette were placed in the sample compartment of the spectrophotometer, and scanned. Repeated scanning showed no change in absorbance, which was taken to mean that the sample had reached constant temperature. Since the half life for decarboxylation at this temperature is about 200 h, no significant decarboxylation was anticipated. That none occurred was shown by rescanning the sample after it had cooled to 25°.

Rate Measurements

About 20–30 mg of pyridinecarboxylic acid was dissolved in 50 ml of buffer, and 1.5 ml portions of this solution were sealed in 2 ml serum ampoules. These were thermostatted at 150 ± 0.1° or 95 ± 0.1°, withdrawn at intervals, chilled, and diluted by weight to 25 ml in 1 *M* NaOH. Absorbances were measured at 25 ± 0.1°, using a Beckman DU spectrophotometer, at wavelengths where the carboxylate ion absorbs but the decarboxylation product does not. These were for homarine 273.5 nm, picolinic acid 275 nm, 6-methylpicolinic and quinolinic acids 280 nm, and 5-nitropicolinic acid 285 nm. The p*H* of the last ampoule in each run, after cooling to 25°, did not differ from that of the original reaction mixture by more than 0.008 units. Excellent first-order plots were obtained to three or more half lives.

Isotope Effects

^{13}C-Carboxyl kinetic isotope effects were measured as described previously (13).

The authors are grateful to the National Research Council of Canada for financial support of this project, to Dr. J. M. Charlton for helpful discussions, to Mr. W. D. Buchannon for the mass-spectrometric measurements, and to Mr. W. B. Easterbrook for the design and construction of the sealed cuvettes.

1. P. Dyson and D. L. Hammick. J. Chem. Soc. 1724 (1937).

2. M. F. R. ASHWORTH, R. P. DAFFERN, and D. L. HAMMICK. J. Chem. Soc. 809 (1939).
3. I. ZLOLOWSKI and M. ZIELINSKI. Nukleonika, **5**, 511 (1961).
4. M. ZIELINSKI. Kernenergie, **5**, 351 (1962).
5. B. R. BROWN and D. L. HAMMICK. J. Chem. Soc. 659 (1949).
6. P. HAAKE and J. MANTECÓN. J. Am. Chem. Soc. **86**, 5230 (1964).
7. N. H. CANTWELL and E. V. BROWN. J. Am. Chem. Soc. **74**, 5967 (1952); **75**, 4466 (1953).
8. L. W. CLARK. J. Phys. Chem. **66**, 125 (1962); **67**, 138 (1963); **68**, 3048 (1964); **69**, 2277 (1965).
9. E. V. BROWN and R. J. MOSER. J. Org. Chem. **36**, 454 (1971).
10. V. PALLINI, C. VASCONETTO, and C. RICCI. Boll. Soc. Ital. Biol. Sper. **12**, 41 (1965); Chem. Abstr. **64**, 8619 (1966).
11. K. R. LYNN and A. N. BOURNS. Chem. Ind. London, 782 (1963).
12. J. L. LONGRIDGE and F. A. LONG. J. Am. Chem. Soc. **90**, 3092 (1968).
13. G. E. DUNN and S. K. DAYAL. Can. J. Chem. **48**, 3349 (1970).
14. A. M. LEKO and R. P. SAPER. Glasnik Hem. Drustva Beograd. **25**, 267 (1961); Chem. Abstr. **59**, 1195 (1963).
15. G. E. DUNN and F. L. KUNG. Can. J. Chem. **44**, 1261 (1966).
16. G. E. DUNN and G. K. J. LEE. Can. J. Chem. **49**, 1032 (1971).
17. P. JOHNSON and E. A. MOELWYN-HUGHES. Proc. Roy. Soc. 175 (1940).
18. R. F. EVANS, E. F. G. HERINGTON, and W. KYNASTON. Trans. Faraday Soc. **49**, 1284 (1953).
19. F. HOLMES and W. R. C. CRIMMIN. J. Chem. Soc. 1175 (1955).
20. R. W. GREEN and H. K. TONG. J. Am. Chem. Soc. **78**, 4896 (1956).
21. J. T. EDSALL and M. H. BLANCHARD. J. Am. Chem. Soc. **55**, 2337 (1933).
22. J. A. ZOLTEWICZ and C. L. SMITH. J. Am. Chem. Soc. **89**, 3358 (1967).
23. I. F. TUPITSYN and N. K. SEMENOVA. Tr. Gos. Inst. Prikl. Khim. **49**, 120 (1962); Chem. Abstr. **60**, 6721 (1964).
24. J. S. THOME and H. GOEBEL. Hoppe-Seyler's Z. Physiol. Chem. **288**, 237 (1951).
25. H. NIENBURG. Ber. **68**, 1474 (1935).

Can. J. Chem. Downloaded from www.nrcresearchpress.com by 210.87.254.5 on 09/05/12
For personal use only.

The Synthesis of (±)-Ochrobirine. A New Route to the Spirobenzylisoquinoline System[1]

N. E. CUNDASAWMY AND D. B. MACLEAN

Department of Chemistry, McMaster University, Hamilton, Ontario

Received March 27, 1972

The spirobenzylisoquinoline system has been synthesized from substituted 2-phenyl-1,3-indandiones as starting materials. Ring B of the spiro system was constructed by a modified Pomeranz–Fritsch reaction. The reaction sequence has been applied to the synthesis of an analog of ochrobirine and then to (±)-ochrobirine itself.

Le système spirobenzylisoquinoline a été synthétisé à partir des phényl-2 indanediones-1,3 substituées en tant que produits de départ. Le cycle B du système spirannique a été construit selon une réaction modifiée de Pomeranz–Fritsch. La séquence réactionnelle a été appliquée à la synthèse d'un analogue de l'ochrobirine et de l'ochrobirine (±) elle-même. [Traduit par le journal]

Canadian Journal of Chemistry, **50**, 3028 (1972)

The spirobenzylisoquinoline alkaloids were first isolated some 30 years ago (1) but it was not until 1964 that a structure was assigned to ochotensimine, an alkaloid of this group (2–4). In the intervening years structures have been proposed for other related alkaloids (5–10) and the total synthesis of several of them has been realized. The alkaloids of this family vary in the nature of the substituents present on aromatic ring A and in the type and number of substituents on the spiro ring. The main structural variants are exemplified in ochotensimine, fumaricine, and ochrobirine shown below.

The synthesis of alkaloids related to ochotensimine and fumaricine has been realized by a route in which the key step is a Pictet–Spengler condensation of the appropriately substituted 1,2-indandione with an appropriately substituted phenylethylamine as shown in Scheme 1. The first synthesis of this type was reported by McLean *et al.* (11, 12) for ochotensimine. Several variants of this scheme have since been reported (13–17). By using ninhydrin instead of an indandione in the Pictet–Spengler condensation the groups of Manske and Ahmed (18) and Kametani *et al.* (19) synthesized model compounds in which two oxygens were incorporated into the spiro ring. Both groups have recently completed the total synthesis of (±)-ochrobirine by this method (20, 21). Other routes to the spiro system have been developed by Kametani *et al.* (22) and by Shamma *et al.* (23–25). In the former a phenylpyruvic acid is substituted for the indandione in the Pictet–Spengler reaction and the spiro ring completed by a cyclization of the acid function. In the latter a protoberberine system is rearranged to the spiro system. Here we report a new synthesis of the spirobenzylisoquinolines by a route different from those previously reported. We have used this method to synthesize (±)-ochrobirine. Our method utilizes the readily

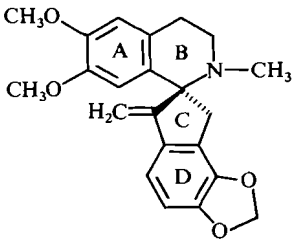

Ochotensimine

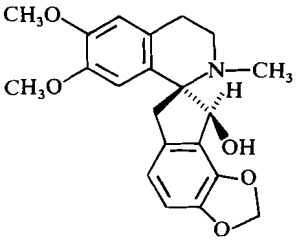

Fumaricine

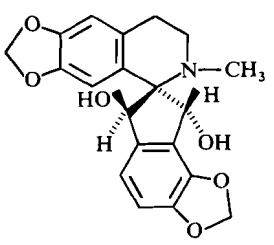

Ochrobirine

[1]Presented in part at the 54th Canadian Chemical Conference of the Chemical Institute of Canada, Halifax, N.S., May, 1971.

Can. J. Chem. Downloaded from www.nrcresearchpress.com by 210.87.254.5 on 09/05/12
For personal use only.

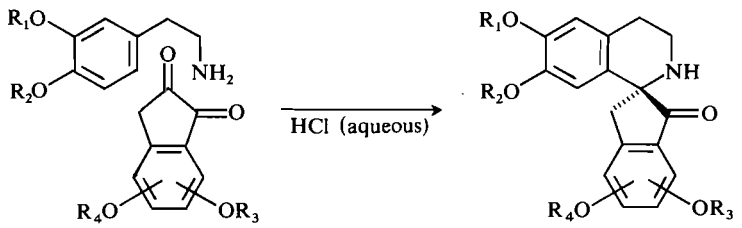

SCHEME 1

available 2-phenyl-1,3-indandiones as starting compounds and completes the synthesis of the spiro system by construction of ring **B** through a modified Pomeranz–Fritsch synthesis as shown in Scheme 2. The scheme was tested using 2-(3,4-dimethoxyphenyl)-1,3-indandione (**1**) before proceeding to the synthesis of (±)-ochrobirine.

2-Phenyl-1,3-indandiones are available by two routes. For example, 3-benzylidenephthalides, prepared by a Perkin condensation of a phthalic anhydride and a phenylacetic acid (26), rearrange in base to 1,3-indandiones (27). In another method, reported by Shapiro *et al.* (28, 29), benzylidenephthalide formation and rearrangement are carried out in the same reaction vessel by interacting a phthalide with an aromatic aldehyde in the presence of an alkoxide and an ester, used as a scavenger to remove the water liberated in benzylidenephthalide formation. Both methods, outlined in Scheme 3, gave high yields of the model compound, 2-(3,4-dimethoxyphenyl)-1,3-indandione (**1**).

The introduction of the nitrogen and the two carbons required to complete the carbon framework was brought about by bromination followed by displacement of bromine by aminoacetaldehyde diethyl acetal. The bromination of 2-phenyl-1,3-indandiones has been studied previously (30) as has the displacement of the bromines with amines (31). Compound **1** brominated readily in glacial acetic acid to 2-bromo-2-(3,4-dimethoxyphenyl)-1,3-indandione (**2**), but the compound proved unstable to heat and light. Purification of **2** was not attempted, therefore, but it was used directly in the next step. The product, 2-(2,2-diethoxyethylamino)-2-(3,4-dimethoxyphenyl)-1,3-indandione (**3**), was obtained in 73% yield based on **1**. These and subsequent steps of the synthesis are outlined in Scheme 4.

Following the procedure of Bobbitt *et al.* (32, 33) the cyclization of **3** in 6 *M* aqueous ethanolic HCl was attempted. Instead of the expected spiroisoquinoline we obtained the dione, **1**, formed by cleavage of the C_2—N bond; glyoxal, as its bis-2,4-dinitrophenyl hydrazone was also isolated. The formation of these products and ammonia is rationalized in Scheme 5 where the driving force for the elimination is postulated to be the protonation at nitrogen. Accordingly, the nitrogen was acetylated and cyclization of the *N*-acetyl compound **4** attempted again. The reaction now proceeded normally to yield **5** (Scheme 4). Reduction of **5** to **6** was brought about with H_2 over Adams catalyst. Hydrolysis of the *N*-acetyl group yielded **7** which had previously been prepared by another route (34).

The identity of the two products was established by comparison of their melting points, their i.r. and their n.m.r. spectra. *N*-methylation of **7** to **8** by the Eschweiler–Clarke procedure proceeded in very low yield

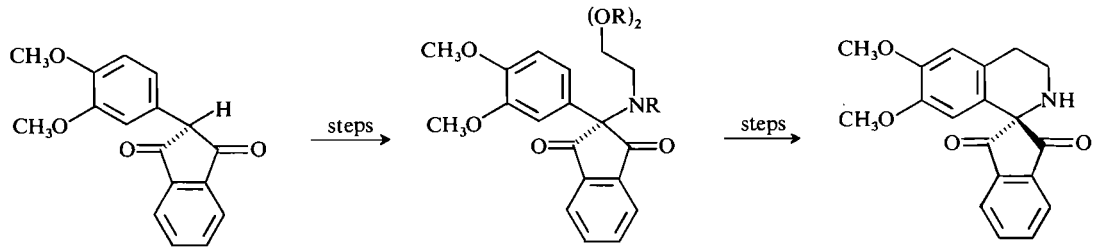

SCHEME 2

Can. J. Chem. Downloaded from www.nrcresearchpress.com by 210.87.254.5 on 09/05/12
For personal use only.

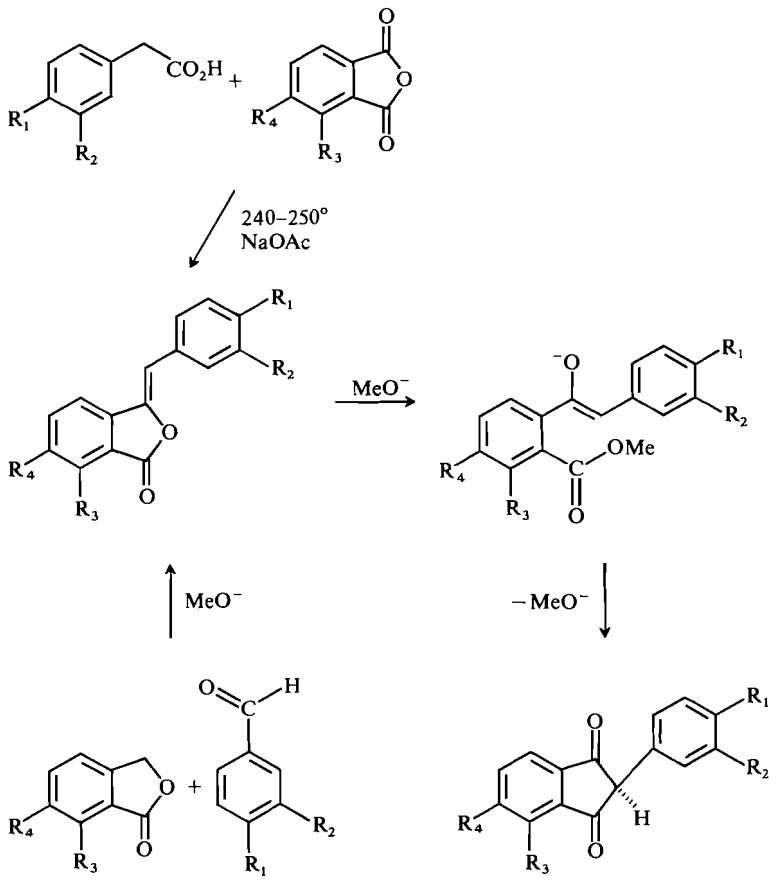

In the model synthesis: $R_1 = R_2 = OCH_3$; $R_3 = R_4 = H$.
In the ochrobirine synthesis: $R_1 + R_2 = R_3 + R_4 = OCH_2O$.

SCHEME 3

which was surprising since this reaction had already been applied successfully to similar systems (18, 34). However the reduction of **8** to the corresponding diol had already been reported (34) and we found that the diol was readily *N*-methylated with formaldehyde and sodium borohydride to **9**. The configuration of the diol was not established in this study. With the successful completion of the model synthesis attention was turned to the synthesis of (±)-ochrobirine.

The starting compounds required for the synthesis of ochrobirine are piperonal and 6,7-methylenedioxyphthalide in one case and 3,4-methylenedioxyphenylacetic acid and 3,4-methylenedioxyphthalic anhydride in the other depending upon the route chosen for the preparation of the substituted 2-phenyl-1,3-indandione. All compounds are available commercially or by procedures described in the literature but it is worthwhile to note that the preparation of the phthalic acid derivatives is lengthy and cumbersome and is a major shortcoming of this synthesis.

The preparation of the 2-phenyl-1,3-indandione in the model series proceeded in high yield by both methods but such was not the case when the methylenedioxy compounds were used. Yields of less than 10% were obtained in both routes. The starting materials were not recovered and the desired product was accompanied by polymeric material. The reasons for the failure in these condensations were not established. However, we found that, when the phenylacetic acid was treated with acetic anhydride, presumably to give an anhydride, prior

Can. J. Chem. Downloaded from www.nrcresearchpress.com by 210.87.254.5 on 09/05/12
For personal use only.

Can. J. Chem. Downloaded from www.nrcresearchpress.com by 210.87.254.5 on 09/05/12
For personal use only.

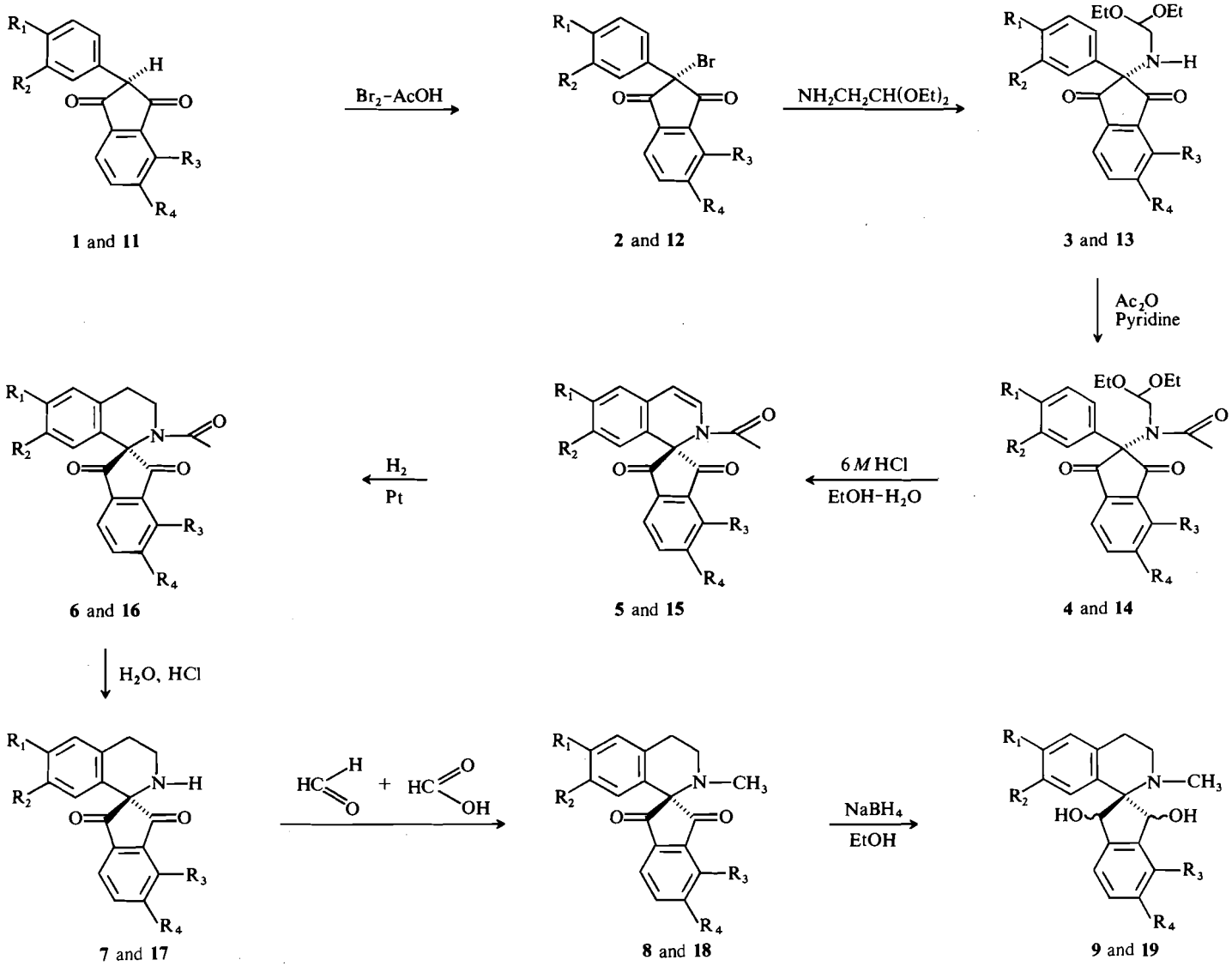

In the model synthesis: $R_1 = R_2 = OCH_3$; $R_3 = R_4 = H$.
In the ochrobirine synthesis: $R_1 + R_2 = R_3 + R_4 = OCH_2O$.

SCHEME 4

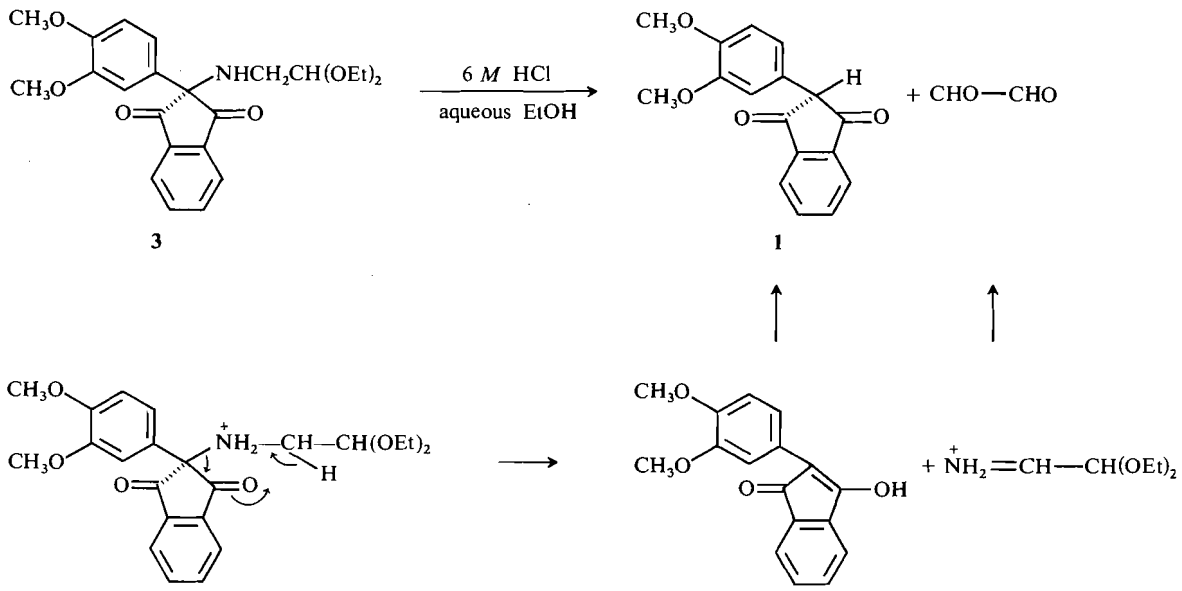

SCHEME 5

to addition of the phthalic anhydride and fused sodium acetate, a satisfactory yield (60–65%) of the benzylidenephthalide (**10**) was obtained. Rearrangement to the dione (**11**) proceeded in nearly quantitative yield. The remainder of the synthesis proceeded in a manner analogous to that in the model series (see Scheme 4) and in satisfactory yield. It was possible, however, to methylate the secondary amine (**17**) by the Eschweiler–Clarke method in satisfactory yield. Compounds **17** and **18** isolated by us have melting points identical with those found by Nalliah *et al.* (21) but considerably higher than those reported by Kametani *et al.* (20 *a*, *b*). Our (±)-ochrobirine melted at nearly the same temperature as that reported for the lower melting modification of Nalliah *et al.* (21). The spectral properties (i.r. and mass spectrum) of synthetic (±)-ochrobirine are identical with those of the natural base. The high degree of specificity found in the borohydride reduction of **18** to **19** was unexpected but has been observed by others (20, 21).

The absolute configuration of (±)-ochrobirine and other alkaloids of this family (35) has recently been established and conforms to that in the formulas.

Experimental

Apparatus, Methods, and Materials

Melting points were recorded on a Köfler micro hot stage apparatus and are uncorrected. Infrared spectra were recorded on a Beckmann IR5 or a Perkin–Elmer 337 spectrophotometer in chloroform solution unless otherwise stated. The p.m.r. spectra were recorded on a Varian A60 or a T60 spectrophotometer in solution in $CDCl_3$ using tetramethylsilane as an internal standard. Chemical shifts are reported in p.p.m. (δ) from TMS. The symbols s = singlet, d = doublet, t = triplet, q = quartet and m = multiplet are used in reporting spectra. Mass spectra were routinely run on all samples to check their molecular weights either on a Hitachi RMU 6A mass spectrometer or on a C.E.C. 21-110B double focusing instrument. High resolution mass spectrometry was used to confirm the composition of several compounds and mass measurements were made by procedures described elsewhere (34).

The microanalyses were performed by Gygli Microanalytical Laboratory, Toronto, Ontario.

3-(3,4-Dimethoxybenzylidene)-phthalide

A mixture of 3,4-dimethoxyphenylacetic acid (0.025 mol), phthalic anhydride (0.021 mol), and freshly fused sodium acetate (150 mg) was rapidly heated in an oil bath to 240–245° and the temperature maintained there until the reaction was complete (1–2 h). The reaction mixture was cooled, dissolved in the minimum amount of hot methanol, and the solution filtered. Upon cooling, yellow crystals of the phthalide were deposited melting at 133–134°; yield, 78%.

Anal. Calcd. for $C_{17}H_{14}O_4$: C, 72.35; H, 4.97. Found: C, 72.13; H, 4.98.

Can. J. Chem. Downloaded from www.nrcresearchpress.com by 210.87.254.5 on 09/05/12
For personal use only.

Can. J. Chem. Downloaded from www.nrcresearchpress.com by 210.87.254.5 on 09/05/12
For personal use only.

I.r.: ν_{max} 1775 cm^{-1}; p.m.r.: 3.80 (3H, s, OCH_3), 3.85 (3H, s, OCH_3), 6.24 (1H, s, benzylic H), and 6.74–6.90 (7H, m, aromatic H's).

*3-(3,4-Methylenedioxybenzylidene)-6,7-methylenedioxyphthalide (**10**)*

The method described above for the preparation of the 3-(3,4-dimethoxybenzylidene)-phthalide gave very low yields when applied to the preparation of the methylenedioxy compound. It was found, however, that the following procedure was satisfactory. A mixture of 3,4-methylenedioxyphenyl acetic acid (0.025 mol) and freshly distilled acetic anhydride (0.05 mol) was heated on a steam bath for 15 min. 3,4-Methylenedioxyphthalic anhydride (0.021 mol) and freshly fused sodium acetate (200 mg) were added and the mixture was heated rapidly to 170–180° until the distillation of acetic acid and other volatile components was complete (45–60 min). The solid was dissolved in hot methanol, the solution filtered and cooled. The bright yellow crystals which separated melted at 259–261°; yield, 60–62%. I.r.: ν_{max} 1772 cm^{-1}.

Anal. Calcd. for $C_{17}H_{10}O_6$: C, 65.80; H, 3.23. Found: C, 65.70; H, 3.33.

*2-(3,4-Dimethoxyphenyl)-1,3-indandione (**1**) from 3-(3,4-Dimethoxybenzylidene)-phthalide (Method A)*

The benzylidenephthalide (0.025 mol) in boiling absolute methanol (200 ml) was treated with a solution of sodium methoxide freshly prepared from sodium (750 mg) and absolute methanol (25 ml). The bright red solution so obtained was heated under reflux for 1 h, cooled, and the solvent removed under vacuum. The red residue was dissolved in water and extracted with ether. The aqueous layer was separated, acidified to p*H* 4 with 10% sulfuric acid and extracted several times with chloroform. The extract was washed several times with water, dried over anhydrous sodium sulfate and evaporated to dryness. The white solid residue was recrystallized from benzene and melted at 196–197°; yield, 92–95%.

Anal. Calcd. for $C_{17}H_{14}O_4$: C, 72.35; H, 4.97. Found: C, 72.51; H, 4.83.

I.r.: ν_{max} 1710, 1745 cm^{-1}; p.m.r.: 3.79 (6H, s, 2 × OCH_3), 4.17 (1H, s, benzylic H), 6.69 (3H, m, aromatic H), 7.73–8.10 (4H, m, aromatic H's).

*2-(3,4-Dimethoxyphenyl)-1,3-indandione (**1**) from 3,4-Dimethoxybenzaldehyde and Phthalide (Method B)*

A boiling mixture of phthalide (0.025 mol), aldehyde (0.025 mol) and freshly distilled methyl formate (12 ml) was treated with a solution of sodium methoxide in methanol prepared from sodium (1.95 g) in anyhydrous methanol (24 ml). The solution, which became red immediately upon addition of the methoxide, was boiled for 1 h under reflux and then worked-up as in the procedure above. Compound **1** was obtained in 95% yield.

*2-(3,4-Methylenedioxyphenyl)-4,5-methylenedioxy-1,3-indandione (**11**)*

This compound was prepared from the phthalide (**10**) by the procedure outlined previously (method A) for the rearrangement of 3-(3,4-dimethoxybenzylidene)-phthalide. Like its analog, this compound was recrystallized from benzene and then melted at 209–210°; yield, 93%. When its preparation from piperonal and 6,7-methylenedioxyphthalide (method B above) was attempted only 5–10% of the desired product was obtained.

Anal. Calcd. for $C_{17}H_{10}O_6$: C, 65.81, H. 3.23. Found: C, 65.66; H, 3.11.

I.r.: ν_{max} 1708, 1740 cm^{-1}; p.m.r.: 4.17 (1H, s, benzylic H), 5.88 (2H, s, OCH_2O), 6.16 (2H, s, OCH_2O), 6.89, 7.46 (2H, AB quartet, $J = 8$ Hz, C-6 and C-7 H's), 6.70–7.42 (3H, m, aromatic H's).

*2-Bromo-2-(3,4-dimethoxyphenyl)-1,3-indandione (**2**)*

A stirred solution of dione **1** (0.005 mol) in glacial acetic acid (100 ml) under an atmosphere of oxygen-free nitrogen at room temperature was treated rapidly with a solution of bromine (0.005 mol) in glacial acetic acid (15 ml). The absorption of bromine was instantaneous but the reaction was stirred for 5 min before removing the glacial acetic acid under vacuum. It was necessary to keep the temperature below 20° at this stage to avoid decomposition of the bromo compound. The residue was a yellow crystalline material melting at 133–134°. In most cases it was used directly in the next step because attempts to recrystallize it resulted in its decomposition. I.r.: ν_{max} 1710, 1745 cm^{-1}; p.m.r.: 3.78 (3H, s, OCH_3), 3.83 (3H, s, OCH_3), 6.70–8.3 (7H, m, aromatic H's).

*2-Bromo-2-(3,4-methylenedioxyphenyl)-4,5-methylenedioxy-1,3-indandione (**12**)*

Compound **11** was brominated by a procedure identical with that used for the preparation of **2**. The crude product melted at 176–178°. I.r.: ν_{max} 1708, 1745 cm^{-1}; p.m.r.: 5.90 (2H, s, OCH_2O), 6.16 (2H, s, OCH_2O), 7.03, 7.57 (AB quartet, $J = 8$ Hz, C-6 and C-7 H's), 6.6–7.3 (3H, m, aromatic H's).

*2-(2,2-Diethoxyethylamino)-2-(3,4-dimethoxyphenyl)-1,3-indandione (**3**)*

A stirred solution of compound **2** (0.01 mol) in anhydrous ether (75 ml) was cooled in an ice bath and to it was added dropwise a solution of freshly distilled aminoacetaldehyde diethyl acetal (0.02 mol) in anhydrous ether (15 ml). The resulting solution was stirred for a total of 15 h under an atmosphere of dry nitrogen. The reaction mixture, containing suspended solids, was washed twice with water, the ether layer separated, dried over anhydrous sodium sulfate, and evaporated to dryness. The yellow gum that resulted was used directly in the next step; yield, 74%. I.r.: ν_{max} 1715, 1750 cm^{-1}; p.m.r.: 1.08 (6H, t, $J = 7$ Hz, 2 × OCH_2CH_3), 2.68 (2H, d, $J = 5$ Hz, N—CH_2—CH), 3.24–3.74 (4H, m, 2 × OCH_2CH_3), 3.72 (3H, s, OCH_3), 3.76 (3H, s, OCH_3), 4.54 (1H, t, $J = 5$ Hz, N—CH_2—CH), 6.7–8.2 (7H aromatic H's).

*2-(2,2-Diethoxyethylamino)-2-(3,4-methylenedioxyphenyl)-4,5-methylenedioxy-1,3-indandione (**13**)*

Compound **13** was prepared from **12** in a manner identical with the preparation of **3** from **2** above; yield, 71–73%. I.r.: ν_{max} 1710, 1748 cm^{-1}; p.m.r.: 1.14 (6H, t, $J = 6$ Hz, 2 × OCH_2CH_3), 2.64 (2H, d, $J = 5$ Hz, N—CH_2CH), 2.30 (1H, broad s, NH), 3.27–3.74 (4H, complex m, 2 × O—CH_2—CH_3), 4.57 (1H, t, $J = 5$ Hz, N—CH_2—CH), 5.87 (2H, s, OCH_2O), 6.15 (2H, s, OCH_2O), 6.87, 7.44 (AB quartet, $J = 8$ Hz, C-6 and C-7 H's), and 6.70–7.00 (3H, m, aromatic H's).

Can. J. Chem. Downloaded from www.nrcresearchpress.com by 210.87.254.5 on 09/05/12
For personal use only.

Treatment of **3** *with 6 M Aqueous Ethanolic Hydrochloric Acid*

A solution of 0.005 mol of **3** in 75 ml of 6 *M* aqueous ethanolic hydrochloric acid was stirred for 16 h at room temperature. The resulting mixture contained a white precipitate. The solvent was removed under vacuum and the white residue so obtained was washed with water and filtered. Recrystallization from benzene afforded 1.35 g of needle-like crystals, m.p. 194–196°. A mixture melting point of the product and compound **1** showed no depression. The i.r. spectrum in $CHCl_3$ and the p.m.r. spectrum in $CDCl_3$ were superimposable on those of compound **1**.

The filtrate was concentrated to about 10 ml and was treated with a solution of 2,4-dinitrophenylhydrazine in ethanol and allowed to stand at room temperature for 15 min. The reddish precipitate that formed was filtered, washed with water, and air dried. Recrystallization from aqueous ethanol gave orange crystals which melted at 328–330°. Authentic glyoxal bis-2,4-dinitrophenylhydrazone is reported to melt at 328° (36).

*N-Acetyl-2-(2,2-diethoxyethylamino)-2-(3,4-dimethoxyphenyl)-1,3-indandione (***4***)*

A mixture of amine **3** (0.001 mol) in anhydrous pyridine (1 ml) and freshly distilled acetic anhydride (3 ml) was stirred at room temperature for 48 h. The solution was added to water and the mixture extracted several times with chloroform. The chloroform extract was washed several times with cold aqueous hydrochloric acid and with water, dried over anhydrous sodium sulfate, and evaporated to dryness. The residue was adsorbed on basic alumina and the column eluted with chloroform. After removal of chloroform from the eluant a crystalline residue was obtained which, after recrystallization from ethanol, melted at 132–133°; yield, 83%.

Anal. Calcd. for $C_{25}H_{29}NO_7$: C, 65.94; H, 6.37; N, 3.08. Found: C, 66.02; H, 6.63; N, 3.12.

I.r.: ν_{max} 1635 (amide), 1712, 1748 cm^{-1}; p.m.r.: 0.97 (6H, t, $J = 6$ Hz, $2 \times OCH_2CH_3$), 2.09 (3H, s, $COCH_3$), 3.04–3.60 (6H, m, $2 \times OCH_2{-}CH_3 + N{-}CH_2{-}CH$), 3.61 (3H, s, OCH_3), 3.67 (3H, s, OCH_3), 4.37 (1H, t, $J = 5$ Hz, $N{-}CH_2{-}CH$), 6.6–7.9 (7H, m, aromatic H's).

*N-Acetyl-2-(2,2-diethoxyethylamino)-2-(3,4-methylenedioxyphenyl)-4,5-methylenedioxy-1,3-indandione (***14***)*

Compound **14** was prepared from **13** in a manner analogous to the preparation of **4** above. After recrystallization from ethanol it melted at 172–174°; yield, 80%.

Anal. Calcd. for $C_{25}H_{25}NO_9$: C, 62.12; H, 5.18; N, 2.90. Found: C, 62.37; H, 5.30; N, 3.08.

I.r.: ν_{max} 1640, 1710, 1740 cm^{-1}; p.m.r.: 1.13 (6H, t, $J = 6$ Hz, $2 \times OCH_2CH_3$), 2.24 (3H, s, $COCH_3$), 3.27, 3.74 (6H, complex m, $2 \times OCH_2CH_3 + N{-}CH_2CH$), 4.47 (1H, t, $J = 5$ Hz, $N{-}CH_2{-}CH$), 5.90 (2H, s, OCH_2O), 6.17 (2H, s, OCH_2O), 6.87, 7.44 (2H, AB quartet, $J = 8$ Hz, C-6 and C-7 H's), and 6.97–7.10 (3H, m, aromatic H's).

*2-Acetyl-6,7-dimethoxy-1,2-dihydroisoquinoline-1-spiro-2'-(1',3'-indandione) (***5***)*

A mixture of **4** (0.003 mol) in 6 *M* aqueous ethanolic hydrochloric acid (50 ml) was stirred at room temperature for 18 h. The ethanol was removed under vacuum, the aqueous acid solution neutralized with ammonia, and the solution extracted twice with chloroform. The chloroform extract was dried over anhydrous sodium sulfate and then evaporated to give a reddish brown residue which was purified by chromatography over basic alumina using chloroform as eluant. Evaporation of the chloroform gave an orange solid which crystallized readily from hot ethanol, m.p. 263–264°; yield, 47–52%.

Anal. Calcd. for $C_{21}H_{17}NO_5$: C, 69.42; H, 4.68; N, 3.86. Found: C, 69.39: H, 5.02; N, 3.96.

I.r.: ν_{max} 1642 ($N{-}COCH_3$), 1668 ($\geq C{=}C \leq$), 1715, 1750 cm^{-1}; p.m.r.: 2.26 (3H, s, $COCH_3$), 3.37 (3H, s, OCH_3), 3.81 (3H, s, OCH_3), 5.64, 6.77 (2H, AB quartet, $J = 8$ Hz, C-3 and C-4 H's), 5.90 (1H, s, C-8 H),[2] 6.60 (1H, s, C-5 H), 7.80–8.15 (4H, m, aromatic H's).

*2-Acetyl-6,7-methylenedioxy-1,2-dihydroisoquinoline-1-spiro-2'-(4',5'-methylenedioxy-1',3'-indandione) (***15***)*

This compound was prepared from **14** in a manner analogous to the preparation described above of **5** from **4**. After recrystallization from hot ethanol the compound melted at 305–308°; yield, 57–61%.

Anal. Calcd. for $C_{21}H_{13}NO_7$: C, 64.44; H, 3.33; N, 3.58. Found: C, 64.33; H, 3.30; N, 3.49.

I.r.: ν_{max} 1640 ($N{-}COCH_3$), 1675 ($\geq C{=}C \leq$), 1715 and 1745 cm^{-1}; p.m.r.: 2.17 (3H, s, $N{-}COCH_3$), 5.54, 6.71 (2H, AB quartet, $J = 8$ Hz, C-3 H and C-4 H's), 5.81 (2H, s, OCH_2O), 6.24 (2H, s, OCH_2O), 6.05 (1H, s, C-8 H), 6.54 (1H, s, C-5 H), 7.21, 7.61 (2H, AB quartet, $J = 8$ Hz, C-6' H and C-7' H's).

*2-Acetyl-6,7-dimethoxy-1,2,3,4-tetrahydroisoquinoline-1-spiro-2'-(1',3'-indandione) (***6***)*

Compound **5** (0.001 mol) dissolved in acetic acid (20 ml) was shaken with hydrogen at 35 p.s.i.g., in the presence of Adams catalyst (25 mg) for 1 h. The catalyst was removed by filtration and the acetic acid evaporated under vacuum. The pale yellow residue was recrystallized from ethanol and melted at 238–240°; yield, 95%.

Anal. Calcd. for $C_{21}H_{19}NO_5$: C, 69.23; H, 5.22; N, 3.85. Found: C, 69.40; H, 5.37; N, 3.85.

I.r.: ν_{max} 1640 ($N{-}COCH_3$), 1718 and 1750 cm^{-1}; p.m.r.: 2.35 (3H, s, $COCH_3$), 3.15, 3.94 (4H, A_2B_2m, C-3 and C-4 H's); 3.55 (3H, s, OCH_3), 3.85 (3H, s, OCH_3), 6.01 (1H, s, C-8 H), 6.85 (1H, s, C-5 H), 7.85–8.1 (4H, m, aromatic H's).

*2-Acetyl-6,7-methylenedioxy-1,2,3,4-tetrahydroisoquinoline-1-spiro-2'-(4',5'-methylenedioxy-1',3'-indandione) (***16***)*

This compound was prepared from **15** in the same way that **6** was prepared from **5**. Recrystallization from ethanol gave yellow crystals melting at 300–301°, yield, 91%.

Anal. Calcd. for $C_{21}H_{15}NO_7$: C, 64.27; H, 3.87; N, 3.56. Found: C, 64.33; H, 3.76; N, 3.56.

I.r.: ν_{max} 1640 ($N{-}COCH_3$), 1715 and 1740 cm^{-1}; p.m.r.: 2.13 (3H, s, $N{-}COCH_3$), 3.01, 3.85 (4H, A_2B_2m, C-3 and C-4 H's), 5.82 (2H, s, OCH_2O), 6.20 (2H, s, OCH_2O), 6.18 (1H, s, C-8 H), 6.67 (1H, s, C-5 H), 7.16, 7.55 (2H, AB quartet, $J = 8$ Hz, C-6 H and C-7' H's).

[2]Assignment of the high field aromatic singlet of ring A to C-8 H is based on analogy with other spirobenzylisoquinoline systems (6, 7, 8). Moreover, the signal assigned to C-8 H is sharper than that assigned to C-5 H because the para benzylic coupling between C-8 H and the protons at C-4 is smaller than the ortho benzylic coupling between C-5 H and the protons at C-4.

Can. J. Chem. Downloaded from www.nrcresearchpress.com by 210.87.254.5 on 09/05/12
For personal use only.

6,7-Dimethoxy-1,2,3,4-tetrahydroisoquinoline-1-spiro-2'-(1',3'-indandione) (7)

The amide **6** (0.5 mmol) was boiled under reflux with 6 *M* ethanolic-aqueous HCl (25 ml) for 2 h. The mixture was taken to dryness, water added, the solution basified, and extracted with chloroform. The extract was washed, dried, and evaporated to a residue which crystallized from ether–hexane and melted at 180–182°; yield, 80%.

Anal. Calcd. for $C_{19}H_{17}NO_4$: C, 70.60; H, 5.26; N, 4.64. Found: C, 70.52; H, 5.30; N, 4.50.

I.r.: ν_{max} 1715 and 1750 cm^{-1}; p.m.r.: 2.79, 3.48 (4H, A_2B_2m, C-3 and -4 H's), 3.50 (3H, s, OCH_3), 3.81 (3H, s, OCH_3), 5.92 (1H, s, C-8 H), 6.71 (1H, s, C-5 H), 7.8–8.2 (4H, m, aromatic H's).

6,7-Methylenedioxy-1,2,3,4-tetrahydroisoquinoline-1-spiro-2'-(4',5'-methylenedioxy-1',3'-indandione) (17)

The amide **16** was hydrolyzed in the same way that **6** was converted to **7**. The resulting amine was recrystallized from ether–hexane and melted at 198–199°; yield, 82–84%.

Anal. Calcd. for $C_{19}H_{13}NO_6$: mol. wt. 351.074; C, 64.95; H, 3.70; N, 3.99. Found: mol. wt. 351.071 (high resolution mass spectrum); C, 64.91; H, 3.91; N, 4.04.

I.r.: ν_{max} 1715 and 1748 cm^{-1}; p.m.r.: 2.74, 3.37 (4H, A_2B_2m, C-3 and -4 H's), 5.78 (2H, s, OCH_2O), 6.28 (2H, s, OCH_2O), 5.99 (1H, s, C-8 H), 6.60 (1H, s, C-5 H), 7.20, 7.64 (2H, AB quartet, $J = 8$ Hz, C-6' and C-7' H's).

2-Methyl-6,7-methylenedioxy-1,2,3,4-tetrahydroisoquinoline-1-spiro-2'-(4',5'-methylenedioxy-1',3'-indandione) (18)

Amine (**17**) (100 mg), 92% formic acid (2 ml), and formaldehyde (2 ml) were heated on a steam bath for 10 h. Water was added to the mixture which was then basified with sodium bicarbonate solution and extracted twice with chloroform. The chloroform extract was washed with water, dried over sodium sulfate, and evaporated to dryness. The yellow residue after recrystallization from ether–hexane melted at 195–196°; yield, 79%.

Anal. Calcd. for $C_{20}H_{15}NO_6$: mol. wt. 365.090; C, 65.75; H, 4.10; N, 3.84. Found: mol. wt. 365.089 (high resolution mass spectrum); C, 65.52; H, 4.03; N, 3.88.

I.r.: ν_{max} 1705 and 1737; p.m.r.: 2.41 (3H, s, N—CH_3), 2.97–3.47 (4H, complex m, C-3 and -4 H's), 5.81 (2H, s, OCH_2O), 6.31 (2H, s, OCH_2O), 5.96 (1H, s, C-8 H), 6.62 (1H, s, C-5 H), 7.24, 7.64 (2H, AB quartet, $J = 8$ Hz, C-6' and C-7' H's).

2-Methyl-6,7-dimethoxy-1,2,3,4-tetrahydroisoquinoline-1-spiro-2'-(1',3'-indandiol) (9)

6,7-Dimethoxy-1,2,3,4-tetrahydroisoquinoline-1-spiro-2'-(1',3'-indandiol) (410 mg) obtained by reduction of **7** with sodium borohydride (34) was treated without purification with 2.5 ml of formalin (37%) at reflux for 2 h. The mixture was taken to dryness under vacuum, the residue so obtained was dissolved in methanol (5 ml), the solution cooled in ice, and then treated with 200 mg of $NaBH_4$. The mixture was stirred for 30 min, the solvent removed under reduced pressure, water added, and the resulting mixture extracted with methylene chloride. The dry methylene chloride solution was evaporated to dryness and crystallized from benzene–petroleum ether gave an analytical sample melting at 161–162°.

Anal. Calcd. for $C_{20}H_{23}NO_4$: C, 70.29; H, 6.73; N, 4.10. Found: C, 70.57; H, 6.81; N, 3.99.

P.m.r.: 2.04 (2H, broad s, 2 × O*H*); 2.65 (3H, s, N—CH_3), 2.78 (2H, t, N—CH_2), 3.48 (2H, t, Ar—CH_2), 3.27 (3H, s, OCH_3), 3.83 (3H, s, OCH_3), 5.35 (2H, broad s, 2 × C*H*—OH), 5.92 (1H, s, C-8 H), 6.67 (1H, s, C-5 H), 7.4 (4H, m, aromatic H's). The two proton singlet at 2.04 δ disappeared in the presence of D_2O.

(±)-Ochrobirine (19)

Compound **18** (32 mg) in absolute ethanol (35 ml) was treated with sodium borohydride (90 mg) and the mixture was stirred at room temperature for 15 h. The solvent was then removed under reduced pressure, the residue taken up in H_2O, and extracted with ether. The ether extract was dried over anhydrous sodium sulfate and evaporated to dryness giving 26 mg of white residue. Examination by t.l.c. showed the presence of two components, one of which (the major one) had the same R_f value as natural ochrobirine. Crystallization from benzene–hexane gave 21 mg of crystalline product melting at 210–212° which on t.l.c. showed only traces of the minor component noted above. Recrystallization from methanol removed the traces of impurity without altering the melting point. The i.r. spectrum in chloroform, the p.m.r. spectrum in $CDCl_3$, and the mass spectrum of the synthetic sample were identical with those of natural ochrobirine.

Mol. Wt. Calcd. for $C_{20}H_{19}NO_6$: 369.121. Found (high resolution mass spectrum): 369.120.

We thank the National Research Council of Canada for financial support of this work and Dr. V. Smula of this laboratory for preparation of compound **9**.

1. R. H. F. MANSKE. Can. J. Res. B**14**, 354 (1936).
2. S. MCLEAN and M.-S. LIN. Tetrahedron Lett. 3819 (1964).
3. S. MCLEAN, M.-S. LIN, and R. H. F. MANSKE. Can. J. Chem. **44**, 2449 (1966).
4. S. MCLEAN, M.-S. LIN, A. C. MACDONALD, and J. TROTTER. Tetrahedron Lett. 185 (1966).
5. D. B. MACLEAN, R. A. BELL, J. K. SAUNDERS, C.-Y. CHEN, and R. H. F. MANSKE. Can. J. Chem. **47**, 3593 (1969).
6. R. H. F. MANSKE, R. RODRIGO, D. B. MACLEAN, D. E. F. GRACEY, and J. K. SAUNDERS. Can. J. Chem. **47**, 3585 (1969).
7. R. H. F. MANSKE, R. G. A. RODRIGO, D. B. MACLEAN, D. E. F. GRACEY, and J. K. SAUNDERS. Can. J. Chem. **47**, 3589 (1969).
8. M. CASTILLO, J. K. SAUNDERS, D. B. MACLEAN, N. M. MOLLOV, and G. I. YAKIMOV. Can. J. Chem. **49**, 139 (1971).
9. C. K. YU, J. K. SAUNDERS, D. B. MACLEAN, and R. H. F. MANSKE. Can. J. Chem. **49**, 3020 (1971).
10. (*a*) I. A. ISRAILOV, M. S. YUNSOV, and S. YU. YUNSOV. Chem. Abstr. **74**, 28827*b* (1971); Khim. Prir. Soedin, **6**, 493 (1970). (*b*) D. A. FESENKO and M. E. PEREL'SON. Chem. Abstr. **75**, 49381*n* (1971); Khim. Prir. Soedin, **7**, 166 (1971).
11. S. MCLEAN, M.-S. LIN, and J. WHELAN. Tetrahedron Lett. 2425 (1968).

12. S. McLEAN, M.-S. LIN, and J. WHELAN. Can. J. Chem. **48**, 948 (1970).
13. B. A. BECKETT and R. B. KELLY. J. Heterocycl. Chem. **5**, 685 (1968).
14. R. B. KELLY and B. A. BECKETT. Can. J. Chem. **47**, 2501 (1969).
15. H. IRIE, T. KISHIMOTO, and S. UYEO. J. Chem. Soc. C, 3051 (1968).
16. T. KISHIMOTO and S. UYEO. J. Chem. Soc. C, 2600 (1969).
17. T. KISHIMOTO and S. UYEO. J. Chem. Soc. C, 1644 (1971).
18. R. H. F. MANSKE and Q. A. AHMED. Can. J. Chem. **48**, 1280 (1970).
19. T. KAMETANI, S. TAKANO, and S. HIBINO. J. Pharm. Soc. Jap. **88**, 1123 (1969).
20. (*a*) T. KAMETANI, S. HIBINO, and S. TAKANO. Chem. Commun. 925 (1971). (*b*) T. KAMETANI, S. HIBINO, and S. TAKANO. J. Chem. Soc. Perkin I, 391 (1972).
21. B. NALLIAH, Q. A. AHMED, R. H. F. MANSKE, and R. RODRIGO. Can. J. Chem. **50**, 1819 (1972).
22. T. KAMETANI, S. TAKANO, S. HIBINO, and T. TERUI. J. Heterocycl. Chem. **6**, 49 (1969).
23. M. SHAMMA and C. D. JONES. J. Am. Chem. Soc. **91**, 4009 (1969).
24. M. SHAMMA and C. D. JONES. J. Am. Chem. Soc. **92**, 4943 (1970).
25. M. SHAMMA and J. F. NUGENT. Tetrahedron Lett. 2625 (1970).
26. R. WEISS. Org. Syn. Coll. Vol. **2**, 61 (1943).
27. F. NATHANSON. Chem. Ber. **26**, 2576 (1893).
28. S. L. SHAPIRO, K. GEIGER, and L. FREEDMAN. J. Org. Chem. **25**, 1860 (1960).
29. S. L. SHAPIRO, K. GEIGER, J. YOULUS, and L. FREEDMAN. J. Org. Chem. **26**, 3580 (1961).
30. G. VANAGS and A. ARENS. Zhur. Obshchei. Khim. **27**, 1358 (1957).
31. A. ARENS, U. RODE, M. ARTJUKH, and D. CIRULE. Latv. PSR Zinat. Akad. Vestis, Kim. Ser. **3**, 342 (1966).
32. J. M. BOBBITT, J. M. KIELY, K. L. KHANNA, and R. EBERMANN. J. Org. Chem. **30**, 2247 (1965).
33. J. M. BOBBITT, D. N. ROY, A. MARCHAND, and C. W. ALLEN. J. Org. Chem. **32**, 2225 (1967).
34. C. K. YU and D. B. MACLEAN. Can. J. Chem. **49**, 3025 (1971).
35. M. SHAMMA, J. L. MONIOT, R. H. F. MANSKE, W. K. CHAN, and K. NAKANISHI. Chem. Commun. 310 (1972).
36. A. I. Vogel. Elementary practical organic chemistry. Part II. Longmans. 1957. p. 582.

Can. J. Chem. Downloaded from www.nrcresearchpress.com by 210.87.254.5 on 09/05/12
For personal use only.

An ^{129}I Mössbauer Study of Novel Polyhalogen Ions Formed by Radioactive Decay in the Tellurium Halides

J. J. JOHNSTONE, C. H. W. JONES, AND P. VASUDEV

Chemistry Department, Simon Fraser University, Burnaby 2, British Columbia

Received March 16, 1972

The ^{129}I Mössbauer emission spectra of the compounds $(NH_4)_2{}^{129m}TeX_6$ and $^{129m}TeX_4$ (X = Cl, Br, I) have been reported against a $Na^{129}I$ absorber at 4 °K. The spectra give evidence in the case of the $(NH_4)_2TeX_6$ compounds for the formation in the radioactive decay of the octahedral ions ICl_6^-, IBr_6^-, and II_6^-. In the TeX_4 compounds, the emission spectra are much more complex and indicate that the ^{129}I atoms are not found in an environment iso-structural and iso-electronic with that of the parent.

The ^{125}Te Mössbauer absorption spectra of the parent compounds were studied to aid in their identification, and the parameters obtained are compared with those in the literature. The ^{125}Te isomer shifts for the TeX_6^{2-} anions are interpreted in terms of pure p-bonding and, in conjunction with data from the emission spectra and data from previously reported n.q.r. work, an isomer shift *vs.* p-hole density relationship is established for tellurium.

Nous rapportons le spectre d'émission Mössbauer de ^{129}I des composés $(NH_4)_2{}^{129m}TeX_6$, et $^{129m}TeX_4$ (X = Cl, Br, I) en fonction d'un absorbant $Na^{129}I$ à 4 °K. Le spectre prouve, dans le cas des composés $(NH_4)_2TeX_6$, la formation des ions octaédriques ICl_6^-, IBr_6^-, et II_6^- durant la désintégration radioactive. Les spectres d'émission des composés TeX_4 sont beaucoup plus complexes et indiquent qu'on ne trouve pas les atomes de ^{129}I dans l'environnement iso-structural et isoélectronique où se trouvent leurs analogues.

Nous avons étudié le spectre d'absorption Mössbauer du ^{125}Te des composés analogues afin de faciliter leur identification; nous avons ensuite comparé les paramètres obtenus avec ceux de la littérature. Nous interprétons les déplacements d'isomère ^{125}Te pour les anions TeX_6^{2-} en termes de liaisons p pures et, en plus des données tirées des spectres d'émission et celles venant d'un travail de n.q.r. rapporté antérieurement, nous établissons la relation entre le déplacement d'isomère et la densité de trous p pour le tellure.

[Traduit par le journal]

Canadian Journal of Chemistry, **50**, 3037 (1972)

Introduction

In a previous publication (1), the ^{129}I Mössbauer emission spectrum of $(NH_4)_2{}^{129m}TeCl_6$ as measured against a $Na^{129}I$ absorber at 80 °K was reported. It was observed that in a large fraction of the radioactive decay events, the daughter ^{129}I atoms remained bonded to the chlorine ligands over the lifetime of the Mössbauer transition, with the formation of the octahedral ICl_6^- ion. This was evidenced by the presence in the spectrum of a single line with an isomer shift corresponding to a large positive value in an absorption experiment. It was shown that the isomer shift for this ion was in good agreement with that to be expected for an ICl_6^- ion from the previously reported Mössbauer data for the ICl_2^- and ICl_4^- ions.

In the present work the investigation was extended to study the three $(NH_4)_2{}^{129m}TeX_6$ (X = Cl, Br, I) compounds at 4 °K and evidence was found for the formation of the octahedral ions IX_6^- in each case. However, in the $(NH_4)_2TeI_6$ lattice the radioactive decay was also found to produce molecular rearrangement in a large fraction of events with the formation of another ^{129}I labelled product.

The $^{129}TeX_4$ compounds (X = Cl, Br, I) have also been studied and the Mössbauer emission spectra again recorded against a $Na^{129}I$ absorber at 4 °K. Here it was found that effectively none of the ^{129}I daughter atoms remained bonded in a lattice environment isoelectronic or isostructural with that of the parent tellurium. In each lattice, the decay was evidently accompanied by molecular rearrangement with the formation of a number of ^{129}I products. The resulting spectra were complex showing the presence of several very broad, unresolved lines. These spectra are tentatively interpreted as showing the presence of the $^{129}IX_4^-$ square planar ions among other products.

A further point of interest lay in the ^{125}Te Mössbauer absorption spectra of the parent TeX_6^{2-} and TeX_4 compounds (X = Cl, Br, I) used in this work. The Mössbauer parameters reported in the literature for these compounds

Can. J. Chem. Downloaded from www.nrcresearchpress.com by 210.87.254.6 on 09/05/12
For personal use only.

Can. J. Chem. Downloaded from www.nrcresearchpress.com by 210.87.254.6 on 09/05/12
For personal use only.

TABLE 1. The Raman spectra of sample preparations of the compounds studied

Compound	Raman spectra (cm^{-1})*				
$TeCl_4$ white solid	375s	348s	341s	150w	
$TeBr_4$ orange solid	245s	231s	224s	133vw	124vw
$(NH_4)_2TeCl_6$ yellow solid	299s	250s	143s		
$(NH_4)_2TeBr_6$ orange solid	178s	155s	91s	75w	
$(NH_4)_2TeI_6$ black solid		108vw	74vw	59vw	

*s = strong, w = weak, vw = very weak.

vary widely and it was important to attempt to define these parameters more closely. Thus, a comparison of the isomer shifts for ^{125}Te and ^{129}I could then be used in attempting to identify the products of the $^{129}Te \rightarrow {}^{129}I$ decay in the solids.

Experimental

The techniques used were essentially as described previously (2). Mössbauer spectra were recorded as 2×256 channel spectra using an NSEC AM1 constant acceleration spectrometer fitted with a Texas Instruments cryoflask and coupled to a Nuclear Data 2000 series 1024 channel analyzer.

The ^{125}Te spectra were recorded with the source and absorber at 80 °K using an $^{125}I/Cu$ (N.E.N.) source of *ca.* 20 mCi, and a Xe/CO_2 proportional detector gated on the 6 keV escape peak of the 35.5 keV γ-ray. The absorbers (5–10 mg cm^{-2} ^{125}Te) were prepared from enriched ^{125}Te and were mounted in Teflon holders with thin windows. The ^{129}I emission spectra were recorded against a $Na^{129}I$ absorber, which was confirmed as a single line absorber against a $Zn^{129m}Te$ source. The source and absorber were at ca. 4 °K. A NaI/Tl scintillation detector was used. The mirror-image spectra were computed separately, using a program kindly provided by Stone (3), and the average value of the δ and e^2qQ values obtained from the computed fits. The spectrometer was routinely calibrated using a variety of Fe standards (4) including $Na_2[Fe(CN)_5NO]2H_2O$ ($\delta = 0.442$ mm s^{-1}, $\Delta = 1.712$ mm s^{-1}) Fe metal foil and α-Fe_2O_3, the spectra being recorded at room temperature against a $^{57}Co/Pd$ source.

The tellurium compounds studied in this work were synthesized using standard techniques (5). The $(NH_4)_2TeX_6$ compounds were obtained by dissolving $^{125}TeO_2$ in HX and adding the appropriate ammonium salt in excess. The TeX_4 compounds were generally prepared by precipitation from a solution of TeO_2 in HX by the addition of a large excess of concentrated H_2SO_4. Several samples of TeI_4 were also prepared by heating tellurium metal with iodine in a sealed evacuated tube. These samples gave identical results to those obtained from aqueous solution preparations. The compounds TeX_4 are readily hydrolyzed and anhydrous preparations throughout would have been preferable. However a simple, very rapid preparation was required to allow the study of both ^{129}Te (69 min) and ^{129m}Te sources where possible. The samples of TeX_4 obtained by precipitation with concentrated H_2SO_4 were filtered off and immediately used in Mössbauer experiments at 80 or 4 °K.

The compounds were characterized by their Raman spectra (Table 1), although a spectrum could not be obtained for TeI_4. These spectra are in good agreement with those reported in the literature (11). Chemical analyses were performed on sample preparations of the compounds shown in Table 2. Analyses were not obtained for the more unstable $TeCl_4$ and $TeBr_4$ compounds.

Results and Discussion

The ^{125}Te Mössbauer Absorption Spectra

The ^{125}Te absorption parameters are shown in Table 3 in comparison with the values reported in the literature. For the $(NH_4)_2TeX_6$ compounds the values of the present work are in reasonable agreement with those reported by Gukasyan *et al.* (9). It should be noted that while the data of Gibb *et al.* (10) were reported as being relative to an $^{125}I/Cu$ source, their isomer shift values, not only for the tellurium hexahalides but also for ZnTe, and H_6TeO_6, show a systematic shift with respect to the data of other workers. It would appear that their

TABLE 2. Chemical analyses of several of the compounds studied

	Analysis (%)			
	Te		X	
Compound	Calculated	Observed*	Calculated	Observed*
TeI_4	20.09	19.79	79.91	79.80
$(NH_4)_2TeCl_6$	34.36	34.22	57.28	56.39
$(NH_4)_2TeBr_6$	20.00	20.16	75.14	74.44
$(NH_4)_2TeI_6$	13.87	13.98	82.77	82.14

*Bernhardt Mikroanalytical Laboratory, Mülheim.

Can. J. Chem. Downloaded from www.nrcresearchpress.com by 210.87.254.6 on 09/05/12
For personal use only.

TABLE 3. The ^{125}Te Mössbauer absorption parameters of the parent compounds with values from the literature

Compound	$^{125}\delta$* mm s^{-1}	Δ† mm s^{-1}	Reference
$TeCl_4$	+1.0 ±0.3	6.0+0.2	This work
	+1.2 ±0.1	4.0±1.6	6
	+2.7 ±0.4	5.4±0.8	7
$TeBr_4$	+1.1 ±0.2	2.8±0.2	This work
	+1.1 ±0.1	3.8±4.0	6
	+1.6 ±0.3	5.0±1.4	7
TeI_4	+1.0 ±0.2	2.7±1.0	This work
	+1.8 ±0.9	~4	6
	+1.0 ±0.6	6.0±1.0	8
$(NH_4)_2TeCl_6$	+1.70±0.10	0.0	This work
	+1.63±0.05	0.0	9
	+1.95±0.05	0.0	10
$(NH_4)_2TeBr_6$	+1.40±0.10	0.0	This work
$[K_2TeBr_6]$	+1.45±0.05	0.0	9
	+1.73±0.04	0.0	10
$(NH_4)_2TeI_6$	+1.10±0.10	0.0	This work
	+1.17±0.08	0.0	9
	+1.54±0.09	0.0	10
ZnTe	−0.07±0.07	0.0	This work

*With respect to an ^{125}I/Cu source.
†Conversion into $e^2qQ(1+\eta^2/3)^{1/2}$ in Mc s^{-1} is obtained by multiplying by 57.4.

source gave considerably more positive isomer shifts than observed in other studies. Erickson and Maddock (12) have commented on the wide variations in ^{125}Te isomer shifts reported by different workers for the same compounds and which apparently arise from differences in ostensibly the same sources.

The values for δ and Δ for $TeCl_4$, $TeBr_4$, and TeI_4 reported here are in reasonable agreement with those of Jung and Trifsthäuser (6). The large errors in the isomer shifts and quadrupole splittings for these compounds, and particularly for TeI_4, reflect the low % resonance absorption at 80 °K and the fact that the broad natural line-widths lead to unresolved lines for small quadrupole splittings.

It is apparent that $TeCl_4$ has a relatively small quadrupole splitting and that the values for $TeBr_4$ and TeI_4 are even smaller. The crystal structure of $TeCl_4$ has been reported (13) and is shown in Fig. 1. Each tellurium forms three short bonds to chlorine atoms and three long bonds to bridging chlorines. The tellurium then exhibits a quadrupole coupling characteristic of the $TeCl_3^+$ unit modified by the three

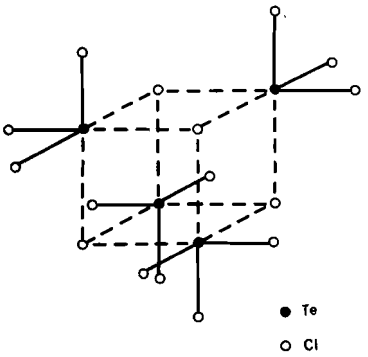

FIG. 1. A representation of the crystal structure of $TeCl_4$ (13).

long Cl^- contacts. Assuming similar structures for the other tetrahalides, the smaller quadrupole splittings in $TeBr_4$ and TeI_4 may then reflect the decreasing electronegativity of the ligand. The environment around the tellurium may approach octahedral symmetry in TeI_4, the "short" and "long" Te—I bonds now being very similar in length.

The ^{129}I Emission Spectra of the $(NH_4)_2TeX_6$ Compounds

The spectra were recorded for several independently prepared sources for each compound and sample spectra are shown in Fig. 2. It is apparent that for $(NH_4)_2{}^{129m}TeCl_6$ and $(NH_4)_2{}^{129m}TeBr_6$ an intense single line was observed in the spectra, with a large negative isomer shift (corresponding to a positive isomer shift for an absorption experiment), indicating a high s-electron density at the iodine nucleus in these decay events. These emission lines are identified as arising from the $^{129}ICl_6^-$ and $^{129}IBr_6^-$ ions formed in the respective matrices in the radioactive decay. The computed Mössbauer parameters are shown in Table 4. In addition to the intense single line in these spectra, other resonance absorption lines were also observed. However, these lines were of such low intensity that an unequivocal assignment could not be made. A brief discussion of the possible origin of these lines is presented later in the paper and reference is made at that point to the tentative assignments shown for the low intensity lines in the $(NH_4)_2TeCl_6$ and $(NH_4)_2TeBr_6$ spectra.

For $(NH_4)_2{}^{129m}TeI_6$ it is apparent that the spectrum comprised a number of lines of about

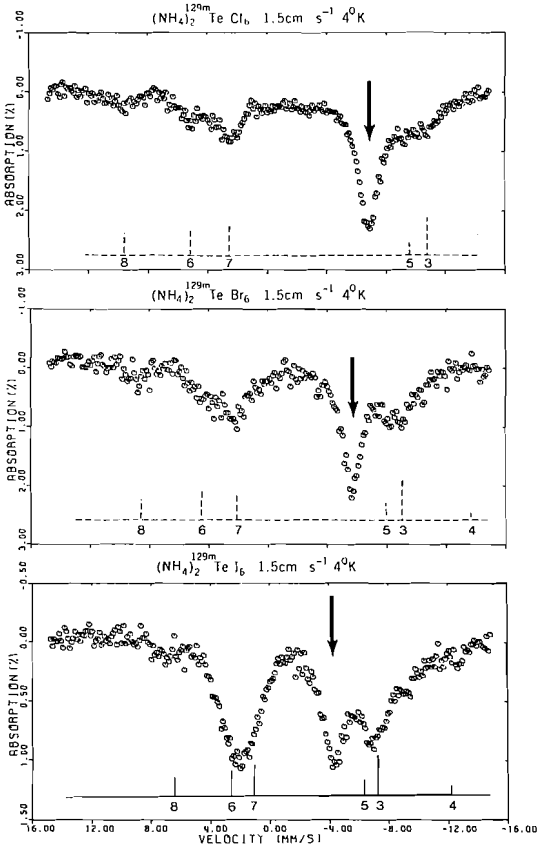

FIG. 2. The ^{129}I Mössbauer emission spectra of the $(NH_4)_2{}^{129m}TeX_6$ compounds measured at *ca.* 4 °K against a $Na^{129}I$ absorber. The arrows denote the emission lines corresponding to the proposed $^{129}IX_6^-$ ions.

TABLE 4. The ^{129}I Mössbauer parameters of the $(NH_4)_2{}^{129m}TeX_6$ compounds

Source	Proposed decay product	$^{129}\delta$* (mm s^{-1})	2Γ (mm s^{-1})
$(NH_4)_2{}^{129m}TeCl_6$	$^{129}ICl_6^-$	$+6.23\pm0.08$	1.5
$(NH_4)_2{}^{129m}TeBr_6$	$^{129}IBr_6^-$	$+5.08\pm0.09$	1.7
$(NH_4)_2{}^{129m}TeI_6$	$^{129}II_6^-$	$+3.56\pm0.08$	2.3

*With respect to ZnTe in an absorption experiment. The parameters obtained in an emission experiment were converted into those of an absorption experiment by adding 0.46 mm s^{-1} and reversing the sign (1). (Note: ref. 2 should have read by *adding* 0.46 mm s^{-1}.)

equal intensity. However, even here it is possible to identify a single line with a large negative isomer shift, which probably arises from the octahedral II_6^- ion. The remaining lines in the spectrum may be identified with a single quadrupole split species with the (absorption) parameters $\delta = 1.9 \pm 0.4$ mm s^{-1} and $e^2qQ = 1242 \pm 123$ Mc s^{-1}, the large errors arising from the unresolved nature of the spectrum.

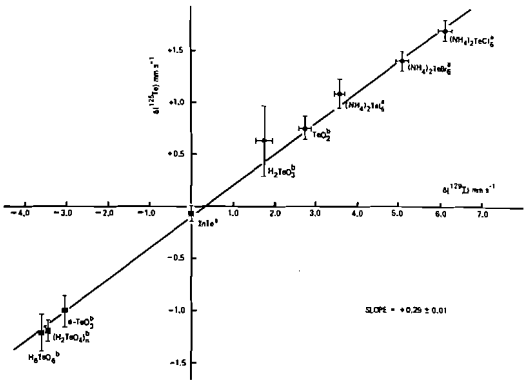

FIG. 3. A plot of the ^{125}Te isomer shifts, relative to an $^{125}I/Cu$ source, *vs.* the ^{129}I isomer shifts, relative to ZnTe, obtained in the same tellurium lattice in emission experiments; (*a*) this work; (*b*) ref. 2.

In support of the above proposal that the single lines of large isomer shift arise from the $^{129}IX_6^-$ ions we may examine the relationship between the ^{125}Te isomer shifts for the parent compounds and the ^{129}I isomer shifts. In a previous publication (2), we have reported a plot of $^{125}\delta$, measured in an absorption experiment, against $^{129}\delta$, measured in an emission experiment in the same matrix, for a series of tellurium oxycompounds. It was observed that a straight line relationship was obtained, of slope $^{125}\delta/^{129}\delta = 0.29$, in reasonable agreement with the isomer shift ratio obtained by Ruby and Shenoy (14). It was concluded that in these oxycompounds the tellurium and daughter iodine were in isoelectronic and isostructural environments. Some of the data for those compounds are reproduced in Fig. 3 together with the $^{125}\delta$ and $^{129}\delta$ values for the $(NH_4)_2TeX_6$ compounds of the present work. The slope of the plot $^{125}\delta/^{129}\delta = 0.29$. It is concluded that the isomer shifts of the single lines indicated in Fig. 2 are indeed consistent with the IX_6^- anions and that these ions are isoelectronic and isostructural with the parent TeX_6^{2-} ions.

It should also be noted that the isomer shift of the proposed ICl_6^- ion is consistent with that to be expected on the basis of the Mössbauer spectra of $^{127}ICl_2^-$ and $^{127}ICl_4^-$. This point was discussed at length in the previous paper (1).

Can. J. Chem. Downloaded from www.nrcresearchpress.com by 210.87.254.6 on 09/05/12
For personal use only.

Can. J. Chem. Downloaded from www.nrcresearchpress.com by 210.87.254.6 on 09/05/12
For personal use only.

It must be emphasized that the formation of the IX_6^- ions is only observed over the lifetime of the Mössbauer transition ($t_{1/2} = 15$ ns). These ions may be chemically unstable over longer times. The linewidths in the emission spectra were observed to be in the range $2\tau = 1.5$ to 2.3 mm s^{-1} and these compare with a linewidth of 1.1 mm s^{-1} observed for the $Na^{129}I$ absorber against a $Zn^{129m}Te$ source at 4 °K. The broadened linewidths in the emission spectra may be evidence of a change in the chemical form of the ^{129}I atoms over the lifetime of the Mössbauer transition. Certainly the spectra at 4 °K indicated the presence of some ^{129}I species other than that of the IX_6^- ion, this being most pronounced in the case of the TeI_6^{2-} lattice.

The fact that ^{129m}Te sources rather than ^{129}Te sources were used in these experiments introduces a further degree of uncertainty in the interpretation of the results. The $^{129m}Te \rightarrow {}^{129}Te$ isomeric transition is highly internally converted, and it is known (2) that Auger charging accompanying the decay can lead to extensive molecular decomposition in, for example, $H_6{}^{129m}TeO_6$. Thus the products other than the IX_6^- ions observed in the TeX_6^{2-} lattices as shown in Fig. 2 may have originated from decomposition products formed in the $^{129}Te \rightarrow {}^{129}Te$ isomeric transition rather than as a result of the chemical instability of the IX_6^- ions themselves. This point could have been checked if it had been possible to prepare the ^{129}Te labelled $(NH_4)_2TeX_6$ compounds. However, the short half-life of ^{129}Te (69 min) and the time involved in the chemical preparation and cooling the sample and Dewar to 4 °K precluded these measurements.

The firm conclusion to be drawn from the above is that there is evidence for the formation of the IX_6^- ions in the radioactive decay, over the lifetime of the Mössbauer transition. This is of some interest since the ICl_6^-, IBr_6^-, and II_6^- (octahedral) ions have not previously been observed (15). Compounds of the form $N(C_2H_5)_4I_7$ are known to contain a three-dimensional array of I_3^- ions and I_2 in which the I_3^- ion is surrounded by four I_2 molecules and each I_2 molecule by two I_3^- ions.

A Comparison of the Charges on Te and I in the TeX_6^{2-} and IX_6^- Ions

Perlow and Perlow (16) have studied the effects of the $^{129}I \xrightarrow{\beta^-} {}^{129}Xe$ radioactive decay in compounds containing the ICl_2^- and ICl_4^- ions. They observed that the xenon analogs of these iodine molecules were stable over the lifetime of the Mössbauer transition. They were able to calculate the charge on the iodine and on the daughter xenon following the decay and observed that following the decay the increased electronegativity of the daughter atom led to an increased electron withdrawal from the Cl ligand. In ICl_4^- the charge on iodine before the decay was +0.39 and following the decay the xenon had a net charge of +1.0 rather than +1.4 *i.e.*, 0.4 electrons had been recalled from the ligands. It is possible to carry out a similar analysis for the present work, using previously reported n.q.r. data to determine the charge on the parent tellurium and the Mössbauer emission data to determine the charge on iodine following the decay.

TABLE 5. The charge on tellurium in the TeX_6^{2-} anions, obtained from n.q.r. data, and the charge on the daughter iodine

Anions	Charge on Te*		Charge on I†
	a	*b*	
$TeCl_6^{2-}$	+2.08	+2.38	
$[ICl_6^-]$			+3.5±0.1
$TeBr_6^{2-}$	+1.48	+1.90	
$[IBr_6^-]$			+2.7±0.1
TeI_6^{2-}	+0.88	+1.36	
$[II_6^-]$			+1.7±0.1

*Determined from the halogen n.q.r. data of Nakamura *et al.* (17) with (*a*) assuming 15% s-bonding character on the halogen and (*b*) assuming pure p-character on the halogen.
†Determined from the Mössbauer emission data.

Thus Nakamura *et al.* (17) have studied the halogen n.q.r. spectra of the tellurium hexahalides. Using the theory of Townes and Dailey they were able to calculate the number of p-electrons on the ligand halogen whose participation in bonding would be required to produce the observed quadrupole coupling. They then assumed that the ligand halogen employs 15% s-character in bonding and calculated the effective charge on the central tellurium atom. The results are shown in Table 5.

A number of workers have shown that, with the exception of IF_5 and IF_7, the iodine Möss-

Can. J. Chem. Downloaded from www.nrcresearchpress.com by 210.87.254.6 on 09/05/12
For personal use only.

bauer data of the interhalogen compounds may be interpreted in terms of pure p-bonding by the iodine, the $[\Psi_s(0)]^2$ at the iodine nucleus increasing linearly with the removal of 5p electrons. Bukshpan *et al.* (18) have established the relationship

$$\delta(^{129}\mathrm{I}) = 1.50\ \mathrm{hp} - 0.54$$

where $\delta(^{129}\mathrm{I})$ is the isomer shift in mm s^{-1} with respect to ZnTe and hp is the number of holes in the closed $5p^6$ I^- configuration. If we assume pure p-bonding by the central iodine in the IX_6^- anions then the Mössbauer isomer shifts of Table 4 may be used to calculate the charge on the iodine, as reported in Table 5. Since we are assuming that the iodine does not employ any s-character in bonding, this calculation yields the smallest net charge that may reside on the central iodine. It should be emphasized that the charge calculated in this way for the ICl_6^- ion is in agreement with the ^{127}I Mössbauer and n.q.r. data for ICl_2^- and ICl_4^-.

A comparison of the charges calculated for the tellurium and iodine (Table 5) indicates that there is a discrepancy, since the charge on the daughter iodine appears to be more than +1 unit greater than that on the tellurium, and this is not to be expected in the light of the increased electronegativity of the central atom. A possible explanation for part of this discrepancy may lie in the assumption by Nakamura *et al.* (17) that the ligand halogen in the TeX_6^{2-} ions employs 15% s-character in bonding. If this assumption is not made, then the charges on the central tellurium increase to the values shown in column *b* of Table 5. In the present context these would appear to be more realistic charges for the tellurium, but even then there is no measurable "recall" in the $TeCl_6^{2-} \rightarrow ICl_6^-$ transition while in the case of $TeBr_6^{2-}$ and TeI_6^{2-} there is recall of 0.23 and 0.64 electrons in each case.

The ^{125}Te Isomer Shifts

As discussed above, Bukshpan *et al.* (18) have established a linear relationship between isomer shifts and hp values for ^{129}I. The question arises whether a similar relationship may be derived for tellurium (19). There has been much discussion in the past of the nature of the bonding in the tellurium hexahalides and, notwithstanding the experiments of Couch *et al.* (20), the general conclusion arrived at is that the tellurium employs essentially pure p-orbitals in bonding, the $5s^2$ electrons being stereochemically nonactive. Thus the TeX_6^{2-} ions are octahedral (21), have relatively long weak Te—X bonds and the ^{125}Te Mössbauer isomer shifts show a simple trend of increasing positive values (increasing $|\Psi_s(0)|^2$ assuming $\Delta R/R$ is positive) with increasing electronegativity of the ligand. We have therefore used the data of Nakamura *et al.* (17) to determine hp on tellurium in the TeX_6^{2-} ions and have plotted these against the Mössbauer isomer shifts of Table 4. The plots are shown in Fig. 4. The additional data point is that for CaTe ($^{125}\delta_{1/Cu} = -0.14 \pm 0.07$ mm s^{-1}), where it is assumed hp = 0. The plots yield:

$$^{125}\delta = 0.45 \pm 0.01\ \mathrm{hp} - 0.15 \pm 0.03$$

Nakamura charges

$$^{125}\delta = 0.41 \pm 0.03\ \mathrm{hp} - 0.16 \pm 0.10$$

Modified charges

It is interesting that if we take Bukshpan's expression (18) for ^{129}I, $^{129}\delta = 1.50\ \mathrm{hp} - 0.54$ (with respect to ZnTe), and $^{125}\delta/^{129}\delta = +0.29$,

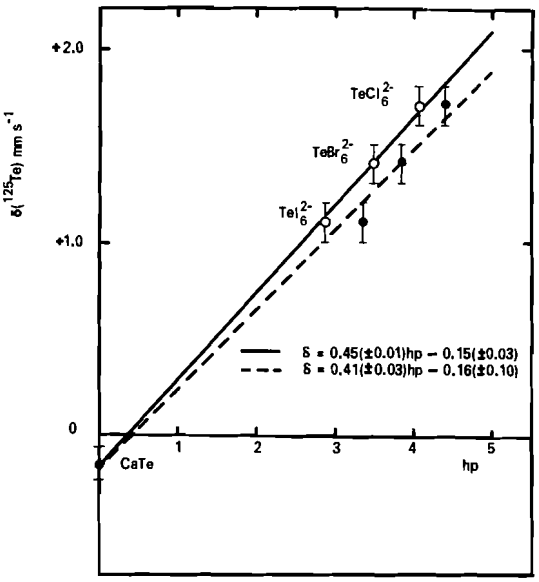

FIG. 4. A plot of the ^{125}Te isomer shifts *vs.* the hp values on tellurium arrived at from n.q.r. data (17). The solid line corresponds to hp values derived assuming 15% s-character on the ligand halogen, while the dotted line corresponds to hp values with no s-character (see Table 5).

Can. J. Chem. Downloaded from www.nrcresearchpress.com by 210.87.254.6 on 09/05/12
For personal use only.

then it is found that

$$^{125}\delta = 0.44 \pm 0.01 \text{ hp} - 0.16 \pm 0.01$$

(with respect to ZnTe)

and

$$^{125}\delta = 0.44 \pm 0.01 \text{ hp} - 0.23 \pm 0.01$$

(with respect to I/Cu)

Within the very large errors involved these different expressions are rather similar. To determine unequivocally whether or not the ligand halogen in TeX_6^{2-} employs any s-character in bonding it will be necessary to measure this parameter in a more direct way. For example the ^{129}I Mössbauer absorption spectrum of $(NH_4)_2Te^{129}I_6$ would provide some evidence for or against s-participation. It may be noted that no evidence was found (22) for s-participation in the ^{129}I spectrum of *trans*-Te(ethylenethiourea)$_2{}^{129}I_2$.

The ^{129}I Emission Spectra of the TeX_4 Compounds

Figure 5 *i* shows the emission spectrum for $^{129m}TeCl_4$. In this instance it was found possible to prepare and study the $^{129}TeCl_4$ source and the spectrum is shown in Figure 5 *ii*. In discussing the possible products of the radioactive decay in this solid, it is first necessary to predict the line positions which would be expected in the ^{129}I emission spectrum for an iodine species isoelectronic and isostructural with that of the parent tellurium. This requires not only a comparison of the isomer shifts for the two nuclides ($^{125}\delta/^{129}\delta = +0.29$) but also a comparison of the quadrupole couplings. Pasternak and Bukshpan (23) observed that

$$(e^2q^{125}Q/e^2q^{129}Q)(1 + n^2/3)^{1/2} = 0.40$$

while Warren *et al.* (2) observed a value of 0.5. The line positions for the emission spectrum were calculated using a value of 0.45 and, since the sign of $e^2q^{125}Q$ in $TeCl_4$ is not immediately apparent, the sets of lines corresponding to both positive and negative $e^2q^{129}Q$ were computed. These line positions are shown on Fig. 5 *i* and it is immediately apparent that the observed and predicted line positions do not coincide. Thus in $^{129m}TeCl_4$ and $^{129}TeCl_4$, the ^{129}I formed in the radioactive decay is not found in an environment isoelectronic or isostructural with

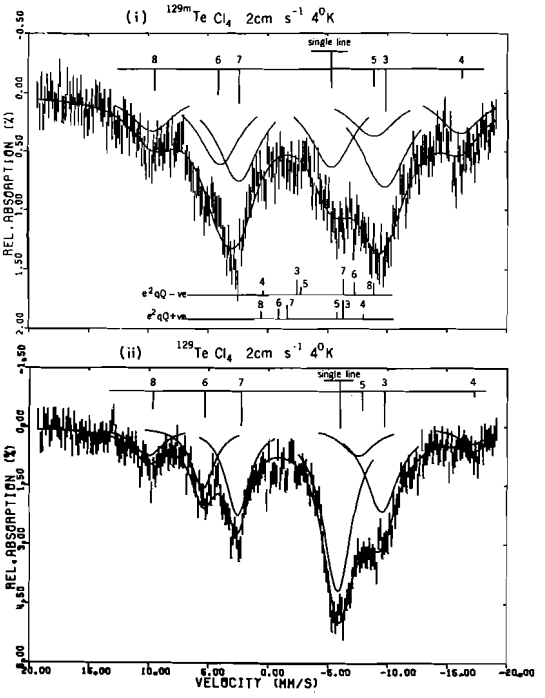

FIG. 5. The ^{129}I emission spectra of the (*i*) $^{129m}TeCl_4$ and (*ii*) $^{129}TeCl_4$ sources measured at *ca.* 4 °K against a $Na^{129}I$ absorber. The predicted line positions for the isoelectronic and isostructural iodine molecule are also shown in (*i*) assuming $\eta = 0$ and following ref. 23.

that of the tellurium and rearrangement must accompany the decay in a large fraction of events. A similar observation was made for $^{129m}TeBr_4$ and $^{129m}TeI_4$.

The question arises as to the identity of the iodine species formed in the TeX_4 lattices. The complex spectra obtained in all instances were so poorly resolved and the line-widths so broad as to make an unequivocal identification of the iodine species present extremely difficult. However, it was found possible to fit the spectra in each case, assuming the presence of a quadrupole split component and one additional single line. Such fits are shown in Fig. 5. The spectra of Fig. 5 lend support to such an interpretation since the single line appears to vary in intensity in the two sources. The computed parameters obtained for the $^{129m}TeCl_4$, $^{129m}TeBr_4$, and $^{129m}TeI_4$ sources are shown in Table 6 and the very large errors reflect the poor quality of the spectra. The parameters for the quadrupole split component in $^{129m}TeCl_4$ *i.e.*,

TABLE 6. The ^{129}I Mössbauer parameters of the $^{129m}TeX_4$ compounds

Source	Proposed decay product	$^{129}\delta$*‡ (mm s^{-1})	e^2qQ†‡ (Mc s^{-1})	hp	U_p
$^{129m}TeCl_4$	$^{129}ICl_4^-$	+3.5±0.7	+2100±120	2.7±0.5	−1.3±0.1
	Unidentified	+5.2±0.8	0		
$^{129m}TeBr_4$	$^{129}IBr_4^-$	+3.0±0.4	+1850±120	2.4±0.3	−1.2±0.1
	Unidentified	+4.4±0.2	0		
$^{129m}TeI_4$	$^{129}II_4^-$	+2.9±0.4	+1400±140	2.3±0.3	−0.9±0.1
	Unidentified	+2.7±0.7	0		

*With respect to ZnTe in an absorption experiment.
†Quoted as parameters for an absorption experiment.
‡The quadrupole split components were computed using the analysis described in ref. 23. Within the large errors $\eta = 0$ in all cases.

δ and the sign and magnitude of e^2qQ, are observed to be very similar to those for the square planar iodine in I_2Cl_6. Moreover for a square planar iodine molecule in which the iodine uses only p-orbitals in bonding, then the isomer shift and quadrupole splitting can be shown to be simply related (23). Thus

$$\delta = 1.50\ \text{hp} - 0.54$$

and

$$\text{hp} = 6 - (U_x + U_y + U_z)$$
$$= 4 - 2U_x$$

where U_x, U_y, and U_z are the populations of the x, y, and z orbitals, and for a square plane with 2 non-bonding electrons in the out-of-plane orbital $U_z = 2$, and $U_x = U_y$.

$$U_p = \frac{-e^2qQ\ \text{mol}}{e^2qQ\ \text{atom}}$$

and

$$U_p = -U_z + \frac{U_x + U_y}{2}$$
$$= -2 + U_x$$

where e^2qQ atom is the quadrupole coupling for 1 p_z electron on iodine ($= +1607$ Mc s^{-1}) and e^2qQ mol is the measured quadrupole coupling for a molecule. Thus hp can be calculated from δ and U_p from e^2qQ mol. But from the above

$$\text{hp} = -2U_p$$

Thus for a square planar daughter ion this simple relationship between the two parameters should be observed. Table 6 shows that, within the large errors involved, this is so for the quadrupole split iodine component in the TeX_4 lattices. We may therefore tentatively identify this fragment in each case as the IX_4^- ion.

The identification of the single line in the spectrum is far from clear. The isomer shift does not appear to correspond to an IX_6^- ion. However, it can not be ruled out that IX_6^- is not formed since it may have a somewhat different isomer shift in the TeX_4 lattice than in the $(NH_4)_2TeX_6$ lattice.

Returning to the discussion of the $(NH_4)_2$-$^{129m}TeI_6$ spectrum, the product observed in addition to the proposed II_6^- ion may have been the square planar II_4^- ion, since the computed parameters were somewhat similar to those observed in $^{129m}TeI_4$. If the structure of TeI_4 is indeed like that of $TeCl_4$, but with a more octahedral environment about the tellurium, then it would not be surprising if the products of radioactive decay in $(NH_4)_2TeI_6$ and TeI_4 were similar. The low intensity lines in the $(NH_4)_2TeCl_6$ and $(NH_4)_2TeBr_6$ spectra may also have arisen from the square planar IX_4^- ions. The tentative assignments shown in Fig. 2 in fact correspond to the line-positions for quadrupole split species with δ and e^2qQ the same as those observed in the $^{129m}TeCl_4$ and $^{129m}TeBr_4$ experiments.

The authors wish to thank Dr. F. Brown, Head Solid State Research Branch, AECL, Chalk River, for his considerable help and co-operation in carrying out the many reactor irradiations.

A grant from the National Research Council of Canada is gratefully acknowledged.

1. C. H. W. JONES and J. L. WARREN. J. Chem. Phys. **53**, 1740 (1970).

Can. J. Chem. Downloaded from www.nrcresearchpress.com by 210.87.254.6 on 09/05/12
For personal use only.

2. J. L. WARREN, C. H. W. JONES, and P. VASUDEV. J. Phys. Chem. **75**, 7867 (1971).
3. A. J. STONE. *Appendix to* G. M. BANCROFT, W. K. ONG, A. G. MADDOCK, R. H. PRINCE, and A. J. STONE. J. Chem. Soc. (A), 1966 (1967).
4. A. M. MUIR, K. J. ANDO, and H. M. COOGAN (*Editors*). Mössbauer effect data index 1958–1965. Interscience, New York. 1966. p. 26.
5. K. W. BAGNALL. Chemistry of selenium, tellurium, and polonium. Elsevier, Amsterdam. 1966. p. 106.
6. P. JUNG and W. TRIFTSHÄUSER. Phys. Rev. **175**, 512 (1968).
7. M. UNLAND. J. Chem. Phys. **49**, 4514 (1968).
8. C. E. VIOLET, R. BOOTH, and F. WOOTEN. Phys. Lett. **5**, 230 (1963).
9. S. E. GUKASYAN, B. F. IOFA, A. N. KARASEV, S. I. SEMENOV, and V. S. SHPINEL. Phys. Stat. Solidii. **37**, 91 (1970).
10. T. C. GIBB, R. GREATREX, N. N. GREENWOOD, and A. C. SARMA. J. Chem. Soc. (A), 212 (1970).
11. (*a*) P. J. HENDRA and Z. JOVIC. J. Chem. Soc. (A), 600 (1968); (*b*) G. C. HAYWARD and P. J. HENDRA. J. Chem. Soc. (A), 643 (1967).
12. N. E. ERICKSON and A. G. MADDOCK. J. Chem. Soc. (A), 1665 (1970).
13. B. BUSS and B. KREBS. Inorg. Chem. **10**, 2795 (1971).
14. S. L. RUBY and G. K. SHENOY. Phys. Rev. **186**, 326 (1969).
15. E. H. WIEBENGA, E. E. HAVINGA, and K. H. BOSWIJK. Adv. Inorgchem. Radiochem. **3**, 133 (1961).
16. G. J. PERLOW and M. R. PERLOW. J. Chem. Phys. **45**, 2193 (1966).
17. D. NAKAMURA, K. ITO, and M. KUBO. J. Am. Chem. Soc. **84**, 163 (1962).
18. S. BUKSHPAN, C. GOLDSTEIN, and J. SORIANO. J. Chem. Phys. **51**, 3976 (1969).
19. B. M. CHEYNE, J. J. JOHNSON, and C. H. W. JONES. Chem. Phys. Lett. **14**, 545 (1972).
20. D. A. COUCH, C. J. WILKINS, G. R. ROSSMAN, and H. B. GRAY. J. Am. Chem. Soc. **92**, 307 (1970).
21. I. D. BROWN. Can. J. Chem. **42**, 2758 (1964).
22. B. M. CHEYNE, C. H. W. JONES, and P. VASUDEV. Can. J. Chem. To be published.
23. M. PASTERNAK and T. SONNINO. J. Chem. Phys. **48**, 1997 (1968).

Can. J. Chem. Downloaded from www.nrcresearchpress.com by 210.87.254.6 on 09/05/12
For personal use only.

A Low Temperature Dielectric Cell and the Permittivity of Hexagonal Ice to 2 K[1]

S. R. GOUGH

Division of Chemistry, National Research Council of Canada, Ottawa, Canada K1A 0R9

Received April 28, 1972

The limiting high frequency permittivity ε_∞ of hexagonal ice, measured using a coaxial three terminal dielectric cell designed to minimize errors arising from differential thermal contraction, varies from 3.093 ± 0.003 at 2 K to 3.15 ± 0.02 at 200 K. The result is discussed in relation to the translational lattice vibrations and a comparison is made with other ices.

La permittivité limite à haute fréquence ε_∞ des cristaux de glace hexagonaux, mesurée en se servant d'une cellule diélectrique coaxiale à trois bornes coaxiales, conçue pour minimiser les erreurs provenant de la contraction thermique différentielle, varie de 3.093 ± 0.003 à 2 K à 3.15 ± 0.02 à 200 K. On discute du résultat en relation aux les vibrations translationnelles de réseau et on fait la comparaison avec d'autres formes crystallographiques de glace. [Traduit par le journal]

Canadian Journal of Chemistry, **50**, 3046 (1972)

Can. J. Chem. Downloaded from www.nrcresearchpress.com by 210.87.254.5 on 09/05/12
For personal use only.

In accord with publications (1–3) from this laboratory concerning molecular motion in clathrate hydrate systems, the dielectric properties of hexagonal ice are of great interest. The static permittivity and relaxational behavior of hexagonal ice are well known to temperatures near −100 °C (4). The limiting high frequency permittivity ε_∞ is less well known, particularly its temperature dependence. Although general agreement exists in the literature that the radio frequency permittivity of hexagonal ice lies in the range 3.1 to 3.2 (5–9) and that a decrease occurs with decreasing temperature (6) contrary to that predicted by the Clausius–Mossotti relation, the situation is not well defined. The need for a precise determination is indicated.

In addition, the origin of a small but significant radio frequency dielectric absorption, observed near 4 K in all the clathrate hydrates so far examined (2), warrants investigation. This absorption, which probably does not arise from guest or host molecule reorientation since the molecules are apparently frozen (2) at these temperatures, is most probably associated with guest molecule librational motion rather than with the host lattice itself. Nevertheless, a low temperature examination of the related guest-free hexagonal ice lattice is certainly relevant.

The results presented below describe the temperature dependence of the limiting high frequency permittivity of hexagonal ice in the range 2 to 270 K. A dielectric cell is described also. Its design minimizes the usually deleterious effects of differential thermal contraction of the dielectric and electrode structure.

[1]NRCC No. 12703.

Experimental Method

(a) General Considerations

The major difficulties involved in the accurate permittivity measurement of a solid dielectric at low temperatures arise from the development of cracks in the dielectric and from loss of electrode contact. Both are caused by differential thermal contraction of the dielectric, electrodes, and the electrode-supporting structure. Correction may be made for an ideal series air-gap at the dielectric–electrode interface but the effect is large for high values of permittivity. For an example, see ref. 10.

The concept of utilizing the larger thermal contraction of Teflon to force an electrode system to follow smaller dimensional changes of a dielectric and so eliminate series-gap formation is due to Cole and co-workers (11). Their method, as used previously in this laboratory (2), involves supporting a parallel plate electrode system by two Teflon discs. Experience has shown that with this design the cell constant is generally not reproducible after large temperature excursions to better than a few percent. Also, the cell constant varies as both the sample thickness and the electrode area vary with temperature.

A coaxial electrode system has the advantage that its cell constant varies only with the electrode length, the electrode radius ratio being temperature independent for electrodes of the same material. The present cell, described in detail below, is a coaxial three-terminal device, the outer electrode being a very thin brass sleeve supported externally by a hollow Teflon cylinder. As before, the larger thermal contraction of Teflon is utilized to force the outer electrode to follow the radial dimensional changes of the dielectric.

Can. J. Chem. Downloaded from www.nrcresearchpress.com by 210.87.254.5 on 09/05/12
For personal use only.

The electrode radius ratio is affected ideally only to the extent that the expansivity of the dielectric is different from that of the electrode material.

Such an electrode system has been briefly described recently (12). The present design offers about a ten-fold increase in reproducibility of the measured capacitance after large thermal excursions and has the advantage that measurements may be made on the same sample over the complete temperature range of interest from 2 K upwards.

(b) The Dielectric Cell

The cell, shown schematically in Fig. 1, consisted of a central cylindrical brass electrode G, guarded by brass supports D and I and insulated by Teflon discs, and an outer electrode sub-system which comprised a hollow cylinder E of Teflon containing a brass liner F a few thousandths of an inch thick which served as the high potential electrode. The two electrode sub-systems were contained in the brass can H of 1/8 in. wall thickness and were supported by the screw I and the top plug B. The latter, held in place by screws C, served as anchorage, heat sink and shielding for the Microdot coaxial electrode leads A, electrode connections, and the various temperature sensors, K, L, and M. It was covered by the cap piece N. The whole was bifilarly wound with a 20 Ω heater winding O and was contained in a Teflon lined copper enclosure P. The assembly was suspended by thin stainless steel supports in an Andonian Associates cryogenic Dewar with leads brought out through vacuum seals.

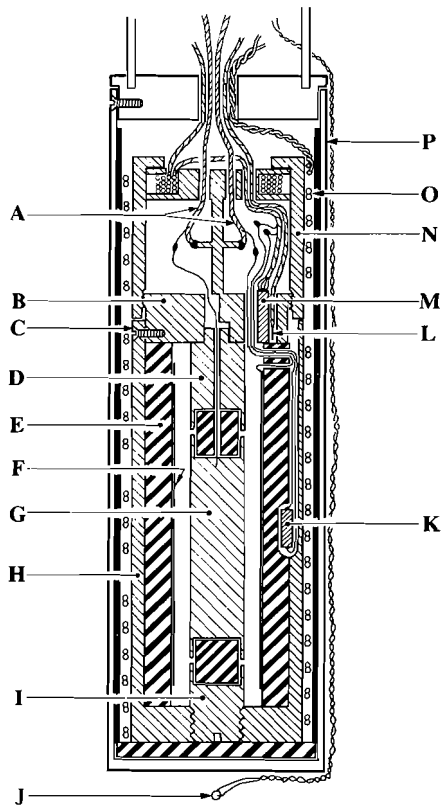

FIG. 1. Schematic of dielectric cell assembly.

(c) Electrical Measurements

Capacitance and conductance were measured below 60 kHz as described previously (27). Measurements at 1 MHz were made using a General Radio five-terminal automatic capacitance bridge whose readings were corrected to compensate for the effects of the Microdot cables leading into the cryostat system.

(d) Temperature Control

Precise temperature control was achieved by adjustment of the flow of liquid helium into the sample chamber of the Dewar and by proportional control of the energy supplied to both the Dewar's helium vaporization heater and to the heater O built into the cell. Heater control was achieved in each case by directly amplifying the voltage differences between reference e.m.f.s. and those produced by currents flowing through the appropriate carbon resistor sensors J and K. The amplified control signals drove d.c. power amplifiers which provided the proportionally regulated heater currents.

Actual temperatures were measured using a calibrated germanium resistance thermometer M below 100 K and a calibrated copper–constantan thermocouple L, referred to the ice point, above 77 K. The measuring thermocouple also served at the higher temperatures to provide a control e.m.f. (in place of the now insensitive carbon sensor K) to drive the sample heater system. Control was better than $\pm 0.01°$ at all temperatures and measurement at the site of the sensors L and M was within $\pm 0.01°$ below 20 K and $\pm 0.1°$ above 77 K.

(e) Determination of the Cell Constant

The basic requirement, to know the geometric capacitance (cell constant, C_0) at the temperature at which freezing of the ice sample took place, was met as follows. The capacitance of the empty cell was measured over the temperature range -5 to $+20$ °C, the cell was filled carefully from the bottom via a piece of Teflon spaghetti, cooled and held at -3 °C until capacitance measurements indicated the nucleation of ice. Then the temperature was raised and held at -1 °C overnight to slowly freeze and anneal the sample. It was assumed that this procedure resulted in no distortion of the outer electrode and that the true cell constant was that corresponding to the freezing temperature. Since two independent experiments, one using a relatively flimsy outer electrode of 0.001 in. brass shim stock stuck to the inside of the Teflon cylinder by silicone grease and the other using a much stronger machined hollow brass cylinder of about 0.005 in. wall thickness that was a push fit into the Teflon cylinder, gave permittivity results agreeing to within 0.1%, it was presumed that the procedures adopted were reliable.

The temperature variation of C_0 was calculated using the data compiled by Eisenberg and Kauzmann (13) for ice and by White (14) for brass. Two thermal effects dominate: (*1*) the change in the electrode radius ratio because ice contracts faster than brass above 100 K leading to an increase in C_0 as the temperature decreases, and (*2*) longitudinal contraction of the low-potential guarded electrode which reduces C_0. The net effect is illustrated in

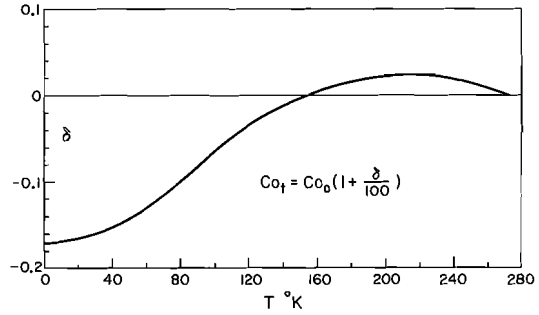

FIG. 2. Calculated temperature variation of the cell constant C_0.

Fig. 2, the maximum estimated deviation in C_0 produced by cooling being about -0.2%.

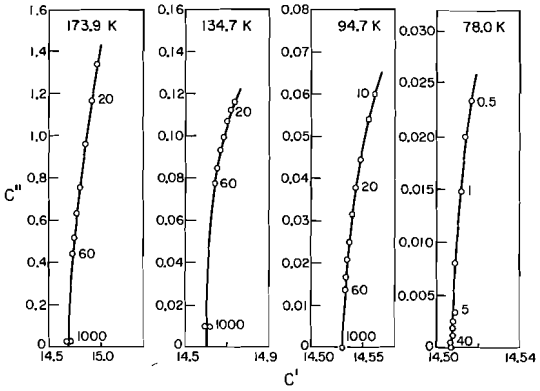

FIG. 3. Determination of the limiting high frequency capacitance C_∞ from the complex capacitance Cole–Cole plot. The numbers on the figures are frequencies in kHz.

Results

Capacitance and conductance measurements were made on three different samples at fixed temperatures over a range of frequency such that the high frequency intercepts of the Cole–Cole arcs could be defined by extrapolation of the data, as illustrated in Fig. 3. The intercepts C_∞ so obtained gave the corresponding limiting permittivity ε_∞. At the highest temperatures, where Debye semicircles were drawn, the data were consistent with those reported previously, however, the extrapolations to C_∞ were the largest and, therefore, the uncertainties greatest. At the lowest temperatures the C_∞ values were read directly from the bridge dials, the uncertainty in ε_∞ being regarded as essentially no worse than 0.2%

Error arising from plastic flow of the sample out of the electrode region caused by the inhomogeneous stress generated by contraction of the Teflon cylinder seems unlikely. Temperature excursions showed no significant hysteresis in ε_∞ (compare points ◇ and ○, Fig. 4) and different samples, despite different thermal histories once frozen and annealed, gave almost identical results. The effect of the unknown stress on the sample was probably small (15) and was neglected.

The permittivity results are illustrated in Fig. 4, where, to preserve clarity, the estimated uncertainty is indicated only for selected points. The curved line is represented by

$$\varepsilon_\infty = 3.093 \pm 0.003 + (0.72 \pm 0.60)10^{-4}T + (0.11 \pm 0.02)10^{-5}T^2$$

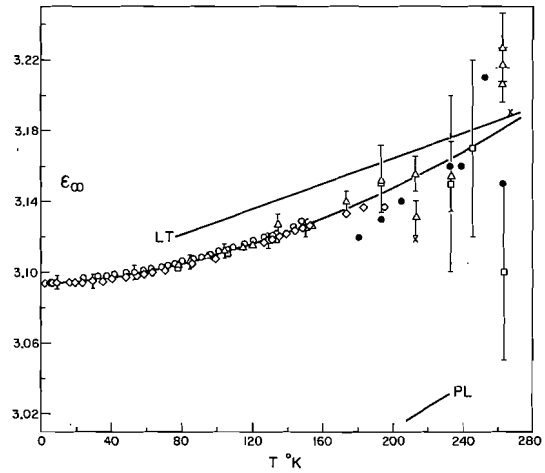

FIG. 4. Temperature variation of the limiting high frequency permittivity of hexagonal ice. Open points, this work; ●, ref. 9; ×, ref. 8; LT, ref. 6; PL, ref. 16.

where the errors quoted are standard deviations and T is the absolute temperature.

At 1 MHz no significant dielectric absorption was observed at any temperature below 100 K and, at 4.2 K, no absorption was observed whatsoever in the frequency range available.

Discussion

The present results are compared in Fig. 4 with those of four other studies of hexagonal ice. The agreement of the data (LT) of Lamb and Turney (6) is excellent considering their estimated uncertainty ($\pm 2\%$) and their dismissal of an observed temperature dependence as

Can. J. Chem. Downloaded from www.nrcresearchpress.com by 210.87.254.5 on 09/05/12
For personal use only.

TABLE 1. High frequency permittivity of various ices at 150 and 220 K

Ice	T (K)	ε_∞	$10^3\delta\varepsilon/\delta T$	ν (cm^{-1})	Reference
I	150	3.12_5	0.37	225	This work, 21
II	150	3.5_2	1.6_6	170	20, 23
IX	150	3.7_2	1.0	190	20, 23
I	220	3.16	0.52	219	This work, 21
I	220	3.02_4	0.54	219	16, 21
N_2 Hydrate	220	2.8_2	$1._2$	—	10
CP Hydrate*	220	2.8_6	$1._2$	—	25
SF_6 Hydrate†	220	2.9_3	$2._0$	—	26

*CP ≡ cyclopropane.
†Structure II hydrate, others structure I.

a nugatory experimental effect. The recent results (PL) of Le Petit and Lafargue (16) show nearly the same slope but differ appreciably in magnitude in spite of their claimed high precision. Their results, obtained for samples of freshly frozen super-cooled water, illustrate the need for adequate conditioning before reliable permittivity measurements of ices can be made. The uncorrected[2] results (solid circles) of von Hippel *et al.* (9) referring to their sample ζ, are quite consistent with the present data. Also, Evans (8), in a review, quotes two results (crosses) of Westphal for a sample of Greenland glacier ice which are in accord with the above. The result of a recent microwave study (17) indicating an ε_∞ of 1.9 at 35.3 and 94.5 GHz is incompatible (18) with published infrared (21) and dielectric data.

The temperature dependence (Fig. 4) of the ε_∞ of hexagonal ice is similar to that of several ionic crystals in which strong lattice vibrations also occur at low infrared frequencies. The alkali halides have been extensively examined in this regard (19). The behavior of some of the other ice phases is known to be similar also (20). Since the contribution to the refractive index of a given infrared band is inversely proportional to the square of the frequency, the low lying lattice modes make the largest contribution to ε_∞. (It has been shown (21) that for hexagonal ice, the translational mode, centered near 229 cm^{-1} at 100 K, contributes about 74% of the difference between the microwave permittivity (3.11) and the square (1.74) of the optical refractive index). The observed temperature dependence of ε_∞, therefore, arises primarily from the anharmonicity of the translational lattice vibrations since it is the anharmonicity that causes the infrared absorption frequencies to be temperature dependent. The effect of density variation on ε_∞ (Clausius–Mossotti function) is much smaller and is in the opposite sense.

Provided the absorptivity is unaffected by temperature, the observed change in ε_∞ suggests a decrease in frequency of about 5 cm^{-1} over the temperature range 0 to 200 K for the 229 cm^{-1} translational band. Extrapolation of the reported (22) temperature dependence of this band indicates an actual decrease of about 13 cm^{-1} over the same temperature interval. The discrepancy implies a change in the band contour with temperature. The calculated frequency shift is hardly affected by correction of the data to constant volume.

The far infrared spectra of most of the phases of ice have been recorded (21, 23, 24) and for some the permittivity is known (20) at several temperatures. Table 1 contains the relevant data. The frequencies given are those about which the absorbence of the translational vibrational bands is centered. However, ices II and IX are orientationally ordered (20) and hence show fairly well resolved spectral features (23). Ice I, in contrast, is orientationally disordered, has all vibrations active, and hence has comparatively poorly defined spectral features (21). Nevertheless, the gross shapes of the translational bands of the three ices are reasonably similar. A qualitative comparison of the data therefore seems justifiable.

For the ices proper, the slope $\delta\varepsilon_\infty/\delta T$ shows a linear correlation with $1/\nu^2$ as may be expected since the lower the frequency the greater the

[2]Uncorrected for non-uniform field.

Can. J. Chem. Downloaded from www.nrcresearchpress.com by 210.87.254.5 on 09/05/12
For personal use only.

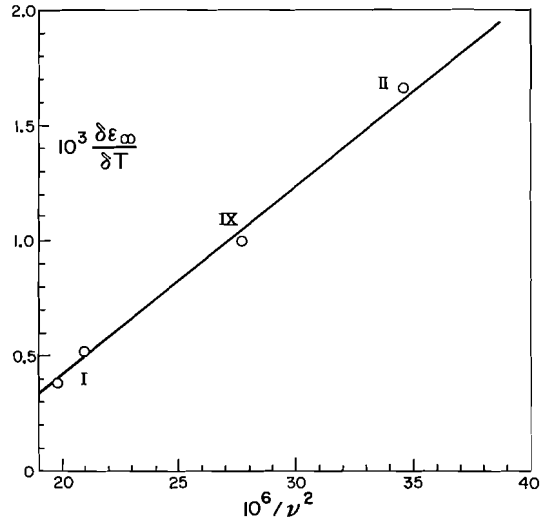

FIG. 5. Empirical correlation between the permittivity temperature dependence and the translational lattice vibrations of ices I, II, and IX.

contribution to ε_∞ and, therefore, the stronger the temperature dependence. The correlation is illustrated in Fig. 5. The line drawn must be regarded, however, as a very approximate representation since its slope depends markedly on the criterion used to establish the tabulated frequencies. Nevertheless, the linear correlation remains. The proportionality implies that the anharmonicities and therefore the potential functions describing translational displacements of the water molecules are similar for these three ices.

The three clathrate hydrates listed each contain a non polar guest and so for these hydrates the ε_∞ of the water lattice dispersion is a "true ε_∞", *i.e.*, it contains no orientational polarization contribution from the guest molecules. Thus the ε_∞ for these hydrates should behave similarly to that of ice. The lower values of permittivity reported (10, 25, 26) for the two hydrate structures are quite consistent with their lower water molecule number densities compared to the number density of ice, provided a small contribution ($\simeq 0.1$) arising from the polarizability of the guest molecules is included (10). The larger slope $\delta\varepsilon_\infty/\delta T$ observed for the two clathrate hydrate structures suggests that their translational lattice modes absorb at somewhat lower frequencies than that of ice I.

It is worth noting that none of the C′–C″ curves, some of which are illustrated in Fig. 3, approach the C′ axis as steeply as required by Debye behavior (note the vertical scales of Fig. 3 are stretched).[3] It has been suggested previously (4) that the extra high frequency absorption giving rise to this behavior is caused by somewhat faster relaxation of the water molecules adjacent to impurity centers. Analysis of the data in terms of multiple Debye-like processes (9) seems hardly justifiable if this suggestion is true.

The technical assistance of R. E. Hawkins who fabricated the cell and the advice and encouragement of Dr. D. W. Davidson are greatly appreciated.

1. D. W. DAVIDSON. Can. J. Chem. **49**, 1224 (1971).
2. B. MORRIS and D. W. DAVIDSON. Can. J. Chem. **49**, 1243 (1971).
3. S. R. GOUGH and D. W. DAVIDSON. Can. J. Chem. **49**, 2691 (1971).
4. S. R. GOUGH and D. W. DAVIDSON. J. Chem. Phys. **52**, 5442 (1970).
5. R. P. AUTY and R. H. COLE. J. Chem. Phys. **20**, 1309 (1952).
6. J. LAMB and A. TURNEY. Proc. Phys. Soc. (London), **B62**, 272 (1949).
7. W. A. CUMMING. J. Appl. Phys. **23**, 768 (1952).
8. S. EVANS. J. of Glaciol. **5**, 773 (1965).
9. A. VON HIPPEL, D. B. KNOLL, and W. B. WESTPHAL. J. Chem. Phys. **54**, 134 (1971).
10. S. R. GOUGH, E. WHALLEY, and D. W. DAVIDSON. Can. J. Chem. **46**, 1673 (1968).
11. R. W. SWENSON and R. H. COLE. J. Chem. Phys. **22**, 284 (1954).
12. S. K. GARG, B. MORRIS, and D. W. DAVIDSON. J. Chem. Soc. Faraday Trans. **268**, 481 (1972).
13. D. EISENBERG and W. KAUZMANN. The structure and properties of water. Oxford University Press, Oxford, England. 1969.
14. G. K. WHITE. Experimental techniques in low temperature physics. 2nd ed. Oxford University Press, Oxford, England. 1968.
15. R. K. CHAN, D. W. DAVIDSON, and E. WHALLEY. J. Chem. Phys. **43**, 2376 (1965).
16. J. P. LE PETIT and C. LAFARGUE. C.R. **273**, Ser. B, 421 (1971).
17. J. W. PERRY and A. W. STRAITON. J. Appl. Phys. **43**, 731 (1972).
18. S. R. GOUGH. Comment submitted to J. Appl. Phys.
19. R. P. LOWNDES and D. H. MARTIN. Proc. Roy. Soc. (London), **A316**, 351 (1970).
20. E. WHALLEY, J. B. R. HEATH, and D. W. DAVIDSON. J. Chem. Phys. **48**, 2362 (1968).

[3]Debye behavior dictates that the complex plane locus meets the capacitance axis at right angles when the axis scales are of equal dimension.

Can. J. Chem. Downloaded from www.nrcresearchpress.com by 210.87.254.5 on 09/05/12
For personal use only.

21. J. E. BERTIE, H. J. LABBÉ, and E. WHALLEY. J. Chem. Phys. **50**, 4501 (1969).
22. R. ZIMMERMAN and G. C. PIMENTEL. Advances in molecular spectrosc. Vol. 2. *Edited by* Mangini. Pergamon. 1962.
23. J. E. BERTIE, H. J. LABBÉ, and E. WHALLEY. J. Chem. Phys. **49**, 775 (1968).
24. J. E. BERTIE, H. J. LABBÉ, and E. WHALLEY. J. Chem. Phys. **49**, 2141 (1968); E. WHALLEY and H. J. LABBÉ. J. Chem. Phys. **51**, 3120 (1969).
25. Y. A. MAJID, S. K. GARG, and D. W. DAVIDSON. Can. J. Chem. **47**, 4697 (1969).
26. Y. A. MAJID, S. K. GARG, and D. W. DAVIDSON. Can. J. Chem. **46**, 1683 (1968).
27. A. D. POTTS and D. W. DAVIDSON. J. Phys. Chem. **69**, 996 (1965).

Can. J. Chem. Downloaded from www.nrcresearchpress.com by 210.87.254.5 on 09/05/12
For personal use only.

Electron Spin Resonance Study of the Self-disproportionation of some Semiquinone Radicals in Solution

S. K. WONG, W. SYTNYK, AND J. K. S. WAN
Department of Chemistry, Queen's University, Kingston, Ontario

Received May 10, 1972

The photolysis of 1,4-benzoquinone, duroquinone, and 1,4-naphthoquinone in isopropanol and in dioxane leads to the observation of e.s.r. spectra of the corresponding semiquinone radicals. The rates of the self-disproportionation of these radicals were measured by the rotating-sector technique. In the case of 1,4-naphthoquinone, unexpected e.s.r. emission was initially observed by photochemically induced dynamic electron polarization of the semiquinone radicals. Photolysis of anthraquinone in isopropanol gives e.s.r. spectra of the anthrasemiquinone radical anions. Their rate of decay was measured and a mechanism for the decay was suggested. The neutral anthrasemiquinone radical, however, was observed when photolyzed in dioxane.

La photolyse de la benzoquinone-1,4,duroquinone et naphtoquinone-1,4 dans l'isopropanol et dans le dioxane, permet d'observer les spectres r.p.e. des radicaux semiquinone correspondants. Les vitesses d'auto-dismutation de ces radicaux ont été mesurées par la technique du secteur tournant. Dans le cas de la naphtoquinone-1,4, on a observé initialement un spectre d'émission r.p.e. inattendu expliqué par une polarisation électronique dynamique, induite par voie photochimique, des radicaux semiquinone. La photolyse de l'anthraquinone dans l'isopropanol donne des spectres r.p.e. des radicaux anions anthrasemiquinone. Leur durée de vie a été mesurée et un mécanisme de leur extinction suggéré. Cependant, le radical neutre anthrasemiquinone a été observé par photolyse dans le dioxane.

[Traduit par le journal]

Canadian Journal of Chemistry, **50**, 3052 (1972)

Introduction

A continuing interest in the photochemistry of the simple quinones is closely associated with the photobiological functions of the more complex, naturally occurring quinones (1–3). The kinetics of photochemical reactions of quinones has been a topic of considerable interest in recent years (3–6). In these studies both the conventional and laser flash photolyses with optical detection have been used. While the assignment of the triplet state absorption and the confirmation of the triplet state as the precursor of the semiquinone radical have been established for duroquinone (3–6), additional e.s.r. spectroscopic information would prove to be desirable. For example, optical studies very often suffer from overlapping, unresolved transient spectra, which have caused some controversies. E.s.r. spectroscopy provides an alternate method of detecting the paramagnetic species and obtains more information about its assignment and structure (7). For kinetic studies, the absolute concentration of the paramagnetic species can be measured by e.s.r. to give the absolute rate constant.

We have undertaken an e.s.r. kinetic study of the photochemistry of 1,4-benzoquinone, duroquinone, 1,4-naphthoquinone, and anthraquinone in isopropanol and in dioxane. Steady-state e.s.r. spectra of the 1,4-benzosemiquinone radical and the durosemiquinone radical in various solvents have been studied by Gough and co-workers (8, 9). A flash photolytic study of *p*-tetrachlorobenzoquinone in alcohol by e.s.r. has recently been reported by Hales and Bolton (10). In this paper, particular attention is given to the disproportionation of the semiquinone radicals, using the increasingly popular rotating sector technique (11, 12). In another report (13) we have studied in detail the photochemistry of *p*-tetrachlorobenzoquinone in dioxane by a combination of various techniques, including the flash photolysis and the rapid scan e.s.r. methods.

Experimental

1,4-Benzoquinone (BDH), duroquinone (Aldrich), 1,4-naphthoquinone (Eastman), and anthraquinone (Matheson) were recrystallized from benzene. Isopropanol and dioxane were spectranalyzed grade from Fisher. The solutions were made to 0.5 *M* or otherwise saturated. The samples in either Pyrex or Suprasil tubes (3 mm to 0.9 mm o.d.) were degassed to less than 10^{-4} Torr by the freeze–pump–thaw method before irradiation.

A varian 4502 e.s.r. spectrometer operating at a fixed frequency of about 9400 MHz and employing 100 KHz modulation was used. The sample temperature was controlled using a V-4557 variable temperature accessory. An

Can. J. Chem. Downloaded from www.nrcresearchpress.com by 210.87.254.40 on 09/05/12
For personal use only.

TABLE 1. Hyperfine splitting constants for semiquinone radicals in solution

Radical	Solvent	HFS (G)
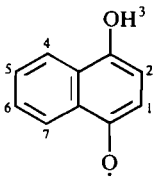 (BSQ)	Isopropanol	$a_1 = 6.92$ $a_2 = 0.35$ $a_3 = a_5 = a_7 = 1.70$ $a_4 = a_6 = 0.18$
	Dioxane	$a_1 = 7.67$ $a_2 = 0.80$ $a_3 = 1.25$ $a_4 = 0.40$ $a_6 = 0.52$ $a_5 = a_7 = 1.85$
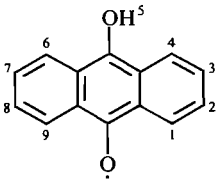 (DSQ)	Dioxane	$a_1 = a_3 = a_7 = a_9 = 3.28$ $a_2 = a_4 = a_6 = a_8 = 0.44$ $a_5 = 0.88$

optical transmission cavity was used for the photolysis experiments.

The light source was an unfiltered 200 W super-pressure mercury DC lamp. The reproducible light pulses were provided by a rotating disk capable of varying the dark-to-light ratio between 20 to 200 and the light period being as short as 200 μs. A Fabri-Tek 1074 signal averager with pre-triggering by means of a miniature photocell was employed to measure the changes in e.s.r. signal amplitude during the intermittent illumination. Generally 10^3–10^4 sweeps were required for a decay curve.

Radical Concentration Measurements

Radical concentrations were calibrated with standard pitch samples, which were in turn standardized against weighed DPPH in benzene. The intensity I was calculated according to

$$[1] \qquad I = KW^2H$$

where W is the peak separation of the derivative curve and H is the height of the resonance. The constant K is determined by the line shape. K for pitch has been determined to be 2.73, and for the present experimental spectra with assumed Lorentzian shape, K equals 1.81 (14). This method was checked against a computer-performed double integration of the spectra for the 1,4-benzosemiquinone radical (BSQ), $C_6H_5\dot{O}_2$, and the durosemiquinone radical (DSQ), $C_{10}H_{13}\dot{O}_2$, in isopropanol and dioxane at 20 °C, and was found to be within 20% agreement.

Analysis for Kinetic Data

The second-order rate constants were obtained from plotting the inverse of concentration against time:

$$[2] \qquad \frac{1}{[SQ]} = \frac{1}{[SQ]_0} + 2k_t \cdot t$$

where $[SQ]_0$ and $[SQ]$ are initial concentration and concentration of semiquinone radicals at time t, respectively; k_t is the second-order rate constant. In the case of 1,4-naphthosemiquinone radical (NSQ), $C_{10}H_7\dot{O}_2$, and anthrasemiquinone radical (ASQ), $C_{14}H_9\dot{O}_2$, in dioxane where the signal-to-noise ratio was not good enough to allow analysis using eq. 2, a half-life method was used which involved greater errors. The Arrhenius parameters were obtained from the plot of log $2k_t$ against $1/T$:

$$[3] \qquad \log 2k_t = \log A - E_a/2.303\ RT$$

The temperature range studied was from 0 to 50 °C.

Results

Electron Spin Resonance Spectra

The photolyses of 1,4-benzoquinone, duroquinone, naphthoquinone, and anthraquinone in isopropanol and dioxane gave the expected e.s.r. spectra of the corresponding semiquinone radicals except in the case of anthraquinone in isopropanol where the anthrasemiquinone radical anions were the major species. The hyperfine splittings of 1,4-benzosemiquinone radical and durosemiquinone radical in the two solvents are in agreement with the reported values (8, 9). Since the e.s.r. hyperfine splitting constants of the 1,4-naphthosemiquinone radical and the anthrasemiquinone radical have not been reported previously, they are given in Table 1.

In the course of the study of temperature dependence of rate constants of DSQ in isopro-

Can. J. Chem. Downloaded from www.nrcresearchpress.com by 210.87.254.40 on 09/05/12
For personal use only.

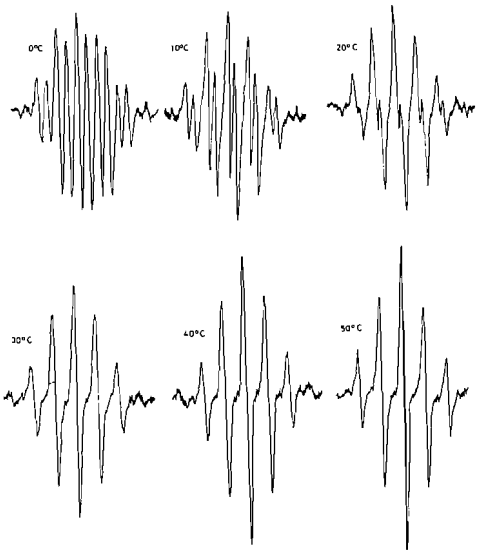

FIG. 1. E.s.r. spectra of the durosemiquinone radical in isopropanol at various temperatures (only the central portion of the spectra are shown here).

panol, it was observed that the e.s.r. spectra changed drastically from 0 to 50 °C (Fig. 1). This can be explained as being due to rapid proton exchange of the hydroxyl group with the solvent, since the doublet splitting of this proton collapsed to a singlet at higher temperatures.

Decay of Radicals

A typical time dependence of radical decay is shown in Fig. 2, indicating also the signal-to-noise ratio. Analyses of these decays show a good second order decay (Fig. 2). The rate constants $2k_t$, measured in this work at 20 ± 2 °C are listed in Table 2 together with the range in initial radical concentrations. The temperature dependence of rate constants of BSQ and DSQ radicals in isopropanol and dioxane has been recorded and is listed in Table 3.

When the radical decay of NSQ was measured during and immediately after the light pulse, the e.s.r. signal was unexpectedly found to be in the form of emission which reverted to the normal absorption mode with a time constant of about 300 μs, as the light pulse decayed (Fig. 3). The e.s.r. absorption further decayed according to a second order kinetics. Since the spin–lattice relaxation time is much shorter than the half-life of the radicals at this concentration, no correction for the concentration is necessary. The novel aspect of this observation has been reported in a preliminary communication (15) in which we proposed that initially the naphthoquinone triplet states are optically spin-polarized and their subsequent abstraction reaction with retention of electron polarization thus leads to the observed e.s.r. emission for the resultant radicals.

Discussion

In the flash photolysis of some quinones, *e.g.* duroquinone and *p*-chloranil, it has been established that the first-order build-up of semiquinone radicals (3, 6) follows closely to the first-order decay of the parent triplets. It should be noted that the lowest triplet state for 1,4-benzoquinone, 1,4-naphthoquinone and anthra-

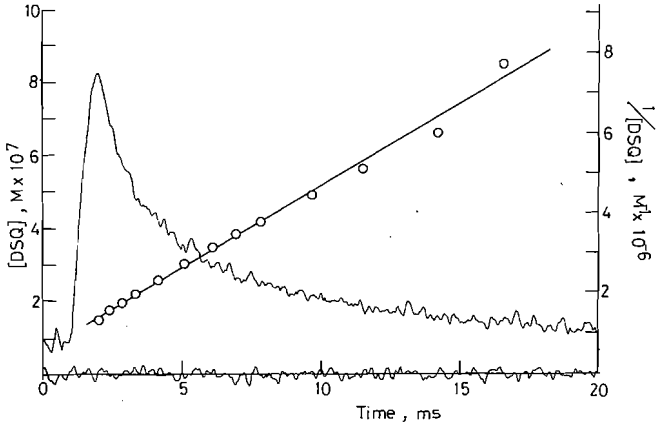

FIG. 2. Decay of the durosemiquinone radical in isopropanol and the corresponding second order kinetic plot.

Can. J. Chem. Downloaded from www.nrcresearchpress.com by 210.87.254.40 on 09/05/12
For personal use only.

TABLE 2. Rate constants for the bimolecular disproportionation of some semiquinone radicals at 20 ± 2 °C

Radicals	Initial concentration ($\times 10^8$ M)	Solvent	$2k_t \times 10^{-9}$ M^{-1} s^{-1}	k(dioxane)/ k(isopropanol)
BSQ	8–20	Isopropanol	1.5±0.2	3.7
	5–14	Dioxane	5.4±0.8	
DSQ	40–105	Isopropanol	0.73±0.06	4.0
	20–40	Dioxane	2.9±0.3	
NSQ	80–100	Isopropanol	0.23±0.04	3.8
	150–300	Dioxane	0.90±0.30	
ASQ	100–200	Dioxane	1.2±0.4	
TCBSQ	25–45	Isopropanol	0.17±0.02	4.6
	50–100	Dioxane	0.76±0.04	
ASQ^-	20–40	Isopropanol	0.049±0.008	

TABLE 3. Arrhenius parameters for the disproportionation of some semiquinone radicals (0–50 °C)

Radicals	Solvents	log A	E_a
BSQ	Isopropanol	11.8	3.7±0.3
BSQ	Dioxane	12.6	3.9±0.4
DSQ	Isopropanol	11.0	3.3±0.3
DSQ	Dioxane	12.3	3.8±0.4

quinone is probably n–π^* in character (16–18), whereas the triplet duroquinone and triplet p-chloranil are probably π–π^* in character (3, 17, 19). In all cases, it is reasonable to assume that the precursors of the semiquinone radicals are the lowest triplet states of the corresponding quinones.

While ketyl radicals are known to dimerize to form pinacols, semiquinone radicals react via self-disproportionation to yield the hydroquinone (HQ) and the quinone (Q) as products (20–22):

$$[4] \qquad 2\dot{S}Q \xrightarrow{k_t} HQ + Q$$

The observed second-order kinetics of the semiquinone radical decay in this study is consistent with this mechanism. In general, it was found that the self-reaction rates in dioxane solvent are about four times greater than those in isopropanol for the same semiquinone radical. Similar observation has also been made in the photolysis of p-chloranil (23). This solvent effect could be partially due to the difference in viscosity of the solvents, provided the self-reaction is mainly diffusion-controlled. It is

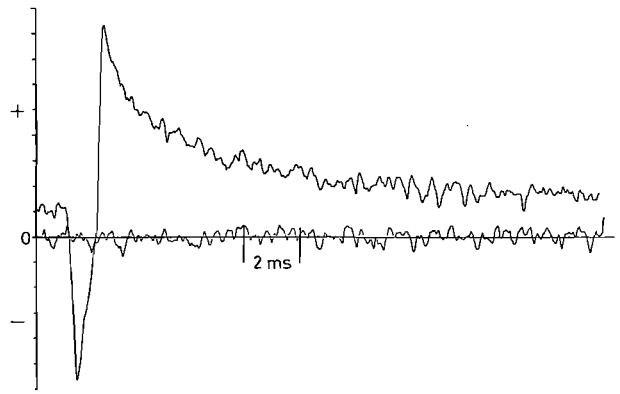

FIG. 3. Decay of the naphthosemiquinone radical in isopropanol exhibiting the conversion of the e.s.r. signal from an initial emission to an absorption mode.

Can. J. Chem. Downloaded from www.nrcresearchpress.com by 210.87.254.40 on 09/05/12
For personal use only.

Can. J. Chem. Downloaded from www.nrcresearchpress.com by 210.87.254.40 on 09/05/12
For personal use only.

well known that alcohols generally have higher viscosities than those of their corresponding ethers. On the other hand, proton exchange between the DSQ radicals and the isopropanol solvent has been observed by e.s.r. (Fig. 1) and such exchange probably involves hydrogen bonding between the semiquinone radicals and the alcohol. Such property in alcohol solvent may account partially for the slower rates of the semiquinone radical reactions. It should be pointed out, however, that the proton exchange rates are about three orders magnitude faster than the chemical decay rates.

While the experimental data at the present time do not lead to conclusive evidence that the self-reaction of the semiquinone radicals is diffusion-controlled, it is perhaps worthwhile to consider briefly the modified Debye equation (24, 25) which has been used to estimate diffusion-controlled rate-constants for like species. The equation is given in the form:

$$[5] \qquad k_{\text{diff}} = \tfrac{1}{2}(8RT/3 \times 10^3\eta)$$

where η is the viscosity of the solvent. A sample calculation using the available viscosity data for isopropanol at 20 °C gives an estimated value of $k_{\text{diff}} = 1.3 \times 10^9\ M^{-1}\ s^{-1}$ at 20 °C. This value is obviously greater than all the experimentally determined rate-constants in isopropanol as listed in Table 2. However, the modified Debye equation implies that the diffusion-controlled rate constant for a bimolecular reaction is independent of the size and nature of the reactant. This assumption is probably not valid in the present study involving fairly large radicals. Apparently the increase of the size of the radicals as indicated by their molecular weights seems to slow down the reaction rates (26, 27).

Another general criterion for diffusion-controlled reactions is that they should have an activation energy of about 3 kcal/mol in systems with most common solvents (25, 28). It should be pointed out that activation energy for viscosity variation in various solvents may be temperature dependent, particularly for solvents with hydrogen-bonding property (29). Since no data for such temperature–viscosity variation are available, it is not worthwhile to compare the experimental values of activation energy obtained in the two different solvents.

Weiner (30) has quoted that the radical termination rate constant ($2k_t$) for BSQ radicals in isopropanol is $1.2 \times 10^8\ M^{-1}\ s^{-1}$ at 30 °C. The large difference between this value and ours (Table 2) is not understood. Bridge and Porter (4) have reported a value of $1.6 \times 10^9\ M^{-1}\ s^{-1}$ for DSQ disproportionation rate constant ($2k_t$) in ethanol/water solution at ~20 °C by flash photolysis and their result is in reasonable agreement with ours (Table 2).

Next we discuss briefly the formation of anthrasemiquinone anion (ASQ^-) and its kinetic behavior in isopropanol. It is rather surprising that ASQ^- is the major photoparamagnetic species observed in the anthraquinone/isopropanol system. The e.s.r. identification of ASQ^- is reasonable from its spectrum which consists of 15 lines with splittings due to two sets of four nearly-equivalent protons (0.96 and 0.48 G) (31, 32). It has been demonstrated that semiquinone neutral radicals convert rapidly to anions in alkaline solutions (4, 18, 33); in fact the pK_a of the equilibrium of durosemiquinone radicals and the anions in ethanol/water was found to be 5.9 (4):

[6] 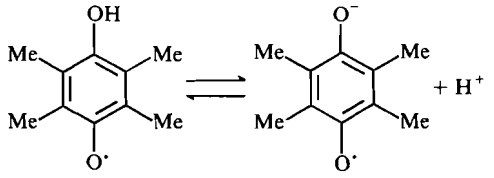

Although the pK_a value is not known for the ASQ^- system, it is possible that the equilibrium in isopropanol lies well to the right. The observation of ASQ^- as a transient species has been reported in the flash photolysis of anthraquinone in ethanol (4). The second order kinetics of ASQ^- is consistent with the following mechanism:

$$[7] \qquad 2ASQ^- \rightarrow AQ^{2-} + AQ$$

However, Bridge and Porter (4) reported in their flash photolysis study that DSQ^- has a bimolecular rate constant of $4.6 \times 10^6\ M^{-1}\ s^{-1}$ in the pH range 7.9–9.1, but a much greater rate constant of $6 \times 10^7\ M^{-1}\ s^{-1}$ was obtained at pH 6.9. They believe that in the strong alkaline solution, chemical reaction analogous to eq. 7 predominates for the decay of DSQ^-, whereas in near neutral solution the following reaction

mechanism accounts for the bimolecular decay:

$$[8] \qquad DSQ^- + H^+ \overset{K_a}{\rightleftharpoons} DSQ$$

$$[9] \qquad 2DSQ \longrightarrow DQ + HDQ$$

Thus, the differential rate equation for the disappearance of DSQ^- would be second order:

$$[10] \qquad \frac{d[DSQ^-]}{dt} = \frac{k_9[H^+]}{K_a}[DSQ^-]^2$$

where k_9 is the bimolecular disproportionation rate constant of DSQ. It follows that such a mechanism could occur also for the decay of ASQ^-.

The authors are grateful to the National Research Council of Canada for financial support. We also wish to thank Mr. Terry Blake for the expert construction of the rotating sector.

1. D. I. Arnon and F. L. Crane. Biochemistry of quinones. *Edited by* R. A. Morton. Academic Press, London. 1965. p. 433.
2. F. L. Crane. Biological oxidation. *Edited by* T. P. Singer. Interscience, New York. 1968. p. 533.
3. D. R. Kemp and G. Porter. Proc. Roy. Soc. London, **A326**, 131 (1972).
4. N. K. Bridge and G. Porter. Proc. Roy. Soc. London, **A244**, 259, 276 (1958); N. K. Bridge. Trans. Faraday Soc. **56**, 1001 (1960).
5. F. Wilkinson, G. M. Seddon, and K. Tickle. Ber. Bunsenges. Phys. Chem. **72**, 315 (1968).
6. D. R. Kemp and G. Porter. Chem. Commun. 1029 (1969).
7. J. K. S. Wan. *In* Advances in photochemistry. To be published.
8. T. E. Gough. Trans. Faraday Soc. **62**, 2321 (1966).
9. T. A. Claxton, T. E. Gough, and M. C. R. Symons. Trans. Faraday Soc. **62**, 279 (1966).
10. B. J. Hales and J. R. Bolton. Photochem. Photobiol. **12**, 239 (1970).
11. S. A. Weiner and G. S. Hammond. J. Am. Chem. Soc. **91**, 986 (1969).
12. K. Adamic, D. F. Bowman, T. Gillan, and K. U. Ingold. J. Am. Chem. Soc. **93**, 902 (1971).
13. L. J. Fabes. Ph.D. Thesis. Queen's University, Kingston, Ontario, 1971; L. J. Fabes, S. K. Wong, and J. K. S. Wan. To be published.
14. Varian Associates. Publication 87-114-401.
15. S. K. Wong and J. K. S. Wan. J. Am. Chem. Soc. To be published.
16. F. Wilkinson. J. Phys. Chem. **66**, 2569 (1962).
17. N. A. Shcheglava, D. N. Shigorin, G. G. Yakobson, and L. Sh. Tushishvili. Russ. J. Phys. Chem. **43**, 1112 (1969).
18. H. H. Dearman and A. Chan. J. Chem. Phys. **44**, 416 (1966).
19. J. A. Barltrop and B. Hesp. J. Chem. Soc. C, 1625 (1967).
20. J. L. Bolland and H. R. Cooper. Proc. Roy. Soc. London, **A225**, 405 (1954).
21. K. Tickle and F. Wilkinson. Trans. Faraday Soc. **61**, 1981 (1965).
22. H. Herman and G. O. Schenck. Photochem. Photobiol. **8**, 255 (1968).
23. S. K. Wong, L. J. Fabes, and J. K. S. Wan. J. Chem. Soc. Faraday II. To be published.
24. P. Debye. Trans. Electrochem. Soc. **82**, 265 (1942).
25. J. G. Calvert and J. N. Pitts, Jr. Photochemistry. John Wiley, New York. 1966. p. 627.
26. L. Bertrand, G. R. DeMare, G. Huybrechts, J. Albregts, and M. Toth. Chem. Phys. Lett. **5**, 183 (1970).
27. G. B. Watts and K. U. Ingold. J. Am. Chem. Soc. **94**, 491 (1972).
28. A. M. North. The collision theory of chemical reactions in liquids. Methuen, London. 1964.
29. S. Glasstone, K. J. Laidler, and H. Eyring. The theory of rate processes. McGraw-Hill, New York. 1941. Chapt. IX.
30. S. A. Weiner. J. Am. Chem. Soc. **94**, 581 (1972).
31. M. Adams, M. S. Blois, Jr., and R. H. Sands. J. Chem. Phys. **28**, 774 (1958).
32. G. Vincow and G. K. Fraenkel. J. Chem. Phys. **42**, 1350 (1965).
33. T. Gough and M. C. R. Symons. Trans. Faraday Soc. **62**, 269 (1966).

Can. J. Chem. Downloaded from www.nrcresearchpress.com by 210.87.254.40 on 09/05/12
For personal use only.

Metals Intercalated in Graphite. I. Reduction and Oxidation

J.-M. LALANCETTE, G. ROLLIN, AND P. DUMAS

Département de Chimie, Faculté des sciences, Université de Sherbrooke, Sherbrooke, Québec

Received April 10, 1972

Potassium in graphite shows distinctive reducing properties towards carbonyls. The reaction products can be related to a mechanism similar to electrochemical reduction. The steric orientation of the reduction can be explained by the particular structure of potassium–graphite.

Chromic anhydride in graphite offers a new selective method of preparation of aldehydes from the corresponding primary alcohol. This method is characterized by its specificity, high yields and a simple experimental procedure.

Le potassium inséré dans le graphite présente des propriétés réductrices particulières. Les produits de réduction peuvent être expliqués par un mécanisme de type électrochimique. La stéréochimie de la réduction s'explique par la structure du potassium–graphite.

L'anhydride chromique inséré dans le graphite offre une nouvelle méthode d'oxydation sélective des alcools primaires en aldéhydes. Cette méthode est caractérisée par sa spécificité et la simplicité des opérations.

Canadian Journal of Chemistry, **50**, 3058 (1972)

Can. J. Chem. Downloaded from www.nrcresearchpress.com by 210.87.254.42 on 09/05/12
For personal use only.

Metals intercalated in graphite present interesting features (1). First, the metal crystalline is broken into atomic particles, the distance between each atom being of the order of 5 Å or more. Secondly, the distance between the planes of graphite holding a layer of metal is from 6 to 7 Å. Such an arrangement would allow, we believe, the selective diffusion of molecules of proper geometry within the lattice of graphite, where reactions with metal atoms will be greatly enhanced. Also, when transition metals, either at zero or at low oxidation state are held between the planes of graphite, the electronic system of graphite can participate to the build-up of coordinated entities that should be quite reactive, in a way similar to dicyclopentadienyltitanium for example.

Potassium–graphite can be obtained very easily by heating a mixture of the two elements, in the absence of air, at 70°. The structure of potassium–graphite is well known from the study of Schleede and Wellmann (2). The stoichiometry of the compounds of potassium can be adjusted quite easily by the relative pressure of potassium to give C_8K, $C_{24}K$, $C_{36}K$, $C_{48}K$ corresponding to one, two, three or more layers of carbons between each plane of potassium atoms. A three dimensional representations of C_8K (3) is given in Fig. 1. Potassium–graphite has been used as catalyst for polymerization (4), alkylation (5), and Wurtz reactions (6). The reduction of carbonyls remained to be examined and it could be expected that the presence of the metal within the structure of graphite would markedly influence the reactivity of the 4s potassium electron. When potassium is inserted in graphite, the planar distance of graphite is increased from 3.35 to 5.40 Å. Since the covalent radius of potassium is 2.03 Å, it is then possible to have interaction and even partial delocalization of this electron within the conduction band of graphite. The heat of insertion of potassium is 7.8 kcal/mol (7), much too low for a quantitative formation of a truly ionic entity like K^+: the heat of insertion would then have to be of the order of 100 kcal/mol for such a complete reaction. But paramagnetic (8) and electric (9) properties have been interpreted as an indication that there is a partial transfer of the 4s electron to the π electronic system of graphite in C_8K. This should influence the mobility and accessibility of the 4s electron, the active species in the initial step of the reduction of a carbonyl.

Reduction

Several saturated and conjugated ketones have been reduced with potassium–graphite. The results of these reductions are reported in Table 1. These results must be examined in relation with the reducing capacity of alkali metals in alcohol (10, 13, 15) and the electrochemical reduction (11, 12, 14, 16). It can be noted that the reaction products obtained from

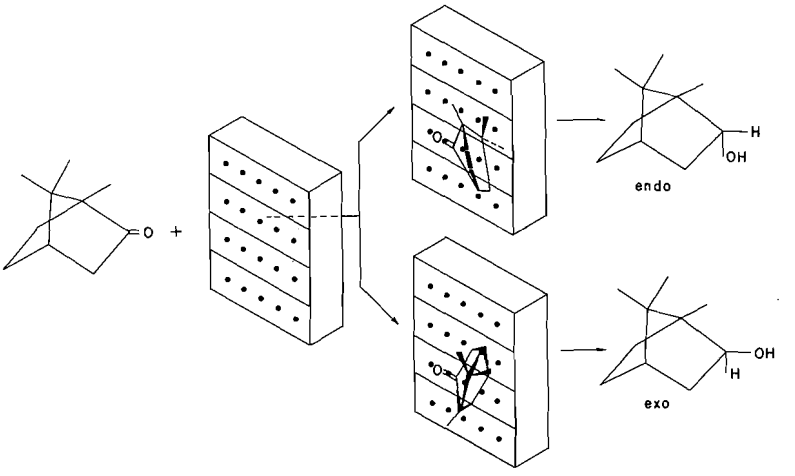

FIG. 1. Stereochemistry of reduction with C_8K.

C_8K and conjugated ketones suggest a mechanism closer to electrochemical reduction than alkali–alcohol reduction. This can be interpreted as an indication that the availability of the 4s electron of potassium in C_8K is more to the electrochemical reduction than the alkali–alcohol system. The stereochemistry of the reduction of camphor, a sterically hindered ketone, is inverted in relation with the reduction product of the alkali–alcohol reduction.

We explain the nature of the observed reduction products and the stereochemistry of the reduction of camphor with C_8K by a mechanism which is similar to the reduction at the surface of an electrode (17). With acetophenone, for example (eq. 1), the electrons of potassium are readily available at the edges of C_8K crystallites, to give the corresponding radical anion. This first intermediate can be desorbed or can abstract a second electron from C_8K to give a dianion. The hydrolysis of these intermediates leads to the corresponding pinacol or alcohol. The reduction of camphor with sodium in alcohol or with potassium, in the presence of graphite, but not intercalated in tetrahydrofuran (THF), gives predominantly the *endo* alcohol. With potassium in graphite, however, the predominant product is the *exo* alcohol. We believe that this inverted orientation can be explained by the necessity for the ketone to be adsorbed at the surface of C_8K crystallite in order to be subject to reduction. And because

[1]

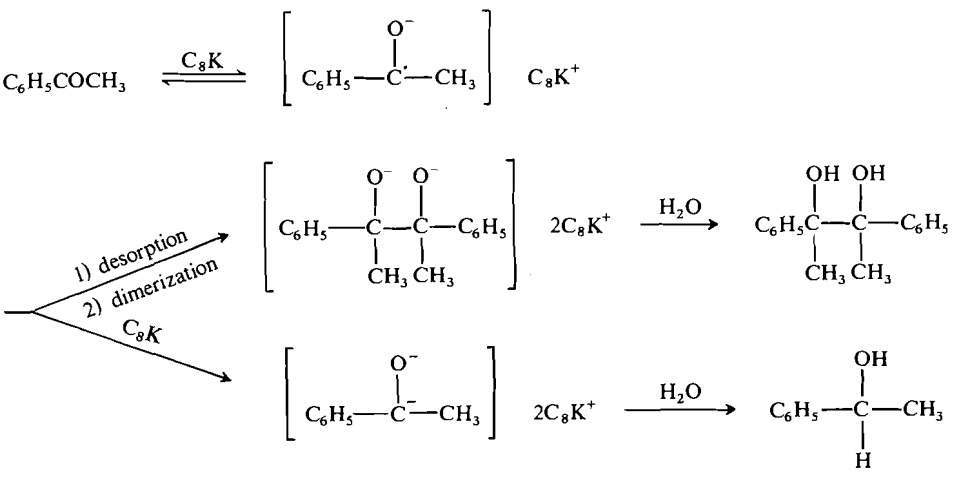

Can. J. Chem. Downloaded from www.nrcresearchpress.com by 210.87.254.42 on 09/05/12
For personal use only.

TABLE 1. Reduction of ketones with C_8K

Ketones	Product	Yield
Benzophenone	Alcohol	98
Acetophenone	Alcohol	45
	Pinacol	45
Cycloheptanone	Alcohol	92
Cyclohexanone	Alcohol	75
Camphor	Alcohol	60 (*exo*)
		40 (*endo*)
4-Phenylbutenone	Saturated ketone	75
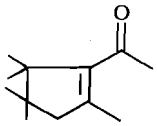	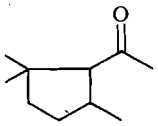	75
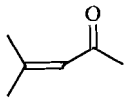	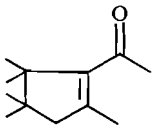	40
	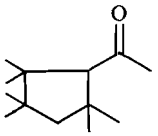	40
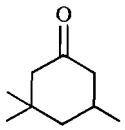	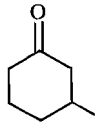	40
	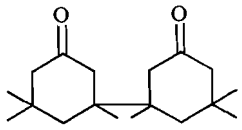	40

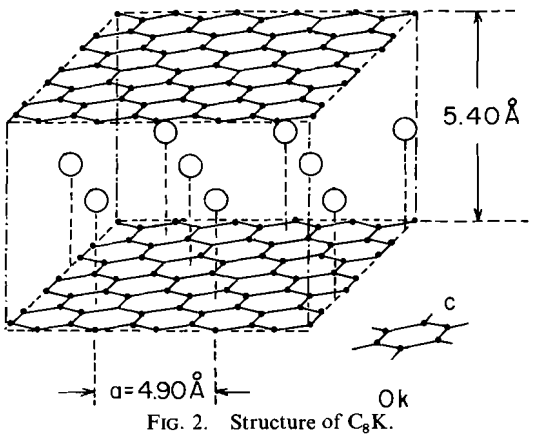

FIG. 2. Structure of C_8K.

this adsorption is easier in a position more favorable for the formation of the *exo* alcohol, this isomer is formed, predominantly, in spite of less favorable thermodynamic factors (Fig. 2).

The results of these reductions with C_8K can be interpreted simply if the structure of C_8K is taken into consideration. This reducing agent shows distinctive properties offering interesting synthetic alternatives to the existing methods of reduction.

Oxidation

Chromic acid can be intercalated in graphite. Several methods can be used to achieve the

Can. J. Chem. Downloaded from www.nrcresearchpress.com by 210.87.254.42 on 09/05/12
For personal use only.

TABLE 2. Oxidation of alcohols with CrO_3–graphite

Alcohol	Contact time (h)	Yield of aldehyde or ketone (%)	Analysis
1-Hexadecanol	24	95	v.p.c., 2,4-d, titration§
Benzyl alcohol	24	98	v.p.c., 2,4-d
Cinnamyl alcohol	96	100	v.p.c., 2,4-d, titration
Furfuryl alcohol	48	72	v.p.c., titration
Citronellol†	24	90	v.p.c., titration
1,6-Hexanediol*	24	60	v.p.c., 2,4-d, titration
Phenylethanediol‡	24	80	v.p.c., 2,4-d, titration
Cyclohexylmethanol	48	52	v.p.c., 2,4-d, titration
Cyclohexanol	24	2	v.p.c.
t-Amyl alcohol	24	0	v.p.c.
Isopulegol	24	0	v.p.c.

*The reaction product was the monohydroxy aldehyde.
†This yield of aldehyde was observed where a trace of pyridine was added to the system, in order to prevent cyclization.
‡The aldehyde observed was benzaldehyde.
§By Smith–Mitchell method.

insertion, calling for the use of acetic acid as solvent (18) or the diffusion of the vapors of CrO_3 in the lattice of graphite at reduced pressure and high temperature (19). We have found that by heating a mixture of chromic anhydride and graphite under reduced pressure, the intercalation was easy, the end product is of constant composition and without any contaminant. Consequently, this method was adopted for the present work. The insertion (55 to 60% by weight of CrO_3) was verified by X-Ray diffraction and the concentration of CrO_3 in the lattice determined by titration (20).

We have investigated the oxidizing capacity of this reagent towards various alcohols. A selection of primary, secondary, and tertiary alcohols were submitted to oxidation under various experimental conditions. Results are reported in Table 2.

From these results, it can be noted that the intercalated chromic anhydride is a very specific oxidizing agent for the conversion of primary alcohols to the corresponding aldehydes. The yields of the reaction are always good, even with sensitive structures like terpenes or allylic systems. With 1,2-diols, there is a rupture of the carbon chain, giving the corresponding aldehydes. Secondary and tertiary alcohols are not oxidized.

Experimentally, the oxidation is very simple. After contact of the alcohol with chromic anhydride–graphite, the aldehyde is obtained by filtration and evaporation of the solvent. There is no problem with chromium salts or solvents difficult to eliminate, *e.g.*, pyridine. The internal mechanism for the oxidation must be close to scheme "B" suggested by Wiberg and Schafer (21) since no internal base is involved.

The good selectivity of the reagent for primary alcohols and the very high yields of aldehydes observed with fatty alcohols must be related to its particular structure, the access to CrO_3 being restricted by the planes of graphite. After oxidation, the resulting aldehyde must be desorbed and be less prone to reenter the lattice, thus explaining the high yield of aldehyde, without secondary product. The residual chromium salts remain in the lattice of graphite under the experimental conditions used in the absence of water, thus eliminating cumbersome purification steps and undesirable secondary reactions.

Consequently, chromic anhydride intercalated in graphite has proved to be a choice reagent for specific oxidation of primary alcohols to the corresponding aldehyde. The yields are comparable to those observed with dipyridine–chromium(VI) complex (22) but a better selectivity is possible.

Experimental

The n.m.r. measurements were made with a Varian A60 apparatus. The i.r. measurements were made with a Perkin–Elmer, model 137 spectrophotometer. The v.p.c. measurements were made with a Microteck, model B.C.2000R apparatus, using an Se30, 4 ft column. Mass spectrometry measurements were performed on a Hitachi Perkin–Elmer instrument, model RMU-6

Preparation of C_8K

A three-necked 1 l flask was flushed with dry helium and briefly heated to around 300°, in order to dry the surface of the flask. After cooling, in an atmosphere of helium, 21 g

Can. J. Chem. Downloaded from www.nrcresearchpress.com by 210.87.254.42 on 09/05/12
For personal use only.

(1.85 mol) of graphite was added and the heating repeated in order to desorb any oxygen or water from the graphite. The graphite used, supplied by Fisher Scientific, was of the Acheson type and contained 99.99% of carbon by elementary analysis. It showed an interlayer spacing of 3.35 Å (no interlayer spacing of 3.44 Å). After cooling, a magnetic stirrer was introduced in the flask and the system heated at 100° with a metal bath. Potassium previously washed with *n*-pentane (8.6 g, 0.22 mol) was then added in small portions, over a period of 40 min, the reaction mixture being continuously stirred. Under these conditions, the insertion was instantaneous, the product being a bronze-colored solid. C_8K, a highly pyrophoric substance was used *in situ* by addition, after cooling, of THF and the ketone to be reduced.

Reduction with C_8K

The reduction of benzophenone can be presented as a typical reduction. To the suspension, of 0.2 mol (27 g) of C_8K in 250 ml of anhydrous THF, 18.2 g (0.1 mol) of benzophenone were added at 25°, during a period of 10 min. The stirring at 25° was continued for 2 h. Then, 20 ml of methanol was added followed by 10 ml of water. After a further stirring of 15 min, the reaction mixture was filtered, the volume of the filtrate was doubled with ether, dried and distilled, giving 18 g of benzhydrol, a quantitative yield.

A similar technique was used for the reduction of ketones reported in Table 1. The identification of the resulting alcohols was done by n.m.r., i.r., and mass spectrometric measurements and by comparison with authentic samples.

Preparation of CrO_3–Graphite[1]

In a thick walled Pyrex tube 4 × 30 mm a 20 g portion of graphite was heated under reduced pressure, at 200°, for 24 h in order to remove any adsorbed gas. After cooling, 40 g of CrO_3 was added. The tube was then sealed under reduced pressure and heated at 200° for 48 h. After cooling, the tube was opened (carefully) and the intercalated product washed with 1 l of distilled water, 500 ml of 10% HCl, and 500 ml of distilled water. After a last washing with 1 l of acetone, the product was dried at 100° to a constant weight. By analysis (20), the content of CrO_3 in the graphite was 55%, in accordance to the value published by Croft (19).

Oxidation of a Typical Alcohol

In a 125 ml flask were added 25 ml of toluene, 10 g of CrO_3–graphite prepared as above, and 0.67 g (0.005 mol) of cinnamyl alcohol. After a reflux of 24 h, the cooled mixture was filtered on an asbestos pad. Evaporation of the solvent gave a quantitative yield of cinnamaldehyde. The molar ratio of CrO_3–alcohol was 10 to 1 in this experiment. Comparable yields were observed with a 4 to 1 ratio.

A similar technique was used with other alcohols and the determination of the yield was done by preparation of the corresponding 2,4-dinitrophenylhydrazone, by v.p.c. analysis, and by titration according to the procedure of Smith and Mitchell (23). The yields as observed with these methods were in agreement within 3%.

[1]Available commercially at Ventron Corporation, Beverly, Mass.

1. M. Sudo, M. Ichikawa, M. Soma, T. Onishi, and K. Tamaru. J. Phys. Chem. **73**, 1174 (1969).
2. A. Schleede and M. Wellmann. Z. Physik. Chem. **B18**, 1 (1932).
3. P. Pascal. Nouveau traité de chimie minérale. Vol. VIII. Masson et Cie, Paris. 1968. p. 388.
4. H. Podall, W. E. Foster, and A. D. Giraitis. J. Org. Chem. **23**, 82 (1958).
5. H. Podall and W. E. Foster. J. Org. Chem. **23**, 401 (1958).
6. F. Glockling and D. Kingston. Chem. and Ind. 1037 (1961).
7. L. Quarterman and W. Primak. J. Am. Chem. Soc. **74**, 806 (1952).
8. G. R. Hennig. Progress in inorganic chemistry. Vol. I. Interscience Publishers, New York. 1959. p. 125.
9. F. R. M. McDonnell, R. C. Pink, and A. R. Ubbelohde. J. Chem. Soc. 191 (1951).
10. W. E. Bachmann. J. Am. Chem. Soc. **55**, 1179 (1933).
11. T. Arai. Chem. Abstr. **62**, 15760 (1965).
12. B. Sakurai and T. Arai. Bull. Chem. Soc. Jap. **28**, 93 (1955).
13. J. Frederick, J. Dippy, and R. L. Lewis. Rec. trav. chim. **56**, 1000 (1937).
14. G. Shima. Chem. Abstr. **24**, 2118 (1930).
15. M. Larcheveque. Ann. Chim. **14** (**5**), 129 (1970).
16. J. Wiemann and M. L. Bouguerra. Ann. Chim. **14** (**2**), 35 (1967).
17. F. D. Popp and H. P. Schultz. Chem. Rev. **62**, 19 (1962).
18. N. Platzer and B. de la Martiniere. Bull. Soc. Chim. Fr. 177 (1961).
19. R. C. Croft. Aust. J. Chem. **9**, 201 (1956).
20. A. I. Vogel. Quantitative inorganic analysis. 3rd ed. Longmans, London. 1961. p. 286, 308.
21. K. B. Wiberg and H. Schafer. J. Am. Chem. Soc. **91**, 933 (1969).
22. J. C. Collins, W. W. Hess, and F. J. Frank. Tetrahedron Lett. **30**, 3363 (1968).
23. D. M. Smith and J. Mitchell, Jr. Anal. Chem. **22**, 750 (1950).

Can. J. Chem. Downloaded from www.nrcresearchpress.com by 210.87.254.42 on 09/05/12
For personal use only.

Benzene Complexes of Ruthenium(II)

R. A. ZELONKA AND M. C. BAIRD
Department of Chemistry, Queen's University, Kingston, Ontario
Received April 19, 1972

The complexes $[\pi\text{-}C_6H_6RuX_2]_2$ (X = Cl, Br, I, SCN) have been prepared and characterized. They react with phosphorus donors to give the monomeric $\pi\text{-}C_6H_6RuX_2PR_3$, and with cyanide and hydride ions to give cyclohexadienyl and cyclohexadiene complexes.

Les complexes du type $[\pi\text{-}C_6H_6RuX_2]_2$ (X = Cl, Br, I, SCN) ont été préparés et caractérisés. Ils réagissent avec les phosphores donneurs pour conduire au $\pi\text{-}C_6H_6RuX_2PR_3$ monomère et avec les ions cyanure et hydrure pour donner les complexes cyclohexadiènyle et cyclohexadiène.

[Traduit par le journal]

Canadian Journal of Chemistry, **50**, 3063 (1972)

Can. J. Chem. Downloaded from www.nrcresearchpress.com by 210.87.254.105 on 09/05/12
For personal use only.

Introduction

In recent years, π-arene metal complexes have generated considerable interest because of their potential roles as homogeneous catalysts. Much of the earlier work was concerned with complexes of zerovalent metals (1), and it was found that although the hydrocarbon ligands retain their aromatic character, they are generally deactivated toward electrophilic attack and activated toward nucleophilic attack relative to the free ligands.

In 1967, Winkhaus and Singer (2) reported the preparation of the insoluble, presumably polymeric $\pi\text{-}C_6H_6RuCl_2$, as well as the apparently dimeric $[\pi\text{-}C_6H_6RuCl_2PBu_3]_2$. The benzene rings were postulated to be bidentate in both cases, an unexpected mode of bonding for ruthenium(II), although well-established for complexes of silver(I) (3).

Aside from their rather novel structures, these compounds also seemed interesting because they offered an opportunity to investigate reactions of aromatic molecules coordinated to metal ions in relatively high oxidation states. Furthermore, although the role of such complexes in the platinum metal-catalyzed H–D exchange of aromatics has been postulated (4), few stable derivatives have previously been available for careful study.

A preliminary report of this work has appeared (5).

Experimental

$[\pi\text{-}C_6H_6RuCl_2]_2$

A soluble dimeric form of this compound was prepared by adding 6 ml of 1,3-cyclohexadiene to a solution of 1.70 g (6.5×10^{-3} mol) of $RuCl_3 \cdot 3H_2O$ in 100 ml of 90% aqueous ethanol. The solution was heated to 45° for 3 h, after which the volume of the solution was reduced to 30 ml. The resulting red precipitate was collected, washed with ethanol, and dried in vacuo (yield 85%). Analytical data are shown in Table 1.

The dimeric nature of the compound was inferred from its far i.r. spectrum (see below). The previously reported (2) brown, insoluble form was rather unreactive.

$[\pi\text{-}C_6H_6Ru(C_6H_8)][Hg_3Cl_6]_{1/2}$

Solid $HgCl_2$ was added to the filtrate obtained from the preparation of $[\pi\text{-}C_6H_6RuCl_2]_2$, yielding a pale yellow precipitate. The material was recrystallized by dissolving in DMSO, adding 1:1 ethanol–ether, and cooling (yield 10%).

Although attempts to prepare this compound by treating $[\pi\text{-}C_6H_6RuCl_2]_2$ with 1,3-cyclohexadiene were unsuccessful, a similar tetraphenylborate complex was precipitated on adding $NaBPh_4$ to the filtrate from the preparation of $[\pi\text{-}C_6H_6RuCl_2]_2$. Although this material was too unstable to purify, its i.r. and n.m.r. spectra confirmed its identity as a benzene 1,3-cyclohexadiene complex, $[\pi\text{-}C_6H_6RuCl(C_6H_8)][BPh_4]$.

$[\pi\text{-}C_6H_6RuCl(CH_3CN)_2][HgCl_3]$

Solid $HgCl_2$ (1.07 g, 4.0×10^{-3} mol) was added to a solution of $[\pi\text{-}C_6H_6RuCl_2]_2$ (0.20 g, 8.0×10^{-4} mol) in 10 ml of 80% aqueous ethanol and the mixture was stirred for 30 min. The resulting yellow–orange precipitate was collected, washed with ether, dissolved in acetonitrile and reprecipitated to give the yellow–orange crystalline product (yield 80%).

$[\pi\text{-}C_6H_6RuX_2]_2$ (X = Br, I, SCN)

Solid NaBr, NaI, or NaSCN was added to saturated solutions of the chloro compound in water. The blood-red bromide, violet iodide, and yellow thiocyanate rapidly precipitated, were collected, washed with water, and dried in vacuo at room temperature for 20 h (yield 80, 95, and 75%, respectively). They were too insoluble to be recrystallized.

$\pi\text{-}C_6H_6RuCl_2L$ (L = PPh_3, PPh_2Me, $PPhMe_2$, PEt_3, PBu_3, $P(OPh)_3$, $P(OMe)_3$, $P(OEt)_3$, $AsPh_3$)

$[\pi\text{-}C_6H_6RuCl_2]_2$ (0.20 g) was added to 2–3 ml of neat ligand and the mixture was warmed to 35° for 20 min. Petroleum ether (40 ml, b.p. 40–60°) was added to pre-

Can. J. Chem. Downloaded from www.nrcresearchpress.com by 210.87.254.105 on 09/05/12
For personal use only.

TABLE 1. Analytical data

Compound	Decomposition point (°C)*	Analysis							
		Calculated				Observed			
		C(%)	H(%)	X(%)	Molecular weight	C(%)	H(%)	X(%)	Molecular† weight
$[Ru(\pi\text{-}C_6H_6)Cl_2]_2$	249	28.82	2.42	28.35 (Cl)	500	28.9	2.75	28.2 (Cl)	232‡
$Ru(\pi\text{-}C_6H_6)(C_6H_8)(Hg_3Cl_6)_{1/2}$	134	21.62	2.12	15.95 (Cl)	—	21.9	2.20	15.7 (Cl)	—
$[Ru(\pi\text{-}C_6H_6)Cl(CH_3CN)_2][HgCl_3]$	118	19.90	2.01	—	604	20.2	2.45	—	§
$[Ru(\pi\text{-}C_6H_6)Br_2]_2$‖	238	21.26	1.78	47.14 (Br)	678	22.6	2.35	46.3 (Br)¶	§
$[Ru(\pi\text{-}C_6H_6)I_2]_2$‖	233	16.64	1.40	58.62 (I)	866	16.6	1.89	56.9 (I)	§
$[Ru(\pi\text{-}C_6H_6)(SCN)_2]_2$	163	32.53	2.05	—	591	32.4	2.03	—	§
$Ru(\pi\text{-}C_6H_6)Cl_2PPh_3$	186	56.26	4.13	—	512	56.1	4.10	—	591
$Ru(\pi\text{-}C_6H_6)Cl_2PPh_2Me$	191	50.67	4.25	—	450	50.7	4.35	—	470
$Ru(\pi\text{-}C_6H_6)Cl_2PPhMe_2$	181	43.41	4.41	—	388	43.4	4.53	—	422
$Ru(\pi\text{-}C_6H_6)Cl_2PBu_3$	212	47.79	7.35	—	453	47.7	7.39	—	470
$Ru(\pi\text{-}C_6H_6)Cl_2PEt_3$	185	39.14	5.75	—	368	39.1	5.85	—	403
$Ru(\pi\text{-}C_6H_6)Cl_2P(OPh)_3$	149	51.44	3.78	—	560	51.4	4.13	—	573
$Ru(\pi\text{-}C_6H_6)Cl_2P(OEt)_3$	138	34.62	5.09	—	416	35.0	5.29	—	434
$Ru(\pi\text{-}C_6H_6)Cl_2P(OMe)_3$	129	28.89	4.04	—	374	29.1	4.23	—	378
$Ru(\pi\text{-}C_6H_6)Cl_2AsPh_3$	224	51.81	3.80	—	556	51.6	3.73	—	568
$Ru(\pi\text{-}C_6H_6)I_2PPh_3$	196	41.46	3.04	—	695	41.0	3.18	—	738
$Ru(\pi\text{-}C_6H_6)Br_2PPh_3$	202	47.94	3.52	—	601	48.2	3.73	—	618
$Ru(\pi\text{-}C_6H_6)(SCN)_2PPh_3$	176	56.00	3.80	—	558	56.7	3.75	—	548
$Ru(\pi\text{-}C_6H_6)Cl_2(Ph_2PCH_2PPh_2)$	191	58.68	4.45	—	635	58.1	4.87	—	652
$[Ru(\pi\text{-}C_6H_6)Cl_2]_2Ph_2P(CH_2)_4PPh_2$	180	51.85	4.35	—	—	52.1	4.59	—	—

*All compounds decompose without melting. Error ~ ±3 °C.
†In $CHCl_3$ unless otherwise stated.
‡In CH_3CN.
§Ionization in CH_3CN.
‖Unrecrystallized samples.
¶Analysis, Br:Cl ratio 1:0.

TABLE 2. Conductivity data (concentrations $\approx 10^{-3}$ *M*) and ruthenium–halogen stretching frequencies (cm^{-1})

Complex	Molar conductance, Λ (Ω^{-1} cm^2 mol^{-1})			ν_{RuX}
	H_2O	CH_3CN	DMSO	
$[\pi\text{-}C_6H_6RuCl_2]_2$	274	16	1.3	294, 256, 248 (sh)
$[\pi\text{-}C_6H_6RuBr_2]_2$	305	55	2.9	203, 182
$[\pi\text{-}C_6H_6RuI_2]_2$	*	100	3.1	170
$[\pi\text{-}C_6H_6Ru(SCN)_2]_2$	*	76	43	
$[\pi\text{-}C_6H_6RuCl_2]_2 + HgCl_2$ (molar ratio 1:1)	277	122	—	
$[\pi\text{-}C_6H_6RuCl(CH_3CN)_2][HgCl_3]$†	*	133	—	274
$\pi\text{-}C_6H_6RuCl_2PPh_3$	—	—	—	290, 277
$\pi\text{-}C_6H_6RuCl_2P(OEt)_3$	—	—	—	290, 275
$\pi\text{-}C_6H_6RuCl_2PEt_3$	*	15	—	284, 268
$\pi\text{-}C_6H_6RuCl_2PEt_3 + HgCl_2$ (2:1)	—	73	—	
$\pi\text{-}C_6H_6RuCl_2PEt_3 + HgCl_2$ (1:1)	—	116	—	
$\pi\text{-}C_6H_6RuCl_2PEt_3 + HgBr_2$ (2:1)	—	74	—	
$\pi\text{-}C_6H_6RuCl_2PEt_3 + HgBr_2$ (1:1)	—	117	—	
$HgCl_2$	—	3	—	
$HgBr_2$	—	4	—	

*Solubility too low for measurement.
†The spectrum also contains a band at 286 cm^{-1} which is assigned to the $HgCl_3^-$ anion (6).

cipitate the products, which were collected, recrystallized from CH_2Cl_2–hexane, and dried in vacuo at room temperature to give 70–85% yields of orange–red products.

In the cases of the solid ligands, the reaction was carried out with a three-fold excess of the ligand in benzene for up to 4 h. Similar reactions with nitrogen donors resulted only in decomposition.

$\pi\text{-}C_6H_6RuX_2PPh_3$ (X = Br, I, SCN)

A mixture of $[\pi\text{-}C_6H_6RuX_2]_2$ (4.0×10^{-4} mol) and 0.21 g PPh_3 (8.0×10^{-4} mol) in 15 ml acetonitrile was stirred at room temperature for 1 h. The solution was filtered, 30 ml of ether were added, and the mixture was cooled to give crystals of the products (yield 80–90%).

$\pi\text{-}C_6H_6RuCl_2(Ph_2PCH_2PPh_2)$

A mixture of $[\pi\text{-}C_6H_6RuCl_2]_2$ (8×10^{-4} mol) and $Ph_2PCH_2PPh_2$ (8×10^{-4} mol) in 30 ml of acetonitrile was stirred at 45° for 1 h. As the reaction proceeded, some product precipitated, and 30 ml of ether were finally added to effect further precipitation. The orange product was collected, recrystallized from acetonitrile–ether, and dried in vacuo at room temperature (yield 76%).

$[\pi\text{-}C_6H_6RuCl_2]_2[Ph_2P(CH_2)_4PPh_2]$

The complex was prepared by the same procedure as the previous derivative (yield 87%). It appears to be completely insoluble in all solvents.

Physical Measurements

Infrared spectra were obtained on Beckman IR-10 and Perkin–Elmer 180 i.r. spectrometers, optical spectra on a Unicam SP820 spectrophotometer, mass spectra on a Jeolco JMS-01SC high resolution mass spectrometer, and n.m.r. spectra on a Bruker HX60 spectrometer with internal TMS lock. Melting points were determined using a Gallenkamp melting point apparatus and are corrected. Molecular weights were determined in chloroform or acetonitrile using a Hewlett–Packard 302B vapor pressure osmometer operating at 37 °C. Conductivity measurements of solutions were carried out using a Philips PR9501 conductivity bridge. Polarograms were obtained using a dropping electrode at negative potentials, a graphite electrode at positive potentials and a saturated calomel electrode as reference with $LiNO_3$ as base electrolyte.

Results and Discussion

Substitution Reactions

As reported by Winkhaus and Singer (2), reaction between ruthenium trichloride and 1,3-cyclohexadiene yields primarily a complex of stoichiometry $\pi\text{-}C_6H_6RuCl_2$. The red material obtained from 90% aqueous ethanol is slightly soluble in the strongly coordinating solvents water, DMSO, and acetonitrile, and undergoes metathetical reactions with bromide, iodide, and thiocyanate salts to give the corresponding bromo, iodo, and thiocyanato compounds. Similar reactions with neutral ligands L can give the adducts $\pi\text{-}C_6H_6RuX_2L$, although forcing conditions cause displacement of the benzene from the metal.

The compounds $\pi\text{-}C_6H_6RuX_2L$ are clearly monomeric in chloroform, in contrast to the conclusions of Winkhaus and Singer (2). The monomeric structures are also suggested by the presence of molecular ion clusters in the mass spectra of $\pi\text{-}C_6H_6RuCl_2PEt_3$ and $\pi\text{-}C_6H_6RuCl_2P(OEt)_3$, and by the far i.r. spectra (Table 2),

Can. J. Chem. Downloaded from www.nrcresearchpress.com by 210.87.254.105 on 09/05/12
For personal use only.

Can. J. Chem. Downloaded from www.nrcresearchpress.com by 210.87.254.105 on 09/05/12
For personal use only.

which contain two bands assignable to symmetric and asymmetric terminal ruthenium–chlorine stretching modes. On this basis, the band at 294 cm^{-1} in the spectrum of $[\pi\text{-}C_6H_6RuCl_2]_2$ may also be assigned to a terminal ruthenium–chlorine stretching mode, while the bands at 256 and 248 cm^{-1} are likely bridging chlorine modes, suggesting a dimeric structure. Similar frequencies have been reported elsewhere for terminal (7) and bridging (8) ruthenium–chlorine stretching modes.

The thiocyanate complex exhibits two CN stretching frequencies in the solid state at 2150 and 2101 cm^{-1}, the former in the region assigned to bridging thiocyanate groups (9). The infrared spectrum also shows C—S stretching modes at 822 and 714 cm^{-1} and SCN bending modes at 457 and 430 cm^{-1}, which may be attributed to the presence of both N-bonded and S-bonded thiocyanate groups, respectively (9).

Thus the two series of complexes in the solid state are probably to be formulated as octahedral complexes of ruthenium(II) (**1** and **2**).

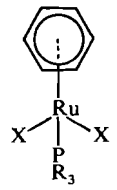

1

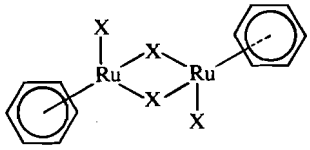

2

The complex cation $[\pi\text{-}C_6H_6RuCl(CH_3CN)_2]^+$ is presumably also octahedral. The C–N stretching modes are observed at approximately 2300 cm^{-1}, as compared to 2250–2315 cm^{-1} for complexes of the type $RuCl_2(PPh_3)_2(RCN)_2$ (10).

The infrared spectrum of $[\pi\text{-}C_6H_6RuCl_2]_2$ in the region 300–4000 cm^{-1} corresponds very closely to that reported by Winkhaus and Singer (2) for the polymeric form of the compounds. Interestingly, the two ν_{CH} at 3083 and 3042 cm^{-1} and the two $\nu_{C=C}$ at 1438 and 839 cm^{-1} are rather intense bands, similar in intensities to the corresponding bands in the spectrum of benzene (11), but in contrast to the spectra of $\pi\text{-}C_6H_6M(CO)_3$ (M = Cr, Mo, W), where the corresponding bands are relatively weak (12–14).

Although dimeric in the solid state, $[\pi\text{-}C_6H_6RuCl_2]_2$ is monomeric in acetonitrile, and presumably also in DMSO and water. Although the solubilities of this compound, as well as of the bromide, iodide, and thiocyanate are very low in these solvents, the six equivalent protons of the coordinated benzene ring give a sufficiently intense line in the n.m.r. spectrum that reactions in solution can be monitored by n.m.r. Comparison of conductivity measurements (Table 2) and n.m.r. spectra (Tables 3 and 4) are very useful in determining the species present in solution.

In accord with the molecular weight measurement (Table 1), conductivity measurements indicate that $\pi\text{-}C_6H_6RuCl_2$ is a non-electrolyte in acetonitrile and DMSO (15) (Table 2). Presumably the sixth position in the octahedron is occupied by a solvent molecule; the DMSO complex has been reported (16). Addition, however, of one molar equivalent of the good Lewis acid $HgCl_2$, itself a non-electrolyte, causes an increase in conductivity to that expected for a 1:1 electrolyte (15). From the solution, the solvated complex $[\pi\text{-}C_6H_6RuCl(CH_3CN)_2][HgCl_3]$ can be isolated.

In accord with the conductivity data, the n.m.r. spectrum of $\pi\text{-}C_6H_6RuCl_2$ in CD_3CN shows the presence of only one benzene resonance. This is assigned to the complex $\pi\text{-}C_6H_6RuCl_2(CD_3CN)$. On adding $HgCl_2$, a second resonance also appears, which may be assigned to the cation, $[\pi\text{-}C_6H_6RuCl(CD_3CN)_2]^+$. There is a downfield shift of 0.31 p.p.m. on going from the neutral complex to the cationic species.

A similar situation is observed in DMSO-d_6, where the resonance at τ4.07 undoubtedly corresponds to the neutral complex, $\pi\text{-}C_6H_6RuCl_2$(DMSO-d_6). In this case the addition of $HgCl_2$ yielded two complexes with lower benzene chemical shifts, presumably the ions $[\pi\text{-}C_6H_6RuCl(DMSO\text{-}d_6)_2]^+$ and $[\pi\text{-}C_6H_6Ru(DMSO\text{-}d_6)_3]^{2+}$.

In water, the conductivity data suggest complete ionization to give $[\pi\text{-}C_6H_6Ru(H_2O)_3]^{2+}$ at mM concentrations. The addition of $HgCl_2$ did not result in increased conductivity. At the higher concentrations ($\sim 10^{-2}$ M) necessary for n.m.r. studies, however, there are two species present. Addition of $HgCl_2$ results in disappearance of the high field line, while addition of NaCl results in disappearance of the low-field line. On the basis of these data, the complexes present are probably $[\pi\text{-}C_6H_6RuCl(D_2O)_2]^+$

TABLE 3. Nuclear magnetic resonance data

Complex	τ (C_6H_6) (relative intensity)		
	CD_3CN	DMSO-d_6	D_2O
$[\pi\text{-}C_6H_6RuCl_2]_2$	4.30	4.07	4.07 (7.1), 3.97 (2.9)
$[\pi\text{-}C_6H_6RuCl_2]_2 + HgCl_2$	4.30, 3.99	4.07, 3.88, 3.53	3.97
$[\pi\text{-}C_6H_6RuCl_2]_2 + NaCl$	—	—	4.07
$[\pi\text{-}C_6H_6RuCl(CH_3CN)_2][HgCl_3]$	3.99	4.07 (3.2), 3.88 (1.3), 3.53 (5.5)	—
$[\pi\text{-}C_6H_6RuBr_2]_2$	4.38 (7.9), 4.28 (2.1)	4.09	4.05 (5.4), 3.97 (4.6)
$[\pi\text{-}C_6H_6RuI_2]_2$	4.30 (8.2), 4.20 (1.8)	4.13	—
$[\pi\text{-}C_6H_6Ru(SCN)_2]_2$	4.13 (1.3), 4.22 (1.0), 4.27 (2.3), 4.30 (2.9), 4.33 (2.5)	3.82 (3.0), 3.92 (3.2), 4.17 (1.3), 4.23 (1.5), 4.28 (1.0)	—

TABLE 4. N.m.r. data for complexes of the type $Ru(\pi\text{-}C_6H_6)Cl_2L$* in $CDCl_3$

Complex	Benzene chemical shift (τ)	J_{H-P} (Hz)	Other resonances (τ), ^{31}P coupling constants
$Ru(\pi\text{-}C_6H_6)Cl_2PPh_3$	4.62 (d)	0.5	C_6H_5 2.42 (m)
$Ru(\pi\text{-}C_6H_6)Cl_2PPh_2Me$	4.60 (d)	0.9	C_6H_5 2.42 (m), CH_3 8.07 (d, $J = 12.1$ Hz)
$Ru(\pi\text{-}C_6H_6)Cl_2PPhMe_2$	4.63 (d)	1.0	C_6H_5 2.33 (m), CH_3 8.32 (d, $J = 11.8$ Hz)
$Ru(\pi\text{-}C_6H_6)Cl_2PEt_3$	4.40 (d)	0.6	CH_2 7.97 (o, $J = 9.7$ Hz), CH_3 8.87 (q, $J = 7.9$ Hz)
$Ru(\pi\text{-}C_6H_6)Cl_2PBu_3$	4.40 (d)	0.8	Butyl 8.08 (m), 8.58 (m), 9.07 (m)
$Ru(\pi\text{-}C_6H_6)Cl_2P(OPh)_3$	4.47 (d)	0.3	C_6H_5 2.62 (d)
$Ru(\pi\text{-}C_6H_6)Cl_2P(OEt)_3$	4.28 (d)	0.3	CH_2 5.82 (q), CH_3 8.68 (t)
$Ru(\pi\text{-}C_6H_6)Cl_2P(OMe)_3$	4.25 (s)	—	CH_3 6.17 (d, $J = 11.1$ Hz)
$Ru(\pi\text{-}C_6H_6)Cl_2AsPh_3$	4.50 (s)	—	C_6H_5 2.47 (m)
$Ru(\pi\text{-}C_6H_6)I_2PPh_3$	4.47 (d)	0.5	C_6H_5 2.57 (m)
$Ru(\pi\text{-}C_6H_6)Br_2PPh_3$	4.55 (d)	0.6	C_6H_5 2.58 (m)
$Ru(\pi\text{-}C_6H_6)(SCN)_2PPh_3$	4.36 (d), 4.46 (d), 4.51 (d)	0.6	C_6H_5 2.53 (m)
$Ru(\pi\text{-}C_6H_6)Cl_2Ph_2PCH_2PPh_2$	4.64 (d)	0.8	C_6H_5 2.90 (m), 2.68 (m), 2.10 (m), CH_2 6.58 (dd, $J = 9.3, 1.3$)
$Ru(\pi\text{-}C_6H_6)Cl_2Ph_2P(CH_2)_4PPh_2$†	4.40 (d)	0.8	C_6H_5 2.43 (m), CH_2 ~8.1 (m), ~8.8 (m)

*s = singlet, d = doublet, t = triplet, q = quintet, o = octet, m = multiplet.
†In CH_3CN with $HgCl_2$ added.

(τ 4.07) and $[\pi\text{-}C_6H_6Ru(D_2O)_3]^{2+}$ (τ 3.97), although a combination of one of these cations and the neutral complex, $\pi\text{-}C_6H_6RuCl_2(D_2O)$, cannot be excluded.

The conductivity and n.m.r. data show that bromo, iodo, and thiocyanato compounds ionize to a greater extent than the chloro, the apparent relative affinity for the benzene–ruthenium(II) species being $I^- < SCN^- < Br^- < Cl^-$ in acetonitrile. The species present in CD_3CN are probably $\pi\text{-}C_6H_6RuX_2(CD_3CN)$ and $[\pi\text{-}C_6H_6RuX(CD_3CN)_2]^+$, while the species in D_2O are probably $[\pi\text{-}C_6H_6RuX(D_2O)_2]^+$ and $[\pi\text{-}C_6H_6Ru(D_2O)_3]^{2+}$.

The n.m.r. spectra of $[\pi\text{-}C_6H_6Ru(SCN)_2]_2$ in both acetonitrile and dimethylsulfoxide contain five lines; two attributable to ionized species and three attributable to neutral species. The solution infrared spectrum in CH_3CN shows a broad CN stretching mode at about 2120 cm^{-1}. As shown above, both N-bonded and S-bonded isomers exist for this system in the solid state and, if exchange is slow on the n.m.r. time scale, three isomers would be expected for the neutral species and two for the ionized in solution. The observation of five lines in the n.m.r. spectrum suggests strongly the presence of linkage isomers in solution also.

Addition of potassium cyanide and sodium hydroxide to aqueous (D_2O) solutions of $\pi\text{-}C_6H_6RuCl_2$ results in the formation of new species with resonances at τ 4.23, and τ 4.57

Can. J. Chem. Downloaded from www.nrcresearchpress.com by 210.87.254.105 on 09/05/12
For personal use only.

Can. J. Chem. Downloaded from www.nrcresearchpress.com by 210:87.254.105 on 09/05/12
For personal use only.

and 4.42, respectively. The compounds are unstable, however, as decomposition is suggested by the appearance of the resonance of free benzene.

The n.m.r. spectra of the phosphine and arsine adducts are listed in Table 4; in most cases, coupling of the benzene protons to ^{31}P was observed. The spectrum of π-$C_6H_6Ru(SCN)_2PPh_3$ contains three resonances for the benzene ring which can be attributed to the presence of S-bonded and N-bonded isomers. The spectrum of π-$C_6H_6RuCl_2PBu_3$ was independent of temperature down to -70 °C, there being no indication of the broadening which might be expected if the benzene ring were not bonded symmetrically.

Although a non-electrolyte in acetonitrile, π-$C_6H_6RuCl_2PEt_3$ does react with mercuric salts to give, presumably, the cation, $[\pi$-$C_6H_6RuCl(CH_3CN)PEt_3]^+$. The observed increase in conductivity is accompanied by a decrease in the intensity of the benzene resonance of the neutral molecule at τ 4.43 and the appearance of a new resonance at τ 4.10. Reactions with nucleophiles also yield new species. Tetraphenylarsonium cyanide reacts in CD_3CN to give a new resonance at τ 4.28, and in $CDCl_3$ to give new resonances at τ 4.30, 4.15 and 3.87. Sodium iodide and hydroxide in CD_3CN give species with resonances at τ 4.38 and 4.10, and τ 4.10, respectively. Although the identities of these new species are not known, coupling to ^{31}P is observed in all cases ($J = 0.8$ Hz), and thus substitution of the neutral ligands is not occurring. In no cases were cationic phosphine complexes isolated.

Structurally, the bis(diphenylphosphino)methane and bis(diphenylphosphino)butane adducts are of interest. The latter is highly insoluble and is formulated as $[\pi$-$C_6H_6RuCl_2]_2Ph_2P(CH_2)_4PPh_2$ with the diphos acting as a bidentate ligand. The solubility in acetonitrile can be increased by the addition of $HgCl_2$ to induce ionization of the complex, the n.m.r. of the solution indicating a ratio of 10:6 for phenyl protons relative to the π-arene protons. The phenyl protons appear as a single multiplet indicating equivalence of the phenyl groups.

In the bis(diphenylphosphino)methane complex, the phosphine acts as a monodentate ligand. The methylene resonance of the free ligand appears at τ 7.23, $J_{PH} = 1.5$ Hz (17), while the phenyl protons appear as a multiplet at τ 2.73. In the spectrum of the complex, the methylene protons appear at τ 6.58 as a double doublet, while the phenyl protons appear as three well-separated multiplets, indicating non-equivalence of the phenyl groups. The observed coupling between phosphorus and the methylene protons is 9.3 Hz (coordinated P) and 1.3 Hz (non-coordinated P). These assignments were confirmed by ^{31}P decoupling. The π-C_6H_6 doublet also collapses into a singlet on decoupling of the coordinated phosphorus while decoupling of the non-coordinated phosphorus has no effect on the π-C_6H_6 doublet.

Although π-$C_6H_6RuCl_2$ does not react with molecular nitrogen in acetonitrile, on bubbling carbon monoxide through a solution, the benzene resonance at τ 4.30 decreases in intensity and a new resonance at τ 3.98 appears. The new compound, presumably π-$C_6H_6RuCl_2CO$, is very unstable, however, and the latter line decays within minutes at room temperature to give a free benzene resonance. The i.r. spectrum of the final solutions shows a carbonyl mode at 1991 cm^{-1}, attributable to a ruthenium carbonyl complex.

The isolation of the complex π-$C_6H_6Ru(C_6H_8)(Hg_3Cl_6)_{1/2}$, obtained by adding $HgCl_2$ to the mother liquor from the preparation of $[\pi$-$C_6H_6RuCl_2]_2$, was quite unexpected. The analytical results from three determinations are consistent, and the i.r. spectrum in the region 1400–1500 cm^{-1} clearly shows the presence of both coordinated benzene and 1,3-cyclohexadiene. The mass spectrum shows lines for the ions $C_6H_6RuC_6H_8^+$ and $C_6H_6Ru^+$, as well as for $C_6H_8^+$, $C_6H_6^+$, and $HgCl_2^+$.

The complex is slightly soluble in DMSO-d_6, the solubility increasing markedly on the addition of $HgCl_2$. The fact that the n.m.r. spectrum does not change on interaction with $HgCl_2$ suggests that the species in solution is not identical with that in the solid state. However, the spectrum (Fig. 1) is nevertheless very helpful in deducing the structure. There is a singlet of relative intensity six at τ 3.53, consistent with the presence of a benzene ring coordinated to ruthenium(II), and three groups of lines with relative intensities 2:2:4, which may be attributed to the coordinated diene (3).

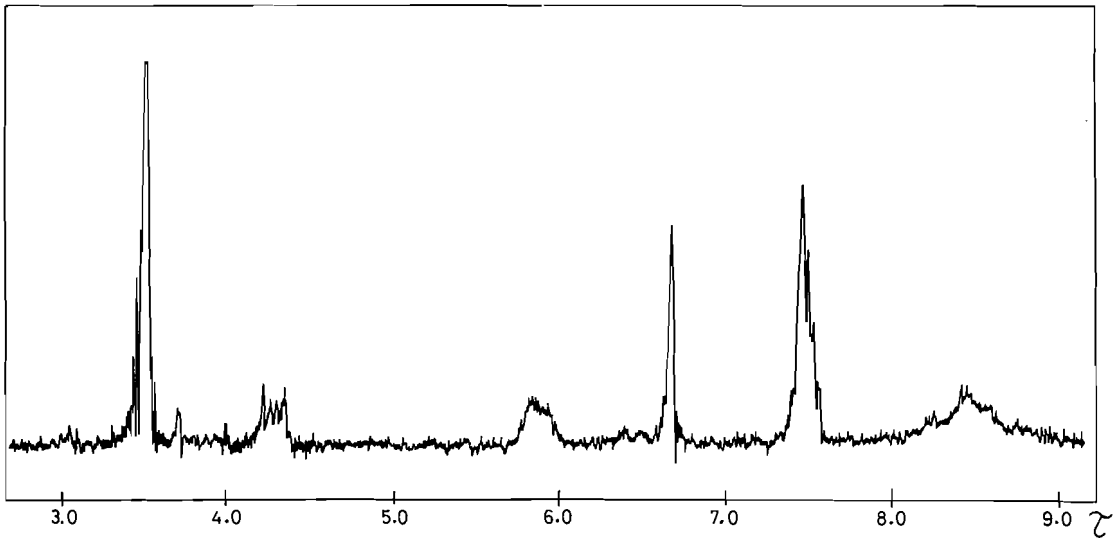

FIG. 1. N.m.r. spectrum of the π-benzenecyclohexadieneruthenium complex in DMSO-d_6.

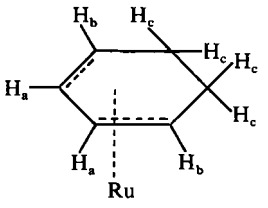

3

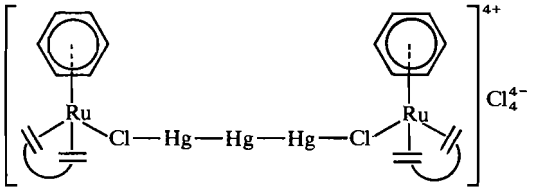

4

The 1:1:1:1 quartet at τ 4.32 can be assigned to H_a, the coupling constants to the two H_b, calculated on a first-order basis, being approximately 2.2 and 5.0 Hz. The unresolved multiplets centered at approximately τ 5.88 and 8.45 are assigned to H_b and H_c, respectively. The resonances at τ 6.68 and 7.47 are attributed to water and residual solvent protons, respectively. Decoupling H_b causes collapse of the resonances of H_a and H_c to singlets, while decoupling H_a causes the H_b resonance to become a broad singlet. The spectrum is very similar to that of 1,3-cyclohexadieneiron tricarbonyl (18).

The structure of the mercury-containing moiety is unknown, but may involve a linear Hg_3^{2+} group (19–21), in which the mercury would have the formal oxidation state +2/3. By analogy with other compounds containing this unusual cation (19–21), a reasonable structure for the complex would be **4**.

A similar complex can be prepared as a tetraphenylborate salt by adding $NaBPh_4$ to the mother liquor, although it is too unstable to recrystallize. The n.m.r. spectrum shows quite clearly the presence of coordinated benzene (τ 3.78) and 1,3-cyclohexadiene (τ 4.88, 7.1, 9.2), while integrations indicate the presence of one BPh_4^- ion per benzene. The far i.r. spectrum shows only one ν_{RuCl} at 249 cm^{-1} in the bridging chloride region, and thus the structure of the complex perhaps should be formulated as $[(C_6H_6)(C_6H_8)Ru^{II}—Cl—Ru^{II}(C_6H_8)(C_6H_6)]^{3+}$. On standing in solution for 30 min, the complex decomposed completely and the n.m.r. spectrum showed only free benzene and 1,3-cyclohexadiene.

Reactions of the Coordinated Benzene

It has long been known (1) that aromatic molecules bonded to zerovalent metal atoms are deactivated toward electrophilic attack, but activated toward nucleophilic attack. Kursanov *et al.* (22, 23) have shown, for instance, that acid-catalyzed H–D exchange of π-C_6H_6Cr-

Can. J. Chem. Downloaded from www.nrcresearchpress.com by 210.87.254.105 on 09/05/12
For personal use only.

Can. J. Chem. Downloaded from www.nrcresearchpress.com by 210.87.254.105 on 09/05/12
For personal use only.

$(CO)_3$ occurs seven orders of magnitude more slowly than does exchange of benzene under the same conditions (22). In contrast, the same complex undergoes ethoxide-catalyzed H–D exchange in ethanol-d_1, conditions under which free benzene does not exchange (23).

On going to the benzene–ruthenium(II) system, it would be expected that the inductive effects of the divalent metal ion would emphasize these effects even further. Not surprisingly, therefore, π-$C_6H_6RuCl_2PMe_2Ph$ is inert to acetic anhydride at 60° in purified nitrobenzene, conditions under which free benzene is readily acetylated (24). Moreover, both π-$C_6H_6RuCl_2PEt_3$ and $[\pi$-$C_6H_6RuCl_2]_2$ are completely unaffected in solution in deuterated trifluoroacetic acid and concentrated sulfuric acid-d_2, respectively. The coordinated benzene resonances appear at τ 4.27 and 4.20, respectively, and there is no indication of either H–D exchange or sulfonation after prolonged heating at 80–100°. Free benzene in 51 mol% D_2SO_4 readily undergoes H–D exchange at room temperature, and undergoes sulfonation at higher temperatures (25).

Furthermore, there is no indication of protonation of the metal in concentrated acids as has been reported for some isoelectronic molybdenum(0) benzene complexes (26).

$[\pi$-$C_6H_6RuCl_2]_2$ does undergo H–D exchange under basic conditions. In NaOD–D_2O solution, decomposition is too rapid to give meaningful results. However, in a 4.0% solution of NaOEt in 1:1 ethanol-d_1–DMSO-d_6 ($NaOEt:Ru^{II} = 20:1$), H–D exchange of the coordinated benzene does occur at room temperature. The course of the reaction is readily followed by n.m.r. using toluene as an internal reference for integrations (free aromatics do not exchange under these conditions).

Initially, the coordinated benzene resonance at τ 4.05 broadened and shifted downfield to τ 3.77, where it became narrow again. Presumably substitution by alkoxide ion was occurring. Equilibrium was eventually reached after about 3 h, by which time 57% deuteration had occurred and 21% of the complex had decomposed, as shown by the formation of a free benzene resonance.

Kang and Maitlis (27) have recently observed base-catalyzed H–D exchange of the methyl protons of $[(CH_3)_5C_5Rh]_2(OH)_3Cl$, and suggested a mechanism involving reversible proton abstraction from the methyl groups by base. This type of mechanism is widely accepted for the base-catalyzed H–D exchange of hydrocarbons (28). Thus the activating effect of the ruthenium ion is readily understood. The strongly electron-withdrawing metal ion would increase the acidity of the benzene protons, thus increasing the rate of reaction with base.

Garnett (4) has shown that platinum(II) salts in acidic media catalyze H–D exchange of aromatics. Our results are in accord with his postulate that, although a π-benzene complex is probably an intermediate in the exchange reaction, it is not a π-benzene complex which actually undergoes exchange.

Although nucleophilic attack by strong bases in water or acetonitrile generally led to substitution and/or decomposition, reactions involving nucleophilic attack on the coordinated benzene ring were observed in DMSO-d_6. The products were, however, too unstable to isolate, and the course of the reactions could only be inferred from n.m.r.

On adding KCN to a solution of $[\pi$-C_6H_6-$RuCl_2]_2$ in DMSO-d_6, the color rapidly changed from deep red to pale yellow. In addition, the coordinated benzene resonance disappeared completely and was replaced by the series of resonances shown in Fig. 2, consistent with a cyclohexadienyl complex (**5**).

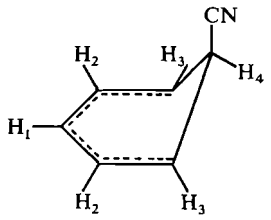

5

The resonance of H_1 appears as an unresolved multiplet at τ 4.00, while H_2 and H_3 appear as 1:2:1 triplets at τ 4.95 and 7.12, respectively, as a result of overlap of two doublets. The resonance of H_4 appears as a triplet at τ 6.17. These assignments were confirmed by decoupling experiments. Decoupling of H_1 resulted in the resonance of H_2 appearing as a 1:1 doublet, while decoupling H_2 caused collapse of the resonance of H_1 to a broad singlet and changed the resonance of H_3 to a doublet.

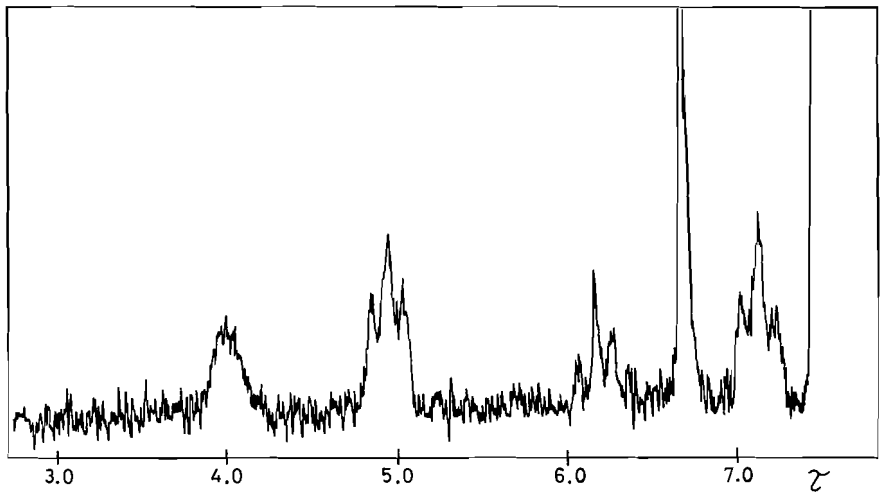

FIG. 2. N.m.r. spectrum of the cyclohexadienylruthenium complex in DMSO-d_6.

Decoupling H_3 changed the resonance of H_1 to a 1:2:1 triplet, that of H_2 to a doublet, and that of H_4 to a singlet. Decoupling H_4 changed the resonance of H_3 to a doublet. Analysis of the spectrum gave $J_{12} = 5.0$, $J_{23} = 5.7$, and $J_{34} = 6.0$ Hz. A very similar spectrum has been reported for the cyanide adduct of $[\pi\text{-}C_6H_6\text{-}Mn(CO)_3]^+$ (29).

A similar, very unstable hydroxycyclohexadienyl complex was also obtained by treating $[\pi\text{-}C_6H_6RuCl_2]_2$ in DMSO-d_6 with sodium hydroxide. The chemical shifts were: H_1, τ 4.55; H_2, τ 5.13; H_3, τ 6.83; H_4, τ 6.22.

Reaction with hydride, as $LiAlH_4$ or $NaBH_4$, in DMSO-d_6 gave yellow solutions whose n.m.r. spectra showed a transient, extremely weak cyclohexadienyl pattern. The main product, however, appeared to be a complex of 1,3-cyclohexadiene (**3**). Protons H_a appeared at τ 5.18 as a 1:1:1:1 quartet, characteristic of the AA′ part of an AA′XX′ system, while H_b and H_c appeared as multiplets at τ 7.95 and 8.52, respectively. Decoupling of H_a caused collapse of the resonance of H_b to a broadened singlet, while decoupling of H_b caused the resonance of H_a to collapse to a sharp singlet. The pattern is similar to those of $[\pi\text{-}C_6H_6Ru(C_6H_8)]^{2+}$ (see above) and $C_6H_8Fe(CO)_3$ (30). Extraction of a reaction mixture with cyclohexane after excess $NaBH_4$ had been added showed (n.m.r.) the presence of free benzene and both 1,3- and 1,4-cyclohexadiene.

There are several precedents in the literature for reactions of the types described here. For instance, the cation $[(\pi\text{-}C_6H_6)Fe^{II}(\pi\text{-}C_5H_5)]^+$ is reduced by hydride ion to the dienyl complex, $\pi\text{-}C_5H_5Fe^{II}(C_6H_7)$ (31), while the cyclohexadienyl complex, $[C_6H_7Fe^{II}(CO)_3]^+$, is reduced to the 1,3-cyclohexadiene complex, $C_6H_8Fe^0(CO)_3$ (30). Also, the cation $[(\pi\text{-}C_6H_6)_2Ru^{II}]^{2+}$ is reduced by $NaBH_4$ to a mixture of two isomers of the empirical formula $C_{12}H_{14}Ru$, benzenecyclohexa-1,3-dieneruthenium(0) and dicyclohexadienylruthenium(II) (31).

Surprisingly, $[\pi\text{-}C_6H_6RuCl_2]_2$ and $\pi\text{-}C_6H_6RuCl_2PEt_3$ appear to be inert to attack by alkyl–lithium and Grignard reagents in ethers, although attack on coordinated arenes in other systems is well-known (32–34). In the case of the dimer, the lack of reaction may be a result of the low solubility of the compound. The phosphine complex is quite soluble in tetrahydrofuran, however, and it is possible that the arene ring is deactivated toward nucleophilic attack because of the presence of the strongly donating phosphine. Substitution of the chlorides by carbanions in this low spin d^6 system must be slow for kinetic reasons, as complexes of the type $\pi\text{-}C_6H_6RuClRPPh_3$ (R = alkyl, aryl) can be prepared by other methods and are quite stable (35).

Miscellaneous

Few redox reactions of $[\pi\text{-}C_6H_6RuCl_2]_2$ have been studied. As described above, reduction with $NaBH_4$ causes destruction of the complex

Can. J. Chem. Downloaded from www.nrcresearchpress.com by 210.87.254.105 on 09/05/12
For personal use only.

to unidentifiable products. Reduction by the complex of hydrogen peroxide in water appears to be catalytic, but the resonance of free benzene appears in the n.m.r. spectrum of a carbon disulfide extract of the reaction mixture, and thus the peroxide appears to oxidize the metal rather than the arene ring.

Polarographic studies showed that $[\pi\text{-}C_6H_6RuCl_2]_2$ undergoes reduction at $E_{1/2} = -0.80$ V *vs.* s.c.e. in aqueous solution, but no oxidation wave was observed in the range +2.0 to −2.0 V. In DMSO, however, using a carbon electrode, an oxidation wave at $E_{1/2} = +0.65$ V and a reduction wave at $E_{1/2} = -1.03$ V were observed.

The π-arene–ruthenium complexes also form charge-transfer complexes with tetracyanoethylene (TCNE), apparently of the same type as does benzene (36). In acetonitrile, charge-transfer bands appear at 355, 401, and 409 mμ for benzene, $\pi\text{-}C_6H_6RuCl_2PEt_3$, and $[\pi\text{-}C_6H_6RuCl_2]_2$, respectively, on interacting with TCNE. Using standard procedures (37), equilibrium constants of 1.1 ± 0.2, 4.4 ± 0.5, and 10 ± 2 l mol^{-1} were calculated for the interactions of TCNE with benzene, $\pi\text{-}C_6H_6RuCl_2PEt_3$, and $[\pi\text{-}C_6H_6RuCl_2]_2$, respectively.

Assuming that TCNE is behaving as Lewis acid, coordination of benzene to ruthenium(II) should decrease its ability to take part in a charge-transfer interaction. We have no explanation for the observed trend, although the errors in the cases of the two complexes may be rather large because of partial overlap of the charge-transfer bands with bands in the spectra of the complexes.

We thank the National Research Council of Canada for financial assistance and the International Nickel Company of Canada for a scholarship to R.A.Z. We also thank Mr. Clint Smith for assistance with the electrochemistry.

1. H. Zeiss, P. J. Wheatley, and H. J. S. Winkley. Benzenoid–metal complexes. The Ronald Press Co. New York. 1966.
2. G. Winkhaus and H. Singer. J. Organomet. Chem. 7, 487 (1967).
3. E. A. H. Griffith and E. L. Amma. J. Am. Chem. Soc. **93**, 3167 (1971), and references therein.
4. J. L. Garnett. Catal. Rev. **5**, 229 (1971).
5. R. A. Zelonka and M. C. Baird. J. Organomet. Chem. **35**, C43 (1972).
6. T. Blackmore, M. I. Bruce, and F. G. A. Stone. J. Chem. Soc. A, 2376 (1971).
7. J. D. Gilbert, M. C. Baird, and G. Wilkinson. J. Chem. Soc. A, 2198 (1968).
8. J. Powell and B. L. Shaw. J. Chem. Soc. A, 159 (1968).
9. K. Nakamoto. Infrared spectra of inorganic and coordination compounds. 2nd ed. Wiley–Interscience, New York. 1970. p. 187.
10. J. D. Gilbert and G. Wilkinson. J. Chem. Soc. A, 1749 (1969).
11. R. D. Nair and D. F. Hornig. J. Chem. Phys. **17**, 1236 (1949).
12. H. P. Fritz and J. Manchot. Spectrochim. Acta, **18**, 171 (1962).
13. H. P. Fritz and J. Manchot. Z. Naturforsch. **17***b*, 710 (1962).
14. D. M. Adams and A. Squire. J. Chem. Soc. A, 814 (1970).
15. W. J. Geary. Coord. Chem. Rev. 7, 81 (1971).
16. I. Ogata, R. Iwata, and Y. Ikeda. Tetrahedron Lett. 3011 (1970).
17. A. J. Carty and R. K. Harris. Chem. Commun. 234 (1967).
18. R. Burton, L. Pratt, and G. Wilkinson. J. Chem. Soc. 594 (1961).
19. G. Torsi, K. W. Fung, G. M. Begun, and G. Manatov. Inorg. Chem. **10**, 2285 (1971).
20. C. G. Davies, P. A. W. Dean, R. J. Gillespie, and P. K. Ummat. Chem. Comm. 782 (1971).
21. R. D. Ellison, H. A. Levy, and K. W. Fung. Inorg. Chem. **11**, 833 (1972).
22. D. N. Kursanov, V. N. Setkina, N. K. Baranetskaya, V. I. Zdanovich, and K. N. Anisimov. Dokl. Akad. Nauk. **190**, 127 (1970).
23. V. N. Setkina, N. K. Baranetskaya, K. N. Arnisimov, and D. N. Kursanov. Bull. Acad. Sci. USSR, 1772 (1964).
24. R. Adams, J. R. Johnson, and C. F. Wilcox. Laboratory experiments in organic chemistry. Macmillan Company, New York. 1965.
25. C. K. Ingold, C. G. Raisin, and B. Topley. J. Chem. Soc. 915 (1936).
26. M. L. H. Green, L. C. Mitchard, and W. E. Silverthorn. J. Chem. Soc. A, 2929 (1971).
27. J. W. Kang and P. M. Maitlis. J. Organomet. Chem. **30**, 127 (1971).
28. A. Steitweiser and J. H. Hammons. Prog. Phys. Org. Chem. **3**, 41 (1965).
29. P. J. C. Walker and R. J. Mawby. Inorg. Chem. **10**, 404 (1971).
30. E. O. Fischer and R. D. Fischer. Angew. Chem. **72**, 919 (1960).
31. D. Jones, L. Pratt, and G. Wilkinson. J. Chem. Soc. 4458 (1962).
32. I. U. Khand, P. L. Pauson, and W. E. Watts. J. Chem. Soc. C, 2024 (1969).
33. J. F. Helling and D. M. Braitsch. J. Am. Chem. Soc. **92**, 7207 (1970).
34. C. White and P. M. Maitlis. J. Chem. Soc. A, 3322 (1971).
35. R. A. Zelonka and M. C. Baird. Unpublished results.
36. W. H. Baddley. Inorg. Chim. Acta Rev. **2**, 7 (1968).
37. C. K. Ke and N. C. Li. J. Inorg. Nucl. Chem. **28**, 2255 (1966).

Can. J. Chem. Downloaded from www.nrcresearchpress.com by 210.87.254.105 on 09/05/12
For personal use only.

Can. J. Chem. Downloaded from www.nrcresearchpress.com by 210.87.254.5 on 09/05/12
For personal use only.

Solvent Structure Effects and Diffusion Control in the Reaction Between Solvated Electrons and Solvated Protons in Alcohols and Water[1]

K. N. JHA, G. L. BOLTON, AND G. R. FREEMAN
Chemistry Department, University of Alberta, Edmonton 7, Alberta

Received April 4, 1972

The rates of reactions 1 and 2 are diffusion controlled in alcohols

[1] $e^-_{solv} + H^+_{solv} \rightarrow$ neutralization

[2] $RO^-_{solv} + H^+_{solv} \rightarrow ROH$

In water reaction 1 is slower and reaction 2 (where RO^- is HO^-) is faster than one would estimate from the Debye equation for diffusion controlled reactions. The solvent dependence of the relative values of k_1 and k_2 is attributed to the solvent dependence of the structures of H^+_{solv}, RO^-_{solv}, and e^-_{solv}; H^+ and RO^- are strong solvent structure makers in alcohols and in water, whereas e^- is a weak solvent structure maker in alcohols and a strong structure breaker in water. Effects of the solvent structure making and breaking properties of ions on their reaction rates have been proposed by Gurney and Frank.

Les vitesses des réactions 1 et 2 dans les alcools sont contrôlées par la diffusion

[1] $e^-_{solv} + H^+_{solv} \rightarrow$ neutralization

[2] $RO^-_{solv} + H^+_{solv} \rightarrow ROH$

Dans l'eau reaction 1 est moins rapide et réaction 2 (où RO^- est HO^-) est plus rapide que la vitesse estimée à partir de l'équation de Debye pour les réactions contrôlées par la diffusion. L'effet du solvant sur les valeurs relatives de k_1 et k_2 est attribué à la configuration de solvatation des ions H^+_{solv}, RO^-_{solv}, et e^-_{solv}: H^+ et RO^- augmentent la structure locale du solvant dans le voisinage des ions; e^- pourrait augmenter un peu la structure dans un alcool, mais il la detruit dans l'eau. Gurney et Frank ont proposé un effet des ions sur la structure du solvant qui augmenterait ou diminuerait la vitesse "normale" d'une réaction.

Canadian Journal of Chemistry, **50**, 3073 (1972)

The values of the rate constant of reaction 1

[1] $e^-_{solv} + H^+_{solv} \rightarrow$ neutralization

in water and alcohols were measured by kinetic spectroscopy several years ago (1) and found to be only about half as large as diffusion controlled values would be (2). The result was interpreted as a reluctance of the solvated proton to accept an electron (3). However, the rate constants have recently been measured in alcohols by an electrical conductance technique (4–6) and found to equal the diffusion controlled values (Table 1). This important result warrants checking by kinetic spectroscopy. Knowledge of the correct values of k_1 is important to the development of the theory of radiolysis kinetics because both e^-_{solv} and H^+_{solv} are intermediate products in the radiolysis systems. We have therefore measured the effect of acid concentration on the decay rate of the optical absorption of solvated electrons in ethanol, methanol and water in an attempt to resolve the conflicting information.

Absolute reagent quality U.S.P. ethyl alcohol was used as received from the U.S. Industrial Chemical Co. It is the highest purity ethanol that has been obtained by any method in this laboratory (7). Absolute methanol, analyzed reagent spectrophotometric grade from Baker Chemical Co. was refluxed for 12 h after addition of 2 g of 2,4-dinitrophenylhydrazine and 0.5 g of concentrated sulfuric acid to 1 l of the alcohol. The refluxing system was flushed with ultrahigh purity argon (Matheson) before and during the treatment. The alcohol was then

[1]Supported by the National Research Council of Canada.

TABLE 1. $k(e^-_{solv} + H^+_{solv})$ measured by optical and conductance methods

Solvent	T (K)	$k(10^{10}\ M^{-1}\ s^{-1})$ Optical absorption Reference 1	Optical absorption Present	Electrical conductance	Diffusion controlled (calcd)*
C_2H_5OH	298	2.0±0.4		4.5±0.4[5]	4.1
	293		3.6±0.2†	3.9±0.4[5]	3.6
	290?			5.4±0.2[6]	
CH_3OH	298	3.9±0.9		7.1±0.3[5]	6.9
	293		6.5‡	6.5±0.3[5]	6.3
H_2O	296	2.3±0.2		2.7±0.2[4]	7.5
	293	2.1±0.1	2.2‡	2.6±0.2[4]	7.2

*Calculated from data in refs. 5 and 6.
†Average of results from six series with separate preparations of solvent and solutions.
‡Two series with separate preparations of solvent and solutions gave the same results.

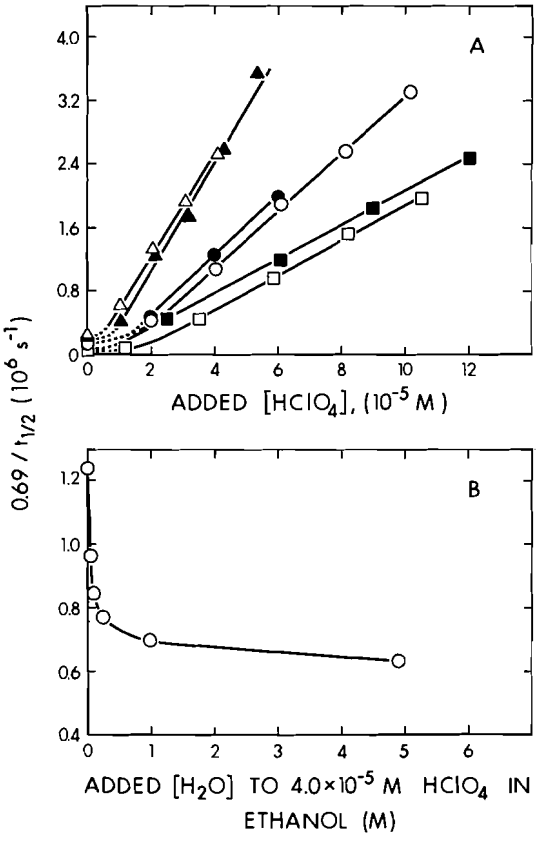

FIG. 1. (*A*) $0.69/t_{1/2}$ at 293 K as a function of $HClO_4$ concentration added to: ○, ● ethanol; △, ▲ methanol; □, ■ water. Open and closed points distinguish results from separate series of experiments. (*B*) $0.69/t_{1/2}$ as a function of water concentration added to a solution of 4.0×10^{-5} *M* $HClO_4$ in ethanol at 293 K.

distilled and the center 50% collected. Water was distilled from a Barnsted still, then from alkaline permanganate, then from a Pyrex still and collected in a quartz reservoir.

Stock solutions of perchloric acid (Baker and Adamson Analytical Reagent, mole ratio $HClO_4/H_2O = 1/2$) were prepared by weighing. The final solutions were de-oxygenated in the Spectrasil optical cells by bubbling for 20 min with the ultrapure argon.

The radiation pulses were 100 ns of 1.7 MeV electrons, giving a dose of 3×10^{16} eV/cm^3. The response time of the optical measuring system was 35 ns.

Typical results are shown in Fig. 1 (*A*). In all cases the plots of $0.69/t_{1/2}$ against added acid concentration were linear, but they extrapolated to intercepts on the "wrong" axis. Some acid was evidently removed from the solution by adsorption on the cell walls. The values of k_1 obtained from the linear slopes are listed in Table 1. The results from the optical and the conductance techniques now agree with each other, within experimental error.

The early values reported for the alcohols (1) are low by a factor of two. The error might have been caused by assuming that a plot such as those in Fig. 1 (*A*) would be linear and have an intercept at $0.69/(t_{1/2}$ pure alcohol). It should also be mentioned that the presence of water in the alcohol reduces the value of the rate constant (Fig. 1 (*B*)), due to a decrease in the diffusion coefficient of the protons (5, 8, 9).

Reaction 1 is diffusion controlled in both

Can. J. Chem. Downloaded from www.nrcresearchpress.com by 210.87.254.5 on 09/05/12
For personal use only.

alcohols, but not in water (Table 1). The reason for this difference is related to the difference in the structures of e^-_{solv} and H^+_{solv} in the different solvents, which are in turn related to the structures of the liquids. There is no reluctance of $H^+(ROH)_n$ to accept an electron from $e^-(ROH)_m$, although there seems to be for $H^+(H_2O)_n$ to accept one from $e^-(H_2O)_m$.

The fact that reaction 2 is diffusion controlled

[2] $$H^+_{solv} + RO^-_{solv}(OH^-_{solv}) \rightarrow ROH_{solv}(H_2O_{solv})$$

in alcohols (5) but is apparently *faster* in water ($k_2 = 11.2 \times 10^{10}\ M^{-1}\ s^{-1}$ (5)) than one would calculate from the bulk diffusion coefficients of H^+_{aq} and OH^-_{aq} ($7.9 \times 10^{10}\ M^{-1}\ s^{-1}$ (5)) is probably also related to the structure of the solvents in the vicinity of the ions. The relative rates of reactions 1 and 2 in water and in alcohols are consistent with the suggestion (10) that e^-_{solv} is a solvent structure breaker in water and a weak structure maker in alcohols; H^+, OH^-, and RO^- are strong structure makers in water and alcohols (ref. 11, pp. 168, 176, 183). A structure-making ion such as H^+_{aq} has difficulty approaching one that breaks structure, such as e^-_{aq}, so there is a sort of repulsion between the two species in solution (ref. 11, chap. 16, 12). This offers at least a partial explanation of why k_1 in water is smaller than would be expected from the Debye equation (2). Conversely, two strong structure makers approach each other more rapidly than "normal" at close distances. This, combined with the structure dependent proton jumping mechanism of migration of both H^+ and OH^- in water, may explain why k_2 in water is greater than would be expected from the Debye equation.

1. L. M. Dorfman and M. S. Matheson. Prog. React. Kinet. **3**, 237 (1965).
2. P. Debye. Trans. Electrochem. Soc. **82**, 265 (1942).
3. M. Anbar. Adv. Chem. Ser. **50**, 55 (1965).
4. G. C. Barker, P. Fowles, D. C. Sammon, and B. Stringer. Trans. Faraday Soc. **66**, 1498 (1970).
5. P. Fowles. Trans. Faraday Soc. **67**, 428 (1971).
6. J. Rabani, M. Grätzel, and S. A. Chandhri. J. Phys. Chem. **75**, 3893 (1971).
7. S. M. S. Akhtar and G. R. Freeman. J. Phys. Chem. **75**, 2756 (1971).
8. B. E. Conway. Electrochemical data. Elsevier Publishing Co., Amsterdam. 1952.
9. H. Strehlow. Z. Phys. Chem. (N.F.) **24**, 240 (1960).
10. K. N. Jha and G. R. Freeman. J. Chem. Phys. **48**, 5480 (1968).
11. R. W. Gurney. Ionic processes in solution. McGraw–Hill Book Co., New York. 1953.
12. H. S. Frank and M. S. Tsao. Ann. Rev. Phys. Chem. **5**, 43 (1954).

A New Synthesis of 6-Hydroxydopamine

Pius A. Wehrli,[1] F. Pigott, and V. Chu

Chemical Research Department, Hoffmann-La Roche Inc., Nutley, N.J. 07110

Received March 23, 1972

An efficient synthesis of 6-hydroxydopamine is described. The key step involves oxidation of an *N*-protected 3-hydroxy-4-methoxyphenethylamine to the corresponding *p*-quinone by means of Fremy's salt.

On décrit une synthèse efficiente de 6-hydroxydopamine. Le pas décisif entraîne l'oxydation au moyen de sel de Fremy d'un *N*-protégé 3-hydroxy-4-méthoxyphènéthylamine au *p*-quinone correspondant.

Canadian Journal of Chemistry, **50**, 3075 (1972)

Introduction

In 1967 Tranzer and Theonen (1) recognized in 6-hydroxydopamine (7) the capacity for selectively destroying adrenergic nerve terminals. The compound was previously described and synthesized by Harley-Mason (2) and Lee and Dickson (3), starting from 2,4,5-trimethoxy- and 2,4,5-tribenzyloxybenzaldehyde respectively. Senoh and Witkop's multistep synthesis (4) involves the addition of methanol to a suitable *o*-quinone intermediate. Because of the generally low yields and the relatively involved pro-

[1]To whom correspondence should be addressed.

Can. J. Chem. Downloaded from www.nrcresearchpress.com by 210.87.254.5 on 09/05/12
For personal use only.

alcohols, but not in water (Table 1). The reason for this difference is related to the difference in the structures of e^-_{solv} and H^+_{solv} in the different solvents, which are in turn related to the structures of the liquids. There is no reluctance of $H^+(ROH)_n$ to accept an electron from $e^-(ROH)_m$, although there seems to be for $H^+(H_2O)_n$ to accept one from $e^-(H_2O)_m$.

The fact that reaction 2 is diffusion controlled

[2] $$H^+_{solv} + RO^-_{solv}(OH^-_{solv}) \rightarrow ROH_{solv}(H_2O_{solv})$$

in alcohols (5) but is apparently *faster* in water ($k_2 = 11.2 \times 10^{10}\ M^{-1}\ s^{-1}$ (5)) than one would calculate from the bulk diffusion coefficients of H^+_{aq} and OH^-_{aq} ($7.9 \times 10^{10}\ M^{-1}\ s^{-1}$ (5)) is probably also related to the structure of the solvents in the vicinity of the ions. The relative rates of reactions 1 and 2 in water and in alcohols are consistent with the suggestion (10) that e^-_{solv} is a solvent structure breaker in water and a weak structure maker in alcohols; H^+, OH^-, and RO^- are strong structure makers in water and alcohols (ref. 11, pp. 168, 176, 183). A structure-making ion such as H^+_{aq} has difficulty approaching one that breaks structure, such as e^-_{aq}, so there is a sort of repulsion between the two species in solution (ref. 11, chap. 16, 12). This offers at least a partial explanation of why k_1 in water is smaller than would be expected from the Debye equation (2). Conversely, two strong structure makers approach each other more rapidly than "normal" at close distances. This, combined with the structure dependent proton jumping mechanism of migration of both H^+ and OH^- in water, may explain why k_2 in water is greater than would be expected from the Debye equation.

1. L. M. Dorfman and M. S. Matheson. Prog. React. Kinet. **3**, 237 (1965).
2. P. Debye. Trans. Electrochem. Soc. **82**, 265 (1942).
3. M. Anbar. Adv. Chem. Ser. **50**, 55 (1965).
4. G. C. Barker, P. Fowles, D. C. Sammon, and B. Stringer. Trans. Faraday Soc. **66**, 1498 (1970).
5. P. Fowles. Trans. Faraday Soc. **67**, 428 (1971).
6. J. Rabani, M. Grätzel, and S. A. Chandhri. J. Phys. Chem. **75**, 3893 (1971).
7. S. M. S. Akhtar and G. R. Freeman. J. Phys. Chem. **75**, 2756 (1971).
8. B. E. Conway. Electrochemical data. Elsevier Publishing Co., Amsterdam. 1952.
9. H. Strehlow. Z. Phys. Chem. (N.F.) **24**, 240 (1960).
10. K. N. Jha and G. R. Freeman. J. Chem. Phys. **48**, 5480 (1968).
11. R. W. Gurney. Ionic processes in solution. McGraw–Hill Book Co., New York. 1953.
12. H. S. Frank and M. S. Tsao. Ann. Rev. Phys. Chem. **5**, 43 (1954).

A New Synthesis of 6-Hydroxydopamine

Pius A. Wehrli,[1] F. Pigott, and V. Chu

Chemical Research Department, Hoffmann-La Roche Inc., Nutley, N.J. 07110

Received March 23, 1972

An efficient synthesis of 6-hydroxydopamine is described. The key step involves oxidation of an *N*-protected 3-hydroxy-4-methoxyphenethylamine to the corresponding *p*-quinone by means of Fremy's salt.

On décrit une synthèse efficiente de 6-hydroxydopamine. Le pas décisif entraîne l'oxydation au moyen de sel de Fremy d'un *N*-protégé 3-hydroxy-4-méthoxyphènéthylamine au *p*-quinone correspondant.

Canadian Journal of Chemistry, **50**, 3075 (1972)

Introduction

In 1967 Tranzer and Theonen (1) recognized in 6-hydroxydopamine (7) the capacity for selectively destroying adrenergic nerve terminals. The compound was previously described and synthesized by Harley-Mason (2) and Lee and Dickson (3), starting from 2,4,5-trimethoxy- and 2,4,5-tribenzyloxybenzaldehyde respectively. Senoh and Witkop's multistep synthesis (4) involves the addition of methanol to a suitable *o*-quinone intermediate. Because of the generally low yields and the relatively involved pro-

[1]To whom correspondence should be addressed.

Can. J. Chem. Downloaded from www.nrcresearchpress.com by 210.87.254.5 on 09/05/12
For personal use only.

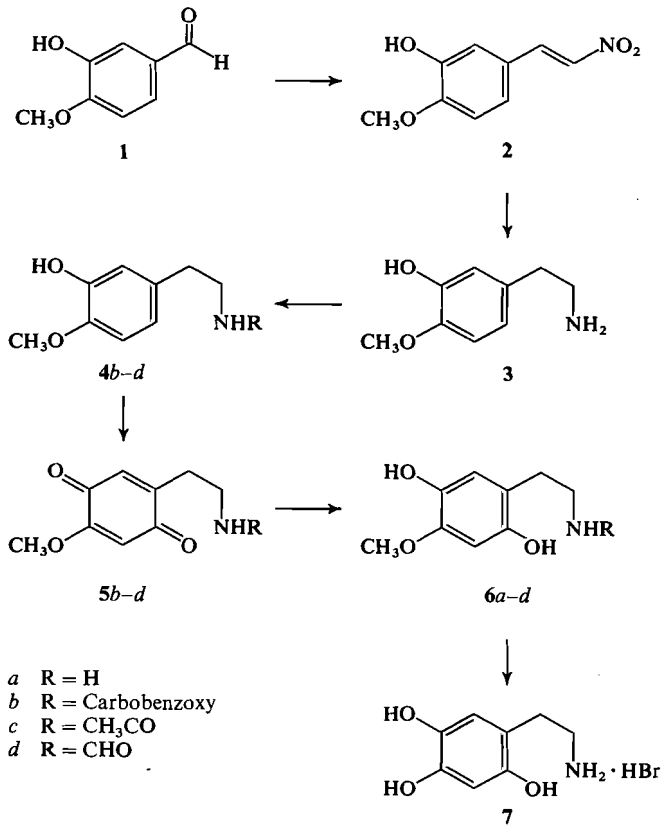

SCHEME 1

cedures, we now wish to report an efficient alternate scheme for the synthesis of this pharmacologically fascinating compound (see Scheme 1).

Starting from isovanillin (**1**), the corresponding phenethylamine **3** was prepared via the known nitrostyrene **2** (5) in about 60% overall yield. The projected central step in our scheme was a Fremy's salt oxidation (6) of 3-hydroxy-4-methoxyphenethylamine (**3**) to the corresponding *p*-quinone **5***a*, but a number of attempts to oxidize **3** failed to give identifiable products. It was only after the amino function was protected by carbobenzoxylation, acetylation, or formylation that the Teuber reaction (7) could be effected successfully. Almost quantitative yields of the corresponding *p*-quinones were obtained with the *N*-carbobenzoxy derivative **4***b* and the *N*-acetyl derivative **4***c*. Why a lower yield was obtained with the *N*-formyl substrate **4***c* is uncertain, but it may have been due to appreciable hydrolysis of the protecting group. Catalytic reduction to the corresponding hydroquinone derivatives **6***a–d* proceeded as expected. Cleavage of the aromatic methoxyl group was effected in good yield with refluxing 48% HBr, 6-hydroxydopamine hydrobromide (**7**) being obtained as pure white crystals. The hydrobromide **7** was obtained directly from the *N*-acetyl derivative **6***c*. Based on isovanillin, **7** was obtained in an overall yield of 40% in our best experiments via the sequence **1** → **2** → **3** → **4***b* → **5***b* → **6***a*·HOAc → **7**.

Experimental

Melting points are uncorrected and were taken in capillary tubes with a Thomas-Hoover apparatus. Infrared spectra were recorded on a Perkin-Elmer 21 spectrophotometer. The symbols s, m, and w refer to strong, medium, and weak bands respectively. All u.v. spectra were recorded on a Carey Model 14 spectrophotometer and the n.m.r. spectra were measured with a Varian A-60 apparatus. Unless otherwise indicated, all t.l.c. was done on silica gel plates.

Can. J. Chem. Downloaded from www.nrcresearchpress.com by 210.87.254.5 on 09/05/12
For personal use only.

Can. J. Chem. Downloaded from www.nrcresearchpress.com by 210.87.254.5 on 09/05/12
For personal use only.

3-Hydroxy-4-methoxy-β-nitrostyrene (2)[2]

A methanolic buffer solution of methyl ammonium acetate was prepared by adding 2.6 g (0.0245 mol) of anhydrous sodium carbonate to a solution of 1.65 g (0.0245 mol) of methylamine hydrochloride in 25 ml of methanol. After stirring for 30 min, the suspension was filtered directly into a solution of 2.2 g (0.0365 mol) of acetic acid in 25 ml of methanol. The p*H* of this buffer solution must be *5.8–6.0*[3] (measured with a glass electrode). Meanwhile 50 g (0.33 mol) of isovanillin was dissolved in 200 ml of warm methanol and then cooled to room temperature.[4] Nitromethane (20 g, 0.33 mol) was added and mixed well and the reaction flask (1 l Erlenmeyer flask) was then wrapped with aluminum foil. The previously prepared methylamine buffer solution was added dropwise with mechanical stirring to the isovanillin–nitromethane mixture over a period of 30 min. The reaction mixture was allowed to stand in the *dark* for 88 h. The resulting yellow crystals were filtered, washed with 25 ml of cold methanol and air dried to give 49 g (76%) of **2**, m.p. 154–155°; λ_{max} (CH_3OH) 243 (sh, ε 6430), 260 (ε 8360), 320 (infl, ε 6400), 367–368 mμ (ε 16 200); δ(DMSO) 3.9 (s, 3H), 6.85–7.3 (m, 3H), 7.8 (s, 2H), 9.9 (s, 1H); R_f 0.55 (EtOAc:C_6H_6, 1:1, u.v. light; R_f 0.45 for isovanillin).

Anal. Calcd. for $C_9H_9NO_4$: C, 55.38; H, 4.65; N, 7.18. Found: C, 55.68; H, 4.58; N, 7.18.

3-Hydroxy-4-methoxyphenethylamine (3)

The nitrostyrene **2** (260 g, 1.33 mol) was suspended in a mixture of 1 l of water and 260 ml of concentrated hydrochloric acid. The volume was adjusted to 3.5 l with water, 50 g of 10% Pd–C catalyst was added, and the heterogeneous mixture was hydrogenated in a glass-lined, rocking autoclave at 80°, initial pressure 800 p.s.i., for 6 h. Most of the hydrogen was absorbed in the first hour. After cooling for 16 h, the catalyst was filtered and the colorless filtrate was evaporated with a rotary evaporator. The solid residue was scraped loose and 360 ml of concentrated ammonium hydroxide was added with ice-cooling. The white salt dissolved gradually and the amine precipitated simultaneously. The crystalline solid was then slurried mechanically for 1 h, filtered, washed with ice-water, and dried *in vacuo* at room temperature. The yield of crude **3** was 173 g (78%), m.p. 144–148° (5). This material was used for further transformation.

N-(3-Hydroxy-4-methoxyphenethyl)carbamic Acid Benzyl Ester (4b)

To a 500-ml resin jar equipped with a stirrer, nitrogen inlet tube, p*H* electrode, two dropping funnels, and an ice bath were added 200 ml of distilled water and 11.03 g (0.066 mol) of amine **3**. The p*H* of this suspension was 9.2. Benzyl chloroformate (9.15 ml) and 1 *N* sodium hydroxide were added simultaneously over 20 min, the p*H* reaching a maximum of 11.3. After stirring for 1 h, the p*H* was 9.6, the solid was filtered, washed well with water, and air-dried; yield 16.64 g (84%), m.p. 113°. Purification was effected by slurrying the crystals with 100 ml of a 1:1 hexane–ether mixture followed by the addition of 200 ml of hexane prior to filtration. The product was washed with hexane and dried *in vacuo*; yield, 13.5 g (68%), m.p. 114.5°; δ($CDCl_3$) 2.70 (t, $J = 6$ Hz, 2H), 3.42 (q, $J = 6$ Hz, 2H), 3.83 (s, 3H), *ca.* 4.8 (broad, 1H), 5.1 (s, 2H), 5.72 (s, 1H), 6.7–6.9 (m, 3H), 7.35 (s, 5H); *m/e* 301 (M^+), 166, 150, 137, 91 (P); R_f 0.7 (EtOAc:$CHCl_3$, 1:1, u.v. light).

Anal. Calcd. for $C_{17}H_{19}NO_4$: C, 67.76; H, 6.36; N, 4.65. Found: C, 67.94; H, 6.37; N, 4.60.

N-(3-Hydroxy-4-methoxyphenethyl)acetamide (4c)

Amine **3** (25.05 g, 0.15 mol) was heated in 15.3 g (0.15 mol) of acetic anhydride for 2 h under nitrogen with stirring at 145° in an oil bath. The reaction mixture was cooled to room temperature and the acetic acid was removed with a rotary evaporator at 50°. To the brown oily residue was added 10 ml of ethyl acetate and, on seeding, the solution turned into an almost solid mass of crystals. It was then crushed, filtered, and washed with three 10 ml-portions of ethyl acetate to give, after drying *in vacuo*, 25 g (80%) of white crystals, m.p. 123°. This material was characterized without further purification; λ_{max} ($CHCl_3$) 3550 (m), 3450 (m), 1670 (s), 1515 (s), 1275 (s) cm^{-1}; δ (DMSO) 1.54 (s, 3H), 2.5 (m, 2H + DMSO), 3.25 (m, 2H), 3.75 (s, 3H), 6.0 (m, 3H), 7.8 (broad, 1H), 8.7 (s, 1H); R_f 0.75 (EtOAC:MeOH, 2:1).

Anal. Calcd. for $C_{11}H_{15}NO_3$: C, 63.14; H, 7.03; N, 6.69. Found: C, 63.22; H, 7.21; N, 6.60.

N-(3-Hydroxy-4-methoxyphenethyl)formamide (4d)

Amine **3** (50 g, 0.3 mol) was refluxed for 21 h with stirring in 250 ml of methyl formate. The reaction mixture was turbid for the duration of the reaction. Before filtering and washing the crystals with some methyl formate, the batch was cooled to 0° and stirred at this temperature for 2 h. After drying *in vacuo* at room temperature the white crystals weighed 44.5 g (76%), m.p. 111–113°. The product was characterized without purification: δ (DMSO) 2.65 (t, $J = 7$ Hz, 2H), 3.3 (q, $J = 7$ Hz, 2H), 3.8 (s, 3H), 6.5–6.9 (m, 3H), *ca.* 7.9 (broad, 1H), 8.1 (s, broad, 1H), 8.5 (s, broad, 1H); R_f 0.1 (EtOAc:$CHCl_3$, 1:1).

Anal. Calcd. for $C_{10}H_{13}NO_3$: C, 61.52; H, 6.71; N, 7.18. Found: C, 61.35; H, 6.78; N, 7.01.

N-[2-(4-Methoxy-3,6-dioxo-1,4-cyclohexadien-1-yl)-ethyl] carbamic Acid Benzyl Ester (5b)

In a 1 l round-bottomed flask, equipped with a mechanical stirrer, dropping funnel, and ice water bath were placed 500 ml of 0.028 *M* aqueous sodium dihydrogen phosphate and 135 g (0.5 mol) of Fremy's salt (8). While stirring vigorously in an ice bath, 37 g (0.123 mol) of **4**, dissolved in 350 ml of acetone, was added within *ca.* 5 min and the suspension was stirred for 68 h. This was over a weekend and may not be necessary; the course of the reaction may be conveniently followed by t.l.c. The heterogeneous mixture was diluted to 6 l with water and extracted with a total of 2.5 l of ethyl acetate. The organic phases were combined and washed once with 250 ml of saturated sodium bi-

[2]The procedure of Ramirez and Burger (5) gave erratic results.

[3]Use of buffers with p*H* > 6.5 promoted the formation of an undesired substance (no movement on t.l.c., ethyl acetate–benzene (1:1), short u.v.) whereas buffers with p*H* < 5.6 tended to keep the reaction from going to completion.

[4]Some isovanillin may crystallize. This can be minimized by adding the other reagents as soon as room temperature is reached. Poorer results are obtained if the reaction is carried out at higher temperatures.

Can. J. Chem. Downloaded from www.nrcresearchpress.com by 210.87.254.5 on 09/05/12
For personal use only.

carbonate solution followed by two 250 ml-portions of water. The yellow solution was dried over sodium sulfate, filtered, and concentrated to *ca.* 250 ml. After cooling with ice, the crystals were filtered and washed with 25 ml of cold ethyl acetate. The mother liquor was evaporated to 25 ml, chilled, filtered, and washed with cold ethyl acetate. The product was obtained in two crops: 32.6 g (m.p. 130°) and 3.2 g (m.p. 125°); total yield, 35.8 g (92%).

A sample of the first crop was analyzed without further purification; λ_{max} (isopropanol) 259 (ε 8700), 360–362 mμ (ε 450); λ_{max} ($CHCl_3$) 3450 (m), 1720 (s), 1680 (s), 1655 (s), 1610 (s) cm^{-1}; δ ($CDCl_3$) 2.65 (t, $J = 7$ Hz, 2H), 3.43 (q, $J =$ 7Hz, 2H), 3.75 (s, 3H), 5.1 (s, 2H), *ca.* 5.4 (broad, 1H), 5.9 (s, 1H), 6.55 (broadened singlet, 1H), 7.3 (s, 5H); *m/e* 317 ($M^+ + 2H$), 315 (M^+), 313 ($M^+ - 2H$), 91 (P); R_f 0.4 ($CHCl_3$:EtOAc, 9:1, u.v. light).

Anal. Calcd. for $C_{17}H_{17}NO_5$: C, 64.75; H, 5.43; N, 4.44. Found: C, 64.88; H, 5.40; N, 4.43.

2-(2-Acetamidoethyl)-5-methoxy-p-benzoquinone (5c)

In a 250-ml one neck round-bottomed flask, equipped with stirrer and ice bath were placed 12.54 g (0.06 mol) of **4***c*, 160 ml of 0.056 *M* aqueous NaH_2PO_4 buffer, and 40 g (0.149 mol) of Fremy's salt. The heterogeneous reaction mixture was stirred well in an ice bath for 3.5 h (completeness of the reaction is monitored by t.l.c.: EtOAc, u.v. light, followed by phosphomolybdic acid spray). It was worked-up by extracting with a total of 2.1 l of ethyl acetate (this large amount of solvent is necessary, because the quinoid material is somewhat water soluble). The combined yellow extracts were then dried over $MgSO_4$ and evaporated *in vacuo* at 40° to give 13.4 g (100%) of bright yellow crystals. T.l.c. of this material showed only trace impurities.

For characterization purposes a similarly prepared sample was recrystallized from acetone, m.p. 140–142°; λ_{max} ($CHCl_3$) 3450 (m), 1680 (s), 1660 (s), 1610 (s), 1180 (s) cm^{-1}; λ_{max} (MeOH) 261 (ε 13 600), 360 (ε 620) mμ; δ ($CDCl_3$) 1.93 (s, 3H), 2.68 (t, $J = 7$ Hz, 2H, signals slightly split $J \sim 1$ Hz), 3.46 (q, $J = 7$ Hz, 2H), 3.82 (s, 3H), 5.95 (s, 1H), *ca.* 6.2 (broad, 1H), 6.6 (t, $J = \sim 1$ Hz, 1H); *m/e* 225 ($M^+ + 2H$), 223 (M^+), 221 ($M^+ - 2H$), 43 (P); R_f 0.07 (EtOAc, u.v. light).

Anal. Calcd. for $C_{11}H_{13}NO_4$: C, 59.18, H, 5.87; N, 6.28. Found: C, 59.00; H, 5.71; N, 6.53.

N-[2-(4-Methoxy-3,6-dioxo-1,4-cyclohexadien-1-yl)-ethyl] formamide (5d)

Formamide **4***d* (4.88 g, 0.025 mol) was stirred vigorously for 4 h at 0° in a slurry of 20 g (*ca.* 0.075 mol) of wet, water-washed Fremy's salt in 55 ml of 1 *M* NaH_2PO_4 solution. The lemon yellow reaction mixture was filtered (very slow filtration), washed with a total of 120 ml of ice water, and dried overnight *in vacuo* to give 13 g of crude product. The organic material was dissolved by refluxing in 250 ml of ethyl acetate. The hot solution was filtered over a bed of Celite and washed with 50 ml of hot ethyl acetate. The clear filtrate was refrigerated overnight, the crystals were filtered and washed with a small amount of cold ethyl acetate to give after drying *in vacuo* at room temperature, 2.85 g (54%) **5***d*, m.p. 135–138°; λ_{max} ($CHCl_3$) 3450 (m), 1690 (s), 1655 (s), 1603 (s), 1175 (s) cm^{-1}; λ_{max} (EtOH) 260–261 (ε 14 420), 360–370 (ε 780) mμ; δ ($CDCl_3$ + DMSO) 2.6 (t, signals slightly split, $J = 7$ Hz, 2H), 3.4 (q, $J = 7$ Hz, 2H), 3.82 (s, 3H), 6.0 (s, 1H), 6.65 (s, slightly split, $J \sim 0.5$ Hz, 1H), 7.75 (broad, 1H), 8.05 (d, $J \sim 1$ Hz, 1H).

Anal. Calcd. for $C_{10}H_{11}NO_4$: C, 57.41; H, 5.30; N, 6.70. Found: C, 57.16; H, 5.31; N, 6.66.

2,5-Dihydroxy-4-methoxyphenethylamine acetate (6a·HOAc)

The yellow quinone **5***b* (10 g, 0.0318 mol) was dissolved in 200 ml of methanol. Acetic acid (2.5 ml, 0.0438 mol) and 1.5 g of 10% Pd–C was added and the mixture was hydrogenated for 3 h at room temperature, initial pressure 300 p.s.i., in a glass lined rocking autoclave. After filtering the catalyst, the faintly reddish solution was evaporated with a rotary evaporator at 50° to give a light brown oily residue which was dissolved in 30 ml of isopropanol. The product crystallized on cooling for 2 h at 0°. After filtering, washing with cold isopropanol followed by ether, and drying *in vacuo* there was obtained 5.2 g (68%) of off-white crystals, m.p. 183–185°. An analytically pure sample was prepared by recrystallization from methanol; λ_{max} (Nujol) 3350 (m), 1640 (m), 1530 (m), 1270 (s), 1220 (s), 1195 (s), 1170 (s), 1155 (s), 870 cm^{-1} (s, doublet); λ_{max} (EtOH) 220 (infl. ε 5980), 294–295 (ε 5640) mμ; δ (DMSO) 1.8 (s, 3H), 2.8 (m, 4H), 3.7 (s, 3H), 6.47 (s, 1H), 6.50 (s, 1H), 8.15 (s, 5H); *m/e* 183 (M^+ for free base), 166, 154, 60 (HOAc), 30 (P).

Anal. Calcd. for $C_9H_{13}NO_3 \cdot C_2H_4O_2$: C, 54.31; H, 7.04; N, 5.76. Found: C, 54.40; H, 6.92; N, 5.78.

N-(2,5-Dihydro-4-methoxyphenethyl)carbamic Acid Benzyl Ester (6b)

The hydroquinone **6***b* was obtained from an uncontrolled reaction. Catalyst (10% Pd–C) was added to a methanolic solution of the quinone starting material under nitrogen. An exothermic reaction resulted which brought the mixture almost to the reflux temperature. After cooling to room temperature, the catalyst was filtered, and on standing for several hours, small needles crystallized from the filtrate. This product was collected, washed with methanol, dried *in vacuo*, and analyzed without further purification; m.p. 135.5–138°; δ (DMSO) 2.64 (t, broad, 2H), 3.25 (t, broad, 2H), 3.7 (s, 3H), 5.05 (s, 2H), 6.5 (s, 1H), 6.6 (s, 1H), 7.1 (broad, 1H), 7.33 (s, 5H), 8.0 (s, 1H), 8.57 (s, 1H); *m/e* 317 (M^+), 153, 91 (P); R_f 0.15 (EtOAc:$CHCl_3$, 1:9, phosphomolybdic acid spray).

Anal. Calcd. for $C_{17}H_{19}NO_5$: C, 64.34; H, 6.03; N, 4.41. Found: C, 64.32; H, 5.91; N, 4.30.

N-(2,5-Dihydroxy-4-methoxyphenethyl)acetamide (6c)

Quinone **5***c* (6.19 g, 0.0278 mol) was dissolved in 50 ml of methanol and hydrogenated over 120 mg of 10% Pd–C in a Brown hydrogenator.[5] After filtration, evaporation of the filtrate gave 6.3 g (100%) of tan solid; 2.5 g was recrystallized from 250 ml of ethyl acetate to give 1.92 g of the hydroquinone **6***c*, m.p. 158–159°; δ (D_2O) 2.2 (s, 3H), 2.95 (t, broad, 2H), 3.65 (t, broad, 2H), 4.1 (s, 3H), 6.86 (s, 1H), 7.0 (s, 1H); *m/e* 225 (M^+), 166 (P), 153 ($M - CH_2NHAc$); R_f 0.05 (polyamide, $CHCl_3$, phosphomolybdic acid spray).

Anal. Calcd. for $C_{11}H_{15}NO_4$: C, 58.65; H, 6.71; N, 6.22. Found: C, 58.91; H, 6.71; N, 6.09.

[5]Delmar Scientific Laboratories, 317 Madison Street, Maywood, Ill.

N-(2,5-Dihydroxy-4-methoxyphenethyl)formamide (6d)

Quinone **5d** (1.0 g) was dissolved in 30 ml of methanol and hydrogenated in a Brown hydrogenator with 100 mg of 10% Pd–C catalyst. Hydrogen uptake ceased after 10 min. The mixture was stirred 20 min longer and then it was filtered over a bed of filter aid. Evaporation and recrystallization of the solid residue from 3 ml of methanol and 10 ml of ethyl acetate yielded 600 mg of tan-colored, *i.e.* air sensitive crystals, m.p. 129–131°. This material was analyzed without further purification: λ_{max} (EtOH) 220 (ε 6700), 293 (ε 4990) mμ; δ (DMSO) 2.55 (t, $J = 8$ Hz, 2H), 3.25 (q, $J = 8$ Hz, 2H), 3.7 (s, 3H), 6.42 (s, 1H), 3.48 (s, 1H), *ca.* 7.9 (broad, 1H), 8.0 (s, 2H), 8.53 (s, 1H); *m/e* 211 (M^+), 166, 153.

Anal. Calcd. for $C_{10}H_{13}NO_4$: C, 56.86; H, 6.20; N, 6.63. Found: C, 56.67; H, 6.27; N, 6.50.

6-Hydroxydopamine Hydrobromide (7)

(a) From 2,5-Dihydroxy-4-methoxyphenethylamine Acetate (6a·HOAc)

Compound **6a** (11.5 g, 0.0473 mol) was refluxed for 5 h in 62.5 ml of 48% hydrobromic acid under nitrogen. The light brown reaction mixture was seeded, cooled to 0°, filtered, washed with three 20 ml-portions of isopropanol followed by three 20 ml-portions of hexane. After drying *in vacuo* the white, crystalline 6-hydroxydopamine hydrobromide (**7**) weighed 11.31 g (95%), m.p. 211–212°.[6]

(b) From N-(2,5-Dihydroxy-4-methoxyphenethyl) acetamide (6c)

In a 100 ml flask, equipped with a stirrer and a nitrogen inlet, was placed 5.04 g (0.0224 mol) of **6c** and 10 ml of 48% hydrobromic acid. After refluxing for 4 h under nitrogen, the brown reaction mixture was evaporated with a rotary evaporator. The brown crystals were slurried with isopropanol, filtered, and washed with the same solvent to give 2.16 g (31%) of tan-colored **7** which was identical (i.r. and t.l.c.) with the material obtained in section *a*.

[6]The reported melting points for 6-hydroxydopamine hydrobromide are 218–219° (see lit. ref. (2)) and 216–218° (see lit. ref. (4)).

We are indebted to the staff of our Physical Chemistry Department directed by Dr. R. P. W. Scott. In particular thanks are due to Dr. H. Wyss for i.r., Dr. V. Toome for u.v., Dr. T. Williams for n.m.r., and Dr. W. Benz for mass spectra. Dr. F. Scheidl carried out the microanalyses and Mr. D. Wagner, of our hydrogenation laboratory, was most helpful in carrying out the high pressure reductions. Dr. A. I. Rachlin's help in preparing the manuscript is greatly appreciated.

1. J. P. Tranzer and H. Thoenen. Naunyn-Schmiedeberg's Arch. exp. Path. Pharmak. **257**, 343 (1967).
2. J. Harley-Mason. J. Chem. Soc. 200 (1953).
3. F. G. H. Lee and D. E. Dickson. J. Med. Chem. **14**, 266 (1971).
4. S. Senoh and B. Witkop. J. Am. Chem. Soc. **81**, 6222 (1959), J. Daly, L. Horner, and B. Witkop. J. Am. Chem. Soc. **83**, 4787 (1961).
5. F. A. Ramirez and A. Burger. J. Am. Chem. Soc. **72**, 2781 (1950).
6. H. J. Teuber and O. Glosauer. Chem. Ber. **98**, 2648 (1965).
7. H. Zimmer, D. C. Lankin, and S. W. Horgan. Chem. Rev. **71**, 229 (1971).
8. P. A. Wehrli and F. Pigott. Inorg. Chem. **9**, 2614 (1970).

Five-membered Heterocyclic Thiones. Part I. 1,3,4-Oxadiazole-2-thione

D. E. Horning and J. M. Muchowski[1]

Bristol Laboratories of Canada, Candiac, Quebec

Received April 17, 1972

1,3,4-Oxadiazole-2-thione was prepared by decarboxylation of the corresponding 5-carboxylic acid. Spectral data supported the predominant, if not exclusive, existence of the thione form in solution.

L'oxadiazole-1,3,4 thione-2 a été préparée par décarboxylation de l'acide carboxylique-5 correspondant. Les données spectrales viennent à l'appui de l'existence prédominante, voire exclusive, de la forme thione en solution. [Traduit par le journal]

Canadian Journal of Chemistry, **50**, 3079 (1972)

Although numerous 5-substituted-1,3,4-oxadiazole-2-thiones have been prepared (1, 2) the parent member, to our knowledge, has not been described. The synthesis of that compound constitutes the subject of this publication.

The formation of 1,3,4-oxadiazole-2-thiones from potassium-3-acyldithiocarbazates was first observed by Hoggarth (3). This synthesis,

[1]To whom enquiries concerning this paper should be addressed at: Syntex, S. A., Division de Investigacion, Calle Carretera Mexico-Toluca No. 2822, Apartado Postal 10-820, Mexico 10, D.F.

Can. J. Chem. Downloaded from www.nrcresearchpress.com by 210.87.254.5 on 09/05/12
For personal use only.

N-(2,5-Dihydroxy-4-methoxyphenethyl)formamide (6d)

Quinone **5d** (1.0 g) was dissolved in 30 ml of methanol and hydrogenated in a Brown hydrogenator with 100 mg of 10% Pd–C catalyst. Hydrogen uptake ceased after 10 min. The mixture was stirred 20 min longer and then it was filtered over a bed of filter aid. Evaporation and recrystallization of the solid residue from 3 ml of methanol and 10 ml of ethyl acetate yielded 600 mg of tan-colored, *i.e.* air sensitive crystals, m.p. 129–131°. This material was analyzed without further purification: λ_{max} (EtOH) 220 (ε 6700), 293 (ε 4990) mμ; δ (DMSO) 2.55 (t, $J = 8$ Hz, 2H), 3.25 (q, $J = 8$ Hz, 2H), 3.7 (s, 3H), 6.42 (s, 1H), 3.48 (s, 1H), *ca.* 7.9 (broad, 1H), 8.0 (s, 2H), 8.53 (s, 1H); *m/e* 211 (M^+), 166, 153.

Anal. Calcd. for $C_{10}H_{13}NO_4$: C, 56.86; H, 6.20; N, 6.63. Found: C, 56.67; H, 6.27; N, 6.50.

6-Hydroxydopamine Hydrobromide (7)

(a) From 2,5-Dihydroxy-4-methoxyphenethylamine Acetate (6a·HOAc)

Compound **6a** (11.5 g, 0.0473 mol) was refluxed for 5 h in 62.5 ml of 48% hydrobromic acid under nitrogen. The light brown reaction mixture was seeded, cooled to 0°, filtered, washed with three 20 ml-portions of isopropanol followed by three 20 ml-portions of hexane. After drying *in vacuo* the white, crystalline 6-hydroxydopamine hydrobromide (**7**) weighed 11.31 g (95%), m.p. 211–212°.[6]

(b) From N-(2,5-Dihydroxy-4-methoxyphenethyl) acetamide (6c)

In a 100 ml flask, equipped with a stirrer and a nitrogen inlet, was placed 5.04 g (0.0224 mol) of **6c** and 10 ml of 48% hydrobromic acid. After refluxing for 4 h under nitrogen, the brown reaction mixture was evaporated with a rotary evaporator. The brown crystals were slurried with isopropanol, filtered, and washed with the same solvent to give 2.16 g (31%) of tan-colored **7** which was identical (i.r. and t.l.c.) with the material obtained in section *a*.

[6]The reported melting points for 6-hydroxydopamine hydrobromide are 218–219° (see lit. ref. (2)) and 216–218° (see lit. ref. (4)).

We are indebted to the staff of our Physical Chemistry Department directed by Dr. R. P. W. Scott. In particular thanks are due to Dr. H. Wyss for i.r., Dr. V. Toome for u.v., Dr. T. Williams for n.m.r., and Dr. W. Benz for mass spectra. Dr. F. Scheidl carried out the microanalyses and Mr. D. Wagner, of our hydrogenation laboratory, was most helpful in carrying out the high pressure reductions. Dr. A. I. Rachlin's help in preparing the manuscript is greatly appreciated.

1. J. P. Tranzer and H. Thoenen. Naunyn-Schmiedeberg's Arch. exp. Path. Pharmak. **257**, 343 (1967).
2. J. Harley-Mason. J. Chem. Soc. 200 (1953).
3. F. G. H. Lee and D. E. Dickson. J. Med. Chem. **14**, 266 (1971).
4. S. Senoh and B. Witkop. J. Am. Chem. Soc. **81**, 6222 (1959), J. Daly, L. Horner, and B. Witkop. J. Am. Chem. Soc. **83**, 4787 (1961).
5. F. A. Ramirez and A. Burger. J. Am. Chem. Soc. **72**, 2781 (1950).
6. H. J. Teuber and O. Glosauer. Chem. Ber. **98**, 2648 (1965).
7. H. Zimmer, D. C. Lankin, and S. W. Horgan. Chem. Rev. **71**, 229 (1971).
8. P. A. Wehrli and F. Pigott. Inorg. Chem. **9**, 2614 (1970).

Five-membered Heterocyclic Thiones. Part I. 1,3,4-Oxadiazole-2-thione

D. E. Horning and J. M. Muchowski[1]

Bristol Laboratories of Canada, Candiac, Quebec

Received April 17, 1972

1,3,4-Oxadiazole-2-thione was prepared by decarboxylation of the corresponding 5-carboxylic acid. Spectral data supported the predominant, if not exclusive, existence of the thione form in solution.

L'oxadiazole-1,3,4 thione-2 a été préparée par décarboxylation de l'acide carboxylique-5 correspondant. Les données spectrales viennent à l'appui de l'existence prédominante, voire exclusive, de la forme thione en solution. [Traduit par le journal]

Canadian Journal of Chemistry, **50**, 3079 (1972)

Although numerous 5-substituted-1,3,4-oxadiazole-2-thiones have been prepared (1, 2) the parent member, to our knowledge, has not been described. The synthesis of that compound constitutes the subject of this publication.

The formation of 1,3,4-oxadiazole-2-thiones from potassium-3-acyldithiocarbazates was first observed by Hoggarth (3). This synthesis,

[1]To whom enquiries concerning this paper should be addressed at: Syntex, S. A., Division de Investigacion, Calle Carretera Mexico-Toluca No. 2822, Apartado Postal 10-820, Mexico 10, D.F.

Can. J. Chem. Downloaded from www.nrcresearchpress.com by 210.87.254.40 on 09/05/12
For personal use only.

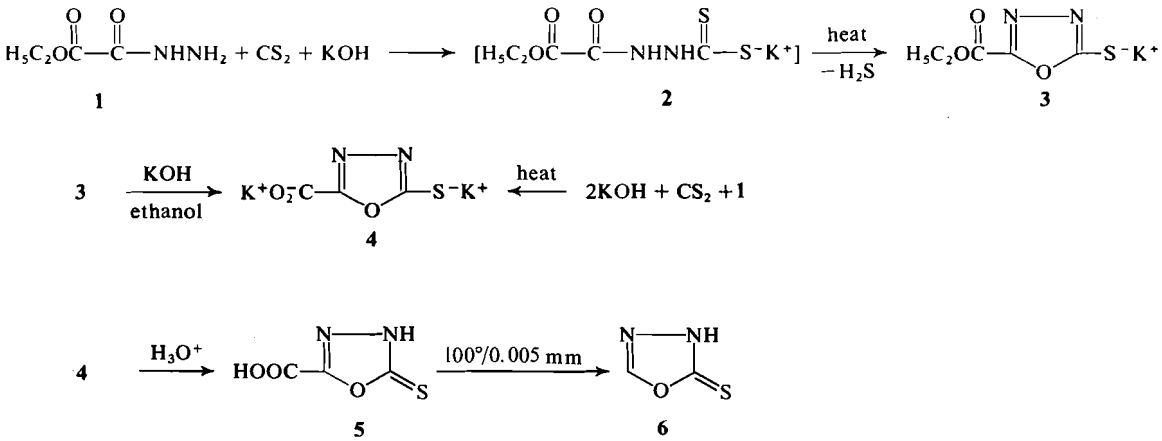

Can. J. Chem. Downloaded from www.nrcresearchpress.com by 210.87.254.40 on 09/05/12
For personal use only.

though extraordinarily versatile (see ref. 1, p. 532) is reported (4) to be unsuccessful when applied to formic acid hydrazide, the only product obtained in this instance being 1,3,4-thiadiazole-2,5-dithione.

It occurred to us that 1,3,4-oxadiazole-2-thione (**6**) might be prepared by decarboxylation of the corresponding 5-carboxylic acid **5**. The synthesis of the latter compound was accomplished in the following manner. Ethyl oxalyl hydrazine (**1**) was converted to the potassium dithiocarbazate **2**, which on heating in ethanol containing a small amount of dimethyl sulfoxide (DMSO),[2] was transformed into the potassium salt **3**. This salt was not purified, instead, it was converted, under remarkably mild conditions, to the dipotassium salt **4**, by titration with 1 equiv of alcoholic potassium hydroxide. Alternatively, **4** could be obtained directly from **1**, carbon disulfide, and 2 equiv of potassium hydroxide. As expected, 1,3,4-oxadiazole-2-thione-5-carboxylic acid (**5**), when heated to its melting point *in vacuo*, lost the elements of carbon dioxide to give the parent thione.

1,3,4-Oxadiazole-2-thione was a stable solid with physical properties (see Table 1) which closely resembled those of the 5-methyl derivative. On the basis of i.r. (4) and u.v. (5) spectral data, it has been concluded that 5-methyl-1,3,4-oxadiazole-2-thione existed in solution in the thione rather than the thiol form. The near identity of the u.v. spectrum of **6** to that of 5-methyl-1,3,4-oxadiazole-2-thione and its 3-*N*-methyl derivative, and the absence of i.r. absorptions in the 2600–2550 cm^{-1} region,[3] indicated that **6** also existed as the thione in solution.

1,3,4-Oxadiazole-2-thione was an acidic substance ($pK'_a = 3.85$) *ca.* four times stronger than the 5-methyl derivative. The reduced acidity of the latter compound was consistent with the known acid weakening effect of a methyl group (8).

Experimental

The melting points were determined in a Gallenkamp melting point apparatus and are not corrected. The n.m.r. spectra were recorded with a Varian A-60A spectrometer in perdeuteriodimethylsulfoxide and are expressed in p.p.m. (δ) from internal tetramethylsilane. The i.r. spectra were recorded with a Unicam SP-200G i.r. spectrometer and the u.v. spectra were measured with a Unicam SP-800 u.v. spectrometer.

Ethyl oxalyl hydrazine was prepared from hydrazine hydrate and diethyl oxalate according to the method of Curtius and Hochschwender (9).

Ethyl-1,3,4-oxadiazole-2-thione-5-carboxylate Potassium Salt (3)

To a stirred solution of ethyl oxalyl hydrazine (35.3 g, 260 mmol) in absolute alcohol (250 ml) was added carbon disulfide (70 ml) followed by a solution of potassium hydroxide (16.5 g of 88% KOH, 260 mmol) in absolute ethanol (150 ml). The mixture was heated to reflux temperature, dry DMSO (40 ml) was added, and the mixture was then main-

[2]The conversion of potassium-3-acyldithiocarbazates to the corresponding oxadiazole thiones is known (4) to require reaction periods of up to 1 week in boiling ethanol. The addition of DMSO to the mixture accelerated the above transformation to such an extent that most reactions were completed in less than 2 days. For example, in ethanol containing *ca.* 10 vol. % DMSO, the potassium salt of 5-methyl-1,3,4-oxadiazole-2-thione (m.p. 230–232°) was obtained in 85% yield (pure) after 36 h under reflux.

[3]The S—H stretching absorption of thiophenols is reported (6) to occur in this region. 2-Methyl-1,2,3-triazole-4-thiol has a strong absorption at 2540 cm^{-1} (7).

TABLE 1. Properties of some 1,3,4-oxadiazole-2-thiones

	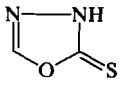	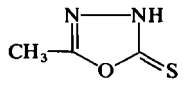
Melting point (°C)	89–91	76–78[a]
pK_a' (water—25°)	3.85	4.45[b]
N.m.r. (δ, p.p.m.)[c] thiol	14.52(w_H = 6 Hz), 8.88	14.30(w_H = 16 Hz), 2.42
S-Methyl ether	9.42, 2.80[d]	2.69, 2.49[e]
U.v.[λ_{max} (log ε)][f] thiol	260(4.12), 208(3.58)	262(4.16), 208(3.57)[g]
S-Methyl ether	—	232(3.74),[h] 221(3.92)[i]
3(*N*)-Methyl	—	263(4.20)[j]
I.r. ($CHCl_3$) (cm^{-1})	3430, 3170, 3140, 2785, 2755 2650(w), 1575, 1489, 1461	3440, 3140(br) 2770, 1634, 1508, 1478

[a]Literature (3) m.p. 78°. A sample of this thione was obtained from Dr. D. N. McGregor, Bristol Laboratories, Syracuse, N.Y.
[b]Sandstrom and Wennerbeck (5) reported pK_a = 5.01 under the same conditions.
[c]Measured in perdeuteriodimethylsulfoxide.
[d]Prepared *in situ* from the potassium salt and methyl iodide.
[e]It is not known which resonance is due to the *C*-methyl group. In the *S*-ethyl derivative (prepared *in situ* from ethyl iodide and the potassium salt) this absorption occurs at δ 2.55.
[f]Measured in 95% ethanol.
[g]Literature (5), λ_{max} (ethanol) 262 (log ε 4.15).
[h]Shoulder.
[i]Literature (5), λ_{max} (ethanol) 219.5 (log ε 3.92).
[j]Data taken from ref. 5.

tained at reflux temperature until the evolution of hydrogen sulfide had become slow (26 h). A small amount of a solid was removed by filtration and the filtrate was evaporated *in vacuo*. The syrup thus obtained was shaken vigorously with several portions (100 ml) of ether to remove DMSO. The ether extracts were discarded, the residue was evaporated *in vacuo* and then dried at room temperature and 0.01 mm for 24 h. The viscous residue (36.0 g) had i.r. (neat) absorptions at 1732 and 1594 (w) cm^{-1}, and n.m.r. bands at δ 1.33 (t, 3H, J = 7.2 Hz), 2.60(s, 10.8 H), 4.37(q, 2H, J = 7.2 Hz). The singlet at δ 2.60 was due to DMSO (1.8 mol/mol of product) which had not been removed. The yield of the potassium salt of the product was therefore 21.7 g (39%). It was not readily purified further and was used as such in subsequent reactions.

1,3,4-Oxadiazole-2-thione-5-carboxylic Acid Dipotassium Salt (4)

(a) From Ethyl-1,3,4-oxadiazole-2-thione-5-carboxylate Potassium Salt (3)

A stirred solution of the crude potassium salt (15.0 g, 42.6 mmol) in ethanol (150 ml) was treated in a dropwise manner with 45 wt. % aqueous potassium hydroxide (6.23 g, 50 mmol). The precipitated solid (9.5 g, 100%) was collected by filtration and dried *in vacuo*. The product, m.p. 250–252° dec., on crystallization from aqueous ethanol (1:2) gave material with m.p. 255° dec.

Anal. Calcd. for $C_3K_2N_2O_3S$: C, 16.21; N, 12.60; S, 14.42. Found: C, 16.16; N, 12.57; S, 14.37.

The i.r. spectrum (Nujol mull) had an intense band at 1622 cm^{-1} and a medium intensity absorption at 1547 cm^{-1}.

(b) From Ethyl-1,3,4-oxadiazole-2-thione-5-carboxylate

A solution of crude **3** (10.0 g) in water was made acidic with hydrochloric acid and then saturated with sodium chloride. The thiol was extracted into ethyl acetate, the extract was dried over sodium sulfate and evaporated *in vacuo* leaving a yellow oil (7.14 g) which solidified on standing. The i.r. spectrum (neat) had a series of strong broad absorptions at 2300–3300 cm^{-1}, an intense band at 1752 cm^{-1}, and a weak absorption at 1593 cm^{-1}. The crude ester (7.14 g) in alcohol (100 ml) was treated as above with 45% potassium hydroxide solution (8.1 g, 65 mmol). The product (6.3 g, 100%) which had m.p. 251–252° was identical to the dipotassium salt described above.

(c) From Ethyl Oxalylhydrazine, Carbon Disulfide, and 2 mol KOH

A solution of the hydrazide (19.7 g, 145 mmol) in alcohol (150 ml) containing carbon disulfide (41 ml) was treated in the usual way with potassium hydroxide (19.2 g of 88% KOH, 291 mmol) in ethanol (150 ml). To the boiling mixture was added DMSO (30 ml) and two further portions (30 ml) of DMSO were added at the end of 5 and 22 h under reflux. After 48 h, the reaction mixture was worked-up in the usual manner to give a solid which was slurried with ethanol (300 ml), diluted with ether (1 l), and the gummy solid was collected by filtration. A solution of this material in water was made basic with sodium carbonate solution (200 g/l, 50 ml) and extracted with ethyl acetate. The aqueous phase was saturated with salt, made acidic with hydrochloric acid, and extracted with ethyl acetate. The extract was dried over sodium sulfate and then evaporated *in vacuo* to give a yellow solid (12.75 g). An ethanol (150 ml) solution of this solid was treated in the usual way with 45% potassium hydroxide (21.8 g) to give a solid (10.3 g, 32% yield based on the hydrazide), m.p. 248–250° dec. identical to the dipotassium salt obtained by methods *a* or *b*.

Can. J. Chem. Downloaded from www.nrcresearchpress.com by 210.87.254.40 on 09/05/12
For personal use only.

1,3,4-Oxadiazole-2-thione

A solution of the dipotassium salt (10.0 g, 45.1 mmol) in water was made acidic with dilute hydrochloric acid, extracted with ethyl acetate (3 × 100 ml), the extract was dried over sodium sulfate and then evaporated *in vacuo*. The residual 1,3,4-oxadiazole-2-thione-5-carboxylic acid (m.p. 88–91° dec., i.r. (Nujol mull), 3285, 2200–3200 (broad, structureless), 1715, 1603, and 1589 cm^{-1}) was placed in a short path distillation apparatus and then heated to 95–100°/0.005 mm. When gas evolution had ceased, the bath temperature was raised to 140–150° and the product was distilled over as rapidly as possible by heating the stillhead with a free flame. The material which had solidified in the condenser was crystallized from benzene to give 1,3,4-oxadiazole-2-thione (2.91 g, 64.5%) with m.p. 88–91°. On recrystallization, material with m.p. 89–91° was obtained.

Anal. Calcd. for $C_2H_2N_2OS$ (equiv. wt. 102.18): C, 23.53; H, 1.97; N, 27.44. Found (101): C, 23.78; H, 2.00; N, 27.51.

We thank Dr. D. N. McGregor of Bristol Laboratories, Syracuse, N.Y. for a generous gift of 5-methyl-1,3,4-oxadiazole-2-thione.

1. J. H. BOYER. Heterocyclic compounds. Vol. 7. *Edited by* R. C. Elderfield. John Wiley and Sons Inc. New York. 1961. pp. 528–532.
2. L. C. BEHR. The chemistry of heterocyclic compounds. Five- and six-membered compounds with nitrogen and oxygen. *Edited by* R. H. Wiley. Interscience Publishers. New York. 1962. pp. 272–274.
3. E. HOGGARTH. J. Chem. Soc. 4811 (1952).
4. C. AINSWORTH. J. Am. Chem. Soc. **78**, 4475 (1956).
5. J. SANDSTROM and I. WENNERBECK. Acta Chem. Scand. **20**, 57 (1966).
6. L. J. BELLAMY. The infrared spectra of complex molecules. 2nd ed. Methuen and Co. Ltd. London. 1958. p. 350.
7. J. P. DARIS and J. M. MUCHOWSKI. Unpublished observation.
8. J. F. KING. *In* Technique of organic chemistry. A. Weissberger, Editor. Vol. XI. Elucidation of structures by physical and chemical methods. Part one. *Edited by* K. W. Bentley. Interscience Publishers. New York. 1963. pp. 325–335.
9. TH. CURTIUS and K. HOCHSCHWENDER. J. Prakt. Chem. **91**, 415 (1915).

Five-membered Heterocyclic Thiones. Part II.[1] Oxazole-2-thione

G. LACASSE AND J. M. MUCHOWSKI[2]
Bristol Laboratories of Canada, Candiac, Quebec

Received April 17, 1972

Oxazole-2-thione was prepared by the condensation of glycolic aldehyde and thiocyanic acid. It was shown by i.r. spectroscopy that oxazole-2-thione, as well as its 4-methyl- and 4,5-dimethyl derivatives, existed as the thione form in solution.

L'oxazole thione-2 a été préparée par condensation de l'aldéhyde glycolique sur l'acide thiocyanique. La spectroscopie i.r. montre que l'oxazole thione-2 ainsi que ses dérivés méthyl-4 et diméthyl-4,5, existent sous la forme thione en solution. [Traduit par le journal]

Canadian Journal of Chemistry, **50**, 3082 (1972)

Oxazole-2-thiones (**2**) are usually prepared by the condensation of α-ketols and thiocyanic acid (2). Although this method is quite general (3, 4) it has not heretofore been applied to the synthesis of the parent compound (**2**, R = R′ = H). This note shows that oxazole-2-thione is also preparable by the above method.

The reaction of glycolic aldehyde (**1**, R = R′ = H) with thiocyanic acid according to the

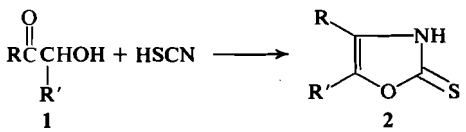

1 **2**

method of Willems and Vandenberghe (2) produced a stable, base-soluble, solid, the elemental analysis and spectral properties (see Table 1) of which were consistent with those expected for oxazole-2-thione.

Gomper and Herlinger (5) have concluded that 3,4-diaryloxazole-2-thiones exist in the thione form from a comparison of their u.v. and fluorescence spectra with those of the

[1]For Part I, see ref. 1.

[2]To whom enquiries concerning this paper should be addressed, at: Syntex, S. A., Division de Investigacion, Calle Carretera Mexico-Toluca No. 2822, Apartado Postal 10-820, Mexico 10, D.F.

Can. J. Chem. Downloaded from www.nrcresearchpress.com by 210.87.254.40 on 09/05/12
For personal use only.

1,3,4-Oxadiazole-2-thione

A solution of the dipotassium salt (10.0 g, 45.1 mmol) in water was made acidic with dilute hydrochloric acid, extracted with ethyl acetate (3 × 100 ml), the extract was dried over sodium sulfate and then evaporated *in vacuo*. The residual 1,3,4-oxadiazole-2-thione-5-carboxylic acid (m.p. 88–91° dec., i.r. (Nujol mull), 3285, 2200–3200 (broad, structureless), 1715, 1603, and 1589 cm^{-1}) was placed in a short path distillation apparatus and then heated to 95–100°/0.005 mm. When gas evolution had ceased, the bath temperature was raised to 140–150° and the product was distilled over as rapidly as possible by heating the stillhead with a free flame. The material which had solidified in the condenser was crystallized from benzene to give 1,3,4-oxadiazole-2-thione (2.91 g, 64.5%) with m.p. 88–91°. On recrystallization, material with m.p. 89–91° was obtained.

Anal. Calcd. for $C_2H_2N_2OS$ (equiv. wt. 102.18): C, 23.53; H, 1.97; N, 27.44. Found (101): C, 23.78; H, 2.00; N, 27.51.

We thank Dr. D. N. McGregor of Bristol Laboratories, Syracuse, N.Y. for a generous gift of 5-methyl-1,3,4-oxadiazole-2-thione.

1. J. H. BOYER. Heterocyclic compounds. Vol. 7. *Edited by* R. C. Elderfield. John Wiley and Sons Inc. New York. 1961. pp. 528–532.
2. L. C. BEHR. The chemistry of heterocyclic compounds. Five- and six-membered compounds with nitrogen and oxygen. *Edited by* R. H. Wiley. Interscience Publishers. New York. 1962. pp. 272–274.
3. E. HOGGARTH. J. Chem. Soc. 4811 (1952).
4. C. AINSWORTH. J. Am. Chem. Soc. **78**, 4475 (1956).
5. J. SANDSTROM and I. WENNERBECK. Acta Chem. Scand. **20**, 57 (1966).
6. L. J. BELLAMY. The infrared spectra of complex molecules. 2nd ed. Methuen and Co. Ltd. London. 1958. p. 350.
7. J. P. DARIS and J. M. MUCHOWSKI. Unpublished observation.
8. J. F. KING. *In* Technique of organic chemistry. A. Weissberger, Editor. Vol. XI. Elucidation of structures by physical and chemical methods. Part one. *Edited by* K. W. Bentley. Interscience Publishers. New York. 1963. pp. 325–335.
9. TH. CURTIUS and K. HOCHSCHWENDER. J. Prakt. Chem. **91**, 415 (1915).

Five-membered Heterocyclic Thiones. Part II.[1] Oxazole-2-thione

G. LACASSE AND J. M. MUCHOWSKI[2]
Bristol Laboratories of Canada, Candiac, Quebec

Received April 17, 1972

Oxazole-2-thione was prepared by the condensation of glycolic aldehyde and thiocyanic acid. It was shown by i.r. spectroscopy that oxazole-2-thione, as well as its 4-methyl- and 4,5-dimethyl derivatives, existed as the thione form in solution.

L'oxazole thione-2 a été préparée par condensation de l'aldéhyde glycolique sur l'acide thiocyanique. La spectroscopie i.r. montre que l'oxazole thione-2 ainsi que ses dérivés méthyl-4 et diméthyl-4,5, existent sous la forme thione en solution. [Traduit par le journal]

Canadian Journal of Chemistry, **50**, 3082 (1972)

Oxazole-2-thiones (**2**) are usually prepared by the condensation of α-ketols and thiocyanic acid (2). Although this method is quite general (3, 4) it has not heretofore been applied to the synthesis of the parent compound (**2**, R = R′ = H). This note shows that oxazole-2-thione is also preparable by the above method.

The reaction of glycolic aldehyde (**1**, R = R′ = H) with thiocyanic acid according to the

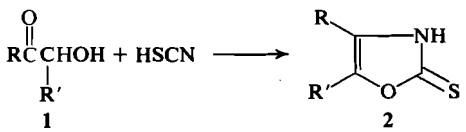

1 **2**

method of Willems and Vandenberghe (2) produced a stable, base-soluble, solid, the elemental analysis and spectral properties (see Table 1) of which were consistent with those expected for oxazole-2-thione.

Gomper and Herlinger (5) have concluded that 3,4-diaryloxazole-2-thiones exist in the thione form from a comparison of their u.v. and fluorescence spectra with those of the

[1]For Part I, see ref. 1.

[2]To whom enquiries concerning this paper should be addressed, at: Syntex, S. A., Division de Investigacion, Calle Carretera Mexico-Toluca No. 2822, Apartado Postal 10-820, Mexico 10, D.F.

Can. J. Chem. Downloaded from www.nrcresearchpress.com by 210.87.254.5 on 09/05/12
For personal use only.

TABLE 1. Properties of some oxazole-2-thiones

	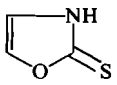	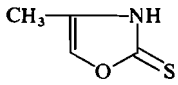	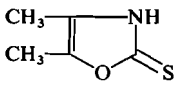
Melting point (°C)	147	150–152[a]	135–137[b]
N.m.r. (δ, p.p.m.)[c]	12.88(1H, $w_H = 19$)[d] 7.73(d, 1H, $J = 1.8$) 7.34(d, 1H, $J = 1.8$)	12.82(1H, $w_H = 20$) 7.44(q, 1H, $J = 1.4$) 3.70(d, 3H, $J = 1.4$)	12.74(1H, $w_H = 40$) 3.64(3H, q, $J \sim 1$) 3.48(3H, q, $J \sim 1$)
U.v. [λ_{max} (log ε)][e]	268(4.17), 211(3.64)	271(4.19), 209(3.65)	275(4.13), 208(3.64)[f]
I.r. ($CHCl_3$)[g] (cm^{-1})	3445, 3165, 3105, 2755, 1595, 1490, 1463	3400, 3160, 2745, 2660, 1660, 1500, 1456	3410, 3110, 2800, 2750, 2660, 1703(w), 1518, 1486, 1453

[a]Literature (3) m.p. 150–152°.
[b]Literature (2) m.p. 137°.
[c]Recorded with a Varian A-60A spectrometer in perdeuteriodimethylsulfoxide containing tetramethylsilane as an internal standard.
[d]d, doublet; q, quartet; other absorptions had singlet multiplicity. The *J*-values and peak widths at half height are given in Hz.
[e]Measured in 95% ethanol on a Unicam SP800 u.v. spectrophotometer.
[f]3-Phenyl-3,4-di-*n*-propyloxazole-2-thione is reported (5) to have λ_{max} 285 (log ε 4.09).
[g]Recorded in chloroform with a Unicam SP-200G i.r. spectrophotometer.

N- and *S*-alkyl derivatives. A similar conclusion was reached from i.r. spectroscopic data (6, 7). On the basis of the i.r. spectral data given in Table 1, in particular the absence of absorptions in the 2600–2500 cm^{-1} region,[3] it is apparent that oxazole-2-thione, and its 4-methyl and 4,5-dimethyl derivatives all exist in solution in the thione rather than the thiol form.

Experimental

4-Methyloxazole-2-thione and 4,5-dimethyloxazole-2-thione were prepared by the method of Willems and Vandenberghe (2).

Oxazole-2-thione

A solution of dihydroxymaleic acid (10) (19.0 g, 128 mmol) in water (300 ml) was maintained at 60° until carbon dioxide evolution had ceased (*ca.* 20 min). A thiocyanic acid solution was prepared in a separate vessel by adding concentrated hydrochloric acid (15 ml) to a solution of potassium thiocyanate (16.5 g, 170 mmol) in absolute alcohol (375 ml) and then filtration to remove the precipitated potassium chloride. The glycolic aldehyde solution (11) and the thiocyanic acid solution were combined and heated under reflux in a nitrogen atmosphere for 16 h. The solvent was removed *in vacuo* ($\leqslant 40°$) and the solid residue was heated with 5% methanolic chloroform (100 ml). The mixture was filtered through anhydrous sodium sulfate (50 g), the filtrate was placed on a dry packed column of silica gel (Brinkman, Activity II, 350 g), and the column was developed with 5% methanolic chloroform. The first 600 ml of the eluate was discarded, the next 600 ml contained the product. After crystallization from dichloromethane a white solid (4.5 g, 35%), m.p. 145° dec. was obtained. One crystallization from benzene gave the analytical specimen with m.p. 147° dec.

Anal. Calcd. for C_3H_3NOS: C, 35.63; H, 2.99; N, 13.85. Found: C, 35.65; H, 2.95; N, 13.74.

[3]The S—H stretching band for thiophenols is reported (8) to occur at 2600–2550 cm^{-1}, while thiophene-2- and 3-thiols absorbed in the 2540–2510 cm^{-1} region (9).

1. D. E. HORNING and J. M. MUCHOWSKI. Can. J. Chem. This issue.
2. J. F. WILLEMS and A. VANDENBERGHE. Bull. Soc. Chim. Belg. **70**, 745 (1961); Chem. Abstr. **57**, 12457 (1962).
3. C. K. BRADSHER and W. J. JONES. J. Org. Chem. **32**, 2079 (1967).
4. P. NAHN and G. WAGNER. Arch. Pharm. **301**, 186 (1968); Chem. Abstr. **69**, 77686*k* (1968).
5. R. GOMPER and H. HERLINGER. Chem. Ber. **89**, 2816 (1956).
6. R. GOMPER and H. HERLINGER. Chem. Ber. **89**, 2825 (1956).
7. F. WEYGAND, H-J. BESTMANN, and F. STEDEN. Chem. Ber. **91**, 2537 (1958).
8. L. J. BELLAMY. The infrared spectra of complex molecules. 2nd ed. Methuen and Co. Ltd. London. 1958. p. 350.
9. S. GRONOWITZ, P. MOSES, and A-B. HORNFELDT. Arkiv. Kemi. **17**, 237 (1961).
10. H. O. L. FISCHER and L. FELDMANN. Chem. Ber. **62**, 854 (1929).
11. H. J. H. FENTON. J. Chem. Soc. **65**, 902 (1894); **67**, 774 (1895).

Can. J. Chem. Downloaded from www.nrcresearchpress.com by 210.87.254.5 on 09/05/12
For personal use only.

Electrochemical Oxidation of Trifluoroacetic Acid in an Organic Medium. I. Synthesis of Trifluoroethane-1,1,1-d_3 and Pentafluoropropane-1,1,1-d_3 [1]

R. N. RENAUD AND D. E. SULLIVAN[2]

Division of Chemistry, National Research Council of Canada, Ottawa, Canada K1A 0R6

Received June 8, 1972

"Crossed" Kolbe reactions are generally not very appropriate for the synthesis of short-chain hydrocarbons. However, trifluoroethane-d_3 and pentafluoropropane-d_3 were prepared in high yields by electrolysis of mixtures of the corresponding perfluoro-acids and acetic-d_3 acid under specific conditions.

La réaction de Kolbe est rarement employée pour la préparation d'hydrocarbures à courte chaîne à partir de deux acides carboxyliques différents. Par contre, le trifluoroéthane-d_3 et le pentafluoropropane-d_3 ont été obtenus en bons rendements à partir de mélanges d'acides perfluorés correspondants et d'acide acétique-d_3 en suivant des conditions expérimentales bien spécifiques.

Canadian Journal of Chemistry, **50**, 3084 (1972)

Can. J. Chem. Downloaded from www.nrcresearchpress.com by 210.87.254.6 on 09/05/12
For personal use only.

Deuterio-fluorohydrocarbons were needed for spectroscopic studies (1) and the only reported synthesis in the literature is that of trifluoroethane-1,1,1-d_3 (2). It was obtained by fluorination of trichloroethane-1,1-1-d_3 with antimony trifluoride (3). This reaction has the disadvantage of being conducted in a metal container under very specific conditions in order to obtain a yield of 30%. Also, the starting material can only be prepared with an overall yield of 40% from dichloroethylene by a four-step synthesis (4). Hasek *et al.* (5) described a method for the synthesis of trifluoroethane, in 50% yield, which could be applied to the preparation of the deuterated analogue. It consists of fluorinating acetic anhydride in the presence of sulfur tetrafluoride, carried out in a stainless steel pressure tube and shaken at 300 °C. Great care must be exercized in working with the poisonous compounds employed in this reaction.

In general "crossed" Kolbe reaction cannot be employed with satisfaction for the synthesis of low molecular weight hydrocarbons. The three possible hydrocarbons formed are difficult to separate (6). Petersen *et al.* (7) obtained only hexafluoroethane from the electrolysis of a mixture of trifluoroacetic acid in acetic acid and concluded that the very high ionization of trifluoroacetic acid was responsible for this result. Acetate ions, which are necessary for the success of the Kolbe reaction, were not present in the solution. However, it was found that controlled concentration of trifluoroacetic acid in the presence of an excess of acetate anions in acetic acid favored the formation of trifluoroethane in 68% yield, and completely eliminated the formation of hexafluoroethane. The only other product formed was ethane, which could be easily separated by a vacuum line distillation at −120 °C.

Pentafluoropropane was prepared in yields of over 75% under the same experimental conditions using pentafluoropropionic acid instead of trifluoroacetic acid.

Experimental

Trifluoroethane-1,1,1-d_3

A solution of trifluoroacetic acid (5.3 g) in acetic-d_3 acid (3.5 ml) was added dropwise during a period of 7 h to a solution of potassium acetate-d_3 (4.5 g) in acetic-d_3 acid (75 ml) at 45° in a 100 ml round-bottom flask equipped with a pressure equilibrated separatory funnel, a thermometer, a reflux condenser, a magnetic bar stirrer and two pieces of smooth platinum foil (1.4 × 1.9 cm) 3 mm apart. The electrodes were sealed into glass tubings which were extended down from a 24/40 glass head. At the top of the condenser, attached in series, was a gas washing bottle containing a 20% solution of sodium hydroxide, a Drierite U tube, a Stock trap and a gas bubbler. The system was flushed continuously with a slow stream of nitrogen from a gas inlet attached at the top of the separatory funnel. The electrolysis was carried out at a current density of 0.34 A/cm^2 and the gaseous materials formed were collected in the Stock trap in liquid nitrogen. The electrolysis was continued for an additional 0.5 h after the addition.

The trap was attached to a vacuum line and the high

[1]NRCC No. 12714.

[2]NRCC Summer Student, 1971.

vapor pressure fraction at $-120°$ (mostly ethane) was collected in a trap in liquid nitrogen. The distillation was continued until the vapor pressure dropped to nearly zero. The solid residue at $-120°$ proved on analysis by v.p.c. and mass spectrometry to be nearly pure trifluoroethane-d_3 (m.p. -105 to $-108°$, lit. $-107°$) (8). The yield based on the trifluoroacetic acid was 68% (2.7 g).

The deuterio-acetic acid remaining in the cell can either be recovered by distillation or kept in the cell for the generation of more trifluoroethane as needed.

Pentafluoropropane-1,1,1-d_3

When the reaction was repeated with pentafluoropropionic acid in place of trifluoroacetic acid, pentafluoropropane-1,1,1-d_3 was obtained in 75% yield.

1. H. J. BERNSTEIN and S. MOHANTY. J. Mag. Res. In press.
2. T. R. STENGEL and R. C. TAYLOR. J. Mol. Spectrosc. **34**, 33 (1970).
3. A. L. HENNE and M. W. RENOLL. J. Am. Chem. Soc. **58**, 889 (1936).
4. J. E. FRANCIS and L. C. LEITCH. Can. J. Chem. **35**, 348 (1957).
5. W. R. HASEK, W. C. SMITH, and V. A. ENGELHARDT. J. Am. Chem. Soc. **82**, 543 (1960).
6. G. E. SVADKOUSKAYA and S. A. VOITKEVICH. Russ. Chem. Rev. **29**, 161 (1960).
7. R. C. PETERSEN, M. FINKELSTEIN, and S. D. ROSS. J. Org. Chem. **32**, 564 (1967).
8. F. SWARTS. Compt. Rend. **197**, 1261 (1933).

Can. J. Chem. Downloaded from www.nrcresearchpress.com by 210.87.254.6 on 09/05/12
For personal use only.

Erratum: A Kinetic Study of the Oxidative Addition of Substituted Benzenethiols Towards *trans*-Halocarbonylbis(triphenylphosphine)iridium(I)

J. R. GAYLOR AND C. V. SENOFF
Department of Chemistry, University of Guelph, Guelph, Ontario

Received August 10, 1972
(Ref.: Can. J. Chem. **50**, 1868 (1972))

Canadian Journal of Chemistry, **50**, 3085 (1972)

Figure 1, but not its caption, was omitted during preparation and printing of this article. The proper Fig. 1, along with its caption, is reproduced below. The material which appears above the caption of Fig. 1 in the article as printed should have followed the second last paragraph of the article (p. 1872).

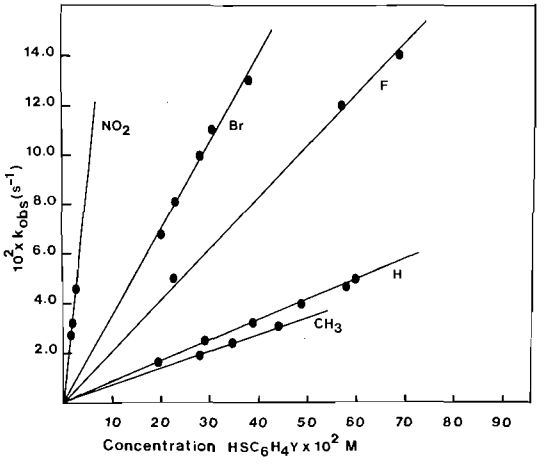

FIG. 1. Plot of k_{obs} *vs.* $[HSC_6H_4Y]$ for *trans*-$[IrCl(CO)(Ph_3P)_2]$ at 25°.

Erratum: The Stereochemistry of the Addition of Two Diazoalkanephosphonates to Norbornene and Norbornadiene; Photolysis of the Adducts. An Entry into the Dimethyl tricyclo[2.1.1.$0^{2,4}$]octyl Phosphonate System

HENRY J. CALLOT AND CLAUDE BENEZRA
Department of Chemistry, University of Ottawa, Ottawa, Canada K1N 6N5

(Ref.: Can. J. Chem. **50**, 1078 (1972))
Received June 27, 1972
Canadian Journal of Chemistry, **50**, 3086 (1972)

The second sentence in the title should read: An entry into the dimethyl tricyclo[3.2.1.$0^{2,4}$]octyl phosphonate system.

Can. J. Chem. Downloaded from www.nrcresearchpress.com by 86.111.144.194 on 09/06/12
For personal use only.

Can. J. Chem. Downloaded from www.nrcresearchpress.com by 210.87.254.40 on 09/05/12
For personal use only.

Canadian Journal of Chemistry

Published by THE NATIONAL RESEARCH COUNCIL OF CANADA

VOLUME 50 OCTOBER 1, 1972 NUMBER 19

N.M.R. Study of Base-Catalyzed Hydrolysis of Trimethylfluorosilane

J. A. GIBSON[1] AND A. F. JANZEN

Department of Chemistry, University of Manitoba, Winnipeg, Manitoba, R3T 2N2

Received April 13, 1972

The diethylamine catalyzed hydrolysis of trimethylfluorosilane in acetonitrile solution has been studied by the nuclear magnetic resonance technique. The concentration and temperature dependence of the pre-exchange lifetime of a fluorine in the exchange reaction was determined from the collapse of the trimethylfluorosilane doublet. The order with respect to trimethylfluorosilane, water, and diethylamine was experimentally determined. Approximate values of the equilibrium constant for the hydrolysis reaction were obtained at several temperatures.

L'hydrolyse catalysée par la diéthylamine, du triméthylfluorosilane en solution dans l'acétonitrile, a été étudiée par la technique r.m.n. L'influence de la concentration et de la température sur la durée de vie de prééchange d'un fluor, dans la réaction d'échange, a été déterminée à partir de la coalescence du doublet du triméthylfluorosilane. L'ordre par rapport au triméthylfluorosilane, eau et diéthylamine a été déterminé expérimentalement. Les valeurs approchées de la constante d'équilibre pour la réaction d'hydrolyse, ont été obtenues à des températures diverses. [Traduit par le journal]

Canadian Journal of Chemistry, **50**, 3087 (1972)

The kinetics of hydrolysis and alcoholysis of organosilicon fluorides and chlorides have been studied by a variety of techniques (1 and references therein, 2). Despite these studies, a number of unresolved features remain, among them: (*a*) the variable order with respect to water, (*b*) order with respect to base catalyst, and (*c*) the negative temperature coefficients. We have applied the nuclear magnetic resonance technique and studied the diethylamine catalyzed hydrolysis of trimethylfluorosilane in acetonitrile solution as a function of trimethylfluorosilane, water, and diethylamine concentration and temperature.

Hydrolysis of $(CH_3)_3SiF$ yields an equilibrium system

$$[1] \qquad (CH_3)_3SiF + H_2O \rightleftarrows (CH_3)_3SiOH + HF$$

with an equilibrium constant $K_{eq} = [(CH_3)_3SiOH][HF]/[(CH_3)_3SiF][H_2O]$ of about 3.7×10^{-3} at $-10°$ and 1.0×10^{-3} at 25° (extrapolated). The equilibrium constant may be roughly estimated from the n.m.r. spectrum by integrating the $(CH_3)_3SiOH$ and $(CH_3)_3SiF$ peaks at low temperature under conditions of slow exchange (see Experimental). Similar equilibrium systems exist for other R_3SiF compounds where K_{eq} has been found to vary between 10^{-2} and 10^{-4} (ref. 2, p. 140).

Trimethylsilanol is converted to hexamethyldisiloxane (3)

$$[2] \qquad 2(CH_3)_3SiOH \rightarrow (CH_3)_3SiOSi(CH_3)_3 + H_2O$$

and, in the presence of diethylamine, hydrogen fluoride is complexed as diethylammonium fluoride and bifluoride. However, the condensation reaction (eq. 2) was monitored by n.m.r. and found to be too slow to interfere with the fluorine exchange studies based on eq. 1.

The fluorine involved in the exchange reaction gives rise to a spin–spin doublet ($J = 7.5$ Hz) in the proton n.m.r. spectrum under conditions of very slow fluorine exchange. As exchange increases, the spin–spin doublet collapses to a single peak. Collapse of the doublet due to intermolecular methyl exchange as found, for

[1]Holder of NRCC post-graduate scholarship.

Can. J. Chem. Downloaded from www.nrcresearchpress.com by 210.87.254.40 on 09/05/12
For personal use only.

example, in organoaluminum (4) or organothallium (5) compounds, is unlikely since CH_3–^{29}Si coupling is unaffected by the exchange process. On the other hand, collapse of the doublet is accompanied by loss of ^{19}F–^{29}Si coupling, consistent with intermolecular fluorine exchange represented by eq. 1.

An alternative mechanism of exchange, represented by eq. 3,

[3] $(CH_3)_3SiF + (C_2H_5)_2NH \rightleftarrows (CH_3)_3Si—N(C_2H_5)_2 + HF$

was considered, but eliminated by the following experiments: firstly, no exchange occurred before addition of water; secondly, if rapid exchange (single n.m.r. peak) was observed in a sample containing $(CH_3)_3SiF$, H_2O, and $(C_2H_5)_2NH$, then addition of $(CH_3)_3Si—N(C_2H_5)_2$ immediately stopped exchange (n.m.r. doublet). Evidently, reaction 3 is displaced essentially to the left, and the effect of adding $(CH_3)_3Si—N(C_2H_5)_2$ must be to stop the fluorine exchange of reaction 1 by removing HF.

In the n.m.r. method, kinetic and activation parameters may be obtained by studying the variation of the pre-exchange lifetime of fluorine with concentration and temperature, as described in recent review articles (6, 7). Following the description by Ham and Mole (7) we express the pre-exchange lifetime of $(CH_3)_3SiF$ by

$$(f\tau')^{-1} = \frac{-1}{[(CH_3)_3SiF]} \frac{d[(CH_3)_3SiF]}{dt}$$

where f is the appropriate statistical factor which converts the pre-exchange lifetime of a nucleus to that of the molecule undergoing exchange. In this case $f = \frac{1}{2}$ since after exchange the fluorine may have spin state $+\frac{1}{2}$ or $-\frac{1}{2}$.

If

$$1/\tau = (\tau'/2)^{-1}$$

then

$$1/\tau = k[(CH_3)_3SiF]^{n-1}F([\text{other species}])$$

where k is the specific rate constant, n is order of reaction in $(CH_3)_3SiF$, and $F([\text{other species}])$ describes the dependence of rate on concentration of other species. If concentration of other species is kept constant, $1/\tau$ should be independent of $[(CH_3)_3SiF]$ for a reaction first order in $(CH_3)_3SiF$.

Figure 1 shows a plot of $1/\tau$ *vs.* $[(CH_3)_3SiF]$ at constant $[H_2O]$ and $[(C_2H_5)_2NH]$ at 38°. The slope, by least-squares method, is 0.05, hence $1/\tau$ is independent of $[(CH_3)_3SiF]$ within experimental error[2] and the reaction is first order in $(CH_3)_3SiF$.

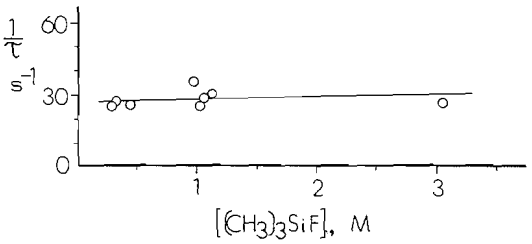

FIG. 1. A plot of $1/\tau$ *vs.* $[(CH_3)_3SiF]$ at 38° at constant $[H_2O] = 0.033$ *M* and $[(C_2H_5)_2NH] = 0.67$ *M*.

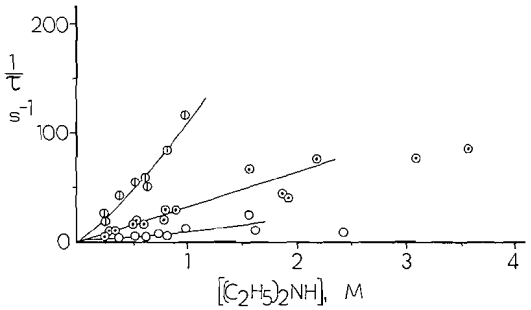

FIG. 2. Plot of $1/\tau$ *vs.* $[(C_2H_5)_2NH]$ at 38°: ○, $[H_2O] = 0.014$ *M*; ⊙, $[H_2O] = 0.028$ *M*; ⊕, $[H_2O] = 0.055$ *M*. $[(CH_3)_3SiF]$ was varied randomly between 0.16 and 0.79 *M*.

Figure 2 shows a plot of $1/\tau$ *vs.* $[(C_2H_5)_2NH]$ as a function of $[H_2O]$ at 38°. Since $1/\tau$ is independent of $[(CH_3)_3SiF]$ the concentration of $(CH_3)_3SiF$ was varied randomly between 0.16 and 0.79 *M*. The zero intercept, within experimental error, suggests that solvent acetonitrile is not an effective catalyst for hydrolysis of $(CH_3)_3SiF$.

If the data of Fig. 2 are re-plotted as ln $1/\tau$ *vs.* ln $[(C_2H_5)_2NH]$, a linear plot is obtained over the concentration range $[(C_2H_5)_2NH] < 1.6$ *M*, and the order with respect to $(C_2H_5)_2NH$ is 1.0, within experimental error, as shown in Table 1. At $[(C_2H_5)_2NH] > 1.6$ *M*, the ln $1/\tau$ *vs.* ln $[(C_2H_5)_2NH]$ plot departs from linearity and ln $1/\tau$ decreases with increasing ln $[(C_2H_5)_2$-

[2]Standard deviations are not quoted since the n.m.r. method generally involves larger errors (6, 7). We assume that our maximum errors are within ±10% of the values quoted in the text.

Can. J. Chem. Downloaded from www.nrcresearchpress.com by 210.87.254.40 on 09/05/12
For personal use only.

TABLE 1. Order with respect to $(C_2H_5)_2NH$ as a function of H_2O concentration at 38°

$[H_2O]$ (M)	n*
0.055	1.07
0.028	1.07
0.014	0.95

*Least-squares slope from plot of ln $1/\tau$ *vs.* ln $[(C_2H_5)_2NH]$ using data of Fig. 2 for $[(C_2H_5)_2NH] < 1.6$ M. $[(CH_3)_3SiF]$ varied randomly between 0.16 and 0.79 M.

TABLE 2. Order with respect to H_2O as a function of $(C_2H_5)_2NH$ concentration at 38°

$[(C_2H_5)_2NH]$ (M)	n*
0.24	1.9
0.51	1.7
1.56	1.5
4.66	1.0

*Least squares slope from plot of ln $1/\tau$ *vs.* $[H_2O]$ using data of Fig. 3. $[(CH_3)_3SiF]$ varied randomly between 0.49 and 1.18 M.

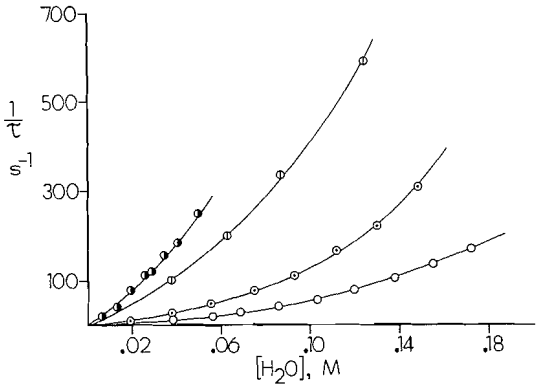

FIG. 3. Plot of $1/\tau$ *vs.* $[H_2O]$ at 38°: ○, $[(C_2H_5)_2NH] = 0.24$ M; ⊙, $[(C_2H_5)_2NH] = 0.51$ M; ◑, $[(C_2H_5)_2NH] = 1.56$ M; ●, $[(C_2H_5)_2NH] = 4.66$ M. $[(CH_3)_3SiF]$ was varied randomly between 0.49 and 1.18 M.

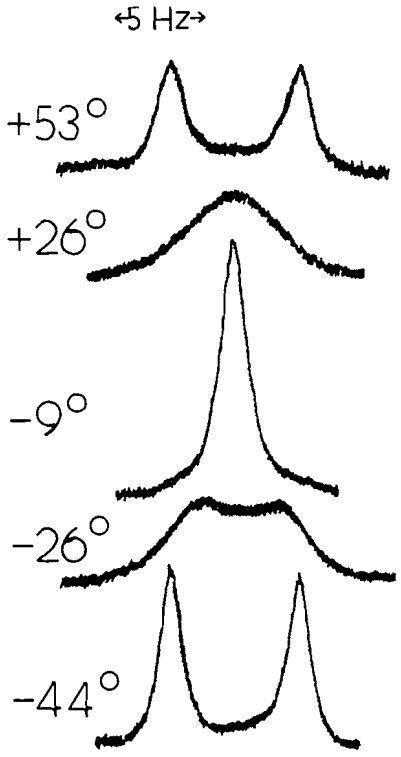

FIG. 4. Typical temperature dependent proton n.m.r. spectra: $[(CH_3)_3SiF] = 0.29$ M, $[H_2O] = 0.038$ M, $[(C_2H_5)_2NH] = 0.35$ M.

NH], resulting in an apparent decrease in order with respect to $(C_2H_5)_2NH$. The anomalous behavior at $[(C_2H_5)_2NH] > 1.6$ M is most readily explained by a decrease in rate of hydrolysis resulting from a decrease in the order with respect to water at high $(C_2H_5)_2NH$ concentration (*cf.* Fig. 3 and Table 2).

Figure 3 shows a plot of $1/\tau$ *vs.* $[H_2O]$ as a function of $(C_2H_5)_2NH$ concentration at 38°. $[(CH_3)_3SiF]$ was varied randomly between 0.49 and 1.18 M. The zero intercept is important since it confirms the absence of adventitious moisture in solvent and reagents.

If the data of Fig. 3 are re-plotted as ln $1/\tau$ *vs.* ln $[H_2O]$, linear plots are obtained and the least-squares slopes are shown in Table 2. The order with respect to H_2O varies between 1.0 and 1.9 and the order is seen to decrease with increasing $(C_2H_5)_2NH$ concentration.

The effect of temperature on rate of hydrolysis was studied and Fig. 4 shows typical temperature dependent spectra. Initial cooling from +53 to −9° results in collapse of the doublet and increase in rate of fluorine exchange. On further cooling below −9°, however, the rate decreases and at −44° the doublet re-appears.

The initial increase in rate of fluorine exchange with decreasing temperature was confirmed for various mixtures of $(CH_3)_3SiF$, $(C_2H_5)_2NH$,

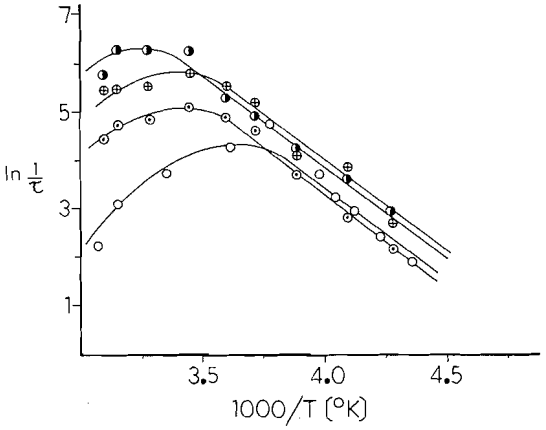

FIG. 5. Plot of $1/\tau$ *vs.* $1/T$: ○, $[(CH_3)_3SiF] = 0.29$ *M*, $[(C_2H_5)_2NH] = 0.35$ *M*, $[H_2O] = 0.038$ *M*; ⊙, $[(CH_3)_3SiF] = 0.66$ *M*, $[(C_2H_5)_2NH] = 0.39$ *M*, $[H_2O] = 0.084$ *M*; ⊕, $[(CH_3)_3SiF] = 0.46$ *M*, $[(C_2H_5)_2NH] = 0.86$ *M*, $[H_2O] = 0.090$ *M*; ◑, $[(CH_3)_3SiF] = 0.48$ *M*, $[(C_2H_5)_2NH] = 0.74$ *M*, $[H_2O] = 0.084$ *M*.

and H_2O, as shown in the Arrhenius plot of $\ln 1/\tau$ *vs.* $1/T$ (Fig. 5). If all the points from the low temperature straight line portion of the Arrhenius plot of Fig. 5 are used to calculate a least-squares slope, an activation energy of 7.8 kcal/mol is obtained for the low temperature process.

Possible Intermediates in Hydrolysis Reaction

Any proposed mechanism must be consistent with the rate expression which, at 38°, is given by

$$R = k[(CH_3)_3SiF][(C_2H_5)_2NH][H_2O]^n$$

where n varies from 1.0 to 1.9, depending on $(C_2H_5)_2NH$ concentration (Table 2), and also consistent with the temperature effects in the Arrhenius plot (Fig. 5).

A mechanism has been proposed by Allen and Modena (8) and others (9) to account for hydrolysis and alcoholysis of organosilicon chlorides, involving a rate-controlling transition

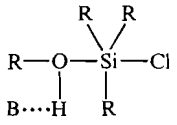

state in which B is a base capable of assisting proton removal from ROH. Chipperfield and Prince (10) studied the hydrolysis of organosilicon and organogermanium chlorides and suggested a transition state involving a water aggregate, *i.e.* $ROH{=}H_2O$ and $B = [H_2O]_{n-1}$, to explain the multiple order in H_2O and the negative temperature coefficient, the latter effect arising from the heat of association of $[H_2O]_n$.

Although the mechanism of Chipperfield and Prince could, in theory, also account for the hydrolysis of $(CH_3)_3SiF$, we do not favor such an explanation for several reasons. Firstly, the order in H_2O in our study does not exceed 1.9, despite variation in H_2O concentration from 0.06 to 0.18 *M*, and $(C_2H_5)_2NH$ from 0.24 to 4.66 *M*, hence the postulate of a water aggregate $(H_2O)_n$ where $n > 2$ is unnecessary. Secondly, the variation in order in H_2O is seen to be inversely proportional to $(C_2H_5)_2NH$ concentration (Fig. 2) and the postulate of a water aggregate with variable n is unnecessary. Thirdly, although the deviation in the Arrhenius plot may be explained in terms of the heat of association of $(H_2O)_n$, a variety of other effects summarized by Hulett (11) may also explain deviations from the Arrhenius equation.[3]

Of the effects discussed by Hulett, the most consistent with the well known tendency of silicon and other group IV elements to form five or six coordinate complexes of the type SiX_4.base and SiX_4.2base (12, 13) would appear to be a change in mechanism with temperature, either involving two (or more) processes of different activation energies with five or six coordinate intermediates, or a reaction involving a pre-equilibrium in which the equilibrium constant varies with temperature.

At 38° the rate law with $n = 1$ is consistent with the five coordinate transition state proposed by Allen and Modena.

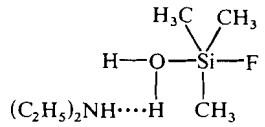

[3]It is of interest that Chipperfield and Prince observed a negative temperature effect for chlorosilanes but not triphenylchlorogermane; however, since they report rate constants for the latter at only two temperatures, 25 and 40°, it is not clear whether their results are real or fortuitous. Only a rate study over wider temperature range would determine whether chlorogermanes differ from chlorosilanes, or whether the behavior parallels that of trimethylfluorosilane shown in Fig. 5.

Can. J. Chem. Downloaded from www.nrcresearchpress.com by 210.87.254.40 on 09/05/12
For personal use only.

Can. J. Chem. Downloaded from www.nrcresearchpress.com by 210.87.254.40 on 09/05/12
For personal use only.

The increase in order in H_2O to 1.9 suggests a second reaction pathway with a six coordinate transition state in which two water molecules are coordinated to silicon.

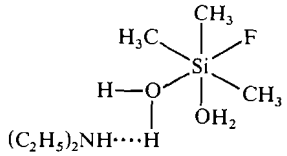

A possible explanation for the decrease in order in H_2O with increasing $(C_2H_5)_2NH$ concentration may be as follows: H_2O and $(C_2H_5)_2NH$ may compete for the sixth coordinate site around silicon, therefore at high $[(C_2H_5)_2NH]$ the order in H_2O decreases to 1.0, whereas at low $[(C_2H_5)_2NH]$ the order increases to 1.9. However, only the transition state in which H_2O occupies the sixth coordinate site is involved in the rate controlling step since the order in $(C_2H_5)_2NH$ does not exceed 1.0 (Table 1).

The fluorine exchange reaction does not appear to be catalyzed by hydroxide ion, since addition of small amounts of solid or aqueous sodium hydroxide to trimethylfluorosilane in acetonitrile solution did not broaden the trimethylfluorosilane doublet (however, condensation of trimethylsilanol is accelerated by addition of hydroxide ion). This result argues against a mechanism involving a pre-equilibrium of $(C_2H_5)_2NH$ and H_2O to give $(C_2H_5)_2NH_2^+$ and HO^- ions.

Other five or six coordinate intermediates, $(CH_3)_3SiF{\cdot}NH(C_2H_5)_2$ or $(CH_3)_3SiF{\cdot}2NH(C_2H_5)_2$ (probably of lower stability than $SiX_4{\cdot}$base and $SiX_4{\cdot}2$base where X = halogen, since the effect of replacing halogen with alkyl groups is known to decrease the stability of the complex (14)), seem reasonable, but their effect on the mechanism is unknown.

To suggest a more detailed mechanism for this complex reaction is not justified at this stage, particularly in view of the generally low precision of kinetic results obtained by the n.m.r. method.

Experimental

Moisture was rigorously excluded from chemicals and equipment. A conventional glass vacuum manifold was dried by silylation (with $(CH_3)_3Si{-}N(C_2H_5)_2$), evacuated, and thoroughly flamed out. Acetonitrile (Spectroquality, Matheson, Coleman and Bell) was redistilled and stored over P_2O_5 in the vacuum manifold. Trimethylfluorosilane (Peninsular Chem Research) was purified by trap-to-trap distillation and stored over activated molecular sieves and diethylamine (Reagent, Fisher) was redistilled twice and stored over sodium amalgam in the vacuum manifold.

N.m.r. tubes were dried at 400° for several days and flamed out under vacuum. Reagents were condensed into the n.m.r. tubes, which were flame sealed, and average concentrations determined by at least five n.m.r. peak integrations. N.m.r. tubes were then opened and capped with silicone rubber septum caps. Solutions made up by this method had negligible moisture content since a plot of $1/\tau$ *vs.* H_2O concentration had zero intercept (Fig. 3). Furthermore, even at high diethylamine concentration, no collapse of the trimethylfluorosilane doublet was observed before addition of water.

Small amounts of water were then added by means of dilute water–acetonitrile solutions of known concentration using 10 or 50 μl syringe and injecting through n.m.r. caps. Samples were shaken and allowed to equilibrate in the n.m.r. probe (38°) for at least 5 min. Blank determinations showed that negligible amounts of adventitious moisture were introduced by this technique.

All proton n.m.r. spectra were recorded using Varian A-56/60A spectrometer at 60 MHz equipped with variable temperature probe. For the temperature runs, n.m.r. tubes were flame sealed to prevent possible moisture condensation. Temperatures were calibrated with the aid of a methanol temperature *vs.* chemical shift chart (15) and are accurate to ±1°.

Theoretical values of τ', the pre-exchange lifetime of a fluorine in the exchange reaction, were obtained for different values of τ', using a program written by B. W. Goodwin of this department, based on the McConnell formulation of the Bloch equations (16). For particular τ' values, the program tabulated peak separation, half-height peak width, ratio of maximum to minimum intensity, and half-height width of collapsed peak (for fast exchange region). These values were then compared with the observed spectra. One component of the $(CH_3)_3SiF$ doublet (in degassed acetonitrile solution) was used to estimate that $T_2 = 1.06$ s.

The end products of hydrolysis after about 8 days at room temperature were $(CH_3)_3SiOSi(CH_3)_3$, identified by comparison with n.m.r. spectrum of an authentic sample, and mixture of diethylammonium fluoride and bifluoride. The latter were precipitated from CH_2Cl_2 solution and identified by elemental analysis (A. Bernhardt, West Germany).

Anal. Calcd. for 1:4 molar ratio of $(C_2H_5)_2NH_2F$: $(C_2H_5)_2NH_2HF_2$: C, 44.0; H, 11.8; N, 12.8. Found: C, 44.27; H, 11.14; N, 12.70.

Estimate of Equilibrium Constant of Hydrolysis Reaction

The diethylamine catalyzed hydrolysis in acetonitrile is

$$(CH_3)_3SiF + H_2O \rightleftarrows (CH_3)_3SiOH + HF$$

rapid at 38° but is slowed down at low tem-

TABLE 3. Values of K_{eq} at various temperatures

T (°K)	$[(CH_3)_3SiF]$ (M)	$[H_2O]$ (M)	$[(CH_3)_3SiOH] = [HF]$ (M)	K_{eq}
263	1.01	0.060	0.015	3.7×10^{-3}
252	1.01	0.057	0.018	5.6×10^{-3}
240	1.01	0.051	0.024	1.12×10^{-2}

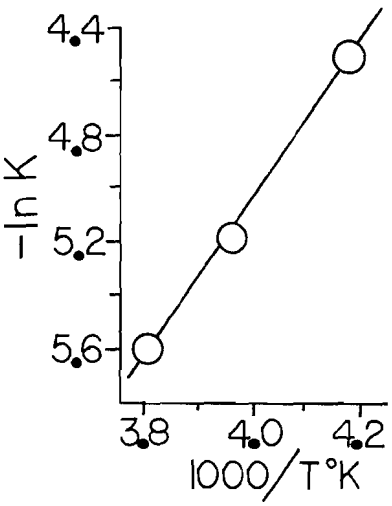

FIG. 6. Plot of ln K_{eq} *vs.* $1/T$ for hydrolysis of trimethylfluorosilane.

perature and a separate n.m.r. peak of low intensity is observed which may be assigned to $(CH_3)_3SiOH$ by comparison with the chemical shift of an authentic sample of $(CH_3)_3SiOH$ prepared by hydrolysis of $(CH_3)_3SiCl$ (17). The equilibrium constant $K_{eq} = [(CH_3)_3SiOH][HF]/[(CH_3)_3SiF][H_2O]$ was estimated at several temperatures by integrating n.m.r. peaks and assuming $[(CH_3)_3SiOH] = [HF]$ (Table 3).

From the relation $d \ln K/d(1/T) = -\Delta H/R$ it is possible to obtain ΔH, the heat of reaction, by plotting ln K *vs.* $1/T$ (18). As shown in Fig. 6, the plot is linear and gives $\Delta H = -6.0$ kcal/mol. Extrapolating K_{eq} to 25° gives K_{eq} $(25°) = 1.0 \times 10^{-3}$. Although values for K_{eq} and ΔH may be obtained quite readily by the n.m.r. method, the numerical results are only approximate estimates.

The financial assistance of the National Research Council of Canada is gratefully acknowledged. We wish to thank Dr. C. E. Burchill for many helpful discussions.

1. A. D. ALLEN and S. J. LAVERY. Can. J. Chem. **47**, 1263 (1969); C. G. SWAIN, R. M. ESTERE, JR., and R. H. JONES. J. Am. Chem. Soc. **71**, 965 (1949).
2. L. H. SOMMER. Stereochemistry, mechanism and silicon. McGraw–Hill, New York, N.Y. 1965.
3. C. EABORN. Organosilicon compounds. Butterworths, London. 1960. pp. 227–268.
4. K. C. WILLIAMS and T. L. BROWN. J. Am. Chem. Soc. **88**, 5460 (1966).
5. J. P. MAHER and D. F. EVANS. J. Chem. Soc. 5534 (1963).
6. C. S. JOHNSON, JR. Adv. Magn. Resonance, **1**, 33 (1965); L. W. REEVES. Adv. Phys. Org. Chem. **3**, 187 (1965); A. ALLERHAND, H. S. GUTOWSKY, J. JONAS, and R. A. MEINZER. J. Am. Chem. Soc. **88**, 3185 (1966).
7. N. S. HAM and T. MOLE. Progress in NMR Spectroscopy, Vol. 4. *Edited by* J. W. Emsley, J. Feeney, and L. H. Sutcliffe. Pergamon Press, New York, N.Y. 1969. p. 91.
8. A. D. ALLEN and G. MODENA. J. Chem. Soc. 3671 (1957).
9. G. SCHOTT, H. KELLING, and R. SCHILD. Chem. Ber. **99**, 291 (1966).
10. J. R. CHIPPERFIELD and R. H. PRINCE. J. Chem. Soc. 3567 (1963).
11. J. R. HULETT. Quart. Rev. **18**, 227 (1964).
12. I. R. BEATTIE. Quart. Rev. **17**, 382 (1963).
13. J. G. A. LUIJTEN, F. RIJKENS, and G. J. M. VAN DER KERK. *In* Advances in Organometallic Chemistry. Vol. 3. *Edited by* F. G. A. Stone and R. West. Academic Press, New York, N.Y. 1965. p. 397.
14. F. KLANBERG and E. L. MUETTERTIES. Inorg. Chem. **7**, 155 (1968).
15. A. L. VAN GEET. Anal. Chem. **42**, 679 (1970).
16. H. M. MCCONNELL. J. Chem. Phys. **28**, 430 (1958).
17. L. H. SOMMER, E. W. PIETRUSZA, and F. C. WHITMORE. J. Am. Chem. Soc. **68**, 2282 (1946).
18. S. GLASSTONE and D. LEWIS. Elements of physical chemistry. *2nd ed.* Van Nostrand Co., Princeton, New Jersey. 1960. p. 316.

Can. J. Chem. Downloaded from www.nrcresearchpress.com by 210.87.254.40 on 09/05/12
For personal use only.

Ammine Complexes of Osmium(II)

A. D. ALLEN AND J. R. STEVENS
Lash Miller Chemical Laboratories, University of Toronto, Toronto 181, Ontario

Received March 27, 1972

Several ammine complexes of osmium(II) containing one or two π-acceptor ligands have been prepared. They have been characterized by analytical techniques and their infrared and electronic spectra have been recorded and assignments proposed. Comparison with similar ruthenium(II) complexes has been made when possible.

Plusieurs complexes entre l'amine et l'osmium(II) contenant un ou deux ligands π-accepteurs ont été préparés. Ils ont été caractérisés par les techniques analytiques, leurs spectres infrarouge et électronique ont été enregistrés et des attributions proposées. Une comparaison avec les complexes analogues du Ruthénium(II) a été faite quand c'était possible. [Traduit par le journal]

Canadian Journal of Chemistry, **50**, 3093 (1972)

Can. J. Chem. Downloaded from www.nrcresearchpress.com by 210.87.254.42 on 09/05/12
For personal use only.

Introduction

Following the publication of the preparation of $[Ru(NH_3)_6]^{2+}$ in 1959 (1) and of $[Ru(NH_3)_5(N_2)]^{2+}$ in 1965 (2), the investigation of ruthenium(II) ammine complexes has increased rapidly (3). A large number of octahedral complexes containing four or five ammonia ligands with a wide variety of ligands in the remaining coordination sites have been prepared. Although the chemistry of divalent osmium generally parallels that of divalent ruthenium (4), no osmium(II) ammine complexes had been prepared prior to 1967.

We reported the preparation of $[Os(NH_3)_5(N_2)]X_2$ (X = Cl, Br, I, BF_4, ClO_4, and $B(C_6H_5)_4$ in 1967 (5) and subsequently *cis*-$[Os(NH_3)_4(N_2)_2]X_2$ (X = Cl, Br, and I) was prepared by diazotization of the former cation (6). We now report the detailed preparation and characterization of halide salts of the ions $[Os(NH_3)_5(N_2)]^{2+}$, $[Os(NH_3)_5CO]^{2+}$, and *cis*-$[Os(NH_3)_4CO(N_2)]^{2+}$.

Experimental

The instruments used in this work were Perkin–Elmer 521 and 180 spectrophotometers for the infrared studies (Nujol mulls between KBr plates) and a Bausch and Lomb 505 spectrophotometer for the electronic spectra (1 cm fused silica cells). Magnetic measurements were made using a Gouy balance. Microanalyses (Table 1) were performed by A. B. Gygli, Toronto or Huffman Laboratories, Wheatridge, Colorado. Halide was determined potentiometrically following the method of Lingane (7).

Preparations

1. Nitrogenpentaammineosmium(II) Chloride, $[Os(NH_3)_5(N_2)]Cl_2$

Two g of ammonium hexachloroosmate were slowly added to 25 ml of ice-cold 85% hydrazine hydrate being rapidly stirred in a single necked flask. Two ml of water were used to rinse the neck of the flask and the solution was refluxed for 15 h. It was then cooled to 0° and the yellow precipitate collected, washed with 95% ethanol and diethyl ether, and air-dried. The product was recrystallized by dissolution in cold dilute hydrochloric acid and reprecipitated by the addition of concentrated hydrochloric acid. Yield of the pale yellow powder 1.1 g (65%).

2. Nitrogenpentaammineosmium(II) Bromide, $[Os(NH_3)_5(N_2)]Br_2$, and Iodide, $[Os(NH_3)_5(N_2)]I_2$

These salts were prepared by metathetical reactions of the chloride salt of the cation with the appropriate sodium salt of the anion. $[Os(NH_3)_5(N_2)]Cl_2$ (0.25 g) was dissolved in 75 ml of water at 20 °C and 10 ml of a saturated solution of sodium bromide or iodide were added. The precipitate was collected, redissolved in the minimum amount of water at 20 °C, and reprecipitated by the further addition of saturated sodium halide solution. The bromide salt is very pale yellow in color and the iodide salt is off-white.

3. cis-Bisnitrogentetraammineosmium(II) Bromide, cis-$[Os(NH_3)_4(N_2)_2]Br_2$

This salt was prepared as previously reported (6).

4. Carbonylpentaammineosmium(II) Halide, $[Os(NH_3)_5CO]X_2$ (X = Cl, Br, I)

Chloropentaammineosmium(III) chloride (0.2 g) was added to 20 ml of approximately 5 *M* formic acid. Freshly amalgamated mossy zinc (3–5 g) was added and carbon monoxide was passed through the solution. The solid slowly dissolved to form a yellow solution which gradually became colorless. After 20 h the zinc was filtered off and the required salt of the carbonylpentaammineosmium(II) cation was precipitated by the addition of the appropriate potassium halide to the filtrate. The complexes were purified by dissolution in cold dilute ammonium hydroxide and reprecipitated as white powders by the addition of a saturated solution of the appropriate potassium halide. Yield of the chloride salt 0.13 g (75%).

5. cis-Carbonylnitrogentetraammineosmium(II) Halides, cis-$[Os(NH_3)_4CO(N_2)]X_2$ (X = Cl, Br, I)

Carbonylpentaammineosmium(II) chloride (0.4 g) and sodium nitrite (0.075 g) were dissolved in 75 ml of water and argon was passed through the solution for 15 min. Ten ml of 1 *M* hydrochloric acid were slowly added to the

TABLE 1. Analytical results

Complex	% N		% H		% C		% Halide	
	Calculated	Found	Calculated	Found	Calculated	Found	Calculated	Found
$[Os(NH_3)_5(N_2)]Cl_2$	26.20	25.79	4.01	4.23	—	—	19.0	18.8
$[Os(NH_3)_5(N_2)]Br_2$	21.17	21.12	3.24	3.52	—	—	34.6	33.8
$[Os(NH_3)_5(N_2)]I_2$	17.59	17.54	2.69	2.98	—	—	45.6	45.3
$[Os(NH_3)_5CO]Cl_2$	18.72	18.42	4.01	4.20	3.21	3.21	19.0	18.6
$[Os(NH_3)_5CO]Br_2$	15.12	15.10	3.24	3.17	2.59	2.56	34.6	33.9
$[Os(NH_3)_5CO]I_2$	12.57	13.20	2.69	2.99	2.15	2.04	45.6	44.2
cis-$[Os(NH_3)_4CO(N_2)]Cl_2$	21.82	21.68	3.12	3.76	3.12	3.28	18.4	18.4
cis-$[Os(NH_3)_4CO(N_2)]Br_2$	17.72	17.77	2.53	2.55	2.53	2.93	33.8	33.6
cis-$[Os(NH_3)_4CO(N_2)]I_2$	14.79	15.60	2.11	2.24	2.11	2.36	44.7	44.2

solution which was being rapidly stirred at 25 °C under argon. Considerable gas evolution was observed and after this had subsided (15 min) the solution was saturated with the appropriate potassium halide. The resulting precipitate, pale pink in color, was collected, washed with 95% ethanol and diethyl ether, then air-dried. When reprecipitated from dilute ammonium hydroxide solution, the products were a light cream color. Yield of the chloride salt, 0.15 g (25%).

Results and Discussion

The preparation of the $[Os(NH_3)_5(N_2)]^{2+}$ ion has been reported previously (5). Attempts to replace the N_2 ligand with CO by direct reaction were unsuccessful. In the synthesis of the $[Os(NH_3)_5CO]^{2+}$ ion via reduction of the trivalent complex, $[Os(NH_3)_5Cl]^{2+}$, by amalgamated zinc in formic acid under carbon monoxide, the formic acid is required for formation of the product but the carbon monoxide is not. The reaction proceeds equally well under nitrogen or argon.

No evidence has been obtained for the formation of $[Os(NH_3)_5(N_2)]^{2+}$ or $[(NH_3)_5OsN_2Os(NH_3)_5]^{4+}$ from the reduction of $[Os(NH_3)_5Cl]^{2+}$ in sulfuric or fluoroboric acid under nitrogen. Similarly, $[Os(NH_3)_5CO]^{2+}$ cannot be prepared by reduction of $[Os(NH_3)_5Cl]^{2+}$ in sulfuric acid under carbon monoxide. It thus appears that a reactive intermediate, analogous to the $[Ru(NH_3)_5H_2O]^{2+}$ ion in the ruthenium system which is known to react with CO (14) and N_2 (8), is not formed in the osmium system. During the preparation of $[OsCl_5CO]^{3-}$ from formic acid and $[OsCl_6]^{2-}$, Cleare and Griffith (9) noticed formato intermediates of unspecified osmium oxidation states. However, formic acid and $[Os(NH_3)_5Cl]^{2+}$ do not react even after prolonged heating. This suggests that in the reaction which produces an osmium–carbonyl complex, the osmium is first reduced by the zinc and then a formate group replaces the chloride to form a formato–osmium(II) species which decomposes to $[Os(NH_3)_5CO]^{2+}$. Formate ion may react with the osmium(II) species when N_2 and CO do not because it is a better nucleophile. The decarbonylation of the formate group occurs because it results in the formation of a strong osmium—carbon bond and stabilization of the divalent osmium state.

The diazotization reaction used to prepare *cis*-$[Os(NH_3)_4(N_2)_2]^{2+}$ from $[Os(NH_3)_5(N_2)]^{2+}$ also produces *cis*-$[Os(NH_3)_4CO(N_2)]^{2+}$ from $[Os(NH_3)_5CO]^{2+}$. Since this type of reaction usually involves an unprotonated primary amine, it implies that a definite concentration of a coordinated amido species is present. Curiously the reaction does not succeed with $[Ru(NH_3)_5(N_2)]^{2+}$ (6). One possible explanation of this difference is an equilibrium of the type

$$[1] \quad [Os(NH_3)_5L]^{2+} \rightleftharpoons [Os(NH_3)_4(NH_2)HL]^{2+} \quad (L = N_2, CO)$$

where one of the ammonia protons can bind to the osmium producing formally an osmium(IV) hydride complex. This can be regarded as an intramolecular protonation of a filled metal d-orbital. Since two of the filled d-orbitals of the osmium are involved in π-bonding with the π^*-orbitals of the ligand L, the third orbital at right angles to the molecular axis would be most readily protonated. Thus the protons on the ammonias *cis* to the ligand L are most favorably located to shift to the metal orbital, and the amide ligand, the site of the electrophilic attack in the diazotization reaction,

Can. J. Chem. Downloaded from www.nrcresearchpress.com by 210.87.254.42 on 09/05/12
For personal use only.

Can. J. Chem. Downloaded from www.nrcresearchpress.com by 210.87.254.42 on 09/05/12
For personal use only.

would be *cis* to the ligand L. The resulting complexes thus have a *cis* stereochemistry. Attempts to identify a *trans* species such as *trans*-$[Os(NH_3)_4(N_2)_2]^{2+}$ or *trans*-$[Os(NH_3)_4(H_2O)(N_2)]^{2+}$ as a minor product in the reaction have not been successful.

An interaction of this kind was previously suggested by Palmer and Basolo (10) to explain the slower rate of proton exchange of $[Ir(NH_3)_6]^{3+}$ compared to $[Rh(NH_3)_6]^{3+}$. More recently Taube and co-workers (11) have proposed the protonation of a d-orbital of $[Ru(NH_3)_6]^{2+}$ to explain the dependence on acid concentration of the rate of aquation of this ion. Attempts to prepare $[Os(NH_3)_5(H_2O)]^{2+}$ by electrochemical reduction of $[Os(NH_3)_5Cl]^{2+}$ have been unsuccessful.[1] The reduced species appear to reduce the solvent, probably via interaction of solvent protons with the filled osmium(II) d-orbitals, which reflects the greater basicity of these orbitals on osmium relative to ruthenium, for which complex the reduction proceeds smoothly. Thus $[Ru(NH_3)_5(N_2)]^{2+}$ is not diazotized because the ruthenium d-orbitals are not sufficiently basic to form $[Ru(NH_3)_4(NH_2)H(N_2)]^{2+}$ while $[Ru(NH_3)_6]^{2+}$ is in fact oxidized by nitrous acid, probably via attack of NO^+ on a d-orbital.

$$[2] \quad [Ru(NH_3)_6]^{2+} + NO^+ \rightarrow [Ru(NH_3)_6]^{3+} + NO$$

In this case the ammonia protons are not sufficiently acidic to protonate the d-orbital since the NH_3 ligands are not sufficiently strongly bound to the metal (ν(Ru-NH_3) < 250 cm^{-1} (12), *cf.* ν(Os—NH_3) at 549 cm^{-1} in $[Os(NH_3)_5(N_2)]Cl_2$). Thus it is only in complexes in which highly basic d-orbitals are accompanied by strong metal–ammonia bonds, leading to acidic ammine protons, that intramolecular protonation occurs to a sufficient extent to permit the diazotization reaction.

The presence of a single π-acceptor ligand is probably a necessary requirement to meet these conditions. A ligand of this type would help to provide a low oxidation state and hence basic d-orbitals but, because it affects the d-orbitals differently, it leaves one exposed. It also strengthens the metal–ammonia bonds. With two *cis* π-acceptor ligands all the d-orbitals will be contracted and further diazotization is inhibited.

[1]Personal communication from J. A. Page and J. Gulens.

The infrared vibrational frequencies and their assignments for the complexes prepared in this work are listed in Tables 2, 3, and 4. The data for two ruthenium complexes are listed for comparison. The assignment of the NH_3 frequencies was made via a straightforward comparison with other ammine complexes (13, 14). All three series exhibit small to moderate dependence of the NH_3 vibrations due to the counter-ion, which can be attributed to different degrees of hydrogen bonding between the ammonia-hydrogens and the anions (15). The pentaammine complexes exhibit lower $\rho(NH_3)$ frequencies than do the tetraammine complexes of the corresponding halide. This is indicative of an increased effective electronegativity of the osmium in the tetraammines (16) reflecting electron withdrawal from the metal by the second π-acceptor ligand.

The carbonylpentaammine salts exhibit correlation coupling of the ν(CO) mode similar to that observed with ν(NN) of $[Os(NH_3)_5(N_2)]X_2$ (5, 17). The low energy spike on the ν(CO) band, which is also prominent in the spectra of the analogous ruthenium complexes, can be assigned to the ^{13}CO component. Its appearance from only 1% of the material is an indication of the extreme intensity of the carbonyl absorption. It is also present as a weak shoulder in the spectra of the chloride and bromide salts of the *cis*-$[Os(NH_3)_4CO(N_2)]^{2+}$ ion. The bands at ~2180 and ~1960 cm^{-1} in the spectra of this ion cannot strictly be assigned to ν(NN) and ν(CO) because of mutual interaction, but the higher energy one is almost certainly basically ν(NN). In the spectrum of the bromide salt it occurs at a similar frequency to the higher energy ν(NN) band of *cis*-$[Os(NH_3)_4(N_2)_2]Br_2$. The carbon-13 shoulder appears on the lower energy band of *cis*-$[Os(NH_3)_4CO(N_2)]^{2+}$ confirming its assignment as basically ν(CO). The frequency of this band is about 75 cm^{-1} higher than in the $[Os(NH_3)_5CO]^{2+}$ salts, suggesting a decrease in the π-back bonding from the osmium to the carbonyl ligand. This results from the π-bonding requirements of the π-acceptor N_2 ligand.

The far infrared spectra of the carbonyl complexes exhibit a different pattern from those of the nitrogen complexes. The moderately intense band(s) at 590–608 cm^{-1} can be assigned to δ(Os—C—O) and the weak band at 557–569

Can. J. Chem. Downloaded from www.nrcresearchpress.com by 210.87.254.42 on 09/05/12
For personal use only.

TABLE 2. Infrared spectral data of N_2 complexes

	Frequency (cm^{-1})			
	$[Os(NH_3)_5(N_2)]X_2$ for X =			
Assignment	Cl	Br	I	$[Ru(NH_3)_5(N_2)]Br_2$*
ν(N—H)	3270s 3170s	3270s 3170sh	3250s 3170s	3350–3100†
ν(N≡N)	2031sh 2022vs 2009vs	2035sh 2027vs 2020vs	 2043vs 2033vs	 2114
$\delta(NH_3)_{deg}$	1645m	1635m	1616m	1618
$\delta(NH_3)_{sym}$	1330m 1313s 1278w	1328w 1311vs 1286w	 1310vs	 1266
$\rho(NH_3)$	827m	821m	803m	788
δ(M—N—N)	524m	515m	499m	499
ν(M—NH_3)	549m 493w 455w 447w	544m 484w 443w	533m 471w 431m	458w 432sh 423

*See ref. 13.
†A region of broad absorption: s = strong; v = very; m = medium; w = weak; sh = shoulder.

TABLE 3. Infrared spectral data of CO complexes

	Frequency (cm^{-1})			
	$[Os(NH_3)_5CO]X_2$ for X =			
Assignment	Cl	Br	I	$[Ru(NH_3)_5CO]Br_2$*
ν(N—H)	3280s, b 3160s, b	3265s, b 3160s, b	3255s,b 3165s,b	3280s, b 3215s, b 3170s, b
ν(C—O)	1890sh 1875vs 1823w	1895sh 1883vs 1830w	1907vs 1898vs 1847w	 1932vs 1878sh
$\delta(NH_3)_{deg}$	1644m, b	1635m, b	1625m, b	1608m
$\delta(NH_3)_{sym}$	1313s 1307s 1260m	 1309s 1265m	 1310s 1285m	 1278s 1250m
$\rho(NH_3)$	828m 815m	819m	801m 788m	790m
δ(M—C—O)	608m 596m	595m	590m	578m
ν(M—C)	569w	561w	557w	532w
ν(Os—NH_3)	450w	439w	433w	

*See ref. 14.

TABLE 4. Infrared spectral data of some osmium tetraammine complexes

	Frequency (cm^{-1})			
		cis-$[Os(NH_3)_4CO(N_2)]X_2$ for X =		
Assignment	*cis*-$[Os(NH_3)_4(N_2)_2]Br_2$	Cl	Br	I
ν(N—H)	3240vs 3155vs	3250s, b 3150s, b	3250s, b 3160s, b	3240s 3165s
ν(N—N)	2170s 2115vs	2179s	2174s	2189s
ν(C—O)		1952vs 1913sh	1956s, b 1918sh	1975vs
$\delta(NH_3)_{deg}$	1580m, b	1575m, b	1610–1575b	1605m, b
$\delta(NH_3)_{sym}$	1342w 1316s	1347w 1322s 1318s	1345w 1319s	1349w 1324s 1310sh
$\rho(NH_3)$	846m	860m	850m	839m
δ(M—C—O)		606s 595s	601s 591s	594s 584s
Other bands	522m 514m 499vw 479w 456s 433w 408m	537m 512w 492vw 470m 462m 413m	531m 502w 486w 461m 403m	523m 491vw 475vw 452m 393m

cm^{-1} to ν(Os—C) by analogy with other carbonyl complexes (9, 14). This leaves a single weak absorption above 400 cm^{-1} at 433–450 cm^{-1} assignable to ν(Os—NH_3). By contrast, the $[Os(NH_3)_5(N_2)]^{2+}$ ion exhibits a moderate intensity band at 499–524 cm^{-1} assigned by Borod'ko *et al.* (17) to ν(Os—N_2), but by comparison with carbonyl and nitrosyl complexes, more likely to be δ(Os—N—N). A weak band appears in these spectra similar to that assigned to ν(Os—NH_3) in the carbonyl complexes. In addition a more intense band at much higher energy (533–549 cm^{-1}), exhibiting a large isotope shift on deuterium substitution and assigned to ν(Os—NH_3) is also found. Neither this band nor a very weak band at 471–493 cm^{-1} have counterparts in the spectra of the carbonyl complexes.

Comparison of the infrared spectra of $[Os(NH_3)_5CO]^{2+}$ and *cis*-$[Os(NH_3)_4(N_2)_2]^{2+}$ with those of *cis*-$[Os(NH_3)_4CO(N_2)]^{2+}$ enables the two peaks ~600 cm^{-1} in the latter ion, to be assigned to δ(Os—C—O). The degeneracy of this mode has been removed since in-plane bending is now different from out-of-plane bending because of the N_2 ligand. This would not be the case if the CO and N_2 ligands were mutually *trans*. The remainder of the far infrared spectrum (to 400 cm^{-1}) cannot be assigned with certainty.

The electronic spectral data for the complexes prepared in this work and several similar ruthenium complexes are listed in Table 5. Previous studies of the ruthenium complexes have assigned the single peak in the spectrum of $[Ru(NH_3)_5(N_2)]^{2+}$ to a metal to ligand ($d_\pi \rightarrow \pi^*(N_2)$) charge transfer transition (18) and the 36 100 cm^{-1} peak in the spectrum of $[Ru(NH_3)_5(CO)]^{2+}$ to this transition (19). The weaker peak in the latter complex was considered to be the $^1A_1 \rightarrow {}^1T_1$ ligand field transition. The analogous osmium complexes exhibit very similar spectral features. The 48 100 cm^{-1} band in the spectrum of $[Os(NH_3)_5(N_2)]^{2+}$ can be assigned to a $d_\pi \rightarrow \pi^*(N_2)$ transition. It occurs at higher energy than in the ruthenium complex because the N_2 ligand is more strongly bonded to the osmium atom causing the antibonding π^* orbitals to be destabilized to a greater degree than in the ruthenium complex.

Can. J. Chem. Downloaded from www.nrcresearchpress.com by 210.87.254.42 on 09/05/12
For personal use only.

TABLE 5. Electronic spectral frequencies*

Complex	Frequency (cm^{-1})		
	$d_\pi \rightarrow \pi^*$	Ligand field transitions	
$[Os(NH_3)_5(N_2)]^{2+}$†	48 100(25)		
$[Os(NH_3)_5CO]^{2+}$†		40 200(0.73)	31 600(0.065)
cis-$[Os(NH_3)_4(N_2)_2]^{2+}$	45 000(20)		
cis-$[Os(NH_3)_4CO(N_2)]^{2+}$	48 300(12)	38 900(1.69)	35 700(1.05)
$[Ru(NH_3)_5(N_2)]^{2+}$‡	45 250(16)		
$[Ru(NH_3)_5CO]^{2+}$§		36 100(0.26)	27 800(0.017)

*Molar extinction coefficients ($\times 10^{-3}$) in parentheses.
†Reference 6.
‡Reference 8.
§Reference 19.

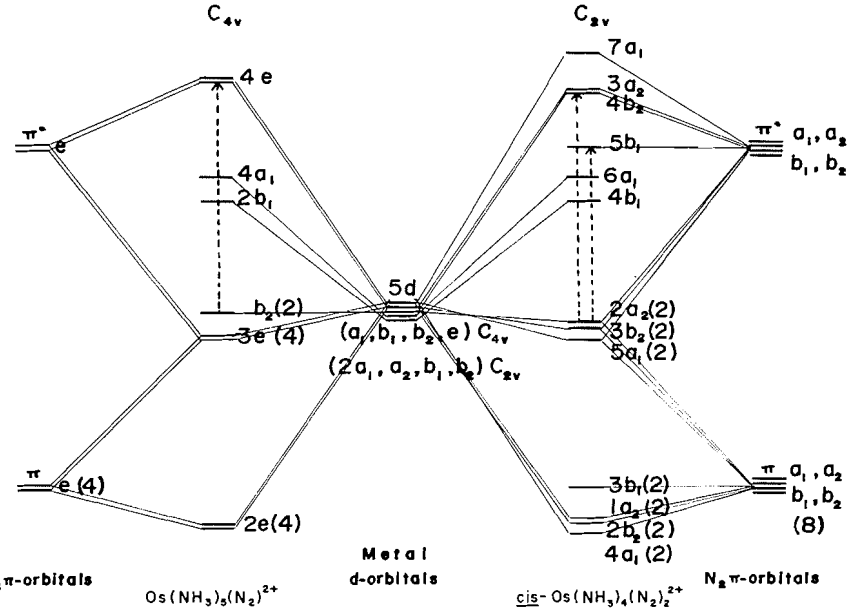

FIG. 1. Schematic diagram of ligand π-orbitals and osmium d-orbitals of osmium(II) nitrogen complexes.

In Fig. 1 it can be seen that the lowest energy charge transfer transition of the *cis*-$[Os(NH_3)_4(N_2)_2]^{2+}$ ion involves the $5b_1$ orbital which is not involved in bonding with the metal. A second transition is expected at higher energy but is not observed below 50 000 cm^{-1}. Mulliken has shown that the π^* orbitals of CO lie at higher energy than the π^* orbitals of N_2 (20). Thus in the *cis*-$[Os(NH_3)_4CO(N_2)]^{2+}$ ion, the first charge transfer band occurs at higher energy than in the *cis*-$[Os(NH_3)_4(N_2)_2]^{2+}$ ion because the upper level is partially formed from π^* (CO) in place of $\pi^*(N_2)$.

Caulton *et al.* (21) have calculated that CO interacts more strongly than N_2 with a low-spin d^6 metal ion because of the synergic effect of the larger σ-bonding capability of CO. Thus the π^* orbitals in the complexes will lie at higher energy in the $[M(NH_3)_5CO]^{2+}$ ions than in the $[M(NH_3)_5(N_2)]^{2+}$ ions (M = Os, Ru). The $d_\pi \rightarrow \pi^*$ transition would thus be expected to occur at higher energy in the CO complexes and in fact is not observed below 50 000 cm^{-1} for either metal. Stanko and Starinshak (19) noted a strong absorption up to the limit of their spectrophotometer and a similar absorption is present in the spectrum of $[Os(NH_3)_5CO]^{2+}$. This probably represents the $d_\pi \rightarrow \pi^*$ transition.

Can. J. Chem. Downloaded from www.nrcresearchpress.com by 210.87.254.42 on 09/05/12
For personal use only.

Can. J. Chem. Downloaded from www.nrcresearchpress.com by 210.87.254.42 on 09/05/12
For personal use only.

The less intense bands in the electronic spectra of the carbonyl complexes probably represent the two spin allowed ligand field transitions, $^1A_{1g} \rightarrow {}^1T_{1g}$ and $^1A_{1g} \rightarrow {}^1T_{2g}$ of an octahedral low-spin d^6 ion. The reason for the wide difference in intensity between the two absorptions is not known although similar behavior is found for the $[Ru(NH_3)_6]^{2+}$ ion (22).

Representative salts ($[Os(NH_3)_5(N_2)]Cl_2$, $[Os(NH_3)_5CO]Br_2$, and *cis*-$[Os(NH_3)_4CO(N_2)]Br_2$) of the complexes were found to be diamagnetic at room temperature as expected for spin-paired octahedral osmium(II) ions.

The chemistry of these osmium(II) complexes is characterized by their extreme inertness. There is little obvious labilization of the *trans*-NH_3 in the $[Os(NH_3)_5(CO)]^{2+}$ ion. Both $[Ru(NH_3)_5CO]^{2+}$ and *cis*-$[Ru(NH_3)_4(H_2O)CO]^{2+}$ lose the NH_3 *trans* to the carbonyl in acidic solutions (14) but $[Os(NH_3)_5CO]^{2+}$ is unaffected by prolonged treatment with hydrochloric acid at elevated temperatures. Hydrazine hydrate does not react with $[Os(NH_3)_5CO]^{2+}$, even to produce $[Os(NH_3)_5(N_2)]^{2+}$, although the latter ion is formed from the reaction of $[Os(NH_3)_5Cl]^{2+}$ with hydrazine hydrate and is the end product (contaminated with *cis*-$[Os(NH_3)_4(N_2)_2]^{2+}$ (17)) in the reaction of osmium(IV) chloro complexes with hydrazine hydrate. Neither carbon monoxide nor sulfur dioxide displace the N_2 ligand from $[Os(NH_3)_5(N_2)]^{2+}$ and likewise this ion is unaffected by prolonged treatment with aqueous ammonia or pyridine in the absence of oxygen. This behavior may be contrasted with that of $[Ru(NH_3)_5(N_2)]^{2+}$ which undergoes several substitution reactions in which the N_2 is displaced (12).

The authors would like to thank the National Research Council of Canada for their financial assistance and the Province of Ontario for a fellowship (J.R.S.).

1. F. M. Lever and A. R. Powell. Chem. Soc. Spec. Publ. No. 13, 135 (1959).
2. A. D. Allen and C. V. Senoff. Chem. Commun. 621 (1965).
3. P. C. Ford. Coordin. Chem. Rev. **5**, 75 (1970).
4. W. P. Griffith. The chemistry of the rarer platinum metals. Interscience, London. 1967. p. 44.
5. A. D. Allen and J. R. Stevens. Chem. Commun. 1147 (1967).
6. H. A. Scheidegger, J. N. Armor, and H. Taube. J. Am. Chem. Soc. **90**, 3263 (1968).
7. J. J. Lingane. Electronanalytical chemistry. 2nd ed. Interscience, New York. 1958.
8. D. F. Harrison, E. Weissberger, and H. Taube. Science, **159**, 320 (1967).
9. M. J. Cleare and W. P. Griffith. J. Chem. Soc. (A), 372 (1969).
10. J. W. Palmer and F. Basolo. J. Inorg. and Nucl. Chem. **15**, 279 (1960).
11. P. C. Ford, J. R. Kuempel, and H. Taube. Inorg. Chem. **7**, 1976 (1968).
12. A. D. Allen and C. V. Senoff. Can. J. Chem. **45**, 1337 (1967).
13. A. D. Allen, F. Bottomley, R. O. Harris, V. P. Reinsalu, and C. V. Senoff. J. Am. Chem. Soc. **89**, 5595 (1967).
14. A. D. Allen, T. Eliades, R. O. Harris, and P. Reinsalu. Can. J. Chem. **47**, 1605 (1969).
15. K. Nakamoto. Infrared spectra of inorganic and coordination compounds. 2nd ed. Wiley–Interscience, New York. 1970. p. 151.
16. J. K. Wilmshurst. Can. J. Chem. **38**, 467 (1960).
17. Yu. G. Borod'ko, G. I. Kozub, and Yu. P. Myagkov. Russ. J. Phys. Chem. (English), **44**, 643 (1970).
18. I. M. Treitel, M. T. Flood, R. E. Marsh, and H. B. Gray. J. Am. Chem. Soc. **91**, 6512 (1969).
19. J. A. Stanko and T. W. Starinshak. Inorg. Chem. **8**, 2156 (1969).
20. R. S. Mullikan. Can. J. Chem. **36**, 10 (1958).
21. K. G. Caulton, R. L. Dekock, and R. F. Fenske. J. Am. Chem. Soc. **92**, 515 (1970).
22. H. H. Schmidtke and D. Garthoff. Helv. Chim. Acta, **49**, 2039 (1966).

Thermal Transformation in Anhydrous Rare Earth Acetates

G. ADACHI AND E. A. SECCO

Department of Chemistry, St. Francis Xavier University, Antigonish, Nova Scotia

Received February 7, 1972

The thermal transformation in anhydrous acetates of Sm, Eu, Gd, Tb, Dy, Ho, Er, Tm, Yb, Lu, and Y has been studied by thermal analysis. The enthalpy change, ΔH, and the entropy change, ΔS, accompanying the transformation process are reported and related to ionic radius of the rare earth element.

The acetates of the rare earth elements, La, Pr, and Nd did not exhibit the thermal transformation property.

La transformation thermique dans les acétates anhydres de Sm, Eu, Gd, Tb, Dy, Ho, Er, Tm, Yb, Lu et Y a été étudiée par analyse thermique. On a determiné les changements d'enthalpie ΔH et d'entropie ΔS, qui accompagnent le processus de transformation et établi la relation au rayon ionique de la terre rare.

Les acétates de terre rare La, Pr, et Nd ne démontrent aucune propriété de transformation thermique.

Canadian Journal of Chemistry, **50**, 3100 (1972)

Can. J. Chem. Downloaded from www.nrcresearchpress.com by 210.87.254.5 on 09/05/12
For personal use only.

Introduction

The mode of thermal decomposition of the anhydrous rare earth acetates has already been reported (1, 2) to occur via the oxycarbonate above 300 °C leading to the oxide as the final residue. The rare earth acetate hydrate was stated to release an appreciable amount of water at ~200 °C (2) as evidenced by an endotherm on the DTA heating curve.

The purpose of this paper is to report the results of a more detailed investigation of the dehydration process in the rare earth acetate hydrates up to 300 °C.

Experimental

All the rare earth acetates used in this study were prepared in this laboratory by dissolving the oxides (American Potash and Chemical Corp., Rare Earth Division, with stated purities ranging from 99.999% for Eu, 99.99% for Nd and La, to 99.9% for the remaining members of the group) in dilute acetic acid, Fisher Reagent Grade, and evaporating the solution to dryness (3). The crude acetate precipitate was recrystallized in de-ionized water followed by drying in air or vacuum.

The heating traces for thermogravimetry, differential thermal analysis, and calorimetry were recorded on a duPont Thermal Analyser, DTA-900 and TGA-950 with the appropriate accessories and programming adjustments, as previously described (4, 5). The heating rate used for the heating curves was 20 °C/min; an ambient atmosphere of dry N_2 (Matheson prepurified grade with stated impurity of 0.003% oxygen) was maintained during all the experiments except where otherwise specified.

The X-ray diffraction patterns of the samples were recorded on a Norelco X-ray diffractometer unit using CuK_α radiation or MoK_α radiation (6).

The infrared spectra were obtained by using the standard KBr and CsI disc technique in a Perkin–Elmer 180 spectrophotometer equipped with a high temperature cell, maximum 350 °C.

Results and Discussion

The results described below for $Eu(CH_3COO)_3$ are representative of the rare earth acetate group studied.

A table of results of thermogravimetry leading to the three product stages (Table 1) is placed with the Depository of Unpublished Data;[1] the agreement between the calculated and observed percentage weight losses is within the expected experimental limits. A typical TG curve of the rare earth acetate hydrate is represented by $Eu(CH_3COO)_3 \cdot H_2O$) in Fig. 1. The trace shows that after the initial dehydration process, a plateau persisted over two heat–cool cycles in a static atmosphere of the dehydrated gaseous products in the temperature interval 50–250 °C. Furthermore, no weight change is indicated in N_2 atmosphere between 170 and 350 °C.

The DTA behavior of the acetate hydrates up to 250 °C is also represented by $Eu(CH_3COO)_3 \cdot H_2O$ in Fig. 2. The first heating cycle revealed an asymmetric endotherm doublet at 100 °C and a less intense second endotherm at 155 °C, curve 1; no thermal effect appeared on cooling from 180 °C, curve 1′. The weak endotherm at 155 °C was not reproducible and was ascribed to the release of occluded H_2O re-

[1] A complete set of tables is available, at a nominal charge, from the Depository of Unpublished Data, National Science Library, National Research Council of Canada, Ottawa, Canada K1A OS2.

Can. J. Chem. Downloaded from www.nrcresearchpress.com by 210.87.254.5 on 09/05/12
For personal use only.

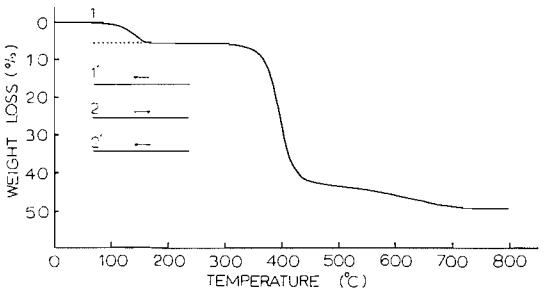

FIG. 1. Thermogravimetric trace of $Eu(CH_3COO)_3 \cdot H_2O$. Curve *1*: first heating cycle stopped at 250 °C; curve *1'*: cooling cycle; curve *2*: second heating cycle; curve *2'*: second cooling cycle; curve (···—): third heating cycle carried to 800 °C.

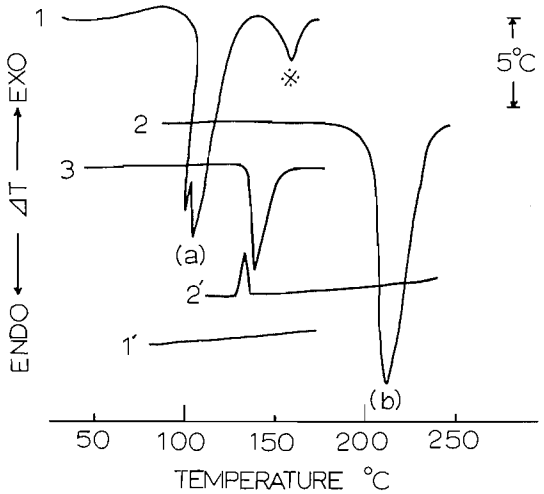

FIG. 2. Differential thermal analysis of $Eu(CH_3COO)_3 \cdot H_2O$. Curve *1*: first heating cycle; curve *1'*: cooling cycle; curve *2*: second heating cycle; curve *2'*: cooling cycle; curve *3*: third heating cycle; peak (*a*): dehydration; peak ·※·: occluded H_2O; peak (*b*): polymeric → monodentate transition.

sulting from dehydration; this endotherm was assessed to be a function of physical factors, such as sample packing, quantity of sample, etc. The second heating cycle, curve 2, showed an intense endotherm at 220 °C which was previously attributed to the final dehydration state (2); cooling the sample from 250 °C revealed a weak exotherm at 130 °C, curve 2'. The third heating cycle, curve 3, showed the reversible thermal effect near 130 °C.

To identify the origin of the endotherms at 155 and 220 °C, the i.r. spectra of the acetate hydrate were recorded at different temperatures

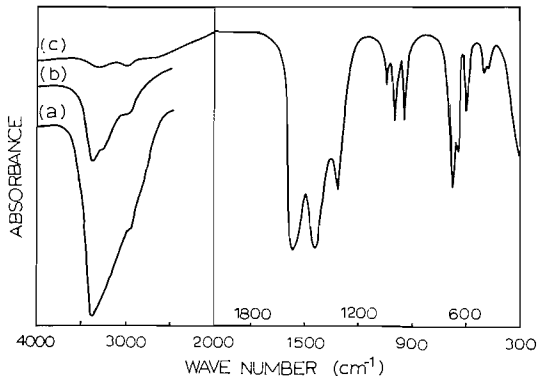

FIG. 3. Infrared spectra of $Eu(CH_3COO)_3 \cdot H_2O$ in high temperature cell. (*a*) room temperature; (*b*) 120 °C; (*c*) 175 °C.

and displayed in Fig. 3. There is no evidence of the characteristic water absorption bands in the spectrum at 175 °C. The assignment of dehydration to the 220 °C must be ruled out on the basis of i.r. and thermogravimetry. No melting action or gas evolution was discernible on the melting point apparatus up to 270 °C. The endotherm at 220 °C was determined by calorimetry to have an enthalpy value of 7.1 ± 0.2 kcal/mol.

The reversible thermal effect at 130–140 °C, hitherto unreported in the literature, attracted our attention; this effect was invariably preceded by the 220 °C endotherm for $Eu(CH_3COO)_3$. This reversible DTA effect was observed in the rare earth acetate series from Sm to Lu excepting Pm; the acetates of La, Pr, and Nd did not display this thermal effect.

X-Ray diffraction patterns of $Eu(CH_3COO)_3$ hydrate, after heating to 200 °C, taken at room temperature were similar to that reported by Karraker (8). However, all the characteristic diffraction peaks disappeared after subsequent heating to 220 °C suggesting a structural transition to an amorphous state. Examination of the sample on the melting apparatus exhibited no discernible melting action.

The i.r. spectra of anhydrous $Eu(CH_3COO)_3$ dried at 200 °C, recorded during some heat–cool cycles, are presented in Fig. 4. The faint doublet on trace (1) at room temperature merges into a single band at 80–90 °C, trace (2). Heating the sample to 220 °C shifts the peak by 10 cm^{-1}, trace (3). Trace (4) is the spec-

Can. J. Chem. Downloaded from www.nrcresearchpress.com by 210.87.254.5 on 09/05/12
For personal use only.

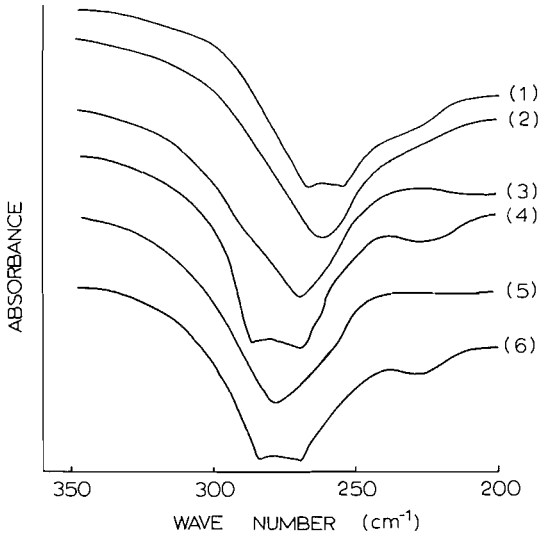

FIG. 4. Infrared spectra of $Eu(CH_3COO)_3$ in frequency region where effect of heat treatment is observed. (*1*) room temperature, after heating to 200 °C; (*2*) 80–90 °C; (*3*) 220 °C; (*4*) room temperature, after heating to 220 °C; (*5*) 160–170 °C; (*6*) room temperature, after heating to 160–170 °C.

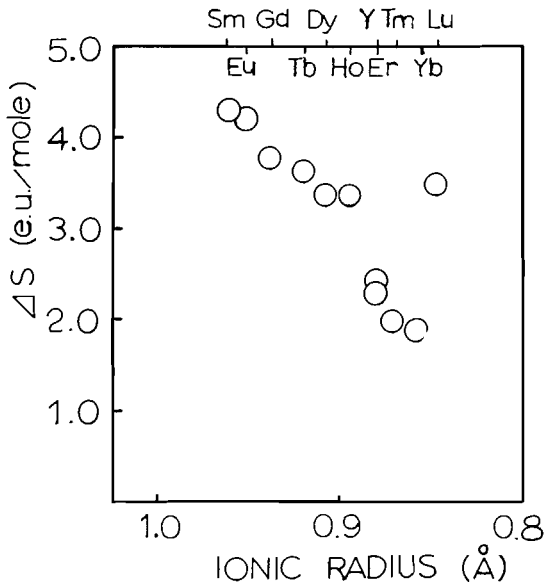

FIG. 5. Plot of ΔS *vs.* ionic radius of rare earth element ion.

trum at room temperature after heating to 220 °C. Trace (5) is the spectrum at 160–170 °C and trace (6) is the room temperature spectrum after heating to 160–170 °C.

The peak temperatures of the exo- and endotherms, along with the enthalpy and entropy values accompanying the transformation were determined. A table of these numerical results (Table 2) is placed with the Depository of Unpublished Data.[1] The plot of ΔS *vs.* ionic size, Fig. 5, shows a direct relationship, with discontinuities discernible (*i*) between Ho and Er, and (*ii*) at Lu. These discontinuities are consistent with the differences in coordination number of the central ions (8).

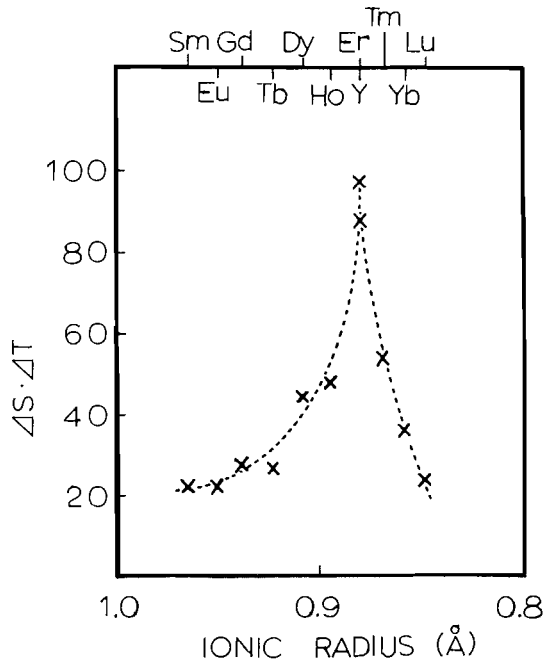

FIG. 6. Plot of $\Delta T.\Delta S$ *vs.* ionic radius of rare earth element ion.

The reported peak temperatures[1] of the exo- and endotherms show thermal hysteresis effects, ΔT characteristic of many reversible transformations, $\Delta T = T_p^f - T_p^r$, where T_p^f represents the peak temperature on heating and T_p^r the peak temperature on cooling. It has been pointed out (7) that hysteresis is a necessary consequence of the coexistence mechanism of continuous transformations with the main factor controlling the hysteresis being the strain energy E_s and that thermodynamic considerations relate the strain energy to $\Delta T.\Delta S$, *i.e.*, $E_s \propto \Delta T.\Delta S$. The plot of $\Delta T.\Delta S$ *vs.* ionic size, Fig. 6, exhibits a lambda-type relationship with a maximum at Er and Y. This maximum in strain energy could be interpreted in terms of a mixed coordination number in Er and Y

acetates consistent with previously reported observations (8).

Infrared evidence does not support an intramolecular configurational rearrangement as in tautomerism for the reversible phenomenon at 130–140 °C. The alteration in the i.r. absorption bands does suggest, however, the possibility of a polymeric–bidentate–monodentate transition phenomenon as postulated by Karraker (8). The observed transitions are assigned to $M(CH_3COO)_3$ as follows:

(1) Irreversible endotherm occurring at 220 °C involving 7.1 kcal/mol

polymeric ⟶ monodentate

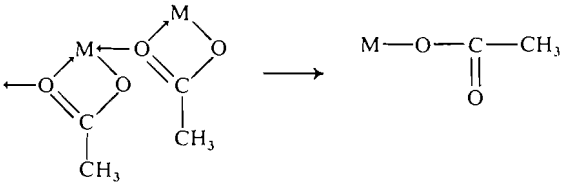

(2) Reversible endotherm occurring at 140 °C involving 1.7 kcal/mol

monodentate $\underset{\text{heating}}{\overset{\text{cooling}}{\rightleftharpoons}}$ bidentate

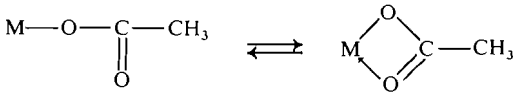

The rupture of the inter-and intramolecular O → M bonds is the critical action on heating to 220 °C and the subsequent formation of the intramolecular O → M on cooling. The change in i.r. band profile and shift of 10–25 cm^{-1} may be expected for ν_{O-M} and δ_{O-M-O} in the polymeric–bidentate–monodentate transition.

On the basis of the transformation enthalpy values, *viz.* 7.1 ± 0.2 kcal/mol at 220 °C and 1.7 ± 0.1 kcal/mol at 140 °C, we assess the multiplicity of the polymeric state to be *ca.* 4.

The authors are indebted to the National Research Council of Canada and St. Francis Xavier University Council of Research for financial support of this research program.

1. I. Mayer and F. Kassierer. J. Inorg. Nucl. Chem. **28**, 2430 (1966).
2. K. C. Patil, G. V. Chandrashekhar, M. V. George, and C. N. R. Rao. Can. J. Chem. **46**, 257 (1968).
3. J. R. Witt and E. I. Onstott. J. Inorg. Nucl. Chem. **24**, 637 (1962).
4. P. Ramamurthy and E. A. Secco. Can. J. Chem. **46**, 3605 (1968).
5. O. K. Srivastava and E. A. Secco. Can. J. Chem. **45**, 579, 1375 (1967).
6. E. A. Secco. Can. J. Chem. **42**, 2143 (1964).
7. C. N. R. Rao and K. J. Rao. Progress in solid state chemistry. *Edited by* H. Reiss. **4**, 131 (1967).
8. D. G. Karraker. J. Inorg. Nucl. Chem. **31**, 2815 (1969).

Can. J. Chem. Downloaded from www.nrcresearchpress.com by 210.87.254.5 on 09/05/12
For personal use only.

A Novel Solution to the Master Equation for Chemical Reaction

R. K. BOYD

Chemistry Department, University of Guelph, Guelph, Ontario

Received May 8, 1972

It was found by McElwain and Pritchard (1*c*), as a result of numerical experiments on the transport matrix for the dissociation of H_2, that an apparent correspondence existed between the eigenvalues λ_i and the pairs of transition probabilities $(A_{i,i-1}; A_{i-1,i})$. In the present work, a qualitative understanding of this result is attempted, using an unusual form of solution of the master equation.

McElwain et Pritchard (1*c*) ont trouvé qu'il existe une correspondance apparente entre les valeurs quantifiées λ_i et les paires de probabilités de transition $(A_{i,i-1}; A_{i-1,i})$, à la suite de nombreuses expériences sur la matrice de transport de la dissociation de H_2. Nous tentons, dans ce présent travail, d'illustrer ce résultat de façon qualitative, au moyen d'une forme inhabituelle de solution de l'équation principale.

[Traduit par le journal]

Canadian Journal of Chemistry, **50**, 3104 (1972)

Pritchard and his collaborators (1) have devised very efficient computer techniques for obtaining numerical solutions to the master equation for dissociation of a diatomic gas dispersed in high dilution in some inert gas M. The development of these techniques has permitted various numerical experiments to be performed, which have led to an increased understanding of such problems as the bottleneck phenomenon (1*d*). The intention of the present work is to attempt to improve the qualitative understanding of one particular result obtained by these workers (1*c*).

For present purposes, it is sufficient to consider a simplified system of n interconverting levels, with one level (say level n) designated a no-return level; it will prove convenient to assume that these levels are numbered in order of increasing energy. Then the master equation for levels 1 to $(n-1)$ may be written as

$$\frac{\mathrm{d}}{\mathrm{d}t}\begin{pmatrix} x_1 \\ x_2 \\ \cdot \\ \cdot \\ \cdot \\ \cdot \\ x_n \end{pmatrix} = \begin{pmatrix} -\alpha_1 & A_{12} & \cdot & \cdot & \cdot & \cdot & A_{n-1,1} \\ A_{21} & -\alpha_2 & & & & & \cdot \\ \cdot & & \cdot & & & & \cdot \\ \cdot & & & \cdot & & & \cdot \\ \cdot & & & & \cdot & & \cdot \\ \cdot & & & & & \cdot & \cdot \\ A_{n-1,1} & \cdot & \cdot & \cdot & \cdot & \cdot & -\alpha_n \end{pmatrix} \begin{pmatrix} x_1 \\ x_2 \\ \cdot \\ \cdot \\ \cdot \\ \cdot \\ x_n \end{pmatrix} \qquad [1]$$

where $x_i(t)$ is the instantaneous concentration of molecules in level i, A_{ij} is the pseudo-first-order rate constant for $j \rightarrow i$ transitions, and

$$\alpha_i = \sum_{\substack{j=1 \\ \neq i}}^{n} A_{ji},$$

the total rate constant for depopulation of level i; clearly, $x_i(\infty) = 0$, in this model, for $i < n$. By defining $\xi_i(t) = x_i/\tilde{x}_i$, where $\tilde{x}_i$ is the local equilibrium population (*i.e.*, the equilibrium population in the limit where transitions into level n are not permitted), and using detailed balance, eq. 1 may

Can. J. Chem. Downloaded from www.nrcresearchpress.com by 210.87.254.105 on 09/05/12
For personal use only.

be rewritten (1) as

$$\frac{\mathrm{d}}{\mathrm{d}t}\begin{pmatrix}\xi_1\\ \xi_2\\ \cdot\\ \cdot\\ \cdot\\ \cdot\\ \xi_n\end{pmatrix}=\begin{pmatrix}-\alpha_1 & A_{21} & \cdot & \cdot & \cdot & \cdot & A_{n-1,1}\\ A_{12} & -\alpha_2 & & & & & \cdot\\ \cdot & & \cdot & & & & \cdot\\ \cdot & & & \cdot & & & \cdot\\ \cdot & & & & \cdot & & \cdot\\ \cdot & & & & & \cdot & \cdot\\ A_{1,n-1} & \cdot & \cdot & \cdot & \cdot & \cdot & -\alpha_{n-1}\end{pmatrix}\begin{pmatrix}\xi_1\\ \xi_2\\ \cdot\\ \cdot\\ \cdot\\ \cdot\\ \xi_n\end{pmatrix}$$

or, in matrix notation

$$[2]\qquad (\mathrm{d}/\mathrm{d}t)|\xi\rangle = \mathbf{A}_0|\xi\rangle$$

The usual analytic solution to this equation is

$$[3]\qquad \xi_i(t) = \sum_{r=1}^{n-1} C_r\phi_r^0(i)\exp(\lambda_r^0 t)$$

where the C_r are constants determined by the initial conditions, $\phi_r^0(i)$ is the ith component of the rth eigenvector of $\mathbf{A}_0$, and λ_r^0 is the rth eigenvalue. The λ_r are real and negative, and are hereinafter assumed to be labelled in order of increasing absolute magnitude, *i.e.*, $|\lambda_1| < |\lambda_2|$, etc.

The unexpected result obtained by McElwain and Pritchard (1*c*), referred to above, involved an approximate one-to-one correspondence between the eigenvalues λ_r^0, and the pairs of rate constants $(A_{r,r-1}; A_{r-1,r})$. Thus, scaling the latter by some factor resulted (1*c*) in similar scaling of the corresponding eigenvalue, with only mild perturbations of neighboring eigenvalues; this correspondence was not exact, and became less apparent for the highest-energy levels, from which dissociation could occur directly (1). That the qualitative meaning of this *numerical* result is unclear may be conveniently shown as follows; let the pair of rate constants $(A_{i,i-1}; A_{i-1,i})$ be increased by the *same* factor $(b+1)$ (thus preserving detailed balance), so that the new perturbed transport matrix may be written as

$$\mathbf{A} = \mathbf{A}_0 + \mathbf{A}'$$

where $\mathbf{A}_0$ is as given in eq. 2, and

$$\mathbf{A}' = \begin{pmatrix}\cdot & & & & & & 0 & & \\ & \cdot & & & & & & & \\ & & \cdot & & & & & & \\ & & & 0 & & & & & \\ & & & 0 & (-bA_{i,i-1}) & (bA_{i,i-1}) & 0 & & \\ & & & 0 & (bA_{i-1,i}) & (-bA_{i-1,i}) & 0 & & \\ & & & & & & 0 & & \\ & & & & & & & \cdot & \\ & & & & & & & & \cdot \\ & & 0 & & & & & & \cdot\end{pmatrix}$$

The first-order perturbation correction to λ_r^0 is

$$[4]\qquad \lambda_r' = \langle\phi_r^0|\mathbf{A}'\phi_r^0\rangle = b[\phi_r^0(i) - \phi_r^0(i-1)][A_{i,i-1}\phi_r^0(i-1) - A_{i-1,i}\phi_r^0(i)]$$

Can. J. Chem. Downloaded from www.nrcresearchpress.com by 210.87.254.105 on 09/05/12
For personal use only.

Can. J. Chem. Downloaded from www.nrcresearchpress.com by 210.87.254.105 on 09/05/12
For personal use only.

Equation 4 gives an accurate estimate of λ'_r provided b is sufficiently small; this was not true of the factors used by McElwain and Pritchard (1*c*), but the qualitative difficulty is now more explicit, *viz.* how can the results $\lambda'_i \approx b\lambda_i^0$ and $\lambda'_{r\neq i} \approx 0$, be accounted for, bearing in mind that each of the $\phi_r(i)$ is a complicated function of *all* the A_{ij}?

It should first be noted that scaling the pair of rate constants $(A_{i,i-1}; A_{i-1,i})$ by a factor $(b+1)$ implies that

$$\alpha_i = \sum_{\substack{j=1 \\ \neq i}}^{n} A_{ji}$$

is approximately scaled by $(b+1)$, while α_{i-1} is only mildly perturbed. This is because $(A_{i-1,i}/A_{i,i-1}) \gg 1$, due to the large Boltzmann factors corresponding to the vibrational spacings in H_2 at 2000 to 3000 °K (1); in addition, the rate constants for multiple-quantum transitions were considerably smaller (1) than those for nearest-neighbor transitions. Thus, to this degree of approximation, what is sought is a correspondence between the α_i and the λ_i^0. The most obvious mathematical condition under which this correspondence would be *exact* requires $\mathbf{A}_0$ to be a triangular matrix, since the α_i form the main diagonal elements. If $\mathbf{A}_0$ were, for example, a lower triangular matrix, with $A_{ij} = 0$ for $j \leqslant i$, the corresponding physical picture would be a completely irreversible one-way cascade, with no upward transitions; the λ_r^0 in eq. 3 could then be replaced by the entirely equivalent $(-\alpha_r)$.

This same result for this very special case will now be derived by an alternative method due to Curtis (2); this method, which bears a certain resemblance to the "many-shot" expansion technique of Serauskas and Schlag (3), will be briefly applied to the one-way cascade model (2), to establish notation, and then extended to the present, more general, problem. For the special case of a one-way downwards cascade, eq. 2 may be rewritten as

$$0 = [1]\, d\xi_i + \left[\sum_{j=i+1}^{n-1} A_{ji}\xi_j(t) - \alpha_i\xi_i\right] dt$$

which is readily integrated, using $\exp(\alpha_i t)$ as an integrating factor (2), to give

$$[5] \qquad \xi_i(t) = \xi_i(0)\exp(-\alpha_i t) + \sum_{j=i+1}^{n-1}\left[A_{ji}\int_{t'=0}^{t}\exp(\alpha_i t')\xi_j(t')\,dt'\right]$$

where

$$\alpha_i = \sum_{j=1}^{i-1} A_{ji}$$

for the present one-way model. Since ξ appears on both sides of eq. 5, it may be successively iterated (2) to yield a series of nested sums and nested integrals

$$[6] \quad \xi_i(t) = \exp(-\alpha_i t)\left\{\xi_i(0) + \sum_{j=i+1}^{n-1}\xi_j(0)A_{ji}\int_{t'=0}^{t}\exp[(\alpha_i-\alpha_j)t']\,dt' + \sum_{j=i+1}^{n-1}\sum_{k=j+1}^{n-1}\xi_k(0)A_{ji}A_{kj}\int_{t'=0}^{t}\exp[(\alpha_i-\alpha_j)t']\int_{t''=0}^{t'}\exp[(\alpha_j-\alpha_k)t'']\,dt''\,dt' + \cdots\right\}$$

Due to the completely irreversible nature of the one-way cascade, this series terminates when the upper and lower limits of the most interior summation coincide. Each order of the series contains all those cascades which move from initial levels to the level of interest in a number of steps equal to the order of the term (2). Furthermore, the integrals are all straightforward, and may be performed exactly. Thus, for example, the contribution to $\xi_i(t)$ by a two-step cascade into level i is given by

$$[7] \qquad \{k \to j \to i\} = \xi_k(0)A_{kj}A_{ji}\left[\frac{\exp(-\alpha_k t)}{(\alpha_j-\alpha_k)(\alpha_i-\alpha_k)} + \frac{\exp(-\alpha_j t)}{(\alpha_k-\alpha_j)(\alpha_i-\alpha_j)} + \frac{\exp(-\alpha_i t)}{(\alpha_k-\alpha_i)(\alpha_j-\alpha_i)}\right]$$

For this completely irreversible case (2), the general contribution to $\xi_i(t)$ is

$$[8] \quad \{v \to u \to \cdots \to k \to j \to i\} = \xi_v(0)\left[\prod_{(x,y)=(u,v)}^{(j,i)} (A_{x,y})\right]\left\{\sum_{z=v}^{i}\left[\exp(-\alpha_z t)\Big/\prod_{\substack{w=v \\ \neq z}}^{i}(\alpha_w - \alpha_z)\right]\right\}$$

By collecting together terms involving $\exp(-\alpha_r t)$ for each r, an expression for $\xi_i(t)$ of the form [3], with each eigenvalue λ_r^0 replaced by the corresponding $(-\alpha_r)$, is obtained as required.

When a more realistic case is considered, wherein both upward and downward transitions are allowed, the matrix $\mathbf{A}_0$ is no longer triangular, and the problem exemplified by eq. 4 remains. However, it is still possible to obtain a solution for $\xi_i(t)$ analogous to eq. 5, since $\exp(\alpha_i t)$ is again an integrating factor; the difference lies in the limits of the nested sums. Whereas in eq. 6 the lower limits of the sums progressively approached the upper limit (reflecting the one-way nature of the model), the summations are now all unrestricted. The expansion of $\xi_i(t)$ thus does not terminate, but this occurs in a particular fashion; eq. 8, derived for the one-way cascade, still holds provided no two of the states $\{v, u, \ldots, k, j, i\}$ are identical. When a state is repeated in the sequence, the coefficient of the corresponding exponential contains time explicitly. Thus, the simplest conceivable example of such a repetition is

$$\{i \to j \to i\} = \xi_i(0)A_{ji}A_{ij}\left[\frac{\exp(-\alpha_j t)}{(\alpha_i - \alpha_j)^2} + \frac{\exp(-\alpha_i t)}{(\alpha_j - \alpha_i)(\alpha_i - \alpha_j)} + \frac{\exp(-\alpha_i t)}{(\alpha_j - \alpha_i)}\,t\right]$$

In general, the highest power of t in the coefficient of an exponential corresponds to the number of repetitions of the corresponding level in the sequence. Some examples are

$$\{j \to i \to j \to i\} = \xi_j(0)A_{ji}^2 A_{ij}\left[\frac{2\exp(-\alpha_j t)}{(\alpha_j - \alpha_i)^3} + \frac{2\exp(-\alpha_i t)}{(\alpha_i - \alpha_j)^3} + \frac{\exp(-\alpha_j t)}{(\alpha_i - \alpha_j)^2}\,t + \frac{\exp(-\alpha_i t)}{(\alpha_j - \alpha_i)^2}\,t\right]$$

$$\{i \to l \to i \to j \to i\} = \xi_i(0)A_{ji}A_{ij}A_{li}A_{il}\left[\frac{\exp(-\alpha_i t)}{(\alpha_l - \alpha_i)}\left\{\frac{t^2}{2(\alpha_j - \alpha_i)} + \frac{t}{(\alpha_l - \alpha_i)(\alpha_i - \alpha_j)} + \frac{t}{(\alpha_j - \alpha_i)(\alpha_i - \alpha_j)}\right.\right.$$
$$\left.\left. + \frac{1}{(\alpha_l - \alpha_i)^2(\alpha_j - \alpha_l)} + \frac{(\alpha_l - \alpha_i)}{(\alpha_j - \alpha_i)^3(\alpha_l - \alpha_j)}\right\} + \frac{\exp(-\alpha_l t)}{(\alpha_i - \alpha_l)^3(\alpha_j - \alpha_l)} + \frac{\exp(-\alpha_j t)}{(\alpha_i - \alpha_j)^3(\alpha_l - \alpha_j)}\right]$$

$$\{i \to m \to i \to l \to i \to j \to i\} = \xi_i(0)A_{ji}A_{ij}A_{li}A_{il}A_{mi}A_{im}$$
$$\times\left\{\frac{\exp(-\alpha_i t)}{(\alpha_m - \alpha_i)}\left[\frac{t^3}{6(\alpha_l - \alpha_i)(\alpha_j - \alpha_i)} + \frac{t^2}{2(\alpha_j - \alpha_i)^2(\alpha_i - \alpha_l)} + \frac{t^2}{2(\alpha_l - \alpha_i)^2(\alpha_i - \alpha_j)}\right.\right.$$
$$\left.\left. + \frac{t^2}{2(\alpha_i - \alpha_m)(\alpha_l - \alpha_i)(\alpha_j - \alpha_i)} + (\text{terms in } t) + (\text{terms independent of } t)\right] + (\text{other exponentials})\right\}$$

Thus, although $\xi_i(t)$ may still be expanded as a sum of exponentials $\exp(-\alpha_r t)$, the coefficients of these exponentials are explicit functions of time, unlike eq. 3, the expansion in terms of the eigenvalues. Any correspondence between the α_r and λ_r^0 can now be only approximate, and its existence will clearly depend on whether or not the coefficients of the $\{\exp(-\alpha_r t)\}$ converge to limiting values more rapidly than the exponentials themselves. If such were true, so that the time-dependence of the coefficients was relatively weak, an approximate correspondence between the α_r and λ_r^0 should exist, since the two expansions for $\xi_i(t)$ must be identical for all times and for all initial conditions. The physical meaning of this required weak time-dependence may be seen from the above discussion; the time-dependence arose from the repetition of levels along a given sequence. Any factor tending to make such a repetition less likely should weaken the time-dependence of the coefficients, and thus strengthen the correspondence between the α_r and λ_r^0. On purely statistical grounds, an increase in the number of levels considered would presumably create such an effect. On the other hand, a general equalization of the A_{ij} would tend to produce

Can. J. Chem. Downloaded from www.nrcresearchpress.com by 210.87.254.105 on 09/05/12
For personal use only.

the opposite effect, since the probability of a return to a given level would be thereby increased; an increase in temperature, or increase in the number of levels for a given dissociation energy, (*e.g.* D_2 instead of H_2) would cause such an equalization. At the opposite extreme is the one-way model (2), where the transition probabilities are completely imbalanced, and the correspondence is exact.

It has been pointed out by a referee that certain general aspects of the present problem were considered some time ago by Carrington (4). In particular, Carrington discussed the effect of a perturbation of the transport matrix, similar to that described here, on the (observable) population distribution; the extremely important converse problem of the effect of small differences, in observed populations, on the deduced transition probabilities, was also treated in detail (4). However, the present, rather more specialized, problem was not treated (4), as the numerical results of Pritchard and co-workers (1) were not then available.

As observed above, the expansion technique of Curtis (2), as applied and extended here, bears some resemblance to the many-shot expansion (3); this relationship may be summarized, in very general terms, by the observation that the latter is essentially an expansion around the strong collision (one-shot) approximation, while the former expands around the one-way cascade.

Financial support by the National Research Council of Canada is gratefully acknowledged.

1. (*a*) V. A. LoDato, D. L. S. McElwain, and H. O. Pritchard. J. Am. Chem. Soc. **91**, 7688 (1969). (*b*) D. L. S. McElwain and H. O. Pritchard. J. Am. Chem. Soc. **91**, 7693 (1969). (*c*) D. L. S. McElwain and H. O. Pritchard. Thirteenth International Symposium on Combustion, The Combustion Institute, 1971. p. 35. (*d*) E. Kamaratos and H. O. Pritchard. Can. J. Chem. **49**, 2617 (1971). (*e*) D. L. S. McElwain and H. O. Pritchard. Can. J. Chem. **49**, 3915 (1971). (*f*) D. L. S. McElwain and H. O. Pritchard. Can. J. Chem. **50**, 897 (1972).
2. L. J. Curtis. Amer. J. Phys. **36**, 1123 (1968).
3. R. V. Serauskas and E. W. Schlag. J. Chem. Phys. **42**, 3009 (1965).
4. T. Carrington. J. Chem. Phys. **35**, 807 (1961).

Can. J. Chem. Downloaded from www.nrcresearchpress.com by 210.87.254.105 on 09/05/12
For personal use only.

Free Radical Bromination of Saturated Hydrocarbons using Bromine and Mercuric Oxide

N. J. BUNCE

Department of Chemistry, University of Guelph, Guelph, Ontario

Received March 14, 1972

The reaction of alkanes with a mixture of bromine and mercuric oxide gives alkyl bromides in preparatively useful yields. The reagent is significantly more reactive than elemental bromine, and it is believed that bromine monoxide, formed *in situ* by the interaction of bromine and mercury oxide, is the reactive intermediate. Bromination by bromine monoxide is a free radical chain process in which hydrogen abstraction is carried out predominantly by bromoxy (BrO·) radicals, and to a lesser extent by bromine atoms.

La réaction des alcanes sur un mélange de brome et d'oxyde mercurique, conduit aux bromures d'alkyles avec des rendements utiles à l'échelle préparative. Le réactif possède une réactivité nettement plus grande que le brome élémentaire et on pense que l'intermédiaire réactif est le monoxyde de brome formé *in situ* dans la réaction du brome sur l'oxyde mercurique. La bromation par le monoxyde de brome est un processus en chaîne par radicaux libres, dans lequel l'arrachement de l'hydrogène est réalisé de façon prédominante par les radicaux bromoxy (BrO·) et à une échelle moindre, par les atomes de brome.

Canadian Journal of Chemistry, **50**, 3109 (1972)

Can. J. Chem. Downloaded from www.nrcresearchpress.com by 210.87.254.40 on 09/05/12
For personal use only.

In the course of extending our studies on the bromodecarboxylation of carboxylic acids using bromine and mercuric oxide (1), it was observed that treatment of acid chlorides (2) with bromine and mercuric oxide in tetrachloroethane solution led to consumption of the bromine without the formation of any decarboxylated products. Control experiments showed that bromine is not appreciably reactive towards refluxing tetrachloroethane, but that addition of mercuric oxide to the hot solution causes a vigorous reaction to ensue with the production of bromotetrachloroethane. It was thus apparent that bromine and mercuric oxide constitute a brominating agent more reactive than elemental bromine alone, and the present study was undertaken to investigate the synthetic scope of the reaction and to try to elucidate details of its mechanism.

Synthesis of Alkyl Bromides

Photobromination of alkanes as a synthetic procedure has the disadvantages of giving an obnoxious byproduct, HBr, and of being inconveniently slow for many substrates. Attack on methyl groups is particularly slow, and alkanes such as neopentane are essentially unreactive except above 100° (3). Alkanes bearing electron withdrawing polar substituents also react very sluggishly, an extreme case being chloroform (4) for which bromination is reversible, the equilibrium favoring bromotrichloromethane only slightly. Using mercury oxide and bromine, however, chloroform reacts rapidly at reflux giving a good yield of bromide, and even 2,2,3,3-tetramethylbutane gives the corresponding primary bromide easily. Since no hydrogen bromide is evolved in these reactions, they may be carried out successfully in the open laboratory.

More reactive substrates such as cyclohexane react quite violently at reflux, and within a few minutes at room temperature if the alkane is in excess and the mixture is well stirred. For this substrate the stoichiometry of the reaction is represented approximately by eq. 1, although as may be seen from the results of quantitative experiments listed in Table 1, additional mercuric bromide is consistently formed at the expense of some of the alkyl bromide.

$$[1] \quad 2RH + 2Br_2 + HgO \rightarrow 2RBr + H_2O + HgBr_2$$

The yield of bromide is little affected by changes in reaction temperature or concentration of reagents and better than 90% of the initial bromine concentration can consistently be accounted for. The expense of using mercuric oxide as a reagent is offset by its ease of recovery from the mercuric oxide/mercuric bromide residue (5).

While the reaction is thus applicable to substitution of primary and secondary C—H

Can. J. Chem. Downloaded from www.nrcresearchpress.com by 210.87.254.40 on 09/05/12
For personal use only.

TABLE 1. Products of the reaction of cyclohexane with HgO/Br_2 in CCl_4*†

Temperature	Br_2 (M)	$C_6H_{11}Br$ (mol/mol Br_2)	$HgBr_2$ (mol/mol Br_2)
Reflux	0.25	0.76	0.57
25°	0.25	0.78	0.57
25°	0.25§	0.34	0.45
Reflux	1.01	0.91	0.53
25°	1.01	0.89	0.51
25°	1.76‡	0.69	0.58

*Reported values are the average of three independent experiments; agreement from run to run was ±2%.
†Water was detected qualitatively by its development of a blue color with anhydrous $CuCl_2$.
‡At this concentration, the heat evolved caused the reaction mixture to reach reflux.
§Not stirred.

TABLE 2. Yields of bromides from reaction of hydrocarbons with HgO/Br_2

Substrate	Solvent	Temperature	RBr (%)*
Cyclohexane	Neat	Reflux	80†
2,3-Dimethylbutane	CCl_4	25°	5‡
Tetramethylbutane	CCl_4	Reflux	72
t-Butylbenzene	CCl_4	Reflux	None§
p-Xylene	CCl_4	Reflux	4‖
p-Nitrotoluene	CCl_4	Reflux	35†
Chloroform	Neat	Reflux	70
Tetrachloroethane	Neat	Reflux	40

*Yield of isolated material from reactions on a 10–50 mmol scale.
†Similar results were obtained in a run at room temperature.
‡Several products formed.
§Major product *p*-bromo-*t*-butyl benzene.
‖Major product 2-bromo-*p*-xylene.

bonds, bromination at tertiary positions is less successful. For example 2,3-dimethylbutane affords almost no 2-bromo-2,3-dimethylbutane, but gives a complex mixture in which 2,3-dibromo-2,3-dimethylbutane predominates. A similar problem attends the bromination of this substrate with elemental bromine (6) where it is believed that the first formed monobromide undergoes a subsequent dark reaction with molecular bromine.

Something of the scope of the new reaction is seen from Table 2, where the action of bromine and mercuric oxide is documented for several substrates.[1] Alkylbenzenes are unsuitable for side chain attack with this reagent as nuclear bromination occurs rather readily. Thus *t*-butylbenzene exclusively, and *p*-xylene chiefly afford the aryl bromide, although *p*-nitrotoluene, being less susceptible to electrophilic substitution, gives a moderate yield of the benzylic bromide. This competing reaction is not a serious limitation since benzylic groups may be brominated conveniently using either elemental bromine or *N*-bromosuccinimide (NBS) (7–10). The nuclear bromination was not further investigated since the reaction appears to offer no advantage over conventional (11) methods of electrophilic bromination.

[1]An attempt to extend the reaction to the synthesis of alkyl iodides using iodine and mercuric oxide was unsuccessful.

TABLE 3. Time for reaction of cyclohexane with HgO/Br_2 in CCl_4 under different conditions

Conditions	Time (min) For 95% reaction	Time (min) For 100% reaction
Dark	47	90
Diffuse light*	10	46
Strong light†	5	19
Diffuse light, N_2 flush	10	50
Diffuse light, O_2 flush	25	70
Diffuse light, I_2 (13 mg)	39	100
Diffuse light, galvinoxyl (10 mg)	49	115
Diffuse light, *t*-BuSH (15 mg)	37	85

*Light of the laboratory.
†One 100 W tungsten lamp placed 3 in. from the reaction flask.

Possible Reaction Mechanisms

The observation of short induction periods in some of the reactions already described suggests a free radical chain mechanism. Confirmation of this idea was obtained in a qualitative study of the rate of bromination of cyclohexane under various conditions, see Table 3. While light acts as a promoter for the reaction, oxygen, iodine,[2] galvinoxyl, and *t*-butyl mercaptan are inhibitors.

Two distinct free radical chain pathways can be proposed for the reaction, and are represented as mechanisms A and B.

Mechanism A

[2] $$Br_2 + RH \rightarrow HBr + RBr$$

[3] $$2HBr + HgO \rightarrow HgBr_2 + H_2O$$

[2]On the assumption that the inhibiting action of iodine is by way of the reaction $R^{\cdot} + I_2 \rightarrow RI + I^{\cdot}$, an attempt was made to prepare iodocyclohexane using cyclohexane, mercuric oxide, and a mixture of iodine and bromine; *cf.* the method of Speier (12) for bromination using a mixture of chlorine and bromine. No iodocyclohexane was obtained.

Can. J. Chem. Downloaded from www.nrcresearchpress.com by 210.87.254.40 on 09/05/12
For personal use only.

Mechanism B

[4] $2Br_2 + HgO \rightarrow HgBr_2 + Br_2O$

[5] $Br_2O + 2RH \rightarrow 2RBr + H_2O$

In mechanism A, bromination is envisioned as a normal free radical bromination where reaction 2 is comprised of the sequence [2*a*], [2*b*], and the mercury oxide serves simply to remove the hydrogen bromide formed in reaction 2.

[2*a*] $Br^{\cdot} + RH \rightleftharpoons HBr + R^{\cdot}$

[2*b*] $R^{\cdot} + Br_2 \rightarrow RBr + Br^{\cdot}$

This sequence could account for the increased reactivity of the reagent over elemental bromine as follows. Abstraction of hydrogen by bromine atoms is well known to be reversible (10, 13–16); the reverse of reaction 2*a* serves both to slow the reaction down and to increase the proportion of products derived from more stable radicals at the expense of those formed from less stable radicals (17). If the removal of hydrogen bromide by mercuric oxide were fast, the reverse of hydrogen abstraction would be suppressed with a corresponding increase in the apparent reactivity of the reagent.

In mechanism B, it is proposed that bromine and mercury oxide first interact to form bromine monoxide, a precedented process (18, 19). Bromination of the alkane is then effected by bromine monoxide rather than molecular bromine; again this will result in increased reactivity if bromine monoxide is a more reactive brominating agent than bromine itself. Although this seems a plausible argument, there are no data reported for bromine monoxide, the closest analogy being the reaction of chlorine monoxide with alkanes (20, 21). A detailed study by Tanner and Nychka (21) indicated that in CCl_4 solution chlorine monoxide chlorinates by way of the chain sequence [6]–[11] where hydrogen abstraction is accomplished by $Cl^{\cdot}$ and $ClO^{\cdot}$ radicals.

[6] $RH + ClO^{\cdot} \rightarrow HOCl + R^{\cdot}$

[7] $R^{\cdot} + Cl_2O \rightarrow RCl + ClO^{\cdot}$

[8] $RH + Cl^{\cdot} \rightarrow R^{\cdot} + HCl$

[9] $HCl + HOCl \rightarrow Cl_2 + H_2O$

[10] $R^{\cdot} + Cl_2 \rightarrow RCl + Cl^{\cdot}$

[11] $2HOCl \rightleftharpoons Cl_2O + H_2O$

Previously Phillips and Shaw (20) had found that in the gas phase at 100° the sequence [6]–[7] accounted for the reaction at low conversions of chlorine monoxide. Likewise Tanner and Nychka found that the product distribution from the chlorination of 1-chloropropane by chlorine monoxide in CCl_4 varied with percentage conversion. This also may be interpreted to mean that reactions 6 and 7 predominate early in the reaction when little HOCl has become available to undergo steps [9] and [11] of the complete scheme.

Distinction between mechanisms A and B is difficult for the following reasons. For mechanism A there is the problem of determining the "true" reactivity of the bromine atom in the absence of reversible hydrogen abstraction, for comparison with the new reagent. In this paper data on bromine atom abstraction have been taken from the literature only when it is clear whether or not abstraction was reversible. For mechanism B where bromine monoxide is the brominating agent there is the difficulty that no data on Br_2O are available, and it is not known, moreover, whether bromination by bromine monoxide would be mechanistically similar to chlorination by chlorine monoxide.

TABLE 4. Relative reactivity of several substrates towards HgO/Br_2 in Freon 113 at 25°

Substrate	Relative reactivity†
Cyclohexane	1.00*
Hexane	0.71±0.04
2,3-Dimethylbutane	2.37±0.08
Bicyclo[2.2.1]heptane	0.85±0.02
Toluene	8.5±0.14
1-Chlorobutane	0.23±0.02
1-Chlorobutane	1.00*
Cyclohexane-d_{12}	1.71±0.02
Chloroform	0.80±0.01
Tetramethylbutane	0.23±0.02
Tetramethylbutane	1.00*
Chloroform-*d*	0.50±0.07

*Assumed.
†Average values from at least three independent experiments.

Reactivity of the Hydrogen Abstracting Agent

The reactivity of the new reagent towards substrates of varied structure was determined using the competitive technique. The results are shown in Table 4, as reactivities per molecule relative to cyclohexane. A more convenient

TABLE 5. Selectivity of the HgO/Br_2 reagent compared with other halogenating agents

Reagent	Conditions	Abstracting radical	Relative selectivity per Hydrogen			Reference
			Primary	Secondary	Tertiary	
HgO/Br_2	F_{113}, 25°	$BrO^{\cdot} + Br^{\cdot}$	1	28*	400	This work
Br_2	Gas phase, 98°	$Br^{\cdot}$	1	250	6300	22
NBS	F_{113}, 25°†	$Br^{\cdot}$	1	200	6000‡	This work
CCl_3Br	Gas phase, 190°	$CCl_3^{\cdot}$	1	80	2300	23
Br_2O	F_{113}, 25°	$BrO^{\cdot} + Br^{\cdot}$	1	30	200	This work
Cl_2O	Gas phase, 100°	$ClO^{\cdot}$	1	21	—	20
Cl_2O	CCl_4, 40°	$Cl^{\cdot} + ClO^{\cdot}$	1	11.5	24	21
t-BuOCl	CCl_4, 40°	*t*-$BuO^{\cdot}$	1	7.9	44	24
CH_3ONO	Gas phase, 250°	$MeO^{\cdot}$	1	8	27	25*a*
$(CH_3)_2NC_6H_4NO$	H_2O	$HO^{\cdot}$	1	8	23	25*b*
H_2O_2	H_2O, 17.5°	$HO^{\cdot}$	1	4.7	9.8	26
Cl_2	Neat alkane, 0°	$Cl^{\cdot}$	1	3.1	5.0	27

*Direct bromination of hexane gave $k_s/k_p = 20$ both at reflux and at 25°.
†Photoinitiated reaction with 100 W tungsten lamp.
‡Competitive photobromination of hexane and 2,3-dimethylbutane in CH_3CN at 50° using NBS gave $k_t/k_s = 32$. These reactions were carried out in sealed evacuated Pyrex glass ampoules.

method of comparing the reactivities of different hydrogen abstracting radicals is through their selectivities, defined as the ratio per hydrogen of the rate constants for attack on hydrogen atoms in primary, secondary, and tertiary environments. The data for HgO/Br_2, calculated from Table 4 and from the isomer ratio in the bromination of *n*-hexane, are given in Table 5, together with data for other reagents.

From Table 5 it is clear that the abstracting species from the HgO/Br_2 reagent is of intermediate reactivity, along with typical oxyradicals. It is neither as reactive as atomic chlorine, nor as selective as the trichloromethyl radical or the bromine atom.[3]

It was demonstrated that hydrogen abstraction by the new reagent is not significantly reversible. A mixture of cyclohexane and cyclohexane-d_{12} was brominated with HgO/Br_2; the excess of the alkane mixture was recovered and shown by mass spectrometry not to have undergone any scrambling of the protium and deuterium (17).

$$[12] \qquad Br^{\cdot} + RH \rightarrow HBr + R^{\cdot}$$

$$[13] \qquad HBr + (CH_2CO)_2NBr \rightarrow Br_2 + (CH_2CO)_2NH$$

$$[14] \qquad R^{\cdot} + Br_2 \rightarrow RBr + Br^{\cdot}$$

[3]The data on bromine atoms were obtained using NBS as the brominating agent, to minimize reversible hydrogen abstraction. From the accepted (10) mechanism for NBS brominations, the hydrogen bromide is removed by reaction with NBS, and is thus unavailable for reversal with $R^{\cdot}$.

The selectivity of the HgO/Br_2 reagent was also compared with that due to bromine monoxide, and found to be closely similar. Both reagents however exhibit a selectivity rather greater than that of other typical oxyradical abstractors, and it would be reasonable to suppose that a mechanism analogous to eq. 6–11 would account for this, with abstraction by the more reactive bromoxy ($BrO^{\cdot}$) radical predominating over the unreactive bromine atom.

Another measure of the reactivity of a free radical is the primary deuterium isotope effect for hydrogen abstraction. For the HgO/Br_2 reagent k^H/k^D was found to be 2.6 for cyclohexane, and 7.0 for the less reactive substrate, chloroform (Table 6). This increase in k^H/k^D for a deactivated substrate is expected because of the larger activation energy for abstraction from the less reactive material (28), and makes comparison of the HgO/Br_2 data with those reported for other radicals difficult, since not all investigators have used the same hydrocarbon substrate. Thus we would expect that for bromine atom abstractions k^H/k^D (cyclohexane) would be larger than the value observed for toluene because toluene is the more reactive substrate towards this radical (29). For the *t*-butoxy radical k^H/k^D for cyclohexane is smaller than the value reported for toluene (30) since in this case cyclohexane is the more reactive hydrocarbon (32).

Can. J. Chem. Downloaded from www.nrcresearchpress.com by 210.87.254.40 on 09/05/12
For personal use only.

TABLE 6. Primary deuterium isotope effects for the HgO/Br_2 reagent compared with other abstracting agents

Reagent	Abstracting radical	Conditions	Substrate	k^H/k^D	Reference
HgO/Br_2	$BrO^{\cdot} + Br^{\cdot}$	F_{113}, 25°	Cyclohexane	2.6	This work
HgO/Br_2	$BrO^{\cdot} + Br^{\cdot}$	F_{113}, 25°	Chloroform	7.0	This work
Br_2	$Br^{\cdot}$	CCl_4, 77°	Toluene	4.6	16
t-BuOCl	*t*-$BuO^{\cdot}$	CCl_4	Toluene	5.5	30
t-BuOCl	*t*-$BuO^{\cdot}$	CCl_4, 0°	Cyclohexane	4.5	This work
H_2O/γ rays	$HO^{\cdot}$	H_2O	CH_3OH	2.0	25
Cl_2	$Cl^{\cdot}$	Neat alkane, 0°	Cyclohexane	1.3	31
Cl_2	$Cl^{\cdot}$	CCl_4, 77°	Toluene	1.3	16

TABLE 7. Isomer distributions in the halogenation of haloalkanes with HgO/Br_2 compared with other reagents

Reagent	Abstracting radical	Solvent	Temperature	Reference			
					CH_3*—CH_2—CH_2—Cl		
HgO/Br_2	$Br^{\cdot} + BrO^{\cdot}$	Neat	25°	This work	0.17	1.00	1.53
Br_2	$Br^{\cdot}$	Neat	Reflux	This work	—	1.00	0.66
Br_2O	$Br^{\cdot} + BrO^{\cdot}$	F_{113}	25°	This work	0.14	1.00	2.11
Cl_2O†	$ClO^{\cdot}$	CCl_4	40°	21	0.17	1.00	1.82
Cl_2O‡	$ClO^{\cdot} + Cl^{\cdot}$	CCl_4	40°	21	0.35	1.00	1.01
t-BuOCl	*t*-$BuO^{\cdot}$	CCl_4	40°	24	0.26	1.00	1.15
Cl_2	$Cl^{\cdot}$	CCl_4	40°	21	0.53	1.00	0.21
					CH_3*—CH_2—CH_2—CH_2—Cl		
HgO/Br_2	$Br^{\cdot} + BrO^{\cdot}$	Neat	25°	This work	0.11	1.00	0.35	0.56
Br_2	$Br^{\cdot}$	Neat	60°	35	—	1.00	0.49	0.44
Cl_2O	$Cl^{\cdot} + ClO^{\cdot}$	CCl_4	40°	21	0.17	1.00	0.37	0.43
t-BuOCl	*t*-$BuO^{\cdot}$	CCl_4	40°	24	0.35	1.00	0.44	0.48
Cl_2	$Cl^{\cdot}$	CCl_4	34°	27	0.36	1.00	0.46	0.13
					CH_3*—CH_2—CH_2—CH_2—Br		
HgO/Br_2	$Br^{\cdot} + BrO^{\cdot}$	Neat	25°	This work	0.11	1.00	0.63	0.59
Br_2	$Br^{\cdot}$ (reversible)	Neat	60°	35	—	1.00	5.78	0.06
NBS	$Br^{\cdot}$ (irreversible)	CH_3CN	40°	36	—	1.00	0.30	0.27

*These reported values are distributions of isomers and are not normalized per hydrogen.
†Early stages of reaction.
‡Completion of reaction.

Although fewer comparative data are available for isotope effects than for selectivity, it is again clear from Table 6 that the new reagent is more reactive than atomic bromine, comparably reactive with an oxyradical, and less reactive than atomic chlorine.

Polar Effects

The response of a radical to a polar effect, exemplified by discrimination against abstraction of hydrogens close to an electron-withdrawing substituent, depends on the deficiency of charge at the C—H bond under attack, and on the electronegativity of the attacking radical. It is thus a characteristic of the radical different from its selectivity or deuterium isotope effect, where bond energy considerations predominate (33). Thus the reactive but electrophilic chlorine atom attacks propionic acid mainly at the methyl group (34).

The response of the HgO/Br_2 reagent to such polar effects was measured for three substrates, 1-chloropropane, 1-chlorobutane, and 1-bromobutane. The results are presented in Table 7, with comparative data for other reagents. For all three substrates the polar effect is quite

Can. J. Chem. Downloaded from www.nrcresearchpress.com by 210.87.254.40 on 09/05/12
For personal use only.

Can. J. Chem. Downloaded from www.nrcresearchpress.com by 210.87.254.40 on 09/05/12
For personal use only.

different from that due to molecular bromine. The case of 1-bromobutane is of interest since this substrate has recently been shown (15, 36) to suffer attack by bromine atoms quite differently according to whether abstraction by Br· is reversible or irreversible. The fact that the HgO/Br_2 reagent shows a polar effect unlike either of these two situations finally excludes abstraction by atomic bromine as the major abstraction mode.

With 1-chloropropane both the HgO/Br_2 reagent and bromine monoxide show similar polar effects, which are also strikingly similar to that observed for chlorine monoxide at low percentage conversions (21). As already mentioned, it is believed that at low conversions the chloroxy (ClO·) radical is the major hydrogen abstractor, and the polar effect thus reinforces the earlier conclusion that the HgO/Br_2 reagent and bromine monoxide both involve bromoxy radicals as the predominant hydrogen abstracting agents.

Conclusions

The reaction of alkanes with bromine and mercuric oxide appears to be a reaction of some synthetic promise; the new reagent is more reactive than elemental bromine or NBS, and might thus find application where these latter reagents are insufficiently vigorous. The reaction appears to involve bromine monoxide as the reactive brominating agent, since solutions of this substance have a reactivity very similar to that of the HgO/Br_2 reagent. Comparison of the reactivity of the reagent towards C—H bonds of different strengths, and its response to polar effects show that the reactivity is greater than that of the bromine atom, but less than that of various oxyradicals. It seems reasonable to conclude that hydrogen abstraction, which has been shown to be irreversible, is carried out mainly by bromoxy radicals, with a smaller contribution from bromine atoms. The reaction mechanism is thus analogous to that previously proposed for chlorination by Cl_2O involving chlorine atoms and chloroxy radicals. Both the selectivity and the polar effects of HgO/Br_2 and of Cl_2O are strikingly similar under conditions where the latter reagent chlorinates by way of chloroxy radicals abstracting.

The proposed mechanism permits the explanation of the deviation of the stoichiometry of bromination from that of eq. 1. Since bromine monoxide is known (18) to be thermally unstable, bromination is in competition with decomposition of the reagent. By analogy with chlorine monoxide (5) this is most likely to give bromine and oxygen. The bromine released may then be reoxidized by mercuric oxide, the result being that mercuric bromide is produced in excess of that required by eq. 1, while alkyl bromide formation is reduced. For unreactive compounds *e.g.* *p*-nitrotoluene, relatively more decomposition of the reagent occurs, with a corresponding decrease in the yield of bromide.

Experimental

Solvents and substrates were reagent grade materials whose purities were checked by vapor phase chromatography (v.p.c.) before use. Freon 113 was obtained from Matheson, and Freon 112 was a gift from E. I. Du Pont de Nemours Co. Inc. Cyclohexane-d_{12} was obtained from Stohler Isotope Chemicals; chloroform-*d* from British Drug Houses Ltd.

Quantitation of products by v.p.c. was as described previously (37). Mass spectra were run on a Varian MAT model CH7; for g.c./m.s. work (gas chromatography with mass spectrometry) the mass spectrometer was interfaced through a Biemann–Watson helium separator to a Varian Aerograph Model 1700 v.p.c. equipped with $\frac{1}{8}$ in. stainless steel columns.

Reactions were carried out either at room temperature with stirring or at reflux in round bottomed flasks equipped with reflux condensers, under normal laboratory illumination except as noted. Normally the reactions were carried out in triplicate, and reported values are the average with the deviations calculated as probable statistical errors (38). Mercuric oxide was recovered from the residues for further use (5).

Reaction of Cyclohexane with Bromine and Mercuric Oxide (Table 1)

The following experiment is typical.

A mixture of mercuric oxide (2.0 g) and cyclohexane (4 ml) was stirred at room temperature in a 25 ml roundbottomed flask equipped with reflux condenser: 2.0 ml of a 2.02 *M* solution of bromine in carbon tetrachloride was added and the mixture was stirred for 20 min by which time the color of bromine was discharged. When the reaction was over, 2.0 ml of a 1.97 *M* solution of bromobenzene in carbon tetrachloride was added as a v.p.c. standard. V.p.c. analysis (10 ft × $\frac{1}{4}$ in. 10% SE30 on acid washed Chromosorb W, 105°) indicated that 1.58 mmol (79%) of bromocyclohexane had been formed. The solution was decanted from the solids at the bottom of the flask, washed with fresh CCl_4 and decanted again. The residue was extracted twice with 25 ml portions of acetone to dissolve mercuric bromide, then filtered with suction through a sintered glass filter of 10–20 μ porosity. Evaporation of the acetone

Can. J. Chem. Downloaded from www.nrcresearchpress.com by 210.87.254.40 on 09/05/12
For personal use only.

afforded 0.736 g (2.04 mmol) of mercuric bromide as off-white crystals m.p. 226–232° (lit. (38) 236°).

Small Scale Preparations of Alkyl Bromides using HgO/Br_2 (Table 2)

The reactions were carried out on a scale of 10–50 mmol using at least a 50% molar excess of mercuric oxide as exemplified below.

p-Nitrobenzyl Bromide:

A mixture of *p*-nitrotoluene (2.0 g), mercuric oxide (6 g) and bromine (5 g) in CCl_4 (60 ml) was heated to reflux for 1.5 h. The hot solution was filtered, and on cooling 0.1 g of an unidentified material of m.p. 145–50° was deposited. V.p.c. (SE30, 250°) indicated that only one compound was present besides starting material. Removal of the solvent and two recrystallizations from ethanol afforded *p*-nitrobenzyl bromide 0.7 g m.p. 96–98° (lit. (38) 99°) and 0.3 g of less pure material m.p. 80–85°.

1-Bromo-2,2,3,3-tetramethylbutane:

A mixture of 2,2,3,3-tetramethylbutane (3.0 g), mercuric oxide (8 g), bromine (1.9 g) and CCl_4 (60 ml) was heated to reflux for 0.5 h. Filtration and removal of solvent and excess alkane afforded a residue of the desired bromide (1.7 g), which was purified by preparative v.p.c. (SE30, 135°). N.m.r. (CCl_4): δ 0.90 ($(CH_3)_3C$—); 0.95 ($(CH_3)_2C<$); 3.45 (CH_2Br).

Reaction of Cyclohexane with HgO/Br_2 in the Presence of other Reagents (Table 3)

The reaction mixtures consisted of 5 ml aliquots of a 80:20 v/v mixture of CCl_4 and cyclohexane, to which were added the appropriate reagents, mercuric oxide (2.0 g), and 1.0 ml of a 1.5 *M* solution of bromine in CCl_4. The contents of the flasks were stirred, or agitated by a gaseous flush as appropriate. Reaction times were estimated (*i*) by comparing the color of the mixture visually with the color of a reaction mixture containing no alkane and 5% of the normal quantity of bromine and (*ii*) when the bromine color was completely discharged.

Competitive Reaction of Hydrocarbon Substrates with HgO/Br_2 (Table 4)

The reactions were carried out in Freon 113 solution using flasks equipped with reflux condensers. Carbon tetrachloride and Freon 112 were used as inert internal standards as appropriate for v.p.c. analysis on SE30 or diisodecyl phthalate (DIDP) columns. The reactions were carried out in at least triplicate, and the reactivities were evaluated as described previously (31). From the results obtained (Table 4) were calculated the data of Tables 5 and 6 pertaining to the HgO/Br_2 reagent.

Reaction of HgO/Br_2 with a Mixture of Cyclohexane and Cyclohexane-d_{12}

A mixture of cyclohexane (0.753 g) and perdeuteriocyclohexane (0.763 g) was made up to 5 ml with Freon 113. Reaction mixtures were prepared containing HgO (1.0 g), Freon 113 (3 ml), bromine (0.5 g), and 1.0 ml of the substrate solution, and stirred until colorless. G.c./m.s. (SE30, 35°) was used to determine the isotopic composition of the alkane mixture before and after reaction. Several mass spectra were run for the control mixture and for each of three reaction mixtures. In no case was there any enhancement of the peaks at m^+/e 85 relative to 84, or of m^+/e 94 and 95 relative to 96.

Selectivity of NBS towards Alkanes (Table 5)

The primary:secondary selectivity was obtained from bromination of hexane (3 ml) with NBS (0.5 g) under the illumination of one 100 W tungsten lamp with stirring. The mixtures were analyzed by v.p.c. (SE30, 100°). The major component was assigned as a mixture of a 2-bromohexane and 3-bromohexane, since photobromination of hexane with Br_2 gave this product exclusively. The minor product, which eluted later, had a retention time identical to that of 1-bromohexane, prepared by the degradation of heptanoic acid with Br_2/HgO (1). The ratio of (2 + 3)-bromohexane to 1-bromohexane was 1: 0.0037 ± 0.0002.

The secondary to tertiary selectivity was obtained by competitive photoinitiated bromination of 2,3-dimethylbutane and *n*-hexane by NBS using CCl_4 as the inert standard and Freon 113 as solvent. V.p.c. analysis of the alkane before and after the reaction (SE30, 50°) gave k(hexane) to k(2,3-dimethylbutane) as 1:7.5 ± 0.9 (six determinations).

The secondary to tertiary selectivity was also determined in homogeneous acetonitrile solutions at 50°. These reactions were conducted in sealed evacuated ampoules, irradiated to initiate the reaction. V.p.c. analysis (DIDP, 75°) gave k(hexane) to k(2,3-dimethylbutane) as 1:7.9 ± 1.5.

Selectivity of Br_2O towards Alkanes

The selectivity per hydrogen was measured by direct bromination of butane and of isobutane with bromine monoxide. A convenient preparation of a bromine monoxide solution was as follows. A mixture of 20 g mercuric oxide and 20 ml of 1 *M* bromine in Freon 113 was swirled for 3 min in a stoppered flask with light excluded. After this time filtration gave a solution that was usually ~0.9 *M* in bromine and ~0.05 *M* in Br_2O (5). For the selectivity experiments 10 ml of such a solution was filtered through a glass sinter of 10–20 μ porosity directly on to *ca.* 1 ml of either butane or isobutane previously condensed. The mixtures were allowed to warm to 0° and after 10 min in the dark, they were quenched with aqueous sodium thiosulfate solution. Control experiments showed that elemental bromine did not react with the alkanes under these conditions. The reaction mixtures were analyzed by v.p.c. (DIDP, 80°) for the appropriate isomeric bromobutanes, whose rentention times were identical with those of authentic samples. Butane gave 1-bromobutane and 2-bromobutane in the ratio 1: 20.0 ± 0.3; isobutane gave isobutyl bromide and *tert*-butyl bromide in the ratio 1: 22.1 ± 0.2.

Kinetic Isotope Effect for t-Butoxy Radical Abstraction

Mixtures of cyclohexane, *n*-hexane, and Freon 113 (standard), each ~1 *M* in CCl_4 were allowed to react with *t*-butyl hypochlorite in sealed degassed ampoules at 0° using photoinitiation. After reaction, the mixtures were analyzed by v.p.c. (DIDP, 50°); $k_{C_6H_{12}}/k_{C_6H_{14}}$ was found to be 2.05 ± 0.02; $k_{C_6D_{12}}/k_{C_6H_{14}}$ was 0.45 ± 0.01.

Reaction of HgO/Br_2 with Haloalkanes (Table 7)

These reactions were all carried out in duplicate using the haloalkane as its own solvent.

1-Chloropropane

Four products were obtained (DIDP, 80°) of which the last to elute comprised about 3% of the total product

Can. J. Chem. Downloaded from www.nrcresearchpress.com by 210.87.254.40 on 09/05/12
For personal use only.

mixture. The first three products were shown to be bromochloropropanes by g.c./m.s. (DIDP, 55°). Of these three products, the third to elute was assigned to 3-bromo-1-chloropropane, because it was absent from the mixture obtained by bromination of 1-chloropropane with elemental bromine alone. The second product was assigned as 2-bromo-1-chloropropane, since it had retention time identical with that of the major product of photo-chlorination of 2-bromopropane. By elimination, the first product was 1-bromo-1-chloropropane.

1-Chlorobutane

Four products were obtained, and were shown to be bromochlorobutanes by g.c./m.s. (SE30, 50°). The elution order was the same using either SE30, 80° or DIDP, 125°, and was concluded to be 1,1-; 1,2-; 1,3-; 1,4-chloro-bromobutane from previously reported studies (39).

1-Bromobutane

The four products obtained on v.p.c. analysis (SE30, 100°) were shown to be dibromobutanes by g.c./m.s. (SE30, 80°). The elution order has previously (15) been shown to be 1,1-; 1,2-; 1,3-; 1,4-dibromobutane.

Reaction of Bromine with Mercuric Oxide with no Added Substrate

A mixture of bromine (0.8 g), mercuric oxide (4 g) and CCl_4 (10 ml) was heated to reflux for 12 h by which time the color due to bromine was discharged. The CCl_4 solution and the solid residue were each treated with an acidified sodium iodide solution. The CCl_4 phase was unreactive, while the residuum gave a deposit of mercuric iodide. In neither case an oxidant was present to liberate molecular iodine.

The author wishes to thank the National Research Council of Canada for supporting this work financially. Thanks are also due to E. I. Du Pont de Nemours Co. Inc. for a gift of Freon 112, and to Miss Linda MacDonald of this department for running the mass spectrometer.

1. N. J. BUNCE. J. Org. Chem. **37**, 664 (1972).
2. F. A. H. RICE. J. Am. Chem. Soc. **78**, 3173 (1956); F. A. H. RICE and W. MORGANROTH. J. Org. Chem. **21**, 1388 (1956).
3. M. S. KHARASCH and M. Z. FINEMAN. J. Am. Chem. Soc. **63**, 2776 (1941).
4. J. H. SULLIVAN and N. DAVIDSON. J. Chem. Phys. **19**, 143 (1951).
5. G. H. CADY. Inorg. Synth. **5**, 156 (1957).
6. G. A. RUSSELL and H. C. BROWN. J. Am. Chem. Soc. **77**, 4025 (1955).
7. G. H. COLEMAN and G. E. HONEYWELL. Org. Synth. Coll. Vol. **2**, 443 (1943).
8. E. F. M. STEPHENSON. Org. Synth. Coll. Vol. **4**, 984 (1963).
9. R. B. WAGNER and H. D. ZOOK. Synthetic organic chemistry. John Wiley & Sons Inc., New York. 1953. p. 98.
10. R. E. PEARSON and J. C. MARTIN. J. Am. Chem. Soc. **85**, 3142 (1963).
11. P. B. D. DE LA MARE and J. H. RIDD. Aromatic substitution, nitration and halogenation. Butterworths, London. 1959. Ch. 8–10.
12. J. L. SPEIER. J. Am. Chem. Soc. **73**, 826 (1951).
13. H. R. ANDERSON, H. A. SCHERAGA, and E. R. VAN ARTSDALEN. J. Chem. Phys. **21**, 1258 (1953).
14. D. D. TANNER, M. W. MOSHER, and N. J. BUNCE. Can. J. Chem. **47**, 4709 (1969).
15. D. D. TANNER, D. DARWISH, M. W. MOSHER, and N. J. BUNCE. J. Am. Chem. Soc. **91**, 7398 (1969).
16. K. B. WIBERG and L. H. SLAUGH. J. Am. Chem. Soc. **80**, 3033 (1958).
17. D. D. TANNER and N. J. BUNCE. J. Am. Chem. Soc. **91**, 3028 (1969).
18. W. BRENSCHEDE and H. J. SCHUMAKER. Z. Physik. Chem. **29B**, 356 (1935); Z. Anorg. Chem. **226**, 370 (1936).
19. P. W. JENNINGS and T. D. ZIEBARTH. J. Org. Chem. **34**, 3216 (1969).
20. L. PHILLIPS and R. SHAW. Proc. Chem. Soc. 294 (1962).
21. D. D. TANNER and N. NYCHKA. J. Am. Chem. Soc. **89**, 121 (1967).
22. G. C. FETTIS, J. H. KNOX, and A. F. TROTMAN-DICKENSON. J. Chem. Soc. 4177 (1960); see also ref. 26.
23. B. P. MCGRATH and J. M. TEDDER. Bull. Soc. chim. Belges, **71**, 772 (1962).
24. C. WALLING and B. B. JACKNOW. J. Am. Chem. Soc. **82**, 6108, 6113 (1960).
25. (*a*) R. SHAW and A. F. TROTMAN-DICKENSON. J. Chem. Soc. 3210 (1960); (*b*) M. ANBAR, D. MEYERSTEIN, and P. NETA. J. Chem. Soc. (B), 742 (1966).
26. T. BÉRCES and A. F. TROTMAN-DICKENSON. J. Chem. Soc. 4281 (1961).
27. C. WALLING and M. F. MAYAHI. J. Am. Chem. Soc. **81**, 1485 (1959).
28. K. B. WIBERG. Chem. Rev. **55**, 713 (1955).
29. G. A. RUSSELL and H. C. BROWN. J. Am. Chem. Soc. **77**, 4518 (1955).
30. C. WALLING and J. A. MCGUINNESS. J. Am. Chem. Soc. **91**, 2053 (1969).
31. M. W. MOSHER and N. J. BUNCE. Can. J. Chem. **49**, 28 (1971).
32. C. WALLING. Pure and Appl. Chem. **15**, 69 (1967).
33. J. M. TEDDER. Quart. Rev. **14**. 336 (1960).
34. A. BRUYLANTS, M. TITS, C. DIEU, and R. GAUTHIER. Bull. Soc. chim. Belges, **61**, 266 (1952).
35. W. THALER. J. Am. Chem. Soc. **85**, 2607 (1963).
36. D. D. TANNER, M. W. MOSHER, N. C. DAS, and E. V. BLACKBURN. J. Am. Chem. Soc. **93**, 5846 (1971).
37. N. J. BUNCE and N. G. MURRAY. Tetrahedron, **27**, 5323 (1971).
38. Handbook of chemistry and physics, R. C. Weast (*editor*). 49th ed. Chemical Rubber Co., Cleveland, Ohio. 1968.
39. P. S. FREDRICKS and J. M. TEDDER. J. Chem. Soc. 144 (1960).

Etude cinétique des systèmes Cu(II).Adénosine et Cu(II).D-Ribose

G. BOIVIN ET M. ZADOR
Département de Chimie, Université de Montréal, Montréal, Québec

Reçu le 27 avril 1972

La cinétique de formation et de dissociation des complexes entre le Cu(II) et l'adénosine a été étudiée en milieu acide ainsi qu'en milieu basique. En milieu acide, les paramètres cinétiques ont été obtenus par la méthode de relaxation et ils correspondent au complexe formé avec le groupement adénine. En milieu basique seule la dissociation des complexes a pu être étudiée par la méthode du "flux stoppé", en utilisant l'EDTA ou un acide fort pour dissocier les complexes, formés dans ce cas avec les groupes hydroxyles du ribose. A titre de comparaison, le D-ribose a été également étudié dans ces conditions. Le mécanisme de ces réactions est discuté.

The kinetics of the formation and dissociation of Cu(II) complexes of adenosine have been determined in acidic and basic medium. In acidic medium, the complex is formed between the Cu(II) and the adenine base and the kinetic parameters have been obtained in this case using a temperature jump method. In basic medium, only the dissociation of the complexes could be studied by a stopped-flow method, by addition of EDTA or strong acid solutions. In these complexes, Cu(II) is bridged with ribose hydroxyls. Finally, D-ribose has also been studied for comparison in the same conditions. The mechanism of these reactions is discussed.

Canadian Journal of Chemistry, **50**, 3117 (1972)

Can. J. Chem. Downloaded from www.nrcresearchpress.com by 210.87.254.6 on 09/05/12
For personal use only.

Introduction

Pendant les deux dernières décades, la biochimie du cuivre a pris une importance considérable surtout par la mise en évidence du cuivre dans certains enzymes et certaines protéines jouant un rôle de premier plan dans les organismes vivants (1).

Plus que tout autre ion métallique, le cuivre forme des chélates très stables avec les substances biologiquement actives (2). Une partie du cuivre contenu dans l'organisme se trouve liée à l'ADN. On a pu démontrer *in vitro* que l'ion cuivrique a la propriété de dénaturer l'ADN en formant des chélates avec les bases puriques telles l'adénine et la guanine (3).

Les nombreux travaux effectués dans ce domaine concernent le site de fixation du cuivre dans l'ADN et la détermination des constantes de stabilité avec l'ADN, ses nucléosides et ses bases constituantes (3, 4).

La nature des complexes du cuivre avec l'adénosine et l'adénine dépend de l'acidité du milieu réactionnel. Ainsi, on a montré qu'il pouvait être lié au groupement adénine en milieu acide ou neutre sans départ de proton (5). Dans le cas de l'adénosine, il pouvait également former deux types de complexes en milieu basique (6, 7). La complexation se faisait alors avec le départ d'un ou de deux protons des groupements hydroxyles du ribose.

La détermination des constantes de stabilité des complexes a été effectuée principalement par potentiométrie (5, 6), par spectrophotométrie (8) et par une méthode cinétique indirecte de dosage du cuivre basée sur son action catalytique dans une réaction d'oxydation (9).

Jusqu'à présent, très peu de travaux cinétiques ont été effectués sur la formation de complexes de l'ion cuivrique avec les bases puriques. Les seules études existantes portent sur la cinétique de formation des complexes avec l'ADP et l'ATP, mais dans ces cas, le cuivre se trouve principalement lié au groupement polyphosphate (10).

Dans ce travail, nous nous sommes proposés d'étudier le mécanisme de formation des complexes du Cu(II) avec l'adénosine et le sucre constituant le D-ribose.

Partie expérimentale

Les réactifs

L'adénosine et le D-ribose sont des produits de Nutritional Biochemicals Co. Le perchlorate cuivrique a été obtenu en dissolvant l'oxyde cuivrique dans l'acide perchlorique. La solution stock a été dosée par iodométrie et par absorption atomique. L'EDTA est un produit Fisher Scientific Co. Les solutions d'adénosine et de D-ribose ont été fraîchement préparées avant chaque série d'expériences. La force ionique des solutions a été maintenue constante à l'aide du perchlorate de sodium.

Appareillage

La cinétique des réactions a été étudiée par les méthodes

Can. J. Chem. Downloaded from www.nrcresearchpress.com by 210.87.254.6 on 09/05/12
For personal use only.

de la relaxation thermique et du "flux stoppé", dont les principes ont déjà été décrits dans la littérature (11).

L'appareil de relaxation provient de Messanlagen Studiengessellschaft m.b.H., Göttingen, Allemagne. L'appareil du "flux stoppé" est constitué d'un système à mélange rapide Durrum–Gibson et d'un monochromateur Jarrel Ash 0.25 m. Dans chaque cas, les variations de densité optique ou de transmission des solutions sont enregistrées sur un oscillographe cathodique et le signal obtenu est photographié. Les spectres visibles et ultraviolets ont été mesurés sur un spectrophotomètre Cary-14. Les cellules réactionnelles sont thermostatées et, dans le cas de la relaxation, la température est mesurée avant chaque expérience à l'intérieur de la cellule à l'aide d'un thermocouple. Le pH des solutions a été controlé à l'aide d'un pH-mètre Radiometer-26.

Méthodes cinétiques

La cinétique de relaxation du système Cu(II).adénosine en milieu acide a été suivie par la diminution de l'absorption sur une des extrémités de la bande de l'adénosine, c'est-à-dire à des longueurs d'onde variant de 280 à 310 nm. Dans ces conditions, il est possible de travailler à des concentrations suffisamment grandes pour étudier la formation du complexe. La dissociation des complexes en milieu basique est étudiée par la méthode du "flux stoppé", on choisit une longueur d'onde où la variation de l'absorption est la plus grande possible entre l'état initial et final du système étudié. Dans les cas où l'on suit la cinétique à une longueur d'onde où le complexe absorbe, on enregistre la diminution de l'absorption; dans quelques cas c'est l'apparition du complexe Cu(II).EDTA qui a été mesurée, on avait alors une augmentation de l'absorption. Les solutions ont été dégazées pour empêcher la formation de bulles. Les solutions à mélanger ont la même force ionique pour éviter des phénomènes provoqués par une chaleur de mélange. Dans chaque cas, des vérifications ont été faites pour s'assurer qu'un des réactifs seul ne présentait pas de relaxation.

Résultats et discussion

Relaxation du système Cu(II)–Adénosine en milieu acide

L'adénosine en milieu acide est protonée selon l'équilibre [1],

$$[1] \qquad AH_2^+ \rightleftharpoons AH + H^+$$

$$pK_{a_1} = 3.51 \text{ à } 25\ ^\circ\text{C (12)}$$

et en milieu basique, elle se dissocie d'après [2],

$$[2] \qquad AH \rightleftharpoons A^- + H^+$$

$$pK_{a_2} = 12.35 \text{ à } 25\ ^\circ\text{C (13)}$$

où AH représente l'adénosine.

Nous avons travaillé en excès de cuivre par rapport à l'adénosine. Ceci permet d'obtenir des cinétiques plus simples étant donné que la concentration en adénosine libre n'intervient pas dans l'équation donnant le temps de relaxation.

TABLEAU 1. Temps de relaxation du système $Cu^{2+} + AH \rightleftharpoons CuAH^{2+}$*

$[Cu^{2+}]$ (M)	τ (ms) 9 °C	21 °C	31 °C
0.20	2.4	1.6	1.1
0.30	2.0	1.2	0.9
0.40	1.6	1.0	0.7
0.50	1.4	0.85	0.6

*[AH] = 0.01 à 0.02 M, pH = 4.0, force ionique = 1.5 M. Les temps de relaxation correspondent à une moyenne de plusieurs expériences et la reproductibilité est meilleure que 10%.

En milieu acide, on observe une relaxation que l'on peut attribuer à la formation du complexe $Cu.AH^{2+}$, suivant la réaction:

$$[3] \qquad AH + Cu^{2+} \underset{k_d}{\overset{k_f}{\rightleftharpoons}} (Cu.AH)^{2+}$$

Les temps de relaxation, τ, obtenus dans différentes conditions expérimentales sont groupés dans le tableau 1. Ils sont indépendants de la concentration en adénosine et du pH. A cause de la faible stabilité du complexe, les mesures de relaxation à une concentration inférieure à 0.2 M en Cu(II) ne sont pas significatives puisque nous sommes à la limite de sensibilité de l'appareil.

Les résultats peuvent être interprétés par une équation de vitesse simple découlant de l'équilibre [3],

$$[4] \qquad 1/\tau = k_f([\overline{Cu(II)}] + [\overline{AH}]) + k_d$$

où les concentrations sont celles à l'équilibre. Avec un grand excès de Cu(II) on obtient l'équation 5.

$$[5] \qquad 1/\tau = k_f[Cu(II)] + k_d$$

La fig. 1 montre que l'éq. 5 est vérifiée et permet d'obtenir les valeurs de k_d et de k_f à diverses températures.

La constante d'équilibre de l'équation 3, se définissant comme suit: $K = [Cu.AH]^{2+}/[Cu^{2+}][AH]$, peut être calculée en faisant le rapport des constantes de vitesse de formation et de dissociation, $K = k_f/k_d$. Le tableau 2 représente les différentes constantes de vitesse et d'équilibre ainsi que les énergies d'activation correspondantes.

Les résultats montrent clairement que le phénomène observé correspond à la réaction

Can. J. Chem. Downloaded from www.nrcresearchpress.com by 210.87.254.6 on 09/05/12
For personal use only.

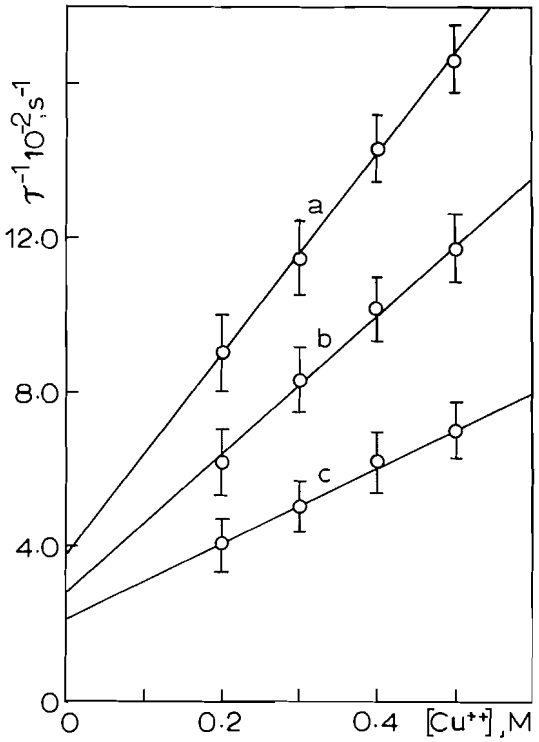

FIG. 1. Variation de τ^{-1} en fonction de la concentration en Cu^{2+}: [adénosine] = 0.01 à 0.02 *M*, p*H* = 4.0, force ionique = 1.5 *M*; (*a*) *T* = 31 °C, (*b*) *T* = 21 °C, (*c*) *T* = 9 °C.

3 et non pas à celle où la formation du complexe s'accompagne du départ d'un proton, ce qui a été mis en évidence à des p*H* plus élevés.

Les énergies d'activation sont du même ordre de grandeur que celles mises en évidence par l'étude r.m.n. des complexes du Cu(II) avec l'éthylènediamine (14).

La valeur de la constante d'équilibre de formation du complexe ($K = 7 \pm 2$) est plus forte que celle du complexe Ni(II).adénosine (15), ce qui est en accord avec la série Irving–Williams (16). Cette valeur correspond bien à celles déterminées dans la littérature par des méthodes différentes. Brintzinger et coll. (8) ont trouvé par spectrophotométrie une constante d'équilibre de 7.0 à 20 °C. Fiskin et Beer (5) en observant par potentiométrie le déplacement de l'équilibre [1], ont trouvé comme constante d'équilibre 5.0 ± 2.3 à 20 °C.

TABLEAU 2. Constantes de vitesse de formation et de dissociation du complexe $CuAH^{2+}$ et les énergies d'activation correspondantes*

T (°C)	k_f (M^{-1} s^{-1})	k_d (s^{-1})	*K* (M^{-1})
9	1100	200	5.5
21	1800	270	7.0
31	2680	340	8.0

*$E_f = 7 \pm 2$ kcal/mol; $E_d = 5 \pm 2$ kcal/mol.

*Etude des constantes de vitesse de dissociation des complexes Cu(II).adénosine et Cu(II).*D*-ribose en milieu basique*

Sur les spectres d'absorption, on observe la présence de deux complexes, le premier apparaissant vers p*H* 10 est de couleur vert pâle tandis que le deuxième vers p*H* 12 a une couleur bleu foncé. La nature exacte de ces complexes n'est pas connue avec certitude, des études potentiométriques montrent néanmoins qu'ils se font par départ de un ou de deux protons (12, 17).

La structure proposée par Reinert et Weiss (17) implique la formation de complexes contenant des ligands hydroxydés du type: $(CuA)_I \equiv CuA(OH)_2^-$, complexe vert et $(CuA)_{II} \equiv CuA(OH)_2^{2-}$, complexe bleu, dans lesquels l'adénosine a perdu un et deux protons respectivement. Ces protons viennent des groupements hydroxyles 2′ et 3′ du ribose. Ceci est confirmé par le fait que le D-ribose forme dans les mêmes conditions des complexes ayant des caractéristiques spectrales identiques, donc un complexe vert, $(CuR)_I$ et un complexe bleu, $(CuR)_{II}$.

Dissociation du complexe bleu $(CuA)_{II}$ par l'EDTA

A p*H* élevé (p*H* > 5) il y a formation d'un hydroxyde très peu soluble. On ne peut obtenir une solution homogène que si la formation des complexes est complète. Dés lors, il est impossible d'utiliser des méthodes de relaxation. Notamment, il n'y a pratiquement plus de perturbation des concentrations à l'équilibre et, de plus, à cause des concentrations élevées, les réactions deviennent trop rapides pour être mesurées. On peut néanmoins étudier la dissociation des complexes par la méthode du "flux stoppé".

Il est possible de dissocier les complexes au moyen d'un ligand formant des chélates encore plus stables avec le Cu(II), tel que l'EDTA. En effet, le complexe Cu(II).EDTA est bien connu; on a déterminé sa constante de stabilité (log

Can. J. Chem. Downloaded from www.nrcresearchpress.com by 210.87.254.6 on 09/05/12
For personal use only.

TABLEAU 3. Constantes de vitesse expérimentales des complexes $(CuA)_I$, $(CuA)_2$, et $(CuR)_{II}$*

[EDTA] (M)	k_{exp} (s^{-1})		
	$(CuA)_I$†	$(CuA)_{II}$‡	$(CuR)_{II}$§
0.080	210	5.3	0.073
0.063	170	4.3	0.062
0.050	125	3.6	0.055
0.025	70	2.2	0.042

*$[Cu^{2+}] = 2.5\ 10^{-3}$ M, $T = 25$ °C, force ionique = 0.5 M.
†Complexe vert du Cu(II).adénosine, $[AH] = 2.5 \times 10^{-2}$ M, pH = 10.2, λ = 360 et 730 nm.
‡Complexe bleu du Cu(II).adénosine, $[AH] = 2.5 \times 10^{-2}$ M, pH = 12.5, λ = 360 et 730 nm.
§Complexe bleu du Cu(II).D-ribose, $[R] = 5 \times 10^{-3}$ M, pH = 11.0, λ = 360 nm.

$\beta_1 = 18.8$) (18) et, de plus, la formation de ce complexe est très rapide (19). Par conséquent, cette réaction d'échange conduit à la disparition totale des complexes du Cu(II) avec l'adénosine ou le D-ribose.

L'étude de la dissociation du complexe avec l'EDTA permet de travailler à pH constant; ceci élimine la formation intermédiaire du complexe $(CuA)_I$, présent à pH plus bas et facilite l'interprétation des résultats.

En utilisant un excès d'EDTA par rapport au complexe, nous obtenons une cinétique d'ordre un. Le tableau 3 groupe les constantes de vitesse expérimentales en fonction de la concentration en EDTA. La constante expérimentale d'ordre un varie avec la concentration en EDTA. Si nous portons graphiquement les constantes expérimentales en fonction de la concentration en EDTA, nous obtenons une droite avec une ordonnée à l'origine non nulle.

Ceci correspond à deux réactions simultanées: (*i*) la dissociation du complexe $(CuA)_{II}$, suivie d'une réaction très rapide du Cu(II) formé, avec l'EDTA (étapes [6] et [7]), et (*ii*) la réaction d'échange direct, de type S_N2, entre le complexe et l'EDTA (étape [8]).

$$[6] \qquad (CuA)_{II} \xrightarrow[\text{lente}]{k_d} AH + Cu(II)$$

$$[7] \qquad Cu(II) + EDTA \xrightarrow[\text{rapide}]{} (Cu.EDTA)$$

$$[8] \qquad (CuA)_{II} + EDTA \xrightarrow[\text{lente}]{k_{EDTA}} AH + (Cu.EDTA)$$

La vitesse de disparition du complexe est donnée par:

$$[9] \qquad V = k_d[(CuA)_{II}] + k_{EDTA}[(CuA)_{II}][EDTA]$$

TABLEAU 4. Constantes de vitesse des réactions des complexes avec l'EDTA*

Complexe	k_d (s^{-1})	k_{EDTA} (M^{-1} s^{-1})
$(CuA)_I$	<20	2500
$(CuA)_{II}$	0.80	57
$(CuR)_{II}$	0.03	0.52

*$T = 25$ °C, force ionique = 0.5 M.

et la constante de vitesse expérimentale par:

$$[10] \qquad k_{exp} = k_d + k_{EDTA}[EDTA]$$

Les deux constantes de l'éq. 10 peuvent être déterminées graphiquement (fig. 2(*b*)). La réaction bimoléculaire, [8], se fait probablement en plusieurs étapes dont la première serait la complexation d'un site de coordination du cuivre du complexe $(CuA)_{II}$.

La formation intermédiaire de complexes mixtes CuA.(EDTA) est une étape possible. Expérimentalement la disparition totale de la bande $(CuA)_{II}$ indiquerait que la concentration de ce complexe devrait être faible, ce qui est raisonnable étant donné la très grande stabilité du complexe Cu(II).EDTA qui devient l'espèce prédominante.

Il est à noter que cette méthode ne peut être appliquée au complexe prépondérant à p$H < 5$, CuA^{2+}, la valeur des constantes de vitesse impliquées étant trop élevée pour une méthode de "flux stoppé".

Dissociation du complexe $(CuR)_{II}$ par l'EDTA

Le complexe bleu avec le D-ribose prédomine en milieu basique à p$H > 9$. La dissociation de ce complexe par l'EDTA peut être étudiée de la même manière que celle du $(CuA)_{II}$. Les résultats sont présentés dans le tableau 3.

L'interprétation des résultats est analogue à celle faite précédemment, (fig. 2(*c*)). Les constantes de vitesse obtenus sont toutefois plus faibles d'un facteur de 50–100 que dans le cas de l'adénosine (tableau 4).

Dissociation du complexe vert, $(CuA)_I$

Le complexe vert, $(CuA)_I$, peut être aussi dissocié en utilisant l'EDTA. Les résultats obtenus à pH 10.2 sont présentés au tableau 3. Les valeurs des constantes de vitesse expérimentales sont d'environ 50 fois plus grandes que pour $(CuA)_{II}$; ceci montre bien que les deux phénomènes peuvent être séparés et que les cons-

Can. J. Chem. Downloaded from www.nrcresearchpress.com by 210.87.254.6 on 09/05/12
For personal use only.

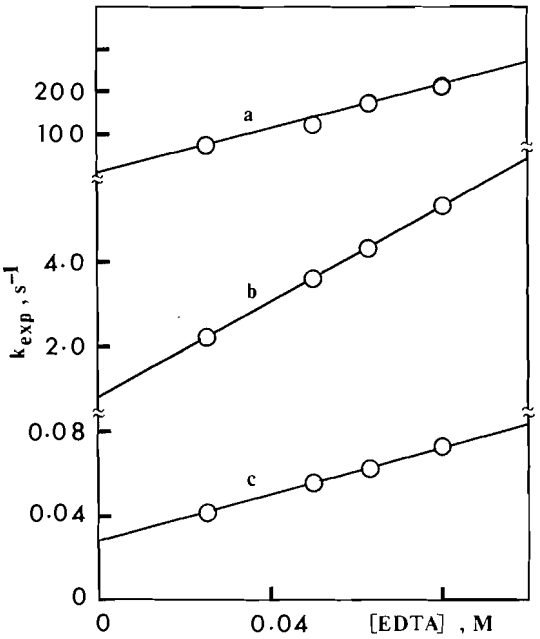

FIG. 2. Variation de la constante de vitesse expérimentale de dissociation des complexes $(CuA)_I$, $(CuA)_{II}$, et $(CuR)_{II}$ en fonction de la concentration en EDTA: $[Cu^{2+}] = 2.5 \times 10^{-3}$ *M*, force ionique 0.5 *M*, $T = 25$ °C; (*a*) complexe $(CuA)_I$: [adénosine] $= 2.5 \times 10^{-2}$ *M*, p*H* = 10.2; (*b*) complexe $(CuA)_{II}$: [adénosine] $= 2.5 \times 10^{-2}$ *M*, p*H* = 12.5; (*c*) complexe $(CuR)_{II}$: [D-ribose] $= 5.0 \times 10^{-3}$ *M*, p*H* = 11.0.

tantes pour $(CuA)_{II}$ sont significatives. L'interprétation graphique est représentée par la fig. 2(*a*). On note que l'ordonnée à l'origine de la droite obtenue est très petite par rapport aux constantes de vitesse expérimentales. Ceci implique que dans ce cas particulier le mécanisme correspondant aux éq. 6 et 7 est quasi négligeable par rapport à celui de l'éq. 8 correspondant à la réaction bimoléculaire avec l'EDTA. La valeur de k_d du tableau 4 ne représente qu'une limite supérieure.

Dans le cas du complexe $(CuA)_I$, on peut utiliser un acide fort pour étudier la dissociation. L'addition de l'acide permet de déplacer les équilibres [1] et [2] vers la formation de AH^+, ce qui entraîne la dissociation du complexe. Dans ce cas là on dissocie le complexe en captant l'adénosine, alors qu'en utilisant l'EDTA on captait le Cu(II).

Cette méthode a déjà été utilisée dans d'autres cas (15, 20, 21). On remarque que la constante de vitesse expérimentale de dissociation augmente avec l'acidité. Les résultats du tableau 5 peuvent être interprétés par un schéma analogue aux éqs. 6, 7, et 8.

TABLEAU 5. Constante de vitesse de dissociation de $(CuA)_I$ en fonction de l'acidité*

$[HClO_4]$ (*M*)	k_{exp} (s^{-1}) $(CuA)_I$
0.25	410
0.20	345
0.15	255
0.10	190
0.05	90
0.037	75

*$k_d < 20$ s^{-1}, $k_{H^+} = 1750$ M^{-1} s^{-1}. $[Cu^{2+}] = 2.5 \times 10^{-3}$ *M*, $[AH] = 5 \times 10^{-3}$ *M*, force ionique = 0.5 *M*, $T = 25$ °C, p*H* initial = 10.2, $\lambda = 750$ nm.

$$[11] \qquad (CuA)_I \xrightarrow[\text{lente}]{k_d} A^- + Cu(II)$$

$$[12] \qquad A^- + 2H^+ \xrightarrow[\text{rapide}]{} AH_2^+$$

$$[13] \qquad (CuA)_I + H^+ \xrightarrow[\text{lente}]{k_{H^+}} Cu(II) + AH$$

$$[14] \qquad AH + H^+ \xrightarrow[\text{rapide}]{} AH_2^+$$

L'ensemble de ces équations conduit à l'expression suivante pour la constante de vitesse expérimentale de disparition du complexe:

$$k_{exp} = k_d + k_{H^+}[H^+]$$

L'influence de l'acidité s'explique bien en admettant la protonation du ligand, ce qui diminue la stabilité du complexe. Ceci conduirait, à acidité très élevée, vers une valeur limite correspondant à la protonation complète et dans certains cas cette valeur limite est atteinte (20).

Bien que la valeur faible de l'ordonnée à l'origine, (fig. 3), implique que la réaction 11 est peu importante, comme avec l'EDTA, cela n'exclue pas la généralité du mécanisme. En effet, Wilkins (20) a trouvé que la dissociation des complexes du Cu(II) avec quelques composés diaminés, était fonction de l'acidité dans une certaine gamme de p*H*, mais que le p*H* n'avait pas d'influence entre p*H* 4 et 7. Dans le cas de l'adénine un comportement analogue fut observé (résultats non publiés). Il faut aussi noter que les valeurs des constantes de vitesse expéri-

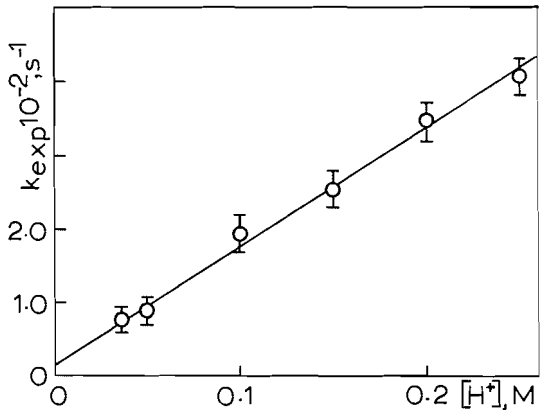

FIG. 3. Variation de k_{exp} du complexe $(CuA)_I$ en fonction de la concentration en acide: [adénosine] = 5×10^{-3} *M*, $[Cu^{2+}] = 2.5 \times 10^{-3}$ *M*, force ionique = 0.5 *M*, p*H* initial = 10.2, *T* = 25 °C.

mentales de dissociation obtenues à acidité élevée n'ont pas la signification d'une vraie constante de dissociation et certains résultats publiés, sans une interprétation adéquate, doivent être considérés avec précaution (20).

Bien que la valeur de k_d obtenue soit entachée d'une erreur importante, il y a au moins accord entre les deux séries de résultats quant à la valeur limite.

On a envisagé l'étude du complexe vert $(CuR)_I$. Ce dernier est prépondérant entre p*H* 5 et 9. A ces p*H* il se forme des précipités d'hydroxyde de cuivre, étant donné que la stabilité de ce complexe n'est pas assez grande pour empêcher leur formation (à p*H* 7, $K = 60$ (9)). Pour cette raison il n'est pas possible d'étudier ce complexe.

Conclusion

Les études sur le site de coordination et sur la stabilité des complexes formés entre le Cu(II) et l'adénosine ont déjà permis de montrer qu'il y avait plusieurs complexes. Nos résultats montrent que ceux-ci se différencient également quant à la cinétique de leur formation et de leur dissociation.

Les constantes de vitesse du complexe en milieu acide, impliquant comme ligand le groupe adénine, sont de loin plus grandes que celles de la dissociation des complexes avec les groupes hydroxyles du ribose, mesurées en milieu basique. Ces derniers sont prépondérants aux p*H* physiologiques. Il est à noter que dans les cas où des groupes desoxyriboses sont impliqués (17), il n'y a pas de formation de complexe avec ce groupement et alors, le complexe avec le groupe adénine est présent même à p*H* = 7 avec ses caractéristiques cinétiques propres.

Les résultats obtenus pour le D-ribose pourraient probablement être appliqués à d'autres sucres possédant deux groupements hydroxyles en position similaire.

Finalement la dissociation des complexes en présence d'EDTA en milieu basique se fait par deux mécanismes simultanés: dissociation unimoléculaire suivie de la formation du complexe Cu(II).EDTA et par une réaction bimoléculaire entre le complexe et l'EDTA. La connaissance du mécanisme de cette réaction est importante pour la compréhension de l'influence de l'EDTA sur l'action physiologique du cuivre.

Par exemple, l'effet inhibiteur de l'EDTA sur certaines réactions enzymatiques (p. 27 réf. 2), est reconnu comme étant dû à son affinité pour les ions métalliques, en particulier les ions cuivriques.

Les auteurs remercient le Ministère de l'Education du Québec pour la subvention de recherche accordée pour la réalisation de ces travaux. Le Conseil National de Recherches du Canada est remercié pour la bourse d'entretien accordée (G.B.).

1. E. FRIEDEN. The complex copper of Nature. *In* Horizons in biochemistry. Albert Szent-Györgyi Dedicatory Volume. *Edited by* Mickael Kaska and Bernard Pullman. Academic Press. 1962; Mineral metabolism. *Edited by* C. L. Comar and F. Bronner. Academic Press. 1960, 1964. P. AISEN, W. BLUMBER, et J. PEISACH. The biochemistry of copper. Academic Press, New York. 1966.
2. J. SCHUBERT. Copper and peroxides in radiobiology and Medicine. Charles C. Thomas, Publisher. 1964.
3. S. HIAI. J. Mol. Biol. **11**, 679 (1965).
4. S. E. BRYAN et E. FRIEDEN. Biochem. **6**, 2728 (1967). G. L. EICHHORN, P. CLARK, et E. D. BECKER. Biochem. **5**, 245 (1966). CH. ZIMMER, G. LUCK, H. FRITZSCHE, et H. TRIEBEL. Biopolym. **10**, 441 (1971). H. VENNER et CH. ZIMMER. Biopolym. **4**, 321 (1966). K. B. YATSIMIRSKII, E. E. KRISS, et T. I. AKHRAMEEVA. DOKL. Akad. Nauk USSR, **168**, 840 (1966). R. PHILLIPS. Chem. Rev. **66**, 501 (1966). R. M. IZATT, J. J. CHRISTENSEN, et J. H. RYTTING. Chem. Rev. **71**, 439 (1971).
5. A. M. FISKIN et M. BEER. Biochem. **4**, 1289 (1965).
6. J. PRADEL et R. P. MARTIN. C.R. Acad. Sc. Paris, **270**, 1863 (1970).
7. R. WEISS et H. VENNER. Hoppe-Seyler's Z. Phys. Chem. **333**, 169 (1963).

Can. J. Chem. Downloaded from www.nrcresearchpress.com by 210.87.254.6 on 09/05/12
For personal use only.

8. P. W. SCHNEIDER, H. BRINTZINGER, et H. ERLENMEYER. Helv. Chem. Acta, **47**, 992 (1964).
9. E. E. KRISS et K. B. YATSIMIRSKII. Russ. J. Inorg. Chem. **13**, 1223 (1968).
10. M. EIGEN et G. G. HAMMES. J. Am. Chem. Soc. **82**, 5951 (1960). G. G. HAMMES et S. A. LEVISON. Biochem. **3**, 1504 (1964). H. STERNLIGHT, D. E. JONES, et K. KUSTIN. J. Am. Chem. Soc. **90**, 7110 (1968).
11. M. EIGEN et L. DEMAEYER. Technique of organic chemistry. Vol. 8. *Edited by* A. Weissberger. Interscience, New York. 1963. G. H. CZERLINSKI. Chemical relaxation. Marcel Dekker Inc., New York. 1966.
12. T. HARKINS et H. FREISER. J. Am. Chem. Soc. **80**, 1132 (1958).
13. R. M. IZATT, L. D. HANSEN, J. H. RYTTING, et J. J. CHRISTENSEN. J. Am. Chem. Soc. **87**, 2760 (1965).
14. R. G. PEARSON et R. D. LANIER. J. Am. Chem. Soc. **86**, 765 (1964).
15. G. BOIVIN et M. ZADOR. Bull. Soc. Chim. Fr. 4279 (1971).
16. L. INGRAHAM. Biochemical mechanisms. John Wiley & Sons, Inc., New York. 1962.
17. H. REINERT et R. WEISS. Hoppe-Seyler's Z. Physiol. Chem. **350**, 1321 (1969).
18. A. E. MARTELL. Stability constants of metal-ion complexes. The Chemical Society, Burlington House, London. 1964.
19. N. TANAKA, H. OSAWA, et M. KANAKA. Bull. Chem. Soc. Jap. **36**, 530 (1963). D. C. OLSON et D. W. MARGERUM. J. Am. Chem. Soc. **85**, 297 (1963).
20. R. G. WILKINS. J. Chem. Soc. 4475 (1962).
21. R. G. WILKINS et G. A. NELSON. J. Chem. Soc. 2662 (1962).

Can. J. Chem. Downloaded from www.nrcresearchpress.com by 210.87.254.6 on 09/05/12
For personal use only.

Aqueous Nonelectrolyte Solutions. Part XI. Mercury Solubility in 6.10 molal Sodium Chloride[1]

D. N. GLEW AND D. A. HAMES

Research and Development Department, Dow Chemical of Canada, Limited, Sarnia, Ontario

Received March 1, 1972

The solubility of mercury in aqueous 6.10 *m* NaCl has been determined between 5 and 70 °C. Solubility equations and thermodynamic functions are derived and compared with those for mercury in water. Salting-out constants are given.

La solubilité du mercure dans une solution aqueuse de NaCl 6.10 *m* a été déterminée entre 5 et 70 °C. Les équations de solubilité et les fonctions thermodynamiques ont été dérivées et comparées à celles du mercure dans l'eau. Les constantes de relargage sont données. [Traduit par le journal]

Canadian Journal of Chemistry, **50**, 3124 (1972)

Can. J. Chem. Downloaded from www.nrcresearchpress.com by 210.87.254.5 on 09/05/12
For personal use only.

Introduction

The solubility equilibrium of liquid mercury with air-free water has been reported recently (1). In this work the solubility equilibrium of liquid mercury has been determined with concentrated sodium chloride solutions between 5 and 70 °C.

Experimental

Material

Mercury of technical electrolytic grade was purified as follows: agitated with a stream of air and washed with (*i*) 10% NaOH, (*ii*) distilled water, (*iii*) 5% HNO_3 and filtered through a gold foil, rewashed with (*iv*) 5% HNO_3, (*v*) distilled water and then distilled three times. A.C.S. grade sodium chloride, supplied by Fisher Scientific Company, was dried by evacuation before use. Technical grade hydrazine hydrate was supplied by Matheson, Coleman and Bell, Grade A helium and Hi-Pure nitrogen by Liquid Carbonic Canadian Corporation, and reagent grade mercuric chloride by Fisher Scientific Company. Water was laboratory distilled.

Method

The solubility cell and temperature measuring equipment have been described elsewhere (1, 2).

The water and mercury were distilled into the evacuated solubility cell as described earlier (1) and sufficient sodium chloride was added under helium to make the solution about 6.1 *m* NaCl. Approximately 0.001 *m* hydrazine hydrate was added to ensure that no mercury was oxidized by residual trace amounts of air. The solubility cell was stoppered, evacuated, and restored to a slight positive pressure with helium. As in the earlier work the solubility cell was continuously stirred and mercury solubilities were determined at preselected temperatures starting from both above and below saturation. The stirrer was stopped 2 h before sampling and 5 to 15 g samples of solution were expressed into a tared flask containing 1 ml 2% $K_2Cr_2O_7$ and 1 ml 20% H_2SO_4. The flask was reweighed and heated to boiling.

Analysis

The train for the flameless atomic absorption analysis of mercury consisted of a gas washing bottle series-connected to an empty trap to catch water droplets, a drying tube containing molecular sieves, and a 10 cm path-length quartz absorption cell (3).[2]

After cooling to room temperature, the sample was transferred quantitatively to the 150 ml gas washing bottle, and was diluted to 60 ml with distilled water. Two ml of 10% $SnCl_2$ was added to reduce the dichromate and ionic mercury and the sparger was replaced in the gas washing bottle. A constant air flow of 1.5 standard cubic ft per h was immediately redirected through the sparger of the gas washing bottle where the finely divided metallic mercury was vaporized. The mercury vapor was carried with the air stream through the quartz cell where it was detected using a Techtron AA 120 atomic absorption spectrophotometer. The spectrophotometer signal was traced on a Varian G-2000 strip-chart recorder. The spectrophotometer parameters were mercury hollow-cathode lamp current 3 mA, slit height 10 mm, slit width 0.10 mm, and wavelength 253.6 nm.

Standard solutions containing 500 p.p.m. (by weight) Hg were prepared from mercuric chloride. Comparison of old and fresh standards showed that they were stable for at least 6 months. A 1.0 p.p.m. Hg standard was prepared daily by dilution of the 500 p.p.m. Hg standard. The spectrophotometer was calibrated with salt solutions containing 0.10 to 1.0 μg Hg, which were prepared using aliquots of the 1.0 p.p.m. Hg standard and the same weight of 6.1 *m* NaCl as in the unknown to be determined. The linear peak height – concentration calibration curve was used to determine the unknown mercury solubility in the NaCl brine.

In this work acid dichromate was used as the oxidizing agent for mercury in preference to the acid permanganate used previously (1) because it does not require the addition of hydroxylamine hydrochloride (3). Identical results were obtained by both techniques.

[1]Contribution No. 195.

[2]Method for determination of mercury in effluent and process streams from a mercury-cell chlorine plant (atomic absorption flameless method). This report is available on request from the company.

TABLE 1. Aqueous solubility of mercury

Temperature (°C)	$S^0 \times 10^8$ (*m*)	[NaCl] (*m*)	$S \times 10^8$ (*m*)	$S' \times 10^8$ (*m*)
5.24	21.8	6.10	5.05	5.05
5.24		6.10	5.25	5.25
5.24		6.10	5.65	5.65
5.24		6.10	6.35	6.35
5.35	21.8	6.10	5.89	5.89
10.17	23.1	6.10	7.40	7.40
10.17		6.10	7.49	7.49
10.17		6.10	7.61	7.61
15.01	24.7	6.12	10.8	10.8
15.01		6.12	11.2	11.2
19.92	26.8	6.13	13.1	13.1
19.92		6.13	13.7	13.7
19.92		6.13	15.1	15.2
19.92		6.13	15.2	15.2
25.02	29.3	6.14	15.6	15.7
25.02		6.14	15.6	15.7
25.02		6.14	16.7	16.8
25.02		6.14	16.9	17.0
30.27	32.5	6.09	18.7	18.7
30.27		6.09	19.6	19.6
30.27		6.09	20.4	20.4
30.27		6.09	20.4	20.4
34.96	36.0	6.18	25.1	25.2
34.96		6.18	26.3	26.4
34.96		6.18	27.5	27.6
34.96		6.18	27.6	27.7
40.02	40.3	6.21	31.3	31.4
40.02		6.21	32.9	33.1
44.86	45.4	6.18	37.1	37.2
44.86		6.18	38.8	38.9
44.86		6.18	41.2	41.3
50.07	51.8	6.09	46.5	46.5
50.07		6.09	49.8	49.8
54.99	59.1	6.29	58.9	58.9
54.99		6.29	61.9	61.8
54.99		6.29	67.4	67.1
54.99		6.29	68.7	68.4
54.99		6.29	68.9	68.6
60.12	68.1	6.18	74.3	74.2
60.12		6.18	76.0	75.9
65.28	79.1	6.18	96.8	96.5
65.28		6.18	97.5	97.2
69.77	90.4	6.18	112	111
69.77		6.18	119	119

The concentration of sodium chloride in the solubility cell was determined by potentiometric titration with silver nitrate.

All equilibrium equations were derived by least-squares using the Clarke–Glew method (4) assuming that the logarithms of the solubilities were normally distributed: this was consistent with the experimental determination of *S*, which was known with a constant percentage experimental error. In contrast with our earlier study (1) all mercury solubilities reported in this work are expressed in molality units, mol Hg/1000 g H_2O.

Results

The solubility of mercury in water, S^0 (mol Hg/1000 g H_2O), between 0 and 120 °C derived from our earlier measurements (1) is best represented by the equation

$$[1] \quad \log_{10} S^0 = -126.345 + 4715.2/T + 42.0288 \log_{10} T$$

Can. J. Chem. Downloaded from www.nrcresearchpress.com by 210.87.254.5 on 09/05/12
For personal use only.

Can. J. Chem. Downloaded from www.nrcresearchpress.com by 210.87.254.5 on 09/05/12
For personal use only.

TABLE 2. Solubility of mercury in 6.10 *m* NaCl and salting-out constant

Temperature (°C)	$S' \times 10^8$ (*m*) Value	σ	k (m^{-1}) Value	σ
0.0	4.31	0.10	0.1120	0.0028
5.0	5.75	0.12	0.0950	0.0020
10.0	7.58	0.14	0.0795	0.0014
15.0	9.91	0.16	0.0654	0.0012
20.0	12.8	0.17	0.0528	0.0011
25.0	16.5	0.20	0.0413	0.0011
30.0	21.0	0.24	0.0311	0.0012
35.0	26.5	0.30	0.0220	0.0012
40.0	33.2	0.39	0.0140	0.0012
45.0	41.3	0.54	0.0069	0.0011
50.0	51.1	0.74	0.0008	0.0011
55.0	62.8	1.0	−0.0044	0.0012
60.0	76.7	1.4	−0.0089	0.0015
65.0	93.1	1.9	−0.0125	0.0019
70.0	112	2.5	−0.0153	0.0024

where T is the absolute temperature (273.15 K = 0 °C (11)). This equation is equivalent to eq. 2 of ref. 1. The standard thermodynamic function changes with their standard errors at 25 °C, derived from eq. 1, are $\Delta G_2^0(l_2 \rightarrow l_1) = 8912 \pm 9$ cal, $\Delta H_2^0(l_2 \rightarrow l_1) = 3326 \pm 150$ cal, $\Delta S_2^0(l_2 \rightarrow l_1) = -18.7 \pm 0.5$ cal/deg, and $\Delta C_{p2}^0(l_2 \rightarrow l_1) = 83.5 \pm 5.6$ cal/deg and correspond with the transfer of 1 mol of mercury from the liquid metallic phase l_2 into the water phase l_1 at unit mercury activity. Values of solubility S^0 given in Table 1 were calculated from eq. 1 at those temperatures used for determination of the mercury solubility in salt solutions.

Experimental values for the solubility S (mol Hg/1000 g H_2O) of mercury in brine between 5 and 70 °C are given in column 4 of Table 1; the sodium chloride molality c varied between 6.09 and 6.29 *m* NaCl and is given in column 3. Salting-out constants, $k = (\log_{10} S^0/S)/c$, were evaluated from each of the solubility determinations and were used to calculate corrected mercury solubilities S' in 6.10 *m* NaCl. Values of S' are given in column 5.

The temperature dependence of the mercury solubility in 6.10 *m* NaCl between 5 and 70 °C is represented by the equation

$$[2] \quad \log_{10} S' = -6.043 - 1639.8/T + 1.9230 \log_{10} T$$

The standard error on a single determination of S′ assessed from eq. 2 is 7.7%, which agrees well with the 7.5% error assessed from analogous measurements in water between 4 and 72 °C (1). The standard thermodynamic function changes and standard errors derived from eq. 2 at 25 °C are $\Delta G_2^0(l_2 \rightarrow l_1) = 9256 \pm 9$ cal, $\Delta H_2^0(l_2 \rightarrow l_1) = 8642 \pm 148$ cal, $\Delta S_2^0(l_2 \rightarrow l_1) = -2.1 \pm 0.5$ cal/deg, and $\Delta C_{p2}^0(l_2 \rightarrow l_1) = 3.8 \pm 11.9$ cal/deg and correspond with the transfer of 1 mol of mercury from phase l_2 into the aqueous 6.10 *m* NaCl phase l_1 at unit mercury activity.

Since the regression coefficient of $\log_{10} T$ in eq. 2 is small and indistinguishable from zero, the temperature dependence of S' between 5 and 70 °C can be represented by

$$[3] \quad \log_{10} S' = -0.424 - 1895.9/T$$

The standard error, assessed from eq. 3, on a single S' determination is 7.6%, essentially the same as assessed from eq. 2.

The mercury solubility in 6.10 *m* NaCl together with its standard error evaluated from eq. 3 is given in Table 2 and shown by the solid line in Fig. 1. The solubility in water evaluated from eq. 1 is shown by the dashed line.

The temperature dependence between 5 and 70 °C for the salting-out constant, k (m^{-1}), derived from each of the experimental solubilities S, is given by

$$[4] \quad k = -20.373 + 1072.2/T + 6.7966 \log_{10} T$$

The standard error on a single determination of k is 0.0054 m^{-1}. Salting-out constants and their standard errors from eq. 4 are given in Table 2. The salting-out constants decrease rapidly with increasing temperature and change sign at 50.8 ± 1.0 °C. At higher temperatures the mercury solubility in 6.10 *m* NaCl is greater than in water.

Discussion

The standard thermodynamic function changes for mercury transfer into 6.10 *m* NaCl and into water, evaluated from eqs. 2 and 1, are compared in Fig. 2.

In aqueous 6.10 *m* NaCl all standard thermodynamic function changes vary little between 5 and 70 °C. The large, slowly varying $\Delta G_2^0(l_2 \rightarrow l_1)$ arises predominantly from the large $\Delta H_2^0(l_2 \rightarrow$

Can. J. Chem. Downloaded from www.nrcresearchpress.com by 210.87.254.5 on 09/05/12
For personal use only.

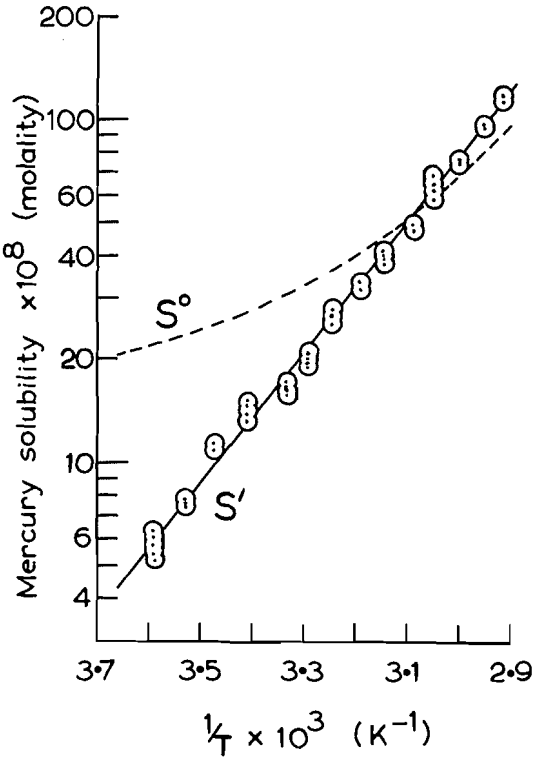

FIG. 1. The temperature dependence of mercury solubility in water, S^0, and in 6.10 *m* NaCl, S'.

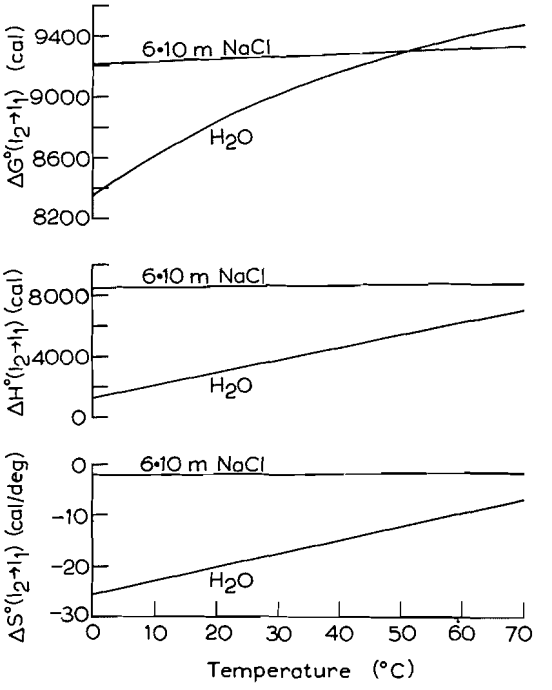

FIG. 2. Standard thermodynamic function changes for the transfer of mercury into water and into 6.10 *m* NaCl.

l_1), with only a small contribution from $\Delta S_2^0(l_2 \rightarrow l_1)$. The small temperature dependence of $\Delta H_2^0(l_2 \rightarrow l_1)$ and $\Delta S_2^0(l_2 \rightarrow l_1)$ correspond with the small positive value of $\Delta C_{p2}^0(l_2 \rightarrow l_1)$. The nearly temperature-invariant thermodynamic function changes probably occur because all of the water in the 6.10 *m* NaCl is in the primary hydration shell of the sodium and chloride ions, and the structure of this tightly bound water is relatively unaffected by the 5 to 70 °C change of temperature.

In contrast in water the free energy, enthalpy, and entropy changes are highly temperature sensitive with a large value for the heat capacity change. The large temperature dependence of the standard thermodynamic function changes probably occurs because of the rapid variation of water structure with temperature (1).

In 6.10 *m* NaCl and water the standard changes of free energy are equal at 50.8 °C, of enthalpy equal at 92 °C, and of entropy equal at 94 °C. Thus it is found that the enthalpy and entropy for mercury transfer into 6.10 *m* NaCl between 5 and 70 °C are similar to those for transfer into water at about 90 °C. The value of $\Delta C_{p2}^0(l_2 \rightarrow l_1)$ is very sensitive to sodium chloride concentration changing from 83.5 ± 5.6 in water to 3.8 ± 11.9 cal/deg in 6.10 *m* NaCl.

The sodium chloride salting-out constant for mercury in water is of the same order of magnitude, but smaller than those found for the inert gases at ambient temperatures (5–7). The high sodium chloride concentration used in this study would result in smaller salting-out constants than obtained for dilute sodium chloride solutions (8, 9). The change of the salting-out constant with temperature is 0.002 m^{-1} deg^{-1} at 25 °C for this work compared with approximately 0.001 from earlier work with nitrous oxide (9, 10) and the inert gases (6). The value of dk/dT falls as temperature is increased, as shown previously (9).

1. D. N. GLEW and D. A. HAMES. Can. J. Chem. **49**, 3114 (1971).
2. D. N. GLEW and D. A. HAMES. Can. J. Chem. **47**, 4651 (1969).
3. J. M. COLEMAN. Dow Chemical of Canada, Limited.

4. E. C. W. CLARKE and D. N. GLEW. Trans. Faraday Soc. **62**, 539 (1966).
5. G. AKERLOF. J. Am. Chem. Soc. **57**, 1196 (1935).
6. A. EUCKEN and G. HERTZBERG. Z. phys. Chem. **195**, 1 (1950).
7. T. J. MORRISON and N. B. B. JOHNSTONE. J. Chem. Soc. 3655 (1955).
8. T. J. MORRISON and F. BILLETT. J. Chem. Soc. 3819 (1952).
9. A. E. MARKHAM and K. A. KOBE. J. Am. Chem. Soc. **63**, 449 (1941).
10. F. A. LONG and W. F. MCDEVIT. Chem. Rev. **51**, 119 (1952).
11. Nat. Bur. Std. Tech. News Bull. **47**, 175 (1963).

Can. J. Chem. Downloaded from www.nrcresearchpress.com by 210.87.254.5 on 09/05/12
For personal use only.

The Oxidation of Tetrahydrofuran by Ruthenium Tetroxide

DONALD G. LEE AND MATTHIJS VAN DEN ENGH[1]

Department of Chemistry, The University of Saskatchewan Regina Campus, Regina, Saskatchewan

Received March 23, 1972

The kinetics of the oxidation of tetrahydrofuran by ruthenium tetroxide in aqueous perchloric acid solutions have been investigated. The rate of reaction is found to be directly dependent on the concentrations of oxidant and reductant, but inversely dependent on the acidity of the medium. A mechanism involving hydride abstraction in the rate determining step was found to be consistent with the evidence obtained from isotopic labeling and an analysis of the activation parameters ($\Delta H^* = 14.0$ kcal/mol, $\Delta S^* = -18.4$ e.u.) of the reaction. This conclusion is further substantiated by noting the similarity between the reactions of ruthenium tetroxide with alcohols and ethers.

Les cinétiques de l'oxydation du Tétrahydrofurane par le tétroxyde de Ruthénium, dans des solutions aqueuses d'acide perchlorique, ont été étudiées. La vitesse de la réaction dépend directement des concentrations de l'oxydant et du réducteur et inversément de l'acidité du milieu. Le mécanisme faisant intervenir un arrachement d'hydrure dans l'étape déterminante de la cinétique est prouvé compatible avec le marquage isotopique et l'analyse des paramètres d'activation de la réaction ($\Delta H^* = 14.0$ kcal/mol, $\Delta S^* = -18.4$ e.u.). Cette conclusion est confirmée par la suite, en notant la similitude entre les réactions du tétroxyde de Ruthénium avec les alcools et les éthers. [Traduit par le journal]

Canadian Journal of Chemistry, **50**, 3129 (1972)

Can. J. Chem. Downloaded from www.nrcresearchpress.com by 210.87.254.105 on 09/05/12
For personal use only.

The oxidation of aliphatic ethers to the corresponding esters (or lactones in the case of cyclic ethers) can be accomplished by the use of chromium trioxide, lead tetraacetate, or ruthenium tetroxide as oxidants (1). The most effective of these reagents, ruthenium tetroxide, has been used in the oxidation of a variety of acyclic, cyclic, and bicyclic ethers (2–4). The reaction, which can be carried out either in aqueous solutions or in non-oxidizable, non-polar solvents (*e.g.*, carbon tetrachloride or chloroform), is free of side reactions and usually gives quantitative yields of pure products.

Despite the apparent utility of this procedure little attention has been paid to the mechanism of this and other related oxidation reactions involving the use of ruthenium tetroxide. Consequently we have undertaken a detailed study of these reactions and wish to report the results obtained from an investigation into the mechanism whereby tetrahydrofuran is converted into γ-butyrolactone in aqueous perchloric acid solutions (reaction 1).

[1] 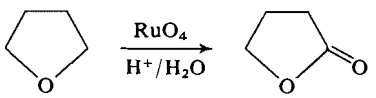

[1]NRCC Scholarship holder 1969–1971.

Experimental

Reagents

Ruthenium tetroxide was prepared by the oxidation of hydrated ruthenium dioxide (0.5 g) obtained from Engelhard Industries Inc., with a solution of sodium periodate (2 g) in 25 ml of water. The mixture was shaken until the reaction was complete (as evidenced by the disappearance of the insoluble black ruthenium dioxide). The bright yellow product of this reaction, ruthenium tetroxide, was extracted into carbon tetrachloride and stored over sodium periodate. Just prior to a kinetic experiment an aliquot of the solution was removed and the ruthenium tetroxide extracted into an aqueous perchloric acid solution of the desired molarity.

Tetrahydrofuran and tetrahydrofuran-d_8 were obtained commercially and purified just prior to use by g.l.c. A diethylene glycol column was found to be satisfactory for this purpose.

Perchloric acid solutions were prepared by the dilution of 70% perchloric acid with doubly distilled water (5).

Kinetic Measurement

In a typical kinetic experiment 3.0 ml of a perchloric acid solution containing a specified amount of ruthenium tetroxide were pipetted into a cuvet which was placed in a thermostated cuvet holder for about 20 min. Then the desired quantity of tetrahydrofuran was added using a microsyringe. The timer was started immediately and the absorption at 310 nm was recorded periodically using a Unicam SP500 Spectrophotometer. As the reaction proceeded the color of the solution changed from bright yellow to brown. The absorption spectrum of ruthenium tetroxide can be shown to obey the Beer–Lambert law in aqueous perchloric acid solutions (Fig. 1); consequently the decrease in absorbance could be taken as a measure of the extent of reaction.

The data obtained in this way were analyzed by a differen-

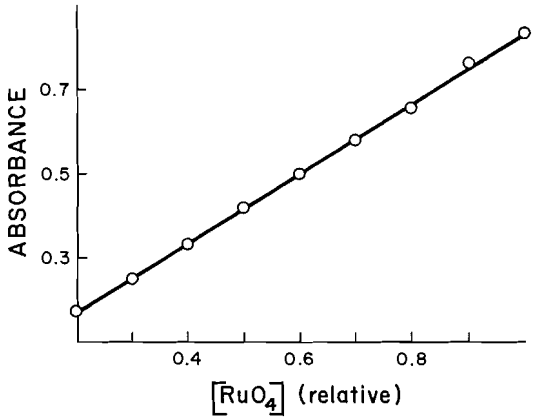

FIG. 1. Verification of Beer's law for ruthenium tetroxide.

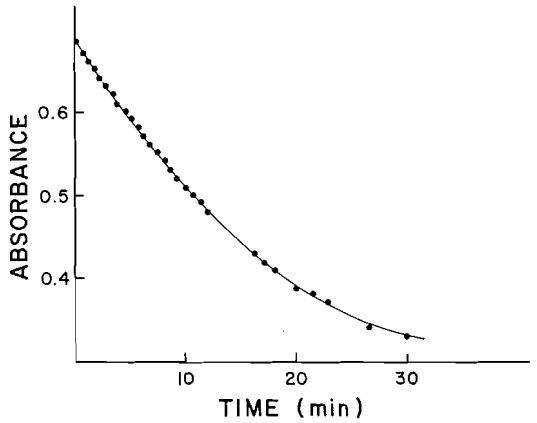

FIG. 2. Typical rate plot for the oxidation of tetrahydrofuran by ruthenium tetroxide in 1.94 M $HClO_4$.

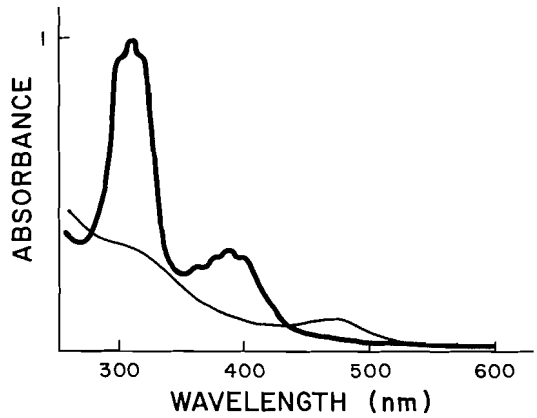

FIG. 3. Absorption spectra before (top) and 2 h after (bottom) addition of an excess of tetrahydrofuran to a solution of ruthenium tetroxide in 2.89 M $HClO_4$.

tial method, which involved the use of initial rates as determined from the initial slopes of plots of absorbance *vs.* time. (A typical plot has been reproduced in Fig. 2.) An integral method of analysis was not satisfactory under these conditions because the products of the reaction also absorb in the same region of the spectrum (Fig. 3). Under such conditions it is more reliable to use initial rates where the concentrations of products will be negligibly small, than to attempt to use an integral method which requires larger corrections (6).

All rates and rate constants reported herein are the average of at least two determinations which agreed to within $\pm 5\%$ or less.

Results

Rate Law

The order of the reaction with respect to oxidant was determined by following the rate of reaction at several different initial concentrations of ruthenium tetroxide while holding the concentration of tetrahydrofuran at a high constant excess. Under these conditions the rate of the reaction can be expressed as in eq. 2.

$$[2] \qquad \frac{d[RuO_4]}{dt} = k[RuO_4]^x$$

Since the concentration of ruthenium tetroxide is approximately proportional to absorbances in the initial stages of the reaction eq. 2 can be expressed as eq. 3.

$$[3] \qquad \frac{d(\text{initial absorbance})}{dt} = k\,(\text{initial absorbance})^x$$

By noting that the first term of eq. 3 is just the initial slope and taking logarithms eq. 4 is obtained.

$$[4] \qquad \log(\text{initial slope}) = x \log(\text{initial absorbance}) + \log k$$

Consequently the order of the reaction with respect to ruthenium tetroxide can be obtained from a plot of log (initial slope) *vs.* log (initial absorbance). Several such plots were prepared and found to be linear with slopes ranging from 0.95 to 1.10. A typical example has been reproduced in Fig. 4. Hence the order of the reaction with respect to ruthenium tetroxide is unity.

The order of the reaction with respect to ether was then determined by observing the change in initial slope when the concentration of tetrahydrofuran was varied at constant ruthenium

Can. J. Chem. Downloaded from www.nrcresearchpress.com by 210.87.254.105 on 09/05/12
For personal use only.

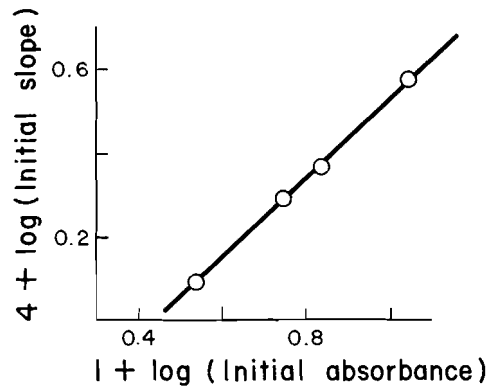

FIG. 4. Plot for determining the order with respect to ruthenium tetroxide.

TABLE 1. Dependence of second order rate constants on the acidity of the medium*

$HClO_4$ (M)	$-H_0$†	$k_2 \times 10^2$‡ (M^{-1} s^{-1})
2.89	1.25	3.19
2.52	1.09	3.38
1.94	0.82	4.01
1.49	0.59	4.33
0.90	0.25	5.38

*[Tetrahydrofuran] = 2.05×10^{-2} M.
†The H_0 values are those reported by Yates and Wai (15).
‡Average of at least three different experiments. The largest deviation from the mean was ±2%.

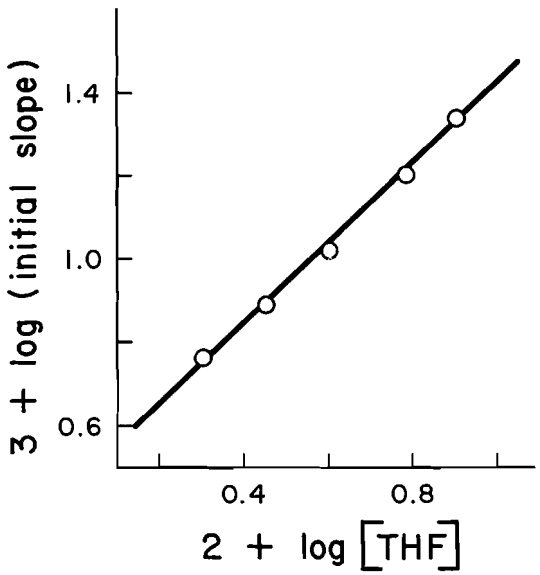

FIG. 5. Plot for determining the order with respect to tetrahydrofuran.

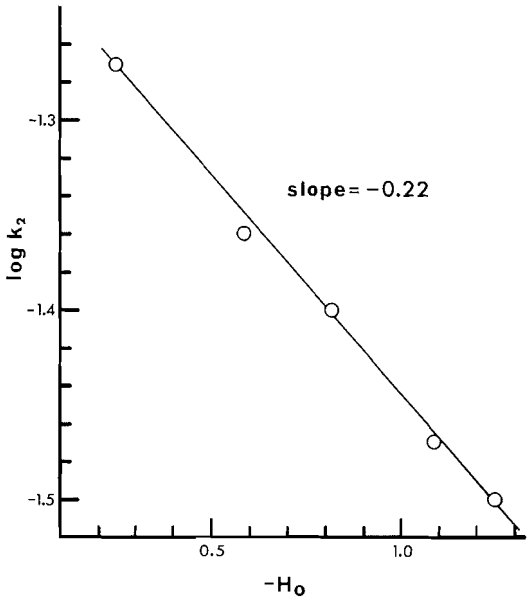

FIG. 6. Variation of rate with acidity.

tetroxide concentrations. As Fig. 5 shows, a plot of log (initial slope) *vs.* log [tetrahydrofuran] was found to be linear with a slope of 0.95. Hence the order with respect to the ether is also unity and the rate law for the reaction can be expressed as in eq. 5.

$$[5] \qquad v = k_2[RuO_4][THF]$$

However, the calculated second order rate constants, k_2, were also found to be dependent on the acidity of the solution. As indicated by the data summarized in Table 1 the rate of reaction decreases as the concentration of perchloric acid increases. A plot of the logarithms of the second order rate constants *vs.* the Hammett acidity function ($-H_0$) gives a straight line with a slope of -0.22 as indicated in Fig. 6. Consequently the complete empirical rate law for the reaction in aqueous perchloric acid could be expressed in the form of eq. 6.

$$[6] \qquad v = k_3[RuO_4][THF]h_0^{-0.22}$$

Isotope Effects

When the oxidation of tetrahydrofuran-d_8

Can. J. Chem. Downloaded from www.nrcresearchpress.com by 210.87.254.105 on 09/05/12
For personal use only.

TABLE 2. Comparison of the rate of oxidation of tetrahydrofuran and tetrahydrofuran-d_8

THF* ($M \times 10^2$)	Hydrogen isotope	$k_2 \times 10^2$ (M^{-1} s^{-1})
2.05	H	3.52
2.05	H	3.41
2.05	H	3.34
1.85	D	2.34
1.85	D	2.46
1.85	D	2.07

*[$HClO_4$] = 1.49 M; Temperature = 25.0 ± 0.1°.

TABLE 3. Data for calculation of activation parameters*

Temperature†	$k_2 \times 10^2$‡ (M^{-1} s^{-1})
10.0	0.798
20.0	1.84
30.0	5.00
40.0	9.82
50.0	20.1

*[$HClO_4$] = 3.08 M; [THF] = 2.05 × 10^{-2} M.
†The temperature was controlled to within ±0.1°.
‡Average of at least three experiments with agreement to within ±5% or less.

was compared with that of unlabeled tetrahydrofuran the rate of reaction was found to decrease by a factor of about 33% (Table 2). This could be either a very large secondary isotope effect or a rather small primary isotope effect. Although it is not possible, on the basis of the available evidence, to distinguish between these two the latter is most probably the case, thus indicating that carbon–hydrogen bond cleavage is involved in the rate determining step.

Activation Parameters

The activation parameters, $\Delta H^{\ddagger}$ and $\Delta S^{\ddagger}$, were obtained by determining the rate constants at several temperatures and plotting ln k_2/T *vs.* $1/T$. The results, summarized in Table 3 and Fig. 7, give $\Delta H^{\ddagger} = 14.0 \pm 0.5$ kcal/mol and $\Delta S^{\ddagger} = -18.4 \pm 1.2$ e.u.

Discussion

The results presented in the previous section are all consistent with a mechanism that involves the transfer of a hydride ion to the oxidant in the rate limiting step. The isotope effect indicates

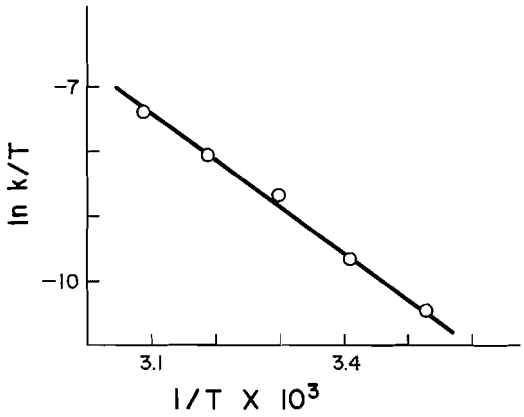

FIG. 7. Plot for determination of activation parameters. Slope = -7070 ± 252 °K^{-1}; intercept = 14.5 ± 0.1; correlation coefficient = 0.998.

that the α-carbon–hydrogen bond is cleaved in the rate determining step and the activation parameters are very similar to those obtained for other reactions which are known to proceed via similar mechanisms (7). Furthermore it has been observed that under similar conditions the oxidations of tetrahydrofuran and 2-propanol by ruthenium tetroxide proceed at comparable rates and exhibit almost identical activation parameters (8). Consequently it appears that the oxidation of ethers is very similar to that of alcohols where it has also been suggested that the rate limiting step involves a hydride ion transfer (8). The proposed mechanism has been outlined in Scheme 1.

The suggestion that the carbonium ion and ruthenium(VI) species recombine to give an ester as indicated in Scheme 1 has not been established, but it would seem to be a logical step. Other work has shown that tetrahydrofuran is not rapidly oxidized by ruthenium(VI) under basic conditions (9); however, the carbonium ion would in all probability be more susceptible to attack.

The inverse dependence of rate on acidity that is indicated by Fig. 6 could be a consequence of either the decrease in water concentration in highly acidic solutions or the protonation of tetrahydrofuran. The oxonium ions formed by protonation of tetrahydrofuran would not readily undergo a hydride transfer, since such a process would create a dipositive species. Hence extensive protonation of the ether would de-

Can. J. Chem. Downloaded from www.nrcresearchpress.com by 210.87.254.105 on 09/05/12
For personal use only.

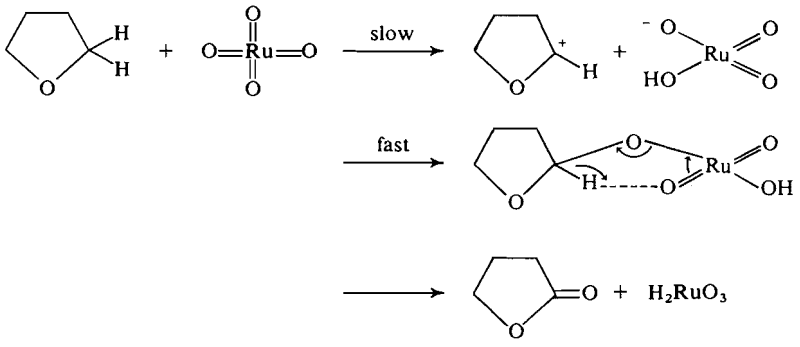

SCHEME 1

crease the rate of reaction; however, calculations show that tetrahydrofuran would *not* be extensively protonated under these conditions and that decreases in substrate concentration through formation of the corresponding oxonium ions can be neglected (10).

The decrease in water concentration (or activity) over the range of acidities studied is substantial and could account for the decrease in rate if the transition state were more highly solvated than the ground state. Such a possibility is not unlikely since it is known from spectral evidence that ruthenium tetroxide is not highly solvated (11), but that the reduced forms of ruthenium are strongly hydrated (12). Thus it is not unreasonable to expect that the transition state, which would contain a reduced ruthenium species, would have a higher demand for solvation than the ground state of the reaction.

In Figs. 8 and 9 $\log k_2$ has been plotted against $\log a_{H_2O}$ and $\log [H_2O]$. Both plots indicate that the rates of reaction are proportional to the amount of available water and the latter suggests an alternative rate law for the reaction (eq. 7) which would be equivalent to eq. 6, but more descriptive of the actual process.

$$[7] \qquad v = k_4[RuO_4][THF][H_2O]^6$$

The approximately linear plot obtained using the concentration of water is similar to that observed for the oxidation of 2-propanol by ruthenium tetroxide (8). Such linear plots have been observed for other reactions (13) and the slopes have generally been taken as an indication

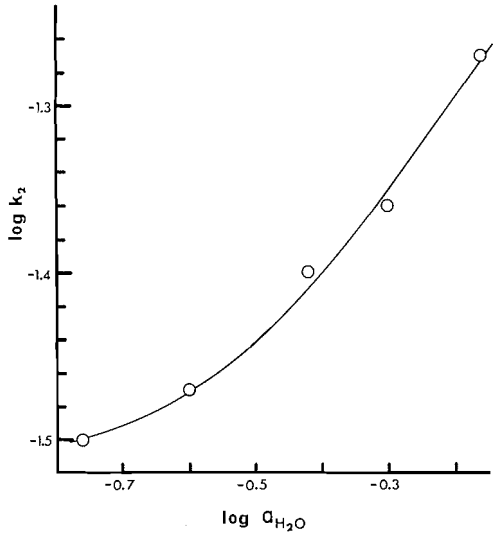

FIG. 8. Variation of rate with the activity of water.

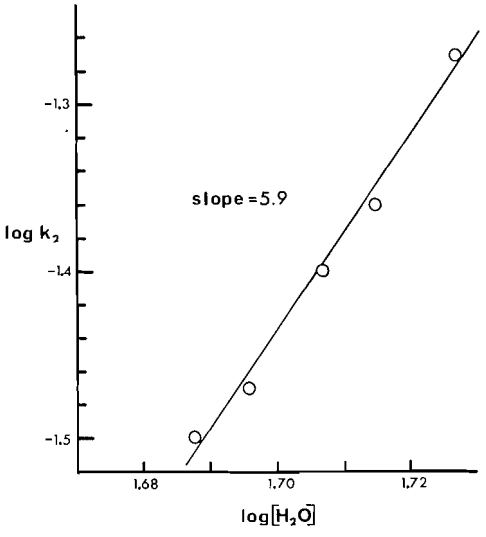

FIG. 9. Variation of rate with water concentration.

Can. J. Chem. Downloaded from www.nrcresearchpress.com by 210.87.254.105 on 09/05/12
For personal use only.

of the additional number of water molecules required to solvate the transition state. If such an interpretation is correct in this case it would mean that the transition state is highly polar, probably resembling the products of the first step in Scheme 1.

A transition state in which the carbon–hydrogen bond has been extensively cleaved is also consistent with the observed small isotope effect (14).

The authors are grateful to the National Research Council of Canada for the award of an operating grant (D.G.L.) and scholarship (M.E.) which supported this work.

1. D. G. LEE. Oxidation, techniques and applications in organic syntheses. Vol. 1. *Edited by* R. L. Augustine. Marcel Dekker Inc., New York. 1969. pp. 54–56.
2. L. M. BERKOWITZ and P. N. RYLANDER. J. Am. Chem. Soc. **80**, 6682 (1958).
3. R. M. MORIARTY, H. GOPAL, and T. ADAMS. Tetrahedron Lett. 4003 (1970).
4. P. N. RYLANDER and L. M. BERKOWITZ. Engelhard Industries Inc., U.S. 3, 278, 558. October 11, 1966. J. WEINSTOCK and M. E. WOLFF. Smith, Kline and French Laboratories, U.S. 2, 960, 503. November 15, 1960. A. WETTSTEIN *et al.* Ciba Corp., U.S. 3, 385, 858. May 28, 1968; Engelhard Industries, Inc., Brit. Pat. 900, 107. July 4, 1962.
5. I. M. KOLTHOFF and E. B. SANDELL. Textbook of quantitative inorganic analysis. The MacMillan Company, New York. 1952. p. 181.
6. K. J. LAIDLER. Chemical kinetics. McGraw-Hill, Toronto, Ontario. 1950. pp. 17, 18.
7. R. M. BARTER and J. S. LITTLER. J. Chem. Soc. (B), 205 (1967). E. J. STROJNY, R. T. IWAMASA, and L. K. FREVEL. J. Am. Chem. Soc. **93**, 1171 (1971). P. AUKETT and I. R. L. BARKER. Chem. Ind. 193 (1967).
8. M. VAN DEN ENGH. Ph.D. Thesis. The University of Saskatchewan Regina Campus, Regina, Saskatchewan, 1971. D. G. LEE and M. VAN DEN ENGH. Can. J. Chem. **50**, 2000 (1972).
9. D. G. LEE and D. HALL. Unpublished results.
10. D. G. LEE and R. CAMERON. Can. J. Chem. **50**, 445 (1972).
11. G. B. BARTON. Spectrochim. Acta, **19**, 1619 (1963).
12. R. E. CONNICK and D. A. FINE. J. Am. Chem. Soc. **82**, 4187 (1960).
13. R. P. BELL, J. P. MILLINGTON, and J. M. PINK. Proc. Roy. Soc. A, **303**, 1 (1968).
14. F. H. WESTHEIMER. Chem. Rev. **61**, 265 (1961).
15. K. YATES and H. WAI. J. Am. Chem. Soc. **86**, 5408 (1964).

Can. J. Chem. Downloaded from www.nrcresearchpress.com by 210.87.254.105 on 09/05/12
For personal use only.

Analysis of a First-order Perturbation Theory for the Direct Correlation Function of Dense Fluids

S. W. BRELVI AND J. P. O'CONNELL

Department of Chemical Engineering, University of Florida, Gainesville, Florida 32601

Received April 10, 1972

An approximate expression for the direct correlation function of a real fluid in terms of its intermolecular potential and hard-sphere distribution functions is examined. Calculations for argon using the Percus–Yevick hard-sphere distribution functions are compared with molecular correlation functions from X-ray scattering data and the macroscopic integral of the correlation function related to the isothermal compressibility. The results are not satisfactory for any pair potential unless the parameters are made state dependent. However, since partial compensation occurs on integration, fairly good correlation of the isothermal compressibility can be obtained up to twice the critical density (except near the critical point itself) using Lennard–Jones (6–12) potential parameters obtained from second virial coefficient data and the Barker–Henderson hard-sphere diameter.

Nous utilisons une expression approximative dans le but de déterminer la fonction de corrélation directe d'un fluide réel en termes de potentiel intermoléculaire et de fonctions de distribution de sphère rigide. Nous comparons les calculs pour l'argon, effectués à partir des fonctions de distribution de Percus–Yevick pour des sphères rigides aux fonctions de corrélation moléculaires tirées de résultats de diffraction de rayons-X; nous établissons ensuite la relation entre l'intégrale macroscopique de la fonction de corrélation et la compressibilité isotherme. Les résultats ne sont pas satisfaisants pour toute paire de potentiel, à moins que les paramètres dépendent de l'état. Toutefois, puisqu'une compensation partielle se produit durant l'intégration, nous pouvons obtenir une assez bonne corrélation de la compressibilité isotherme, jusqu'au double de la densité critique (à l'exception des environs du point critiqué), en utilisant les paramètres de potentiel (6–12) de Lennard–Jones, obtenus à partir du second coëfficient du viriel et du diamètre de la sphère rigide de Barker–Henderson. [Traduit par le journal]

Canadian Journal of Chemistry, **50**, 3135 (1972)

Can. J. Chem. Downloaded from www.nrcresearchpress.com by 210.87.254.6 on 09/05/12
For personal use only.

In statistical thermodynamic studies of fluids, the structure of a real fluid state can be approximated as a perturbation about a reference state whose properties are known (1–3, 12). The relation between the properties in the two states is then found in terms of a perturbation parameter. Most work in this area has been directed towards describing the radial distribution function of the real fluid. Barker and Henderson (3, 12) have successfully used their perturbation theory to model the real fluid as a perturbation about the rigid sphere fluid. They have calculated the radial distribution function and thermodynamic properties to a high degree of accuracy. However, little attention has been given to determining a satisfactory expression for the direct correlation function which is of shorter range than the radial distribution function and could lead to more accurate thermodynamic properties. In this paper we have analyzed an analytical expression for the direct correlation function which is an approximation of a perturbation expression based on the Percus–Yevick functional (4). The real fluid direct correlation function is described only qualitatively; for quantitative agreement state dependent potential parameters are necessary. However, the isothermal compressibility of the fluid can be fairly well correlated up to twice the critical density with potential parameters obtained from second virial coefficients.

Derivation of Expressions

The central expression of the first order perturbation theory (4) is

$$[1] \quad g^{rf}(r)\, e^{\beta\phi^{rf}(r)} = g^{hs}(r)[1 + g^{rf}(r) - g^{hs}(r) - c^{rf}(r) + c^{hs}(r)]$$

where $g^{rf}(r)$, $c^{rf}(r)$, $\phi^{rf}(r)$ are the radial distribution function, the direct correlation function, and the intermolecular pair potential for the real fluid; $g^{hs}(r)$ and $c^{hs}(r)$ are the corresponding properties for the hard-sphere fluid. Equation 1 holds in the region $r \geqslant a$, where "a" is the hard-sphere diameter. For distances $r < a$, the real fluid functions are the same as those of the hard-sphere fluid. This equation

Can. J. Chem. Downloaded from www.nrcresearchpress.com by 210.87.254.6 on 09/05/12
For personal use only.

TABLE 1. Potential parameters for modeling direct correlation function of argon, $\sigma = 3.375$ Å

Temperature (°K)	Density (g/cc)	Hard-sphere diameter a (Å)	Well depth ε/k (°K)
163.15	0.536	2.942	100.6
	0.78	2.917	90.3
153.15	0.536	2.906	97.0
	0.78	2.901	86.6
	0.91	2.911	83.4
148.15	0.28	2.901	117.9
	0.78	2.909	86.8
	0.91	2.919	81.1
	0.982	2.919	80.1
143.15	0.91	2.950	79.4
	0.982	2.950	75.1

has been shown to agree more closely with the molecular dynamics calculations of $g^{rf}(r)$ for all r at state points in the liquid region of a Lennard–Jones (6–12) fluid than does the usual first order Percus–Yevick eq. 4. For the purposes of these calculations, the hard-sphere functions will be those given by a modified solution of the first-order Percus–Yevick theory (5, 6). Equation 1 is a relation between the real fluid properties and those of the hard-sphere fluid. For another independent relation between the real fluid properties, we make the assumption of the first-order Percus–Yevick equation for the real fluid (7)

$$[2] \qquad c^{rf}(r) = g^{rf}(r)[1 - e^{\beta\phi^{rf}(r)}]$$

This leads to

$$[3] \quad c^{rf}(r) = \frac{[1 + c^{hs}(r) - g^{hs}(r)][e^{-\beta\phi^{rf}(r)} - 1]g^{hs}\, e^{\beta\phi^{hs}(r)}}{[1 - g^{hs}\, e^{\beta\phi^{hs}(r)}]}$$

giving

$$[4] \quad c^{rf}(r) = \frac{g^{hs}(r)[1 + c^{hs}(r) - g^{hs}(r)][e^{-\beta\phi^{rf}} - 1]}{[1 - g^{hs}(r)]}$$

for $r \geqslant a$. For $r < a$ we have

$$[5] \qquad c^{rf}(r) = c^{hs}(r)$$

Finally, assumption of a functional form for the intermolecular potential will specify the real fluid direct correlation function in terms of hard sphere properties only. While this expression suffers the disadvantages of the normal first-order Percus–Yevick theory through use of eq. 2, use of eq. 3 allows several tests to be made of the applicability of this first-order perturbation about rigid-sphere fluids. First, there is the direct comparison with the experimental direct correlation function. Second, since a fluid with a spherically symmetric intermolecular potential has the compressibility equation of state

$$[6] \qquad \frac{1}{kT}\left(\frac{\partial P}{\partial \rho}\right) = 1 - 4\pi\rho \int_0^\infty r^2 c(r)\, dr$$

comparisons for the integrated form of eq. 3 with macroscopic data can be made.

Comparison with Direct Correlation Functions of Argon

The microscopic direct correlation function data for liquid argon (Mikolaj and Pings (8)) were used to test eq. 3. For this comparison, the hard-sphere diameter, and the intermolecular potential function with its parameters must be chosen. The hard-sphere diameter, a, was determined by fitting the experimental curve of $r^2c(r)$ to one calculated from the first-order Percus–Yevick direct correlation function for hard spheres (5):

$$[7] \quad c(x) = -\frac{1}{(1-\eta)^4} \times \left[(1+2\eta)^2 - \frac{3\eta}{2}(2+\eta)^2 x + \frac{\eta}{2} x^3 (1+2\eta)^2\right] \quad \text{for } x \leqslant 1$$

$$= 0 \quad \text{for } x > 1$$

$$x = \frac{r}{a}; \qquad \eta = \frac{\pi}{6}\rho a^3$$

The desired value of a was that giving the best possible agreement in the minima of the experimental and calculated curves. This usually occurred at values of x from 0.85 to 0.95 in eq. 7, but varied significantly with temperature and slightly with density. Table 1 shows the values obtained. Then eq. 4 was used to determine the potential energy function. The form of this function was modelled by the Dymond and Alder (9) potential with two parameters. However, although the zero potential distance

Can. J. Chem. Downloaded from www.nrcresearchpress.com by 210.87.254.6 on 09/05/12
For personal use only.

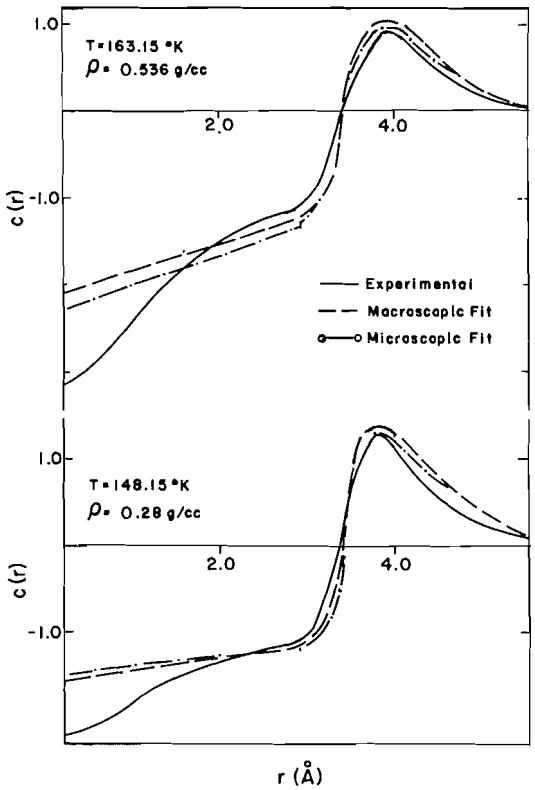

FIG. 1. Direct correlation function of argon from (*i*) experimental compressibility (macroscopic), and (*ii*) experimental direct correlation function (microscopic).

(3.375 Å) was essentially independent of temperature and density, the well depth ε/k varied significantly with density, and somewhat with temperature. (Similar observations were made by Mikolaj and Pings (10) in applying the first-order Percus–Yevick result, eq. 2, directly to the data for the radial distribution function and the direct correlation function. These have been attributed to nonadditivity of the potential.) Figure 1 shows a comparison of the experimental and calculated direct correlation functions. The major discrepancies appear at very short distances where the hard sphere direct correlation function does not vary as much with distance, and in the region between the hard-sphere diameter and the minimum in the well. Although some of this latter difference is due to the choice of the Dymond and Alder potential model, similar differences were observed with the Lennard–Jones 6–12 potential, and apparently the rapid variation of the hard sphere radial distribution function is the major reason for the erroneous steep slope in this region.

Direct Comparison of First-Order Theory with Compressibility of Argon

The Strobridge equation of state for argon (11) was used for macroscopic testing of the theory. The state points covered were in the range $\rho_c \leqslant \rho \leqslant 2\rho_c$. In these determinations, however, the hard-sphere diameter corresponding to a given macroscopic state was obtained by matching the calculated and experimental values of the integral of eq. 6, *i.e.*,

$$[8] \qquad \int_0^a r^2 c(r)\,dr = \int_0^a r^2 c_{py}^{hs}(r)\,dr$$

Again, the hard-sphere size was found to depend primarily on temperature. This variation was correlated by the equation

$$[9] \qquad a_R = 0.137 + \frac{0.657}{T_R} - \frac{0.200}{T_R^2}$$

where $a_R = N_0 a/V_c^{1/3}$; $T_R = T/T_c$. N_0 is Avogadro's number, V_c is the critical volume and T_c is the critical temperature. Although there was a slight density dependence of a, mean values were chosen at each temperature. The zero potential distance was again held constant at 3.375 Å. The best value of ε/k at each macroscopic state was determined by fitting calculated isothermal compressibilities from eq. 6 to experimental compressibilities. In the critical region, the compressibility is extremely sensitive to small errors in the integral, so a weighting factor of $1/\Delta I_c$ was used in the fitting, where ΔI_c is the change in the integral which results in a 100% change in the calculated value of the compressibility. The final equation was

$$[10] \qquad \frac{\varepsilon}{kT_c} = 0.3177 + \frac{3.2148}{\rho_R} - \frac{2.8136}{\rho_R^{1.084}}$$

where $\rho_R = \rho/\rho_c$ and ρ_c is the critical density. The results for the above calculations for reduced densities up to about 2 are summarized in Table 2. While the agreement of the calculated compressibility with the Strobridge compressibility is not within experimental error, it is at least as good as that obtained by numerical

TABLE 2. Comparison of isothermal compressibilities of argon

Temperature (°K)	Density (g/cc)	Well depth* ε/k (°K)	Hard-sphere diameter a (Å)	I (Å)^3 Eq. 12	I (Å)^3 Exp.	ΔI_c (Å)^3	K (atm^{-1} × 10^2) Eq. 12	K (atm^{-1} × 10^2) Exp.	K (atm^{-1} × 10^2) Scattering† data
163.15	0.536	108.44	2.857	8.2	8.1	1.75	3.3	3.10	2.5
163.15	0.78	98.72	2.857	2.8	2.5	4.28	0.65	0.60	0.46
158.15	0.536	108.44	2.897	9.2	8.8	1.05	8.79	5.37	2.10
153.15	0.536	108.44	2.939	9.6	9.5	0.33	24.02	17.47	3.60
153.15	0.78	98.72	2.939	3.1	4.4	2.38	0.75	1.15	0.48
153.15	0.91	94.64	2.939	−0.6	−1.4	7.15	0.32	0.28	0.27
148.15	0.28	117.40	2.982	16.5	16.5	2.35	9.44	9.40	
148.15	0.78	98.72	2.982	4.2	5.4	1.35	1.11	2.11	0.99
148.15	0.91	94.64	2.982	−0.2	−0.2	5.94	0.35	0.35	0.38
148.15	0.982	92.65	2.982	−1.3	−5.1	10.45	0.27	0.17	0.19
143.15	0.91	94.64	3.024	−0.4	−1.2	4.64	0.35	0.46	0.57
138.15	0.982	92.65	3.067	−1.9	−2.3	7.65	0.27	0.25	

*Dymond–Alder potential.
†Numerical integration of Mikolaj and Pings scattering data up to $r = 20$ Å.

integration of the experimental scattering data. The latter result is subject to some error since the long distance tail of $c(r)$ is difficult to estimate. Apparently, however, the density dependence of the hard-sphere diameter or second order terms are of considerable consequence.

The present calculations were extended to other temperature and density regions to determine the limits on the model. Figure 2 shows the comparisons of the second virial coefficient as a function of temperature. The agreement (r.m.s. deviation 1.2 cc/g mol) indicates that the temperature dependence for the hard-sphere diameter is essentially correct for this property

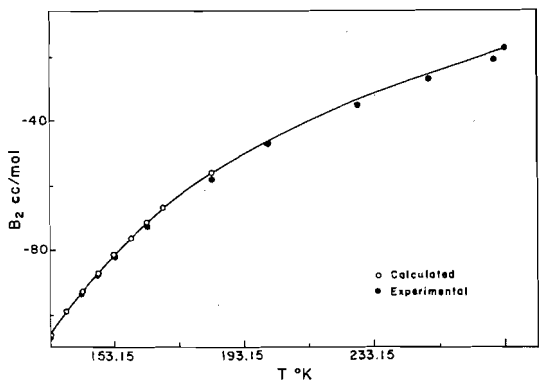

FIG. 2. Second virial coefficient of argon from temperature dependent hard-sphere diameter (eq. 9) and Dymond and Alder potential function ($\varepsilon/k = 115.2$ °K).

and that the energy parameter is not sufficiently sensitive to temperature to affect the calculation.

Comparison with Compressibilities Using Second Virial Coefficient Parameters and Temperature Dependent Hard-Sphere Diameter

The results of calculations in the preceding section fail to distinguish whether the errors of the theory are in the perturbation method or in the choice of intermolecular potential. An alternative to strict correlation of the compressibility is to use a result of the Barker and Henderson perturbation theory (12) for modifying the hard-sphere diameter with temperature and obtain the potential parameters σ and ε/k from a potential model and second virial coefficient data. An additional motivation for this test is to see how accurately the compressibility can be determined from these relatively simple parameter requirements and be applicable to other fluids through corresponding states relations. The numerical values of the potential parameters used are summarized in Table 3.

The dependence of the hard-sphere diameter on temperature is through the intermolecular potential, *i.e.*,

$$[11] \qquad a^* = \frac{a}{\sigma} = \int_0^1 [1 - e^{-\phi(x)/kT}]\, dx$$

where x is the reduced distance r/σ.

Can. J. Chem. Downloaded from www.nrcresearchpress.com by 210.87.254.6 on 09/05/12
For personal use only.

Can. J. Chem. Downloaded from www.nrcresearchpress.com by 210.87.254.6 on 09/05/12
For personal use only.

TABLE 3. Intermolecular potential parameters

	Lennard–Jones 6–12 potential		Dymond and Alder potential	
	Potential zero distance (Å)	Well depth ε/k (°K)	Potential zero distance (Å)	Well depth ε/k (°K)
Argon	3.405*	119.8	3.28†	138.2
Krypton	3.6*	171.	3.476†	196.
Oxygen	3.46	118.	3.275‡	141.67‡

*Reference 16.
†Reference 17.
‡These parameters were derived from two-parameter corresponding states relations, using parameters for krypton.

For purposes of numerical computation, the compressibility integral is separated into two parts, a hard-sphere contribution and a perturbed, or soft-sphere, contribution.

$$[12] \quad I = \int_0^\infty c(r)r^2\,dr = \int_0^a c^{hs}(r)r^2\,dr + \int_0^\infty c^{ss}(r)r^2\,dr$$

The hard-sphere contribution was determined from two separate theoretical equations to test its effect on the total integral. The first was the direct analytical integration of eq. 7, which is the first-order Percus–Yevick solution for the hard-sphere direct correlation function. The second method was to use the Carnahan and Starling (13) equation of state for hard spheres to calculate the total compressibility integral for the hard-sphere fluid,

$$[13] \quad I^{hs} = \int_0^a c^{hs}(r)r^2\,dr + \int_a^\infty c^{hs}(r)r^2\,dr$$

Since the quantity of interest was the first integral in eq. 13, when I^{hs} is substituted into eq. 12, a small correction must be made to the integrand in the second term there.

The effect of varying the perturbation (or soft sphere) potential was studied by using the Lennard–Jones 6–12 and the Dymond and Alder potentials in two corresponding sets of calculations. The fluids chosen for study were argon, krypton, and oxygen. To extend the reduced density range and determine an upper limit on the applicability of this method, experimental data for Kr in the reduced density range $1.43 \leqslant \rho^* \leqslant 2.48$ were taken from Trappeniers *et al.* (14) and data for O_2 in the reduced density range $2.0 \leqslant \rho^* \leqslant 2.5$ from Weber (15). The numerically computed compressibility integrals for argon, krypton, and oxygen are shown in Tables 4, 5, and 6 and compared with experimental values. Figure 3 shows the integrals for argon and krypton plotted as functions of temperature and density. An overall appraisal of the results indicates that the isothermal compressibility may be determined to about 10% accuracy up to twice the critical density when one uses the Lennard–Jones potential as the attractive potential. The integrals incorporating the Dymond and Alder potential are too positive, *i.e.*, there is a net positive contribution due to the width of the attractive bowl. The shallower and narrower bowl of the Lennard–Jones potential is appar-

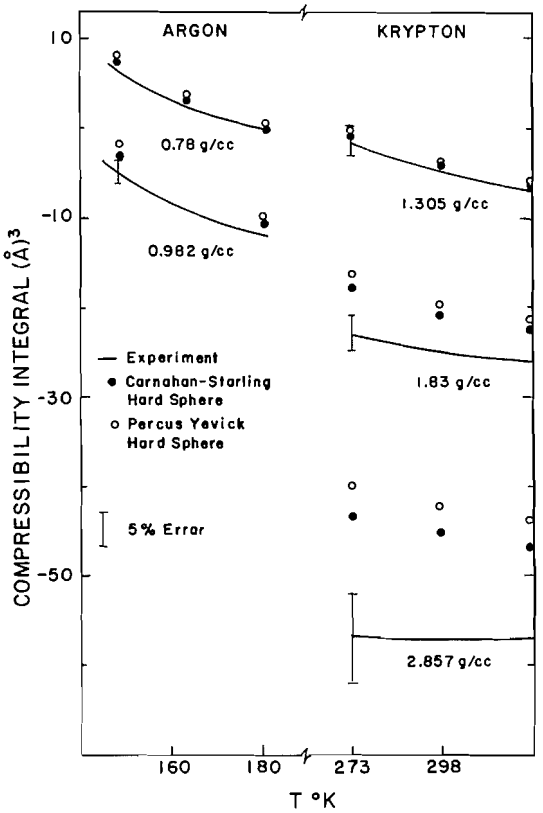

FIG. 3. Compressibility integrals from first-order expression for $c(r)$ (eq. 3) and Lennard–Jones 6–12 potential parameters with (*i*) Percus–Yevick hard-sphere integral, (*ii*) Carnahan and Starling hard-sphere integral.

Can. J. Chem. Downloaded from www.nrcresearchpress.com by 210.87.254.6 on 09/05/12
For personal use only.

TABLE 4. Calculations for isothermal compressibility of argon – effect of varying attractive potentials and hard-sphere direct correlation function

		Attractive potential L.J. 6–12 $\varepsilon/k = 119.8\,^{\circ}K$, $\sigma = 3.405$ Å					Attractive potential Dymond–Alder $\varepsilon/k = 138.2\,^{\circ}K$, $\sigma = 3.28$ Å					
			I_{py}^{hs}		I_{cs}^{hs}			I_{py}^{hs}		Experimental*		
Temperature (°K)	Density (g/cc)	HS diameter a (Å)	I (Å)^3	K (atm^{-1} $\times 10^4$)	I (Å)^3	K (atm^{-1} $\times 10^4$)	HS diameter a (Å)	I (Å)^3	K (atm^{-1} $\times 10^4$)	I (Å)^3	K (atm^{-1} $\times 10^4$)	ΔI_c
181.03	0.78	3.282	−0.19	33.5	0.18	35.4	3.201	4.43	100.2	−0.38	32.6	7.14
	0.91	3.282	−6.10	14.4	−5.38	15.3	3.201	0.15	30.4	−6.49	13.9	12.3
	0.982	3.282	−10.17	9.5	−9.15	10.1	3.201	−2.77	18.1			
163.15	0.536	3.293	11.11	†	11.19	†	3.208	14.07	†	8.09	312.7	1.75
	0.78	3.293	3.57	80.9	3.96	92.2	3.208	8.77	†	2.49	60.4	4.28
	0.91	3.293	−2.46	23.9	−1.70	25.4	3.208	4.51	148.0	−3.46	20.5	9.25
148.15	0.536	3.296	15.31	†	15.38	†	3.213	18.73	†			
	0.78	3.296	7.88	†	8.29	†	3.213	13.62	†	5.41	220.0	1.35
	0.91	3.296	1.89	53.7	2.67	67.0	3.213	9.42	†	−0.15	35.2	5.94
	0.982	3.296	−2.27	23.5	−1.18	27.4	3.213	6.50	†	−5.08	17.2	10.45
143.15	0.91	3.299	3.50	94.4	4.29	144.0	3.214	11.37	†	1.16	46.0	4.64
	0.982	3.299	−0.69	30.7	0.42	37.5	3.214	8.47	†	−3.74	20.4	9.11

*Reference 11.

†The direct correlation function integral has too large a positive value, *i.e.*, $4\pi\rho \int_0^\infty c(r) \cdot r^2 \, dr > 1$; See eq. 14.

Can. J. Chem. Downloaded from www.nrcresearchpress.com by 210.87.254.6 on 09/05/12
For personal use only.

TABLE 5. Calculations for isothermal compressibility of krypton – effect of varying attractive potentials and hard-sphere direct correlation function

		Attractive potential Lennard–Jones 6–12 $\varepsilon/k = 171\,^\circ$K, $\sigma = 3.6$ Å					Attractive potential Dymond and Alder $\varepsilon/k = 196\,^\circ$K, $\sigma = 3.476$ Å					
			I_{py}^{hs}		I_{cs}^{hs}			I_{py}^{hs}		Experiment*		
Temperature (°K)	Density (g/cc)	HS diameter a (Å)	I (Å)^3	K (atm^{-1} $\times 10^4$)	I (Å)^3	K (atm^{-1} $\times 10^4$)	HS diameter a (Å)	I (Å)^3	K (atm^{-1} $\times 10^4$)	I (Å)^3	K (atm^{-1} $\times 10^4$)	ΔI_c
323.15	1.305	3.451	−5.7	14.4	−5.9	14.3	3.378	−2.1	19.4	−6.3	13.9	14.7
	1.83	3.451	−33.5	3.6	−21.6	3.8	3.378	−14.9	5.0	−26.3	3.2	32.4
	2.257	3.451	−46.3	1.3	−43.2	1.4	3.378	−32.7	1.8	−57.3	1.1	62.2
298.15	1.305	3.457	−3.3	18.8	−3.5	18.7	3.384	0.6	28.0	−4.3	17.3	12.8
	1.83	3.457	−20.3	4.3	−19.5	4.5	3.384	−12.4	6.1	−25.0	3.6	31.0
	2.257	3.457	−44.7	1.5	−41.5	1.6	3.384	−30.5	2.1	−57.8	1.1	62.7
273.15	1.305	3.469	−0.5	27.1	−0.5	27.1	3.386	4.0	54.0	−2.0	23.0	10.5
	1.83	3.469	−18.0	5.1	−16.7	5.5	3.386	−8.9	8.3	−23.2	4.2	29.2
	2.257	3.469	−43.4	1.7	−39.3	1.8	3.386	−27.0	2.5	−58.2	1.2	62.7

*Reference 14.

TABLE 6. Calculations for isothermal compressibility of oxygen – effect of varying attractive potential and hard-sphere direct correlation function

		Attractive potential Lennard–Jones 6–12 $\varepsilon/k = 118\,^\circ$K, $\sigma = 3.46$ Å					Attractive potential Dymond and Alder $\varepsilon/k = 141.67\,^\circ$K, $\sigma = 3.275$ Å					
			I_{py}^{hs}		I_{cs}^{hs}			I_{py}^{hs}		Experiment*		
Temperature (°K)	Density (g/cc)	HS diameter a (Å)	I (Å)^3	K (atm^{-1} $\times 10^4$)	I (Å)^3	K (atm^{-1} $\times 10^4$)	HS diameter a (Å)	I (Å)^3	K (atm^{-1} $\times 10^4$)	I (Å)^3	K (atm^{-1} $\times 10^4$)	ΔI_c
100	1.116	3.376	−39.9	3.0	−31.7	3.7	3.226	12.8	†	−40.9	2.9	44.6
120	1.015	3.365	−27.8	4.2	−23.0	4.9	3.218	5.8	†	−32.8	3.6	37.0
140	0.892	3.355	−15.9	7.2	−13.6	8.0	3.212	5.0	†	−16.1	7.1	20.8
120	1.076	3.365	−41.9	2.6	−36.0	2.9	3.218	−1.2	23.2	−47.0	2.3	50.9
140	0.991	3.355	−31.6	3.3	−28.0	3.7	3.212	−3.3	15.8	−33.0	3.2	37.3

*Reference 15.
†See second footnote, Table 4.

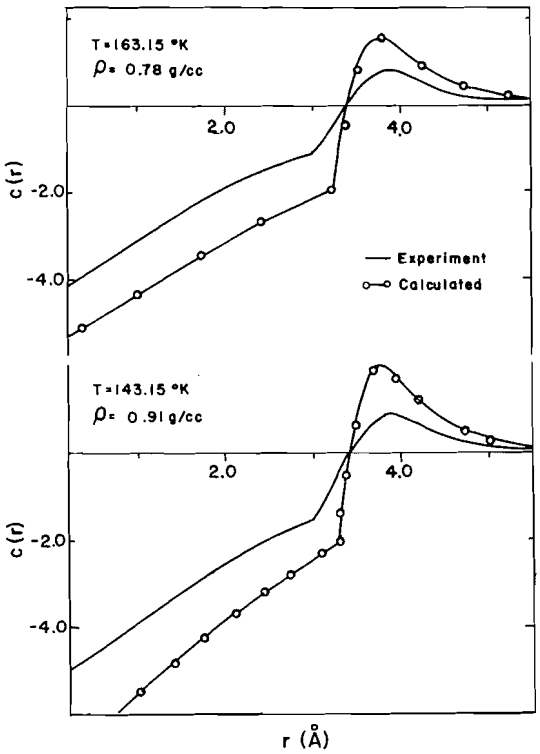

FIG. 4. Direct correlation function of argon from first-order expression for $c(r)$ (eq. 3) and Lennard–Jones 6–12 potential.

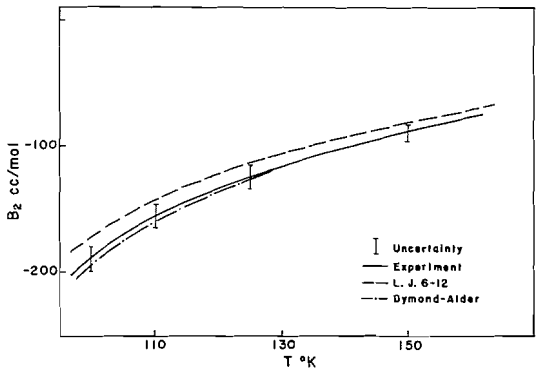

FIG. 5. Second virial coefficient of oxygen from temperature dependent hard-sphere diameter (eq. 11) and (*i*) Lennard–Jones 6–12 potential, (*ii*) Dymond and Alder potential. Experimental values from ref. 18.

ently more representative of the effective intermolecular potential. At the lower densities there is little to choose between the hard-sphere contributions of the Percus–Yevick and the Carnahan and Starling equations; at higher densities the Percus–Yevick hard-sphere contribution is significantly better.

A comparison of the calculated direct correlation function with the experimental data for argon using the Lennard–Jones potential is instructive. These are shown plotted in Fig. 4. It is apparent that the microscopic function is modeled only qualitatively; quantitative agreement would not be obtained except by a simultaneous dependence of both hard-sphere diameter and ε/k on temperature and density. On the other hand, significant cancellation of errors occurs in the integration of this correlation function since the calculations for compressibilities are in reasonable agreement with experiment. The calculated second virial coefficients for oxygen are compared with experimental values in Fig. 5. The values calculated with the Dymond–Alder potential are within experimental error (r.m.s. deviation 2.14 cc/g mol) indicating that the temperature variation of the hard-sphere diameter is accurate for this potential. The second virial coefficient from the Lennard–Jones potential is less accurate (r.m.s. deviation = 11.8 cc/g mol) but this is typical of the inadequacy of this potential for second virial coefficients at low temperatures.

Conclusions

Calculations indicate that the present first-order perturbation theory about a hard-sphere base is not adequate for microscopic modeling of a real fluid in a dense state. The difficulty is shown in attempting to separate the intermolecular potential parameters into density dependent and temperature dependent quantities. Although the temperature dependence of the hard-sphere diameter is well described (as shown by the calculations for second virial coefficients), the density dependence of the microscopic property $c(r)$ cannot be completely defined by a density dependent ε/k and the hard-sphere correlation functions. The errors are sensitive to the potential model but it is likely that second order terms are also important.

With the method of the last section, one can use low density intermolecular potential parameters to describe the temperature variation of the isothermal compressibility. Quantitative agreement with experiment (up to 15% error) appears possible up to about twice the critical density.

Can. J. Chem. Downloaded from www.nrcresearchpress.com by 210.87.254.6 on 09/05/12
For personal use only.

However, precise agreement with experimental results is not attainable at higher densities. Apparently, a first-order theory requires a density-dependent hard-sphere diameter before it can properly model the microscopic, as well as the macroscopic, state of the dense liquid.

The authors are grateful to the Donors of the Petroleum Research Fund for partial financial support and to the University of Florida Computing Center for use of its facilities.

1. J. S. ROWLINSON. Rept. Prog. Phys. **28**, 169 (1965).
2. H. C. LONGUET-HIGGINS and B. WIDOM. Mol. Phys. **8**, 549 (1964).
3. J. A. BARKER and D. HENDERSON. J. Chem. Phys. **47**, 2856 (1967).
4. S. W. BRELVI and J. P. O'CONNELL. Phys. Fluids. In press.
5. M. S. WERTHEIM. Phys. Rev. Lett. **10** (8), 321 (1963).
6. R. O. WATTS and D. HENDERSON. Mol. Phys. **16** (3), 217 (1969).
7. J. K. PERCUS. *In* Classical fluids. *Edited by* Frisch and Lebowitz, Benjamin, New York. 1964.
8. P. G. MIKOLAJ and C. J. PINGS. J. Chem. Phys. **46**, 1401 (1967).
9. J. H. DYMOND and B. J. ALDER. J. Chem. Phys. **51**, 309 (1969).
10. P. G. MIKOLAJ and C. J. PINGS. J. Chem. Phys. **46**, 1412 (1967).
11. A. L. GOSMAN, R. D. MCCARTY, and J. G. HUST. Thermodynamic properties of argon. NSRDS-NBS 27, U.S. Dept. of Commerce, NBS, Washington, D.C.
12. J. A. BARKER and D. HENDERSON. J. Chem. Phys. **47**, 4714 (1967).
13. N. F. CARNAHAN and K. E. STARLING. J. Chem. Phys. **51**, 635 (1969).
14. N. J. TRAPPENIERS, T. WASSENAAR, and G. J. WOLKERS. Physica, **32**, 1503 (1966).
15. L. A. WEBER. J. Res. NBS. A. Phys. and Chem. **74A**, 93 (1970).
16. J. O. HIRSCHFELDER, C. F. CURTISS, and R. B. BIRD. Molecular theory of gases and liquids. Wiley, New York. 1954.
17. J. H. DYMOND. J. Chem. Phys. **54**, 3675 (1971).
18. J. H. DYMOND and E. B. SMITH. The virial coefficients of gases. Clarendon Press, Oxford. 1969.

Can. J. Chem. Downloaded from www.nrcresearchpress.com by 210.87.254.6 on 09/05/12
For personal use only.

Homogeneous Catalysis of D_2–H_2O Isotope Exchange by Pentacyanocobaltate(II)[1]

G. G. STRATHDEE AND M. J. QUINN

Research Chemistry Branch, Whiteshell Nuclear Research Establishment, Atomic Energy of Canada Limited, Pinawa, Manitoba, R0E 1L0

Received April 4, 1972

The rate of exchange of deuterium between hydrogen gas and water catalyzed by pentacyanocobaltate(II) has been measured as a function of pressure and temperature at a constant total cobalt concentration, 0.05 *M*, and ionic strength, 1 *M*. The rates of evolution of hydrogen from solutions of hydridopentacyanocobaltate(III) have been determined under identical conditions. These data have been employed to test the validity of a mechanism for the $Co(CN)_5^{3-}$-catalyzed isotope exchange reaction, and to clarify the controversy over the magnitude of the specific rate for the deuterium transfer step

$$DCo(CN)_5^{3-} + H_2O \xrightarrow{k_3} HCo(CN)_5^{3-} + HDO$$

Calculations show that kinetic isotope and ion pairing effects are significant.

La vitesse d'échange du deutérium entre l'hydrogène gazeux et l'eau, catalysée par le pentacyanocobaltate(II), a été mesurée en fonction de la pression et de la température pour une concentration totale et constante en cobalt de 0.05 *M* et une force ionique de 1 *M*. Les vitesses de dégagement d'hydrogène à partir des solutions d'hydridopentacyanocobaltate(III) ont été déterminées dans des conditions identiques. Ces données ont été utilisées pour contrôler la validité d'un mécanisme d'échange isotopique catalysé par $Co(CN)_5^{3-}$ et pour clarifier la controverse sur la grandeur de la vitesse spécifique dans l'étape de transfert du deutérium:

$$DCo(CN)_5^{3-} + H_2O \xrightarrow{k_3} HCo(CN)_5^{3-} + HDO$$

Les calculs montrent l'importance des effets isotopiques sur la cinétique et appariement des ions.

[Traduit par le journal]

Canadian Journal of Chemistry, **50**, 3144 (1972)

Introduction

Several investigations of isotope exchange between D_2 and water homogeneously catalyzed by pentacyanocobaltate(II), $Co(CN_5^{3-}$, have been reported (1–3) but the validity of the mechanism suggested by Kemball and coworkers (5) and Schindewolf (2) for deuterium exchange has not been demonstrated.

A number of studies have been focussed upon the reactions incorporated in this mechanism. For example, the rates of activation of hydrogen by $Co(CN)_5^{3-}$ (1, 5, 7–10):

$$[1] \qquad H_2 + 2Co(CN)_5^{3-} \xrightarrow{k_1} 2HCo(CN)_5^{3-}$$

and the evolution of hydrogen from solutions of $HCo(CN)_5^{3-}$ (5, 10):

$$[2] \qquad 2HCo(CN)_5^{3-} \xrightarrow{k_2} H_2 + 2Co(CN)_5^{3-}$$

have been measured. In addition, the magnitude of the equilibrium constant for reversible hydrogen absorption has been determined by both hydrogen uptake and spectroscopic techniques (5, 8, 9).

Reversible homolytic activation of D_2 is not sufficient to cause exchange of deuterium between D_2 and water, and the transfer reaction 3 must occur

$$[3] \qquad DCo(CN)_5^{3-} + H_2O \xrightarrow{k_3} HCo(CN)_5^{3-} + HDO$$

However, there is some uncertainty in the magnitude of the specific rate constant k_3. For example, Kemball has used the fact that since a ^1H resonance for $HCo(CN)_5^{3-}$ prepared by reaction of $Co(CN)_5^{3-}$ with H_2 in D_2O was not detectable, then the rate of the transfer step between $HCo(CN)_5^{3-}$ and D_2O must be fast on the n.m.r. time scale (5). The broad ^1H resonance and the lack of ^1H–^{13}C coupling in the spectrum of $HCo(CN)_5^{3-}$ in H_2O would support this claim, but these observations are more likely due to fast cyanide exchange or the presence of paramagnetic Co(II) species (4, 6). In contrast, the observation of HD in the gas phase during D_2–H_2O exchange experiments

[1]AECL No. 4289.

Can. J. Chem. Downloaded from www.nrcresearchpress.com by 210.87.254.42 on 09/05/12
For personal use only.

Can. J. Chem. Downloaded from www.nrcresearchpress.com by 210.87.254.42 on 09/05/12
For personal use only.

(1) did not appear to us to be consistent with a rapid transfer step. Since the rate determining step in the overall exchange scheme is believed to be the dehydrogenation reaction 2, which is slow, HD should only be observed in the gas phase if the rate of transfer step 3 is comparable to or slower than that of [2]. If [3] is as rapid as has been suggested, predominantly H_2 should be evolved. This is not normally the case.

In this paper, a more comprehensive study is presented of the pressure and temperature dependence of the D_2–H_2O exchange catalyzed by $Co(CN)_5^{3-}$, and the H_2 evolution reaction 2, than has previously been reported (1–3). In addition, the effect of ionic strength on the overall D_2–H_2O exchange and the aging reaction

$$[4]\quad 2Co(CN)_5^{3-} + H_2O \rightarrow HCo(CN)_5^{3-} + (HO)Co(CN)_5^{3-}$$

has been re-examined under our experimental conditions. These data are employed to test the validity of the mechanism which has been proposed to explain D_2–H_2O exchange catalyzed by $Co(CN)_5^{3-}$, and to attempt to resolve the inconsistency in current estimates of the specific rate of the transfer reaction 3.

Experimental

Pentacyanocobaltate(II) solutions were prepared in the reaction flask by injecting the required amounts of degassed aqueous solutions of cobalt(II) chloride, and potassium cyanide containing potassium chloride to adjust the ionic strength. Reactions were conducted in jacketted Pyrex glass cells of typically 100 ml capacity. Solutions were magnetically stirred, usually at 3000 r.p.m., with a Teflon-covered bar in the cell. Temperature was controlled to better than 0.1 °C.

Hydrogen was purified by passing the gas through an Engelhard Deoxo unit and molecular sieve drier. Deuterium was evolved at 450 °C from uranium deuteride which had been prepared from uranium turnings and D_2 at 225 °C. Other reagents were used as received.

The evolution of H_2 from solutions of $HCo(CN)_5^{3-}$ prepared by hydrogenation of $Co(CN)_5^{3-}$ was followed by observing the increase in pressure in a calibrated cell, after pumping off the excess H_2, by means of a Viatran Corporation Model 103 pressure transducer. The output was variably biased to permit a maximum recorder sensitivity of about 25 Torr on the 1 mV scale. Experiments without $Co(CN)_5^{3-}$ demonstrated that the cell was re-saturated with water vapor within a few seconds and therefore did not affect initial rates of evolution calculated from the slopes of pressure–time data.

Rates of the decomposition of aging reaction 4 were determined spectroscopically by observation of the 980 nm band of $Co(CN)_5^{3-}$ with a Unicam SP700 spectrophotometer while the solution was rapidly circulated through a 0.1 cm pathlength optical cell by means of a peristaltic pump.

Exchange experiments were conducted with solutions 0.05 *M* in cobalt, $CN^-:Co^{2+} = 6$, and ionic strength = 1 *M* unless noted otherwise. These solutions were reacted with either excess D_2 (pre-deuteration) or excess H_2 (pre-hydrogenation) for about 30 min at the pressure of the subsequent exchange experiment. Thirty ml of those deuterated or hydrogenated solutions were transferred by syringe to a reaction vessel containing D_2 at the appropriate pressure. Samples of the resultant D_2, HD, and H_2 gas mixtures were removed from the flask with a gas-tight syringe and analyzed with a CEC-21-130 mass spectrometer. Initial exchange rates were calculated with the relation

$$[5]\quad -d(D_2)/dt = \ln[(\theta_0 - \theta_e)/(\theta_t - \theta_e)]A/t = k_x A$$

where θ_0, θ_t, and θ_e represent the mole percent D_2 at $t = 0$, $t = t$ s, and at equilibrium, and A is the effective solubility, moles per liter, = initial D_2, m mole ÷ the volume of the solution, ml. The experimental specific rate k_x was obtained from the slope of log $D_2 - t$ plots.

Results

Data from a typical D_2–H_2O exchange experiment are shown in Fig. 1. In this example, the $Co(CN)_5^{3-}$ solution was initially pre-deuterated. The slow disappearance of D_2 in the first 1000 s is characteristic of this type of experiment and reflects the relatively slow rate of the transfer reaction 3. This is discussed below. In comparison, exchange reactions preceded by hydrogenation rather than deuteration did not exhibit this curvature in the disappearance of D_2, and relative initial HD:H_2 yields were lower. If the reactions were followed for sufficient time, maximum HD concentrations were observed in the range 35 to 45 mol%. The ratio of initial rates of evolution of HD and H_2 was obtained from the slopes of plots of mol% HD and H_2 against time which were linear at less than 20% D_2 conversion.

The rates of D_2–H_2O exchange at 0, 15, and 30 °C as a function of total hydrogen pressure are shown in Fig. 2, along with curves calculated by the method discussed later in this section. All solutions of $Co(CN)_5^{3-}$ were pre-deuterated except for those experiments at 30 °C, distinguished by filled circles and a dashed calculated line in the figure, in which $Co(CN)_5^{3-}$ solutions were hydrogenated prior to exchange with D_2. Although experimental data are scattered, calculations suggest pre-hydrogenation gives higher initial rates of exchange than does pre-deuteration. Rates of exchange decrease

Can. J. Chem. Downloaded from www.nrcresearchpress.com by 210.87.254.42 on 09/05/12
For personal use only.

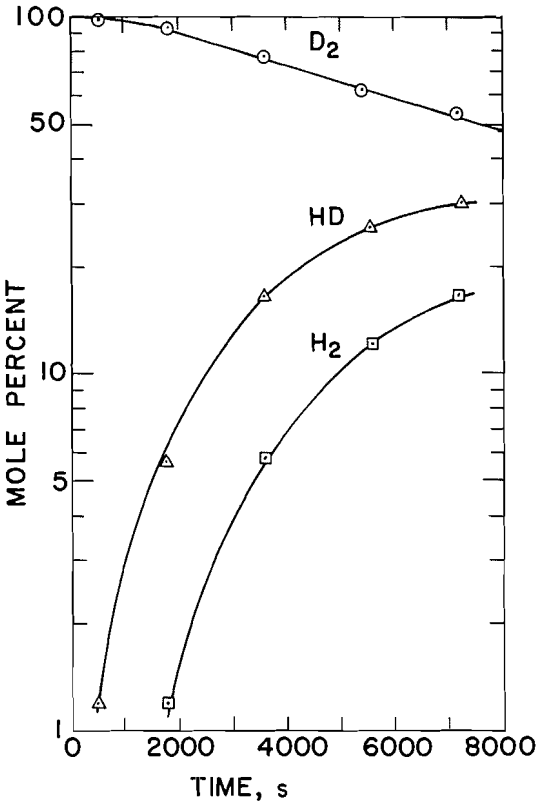

FIG. 1. Typical D_2–H_2O exchange data. Total cobalt: 0.05 *M*; initial D_2: 300 Torr; ionic strength: 1.0 *M*; T = 30 °C; V_G: 75 ml; V_L: 30 ml.

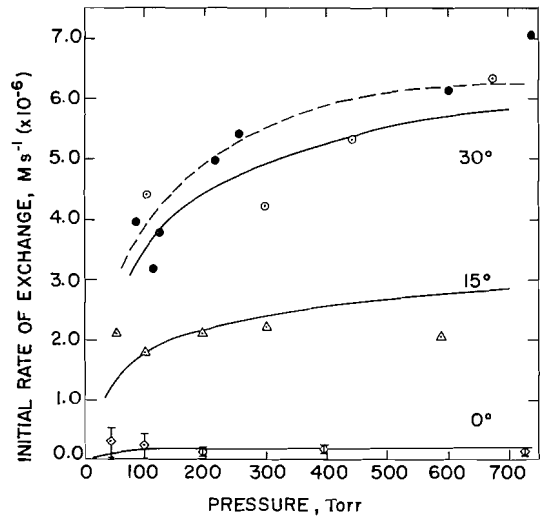

FIG. 2. Initial rates of D_2–H_2O exchange. Total cobalt 0.05 *M*; ionic strength: 1.0 *M*. Predeuteration, —; prehydrogenation ---.

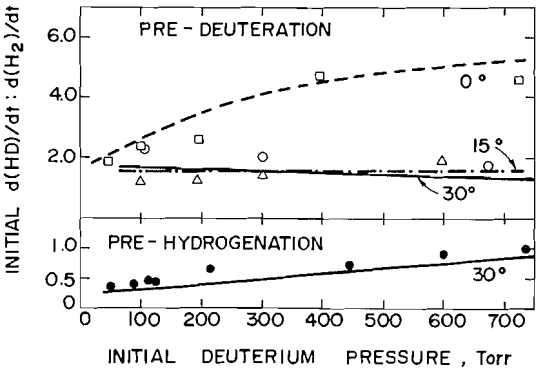

FIG. 3. Initial rate ratio HD:H_2. Total cobalt: 0.05 *M*; ionic strength: 1.0 *M*.

gradually with decreasing pressure. This is similar to the change in rate with pressure expected for the component reactions 1 and 2 in the overall hydrogen uptake equilibrium.

The ratio of initial rates of formation of HD and H_2 are plotted in Fig. 3, and these data are compared with calculated curves. It may be seen that the HD:H_2 initial rate ratios decrease significantly with increasing temperature. Prehydrogenation gives a lower ratio than does pre-deuteration, primarily due to the higher initial rate of evolution of H_2. A relatively greater concentration of $HCo(CN)_5^{3-}$ compared to $DCo(CN)_5^{3-}$ must therefore exist in solution upon pre-hydrogenation rather than pre-deuteration. These observations qualitatively suggest that the rate of the transfer reaction 3 is slower than, but of comparable magnitude to, the rate of the de-hydrogenation reaction 2.

The rates of evolution of H_2 from hydrogenated solutions of $Co(CN)_5^{3-}$ are shown in Fig. 4, together with fitted curves. These results have the same general pressure-dependence as do exchange rate data, indicating the common dependence of these observations on the dehydrogenation reaction 2. However, the rates of evolution of hydrogen are about a factor of three greater than the rates of D_2–H_2O exchange. This is another indication that the rate of reaction 3 is less than that of reaction 2.

The decomposition or aging of 0.05 *M* $Co(CN)_5^{3-}$, reaction 4, increased with ionic strength. Second order plots, $1/[Co(CN)_5^{3-}]$ *vs.* time, were linear at 1.0 *M* ionic strength, but showed curvature at higher ionic strengths. A comparison of apparent specific aging rates at 30 °C, k_4

Can. J. Chem. Downloaded from www.nrcresearchpress.com by 210.87.254.42 on 09/05/12
For personal use only.

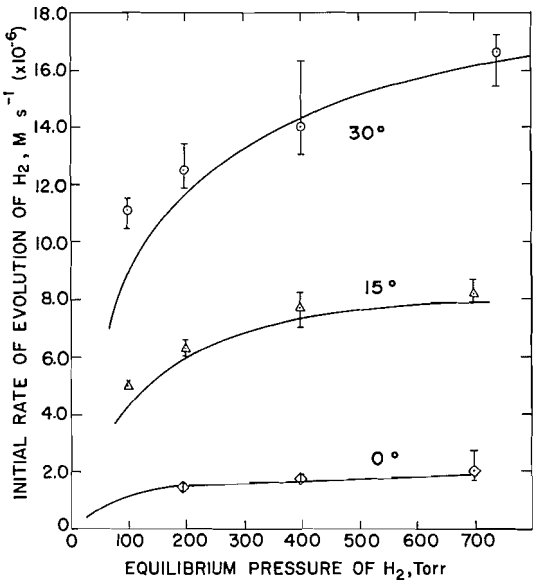

FIG. 4. Initial rates of evolution of H_2. Total cobalt: 0.05 *M*; ionic strength: 1.0 *M*.

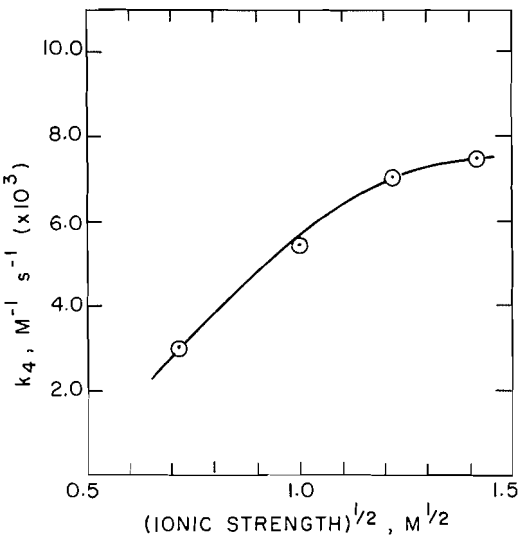

FIG. 5. Effect of ionic strength on the specific rate of aging. Decomposition of $Co(CN)_5^{3-}$.

$= d(1/[Co(CN)_5^{3-}])/dt$, evaluated at 200 s after mixing the reagents is shown in Fig. 5.

Increasing the ionic strength also accelerates the initial D_2–H_2O exchange and increases the HD:H_2 initial yield ratio, Fig. 6. For this dependence to be observed, the effect of ionic strength on the rates of reactions 2 and 3 must differ.

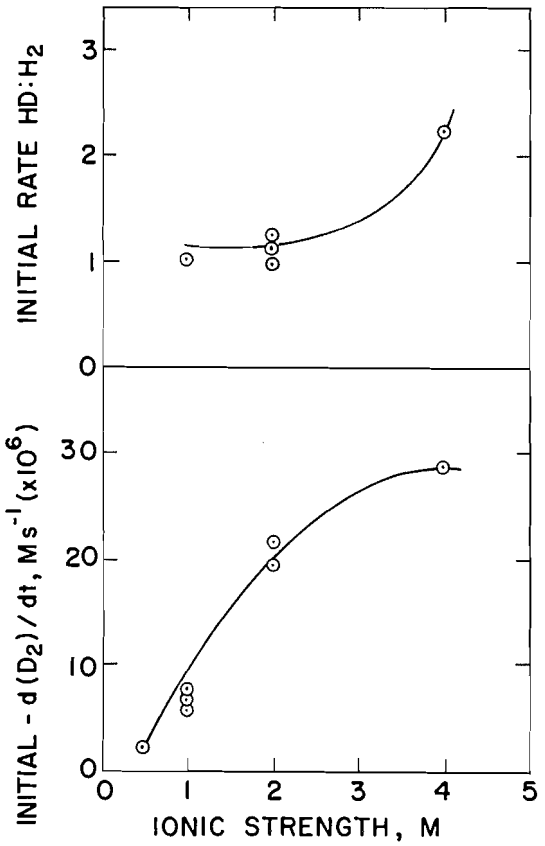

FIG. 6. Effect of ionic strength on the initial rate of isotope exchange and the initial HD:H_2 rate ratio. Initial D_2: 700 Torr. *T*: 30 °C.

Although expressions which describe the effect of ionic strength (11) on rate constants are not generally applicable at the high electrolyte concentrations used in our experiments, it is interesting to note that the rate of exchange increases more rapidly than would be predicted for the enhancement of reaction rate of two triply charged anions by ionic strength. The possible influence of ion–pair formation in this system is discussed later.

The full set of reactions included in the mechanism for D_2–H_2O exchange are shown in Table 1. Isotope exchange and hydrogen evolution experiments were simulated by numerical integration of the seven differential equations shown in Table 2 by a modified Hammings predictor–corrector method.[2] The term (1 +

[2]IBM 360 system subroutine 17HPCG.

TABLE 1. D_2–H_2O Exchange reaction mechanism

Activation of Hydrogen

[1*a*] $D_2 + 2Co(CN)_5^{3-} \xrightarrow{k_1} 2DCo(CN)_5^{3-}$

[1*b*] $HD + 2Co(CN)_5^{3-} \xrightarrow{k_1} HCo(CN)_5^{3-} + DCo(CN)_5^{3-}$

[1*c*] $H_2 + 2Co(CN)_5^{3-} \xrightarrow{k_1} 2HCo(CN)_5^{3-}$

Evolution of Hydrogen

[2*a*] $2\,DCo(CN)_5^{3-} \xrightarrow{k_2} D_2 + 2\,Co(CN)_5^{3-}$

[2*b*] $HCo(CN)_5^{3-} + DCo(CN)_5^{3-} \xrightarrow{k_2} HD + 2\,Co(CN)_5^{3-}$

[2*c*] $2\,HCo(CN)_5^{3-} \xrightarrow{k_2} H_2 + 2\,Co(CN)_5^{3-}$

Transfer

[3] $DCo(CN)_5^{3-} + H_2O \xrightarrow{k_3} HCo(CN)_5^{3-} + HDO$

Aging

[4] $2\,Co(CN)_5^{3-} + H_2O \xrightarrow{k_4} HCo(CN)_5^{3-} + (HO)Co(CN)_5^{3-}$

TABLE 2. Reaction rate expressions for D_2–H_2O exchange catalyzed by $Co(CN)_5^{3-}$*

$dc_1/dt = (-0.5k_1c_1c_4^2 + 0.5k_2c_5^2)/(1 + V_G/RTV_LH)$
$dc_2/dt = (-0.5k_1c_2c_4^2 + 0.5k_2c_5c_6)/(1 + V_G/RTV_LH)$
$dc_3/dt = (-0.5k_1c_3c_4^2 + 0.5k_2c_6^2)/(1 + V_G/RTV_LH)$
$dc_4/dt = -k_1c_3c_4^2 + k_2c_6^2 - k_1c_2c_4^2 + k_2c_5c_6 - k_1c_1c_4^2 + k_2c_5^2 - k_4c_4^2$
$dc_5/dt = k_1c_1c_4 + 0.5k_1c_2c_4^2 - k_2c_5^2 - 0.5k_2c_5c_6 - k_3c_5$
$dc_6/dt = 0.5k_1c_2c_4^2 + k_1c_3c_4^2 - k_2c_6^2 - 0.5k_2c_5c_6 + k_3c_5 + 0.5k_4c_4^2$
$dc_7/dt = 0.5k_4c_4^2$

*$c_1 = [D_2]$, $c_2 = [HD]$, $c_3 = [H_2]$, $c_4 = [Co(CN)_5^{3-}]$, $c_5 = [DCo(CN)_5^{3-}]$, $c_6 = [HCo(CN)_5^{3-}]$, $c_7 = [(HO)Co(CN)_5^{3-}]$. H = Henry's Law constant for H_2 in water, in mol l^{-1} atm^{-1}, R = gas constant, T = absolute temperature, V_G = volume of gas phase, in l, V_L = volume of solution, in l.

$V_G/RT\,V_LH$) accounts for the transfer of D_2, HD, and H_2 between the gas and solution phases. These assumptions were made: (*i*) the gas phase and dissolved hydrogen mixtures were in continuous equilibrium, (*ii*) kinetic isotope effects could be neglected, therefore reactions in sets [1*a*–*c*] and [2*a*–*c*], shown in Table 1, have specific rates k_1 and k_2 respectively, and (*iii*) the aging reaction 4 is irreversible. Reversal of the transfer step 3 under our experimental conditions was insignificant and related differential terms were omitted from equations in Table 2. Rate constants were expressed in terms of moles of cobalt species. The solubility of hydrogen in 1 *M* KCl (12) and an enthalpy of solution for H_2 in water of 1.29 kcal mol^{-1} calculated from published data (13) gave these hydrogen solubilities in our 1 *M* electrolyte: 0°: 0.76; 15°: 0.67; 30°: 0.60 *M* ($\times 10^3$).

The characteristic shape of the D_2–H_2O exchange and hydrogen evolution rate curves included in Figs. 2 and 4, respectively, is determined by the common dependence of these rates on the overall concentration of $HCo(CN)_5^{3-}$ and its deuterated analogue. Since the hydrogenation equilibrium has been assumed to hold:

[6] $H_2 + 2Co(CN)_5^{3-} \overset{K}{\rightleftharpoons} 2\,HCo(CN)_5^{3-}$

Can. J. Chem. Downloaded from www.nrcresearchpress.com by 210.87.254.42 on 09/05/12
For personal use only.

Can. J. Chem. Downloaded from www.nrcresearchpress.com by 210.87.254.42 on 09/05/12
For personal use only.

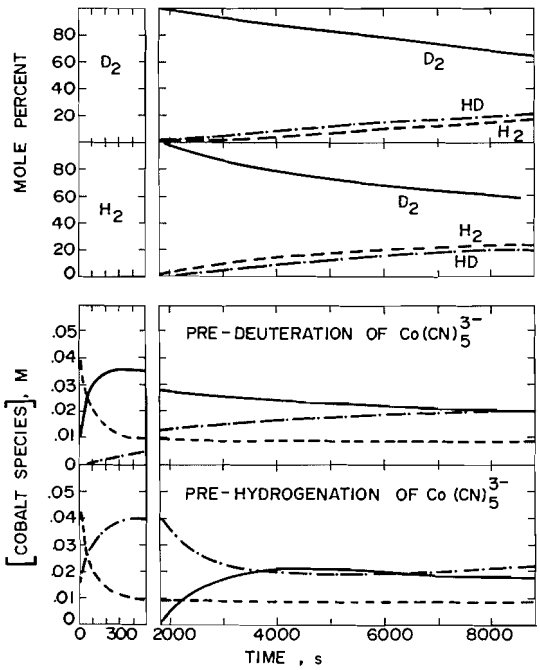

FIG. 7. Comparison of calculated change in composition of gas phase and solution components during D_2–H_2O exchange. Cobalt species: --- $Co(CN)_5^{3-}$; —$DCo(CN)_5^{3-}$; ·-·- $HCo(CN)_5^{3-}$. Total hydrogen: 700 Torr. T: 30 °C. V_G: 75 ml. V_L: 30 ml.

the concentration of $HCo(CN)_5^{3-}$ plus $DCo(CN)_5^{3-}$ is given by the expression

$$[7] \quad [HCo(CN)_5]^{3-} = [Co]_T \frac{K[H_2]_T}{1 + K[H_2]_T}$$

where $[Co]_T$ = total cobalt, $[H_2]_T$ = total hydrogen, if the aging reaction 4 is neglected. The curves through our data are therefore determined by the model we have employed and are representative within the errors discussed here.

The calculated variation with time of the three catalytically important species $Co(CN)_5^{3-}$ and $HCo(CN)_5^{3-}$ is illustrated in Fig. 7 for both pre-deuteration and pre-hydrogenation of 0.05 M $Co(CN)_5^{3-}$ at 700 Torr and 30 °C prior to isotope exchange. The corresponding change in the composition of the gas phase is also shown. The first segment of the figure shows calculated concentration changes when 30 ml of solution contacted 600 ml of either D_2 or H_2 gas. The second segment shows the effect on these concentrations when 30 ml of these solutions exchange deuterium with 75 ml of D_2 gas.

The course of exchange reactions is significantly dependent on the pre-treatment. Pre-deuteration yields mainly $DCo(CN)_5^{3-}$, the concentration of which decreases slowly as the transfer 3 and evolution reactions 2*a* and *b* occur. The initially high D:H ratio of the gas reservoir maintains the concentration of $DCo(CN)_5^{3-}$ by reactions 1*a* and *b*. In contrast, pre-hydrogenation gives a high initial concentration of $HCo(CN)_5^{3-}$ which disappears relatively rapidly due to evolution reactions 2*b* and 2*c*. Absorption of D_2 and HD, reactions 1*a* and *b*, causes an increase in the concentration of $DCo(CN)_5^{3-}$ which then decays at a rate similar to that in the case of the pre-deuteration. If the exchange reaction is examined at reduced pressure, the amount of isotopic hydrogen in the gas phase is proportionally decreased, and the changes described in Fig. 7 occur more rapidly.

Discussion

The objectives of this study were to test the validity of the simple mechanism which has been proposed to explain the manner in which D_2–H_2O exchange is catalyzed by $Co(CN)_5^{3-}$, and to obtain a reliable estimate of the specific rate for the deuterium transfer reaction 3. In view of the many reports on the reversible hydrogenation of $Co(CN)_5^{3-}$ (1, 5, 8–10, 13, 14, 16) it was evident that the kinetics of the two basic reactions had been satisfactorily established. However, rate constants reported in the literature for the component reactions 1*c* and 2*c* of the scheme shown in Table 1 could not satisfactorily be employed in a computer simulation of the D_2–H_2O exchange process. Principally, the quantitative effects of ionic strength and electrolyte on k_2 and k_3 were unknown. We therefore measured the rates of H_2 evolution and D_2–H_2O exchange, under comparable conditions of solution composition and reactor configuration, from which the magnitudes of k_2 and k_3 could be derived. These conditions have been specified in the Experimental section.

The major assumptions (*i*) that the dissolved hydrogen mixture is in continuous equilibrium with that in the gas phase, (*ii*) that kinetic isotope effects could be neglected, and (*iii*) that the decomposition reaction 4 is irreversible are conservative. In our experiments the half-life of the overall exchange reaction was con-

Can. J. Chem. Downloaded from www.nrcresearchpress.com by 210.87.254.42 on 09/05/12
For personal use only.

TABLE 3. Specific rate constants

Constant	Value at 0°	Value at 15°	Value at 30°
k_1 M^{-2} s^{-1}	614	606	600
k_2 M^{-1} s^{-1} ($\times 10^3$)	1.6	8.5	20.0
k_3 s^{-1} ($\times 10^5$)	2.5	15.0	33.0
k_4 M^{-1} s^{-1} ($\times 10^3$)	0.9	2.2	5.0

siderably greater than expected for dissolution of hydrogen in water under conditions of turbulent mixing (*e.g.* hours compared to seconds). Multiple exchange processes of the type described by Halpern and James (17) were therefore considered unlikely to occur. Kinetic hydrogen–deuterium isotope effects undoubtedly exist for reactions 1–3. Partly for simplicity, but mainly because of lack of supporting data, assumption (*ii*) is made for reactions 1 and 2. Under our conditions the reverse of reaction 3 is not significant, therefore neglect of this isotope effect is valid. Additional comment on these topics is included later in this discussion.

The rate constant parameters which yielded the fits to our data in Figs. 2–4 are shown in Table 3. The manner in which these values were determined requires some discussion: The magnitude of k_1 was based on available data; k_2 was varied until the fits to hydrogen evolution data shown in Fig. 4 were obtained; k_3 was then adjusted to provide the fits to exchange results shown in Figs. 2 and 3; k_4 was based on our measurement of the rate of aging. It should be noted that k_3 was established subsequent to and independently of the evaluation of k_2. Within the framework of the calculation the estimated error in k_2 is $\pm 10\%$ and in k_3 is $\pm 20\%$. A discussion of each rate constant follows:

Activation, k_1

A value for the specific rate of hydrogen activation at 30 °C of 600 M^{-2} s^{-1} was selected and an enthalpy of activation of -0.7 kcal mol^{-1} was used to calculate k_1 at 0 and 15 °C (8, 9). This may be compared with values found by Burnett *et al.* (5), 620 M^{-2} s^{-1} at $\mu = 0.51$ M, and DeVries (8), 830 M^{-1} s^{-1} at $\mu = 1.0$ M and 25 °C. There is evidence that k_1 may be somewhat lower under our conditions.[3] In general, data in the literature shows that k_1 increases with the ionic strength of the solution (5, 8, 9). Mills has reported that k_1 is dependent on the square root of the ionic strength, but is not a function of the electrolyte used. However, mass transport of hydrogen may have influenced these results, and the validity of this correlation has not been checked under chemical rate limiting conditions. Since our calculations showed the D_2–H_2O exchange rate was only slightly dependent on k_1, re-determination of k_1 for our conditions was considered unnecessary. For example, a 3.5-fold increase of this parameter to 2100 M^{-2} s^{-1} increased the calculated exchange rate by only 12% at 700 Torr and 30 °C.

[3]W. J. Wallace. Personal communication.

Evolution, k_2

Our value of 16×10^{-3} M^{-1} s^{-1} at 25 °C for 1 M ionic strength taken from Fig. 8, an Arrhenius plot of k_2 and k_3 data, is somewhat higher than the 4.5×10^{-3} M^{-1} s^{-1} Burnett *et al.* have reported for k_2 at 0.51 ionic strength (5). However, it may be seen in Fig. 6 that the rate of initial D_2–H_2O exchange at 30 °C and 700 Torr initial D_2 pressure increases by a factor of about four when the ionic strength is increased from 0.5 to 1.0 M. Since the HD:H_2 rate ratio does not change within this range, the dependence of the exchange rate on ionic strength must reflect the change in k_2. Therefore if our value for k_2 quoted above is lowered by this factor of four to 4×10^{-3} M^{-1} s^{-1}, it agrees with that of Burnett *et al.*

Transfer, k_3

Previous exchange studies have provided no quantitative estimate of k_3. However, our value of k_3 at 20 °C, 1.5×10^{-4} s^{-1}, for first-order decay of $DCo(CN)_5^{3-}$ may be compared with the rate of OH^- catalyzed deprotonation of $HCo(CN)_5^{3-}$ discussed by Venerable and Halpern (18). Using their value of k_{-2} (their notation) = 0.12 M^{-1} s^{-1} for the reaction

$$[8] \qquad HCo(CN)_5^{3-} + OH^- \underset{k_2}{\overset{k_{-2}}{\rightleftharpoons}} Co(CN)_5^{4-} + H_2O$$

the pseudo first-order constant $k_{-2}[OH^-]$ in the solutions of pH 11.5–12.0 which we employed would be about 1×10^{-3} s^{-1}. If a relatively large H–D isotope effect exists for the OH^- catalyzed dissociation of the hydrido

Can. J. Chem. Downloaded from www.nrcresearchpress.com by 210.87.254.42 on 09/05/12
For personal use only.

compared to the deuterido complex (the maximum would be about 5), then the agreement between our value of k_3 and Venerable's $k_{-2}[OH^-]$ would considerably improve. In view of the relatively slow rate of this transfer step, it is surprising that the ^1H resonance of $HCo(CN)_5^{3-}$ prepared by reaction of H_2 and $Co(CN)_5^{3-}$ in D_2O solution has not been observed at the intensity expected (4, 5). If no gaseous H_2 is present, or if gas–liquid equilibration of H_2 is slow as might be the case in an n.m.r. tube, $HCo(CN)_5^{3-}$ could decay with a half-life of about 10^3 s. This could be sufficiently rapid to make direct observation of the transfer reaction difficult by n.m.r.

Decomposition, k_4

We used our measured value of the specific rate of the aging reaction 4 at 30 °C, 5×10^{-3} M^{-1} s^{-1}, and calculated the values at 0 and 15 °C shown in Table 2 with an activation energy of 9.8 kcal mol^{-1} obtained by Sokol and Brubaker (19). They measured $k_4 = 1.35 \times 10^{-3}$ M^{-1} s^{-1} for 0.17 M $Co(CN)_5^{3-}$, and DeVries obtained 1.5×10^{-3} M^{-1} s^{-1} at $\mu =$ 0.86 M and 30 °C (8). Measurements of k_4 by Burnett *et al.* were erratic (5). The aging reaction did not greatly affect the results of exchange reaction calculations, except at pressure below about 100 Torr where the effect of reaction 4 noticeably increased the concentration of $(HO)Co(CN)_5^{3-}$ which we have assumed to be catalytically inactive. In general, competition by the aging reaction was not significant.

The temperature-dependence of the rate constants k_2 and k_3, reported in Table 3, are shown in an Arrhenius plot in Fig. 8. The curvature of each parameter with T^{-1} is considered real. By bracketting hydrogen evolution and deuterium exchange data with calculated curves, the errors in k_2 and k_3 are estimated to be less than 10% and less than 20%, respectively. This is not enough to introduce the curvature shown in Fig. 8. We suggest that this deviation from linearity may be due to ion pair formation between potassium cations and cobalt complex anions. If it is assumed that the specific rate constants for the de-hydrogenation and transfer steps are higher for the ion-paired compared to the "free" $DCo(CN)_5^{3-}$ and $HCo(CN)_5^{3-}$ species, then the relative decrease in stability

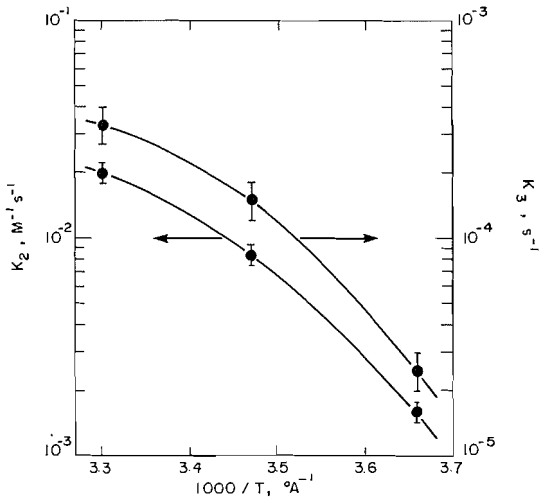

FIG. 8. Temperature dependence of constants k_2 and k_3.

of the ion-paired species with increasing temperature would result in a non-linear dependence of k_2 and k_3 on $1/T$ as observed. There is spectroscopic evidence for ion pair formation with $Co(CN)_5^{3-}$ in concentrated electrolyte solutions (15, 20), and pentacyanocobaltate(I) is believed to exist as a dimer possessing a proton bridge (21). Piringer and Farcas (10) have also implied that ion-pairing is important.

The activation enthalpies for k_2 and k_3 do not differ greatly. Tangents to the curves in Fig. 8 at 15 °C give values of about 12 kcal mol^{-1}. This agrees with the enthalpy of activation for k_2 of about 11 kcal mol^{-1} suggested by DeVries' data (8). Since the temperature dependence of the overall exchange reaction rate is governed by $\Delta H^{\neq}$ for k_2 and k_3 and must be at least as large as the lowest $\Delta H^{\neq}$, the 7 kcal mol^{-1} reported by Schindewolf (2) and by Piringer and Farcas (3, 10) appears somewhat low.

The isotope effect for the overall exchange was in the sequence $k_{D_2} > k_{HD} > k_{H_2}$. This is based on the experimental fact that the maximum in the HD yield was 5–10% higher than the maximum calculated assuming no H–D isotope effect for rate constants k_1 and k_2. The effect must originate with reactions 1 and 2 of the hydrogen absorption equilibrium. It is suggested that either an inverse sequence of specific rates for activation of D_2, HD, and H_2, $k[1a] > k[1b] > k[1c]$, or a normal sequence for

Can. J. Chem. Downloaded from www.nrcresearchpress.com by 210.87.254.42 on 09/05/12
For personal use only.

evolution of H_2, HD, and D_2, $k[2c] > k[2b] > k[2a]$, or both possibilities could account for this observation. Schindewolf (2) has argued that $k(H_2):k(D_2)$ is 1.5, based on the relative rate of para–ortho hydrogen conversion to D_2–H_2O isotope exchange catalyzed by $Co(CN)_5^{3-}$. By comparing our data in Figs. 2 and 4 it may be seen that under our conditions the rate of H_2 evolution, presumably representative of para-ortho conversion, is three times as great as the rate of D_2–H_2O exchange. The latter data are, of course, dependent on pH. In view of the complex dependence of the rate of D_2–H_2O exchange on k_1, k_2, and k_3 the applicability to our system of the isotope effect discussed by Schindewolf is doubtful.

In general, other homogeneous catalysts which activate hydrogen exhibit isotope effects, $k(H_2):k(D_2)$, in the range 1.0 ± 0.3 (17, 22–24). Because of the uncertainty in the value for the $Co(CN)_5^{3-}$ system, we chose to exclude this effect as a parameter in the calculations. Accordingly, it must be kept in mind that the rate constants quoted here have been evaluated with the basic assumption that the deuterium isotope effect may be neglected. The error limits assigned to k_2 ($\pm 10\%$) and k_3 ($\pm 20\%$) define the degree of fit to our data within this framework. Also, the different solubilities of D_2, HD, and H_2 will affect the corresponding equilibria, but information is not available on the magnitude of this effect in concentrated electrolyte solutions. Further refinement of specific rates k_1 and k_2 requires experimental evaluation of the deuterium isotope effect for reactions 1 and 2. Gross departures from the values quoted in Table 3 are not expected.

The equilibrium constant for absorption of hydrogen by $Co(CN)_5^{3-}$ obtained from the ratio of our rate constants $K = k_1/k_2$ is 0.4×10^5 M^{-1} at 25 °C and 1 M ionic strength. This is about a factor of three lower than has already been reported (5, 8, 16) at an ionic strength of 0.5 M. Since our data for the rate of the hydrogen evolution reaction have enabled the estimation of k_2 with an error of about 10%, the apparent discrepancy between these values for K must arise with k_1. It has already been noted that there is no experimental evidence for k_1 being greater than 830 M^{-1} s^{-1} at 1.0 M ionic strength. On the basis of present information we must conclude that K for the overall hydrogenation equilibrium in concentrated electrolytes decreases with increasing ionic strength.

It is clear that while the mechanism which has been proposed to explain D_2–H_2O exchange catalyzed by $Co(CN)_5^{3-}$ adequately accounts for the general features of our experimental data, discrepancies do exist. The non-linearity of k_2 and k_3 with T^{-1}, and the comparatively low value of K predicted by our results have been attributed to ion-pair equilibria not included in the simple scheme. The assumption that kinetic and thermodynamic isotope effects may be neglected does not seem justified. However, further experimental investigation of these topics is required before alternative or additional mechanisms will displace the present model.

The authors wish to thank their colleagues for helpful discussions, particularly Dr. Norman Sagert and Dr. Allan Symons. We also thank David Bell and the mass spectrometry section for completing all the isotopic analyses, and Mrs. D. Wuschke for programming and assistance.

1. G. A. MILLS, S. W. WELLER, and A. WHEELER. J. Phys. Chem. **63**, 403 (1959); G. A. MILLS, S. W. WELLER, and L. W. WRIGHT. U.S. Pat. 2 967 089 (1961).
2. U. SCHINDEWOLF. Ber. Bunsenges. Phys. Chem. **67**, 219 (1963); J. Chim. Phys. **60**, 124 (1963).
3. O. PIRINGER and A. FARCAS. Nature **206**, 1040 (1965); O. PIRINGER, A. FARCAS, and U. LUCA. International Conference on Coordination Chemistry.
4. W. P. GRIFFITH and G. WILKINSON. J. Chem. Soc. 2757 (1959).
5. M. G. BURNETT, P. J. CONNOLLY, and C. KEMBALL. J. Chem. Soc. A, 800 (1967).
6. G. M. WHITESIDES and G. MAGLIO. J. Am. Chem. Soc. **91**, 4980 (1969).
7. M. IGUCHI. J. Chem. Soc. Jap. **63**, 534 (1942).
8. B. DEVRIES. J. Catal. **1**, 489 (1962).
9. J. HALPERN and M. PRIBANIC. Inorg. Chem. **9**, 2616 (1970).
10. O. PIRINGER and A. FARCAS. Zeit. Phys. Chem. Neue Folge, **46**, 190 (1965).
11. F. BASOLO and R. G. PEARSON. Mechanisms of inorganic reactions. Wiley, New York. 1967. p. 36.
12. International critical tables, Vol. 3. McGraw-Hill, New York. 1928. p. 272.
13. H. STEPHEN and I. STEPHEN. Vol. 1, Part I. Solubilities of inorganic and organic compounds. MacMillan, New York. 1963. p. 80.
14. N. K. KING and M. E. WINFIELD. J. Am. Chem. Soc. **83**, 3366 (1961).
15. R. G. S. BANKS and J. M. PRATT. J. Chem. Soc. A, 854 (1968).
16. R. G. S. BANKS, P. K. DAS, H. A. O. HILL, J. M. PRATT, and R. J. P. WILLIAMS. Discuss. Faraday Soc. **46**, 80 (1968).

17. J. HALPERN and B. R. JAMES. Can. J. Chem. **44**, 671 (1966).
18. G. D. VENERABLE, II and J. HALPERN. J. Am. Chem. Soc. **93**, 2176 (1971).
19. C. S. SOKOL and C. H. BRUBAKER. J. Inorg. Nucl. Chem. **30**, 3267 (1968).
20. J. M. PRATT and R. J. P. WILLIAMS. J. Chem. Soc. A, 1291 (1967).
21. N. MAKI and Y. ISHIUCHI. Bull. Chem. Soc. Jap. **44**, 1721 (1971).
22. J. HALPERN. Ann. Rev. Phys. Chem. **16**, 103 (1965).
23. J. HALPERN, J. F. HARROD, and B. R. JAMES. J. Am. Chem. Soc. **88**, 5150 (1966).
24. P. B. CHOCK and J. HALPERN. J. Am. Chem. Soc. **88**, 3511 (1966).

Can. J. Chem. Downloaded from www.nrcresearchpress.com by 210.87.254.42 on 09/05/12
For personal use only.

Electrical Conductivity of Pure and Doped Ammonium Perchlorate Crystals

P. W. M. JACOBS, FRANCES E. LOVATT, and WEE LAM NG[1]

Department of Chemistry, The University of Western Ontario, London 72, Ontario

Received March 23, 1972

The conductivity of single crystals of pure ammonium perchlorate and of ammonium perchlorate doped with Ba^{2+} and with SO_4^{2-} ions has been measured at a frequency of 1591 Hz between room temperature and 260 °C. All three systems display a marked increase in conductivity at the temperature of the orthorhombic → cubic phase transition. It is suggested that this sudden increase in conductivity is more probably due to secondary effects (specifically, dislocation generation) than to the actual change in crystal structure. The general similarity between the results for pure and doped crystals tends to support a proton transfer mechanism for a.c. conductivity that does not involve vacancies. However, vacancies may be important in d.c. conductance mechanisms.

Nous avons mesuré la conductivité de cristaux uniques du perchlorate d'ammonium pur et contaminé avec des ions Ba^{2+} et SO_4^{2-}, à la fréquence de 1591 Hz, de la température de la pièce à 260 °C. Les trois systèmes montrent une augmentation sensible de la conductivité à la température de la transition orthorhombique → cubique. On suggère que cette soudaine augmentation de conductivité est probablement due à des effets secondaires (plus spécialement à la naissance de dislocation) plutôt qu'à des changements de la structure cristalline comme telle. La ressemblance générale entre les résultats pour les cristaux purs et contaminés suppose un mécanisme de transfert de proton pour la conductivité a.c., ce qui n'implique pas d'absences. Toutefois, les absences peuvent devenir un facteur important dans les mécanismes de conductance d.c.

[Traduit par le journal]

Canadian Journal of Chemistry, **50**, 3154 (1972)

Can. J. Chem. Downloaded from www.nrcresearchpress.com by 210.87.254.105 on 09/05/12
For personal use only.

The electrical conductivity of both compressed pellets and single crystals of ammonium perchlorate has been investigated before (1–5) but there have been no previous attempts to examine the effect on the conductivity of doping with divalent cation or anion impurities. A recent detailed study (5) of the effects of annealing, partial decomposition, and the adsorption of water and ammonia on the a.c. conductivity led to a proposed mechanism for charge transport involving proton transfer from NH_4^+ ions to proton defects (NH_3 molecules) on normal lattice sites in the cation sub-lattice. The proton defects were considered to be formed by proton transfer from NH_4^+ ions to water or ammonia molecules either on the surface or inside the crystal in voids or at dislocations. It was also suggested that in very thoroughly annealed crystals which had, however, not been heated to a temperature sufficient to induce thermal decomposition, proton defects would be formed by transfer of a proton from NH_4^+ to ClO_4^-. It was considered that these molecular defects would form primarily at the surface and at dislocations and internal boundaries. Of course, a surface NH_3 can be rapidly converted to a proton defect in the bulk by the process

$$[1] \qquad NH_4^+ (l) + NH_3 (s) \rightarrow \boxed{NH_3}_+ + NH_4^+ (s)$$

where (l) denotes a normal lattice site, $\square_+$ a cation vacancy, $\boxed{NH_3}_+$ a cation vacancy occupied by an ammonia molecule (= proton defect), and (s) the site where the ammonia molecule is first formed, adjacent to the surface or a dislocation. The migration of proton holes in the bulk we represent similarly by

$$[2] \qquad NH_4^+ (l) + \boxed{NH_3}_+ \rightleftharpoons \boxed{NH_3}_+ + NH_4^+ (l)$$

In unannealed crystals the role of NH_3 (s) as a proton acceptor in eq. 1 is assumed by water molecules present in the virgin crystal or deliberately introduced by exposure to water vapor (5). The main differences between pellets and single crystals arise from the dominance of surface effects in the former, *i.e.*, it is the water or ammonia adsorbed on the surface rather than that sorbed into the bulk that functions as a proton acceptor.

The activation energy E for proton migration, process 2, appears to be very small (5); that for the formation of proton defects depends on the acceptor and lies on the range 0.5–1.0 eV. For the formation of instrinsic molecular defects

$$[3] \qquad NH_4^+ (s) + ClO_4^- (s) \rightleftharpoons \boxed{NH_3}_+ (s) + \boxed{HClO_4}_- (s)$$

[1]Present address: Surface Physics, Cavendish Laboratory, Cambridge, England.

Can. J. Chem. Downloaded from www.nrcresearchpress.com by 210.87.254.105 on 09/05/12
For personal use only.

followed by process 1, E appears to be close to 0.85 eV (5). When (s) is a surface site, reaction 3 is the first step in the sublimation process. Such molecular defects are believed to be responsible for the anomalous thermodynamic properties of ammonium chloride (6). The conductivity of ammonium chloride has been investigated by Herrington and Staveley (6) and by Fuller and Patten (7). Isotope effects (7) indicate that protons are the charge carriers. Herrington and Staveley (6) proposed a three-stage mechanism for proton conduction in ammonium chloride which involves the participation of either cation or anion vacancies. These stages are: (*i*) proton transfer from NH_4^+ to Cl^- adjacent to a vacancy; (*ii*) the jump of either the NH_3 molecule into a cation vacancy, or the HCl molecule into an anion vacancy, depending on which type is present; (*iii*) proton transfer from HCl to NH_3. Since step (*iii*) involves a species that has interchanged with a vacancy, the final configuration differs from the initial one in that the cation or anion vacancy has moved one lattice site on its own sub-lattice. This mechanism is supported by the appearance of a low-temperature extrinsic region in NH_4Cl crystals doped with Cd^{2+} (6).

Our mechanism (5) for conduction in ammonium perchlorate via proton defects does not rely on the presence of cation or anion vacancies. However, it is possible to envisage cation vacancies acting as proton acceptors

[4] $$NH_4^+ (l) + \square_+ \rightarrow \boxed{NH_3}_+ + H^+ (l)$$

and it would seem important, therefore, to examine the effect of doping ammonium perchlorate with divalent cations or anions. An increase in conductivity on doping with either divalent cations or anions would support the Staveley mechanism, whereas an increase in σ on doping with cations and a decrease on doping with anions would support process 4. The absence of a significant effect would, by default, tend to support the charge transport mechanism based on process 2, plus either process 1 or 3, as the case might be.

The work described in this paper comprises measurements of the conductivity of ammonium perchlorate single crystals doped with Ba^{2+} and with SO_4^{2-} together with further measurements on pure ammonium perchlorate. A subsidiary aim was to look for any effects that could be ascribed to the orthorhombic → cubic phase transformation that occurs at around 240 °C. In previous work (5) such effects had not been carefully distinguished from those connected with thermal decomposition which occurs in the same temperature range.

Experimental

Ammonium perchlorate of 99.99% purity was purchased from the Fisher Scientific Co. Large single crystals of average size 12 × 12 × 4 mm were grown by slow cooling of a saturated solution of ammonium perchlorate containing seed crystals mounted on the arms of a glass crystal "tree" which was rotated continuously in alternate directions for 3½ revolutions by a 25 r.p.m. motor via a rack and pinion gear. Doped crystals were grown in a similar manner from solutions containing 0.1 mol% $(NH_4)_2SO_4$ or 1.0 mol% $Ba(ClO_4)_2$, respectively. It was expected that the crystals would contain much smaller concentrations of the foreign ions. Crystals were analyzed amperometrically with 0.001 M Pb^{2+} for SO_4^{2-} and 0.0018 M SO_4^{2-} for Ba^{2+}. Trial analyses with standard solutions showed that SO_4^{2-} down to 10^{-5} M and Ba^{2+} down to 10^{-3} M could be analyzed by this method. However, the crystal analyses were negative showing that they contained $< 10^{-2}$ mol% SO_4^{2-} and < 1 mol% Ba^{2+}, respectively. Nevertheless, the crystals did contain sufficient of these impurities to affect significantly their rate of thermal decomposition for the overall reaction time was shortened for both Ba^{2+}- and SO_4^{2-}-doped crystals. For example, the time to reach 50% decomposition at 230 °C was 350 min for the pure crystal, 200 min for the SO_4^{2-}-doped, and only 50 min for the Ba^{2+}-doped ammonium perchlorate.

The crystals were mounted in a conductivity cell similar to that described previously (8) except that a grounded guard ring electrode was employed. Conductance measurements were made at a frequency of 1591 Hz using a Wayne Kerr B221 transformer ratio arm bridge. The temperature of the crystal was measured by two Pt/Pt + 13% Rh thermocouples in contact with each of the Pt electrodes. The vacuum line included provision for admitting pure dry nitrogen to the conductance cell.

Results

Ammonium Perchlorate Containing Ba^{2+}

The dependence on temperature (T) of the specific conductance (σ) of a crystal doped with Ba^{2+} ions is shown in Fig. 1 in the form of a plot of log σT *vs.* T^{-1}. These data were obtained after a preliminary annealing procedure. After mounting the crystal in the conductance cell, the cell was evacuated to a pressure of $\sim 10^{-6}$ Torr and the temperature of the crystal was then raised slowly to 103 °C. It was annealed at 103 °C under vacuum for 21 h and then cooled slowly to room temperature (r.t.). After a further 16 h at r.t. dry nitrogen gas was admitted at a pressure of 400 Torr and the

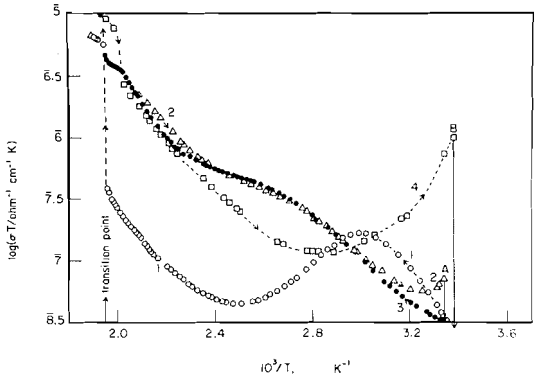

FIG. 1. Conductivity of a Ba^{2+}-doped ammonium perchlorate crystal. The numbers on the curves show the order in which the runs were performed. Arrows on the curves show whether measurements were made on heating or cooling. Vertical arrows (full lines) indicate conductivity changes on annealing in vacuum. Vertical arrows (broken lines) indicate the sudden increase in σ at the transition point.

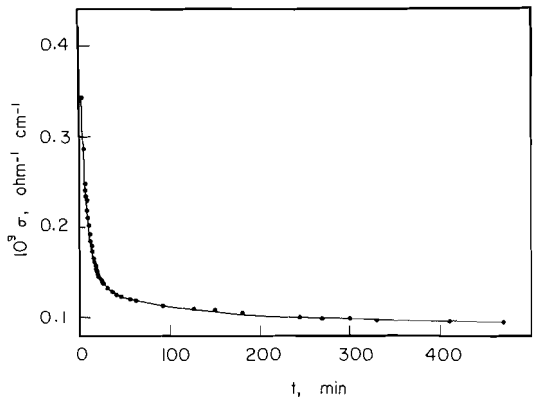

FIG. 2. Time-dependence of the specific conductance of an ammonium perchlorate crystal doped with Ba^{2+} during annealing at room temperature after partial thermal decomposition under 400 Torr nitrogen. The conductivity change corresponds to arrow B in Fig. 1.

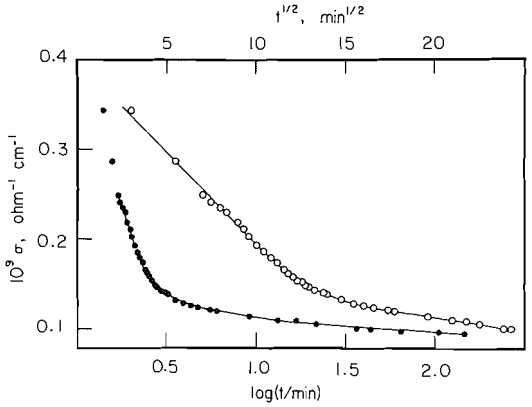

FIG. 3. Kinetics of the isothermal conductivity change shown in Fig. 2. ●, σ *vs.* $t^{1/2}$; ○, σ *vs.* log t.

measurements recorded in Fig. 1 were then made. Curve 1 shows the changes in conductivity that occurred on heating up to 255 °C. The conductivity at first increases, passes through a maximum at ~65 °C, and then decreases with further increase in temperature passing through a minimum at ~130 °C after which it increases steadily. This discontinuity in σ close to 240 °C appears to be associated with the orthorhombic → cubic phase change in ammonium perchlorate (9). However, on cooling (run 2) the conductivity remains an order of magnitude greater than, but roughly parallel to, curve 1. The low-temperature maximum has also disappeared. On reaching r.t. the nitrogen was pumped out and the apparatus evacuated continuously for 65 h during which time the conductivity fell by a factor of 2.2 (arrow A). On re-heating in 400 Torr dry nitrogen the conductivity curve (run 3) follows the cooling curve 2 rather closely from 60 to 150 °C. It then lies slightly below curve 2 and goes through a smaller increase than curve 1 around the transition point. On cooling (run 4) the conductivity follows curve 3 at first but then goes through a minimum, increasing steadily down to r.t. at which point it is a factor of 20 greater than before the heating cycle. On pumping for 26 h at r.t. the conductivity fell (arrow B) thus recovering its value before run 3. At this stage oxygen at a pressure of 400 Torr was admitted to the cell but no change in σ occurred.

The kinetics of the change in σ during the last evacuation at room temperature (arrow B in Fig. 1) were followed. The plot of σ against time t (Fig. 2) has a hyperbolic character. In Fig. 3 are shown plots of σ against log t and σ against $t^{1/2}$ to test if the rate-controlling step is desorption or a diffusion process. There are evidently two processes involved with widely different relaxation times. At short times the logarithmic function appears to give the better fit but at long times $\sigma \propto t^{1/2}$ is a better representation of the data.

Can. J. Chem. Downloaded from www.nrcresearchpress.com by 210.87.254.105 on 09/05/12
For personal use only.

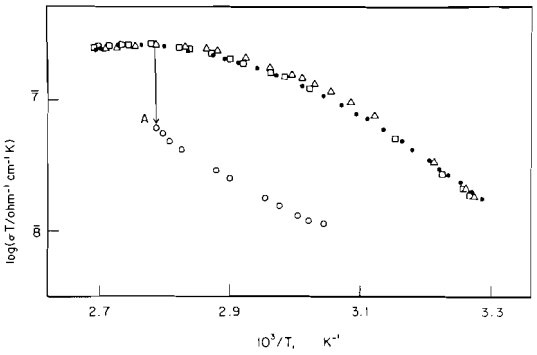

FIG. 4. Conductivity of a SO_4^{2-}-doped ammonium perchlorate crystal on thermal cycling between r.t. and 100 °C. After an initial anneal, as described in the text, the conductivity is reproducible provided the crystal is not heated to higher temperatures or suffers a prolonged anneal. If it is annealed, the conductivity decreases, arrow A; ●, run 1, heating; △, run 2, cooling; □, run 3, heating; ○, run 4, cooling.

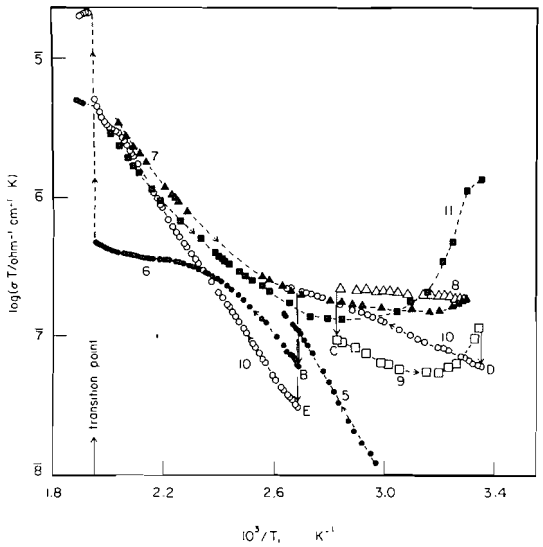

FIG. 5. Conductivity of a SO_4^{2-}-doped ammonium perchlorate crystal. The numbers indicate the order in which the runs were performed. Vertical arrows (full lines) indicate conductivity changes on annealing isothermally. Vertical lines (broken lines) indicate the increase in conductivity that occurs at the transition point.

Ammonium Perchlorate Containing SO_4^{2-}

The temperature dependence of the conductivity of a SO_4^{2-}-doped ammonium perchlorate crystal is shown in Figs. 4 and 5. Figure 4 shows the effects of thermal cycling between r.t. and ~100 °C. The crystal was first heated slowly in vacuum from r.t. to 102 °C and then annealed at this temperature in vacuum for 65 h. The crystal was then cooled slowly to r.t. and the conductivity measured during slow heating to 98 °C (run 1, Fig. 4). Below 50 °C, σT obeys the Arrhenius equation with an activation energy E of 0.70 eV. At higher temperatures the slope of the curve decreases and it passes through a very flat maximum at ~90 °C (*cf.* run 1, Fig. 1). On cooling (run 2) the curve is re-traced with fair reproducibility. At r.t., 400 Torr nitrogen was introduced into the cell and on reheating (run 3) curve 1 was again reproduced, showing that the crystal is in a reproducible state after the initial anneal and also that the conductivity is independent of whether the crystal is in vacuum or in a nitrogen atmosphere. The crystal was now annealed in nitrogen for a further 88 h at 98 °C when the conductivity fell by a factor of 4 (arrow A). The activation energy over the linear section (run 4) is 0.65 eV.

Further experiments, involving heating to higher temperatures, are shown in Fig. 5. The crystal was reheated to 106 °C (run 5, $E = 0.65$ eV) and on further annealing for 18 h at 100 °C, σ fell by 70% (arrow B). Run 6 shows the variation in σT as the crystal was heated from 100 °C (point B in Fig. 5). Between 185 and 225 °C the conductivity increases very slowly with temperature, the slope at the point of inflection corresponding to $E = 0.04$ eV. Above 225 °C σ increases somewhat and then it increases suddenly by a factor of 10 at the transition point. On cooling, run 7, the low temperature conductivity is much larger than previously (*cf.* Fig. 4). On re-heating the conductivity is substantially independent of temperature up to 79 °C but on annealing at this temperature (still under nitrogen) for 16 h, σ fell by a factor of 2.5 (arrow C). The significant feature on cooling again to r.t. (run 9) was the increase in σ that occurred at low temperatures. (This is also evident, but less marked, in run 7.) The system was then evacuated for 28 h at r.t. and the conductivity fell by 80% (arrow D). The crystal was then heated in nitrogen to 100 °C, annealed there for 64 h (run 10, arrow E), and then heated to 253 °C ($E = 0.62$ eV, over the range 110–135 °C). There was again a sudden marked increase in σ at the transition point. On cooling

Can. J. Chem. Downloaded from www.nrcresearchpress.com by 210.87.254.105 on 09/05/12
For personal use only.

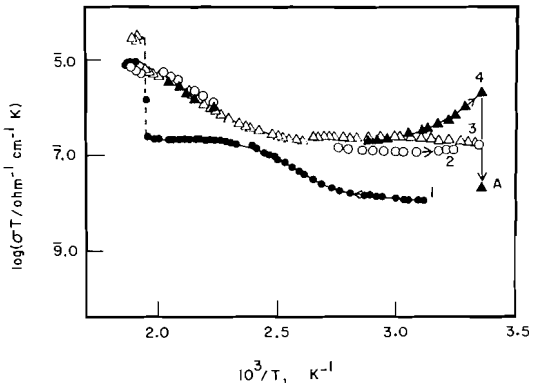

FIG. 6. Conductivity of a pure ammonium perchlorate crystal after a very thorough anneal at 116 °C. The numbers indicate the order in which the runs were performed. The vertical arrow A shows the decrease in conductivity that occurs on pumping at room temperature after partial thermal decomposition and the vertical lines (broken lines) show the increase in σ that occurs at the transition point.

(run 11) the significant feature is the big increase in σ at low temperatures.

Pure Ammonium Perchlorate

The conductivity plot for a pure ammonium perchlorate crystal is shown in Fig. 6. This crystal had been subjected to thermal cycling between r.t. and 116 °C and had also been very thoroughly annealed at 116 °C but had not been heated above this temperature prior to the first run shown (1 in Fig. 6). The conductivity is at first practically independent of temperature, increases above the anneal temperature and is again almost constant from 160 °C to the transition point. In this run it was possible to fix the sharp increase in σ quite precisely since the conductivity changed by a factor of 21 between 238.6 and 239.6 °C. The crystal was again under 400 Torr of nitrogen during this experiment. The curves 2, 3, and 4 show the conductivity changes during successive cooling, heating, and cooling cycles. As with the SO_4^{2-}-doped crystal there was a second but smaller increase in σ at the transition point on heating the crystal above 240 °C for the second time, (run 3). Again, there is a marked increase in σ on cooling to r.t. (run 4). However, the conductivity fell by two orders of magnitude on pumping at r.t. for 18 h.

The time-dependence of σ on annealing a pure (undecomposed) ammonium perchlorate crystal at 89 and 114 °C had been studied previously (5). Plots of σ against $t^{1/2}$ were linear and showed only a single relaxation time, in contrast to Fig. 3. Again in contrast to Fig. 3 plots of σ against log t showed a decided curvature.

Discussion

Ammonium perchlorate at room temperature belongs to the space group *Pnma* which also includes barium sulfate. Indeed the orthorhombic crystal structures and lattice parameters are so similar that Ba^{2+} and SO_4^{2-} were chosen as the divalent impurities to be incorporated in the ammonium perchlorate crystals. The NH_4^+ ions are freely rotating down to very low temperatures, at least 20 K (9), thus indicating the absence of significant hydrogen-bonding (10). The phase transition to the cubic form is accompanied by the onset of free rotation of the perchlorate anions. The temperature generally quoted for the phase transition is 240 °C (9).

The effect on its conductivity of doping a uni-univalent ionic salt with divalent ions is well understood when charge transport proceeds by the motion of vacancies or interstitial ions. One anticipates the low temperature will be increased by doping and that a sufficiently high temperature (depending on the impurity concentration) the conductivity of the pure and doped crystals will all follow the same (intrinsic) curve. Unfortunately, there is no such thing as truly intrinsic behavior for ammonium perchlorate single crystals although both compressed pellets and single crystals will yield reproducible results on the same sample if it is carefully annealed. (It should be stressed here that these remarks apply to a.c. conductance measurements. We have made no d.c. measurements and it is possible for these to yield different results if, for example, there should be a substantial orientational polarization.) Thus one should not expect different crystals to show even qualitatively the same behavior. This is due to the very important role played by adsorbed or occluded water in the a.c. conductance mechanism.

The experimental results for pure and doped ammonium perchlorate crystals (Figs. 1, 4, 5, and 6) can be understood in terms of the proton

Can. J. Chem. Downloaded from www.nrcresearchpress.com by 210.87.254.105 on 09/05/12
For personal use only.

Can. J. Chem. Downloaded from www.nrcresearchpress.com by 210.87.254.105 on 09/05/12
For personal use only.

defect mechanism advanced previously (5) without any need to invoke a mechanism involving vacancies. It may be, in view of the low doping levels achieved, that there are some minor effects due to vacancies but the present results are dominated by water in the crystals. If ammonium perchlorate is thoroughly annealed at about 100 °C then reproducible results are obtained on thermal cycling (Fig. 4). The broad maximum indicates that saturation of carriers has been achieved, *i.e.*, that all the available water has been utilized as a proton acceptor. On either prolonged annealing (Fig. 4, A; Fig. 5, B and E) or further increase in temperature (Fig. 1, run 1) the conductivity decreases as water is driven off, evidently from inside the crystal as the kinetics are diffusion controlled (5). The apparent differences between the annealing kinetics of Ba^{2+}-doped ammonium perchlorate (Figs. 2, 3) and pure ammonium perchlorate arise because the experiments described in ref. 5 refer to undecomposed crystals that had never been heated above 120 °C. Hence diffusion processes prevail over desorption. The experiment described here was performed on a partially decomposed crystal. Now decomposition causes the crystal to become porous (11) and the resultant increase in (internal) surface area results in detectable desorption of water. This is followed by the slower loss of water by diffusion out of the crystal and hence two processes are observed (Figs. 2, 3). On further heating (*e.g.* runs 6 and 10, Fig. 5, or run 1 in Fig. 1) the conductivity again increases. In run 10 of Fig. 5 there is reasonable Arrhenius behavior up to 185 °C with $E = 0.62$ eV, indicating proton transfer to water, not intrinsic behavior.

Why does the conductivity in run 6 saturate while that in run 10 goes on increasing? Because in the latter there is more water available, this having come from the occlusion of water formed by thermal decomposition of the crystal during run 6. Notice that in runs 7, 9, and 11 the conductivity increases at low temperature as more water is adsorbed by the crystal from the gas phase. Some of this water can be removed by pumping (D in Fig. 5). These results are not specific to the SO_4^{2-}-doped crystals and broadly similar behavior can be seen in Figs. 1, 5, and 6.

The phase transition is clearly marked by a sudden increase in σ, runs 1 and 3 in Fig. 6, runs 6 and 10 in Fig. 5, and runs 1 and 3 in Fig. 1. However, there is substantial hysteresis and the conductivity does not follow the heating curve. There are at least three possible explanations for this: (*a*) the cubic phase might be metastable and revert only slowly to the orthorhombic structure; (*b*) the lattice reorganization during the phase change might re-distribute sufficient water within the crystal or generate a sufficient number of dislocations to increase the conductivity permanently; (*c*) the water formed by concomitant thermal decomposition might be responsible for the observed increase in σ. The increase in conductivity on heating is too sharp to be accounted for entirely by thermal decomposition. Thus the phase transition undoubtedly does increase the conductivity substantially but whether this is a direct result of the change in crystal structure is unclear. It could be due to re-location of water, generation of dislocations or due to the onset of free rotation of the perchlorate anions facilitating the transfer of protons from NH_4^+ to ClO_4^-.

Conclusion

Although ammonium perchlorate crystals doped with Ba^{2+} or SO_4^{2-} show substantially different characteristics to pure crystals on thermal decomposition (12), there are no differences in their a.c. electrical conductivity that can be ascribed directly to the presence of vacancies in the doped crystals. The changes in the conductivity of these crystals on thermal cycling can be explained in terms of charge transport via proton defects. Proton defects (NH_3 molecules) are formed by transfer of a proton from an NH_4^+ lattice cation to water molecule or to a ClO_4^- anion. Defect formation occurs initially at special sites such as the surface or in the neighborhood of dislocations.

Finally, it should be emphasized that all the measurements described in this paper were made at the single frequency of 1591 Hz and it is certainly possible that at this frequency other dielectric loss mechanisms are operative in addition to conductance losses.

We wish to thank the National Research Council of Canada for financial support of this work.

1. P. ZIRKIND and E. S. FREEMAN. Nature, **199**, 1280 (1963).
2. H. WISE. J. Phys. Chem. **71**, 2843 (1967).
3. J. N. MAYCOCK, V. R. PAI VERNEKER, and C. S. GORZYNSKI. Solid State Commun. **5**, 225 (1967).
4. V. V. BOLDYREV. Dokl. Akad. Nauk SSSR, **181**, 1406 (1968).
5. P. W. M. JACOBS and WEE LAM NG. J. Phys. Chem. Solids. In press.
6. THELMA M. HERRINGTON and L. A. K. STAVELEY. J. Phys. Chem. Solids, **25**, 921 (1964).
7. R. G. FULLER and F. W. PATTEN. J. Phys. Chem. Solids, **31**, 1539 (1970).
8. A. R. ALLNATT and P. W. M. JACOBS. Trans. Faraday Soc. **58**, 116 (1962).
9. P. W. M. JACOBS and H. M. WHITEHEAD. Chem. Rev. **69**, 551 (1969).
10. R. E. RICHARDS and T. SCHAEFER. Trans. Faraday Soc. **57**, 210 (1961).
11. P. J. HERLEY, P. W. M. JACOBS, and P. W. LEVY. Proc. Roy. Soc. Lond. A, **318**, 197 (1970).
12. P. W. M. JACOBS and WEE LAM NG. J. Solid State Chem. To be published.

Can. J. Chem. Downloaded from www.nrcresearchpress.com by 210.87.254.105 on 09/05/12
For personal use only.

Model Calculations on the Influence of Mechanical and Electrical Anharmonicity on Infrared Intensities: Relation to Hydrogen Bonding

THÉRÈSE DI PAOLO,[1] C. BOURDÉRON, AND C. SANDORFY
Département de Chimie, Université de Montréal, Montréal, Québec

Received April 20, 1972

The influence of mechanical and electrical anharmonicity on the intensity of X—H stretching vibrations is investigated by means of model calculations in relation to hydrogen bonding. It is found that while both kinds of anharmonicities have a significant effect on the intensity, they cannot explain the characteristic increase in intensity of the fundamental and the equally characteristic decrease in the intensity of the first overtone. It is shown that not only the first but both these phenomena are due to the large value of the first derivative of the dipole moment in hydrogen bonded systems. This is linked to the possibility that the effect of electrical anharmonicity ($d^2\mu/dQ^2$) might be cancelled by a high value of $(d\mu/dQ)_e$ in the expression of the overtone intensity.

L'influence des anharmonicités mécanique et électrique sur l'intensité des vibrations de valence X—H est étudiée à l'aide de calculs de modèle en relation avec la liaison hydrogène. On trouve que les deux types d'anharmonicité ne peuvent pas expliquer l'augmentation caractéristique de l'intensité de la fondamentale et la diminution également caractéristique de l'intensité de la première harmonique même si elles ont un effet significatif sur l'intensité. On montre que ces deux phénomènes sont dûs à la grande valeur de la première dérivée du moment dipolaire dans les liaisons hydrogènes. L'effet de l'anharmonicité électrique ($d^2\mu/dQ^2$) peut être compensé par une grande valeur de $(d\mu/dQ)_e$ dans l'expression de l'intensité de l'harmonique.

Canadian Journal of Chemistry, **50**, 3161 (1972)

Can. J. Chem. Downloaded from www.nrcresearchpress.com by 210.87.254.40 on 09/05/12
For personal use only.

Introduction

The formation of hydrogen bonds has a marked influence on the frequency, intensity, and width of infrared X—H stretching bands. (X is O or N in the most important cases). It has been concluded, in previous publications from this laboratory (1, 2), that the increase in mechanical anharmonicity accounts for a large part of the frequency shift which occurs when the OH groups of alcohols are engaged in hydrogen bonding, and that it is also an important factor causing the great width of the hydrogen bonded OH stretching bands. These studies concerned mainly the so called "polymer" band of alcohols.

The influence of mechanical anharmonicity on the intensities has not been studied systematically. On the other hand electrical anharmonicity has been linked (3, 4), to the surprising weakness of the first polymer overtone (5).

The purpose of the present study was to obtain an insight into the effect of mechanical and electrical anharmonicity on the intensity of the fundamental and the first overtone of X—H stretching bands. An explanation was sought for the increase in the intensity of the fundamental by about an order of magnitude (*cf.* 6), and for the decrease in the intensity of the first overtone, characteristic of many hydrogen bonded systems. This has been attempted through model calculations. A somewhat similar study of the frequencies was carried out previously by Foldes and Sandorfy (7).

The transition moment for a vibrational transition of a diatomic oscillator can be given by:

$$R^{v'v''} = \int \Psi^*_{v'} \mu \Psi_{v''} \, d\tau \qquad [1]$$

where v' and v'' are the vibrational quantum numbers for the upper and lower vibrational states. The potential will be represented to the second order by the usual expansion

$$V = \tfrac{1}{2}kQ^2 + k_3Q^3 + k_4Q^4 \qquad [2]$$

where k, k_3, and k_4 are the harmonic, cubic, and quartic potential constants, respectively, and Q is the normal coordinate. The variable dipole moment will be taken to be

$$\mu(Q) = \mu_e + \mu_1 Q + \mu_2 Q^2 \qquad [3]$$

where μ_e is the equilibrium dipole moment,

$$\mu_1 = \left(\frac{d\mu}{dQ}\right)_e, \qquad \mu_2 = \tfrac{1}{2}\left(\frac{d^2\mu}{dQ^2}\right)_e \qquad [4]$$

[1]Holder of NRCC postgraduate scholarship 1970–1972.

Can. J. Chem. Downloaded from www.nrcresearchpress.com by 210.87.254.40 on 09/05/12
For personal use only.

and we have neglected higher terms. The effect of the next term in the expansion of μ ($\mu_3 Q^3$) will be examined in a separate note (8). Then

$$[5] \qquad R^{v'v''} = \mu_1 R_1^{v'v''} + \mu_2 R_2^{v'v''}$$

where

$$R_1^{v'v''} = \int \Psi_{v'}^* Q \Psi_{v''} \, d\tau$$

and

$$R_2^{v'v''} = \int \Psi_{v'}^* Q^2 \Psi_{v''} \, d\tau$$

The Ψ_v will be harmonic oscillator wave functions perturbed to the second order. The expressions for the R_i were given by Herman and Shuler (9) and will not be reproduced here.[2] The intensities of the fundamental and the first overtone are, from Herman and Shuler's equation [10]:

$$[6] \quad A^{1,0} = \left(\frac{8\pi^3 N_{v^0}}{3hc}\right) \times \omega^{1,0} \left\{\mu_1\left(\frac{1}{\sqrt{2}} - \frac{3}{2\sqrt{2}} g + \frac{11}{4\sqrt{2}} b^2\right) + \mu_2\left(-\frac{5b}{\sqrt{2}} + \frac{88}{\sqrt{2}} bg - \frac{715}{12\sqrt{2}} b^3\right)\right\}^2$$

$$[7] \quad A^{2,0} = \left(\frac{8\pi^3 N_{v^0}}{3hc}\right) \times \omega^{2,0} \left\{\sqrt{2}\mu_1\left(\frac{b}{2} - \frac{111}{8} bg - \frac{71}{48} b^3\right) + \frac{\mu_2}{\sqrt{2}}\left(1 - \frac{15}{4} g + \frac{3}{8} b^2\right)\right\}^2$$

where ω is the wave number in cm^{-1}; $b \equiv k_3/\omega_e$, $g \equiv k_4/\omega_e$, and N_{v^0} is the number of molecules per cm^3 in the lower vibrational level. (The validity of eqs. 6 and 7 is not linked to the choice of these units, however).

Outline of the Work

(*I*) As a starting point, we needed reasonable representative values for k_3, k_4, and the first and second derivatives of the dipole moment for a band not perturbed by hydrogen bonding. We choose the *free* OH stretching mode of 2,6-ditertiary-butyl-paracresol, which, for steric reasons, does not enter into any association at room temperature. We measured the band due to the fundamental on a Perkin–Elmer model 621 spectrometer and the first overtone on a Cary 17 instrument. We computed the anharmonicity constant from the observed frequencies and, from these, the potential constants (see below). We then determined the intensities from the band areas, through the Lorentz (Cauchy) formula. Thus, having $A^{1,0}$, $A^{2,0}$, k_3, and k_4, we could compute the squares of μ_1 and μ_2 from eqs. 6 and 7. We then examined the influence of k_3, k_4, μ_1, and μ_2 on the absorption intensities of 2,6-ditertiary-butyl-paracresol. We successively put each of these parameters equal to zero while keeping the others unchanged, and computed $A^{1,0}$, $A^{2,0}$ in each case.

(*II*) In the second part of our work we varied k_3, k_4, μ_1, and μ_2 separately between *wide limits* in order to approach conditions prevailing in hydrogen bonded systems. We then attempted to explain the usually large increase in the intensity of the fundamental and the decrease in the intensity of the first overtone.

Results of the Calculations

(*I*) Second order perturbation theory is known to be valid when applied to the free OH stretching vibration (10). This implies that k_4 is very small, and we therefore neglected it, since our aim was merely to obtain starting values. k_3 can then be obtained from the expression of the first anharmonicity constant ($X = (15k_3^2/4\omega_e) - (3/2)\,k_4$ in cm^{-1}). We thus found from

$$X = \nu_{01} - \frac{\nu_{02}}{2} = \frac{\nu_{02}}{2} - \frac{\nu_{03}}{3} = \frac{\nu_{03}}{3} - \frac{\nu_{04}}{4}$$

$X = 88\ cm^{-1}$, $\omega_e = 3826\ cm^{-1}$, $k_3 = -300\ cm^{-1}$. (The measured values of ν_{03} and ν_{04} were 10 418 and 13 540 cm^{-1}. As to the value of k_3 in similar cases see, for example, ref. 11 or 12.)

Experimentally we found

$$A^{1,0} = 12\,800\ l\ mol^{-1}\ cm^{-2}$$

$$A^{2,0} = \quad 310\ l\ mol^{-1}\ cm^{-2}$$

We fed these values of the band areas and k_3 and k_4 into eqs. 6 and 7 to compute μ_1 and μ_2. In order to circumvent the difficulty due to the presence of cross terms in these equations, we first took their square roots. The values of the μ_i

[2] A more elaborate treatment was given by Toth *et al.* (15) and should be used, if quantitative results were sought for given molecules.

Can. J. Chem. Downloaded from www.nrcresearchpress.com by 210.87.254.40 on 09/05/12
For personal use only.

obtained with the two possible different combinations of signs are given in Table 1.

Since we have no sure way of determining their signs we had to consider both these combinations ((+ +) and (+ −)) where the signs relate to eqs. 6 and 7, respectively, in each bracket. (The two other combinations in which all + are replaced by − and *vice versa* yield the same results with opposite signs.) We are going to describe the results obtained with each of these two combinations of signs in the hope of being led to the right combination by making comparisons with experiment. Table 2 contains the results.

In order to assess the contribution of mechanical anharmonicity to the intensities given in Table 2, we carried out another set of calculations in which mechanical anharmonicity was neglected (that is $k_3 = k_4 = 0$); and harmonic oscillator wave functions were used for obtaining the expressions of $A^{1,0}$ and $A^{2,0}$. (The matrix components needed for this and the previous calculations were given, for example, by Barchewitz (13)). The results are shown in Table 3.

Tables 2 and 3 show that the influence of electrical and mechanical anharmonicity on the intensity of the fundamental is small. The difference between (+ +) and (+ −) is much greater without mechanical anharmonicity than with it. Furthermore, without electrical anharmonicity the overtone is much weaker.

(*II*) We varied separately k_3, k_4, and μ_2 while keeping the values of the others unchanged and then we varied them jointly.

The fixed values were, as before,

$$k_3 = -300\ \text{cm}^{-1}, \qquad k_4 = 0$$

and the fixed values of μ_2 were as given before for the two different combinations of signs (Table 1).

We varied k_3 from -200 to $-400\ \text{cm}^{-1}$. This corresponds to anharmonicity constants (X) equal to 50 and 200 cm^{-1}. All the anharmonicity constants for associated alcohols, amines, etc. fall into this range (2, 14).

$A^{1,0}$ kept increasing from $k_3 = -200$ to $k_3 = -400\ \text{cm}^{-1}$ but in no case did the total variation exceed 10%. This is true even if $\mu_2 = 0$ and even if k_4 varies from $+k_3/10$ to $-k_3/10$ for both (+ +) and (+ −).

TABLE 1. Values of the first and second derivatives of the dipole moment for the OH stretching vibration of 2,6-di-tert-butylparacresol for the two possible selection of signs in the square roots of eqs. 6 and 7

	μ_1 (e.s.u. cm)	μ_2 (e.s.u. cm)
(+ +)	1.53×10^{-19}	3.03×10^{-20}
(+ −)	1.67×10^{-19}	-5.72×10^{-21}

TABLE 2. The influence of electrical anharmonicity on the intensities of the fundamental and first overtone of the OH stretching vibration of 2,6-di-tert-butylparacresol: $k_3 = -300\ \text{cm}^{-1}$, $k_4 = 0$

	$A^{1,0}$ (l $\text{mol}^{-1}\ \text{cm}^{-2}$)	$A^{2,0}$ (l $\text{mol}^{-1}\ \text{cm}^{-2}$)
(*a*) Case (+ +)		
$\mu_1 = 1.53 \times 10^{-19}$ e.s.u. cm	12 800	310
$\mu_2 = 3.03 \times 10^{-20}$ e.s.u. cm		
$\mu_1 = 1.53 \times 10^{-19}$ e.s.u. cm	11 000	120
$\mu_2 = 0$		
(*b*) Case (+ −)		
$\mu_1 = 1.67 \times 10^{-19}$ e.s.u. cm	12 800	310
$\mu_2 = -5.72 \times 10^{-21}$ e.s.u. cm		
$\mu_1 = 1.67 \times 10^{-19}$ e.s.u. cm	13 200	150
$\mu_2 = 0$		

TABLE 3. The influence of electrical anharmonicity on the intensities of the fundamental and first overtone of the OH stretching vibration of 2,6-di-tert-butylparacresol: $k_3 = 0$, $k_4 = 0$

	$A^{1,0}$ (l $\text{mol}^{-1}\ \text{cm}^{-2}$)	$A^{2,0}$ (l $\text{mol}^{-1}\ \text{cm}^{-2}$)
(*a*) Case (+ +)		
$\mu_1 = 1.53 \times 10^{-19}$ e.s.u. cm	10 600	820
$\mu_2 = 3.03 \times 10^{-20}$ e.s.u. cm		
$\mu_1 = 1.53 \times 10^{-19}$ e.s.u. cm	10 600	0
$\mu_2 = 0$		
(*b*) Case (+ −)		
$\mu_1 = 1.67 \times 10^{-19}$ e.s.u. cm	12 800	30
$\mu_2 = -5.72 \times 10^{-21}$ e.s.u. cm		
$\mu_1 = 1.67 \times 10^{-19}$ e.s.u. cm	12 800	0
$\mu_2 = 0$		

The intensity of the first overtone decreases steadily from $k_3 = -200$ to $k_3 = -400\ \text{cm}^{-1}$, the total variation being about 40% for (+ +) and 50% for (+ −).

In the case of (+ +) if μ_2 is varied from 1.5×10^{-20} e.s.u. cm to 6.0×10^{-20} while k_3 and k_4 are kept constant, $A^{1,0}$ varies by about $\pm 20\%$ with respect to its previous value of 12 800. $A^{2,0}$ is

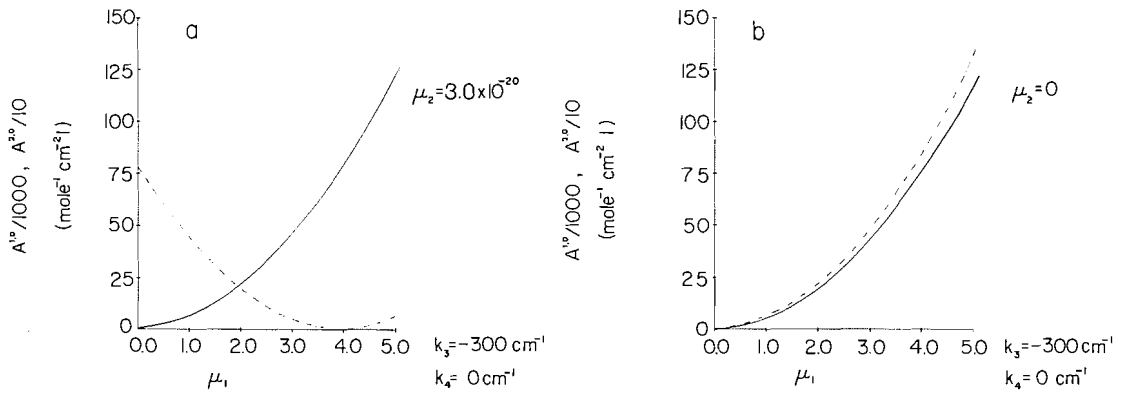

FIG. 1. Variation of the intensities of the fundamental — and the first overtone ····· as a function of $\mu_1 = d\mu/dQ$ for case (+ +); (*a*) for $\mu_2 = 3.0 \times 10^{-20}$ e.s.u. cm; (*b*) for $\mu_2 = 0$. The numbers on the abscissa should be multiplied by 10^{-19} e.s.u. cm.

practically zero for 1.5×10^{-20} and, for 6.0×10^{-20} it increases by an order of magnitude with respect to its value at 3.0×10^{-20} e.s.u. cm (30). For (+ −) the variations are very slight for both the fundamental and the overtone. This is expected in view of the small value of μ_2 which we have obtained in this case. The simultaneous variation of k_3, k_4, and μ_2 between the limits indicated above leads only to slight departures from these results.

On the whole we can say that variation of the mechanical and electrical anharmonicities between reasonable limits varies $A^{1,0}$ by about 20% at most.

(*III*) These results would have a certain interest if we were dealing with infrared intensities in general, but do not explain the intensity changes observed with hydrogen bonded systems.

So we varied μ_1 from zero to about six times its original fixed value. Figure 1*a* shows the obtained variation of the intensities $A^{1,0}$ and $A^{2,0}$ for the case (+ +) while k_3 was equal to $-300\ \text{cm}^{-1}$, k_4 to 0, and μ_2 had its fixed value. It is a striking result. Whereas the intensity of the fundamental undergoes a rapid increase when μ_1 increases, the intensity of the first overtone decreases rapidly in accord with experimental observation.

If we set $\mu_2 = 0$, that is, if we have no electrical anharmonicity, the picture changes completely and $A^{1,0}$ and $A^{2,0}$ exhibit a parallel increase with increasing μ_1 (Fig. 1*b*).

The reason for this is found if we take a closer look at the expression of $A^{2,0}$ (eq. 7). While the coefficient of μ_1 is normally small in this expression, and μ_2 is the main factor in determining the intensity of the first overtone, a very large value of μ_1 can cancel the contribution of μ_2 because of the negative value of the first term in eq. 7. For (+ −) the intensities of both the fundamental and first overtone increase with increasing μ_1 (Fig. 2*a*, *b*), whether μ_2 is different from zero or not. This is contradictory to what is observed in the case of hydrogen bonds and it leads to (+ +) as the right combination of signs in eqs. 6 and 7.

It is then clear that the decrease in intensity of the first overtone does not necessarily imply a decrease in electrical anharmonicity as might have been thought (4). It is connected with the high value of μ_1, making a compensation possible between the terms containing μ_1 and μ_2 in eq. 7.

It can be equally seen from eq. 7 that mechanical anharmonicity is needed to give μ_1 an appreciable coefficient. As we ascertained, any value of k_3 from -200 to $-400\ \text{cm}^{-1}$ would be sufficient.

Discussion and Conclusions

It follows from the above results that neither mechanical nor electrical anharmonicity can explain the most important intensity changes that occur upon hydrogen bond formation; the large increase in the intensity of the fundamental and a large decrease in the intensity in the first

Can. J. Chem. Downloaded from www.nrcresearchpress.com by 210.87.254.40 on 09/05/12
For personal use only.

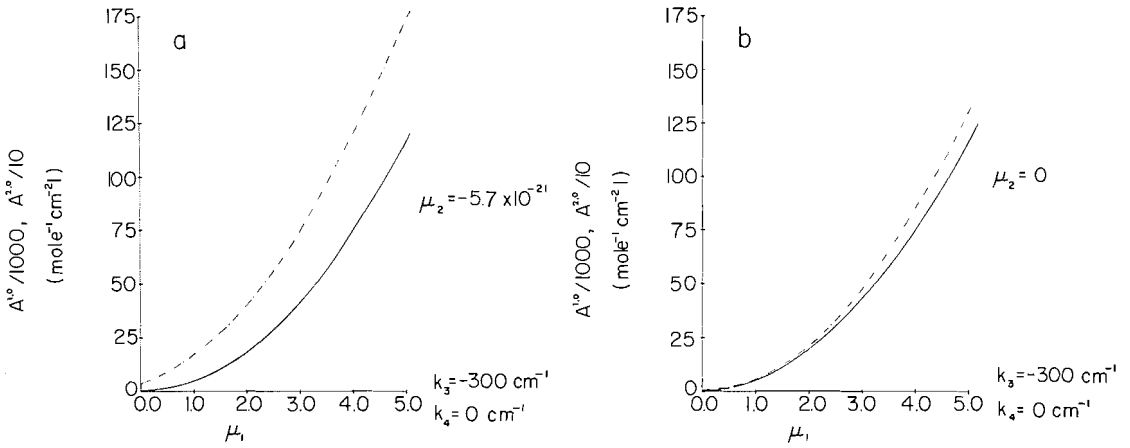

FIG. 2. Variation of the intensities of the fundamental — and the first overtone ····· as a function of $\mu_1 = d\mu/dQ$ for case (+ −); (*a*) for $\mu_2 = -5.7 \times 10^{-21}$ e.s.u. cm; (*b*) for $\mu_2 = 0$. The numbers on the abscissa should be multiplied by 10^{-19} e.s.u. cm.

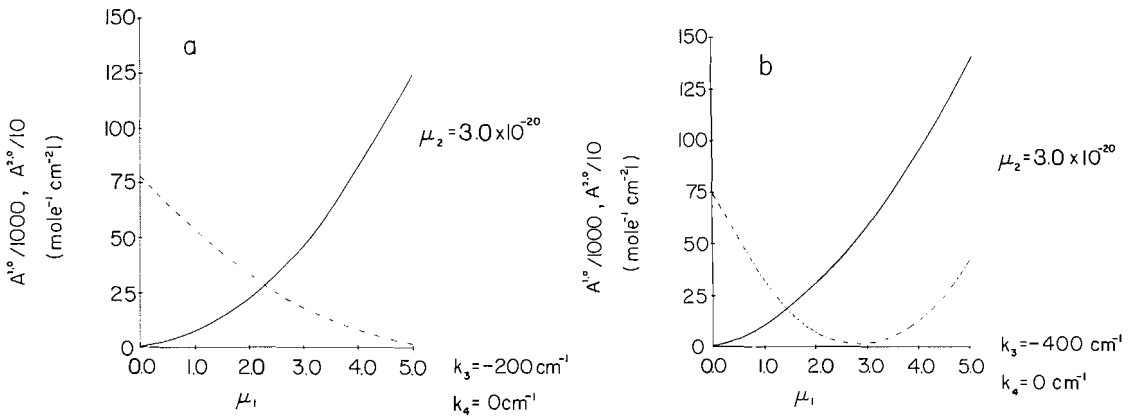

FIG. 3. Variation of the intensities of the fundamental — and the first overtone ····· as a function of $\mu_1 = d\mu/dQ$ for case (+ +) with $\mu_2 = 3.0 \times 10^{-20}$ e.s.u. cm; (*a*) $k_3 = -200\,\text{cm}^{-1}$; (*b*) $k_3 = -400\,\text{cm}^{-1}$. The numbers on the abscissa should be multiplied by 10^{-19} e.s.u. cm.

overtone. We need, of course, the large variation of the dipole moment (μ_1) to explain the high intensity of the fundamental. We have now shown that a high value of μ_1 equally explains the low intensity of the first overtone with any reasonable values of the anharmonicities. It is important to point out that agreement with the experimental facts requires that μ_1 and μ_2 have the same sign.

We might go a step further. It has been found previously (3) in the case of self-associated alcohols that only the polymer bands (OH bonds in inner positions, not in small rings) show the above mentioned two main intensity changes; dimers and oligomers (like cyclic trimers and tetramers) have weaker fundamentals and relatively strong overtones. This is actually helpful in ascertaining the presence of certain associated species in liquid or dissolved alcohols and amines (14). Now, in looking at Fig. 1*a* we see that a relatively small change in μ_1 can bring about large differences in the relative intensities of the fundamental and its first overtone, giving a qualitative explanation of the different behavior of oligomer bands and polymer bands.

We acknowledge financial assistance from the National Research Council of Canada.

Can. J. Chem. Downloaded from www.nrcresearchpress.com by 210.87.254.40 on 09/05/12
For personal use only.

1. A. FOLDES and C. SANDORFY. J. Mol. Spectrosc. **20**, 62 (1966).
2. M. ASSELIN and C. SANDORFY. J. Mol. Struct. **8**, 145 (1971).
3. C. BOURDÉRON, J.-J. PÉRON, and C. SANDORFY. J. Phys. Chem. **76**, 864 (1972).
4. J.-J. PÉRON, C. BOURDÉRON, and C. SANDORFY. Can. J. Chem. **49**, 3901 (1971).
5. W. A. P. LUCK and W. DITTER. J. Mol. Struct. **1**, 261 (1967–68).
6. S. BRATOS and D. HADZI. J. Chem. Phys. **27**, 991 (1957).
7. A. FOLDES and C. SANDORFY. Can. J. Chem. **49**, 505 (1971).
8. C. BOURDÉRON. To be published.
9. R. C. HERMAN and K. E. SHULER. J. Chem. Phys. **22**, 481 (1954).
10. G. DUROCHER and C. SANDORFY. J. Mol. Spectrosc. **15**, 22 (1965).
11. G. HERZBERG. Molecular spectra and molecular structure. Vol. 1. Spectra of diatomic molecules. D. Van Nostrand Company, New York. 1950. p. 90.
12. B. T. DARLING and D. M. DENNISON. Phys. Rev. **57**, 128 (1940).
13. P. BARCHEWITZ. Spectroscopie infrarouge. Vol. 1. Vibrations moléculaires. Gauthier–Villars, Paris. 1961.
14. M.-C. BERNARD and C. SANDORFY. J. Chem. Phys. **56**, 3412 (1972).
15. R. A. TOTH, R. H. HUNT, and E. K. PLYLER. J. Mol. Spectrosc. **23**, 74 (1969).

Can. J. Chem. Downloaded from www.nrcresearchpress.com by 210.87.254.40 on 09/05/12
For personal use only.

A Comparative Study of Bu_4NBr, $NaBPh_4$, Ph_4PCl, and Ph_4AsCl in Water and Methanol at 25 °C: Partial Molal Volumes, Heat Capacities, and Viscosities

C. JOLICOEUR, P. R. PHILIP, G. PERRON, P. A. LEDUC, AND J. E. DESNOYERS

Département de chimie, Université de Sherbrooke, Sherbrooke, Québec

Received March 29, 1972

The apparent molal volumes (ϕ_v) and heat capacities (ϕ_c) of Bu_4NBr, $NaBPh_4$, Ph_4PCl, and Ph_4AsCl have been measured in water and methanol at 25 °C in the concentration range 0.01–0.2 *M*. The viscosity of aqueous $NaBPh_4$ and Ph_4AsCl have also been measured at 25 °C and in the same concentration range. Individual ionic values have been estimated for most of these properties. A comparison of these values for the quaternary ions Bu_4N^+, BPh_4^-, Ph_4P^+, Ph_4As^+ illustrates sizable differences in the solute–solvent interactions of alkyl and aryl substituted ions. Some specificity is also suggested in the solvation of the tetraphenyl ions, as shown by a comparison of the properties which should reflect directly the size of the ions (r_{Stokes}, $\bar{V}^0$, and B_η) and also in ($H_2O \rightarrow CH_3OH$) transfer functions.

Le volume apparent molaire (ϕ_v) et la capacité calorifique apparente molaire (ϕ_c) de Bu_4NBr, $NaBPh_4$, Ph_4PCl, et Ph_4AsCl ont été mesurés dans l'eau et dans le méthanol à 25 °C, dans un domaine de concentration variant de 0.01 à 0.2 *M*. Egalement, la viscosité de solutions aqueuses de $NaBPh_4$ et Ph_4AsCl a été déterminée. Pour la majorité de ces propriétés, des valeurs ioniques individuelles ont pu être estimées. La comparaison de ces valeurs pour les différents ions quaternaires met en évidence une différence significative entre les interactions soluté–solvant des ions quaternaires, selon que les substituants sont aliphatiques ou aromatiques. Dans la série BPh_4^-, Ph_4P^+, et Ph_4As^+, une certaine spécificité dans la solvatation est également apparente, particulièrement dans les propriétés qui reflètent directement la dimension des ions (r_{Stokes}, $\bar{V}^0$, et B_η) et dans les fonctions thermodynamiques de transfert ($H_2O \rightarrow CH_3OH$).

Canadian Journal of Chemistry, **50**, 3167 (1972)

Can. J. Chem. Downloaded from www.nrcresearchpress.com by 210.87.254.5 on 09/05/12
For personal use only.

Introduction

In the study of aqueous hydrophobic solutes, molecules or ions containing unsaturated side chains are usually avoided because of ill-defined interactions between water molecules and π-electron systems, and also because there are no convenient homologous series such as those found in the aliphatic substituents. Differences between the water–solute interactions of aliphatic and aromatic solutes have been suggested for some time[1] and recently emphasized by systematic transfer studies (2). It has been possible to illustrate these differences in solute–solvent interactions from an investigation of the near-i.r. spectra of water in solutions containing alkyl and aryl substituted quaternary ions (3). While Bu_4N^+ changed the water spectrum in a way similar to a decrease in temperature, Ph_4As^+, Ph_4P^+, and BPh_4^- all produced spectral changes which could not be correlated with simple structural modifications of water. Furthermore, it could be inferred from the spectra that BPh_4^- and Ph_4As^+ or Ph_4P^+ behave quite differently in their interactions with water. In spite of the *a priori* similarity of the latter ions, indications of specific behavior were also found in their heats of transfer between protic and aprotic solvents (4), their apparent molal expansitivities (5),[2] and also in their effects on the electron spin relaxation of stable nitroxide radicals (6). Since this work was completed, solvent chemical shifts in solutions of Ph_4AsCl, Ph_4PCl, and $NaBPh_4$ have also shown specific solvation effects for Ph_4P^+, Ph_4As^+, and BPh_4^- (7).

Knowledge of the effects of hydrophobic solutes on the structure of water, and on the interactions among hydrophobic solutes, was originally (and frequently since) inferred from thermodynamic properties (8–11) and viscosity data (9, 10). It thus seemed appropriate to use these properties to try to confirm and specify differences between alkyl and aryl substituted ions, and between various ions in the latter

[1]See for example the different apparent molal expansitivities (ϕ_E) of benzene and CH_4, C_2H_6, or C_3H_8 in water (ref. 1).

[2]For $NaBPh_4$ and Ph_4AsCl, ϕ_E^0 and $d\phi_E^0/dT$ are quite different; also, $d\phi_E^0/dT$ for these salts is of opposite sign to that of Bu_4NCl.

Can. J. Chem. Downloaded from www.nrcresearchpress.com by 210.87.254.5 on 09/05/12
For personal use only.

group. In the present comparative study of Bu_4NBr, $NaBPh_4$, Ph_4PCl, and Ph_4AsCl we have chosen to investigate apparent molal volumes (ϕ_v), apparent molal heat capacities (ϕ_c) and viscosities (η); for simple electrolytes, these properties are sometimes rather well correlated (12). Measurements in methanol were carried out in an attempt to resolve specific interactions between water and aromatic substituents from the influence of hydrophobic solutes on the water structure. Some measurements were also carried out on benzene and triphenylmethane for the purpose of comparing the behavior of the neutral molecules with that of the tetraphenyl ions.

Experimental

(a) Materials

The solvents and other materials required in this work were: water doubly distilled over alkaline $KMnO_4$ in a glass still; methanol (see discussion below); hexane and benzene Fisher spectranalyzed; $NaBPh_4$, Ph_4AsCl, Ph_4PCl, and Ph_3CH, K and K. The salts were purified following procedures described elsewhere (3, 6*b*) and triphenylmethane was recrystallized from anhydrous ether. All solutions were filtered immediately prior to their use.

(b) Measurements

Since it is very difficult to obtain anhydrous methanol, several tests were conducted in order to evaluate the effect of the water content on the partial molal volumes and heat capacities of solutes in this solvent. For different lots Karl Fisher titrations gave the following water contents: 500 p.p.m. or less for Fisher certified methanol and 500–1000 p.p.m. for Spectrograde methanol. Distillation of Fisher certified material over $MgSO_4$ under a dry nitrogen atmosphere yielded methanol containing less than 100 p.p.m. H_2O. Between 100–500 p.p.m. H_2O content it was not possible to establish a significant influence of water on the properties investigated. The tests were more convincing for partial molal volumes than for partial molal heat capacities; the latter bear larger uncertainties, because of other problems encountered as discussed below. The results given here were all obtained using Fisher certified grade methanol containing less than 300 p.p.m. H_2O.

Density measurements were carried out with a buoyancy densitometer (described in detail elsewhere, ref. 13) which is capable of an accuracy of 2×10^{-6} g cm^{-3}. With solutions in methanol, evaporation of the solvent increased the uncertainty to 10^{-5} g cm^{-3}. For these, density measurements were also carried out using a digital densitometer, DMA (Anton Parr, Austria); both methods yielded values agreeing to within 10^{-5} g cm^{-3}.

The specific heats of the solutions were obtained using a differential flow microcalorimeter reported recently by Picker *et al.* (14). The instrument measures directly the ratio of the volumetric specific heats (σ) of a solution relative to that of its solvent. For aqueous solutions, the detection limit of the instrument is typically 2×10^{-5} cal K^{-1} cm^{-3} when using a temperature increment of ~ 1.5 K. As mentioned above, additional problems were encountered with solutions in methanol due to its high vapor pressure, its high fluidity and its ability to dissolve sealing materials. The constant rate of flow required for the specific heat measurements was thus very difficult to achieve. The viscosity of the solutions was determined with a flow viscometer also described previously (15); with water at 25 °C, the flow time of the instrument was 811.05 s with a reproducibility of ± 0.05 s. For the quaternary salts (except Ph_4PCl) in water and methanol, the concentration range investigated was 0.01–0.2 *M*. In methanol, measurements at two or three concentrations only were carried out, repeating each measurement 4–6 times.

The specific heat of aqueous benzene solutions was measured at the saturation concentration only (0.0231 *m* at 25 °C (1)). Similarly the density and specific heat of Ph_3CH in hexane and methanol were obtained for a single low concentration: 0.03635 and 0.03022 *m*, respectively. In the above instances, the results are assumed to correspond to infinite dilution values.

Results

The apparent molal volumes (ϕ_v) were calculated from the density measurements using standard equations (*e.g.* ref. 15); the density of water, methanol, and hexane at 25 °C were taken respectively as 0.997044, 0.78636, and 0.66265 g cm^{-3};[3] the data were fitted to the Redlich–Meyer equation (17)

$$[1] \qquad \phi_v = \phi_v^0 + A_v c^{1/2} + B_v c$$

where $A_v = 1.868$ (17) in water and 15.77 in MeOH (18). The results obtained for aqueous solutions of $NaBPh_4$, Ph_4PCl, and Ph_4AsCl are given in Table 1 and some of the results are plotted in Fig. 1.

The densities of methanol solutions and the calculated ϕ_v of Bu_4NBr, $NaBPh_4$, Ph_4PCl, Ph_4AsCl, and Ph_3CH are reported in Table 2.

The parameters ϕ_v^0 and B_v of eq. 1 for the aqueous solutions are given in Table 3 along with ϕ_v^0 of the solutes in methanol.

Specific heats (cal K^{-1} g^{-1}) are readily obtained from the relative increment of the volumetric specific heats ($\Delta\sigma/\sigma_0$ cal K^{-1} cm^{-3}) using the densities of the solution (d) and that of the solvent (d_0):

$$[2] \qquad \frac{c_p}{c_p^0} = \left(1 + \frac{\Delta\sigma}{\sigma_0}\right)\frac{d_0}{d}$$

[3]Density of H_2O taken from ref. 16; density of methanol and hexane measured using a buoyancy densitometer.

TABLE 1. Summary of data on aqueous solutions of $NaBPh_4$, Ph_4PCl, and Ph_4AsCl at 25 °C

	m (mol (kg H_2O)$^{-1}$)	$1000(d-d_0)$ (g l^{-1})	ϕ_v (cm^3 mol^{-1})	$10^3(\Delta\sigma/\sigma_0)$	ϕ_c (cal K^{-1} mol^{-1})	η/η_0
$NaBPh_4$	0.01006	0.664_7	276.6_1			1.01348
	0.01997	1.309_5	276.9_0	-0.21_0	265.2	1.02604
	0.04123	2.693	276.7_8	-0.40_6	265.7	1.05373
	0.07390	4.798	276.5_9	-0.82_0	264.2	1.09680
	0.10521	6.802	276.3_1	-1.27_2	262.7	1.13930
	0.18430	11.697	276.1_6	−2.86	258.7	1.25458
Ph_4PCl	0.01141	0.741_1	310.3_7	−0.585	257.7	
	0.02076	1.346_5	310.3_1	-1.09_4	256.2	
	0.42250	2.720	310.3_7	-2.45_0	250.5	
Ph_4AsCl	0.00984	0.984_2	319.0_7	-0.46_2	270.7	1.01323
	0.02000	1.991	319.2_7	-1.10_0	262.6	1.02283
	0.04171	4.118	319.4_1	−2.42	259.6	1.04747
	0.06343	6.227	319.2_8	−4.03	253.2	1.07178
	0.08342	8.140	319.2_8	−5.66	248.4	1.09428
	0.09988	9.710	319.1_4	−6.87	247.0	1.11209
	0.15727	15.046	318.7_9	−11.97	237.8	1.18060
	0.20582	19.445	318.7_9	−16.88	230.2	1.24296

TABLE 2. Apparent molal volumes and heat capacities of Bu_4NBr, $NaBPh_4$, Ph_4PCl, Ph_4AsCl, and Ph_3CH in methanol at 25 °C

	Molality	$1000(d-d_0)$ (g l^{-1})	ϕ_v (cm^3 mol^{-1})	$10^3\,\Delta\sigma/\sigma_0$	ϕ_c (cal K^{-1} mol^{-1})
Bu_4NBr	0.05013	3.702	289.2	−1.29	122.0
	0.07556	5.488	290.5	−1.77	123.9
	0.10040	7.236	290.7	−2.18	125.0
$NaBPh_4$	0.01833	2.171	243.0	0.70_0	139.1
	0.03646	4.233	246.1	0.531	142.8
	0.07250	8.371	245.9	3.929	150.4
Ph_4PCl	0.01002	1.243	275.5		
	0.02064	2.509	279.3	−0.754	110.7
	0.04169	5.004	280.8	−1.125	117.2
	*0.02826	3.412	280.2		
	*0.03667	4.465	278.2		
	*0.05817	6.933	231.5		
Ph_4AsCl	0.02561	3.894	285.3		
	0.04915	7.269	290.7	−1.235	123.0
	0.07497	11.211	286.7	−1.487	124.3
	*0.03372	5.101	286.1		
	*0.05531	7.973	287.8		
	*0.06643	9.875	288.5		
Ph_3CH	0.03868	2.135	220.9	0.103	106.8
Ph_3CH in Hexane	0.05529	3.613	218.7	0.525	83.9
C_6H_6 in Water	0.0231 (refs. 27, 40)			1.14	132

*Measurements carried out with a digital densitometer.

Can. J. Chem. Downloaded from www.nrcresearchpress.com by 210.87.254.5 on 09/05/12
For personal use only.

Can. J. Chem. Downloaded from www.nrcresearchpress.com by 210.87.254.5 on 09/05/12
For personal use only.

TABLE 3. Summary of the data on partial molal volumes and heat capacities of Bu_4NBr, $NaBPh_4$, Ph_4PCl, Ph_4AsCl, and Ph_3CH in water and methanol at 25 °C

		ϕ_v^0 ($cm^3\ mol^{-1}$)	B_v	ϕ_c^0 (cal $K^{-1}\ mol^{-1}$)	B_c	B_η
Bu_4NBr	H_2O	(300.5, ref. 21)	−11.0	(289.1, ref. 19)	(−10, ref. 19)	(1.15, ref. 20) (1.28, refs, 23, 24)
	CH_3OH	286.5 (285.9, ref. 18)		116		
$NaBPh_4$	H_2O	276.6 (276.4, ref. 5)	−7.9	266.3 (264, ref. 22)	−55	1.21
	CH_3OH	241		128		
Ph_4PCl	H_2O	310.0	2.3	$260._5$	−270	
	CH_3OH	277		107		
Ph_4AsCl	H_2O	319.1 (318.5, ref. 5)	−6.2	$266._7$	−227	1.08
	CH_3OH	283		118		

Can. J. Chem. Downloaded from www.nrcresearchpress.com by 210.87.254.5 on 09/05/12
For personal use only.

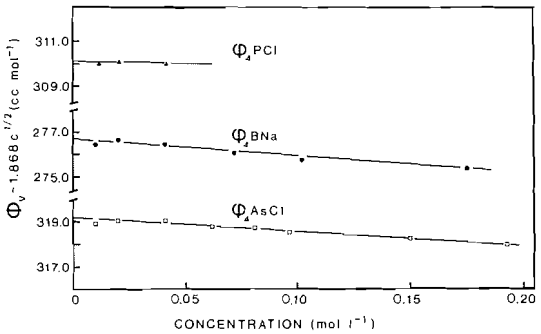

FIG. 1. Apparent molal volumes of $NaBPh_4$, Ph_4PCl, and Ph_4AsCl in water at 25 °C, corrected for the Debye–Hückel limiting slope.

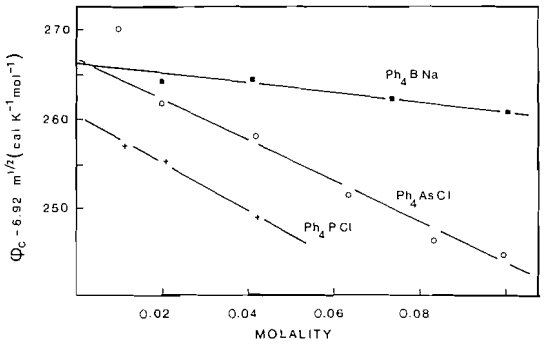

FIG. 2. Apparent molal heat capacities of aqueous $NaBPh_4$, Ph_4PCl, and Ph_4AsCl at 25 °C, corrected for the Debye–Hückel limiting slope.

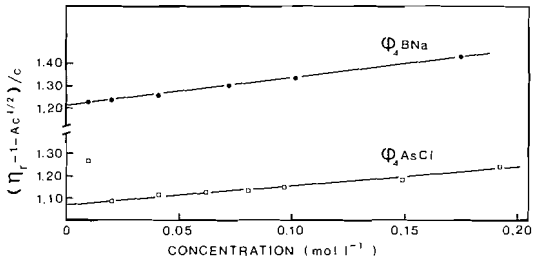

FIG. 3. Changes in the relative viscosity of aqueous solutions of $NaBPh_4$ and Ph_4AsCl corrected for long range coulombic forces.

The apparent molal heat capacities, ϕ_c, are then calculated in the usual way:

$$[3] \qquad \phi_c = Mc_p + 1000\,\frac{(c_p - c_0^0)}{m}$$

where M is the formula weight of the solute. The specific heats of the solvents used were taken as: water, 0.99888; methanol, 0.6056; hexane, 0.54220 cal K^{-1} g^{-1}.[4]

The calculated ϕ_c's of aqueous $NaBPh_4$, Ph_4PCl, and Ph_4AsCl were fitted to the equation

$$[4] \qquad \phi_c = \phi_c^0 + A_c m^{1/2} + B_c m$$

where A_c can be evaluated as 6.92 for ϕ_c given in cal K^{-1} mol^{-1} (26). For solutions in MeOH, the magnitude of A_c is not available and ϕ_c^0 was estimated from a plot of ϕ_c *vs.* m. The values of $\Delta\sigma/\sigma_0$ and ϕ_c for aqueous systems are given in Table 1, and in Table 2 for the other solvent systems; the derived ϕ_c^0's and B_c's are reported in Table 3. Figure 2 shows $(\phi_c - 6.92\,m^{1/2})$ plotted against m for the above salts in aqueous solutions.

Data for volume and heat capacity of Ph_3CH at low concentration in MeOH and hexane are included in Table 2, along with the heat capacity of aqueous benzene. For the latter, the results were obtained at saturation concentration and in both cases the concentration dependence was assumed negligible.

The apparent molal volumes of benzene was taken as 83.2 cm^3 mol^{-1} (1) and its ϕ_c was determined as 132 ± 3 cal K^{-1} mol^{-1}, in close agreement with that calculated from the $\Delta\bar{C}_p$ of solution measured by Franks *et al.* (27): 129 cal K^{-1} mol^{-1}.[5]

The viscosity of aqueous solutions of $NaBPh_4$ and Ph_4AsCl were fitted to the equation:

$$[5] \qquad \frac{\eta}{\eta_0} = 1 + A_\eta c^{1/2} + B_\eta c + D_\eta c^2$$

The data are shown on Fig. 3 where $(\eta/\eta_0 - 1 - Ac^{1/2})/c$ is plotted against c (15). The B_η and D_η coefficients are obtained from this plot though, for the present discussion, only B_η is used (Table 3).[6] The A_η coefficients required to subtract the effect of the long-range coulombic forces on the viscosity (24) were calculated from the conductance data (24, 28, 29).

Uncertainties

The uncertainties of the various ϕ_v^0 and ϕ_c^0 data were estimated as follows: ϕ_v^0 in aqueous

[4]Data for H_2O taken from ref. 25; data for methanol and hexane interpolated from values reported in ref. 45.

[5]The specific heat of liquid benzene was taken as 0.4178 cal K^{-1} g^{-1} (ref. 46).

[6]Though these coefficients are known to account for solute–solute interactions, in the R_4NX and alkali halides series they have no simple interpretation; see ref. 20.

TABLE 4. Summary of the Stokes radii and some ionic properties of the quaternary ions in H_2O and CH_3OH at 25 °C*

	H_2O				CH_3OH
	r_s (Å)	$\bar{V}^0$(ion) (cm^3 mol^{-1})	B_η(ion) (l mol^{-1})	$\bar{C}_p^0$(ion) (cal K^{-1} mol^{-1})	$\bar{V}^0$(ion) (cm^3 mol^{-1})
Bu_4N^+	(4.74, ref. 24)	270.0	(1.19, ref. 20) (1.28, refs. 23, 24)	304, 350	267
BPh_4^-	(4.62, ref. 28)	283.6	1.12	275, 229	257
Ph_4P^+	(4.60, ref. 29)	286.3		275, 320	264
Ph_4As^+	(4.70, ref. 29)	295.5	1.09	280, 326	270
$\frac{4}{3}(Ph_3CH)$					295

* $\bar{V}^0 = \phi_v^0$, $\bar{C}_p^0 = \phi_c^0$; for the $\bar{C}_p^0$(ion) the first value given was obtained from an ionic scale proposed by Noyes (30); the other values follow from a scale suggested by Criss and Cobble (31) (see text).

solutions, ± 0.1 cm^3 mol^{-1}; in methanol solutions, ± 1 cm^3 mol^{-1}; ϕ_c^0 in aqueous solutions, ± 1 cal K^{-1} mol^{-1}; in methanol solutions, $\pm$ 5 cal K^{-1} mol^{-1}. Data obtained in *n*-hexane bear the same uncertainty as those obtained for solutions in methanol. The uncertainty on B_η is ± 0.01 l mol^{-1}. For the data on aqueous solutions, the error assigned to the intercepts and slopes was the calculated standard deviations. For solutions in methanol, the uncertainties reported were estimated from the extrema of the graphical intercepts, taking into account the standard deviation in a series of measurements at each concentration.

Ionic Values

The purpose of this work being to compare the properties of quaternary ions, ionic contributions to the infinite dilution properties are most appropriate. Table 4 lists various ionic properties to be used in the following discussion; the values reported are those which could be estimated with reasonable certainty. For ionic ϕ_c^0 values, two widely different scales have been proposed so the results obtained by the two methods are included in Table 4.

The individual ionic volumes are based on the scale determined by Conway *et al.* (21) which gives $\bar{V}^0$ $(H^+) = -5.5$ cm^3 mol^{-1}. Although other means of estimating $\bar{V}^0$ (ions) have been proposed (32, 33), the differences in the various scales only amount to 1 or 2 cm^3 mol^{-1}.

In methanol, $\bar{V}^0$ (Br^-) has also been obtained by Conway's method using data from Padova and Abrahamer (18), *i.e.* plotting $\bar{V}^0(R_4NBr)$ against number of carbon atoms of the cations. $\bar{V}^0(Br^-)$ was found as 19 ± 5 cm^3 mol^{-1} which compared reasonably well with 16.6 cm^3 mol^{-1} obtained by Millero (35) using a different method. For the present purpose, the former value is used throughout.

Ionic contributions to $\bar{C}_p^0$ of electrolytes have been assigned following two methods or assumptions. The ionic scale of $\bar{C}_p^0$ tabulated by Noyes (30) assumes that $\bar{C}_p^0(K^+) = \bar{C}_p^0(F^-)$, which gives $\bar{C}_p^0(H^+) = -14.5$ cal K^{-1} mol^{-1}. It is now rather well established that the structure-breaking effects of the larger alkali and halide ions contribute significantly to their $\bar{C}_p^0$ in water (19); however there is no way of ensuring that the overall structural effects around F^- and K^+ should lead to identical contributions to $\bar{C}_p^0$. From a "correspondence principle", Criss and Cobble (31) derived a scale of ionic $\bar{C}_p^0$ from which $\bar{C}_p^0(H^+) = 28$ cal K^{-1} mol^{-1}. On the latter scale, all halide ions have negative $\bar{C}_p^0$ while those of the alkali metal ions are all positive. In view of the known structure-breaking influences of both the larger anions and cations, *e.g.*, I^-, Cs^+, such different values seem unacceptable.

It should be mentioned that a plot of $\bar{C}_p^0(R_4NBr$, $R = Me \rightarrow Bu)$ *vs.* formula weight of cation (19) is nearly linear and, upon extrapolation to zero cation mass, gives $\bar{C}_p^0(Br^-) = -65 \pm 10$ cal K^{-1} mol^{-1}; on this scale, $\bar{C}_p^0(H^+) = 31$ cal K^{-1} mol^{-1}. However good the agreement with the estimate of Criss and

Can. J. Chem. Downloaded from www.nrcresearchpress.com by 210.87.254.5 on 09/05/12
For personal use only.

Can. J. Chem. Downloaded from www.nrcresearchpress.com by 210.87.254.5 on 09/05/12
For personal use only.

Cobble (31), there is reason to expect that the extrapolation procedure used for $\bar{V}^0$ (21) will not be valid for $\bar{C}_p^0$: structure-making ions such as Bu_4N^+ will increase $\bar{C}_p^0$, whereas structure-breaking ions such as Me_4N^+ will decrease $\bar{C}_p^0$ (19, 34); these combined effects will lead to an extrapolated $\bar{C}_p^0(Br^-)$ being much too negative. Since none of these scales of $\bar{C}_p^0$ can, at present, be considered reliable, we included in Table 4 the $\bar{C}_p^0$ of the quaternary ions computed from both the Noyes assumption and the correspondence principle.

The ionic contributions to the B_η coefficients, given in Table 4, are based on Kaminsky's method of separation (12) which yields $B_\eta(Br^-) = -0.04$; other estimates of ionic B_η have been shown to be in good agreement with the one used here (20). The Stokes radii were taken from the literature as calculated from limiting ionic conductances (21, 28, 29). Most of the individual ionic values in aqueous solutions are collected on Fig. 4 where we have plotted the ionic B_η, $\bar{V}^0$, and $\bar{C}_p^0$ (two sets) against the formula weight of the quaternary ions.

Nonelectrolytes

Together with the results given in previous tables, additional data for nonelectrolytes in water were also found desirable. The apparent molal volume of butane in water was extrapolated from data for methane, ethane, and propane (1) which gave $\bar{V}^0(\text{butane}) = 82\,\text{cm}^3\,\text{mol}^{-1}$. The apparent molal heat capacity of butane was calculated as $125._3$ cal K^{-1} mol^{-1} from the $\Delta\bar{C}_p$ of solution measured by Kresheck *et al.* (36).[7]

Discussion

In the following sections we will attempt to bring forward the aspects of the above results which, as in the case of previous spectral investigations (3, 7), can help to establish specific solvation behavior among the various quaternary ions studied.

(*a*) *Effective Ionic Sizes*

The interpretation of differences in the properties of the hydrophobic ions studied first requires an examination of their relative sizes

[7]The specific heat of butane was taken as 0.40261 cal $K^{-1}g^{-1}$ (ref. 47). The correction from 1 atm. to 1 mm Hg required to compare with values for benzene was found negligible.

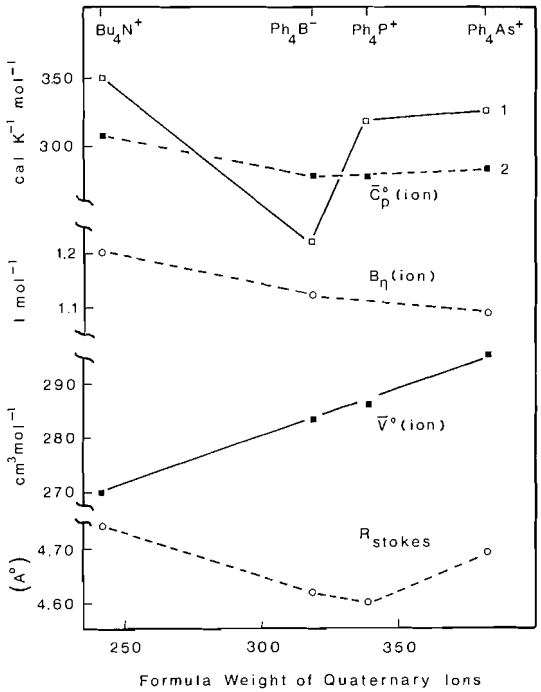

FIG. 4. Estimated ionic contributions to the viscosity B_η coefficients and partial molal volumes and heat capacities at infinite dilution ($\bar{V}^0$ and $\bar{C}_p^0$) and 25 °C. The two sets of data for $\bar{C}_p^0$ were obtained by different methods of assignment: (*1*) —, Criss and Cobble (31); (*2*) ---, Noyes (30).

in solution, and of the properties most directly related to the size. As can be seen from Fig. 4, a comparison of r_s, B_η, and $\bar{V}^0$ clearly shows irregularities in the behavior of the various ions studied. In the tetraphenyl series, the radii of the ions should increase as the size of the central atom, X, increases through X = B, P, As; as can be seen from Table 4, the Stokes radii agree reasonably with such an order and so does $\bar{V}^0$ for these ions in water (Fig. 4).

The same trend does not, however, carry on for Bu_4N^+ which has a larger r_s and a smaller $\bar{V}^0$, in spite of the similar $\bar{V}^0$(aq) of butane and benzene. To explain this observation we can adopt the proposed view (for further discussion and references, see ref. 37) that, while the alkyl groups stabilize hydrogen-bonded networks in water (increasing local viscosity and thus r_s), they occupy some of the void space in these networks (decreasing $\bar{V}^0$). The comparisons of $\bar{V}^0$ and r_s then suggests that the aryl substituted ions do not perform structure stabilization to

Can. J. Chem. Downloaded from www.nrcresearchpress.com by 210.87.254.5 on 09/05/12
For personal use only.

the same extent or in the same fashion as Bu_4N^+ does.[8]

Effective radii, such as r_s, are usually a combined measure of the particle size and of the effect of the particle on the surrounding solvent (solute–solvent interactions and structural effects). Similarly, viscosity B_η coefficients include both a size effect and a contribution arising from changes in the local viscosity around the solutes (24, 38). Therefore, r_s and B_η should follow the same pattern in the series of ions studied here. Indeed, B_η is largest for Bu_4N^+ (Fig. 4); however, for BPh_4^- and Ph_4As^+, the relative magnitude of B_η is opposite to that observed for r_s. Though the difference is small, this suggests different solute–solvent interactions for BPh_4^- and Ph_4As^+, which is consistent with previous spectral studies of these ions (3, 7).

Desnoyers and Perron (20) have used the deviation from the Einstein hydrodynamic model, *i.e.* $B_\eta = 0.0025V$ (24), as a criterion of overall structural influence of a solute, when the hydrodynamic volume is replaced by $\bar{V}^0$. For the ions examined, $(B_\eta - 0.0025\bar{V}^0)$ is found as 0.52, 0.41, and 0.35 for Bu_4N^+, BPh_4^-, and Ph_4As^+, respectively. These large positive deviations suggest that all of these ions have overall structure-making influences, decreasing in the order Bu_4N^+, BPh_4^-, Ph_4As^+.

(b) $\bar{V}^0$ and $\bar{C}_p^0$ in Water

As can be seen from Fig. 4, the relation between $\bar{V}^0$ of the quaternary ions in aqueous solution and their molecular weight is very nearly linear. As mentioned earlier, the larger volume of BPh_4^- compared to Bu_4N^+ can be the result of packing effects. On the other hand, the increase in $\bar{V}^0$ of the tetraphenyl ions with formula weight is of the same order as the increase in volume of the central atom, calculated from the covalent radii. Thus, for these salts, little can be learned on specific solute–solvent interactions from the $\bar{V}^0$ data in water only.

In comparing the $\bar{C}_p^0$ values of the quaternary ions in the series shown on Fig. 4, an additional problem arises because of the uncertainty on the intrinsic heat capacity of the organic ions. Specific heat data are not available for all the salts studied here, but the molar heat capacities of solid Bu_4NBr and $NaBPh_4$ have been estimated as 114 and 102 cal K^{-1} mol^{-1}.[9] Thus, the corresponding $\Delta\bar{C}_p^0$ (*i.e.*, $\bar{C}_p^0 - \bar{C}_p^0(s)$) would be 175 and 164 cal K^{-1} mol^{-1}. Since the water structure-breaking effects of ions contributes a negative quantity to $\bar{C}_p^0$ (19), and since Br^- consistently appears as a more effective structure breaker than Na^+, ionic values of $\Delta\bar{C}_p^0$ for Bu_4N^+ and BPh_4^- would be even more different. In terms of the current interpretation of the large positive $\Delta\bar{C}_p^0$ (34), all the quaternary ions studied here appear to promote water structure to a high degree. From either $\bar{C}_p^0$ (ionic) or $\Delta\bar{C}_p^0$ (salts), a clear distinction is seen between BPh_4^- and Bu_4N^+, the latter being a more efficient structure promoter. Unfortunately, from the $\bar{C}_p^0$ alone, nothing can be inferred on the relative hydration of the three aryl substituted ions. Following the above discussion on ionic $\bar{C}_p^0$ scales, one can anticipate that true ionic $\bar{C}_p^0$ will also reflect specific solvation effects amongst the tetraphenyl ions. On the other hand, the small degree of specificity of $\bar{C}_p^0$ towards the different ions studied here may be a coincidence, similar to that observed with the partial molal expansitivities (ϕ_E^0). Millero (5) has shown that the temperature coefficient of ϕ_E^0's has opposite sign for Bu_4NCl and Ph_4AsCl (or $NaBPh_4$), though at 25 °C, ϕ_E^0 for these salts are all of similar magnitude. If the same is true for the partial molal heat capacities, then a study of the temperature coefficient of $\bar{C}_p^0$ would help elucidate the specific solvation effects.

(c) Additivity of Side Chain Contributions to $\bar{V}^0$ and $\bar{C}_p^0$ in Water

The additivity of chain contributions to the heats of transfer $R_{4-n}NH_n^+$ has been thoroughly investigated in water and in aprotic solvents (39). There, as with other properties, (*e.g.* salting-in of benzene by the quaternary salts (40)), additivity of group contributions to the properties of aqueous solutes is not found. In the present case, a different kind of additivity can be examined if we compare the properties ($\bar{V}^0$, $\bar{C}_p^0$) of the aqueous hydrocarbons (side chains) and the quaternary ions. We can define

[8]Compared to *e.g.* Ph_4P^+, the r_s of Bu_4N^+ is expected to be smaller if folding of the butyl chains is significant.

[9]The molar heat capacity of solid $NaBPh_4$ had been estimated as 102 ± 2 cal K^{-1} mol^{-1} (22). From the data in ref. 34, we can calculate the heat capacity of solid Bu_4NBr as 114 cal K^{-1} mol^{-1}.

Can. J. Chem. Downloaded from www.nrcresearchpress.com by 210.87.254.5 on 09/05/12
For personal use only.

TABLE 5. Non-additivity of side-chain contributions to $\bar{V}^0$ and $\bar{C}_p^0$ in aqueous solutions, as defined in eq. 6

	$\delta\bar{V}^0$ ($cm^3\ mol^{-1}$)	$\delta\bar{V}^0/\bar{V}^0$	$*\delta\bar{C}_p^0$ (cal K^{-1} mol^{-1})	$\delta\bar{C}_p^0/\bar{C}_p^0$
Bu_4N^+	58	0.22	197	0.65
BPh_4^-	49	0.17	253	0.92
Ph_4P^+	47	0.16	253	0.92
Ph_4As^+	37	0.13	248	0.89

*Using the ionic scale of Noyes (30).

the non-additivity for property X as $\delta\bar{X}^0$ where

[6] $\delta\bar{X}^0 = 4\bar{X}^0$(hydrocarbon) $- \bar{X}^0$(quaternary ion)

where $\bar{X}^0$ is a thermodynamic property for which the hydrocarbon and the quaternary ions have identical reference states. $\delta\bar{V}^0$ and $\delta\bar{C}_p^0$ were calculated from $\bar{V}^0$ and $\bar{C}_p^0$ for several quaternary ions in water and the data on aqueous butane and benzene solutions. The results are shown in Table 5.

As in previous studies mentioned above the non-additivity of side chain contributions is marked, and much more important for $\bar{C}_p^0$ than for $\bar{V}^0$. In spite of the additional volume of the central atom, $\delta\bar{V}^0$ is positive and must result from interference of the substituents. $\delta\bar{V}^0$ is maximum for Bu_4N^+ and decreases with formula weight of the quaternary ions; at least for the tetraphenyl ions, this might be expected since side-chain interference should decrease as the size of the central atom increases. (Using data in the literature (1, 21) one finds that in the series R_4N^+ (R = Me → Bu), $\delta\bar{V}^0$ is independent of chain length for R > Me; this suggests that folding of the longer side chains, *e.g.* Bu, does not contribute significantly to the larger $\delta\bar{V}^0$ observed for Bu_4N^+.)

The comparison of the various $\delta\bar{C}_p^0$ is more rewarding; the data in Table 5 confirm that $\bar{C}_p^0$ is much more sensitive than $\bar{V}^0$ to changes in solute–solvent interactions and packing effects.[10] Because of the uncertainty in the assignments of ionic $\bar{C}_p^0$, no conclusion can be firmly drawn from a comparison among the tetraphenyl ions, but $\delta\bar{C}_p^0$ shows a pronounced difference between these and Bu_4N^+. In the simplest picture, one can say that Bu_4N^+ is the one that retains, to the largest extent, the hydrophobic (structure-making) character of the hydrocarbon substituents.

[10] $\delta\bar{C}_p^0$ also contains a contribution from the normal modes of the quaternary ion; however, it seems reasonable to assume that these will be similar in all the ions considered here.

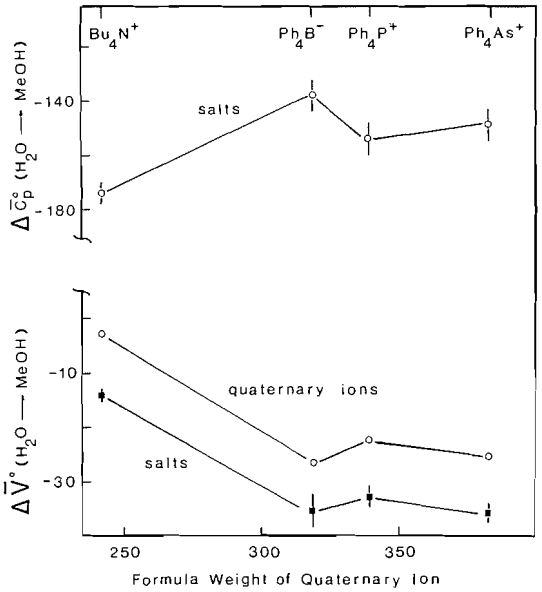

FIG. 5. Change in $\bar{V}^0$ and $\bar{C}_p^0$ of the quaternary ions (or salts) for ($H_2O \rightarrow CH_3OH$) transfer at 25 °C.

(*d*) *$H_2O \rightarrow CH_3OH$ Transfers*

The change in apparent molal volumes and heat capacities observed when the ions are transferred from water to methanol should provide some clues to the relative importance of the water structure stabilization by the organic ions and the solute–solvent interactions particularly of the type Ph · · · H—O—R. In methanol, the effect of large organic ions on the solvent structure has been shown to be much less than in water (42); on the other hand, solute–solvent interactions involving the —OH group should be possible to similar degrees in both solvents. Figure 5 shows $\Delta\bar{V}^0(H_2O \rightarrow CH_3OH)$ for quaternary ions and their salts and $\Delta\bar{C}_p^0$ ($H_2O \rightarrow CH_3OH$) for the salts only, since we have no reliable means of assigning ionic values to $\bar{C}_p^0$(MeOH). Clearly the transfer $\Delta\bar{V}^0$ and $\Delta\bar{C}_p^0$ are inversely related, and the distinction between Bu_4N^+ and the tetraphenyl salts is neatly established; also, some discrimination between BPh_4^-, Ph_4P^+, and Ph_4As^+ now seems apparent.

Can. J. Chem. Downloaded from www.nrcresearchpress.com by 210.87.254.5 on 09/05/12
For personal use only.

To estimate the importance of the Ph · · · H—O—R interactions with the tetraphenyl ions in methanol, we can examine the results obtained with Ph_3CH (Table 2); as a rough approximation to the behavior of a neutral tetraphenyl molecule, we multiply the data for Ph_3CH throughout by 4/3.[11] For this hypothetical Ph_4C molecule, the $\Delta\bar{V}^0$(*n*-hexane → MeOH) is found as $+3\ cm^3\ mol^{-1}$ and the $\Delta\bar{C}_p^0$(*n*-hexane → MeOH) as $+30\ cal\ K^{-1}\ mol^{-1}$. Thus, for such a molecule, hydrogen-bonding type interactions of —OH groups with the phenyl rings do not appear as a major contributor to $\bar{V}^0$ and $\bar{C}_p^0$ in methanol. A comparison of $\frac{4}{3}\bar{V}^0(Ph_3CH)$ and $\bar{V}^0$(tetraphenyl ions) in methanol (Table 4) would suggest that the charging process decreases $\bar{V}^0$ significantly; the same is true for $\bar{C}_p^0$ unless $\bar{C}_p^0(Na^+)$ and $\bar{C}_p^0(Cl^-)$ are both strongly negative in methanol.

The $(H_2O \rightarrow CH_3OH)$ transfers of the salts studied are readily interpreted, at least for the trends observed. $\Delta\bar{C}_p^0(H_2O \rightarrow CH_3OH)$ is largest for Bu_4NBr, as expected if Bu_4N^+ is the most hydrophobic: contributions arising from the structure-promoting phenomenon will be much weaker in MeOH (42). On the other hand, $NaBPh_4$ has the smallest $\Delta\bar{C}_p^0(H_2O \rightarrow CH_3OH)$ which is also readily understood if the hydrophobic character of BPh_4^- is less than that of the other ions. An equivalent statement would be that the solute–solvent interactions of BPh_4^- in methanol more closely resemble those in water.

The $\Delta\bar{V}^0(H_2O \rightarrow CH_3OH)$ for Bu_4N^+ (Bu_4NBr) is very small, much less than for the tetraphenyl ions. If the $\Delta\bar{V}^0(H_2O \rightarrow CH_3OH)$ was dominated by molecular packing effects, one might expect that the tetraphenyl ions would have a more positive $\bar{V}^0$ in MeOH, *i.e.*, since the aryl chains are not as flexible as the alkyl chains, the larger solvent molecules would lead to more free space around the tetraphenyl ions (see also a discussion by Coetzee and Sharpe (7)). It thus seems logical to infer that in water, there is more free space around the tetraphenyl ions than around Bu_4N^+, which is in agreement with the earlier statement of water structure promotion and void occupancy by the alkyl chains.

[11]This approach is similar to that used by Grunwald *et al.* (41) who compared tetraphenyl methane with BPh_4^- and Ph_4As^+ in dioxane–water mixtures.

Though we believe the differences in $\bar{V}^0$ among the tetraphenyl ions in MeOH to be beyond experimental error, their significance is not readily established.

(e) Concentration Dependences

In aqueous solutions of electrolytes containing large hydrophobic ions, negative deviations to the Debye–Hückel limiting law (DHLL) have often been interpreted on the basis of structural interactions between the hydrophobic ions (37, 43). The observed concentration dependence of ϕ_v in water, corrected for the DHLL, is negative for all the salts studied; the B_v parameter (Table 3) is increasingly negative in the order Ph_4PCl, Ph_4AsCl, $NaBPh_4$, Bu_4NBr. Following the above discussion, it seems unlikely that this situation reflects mainly the order of the hydrophobic character of the organic ions, as for instance, in the series R_4NX where R is changed from Me to Bu (43). Similarly, in aqueous solutions, the observed deviations from the DHLL of ϕ_c are also negative (B_c, Table 3); however, the trend among the B_c coefficients is exactly opposite to that observed with the B_v parameters. On the basis of a structural interaction model, it thus appears that anion–cation structural interactions (37, 43) contribute significantly to the excess volumes and heat capacities, and in different ways for the different salts. More extensive measurements, together with a quantitative account of the size effects (44) should lead to a better understanding of the deviations from a limiting theory of the various excess functions.

Conclusion

The comparative study of the large organic ions Bu_4N^+, BPh_4^-, Ph_4P^+, and Ph_4As^+, using different thermodynamic methods and (water → methanol) transfer properties, illustrates some of the points made in earlier work. Differences in the solvation of alkyl and aryl substituted quaternary ions are emphasized in most of the properties examined. Within the series of tetraphenyl ions, some specific solvation effects are suggested in comparing properties which depend most directly on the size of the solute particles (r_s, $\bar{V}^0$, and B_η) and in $(H_2O \rightarrow CH_3OH)$ transfers.

A comparison of the results for Bu_4N^+ with

Can. J. Chem. Downloaded from www.nrcresearchpress.com by 210.87.254.5 on 09/05/12
For personal use only.

those for the tetraphenyl ions shows consistently that Bu_4N^+ is more hydrophobic than the $Ph_4X^{\pm}$, *i.e.*, in the sense currently employed, water structure promotion by Bu_4N^+ is more extensive than by the others. Also, the results are consistent with the view that occupancy of the void space in water hydrogen-bonded networks by the solute side chains is more effective with aliphatic substituents than aromatic groups.

Among the tetraphenyl ions, mild differences in behavior are observed, particularly in $H_2O \rightarrow CH_3OH$) transfer. However, the discrimination is not nearly as sharp as has been found in spectral studies of solvation (3, 7). It should be remarked, on the other hand, that spectral studies of solvation in which the properties of the protons are examined (*i.e.*, OH stretching frequencies or H chemical shifts) are expected to distinguish more efficiently between anions and cations, if water (or methanol) molecules are oriented differently in each case. The leading contributions to the spectral properties and the thermodynamic properties need not, therefore, result from the same effects, which indeed appears to be the case with the large organic ions studied here.

Financial support from the National Research Council of Canada through grants to C.J. and J.E.D. is gratefully acknowledged. The extensive help of Mr. P. Picker with many experimental problems is acknowledged with pleasure. We also acknowledge the help of Professor A. Hade of the Université du Québec, Montreal, who kindly lent us a Digital Densitometer.

1. W. L. MASTERTON. J. Chem. Phys. **22**, 1830 (1954).
2. C. V. KRISHNAN and H. L. FRIEDMAN. J. Phys. Chem. **74**, 2356 (1970); **73**, 3934 (1969).
3. C. JOLICOEUR, N. D. THÉ, and A. CABANA. Can. J. Chem. **49**, 2008 (1971).
4. C. V. KRISHNAN and H. L. FRIEDMAN. J. Phys. Chem. **75**, 3606 (1971).
5. F. J. MILLERO. J. Chem. Eng. Data, **15**, 562 (1970); **16**, 229 (1971).
6. (*a*) C. JOLICOEUR and H. L. FRIEDMAN. J. Phys. Chem. **75**, 165 (1971); (*b*) C. JOLICOEUR and H. L. FRIEDMAN. Ber. Bunsenges. Physik. Chem. **75**, 248 (1971).
7. J. F. COETZEE and W. R. SHARPE. J. Phys. Chem. **75**, 3141 (1971).
8. H. S. FRANK and M. EVANS. J. Chem. Phys. **13**, 507 (1945).
9. H. S. FRANK and W. Y. WEN. Discuss. Faraday Soc. **24**, 133 (1957).
10. H. S. FRANK. *In* Chemical physics of ionic solutions. *Edited by* B. E. Conway and R. G. Barradas. John Wiley and Sons, Inc., New York. 1966. p. 53.
11. W. KAUZMANN. Advances in protein chemistry. Vol. 14. *Edited by* C. B. Anfinsen Jr., M. L. Anson, J. T. Edsall, and F. M. Richards. Academic Press, N.Y. 1959. p. 1.
12. M. KAMINSKY. Discuss. Faraday Soc. **24**, 171 (1957).
13. J. E. DESNOYERS and M. AREL. Can. J. Chem. **45**, 359 (1967).
14. P. PICKER, P. A. LEDUC, P. R. PHILIP, and J. E. DESNOYERS. J. Chem. Thermodyn. **3**, 631 (1971).
15. J. E. DESNOYERS, M. AREL, and P. A. LEDUC. Can. J. Chem. **47**, 547 (1969).
16. Handbook of chemistry and physics. 49th ed. The Chemical Rubber Publishing Co., Cleveland, Ohio.
17. O. REDLICH and D. M. MEYER. Chem. Rev. **64**, 221 (1964).
18. J. PADOVA and I. ABRAHAMER. J. Phys. Chem. **71**, 2113 (1967).
19. P. R. PHILIP and J. E. DESNOYERS. J. Solution Chem. In press.
20. J. E. DESNOYERS and G. PERRON. J. Solution Chem. In press.
21. B. E. CONWAY, R. E. VERRALL, and J. E. DESNOYERS. Trans. Faraday Soc. **62**, 2738 (1966).
22. S. SUBRAMANIAN and J. C. AHLUWALIA. J. Phys. Chem. **72**, 2525 (1968).
23. R. L. KAY and D. F. EVANS. J. Phys. Chem. **70**, 2325 (1966).
24. R. KAY, T. VITTUCCIO, C. ZAWOYSKI, and D. F. EVANS. J. Phys. Chem. **70**, 2336 (1966).
25. H. F. STIMSON. Am. J. Phys. **23**, 614 (1955).
26. G. N. LEWIS and M. RANDALL. Thermodynamics. 2nd ed., *Revised by* K. S. Pitzer and L. Brewer. McGraw-Hill, New York. 1961. Chap. 23. pp. 338–339.
27. F. FRANKS, M. GENT, and H. H. JOHNSON. J. Chem. Soc. 2716 (1963).
28. J. F. SKINNER and R. M. FUOSS. J. Phys. Chem. **68**, 1882 (1964).
29. G. KALFOGLOU and H. L. BOWEN. J. Phys. Chem. **73**, 2728 (1969).
30. R. M. NOYES. J. Am. Chem. Soc. **86**, 971 (1964).
31. C. M. CRISS and J. M. COBBLE. J. Am. Chem. Soc. **86**, 5390 (1964).
32. M. H. PANCKHURST. Rev. Pure. Appl. Chem. **19**, 45 (1969).
33. F. J. MILLERO. Chem. Rev. **71**, 147 (1971).
34. E. M. ARNETT and J. J. CAMPION. J. Am. Chem. Soc. **92**, 7097 (1970).
35. F. J. MILLERO. J. Phys. Chem. **73**, 2417 (1969).
36. G. C. KRESHECK, H. SCHNEIDER, and H. A. SCHERAGA. J. Phys. Chem. **69**, 3132 (1965).
37. J. E. DESNOYERS and C. JOLICOEUR. Modern aspects of electrochemistry. Vol. 5. *Edited by* J. O'M. Bockris and B. E. Conway. Plenum Publishing Corp., New York. 1969. p. 1.
38. R. W. GURNEY. Ionic processes in solution. Dover, N.Y. 1962. Chap. 9.
39. C. V. KRISHNAN and H. L. FRIEDMAN. J. Phys. Chem. **74**, 3900 (1970).
40. J. E. DESNOYERS, G. E. PELLETIER, and C. JOLICOEUR. Can. J. Chem. **43**, 3232 (1965).

41. E. GRUNWALD, G. BAUGHMAN, and G. KOHNSTAM. J. Am. Chem. Soc. **82**, 5801 (1960).
42. C. V. KRISHNAN and H. L. FRIEDMAN. J. Phys. Chem. **75**, 388 (1971).
43. J. E. DESNOYERS, M. AREL, G. PERRON, and C. JOLICOEUR. J. Phys. Chem. **73**, 3346 (1969).
44. H. L. FRIEDMAN, C. V. KRISHNAN, and C. JOLICOEUR. Ann. New York Acad. Sci. To be published.
45. Physico-chemical constants of pure organic compounds. *Edited by* J. Timmermans. Elsevier Publishing Co., New York. (1950).
46. Physical properties of chemical compounds. Advanced Chemical Series. Vol. 15. A.C.S. Washington. 1955. p. 11.
47. Physical properties of chemical compounds. Advanced Chemical Series. Vol. 22. A.C.S. Washington. 1959. p. 14.

Can. J. Chem. Downloaded from www.nrcresearchpress.com by 210.87.254.5 on 09/05/12
For personal use only.

Rearrangement Studies with ^{14}C. XXXVII. The Treatment of 1-^{14}C-1-Chlorobutane with Aluminum Chloride

C. C. Lee and I. Y. Zea Ponce

Department of Chemistry and Chemical Engineering, University of Saskatchewan, Saskatoon, Saskatchewan

Received September 3, 1971[1]

After treatment of 1-^{14}C-1-chlorobutane with anhydrous $AlCl_3$ at 20° for 20, 60, or 120 min, the isomeric chlorobutanes recovered were mainly *n*-butyl and *sec*-butyl, with small amounts of *t*-butyl and *iso*-butyl chlorides. Degradations showed only 0.2–0.4% rearrangement of the ^{14}C-label from C-1 to -2 in the recovered ^{14}C-1-chlorobutane, while extensive scramblings over all four carbon positions were noted for the recovered ^{14}C-2-chlorobutane. Successive 1,2-hydride shifts interconverting the 2-butyl cations or ion-pairs were found to play a major role in accounting for the scrambling data. It was concluded that processes involving protonated methylcyclopropanes could not be the main pathway for the rearrangement of the label into C-2 and -3 of the ^{14}C-2-chlorobutane. 1,2-Ethyl followed by 1,2-hydrogen shifts giving rise to encumbered 2-butyl cations with different structural features appeared to be required to explain the ^{14}C-contents in the C-2 and -3 positions.

Le traitement du ^{14}C-chloro-1 butane par $AlCl_3$ anhydre à 20° pendant 20, 60 et 120 min, conduit aux chlorobutanes isomères dont les principaux sont les chlorures de *n*-butyle et de *sec*-butyle, avec de petites quantités de chlorures de *t*-butyle et d'*iso*-butyle. Les dégradations montrent seulement un réarrangement de 0.2–0.4% du ^{14}C de la position C-1 à -2 dans le ^{14}C-chloro-1 butane retrouvé tandis qu'un mélange important de marquage a été trouvé à travers les quatre carbones dans le ^{14}C-chloro-2 butane final. Les déplacements-1,2 successifs d'hydrure, interconvertissant les cations butyl-2 ou les paires d'ions, jouent un rôle majeur permettant de rendre compte des données de ce mélange. On a conclu que les transformations faisant intervenir les méthylcyclopropanes protonés ne pouvaient être le processus réactionnel principal dans le réarrangement en C-2 et -3 du ^{14}C-chloro-2 butane marqué. Les déplacements-1,2 d'éthyle puis d'hydrogène conduisant à des cations butyl-2 encombrés avec diverses caractéristiques structurales, apparaissent nécessaires pour expliquer les teneurs en ^{14}C sur les positions C-2 et -3. [Traduit par le journal]

Canadian Journal of Chemistry, **50**, 3179 (1972)

Protonated cyclopropanes as reaction intermediates are of some current interest and much of the work in this area has dealt with unsubstituted protonated cyclopropane, $C_3H_7^+$ (1, 2). Recently, Deno and coworkers (3) have obtained evidence suggesting a role for protonated cyclopropane intermediates in the reaction of D_2SO_4 with suitably substituted cyclopropanes such as cyclopropanecarboxylic acid and its 1-methyl derivative. However, the addition of DCl to methylcyclopropane (4) and the deamination of various *d*-labeled 1-butylamines (5) failed to give any isotopic scrambling data in support of the intermediacy of protonated methylcyclopropane. On the other hand, proton scramblings in the 2-butyl cation observed by n.m.r. (6) and the $HF–SbF_5$ catalyzed isomerization of 1-^{13}C-butane to 2-^{13}C-butane (7) were interpreted as proceeding via protonated methylcyclopropane. In the present work the study on the involvement of protonated cyclopropane intermediates in the treatment of 1-^{14}C-1-chloropropane with $AlCl_3$ (8) was extended to include an investigation of the rearrangements induced by treatment of 1-^{14}C-1-chlorobutane (**1**-Cl-1-^{14}C) with $AlCl_3$ in an attempt to ascertain whether protonated methylcyclopropane intermediates would play a role in the reaction.

Results and Discussion

1-Cl-1-^{14}C (10.0 g) and anhydrous $AlCl_3$ (1.0 g) were stirred at 20° for 20, 60, or 120 min and then quenched by the addition of ice-water. The recovered material was converted to the Grignard reagent and treated with oxygen (9). Inactive *n*-, *sec*-, *t*- and *iso*-butyl alcohols (**1**-OH, **2**-OH, **3**-OH, and **4**-OH, respectively) were added as carriers and the four diluted alcohols were recovered by preparative v.p.c. Isotope dilution calculations gave the relative amounts of these isomeric alcohols derived from the original mixture of butyl chlorides in the recovered product. The results are given in Table 1.

The **1**-OH-^{14}C and **2**-OH-^{14}C, purified by preparative v.p.c., were degraded to give the

[1]Revision received June 16, 1972.

Can. J. Chem. Downloaded from www.nrcresearchpress.com by 210.87.254.42 on 09/05/12
For personal use only.

TABLE 1. Relative yields (%) of isomeric butyl alcohols derived from the corresponding chlorides recovered after treatment of 1-^{14}C-1-chlorobutane (**1**-Cl-1-^{14}C) with $AlCl_3$*

	Contact time (min)								
	60					20		120	
Alcohol	Expt. 1†	Expt. 2	Expt. 3	Expt. 4	Expt. 5	Expt. 6	Expt. 7	Expt. 8	Expt. 9
n-BuOH	94.2	71.1	71.4	71.1	67.5	66.4	69.7	67.3	65.3
sec-BuOH	5.3	27.3	25.2	26.2	30.5	30.4	26.8	26.8	27.7
t-BuOH	0.3	1.2	2.9	2.4	1.7	2.6	2.9	5.0	5.8
iso-BuOH	0.2	0.3	0.3	0.3	0.3	0.6	0.5	0.9	1.2

*Obtained by isotope dilution calculations; the ^{14}C-activities were determined on the v.p.c. purified *t*-BuOH and on the α-naphthylurethanes of the other alcohols. The lowest activities measured were about 1100 c.p.m./mmol for the diluted *iso*-BuOH from the experiments with 60 min contact time. Different batches of $AlCl_3$ were used for the 60 min and for the 20 and 120 min experiments.
†The **1**-Cl-1-^{14}C used as reactant was contaminated by about 5–10% diethyl ether, which apparently deactivated the catalyst.

isotopic distributions in the butyl group. **1**-OH-^{14}C was oxidized to butyric acid, converted to 1-propylamine, and then oxidized to propionic acid (10), which in turn was degraded by conversion to acetic acid and then to methylamine (11). The **2**-OH-^{14}C was treated with Br_2–NaOH to give CBr_4 and propionic acid (9), the latter again being degraded to acetic acid and methylamine. The activities of appropriate solid derivatives of the degradation products gave the ^{14}C-distributions. The results indicate that for the recovered 1-butyl product, there was only about 0.2–0.4% rearrangement of the ^{14}C-label from C-1 to -2, and essentially none to C-3 and -4. Extensive scrambling of the label was found in the **2**-OH-^{14}C, the data being summarized in Table 2.

In previous studies on the deamination of various *d*-labeled 1-butylamines (5, 12), no isotope position rearrangement was found in the 1-butanol product and this was interpreted as evidence eliminating the possibility of a 1,2-ethyl shift. The presently observed 0.2–0.4% rearrangement of the ^{14}C-label from C-1 to -2 in the 1-butyl product, though small, is believed to be real since the activities observed for C-2 were beyond experimental errors. Also in the deamination studies (5), it was noted that the only isotope position isomers observed in the 2-butanol product were attributable to successive 1,2-hydride shifts involving interconversions between 2-butyl cations. Similarly, in earlier work with ^{14}C-labeled 2-butyl systems (9, 13), only 1,2-hydride shifts interconverting the 2-butyl cations were reported. Such processes operating in the present system would only scramble the ^{14}C-label over the C-1 and -4 positions of the recovered **2**-Cl-^{14}C. The rearrangements of the ^{14}C-label into C-2 and -3 in the 2-butyl product (Table 2), which have not been observed previously, would require some explanation other than successive 1,2-hydride shifts.

A possible route involving protonated methylcyclopropane intermediates could lead to the scrambling of the ^{14}C-label into C-2 and -3 of the **2**-Cl-^{14}C. Much of the recent discussion on protonated cyclopropanes has been concerned with edge- and corner-protonations (1, 2, 8, 14). Equilibration of protonated methylcyclopropanes could proceed via edge-protonated species **5***a–c* and corner-protonated species **6***a–c*. **2**-Cl-3-^{14}C could be formed from **5***b* or **6***b*, and under the reaction conditions, **2**-Cl-3-^{14}C could give rise to **2**-Cl-2-^{14}C. Such processes would lead to the expectation that shorter contact times between the reactants should give more **2**-Cl-3-^{14}C than **2**-Cl-2-^{14}C, but this is opposite to what was observed (Table 2).

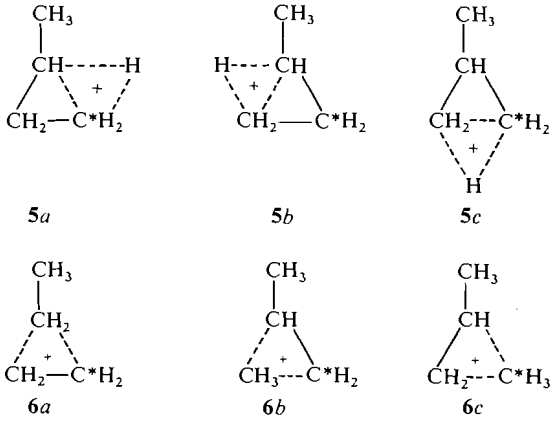

Can. J. Chem. Downloaded from www.nrcresearchpress.com by 210.87.254.42 on 09/05/12
For personal use only.

Can. J. Chem. Downloaded from www.nrcresearchpress.com by 210.87.254.42 on 09/05/12
For personal use only.

TABLE 2. ^{14}C-Distribution in the 2-butyl product recovered after treatment of 1-^{14}C-1-chlorobutane (**1**-Cl-1-^{14}C) with $AlCl_3$

Contact time (min)	Expt.	Specific activity (c.p.m./mmol)*					^{14}C-Distribution (%)†			
		$CH_3CH_2CHOHCH_3$‡	CBr_4	CH_3CH_2COOH§	CH_3COOH‖	CH_3NH_2¶	C-1	C-2	C-3	C-4
60	1**		4 200	7 900	4 800	4 100	34.7	25.6	5.7	33.9
	2	12 900	5 300	7 400	5 500	4 600	41.7	15.0	7.1	36.2
	3	32 400	14 200	18 000	13 500	11 300	44.1	14.0	6.8	35.1
	4	16 100	6 900	9 100	6 800	5 700	43.1	14.4	6.8	35.7
	5	22 600	9 700	12 800	9 600	8 000	43.1	14.2	7.1	35.6
20	6		28 200	35 600	21 900	19 400	44.2	21.5	3.9	30.4
	7		30 700	40 000	25 200	22 600	43.4	21.0	3.6	32.0
120	8		25 400	33 000	26 900	21 000	43.5	10.5	10.0	36.0
	9		15 400	20 800	17 400	13 600	42.5	9.5	10.4	37.6

*Measured by a liquid scintillation counter and corrected for quenching.
†The sum of the specific activities of CBr_4 and CH_3CH_2COOH was taken as 100%.
‡Assayed as the α-naphthylurethane.
§Assayed as the *S*-benzylisothiouronium salt.
‖Assayed as the *p*-nitrobenzyl ester.
¶Assayed as the *p*-toluenesulfonamide.
**The 1-Cl-1-^{14}C used as reactant was contaminated by about 5–10% diethyl ether, which apparently deactivated the catalyst.

Can. J. Chem. Downloaded from www.nrcresearchpress.com by 210.87.254.42 on 09/05/12
For personal use only.

Pertinent to the above representation of protonated methylcyclopropanes as **5***a–c* or **6***a–c* are the recently reported calculations of Radom and coworkers (15) on the $C_3H_7^+$ cations. These workers concluded that besides the stable 2-propyl cation, a "methyl eclipsed 1-propyl cation" with distorted geometry, which could be regarded as a distorted corner-protonated cyclopropane (the term "partially-bridged" structure was also used in a private communication from Professor P. v. R. Schleyer), may well be the only other potential minimum in the complete $C_3H_7^+$ surface. If partially-bridged structures **7***a* and *b* were stable species, equilibrating through **6***a* as a transition state, 1,3-hydride shifts could give rise to **2**-Cl-4-^{14}C and

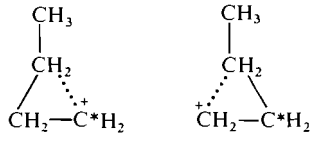

7a *7b*

2-Cl-3-^{14}C, respectively, from **7***a* and *b* via **5***a* and *b* as transition states. As pointed out in the preceding paragraph, such a route would also be expected to give more **2**-Cl-3-^{14}C than **2**-Cl-2-^{14}C with shorter contact time between the reactants, and this does not agree with the observed results.

The above considerations thus suggest that protonated methylcyclopropane intermediates would not likely be involved in the main pathway leading to the rearrangement of the isotopic label into the C-2 and -3 positions of the recovered **2**-Cl-^{14}C. However, the possibility of minor involvements of protonated methylcyclopropanes could not be unequivocally eliminated. The formation of *i*-BuCl (**4**-Cl) (Table 1) via only classical ions is unlikely as this would require the unfavorable rearrangement of *sec*-butyl to isobutyl cations. Bimolecular reactions followed by rearrangement and fragmentation (16, 17) conceivably could give rise to *t*-BuCl (**3**-Cl) and *i*-BuCl (**4**-Cl), with **3**-Cl dominating. Alternatively, **4**-Cl could be derived from protonated methylcyclopropanes **5***c* or **6***b* and *c*, and subsequent effects of the $AlCl_3$ would convert much of the **4**-Cl to **3**-Cl. It is of interest to note that more than a decade ago, Roberts and coworkers (18, 19) had observed that at relatively high temperatures of 80 or 100°, $AlCl_3$ could induce the isomerization of *sec*-butylbenzene to isobutylbenzene, and these workers have attributed the process to the intervention of an intermediate π-complex between the benzene ring and a methyl-bridged cation (corner-protonated methylcyclopropane) analogous to **6***b* and *c*.

An alternative route for the scrambling of the ^{14}C-label into C-2 and -3 of the recovered **2**-Cl-^{14}C could involve 1,2-shifts in the classical 1-butyl and 2-butyl cations. A simple scheme might be as depicted in Scheme 1. A significant role is assigned to the 1,2-ethyl shift, and if product formation from the primary 1-butyl cation to give **1**-Cl were relatively slow compared to its rearrangement to the 2-butyl cation, only very small amounts of **1**-Cl-2-^{14}C would be formed as was observed. The processes would predict more **2**-Cl-2-^{14}C than **2**-Cl-3-^{14}C with shorter contact time as was also observed. Such a scheme, however, is not adequate as a complete explanation of the data in Table 2. If the ions were free and unencumbered as depicted, and if the ^{14}C isotope effects were relatively minor and negligible, **8**-1-^{14}C and **8**-2-^{14}C should behave in the same way as they differ only in the location of the isotopic label. Therefore, the scrambling between C-1 and -4 should be related

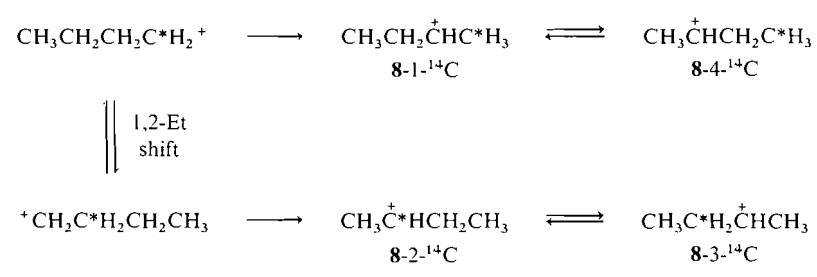

SCHEME 1

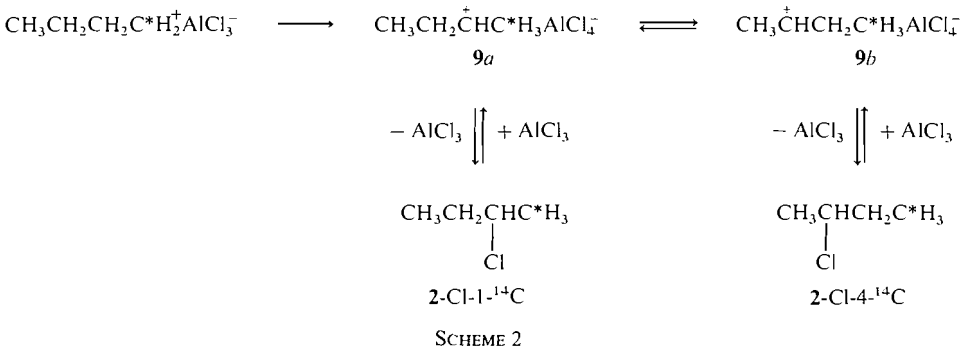

SCHEME 2

to the scrambling between C-2 and -3 so that, in a given experiment, the ratio of **2**-Cl-1-^{14}C to **2**-Cl-4-^{14}C must be equal to the ratio of **2**-Cl-2-^{14}C to **2**-Cl-3-^{14}C, and this was not observed. From Table 2, it can be seen that in the recovered **2**-Cl-^{14}C, the ratio of the ^{14}C-contents for C-2/C-3 is greater than that for C-1/C-4 in the experiments with contact times of 20 or 60 min. On the other hand, with a longer contact time of 120 min, apparently complete equilibration between C-2 and -3 has been achieved, while the ^{14}C ratio for C-1/C-4 is still greater than unity. To account for these differences, modifications of the simple classical ion scheme appear to be necessary.

Firstly, there must be a fast process leading from reactant to **2**-Cl-1-^{14}C and **2**-Cl-4-^{14}C, and which could eventually equilibrate these two isotope position isomers. Successive 1,2-hydride shifts, probably involving ion-pairs which gave the final product only upon quenching, as depicted in Scheme 2, would be adequate in

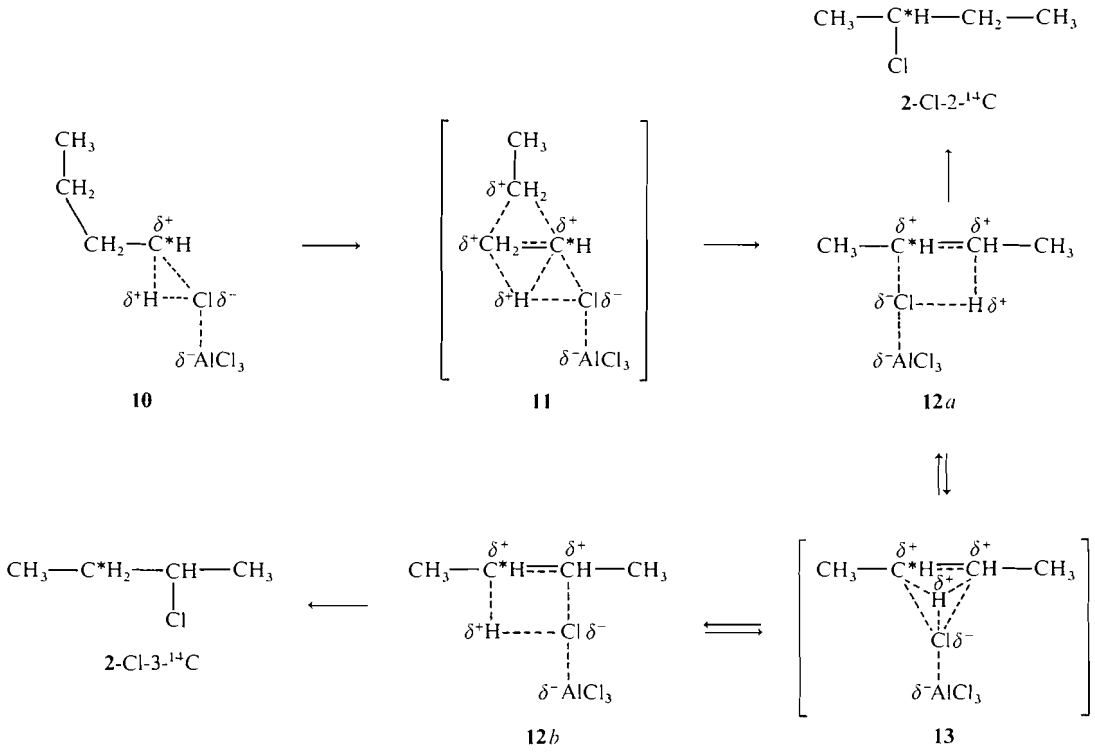

SCHEME 3

Can. J. Chem. Downloaded from www.nrcresearchpress.com by 210.87.254.42 on 09/05/12
For personal use only.

Can. J. Chem. Downloaded from www.nrcresearchpress.com by 210.87.254.42 on 09/05/12
For personal use only.

accounting for this scrambling of the label between C-1 and -4.

Secondly, there must be another process, fairly fast but slower than the first one, leading from reactant to **2**-Cl-2-^{14}C and **2**-Cl-3-^{14}C. Initially, this process would give mostly **2**-Cl-2-^{14}C with little, if any, **2**-Cl-3-^{14}C, but eventually, **2**-Cl-2-^{14}C would equilibrate with **2**-Cl-3-^{14}C and this would have to take place at a rate faster than the equilibration between **2**-Cl-1-^{14}C and **2**-Cl-4-^{14}C in order to account for the results observed with a contact time of 120 min (Table 2). Thus the intermediates responsible for the formation of **2**-Cl-2-^{14}C and **2**-Cl-3-^{14}C would have to be different structurally, and hence behave differently, from ion-pairs **9***a* and *b*. A possible representation of these intermediate species with different structural features could be encumbered butyl cations, as depicted in Scheme 3, involved in the 1,2-ethyl and the subsequent 1,2-hydrogen shifts.

It might be visualized that under the influence of the $AlCl_3$, stretching of the C—Cl bond of the reactant, **1**-Cl-1-^{14}C, could impart positive characteristics to the C-1 carbon and hydrogen atoms, allowing the chlorine atom to be hydrogen-bonded to give **10**. Ethyl and hydrogen shifts could then occur as shown in Scheme 3, giving rise to **12***a* and *b* with **11** and **13** as transition states. Formation of the products, **2**-Cl-2-^{14}C and **2**-Cl-3-^{14}C, would take place only upon quenching; otherwise, if these isotope position isomers were formed during the reaction, they would behave and equilibrate similarly as **2**-Cl-1-^{14}C and **2**-Cl-4-^{14}C. The essential assumption that **9***a*, *b* and **12***a*, *b* could behave differently would also suggest that these species could undergo side reactions, such as elimination, at different rates. This would provide an explanation for the observation of a lesser percentage of rearrangement of the ^{14}C-label into C-2 and -3 in the experiments with longer contact time, as recorded in Table 2.

Experimental

*1-^{14}C-1-Chlorobutane (**1**-Cl-1-^{14}C)*

The reaction of 1-propylmagnesium chloride with $^{14}CO_2$ to give 1-^{14}C-butyric acid, followed by $LiAlH_4$ reduction to 1-^{14}C-1-butanol and conversion of the latter to 1-^{14}C-1-butyl tosylate (**1**-OTs-1-^{14}C), b.p. 134–135° at 2.5 mm (lit. (20) b.p. 135° at 2.5 mm) were carried out according to standard procedures. Conversion of the **1**-OTs-1-^{14}C to **1**-Cl-1-^{14}C was effected in 75% yield by a displacement reaction with $CaCl_2$ in ethylene glycol in the same manner as previously described for the preparation of 1-^{14}C-1-chloropropane (21). The **1**-Cl-1-^{14}C was purified by preparative v.p.c. using a Pye Automatic Preparative Chromatograph with a 15 ft × 3/8 in. copper column packed with 25% β,β'-oxydipropionitrile on 60/80 mesh chromosorb P. Degradation (see below) of the **1**-Cl-1-^{14}C so obtained gave inactive 1-propylamine, indicating that all of the ^{14}C-label was located at C-1.

*Treatment of **1**-Cl-1-^{14}C with $AlCl_3$*

In a 100-ml round-bottom flask, equipped with magnetic stirrer and reflux condenser, 10.0 g (108 mmol) of **1**-Cl-1-^{14}C and 1.0 g (7.5 mmol) of anhydrous $AlCl_3$ were stirred at 20° for 20, 60, or 120 min. Ice-water was then added. The organic layer was separated, washed successively with 10% NaOH solution and with water, and then dried over anhydrous $MgSO_4$. The recoveries of organic material from the various experiments ranged between 61–71%.

The recovered material was converted to the Grignard reagent and treated with oxygen as previously described (9) to give a mixture of isomeric butyl alcohols. A small sample of this mixture of alcohols was separated by preparative v.p.c. (Aerograph Autoprep with a 10 ft × 3/8 in. copper column packed with 20% Carbowax 20 M on 60/80 mesh chromosorb P) to give pure, undiluted **1**-OH-^{14}C whose specific activity would be equal to the specific activity of any one of the four undiluted, isomeric butyl alcohols. To another small sample of the mixture of alcohols (usually about 0.4–0.5 g), appropriate amounts of ordinary *n*-, *sec*-, *t*-, and *iso*-butyl alcohols (**1**-OH, **2**-OH, **3**-OH, and **4**-OH, respectively) were added as carriers and pure samples of the four diluted alcohols were recovered by preparative v.p.c. using the Carbowax column. Knowing the weights of the carriers and the specific activities of the undiluted and diluted alcohols, the yields of the undiluted alcohols were calculated. The following actual data from experiment 2 will serve as an illustration of the calculations.

The specific activity of the isomeric butyl alcohols before isotopic dilution, as measured by the α-naphthylurethane of the v.p.c. purified, undiluted **1**-OH-^{14}C, was 726 000 c.p.m./mmol.

The weights of inactive **1**-OH, **2**-OH, **3**-OH, and **4**-OH added as carriers were, respectively, 501.0, 690.7, 624.6, and 662.4 mg, and the specific activities of these four diluted alcohols (measured as the α-naphthylurethanes except for 3-OH) were, respectively, 231 900, 83 600, 4740, and 1140 c.p.m./mmol.

If x = the yield of **1**-OH-^{14}C in mg, then (726 000 c.p.m./mmol) (x/74.12 mmol) = (231 900 c.p.m./mmol)[(x + 501.0)/74.12 mmol]; x = 234 mg.

Similarly, the yields of **2**-OH-^{14}C, **3**-OH-^{14}C, and **4**-OH-^{14}C were calculated to be 89.8, 4.1 and 1.0 mg, respectively.

Hence for experiment 2, the relative percentage yields of **1**-OH-^{14}C, **2**-OH-^{14}C, **3**-OH-^{14}C, and **4**-OH-^{14}C, respectively, were 71.1, 27.3, 1.2, and 0.3%, as given in Table 1.

Degradation Procedures

The main products, **1**-OH-^{14}C and **2**-OH-^{14}C, derived from the above treatments, were purified by preparative v.p.c. and diluted with inactive carriers to provide sufficient quantities of material for the degradations.

The 1-OH-^{14}C was oxidized to butyric acid in alkaline $KMnO_4$. A typical run is as follows. A solution of 5.0 g (68 mmol) of 1-OH-^{14}C in 300 ml of 20% NaOH was stirred and cooled in an ice-bath. With the temperature kept below 15°, 25 g (158 mmol) of $KMnO_4$ was added in small portions over a period of 2 h. The mixture was left at room temperature overnight and then filtered to remove the MnO_2. Acidification of the filtrate with H_2SO_4, followed by steam distillation, neutralization, and evaporation gave 5.7 g (76%) of the sodium salt of butyric acid, part of which was converted, for ^{14}C-determination, to the solid derivative, *S*-benzylisothiouronium butyrate, m.p. 148–149° (lit. (22*a*) m.p. 149°).

The sodium butyrate was converted by a Schmidt reaction (11, 23) to 1-propylamine, benzamide derivative, m.p. 84° (lit. (22*b*), m.p. 84°) or α-naphthylurea derivative, m.p. 195–196° (lit. (24) m.p. 196°). The 1-propylamine was oxidized to propionic acid by alkaline $KMnO_4$ according to the method of Mosbach and coworkers (10) and the propionic acid, in turn, was degraded to acetic acid and then to methylamine as previously described (11).

The 2-OH-^{14}C was converted to CBr_4 and propionic acid by treatment with Br_2–NaOH (9) and the propionic acid was similarly degraded to acetic acid and methylamine (11).

Valuable comments and suggestions made by Professor Arthur Fry, who suggested the explanation given in Scheme 3, and the financial support given by the National Research Council of Canada are gratefully acknowledged.

1. C. J. COLLINS. Chem. Rev. **69**, 543 (1969).
2. C. C. LEE. *In* Progress in physical organic chemistry. Vol. 7. A. Streitwieser, Jr. and R. W. Taft, *editors*. Interscience Publishers, New York. 1970. pp. 129–187.
3. N. C. DENO, W. E. BILLUPS, D. LAVIETES, P. C. SCHOLL, and S. SCHNEIDER. J. Am. Chem. Soc. **92**, 3700 (1970).
4. N. C. DENO, D. LAVIETES, J. MOCKUS, and P. C. SCHOLL. J. Am. Chem. Soc. **90**, 6457 (1968).
5. G. J. KARABATSOS, R. A. MOUNT, D. O. RICKTER, and S. MEYERSON. J. Am. Chem. Soc. **92**, 1248 (1970).
6. M. SAUNDERS, E. L. HAGEN, and J. ROSENFELD. J. Am. Chem. Soc. **90**, 6882 (1968).
7. D. M. BROUWER. Rec. Trav. Chim. **87**, 1438 (1968).
8. C. C. LEE and D. J. WOODCOCK. J. Am. Chem. Soc. **92**, 5992 (1970).
9. C. C. LEE, J. W. CLAYTON, D. G. LEE, and A. J. FINLAYSON. Tetrahedron, **18**, 1395 (1962).
10. E. G. MOSBACH, E. F. PHARES, and S. F. CARSON. Arch. Biochem. Biophys. **33**, 179 (1951).
11. C. C. LEE and J. E. KRUGER. Tetrahedron, **23**, 2539 (1967).
12. A. STREITWIESER, JR. and W. D. SCHAEFFER. J. Am. Chem. Soc. **79**, 2888 (1957).
13. J. D. ROBERTS, W. BENNETT, R. E. MCMAHON, and E. W. HOLROYD, JR. J. Am. Chem. Soc. **74**, 4283 (1952).
14. G. J. KARABATSOS, C. E. ORZECH, JR., J. L. FRY, and S. MEYERSON. J. Am. Chem. Soc. **92**, 606 (1970).
15. L. RADOM, J. A. POPLE, V. BUSS, and P. v. R. SCHLEYER. J. Am. Chem. Soc. **94**, 311 (1972).
16. G. J. KARABATSOS and F. M. VANE. J. Am. Chem. Soc. **85**, 729 (1963).
17. G. J. KARABATSOS, F. M. VANE, and S. MEYERSON. J. Am. Chem. Soc. **85**, 733 (1963).
18. R. M. ROBERTS, Y. W. HAN, C. H. SCHMID, and D. A. DAVIS. J. Am. Chem. Soc. **81**, 640 (1959).
19. R. M. ROBERTS and D. SHIENTHONG. J. Am. Chem. Soc. **82**, 732 (1960).
20. K. L. SERVIS and J. D. ROBERTS. J. Am. Chem. Soc. **86**, 3773 (1964).
21. C. C. LEE, B. S. HAHN, K. M. WAN, and D. J. WOODCOCK. J. Org. Chem. **34**, 3210 (1969).
22. A. I. VOGEL. Elementary practical organic chemistry. Part II. Qualitative organic analysis. Longman, Green and Co., London. 1957. (*a*) p. 592; (*b*) p. 616.
23. O. A. REUTOV and T. N. SHATKINA. Tetrahedron, **18**, 237 (1962).
24. M. FRANKEL and S. PATAI. Tables for identification of organic compounds, 2nd ed. Chemical Rubber Co., Cleveland, Ohio. 1964. p. 213.

Can. J. Chem. Downloaded from www.nrcresearchpress.com by 210.87.254.42 on 09/05/12
For personal use only.

Thermal Routes to Substituted Cyclopentadienes

D. M. FINDLAY, MARIE LESSARD ROY, AND STEWART MCLEAN
Department of Chemistry, University of Toronto, Toronto 181, Ontario

Received April 19, 1972

An investigation has been made with the aim of finding a route to cyclopentadienes, particularly those with a single substituent at the 5-position, in which the final step is a thermal process of low enough activation energy that the cyclopentadiene produced does not undergo rearrangement by hydrogen migration under the reaction conditions. In the routes studied the final intermediates have been suitably substituted norbornenes which can lead to the required cyclopentadiene and an aromatic fragment by a retro-Diels–Alder reaction. In one series the intermediate was a phenyl azide adduct of norbornadiene which fragmented to cyclopentadiene and phenyltriazole, but the temperature required for this was clearly too high to allow substituted cyclopentadienes to be isolated before they had rearranged. In the course of this work, in addition to the *exo*-adduct of phenyl azide, the *endo*-adduct and a number of bisadducts were obtained and studied. In another series, adducts of tetraphenylcyclopentadienone and dimethyldiphenylcyclopentadienone with norbornadiene and 7-phenylnorbornadiene were prepared and studied. Decarbonylation of the adducts was effected both thermally and photochemically; in the latter case the reaction could be carried out at low temperature and the dihydrobenzene (a dihydrobenzonorbornadiene) produced was isolable. With or without isolation, the dihydrobenzene underwent a subsequent retro-Diels–Alder reaction to provide the cyclopentadiene and a substituted benzene. Kinetic studies showed that the activation energy for this process was almost but not quite low enough to satisfy the conditions stipulated, and in no case was a 5-substituted cyclopentadiene isolated before it had rearranged.

Une voie d'accès aux cyclopentadiènes a été étudiée (particulièrement ceux possédant un seul substituant en position 5) dans laquelle l'étape finale est un processus thermique d'énergie d'activation suffisamment basse pour que le cyclopentadiène formé ne subisse pas de réarrangement par migration d'hydrogène, dans les conditions de la réaction. Dans les voies d'accès envisagées, les intermédiaires finals ont été des norbornènes convenablement substitués pouvant mener au cyclopentadiène voulu plus un fragment aromatique résultant d'une réaction du type "rétro-Diels–Alder". Dans une série, l'intermédiaire qui résulte de l'addition entre un phénylazide et le norbornadiène, se fragmente en cyclopentadiène et phényltriazole mais la température utilisée nettement trop élevée, n'a pas permis d'isoler les cyclopentadiènes substitués avant leur réarrangement. Au cours de ce travail, en plus du composé d'addition *exo* du phénylazide, le produit *endo* et un certain nombre de composés de bis-addition ont été obtenus et examinés. Dans une autre série, on a préparé et étudié les produits d'addition entre les tétraphénylcyclopentadiènone et diméthyldiphénylcyclopentadiènone et le norbornadiène et phényl-7 norbornadiène. La décarbonylation des produits résultants a été effectuée à la fois par voie thermique et photochimique, dans ce dernier cas, la réaction effectuée à basse température a permis d'isoler le dihydrobenzène (dihydrobenzonorbornadiène). Celui-ci, isolé ou non, subit une réaction subséquente de "rétro-Diels–Alder" et donne le cyclopentadiène plus un benzène substitué. Les études cinétiques montrent que l'énergie d'activation de ce processus est presque suffisamment (mais pas tout à fait) basse pour satisfaire aux conditions stipulées; par conséquent, l'isolement d'un cyclopentadiène substitué en 5 avant son réarrangement n'a pas été possible dans aucun cas.

[Traduit par le journal]

Canadian Journal of Chemistry, **50**, 3186 (1972)

In general, 5-monosubstituted cyclopentadienes (**1** where R represents an organic substituent) are less stable than their positional isomers (**2** and **3**) and constitute a small fraction of the equilibrium mixture. Equilibrium can be established through a base-catalyzed process or through a purely thermal 1,5-sigmatropic migration of a hydrogen atom, the latter process being so facile that it takes place at an appreciable rate even at room temperature, at least in the cases that have been studied (1). Our interest in studying this rearrangement in more detail, and particularly how varying the group R affects it, led us to seek a general synthesis of molecules of formula **1**. (The route used previously, requiring a nucleophilic displacement by a cyclopentadienide ion, can not be generalized to include, for example, cases where R is an aryl group.) The extremely facile rearrangement of **1** clearly imposes severe constraints on a synthetic scheme, since it can be expected that **1** will not be isolable if the step which generates it requires basic conditions or heat, with room temperature representing a probable upper limit even in favorable cases. We have, therefore, sought a route by which **1** is formed under neutral conditions in a

Can. J. Chem. Downloaded from www.nrcresearchpress.com by 210.87.254.6 on 09/05/12
For personal use only.

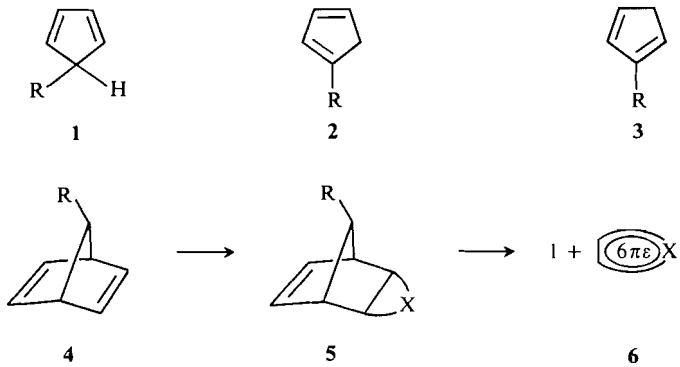

thermal process of such low activation energy that the reaction takes place below room temperature. Although we have not yet succeeded in achieving this goal, we describe here the progress we have made in developing synthetic sequences which generate cyclopentadienes in reactions of low activation energy.

The synthetic plan envisaged the conversion of a 7-substituted norbornadiene (**4**), to which a general synthetic route is available (2), into a derivative (**5**) which could undergo a retro-Diels–Alder reaction to afford the cyclopentadiene and a fragment (**6**) that had aromatic character. It was hoped that the aromatic stabilization of **6** would provide a driving force for the reaction and lower its activation energy sufficiently to meet our requirements.

Since a 1,3-dipolar cycloaddition reaction of **4** to form **5** offered a reaction that could be used to develop this plan, the reaction of the model compound norbornadiene itself (**4***a*) with phenyl azide was investigated. It was found, however, that the cycloaddition reaction took place at an appreciable rate in cyclohexane solution only above 60° and that the adduct (**7**) required even higher temperatures (at least 80°) in order to undergo the required retro-Diels–Alder reaction to afford the anticipated cyclopentadiene and 1-phenyl-1,2,3-triazole. It is obvious, therefore, that these conditions are too vigorous to offer any hope of using them to isolate thermally labile cyclopentadienes.

In the course of our investigation of the conditions required to effect the reaction of norbornadiene with phenyl azide, we discovered that, in addition to the expected *exo*-adduct **7**, the *endo*-adduct (**8**) was also formed, apparently the first example of an adduct formed with this stereochemistry in such reactions. Moreover, when phenyl azide was allowed to react with a deficiency of norbornadiene or with preformed monoadduct, four (**9**, **10**, **11**, **12**) of the possible stereoisomeric bisadducts were formed, and only the *endo–endo*-bisadducts (**13**, **14**) appeared to be absent in the products. We have reported the isolation and characterization of these adducts in a preliminary communication (3) and the significance of these results with respect to the general question of the orientation of azide additions has been commented on by others (4). Structural assignments were based on an analysis of the n.m.r. spectrum and a determination of the molecular composition of each adduct. In the mass spectrum, the monoadducts showed a low intensity parent ion and readily lost N_2, while the highest mass peak observed for the bisadducts was a low intensity peak at $M - N_2$, and the loss of a further N_2 fragment was also apparent. The photochemical behavior of the adducts was also investigated briefly: both *exo–exo*-adducts (**9**, **10**) were converted cleanly to the same bisaziridine on exposure to sunlight, the *exo–endo*-adducts (**11**, **12**) also appeared to form a bisaziridine under the same conditions, but the product was not isolated or properly characterized. The *exo*-monoadduct (**7**) did not give a characterizable product under these conditions; however, it has been reported recently (5) that the latter adduct is also converted to an aziridine by photolysis under the appropriate conditions.

Since the elimination of a triazole by a retro-Diels–Alder reaction did not appear to offer a route of sufficiently low activation energy to meet our requirements, we turned to a corresponding reaction in which the fragment **6**

Can. J. Chem. Downloaded from www.nrcresearchpress.com by 210.87.254.6 on 09/05/12
For personal use only.

Can. J. Chem. Downloaded from www.nrcresearchpress.com by 210.87.254.6 on 09/05/12
For personal use only.

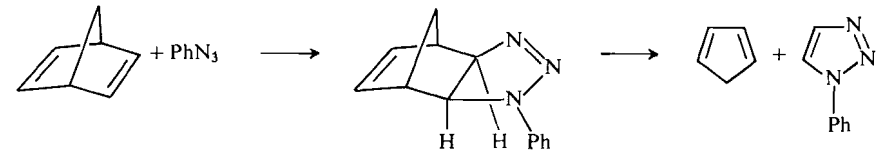

4a 7

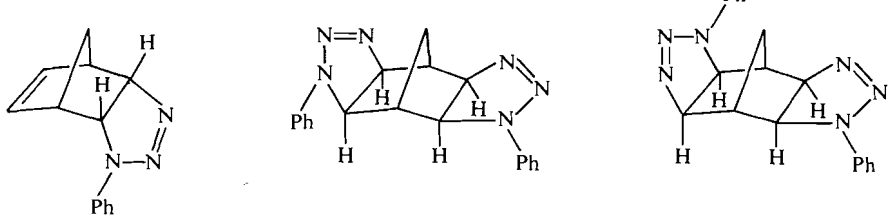

8 9 10

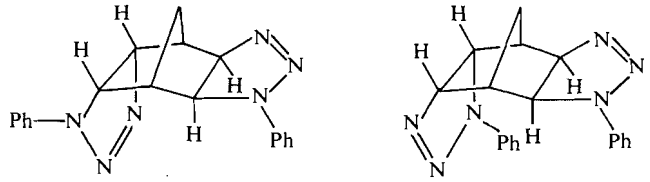

11 12

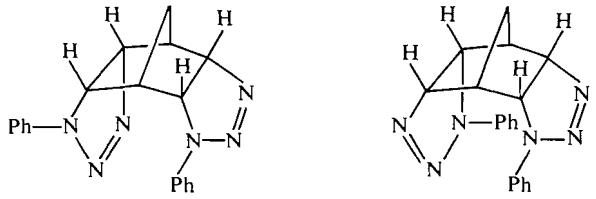

13 14

eliminated is a benzene. The proposed route for this required the addition of a cyclopentadienone to a norbornadiene (**4**), followed by decarbonylation of the intermediate **15** to provide the dihydrobenzene (**16**) which would be expected to undergo the retro-Diels–Alder reaction readily.

It had been reported (6) that norbornadiene does in fact react with tetraphenylcyclopentadienone (tetracyclone) in the expected manner when the components are heated together, but that the subsequent steps also take place under these conditions and the products obtained are cyclopentadiene and tetraphenylbenzene. However, when we examined the reaction by allowing norbornadiene (**4***a*) to react with tetracyclone in refluxing chloroform or benzene, the ketone **15***a* was obtained in excellent yield and was moderately stable to prolonged exposure to the reaction conditions; this Diels–Alder reaction was also markedly accelerated by aluminum chloride (7). The product was assigned structure **15***a* from its spectroscopic characteristics, which included in the i.r. spectrum a carbonyl absorption at 5.63 μ and, in the n.m.r. spectrum, two one-proton doublets with $J = 9.5$ Hz at τ 7.35 and 8.59 and a sharp peak at τ 7.14 associated with the two protons on the carbon atoms involved in the ring fusion. The lack of coupling exhibited by the latter protons indicates that the

Can. J. Chem. Downloaded from www.nrcresearchpress.com by 210.87.254.6 on 09/05/12
For personal use only.

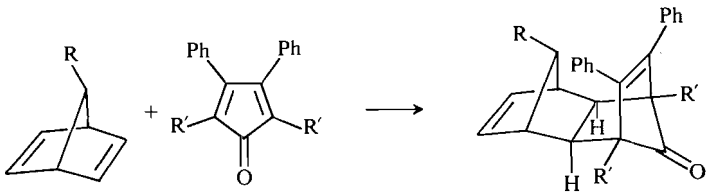

4 15

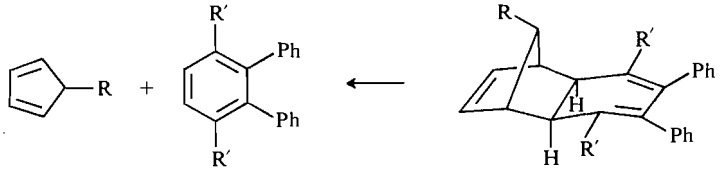

1 16

Substituents (if specified)
(*a*) R = H; R′ = Ph (*c*) R = Ph; R′ = Me
(*b*) R = Ph; R′ = Ph (*d*) R = H; R′ = Me

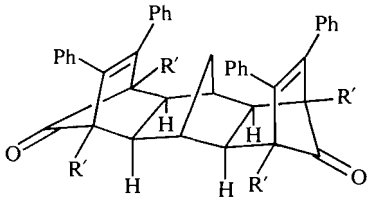

17

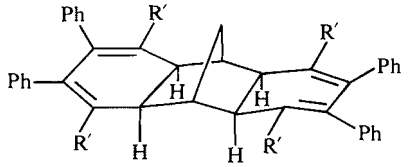

18

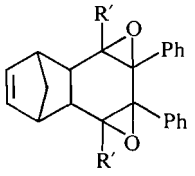

19

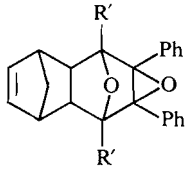

20

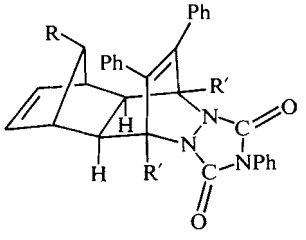

21

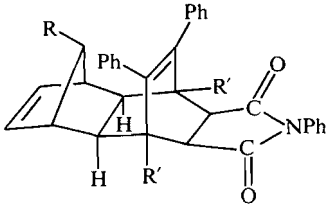

22

Can. J. Chem. Downloaded from www.nrcresearchpress.com by 210.87.254.6 on 09/05/12
For personal use only.

stereochemistry of **15***a* results from the expected *exo*-addition to the norbornadiene and the considerable difference in the chemical shifts of the two protons on the one-carbon bridge of the bicycloheptene points to the stereochemistry assigned, with one of these protons in close proximity to the diphenylethylene moiety (8). Additional support for the latter assignment was provided by the observation that chemical shifts of the bridge methylene protons were not significantly changed when the ketone was reduced to the corresponding alcohol. When the Diels–Alder reaction was carried out with norbornadiene and excess tetracyclone, a small amount of an insoluble, high-melting solid was obtained which, although it was not characterized completely, is believed to be the bisadduct **17***a*, resulting from the reaction at both double bonds of norbornadiene.

The isolation of monoadduct **15***a* showed that it did not readily undergo decarbonylation at the temperature required for its formation; consequently, the application of this route to the synthesis of a thermally labile cyclopentadiene appeared unpromising. There is more quantitative support for this pessimism in the activation energies that have been determined from recent kinetic studies of the thermal decarbonylation of related molecules (8). In fact, **15***a* was even more thermally stable in our hands than we had been led to expect (6), decomposing only slowly in refluxing chloroform, and we used refluxing toluene to effect its complete decomposition to cyclopentadiene and tetraphenylbenzene. Thermal decomposition of the bisadduct **17***a*, on the other hand, appeared to stop at the decarbonylation (double) stage, and a hydrocarbon believed to be **18***a*, a bis(dihydrobenzene) not susceptible to the retro-Diels–Alder fragmentation, was isolated. The n.m.r. spectrum showed the absence of significant coupling between non-aromatic protons, providing evidence for the stereochemical assignment shown in **18***a*, and supporting the stereochemistry proposed for the precursor **17***a*.

In the hope that it was only the thermal decarbonylation reaction that had too high an activation energy and that the subsequent retro-Diels–Alder reaction might still meet our requirements, we examined the photolysis of the model adduct **15***a*, since only the decarbonylation step should be photochemically activated. (Subsequent evidence (9) suggests that this assumption may not be completely justified.) Irradiation of a solution of **15***a* at room temperature converted it to cyclopentadiene and tetraphenylbenzene in good yield, and it appeared likely, therefore, that the photochemical decarbonylation had been followed by a facile thermal retro-Diels–Alder reaction. It may be noted that if oxygen was not thoroughly removed from the reaction mixture, an oxidized photoproduct was obtained, and if oxygen was deliberately bubbled through the solution during photolysis, this material was the major product isolated. Its composition corresponds to a molecule of formula **16***a* plus O_2, and its spectroscopic characteristics indicate that it is the conjugated diene part of **16***a* that has been affected by the oxidation. The product is thermally stable and catalytic hydrogenation over palladium reduces only its isolated double bond in the norbornene system. Two structures, **19***a* and **20***a*, may be considered for the oxidized photoproduct; a decision between these can not be made on the basis of the experimental evidence available at present, but there is precedent (10) for favoring **19***a*.

Results closely paralleling those just described and leading to the corresponding products (**15***d*–**19***d*) were obtained if the sequence was carried out with 2,5-dimethyl-3,4-diphenylcyclopentadienone in place of tetracyclone in the Diels–Alder reaction with norbornadiene.

Since the Diels–Alder reaction–photodecarbonylation–retro-Diels–Alder reaction sequence described for the model series gave promising results, we examined this sequence for the case of 7-phenylnorbornadiene (**4***b*). Reaction of **4***b* with tetracyclone at 70° afforded the corresponding adduct **15***b*, but the yield was very low and was not improved by the addition of aluminum chloride. Reactions of this kind must be carried out within a strictly limited range of temperatures; at temperatures below this "window" the rate of adduct formation is impracticably low, while at temperatures above it the adduct suffers decarbonylation before it can be isolated. In the case of **15***b* this window was even narrower than in the model series; the adduct was isolated only at 70°, and even then the reaction afforded a mixture consisting mainly

Can. J. Chem. Downloaded from www.nrcresearchpress.com by 210.87.254.6 on 09/05/12
For personal use only.

of unchanged starting materials and products resulting from the subsequent decomposition of **15***b* (tetraphenylbenzene and tetracyclone adducts of phenylcyclopentadiene). However, replacing tetracyclone with 2,5-dimethyl-3,4-diphenylcyclopentadienone allowed the adduct **15***c* to be obtained in satisfactory yield. The stereochemistry shown for **15***b* and *c* is based on analogy with **15***a* and the expectation that addition to the norbornadiene had taken place on the side opposite to the phenyl substituent, and this is supported by the low field position (8) of the n.m.r. signal for the proton on the one-carbon bridge in the products; direct evidence that *exo*-addition to the norbornadiene had taken place was also given by the n.m.r. spectra of the adducts, which showed the absence of significant coupling involving non-aromatic protons.

When a dilute solution of **15***c* at between −40 and 0° was irradiated with u.v. light, the decarbonylation product **16***c* was obtained and could be trapped as its adduct **21***c* with 4-phenyl-1,2,4-triazoline-3,5-dione; the stereochemistry shown for **21***c* is that expected for adduct formation with the assumed intermediate **16***c*, but supporting evidence for the stereochemical features not present in the precursor is found only in the observation that the chemical shift of the benzylic proton corresponds closely to that assigned to the corresponding proton in **15***c*. If care was taken to keep the temperature as low as possible at all times, **16***c* itself could be observed as a product of the photolysis. The tetracyclone adduct **15***b* of norbornadiene could be converted in the same way to the analogous products **16***b* and **21***b*. At room temperature both dihydrobenzenes, (**16***b* and *c*) underwent the expected retro-Diels–Alder reactions and phenylcyclopentadiene was produced and isolated as its *N*-phenylmaleimide adduct; the adduct isolated was that of 1-phenylcyclopentadiene (**2***b*), presumably since the 5-phenylcyclopentadiene (**1***b*) originally obtained rearranged under the reaction conditions. Our failure to obtain any of the adduct of 2-phenylcyclopentadiene (**3***b*) may be significant but the scale of these reactions makes this less certain, since the latter is the less abundant isomer at equilibrium; our investigation of the distribution of isomers obtained when an equilibrium mixture of phenylcyclopentadienes was prepared (11) and allowed to react with *N*-phenylmaleimide indicated, in agreement with a recent report (12), that the diene mixture was composed of the 1-phenyl and 2-phenyl isomers in a ratio of about 7:1. Attempts to use *N*-phenylmaleimide to trap the 5-phenylcyclopentadiene as soon as it was formed in the thermolysis of the dihydrobenzenes (**16***b* and *c*) were frustrated because the dihydrobenzenes themselves formed *N*-phenylmaleimide adducts (**22***b* and *c*) too readily. The stereochemistry shown for these adducts is that expected to result from the Diels–Alder reaction, but no supporting experimental evidence was obtained for those features not present in the precursor.

It appears then that, although the thermal fragmentation of the dihydrobenzenes is a process of relatively low activation energy, it takes place at a significant rate only in a temperature range in which the rearrangement of the 5-phenylcyclopentadiene produced is too fast to allow the unrearranged 5-phenyl isomer to be trapped or observed spectroscopically. In order to obtain a slightly more precise estimate of the activation energy for the thermolysis of the dihydrobenzenes, we have used n.m.r. spectroscopy to follow their decay in the relatively limited temperature range accessible to us. The kinetic results, which are expected to be only approximate, show that both dihydrobenzenes decay according to the first order rate law and that the E_a value is 28 kcal/mol for **16***b*, and 24 kcal/mol for **16***c*. These results lead to a half-life at 33° of 130 min for **16***c*, and when this is compared with the value of 19 min reported recently (9) for the thermolysis of **16***d* at the same temperature, it appears that the phenyl substituent on the one-carbon bridge of **16***c* retards the rate of the retro-Diels–Alder reaction, but no good explanation for this effect has yet been recognized.

Although the kinetic results are only approximate, they serve to show that we have come close to, but not reached, our goal of a thermal route to cyclopentadienes that has an activation energy low enough to be of general applicability to the synthesis of thermally unstable isomers. Even if a more precise determination of the activation energy were made we would not be able to state quantitatively how close we have

Can. J. Chem. Downloaded from www.nrcresearchpress.com by 210.87.254.6 on 09/05/12
For personal use only.

come to the goal since it is impossible to define the goal precisely in terms of energy; the kinetic parameters for the thermal rearrangement of substituted cyclopentadienes have been determined in only a few cases, 5-methylcyclopentadiene with E_a of 20 kcal/mol (1) providing a representative example, but they must be guessed at for others, including 5-phenylcyclopentadiene, the case appropriate to the present discussion.

Experimental

Melting points were determined on a calibrated Thomas–Kofler micro hot stage. Unless otherwise indicated, chloroform solutions were used to obtain i.r. spectra and the wavelengths of significant absorptions are reported in μ, solutions in 95% ethanol were used to obtain u.v. spectra and the wavelengths of maximum absorption (λ_{max}) are reported in mμ followed by the extinction coefficient (ε) in parentheses, and chloroform-*d* solutions with tetramethylsilane as an internal standard were used to obtain n.m.r. spectra and chemical shifts are reported on the τ scale followed in parentheses with an indication of the multiplicity of the signal and the number of protons associated with it. Spectrometers used were a Perkin–Elmer 237B for i.r. spectra, a Unicam SP.800A for u.v. spectra, and a Varian HA-100 for n.m.r. spectra (unless otherwise indicated). Routine mass spectra were determined at 70 eV on a CEC 21–490 or an AEI MS-902 spectrometer and the *m/e* values of significant ions are reported followed in parentheses with a figure showing the height of the peak relative to that of the base peak (100%); accurate mass measurements were made on the AEI MS-902 spectrometer.

Phenyl Azide Adducts of Norbornadiene

(1) Preparation

(a) Phenyl azide and excess norbornadiene. The solution obtained by dropwise addition of phenyl azide (1.8 g) in 0.5 ml of cyclohexane to 20 ml of norbornadiene was heated to 60–65° for 2 h. A small amount of precipitate (29 mg) formed and was collected by filtration; it proved to be the *exo–exo–trans*-bisadduct **10** (see below). The filtrate was taken to dryness, the residue was dissolved in ether, and pentane was added to the solution, which was then cooled to −20°. The crystals (2.13 g; 67%) obtained were subjected to fractional crystallization from ether and then ether–carbon tetrachloride.

The first component obtained was the *endo*-monoadduct **8** (150 mg; 5%), m.p. 123–124°.

Anal. Calcd. for $C_{13}H_{13}N_3$: C, 73.90; H, 6.20; N, 19.89. Found: C, 73.81; H, 6.10; N, 19.83.

U.v. 281 (shoulder; 6100), 289 (7900), 308 (8400); n.m.r. 2.5–3.1 (complex; 5), 4.01 (d of d, $J = 6.0$, 3.5 Hz; 1), 4.20 (d of d, $J = 6.0$, 3.5 Hz; 1), 4.67 (d of d, $J = 10.5$, 4.5 Hz; 1), 5.67 (d of d, $J = 10.5$, 3.5 Hz; 1), 6.35 (unresolved; 1), 6.53 (unresolved; 1), 8.46 (d, $J = 9.5$ Hz, further fine splitting; 1), 8.64 (d, $J = 9.5$ Hz; 1); mass spectrum 211 (2), 183 (64), 182 (67), 117 (78), 104 (87), 91 (62), 77 (100).

The second component obtained was the *exo*-monoadduct **7** (1.77 g; 56%), m.p. 54.5–55°.

Anal. Calcd. for $C_{13}H_{13}N_3$: C, 73.90; H, 6.20; N, 19.89. Found: C, 73.84; H, 6.12; N, 19.95.

U.v. 281 (shoulder; 6300), 289 (7600), 308 (8000); n.m.r. 2.4–3.1 (complex; 5), 3.74 (d of d, $J = 6.0$, 3.0 Hz; 1), 3.84 (d of d, $J = 6.0$, 3.0 Hz; 1), 5.14 (d, $J = 9.5$ Hz, very fine further splitting; 1), 6.03 (d, $J = 9.5$ Hz, very fine further splitting; 1), 6.60 (narrow unresolved m; 1), 6.71 (narrow unresolved m; 1), 8.53 (d, $J = 10.0$ Hz, further fine splitting; 1), 8.77 (d, $J = 10.0$ Hz; 1); mass spectrum 211 (1), 183 (5), 182 (45), 117 (55), 104 (72), 91 (46), 77 (100), 66 (86).

(b) Norbornadiene and excess phenyl azide. The solution obtained by dropwise addition of norbornadiene (2.78 g) in 25 ml of cyclohexane to phenyl azide (8.90 g) in 10 ml of cyclohexane was heated to 60–70° for 2 h. The products obtained were separated by a series of fractional crystallizations. The first component obtained was the *exo–exo–trans*-bisadduct **10** (5.75 g; 58%) which separated from the reaction mixture and was insoluble in most common solvents. Recrystallization from pyridine afforded a pure sample, m.p. 226° (dec.) (lit. (13) 236–238° (dec.)).

Anal. Calcd. for $C_{19}H_{18}N_6$: C, 69.07; H, 5.49; N, 25.44. Found: C, 68.95; H, 5.49; N, 25.60.

U.v. (absolute EtOH) 280 (shoulder; 10 000), 288 (10 800), 305 (10 800); n.m.r. (pyridine-d_5) 2.3–2.9 (complex; 10), 4.91 (d, $J = 9.5$ Hz; 2), 5.82 (d, $J = 9.5$ Hz; 2), 6.78 (unresolved m; 2), 8.92 (unresolved m; 2); mass spectrum 302 (2), 274 (26), 273 (23), 182 (62), 156 (49), 119 (41), 104 (73), 28 (100).

The second component obtained was the *exo–exo–cis*-bisadduct **9** (2.34 g; 23%), m.p. 164–166° (dec.), which was recrystallized from ether–carbon tetrachloride.

Anal. Calcd. for $C_{19}H_{18}N_6$: C, 69.07; H, 5.49; N, 25.44. Found: C, 69.12; H, 5.65; N, 25.46.

U.v. (absolute EtOH) 280 (shoulder; 9800), 288 (10 700), 304 (10 600); n.m.r. 2.4–3.1 (complex; 10), 5.17 (d, $J = 9.5$ Hz; 2), 6.05 (d, $J = 9.5$ Hz; 2), 6.71 (broadened s; 1), 6.96 (broadened s; 1), 8.87 (broadened s; 2); mass spectrum 302 (1), 274 (2), 273 (4), 182 (17), 156 (18), 119 (100).

The remaining crystalline material (1.0 g) appeared, on the basis of its n.m.r. spectrum, to contain a further small amount of **9**, a mixture of the *exo–endo*-adducts **11** and **12** (described below), and possibly a small amount of the monoadducts 7 and **8**. Further fractional crystallization was only partially successful.

(c) endo-Monoadduct and phenyl azide. A solution of phenyl azide (500 mg) and the *endo*-monoadduct **8** (125 mg) in 10 ml of cyclohexane was heated to 50–60° for 4 h. After solvent and excess phenyl azide had been removed by vacuum distillation, the residue was dissolved in hot carbon tetrachloride–chloroform (3:1), and allowed to crystallize. The material obtained (159 mg; 81%) melted in the range 157–170° and appeared from its n.m.r. spectrum to be a 2:3 mixture of *exo–endo–cis*-bisadduct **11** and its *trans* isomer **12**. A pure sample of the *exo–endo–trans*-bisadduct **12** (34 mg), m.p. 230° (dec.), was obtained by continued recrystallization.

Anal. Calcd. for $C_{19}H_{18}N_6$: C, 69.07; H, 5.49; N, 25.44. Found: C, 69.35; H, 5.30; N, 25.21.

U.v. (absolute EtOH) 280 (shoulder; 8700), 288 (9800), 304 (10 500); n.m.r. 2.4–3.1 (complex; 10), 4.78 (d of d, $J = 12.5$, 5.5 Hz; 1), 5.55 (d, $J = 9.0$ Hz with further fine splitting; 1), 5.71 (d of d, $J = 12.5$, 5.0 Hz; 1), 6.11 (d, $J = 9.0$ Hz with further fine splitting; 1), 6.65 (two superimposed

Can. J. Chem. Downloaded from www.nrcresearchpress.com by 210.87.254.6 on 09/05/12
For personal use only.

multiplets; 2), 8.46 (d, $J = 12.0$ Hz with further fine splitting; 1), 8.62 (d, $J = 12.0$ Hz with further fine splitting; 1).

A pure sample of the *exo–endo–cis*-bisadduct **11** could not be obtained, but the n.m.r. spectrum of a sample of the mixture of isomers enriched in **11** included the following signals assigned to **11**: 4.74 (d of d, $J = 12$, 5 Hz), 5.40 (broadened d, $J = 9.5$ Hz), 5.71 (d of d, $J = 12$, 5 Hz), 6.51 (broadened d, $J = 9.5$ Hz, superimposed on m), 6.91 (m).

(2) Thermolysis and Photolysis

The *exo*-monoadduct **7** in xylene was heated in a flask fitted with a distilling head. At 120° the presence of cyclopentadiene in the distillate was demonstrated by v.p.c. and, after 2 h, phenyltriazole (79%) was recovered from the flask.

A saturated solution of the *exo–exo–trans*-bisadduct **10** in ethanol was exposed to indirect sunlight for several days (depending on the weather). The bisaziridine (corresponding to 60% conversion) was isolated from the reaction mixture and obtained, after recrystallization from cyclohexane–carbon tetrachloride, as crystals, m.p. 182–186°.

Anal. Calcd. for $C_{19}H_{18}N_2$: C, 83.15; H, 6.61; N, 10.21. Found: C, 82.95; H, 6.73; N, 10.20.

U.v. 244 (23 600), 280 (1750); n.m.r. 2.6–3.4 (complex; 10), 7.06 (broadened s; 2), 7.57 (broadened s; 4); 8.62 (broadened s; 2); mass spectrum 274 (2), 273 (2), 182 (87), 181 (69), 180 (72), 170 (81), 169 (66), 157 (69), 156 (100), 143 (76), 130 (54), 104 (71). The *exo–exo–cis*-bisadduct **9** was converted to the same product (34% yield) in the same way.

Adducts of Norbornadiene with Cyclopentadienones

(1) Preparation

(a) Tetracyclone with excess norbornadiene. A solution of tetracyclone (3.24 g) and 25 ml of norbornadiene in 65 ml of chloroform was refluxed until the red color disappeared (21 h). The ketone **15***a* (3.89 g; 91%) contaminated with a small amount of tetraphenylbenzene (isolated in 7% yield) was obtained from the reaction mixture and purified by recrystallization from acetone–benzene; crystals were obtained which melted with decomposition at 160–162° (and recrystallized to form plates, m.p. 194–195°).

Anal. Calcd. for $C_{36}H_{28}O$: C, 90.72; H, 5.92. Found: C, 90.59; H, 5.95.

U.v. 225 (shoulder; 26 100), 260 (10 500); i.r. 5.63; n.m.r. 2.5–3.2 (complex; 20), 3.46 (t, $J = 1.5$ Hz; 2), 6.56 (t, $J = 1.5$ Hz; 2), 7.14 (s; 2), 7.35 (d, $J = 9.5$ Hz, slightly broadened; 1), 8.59 (d, $J = 9.5$ Hz, slightly broadened; 1); mass spectrum 410 (4), 382 (100). The same product was obtained in less than 1 h when the reaction was carried out in benzene at room temperature in the presence of a slight excess of aluminum chloride (on a molar basis with respect to tetracyclone), but the work-up was more difficult and the yield was lower.

A sample of the ketone **15***a* was reduced with lithium aluminum hydride to the corresponding alcohol (81% yield), m.p. 200–201°.

Anal. Calcd. for $C_{36}H_{30}O$: C, 90.34; H, 6.32. Found: C, 90.34; H, 6.52.

I.r. 2.81 (sharp), 2.94 (broad); n.m.r. 2.5–3.4 (complex; 20), 3.53 (narrow unresolved m; 2), 5.41 (s; 1), 6.90 (broadened s; 2), 6.97 (broadened s; 2), 8.21 (s; 1; removed by D_2O), 7.35 (d, $J = 9.0$ Hz, slightly broadened; 1), 8.57 (d, $J = 9.0$ Hz, slightly broadened; 1); mass spectrum 478 (8), 412 (27), 386 (69), 382 (100), 233 (46), 221 (32), 191 (42).

(b) Norbornadiene with excess tetracyclone. A solution of norbornadiene (300 mg) and tetracyclone (4.22 g) in 50 ml of chloroform was refluxed for 3 days. The insoluble product appeared to be the bisadduct **17***a*, which decomposed slowly above 320°; i.r. (KBr disc), 5.63; mass spectrum 422 (21), 384 (6), 371 (9), 156 (16), 28 (100).

(c) Norbornadiene with 2,5-dimethyl-3,4-diphenylcyclopentadienone. A solution of norbornadiene (5.13 g) and the dienone (dimer (14)) (4.88 g) in 60 ml of benzene was refluxed for 45 h. The reaction mixture yielded the monoadduct **15***d* (4.66 g; 67%) m.p. 171.5–172° (lit. (15) 173°); u.v. 260 (9400); i.r. 5.65; n.m.r. 2.7–3.2 (complex; 10), 3.75 (t, $J = 1.5$ Hz; 2), 6.96 (narrow m; 2), 8.01 (s; 2), 7.50 (d, $J = 9.5$ Hz; 1), 8.74 (s; 6), 8.76 (d, $J = 9.5$ Hz; 1). The mother liquor afforded a further product which appeared to be the bisadduct **17***d* which was obtained as crystals, m.p. 219–223°, from ethanol–chloroform; i.r. 5.63; n.m.r. 2.6–3.2 (complex; 20), 7.5–8.2 (complex; 8), 8.68 (s; 12); mass spectrum 298 (22), 258 (100).

(d) 7-Phenylnorbornadiene with 2,5-dimethyl-3,4-diphenylcyclopentadienone. A solution of 7-phenylnorbornadiene (2) (4.78 g) and the dienone (4.95 g) in 60 ml of benzene was refluxed for 36 h. The reaction mixture yielded the monoadduct **15***c* (4.51 g; 55%), m.p. 170–171.5° (dec.) after recrystallization from methanol–ether.

Anal. Calcd. for $C_{32}H_{28}O$: C, 89.68; H, 6.59. Found: C, 89.71; H, 6.51.

U.v. 263 (8900); i.r. 5.65; n.m.r. 2.6–3.2 (complex; 15), 3.90 (t, $J = 2.0$ Hz; 2), 5.39 (broadened s; 1), 6.57 (narrow m; 2), 7.84 (s; 2), 8.63 (s; 6); mass spectrum 258 (100), 243 (23), 228 (8), 142 (50), 116 (16).

(e) 7-Phenylnorbornadiene with tetracyclone. The reaction between these components under conditions similar to those described above led to the formation of adducts of phenylcyclopentadienes with tetracyclone as the principal isolable products. No improvement was observed when aluminum chloride was present. When the reaction was carried out at 70° for 3 days a small yield (9%) of the desired adduct **15***b* was isolated, m.p. 162–164° (dec.); u.v. (absolute EtOH), 220 (shoulder), 260 (9600); i.r. (KBr disc) 5.62; n.m.r. 2.8–3.2 (complex; 25), 3.65 (narrow m; 2), 5.25 (broadened s; 1), 6.22 (narrow m; 2), 6.98 (s; 2).

Reference samples of the adducts of phenylcyclopentadiene (11) and tetracyclone were prepared in the usual manner. The principal product was the adduct of 1-phenylcyclopentadiene, m.p. 183–185°.

Anal. Calcd. for $C_{40}H_{30}O$: C, 91.22; H, 5.74. Found: C, 91.13; H, 5.79.

U.v. (absolute EtOH) 260 (21 900); i.r. (KBr disc) 5.62; n.m.r. 2.2–3.4 (complex; 25), 3.46 (d, $J = 2$ Hz; 1), 5.59 (d of d, J values 8, 2 Hz; 1), 6.29 (m; 1), 6.85 (complex; 2).

A very small amount of a second product, m.p. 180–181°, was considered to be the adduct of 2-phenylcyclopentadiene.

(2) Thermolyses

*(a) Norbornadiene-tetracyclone adduct **15***a*.* A solution of the adduct **15***a* (250 mg) in 70 ml of toluene was refluxed for 3 days. Removal of the solvent and recrystallization of the residue provided 1,2,3,4-tetraphenylbenzene (193 mg; 96%), m.p. 194–195° (lit. (6) 191°). The corresponding reaction in refluxing chloroform afforded tetraphenylbenzene (11%) and unchanged **15***a* (73%) after 50 h.

*(b) Norbornadiene-tetracyclone bisadduct **17***a*.* The bis-

Can. J. Chem. Downloaded from www.nrcresearchpress.com by 210.87.254.6 on 09/05/12
For personal use only.

adduct **17***a* (104 mg) was suspended in 25 ml of anisole, which was refluxed until solution was complete (about 1.5 h). About 15 ml of anisole was removed under vacuum, a brown gum which had formed was removed by filtration, ether was added to the filtrate, and the solution was cooled. The product (**18***a*) (52 mg; 53%) was collected, recrystallized from benzene–cyclohexane, and obtained as crystals, m.p. 336°.

Anal. Calcd. for $C_{63}H_{48}$: C, 93.71; H, 6.29. Found: C, 93.85; H, 6.27.

U.v. 262 (33 900), 309 (19 200); n.m.r. 2.9–3.4 (complex; 40), 6.79 (s; 4), 7.54 (broadened s; 2), 7.68 (broadened s; 2); mass spectrum 422 (100), 395 (34), 382 (37), 329 (27).

(c) Dimethyldiphenylcyclopentadienone adducts. After a solution of the norbornadiene adduct **15***d* in toluene had been refluxed for 24 h, 1,4-dimethyl-2,3-diphenylbenzene (14) (64%) was isolated. Under similar conditions the 7-phenylnorbornadiene adduct **15***c* gave the same product in 48% yield.

(3) Photolyses

Photolyses were carried out with a 450 W Hanovia high-pressure mercury lamp in a quartz immersion well.

(a) Norbornadiene-tetracyclone adduct 15a. A solution of the adduct **15***a* (356 mg) in 230 ml of 1:6 tetrahydrofuran–cyclohexane continuously purged with a stream of oxygen-free nitrogen was photolyzed at room temperature for 24 h. Solvent and volatile products were distilled on to *N*-phenylmaleimide which trapped the cyclopentadiene formed as its adduct (137 mg; 77%), m.p. 140–142°; the residue afforded 1,2,3,4-tetraphenylbenzene (229 mg; 81%), m.p. 193–195°.

Irradiation of the adduct **15***a* (138 mg) in 75 ml of 1:4 benzene–hexane agitated by a stream of oxygen at room temperature for 12 h yielded a precipitate (74 mg; 57%) which was purified by t.l.c. and recrystallization from benzene–cyclohexane, and obtained as crystals, m.p. 288–289°.

Anal. Calcd. for $C_{35}H_{28}O_2$: C, 87.47; H, 5.87. Found: C, 87.39; H, 6.26.

U.v. 260 (1200); n.m.r. 2.56–3.25 (complex; 20), 3.91 (t, $J = 2.0$ Hz; 2), 7.09 (t, $J = 2.0$ Hz; 2), 7.64 (d, $J = 2.0$ Hz; 2), 7.78 (broadened d, $J = 8.5$ Hz; 1), 8.37 (broadened d, $J = 8.5$ Hz; 1); mass spectrum 480 (5), 479 (15), 413 (29), 382 (5), 375 (21), 360 (12), 309 (100), 279 (26), 255 (10), 178 (34), 105 (53); mass measurement 479.1969 (calcd. for $C_{35}H_{27}O_2$: 479.2011), 309.1281 (calcd. for $C_{23}H_{17}O$: 309.1279).

Hydrogenation of the photo-oxidation product (94 mg) in 50 ml of ethyl acetate over 10% palladium-on-carbon converted it to a product (86 mg), m.p. 289–295°; u.v. 260 (1100); n.m.r. 2.5–3.4 (complex; 20), 7.51 (d, $J = 1.5$ Hz; 2), 7.62 (m; 2), 7.88 (broadened d, $J = 11$ Hz; 1), 8.4–9.0 (complex; 5); mass spectrum 482 (5), 377 (23), 361 (16), 309 (18), 272 (10), 231 (23), 178 (53), 105 (100).

(b) 7-Phenylnorbornadiene-dimethyldiphenylcyclopentadienone adduct **15***c*. A solution of the adduct **15***c* (228 mg) in 240 ml of 1:5 ether–hexane[1] was purged with nitrogen, cooled in an ice-salt bath, and irradiated for 3 h. The solution was transferred to a flask equipped with a septum cap and cooled in Dry Ice. A solution of freshly prepared 4-phenyl-1,2,4-triazoline-3,5-dione (17) in methylene chloride was added dropwise through a syringe until the red color of the dione persisted in the reaction mixture. Evaporation of the solution and purification of the product by t.l.c. and recrystallization from benzene–cyclohexane provided the crystalline adduct **21***c* (174 mg; 57%), m.p. 250–253° (dec.).

Anal. Calcd. for $C_{39}H_{33}N_3O_2$: C, 81.36; H, 5.78; N, 7.30. Found: C, 81.44; H, 5.69; N, 7.53.

U.v. (absolute EtOH) 250 (8700); i.r. 5.67, 5.87; n.m.r. 2.4–3.3 (complex; 20), 3.83 (narrow m; 2), 5.40 (broadened s; 1), 6.65 (broadened s; 2), 7.58 (s; 2), 8.03 (s; 6); mass spectrum 575 (2), 407 (3), 322 (3), 258 (100), 243 (35), 228 (18), 142 (50), 119 (28).

When, instead of treatment of the photolyzed solution with the triazolinedione, distillation of the solvent was carried out under vacuum while the reaction mixture was maintained at a temperature of 0° or lower, a solid was obtained (the yield varied considerably from one run to another) which, after it had been washed with cold cyclohexane, was a fairly pure sample of the cyclohexadiene **16***c*; n.m.r. (60 MHz) 2.5–3.4 (complex; ~15), 3.87 (narrow m; 2), 6.15 (broadened s; 1), 6.52 (narrow m; 2), 7.44 (s; 2), 8.33 (s; 6).

When *N*-phenylmaleimide in carbon tetrachloride was added to the product **16***c* and the solution was allowed to warm to room temperature, the adduct **22***c*, m.p. 297–299° (dec.) was isolated; i.r. 5.63, 5.85; n.m.r. 2.3–3.4 (complex; 20), 3.86 (narrow m; 2), 5.30 (broadened s; 1), 6.57 (narrow m; 2), 6.98 (s; 2), 7.81 (s; 2), 8.36 (s; 6); mass spectrum 573 (12), 431 (5), 405 (8), 400 (2), 399 (2), 320 (9), 258 (100), 243 (23), 173 (18); mass measurement 573.2667 (calcd. for $C_{41}H_{35}NO_2$, 573.2668).

When the photolysis of **15***c* was carried out in the usual manner but the reaction mixture was then left untreated at room temperature for 6 h, 1,4-dimethyl-2,3-diphenylbenzene (67%), m.p. 106–107°, was isolated, and addition of *N*-phenylmaleimide to the reaction mixture led to the isolation of its adduct with 1-phenylcyclopentadiene (39%), m.p. 176.5–177.5°.

Reference samples of the adducts of phenylcyclopentadiene (11) and *N*-phenylmaleimide were prepared in the usual way. The major product isolated (54%) was the adduct of 1-phenylcyclopentadiene, m.p. 176.5–177.5°.

[1]Hexane was treated before use with potassium permanganate–sulfuric acid to remove alkenes, and dried (16). When untreated "Certified ACS" grade hexane was used the major product at a later stage of this procedure was a solid, m.p. 119–125°, which was shown to be the product of the following reaction:

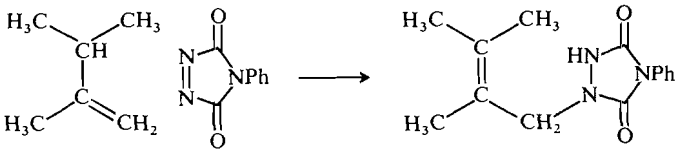

The same product was isolated when a solution of the triazolinedione in untreated hexane was left standing.

Can. J. Chem. Downloaded from www.nrcresearchpress.com by 210.87.254.6 on 09/05/12
For personal use only.

Anal. Calcd. for $C_{21}H_{17}NO_2$: C, 79.98; H, 5.43; N, 4.44. Found: C, 79.85; H, 5.59; N, 4.48.

I.r. (KBr disc) 5.65, 5.82; n.m.r. 2.3–2.9 (complex; 10), 3.58 (m; 2), 6.45 (narrow unresolved band; 3), 8.00 (almost collapsed AB pattern, $J \sim 9$ Hz; 2).

The minor product (8%) was the adduct of 2-phenylcyclopentadiene, m.p. 160.5–162°.

Anal. Calcd. for $C_{21}H_{17}NO_2$: C, 79.98; H, 5.43; N, 4.44. Found: C, 80.02; H, 5.79; N, 4.58.

I.r. 5.63, 5.86; n.m.r. 2.4–3.4 (complex; 10), 3.50 (narrow m; 1), 6.05 (narrow m; 1), 6.47 (narrow unresolved band; 3), 8.09 (d, $J = 8.5$ Hz; 1), 8.33 (d, $J = 8.5$ Hz; 1).

(c) 7-Phenylnorbornadiene-tetracyclone adduct **15***b*. Photolysis of the adduct **15***b* under the conditions described for **15***c* gave results paralleling those described in section *b*. The cyclohexadiene **16***b* was isolated; n.m.r. (60 MHz) 2.4–3.4 (complex; ~25), 4.07 (narrow m; 2), 5.74 (broadened s; 1), 6.70 (narrow m; 2), 6.88 (s; 2). It was also trapped as its phenyltriazolinedione adduct **21***b*, m.p. 141.5–143°.

Anal. Calcd. for $C_{49}H_{37}N_3O_2$: C, 84.09; H, 5.33; N, 6.01. Found: C, 83.52; H, 5.33; N, 6.23.

I.r. 5.67, 5.84; n.m.r. 2.4–3.2 (complex; 30), 3.72 (narrow m; 2), 5.38 (broadened s; 1), 6.44 (broadened s; 2), 6.90 (s; 2); mass spectrum 382 (87), 142 (100), 115 (25).

When **15***b* was allowed to decompose at room temperature, tetraphenylbenzene (78%) was isolated and phenylcyclopentadienes (49%) were trapped as their *N*-phenylmaleimide adducts.

(4) Kinetic Studies

Solutions of the cyclohexadienes **16***b* and *c* in chloroform-*d* were prepared and stored in Dry Ice. Samples were placed in the calibrated variable-temperature probe of a Varian A 56/60 n.m.r. spectrometer and the rate of decay of the cyclohexadiene was measured by repeated integration of the characteristic signals through at least two half lives. For **16***b* the decay of the peak at τ 6.88 was monitored and for **16***c* the decay of the methyl signal at τ 8.33 and the growth of the methyl signal at τ 7.92 of the 1,4-dimethyl-2,3-diphenylbenzene were used together. Runs were carried out with both series before instrument settings were changed; measurements were made at 33.5, 41.0, 43.5, and 48.0 °C. Data were analyzed by a standard least squares routine.

We thank the National Research Council of Canada for an operating grant supporting this work and for a Graduate Scholarship (to D.M.F., 1968–1971).

1. S. McLean and P. Haynes. Tetrahedron **21**, 2329 (1965). S. McLean, C. J. Webster, and R. J. D. Rutherford. Can. J. Chem. **47**, 1555 (1969).
2. P. R. Story and S. R. Fahrenholtz. J. Org. Chem. **28**, 1716 (1963).
3. S. McLean and D. M. Findlay. Tetrahedron Lett. 2219 (1969).
4. R. S. McDaniel and A. C. Oehlschlager. Can. J. Chem. **48**, 345 (1970).
5. B. Halton and A. D. Woolhouse. Tetrahedron Lett. 4877 (1971).
6. K. Mackenzie. J. Chem. Soc. 473 (1960).
7. C. F. H. Allen, R. W. Ryan, and J. A. Van Allan. J. Org. Chem. **27**, 778 (1962). P. Yates and P. Eaton. J. Am. Chem. Soc. **82**, 4436 (1960).
8. R. McCulloch, A. R. Rye, and D. Wege. Tetrahedron Lett. 5163, 5231 (1969).
9. W. S. Wilson and R. N. Warrener. Tetrahedron Lett. 5203 (1970).
10. K. K. Maheshwari, P. De Mayo, and D. Wiegand. Can. J. Chem. **48**, 3265 (1970). W. Herz, R. C. Ligon, H. Kanno, W. H. Schuller, and R. V. Lawrence. J. Org. Chem. **35**, 3338 (1970).
11. R. Riemschneider and R. Nehrin. Monatsh. Chem. **91**, 829 (1960).
12. D. Schoenleber. Chem. Ber. **102**, 1789 (1969).
13. R. Huisgen, L. Moebius, G. Mueller, H. Stangl, G. Szeimies, and J. M. Vernon. Chem. Ber. **98**, 3992 (1965).
14. C. F. H. Allen and J. Van Allan. J. Am. Chem. Soc. **64**, 1260 (1942). T. W. Gray. J. Chem. Soc. **95**, 2131 (1909).
15. C. M. Anderson, J. B. Bremner, H. H. Westberg, and R. N. Warrener. Tetrahedron Lett. 1585 (1969).
16. A. I. Vogel. Practical organic chemistry. 3rd Ed. Longmans, London. 1956. p. 174.
17. J. C. Stickler and W. H. Pirkle. J. Org. Chem. **31**, 3444 (1966).

Metallation of *N*-Substituted β-Lactams. A Method for the Introduction of 3-Substituents into β-Lactams

T. DURST AND M. J. LEBELLE

Department of Chemistry, University of Ottawa, Ottawa, Canada, K1N 6N5

Received November 1, 1971[1]

N-Alkyl and *N*-aryl β-lactams yield lithio carbanions upon reaction with lithium diisopropylamide in tetrahydrofuran at −78°. These lithio salts react with a variety of electrophiles (*e.g.* ketones, esters, reactive alkyl halides) to give the 3-substituted derivatives in fair to good yield. The procedure is useful for the preparation of rather complex 3-substituted β-lactams from readily available simple derivatives.

Les β-lactames *N*-alkyle et *N*-aryle donnent des lithiocarbanions en réagissant avec le lithium diisopropylamide dans le tetrahydrofuranne à −78°. Ces sels de lithium réagissent avec divers électrophiles (par exemple cétones, esters, halogénures d'alkyles, réactifs) pour conduire aux dérivés substitués en -3, avec des rendements moyens ou bons. Cette méthode est utile pour la préparation des β-lactames complexes substitués en -3, à partir de dérivés simples, facilement accessibles. [Traduit par le journal]

Canadian Journal of Chemistry, **50**, 3196 (1972)

A number of authors have recently reported that the reaction of *N*,*N*-disubstituted alkyl amides *e.g.* **1** with strong bases such as $NaNH_2$ (1, 2), *n*-BuLi (3) or lithio *s*-trithiane (3) leads to carbanions which can be alkylated with a variety of alkyl halides or condensed with carbonyl compounds. *e.g.* eq. 1.

The problems encountered in the synthesis of complex β-lactams either via cyclization of acyclic precursors or cycloaddition reactions (4), prompted us to investigate the synthesis of a variety of 3-substituted β-lactams from more readily available simple lactams via the carbanion route.

The formation of β-lactam carbanions in the penicillin and cephalosporin series has been investigated by a number of groups (5). In these examples two types of reactions have generally been observed (*a*) epimerization of the naturally occurring *cis*-β-lactam to the more stable *trans* configuration and (*b*) β-elimination of the thiolate moiety followed by further rearrangements (Scheme 1).

Several recent reports have indicated some of the synthetic potential of β-lactam carbanions. The first, by Kaiser *et al.* (6), showed that treatment of the allyldimethylammonium salt **2** with NaH in dimethylformamide–benzene resulted in the intramolecular migration of the allyl group from nitrogen to carbon thereby forming **3** (eq. 2).

More pertinent to the work discussed in this paper are the results of Böhme *et al.* (7) who were able to transform methyl *N*-benzylidene-6-aminopenicillanate (4) into a mixture of the epimeric-6-methyl derivatives **5** and **6** upon reaction with CH_3I/NaH in dimethoxyethane at 0° (eq. 3). In this case the ease of carbanion formation is undoubtedly due in large part to the additional stabilization afforded by the neighboring N=CHPh group. A similar reaction was also carried out on the analogous cephalosporin derivative.

More recently, Firestone and coworkers (8) have shown that the imine prepared from 6-aminopenicillanic acid benzyl ester and *p*-

[1] $CH_3\overset{O}{\overset{\|}{C}}N(CH_3)_2$ (**1**) $\xrightarrow[NH_3]{NaNH_2}$ $Na\overset{O}{\overset{\|}{C}}H_2N(CH_3)_2$ $\xrightarrow{CH_3I}$ $CH_3CH_2\overset{O}{\overset{\|}{C}}N(CH_3)_2$

[1]Revision received May 29, 1972.

Can. J. Chem. Downloaded from www.nrcresearchpress.com by 210.87.254.5 on 09/05/12
For personal use only.

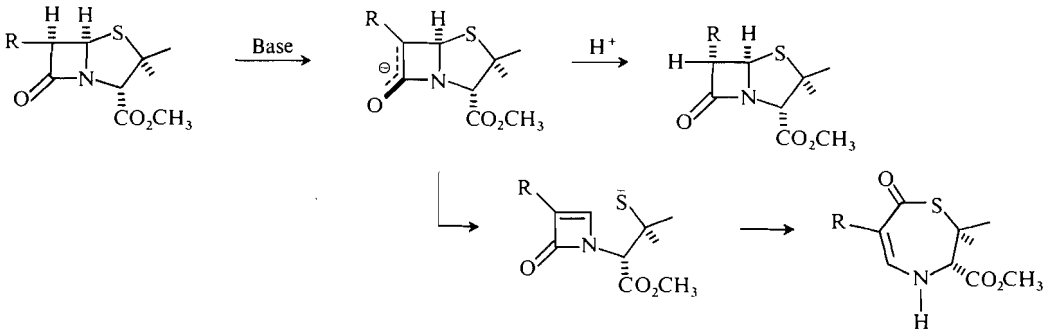

R = phthaloylamino

SCHEME 1

[2]

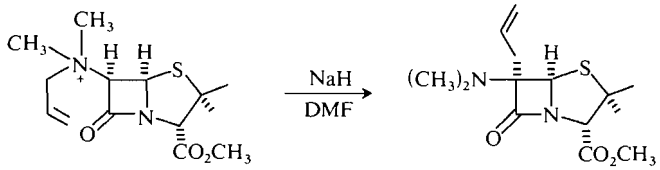

2 3

nitrobenzaldehyde readily yielded a carbanion upon treatment with phenyllithium in tetrahydrofuran at −78°. Alkylation of this carbanion with methyl and ethyl iodide gave the 6α alkylated isomers.

We have found that simple monocyclic *N*-methyl[2] or *N*-phenyl β-lactams readily form lithio derivatives upon addition to an equimolar amount of lithium diisopropylamide in tetrahydrofuran at −78°. These species are reasonably stable at −78° and react readily with a variety of electrophiles to yield the 3-substituted derivatives in fair to good yield (eq. 4, Table 1).

Thus the lithio salt **7***a* reacted with acetone or methyl iodide to afford the products **11** and **12** in 80 and 59% yield respectively. The i.r. spectrum of each product showed a strong band in the 1730–1750 cm^{-1} region which confirmed that the β-lactam ring had been retained (9). In the n.m.r. spectrum of each product the coupling between the two remaining ring protons was <2.5 Hz, indicative of the *trans*-configuration (10). No evidence of the presence of the *cis* isomers of **11** and **12** was detected in the n.m.r. spectra of the total crude products. The other spectroscopic features were as expected and are recorded in the Experimental. The lithio salts of the β-lactams **9** and **10** also yielded only one product on reaction with the various electrophiles. These were also shown by n.m.r. to have the *trans* configuration. Not unexpectedly, diastereomeric mixtures were obtained from the lithio salt of **8**. No attempts were made to separate these diastereomers.

The 3-methyl-β-lactam **12** also yielded a lithio derivative (**12***a*) which was trapped with benzophenone to give **13** in a 30% yield. When **12***a* was quenched with H_2O, **12** was regen-

[3]

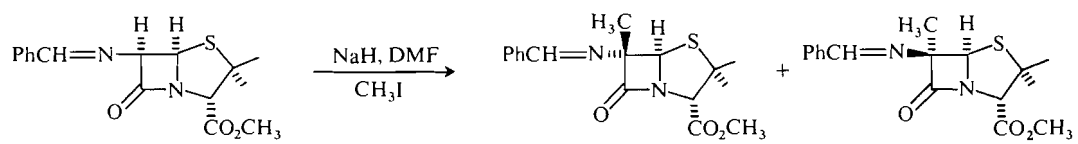

4 5 (5%) 6 (α isomer, 90%)

[2]Methylation of *N*-unsubstituted β-lactams was carried out by dissolving such lactams in excess CH_3I at 0–10° and slowly adding 1 equiv dry, powdered KOH. The yield of *N*-methylated β-lactams was generally over 80%. This alkylation procedure was also successful with other reactive halides such as benzyl or allyl bromide, but not with ethyl bromide or isopropyl iodide. In the latter experiments polymerization of the β-lactam occurred.

Can. J. Chem. Downloaded from www.nrcresearchpress.com by 210.87.254.5 on 09/05/12
For personal use only.

Can. J. Chem. Downloaded from www.nrcresearchpress.com by 210.87.254.5 on 09/05/12
For personal use only.

[4] 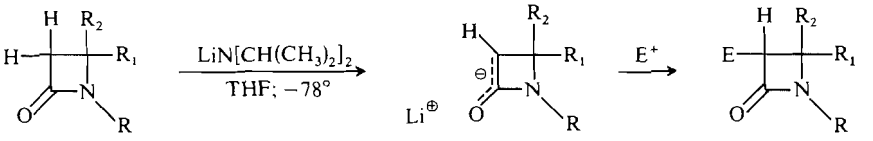

7–10 7a–10a

	R	R_1	R_2
7	CH_3	$CH{=}CH_2$	H
8	CH_3	$CH{=}CH_2$	CH_3
9	CH_3	Ph	H
10	Ph	Ph	H

TABLE 1. Introduction of a 3-substituent into 2-azetidinones

Lithio salt	Electrophile	Yield %	
7*a*	Acetone	80	(11)
7*a*	Methyl iodide	59	(12)
7*a*	Methyl benzoate	28	(14)
		50	(15)
8*a*	Acetone	77	
8*a*	Benzophenone	75	
8*a*	*n*-Butylbromide	0	
9*a*	Benzophenone	50	
10*a*	Cyclohexanone	41	
10*a*	Acetone	58	
10*a*	Iodine	29	
10*a*	Methyl benzoate	61	
12*a*	Benzophenone	30	(13)

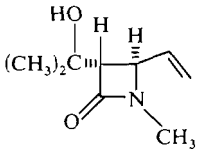

11

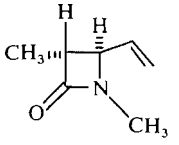

12

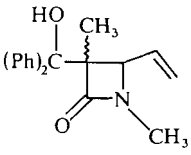

13

erated; no evidence of isomerization to the *cis* isomer was detected by n.m.r.

Reaction of 7*a* with methyl benzoate led to the formation of the phenacyl lactam **14** (i.r. 1750 and 1680 cm^{-1}) in 28% yield. The *trans* stereochemistry is assigned by analogy with **11** and **12** but could not be verified by n.m.r. In addition to the above material, a second product was obtained in 50% yield to which is tentatively assigned the dilactam structure **15**. The material had a broad m.p. (128–151°) and is probably a mixture of diastereomers. The i.r. spectrum of **15** showed bands at 3580 and 3400 (free and bonded OH), 1740 (C=O), 988, and 930 cm^{-1} (terminal vinyl). N.m.r. bands occurred at δ 2.4–2.8 (three sharp lines, total 6H, due to the NCH_3 group of the various diastereomers), 3.1 (s, 1H, OH), 3.5–4.0 (m, 4H, ring H), 4.8–6.0 (m, 6H, vinyl), and 7.2–7.7 (m, 5H, aromatic).

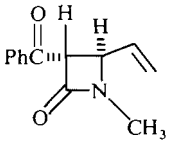

14

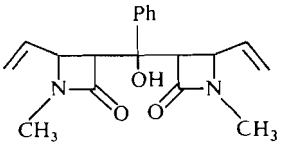

15

In addition to the adducts derived from the lithio salt of **10***a*, we generally observed the formation of a small amount of bi-product which was identified as **16** (see Experimental for spectroscopic data). The yield of **16** can be increased to about 27% by allowing a solution of **10***a* to warm to room temperature in the absence of a trapping agent. Its mode of formation is suggested in eq. 5. Products analogous to **16** were not observed in the reaction of the lithio salts of the *N*-alkyl-β-lactams.

[5] **10***a* + **10** ⟶ 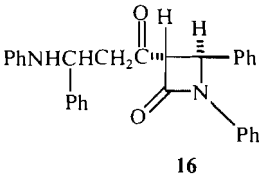

16

Experimental

N.m.r. spectra were recorded as $CHCl_3$ solutions using Varian T-60 and HA-100 spectrometers; peak positions are quoted in δ units. I.r. spectra were recorded in $CHCl_3$

Can. J. Chem. Downloaded from www.nrcresearchpress.com by 210.87.254.5 on 09/05/12
For personal use only.

solution, unless otherwise indicated, on a Beckman IR-20 spectrophotometer. Melting points and boiling points are uncorrected. For the sake of unambiguous designations, the 2-azetidinone nomenclature is used in this part of the paper.

1,4-Diphenyl-2-azetidinone

This 2-azetidinone was prepared by the method of Gilman and Speeter (11) as found in ref. 12.

4-Vinyl-2-azetidinone and 2-Methyl-4-vinyl-2-azetidinone

These 2-azetidinones were prepared by the method of Moriconi and Meyer (13) except that reduction of the 1-chlorosulfonyl-2-azetidinones was carried out with sodium sulfite (14).

4-Phenyl-2-azetidinone

This compound was obtained from the reaction of styrene and chlorosulfonyl isocyanate in methylene chloride followed by sodium sulfite reduction of the crude *N*-chlorosulfonyl β-lactam; m.p. 106–108°; lit. m.p. 108–109° (15).

N-Methylation of 2-Azetidinones. General Procedure

The 2-azetidinone was mixed with an excess of methyl iodide. The mixture was cooled to 0° and 1 equiv of freshly powdered dry potassium hydroxide was added with stirring. The mixture was then stirred at the temperatures and for the times indicated. The work-up consisted of adding methylene chloride and filtering the mixture. The methylene chloride was dried over magnesium sulfate and evaporated to give almost pure products.

1-Methyl-4-vinyl-2-azetidinone

4-Vinyl-2-azetidinone (4.01 g, 41 mmol) and 11.4 g of methyl iodide were stirred with 2.36 g of potassium hydroxide. Work-up gave 3.8 g (83%) of product, b.p. 34–35°/0.35 mm. The n.m.r. spectrum showed peaks at δ 2.75 (s, 3H), 2.45–3.39 (m, 2H), 3.78–4.09 (m, 1H), and 5.12–6.18 (m, 3H). The i.r. spectrum showed bands at 1735 (s), 1410 (m), 1390 (m), 990 (m), and 930 (m). The mass spectrum gave a molecular ion at *m/e* 111.

1,4-Dimethyl-4-vinyl-2-azetidinone

4-Methyl-4-vinyl-2-azetidinone (2.65 g, 23.8 mmol) and 6.8 g (48 mmol) of methyl iodide were stirred with 1.34 g (24 mmol) of potassium hydroxide for 10 min. Work-up gave 2.78 g of yellow oil (90%) which was pure by n.m.r. The product was distilled and gave a colorless liquid b.p. 40–50°/0.35 mm. The n.m.r. spectrum indicated peaks at δ 1.75 (s, 3H), 2.69 (s, 3H), 2.81 (s, 2H), and 5.00–6.21 (m, 3H). The i.r. spectrum showed bands at 1735 (s), 1410 (m), 1390 (m), 995 (m), and 930 (m) cm^{-1}.

1-Methyl-4-phenyl-2-azetidinone

To a solution of 4-phenyl-2-azetidinone (7.5 g, 51 mmol) in 60 ml CH_3I was added slowly 3.1 g of powdered KOH. The reaction mixture was stirred overnight at room temperature. The precipitate was filtered and washed with 50 ml of CH_2Cl_2. The solvents were evaporated and the product distilled. The yield of methylated β-lactam, b.p. 86–90°/0.2 mm, was 6.4 g (78%). The i.r. spectrum showed the β-lactam carbonyl at 1740 cm^{-1}. The n.m.r. spectrum showed the following peaks: δ 2.72 (s, 3H), 2.79 (d of d, J = 16, 2.5 Hz, 1H), 3.04 (d of d, J = 16 Hz, 4.5H), 4.47 (d of d, J = 4.5 Hz, 2.5), and 7.32 (s, 5H). The mass spectrum showed the parent peak at *m/e* = 161.

Formation of 3-Substituted-2-azetidinones. General Procedure

To a tetrahydrofuran solution of 1.1 equiv of diisopropylamine under nitrogen atmosphere at −78° was added 1.0–1.1 equiv of *n*-butyllithium (Foote Mineral Co., 1.6 *M* in hexane). After 5 min a tetrahydrofuran solution of the 2-azetidinone which had been cooled to −78° was added to the first solution and this was stirred for 0.5–1.5 min. A selected electrophile was then added, either neat if liquid, or as a tetrahydrofuran solution if solid. The reaction was stirred at −78° for the time specified. The solution was then poured into water and the aqueous phase saturated with sodium chloride. The products were extracted with methylene chloride and dried over magnesium sulfate. The products were usually purified by preparative t.l.c. or column chromatography. Yields refer to purified materials.

Formation of 3-Derivatives of 1-Methyl-4-vinyl-2-azetidinone

*(a) Acetone Derivative (**11**)*

To a solution of 3.88 mmol of the lithio salt of **7** was added 3 ml (40 mmol) of acetone. The reaction mixture was stirred for 5 min at −78°. Work-up gave 704 mg of a colorless oil from which 522 mg (80%) of **11** was isolated as a pale yellow oil by preparative t.l.c. using 5% CH_3OH in $CHCl_3$ as eluent. The i.r. spectrum showed strong bands at 3440 and 1730 cm^{-1}; n.m.r. peaks occurred at δ 1.24 (s, 3H), 1.43 (s, 3H), 2.60 (s, 1H, O—H), 2.75 (s, 3H), 2.88 (d, J=2.0 Hz, 1H), 3.90 (d of d, J=2.0 and 8.0 Hz, 1H), and 5.2–6.1 (m, 3H).

Anal. Calcd. for $C_9H_{15}NO_2$: C, 63.88; H, 8.94; N, 8.28. Found: C, 63.79; H, 8.97; N, 8.40.

*(b) 3-Methyl Derivative (**12**)*

A solution of 8.5 mmol of **7***a* and 3 ml (50 mmol) of methyl iodide was allowed to react for 10 min. Work-up followed by purification by preparative t.l.c. gave 630 mg (59%) of **12** as an oil. The n.m.r. spectrum showed peaks at δ 1.30 (d, J=7.5 Hz, 3H), 2.73 (s, 3H), 2.66–2.94 (m, 1H), 3.50 (d of d, J = 8.0 and 2.0 Hz, 1H), 5.10–6.10 (m, 3H).

Anal. Calcd. for $C_7H_{11}NO$: C, 67.17; H, 8.86; N, 11.19. Found: C, 66.89; H, 9.01; N, 11.02.

*(c) Benzoyl Derivatives (**14** and **15**)*

From the reaction of 4.1 mmol of **7***a* and 550 mg (4.5 mmol) of methyl benzoate was obtained 862 mg of crude product. Preparative t.l.c. gave two products on development with 5% methanol in chloroform. The upper fraction was obtained as a yellowish solid, 240 mg (28%), and was recrystallized from ether–pentane to give white needles, m.p. 66.5–67.5°. The i.r. spectrum showed strong bands at 1750 and 1680 cm^{-1}; the n.m.r. spectrum showed peaks at δ 2.80 (s, 3H), 4.50–4.70 (m, 2H), 5.24–6.00 (m, 3H), 7.24–7.29 (m, 3H), and 7.91–8.24 (m, 2H).

Anal. Calcd. for $C_{13}H_{13}NO_2$: C, 72.54; H, 6.09; N, 6.51. Found: C, 72.48; H, 6.01; N, 6.51.

A lower fraction was extracted from the plate to yield 336 mg (50%) of white solid, m.p. 128–151° (methylene chloride–ether–pentane) to which we have assigned structure **15**. The i.r. spectrum showed bands at 3580 (w), 3400 (b), 1740 (s), 1542 (w), 988 (m), and 930 (m) cm^{-1}. The n.m.r. spectrum is described in the text.

Anal. Calcd. for $C_{19}H_{22}N_2O_3$: C, 69.92; H, 6.79; N, 8.58. Found: C, 69.95; H, 6.80; N, 8.60.

Can. J. Chem. Downloaded from www.nrcresearchpress.com by 210.87.254.5 on 09/05/12
For personal use only.

Formation of 3-Derivatives of 1,4-Dimethyl-4-vinyl-2-azetidinone

(a) Acetone Derivative

A solution of the lithio salt **8***a*, prepared from 334 mg (2.7 mmol) of **8**, was reacted with 3 ml of acetone for 5 min, at −78°. Work-up gave 538 mg of colorless oil which after purification by preparative t.l.c. gave 377 mg (77%) of white solid, m.p. 64.5–70.5° (methylene chloride–ether–pentane). The n.m.r. spectrum showed peaks at δ 1.16–1.75 (m, 9H), 2.42–3.09 (m, 5H), and 5.00–6.45 (m, 3H). The i.r. spectrum showed bands at 3580 (m), 3440 (b), 2980 (s), 1730 (s), 1375 (s), 999 (m), and 925 (m).

Anal. Calcd. for $C_{10}H_{17}NO_2$: C, 65.54; H, 9.35; N, 7.64. Found: C, 65.45; H, 9.16; N, 7.62.

(b) Benzophenone Derivative

To a solution of 3.0 mmol of the lithio salt **8***a* was added 550 mg (3.0 mmol) of benzophenone. The reaction was worked-up after 5 min to yield 850 mg of crude product. Column chromatography (silica gel, chloroform–methanol) gave 683 mg (75%) of adduct as a mixture of diastereomers, m.p. 147–152° (methylene chloride–ether). The n.m.r. spectrum showed peaks at δ 1.05 and 1.37 (two singlets, 3H), 2.66 and 2.67 (2 singlets, 3H), 2.81 and 3.03 (two singlets, 1H), 4.23 (s, 1H, exchangeable with D_2O), 4.83–5.93 (m, 3H), and 7.00–7.80 (m, 10 H). The i.r. spectrum showed bands at 3420 (b), 1730 (s), 980 (w), and 920 (w) cm^{-1}.

Anal. Calcd. for $C_{20}H_{21}NO_2$: C, 78.14; H, 6.89; N, 4.56. Found: C, 78.03; H, 6.96; N, 4.53.

Benzophenone Adduct of 1-Methyl-4-phenyl-2-azetidinone

A solution of the lithio salt **9***a* was prepared by reacting 371 mg (2.3 mmol) of **9** with 2.5 mmol of lithium diisopropylamide for 1 min. Benzophenone (420 mg, 2.6 mmol) was then added and the reaction mixture stirred for 6 min. Work-up gave 750 mg of an orange solid from which 390 mg (50%) of adduct was obtained as a white powder, m.p. 216–217° (methylene chloride–ether). The i.r. spectrum had bands at 3560 (w), 3360 (broad), and 1730 (s) cm^{-1}. The n.m.r. peaks occurred at 2.75 (s, 3H), 4.00 (broad singlet, 1H), 4.33 (d, J=2.0 Hz, 1H), and 7.00–7.66 (m, 15 H). The OH absorption could not be seen in the n.m.r.

Anal. Calcd. for $C_{23}H_{21}NO_2$: C, 80.44; H, 6.16; N, 4.08. Found: C, 80.32; H, 6.01; N, 4.07.

Benzophenone Derivative of 1,3-Dimethyl-4-vinyl-2-azetidinone

A solution of 220 mg (1.76 mmol) of **12** was added to 1.1 equiv of lithium diisopropylamide and 320 mg (1.0 equiv) of benzophenone was added after 1.25 min. The reaction was stirred for a further 10 min. Work-up gave 558 mg of crude product which was recrystallized to give 162 mg (30%) of pure **13**, m.p. 171–172.5° (methylene chloride–ether–pentane). The i.r. spectrum showed bands at 3600 (w), 3460 (broad), 1735 (s), 1020 (w), and 925 (w) cm^{-1}. The n.m.r. showed peaks at δ 1.30 (s, 3H), 2.46 (s, 3H), 3.36 (broad singlet, 1H), 3.90 (d, J=7 Hz, 1H), 5.03–6.06 (m, 3H), and 7.12–7.69 (m, 10 H).

The mass spectrum of the compound indicated the parent peak at m/e=307, calcd for $C_{21}H_{20}NO_2$=307.

3-Derivatives of 1,4-Diphenyl-2-azetidinone

(a) 3-Iodo Derivative

A solution of 2.23 g (0.01 mol) of 2-azetidinone and 1.1 equiv of lithium diisopropylamide was stirred for 3 min. Iodide (2.54 g, 1 equiv was added; the reaction was stirred for a further 30 min. The work-up was carried out as usual except that the aqueous layer was saturated with sodium sulfite. Column chromatography (pentane–ether) of the crude product yielded 1.022 g grey solid (29%), m.p. 106.5–108° (ether–pentane). The n.m.r. spectrum indicated peaks at δ 4.72 (d, J = 2.0 Hz, 1H), 5.14 (d, J = 2.0 Hz, 1H), 7.04–7.47 (m, 10 H). The i.r. spectrum showed bands at 1755 (s), 1600 (m), and 1374 (m) cm^{-1}. The mass spectrum of the compound indicated the parent peak at m/e = 349. Since the compound tended to decompose, it was not analyzed.

(b) Cyclohexanone Derivative

To a solution of 3.14 mmol of the lithio salt of 1,4-diphenyl-2-azetidinone was added cyclohexanone (310 mg, 3.14 mmol) and the reaction stirred for 10 min. Column chromatography of the 700 mg of crude product gave 416 mg (41%) of pale yellow solid. Recrystallization from methylene chloride–ether–pentane gave white needles, m.p. 163–164°. The i.r. spectrum showed bands at 3580 (w), 3430 (b), 2940 (s), 1735 (s), 1600 (m), 1495 (m), 1380 (m), and 1145 (m) cm^{-1}. The n.m.r. spectrum showed peaks at δ 1.06–2.10 (m, 11 H), 3.16 (d, J = 2.5 Hz, 1H), 5.06 (d, J = 2.5 Hz, 1H), and 7.00–7.48 (m, 10H).

Anal. Calcd. for $C_{21}H_{23}NO_2$: C, 78.47; H, 7.21. Found C, 78.35; H, 7.21.

(c) Acetone Derivative

1,4-Diphenyl-2-azetidinone (3.97 mmol) was stirred with 1.0 equiv of lithium diisopropylamide for 30 s and 3 ml (10 equiv) of acetone was added. The reaction was stirred for 10 min. Work-up gave 1.18 g of yellow solid. Column chromatography yielded 643 mg (58%) white solid, m.p. 148–149.5° (methylene chloride–ether–pentane). The n.m.r. spectrum showed peaks at 1.32 and 1.43 (two singlets, 6H), 1.87 (s, 1H), 2.10 (d, J = 2.5 Hz, 1H), 5.00 (d, J = 2.5 Hz, 1H), and 7.00–7.45 (m, 10H). The i.r. spectrum showed bands at 3580 (w), 3460 (b), 1725 (s), 1600 (m), 1350 (m), and 1375 (m) cm^{-1}.

Anal. Calcd. for $C_{18}H_{19}NO_2$: C, 76.84; H, 6.81; N, 4.97. Found: C, 76.25; H, 6.77; N, 4.90.

(d) Benzoyl Derivative

1,4-Diphenyl-2-azetidinone (1.22 g, 5.49 mmol) was stirred with 1.05 equiv of lithium diisopropylamide for 30 s and 1 equiv of methyl benzoate was added. After 10 min the reaction was worked-up to give 1.85 g of yellow solid. Column chromatography yielded 1.1 g (61%) of white solid, m.p. 133–136° (methylene chloride–ether–pentane). The n.m.r. spectrum showed peaks at δ 4.80 (d, J = 2.0 Hz, 1H), 5.75 (d, J = 2.0 Hz, 1H), 6.95–7.61 (m, 13 H), 8.05–8.25 (m, 2H). The i.r. spectrum showed bands at 1740 (s), 1682 (s), and 1600 (m) cm^{-1}.

Anal. Calcd. for $C_{22}H_{17}NO_2$: C, 80.71; H, 5.24; N, 4.28. Found: C, 80.48; H, 5.47; N, 4.20.

*Decomposition of the Lithio Salt of 1,4-Diphenyl-2-azetidinone (**10***a*)

To a solution of 1.1 equiv of lithium diisopropylamide was added 2.80 mmol of 2-azetidinone and the solution allowed to warm to room temperature over 20 min. Work-up yielded 630 mg of crude material which was recrystallized from methylene chloride–ether to give 167 mg (27%)

of **17** as a white solid, m.p. 182–183°. The i.r. spectrum (KBr pellet) showed bands at 3380 (w), 1740 (s), 1710 (s), 1600 (m), 1490 (m), 1360 (m), 750 (m), and 690 (m) cm^{-1}. The n.m.r. spectrum (DMSO-d_6) showed peaks at 2.78–3.48 (m, 2H), 4.57 (d, $J = 2.5$ Hz, 1H), 4.72–5.08 (m, 1H), 5.42 (d, $J = 2.5$ Hz, 1H), 6.06 (d, $J = 7.5$ Hz, 1H), 6.48 (d, $J = 6.5$ Hz, 2H), 6.82–7.60 (m, 18 H).

Anal. Calcd. for $C_{30}H_{26}N_2O_2$: C, 80.69; H, 5.87; N, 6.27. Found: C, 80.58; H, 5.95; N, 6.25.

Financial Assistance by Bristol Laboratories, Syracuse, and by the National Research Council of Canada is gratefully acknowledged.

1. P. G. GASSMAN and B. L. FOX. J. Org. Chem. **31**, 982 (1966).
2. H. L. NEEDLES and R. E. WHITFIELD. J. Org. Chem. **31**, 989 (1966).
3. D. N. CROUSE and D. SEEBACH. Ber. **101**, 3113 (1968).
4. (*a*) J. C. SHEEHAN and E. J. COREY. Org. React. **9**, 388 (1957). (*b*) J. A. MOORE. *In* The chemistry of heterocyclic compounds. Vol. 19, Part II. *Edited by* A. Weissberger. Interscience Publishers, Inc. New York, N.Y. 1964. pp. 916–941. (*c*) R. GRAF. Ann. **661**, 123 (1963); (*d*) H. BESTIAN, H. BIENER, K. CLAUS, and H. HEYN. Ann. **718**, 94 (1968).
5. (*a*) S. WOLFE and W. S. LEE. Chem. Commun. 242, 1968 (*b*) R. D. G. COOPER, P. V. DEMARCO, and D. O. SPRY. J. Am. Chem. Soc. **91**, 1528 (1969). (*c*) O. K. J. KOVACS, B. EKSTRÖM, and B. SJÖBERG. Tetrahedron Lett. 1863 (1969). (*d*) J. P. CLAYTON, J. H. C. NAYLOR, R. SOUTHGATE, and E. R. STOVE. Chem. Commun. 129 (1969). (*e*) M. L. SASSIVER and R. G. SHEPHERD. Tetrahedron Lett. 3993 (1969). (*f*) G. E. GUTOWSKI. Tetrahedron Lett. 1779 (1970). (*g*) J. R. JACKSON and R. J. STOODLEY. Chem. Commun. 647 (1971). (*h*) B. G. RAMSEY and R. J. STOODLEY. Chem. Commun. 450 (1971).
6. G. V. KAISER, C. W. ASHBROOK and J. E. BALDWIN. J. Am. Chem. Soc. **93**, 2342 (1971).
7. E. H. W. BÖHME, H. E. APPLEGATE, B. TOEPLITZ, J. E. DOLFINI, and J. Z. GOUGOUTAS. J. Am. Chem. Soc. **93**, 4324 (1971).
8. R. A. FIRESTONE, N. SCHELECHOW, D. B. R. JOHNSTON, and B. G. CHRISTENSEN. Tetrahedron Lett. 375 (1972).
9. E. J. MORICONI and J. F. KELLY. J. Org. Chem. **33**, 3046 (1968).
10. D. A. JOHNSON and D. MANIA. Tetrahedron Lett. 267 (1969).
11. H. GILMAN and M. SPEETER. J. Am. Chem. Soc. **65**, 2255 (1943).
12. J. C. SHEEHAN and E. J. COREY. Org. React. **9**, 394 (1957).
13. E. J. MORICONI and W. C. MEYER. Tetrahedron Lett. 3823 (1968).
14. T. DURST and M. J. O'SULLIVAN. J. Org. Chem. **35**, 2043 (1970).
15. R. GRAF. Ann. **661**, 111 (1963).
16. F. F. BLICKE and W. A. GOULD. J. Org. Chem. **23**, 1102 (1958).

Can. J. Chem. Downloaded from www.nrcresearchpress.com by 210.87.254.5 on 09/05/12
For personal use only.

Ambident Ligands. I. Phenylsulfoxyacetic Acid

N. J. GOGAN, M. J. NEWLANDS, AND BECK-YU TAN (NÉE YAP)[1]

Department of Chemistry, Memorial University of Newfoundland, St. John's, Newfoundland

Received October 18, 1971[2]

Phenylsulfoxyacetic acid, $C_6H_5S(O)CH_2CO_2H$, a potential ambident ligand, forms simple salts with magnesium(II), calcium(II), barium(II), manganese(II), cobalt(II), nickel(II), copper(II), zinc(II), silver(I), and mercury(I). With cadmium(II) it forms a simple salt and a complex, oxygen-bonded to the sulfoxide group. With platinum(II) it gives complexes which are sulfur-bonded to the sulfoxide group.

L'acide phénylsulfoxyacétique, $C_6H_5S(O)CH_2CO_2H$, ligand ambidentique à l'état potentiel, forme des sels simples avec le magnésium(II), calcium(II), barium(II), manganèse(II), cobalt(II), nickel(II), cuivre(II), zinc(II), argent(I), et mercure(I). Avec le cadmium(II), il forme un sel simple et un complexe, lié à l'oxygène du groupe sulfoxyde. Avec le platine(II), on obtient des complexes liés au soufre du groupe sulfoxyde.

[Traduit par le journal]

Canadian Journal of Chemistry, **50**, 3202 (1972)

Introduction

An interest in competition between donor sites in ligands is of relatively recent origin (1) although linkage isomerism has been known for a long time (2). Current interest stems in part from improved methods for determining the structures of complexes and in part from attempts to place observed stabilities of complexes on a more rational basis (3). The present work is part of a larger study of internal competition between donor sites in ligands which has as its long-term objective a more detailed understanding of the factors involved in such competition during complex formation.

Discussion

The ligand **1** studied in the present work has three potential donor sites, the sulfur and oxygen atoms of the SO group and the oxygen atoms of the carboxylate group. The ligand is also potentially a chelating agent, giving a five-membered chelate ring if the carboxylate group and the sulfur of the SO group are involved, and a six-membered chelate ring if the carboxylate group and the oxygen atom of the SO group are involved.

Detailed i.r. studies of sulfoxides (4), confirmed in some cases by X-ray crystallography (5–7), have shown that $\Delta\nu(S{-}O)$, $(\nu(S{-}O)_{ligand} - \nu(S{-}O)_{complex})$, is negative when coordination is via sulfur and positive when coordination is via oxygen.[3] Similar studies permit distinction between carboxylate salts and mono and bidentate carboxylate complexes (8).

1

The i.r. spectral data for the products of the reaction of phenylsulfoxyacetic acid **1** with the carbonates, basic carbonates or hydroxides of some group II metals, zinc(II), Ag(I) and some first row transition metals are given in Table 1. The data for the product of the reaction of mercurous nitrate and sodium phenylsulfoxyacetate are also given. The data for the parent acid and its sodium salt are also included for comparison. It is seen that $\Delta\nu(CO_2)$ is similar to the sodium salt for all these metal compounds indicating that the carboxylate–metal bonding is essentially ionic. The position of the SO stretching frequency is almost the same as for the parent acid and its sodium salt which indicates no bonding of the SO group to the metal. These compounds are therefore classified as simple salts. The i.r. spectra were the same before and after drying except for the presence of $\nu OH(H_2O)$ in some compounds before drying. The copper, zinc, and magnesium compounds still showed broad $\nu OH(H_2O)$ bands, at about 3010, 3250,

[1]Taken in part from the M.Sc. thesis of Beck-Yu Yap, Memorial University of Newfoundland, 1970.

[2]Revision received June 27, 1972.

[3]Recently (15) a case has been reported where bonding to SO takes place without a change in $\nu(S{-}O)$. However, in all cases so far tested a significant shift in $\nu(S{-}O)$ has indicated definite bonding.

Can. J. Chem. Downloaded from www.nrcresearchpress.com by 210.87.254.40 on 09/05/12
For personal use only.

TABLE 1. I.r. absorptions of sulfoxy and carbonyl stretching frequencies of phenylsulfoxyacetates in KBr discs*

Compound	Frequency (cm^{-1})				
	ν(S—O)	$\nu_{asym}(CO_2)$	$\nu_{sym}(CO_2)$	$\Delta\nu(CO_2)$	$\Delta\nu$(S—O)
$C_6H_5SOCH_2CO_2H$	1008(s)	1720(s)	1240(s)	480	0
$C_6H_5SOCH_2CO_2Na$	1010(s)	1605(s)	1385(s)	220	−2
$(C_6H_5SOCH_2CO_2)_2Mg\cdot 2H_2O$	1018(s)	1610(s) 1585(s)	1378(s)	232	−10
$(C_6H_5SOCH_2CO_2)_2Ca$	1012(s)	1595(s)	1395(s)	200	−4
$(C_6H_5SOCH_2CO_2)_2Ba$	1018(s)	1580(s)	1395(s)	185	−10
$(C_6H_5SOCH_2CO_2)_2Mn$	1008(s)	1588(s)	1398(s)	190	0
$(C_6H_5SOCH_2CO_2)_2Co$	1018(s)	1590(s)	1395(s)	195	−10
$(C_6H_5SOCH_2CO_2)_2Ni$	1012(s)	1580(s)	1395(s)	205	−4
$(C_6H_5SOCH_2CO_2)_2Cu\cdot H_2O$	1030(s)	1600(s)	1400(s)	190	−22
$(C_6H_5SOCH_2CO_2)_2Cu\cdot 3/2H_2O$	1008(s)	1595	1402(s) 1380(s)	193 215	0
$(C_6H_5SOCH_2CO_2)_2Zn\cdot 2H_2O$	1015(s)	1600(s)	1372(s)	228	−7
$C_6H_5SOCH_2CO_2Hg$	1015(s)	1580(s)	1305(s)	275	−7
$C_6H_5SOCH_2CO_2Ag$	1012(s)	1598† 1552(s)	1378(s)	174	−4

*s = strong, ν(OH) region was examined in Nujol or HCB nulls.
†Absent in Nujol null.

and 3320 cm^{-1}, respectively, after drying for several hours under vacuum at 70°. In the case of all the other compounds these bands were absent after similar drying. This is in agreement with the elemental analyses (Table 4). When the copper salt was dried at 90° for several hours under vacuum it lost some of its water and the color changed from blue to green. The SO stretching frequency also changed. The value of $\Delta\nu$(SO), −22 cm^{-1}, for the green copper compound might indicate some interaction between the copper and the sulfur of the SO group but it is hardly large enough to be definitive for sulfur–copper bonding.

Reaction of the acid, **1**, with cadmium carbonate gave a dihydrate $Cd(C_6H_5SOCH_2CO_2)_2\cdot 2H_2O$. When crystallized from water this product has $\Delta\nu(SO) = +48$ cm^{-1} indicative of bonding through the oxygen of the SO group. The $\Delta\nu(CO_2)$ value of 210 cm^{-1} is similar to that of the sodium salt so there appears to be no covalent bonding between the $-CO_2$ groups and the cadmium. When the product was recrystallized from 95% ethanol a product with the same empirical formula but with a different i.r. spectrum was obtained. The $\Delta\nu$(SO) value is −12 cm^{-1} indicating no significant interaction between the metal and the SO group. The $\Delta\nu(CO_2)$ value, 167 cm^{-1}, is again similar to the sodium salt. The differences in the two compounds were further investigated. The X-ray powder diffraction patterns are quite different. Their melting points are also different. The properties in solution for the two compounds seem to be very similar. The molar conductance[3] is 147.28 Ω^{-1} cm^2 for the water crystallized product and 151.75 Ω^{-1} cm^2 for the product crystallized from 95% ethanol. The ^1H n.m.r. spectra in D_2O are the same for both products showing the phenyl protons and the AB system of the methylene group. It would thus appear that the two compounds are different in the solid but dissociate in solution to give the same ions. The compound recrystallized from 95% ethanol seems to be a simple salt whereas that crystallized from water seems to be a complex. The water-crystallized product shows bands below 500 cm^{-1} at 475, 380, and 300 cm^{-1}, the region where M—O stretching frequencies are expected. The ethanol crystallized product has no band in this region. The structure, therefore, of the water crystallized product would seem to be a tetra-coordinate complex with the oxygen of two phenylsulfoxyacetate ions and of two water molecules coordinated onto the metal. The carboxylate groups would presumably be outside the coordination sphere. However, ionic structures such as $[Cd(H_2O)_4]^{2+}[Cd(PhSOCH_2CO_2)_4]^{2-}$ cannot be ruled out on the above evidence.[4]

[4]We thank one of the referees for suggesting this ionic structure.

Can. J. Chem. Downloaded from www.nrcresearchpress.com by 210.87.254.40 on 09/05/12
For personal use only.

TABLE 2. I.r. spectra of complexes: ν(SO) and $\nu(CO_2)$ regions*

Compound	Absorption (cm^{-1}). ν(SO)	$\nu_{asym}(CO_2)$	ν_{sym}	$\Delta\nu(CO_2)$†	$\Delta\nu$(SO)‡
$H[Pt(PhSOCH_2CO_2)Cl_2]$	1120s	1665s	1305s	360	−112
$K[Pt(PhSOCH_2CO_2)Cl]$	1120s	1668s	1305s	363	−112
$Cs[Pt(PhSOCH_2CO_2)Cl_2]$	1120s	1660s	1305s	355	−112
$[Pt(PhSOCH_2CO_2H)Cl_2]_2$	1135s	1718s	1300mbr	418	−127
$(PhSOCH_2CO_2)_2Cd\cdot 2H_2O$§	960s	1590s	1380s	210	+48
$(PhSOCH_2CO_2)_2Cd\cdot 2H_2O$¶	1020s	1565s	1398s	167	−12

*KBr discs; s = strong, m = medium, br = broad.
†$\Delta\nu(CO_2) = \nu_{asym} - \nu_{sym}$.
‡$\Delta\nu(SO) = \nu(SO)_{(ligand)} - \nu(SO)_{(complex)}$.
§Crystallized from water.
¶Crystallized from ethanol.

TABLE 3. I.r. spectra: 600–250 cm^{-1} range*

Compound	Absorption (cm^{-1})	Pt—Cl
2 M = H	550m, 528s, 515s, 444w, 405m,† 375w	338m, 318s
M = K	552w, 530m, 518s, 445w, 407m†	340m, 318s
M = Cs	550m, 530s, 515s, 442w, 405m†	340m, 318s
3	580m, 528s, 502s, 448w, 305w†	338s, 315msh, 280w
$\{Pt[P(OEt)_3]Cl_2\}_2$‡		361vs, 354sh, 325m
$\{Pt(PEt_3)Cl_2\}_2$‡		353vs, 345sh, 325m, 266s

*s = strong, m = medium, w = weak, v = very, sh = shoulder.
†KBr discs.
‡Reference 11.

These structures are in keeping with the fact that most complexes of cadmium are tetra-coordinate complexes.

Reaction of the acid **1** with potassium tetrachloroplatinate(II) with or without the presence of an alkali metal chloride gave the compounds **2**, $M[Pt(PhSOCH_2CO_2)Cl_2]$ (M = H, K, or Cs). The i.r. spectral data given in Table 2 indicate that the ligand is attached to platinum via sulfur of the sulfoxide group. A shift of $\nu_{asym}(CO_2)$ from that of the acid (1720 cm^{-1}) indicates coordination via the carboxylate group and the large value of $\Delta\nu(CO_2)$ suggests monodentate coordination (8). All the compounds, **2**, show a medium intensity band at about 405 cm^{-1} (Table 3), which is believed to be ν(Pt—O) (*cf.* 388 and 407 cm^{-1} attributed to ν(Pt—O) in glycinate complexes of platinum(II) (9)).

The reaction of the acid, **1**, with potassium tetrachloroplatinate(II) in the presence of cesium chloride yielded, in addition to **2** (M = Cs), a compound with empirical formula $PtCl_2(C_6H_5SOCH_2CO_2H)$. This has $\Delta\nu$(SO) = −127 cm^{-1} indicating bonding of the SO group to the metal via the sulfur atom. However, the carbonyl stretching frequencies are close to that of the parent acid, indicating that the carboxylic group is not bonded to the metal. This information suggests the binuclear chlorine bridged structure shown in **3**. This structure is also supported by other evidence. The νOH(—COOH) is observed at about 2900 cm^{-1} (compared to

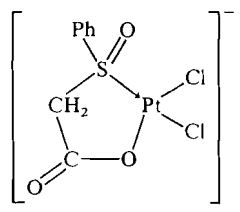

2

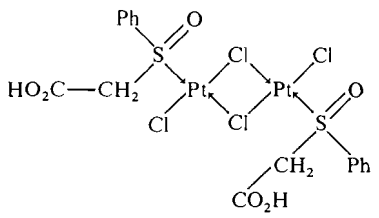

3

Can. J. Chem. Downloaded from www.nrcresearchpress.com by 210.87.254.40 on 09/05/12
For personal use only.

TABLE 4. Analytical data for phenylsulfoxyacetates

Compound	Melting point (°C)	Analysis (%) C Found	C Calcd.	H Found	H Calcd.	S Found	S Calcd.	Metal Found	Metal Calcd.
$(C_6H_5SOCH_2CO_2)_2Mg\cdot 2H_2O$	180–181	44.09	45.03	4.02	3.78	14.90	15.03	5.68	5.79
$(C_6H_5SOCH_2CO_2)_2Ca$	140 (dec.)	47.13	47.29	3.65	3.47	15.67	15.78	9.70	9.86
$(C_6H_5SOCH_2CO_2)_2Ba$	154	38.30	38.15	2.98	2.80	12.57	12.73	27.51	27.26
$(C_6H_5SOCH_2CO_2)_2Mn$	148.5 (dec.)	45.49	45.60	3.74	3.35	15.10	15.22	13.00	13.05
$(C_6H_5SOCH_2CO_2)_2Co$	167 (dec.)	45.10	45.20	3.53	3.32	15.26	15.08	13.20	13.86
$(C_6H_5SOCH_2CO_2)_2Ni$	170	45.06	45.21	3.51	3.32	15.02	15.09	13.28	13.81
$(C_6H_5SOCH_2CO_2)_2Cu\cdot H_2O$	142 (dec.)	42.84	42.89	3.80	3.59	14.21	14.32	14.00	14.21
$(C_6H_5SOCH_2CO_2)_2Cu\cdot 3/2H_2O$	130 (dehydration) 150 melt	42.74	42.06	3.78	3.75	14.12	14.04	13.11	13.91
$(C_6H_5SOCH_2CO_2)_2Zn\cdot 2H_2O$	140 (dec.)	41.17	41.09	3.81	3.88	13.72	13.71	13.27	13.96
$(C_6H_5SOCH_2CO_2)Ag$	167	33.26	33.01	2.62	2.42	10.85	11.01	37.01	37.08
$(C_6H_5SOCH_2CO_2)Hg$	184	26.14	25.01	1.98	1.84	8.52	8.35		

2920 cm^{-1} for the parent acid). The compound dissociates in water to give highly conducting solutions. The molar conductance is 755 Ω^{-1} cm^2 compared to 163–198 Ω^{-1} cm^2 for compounds **2**. The ^1H n.m.r. in acetone-d_6 shows the phenyl ring resonances as complex multiplets at 1.85 and 2.32 τ and an AB system ($J = 15$ Hz) of the methylene group at 5.38 τ. The absence of the $—CO_2H$ proton resonance indicates rapid exchange.

All compounds **2** and **3** show bands in the 310–340 cm^{-1} region which are probably assignable to ν(Pt—Cl) (10). The presence of two bands and the relatively large difference between them in **2** suggests that the Pt—Cl are *cis* to one another.

The situation with **3** is not so clear. There are three possible ν(Pt—Cl) and these could be assigned as terminal (338 cm^{-1}) and bridging (315 and 280 cm^{-1}) (11, 12) but the lowest energy band is somewhat weak. Nevertheless the general pattern of bands is very similar to that for $Pt_2(PEt_3)_2Cl_4$ discussed by Adams *et al.* (11). This evidence would suggest that **3** is a chlorine-bridged dimer.

Thus phenylsulfoxyacetic acid does behave as an ambident ligand, bonding to class "a" acceptors via oxygen and to class "b" acceptors via sulfur of the sulfoxy group. It does not appear to be as good a donor as an unsubstituted sulfoxide.

Experimental

Phenylsulfoxyacetic acid was prepared from commercial phenylthioacetic acid (Aldrich) by oxidation with hydrogen peroxide in ethanol (13). Metal salts were commercially available materials except where otherwise specified. I.r. spectra as Nujol or hexachlorobutadiene (HCB) mulls or KBr discs were recorded with a Perkin-Elmer Model 457 spectrometer (4000–250 cm^{-1}), X-ray powder diffraction patterns were recorded in the Department of Geology. Conductivity measurements were made in aqueous solution with a Beckman RC-18 conductivity bridge using standard KCl solutions as calibrant. ^1H n.m.r. spectra were recorded with a Varian A-60 spectrometer. Element analyses (C, H, S, Cl) were carried out by the Alfred Bernhardt Microanalytical Laboratory, West Germany. Metal analyses were obtained by standard methods (Ca, Mn, Co, and Cu by atomic absorption; Mg, Ni, Zn, and Cd by complexometry, Ag and Ba by gravimetry).

Salts of Phenylsulfoxyacetic Acid

(*a*) An aqueous solution of phenylsulfoxyacetic acid (3.680 g, 20.0 mmol in 100 ml) was added to heavy basic magnesium carbonate, $3MgCO_3\cdot Mg(OH)_2\cdot 3H_2O$, (0.9134 g, 2.5 mmol) and the reaction mixture was stirred until it was no longer acidic. Excess magnesium carbonate was filtered off, the solvent was removed under reduced pressure, and the residue was recrystallized from aqueous acetone and dried at 70° to give magnesium phenylsulfoxyacetate dihydrate (4.16 g, 97.5%). Salts of Ca(II), Ba(II), Mn(II), Ni(II), Cu(II), Zn(II), and Ag(I) were prepared by the same method from the corresponding carbonates, hydroxides, or basic carbonates.

(*b*) An aqueous solution of sodium phenylsulfoxyacetate (2.06 g, 10.0 mmol in 5 ml) was added to acidic aqueous mercury(I) nitrate solution (2.806 g, 10.0 mmol in 15 ml) in the dark. The white precipitate, which began to form immediately, was filtered off after 2 h and dried *in vacuo* at 70° to give mercury(I) phenylsulfoxyacetate (3.15 g, 82.0%).

Complexes of Phenylsulfoxyacetic Acid

(a) With Cadmium(II)

An aqueous solution of phenylsulfoxyacetic acid (3.680 g, 20.0 mmol in 100 ml) was added with stirring to an excess of freshly prepared cadmium carbonate (14). Stirring was continued at 50° until the solution became neutral. The

Can. J. Chem. Downloaded from www.nrcresearchpress.com by 210.87.254.40 on 09/05/12
For personal use only.

Can. J. Chem. Downloaded from www.nrcresearchpress.com by 210.87.254.40 on 09/05/12
For personal use only.

excess of cadmium carbonate was filtered off, the solvent was evaporated under reduced pressure, and the residue solidified by the addition of ethyl ether. Recrystallization from water gave the complex $[C_6H_5S(O)CH_2CO_2]_2Cd{\cdot}2H_2O$, m.p. 124–125° (4.230 g, 88.5%).

Anal. Calcd. for $C_{16}H_{18}O_8S_2Cd$: C, 37.33; H, 3.52; S, 12.46. Found: C, 37.37; H, 3.61; S, 12.26.

X-Ray powder diffraction pattern $d(I/I_{10})$; 1.77(5), 2.16(5), 2.44(5), 2.50(5), 2.68(6), 2.90(5), 3.08(4), 3.31(8), 3.47(8), 3.92(7), 4.17(6), 4.50(1), 4.91(1), 5.50(10), 7.76(3). Recrystallization from 95% ethanol gave a simple salt dihydrate with the same formula, m.p. 131–132°.

Anal. Calcd. for $C_{16}H_{18}O_8S_2Cd$: C, 37.33; H, 3.52; S, 12.46. Found: C, 37.62; H, 3.37; S, 12.23.

X-Ray powder diffraction pattern $d(I/I_{10})$; 2.32(5), 2.59(3), 2.91(7), 3.38(6), 3.62(5), 3.88(10), 4.32(8), 4.91(1), 5.37(8), 5.93(8).

(b) Hydrogen Dichloromono(phenylsulfoxyacetato)-platinate(II)

An aqueous solution of potassium tetrachloroplatinate(II) (0.4152 g, 1.00 mmol in 3 ml) was added to an aqueous solution of phenylsulfoxyacetic acid (0.1840 g, 1.00 mmol in 5 ml) to give a yellow precipitate which began to form after 5 h at 45°. The precipitate was filtered off, washed with water and dried *in vacuo* to give the title product, m.p. 230° (dec.), (0.3378 g, 75.0%).

Anal. Calcd. for $C_8H_8Cl_2O_3SPt$: C, 21.34; H, 1.79; S, 7.12; Cl, 15.75. Found: C, 21.26; H, 1.69; S, 7.04; Cl, 15.45.

(c) Potassium Dichloromono(phenylsulfoxyacetato)-platinate(II)

An aqueous solution of potassium tetrachloroplatinate(II) (0.8304 g, 2.00 mmol in 3 ml) was added to an aqueous solution of potassium phenylsulfoxyacetate prepared by neutralizing the acid (0.3680 g, 2.00 mmol in 10 ml) with the stoichiometric amount of potassium carbonate. Stirring was continued at room temperature until the initially reddish solution turned yellow. Cooling caused crystallization of a yellow material which was washed with cold water and cold 95% ethanol and then dried *in vacuo* to give the title compound, m.p. 260° (dec.) (0.2363 g, 24.2%).

Anal. Calcd. for $C_8H_7Cl_2O_3SKPt$: C, 19.68; H, 1.65; S, 6.56; Cl, 14.52. Found: C, 19.89; H, 1.56; S, 6.82; Cl, 14.17.

(d) Cesium Dichloromono(phenylsulfoxyacetato)-platinate(II) and Di-μ-chlorodichlorobis-(phenylsulfoxyacetic acid)diplatinum(II)

A mixture of potassium tetrachloroplatinate(II) (0.4152 g, 1.00 mmol), phenylsulfoxyacetic acid (0.1840 g, 1.00 mmol) and cesium chloride (0.1684 g, 1.00 mmol) was dissolved in water (10 ml) and stirred at room temperature for 14 h.

The yellow precipitate was filtered off, washed with cold water, and dried *in vacuo* to give the cesium salt, $Cs[Pt(C_6H_5SOCH_2CO_2)Cl_2]$, m.p. 230° (dec.) (0.2268 g, 39.1%).

Anal. Calcd. for $C_8H_7Cl_2O_3SCsPt$: C, 16.51; H, 1.21; S, 5.51; Cl, 14.52. Found: C, 16.34; H, 1.31; S, 5.34; Cl, 14.17.

Yellow acicular crystals of the chlorine-bridged dimer separated from the mother liquors after 3 days at 0°, m.p. 125° (0.1520 g, 33.8%).

Anal. Calcd. for $C_{16}H_{16}O_6Cl_4S_2Pt_2$: C, 21.34; H, 1.79; S, 7.12; Cl, 15.75. Found: C, 21.19; H, 1.81; S, 7.39; Cl, 15.80.

Unsuccessful Experiments

Attempts to isolate pure compounds of chromium, cobalt, iron, and molybdenum using standard methods were unsuccessful.

We thank the National Research Council of Canada for financial support and Dr. V. S. Papezik of the Department of Geology for obtaining the X-ray powder diffraction patterns.

1. A. H. Norbury and A. I. P. Sinha. Quart. Rev. **24**, 69 (1970).
2. F. A. Cotton and G. Wilkinson. Adv. Inorg. Chem. Interscience, 2nd Ed., New York. p. 149.
3. S. Ahrland, J. Chatt, and N. R. Davies. Quart. Rev. **12**, 265 (1958); R. G. Pearson. J. Am. Chem. Soc. **85**, 3533 (1963).
4. J. Gopalakrishnan and C. C. Patel. J. Sci. Ind. Res. **27**, 475 (1968); W. L. Reynolds. Progr. Inorg. Chem. **12**, 1 (1970) and references cited therein.
5. M. J. Bennett, F. A. Cotton, and D. L. Weaver. Acta Cryst. **23**, 581 (1967); M. J. Bennett, F. A. Cotton, D. L. Weaver, R. J. Williams, and W. H. Watson. Acta Cryst. **23**, 788 (1967).
6. D. A. Langs, C. R. Hare, and R. G. Little. Chem. Commun. 1080 (1967).
7. M. McPartlin and R. Mason. Chem. Commun. 545 (1967); N. W. Isaacs, C. H. L. Kennard, and W. Kitching. Chem. Commun. 820 (1968).
8. N. Nakamoto. Infrared spectra of inorganic and coordination compounds. John Wiley, New York. 1963. pp. 197–215.
9. J. A. Kieft and N. Nakamoto. J. Inorg. Nucl. Chem. **29**, 2561 (1967).
10. D. M. Adams, J. Chatt, J. Geratt, and A. D. Westland. J. Chem. Soc. 734 (1964).
11. D. M. Adams and P. J. Chandler. J. Chem. Soc. A, 588 (1969).
12. A. Pidcock, R. E. Richard, and L. M. Venanzi. J. Chem. Soc. A, 1970 (1968); C. V. Senoff. Can. J. Chem. **46**, 3287 (1968).
13. P. Golding. M.Sc. Thesis, Memorial University of Newfoundland. 1968. p. 31.
14. G. Brauer. Handbook of preparative inorganic chemistry. Vol. II. Academic Press, New York. 1965. p. 1104.
15. C. V. Senoff, E. Maslowsky, and R. G. Goel. Can. J. Chem. **49**, 3585 (1971).

Chaleurs de mélange du système éthyl-3 pentanol-3 tétrachlorure de carbone

H. Brusset, M. Desgranges, et J. C. Lecoq

Laboratoire de Recherches de Chimie systématique, Ecole Normale Supérieure, 24 rue Lhomond et Université Paris VI, Bâtiment F 8, rue Cuvier Paris V°

Reçu le 7 décembre, 1971

Les enthalpies de mélange du système éthyl-3 pentanol-3 tétrachlorure de carbone ont été mesurées par microcalorimétrie. La théorie classique des solutions associées conduit à une expression de l'enthalpie d'excès que nous avons simplifiée par l'introduction de la chaleur à dilution infinie de l'alcool. L'expression obtenue permet de calculer l'enthalpie de formation d'une liaison hydrogène en utilisant des résultats calorimétriques et tonométriques.

Le calcul permet de vérifier que cette enthalpie est indépendante de la concentration de la solution (jusqu'à 0.45 en fraction molaire). La valeur obtenue est en bon accord avec les résultats de la littérature.

The enthalpies of mixing in the system 3-ethyl-3 pentanol–carbon tetrachloride were measured by microcalorimetry. The classic theory of associated solutions leads to an expression for the excess enthalpy which we have simplified by introducing the heat at infinite dilution for the alcohol. The resulting expression allows the enthalpy of formation of a hydrogen bond to be calculated using calorimetric and tonometric results. The calculations show that this enthalpy is independent of the concentration of the solution (up to 0.45 in molar fraction) and is in agreement with the literature.

Canadian Journal of Chemistry, **50**, 3207 (1972)

Can. J. Chem. Downloaded from www.nrcresearchpress.com by 210.87.254.40 on 09/05/12
For personal use only.

Introduction

La mesure des enthalpies de mélange du système éthyl-3 pentanol-3 tétrachlorure de carbone a déjà été effectuée à 3 températures (25, 40, 50 °C) en utilisant un microcalorimètre de type Calvet (1).

Dans le présent article, nous complétons l'étude de ce système à 60 °C.

Nous avons ensuite effectué le lissage des courbes expérimentales. L'utilisation de la théorie classique des mélanges associés nous permet de calculer, à partir de nos résultats calorimétriques, combinés à ceux déduits de mesures tonométriques, l'énergie d'association de l'alcool.

Etude expérimentale

Le dispositif expérimental permettant de réaliser le mélange des deux constituants du système est détaillé dans la référence 1. Rappelons simplement que l'un des constituants du mélange est contenu dans une ampoule de verre soufflé aussi mince que possible. Le second constituant du mélange occupe la partie supérieure d'un cloche de verre. L'ampoule terminée par un capillaire est maintenue dans la cloche de verre par un bouchon de liège d'où dépasse légèrement le capillaire. Tout le système ampoule–cloche est contenu dans la cellule de mesure. Les 2 constituants ne sont surmontés d'aucune atmosphère, tout le reste de l'espace étant occupé par du mercure. En faisant descendre la cloche de verre, l'extrémité inférieure du capillaire de l'ampoule vient buter au fond de la cellule; l'ampoule remonte et vient se briser sur l'extrémité pointue d'un petit agitateur en acier, les 2 liquides se mélangent. L'homogénéité du mélange est réalisée par quelques va-et-vient de l'agitateur.

Le contrôle de la température de l'enceinte est assuré par un régulateur de température RT 64 de Setaram (France).

L'utilisation de ce dispositif nous a permis de mesurer les enthalpies de mélange de l'éthyl-3 pentanol-3 dans le tétrachlorure de carbone à 4 températures. Les résultats obtenus sont donnés dans le tableau 1. Les courbes de la fig. 1 représentent l'enthalpie de mélange H^E en ordonnée en fonction de la fraction molaire d'alcool x_A.

Pour les faibles concentrations en l'un ou l'autre des constituants ($x_A < 0.15$ et $x_A > 0.85$) l'erreur expérimentale sur H^E est estimée à 2.5%. Pour les concentrations intermédiaires ($0.15 < x_A < 0.85$) cette erreur est inférieure à 2%.

L'incertitude sur la fraction molaire d'alcool varie de 0.05% aux fortes concentrations jusqu'à 1% aux faibles concentrations.

Le phénomène observé est endothermique. Ceci est normal puisque la mise en solution de l'alcool dans le solvant provoque essentiellement la désassociation partielle de

Tableau 1. Enthalpies de mélange du système éthyl-3 pentanol-3 tétrachlorure de carbone à 25, 40, 50, et 60 °C obtenues par lissage

	H^E (J)			
x_A	25 °C	40 °C	50 °C	60 °C
0.1	799	837	814	888
0.2	1102	1149	1194	1248
0.3	1182	1242	1320	1370
0.4	1162	1234	1306	1372
0.5	1081	1152	1212	1291
0.6	944	998	1063	1131
0.7	752	783	862	907
0.8	518	537	608	642
0.9	263	285	308	352

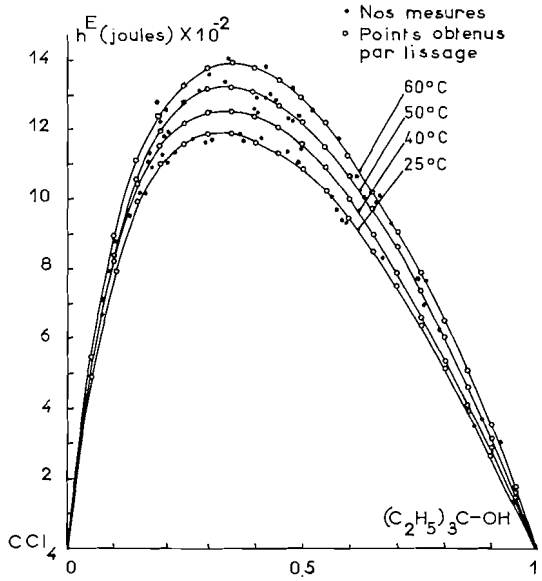

FIG. 1. Chaleurs de mélange du système éthyl-3 pentanol-3 tétrachlorure de carbone à 25, 40, 50, et 60 °C.

TABLEAU 2. Coefficients des expressions analytiques des courbes d'enthalpies de mélange à 25, 40, 50, et 60 °C

Température (°C)	Coefficients	Dispersion moyenne	Erreurs statistiques Δa_i
25	11 912	16.1	814
	−36 799		8 483
	80 808		28 818
	−67 030		39 486
	23 843		18 816
40	12 716	14.9	527
	−42 387		7 120
	91 777		26 184
	−99 019		38 053
	40 300		18 894
50	11 110	14.0	433
	−23 374		2 963
	28 230		6 215
	−13 047		4 007
60	13 124	19.2	1 105
	−40 061		11 745
	83 548		40 651
	−88 695		55 994
	36 321		26 493

l'alcool et que cet effet est endothermique. L'enthalpie de mélange croît avec la température (2).

Lissage des courbes expérimentales

Nous avons lissé nos courbes expérimentales suivant un développement polynômial de Redlich–Kister (3) couramment utilisé (4, 5)

$$[1] \qquad H^E = x_A(1 - x_A)(a_1 + a_2x_A + a_3x_A^2 + \ldots)$$

où H^E est l'enthalpie de mélange (ou d'excès) par mole de mélange, et x_A la fraction molaire en alcool.

La méthode de lissage employée est celle des moindres carrés.

Le nombre des coefficients du développement (éq. 1) que nous utilisons n'est pas fixé *a priori*; pour le déterminer, nous employons un critère proposé par Mme Duboc (6) et que nous rappelons brièvement.

Pour une courbe donnée, nous effectuons le lissage suivant les développements successifs à 2, 3, ..., n coefficients. Pour chaque développement nous calculons la dispersion moyenne δ des points expérimentaux autour de la courbe lissée ainsi que les erreurs statistiques Δa_i sur les coefficients a_i. Nous constatons que lorsque le nombre de coefficients a_i croît, la dispersion δ décroît, passe par un minimum pour m coefficients, puis se met à croître. D'autre part, certaines erreurs statistiques Δa_i deviennent supérieures aux coefficients a_i pour un développement à $m + 1$ coefficients. Ainsi, nous sommes conduits à adopter le développement à m coefficients pour lequel la dispersion moyenne δ est minimum.

Les coefficients obtenus pour l'ensemble des courbes étudiées sont donnés dans le tableau 2. Dans ce tableau nous ne donnons que les coefficients que nous sommes conduits à adopter compte tenu du critère indiqué précédemment.

Les courbes lissées sont données sur la fig. 1.

Le premier terme a_1, des développements obtenus, représente la pente de la tangente à l'origine de la courbe considérée, ou encore la chaleur à dilution infinie $H^E_\infty = \lim (H^E/x_A)_{x_A \to 0}$ de l'alcool dans le solvant.

Application de la théorie classique des mélanges idéaux associés et résultats

Nous donnons tout d'abord la liste des symboles utilisés dans les équations qui vont suivre. H^E, enthalpie d'excès par mole de mélange; H^E_∞, enthalpie molaire à dilution infinie de l'alcool dans le solvant; x_A, fraction molaire stoechiométrique de l'alcool; x_S, fraction molaire du constituant non associé du mélange; $x^e_{A_i}$, fraction molaire effective (mélange considéré comme constitué de monomères et de polymères) du polymère d'ordre i à l'équilibre; $x^{0e}_{A_i}$, fraction molaire effective du complexe A_i dans l'alcool pur; ΔH^0, enthalpie de formation d'une liaison hydrogène; ΔH^0_p, enthalpie de formation d'une liaison hydrogène dans l'alcool pur.

La théorie classique des mélanges idéaux associés (7, 8) pose, comme hypothèse, que l'enthalpie de mélange observée n'est due qu'au phénomène de désassociation.

Les hypothèses qui permettent d'obtenir une expression de l'enthalpie d'excès H^E par mole de mélange (7, 8, 9) sont les suivantes:

Can. J. Chem. Downloaded from www.nrcresearchpress.com by 210.87.254.40 on 09/05/12
For personal use only.

Can. J. Chem. Downloaded from www.nrcresearchpress.com by 210.87.254.40 on 09/05/12
For personal use only.

(*a*) Tout au moins pour des solutions suffisamment diluées d'alcool dans un solvant inerte, l'enthalpie de formation d'une liaison hydrogène a une valeur constante ΔH^0 indépendante des espèces dans lesquelles elle est engagée. Pour l'alcool pur, cette valeur peut être différente et nous l'appelons ΔH^0_p.

(*b*) L'association est linéaire, ou tout au moins les cycles sont très peu nombreux.

(*c*) L'enthalpie de mélange n'est due qu'à la désassociation de l'alcool.

Le calcul de l'enthalpie d'excès se mène alors de la façon suivante:

Par mole stoechiométrique d'alcool en solution (mole correspondant à la formule chimique R—OH de l'alcool), il y a n_{A_1} monomères, n_{A_2} dimères, ..., n_{A_i} polymères d'ordre i, et dans l'hypothèse de polymères linéaires, il y a donc $\sum_{i=2}(i-1)n_{A_i}$ liaisons hydrogène par mole stoechiométrique d'alcool pur.

L'enthalpie d'excès H^E par mole de mélange a pour expression:

$$[2]\quad H^E = \left(\sum_{i=2}(i-1)n_{A_i}\Delta H^0 - \sum_{i=2}(i-1)n^0_{A_i}\Delta H^0_p\right)x_A$$

En remplaçant dans cette expression les n_{A_i} par leurs valeurs en fonction des fractions molaires effectives $x^e_{A_i}$, puis en formant l'expression $\sum_{i=1} ix^e_{A_i}$ et tenant compte de $\sum_{i=1} in_{A_i} = 1$, l'expression 2 devient:

$$[3]\quad H^E = \left(\frac{\sum_{i=2}(i-1)\Delta H^0 x^e_{A_i}}{\sum_{i=1} ix^e_{A_i}} - \frac{\sum_{i=2}(i-1)\Delta H^0_p x^{0e}_{A_i}}{\sum_{i=1} ix^{0e}_{A_i}}\right)x_A$$

Expression dans laquelle ne figurent plus les n_{A_i} mais les fractions molaires effectives.

Cette expression 3 est plus connue sous la forme suivante (7):

$$[4]\quad H^E = \frac{\sum_{i=2}(i-1)\Delta H^0 x^e_{A_i}}{1+\sum_{i=2}(i-1)x^e_{A_i}} - \frac{\sum_{i=2}(i-1)\Delta H^0_p x^{0e}_{A_i}}{1+\sum_{i=2}(i-1)x^{0e}_{A_i}}x_A$$

Mais nous l'avons obtenue par une approche différente.

Cette forme est identique à éq. 3, car un calcul algébrique simple, mais un peu long, permet de montrer que:

$$\sum_{i=1} ix^e_{A_i} = x_A\left(1+\sum_{i=2}(i-1)x^e_{A_i}\right)$$

Ce qui donne pour l'alcool pur:

$$\sum_{i=1} ix^{0e}_{A_i} = 1+\sum_{i=2}(i-1)x^{0e}_{A_i}$$

Nous pouvons, grâce à l'introduction de la chaleur à dilution infinie H^E_∞ de l'alcool, éliminer les paramètres se rapportant à l'alcool pur (2ème partie de l'équation 3). Cette méthode a déjà été utilisée par Stokes (10). Nous avons vu que

$$H^E_\infty = \lim\left(\frac{H^E}{x_A}\right)_{x_A\to 0}$$

Formons H^E/x_A à partir de l'éq. 3.

$$[5]\quad \frac{H^E}{x_A} = \frac{\sum_{i=2}(i-1)\Delta H^0 x^e_{A_i}}{\sum_{i=1} ix^e_{A_i}} - \frac{\sum_{i=2}(i-1)\Delta H^0_p x^{0e}_{A_i}}{\sum_{i=1} ix^{0e}_{A_i}}$$

A dilution infinie ($x_A \to 0$), nous supposons qu'il ne reste plus que des monomères (11, 12). Dans ces conditions, le numérateur du 1er terme de l'éq. 5 est nul et

$$[6]\quad H^E_\infty = \frac{-\sum_{i=2}(i-1)\Delta H^0_p x^{0e}_{A_i}}{\sum_{i=1} ix^{0e}_{A_i}}$$

En formant [6] – [5] il vient:

$$[7]\quad H^E_\infty - \frac{H^E}{x_A} = \frac{-\sum_{i=2}(i-1)\Delta H^0 x^e_{A_i}}{\sum_{i=1} ix^e_{A_i}}$$

Cette équation a l'avantage de ne plus présenter de termes relatifs à l'alcool pur.

Par ailleurs, une étude tonométrique (13, 14) a permis, dans le cadre de la théorie des solutions idéales associées (8), de déterminer les constantes d'équilibre entre les polymères de l'alcool et de calculer les fractions molaires effectives $x^e_{A_i}$ des divers polymères, jusqu'à une fraction

TABLEAU 3. Répartition des polymères du système éthyl-3 pentanol-3 tétrachlorure de carbone à 25 °C (réf 14)

x_A	$x^e_{A_1}$	$x^e_{A_2}$	$x^e_{A_3}$	$x^e_{A_4}$	$x^e_{A_5}$	$x^e_{A_6}$	$x^e_{A_7}$
0.05	0.038	0.003	0.001	0.001	0.001	0.001	0.001
0.10	0.072	0.013	0.003	0.001	0.001	0.001	0.001
0.15	0.095	0.022	0.006	0.002	0.001	0.001	0.001
0.20	0.112	0.031	0.010	0.003	0.001	0.001	0.001
0.25	0.126	0.039	0.014	0.005	0.002	0.001	0.001
0.30	0.137	0.047	0.018	0.007	0.003	0.001	0.001
0.35	0.148	0.055	0.023	0.010	0.004	0.002	0.001
0.40	0.158	0.062	0.028	0.013	0.006	0.003	0.001
0.45	0.175	0.077	0.033	0.019	0.010	0.005	0.001

stoechiométrique d'alcool de 0.45 (domaine de validité de la théorie) et à 25 °C (tableau 3).

Rappelons simplement que cette étude tonométrique utilise la théorie des solutions idéales associées et un modèle à 2 constantes d'équilibre. La première constante K_1 est relative aux équilibres du type $A_1 + A_1 \rightleftarrows A_2$ où A_1 est un monomère d'alcool et A_2 un dimère.

La seconde constante K_2 est commune à tous les équilibres du type $A_i + A_1 \rightleftarrows A_{i+1}$ $(i \geqslant 2)$.

Ce modèle conduit à l'équation classique (8, 13, 14)

$$\frac{1}{P_A} = \frac{K_2}{P^0_A L} + \frac{1}{P^0_A L}\sqrt{\frac{K_1}{f_B - 1}}$$

P_A, pression partielle d'alcool; P^0_A, tension de vapeur de l'alcool pur à la température considérée; f_B, coefficient d'activité du solvant dans le mélange; L, limite du coefficient d'activité f_A de l'alcool quand $x_A \to 0$.

Le tracé de la droite $1/P_A = f(1/\sqrt{f_B - 1})$ permet de calculer sa pente $\sqrt{K_1}/P^0_A L$ et son ordonnée à l'origine $K_2/P^0_A L$.

P^0_A est connu et les mesures tonométriques permettent la détermination de L. Pour le système envisagé ici il a été trouvé à 25 °C: $K_1 = 2.5$ et $K_2 = 2.9$.

A partir de K_1 et K_2 et en appliquant la loi d'action de masse aux équilibres entre polymères indiqués précédemment, on en déduit la répartition des polymères de l'alcool en fonction de la fraction molaire stoechiométrique x_A d'alcool.

L'étude tonométrique (13, 14) a montré que, pour les mélanges d'éthyl-3 pentanol-3 dans le tétrachlorure de carbone et jusqu'à $x_A = 0.45$, la polymérisation de l'alcool est limitée pratiquement à l'ordre 6 (voir tableau 3).

TABLEAU 4. Système éthyl-3 pentanol-3 tétrachlorure de carbone: enthalpie de formation de la liaison hydrogène à 25 °C

x_A	ΔH^0 (J)
0.05	−22 978
0.10	−22 081
0.15	−21 934
0.20	−22 087
0.25	−21 610
0.30	−22 242
0.35	−21 687
0.40	−21 437
0.45	−20 687

L'utilisation de ces résultats et de ceux que nous avons obtenus par microcalorimétrie, nous permet grâce à l'éq. 7 de calculer ΔH^0 pour chaque concentration.

$$[8] \qquad \Delta H^0 = -\left(H^E_\infty - \frac{H^E}{x_A}\right)\frac{\sum_{i=1} i x^e_{A_i}}{\sum_{i=2}(i-1)x^e_{A_i}}$$

Les résultats obtenus sont donnés dans le tableau 4. (*i*) L'examen du tableau 4 nous montre que ΔH^0 est pratiquement indépendant de la concentration en alcool, dans le domaine exploré. Nous vérifions là, une hypothèse assez souvent faite (9, 10). (*ii*) La valeur moyenne de ΔH^0 est $\Delta H^0 = -21860$ J. L'écart maximum entre cette moyenne et les valeurs du tableau 4 est de 5.3%. (*iii*) Des mesures de r.m.n., exploitées à l'aide d'un modèle d'association linéaire (15), ont conduit, pour le même système, à la même température à une enthalpie de dimérisation de −24 244 J. Cette valeur diffère d'à peu près 10% de celle que nous trouvons. (*iv*) D'autres auteurs (16) utilisant un modèle un peu

Can. J. Chem. Downloaded from www.nrcresearchpress.com by 210.87.254.40 on 09/05/12
For personal use only.

différent du modèle classique des mélanges associés, font l'hypothèse de l'existence de 2 valeurs différentes de la chaleur de formation d'une liaison hydrogène; ils trouvent pour la première relative aux dimères $-17\,974$ J, pour la seconde, relative aux liaisons hydrogène de tous les autres polymères: $-20\,900$ J. Ces valeurs ne sont pas très éloignées de celle que nous avons calculée.

Conclusion

Les enthalpies de mélanges élevées du système éthyl-3 pentanol-3 tétrachlorure de carbone sont dues presque essentiellement à la désassociation de l'alcool.

La théorie classique des solutions associées conduit à une expression de l'enthalpie d'excès que nous avons pu notablement simplifier par l'introduction de la chaleur à dilution infinie de l'alcool. La nouvelle expression obtenue permet alors de calculer l'enthalpie de formation ΔH^0 d'une liaison hydrogène en utilisant des résultats calorimétriques et tonométriques.

Le calcul nous a permis de vérifier que ΔH^0 est pratiquement indépendant de la concentration de la solution tout au moins sur un certain domaine (jusqu'à 0.45 en fraction molaire).

Enfin, la valeur obtenue ($-21\,860$ J) est en bon accord avec les résultats donnés dans la littérature (15, 16).

1. H. Brusset, J. C. Lecoq, M. C. Milot, et M. Desgranges. Bull. Soc. Chim. Fr. **2**, 397 (1969).
2. C. Cachet. Thèse de 3ème Cycle, Marseille, France, 1964.
3. O. Redlich et A. T. Kister. Ind. Eng. Chem. **40**, 345 (1948).
4. J. P. Grolier et A. Viallard. C.R. Acad. Sci. Paris, Sér. C. **265**, 953 (1967).
5. F. Mato et J. Coca. An. Quim. **65** (1), 1 (1969).
6. C. Duboc. Chim. Ind., Génie Chim. **101** (5), 589 (1969).
7. H. Kehiaian et A. Treszczanowicz. Bull. Soc. chim. Fr. **5**, 2561 (1969).
8. I. Prigogine et R. Defay. Thermodynamique chimique. Editions DESOER, Liège. 1950.
9. H. Renon et J. M. Prausnitz. Chem. Eng. Sci. **22**, 299 (1967); Errata, Chem. Eng. Sci. **22**, 1891 (1967).
10. R. H. Stokes. Aust. J. Chem. **21** (5), 1343 (1968).
11. J. Dos Santos, P. Pineau, et M. L. Josien. J. Chim. Phys. **62**, 628 (1965).
12. C. Duboc. Bull. Soc. Chim. Fr. **7**, 2260 (1969).
13. H. Brusset, P. Delvalle, et M. Philoche-Levisalles. Bull. Soc. Chim. Fr. **9**, 3024 (1969).
14. M. Philoche. Thèse de Docteur Ingénieur. Paris, France, 1968.
15. J. Martin. C. R. Acad. Sci., Paris, Sér. C. **256** (17), 3651 (1963).
16. J. Biais, B. Lemanceau, et C. Lussan. J. Chim. Phys. **64** (6), 1019 (1967).

Can. J. Chem. Downloaded from www.nrcresearchpress.com by 210.87.254.40 on 09/05/12
For personal use only.

Preparation, Mössbauer and Vibrational Spectra of some Penta- and Hexacoordinated Addition Compounds of Dimethyl and Diphenyltin(IV) Dichloride

B. V. LIENGME

Department of Chemistry, St. Francis Xavier University, Antigonish, Nova Scotia

AND

R. S. RANDALL AND J. R. SAMS[1]

Department of Chemistry, University of British Columbia, Vancouver 8, British Columbia

Received July 29, 1971[2]

A number of both mono and bis addition compounds of dimethyl- and diphenyltin dichloride with oxygen donor molecules of the general type R_nEO (E = C, N, P, S) have been prepared and characterized by Mössbauer, infrared, and Raman spectroscopies. In the solid state the bis derivatives all have *trans* methyl or phenyl groups, and with the sole exception of $Me_2SnCl_2 \cdot 2C_5H_5NO$, all appear to have *cis*-chlorines and *cis*-donor molecules. Considerable distortions of the Ph_2Sn groups from linearity are suggested. The rather unusual $R_2SnCl_2 \cdot L$ complexes appear to have trigonal bipyramidal structures in which the R groups and one Cl atom occupy equatorial positions, with the donor molecule and second Cl atom in apical positions. Again the C_5H_5NO adduct of Me_2SnCl_2 seems to be an exception, with both apices apparently occupied by Cl atoms.

Un certain nombre de composés de mono et de bis addition du dichlorure de diméthyl- et de diphénylétain avec des donneurs d'oxygène de type général R_nEO (E = C, N, P, S) ont été préparés et caractérisés par spectroscopie Mössbauer, infrarouge et Raman. A l'état solide, les dérivés bis ont tous les groupes méthyle ou phényle en *trans* et à l'exception de $Me_2SnCl_2 \cdot 2C_5H_5NO$ seul, tous apparaissent avoir les chlores en *cis* et les molécules du donneur en *cis*. Des distorsions considérables par rapport à la linéarité des groupes Ph_2Sn sont suggérées. Les complexes peu usuels du type $R_2SnCl_2 \cdot L$ apparaissent posséder des structures trigonales bipyramidales dans lesquelles on trouve les groupes R et un atome de Cl en position équatoriale, la molécule du donneur et le second atome de Cl étant disposés au sommet. Le composé d'addition de Me_2SnCl_2 avec C_5H_5NO semble être encore une exception, les deux sommets sont occupés apparamment par des atomes de Cl.

[Traduit par le journal]

Canadian Journal of Chemistry, 50, 3212 (1972)

Introduction

Most addition compounds of diorganotin(IV) dihalides with monodentate Lewis bases reported thus far have the expected 1:2 stoichiometry (1) *i.e.*, $R_2SnX_2 \cdot 2L$ (R = alkyl, aryl; X = halogen; L = monodentate ligand), with hexacoordination about the tin atom. Scattered reports of a few complexes of the type $R_2SnX_2 \cdot L$ have appeared (2–6), but no systematic study of these latter derivatives has been made.

We felt it would be of interest to try to prepare a number of $R_2SnX_2 \cdot L$ complexes and to investigate their Mössbauer and vibrational spectroscopic properties. In a trigonal bipyramidal structure it is expected that the more electropositive organic groups should occupy equatorial positions, as observed (7) for the $Me_2SnCl_3^-$ ion. Of the remaining ligands, those of highest electronegativity will presumably occupy axial locations. There is thus the possibility of competition between the halogens and the donor molecule for one of the apical positions, with the occurrence of structure **1** or **2** presumably depending upon the nature of the Lewis base. For example, it is reported that

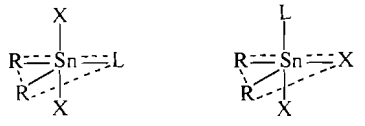

1 2

$Me_2SnCl_2 \cdot DMF$ shows two infrared-active Sn—Cl stretching bands (3), but only one Sn—Cl absorption is found for $Me_2SnCl_2 \cdot Me_2SeO$ (4). From these results, it was concluded (3, 4) that the DMF adduct has structure **2**, while the selenoxide derivative has structure **1**.

Addition compounds of 1:2 stoichiometry

[1]To whom correspondence to be addressed.

[2]Revision received May 25, 1972.

Can. J. Chem. Downloaded from www.nrcresearchpress.com by 210.87.254.40 on 09/05/12
For personal use only.

Can. J. Chem. Downloaded from www.nrcresearchpress.com by 210.87.254.40 on 09/05/12
For personal use only.

are also of some structural interest. X-Ray data for $Me_2SnCl_2 \cdot 2Me_2SO$ (8) and $Me_2SnCl_2 \cdot 2PyO$ (9) ($PyO = C_5H_5NO$) show *cis* and *trans* arrangements, respectively, of the chlorine atoms, with the methyl groups *trans* in both complexes. The factors governing the occurrence of one or the other arrangement are by no means clear. Furthermore, recent work by Fitzsimmons *et al.* (10) on some organotin dithiocarbamates has raised the possibility that corresponding methyl- and phenyltin derivatives might not necessarily be isostructural. For compounds of the type $R_2Sn(S_2CNR'_2)_2$ *trans*-octahedral structures are observed for $R = CH_3$ and n-C_4H_9, but a *cis*-octahedral configuration is indicated for $R = C_6H_5$.

In this paper we report the preparation of a number of 1:1 adducts of Me_2SnCl_2 and Ph_2SnCl_2 with Lewis bases in which coordination to tin is via an oxygen atom. Mössbauer, infrared, and Raman spectra are used to deduce the probable structures of these derivatives, and of the corresponding 1:2 complexes. A preliminary report on some of the sulfoxide complexes of Ph_2SnCl_2 has appeared (11).

Experimental

Materials

Diethyl sulfoxide (Et_2SO) was obtained by oxidation of diethyl sulfide with nitric acid, followed by distillation under reduced pressure. The purity of the compound was checked by microanalysis and by its infrared spectrum. The other Lewis bases employed were purchased from Eastman Organic Chemicals, Aldrich Chemical Company, or Fisher Scientific Co., and were used without further purification. Diphenyltin dichloride from Alfa Inorganics was recrystallized from methanol, and dimethyltin dichloride from Columbia Organic Chemicals Co. was recrystallized from carbon tetrachloride and dried *in vacuo* prior to use. All solvents were reagent grade.

Preparation of Complexes

The 1:1 addition compounds were prepared by adding a solution of dimethyl- or diphenyltin dichloride in a suitable solvent to a stoichiometric quantity of the appropriate Lewis base dissolved in the same solvent employed for the tin compound. In the case of the $Ph_2SnCl_2 \cdot Ph_3PO$ derivative, precipitation occurred immediately on mixing the solutions, and the product was suction-filtered and dried in air. For the other 1:1 complexes, the solvent was removed under reduced pressure and the products dried *in vacuo*. Preparation of the 1:2 derivatives followed a similar route, except that 100% excess of base was used. In most cases essentially quantitative yields of the pure complexes resulted, but where necessary the products were recrystallized from chloroform or carbon tetrachloride.

With the exception of the four PyO derivatives which were obtained as buff colored powders, and $Me_2SnCl_2 \cdot (CH_2)_4SO$ which is an oil at room temperature, all the complexes precipitated as white crystalline products. Analytical data, melting points, and solvent employed are given in Table 1.

Mössbauer Spectra

The Mössbauer spectrometer has been described in detail (12). The polycrystalline powders were contained in brass cells fitted with Mylar windows. A sample thickness of ~ 1 mm was maintained by use of a Teflon spacer in the cell. All measurements were made in transmission geometry with the absorber at 80 ± 2 K and the $Ba^{119m}SnO_3$ source at 295 ± 2 K. In the case of $Me_2SnCl_2 \cdot (CH_2)_4SO$, the sample was applied dropwise from a syringe onto a Mylar window maintained at liquid nitrogen temperature. Isomer shifts are reported relative to an SnO_2 absorber at 80 ± 2 K. The data were computer-fitted to Lorentzian line shapes; no constraints were imposed. We estimate the precision of the Mössbauer measurements to be ± 0.03 mm s^{-1}.

Infrared Spectra

In the 2000–250 cm^{-1} region the infrared spectra were obtained on a Perkin–Elmer 457 grating spectrophotometer, and between 600–180 cm^{-1} on a Perkin–Elmer 180 instrument. The samples were run as Nujol mulls on CsI plates, except $Me_2SnCl_2 \cdot (CH_2)_4SO$ which was run as a thin film. Comparison spectra of the Lewis base ligands, either neat or as Nujol mulls, were also recorded.

Raman Spectra

A Cary 81 instrument, fitted with a Spectra Physics Corp. Model 125 He–Ne laser, was employed. The 6328 Å line was used as exciting light. The solid samples were contained in 5 mm o.d. flat-bottomed Pyrex tubes.

Results and Discussion

There generally seems to be little difficulty in obtaining both 1:1 and 1:2 adducts of Me_2SnCl_2 and Ph_2SnCl_2 with the oxygen donors employed here. However, we have been unable to obtain 1:1 complexes of Me_2SnCl_2 with Ph_2SO and Ph_3PO, although Ph_2SnCl_2 readily yields 1:1 adducts with these bases and $Me_2SnCl_2 \cdot (PhCH_2)_2SO$ has been reported (5). Similarly, we have not isolated $Ph_2SnCl_2 \cdot DMF$, although the existence of $Me_2SnCl_2 \cdot DMF$ has been claimed (2, 3) and confirmed here. In each case several different solvent systems were tried, but i.r. spectra always showed the presence of the bis derivative. All our attempts to prepare $Ph_2SnCl_2 \cdot 2Ph_3PO$ afforded only the mono-addition compound, despite the reported (13) preparation of the 1:2 complex. Mullins (6) has also been unable to obtain the bis-adduct.

Both 1:1 and 1:2 derivatives appear to be air stable and to offer no survival problems, except $Me_2SnCl_2 \cdot Bu_2SO$ and $Ph_2SnCl_2 \cdot PyO$.

TABLE 1. Analytical data and melting points for complexes of Me_2SnCl_2 and Ph_2SnCl_2*

Compound	Solvent	Calcd (%) C	Calcd (%) H	Found (%) C	Found (%) H	Melting point (°C)
$Ph_2SnCl_2 \cdot Me_2SO$	Petroleum ether	39.8	3.8	39.9	3.8	80–82
$Ph_2SnCl_2 \cdot Et_2SO$	$CHCl_3$	42.7	4.5	43.1	4.7	102–104
$Ph_2SnCl_2 \cdot Pr_2SO$	Petroleum ether	45.2	5.1	45.0	5.1	75–77
$Ph_2SnCl_2 \cdot Bu_2SO$	Petroleum ether	47.4	5.6	47.5	5.4	100–102
$Ph_2SnCl_2 \cdot Ph_2SO$	Petroleum ether	52.8	3.7	53.5	4.0	92–95
$Ph_2SnCl_2 \cdot (CH_2)_4SO$	Petroleum ether	42.9	4.1	42.7	4.2	106–108
$Ph_2SnCl_2 \cdot PyO$	CH_3OH	46.7	3.4	46.0	3.7	<23
$Ph_2SnCl_2 \cdot Ph_3PO$	CH_3OH	57.8	4.1	57.3	4.1	166–168 (lit. 173–175, (6))
$Ph_2SnCl_2 \cdot 2Me_2SO$	$CHCl_3$	38.4	4.4	38.0	4.3	132–135
$Ph_2SnCl_2 \cdot 2Et_2SO$	$CHCl_3$	43.2	5.4	42.9	5.1	97–98
$Ph_2SnCl_2 \cdot 2Pr_2SO$	Petroleum ether	47.1	6.3	47.2	6.1	105–108
$Ph_2SnCl_2 \cdot 2Bu_2SO$	Petroleum ether	50.3	6.9	49.7	6.6	109–111
$Ph_2SnCl_2 \cdot 2Ph_2SO$	Petroleum ether	57.8	4.0	57.5	4.2	62–64
$Ph_2SnCl_2 \cdot 2(CH_2)_4SO$	Petroleum ether	43.5	4.8	43.3	5.0	131–134
$Ph_2SnCl_2 \cdot 2PyO$	CH_3OH	49.6	3.8	50.3	3.6	158–160
$Ph_2SnCl_2 \cdot 2DMF$	$CHCl_3$	44.1	4.9	43.2	4.8	64–66
$Me_2SnCl_2 \cdot Me_2SO$	$CHCl_3$	16.1	4.0	16.2	4.2	49–51
$Me_2SnCl_2 \cdot Et_2SO$	$CHCl_3$	22.1	5.0	21.6	5.0	45–48
$Me_2SnCl_2 \cdot Pr_2SO$	$CHCl_3$	27.2	5.7	26.5	5.5	65–68
$Me_2SnCl_2 \cdot Bu_2SO$	$CHCl_3$	31.5	6.3	31.0	6.2	†
$Me_2SnCl_2 \cdot (CH_2)_4SO$	$CHCl_3$	22.3	4.4	21.9	4.1	‡
$Me_2SnCl_2 \cdot PyO$	$CHCl_3$	26.7	3.5	26.7	3.4	114–116
$Me_2SnCl_2 \cdot DMF$	$CHCl_3$	20.5	4.5	19.8	4.3	52–55 (lit. 56–58, (2))
$Me_2SnCl_2 \cdot 2Me_2SO$	$CHCl_3$	19.2	4.8	20.2	4.7	108–110 (lit. 110, (19))
$Me_2SnCl_2 \cdot 2Et_2SO$	$CHCl_3$	27.8	6.1	26.9	6.0	81–83
$Me_2SnCl_2 \cdot 2Pr_2SO$	$CHCl_3$	34.5	7.0	34.1	6.9	98–100
$Me_2SnCl_2 \cdot 2Bu_2SO$	$CHCl_3$	39.7	7.8	39.4	7.7	73–76
$Me_2SnCl_2 \cdot 2(CH_2)_4SO$	$CHCl_3$	28.2	4.5	28.6	4.4	59–62
$Me_2SnCl_2 \cdot 2Ph_2SO$	$CHCl_3$	50.0	4.2	50.3	4.0	93–95
$Me_2SnCl_2 \cdot 2PyO$	CH_3OH	35.2	3.9	34.6	3.9	128–130 (lit. 135–136, (22))
$Me_2SnCl_2 \cdot 2DMF$	$CHCl_3$	26.3	5.5	25.7	5.6	82–84 (lit. 84–85, (2))
$Me_2SnCl_2 \cdot 2Ph_3PO$	CH_3OH	58.8	4.7	58.5	4.6	133–135

*Me = CH_3, Et = C_2H_5, Pr = n-C_3H_7, Bu = n-C_4H_9, Ph = C_6H_5, PyO = C_5H_5NO, DMF = Me_2NCHO.
†Semi-solid at room temperature.
‡Oil at room temperature. After freezing to 80 K and re-warming, m.p. = 51–53° and analytical data unchanged.

These slowly decompose on standing at room temperature and are best stored under refrigeration.

$Me_2SnCl_2 \cdot (CH_2)_4SO$ was originally isolated as an oil which failed to yield a solid product on trituration, on cooling in an ice bath, or after prolonged evacuation. When a sample of this compound was frozen at 80 K to record its Mössbauer spectrum and warmed again to room temperature, it reverted to an oil which then solidified over a period of several hours. The solid and liquid products show significant differences in their Mössbauer and i.r. spectra, as discussed below.

Mössbauer Spectra

^{119}Sn Mössbauer isomer shifts (δ), quadrupole splittings (Δ), and linewidths (Γ = FWHM) are given in Table 2 for all complexes prepared here. For all the 1:2 adducts of both Me_2SnCl_2 and Ph_2SnCl_2, the large Δ values clearly establish *trans*-R_2 configurations, as a *cis* arrangement of the organic groups would give a splitting no larger than *ca.* 2 mm s^{-1}

Can. J. Chem. Downloaded from www.nrcresearchpress.com by 210.87.254.40 on 09/05/12
For personal use only.

Can. J. Chem. Downloaded from www.nrcresearchpress.com by 210.87.254.40 on 09/05/12
For personal use only.

TABLE 2. Mössbauer parameters (at 80 K) for Me_2SnCl_2 and Ph_2SnCl_2 complexes

Compound	δ* (mm s^{-1})	Δ (mm s^{-1})	Γ_1 (mm s^{-1})	Γ_2 (mm s^{-1})
Me_2SnCl_2	1.55	3.60	1.05	1.08
$Me_2SnCl_2 \cdot Me_2SO$	1.44	3.70	1.11	1.15
$Me_2SnCl_2 \cdot Et_2SO$	1.38	3.60	1.14	1.19
$Me_2SnCl_2 \cdot Pr_2SO$	1.51	4.07	0.99	1.06
$Me_2SnCl_2 \cdot Bu_2SO$	1.51	3.94	1.06	1.12
$Me_2SnCl_2 \cdot (CH_2)_4SO$†	1.44	3.81	1.22	1.39
‡	1.40	3.62	1.07	1.10
$Me_2SnCl_2 \cdot PyO$	1.33	3.97	1.06	1.04
$Me_2SnCl_2 \cdot DMF$	1.51	3.99	1.06	1.12
$Me_2SnCl_2 \cdot 2Me_2SO$	1.43	4.18	0.88	0.90
$Me_2SnCl_2 \cdot 2Et_2SO$	1.34	4.12	1.13	1.17
$Me_2SnCl_2 \cdot 2Pr_2SO$	1.35	4.14	1.01	1.03
$Me_2SnCl_2 \cdot 2Bu_2SO$	1.36	4.11	1.01	1.04
$Me_2SnCl_2 \cdot 2(CH_2)_4SO$	1.44	4.11	1.00	1.01
$Me_2SnCl_2 \cdot 2Ph_2SO$	1.47	4.19	1.02	0.98
$Me_2SnCl_2 \cdot 2PyO$	1.35	4.02	1.05	1.03
$Me_2SnCl_2 \cdot 2DMF$	1.45	4.25	1.02	1.04
$Me_2SnCl_2 \cdot 2Ph_3PO$	1.44	4.23	0.93	0.87
Ph_2SnCl_2	1.37	2.83	0.78	0.79
$Ph_2SnCl_2 \cdot Me_2SO$	1.21	3.06	0.90	0.91
$Ph_2SnCl_2 \cdot Et_2SO$	1.21	2.92	0.99	0.99
$Ph_2SnCl_2 \cdot Pr_2SO$	1.27	3.01	0.83	0.86
$Ph_2SnCl_2 \cdot Bu_2SO$	1.25	3.20	0.96	0.98
$Ph_2SnCl_2 \cdot Ph_2SO$	1.25	3.11	1.18	1.10
$Ph_2SnCl_2 \cdot (CH_2)_4SO$	1.23	2.91	0.87	0.83
$Ph_2SnCl_2 \cdot PyO$	1.23	2.93	1.04	1.09
$Ph_2SnCl_2 \cdot Ph_3PO$	1.20	3.05	1.15	1.17
$Ph_2SnCl_2 \cdot 2Me_2SO$	1.30	3.86	0.75	0.82
$Ph_2SnCl_2 \cdot 2Et_2SO$	1.22	3.70	0.87	0.83
$Ph_2SnCl_2 \cdot 2Pr_2SO$	1.24	3.68§	0.88	0.82
$Ph_2SnCl_2 \cdot 2Bu_2SO$	1.20	3.65	0.87	0.84
$Ph_2SnCl_2 \cdot 2Ph_2SO$	1.28	3.73	1.12	1.02
$Ph_2SnCl_2 \cdot 2(CH_2)_4SO$	1.24	3.76	0.76	0.67
$Ph_2SnCl_2 \cdot 2PyO$	1.26	3.47	1.02	1.19
$Ph_2SnCl_2 \cdot 2DMF$	1.28	3.59	1.16	1.19

*Relative to SnO_2 at 80 K.
†Oil at room temperature.
‡Solid at room temperature.
§Owing to a typographical error in ref. (11), this value was incorrectly given as 3.86 mm s^{-1}.

(10, 14). On the other hand, *cis* and *trans* arrangements of donor molecules are effectively degenerate as regards the electric field gradient (EFG), so that no further structural conclusions are possible on the basis of these data. There is no systematic variation of Δ with changes in Lewis base, nor is any anticipated in view of the fact that the organic ligands control the sign, and to a large extent the magnitude of the EFG at tin (15). All the 1:2 complexes have slightly lower δ values than the parent organotin halide. This may be due to shielding of the s electrons resulting from donation into the vacant 5d orbitals of tin. The somewhat smaller δ and Δ values for the phenyl- as compared to methyltin compounds are expected from electronegativity considerations and are consistent with trends observed in other systems (16).

The $Ph_2SnCl_2 \cdot L$ derivatives show Δ values lying between those for Ph_2SnCl_2 and the corresponding 1:2 adducts with no significant line broadening, thus confirming they are true addition compounds. The large difference in splittings observed for Ph_2SnCl_2 and the 1:2 complexes requires that equimolar mixtures of the two should show either four-line Mössbauer spectra or extremely broad apparent doublets. Although the 1:1 adducts of Me_2SnCl_2 generally

Can. J. Chem. Downloaded from www.nrcresearchpress.com by 210.87.254.40 on 09/05/12
For personal use only.

have Δ values intermediate between those for the parent compound and the corresponding 1:2 complexes, the distinction is not as clear as that for the phenyltin derivatives. This is probably due to the fact that Me_2SnCl_2 has a considerably larger Δ than does Ph_2SnCl_2, so there is a relatively smaller change in Δ on forming a pentacoordinate adduct. However, these data, together with melting points and vibrational spectra, leave little doubt that all the 1:1 derivatives are formulated correctly.

When the $Me_2SnCl_2 \cdot (CH_2)_4SO$ product originally isolated as an oil was frozen at ~ 80 K, a doublet with unusually broad lines and $\Delta \simeq 3.8$ mm s^{-1} was observed. After the sample melted and resolidified at room temperature as described above, it was again cooled to 80 K and its Mössbauer spectrum redetermined. The splitting had now decreased by 0.2 mm s^{-1}, and the lines were significantly narrower. The latter spectrum is quite "clean" and cannot be interpreted in terms of an equimolar mixture of Me_2SnCl_2 and $Me_2SnCl_2 \cdot 2(CH_2)_4SO$. Because of the broad lines and the magnitude of the splitting observed in the initial spectrum, we cannot rule out the possibility that the *oil* is a mixture of neat Me_2SnCl_2 and the 1:2 adduct. However, such a suggestion does not seem to be supported by the infrared spectrum (*vide infra*). We think the oil is probably a metastable state, and that the line-broadening may arise from difficulties in controlling sample thickness when freezing the oil.

Vibrational Spectra

With the exception of the element–oxygen stretching frequencies ν(E—O) of the donor molecules, all bands of structural significance lie below 600 cm^{-1} for the methyltin complexes and below 500 cm^{-1} for the phenyltin derivatives. Thus we do not tabulate bands above these regions except for ν(E—O). It was difficult to obtain satisfactory Raman spectra in the 600–180 cm^{-1} region owing to the high background of Rayleigh scattering, and the spectra were not of particularly high quality. Our structural conclusions are therefore based primarily on the i.r. data. To facilitate discussion we consider the mono and bis adducts separately.

(i) $Ph_2SnCl_2 \cdot 2L$ Complexes

Observed vibrational frequencies and assignments are given in Table 3. Not listed are certain characteristic bands common to all the phenyltin compounds (1:1 and 1:2 adducts and neat Ph_2SnCl_2) which we mention briefly. There are two bands of weak-to-medium intensity at 1068 ± 3 and 1022 ± 1 cm^{-1} which we attribute to a phenyl in-plane C—H deformation mode, and a ring vibration at 1000 ± 3 cm^{-1}, usually of medium intensity. Strong bands assigned as out-of-plane C—H deformations (17) occur at 735 ± 6 and 695 ± 4 cm^{-1}, the former band being split in several of the compounds. There is also a strong absorption at 460 ± 5 cm^{-1} which Poller (18) attributes to the substituent-sensitive 16*b* mode of a mono-substituted benzene. This band is split in the bis-Me_2SO complex and in all the 1:1 adducts.

The general features of most of the i.r. spectra of the bis complexes can be discussed conveniently in terms of that of $Ph_2SnCl_2 \cdot 2Me_2SO$. Tanaka (19) has published i.r. data for this compound, but we disagree with several of his assignments. For example, the 1021 cm^{-1} band mentioned above is assigned as a methyl rocking mode by Tanaka (19), although this band is observed in all the phenyltin compounds reported here, and is clearly not associated with methyl rocking in Me_2SO. Both Tanaka (19) and we assign the strong, broad absorption at 420 cm^{-1} in the Me_2SO derivative as ν(Sn—O). (This is the only band involving a tin—substituent vibration which shows appreciable variation in position amongst these complexes, and we return to this point below.) The intense band at 294 cm^{-1} is not specifically assigned by Tanaka (19), and the 264 cm^{-1} band is ascribed to the asymmetric Sn—Ph stretching mode. Since all the complexes in Table 3 show strong bands in the former region but not the latter, we assign the 294 cm^{-1} absorption to ν_{as}(Sn—Ph). Further support for this assignment comes from a recent study of diphenyltin halide complexes with nitrogen donors (20), where ν_{as}(Sn—Ph) is always found in the 290–280 cm^{-1} region. However, we are unable to give a definite assignment for the 264 cm^{-1} band. Our assignments of the bands at 244 and 226 cm^{-1} (see Table 3) are just the reverse of Tanaka's (19). Our choice is based primarily on the fact that similar complexes of Ph_2SnCl_2 with N-donors show strong bands at ~ 250 and ~ 230 cm^{-1}, but the former are absent in corresponding derivatives of Ph_2SnBr_2 (20). Finally, all the

TABLE 3. Relevant vibrational bands and assignments for the complexes $Ph_2SnCl_2 \cdot 2L$*

Vibrational bands (cm^{-1}) for L =								
Me_2SO	Et_2SO	Pr_2SO	Bu_2SO†	Ph_2SO	$(CH_2)_4SO$†	PyO	DMF†	Assignment
946s 934s	937vs 929vs	938vs,br	935vs,br 925s,sh	988ms 929ms	953s 950s	1209s 1200s	1640s,br	ν(E—O)
[101,113	84,92	80	93,103	48,67	67,70	35,44	30]	$\Delta\nu$(E—O)‡
420s 409ms,sh (423w)	412s 409ms,sh (415m)	421s 418s (422w)	423s 411ms,sh	273s,sh 268s 261s,sh (270mw)	377s 375s,sh	340vs,br (344m)	272s 260s,sh	ν(Sn—O)
294s (—)	288s (—)	285s (—)	285ms	289ms (—)	289s	282s (285w)	288s,sh	ν_{as}(Sn—Cl)
244ms,sh (242ms)	244ms (245s)	244m,sh (239s)	246ms,sh	246m,sh (247s)	248s,sh	242ms (239s)	244ms,sh	ν_{as}(Sn—Cl)
226s (229s)	220s,sh 216s (226m)	224s 216m,sh (221m)	226s	228ms 224sh (234m)	225s	222s,sh 218s (220mw)	230s	ν_s(Sn—Ph)
201sh 198ms (202m)	206s (203m)	203ms 196ms (210mw) (206sh)	204s	201s (196mw)	195m	195s (194m)	205m	ν_s(Sn—Cl)
378m (361m) 360m (345m)	(493ms) 489s (358w) 312m	(310m) (263mw)		479s (359m) (310mw)	255s	(416mw) 400w (303w)	449ms 408ms,br 380s 346s	Ligand and other vibrations between 500–180 cm^{-1}
343m (315w) 313mw 264s (261s) (215w)	(306mw) 300m (215m)							Ligand and other vibrations between 500–180 cm^{-1}

*Raman bands in parentheses; s = strong, m = medium, w = weak, v = very, br = broad, sh = shoulder.
†Raman spectrum not recorded.
‡$\Delta\nu$(E—O) is ν(E—O) for the free ligand minus ν(E—O) for the complex.

compounds in Table 3 show a fairly strong band near 200 cm^{-1} which we attribute to another Sn—Cl vibrational mode, in agreement with Tanaka (19).

The R_2SO complexes for R = Me, Et, *n*-Pr, and *n*-Bu show strong bands at ~420 cm^{-1}, which we can safely attribute to ν(Sn—O). However, for R = $(CH_2)_4SO$ this band is lowered to 377 cm^{-1}, suggesting slightly weaker Sn ← O coordination. This is born out by the somewhat smaller shift in ν(S—O) observed for this complex. Our assignment of ν(Sn—O) at 340 cm^{-1} in the bis-PyO adduct is similar to those of Clark and Wilkins (321 cm^{-1}) (21) and Kawasaki *et al.* (325 cm^{-1}) (22) for the corresponding vibration in $Me_2SnCl_2 \cdot 2PyO$. The only cases where there may be some ambiguity in assigning ν(Sn—O) are in the Ph_2SO and DMF complexes. In the former, the comparatively small shift in ν(S—O) indicates relatively weak complexation, and we feel the only reasonable assignment for ν(Sn—O) is the strong and rather complex absorption envelope centered at 268 cm^{-1}. For the bis-DMF adduct there are three fairly strong bands at 408, 380, and 346 cm^{-1} in addition to the band at 272 cm^{-1}. The 408 and 346 cm^{-1} bands probably correspond to deformation and wagging modes of the Me_2N fragment, observed in DMF itself at 405 and 350 cm^{-1} (23), but assignment of the 380 cm^{-1} absorption is in doubt. However, DMF is a weak Lewis base, and we prefer the band at 272 cm^{-1} for ν(Sn—O).

It is interesting that both asymmetric and

Can. J. Chem. Downloaded from www.nrcresearchpress.com by 210.87.254.40 on 09/05/12
For personal use only.

TABLE 4. Relevant vibrational bands (in cm^{-1}) and assignments for the complexes $Me_2SnCl_2 \cdot 2L$*

Vibrational band (cm^{-1}) for L =									Assignment
Me_2SO	Et_2SO	Pr_2SO	Bu_2SO	Ph_2SO	$(CH_2)_4SO$	PyO	DMF	Ph_3PO	
947s,sh 941vs	936vs,br	950s,sh 945vs 939s,sh	947vs,br	990vs,br	943vs,br	1208s 1198s	1640s,br	1151s	ν(E—O)
[100,106	85	68–79	81	46	77	36,46	30	38]	$\Delta\nu$(E—O)†
572s (575w)	569s (—)	573s (—)	569ms (—)	577ms (582w)	572s (574vw)	571ms (—)	577ms (583w)	575ms (—)	ν_{as}(Sn—Me)
514w (512s)	— (504s)	— (508s)	— (508s)	513vw (516s)	504w (508s)	— (508s)	511mw (515s)	507w (509s)	ν_s(Sn—Me)
418vs,sh 412vs (416mw)	420vs 408s (409w)	440s 428vs (439sh) (431m)	426s,sh 420vs (417sh) (410mw)	268s,sh 263vs 258s,sh (262m) (258sh)	365s 359s,sh (365m)	324vs (—)?	269s,sh 264s (258m)	264m,sh 258s (256m)	ν(Sn—O)
252s,sh 247vs 240vs 232s,sh (249mw)	250m,sh 236s,br (230w)	237vs 234s,sh (237mw)	233s 230s,sh (228w)	232ms 228m,sh (238w)	256s 248s,br 239s,sh (245w)	234s,sh 229vs (—)?	249s 240s,sh (238w)	248s 242s,sh (244sh)	ν(Sn—Cl)
(342s) 340s (314s) 310ms 187sh	(357m) 351vw 322vw 279w	(543mw) (355w) 354w 302w (292ms)	(526w) 454m (339w) (287w) 282w	541vs 498s (468m) 464s 430m 397vw (375w) 372vw (308m) 304w 198m	(554w) 551ms (373w) 328m 263s,sh	554vs 464s	(413m) 407m (388w) 380s (361w) 359s	(544w) 541vs 537vs 454m 446m 396w 311w (298w) 291w 204vw	Ligand and other vibrations between 600–180 cm^{-1}

*Raman bands in parentheses.
†$\Delta\nu$(E—O) is ν(E—O) for the free ligand minus ν(E—O) for the complex.

symmetric Sn—Ph vibrations appear as strong bands in the i.r., as also found for similar complexes with nitrogen donors (20). Since the Mössbauer data demand a structure with *trans*-phenyl groups, these results seem to require appreciable distortion of the C—Sn—C angle from 180°. That two Sn—Cl stretching frequencies are both infrared and Raman active leads us to assign a *cis*-chlorine arrangement in all the 1:2 adducts of Ph_2SnCl_2 reported here. We therefore conclude that these complexes have structure **3** rather than **4**:

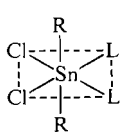

3

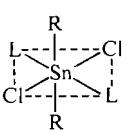

4

(ii) $Me_2SnCl_2 \cdot 2L$ Complexes

Table 4 lists observed vibrational frequencies and assignments for these complexes. Tanaka (19) has also given quite a complete assignment of the i.r. spectrum of $Me_2SnCl_2 \cdot 2Me_2SO$, and except for minor details we are in excellent agreement with this author for both band positions and assignments.

In all cases ν_{as}(Sn—Me) produces a fairly strong band at $\sim 570\ cm^{-1}$ in the i.r., whereas ν_s(Sn—Me) is either absent or appears as a weak absorption at $\sim 510\ cm^{-1}$. These intensities are reversed in the Raman spectra. While consistent with the *trans*-dimethyl arrangements deduced from the Mössbauer spectra, these results are of no help in deciding the dispositions of the remaining four ligands.

Strong similarities in the positions of ν(E—O)

Can. J. Chem. Downloaded from www.nrcresearchpress.com by 210.87.254.40 on 09/05/12
For personal use only.

Can. J. Chem. Downloaded from www.nrcresearchpress.com by 210.87.254.40 on 09/05/12
For personal use only.

between corresponding methyl- and phenyltin derivatives (see Table 3) are found, suggesting similar strengths of complexation to the two organotin chlorides. Moreover, there is close agreement in ν(Sn—O) for corresponding methyl- and phenyltin adducts, and except for the DMF and Ph_3PO complexes our assignments of this band require no comment. For $Me_2SnCl_2 \cdot 2DMF$, Matsubayashi *et al.* (2) assign very strong bands at 272 and 250 cm^{-1} to ν(Sn—Cl) and attribute a medium-intensity band at 191 cm^{-1} (not observed by us) to ν(Sn—O). We prefer our assignments on the basis of (*a*) band intensities; (*b*) comparison with the spectrum for $Ph_2SnCl_2 \cdot 2DMF$; (*c*) the fact that in all other 1:2 adducts studied here ν(Sn—Cl) never lies above 256 cm^{-1}; and (*d*) the fact that we find no bands whatever in the 230–180 cm^{-1} region either in the i.r. or Raman spectra. Clark and Wilkins (21) have reported some i.r. data (600–200 cm^{-1}) for $Me_2SnCl_2 \cdot 2Ph_3PO$, and assign Sn—Cl vibrations at 261 and 246 cm^{-1}. They suggest (21) that ν(Sn—O) in this complex "probably lies close to ligand bands in the range 400–300 cm^{-1}". However, in the 440–280 cm^{-1} region we find only three weak bands at 396, 311, and 291 cm^{-1}, none of which can be reasonably assigned to ν(Sn—O). We suggest that the higher lying strong band in the 270–240 cm^{-1} region is probably ν(Sn—O), but this assignment is tentative.

All the bis derivatives have strong i.r. bands in the range 250–230 cm^{-1} which we attribute to ν(Sn—Cl). Where comparison is possible our assignments in this region are in agreement with those of other workers (2, 19, 21, 22), except as noted above.

In the Raman spectra we find bands in the Sn—O region usually of medium intensity, while lines assignable to ν(Sn—Cl) are generally weak. It is interesting to note that in all the 1:2 adducts the only strong Raman band of structural significance is ν_s(Sn—Me). Surprisingly, neither ν_s(Sn—Cl) nor ν_s(Sn—O) appears even weakly in the Raman spectrum of $Me_2SnCl_2 \cdot 2PyO$, although both modes are allowed.

We now attempt to assign structures to these complexes, it being remembered that $Me_2SnCl_2 \cdot 2Me_2SO$ is known (8) to have structure **3** and $Me_2SnCl_2 \cdot 2PyO$ to have structure **4** (9). It appears that little structural information is obtainable from i.r. spectra in the ν(Sn—Cl) region, since in all cases this band is either split or has one or more shoulders. It is possible that the 234 cm^{-1} shoulder in the PyO derivative is due to the NO out-of-plane deformation mode found at 233 cm^{-1} in the neat ligand (24). The main difference in structurally significant i.r. bands between $Me_2SnCl_2 \cdot 2PyO$ and the other 1:2 adducts is the degree of complexity of ν(Sn—O). (The *position* of this band does not distinguish between *cis* and *trans* donor molecules.) Only in the PyO complex is this mode both unsplit and without apparent shoulders. These results lead us to suggest that all the 1:2 sulfoxide derivatives of Me_2SnCl_2 have structure **3**. From i.r. results for the bis-DMF and -Ph_3PO complexes it is difficult to draw any definite conclusions, although we favor structure **3** on the basis of the Raman spectra.

(iii) $Ph_2SnCl_2 \cdot L$ Complexes

Infrared and Raman data are collected in Table 5. All these compounds show strong absorptions at ~283 and ~235 cm^{-1} in the i.r., assigned to ν_{as}(Sn—Ph) and ν_s(Sn—Ph), respectively. Both modes are also Raman-active, the latter usually having greater intensity.

The bands assigned to ν(E—O) and ν(Sn—O) are very similar in position to those in the corresponding 1:2 compounds, implying little difference in donor–acceptor interaction strengths between 1:1 and 1:2 adducts with a given base. Intense absorptions are also observed for all 1:1 derivatives at ~325 and ~270 cm^{-1}, which can be attributed to Sn—Cl vibrations. In the Raman spectra the former band is also strong while the latter is of medium-to-weak intensity. These results argue against structure **1**, in which the Cl—Sn—Cl arrangement is expected to be nearly linear, and suggest **2** is much more likely for these complexes. Mullins (6) has assigned structure **2** to $Ph_2SnCl_2 \cdot L$ (L = Ph_3PO, Ph_3AsO) in solution on the basis of dipole moment measurements.

(iv) $Me_2SnCl_2 \cdot L$ Complexes

Relevant vibrational data are given in Table 6. Both ν_s(Sn—Me) and ν_{as}(Sn—Me) appear in the i.r. with similar intensities in all the compounds. The former is also strongly active in the Raman spectra, but the latter is surprisingly weak. The positions of ν(E—O) and ν(Sn—O)

TABLE 5. Relevant vibrational bands (in cm^{-1}) and assignments for the complexes $Ph_2SnCl_2 \cdot L$*

Vibrational bands (cm^{-1}) for L =								
Me_2SO	Et_2SO	Pr_2SO	Bu_2SO†	Ph_2SO	$(CH_2)_4SO$†	PyO	Ph_3PO†	Assignment
958s,sh 951vs 946s,sh	959vs 950vs	952s,sh 939vs,br	936vs 933vs 924s,sh	967vs,br	951s,sh 940vs,br	1211s	1137s	ν(E—O)
[89–103	62,71	66,79	92–104	69	69,80	33	52]	$\Delta\nu$(E—O)‡
419s,br (420w)	427ms,br (428m) (425sh)	439s,sh 423m (429mw)	424s 420s 412ms,sh	256ms (254mw)	383ms 381ms	352s 349s,sh (356mw)	258s,sh(?)	ν(Sn—O)
334vs 330s,sh (345s)	333s 328s,sh (341s)	335vs 328vs (335s)	335ms 329ms 324m,sh	336s 330s,sh (342s)	341vs 334s,sh	331vs 326s,sh (335s)	336s 329ms,sh	ν(Sn—Cl)
280s (281w)	281s,sh (288w)	285s,sh (292m)	286s	280s,sh (280w)	282vs	283s (283w)	282s	ν_{as}(Sn—Ph)
268vs,br (270w)	272vs,br (270m)	275vs (272w)	275s	271vs (275m)	264vs,br	265vs (264s)	268vs	ν(Sn—Cl)
238s,sh 232s 225m,sh (234ms)	240s (234mw)	233ms,sh 227s (234m)	232s,sh 227vs	232s,br (228mw)	225s 219s,sh	232s 221m,sh (234mw)	235s 220m	ν_s(Sn—Ph)
443m 317m (311m) (252mw) (223w) (212s) 201m	481mw (380m) 379w (365mw) (246mm) (220s) (209w) 195m (193w)	480m (313ms) 307w (216s) 203ms	484w 308s	488s 474w 443s 420w (370mw) 369w (216s) 206ms 192ms	421vw 206m,sh	(477mw) 443s (224s) (213mw) 206m (203s)	412m 321ms 304ms 193m	Ligand and other vibrations between 500–180 cm^{-1}

*Raman bands in parentheses.
†Raman spectrum not recorded.
‡$\Delta\nu$(E—O) is ν(E—O) for the free ligand minus ν(E—O) for the complex.

are again very similar to those in the corresponding 1:2 adducts.

With the exception of the PyO complex, all 1:1 derivatives have intense i.r. absorptions between ~340–300 cm^{-1} and in the range 255–225 cm^{-1}, which we attribute to Sn—Cl vibrations. As for the $Ph_2SnCl_2 \cdot L$ compounds, we therefore suggest structure **2** for these 1:1 adducts.

However, $Me_2SnCl_2 \cdot PyO$ is an apparent exception. By analogy with the 1:2 adduct the very strong absorption at 324 cm^{-1} (weak at 327 cm^{-1}, Raman) is assigned to ν(Sn—O). There are only three i.r. active bands lying below this, one of which (304 cm^{-1}) is in the appropriate range for ν_{as}(Sn—Cl), but is weaker than expected for this band. Morevoer, ν_{as}(Sn—Cl) is of medium-to-strong Raman intensity in the other 1:1 derivatives studied, but no Raman band is observed for $Me_2SnCl_2 \cdot PyO$ between 327 and 245 cm^{-1}. Of the two remaining bands, the one at 232 cm^{-1} (absent in Raman) may be due to the NO out-of-plane deformation in PyO, whilst that at 252 cm^{-1} (245 cm^{-1}, vw, in Raman) can reasonably be assigned to a Sn—Cl vibration. We suggest, therefore, that $Me_2SnCl_2 \cdot PyO$ may be structurally dissimilar to the other 1:1 derivatives reported here, and probably has structure **1**.

The 1:1 $(CH_2)_4SO$ derivative exhibited unusual behavior. Except for the band at 270 cm^{-1} the i.r. results for the oil originally obtained are entirely consistent with those expected from data on the other 1:1 sulfoxide adducts. After solidification was induced as described above, the spectrum underwent several interesting

Can. J. Chem. Downloaded from www.nrcresearchpress.com by 210.87.254.40 on 09/05/12
For personal use only.

TABLE 6. Relevant vibrational bands (in cm^{-1}) and assignments for the complexes $Me_2SnCl_2 \cdot L$*

Vibrational bands (cm^{-1}) for L =								
				$(CH_2)_4SO$†				
Me_2SO	Et_2SO	Pr_2SO	Bu_2SO†	Oil‡	Solid	PyO	DMF	Assignment
947s,sh 940s	948vs,br	954vs,br	950vs,br	961vs,br	937vs,br	1213s 1200s	1653s,sh 1646s,br	ν(E—O)
[100,107	73	64	78	59	83	31,44	17,24]	$\Delta\nu$(E—O)§
571s (572w)	569s (572w)	576s (574w)	568s	567s	574ms 567s	570ms (566w)	575s (580mw)	ν_{as}(Sn—Me)
516ms (519s)	518ms (521s)	507m (512s)	517ms	519ms	518ms 511ms	508ms (506s)	516ms (520vs)	ν_s(Sn—Me)
420s,sh 415vs (421w)	417s 403s (414vw)	436s 422vs (421w)	427s,sh 418vs 412s,sh	383ms,sh 374ms 369ms,sh	390s,sh 385s 382s,sh	324vs 320s,sh (327w)	267s,sh 260vs (258w)	ν(Sn—O)
334s,sh 323vs 316s,sh (322s)	321vs 315s,sh (316m)	308vs 304vs (310m)	338s,sh 332vs 322vs 315s,sh	334s,sh 326vs 321vs 314s,sh	320s,sh 313vs 309vs 304s,sh	— (—)	310s,sh 306vs (308ms)	ν(Sn—Cl)
248vs 245vs (240vw)	254s,sh 249vs (?)	235s,sh 228s (248vw)	244ms,sh 239s	270s(?)	254vs 247s,sh	252ms (245vw)	254vs 247s,sh (250w,sh)	ν(Sn—Cl)
340m,sh 309m,sh	(358w) 348vw 271w,sh	493w 355mw (297m) 285w 250w,sh	490w 453m 397m,sh 273ms	536m	534ms 341w	561m,sh 551vs (550w) (463mw) 462s (455mw)	407m 378s (366w) 363s (350w) 193vw	Ligand and other vibrations between 600–180 cm^{-1}
						451ms 350m,sh 304m 232s (195w)		Ligand and other vibrations between 600–180 cm^{-1}

*Raman bands in parentheses.
†Raman spectrum not recorded.
‡I.r. spectrum not recorded below 250 cm^{-1}.
§$\Delta\nu$(E—O) is ν(E—O) for the free ligand minus ν(E—O) for the complex.

changes (see Table 6). ν(S—O) decreased by 24 cm^{-1} and ν(Sn—O) rose by 11 cm^{-1}, both of which indicate strengthening of the O → Sn coordinate bond. Both Sn—Cl bands were lowered by ~13 cm^{-1}, and a weak band at 341 cm^{-1} (which may have been obscured in the oil) appeared. Most surprising was the apparent splitting of both ν_s(Sn—Me) and ν_{as}(Sn—Me), which seems difficult to explain. Neither i.r. nor Mössbauer spectrum is consistent with disproportionation according to

$$2Me_2SnCl_2 \cdot (CH_2)_4SO \rightarrow Me_2SnCl_2 \cdot 2(CH_2)_4SO + Me_2SnCl_2$$

The existence of solid-state isomers is a possibility, but there is no direct evidence at present bearing upon this point.

Conclusions

The two PyO derivatives of Me_2SnCl_2 appear to be unique amongst all the adducts of diorganotin dihalides for which structural information is available, in having structures **1** and **3**. We are aware of no other 1:2 adduct of R_2SnCl_2 to which **3** can be assigned without serious reservations, and the only other suggested example of **1** is $Me_2SnCl_2 \cdot Me_2SeO$ (4). This compound, however, was not isolated in pure form, but obtained only as a mixture with the

Can. J. Chem. Downloaded from www.nrcresearchpress.com by 210.87.254.40 on 09/05/12
For personal use only.

1:2 adduct. Since it has not been well characterized, we feel its structure is open to doubt.

It seems reasonable to expect the two ligands of greatest electronegativity to occupy the apical positions in a trigonal bipyramidal structure. In Lewis bases of the R_nEO type studied here, the effective electronegativity of the oxygen atom depends not only on the nature of E, but also on the nature of the R groups, which affects the degree of E—O multiple bonding and the stabilization of various resonance structures. If these ideas are correct, then PyO appears to be the only ligand studied here for which the effective electronegativity of oxygen may be less than that of chlorine. This could be due both to the fact that N has a higher electronegativity than C, S, or P, and that PyO is the only ligand studied in which E is part of a delocalized π-system. However, such an argument does not explain the observed difference between the PyO adducts of Me_2SnCl_2 and Ph_2SnCl_2. In this connexion a study of PyO complexes with other R_2SnCl_2 molecules might prove helpful.

We thank the National Research Council of Canada for financial support, and Mrs. A. Sallos for technical assistance.

1. H. C. Clark and R. G. Goel. J. Organomet. Chem. **7**, 263 (1967).
2. G. Matsubayashi, T. Tanaka, and R. Okawara. J. Inorg. Nucl. Chem. **30**, 1831 (1968).
3. G. Matsubayashi, N. Nishii, and T. Tanaka. Bull. Chem. Soc. Jap. **42**, 2369 (1969).
4. T. Tanaka and T. Kamitani. Inorg. Chim. Acta, **2**, 175 (1968).
5. W. Kitching, C. J. Moore, and D. Doddrell. Aust. J. Chem. **27**, 1149 (1969).
6. F. P. Mullins. Can. J. Chem. **49**, 2719 (1971).
7. F. B. Einstein and B. R. Penfold. J. Chem. Soc. A, 3019 (1968).
8. N. W. Isaacs and C. H. L. Kennard. J. Chem. Soc. A, 1257 (1970).
9. E. A. Blom, B. R. Penfield, and W. T. Robinson. J. Chem. Soc. A, 912 (1969).
10. B. W. Fitzsimmons, A. A. Owusu, N. J. Seeley, and A. W. Smith. J. Chem. Soc. A, 935 (1970).
11. R. S. Randall, R. W. J. Wedd, and J. R. Sams. J. Organomet. Chem. **30**, C19 (1971).
12. P. A. Yeats, B. F. E. Ford, J. R. Sams, and F. Aubke. J. Chem. Soc. A, 2188 (1970).
13. V. G. Kumar Das and W. Kitching. J. Organomet. Chem. **13**, 523 (1968).
14. B. W. Fitzsimmons, N. J. Seeley, and A. W. Smith. J. Chem. Soc. A, 143 (1969).
15. R. V. Parish and C. E. Johnson. J. Chem. Soc. A, 1906 (1971).
16. R. C. Poller and J. N. R. Ruddick. J. Chem. Soc. A, 2273 (1969).
17. R. C. Poller. J. Inorg. Nucl. Chem. **24**, 593 (1962).
18. R. C. Poller. Spectrochim. Acta, **22**, 935 (1966).
19. T. Tanaka. Inorg. Chim. Acta, **1**, 217 (1967).
20. R. C. Poller, J. N. R. Ruddick, M. Thevarasa, and W. R. McWhinnie. J. Chem. Soc. A, 2327 (1969).
21. J. P. Clark and C. J. Wilkins. J. Chem. Soc. A, 871 (1966).
22. Y. Kawasaki, M. Hori, and K. Uenaka. Bull. Chem. Soc. Jap. **40**, 2463 (1967).
23. G. Durgaprasad, D. N. Sathyanarayana, and C. C. Patel. Bull. Chem. Soc. Jap. **44**, 316 (1971).
24. S. Kida, J. V. Quagliano, J. A. Walmsley, and S. Y. Tyree. Spectrochim. Acta, **19**, 189 (1963).

Can. J. Chem. Downloaded from www.nrcresearchpress.com by 210.87.254.40 on 09/05/12
For personal use only.

The Chlorination of Pyrroles. Part III[1]

D. G. DURHAM, C. G. HUGHES, AND A. H. REES
Department of Chemistry, Trent University, Peterborough, Ontario

Received April 13, 1972

The chlorination and subsequent demethylation of 2-(2′-methoxybenzoyl) and 2-(2′,6′-dimethoxybenzoyl)-pyrroles are described, giving deoxypyoluteorin and pyoluteorin as main products. A number of minor products of under- and overchlorination have been characterized. Alternative syntheses of some of these antibiotics are detailed. Two routes to 2,3-dichloropyrrole are given and the Friedel–Crafts reaction of this compound utilized in synthesizing deoxypyoluteorin and pyoluteorin. A number of analogs have been made and their microbiological activities compared. The monodeoxy series is generally more active.

La chloration et la déméthylation ultérieure des (méthoxy-2′ benzoyl)-2 et (diméthoxy-2′,6′ benzoyl)-2 pyrroles sont décrites et conduisent aux déoxypyolutéorine et pyolutéorine comme produits majeurs. Un certain nombre de produits mineurs, issus de la sous-et de la surchloration, ont été caractérisés. Des synthèses possibles de quelques uns de ces antibiotiques sont données en détails. Deux voies d'accès au dichloro-2,3 pyrrole sont citées et la réaction de Friedel–Crafts sur ce composé a été utilisée dans la synthèse de la déoxypyolutéorine et de la pyolutéorine. Des composés analogues ont été synthétisés et leurs activités microbiologiques comparées. La série monodéoxy est généralement plus active.

[Traduit par le journal]

Canadian Journal of Chemistry, **50**, 3223 (1972)

Can. J. Chem. Downloaded from www.nrcresearchpress.com by 210.87.254.6 on 09/05/12
For personal use only.

We give practical details of our original synthesis of monodeoxypyoluteorin (**1***a*) (1) from 4,5-dichloropyrrole-1-carboxylic acid. Chlorination of 2-(2′-methoxybenzoyl) pyrrole (**2***b*) affords another route as does the Friedel–Crafts reaction of 2-anisoyl chloride on 2,3-dichloropyrrole (2). We also describe the synthesis of the bromine **3***a* and iodine **4***a* analogs and compare their activities (Table 1). The beneficial effect of a chlorine atom in the phenolic ring is seen in the activity of 5′-chlorodeoxypyoluteorin **5***a* (Table 1). No activity was found in compound **10** (X = Y = Cl), made by chlorination of 2-picolinylpyrrole (**10**) (X = Y = H).

To investigate the structure/activity relationship, we reduced the ketone **1***a* to the alcohol with borohydride. On work-up, an indicating solution was obtained which was red in acid and yellow in base. We suspect this was due to the dehydra-compound **11** as on isolation, an insoluble product was obtained, thought from its mass spectrum to be a dimer of **11**.

Chlorination of 2-(2′,6′-dimethoxybenzoyl)-pyrrole (**12***b*), followed by demethylation, gives pyoluteorin (**14***a*). Slight overchlorination gives a potentially very useful mixture containing 3′-chloropyoluteorin (**15***a*) which is more active against *Staph. aureus* than pyoluteorin itself.

[1]See ref. 8 for Part II.

The potentially insecticidal chloro-analog of pyoluteorin, 4,5-dichloro-2-(2′,6′-dichlorobenzoyl)pyrrole (**17**) was also made but found to be microbiologically inactive, indicating that under test conditions, hydrolysis via **18** was not significant.

Chlorination of pyrrole-2-carboxylic acid-3-carboxylic ester gave a good yield of the 4,5-dichloro-derivative **19** which was converted smoothly to 2,3-dichloropyrrole and hence to pyoluteorin.

Since monodeoxypyoluteorins are generally the more active (3), we prepared some pyolu-

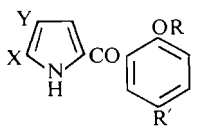

1 X = Y = Cl; R′ = H
2 X = Y = R′ = H
3 X = Y = Br; R′ = H
4 X = Y = I; R′ = H
5 X = Y = R′ = Cl
6 X = R′ = H; Y = Cl
7 X = Y = 3 = Br; R′ = H
8 X = Y = 3 = Cl; R′ = H
9 X = Y = H; R′ = Cl
a) R = H
b) R = Me

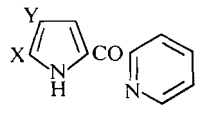

10

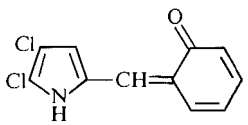

⇅ **11**

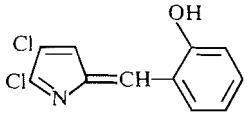

TABLE 1. Comparison of activities of pyoluteorin compounds*

Organism	Complete inhibition (μg/ml)					
	1*a*	**3***a*	**4***a*	**5***a*	**14***a*	**15***a*
Staph. aureus 209-P	3.1	6.2	25	0.4	6.2	1.5
Staph. aureus (resistant)	3.1	6.2	—	0.8	6.2	0.8
Shig. flexneri	—	—	—	—	6.2	6.2
Shig. flexneri (resistant)	—	—	—	—	6.2	12.5
Tricophyton asteroides	6.2	6.2	25	<1.5	50	—
Tricophyton interdigitale	12.5	6.2	—	<1.5	50	—
Tricophyton rubrum	3.1	6.2	6.2	<1.5	50	—

*Plate method, solvent acetone (maximum concentration 10%) nutrient agar medium; culture temperature 37 and 27°; incubation time 18 h.

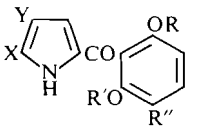

12 X = Y = R″ = H
13 Y = Cl, R″ = X = H
14 X = Y = Cl, R″ = H
15 X = Y = R″ = Cl
16 X = H, Y = R″ = Cl
a) R = R′ = H
b) R = R′ = Me
c) R = Me, R′ = H

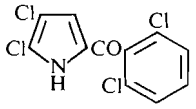

17

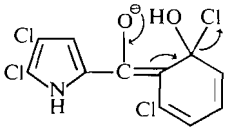

18

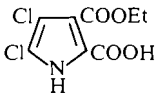

19

teorin monomethyl ethers but these were less active.

The mass spectra of pyoluteorins follow from the typical pattern for aromatic ketones, showing α-cleavage, partly with hydrogen transfer from the nearby functional group.

Experimental

*Synthesis of 2-(2′-Methoxybenzoyl)pyrrole (**2b**)*

(*i*) Sodium pyrrole-2-carboxylate, 1.75 g, was heated (4) with 1 equiv 2-methoxybenzoyl chloride at 160° for 1 h. The product was extracted with ethyl acetate and this solution washed with sodium bicarbonate solution then with water, dried ($MgSO_4$), and concentrated. Preparative t.l.c. on silica, using ether/light petroleum, 1:1, gave 2-(2′-methoxybenzoyl)pyrrole (**2***b*) as a band at R_f 0.3 which was extracted with ethyl acetate, 170 mg crystallized from benzene/light petroleum, colorless plates; m.p. 130–132°; n.m.r. Table 2; i.r. ν_{max}(Nujol) 1610, 1595 cm^{-1}; u.v. max 301 mμ (ε 16 830).

Anal. Calcd. for $C_{12}H_{11}NO_2$: C, 71.6; H, 5.5; N, 7.0. Found: C, 70.6; H, 4.8; N, 7.3.

(*ii*) By the method described below for 2,6-dimethoxybenzoyl chloride, 2-methoxybenzoyl chloride and pyrrole gave **2***b* in 60% yield.

Preparation of 4,5-Dichloropyrrole-2-carboxylic Acid

(*i*) Methyl pyrrole-2-carboxylate, 6 g in 100 ml acetic acid, was treated with 2.5 mol equiv chlorine (1.5 *N* solution) in acetic acid. After 24 h, evaporation and recrystallization gave 3.7 g 4,5-dichloro-ester, shown by g.l.c. and n.m.r. to contain traces of the 3,4,5-trichloro-ester but none of the 3,5-dichloro-isomer.

The 4,5-dichloro-ester above, 4.2 g, in 200 ml of methanol, was refluxed 5 h with 110 ml 30% potassium hydroxide solution. Evaporation and careful acidification of the residue gave 3.6 g dichloro-acid, shown later to contain traces of trichloro-acid.

(*ii*) Pyrrole-2-carboxylic acid, 7.15 g, in 300 ml acetic acid, was stirred and 2 mol equiv of chlorine in acetic acid added dropwise at 20°. After 10 h, the solvent was removed and the resulting 4,5-dichloro-pyrrole-2-carboxylic acid was crystallized from benzene until it was free (n.m.r. in NaOD) from impurities, yield 2.8 g, 24%.

*Synthesis of 4,5-Dichloro-2-(2′-Methoxybenzoyl)pyrrole (**1b**)*

(*a*) 4,5-Dichloropyrrole-2-carboxylic acid, 2.2 g from synthesis (*i*) above, as the sodium salt, was reacted with *o*-methoxybenzoyl chloride (from 1.8 g acid) by the method described above. The same isolation procedure gave 85 mg 4,5-dichloro-2-(2′-methoxybenzoyl)pyrrole, m.p. 171–173°, crystallized from benzene/light petroleum, ν_{max} (Nujol) 1630, 1600, 1585 cm^{-1}; u.v. max 310 mμ; pK_a 9.8.

Anal. Calcd. for $C_{11}H_7NO_2Cl_2$: C, 51.55; H, 2.76; Cl, 27.7; N, 5.5. Found: C, 51.3; H, 2.8; Cl, 28.0; N, 5.55.

A minor band at R_f 0.5 was extracted with ethyl acetate and the compound crystallized from benzene/light petro-

Can. J. Chem. Downloaded from www.nrcresearchpress.com by 210.87.254.6 on 09/05/12
For personal use only.

Can. J. Chem. Downloaded from www.nrcresearchpress.com by 210.87.254.6 on 09/05/12
For personal use only.

TABLE 2. N.m.r. spectra of monodeoxypyoluteorins (τ)

Compound		Pyrrole ring position						
a	*b*	1	3	4	5	OH	OMe	Solvent*
1		−3.3	3.26	Cl	Cl	−0.5		d
	1	−0.3	3.48	Cl	Cl		6.17	c
2		−1.9	Under aromatic	3.55	Under aromatic	−0.1		c
	2	Under aromatic	3.35	3.75	3.1		6.17	c
3		−1.33	3.0	Br	Br	−0.42		c
	3	−3.2	3.47	Br	Br		6.22	d
4		−2.67	3.33	I	I	−0.8		d
	4	−2.7	3.65	I	I		6.3	d
5		−3.07	3.37	Cl	Cl	−0.1		d
	5	−4.7	3.53	Cl	Cl		6.3	d
6		−2.07	3.4	Cl	2.83	−0.4		d
			← $J_{3,5} = 1.6$ Hz →					
	6	−0.33	3.58	Cl	3.1		6.23	c
7		Solution too weak	Br	Br	Br	+0.6		c
	8	Under aromatic	Cl	Cl	Cl		6.18	c
9		−1.75	3.47	3.9	2.95	−0.2		d
	9	−0.1	3.4	3.83	2.98		6.27	c

*Solvent: c, $CDCl_3$; d. d_6DMSO.

TABLE 3. Mass spectra of monodeoxypyoluteorins "*a*"*

	1		**2**		**3**		**4**		**5**		**6**		**7**		**9**	
Ion	*m/e*	%	*m/e*	%	*m/e*	%	*m/e*	%	*m/e*	%	*m/e*	%	*m/e*	%	*m/e*	%
M^+	255	32	187	70	343	10	439	95	289	38	221	60	421	4	221	65
20	135	18	67	100		—	319	100	135	85	101	40		—	67	100
21	134	2	66	16		—	318	5	134	6	100	8		—	66	14
22	121	100	121	46	121	100	121	84	155	100	121	100	121	100	155	16

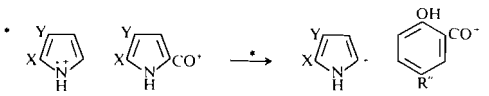

20 **21** **22**

leum, needles m.p. 143°; ν_{max} 3600, 1635, 1600, 1585 cm^{-1}; u.v. max 307 mμ. The n.m.r. and mass spectra showed this compound to be 2-(2′-methoxybenzoyl)-3,4,5-trichloropyrrole.

(b) Chlorination of 2-(2′-Methoxybenzoyl)pyrrole (**2***b*): *(i)* 200 mg of the above pyrrole was chlorinated (2) using 2 mol equiv *t*-butyl hypochlorite, giving the 4,5-dichloro derivative, m.p. 168–170°, crystallized from benzene/light petroleum. A by-product, 9 mg, was later shown to be the 4-monochloro compound **6***b*.

(ii) Using only 1 mol equiv of chlorinating agent, 500 mg of the above pyrrole gave 85 mg 4,5-dichloroderivative, 340 mg 4-chloro derivative, m.p. 122–123°, and 30 mg starting material.

The orientation of the 4-chloro compound follows from the n.m.r. (Table 2) and mass spectrum (Table 3).

Anal. Calcd. for $C_{12}H_{10}ClNO_2$: C, 61.15; H, 4.27; Cl, 15.05; N, 5.94. Found: C, 61.0; H, 4.22; Cl, 15.2; N, 5.85.

(c) The Friedel-Crafts reaction (2) of 2,3-dichloropyrrole and *o*-methoxybenzoyl chloride gave 52% 4,5-dichloro-2-

TABLE 4. Demethylation of monodeoxypyoluteorin methyl ethers "*b*" by boron trichloride (4)

Products "*a*"	M.p. (°C)	Yield (%)		Microanalysis C	H	N	Halide
1	174–176	72	Calcd.	51.55	2.75	5.5	27.7
			Found	51.3	2.8	5.5	28.0
2	74	>70	Calcd.	70.6	4.85	7.5	—
			Found	70.6	4.80	7.5	
3	151–152	89	Calcd.	38.3	2.05	4.05	46.3
			Found	38.6	2.05	3.95	46.0
4	190–196	75	Calcd.	30.1	1.6	3.2	57.8
			Found	30.1	1.65	3.3	57.8
5	191–193	80	Calcd.	45.5	2.1	4.8	36.6
			Found	45.65	2.05	4.8	36.6
6	160–162	80	Calcd.	59.6	3.6	6.3	16.0
			Found	59.5	3.5	6.5	16.2
9	136–137	80	Calcd.	59.6	3.6	6.3	16.0
			Found	59.4	3.7	6.3	16.0

(2′-methoxybenzoyl)pyrrole (**1***b*), spectroscopically identical with material from syntheses (*a*) and (*b*) above.

*Bromination of 2-(2′-Methoxybenzoyl)pyrrole (**2***b*)*

To the pyrrole, 1.5 g in chloroform, was added 0.84 g bromine in chloroform, with stirring. After 42 h the red solution was washed with sodium thiosulfate solution then with water. The dried solution was then evaporated and the residue crystallized from benzene/light petroleum giving 1.68 g 4,5-dibromo derivative, m.p. 192–193°, **3***b*.

Anal. Calcd. for $C_{11}H_7Br_2NO_2$: C, 38.3; H, 2.05; Br, 46.3; N, 4.05. Found: C, 38.6; H, 2.1; Br, 46.0; N, 3.95.

From the mother liquor, after demethylation, a compound m.p. 165–170° was separated by t.l.c. on silica using benzene/ethanol 95:5 and shown by m.s. and n.m.r. to be 2-(2′-hydroxybenzoyl)-3,4,5-tribromopyrrole (**7***a*).

*Iodination of 2-(2′-Methoxybenzoyl)pyrrole (**2***b*)*

A mixture of 0.2 g of the above pyrrole, 0.5 g iodine, and 0.4 g mercuric oxide was stirred 18 h in benzene at 20°, then filtered. The filtrate was washed with sodium thiosulfate solution, then water and dried. Evaporation of the solvent and crystallization of the residue from benzene/light petroleum gave 0.32 g 4,5-di-iodo derivative, m.p. 218–225°, **4***b*.

Anal. Calcd. for $C_{12}H_9NI_2O_2$: C, 31.8; H, 2.0; I, 56.05; N, 3.1. Found: C, 31.9; H, 1.9; I, 56.0; N, 2.95.

*Preparation and Chlorination of 2-(5′-Chloro-2′-methoxybenzoyl)pyrrole (**9***b*)*

The Friedel–Crafts method, above, of pyrrole and 5-chloro-anisoyl chloride gave 31% of the above ketone, m.p. 104–105°, crystallized from benzene/light petroleum.

Anal. Calcd. for $C_{12}H_{10}ClNO_2$: C, 61.15; H, 4.27; Cl, 15.05; N, 5.95. Found: C, 61.3; H, 4.2; Cl, 15.1; N, 5.9.

Chlorination by 2 mol equiv of *t*-butyl hypochlorite, as described above, gave the 4,5-dichloro derivative, m.p. 190–195°, crystallized from light petroleum (b.p. 100–120°).

Anal. Calcd. for $C_{12}H_8Cl_3NO_2$: C, 47.3; H, 2.65; Cl, 34.9: N, 4.6. Found: C, 47.5; H, 2.7; Cl, 34.3; N, 4.6.

*Preparation and Chlorination of 2-Picolinylpyrrole (**10**)*

In a modification of the published synthesis (5) which failed, we refluxed 5 g picolinic acid and 13 ml pure thionyl chloride in 100 ml dry benzene for 2 h. The solvent was then removed and the residue sublimed in vacuum giving 3.2 g acid chloride which was used at once.

The Friedel–Crafts reaction, as described above, of 3.2 g picolinyl chloride and 4 ml pyrrole gave 0.8 g 2-picolinylpyrrole, m.p. 69–70°, crystallized from light petroleum, m.s. *m/e* 172 (100%, M^+).

Anal. Calcd. for $C_{10}H_8N_2O$: C, 69.75; H, 4.7; N, 16.3. Found: C, 69.8; H, 4.5; N, 16.2.

Dichlorination with hypochlorite ester, as described above, gave a product, m.p. 205–209°, which from the m.s. contained some mono-chloro compound from which it was not easily separable. The crude material was found to be microbiologically inactive so it was not investigated further.

Demethylation of 2-(2′-Methoxybenzoyl)pyrroles

Table 4 lists the monodeoxypyoluteorins obtained, **1***a*–**7***a* with their m.p.'s and analyses.

*Borohydride Reduction of Monodeoxypyoluteorin (**1***a*)*

Excess aqueous sodium borohydride solution was added slowly to 80 mg 3,4-dichloro-2-(2′-hydroxybenzoyl)pyrrole in cold methanol. Within a few minutes, the yellow solution became colorless. Dilute sulfuric acid was added slowly when a red color developed which became yellow on addition of alkali. Chloroform extraction at p*H* 7 gave, after evaporation of the dried solution, an insoluble dark solid which deposited as the solution became concentrated.

Mass spectrometry showed the mol. wt. to be 486 with a pattern for four chlorine atoms, indicating that a dimer of **11** was obtained. The same result was obtained when water, not acid was used in the work-up.

*New Synthesis of 2-(2′,6′-Dimethoxybenzoyl)pyrrole (**12***b*)*

Pyrrole, 0.9 g was dissolved in 100 ml dry methylene chloride containing 2.7 g 2,6-dimethoxybenzoyl chloride

Can. J. Chem. Downloaded from www.nrcresearchpress.com by 210.87.254.6 on 09/05/12
For personal use only.

TABLE 5. N.m.r. spectra (τ) of new analogs of pyoluteorin

Solvent	1	3	4	5	2′		6′		3′	4′	5′
DMSO-d_6	−3.3	3.3d	Cl	Cl	OMe	6.3	OH	0.0	Cl	2.35s	Cl
$CDCl_3$	−0.45	3.63d	Cl	Cl	OMe	6.22	OMe	6.3	Cl	2.73d	3.4d
$CDCl_3$	−0.5	3.65	Cl	3.08	OMe	6.6	OMe	6.7	Cl	2.75d	3.42d
$CDCl_3$	−1.2	3.6m	3.9m	3.05m	OMe	6.24	OMe	6.37	Cl	2.8d	3.4d
DMSO-d_6	−2.9	3.67	Cl	Cl	OH	0.45	OH	0.88	Cl	2.98	3.73
DMSO-d_6	−1.97	3.8	Cl	2.95	OH	0.68	OMe	6.43	Cl	2.8	3.53
		←		→							
		J=1.6 Hz									
$CDCl_3$	−0.23	3.55m	3.8m	2.9m	Cl		Cl		2.77	2.77	2.77
$CDCl_3$	0.2	3.62d	Cl	Cl	Cl		Cl		2.73	2.73	2.73

and the mixture was added to a stirred solution of 3.5 ml stannic chloride in 50 ml methylene chloride at room temperature and the system was kept at 60–70° for 2 h during which a yellow solid precipitated. After adding excess dilute sulfuric acid, the organic layer was separated, washed with water, then dried. The solution was concentrated and chromatographed on a 25 × 2 cm column of alumina, eluting with chloroform/light petroleum (4:1). The following fractions were obtained: (*i*) an oil, probably resorcinol dimethyl ether; (*ii*) a solid, m.p. 128–129°, identical with a compound obtained by Bailey and Rees (unpublished) and shown by spectroscopy to be 2,2′,4,6′-tetramethoxybenzophenone ν_{max} (Nujol) 3500 v.w., br., 1645, 1598 br., 1285, 1275, 1255, 1210, 1108, 1030, 945, 835, 790 cm^{-1}; n.m.r. ($CDCl_3$) 5.2 (3H, s, *p*-MeO), 5.33 (9H, s, 3*o*-MeO)τ; m.s. *m/e* 302 (M^+, 37%), 165 (100%); (*iii*) 1.6 g (50%) 2-(2′,6′-dimethoxybenzoyl)pyrrole, m.p. 191–193°, crystallized from benzene/light petroleum, lit. (6) m.p. 187–188° and (7) 193–196°; (*iv*) a minor product having an n.m.r. spectrum consistent with 2,4-di-(2′,6′-dimethoxybenzoyl)pyrrole contaminated with some of fraction *iii*.

Aluminum chloride could also be used for this preparation but the condition of the catalyst was important. High quality material gave 2-(2′-hydroxy-6′-methoxybenzoyl)-pyrrole, m.p. 128–130°, lit. m.p. (8) 129°. Less active catalyst did not cause monodemethylation.

Preparation of 4,5-Dichloro-2-(3′,5′-dichloro-2′-hydroxy-6′-methoxybenzoyl)pyrrole

A solution of 0.6 g chlorine in 26 ml acetic acid was added dropwise to a solution of 0.44 g 2-(2′-hydroxy-6′-methoxybenzoyl)pyrrole (**12***c*). After 4 h stirring, the solvent was removed and the residue crystallized from light petroleum giving 0.51 g tetrachloro compound, m.p. 179–181°; n.m.r., Table 5.

Anal. Calcd. for $C_{12}H_7Cl_4NO_3$: C, 40.6; H, 2.0; Cl, 40.0; N, 3.9. Found: C, 40.9; H, 2.1; Cl, 40.0; N, 3.8.

*Chlorination of 2-(2′,6′-Dimethoxybenzoyl)pyrrole (**12***b*)*

To 116 mg of the above pyrrole in 20 ml chloroform was added 2 mol equiv *t*-butyl hypochlorite in carbon tetrachloride. The mixture was stirred 3 h at 20° and the solvents removed. Preparative t.l.c. of the residue on silica HF_{254} with ether/petrol (3:1) gave the following compounds in order of decreasing R_f values: (*i*) 3′-Chloropyoluteorin dimethyl ether, (**15***b*), 51 mg, m.p. 174–176° crystallized from benzene/light petroleum; n.m.r. Table 5.

Anal. Calcd. for $C_{13}H_{10}Cl_3NO_3$: C, 46.7; H, 3.0; Cl, 32.1. Found: C, 46.8; H, 3.0; Cl, 31.6; N, 4.4.

TABLE 6. Mass spectra of pyoluteorin (**14***a*) and 3′-chloropyoluteorin (**15***a*)*

		M^+	**20**	**23**	**24**
14*a*	*m/e*	271	135	137	136
	%	20	20	100	58
15*a*	*m/e*	305	135	171	170
	%	22	43	90	100

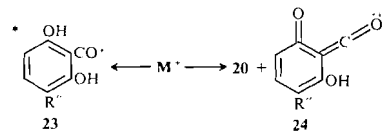

23 24

(*ii*) 4-Chloro-2-(3′-chloro-2′,6′-dimethoxybenzoyl)pyrrole (**16***b*), n.m.r. Table 5, 55 mg, containing pyoluteorin dimethyl ether (**14***b*) from which it was not separable prior to demethylation. (*iii*) 5-Dechloropyoluteorin dimethyl ether (8), (**13***b*), 10 mg. (*iv*) Starting material, 5 mg.

Chlorination (1 equiv) at −70° gave (half scale): (*ii*) 12 mg mixture as above, 17%; (*iia*) 13 mg crude material shown by n.m.r. (Table 5) to be 2-(3′-chloro-2′,6′-dimethoxybenzoyl)pyrrole, 20%; (*iii*) 20 mg, 30%; (*iv*) 10 mg, 17%.

*3′-Chloropyoluteorin (**15***a*)*

The dimethyl ether above was treated with boron trichloride (4) giving 3′-chloropyoluteorin, m.p. 200–205° (erroneously reported (2) as its monomethyl ether); n.m.r. Table 5, m.s. Table 6.

Anal. Calcd. for $C_{11}H_6Cl_3NO_3$: C, 43.1; H, 2.0; Cl, 34.7; N, 4.6. Found: C, 43.3; H, 2.0; Cl, 35.0, N, 4.7.

*Demethylation of Mixture of Dimethylpyoluteorin (**14***b*) and 3′,4-Dichloro Isomer (**16***b*)*

The crude mixture, 220 mg, after treatment with boron trichloride (4) gave a product separated by t.l.c., benzene/ethanol (9:1) into pyoluteorin 32 mg, 15% and 130 mg, 60% of 4-chloro-2-(3′-chloro-2′-hydroxy-6′-methoxybenzoyl)-pyrrole (**16***c*), m.p. 170–172°, crystallized from benzene/light petroleum as pale yellow needles; n.m.r. Table 5.

Anal. Calcd. for $C_{12}H_9Cl_2NO_3$: C, 50.4; H, 3.1; Cl, 24.8; N, 4.9. Found: C, 50.2; H, 3.2; Cl, 24.8; N, 5.0.

2,6-Dichlorobenzoylation of Pyrrole

2,6-Dichlorobenzoyl chloride, 10 g and 3.5 g pyrrole in methylene chloride were treated with excess stannic chloride

Can. J. Chem. Downloaded from www.nrcresearchpress.com by 210.87.254.6 on 09/05/12
For personal use only.

at 50–60° for 2 h. Column chromatography on alumina gave on elution with ether/light petroleum (3:1) 1.1 g, 2-(2′,6′-dichlorobenzoyl)pyrrole, needles, m.p. 165–167°, crystallized from benzene/light petroleum; n.m.r. Table 5, m.s. *m/e* 239 (43%, M^+), 94 (100%).

Anal. Calcd. for $C_{11}H_7Cl_2NO$: C, 55.0; H, 2.95; Cl, 29.5; N, 5.8. Found: C, 55.2; H, 2.85; Cl, 29.4; N, 5.7.

Further elution gave 2,4-di-(2′,6′-dichlorobenzoyl)pyrrole, 1.5 g pale yellow cubes, m.p. 284–286°, crystallized from benzene; n.m.r. (DMSO-d_6) H3 3.34, H5 2.4, H arom. 2.52 (3H) and 2.57 (3H), NH −3.02; m.s. *m/e* 411 (45%, M^+), 266 (100%).

Anal. Calcd. for $C_{18}H_9Cl_4NO_2$: C, 52.35; H, 2.2; Cl, 34.3; N, 3.4. Found: C, 52.7; H, 2.2; Cl, 34.0; N, 3.6.

Chlorination of 2-(2′,6′-Dichlorobenzoyl)pyrrole

The above pyrrole, 0.24 g in methylene chloride was treated with 2 mol equiv *t*-butyl hypochlorite at 20°. After 2.5 h the solvent was removed and the residual 4,5-dichloro derivative **17** crystallized from light petroleum (b.p. 100–120°), 220 mg, m.p. 186–190°; n.m.r. Table 5, m.s. *m/e* 307 (80%, M^+), 309 (100%, M + 2).

Anal. Calcd. for $C_{11}H_5Cl_4NO$: Cl, 45.9; N, 4.5. Found: Cl, 45.6; N, 4.5.

Chlorination of Ethyl Pyrrole-2-carboxylic Acid-3-carboxylate

The half ester (9), 9.2 g in acetic acid, was stirred while adding a solution of 2 mol equiv chlorine in acetic acid at room temperature. After 24 h the solvent was removed and the residue crystallized from aqueous ethanol (charcoal) to give the 4,5-dichloro derivative, 9.3 g white needles, m.p. 193–195°.

Anal. Calcd. for $C_8H_7Cl_2NO_4$: C, 38.1; H, 2.8; Cl, 28.1; N, 5.55. Found: C, 38.3; H, 2.7; Cl, 28.1; N, 5.8.

Preparation of Ethyl 2,3-Dichloropyrrole-4-carboxylate

The above dichloropyrrole half ester, 1 g, was refluxed 1 h in dimethylformamide. The cold solution was poured into ice water and extracted with ether. The latter solution was extracted with sodium bicarbonate solution then washed with water and evaporated leaving the dichloroester, m.p. 141–144°, crystallized from light petroleum, needles, 550 mg; n.m.r. ($CDCl_3$) 2.95d ($J_{1,2} = 1.7$ Hz) 5H, 1.2., NH.

Anal. Calcd. for $C_7H_7Cl_2NO_2$: C, 40.4; H, 3.4; Cl, 34.1; N, 6.75. Found: C, 40.55; H, 3.4; Cl, 33.9; N. 6.9.

Preparation and 2,6-Dimethoxybenzoylation of 2,3-Dichloropyrrole

The dichloropyrrole half ester above, 2 g in 50 ml diethylene glycol was refluxed 1 h with stirring. The solution was then shown by t.l.c. to contain the dichloroester above. A solution of 2 g sodium hydroxide in 6 ml water was then added and refluxing continued 3 h when the mixture was cooled, poured into ice water, and the aqueous solution extracted with benzene, washed and dried.

To this solution of 2,3-dichloropyrrole was added 1.8 g 2,6-dimethoxybenzoyl chloride and 2.2 g stannic chloride. The mixture was kept at 50–60° for 2 h then cooled and treated with dilute sulfuric acid. Water and chloroform were added and the organic layer was separated, washed with water and dried. Evaporation of the solvent left a residue which was extracted with hot petrol (b.p. 100–120°) containing charcoal, giving 0.9 g dimethyl pyoluteorin (7), m.p. 196–198°, **14***b*.

We thank the National Research Council of Canada for financial support and the Sankyo Co. Ltd. of Tokyo for the microbiological results.

1. D. G. DURHAM. M.Sc. Thesis. Trent University, Peterborough, Ontario, 1969.
2. G. R. BIRCHALL, C. G. HUGHES, and A. H. REES. Tetrahedron Lett. 4879 (1970).
3. K. BAILEY, G. R. BIRCHALL, D. G. DURHAM, C. G. HUGHES, and A. H. REES. Abstracts of XXIIIrd Int. Union of Pure and Appl. Chem. 73 (1971).
4. K. BAILEY and A. H. REES. J. Chem. Soc. D, 1284 (1969); Can. J. Chem. **48**, 2257 (1970).
5. E. SPATH and H. SPITZER. Ber. **59**, 1481 (1926).
6. R. TAKEDA. Bull. Agric. Chem. Soc. Jap. **23**, 126 (1959).
7. A. J. BIRCH, P. HODGE, R. W. RICKARDS, R. TAKEDA, and T. R. WATSON. J. Chem. Soc. 2641 (1964).
8. G. R. BIRCHALL and A. H. REES. Can. J. Chem. **49**, 919 (1971).
9. G. A. SWAN and A. WAGGOTT. J. Chem. Soc. C, 285 (1970).

Can. J. Chem. Downloaded from www.nrcresearchpress.com by 210.87.254.6 on 09/05/12
For personal use only.

Acetate-catalyzed Bromination and Exchange Reactions of 2-Butanone

J. W. THORPE AND J. WARKENTIN

Department of Chemistry, McMaster University, Hamilton, Ontario

Received December 21, 1970[1]

Products from bromination of 2-butanone in an aqueous acetate buffer were studied in order to compare the regiochemistry of monobromination with that of deuterium exchange. The good agreement found suggests that direct reaction of Br_2 with unenolized ketone, for which there have been claims in the literature recently, is unimportant or absent under the conditions of the experiments.

Les produits issus de la bromation de la butanone-2 dans une solution aqueuse tamponnée à l'acétate, ont été étudiés en vue de comparer la régiochimie de la monobromation avec celle de l'échange au deutérium. Le bon accord trouvé laisse penser que l'action directe du brome sur la cétone non énolisée, proclamée récemment dans la littérature, n'est pas importante voire absente dans les conditions expérimentales.

[Traduit par le journal]

Canadian Journal of Chemistry, **50**, 3229 (1972)

Introduction

The generally-accepted mechanism of racemization, hydrogen isotope exchange, and halogenation of carbonyl compounds is rate-determining enolization followed by fast reaction of the enol or enolate ion. Evidence for that mechanism has come mainly from kinetic studies. Halogenation rates were found to be independent of both the concentration[2] and the identity of the halogen (2–4) and in several cases the rate of racemization of an optically-active ketone was shown to be identical to the rate of its halogenation or hydrogen–deuterium exchange under similar conditions (5–6).

In spite of the accumulated evidence for a common mechanism, the recent literature contains claims for additional halogenation mechanisms (7) other than that involving rate-limiting enol- or enolate-formation.[3] Rappe has claimed, for example, that bromination of 2-butanone can result in a ratio of monohalides (**3**-Br/**1**-Br = 7–7.5) quite different from that predicted on the basis of relative exchange rates (CH_2/CH_3 = 0.6–0.7) under similar conditions (*7c*). Such a result is clearly not compatible with a common rate-determining step for the two reactions and to account for the discrepancy, Rappe (*7b–e*) postulated reaction of unenolized ketone with brominating agent. If that were the case, a substantial contribution from a term in bromine concentration would have to be present in a kinetic description of the overall process but such evidence has not yet been provided to support the product studies. On the other hand there is a claim, based on kinetics, for direct reaction between acetone and bromine. Sytilin reported that initial rates of acid-catalyzed bromination of acetone depend on the concentration of bromine (8).

In view of these challenges of the long-accepted mechanisms of important reactions, we have continued to investigate reactions of ketones, including kinetic studies and product studies. This account deals with the composition of the products from acetate-catalyzed[4] bromination of 2-butanone. We refer to the bromination process in aqueous acetic acid buffer as acetate-catalyzed, although that description encompasses several mechanisms, differing in the degree to which carbonyl oxygen is protonated according to the acid (water or acetic acid) involved there. The relative contributions of various mechanisms need not be known for our purpose because bromination and exchange can be studied in virtually identical conditions.

[1]Revision received June 21, 1972.

[2]For halogen concentrations exceeding 10^{-5}–10^{-6} M (1).

[3]Although the enol and enolate mechanisms are different, they are treated together here because they have in common the zero-order dependence on halogen except at very low ($<10^{-5}$ M) halogen concentrations (1). We are not concerned here with such low concentrations, for the last part of a bromination run, from $[Br_2] \simeq 10^{-6}$ to $[Br_2] = 0$ M, must have an immeasurably small effect on product ratios if the initial bromine concentration is relatively high.

[4]Base-promoted halogenation of a ketone consumes 1 equiv of base. The reaction is therefore not really catalyzed, unlike exchange. Because we are comparing halogenation and exchange it is convenient to waive the distinction.

Can. J. Chem. Downloaded from www.nrcresearchpress.com by 210.87.254.105 on 09/05/12
For personal use only.

TABLE 1. Substitution products from butanone*

	Yields (%)†									
	1-Substituted butanones				3-Substituted butanones			Other		
$[Br_2]$ (M)	Br§	OAc	Br_2	Br_3	Br	OAc	Br_2	Br_4	$CHBr_3$	X‡
0.010	16	20	2.9	7.3	21	25	1.2	trace	6.9	1.0
0.010	16	21	2.7	6.9	22	25	1.2	trace	5.3	1.0
0.030	14	17	3.5	7.7	18	26	1.8	3.2	9.1	1.1
0.046	11	19	4.1	9.4	14	23	2.0	5.8	11	0.90
0.050	11	19	4.3	9.9	14	22	2.1	5.7	12	0.86
0.050	11	17	4.7	9.7	15	23	2.2	7.3	11	0.95
0.081	8.1	16	6.0	12	12	17	2.9	9.5	17	0.76
0.100	4.8	15	7.6	13	7.9	16	3.9	10	23	0.69

*Butanone (2 M) in aqueous HOAc (1 M) containing AcO^- (1 M).
†Relative yields determined by g.l.p.c. with a QF-1 column. The same relative yields were obtained using a SE30 column, suggesting that all peaks in the g.l.p.c. traces correspond to single components of the mixture.
‡The ratio X is defined in the text and in eq. 1.
§Substituted ketones are coded by kind and number of substituents. 1,1,1,3-Tetrabromo-2-butanone is coded Br_4.

Methods and Results

In principle it is a simple matter to determine whether or not the regiochemistry of halogenation of 2-butanone is the same as that of hydrogen–deuterium exchange under similar conditions. The selectivity of exchange is readily established by following the disappearance of the appropriate signals in the p.m.r. spectrum. That of bromination would follow directly from the ratio of monobromoketones formed, if these were the only products. It is not possible to keep the product mixture so simple, however. Even with a large butanone:bromine ratio (200:1), acetate-catalyzed bromination leads to at least six of the eleven bromoketones, $CH_{(3-n)}Br_nCOCH_{(2-m)}Br_mCH_3$, to bromoform, and to the acetoxyketones resulting from S_N2 reaction of monobromoketones. A rigorous determination of the regiochemistry of monobromination requires division of the haloform yield and of some polyhalo ketone yields into fractions arising from initial 1- and 3-halogenation.

We have used an approximate method for determining the ratio of monobromination rates of butanone. If butanone is used in large excess over bromine, the yields of bromoform and of highly-brominated ketones can be kept relatively low. The method consists of determining the ratio (X) of sums of relative yields of those products whose origin (either initial 1-halogenation or initial 3-halogenation) is assignable, eq. 1. If X is near unity and if the unassigned products constitute a minor fraction of the total and if the materials balance is good, then X cannot be very different from the

$$[1] \qquad X = \frac{\sum \text{yields of 3-products}}{\sum \text{yields of 1-products}}$$

$$[2] \quad 2k_3/3k_1 = \frac{\sum (\text{yields of 3-products}) + Z'}{\sum (\text{yields of 1-products}) + Z}$$

ratio $2k_3/3k_1$ of eq. 2, in which Z' and Z represent the yields of all unassigned products arising from 3-bromobutanone and 1-bromobutanone, respectively. Assignable 2-butanones were: (*a*) 3-bromo, 3-acetoxy, 3,3-dibromo-, (*b*) 1-bromo, 1-acetoxy, 1,1-dibromo, and 1,1,1-tribromo. Unassignable products were 1,1,1,3-tetrabromo-2-butanone and bromoform. The assumed initial reactions and the definitions of rate constants[5] are shown in eq. 3. Results of applying the approximate method described above are in Table 1.

Discussion

Values of X show a downward trend from about 1.0–0.69 with increases in the initial bromine:ketone ratio from 1:200–1:20. This trend is presumably largely the result of the corresponding increases in the relative amounts of

[5]Rate constants are defined on the *per hydrogen* basis, as was done previously (9). Rate constants *per group* are obtained by multiplying by the appropriate statistical factor.

Can. J. Chem. Downloaded from www.nrcresearchpress.com by 210.87.254.105 on 09/05/12
For personal use only.

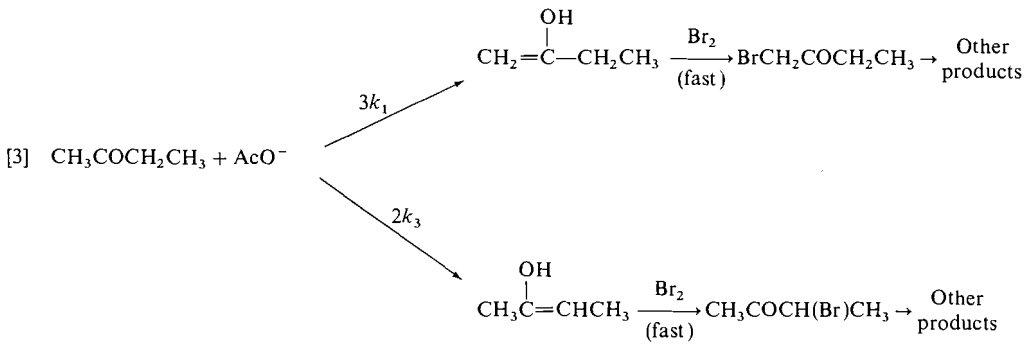

unassigned products. Seven of the eight sets of data are fitted fairly well to a straight line, $X = m[Br_2] + X_0$ which extrapolates to $X_0 \simeq 1.05$ at $[Br_2]_{initial} = 0$. This is a minimum value since either weighting the other set of data in drawing the line or else nonlinear extrapolation gives a higher value. Therefore the minimum ratio of rate constants, based on the assumption that bromination proceeds exclusively by the enolization mechanism (eq. 3) and based on analysis of the product composition rather than on kinetics, is $\frac{3}{2}X = 1.58$.

The regioselectivity of deuterium exchange, in the same medium at 54.8°, was obtained by p.m.r. as described in the accompanying note (10). The ratio of observed rate constants, $k_{CH_2}^{obsd.}/k_{CH_3}^{obsd.}$, which is equal to the ratio of rate constants, k_3/k_1 (exchange), defined on the *per hydrogen* basis, was 1.69. This rate ratio for hydrogen isotope exchange of butanone can be confidently equated with the rate ratio for enolization[6] although the magnitude of the ratio, and particularly its dependence on the conditions, has been the subject of some controversy (7*c*, 11). It is very probable then that the ratio of enolization rate constants, k_3/k_1, of butanone is near 1.7 at 54.8°, in the medium used for the bromination studies. The differential effect on the two rate constants, of changing from D_2O (exchange) to H_2O (bromination), must be very small. The good agreement (1.58 *vs.* 1.69) between the two estimates of k_3/k_1 means that, contrary to recent claims (7), the product composition in bromination of butanone, like the kinetics (2–4, 12), is compatible with the enolization mechanism. Although direct reaction between bromine and butanone may occur under other conditions, it seems preferable to retain the enolization mechanism generally, unless there is compelling evidence against its applicability.

[6]The mechanism of exchange, unlike that of halogenation, appears still to be universally accepted as involving an enol or enolate intermediate. We have shown (10) that direct reaction between D_2O and butanone is extremely slow.

Experimental

Chemicals

Reagent grade acetic acid and butanone were distilled once before use. Sodium acetate was dried at 150° to obtain the anhydrous material, which was kept in a desiccator.

Products

The products obtained in this work were isolated by g.l.p.c. from preparative-scale brominations of 2-butanone and were identified through their refractive indices and their proton and mass spectra. These are: *3-bromo-2-butanone*, n_D^{22} 1.4560 (lit. (13) n_D^{20} 1.4571); n.m.r. (CCl_4) δ 4.40 (q, 1, $J = 7$ Hz, C*H*Br), 2.32 (s, 3, CH_3CO), 1.72 (d, 3, $J = 7$ Hz, CHBrCH_3); *1-bromo-2-butanone*, n_D^{22} 1.4658 (lit. (13) n_D^{20} 1.4670); n.m.r. (CCl_4) δ 3.85 (s, 2, $BrCH_2CO$), 2.68 (q, 2, $J = 7$ Hz, $COCH_2$), 1.08 (t, 3, $J = 7$ Hz, CH_2CH_3); *3-acetoxy-2-butanone*, n_D^{22} 1.4118 (lit. (14) n_D^{20} 1.4129); n.m.r. (CCl_4) δ 4.95 (q, 1, $J = 7$ Hz, C*H*(OAc)CH_3), 2.04 (s, 6, $CH_3COCH(OCOCH_3)$), 1.30 (d, 3, $J = 7$ Hz, CH(OAc)-CH_3); *1-acetoxy-2-butanone*, n_D^{22} 1.4177 (lit. (15) n_D^{19} 1.4190); n.m.r. (CCl_4) δ 4.52 (s, 2, CH_2OAc), 2.40 (q, 2, $J = 7$ Hz, $COCH_2$), 2.10 (s, 3, $OCOCH_3$), 1.07 (t, 3, $J = 7$ Hz, CH_2CH_3); *1,1-dibromo-2-butanone*, n_D^{22} 1.5126 (lit. (16) n_D^{25} 1.5112); n.m.r. (CCl_4) δ 6.15 (s, 1, C*H*Br_2), 3.15 (q, 2, $J = 8$ Hz, $COCH_2$), 1.42 (t, 3, $J = 8$ Hz, CH_2CH_3); mol. *wt. m/e* 230 (triplet); *3,3-dibromo-2-butanone*, n_D^{21} 1.5072 (lit. (17) n_D^{25} 1.5050); n.m.r. (CCl_4) δ 2.62 (s, 3, CBr_2CH_3), 2.47 (s, 3, $COCH_3$); mol. wt. *m/e* 230 (triplet); *1,1,1-tribromo-2-butanone*, n_D^{21} 1.5647 (lit. (18) n_D^{25} 1.5626); n.m.r. (CCl_4) δ 3.51 (q, 2, $J = 8$ Hz, $COCH_2$), 1.64 (t, 3, $J = 8$ Hz, CH_2CH_3); mol. wt. *m/e* 309 (quartet); *1,1,1,3-*tetrabromo-2-butanone, n_D^{22} 1.6341; n.m.r. (CCl_4) δ 5.42 (q, 1, $J = 7$ Hz, COC*H*Br), 2.18 (d, 3, $J = 7$ Hz, CHBrCH_3); mol. wt. *m/e* 388 (quintet); and *bromoform*, n_D^{22} 1.5965 (lit. (19) n_D^{20} 1.5976); n.m.r. (CCl_4) δ 7.24 (s); mol. wt. *m/e* 253 (quartet). These compounds are numbered in the above order, from **1**–**9** in the following descriptions of elution order: 20% SE-30 column (10 ft × 1/8 in.), **1**, **2**, **3**, **9**, **6**, **4**, **5**,

Can. J. Chem. Downloaded from www.nrcresearchpress.com by 210.87.254.105 on 09/05/12
For personal use only.

7, and **8**; 12% QF-1 column (10 ft × 1/8 in.), **9**, **1**, **6**, **2**, **5**, **3**, **4**, **7**, and **8**.

A rough material balance for bromination of butanone was obtained as follows. A calibration constant for a given component was obtained by injecting different known volumes of a solution of known concentration, prepared by dissolving a weighed sample of the component in carbon tetrachloride. The constant related the integral peak area observed to the known molar quantity of material injected, for the different volumes injected showed that the calibration number was independent of sample size in the size range that was used. The peaks corresponding to the monobromides, the acetoxyketones, and bromoform were calibrated in this way. Isomers gave the same detector response (same calibration constant) and the difference between the constants for acetoxyketones and bromoform was only 14%. The higher bromoketones were assigned the same factors as monobromoketones. Knowledge of the volume of the CCl_4 solution containing the products from a bromination of butanone permitted calculation of approximate concentrations and yields. The material balance was based on bromine by assuming that one mole of bromine produces Avogadro's number of C—Br bonds in the reactions. Thus, acetoxyketones were weighted as one because they arise from bromoketones, a dibromoketone was weighted two, and bromoform was given a weight of three. In a typical small scale run (Table 1, first entry) the balance on Br was about 90%. The small fraction of bromine unaccounted for is probably in the form of bromoacids from the haloform reaction.

Bromination of Butanone

2-Butanone (7.2 g, 0.100 mol), acetic acid (3.00 g, 0.0500 mol), and sodium acetate (4.10 g, 0.0500 mol) in a volumetric flask were dissolved in distilled water to make 50 ml of solution. A stirring bar was added, the flask was placed in a bath (54.8 ± 0.04°) containing a submerged stirrer and after time for equilibration, bromine (0.080 g, 5.00×10^{-4} mol) was added. As soon as decolorization occurred the solution was poured into 50 ml of ice water in a separatory funnel and the cold mixture was extracted six times with 5 ml portions of carbon tetrachloride. The combined extract was dried over anhydrous sodium sulfate before the bulk of the solvent was evaporated at the water pump. The residue was analyzed by g.l.p.c. (average of five injections), using a 10 ft × 1/8 in., 12% QF-1 column in a Varian Aerograph Model 204-B instrument equipped with flame ionization detector and with a Varian Aerograph Model 476 digital integrator.

Relative yields of products were (%): 1-Br, 16; 1-OAc, 20; 3-Br, 21; 3-OAc, 25; 1,1-dibromo-2-butanone, 2.9; 1,1,1-tribromo-2-butanone, 7.3; 3,3-dibromo-2-butanone, 1.2; 1,1,1,3-tetrabromo-2-butanone, trace; and bromoform 6.9.

Financial support from the National Research Council of Canada is gratefully acknowledged. We are also indebted to the Ontario Department of University Affairs for an Ontario Graduate Fellowship to one of us (J.W.T.).

1. K. YATES and W. V. WRIGHT. Can. J. Chem. **41**, 2882 (1963).
2. P. D. BARTLETT. J. Am. Chem. Soc. **56**, 967 (1934).
3. R. P. BELL and H. C. LONGUET-HIGGINS. J. Chem. Soc. 636 (1946).
4. R. P. BELL and K. YATES. J. Chem. Soc. 1927 (1962).
5. S. K. HSÜ and C. L. WILSON. J. Chem. Soc. 623 (1936).
6. S. K. HSÜ, C. K. INGOLD and C. L. WILSON. J. Chem. Soc. 78 (1938).
7. (*a*) C. RAPPE. Acta Chem. Scand. **20**, 376 (1966); (*b*) **20**, 1721 (1966); (*c*) **20**, 2236 (1966); (*d*) **21**, 2857 (1967); (*e*) **21**, 1823 (1967); (*f*) **22**, 219 (1968).
8. M. S. SYTILIN. Zhur. Fiz. Khim. **41**, 1200 (1967); Russ. J. Phys. Chem. **41**, 640 (1967).
9. J. WARKENTIN and C. BARNETT. J. Am. Chem. Soc. **90**, 4629 (1968).
10. R. A. COX, J. W. THORPE, and J. WARKENTIN. Can. J. Chem. This issue.
11. C. RAPPE. Acta Chem. Scand. **23**, 2305 (1969).
12. R. A. COX and J. WARKENTIN. Can. J. Chem. This issue.
13. J. R. CATCH, D. F. ELLIOT, D. H. HEY, and E. R. H. JONES. J. Chem. Soc. 272 (1948).
14. G. F. HENNION and W. S. MURRAY. J. Am. Chem. Soc. **64**, 1220 (1942).
15. J. J. RIEHL and M. M. DELEPINE. C. R. Acad. Sci. Paris, Ser. C, **250**, 4174 (1960).
16. C. RAPPE. Ark. Kemi. **24**, 73 (1965).
17. C. RAPPE and R. KUMAR. Ark. Kemi. **23**, 475 (1965).
18. C. RAPPE. Ark. Kemi. **21**, 503 (1963).
19. R. C. WEAST, editor. Handbook of chemistry and physics. 51st ed. The Chemical Rubber Company, Cleveland, Ohio. 1970. p. C-369.

Can. J. Chem. Downloaded from www.nrcresearchpress.com by 210.87.254.105 on 09/05/12
For personal use only.

Kinetics of Bromination of Acetone, Bromoacetone, and 1,1-Dibromoacetone

ROBIN A. COX AND JOHN WARKENTIN
Department of Chemistry, McMaster University, Hamilton, Ontario

Received December 21, 1970[1]

The rate of bromine consumption in acetate-promoted bromination of acetone is not measurably dependent on bromine concentration, in confirmation of earlier work. This result casts doubt on the existence of recently-reported, nonenolic mechanisms for bromination of butanone under similar conditions. The effects of alpha bromine substituents on rates of enolization of acetone are reported.

La vitesse de disparition de brome lors de la bromation de l'acétone amorcée par l'acétate, n'est pas mesurable par rapport à la concentration en brome; ce qui confirme un travail antérieur. Ce résultat met en doute l'existence récemment rapportée d'un mécanisme non-énolique lors de la bromation de la butanone dans des conditions semblables. Les effets des substituants bromo en α sur les vitesses d'énolisation de l'acétone sont donnés. [Traduit par le journal]

Canadian Journal of Chemistry, **50**, 3233 (1972)

Can. J. Chem. Downloaded from www.nrcresearchpress.com by 210.87.254.6 on 09/05/12
For personal use only.

Introduction

After many years of unchallenged acceptance (1) the enolization mechanism for alpha halogenation of carbonyl compounds was recently called into question by two independent investigators. Rappe (*2a–d*) claimed a large disparity between the experimental ratio of monobromides from butanone and the ratio calculated from base-catalyzed deuterium exchange rates under comparable conditions. Sytilin (3) claimed that the initial rate of bromination of acetone, catalyzed by acid, is dependent on the concentration of bromine.

In the preceding paper (4) evidence is presented for a reasonable agreement between product data pertaining to bromination of butanone and kinetic exchange data (5) for one set of conditions. This account deals with the kinetics of bromination of acetone under the same conditions. Butanone bromination proved to be too complex for analysis but a fundamental difference in mechanism between acetone and butanone reactions is so unlikely that the results for acetone can be applied directly to reactions of butanone.

Methods and Results

The concentration most easily followed in bromination of a ketone is that of bromine. In this work the potential of the Br_2, Br^- half cell, relative to that of the glass electrode, was measured with a platinum electrode in a buffered medium. Low concentrations of bromine, in the range 10^{-3}–10^{-7} *M*, were readily measured. The analysis was simplified by beginning with $[Br^-] = 0.1$, $[CH_3COCH_3] = 0.3$, and $[Br_2] = 10^{-3}$–10^{-4} *M*, so as to keep the concentrations of bromide and acetone effectively constant during the course of the reaction. Further simplification resulted from the use of a large excess (1 *M*) of acetate, which should keep the rate of enolization, if that is the mechanism, effectively constant throughout the course of bromination.

For the electrochemical reaction, $Br_2 + 2e \rightarrow 2Br^-$, the potential is given by the Nernst equation, which can be approximated as eq. 1

$$[1] \qquad E = E^0 - \frac{RT}{2F} \ln \frac{[Br^-]^2}{[Br_2]}$$

by writing concentrations instead of activities. Taking into account the constancy of $[Br^-]$, the potential of the glass electrode and any other concentrations (except $[Br_2]$) that could affect the potential but remain constant during the reaction, we can write eq. 2, in which E'

$$[2] \qquad E = E' + \frac{RT}{2F} \ln [Br_2]$$

contains all the constant terms. Its value was determined experimentally, with titrimetrically determined bromine solutions, for 5° temperature increments from 20–40°, inclusive. Initial concentrations of $[Br_2]$ in solutions used for brominating acetone could then be deter-

[1]Revision received October 8, 1971. Publication delayed at authors' request.

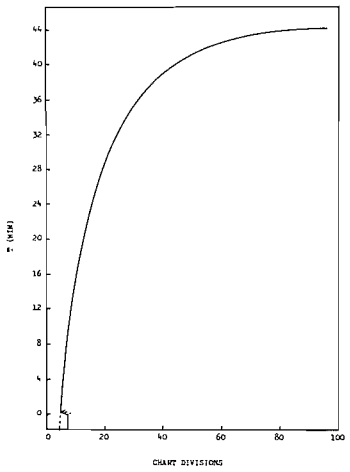

FIG. 1. Sample chart trace, acetone.

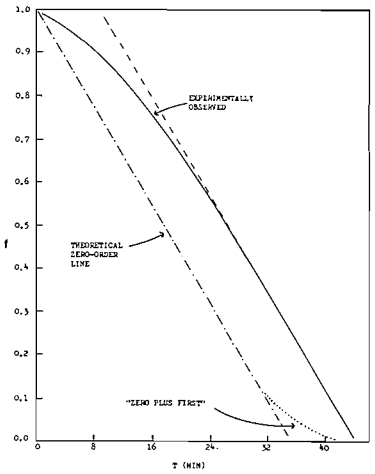

FIG. 2. Concentration/time graph for the bromination of acetone at 40°.

mined potentiometrically from the known value of E' using eq. 3.

$$[3]\quad [Br_2]_0 = \text{antilog}\left(\frac{E - E'}{C_t}\right), \text{ where}$$

$$C_t = 2.3026\,\frac{RT}{2F}$$

Potentials were read with a pH-meter and recorded with a chart recorder. The pH-meter reading (E) was linearly related to the chart paper reading (Ch) according to eq. 4.

$$[4]\quad E = -(0.760 \pm 0.001)Ch + (73.79 \pm 0.03)$$

Combining eqs. 2 and 4 gives eq. 5

$$[5]\quad [Br_2] = \exp\left(\frac{Ch' - Ch}{C_t'}\right), \text{ where}$$

$$C_t' = \frac{RT}{2(0.760F)}$$

which leads to eq. 6 if one defines an arbitrary zero such that

$$[Br_2]_0 = \exp\left(\frac{Ch' - Ch_0}{C_t'}\right)$$

Equation 6 could be used to determine f, the relative bromine concentration, at any

$$[6]\qquad f = \frac{[Br_2]}{[Br_2]_0} = \exp\left(\frac{Ch_0 - Ch}{C_t'}\right)$$

time directly from chart traces. The number f, together with $[Br_2]_0$ from eq. 3, permits calculation of $[Br_2]$ at any time from the chart trace.

The form of eq. 6 indicates that the chart trace will be a straight line of slope kC_t', if bromine consumption follows first order kinetics ($f = f_0 \exp(-kt)$). On the other hand, zero-order bromine consumption would result in a curved chart trace but a straight line plot of f against time. A typical chart trace is reproduced as Fig. 1. Figure 2 shows the expected shapes of f *vs.* t plots, as well as the actual time dependence of the relative bromine concentration. Bromine consumption does not follow the theoretical "zero-order" line,[2] Fig. 2, but it does become linear after initial acceleration of the rate and the final slope approaches that of the zero-order line. The initial increase in rate is caused by the formation of bromoacetones, which react faster than acetone but not fast enough to result in an initial stoichiometry of $3Br_2$ per molecule of ketone. The meaning of the limiting slope is discussed below.

An important feature of the f *vs.* t plot (Fig. 2) is the absence of tailing of the experimental curve toward the end of a run; a feature expected if there were a first-order (in $[Br_2]$) component superimposed on zero-order kinetics. Such tailing can be observed if the Br_2 concentration is followed to values below 10^{-5}–10^{-6} M where halogenations are known to be first order in halogen (6). They can become first order in that

[2]The zero-order line is drawn with the assumption that all brominations after the first are fast. Therefore $-d[Br_2]/dt = 3k_1[\text{ketone}][AcO^-]$.

Can. J. Chem. Downloaded from www.nrcresearchpress.com by 210.87.254.6 on 09/05/12
For personal use only.

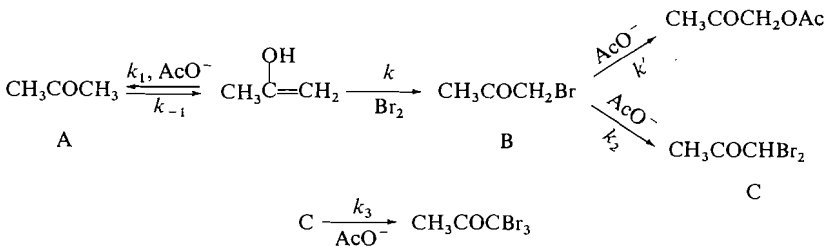

SCHEME 1

concentration range not because of direct reaction between ketone and halogen, but because k[enol][Br_2] no longer greatly exceeds k_{-1}[enol] (Scheme 1). That part of a bromination run, which was readily observed on the chart traces, was not detailed in graphs of f *vs.* t, where it would occupy the section of the f-scale between about 0.01 and 0 (Fig. 2). What is demonstrated then is that there is no detectable first-order consumption of bromine by acetone during about 99% of the reaction.

Rate constants can be extracted from f and t data by means of the equations developed below. From Scheme 1 the rate of bromine consumption is given by eq. 7, in which the rate

$$[7] \quad -\frac{d[Br_2]}{dt} = k_1[A] + k_2[B] + k_3[C]$$

constants are pseudo-first-order constants, including the constant concentration of acetate. The concentration of acetone, [A], was also held constant leaving [B] and [C], the concentration of bromoacetone and dibromoacetone, respectively, to be evaluated.

The value of [B], in terms of rate constants and known concentrations (eq. 9), is obtained by integrating differential eq. 8.

$$[8] \quad \frac{d[B]}{dt} = k_1[A] - k_2'[B], \quad \text{where} \quad k_2' = k_2 + k'$$

$$[9] \quad [B] = \frac{k_1}{k_2'}[A](1 - e^{-k_2't})$$

The value of [C] is determined as outlined below. The first-order differential equation (eq. 10) can be solved by assuming a solution, differentiating it, and equating coefficients.[3] This process leads to eq. 11.

[3]Details are not given here because the final result can be checked by differentiation. Readers interested in the particulars may obtain these by writing to the authors.

$$[10] \quad \frac{d[C]}{dt} = k_2[B] - k_3[C]$$

$$= \frac{k_1k_2}{k_2'}[A](1 - e^{-k_2't}) - k_3[C]$$

$$[11] \quad [C] = -\frac{k_1k_2[A]\,e^{-k_2't}}{k_2'(k_3 - k_2')} + \frac{k_1k_2[A]\,e^{-k_3t}}{k_3(k_3 - k_2')} + \frac{k_1k_2[A]}{k_2'k_3}$$

With [B] and [C] evaluated we can return to eq. 7 to express the measured variable, [Br_2], in terms of [A], rate constants and time. Integration between the limits $[Br_2]_0$ at $t = 0$ and $[Br_2]_t$ at $t = t$ yields eq. 12, which on division by $[Br_2]_0$ gives eq. 13.

$$[12] \quad [Br_2]_0 - [Br_2]_t = k_1[A]t + \frac{2k_1k_2[A]t}{k_2'} - \frac{k_1k_2(2k_3 - k_2')[A](1 - e^{-k_2't})}{(k_2')^2(k_3 - k_2')} + \frac{k_1k_2[A](1 - e^{-k_3t})}{k_3(k_3 - k_2')}$$

$$[13] \quad f = 1 - \frac{k_1[A]}{[Br_2]_0}\left[\left(1 + \frac{2k_2}{k_2'}\right)t + \frac{k_2(2k_3 - k_2')(1 - e^{-k_2't})}{k_2'^2(k_3 - k_2')} - \frac{k_2(1 - e^{-k_3t})}{k_3(k_3 - k_2')}\right]$$

The initial slope of the f *vs.* t plot is, therefore:

$$\left(\frac{df}{dt}\right)_{t=0} = -k_1\frac{[A]}{[Br_2]_0}$$

That is, the initial rate of change of f depends on the rate constant (pseudo-first-order) for enolization of acetone and on the initial ketone to bromine concentration ratio, as it should. It

Can. J. Chem. Downloaded from www.nrcresearchpress.com by 210.87.254.6 on 09/05/12
For personal use only.

$$[14]\quad \left(\frac{df}{dt}\right)_{t\to\infty} = -k_1\frac{[A]}{[Br_2]_0}\left(1+\frac{2k_2}{k_2'}\right)$$

$$[15]\quad \left(\frac{df}{dt}\right)_{t\to\infty} \simeq -3k_1\frac{[A]}{[Br_2]_0}$$

$$[16]\quad f = 1-\frac{k_2[B]_0}{[Br_2]_0} \times\left\{\frac{(2k_3-k_2')}{k_2'(k_3-k_2')}(1-e^{-k_2't})+\frac{1-e^{-k_3t}}{k_3-k_2'}\right\}$$

$$[17]\quad f = 1-\frac{[C]_0}{[Br_2]_0}(1-e^{-k_3t})$$

was used to evaluate k_1.[4] The limiting slope of the f *vs.* t graph is given by eq. 14, which, because $k_2' = k_2 + k'$, reduces to eq. 15 if k' is small relative to k_2. Thus, in the absence of the S_N2 reaction, the ratio of final to initial slopes of f *vs.* t would be the stoichiometric factor (three) for bromine consumption.[5] Rate constants for enolization of acetone and of bromoacetones could, in principle, be evaluated directly by computer fitting of the f *vs.* t graph. Errors rapidly become large, however, if such fitting is used to evaluate rate constants beyond that of the first step. The rate constants k_2 and k_3 were therefore obtained from separate experiments, in which bromoacetone (B) and 1,1-dibromoacetone (C) were the starting materials. The kinetic analysis is analogous to that outlined above, except that the bromoketones can not be used in large excess because of their limited solubility. Relationships between f and t for the bromoketones are given below as eqs. 16 and 17.

Discussion

Despite the need to include the rates of "fast" reactions (8) in the overall kinetic analysis of acetone bromination, it is clear that rate-determining enolization is a satisfactory mechanism, for f *vs.* t graphs (Fig. 2) meet the time

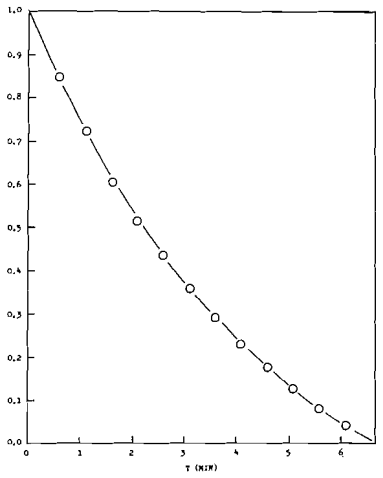

FIG. 3. Graph of f *vs.* t for the bromination of dibromoacetone at 30°.

axis without any evidence of tailing. The shape of the graph is a qualitative test for kinetic dependence on bromine concentration. Acetone is not a good system for quantitative comparison of theory with experiment because of S_N2 reaction of bromoacetone and because of bromination of 1,1,1-tribromoacetone. A reasonable fit is therefore assured, with so many adjustable (within the limits of error) rate constants available.

A quantitative comparison was possible in less complex systems. Bromination of 1,1-dibromoacetone is relatively simple, because bromination of 1,1,1-tribromoacetone is slower than that of its precursor. In Fig. 3, the solid line is that described by eq. 17, with $k_3 = 5.05 \times 10^{-3}\ M^{-1}\ s^{-1}$. The points, which are experimental values of f and t,[6] fit the theoretical curve well considering the approximations that bromination of tribromoacetone can be neglected and that enolization at the CH_3 group of dibromoacetone can be neglected.

A qualitative and a semi-quantitative fit of kinetic data to schemes based on assumed rate-determining enolization means that the mechanism is acceptable for ketones with considerably different chemical properties. It follows that 2-butanone bromination must also go by the

[4]Bell *et al.* reported $k_1 = 4.0 \times 10^{-8}\ M^{-1}\ s^{-1}$, statistically corrected at 25° (7). Our initial slope gave $k_1^{25°} = 3.96 \times 10^{-8}\ M^{-1}\ s^{-1}$.

[5]This analysis is based on the assumed Scheme 1. The one approximation in Scheme 1 is that 1,1,1-tribromoacetone does not consume an appreciable quantity of the available bromine. It turns out that the ratio of final to initial slopes is very nearly three, because bromine consumption by tribromoacetone is compensated, fortuitously, by the S_N2 reaction.

[6]The reader is reminded that f *vs.* t curves, for relatively insoluble ketones like 1,1-dibromoacetone, do not have a linear portion because the substrate concentration changes with time.

Can. J. Chem. Downloaded from www.nrcresearchpress.com by 210.87.254.6 on 09/05/12
For personal use only.

TABLE 1. Acetate-catalyzed enolization at 30°

Ketone	k^H (M^{-1} s^{-1})*	$k^H_{ketone}/k^H_{acetone}$
CH_3COCH_3	7.38×10^{-8}	1.0
CH_3COCH_2Br	3.27×10^{-4}	4.43×10^3
$CH_3COCHBr_2$	5.05×10^{-3}	6.83×10^4

*Statistically corrected rate constants. The bromoketone rate constants are not corrected for reaction at the CH_3 group.

enolization mechanism under the same conditions. The kinetics of bromine consumption by that ketone are quite complex[7] but there the ratio of monobromo ketones was shown to be in agreement with data from hydrogen isotope exchange (4); a process which can not involve reaction between unenolized ketone and D_2O (5).

It is possible, of course, that there is some direct reaction between ketones and bromine. Our results indicate that such reaction, if any, is not competitive enough to make itself manifest in either kinetics or products. The older literature contains numerous examples of ketone reaction under other conditions, which are adequately accommodated by the general enolization mechanism. Hence there appears to be no need for the extra halogenation mechanisms proposed recently (*2a–d*).

The effects of bromine substituents on acetate-promoted bromination are shown in Table 1. Bromine enhances the rate of enolization at the bromine-bearing carbon through its polar effect which overcomes an opposing steric effect. The overall effects of Br are not additive; two bromines being less than twice as effective as one in enhancing rate. The steric effect should reduce the reactivity of methylene protons of bromoacetone about two-fold, and that of the methine proton of 1,1-dibromoacetone about 40-fold, relative to that of a proton of acetone. These are rough estimates, based on the overall effects of CH_3 groups on deuterioxide-catalyzed exchange of ketones (9) and on the assumption that the steric requirements of CH_3 and Br are the same. Adjustment of the overall effects of Br substituents for the probable steric effect leaves a polar effect which is also not additive.

The effects of bromine substituents on enolization rates, at either alpha site of a ketone, are discussed in more detail in an accompanying paper.

[7]There are 13 enolization rate constants to consider in formation of pentabromobutanone as well as at least two rate constants for bimolecular substitution.

Experimental

Apparatus

The experimental setup was essentially that of Bell and Robinson (10). The reaction vessel was a cylindrical glass cell of about 120 ml capacity. It was fitted with one B-14 and two B-19 outer glass joints. The larger necks held a glass electrode (Fisher, cat. no. 13-639-1) and a platinum electrode (Johnson, Matthey and Mallory, 13 × 31 mm cylinder, type C Unimesh) each of which was sealed with epoxy resin to a B-19 inner glass joint. A 1 in., Teflon-coated bar magnet in the cell was driven by a magnetic stirrer (TRI-R Instruments, Jamaica, N.Y.) immersed in a constant temperature bath controlled to ±0.03°. Temperatures were measured with calibrated thermometers.

The lead of the platinum electrode was connected to the input terminal of a p*H*-meter (Fisher Accumet, model 310, expanded scale) and the glass electrode was hooked up to the reference terminal. Potential in millivolts could be read from the p*H*-meter which was itself connected to a chart recorder to obtain a record of potential against time. It was necessary to use shielded cable, to screen the cell with grounded copper gauze, and to use an aluminum-foil-covered, grounded shield between the apparatus and passersby in order to achieve stable, reproducible potentials. Polarization of the platinum electrode was not a problem as indicated by lack of dependence of potential on stirring speed.

Ketones and Solvents

Bromoketones had to be highly pure and especially free of more reactive higher bromoketones. Fractional distillation was unsatisfactory and all bromoketones were purified by repeated g.l.p.c. in a 10 ft × 3/8 in. QF-1 (10%) column. Pure compounds used for kinetics gave only one g.l.p.c. peak with three analytical columns: 10 ft × 1/8 in. QF-1 (12%), 5 ft × 1/8 in. FFAP (10%), and 10 ft × 1/8 in. SE-30 (20%), all on 60/80 mesh Chromosorb W. They were clear, colorless liquids with n.m.r. spectra (Varian T60) free of extraneous signals. They could be stored safely in sealed tubes at about −10° in a freezer.

Bromoacetone was prepared by the potassium chlorate method (11). A pure sample gave n_D^{25} 1.4680, lit. (12) n_D^{25} 1.4739; n.m.r. (CCl_4): δ 2.30, s, 3, CH_3CO; 3.78, s, 2, $BrCH_2CO$.

1,1-Dibromoacetone was obtained as a by-product from the preparation of bromoacetone. A pure sample had n_D^{25} 1.5232, lit. (12) n_D^{25} 1.5237; n.m.r. (CCl_4): δ 2.51, s, 3, CH_3CO; 5.67, s, 1, Br_2CHCO.

Dioxane (Fisher, Certified Grade) was purified by refluxing, first with hydrochloric acid and then with sodium, according to the procedure described by Fieser (13).

Solutions

Stock solutions were KBr (0.3333 *M*), NaOAc (2.00 *M*), HOAc (1.0 *M*), all in water and Br_2 (*ca.* 5×10^{-2} *M*) in 0.3333 *M* KBr solution. Solutions of ketones were prepared by weighing them into volumetric flasks, dissolving in dioxane, and filling with water to the mark. In the case of acetone, dioxane was omitted. Such solutions had a total

Can. J. Chem. Downloaded from www.nrcresearchpress.com by 210.87.254.6 on 09/05/12
For personal use only.

organic content (ketone plus dioxane) of 20% v/v and remained homogeneous on addition to the buffer solution in the cell.

Procedure

In a typical run, 50 ml of 2 *M* sodium acetate solution, 25 ml of 0.3333 *M* potassium bromide solution, and 10 ml of 1 *M* acetic acid solution were pipetted into the vessel. The electrodes were inserted and the vessel was positioned in the thermostat. After 10 or 15 min, the stock solution of bromine (5 ml) was pipetted in, the last neck was closed, and the system was left to equilibrate until the potential was absolutely steady, with the p*H*-meter in the expanded-scale mode. This generally took 0.5–1 h. During this time the ketone solution was brought to the bath temperature in another vessel.

The initial steady potential was recorded and used to calculate the bromine concentration (eq. 3, text). The recorder pen was then placed at the minimum reading by adjusting the p*H*-meter's standardizing potentiometer. Ketone solution (10 ml) was pipetted into the cell, bringing the total volume in the latter to 100 ml and the concentrations to: NaOAc, 1 *M*; HOAc, 0.1 *M*; KBr, 0.1 *M*; dioxane plus ketone, 2% v/v; acetone, 0.2–0.3 *M*; sparingly-soluble ketones, *ca.* 10^{-3} *M*; Br_2, 10^{-3}–10^{-4} *M*. Reaction was followed until the pen had traversed the 10 in. chart (end), a range of bromine concentrations of just over two powers of ten. At that point the p*H*-meter was returned to normal mode, at which setting the chart width represented some 20 powers of ten in bromine concentration. Reaction was followed a little longer, just to ensure that, at the nominal end of the run, the bromine concentration had not passed into the concentration range where ketonization of enols competes with their bromination (6).

A chart trace was treated as follows. The early, almost straight, part of the curve was extrapolated back through the irregularities (Fig. 1) caused by addition of ketone solution, to give Ch_0, eq. 6. Chart readings (Ch between 15 and 30 points), corrected for any blank reaction, and corresponding values of time were read from the trace. Values of $(Ch - Ch_0)$ and time (t) were then treated by computer, as outlined below, to obtain enolization rate constants k_1. The rate expression of the form $f = 1 + \alpha t + \beta(1 - e^{-k_2' t}) + \gamma(1 - e^{-k_3 t})$ was rewritten as a polynomial in t, $f = a_1 + a_2 t + a_3 t^2 + a_4 t^3 + \cdots$, by expanding the exponential terms as power series. The computer program solved the polynomial expression and printed out values of the coefficients. These coefficients could be expressed in terms of rate constants by substituting appropriate values of α, β, and γ from the rate expressions. The first four coefficients are: $a_1 = 1$; $a_2 = \alpha + k_2'\beta + k_3\gamma$; $a_3 = -(\beta k_2'^2 + k_3^2)/2!$; $a_4 = (\beta k_2'^3 + \gamma k_3^3)/3!$. The first coefficient is always unity, because of the treatment in terms of relative bromine concentration. The second coefficient, a_2, contains only terms in t and is the equivalent of the expression obtained by differentiating the rate expression and setting $t = 0$. Thus a_2 is always the initial slope of the f *vs.* t graph and it contains only the first enolization rate constants for the ketone under study. Details may be obtained from the authors.

Financial support from the National Research Council of Canada is gratefully acknowledged. We are indebted also to the Ontario Department of University Affairs for an Ontario Graduate Fellowship to R.A.C.

1. A. LAPWORTH. J. Chem. Soc. **85**, 30 (1904).
2. (*a*) C. RAPPE. Acta Chem. Scand. **20**, 1721 (1966); (*b*) **20**, 2236 (1966); (*c*) **21**, 857 (1967); (*d*) **21**, 1823 (1967).
3. M. S. SYTILIN. Zhur. Fiz. Khim. **41**, 1200 (1967); Russ J. Phys. Chem. **41**, 640 (1967).
4. J. W. THORPE and J. WARKENTIN. Can. J. Chem. This issue.
5. R. A. COX, J. W. THORPE, and J. WARKENTIN. Can. J. Chem. This issue.
6. K. YATES and W. V. WRIGHT. Can. J. Chem. **41**, 2882 (1963).
7. R. P. BELL, G. R. HILLIER, J. W. MANSFIELD, and D. S. STREET. J. Chem. Soc. B, 827 (1967).
8. R. P. BELL and K. YATES. J. Chem. Soc. 1927 (1962). These authors found it necessary to include rates of chlorination of chloroacetone and of dichloroacetone in order to fit the overall rate of chlorine consumption during chlorination of acetone.
9. J. WARKENTIN and C. BARNETT. J. Am. Chem. Soc. **90**, 4629 (1968).
10. R. P. BELL and R. R. ROBINSON. Proc. Roy. Soc. Ser. A, **270**, 411 (1962).
11. J. R. CATCH, D. F. ELLIOTT, D. H. HEY, and E. R. H. JONES. J. Chem. Soc. 272 (1948).
12. C. RAPPE. Arkiv. Kemi. **21**, 503 (1963).
13. L. F. FIESER. Experiments in organic chemistry. D. C. Heath and Co., Boston, Mass. 1955. p. 285, procedure a.

Can. J. Chem. Downloaded from www.nrcresearchpress.com by 210.87.254.6 on 09/05/12
For personal use only.

Hydrogen Isotope Exchange in 2-Butanone. Further Measurements and Some Comments

R. A. Cox, J. W. Thorpe, and J. Warkentin

Department of Chemistry, McMaster University, Hamilton, Ontario

Received December 21, 1970[1]

The ratio of rate constants for exchange at the methylene and methyl positions of butanone, $k^H_{CH_2}/k^H_{CH_3}$, is shown to be near 1.69 in 1:1 acetic acid–acetate buffer; nearly twice the value (0.86) for deuterioxide catalysis at 54.8°. Methods of obtaining rate constants for acetate catalysis from composite rates (acetate and deuterioxide), or from rates in buffered media, are shown to be adequate for estimating rate ratios.

Detailed temperature dependence of the relative rate constants for either system is not yet available but the effects are known to be small. For butanone enolizations the isokinetic temperature is in the neighborhood of 35°, when reaction is catalyzed by deuterioxide in aqueous media.

Le rapport des constantes de vitesse de l'échange aux positions méthylène et méthyl de la butanone, $k^H_{CH_2}/k^H_{CH_3}$, est près de 1.69 dans un tampon 1:1 acide acétique–acétate et près de deux fois cette valeur (0.86) dans le cas de la catalyse par l'oxyde de deutérium à 54.8°. Les méthodes permettant d'obtenir les constantes de vitesse pour la catalyse par acétate à partir de vitesses combinées (acétate et oxyde de deutérium) ou de vitesses en milieu tamponné sont estimées adéquates pour la détermination des rapports de vitesse.

La dépendance de la température sur les constantes de vitesse relatives de ces systèmes n'a pas été approfondie, mais les effets sont reconnus comme étant faibles. Dans le cas des énolisations de la butanone, la température isocinétique se situe aux environs de 35° lorsque la réaction est catalysée par l'oxyde de deutérium en milieu aqueux. [Traduit par le journal]

Canadian Journal of Chemistry, **50**, 3239 (1972)

Can. J. Chem. Downloaded from www.nrcresearchpress.com by 210.87.254.40 on 09/05/12
For personal use only.

Discussion and Results

In order to compare the ratio of hydrogen isotope exchange rates in butanone with the ratio of bromoketones formed in comparable circumstances (1) it was desirable to redetermine the former. There is some controversy (2) with regard to the magnitude of the reactivity ratios for exchange $(k^H_{CH_2}/k^H_{CH_3})$[2] and concerning the effect of changing the catalyzing base from hydroxide to acetate.

We have made two more measurements of the relative rates of exchange in butanone at 54.8°. The media for these studies were 1:1 acetic acid–acetate buffers in D_2O and exchange was followed by n.m.r., with two different n.m.r. spectrometers. The results,

$$(k^H_{CH_2}/k^H_{CH_3})^{54.8}_{HOAc,\,AcO^-} = 1.70 \pm 0.10 \quad \text{and} \quad 1.68 \pm 0.12$$

are in good agreement with the average ratio (1.85) obtained recently (4) for butanone exchange in aqueous buffer ($HOAc/AcO^- = 0.726$) at 41.8°. The latter measurement came from mass spectrometric monitoring of the exchange process and provides support for the reliability of the n.m.r. method.

We have previously published two estimates of the reactivity ratio for acetate alone. In unbuffered, aqueous acetate the following average *observed* ratios, $k^H_{CH_2}/k^H_{CH_3}$, for exchange have been reported: 1.4 for 1 *M* acetate at 59.2° (5), 1.4 for 2.5–5.0 *M* acetate at 50° (6), and 1.05 for 0.5 *M* acetate at 30° (7). These ratios are composite values, however, because hydrolysis of acetate in unbuffered systems produces appreciable concentrations of HO^-, which has a much larger catalytic coefficient (by a factor greater than 10^5) than acetate. We used an extrapolation technique (5) to isolate the catalytic coefficients of acetate toward butanone and obtained the ratio $(k^H_{CH_2}/k^H_{CH_3})^{59.2°}_{AcO^-} = 2.16 \pm 0.36$. This number was checked by using buffer solutions (8) in which the buffer ratios ($HOAc/AcO^- = 0.0469$ and 0.0936) were low enough to leave acid-catalysis terms undetectable by n.m.r. That method gave 1.90 ± 0.17 at 54.8°.[3]

[1]Revision received October 8, 1971. Publication delayed at authors' request.

[2]All ratios cited in this paper are statistically corrected; *per hydrogen* (3).

[3]The temperature dependence of enolization rate ratios is not known quantitatively for any of the systems discussed

Can. J. Chem. Downloaded from www.nrcresearchpress.com by 210.87.254.40 on 09/05/12
For personal use only.

Although the present results are for 1:1 buffer ratios they are roughly comparable with the others since catalysis involving HOAc is unimportant compared to catalysis by AcO^-, not only in enolization of butanone (8) but also in enolization of methoxyacetone (9). It is noteworthy also that our ratios for buffer systems are not greatly different from some ratios reported for acid catalysis; 2.1 at 50° (6) and 1.9 at 40.2° (10). A small component from acetic acid catalysis would therefore not be expected to change the observed site selectivity appreciably.

Catalysis by a strong base, HO^-, does appear to involve a different selectivity. We reported (8) $(k^H_{CH_2}/k^H_{CH_3})^{54.8°}_{OD^-} = 0.86$, and somewhat larger values (1.1–1.2) for that ratio in the temperature range 0–32° (3, 5). Rappe reported 1.05 for 30° (7) and 0.91 for 40° (11) and calculated (2) the value 0.84 from our 59.2° data, in an effort to discredit the extrapolation technique (5) referred to above. The agreement between this calculated value and the measured values (above) is quite satisfactory, when the corrections for the different temperatures are made,[3] and tends to support, rather than to undermine, the extrapolation method.[4] The disagreement then, concerns the value of the rate ratio for enolization by acetate as the major basic catalyst. Although Rappe's observed ratios, 1.2–1.4 (2, 7), are a little smaller than ours, 1.4–1.9 (5, 8), or that of Bothner-By and Sun, 1.4 (6), all measurements pertaining to 50–59.2°, it is noteworthy that his own measurements indicate a still lower value for hydroxide catalysis in the same range of temperatures. As was already pointed out, the difference between *observed* rate ratios for an unbuffered acetate medium and one containing only HO^- must be a minimum value for the relative selectivities of the two bases, because data from unbuffered acetate systems are composite values of hydroxide and acetate catalysis. Rappe's data therefore are reasonably consistent with our claim that $k^H_{CH_2}/k^H_{CH_3}$ for acetate ion has nearly twice the value that it has for hydroxide in the neighborhood of 55° (5, 8).

In summary, the rate ratio reported here and used in the accompanying paper, for exchange of butanone in $HOAc/AcO^-$ buffers, is in good agreement with that obtained by a different method (4). It is also roughly the same as the rate ratio estimated for catalysis by AcO^- alone but greater than the rate ratio pertaining to catalysis by HO^-. Our findings are therefore more in harmony with those of Hine and coworkers (9), who reported that the selectivity in exchange of methoxyacetone is base dependent, than with those of Rappe (2). Exchange must involve catalyzed enolization, since a sample of pure butanone in D_2O (8), in a carefully cleaned, sealed n.m.r. tube is still not detectably exchanged after $2\frac{1}{2}$ years at room temperature.

Experimental

A buffer solution was prepared by adding anhydrous sodium acetate (0.832 g, 0.0101 mol) and acetic acid (twice distilled, 0.609 g, 0.0101 mol) to deuterium oxide (99.5 %D, 8.20 ml). To 0.82 ml of this solution in an n.m.r. tube was added 2-butanone (0.18 ml) from a calibrated pipette. Three samples in three tubes were prepared in this way, one of which was kept cold and was used for recording the initial p.m.r. spectrum. The others were sealed and were placed in a bath kept at 54.8 ± 0.04 °C. Concentrations in each tube, neglecting volume changes on mixing, were: acetic acid and sodium acetate, 0.832 *M*; 2-butanone, 2.00 *M*. The initial ratio of deuterium to exchangeable protium was about 8:1.

Exchange was followed to at least one half-life by integrating the signals from the α-protons in the p.m.r. spectrum, relative to that of the non-exchanging β-methyl group as internal standard. The CH_3 signal from the buffer components was sufficiently separated; it did not interfere with integration. Each analysis was the average of six integrations with a Varian A-60 instrument. Analyses were performed at different times by removing a tube from the bath, plunging it into ice water to reduce exchange rates to negligible levels, and transferring the cold tube to the instrument. Time outside the bath was not counted.

A second pair of samples, in which the buffer ratio was also 1:1 but the buffer concentration was 0.610 *M*, was treated in exactly the same way, except that analyses were done with a Varian T-60 instrument.

Observed rate constants were obtained from pseudo-first-order plots of $\log I_t$ against time, where I_t is the

---

here. Its small magnitude and the direction of change to be expected are illustrated for the case of hydroxide catalysis. The ratio, $(k^H_{CH_2}/k^H_{CH_3})_{OD^-}$, changes from about 0.86 at 54.8° to about 1.2 at 0°; an average increment less than 0.04 per 5°. Comparisons of data pertaining to different temperatures can therefore be drawn, as long as the difference in temperature is only 5–10°.

[4]Absolute values of rate constants from the extrapolation technique are likely to be in greater error than the ratios. A fortuitous equality of rate constants for acetate catalysis at 59.2 and 54.8° has been pointed out (2). That temperature difference should have meant rate factors near 1.6, for a given site, as estimated from activation parameters for enolization of acetone. The extrapolation method may well be at fault where actual rate constants, rather than their ratios, are concerned.

normalized integral of a given signal at time t. Straight lines were obtained, the slopes of which agreed with computer-fitted values to 3% or better. Rate constants and their standard deviations are: $k_{CH_3}^{obsd} = 6.85 \pm 0.16 \times 10^{-7}\ s^{-1}$; $k_{CH_2}^{obsd} = 11.64 \pm 0.44 \times 10^{-7}\ s^{-1}$ for buffer concentration 0.832 M; $k_{CH_3}^{obsd} = 4.10 \pm 0.13 \times 10^{-7}\ s^{-1}$; $k_{CH_2}^{obsd} = 6.89 \pm 0.28 \times 10^{-7}\ s^{-1}$ for buffer concentration 0.0610 M. Errors are indicative only of the quality of the fit to pseudo-first-order kinetics and of the probable reliability of rate ratios from a given run. Absolute values of rate constants are much less certain, being subject to errors in concentration and temperature that cancel out in the ratios. For the two runs described above, second order rate constants for a given site differ by roughly 20%.

This work was supported by a grant from the National Research Council of Canada. The Ontario Department of University Affairs provided assistance in the form of Ontario Graduate Fellowships to R.A.C. and J.W.T.

1. J. W. THORPE and J. WARKENTIN. Can. J. Chem. This issue.
2. C. RAPPE. Acta Chem. Scand. **23**, 2305 (1969).
3. J. WARKENTIN and C. BARNETT. J. Am. Chem. Soc. **90**, 4629 (1968).
4. J. JULLIEN and NGYUEN-THOI-LAI. Bull. Soc. Chim. Fr. 3948 (1970).
5. J. WARKENTIN and O. S. TEE. J. Am. Chem. Soc. **88**, 5540 (1966).
6. A. A. BOTHNER-BY and C. SUN. J. Org. Chem. **32**, 492 (1967).
7. C. RAPPE. Acta Chem. Scand. **20**, 2236 (1966).
8. J. WARKENTIN and R. A. COX. J. Org. Chem. **33**, 1301 (1968).
9. J. HINE, K. G. HAMPTON, and B. C. MENON. J. Am. Chem. Soc. **89**, 2664 (1967).
10. C. RAPPE and W. H. SACHS. J. Org. Chem. **32**, 3700 (1967).
11. C. RAPPE and W. H. SACHS. J. Org. Chem. **32**, 4127 (1967).

Can. J. Chem. Downloaded from www.nrcresearchpress.com by 210.87.254.40 on 09/05/12
For personal use only.

Effects of Bromine Substituents on Rates of Acetate-promoted Enolization of Ketones

R. A. Cox and J. Warkentin

Department of Chemistry, McMaster University, Hamilton, Ontario

Received November 25, 1971[1]

Effects of bromine substituents on rates of acetate-catalyzed bromination of ketones are reported. Approximate polar contributions to the rates were obtained, based on the approximation that the steric effects of bromine and methyl are identical. Such polar substituent effects are quite large at the α′-position of an α-bromo ketone, leading to the conclusion that the carbonyl group is much better than the methylene group in transmitting polar effects.

Rate enhancements caused by α-bromine substituents are largely entropic in origin and rates correlate well with ionization constants of α-bromo acids. These results are interpreted as indicative of an enolate-like transition state for acetate-catalyzed enolization.

Les effets des substituants brome sur les vitesses de bromation des cétones, catalysée par l'acétate, sont rapportés. Les contributions polaires approximatives aux vitesses sont obtenues, fondées sur l'approximation que les effets stériques du brome et du méthyle sont identiques. De tels effets polaires de substituants sont très accentués sur la position α′ d'une α-bromo cétone permettant de conclure que le groupe carbonyle est de deux fois environ aussi bon que le groupe méthylène, dans la transmission des effets polaires. Les accroissements de vitesse dûs aux substituants α bromés sont grandement d'origine entropique et les vitesses sont en relation avec les constantes d'ionisation des α-bromoacides. L'interprétation de ces résultats révèle un état de transition du type énolate dans l'énolisation catalysée par l'acétate.

[Traduit par le journal]

Canadian Journal of Chemistry, **50**, 3242 (1972)

Introduction

It has been known for a long time that most α-halo ketones are enolized more rapidly than simple ketones in the presence of base (1). In acetate-catalyzed iodination at 25°, chloroacetone and bromoacetone were reported to be 45.8 and 75.0 times as fast, respectively, as acetone (2) and acetate-catalyzed α-hydrogen exchange of chloroacetone at 41.8° was found to be about 580-fold faster than exchange of acetone (3). For the alkyl, aryl ketones $C_6H_5COCH_3$, $C_6H_5COCH_2Br$, and $C_6H_5COCHBr_2$, relative acetate-catalyzed bromination rates were reported to be 1:53:104 (4), statistically corrected. The success of the iodoform reaction (5) and of haloform reactions in general, has been attributed to fast halogenation of a first-formed halo ketone at the already-halogenated α-site (6–9).

Exceptions to the general rule are found in systems with sterically-hindered α-sites. For example, α-bromobenzyl phenyl ketones are brominated more slowly than the parent ketones in the presence of acetate (10) and 2-bromo-2,4-dimethyl-3-pentanone is less reactive toward hydroxide ion than 2,4-dimethyl-3-pentanone (11).

Greater reactivity of a halo ketone, relative to that of the parent ketone, was first attributed to an enhanced rate of enolization at the substituted α-site alone rather than to greater reactivity at both α-sites. This rationale was no doubt based on the findings that unsymmetrical halogenation of acetone in basic solutions is preferred (6), that the haloform reaction yields primarily halogen-free carboxylic acid (12, 13), and on the expectation that the carbonyl group would effectively insulate the remote α-position from the polar effect of α-halogen (14). Indications that both α-positions may have their reactivity enhanced came from the finding that α-halo acids are formed in haloform reactions (7, 8), albeit in low yield, and from measurements of hydrogen isotope exchange rates (3, 15). The latter work indicates that α-chlorine enhances acetate-promoted α′-enolization rates by factors ranging from about 4.4 (methyl-α-chlorobenzyl ketone) to 19 (chloroacetone), with the effect in α-chlorocyclohexanone intermediate at 5.1. In the case of α-fluorine substituents the rate enhancement is actually larger at the unsubstituted α-position. Fluoroacetone is exchanged about 3.5 times as

[1]Revision received May 31, 1972. Publication delayed at authors' request.

Can. J. Chem. Downloaded from www.nrcresearchpress.com by 210.87.254.42 on 09/05/12
For personal use only.

Can. J. Chem. Downloaded from www.nrcresearchpress.com by 210.87.254.42 on 09/05/12
For personal use only.

fast as acetone in aqueous acetate buffer but the CH_3 group is 5.2 times as reactive as the CH_2F group, statistically corrected (3, 15).

In this article we discuss quantitative estimates of the polar effect of α-bromine substituents on rates of acetate-catalyzed enolization of ketones. A correlation between rate constants in that reaction and acidity constants of carboxylic acids is also presented.

Methods

Brominations were carried out in homogeneous media consisting of aqueous acetic acid–acetate buffer (1:10; 1 *M* in AcO^-) and dioxane (5% v/v). Reactions were pseudo-first-order; acetate being present in large excess over Br_2. All rates reported are for reactions of zero order in Br_2; that is, the bromine concentration range always exceeded the limit, *ca.* 10^{-5} -10^{-6} *M*, below which ketone bromination becomes first order in bromine (16). The overall rate of bromine consumption could therefore be equated to the overall rate of enolization. In the buffer medium employed, most of that enolization must be effected by acetate ions since catalysis by HOAc is not detectable in 1:10 (HOAc:OAc^-) buffer (17).

Enolization was followed by measuring the concentration of bromine via the redox potential of the medium, as described elsewhere (18). The method is sensitive to impurities which consume bromine and hence all ketones were checked by g.l.p.c. and were purified by preparative g.l.p.c. The shapes of graphs of relative bromine concentrations against time and the methods and equations for extracting rate constants from such data are described elsewhere (18).

Results and Discussion

To separate polar effects from steric effects, advantage was taken of the approximately equal steric requirements of methyl and bromine substituents. The steric substituent parameters (E_s) and the Van der Waals radii of Br and CH_3 are essentially the same (19). Therefore any consequence of interchanging the two substituents should be primarily the result of the difference in their inductive effects.

Table 1 contains kinetic data for the bromination of three sets of ketones. In the first set, successive substitution of bromine for methyl groups keeps the substrates sterically equivalent and rate factors therefore give a measure of the polar effect of α-bromine on α-enolization and on α′-enolization. Rate factors are of the order 780 and 92 at the α- and α′-sites, respectively, taking the corrected (bracketed) value in the second row. The value 8.0×10^{-5} M^{-1} s^{-1} for 1-bromo-2-butanone is the observed rate constant adjusted for a statistical factor of two. It is a crude value of the CH_2Br reactivity, based on the assumption that reaction at CH_3 can be neglected. The bracketed value includes a correction (see footnote to Table 1) for CH_3 reactivity.

The second set of ketones provides another measure of the α- and α′-effects. Again the effect of α-bromine is to enhance α′-reactivity by a factor near 10^3. A steric effect is introduced in going from $CH_3COC(CH_3)_3$ to $BrCH_2COC(CH_3)_3$ but that factor is known to be small compared to 10^3 (20). The second and third entries of set 2 are sterically equivalent and

TABLE 1. Rates of acetate-catalyzed enolization of ketones at 30°

Ketone	k^H (M^{-1} s^{-1})[a]	$\Delta\Delta G^*$ (kcal mol^{-1})[b]
$CH_3CH_2COCH_2CH_3$	9.4×10^{-8}	0.0
$CH_3CH_2COCH_2Br$	$8.0(7.3) \times 10^{-5}$[c]	4.1
$BrCH_2COCH_2Br$	6.7×10^{-3}	2.6
$(CH_3)_3CCOCH_3$	6.3×10^{-8}	0.0
$(CH_3)_3CCOCH_2Br$	5.8×10^{-5}	4.1
$(CH_3)_2CBrCOCH_2Br$	2.7×10^{-3}	2.3
$CH_3COC(CH_3)_3$	6.3×10^{-8}	0.0
$CH_3COCBr(CH_3)_2$	7.0×10^{-6}	2.8
$CH_3COCBr_2CH_3$	7.6×10^{-5}	1.5
CH_3COCBr_3	1.9×10^{-4}	0.5

[a]Statistically corrected. The statistical factors by which observed rate constants were divided are (starting with the top row): 4, 2, 4, 3, 2, 2, 3, 3, 3, and 3.

[b]In each set the difference between ΔG^* for that ketone and the one immediately above it, except in case of the first member of a set, which is taken as the reference compound for that set. The numbers are therefore increments in ΔG^* at 30° caused by the change in substituents. Values of ΔG^* were calculated from the equation

$$\ln k_{rate} = \ln \frac{kT}{h} - \frac{\Delta G^*}{RT}$$

[c]Based on the assumption that all enolization occurred at the CH_2Br group. The number in parentheses is the calculated CH_2Br reactivity obtained by correcting the observed rate for reaction at the other methylene group. The estimated rate for that group is 7.0×10^{-6} M^{-1}, s^{-1}, obtained by subtracting 2.6 kcal mol^{-1} from ΔG^* (observed). The equation $8.0 \times 10^{-5} = k^H_{CH_2Br} + k^H_{CH_2CH_3}$ was then applied.

Can. J. Chem. Downloaded from www.nrcresearchpress.com by 210.87.254.42 on 09/05/12
For personal use only.

again show that the effect of α-Br is also substantial (47-fold) on α′-reactivity.

In the third set of ketones the effects of one, two, and three α-bromines on α′-enolization rates of sterically-equivalent compounds are indicated. One bromine increases reactivity at the other α-site by the factor 111, compared to 92 and 47 in sets 1 and 2, respectively. A second and third bromine cause the much smaller factors 10.9 and 2.5, respectively, showing that the α-effects are far from cumulative.

The most striking result is that the polar effect of bromine is transmitted so well through the carbonyl group. The factor by which CH_2 groups attenuate inductive effects is about 2.8 per group intervening between the dipole and the carbon atom of interest (21). Therefore α′-substituents of halo ketones, which are insulated from the effect of α-halogen by two carbons, should see that effect attenuated by the factor 7.8 (*i.e.* 2.8^2). From the data of Table 1 we can calculate the actual insulating factor applicable to α′-substituents. It is given by $\log (k^{\alpha}_{Br}/k^{\alpha}_{H})/\log k^{\alpha'}_{Br}/k^{\alpha'}_{H}$, in which the ratio in the numerator is that for α-enolizations, with and without α-Br, while that in the denominator compares α′-enolizations, with and without α-Br. An equivalent expression is $\Delta\Delta G^{\ddagger}_{\alpha}/\Delta\Delta G^{\ddagger}_{\alpha'}$. The numerator is about 4.1 kcal mol^{-1} and the denominator is 2.8 or 2.3 kcal mol^{-1}, depending on the set of ketones chosen (Table 1). Thus we estimate the attenuation factor for α′-substituents to be only 1.3–1.8 compared to 7.8 calculated for two CH_2 groups. An attenuation factor below 2.8 indicates that the reactions from which that number was derived (21) are not perfect models for the systems in question here, in which the insulating group contains π-electrons.[2] Nevertheless, although we cannot assign a number to the CO component of the CH_2CO group, the small composite attenuation factor indicates that the carbonyl group is a very good transmitter of polar effects.

Although the effects of α- and α′-bromine are roughly additive (compare third, sixth, and eighth entries in $\Delta\Delta G^{\ddagger}$ column of Table 1) it is clear that the second and third halogens at a given α-site are much less effective than the first. Such lack of additivity is not new; it shows up also in the ionization constants of α-bromocarboxylic acids. In fact there is a good correlation between the pK_a values of some model acids, chosen because their pK_a values are known (22), and acetate-catalyzed enolization rate constants of corresponding bromo ketones (Fig. 1). The correlation coefficient is −0.995 and the slope of the line is -0.87 ± 0.02. This correlation suggests that the transition state for enolization is enolate-like although the extent to which negative charge is developed cannot be inferred from the slope. In a series of phenyl benzyl ketones the fractional charge developed in the ketone moiety at the transition state for acetate-catalyzed enolization was estimated to be 64% (23).

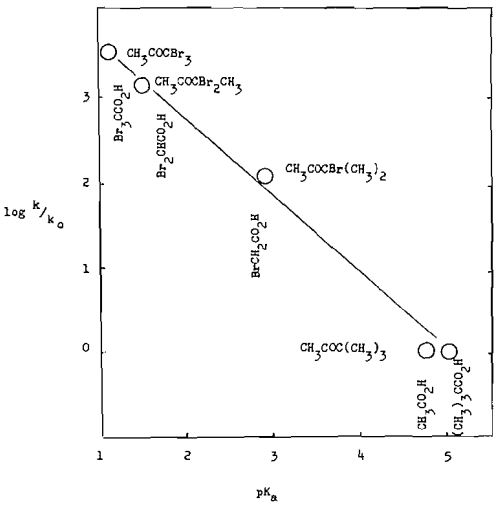

FIG. 1. Correlation of $\Delta G^{\ddagger}$ for enolization with ΔG^{0} for ionization.

Activation parameters found for acetone and bromoacetones (Table 2) are in keeping with an enolate-like transition state. For reaction at room temperature over half of the substituent effect of bromines is entropic. A likely way in which bromines increase the activation entropy is through their effect on solvation. A bromo enolate must be less solvation-dependent than an unsubstituted enolate because it can partly disperse charge internally into the polar C—Br bond. Consequently, for a given degree of charge development in an enolate-like transition state, bromine substituents should decrease the extent of solvent electrostriction.

[2]The minimum factor for the insulating unit $CH_2C{=}O$, assuming that CO transmits perfectly (attenuation of CO = 1), would be 2.8 × 1.

TABLE 2. Activation parameters of acetate-catalyzed enolization of acetone and bromoacetones

Ketone	CH_3COCH_3	CH_3COCH_2Br	$CH_3COCHBr_2$
k^H, [a] 20°	2.0×10^{-8}	9.1×10^{-5}	1.7×10^{-3}
25°	4.0×10^{-8}		
30°	7.4×10^{-8}	3.3×10^{-4}	5.1×10^{-3}
35°	1.3×10^{-7}		
40°	2.4×10^{-7}	8.3×10^{-4}	1.5×10^{-2}
ΔH^* (kcal mol^{-1})[b]	22.0 ± 0.3	19.6 ± 0.7	19.3 ± 0.4
ΔS^* (e.u.)[b]	-18.5 ± 0.6	-10.0 ± 2.0	-5.4 ± 1.0

[a]Statistically corrected second order rate constants (M^{-1} s^{-1}).
[b]From the equation $\ln k_{rate}/T = \ln k/h - \Delta H^*/RT + \Delta S^*/R$. Errors in the activation parameters came from root-mean-square errors in the slope and intercept of a computer-fitted line.

The charge in the ketone moiety at the transition state need not be increased by Br-substituents, for the more acidic α-bromo ketones must have more reactant-like transition states than the parent ketones (24).

A rationale for the non-cumulative effects of Br-substituents on either pK_a values or enolization rates is based on conformational preferences. An α-halo carboxylate ion (**1**)

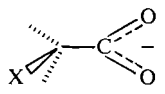

1

probably has a preferred conformation in which the C—X dipole is perpendicular to the carboxylate plane, as drawn. Such an arrangement should lead to the minimum dipole–ion repulsions. A second halogen cannot also adopt that arrangement and consequently the net inductive withdrawing effect per halogen would be reduced through a repulsive ion–dipole interaction. The argument for an enolate-like transition state is strictly analogous.

There is one problem with regard to the enolate-like transition state for catalysis of enolization by a weak base like acetate. 2-Butanone enolizes more slowly than acetone but its reactivity per hydrogen is higher at the methylene than at the methyl group (17, 25). One way of accounting for this is to postulate predominant steric retardation with a small polar rate enhancement at CH_2 superimposed. For an enolate-like transition state that effect would have to be one of electron-withdrawal, contrary to the effect of para CH_3 on benzoic acid acidity. Because of this problem we suggested (20) that the transition state might be enol-like, at least for the more highly endothermic enolizations involving weak bases. However, this concerted mechanism, originally postulated by Swain (26) to account for a termolecular term in the kinetics of enolization of acetone (27, 28) has little support as a general mechanism, although it may be important in carboxylic acid–carboxylate anion catalyst systems (29). Moreover, Brönsted correlations (30) indicate that the transition state for enolization of acetone by weak bases is highly enolate-like ($\beta \simeq 0.8$). Our present results are more readily rationalized in terms of transition states with enolate character but do not clarify the anomalous methylene reactivity of 2-butanone toward weak bases.

It should be emphasized, in summary, that it is probably unsafe to extrapolate the reactivity trends reported here. Although the effects of I, Br, and Cl may be qualitatively the same, fluorine- (16, 31) and methoxy-substituted (32) ketones do not fit expectations based on the inductive effects of those substituents. It has been suggested (33) that polarizability of the substituent may be a controlling factor. Furthermore the quantitative relationships between α- and α′-reactivity are no doubt functions not only of the base and the substituent but also of the medium and the temperature.

Experimental

Purification of Bromoketones

The general procedure involved rapid distillation, at reduced pressure, of a CCl_4 extract of the crude bromo ketone mixture obtained from the appropriate synthesis

Can. J. Chem. Downloaded from www.nrcresearchpress.com by 210.87.254.42 on 09/05/12
For personal use only.

Can. J. Chem. Downloaded from www.nrcresearchpress.com by 210.87.254.42 on 09/05/12
For personal use only.

(see below). The fraction shown (by n.m.r.) to contain most of the desired product was stabilized by addition of magnesium oxide, which removes traces of HBr, before it was subjected to preparative g.l.p.c. 1,1,1-Tribromoacetone was partly isomerized to 1,1,3-tribromoacetone on distillation. Consequently it was isolated by g.l.p.c. of the crude CCl_4 extract directly.

Preparative g.l.p.c. was done with a 10 ft × 3/8 in. silicone QF-1 column (10%, on 60/80 mesh, non-acid-washed, Chromosorb W) in a Varian Aerograph A90-P3 instrument. The column was operated at 110–130° with helium flow rates between 50 and 100 ml/min. Compounds collected from the column were rechromatographed at least once or until they appeared to be homogeneous on three different analytical columns (10 ft × 1/8 in. QF-1, 12%; 5 ft × 1/8 in. FFAP, 10%; and 10 ft × 1/8 in. SE-30, 20%; all on 60/80 mesh Chromosorb W) and showed only the expected n.m.r. signals. Such samples were water-white and stable when stored at about −10°, without added MgO.

N.m.r. spectra were recorded on a Varian T-60 instrument.

Bromoacetone

The method of Catch and coworkers (34), in which acetone is brominated in the presence of potassium chlorate, was used. The crude product contained chloroacetone, presumably from substitution on bromoacetone by chloride generated from chlorate, and 1,1-dibromoacetone. Purification by g.l.p.c., as described above, gave bromoacetone: n_D^{25} 1.4680 (lit. (35), n_D^{25} 1.4739, (33), n_D^{15} 1.4697); n.m.r. (CCl_4) δ 2.30 (s, 3, CH_3), 3.78 (s, 2, CH_2).

1,1-Dibromoacetone

1,1-Dibromoacetone was obtained as a byproduct from the synthesis of bromoacetone (above) and from the preparation of 1,1,1-tribromoacetone (below). Pure material (g.l.p.c.) had n_D^{25} 1.5232 (lit. (35) n_D^{25} 1.5237); d_4^{23} 2.063; n.m.r. (CCl_4) δ 2.51 (s, 3, CH_3), 5.67 (s, 1, CH).

1,1,1-Tribromoacetone

1,1-Dibromoacetone (2.81 g, 0.013 mol) and *N*-bromosuccinimide (NBS) (2.32 g, 0.013 mol) were refluxed in CCl_4 (14 ml) under illumination from a 75 W tungsten spot lamp. After 12 h, the yield was 91%, estimated by n.m.r. Chromatography as described above gave pure tribromoacetone: n_D^{25} 1.5708 (lit. (35) n_D^{25} 1.5689); d_4^{20} 2.334; n.m.r. (CCl_4) δ 2.76 (s, CH_3).

1,1-Dibromoacetone was also prepared from NBS and acetone and by bromination of acetone with Br_2 in glacial acetic acid containing sodium acetate. These procedures were less satisfactory in our hands and are therefore not described in detail.

1,3-Dibromoacetone and 1,3-Dibromo-3-methyl-2-butanone

These compounds were prepared by the method of Wagner and Moore (36). The appropriate ketone (0.5 mol) in a 250 ml, three-necked flask fitted with gas inlet tube, magnetic stirrer, pressure-equalizing dropping funnel, and a reflux condenser was cooled with ice while bromine (53 ml, 1 mol) was added gradually from the funnel. Reaction was initiated with the light from a tungsten lamp when a few drops of Br_2 had been added; the rest of the Br_2 was then dropped in over a period of 2 h. When addition was complete nitrogen was bubbled through the solution overnight to sweep out HBr. The product was distilled from the flask at low pressure and chromatographed as described. From acetone was obtained 1,3-dibromoacetone: m.p. 28–28.5°; b.p. 80°, (lit. (35) m.p. 25.5–27.0°, b.p. 79.5–80.5 (9 mm)); n.m.r. (CCl_4) δ 4.10 (s, CH_2). Methyl isopropyl ketone gave 1,3-dibromo-3-methyl-2-butanone: m.p. 13–14°; b.p. 68–72° (3 mm); n_D^{25} 1.5154 (lit. (36) m.p. 10–12°, b.p. 111° (15 mm), n_D^{25} 1.5178); n.m.r. (CCl_4) δ 1.94 (s, 6, CH_3), 4.31 (s, 2, CH_2).

1-Bromo-2-butanone

1-Diazo-2-butanone was treated with HBr according to the procedure of Catch and coworkers (37) to afford the title compound: b.p. 44–45° (10 mm); n_D^{25} 1.4670 (lit. (34) b.p. 49° (10 mm), lit. (37) n_D^{20} 1.4670); n.m.r. (CCl_4) δ 1.08 (t, 3, $J = 7$ Hz, CH_3), 2.64 (q, 2, $J = 7$ Hz, CH_3CH_2), 3.76 (s, 2, $BrCH_2$).

3-Bromo-3-methyl-2-butanone

This ketone was synthesized from methyl isopropyl ketone by the method of Catch and coworkers (38) and was purified by g.l.p.c.: n_D^{25} 1.4554, (lit. (39) n_D^{25} 1.4510); d_4^{20} 1.334; n.m.r. (CCl_4) δ 1.80 (s, 6, $(CH_3)_2C$), 2.36 (s, 3, CH_3CO).

3,3-Dibromo-2-butanone

2-Butanone (7.2 g, 0.1 mol) and NBS (35.6 g, 0.2 mol) were refluxed in CCl_4 (150 ml) under illumination from a 75 W tungsten spot lamp (39). After $1\frac{1}{2}$ h the reaction was complete and the yield (n.m.r.) of the title compound was about 95%. Distillation followed by preparative g.l.p.c. gave pure 3,3-dibromo-2-butanone: n_D^{25} 1.5053 (lit. (39) n_D^{25} 1.5050); d_4^{22} 1.827; n.m.r. (CCl_4) δ 2.50 (s, CH_3CO), 2.67 (s, 3, CH_3CBr_2).

1-Bromo-3,3-dimethyl-2-butanone (Bromopinacolone)

Pinacolone (10.02 g, 0.1 mol) and NBS (17.8 g, 0.1 mol) in CCl_4 (100 ml) were heated and irradiated with the light from a 75 W tungsten spot lamp. After 24 h of refluxing, the solution contained pinacolone (70%), bromopinacolone (15%), and dibromopinacolones (15%), as estimated by n.m.r. The mixture was cooled with ice, the insoluble solids were filtered off, and the solution was concentrated on a rotary evaporator. Distillation gave a fraction boiling at 55–60° (4 mm) which contained at least 50% 1-bromo-3,3-dimethyl-2-butanone (n.m.r.) along with $(CH_3)_3CCOCHBr_2$, $BrCH_2(CH_3)_2CCOCH_3$, and $BrCH_2(CH_3)_2CCOCH_2Br$. The desired ketone was purified by g.l.p.c. as described above: n_D^{25} 1.4630 (lit. (40) n_D^{25} 1.4659, (41) n_D^{20} 1.4640); n.m.r. (CCl_4) δ 1.21 (s, 9, $(CH_3)_3C$), 4.01 (s, 2, $BrCH_2$).

Other Ketones

Acetone, butanone, and 3-pentanone were commercial, reagent-grade materials distilled in a 20 × 2 cm glass still packed with 3 mm single-turn glass helices. Center cuts showed only the expected n.m.r. signals and only a single peak on analytical g.l.p.c. columns.

Pinacolone (Aldrich, reagent grade) was purified by preparative g.l.p.c., as described above for bromo ketones. The product used was homogeneous on three analytical g.l.p.c. columns and there were no impurities detectable by n.m.r.

Procedure

The apparatus and the procedure are described elsewhere (18).

We are grateful to the National Research Council of Canada for financial support and to Mr. J. W. Thorpe for samples of some of the bromo ketones. One of us (R.A.C.) was the grateful recipient of an Ontario Graduate Fellowship.

1. R. P. BELL and O. M. LIDWELL. Proc. Roy. Soc. Ser. A, **176**, 88 (1940).
2. R. P. BELL, G. R. HILLIER, J. W. MANSFIELD, and D. G. STREET. J. Chem. Soc. B, 827 (1967), and refs. cited therein.
3. J. JULLIEN and T-L. NGUYEN. Bull. Soc. Chim. Fr. 4669 (1968).
4. E. S. LEWIS, J. D. ALLEN, and E. T. WALLICK. J. Org. Chem. **34**, 255 (1969).
5. K. J. MORGAN, J. BARDWELL, and C. F. CULLIS. J. Chem. Soc. 3190 (1950).
6. P. D. BARTLETT. J. Am. Chem. Soc. **56**, 967 (1934).
7. C. F. CULLIS and M. H. HASHMI. J. Chem. Soc. 2512 (1956).
8. C. F. CULLIS and M. H. HASHMI. J. Chem. Soc. 1548 (1957).
9. P. SYKES. A guidebook to mechanism in organic chemistry. Longmans, Green and Co., Ltd., London. 1961. pp. 204–207.
10. A. FISCHER, J. PACKER, and J. VAUGHAN. J. Chem. Soc. 226 (1963).
11. J. R. HULETT. J. Chem. Soc. 430 (1965).
12. J. L. SIMONSEN. J. Chem. Soc. **121**, 2292 (1922).
13. F. W. SEMMLER and H. VON SCHILLER. Chem. Ber. **60**, 1591 (1927).
14. J. A. FEATHER and V. GOLD. J. Chem. Soc. 1752 (1965).
15. J. JULLIEN and T-L. NGUYEN. Bull. Soc. Chim. Fr. 3948 (1970).
16. K. YATES and W. V. WRIGHT. Can. J. Chem. **41**, 2882 (1963).
17. J. WARKENTIN and R. A. COX. J. Org. Chem. **33**, 1301 (1968).
18. R. A. COX and J. WARKENTIN. Can. J. Chem. This issue.
19. R. W. TAFT, JR. Steric effects in organic chemistry. M. S. Newman, Editor. John Wiley and Sons, Inc., New York, N.Y. 1956. p. 601.
20. J. WARKENTIN and C. BARNETT. J. Am. Chem. Soc. **90**, 4629 (1968).
21. R. W. TAFT, JR. Steric effects in organic chemistry, M. S. Newman, Editor. John Wiley and Sons, Inc., New York, N.Y. 1956. p. 592 and refs. cited therein.
22. J. E. LEFFLER and E. GRUNWALD. Rates and equilibria of organic reactions. John Wiley and Sons, Inc., New York, N.Y. 1963. p. 372.
23. J. F. GRUNWELL. Ph.D. Thesis. Massachusetts Institute of Technology, Boston, Mass., 1968.
24. G. S. HAMMOND. J. Am. Chem. Soc. **77**, 334 (1955).
25. R. A. COX, J. W. THORPE, and J. WARKENTIN. Can. J. Chem. This issue.
26. C. G. SWAIN. J. Am. Chem. Soc. **72**, 4578 (1950).
27. H. M. DAWSON and E. SPIVEY. J. Chem. Soc. 2180 (1930).
28. R. P. BELL and P. JONES. J. Chem. Soc. 88 (1953).
29. C. G. SWAIN, A. J. DIMILO, and J. P. CORDNER. J. Am. Chem. Soc. **80**, 5983 (1958).
30. C. G. SWAIN and A. S. ROSENBERG. J. Am. Chem. Soc. **83**, 2154 (1961).
31. J. CANTACUZÈNE, M. ATLANI, and J. ANIBIE. Tetrahedron Lett. 2335 (1968).
32. J. HINE, K. G. HAMPTON, and B. C. MENON. J. Am. Chem. Soc. **89**, 2664 (1967).
33. M. CHEVALLIER, J. JULLIEN, and T-L. NGUYEN. Bull. Soc. Chim. Fr. 3332 (1969).
34. J. R. CATCH, D. F. ELLIOTT, D. H. HEY, and E. R. H. JONES. J. Chem. Soc. 272 (1948).
35. C. RAPPE. Arkiv Kemi, **21**, 503 (1963).
36. R. B. WAGNER and J. A. MOORE. J. Am. Chem. Soc. **72**, 974 (1950).
37. J. R. CATCH, D. F. ELLIOTT, D. H. HEY, and E. R. H. JONES. J. Chem. Soc. 278 (1948).
38. J. R. CATCH, D. H. HEY, E. R. H. JONES, and W. WILSON. J. Chem. Soc. 276 (1948).
39. C. RAPPE and R. KUMAR. Arkiv Kemi, **23**, 475 (1965).
40. J. H. BOYER and D. STRAW. J. Am. Chem. Soc. **74**, 4506 (1952).
41. V. WOLF and H. PIATER. Ann. Chem. **696**, 90 (1966).

Can. J. Chem. Downloaded from www.nrcresearchpress.com by 210.87.254.42 on 09/05/12
For personal use only.

Oxidation of Semicarbazones of Ketones. Improved Synthesis of Δ^3-1,3,4-Oxadiazolin-2-ones

P. KNITTEL, S. L. LEE, AND J. WARKENTIN

Department of Chemistry, McMaster University, Hamilton, Ontario

Received May 31, 1972

Oxidation of readily-available semicarbazones of ketones with lead tetraacetate, followed by hydrolysis (*in situ*) of the products, makes novel Δ^3-1,3,4-oxadiazolin-2-ones easily accessible. Spectra of the compounds are discussed and some of their potential for synthesis is indicated.

L'oxydation des semicarbazones de cétones, facilement disponibles, par le tétracétate de plomb suivie de l'hydrolyse (*in situ*) des produits constitue une voie d'accès simple et nouvelle aux Δ-3 oxadiazoline-1,3,4 ones-2. Les spectres des composés sont discutés et quelques unes de leurs utilisations potentielles en synthèse sont indiquées. [Traduit par le journal]

Canadian Journal of Chemistry, **50**, 3248 (1972)

Can. J. Chem. Downloaded from www.nrcresearchpress.com by 210.87.254.5 on 09/05/12
For personal use only.

Oxidation of carbonyl derivatives of aldehydes and ketones has been studied extensively and includes, among a variety of pathways, a useful route to heterocyclic compounds (1). Aldehyde semicarbazones are cyclized to 2-amino-1,3,4-oxadiazoles (**1**) (2), possibly via 2-imino-Δ^3-1,3,4-oxadiazolines (**2***a*) which are isomerized under the reaction conditions. 4-Substituted ketone semicarbazones can be cyclized (3) to oxadiazolines **2***b*, some of which have been hydrolyzed (4) to the corresponding Δ^3-1,3,4-oxadiazolin-2-ones (**3**).

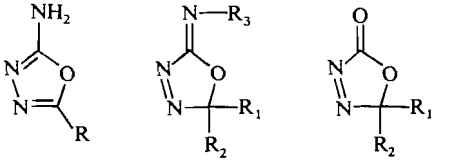

1 **2** **3**

2*a* $R_1 = R_3 = H$; R_2 = alkyl or aryl
2*b* $R_1 = R_2 = R_3$ = alkyl or aryl
2*c* $R_1 = R_2$ = alkyl or aryl; $R_3 = H$

There are no reports in the literature of oxidation of unsubstituted semicarbazones of ketones to 2-imino-Δ^3-1,3,4-oxadiazolines (**2***c*), possibly because such compounds are themselves sensitive to oxidants or because they are easily hydrolyzed. In this paper we report a convenient synthesis of oxadiazolinones **3** by oxidative cyclization of ketone semicarbazones with lead tetraacetate, followed by hydrolysis, *in situ*, of the presumed intermediates, **2***c*.

Discussion

Table 1 lists spectra and physical properties of five new oxadiazolinones. 5,5-Dimethyl-Δ^3-1,3,4-oxadiazolin-2-one, which was prepared earlier by an analogous but longer route (4), was also synthesized from its semicarbazone by the simpler method in 67% yield.

Yields of crude products were near 60% in all cases; those of analytically-pure products were typically near 40%. Considering the ease with which many semicarbazones can be prepared and the simplicity of the present procedure (see Experimental), it is evident that many oxadiazolinones **3** are now within easy reach.

Oxadiazolinones **3** are α,β-unsaturated-α,β-diaza-γ-lactones which may be compared to their carbon analogs, α,β-unsaturated-γ-lactones. A striking effect of the azo function is to raise the carbonyl stretching frequency of the lactone function. Thus, whereas α,β-unsaturated-γ-lactones absorb near 1750 cm^{-1}, oxadiazolinones **3** absorb near 1835 cm^{-1}. The azo substituent probably exerts its influence both directly at the carbonyl carbon, where sp^2 nitrogen acts inductively somewhat like a halogen atom, and indirectly at the γ-carbon, which transmits an inductive effect to the ether oxygen. An electronegative γ-substituent in a γ-lactone is known to raise ν_{CO} substantially; from about 1770 cm^{-1} in γ-valerolactone to 1797 cm^{-1} in γ-acetoxy-γ-valerolactone (5). Compounds **3**, like γ-lactones in general (5), do not change carbonyl frequency appreciably as a result of the

TABLE 1. 5,5-Disubstituted-Δ^3-1,3,4-oxadiazolin-2-ones (3)

Compound	M.p. or N_D^{25} (Purification)*	I.r. (cm^{-1})†	U.v. (λ_{max}, nm; ε)‡	N.m.r. (δ)§	Analysis‖ C	H	N
$R_1 = R_2 = (CH_2)_5$	59–60° (s, 10^{-2})	1826 1540	215(3501) 362(286) 375(320)	1.85, m	54.54 54.71	6.54 6.64	18.17 18.18
$R_1 = R_2 = (CH_2)_4$	1.4754 (d, 40°, 10^{-2})	1840 1538	223(3608) 360(287) 364(318) 370(369) 377(246)	2.10, m	51.42 51.61	5.75 5.84	19.99 20.19
$R_1 = CH_3$; $R_2 = (CH_3)_2CH$	1.4345 (d, 42°, 10^{-1})	1836 1542	219(3128) 369(275) 376(303) 382(190)	0.99, d, 3 1.12, d, 3 1.64, s, 3 2.34, m, 1	50.69 50.71	7.09 7.04	19.71 19.86
$R_1 = CH_3$; $R_2 = CH_2CH_2CH_3$	1.4327 (d, 40°, 10^{-2})	1835 1544	216(2940) 367(247) 374(276) 381(167)	1.08, m, 5 1.73, s, 3 2.20, m, 2	50.69 50.72	7.09 6.83	19.71 19.31
$R_1 = CH_3$; $R_2 = C_6H_5CH_2$	49–50° (s, 10^{-2})	1831 1539	206(9489) 210(9050) 365(241) 373(252) 379(176)	1.66, s, 3 3.32, s, 2 7.51, m, 5	63.15 63.27	5.30 5.35	14.73 14.97

*For solids at room temperature the m.p. is given. For an oil the refractive index at 25° is tabulated instead. Purification procedure is abbreviated as follows: s = sublimation at ambient temperature and at the pressure indicated (Torr), d = bulb-to-bulb distillation at the pot temperature and the pressure indicated, with the receiver in liquid N_2.

†Solutions in CCl_4.

‡In hexane. The $n \rightarrow \pi^*$ band shows fine structure in this solvent; individual maxima of that band are tabulated. In ethanol the first compound listed has $\lambda_{max} = 227$ (3521) and 368 nm (255), the latter band without fine structure.

§CCl_4, internal TMS. Chirality of the unsymmetrically-substituted members complicates some of the spectra. The third compound listed, for example, has magnetically non-equivalent methyls in the isopropyl substituent. Abbreviations are d = doublet, m = multiplet, s = singlet, and numbers following such symbols are relative integrals.

‖Calculated figures in the upper rows; analytical results in the lower rows.

extra rigidity imposed by spirocyclic geometry (Table 1).

A band near 1540 cm^{-1} is present in the i.r. spectra of all the oxadiazolinones (Table 1). This band is strong except in the spectrum of the benzyl-substituted member (last row), where it is of medium intensity. The most likely source of this band is the N=N stretching mode of the *cis*-azo function; high intensity being the result of the unsymmetric substitution of that group. Azo stretching bands, although weak or altogether absent in highly symmetric azo compounds, are reported to be near 1575 cm^{-1} (6) in general, and five-membered cyclic models, the 3-acetoxy-1-pyrazolines, have the N=N band at 1565 cm^{-1} (7).

U.v. spectra of oxadiazolinones **3** consist of a $\pi \rightarrow \pi^*$ band (λ_{max} near 217 nm) of medium intensity and a $n \rightarrow \pi^*$ band (λ_{max} near 370 nm) of low intensity (Table 1). The former is red-shifted if the solvent is changed from hexane to ethanol, as is common for $\pi \rightarrow \pi^*$ bands (8). The latter is also slightly red-shifted, from about 362 nm in hexane to about 368 nm in ethanol, in the case of the cyclohexanespiro compound. In contrast $n \rightarrow \pi^*$ bands of ketones are blue-shifted if solvent polarity is increased; a consequence of the decreased polarity of the excited state relative to that of the ground state (8). A red shift must therefore be indicative of greater excited state polarity and in the present case indicates that the 370 nm band arises from excitation of the n-electrons from nitrogen rather than of the n-electrons from the carbonyl oxygen.

Chemical properties of oxadiazolinones **3** indicate some potential as reagents in synthesis. Their thermal decomposition, in either polar or

Can. J. Chem. Downloaded from www.nrcresearchpress.com by 210.87.254.5 on 09/05/12
For personal use only.

non-polar solvents (9), to CO_2 and disubstituted diazomethanes makes them convenient sources of the latter, which can be caused to react *in situ* with a substrate. Esters, ethers, and cyclopropanes, for example, can be prepared by heating oxadiazolinones with carboxylic acids, phenols, or olefins, respectively. Another advantage of generating diazomethanes this way, rather than by a base-catalyzed oxidation of hydrazones with mercuric oxide or silver oxide (10), is the absence of metallic impurities (Hg or Ag) which strongly catalyze decomposition (10). Hydrazones are not very convenient starting materials in any case because, although they are not particularly difficult to prepare (10–12), they are prone to disproportionation (10, 12) during storage or distillation.

The utility of oxadiazolinones **3** as reagents for synthesis is under investigation and details will be published separately.

Experimental

I.r. spectra were taken with a Perkin–Elmer Model 521 instrument, using solutions (CCl_4) in 0.1 mm cells. U.v. and p.m.r. spectra were obtained with Cary Model 14 and Varian Associates Model T60 instruments, respectively. A typical synthesis is described in detail below.

Cyclohexanespiro-5′(Δ³-1′,3′,4′-Oxadiazolin-2′-one)[1]

To cyclohexanone semicarbazone (5.0 g, 0.033 mol) in 300 ml of well-stirred, ice-cooled CH_2Cl_2, with nitrogen (L-Grade) bubbling through, was added 30 g (0.068 mol) of $Pb(OAc)_4$. After 30 min, ice water (300 ml) was added followed by 2.4 *M* HCl (20 ml). The mixture, still in the ice bath, was stirred for 20 min more. After a heavy brown sludge was removed by filtering the entire mixture through a bed of Celite, the organic layer was separated, washed twice with ice water (200 ml), and dried over magnesium sulfate. Removal of the solvent with a rotary evaporator left 2.8 g (56%) of solid, crude product. Recrystallization from petroleum ether (40–60°) followed by sublimation at ambient temperature and 10^{-2} Torr gave analytically pure material (1.86 g, 38%) melting at 59–60°.

[1]Nomenclature of this compound is according to IUPAC Rule B-11 in Nomenclature of Organic Chemistry, Sections A and B. 2nd ed. 1966.

This work was supported by the National Research Council of Canada.

1. Recent reviews of the literature: (*a*) R. N. BUTLER. Chem. Ind. 437 (1968); (*b*) J. WARKENTIN. Synth. 279 (1970).
2. (*a*) G. VALENTI and F. MAGGIO. Ann. Chim. (Rome), **42**, 18 (1952); (*b*) F. MAGGIO, G. WERBER, and G. LOMBARDO. Ann. Chim. (Rome), **50**, 491 (1960); (*c*) M. S. GIBSON. Tetrahedron, **18**, 1377 (1962); (*d*) H. GEHLEN and K. MÖCKEL. Ann. Chem. **651**, 133 (1962); (*e*) T. M. LAMBE, R. N. BUTLER, and F. L. SCOTT. Chem. Ind. 996 (1971).
3. A. M. CAMERON, P. R. WEST, and J. WARKENTIN. J. Org. Chem. **34**, 3230 (1969).
4. S. L. LEE, G. B. GUBELT, A. M. CAMERON, and J. WARKENTIN. Chem. Commun. 1074 (1970).
5. L. J. BELLAMY. The infrared spectra of complex molecules. Methuen and Co. Ltd., London. 1960. Chapt. 11.
6. D. H. WILLIAMS and I. FLEMING. Spectroscopic methods in organic chemistry. McGraw-Hill Publishing Co. Ltd., Berkshire, England. 1966. p. 65.
7. J. P. FREEMAN. J. Org. Chem. **29**, 1379 (1964).
8. D. H. WILLIAMS and I. FLEMING. Spectroscopic methods in organic chemistry. McGraw-Hill Publishing Co. Ltd., Berkshire, England. 1966. p. 12.
9. S. L. LEE, A. M. CAMERON, and J. WARKENTIN. Can. J. Chem. **50**, 2326 (1972).
10. A. C. DAY, P. RAYMOND, R. M. SOUTHAM, and M. C. WHITING. J. Chem. Soc. C, 467 (1966).
11. D. H. R. BARTON, R. E. O'BRIEN, and S. STERNHELL. J. Chem. Soc. 470 (1962).
12. G. R. NEWKOME and D. L. FISHEL. J. Org. Chem. **31**, 677 (1966).

Can. J. Chem. Downloaded from www.nrcresearchpress.com by 210.87.254.5 on 09/05/12
For personal use only.

Can. J. Chem. Downloaded from www.nrcresearchpress.com by 210.87.254.105 on 09/05/12
For personal use only.

Assessment of Free Radical Catalysis in Thermal Methyl Isocyanide Isomerization. Variation of Inert Gas Efficiency with k/k_∞ [1]

T. FUJIMOTO,[2] F. M. WANG, AND B. S. RABINOVITCH

Department of Chemistry, University of Washington, Seattle, Washington 98195

Received May 1, 1972

Experiments have been made to assess the importance of radical chain effects in thermal isomerization of methyl isocyanide. Three bath gases, propylene, propane, and hexafluoroethane were studied at 230 °C over a small region of fall-off. The relative dilution with propane was varied widely. A negative search was made for possible secondary radical products. The values of k_∞ accord with earlier results in the pure system. It is believed that radical catalysis is minor. The observed collisional efficiency of the inert gases $\bar{\beta}_\omega(\infty)$ decreases with increase of k/k_∞, in accord with previous theoretical predictions.

Nous avons effectué certains travaux dans le but de souligner l'importance des effets de chaînes radicalaires dans l'isomérisation de l'isocyanure de méthyle. Trois gaz porteurs ont été étudiées à 230 °C dans une mince région de retombée, sort le propylène, le propane et l'hexafluoroéthane. La dilution relative avec le propane variait considérablement. Les recherches dans le but de trouver des produits secondaires radicalaires possibles se sont avérées négatives. Les valeurs de k_∞ sont en accord avec les résultats précédents avec le système pur. On croit que la catalyse radicalaire est minime. L'efficacité de collision observée des gaz inertes, $\bar{\beta}_\omega(\infty)$ diminue avec l'augmentation de k/k_∞, en accord avec les prédictions théoriques précédentes.
[Traduit par le journal]

Canadian Journal of Chemistry, **50**, 3251 (1972)

Introduction

Yip and Pritchard (1) have proposed a concurrent free-radical catalyzed process for thermal unimolecular methyl isocyanide isomerization. This proposal was based on the experimental finding of small amounts of methane and hydrogen cyanide side products, and on the observation that the rate appeared to be reduced when the system was pressurized with increasing amounts of propane, and unaffected when pressurized with carbon dioxide. This was suggested to be due to propane inhibition of a (methyl) free radical chain catalysis (2), $CH_3 + CH_3NC \rightarrow CH_3 + CH_3CN$. This implies, of course, that the transfer radical, n-C_3H_7 or i-C_3H_7, does not propagate the chain as efficiently as methyl. A steady-state treatment led to a divergently increasing rate constant with increasing concentration of methyl isocyanide. These studies were performed at 200 °C at high total pressures, from one to 100 atm of added propane "inert" gas and 1.3 atm of isocyanide.[3]

Complications may arise at higher pressures, and in any case it has appeared desirable to investigate this subject at pressures near and below 1 atm, where most of the earlier work on unimolecular behavior has been performed (3–5). Wider variation of the nature of the inert gas and of its proportion to isocyanide is also desirable.

In this note we report the studies which we have made to assess the importance of the radical chain effect in the unimolecular isomerization of methyl isocyanide. We have examined the relative rates and inhibition by three species, propylene, propane, and hexafluoroethane, whose radical trapping abilities are in decreasing order. We have searched for possible secondary radical products in the presence of propane. We have examined the effect of variation of the dilution ratio on the rate constant for isomerization at constant

[1]This work was supported by the National Science Foundation.

[2]Present address: Department of Polymer Chemistry, Kyoto University, Kyoto, Japan.

[3]Professor Pritchard informs us that the base amount of isocyanide used in (1) was 4×10^{-4} mol and not 4×10^{-5} as reported.

Can. J. Chem. Downloaded from www.nrcresearchpress.com by 210.87.254.105 on 09/05/12
For personal use only.

total pressure, with propane as the inert gas. Finally, we have determined rate constants close to $p = \infty$ for the three inert gases used.

Experimental

The preparation and purification of methyl isocyanide, together with most of the experimental method has been described previously (3, 4). Matheson propane and hexafluoroethane were purified by repeated bulb-to-bulb distillation; the former contained a small amount of methane; Phillips propylene (research grade) was used without further purification. All runs were made at 230.5 °C.

The fall-off behavior of inert gases were studied in a 100 ml Pyrex reactor. Approximately 4.0×10^{-6} mol of methyl isocyanide was used in each run (~1.25 Torr); the pressure of inert gases ranged from 43 to 1700 Torr. Several higher-pressure dilution experiments were carried out in a 0.5 ml glass tube at a constant total pressure around 2000 Torr; the ratio of C_3H_8/CH_3NC was varied from 1:3.4 to 10:1. In all cases, propionitrile was added (10% of the methyl isocyanide used) as an internal analytical standard. Reaction was carried to around 25–35% conversion.

The search for radical products was made mainly in runs in 100 ml reactor and in several experiments in the glass tube. The quantity of methyl isocyanide varied from 4×10^{-6} to 65×10^{-6} mol in these experiments. Dilution ratios of propane varied from 130- to 170-fold excess over the parent substrate. The extent of reaction was allowed to range from 15 to 90%.

The bulk of the inert gas, trapped with run products at −196 °C, was removed while raising the temperature up to −145 °C. The products were fractionated into high and low boiling fractions by distillation at −95 °C. They were analyzed by using a 15 ft tricresylphosphate/chromosorb column for nitriles, and a tricresylphosphate/chromosorb–silver nitrate/fire-brick series column for hydrocarbons. In a few runs, a special search was made for CH_4 by trapping with silica gel at −196 °C.

Results and Discussion

Side Products

Traces of hydrogen cyanide and methane were found at higher degrees of conversion, especially at higher concentrations of isocyanide. They occurred to the extent of about 0.01 and 0.8%, respectively, of the acetonitrile produced at 80% reaction. No ethane or isomers of C_3H_7CN and C_4H_9CN were ever found within the detection limit, which was $\leqslant 0.001\%$ of the acetonitrile formed.

Nor could any hexanes, *e.g.*, *n*-hexane, 2-methylpentane, 2,3-dimethylbutane, or higher hydrocarbons be detected. In one case, a trace of *n*-butane (but *not* *i*-butane) was observed; this was evidently a line impurity. There was no evidence for the presence of C_2N_2. To this point we agree with Yip and Pritchard (1).

If isomerization were catalyzed by a concurrent free radical (CH_3) process, one would expect to find secondary radical products when the system is inhibited by a radical scavenger such as propane, even if the chain length were as large as 50 (1). Our inability to detect products of *i*-Pr or, less likely, *n*-Pr radical, whether hydrocarbons or nitriles, suggests that the radical effect does not play an important role in the isomerization of methyl isocyanide.

Rate Constants in the Fall-off and High Pressure Regions; Inert Gas Efficiency

The previous conclusion is also supported by the close coincidence of the high pressure ($> 10^3$ Torr) rate constant values for the two getter bath gases, propylene and propane, and for the inert gas C_2F_6, as well (Fig. 1).

The shapes and position of the fall-off curves below 10^3 Torr for all three collisional activation bath species are compatible with that of the parent substrate, as shown in Fig. 1. Propylene and propane fall on the same fall-off curve, within experimental error. The collisional activation efficiencies of these gases at infinite dilution in the second order, low pressure region, $\bar{\beta}_0(\infty)$, have been determined previously (5) at 280 °C to be virtually identical (0.61), which accords with their close superposition in the figure; at 230 °C, the efficiency value would be increased a little to ~0.63 (6).

Earlier, Tardy and Rabinovitch (7) have shown that $\bar{\beta}_\omega(\infty)$ decreases with increasing value of the collision rate ω, *i.e.*, with increase of k/k_∞. On referring to the universal curve, Fig. 7 (I) of ref. 6, it is seen that the value $\bar{\beta}_0(\infty) = 0.63$ corresponds to a reduced parameter $E' = 2.0$, where E' is defined as $E' = \langle \Delta E \rangle / \langle E^+ \rangle$; $\langle \Delta E \rangle$ is the average amount of energy lost per collision and $\langle E^+ \rangle$ is the average excess energy above threshold in the low pressure regime. $\langle E^+ \rangle$ has been calculated (8) for methyl isocyanide and is 425 cm^{-1}, whence $\langle \Delta E \rangle$ is found to be 850 cm^{-1} for propylene and propane. Then from the theoretical curves for the variation of $\bar{\beta}_\omega(\infty)$ with k/k_∞, given in Fig. 12*a* of ref. 6 for a range of E' values, it is found that $\bar{\beta}_\infty(\infty)$ declines monotonically to 0.47 as k/k_∞ approaches to unity. The values are summarized in Table 1, together with values for C_2F_6 which were obtained in the same way from the same sources.

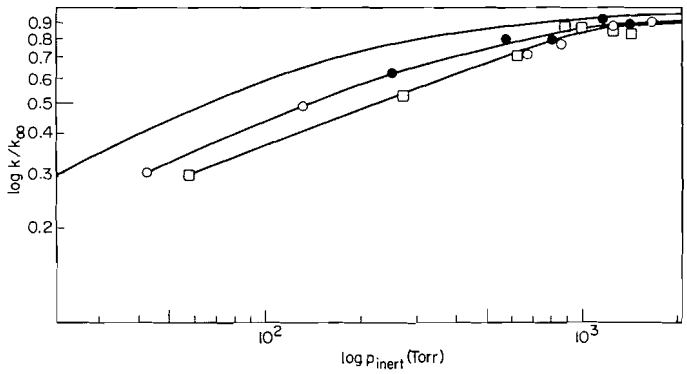

FIG. 1. Fall-off plots for CH_3NC; solid curve is plot of Schneider and Rabinovitch; ○, C_3H_8; ●, C_3H_6; □, C_2F_6.

TABLE 1. Some collisional efficiency parameters

	$\bar{\beta}_0(\infty)$* obs.†	E'	$\langle\Delta E\rangle$ (cm^{-1})	$\bar{\beta}_{0.3}(\infty)$ theor.‡	obs.	$\bar{\beta}_{0.6}(\infty)$ theor.‡	obs.	$\bar{\beta}_{1.0}(\infty)$ theor.‡
C_3H_8 / C_3H_6	0.63	2.0	850	0.56	0.49	0.50	0.43	0.47
C_2F_6	0.45	1.6	680	0.37	0.35	0.31	0.28	0.27

*The subscript on $\bar{\beta}$ refers to k/k_∞ value
†Reference 5.
‡Reference 7.

A comparison (Table 1) at several values of k/k_∞, of the pressure displacement factor (equal theoretically to $1/\bar{\beta}_\omega(\infty)$) for the C_3H_6–C_3H_8 curve, and for the C_2F_6 curve, relative to the parent strong collider curve of Schneider and Rabinovitch (3) gives reasonable numerical agreement with these predictions. But in view of the cursory nature of the comparison afforded by the present rather limited data on variation of $\bar{\beta}_\omega(\infty)$ with the region of fall-off, it is enough to claim that the agreement of the experimental results with the theoretical predictions is qualitatively correct and is quantitatively as good as may be expected for the limited data. More systematic examination of this effect is being made for the more favorable case of (inefficient) helium as the inert collider.

One may also note in Fig. 1 that not only is the relative collisional efficiency of propylene quite close to that of propane, but any difference between them at the highest pressures (the propylene rate is a little higher) is in the opposite direction to that which would be predicted for the more efficient scavenger if a radical scheme entered. At 2000 Torr, the (extrapolated) k/k_∞ values for propylene–propane and hexafluoroethane are 0.92 and 0.85, respectively. *These values agree* (as well as can be read from the curves) *with the parent molecule values* at 940 (corresponding to $\bar{\beta} = 0.47$) and 580 Torr ($\bar{\beta} \simeq 0.29$), respectively.

We believe that the data of Schneider and Rabinovitch (3) show no real indication that the values of k/k_∞ diverge from unity at still higher pressures (up to 14 atm) of isocyanide, as has been suggested (1, 2) could occur if radical catalysis enters. The reader can make up his own mind by examination of the data.

Dilution Effect at Constant Pressure

Several runs were made at a constant total pressure of 2000 Torr and variable proportions of CH_3NC–C_3H_8. The pressure chosen, 2000 Torr, was the highest practical one; it was desired to work as close to P_∞ as possible so as to minimize the effect of the differing collision efficiencies of CH_3NC and C_3H_8 on the observed k values. These experiments gave a rate constant of $83.5(\pm 1.5) \times 10^{-5}$ s^{-1}; the variation is within experimental error, although the

Can. J. Chem. Downloaded from www.nrcresearchpress.com by 210.87.254.105 on 09/05/12
For personal use only.

TABLE 2. Variation of observed rate with dilution at constant total pressure (2000 Torr)

Dilution ratio	Effective pressure (Torr)	$k \times 10^5$, s^{-1}	Parent rate at effective pressure* $k \times 10^5$ (s^{-1})
1:3.4	1881	85.1	87.1
3:1	1252	83.3	84.0
10:1	1120	82.1	83.5
1600:1	940	84.3	81.5

*From data of ref. 3.

decline with dilution may be real (Table 2). Moreover, extrapolation of the propane fall-off curve (Fig. 1) to 2000 Torr, which is at very high dilution of 1600:1, yields the concordant value, 84.3×10^{-5} s^{-1}. Although Yip and Pritchard found also that adding 1 atm of propane (at a dilution of roughly unity) did not decrease their rate, it should be noted that our dilutions extend over a range of 5×10^3 at constant pressure. It was for the purpose of increasing their dilution that they extended their propane pressures to 100 atm.

Conclusion

We conclude that (*1*) the presence of traces of methane and hydrogen cyanide does not imply an important concurrent radical process, (*2*) the rate constant of the isomerization in the region of 1 atm and below represents an elementary process, and (*3*) this system provides support for the theoretically predicted variation of the inert gas activation efficiency $\bar{\beta}(\infty)$ with fall-off region.

Our study provides no reason to doubt that the methyl isocyanide system continues as a good test for the theory of unimolecular reactions. We have no definite explanation for the very high pressure results of ref. 1. We have had some indication that some radical effect *may* enter for the thermal C_2H_5NC system, and *may* become important for n-C_3H_7NC system, but this is not definitely established.

1. C. K. YIP and H. O. PRITCHARD. Can. J. Chem. **48**, 2942 (1970).
2. D. H. SHAW and H. O. PRITCHARD. Can. J. Chem. **45**, 2749 (1967).
3. F. W. SCHNEIDER and B. S. RABINOVITCH. J. Am. Chem. Soc. **84**, 4215 (1962).
4. S. C. CHAN, J. T. BRYANT, and B. S. RABINOVITCH. J. Phys. Chem. **74**, 2058 (1970).
5. S. C. CHAN, B. S. RABINOVITCH, J. T. BRYANT, L. D. SPICER, T. FUJIMOTO, Y. N. LIN, and S. P. PAVLOU. J. Chem. **74**, 3160 (1970).
6. S. C. CHAN, J. D. BRYANT, and B. S. RABINOVITCH. J. Phys. Chem. **74**, 2055 (1970).
7. D. C. TARDY and B. S. RABINOVITCH. J. Chem. Phys. **48**, 1282 (1968).
8. D. C. TARDY and B. S. RABINOVITCH. J. Chem. Phys. **45**, 3720 (1966).

Can. J. Chem. Downloaded from www.nrcresearchpress.com by 210.87.254.105 on 09/05/12
For personal use only.

Can. J. Chem. Downloaded from www.nrcresearchpress.com by 210.87.254.40 on 09/05/12
For personal use only.

Oriented Polycrystal Formation of Halogen-containing Organic Molecules on Alkali Halide Windows and their Usefulness in Vibrational Spectroscopic Studies

J. E. KATON, DEEPALI SINHA, M. G. GRIFFIN, AND D. A. CONDIT
Department of Chemistry, Miami University, Oxford, Ohio 45056

Received June 14, 1972

It has been found that several halogen-containing organic molecules *normally* crystallize as oriented polycrystals when in contact with alkali halide windows. This effect can lead to erroneous interpretation of crystal film spectra if it is not recognized, but can be very useful for determining molecular and/or crystal structures if the spectra are properly analyzed.

On a constaté que plusieurs molécules organiques contenant un halogène, cristallisent normalement sous forme de polycristaux orientés lorsqu'elles sont en contact avec des halogénures alcalins. Cet effet, s'il n'est pas reconnu, peut mener à une interprétation erronée des spectres de film cristallin mais peut également être très utile dans la détermination des structures moléculaires et (ou) cristallines si les spectres sont analysés correctement. [Traduit par le journal]

Canadian Journal of Chemistry, **50**, 3255 (1972)

It has been known for many years that polarized infrared spectra of single crystals or oriented samples are very useful both for detailed spectroscopic assignments and for deducing the details of molecular and crystal structure (1). Sample preparation for such studies is usually very tedious at best, however. A few years ago one of the present authors reported that both cyclopropylcarbonyl chloride and cyclopropylcarbonyl bromide appeared to form oriented polycrystals on cooling, as indicated by infrared polarization effects (2). The equipment available at that time was not very suitable for such studies and the results were thought to be unusual.

We have now found that several additional halogen-containing organic compounds can be very readily induced to form polycrystals which are highly oriented when grown between alkali halide plates. This phenomenon occurs when a capillary liquid film of the material between two alkali halide windows is cooled. The cooling need not be very slow, since it normally occurs when liquid nitrogen is slowly added to a Dewar bearing the infrared cell. Compounds which have been crystallized in this fashion to date are: methyl chloroformate ($ClCO_2CH_3$) and methyl chloroformate-d_3; benzoyl chloride (C_6H_5COCl), benzoyl chloride-d_5, and benzoyl bromide; γ-chloroacetic acid (3); and methyl chloroacetate ($ClCH_2CO_2CH_3$) and methyl chloroacetate-d_3.

A striking example is furnished by methyl chloroformate, whose polarized infrared spectra are reproduced in Fig. 1. This sample was loaded into a low temperature cell as a capillary film and immediately cooled with liquid nitrogen. The spectra were recorded on a Perkin–Elmer Model 180 infrared spectrophotometer utilizing the standard accessory wire grid polarizer on a AgBr substrate. The results indicate that the molecule crystallizes with a plane of symmetry (C_s point group) and the planes are all parallel to the incident beam of the spectrometer. As a result, those absorption bands evident in the upper spectrum are due to vibrations of A' symmetry while those evident in the lower spectrum are those due to vibrations of A'' symmetry. An indication of the usefulness of such results in vibrational assignment studies is given by the band near 1449 cm^{-1} in both spectra. Upon careful observation it is noted that the frequency of this band is 1448.6 ± 0.1 cm^{-1} in the upper spectrum and 1449.2 ± 0.1 cm^{-1} in the lower. It is due to the CH_3 bending mode which is degenerate under the C_{3v} symmetry of the uncoupled CH_3 group, but splits into one A' and one A'' component under C_s symmetry. The use of polarized radiation allows

Can. J. Chem. Downloaded from www.nrcresearchpress.com by 210.87.254.40 on 09/05/12
For personal use only.

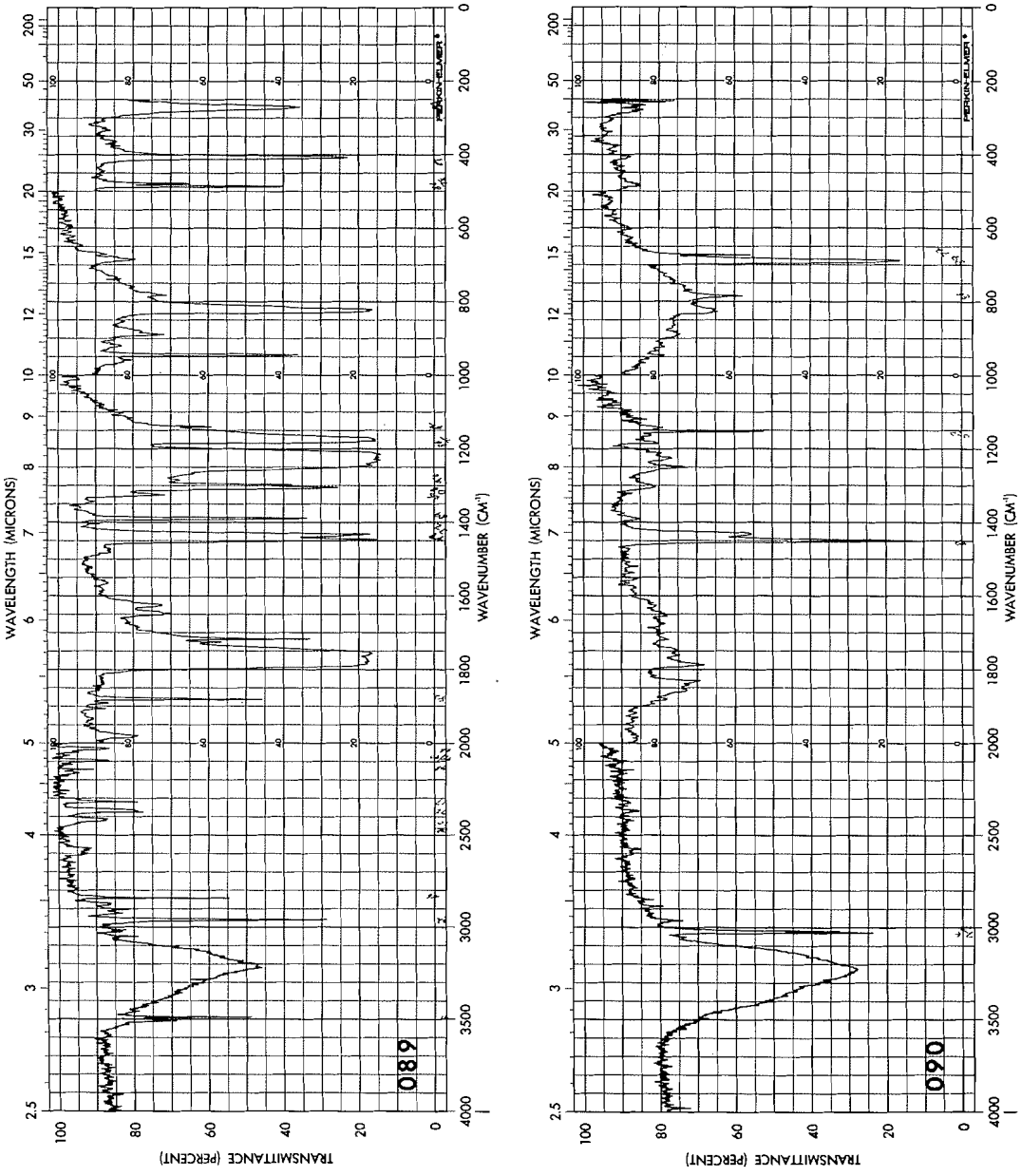

FIG. 1. Infrared Spectra of an oriented polycrystalline film of methyl chloroformate at about 100 °K. The polarizer settings differ by 90° in the two spectra.

the ready resolution of these two bands which are at best resolvable only with difficulty under other conditions. No crystal splitting is observable in the spectra. This is very unusual in our experience for such a polar material under these experimental conditions. Such data is consistent only with certain crystal structures (4).

Methyl chloroacetate when treated in the same way yields polarized infrared spectra which indicate that the molecule crystallizes with no symmetry (C_1 point group). Each fundamental appears to be crystal split into two components, however, which have transition moments perpendicular to one another. Again, such results are consistent with only a few possible crystal structures.

The results with γ-chloroacetic acid were obtained by melting the material between sodium chloride windows and allowing the sample to cool to room temperature. This indicates that such behavior can also be obtained with normally solid materials.

The generality of this behavior is not yet known, but our results indicate that it is more common than might be expected. To date, the effect has occurred with every organic halogen-containing compound which we have studied. They also indicate that one must be very careful in interpreting ordinary low temperature solid-state infrared spectra due to the inherent polarization properties of grating monochromators. Such spectra may be partially polarized unless the crystals are truly randomly oriented. On the other hand, the behavior is very valuable since it allows one to draw a good deal more information from the spectrum than can ordinarily be obtained.

1. S. KRIMM. *In* Infra-red spectroscopy and molecular structure. *Edited by* M. Davies. Elsevier, New York. 1963. Chap. 8.
2. J. E. KATON, W. R. FEAIRHELLER, JR., and J. T. MILLER, JR. J. Chem. Phys. **49**, 823 (1968).
3. S. U. PICKERING. J. Chem. Soc. **67**, 644 (1895).
4. W. G. FATELEY, N. T. MCDEVITT, and F. F. BENTLEY. Appl. Spectrosc. **25**, 155 (1971).

Can. J. Chem. Downloaded from www.nrcresearchpress.com by 210.87.254.40 on 09/05/12
For personal use only.

Can. J. Chem. Downloaded from www.nrcresearchpress.com by 210.87.254.40 on 09/05/12
For personal use only.

Canadian Journal of Chemistry

Published by THE NATIONAL RESEARCH COUNCIL OF CANADA

VOLUME 50 OCTOBER 15, 1972 NUMBER 20

Transient Response of the System Al/Al_2O_3/Electrolyte. Part I. Galvanostatic Transients

D. G. W. GOAD[1] AND M. J. DIGNAM

Department of Chemistry, University of Toronto, Toronto 181, Ontario

Received October 13, 1971[2]

Voltage transients under galvanostatic conditions are investigated for the system Al/Al_2O_3/electrolyte (glycol–borate) and the results, along with similar results obtained by Dewald for the system Ta/Ta_2O_5/electrolyte (0.1 N H_2SO_4), are analyzed according to the dielectric relaxation model due to Dignam. This model accounts for the general form of the transients, but systematic discrepancies are apparent. Modification of the model to include two independent ion-current-driven dielectric relaxation processes gives essentially exact agreement with the data and values for the constants in accord with those obtained earlier from potentiostatic transient measurements.

Nous étudions les transitions de voltage sous des conditions galvanostatiques pour le système Al/Al_2O_3/électrolyte (glycol–borate) et nous analysons les résultats, de même que les résultats similaires obtenus par Dewald pour le système Ta/Ta_2O_5/électrolyte (0.1 N H_2SO_4), selon le modèle de relaxation diélectrique de Dignam. Ce modèle tient compte de la forme générale des transitions, mais souffre quand même de certains défauts. Nous apportons une modification au modèle qui permet d'obtenir un excellent accord avec les données, les valeurs des constantes et les résultats précédents tirés de mesures de transition potentiostatique.
[Traduit par le journal]

Canadian Journal of Chemistry, **50**, 3259 (1972)

Introduction

The kinetics of anodic oxidation of the valve metals (Al, Nb, Ta, and others) has been the subject of extensive investigation in the last 20 years (1–3). Under galvanostatic conditions, a steady-state situation is fairly rapidly achieved in which the differential field strength, E, defined as the derivative of the cell overpotential with respect to film thickness, is independent of time. Under these conditions, the relation between the ion current density, i, and the differential field strength is given by (4)

$$[1] \qquad i = A \exp [-W_s(E)/kT]$$

where $W_s(E)$ can be regarded as the effective net activation energy for anodic film growth, while A is a constant. Data for the steady-state anodic oxidation of Ta, Nb, and Al are represented extremely well by eq. 1 on expanding $W_s(E)$ as a quadratic function of the field strength a point first noted by Young (1), *viz.*

$$[2] \qquad W_s(E) = \phi - \mu_s^* E(1 - \mu_s^* E/C\phi)$$

where ϕ is the effective activation energy at zero field strength, μ_s^* the effective activation dipole (or charge-activation distance product) in the low field limit, and C a dimensionless constant. The origin of the quadratic field term is discussed at length in ref. 4. For measurements made at a single temperature, the field strength need only be varied by a few percent to cover the experimentally accessible range of current densities, so that to a good approximation $\ln i$ may be represented as a linear function of E,

$$[3] \qquad i \simeq \alpha \exp (\beta_s E)$$

where

$$\beta_s = \mu_s^*(1 - 2\mu_s^* \bar{E}/C\phi)/kT$$

[1]Present address: ALCAN International Ltd., Research Centre, Kingston, Ontario.

[2]Revision received June 23, 1972.

Can. J. Chem. Downloaded from www.nrcresearchpress.com by 210.87.254.40 on 09/05/12
For personal use only.

and

$$\alpha = A \exp\left[-(\phi - (\mu_s^* \bar{E})^2/C\phi)/kT\right]$$

$\bar{E}$ being the mean value of E over the range of experimental interest.

Under galvanostatic conditions, E is found to be independent of film thickness over the range of a few tens of Ångstroms to several thousand Ångstroms, beyond which electrical breakdown occurs (1). This result requires that any space charge within the film either be negligible, in which case ion transport must be controlled at an interface, or be confined to a region of the order of a few tens of Ångstroms near one or both of the interfaces, in which case bulk control of ion transport becomes the probable mechanism.

There is a number of models which can account satisfactorily for the form of the steady-state kinetics. In fact almost any model involving the field assisted migration of ionic species across one or more activation barriers will, under certain conditions, lead to steady-state kinetics in accord with [1] and [2]. To differentiate among the possible mechanisms, data obtained under transient conditions must be examined. The purpose of Parts I and II of these articles is to obtain and analyze such data for the system Al/Al_2O_3/electrolyte.

Potentiostatic transients for this system have been measured and analyzed by Dignam and Ryan (5). However, galvanostatic transient data and complete a.c. impedance data have not been reported for this system. In Part I, the results of galvanostatic transient measurements are presented, with a.c. impedance measurements being presented in Part II. For systems where kinetics are characterized by a set of linear equations, the various forms of transient measurements are equivalent. For the valve metal systems, however, i and E are not linearly related.

Experimental

Introduction

Galvanostatic transient measurements were performed in the manner of Dewald (6). His procedure was to form an anodic film under steady-state conditions corresponding to a current density, I_1, and field strength E_1. The current density was then switched rapidly from I_1 to a value $I_2 \neq I_1$, thus initiating the transient. The electrode potential was monitored following initiation of the transient, from which the time dependence of the "excess field", $\Delta E = E - E_2$, was calculated, E being the instantaneous value of the field strength, and E_2 its steady-state value corresponding to $I = I_2$.

In the present study, the procedure was modified slightly in order to eliminate both that part of the measured potential change arising from film growth during the transient, and that arising from possible current dependent interfacial potentials. Films were formed by increasing the aluminum/oxide electrode potential at a constant rate, corresponding to film formation at a steady-state current density I_1 (7). At a given electrode potential, V_1, the current was changed by a factor equal to I_2/I_1, and the voltage recorded as a function of time. The experiment was then repeated on the same electrode after forming the film at the same constant rate of voltage rise to a potential $V_2 > V_1$. Subtraction of the voltage data at corresponding times after initiating the transients gives ΔV from which $E/E_1 = \Delta V/(V_2 - V_1)$ may be calculated.

Film formation at a constant rate of voltage rise (which corresponds to a constant current density) rather than at constant current, eliminates the effect which any change in electrode area with film thickness would otherwise have on the measured potential differences.

The Cell and Electrodes

The cell has been described previously (7). The anodes were of aluminum sheet (99.99% Al, 0.04 in. thick), which was formed into paddle-shaped electrodes of dimensions 1 in. × 0.25 in. for the paddle, 1 in. × 0.006 in. for the tab. Following routine cleaning procedures, they were electropolished at about 0.2 A/cm^2 and 25 °C in 5 parts ethanol to 1 part 70% perchloric acid by volume (8). The electrodes were rinsed briefly in ethanol, then for 1 min in running distilled water, dried in a clean air jet, and stored in a desiccator over activated alumina. The reference electrode was a mercury/mercuric oxide electrode prepared as described by Cahan *et al.* (9). It was located in a compartment which contained a 20% aqueous solution of ammonium pentaborate. Connection to the reference electrode compartment was made by a side tube which ended in a capillary tip brought up underneath the anode and sealed by a membrane permeable to cations only (10). This configuration was chosen to minimize the impedance of the reference electrode system in order that fast response times could be achieved. The entire cell was kept in an air thermostated metal box. A 30% by weight solution of ammonium pentaborate in ethylene glycol was used as electrolyte as this gives high current efficiencies for film formation over a wide range of current density (11).

Electrical Circuit

The circuit employed (Fig. 1) operates as follows. Initially the switches S_1 and S_2 are in positions 1, and a voltage, e, applied to the input of amplifier 1 produces a linearly increasing voltage, e_1, at the output. Amplifier 3 measures the difference between e_1 and $(e_{Al} - e_{ref})$ and applies this through the integrator amplifier 5 to the resistor R_2, which causes the cell current to change until $(e_{Al} - e_{ref})$ is equal to e_1. The output of amplifier 3, e_3, is then zero and the output of amplifier 5 constant. The cell current, i', is now given by $-e_5/R_2$. Any changes in electrode area with increasing film thickness results in a change in i' until $(e_{Al} - e_{ref})$ is once again equal to e_1.

Can. J. Chem. Downloaded from www.nrcresearchpress.com by 210.87.254.40 on 09/05/12
For personal use only.

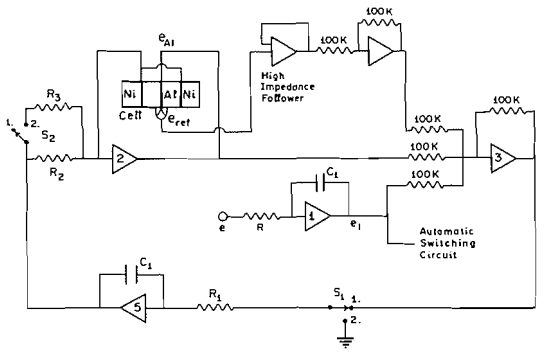

FIG. 1. Circuit used for the study of galvanostatic transients.

The transient is initiated when e_1 reaches a value determined by the input to the automatic switching circuit. The relay switches (Clair mercury wetted type) then adopt positions 2. The input to amplifier 5 is grounded and the output has a constant value of $-i'R_2$ where i' is the initial cell current. The new cell current is consequently $-e_5(R_2 + R_3)/R_2R_3$ or $(R_2 + R_3)i'/R_3$, so that $I_2/I_1 = (R_2 + R_3)/R_3$. A reversal of the initial and final switch positions in S_2 allows a decrease in cell current to be achieved on switching, *i.e.*, $I_2/I_1 = R_3/(R_2 + R_3)$.

Procedures

The automatic switching circuit, in addition to initiating the transient, triggers the oscilloscope which records the voltage $-e_3 = V_m = (e_{Al} - e_{ref}) - e_1$. Subtraction of V_m for the first transient initiated from that for the second, at corresponding times, gives $\Delta V_m = \Delta V - (V_2 - V_1) = (V_2 - V_1)\cdot(E/E_1 - 1)$. For large times, when the transient has died away, $E = E_2$ and ΔV_m takes on the constant value $\Delta V_m^\infty = (V_2 - V_1)(E_2/E_1 - 1)$. The normalized excess field can therefore be calculated from the measured potentials according to the equation

$$(E - E_2)/(E_2 - E_1) = \Delta V_m/\Delta V_m^\infty - 1$$

All of the results reported were calculated from this equation.

Although the field strengths and current densities are not required for the analysis of the data, they were nevertheless calculated as follows. The output of amplifier 1 was recorded at intervals prior to initiating the transient, from which the time derivative of the electrode potential was obtained by a linear regression analysis. From this derivative the formation current density, I_1, and field strength, E_1, were calculated using the steady-state parameters reported by Dignam, Goad, and Sole (11).

For all the runs reported, the two transients comprising a single run were initiated at times corresponding to anodic overpotentials of approximately 40 and 80 V, respectively. For one run, however, transients were initiated at 40, 60, and 80 V, allowing the ΔV_m values obtained from the 40–60 V data to be compared with those from the 60–80 V data. Within experimental error, the values were indistinguishable.

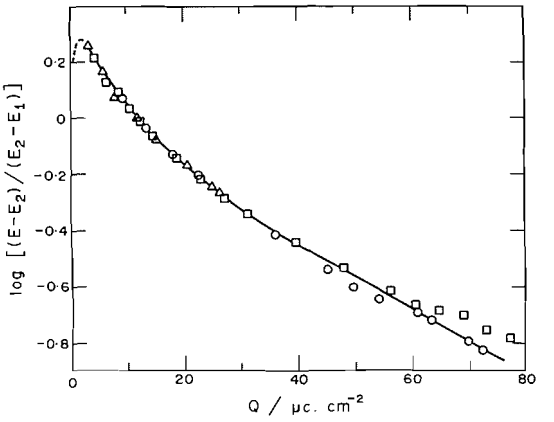

FIG. 2. Decay of the excess field, $E - E_2$, following initiation of galvanostatic transients: ○, $I_1 = 40.9\ \mu A/cm^2$, $E_1 = 8.19 \times 10^6$ V/cm, $I_2/I_1 = 11$; □, $I_1 = 208\ \mu A/cm^2$, $E_1 = 8.56 \times 10^6$ V/cm, $I_2/I_1 = 2$; △, $I_1 = 207.5\ \mu A/cm^2$, $E_1 = 8.56 \times 10^6$ V/cm, $I_2/I_1 = 0.5$; the solid line was calculated from [4] using the values for the parameters listed.

Results

Experiments were carried out for final to initial current ratios, I_2/I_1 of 0.5, 2.0, and 11.0. In Fig. 2, the results of these experiments are displayed in the form log $[(E - E_2)/(E_2 - E_1)]$ *vs.* $Q = I_2t$, the charge passed per unit area following initiation of the transient. Apart from scaling factors, the graphs represent the time decays of the "excess field", $E - E_2$. Presenting the data in this form illustrates an important feature of the kinetics of the decay process. It is characterized by the charge passed per unit area, Q, not the time elapsed. This behavior was first noted by Dewald (6) for the system Ta/Ta_2O_5/dilute aqueous H_2SO_4. In fact, the results of Fig. 2 are of the same general form as those obtained by Dewald.

The field values before the maximum in E is reached are not shown, being difficult to measure accurately because of the very rapid rate of change of E in this region. Presumably the finite rate of approach of the field to its maximum value following initiation of the transient is a consequence of having to alter the charge on the Al/Al_2O_3/electrolyte capacitor.

The solid line in Fig. 2 is the result of fitting the data to a pair of exponential functions in Q, *i.e.*

$$[4]\quad (E - E_2)/(E_2 - E_1) = M_1 \exp(m_1Q) + M_2 \exp(m_2Q)$$

Can. J. Chem. Downloaded from www.nrcresearchpress.com by 210.87.254.40 on 09/05/12
For personal use only.

The values of the constants which minimize the variance in E are given below:

$$M_1 = 1.32$$

$$M_2 = 1.03$$

$$m_1 = -1.44 \times 10^5 \text{ cm}^2/\text{C}$$

$$m_2 = -0.266 \times 10^5 \text{ cm}^2/\text{C}$$

A single exponential function will not represent the data well since $\log [(E - E_2)/(E_2 - E_1)]$ is not a linear function of Q.

Discussion

Four different mechanisms have been offered to account for the existence of transients in connection with the anodic oxidation of the valve metals (1, 2). The first, due to Bean, Fisher, and Vermilyea (12), and elaborated upon by Dewald (6), is based upon the assumption that ion transport is controlled within the film through a mechanism involving the field assisted generation of defect pairs. This model, frequently referred to as the high field Frenkel defect model (1), was examined recently in some detail by Dignam and Taylor (13). Using an argument based on the magnitude of the mean distance travelled by a mobile defect in the field direction following its formation. Dignam and Taylor conclude that the high field Frenkel defect model cannot apply to thin films. They further conclude that any mechanism involving both rate control within the film and the homogeneous generation of defect pairs, in which the mobile defect concentration is field or current dependent, is highly improbable for thin films. Young (14) has recently pointed out an error in their reasoning. It is the magnitude of the characteristic space charge length for the model, not the mean distance travelled by a defect (15), which should have been used in the argument advanced by Dignam and Taylor. As these two quantities are closely related (both are inversely proportional to the mobile defect concentration (15)), their original conclusions remain essentially intact. Furthermore, although the high field Frenkel defect model accounts moderately well for galvanostatic transients for the Ta system (6), it was shown first by Young for Ta (16), then by Dignam and Ryan for Al (5), that it predicts potentiostatic transients of the wrong form.

Adams, van Rysselberghe, and Willis (ref. 1 sec. 20.05) suggest a mechanism based on control at the metal/oxide interface, the number of metal ions suitably located for entry into the oxide varying with current density due, for example, to the characteristics of the screw dislocations terminating at the metal surface. This model has not been developed in a mathematical form.

Young (14, 16) has proposed a model based on rate control by ion transport within the film in which, under galvanostatic conditions, the concentration of mobile defects is assumed to approach its steady-state value at a rate proportional to i^2. The model appears to require the interaction of ionic defects in motion to create additional defects, a sort of second order avalanche mechanism. It has only been developed for the particular case of potentiostatic conditions.

The most recent models are due to one of us (M.J.D.) (4, 17, 18). In the first model (17) the oxide film was assumed to be composed of small crystallites or polymeric units, with the principal rate controlling step being ion transport between such units. It now seems unlikely that this is even approximately correct, since films only 10 to 20 Å in thickness give rise to the same transient phenomena as do much thicker films (19). Indeed, this result argues against any model involving kinetic control within the film, rather than at its boundaries. However, essentially the same set of equations as were obtained using the original model can be derived from a model involving interfacial control (4, 18). The principal features of this model are that the rate is controlled at an interface (we shall choose the oxide/electrolyte interface), with transients arising as a result of dielectric relaxation processes within the film. (Changes in the polarization of the oxide film will bring about changes in the distribution of the potential between the film and interfacial regions.) A more detailed development of the model follows. We note at this point, however, that the equations arising from this model are in accord with both steady-state data and ion current transient data obtained under potentiostatic conditions (5, 7).

Dielectric Relaxation Model

Assuming the rate to be controlled near the electrolyte/film interface, the anodic overpoten-

Can. J. Chem. Downloaded from www.nrcresearchpress.com by 210.87.254.40 on 09/05/12
For personal use only.

tial, η, may be divided into a film portion, η_x, and an electrolyte-oxide double-layer portion, η_d. Provided that the free charge at the oxide/double-layer interface, as well as that within the oxide, is negligible compared with that on the electrolyte phase, or the metal/oxide interface, the normal component of the electric displacement will be effectively constant throughout the oxide film and the double-layer, so that

$$[5] \qquad \varepsilon_0 E + P = \varepsilon_0 K_d E_d = \varepsilon_0 K_d \eta_d / d$$

where ε_0 is the permittivity of free space, E and P are the field strength and polarization in the oxide, K_d and d the effective dielectric constant and thickness of the double-layer, and E_d the field in the double-layer. Assuming the rate controlling interfacial reaction to involve the field assisted migration of ionic species of fixed boundary concentration across an activation barrier, then for E_d large (4) $i = A \exp[-W(E_d)/kT]$ where $W(E_d)$ is the net activation energy for the barrier crossing and can be expanded in the same form as was $W_s(E)$ (*cf.* [1] and [2]). Making the same approximation as was used to obtain [3], this equation can be written as

$$[6] \qquad i \simeq \alpha \exp \beta E_d$$

where for isothermal conditions, α and β can be treated as constants. Under steady-state conditions, P is assumed to take the usual form, *i.e.* $P = \varepsilon_0(K_s - 1)E$ where K_s is the static (or steady-state) dielectric constant of the film, which with [5] and [6] leads to [3] with

$$[7] \qquad \beta_s = (K_s/K_d)\beta$$

Dividing P into a component P_1 which follows the field, and a component P_2 which gives rise to the relaxation process (and hence to the transients), we may write

$$[8] \qquad P = P_1 + P_2$$

$$[9] \qquad P_1 = \varepsilon_0(K_1 - 1)E$$

where K_1 is the dynamic or high frequency dielectric constant. In this model, the form of the transients is determined almost entirely by the choice of the form of the time dependence of P_2. If dP_2/dt has the usual form for a thermally activated relaxation process, *i.e.* $dP_2/dt = (1/\Upsilon)(\varepsilon_0\chi_2 E - P_2)$ where Υ is the relaxation time and $P_2 = \varepsilon_0\chi_2 E$ under steady-state conditions, then the decay of the excess field during a galvanostatic measurement also takes this form, contrary to observation. The simplest assumption one can make which will lead to the correct form for the transients is that dP_2/dt is given by

$$[10] \qquad dP_2/dt = Bi(\varepsilon_0\chi_2 E - P_2)$$

where B is a constant. Equation 10 may be rationalized by assuming that ion transport through the vitreous oxide involves the co-operative motion of groups of atoms, and consequently leads to small irreversible displacements of the atoms close to the path of motion of the ionic defect. Such irreversible displacements will constitute, in general, polarization changes. Alternatively (or additionally), local vibrational excitation along the path of motion of a defect might induce the establishment of local equilibrium polarization, leading again to an equation of the form of [10]. In either case, the effect may be approximated by assuming that defect motion brings about equilibrium polarization within a distance r of the moving defect, in which case $B = \pi r^2/q$ where q is the charge on the mobile defect. Finally we note that [10] can only be a good approximation for conditions in which i is not too small, since conventional mechanisms involving thermal activation must contribute significantly to dP_2/dt for i sufficiently small (1).

Analysis of the Results

Equations 5 to 10 constitute a description of the dielectric relaxation model for the transients. Unfortunately, an exact analytical solution of these equations for the conditions of the experiments has not been discovered. The difficulty arises from the fact that the ion current density, i, and the total current density, I, are not in general the same, but differ by the charging current density $i^c = \varepsilon_0 dE/dt + dP/dt = I - i$. It can be shown, however, that beyond the maximum in the normalized excess field, $(E - E_2)/(E_2 - E_1)$, (*cf.* Fig. 2) the charging current may be neglected in comparison with I (see Appendix). Solving the equations in this approximation, the boundary conditions become

$$i = I_1 = \alpha \exp \beta_s E_1 = \text{constant for } t < 0$$

$$[11] \qquad i \simeq I_2 = \alpha \exp \beta_s E_2 = \text{constant for } t \geqslant 0$$

$$P_2(t = 0) \simeq P_2(t < 0)$$

The final condition arises from neglecting the change in P_2 during the charging process in

TABLE 1. Dewald's data (6) for galvanostatic transients obtained for the system $Ta/Ta_2O_5/0.1\ N\ H_2SO_4$; $I_1 \sim 10^{-4}$ A/cm^2, $I_2/I_1 = 2$

Data		Results $(E-E_2)/(E_2-E_1)$	
Q (μC/cm^2)	$(E-E_2)/E_r$*	From data‡	Calculated from [4]
4.5	0.0317	1.512	1.513
10.4	0.0243	1.159	1.155
20.0	0.0166	0.792	0.798
40.0	0.0100	0.477	0.471
54.5	0.00776	0.370	0.365
69.3	0.00610	0.291	0.298
84.8	0.00502	0.239	0.245
100.0	0.00424	0.202	0.205
114.5	0.00369	0.176	0.173
129.3	0.00308	0.147	0.146
143.0	0.00272	0.130	0.125
		Standard deviation	0.005_1

*E_r is the steady-state field required to cause oxide film growth at the rate of 1 Å/s, which Dewald took to be 6.6×10^6 V/cm.
‡For $I_2/I_1 = 2$, $(E_2 - E_1) = (1/\beta_s) \ln 2 = 0.138 \times 10^6$ V/cm (from Young's data (20) for $\bar{E} \simeq 6.6 \times 10^6$ V/cm).

which the reduced excess field reaches its maximum value. The solution of equations [5] to [10] for the conditions [11] takes the form of [4] (see Appendix) with

$$M_1 = (K_s - K_1)/K_1$$
$$M_2 = 0 \qquad [12]$$
$$m_1 = -B(K_s/K_1)$$

Thus, although the model in this form represents the general features of the transients well, it does not provide a good quantitative fit to the data, since the normalized excess field is predicted to decay according to a single, rather than a pair of exponential functions of the charge passed. The situation, however, is easily remedied by introducing a second, independent, dielectric relaxation process. Thus on replacing [8] by

$$P = P_1 + P_2 + P_3 \qquad [13]$$

and [10] by

$$dP_k/dt = B_k i(\varepsilon_0 \chi_k E - P_k) \qquad k = 2,3 \qquad [14]$$

and adding to the conditions [11] the additional condition

$$P_3(t=0) \simeq P_3(t<0) \qquad [15]$$

the equations may be solved (see Appendix) to give once again [4] with m_1 and m_2 being the roots of the equation

$$m^2 + \left[B_2 + B_3 + \frac{B_2\chi_2 + B_3\chi_3}{K_1}\right] m + \frac{B_2 B_3 K_s}{K_1} = 0 \qquad [16]$$

and M_1 and M_2 can be obtained from

$$M_1 + M_2 = (K_s - K_1)/K_1$$
$$(M_1 m_1 + M_2 m_2) = -\frac{K_s}{K_1}\frac{B_2\chi_2 + B_3\chi_3}{K_1} \qquad [17]$$

Using the values of M_1, m_1, M_2, m_2 appearing under [4], [16] and [17] have been solved numerically to give

$$\chi_2 = 1.91\ K_1$$
$$\chi_3 = 0.44\ K_1 \qquad [18]$$
$$B_2 = 1.22 \times 10^4\ \text{cm}^2/\text{C}$$
$$B_3 = 9.32 \times 10^4\ \text{cm}^2/\text{C}$$

The value of K_1 is not known very accurately; taking $K_1 = 8.5$ (7) gives $\chi_2 = 16.2$, $\chi_3 = 3.74$, and $K_s = K_1 + \chi_2 + \chi_3 = 28.5$.

In Table 1, Dewald's galvanostatic transient data for Ta (6) are presented. Fitting this data to [4], the values of the parameters which minimize the variance in E are

$$M_1 = 1.26_6$$
$$M_2 = 0.633$$
$$m_1 = -7.30_2 \times 10^4\ \text{cm}^2/\text{C}$$
$$m_2 = -1.13_2 \times 10^4\ \text{cm}^2/\text{C}$$

from which

$$\chi_2 = 1.30_4 K_1$$
$$\chi_3 = 0.594 K_1 \qquad [19]$$
$$B_2 = 0.657 \times 10^4\ \text{cm}^2/\text{C}$$
$$B_3 = 4.34 \times 10^4\ \text{cm}^2/\text{C}$$

Taking $K_1 = 27.6$ (20) gives $\chi_2 = 36.0$, $\chi_3 = 16.4$, and $K_s = 80.0$.

Comparison of the B_k and χ_k values for Al and Ta does not disclose any obvious relationships; one can say only that the larger χ value is

Can. J. Chem. Downloaded from www.nrcresearchpress.com by 210.87.254.40 on 09/05/12
For personal use only.

Can. J. Chem. Downloaded from www.nrcresearchpress.com by 210.87.254.40 on 09/05/12
For personal use only.

associated with the smaller B value, for both systems.

Comparison with Previous Results

The above values for the parameters will be compared with those obtained previously from measurements of potentiostatic transients. Dignam and Ryan (5) fitted their data for transients obtained under potentiostatic conditions (approximately constant field conditions) for aluminum to the dielectric relaxation model, assuming only one ion-current-driven relaxation process. For Al_2O_3 films formed initially at about 2×10^{-4} A/cm^2 in a glycol–borate electrolyte, a value for B of $(1.22 \pm 0.07) \times 10^4$ cm^2/C was obtained in excellent agreement with the value of B_2 obtained in the present study. However, for films formed at about 2×10^{-6} A/cm^2 in the same electrolyte, a significantly larger value was obtained, namely $(1.46 \pm 0.04) \times 10^4$ cm^2/C. In both instances, the value of B obtained was independent of the field strength employed for the experiment, a point which was not noted in the original publication (5).

It can be shown (21) that for conditions of constant field strength, and negligible charging current, the dielectric relaxation model predicts transients of the following form:

$$[20] \quad \ln [I_{ss}/I] = \sum_k b_k \exp(-B_k Q) \qquad k = 2,3$$

where I_{ss} is the final steady-state current density and the b_k are constants determined by the initial conditions. However, over the region in which eq. 20 should be valid (*i.e.* negligible charging current), eq. 20 may be simplified to

$$[21] \quad \ln [I_{ss}/I] \propto \exp(-B_2 Q)$$

since over the entire region, $B_3 Q \gg 1$. Potentiostatic transient data yield, therefore, only the value for B_2.

As observed previously (5), the value for B_2 appears to depend somewhat on the conditions of film formation, a result expected if the film structure is dependent on formation conditions. Note that the present galvanostatic transient studies were carried out for current densities $\sim 2 \times 10^{-4}$ A/cm^2 and that the value for B_2 obtained from these studies agrees with that obtained from potentiostatic transient studies on films formed at 2×10^{-4} A/cm^2.

Analysis of Young's potentiostatic transient data for tantalum (16) by Dignam and Ryan (5) gave a value for B_2 of 8.0×10^3 cm^2/C. This value is close, but not equal, to that calculated from Dewald's data, which were for films formed in 0.1 N H_2SO_4 and at current densities $\sim 10^{-4}$ A/cm^2. Young's data, on the other hand, were for specimens formed at 100 V (constant potential) for 3.5 hn then annealed in boiling water for 5 min. As for the case of aluminum this small discrepancy is likely due to the different formation conditions employed in the two sets of measurements.

In summary, the dielectric relaxation model, with two independent ion-current-driven relaxation processes, provides a quantitative description of both galvanostatic and potentiostatic transients, a single set of constants reproducing both sets of data for the aluminum system. The same is true for the tantalum system; however, more data is required to show this (21).

Appendix

Decay of Charging Current

The charging current density, $i^c = \varepsilon_0 dE/dt + dP/dt$, on using [5] becomes $i^c = \varepsilon_0 K_d dE_d/dt$ so that the total current density $I = i + i^c$, is given by

$$[A1] \qquad I = i + I\varepsilon_0 K_d dE_d/dQ$$

where $Q = \int_0^t I\, dt$ is the charge passed per unit area of electrode. Substituting for E_d from [6] and re-arranging, [A1] becomes

$$[A2] \qquad \frac{di}{i[1 - i/I]} = \frac{\beta}{\varepsilon_0 K_d} dQ$$

Integrating [A2] for the conditions $i = I_1$ for $Q = 0$, and $I = I_2$ = a constant, gives

$$[A3] \quad \left(\frac{1 - i/I_2}{i/I_2}\right) = \left(\frac{1 - I_1/I_2}{I_1/I_2}\right) \exp\left(-\frac{\beta Q}{\varepsilon_0 K_d}\right)$$

From [7], $\beta/K_d = \beta_s/K_s \simeq 16.5$ Å/V (7) so that $\varepsilon_0 K_d/\beta = 0.54$ μC/cm^3. Thus for values of I_2/I_1 of 0.5, 2.0, and 11, we may calculate from [A3] that $|i^c| = |I_2 - i|$ falls to 1% of I_2 for values of the charge passed of 2.1, 2.5, and 3.7 μC/cm^2, respectively. The approximation $i = I_2$ is therefore a very good one over the region of data analyzed (*cf.* Fig. 2).

Can. J. Chem. Downloaded from www.nrcresearchpress.com by 210.87.254.40 on 09/05/12
For personal use only.

Decay of Excess Field

The problem will be solved in the approximation $i \simeq I_2$ for $Q > 0$, and initially for the more general case of two independent dielectric relaxation processes. Accordingly, [14] may be written

$$[A4] \quad \mathrm{d}[P_k \exp(B_k Q)] = [B_k \varepsilon_0 \chi_k E \exp(B_k Q)]\,\mathrm{d}Q, \quad k = 2,3$$

which on using the boundary conditions [11] and [15] (*i.e.* $P_k(Q=0) = \varepsilon_0 \chi_k E_1$, $k = 2,3$) may be integrated to yield the following expression for P_k

$$[A5] \quad P_k = [\varepsilon_0 \chi_k E_1 + B_k \varepsilon_0 \chi_k \times \int_0^Q E \exp(B_k Q)\,\mathrm{d}Q] \exp(-B_k Q)$$

From [6] and [11], $\beta E_\mathrm{d} = \beta_\mathrm{s} E_2$ for $Q > 0$, so that [5] may be written

$$[A6] \quad \varepsilon_0 E + P = \varepsilon_0 K_\mathrm{d} (\beta_\mathrm{s}/\beta) E_2$$

Eliminating P and then P_1 using [13] and [9], and eliminating β using [7] gives

$$[A7] \quad \varepsilon_0 K_1 E + P_2 + P_3 = \varepsilon_0 K_\mathrm{s} E_2$$

Substituting for P_2 and P_3 from [A5] leads to an integral equation in E. Elimination of the two integrals by the usual method of isolation and differentiation leads to the following second order differential equation in the excess field, $\Delta E = E - E_2$.

$$[A8] \quad \frac{\mathrm{d}^2 \Delta E}{\mathrm{d}Q^2} + \left(B_2 + B_3 + \frac{B_2 \chi_2 + B_3 \chi_3}{K_1}\right) \frac{\mathrm{d}\Delta E}{\mathrm{d}Q} + \frac{B_2 B_3 K_\mathrm{s}}{K_1} \Delta E = 0$$

In deriving [A8], use has been made of the relation $K_1 + \chi_2 + \chi_3 = K_\mathrm{s}$. The solution of [A8] takes the form of [4] with m_1 and m_2 the roots of [16]. The integration constants M_1 and M_2 are evaluated from the boundary conditions that for $Q = 0$, $E = E_1 + (K_\mathrm{s}/K_1)(E_2 - E_1)$ and $\mathrm{d}E/\mathrm{d}Q = -(1/K_1)(B_2 \chi_2 + B_3 \chi_3)(E - E_1)$ (which can be derived in a straightforward manner from [A5] and [A7]) and are given in [17].

Proceeding in an identical manner for the case $B_3 = \chi_3 = P_3 = 0$, $B_2 = B$, one obtains in place of [A8]

$$[A9] \quad \mathrm{d}\Delta E/\mathrm{d}Q + B(K_\mathrm{s}/K_1)\Delta E = 0$$

Using the boundary condition $E = E_1 + (K_\mathrm{s}/K_1)(E_2 - E_1)$ for $Q = 0$, [A9] integrates to give [4] with $M_2 = 0$ and M_1 and m_1 given by [12].

1. L. YOUNG. Anodic oxide films. Academic Press, London. 1961.
2. W. S. GORUK, L. YOUNG, and F. R. ZOBEL. *In* Modern aspects of electrochemistry. No. 4, *Edited by* J. O'M. Bockris. Plenum Press, New York. 1966. Chapt. 3.
3. D. A. VERMILYEA. *In* Advances in electrochemistry and electrochemical engineering. Vol. 3. *Edited by* P. Delahay and Z. Tobias. Interscience, New York. 1963, Chapt. 4.
4. M. J. DIGNAM and D. B. GIBBS. J. Phys. Chem. Solids, **30**, 375 (1969).
5. M. J. DIGNAM and P. J. RYAN. Can. J. Chem. **46**, 549 (1968).
6. J. F. DEWALD. J. Phys. Chem. Solids, **2**, 55 (1957).
7. M. J. DIGNAM and P. J. RYAN. Can. J. Chem. **46**, 535 (1968).
8. P. A. JACQUET. Met. Rev. **1**, 157 (1956).
9. B. D. CAHAN, J. B. OCKERMAN, R. F. AMLIE, and P. RUETSCHI. J. Electrochem. Soc. **107**, 725 (1960).
10. R. J. STEWART and W. F. GRAYDON. J. Phys. Chem. **59**, 86 (1955).
11. M. J. DIGNAM, D. GOAD, and M. SOLE. Can. J. Chem. **43**, 800 (1965).
12. C. P. BEAN, J. C. FISHER, and D. A. VERMILYEA. Phys. Rev. **101**, 511 (1956).
13. M. J. DIGNAM and D. F. TAYLOR. Can. J. Chem. **49**, 416 (1971).
14. L. YOUNG. Can. J. Chem. **50**, 574 (1972).
15. M. J. DIGNAM. *In* Oxides and oxide films: some fundamental aspects. Vol. I. *Edited by* J. W. Diggle. Marcel Dekker, Inc., New York. In press. Chapt. 2, Section V.
16. L. YOUNG. Proc. Roy. Soc. **A263**, 395 (1961).
17. M. J. DIGNAM. J. Electrochem. Soc. **112**, 722 (1965).
18. M. J. DIGNAM. Extended Abstracts. Chemical Institute of Canada, Symposium on Physical Chemistry of Solids, University of Montreal, Quebec, Aug. 29–31, 1966. p. 35. *Also* Extended Abstracts, Dielectric and Insulation Division, Electrochem. Soc., Meeting, Dallas, Texas, May 1967, Vol. 6, No. 1, p. 11.
19. A. TVARUSKO. U.S. At. Energy Comm. NP-16828 (1966).
20. L. YOUNG. Proc. Roy. Soc. **A258**, 496 (1960).
21. D. E. TAYLOR and M. J. DIGNAM. In preparation.

Transient Response of the System Al/Al_2O_3/Electrolyte. Part II. A.c. Impedance Measurements During Steady-State Film Growth

D. G. W. GOAD[1] AND M. J. DIGNAM

Department of Chemistry, University of Toronto, Toronto 181, Ontario

Received October 13, 1971[2]

Experiments are described in which the a.c. impedance of the system Al/Al_2O_3/electrolyte (glycol–borate) is measured under conditions of steady-state film growth. Using an equivalent circuit of a resistive and capacitive element in parallel, the results are presented in the form of the a.c. conductance, σ_{ac}, and effective dielectric constant, K_{eff}, of the oxide film as a function of the d.c. current density, I_0, and angular frequency ω. The results show that σ_{ac}/I_0 and K_{eff} vary with (ω/I_0), but within experimental error are independent of ω and I_0 separately. The dielectric relaxation model, assuming two ion-current-driven relaxation processes and using the constants determined in Part I, reproduces the data almost within experimental scatter. A poorer fit is achieved if only one relaxation process is assumed.

Nous décrivons des expériences au cours desquelles l'impédance ac du système Al/Al_2O_3/électrolyte (glycol–borate) est mesurée dans des conditions de croissance de film à l'état stationnaire. Au moyen d'un circuit équivalent d'éléments de résistance et de capacitance en parralèle, nous présentons les résultats sous forme de conductance ac, σ_{ac} et de constante diélectrique effective, K_{eff}, du film d'oxyde en fonction de la densité du courant d.c., I_0, et de la fréquence angulaire ω. Les résultats démontrent que σ_{ac}/I_0 et K_{eff} varient avec (ω/I_0), mais ils sont indépendants, à l'intérieur de l'erreur expérimentale, de ω et I_0, séparément. Le modèle de relaxation diélectrique, qui suppose deux processus de relaxation produits par un courant d'ion, utilisant les constantes déterminées dans la partie I, reproduit les données presque à l'intérieur de l'éparpillement expérimental. Un ajustement plus grossier est obtenu lorsqu'on suppose un seul processus de relaxation.

[Traduit par le journal]

Canadian Journal of Chemistry, **50**, 3267 (1972)

Introduction

In Part I of this paper (1) galvanostatic transient data for the system Al/Al_2O_3/electrolyte have been obtained and shown to be in accord with the dielectric relaxation model, provided that one postulates the existence of two independent ion-current-driven relaxation processes. Furthermore, the constants obtained from the analysis agree with those calculated earlier from potentiostatic transient data. The purpose of Part II of this paper is to report the results of a.c. impedance measurements made on the same system, during the course of steady-state film growth, and to test whether or not the results are in accord with the dielectric relaxation model.

The method employed is to superimpose a small constant amplitude a.c. current on a constant d.c. formation current. The components of the a.c. part of the electrode potential which are respectively in and out of phase with the a.c. cell current are then measured, from which the effective a.c. conductivity and dielectric constant of the oxide film can be calculated. Experiments of this kind have been carried out for the tantalum and aluminum systems by Winkel *et al.*, using a bridge circuit to measure the a.c. components (2). They did not, however, report data for the out-of-phase component.

In the present study, a lock-in (*i.e.* phase sensitive) amplifier, rather than an a.c. bridge, was used to measure the a.c. component, thus eliminating any problem which might otherwise arise from the presence of higher harmonics of the fundamental frequency. (Since the cell voltage and current are not linearly related, higher harmonics will be generated.)

Experimental

Apparatus

A schematic diagram of the apparatus used to maintain a constant d.c. current through the cell and superimpose a small a.c. current is shown in Fig. 1. The cell forms the feedback element of an operational amplifier (Philbrick model SP2A with 100 V booster), so that the current through the cell is the sum of the currents through the input resistors. One of the resistors is connected to a 15 V regulated, d.c. supply, the other to the output of the lock-in amplifier reference channel, which provides an a.c. signal continuously adjustable from 0 to 1 V and from 1.5 Hz to 10 kHz. Since the aluminum anode of the cell is connected to the

[1]Present address: ALCAN International Ltd., Research Centre, Kingston, Ontario, Canada.

[2]Revision received June 23, 1972.

Can. J. Chem. Downloaded from www.nrcresearchpress.com by 210.87.254.42 on 09/05/12
For personal use only.

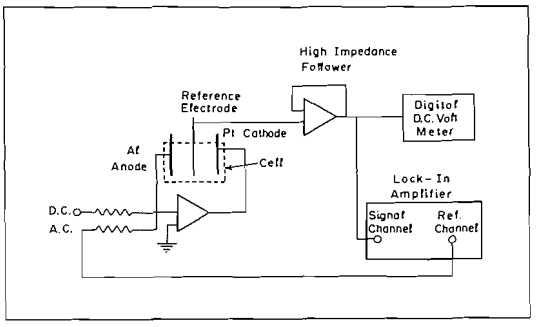

FIG. 1. Schematic diagram of the apparatus for measuring the a.c. impedance of an electrode system under galvanostatic conditions.

amplifier input, it is a virtual ground; thus the anode potential *vs.* the reference electrode is just the negative of the reference electrode potential (measured against ground). The reference electrode potential is fed through a high impedance voltage follower to both a d.c. digital voltmeter and the signal channel input of the lock-in amplifier. Thus both the d.c. and a.c. components of the electrode potential are available for recording.

The anodizing cell and electrolyte were the same in all important respects as those described in Part I (1), except that temperature control was maintained by water circulation (the cell was of double-walled construction) rather than by an air thermostat.

Results

For all the experimental runs, the d.c. electrode potential, V_0, and the two a.c. components V_{in} and V_{out}, were found to increase linearly with the time over the range of 20 to 100 V for V_0, a result expected if space charge within the film is either negligible, or confined to zones close to the oxide boundaries (*cf.* Part I). For values of V_0 less than 20 V, the time derivatives of the potentials vary by a few percent, a behavior which has been noted before in the case of dV_0/dt (3). Over the region in which steady-state conditions obtain (*i.e.* $100\text{ V} > V_0 > 20\text{ V}$), the data for a given run can therefore be represented by the values of the d.c. cell current, the amplitude and frequency of the a.c. cell current, and the time derivatives of the potentials. The derivatives were determined by linear regression analyses of the primary data. The steady-state formation current density, I_0, and corresponding field strength, E_0, were calculated from dV_0/dt as described in Part I. Having obtained I_0 and knowing the total d.c. cell current, the electrode area, and hence the

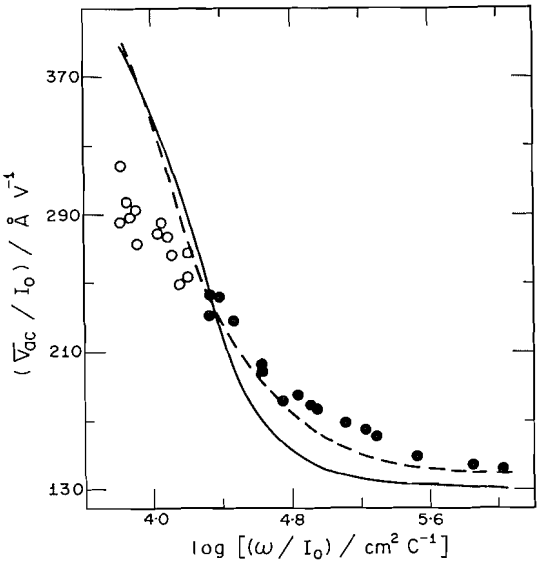

FIG. 2. Graph of $(J_{ac}/I_0) \equiv (I_{in}/E_\omega I_0)$ *vs.* log (ω/I_0). ●, $I_0 \simeq 4 \times 10^{-4}$ A/cm^2, ω varying; ○, I_0 varying, $\omega = 2\pi \times 1.5\ s^{-1}$. The solid line is calculated from [12], the broken line from [10].

amplitude of the a.c. current density, I_ω, was calculated. Finally, since for steady-state conditions there is no d.c. component to the charging current (since E_0 and I_0 are constant) then I_0 is the d.c. ion current density. Thus from Faraday's law, $E_0 = (dV_0/dt)/\Omega I_0$, $E_{in} = (dV_{in}/dt)/\Omega I_0$ and $E_{out} = (dV_{out}/dt)/\Omega I_0$ where E_{in} and E_{out} are the differential field amplitudes corresponding to V_{in} and V_{out}, and $\Omega = W_e/F\rho$, with W_e being the electrochemical equivalent weight of the oxide, ρ its density, and F the Faraday. Thus E_{in} and E_{out} may be calculated from $E_{in} = E_0(dV_{in}/dt)/(dV_0/dt)$ and $E_{out} = E_0(dV_{out}/dt)/(dV_0/dt)$. The results for a single run may therefore be represented by the values for the six quantities, I_0, E_0, I_ω, E_{in}, E_{out}, and ω for that run. A further reduction in the data can be achieved by defining a parallel equivalent a.c. conductivity, σ_{ac}, and dielectric constant, K_{eff}, according to (see Appendix)

$$[1] \qquad \sigma_{ac} = I_\omega E_{in}/(E_{in}^2 + E_{out}^2)$$

$$[2] \qquad \omega\varepsilon_0 K_{eff} = -I_\omega E_{out}/(E_{in}^2 + E_{out}^2)$$

where ε_0 is the permittivity of free space. If the anodic oxide film behaved simply as a lossy dielectric, σ_{ac} and K_{eff} would be the conductivity and dielectric constant of the film (see

Can. J. Chem. Downloaded from www.nrcresearchpress.com by 210.87.254.42 on 09/05/12
For personal use only.

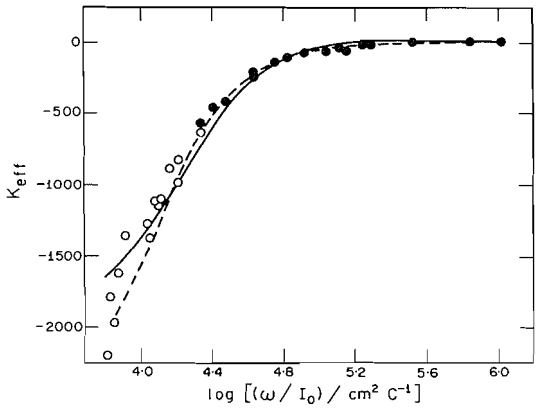

FIG. 3. Graph of $K_{eff} \equiv I_{out}/E_\omega \omega \varepsilon_0$ *vs.* log (ω/I_0). ●, $I_0 \simeq 4 \times 10^{-4}$ A/cm^2, ω varying; ○, I_0 varying, $\omega = 2\pi \times 1.5$ s^{-1}. The solid line is calculated from [13], the broken line from [11].

Appendix). It should be emphasized, however, that the calculation of σ_{ac} and K_{eff} from the primary data does not involve assumptions concerning the mechanism of anodic oxidation.

In Figs. 2 and 3 the results for all the runs are plotted in the form σ_{ac}/I_0 and K_{eff} *vs.* log (ω/I_0). A practical lower limit exists on the ratio $\omega : I_0$ which can be used, since for increasing I_0, the total time available for measurement decreases, and each measurement takes a minimum of several periods, $1/\omega$, to perform. The somewhat larger scatter in the results for small values of ω/I_0 is due to this difficulty.

Discussion

The results, plotted in the form σ_{ac}/I_0 and K_{eff} *vs.* log (ω/I_0) fall on smooth curves within experimental scatter, even though different values for I_0 have been used. Thus σ_{ac}/I_0 and K_{eff} depend on ω/I_0, but appear to be independent of ω and I_0 separately, within experimental error. Such behavior might have been anticipated from the form of the galvanostatic and potentiostatic transients (*cf.* Part I) which were shown not to involve time as a parameter. Thus all three quantities σ_{ac}/I_0, K_{eff}, and (ω/I_0), are dimensionally independent of time.

The large negative value which K_{eff} assumes when ω/I_0 is small appears at first glance to be rather surprising. However, K_{eff} cannot be interpreted simply as the dielectric constant of the oxide film since relaxation processes associated with the kinetics of ionic conduction will contribute to the current component out of phase with the field, and hence to K_{eff}. Thus the behavior of both σ_{ac} and K_{eff} provides information on the kinetics of ionic conduction.

In the following sections, expressions for K_{eff} and σ_{ac} are derived on the basis of the dielectric relaxation model, outlined in Part I, and compared with the experimental results.

Expressions for K_{eff} and σ_{ac} from Dielectric Relaxation Model

We employ at the outset the equations which involve two ion current driven dielectric relaxation processes (*cf.* Part I). Thus from [5] to [14] of Part I,

$$[3] \qquad i = \alpha \exp \beta E_d$$

$$[4] \qquad \varepsilon_0 K_d E_d = \varepsilon_0 E + P$$

$$[5] \qquad P = \varepsilon_0 \chi_1 E + P_2 + P_3$$

$$[6] \qquad dP_k/dt = B_k i(\varepsilon_0 \chi_k E - P_k), \qquad k = 2,3$$

$$[7] \qquad I = i + i^c = i + \varepsilon_0 \, dE/dt + dP/dt$$

where i, i^c, and I are the ion, charging, and total current densities, respectively; E and E_d are the fields in the oxide and oxide/electrolyte double layer, respectively; P is the polarization of the oxide film which is divided into components $\varepsilon_0 \chi_1 E$, P_2, and P_3 with corresponding electric susceptibilities χ_1, χ_2, and χ_3; ε_0 is the permittivity of free space; α, β, B_2, and B_3 are constants associated with the kinetics of ion transport (α and β) and dielectric polarization (B_2 and B_3); and t is time. Next we expand E, i, I, P, P_2, P_3, and E_d in terms of their d.c. and a.c. components, *i.e.*,

$$[8] \quad \begin{aligned} E &= E_0 + E_\omega \exp(j\omega t) + \text{harmonics} \\ i &= I_0 + (i_{in} + j i_{out}) \exp(j\omega t) + \text{harmonics} \\ I &= I_0 + (I_{in} + j I_{out}) \exp(j\omega t) + \text{harmonics} \\ P &= P_0 + (P_{in} + j P_{out}) \exp(j\omega t) + \text{harmonics} \end{aligned}$$

etc.

where $j = \sqrt{-1}$ and the subscripts in and out refer to the components which are in and out of phase, respectively, with the a.c. field of amplitude E_ω. Finally, on making the substitutions [8] into [3] to [7], and equating corresponding components, a total of 18 equations are obtained,

Can. J. Chem. Downloaded from www.nrcresearchpress.com by 210.87.254.42 on 09/05/12
For personal use only.

six in each of the d.c., real, and imaginary a.c. components respectively. Elimination of the d.c. and a.c. components of i, P, P_2, P_3, and E_d leads to the following three independent equations

$$[9] \qquad I_0 = \alpha \exp(\beta_s E_0)$$

$$[10] \quad \frac{\sigma_{ac}}{I_0} = \beta_t + \left(\frac{\beta_s - \beta_t}{1+\Delta}\right)\left[1 + \left(\frac{\omega}{B_2 B_3 I_0}\right)^2 \left(\frac{B_2^2\chi_2 + B_3^2\chi_3}{K_s - K_1}\right)\right] + \frac{\varepsilon_0(\omega/I_0)^2}{B_2B_3(1+\Delta)}\left[(B_2\chi_2 + B_3\chi_3) + \left(\frac{\omega^2}{B_2B_3I_0^2}\right)(B_2\chi_2 + B_3\chi_3)\right]$$

$$[11] \quad K_{eff} = K_1 + \left(\frac{K_s - K_1}{1+\Delta}\right)\left[1 + \left(\frac{\omega}{B_2B_3I_0}\right)^2\left(\frac{B_2^2\chi_2 + B_3^2\chi_3}{K_s - K_1}\right)\right] - \left(\frac{\beta_s}{\varepsilon_0 K_s B_2 B_3 \Delta}\right)\left[(B_2\chi_3 + B_3\chi_2) + \left(\frac{\omega^2}{B_2B_3I_0^2}\right)(B_2\chi_2 + B_3\chi_3)\right]$$

where

$$\sigma_{ac} = I_{in}/E_\omega$$

$$K_{eff} = I_{out}/E_\omega \varepsilon_0 \omega$$

(they are also given by [1] and [2], see Appendix),

$$\Delta = (\omega/B_2B_3I_0)^2(B_2^2 + B_3^2 + \omega^2/I_0^2)$$

$$K_s = 1 + \chi_1 + \chi_2 + \chi_3$$

$$K_1 = 1 + \chi_1$$

$$\beta_s = (K_s/K_d)\beta$$

and

$$\beta_t = (K_1/K_d)\beta$$

Equation 9 is simply the relationship between the steady-state current density and field strength (see Part I), while [10] and [11] are the desired expressions for σ_{ac} and K_{eff} when two ion-current-driven dielectric relaxation processes are considered. The equations appropriate for a single such relaxation process are obtained from [10] and [11] on setting $\chi_3 = 0$, and $B_2 = B$, and are given by

$$[12] \quad \frac{\sigma_{ac}}{I_0} = \beta_t + \left(\frac{\beta_s - \beta_t}{1 + (\omega/BI_0)^2}\right) + \left(\frac{\varepsilon_0}{B}\right)\left(\frac{\omega}{I_0}\right)^2\left(\frac{K_s - K_1}{1 + (\omega/BI_0)^2}\right)$$

$$[13] \quad K_{eff} = K_1 - \left(\frac{(\beta_s - \beta_t)/\varepsilon_0 B}{1 + (\omega/BI_0)^2}\right) + \left(\frac{K_s - K_1}{1 + (\omega/BI_0)^2}\right)$$

In Table 1, the behavior of σ_{ac}/I_0 and K_{eff} in the high and low frequency limits is given. For both cases $K_{eff} = K_1$ in the high frequency limit, and $\sigma_{ac}/I_0 = \beta_s$ in the low frequency limit, as expected.

For both forms of the dielectric relaxation model, the experimental quantities σ_{ac}/I_0 and K_{eff} are predicted to be functions of (ω/I_0), but not of ω or I_0 independently. (This conclusion is based on the assumption that β_s and β_t are independent of E_0, which is not strictly true as noted in Part I, but is a good enough approximation for the present application.) The solid lines in Figs. 2 and 3 were computed from eqs. 12 and 13, by setting $K_1 = 8.5$, $\beta_t = 129$ Å/V, and $\beta_s/\beta_t = 3.1$ (4), then adjusting B to satisfy a weighted least squares criterion for σ_{ac}/I_0 and K_{eff}, the weighting factor being taken to be proportional to the square of the reciprocal of the standard deviation of the individual measurements of σ_{ac}/I_0 and K_{eff}. The value for B found in this way is 1.75×10^4 cm^2/C. It is evident that the fit is only fair.

The broken lines of Figs. 2 and 3 were computed from [10] and [11] using the values for K_s/K_1, χ_2/K_1, B_2, and B_3 determined in Part I of this paper, and adjusting K_1 and β_t to satisfy the same least squares criterion as above. The fit is appreciably better, being within experimental scatter except perhaps for σ_{ac}/I_0 at low (ω/I_0) where the experimental measurements are the most difficult to obtain. Furthermore, the values deduced, $K_1 = 10$ and $\beta_t = 134$ Å/V, agree within experimental error with independent measurements of these parameters (4). Thus from Fig.

Can. J. Chem. Downloaded from www.nrcresearchpress.com by 210.87.254.42 on 09/05/12
For personal use only.

TABLE 1. Expressions for σ_{ac}/I_0 and K_{eff} in the high and low frequency limits

	Single relaxation process	Two independent relaxation processes
$\underset{(\omega/I_0)\to 0}{\text{Limit}}\left(\frac{\sigma_{ac}}{I_0}\right)$	β_s	β_s
$\underset{(\omega/I_0)\to 0}{\text{Limit}}\ (K_{eff})$	$\frac{(\beta_s-\beta_t)}{\varepsilon_0 B}+\{K_s\}^*$	$\frac{(\beta_s-\beta_t)}{\varepsilon_0 B_2}+\frac{\chi_3\beta_t}{\varepsilon_0 K_1}\left(\frac{1}{B_2}-\frac{1}{B_3}\right)+\{K_s\}^*$
$\underset{(\omega/I_0)\to \infty}{\text{Limit}}\left(\frac{\sigma_{ac}}{I_0}\right)$	$\beta_t+\{\varepsilon_0\chi_2 B\}^*$	$\beta_t+\{\varepsilon_0(\chi_2 B_2+\chi_3 B_3)\}^*$
$\underset{(\omega/I_0)\to \infty}{\text{Limit}}\ K_{eff}$	K_1	K_1

*The terms in parentheses make a negligible contribution for the Al/Al_2O_3/electrolyte system.

10, ref. 4, β_t has a value of 134 Å/V for $I_0 \sim 10^{-3}$ A/cm^2, which lies approximately mid way within the range of I_0 values covered in Figs. 2 and 3 (4×10^{-4} to 1.5×10^{-3} A/cm^2). The value of K_1, as distinct from the ratios K_s/K_1 and χ_2/K_1, affects the fit significantly only in the case of K_{eff}, which approaches K_1 for large values of (ω/I_0) (*cf.* Table 1). It is apparent from Fig. 3 that a value for K_1 of 10 is, within experimental accuracy, indistinguishable from the value 8.5 (4).

In summary, the dielectric relaxation model, employing two independent relaxation processes, accounts quantitatively for a.c. impedance measurements, as well as for potentiostatic and galvanostatic transient measurements, performed on the system Al/Al_2O_3/electrolyte, a single set of constants reproducing the data from all three experiments.

Appendix

Defining I_{in} and I_{out} for any circuit element as the components of the a.c. current density, of amplitude I_ω, which are respectively in and out of phase with the a.c. field of amplitude E_ω; and E_{in} and E_{out} as the components of a.c. field which are respectively in and out of phase with the a.c. current density, then

[A1] $E_{in} = E_\omega \cos\delta, \qquad E_{out} = E_\omega \sin\delta$

[A2] $I_{in} = I_\omega \cos\delta, \qquad I_{out} = -I_\omega \sin\delta$

where δ is the phase angle between the a.c. current and field. Solving for I_{in}/E_ω and I_{out}/E_ω gives

[A3] $I_{in}/E_\omega = \sigma_{ac} = I_\omega E_{in}/(E_{in}^2 + E_{out}^2)$

[A4] $I_{out}/E_\omega = \omega\varepsilon_0 K_{eff} = -I_\omega E_{out}/(E_{in}^2 + E_{out}^2)$

where σ_{ac} and K_{eff} are the parallel equivalent conductivity and dielectric constant for the circuit element. Equations A3 and A4 have been used in writing down [1], [2], [10], and [11].

The authors are grateful to the National Research Council of Canada for supporting this research and for a Scholarship (D.G.W.G.). One of us (D.G.W.G.) also wishes to thank Canadian Industries Ltd., for financial assistance in the form of a Fellowship.

1. D. G. W. GOAD and M. J. DIGNAM. Can. J. Chem. This issue.
2. P. WINKEL, C. A. PISTORIUS, and W. CH. VAN GEEL. Phillips Res. Rept. **13**, 277 (1958).
3. M. J. DIGNAM and P. J. RYAN. Can. J. Chem. **41**, 3108 (1963).
4. M. J. DIGNAM and P. J. RYAN. Can. J. Chem. **46**, 549 (1968).

Can. J. Chem. Downloaded from www.nrcresearchpress.com by 210.87.254.42 on 09/05/12
For personal use only.

A Total Synthesis of Cadin-4, 10(15)-dien-3α-ol: Structure of Khusinol

R. B. KELLY AND J. EBER

Department of Chemistry, University of New Brunswick, Saint John, New Brunswick

Received May 23, 1972

A total synthesis of cadin-4,10(15)diene-3α-ol, one of the structures proposed for khusinol, is described. Neither this compound nor its C_3-epimer was identical with khusinol.

La synthèse totale du cadindiène-4,10(15)ol-3α, une des structures proposées pour le khusinol est décrite. Ce composé et son épimère au niveau du C_3 ne sont pas identifiés au khusinol.

[Traduit par le journal]

Canadian Journal of Chemistry, **50**, 3272 (1972)

Can. J. Chem. Downloaded from www.nrcresearchpress.com by 210.87.254.6 on 09/05/12
For personal use only.

The isolation of khusinol from the oil of *Vitiveria zizanioides* (L). Nash was first reported in 1963 and at that time structure **1** (title compound) was assigned to this sesquiterpene alcohol (1). It was also shown, by conversion to (−) γ-cadinene, that khusinol belongs to the naturally occurring antipodal series of cadalenic compounds and is therefore of interest from the point of view of biogenesis (1).

Structure **1** for khusinol was adduced from chemical evidence and, apparently, without the benefit of n.m.r. spectroscopy. More recently, however, a revised structure **2** for khusinol has been proposed (2). The latter proposal was based on further chemical evidence and high resolution n.m.r. spectroscopy. The validity of neither of these structures has been verified by synthesis.

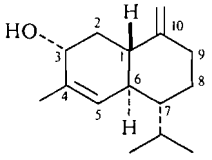

1

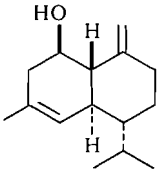

2

Before the proposal of structure **2** for khusinol, we were prompted by the availability in our laboratories of the convenient intermediate **3** to complete a synthesis of **1**. We now wish to give an account of the details of this synthesis (see Scheme 1) and to report that, since neither **1** nor its C_3-epimer (**12**) were identical with khusinol, these structures need no longer be considered for this sesquiterpenoid.[1]

[1]The numbering system shown in **1** is used throughout.

The totally synthetic enone **3** (3) was converted into the crystalline epoxide **4** by treatment with *m*-chloroperbenzoic acid.[2] The assignment of structure **4**, rather than the alternative structure **5**, to the epoxide is based on the following evidence. The epoxide was converted, in 92% yield, into a crystalline bromohydrin in which the bromine atom and the hydroxyl group are *trans* diaxially oriented (4). The n.m.r. signal for the methyl group at C-4 appeared at δ 1.87 in agreement with the presence of the group CH_3—C—Br. Acetylation of the bromohydrin under conditions which could not be expected to acetylate a tertiary alcohol such as **7** and which gave only a monoacetate when applied to the diol **8** (*vide supra*), did, in fact, give a crystalline acetate. Furthermore, the downfield shift (1.17 p.p.m.) of the n.m.r. signal for the C-3 proton as a result of acetylation of the bromohydrin is characteristically associated with the acetylation of a secondary alcohol such as **6** (5). The above evidence establishes structure **6** for the bromohydrin to the exclusion of **7**. Therefore, in accordance with the well established stereospecific manner in

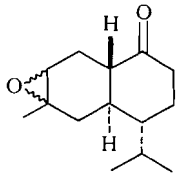

4 β-Epoxide (as in Scheme 1)
5 α-Epoxide

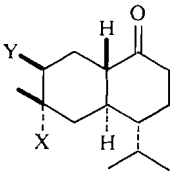

6 Y = OH; X = Br
7 Y = Br; X = OH

[2]The i.r. and n.m.r. spectra of all compounds were consistent with assigned structures; spectral data are given in the Experimental.

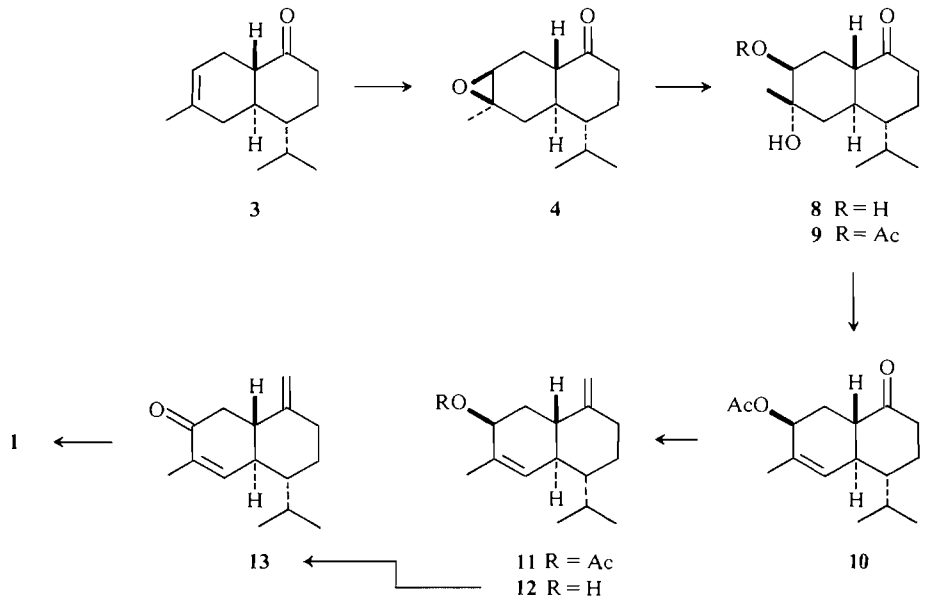

SCHEME 1

which epoxides are cleaved (4), the epoxide which is the precursor of **6** must be assigned structure **4** rather than **5**.

Hydrolysis of the epoxide **4** afforded the crystalline diaxially oriented diol **8** (4). Acetylation of the latter and treatment of the resulting monoacetate **9** with phosphorus oxychloride in pyridine gave the olefin **10**. The fact that the n.m.r. signal for the vinylic proton in **10** appeared as a singlet is proof that the double bond was introduced into the assigned position (3).

The acetate **10** was converted into the diene **11** in 79% yield via a modified Wittig reaction (6). Several cases have been reported where decalones and octalones having the keto group adjacent to a ring junction (such as in **10**), when subjected to the Wittig reaction, have yielded olefins in which the angular carbon atom originally adjacent to the ketone had undergone epimerization (7). This phenomenon has been observed only in the case of *cis*-fused systems. The possibility of this type of epimerization happening in the case of **10** to give a *cis*-fused diene is ruled out by the fact that, in the n.m.r. spectrum of the diene, the signal at δ 5.83 for the vinylic proton at C-5 appeared as a singlet. This requires that the dihedral angle between the C-5 and -6 protons be approximately 90°, a requirement satisfied by the *trans*-fused structure **11** but not by any reasonable conformation of the *cis*-fused diene corresponding to **11**.

Reduction of the acetate **11** with lithium aluminum hydride afforded the alcohol **12** which is the C_3-epimer of the desired compound (**1**).

Oxidation of **12** with activated manganese dioxide (8) gave, in 75% yield, the α,β-unsaturated ketone **13** which, on reduction with lithium aluminum hydride, afforded **1** as a crystalline compound in 98% yield. The broadening of the n.m.r. signal for the C-3 proton by 13 Hz ($w_{1/2}$) as a result of the transformation **12** → **1** is consistent with the conversion of a quasi axial hydroxyl into a quasi equatorial hydroxyl group (5). Comparison of the spectral properties and behavior on t.l.c. of the newly acquired dienol with the corresponding properties of the precursor dienol **12** showed that the two compounds were distinctly different.

Experimental

General

The n.m.r. spectra were determined in deuteriochloroform ($CDCl_3$) solutions with a Varian T-60 instrument. Chemical shifts are expressed in p.p.m. (δ values) downfield from the tetramethylsilane signal as internal standard.

Can. J. Chem. Downloaded from www.nrcresearchpress.com by 210.87.254.6 on 09/05/12
For personal use only.

Can. J. Chem. Downloaded from www.nrcresearchpress.com by 210.87.254.6 on 09/05/12
For personal use only.

Reaction products were isolated by the following procedure. The product was extracted into the specified solvent and the extract was washed two or three times with appropriate aqueous solutions as indicated. The original aqueous layer (if any) and the aqueous washings were extracted three times with the solvent and the combined extracts were dried over anhydrous magnesium sulfate, filtered, and evaporated *in vacuo* on a rotary evaporator.

Brine refers to a saturated solution of sodium chloride.

Petroleum ether refers to the fraction with boiling point range 30–60°.

Keto Epoxide ***4***

A solution of 411 mg of the enone **3** and 454 mg of *m*-chloroperbenzoic acid in 37 ml of chloroform was stirred at room temperature for 1 h. The solution was then treated with 28 ml of 10% aqueous sodium bisulfite solution and stirred for a further 15 min. The reaction mixture was extracted with chloroform and the extract was worked-up in the usual manner by washing with 5% sodium bicarbonate solution and water. The oily residue, on crystallization from pentane afforded 245 mg (55%) of **4**, m.p. 71–73°; ν_{max} (Nujol) 1705 cm^{-1} (ketone); n.m.r. δ 0.75 and 1.00 (doublets, 3H each, $J = 7.0$ Hz, isopropyl group),[3] 1.28 (s, 3H, CH_3—C—O), 3.05 (m, 1H, H—C—O).

Anal. Calcd. for $C_{14}H_{22}O_2$: C, 75.64; H, 9.97. Found: C, 75.44; H, 9.82.

Keto Bromohydrin ***6*** *and its Acetate*

A solution of 33 mg of the epoxide **4** in 2 ml of glacial acetic acid was treated, with cooling in an ice bath, with 0.5 ml of 24% hydrobromic acid in acetic acid. The reaction solution was kept at 0° for 45 min then diluted with 30 ml of methylene chloride. The resulting solution was worked-up in the usual manner by washing with water. The residue, an oil, was crystallized from pentane to give 42 mg (92%) of **6**, m.p. 123–125°; ν_{max} (Nujol) 3420 (OH) and 1685 cm^{-1} (ketone); n.m.r. δ 1.87 (s, 3H, CH_3—C—Br), 4.03 (m, $w_{1/2}$ = 6.5 Hz, 1H, H—C—OH).

The *acetate* was prepared in 72% yield in the usual manner with acetic anhydride in pyridine at room temperature. Crystallized from pentane, it melted at 143–145°, ν_{max} (Nujol) 1740 (acetate) and 1705 cm^{-1} (ketone); n.m.r. δ 1.71 (s, 3H, CH_3—C—Br), 2.00 (s, 3H, acetate), 5.20 (m, $w_{1/2} = 6.5$ Hz, 1H, H—C—OAc).

Anal. Calcd. for $C_{16}H_{25}OBr$: Br, 23.14. Found: Br, 23.02.

Keto Diol ***8***

A mixture of 445 mg of the epoxide **4**, 60 ml of acetone, and 60 ml of water was refluxed for 15 h. The acetone was evaporated *in vacuo* and the remaining aqueous solution was saturated with sodium chloride and extracted with ether. The ether extracts were worked-up in the usual manner by washing with brine. The crude product, an oil, was chromatographed on a column of 15.0 g of silica gel in benzene–ether (1:1). The eluate, on crystallization from ethyl acetate–petroleum ether afforded 237 mg of **8**, m.p. 134°; ν_{max} (Nujol) 3550 and 3350 (hydroxyls) and 1680 cm^{-1} (ketone); n.m.r. δ 1.28 (s, 3H, CH_3—C—OH), 3.63 (m, $w_{1/2} = 6.5$ Hz, 1H, H—C—OH).

Anal. Calcd. for C_{14} $H_{24}O_3$: C, 69.54; H, 10.06. Found: C, 70.20: H, 10.28.

[3]This pair of doublets appears in the n.m.r. spectra of all succeeding compounds.

Acetate ***9***

Treatment of the diol **8** in the usual manner with acetic anhydride in pyridine afforded, in 95% yield, the acetate **9**, m.p. 137°; ν_{max} (Nujol) 3410 (OH) and 1700 cm^{-1} (broad band, ketone and acetate); n.m.r. δ 1.30 (s, 3H, CH_3—C—OH), 2.06 (s, 3H, acetate). 4.82 (m, $w_{1/2} = 6.5$ Hz, 1H, H—C—OAc).

Anal. Calcd. for $C_{16}H_{26}O_4$: C, 68.05; H, 9.28. Found: C, 68.38; H, 9.40.

Enone Acetate ***10***

A solution of 2.03 g of the acetate **9** in 75 ml of pyridine was treated, with cooling on an ice-salt bath, with 16.5 ml of phosphorus oxychloride then left at room temperature for 12 h. The reaction was poured into a mixture of 500 g of ice and water and the resulting cold solution was extracted with ether. The ether extract was worked-up in the usual manner by washing, in the order mentioned, with cold 1 *N* hydrochloric acid, cold saturated sodium bicarbonate solution, and ice water. Evaporation of the ether extracts yielded 2.00 g of yellow oil which was combined with 450 mg of similar material from another run. The oil was chromatographed on a column of 120 g of silica gel impregnated with 20% of silver nitrate. Elution of the column with 25% of ether in petroleum ether, evaporation of the effluent *in vacuo* and crystallization of the residue from pentane afforded 1.40 g (61%) of **10**, m.p. 108–109°; ν_{max} (Nujol), no hydroxyl bands, 1735 (acetate) and 1710 cm^{-1} (ketone); n.m.r. δ 1.71 (s, 3H, vinylic CH_3), 2.03 (s, 3H, acetate), 5.17 (m, $w_{1/2} = 9.5$ Hz; 1H, H—C—OAc), 5.81 (s, 1H, vinylic proton).

Anal. Calcd. for $C_{16}H_{24}O_3$: C, 72.69; H, 9.15. Found: C, 72.56; H, 8.96.

Dienol Acetate ***11***

The Wittig reaction was carried out in an atmosphere of dry, oxygen-free nitrogen as follows. A stirred suspension of 393 mg of the ketone **10** in 3 ml of dimethyl sulfoxide was treated with 3.75 ml of a 0.5 *M* solution of methylenetriphenylphosphorane (6) whereupon a mildly exothermic reaction occurred and the ketone was completely dissolved. The yellow reaction solution was stirred at room temperature for 11 h then poured into 35 ml of water. The aqueous solution was worked-up in the usual manner by extraction with ether, and washing the ether extracts with water. Evaporation of the ether extracts *in vacuo* gave 446 mg of oil which was chromatographed on a column of 15.0 g of silica gel impregnated with 20% of silver nitrate. Elution of the column with 5% of ether in pentane yielded an oil which, after crystallization from pentane, afforded 309 mg (79%) of **11**, m.p. 53–54°; ν_{max} (Nujol) 1740 (acetate), 1684 (olefin), and 890 cm^{-1} with overtone at 1780 cm^{-1} (exocyclic CH_2); n.m.r. δ 1.72 (s, 3H, vinylic CH_3), 2.03 (s, 3H, acetate), 4.47 and 4.63 (singlets, 1H each, exocyclic CH_2), 5.17 (m, $w_{1/2} = 7.0$ Hz, 1H, H—C—OAc), 5.83 (s, 1H, vinylic proton).

Anal. Calcd. for $C_{17}H_{26}O_2$: C, 77.81; H, 9.99. Found: C, 78.01; H, 9.97.

Dienol ***12***

A solution of 519 mg of the dienol acetate **11** in 25 ml of ether was added dropwise to a stirred mixture of 250 mg of lithium aluminum hydride in 25 ml of ether. After stirring for 16 h at room temperature, the reaction mixture was refluxed for 2 h, cooled, and treated with 0.4 ml of brine

and stirred for a further period of 1 h. Removal of the solid material by filtration and evaporation of the filtrate *in vacuo* gave 550 mg of oil. Chromatography of the crude product on 25 g of silica gel impregnated with 20% of silver nitrate using 25% of ether in petroleum ether as solvent gave an oil which, on crystallization from petroleum ether, afforded 348 mg of **12**, m.p. 96°; ν_{max} (Nujol), no carbonyl absorption, 3225 (OH), 1648 (olefin), 880 with overtone at 1760 cm^{-1} (exocyclic CH_2); n.m.r. δ 1.78 (s, 3H, vinylic CH_3), 3.97 (m, $w_{1/2}$ = 7.0 Hz, 1H, H—C—OH), 4.50 and 4.63 (singlets, 1H each, exocyclic CH_2), 5.70 (s, 1H, vinylic proton).

Anal. Calcd. for $C_{15}H_{24}O$: C, 81.76; H, 10.98. Found: C, 81.63; H, 10.71.

Dienone ***13***

A suspension of 251 mg of the dienol **12** and 5.0 g of activated manganese dioxide (8) in 75 ml of pentane was stirred at room temperature for 6 h. Removal of the solid material by filtration and evaporation of the filtrate *in vacuo* afforded an oil which crystallized from pentane to afford 186 mg (74%) of **13**, m.p. 62.5–63°; λ_{max} (EtOH) 238 nm (ε, 9700); ν_{max} (Nujol), no hydroxyl band, 1675 (ketone), 1647 (olefin), 880 with overtone at 1760 cm^{-1} (exocyclic CH_2); n.m.r. δ 1.78 (s, 3H, vinylic CH_3), 4.50 and 4.71 (singlets, 1H each, exocyclic CH_2), 6.81 (s, 1H, vinylic proton).

Anal. Calcd. for $C_{15}H_{22}O$: C, 82.52; H, 10.16. Found: C, 82.84; H, 10.06.

Dienol ***1*** *(Cadin-4, 10(15)-diene-3α-ol)*

A solution of 130 mg of the dienone **13** in 10 ml of ether was added dropwise to a refluxing mixture of 200 mg of lithium aluminum hydride and 10 ml of ether. The reaction mixture was refluxed for 18 h then cooled and treated with 0.4 ml of brine. After stirring for 2 h, the solid material was removed by filtration and the filtrate was evaporated *in vacuo*. Crystallization of the residue from ether–petroleum ether afforded 129 mg of **1**, m.p. 115.5–116.5°; ν_{max} (Nujol) 3350(OH), 1647 (olefin), 880 with overtone at 1760 cm^{-1} (exocyclic CH_2); n.m.r. δ 1.77 (s, 3H, vinylic CH_3), 4.15 (m, $w_{1/2}$ = 20 Hz, 1H, H—C—OH), 4.50 and 4.62 (singlets, 1H each, exocyclic CH_2), 5.57 (s, 1H, vinylic proton).

This compound was separated from authentic khusinol and from the dienol **12** by t.l.c. on silica gel with chloroform as solvent.

Anal. Calcd. for $C_{15}H_{24}O$: C, 81.76; H, 10.98. Found: C, 81.56; H, 11.20.

We are grateful to the National Research Council of Canada for a grant in aid of this work. Also, we thank Dr. K. K. Chakravarti, National Chemical Laboratory, Poona, India, for a sample of khusinol.

1. A. A. Rao, K. L. Surve, K. K. Chakravarti, and S. C. Bhattacharyya. Tetrahedron, **19**, 233 (1963).
2. S. V. Tirodkar, S. K. Paknikar, and K. K. Chakravarti. Sci. and Cult. **35**, 27 (1969).
3. R. B. Kelly and J. Eber. Can. J. Chem. **48**, 2246 (1970).
4. A. Furst and P. A. Plattner. Abstr. Papers 12th Intern. Congress Pure and Appl. Chem. New York. 1951. p. 409.
5. N. S. Bhacca and D. H. Williams. Applications of n.m.r. spectroscopy in organic chemistry. Holden-Day, Inc., San Francisco. 1964. pp. 77–83.
6. R. Greenwald, M. Chaykovsky, and E. J. Corey. J. Org. Chem. **28**, 1128 (1963).
7. C. H. Heathcock and R. Ratcliffe. J. Am. Chem. Soc. **93**, 1746 (1971) and refs. cited therein.
8. J. Attenburrow, A. F. B. Cameron, J. H. Chapman, R. M. Evans, B. A. Hems, A. B. A. Jansen, and T. Walker. J. Chem. Soc. 1094 (1952).

Can. J. Chem. Downloaded from www.nrcresearchpress.com by 210.87.254.6 on 09/05/12
For personal use only.

Synthesis of 8,3′-Thioanhydroguanosine[1]

KELVIN K. OGILVIE, LEWIS A. SLOTIN,[2] DENIS C. K. LIN, AND JOHN B. WESTMORE
Department of Chemistry, University of Manitoba, Winnipeg, Manitoba

Received May 23, 1972

The synthesis of 8,3′-thioanhydroguanosine is described. The anhydro ring is formed by displacement of bromine from position-8 and methanesulfonate from the 3′-position using thiourea in refluxing *n*-butanol. The 8,3′-thioanhydroguanosine is converted by Raney nickel reduction to 3′-deoxyguanosine, an analogue of cordycepin.

La synthèse du 8,3′-thioanhydroguanosine est décrite. Le cycle anhydro est formé par déplacement du brome de la position-8 et du méthanesulfonate de la position-3′, en utilisant la thiourée dans le *n*-butanol à reflux. Le 8,3′-thioanhydroguanosine est transformé en 3′-déoxyguanosine, un analogue de la cordycépine, par réduction au nickel de Raney. [Traduit par le journal]

Canadian Journal of Chemistry, **50**, 3276 (1972)

Can. J. Chem. Downloaded from www.nrcresearchpress.com by 210.87.254.42 on 09/05/12
For personal use only.

Introduction

Anhydronucleosides are important modifications of natural nucleosides. They are easily converted into either the natural ribo or sugar modified nucleosides (1, 2) and have provided an attractive synthetic route to nucleotides, particularly arabinonucleotides (3–5). Recently a thioanhydropurine nucleoside has been used in studies on enzyme specificity (6).

While several papers have recently appeared which present general methods (7–9) for the synthesis of 8,2′-anhydropurine nucleosides, there is still no simple general route to the 8,3′-anhydropurines. Indeed adenosine is the only purine nucleoside for which 8,3′-anhydroderivatives have been described (2, 10). We wish to report the synthesis of 8,3′-thioanhydroguanosine which is readily converted into 3′-deoxyguanosine, an analogue of cordycepin.

Results and Discussion

The synthesis of 8,3′-thioanhydroguanosine is outlined in Scheme 1. N^2-Dimethylaminomethylene-8-bromoguanosine (**1**, 11) was treated with excess trityl chloride at elevated temperatures (12) to produce 2′,5′-di-*O*-trityl-N^2-dimethylaminomethylene-8-bromoguanosine (**2**) in 74% yield. This product was treated with methanesulfonyl chloride in pyridine to introduce the sulfonate group on the 3′-position. Because we anticipated that the N^2- and $O^{2',5'}$-protecting groups would be at least partially hydrolyzed during the step to form the anhydrolinkage, these groups were hydrolyzed directly using hydrazine hydrate solution followed by acetic acid to yield 3′-*O*-methanesulfonyl-8-bromoguanosine (**3**).

The anhydrolinkage was formed by treating **3** with thiourea in refluxing *n*-butanol producing 8,3′-thioanhydroguanosine (**4**) in 37% yield. Compound **4** was identified by mass spectral analysis[3] including a high resolution mass spectrum, of its silylated derivative. Compound **4** was converted to 3′-deoxyguanosine (**5**, 13) using Raney nickel.

Compound **5** was further characterized by acidic hydrolysis (19) to 3-deoxyribose which showed a negative Dische test (16) but positive cysteine (17) and aniline (18) tests. 3′-Deoxyguanosine (3′-dG) has very similar properties (λ_{max} (H_2O) 254 nm 270 (sh) nm, M^+ of the tetrasilyl derivative = 555) to 2′-deoxyguanosine (2′-dG) except for paper chromatography in solvent A where 3′-dG has $R_f = 0.24$ while 2′-dG has $R_f = 0.32$.

3′-Deoxyguanosine is the guanosine analogue of cordycepin, an antibiotic first isolated by Cunningham in 1951 (20). Cordycepin is converted metabolically to the triphosphate which inhibits purine biosynthesis and RNA synthesis (21).

[1]Part VIII in a series on anhydronucleosides.
[2]NRCC Scholarship Holder 1970–present.

[3]A detailed mass spectral analysis of thioanhydropurines will be reported shortly (14), see also Ikehara and coworkers (15).

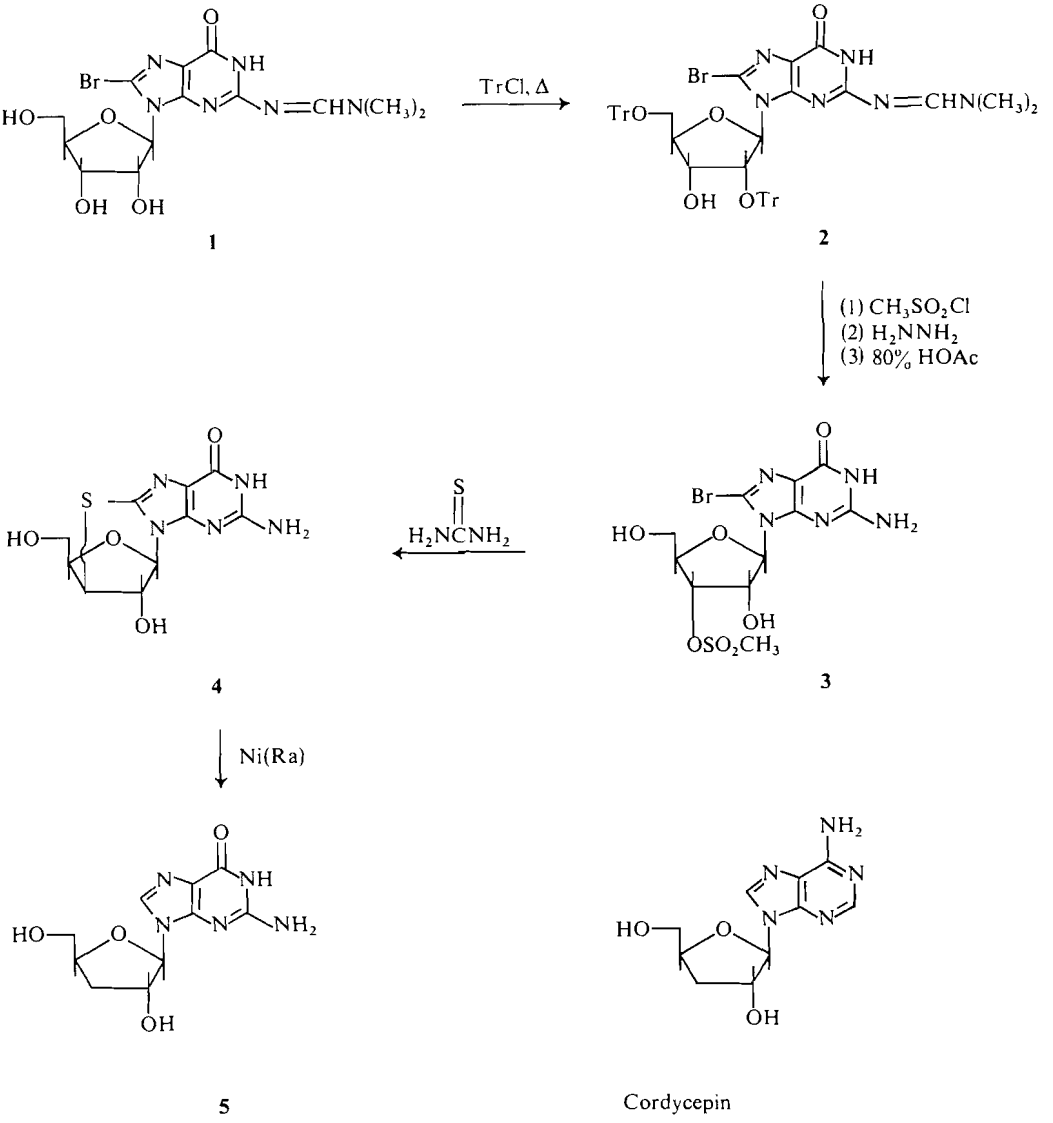

SCHEME 1

Experimental

General Methods

Descending paper chromatography was carried out on Whatman 3MM paper. The solvent systems employed were: solvent A, isopropyl alcohol–concentrated ammonium hydroxide–water (7:1:2); solvent B, ethanol–water (7:3). The solvents were prepared on a volume basis. Thin-layer chromatography was carried out employing the ascending technique. All thin-layer chromatography was run on Eastman Chromagram Sheets 6060 (silica gel with fluorescent indicator) on strips 10 × 2 cm. Thick-layer chromatography was carried out on glass plates (20 × 20 cm) coated with a 2 mm thick layer of silica gel DSF-5 (Mondray Chemicals Ltd.). Nucleosides and their derivatives were detected on paper chromatograms, thin- and thick-layer plates, using a u.v. source (Mineralite output 254 nm). Compounds containing trityl groups were detected on chromatography by spraying with 10% perchloric acid solution and drying them in a stream of warm air.

I.r. spectra were obtained on a Perkin–Elmer 337 recording spectrophotometer using KBr disks for sample preparation. U.v. spectra were obtained on a Cary Model 14 recording spectrophotometer. Mass spectra were obtained on a Hitachi RMU-6D instrument. High resolution mass spectra were obtained on an AEI MS-9 high resolution mass

Can. J. Chem. Downloaded from www.nrcresearchpress.com by 210.87.254.42 on 09/05/12
For personal use only.

Can. J. Chem. Downloaded from www.nrcresearchpress.com by 210.87.254.42 on 09/05/12
For personal use only.

spectrometer. Melting points were determined on a Fisher–Johns melting point apparatus and are reported uncorrected. Elemental analyses were performed by Galbraith Laboratories Inc., Knoxville, Tennessee. Samples submitted to them were prepared by crystallization, lyophilization, or precipitation from tetrahydrofuran with hexane followed by heating in a drying apparatus over P_2O_5.

Reagent grade pyridine was distilled from *p*-toluenesulfonyl chloride, redistilled from calcium hydride, and stored over Linde Molecular Sieve. Reagent grade *N,N*-dimethylformamide (DMF) was dried by distillation from calcium hydride and stored over Linde Molecular Sieve.

*2′,5′-Di-O-trityl-N^2-dimethylaminomethylene-8-bromoguanosine (**2**)*

N^2-Dimethylaminomethylene-8-bromoguanosine (11, 1.95 g, 4.6 mmol) and trityl chloride (3.96 g, 13.95 mmol) were stirred at room temperature in pyridine (25 ml) for 72 h followed by heating at 100 °C for 0.5 h. The solution was cooled and poured into an ice-water (1 l) mixture. The resulting precipitate was collected by filtration, dissolved in chloroform, and dried over sodium sulfate. The solution was collected by filtration and concentrated to a small volume at reduced pressure. Upon addition of hexane the product precipitated as a white solid which was collected and dried (3.5 g, 74%, m.p. 151–153 °C, R_f (THF) 0.60). The u.v. spectrum (95% ethanol) showed λ_{max} at 309 (ε 23 800) and 233 (ε 25 600) with a shoulder at 284 nm (ε 23 100). Prominent bands in the i.r. spectrum occurred at 14.2 (trityl) and 6.5 μ.

Anal. Calcd. for $C_{51}H_{45}N_6O_5Br$: C, 67.92; H, 5.03; Br, 8.86. Found: C, 67.78; H, 4.80; Br, 8.84.

2′,5′-Di-O-trityl-3′-O-methanesulfonyl-N^2-dimethylaminomethylene-8-bromoguanosine and 2′,5′-Di-O-trityl-3′-O-methanesulfonyl-8-bromoguanosine

Compound **2** (3.5 g, 3.88 mmol) was dissolved in pyridine (20 ml) and the solution was cooled to 0 °C. Methanesulfonyl chloride (4 mmol) was added and the solution was kept at 0 °C for 24 h. An additional 4 mmol of methanesulfonyl chloride was added and stirring was continued for a further 24 h at 0 °C. The solution was poured into an ice-water mixture, the precipitate was collected by filtration, dissolved in chloroform, and the resulting solution was dried over sodium sulfate. The chloroform solution was collected by filtration, concentrated to a small volume, and applied to 15 t.l.c. plates which were developed three times in ether. The band at R_f 0.30 was eluted with tetrahydrofuran (THF), the solution was concentrated, and on addition of hexane the product precipitated as a white solid (3 g, 79%), m.p. 144–145 °C. The u.v. spectrum (95% ethanol) showed λ_{max} at 312, 284.5 and 232 nm. The i.r. spectrum showed prominent peaks at 14.2 (trityl) and 8.5 μ (covalent sulfonate).

Without further purification 2 g of this product was dissolved in hydrazine hydrate – acetic acid – water (1:6:24, 10 ml) and the solution was stirred at room temperature for 48 h. The solution was poured into ice-water and the resulting precipitate was collected and dried to yield 1.55 g (85%) of 2′,5′-di-*O*-trityl-3′-*O*-methanesulfonyl-8-bromoguanosine, m.p. >169 °C (dec.); R_f (THF) 0.68. The product showed prominent peaks in the i.r. at 14.2 and 8.5 μ. The u.v. spectrum (95% ethanol) showed λ_{max} at 266 (ε 15 300) with shoulders at 233 (ε 23 600) and 274 nm (ε 13 180).

Anal. Calcd. for $C_{49}H_{42}N_5O_7BrS$: C, 63.63; H, 4.58; Br, 8.64. Found: C, 63.62; H, 4.45; Br, 8.40.

*3′-O-Methanesulfonyl-8-bromoguanosine (**3**)*

2′,5′-Di-*O*-trityl-3′-*O*-methanesulfonyl-8-bromoguanosine (1 g, 1.08 mmol) was dissolved in 80% acetic acid (7 ml) and heated on a steam bath for 15 min. The solution was poured into ice-water and the resulting precipitate was collected, dried, and crystallized from ethanol to give 390 mg (83%) of **3**, m.p. >187 °C (dec.); R_f (A) 0.47, R_f (B) 0.75. The u.v. spectrum (95% ethanol) showed λ_{max} at 261.5 (ε 14 100) and a shoulder at 270 nm (ε 12 500). A peak at 8.5 μ in the i.r. spectrum showed the presence of covalent sulfonate.

Anal. Calcd. for $C_{11}H_{14}N_5O_7BrS$: C, 30.01; H, 3.21. Found: C, 30.11; H, 3.29.

*8,3′-Thioanhydroguanosine (**4**)*

Compound **3** (51 mg, 0.116 mmol) and thiourea (18 mg, 0.23 mmol) were added to *n*-butanol (4 ml) and the solution was heated at reflux for 5 h. The solvent was removed at reduced pressure and the residue was dissolved in DMF–NH_4OH (1:1, 2 ml) and applied to Whatman 3MM paper which was developed in solvent A. The band at R_f (A) 0.32 was eluted with water and lyophilized to yield 13 mg (37%) of **4**, m.p. > 183 °C (dec.); R_f (A) 0.32, R_f (B) 0.58, R_f (EtOH) 0.45. The u.v. spectrum in water showed λ_{max} at 272 (ε 14 410) with a shoulder at 283 nm (ε 10 730).

Mol. Wt. Calcd. for $C_{10}H_7N_5O_4S \cdot 4TMS$: 585.2113. Found: 585.2122.

*3′-Deoxyguanosine (**5**)*

Compound **4** (25 mg, 0.084 mmol) was dissolved in hot water (2 ml) and after addition of a spoonful of Raney nickel the mixture was heated at reflux for 3 h. The mixture was filtered and the clear filtrate was applied to Whatman 3MM paper which was developed in solvent A. The band at R_f (A) 0.24 was eluted with water and lyophilized to yield 4 mg (18%) of 3′-deoxyguanosine (13) m.p. >198 °C (dec.). The mass spectrum of the tetrasilyl derivative showed a parent peak at *m/e* 555. On paper chromatography the product had R_f (A) 0.24 and R_f (B) 0.61 while 2′-deoxyguanosine had R_f (A) 0.32 and R_f (B) 0.61. The u.v. spectrum of compound **5** showed λ_{max} (H_2O) at 253 (ε 13 100) and 270 nm (ε 8900).

3′-Deoxyguanosine was further identified by hydrolysis (19) to 3′-deoxyribose which gave a negative Dische test (16) but positive cysteine (17) and aniline (18) tests.

We wish to acknowledge financial assistance from the National Research Council of Canada. The generous assistance of Dr. A. M. Hogg and Mr. T. Budd of the University of Alberta in obtaining the high resolution mass spectra is gratefully acknowledged.

1. J. J. Fox. Pure and Appl. Chem. **18**, 223 (1969).
2. M. Ikehara. Accts. Chem. Res. **2**, 47 (1969).
3. M. Ikehara, S. Uesugi, and M. Vasumoto. J. Am. Chem. Soc. **92**, 4735 (1970).

4. K. K. OGILVIE and D. IWACHA. Can. J. Chem. **48**, 862 (1970).
5. K. L. NAGPAL and M. M. DHAR. Tetrahedron Lett. 47 (1968).
6. K. K. OGILVIE, L. SLOTIN, and P. RHEAULT. Biochem. Biophys. Res. Commun. **45**, 297 (1971).
7. K. K. OGILVIE and L. SLOTIN. J. Chem. Soc. D, 890 (1971).
8. K. K. OGILVIE, L. SLOTIN, J. B. WESTMORE, and D. LIN. Can. J. Chem. **50**, 2249 (1972).
9. M. IKEHARA and S. TEZUKA. Tetrahedron Lett. 1169 (1972).
10. M. KANEKO, B. SHIMIZU and M. IKEHARA. Tetrahedron Lett. 3113 (1971).
11. K. K. OGILVIE, L. SLOTIN, J. B. WESTMORE and D. LIN. Can. J. Chem. **50**, 1100 (1972).
12. N. C. YUNG and J. J. FOX. J. Am. Chem. Soc. **83**, 3060 (1961).
13. S. R. JENKINS, F. W. HOLLY, and E. WALTON. J. Org. Chem. **30**, 2851 (1965).
14. J. B. WESTMORE and K. K. OGILVIE. In preparation.
15. M. IKEDA, Y. TAMURA, and M. IKEHARA. J. Heterocycl. Chem. **7**, 1377 (1970).
16. J. BUCHANAN. J. Chem. Soc. 3162 (1950).
17. J. BUCHANAN. Nature, **168**, 1091 (1951).
18. S. M. PARTRIDGE. Nature, **164**, 443 (1949).
19. M. IKEHARA and H. TADA. Chem. Pharm. Bull. (Tokyo), **15**, 94 (1967).
20. K. G. CUNNINGHAM, S. A. HUTCHINSON, W. MASON, and F. S. SPRING. J. Chem. Soc. 2299 (1951).
21. M. E. BALIS. Antagonists and nucleic acids. American Elsevier Publishing Company, New York. 1968.

Can. J. Chem. Downloaded from www.nrcresearchpress.com by 210.87.254.42 on 09/05/12
For personal use only.

The Triterpenes of *Lycopodium lucidulum* Michx.

K. ORITO, R. H. MANSKE, AND R. RODRIGO
Department of Chemistry, University of Waterloo, Waterloo, Ontario

Received May 10, 1972

Nine known serratane triterpenoids have been isolated from *Lycopodium lucidulum* Michx. mostly as their acetates. Serratenediol is the major one and is accompanied by significant amounts of serratriol. Moderate quantities of serratenediol-3-acetate, tohogenol, and episerratenediol were present together with minor amounts of 16-oxoserratriol, tohogeninol, and the phlegmanols A and E.

Neuf triterpènoides connus de la série serratane ont été isolés à partir du *Lycopodium lucidulum* Michx, la plupart sous forme d'acétates. Le serratenediol, composé majeur, est accompagné d'une quantité importante de serratriol. De quantités moyennes de serratènediolacétate-3, tohogenol, et épiserratenediol sont présentes en plus de petites quantités d'oxo-16 serratriol, tohogeninol, et phlegmanols A et E.

[Traduit par le journal]

Canadian Journal of Chemistry, **50**, 3280 (1972)

Can. J. Chem. Downloaded from www.nrcresearchpress.com by 210.87.254.105 on 09/05/12
For personal use only.

The elucidation of the structure of serratenediol (**1**) a pentacyclic triterpene from *Lycopodium serratum* was reported by Inubushi *et al.* (1, 14) in 1964. Subsequently intense activity in this field by various research groups has resulted in the discovery of a whole series of such triterpenes having the common structural feature—a seven-membered ring-C. These have been isolated from *Lycopodium serratum* (2–4), *L. clavatum* (2, 4–6), *L. phlegmaria* (7), *L. cernuum*, and *L. inundatum* (8). They have also been found in a fern (9) and in the bark of species of pine (10) and spruce (11). A comprehensive mass-spectrometric study of the group has also been made (13).

We now report the results of our study of the neutral triterpenes of *L. lucidulum* collected in Ontario. While this work was in progress the structure of a phenolic diterpene from the same source was determined (15).

Isolation

The non basic fraction of the methanolic extract of dried plant material was saponified and acetylated and the resulting crystalline mixture of acetates separated essentially by chromatographic techniques.

In another procedure the non-basic material was extracted without prior saponification and the products separated as before.

*Serratenediol (**1**), Serratenediol Diacetate (**2**), Serratenediol-3-acetate (**3**), 21-Episerratenediol Diacetate (**4**), Serratriol Triacetate (**5**), and 16-Oxoserratriol Triacetate (**6**)*

The identities of **1**, **2**, **4**, **5**, and **6** were established by direct comparison with authentic specimens (t.l.c., i.r., and mass spectra) (2, 3, 4, 6*b*, 10, 12).

Serratenediol-3-acetate (**3**) had the expected properties and its identity was confirmed by oxidation to 3β-acetoxy-14-serraten-21-one (**8**) (12) which was hydrolyzed to 3β-hydroxy-14-serraten-21-one (serrateneolone) (**7**) (10).

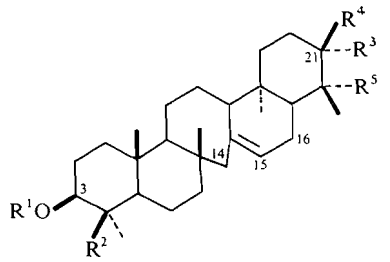

1 Serratenediol ($R^1 = R^4 = H$; $R^2 = R^5 = Me$; $R^3 = OH$)
2 Serratenediol diacetate ($R^1 = Ac$; $R^2 = R^5 = Me$; $R^3 = OAc$; $R^4 = H$)
3 Serratenediol-3-acetate ($R^1 = Ac$; $R^2 = R^5 = Me$; $R^3 = OH$; $R^4 = H$)
4 21-Episerratenediol diacetate ($R^1 = Ac$; $R^2 = R^5 = Me$; $R^3 = H$; $R^4 = OAc$)
5 Serratriol triacetate ($R^1 = Ac$; $R^2 = CH_2OAc$; $R^3 = OAc$; $R^4 = H$; $R^5 = Me$)
6 16-Oxoserratriol triacetate (**5** plus 16=O)
7 3β-Hydroxy-14-serraten-21-one ($R^1 = H$; $R^2 = R^5 = Me$; $R^3 + R^4 = O$=)
8 3β-Acetoxy-14-serraten-21-one ($R^1 = Ac$; $R^2 = R^5 = Me$; $R^3 + R^4 = O$=)
9 Phlegmanol E diacetate ($R^1 = Ac$; $R^2 = Me$; $R^3 = H$; $R^4 = OAc$; $R^5 = CH_2OH$)
10 Phlegmanol E triacetate ($R^1 = Ac$; $R^2 = Me$; $R^3 = H$; $R^4 = OAc$; $R^5 = CH_2OAc$)
11 Phlegmanol A triacetate ($R^1 = CO(CH_2)_2C_6H_3$-3, 4-$(OAc)_2$; $R^2 = R^5 = Me$; $R^3 = OAc$; $R^4 = H$)

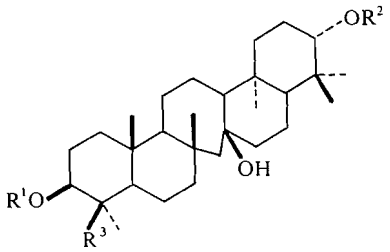

12 Tohogenol ($R^1 = R^2 = H$; $R^3 = Me$)
13 Tohogenol diacetate ($R^1 = R^2 = Ac$; $R^3 = Me$)
14 Tohogeninol triacetate ($R^1 = R^2 = Ac$; $R^3 = CH_2OAc$)

Tohogenol Diacetate (13) and Tohogeninol Triacetate (14)

Tohogenol diacetate (**13**) had a p.m.r. spectrum identical with that already published (3) and showed in its i.r. spectrum the presence of hydroxyl and acetate groups. (ν_{max} (Nujol) 3600, 1730 and 1250 cm^{-1}). Contrary to the earlier report we have found that the compound does display a molecular ion (*m/e* 544, 93%), in its mass spectrum (280 °C) in addition to the fragments characteristic of serratenediol diacetate. The identity of this compound was confirmed by hydrolysis to tohogenol (**12**) and by dehydration (3) to serratenediol diacetate (**2**) identical with an authentic sample.

Tohogeninol triacetate (**14**) was isolated pure in very small quantity after several recrystallizations. However, an impure sample was dehydrated (3) to serratriol triacetate (**5**) identical with an authentic specimen.

Phlegmanol E Diacetate (9) and Phlegmanol A Triacetate (11)

Phlegmanol E diacetate (**9**) had identical spectral properties with those already published (7*b*) and upon acetylation gave phlegmanol E triacetate (**10**), again possessing the expected properties.

Phlegmanol A triacetate (**11**) had properties consistent with its structure (7) and its identity was confirmed by conversion to serratenediol (**1**) and dihydrocaffeic acid dimethyl ether by the published procedure (7).

Experimental

Melting points were determined using a Fischer Meltemp apparatus and are uncorrected. Melting points in parentheses were determined *in vacuo* and are corrected. I.r. spectra were recorded on a Beckmann I.R. 10 spectrometer, samples being dissolved in chloroform or dispersed in Nujol. P.m.r. spectra were determined in deuterochloroform using added TMS on a Varian T-60 instrument. Mass spectra were recorded on a Perkin-Elmer Hitachi RMU-6E spectrometer.

Isolation of the Triterpenoids from L. lucidulum

The dried plant material was extracted with methanol and most of the solvent removed. The residue was acidified with dilute hydrochloric acid and the remaining methanol removed in a current of steam. The water insoluble portion was separated by filtration and washed until the filtrate was colorless and neutral to test paper. The yield was approximately 5% of the dried plant material.

Separation of the Constituents

A suspension of the above material (20 g) was heated under reflux with 5% methanolic potassium hydroxide (200 ml) for 7 h and filtered. The residue was washed, dried, and acetylated with acetic anhydride–pyridine to yield a crystalline product, A (11 g). The filtrate was concentrated and diluted with water (300 ml). The resulting brown precipitate was washed, dried, and similarly acetylated to give another crystalline product, B (3.2 g).

Serratenediol diacetate (2), 21-Episerratenediol Diacetate (4), and Serratriol Triacetate (5)

Product A was dissolved in benzene and chromatographed on neutral alumina (220 g). Elution of the column with benzene gave first a fraction containing **2** (3.9 g), crystallized from chloroform–methanol, m.p. 341–343° (349–350°) (12), followed by a second fraction (**5**) (1.6 g), crystallized from benzene–hexane, m.p. 248–250° (265–266°) (2).

The filtrate from the crystallization of **2** was freed of solvents and the residue upon repeated fractional crystallization from *n*-hexane yielded **4** (92 mg), m.p. 225–228° (228–230°) (3, 6*b*, 10) and **2** (207 mg).

Tohogenol Diacetate (13)

The crystalline product, B, dissolved in benzene was chromatographed as before (neutral alumina, 65 g) to yield **2** (363 mg) and **4** (49 mg) in the first eluates, followed by **13** (443 mg) which was crystallized from benzene–hexane, m.p. 312–313° (330–331°) (3).

Phlegmanol E Diacetate (9), Tohogeninol Triacetate (14), and 16-Oxoserratriol Triacetate (6)

The slower moving fractions from the chromatography of products A and B were eluted with benzene–ether and the combined eluates examined by preparative t.l.c. on silica hexane–benzene–ether (3:3:1). A product of R_f 0.31 appeared to be a mixture of **6** and **14** in the ratio 2:3, as estimated by p.m.r. The mixture was dehydrated and reacetylated (3) to yield a product from which it was possible to isolate, by means of t.l.c. in the same system **6** (12 mg), R_f 0.31, m.p. 313–315° (320–324°) (4), and **5**, (16 mg), R_f 0.43.

Tohogeninol triacetate (**14**), (8 mg), m.p. 263–264° (3), was isolated from another preparation of the initial mixture by repeated crystallization from chloroform–methanol.

A further fraction (R_f 0.4) was also recovered from the silica plates and this, when crystallized from benzene–hexane (37 mg), m.p. 254–256° (267–268°) was identified as **9**.

Serratenediol-3-acetate (3) and Phlegmanol A Triacetate (11)

The crude neutral material (20 g) was extracted without prior saponification in a Soxhlet apparatus, successively

Can. J. Chem. Downloaded from www.nrcresearchpress.com by 210.87.254.105 on 09/05/12
For personal use only.

with ether, chloroform, and chloroform–methanol (4:1). The ether extract (2.5 g) was purified by preliminary chromatography on silica (100 g) followed by t.l.c. on silica plates as before. The faster moving fraction, crystallized from benzene–hexane (510 mg), m.p. 323–324° (335–338°), was identified as **3** (*7b*). The slower moving fraction was identified as **1**, m.p. 293–295° (302–303°) (12).

The chloroform and chloroform–methanol fractions were combined and acetylated and the product (8.7 g) chromatographed in benzene on a column of silica (200 g). The first eluates consisted of **2** (0.67 g) and **5** (0.91 g). The later fractions, with benzene–ether, were collected and purified by t.l.c. on silica plates as before and the major slow moving constituent recovered and crystallized from chloroform–methanol to yield **11** (62 mg), m.p. 297–299° (299–300°) (7).

We wish to thank Dr. D. B. MacLean of McMaster University for mass spectra of several compounds isolated in this work and Dr. Y. Tsuda of the Showa College of Pharmaceutical Sciences, Tokyo for a generous gift of sample triterpenes. Financial support from the National Research Council of Canada is gratefully acknowledged.

1. Y. INUBUSHI, Y. TSUDA, H. ISHII, M. HOSOKAWA, and T. SANO. Yakugaku Zasshi, **82**, 1339 (1962); Chem. Abstr. **59**, 678*h* (1963). Y. INUBUSHI, Y. TSUDA, H. ISHII, T. SANO, M. HOSOKAWA, and T. HARAYAMA. Yakugaku Zasshi, **84**, 1108 (1964); Chem. Abstr. **62**, 5498*b* (1965).
2. Y. TSUDA, T. SANO, A. MORIMOTO, and Y. INUBUSHI. Tetrahedron Lett. 5933 (1966).
3. T. SANO, Y. TSUDA, and Y. INUBUSHI. Tetrahedron, **26**, 2981 (1970).
4. Y. TSUDA, T. FUJIMOTO, and K. KIMPARA. Chem. Commun. 261 (1970).
5. Y. TSUDA and T. FUJIMOTO. Chem. Commun. 260 (1970).
6. (*a*) T. SANO, T. FUJIMOTO, and Y. TSUDA. Chem. Commun. 1274 (1970). (*b*) Y. TSUDA and M. HATANAKA. Chem. Commun. 1040 (1969). Y. TSUDA and T. FUJIMOTO. Chem. Commun. 1042 (1969).
7. (*a*) Y. INUBUSHI, T. HARAYAMA, T. HIBINO, and R. SOMANATHAN. Chem. Commun. 1118 (1970). (*b*) Y. INUBUSHI, T. HIBINO, T. HARAYAMA, T. HASEGAWA, and R. SOMANATHAN. J. Chem. Soc. C, 3109 (1971).
8. Y. INUBUSHI, T. HARAYAMA, T. HIBINO, and M. AKATSU. Yakugaku Zasshi, **91**, 980 (1971); Chem. Abstr. **75**, 148492*j* (1971).
9. G. BERTI, F. BOTTARI, A. MARSILLI, I. MORELLI, and A. MANDELBAUM. Chem. Commun. **50** (1967).
10. J. W. ROWE. Tetrahedron Lett. 2347 (1964); J. W. ROWE and C. L. BOWER. Tetrahedron Lett. 2745 (1965).
11. J. P. KUTNEY, I. H. ROGERS, and J. W. ROWE. Tetrahedron, **25**, 3731 (1969); I. H. ROGERS and L. R. ROZEN. Can. J. Chem. **48**, 1021 (1970).
12. Y. TSUDA, T. SANO, K. KAWAGUCHI, and Y. INUBUSHI. Tetrahedron Lett. 1279 (1964).
13. J. P. KUTNEY, G. EIGENDORF, and I. H. ROGERS. Tetrahedron, **25**, 3753 (1969).
14. Y. INUBUSHI, T. SANO, and Y. TSUDA. Tetrahedron Lett. 1303 (1964); Y. INUBUSHI, Y. TSUDA, T. SANO, Y. KONITA, S. SUZUKI, H. AGETA, and Y. OTAKE. Chem. Pharm. Bull. (Japan), **15**, 1153 (1967).
15. R. H. BURNELL and M. MOINAS. Chem. Commun. 897 (1971).

Can. J. Chem. Downloaded from www.nrcresearchpress.com by 210.87.254.105 on 09/05/12
For personal use only.

A General Relation Between H_0, Acid Concentration, and Water Activity for Strong Acids at Moderate Concentrations

T. T. TENG AND F. LENZI

Département de Génie chimique, École Polytechnique, Université de Montréal, Montréal, Québec

Received January 28, 1972

Values of the Hammett acidity function H_0 can be correlated for strong acid solutions up to $-H_0$ values of 3.5 via a Bascombe and Bell type equation: $-H_0 = \log (C_{H^+}/a^3_{H_2O}) + AC_{H^+}$ taking into account the degree of dissociation of the acids. This can be interpreted according to

$$H_3O^+.3H_2O \rightleftarrows H_3O^+ + 3H_2O$$

and

$$B + H_3O^+ \rightleftarrows BH_3O^+$$

Alternatively, an approach based on the treatment of equilibrium constants in terms of mole-fractions yields

$$-H_0 = 1.46 \log \frac{C^+_H}{a^3_{H_2O}} + 0.148$$

valid for the same acids (H_2SO_4, $HClO_4$, HCl, and HNO_3) and again involving a tri-dehydration of the tetra-hydrated proton. The log of the ratio $(f_{H^+hydr.} Y_{Bhydr.})/(Y_{BH^+hydr.})$ has been found to be proportional to $-H_0$ itself and to be otherwise independent of the nature of the acid anion.

On peut établir la corrélation des valeurs de la fonction d'acidité de Hammett, soit H_0, pour des solutions d'acides forts allant jusqu'à des valeurs de $-H_0$ de 3.5, au moyen d'une équation de type Bascombe et Bell: $-H_0 = \log (C_{H^+}/a^3_{H_2O}) + AC_{H^+}$, tout en tenant compte du degré de dissociation des acides. On peut interpréter ces résultats en se basant sur les équations:

$$H_3O^+.3H_2O \rightleftarrows H_3O^+ + 3H_2O$$

$$B + H_3O^+ \rightleftarrows BH_3O^+$$

D'autre part, une approche basée sur le traitement des constantes d'équilibre en termes de fractions molaires nous donne

$$-H_0 = 1.46 \log \frac{C_{H^+}}{a^3_{H_2O}} + 0.148$$

qui est valide pour les mêmes acides (H_2SO_4, $HClO_4$, HCl, et HNO_3) et qui implique une tridéshydratation du proton tétrahydraté. On découvre que le logarithme du rapport $f_{H^+hydr.} Y_{Bhydr.}/Y_{BH^+hydr.}$ est proportionnel à $-H_0$ et indépendant de la nature de l'anion de l'acide.

[Traduit par le journal]

Canadian Journal of Chemistry, **50**, 3283 (1972)

Introduction

Bascombe and Bell (1) suggested that the rapid rise of effective acidity with increasing concentration of stoichiometric acid in aqueous acid solutions is mainly due to proton hydration. They re-wrote Hammett and Deyrup's (2) equilibrium

$$B + H^+ \rightleftarrows BH^+$$

in the form

$$B + H^+ mH_2O \rightleftarrows BH^+ + mH_2O$$

finding that a value of $m = 4$ fitted the experimental H_0 data for HCl, HBr, $HClO_4$, and H_2SO_4 acid solutions up to 8 *M*. Bascombe and Bell assumed that the hydration of B, BH^+, and the acid anions could be ignored, and that the molar activity coefficients $f_{H^+ mH_2O}$ and f_{BH^+} or f_B and $f^m_{H_2O}$ were approximately equal.

Bascombe and Bell themselves pointed out the approximate nature of their treatment, which has also been criticized elsewhere (3, 28). Although neglect of anionic hydration is probably reasonable[1] (4), the hydration of both B and BH^+ cannot necessarily be neglected *a priori*.

[1]Wyatt (5) and Yates and Wai (13) have shown that H_0 is a common function of the water activity, a_{H_2O}, for H_2SO_4, HCl, $HClO_4$, and HNO_3; this suggests that differential anionic hydration effects would only appear as a_{H_2O} differences.

Can. J. Chem. Downloaded from www.nrcresearchpress.com by 210.87.254.105 on 09/05/12
For personal use only.

Can. J. Chem. Downloaded from www.nrcresearchpress.com by 210.87.254.105 on 09/05/12
For personal use only.

The conjugate acid of the base BH^+ has been found to be mono- or di-hydrated (6); the acidity phenomenon should be more realistically attributed to the hydration difference between H^+ and B on the one hand, and BH^+ on the other (7, 8). In addition strong acids, even at moderate concentrations, cannot be considered as being necessarily completely dissociated (9).

A more general approach (10) gives

[1] $$H^+ mH_2O \overset{K_1}{\rightleftharpoons} H^+(m-n)H_2O + nH_2O$$

[2] $$BtH_2O + H^+(m-n)H_2O \overset{K_2}{\rightleftharpoons} BH^+(m-n-p)H_2O + (t+p)H_2O$$

where m is the average proton hydration.

While it is over-optimistic to assume that unique values of m and $(m-n)$ define the proton hydrates present, it may well be that there is a preponderance of a more hydrated proton species $H^+ mH_2O$ over an appreciable concentration range, and that a less or least hydrated species $H^+(m-n)H_2O$ would be much more reactive than species intermediate between $H^+ mH_2O$ and $H^+(m-n)H_2O$.

It is asserted that K_1 is sufficiently small such that up to moderate acid concentrations most of the hydrated protons will be in the m rather than the $(m-n)$ hydrated form, thus allowing the approximation $C_{H^+} \equiv C_{H^+ mH_2O} \simeq \alpha C_{\text{stoichiometric}}$ where α is the degree of dissociation, $C_{\text{stoichiometric}}$ is the experimental concentration of the acid, and C_{H^+} represents $C_{H^+ mH_2O}$.

Experimental Data Selection

H_0 values were taken from (10–15), those of a_{H_2O} from (10, 16–18, 21, 22) or calculated from density (19) and osmotic coefficient (20) data. Values of α_{HClO_4} were obtained from ref. 23, while those of α_{HNO_3} and α_{HCl} were taken from refs. 24 and 25. As advocated by Edward (26), actual hydrogen-ion concentrations (27) were used for H_2SO_4. The conversion between these and stoichiometric acid concentrations at 25 °C was that of Robertson and Dunford (18).

Modified Bascombe and Bell Treatment

Equilibria 1 and 2 can be combined to give

[3] $$BtH_2O + H^+ mH_2O \overset{K'}{\rightleftarrows} BH^+ kH_2O + hH_2O$$

where $h = t + n + p$ and $k = m - n - p$. Equilibrium 3 has previously been proposed by Edward (26). From [3],

$$K' = \frac{1}{K} = a_{BH^+ kH_2O} a^h_{H_2O} / a_{BtH_2O} a_{H^+ mH_2O}$$

and

$$pK = \log \frac{C_{BH^+ kH_2O} a^h_{H_2O}}{C_{BtH_2O} C_{H^+}} \cdot \frac{f_{BH^+ kH_2O}}{f_{BtH_2O} f_{H^+}}$$

where the a's are activities, C's are concentrations in mol/l, f's are molar activity coefficients and f_{H^+} represents $f_{H^+ mH_2O}$.

Defining H_0 in the usual way

$$H_0 \equiv pK - \log \frac{C_{BH^+ kH_2O}}{C_{BtH_2O}} = -\log \frac{C_{H^+}}{a^h_{H_2O}} \cdot \frac{f_{BtH_2O} f_{H^+}}{f_{BH^+ kH_2O}}$$

whence

[4] $$-H_0 - \log C_{H^+} + h \log a_{H_2O} = \log f_{BtH_2O} + \log f_{H^+} - \log f_{BH^+ kH_2O}$$

The terms on the right of eq. 4 represent the salt effects of the species BtH_2O, $H^+ mH_2O$ and $BH^+ kH_2O$, respectively, giving eq. 5

[5] $$-H_0 - \log C_{H^+} + h \log a_{H_2O} = AC_{H^+}$$

where A is the combined salting-in or salting-out coefficient. Equation 5 has the Bascombe and Bell form, but with h representing $(t+n+p)$ and C_{H^+} standing for the actual hydrated proton concentration. A similar equation has been developed by Dawber (29).

Calculations

Equation 5 has been applied to the actual data originally (1) used for H_2SO_4, $HClO_4$, and HCl. A value of $h \simeq 3$, as opposed to Bascombe and Bell's value of $h \simeq 4$, gives the best fit (least squares) while still leading to reasonable values of "A". H_0 values for $HClO_4$ (13) and H_2SO_4 (14) have been redetermined recently. Equation 5 has been applied to these values as well as H_0 data for HNO_3 (15) and HCl (10, 11) and similar calculations have been made for different H_0 ranges for all the sets of H_0 data of the four acids.

These calculations show that at low acidity ($-H_0 < 1.5$), optimal h values tend to increase

Can. J. Chem. Downloaded from www.nrcresearchpress.com by 210.87.254.105 on 09/05/12
For personal use only.

with decreasing acid concentration. For intermediate $-H_0$ ranges ($\simeq 1.5$ to 3.5) optimal values of h lie between 2.25 and 3.6, while for $-H_0$ values >3.5 the optimal values of h tend to decrease except for HNO_3.[2]

The results in refs. 10 and 30 confirm this general trend in the case of $HClO_4$ and HCl.

A common value of $h \simeq 3$ gives a good fit for all the data of all the acids up to $-H_0 = 3.5$.

Mole Fraction Treatment

Equilibrium 3 can be expressed in terms of mole-fractions, N_{species}, and rational activity coefficients, Y_{species}:

$$[6] \quad K_x = \frac{N_{BH^+ kH_2O} N^h_{H_2O}}{N_{BtH_2O} N_{H^+ mH_2O}} \cdot \frac{Y_{BH^+ kH_2O} Y^h_{H_2O}}{Y_{BtH_2O} Y_{H^+ mH_2O}}$$

Substituting (moles of species/total number of moles) for $N_{BH^+ kH_2O}$ and N_{BtH_2O}, a_{H_2O} for $N_{H_2O} \cdot Y_{H_2O}$, $C_{H^+ mH_2O} f_{H^+ mH_2O} / Y_{H^+ mH_2O}$ for $N_{H^+ mH_2O}$, and considering 1 liter of solution, yields

$$[7] \quad K_x = \frac{a^h_{H_2O} C_{BH^+ kH_2O}}{C_{BtH_2O} C_{H^+ mH_2O}} \cdot \frac{Y_{BH^+ kH_2O}}{Y_{BtH_2O} f_{H^+ mH_2O}}$$

where C_{species} is in mol/l of species.

Defining

$$-H_0 \equiv \text{p}\left(\frac{1}{K_x}\right) + \log \frac{C_{BH^+ kH_2O}}{C_{BtH_2O}}$$

$$[8] \quad -H_0 = -H_p + \log \frac{f_{H^+ mH_2O} Y_{BtH_2O}}{Y_{BH^+ kH_2O}},$$

where

$$H_p = -\log \frac{C_{H^+ mH_2O}}{a^h_{H_2O}}$$

Calculation

Plots of $-H_0$ against $-H_p$ have been prepared for the more recent data for $HClO_4$, H_2SO_4, as well as for HNO_3 and HCl using different values of h in the calculation of H_p. For small whole number values of h the points for the different acids lie on a common plot which is approximately linear up to moderately high acidities and passes close to the origin. Such a plot is shown in Fig. 1 for the value $h = 3$ which gives the least deviation up to an acidity of $H_0 = -3.5$.

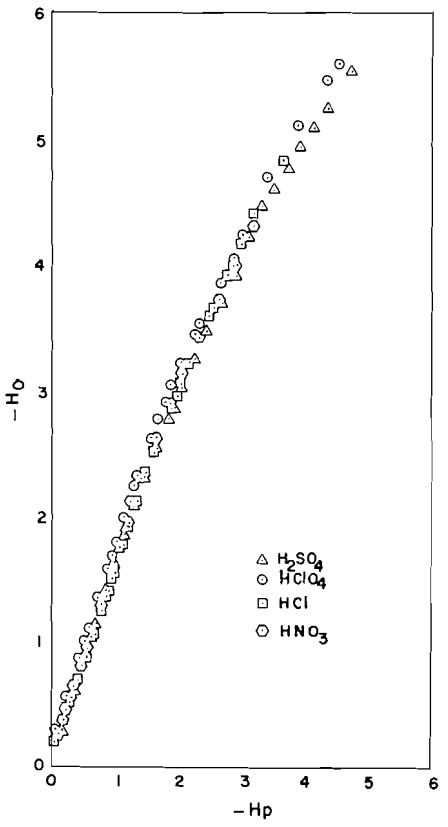

FIG. 1. Plot of $-H_0$ against $-H_p$ for $h = 3$ for the four acids. The "old" data for H_2SO_4 and $HClO_4$ (11) are not shown here to avoid over-cluttering: in fact they show no significant difference from the newer data on this plot.

The plot in Fig. 1 can be represented by

$$[8a] \quad -H_0 = -1.46H_p + 0.148.$$

Values of $-H_0$ calculated via [8*a*] compare with observed values to an average of 0.08, 0.08, 0.07, and 0.05 in H_0 units for H_2SO_4, $HClO_4$, HCl, and HNO_3 respectively. Equation 8*a* is equivalent to

$$[8b] \quad -H_0 = -H_p + (-0.46H_p + 0.148)$$

implying that the second term on the right of eq. 8 is proportional to H_p (or H_0) but is largely independent of the nature of the acid anion.

Table 1 lists the optimal h values for different $-H_0$ ranges for the four acids. Diminishing

[2]This may be due to uncertainties in the degree of dissociation which would affect eq. 5 in both the $\log C_{H^+}$ and the AC_{H^+} terms. As will be seen in Fig. 1 the behavior of HNO_3 is in accord with that of the other acids; this is possibly due to the absence of an AC_{H^+} term in eq. 8*a*.

TABLE 1. Testing of eq. 8 for optimum h for different $-H_0$ ranges for H_2SO_4, $HClO_4$, HCl, and HNO_3

Upper value of $-H_0$ range	Best fit h	Standard deviation for the straight line	Slope of the straight line	Intercept of the line	Standard deviation for $h = 3$
3.99	2.25	0.1131	1.67	0.118	0.1198
3.69	2.50	0.1078	1.59	0.131	0.1105
3.45	3.00	0.0967	1.46	0.148	0.0967
3.04	3.00	0.0930	1.48	0.134	0.0930
2.86	3.25	0.0883	1.42	0.141	0.0885
2.62	3.75	0.0809	1.35	0.138	0.0832
2.32	4.00	0.0777	1.32	0.129	0.0821
2.07	4.00	0.0757	1.32	0.128	0.0784
1.90	4.25	0.0756	1.29	0.132	0.0778
1.75	4.25	0.0731	1.30	0.123	0.0766

values of optimal h with increasing acidity is in accord with some of the results of the modified Bell and Bascombe treatment given above. The fifth column of Table 1 shows that the intercept (or additive constant of value 0.148 in [8*a*]) tends to diminish with decreasing acidity corresponding to the higher values of h. This satisfies the requirement that the additive constant should vanish for [8*a*] to hold in the limit of diminishing acidity, when $a_{H_2O} \rightarrow 1$ and $C_{H^+ mH_2O} \rightarrow 0$. Thus 0.148 can be interpreted as a term compensating for the imposed constancy in h.

The average dehydration h may indeed be higher at lower acidities; eq. 8 is, however, relatively insensitive to the value of h at low acidity when $a_{H_2O} \rightarrow 1$.

The results in Fig. 1 appear to establish an indicator-independent "acidity function", H_p, which is closely related to H_0 up to values of $-H_0 = 3.5$.

Conclusions

Both approaches lead to the result that $h \simeq 3$ gives reasonable correlation between experimental values of H_0, a_{H_2O}, and C_{H^+} up to $-H_0$ values of 3.5 (except for HNO_3 via [5]). At higher acidities a diminution in h, compatible with other data, is indicated. Equation 8*a* contains two empirical but acid-anion independent constants[3] as opposed to [5] which contains only one empirical constant, "A", which is, however, acid-anion dependent.

[3]Of which the additive constant is only important at relatively low acidities; its compensatory nature has been discussed.

Equation 3 can be rewritten as

$$BtH_2O + H^+ mH_2O \rightleftarrows BH^+ kH_2O + 3H_2O$$

Some anilines in the uncharged form have been found to be unhydrated (6), suggesting a value of $t = 0$. It has also been suggested that the conjugate acid of the indicator base may be monohydrated, indicating that $k = 1$ and thus $m = 4$, in accord with the evidence (31) pointing to the existence of the tetrahydrated proton, $H_9O_4^+$, at moderate acid concentrations.

Assuming that the reactive hydrated proton species is the monohydrate, *i.e.* $m - n = 1$, equilibria 1 and 2 can now be rewritten as

[1*a*] $$H_3O^+.3H_2O \rightleftarrows H_3O^+ + 3H_2O$$

[2*a*] $$B + H_3O^+ \rightleftarrows BH_3O^+$$

Equilibrium 1*a* is in fact a combination of hydration equilibria 2, 3, and 4 in the paper of Knewstubb and Tickner (32); [1*a*] has also been invoked in the interpretation of the kinetics of the chloride–chlorate reaction in moderately concentrated solutions of $HClO_4$ and H_2SO_4 (33).

The lower values of h at increasing acidity can be interpreted as a lowering of m, the average hydration number of the proton, while H_3O^+ would still be the reacting species, and conversely for the higher values of h at lower acidity.

The authors wish to thank the National Research Council of Canada for operating grant A-4520.

1. K. N. BASCOMBE and R. P. BELL. Discuss. Faraday Soc. **24**, 158 (1957).
2. L. P. HAMMETT and A. J. DEYRUP. J. Am. Chem. Soc. **54**, 2721 (1932).

Can. J. Chem. Downloaded from www.nrcresearchpress.com by 210.87.254.105 on 09/05/12
For personal use only.

3. G. W. MACH. Ph.D. Thesis. Department of Chemistry, University of Pittsburgh. 1964.
4. (*a*) H. L. FRIEDMAN. J. Am. Chem. Soc. **74**, 5 (1952). (*b*) G. E. WALRAFEN. J. Chem. Phys. **52**, 4176 (1970).
5. P. A. H. WYATT. Discuss. Faraday Soc. **24**, 162 (1957).
6. M. K. CHANTOONI, JR. and I. M. KOLTHOFF. J. Am. Chem. Soc. **92**, 2236 (1970).
7. K. B. WIBERG. Physical organic chemistry. John Wiley and Sons. 1964. p. 298.
8. C. H. ROCHESTER. Acidity functions. Academic Press. 1970. p. 62.
9. E. A. GUGGENHEIM and R. H. STOKES. Equilibrium properties of aqueous solutions of single strong electrolytes. Pergamon Press. 1969. p. 143.
10. D. ROSENTHAL and J. S. DWYER. Can. J. Chem. **41**, 80 (1963).
11. M. A. PAUL and F. A. LONG. Chem. Rev. **57**, 1 (1957).
12. T. G. BONNER and J. C. LOCKHART. J. Chem. Soc. 2840 (1957).
13. K. YATES and H. WAI. J. Am. Chem. Soc. **86**, 5408 (1964).
14. C. D. JOHNSON, A. R. KATRITZKY, and S. A. SHAPIRO. J. Am. Chem. Soc. **91**, 6654 (1969).
15. J. G. DAWBER. J. Chem. Soc. (A), 1532 (1968).
16. R. A. ROBINSON and O. J. BAKER. Trans. Proc. Roy. Soc. New Zealand, **76**, 250 (1946).
17. J. C. SCHUMACHER. Perchlorates. Reinhold Pub. Corp. 1960.
18. E. B. ROBERTSON and H. B. DUNFORD. J. Am. Chem. Soc. **86**, 5080 (1964).
19. Handbook of chemistry and physics. 49th ed. The Chemical Rubber Co. 1968.
20. R. A. ROBINSON and R. H. STOKES. Electrolyte solutions. 2nd ed. Butterworth. 1968.
21. M. R. VANDONI and M. LAUDY. J. Chim. Phys. **49**, 99 (1952).
22. F. A. LONG and M. PURCHASE. J. Am. Chem. Soc. **72**, 3267 (1950).
23. K. HEINZINGER and R. E. WESTON, JR. J. Chem. Phys. **42**, 272 (1965). A. K. COVINGTON, M. J. TAIT, and W. F. K. WYNNE-JONES. Proc. Roy. Soc. London, A **286**, 235 (1965). J. W. AKITT, A. K. COVINGTON, J. G. FREEMAN, and T. H. LILLEY. Trans. Faraday Soc. **65**, 2701 (1969).
24. E. HÖGFELDT. J. Inorg. Nucl. Chem. **17**, 302 (1961).
25. G. C. HOOD and C. A. REILLY. J. Chem. Phys. **32**, 127 (1960).
26. J. T. EDWARD. Trans. Roy. Soc. Can. **2**, 313 (1964).
27. T. F. YOUNG. Rec. Chim. Prog. **12**, 81 (1951).
28. E. HÖGFELDT and P. J. STAPLES. J. Chem. Soc. (A), 2074 (1971).
29. J. G. DAWBER. Chem. Commun. (13), 405 (1966).
30. R. W. DUERST. J. Chem. Phys. **48**, 2275 (1968).
31. (*a*) E. WICKE, M. EIGEN, and TH. ACKERMANN. Z. Physik. Chem. (Frankfurt), **1**, 340 (1954). (*b*) H. L. CLEVER. J. Chem. Educ. **40**, 637 (1963). (*c*) K. E. HAWLETT. Sci. Progr. **53**, 305 (1965). (*d*) M. DEPAZ, S. EHRENSON, and L. FRIEDMAN. J. Chem. Phys. **52**, 3362 (1970). (*e*) M. D. NEWTON and S. EHRENSON. J. Am. Chem. Soc. **93**, 4971 (1971).
32. P. F. KNEWSTUBB and A. W. TICKNER. J. Chem. Phys. **38**, 464 (1963).
33. P. CRISCI and F. LENZI. Can. J. Chem. **49**, 2552 (1971).

Can. J. Chem. Downloaded from www.nrcresearchpress.com by 210.87.254.105 on 09/05/12
For personal use only.

The Pyrolysis of some Neopentyl Xanthates: a Competitive Formation of Olefins and Dithiolcarbonates

K. G. RUTHERFORD, B. K. TANG, L. K. M. LAM, AND D. P. C. FUNG[1]

Department of Chemistry, University of Windsor, Windsor, Ontario

Received April 28, 1972

A study of the pyrolysis of a series of neopentyl-type xanthate esters was carried out at 250 °C. The formation of olefins and dithiolcarbonates were found to be two competing processes. The olefin formation process became more important when the number of β-phenyl groups increased and when there was an electron donating group substituted at the para-position of the β-phenyl ring. Kinetics studies supported the proposal that the transition state of the olefin formation process involved a stabilized phenonium ion. However the dithiolcarbonate formation became more important when there was the least number of β-phenyl substituents and this rearrangement appeared to proceed through a concerted four-membered cyclic transition state.

Nous avons entrepris une étude de pyrolyse sur une série d'esters xanthates de type néopentyl à 250 °C. Nous trouvons que la formation d'oléfines et de dithiolcarbonates s'effectue selon deux processus compétitifs. Le processus de formation d'oléfines prend de l'importance lorsque le nombre de groupe β-phényl augmente et qu'un groupe donneur d'électrons est substitué en position para du cycle β-phényl. Les études cinétiques appuient la proposition que l'état de transition du procédé de formation d'oléfines implique un ion phénonium stabilisé. La formation de dithiolcarbonate prédomine lorsqu'il y a un nombre minimum de substituants β-phényl et ce réarrangement se produit en passant par un état de transition cyclique concerté impliquant quatre membres. [Traduit par le journal]

Canadian Journal of Chemistry, **50**, 3288 (1972)

Can. J. Chem. Downloaded from www.nrcresearchpress.com by 210.87.254.6 on 09/05/12
For personal use only.

Introduction

The formation of olefin(s) by the pyrolysis of xanthate esters is called the Chugaev reaction (for reviews, see ref. 1). The mechanism of this reaction has generally been agreed to involve a concerted six-membered cyclic transition state (2–5). However, other mechanisms have been proposed (6, 7).

A rather interesting side reaction observed in the pyrolysis of some *S*-methyl xanthate esters involves the formation of dithiolcarbonates. For example, in the pyrolysis of the xanthate ester of 1-cyclopropylethanol, Overberger and Borchert (8) reported yields of 45% of the olefins and 35% of the dithiolcarbonates, of which the major component was identified as 1-cyclopropylethyl dithiolcarbonate. A concerted four-membered cyclic transition state was suggested (Scheme 1).

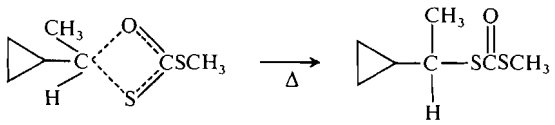

SCHEME 1. A cyclic transition state proposed for the dithiolcarbonate formation from pyrolysis of 1-cyclopropylethyl xanthate.

Recently, this rearrangement reaction was studied by Taguchi and co-workers (9–11) who found that the pyrolysis of *trans*-2-dimethylaminocyclohexyl xanthate gave only the corresponding dithiolcarbonate while the *cis* isomer underwent the expected elimination. Participation by the neighboring amino group was suggested in an ion-pair transition state (Scheme 2).

In a study of the pyrolysis of some neopentyl xanthate esters, Laakso (12) reported no olefin formation whatsoever (Scheme 3).

The corresponding dithiolcarbonates were found in 70–80% yield. These results would appear to indicate that xanthate–dithiolcarbonate rearrangement is a true case of the classic cyclic S_Ni mechanism since one would surely expect in a neopentyl-type system at least some olefin formation would be observed from Wagner–Meerwein rearrangement (13) if an ion-pair intermediate was involved. A study was carried out to pyrolyze a series of neopentyl-type xanthates in order to investigate if Laakso's result was a general phenomenon.

[1]Present address: Eastern Forest Products Laboratory, Canada Department of the Environment, Ottawa 7, Canada.

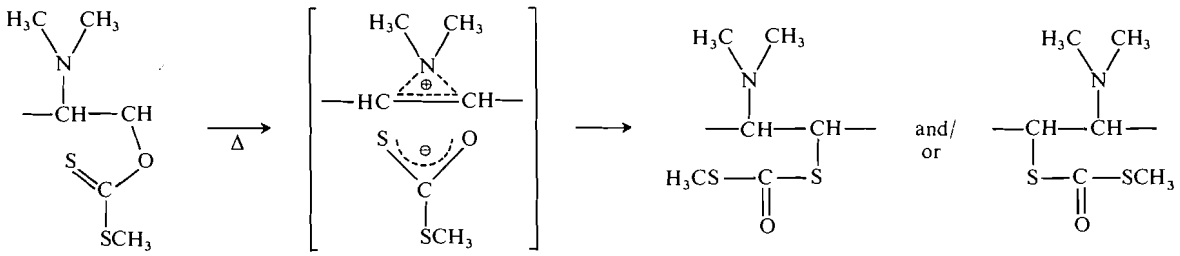

SCHEME 2. A proposed ion-pair transition state for the dithiolcarbonate formation from the pyrolysis of *trans*-2-dimethylaminocyclohexyl xanthate.

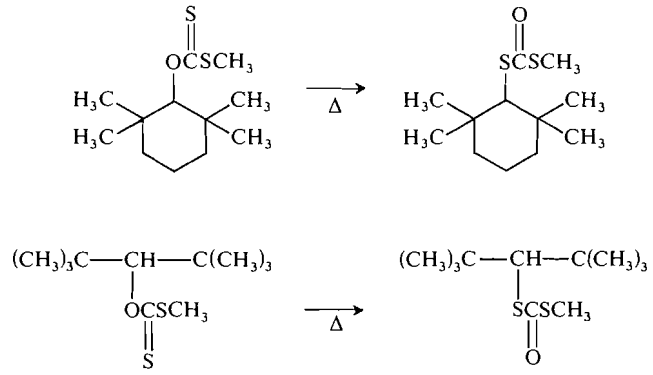

SCHEME 3. Pyrolysis of some neopentyl xanthate esters.

Results and Discussion

Synthesis of Xanthates

A series of *S*-methyl xanthate esters of neopentyl-type alcohols were synthesized. All xanthates prepared shown in Table 1, were relatively stable. Thus these xanthates could be purified by distillation and/or recrystallization. They were synthesized according to procedures developed in this laboratory (14).

As shown in Table 1 boiling points and melting points of this series increase as the formula weight increases and as the number of β-phenyl substituents increases. It is interesting to note that neopentyl xanthate did not decompose even at reflux temperature for 24 h. Again while an electron-withdrawing group at the para-position of the β-phenyl group raises the decomposition temperature, an electron-donating group decreases it. The increasing number of β-phenyl groups also reduces the decomposition temperature of a xanthate ester.

TABLE 1. Xanthate derivative

Xanthate*	M.p. (°C)	B.p. (°C)	Decomposition temperature (°C)
$(CH_3)_3CCH_2OX$		217 (760 mm)	†
p-$BrC_6H_4(CH_3)_2CCH_2OX$		135 (0.1 mm)	300
$C_6H_5(CH_3)_2CCH_2OX$		105 (0.2 mm)	280
p-$CH_3C_6H_4(CH_3)_2CCH_2OX$		122 (0.3 mm)	270
$(C_6H_5)_2(CH_3)CCH_2OX$	52–53		245
$(C_6H_5)_3CCH_2OX$	97–98		210

*X = —CSCH$_3$.
†No decomposition at boiling temperature.

Can. J. Chem. Downloaded from www.nrcresearchpress.com by 210.87.254.6 on 09/05/12
For personal use only.

Can. J. Chem. Downloaded from www.nrcresearchpress.com by 210.87.254.6 on 09/05/12
For personal use only.

TABLE 2. Pyrolysis of neopentyl-type xanthate at 250 °C

Xanthate*	Time (h)	Product distribution (%)				
		Unreacted xanthate	Dithiol-carbonate	Olefin yield	Olefin distribution	Unknown
$(CH_3)_3CCH_2OX$	0.5	99	1	0		
	20.0	64	35	0		1
	40.0	57	42	0		1
$C_6H_5(CH_3)_2CCH_2OX$	0.5	75	8	17	11.5 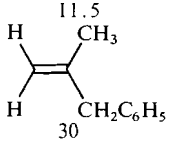 5.5 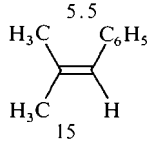	
	2.0	32	22	45	30 15	
$CH_3(C_6H_5)_2CCH_2OX$	0.5	8		88	43 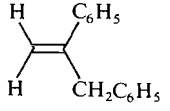 35 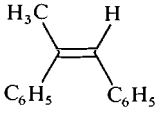 10 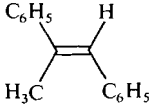	4
$(C_6H_5)_3CCH_2OX$	0.5	0	0	100	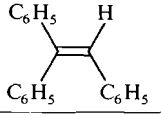	

*$X = -\overset{S}{\overset{\|}{C}}SCH_3$.

Can. J. Chem. Downloaded from www.nrcresearchpress.com by 210.87.254.6 on 09/05/12
For personal use only.

It was decided to study the pyrolytic products in detail because the decomposition of these xanthates suggested that Wagner–Meerwein rearrangement may be occurring. The pyrolytic temperature was chosen to be 250 °C which represents a median decomposition temperature for this series.

Product Studies

Weighed amounts of xanthate were heated at 250 °C for 30 min and/or several hours when required. Olefins were separated by g.l.c. and were identified by standard procedures. The relative amounts of olefinic products were determined by the use of g.l.c. and by n.m.r. spectroscopy. The residues were analyzed by similar methods. A summary of product distributions is shown in Table 2.

To summarize the results of Table 2 the following salient points should be noted:

(*1*) Neopentyl xanthate undergoes only rearrangement to the dithiolcarbonate. No evidence of methyl group participation was observed.

(*2*) Increasing β-phenyl substitution leads to increasing amounts of olefin formation. The olefinic products are derived only from phenyl migration. No xanthate–dithiolcarbonate rearrangement was observed at all in the pyrolysis of 2,2,2-triphenylethyl xanthate and only a small amount (<4%) of dithiolcarbonate was observed in the diphenylpropyl system.

(*3*) There is a predominance of terminal olefins.

(*4*) No skeletally rearranged dithiolcarbonate was observed.

These observations prompted a further study into the course and nature of the pyrolysis of the xanthates under investigation.

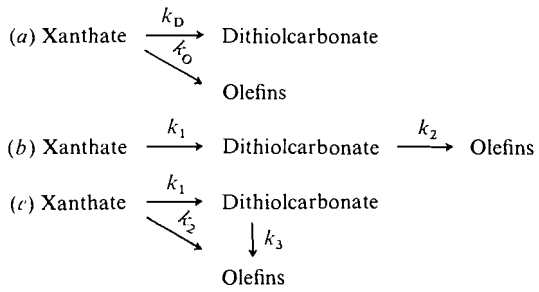

SCHEME 4. The probable courses of reaction for the pyrolysis of neopentyl-type xanthates.

There are three probable ways to account for the products: (*a*) two competing processes to afford both olefin(s) and dithiolcarbonate; (*b*) a consecutive process, and (*c*) a competing–consecutive process (Scheme 4). A kinetic study of the pyrolysis of these xanthates was undertaken in the hope that the results would help to differentiate between the above processes.

Kinetic Studies

Small samples of the xanthates placed in loosely-corked test tubes or sealed tubes (under a nitrogen atmosphere) were suspended in a constant temperature silicone oil bath. At set intervals, reaction was quenched in ice and samples were analyzed by n.m.r. spectroscopy. Using methyl benzoate as an internal standard, the *S*-methyl groups of both the xanthate and the dithiolcarbonate were compared with the methyl group of methyl benzoate and the percent of reaction was calculated.

The rate constants of disappearance of the xanthates (k_t) were determined from the first order rate equation and are listed in Table 3.

If a given reaction occurs by two first-order

TABLE 3. Pyrolysis of neopentyl-type xanthate at 250 °C

Xanthate	k_t (s^{-1})*	k_D (s^{-1})†
$(CH_3)_3CCH_2OX$	$(6.2\pm0.7)\times10^{-6}$	$(5.9\pm0.7)\times10^{-6}$
p-$BrC_6H_4(CH_3)_2CCH_2OX$	$(9.1\pm0.7)\times10^{-5}$	$(3.4\pm0.7)\times10^{-5}$
$C_6H_5(CH_3)_2CCH_2OX$	$(16\ \pm0.7)\times10^{-5}$	$(5.0\pm0.7)\times10^{-5}$
p-$CH_3C_6H_4(CH_3)_2CCH_2OX$	$(7.0\pm0.7)\times10^{-4}$	‡
$CH_3(C_6H_5)_2CCH_2OX$	$(15\ \pm0.7)\times10^{-4}$	‡
$(C_6H_5)_3CCH_2OX$	$(9.2\pm0.7)\times10^{-3}$§	0

*k_t = Rate constant of disappearance of xanthate.
†k_D = Rate constant of formation of dithiolcarbonate.
‡Not available.
§Calculated value.

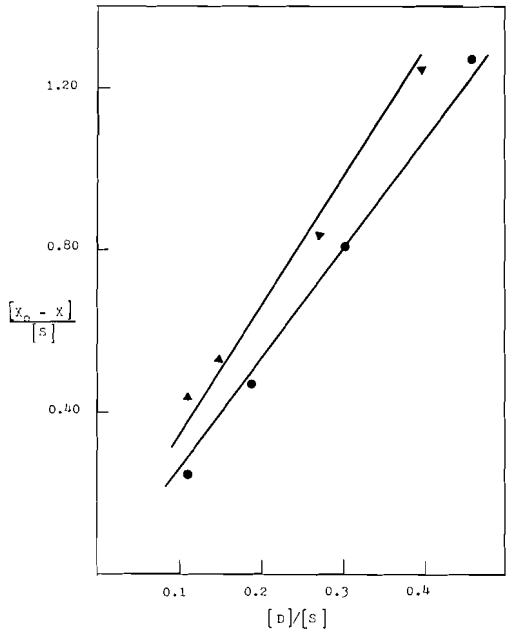

FIG. 1. The rate of disappearance of *p*-bromoneophyl (●) and neophyl (▲) xanthates against the rate of formation of the corresponding dithiolcarbonates; [S] = concentration of the internal standard.

competing processes as shown in (*a*) in Scheme 4, then

$$[1] \qquad [X] = [X_0]e^{-k_t(t)}$$

$$[2] \qquad [D] = -\frac{k_D}{k_t}[X - X_0]$$

$$[3] \qquad [O] = -\frac{k_O}{k_t}[X - X_0]$$

$$[4] \qquad k_t = k_D + k_O$$

where k_t = rate constant of disappearance of xanthate; k_D = rate constant of dithiolcarbonate formation; k_O = rate constant of olefin formation; [X] = concentration of xanthate at time t; $[X_0]$ = concentration of xanthate at time zero; [D] = concentration of dithiolcarbonate; [O] = concentration of olefin(s). Thus for two competing processes the plot of [D] *vs.* $[X - X_0]$ should be a straight line as predicted by eq. 2. If so, eq. 4 is also satisfied.

Figure 1 confirms the linear relationship between [D] and $[X_0 - X]$ for both neophyl and *p*-bromoneophyl xanthates. The rates of dithiolcarbonate formation (k_D) were calculated from the slopes of these lines and are shown in Table 3. Thus the production of olefin and dithiolcarbonate are two competitive processes in the pyrolysis of these two compounds. This result indicates that the relationship in eq. 4 is also true.

Further studies showed that there was no olefin formation from the pyrolysis of neopentyl and neophyl dithiolcarbonates under similar experimental conditions. On this basis, the consecutive process and the competing–consecutive process can be eliminated.

Wagner–Meerwein Rearrangement Leading to Olefin Formation

The rate constants of olefin formation (k_O) were calculated according to eq. 4. For 2,2-diphenylpropyl, *p*-methylneophyl and 2,2,2-triphenylethyl xanthates, it was assumed that $k_O = k_t$ because less than 5% of dithiolcarbonate was observed after 70% completion of pyrolysis.

Table 4 shows that the rate of olefin formation increases with increasing number of β-phenyl substituents. Furthermore, the rate was also increased by electron-donating groups substituted at the para-position of the benzene ring. A similar observation was obtained in the acetolysis of neopentyl-type brosylates (15).

TABLE 4. Rates of acetolysis of neopentyl-type brosylates (k_s) at 75 °C and calculated rates of olefin formation in the pyrolysis of neopentyl-type xanthates (k_O) at 250 °C

	Pyrolysis of xanthates		Acetolysis of brosylates	
	k_O (s^{-1})	$-\log k_O$	k_s (s^{-1})	$-\log k_s$
p-$BrC_6H_4(CH_3)_2CCH_2OH$	$(5.7+0.7)\times10^{-5}$	4.2–4.3	1.09×10^{-5}	4.96
$C_6H_5(CH_3)_2CCH_2OH$	$(11+0.7)\times10^{-5}$	3.9–4.0	6.84×10^{-5}	4.12
p-$CH_3C_6H_4(CH_3)_2CCH_2OH$	$(7.0+0.7)\times10^{-4}$	3.1–3.2	5.00×10^{-4}	3.30
$CH_3(C_6H_5)_2CCH_2OH$	$(15+0.7)\times10^{-4}$	2.8–2.9		
$(C_6H_5)_3CCH_2OH$	$(9.2+0.7)\times10^{-3}$	2.0–2.1	1.06×10^{-3}	2.98

Can. J. Chem. Downloaded from www.nrcresearchpress.com by 210.87.254.6 on 09/05/12
For personal use only.

Can. J. Chem. Downloaded from www.nrcresearchpress.com by 210.87.254.6 on 09/05/12
For personal use only.

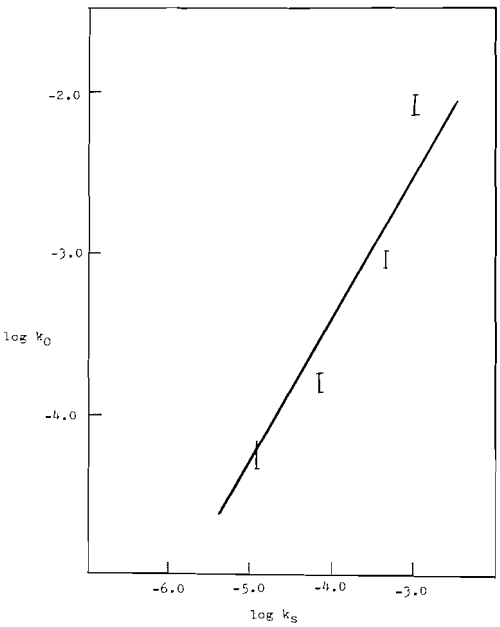

FIG. 2. The linear free energy plot of the rates of pyrolysis of neopentyl-type xanthates (k_O) and the rates of acetolysis of neopentyl-type brosylates (k_s).

Figure 2 shows a linear free energy relationship between the two reactions. The straight line relationship suggests that there is a considerable parallelism between mechanisms of the two reactions (16). It has been demonstrated that the rates of acetolysis of neophyl brosylates were moderately sensitive to substituent effects. A Hammett plot of log k_s *vs.* σ^+ values gave a ρ-value of -2.96 for the reaction. Based on these observations, it was concluded that ionization with phenyl participation was the rate determining step in the acetolysis of neophyl brosylates. This author further proposed that acetolysis of 2,2-diphenylethyl brosylate and 2,2,2-triphenylethyl brosylate should also proceed with the same mechanism (15).

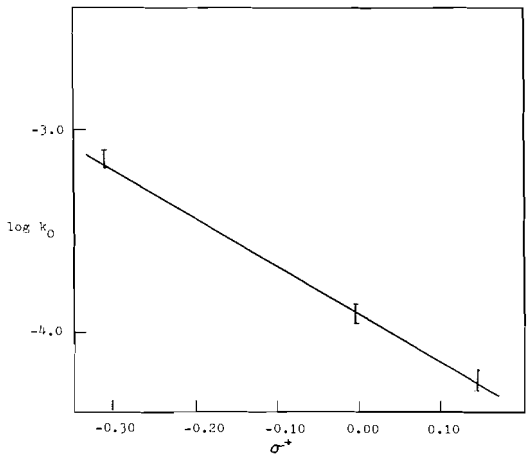

FIG. 3. Plot of log k_O for the pyrolysis of para-substituted neophyl xanthates at 250 °C against σ^+ values: -0.306 for p-CH_3; 0.00 for p-H; $+0.148$ for p-Br.

In our studies, the decomposition rates of the substituted neophyl xanthates were also found to be moderately sensitive to the nature of substituents. This observation, coupled with the apparent similarity between the two systems, suggests that a phenonium ion transition state is also involved in the olefin formation during the neophyl-type xanthate pyrolysis process as shown in Scheme 5.

Figure 3 shows a Hammett–Taft plot of calculated rate constants of olefin formation of three substituted neophyl xanthates *vs.* the corresponding σ^+ values of the substituents. A reasonably good straight line relationship was obtained. The ρ-value for the reaction was calculated to be -2.42. This further supports the proposed involvement of the phenonium ion transition state.

It is interesting to note that there is a predominance of the Hofmann-type olefins in the product. In the acetolysis of neophyl brosylate, the 2-benzylpropene to 2,2-dimethylstyrene

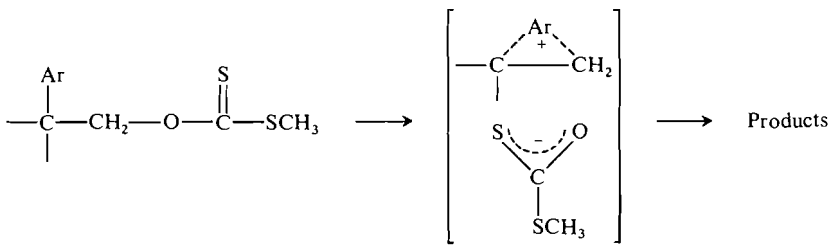

SCHEME 5. Proposed transition state for the olefin(s) formation process.

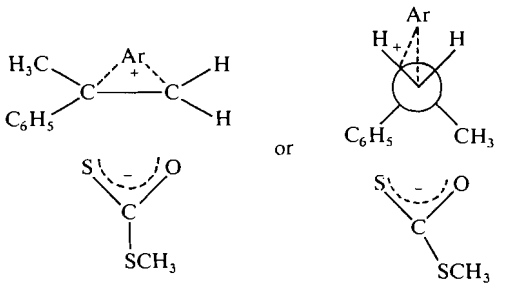

SCHEME 6. The proposed transition state of the pyrolysis of diphenylpropyl xanthate.

ratio was 1:1 (15). Kwart and co-workers (17, 18) reported a ratio of 2.2:1 of 2-benzylpropene to 2,2-dimethylstyrene in the pyrolysis of neophyl acetate in the gas phase at 575 °C. Statistically speaking, the ratio of the two olefins should be 3:1. Since in the pyrolysis of neophyl xanthate the observed ratio is 2:1, the larger than statistically predicted amount of conjugated olefin formed in the reaction suggests that both statistical and thermodynamic effects are important.

The 1-benzylstyrene (**1**) to methylstilbene (**2**) ratio should be 3:2 in the pyrolysis of 2,2-diphenylpropyl xanthate if statistics were the only controlling factor. Experimentally, the ratio was found to be 1:1. If isomerization of **1** to **2** was unimportant under the reaction conditions,[2] the larger than statistically predicted amount of fully conjugated olefin, **2**, again indicated that both statistic and thermodynamic effects are important during the olefin formation process. On the other hand, if all the methyl-*trans*-stilbene formed were considered to come from the isomerization of 1-benzylstyrene, the **1** to **2** ratio is 3:2, exactly as predicted by the statistical consideration. The reasons for a predominant formation of methyl-*cis*-stilbene over that of the *trans* isomer (3.5:1) is not entirely clear (Scheme 6).

Dithiolcarbonate Formation

In the dithiolcarbonate formation process, both neopentyl and neophyl xanthate gave considerable yields of dithiolcarbonates without skeletal rearrangement. The absence of skeletally rearranged dithiolcarbonates indicates that the reaction might have proceeded through a non-assisted tight ion-pair or a cyclic S_Ni mechanism as shown in Scheme 7. In case of an ion-pair, electron-donating groups at the tertiary carbon should stabilize the ion-pair while electron-withdrawing groups should destabilize it. Thus it is expected that the rate of rearrangement would be faster when $R = CH_3$ than when R = aryl. The rate of formation of neophyl dithiolcarbonate was almost nine times faster than that of the neopentyl dithiolcarbonate as shown in Table 3. Therefore a mechanism involving the formation of a non-assisted tight ion-pair intermediate during the xanthate–dithiolcarbonate rearrangement appears to be in contradiction to the observed results. On the other hand, a concerted S_Ni mechanism involves little charge development in the cyclic transition state. The presence of electron-withdrawing groups at the tertiary carbon atom will enhance the electrophilicity of the methylene carbon, and this increases the rate of dithiolcarbonate formation. This explains the observed faster rate of neophyl dithiolcarbonate formation over that of neopentyl dithiolcarbonate. Moreover, the smaller rate of formation of *p*-bromoneophyl dithiolcarbonate than that of neophyl dithiolcarbonate also supports this argument. Thus, the mechanism of the dithiolcarbonate formation may involve a concerted four-membered cyclic transition state.

Summary and Conclusions

The olefin formation and the dithiolcarbonate formation in the pyrolysis of neophyl xanthates are found to be two competing processes. The Wagner–Meerwein rearrangement becomes more important when the number of β-phenyl groups increases and when there is an electron-donating group substituted at the para-position of the β-phenyl ring. The transition state of the olefin formation process is best represented by a stabilized phenonium ion. The driving force of the rearrangement appears to be mainly electronic in nature, however, release of steric crowding at the ground state could also play an importante role. The dithiolcarbonate is thermally more stable than the corresponding xanthate and its formation becomes more important when the number of β-phenyl substituents is the least. This rearrangement

[2]Under the reaction conditions, it was found that 1-benzylstyrene isomerized up to 48% to methyl-*trans*-stilbene but gave no methyl-*cis*-stilbene. No *cis–trans* isomerization of stilbenes was observed.

Can. J. Chem. Downloaded from www.nrcresearchpress.com by 210.87.254.6 on 09/05/12
For personal use only.

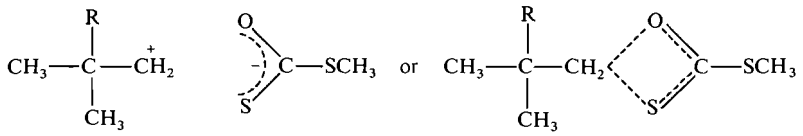

SCHEME 7. The possible transition state of the xanthate–dithiolcarbonate rearrangement. (R = CH_3, aryl).

TABLE 5. Element of analysis of xanthates

Xanthate	Theoretical (%)			Found (%)		
	Carbon	Hydrogen	Bromine	Carbon	Hydrogen	Bromine
$(CH_3)_3CCH_2OX$	47.15	7.91		47.11	8.16	
p-$BrC_6H_4(CH_3)_2CCH_2OX$	45.14	4.74	25.01	45.46	4.87	25.04
$C_6H_5(CH_3)_2CCH_2OX$	59.86	6.71		60.08	6.73	
p-$CH_3C_6H_4(CH_3)_2CCH_2OX$	61.37	7.13		61.65	6.88	
$CH_3(C_6H_5)_2CCH_2OX$	67.51	6.00		67.34	5.99	
$(C_6H_5)_3CCH_2OX$	72.49	5.53		72.15	5.41	

appears to proceed through a concerted four-membered cyclic transition state.

Experimental

Synthesis of Xanthates

All Xanthates were synthesized according to procedures developed in this laboratory (14).[3] Elemental analyses of these xanthates are summarized in Table 5. The i.r. and n.m.r. spectral data of these compounds all supported the desired xanthate structures.

Pyrolysis of Neopentyl Xanthate

Neopentyl xanthate (5 g) was refluxed under nitrogen for 48 h. No decomposition was observed as the i.r. spectrum of the product was identical with that of neopentyl xanthate. Another attempted decomposition was carried out in sealed tube at higher temperature. The xanthate, 1 g, was sealed in a 4 ml micro test tube under nitrogen and was kept at 270 °C for 5 h. The product was analyzed by g.l.c. (8 ft Lac-728 column, 120 °C, 60 cc helium/min) and gave two peaks. The first peak (retention time, 32 min; 60%) was identified as unreacted neopentyl xanthate. The second peak (retention time, 38 min; 40%) was identified as neopentyl dithiolcarbonate: i.r. (10%, CCl_4) 2960 and 2870 (s, C—H), 1650 (s, C=O), 1365 (m, C—H), 860 (s, S—CO—S); n.m.r. (10%, $CDCl_3$) 0.97 (s, 9, $C(CH_3)_3$), 2.48 (s, 3, SCH_3), 3.07 (s, 2, SCH_2).

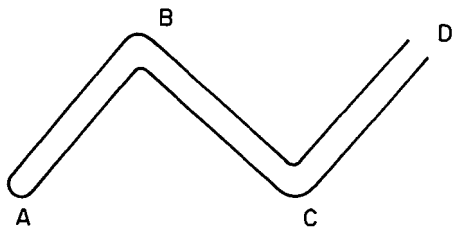

FIG. 4. An N-tube for pyrolysis.

[3]In the synthesis of para-bromoneophyl xanthate, sodium hydride was used instead of potassium metal to generate the sodium salt from the corresponding alcohol.

In an attempt to detect olefin formation, this xanthate (200 mg) was sealed in an n.m.r. tube and heated in a silicone oil bath at 250 °C. A spectrum was run every 4 h. After 40 h no olefin was observed and the corresponding dithiolcarbonate was the only product in 42% yield.

Pyrolysis of Neopentyl Dithiolcarbonate

The dithiolcarbonate (200 mg) in a sealed n.m.r. tube was kept in a silicone oil bath at 250 °C. An n.m.r. spectrum was run every 10 h. After a duration of 40 h, no decomposition was observed. The i.r. spectrum of the resultant liquid was identical to that of the starting dithiolcarbonate.

Pyrolysis of Neophyl Xanthate

Decomposition of a small amount of the xanthate (0.5 g, 2.1 mmol) was carried out in an N-tube (Fig. 4) in a silicone oil bath at 250 °C. The xanthate was pipetted into a straight tube AD 12 cm × 7 mm which was bent to an N-shape as shown in Fig. 4. Part A of the tube was immersed in an oil bath while part C was cooled. The advantage of this N-tube is to allow easy separation of olefin from the residue and also only small amounts of xanthate are required by this method. After heating for 2 h, part A was cooled and was separated from part C. The olefins in part C weighed 127 (9.5 mmol, 45%) while the residue in part A weighed 270 mg. The loss of material was due to escape of gaseous products.

Analysis of the Olefins

The olefins were separated by g.l.c. (8 ft Lac-728 column, 125 °C, 60 cc helium/min). On the chromatogram two peaks appeared with retention times of 5.5 (67%) and 7.5 min (33%). The first peak was identified as 2-benzylpropene: n_D^{25} 1.5050 (lit. (30) 1.5057); i.r. (10%, CCl_4) 3080 (s, C=CH), 3020 (s, Ar—H), 2980 and 2970 (s, C—H), 1645

Can. J. Chem. Downloaded from www.nrcresearchpress.com by 210.87.254.6 on 09/05/12
For personal use only.

Can. J. Chem. Downloaded from www.nrcresearchpress.com by 210.87.254.6 on 09/05/12
For personal use only.

(m, C=C), 1600 and 1490 (w, Ar), 884 (s, C=CH_2), 690 (s, Ar—H); n.m.r. (10%, $CDCl_3$) 1.65 (s, 3, C=C—CH_3), 3.24 (s, 2, C=C—CH_2—Ar), 4.62 (s, 2, C=CH_2), 7.00 (bs, 5, C_6H_5). The second peak was identified as 2-methyl-1-phenylpropene: n_D^{25} 1.5367 (lit. (34) n_D^{20} 1.5400); i.r. (10% CCl_4) 3060 (s, C=CH), 3020 (s, Ar—H), 2970 and 2920 (s, C—H), 1659 (m, C=C), 1600 and 1490 (w, Ar), 825 (m, C=CH), 690 (s, Ar—H); n.m.r. (10%, $CDCl_3$) 1.85 (m, 6, C=$C(CH_3)_2$), 6.10 (m, 1, C=CH), 7.07 (bs, 5, C_6H_5).

Analysis of the olefinic mixture by n.m.r. integration showed a similar product distribution.

Isomerization Study of the Olefins

A 30 mg sample of each of the two olefins was heated separately in an N-tube at 250 °C for 30 min. The n.m.r. spectrum showed that no isomerization occurred for both 2-benzylpropene and 2-methyl-1-phenylpropene.

Analysis of the Residue

The residue was separated by g.l.c. (6 ft Lac-728 column, 200 °C, 60 cc helium/min). On the chromatogram only two peaks appeared at 130 (60%) and 138 min (40%). The compound corresponding to the first peak was identical to the unreacted xanthate. The second component of the residue was identified as the neophyl dithiolcarbonate: n_D^{26} 1.5757; i.r. (10%, CCl_4) 3020 (w, Ar—H), 2950 and 2920 (s, C—H), 1640 (s, C=O), 860 (s, S—CO—S), 690 (s, Ar—H); n.m.r. (10%, $CDCl_3$) 1.34 (s, 6, $C(CH_3)_2$), 2.28 (s, 3, SCH_3), 3.20 (s, 2, SCH_2), 7.00 (bs, 5, C_6H_5).

Analysis of the residue by n.m.r. integration showed a similar product distribution.

Hydrolysis and Reduction of Neophyl Dithiolcarbonate

Neophyl dithiolcarbonate (1 g) was hydrolyzed by sodium hydroxide according to the method of Taguchi and Makao (9) followed by Ra–Ni reduction according to the method of Sondheimer and Rosenthal (19). The resultant reaction mixture was extracted with ether. The organic layer was concentrated and analyzed by g.l.c., i.r., and n.m.r. *t*-Butylbenzene was the only observed product.

Another neophyl xanthate sample (500 mg) was charged to an N-tube which was heated for 30 min. The olefins weighed 42 mg (17%). Analysis by n.m.r. integration showed that 2-benzylpropene and 2-methyl-1-phenylpropene were present in the ratio 67:33. The residue weighed 412 mg and the n.m.r. integration showed that the xanthate to the dithiolcarbonate ratio was 90:10. The loss of material was due to escape of gaseous products.

Pyrolysis of Neophyl Dithiolcarbonate

The dithiolcarbonate (22 mg) was heated in an N-tube at 250 °C for 2 h. No olefin was found. The residue was analyzed by g.l.c., i.r., and n.m.r. and was found to be the starting dithiolcarbonate.

Pyrolysis of p-Bromoneophyl Xanthate

Decomposition of this xanthate (41 mg, 0.13 mmol) was carried out in a 75 × 10 mm test tube at 250 °C for 2 h. The composition of products was analyzed by n.m.r. integration without further purification (methyl benzoate was used as internal standard). The mixture contained 50% of the unreacted xanthate and 17% of the dithiolcarbonate. The olefin portion was not analyzed.

Pyrolysis of p-Methylneophyl Xanthate

Decomposition of this xanthate (33 mg, 0.13 mmol) was carried out in a 75 × 10 mm test tube at 250 °C for 30 min. The composition of products was determined by n.m.r. integration without further purification (methyl benzoate was used as internal standard). The mixture contained 27% of the unreacted xanthate and less than 4% of the dithiolcarbonate. The olefin portion was not analyzed.

Pyrolysis of 2,2-Diphenylpropyl Xanthate

Decomposition of this xanthate (500 mg, 1.65 mmol) was carried out in an N-tube in a silicone oil bath at 250 °C for 30 min. No olefin was found in part C of the tube. The product was analyzed in the following manner.

Analysis of Olefins

The olefins were separated from the reaction mixture by liquid column chromatography (silica gel, petroleum ether (b.p. 30–60 °C)) and weighed 280 mg (88%). Olefins were further separated by g.l.c. (6 ft 10% SE-30, 170 °C, 60 cc helium/min). On the chromatogram three peaks appeared with retention times of 6.4 (39%), 7.4 (49%), and 10.8 min (12%). Analysis of the olefinic mixture by n.m.r. integration showed a similar product distribution. The first peak was identified as methyl-*cis*-stilbene: m.p. 46–47 °C (lit. (20) m.p. 48 °C); i.r. (10%, CCl_4) 3060 (s, C=CH), 3020 (s, Ar—H), 2970 and 2920 (w, C—H), 1600 and 1490 (m, Ar), 849 (m, C=CH), 690 (s, Ar—H); n.m.r. (10%, CCl_4) 2.11 (d, 3, $J = 2$ Hz, C=CCH_3), 6.21 (m, 1, C=CH), 6.70–7.10 (bd, 10, $C(C_6H_5)_2$). The second peak was identified as 1-benzylstyrene: n_D^{24} 1.5893 (lit. (21) n_D^{25} 1.5891); i.r. (10%, CCl_4) 3060 (s, C=CH), 3020 (s, Ar—H), 2910 (m, C—H), 1625 (m, C=C), 1600 and 1490 (m, Ar), 890 (s, C=CH_2), 690 (s, Ar—H); n.m.r. (10%, CCl_4) 3.65 (s, 2, C=CCH_2Ar), 4.80 (bd, 1, C=CH), 5.25 (bd, 1, C=CH), 6.90–7.10 (bs, 10, $C(C_6H_5)_2$). The third peak was identified as methyl *trans*-stilbene: m.p. 81–82 °C (lit. (20) m.p. 82 °C); i.r. (10%, CCl_4) 3060 (s, C=CH), 3020 (s, Ar—H), 2980 and 2940 (w, C—H), 1600 and 1490 (m, Ar), 849 (m, C=CH), 690 (s, Ar—H); n.m.r. (10%, CCl_4) 2.17 (d, 3, $J = 2$ Hz, C=CCH_3), 6.65 (m, 1, C—CH), 6.90–7.20 (m, 10, $C(C_6H_5)_2$).

Olefin Isomerization Study

A 30 mg sample of each of the three olefin products was heated separately in three micro test tubes at 250 °C for 30 min. The n.m.r. analysis showed that no isomerization occurred between *trans*- and *cis*-stilbenes. However, 48% of benzylstyrene was isomerized to methyl-*trans*-stilbene.

Analysis of Other Products

The remaining material on the chromatography column weighed 60 mg. The i.r. spectrum showed characteristic xanthate bands and dithiolcarbonate bands at 1645 and 860 cm^{-1}. The n.m.r. spectrum showed that the mixture contained 66% of the unreacted xanthate. Attempts to isolate the dithiolcarbonate were unsuccessful.

Pyrolysis of 2,2,2-Triphenylethyl Xanthate

Decomposition of this xanthate (1g, 2.7 mmol) was carried out in a micro test tube in a silicone oil bath at 250 °C for 30 min. The product weighed 700 mg (2.7 mmol). The t.l.c. analysis (silica gel, pentane) showed only one spot corresponding to triphenylethylene: m.p. 88–89 °C. The i.r. spectrum was identical to an authentic sample.

An Attempt to Detect Dithiolcarbonate Formation

The *S*-methyl xanthate ester of 2,2,2-triphenylethanol

(0.5 g) in an n.m.r. tube was heated in a silicone oil bath at 200 °C. An n.m.r. spectrum was run every 30 min for a period of 2 h. No dithiolcarbonate formation was observed. Another sample was heated in an oil bath at 160 °C. An n.m.r. spectrum was run every 6 h for a period of 36 h. Again, no dithiolcarbonate formation was observed.

Kinetic Studies

Kinetic studies of the pyrolysis of xanthate esters were carried out on neat samples. An accurately weighed sample (30 mg) of the solid xanthate ester to be studied was placed in a 75 × 10 mm test tube. For liquid xanthate esters, a 30 μl sample was introduced into the test tubes by means of a constant volume addition syringe and then it was weighed accurately. The test tubes were loosely corked or sealed under a nitrogen atmosphere and were suspended in a constant temperature silicone oil bath at the desired temperature. Samples were removed at set intervals and were immediately cooled in ice-water. The samples were analyzed by n.m.r. using methyl benzoate as an internal standard. The relative amounts of xanthate left unreacted and the relative amounts of products formed at each interval were estimated by n.m.r. integrations. The maximum error in integration was estimated to be about 5%.

1. C. H. DEPUY and R. W. KING. Chem. Revs. **60**, 431 (1960); H. R. NACE. *In* Organic reactions. Vol. XII. John Wiley and Sons, Inc., New York, N.Y. 1962. p. 58.
2. J. MARCH. *In* Advances in organic chemistry. McGraw-Hill, Inc., New York, N.Y. 1968. p. 757.
3. F. F. BORDWELL and P. S. LANDIS. J. Am. Chem. Soc. **80**, 6379 (1958).
4. D. J. CRAM. J. Am. Chem. Soc. **71**, 3883 (1949).
5. R. F. W. BADER and A. N. BOURNS. Can. J. Chem. **39**, 348 (1961).
6. C. DJERASSI and W. S. BRIGGS. J. Org. Chem. **33**, 1625 (1968).
7. R. E. GILMAN, J. D. HENION, S. SHAKSHOSKI, J. I. H. PATTERSON, M. J. BOGDANOWICZ, R. J. GRIFFITH, D. E. HARRINGTON, R. K. RANDALL, and K. T. FINLEY. Can. J. Chem. **48**, 970 (1970).
8. C. G. OVERBERGER and A. E. BORCHERT. J. Am. Chem. Soc. **82**, 4896 (1960).
9. T. TAGUCHI and M. MAKAO. Tetrahedron, **18**, 245 (1962).
10. T. TAGUCHI, Y. KAWAZOE, and M. MAKAO. Tetrahedron Lett. 131 (1963).
11. T. TAGUCHI, Y. KAWAZOE, K. YOSHIHIRA, H. KANAYAMA, M. MORI, K. TABATA, and K. HARANO. Tetrahedron Lett. 2717 (1965).
12. P. V. LAAKSO. Suomen Kemi, **13B**, 8 (1940); Chem. Abstr. **34**, 5059 (1940).
13. P. DE MAYO. *In* Molecular rearrangements. Vol. I. Interscience, New York, N.Y. 1963. pp. 6–15.
14. K. G. RUTHERFORD, R. M. OTTENBRITE, and B. K. TANG. J. Chem. Soc. C, 582 (1971).
15. S. WINSTEIN and R. HECK. J. Am. Chem. Soc. **79**, 3432 (1957).
16. H. C. BROWN, R. BERNHEIMER, and K. J. MORGAN. J. Am. Chem. Soc. **87**, 1280 (1965).
17. H. KWART and D. HOSTER. Chem. Commun. 1155 (1967).
18. H. KWART and H. G. LING. Chem. Commun. 302 (1969).
19. F. SONDHEIMER and D. ROSENTHAL. J. Am. Chem. Soc. **80**, 3995 (1958).
20. E. ELLINGBOE and R. C. FUSON. J. Am. Chem. Soc. **55**, 2964 (1933).
21. D. H. HUNTER and D. J. CRAM. J. Am. Chem. Soc. **88**, 5499 (1966).

Can. J. Chem. Downloaded from www.nrcresearchpress.com by 210.87.254.6 on 09/05/12
For personal use only.

Spectrofluorometric Studies. XI. Some Aspects of the Photochemistry of Ortho-fused Benzocycloalkenes

M. GROSSMAN, R. KUBELA, G. P. SEMELUK, AND I. UNGER

Department of Chemistry, The University of New Brunswick, Fredericton, New Brunswick

Received July 13, 1971[1]

Fluorescent yields of 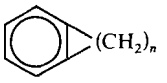 $n = 2, 3, 4, 5, 6$

excited in the 2500 Å region in cyclohexane solution have been examined. There is a general trend of fluorescent yields decreasing with increasing alkene ring size. The sum of the fluorescent and triplet yields decreases with increasing ring size. Triplet energies, obtained by Evans' method and roughly confirmed by phosphorescent emission spectra at 77 °K, do not vary greatly.

Les rendements en fluorescence de $n = 2, 3, 4, 5, 6$

excité dans la région 2500 Å en solution dans le cyclohexane, ont été examinés. Les rendements en fluorescence tendent généralement à décroître lorsque la taille du cycle alcène croît. La somme des rendements triplet et fluorescence décroît avec la taille du cycle. Les énergies triplet, obtenues par la méthode d'Evans et confirmées de façon approchée par les spectres d'émission de phosphorescence à 77 °K, ne varient pas de façon prononcée. [Traduit par le journal]

Canadian Journal of Chemistry, **50**, 3298 (1972)

Introduction

That benzene (1) and benzene derivatives (2–4) may on photoexcitation undergo intramolecular rearrangement has now been well established. Intermediates in such reactions can be prismane (5), fulvene (6), Dewar benzene (2), or benzvalene (7). When one of the above intermediates results from the excitation of an ortho-derivative of benzene, the meta- and para-derivatives may be produced on rearomatization. Ortho-xylene, which may be considered as an ortho-fused benzocycloalkene with an infinitely large ring, does in fact show this type of behavior in the gas phase (8) and also in liquid phase, but in much smaller yield (9). Should this also occur for other members in the ortho-fused benzocycloalkene series then one would in principle have a novel reaction for the formation of meta- and para-bridged compounds. Prior to starting a study of this type, however, it is necessary to examine the simple photochemistry of these compounds *i.e.*, to determine the singlet and triplet yields of these molecules and the effect of various parameters on these yields.

[1]Revision received June 19, 1972.

Experimental

Materials

The cyclohexane and EPA (ethyl ether, isopentane, and ethyl alcohol; 5:5:2) were Hartman–Leddon Company fluorometric grade materials and were used without further purification. The benzene was obtained from Aminco; benzocyclopentene (indane) was from Columbia Organic Chemicals. The ortho-xylene and the benzocyclohexene (1,2,3,4-tetrahydronaphthalene) were API (American Petroleum Institute) standard samples.

Benzocyclobutene (Bicyclo[4.2.0]octa-1,3,5-triene)

This cyclobutene was prepared by gas phase pyrolysis of 1,3-dihydroisothianaphthene-2,2-dioxide as described by Cava and Deana (10), except the apparatus in which the pyrolysis was carried out was slightly different. Instead of the Pyrex sleeve with the Nichrome coil, a 2 ft long Quartz glass tube (i.d. = 9 mm) was used which was heated from outside to 600 °C. Yield of the crude distilled hydrocarbon was 60%; b.p. 149–150 °C uncorrected at atmospheric pressure. It was further purified by v.p.c. using a column with 20% Carbowax 20 M on chromosorb W, and helium carrier.

Can. J. Chem. Downloaded from www.nrcresearchpress.com by 210.87.254.6 on 09/05/12
For personal use only.

Can. J. Chem. Downloaded from www.nrcresearchpress.com by 210.87.254.6 on 09/05/12
For personal use only.

Benzosuberan (1,2-Benzocyclohept-1-ene)

Benzosuberan was prepared by Clemmensen reduction of the corresponding 1-ketone (11). The obtained liquid was distilled from metallic potassium and hydrogenated over 5% palladium on charcoal in methanol at atmospheric pressure. The colorless oil, which distilled at 96–97 °C (uncorrected, 12 Torr), was purified by v.p.c. using a 15% Carbowax 20 M on chromosorb W column and helium carrier.

Benzocyclooctene (1,2-Benzo-cyclo-oct-1-ene)

This cyclooctene was prepared by Friedel–Crafts cyclization of ε-phenyl-*n*-caproyl chloride, followed by Wolff–Kishner reduction of the obtained ketone to give the crude hydrocarbon (12). The b.p. after repeated distillation was 92–100 °C (uncorrected) at 2 Torr. The material was finally purified by passing through a v.p.c. column containing 20% SE-30 on chromosorb M, using helium carrier.

Purity checks using v.p.c., absorption and fluorescence spectra indicated all the materials, with the exception of benzocyclohexene and benzocyclobutene to contain negligible impurities. The solution spectra in the first absorption region were in agreement with absorptivity measurements reported by Moore *et al.* (13, 14), as noted in a previous publication (15).

The benzocyclohexene contained <0.2 mol % of an impurity which appeared to be naphthalene, a contaminant commonly found in samples of this compound. The indirect identification and the effect of the impurity of the fluorescence measurements made in this study are ascertained by adding varying amounts of naphthalene (up to 1 mol %) to both benzocyclohexene and benzocyclopentene. Fluorescence was excited by irradiation in the wavelength regions corresponding to that for the compound under study, and to that for naphthalene. In the case of benzocyclohexene, it was found that the impurity fluorescence spectra excited in the naphthalene region did not change in appearance, but did increase in intensity for increasing amounts of added naphthalene. The quantum yield of benzocyclohexene fluorescence was not changed, however, by the presence of added naphthalene. The same was true in the case of benzocyclopentene solutions with added naphthalene, except in this case the intensity of naphthalene fluorescence, originally zero for solutions of the pure compound, increased proportionately to the quantity of added naphthalene. In the case of benzocyclohexene phosphorescence emission from EPA glass, there was some evidence of the presence of naphthalene. This occurred on the long wavelength side of benzocyclohexene phosphorescence spectra, and does not affect conclusions regarding the position of the short wavelength tail, which was used to give a rough indication of the singlet–triplet energy spacing. Although these experiments may not be conclusive, they do indicate that it is quite unlikely that the impurity in benzocyclohexene has any significant effect on the measurements made on this compound.

In addition to undergoing photodecomposition, benzocyclobutene is subject to slow thermal decomposition at room temperature, which might be due to its strained structure. The measured (low) fluorescent yield was independent of the age of sample (up to 6 months), suggesting that either the unknown decomposition products are not effective quenchers, or that they are so effective that the concentration level reached during the few days intervening between purification and measurement is sufficient to cause a saturated quenching effect. Although it is not possible at this time to choose between the alternatives, the low fluorescent yield is consistent with the expectation that the strained structure may provide a reaction pathway having a rate competitive with fluorescence.

Procedure

Room temperature fluorescent spectra of dilute solutions (~ 0.002 *M*) in cyclohexane were taken with an Aminco–Bowman spectrophotofluorometer (SPF) modified to include, (*a*) an adjustable entrance slit to the exciting monochromator, (*b*) an optical system involving mirrors and condensing lens to focus the resultant higher intensity exciting radiation on this slit, and (*c*) a phototube to monitor the transmitted radiation which allows measurements of absorbed intensity. Additional experimental details have been given previously (16, 17).

The standard phosphorescence attachment and rotating shutter were used to record phosphorescence spectra, which were observed at liquid nitrogen temperatures from EPA glassy matrix. The u.v. absorption spectra were observed in cyclohexane solution with a Hitachi Coleman Model EPS-3T recording spectrometer. Solutions used for fluorescence and phosphorescence measurements were degassed and hermetically sealed in the appropriate measuring cells. Optical quality quartz cuvette-type cells of 1 cm path length, obtained from Hellma (Canada) Limited were used for measurements involving both fluorescence and absorption. A number of fluorescence measurements were made in cylindrical quartz cells of 10 mm i.d. These were not greatly different from measurements obtained using the cuvette-type cells when care was taken to maintain a standard orientation and position in the cell holder. Aminco cylindrical quartz cells 3 mm o.d., and one constructed in this laboratory, were used for the phosphorescence experiments.

Evans' high pressure oxygen perturbation method was used to obtain singlet–triplet absorption spectra in chloroform solution of a few members of the series. Experimental details of the procedure have been given previously (18).

Triplet yields were estimated by the *cis–trans* isomerization technique (19, 20) using *cis*-butene-2. These yields are based on a value of 0.28 for the ortho-xylene triplet yield (21).

All fluorescent quantum yields are based on the ortho-xylene fluorescent yield being 0.19 (22). Since all of the fluorescent spectra cover the same spectral region, corrections for the photomultiplier tube response were unnecessary. This coincidence of spectral region was also true for the phosphorescent emission spectra.

Results and Discussion

Typical fluorescent emission spectra obtained with exciting wavelengths ranging from 230 to about 275 nm are given in Fig. 1. At wavelengths greater than ~ 275 nm no significant emission was observed, except for benzocyclohexene which had a small impurity concentration, as evidenced by the appearance of a new

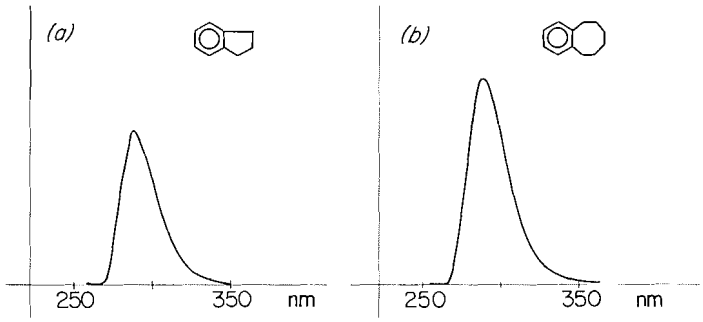

FIG. 1. (*a*) Fluorescent spectrum (uncorrected) of benzocyclopentene: 1.2×10^{-4} *M* in cyclohexane, 298 °K; $\lambda_{ex} = 250$ nm. (*b*) Fluorescent spectrum (uncorrected) of benzocyclooctene: 6.1×10^{-4} *M* in cyclohexane, 298 °K; $\lambda_{ex} = 270$ nm.

emission band covering a different spectral region. For benzocyclobutene, emission in a different spectral region was observed at the shorter wavelengths within the 230 to 275 nm absorption band, also indicating a small impurity concentration. In the case of benzocyclohexene the impurity appeared to be naphthalene, while in the other case it was not identified.

Except for the case of benzene, concentrations of sample and reference solutions were adjusted so that the absorbance (*A*) was approximately the same for both solutions at the comparison wavelengths, in order to minimize as much as possible inner filter and "around the corner" effects (23). For many pairs this adjustment at one comparison wavelength resulted in $A_{reference} \sim A_{sample}$ for all the comparison wavelengths. In these cases this was obviously a consequence of the experimental detail: (*1*) a relatively large irradiation band width (9 nm); (*2*) solution broadened absorption bands; (*3*) absorption bands covering the same wavelength range and having similar shapes.

For samples and reference having different absorbance, quantum yield measurements were corrected by a previously described procedure (23). Inner filter effects, which were self-cancelling, were found to be negligible. The results of the fluorescent quantum yield measurements are summarized in Tables 1 and 2.

The data in Table 1 represent a selection of solutions for which the absorbance match with the reference *o*-xylene solutions was very good, and for which the geometrical considerations were the most favorable. In Table 2 *all* the data obtained has been averaged; that obtained in cases of poor absorbance matches with corrections made as noted (23), that obtained in cases of good absorbance matches, and that derived from the cylindrical cells. It is to be noted that the trend in Table 1 for each excitation wavelength, is preserved in the averages summarized in Table 2.

In general there is a trend of decreasing fluorescent yield with increasing alkene ring size. Benzocyclobutene, one of the exceptions to this trend, appears to be different in other respects also, particularly with respect to its lack of stability, and so should be treated as a special case. On the other hand benzocycloheptene provides an interesting anomaly. It has previously been noted (13, 14) that the maximum molar absorbancy index of benzocycloheptene solutions in cyclohexane is an exception to a generally decreasing trend of maximum absorbancy indices with increasing ring size. However, this is *not* observed in gas phase spectra (15), suggesting some type of specific interaction with the solvent. The reasons for this are not obvious.

Several values have been reported for the fluorescent quantum yield of ortho-xylene (22, 24, 25). The value given by Berlman was chosen as our standard reference value after a careful comparison of methods and techniques used by the various authors. As a check, the fluorescent yield for benzene was determined, and found to be in good agreement with values obtained under similar conditions (26) and not too different from that reported by Berlman (22). Hence the quantum yields given in Tables 1 and 2, although not determined by an absolute method, should be fairly accurate. Triplet

Can. J. Chem. Downloaded from www.nrcresearchpress.com by 210.87.254.6 on 09/05/12
For personal use only.

TABLE 1. Fluorescent yields of some ortho-fused benzocycloalkenes in cyclohexane solutions. Determinations made in square cross-section cuvettes, with good absorbancy matches to ortho-xylene reference solutions

Compound	$c \times 10^4$ (mol/l)	Fluorescent yield*		
		260 nm	265 nm	270 nm
Benzocyclooctene	4.5 (except: 270 nm; 29)	0.20	0.22	0.20
Benzocycloheptene	7.0	0.14	0.15	0.14
Benzocyclohexene	2.5	0.29	0.24	0.25
Benzocyclopentene	2.0	0.34	0.37	0.39
Benzocyclobutene	0.7	0.06	0.04	0.08

*Based on ortho-xylene fluorescent yield taken as 0.19 (Berlman (22)).

TABLE 2. Summary of fluorescent yield averages of some ortho-fused benzocycloalkenes in cyclohexane solutions

Compound	Excitation wavelength region (nm)	Concentration range ($\times 10^4$ M)	Fluorescent yield*
Benzocyclooctene	250–270	4.5–29	0.197 ±0.008
Benzocycloheptene	250–270	6.0–12	0.15 ±0.01
Benzocyclohexene	250–270	2.5–15	0.24 ±0.02
Benzocyclopentene	250–270	1.3–29	0.38 ±0.02
Benzocyclobutene	260–270	0.7–10	0.05 ±0.02
Benzene†	265	34.0–39	0.06

*Based on ortho-xylene fluorescent yield taken as 0.19 (Berlman (22)).
†Determined as a check on the procedure. Berlman's value is 0.07.

yield results on benzocycloheptene, benzocyclohexene, and benzocyclopentene are summarized in Table 3, as are the "quantum deficits". Inspection of Table 3 shows that there is a trend of increasing quantum deficit with increasing ring size, which suggests processes other than fluorescence and intersystem crossover to triplet, become progressively more favored. The principal alternate processes are internal conversion to the ground state and intramolecular isomerization. Unfortunately it was not possible under our experimental conditions to detect with any certainty whether or not any valence isomers were present. In another series of experiments it was found that no meta and para isomers are produced photochemically until the ring size exceeds $n = 12$. The evidence so far obtained, then, leads to the conclusion that the major portion of the quantum deficit is probably accounted for by internal conversion processes.

A single experiment utilizing a high pressure of xenon with benzocyclopentene in the presence of *cis*-butene-2 showed a large increase in isomerization of the olefin. Experiments with meta-fused benzocyclodecahexene in the presence and absence of xenon showed that xenon depresses the formation of the ortho-fused isomer. It therefore appears likely that isomerization, when it can occur, proceeds through the excited singlet.

Typical phosphorescent emission spectra from EPA glassy matrix at 77 °K, obtained with exciting wavelengths corresponding to those used for exciting fluorescence, are shown in Fig. 2. The experimental arrangement is not well suited to the determination of phosphorescent yields, hence no such measurements were attempted.

The apparent coincidence of the spectral region of fluorescent emission for this series of compounds, and the corresponding and similar observation regarding the phosphorescent emission, invites comment, particularly since the behavior of benzene in these respects is very similar also. It strongly suggests that (*a*) the

Can. J. Chem. Downloaded from www.nrcresearchpress.com by 210.87.254.6 on 09/05/12
For personal use only.

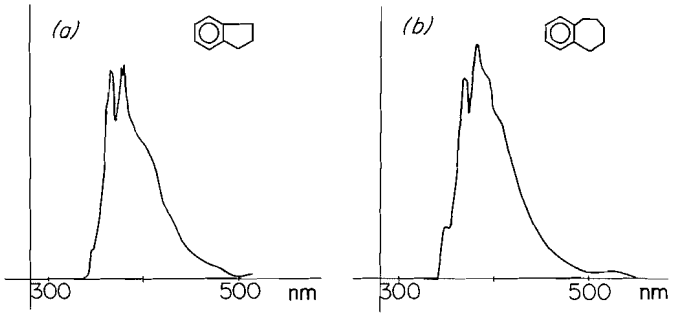

FIG. 2. (*a*) Phosphorescent spectrum (uncorrected) of benzocyclopentene: 1.6×10^{-3} *M* in EPA, 77 °K; shutter speed 2330 r.p.m.; $\lambda_{ex} = 266$ nm. (*b*) Phosphorescent spectrum (uncorrected) of benzocycloheptene: 1.5×10^{-3} *M* in EPA, 77 °K; shutter speed 2550 r.p.m.; $\lambda_{ex} = 265$ nm.

TABLE 3. Summary of triplet yields and quantum deficit for some ortho-fused benzocycloalkenes in methyl cyclohexane solutions at excitation wavelength of 254 nm

Compound	Concentration ($\times 10^4$ *M*)	Triplet yield*	Deficit $1 - (\phi_t + \phi_f)$
Benzocycloheptene	6.16	0.35	0.49
Benzocyclohexene	5.88	0.41	0.35
Benzocyclopentene	6.54	0.31	0.31

*Using the *cis*-butene-2 technique, based on ortho-xylene triplet yield taken as 0.28 (21).

singlet energies of this group of compounds are nearly the same and approximately equal to that of benzene; (*b*) the triplet energies are also the same and not too different from that of benzene. As a consequence, it may be concluded that the presence of the ortho-fused ring does not greatly modify the energies involved in the benzene π–π^* system. The vibrational (and probably rotational) detail is different (15), but the energy spread and location of the first excited singlets and triplets appear to be approximately the same.

Confirmation of the above is provided by the absorption spectra previously obtained (15), and by the oxygen perturbed absorption spectra for a few members of this series. A comparison of these energies obtained from the corresponding O—O bands, is given in Table 4. Some interesting comparisons can be made between the benzocycloalkenes and the fluorinated benzenes. In both series of compounds the singlet and triplet energies, as determined from the O—O bands of the corresponding absorption spectra, are not too different from one another nor from benzene. There is, however, a tremendous difference in the observed Stokes loss. As implied above, the Stokes loss is approximately

TABLE 4. Spectroscopically observed singlet and triplet energies

Compound	Singlet energies		Triplet energies		
	cm^{-1}*	kcal mol^{-1}	From phosphorescent† emission (cm^{-1})	From Evans' method‡ (cm^{-1})	kcal mol^{-1}
Benzene	38086.1	108.9	30300	29400	84.1
Benzocyclobutene	37093	106.1	—	—	—
Benzocyclopentene	36911	105.5	29400	28700	82.2
Benzocyclohexene	36795	105.2	29100	28400	81.3
Benzocycloheptene	37064	105.9	—	—	—
Benzocyclooctene	36943	105.6	—	—	—
o-Xylene	37313	106.7	30300	28650	81.9

*From O—O band gas phase absorption spectra (15) except for benzene which is taken from Herzberg (28).
†From shortest wavelength, in EPA glass at 77 °K, relatively low intensity, low resolution.
‡From O—O band, high pressure oxygen perturbed absorption spectra, in chloroform solution.

Can. J. Chem. Downloaded from www.nrcresearchpress.com by 210.87.254.6 on 09/05/12
For personal use only.

constant in the benzocycloalkenes. In contrast, the greater the fluorine loading of the benzene ring the greater is the Stokes shift, and the further the fluorescent emission "tail" extends towards longer wavelengths.[2] Fluorine substitution appears to exert a far greater influence in benzenoid excited states than it does in the ground electronic state, whereas this is not so for hydrocarbon substituents.

The authors wish to thank the National Research Council of Canada for financial assistance, and to acknowledge the help received from Dr. Z. Valenta of this department during the course of many useful discussions.

1. K. E. WILZBACH, J. S. RITSCHER, and L. KAPLAN. J. Am. Chem. Soc. **89**, 1031 (1967).
2. K. WILZBACH and K. J. RAUSCH. J. Am. Chem. Soc. **92**, 2178 (1970).
3. I. HALLER. J. Am. Chem. Soc. **88**, 2070 (1966).
4. F. LAHMANI and N. IVANOFF. Tetrahedron Lett. 3913 (1967).
5. H. G. VIEHE, R. MERENYI, J. F. M. OTH, J. R. SENDERS, and P. VALANGE. Angew. Chem. Int. Ed. Eng. **3**, 755 (1964).
6. H. R. WARD, J. S. WISHNOK, and P. D. SHERMAN, JR. J. Am. Chem. Soc. **89**, 162 (1967).
7. K. SHINDO and S. LIPSKY. J. Chem. Phys. **45**, 2292 (1966).
8. W. A. NOYES, JR. and C. S. BURTON. Ber. Bunsenges. Physik. Chem. **72**, 146 (1968).
9. R. B. CUNDALL and A. J. R. VOSS. Chem. Commun. 902 (1968).

[2]Unpublished data from this laboratory. Example for pentafluorobenzene given in ref. 27.

10. M. P. CAVA and A. A. DEANA. J. Am. Chem. Soc. **81**, 4266 (1959).
11. P. A. PLATTNER. Helv. Chim. Acta, **27**, 801 (1944).
12. R. HUISGEN and W. RAPP. Chem. Ber. **85**, 826 (1952).
13. W. R. MOORE, E. MARCUS, S. E. FENTON, and R. T. ARNOLD. Tetrahedron, **5**, 179 (1959).
14. H. MEIER, J. HEISS, H. SUHR, and E. MULLER. Tetrahedron, **24**, 2307 (1968).
15. C. M. HUMBY, G. P. SEMELUK, and R. D. S. STEVENS. Spectrosc. Lett. **3**, 99 (1970).
16. F. W. AYER, F. GREIN, G. P. SEMELUK, and I. UNGER. Ber. Bunsenges. Physik. Chem. **72**, 282 (1968).
17. S. H. NG, G. P. SEMELUK, and I. UNGER. Ber. Bunsenges. Physik. Chem. **74**, 29 (1970).
18. G. P. SEMELUK and R. D. S. STEVENS. Can. J. Chem. **49**, 1567 (1971).
19. R. B. CUNDALL and T. F. PALMER. Trans. Faraday Soc. **56**, 1211 (1960).
20. R. B. CUNDALL and D. G. MILNE. J. Am. Chem. Soc. **83**, 3902 (1961).
21. R. B. CUNDALL and A. J. R. VOSS. Chem. Commun. 116 (1969).
22. I. B. BERLMAN. Handbook of fluorescent spectra of aromatic molecules. Academic Press, New York. 1965.
23. J. L. DURHAM, G. P. SEMELUK, and I. UNGER. Can. J. Chem. **46**, 3177 (1968).
24. E. J. BOWEN and A. H. WILLIAMS. Trans. Faraday Soc. **35**, 765 (1939).
25. M. D. LUMB and D. A. WEYL. J. Mol. Spectrosc. **23**, 365 (1967).
26. J. W. EASTMAN. J. Chem. Phys. **49**, 4617 (1968).
27. S. LEM, G. P. SEMELUK, and I. UNGER. Can. J. Chem. **49**, 1569 (1971).
28. G. HERZBERG. Molecular spectra and molecular structure. III. Electronic spectra and electronic structure of polyatomic molecules. D. Van Nostrand Company, N. J. 1966.

Can. J. Chem. Downloaded from www.nrcresearchpress.com by 210.87.254.6 on 09/05/12
For personal use only.

A Kinetic and Electron Spin Resonance Study of the Polymerization of Vinyl Acetate Retarded by 2,4,6-Tri-*t*-butylphenol

H. LILLES, R. D. PARNELL, AND K. E. RUSSELL
Department of Chemistry, Queen's University, Kingston, Ontario

Received March 27, 1972

The effect of 2,4,6-tri-*t*-butylphenol on the rate of polymerization of vinyl acetate and on the degree of polymerization of the resultant polymer has been determined. It is shown that the phenoxy radicals produced by hydrogen transfer do not reinitiate polymerization and that they disappear from solution by reaction with polyvinyl acetate radicals. The chain transfer constant is estimated to be 0.017 ± 0.004 at 45° from molecular weight studies and 0.021 ± 0.004 from rate studies. Stationary state concentrations of phenoxyl of the order of 10^{-7} *M* have been determined by e.s.r. spectroscopy. The rate constant for the reaction of polyvinyl acetate radicals with 2,4,6-tri-*t*-butylphenoxyl is $(6.6 \pm 2.3) \times 10^7$ l mol^{-1} s^{-1} at 45°.

Nous avons déterminé l'influence du 2,4,6-tri-*t*-butylphénol sur la vitesse de polymérisation de l'acétate de vinyle et sur le degré de polymérisation de ce polymère. On montre que les radicaux phénoxy produits par transfert d'hydrogène ne réinitient pas la polymérisation et ils disparaissent de la solution en réagissant avec les radicaux d'acétate de polyvinyle. La constante de transfert de chaîne est estimée à 0.017 ± 0.004 à 45° à partir d'études de poids moléculaires et à 0.021 ± 0.004 à partir d'études de vitesses. Des concentrations de radical phénoxyl à l'état stationnaire de l'ordre de 10^{-7} *M* ont été déterminées par r.p.e. La constante de vitesse de la réaction des radicaux d'acétate de polyvinyl avec le 2,4,6-tri-*t*-butylphénoxyl est $(6.6 \pm 2.3) \times 10^7$ l mol^{-1} s^{-1} à 45°. [Traduit par le journal]

Canadian Journal of Chemistry, **50**, 3304 (1972)

Can. J. Chem. Downloaded from www.nrcresearchpress.com by 210.87.254.40 on 09/05/12
For personal use only.

Introduction

The general objective of our present work is to explore the factors which influence the rates of reaction of radical intermediates in solution and in particular to obtain such information for radical–radical processes. Whenever possible, the concentrations of radical intermediates are directly determined by means of e.s.r. spectroscopy and the results yield estimates of reaction rate constants which cannot be readily obtained by other means.

In earlier studies (1, 2) it was established that the reaction of 2,2-diphenyl-1-picrylhydrazyl (DPPH) with hindered phenols could readily be followed by e.s.r. spectroscopy. The simplest reaction examined in this way was that between DPPH and 2,4,6-tri-*t*-butylphenol in benzene; the DPPH abstracts the hydrogen atom from the OH group to give 2,2-diphenyl-1-picrylhydrazine and the tri-*t*-butylphenoxy radical. The hindered phenoxy radical has a narrow line spectrum compared with that of DPPH and its concentration can be determined in the presence of the second radical. In other work (3), the reactivities of a number of phenols towards the polyvinyl acetate radical were compared. Transfer constants, *i.e.* ratios of rate constants for attack of polyvinyl acetate radicals on phenol and on monomer, were determined, but in the absence of information concerning the relative importance of the various radical–radical termination reactions, the transfer constants could only be quoted to a low accuracy.

The present paper describes a study of the effect of 2,4,6-tri-*t*-butylphenol on the polymerization of vinyl acetate. The phenol reacts with polyvinyl acetate radicals to produce 2,4,6-tri-*t*-butylphenoxyl, a radical which has little or no reactivity towards itself (4) or towards vinyl acetate monomer. The tri-*t*-butylphenoxyl is produced in the chain transfer reaction and is lost only in the cross reaction with polyvinyl acetate radicals. It is thus possible to use measurements of the degree of polymerization to obtain an unambiguous value of the chain transfer constant and to check this value by an independent analysis of the effect of the added phenol on the rate of polymerization of the vinyl acetate (5). The transfer constant yields the rate constant for hydrogen atom abstraction from the phenol by polyvinyl acetate radicals since the propagation rate constant for vinyl acetate polymerization is

Can. J. Chem. Downloaded from www.nrcresearchpress.com by 210.87.254.40 on 09/05/12
For personal use only.

known from independent studies. The dependence of the steady state concentration of tri-*t*-butylphenoxyl upon phenol and initiator concentrations was determined by e.s.r. spectroscopy and the rate constant for the reaction between polymer and phenoxy radicals was derived from these results.

Experimental

Materials

Azobisisobutyronitrile was recrystallized twice from diethyl ether and stored at 0°. 2,4,6-Tri-*t*-butylphenol (Aldrich Chemical Company) was recrystallized three times from methanol in an atmosphere of nitrogen and stored under nitrogen at 0°.

Vinyl acetate was fractionally distilled at atmospheric pressure and the distillate degassed on the vacuum line. The monomer was "prepolymerized" by adding 1 g azobisisobutyronitrile to 500 ml vinyl acetate and irradiating at 0° with near u.v. radiation. The prepolymerization was stopped when the magnetic stirrer indicated that the solution had become fairly viscous. The vinyl acetate was fractionally distilled from the mixture at reduced pressure (b.p. about 18°) and a middle fraction (100 ml) collected. The frozen monomer was stored on the vacuum line in the absence of light. The absorbance of the monomer was less than 0.03 at 275 nm in a 1 cm cell.

Procedure

The polymer samples were prepared as described in an earlier paper (3). Tri-*t*-butylphenol concentrations were in the range 0.002–0.07 *M*. The experiments were performed at 45 °C and the conversion of monomer to polymer was kept below 5%. Degrees of polymerization were estimated from intrinsic viscosities and from osmotic pressures of polymer solutions. The intrinsic viscosities were determined at 25° and degrees of polymerization obtained from eq. 1 (6).

$$[1] \qquad \bar{P}_n = 2.57[\eta_l]^{1.40}$$

$\bar{P}_n$ is the number average degree of polymerization and $[\eta_l]$ is the limiting viscosity number. The values of $\bar{P}_n$ obtained by this method were in good agreement (±8%) with those obtained directly by means of a Hewlett Packard Membrane Osmometer (Model 501) with toluene as solvent at 30°.

E.s.r. spectra of reaction mixtures were obtained by means of a Varian V4502 spectrometer fitted with a variable temperature control unit. The temperature of the solution for a given dial setting was regularly checked in separate calibration experiments. The steady state concentration of tri-*t*-butylphenoxyl was of the order of 10^{-7} *M* and a convenient modulation amplitude for concentration studies was 0.2 G. The microwave power was maintained at a low level in order to minimize saturation; even so, some saturation occurred and a small correction factor, determined in separate saturation studies on DPPH and phenoxy radicals, was applied. In any run the observed spectra were compared with the spectrum of a Mn^{2+} standard contained in a small capillary (7); the Mn^{2+} standard was calibrated by means of a freshly made standard solution of DPPH. All double integrations of first derivative curves were performed manually. Reaction mixtures were prepared *in vacuo* and tri-*t*-butylphenol concentrations were in the range 0.065–0.3 *M*.

Results

Polymerization Rate Studies

The purified vinyl acetate polymerized under given conditions of temperature and initiator at a reproducible rate. The ratio, $R_p/[In]^{1/2}$, where R_p is the overall rate of polymerization and [In] the initiator concentration, was found to be $(39 \pm 2) \times 10^{-4}$ $mol^{1/2}\ l^{-1/2}\ s^{-1}$ at 45°. The ratio did not vary with initiator concentration in the range 0.004–0.06 *M*; the correction for the heating effect (8) in the 5 ml reaction tube is small at 45°. The value of $(39 \pm 2) \times 10^{-4}$ $mol^{1/2}\ l^{-1/2}\ s^{-1}$ at 45° compares with an interpolated ratio of 33×10^{-4} $mol^{1/2}\ l^{-1/2}\ s^{-1}$ obtained by Matheson *et al.* (9) and 31×10^{-4} $mol^{1/2}\ l^{-1/2}\ s^{-1}$ obtained by Bird and Russell (3). Matheson *et al.* showed that a rough check on the purity of the vinyl acetate could be made by measuring the extinction coefficient of the pure monomer in the region of 275 nm since impure monomer absorbs strongly at this wavelength. The extinction coefficient of the monomer used in this work was 0.002–0.003 at 275 nm which compares with an extinction coefficient of approximately 0.0032 derived from spectra given by Matheson *et al.* (9) and Schulz and Stein (10).

The experimentally observed $R_p/[In]^{1/2}$ was used to determine the magnitude of the ratio $(2k_{tc} + 2k_{td})/k_p^2$ at 45°; in this expression $2k_{tc}$, $2k_{td}$ are the rate constants for the disappearance of polyvinyl acetate radicals by mutual combination and disproportionation respectively and k_p is the propagation rate constant. The rate of initiation of polymerization was estimated by coupling the rate constant, k_d, for the decomposition of azobisisobutyronitrile in solution (11), after correcting for solvent effect (12), with the initiator efficiency of 0.54 recently determined by Tüdös and co-workers (8). The resulting value of $(2k_{tc} + 2k_{td})/k_p^2$ is 7.6 ± 1.1 $mol\ l^{-1}\ s$ at 45°; the error limits, ± 1.1 $mol\ l^{-1}\ s$, are based on assumed uncertainties of 10% in k_d, 10% in the initiator efficiency and 5% in $R_p/[In]^{1/2}$.

The effect of tri-*t*-butylphenol on the rate of polymerization of vinyl acetate at 45° is shown

TABLE 1. Dependence of rate of polymerization at 45 °C of added phenol for two series of experiments

Series	10^3[In] (mol l^{-1})	[M] (mol l^{-1})	10^3[XOH] (mol l^{-1})	$10^4 R_p$ (mol l^{-1} s^{-1})	$10^4 R_p/[In]^{1/2}$ (mol$^{1/2}$ $l^{1/2}$ s^{-1})	$\frac{1}{\lambda} - \lambda$
I	5.73	10.44	0	3.00	39.7	0
I	5.18	10.44	0	2.70	37.5	0
I	5.33	10.44	0	2.92	40.0	0
II	6.03	10.44	0	3.06	39.4	0
II	5.65	10.44	0	3.06	40.5	0
I	5.54	10.43	4.52	1.84	24.8	0.94
I	5.01	10.41	7.48	1.15	16.2	1.99
I	5.34	10.40	10.9	1.02	14.0	2.43
II	5.30	10.39	14.1	0.921	12.7	2.84
II	4.86	10.37	19.6	0.690	9.90	3.78
II	5.90	10.34	29.7	0.553	7.20	5.38
II	4.96	10.34	28.8	0.485	6.92	5.61
I	5.34	10.27	52.8	0.280	3.83	9.93
I	4.92	10.22	68.5	0.201	2.86	13.3

in Table 1. The reaction is strongly retarded, the addition of 0.02 M tri-t-butylphenol reducing the rate to less than one quarter of the unretarded rate. The results were analyzed by the method of Jenkins (5) on the assumption that reinitiation of polymerization by phenoxy radicals is negligible and that phenoxy radicals are lost only by a cross termination process. Jenkins defines a parameter λ equal to $R_p[M]_0/R_{p0}[M]$ where R_p, R_{p0} are the rates of the retarded and unretarded polymerization and [M], $[M]_0$ are the corresponding monomer concentrations. A plot of $1/\lambda - \lambda$ *vs.* phenol concentration should be linear and of slope $C_{tr,XOH}k_p^2[M]_0/R_{p0}(k_{tc} + k_{td})$; $C_{tr,XOH}$ is the ratio $k_{tr,XOH}/k_p$ and $k_{tr,XOH}$ is the rate constant for the hydrogen abstraction reaction 2:

[2] $$RM_n^{\cdot} + XOH \rightarrow RM_nH + XO^{\cdot}$$

The values of $1/\lambda - \lambda$ in Table 1 are plotted against phenol concentration in Fig. 1. The transfer constant $C_{tr,XOH}$ derived from these rate studies is 0.021 ± 0.004 at 45°.

Degree of Polymerization Studies

The number average degree of polymerization, $\bar{P}_n$, of the polyvinyl acetate resulting from polymerization of the pure monomer obeys relationship [3]:

[3] $$\frac{1}{\bar{P}_n} = \frac{(k_{tc} + 2k_{td})R_p}{k_p^2[M]^2} + \frac{k_{tr,M}}{k_p}$$

where $k_{tr,M}$ is the rate constant for the transfer reaction of polyvinyl acetate radicals with vinyl acetate monomer; transfer to polymer (13) can be neglected at low conversions of monomer to polymer. A plot of $1/\bar{P}_n$ *vs.* $R_p/[M]^2$

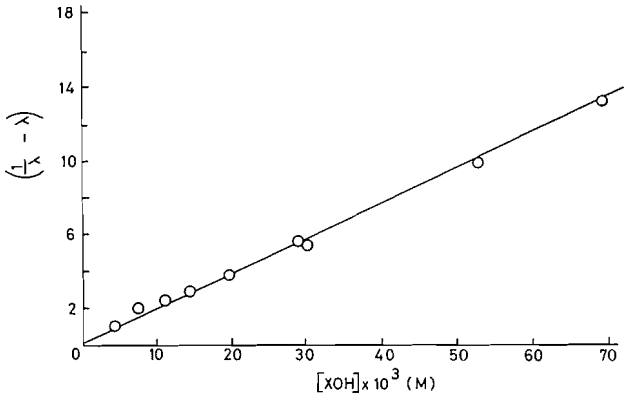

FIG. 1. Plot of $1/\lambda - \lambda$ *vs.* concentration of tri-t-butylphenol for vinyl acetate polymerization at 45°.

Can. J. Chem. Downloaded from www.nrcresearchpress.com by 210.87.254.40 on 09/05/12
For personal use only.

TABLE 2. The effect of phenol concentration on the degree of polymerization of polyvinyl acetate for two series of experiments

Series	10^4[XOH]/[M]	$10^4/\bar{P}_n$	$10^4(1/\bar{P}_n - (k_{tc} + 2k_{td})R_p/k_p^2[M]^2)$
I	0	1.832	1.66
I	0	1.957	1.77
II	0	1.888	1.69
II	0	1.919	1.72
II	7.16	2.057	1.99
I	7.19	1.969	1.90
II	13.5	2.204	2.15
II	18.7	2.439	2.40
II	27.6	2.654	2.62
II	28.5	2.758	2.72
I	31.5	2.874	2.86
I	50.8	3.369	3.35

gives a straight line of slope 7 ± 2 mol l^{-1} s and intercept $(1.72 \pm .05) \times 10^{-4}$ at 45°. The value of 7 mol l^{-1} s for $(k_{tc} + 2k_{td})/k_p^2$ is in fair agreement with the results of Schulz and Roberts-Nowakowska (14) but is much lower than the value used in an earlier study (3), based on kinetic data (9) and the assumption of disproportionation as the predominant termination mechanism (15). The monomer transfer constant, 1.72×10^{-4} at 45°, is in agreement with recent estimates; these include 1.32×10^{-4} at 40° and 1.91×10^{-4} at 60° (14), 2.0×10^{-4} at 45° (3), 1.9×10^{-4} at 60° (16), and 1.88×10^{-4} at 60° (10) (see also the summary by Lindemann (13)).

The degree of polymerization is reduced to a far less extent than the rate of polymerization on the addition of tri-*t*-butylphenol; for example, $\bar{P}_n$ is reduced to three quarters of the unretarded value at 45° by the addition of 0.02 *M* tri-*t*-butylphenol. If phenoxy radicals disappear from solution only by reaction with polyvinyl acetate radicals in a cross termination process, the dependence of $\bar{P}_n$ on phenol concentration should be given by eq. 4.

$$[4] \quad \frac{1}{\bar{P}_n} = \frac{(k_{tc} + 2k_{td})R_p}{k_p^2[M]^2} + \frac{k_{tr,M}}{k_p} + \frac{2k_{tr,XOH}[XOH]}{k_p[M]}$$

Typical results for the effect of phenol concentration on $\bar{P}_n$ at 45° are given in Table 2. A plot of $1/\bar{P}_n - (k_{tc} + 2k_{td})R_p/k_p^2[M]^2$ *vs.* [XOH]/[M] for the results at 45° is shown in Fig. 2. The transfer constant is found from degree of polymerization analysis to be 0.017 ± 0.002 at 45°.

Electron Spin Resonance Studies

A solution of tri-*t*-butylphenoxyl in pure vinyl acetate can be maintained at 45 °C for weeks with only a slight drop in radical concentration (less than 5% per week) as determined by e.s.r. spectroscopy. It is, therefore, confirmed that the phenoxy radical does not attack vinyl acetate monomer at an appreciable rate under the reaction conditions nor does it react with itself.

When tri-*t*-butylphenol (~0.1 *M*) was added to a solution of azobisisobutyronitrile in vinyl acetate at 45°, a stationary concentration of the corresponding phenoxyl was built up. A triplet

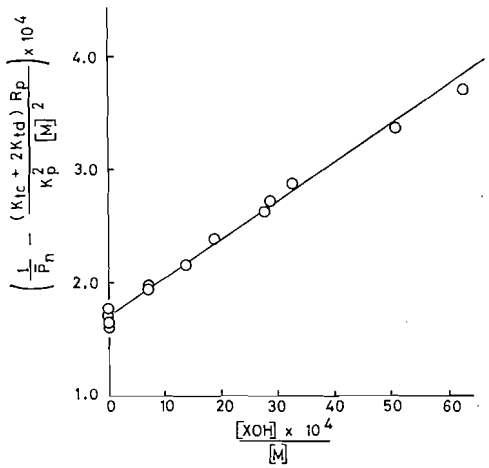

FIG. 2. Plot of $1/\bar{P}_n - (k_{tc} + 2k_{td})R_p/k_p^2[M]^2$ *vs.* [XOH]/[M] for vinyl acetate polymerization at 45°.

Can. J. Chem. Downloaded from www.nrcresearchpress.com by 210.87.254.40 on 09/05/12
For personal use only.

Can. J. Chem. Downloaded from www.nrcresearchpress.com by 210.87.254.40 on 09/05/12
For personal use only.

with peak to peak separation of 1.8 G (17) was readily observed at high gain. The phenoxyl concentration was independent of initiator concentration over the range 0.024–0.15 M at 45° within the limits of experimental error ($\pm 10\%$). When azobiscyclohexanenitrile was used as initiator, the same stationary concentration of phenoxyl was eventually observed. The phenoxyl concentration is thus independent of the initiator and its concentration at a given temperature.

The effect of 2,4,6-tri-*t*-butylphenol concentration on the stationary state concentration of phenoxyl was determined for the retarded polymerization at 45°. The phenoxyl concentration was 1.3×10^{-7} M when [XOH] was 0.065 M and it was proportional to the phenol concentration over the range studied. The mean value of the ratio [XO·]/[XOH] was $(1.9 \pm 0.3) \times 10^{-6}$ at 45°.

Discussion

The rate of free radical polymerization of vinyl acetate is reduced by the addition of alkyl phenols such as tri-*t*-butylphenol. The attack of polymer radicals on the phenol occurs at the OH group of the phenol because very much smaller effects are generally observed when the corresponding deuterated phenols are added at the same concentration (3, 18). The present work shows that a low stationary state concentration of tri-*t*-butylphenoxyl is built up as a result of the transfer process. The phenoxyl does not attack vinyl acetate at an appreciable rate and does not react with itself. The conclusion is therefore reached that effectively all the phenoxy radicals disappear by reaction with polyvinyl acetate radicals.

[5] $$RM_n^{\cdot} + XO^{\cdot} \rightarrow \text{products}$$

It is assumed that the products of reaction 5 are sufficiently inert not to affect the polymerization at the low concentration at which they are formed. If the rate constant of reaction 5 is k_5, the stationary state concentration of phenoxyl is given by [6].

[6] $$[XO^{\cdot}] = k_{tr,XOH}[XOH]/k_5$$

It is observed experimentally that the concentration of phenoxyl is proportional to the phenol concentration and is independent of the rate of initiation, in accord with eq. 6.

The transfer constant, $C_{tr,XOH}$ is estimated to be 0.021 ± 0.004 at 45° from rate measurements and 0.017 ± 0.002 at 45° from degree of polymerization measurements. The error limits in the value derived from rate measurements stem largely from uncertainty in the value of $(k_{tc} + k_{td})/k_p^2$. The agreement between the two estimates is satisfactory and lends further support to the proposed mechanism.

The value of $k_{tr,XOH}$ can be estimated provided that k_p is known at the polymerization temperature. The estimates of k_p in the literature vary widely but there is good agreement between the values of $k_p/(2k_{tc} + 2k_{td})$ obtained by various authors. Thus Matheson *et al.* (9) quote values of 22.6×10^{-6} at 50° and 17.2×10^{-6} at 25°, Bengough *et al.* (19) give a value of 21×10^{-6} at 45° and Bartlett *et al.* (20) a value of 17×10^{-6} at 25°. If $k_p/(2k_{tc} + 2k_{td})$ is assumed to be $(20 \pm 4) \times 10^{-6}$ at 45° and this is combined with the present estimate of $(2k_{tc} + 2k_{td})/k_p^2$, a value of $(6.6 \pm 1.7) \times 10^3$ l mol^{-1} s^{-1} is derived for k_p. The purity of the various monomer samples varied from one study to another and it is possible that larger limits of error should be assigned to k_p. However, if these limits are accepted, the rate constant for the reaction of polyvinyl acetate radicals with 2,4,6-tri-*t*-butylphenol, $k_{tr,XOH}$, is 125 ± 38 l mol^{-1} s^{-1} at 45°.

The mean value for the ratio [XO·]/[XOH] is 1.9×10^{-6} at 45°. The rate constant for the cross termination reaction 5 is given from eq. 6 as $(6.6 \pm 2.3) \times 10^7$ l mol^{-1} s^{-1} at 45°. This high value indicates that the reaction between polyvinyl acetate radicals and tri-*t*-butylphenoxyl is not subject to considerable steric hindrance. The ease of cross termination with hindered phenoxy radicals may mean that cross termination is far more important than mutual termination of phenoxy radicals even when their interaction is less subject to steric hindrance. This suggestion is being investigated by extension of these studies to other phenols, such as 4-methyl-2,6-di-*t*-butylphenol, which give phenoxyls capable of reacting with themselves at an appreciable rate.

The authors are grateful to the National Research Council of Canada for grant support, a bursary to H.L. (1967–1968) and a scholarship to R.D.P. (1969–1971).

1. P. B. AYSCOUGH and K. E. RUSSELL. Can. J. Chem. **43**, 3039 (1965).

2. P. B. AYSCOUGH and K. E. RUSSELL. Can. J. Chem. **45**, 3019 (1967).
3. R. A. BIRD and K. E. RUSSELL. Can. J. Chem. **43**, 2123 (1965).
4. E. MULLER and K. LEY. Ber. **87**, 922 (1954).
5. A. D. JENKINS. Trans. Faraday Soc. **54**, 1885 (1958).
6. N. FUHRMAN and R. B. MESROBIAN. J. Am. Chem. Soc. **76**, 3281 (1954).
7. D. R. GEE, K. E. RUSSELL, and J. K. S. WAN. Can. J. Chem. **48**, 2740 (1970).
8. T. A. BEREZHNYKH-FÖLDES and F. TÜDŐS. Vysokomol. Soed. **6**, 1522 (1964); F. TÜDŐS, T. A. BEREZHNYKH-FÖLDES, and M. SIMONYI. Vysokomol. Soed. **9**, 2284 (1967).
9. M. S. MATHESON, E. E. AUER, B. V. BEVILACQUA, and E. J. HART. J. Am. Chem. Soc. **71**, 2610 (1949).
10. G. V. SCHULZ and D. J. STEIN. Makromol. Chem. **52**, 1 (1962).
11. J. P. VAN HOOK and A. V. TOBOLSKY. J. Am. Chem. Soc. **80**, 779 (1958).
12. C. E. H. BAWN and S. F. MELLISH. Trans. Faraday Soc. **47**, 1216 (1951).
13. M. K. LINDEMANN. *In* Kinetics and mechanisms of polymerization Vol. I. Vinyl polymerization. Part I. *Edited by* G. E. Ham. Marcel Dekker, New York, 1967. Chapt. 4.
14. G. V. SCHULZ and L. ROBERTS-NOWAKOWSKA. Makromol. Chem. **80**, 36 (1964).
15. B. L. FUNT and W. PASIKA. Can. J. Chem. **38**, 1865 (1960).
16. M. MATSUMOTO and M. MAEDA. Kobunshi Kagaku, **12**, 428 (1955).
17. J. K. BECCONSALL, S. CLOUGH, and G. SCOTT. Trans. Faraday Soc. **56**, 459 (1960).
18. M. SIMONYI, F. TÜDŐS, S. HOLLY, and J. POSPISIL. Europ. Polym. J. **3**, 559 (1967).
19. W. I. BENGOUGH, I. T. BROWNLIE, and J. FERGUSON. Soc. Chem. Ind. (London): Monograph No. **20**, 220 (1966).
20. H. KWART, H. S. BROADBENT, and P. D. BARTLETT. J. Am. Chem. Soc. **72**, 1060 (1950).

Can. J. Chem. Downloaded from www.nrcresearchpress.com by 210.87.254.40 on 09/05/12
For personal use only.

Sequence Studies in Biosynthesis: Trichothecin

J. M. FORRESTER AND T. MONEY

Department of Chemistry, The University of British Columbia, Vancouver 8, British Columbia

Received May 8, 1972

An investigation of the precursor activity of α-bisabolol, γ-bisabolene and monocyclofarnesol indicates that these compounds are not intermediates in the biosynthesis of trichothecin.

Une étude sur l'activité du précurseur de l'α-bisabolol, γ-bisabolène et monocyclofarnésol montre que ces composés ne sont pas des intermédiaires dans la biosynthèse de la trichotécine.

[Traduit par le journal]

Canadian Journal of Chemistry, **50**, 3310 (1972)

Can. J. Chem. Downloaded from www.nrcresearchpress.com by 210.87.254.40 on 09/05/12
For personal use only.

The biosynthesis of the trichothecane antibiotics has been the subject of considerable investigation. Results obtained by various research groups have shown that the complex structures (*cf.* **5**) of the group are derived from three molecules of mevalonic acid (1–4) and that farnesyl pyrophosphate (**1**) (2, 5) is an intermediate in this process (see Scheme 1). Beyond this the biosynthetic sequence has not been elucidated although the proposal has been made that cyclization of **1** could lead to γ-bisabolene (**3**) (3, 6–10) via a monocyclic intermediate **2** of undetermined structure. Subsequent cyclization of γ-bisabolene (**3**) to the trichothecane skeleton (*cf.* **4***b*) in addition to oxidation reactions of an undefined nature (3, 7, 8) could produce representative members of this group *e.g.* trichothecin (**5***a*). We have been concerned with the validity of these proposals and recent results by Adams and Hanson (4) which elegantly preclude the intermediacy of γ-bisabolene (**3**) prompt us to record our own observations in this area.

Our first investigations (1968) involved α-bisabolol (**7**) which we considered to be a possible intermediate in the process (*i.e.* equivalent to **2**) (see Scheme 2). Radioactive α-bisabolol (**7**) was obtained from ketodiene (**6**) (11) by treatment with C^{14}-methylmagnesium iodide. An aqueous solution of 9-C^{14}-α-bisabolol (0.37 mCi/mmol) was solubilized with Tween 20 and added to 5-day-old cultures of *Tricothecium roseum*.

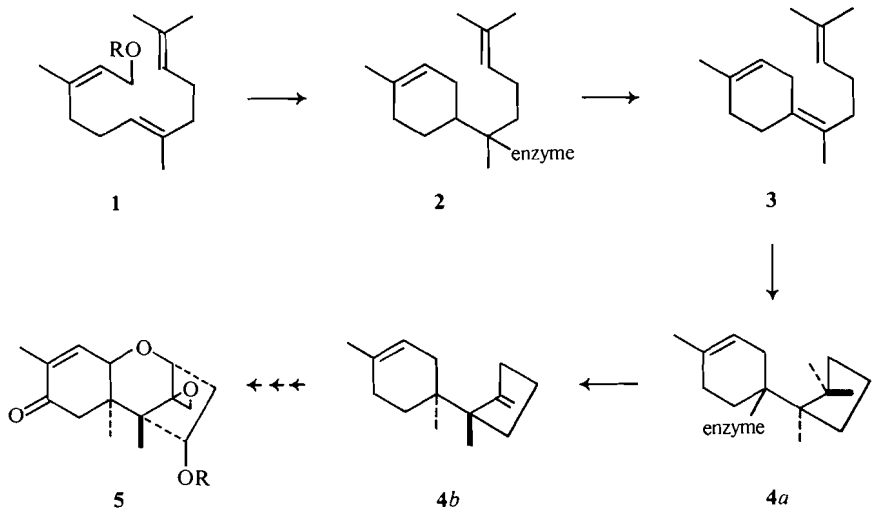

SCHEME 1

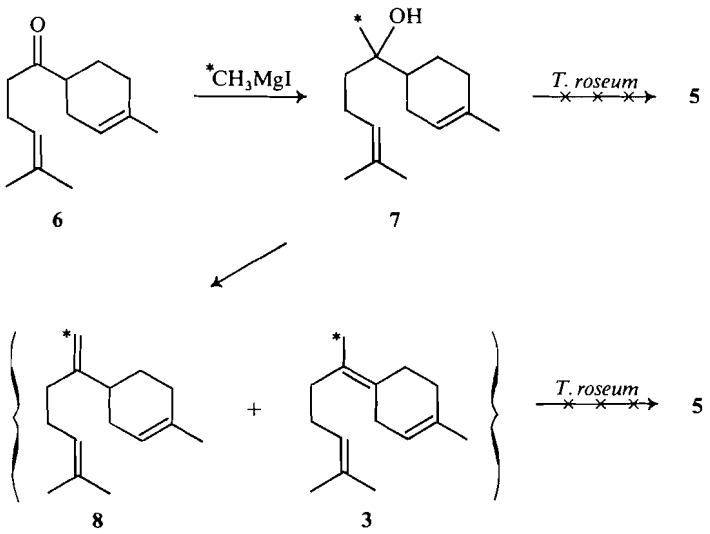

(* = carbon – 14)

SCHEME 2

After a period of three weeks trichothecin was isolated (1) and repeatedly crystallized from petroleum ether (60–80°) until constant radioactivity (5.3×10^{-5} mCi/mmol) had been attained (incorporation 0.014%). Alkaline hydrolysis (KOH/MeOH) of tricothecin (**5***a*) yielded trichothecolone (**5***b*) (3.3×10^{-5} mCi/mmol) possessing only 60% of the original activity. Jones and Lowe have shown (1) that the isocrotonate unit in trichothecin is acetate-derived and our results indicate that extensive degradation of α-bisabolol to radioactive units (acetate?) had occurred prior to incorporation.

We then turned our attention to the precursor activity of γ-bisabolene (**3**). Dehydration of 9-C^{14}-α-bisabolol (**7**) with $POCl_3$/pyridine yielded a mixture of β-bisabolene (**8**) and γ-bisabolene (**3**). The presence of at least 50% γ-bisabolene was determined by g.l.c. and in non-radioactive runs the isomeric bisabolenes were isolated and identified by n.m.r. For the biosynthetic experiment an aqueous solution of the mixture[1] of **8** and **3** (solubilized by Tween 20) was administered to *T. roseum*. Trichothecin was isolated after three weeks and was shown to have specific activity of 1.88×10^{-5} mCi/mmol (specific incorporation 0.005%). Alkaline hydrolysis yielded trichothecolone (1.15×10^{-5} mCi/mmol), possessing only 60% of the original activity present in trichothecin.

The low and non-specific incorporation of α-bisabolol, β-bisabolene, and γ-bisabolene seemed to exclude the intermediacy of these compounds in the biosynthetic process and, as noted earlier, this has been decisively shown by Adams and Hanson (4) using specifically labelled mevalonic acid and geranyl pyrophosphate. It is of interest to note that Nozoe and co-workers (12) have come to a similar conclusion with the cuparene-type sesquiterpene helicobasidin (**13**).

An alternative biosynthetic route to the cuparene type intermediate (**4***a*) has been considered (13). This involves cyclization of monocyclofarnesol (**11**) to a spiro bicyclic intermediate (**12**) (see Scheme 3) reminiscent of the type postulated in the biosynthesis of the chamigrenes (**14**). Subsequent ring contraction could then provide **4***a*. We have evaluated the merit of this biosynthetic proposal by examining the precursor activity of monocyclofarnesol (**11**). The latter compound was synthesized in radioactive form by condensing dihydro-β-ionone (**9**) (14), in a modified Wittig reaction (15, 16), with methyl

[1]Although it would have been more meaningful to have proceeded with studies on pure β- and γ-bisabolene, the separation of small quantities of radioactive samples of these compounds would have resulted in considerable loss of valuable material. In addition we considered that if either or both isomers were on the main biosynthetic route a considerable and specific incorporation would be easily discerned.

Can. J. Chem. Downloaded from www.nrcresearchpress.com by 210.87.254.40 on 09/05/12
For personal use only.

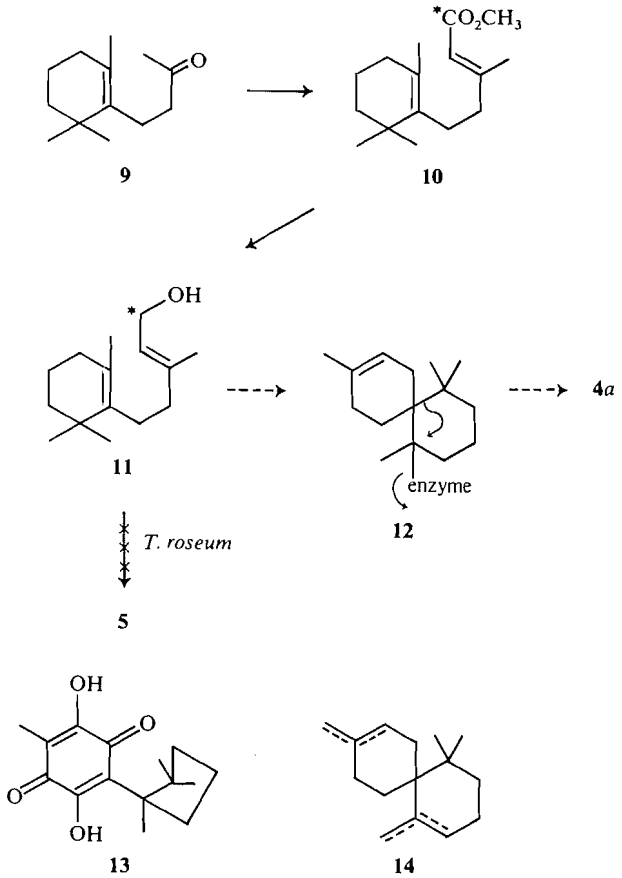

(* = carbon – 14)

SCHEME 3

1-C^{14}-bromoacetate followed by reduction of the intermediate ester **10**. Administration of **11** to *Trichothecium roseum* in the manner described above yielded trichothecin with specific activity 0.867×10^{-5} mCi/mmol (specific incorporation 0.003%). Conversion to trichothecolone (0.237×10^{-5} mCi/mmol) with substantial decrease in radioactivity indicated that monocyclofarnesol (**11**) had been extensively degraded prior to incorporation.

These results would seem to suggest that the biosynthetic route from farnesyl pyrophosphate to trichothecin proceeds directly to intermediate **4***a* and does not involve intermediates of the type previously suggested.[2]

[2]A recent report (20) describes the incorporation of trichodiene (**4***b*) into trichothecin.

Experimental

All melting points were determined on a Kofler block and are uncorrected. I.r. spectra (ν_{max}) were recorded on a Perkin–Elmer Infracord model 137 spectrophotometer. N.m.r. spectra (τ) were determined in carbon tetrachloride or deuteriochloroform solution and recorded on a Varian Associates model T-60 spectrometer. Signal positions are given in the Tiers τ scale, with tetramethylsilane as an internal standard; the multiplicity, coupling constants (where appropriate), and integrated peak areas are indicated in parentheses; s = singlet, br.s = broad singlet, d = doublet, t = triplet, m = multiplet. Mass spectra (M^+) were determined with an AEI model MS9 spectrometer. Microanalyses were determined by Mr. P. Borda, Microanalytical Laboratory, University of British Columbia. T.l.c. results were obtained using silica gel HF^{254} of 0.5 mm thickness. A Nuclear-Chicago Mark 1 model 6860 Liquid Scintillation counter was used for radioactivity measurements.

α-Bisabolol (7)

To a solution of methyl magnesium iodide, prepared from

Can. J. Chem. Downloaded from www.nrcresearchpress.com by 210.87.254.40 on 09/05/12
For personal use only.

Can. J. Chem. Downloaded from www.nrcresearchpress.com by 210.87.254.40 on 09/05/12
For personal use only.

methyl iodide (106.5 mg, 0.75 mmol) and magnesium powder (19.8 mg, 0.83 mmol) in ether (5 ml), was added ketodiene (**6**) (11) (51.5 mg, 0.25 mmol) in ether (2 ml). The mixture was allowed to stir at room temperature for 2 h then worked-up by adding saturated aqueous ammonium acetate solution. The ether layer was separated and the aqueous phase extracted twice with ether. The combined ether layers were washed with brine and dried (Na_2SO_4). Evaporation of the ether gave α-bisabolol (**7**) (55 mg, 100%) as a colorless oil; ν_{max}(liquid film) 3435, 2915, 1440, 1370, 1105, 830, 800 cm^{-1}; τ (CCl_4) 4.67 (s, 1H), 4.90 (t, $J = 7$ Hz, 1H), 7.60–8.23 (m, 7H), 8.37 (s, 9H), 8.50–8.87 (m, 5H), 8.93 (d, $J = 2$ Hz, 3H): M^+ *m/e* 222.

9-C^{14}-α-Bisabolol (7)

α-Bisabolol (**7**) was prepared as above using C^{14}-methyl iodide (213.0 mg, 1.5 mmol, 1 mCi, 0.667 mCi/mmol), magnesium powder (39.6 mg, 1.65 mmol) and ketodiene (**6**) (103 mg, 0.5 mmol). The yield of 9-C^{14}-α-bisabolol (**7**) was 110.0 mg (100%), and the specific activity was determined to be 0.33 mCi/mmol.

Isolation of Trichothecin (5a) from Trichothecium roseum

Trichothecium roseum was grown as described in the literature (17, 18) except that the p*H* was not adjusted. Trichothecin (**5***a*) was isolated as described in the literature (18) except that preparative t.l.c. on silica gel was used in the purification rather than column chromatography on alumina. In a typical experiment 10 flasks of *T. roseum* were allowed to grow for 3 weeks. The broth was then filtered, the mycelia washed with a little water, and the combined washings and broth extracted with carbon tetrachloride (2 × 100 ml). Evaporation of the carbon tetrachloride gave a gum (148.6 mg) which was purified by t.l.c. on silica gel, using petroleum ether–ethyl acetate (1:1). Under u.v. radiation the trichothecin (**5***a*) showed up as a dark band approximately half way up the plate. Extraction of this band with ethyl acetate and subsequent removal of solvent gave trichothecin (**5***a*) (94.3 mg). Crystallization from petroleum ether (60–80°) provided pure trichothecin (**5***a*) as white needles, m.p. 116–118 °C (lit. (17), m.p. 118 °C); ν_{max} ($CHCl_3$) 1715, 1685 cm^{-1}.

Administration of 9-C-^{14}-α-Bisabolol (7) to Trichothecium roseum

To 9-C^{14}-α-bisabolol (**7**) (52 mg, 0.087 mCi) was added water (20 ml) and Tween 20 (2 ml). This well shaken mixture was then evenly distributed among 10 flasks of 5-day-old cultures of *T. roseum* which were then left for a further 20 days. The trichothecin was isolated as before and recrystallized to constant specific activity (5.3×10^{-5} mCi/mmol) (specific incorporation, 0.014%).

Trichothecolone (5b)

Trichothecin (50 mg, 0.15 mmol) was stirred overnight at room temperature in 1 *N* methanolic potassium hydroxide solution (2 ml). Water (1.5 ml) was added and the methanol evaporated *in vacuo*. The aqueous layer was then extracted with chloroform, removal of which gave a colorless gum which slowly crystallized. This was recrystallized from benzene–petroleum ether (2:1) to give trichothecolone (39.8 mg, 100%) as white needles, m.p. 182–184 °C (lit. (19), m.p. 183–184 °C); ν_{max}($CHCl_3$) 3560, 1680 cm^{-1}.

Hydrolysis of C^{14}-Labelled Trichothecin (5a)

C^{14}-Labelled trichothecin (**5***a*) (5.3 mg) was diluted with inactive trichothecin (10.6 mg) and this was hydrolyzed as above to give C^{14}-labelled trichothecolone (**5***b*) (9.5 mg) which was recrystallized to a constant specific activity of 1.1×10^{-5} mCi/mmol, representing loss of 40% of the radioactivity.

γ-Bisabolene (3)

To a solution of α-bisabolol (**7**) (75 mg, 0.3 mmol) in pyridine (1 ml) was added a solution of phosphorus oxychloride (0.5 ml) in pyridine (2 ml). The reaction mixture was stirred overnight, added to ice-water and the aqueous mixture extracted with ether. The combined ether extracts were washed with brine, dried ($MgSO_4$), and the ether evaporated *in vacuo* to give a yellow oil (45.6 mg, 75%). Purification of this oil by preparative g.l.c. on a 30% Carbowax column at 180 °C gave two components with very similar retention times. The less volatile peak (~50%) was shown to be γ-bisabolene (**3**); ν_{max}(liquid film) 2935, 1440, 1370, 1145, 1100, 910, 825, 800 cm^{-1}; τ (CCl_4) 4.67 (br.s, 1H), 4.93 (t, $J = 7$ Hz, 1H), 7.37 (m, 2H); 8.07 (m, 8H), 8.38 (m, 12H). The more volatile peak (~50%) was shown to be β-bisabolene (**8**) plus other unidentified isomers(s), ν_{max} (liquid film) 2940, 1650, 1445, 1375, 920, 890, 830, 800 cm^{-1}; τ (CCl_4) very similar to the n.m.r. spectrum of γ-bisabolene (**3**) but showing signal at 5.3 τ attributable to C=CH_2 group in (**8**).

9-C^{14}-γ-Bisabolene (3)/9-C^{14}-β-Bisabolene (8)

C^{14}-Labelled α-bisabolol (55 mg) was dehydrated as above and the crude product purified by chromatography on alumina to yield 9-C^{14}-γ-bisabolene (**3**) and 9-C^{14}-β-bisabolene (**8**) as a colorless oil (13 mg).

Administration of 9-C^{14}-γ-Bisabolene (3)/9-C^{14}-β-Bisabolene (8) to Trichothecium roseum

A well shaken mixture of 9-C^{14}-γ-bisabolene (**3**) (13 mg, 0.024 mCi), water (5 ml), and Tween (20) (0.5 ml) was evenly distributed among five flasks of 1-week-old cultures of *T. roseum*. After 3 weeks trichothecin was isolated as before and crystallized to constant specific activity (1.88×10^{-5} mCi/mmol) (specific incorporation 0.005%). The remaining trichothecin (**5***a*) was hydrolyzed as described above to give trichothecolone (**5***b*) with specific activity of 1.15×10^{-5} mCi/mmol representing a loss of 40% of the radioactivity originally present in trichothecin.

Dihydro-β-ionone (9)

β-Ionone (19.2 g, 0.1 mol) was hydrogenated in ethanol (50 ml) using Raney nickel (~4 g) as catalyst. After uptake of the theoretical volume of hydrogen the catalyst was removed by filtration, the ethanol removed *in vacuo* and the resulting oil distilled to give dihydro-β-ionone (**9**) (14.0 g, 72%) as a colorless oil, b.p. 115–116 °C (9 mm) (lit. (14), b.p. 122–122.5 °C (12 mm)); ν_{max} 2940, 1725, 1360, 1155 cm^{-1}; τ (CCl_4) 7.68 (m, 4H), 7.94 (s, 3H), 8.43 (s, 3H), 9.00 (s, 6H); M^+ *m/e* 194.

Anal. Calcd. for $C_{13}H_{22}O$: C, 80.35; H, 11.41. Found: C, 80.59; H, 11.48.

Methyl Monocyclofarnesate (10)

Ether washed 50% sodium hydride/oil dispersion (0.48 g, 0.01 mol NaH) was added to dry benzene (50 ml), and tri-

methylphosphonoacetate (1.82 g, 0.01 mol) in benzene (5 ml), added at room temperature. After stirring at room temperature for 0.5 h, dihydro-β-ionone (**9**) (1.35 g, 0.007 mol), in benzene (5 ml) was added dropwise and the solution refluxed for 15 h. On cooling, water was added and the resulting oil extracted three times with ether, the ether was dried ($MgSO_4$) and evaporated *in vacuo*. Distillation gave methyl monocyclofarnesate (**10**) (1.0 g, 57%) as a colorless oil, b.p. 81–83 °C (0.02 mm); ν_{max} 2935, 1720, 1645, 1430, 1355, 1220, 1140 cm^{-1}; τ (CCl_4) 4.37 (br.s, 1H), 6.37 (s, 3H), 7.80 (s, 2H), 7.84 (s, 3H), 8.38 (s, 3H), 8.97 (s, 6H); M^+ *m/e* 250.

Anal. Calcd. for $C_{16}H_{26}O_2$: C, 76.76; H, 10.47. Found: C, 77.16; H, 10.59.

Monocyclofarnesol (11)

Lithium aluminum hydride (30 mg, 0.79 mmol) was added to a solution of methyl monocyclofarnesate (**10**) (300 mg, 1.2 mmol) in ether (10 ml). The resulting solution was stirred overnight and worked-up by adding ice–dilute HCl. The ether layer was separated and the aqueous layer was extracted three times with ether. The combined ether extracts were washed thoroughly with brine, dried ($MgSO_4$) and the ether evaporated *in vacuo* to give monocyclofarnesol (**11**), (252 mg, 95%) as a colorless oil, ν_{max} 3350, 2940, 1670, 1460, 1380, 1110, 1000 cm^{-1}; τ (CCl_4) 4.64 (t, $J = 7$ Hz, 1H), 5.98 (d, $J = 7$ Hz, 2H), 8.99 (s, 6H); M^+ *m/e* 222.

1-C^{14}-Monocyclofarnesol (11)

1-C^{14}-Methyl bromoacetate (306 mg, 2 mmol, 1 mCi, 0.5 mCi/mmol), trimethyl phosphite (248 mg, 2 mmol), and benzene (1 ml) were refluxed for 5 h. On cooling, benzene (4 ml) and pentane washed sodium hydride (50% oil dispersion) (240 mg, 5 mmol) were added and the solution allowed to stir at room temperature for 1.5 h. Dihydro β-ionone (**9**) (388 mg, 2 mmol) in benzene (5 ml) was then added and the solution allowed to reflux overnight. The reaction mixture was worked-up by adding water followed by ether extraction. Removal of the solvents gave a yellow oil which was purified by chromatography on silica. The fraction eluting with petroleum ether–benzene (3:1) consisted of methyl monocyclofarnesate (**10**) (171 mg). Methyl monocyclofarnesate (**10**) (171 mg, 0.68 mmol) was stirred in ether (10 ml) with lithium aluminum hydride (17.1 mg, 0.45 mmol) for 10 h. The reaction mixture was worked-up by adding dilute HCl followed by ether extraction and evaporation of the ether to give 1-C^{14}-monocyclofarnesol (**11**) (110 mg). The specific activity was determined to be 0.29 mCi/mmol.

Administration of 1-C^{14}-Monocyclofarnesol (11) to Trichothecium roseum

A well shaken mixture of 1-C^{14}-monocyclofarnesol (**11**) (55.0 mg, 0.071 mCi), water (18 ml), and Tween 20 (2 ml) was evenly distributed among 10 flasks of 7-day-old cultures of *T. roseum*. After a further 24 days the trichothecin (**5***a*) was isolated in the usual manner and recrystallized to constant specific activity (0.867×10^{-5} mCi/mmol), representing an incorporation of 0.003%. The remaining trichothecin was hydrolyzed as above to give trichothecolone (**5***b*) with specific activity of 0.237×10^{-5} mCi/mmol.

We are grateful to the National Research Council of Canada for generous financial support (NRCC A2267).

1. E. R. H. Jones and G. Lowe. J. Chem. Soc. 3959 (1960).
2. B. A. Achilladelis, P. M. Adams, and J. R. Hanson. Chem. Commun. 511 (1970), and refs. cited therein.
3. R. Achini, B. Muller, and Ch. Tamm. Chem. Commun. 404 (1971).
4. P. M. Adams and J. R. Hanson. Chem. Commun. 1414 (1971).
5. B. A. Achilladelis and J. R. Hanson. Chem. and Ind. 1643 (1967).
6. L. Ruzicka. Pure Appl. Chem. **6**, 512 (1963).
7. W. Parker, J. S. Roberts, and R. Ramage. Q. Rev. **21**, 331 (1967).
8. P. M. Adams and J. R. Hanson. Chem. Commun. 1569 (1970).
9. W. O. Godtfredson and S. Vangedal. Acta Chem. Scand. **19**, 1068 (1965).
10. W. Zurcher, J. Gutzwiller, and Ch. Tamm. Helv. Chim. Acta, **48**, 839 (1965).
11. A. Manjarrez and A. Guzman. J. Org. Chem. **31**, 348 (1966).
12. S. Nozoe, M. Marisaki, and H. Matsumoto. Chem. Commun. 926 (1970); *cf.* R. Bentley and D. Chen. Phytochem. **8**, 2171 (1969).
13. S. Ito, K. Endo, T. Yoshida, M. Yatagai, and M. Kodama. Chem. Commun. 186 (1967); J. J. Sims, W. Fenical, R. M. Wing, and P. Radlick. J. Am. Chem. Soc. **93**, 3774 (1971).
14. A. Caliezi and H. Schinz. Helv. Chim. Acta, **33**, 1129 (1950).
15. W. S. Wadsworth, Jr. and W. D. Emmons. J. Am. Chem. Soc. **83**, 1733 (1961).
16. T. Kato, S. Kanno, and Y. Kitahara. Tetrahedron, **26**, 4287 (1970).
17. G. G. Freeman and R. I. Morrison. Biochem. J. **44**, 1 (1949).
18. G. G. Freeman. J. Gen. Microbiol. **12**, 213 (1955).
19. G. G. Freeman, J. E. Gill, and W. S. Waring. J. Chem. Soc. 1105 (1959).
20. Y. Machida and S. Nozoe. Tetrahedron Lett. 1969 (1972).

Can. J. Chem. Downloaded from www.nrcresearchpress.com by 210.87.254.40 on 09/05/12
For personal use only.

The Effect of Bridge Size on the Sigmatropic Rearrangement of 2,3-Dibenzoyl-2,3-diazabicyclo[2.2.*n*]alk-5-enes

MISS C. Y-J. CHUNG, DONALD MACKAY, AND T. D. SAUER
Department of Chemistry, University of Waterloo, Waterloo, Ontario

Received April 6, 1972

The thermal isomerization of the title compounds **3***a–d* to the bicyclic oxadiazines **4***a–d* becomes increasingly difficult with bridge size *n* and could not be detected in the case of **3***d*. The reversibility of the isomerization has been demonstrated for **3***c* ⇄ **4***c*.

Cyclooctadiene behaves both as a diene and as a dienophile in its reaction with azodibenzoyl.

L'isomérisation thermique des composés 3*a–d* en oxadiazines bicycliques 4*a–d*, devient de plus en plus difficile avec la taille *n* du pont et ne peut être détectée dans le cas de 3*d*. La réversibilité de l'isomérisation a été démontrée pour 3*c* ⇄ 4*c*. Le cyclooctadiène se comporte à la fois comme un diène et un diénophile dans sa réaction avec l'azodibenzoyle. [Traduit par le journal]

Canadian Journal of Chemistry, **50**, 3315 (1972)

Can. J. Chem. Downloaded from www.nrcresearchpress.com by 210.87.254.105 on 09/05/12
For personal use only.

The thermal isomerization of the [2.2.1] bicyclic adducts **1** of *cis*-hex-3-ene-2,5-dione and fulvenes to the dihydropyrans **2** has been recognized as a [3,3]-sigmatropic process (1). Two factors were implicated as driving forces, the exocyclic double bond which becomes conjugated in the product and the relief of angle strain in going from the [2.2.1] to the [3.3.0] bicyclic system (1).

We have subsequently shown (2) in the completely analogous isomerizations of the adduct, **3***a*, of azodibenzoyl with cyclopentadiene and, more recently (3), of its adduct, **3***b*, with 1,3-cyclohexadiene that neither the exocyclic double bond nor the relief of large amounts of strain are strict requirements, at least for the [2.2.1] diazabicyclo system.[1] We now wish to describe in detail the effect of variation in bridge size on the ease and reversibility of this isomerization in the homologous series **3***a–d*.

Azodibenzoyl reacted with an excess of 1,3-cycloheptadiene in refluxing benzene to give the Diels–Alder adduct **3***c*, m.p. 203–204°, in an almost quantitative yield. With 1,3-cyclooctadiene, however, it gave only a moderate yield (37%) of the adduct **3***d*, m.p. 207–208°, along with lesser amounts (10%) of the isomeric oxadiazine **4***d*, m.p. 145.5–146°, and much NH-containing material which was not examined further. Compounds **3***d* and **4***d* were separated by chromatography on alumina.

The structures of **3***c* and *d* follow from the similarity of all their spectra to those of **3***a*, (2) (Table 1), with the notable difference that the n.m.r. absorptions of their tertiary protons (and to a lesser extent the vinyl) were chemically shifted from one another, like those of **3***b* (3), and unlike those of **3***a* which are isochronous. This chemical shift difference was observable in a wide range of solvents, the values in pyridine-d_5

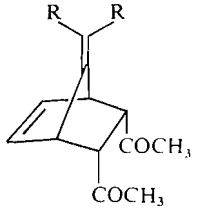

1

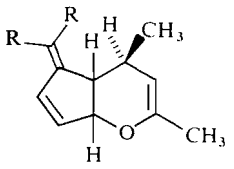

2

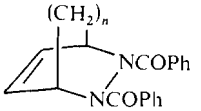

3

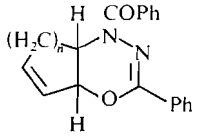

4

a, $n=1$; *b*, $n=2$; *c*, $n=3$; *d*, $n=4$;

[1]The adduct of dimethylfulvene and dimethyl azodicarboxylate has been reported (4) as very easily isomerized to a mixture of products, one of which was tentatively assigned an oxadiazine structure. Several pathways may thus be involved.

Can. J. Chem. Downloaded from www.nrcresearchpress.com by 210.87.254.105 on 09/05/12
For personal use only.

TABLE 1. Diels–Alder adducts of azodibenzoyl and 4-phenyl-1,2,4-triazoline-3,5-dione

Compound	Yield (%)	M.p.* (°C)	$\nu_{C=O}$(Nujol) (cm^{-1})	$\lambda_{max}(\varepsilon \times 10^{-4})$ (EtOH; nm)	τ($CDCl_3$) Aryl	Vinyl	*tert*	Methylene†	Analysis Calcd: Found:	C	H	N
3*a*	100	138–139	1682, 1658	255 (1.4)	1.9–2.7	3.55	4.81	7.99, 8.27q	ref. 2			
3*b*	60	157–158	1671, 1626, 1612	255 (0.79)	2.2–2.8	3.50b	4.6b, 5.2b‡	7.7b, 8.5, 8.7q	ref. 3			
3*c*	94	203–204(*a*)	1677, 1636, 1617	255 (0.80)	2.2–3.1	3.90b	4.55b, 5.50b	7.7–8.8	$C_{21}H_{20}N_2O_2$	75.9	6.1	8.4
										76.2	6.2	8.3
3*d*	37	207–208(*a*)	1676, 1654, 1635	255 (0.72)	2.0–3.1	4.00m	4.70b, 5.56b	7.0–8.7	$C_{22}H_{22}N_2O_2$	76.3	6.4	8.1
										76.2	6.4	8.2
8*a*	100	172.5–174.5(*b*)	1762, 1707	220sh (0.95)	2.4–2.8	3.50t	5.06b	7.5–8.5	$C_{14}H_{13}N_3O_2$	65.9	5.1	16.5
				251 (0.46)						66.2	5.4	16.4
8*b*	100	203.5–206.5(*c*)	1752, 1691	220sh (1.3)	2.2–2.9	3.87q	5.03b	7.4–8.8	$C_{16}H_{17}N_3O_2$	67.8	6.0	14.8
										67.4	5.9	14.6

*Crystallization from: (*a*) aqueous EtOH; (*b*) benzene–hexane; (*c*) benzene–CCl_4.
†τ-values separated by a dash are at the extreme limits of the absorption; q, quartet; b, broad; m, multiplet; t, triplet.
‡Overlapping.

TABLE 2. Rate data for coalescence and isomerization of adducts 3*a–d*

Compound	τ^* (C_5D_5N)	T_c (°C)	k_c (s^{-1})	$\Delta G_c^{\ddagger}$ (kcal mol^{-1})†	T_{isom} (°C)	k_{isom} (s^{-1})	$\Delta G_{isom}^{\ddagger}$ (kcal mol^{-1})
3*a*					62	1.73×10^{-5}‡	26.9
3*b*	4.46, 5.19	49±1	162±2	15.6±0.1	62	4.4×10^{-10}‡	33.9
					258	2.2×10^{-2}	35.6
3*c*	4.40, 5.43	111±2	227±4	18.5±0.1	258	1.1×10^{-4}	41.2
3*d*	4.49, 5.48	156±4	219±2	20.8±0.2	258§	$<1.8\times10^{-6}$	>45.5

*Values at maximum separation, observed at 10° for 3*b* and at room temperature for 3*c* and *d*.
†Values and implied accuracy from the usual formulae, see *e.g.* ref. 13. The protons, while not coupled to one another, are coupled to other protons and appear as broad symmetrical peaks. The values may be approximate.
‡From ref. 3.
§Isomerization not detected.

(0.73 for 3*b*, 1.03 for 3*c* and 0.99 p.p.m. for 3*d*) being typical. Heating of the solutions of 3*b–d* in pyridine-d_5 caused coalescence of the absorptions at temperatures which increased with the bridge size (Table 2). The associated increase in the free energy of activation ($\Delta G_c^{\ddagger}$) for this exchange phenomenon parallels exactly the trend observed (5) for the related adducts of dimethyl azodicarboxylate (structures 3*b–d* with OCH_3 in place of Ph). Like these, 3*b–d* evidently exist in the twist conformation **5** in which the tertiary protons are diastereotopic. Slow interconversion of **5** with its enantiomer through a symmetric transition state exchanges the identity of these protons.

The strain-free twist forms of 3*b–d* permit a closer approach of the appropriate reacting oxygen and carbon atom pairs than does the symmetric and rigid adduct 3*a*,[2] suggesting that isomerization rates might be greater for these flexible systems than for 3*a*. Such an approach, however, would lead to a six-centered skew boat transition state, rather than to the symmetric boat form, and hence the symmetric bicyclic framework, **6**, ideally required by orbital symmetry considerations. The latter should dictate that the isomerization rates, like the exchange rates, would decrease in the order of increasing bridge size. This is indeed the case.

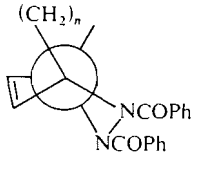

5

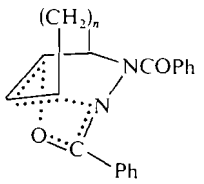

6

As reported earlier 3*a* isomerized rapidly at 100° (2) but 3*b* was stable up to 150°; at 200° the isomerization of 3*b* was complete in 1.5 h (3). By contrast 3*c* was stable indefinitely at 200°,[3] but g.l.c. analysis showed that in refluxing diphenyl ether (258°) it isomerized to 4*c*, which in turn slowly decomposed to a number of minor products. The ratio of 4*c*:3*c* rose to a maximum of 1.9:1 after 8 h and thereafter remained the same, indicating that the isomerization was reversible. The mixture, after refluxing for 6 h, was separated by conventional crystallization techniques giving unreacted 3*c* and its isomer 4*c*, m.p. 131–132°, which had all the properties expected of an oxadiazine (2, 3, 6). The reversibility was confirmed by re-heating pure 4*c* in diphenyl ether for 4 h, when the ratio of 4*c*:3*c* was about 3:1 and before much by-product had accumulated; again a mixture of 3*c* and 4*c* was obtained from which pure 3*c* was isolated by chromatography on silica gel.

The retro rearrangement of the 2-phenyl-4-benzoyl-1,3,4-oxadiazine to the *N,N'*-dibenzoylpyridazine derivative, involving in essence the synthesis of an amide group by a sigmatropic process, is thus established. It has parallels in the Claisen type rearrangement of allyloxytetrazoles, -benzoxazoles, -benzothiazoles (7), and -benzimidazoles (8). In these reactions, however, the group migrating to nitrogen is exocyclic and the reactions are irreversible.

In the non-degenerate Cope reaction with its six-carbon transition state framework the co-

[2]This is easily seen with models. The other oxygen and carbon pair are of course further apart, at their closest, than they are in 3*a*.

[3]Samples were heated in sealed evacuated tubes.

Can. J. Chem. Downloaded from www.nrcresearchpress.com by 210.87.254.105 on 09/05/12
For personal use only.

Can. J. Chem. Downloaded from www.nrcresearchpress.com by 210.87.254.105 on 09/05/12
For personal use only.

existence of both isomers in comparable amounts has been frequently noted (9, 10). In hetero-Cope reactions electronegativity differences in the atoms of the transition state must be expected to lead to significant bond energy differences between the two isomers into which it can pass. This in large measure must dictate that there should be considerable free energy differences between the isomers, especially when there is more than one hetero atom in the transition state, and hence several different bond types in the two isomers. In the large literature of Claisen rearrangements, though reversibility has been well established (9), examples in which isomerization is incomplete are rare (11, 12). The favorable equilibrium observed in **3***c* ⇄ **4***c* (a "di-hetero-Cope" system) must be considered fortuitous.

The adduct **3***d* was stable up to 320°,[3] thus ruling out the possibility that the formation of the oxadiazine **4***d*, isolated from the reaction of azodibenzoyl with an excess of 1,3-cyclooctadiene, noted earlier, could have arisen by isomerization of **3***d*. At 320° **4***d* was in fact shown to be completely degradable. Its decomposition set in about 310°, but the presence of **3***d* among the products could not be conclusively detected. Thus the thermal interconversion of **3***d* and **4***d* in either direction has not been demonstrated. Attempts to facilitate the isomerization by acid catalysis (3) also failed; **3***d* was unaffected when refluxed for 12 h in dioxan containing *p*-toluenesulfonic acid or for 1 day in pyridine containing sulfuric acid.

The free energy of activation for isomerizatio, $\Delta G^{\ddagger}_{isom}$, has already been estimated as 7 kcal mol^{-1} higher for **3***b* than for **3***a*, by comparison of their acid-catalyzed isomerizations under identical conditions (3). A direct comparison of the isomerization rates of **3***b* and *c* in refluxing diphenyl ether was obtained by g.l.c. analysis. The isomerization of **3***b* was rapid, clean, and quantitative with a first order rate constant of 2.2×10^{-2} s^{-1} ($\Delta G^{\ddagger}_{isom} = 35.6$ kcal mol^{-1}) (Table 2). The determination for **3***c* was complicated by the reversibility of the isomerization and the instability of the product **4***c* (the overall process is of the type A ⇄ B → C + D + -- and is thus kinetically complex). In the early stages (up to 3 h) of the reaction however, before by-product accumulation was significant, the concentration of **3***c* could be obtained directly from the ratio of the peak areas of **3***c* and **4***c*.[4] A plot of the concentration of **3***c* against time gave an initial slope from which the rate constant was estimated as 1.1×10^{-4} s^{-1} ($\Delta G^{\ddagger}_{isom} = 41.2$ kcal mol^{-1}).[5]

Only a lower limit can be placed on $\Delta G^{\ddagger}_{isom}$ for **3***d*. When **3***d* was refluxed for 8 h in diphenyl ether and the solution evaporated the n.m.r. spectrum of the residue was completely unchanged. If the detection limit of the isomer **4***d* is set at 5% then the rate constant is less than 1.8×10^{-6} s^{-1} representing a $\Delta G^{\ddagger}_{isom}$ value >45.5 kcal mol^{-1}.

As Table 2 shows, a direct comparison of the differences in free energy of activation for ring twisting ($\Delta\Delta G^{\ddagger}_{c}$) with the $\Delta\Delta G^{\ddagger}_{isom}$ values cannot be made[6] for successive members of the adducts **3**, but it is evident that they are perhaps half as large. This suggests that a considerable portion of the free energy of activation for isomerization can be identified with that for ring twisting as having a common origin, the requirement of a transition state with local C_s symmetry.

The increasing stability of the adducts **3** with bridge size *n* is related to an increasing twist angle. It might be expected to reach a limit when the twist angle corresponds to that of the pseudo boat form of an unbridged tetrahydropyridazine. Further increase in *n* could permit the tetrahydropyridazine to pass into the lower energy pseudo chair form, which would then resemble in stability the simple unbridged adduct **7** of butadiene. All efforts to isomerize **7** (14), alone or in the presence of acid, at temperatures up to 350° failed (above this it charred and decomposed). The thermal stability of **7** seems reasonable in the light of the known (15) high barrier to ring inversion for this ring system (~15 kcal mol^{-1}), which must be surmounted as a prerequisite to the boat form from which reaction can be initiated.

The flexibility of the [2.2.*n*]diazabicyclo

[4]The ratio of the peak areas of pure **3***c* and **4***c* was shown to be identical with the ratio of their concentrations.

[5]The early points on a plot of ln concentration of adduct against time gave a straight line fit from which the value of the rate constant could also be determined. The two values were within 10% of one another.

[6]Other activation parameters would be needed to correlate them at a common temperature. It is a safe guess that $\Delta S^{\ddagger}$ values for both processes for the adducts **3** are small and negative (13, 2). Thus $\Delta G^{\ddagger}$ values would increase slightly with temperature.

Can. J. Chem. Downloaded from www.nrcresearchpress.com by 210.87.254.105 on 09/05/12
For personal use only.

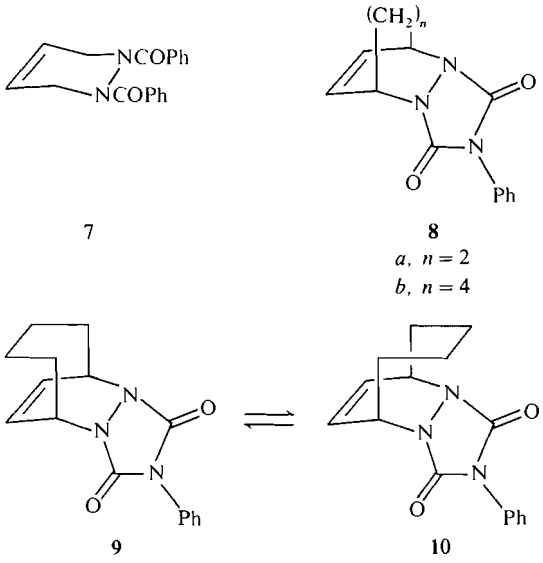

system in **3***b–d* is lost in the adducts derived from the cyclic azo compound 4-phenyl-1,2,4-triazoline-3,5-dione. Cyclohexadiene and cyclooctadiene gave quantitatively the adducts **8***a*, m.p. 172.5–174.5°, and **8***b*, m.p. 203.5–206.5°, in which the urazole ring is probably planar by analogy with related structures (16). Their room temperature n.m.r. spectra were very similar, apart from the differences expected in the methylene region. The vinyl and the tertiary protons in each were isochronous, the former as sharp multiplets (basically a triplet in **8***a* and a quartet in **8***b*) and the latter rather broadened. Ring inversional effects associated with the cycloalkene portion of the adduct **8***b*, *e.g.* **9** ⇄ **10**, are evidently fast at room temperature.

The formation of **4***d* from cyclooctadiene is of interest. Its identity follows by comparison of its spectroscopic properties in general with those of **4***a* (2), *b* (3) and *c* (Experimental), and its stereochemistry in particular from the n.m.r. absorption pattern of its tertiary protons. Its formation along with **3***d* in two competing Diels–Alder reactions represents, we believe, the first example in which a simple conjugated diene reacts as a dienophile with an azodicarbonyl compound as a heterodiene, though such a role for the latter towards other types of olefins is now well established (17–20).

Experimental

The i.r. spectra were taken on a Beckman IR10 or a Perkin–Elmer 457 spectrometer and the u.v. spectra on a Coleman EPS-3T Hitachi spectrometer. The n.m.r. spectra were run routinely on a Varian T-60, absorption values being measured against tetramethylsilane as internal standard. The coalescence temperatures for the adducts **3***b–d* were determined on a Varian HA-100 spectrometer with ethylene glycol as temperature calibration standard.

Solvents were purified by conventional means. Anhydrous magnesium sulfate was used as drying agent for solutions in organic solvents. Melting points are uncorrected.

1,3-Cycloheptadiene was made by the method of Hafner and Rellensmann (21), and 1,3-cyclooctadiene was purchased from Aldrich Chemical Co. The oxidation technique of Stickler and Pirkle (22) was used to prepare 4-phenyl-1,2,4-triazoline-3,5-dione.

6,7-Dibenzoyl-6,7-diazabicyclo[3.2.2]non-9-ene (3c)

A solution of azodibenzoyl (1.0 g, 4.2 mmol) and 1,3-cycloheptadiene (a two-fold excess) in carbon tetrachloride (25 ml) was refluxed for 16 h in the dark. The solution became almost colorless and a precipitate developed in the later stages. The solvent was removed and the residue was triturated with cold benzene (25 ml) to give the adduct (1.30 g, 94%) which had m.p. 199–201° directly. Recrystallization from carbon tetrachloride–hexane and finally from aqueous ethanol gave dense prisms, m.p. 203–204°; mass spectrum 332 (M^+, 77), 105 ($PhCO^+$, 100), 77 (Ph^+, 68); see Table 1 for other analytical data.

Isomerization of 3c to (±) cis-4-benzoyl-4,4a,5,6,9,9a-hexahydro-2-phenylcyclohepta-1,3,4-oxadiazine (4c)

Samples of the adduct **3***c* were stable indefinitely when heated at 200° in sealed evacuated tubes.

A solution of **3***c* (1.1 g, 3.2 mmol) in diphenyl ether (55 ml) was refluxed for 6 h. The solvent was distilled at 160° under reduced pressure, the final traces being removed by a stream of nitrogen at 100°. The dark residue was extracted with a large amount of hot petroleum ether (b.p. 35–60°), from which unreacted **3***c* crystallized and was removed on cooling. Evaporation of the mother liquor and crystallization of the residue from aqueous methanol gave the *oxadiazine* (17%), which was recrystallized to a constant m.p. of 131–132° from aqueous methanol; ν (CCl_4) 1643 cm^{-1} (C=O, C=N); ν (Nujol) 1630 cm^{-1} (C=O, C=N); λ_{max}(EtOH) 220, 295 nm (ε 17 600, 15 100); τ ($CDCl_3$) 2.0–2.8 (10 phenyl H), 3.5–4.3 (2 vinyl **H**, overlapping, nine lines), 4.93 (C_{4a}–H, broad, complex), 5.17 (C_{9a}–H, doublet, much further split), 7.5–8.7 p.p.m. (6 methylene H).

Anal. Calcd. for $C_{21}H_{20}N_2O_2$: C, 75.9; **H**, 6.1; N, 8.4. Found: C, 76.2; **H**, 6.3; N, 8.2.

Thin layer chromatography established the presence of at least two other minor products in the original reaction mixture.

Isomerization of 4c to 3c

The oxadiazine **4***c* (95 mg) was refluxed in diphenyl ether (5 ml) for 4 h and the solvent was removed under reduced pressure. The residue was chromatographed on silica gel from chloroform–hexane (1:1), elution with this solvent mixture giving a crystalline solid (48 mg) whose i.r. spectrum showed it to be mainly unchanged oxadiazine. Further elution with chloroform gave crystalline **3***c* (22 mg) which on recrystallization from carbon tetrachloride–hexane had m.p. 202–203°, alone or in admixture with **3***c* synthesized as described above.

Can. J. Chem. Downloaded from www.nrcresearchpress.com by 210.87.254.105 on 09/05/12
For personal use only.

Cycloaddition Reactions of Azodibenzoyl and 1,3-Cyclooctadiene

A solution of azodibenzoyl (4.0 g, 16 mmol) and 1,3-cyclooctadiene (40 ml) became almost colorless when heated at 100° for 5 h. The solution was evaporated and the residue was digested with hot benzene (40 ml) and then cooled and filtered. The small amount of insoluble material, which contained NH absorption in its i.r. spectrum, was not further examined and the benzene filtrate was chromatographed on neutral alumina. Elution first with benzene gave *(±)cis-1-benzoyl-4a,7,8,9,10,10a-hexahydro-3-phenyl-cyclo-octa-1 H-4,1,2-oxadiazine* (**4***d*) (0.59 g, 10%) and then with benzene–ether (19:1) gave *7,8-dibenzoyl-7,8-diaza-bicyclo[4.2.2]dec-9-ene* (**3***d*) (2.15 g, 37%). Further elution with benzene–ether (9:1) gave more NH-containing fractions (1.1 g).

The adduct **3***d* was twice crystallized from 90% ethanol as prisms, m.p. 207–208° (see Table 1).

The adduct **4***d* after two crystallizations from aqueous ethanol had m.p. 145.5–146°; ν (CCl_4) 1647 cm^{-1} (C=O, C=N); ν (Nujol) 1639, 1624 cm^{-1} (C=O, C=N); λ_{max}(EtOH) 220, 295 nm (ε 20 700, 17 100); τ ($CDCl_3$) 1.9–2.8 (10 phenyl H), 3.7–4.3 (2 vinyl H, overlapping, complex), 4.80 (C_{10a}—H, broad, complex), 5.08 (C_{4a}—H, multiplet), 6.7–9.1 p.p.m. (8 methylene H).

Anal. Calcd for $C_{22}H_{22}N_2O_2$: C, 76.3; H, 6.4; N, 8.1. Found: C, 76.1; H, 6.5; N, 8.2.

Attempted Thermal Isomerization of 3d and of 4d

Refluxing of either adduct for 10 h in decalin (187°) or 8 h in diphenyl ether (258°) caused no isomerization. Evaporation of the solvents at 100° in a stream of nitrogen led to the recovery of pure starting material.

Samples of each adduct (50 mg) were then heated in sealed evacuated tubes at various higher temperatures. At 305° **4***d* was unchanged after heating for 2 h, but at 320° it was converted into a dark gummy substance with a complex i.r. spectrum showing N—H absorption; evidence for the presence of **3***d* among the products, either in the spectrum or by t.l.c. analysis, was inconclusive. **3***d* was recovered with only slight discoloration and no change in its i.r. spectrum after heating for 2 h at 320°.

Attempted Acid-catalyzed Isomerization of 3d

A sample of **3***d* (50 mg) was refluxed for 12 h in dioxan (5 ml) containing *p*-toluenesulfonic acid (10 mg). Evaporation, addition of ether, and extraction of the solution with aqueous sodium hydrogen carbonate led to the recovery of pure **3***d* from the ethereal solution (n.m.r. spectrum).

Similarly **3***d* (50 mg) was refluxed for 1 day in pyridine (5 ml) containing a few drops of concentrated sulfuric acid. Evaporation and extraction of the residue with chloroform-*d* gave a solution whose n.m.r. spectrum was that of pure **3***d*.

Determination of Isomerization Rates by Gas–liquid Chromatographic Analysis

The analysis was carried out on a Varian Aerograph (series 1520) dual flame instrument using 1/8 in. columns of XE-60 on Varoport 30. A 1½ ft column with 1% stationary phase at 140° was used for the analysis of the product mixture **3***b* and **4***b* (**3***b* was unstable above 150°), and a 5 ft column with 3% stationary phase at 240° for **3***c* and **4***c*.

3*b* (20 mg) was added all at once to refluxing diphenyl ether (2 ml) and samples of the solution were withdrawn with pre-heated Pasteur pipettes at intervals over the next 2 min. The samples were diluted with acetone and chromatographed, peak areas being determined by photocopying (three times), cutting out and weighing. The first order rate constant was determined directly from the area ratios.

Similarly solutions of **3***c* and **4***c* (10 mg in each case) were refluxed in diphenyl ether (1 ml). Samples were withdrawn over a period of 30 h, diluted with acetone, and analyzed as above. Since several peaks due to by-products appeared in the later chromatograms, and since the reaction was reversible, only the early ratios of **3***c*:**4***c* were used to estimate the first order rate constant for the isomerization of **3***c*. An initial slope for the plot of concentration of **3***c* against time was used in the calculation.

Adducts of 1,3-Cyclohexadiene and 1,3-Cyclooctadiene with 4-Phenyl-1,2,4-triazoline-3,5-dione

In each case the azo compound (263 mg, 15 mmol) was added to a solution of the diene (0.5 ml) in benzene (5 ml) at room temperature. The cyclohexadiene solution became colorless instantaneously and the cyclooctadiene one within 5 min, both reactions being markedly exothermic. Evaporation gave straw-colored quantitative residues of **8***a* and *b* which crystallized. They had i.r. spectra identical with those of the adducts after recrystallization, **8***a*, m.p. 172.5–174.5° (dec.) from benzene–hexane, and **8***b*, m.p. 203.5–206.5° (dec.) from benzene–carbon tetrachloride, both as dense colorless prisms (Table 1).

Attempted Isomerization of 1,2-Dibenzoyl-1,2,3,6-tetrahydropyridazine (7)

(a) Thermal

A solution of **7** (50 mg) was refluxed in diglyme (2 ml, 222°) for 2 h. Water and ether were then added and the ether layer shaken out thoroughly with water. The residue from the ether layer was essentially pure **7** (i.r. spectrum).

A sample (50 mg) was heated in a sealed evacuated tube at 350° for 1½ h. The dark product was washed out of the tube with ether and decolorized with charcoal in the ether solution. Evaporation gave colorless, crystalline **7**, whose i.r. was that of analytically pure starting material.

(b) Acid-catalyzed

A sample (50 mg) was refluxed in heptane (50 ml) containing 2% trifluoroacetic acid for 14 h. The solution was evaporated and the residue washed with cold very dilute methanol, which induced crystallization. The product was pure **7** (i.r. spectrum).

We wish to thank Mr. R. F. Hobson of this department for the determination of the coalescence temperatures of the adducts **3***b–d*. The financial assistance of the National Research Council of Canada is acknowledged.

1. M. T. Hughes and R. O. Williams. Chem. Commun. 587 (1968).
2. D. Mackay, J. A. Campbell, and C. P. R. Jennison. Can. J. Chem. **48**, 81 (1970).
3. C. Y-J. Chung, D. Mackay, and T. D. Sauer. Can. J. Chem. **50**, 1568 (1972).
4. J. Tufariello and J. J. Spadaro, Jr. Tetrahedron Lett. 3935 (1969).

5. J. M. LEHN and J. WAGNER. Tetrahedron, **25**, 677 (1969).
6. J. A. CAMPBELL, D. MACKAY, and T. D. SAUER. Can. J. Chem. **50**, 371 (1972).
7. J. K. ELWOOD and J. W. GATES, JR. J. Org. Chem. **32**, 2956 (1967).
8. K. M. KRIVOZHEIKO, M. B. KOLESOVA, and A. V. EL'TSOV. Biol. Activ. Soldin. 300 (1968). Chem. Abstr. **72**, 21660 (1970).
9. S. J. RHOADS. *In* Molecular rearrangements. *Edited by* P. de Mayo. Part 1. Rearrangements through "no mechanism" pathways. Interscience Publishers, Inc., New York. 1963. Chapt. 11.
10. H. M. FREY and R. K. SOLLY. Trans. Faraday Soc. **64**, 1858 (1968).
11. J. GREEN and D. MCHALE. Chem. Ind. 1801 (1964).
12. M. REY and A. S. DREIDING. Helv. Chim. Acta, **48**, 1985 (1965).
13. J. E. ANDERSON and J. M. LEHN. Tetrahedron, **24**, 137 (1968).
14. D. MACKAY, U. F. MARX, and W. A. WATERS. J. Chem. Soc. 4793 (1964).
15. B. PRICE, I. O. SUTHERLAND, and F. G. WILLIAMSON. Tetrahedron, **22**, 3477 (1966).
16. A. B. EVNIN, D. R. ARNOLD, L. A. KARNISCHKY, and E. STROM. J. Am. Chem. Soc. **92**, 6218 (1970).
17. J. J. TUFARIELLO, T. F. MICH, and P. S. MILLER. Tetrahedron Lett. 2293 (1966).
18. J. FIRL and S. SOMMER. Tetrahedron Lett. 1925; 1929 (1970).
19. C. F. HUEBNER, E. M. DONOGHUE, C. J. NOVAK, L. DORFMAN, and E. WENKERT. J. Org. Chem. **35**, 1149 (1970).
20. E. K. VON GUSTORF, D. V. WHITE, B. KIM, D. HESS, and J. LEITICH. J. Org. Chem. **35**, 1155 (1970).
21. K. HAFNER and W. RELLENSMANN. Ber. **95**, 2567 (1962).
22. J. C. STICKLER and W. H. PIRKLE. J. Org. Chem. **31**, 3444 (1966).

Can. J. Chem. Downloaded from www.nrcresearchpress.com by 210.87.254.105 on 09/05/12
For personal use only.

A Convenient Synthesis of L(+)-Muscarine

J. WHITING, Y.-K. AU-YOUNG, AND B. BELLEAU[1]

Department of Chemistry, University of Ottawa, Ottawa, Canada

Received May 1, 1972

A new total synthesis of L(+)-muscarine is described. Performic acid oxidation of *N*-acetylcrotylglycine gave the corresponding 4,5-diol which was resolved at the α-carbon by stereospecific hydrolysis of the *N*-acetyl group of the L-isomer with hog kidney acylase I. The resulting α-L(+)-aminoacid diol (**3**: Chart 1) was deaminated with nitrous acid to give 4-hydroxy-5-methyl-2-tetrahydrofuran carboxylic acid with retention of configuration at position 2. Reaction of the corresponding methyl ester with dimethylamine gave two major amide constituents in 65% yield. Reduction of these two *N*,*N*-dimethylamides (**5***a* and *b*) with lithium aluminum hydride followed by quaternization with methyl iodide afforded a pure isomer of L(+)-muscarine (**6***a*) and L(+)-muscarine (**6***b*) in high yields. The biological activity of the latter was the same as that of the natural alkaloid.

Une nouvelle synthèse totale de la L(+)-muscarine est décrite. L'oxydation par l'acide performique du *N*-acétyl crotylglycine donne le diol-4,5 correspondant qui a été résolu au niveau du carbone α par hydrolyse stéréospécifique du groupe *N*-acétyle de l'isomère L par l'acylase I, provenant de rein de porc. L'α-L-(+)amino acide diol (**3**, partie I) résultant, après désamination par l'acide nitreux, conduit à l'acide hydroxy-4 méthyl-5 tétrahydrofurane-2 carboxylique avec rétention de configuration sur le carbone 2. La réaction de l'ester méthylique correspondant avec la diméthylamine donne essentiellement deux composés amides avec un rendement de 65%. La réduction de ces deux *N*,*N*-diméthylamides (**5***a* et *b*) par l'hydrure de lithium d'aluminum suivie d'une transformation en sel quaternaire par l'iodure de méthyle, a permis l'obtention d'un isomère pur de la L(+) muscarine (**6***a*) et de la L(+) muscarine (**6***b*), avec de bons rendements. L'activité biologique de cette dernière est la même que celle de l'alcaloide naturel.

[Traduit par le journal]

Canadian Journal of Chemistry, **50**, 3322 (1972)

Introduction

As part of our research studies on the nature and function of the acetylcholine receptor protein of excitable membranes (1, 2, 3), access to the potent cholinomimetic alkaloid L(+)-muscarine (**6***b*; Chart 1) (4) and its radioactive form became essential in order to discriminate between pharmacologically specific and non-specific binding sites. Extraction of the alkaloid from natural sources (5) is impractical at best and most of the recent biological studies with this quaternary base and its stereoisomers have been carried out with totally synthetic materials (6). The synthesis, chemistry, and stereochemistry of muscarine have been reviewed by Wilkinson (7) and also by Eugster (8) who has pioneered much of the relevant work in this fundamental area of medicinal chemical research. The X-ray structure and absolute configuration of the alkaloid have been elucidated by Jellinek (9). Subsequently, Pauling (10) has drawn analogies between its conformation and that of acetylcholine in the crystalline states. We wish to report on a new synthetic approach which provides access to L(+)-muscarine more conveniently and efficaciously than before. Adaptation of the method to the preparation of the radioactive analog can be readily visualized.

The synthetic scheme illustrated in Chart 1 was adopted because of the following broad advantages that it offers: (*a*) the intermediacy of an *N*-acylated α-aminoacid provides for ready enzymatic resolution to an optically pure L(+)-aminoacid (11); (*b*) nitrous acid deamination of α-aminoacids proceeds with complete rentention of configuration (11) and, in a favorable case such as **3** (Chart 1), ring closure to a tetrahydrofuran ring should compete favorably with α-substitution by the solvent (12). In this manner, the desired natural absolute configuration about C-2 of **4** (Chart 1) would be secured without ambiguity or difficulty. From there, it should be a simple matter of adapting Eugster's techniques (8).

Performic acid oxidation of predominantly *trans*-*N*-acetyl-DL-crotylglycine (**1**) (13) followed by mild alkaline hydrolysis gave **2** in high yield as a mixture of stereoisomers. Incubation of the latter mixture at p*H* 8 with

[1]Author to whom correspondence should be addressed, Department of Chemistry, McGill University, Montreal, Quebec.

Can. J. Chem. Downloaded from www.nrcresearchpress.com by 210.87.254.42 on 09/05/12
For personal use only.

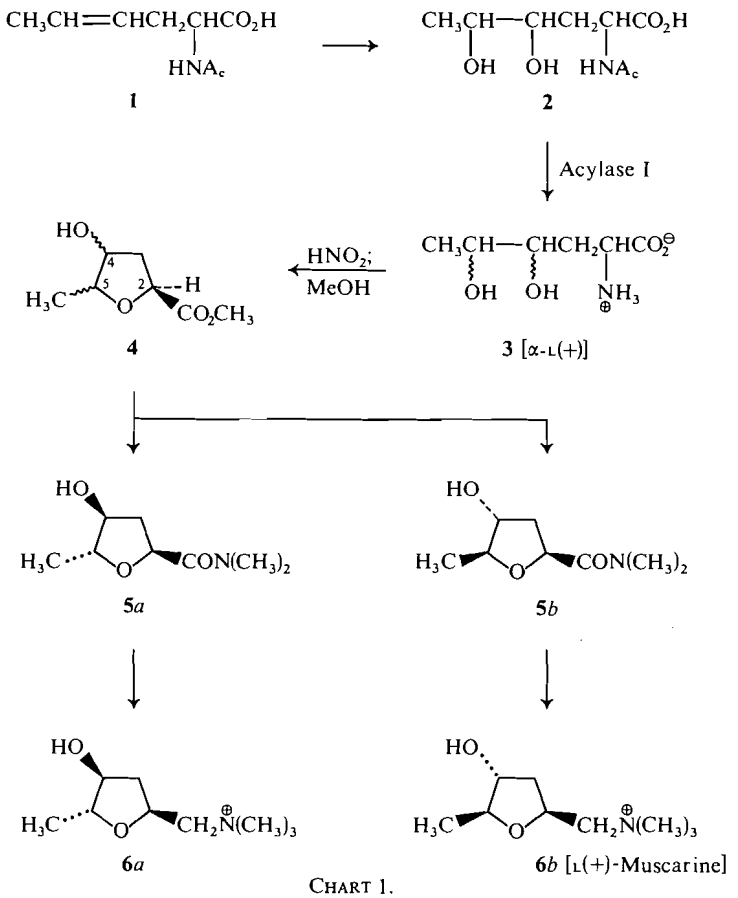

CHART 1.

hog kidney acylase I led to the isolation in 25% yield of a pure crystalline L(+)-α-aminoacid (**3**) unresolved about its hydroxyl bearing carbons. This optically active mixture of predominantly *threo*-diols was treated with nitrous acid and the resulting ring-closed acid esterified with methanolic hydrogen chloride to give optically active **4** as a clear oil in 42% yield (based on **3**). Reaction of the latter with ethanolic dimethylamine according to the literature (8 and refs. cited therein) gave a mixture of amides in good yield. Given that configurational integrity is retained at position 2, there are four possible stereoisomers about C-4 and -5 but two should predominate since *trans*-**1** should yield mostly *threo*-diols. All four were actually detected and isolated by chromatography on silicic acid but only two major crystalline fractions (**5***a* and *b*) in 1:1 ratio accounted for 65% of the total amide mixture. These two predominant isomers were reduced with lithium aluminum hydride and the resulting amines converted to their corresponding crystalline quaternary iodides. The first major isomer (from **5***a*) was shown to possess structure **6***a* by high resolution n.m.r. spectroscopy (220 MHz) (see Fig. 1). However, the relative configuration about positions 4 and 5 was not determined although we are inclined to favor the *allo*-arrangement (**6***a*) on the basis that the predominantly *trans*-configuration of the starting crotylglycine (**1**) should lead to a predominance of the DL-*threo*-diol (**2**) which in turn should ultimately give equal amounts of the two possible *trans*-enantiomers about positions 4 and 5 as the major products. In agreement with this expectation, Mr. Bruce Lippert of our laboratories established that, whereas the first major isomer **6***a* possessed very weak activity on the guinea-pig ileum (in

Can. J. Chem. Downloaded from www.nrcresearchpress.com by 210.87.254.42 on 09/05/12
For personal use only.

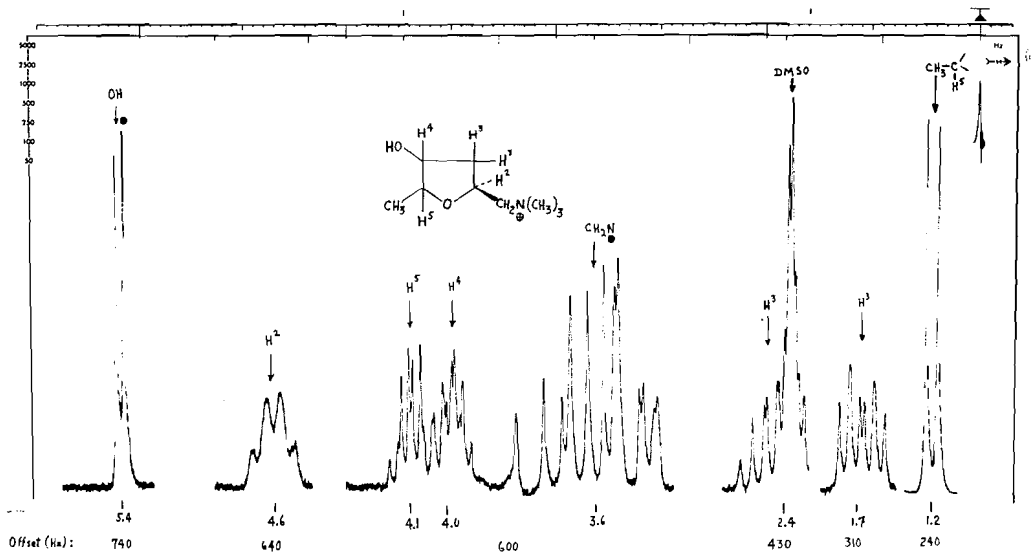

FIG. 1. The n.m.r. spectrum of **6***a* at 220 MHz in 1:1 DMSO–benzene (sweep time 100 s; sweep width 500 Hz; sweep offset variable as indicated). In the absence of benzene, H^4 and H^5 are poorly resolved. Irradiation of H^4 collapsed the OH to a singlet but irradiation of H^5 did not. Irradiation of OH caused partial collapse of H^4 but not of H^5. Only structure **6***a* is consistent with these data (supplied by Dr. A. H. Grey of the Canadian 220 MHz n.m.r. center at Sheridan Park, Ontario).

agreement with published data for DL-allomuscarine (6)), the other major isomer **6***b* surpassed acetylcholine in potency by a factor of 2. Since of all the possible stereoisomers of muscarine only the natural alkaloid displays such uniquely high activity (6), it follows that the second major isomer is L(+)-muscarine (**6***b*). Therefore, the other major isomer may be tentatively assigned the *allo*-configuration **6***a* which is enantiomeric with **6***b* at positions 4 and 5. Access to the rare L(+)-muscarine has become significantly easier than before.

Experimental

2-Acetamido-4,5-dihydroxyhexanoic Acid (2)

To a warm solution of 5.5 g of *N*-acetyl crotylglycine (13) in 22 ml of 98% formic acid was added slowly 5.5 ml of 30% hydrogen peroxide. After the addition was completed, the mixture was stirred for *5 h at 40–50° and then evaporated to dryness in vacuo*. The residue was dissolved in 25 ml of 10% aqueous sodium carbonate, the solution allowed to stand 15–17 h, followed by acidification and evaporation to dryness *in vacuo*. The residue was extracted with 2-propanol and the combined extracts treated with 25 g of Dowex 50W × 8 resin. After vigorous shaking for 30 min, the mixture was filtered and the filtrate evaporated to dryness *in vacuo* to yield a viscous yellowish oil (5 g) whose n.m.r. spectrum was consistent with structure **2** or the corresponding lactones. A substantial proportion was in the lactone form as judged from the i.r. spectrum.

Enzymatic Resolution of **2**

A solution of 4 g of the preceding material in 290 ml of pure water was treated with 2 *N* LiOH until the p*H* remained constant at 8.0 (lactone opening is gradual so that LiOH is consumed over a period of several minutes). A 5 mg portion of hog kidney acylase I (sigma) was added and the volume of the solution brought to 1600 ml and gently stirred at 38° for 20 h while adding appropriate quantities of 2 *N* LiOH so as to keep the p*H* as close to 8 as possible. The p*H* of the solution was then adjusted to 5 with acetic acid, the mixture filtered through Norit, and the filtrate concentrated *in vacuo* to a volume of about 800 ml followed by treatment with 100 g of Dowex 50W × 8 (50–100 mesh) resin in the acid form. After shaking for 30 min, the suspension was filtered, the resin washed with water, and then suspended in 200 ml of a 2 *M* solution of triethylamine in 20% aqueous methanol. The suspension was filtered, the resin washed with another 200 ml portion of the same solution and the combined filtrates evaporated to dryness *in vacuo*. The residue was first crystallized from 2-propanol and then from ethanol–water to give 1.0 g of white crystals, m.p. 185–187° (dec.), $[\alpha]_D^{25}$ 4.3° (H_2O).

Anal. Calcd. for $C_6H_{13}NO_4$: C, 44.17; H, 8.00. Found: C, 44.31; H, 7.88.

The filtrate from the Dowex resin was evaporated to dryness *in vacuo* and the residue crystallized from methanol–ether to give 1.0 g of white needles, m.p. 182–185°; $[\alpha]_D^{25}$ 43.2° (H_2O). This compound proved to be the unhydrolyzed *N*-acetyl derivative enriched in the D-isomer.

Can. J. Chem. Downloaded from www.nrcresearchpress.com by 210.87.254.42 on 09/05/12
For personal use only.

Can. J. Chem. Downloaded from www.nrcresearchpress.com by 210.87.254.42 on 09/05/12
For personal use only.

Anal. Calcd. for $C_8H_{15}NO_5$: C, 46.83; H, 7.31. Found: C, 46.61; H, 7.42.

Ring Closure to ***4***

To a solution of 7.1 g of the preceding L(+)-aminoacid in 18 ml of water containing 8.5 g of silver nitrite was added dropwise 56 ml of 1 *N* HCl while stirring vigorously at 0°. After 1 h, the mixture was allowed to warm to room temperature and continuously stirred for 15–17 h. A few drops of dilute HCl were added and the silver chloride filtered off. The filtrate was evaporated to dryness *in vacuo* and the residue dissolved in dry methanolic hydrogen chloride. After 15 h at room temperature, the solution was evaporated and the product distilled to give 2.90 g (42% yield) of a colorless oil, b.p. 94–95°/0.4 mm; i.r.: 3440 ν(OH), 1720 ν(C=O), 1190 and 1050 cm^{-1} ν(C—O); $[\alpha]_D^{25}$ −10.4° (H_2O).

Anal. Calcd. for $C_7H_{12}O_4$: C, 52.50; H, 7.50. Found: C, 52.36; H, 7.62.

Aminolysis of ***4*** *to* ***5***

A solution of 8.5 g of the preceding ester in 125 ml of a 33% ethanolic solution of dry dimethylamine was heated at 100° in a steel bomb for 24 h. The solution was evaporated *in vacuo* and the residual oil extracted repeatedly with ether. The ether was evaporated and the light brown oil applied in a little chloroform to a column of 1800 g of Silicar CC7 (chromatographic grade). Elution with chloroform (several liters) led to separation (as continuously monitored by t.l.c.) of the crude amide into four fractions: first to be eluted was ~0.9 g of an oil followed in sequence by two major crystalline fractions of 2.2 g each and finally by an impure oily fourth fraction. The first major fraction (**5**) was recrystallized from ether to give colorless needles, m.p. 63–65°; $[\alpha]_D^{25}$ 46.4° (EtOH) (homogeneous by t.l.c. and n.m.r.).

Anal. Calcd. for $C_8H_{15}NO_3$: C, 55.47; H, 8.73; N, 8.09. Found: C, 55.36; H, 8.57; N, 7.81.

The second major fraction (**5***b*) was recrystallized from ether to give colorless needles, m.p. 57° (sublimation); $[\alpha]_D^{25}$ 4.5° (EtOH) (homogeneous by t.l.c. and n.m.r.).

Anal. Calcd. for $C_8H_{15}NO_3$: C, 55.47; H, 8.73; N, 8.09. Found: C, 55.63; H, 8.62; N, 7.91.

L(+)-*Muscarine and* L(+)-*Allomuscarine*

The preceding amides **5***a* and *b* (300 mg) were added in 15 ml of ether, after heating under reflux for 2 h, to suspensions of 1.2 g of $LiAlH_4$ in 60 ml of ether; the mixtures were hydrolyzed at 0° with 12 ml of 30% aqueous KOH. After work-up in the usual manner, the colorless oil amines were treated with excess methyl iodide in ether whereupon white crystals of **6***a* iodide and **6***b* iodide (95 and 97% yields respectively) separated. They were recrystallized from acetonitrile–acetone and dried over P_2O_5 at 100° for up to 24 h. The m.p. varied considerably (from 131–150°) depending on crystal form and drying time. For **6***a*, the m.p. was 131–132° on several occasions; $[\alpha]_D^{25}$ 29° (EtOH); its n.m.r. spectrum (220 MHz) confirmed the structural assignment (Fig. 1).

Anal. Calcd. for $C_9H_{20}INO_2$: C, 35.89; H, 6.69; N, 4.64. Found: C, 35.68; H, 6.51; N, 4.31.

For **6***b* iodide, the m.p. was 148–150° (lit. (6) 149°); $[\alpha]_D^{25}$ 3.1 (EtOH) (lit. (6) for the chloride, 6.7 (H_2O)): the n.m.r. spectrum showed the product to be homogeneous and was consistent in every detail with the structure.

Anal. Calcd. for $C_9H_{20}INO_2$: C, 35.89; H, 6.69; N, 4.64. Found: C, 35.92; H, 6.76; N, 4.47.

The cholinomimetic activity (guinea-pig ileum) of this isomer was identical to that reported for L(+)-muscarine iodide (6).

We are grateful to the National Research Council of Canada and Bristol Laboratories of Canada for the financial support of this work. The skilful assistance of A. Gauthier in the preliminary phases of this work was highly appreciated. We are also indebted to Dr. A. H. Grey of the Canadian 220 MHz n.m.r. center (Sheridan Park) and Dr. Arthur Perlin for the n.m.r. spectra and their interpretation.

1. B. BELLEAU. Advances in chemistry series 108. R. F. Gould, editor. American Chemical Society, 1971, p. 141.
2. B. BELLEAU and V. DITULLIO. Can. J. Biochem. **49**, 1131 (1971).
3. B. BELLEAU. *In* Fundamental concepts in drug-receptor interactions. J. F. Danielli, J. F. Moran, and D. J. Triggle, editors. Academic Press, New York. 1970. p. 121.
4. C. H. EUGSTER and P. WASER. Experientia, **10**, 298 (1954).
5. C. H. EUGSTER. Helv. Chim. Acta, **39**, 1002 (1956).
6. P. G. WASER. Pharmacol. Rev. **13**, 465 (1961).
7. S. WILKINSON. Quart. Rev. **15**, 153 (1961).
8. C. H. EUGSTER. Adv. Org. Chem. **2**, 427 (1960).
9. F. JELLINEK. Acta Cryst. **10**, 277 (1959).
10. P. PAULING. *In* Structural chemistry and molecular biology. A. Rich and N. Davidson, editors. Freeman, San Francisco. 1968. p. 555.
11. J. Greenstein and M. Winitz. Chemistry of amino acids. John Wiley, New York. 1961.
12. E. HARDEGGER and F. LOHSE. Helv. Chim. Acta, **40**, 2383 (1957).
13. C. G. SKINNER, J. EDELSON, and W. SHIVE. J. Am. Chem. Soc. **83**, 2284 (1961).

The Preparation, Properties, and some Complexes of Anhydrous Manganese(III) Nitrate

D. W. JOHNSON AND D. SUTTON[1]

Department of Chemistry, Simon Fraser University, Burnaby 2, British Columbia

Received May 4, 1972

Manganese(III) nitrate and its dinitrogen pentoxide "adduct" have been prepared by the reaction of N_2O_5 with MnF_3. Infrared spectra and magnetic susceptibility measurements show these compounds to contain high-spin manganese(III) coordinated by nitrate groups and the "adduct" to be the nitronium salt, $[NO_2]^+[Mn(NO_3)_4]^-$. The syntheses of complexes of $Mn(NO_3)_3$ with some organic ligands, *e.g.*, 2,2′-bipyridyl, *o*-phenanthroline, acetonitrile, and triphenyl phosphine oxide are described.

Nous avons préparé le nitrate de manganèse(III) et son dérivé pentoxyde dinitré par réaction de N_2O_5 avec MnF_3. Les spectres infrarouges et les mesures de susceptibilité magnétique révèlent un manganèse(III) à spin élevé, coordonné par les groupes nitrate; de la même façon on apprend que le dérivé est un sel nitronium, $[NO_2]^+[Mn(NO_3)_4]^-$. Nous décrivons aussi la synthèse de complexes de $Mn(NO_3)_3$ avec quelques ligands organiques, c'est-à-dire 2,2′-bipyridyl, *o*-phénanthroline, acétonitrile et l'oxyde de triphényl phosphine.

[Traduit par le journal]

Canadian Journal of Chemistry, **50**, 3326 (1972)

Introduction

One of the most obvious features of the chemistry of manganese(III) is the small number of well established simple anhydrous compounds. These are limited to the oxide, Mn_2O_3 (1), the hydroxide, Mn(OH)O (2), and the fluoride (3). Prior to this study, manganese(III) nitrate, or its hydrate, and complexes of manganese(III) containing coordinated nitrates were all unknown. The anhydrous trivalent nitrates of the neighboring 3d elements chromium, iron, and cobalt (4–6) have all been reported in recent years. Both the chromium and iron compounds have low thermal stability and are involatile (and presumably polymeric) solids. By contrast, $Co(NO_3)_3$ is volatile and monomeric (6). Again, anhydrous iron(II) and chromium(II) nitrates and their complexes are unknown, whereas the ease of formation of the (II) oxidation state complicates the synthesis of cobalt(III) nitrato-complexes (7). We were therefore interested in determining whether the remaining member of this sequence, $Mn(NO_3)_3$, could be synthesized, bearing in mind the existence of stable manganese(II) nitrate.

We now give the details of the syntheses and properties of $Mn(NO_3)_3$, and related nitratomanganate complex anions and describe some reactions that lead to complexes with organic donor ligands.

[1]To whom correspondence should be addressed.

Experimental

Preparation of Compounds

Manganese(III) Nitrate

A large excess (20 g, 0.185 mol) of dinitrogen pentoxide was condensed onto anhydrous red manganese(III) fluoride (1.0 g, 8.9 mmol) at −78 °C. The solids were mixed and allowed to warm to room temperature to liquefy the N_2O_5; liquid N_2O_4 (20 ml) was then added and the mixture was stirred at 5 °C under a dry atmosphere for 3 days, the flask being vented to the atmosphere by a phosphoric oxide guard tube. During that time a reaction took place producing a dark brown oil which was then filtered from unreacted MnF_3. Careful removal of the volatiles (mainly N_2O_4) *in vacuo* at room temperature gave a dark brown hygroscopic solid. Extreme care had to be taken to avoid excess pumping on this because the eventual product, $Mn(NO_3)_3$, has low thermal stability, and evolves N_2O_4 at room temperature also. The procedure adopted was to isolate the sample from the pump as soon as all liquid had disappeared and then to continue pumping cautiously until an infrared spectrum of the product exhibited no bands assignable to nitrogen oxides, NO^+ or NO_2^+. Samples were sealed in glass ampoules and kept at −14 °C in a refrigerator. Manipulations were carried out quickly in a dry-box, using cooled apparatus where necessary.

Anal. Calcd. for $Mn(NO_3)_3$: Mn, 22.8; N, 17.4. Found: Mn, 22.5; N, 17.4.

The same compound could be synthesized using N_2O_5 alone, but the use of N_2O_4 as a solvent enabled the reaction to proceed more quickly and minimized the evaporation of N_2O_5. Anhydrous MnF_3 was obtained from Alfa Inorganics Inc., Beverly, Mass., U.S.A. Dinitrogen pentoxide was synthesized by the action of fuming nitric acid on phosphorus(V) oxide under a stream of ozone, and dried by passage through further phosphorus(V) oxide.

Nitronium Tetranitratomanganate(III)

When the filtrate from a reaction identical to that above

Can. J. Chem. Downloaded from www.nrcresearchpress.com by 210.87.254.105 on 09/05/12
For personal use only.

Can. J. Chem. Downloaded from www.nrcresearchpress.com by 210.87.254.105 on 09/05/12
For personal use only.

was cooled in liquid nitrogen, evacuated and the nitrogen bath removed so that the volatiles sublimed *in vacuo*, a residue of the brown hygroscopic nitronium salt $[NO_2]^+[Mn(NO_3)_4]^-$ remained.

Anal. Calcd. for $[NO_2]^+[Mn(NO_3)_4]^-$: Mn, 15.7; N, 20.1. Found: Mn, 15.8; N, 20.2.

Hydrolysis, followed by ceric sulfate titration indicated the absence of nitrite, precluding formulation as an N_2O_4 adduct or nitrosonium salt. Storage of this salt at room temperature for one week showed no observable evolution of nitrogen oxides.

The oxidation state of the metal in each compound was confirmed by the consumption of one equivalent of KI on titration in aqueous solution, and by the formation of a characteristic red solution ($\nu_{max} \sim 19.7$ kcm^{-1}) in 6 *M* H_2SO_4.

Potassium Tetranitratomanganate(II)

Stirring potassium permanganate (1.0 g, 6.4 mmol) with N_2O_4 (20 ml, 0.31 mol) in nitromethane or acetonitrile (20 ml) for 2 h produced a yellow precipitate of $K_2[Mn(NO_3)_4]$.

Anal. Calcd. for $K_2Mn(NO_3)_4$: K, 20.5; Mn, 14.4; N, 14.7. Found: K, 20.0; Mn, 14.9; N, 14.5.

Also produced was a dark "brown solution", to which we shall refer in some of the syntheses below. Carbon and hydrogen analyses and i.r. spectroscopy confirmed the absence of solvent in the precipitate. Evaporation of the brown solution produced a brown gum of indefinite composition.

Sodium Tetranitratomanganate(II)

A similar reaction using $NaMnO_4$ gave a pale yellow precipitate of $Na_2Mn(NO_3)_4$.

Anal. Calcd. for $Na_2Mn(NO_3)_4$: Na, 13.2; Mn, 15.7. Found: Na, 13.1; Mn, 15.9.

Trinitrato-2,2′-bipyridylmanganese(III)

Addition of 2,2′-bipyridyl to a nitromethane solution of $Mn(NO_3)_3$ at 5 °C in a 1:1 mole ratio gave a low yield (~20%) of dark red crystals. The same complex was also obtained by adding solid 2,2′-bipyridyl (0.32 g, 2.0 mmol) to a freshly filtered portion of the "brown solution" in nitromethane calculated to contain 2.0 mmol of manganese. Within 24 h at 5 °C large crystals of $Mn(NO_3)_3 \cdot bipy$ crystallized from the mixture in good yield (~80%). The compounds prepared by each method were shown to be identical by elemental analysis and i.r. spectroscopy.

Anal. Calcd. for $Mn(NO_3)_3 \cdot C_{10}H_8N_2$: Mn, 13.8; C, 30.2; H, 2.03; N, 17.6. Found: Mn, 13.8; C, 30.0; H, 2.08; N, 17.5.

Trinitrato-o-phenanthrolinemanganese(III)

This brick red crystalline complex was similarly prepared by both methods used for the bipyridyl complex.

Anal. Calcd. for $Mn(NO_3)_3 \cdot C_{12}H_8N_2$: Mn, 13.0; C, 34.2; H, 1.91; N, 16.6. Found: Mn, 12.8; C, 34.3; H, 1.87; N, 16.2.

Trinitratomanganese(III)·acetonitrile

Acetonitrile was used instead of nitromethane as the solvent in producing the "brown solution". Evaporation of this solution *in vacuo* gave a dark brown solid containing both $Mn(NO_3)_3$ and coordinated acetonitrile. Although reproducible analyses could not be obtained, a composition between $Mn(NO_3)_3 \cdot 1.5CH_3CN$ and $Mn(NO_3)_3 \cdot 2.0MeCN$. was indicated.

Trinitratomanganese(III)·bistriphenylphosphineoxide

Addition of triphenylphosphine oxide (1.28 g, 4.6 mmol) to the "brown solution" in nitromethane (2:1 mole ratio) yielded dark red crystals of $Mn(NO_3)_3 \cdot 2Ph_3PO$.

Anal. Calcd. for $Mn(NO_3)_3 \cdot C_{36}H_{30}P_2O_2$: Mn, 6.9; C, 54.2; H, 3.29; N, 5.3. Found: Mn, 6.9; C, 53.2; H, 3.65; N, 4.8.

Spectroscopic Measurements

Infrared spectra (4000–350 cm^{-1}) were recorded on Perkin–Elmer 457 or Beckman IR-12 spectrophotometers, using silver chloride cells. The spectra were obtained as Nujol and Fluorolube mulls. Reaction with Nujol was observed for $Mn(NO_3)_3$ and $[NO_2]^+[Mn(NO_3)_4]^-$ and the spectra are corrected. Electronic spectra were recorded on a Unicam S.P. 800 or a Cary 14 spectrophotometer.

Magnetic Measurements

Magnetic susceptibilities were measured at 22 or 0 °C by the Faraday method using $Hg[Co(NCS)_4]$ as a calibrant. Samples were manipulated, and measurements made, in a dry argon atmosphere.

Analyses

Manganese was determined by both atomic absorption spectroscopy and volumetrically following bismuthate oxidation. Sodium and potassium were determined by atomic absorption spectroscopy. Nitrogen was determined by Kjeldahl's method or in conjunction with carbon and hydrogen by the S.F.U. micro-analytical laboratory.

Results and Discussion

Manganese(III) Nitrate, $Mn(NO_3)_3$

This compound is stable indefinitely below −14 °C in a dry atmosphere, but evolves N_2O_4 rapidly at room temperature and fumes in moist air. This makes $Mn(NO_3)_3$ the least thermally stable of any of the known first row transition metal trinitrates.

Chromium(III) nitrate (4) and $Fe(NO_3)_3$ (5) decompose rapidly at 60 and 70 °C, respectively, whereas $Co(NO_3)_3$ (6) sublimes readily *in vacuo* with little decomposition at 40 °C. $Mn(NO_3)_3$ is slowly reduced to $Mn(NO_3)_2 \cdot N_2O_4$ by pure liquid dinitrogen tetroxide. Fereday (8) observed similar reduction of $Co(NO_3)_3$ in contact with N_2O_4. It is interesting to note that when a stream of dry argon is passed over the $Mn(NO_3)_3$ to remove the N_2O_4 we find that the $Mn(NO_3)_3$ decomposes with the loss of exactly 108 mol. wt. units to give a tan colored compound of formula $MnO(NO_3)$, which is stable at room temperature in a dry atmosphere ($\chi_M^{corr} = 8670 \times 10^{-6}$ c.g.s.u. at 22 °C, $\mu_{eff} = 4.52 \pm 0.1$ B.M.).

For $Mn(NO_3)_3$ the molar magnetic susceptibility at 0 °C is $\chi_M^{corr} = 8150 \times 10^{-6}$ c.g.s.u.

Can. J. Chem. Downloaded from www.nrcresearchpress.com by 210.87.254.105 on 09/05/12
For personal use only.

TABLE 1. Infrared spectra of $Mn(NO_3)_3$ and $[NO_2]^+[Mn(NO_3)_4]^-$ (cm^{-1})

Assignment†	$Mn(NO_3)_3$	$[NO_2]^+[Mn(NO_3)_4]^-$
$\nu_3[NO_2]^+$		2380 m 2358 m 1685 m‡
$\nu_1; A_1[\nu(NO^*)]$	1540 s,br	1532 s,br
$\nu_4; B_1[\nu(NO_2)]$	1270 s 1255 s	1298 s,br
$\nu_2; A_1[\nu(NO_2)]$	977 s	1010 s 912 w
$\nu_3; A_1$[ring def] and $\nu_6; B_2[\pi O_2NO^*]$	794 m,sp 768 m 743 sh	797 m,sp 755 m 740 m
$\nu_2[NO_2]^+$		560 b

*Signifies the uncoordinated oxygen atom.
†Nitrate bands assigned assuming local C_{2v} symmetry of bidentate or bridging (for $Mn(NO_3)_3$) nitrate groups.
‡Due to a reaction product with Nujol.

which gives $\mu_{eff} = 4.4 \pm 0.1$ B.M.; a value which is reduced somewhat below the theoretical "high-spin" value (*cf.*, $Fe(NO_3)_3$ (5) and $FeO(NO_3)$ (9)), and is probably due to the compound being magnetically non-dilute.

The i.r. absorption bands of $Mn(NO_3)_3$ are listed in Table 1 and are generally similar to those reported for $Cr(NO_3)_3$ (4) and $Fe(NO_3)_3$ (5). No Raman spectrum was obtained due to absorption of the He–Ne line; we have therefore made only a tentative assignment. The relative insolubility of $Mn(NO_3)_3$ in common solvents makes it seem likely that it is a polymeric compound in which some or all of the nitrates are bridging and the assignment in Table 1 is therefore arbitrarily made on C_{2v} local symmetry with two coordinated oxygen atoms. As has been noted in other nitrates (6, 10) there is apparently no observed absorption band corresponding to the out-of-plane bend.

$Mn(NO_3)_3$ is an extremely vigorous oxidizing agent. It dissolves in water rapidly evolving oxygen, to give a yellow-brown solution together with a brown precipitate, presumably representing disproportionation to Mn(II) and Mn(IV). When an ampoule of $Mn(NO_3)_3$ is broken under aqueous potassium iodide solution, the iodide is oxidized quantitatively. $Mn(NO_3)_3$ reacts violently with diethyl ether, and readily with hydrocarbons such as Nujol. This behavior is frequently displayed by complexes containing bidentate nitrate groups coordinated to a high oxidation state metal. It is sparingly soluble in nitromethane, decomposes in water, acetone, acetonitrile, and other polar solvents, and is insoluble in chloroform, carbon tetrachloride, and benzene. Reactions with a number of donor ligands have been studied and yield complexes which are discussed below.

Nitronium Tetranitratomanganate(III)

The structure of the compound obtained by reaction between N_2O_5 and MnF_3 in liquid N_2O_4 and subsequent removal of the volatile materials by sublimation is $[NO_2]^+[Mn(NO_3)_4]^-$. This formulation, rather than as a nitrosonium salt, N_2O_4 adduct, or N_2O_5 adduct, is based on the analyses and the following observations: (*a*) bands occur in the i.r. spectrum at 2380 and 2358 cm^{-1} ($\nu_3[NO_2]^+$) and 560 cm^{-1} ($\nu_2[NO_2]^+$); (*b*) no bands attributable to N_2O_4, N_2O_5, NO^+, or ionic nitrate were observed, and (*c*) the remaining i.r. bands are characteristic of coordinated nitrates (Table 1).

Tetranitrato anions are known for a wide range of metals (11–18), but this is the first instance where the tetranitrato anion exists for two oxidation states of the same metal (15, 16). The manganese(II) analog $[Mn(NO_3)_4]^{2-}$ (16) and the neighboring iron(III) complex ion $[Fe(NO_3)_4]^-$ (18) have both been shown in the compounds studied by X-ray crystallography, to be eight coordinate D_{2d} complexes containing four bidentate nitrate groups. The structure of $[Mn(NO_3)_4]^-$ is probably similar, though it might be expected to contain asymmetric bidentate nitrate groups on account of the non-spherical d-electron configuration (19).

$[NO_2]^+[Mn(NO_3)_4]^-$ is thermally more stable than $Mn(NO_3)_3$ and shows no evolution of nitrogen oxides at room temperature within one week. Thermal decomposition commences at 60 °C and does not yield $Mn(NO_3)_3$, since the decomposition temperature is above that of the nitrate itself. Similar enhanced thermal stability over that of the parent nitrate is also observed for $Cr(NO_3)_3 \cdot 2N_2O_4$ (4), $[NO]^+[Fe(NO_3)_4]^-$ and $[NO_2]^+[Fe(NO_3)_4]^-$ (12). The only point in the thermogravimetric curve where there is a sharp decrease in decomposition rate occurs at approximately 600° and at a mass loss which corresponds approximately to the composition $MnNO_6$. No analysis of this

TABLE 2. Infrared and Raman spectra of $Na_2Mn(NO_3)_4$ and $K_2Mn(NO_3)_4$ (cm^{-1})

Assignment†	$Na_2Mn(NO_3)_4$		$K_2Mn(NO_3)_4$		$[Mn(NO_3)_4]^{2-}$‡
	Infrared	Raman	Infrared	Raman	infrared
$2 \times \nu_6$				1630 w	
$\nu_1; A_1[\nu(NO^*)]$	1490 s	1505 w	1480 s,br	1485 s	1463
$\nu_4; B_1[\nu(NO_2)]$	1280 s,br	1335 w	1290 s,br	1290 s	1283
		1290 w		1225 w	
$\nu_2; A_1[\nu(NO_2)]$	1041 sh	1052 vs	1048 sp	1046 vs	1028
	1036 sp	1043 m,sh	1044 sp		
$\nu_6; B_2[\pi O_2NO^*]$	820 m		831 m		
	812 m		813 sp		813
	807 m				
$\nu_3; A_1$[ring def]	765 sh	744 m	755 m	750 m	
	750 s,sp		748 sh		
$\nu_5; B_1[\delta ONO^*]$		719 m	710 w	708 m	

*Signifies the uncoordinated oxygen atom.
†Assuming local C_{2v} symmetry of individual bidentate NO_3 groups.
‡Taken from ref. 15.

material was attempted. While the material may be a polymeric nitrate species it is extremely unlikely that it is the molecular oxide nitrate $MnO_3(NO_3)$. Compounds MnO_3X (*e.g.*, X = F) are molecular and unstable and few examples are known; attempts by Chapman to prepare the species $MnO_3(NO_3)$ by reaction of $KMnO_4$ or Mn_2O_7 with N_2O_5 produced a highly unstable product which eluded identification as $MnO_3(NO_3)$ with certainty (20).

The molar susceptibility of $[NO_2]^+[Mn(NO_3)_4]^-$ is $\chi_M^{corr} = 9960 \times 10^{-6}$ c.g.s.u. at 22 °C; $\mu_{eff} = 4.9 \pm 0.1$ B.M. This value is identical with the calculated spin only value of 4.90 B.M. corresponding to Mn^{3+} with four unpaired electrons. The compound is soluble in nitromethane to give a green solution, and brown solutions in acetonitrile and ethyl acetate. Decomposition occurs in water and acetone. It is insoluble in benzene and carbon tetrachloride. The molar conductivity of a saturated (2×10^{-4} *M*) nitromethane solution is exceedingly low (16.9 ohm^{-1} cm^2). A low value was also observed for $[NO_2]^+[Fe(NO_3)_4]^-$ and explained in terms of a proposed solution equilibrium with non-electrolytes such as $Fe(NO_3)_3N_2O_5$ or its dissociated and solvated components (12).

Sodium and Potassium Tetranitratomanganate(II)

Both compounds have a magnetic susceptibility of $\chi_M^{corr} = 15\,400 \times 10^{-6}$ c.g.s.u.; $\mu_{eff} = 6.0 \pm 0.1$ B.M., as is expected for high spin d^5 species. The structure of $[Ph_4As]_2[Mn(NO_3)_4]$ has been determined (16) and shows that the anion exhibits approximately D_{2d} symmetry, with all the nitrates coordinating as bidentate ligands. The infrared and Raman spectra of the sodium and potassium salts are presented in Table 2, along with that obtained by Straub *et al.* (15) for $[Ph_3CH_3As]_2[Mn(NO_3)_4]$. The assignments given in the Table refer to the C_{2v} local symmetry of the bidentate nitrate groups; splitting of the main regions of absorption observed in some cases may be due to coupling of nitrate vibrations under the full molecular symmetry (6, 10) or to crystal site-symmetry splitting. The compounds are soluble in water but are either insoluble or decompose with precipitation of some alkali metal nitrate in most organic solvents studied. Thus, where solution does occur, partial dissociation of the complex anion to give solvated $Mn(NO_3)_2$ and NO_3^- takes place, as observed by Fereday (8) for alkali metal nitrato cobaltates (II).

Trinitrato-2,2'-bipyridyl Manganese(III)

In view of the numerous possibilities for the molecular structure of this complex, bearing in mind the various coordinating modes open to the nitrate group, the crystal structure of this complex was determined, and is reported in the following paper (21). The complex is molecular and monomeric. The manganese atom has an approximate pentagonal bipyramidal coordina-

Can. J. Chem. Downloaded from www.nrcresearchpress.com by 210.87.254.105 on 09/05/12
For personal use only.

TABLE 3. Infrared spectra of some complexes of $Mn(NO_3)_3$* (cm^{-1})

$Mn(NO_3)_3$·bipy	$Mn(NO_3)_3$·*o*-phen	$Mn(NO_3)_3$·2Ph_3PO	$Mn(NO_3)_3$·*x*MeCN
1518 s	1555 sh	1552 sh	1555 s,br
1500 s	1535 s,br‡	1520 s,br	
1285 s	1243 s	1265 s	1270 s,br
1265 s	1230 sh		
	1210 s		
923 s	948 m	968 s	972 s
		953 sh	
802 m	800 w	798 m,sp	791 m
		787 m,sp	
747 m	752 m	†	†

*Only the nitrate absorptions are listed.
†This region of the spectrum is obscured by ligand bands.
‡May be partially overlapped by a band due to *o*-phen.

tion environment, with the four oxygen atoms of one symmetric and one asymmetric bidentate nitrate group and one bipyridyl nitrogen atom defining the equatorial plane. The remaining bipyridyl nitrogen atom, and the oxygen atom of a unidentate nitrate group are at the apices.

The infrared spectrum (Table 3) confirms the absence of nitrate ions and the presence of coordinated bipyridyl, but without the complementary Raman spectrum it is difficult to assign the i.r. spectrum with confidence in terms of discrete vibrations associated with unidentate and bidentate nitrate groups. We have attempted to observe the combination frequencies in the 1700–1900 cm^{-1} regions to aid the assignment (22) but find these to be too weak to locate with certainty. On the basis of the generalization that where a bidentate and a unidentate nitrate group are coordinated to the same or similar metal atoms in comparable oxidation states the separation of the two highest nitrate fundamental stretching frequencies will be greater for the bidentate group than for the unidentate group (19, 23), we very tentatively assign the bands at 1518 and 1265 cm^{-1} to bidentate nitrate vibrations, and those at 1500 and 1285 cm^{-1} to the unidentate nitrate group. Despite the inequivalence of the three nitrate groups in the molecule only a single band is observable in the third and lowest fundamental nitrate stretching region and is at an extremely low position, 923 cm^{-1}. This is close to the lowest value so far reported for this band, at 920 cm^{-1} in the unidentate nitrate complex $K[Au(NO_3)_4]$ (19).

$Mn(NO_3)_3$·bipy is a high spin complex having $\chi_M^{corr} = 10\,530 \times 10^{-6}$ c.g.s.u. at 22 °C, $\mu_{eff} = 5.0 \pm 0.1$ B.M. The room temperature diffuse-reflectance spectrum of a powdered sample shows a band at 19.7 kcm^{-1} assigned to a d–d transition. No complexes containing a greater proportion of bipyridyl (or *o*-phenanthroline) could be obtained even upon increasing the excess of ligand up to threefold. Thus the complexes of 1:1.5 stoichiometry formed with $Co(NO_3)_3$ (6) and InX_3 (X = Cl, Br, I, NCS) (24, 25), are apparently not formed in the case of $Mn(NO_3)_3$, under these conditions. The compound is soluble in acetonitrile sparingly in acetone to give a yellow solution, and decomposes in water to give a yellow-brown solution. It is insoluble in benzene, carbon tetrachloride, ethyl acetate, and nitromethane.

Trinitrato-o-phenanthroline Manganese(III)

The stoichiometry of this compound suggests that this complex could have a similar molecular structure to that of the bipyridyl complex. The infrared spectrum (Table 3) is similar, where bands can be discerned from *o*-phenanthroline absorption, but there are small shifts in band positions. A comparison of the X-ray powder patterns of the bipyridyl and *o*-phenanthroline complexes indicates that they are not isomorphous, although the patterns are quite similar at low angles. Thus, no definite conclusion as to the molecular structure of the *o*-phenanthroline complex can be drawn at this time. Magnetic measurements give $\chi_M^{corr} = 10\,830 \times 10^{-6}$ c.g.s.u.; $\mu_{eff} = 5.0 \pm 0.1$ B.M. at 22 °C.

Can. J. Chem. Downloaded from www.nrcresearchpress.com by 210.87.254.105 on 09/05/12
For personal use only.

The compound shows solubility properties like those of the bipyridyl complex.

Complexes with Triphenylphosphine Oxide and Acetonitrile

Triphenyl phosphine oxide forms the high-spin complex $Mn(NO_3)_3$ $(Ph_3PO)_2$ having $\chi_M^{corr} = 10\,150 \times 10^{-6}$ c.g.s.u. and $\mu_{eff} = 4.9 \pm 0.1$ B.M. The infrared spectrum shows the nitrate bands listed in Table 3 as well as bands typical of complexed Ph_3PO (*e.g.*, ν(P=O) 1150 cm^{-1} (26)). The structure of this complex is not known. The complex dissolves in benzene and acetonitrile to give yellow solutions and is insoluble in carbon tetrachloride, nitromethane and water.

The acetonitrile complex shows infrared bands typical of coordinated nitrate groups and coordinated acetonitrile (ν(C≡N) 2291 cm^{-1}). A strong band also occurs at 415 cm^{-1} which is absent from the spectra of the other complexes and therefore is presumably not due to a Mn—O mode; it may be the Mn—N stretch of the coordinated acetonitrile though such modes have been difficult to assign with certainty (23). For this compound $\chi_M^{corr} = 11\,400 \times 10^{-6}$ c.g.s.u. $\mu_{eff} = 5.2$ B.M., assuming the formula contains two molecules of CH_3CN.

The authors wish to thank the National Research Council of Canada for support of this work through operating grants.

1. R. Norrestam. Acta Chem. Scand. **21**, 2871 (1967).
2. R. L. Collin and W. N. Lipscomb. Acta Cryst. **2**, 104 (1949).
3. G. Brauer. Handbook of preparative inorganic chemistry. 2nd ed. **1**, 263 (1963).
4. C. C. Addison and D. J. Chapman. J. Chem. Soc. 539 (1964).
5. D. J. Lovejoy and A. J. Vosper. Chem. Commun. 1208 (1968).
6. R. J. Fereday, N. Logan, and D. Sutton. J. Chem. Soc. (A), 2699 (1969).
7. R. J. Fereday and D. Sutton. Chem. Commun. 510 (1966).
8. R. J. Fereday. Thesis. University of Nottingham, 1968.
9. C. C. Addison, B. F. G. Johnson, and N. Logan. J. Chem. Soc. 4490 (1965).
10. C. C. Addison, D. W. Amos, W. H. H. Hoyle, and D. Sutton. J. Chem. Soc. (A), 1497 (1967).
11. C. C. Addison and D. Sutton. Prog. in Inorg. Chem. **8**, 195 (1967) and references therein.
12. C. C. Addison, P. M. Boorman, and N. Logan. J. Chem. Soc. 4978 (1965).
13. G. N. Shirokova and V. Ya. Rosolovskii. Russ. J. Inorg. Chem. **16**, 1106 (1971).
14. D. W. Amos. Chem. Commun. 20 (1970).
15. D. K. Straub, R. S. Drago, and J. T. Donoghue. Inorg. Chem. **1**, 848 (1962).
16. J. Drummond and J. S. Wood. J. Chem. Soc. (A), 226 (1970).
17. D. Bowler and N. Logan. Chem. Commun. 582 (1971).
18. T. J. King, N. Logan, A. Morris, and S. C. Wallwork. Chem. Commun. 554 (1971).
19. C. C. Addison, N. Logan, S. C. Wallwork, and C. D. Garner. Q. Rev. (London), **25**, 289 (1971).
20. D. J. Chapman. Thesis. University of Nottingham, 1965.
21. D. W. Johnson and D. Sutton. Can. J. Chem. Following paper.
22. A. B. P. Lever, E. Mantovani, and B. S. Ramaswany. Can. J. Chem. **49**, 1957 (1971).
23. F. W. B. Einstein, E. Enwall, D. M. Morris, and D. Sutton. Inorg. Chem. **10**, 678 (1971).
24. A. J. Carty and D. G. Tuck. J. Chem. Soc. (A), 1081 (1966).
25. S. J. Patel, D. B. Sowerby, and D. G. Tuck. J. Chem. Soc. (A), 1187 (1967).
26. J. D. Donaldson and D. G. Nicholson. J. Chem. Soc. (A), 145 (1970).

Can. J. Chem. Downloaded from www.nrcresearchpress.com by 210.87.254.105 on 09/05/12
For personal use only.

The Crystal and Molecular Structure of Trinitrato-2,2′-bipyridylmanganese(III): A Complex with Three Distinctly Different Nitrate Ligands

F. W. B. EINSTEIN, D. W. JOHNSON, AND D. SUTTON[1]

Department of Chemistry, Simon Fraser University, Burnaby, British Columbia

Received May 4, 1972

The 2,2′-bipyridyl complex of manganese trinitrate, $Mn(NO_3)_3 \cdot bipy$, forms monoclinic crystals, space group $P2_1/c$ with four molecules in a unit cell with dimensions of $a = 7.311(3)$, $b = 18.022(7)$, $c = 11.704(4)$ Å, and $\beta = 108.73(3)°$. The manganese atom is seven co-ordinate, with approximate pentagonal bipyramidal geometry. The equatorial ligand atoms consist of one nitrogen of the bipyridyl group and four oxygens from two bidentate nitrate groups; the remaining bipyridyl nitrogen and the coordinated oxygen of the unidentate nitrate group are at the apices. This is the first nitrato-complex to be shown by crystallography to possess three distinctly different coordinated nitrate groups. One nitrate group is unidentate with Mn—O = 1.896(8) Å, one is symmetrical bidentate with Mn—O = 2.236(8) and 2.201(8) Å and one asymmetric bidentate with Mn—O = 2.112(8) and 2.400(9) Å.

Le complexe de trinitrate de manganèse avec le radical 2,2′-bipyridyl, $Mn(NO_3)_3 \cdot bipy$, forme des cristaux monocliniques, dont le groupe spatial est $P2_1/c$, avec quatre molécules par maille de dimensions: $a = 7.311(3)$, $b = 18.022(7)$, $c = 11.704(4)$ Å, et $\beta = 108.73(3)°$. L'atome de manganèse, possède un nombre de coordination de sept, avec une géométrie approximative de bipyramide pentagonale. Les atomes de ligands équatoriaux consistent en un azote du groupe bipyridyl et de quatre oxygènes provenant des deux groupes nitrate bidentés; l'azote du groupe bipyridyl et l'oxygène coordonné du groupe nitrate monodenté constituent les sommets. C'est la première fois en cristallographie, qu'on étudie un complexe nitrato possédant trois groupes nitrate différemment coordonnés. En effet, un groupe nitrate est monodenté avec la liaison Mn—O = 1.896(8) Å, le second est symétriquement bidenté Mn—O = 2.236(8) et 2.201(8) Å et le troisième asymétriquement bidenté avec Mn—O = 2.112(8) et 2.400(9) Å. [Traduit par le journal]

Canadian Journal of Chemistry, **50**, 3332 (1972)

Can. J. Chem. Downloaded from www.nrcresearchpress.com by 210.87.254.5 on 09/05/12
For personal use only.

In the preceding paper (1) we reported the synthesis of 1:1 high-spin complexes of manganese(III) nitrate with bidentate nitrogen bases such as 2,2′-bipyridyl and *o*-phenanthroline. The solid state structure of such compounds is of interest in view of the diversity of possibilities which exist. There have been few structural determinations of high-spin manganese(III) compounds, some recent examples being $MnCl_5^{2-}$, $(NH_4)_2MnF_5$, and $K_2Mn(SO_4)F_3$ (2–4). Although the first of these is pentacoordinate, the other examples exhibit ligand bridging and octahedrally coordinated manganese(III). The nitrate group is capable of considerable versatility as a ligand toward metal ions (5, 6) and frequently acts as a bidentate ligand thereby inducing rather high coordination numbers. Thus eight-coordinate nitrato-complexes of 3d metals have been established for a range of oxidation states, *e.g.*, $Mn(NO_3)_4^{2-}$ (7), $Fe(NO_3)_4^-$ (8), and $Ti(NO_3)_4$ (9). If all the nitrate groups were to be bidentate in $Mn(NO_3)_3 \cdot bipy$ an eight-coordinate molecular complex could result in this case also; however, the steric requirements of the bipyridyl might hinder this arrangement. Conversely, wholly unidentate nitrate coordination could yield a pentacoordinate species. Between these extremes there exist numerous structural possibilities which might arise from a combination of unidentate, bidentate or bridging coordination. One alternative is ruled out on infrared spectral evidence (1); the structure cannot contain uncoordinated nitrate ions. Finally the possibility of octahedrally coordinated manganese(III) occurring has its own special interest regarding the possible mechanism for the removal of the degeneracy of the ground state in the d^4 configuration (Jahn–Teller effect). In tris-(acetylacetonato) manganese(III) this occurs by angular distortion (10, 11) whilst in acetylacetonato-bis(*N*-phenylamino-troponiminato) manganese(III) there are unequal bond lengths (12). For a variety of reasons, therefore, we considered the X-ray crystal structure determination of $Mn(NO_3)_3 \cdot bipy$ to be of interest.

[1]To whom correspondence should be addressed.

Can. J. Chem. Downloaded from www.nrcresearchpress.com by 210.87.254.5 on 09/05/12
For personal use only.

Experimental

Trinitrato-2,2'-bipyridylmanganese(III) was prepared according to the method reported previously (1). The crystals are dichroic, appearing dark red to reflected light and dark green to transmitted light. One crystal, a parallelepiped, approximately 0.28 mm × 0.24 mm × 0.18 mm in dimension was sealed in a Lindemann glass capillary in a dry box and was used for the entire crystallographic data collection.

Weissenberg photographs of the reciprocal lattice layers $0kl$ and $1kl$, and precession photographs of the $h0l$ and $hk0$ layers were taken using Cu radiation ($\lambda = 1.5418$ Å). The systematic absences $h0l$, $l = 2n + 1$, and $0k0$, $k = 2n + 1$ together with the Laue symmetry $(2/m)$ allowed the space group to be deduced unequivocally as $P2_1/c$.

Cell dimensions were determined from accurate counter measurement of 23 of the strongest reflections having $2\theta > 30°$, using a Picker FACS-1 computer-controlled four-circle diffractometer and Mo $K\alpha_1$ radiation ($\lambda = 0.70926$ Å) with a 1.0° takeoff angle. The crystal was in a general orientation. Crystal data are as follows:

$Mn(NO_3)_3 \cdot C_{10}H_8N_2$ mol. wt. = 397.15

Monoclinic, $P2_1/c$, $a = 7.311(3)$, $b = 18.022(7)$, $c = 11.704(4)$ Å, $\beta = 108.73(3)$, $V = 1461$ Å^3, $\rho_o = 1.82(2)$ g/cc (flotation), $\rho_c = 1.81$ g/cc, $Z = 4$, $\mu = 10.6$ cm^{-1}, Mo $K\alpha$ = 0.7107 Å, $T = 20$ °C.

Reflection intensities for the unique set of data were collected by peak-top counting using niobium filtered Mo $K\alpha$ radiation, and a scintillation counter with pulse height analysis. The take-off angle was 3.5°. Each reflection with $2\theta \leqslant 45°$ was measured for 20 s with two background counts of 10 s each taken 2.0° apart plus allowance for dispersion. Every hour two standard reflections were measured; their variation was ±5% over the entire data collection. The net intensities were corrected for Lorentz and polarization effects; absorption was neglected since we estimate it would introduce a maximum error of ±1%. A reflection was considered unobserved if the net count was less than 3.0 σ, $\sigma = (\text{total count} + \text{background})^{1/2}$. 1914 reflections were measured of which 1119 were regarded as observed.

Structure Determination

An examination of the three-dimensional Patterson function based on the data in the range $2\theta \leqslant 30°$ allowed the determination of the position of the manganese atom and six other atoms. Refinement of the scale and the atomic coordinates gave $R = 38.8\%$, where $R = \Sigma(|F_o| - |F_c|)/\Sigma|F_o|$. A Fourier synthesis on these data revealed all the non-hydrogen atoms. Refinement of the structure, incorporating the remaining data in the range $45° \geqslant 2\theta \geqslant 30°$, and allowing anisotropic temperature parameters for only Mn, N(1), O(12), and O(13) reduced R to 6.7%. In the latter stages, all the hydrogen atoms were visible in an electron density difference map and were included at calculated positions (d(C—H) = 0.98 Å) (13).

The principal discrepancies at this stage were in the region of the unidentate nitrate group, notably the uncoordinated oxygen atoms. However, further refinement of this group (with fixed contributions from the remaining atoms) on the basis of models in which one or both of the uncoordinated oxygen atoms were described by two "fractional atom" positions with various occupancies gave no significant improvement in agreement. Instead, continued refinement of the whole structure, now incorporating anisotropic thermal parameters for all non-hydrogen atoms gave a final $R = 5.9\%$. This improvement was somewhat surprising as the major features (peaks and troughs up to $\rho = 0.7(2)$ e$^-$/Å^3) in an electron density difference map were still in the region of the unidentate nitrate group, but the high correlation coefficients (~0.3) between the x and z parameters of the uncoordinated oxygen atoms of this group may indicate indeterminacy between these parameters in the least squares procedure.[2]

Initially, constant weights were used in the refinement; in the final stages weights $w(= 1/\sigma^2)$ were given in terms of $\sigma = (A \cdot B/F_o)^{1/2}$ for $B < F_o$ and $\sigma = (A \cdot F_o/B)^{1/2}$ for $F_o \leqslant B$, where $A = 3.1$ and $B = 20$. The function minimized was $\Sigma w\{||F_o| - |F_c||\}^2$.

In the structure factor calculations, the atomic scattering factors for Mn, O, N, and C were taken from ref. 14 and that of Mn was corrected for anomalous dispersion. The final atomic coordinates and temperature factors are listed in Table 1, and the interatomic distances and angles in Table 2, along with the estimated standard deviations. Mean planes through appropriate groups of atoms are presented in Table 3. Crystallographic computer programs used in this work have been cited elsewhere (15).

Discussion

$Mn(NO_3)_3 \cdot$bipy is a monomeric, molecular, seven coordinate complex. The molecular configuration (Fig. 1) is that of an irregular pentagonal bipyramid. The manganese atom is coordinated in the equatorial plane to N(5) of the bipyridyl group and the four oxygen atoms O(21), O(22), O(31), and O(32) of two bidentate nitrate groups. The apical atoms are N(4) of the bipyridyl group and O(11), the coordinated atom of a unidentate nitrate group. The pentagon has pseudo m symmetry along Mn—N(5), and is slightly puckered. As expected, there are shorter distances between the coordinating oxygen atoms within each bidentate nitrate group compared with the non-bonded contacts between nitrate and bipyridyl groups.

The observed seven-coordinate environment of manganese(III) was rather unexpected. Whilst seven-coordinate compounds of 3d metals are not unknown, they do not occur commonly (16), and to our knowledge this is the first established instance of this geometry occurring for Mn(III). Also intriguing is the observation that the two bidentate nitrate groups are quite dissimilar,

[2]Complete set of tabular data is available, at a nominal charge, from the Depository of Unpublished Data, National Science Library, National Research Council of Canada, Ottawa, Canada, K1A 0S2.

Can. J. Chem. Downloaded from www.nrcresearchpress.com by 210.87.254.5 on 09/05/12
For personal use only.

TABLE 1. Final fractional coordinates and thermal parameters†‡

Atom	x	y	z	U_{11}	U_{22}	U_{33}	U_{12}	U_{13}	U_{23}
Mn	0.0636(2)	0.1447(1)	0.2780(1)	0.049(1)	0.042(1)	0.044(1)	0.001(1)	0.011(1)	0.001(1)
O11	−0.1395(12)	0.1517(6)	0.1332(7)	0.095(7)	0.116(8)	0.052(5)	0.008(6)	0.008(4)	−0.017(5)
O12	−0.2578(23)	0.1442(9)	−0.0590(9)	0.231(15)	0.208(15)	0.047(6)	0.070(3)	−0.014(8)	0.027(8)
O13	−0.0810(28)	0.0659(11)	0.0346(14)	0.238(20)	0.198(16)	0.140(13)	0.028(15)	−0.014(12)	−0.061(12)
N1	−0.1579(19)	0.1272(8)	0.0310(11)	0.107(9)	0.106(10)	0.061(8)	0.042(5)	0.014(7)	−0.003(7)
O21	−0.0835(11)	0.0669(4)	0.3502(7)	0.067(5)	0.056(5)	0.077(5)	−0.005(4)	0.028(4)	−0.011(4)
O22	−0.1789(12)	0.1771(5)	0.3653(8)	0.087(7)	0.048(5)	0.112(7)	−0.002(4)	0.036(5)	0.010(5)
O23	−0.3086(13)	0.0847(5)	0.4303(8)	0.081(6)	0.115(8)	0.087(6)	−0.021(6)	0.050(5)	0.007(5)
N2	−0.1962(15)	0.1104(6)	0.3845(8)	0.069(7)	0.060(6)	0.046(5)	−0.002(5)	0.016(5)	0.001(5)
O31	0.2103(13)	0.0392(4)	0.2604(7)	0.097(7)	0.072(5)	0.085(6)	−0.023(5)	0.058(5)	−0.007(5)
O32	0.2935(13)	0.1384(5)	0.1969(7)	0.118(7)	0.053(5)	0.086(6)	0.016(5)	0.053(5)	0.010(5)
O33	0.4286(13)	0.0369(5)	0.1721(7)	0.094(6)	0.096(7)	0.076(6)	0.037(5)	0.042(5)	0.005(5)
N3	0.3162(14)	0.0698(5)	0.2088(8)	0.063(6)	0.058(6)	0.055(6)	0.012(5)	0.020(5)	−0.003(5)
N4	0.2596(11)	0.1567(4)	0.4410(6)	0.052(5)	0.037(5)	0.039(4)	0.002(4)	0.018(4)	0.009(4)
N5	0.1080(11)	0.2592(4)	0.2814(7)	0.051(5)	0.046(5)	0.037(4)	0.010(4)	0.013(4)	0.006(4)
C1	0.3256(15)	0.1002(5)	0.5165(9)	0.053(6)	0.043(6)	0.051(6)	0.005(5)	0.016(5)	0.012(5)
C2	0.4611(16)	0.1115(7)	0.6287(10)	0.048(7)	0.077(8)	0.055(7)	0.016(6)	0.020(6)	0.024(6)
C3	0.5302(16)	0.1808(7)	0.6614(10)	0.052(7)	0.090(9)	0.045(7)	0.002(7)	0.015(5)	−0.002(6)
C4	0.4645(15)	0.2393(6)	0.5838(9)	0.062(7)	0.060(7)	0.040(6)	−0.001(6)	0.005(6)	−0.001(5)
C5	0.3284(14)	0.2268(5)	0.4738(9)	0.054(6)	0.041(6)	0.042(6)	0.003(5)	0.022(5)	0.006(4)
C6	0.2376(14)	0.2845(5)	0.3842(8)	0.053(6)	0.042(6)	0.039(6)	0.005(5)	0.020(5)	0.006(5)
C7	0.2757(16)	0.3588(6)	0.4030(9)	0.083(8)	0.046(6)	0.057(6)	−0.007(6)	0.027(6)	−0.004(6)
C8	0.1755(21)	0.4083(6)	0.3141(11)	0.118(11)	0.039(6)	0.064(8)	0.005(7)	0.044(8)	0.002(6)
C9	0.0477(18)	0.3824(6)	0.2112(11)	0.077(8)	0.054(7)	0.061(8)	0.013(6)	0.027(6)	0.024(6)
C10	0.0160(16)	0.3070(6)	0.1960(9)	0.069(8)	0.053(6)	0.046(6)	0.002(6)	0.014(6)	0.017(5)

Atom	x	y	z	U
H1	0.279	0.050	0.492	0.061
H2	0.507	0.069	0.684	0.073
H3	0.624	0.188	0.741	0.073
H4	0.514	0.289	0.608	0.066
H5	0.371	0.377	0.477	0.073
H6	0.196	0.461	0.325	0.067
H7	−0.020	0.417	0.146	0.073
H8	−0.078	0.288	0.120	0.067

†For the expression $\exp -2\pi^2(a^{*2}h^2U_{11} + b^{*2}k^2U_{22} + c^{*2}l^2U_{33} + 2a^*b^*hkU_{12} + 2a^*c^*hlU_{13} + 2b^*c^*klU_{23})$, U is in Å^2.
‡Estimated standard deviations in the last significant figures are given in parentheses in this and subsequent tables.

one being symmetrically, the other asymmetrically, bonded to manganese. Thus, the structure contains three dissimilarly coordinated nitrate groups, the first time this has been reported.

An explanation for this structure probably lies in the different stereochemical requirements of nitrate and bipyridyl ligands, and for comparison we can view the complex as formally derived from $Mn(NO_3)_4^-$ by replacement of NO_3^- by bipyridyl. By comparison with $Mn(NO_3)_4^{2-}$ (7) and $Fe(NO_3)_4^-$ (8) we may assume the $Mn(NO_3)_4^-$ ion to be eight-coordinate involving four bidentate nitrate groups, each subtending an angle of about 60° at the manganese. Replacement of a nitrate group by

TABLE 2. Interatomic distances and angles

(*a*) Interatomic bonded contacts

Bond	Distance (Å)		Bond	Distance (Å)
Mn—O(11)	1.864(8)	1.896(8)*	N(4)—C(1)	1.333(11)
—O(21)	2.102(8)	2.112(8)	—C(5)	1.368(12)
—O(22)	2.386(9)	2.400(9)	N(5)—C(6)	1.350(11)
—O(31)	2.225(8)	2.237(8)	—C(10)	1.327(12)
—O(32)	2.183(8)	2.201(8)	C(1)—C(2)	1.383(15)
—N(4)	1.997(7)	1.993(8)	C(2)—C(3)	1.355(15)
—N(5)	2.088(8)	2.086(8)	C(3)—C(4)	1.374(15)
N(1)—O(11)	1.241(13)		C(4)—C(5)	1.370(13)
—O(12)	1.115(14)	1.233(17)	C(5)—C(6)	1.474(12)
—O(13)	1.234(18)	1.332(21)	C(6)—C(7)	1.371(14)
N(2)—O(21)	1.291(12)		C(7)—C(8)	1.387(15)
—O(22)	1.237(11)		C(8)—C(9)	1.349(16)
—O(23)	1.209(11)		C(9)—C(10)	1.379(15)
N(3)—O(31)	1.253(11)			
—O(32)	1.248(11)			
—O(33)	1.200(11)			

*Figures in this column are corrected for thermal motion, the second atom assumed to ride on the first.

(*b*) Interatomic angles

Bonds	Angle (deg)	Bonds	Angle (deg)
O(11)—Mn—O(21)	92.8(4)	C(1)—N(4)—C(5)	119.8(8)
—O(22)	83.6(4)	Mn —N(4)—C(1)	123.0(7)
—O(31)	103.9(4)	Mn —N(4)—C(5)	117.1(6)
—O(32)	96.2(4)	Mn —N(5)—C(6)	114.2(6)
—N(4)	168.3(4)	Mn —N(5)—C(10)	126.1(7)
—N(5)	91.4(4)	C(6)—N(5)—C(10)	119.6(8)
O(21)—Mn—O(22)	56.3(3)	Mn —O(11)—N(1)	131.3(8)
—O(31)	78.0(3)	Mn —O(21)—N(2)	100.4(6)
—N(4)	89.5(3)	Mn —O(22)—N(2)	88.4(7)
O(22)—Mn—N(4)	88.2(3)	Mn —O(31)—N(3)	93.4(6)
—N(5)	83.2(3)	Mn —O(32)—N(3)	95.5(6)
O(31)—Mn—O(32)	56.9(3)	N(4)—C(1)—C(2)	120.9(10)
—N(4)	87.8(3)	C(1)—C(2)—C(3)	119.5(9)
O(32)—Mn—N(4)	90.2(3)	C(2)—C(3)—C(4)	120.1(10)
—N(5)	85.6(3)	C(3)—C(4)—C(5)	119.3(10)
N(4) —Mn—N(5)	79.3(3)	C(4)—C(5)—C(6)	125.3(9)
O(11)—N(1)—O(12)	130.3(14)	C(5)—C(6)—C(7)	123.6(9)
—O(13)	112.2(14)	C(6)—C(7)—C(8)	118.5(10)
O(12)—N(1)—O(13)	115.6(15)	C(7)—C(8)—C(9)	119.6(10)
O(21)—N(2)—O(22)	114.9(10)	C(8)—C(9)—C(10)	119.7(10)
—O(23)	119.9(10)	C(9)—C(10)—N(5)	121.2(10)
O(22)—N(2)—O(23)	125.2(11)		
O(31)—N(3)—O(32)	114.2(9)		
—O(33)	123.7(10)		
O(32)—N(3)—O(33)	122.1(10)		

Can. J. Chem. Downloaded from www.nrcresearchpress.com by 210.87.254.5 on 09/05/12
For personal use only.

Can. J. Chem. Downloaded from www.nrcresearchpress.com by 210.87.254.5 on 09/05/12
For personal use only.

TABLE 2 (*Concluded*)
(*c*) Selected intramolecular nonbonded contacts

Atoms	Distance (Å)	Atoms	Distance (Å)
Mn—O(13)	3.05(1)	O(21)—O(22)	2.13(2)
—N(1)	2.84(1)	—O(23)	2.16(2)
—N(2)	2.66(1)	—O(31)	2.71(3)
—N(3)	2.62(1)	—N(4)	2.89(3)
O(11)—O(12)	2.14(3)	—C(1)	3.06(4)
—O(13)	2.06(3)	O(22)—O(23)	2.17(2)
—O(21)	2.88(3)	—N(4)	3.06(3)
—O(22)	2.86(3)	—N(5)	2.98(3)
—O(31)	3.23(4)	O(31)—O(32)	2.09(2)
—O(32)	3.02(3)	—O(33)	2.16(2)
—N(5)	2.83(3)	—N(4)	2.93(3)
—C(10)	3.02(3)	O(32)—O(33)	2.14(2)
O(12)—O(13)	1.99(2)	—N(4)	2.96(3)
O(13)—O(31)	2.85(3)	—N(5)	2.90(3)
—O(32)	3.08(3)	N(4)—N(5)	2.61(3)
		C(4)—C(7)	3.03(4)

(*d*) Intermolecular contacts shorter than 3.5 Å, excluding H atoms

Atoms	Distance (Å)	Atoms	Distance (Å)
O(11)—C(4)	3.39(4) (*2*)*	O(23)—C(1)	3.40(3) (*4*)*
O(12)—O(22)	3.44(4) (*2*)	O(31)—C(9)	3.47(3) (*3*)
—C(7)	3.30(3) (*2*)	O(32)—C(4)	3.04(3) (*2*)
O(13)—O(13)	2.88(5) (*4*)	—C(7)	3.40(3) (*2*)
—O(33)	3.43(5) (*4*)	O(33)—C(2)	3.47(3) (*4*)
O(21)—C(8)	3.39(3) (*3*)	C(2) —C(8)	3.48(3) (*2*)
—C(9)	3.43(3) (*3*)	—C(9)	3.46(3) (*2*)
		C(3) —C(10)	3.45(3) (*2*)

*Figures in this column refer to the following symmetry transformations with respect to atoms in column two: (*1*) x, y, z; (*2*) $x, \frac{1}{2}-y, \frac{1}{2}+z$; (*3*) $1-x, \frac{1}{2}+y, \frac{1}{2}-z$; (*4*) $1-x, 1-y, 1-z$.

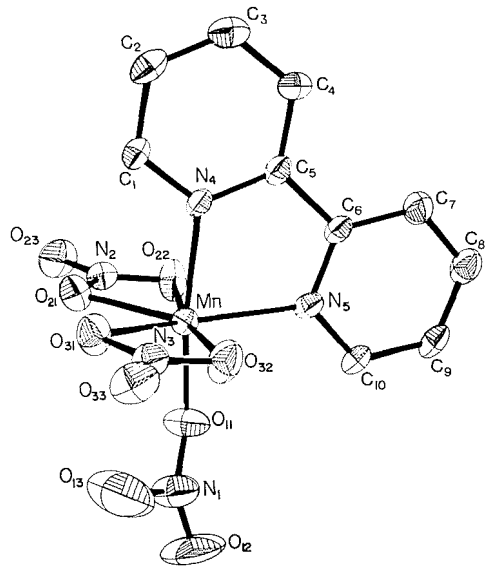

FIG. 1. The molecular configuration of $Mn(NO_3)_3 \cdot bipy$.

bipyridyl which subtends a larger interbond angle of $\sim 80°$ at manganese presumably introduces steric crowding which is relieved by one nitrate group having to adopt the unidentate configuration. It is more difficult to judge whether the coordination difference between the two remaining bidentate nitrate groups is also merely a consequence of crowding or whether it originates, at least partially, in the electronic configuration of the manganese atom, which is non-spherically symmetrical high-spin d^4. Unlike the more "regular" tetranitrato complexes for which the possibility of electronically induced distortions have been discussed (5), the inequivalence of the residual ligands in this complex may well be the main reason for the apparent differences in the bidentate nitrates. It may be noted, however, (*a*) that the long Mn—O(22) bond is *not trans* to a bipyridyl nitrogen, and (*b*) atom O(22) is one of four almost coplanar atoms in the equatorial

Can. J. Chem. Downloaded from www.nrcresearchpress.com by 210.87.254.5 on 09/05/12
For personal use only.

TABLE 3. Mean planes as $AX + BY + CZ + D = 0$ where X, Y, and Z are expressed in Å and are parallel to a, b, and c^*

Plane	Atoms in the plane with their deviations (Å)	A	B	C	D	χ^2	Distance of Mn from plane (Å)
1	N(1) O(11) O(12) O(13) (0.069) (−0.010) (−0.029) (−0.035)	0.8544	0.5132	−0.0819	0.006	25.9*	0.596
2	N(2) O(21) O(22) O(23) (−0.007) (0.001) (0.002) (0.002)	−0.4249	−0.0823	−0.9015	2.778	0.64	0.032
3	N(3) O(31) O(32) O(33) (−0.003) (0.001) (0.001) (0.001)	−0.4507	−0.1313	−0.8830	2.892	0.13	0.090
4	N(4) C(1) C(2) C(3) C(4) C(5) (−0.002) (0.007) (−0.006) (−0.003) (0.007) (−0.003)	0.9039	−0.1581	−0.3975	2.171	1.09	0.010
5	N(5) C(6) C(7) C(8) C(9) C(10) (−0.004) (−0.001) (0.010) (−0.10) (−0.001) (0.009)	0.9060	−0.0709	−0.4172	1.872	1.89	0.124
6	N(5) O(21) O(22) O(31)† (−0.012) (−0.027) (0.031) (0.018)	−0.3605	−0.0261	−0.9324	2.932	28.7*	0.194

*As noted in the text, these atoms are statistically not coplanar.
†O(32) is 0.317 Å out of the plane.

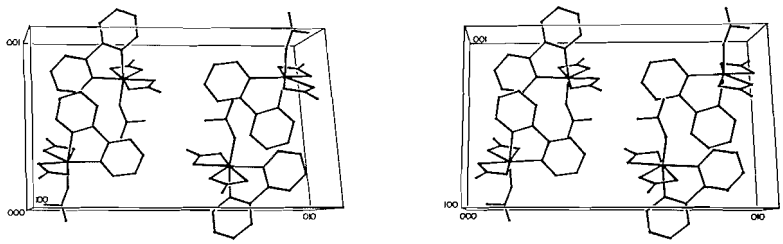

FIG. 2. A stereoscopic view showing the molecular packing.

pentagon (maximum deviation 0.03 Å), whereas the fifth atom, O(32), deviates from this "plane" by 0.32 Å (see Table 3, Plane *6*). It may well be that both nitrates are potentially symmetric but that O(22) cannot relieve crowding by a large out of plane displacement and has to do so by additional lengthening of the Mn—O(22) bond. This is consistent with the non-bonded contacts from O(22) and O(32) to the apical atoms O(11) and N(4) shown in Table 2*c*; the distances and angles to N(4) are similar but O(11) is angled towards O(22) and is closer to it than to O(32). The effect of a dissimilar ligand in a 7-coordinate complex is well illustrated in $CH_3Sn(NO_3)_3$ where all the nitrates are unsymmetrically bidentate (17), a dramatic change from four symmetric bidentate nitrates in the structure of $Sn(NO_3)_4$ (18). By contrast, the bidentate nitrate groups in the seven-coordinate molecule $VO(NO_3)_3CH_3CN$ (19) are symmetric, despite the dissimilar nature of the remaining ligands.

The latter compound offers the only other example in which the dimensions of bidentate and unidentate nitrate groups may be compared within the same molecule, and similarities with the present structure are evident. The unidentate nitrate groups are coordinated with almost identical metal–oxygen bond lengths which are significantly shorter than those to the bidentate nitrate groups.

The dimensions within the unidentate and bidentate nitrate groups are according to expectations (5). The unidentate group is the least well defined feature of the structure, due to its rather large thermal motion, but the long manganese–oxygen contact to the nearest uncoordinated oxygen atom O(13), 3.05(1) Å shows that there is no question as to the unidentate character of this nitrate group. The apparently large departure from planarity probably reflects positional inaccuracies of the uncoordinated oxygen atoms arising from both high correlation between parameters and large thermal motion. The remaining nitrate groups are each planar. The two heterocyclic rings of the bipyridyl group are planar with a dihedral angle of 5.1°.

The molecular packing illustrated in Fig. 2 is somewhat unexpected. The shortest intermolecular contact is O(13) ... O(13) = 2.88(5) Å, (see Table 2*d*) equal to the sum of Van der Waals radii. This is contrary to the anticipated "head-to-tail" packing to be expected if molecular dipolar forces dominate, and suggests that Van der Waals attraction is likely to be the main packing force.

We thank the National Research Council of Canada for support of this work through operating grants.

1. D. W. JOHNSON and D. SUTTON. Can. J. Chem. This issue.
2. I. BERNAL, N. ELLIOTT, and R. LABANCETTE. Chem. Commun. 803 (1971).
3. D. R. SEARS and J. L. HOARD. J. Chem. Phys. **50**, 1066 (1969).
4. A. J. EDWARDS. J. Chem. Soc. (A), 3074 (1971).
5. C. C. ADDISON, N. LOGAN, S. C. WALLWORK, and C. D. GARNER. Q. Rev. **25**, 289 (1971).
6. C. C. ADDISON, and D. SUTTON. Prog. Inorg. Chem. **8**, 195 (1967).
7. J. DRUMMOND and J. S. WOOD. J. Chem. Soc. (A), 226 (1970).
8. T. J. KING, N. LOGAN, A. MORRIS, and S. C. WALLWORK. Chem. Commun. 554 (1971).
9. C. D. GARNER and S. C. WALLWORK. J. Chem. Soc. (A), 1496 (1966).
10. B. MOROSIN and J. R. BRATHEVODE. Acta. Cryst. **17**, 705 (1964).
11. T. S. DAVIS, J. P. FACKLER, and M. J. WEEKS. Inorg. Chem. **7**, 1994 (1968).
12. (*a*) M. BARTLETT and G. J. PALENIK. Chem. Commun. 416 (1970). (*b*) P. M. PLAKSIN, R. C. STOUFER, M. MATHEW, and G. J. PALENIK. J. Am. Chem. Soc. **94**, 2121 (1972).
13. R. F. STEWART, E. F. DAVIDSON, and W. T. SIMPSON J. Chem. Phys. **42**, 3175 (1965).

Can. J. Chem. Downloaded from www.nrcresearchpress.com by 210.87.254.5 on 09/05/12
For personal use only.

14. International tables for X-ray crystallography. Vol. III Kynoch Press, Birmingham. 1962. p. 202.
15. L. Y. Y. CHAN and F. W. B. EINSTEIN. Can. J. Chem. **49**, 418 (1971).
16. E. L. MUETTERTIES and C. M. WRIGHT. Q. Rev. **21**, 109 (1967).
17. G. S. BROWNLEE, A. WALKER, S. C. NYBURG, and J. T. SZYMANSKI. Chem. Commun. 1073 (1971).
18. C. D. GARNER, D. SUTTON, and S. C. WALLWORK. J. Chem. Soc. (A), 1949 (1967).
19. F. W. B. EINSTEIN, E. ENWALL, D. M. MORRIS, and D. SUTTON. Inorg. Chem. **10**, 678 (1971).

Can. J. Chem. Downloaded from www.nrcresearchpress.com by 210.87.254.5 on 09/05/12
For personal use only.

Charge-transfer Complexes with Nitrate Esters as Electron Acceptors

T. URBAŃSKI
Chemical Faculty, Warsaw Institute of Technology, Warsaw 10, Poland
AND
B. HETNARSKI AND W. POŁUDNIKIEWICZ
Institute of Organic Chemistry, Polish Academy of Sciences, Warsaw, Poland

Received December 29, 1971

Nitrate esters of alcohols, containing from one to six *O*-nitro groups, react with tetramethyl-*p*-phenylenediamine (TMPD) in non-polar solvents to yield Wurster cation. The number of *O*-nitro groups necessary to produce 1 mol of Wurster cation is at least three. This is now explained in terms of the enthalpy of the reaction related to the electron affinity of nitrate esters; esters with five to six *O*-nitro groups show a relatively high enthalpy manifested by their ability to form charge-transfer complexes. Initially an unstable complex A is formed which then gives Wurster cation, both reactions being fast. A slow transformation then occurs into more stable complex B having the composition: 1 mol TMPD–2 mol of pentanitrates or 1 mol TMPD–1 mol of hexanitrate. TMPD in complex B was transformed into tetramethyl-*p*-quinonediimine dication.

That all nitrate esters with one to four *O*-nitro groups do not form complexes A and B may be due either to their relatively low enthalpy (and electron affinity), or to more favorable structures of complexes A and B of pentanitrates of D-xylitol and penta- and hexanitrates of hexitols with TMPD.

Les esters nitrates d'alcools, contenant de un à six *O*-nitro groupements, réagissent avec le tétraméthyl-*p*-phénylènediamine (TMPD) en solvants apolaires pour donner le cation de Wurster. Un minimum de trois groupes *O*-nitro est nécessaire pour produire 1 mol de cation de Wurster. On explique ceci en termes d'enthalpie de réaction reliée à l'affinité électronique des esters nitrates; les esters comprenant de cinq à six groupes *O*-nitro possèdent une enthalpie relativement élevé qui se manifeste par une certaine facilité à former des complexes de transfert de charge. Un complexe instable A est formé initialement et se transforme ensuite en cation de Wurster et ces deux réactions s'accomplissent rapidement. On observe ensuite une réaction lente en un complexe B plus stable, dont la composition est la suivante: 1 mol de TMPD–2 mol de pentanitrates ou 1 mol de TMPD–1 mol d'hexanitrate. Le TMPD du complexe B est transformé en tétraméthyl-*p*-quinonediimine (TMPQD).

Le fait que tous les esters nitrates comprenant de un à quatre groupes *O*-nitro ne forment pas les complexes A et B peut être dû, soit à leur enthalpie relativement faible (et leur électroaffinité) ou encore à des structures plus favorables des complexes A et B de pentanitrates de D-xylitol et de penta- et d'hexanitrates d'hexitols avec TMPD. [Traduit par le journal]

Canadian Journal of Chemistry, **50**, 3340 (1972)

One of the authors of the present paper (1) and his co-worker (2) have shown by way of thermal analysis that some *O*-nitro compounds, such as D-mannitol hexanitrate and erythritol tetranitrate can form addition complexes with aromatic nitro compounds. Recently, preliminary reports were published (3–5) on charge-transfer complexes between nitrate esters and tetramethyl-*p*-phenylenediamine (TMPD). Further experiments carried out with pentanitrates of D-mannitol and D-xylitol confirmed our former statement that a fast reaction of nitrate esters with TMPD in the absence of daylight leads to formation of the bluish-violet colored radical-ion, known as Wurster cation (6). The short time of irradiation of the samples in the spectrophotometer did not speed up the formation of the cation.

More detailed examination of the electronic spectra of pentanitrates of D-xylitol and D-mannitol and hexanitrates of hexitols with TMPD in 1,2-dichloroethane has shown rapid formation of a low intensity, transitory band between 909 and 1030 nm, in addition to the formerly reported bands at 570 and 620 nm (curve 1, Fig. 1) known to be typical of Wurster cation. For pentanitrates of D-xylitol and D-mannitol, the long wave bands were at 909 and 980 nm respectively, for hexanitrates of D-mannitol, D-sorbitol, dulcitol, and *myo*-inositol the wavelengths were 1030, 917, 926, and 990 nm respectively. The bands are of similar wave-

Can. J. Chem. Downloaded from www.nrcresearchpress.com by 210.87.254.42 on 09/05/12
For personal use only.

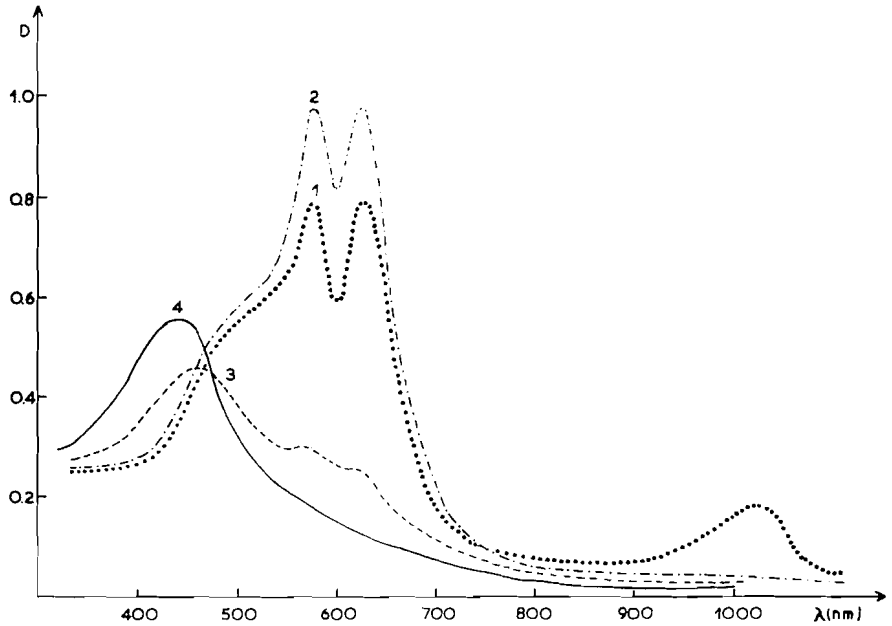

FIG. 1. General shape of electronic spectra of nitrate esters and tetramethyl-*p*-phenylenediamine (TMPD) in 1,2-dichloroethane at 23 °C.

(1) Pentanitrates of D-xylitol and D-mannitol and hexanitrates of hexitols immediately after mixing with TMPD; (2) pentanitrates of D-xylitol and D-mannitol and hexanitrates of hexitols 15 min after mixing with TMPD, and nitrate esters of alcohols with one to four *O*-nitro groups 24 h after mixing with TMPD; (3 and 4) the pentanitrates and hexanitrates (as above) 1 and 2 h, respectively, after mixing with TMPD.

lengths to the rather elusive ones described already in the literature and characteristic of some charge-transfer complexes (7).

The shape of the electronic spectra of systems with nitrate esters containing different numbers of *O*-nitro groups and carbon atoms varies considerably. All esters examined can be classified into two categories according to their behavior in 1,2-dichloroethane as a solvent:

(*a*) Substances which give curves of type 2 (Fig. 1), stable for a few days. They are obtained from nitrate esters with between one and four nitro groups (butyl nitrates, glycerol trinitrate, erythritol tetranitrate, pentaerythritol tri- and tetranitrates).

(*b*) Substances which initially give curves of type 1 but which, after 5 min, lose the band near 1000 nm; the absorption curve 1 changes into 2. The bands near 1000 nm characterize the transient charge-transfer complex A (Schemes 1 and 2) and should be considered as CT-bands. During the next 2 h, the absorption curve gradually changes into curve 4 with the maximum at 450 nm characterizing the yellow colored relatively stable complex B (Fig. 1). Nitrate esters containing five to six *O*-nitro groups and five to six carbon atoms belong to this group. They are pentanitrates of D-xylitol, D-mannitol, hexanitrates of D-mannitol, D-sorbitol, dulcitol, and *myo*-inositol.

The complexes formed from substances *b* show very strong absorption at 620 nm during the initial 30 min. The intensity of this absorption, D_{620}, is 10–60 times larger than the absorption at the same wavelength of mono-, di-, tri-, and tetranitrates, as partly reported in the preliminary communication (3).

Analysis of Curves 1 and 2

A few conclusions can be drawn from the analysis of curves 1 and 2.

By using as before (3–5) the Job method (8) of continuous changes related to absorption bands 909–1030 nm, we established that complex A was composed of 1 mol of D-xylitol or D-mannitol pentanitrate and 1 mol of TMPD, or of 1 mol of hexanitrates of hexitols combined with 2 mol of TMPD. This confirms the formerly

Can. J. Chem. Downloaded from www.nrcresearchpress.com by 210.87.254.42 on 09/05/12
For personal use only.

Can. J. Chem. Downloaded from www.nrcresearchpress.com by 210.87.254.42 on 09/05/12
For personal use only.

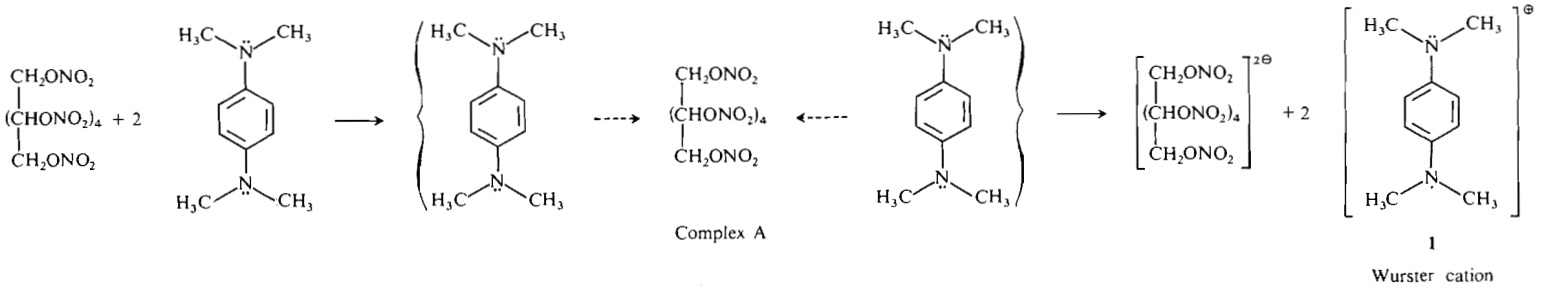

Complex A

1

Wurster cation

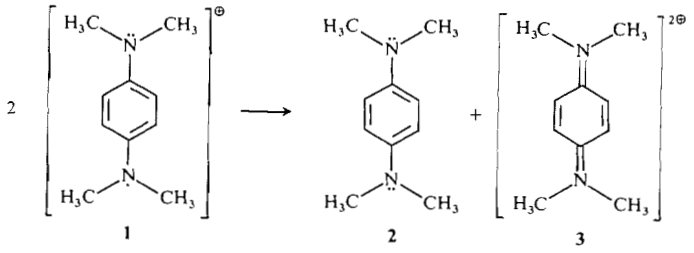

1 2 3

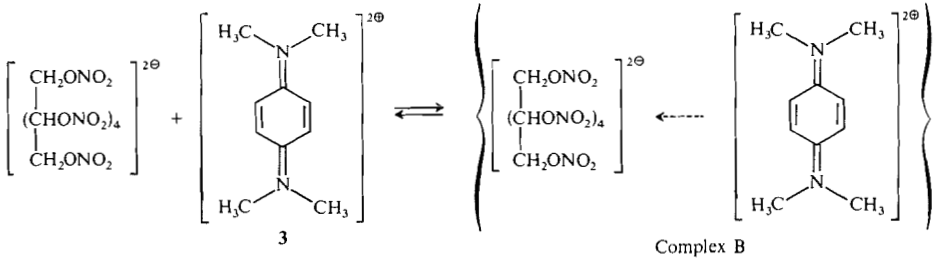

3

Complex B

SCHEME 1

Can. J. Chem. Downloaded from www.nrcresearchpress.com by 210.87.254.42 on 09/05/12
For personal use only.

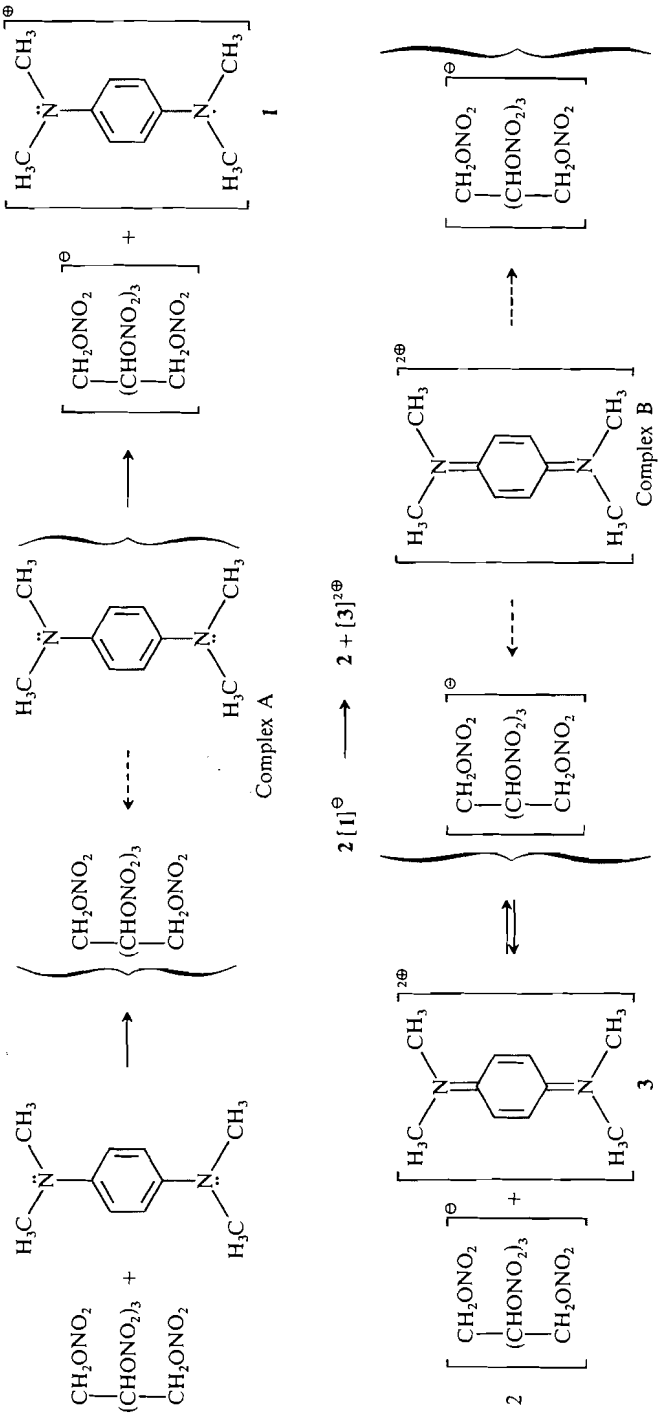

SCHEME 2

established rule that at least three ONO_2 groups are needed to withdraw one electron from TMPD (3, 4) and allows the formula of complex A to be shown as

$$\{x[R(ONO_2)_n] \leftarrow y[TMPD]\}$$

when $n = 5$; $x = y = 1$
and $n = 6$; $x = 1$; $y = 2$

The rule also holds for the formation of Wurster cation from penta-*O*-nitro compounds and TMPD: 1 mol of D-xylitol or D-mannitol pentanitrates forms 1 mol of Wurster cation.

The question arises as to why not less than three *O*-nitro groups are needed to withdraw one electron from 1 mol of TMPD in order to form complex A or Wurster cation. The answer may be found, at least in part, in the enthalpy ($-\Delta H$) of formation of Wurster cation. Since the enthalpy can serve as a measure of the electron affinity, the *comparative* values of electron affinities may be a measure of the ability to form Wurster cation.

The enthalpy was calculated from the well-known thermodynamic equation $-\Delta H = RT^2$ d ln K/dT. Assuming that the equilibrium constant K is equal to the concentration constant K_c we could use the equation

$$-\Delta H = \frac{RT_1T_2}{T_1 - T_2} \ln \frac{K_c'}{K_c''}$$

where K_c' and K_c'' are concentration constants at temperature T_1 and T_2 respectively. The concentration constants were determined from the absorbance of the band 620 nm at two temperatures, 0 and 23 °C. Since a higher temperature could not be used owing to the ease of decomposition of nitrate esters under the influence of bases, 23 °C was chosen as the upper safe limit. Temperatures lower than 0 °C were not used because we required a relatively narrow temperature range which would not necessitate taking into consideration the influence of the change of density of the solvent and the compounds with temperature, and which would guarantee that the course of the reaction was unchanged.

Obviously, examining the absorbance at only these two temperatures makes the figures less accurate so they have comparative value only. It was pointless to determine another value between 0 and 23 °C, as the absorbance would not differ sufficiently from those at these two temperatures.

Reaction of Nitrate Esters with One to Four O-Nitro Groups

The expressions describing the equilibria depend on the number of *O*-nitro groups in the molecule. Thus for *n*-, *sec*-, and *t*-butyl nitrates and ethylene glycoldinitrate where 3 mol of ester were necessary to produce 1 mol of the Wurster cation, eq. 1 was used:

$$[1] \quad 3\,RN^{I} + TMPD \underset{}{\overset{K_{c,3/1}}{\rightleftharpoons}} 3\,RN^{I\ominus} + TMPD^{\oplus}$$

where RN^{I} denotes the above mentioned nitrates. The initial concentrations of esters and TMPD are $[RN^{I}]_0 = 3a$ and $[TMPD] = a$, respectively, and the concentrations at equilibrium are $[RN^{I\ominus}]_e = [TMPD^{\oplus}]_e = x$. Hence

$$[2] \quad K_{c,3/1} = \frac{x^2}{27(a-x)^4}$$

The concentration x of the cation $TMPD^{\oplus}$ at equilibrium was calculated from the equation:

$$x = \frac{D_{620}}{E_{620} \cdot I}$$

where: D_{620} is absorption of the cation $TMPD^{\oplus}$ at $\lambda = 620$ nm; E_{620} is the molar extinction coefficient of the cation $TMPD^{\oplus}$ at $\lambda = 620$ nm, and equal to 12.5×10^3; and I is the thickness of the examined layer in cm.

When tri- and tetra-*O*-nitro compounds were examined, eq. 3 was applied:

$$[3] \quad RN^{III} + TMPD \underset{}{\overset{K_{c,1/1}}{\rightleftharpoons}} RN^{III\ominus} + TMPD^{\oplus}$$

where RN^{III} denotes glycerol trinitrate, erythritol tetranitrate, pentaerythritol tri- and tetranitrates. The initial concentrations of the esters and TMPD were $[RN^{III}]_0 = [TMPD]_0 = a$, and at equilibrium, $[RN^{III\ominus}]_e = [TMPD^{\oplus}]_e = x$.

$$[4] \quad K_{c,1/1} = \frac{x^2}{(a-x)^2}$$

The measurements of D_{620} (see Table 1 of our previous publication (3)) in 1,2-dichloroethane solution at concentrations 0.01–0.2 mol/l were taken 24 h after mixing the ester with TMPD, to ensure a constant concentration of $TMPD^{\oplus}$. A few conclusions can be drawn from the figures thus obtained:

(*a*) The values of D_{620}, K_c, and ΔH increase with the number of ONO_2 groups. The only exception is in the case of pentaerythritol tetra-

Can. J. Chem. Downloaded from www.nrcresearchpress.com by 210.87.254.42 on 09/05/12
For personal use only.

TABLE 1. Equilibrium constants at 0 and 23 °C, and calculated values of enthalpy of formation ($-\Delta H$) of Wurster cation from nitrate esters with one to four *O*-nitro groups in 1,2-dichloroethane

Electron acceptor	Concentrations* (mol/l)	K_c		$-\Delta H$ (kcal/mol)	
		0°	23°	For the whole molecule	For one ONO_2 group
n-Butyl nitrate	0.08 –0.15	$(2.56\pm0.02)\times10^{-8}$	$(2.37\pm0.02)\times10^{-8}$	0.47	0.47
sec-Butyl nitrate	0.08 –0.15	$(6.44\pm0.02)\times10^{-8}$	$(5.88\pm0.02)\times10^{-8}$	0.54	0.54
tert-Butyl nitrate	0.08 –0.15	$(7.36\pm0.02)\times10^{-8}$	$(6.66\pm0.02)\times10^{-7}$	0.61	0.61
Ethylene glycol dinitrate	0.08 –0.15	$(4.32\pm0.01)\times10^{-7}$	$(3.99\pm0.01)\times10^{-7}$	0.58	0.29
Glycerol trinitrate	0.015–0.020	$(1.70\pm0.01)\times10^{-6}$	$(1.47\pm0.01)\times10^{-6}$	0.91	0.30
Pentaerythritol trinitrate	0.018–0.025	$(1.32\pm0.02)\times10^{-6}$	$(1.15\pm0.01)\times10^{-6}$	0.84	0.28
meso-Erythritol tetranitrate	0.018–0.022	$(2.32\pm0.02)\times10^{-5}$	$(1.88\pm0.01)\times10^{-5}$	1.28	0.32
Pentaerythritol tetranitrate	0.008–0.012	$(1.76\pm0.01)\times10^{-7}$	$(1.60\pm0.01)\times10^{-7}$	0.58	0.14

*Thickness of the layer 1 cm. The values of D_{620} were partly reported in a previous publication (3).

nitrate and can be attributed to the relatively symmetrical structure of the compound and resulting low dipole moment ($\mu = 2.5$ D in dioxane (11)) which is much lower than the 3.3 D for erythritol tetranitrate found by us, in the same solvent. One of the authors of the present paper has suggested (12) that high dipole moments favor the formation of addition complexes.

(*b*) Nitrate esters of similar polarity, *e.g.* ethylene glycol, dinitrate glycerol trinitrate, and *meso*-erythritol tetranitrate (dipole moments 3.3, 3.2 (13), and 3.3 D (14), respectively) show a very similar enthalpy calculated for one ONO_2 group.

(*c*) The enthalpies of the reactions of nitrate esters with TMPD to form $TMPD^{\oplus}$ can be used to explain the mole ratio of reactants, in most cases. Thus they explain why ethylene glycol dinitrate gives the same ratio (3/1) as butyl nitrates in spite of the presence of two *O*-nitro groups: the total value of ΔH (and also K_c) in ethylene glycol dinitrate is of the same magnitude as in butyl monoesters.

Tri-*O*-nitro compounds and *meso*-erythritol tetranitrate have much higher values of ΔH and K_c, thus explaining the ratio 1/1. Pentaerythritol tetranitrate behaves in the same way as the trinitrates and erythritol tetranitrate in spite of the relatively low figures for ΔH and K_c. Also the figures for pentaerythritol trinitrate are lower than those for glycerol trinitrate. The low figures for pentaerythritol derivatives can probably be attributed to the structure of pentaerythritol which differs considerably from the rest of the alcohols in its central carbon atom and higher symmetry.

Reaction of Nitrate Esters with Five to Six O-Nitro Groups

The equilibria take the form shown in eqs. 5 and 6

$$[5]\quad RN^{V} + TMPD \underset{}{\overset{K_{c,1/1}}{\rightleftharpoons}} RN^{V\ominus} + TMPD^{\oplus}$$

$$[6]\quad RN^{VI} + 2\,TMPD \underset{}{\overset{K_{c,1/2}}{\rightleftharpoons}} RN^{VI\ominus} + 2\,TMPD^{\oplus}$$

where RN^{V} and RN^{VI} are pentanitrate and hexanitrate esters respectively. Equation 5 is identical with [3] and the concentration constant for pentanitrates can therefore be calculated from eq. 4.

For hexanitrates the concentrations of the components initially and at equilibrium are $[RN^{VI}]_0 = a$, $[TMPD]_0 = 2a$; and $[RN^{VI\ominus}]_e = x/2$, $[TMPD^{\oplus}]_e = x$, respectively. Hence

$$K_{c,1/2} = \frac{x^3}{(2a-x)^3}$$

The results are collected in Table 2.

Can. J. Chem. Downloaded from www.nrcresearchpress.com by 210.87.254.42 on 09/05/12
For personal use only.

TABLE 2. Equilibrium constants at 0 and 23 °C, and calculated values of enthalpy of formation of Wurster cation from nitrate esters with five to six *O*-nitro groups in 1,2-dichloroethane*

Electron acceptor	K_c		$-\Delta H$ (kcal/mol)	
	0°	23°	For the whole molecule	For one ONO_2 group
D-Xylitol pentanitrate	$(3.98\pm0.02)\times10^{-5}$	$(2.73\pm0.01)\times10^{-5}$	2.28	0.46
D-Mannitol pentanitrate	$(5.44\pm0.03)\times10^{-4}$	$(3.11\pm0.02)\times10^{-4}$	3.40	0.68
D-Mannitol hexanitrate	$(2.35\pm0.03)\times10^{-4}$	$(1.46\pm0.03)\times10^{-4}$	2.88	0.48
D-Sorbitol hexanitrate	$(1.85\pm0.03)\times10^{-4}$	$(1.18\pm0.01)\times10^{-4}$	2.73	0.455
D-Dulcitol hexanitrate	$(1.70\pm0.01)\times10^{-4}$	$(1.08\pm0.02)\times10^{-4}$	2.75	0.46
myo-Inositol hexanitrate	$(2.92\pm0.02)\times10^{-4}$	$(1.75\pm0.01)\times10^{-4}$	3.10	0.52

*Concentrations 0.002–0.004 mol/l, thickness 0.2 cm. Measurements made 15 and 30 min after the solutions were prepared for hexanitrates and pentanitrates respectively. The values of D_{620} were partly reported before (3).

The main conclusions are as follows:

(*1*) The pentanitrates of D-xylitol and D-mannitol and hexanitrates of hexitols show a very high absorption at 620 nm, and high values of K_c and ΔH.

(*2*) Relatively high values of the enthalpy of penta- and hexanitrates explain the ratio 1:1 of the hexanitrates and TMPD. However they cannot by themselves explain the difference with the pentanitrates where the ratio is 2:1; part of the explanation may be related to conformations as discussed below.

Analysis of Curve 4, Nitrate Esters with Five or Six O-Nitro Groups

The change of intensity of absorption of curve 1, through 2 and 3, leading to curve 4 (Fig. 1), the characteristic electronic spectra arising from D-mannitol, D-sorbitol, dulcitol, and *myo*-inositol hexanitrates, and D-xylitol and D-mannitol pentanitrates, can now be discussed. The change with time of the intensity of band 620 nm, characteristic of Wurster cation, and band 450 nm, characterizing the new complex B, is depicted in Fig. 2. It has been established that this change is typical of solutions in solvents with a low dielectric constant, such as 1,2-dichloroethane, dichloromethane, and benzene. When hexanitrates of hexitols were mixed with TMPD in polar solvents such as methanol, the original bluish-violet color remained unchanged for several days and no yellow complex with band 450 nm was formed. Band 450 nm cannot be assigned to the TMPQD (tetramethyl-*p*-quinonediimine) dication since it is not found in the spectrum of TMPQD diperchlorate (15). Another feature supports the view that the band is produced by a complex and may be a CT-band, namely that the intensity of the band increases with lowering the temperature.

Also in accord with the previous finding, the conductivity of the solution of complex B in *n*-heptane considerably increased when methanol was added, indicating the dissociation of the complex into ions in a polar solvent.

As mentioned before (3, 5) the complex B, in solution in *n*-heptane, showed in the i.r. spectrum the presence of bands corresponding to the quinonoimine structure (**3**, Scheme 1) of the donor moiety of the complex. Also t.l.c. indicated that Wurster cation (**1**), formed originally with pentanitrates of D-xylitol and D-mannitol, and hexanitrates of hexitols, was subject to disproportionation as shown in Scheme 1. The quinonoimine dication (**3**) eventually formed relatively stable complexes with the penta- and hexanitrates.

By using the Job method (8) of continuous changes in the band at *ca.* 450 nm, in 1,2-dichloroethane, dichloromethane, or benzene, 24 h after mixing, the ratio between the penta- and hexanitrates as acceptors and quinonoimine

Can. J. Chem. Downloaded from www.nrcresearchpress.com by 210.87.254.42 on 09/05/12
For personal use only.

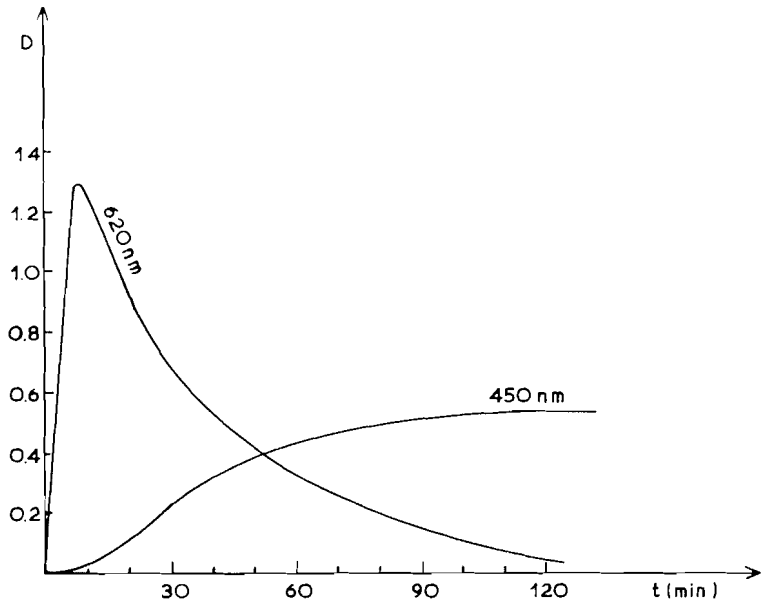

FIG. 2. Change with time of the intensity of band 620 and 450 nm of solutions of D-mannitol hexanitrate and TMPD in 1,2-dichloroethane at 23 °C.

dication was established with the results tabulated in Table 3.

Further confirmation of the ultimate formation of complex B was found in the e.s.r. spectra. Immediately after mixing pentanitrates of D-xylitol and D-mannitol or hexanitrates of hexitols with TMPD in 1,2-dichloroethane the e.s.r. spectrometer registered 13 triplets corresponding to Wurster cation, in agreement with data in the literature (16). After 2 h the signal disappeared and a broad singlet, which we assign to the complex B, was formed (Fig. 3). It was very similar to the e.s.r. signal of complexes of TMPD and chloranils in non-polar solvents (17).

The formation of complex B can be illustrated by two equations:

$$2\ R^{V}(ONO_2)_5 + TMPD \rightleftharpoons [2\ R^{V}(ONO_2)_5^{\ominus} \ldots . TMPQD^{2\oplus}]$$

$$R^{VI}(ONO_2)_6 + TMPD \rightleftharpoons [R^{VI}(ONO_2)_6^{2\ominus} \ldots . TMPQD^{2\oplus}]$$

where $TMPQD^{2\oplus}$ is the tetramethyl-*p*-quinonediimine dication.

The sequence of reactions to form complex A, Wurster cation, and complex B from hexanitrates of hexitols and TMPD is depicted by Scheme 1, those for D-xylitol pentanitrate and TMPD in Scheme 2.

TABLE 3. Ratio of nitrate ester/TMPD on the basis of band 450 nm

Nitrate ester	Ratio	λ_{max} (nm)
D-Xylitol pentanitrate	2:1	446
D-Mannitol pentanitrate	2:1	440
D-Mannitol hexanitrate	1:1	450
D-Sorbitol hexanitrate	1:1	450
Dulcitol hexanitrate	1:1	449
myo-Inositol hexanitrate	1:1	445

Unfortunately, we were unable to isolate the complexes from their solutions. Evaporating the solvent at low temperature and under reduced pressure left only a brown tarry residue showing signs of decomposition with evolution of nitrogen dioxide. This can easily be understood considering the low stability of nitrate esters in the presence of basic compounds. It is well known that even diphenylamine is too basic to be combined with nitroglycerine and similar esters.

Enthalpy of Formation of Complex B

As previously stated (3, 5), we calculated equilibrium constants K_c from the Benesi–Hildebrand equation (18), as modified by Ketelaar and his co-workers (19). From the values for K_c in 1,2-dichloroethane we calcu-

Can. J. Chem. Downloaded from www.nrcresearchpress.com by 210.87.254.42 on 09/05/12
For personal use only.

FIG. 3. E.s.r. signal of the complex B of D-mannitol hexanitrate with TMPQD dication.

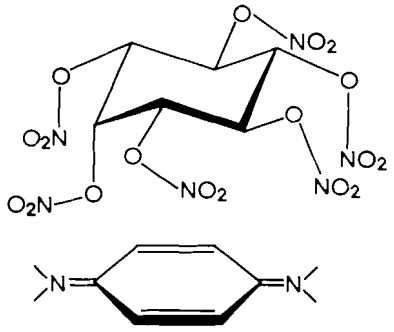

FIG. 4. Suggested structure of the complex B of *myo*-inositol with TMPQD dication.

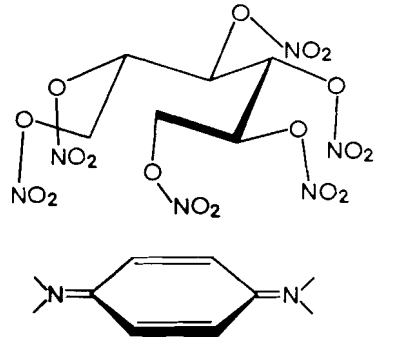

FIG. 5. Suggested structure of the complex B of chain hexitol hexanitrates with TMPQD dication.

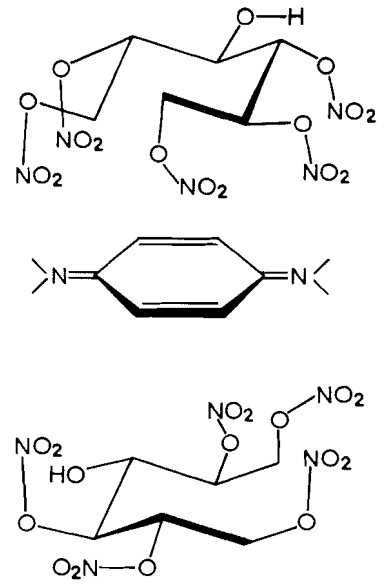

FIG. 6. Suggested structure of the complex B of D-mannitol pentanitrate with TMPQD dication.

lated the enthalpy: $-\Delta H = 5.12$ kcal/mol, a value of the same magnitude as in many $\pi-\pi$ complexes. The complex D-mannitol hexanitrate – tetramethylquinonodiimine may be considered as a $\pi-\pi$ complex. It also follows that *O*-nitro compounds with five or six *O*-nitro groups should be classified as π-electron acceptors.

Possible Structures of Complexes A and B of Nitrate Esters with Five to Six O-Nitro Groups

We attempt to explain the fact that complexes A and B can be formed only by nitrate esters with five to six *O*-nitro groups and five to six carbon atoms, in terms of conformation.

The complex with the six-membered ring of *myo*-inositol has probably the structure of parallel rings: that of the ester and of TMPD or the tetramethylquinonodiimine (Fig. 4). This is in agreement with the results of X-ray examination of classical CT-complexes (20) and in agreement with the "overlap and orientation principle" of Mulliken (21). The fact that only esters with five or six carbon atoms can form complexes A and B can probably be explained in terms of the conformation of these esters. Considering that five- and six-membered rings can readily be formed, it is now suggested that under the action of

Can. J. Chem. Downloaded from www.nrcresearchpress.com by 210.87.254.42 on 09/05/12
For personal use only.

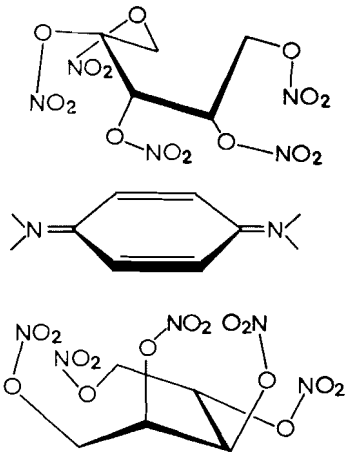

FIG. 7. Suggested structure of the complex B of D-xylitol pentanitrate with TMPQD dication.

TMPD the esters with five or six carbon atoms and five or six *O*-nitro groups are coiled into pseudo-rings. The pseudo-rings could be placed into position parallel to TMPD or the tetramethylquinonodiimine ion (Figs. 5–7).

Further experiments are being carried out with dinitrate esters of ω,ω'-diols containing five or more carbon atoms.

Experimental

Nitrate esters and tetramethyl-*p*-phenylenediamine were prepared as described earlier (4). Tetramethyl-*p*-quinonediimine diperchlorate was prepared according to Hünig and Daum (15). The solvents benzene, methanol, *n*-heptane were of spectroscopic grade. 1,2-Dichloroethane was purified as described in our previous paper (4).

The solutions of nitrate esters and TMPD were prepared away from daylight, and after mixing were kept in darkness. Electronic spectra were examined on a Unicam SP-500 spectrophotometer with thermostated cells of 0.2 and 1.0 cm thickness and concentrations of the nitrate esters varying according to the intensity of the absorbance of the solutions with TMPD, from 0.002 to 0.15 mol/l (Tables 1 and 2). I.r. spectra were measured on Unicam SP-200 and Hilger H-800 spectrophotometers, as previously described (5).

Our thanks are due to the Referees for their valuable comments and discussion.

1. T. URBAŃSKI. Roczniki Chem. **13**, 399 (1933); **14**, 925 (1934); **15**, 191 (1935); **16**, 359 (1936); **17**, 474 (1937).
2. M. WITANOWSKI. Roczniki Chem. **39**, 635 (1965).
3. B. HETNARSKI, W. POŁUDNIKIEWICZ, and T. URBAŃSKI. Tetrahedron Lett. 3 (1970).
4. B. HETNARSKI, W. POŁUDNIKIEWICZ, and T. URBAŃSKI. Bull. Acad. Pol. Sc., série sci. chim. **18**, 385 (1970).
5. T. URBAŃSKI, B. HETNARSKI, and W. POŁUDNIKIEWICZ. Bull. Acad. Pol. Sci., série sci. chim. **18**, 405 (1970).
6. C. WURSTER and B. SCHOBIG. Ber. **12**, 1809 (1879).
7. W. E. WENTWORTH and E. CHEN. J. Phys. Chem. **67**, 2201 (1963); J. H. LUPINSKI. J. Chem. Phys. **67**, 2725 (1963); R. FOSTER and T. J. THOMSON. Trans. Faraday Soc. **59**, 1059 (1963).
8. P. JOB. C.R. **180**, 928 (1925); Ann. Chim. Phys. **9**, 113 (1928).
9. R. S. MULLIKEN. J. Phys. Chem. **56**, 801 (1952).
10. H. O. PRITCHARD. Chem. Rev. **52**, 529 (1953); G. BRIEGLEB and W. LIPTAY. Elektronen-Donator-Acceptor Komplexe. Springer Verlag, Berlin. 1961. p. 161.
11. C. T. MORTIMER, H. SPEDDING, and H. D. SPRINGALL. J. Chem. Soc. 188 (1957).
12. T. URBAŃSKI. Roczniki Chem. **25**, 257 (1951).
13. L. J. DE KREUK. Rec. Trav. Chim. **61**, 819 (1942).
14. Our own measurements.
15. S. HÜNIG and W. DAUM. Chem. Ber. **88**, 1238 (1955).
16. J. W. EASTMAN, G. ENGELSMA, and M. CALVIA. J. Am. Chem. Soc. **84**, 1339 (1962).
17. J. ISENBERG and S. L. BAIRD, JR. J. Am. Chem. Soc. **84**, 3802 (1962).
18. H. A. BENESI and J. H. HILDEBRAND. J. Am. Chem. Soc. **71**, 2703 (1949).
19. J. A. A. KETELAAR, C. VAN DE STOLPE, A. GOUDSMIT, and W. DZCUBAS. Rec. Trav. Chim. **71**, 1104 (1952).
20. *e.g.* D. S. BROWN, S. C. WALLWORK, and A. WILSON. Acta Cryst. **17**, 168 (1964).
21. R. S. MULLIKEN. Rec. Trav. Chim. **75**, 845 (1956).

Can. J. Chem. Downloaded from www.nrcresearchpress.com by 210.87.254.42 on 09/05/12
For personal use only.

Solvolysis of Substituted Nortricyclanes and Norbornenes at 250° [1]

NICK H. WERSTIUK AND T. KADAI

Department of Chemistry, McMaster University, Hamilton, Ontario

Received May 4, 1972

Solvolysis of nortricyclyl bromide (**1***a*), nortricyclyl chloride (**1***b*), nortricyclanol (**1***c*), and 5- and 7-norbornenols (**2***b*, **7**) and *exo*-2,3-epoxybicyclo[2.2.1]heptane (**11**) in 10% v/v acetic acid–water at 250° yields 2-(cyclopentene)acetaldehyde (**3**), 3-(cyclopentene)acetaldehyde (**4**), 3-(cyclohexene)carboxaldehyde (**5**), norcamphor (**6**), and norbornanediols. In each case the diol concentration builds up then decreases as the conversion to **3**, **4**, **5**, and **6** occurs. When the substrates **1***a*, *b*, and *c*, **2***b*, **7**, **10***a*, and **11** are solvolyzed in deuterated medium, deuterium other than α to the carbornyl group is incorporated into the aldehydes and norcamphor.

La solvolyse du bromure de nortricyclyle (**1***a*), chlorure de nortricyclyle (**1***b*) nortricyclanol (**1***c*), norbornénols-5 et -7 (**2***b*, **7**), *exo*-époxy-2,3 bicyclo[2.2.1] heptane (**11**), dans un mélange à 10% en volume d'acide acétique–eau à 250°; conduit au cyclopentène-2 acétaldéhyde (**3**), cyclopentène-3 acétaldéhyde (**4**), cyclohexène-3 carboxaldéhyde (**5**), norcamphre (**6**), et norbonanediols. Dans tous les cas, la concentration en diol croît puis diminue au fur et à mesure que la conversion en **3**, **4**, **5**, et **6** s'effectue. Quand les substrats **1***a*, **1***b*, et *c*, **2***b*, **7**, **10***a*, et **11** sont solvolysés en milieu deutérié, un deutérium autre que celui en α du groupe carbonyle est incorporé dans les aldéhydes et le norcamphre.

[Traduit par le journal]

Canadian Journal of Chemistry, **50**, 3350 (1972)

Can. J. Chem. Downloaded from www.nrcresearchpress.com by 210.87.254.5 on 09/05/12
For personal use only.

Introduction

Solvolysis of 3-substituted nortricyclanes (**1***a* and *b*) and 5-substituted norbornenes in 80% ethanol–water (1), acetic acid (2*a*, *b*), or methanol (3) at 25–55° gives 3-nortricyclyl (**1***e*, *f*, and *g*) and *exo*-5-norbornenyl products (**2***c*, *d*, and *e*) via the cationic species **8** or **9**. Treatment of dehydronorbornyl acetate and nortricyclyl acetate with 50% H_2SO_4–HOAc at 95° gives norbornyl diacetates (4).

We have found that in solvolysis of the nortricyclyl substrates **1***a*, *b*, and *c*, the *endo*-5-, *exo*-5-, *anti*-7-norbornenols, and *exo*-2,3-epoxybicyclo[2.2.1]heptane at 250° in 10% v/v acetic acid–water or water only in the case of the halonortricyclanes, the aldehydes **3**, **4**, and **5** are formed in addition to norcamphor (**6**) (5*a*, *b*). When the solvolyses are carried out in deuterated medium, deuterium is incorporated into **3**, **4**, **5**, and **6**. Table 1 gives the results of our study.

Results and Discussion

Norcamphor and 3-(cyclohexene)carboxaldehyde were identified by comparison of i.r., n.m.r., m.s., and g.l.p.c. retention time data with those of authentic samples. The (cyclopentene)-acetaldehydes were identified in the following manner. That cyclopentenyl and aldehydic moieties were present was indicated by the i.r. of **3** + **4** which showed bands at 3052, 1612, and 2710 cm^{-1} (6). The n.m.r. spectrum showed absorptions at δ 9.50 and 5.68 and supported this premise. Since the 2- and 3-(cyclopentene)-acetaldehydes are not separated by g.l.p.c., the solvolysis method as described by Trahanovsky *et al.* (7) was employed for ratio determination. Reduction of **3** + **4** to the (cyclopentene)-ethanols, preparation of the nosylates of the mixture, followed by acetolysis gave the *exo*-norbornyl (84%), 2-(cyclopentene)ethyl (14%) acetates, and 1% of an unknown as was determined by g.l.p.c. A control experiment with a mixture of **3** + **4**, prepared by ceric ammonia nitrate oxidation of *exo*-norborneol (7) established a ratio 42:58 which compared favorably with the ratio of 48:52 determined for the same mixture by Trahanovsky *et al.* (7). Closer scrutiny showed that i.r. fingerprint spectroscopy is a more direct method for determining the **3**:**4** ratio. A band at 910 cm^{-1} present in the spectrum of 2-(cyclopentene)acetaldehyde (**3**) was present in the i.r. of a mixture of **3** + **4**. The relative area of the peak at 910 to that of the broad doublet at 718 (due to **3**) and 666 (due to **4**) determined for the 42:58 and 14:85 mixtures is 16 and 6%, respectively. Therefore to deter-

[1]Presented in part at the 53rd Canadian Chemical Conference of the Chemical Institute of Canada, Toronto, Ontario, May, 1970.

Can. J. Chem. Downloaded from www.nrcresearchpress.com by 210.87.254.5 on 09/05/12
For personal use only.

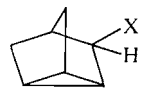

1

a X = Br
b X = Cl
c X = OH
d X = OBs
e X = OEt
f X = OAc
g X = OMe

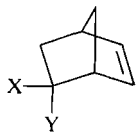

2

a X = OH; Y = H
b X = H; Y = OH
c X = OEt; Y = H
d X = OAc; Y = H
e X = OMe; Y = H

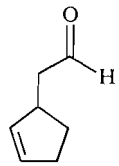

3

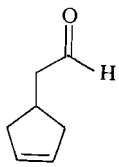

4

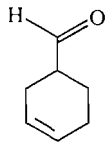

5

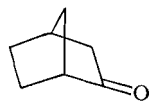

6

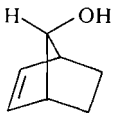

7

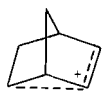

8

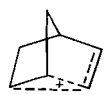

9

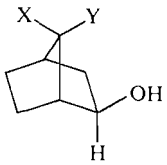

10

a X = H; Y = OH
b X = OH; Y = H

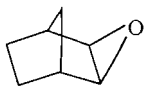

11

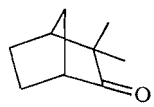

12

mine the percentage of **3** in a mixture of **3** + **4**, the percent area of the 910 peak to the 718–666 doublet is multiplied by 2.6. When the procedure is applied to pure 2-(cyclopentene)acetaldehyde, the area of the 910 peak × 2.6 is within 3% of the area of the 718 peak and thus establishes the validity of the method.

G.l.p.c. analysis of a typical run with nortricyclanol and the nortricyclyl halides showed 10–15 peaks of retention times in the region of authentic samples of *syn*- and *anti*-2,7-norbornandiol. In one run carried out in deuterated medium the diol fraction was converted to the corresponding diacetates with acetic anhydride in pyridine. N.m.r. and mass spectral studies and g.l.p.c. retention time data on a 10 ft × 1/8 in. 10% Carbowax on Chromosorb W column established through the diacetates that the *syn*-7-, *anti*-7-, *exo*-5-, and *endo*-5-*exo*-2-norbornandiols are products. No attempt was made to identify all the components of higher retention time.

The data in Table 1 shows that acid (entries 10, 13–17) and a temperature >200° (entries 5

TABLE 1. Data for solvolysis of nortricyclyl and norbornenyl substrates

		Conditions*			Relative % yields						% Yield†			D/molecule‡		
Substrate	Entry	Solvent	Temperature (°C)	Time	3 + 4	5	6	1*c*	Diols	Other	3 + 4	5	6	3 + 4	5	6
1*a*	1	H^+		4h	t	t	90			10			32			3.2
1*b*	2	H^+		10 min	1	1	2	3	90	3						
	3	H^+		60 min	2	4	80	1	8	5						
	4	D^+		1.3 h	1	2	85	1	5	6						3.6
	5	H_2O	250	1.5 h	t	t	90	—	5	5			38			
	6	H^+	165	1.5 h	—	—	—	5	—	95						
	7	D^+		4 h	—	—	93	—	—	7			30			3.7
1*c*	8	H^+		10 min	1	1	2	45	45	6			40			
	9	H^+		60 min	1	1	2	—	90	5						
	10	H^+		4 h	15§	20	45	—	20	t						
	11	D^+	300	1.5 h									35	2.4	2.2	2.0
	12	D^+		9.5 h	15	23	52	—	8	2	9	15	33	2.2	2.0	1.7
	13	H_2O	250	1.5 h				100								
2*a* + 2*b*	14	H^+		1.5 h	10	15	24	11	13	27						
	15	H_2O	250	1.5 h	—	—	—	11	—	89						
7	16	H^+		1.5 h	3	5	16	t	70	6						
	17	H_2O	250	1.5 h	—	—	—	—	—	100						

*H^+ = 10% v/v HOAc–H_2O at 250°; D^+ = 10% v/v DOAc–D_2O at 250°.
†Preparative g.l.p.c. was used to determine the yields. Each value is corrected for collection losses.
‡Greater than 90% of the enolizable deuterium was washed out.
§A composite of 15% **3**, 84% **4**, and 1% of an unknown.

and 6) is required for the reaction. That is, nortricyclanol, *exo*-2-, *endo*-2-, and *anti*-7-norbornenols are stable in water at 250°. When the reaction is carried out in 10% v/v HOAc–H_2O at temperatures below 200° the conversion to the aldehydes and norcamphor does not occur detectably. Nortricyclyl bromide and nortricyclyl chloride are converted to **3**, **4**, **5**, and **6** in H_2O because HBr and HCl are generated during solvolysis. As shown by entries 1, 5, 10, and control experiments, the aldehydes are unstable in the presence of HCl and HBr and this accounts for the apparent formation of norcamphor only in reactions where HBr and HCl are generated. In the absence of the acids HCl and HBr the aldehydes are reasonably stable in 10% v/v HOAc–H_2O (entries 10 and 12) and are isolated from the nortricyclanol reaction in 20–25% yield. Entries 2, 8, and 9 show that 1*a*,·*b*, and *c* initially yield diols which together with norbornenols are then converted to **3**, **4**, **5**, and **6**. Scheme 1 represents various possible reaction pathways for the formation of the aldehydes and norcamphor. Further work must be done on hydroxy-cation intermediates to elucidate the exact details of the various pathways. The aldehydes and especially **6** therefore act as sinks for appropriately substituted norbornyl systems. Conceivably any appropriately substituted bicyclic system which contains seven ring-carbon atoms and which yields hydroxy-cations on solvolysis or protonation is convertible to the sink-compounds. For example, Crandall (8) has observed the conversion of *exo*-2,3-epoxybicyclo[2.2.1]heptane to 1*c*, **5**, and **6** on a g.l.p.c. column at 200°.

The conversion of 1*c* to **3** + **4** and **5** is one of a relatively small group of reactions involving the formal cleavage of bicyclo[2.2.1]heptyl system. This process provides a unique synthetic route to **3** + **4** and **5** and other unsaturated monocyclic systems (10*a–j*). For example, Jones and Jones (10*g*) have observed the conversion of *anti*-2,2,4,6-tetramethylbicyclo[2.2.1]hept-5-en-7-ol to a mixture of 1,3,5,5-tetramethyl-1-formylcyclohex-4- and -5-ene in refluxing aqueous acetic acid with a trace of H_2SO_4, and Arbusow (10*a*) has shown that treatment of pinene oxide with anhydrous $ZnBr_2$ yields the 3-(2,2,3-trimethylcyclopentene)acetaldehyde.

The solvolysis of suitably alkylated norbornenols, nortricyclanols, norbornene oxides or other bicyclic systems under the conditions described herein is an alternative synthetic method for the preparation of substituted norcamphors and aldehydes.

Can. J. Chem. Downloaded from www.nrcresearchpress.com by 210.87.254.5 on 09/05/12
For personal use only.

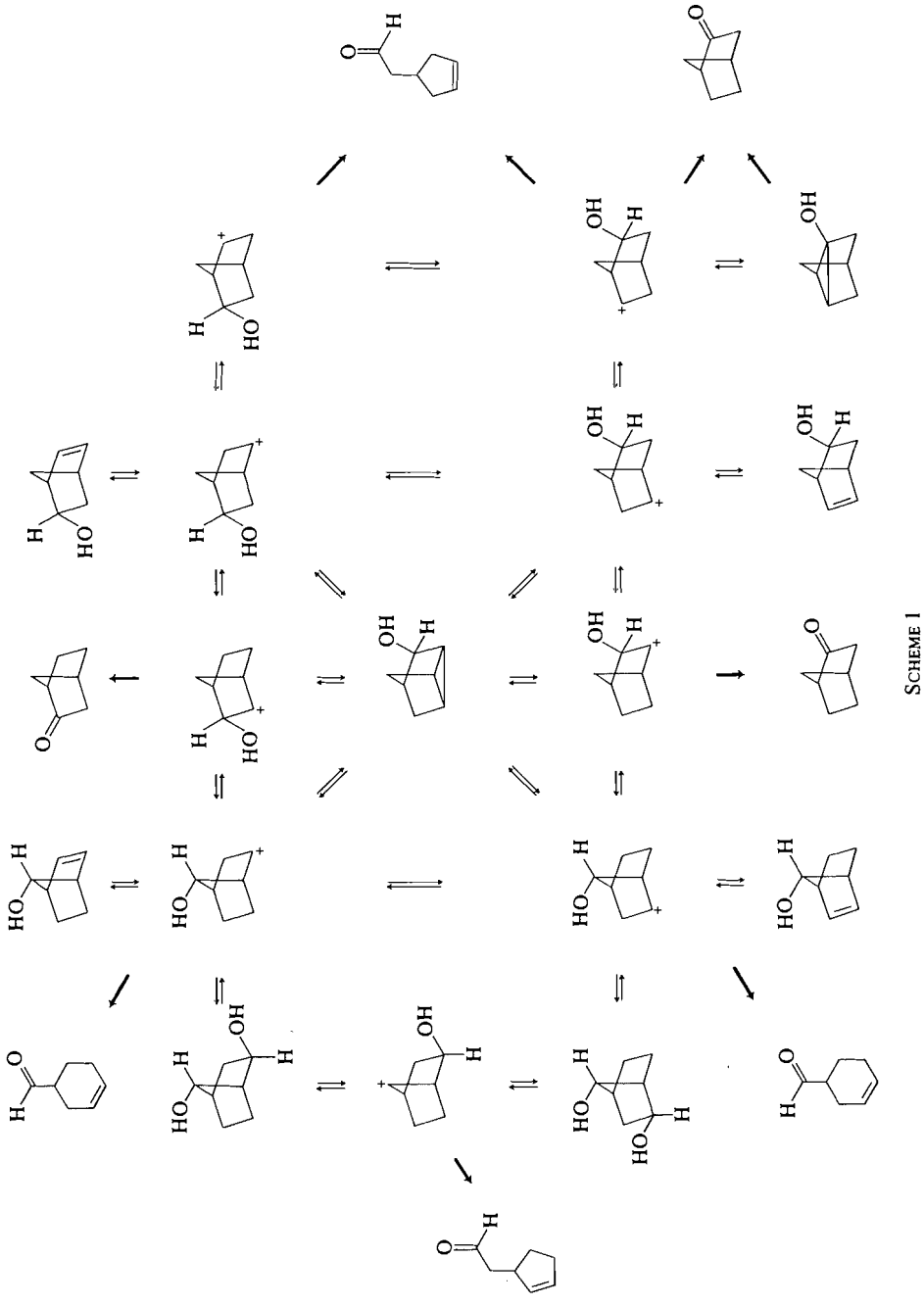

SCHEME 1

Can. J. Chem. Downloaded from www.nrcresearchpress.com by 210.87.254.5 on 09/05/12
For personal use only.

TABLE 2. Deuterium distribution in norcamphor

Substrate	Fraction of one deuterium at *†							
	C-1	C-4	C-5x‡	C-5n	C-6x	C-6n	C-7a	C-7s
1*a*	0.40	0.35	0.50	0.50	0.30	0.40	0.30	0.30
1*b*	0.40	0.30	0.55	0.55	0.55	0.50	0.25	0.60
1*c*	0.20	0.10	0.35	0.45	0.15	0.20	0.15	0.20
2*b*	0.35	0.20	0.20	0.45	0.30	0.45	0.25	0.25
7	0.35	0.30	0.35	0.40	0.25	0.35	0.25	0.50
10*a*	0.20	0.15	0.20	0.25	0.25	0.20	0.15	0.20
11	0.30	0.25	0.35	0.35	0.20	0.25	0.20	0.25

*Rounded to 0.05 of one deuterium.
†C-3-*exo*- and C-3-*endo* are omitted because deuterium is incorporated via acid-catalyzed enolization (usually 1.7 D).
‡x = exo, n = endo, a = anti, s = syn.

Deuterium is incorporated in the aldehydes and norcamphor when **1***a*, *b*, and *c*, **2***b*, **7**, **10***a*, and **11** are solvolyzed in deuterated medium. Mass spectral deuterium analysis of **6** (a composite of up to d_8 species) obtained from **1***a* and *b* and the aldehydes and norcamphor (a composite in each case of up to d_6 species) obtained from **1***c* showed that the amount of deuterium incorporated depends on the acidity of the medium (entries 1, 4, 7, 11, 12). Control experiments in deuterated medium (DOAc–D_2O) show that (*a*) deuterium is not incorporated into the aldehydes **3** + **4** and **5** after they are formed, (*b*) isomerization of the double bond in **3** + **4** and **5** does not occur, and (*c*) deuterium is not incorporated into norcamphor via acid-catalyzed homoenolization (9) or some other pathway which involves HOAc–$^-$OAc. Our attempts to homoenolize camphenilone (**12**) in presence of CF_3COOD at 250° failed.

That protium–deuterium exchange occurs via protonation–deprotonation pathways (Scheme 1) is supported by the fact that deuterium is incorporated into unreacted nortricyclanol and the *syn*- and *anti*-7-*exo*- and *endo*-5-*exo*-2-norbornanediols.

In each case the deuterated norcamphor obtained from the solvolysis of **1***a*, *b*, and *c*, **2***b*, **7**, **10**, and **11** was reduced to *endo*-norborneol and the distribution of deuterium was determined by area integration analysis in the presence of $Eu(DPM)_3$(11, 12). The data are listed in Table 2. Whereas an unsubstituted norbornyl cation undergoes complete exchange under these reaction conditions (13) a hydroxy-cation fragments into the sink-compounds before complete exchange can occur.

Experimental

General

Analytical and preparative g.l.p.c. analyses were performed on Varian Model 204 B and 90 P-3 gas chromatographs with helium as the carrier gas. N.m.r. spectra were obtained in CCl_4 on Varian A-60 and HA-100 instruments with tetramethylsilane as internal standard. Mass spectra were obtained on a Hitachi–Perkin–Elmer RMU-6A spectrometer at 80 and 11 eV. Relative percent yields were obtained by tracing, cutting out, and weighing peaks. Collection losses during preparative g.l.p.c. for the aldehydes **3** and **4**, **5**, and for norcamphor (6) were determined by injecting aliquots of known concentration and determining the collection efficiency. In most experiments the isolated and corrected yields are given. Pentane was stirred over 30% fuming sulfuric acid, washed with bicarbonate solution, dried, and distilled. Pyridine was distilled from barium oxide. All solutions were dried over anhydrous $MgSO_4$ or Na_2SO_4. Nortricyclyl bromide was purchased from Frinton Laboratories, Vineland, New Jersey. Norcamphor, 3-(cyclohexene)-carboxyaldehyde, and 2-(cyclopentene)acetic acid were obtained from Aldrich Chemical Co., Milwaukee.

Acetic Acid-O-d

Acetic acid-O-*d* was prepared by heating equimolar quantities of acetic anhydride (freshly distilled) and deuterium oxide (99.8% d_2) for 12 h on the steam-bath in a flask protected from atmospheric water with a drying tube.

Nortricyclanol

Nortricyclanol, m.p. 107–110° (lit. (14) 108–110°) was prepared from norbornadiene by the procedure of Meinwald *et al.* (14).

Nortricyclyl Chloride

Nortricyclyl chloride, b.p. 48–50° (10 mm) was prepared by the chlorination of norbornene as described by Roberts *et al.* (5*b*).

Solvolysis of Nortricyclanol

Nortricyclanol (15.5 g, 0.14 mol, m.p. 107–110°) and 10% v/v CH_3COOH–H_2O (40 ml) were introduced to a thick-walled glass tube. The solution was degassed three times, the tube was sealed and then heated for 4 h at 250° in a Carius oven. The reaction mixture was neutralized with solid sodium bicarbonate, saturated with NaCl, and extracted

Can. J. Chem. Downloaded from www.nrcresearchpress.com by 210.87.254.5 on 09/05/12
For personal use only.

Can. J. Chem. Downloaded from www.nrcresearchpress.com by 210.87.254.5 on 09/05/12
For personal use only.

with ether (8 × 40 ml). The ether extract was dried and the solvent was removed on the rotatory evaporator to give a viscous mass. Analytical g.l.p.c. on a 5 ft × 1/8 in. 5% SE-30 on Chromosorb W column (165°) showed that the mixture was composed of 40% diols, 50% **3** + **4**, **5**, and **6**, and 10% of products of intermediate retention time. The viscous mass was washed with pentane (4 × 20 ml). G.l.p.c. analysis showed that the aldehydes and norcamphor were extracted preferentially and the viscous material which remained solidified on standing. The aldehydes **3** + **4**, **5**, and norcamphor (**6**) were isolated by preparative g.l.p.c. on a 15 ft × 3/8 in. 15% Carbowax on Chromosorb W column (150°). After six injections, the temperature of the oven was increased to 215–220°, to clean the column of the diols which interfered with the collection of **3** + **4**, **5**, and **6**. **3** + **4**; i.r. (CCl_4), 3052 (C=C^H), 2710 (H—C^{=O}), 1612 (C=C), and 666 cm^{-1} (C=C^H); n.m.r. (CCl_4), δ 9.70 (multiplet, 1H, H—C^{=O}), 5.67 (multiplet, 2H, H_{C=C}H), 2.8–1.8 (multiplet, 7H); m.s., 80 eV, M^+ at *m/e* 110 corresponds to $C_7H_{10}O$. 2,4-DNP; m.p. 120.5–122.5° after two recrystallizations from aqueous ethanol.

Anal. Calcd. for $C_{13}H_{14}N_4O_4$: C, 53.79; H, 4.86; N, 19.30. Found: C, 53.61; H, 4.83; N, 19.29.

Compound **5**; i.r., (CCl_4), 3024 (C=C^H), 2700 (H—C^{=O}), 1730 (C=O), 1655 (C=C), 660 cm^{-1} (C=C^H); n.m.r. (CCl_4), δ 9.55 (s, 1H, H—C^{=O}), 5.68 (multiplet, 2H, H_{C=C}H), 2.2–1.8 (multiplet, 7H). The i.r. and n.m.r. were identical to those obtained for an authentic sample of 3-(cyclohexene)carboxaldehyde. M.s., 80 eV, showed M^+ at *m/e* 110 corresponding to $C_7H_{10}O$. **6**; m.p. 89–91° (lit. (8) 90–91°); m.p. of 2,4-DNP 129–131° (lit. (5*b*) 130–131.5°); n.m.r. (CCl_4), δ 2.70 (multiplet, 1H, C-1 bridgehead), 2.50 (multiplet, 1H, C-4 bridgehead), 2.1–1.5 (multiplet, 8H) was identical to that of an authentic sample; M.s., 80 eV, M^+ at *m/e* 110 corresponding to $C_7H_{10}O$.

No attempt was made to isolate the diol fractions.

Solvolysis of Nortricyclanol in Deuterated Medium

Nortricyclanol (12.1 g, 0.11 mol, m.p. 107–110°) and 10% v/v CH_3COOD–D_2O (35 ml) were introduced into a heavy walled glass tube. The solution was degassed three times, sealed under vacuum, and heated in a Carius oven for 9.5 h at 250°. The dark brown mixture was neutralized with solid sodium bicarbonate, saturated with NaCl, extracted with pentane (10 × 50 ml), and then ether (5 × 50 ml). Gas chromatography of the pentane extract on a 10 ft × 1/8 in. 10% Carbowax on Chromosorb W column (180°) showed that **3** + **4**, **5**, and **6** were extracted preferentially. In addition five minor components (5%) of retention time near **6** and ten components (10%) of retention time in the diol region were present. Gas chromatographic analyses of the ether extract on the same column showed ten components (90%) in the diol region, **3** + **4**, **5**, and **6** and five components in the region of **6** (total (10%). The pentane and ether extracts were decolorized with Norit, dried, and concentrated by distillation through a 12 in. Vigreux column. The concentrated pentane and ether extracts were transferred quantitatively into 10 ml and 5 ml volumetrics respectively, and made up to volume.

Injection of several aliquots (0.05 ml) of the pentane and ether extracts through the 15 ft × 3/8 in. 15% Carbowax on Chromosorb W column (180°) established the yields of the acetaldehydes (**3** + **4**), 3-(cyclohexene) carboxaldehyde (**5**), and norcamphor (**6**) as 0.6 (5%), 1.1 (9%), and 3.2 g (27%) respectively. Correction for collection losses established the actual yields as 1.1 (9%) of **3** + **4**, 1.8 (15%) of **5**, and 4.0 g (33%) of **6**. No attempt was made to isolate materials of longer retention time. However, comparison of retention time data on a 10 ft × 1/8 in. 10% Carbowax on Chromosorb W column with authentic samples of *syn*- and *anti*-7-*exo*-2-norbornandiols indicated that the major components of the ether extract are the 2,7-norbornanediols.

The enolizable deuterium in **3** + **4** and **5** was washed out by three injections of each material through a 5% KOH column (150–170°) as described in the norcamphor homoenolization experiment. The deuterated norcamphor (0.16 g) isolated from the pentane extract (sodium bisulfite extraction was used to remove the aldehydes) was washed three times at 25 ± 3° for 24 h with 4–6 ml portions of a solution made up of methanol (20 ml), water (10 ml), and KOH (1.0 g). Each wash solution was worked-up by the addition of water (5 ml) and extraction with pentane (1 × 10, 4 × 5 ml). In each case the pentane extract was concentrated by distillation through a 2 ft Vigreux column and the norcamphor was isolated by preparative g.l.p.c.

Deuterium assay mass spectrometrically at 11 eV on the samples from which the enolizable deuterium was washed out, established that (*a*) **3** + **4** was composed of 2.5 d_5, 9.5 d_4, 23.5 d_3, 34.7 d_2, 24.7 d_1, and 4.2% d_0 species (2.16 atoms of deuterium); (*b*) **5** was composed of 3.0 d_5, 8.6 d_4, 18.8 d_3, 31.1 d_2, 32.7 d_1, and 4.9% d_0 species (2.00 atoms of deuterium), and (*c*) **6** was composed of 6.9 d_4, 15.6 d_3, 28.2 d_2, 39.0 d_1, and 7.6% d_0 species (1.70 atoms of deuterium).

To determine the location of the deuterium, the deuterio-*endo*-norborneol (0.020 g, 1.70×10^{-4} mol), obtained from lithium aluminum hydride in ether reduction of the norcamphor was subjected to n.m.r. area integral analysis in the presence of $Eu(DPM)_3$ (0.080 g, 1.13×10^{-4} mol) in CCl_4 (11, 12). The analysis established the following deuterium distribution; 0.20 at C-1, 0.10 at C-4, 0.30 at C-5-*exo*, 0.45 at C-5-*endo*, 0.15 at C-6-*exo*, 0.20 at C-6-*endo*, 0.20 at C-7-*syn*, and 0.15 at C-7-*anti* (1.75 atoms of deuterium).

To Check Deuterium Content in Nortricyclanol and Norbornanediols

Nortricyclanol (2.3 g, 0.021 mol, m.p. 107–110°), 10% v/v DOAc–D_2O (18 ml) were introduced into a thick walled tube and sealed under vacuum after degassing three times. The tube was heated in the Carius oven at 250° for 30 min, the reaction mixture was neutralized with solid $NaHCO_3$, and extracted with pentane (3 × 20 ml) and ether (3 × 20 ml). Analytical g.l.p.c. on a 10 ft × 1/8 in. 10% Carbowax on Chromosorb W column (temperature programming 165–220°) showed that the pentane extract was composed primarily (80%) of the aldehydes **3** + **4** and **5**, norcamphor, and nortricyclanol, four unidentified components (10%), and 10% of diols. Gas chromatographic analysis of the ether extract on the same column showed predominantly diols

Can. J. Chem. Downloaded from www.nrcresearchpress.com by 210.87.254.5 on 09/05/12
For personal use only.

(90%) as well as the aldehydes **3** + **4**, and **5**, norcamphor, nortricyclanol, and three minor unidentified peaks (10%). The nortricyclanol was isolated by preparative g.l.p.c. from the concentrated pentane fraction and mass spectrometric deuterium assay showed 1.2 d_4, 2.2 d_3, 13.8 d_2, 67.8 d_1, and 15.0% d_0 species, a total of 1.02 atoms of deuterium per molecule.

The ether extract was concentrated by distillation to yield a two phase liquid and solid mixture. The liquid phase was decanted and to the remaining solid was added pyridine (5 ml) and acetic anhydride (4 ml). The solution was stirred at 25 ± 3° for 24 h and poured onto crushed ice (15 g). After the ice melted the solution was diluted to 65 ml with water and extracted with ether (4 × 15 ml). The ether extract was washed with 3% aqueous HCl (3 × 15 ml), water (2 × 15 ml), and dried. Analytical g.l.p.c. on a 10 ft × 1/8 in. 10% Carbowax column (200°) showed four components (with increasing retention time) in the ratio of 1:1:1:2. Analytical g.l.p.c. of a mixture of *syn*-7-acetoxy-, *anti*-7-acetoxy-, *exo*-5-acetoxy-, *endo*-5-acetoxy-*exo*-2-norbornyl acetates obtained from Frinton Laboratories had identical retention times to the diacetates obtained from the nortricyclanol reaction and established that the diol portion of the nortricyclanol reaction was composed primarily of norbornanediols. The diacetate mixture was separated into three fractions by preparative g.l.p.c. on a 15 ft × 3/8 in. 15% Carbowax on Chromosorb W column. Peaks 3 and 4 separated by analytical g.l.p.c. were not resolved by preparative g.l.p.c. and were collected together. Deuterium assay mass spectrometrically at 11 eV using the $M^+ - 43$ ($CH_3-\overset{\overset{O}{\|}}{C}<$) peaks because the molecular ion intensity was low gave the following data: Peak 1; 14.4 d_2, 80.9 d_1, and 4.7% d_0 species; 1.10 d per molecule; n.m.r. (CCl_4), δ 4.58 (doublet with fine structure, 1H, H—$\overset{|}{C}$—OAc), 4.20 (multiplet, 1H, H—$\overset{|}{C}$—OAc), 2.48 (multiplet, 1H, bridgehead C—H), 2.20 (multiplet, 1H, bridgehead C—H), 1.96 (singlet, 6H, $CH_3—\overset{\overset{O}{\|}}{C}—O—$), 1.90–0.90 (norbornyl envelope). Peak 2; 11.4 d_2, 85.9 d_1, and 2.7% d_0; 1.09 d per molecule; n.m.r. (CCl_4), δ 4.75 (multiplet, 1H, H—$\overset{|}{C}$—OAc). 4.40 (multiplet, 1H, H—$\overset{|}{C}$—OAc), 2.25 (multiplet, 2H, bridgehead C—H), 1.96 (singlet, 6H, $CH_3—\overset{\overset{O}{\|}}{C}—$), 1.90–0.90 (norbornyl envelope). Peak 3; 16.8 d_2, 77.4 d_1, and 5.8% d_0; 1.11 d per molecule; n.m.r., (CCl_4), δ 4.45 (multiplet, 2H, H—$\overset{|}{C}$—OAc), 2.18 (multiplet, 2H, bridgehead C—H), 1.96 (singlet, 6H, $CH_3—\overset{\overset{O}{\|}}{C}—O—$), 1.90–0.90 (norbornyl envelope).

Solvolysis of syn-7-Hydroxy-exo-2-Norborneol in Deuterated Medium

syn-7-Hydroxy-*exo*-2-norborneol (0.34 g) was heated with 10% v/v DOAc–D_2O (6 ml) in a sealed tube for 9.5 h at 250°. Work-up in the usual manner and analytical g.l.p.c. analysis of the ether extract on a 10 ft × 1/8 in. 10% Carbowax on Chromosorb W column (110°) showed **3** + **4** (18%), **5** (21%), and **6** (59%) as well as 2% of three other components. The deuterated norcamphor (0.040 g, 15%) (corrected yield 40%) was isolated by preparative g.l.p.c. on a 15 ft × 3/8 in. 5% KOH + 15% Carbowax on Chromosorb W column. The norcamphor was recollected by preparative g.l.p.c. and reduced with lithium aluminum hydride in ether. N.m.r.–Eu(DPM)$_3$ analysis of the deuterated *endo*-norborneol showed (rounded to 0.05 d) 0.20 d at C-1, 0.15 d at C-4, 0.20 d at C-5-*exo*, 0.25 d at C-5-*endo*, 0.25 d at C-6-*exo*, 0.20 d at C-6-*endo*, 0.15 d at C-7-*anti*, and 0.20 d at C-7-*syn*.

Solvolysis of anti-7-Norbornenol in Deuterated Medium

anti-7-Norbornenol (0.32 g) was heated at 250° with 10% v/v DOAc–D_2O (6 ml) for 9.5 h and worked-up in the usual manner. Analytical g.l.p.c. analysis showed **3** + **4** (3%), **5** (14%), and **6** (71%) as well as 12% of four other components. The deuterated norcamphor was isolated by preparative g.l.p.c. (0.072 g, 23%) (corrected yield 63%) and reduced with lithium aluminum hydride. N.m.r.–Eu(DPM)$_3$ analysis established a deuterium distribution of 0.35 at C-1, 0.30 at C-4, 0.35 at C-5-*exo*, 0.40 at C-5-*endo*, 0.25 at C-5-*exo*, 0.35 at C-6-*endo*, 0.50 at C-7-*syn*, and 0.25 at C-7-*anti*.

Solvolysis of endo-5-Norbornenol in Deuterated Medium

endo-5-Norbornenol (0.45 g) was heated in 10% v/v DOAc–D_2O (7 ml) as described previously. Work-up and g.l.p.c. analysis showed **3** + **4** (12%), **5** (15%), **6** (67%), and 6% of five other components. Preparative g.l.p.c. isolation gave 0.090 g of deuterionorcamphor (19%) (corrected yield 52%). Eu(DPM)$_3$ analysis of the *endo*-norborneol obtained by lithium aluminum hydride reduction established the deuterium distribution of 0.35 d at C-1, 0.20 at C-4, 0.20 at C-5-*exo*, 0.45 at C-5-*endo*, 0.30 at C-6-*exo*, 0.45 at C-6-*endo*, 0.25 at C-7-*anti*, and 0.25 at C-7-*syn*.

Solvolysis of exo-2,3-Epoxybicyclo[2.2.1]heptane in Deuterated Medium

exo-2,3-Epoxybicyclo[2.2.1]heptane (0.6 g, 5.5×10^{-3} mol) was heated in 10% v/v DOAc–D_2O (7 ml) as described previously. Work-up and g.l.p.c. analysis showed **3** + **4** (3%), **5** (10%), and **6** (69%) as well as 18% of three other components. Preparative g.l.p.c. analysis established an isolable yield of 0.22 g (36%) and a corrected yield of 62% for the deuterio norcamphor. The enolizable deuterium in the norcamphor was washed out with three washings of the KOH–MeOH–H_2O solution. The *endo*-norborneol obtained by lithium aluminum hydride reduction was subjected to Eu(DPM)$_3$ analysis which established a distribution of 0.30 d at C-1, 0.25 at C-4, 0.35 at C-5-*exo*, 0.35 at C-5-*endo*, 0.25 at C-6-*exo*, 0.30 at C-6-*endo*, 0.25 at C-7-*syn*, and 0.20 at C-7-*anti*.

$LiAlH_4$ Reduction of (Cyclopentene)acetaldehydes from Nortricyclanol Reaction

The mixture of aldehydes **3** + **4** (0.13 g, 1.2×10^{-3} mol) isolated by preparative g.l.p.c. as described previously was dissolved in ether (70 ml) and reduced with lithium aluminum hydride (0.023 g, 0.6×10^{-3} mol). After a 3 h reflux, 10% NaOH (0.5 ml) and water (0.2 ml) were added dropwise carefully to the cooled reaction flask. The gelatinous precipitate was filtered off and the ethereal filtrate was washed with

Can. J. Chem. Downloaded from www.nrcresearchpress.com by 210.87.254.5 on 09/05/12
For personal use only.

saturated sodium bicarbonate (2 × 5 ml), water (1 × 5 ml), saturated aqueous sodium chloride, and dried. The mixture of (cyclopentene)ethanols (0.071 g, 57%) >99% pure as shown by analytical g.l.p.c. was isolated by preparative g.l.p.c. on a 15 ft × 3/8 in. 15% Carbowax column (170°).

Preparation of (Cyclopentene)ethanol Nosylates

The mixture of (cyclopentene)ethanols (0.071 g, 0.63×10^{-3} mol) was dissolved in dry pyridine (2.5 ml) and the solution was cooled in an ice–salt bath for 30 min. To the cold magnetically stirred solution was added freshly recrystallized (petroleum ether, b.p. 60–100°) *p*-nitro-benzenesulfonyl chloride (0.14 g, 0.64×10^{-3} mol). After stirring for 45 min at 0 to −10° the reaction mixture was poured into a solution made up of 20 ml of ice-water and 3.5 ml concentrated hydrochloric acid. The solid was collected on a sintered glass disc and washed with ice-cold 3% aqueous hydrochloric acid and several 10 ml portions of water and dried under vacuum at room temperature. The nosylate (0.13 g, 71%) had a m.p. of 64–67° (lit. (3) 65–67°).

Preparation of 2- and 3-(Cyclopentene)acetaldehydes. The CAN Oxidation of exo-Norborneol

exo-Norborneol (5.0 g, 44.6×10^{-3} mol) was oxidized with ceric ammonium nitrate (48.9 g, 89.2×10^{-3} mol) according to the procedure of Trahanovsky *et al.* (7). After 30 min at 50° the reaction mixture was cooled, water was added (150 ml) and extracted with pentane (3 × 100 ml). The pentane extract was washed with saturated aqueous sodium bicarbonate (2 × 50 ml), water (2 × 50 ml), saturated aqueous sodium chloride (2 × 50 ml), and dried. Analytical g.l.p.c. analysis on a 10 ft × 1/8 in. 10% Carbowax on Chromosorb W column (165°) showed that the aldehydes comprised 90% of the products. Control experiments showed that pentane extraction separated the aldehydes from the nitro-compound also produced in oxidation. The pentane was removed on the rotary evaporation to give 3.0 g of crude product which was dissolved in ether (60 ml) and added slowly to a stirred solution of lithium aluminum hydride (0.55 g) in ether (200 ml). Work-up gave 2.8 g of crude (cyclopentene)ethanols from which 0.28 g of a 2- and 3-(cyclopentene)ethanol mixture was isolated by preparative g.l.p.c. on a 15 ft × 3/8 in. 15% Carbowax column (170°).

The mixture of (cyclopentene)ethanols (0.28 g) was converted to the mixture of nosylates (0.62 g, m.p. 66–68°) as described previously.

Acetolysis of (Cyclopentene)ethanol Nosylates

The nosylate mixture (0.23 g) was dissolved in anhydrous acetic acid (13 ml) which contained anhydrous sodium acetate (0.065 g). After heating at 100 ± 2° for 13 h, work-up of the reaction mixture gave a pentane solution of acetates. Removal of the pentane gave 0.11 g of an oil. Analytical g.l.p.c. (tracing and weighing peaks) on a 10 ft × 1/8 in. 10% Carbowax column (125°) showed 58% of *exo*-norbornyl acetate and 42% of 2-(cyclopentene)ethyl acetate after comparison of retention times to those of authentic samples.

Acetolysis of Mixture of Nosylates Prepared from Aldehydes Obtained from Nortricyclanol Reaction

The mixture of nosylates (0.073 g, 0.24×10^{-3} mol) obtained previously was dissolved in anhydrous acetic acid (6 ml) containing 0.021 g of anhydrous sodium acetate and the solution was heated for 13 h at 100 ± 2°. Work-up gave a pentane solution of acetates. Removal of the pentane gave 0.034 g (89%) of an oil which when analyzed under the conditions employed previously showed 85% of norbornyl acetate, 14% of 2-(cyclopentene)ethyl acetate, and 1% of an unknown acetate.

Lithium Aluminum Hydride Reduction of 2-(Cyclopentene)acetic Acid

2-(Cyclopentene)acetic acid (8.2 g, 0.065 mol) in ether (50 ml) was added dropwise to a solution of lithium aluminum hydride (2.0 g, 0.052 mol) in ether (150 ml) and then refluxed for 12 h. Work-up as described previously, yielded 2-(cyclopentene)ethanol (7.3 g, 95%).

Silver Carbonate on Celite Oxidation of 2-(Cyclopentene)ethanol

A ten-fold excess of silver carbonate on celite (38 g, 66.2×10^{-3} mol) prepared by the method of Fetizon and coworkers (15) was suspended in benzene (250 ml) and refluxed, collecting any residual water with a Dean–Stark apparatus. After all the water was removed, 2-(cyclopentene)ethanol (0.74 g, 6.62×10^{-3} mol) in benzene (75 ml) was added dropwise. After refluxing for an additional 16 h, the hot reaction mixture was filtered through a fine porosity fritted funnel which contained a thin layer of purified celite. The filtrate was concentrated on the rotary evaporator and the 2-(cyclopentene)acetaldehyde (0.60 g, 32%) was collected by preparative g.l.p.c. on a 15 ft × 3/8 in. 15% Carbowax column (155°). 2,4-DNP; m.p. 98–99.5° after three recrystallizations from methanol (lit. (16) 98–99°; (10*d*) 100–101°).

Infrared Fingerprint Region Assay of 2- and 3-(Cyclopentene)acetaldehyde Mixtures

The i.r. fingerprint region (CS_2) of the **3** + **4** mixtures obtained from CAN oxidation of *exo*-norborneol and solvolysis of nortricyclanol showed a peak at 910 and an unresolved broad doublet with maxima at 718 and 666 cm^{-1}. The i.r. fingerprint region of **3** prepared by Ag_2CO_3 oxidation of 2-(cyclopentene)ethanol showed bands at 910 and 718. Analysis (tracing, cutting, and weighing) showed that the 910 peak was 16 and 6% of the area of the 718–666 doublet for the aldehyde mixtures obtained from the CAN oxidation and the nortricyclanol reactions, respectively. Therefore, to obtain the amount of **3** in a mixture of **3** + **4** to within ±2–3%, the 910 peak area percentage is multiplied by 2.6 (16 × 2.6 = 41.6; 6 × 2.6 = 15.6). Application of the analysis to pure **3** showed that the 910 peak area × 2.6 was within 2% of the 718 peak area, establishing the validity of the method.

Solvolysis of Nortricyclyl Halides

Nortricyclyl chloride (0.88 g, 6.8×10^{-3} mol) and water (20 ml) were introduced into a clean heavy-walled glass tube. The solution was degassed three times, sealed under vacuum, and heated in a Carius oven for 1.5 h at 250°. The dark reaction mixture was neutralized with sodium bicarbonate, saturated with sodium chloride, and extracted with ether (4 × 20 ml). The extract was decolorized with Norit, dried, and concentrated by distillation through a 12 in. Vigreux column and made up to volume in a 2 ml volumetric flask. Injection and collection of aliquots (0.1 ml) on the 15 ft × 3/8 in. 15% Carbowax on Chromosorb W column (155°) established that the isolable and corrected yields of

Can. J. Chem. Downloaded from www.nrcresearchpress.com by 210.87.254.5 on 09/05/12
For personal use only.

norcamphor were 29 and 38% respectively. Only minor amounts <5% of the aldehydes and diols (7 components) could be detected by analytical g.l.p.c. on a 10 ft × 1/8 in. 10% Carbowax on Chromosorb W column (temperature programming 165–220°).

Deuterated Medium

Solvolysis of nortricyclyl chloride (2.4 g, 18.7×10^{-3} mol) in 10% v/v CH_3COOD–D_2O (15 ml) for 4 h at 250° and work-up gave 0.3 g (15%) of deuterated norcamphor. Correction for collection losses (preparative g.l.p.c.) established the actual yield at 30%. The enolizable deuterium was removed by three washings with a methanol–water–KOH solution. Mass spectrometric deuterium assay established the norcamphor as a composite of 3.9 d_8, 9.4 d_7, 12.5 d_6, 13.5 d_5, 13.9 d_4, 15.5 d_3, 15.2 d_2, 13.0 d_1, and 3.1% d_0 species (3.70 atoms of deuterium).

To determine the location of the deuterium, the deuterated *endo*-norborneol (0.020 g, 1.70×10^{-4} mol), obtained from the lithium aluminum hydride in ether reduction of deuterated norcamphor (after the enolizable deuterium was washed out), was subjected to n.m.r., integral analysis in the presence of $Eu(DPM)_3$ (0.85 g, 1.21×10^{-4} mol) in CCl_4 (11, 12). The analysis established the following deuterium distribution; 0.40 *d* C-1, 0.30 *d* C-4, 0.55 *d* C-5-*exo*, 0.55 *d* C-5-*endo*, 0.55 *d* C-6-*exo*, 0.50 *d* C-6-*endo*, 0.60 *d* C-7-*syn*, and 0.25 *d* C-7-*anti* (3.70 atoms of deuterium per molecule).

Solvolysis of nortricyclyl bromide (1.8 g, 9.8×10^{-3} mol) in 10% v/v CH_3COOD–D_2O (15 ml) for 4 h at 250° and work-up gave 0.2 g (13%) of deuterated norcamphor after preparative g.l.p.c. (corrected yield 32%). After the enolizable deuterium was washed out, mass spectrometric deuterium assay established the following distribution, 2.6 d_8, 5.6 d_7, 7.8 d_6, 10.6 d_5, 13.6 d_4, 16.6 d_3, 18.9 d_2, 18.8 d_1, and 5.6% d_0 species (3.20 atoms of deuterium).

The position of deuterium was determined via the deuterated *endo*-norborneol (0.020 g, 1.70×10^{-4} mol) using the $Eu(DPM)_3$ (0.080 g, 1.13×10^{-4} mol. CCl_4 (11, 12)) method. The analysis established the following deuterium distribution; 0.40 *d* C-1, 0.35 *d* C-4, 0.50 *d* C-5-*exo*, 0.50 *d* C-5-*endo*, 0.30 *d* C-6-*exo*, 0.40 *d* C-6-*endo*, 0.30 *d* C-7-*syn*, and 0.30 *d* C-7-*anti* (3.20 atoms of deuterium per molecule).

Treatment of 3-(Cyclohexene)carboxaldehyde Under Solvolysis Conditions

3-(Cyclohexene)carboxaldehyde (0.46 g) and 10% v/v CH_3COOD–D_2O (11 ml) were sealed under vacuum in a thick-walled tube after degassing as described previously. The solution was heated in the oven for 1.5 h at 250° and worked-up in the usual manner. Gas chromatographic analysis on a 10 ft × 1/8 in. 10% Carbowax on Chromosorb W column (temperature programming 170–220°) showed by comparison with authentic samples that norcamphor and the (cyclopentene)acetaldehydes were not formed. Four minor components (<10%), one of retention lower than **5** and three of longer retention time were present. After the enolizable deuterium was washed out by three injections through the 5% KOH + 20% Carbowax on Chromosorb W column (160°), mass spectrometric analysis showed that no deuterium was incorporated into **5**.

Treatment of 3-(Cyclohexene)carboxaldehyde in 18% DOAc–D_2O; 1% HCl

The aldehyde **5** (0.48 g), 18% v/v DOAc–D_2O (15 ml), and concentrated hydrochloric acid (0.4 ml) were introduced into a sealed tube, degassed three times, and sealed under vacuum. The tube was heated at 250° for 1.5 h and worked-up as described previously. Gas chromatographic analysis on a 10 ft × 1/8 in. 10% Carbowax on Chromosorb W column (temperature program 180–230°) showed 12 components, and only a trace <2% of **5**. Norcamphor comprised approximately 15% of the mixture.

Treatment of 2-(Cyclopentene)acetaldehyde under Solvolysis Conditions

2-(Cyclopentene)acetaldehyde (0.58 g, 5.28×10^{-3} mol) and 10% v/v CH_3COOD–D_2O (12 ml) were sealed in a thick-walled glass tube. The tube was heated in a Carius oven for 1.5 h at 250° and worked-up in the usual manner. Gas chromatographic analysis on a 10 ft × 1/8 in. 10% Carbowax on Chromosorb W column showed that only starting material was present. After the enolizable deuterium was washed out by four injections through the 5% KOH + 20% Carbowax on Chromosorb W column (155°), mass spectrometric analysis showed that deuterium was not incorporated into **3**. I.r. analysis of the aldehyde showed that isomerization to **4** did not occur.

Check for Acid-catalyzed Homoenolization

Run 1

Norcamphor (0.5 g, 4.5×10^{-3} mol), 15% v/v DOAc–D_2O (10 ml), and concentrated HCl (0.37 ml) were introduced into a thick walled tube and sealed under vacuum after three degassings. The solution was heated at 260° for 1.5 h, worked-up in the usual manner, and made up to volume in a 4 ml volumetric flask. The norcamphor (42%) (corrected yield 73%) was isolated by preparative g.l.p.c. by injecting aliquots (0.1 ml) through the 5% KOH + 20% Carbowax column (150°). Deuterium assay mass spectrometrically after one, two, and three injections of the same sample gave the following results; one injection, 7.1 d_2, 58.4 d_1, 34.5% d_0; two injections, 1.8 d_2, 24.8 d_1, 73.4% d_0; three injections, 0.8 d_2, 4.4 d_1, 94.8% d_0 species. This established that deuterium is not incorporated into norcamphor via acid-catalyzed homoenolization and that the 5% KOH column removes at least 95% of the two enolizable deuterium from norcamphor after three injections.

Run 2

Camphenilone (0.19 g), 15% v/v DOAc–D_2O (10 ml), and concentrated HCl (0.13 ml) were introduced into a thick-walled glass tube and sealed under vacuum after degassing. The mixture was heated at 250° for 3 h and worked-up as described previously. Mass spectrometric deuterium assay on the camphenilone isolated by preparative g.l.p.c. on the 10 ft × 3/8 in. 5% KOH + 20% Carbowax column (145°) showed 98 d_0 and 2% d_1 species.

A duplicate of run 2 with camphenilone (0.18 g), 15% v/v DOAc–D_2O (10 ml), and concentrated HCl (0.11 ml) that was heated for 18 h at 275° was worked-up and analyzed by analytical g.l.p.c. (5 ft × 1/8 in. 5% SE-30 on chromosorb W column 110°). Less than 5% of the camphenilone remained. There were three major components (80%) of retention time shorter than camphenilone as well as four other minor components (20%).

Run 3

Two sealed tubes, one containing 0.21 g of camphenilone and 2 ml of 10% v/v CF_3COOD–D_2O and the other 0.28 g

in 2 ml of 10% v/v CF_3COOD–D_2O were prepared and heated at 205° for 17 and 120 h respectively. After work-up, deuterium assay on samples isolated by preparative g.l.p.c. on a 10 ft × 3/8 in. 10% Carbowax on Chromosorb W column (185°) showed that in both cases no deuterium had been incorporated into the camphenilone.

We thank the National Research Council of Canada for financial support.

1. J. D. ROBERTS, W. BENNETT, and R. ARMSTRONG. J. Am. Chem. Soc. **72**, 3329 (1950).
2. (*a*) S. WINSTEIN, H. M. WALBORSKY, and K. SCHREIBER. J. Am. Chem. Soc. **72**, 5795 (1950). (*b*) S. J. CRISTOL, T. C. MORRILL, and R. A. SANCHEZ. J. Am. Chem. Soc. **88**, 3087 (1966).
3. S. J. CRISTOL, W. K. SEIFERT, D. W. JOHNSON, and J. B. JURALE. J. Am. Chem. Soc. **84**, 3918 (1962).
4. H. KRIEGER. Ann. Acad. Sci. Fennicae Ser. A II, Chem. No. 109.
5. (*a*) L. SCHMERLING. U.S. Pat. 2 500 385; Chem. Abstr. **44**, 5391 (1950). (*b*) J. D. ROBERTS, F. O. JOHNSON, and R. A. CARBONI. J. Am. Chem. Soc. **76**, 5692 (1954).
6. Applications of spectroscopy to organic chemistry. *Edited by* J. C. D. Brand and G. Eglington. Oldbourne Press, London. 1965.
7. W. S. TRAHANOVSKY, P. J. FLASH, and L. M. SMITH. J. Am. Chem. Soc. **91**, 5068 (1969).
8. J. K. CRANDALL. J. Org. Chem. **29**, 2830 (1964).
9. A. NICKON, J. L. LAMBERT, S.J., R. O. WILLIAMS, and N. H. WERSTIUK. J. Am. Chem. Soc. **88**, 3354 (1966).
10. (*a*) B. ARBUSOW. Ber. **68**, 1430 (1935). (*b*) D. E. GWYNN and L. SKILLERN. Chem. Commun. **9**, 490 (1968). (*c*) C. A. GROB. Gass. Chem. Ital. **92**, 902 (1962). (*d*) L. H. ZALKOW and A. C. OEHLSCHLAGER. J. Am. Chem. Soc. **86**, 4208 (1964). (*e*) S. J. CRISTOL and R. K. BLY. J. Am. Chem. Soc. **82**, 6155 (1960). (*f*) J. M. COXON, E. DANSTED, M. P. HARTSHORN, and K. E. RICHARDS. Tetrahedron, **25**, 3307 (1969). (*g*) L. B. JONES and V. K. JONES. J. Org. Chem. **36**, 1017 (1971). (*h*) C. J. COLLINS, B. M. BENJAMIN, V. F. RAAEN, I. T. GLOVER, and M. D. ECKART. Liebigs. Ann. Chem. 739, 7 (1970). (*i*) J. M. COXON, M. P. HARTSHORN, and A. J. LEWIS. Aust. J. Chem. **24**, 1009 (1971). (*j*) N. H. WERSTIUK and T. KADAI. Chem. Commun. 1613 (1970).
11. C. C. HINCKLEY. J. Org. Chem. **35**, 2834 (1970); J. K. M. SANDERS and D. H. WILLIAM. Chem. Commun. 422 (1970).
12. N. H. WERSTIUK and T. KADAI. Unpublished results.
13. N. H. WERSTIUK and T. KADAI. Chem. Commun. 1349 (1971).
14. J. MEINWALD, J. CRANDALL, and W. E. HYMANS. Org. Syn. **45**, 74 (1965).
15. M. FETIZON et M. GOLFIER. C.R. de l'Academie des Sciences, Series C, 267 (1968); M. FETIZON, V. BALOGH, and M. GOLFIER. J. Org. Chem. **36**, 1339 (1971).
16. C. W. WHITEHEAD, J. J. TRAVERSO, H. R. SULLIVAN, and F. J. MARSHALL. J. Org. Chem. **26**, 2814 (1961).

Can. J. Chem. Downloaded from www.nrcresearchpress.com by 210.87.254.5 on 09/05/12
For personal use only.

Chemistry of Aminochromes. Part XV. The Reaction of Epinochrome with Thiols[1,2]

W. S. POWELL[3,4] AND R. A. HEACOCK[5]

Chemistry Department, Dalhousie University, Halifax, Nova Scotia and Atlantic Regional Laboratory, National Research Council of Canada, Halifax, Nova Scotia

Received April 14, 1972

Epinochrome (**5**) has been shown to react with thioglycollic acid to give mainly 5,6-dihydroxy-1-methylindoline and a 4-thiosubstituted 5,6-dihydroxy-1-methylindoline. The acetyl derivatives of these compounds (*i.e.* **7***b* and **15**), along with that of the corresponding 4-thiosubstituted 5,6-dihydroxyindole (*i.e.* **11**), were isolated after acetylation of the reaction mixture. The latter compound is probably a secondary product of the reaction, having arisen from the 4-thiosubstituted 5,6-dihydroxy-1-methylindoline which is formed initially.

On a montré que l'épinochrome (**5**) réagit avec l'acide thioglycolique pour conduire principalement au dihydroxy-5,6 méthyl-1 indoline et au dihydroxy-5,6 méthyl-1 indoline thiosubstitué en position 4. Les dérivés acétylés de ces composés (c'est-à-dire **7***b* et **15**) de même que ceux qui correspondent au dihydroxy-5,6 indole thiosubstitué en position 4 (par exemple **11**) ont été isolés après acétylation du mélange réactionnel. Le dernier composé est probablement un produit secondaire de la réaction provenant du dihydroxy-5,6 méthyl-1 indoline thiosubstitué en position 4 qui s'est initialement formé.

[Traduit par le journal]

Canadian Journal of Chemistry, **50**, 3360 (1972)

Aminochromes which are substituted in the 3-position by an alkoxyl or hydroxyl group react with thiols to give three types of products: (*i*) aminochrome/thiol addition products in which the thiol residue is attached to the 3*a*-position[6] of the indole nucleus (1, 2), (*ii*) 5,6-dihydroxyindoles (3, 4), and (*iii*) 4-thiosubstituted 5,6-dihydroxyindoles (5, 6). The aminochrome/thiol addition products were the major products formed, at least initially, when the reactions occurred in either neutral or slightly acidic solution, whereas the indolic products predominated at lower p*H*'s.

Very little work has been carried out, however, on the reactions of thiols with aminochromes which are unsubstituted in the 3-position. Bouchilloux and Kodja (7) reported that glutathione (GSH) reacted with dopachrome (**1**) (which they had eluted from a paper chromatogram of dopa oxidation products), to give three major products: 5,6-dihydroxyindole (**2***a*), 2-carboxy-5,6-dihydroxyindole (**2***b*), and a thiosubstituted 5,6-dihydroxyindole which they suggested had either the structure **3***a* or *b*. It was suggested the 5,6-dihydroxyindoles (**2***a* or *b*) were formed by the rearrangement of **1**. The thiosubstituted 5,6-dihydroxyindole was postulated to have arisen as a result of the addition of GSH to either the indolequinone **4***a* or *b* which could have been produced by the oxidation of the corresponding 5,6-dihydroxyindoles (**2***a* or *b*).

The reaction of epinochrome (**5**) with β-mercaptopropionic acid in aqueous solution at slightly acidic p*H*'s has recently been investi-

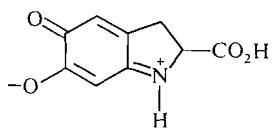

1

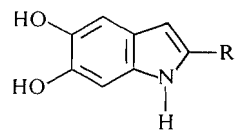

2

a R = H
b R = CO_2H

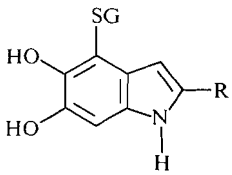

3

a R = H
b R = CO_2H

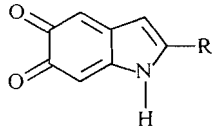

4

a R = H
b R = CO_2H

[1]For Part XIV, see ref. 15.

[2]NRCC No. 12746.

[3]Taken from the Ph.D. Thesis of W. S. Powell, Dalhousie University, 1972.

[4]Holder of NRCC Scholarship, 1967–1971.

[5]Correspondence and reprint requests should be sent to this author (R.A.H.) at the Atlantic Regional Laboratory.

[6]In earlier papers in this series (*cf.* refs. 1, 5, 6, and 15) the older system of numbering the indole nucleus was employed in which the 3*a*-position was referred to as the 9-position.

Can. J. Chem. Downloaded from www.nrcresearchpress.com by 210.87.254.105 on 09/05/12
For personal use only.

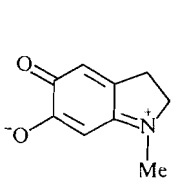

5

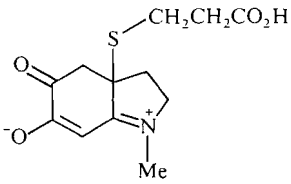

6

gated in these laboratories (2). It has been shown that under these conditions the major product formed initially is 3*a*-*S*-(β-carboxyethylthio)-3*a*, 4-dihydroepinochrome (**6**), which was isolated as its *p*-nitrophenylhydrazone derivative (2).

The reactions of epinochrome (**5**) with some thiols (*i.e.* thioglycollic acid and GSH) under acidic conditions have now been studied. During the course of these investigations it was found that **5** could be obtained in crystalline form more conveniently and in higher yields than by the method previously described (8) by an adaptation of the procedure employed by Heacock *et al.* (9) for the preparation of adrenochrome.

Thin-layer chromatography of the initial products of the reaction between epinochrome (**5**) and some thiols was hampered by the facile autoxidation of some of the products to indoline-5,6-quinone derivatives; this occurred when the excess thiol was separated from the reaction products during the chromatographic process. The chromatographic picture was also complicated by the ready formation of rearrangement products from the quinones described above.

The reaction between **5** and GSH in aqueous buffer at p*H* 3.3 was followed by u.v./visible spectroscopy. The absorption maximum of **5** in the visible region at 476 nm disappeared with time whilst the peak at 307 nm was replaced by a peak of lower intensity at 311 nm. An ether extract of the reaction mixture showed maximum absorption at 309 nm (in aqueous solution) whilst the aqueous phase of the reaction mixture absorbed maximally at 312 nm. It would appear from a consideration of the λ_{max} values of analogous compounds that the ether extractable product could be 5,6-dihydroxy-1-methylindoline (7*a*) and that the main product remaining in the mother liquors may be a 5,6-dihydroxy-1-methylindoline thioether.

In order to obtain more definitive information about the products of a typical interaction of this type an attempt was made to isolate the products of the reaction between epinochrome and thioglycollic acid. Since the initial reaction products were reoxidized very readily by air, they were acetylated directly after formation by acetic anhydride and pyridine.

In view of the fact that it was anticipated that 5,6-diacetoxy-1-methylindoline (7*b*) might be one of the products of this reaction, this hitherto unknown compound was synthesized by a method similar to that employed by Wyler and Chiovini (10) for the preparation of 5,6-diacetoxy-1-acetyl-2-carbomethoxyindoline (**8**).

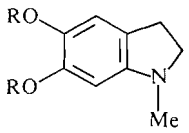

7

a R=H
b R=Ac

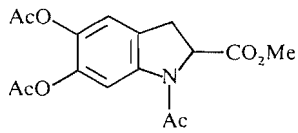

8

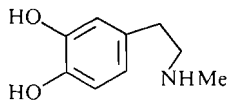

9

Solutions of epinochrome (**5**), prepared by the oxidation of epinine (**9**) by potassium ferricyanide in phosphate buffer were immediately and rapidly reduced with sodium dithionite ($Na_2S_2O_4$) to give 5,6-dihydroxy-1-methylindoline (7*a*), which was stabilized by the addition of hydrochloric acid and isolated as 5,6-diacetoxy-1-methylindoline (7*b*) after acetylation with acetic anhydride and pyridine. It was essential to carry out all the stages in this procedure as quickly as possible to minimize losses due to either the easy reoxidation of the 5,6-dihydroxyindoline reduction product or the facile rearrangement of the aminochrome **5**. The spectroscopic data obtained for 7*b* were consistent with the 5,6-diacetoxy-1-methylindoline structure. The λ_{max} in the u.v. spectrum of this compound (*i.e.* 310 nm) was close to that previously reported for similar 5,6-dihydroxyindoline derivatives (10–14). The signals for the protons at positions 4- and 7- in the p.m.r.

Can. J. Chem. Downloaded from www.nrcresearchpress.com by 210.87.254.105 on 09/05/12
For personal use only.

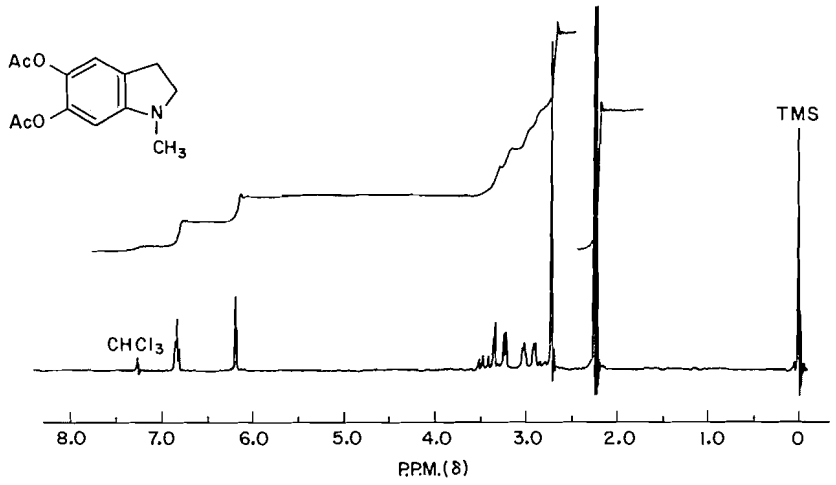

FIG. 1. P.m.r. spectrum (60 MHz) of 5,6-diacetoxy-1-methylindoline (*7b*) in $CDCl_3$ using tetramethylsilane as internal reference.

spectrum of *7b* (shown in Fig. 1) were observed at δ 6.85 and 6.21 respectively with benzylic coupling being observed between the proton in the 4-position and the C_3-methylene protons ($J = 1.1$ Hz). Similar couplings have recently been reported for analogous compounds (11, 12).

The mixture of acetylated products formed after the addition of acetic anhydride and pyridine (1:1) to the epinochrome/thioglycollic acid reaction mixture was examined by t.l.c. 5,6-diacetoxy-1-methylindole (**10**), 6-acetoxy-4-*S*-carboxymethylthio-5-hydroxy-1-methylindole lactone (**11**), and 5,6-diacetoxy-1-methylindoline (*7b*) were used as chromatographic standards.

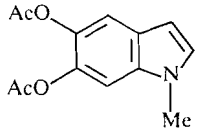

10

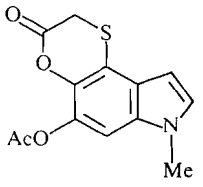

11

The results of this chromatographic examination are given in Table 1.

It appeared that three main products were obtained, two of which were the acetylated indole thioether lactone **11** and 5,6-diacetoxy-1-methylindoline (*7b*). The indoline derivative, however, only gave a positive reaction with the indole chromogenic reagents (*i.e.* Ehrlich's reagent and cinnamaldehyde) when the chromatograms were heated for several minutes after spraying (see Table 1). This may have been due to hydrolysis of the ester linkages of *7b* by the acid present in the chromogenic reagent, upon heating the plates. The resulting 5,6-dihydroxyindoline would readily oxidize in air to the corresponding indoline-5,6-quinone, which would rearrange rapidly to the corresponding 5,6-dihydroxyindole.

The third major product, like *7b*, gave colors with Ehrlich's reagent or cinnamaldehyde only after heating, suggesting that it was also an acetylated 5,6-dihydroxyindoline derivative. In a similar manner to the 4-substituted product **11** it gave a blue-green color with aqueous sodium hydroxide usually observed for 5,6-dihydroxyindoles substituted in the 4-position. In addition to the three major products described above there were a number of minor products formed including one that appeared to be chromatographically the same as 5,6-diacetoxy-1-methylindole (**10**).

The indolic products in the reaction mixture may have been formed as a result of the loss of the protective effect of the —SH group of the excess thioglycollic acid, due to its acetylation by the acetic anhydride/pyridine mixture. Any 5,6-dihydroxyindolines (*cf.* **12**) present at this stage could be oxidized in air to the corresponding indoline-5,6-quinones (*cf.* **13**), which

Can. J. Chem. Downloaded from www.nrcresearchpress.com by 210.87.254.105 on 09/05/12
For personal use only.

Can. J. Chem. Downloaded from www.nrcresearchpress.com by 210.87.254.105 on 09/05/12
For personal use only.

TABLE 1. Thin-layer chromatography* of the acetylated products of the reaction between epinochrome and thioglycollic acid

	R_f values†			Colors with chromogenic reagents§				
	S_1‡	S_2‡	S_3‡	Ehr	Ehr (after heating)	Cin	Cin (after heating)	1 *N* NaOH
Reaction mixture	0.66	0.20	0.63(s)	V	B	R	V	BG
	0.61	0.39	0.37(s)	—	B	—	V	BG
	0.56	0.25	0.51(w)	P	V	O	VBn	Bn
	0.49	0.44	0.08(s)	—	V	—	VBn	V → Bn
6-Acetoxy-4-*S*-carboxymethylthio-5-hydroxy-1-methylindole lactone (**11**)	0.66	0.19	0.62	V	B	R	V	BG
5,6-Diacetoxy-1-methylindole (**10**)	0.56	0.25	0.51	P	V	O	VBn	Bn
5,6-Diacetoxy-1-methylindoline (*7b*)	0.49	0.43	0.08	—	V	—	VBn	V → Bn

*Ascending development on Merck pre-coated silica gel F-254 t.l.c. plates (5 × 20 cm; layer thickness 0.25 mm).
†Several other minor Ehrlich positive products were also present, along with products which appeared to be derived solely from the thioglycollic acid (*i.e.* positive iodine/azide reaction (*cf.* ref. 16)).
‡Solvents: S_1 = benzene/ethyl acetate (8:2); S_2 = hexane/ethyl acetate/pyridine (7:2:1); S_3 = benzene/ethyl acetate/formic acid (33:4:3).
§Abbreviations: Ehr = Ehrlich's reagent; Cin = cinnamaldehyde; s = strong; w = weak; V = violet; B = blue; R = red; G = green; P = pink; O = orange; Bn = brown.

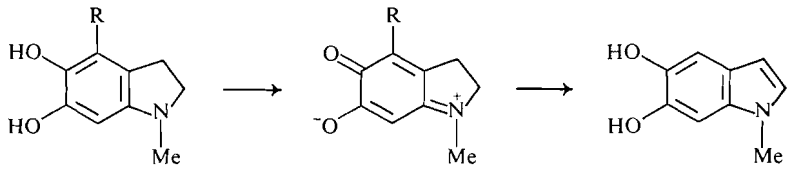

12 **13** **14**

SCHEME 1

would rearrange to 5,6-dihydroxyindoles (*cf.* **14**) in the presence of pyridine (See Scheme 1).

When precautions were taken to exclude air during the course of the acetylation procedure, t.l.c. of the products indicated that, although some 5,6-dihydroxyindoles were still formed, much larger amounts of the 5,6-dihydroxyindoline compounds were obtained.

It was possible to isolate the acetylated lactonized indole thioether **11** from the reaction mixture by column chromatography on silica gel using a neutral eluting solvent system. The product obtained in this manner was identical to samples of 6-acetoxy-4-*S*-carboxymethylthio-5-hydroxy-1-methylindole lactone (**11**) prepared from adrenochrome by the method of Powell *et al.* (**5**).

The two basic 5,6-dihydroxyindoline derivatives were isolated from the crude reaction mixture by column chromatography on silica gel, using a basic eluting system (a hexane/pyridine mixture). They were finally obtained as pure compounds after a second separation on a silica gel column using a neutral eluting solvent system. The major product obtained in this manner was 5,6-diacetoxy-1-methylindoline (*7b*) and was identical to samples of this product obtained by acetylation of the dithionite reduction product of epinochrome (**5**). The second basic product, which was obtained as a white crystalline solid, was shown by mass spectrometry to have a molecular formula of $C_{13}H_{13}NO_4S$. The i.r. spectrum of this compound showed a strong absorption at 1761 cm^{-1}, probably due to the ester and lactone carbonyl groups. The p.m.r. spectrum of this product (Fig. 2) was similar to that of *7b* with the exception of the absence of peaks due to the H_4 proton and one of the acetyl methyl signals. In addition, a peak at δ 3.43, which can be assigned to the —*S*—CH_2— group, was also observed. The peak for the corresponding protons of **11** has been reported to occur at δ 3.50 (5).

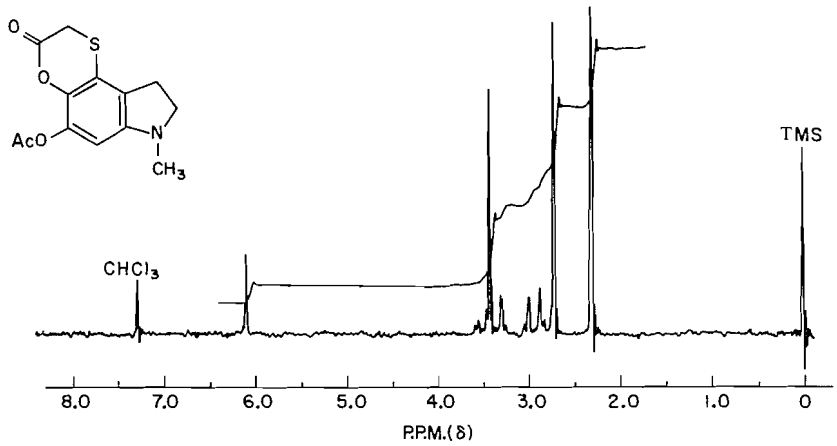

FIG. 2. P.m.r. spectrum (60 MHz) of 6-acetoxy-4-*S*-carboxymethylthio-5-hydroxy-1-methylindoline lactone (**15**) in $CDCl_3$ using tetramethylsilane as internal reference.

These facts show unambiguously that this product is 6-acetoxy-4-*S*-carboxymethylthio-5-hydroxy-1-methylindoline lactone (**15**).

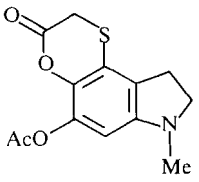

15

The present investigation would suggest that aminochromes which do not have a 3-hydroxyl (or 3-alkoxyl) substituent react with thiols under acidic conditions to give the corresponding 5,6-dihydroxyindoline reduction products (*i.e.* true "leuco" derivatives) as well as 4-thiosubstituted 5,6-dihydroxyindolines. An alternative explanation can now be presented for the formation of the thiosubstituted 5,6-dihydroxyindoles reported to be formed in the reaction between dopachrome (**1**) and GSH which was investigated by Bouchilloux and Kodja (7). The indolic product may have arisen via the oxidation of an initially formed thiosubstituted 5,6-dihydroxyindoline to the thiosubstituted aminochrome. This could then rearrange to the dihydroxyindole (*cf.* Scheme 1).

Experimental

The melting points were determined on either a Leitz Hot Stage instrument or a Fisher–Johns apparatus and are uncorrected. The i.r. spectra were obtained with the aid of a Perkin–Elmer model 237 recording spectrophotometer; the u.v./visible spectra were measured on either a Beckman DK-2 or a Bausch and Lomb "spectronic 505" recording spectrophotometer; the p.m.r. spectra were recorded on a Varian A-60A instrument and the mass spectra were obtained on a DuPont/C.E.C. 21-110B instrument.

Epinochrome (*5*)

Epinine free base[7] (2 g) was suspended in dry methanol (82 ml) and 98% formic acid added dropwise with stirring until a clear solution was obtained. Freshly prepared silver oxide (8.64 g) was added portionwise during a period of 5 min, during which time the reaction temperature was maintained between 16° and 25°. The reaction mixture was then filtered through a Dowex-1 × 8(Cl^-) (200–400 mesh) resin bed[8] (height = 3.5 cm; diameter = 4.5 cm). Dry ether (260 ml) was added to the filtrate and it was kept in a cold room at −30° for 8 h. Upon filtration epinochrome (1.17 g, 60%) was obtained as deep red needles, m.p. 80–83° with decomposition (lit. m.p. 78° (8)); λ_{max} (H_2O) nm (ε): 217 (31 400), 307 (12 600), 476 (4070); ν_{max} (Nujol): 1661, 1652, 1612, 1566 cm^{-1}.

5,6-Diacetoxy-1-methylindoline (*7b*)

A solution of potassium ferricyanide (2 g) in 50 ml of Soerensen phosphate buffer[9] (p*H* 8) was added to a stirred solution of epinine hydrochloride (250 mg) in 75 ml of the same buffer. After 4–5 s, a solution of sodium dithionite (1.36 g) in the same buffer (25 ml) was added, resulting in an almost immediate discharge of the red color of the epinochrome solution. Concentrated HCl (2.5 ml) was added to

[7]The free base of epinine was prepared by the addition of solid K_2CO_3 to a stirred aqueous solution of epinine hydrochloride. After standing in an ice bath for 1.5 h under a stream of nitrogen, the free base was filtered off, washed with water, and dried *in vacuo*.

[8]The Dowex resin was pretreated by the method previously described in the literature (9).

[9]0.5 g KH_2PO_4 and 22.6 g $Na_2HPO_4 \cdot 12H_2O$ per liter.

Can. J. Chem. Downloaded from www.nrcresearchpress.com by 210.87.254.105 on 09/05/12
For personal use only.

Can. J. Chem. Downloaded from www.nrcresearchpress.com by 210.87.254.105 on 09/05/12
For personal use only.

the solution 1–2 s after the addition of the dithionite and the reaction mixture was then concentrated to dryness *in vacuo*, benzene being added during the latter stages to enable complete removal of any water present. A 1:1 mixture of acetic anhydride and pyridine (25 ml) was added to the solid residue which had been broken up with a spatula. The acetylation mixture was left at room temperature for 4 h, filtered, and the residue washed with dichloromethane (3 × 20 ml). The washings and the acetic anhydride/pyridine solution were combined, filtered, and concentrated to dryness *in vacuo* below 50°. The residue was dissolved in a mixture of 0.5 *N* HCl (25 ml) and dichloromethane (25 ml) in a separatory funnel. The organic layer was separated and washed with saturated aqueous sodium bicarbonate solution (4 × 30 ml) and water (2 × 30 ml). The dried (Na_2SO_4) dichloromethane solution was then concentrated to dryness *in vacuo*. The crude product, which also contained a small amount of 5,6-diacetoxy-1-methylindole, was purified on a silica gel (Davison, 100–200 mesh) column (height = 18 cm; diameter = 2.2 cm) with a mixture of hexane/ethyl acetate/pyridine (15:3:2) as eluant. A series of 25 ml fractions were collected. Fractions 6–10 were combined and the solvent removed *in vacuo* below 50° to give a white crystalline solid, from which 5,6-diacetoxy-1-methylindoline (**7***b*) (200 mg) was obtained in colorless rods (m.p. 115–116°) on recrystallization from heptane; λ_{max} (EtOH) nm (ε): 206 (22 200), 257 (9710), 310 (3460); ν_{max} (Nujol): 1765, 1756 cm^{-1}. The p.m.r. δ ($CDCl_3$): 6.85 (1H, t, $J_{3A,4} = J_{3B,4}$ = 1.1 Hz, H_4); 6.20 (1H, s, H_7); 3.54–2.72(4H, m, AA'BB' system centered at 3.13, $—CH_2CH_2—$ of the five-membered ring; the C_3-methylene group, which appears as the upper field half of this system is coupled to H_4, J = 1.1 Hz); 2.72 (3H, s, *N*—CH_3); 2.25 (3H, s, *C*—CH_3); 2.22 (3H, s, *C*—CH_3). Mass spectrum: $M^{+\cdot}$ 249; calcd. for $C_{13}H_{15}NO_4$: 249.

Anal. Calcd. for $C_{13}H_{15}NO_4$: C, 62.64; H, 6.07; N, 5.62. Found: C, 62.72; H, 6.05; N, 5.83.

The Epinochrome–Thioglycollic Acid Reaction

(a) Chromatographic Study of Reaction Products after Acetylation

Epinochrome (50 mg) was added to thioglycollic acid (1 ml) and the mixture shaken until all the solid had dissolved (*ca.* 15 min). A 1:1 mixture (7 ml) of acetic anhydride and pyridine was added and the reaction mixture kept at room temperature for 2 h. Concentration of this solution *in vacuo* gave a dark yellow oil which was dissolved in dichloromethane (25 ml). After washing with a saturated aqueous sodium bicarbonate solution (3 × 25 ml) and water (2 × 25 ml) the organic phase was dried (Na_2SO_4) and its composition investigated by t.l.c. on silica gel (see Table 1).

(b) Isolation of the Reaction Products as their Acetyl Derivatives

Epinochrome (500 mg) was added to thioglycollic acid (5 ml) and the mixture shaken until all the solid had dissolved (*ca.* 45 min). The flask containing the thioglycollic acid solution was then evacuated and nitrogen was bubbled through the reaction mixture. A 1:1 mixture (40 ml) of acetic anhydride and pyridine was added to the thioglycollic acid solution at 0°, the system being maintained under nitrogen at slightly reduced pressure throughout the addition and then for a further 2 h. Half an hour after the addition of the acetic anhydride and pyridine the reaction mixture was allowed to warm up to room temperature and after another 1.5 h it was concentrated to small bulk *in vacuo* below 50°. The residue was dissolved in dichloromethane (50 ml) and this solution was washed with a saturated aqueous solution of sodium bicarbonate (3 × 50 ml) and then with water (3 × 50 ml). A dark yellow oil was obtained upon concentration of the dried (Na_2SO_4) organic layer *in vacuo*, below 30°.

Isolation of 6-acetoxy-4-S-carboxymethylthio-5-hydroxy-1-methylindole lactone (**11**). The dark yellow oil described above (prepared from 500 mg of epinochrome) was purified chromatographically on a silica gel (Davison, 100–200 mesh) column (height = 25 cm; diameter = 2 cm) using benzene (500 ml) followed by benzene/ethyl acetate (97:3; 1000 ml) as eluting solvents. A series of fractions (fraction volume, 17 ml) were collected and these were monitored by t.l.c. on silica gel plates (using benzene/ethyl acetate (8:2) as developing solvent with Ehrlich's reagent and 1 *N* NaOH as chromogenic reagents). Fractions 65–80 were combined and concentrated to dryness *in vacuo* to give 6-acetoxy-4-*S*-carboxymethylthio-5-hydroxy-1-methylindole lactone (**11**) as a white crystalline solid (60 mg, 7.1%), which, after recrystallization from heptane, had a melting point of 160–163°. The identity of this product with samples of the product which had previously been prepared from the reaction of thioglycollic acid with adrenochrome (5) was established by the nondepression of m.p. and by the identity of their i.r., n.m.r., and mass spectral properties.

Isolation of 6-acetoxy-4-S-carboxymethylthio-5-hydroxy-1-methylindoline lactone (**15**) *and 5,6-diacetoxy-1-methylindoline* (**7***b*). A sample of the dark yellow oil obtained after acetylation of the epinochrome/thioglycollic acid reaction mixture (prepared from 500 mg epinochrome) and obtained in the manner described above was chromatographed on a column (height = 20 cm; diameter = 2 cm) of silica gel (Davison, 100–200 mesh) with hexane/pyridine (8:2) as eluant. Once again a series of fractions was collected (fraction volume, 20 ml). A yellow oil was obtained after concentration of fractions 8–20 to dryness *in vacuo* below 35°. This oil was rechromatographed on a column (height = 20 cm; diameter = 2 cm) of silica gel (Davison, 100–200 mesh) with the following solvents as eluants: benzene (500 ml); benzene/ethyl acetate (97:3, 1000 ml). and benzene/ethyl acetate (95:5, 2000 ml). Fractions 95–120 (fraction size, 15 ml) were combined and concentrated to dryness *in vacuo* to give 6-acetoxy-4-*S*-carboxymethylthio-5-hydroxy-1-methylindoline lactone (**15**) as a white crystalline solid (70 mg, 8.2%), which gave colorless needles, m.p. 137–140° after recrystallization from heptane; λ_{max} (EtOH) nm (ε): 225 (sh), 234 (19 700), 262 (9020), 319 (4010); ν_{max} (Nujol); 1761 cm^{-1}. The p.m.r. δ ($CDCl_3$): 6.10 (1H, s, H_7); 3.43 (2H, s, *S*—CH_2—); 3.63–2.71 (4H, m, AA'BB' system centered at 3.17, $—CH_2CH_2—$ of five-membered ring); 2.73 (3H, s, *N*—CH_3); 2.32 (3H, s, *C*—CH_3). Mass spectrum: $M^{+\cdot}$ 279.0561 ± 0.0008; calcd. for $C_{13}H_{13}NO_4S$: 279.0566.

In a similar fashion fractions 150–200 were combined and concentrated to dryness *in vacuo* to give 5,6-diacetoxy-1-methylindoline (**7***b*) as a white crystalline solid (115 mg, 15.1%). Recrystallization from heptane gave colorless rods, m.p. 113–115°. The fact that this product was the same as samples of 5,6-diacetoxy-1-methylindoline which had previously been prepared by the reduction of epinochrome

with sodium dithionite in the manner described above was established by the nondepression of m.p. and the identity of their i.r., p.m.r., and mass spectra.

The authors wish to thank Dr. L. M. Babineau, Directeur, Département de Biochimie, Faculté de Médecine, Université Laval, Québec 10e., Québec for the provision of space and facilities in his department, during the academic year 1969–1970, where the early stages of this work were carried out.

Thanks are accorded to Mr. D. Embree and Dr. W. D. Jamieson of A.R.L. for the mass spectral data.

1. W. S. Powell and R. A. Heacock. Exper. **28**, 124 (1972).
2. W. S. Powell and R. A. Heacock. J. Chem. Soc. In preparation.
3. R. A. Heacock and B. D. Laidlaw. Chem. Ind. (London), 1510 (1958).
4. R. A. Heacock and B. D. Scott. Can. J. Biochem. Physiol. **37**, 1087 (1959).
5. W. Powell, R. A. Heacock, G. L. Mattok, and D. L. Wilson. Can. J. Chem. **47**, 467 (1969).
6. W. Powell, and R. A. Heacock. Can. J. Chem. **47**, 2102 (1969).
7. S. Bouchilloux and A. Kodja. Bull. Soc. Chim. Biol. **42**, 1045 (1960).
8. H. Sobotka and J. Austin. J. Am. Chem. Soc. **73**, 3077 (1951).
9. R. A. Heacock, C. Nerenberg, and A. N. Payza. Can. J. Chem. **36**, 853 (1958).
10. H. Wyler and J. Chiovini. Helv. Chim. Acta, **51**, 1476 (1968).
11. N. Fischer and A. S. Dreiding. Helv. Chim. Acta, **53**, 1937 (1970).
12. U. Wölcke, A. Kaiser, W. Koch, and M. Scheer. Helv. Chim. Acta, **53**, 1704 (1970).
13. G. Piattelli Oriente, S. Sciuto, and M. Piattelli. Gazz. Chim. Ital. **100**, 693 (1970).
14. S. N. Mishra and G. A. Swan. J. Chem. Soc. C, 1424 (1967).
15. W. S. Powell and R. A. Heacock. Can. J. Chem. **49**, 341 (1971).
16. W. E. Dahl and H. L. Pardue. Anal. Chem. **37**, 1382 (1965).

Can. J. Chem. Downloaded from www.nrcresearchpress.com by 210.87.254.105 on 09/05/12
For personal use only.

Addition Reactions in the Nitration of Some Polycyclic Aromatic Compounds

A. FISCHER AND D. R. A. LEONARD
Department of Chemistry, University of Victoria, Victoria, British Columbia

Received April 28, 1972

Reaction of 3-oxo-1,2,3,7,8,9,10,10*a*-octahydrocyclohepta[*de*]naphthalene with nitric acid in acetic anhydride gives two stereoisomeric 4-acetoxy-6*a*-nitro-3-oxo-1,2,3,4,6*a*,7,8,9,10,10*a*-decahydrocyclohepta[*de*]-naphthalenes as well as the expected nitro substitution products. Formation of these adducts from a substrate containing a meta-directing deactivating substituent shows that the 1,4-addition reaction of acetyl nitrate is more general than previously suspected. 1,4-Acetyl nitrate adducts are also formed from tetralin, benzsuberane, 5,6,7,8-tetrahydrocyclohepta[*fg*]acenaphthene, and 1,2,3,4,7,8,9,10-octahydrodicyclohepta-[*de*,*ij*]naphthalene. Decomposition of the last two adducts gives in each case a product with the nitro group substituted into the alicyclic ring.

La réaction de l'oxo-3 octahydro-1,2,3,7,8,9,10,10*a* cyclohepta[*de*]naphtalène avec l'acide nitrique dans l'anhydride acétique conduit aux deux acétoxy-4 nitro-6*a* oxo-3 décahydro-1,2,3,4,6*a*,7,8,9,10,10*a* cyclo-hepta[*de*]naphtalènes stéréoisomères ainsi qu'aux produits de nitration attendus. La formation de ces composés d'addition à partir d'un substrat contenant un substituant désactivant en méta montre que l'addition-1,4 de l'acétylnitrate est plus générale qu'on le pensait antérieurement. Des composés d'addition-1,4 avec l'acétyl-nitrate sont également formés à partir de la tétraline, benzsubérane, tétrahydro-5,6,7,8 cyclohepta[*fg*]acénaph-tène et octahydro-1,2,3,4,7,8,9,10 dicyclohepta[*de*,*ij*]naphtalène. La décomposition de ces deux derniers composés d'addition donne dans chaque cas un produit substitué par le groupe nitro sur le cycle alicyclique.
[Traduit par le journal]

Canadian Journal of Chemistry, **50**, 3367 (1972)

Can. J. Chem. Downloaded from www.nrcresearchpress.com by 210.87.254.40 on 09/05/12
For personal use only.

Nitration in acetic anhydride of *o*- and *p*-xylenes, of 1,2,3-trimethylbenzene (hemimellitene) and of indane has been reported to give diastereoisomeric 1,4-nitro-acetate addition products as well as the normal nitro substitution products (1–3). The 1,4-diene adducts arise by attack of the nitrating electrophile at the position carrying a substituent (*ipso* attack (4)) followed by combination of acetate with the resulting σ-complex, eq. 1. Adducts have only been observed when $X \neq H$. Presumably the normal σ-complex ($X = H$) loses the proton more rapidly than it adds acetate or, alternatively, the adduct once formed undergoes an extremely facile 1,4-elimination of acetic acid, leading in either case to the normal nitration product. Hence, subject only to the restriction that a substituted position must be of comparable reactivity to an unsubstituted position, adduct formation might be expected to be generally observed competing with normal nitration of aromatic compounds. The present study of the nitration of some cyclic compounds supports this hypothesis.

Nitration in acetic anhydride of 3-oxo-1,2,3,-7,8,9,10,10*a*-octahydrocyclohepta[*de*]naphthalene (**1**) gave a pair of diastereoisomeric dienes **2** (39%) and the 4-nitro (26%), 5-nitro (34%), and 6-nitro (1%) substitution products **3**. The presence of nitro and acetoxy groups in the adducts is established by the i.r. spectra and is confirmed by the mass spectra. The adducts cannot be 1,3-dienes as λ_{max} (241 and 241.5 nm) occurs at too short a wavelength. There are potentially 12 structurally isomeric 1,3-diene adducts. λ_{max} for these calculated by Woodward's rules or by analogy with known compounds containing the same chromophoric system is 268 nm or greater (5). There are potentially six (three pairs) structurally isomeric 1,4-diene adducts whose partial structures are shown as **4**, **5**, and **6**. Structure **6** has isolated olefinic and carbonyl double bonds and thus would exhibit only weak carbonyl absorption above 200 nm.

[1]

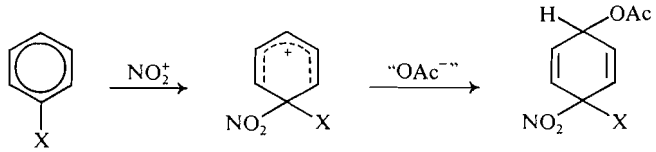

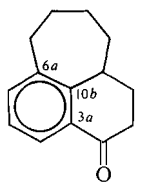

1

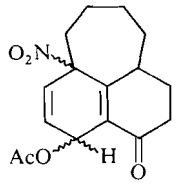

2

a cis
b trans

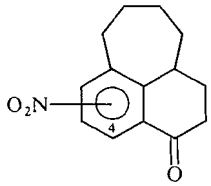

3

a 4-Nitro
b 5-Nitro
c 6-Nitro

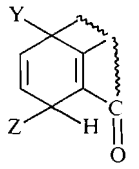

4

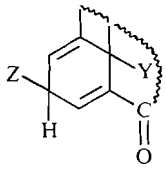

5

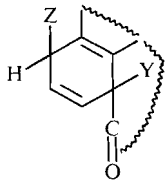

6

a Y = NO_2, Z = OAc
b Y = OAc, Z = NO_2

It is ruled out by the strong u.v. absorption at 241 nm ($\varepsilon \sim 800\ m^2\ mol^{-1}$). Structure **5** is not consistent with the n.m.r. spectra, which establish the presence of adjacent vinylic protons ($J \sim 10$ Hz). Moreover structure **5** requires two approximately equal ^3J couplings of magnitude (6) 2.6–4.6 Hz whereas only one such coupling was observed. The observed coupling (9.6, 4.3, −0.2 and 9.9, 3.6, −1.6 for the two isomers) are consistent only with structure **4**. The calculated λ_{max} for **4** (249 nm) is in acceptable agreement with the observed values (241 and 241.5 nm). On chemical grounds structure **4***a* is much more likely than **4***b*. Structure **4***b* has a proton which is α to a nitro group and which would allow a facile 1,4-elimination of acetic acid under the basic work-up conditions. By analogy with the previously investigated systems we assume that the acetoxy and nitro groups are *cis* in one isomer and *trans* in the other. We are unable to assign the stereochemistry of the two diene products. The dienes contain three asymmetric centers (4, 6a, and 10a) and it is probable that each of the isolated isomers consists of two pairs of enantiomers.

The structures of the nitro substitution products **3** are established by n.m.r. and mass spectra. The 4- and 6-nitro isomers have a distinctive ortho coupling (8 Hz) whereas the 5-nitro isomer exhibits a smaller meta coupling (2.5 Hz). The base peak in the mass spectrum of the 6-nitro isomer is at $m/e = 228$, corresponding to loss of OH. No significant peak at the same mass appeared in the spectrum of the 4-isomer and analogy with the behavior of the nitro-toluenes (7) establishes the position of the nitro group with respect to the methylene group in each compound. Chemical shift differences between the aromatic protons of **1** and **3***a*, *b*, and *c* support the above assignment, *e.g.* **3***b* is clearly identified as the isomer whose aromatic protons are both shifted to the lowest field since both aromatic protons are ortho to a nitro group. Similar arguments can be adduced to support the assignments of **3***a* and *c*.

The relative reactivities of the ring sites of **1** to electrophilic attack (assuming that these are reflected by the product ratios) are $6a > 5 > 4 \gg 6$. No products were observed resulting from attack at 3*a* and 10*b* positions. The preference for *ipso* attack at the 6*a* position, leading to the adducts **4***a*, rather than at the 10*b* position, leading to adducts **5***a*, is explicable in terms of the meta directing effect of the carbonyl function. It should be noticed, however, that the 4-position (ortho to carbonyl) is not much less reactive than the 5-position (meta to carbonyl). The 4-position would be expected to be more reactive than the 6 as found, both because the two methylene substituents might

Can. J. Chem. Downloaded from www.nrcresearchpress.com by 210.87.254.40 on 09/05/12
For personal use only.

Can. J. Chem. Downloaded from www.nrcresearchpress.com by 210.87.254.40 on 09/05/12
For personal use only.

be expected to activate the former position to a greater extent (*cf.* *o*-xylene (8)) and because the electron-withdrawing carbonyl group should favor ortho more than para substitution (9).

The dienes **2***a* and *b* represent the first reported examples of adducts obtained from an aromatic containing a deactivating meta directing substituent. Their formation supports the hypothesis that the addition reaction is a nitration which has been diverted in the second step. Compounds **2***a* and *b* appear to be much more stable than previously isolated dienes, probably because of the presence of the deactivating carbonyl group.

Adducts formed from the other substrates on reaction with nitric acid in acetic anhydride were much more labile and with the exception of the tetralin adduct, decomposed during work-up. However, in each case the characteristic τ 3.5–4.5 p.p.m. absorption in the spectrum of the reaction mixture prepared at low temperatures demonstrated that adducts were formed in good yield. The n.m.r. spectrum of the product mixture from tetralin indicated that two dienes were formed but only one of these was isolated. Benzsuberane likewise gave two adducts but neither was isolated. Comparable yields of diene products, as indicated by the n.m.r. spectra, showed that the fraction of *ipso* attack, leading to adduct formation, is not markedly sensitive to ring size in the series indane (3), tetralin, benzsuberane.

Formation of aryl acetate by elimination of nitrous acid is the common mode of decomposition of the dienes previously studied. However, the dienes from the octahydrodicycloheptanaphthalene **7** and the tetrahydrocycloheptaacenaphthene **8** gave the "side-chain" nitro compounds **9** and **10** as the predominant decomposition products, respectively. In the case of the acenaphthene derivative **10** the nitro group, whose presence is revealed by the i.r. absorption at 1555 cm^{-1}, is substituted into the five-membered ring and not the seven-membered ring. The parent hydrocarbon **8** exhibits a sharp singlet at τ 6.77 p.p.m., similar to the singlet at 6.68 p.p.m. in the spectrum of acenaphthene, and a broader resonance at 6.9 p.p.m., similar to that of octahydrodicycloheptanaphthalene **7** (10). In the spectrum of the product the singlet at 6.77 p.p.m. is replaced by downfield resonances which have vicinal and geminal

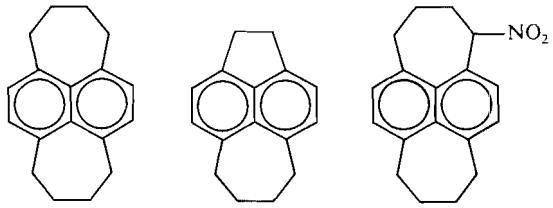

7 8 9

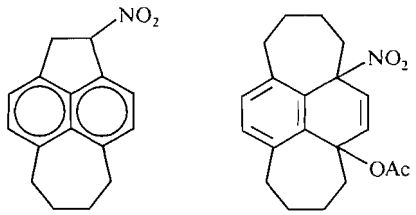

10 11

coupling constants expected for the CH_2CHNO_2 group while the broad higher field resonance attributed to the α-protons of the seven-membered ring still appears. The diene precursor to this product was extremely labile and could only be "isolated" as a minor constituent of largely unreacted starting material. The structure of the diene **11** from octahydrodicycloheptanaphthalene is established by the n.m.r. spectrum which exhibits an AB quartet centered at 4.16 p.p.m. with a coupling constant of 9.5 Hz. Thus the diene must have adjacent vinylic protons as in **11**. Formation of the nitro compounds **9** and **10** obviously parallels the reaction of 1,4-dimethylnaphthalene with nitric acid in acetic anhydride which leads to ω-nitro-1,4-dimethylnaphthalene (11). It has been shown that the dimethylnaphthalene 1,4-acetyl nitrate adducts are intermediates in this reaction (12).

For the isomeric dienes **2***a* and *b* the dihedral angle (ϕ) between the $H^4—C^4—C^5$ and $C^4—C^5—H^5$ planes can be calculated from Garbisch's equations (6), using the three and four bond coupling constants in Table 1. There is excellent agreement between the two values of ϕ (60, 60°) for the isomer (m.p. 105°) whose n.m.r. spectrum when analyzed gave a single solution. For the other isomer, m.p. 120.5°, which gave two n.m.r. solutions there is excellent agreement between the two values of ϕ (47, 48°) for one of these, that with $J_{45} = 4.42$ and $J_{46} = -0.76$ Hz, and this solution is therefore preferred. The other solution gives ϕ as 50 and 39°. The mean values of ϕ for the two isomers

TABLE 1. Computed coupling constants (Hz) and chemical shifts (τ)* for dienes **2***a* and *b*

Compound	M.p. (°C)	J_{45}	J_{46}	J_{56}	ν_4	ν_5	ν_6
2	120.5	4.27	−0.22	9.63	3.85	3.64	3.92
2	120.5	4.42	−0.76	9.49	3.85	3.64	3.92
2	105	3.57	−1.62	9.89	3.89	3.77	3.99

*Two solutions were obtained for the diene **2**, m.p. 120.5°.

(60 and 47 or 44°) imply that the 1,4-hexadiene ring is planar or nearly so. If the ring were in the boat form, as Dreiding models suggest, then ϕ would be either ~93 or ~27°. 1,4-Cyclohexadiene itself is reported to have a planar ring (13).

Experimental

U.v. spectra were determined on a Unicam S.P. 800 spectrometer. I.r. spectra were determined on a Perkin–Elmer model 337 spectrometer calibrated with polystyrene. N.m.r. spectra were determined on a Varian HA-60-IL spectrometer using tetramethylsilane as internal standard. Unless specified otherwise coupling constants cited are apparent values estimated directly from the appropriate spectrum. Mass spectra were determined on an AEI MS-902 instrument. Microanalyses were by Dr. A. D. Campbell, University of Otago, Dunedin, New Zealand. Melting points are uncorrected. Nitric acid was purified by distilling fuming acid (300 cm^3) at 1 mm from urea (10 g) and sulfuric acid (500 cm^3). Alumina was neutral alumina deactivated with $7\frac{1}{2}$% (v/v) of water.

*Nitration of 3-Oxo-1,2,3,7,8,9,10,10a-octahydrocyclohepta[de]naphthalene (**1**) in Acetic Anhydride*

A solution of nitric acid (7.5 g, 0.12 mol) in acetic anhydride (25 cm^3) was added slowly to a stirred suspension of the tricyclic ketone **1** (10 g, 0.05 mol) in acetic anhydride maintained below −50° (10). The temperature of the mixture was allowed to rise to 0° and the solution stirred at this temperature for 3 h. The solution was poured into cold carbon tetrachloride (400 cm^3) and the resulting solution washed with water (3 × 400 cm^3), 0.5 *M* ammonium hydroxide (2 × 400 cm^3), and water. After drying over magnesium sulfate the solvent was evaporated at room temperature to give 18.6 g of residue: i.r. (film) 1735 ($OCOCH_3$), 1705–1675 (C=O), 1545–1520 cm^{-1} (NO_2); n.m.r. ($CDCl_3$) τ 1.3–3.0 (Ar*H*), 3.5–4.1 (vinyl and allylic *H*). The integrals of the aromatic and vinyl–allylic (diene) regions were the same and thus the ratio of aromatic to diene products was 3:2, on the assumption that the aromatic products had two aromatic protons and the diene products three vinyl–allylic protons. G.l.c. of the product on QF-1 and SE-30 columns showed only four peaks of relative areas, in order of retention time, 1.5, 1.5, 55, and 42%. These peaks were shown to correspond to unreacted tricyclic ketone **1** and its 6-NO_2, 5-NO_2, and 4-NO_2 derivatives **3**, respectively. No peaks corresponding to the dienes or to decomposition products, such as aryl acetates, were observed.

Recrystallization of the crude product from carbon tetrachloride followed by successive recrystallizations from methanol and ethanol gave pale yellow needles of 5-nitro-3-oxo-1,2,3,7,8,9,10,10*a*-octahydrocyclohepta[*de*]naphthalene (**3***b*) which were sublimed at 145°/0.002 mm; m.p. 149.5–149.8°; i.r. (Nujol) 1695 (C=O), 1605, 1590 (aromatic ring), 1520 cm^{-1} (aromatic NO_2); u.v. max (95% C_2H_5OH) 202 (ε 2980), 274 (ε 1180), 320 nm (shoulder, ε 360 m^2 mol^{-1}); n.m.r. ($CDCl_3$) τ 1.42 and 1.93 (q, 2, J = 2.5 Hz, 4-*H* and 6-*H*), 6.7 (m, 1, C_6H_2CH), 7.0 (m, 2, $C_6H_2CH_2$), 7.3 (m, 2, $COCH_2$), 7.5–9.0 p.p.m. (m, 8, alicyclic CH_2); mass spectrum (70 eV) *m/e* (relative intensity) 245.1060 (100, M_r ($^{12}C_{14}{}^{1}H_{15}{}^{14}N^{16}O_3$) = 245.1052), 228 (20), 217 (17), 203 (34), 199 (39), 189 (10), 188 (9), 171 (16), 142 (17), 141 (26).

Anal. Calcd. for $C_{14}H_{15}NO_3$: C, 68.55; H, 6.16; N, 5.71. Found: C, 68.44; H, 6.15; N, 5.75.

Concentration of the second methanol mother liquor and five recrystallizations of the residue from ethanol gave colorless crystals of 4-nitro-3-oxo-1,2,3,7,8,9,10,10*a*-octahydrocyclohepta[*de*]naphthalene (**3***a*), which were sublimed at 120°/0.002 mm; m.p. 124.5–125.1°; i.r. (Nujol) 1705 (C=O), 1595 (aromatic ring), 1535 cm^{-1} (aromatic NO_2); u.v. max (95% C_2H_5OH) 215 (ε 1900), 254 (shoulder, ε 650), 304 nm (ε 250 m^2 mol^{-1}); n.m.r. ($CDCl_3$) τ 2.62 and 2.86 (q, 2, J = 8 Hz, 5-*H* and 6-*H*), 6.8 (m, 1, C_6H_2CH), 7.1 (m, 2, $C_6H_2CH_2$), 7.4 (m, 2, $COCH_2$), 7.5–9.0 p.p.m. (m, 8, alicyclic CH_2); mass spectrum (70 eV) *m/e* (relative intensity) 245.1048 (53, M_r ($^{12}C_{14}{}^{1}H_{15}{}^{14}N^{16}O_3$) = 245.1052), 229 (3), 217 (35), 201 (28), 187 (14), 184 (14), 173 (13), 171 (13), 161 (13), 159 (19), 143 (29), 141 (37), 129 (44), 128 (100).

Anal. Calcd. for $C_{14}H_{15}NO_3$: C, 68.55; H, 6.16; N, 5.71. Found: C, 68.93; H, 6.15; N, 5.73.

Concentration of the initial carbon tetrachloride mother liquor and recrystallization of the residue from carbon tetrachloride gave crude diene. Chromatography of this on alumina and elution with pentane and pentane–benzene mixtures gave, in the later fractions, an uncontaminated diene which was recrystallized three times from benzene and once from ether to give colorless crystals of 4-acetoxy-6*a*-nitro-3-oxo-1,2,3,4,6*a*,7,8,9,10,10*a*-decahydrocyclohepta-[*de*]naphthalene (**2***a* or *b*), m.p. 120.5° (dec.); i.r. (Nujol) 1735 ($OCOCH_3$), 1690 (C=C), 1675 (conjugated C=O), 1640 (C=C), 1545 cm^{-1} (NO_2); u.v. max (95% C_2H_5OH) 204.5 (ε 690), 241.5 nm (ε 810 m^2 mol^{-1}); n.m.r. ($CDCl_3$) τ 3.64 (q, 1, J_{56} = 9.5 Hz, J_{45} = 4 Hz, 5-*H*), 3.85 (d, 1, J_{45} = 4 Hz, 4-*H*), 3.92 (d, 1, J_{56} = 9.5 Hz, 6-*H*), 8.01 (s, 3, $OCOCH_3$), 7.0–9.3 p.p.m. (alicyclic CH_2); mass spectrum (70 eV) *m/e* (relative intensity) 259.1340 (<1, M_r ($^{12}C_{16}{}^{1}H_{19}{}^{16}O_3$) = 259.1334, $M^{\cdot} - NO_2$), 245.1051 (5, M_r ($^{12}C_{14}{}^{1}H_{15}{}^{14}N^{16}O_3$) = 245.1052, $M^{\cdot} - HOAc$), 217 (5),

Can. J. Chem. Downloaded from www.nrcresearchpress.com by 210.87.254.40 on 09/05/12
For personal use only.

Can. J. Chem. Downloaded from www.nrcresearchpress.com by 210.87.254.40 on 09/05/12
For personal use only.

216 (4), 201 (11), 200 (65), 185 (6), 172 (13), 159 (22), 158 (100).

Anal. Calcd. for $C_{16}H_{19}NO_5$: C, 62.94; H, 6.27; N, 4.59. Found: C, 62.74; H, 6.23; N, 4.56.

A second diene fraction was obtained by concentration of the carbon tetrachloride mother liquor and recrystallization of the residue from 1:1 benzene–pentane. Chromatography on alumina, using benzene–pentane mixtures as eluant, and recrystallization of the final fractions from 1:1 benzene–pentane gave colorless prisms of a second 4-acetoxy-6*a*-nitro-3-oxo-1,2,3,4,6*a*,7,8,9,10,10*a*-decahydrocyclohepta[*de*]naphthalene (2*b* or *a*), m.p. 104–104.8° (dec.); i.r. (Nujol) 1735 ($OCOCH_3$), 1680 (C=C), 1675 (conjugated C=O), 1635 (C=C), 1545 cm^{-1} (NO_2); u.v. max (95% C_2H_5OH) 205.5 (ε 710), 241 nm (ε 830 m^2 mol^{-1}); n.m.r. ($CDCl_3$) τ 3.77 (q, 1, $J_{56} = 10$ Hz, $J_{45} = 3$ Hz, 5-*H*) 3.89 (d, 1, $J_{45} = 3$ Hz, 4-*H*) 3.99 (d, 1, $J_{56} = 10$ Hz, 6-*H*), 7.98 (s, 3, $OCOCH_3$), 7.0–9.2 p.p.m. (alicyclic CH_2); mass spectrum (70 eV) *m/e* (relative intensity) 259.1328 (4, M_r ($^{12}C_{16}{}^{1}H_{19}{}^{16}O_3$) = 259.1334, $M^{\cdot+} - NO_2$), 245.1058 (10, M_r ($^{12}C_{14}{}^{1}H_{15}{}^{14}N^{16}O_3$) = 245.1052, $M^{\cdot+} - HOAc$), 233 (6), 217 (55), 216 (95), 201 (23), 200 (97), 185 (19), 172 (28), 159 (42), 158 (100).

Anal. Calcd. for $C_{16}H_{19}NO_5$: C, 62.94; H, 6.27; N, 4.59. Found: C, 63.11; H, 6.28; N, 4.53.

The residue obtained by concentrating the first benzene–pentane mother liquor was recrystallized from 1:3 benzene–pentane and gave a mixture of diene and nitro compounds which was discarded. The residue obtained by concentrating the new mother liquor was chromatographed on alumina and eluted with pentane and benzene–pentane mixtures. Unreacted tricyclic ketone **1** was eluted in the first 1:1 benzene–pentane fraction. The third column volume of 1:1 benzene–pentane eluted the 6-nitro ketone **3***c*. The 6-nitro-3-oxo-1,2,3,7,8,9,10,10*a*-octahydrocyclohepta[*de*]-naphthalene (**3***c*) was recrystallized from chloroform–ethanol and twice from ethanol, then sublimed at 65°/0.002 mm: m.p. 68.0–69.8°; i.r. (Nujol) 1695 (C=O), 1595 (aromatic ring), 1530 cm^{-1} (NO_2); u.v. max (95% C_2H_5OH) 213 (ε 1870), 252.5 (ε 930), 307 nm (ε 240 m^2 mol^{-1}); n.m.r. ($CDCl_3$) τ 2.0 and 2.57 (q, 2, $J = 8.5$ Hz, 4-*H* and 5-*H*), 6.7 (m, 1, C_6H_2CH), 7.0 (m, 2, $C_6H_2CH_2$), 7.4 (m, 2, $COCH_2$), 7.5–9.0 p.p.m. (m, 8, alicyclic CH_2); mass spectrum (70 eV) *m/e* (relative intensity) 245.1060 (59, M_r ($^{12}C_{14}{}^{1}H_{15}{}^{14}N^{16}O_3$) = 245.1052), 229 (31), 228 (100), 210 (14), 200 (40), 199 (20), 172 (18), 170 (16), 158 (25).

Anal. Calcd. for $C_{14}H_{15}NO_3$: C, 68.55; H, 6.16; N, 5.71. Found: C, 68.64; H, 6.14; N, 5.70.

Nitration of Tetralin in Acetic Anhydride

A solution of nitric acid (9 g, 0.15 mol) in acetic anhydride (25 cm^3) was added to a mixture of tetralin (13.2 g, 0.1 mol) in acetic anhydride (25 cm^3) at −78°. The mixture was allowed to warm to 0° and stirred at this temperature for 10 h. After standing overnight at −5° the reaction mixture was worked-up as described for the tricyclic ketone. The crude product had i.r. (film) 1735 ($OCOCH_3$), 1545 (aliphatic NO_2), 1520 cm^{-1} (aromatic NO_2). Its n.m.r. indicated that approximately 50% diene was present and that all of the tetralin had reacted. The product was chromatographed on basic alumina deactivated with 5% (v/v) of water. Elution with pentane gave nitrotetralins and elution with ether–pentane mixtures gave, in the 10% ether–pentane fraction, 7-acetoxy-4*a*,7-dihydro-4*a*-nitrotetralin: i.r. 1735 (ester C=O), 1545 cm^{-1} (aliphatic NO_2); n.m.r. (CCl_4) τ 4.03 (s, 2, 5-*H* and 6-*H*), 4.16 (m, 1, 8-*H*), 4.36 (m, 1, 7-*H*), 7.2 (m, 1) 7.65 (m, 2), 7.98 (s, 3, $OCOCH_3$), 8.0–9.0 p.p.m. (m, 5).

Nitration of Benzsuberane

Benzsuberane (3 g; 0.02 mol) was nitrated at −20° for 2 h following the procedure described for tetralin. The crude product had i.r. (film) 1740 ($OCOCH_3$), 1545 (aliphatic NO_2), 1520 cm^{-1} (aromatic NO_2); n.m.r. (CCl_4) τ 1.9–3.0 (Ar*H*), 3.7–4.5 (vinylic and allylic *H*) 7.98 and 8.03 p.p.m. ($OCOCH_3$). The integral ratio of the aromatic and diene regions indicated that 40% of the product was dienes and the integral ratio of the two acetate peaks indicated that the likely stereoisomeric dienes were present in a 3:2 ratio. The dienes decomposed before separation from the product mixture.

*Nitration of 5,6,7,8-Tetrahydrocyclohepta[fg]acenaphthene (**8**)*

Preliminary study of the reaction carried out in an n.m.r. tube at −20° showed that diene was formed (200–290 Hz downfield signal from acetic anhydride) in approximately 50% yield. When the reaction was carried out on the cyclohepta-acenaphthene (prepared by the method of Fieser and Peters (14)) at −20°, following the procedure described for tetralin, a yellow solid (405 mg) was obtained whose i.r. (absence of $OCOCH_3$) and n.m.r. (absence of vinyl–allylic *H*) showed that no diene was present. Recrystallization (× 2) from carbon tetrachloride gave 1-nitro-5,6,7,8-tetrahydrocyclohepta[*fg*]acenaphthene (**10**), m.p. 123.0–123.7°; i.r. (Nujol) 1595 (aromatic ring) 1555 (aliphatic NO_2) 835, 826, 792 cm^{-1} (aromatic C—H bending); n.m.r. (CCl_4) τ 2.51 and 2.76 (q, 2, $J_{9,10} = 7$ Hz, $J_{1,10} = 1.0$ Hz, 10-*H* and 9-*H* respectively), 2.82 (s, 2, 3-*H* and 4-*H*), 3.71 (q, 1, $J_{1,2\alpha} = 7.5$ Hz, $J_{1,2\beta} = 3.0$ Hz, 1-*H*) 5.93 and 6.27 (octet, 2, $J_{2\alpha,2\beta} = 18$ Hz, $J_{1,2\alpha} = 7.5$ Hz, $J_{1,2\beta} = 3.0$ Hz, 2β-H and 2α-H respectively), 6.80 (b, 4, 5-H_2 and 8-H_2), 7.85–8.05 p.p.m. (m, 4, 6-H_2 and 7-H_2); mass spectrum (70 eV) *m/e* (relative intensity) 253 (6, M_r ($^{12}C_{16}{}^{1}H_{15}{}^{14}N^{16}O_2$) = 253), 237 (1), 221 (2), 208 (18), 207 (100), 191 (8), 189 (9), 179 (9), 178 (8), 165 (33). This compound was photosensitive and it decomposed before analysis.

When the nitration reaction was carried out at −78° and the reaction mixture quenched at this temperature by condensing gaseous ammonia into it, the product isolated contained diene as well as nitro-arenes: i.r. (film) 1735 and 1230 ($OCOCH_3$), 1550 (aliphatic NO_2), 1530 cm^{-1} (aromatic NO_2); the n.m.r. showed absorption in the vinyl–allylic region (τ 3.5–4.5). However the diene decomposed before it could be separated from the other products.

*Nitration of 1,2,3,4,7,8,9,10-Octahydrodicyclohepta-[de,ij]naphthalene (**7**)*

Preliminary study of the reaction carried out in an n.m.r. tube at −30° indicated that diene was formed and that it was still present in the reaction mixture at room temperature. The reaction was carried out on the hydrocarbon (0.25 mmol) at −35° for 30 min and the product was isolated following the procedure described for the tricyclic ketone (**1**): i.r. (film) 1745 and 1235 ($OCOCH_3$), 1550 (aliphatic NO_2), 1530 cm^{-1} (aromatic NO_2); n.m.r. (CCl_4) τ 2.60, 2.64, 2.75, 2.81, 2.97, and 3.08 (aromatic *H*), 4.07 and 4.26

(q, integral = 0.5 of aromatic region, $J_{56} = 9.5$ Hz, 5-*H* and 6-*H*), 6.5–8.8 (benzylic and alicyclic H), 8.00, 8.04, and 8.05 p.p.m. (probably two or all three from $OCOCH_3$). The diene, of likely structure **11**, could not be isolated from the other products without decomposition.

Exact Analysis of the Nuclear Magnetic Resonance Spectra of Dienes **2***a and b*

A computer program written by Dr. A. L. Wilkinson and following Castellano and Waugh's method of exact analysis of three spin systems (15) was used to evaluate coupling constants and chemical shifts for the vinyl–allylic protons of the dienes.

In the case of the first diene, two solutions were obtained which satisfied the requirements of a positive *cis* vinyl coupling and three- and four-bond vinyl–allylic couplings within the range predicted by Garbisch's equations (16). For the second diene it was necessary to irradiate in the alicyclic proton range in order to remove a coupling to the 4-proton before a solution from the three spin system could be obtained. Solutions are given in Table 1.

We thank the National Research Council of Canada and the University of Victoria for financial support and Dr. Alan L. Wilkinson for computer analysis of n.m.r. spectra.

1. D. J. BLACKSTOCK, A. FISCHER, K. E. RICHARDS, J. VAUGHAN, and G. J. WRIGHT. Chem. Commun. 641 (1970).
2. D. J. BLACKSTOCK, J. R. CRETNEY, A. FISCHER, M. P. HARTSHORN, K. E. RICHARDS, J. VAUGHAN, and G. J. WRIGHT. Tetrahedron Lett. 2793 (1970).
3. A. FISCHER, C. C. GREIG, D. R. A. LEONARD, and A. L. WILKINSON. Can. J. Chem. **50**, 2211 (1972).
4. C. L. PERRIN and G. A. SKINNER. J. Am. Chem. Soc. **93**, 3389 (1971).
5. A. I. SCOTT. Interpretation of the ultraviolet spectra of natural products. Pergamon Press, Oxford. 1964. Chapt. 2.
6. E. W. GARBISCH, JR. J. Am. Chem. Soc. **86**, 5561 (1964).
7. H. BUDZIKIEWICZ, C. DJERASSI, and D. H. WILLIAMS. Mass spectrometry of organic compounds. Holden-Day Inc. San Francisco. 1967. p. 516.
8. A. FISCHER, J. VAUGHAN, and G. J. WRIGHT. J. Chem. Soc. 368 (1967).
9. R. O. C. NORMAN and R. TAYLOR. Electrophilic substitution in benzenoid compounds. Elsevier, Amsterdam. 1965. p. 306.
10. A. FISCHER, D. R. A. LEONARD, and D. A. R. HAPPER. Can. J. Chem. **48**, 1446 (1970).
11. R. ROBINSON and H. W. THOMPSON. J. Chem. Soc. 2015 (1932).
12. A. L. WILKINSON. Personal communication.
13. E. W. GARBISCH, JR. and M. G. GRIFFIN. J. Am. Chem. Soc. **90**, 3590 (1968).
14. L. F. FIESER and M. A. PETERS. J. Am. Chem. Soc. **54**, 4347 (1932).
15. S. CASTELLANO and J. S. WAUGH. J. Chem. Phys. **34**, 295 (1961).

Can. J. Chem. Downloaded from www.nrcresearchpress.com by 210.87.254.40 on 09/05/12
For personal use only.

Synthesis of 4-*O*-β-D-Glucopyranosyl-L-rhamnopyranose

G. M. BEBAULT AND G. G. S. DUTTON
Chemistry Department, University of British Columbia, Vancouver 8, British Columbia

Received June 1, 1972

4-*O*-(β-D-Glucopyranosyl)-L-rhamnose (scillabiose) has been synthesized in 55% yield by condensation of 2,3,4,6-tetra-*O*-acetyl-α-D-glucopyranosyl bromide with methyl 2,3-*O*-isopropylidene-α-L-rhamnopyranoside using mercuric cyanide in acetonitrile (Helferich reaction). The disaccharide and the derived alditol are both syrups but each forms a crystalline peracetate. A convenient synthesis of 1-deoxy-D-erythritol is described.

4-*O*-(β-D-Glucopyrannosyle)-L-rhamnose (scillabiose) a été synthétisé avec un rendement de 55% par réaction du α-D-tétracétylbromoglucose avec le méthyl 2,3-*O*-isopropylidène-α-L-rhamnopyrannoside en utilisant le cyanure de mercure dans l'acétonitrile (réaction de Helferich). Le disaccharide et l'alditol correspondant sont sirops mais chacun donne un peracétate crystallin. Une nouvelle synthèse de 1-deoxy-D-erythritol est décrite.

Canadian Journal of Chemistry, **50**, 3373 (1972)

Can. J. Chem. Downloaded from www.nrcresearchpress.com by 210.87.254.6 on 09/05/12
For personal use only.

L-Rhamnose is widely distributed in nature and is commonly found as a constituent of plant gums (1), plant glycosides (2), and in bacterial polysaccharides (3). Despite this, no disaccharide having L-rhamnose as the aglycone has been synthesized (4) with the exception of 4-*O*-(3-*O*-methyl-β-D-galactopyranosyl)-L-rhamnose (5). Such disaccharides are invaluable not only for the identification of fragments obtained in structural studies but also for the determination of immunodominant groups in polysaccharides which have antigenic activity (6). The aldobiouronic acid 4-*O*-(β-D-glucopyranosyluronic acid)-L-rhamnose has been isolated from hydrolyzates of *Acrosiphonia centralis* (7), *Ulva lactuca* (8), and *Klebsiella* K9 capsular polysaccharide (9). In the first two cases this acid has been characterized after reduction to the neutral disaccharide.

The synthesis of 4-*O*-(β-D-glucopyranosyl)-L-rhamnose (scillabiose) described here was originally undertaken mainly as a model study for the subsequent synthesis of the D-manno- analog (3) but since the related aldobiouronic acid has now been identified as a component of *Klebsiella* type K9 capsular polysaccharide the preparation of this disaccharide is related to our studies on these bacteria. Scillabiose was first isolated from the glycosides scillarin A and glucoscilliphaeoside obtained from *Scilla maritima* (2, 10) and its identification as 4-*O*-(β-D-glucopyranosyl)-L-rhamnose was subsequently established (11, 12).

Methyl 2,3-*O*-isopropylidene-α-L-rhamnopyranoside (**3**) was prepared most conveniently from methyl α-L-rhamnopyranoside (**1**) by reaction with acetone in the presence of cation exchange resin (13–16) and was purified through the crystalline 4-acetate (**2**). Condensation of this intermediate with 2,3,4,6-tetra-*O*-acetyl-α-D-glucopyranosyl bromide using mercuric cyanide in acetonitrile (17) gave methyl 4-*O*-(2,3,4,6-tetra-*O*-acetyl-β-D-glucopyranosyl)-2,3-*O*-isopropylidene-α-L-rhamnopyranoside (**5**) as a crystalline product (yield 80%).

Initial attempts to prepare scillabiose heptaacetate (**7**) by direct acetolysis of **5** under several different conditions gave only very poor yields (15%) of **7**. This was eventually explained by the fact that direct acetolysis gave a product soluble in water that was thus lost during washing of the organic solvent layer. A search of the literature revealed that in a review Guthrie and McCarthy (18) do not mention any example of acetolysis where an acetal (or ketal) is formed between two secondary hydroxyl groups in a sugar ring. Subsequent to the date of this review acetolysis has been used for benzylidene acetals (19) and isopropylidene ketals (20) but in each case the rings have spanned primary and secondary hydroxyl groups. Acetolysis of isopropylidene ketals formed between two secondary hydroxyl groups has been studied by Sowa (21) in extending an earlier observation made by Jerkeman (22) but these examples involved furanose systems and

Can. J. Chem. Downloaded from www.nrcresearchpress.com by 210.87.254.6 on 09/05/12
For personal use only.

epimerization. Acetolysis of methyl glycosides has been successfully achieved in several cases (18, 19, 23).

Scillabiose heptaacetate (**7**) was obtained in good yield (70%) when the isopropylidene group was removed from the intermediate **5** prior to acetolysis. This was achieved most conveniently by treatment with trifluoroacetic acid (24) and acetolysis was then carried out essentially as described by Aspinall and co-workers (19). Scillabiose heptaacetate (**7**) thus obtained had m.p. 139–140° and n.m.r. showed clearly the presence of seven acetate groups. Neither the melting point nor the optical rotation agree with that given in the literature (2, 10) for "scillabiose hexaacetate". Although satisfactory analytical data are given for a hexaacetate there is no indication why such an acetate should be formed and Bailey (4) has recognized this ambiguity by listing only scillabiose acetate. Deacetylation gave scillabiose as a syrup which was reduced and acetylated to give crystalline scillabiitol octaacetate, m.p. 132–133°. The n.m.r. spectrum of the free disaccharide and the corresponding alditol each in deuterium oxide showed $J_{1,2}$ 7.5 and 7.2 Hz, respectively, consistent with a β-D-linkage (25). Determination of the number of substituent groups in rhamnose disaccharides and intermediates is greatly facilitated by the doublet at about τ 8.70 characteristic of the 6-deoxy group.

Proof of structure of the disaccharide was obtained by periodate oxidation and methylation of the methyl glycoside of the disaccharide. The methyl glycoside (**9**) was prepared by deacetylation of **6**; removal of sodium ion with cation exchange resin was best done in the cold to prevent hydrolysis of the labile methyl glycoside of the 6-deoxy hexose. The disaccharide glycoside consumed 3.0 mol of periodate and successive borohydride reduction and methanolysis gave glycerol and 1-deoxy-D-erythritol identified by g.l.c. and mass spectrometry of their acetate derivatives. When the polyalcohol was hydrolyzed, rather than methanolyzed, one major peak and several smaller ones were obtained on g.l.c., in addition to the peaks expected for glycerol and 1-deoxy-D-erythritol. Methanolysis gave essentially only two peaks with traces of other components. This is a further example of the difficulty of obtaining quantitative hydrolysis of such polyalcohols. This and related problems have been discussed elsewhere (26). 1-Deoxy-D-erythritol was conveniently prepared by a new route involving periodate oxidation of methyl 4-*O*-acetyl-α-L-rhamnopyranoside (**13**).

Methylation (27) of the disaccharide glycoside followed by methanolysis and g.l.c. indicated the presence of methyl 2,3,4,6-tetra-*O*-methyl-D-glucopyranoside and methyl 2,3-di-*O*-methyl-L-rhamnopyranoside. Hydrolysis of the permethylated disaccharide followed by borohydride reduction gave 2,3,4,6-tetra-*O*-methyl-D-glucitol and 2,3-di-*O*-methyl-L-rhamnitol identified by g.l.c. and mass spectrometry (28) of their acetate derivatives. 2,3,4,6-Tetra-*O*-methyl-D-glucose and 2,3-di-*O*-methyl-L-rhamnose are not separable on g.l.c. as their methyl glycosides but can be completely separated by making the trimethylsilyl derivative of the methyl glycosides. This shortens the retention time of the rhamnosides and is a method which has been used with particular success in the mannose series (29, 30). They can also be completely separated as acetate derivatives (31).

Experimental

Melting points were taken between glass slides on a Fisher–Johns apparatus and are uncorrected. Optical rotations were measured with a Perkin–Elmer model 141 polarimeter at 23 ± 1°. N.m.r. spectra were recorded on a Varian XL-100 instrument using tetramethylsilane as internal standard except as noted. Gas–liquid partition chromatography was carried out on an F and M 720 instrument at a gas flow rate of 60 ml/min using columns: (*a*) 2 ft × 1/4 in. 20% SE 30 (F and M Division, Hewlett Packard, Avondale, Pennsylvania), (*b*) 4 ft × 1/4 in. 5% butanediol succinate on 80–100 mesh Diatoport S and (*c*) 6 ft × 1/4 in. 15% OS 138 on 100–120 mesh Gas Chrom Q. T.l.c. was carried out using solvent systems A and B (see below) on silica gel G (EM Reagents). The dried plates were visualized by spraying with 35% ethanolic sulfuric acid and heating to about 150° for 3–5 min. Paper chromatographic separations were carried out on Whatman No. 1 paper using the upper layer of solvent systems C and D (see below) and were visualized using silver nitrate in acetone for non-reducing compounds (32) and *p*-anisidine spray (33) in trichloroacetic acid for reducing sugars. Solvent A, ethyl ether–toluene (2:1); B, butanone–water azeotrope; C, ethyl acetate–pyridine–water (8:2:2); D, 1-butanol–ethanol–water (4:1:5). R_G indicates with respect to 2,3,4,6-tetra-*O*-methyl-D-glucose. Solutions were concentrated below 50° *in vacuo*.

Methyl α-L-Rhamnopyranoside (1)

This compound was prepared essentially as described by Levene and Muskat (34). The glycoside crystallized from

Can. J. Chem. Downloaded from www.nrcresearchpress.com by 210.87.254.6 on 09/05/12
For personal use only.

ethyl acetate immediately upon being seeded; yield 80%. Recrystallization from ethyl acetate gave pure **1**, m.p. 108.5–109°; $[\alpha]_D$ −60.4° (*c* 9.6, water); R_f (solvent B) 0.39; (lit. (35, 36) m.p. 108–109°, $[\alpha]_D$ −62.5° (*c* 9.1, water)); n.m.r. (D_2O, external TMS): τ 5.36 (1H doublet, $J_{1,2}$ = 1.5 Hz, H-1), 6.64 (3H singlet, C-1 OMe), 8.75 (3H doublet, $J_{5,6}$ = 6 Hz, CH_3).

Methyl 4-O-Acetyl-2,3-O-isopropylidene-α-L-rhamnopyranoside (2)

A solution of methyl α-L-rhamnopyranoside (**1**) (5 g) in dry acetone (150 ml) was magnetically stirred in an ice–water bath with 2,2-dimethoxypropane (50 ml) and Amberlite IR 120 H^+ resin (10 ml, freshly regenerated, soaked in acetone overnight) for 5 h. The solution was filtered through a layer of calcium oxide to remove traces of acid and the filtrate was concentrated. T.l.c. (solvent B) showed a major component with R_f 0.69 and a small amount of starting material. The syrupy product was acetylated with pyridine (30 ml) and acetic anhydride (30 ml). The acetate (**2**) was crystallized from ethanol (25 ml); yield 4.9 g. Recrystallization from ethanol gave pure **2**, m.p. 66–67°; $[\alpha]_D$ −16.5° (*c* 2.4, chloroform); (lit. (37) m.p. 61–63°, $[\alpha]_D$ −14.5° (*c* 2.8, chloroform)); n.m.r. ($CDCl_3$): τ 5.10 (1H singlet, H-1), 6.62 (3H singlet, C-1 OMe), 7.92 (3H singlet, C-4 OAc), 8.44, 8.66 (3H singlets, isopropylidene CH_3's), 8.83 (3H doublet, $J_{5,6}$ = 6Hz, CH_3).

Anal. Calcd. for $C_{12}H_{20}O_6$: C, 55.37; H, 7.75; OMe, 11.92. Found: C, 55.73; H, 7.73; OMe, 12.11.

Methyl 2,3-O-Isopropylidene-α-L-rhamnopyranoside (3)

Methyl4-*O*-acetyl-2,3-*O*-isopropylidene-α-L-rhamnopyranoside (**2**) (5.9 g) was dissolved in dry methanol (10 ml) and treated with sodium methoxide (0.2 *N*, 25 ml) for 30 min. Sodium ion was removed from the chilled solution with Amberlite IR 120 H^+ resin and the methanol was evaporated to give a syrupy product **3**; yield 4.9 g. T.l.c. (solvent A) showed one spot with R_f 0.54; $[\alpha]_D$ −16.4° (*c* 3.1, acetone); (lit. (34, 38) $[\alpha]_D$ −15.9° (*c* 1.6, acetone)); n.m.r. ($CDCl_3$); τ 5.14 (1H singlet, H-1), 6.62 (3H singlet, C-1 OMe), 8.70 (3H doublet, $J_{5,6}$ = 6 Hz CH_3), 8.48, 8.65 (3H singlets, *endo-*, *exo*-isopropylidene CH_3 (39)).

2,3,4,6-Tetra-O-acetyl-α-D-glucopyranosyl Bromide (4)

Compound **4** was prepared from anhydrous D-glucose either as reported by Lemieux (40) in 68% yield or more conveniently but in lower yield (55%) by the method of Dale (41). In both cases recrystallization from ether gave pure **4**, m.p. 90.5–91°; $[\alpha]_D$ +199.9° (*c* 2.2, chloroform); (lit. (40) m.p. 88–89°, $[\alpha]_D$ +197.8° (*c* 2, chloroform)).

Methyl 4-O-(2,3,4,6-Tetra-O-acetyl-β-D-glucopyranosyl)-2,3-O-isopropylidene-α-L-rhamnopyranoside (5)

To a solution of methyl 2,3-*O*-isopropylidene-α-L-rhamnopyranoside **3** (4.9 g, 22.5 mmol) and dry mercuric cyanide (5.0 g) in acetonitrile (50 ml, distilled over CaH_2) was added the bromide **4** (15 g) with stirring and the stirring was continued for 5 h. The acetonitrile was removed from the reaction mixture under reduced pressure and the remaining syrup was dissolved in chloroform (150 ml). The chloroform solution was washed with 1 *N* potassium bromide (2 × 75 ml), water (75 ml), saturated sodium bicarbonate (75 ml), and water (2 × 75 ml). The chloroform was removed and the remaining syrup, dissolved in warm ethanol (50 ml), crystallized upon cooling; yield 9.9 g, 18.0 mmol, 80%. Recrystallization from ethanol gave pure **5**, m.p. 158.5–159°; $[\alpha]_D$ −30.6° (*c* 1.7, chloroform); R_f (t.l.c. solvent A) 0.56; n.m.r. ($CDCl_3$): τ 6.66 (3H singlet, C-1 OMe), 7.96–8.03 (12H, OAc's), 8.75 (3H doublet, $J_{5,6}$ = 6 Hz, CH_3), 8.49, 8.67 (3H singlets, isopropylidene CH_3's).

Anal. Calcd, for $C_{24}H_{36}O_{14}$: C, 52.55; H, 6.62. Found: C, 52.63; H, 6.74.

Methyl 4-O-(2,3,4,6-Tetra-O-acetyl-β-D-glucopyranosyl)-α-L-rhamnopyranoside (6)

A solution of methyl 4-*O*-(2,3,4,6-tetra-*O*-acetyl-β-D-glucopyranosyl)-2,3-*O*-isopropylidene-α-L-rhamnopyranoside (**5**) (2.0 g) in chloroform (90 ml) was treated at room temperature for 1 h with trifluoroacetic acid containing 1% water (10 ml). The reaction mixture was concentrated and any remaining trifluoroacetic acid was removed by distillation with toluene. The remaining syrup showed one spot on t.l.c., R_f (solvent A) 0.09 and (solvent B) 0.66; yield 1.83 g; n.m.r. ($CDCl_3$): τ 6.65 (3H singlet, C-1 OMe), 7.93–8.01 (12H, OAc's), 8.70 (3H doublet, $J_{5,6}$ = 6 Hz, CH_3).

4-O-(2,3,4,6-Tetra-O-acetyl-β-D-glucopyranosyl)-1,2,3-tri-O-acetyl-α-L-rhamnopyranose (Scillabiose Heptaacetate) (7)

Methyl 4-*O*-(2,3,4,6-tetra-*O*-acetyl-β-D-glucopyranosyl)-α-L-rhamnopyranoside (**6**) (1.0 g) in acetic anhydride (5 ml) was shaken with concentrated sulfuric acid 2% (v/v) in acetic anhydride (10 ml) for 5 h (19). The reaction mixture was diluted with chloroform (100 ml) and the chloroform solution was washed with water (2 × 100 ml), saturated sodium bicarbonate (2 × 75 ml), and again with water (3 × 100 ml). The recovered syrup was dissolved in 2-propanol (20 ml) and the heptaacetate (**7**) crystallized immediately upon seeding with a crystal obtained from a t.l.c. plate separation (42); yield 0.85 g. T.l.c. (solvent A) showed a major component with R_f 0.34 and only a trace of cleavage products. Recrystallization from 2-propanol gave pure **7**, m.p. 139–140°; $[\alpha]_D$ −62.3° (*c* 2.6, chloroform); n.m.r. ($CDCl_3$): τ 4.04 (1H doublet, $J_{1,2}$ = 1.5 Hz, H-1), 7.86–8.04 (21H, OAc's), 8.70 (3H doublet, $J_{5,6}$ = 6 Hz, CH_3).

Anal. Calcd. for $C_{26}H_{36}O_{17}$: C, 50.32; H, 5.85. Found: C, 50.07; H, 5.84.

4-O-β-D-Glucopyranosyl-L-rhamnopyranose (8)

Scillabiose heptaacetate (**7**) (500 mg) was treated with sodium methoxide (0.2 *N*, 25 ml) for 1 h at room temperature. Sodium ion was removed with Amberlite IR 120 H^+ resin and the methanol was evaporated. The remaining syrup (250 mg) showed one spot on a paper chromatogram (solvent C) with $R_{glucose}$ 1.2; $[\alpha]_D$ −24.2° (*c* 1.1, water); (lit. (10) $[\alpha]_D$ −24.8° (*c* 3.3, water)); n.m.r. (D_2O, external TMS): τ 4.88 (1H doublet, $J_{1,2}$ = 1.5 Hz, H-1 of α-L-form), 5.12 (1H doublet, $J_{1,2}$ = 0.8 Hz, H-1 of β-L-form), 5.26 (1H doublet, $J_{1',2'}$ = 7.5 Hz, H-1'), 8.65 (3H doublet, $J_{5,6}$ = 6 Hz, CH_3).

G.l.c. of the per(trimethylsilyl) disaccharide (column *a* at 250°) gave one peak (73%) at 10.1 min and a second peak at 12.6 min (per(trimethylsilyl) sucrose 12.6 min) (43).

Methyl 4-O-β-D-Glucopyranosyl-α-L-rhamnopyranoside (9)

Methyl 4-*O*-(2,3,4,6-tetra-*O*-acetyl-β-D-glucopyranosyl)-

Can. J. Chem. Downloaded from www.nrcresearchpress.com by 210.87.254.6 on 09/05/12
For personal use only.

α-L-rhamnopyranoside (**6**) (1.83 g) was deacetylated with sodium methoxide (0.2 *N*, 25 ml) for 1 h. Sodium ion was removed from the cold solution with Amberlite IR 120 H^+ resin and the methanol was removed. T.l.c. (solvent B) showed a major component with R_f 0.04 and a small amount of a faster running compound; yield 1.1 g. A portion of the syrupy product was purified by preparative t.l.c. (42) for analytical purposes $[\alpha]_D$ −57.5° (*c* 1.5, methanol); $R_{glucose}$ (solvent C) 2.9; n.m.r. (D_2O, external TMS): τ 5.30 (1H doublet, $J_{1',2'} = 7.7$ Hz, H-1'), 5.32 (1H doublet, $J_{1,2} = 1.5$ Hz, H-1), 6.61 (3H singlet, C-1 OMe), 8.65 (3H doublet, $J_{5,6} = 6$ Hz, CH_3).

Reaction of the methyl glycoside of the disaccharide **9** (0.625 g) with sodium metaperiodate (0.05 *M*, 400 ml) at 5° in the dark showed a rapid uptake of 1 mol with the consumption of periodate becoming constant (3.0 mol) in 48 h (44, 45). Iodate and excess periodate were removed by addition of barium acetate and the residual polyaldehyde was reduced with sodium borohydride (0.6 g). A portion of the polyalcohol (0.1 g), obtained by deionization, distillation with methanol, and concentration, was subjected to methanolysis (3% HCl in methanol, 10 ml, reflux, 6.5 h) and then neutralized with Duolite A 4 OH^- resin. Glycolaldehyde dimethyl acetal and solvents were removed by evaporation and the recovered syrup showed two major spots on paper chromatography (solvent D) corresponding to standard 1-deoxy-D-erythritol and glycerol. A portion was acetylated with pyridine (1 ml) and acetic anhydride (1 ml). Injection in ethyl acetate, onto column *b* at 140° gave peaks identical to authentic standards of the peracetylated derivatives of 1-deoxy-D-erythritol (12 min) and glycerol (18 min). Samples were collected and the mass spectra obtained corresponded to those of the authentic standards.

Methyl glycoside (**9**) (1.1 g) in dry methyl sulfoxide (20 ml) was methylated (46) by reaction with methyl sulfinyl anion (1.5 *M*, 20 ml) for 4 h and then shaking with methyl iodide (6 ml) overnight. The reaction mixture was diluted with water and the product was extracted with petroleum ether (b.p. 65–70°). The recovered syrup (**10**) (1 g) gave one spot on t.l.c. (solvent A) with R_f 0.28; $[\alpha]_D$ −51° (*c* 2.6, methanol); (lit. (7) $[\alpha]_D$ +7° (*c* 2.0, methanol)); n.m.r. ($CDCl_3$): τ 5.26 (1H doublet, $J_{1,2} = 1.5$ Hz, H-1), 5.37 (1H doublet, $J_{1',2'} = 7.7$ Hz, H-1'), 6.36–6.63 (21H, OMe's), 8.68 (3H doublet, $J_{5,6} = 6$ Hz, CH_3). Methanolysis of **10** (300 mg, 3% methanolic HCl, 30 ml, reflux, 8 h) and examination of the methyl glycosides as the trimethylsilyl derivatives on column *b* programmed from 110 to 205° at 2°/min, gave peaks corresponding to methyl 2,3-di-*O*-methyl-L-rhamnopyranosides (6.8, 9.8 min) and methyl 2,3,4,6-tetra-*O*-methyl-D-glucopyranosides (15.4, 20.7 min). The peak corresponding to methyl 2,3,4,6-tetra-*O*-methyl-β-D-glucopyranoside was collected, m.p. 36° (lit. (47) m.p. 39–41°). The mixed melting point with standard was undepressed. Hydrolysis of **10** (300 mg, 2 *N* TFA, 25 ml, 5 ml methanol, reflux, 16 h) gave a 1:1 mixture of 2,3,4,6-tetra-*O*-methyl-D-glucose and 2,3-di-*O*-methyl-L-rhamnose as shown by paper chromatography (solvent D) using authentic standards. They could also be separated by g.l.c. as their acetate derivatives on column *b* programmed from 110 to 210° at 2°/min. The glucose derivatives gave two peaks at 27.9 min (29%) and 30.2 min (21%) while the rhamnose derivatives gave two peaks at 37.0 min (38%) and 40.7 min (4%). Two unidentified peaks at 16.1 min (5%) and 18.5 min (3%) may be rhamnofuranose derivatives. A portion of the hydrolyzate was reduced with sodium borohydride and the resulting alditols acetylated with pyridine and acetic anhydride. Injection in ethyl acetate onto column *b* at any temperature gave one peak but column *c* at 225° gave two peaks identical to authentic standards of 1,4,5-tri-*O*-acetyl-2,3-di-*O*-methyl-L-rhamnitol (38.6 min) and 1,5-di-*O*-acetyl-2,3,4,6-tetra-*O*-methyl-D-glucitol (46.3 min) (28). Samples were collected and the mass spectra obtained corresponded to those of the authentic standards.

*4-O-β-D-Glucopyranosyl-L-rhamnitol (**11**)*

The free disaccharide **8** (200 mg) was reduced with sodium borohydride (50 mg) in water (10 ml) overnight. Passage through cation exchange resin, concentration, and distillation with methanol gave **11**; $R_{glucose}$ (solvent C) 0.8; n.m.r. (D_2O, external TMS): τ 5.37 (1H doublet, $J_{1,2} = 7.2$ Hz, H-1), 8.70 (3H doublet, $J_{5,6} = 6$ Hz, CH_3).

G.l.c. of the per(trimethylsilyl) alditol (column *a* at 250°) gave one peak at 13.3 min (per(trimethylsilyl) sucrose, 16.6 min) (43).

The alditol **11** was acetylated with pyridine (3 ml) and acetic anhydride (3 ml) to give 4-*O*-β-D-glucopyranosyl-L-rhamnitol octaacetate (scillabiitol octaacetate) (**12**) (320 mg, crystallized from ethanol (20 ml)). Recrystallization from ethanol gave pure **12**, m.p. 132–133°; $[\alpha]_D$ −78.6° (*c* 2.0, chloroform); R_f (t.l.c., solvent A) 0.33; n.m.r. ($CDCl_3$): τ 7.84–7.99 (24H, OAc's), 8.66 (3H doublet, $J_{5,6} = 6$ Hz, CH_3).

Anal. Calcd. for $C_{28}H_{40}O_{18}$: C, 50.60; H, 6.07. Found: C, 50.63; H, 6.06.

*Methyl 4-O-Acetyl-α-L-rhamnopyranoside (**13**)*

A solution of methyl 4-*O*-acetyl-2,3-*O*-isopropylidene-α-L-rhamnopyranoside (**2**) (3 g) in chloroform (135 ml) was treated for 1 h at room temperature with trifluoroacetic acid containing 1% water (15 ml). The reaction mixture was concentrated on the rotary evaporator and any remaining TFA removed by distillation with toluene. The remaining syrup crystallized neat (2.5 g). T.l.c. showed one spot with R_f (solvent B) 0.66. It was further purified by recrystallization from ethyl acetate or by sublimation, m.p. 117°; $[\alpha]_D$ −104.1° (*c* 2.2, chloroform), $[\alpha]_D$ −56.0° (*c* 2.8, water); (lit. (37) m.p. 112–116°, $[\alpha]_D$ −55° (*c* 1.8, water)); n.m.r. $CDCl_3$): τ 5.30 (1H doublet, $J_{1,2} = 1.5$ Hz, H-1), 6.64 (3H singlet, C-1 OMe), 7.90 (3H singlet, OAc), 8.80 (3H doublet, $J_{5,6} = 6$ Hz, CH_3).

Anal. Calcd. for $C_9H_{16}O_6$: C, 49.09; H, 7.32. Found: C, 49.22; H, 7.53.

*1-Deoxy-D-erythritol (**14**)*

Reaction of methyl 4-*O*-acetyl-α-L-rhamnopyranoside (**13**) (2.4 g) with sodium metaperiodate (0.05 *M*, 400 ml) at 5° in the dark reached a constant uptake of 1 mol (44, 45) in 20 h. Iodate and excess periodate were removed by addition of barium acetate and the residual polyaldehyde was deacetylated and reduced with sodium borohydride (2 g). The polyalcohol, obtained by deionization, distillation with methanol, and concentration, was subjected to methanolysis (3% HCl, 30 ml, reflux, 6.5 h) and then neutralized with Duolite A 4 OH^- resin. Glycolaldehyde dimethyl

Can. J. Chem. Downloaded from www.nrcresearchpress.com by 210.87.254.6 on 09/05/12
For personal use only.

acetal and solvent were evaporated and the remaining crude syrup (1.1 g) gave $[\alpha]_D$ 0.4° (*c* 1.6, methanol); (lit. (48) $[\alpha]_D$ +7.4° (*c* 2, methanol)); R_f (solvent D) 0.57 (lit. (49) R_f (solvent D) 0.53). A portion was acetylated with pyridine and acetic anhydride and when injected onto column *b* at 140° gave a major peak at 12 min. A sample was collected and the mass spectrum obtained showed *m/e* 43, 44, 70, 71, 86, 87, 103, 115, 117, 130, 145, 159, and 189. Another portion (1 g) was converted to 1-deoxy-D-erythritol tri-(*p*-nitrobenzoate), m.p. 161–162° (acetone, 2.7 g/10 ml); $[\alpha]_D$ 81.9° (*c* 2.2, chloroform); (lit. (49) m.p. 159–160°, $[\alpha]_D$ 81.07° (*c* 2.05, chloroform)).

Anal. Calcd. for $C_{25}H_{19}O_{12}N_3$: C, 54.26; H, 3.46; N, 7.59. Found: C, 54.08; H, 3.31; N, 7.81.

*Methyl 2,3-Di-O-methyl-α-L-rhamnopyranoside (**15**)*

Methyl 4-*O*-acetyl-α-L-rhamnopyranoside (**13**) (500 mg) in dichloromethane (5 ml) was chilled in an ice–salt water bath (−5°). Boron trifluoride etherate solution (1 ml of a solution of 0.4 ml of BF_3 etherate in 10 ml of dichloromethane) was added to the reaction mixture and then diazomethane in dichloromethane (at −78°) was added dropwise while swirling the flask until a faint yellow color persisted. The reaction mixture was kept at −5° for 30 min and then allowed to warm up (50, 51). The solid polymethylene was filtered off and the filtrate was concentrated. T.l.c. (solvent A) showed a major spot at R_f 0.47 with a minor monomethyl component at R_f 0.29. The product was purified by a preparative t.l.c. separation (solvent A) (42); yield 450 mg; n.m.r. ($CDCl_3$): τ 5.25 (1H doublet, $J_{1,2}$ = 1.5 Hz, H-1), 6.49, 6.58, 6.61 (3H singlets, OMe's), 7.93 (3H singlet, OAc), 8.80 (3H doublet, $J_{5,6}$ = 6 Hz, CH_3). Deacetylation of methyl 4-*O*-acetyl-2,3-di-*O*-methyl-α-L-rhamnopyranoside gave a syrup (t.l.c. (solvent A) R_f 0.24) (270 mg); $[\alpha]_D$ −5.6° (*c* 2.0, water); $[\alpha]_D$ −27.8° (*c* 2.0, chloroform); (lit. (52) $[\alpha]_D$ −6° (*c* 2.0, water); (53) $[\alpha]_D$ −14° (*c* 1.97); (54) $[\alpha]_D$ −26.2° (*c* 0.3, chloroform)), n.m.r. ($CDCl_3$): τ 5.24 (1H doublet, $J_{1,2}$ = 1.5 Hz, H-1), 6.52, 6.56, 6.64 (3H singlets, OMe's), 8.68 (3H doublet, $J_{5,6}$ = 6 Hz, CH_3). A portion of **15** (200 mg) gave methyl 2,3-di-*O*-methyl-4-*O*-toluene-*p*-sulfonyl-α-L-rhamnopyranoside (300 mg), m.p. 114° (2-propanol, 100 mg/ml); $[\alpha]_D$ −36.7° (*c* 2.6, chloroform); (lit. (52) m.p. 111°, $[\alpha]_D$ −33° (*c* 2.0 chloroform)); n.m.r. ($CDCl_3$): τ 2.12–2.74 (4H, aromatic protons), 5.30 (1H doublet, $J_{1,2}$ = 1.5 Hz, H-1), 6.56, 6.68, 7.06 (3H singlets, OMe's), 7.58 (3H singlet, toluene CH_3), 8.67 (3H doublet, $J_{5,6}$ = 6 Hz, CH_3).

Anal. Calcd. for $C_{16}H_{24}O_7S$: C, 53.32; H, 6.71. Found: C, 53.11; H, 6.72.

*2,3-Di-O-methyl-L-rhamnose (**16**)*

The methyl glycoside **15** (300 mg) was hydrolyzed (2 *N* TFA, 30 ml, reflux, 5 h), the recovered syrup (260 mg) showed one spot on t.l.c. R_f (solvent B) 0.41 and on paper chromatography gave a reddish-brown spot with R_G (solvent D) 0.85 when sprayed with aniline trichloroacetate spray (lit. (53) R_G 0.83), $[\alpha]_D$ +42.2°(*c* 1.5, water) (lit. (52) $[\alpha]_D$ +40° (*c* 0.7, water)). Reduction of **16** and acetylation gave 1,4,5-tri-*O*-acetyl-2,3-di-*O*-methyl-L-rhamnitol (**17**) (280 mg). Injection of **17** in ethyl acetate onto column *b* programmed from 150 to 200° at 2°/min gave a major peak at 24.4 min and on column *c* at 225° gave a major peak at 38.6 min. A sample was collected and the mass spectrum obtained showed *m/e* 43, 44, 45, 58, 59, 69, 71, 74, 85, 87, 101, 113, 117, 143, 161, and 203 (28).

The authors thank the National Research Council of Canada for the award of a scholarship (to G.M.B.) and for a grant which made this work possible.

1. G. O. ASPINALL. Adv. Carbohydr. Chem., **24**, 333 (1969).
2. A. STOLL, W. KREIS, and A. VON WARTBURG. Helv. Chim. Acta, **35**, 2495 (1952).
3. O. LÜDERITZ, K. JANN, and R. WHEAT. Comp. Biochem. **26A**, 105 (1968).
4. R. W. BAILEY. Oligosaccharides, Pergamon Press, London, 1965.
5. R. J. BEVERIDGE, W. A. SZAREK, and J. K. N. JONES. Carbohydr. Res. **19**, 107 (1971).
6. D. HUNGERER, K. JANN, B. JANN, F. ØRSKOV, and I. ØRSKOV. Eur. J. Biochem. **2**, 115 (1967).
7. J. J. O'DONNELL and E. PERCIVAL. J. Chem. Soc. 2168 (1959).
8. J. P. MCKINNELL and E. PERCIVAL. J. Chem. Soc. 2082 (1962).
9. B. LINDBERG, J. LÖNNGREN, J. L. THOMPSON, and W. NIMMICH. Carbohydr. Res. In press.
10. A STOLL, E. SUTER, W. KREIS, B. B. BUSSEMAKER, and A. HOFMANN. Helv. Chim. Acta, **16**, 703 (1933).
11. G. ZEMPLEN. Math. naturw. Anz. ungar. Akad. Wiss. **57**, 999 (1938); Chem. Abstr. **33**, 4202 (1939).
12. A. STOLL and J. RENZ. Enzymol. **7**, 362 (1939); Chem. Abstr. **34**, 6298 (1940).
13. R. CARRINGTON, G. SHAW, and D. V. WILSON. J. Chem. Soc. 6864 (1965).
14. J. E. CADOTTE, F. SMITH, and D. SPRIESTERSBACH. J. Am. Chem. Soc. **74**, 1501 (1952).
15. F. SMITH and D. SPRIESTERSBACH. J. Am. Chem. Soc. **76**, 4191 (1954).
16. W. H. WADMAN. J. Chem. Soc. 3051 (1952).
17. B. HELFERICH and J. ZIRNER. Chem. Ber. **95**, 2604 (1962).
18. R. D. GUTHRIE and J. F. MCCARTHY. Adv. Carbohydr. Chem. **22**, 11 (1967).
19. G. O. ASPINALL, R. KHAN, and Z. PAWLAK. Can. J. Chem. **49**, 3000 (1971).
20. A. ROSENTHAL and M. SPRINZL. Can. J. Chem. **47**, 3941 (1969).
21. W. SOWA. Can. J. Chem. **49**, 3292 (1971).
22. P. JERKEMAN. Acta Chem. Scand. **17**, 2769 (1963).
23. T. ISIKAWA and H. G. FLETCHER JR. J. Org. Chem. **34**, 563 (1969).
24. A. J. ACHER, Y. RABINSOHN, E. S. RACHAMAN, and D. SHAPIRO. J. Org. Chem. **35**, 2436 (1970).
25. J. N. C. WHYTE. Anal. Biochem. **42**, 476 (1971).
26. G. G. S. DUTTON and K. B. GIBNEY. Carbohydr. Res. In press.
27. S. HAKOMORI. J. Biochem. (Tokyo), **55**, 205 (1964).
28. H. BJÖRNDAL, C. G. HELLERQVIST, B. LINDBERG, and S. SVENSSON. Angew. Chem. Int. Ed. **9**, 610 (1970).
29. Y. C. LEE and C. E. BALLOU. Biochem. **4**, 257 (1965).
30. R. J. YU, C. T. BISHOP, F. P. COOPER, and H. F. HASENCLEVER. Can. J. Chem. **45**, 2205 (1967).

31. G. M. BEBAULT, G. G. S. DUTTON, and R. H. WALKER. Carbohydr. Res. In press.
32. W. E. TREVELYAN, D. P. PROCTER, and J. S. HARRISON. Nature, **166**, 444 (1950).
33. L. HOUGH, J. K. N. JONES, and W. H. WADMAN. J. Chem. Soc. 1702 (1950).
34. P. A. LEVENE and I. E. MUSKAT. J. Biol. Chem. **105**, 431 (1934).
35. E. FISCHER. Ber. **28**, 1145 (1895).
36. J. MINSAAS. Norske Videnskab. Selskab Forhandlinger, **6**, 177 (1933).
37. A. C. RICHARDSON and J. M. WILLIAMS. Tetrahedron, **23**, 1641 (1967).
38. K. BUTLER, P. F. LLOYD, and M. STACEY. J. Chem. Soc. 1531 (1955).
39. R. D. KING and W. G. OVEREND. Carbohydr. Res. **9**, 423 (1969).
40. R. U. LEMIEUX. Methods Carbohydr. Chem. **2**, 221 (1963).
41. J. K. DALE. J. Am. Chem. Soc. **38**, 2187 (1916).
42. D. HORTON and T. TSUCHIYA. Carbohydr. Res. **5**, 426 (1967).
43. E. PERCIVAL. Carbohydr. Res. **4**, 441 (1967).
44. L. MALAPRADE. Bull. Soc. Chim. **43**, 683 (1928); Chem. Abstr. **22**, 3374 (1928).
45. J. C. RANKIN and A. JEANES. J. Am. Chem. Soc. **76**, 4435 (1954).
46. P. A. SANDFORD and H. E. CONRAD. Biochem. **5**, 1508 (1966).
47. W. N. HAWORTH and G. C. LEITCH. J. Chem. Soc. **113**, 188 (1918).
48. G. G. S. DUTTON and A. M. UNRAU. Can. J. Chem. **43**, 1738 (1965).
49. R. CHABY and L. SZABO. Tetrahedron, **27**, 3197 (1971).
50. J. O. DEFERRARI, E. G. GROS, and I. O. MASTRONARDI. Carbohydr. Res. **4**, 432 (1967).
51. W. E. DICK, JR. Carbohydr. Res. **21**, 255 (1972).
52. E. E. PERCIVAL and E. G. V. PERCIVAL. J. Chem. Soc. 690 (1950).
53. F. BROWN, L. HOUGH, and J. K. N. JONES. J. Chem. Soc. 1125 (1950).
54. J. R. EDWARDS and J. A. HAYASHI. Arch. Biochem. Biophys. **111**, 415 (1965).

Can. J. Chem. Downloaded from www.nrcresearchpress.com by 210.87.254.6 on 09/05/12
For personal use only.

Can. J. Chem. Downloaded from www.nrcresearchpress.com by 210.87.254.40 on 09/05/12
For personal use only.

On the Mobility of Quasifree Electrons in Liquid Methane

KENJI FUEKI

Department of Synthetic Chemistry, Faculty of Engineering, Nagoya University, Chikusa-ku, Nagoya, Japan

Received May 30, 1972

A theoretical estimate has been made of the mobility and energy of quasifree electrons in liquid methane. It is shown that the calculated mobility is in agreement with the measured mobility and that the calculated energy is also consistent with a qualitative correlation between the mobility and energy of quasifree electrons in liquid alkanes.

Une estimation théorique sur la mobilité et l'énergie des électrons quasilibres dans le méthane liquide, a été donnée. On a montré que les mobilités calculée et mesurée sont en accord et que l'énergie calculée est également compatible avec une corrélation qualitative existant entre la mobilité et l'énergie des électrons quasilibres dans les alcanes liquides. [Traduit par le journal]

Canadian Journal of Chemistry, **50**, 3379 (1972)

The mobility of quasifree electrons in liquid methane has recently been measured by Fuochi and Freeman (1), who have found that it is very high as compared to the mobilities of electrons in other hydrocarbons and is about the same magnitude as that in liquid argon.

In this note we report a theoretical estimate of the electron mobility in liquid methane by use of the Cohen–Lekner theory (2), which has been successfully applied to semiempirical calculations of the electron mobilities in *n*-hexane and neopentane (3, 4). Since the electron mobility in liquid methane is considerably higher than that in neopentane where the activation energy for the mobility as expressed by the Arrhenius equation is nearly zero (5), it is very likely that the activation energy is zero for the mobility of electrons in liquid methane.

The mobility of quasifree electrons in liquid methane is then given by (2)

$$\mu_0 = \frac{2}{3}\left(\frac{2}{\pi m k T}\right)^{1/2}\left[\frac{e}{n\sigma_1 S(0)}\right]$$

where m is the mass of the electron; k, Boltzmann's constant; T, the absolute temperature; e, the electronic charge; n, the number density of molecules; σ_1, the scattering cross section; and $S(0) = nkT\kappa_T$ (κ_T is the isothermal compressibility). The physical constants used in the calculation are listed in Table 1. The electron scattering cross section is given by $\sigma_1 = 4\pi\bar{a}^2_{CH_4}$, where $\bar{a}_{CH_4}$ is the scattering length in liquid methane. $\bar{a}_{CH_4}$ is estimated to be $\bar{a}_{CH_4} = \bar{a}_{Ne} \times (\zeta_{Ne}/\zeta_{CH_4}) = 1.02$ Å, where $\bar{a}_{Ne}$ (0.556 Å) is the scattering length in liquid neon (6), and ζ_{CH_4} (1.564 a.u.) and ζ_{Ne} (2.879 a.u.) are, respectively, orbital exponents in spherically symmetric one-center wave functions of the methane molecule (7) and of the neon atom (8) which is isoelectronic to the methane molecule. It is assumed that $\bar{a}$ may be related to the orbital exponent, since the orbital exponent is a measure of the spread of the electron cloud in the atom or molecule which determines the hard core radius. The estimated scattering cross section of electrons in liquid methane is three times as great as that in gaseous methane, $\sigma_g = 4.33 \times 10^{-16}$ cm^2 (9). The same ratio between the gas and liquid phase scattering cross sections of electrons was found for *n*-pentane (3).

The calculated mobility of electrons in liquid methane is given in Table 1 together with the measured mobility. The calculated value is in agreement with the experimental value. The momentum mean free path $\Lambda = [n\sigma_1 S(0)]^{-1}$ is 122 Å for liquid methane at 120 °K and it is very close to a value of Λ, 113 Å, for liquid neopentane at 300 °K (4).

Since the methane molecule is spherically symmetric, the Wigner–Seitz model (6) for the excess electron in liquids is considered to be best applicable to liquid methane. Using the

TABLE 1. Physical constants and electron mobility in liquid methane

T (°K)	ρ* (g/cm^3)	κ_T† (cm^2/dyn)	$S(0)$	σ_t (cm^2)	μ_0 (cm^2/V) Calcd.	Expt.‡
120	0.415	1.64×10^{-10}	4.11×10^{-2}	1.32×10^{-15}	270	300

*Reference 11.
†Value at 100 °K, ref. 12.
‡Reference 1.

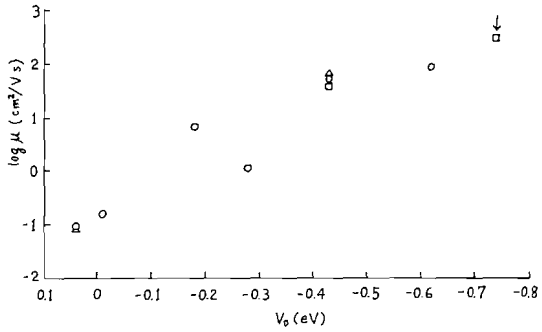

FIG. 1. Plot of V_0 *vs.* logarithm of mobility, μ, for the excess electron in liquid alkanes and tetramethylsilane: ○, mobility values from ref. 13; △, mobility values from ref. 5; □, mobility values from Ref. 1. All the V_0 values were taken from ref. 10 except for liquid methane for which V_0 was calculated in this work.

Wigner–Seitz method, the energy of the quasi-free electron state, V_0, is calculated to be -0.74 eV. This value is somewhat lower than the values of V_0 measured for the alkanes with less molecular sphericity and it is consistent with a qualitative correlation between V_0 and the electron mobilities found for the alkanes (10). Figure 1 shows a plot of V_0 *vs.* logarithm of the mobility for the excess electron in several alkanes and tetramethylsilane. It can be seen in Fig. 1 that the point for liquid methane indicated by the arrow fits with such a qualitative correlation. It should be noted, however, that the estimate of V_0 is sensitive to the choice of $\bar{a}$ for liquid methane and therefore not very accurate. Clearly the direct measurement of V_0 for liquid methane is desirable to test this prediction.

1. P. G. FUOCHI and G. R. FREEMAN. J. Chem. Phys. **56**, 2333 (1972).
2. (*a*) J. LEKNER. Phys. Rev. **158**, 130 (1967); (*b*) M. COHEN and J. LEKNER. Phys. Rev. **158**, 305 (1967).
3. K. FUEKI, D.-F. FENG, and L. KEVAN. Chem. Phys. Lett. **13**, 616 (1972).
4. H. T. DAVIS, L. D. SCHMIDT, and R. M. MINDAY. Chem. Phys. Lett. **13**, 413 (1972).
5. R. M. MINDAY, L. D. SCHMIDT, and H. T. DAVIS. J. Phys. Chem. **76**, 442 (1972).
6. B. E. SPRINGETT, J. JORTNER, and M. H. COHEN. J. Chem. Phys. **48**, 2720 (1968).
7. A. F. SATURNO and R. G. PARR. J. Chem. Phys. **33**, 22 (1960).
8. A. F. SATURNO and R. G. PARR. J. Chem. Phys. **29**, 490 (1958).
9. (*a*) L. G. CHRISTOPHOROU, G. S. HURST, and A. HADJIANTONIOU. J. Chem. Phys. **44**, 3506 (1966); (*b*) L. G. CHRISTOPHOROU, G. S. HURST, and W. G. HENDRICK. J. Chem. Phys. **45**, 1081 (1966).
10. R. A. HOLROYD and M. ALLEN. J. Chem. Phys. **54**, 5014 (1971).
11. R. W. GALLANT. Physical properties of hydrocarbons. Vol. 1. Gulf Publishing Co., Houston, Texas. 1968; Vol. 2. 1970.
12. H. H. LANDOLT and R. BÖRNSTEIN. Zahlenwerte und functionen. 6 Auflage. Mechanisch-thermische Zustandsgrössen. 1 Teil, Springer–Verlag, Berlin. 1971. p. 632.
13. W. F. SCHMIDT and A. O. ALLEN. J. Chem. Phys. **52**, 4788 (1970).

Can. J. Chem. Downloaded from www.nrcresearchpress.com by 210.87.254.40 on 09/05/12
For personal use only.

Partial Photoresolution of Some Chromium (III) Complexes of Phenanthroline and Bipyridine Using Circularly Polarized Laser Irradiation

NOEL A. P. KANE-MAGUIRE AND COOPER H. LANGFORD[1]
Department of Chemistry, Carleton University, Ottawa, Canada K1S 5B6

Received April 13, 1972

Partial photoresolution of $Cr(C_2O_4)phen_2^+$, $Cr(C_2O_4)_2phen^-$, and $Crbipy_3^{3+}$ by irradiation with circularly polarized light from an argon ion laser and 496.5 or 514.5 nm is reported. Steady states corresponding to 1–2% resolution are achieved. They are in agreement with predictions from known circular dichroism and the assumption that differential isomerization is simply a consequence of differential absorptivity of the enantiomers.

Nous rapportons la photorésolution partielle de $Cr(C_2O_4)phen_2^+$, $Cr(C_2O_4)_2phen^-$ et $Crbipy_3^{3+}$ par irradiation au moyen de lumière circulairement polarisée provenant d'un laser à ion d'argon émettant à 496.5 ou 514.5 nm. Nous obtenons les états continus correspondant à une résolution de 1–2%. Ils sont en accord avec les prédictions basées sur des résultats connus de dichroisme circulaire et sur l'hypothèse que l'isomérisation différentielle est simplement une conséquence de l'absorptivité différentielles des énantiomères.
[Traduit par le journal]

Canadian Journal of Chemistry, **50**, 3381 (1972)

Can. J. Chem. Downloaded from www.nrcresearchpress.com by 210.87.254.40 on 09/05/12
For personal use only.

Introduction

There has been a longstanding interest in partial resolution of racemates by irradiation with circularly polarized light. The interest has enjoyed only limited reward. The limitation is a consequence of two factors. First, the only recognized mechanism for steady state resolution is an excess of an isomerization reaction of one enantiomer over the other due to differential absorptivity of circularly polarized light (circular dichroism) and this mechanism depends on the ratio of the circular dichroism ($\Delta\varepsilon$) to the absorptivity ε. Second, it is the unusual system where photoisomerization is efficient enough to prevent competition from thermal racemization functioning as the limit to stationary state resolution. (Of course, there are a few examples of partial resolutions that do not lead to a stationary state at all. They depend on photodecomposition, not photoisomerization.)

One metal complex system, $Cr(C_2O_4)_3^{3-}$ and its aquo derivatives, has been systematically investigated (1, 2, 8). Partial photoresolution stationary states in agreement with circular dichroism and known thermal isomerization kinetics were found. We report here similar success with another family of Cr(III) complexes where we have the added advantage that thermal isomerizations are slow enough to be neglected. (This family came to attention in consequence of observation of a photochemical analog of the Pfeiffer effect where partial resolution was achieved without circular polarization (3)). The complexes are $Cr(C_2O_4)phen_2^+$, $Cr(C_2O_4)_2phen^-$, and $Cr(bipy)_3^{3+}$ – (phen = 1,10-phenanthroline; bipy = bipyridine). The $Cr(phen)_3^{3+}$ complex lacks a favorable dissymmetry factor ($\Delta\varepsilon/\varepsilon$) in the region of its first d–d absorption band.

[1]To whom correspondence should be addressed.

Experimental

The complexes were prepared according to published procedures as chloride or potassium salts (4). They were characterized by their visible spectra. Circular dichroism spectra of the oxalato species are available (5). $Cr(bipy)_3^{3+}$ has not, to our knowledge, been successfully resolved by conventional procedures.

An intense source of elliptically (nearly circularly) polarized light was provided by passing the linearly polarized beam from a Coherent Radiation argon ion laser (lines at 496.5 or 514.5 nm) through a 589 nm 1/4 wave plate. The 1/4 wave plate was adjusted to an angle minimizing the variation of intensity which would pass a linear polarizer placed beyond it. The approximately circularly polarized beam was passed through a diverging lens system (to avoid excess heating in the solution along the laser beam), and into a 10 cm cell containing the solution to be irradiated at 15 °C. The anticipated handedness of the circularly polarized light was confirmed from analogous experiments using a left-hand circular polarizer in place of the 1/4 wave plate. Light intensity was monitored by ferrioxalate actinometry (6).

Optical rotation was measured using a Perkin–Elmer 141 ($\pm 0.001°$) polarimeter.

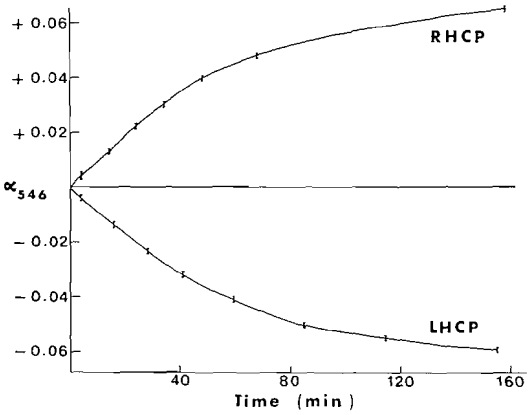

FIG. 1. Observed rotations as a function of irradiation time for $[Cr(C_2O_4)\ phen_2]Cl$ (5.06×10^{-3} *M*) in RHCP and LHCP light at 496.5 nm.

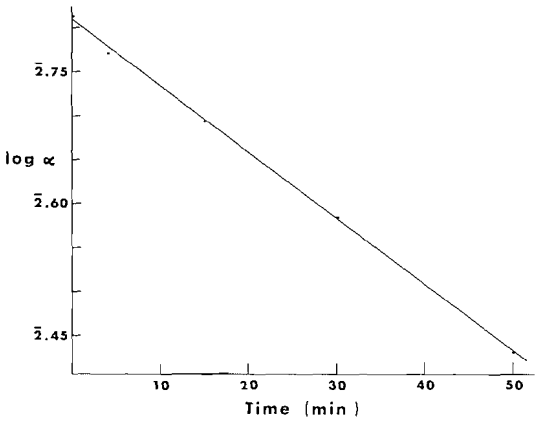

FIG. 2. Photoracemization kinetics at 496.5 nm for photoresolved (+) $Cr(C_2O_4)\ phen_2^+$ sample at 15 °C.

Results

$[Cr(C_2O_4)\ phen_2]\ Cl$

This compound has a favorable dissymmetry factor ($\Delta\varepsilon/\varepsilon$) in its first ligand field band. At 496.5 nm, $\Delta\varepsilon/\varepsilon$ is $2.4/61 = 0.039$. Under 496.5 nm irradiation, the photoreaction is isomerization. (Thermal isomerization has an insignificant rate, $t_{1/2} \simeq 23$ h at 15 °C.)

The consequences of irradiating the racemic ($\pm$) $Cr(C_2O_4)\ phen_2^+$ (5.06×10^{-3} *M* aqueous solution) with alternately right and left circularly polarized light are shown in Fig. 1. It can be seen that a steady state rotation is approached with a half life of approximately 40 min, under a light intensity of 1.8×10^{-7} einstein s^{-2} at 496.5 nm. Steady state rotations (and the corresponding specific rotations) for the three visible wavelengths available on the Perkin–Elmer polarimeter are collected in Table 1. Photoracemization kinetics at 496.5 nm for the photoresolved (+) $- Cr(C_2O_4)\ phen_2^+$ are shown in Fig. 2. These were obtained by removing the 1/4 wave plate, resulting in a 10% increase in light intensity, The half-time for racemization is 40 min and the quantum yield for the process is 0.21.

Photoresolution was also examined with irradiation at 514.5 nm. The results were essentially indistinguishable from the 496.5 nm results, as the similarity of $\Delta\varepsilon/\varepsilon$ values and the wavelength independence of this quantum yield (7) would suggest.

$K[Cr(C_2O_4)_2\ phen]$

This compound has a reasonable $\Delta\varepsilon/\varepsilon$ value of 0.039 at 514.5 nm. Kinetic behavior in a photoresolution experiment is similar to $[Cr(C_2O_4)\ phen_2]Cl$. Detailed kinetic measurements were not made although it was observed that photoinduced optical activity could be eliminated again by photoracemization in unpolarized light. The steady state resolution results are included in Table 1.

$[Cr\ bipy_3]\ (ClO_4)_3$

A value of $\Delta\varepsilon/\varepsilon$ for this complex is not available. However, it was irradiated with the "circularly" polarized light at 488.0 nm. Observed steady state rotations are recorded in Table 2.

Discussion

The kinetics shown in Figs. 1 and 2 are consistent with the nearly inevitable conclusion that isomerization rates of excited enantiomers are the same within experimental precision. The resolution results from differential absorptivity. The steady state fractional resolution should correspond to $\Delta\varepsilon/2\varepsilon$, resulting in a percent resolution of $50\,\Delta\varepsilon/\varepsilon$ (1, 2). The collected results in Table 1 are consistent with this conclusion. The percent resolutions achieved were 1.6% for $Cr(C_2O_4)\ phen_2^+$ and 2.0% for $Cr(C_2O_4)_2\ phen^-$, to be compared with the respective theoretical values of 1.9 and 2.0%. The identity of the partially resolved products is supported by the agreement of the specific rotations at the wavelengths available on the Perkin–Elmer 141 with known o.r.d. spectra. Further, in the case

Can. J. Chem. Downloaded from www.nrcresearchpress.com by 210.87.254.40 on 09/05/12
For personal use only.

TABLE 1. Comparison of steady-state rotation with $A\ (-)_{589}$ $[Cr(C_2O_4)\ phen_2]Cl$ and $B\ (+)_{589}$ $K[Cr(C_2O_4)_2\ phen]$

State	Rotation at λ (nm) = 436	546	578	589
A α steady state (RHCP)*		+0.065	+0.047	+0.042
α steady state (LHCP)		−0.059	−0.044	−0.039
[α] steady state (RHCP)		+21.1	+15.3	+14.0
[α] steady state (LHCP)		−19.2	−14.3	−12.7
[α] (−) $[Cr(C_2O_4)\ phen_2]Cl$	−806	−1320	−975	−880
B α steady state (RHCP)†	−0.049	+0.040	+0.047	+0.041
α steady state (LHCP)	+0.041	−0.034	−0.041	−0.034
[α] steady state (RHCP)	−26.1	+20.7	+25.0	+21.8
[α] steady state (LHCP)	+21.8	−18.1	−21.8	−18.1
[α] (+) $K[Cr(C_2O_4)_2\ phen]$	−1270	+1000	+1240	+850

*Complex concentration = 5.06×10^{-3} *M*.
†Complex concentration of irradiated solution was 8.08×10^{-3} *M*. The rotations listed are for a complex concentration of 4.04×10^{-3} *M* (dilution being necessary because of the high absorbance).

TABLE 2. Steady-state rotations observed on irradiating (±) $[Crbipy_3](ClO_4)_3$ at 488.0 nm

Steady state	Rotation at λ (nm) = 546	578	589
α steady state (RHCP)*	+0.011	+0.009	+0.009
α steady state (LHCP)	−0.006	−0.005	−0.005
[α] steady state (RHCP)	+3.8	+3.1	+3.1
[α] steady state (LHCP)	−2.1	−1.7	−1.7

*Complex concentration = 3.5×10^{-3} *M*.

of $[Cr(C_2O_4)\ phen_2]Cl$, the quantum yield at 496.5 nm for photoracemization of the photoresolved sample (0.21) is essentially identical to that of (−) $[Cr(C_2O_4)phen_2]Cl$ at 15 °C (7).

The absence of any photoinduced activity in the case of $Crphen_3^{3+}$ cannot be ascribed to kinetic factors. Under the conditions used, photoracemization is known to proceed at a rate several orders of magnitude faster than either thermal racemization or photoaquation (7). The explanation may be found in the unfavorable dissymmetry factor in the ligand field region, due to the high ε values (arising from overlap with bands of charge transfer character). Assuming a circular dichroism of similar magnitude for $Crphen_3^{3+}$ and $Crbipy_3^{3+}$, a partial photoresolution of this latter compound might be anticipated (as observed, Table 2), in view of the smaller extinction coefficients found in the d–d region.

1. K. L. STEVENSON and J. F. VERDIECK. J. Am. Chem. Soc. **90**, 2974 (1968).
2. K. L. STEVENSON and J. F. VERDIECK. Mol. Photochem. **1**, 271 (1969).
3. N. A. P. KANE-MAGUIRE, B. DUNLOP, and C. H. LANGFORD. J. Am. Chem. Soc. **93**, 6293 (1971).
4. (*a*) J. A. BROOMHEAD, M. DWYER, and N. A. P. KANE-MAGUIRE. Inorg. Chem. **7**, 1388 (1968); (*b*) J. A. BROOMHEAD. Aust. J. Chem. **15**, 228 (1962); (*c*) F. H. BURSTALL and R. S. NYHOLM. J. Chem. Soc. 3570 (1952).
5. J. FERGUSON, C. J. HAWKINS, N. A. P. KANE-MAGUIRE, and H. LIP. Inorg. Chem. **8**, 771 (1969).
6. C. G. HATCHARD and C. S. PARKER. Proc. Roy. Soc. Sec. A, **235**, 518 (1956).
7. N. A. P. KANE-MAGUIRE and C. H. LANGFORD. J. Am. Chem. Soc. **94**, 2125 (1972).
8. B. NORDEN. Acta Chem. Scand. **23**, 2925 (1969).

Can. J. Chem. Downloaded from www.nrcresearchpress.com by 210.87.254.40 on 09/05/12
For personal use only.

Kinetics of Displacement of Ni(II) by Cu(II) in Bis(dithiocarbamato)nickel(II)

R. R. SCHARFE,[1] V. S. SASTRI, AND C. L. CHAKRABARTI[2]
Department of Chemistry, Carleton University, Ottawa, Canada K1S 5B6

Received June 12, 1972

Rates of displacement of Ni(II) in bis(dithiocarbamato)Ni(II) by Cu(II) with a variety of substituted dithiocarbamic acids in different solvents have been determined and a mechanism of the reaction and potential application of the displacement reaction to spectrophotometric titration of Cu(II) for its quantitative determination are suggested.

Nous avons déterminé les vitesses de déplacement du Ni(II) dans le bis (dithiocarbamato) Ni(II) par Cu(II) avec une variété d'acides dithiocarbamiques substitués dans différents solvants ; nous proposons un mécanisme de réaction de même que l'application possible de la réaction de déplacement au titrage spectrophotométrique de Cu(II) pour sa détermination quantitative. [Traduit par le journal]

Canadian Journal of Chemistry, **50**, 3384 (1972)

Can. J. Chem. Downloaded from www.nrcresearchpress.com by 210.87.254.105 on 09/05/12
For personal use only.

Introduction

For the purpose of quantitative determination of metal ions, complexation reactions of dithiocarbamic acids (DTC) are very useful (1). Recent work in this laboratory has clarified many aspects of the chemistry of dithiocarbamic acids (2–5). During the course of obtaining definitive information on the stability constants (6) and applying these data to spectrophotometric titration of metal ions such as Cu(II) and Ni(II) with dithiocarbamic acids, it was found that information on exchange rates between Cu(II) and $Ni(DTC)_2$ was necessary but lacking in the literature. Thus, the present work has been aimed at the determination of rates of displacement of Ni(II) from $Ni(DTC)_2$ by Cu(II) with respect to factors such as (*i*) effect of the substituent at the nitrogen center on the displacement rates; (*ii*) effect of the nature of solvent medium on the displacement rates.

Experimental

Reagents

Commercially obtained (Anachemia) diethyl dithiocarbamic acid as the sodium salt was used. The dimethyl, di-*n*-propyl, diisopropyl, pyrrolidine, piperidine, and hexamethylene dithiocarbamic acids were synthesized as the sodium salts by chemical reaction of stoichiometric amounts of the amine with CS_2 in a basic medium according to preparative methods described in the literature (7). All dithiocarbamic acids were recrystallized twice from hot ethanol and air-dried. Quantitative determination of the dithiocarbamate content of the reagents was done by amperometric titration with a standard Zn(II) solution at a p*H* of 6–7 by measuring the diffusion current at -1.25 V with respect to Ag/AgCl reference electrode. Spectrophotometric titration of dithiocarbamic acids with standard Cu(II) solutions gave results in agreement with those obtained by the amperometric titration. The water content of the reagents was obtained by Karl Fisher titration. Chemical analysis showed that the dithiocarbamate and water contents of the reagents add up to 100%. All the solvents and metal salts used in this study were of reagent grade purity. There were no detectable side reactions of the ligands with the solvents used in this study.

Apparatus

A modified Bausch and Lomb Spectronic 505 recording spectrophotometer was used, at a fixed wavelength, to study the slow rates of displacement of Ni(II) from $Ni(DTC)_2$ by Cu(II) with 1 cm matched quartz cells at a temperature of 25.0 ± 0.1 °C. Fast displacement rates were studied with a Durram–Gibson stopped-flow spectrophotometer fitted with an oscilloscope.

Procedure

An aliquot of 3 ml of 2.5×10^{-5} *M* $Ni(DTC)_2$ solution in the appropriate solvent was placed in a thermostatted 1 cm quartz cell, and to this was added 0.05 ml of 1.64×10^{-4} *M* Cu(II) solution by means of a Teflon device which was also used as a stirrer (4). The mixing was done with the stirrer and was complete within an average time of 6 s, and the change in absorbance due to formation of $CuDTC^+$ at a wavelength of 430–440 nm as a function of time was recorded. In the case of faster kinetics, the syringes of the stopped-flow spectrophotometer were filled with $Ni(DTC)_2$ and Cu(II) solutions and then mixed in the mixing chamber, and the change in the transmittance was recorded on the oscilloscope. The final spectrum of the product of the reaction agreed well with the spectrum of a synthetic sample of $Cu(DTC)^+$ complex. Plots of log concentration *vs.* time were linear and gave reproducible rate constants ($\pm 5\%$). Typical spectra of $Ni(DTC)_2$ and $Cu(DTC)^+$ and rate curves are given in the literature (8).

Results and Discussion

Data on the rates for the reaction

$$Ni(DTC)_2 + 2Cu^{2+} \rightarrow Ni^{2+} + 2Cu(DTC)^+$$

[1]Taken in part from the M.Sc. thesis of R. R. Scharfe.
[2]To whom all correspondence should be addressed.

TABLE 1. Displacement rates of $Ni(DTC)_2$ with Cu^{2+} for dialkyl DTC chelates ($s^{-1} \times 10^2$)

Solvent	Me_2DTC	Et_2DTC	$n\text{-}pr_2DTC$	$i\text{-}pr_2DTC$
Methyl cellosolve	0.911	0.465	0.287	0.0192
DMSO	0.488	5.82	2.23	0.0871
Acetone	12.4	15.5	19.8	14.3
Methanol	31.5	72.9	23.1	8.66
Ethanol	330	83.4	75.3	67.9
Pyridine	3.15	2.58	2.25	0.845
Acetonitrile	173	—	16.1	13.8

TABLE 2. Displacement rates for cyclic DTC chelates ($s^{-1} \times 10^2$)

Solvent	PyrrDTC	PipDTC	HexaDTC
Methyl cellosolve	5.77	1.24	1.14
DMSO	8.15	4.81	1.26
Acetone	8.34	7.21	2.64
Methanol	>693*	34.6*	49.5
Ethanol	216*	78.7*	124
Pyridine	6.41	2.17	1.57
Acetonitrile	69.3	26.2	8.30

*Decomposed.

for a variety of substituted dithiocarbamic acids in different solvents are presented in Tables 1 and 2. The displacement reaction may take place in two ways, namely, (*a*) $Ni(DTC)_2$ dissociating to make one end of sulfur atom free for attachment to Cu^{2+}; (*b*) Cu^{2+} may be attacking the nitrogen center of DTC part of the nickel complex.

In case (*a*), Cu^{2+} is bonded to the sulfur atom, and in case (*b*), Cu^{2+} is bonded to the nitrogen atom. The displacement rates (Tables 1 and 2) do vary as a function of the nature of the substituent at the nitrogen atom. Steric hindrance at the nitrogen atom due to a bulky substituent results in a decrease in the displacement rate, and this makes (*b*), *i.e.*, the attack of Cu^{2+} at the nitrogen atom more likely than (*a*), *i.e.*, the attack of Cu^{2+} at the sulfur atom, since the sulfur atom is further away from the substituent group.

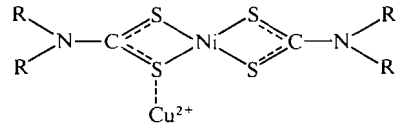

(*a*)

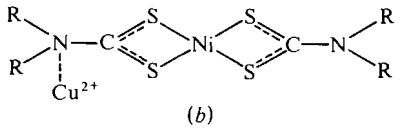

(*b*)

In methyl cellosolve, the order of reactivity is $Me_2 > Et_2 > n\text{-}pr_2 \gg i\text{-}pr_2DTC$ (Table 1). For the cyclic DTC's, the order is pyrr > pip > hexaDTC (Table 2). This trend may be due to variation of the basicity of nitrogen atom in the cyclic dithiocarbamic acids (9). On the basis of the rate data, a fast equilibrium between $Ni(DTC)_2$ and Cu^{2+} ion followed by a slow rearrangement to give $Cu(DTC)^+$, the latter being the rate determining step, is postulated, [I].

The displacement rates show a marked solvent dependence. The order of reactivity for piperidine, hexamethylene, and pyrrolidine DTC's is EtOH > MeOH > acetone > pyridine > DMSO > methyl cellosolve. The dialkyl DTC complexes do not display such a regular dependence on the solvent, and the reason for this is not known at present. The data allow one to advance the view that the solvation of the nitrogen atoms in the DTC ligands bonded to Ni(II) affects the displacement rates of Ni(II) by Cu(II).

The DTC chelates have been used in the quantitative determination of various metal ions (including Cu^{2+}) when only one of the

[I] 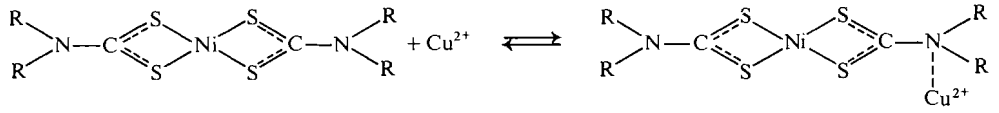

Can. J. Chem. Downloaded from www.nrcresearchpress.com by 210.87.254.105 on 09/05/12
For personal use only.

metal ions is present. The data on the displacement rates of Ni(II) from $Ni(DTC)_2$ by Cu(II) show that it should be feasible to determine quantitatively Cu(II) in the presence of Ni(II) by spectrophotometric titration of Cu(II).

The authors are grateful to the National Research Council of Canada for the financial support of this work.

1. A. HULANICKI. Talanta, **14**, 1371 (1967).
2. K. I. ASPILA, V. S. SASTRI, and C. L. CHAKRABARTI. Talanta, **16**, 1099 (1969).
3. S. J. JORIS, K. I. ASPILA, and C. L. CHAKRABARTI. Anal. Chem. **41**, 1441 (1969).
4. K. I. ASPILA, S. J. JORIS, and C. L. CHAKRABARTI. J. Phys. Chem. **74**, 3625 (1970).
5. V. S. SASTRI, K. I. ASPILA, and C. L. CHAKRABARTI. Can. J. Chem. **47**, 2320 (1969).
6. R. R. SCHARFE, V. S. SASTRI, and C. L. CHAKRABARTI. Anal. Chem. In press.
7. H. L. KLOPPING and G. J. VAN DER KERK. Rec. Trav. Chim. **70**, 917 (1951).
8. R. R. SCHARFE. M.Sc. Thesis. Carleton University, Ottawa, Canada. 1972.
9. R. R. VANDEBEEK. M.Sc. Thesis. Carleton University, Ottawa, Canada. 1971.

Remarks on the Concept of Minimum State Density in the Activated Complex Theory

W. H. WONG

Lash Miller Chemical Laboratory, University of Toronto, Toronto, Ontario

Received April 19, 1972

The concept of minimum state density in the activated complex theory and its relation to the transmission coefficient were discussed by formulating the average reaction cross-section.

Le concept de la densité de l'état minimal dans la théorie du complexe activé et ses relations avec le cöefficient de transmission sont discutés en formulant la section droite moyenne de la réaction.

[Traduit par le journal]

Canadian Journal of Chemistry, **50**, 3386 (1972)

In modern versions of activated-complex theory (ACT) of chemical reaction, the quasi-equilibrium hypothesis is tacitly assumed (1, 2). In these formulations, the activated complex is generally identified as the species in the vicinity of the saddle point on the relevant potential hypersurface. This conventional definition is widely adopted to interpret experimental data (3, 4) in terms of ACT. In a recent theoretical study on the behavior of reaction cross-section, Morokuma *et al.* (5) equated the rate constant from collision theory to that from the conventional ACT, *i.e.* they also assumed that the activated complex had a configuration corresponding to the most prominent topographical point on the potential surface. They found that the reaction cross-section was a diverging function of energy, contrary to the classical trajectory results (6).

For a highly exothermic reaction, this conventional definition of the transition state is even less satisfactory due to the absence of a prominent energy barrier. A suggestion has been made that the "free energy surface" rather than the potential energy surface should be used to define the transition state and that the activated complex should be located at the maximum of the free energy profile along the "reaction co-ordinate" (7). Recently the concept of minimum state density was put forward for choosing the transition state (8). This concept has been shown (8) to be related to the maximum free energy criterion (7) through a Boltzmann weighting factor. In this Note we attempt to amplify the concept in ref. 8 by deducing the average reaction cross-section in a slightly different way.

With the quasi-equilibrium hypothesis and by

Can. J. Chem. Downloaded from www.nrcresearchpress.com by 210.87.254.105 on 09/05/12
For personal use only.

metal ions is present. The data on the displacement rates of Ni(II) from $Ni(DTC)_2$ by Cu(II) show that it should be feasible to determine quantitatively Cu(II) in the presence of Ni(II) by spectrophotometric titration of Cu(II).

The authors are grateful to the National Research Council of Canada for the financial support of this work.

1. A. HULANICKI. Talanta, **14**, 1371 (1967).
2. K. I. ASPILA, V. S. SASTRI, and C. L. CHAKRABARTI. Talanta, **16**, 1099 (1969).
3. S. J. JORIS, K. I. ASPILA, and C. L. CHAKRABARTI. Anal. Chem. **41**, 1441 (1969).
4. K. I. ASPILA, S. J. JORIS, and C. L. CHAKRABARTI. J. Phys. Chem. **74**, 3625 (1970).
5. V. S. SASTRI, K. I. ASPILA, and C. L. CHAKRABARTI. Can. J. Chem. **47**, 2320 (1969).
6. R. R. SCHARFE, V. S. SASTRI, and C. L. CHAKRABARTI. Anal. Chem. In press.
7. H. L. KLOPPING and G. J. VAN DER KERK. Rec. Trav. Chim. **70**, 917 (1951).
8. R. R. SCHARFE. M.Sc. Thesis. Carleton University, Ottawa, Canada. 1972.
9. R. R. VANDEBEEK. M.Sc. Thesis. Carleton University, Ottawa, Canada. 1971.

Remarks on the Concept of Minimum State Density in the Activated Complex Theory

W. H. WONG

Lash Miller Chemical Laboratory, University of Toronto, Toronto, Ontario

Received April 19, 1972

The concept of minimum state density in the activated complex theory and its relation to the transmission coefficient were discussed by formulating the average reaction cross-section.

Le concept de la densité de l'état minimal dans la théorie du complexe activé et ses relations avec le cöefficient de transmission sont discutés en formulant la section droite moyenne de la réaction.

[Traduit par le journal]

Canadian Journal of Chemistry, **50**, 3386 (1972)

Can. J. Chem. Downloaded from www.nrcresearchpress.com by 210.87.254.6 on 09/05/12
For personal use only.

In modern versions of activated-complex theory (ACT) of chemical reaction, the quasi-equilibrium hypothesis is tacitly assumed (1, 2). In these formulations, the activated complex is generally identified as the species in the vicinity of the saddle point on the relevant potential hypersurface. This conventional definition is widely adopted to interpret experimental data (3, 4) in terms of ACT. In a recent theoretical study on the behavior of reaction cross-section, Morokuma *et al.* (5) equated the rate constant from collision theory to that from the conventional ACT, *i.e.* they also assumed that the activated complex had a configuration corresponding to the most prominent topographical point on the potential surface. They found that the reaction cross-section was a diverging function of energy, contrary to the classical trajectory results (6).

For a highly exothermic reaction, this conventional definition of the transition state is even less satisfactory due to the absence of a prominent energy barrier. A suggestion has been made that the "free energy surface" rather than the potential energy surface should be used to define the transition state and that the activated complex should be located at the maximum of the free energy profile along the "reaction co-ordinate" (7). Recently the concept of minimum state density was put forward for choosing the transition state (8). This concept has been shown (8) to be related to the maximum free energy criterion (7) through a Boltzmann weighting factor. In this Note we attempt to amplify the concept in ref. 8 by deducing the average reaction cross-section in a slightly different way.

With the quasi-equilibrium hypothesis and by

Can. J. Chem. Downloaded from www.nrcresearchpress.com by 210.87.254.6 on 09/05/12
For personal use only.

equating the incident flux of the reacting pairs to the flow passing through the dividing hypersurface just outside the activated complex region, the following expression was derived by Marcus (2)

$$[1] \qquad \sum_N g(N)\frac{k^2}{\pi}\sigma_{Np} = \sum_{N^+} g(N^+)\kappa(E_{N^+})$$

where $g(N)$ and $g(N^+)$ are the degeneracy factors of the initial quantum state N and the quantum state N^+ of the activated complex, respectively. The symbol σ_{Np} is the reaction cross-section of a reacting pair in state N and with relative momentum p, κ is the transmission coefficient, and k is the wavenumber. The reaction path degeneracy factor has been omitted for brevity. The energy relation for the reactant is

$$E = E_p + E_N$$

in which E is the total energy, E_p and E_N are the relative translational and internal energies of the reactant, respectively.

Multiplying [1] by $\exp(-\beta E)$ and integrating from zero to infinity we can write

$$[2] \qquad \int_0^\infty \left[\sum_N g(N)\frac{2\mu}{\pi\hbar^2}(E-E_N)\sigma_{Np}\right] \times \exp(-\beta E)\,dE = \int_0^\infty \left[\sum_{N^+} g(N^+)\kappa(E_{N^+})\right]\exp(-\beta E)\,dE$$

One may define an average cross-section as

$$[3] \qquad \sigma(E) = \frac{\sum_N g(N)(E-E_N)\sigma_{Np}}{\sum_N g(N)(E-E_N)H(E-E_N)} = \sum_N g(N)(E-E_N)\sigma_{Np}/f(E)$$

where

$$H(x) = 1 \qquad x > 0$$
$$= 0 \qquad x \leqslant 0$$

and $f(E)$ is the energy density function (5).

Substituting [3] into [2] and making the usual assumption of the ACT,

$$[4] \qquad \kappa = 1 \qquad E - V^{\ddagger} > 0$$
$$= 0 \qquad E - V^{\ddagger} \leqslant 0$$

where $V^{\ddagger}$ is the potential energy of the activated complex, we then have

$$[5] \qquad \frac{2\mu}{\pi\hbar^2}\int_0^\infty f(E)\sigma(E)\exp(-\beta E)\,dE = \sum_{N^+} g(N^+)\int_{V^{\ddagger}}^\infty \exp(-\beta E)\,dE = \sum_{N^+} g(N^+)/\beta \exp(-\beta V^{\ddagger})$$

where μ is the reduced mass of the reactant.

Performing the inverse Laplace transform, we write

$$f(E)\sigma(E) = \frac{\pi\hbar^2}{2\mu}\frac{1}{2\pi i}\int_{c-i\infty}^{c+i\infty}\sum_{N^+} g(N^+)\frac{1}{\beta} \times \exp(\beta V^{\ddagger} + \beta E)\,d\beta = \frac{\pi\hbar^2}{2\mu}\sum_{N^+} g(N^+)H(E-V^{\ddagger}) = \frac{\pi\hbar^2}{2\mu}f^+(E)$$

in which f^+ is just the number of states of the activated complex with total energy equal to or less than E. Therefore

$$[6] \qquad \sigma(E) = \frac{\pi\hbar^2}{2\mu}\frac{f^+(E)}{f(E)}$$

which is the same equation obtained by Morokuma *et al.* (5) by equating directly the rate constant from collision theory to that from ACT. The characteristic frequencies of the activated complex (and hence the function $f^+(E)$) depend on the location of the transition state along the reaction coordinate. The principle of minimum state density requires that the "bottleneck" be located at S^+, given by the solution of

$$\frac{\partial}{\partial S}\left(\frac{df^+(E)}{dE}\right) = 0$$

Since in the derivation of [6], we have chosen the transmission coefficient as unity when $E - V^{\ddagger} > 0$, the boundary dividing the product region from the reactant region in the available phase space of the system should obviously be defined in such a way that the flux density passing through this boundary is a minimum. This can best be illustrated by considering the rate constant from the adiabatic transition state

theory (1, 2, 8) (see Expr. 13 of ref. 8)

$$k_r = \frac{1}{Q\beta h}\int_{E=0}^{\infty} \exp(-\beta E)\frac{df^+(E)}{dE}\,dE$$

in which Q is the partition function of the reactants. From the above expression, it is obvious that the minimization of state density is equivalent to minimizing the rate constant. This procedure is, of course, in the spirit of the variational theory of reaction rates developed by Wigner (9), by Horiuti (10), and by Keck (11), in which attempts were made to define a dividing surface that would eliminate the "recrossing" of the phase space trajectories.

I am grateful to Professor R. A. Marcus for invaluable discussions.

1. M. A. Eliason and J. O. Hirschfelder. J. Chem. Phys. **30**, 1426 (1959); G. L. Hafacker. Z. Naturforsch, **18a**, 607 (1963); R. A. Marcus. J. Chem. Phys. **41**, 2614 (1964); **41**, 2624 (1964); N. S. Snider. J. Chem.Phys. **51**, 1489 (1969).
2. R. A. Marcus. J. Chem. Phys. **45**, 2138 (1966); **45**, 2630 (1966); **46**, 959 (1967).
3. A. A. Westenberg and N. de Haas. J. Chem. Phys. **48**, 4405 (1968).
4. D. J. LeRoy, B. A. Ridley, and K. A. Quickert. Discuss. Faraday Soc. **44**, 92 (1967).
5. K. Morokuma, B. C. Eu, and M. Karplus. J. Chem. Phys. **51**, 5193 (1969); K. Morokuma and M. Karplus. J. Chem. Phys. **55**, 63 (1971).
6. M. Karplus, R. N. Porter, and R. D. Sharma. J. Chem. Phys. **43**, 3259 (1965).
7. K. J. Laidler and J. C. Polanyi. *In* Progress in reaction kinetics. Vol. 3. *Edited by* G. Porter. Pergamon Press. 1965. p. 3.
8. W. H. Wong and R. A. Marcus. J. Chem. Phys. **55**, 5625 (1971).
9. E. Wigner. J. Chem. Phys. **5**, 720 (1937).
10. J. Horiuti. Bull. Chem. Soc. Jap. **13**, 210 (1938).
11. J. C. Keck. Adv. Chem. Phys. **13**, 85 (1967).

Phase Diagrams of Sodium Chloride and of Potassium Chloride in Water-Dioxane

A. N. Campbell and S. Y. Lam

Department of Chemistry, University of Manitoba, Winnipeg, Manitoba R3T 2N2

Received June 1, 1972

The equilibrium conditions, at 25°, of the NaCl–water–dioxane and KCl–water–dioxane systems have been investigated. While water–dioxane mixtures separate into two layers in the presence of certain concentrations of sodium chloride, the system KCl–water–dioxane does not form two layers under any conditions. The LiCl–water–dioxane system has been previously investigated by Lynch (1).

Nous avons étudié les conditions d'équilibre, à 25°, des systèmes: NaCl–eau–dioxanne et KCl–eau–dioxanne. Tandis que les mélanges eau–dioxanne se séparent pour former deux couches en présence d'une certaine concentration de NaCl, le phénomène ne se produit pas lorsqu'on utilise le mélange KCl–eau–dioxanne, dans n'importe quelles conditions. Le système LiCl–eau–dioxanne avait été étudié précédemment par Lynch (1). [Traduit par le journal]

Canadian Journal of Chemistry, **50**, 3388 (1972)

In the course of calorimetric work by Bhatnagar of this Department, it was observed that in the presence of certain concentrations of sodium chloride, mixtures of dioxane and water separated into two layers. A scrutiny of the literature revealed that Lynch (1) had made a study of the LiCl–water–dioxane system. In the presence of lithium chloride, certain water–dioxane mixtures also separate into two layers. Lynch's diagram exhibits two invariant triangles. In one, the equilibrium phases are: liquid I, liquid II, and the solid ternary compound $LiCl.H_2O.(C_2H_4)_2O_2$, liquid I being almost pure dioxane. In the second invariant triangle, the equilibrium phases are the above compound, equilibrium liquid, and $LiCl.H_2O$.

Nothing appeared to be known about the systems comprising sodium and potassium chlorides, respectively, so we thought it worthwhile to spend a little time on their investigation. Little need be said about the technique, except that both liquid and equilibrium "wet"

Can. J. Chem. Downloaded from www.nrcresearchpress.com by 210.87.254.6 on 09/05/12
For personal use only.

theory (1, 2, 8) (see Expr. 13 of ref. 8)

$$k_r = \frac{1}{Q\beta h}\int_{E=0}^{\infty} \exp(-\beta E)\frac{df^+(E)}{dE}\,dE$$

in which Q is the partition function of the reactants. From the above expression, it is obvious that the minimization of state density is equivalent to minimizing the rate constant. This procedure is, of course, in the spirit of the variational theory of reaction rates developed by Wigner (9), by Horiuti (10), and by Keck (11), in which attempts were made to define a dividing surface that would eliminate the "recrossing" of the phase space trajectories.

I am grateful to Professor R. A. Marcus for invaluable discussions.

1. M. A. Eliason and J. O. Hirschfelder. J. Chem. Phys. **30**, 1426 (1959); G. L. Hafacker. Z. Naturforsch, **18a**, 607 (1963); R. A. Marcus. J. Chem. Phys. **41**, 2614 (1964); **41**, 2624 (1964); N. S. Snider. J. Chem.Phys. **51**, 1489 (1969).
2. R. A. Marcus. J. Chem. Phys. **45**, 2138 (1966); **45**, 2630 (1966); **46**, 959 (1967).
3. A. A. Westenberg and N. de Haas. J. Chem. Phys. **48**, 4405 (1968).
4. D. J. LeRoy, B. A. Ridley, and K. A. Quickert. Discuss. Faraday Soc. **44**, 92 (1967).
5. K. Morokuma, B. C. Eu, and M. Karplus. J. Chem. Phys. **51**, 5193 (1969); K. Morokuma and M. Karplus. J. Chem. Phys. **55**, 63 (1971).
6. M. Karplus, R. N. Porter, and R. D. Sharma. J. Chem. Phys. **43**, 3259 (1965).
7. K. J. Laidler and J. C. Polanyi. *In* Progress in reaction kinetics. Vol. 3. *Edited by* G. Porter. Pergamon Press. 1965. p. 3.
8. W. H. Wong and R. A. Marcus. J. Chem. Phys. **55**, 5625 (1971).
9. E. Wigner. J. Chem. Phys. **5**, 720 (1937).
10. J. Horiuti. Bull. Chem. Soc. Jap. **13**, 210 (1938).
11. J. C. Keck. Adv. Chem. Phys. **13**, 85 (1967).

Phase Diagrams of Sodium Chloride and of Potassium Chloride in Water-Dioxane

A. N. Campbell and S. Y. Lam

Department of Chemistry, University of Manitoba, Winnipeg, Manitoba R3T 2N2

Received June 1, 1972

The equilibrium conditions, at 25°, of the NaCl–water–dioxane and KCl–water–dioxane systems have been investigated. While water–dioxane mixtures separate into two layers in the presence of certain concentrations of sodium chloride, the system KCl–water–dioxane does not form two layers under any conditions. The LiCl–water–dioxane system has been previously investigated by Lynch (1).

Nous avons étudié les conditions d'équilibre, à 25°, des systèmes: NaCl–eau–dioxanne et KCl–eau–dioxanne. Tandis que les mélanges eau–dioxanne se séparent pour former deux couches en présence d'une certaine concentration de NaCl, le phénomène ne se produit pas lorsqu'on utilise le mélange KCl–eau–dioxanne, dans n'importe quelles conditions. Le système LiCl–eau–dioxanne avait été étudié précédemment par Lynch (1). [Traduit par le journal]

Canadian Journal of Chemistry, **50**, 3388 (1972)

In the course of calorimetric work by Bhatnagar of this Department, it was observed that in the presence of certain concentrations of sodium chloride, mixtures of dioxane and water separated into two layers. A scrutiny of the literature revealed that Lynch (1) had made a study of the LiCl–water–dioxane system. In the presence of lithium chloride, certain water–dioxane mixtures also separate into two layers. Lynch's diagram exhibits two invariant triangles. In one, the equilibrium phases are: liquid I, liquid II, and the solid ternary compound $LiCl.H_2O.(C_2H_4)_2O_2$, liquid I being almost pure dioxane. In the second invariant triangle, the equilibrium phases are the above compound, equilibrium liquid, and $LiCl.H_2O$.

Nothing appeared to be known about the systems comprising sodium and potassium chlorides, respectively, so we thought it worthwhile to spend a little time on their investigation. Little need be said about the technique, except that both liquid and equilibrium "wet"

Can. J. Chem. Downloaded from www.nrcresearchpress.com by 210.87.254.6 on 09/05/12
For personal use only.

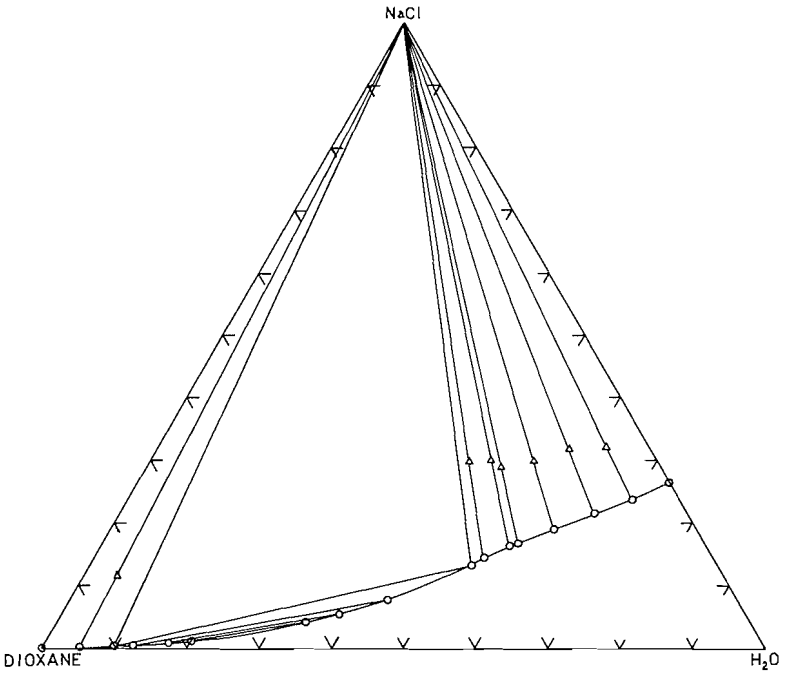

FIG. 1. Phase diagram of the NaCl–water–dioxane system.

TABLE 1. Compositions of liquids in equilibrium in NaCl–water–dioxane system

Liquid I	Liquid II
0.1% NaCl	13.3% NaCl
90.8% Dioxane	34.1% Dioxane
9.1% Water	52.0% Water

solid phases were analyzed by distillation, followed by refractive index measurement of the distillate, and weighing of the solid residue. The salt content of the solutions was also checked by volumetric determination of chloride by Mohr's method.

To summarize the results, in presence of potassium chloride at 25°, water–dioxane mixtures will not separate into two layers for any concentration of salt. The concentration of KCl in solution varies from 26.3% in pure water to zero in pure dioxane. Figure 1 shows the relations in the NaCl–water–dioxane system. For the invariant triangle, the compositions of liquids in equilibrium with pure solid NaCl are shown in Table 1. No compound is formed.

The equilibrium relations in these three systems are in agreement with the well-known facts that the affinities of the ions Li^+, Na^+, and K^+ for water are in the above order: the greater the affinity of an ion for water, the greater the probability of the formation of two layers.

1. C. C. LYNCH. J. Phys. Chem. **46**, 366 (1942).

Can. J. Chem. Downloaded from www.nrcresearchpress.com by 210.87.254.6 on 09/05/12
For personal use only.

Circular Dichroism of *R*-1,2-Propanediamine Complexes of Copper(II)

ROLAND A. HAINES AND E. WENDY CREWS
Department of Chemistry, University of Western Ontario, London, 72, Ontario

Received April 28, 1972

The optical activity associated with solutions containing copper(II) ions and *R*-1,2-propanediamine (*R*-pn) has been examined in detail. Circular dichroism data previously reported for $[Cu(R\text{-pn})_2]^{2+}$ have been found to be in error and new data are reported for this ion, as well as $[Cu(R\text{-pn})]^{2+}$.

L'activité optique associée aux solutions contenant les ions Cu(II) et la *R*-propanediamine-1,2 (*R*-pn) a été examinée en détail. Les données du dichroïsme circulaire citées antérieurement pour $[Cu(R\text{-pn})_2]^{2+}$ ont été trouvées être erronées et des nouvelles valeurs sont rapportées pour cet ion ainsi que pour $[Cu(R\text{-pn})]^{2+}$. [Traduit par le journal]

Canadian Journal of Chemistry, **50**, 3390 (1972)

The circular dichroism (c.d.) spectrum of the bis-(*R*-1,2-propanediamine)copper(II) ion $[Cu(R\text{-pn})_2]^{2+}$ has been reported previously (1) and showed two positive c.d. maxima in the region of the d–d absorption band. Recently, we have found it necessary to examine the circular dichroism associated with this ion in detail and have obtained results which are not consistent with those reported. The results of our investigation are given in this paper.

A sample of $[Cu(R\text{-pn})_2](NO_3)_2$ prepared in our laboratory was found to have a c.d. spectrum consisting of only one positive band with a maximum at 514 nm. However, the spectrum reported had two positive maxima at 510 and 657 nm. Since no experimental details were given in that report, it was decided to examine the changes in optical activity which occur on generating the species *in situ* in an attempt to explain the discrepancy.

The species present in a solution of copper(II) ions and *R*-pn is strongly p*H* dependent. At low p*H* the 1:1 complex $[Cu(R\text{-pn})]^{2+}$ is favored while in more basic solutions the 2:1 species $[Cu(R\text{-pn})_2]^{2+}$ predominates. Detailed thermodynamic data and formation constants have been reported for both complexes (2, 3). In our studies, aqueous solutions containing copper (II) nitrate and *R*-pn·2HCl in a 1:2 molar ratio were prepared. The initial p*H* of these solutions was approximately 2.6 and under these conditions essentially no complex formation occurred. Aqueous NaOH was then added in small amounts and absorption and c.d. spectra were obtained following each addition.

The absorption spectrum initially showed a peak at 805 nm characteristic of the aquo copper(II) ion. As the p*H* was increased, this band was shifted to shorter wavelengths and above p*H* 9.9 the spectrum had a maximum at 555 nm and did not change further. For solutions of p*H* greater than 6.5, a fine white precipitate was formed in small quantities as the base was added. This precipitate is due to hydrolysis of the copper ion and has been noted previously (4). Appropriate corrections (*vide infra*) therefore had to be included in the concentrations of the species present.

For the initial solution, no measurable c.d. was observed. However, as the p*H* was increased, a positive peak was formed at 625 nm and grew in intensity until p*H* = 5.0. Above this p*H* the long tail on the low wavelength side of the c.d. maximum developed into a separate peak at 514 nm and grew at the expense of the 625 nm band. After p*H* 9.9 the c.d. spectrum became constant and consisted only of the peak at 514 nm as shown in Fig. 1(*a*).

The limiting absorption and c.d. spectra above p*H* 9.9 were considered as being characteristic of the $[Cu(R\text{-pn})_2]^{2+}$ ion and were also similar to the spectra obtained for dissolved $[Cu(R\text{-pn})_2](NO_3)_2$. Since some hydrolysis had occurred during the study, it was necessary to obtain a corrected value for the concentration of the species in solution. This was accomplished by carrying out absorption measurements at the isosbestic point (640 nm) which we observed for these solutions above p*H* 4.8. A series of standard solutions showed that at this wavelength the molar extinction coefficient $\varepsilon = 37.5$ l mol^{-1} cm^{-1}. Hence, calculations of the total

Can. J. Chem. Downloaded from www.nrcresearchpress.com by 210.87.254.6 on 09/05/12
For personal use only.

Can. J. Chem. Downloaded from www.nrcresearchpress.com by 210.87.254.6 on 09/05/12
For personal use only.

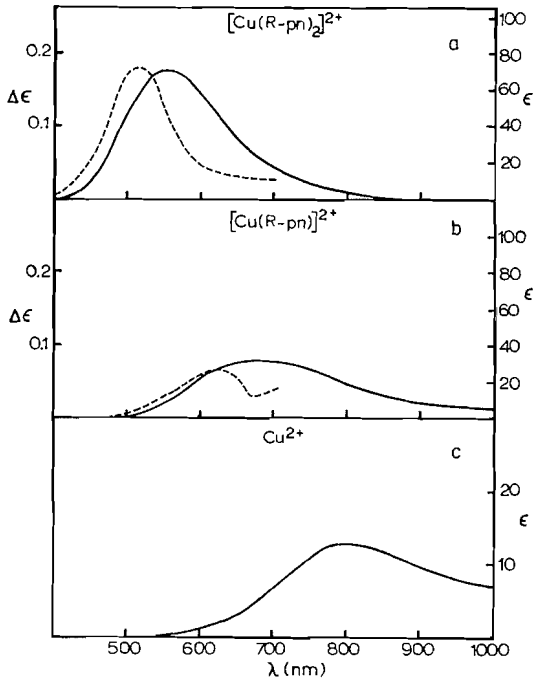

FIG. 1. Absorption (—) and circular dichroism (---) spectra of copper(II)–*R*-pn species.

copper concentration in our solution could be made and applied to both the c.d. and absorption spectra of the limiting $[Cu(R\text{-pn})_2]^{2+}$ species. The resulting values are shown in Fig. 1(*a*).

Data for the 1:1 complex were obtained by generating the species *in situ*. Copper(II) nitrate and *R*-pn·2HCl were mixed in a 20:1 molar ratio and the p*H* was adjusted to 3.6. At this acidity, formation of $[Cu(R\text{-pn})]^{2+}$ is favored and no appreciable amount of $[Cu(R\text{-pn})_2]^{2+}$ is present. The c.d. and absorption spectra determined for $[Cu(R\text{-pn})]^{2+}$ are shown in Fig. 1(*b*). The c.d. spectrum was measured directly while the absorption spectrum was derived by correcting for the absorption of uncomplexed copper(II) ion, whose absorption spectrum is shown in Fig. 1(*c*).

The 2:1 species has an absorption maximum at 555 nm with $\varepsilon = 72.1$ l mol^{-1} cm^{-1} while the c.d. spectrum has a maximum at 514 nm with $\Delta\varepsilon = 0.18$. The 1:1 species shows an absorption maximum at 675 nm with $\varepsilon = 31.5$ and a c.d. maximum at 625 nm where $\Delta\varepsilon = 0.065$. From the data calculated for these species it was possible to determine ratios for the concentrations of these two species in a given solution. Since each species makes a contribution to the total spectrum observed, it is possible to solve a series of simultaneous equations of the type

$$A_\lambda = \varepsilon_\lambda^{2:1} b c^{2:1} + \varepsilon_\lambda^{1:1} b c^{1:1} + \varepsilon_\lambda^{Cu^{2+}} b c^{Cu^{2+}}$$

where A_λ = the observed absorbance at a wavelength λ; ε_λ^x = the molar extinction coefficient of species x at λ, b = the path length in cm; and c^x is the molar concentration of species x. From measurements at three different wavelengths, the concentration of each species can be calculated. For c.d. spectra only two species contribute to the observed spectrum and two simultaneous equations of the type

$$\Delta A_\lambda = \Delta\varepsilon_\lambda^{2:1} b c^{2:1} + \Delta\varepsilon_\lambda^{1:1} b c^{1:1}$$

were solved where ΔA_λ = the observed differential absorbance at wavelength λ and $\Delta\varepsilon_\lambda^x$ is the molar c.d. value of species x at λ. (Quantities b and c^x are defined as before.) Ratios calculated from both sets of data are shown in Table 1.

TABLE 1. Calculated ratios of $[Cu(R\text{-pn})_2]^{2+}$: $[Cu(R\text{-pn})]^{2+}$

	Ratio of $[Cu(R\text{-pn})_2]^{2+}$: $[Cu(R\text{-pn})]^{2+}$	
p*H*	From c.d. spectra	From absorption spectra
4.4	0.22	0.23
4.9	0.64	0.68
5.5	1.2	1.3
6.3	1.4	1.7
6.7	2.6	2.6
7.3	14	20
9.9	$>10^6$	$>10^8$

On the basis of our studies it would appear that the spectra reported by Gillard (1) consisted of a mixture of the 2:1 and 1:1 species, possibly because of a solution which was not sufficiently basic to favor the formation of the 2:1 species. His conclusions concerning the complexity of the c.d. spectrum, however, would still appear to be valid. The tail on the long wavelength side of the c.d. peak for $[Cu(R\text{-pn})_2]^{2+}$ would suggest that more than one component band is present. For the 1:1 complex a second component actually was indicated but unfortunately was located beyond the range of our instrument. Three component transitions make up the large d–d absorption band in most square planar copper(II) complexes and in certain cases more than one com-

ponent has been observed in the c.d. spectra (5). For the *R*-pn complexes studied here, the component bands overlap quite strongly and hence assignment to individual transitions is difficult.

Experimental

R-1,2-Propanediamine dihydrochloride was obtained from Frinton Laboratories, Vineland, N.J. ($[\alpha]_{589} = -34°$ for the free base.) Solutions used in the study were approximately 3×10^{-2} *M* in copper(II) ion and were prepared as indicated in the text.

Circular dichroism spectra were obtained using a Durrum–Jasco Model ORD/UV-5 recording spectropolarimeter with c.d. attachment. Absorption spectra were determined on a Beckman-DK-1 recording spectrophotometer. Measurements of p*H* were carried out using a Sargent Model DR p*H* meter equipped with a combination glass–calomel electrode.

We gratefully acknowledge the financial assistance of the National Research Council of Canada in support of this work.

1. R. D. GILLARD. J. Inorg. Nucl. Chem. **26**, 1455 (1964).
2. H. K. J. POWELL and N. F. CURTIS. J. Chem. Soc. A, 1441 (1967).
3. A. T. ADVANI, D. S. BARNES, and L. D. PETTIT. J. Chem. Soc. A, 2691 (1970).
4. H. OJIMA and K. SONE. Bull. Chem. Soc. Jap. **35**, 298 (1962).
5. C. J. HAWKINS and C. L. WONG. Aust. J. Chem. **23**, 2237 (1970).

Reaction of *N*-Acetyl-2,3-diphenylindole with Nitric Acid

VINOD DAVE[1] AND E. W. WARNHOFF
Department of Chemistry, University of Western Ontario, London, Ontario

Received May 5, 1972

Based on spectroscopic and chemical evidence the 3-hydroxy-6-nitro-2,3-diphenylindolenine structure **8** is assigned to the previously reported *N*-acetyl-2,3-diphenylindole–nitric acid reaction product. The product from the acid-catalyzed rearrangement of **8** is assigned the oxindole structure **12**.

Par des preuves spectrales et chimiques, la structure **8** a été identifiée à l'hydroxy-3 nitro-6 diphényl-2,3 indolénine, produit issu de la réaction entre le *N*-acétyl diphényl-2,3 indole et l'acide nitrique. La structure oxindole **12** a été attribuée au produit issu du réarrangement acidocatalysé de **8**.

[Traduit par le journal]

Canadian Journal of Chemistry, **50**, 3392 (1972)

In a systematic study of the nitration of indoles, spanning a period of 35 years, Plant and his coworkers treated several indolic compounds with nitric acid (1). One such reaction between *N*-acetyl-2,3-diphenylindole (**1**) and nitric acid in acetic acid yielded a colorless compound, m.p. 262° (dec.), to which Fennell and Plant assigned the phenanthrene nitro alcohol structure **2** (2). There are two characteristic features of **2** which argue against it being the nitration product: an unusual oxidative coupling of the phenyl rings in the 2- and 3-positions, and remarkable stability of the carbinolamine moiety in **2** under the acid conditions used. In view of the doubtful structural assignment for the nitration product, the reaction was reinvestigated.

When the reaction was carried out according to the published procedure there was indeed obtained a colorless compound, m.p. 250° (dec.), whose i.r. spectrum showed the presence of N—H and/or O—H and nitro group absorption. Mass spectrometry gave the molecular ion peak at 330, confirming Fennell and Plant's molecular formula. However, the u.v. spectrum lacked the absorption due to a dihydrophenanthrene chromophore (3). Since spectroscopic information was not sufficient to establish the structure,[2] chemical means were resorted to.

On treating the nitration product with *m*-chloroperbenzoic acid (*m*-CPBA) there was obtained a lemon yellow compound, m.p.

[1]Author to whom inquiries should be addressed.

[2]Insolubility problems made it difficult to get a good integration of the n.m.r. spectrum and no exchangeable protons were apparent.

Can. J. Chem. Downloaded from www.nrcresearchpress.com by 210.87.254.6 on 09/05/12
For personal use only.

ponent has been observed in the c.d. spectra (5). For the *R*-pn complexes studied here, the component bands overlap quite strongly and hence assignment to individual transitions is difficult.

Experimental

R-1,2-Propanediamine dihydrochloride was obtained from Frinton Laboratories, Vineland, N.J. ($[\alpha]_{589} = -34^\circ$ for the free base.) Solutions used in the study were approximately 3×10^{-2} *M* in copper(II) ion and were prepared as indicated in the text.

Circular dichroism spectra were obtained using a Durrum–Jasco Model ORD/UV-5 recording spectropolarimeter with c.d. attachment. Absorption spectra were determined on a Beckman-DK-1 recording spectrophotometer. Measurements of p*H* were carried out using a Sargent Model DR p*H* meter equipped with a combination glass–calomel electrode.

We gratefully acknowledge the financial assistance of the National Research Council of Canada in support of this work.

1. R. D. GILLARD. J. Inorg. Nucl. Chem. **26**, 1455 (1964).
2. H. K. J. POWELL and N. F. CURTIS. J. Chem. Soc. A, 1441 (1967).
3. A. T. ADVANI, D. S. BARNES, and L. D. PETTIT. J. Chem. Soc. A, 2691 (1970).
4. H. OJIMA and K. SONE. Bull. Chem. Soc. Jap. **35**, 298 (1962).
5. C. J. HAWKINS and C. L. WONG. Aust. J. Chem. **23**, 2237 (1970).

Reaction of *N*-Acetyl-2,3-diphenylindole with Nitric Acid

VINOD DAVE[1] AND E. W. WARNHOFF
Department of Chemistry, University of Western Ontario, London, Ontario

Received May 5, 1972

Based on spectroscopic and chemical evidence the 3-hydroxy-6-nitro-2,3-diphenylindolenine structure **8** is assigned to the previously reported *N*-acetyl-2,3-diphenylindole–nitric acid reaction product. The product from the acid-catalyzed rearrangement of **8** is assigned the oxindole structure **12**.

Par des preuves spectrales et chimiques, la structure **8** a été identifiée à l'hydroxy-3 nitro-6 diphényl-2,3 indolénine, produit issu de la réaction entre le *N*-acétyl diphényl-2,3 indole et l'acide nitrique. La structure oxindole **12** a été attribuée au produit issu du réarrangement acidocatalysé de **8**.

[Traduit par le journal]

Canadian Journal of Chemistry, **50**, 3392 (1972)

In a systematic study of the nitration of indoles, spanning a period of 35 years, Plant and his coworkers treated several indolic compounds with nitric acid (1). One such reaction between *N*-acetyl-2,3-diphenylindole (**1**) and nitric acid in acetic acid yielded a colorless compound, m.p. 262° (dec.), to which Fennell and Plant assigned the phenanthrene nitro alcohol structure **2** (2). There are two characteristic features of **2** which argue against it being the nitration product: an unusual oxidative coupling of the phenyl rings in the 2- and 3-positions, and remarkable stability of the carbinolamine moiety in **2** under the acid conditions used. In view of the doubtful structural assignment for the nitration product, the reaction was reinvestigated.

When the reaction was carried out according to the published procedure there was indeed obtained a colorless compound, m.p. 250° (dec.), whose i.r. spectrum showed the presence of N—H and/or O—H and nitro group absorption. Mass spectrometry gave the molecular ion peak at 330, confirming Fennell and Plant's molecular formula. However, the u.v. spectrum lacked the absorption due to a dihydrophenanthrene chromophore (3). Since spectroscopic information was not sufficient to establish the structure,[2] chemical means were resorted to.

On treating the nitration product with *m*-chloroperbenzoic acid (*m*-CPBA) there was obtained a lemon yellow compound, m.p.

[1]Author to whom inquiries should be addressed.

[2]Insolubility problems made it difficult to get a good integration of the n.m.r. spectrum and no exchangeable protons were apparent.

Can. J. Chem. Downloaded from www.nrcresearchpress.com by 210.87.254.105 on 09/05/12
For personal use only.

Can. J. Chem. Downloaded from www.nrcresearchpress.com by 210.87.254.105 on 09/05/12
For personal use only.

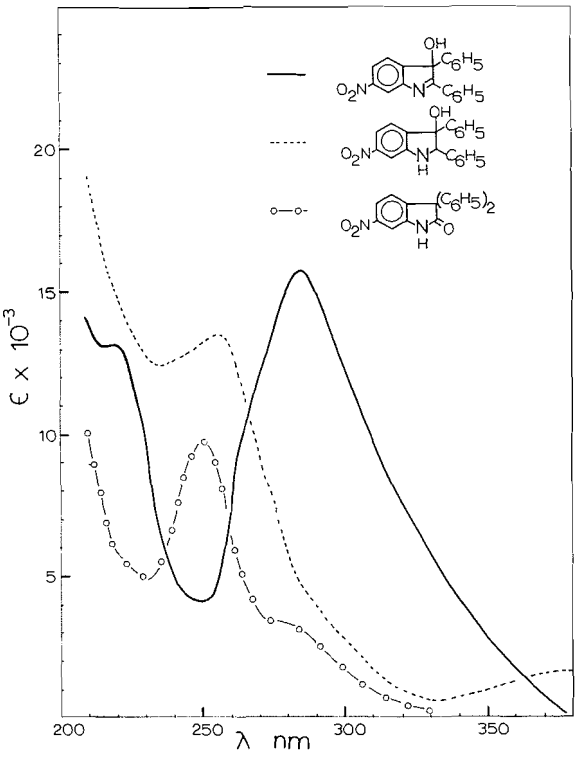

FIG. 1. The u.v. spectra of the nitro alcohol, its reduction product, and its rearrangement product.

192°, whose i.r. spectrum showed the presence of two carbonyl groups, one of which was likely due to an amide, suggesting possible cleavage of a double bond in the pyrrole ring during the peracid reaction. A literature search revealed that the two known nitro indoles **3** and **4** on oxidation gave the ring cleavage products **5** and **6** which were also yellow and had melting points close to that of the lemon yellow compound described above (4, 5).[3] Comparison of the lemon yellow compound from the peracid reaction on the nitration product with authentic samples (Scheme 1) of **5** (4) and **6** (5) showed it to be identical with **5**. The peracid reaction thus proved the presence of an indole or indolenine double bond and established that the nitro group was in the 6-position.

It was tempting to assume that the nitration product was *N*-hydroxy-6-nitro-2,3-diphenylindole (**7**). However, this possibility was discounted for the following reasons: (*a*) since 6-nitro-2,3-diphenylindole is orange in color, the *N*-hydroxy derivative would be expected to be colored, while the nitration product is colorless; (*b*) the compound did not give a positive ferric chloride test (8, 9), and (*c*) it lacked the characteristic bathochromic shift for *N*-hydroxy indoles in its u.v. spectrum in the presence of base (9).

The only structure left which could account for the available information was 3-hydroxy-6-nitro-2,3-diphenylindolenine (**8**). Support for this structure was provided by the following two observations. Firstly, sodium borohydride reduction of the carbon—nitrogen double bond in **8** gave the hydroxyindoline **9** as an orange-red solid.[4] The n.m.r. spectrum of this compound showed the presence of a methine proton at δ 5.1 and the i.r. spectrum showed absorption at 3340 and 3510 cm^{-1} due to NH and OH. The dihydro compound **9** on heating above the melting point gave 6-nitro-2,3-diphenylindole (**3**) as the only product. Secondly, reaction of the "nitro alcohol" with acetic anhydride in pyridine gave a colorless *O*-acetate. The u.v. spectrum of this compound was identical with that of the nitration product and hence the acetate was tentatively assigned the nitroacetoxyindolenine structure **11**.

Attempts to prepare the hydroperoxide **10** from the nitro indole **3** for reduction to **8** were unsuccessful. However, Taylor and his coworkers had treated several indole alkaloids with lead tetraacetate in methylene chloride to obtain 3-acetoxyindolenines (10). This reaction on 6-nitro-2,3-diphenylindole (**3**) gave a colorless compound which was identical with the *O*-acetate obtained from the nitro alcohol–acetic anhydride reaction, thus establishing the 3-acetoxyindolenine structure **11** for the latter and the 3-hydroxy-6-nitro-2,3-diphenylindolenine structure (**8**) for the nitration product.

Fennell and Plant had treated their nitration product with refluxing acetic acid and obtained an isomeric red compound, m.p. 227°, to which no structure was assigned. Repetition of the reaction gave a red-orange compound, m.p. 227–229°, whose i.r. spectrum showed the presence of a carbonyl group at 1720 cm^{-1}. Mass spectrom-

[3]Compounds formed by the double bond cleavage of 4- and 5-nitro-2,3-diphenylindole are colorless (4).

[4]The orange-red color of this dihydro compound is not surprising, since *N*-methyl and *N*-ethyl-*m*-nitroaniline are reddish-yellow in color.

Can. J. Chem. Downloaded from www.nrcresearchpress.com by 210.87.254.105 on 09/05/12
For personal use only.

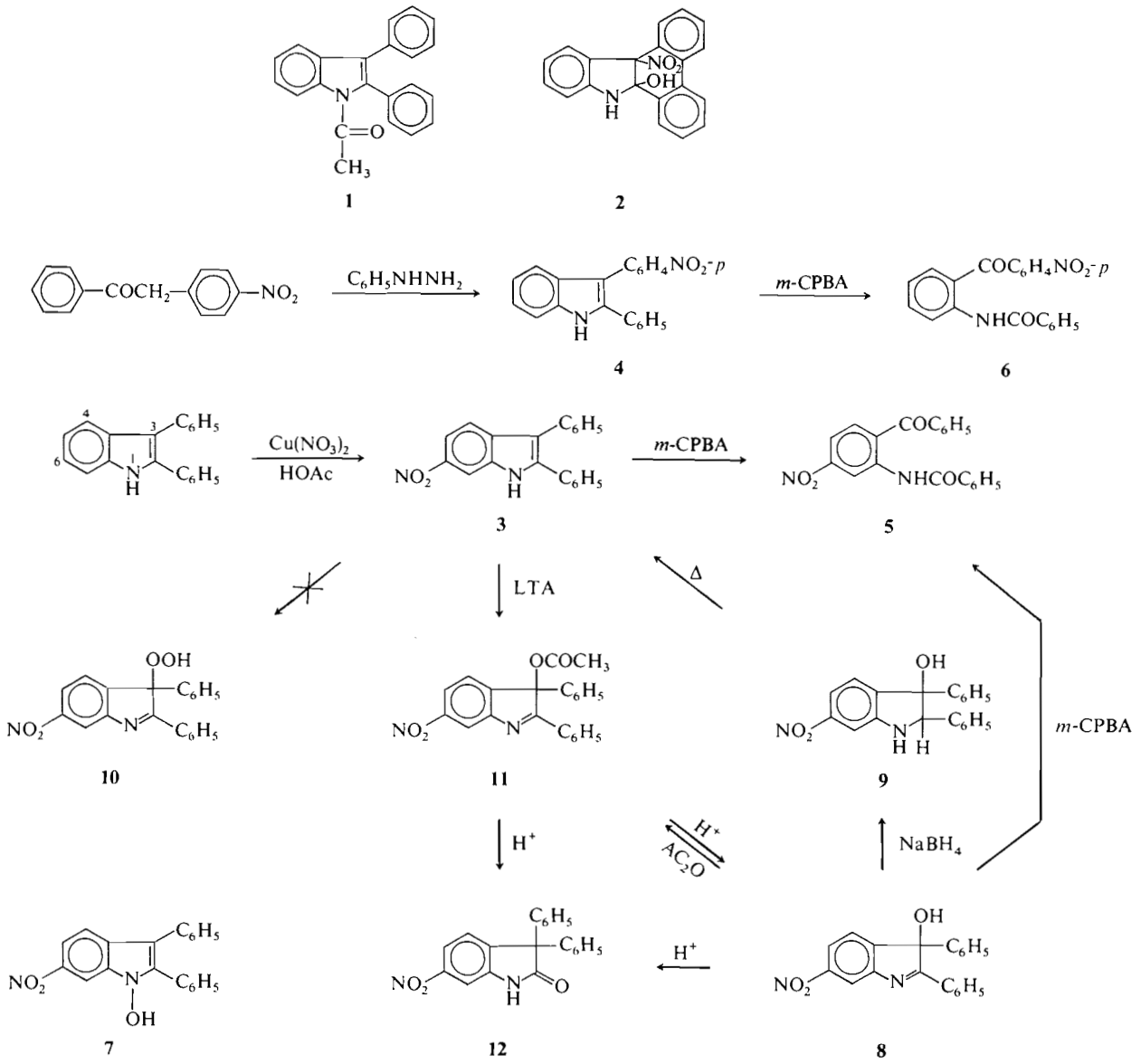

SCHEME 1

Can. J. Chem. Downloaded from www.nrcresearchpress.com by 210.87.254.105 on 09/05/12
For personal use only.

etry gave the molecular ion peak at 330, corresponding to Fennell and Plant's molecular formula. Treatment of 3-acetoxy-6-nitro-2,3-diphenylindolenine (**11**) with hydrochloric acid, Taylor's general method for preparation of oxindole alkaloids (10), gave the same red compound which is therefore 3,3-diphenyl-6-nitrooxindole (**12**). From the acid reaction on 3-acetoxyindolenine **11** there was also obtained, albeit in only 3% yield, Fennell and Plant's nitration product **8**, presumably by acid hydrolysis of the acetate group, confirming the 3-hydroxyindolenine structure **8** for the nitration product.

Formation of 3-hydroxy-6-nitro-2,3-diphenylindolenine (**8**) under the nitration conditions used is understandable. The initial product of the reaction probably is 3,6-dinitro-2,3-diphenylindolenine which on hydrolysis in aqueous acid would give the 3-hydroxyindolenine **8**.[5] One possible mechanism (13) for the peracid reaction of indolenine **8** would involve formation of an oxaziridine followed by cleavage to give **5**.

In view of the present findings, the structures of products from other reactions between nitric acid and *N*-acetyl-2,3-diphenylindole under different conditions for which the basic phenanthrene skeleton have been assumed (2) should be considered suspect.

Experimental[6]

Reaction of N-Acetyl-2,3-diphenylindole with Nitric Acid

The reaction was carried out by the method of Fennell and Plant (2) to give the nitro alcohol **8** as colorless needles (23%), m.p. 250° (dec., sealed capillary) (lit. (2) 262° (dec.)); ν_{max} (Nujol) 3100 (OH) and 1500 cm^{-1} (NO_2); ν_{max} (THF) 3280 (OH) and 1520 cm^{-1} (NO_2); λ_{max} 220 (12 900) and 285 nm (15 600); *m/e* 330 (molecular ion).

Anal. Calcd. for $C_{20}H_{14}N_2O_3$ (330.3): C, 72.72; H, 4.27; N, 8.48. Found: C, 72.62; H, 4.42; N, 8.05.

Reaction of Nitro Alcohol 8 with Peracid

To a stirred solution of nitro alcohol **8** (100 mg) in chloroform (40 ml) was added a solution of *m*-chloroperbenzoic acid (200 mg) in chloroform (2.0 ml). After the pale yellow solution was stirred for 1 h at room temperature, it was first washed with 10% aqueous Na_2SO_3 and then with 5% $NaHCO_3$ solution. The organic layer was washed to neutrality, dried, and concentrated giving a yellow solid. Three recrystallizations from chloroform–petroleum ether gave lemon-yellow needles of **5** (70 mg), m.p. 190–192°; ν_{max} 3310 (NH), 1680, 1640 (—C=O), and 1530 cm^{-1} (NO_2); λ_{max} 255 (10 100) and 272 nm (8900); *m/e* 346 (molecular ion).

Anal. Calcd. for $C_{20}H_{14}N_2O_4$ (346.3); C, 69.36; H, 4.07; N, 8.09. Found: C, 69.35; H, 4.03; N, 7.44.

The compound was identical in all respects with the authentic sample of the keto amide **5** (see below).

Reaction of 6-Nitro-2,3-diphenylindole (3) with Peracid

To a stirred solution of 6-nitro-2,3-diphenylindole (5) (50 mg) in chloroform (4.0 ml) was added a solution of *m*-chloroperbenzoic acid (100 mg) in chloroform (0.5 ml). After the pale yellow solution was stirred at room temperature for 0.5 h, it was worked-up as above to give a yellow solid (52 mg). Two recrystallizations from chloroform–petroleum ether gave the keto amide **5** as lemon-yellow needles (42 mg), m.p. 190–192° (lit. (4) 192–193°).

Reaction of 2-Phenyl-3-(4'-nitrophenyl)indole (4) with Peracid

A solution of the nitroindole **4** (5, 6) (30 mg), *m*-chloroperbenzoic acid (60 mg), and chloroform (5.0 ml) was refluxed for 0.5 h. After cooling, the solution was worked-up as above giving a yellow solid. Three recrystallizations from chloroform–petroleum ether gave the keto amide **6** as yellow needles (26 mg), m.p. 185–188° (lit. (5) 187–189°). The mixed m.p. of this compound with the nitro alcohol–peracid product **5** was depressed to 163–185° and the two compounds had different R_f on t.l.c.; ν_{max} 3280 (NH), 1670, 1630 (—C=O), and 1500 cm^{-1} (NO_2); λ_{max} 257 (5500) and 272 nm (4500); *m/e* 346 (molecular ion).

Reaction of the Nitro Alcohol 8 with Sodium Borohydride

To a stirred colorless solution of the nitro alcohol (100 mg) in methanol (2.5 ml) and tetrahydrofuran (2.5 ml) was added sodium borohydride (200 mg) over a period of 5 min. The solution which immediately became yellow–orange was stirred at room temperature for 20 min, diluted with ether, washed with water, dried, and concentrated to give an orange colored solid (98 mg). The crude material was put on a silica gel preparative layer plate and developed with benzene–ether (90:10). The orange band at R_f 0.48 gave an orange–red solid (86 mg). Two recrystallizations from chloroform–petroleum ether gave the hydroxyindoline **9** as reddish-orange plates (64 mg), m.p. 158–204° (dec.)

[5]Precedent for such ready hydrolysis of a *C*-nitro group is known from the work of Plant (11) and Taylor (12) who treated *N*-acetyl and *N*-benzoyl-2,3-dimethylindole with nitric acid and isolated what was presumably the nitro alcohol **i** which on hydrolysis gave the diol **ii**.

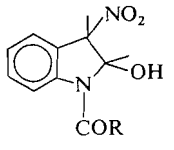

i

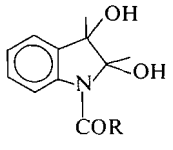

ii

[6]For general experimental methods see ref. 14. Unless otherwise stated i.r. spectra were taken with chloroform solutions, u.v. spectra with methanol, and n.m.r. spectra with deuteriochloroform solutions containing tetramethylsilane as internal standard.

Can. J. Chem. Downloaded from www.nrcresearchpress.com by 210.87.254.105 on 09/05/12
For personal use only.

(see below); ν_{max} 3510 and 3340 cm^{-1} (NH and OH); λ_{max} 255 (13 570) and 385 nm (1590); δ 5.1 (1H, N—CHPh); highest peak in the mass spectrum was at 314 corresponding to 6-nitro-2,3-diphenylindole.

Anal. Calcd. for $C_{20}H_{16}N_2O_3$ (332.4): C, 72.28; H, 4.85; N, 8.43. Found: C, 72.48; H, 4.71; N, 7.78.

The sodium borohydride product (15 mg) was sealed in a glass tube and heated at 180° for 2 h. After cooling, the material was recrystallized twice from chloroform–methanol–petroleum ether giving orange crystals (9 mg), m.p. 229–231°, identical in all respects with the authentic sample of 6-nitro-2,3-diphenylindole (**3**).

Reaction of 6-Nitro-2,3-diphenylindole with Lead Tetraacetate

The method of Taylor *et al.* (10) was slightly modified. To a refluxing solution of 6-nitro-2,3-diphenylindole (106 mg) in methylene chloride (10 ml) was added lead tetraacetate (270 mg). After the solution was refluxed for 3.5 h, it was cooled, filtered, and concentrated to give an oily solid. The material was put on two alumina preparative layer plates and developed with benzene–ether (87:13). The band at R_f 0.41 gave a colorless solid (83 mg). Three recrystallizations from chloroform–petroleum ether gave the nitro acetoxyindolenine **11** as a colorless solid (60 mg), m.p. 210° (dec.); ν_{max} 1770 (sh), 1755 (—CO), and 1520 cm^{-1} (NO_2); λ_{max} 285 nm (20 100); *m/e* 372 (molecular ion).

Anal. Calcd. for $C_{22}H_{16}N_2O_4$ (372.4): C, 70.96; H, 4.33, N, 7.52. Found: C, 70.39; H, 4.18; N, 6.87.

The faintly yellow band from the above plates at R_f 0.70 gave a pale yellow oil (18 mg) which failed to crystallize and was not further investigated.

Reaction of Nitro Alcohol 8 with Acetic Anhydride

A solution of nitro alcohol **8** (40 mg), pyridine (1.0 ml), and acetic anhydride (0.5 ml) was stirred at room temperature for 12 days. After the addition of chloroform, the reaction mixture was washed first with water and then with 5% $NaHCO_3$ solution. The organic layer was washed, dried, and concentrated giving a faintly yellow solid. Two recrystallizations from chloroform–petroleum ether gave the acetoxy compound **11** as colorless crystals (29 mg), identical in all respects with the authentic sample of 6-nitro-3-acetoxy-2,3-diphenylindolenine (**11**).

Reaction of the Nitro Alcohol 8 with Acetic Acid

The reaction was carried out in essentially the same way as reported by Fennell and Plant (2). The crude product was recrystallized from methanol–petroleum ether to give orange-red needles, m.p. 227–230° (lit. (2) 227°); ν_{max} 3410 (NH), 1720, 1700 (sh) (—C=O), and 1510 cm^{-1} (NO_2); λ_{max} 250 (9700), 280 (3200), and 460 nm (860); *m/e* 330 (molecular ion). This compound was identical in all respects with the authentic sample of 3,3-diphenyl-6-nitrooxindole (see below).

Reaction of 3-Acetoxy-6-nitro-2,3-diphenylindolenine (11) with Hydrochloric Acid

The method of Taylor and his coworkers (10) was used. To the refluxing solution of 6-nitro-3-acetoxy-2,3-diphenylindolenine (**11**) (50 mg) in methanol (10 ml) and chloroform (5 ml) was added concentrated HCl (0.5 ml). After the solution was refluxed for 13 h, the solvents were evaporated on the rotary evaporator. The residual orange solid was dissolved in chloroform and washed with water. The organic layer was dried and concentrated to give an orange solid (51 mg). The material was put on a silica gel preparative plate and developed with benzene–ether (95:5). The band at R_f 0.77 gave an orange solid (27 mg). Two recrystallizations from chloroform–petroleum ether gave 3,3-diphenyl-6-nitrooxindole (**12**) as orange–red needles (12 mg), m.p. 228–230°.

The band at R_f 0.42 gave a colorless compound (8 mg). Two recrystallizations from acetone–petroleum ether gave colorless needles (1.5 mg) identical in all respects with the nitro alcohol **8**.

We would like to thank the National Research Council of Canada for financial support.

1. D. A. KINSLEY and S. G. P. PLANT. J. Chem. Soc. 4814 (1956) and previous papers in the series; see also K. SCHOFIELD. Quart. Rev. **4**, 382 (1950).
2. R. C. G. FENNELL and S. G. P. PLANT. J. Chem. Soc. 2872 (1932).
3. G. H. BEAVEN, D. M. HALL, M. S. LESSLIE, and E. E. TURNER. J. Chem. Soc. 854 (1952).
4. K. SCHOFIELD and R. S. THEOBALD. J. Chem. Soc. 1505 (1950).
5. A. DA SETTIMO and M. F. SAETTONE. Tetrahedron, **21**, 823 (1965).
6. E. B. WOMACK, N. CAMPBELL, and G. B. DODDS. J. Chem. Soc. 1402 (1938).
7. B. WITKOP and H. FIEDLER. Ann. **558**, 91 (1947).
8. J. D. LOUDON and I. WELLINGS. J. Chem. Soc. 3462 (1960).
9. M. KAWANA, M. YOSHIOKA, S. MIYAJI, H. KATAOKA, Y. OMOTE, and N. SUGIYAMA. Nippon Kagaku Zasshi. **86**, 526 (1965); Chem. Abstr. **63**, 11479 (1965).
10. N. FINCH, C. W. GEMENDEN, I.H-C. HSU, and W. I. TAYLOR. J. Am. Chem. Soc. **85**, 1520 (1963).
11. S. G. P. PLANT and M. L. TOMLINSON. J. Chem. Soc. 955 (1933); S. G. P. PLANT and W. D. WHITAKER. J. Chem. Soc. 283 (1940).
12. C. M. ATKINSON, J. W. KERSHAW, and A. TAYLOR. J. Chem. Soc. 4426 (1962).
13. B. WITKOP and J. B. PATRICK. J. Am. Chem. Soc. **73**, 2196 (1951).
14. V. DAVE and E. W. WARNHOFF. Can. J. Chem. **49**, 1911 (1971).

Reaction of 2,3-Diphenylindole with Permanganate. Rearrangements of *N,N'*-Dimers

VINOD DAVE
Department of Chemistry, University of Western Ontario, London, Ontario
Received May 5, 1972

Based on spectroscopic and chemical evidence dimeric structure **1** is assigned to the major product from reaction of 2,3-diphenylindole and potassium permanganate. Thermal and acid-catalyzed rearrangements of *N,N'*-dimers **1** and **6** were studied.

Sur des bases spectrales et chimiques, la structure du dimère **1** a été attribuée au produit majeur de la réaction entre le diphényl-2,3 indole et le permanganate de potassium. Les réarrangements thermiques et acido-catalysés des *N,N'*-dimères **1** et **6** ont été étudiés. [Traduit par le journal]

Canadian Journal of Chemistry, **50**, 3397 (1972)

Can. J. Chem. Downloaded from www.nrcresearchpress.com by 210.87.254.105 on 09/05/12
For personal use only.

Over a quarter of a century ago Koelsch (1) reacted 2,3-diphenylindole with potassium permanganate and reported the formation of a compound, $C_{40}H_{28}N_2O + C_6H_6$ (from benzene–ethanol), m.p. 199–200°, to which no structure was assigned. Because of our interest in the chemistry of indole oxidations and rearrangements (2), we have reinvestigated the reaction. When the reaction was carried out according to the procedure of Koelsch,[1] there were obtained three crystalline compounds and a glassy material. The least polar (t.l.c.), major product (30%), dimer A, $C_{40}H_{28}N_2$, had m.p. 204–206° (from chloroform–petroleum ether) and was identical in all respects with a sample recrystallized from benzene–ethanol. Though no direct comparison with Koelsch's sample was made, our compound is probably the same as his sample of m.p. 199–200°. Based on the analytical data and the following spectroscopic and chemical evidence the *N,N'*-dimeric structure **1** is assigned to dimer A.

The compound (molecular ion *m/e* 536) contained the diphenylindole chromophore (u.v.) but only aromatic hydrogen atoms (n.m.r.) and no NH group (i.r.). The above spectroscopic data suggested the probable linking of two diphenylindole molecules by the nitrogen atoms. That this was indeed the case was shown by the reductive cleavage of the nitrogen–nitrogen single bond by lithium aluminum hydride to give 2,3-diphenylindole as the only product. The dimeric indole structure **1** was further supported by the reaction with *m*-chloroperbenzoic acid (4) which gave the *N*-benzoyl-*o*-aminobenzophenone derivative **2**.

The second more polar compound, dimer B, (7%) from the permanganate reaction was a crystalline solid of m.p. 219–221°, isomeric with the *N,N'*-dimer. The third more polar compound from the reaction was a glassy material whose purity was uncertain and which was not further investigated. The most polar compound from the reaction (<1%) was a solid, m.p. 246–248°, whose trimeric nature was proved by molecular weight determination.

The acid-catalyzed and thermal rearrangements of dimer A were examined. Reaction with concentrated hydrochloric acid in refluxing acetone under benzidine rearrangement conditions (5) gave an isomeric dimer (dimer C), m.p. 235° (dec.). Heating the dimer A alone at 240° for 1 h in a sealed tube followed by column chromatography gave four crystalline products, one of which was proved to be 2,3-diphenylindole and the other three were isomeric with dimers A, B, and C. The four compounds in increasing order of polarity on alumina had melting points as follows: 270–271° (dimer D); 113–115° (2,3-diphenylindole); 298° (dec.) (dimer E); and 296° (dimer F).

Though no definite structural assignments for dimers B–F and the trimer are possible, the possibilities can be limited.[2] All the dimers B–F showed i.r. absorption due to the N–H,

[1]It is necessary to add solid permanganate, since as in case of carbazole (3), diphenylindole is recovered largely unchanged if a solution of permanganate in acetone is used (heterogenous reaction?).

[2]Throughout the discussion it has been assumed that the phenyl rings in the 2- and 3-positions remain unreactive; however, the data at hand do not necessarily prove that.

Can. J. Chem. Downloaded from www.nrcresearchpress.com by 210.87.254.105 on 09/05/12
For personal use only.

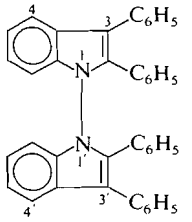

1

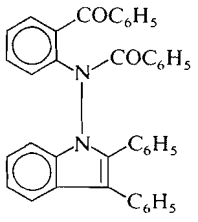

2

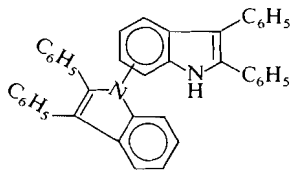

3

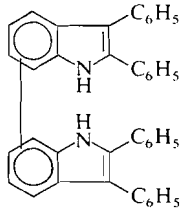

4

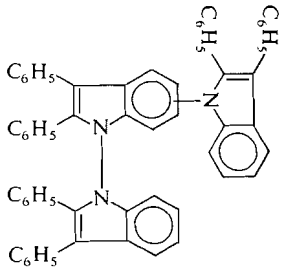

5

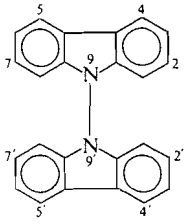

6

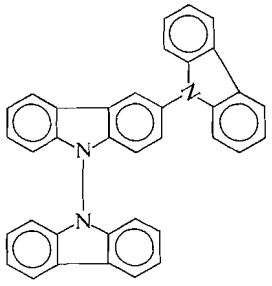

7

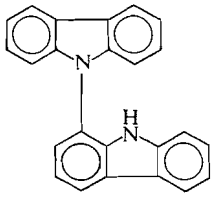

8

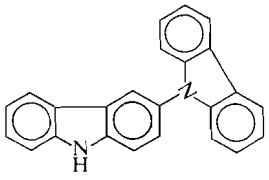

9

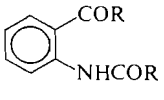

10

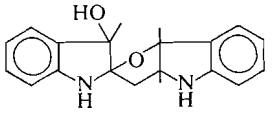

11

while the trimer lacked this absorption. All of the compounds showed the presence of the indole chromophore in their u.v. spectra. Dimer C, the benzidine rearrangement product, failed to react with acetic anhydride but readily gave an *N*-methyl derivative in the presence of sodium hydride – methyl iodide. This *N*-methyl compound lacked N—H i.r. absorption, and hence it must be either the 1,5′- or, more likely in view of the hindrance to acetylation, the 1,7′-linkage product (see **3**). Dimers B and E reacted with acetic anhydride to give monoacetates which lacked i.r. N—H absorption. In view of the fact that radical aromatic substitution takes place in *o*-, *m*-, and *p*-positions (6), combined with the finding that the reaction

Can. J. Chem. Downloaded from www.nrcresearchpress.com by 210.87.254.105 on 09/05/12
For personal use only.

of the benzyl radical with indole gave the 4-substituted indole derivative as one of the products (7), the dimers B and E must be two of the remaining three carbon–nitrogen coupling products (see **3**). Because of the low yields of dimers D and F no derivative preparation was attempted, but in view of the above discussion one or both of them could be the carbon–carbon coupling products (see **4**). The only trimer in the series must have structure **5** because it lacks i.r. N—H absorption.

Reaction of the related compound carbazole with potassium permanganate was reported half a century ago by Perkin and Tucker (8) who isolated two pure compounds from the reaction. The compound of m.p. 220° was proved to be 9,9′-dicarbazolyl (**6**). The compound having m.p. 265° which was reported to be isomeric with 9,9′-dicarbazolyl, but to which no structural assignment was possible, has recently been proved to be the trimer **7** (9, 10). Like *N,N′*-dimer **1**, 9,9′-dicarbazolyl (**6**) underwent thermal rearrangement at 250° to give three products, one of which sublimed during the reaction and was proved to be carbazole. The other two compounds were found to be 1,9′- and 3,9′-dicarbazolyl (**8** and **9**), by comparison with the authentic samples. Unlike dimer **1**, 9,9′-dicarbazolyl (**6**), did not undergo the benzidine rearrangement under the conditions used for rearrangement of **1**.

Reaction of potassium permanganate with indole, 2-methylindole, 3-methylindole, and 2-phenylindole gave largely unreacted starting material or, on longer reaction time gave double bond cleavage product **10**. 3-Phenylindole gave a product which lacked i.r. N—H absorption, but no homogeneous compound could be isolated. 2,3-Dimethylindole, however, reacted with potassium permanganate to give *o*-acetamidoacetophenone (**10**, R=CH_3) and the dimer of 3-hydroxy-2,3-dimethylindolenine (**11**) (2).

Experimental

General

Molecular weight determinations using a Hewlett-Packard model 301A osmometer were carried out with chloroform as solvent. Aluminum oxide PF-254, Type E (Merck, Germany) was used for analytical and preparative layer (20 g, 20 × 20 cm plate) chromatography. For other general experimental methods see ref. 2. Unless otherwise stated i.r. spectra were taken with chloroform solution, u.v. spectra with methanol, and n.m.r. spectra with deuteriochloroform solution containing tetramethylsilane as internal standard.

2,3-Diphenylindole

This starting material was either purchased from the Koch-Light Laboratories Ltd. or was made by Fischer indole synthesis, m.p. 113–115° (lit. (11) 123°).

Reaction of 2,3-Diphenylindole with Potassium Permanganate

To a solution of 2,3-diphenylindole (2.0 g) in acetone (10 ml) was added with stirring potassium permanganate (800 mg) over a period of 15 min. After the mixture was stirred at room temperature for 0.5 h, it was filtered and concentrated giving an amber colored highly viscous mass. This was put on eight silica gel preparative layer plates and developed with petroleum ether–ethyl acetate (75:25). The band at R_f 0.60 gave a pale yellow solid (1.2 g, 60%). Two recrystallizations from chloroform–petroleum ether gave *N,N′*-dimer **1** (dimer A) as a faintly yellow solid (618 mg), m.p. 204–206°; ν_{max} 1600 and 1440 cm^{-1}; λ_{max} 230 (16 650), 252 (10 410), and 300 nm (7910); *m/e* 536 (molecular ion); osmometric molecular weight 511.

Anal. Calcd. for $C_{40}H_{28}N_2$ (536.7): C, 89.52; H, 5.26; N, 5.22. Found: C, 89.38; H, 5.69; N, 5.09.

The more polar material from the above plates was put on four silica gel preparative layer plates and developed twice with benzene. A band at R_f 0.43 gave a pale yellow oil (265 mg, 13%) which gave pale yellow crystals on trituration with petroleum ether (b.p. 30–60°). One recrystallization from ether–petroleum ether (b.p. 30–60°) and two recrystallizations from chloroform–petroleum ether gave dimer B as a very faintly yellow solid (133 mg), m.p. 219–221° (dec.); ν_{max} 3460 (NH) and 1600 cm^{-1}; λ_{max} 227 (18 350), 257 (21 030), and 315 nm (14 320); *m/e* 536 (molecular ion); osmometric molecular weight 560.

Anal. Calcd. for $C_{40}H_{28}N_2$ (536.7): C, 89.52; H, 5.26; N, 5.22. Found: C, 89.26; H, 5.94; N, 5.18.

The more polar material from the above plates was put on two silica gel preparative layer plates, and developed twice using benzene–ether (97.5:2.5). Band at R_f 0.39 gave an almost colorless glassy oil (94 mg, 4.7%). I.r. showed absorption due to trace of —C=O (1690 cm^{-1}) and absence of N—H. The material failed to crystallize and was not further investigated. The band at R_f 0.29 gave an oily solid (74 mg, 3.7%). It was washed twice using ether and then recrystallized once from chloroform–petroleum ether and once from methanol–petroleum ether to give the trimer as an almost colorless solid (15 mg), m.p. 246–248°; ν_{max} 1590 cm^{-1}; λ_{max} (saturated solution) 250, 257, and 300 nm; molecular weight by osmometer 806, *m/e* 803 (molecular ion).

Anal. Calcd. for $C_{60}H_{41}N_3$ (803.9): C, 89.64; H, 5.14; N, 5.23. Found: C, 89.21; H, 5.94; N, 4.83.

Reaction of the N,N′-Dimer A (1) with Lithium Aluminum Hydride

To a stirred solution of dimer A (50 mg) in tetrahydrofuran (2.5 ml) was added lithium aluminum hydride (150 mg). After stirring the mixture at room temperature for 4 h, water was added and the mixture was extracted with ether. The organic layer was dried and concentrated giving an oily solid (50 mg). The crude mixture was put on a silica gel preparative layer plate and developed using petroleum

Can. J. Chem. Downloaded from www.nrcresearchpress.com by 210.87.254.105 on 09/05/12
For personal use only.

ether–ethyl acetate (75:25). The band at R_f 0.44 gave an oily solid (48 mg). Two recrystallizations from chloroform–petroleum ether gave an almost colorless solid (35 mg), identical in all respects with 2,3-diphenylindole.

Reaction of the N,N′-Dimer A (1) with Peracid

To a stirred solution of the dimer A (100 mg) in chloroform (1.0 ml) was added a solution of *m*-chloroperbenzoic acid (120 mg) in chloroform (1.0 ml). After stirring the solution at room temperature for 0.5 h, it was extracted first with 10% sodium sulfite and then with 5% sodium bicarbonate. The organic layer was washed and dried giving an oily solid. This material was put on a silica gel preparative layer plate and developed using petroleum ether–ethyl acetate (70:30). The band at R_f 0.29 gave an oily solid (70 mg). It was recrystallized four times from chloroform–petroleum ether giving amide **2** as a colorless solid (43 mg), m.p. 217–219°; ν_{max} 1640 cm^{-1} (amide C=O); λ_{max} 245 (9481) and 290 nm (3793); *m/e* 568 (molecular ion).

Anal. Calcd. for $C_{40}H_{28}N_2O_2$ (568.7): C, 84.48; H, 4.96; N, 4.93. Found: C, 84.79; H, 5.20; N, 4.74.

Acetate of Dimer B

A mixture of dimer B (150 mg), sodium acetate (300 mg), pyridine (2.0 ml), and acetic anhydride (0.5 ml) was refluxed for 36 h. After cooling, it was taken in chloroform, washed first with water and then with 5% sodium bicarbonate solution. The organic layer was washed with water, dried, and concentrated giving an oil which was put on two silica gel preparative layer plates and developed using benzene–ether (95:5). The band at R_f 0.38 gave a solid (110 mg), which after two recrystallizations from ether gave colorless crystals (63 mg), m.p. 177–181° (dec.); ν_{max} 1700 cm^{-1} (amide C=O); λ_{max} 250 (11 940) and 300 nm (7961); δ 1.95 (N—$COCH_3$); *m/e* 578 (molecular ion).

Anal. Calcd. for $C_{42}H_{30}N_2O$ (578.7): C, 87.17; H, 5.23; N, 4.84. Found: C, 86.78; H, 5.26; N, 5.04.

The above acetate was saponified with NaOH in refluxing methanol to give back dimer B (m.p., t.l.c.).

Reaction of the N,N′-Dimer 1 with HCl

To a refluxing solution of dimer A (250 mg) in acetone (10 ml) was added concentrated HCl (1.0 ml). After refluxing the cherry-red solution for 5.5 h, acetone was distilled on a rotary evaporator. The cooled residue was taken in chloroform, washed with water, dried, and concentrated giving dark brown oil. The crude mixture was put on two silica gel preparative layer plates and developed with benzene–petroleum ether (50:50). The band at R_f 0.49 gave an amber colored oil. This material was put on two alumina preparative layer plates and developed once using petroleum ether–benzene (75:25) and once using petroleum ether–benzene (50:50). The band at R_f 0.76 gave an almost colorless oil. This was boiled with petroleum ether, solvent pipetted out, and the material was dried giving a colorless solid (42 mg), m.p. 231–235° (dec.). Recrystallization from ether–petroleum ether (30–60°) gave dimer C as a colorless crystalline solid (28 mg), m.p. 232–235° (dec.); ν_{max} 3400 (NH) and 1600 cm^{-1}; λ_{max} 247 (18 880), 252 (17 620), and 330 nm (11 740); *m/e* 536 (molecular ion).

Anal. Calcd. for $C_{40}H_{28}N_2$ (536.7): C, 89.52; H, 5.26; N, 5.22. Found: C, 88.86; H, 5.34; N, 5.06.

N-Methyl Derivative of Dimer C

The procedure of Coggins and Benoiton (12) was used. To a hot (70°) solution of dimer C (100 mg), tetrahydrofuran (1.0 ml), and dimethylformamide (1.0 ml) was added sodium hydride (*ca.* 300 mg) and the mixture was heated at 70° for 5 min. To this hot solution was added methyl iodide (1.0 ml) and the mixture was refluxed (bath 70°). Within 15 min most of the mass had solidified. To this was added tetrahydrofuran (1.0 ml) and dimethyl formamide (1.0 ml) and reflux continued. At the end of 1 h, the mixture was cooled and water added. The mass was extracted with ether, washed with water, dried, and concentrated giving a brown oil (93 mg). This was put on a silica gel plate and developed using benzene–petroleum ether (50:50). The band at R_f 0.56 gave a colorless oil (65 mg). T.l.c. of this in above solvent system showed a single spot slightly less polar than dimer C. The compound failed to crystallize; however, adding methanol to an ether solution of the compound gave a solid, which was boiled thoroughly with methanol giving a colorless solid, which lacked any definite crystal structure and changed to glassy material at 172°, ν_{max} 1600 cm^{-1}; λ_{max} (saturated solution) 250 and 330 nm; *m/e* 550 (molecular ion).

Anal. Calcd. for $C_{41}H_{30}N_2$ (550.7): C, 89.51; H, 5.49; N, 5.09. Found: C, 89.49; H, 5.48; N, 4.62.

Thermal Reaction on Diphenylindole N,N′-Dimer 1

Dimer **1** (3.3 g) was sealed in a glass tube and heated at 240° for 1 h. The brown-black mass was allowed to stand at room temperature in acetone over a period of 3 days and the precipitated solid was removed every few hours using centrifugation. This solid was recrystallized twice from acetone giving dimer E as a colorless crystalline solid (543 mg), m.p. 298° (dec.); ν_{max} (Nujol) 3340 (N—H) and 1570 cm^{-1}; λ_{max} 253 (15 570) and 315 nm (9662); *m/e* 536 (molecular ion).

Anal. Calcd. for $C_{40}H_{28}N_2$ (536.7): C, 89.52; H, 5.26; N, 5.22. Found: C, 89.09; H, 5.72; N, 5.26.

The residue left after removal of dimer E was chromatographed on alumina. Fractions in petroleum ether–benzene (92:8) gave a crystalline solid (75 mg). Three recrystallizations from chloroform–petroleum ether gave dimer D as a colorless solid (50 mg), m.p. 270–271°; ν_{max} 3440 (N—H) and 1585 cm^{-1}; λ_{max} (saturated solution) 250, 257, and 310 nm; *m/e* 536 (molecular ion).

Anal. Calcd. for $C_{40}H_{28}N_2$ (536.7): C, 89.52; H, 5.26; N, 5.22. Found: C, 88.98, H, 5.76; N, 5.11.

Fractions in petroleum ether–benzene (86:14) to petroleum ether–benzene (80:20) gave 575 mg of crystalline 2,3-diphenylindole.

Fractions in petroleum ether–benzene (72:28) gave a solid (47 mg). Two recrystallizations from acetone gave colorless crystals (28 mg), identical in all respects with dimer E described above.

Later fractions in petroleum ether–benzene (72:28) gave a solid which was recrystallized five times from acetone–petroleum ether giving dimer F as a colorless crystalline solid (18 mg), m.p. 296° (dec.); ν_{max} 3380 (N—H) and 1590 cm^{-1}; λ_{max} (saturated solution) 245 and 315 nm; *m/e* 536 (molecular ion).

Anal. Calcd. for $C_{40}H_{28}N_2$ (536.7): C, 89.52; H, 5.26; N, 5.22. Found: C, 89.66; H, 5.51; N, 5.04.

T.l.c. of dimers E and F using petroleum ether–benzene (50:50) showed dimer F to be more polar than E, and mixed m.p. was 272–305°.

More polar fractions gave greenish-brown oil which was not investigated further.

Acetate of Dimer E

A mixture of dimer E (100 mg), sodium acetate (200 mg), pyridine (1.0 ml), and acetic anhydride (0.5 ml) was refluxed for 30 h. The cooled mixture was taken in chloroform, washed with 5% sodium bicarbonate, washed with water, dried, and concentrated giving amber colored oily solid. Three recrystallizations from chloroform–petroleum ether gave a colorless crystalline solid (54 mg), m.p. 280–283°; ν_{max} 1705 cm^{-1} (amide C=O); λ_{max} (saturated solution) 257 and 300 nm; δ 1.95 (—N(—$COCH_3$)—); *m/e* 578 (molecular ion).

Anal. Calcd. for $C_{42}H_{30}N_2O$ (578.7): C, 87.17; H, 5.23. Found: C, 87.15; H, 5.23.

The above acetate was saponified to dimer E with NaOH in refluxing methanol.

Thermal Reaction of Carbazole 9,9′-Dimer **6**

Carbazole 9,9′-dimer (8) (2.3 g) was sealed in a glass tube and heated at 250° for 3 h. A colorless crystalline solid (50 mg) had sublimed onto the cooler part of the tube and was proved to be carbazole. The brown–black residue was chromatographed on alumina. Fractions in petroleum ether–benzene (92:8) gave a solid (103 mg). Four recrystallizations from chloroform–petroleum ether gave a colorless crystalline solid (66 mg), m.p. 191–194°; ν_{max} 3440 (NH) and 1575 cm^{-1}; λ_{max} 236 (34 850), 257 (20 770), 287 (11 330), 293 (15 100), 337 (3777), and 349 nm (4155); *m/e* 332 (molecular ion). The compound was identical (m.p., mixed m.p., t.l.c.) with an authentic sample of 1,9′-dicarbazolyl (**8**) supplied by Tomlinson (13).

Fractions in petroleum ether–benzene (84:16) to petroleum ether–benzene (78:22) gave carbazole as a colorless crystalline solid (1.3 g).

Later fractions in petroleum ether–benzene (78:22) gave an oily solid (250 mg). This was put on four silica gel preparative layer plates and developed twice using petroleum ether–benzene (50:50). The band at R_f 0.50 gave a crystalline solid. Three recrystallizations from chloroform–petroleum ether gave a colorless solid (69 mg), m.p. 204–207°; ν_{max} 3480 (NH) and 1590 cm^{-1}; λ_{max} (saturated solution) 236, 257, 287, 293, 337, and 349 nm; *m/e* 332 (molecular ion). This material was identical with authentic sample of 3,9′-dicarbazolyl (**9**).

Preparation of 3,9′-Dicarbazolyl (9)

Modified procedure of Sugita (9) was used. A mixture of trimer **7** (100 mg), HI (1.5 ml, 47.6%), and few drops of 95% ethanol was heated with stirring at 160°. Within a few hours a solid had started subliming into the condenser. After heating the mixture for 50 h, the contents of the flask were cooled, taken in chloroform, and washed with 5% sodium bicarbonate. The organic layer was washed, dried, and concentrated giving a green viscous mass. This was put on a silica gel preparative layer plate and developed twice using benzene–petroleum ether (50:50). The band at R_f 0.52 gave an oily solid. Three recrystallizations from chloroform–petroleum ether gave 3,9′-dicarbazolyl (**9**) as a colorless crystalline solid (19 mg), m.p. 204–206°, (lit. (9) 212–215°). The solid that had sublimed into the condenser was proved to be carbazole.

The author would like to thank Professor E. W. Warnhoff for encouragement and constructive criticism throughout the work. He would also like to thank Professor C. F. Koelsch for details of permanganate experiment, Dr. Muriel L. Tomlinson for an authentic sample of **8**, and the National Research Council of Canada for financial support.

1. C. F. KOELSCH. J. Am. Chem. Soc. **66**, 1983 (1944).
2. V. DAVE and E. W. WARNHOFF. Chem. Commun. 919 (1970); Can. J. Chem. **49**, 1911, 1921 (1971); **50**, 2470 (1972). V. DAVE, J. B. STOTHERS, and E. W. WARNHOFF. Can. J. Chem. **50**, 2475 (1972).
3. H. WIELAND and S. GAMBARJAN. Ber. **39**, 1499 (1906).
4. B. WITKOP and H. FIEDLER. Ann. **558**, 91 (1947).
5. H. J. SHINE. Aromatic rearrangements. p. 126ff. Elsevier Publishing Co., New York, N.Y. 1967.
6. D. H. HEY. Advances in free radical chemistry. G. H. Williams, editor. Vol. 2. Logos Press, London. 1967. p. 47.
7. J. HUTTON and W. A. WATERS. J. Chem. Soc. 4253 (1965).
8. W. H. PERKIN, JR. and S. H. TUCKER. J. Chem. Soc. **119**, 216 (1921).
9. J. SUGITA. Nippon Kagaku Zasshi. **88**, 659 (1967); Chem. Abstr. **69**, 10319z (1968).
10. W. A. WATERS and J. E. WHITE. J. Chem. Soc. C, 740 (1968).
11. R. C. G. FENNEL and S. G. P. PLANT. J. Chem. Soc. 2872 (1932).
12. J. R. COGGINS and N. L. BENOITON. Can. J. Chem. **49**, 1968 (1971).
13. A. C. GEALE, J. M. G. LINNELL, and M. L. TOMLINSON. J. Chem. Soc. 1124 (1956).

Can. J. Chem. Downloaded from www.nrcresearchpress.com by 210.87.254.105 on 09/05/12
For personal use only.

Can. J. Chem. Downloaded from www.nrcresearchpress.com by 210.87.254.105 on 09/05/12
For personal use only.

The Importance of Conformation in the Ozonolysis of Acetals[1]

PIERRE DESLONGCHAMPS,[2] CLAUDE MOREAU, DANIEL FRÉHEL, AND PAUL ATLANI[3]
Laboratoire de synthèse organique, Département de chimie, Université de Sherbrooke, Sherbrooke, Québec

Received July 10, 1972

Six gauche conformations are theoretically possible for an acetal function and only three of them are reactive toward ozone. Each oxygen of the acetal function must have an electron pair orbital oreitned antiperiplanar to the C—H bond in order to be reactive toward ozone.

Il y a six conformations gauches pour une fonction acétal dont trois seulement sont réactives avec l'ozone. Chaque atome d'oxygène de la fonction acétal doit posséder une orbitale d'électrons libres orientée de manière antipériplanaire par rapport au lien C—H pour qu'elle soit réactive avec l'ozone.

Canadian Journal of Chemistry, **50**, 3402 (1972)

We have recently reported (1) that acetals are smoothly oxidized by ozone yielding the corresponding ester and alcohol in high yield.

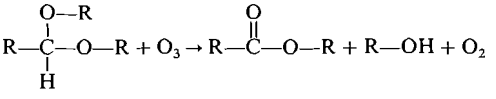

We have also described that conformationally rigid β-glycosides (methyl 2,3,4,6-tetra-*O*-acetyl-β-D-glucopyranoside and methyl 2-deoxy-3,4,6-tri-*O*-acetyl-β-D-glucopyranoside) are oxidized (O_3, Ac_2O–AcONa) to their corresponding aldonic acid methyl ester whereas the α-glycosides (methyl 2,3,4,6-tetra-*O*-acetyl-α-D-glucopyranoside and methyl 2-deoxy-3,4,6-tri-*O*-acetyl-α-D-glucopyranoside) are inert toward ozone. Cyclic acetals (1,3-dioxolane and 1,3-dioxane) are also very readily oxidized. These results led us to postulate that an acetal would react with ozone only if it can take a conformation in which each oxygen of the acetal function can have an electron pair orbital oriented antiperiplanar to the C—H bond (1).

Scheme 1 shows the nine gauche conformers that are theoretically possible for an acetal function. However, conformers **A′**, **B′**, and **D′** are respectively mirror image of conformer **A**, **B** and **D**. Consequently, there are only six different gauche conformers (**A**, **B**, **C**, **D**, **E** and **F**) for an acetal function and of those, only the conformer having an orbital on each oxygen oriented antiperiplanar to the C—H bond should be reactive. Thus, **A**, **C** and **F** should be reactive, whereas **B**, **D** and **E** should be inert toward ozone. We wish to report experimental results which support this hypothesis.

Scheme 2 shows the conformers of Scheme 1 in which a six-membered ring has been incorporated. In this manner, conformers **A**, **B** and **C** represent the three conformers of a conformationally rigid β-glycoside while conformers **D**, **E** and **B′** correspond to the three conformers of a rigid α-glycoside (2).

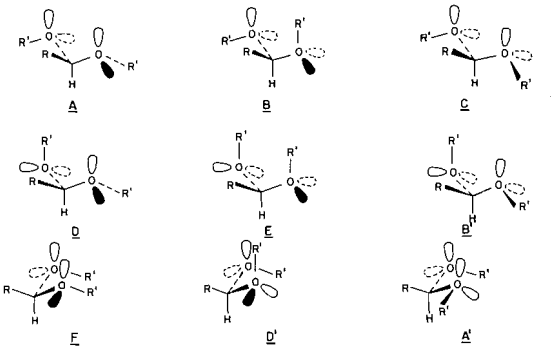

SCHEME 1

[1]Support for this work by the National Research Council of Canada, the Alfred P. Sloan Foundation, and by the "Ministère de l'Education" Québec, is gratefully acknowledged.

[2]A. P. Sloan Fellow, 1970–1972. To whom all correspondence should be addressed.

[3]Holder of a "bourse postdoctorale France-Québec", 1971–1972.

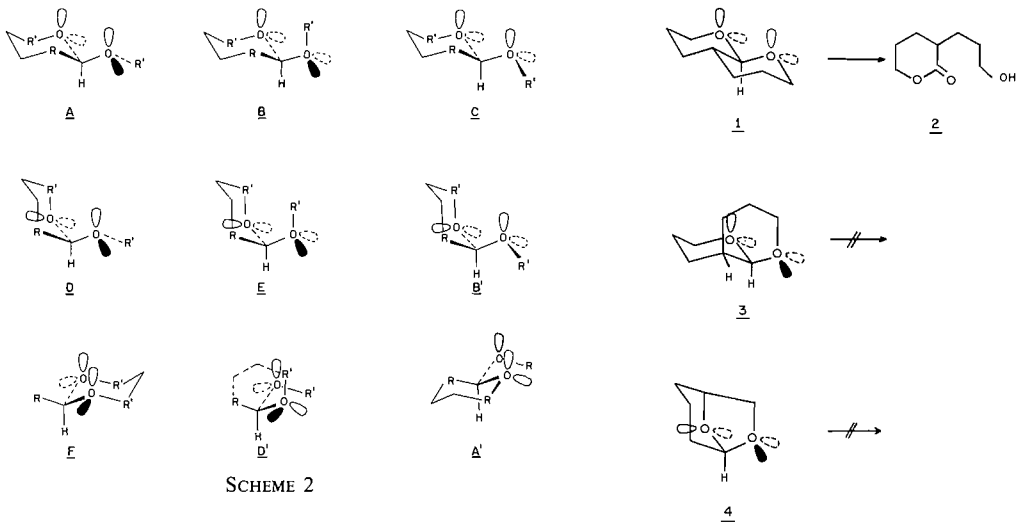

SCHEME 2

Conformationally rigid α-glycosides are inert toward ozone, conformers **D**, **E** and **B′** are therefore not reactive. Conformer **B′** is an equivalent of **B** (mirror image in Scheme 1), **B** is therefore not reactive and the same conclusion is also valid for **D′**. 1,3-Dioxane acetals represent a good model for conformer **F** and since they react with ozone, **F** is a reactive conformer. Compound **1** (*trans*-1,8-dioxaoctahydronaphthalene, (3)), a rigid model for conformer **C**, is readily oxidized into hydroxylactone[4] **2** (EtOAc, −78°, 1.5 h, 100%). Compound **3** (*cis*-1,8-dioxaoctahydronaphthalene, (3)) and compound **4** (6,8-dioxabicyclo [3.2.1] octane, (4)) are respectively rigid models for conformers **B** and **E** and they were unchanged by ozone treatment. Consequently, oxidation studies have been carried out on rigid models for conformers **B**, **C**, **E**, and **F**.

Conformer **D** represents the most stable conformation for an α-glycoside (2); since they are not reactive, **D** can be eliminated as a reactive conformer. Conformer **A** or its mirror image **A′** represents the more stable conformation for a β-glycoside; since they react with ozone, it is very likely that **A** is a reactive conformer.[5]

The preceding findings are confirmed by the observations that methyl tetra-*O*-acetyl-β-D-mannopyranoside (**5**) and β-D-galactopyrano-

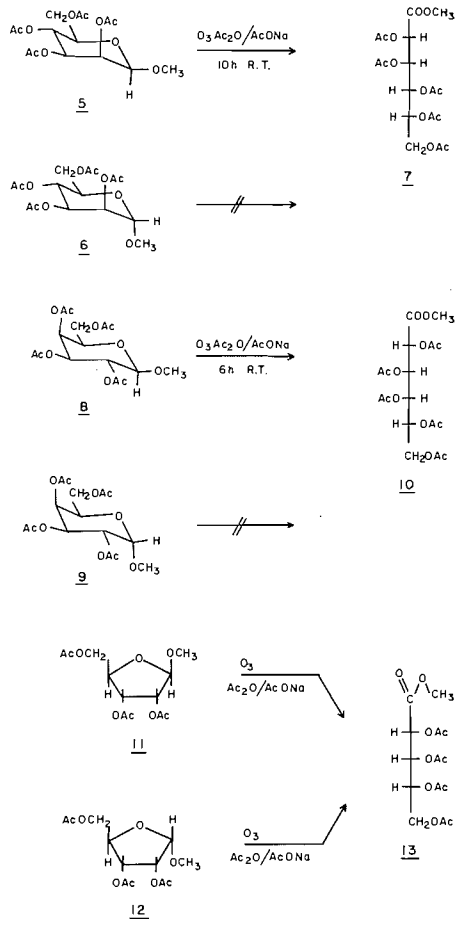

[4]This compound gave satisfactory analytical data.

[5]Work is now in progress towards the synthesis of a rigid model for conformer **A**.

Can. J. Chem. Downloaded from www.nrcresearchpress.com by 210.87.254.105 on 09/05/12
For personal use only.

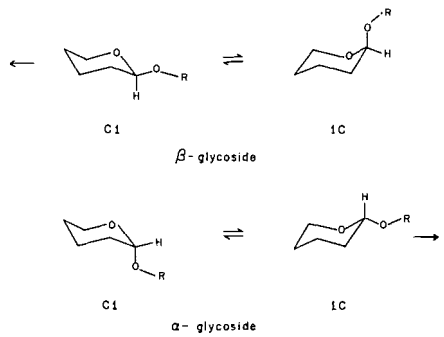

SCHEME 3

side (**8**) are converted in high yield into their corresponding penta-*O*-acetyl aldonic acid methyl ester **7**[4] and **10**[4] whereas the corresponding α-anomers **6** and **9** are inert. Those sugars represent further examples of conformationally rigid β- and α-glycosides.

There are some α- and β-methyl glycosides which are known to be conformationally labile and in such cases, both anomers should be reactive. Their respective rate of reaction should depend mainly on the population of the C1 conformation for the β anomer and the 1C conformation for the α anomer (Scheme 3). Methyl 2,3,4-tri-*O*-acetyl-β-D-xylopyranoside (81% in conformation C1, (5)) is converted into methyl 2,3,4,5-tetra-*O*-acetyl-β-D-xylonate[4] in 8 h whereas only 92% conversion was observed after 71 h of reaction with methyl 2,3,4-tri-*O*-acetyl-α-D-xylopyranoside (<2% in conformation 1C, (5)). Only 76% of methyl 2,3,4-tri-*O*-acetyl-β-D-arabinopyranoside (3% in conformation C1, (5)) is converted into methyl 2,3,4,5-tetra-*O*-acetyl-D-arabinonate[4] after 75 h of reaction whereas methyl 2,3,4-tri-*O*-acetyl-α-D-arabinopyranoside (83% in conformation 1C, (5)) is completely transformed after 7 h. The last two examples represent the first case of an α-glycoside being more reactive than the corresponding β-glycoside. Since no conformational rigidity exists in α- and β-glycofuranoside, both anomers should be reactive with ozone. Methyl 2,3,5-tri-*O*-acetyl-β- and -D-ribofuranoside (**11**, **12**) are both converted into methyl 2,3,4,5-tetra-*O*-acetyl-D-ribonate[4] (**13**) at approximately the same rate (16 h, r.t., 85%).

1. P. DESLONGCHAMPS and C. MOREAU. Can. J. Chem. **49**, 2465 (1971).
2. R. U. LEMIEUX. Molecular rearrangements, Pt. 2 *Edited by* Paul de Mayo. Interscience, New York. 1964; R. U. LEMIEUX. Abstract of Papers, Am. Chem. Soc. **135**, 5E (1959); R. U. LEMIEUX. Pure Appl. Chem. **25**, 527 (1971).
3. Y. BAHUREL, M. LISSAC-CAHU, G. DESCOTES, M. GELIN, J. DESMAU, and J. DUPLAN. Bull. Soc. Chim. Fr. 4006 (1970).
4. T. P. MURRAY, C. S. WILLIAMS, and R. K. BROWN. J. Org. Chem. **36**, 1311 (1971).
5. P. L. DURETTE and D. HORTON. Carbohydr. Res. **18**, 403 (1971).

Can. J. Chem. Downloaded from www.nrcresearchpress.com by 210.87.254.105 on 09/05/12
For personal use only.

The Importance of Conformation of the Tetrahedral Intermediate in the Hydrolysis of Esters. Selective Cleavage of the Tetrahedral Intermediate Controlled by Orbital Orientation[1]

PIERRE DESLONGCHAMPS,[2] PAUL ATLANI,[3] DANIEL FRÉHEL, AND ALAIN MALAVAL

Laboratoire de synthèse organique, Département de chimie, Université de Sherbrooke, Sherbrooke, Québec

Received July 10, 1972

The hydrolysis or the transesterification of esters proceeds via a hemi-orthoester tetrahedral intermediate. There are nine different gauche conformers possible for such a tetrahedral intermediate and it is proposed that each of them should decompose in a highly selective manner. It is further proposed that the lone pair orbitals of the oxygen atoms control this selective decomposition.

L'hydrolyse ou la transestérification d'un ester procède par un intermédiaire tétrahédrique du type hemi-orthoester. Il y a 9 conformères gauches possibles pour un hemi-orthoester et il est proposé que chaque conformère se décompose d'une manière très sélective. Il est de plus avancé que les orbitales d'électrons non-liés des atomes d'oxygène contrôlent cette décomposition sélective.

Canadian Journal of Chemistry, **50**, 3405 (1972)

The hydrolysis or the transesterification of esters proceeds normally via a hemi-orthoester tetrahedral intermediate. In principle, in a transesterification reaction, such intermediate **1** (Scheme 1) can lead to the *cisoïde* ester **2A**, the *transoïde* ester **2B**, the *cisoïde* ester **3A**, or the *transoïde* ester **3B**.

Theoretically, there are nine different gauche conformers[4] for a tetrahedral intermediate such as **1** (Scheme 2). We want to disclose experimental evidence which permits us to propose that each conformer should cleave in a specific manner to yield either one or two of the four possible esters **2A**, **2B**, **3A**, or **3B**. We would like further to propose that the lone pair orbitals on the oxygen atoms in the nine different conformers of **1** govern this remarkable selective decomposition; specific cleavage of a C—O alkyl bond in a tetrahedral conformer being allowed only if the other two oxygens of this tetrahedral conformer have each an orbital oriented antiperiplanar to the C—O alkyl bond to be broken.

For example, conformer **A** can give only the *transoïde* ester **2B** since the C—OCH_3 bond can be easily cleaved because the negative oxygen and the OR oxygen have each an orbital oriented antiperiplanar to the C—OCH_3 bond, yielding specifically the *transoïde* ester **2B**, the OR group being antiperiplanar to the C—R′ bond (Scheme 3). Cleavage of the C—OR bond

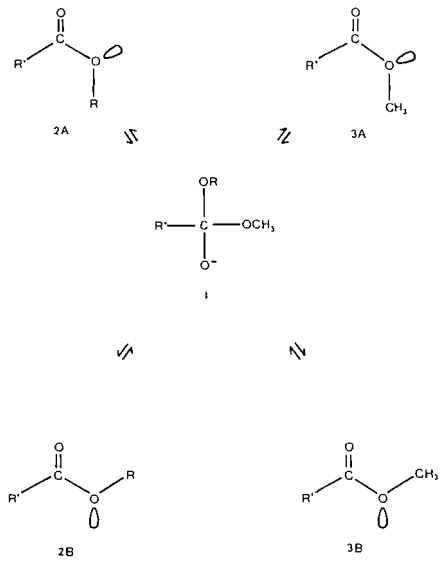

SCHEME 1

[1]Support for this work by the National Research Council of Canada, the Alfred P. Sloan Foundation, and by the "Ministère de l'Education", Québec, is gratefully acknowledged.

[2]A. P. Sloan Fellow, 1970–1972. To whom all correspondence should be addressed.

[3]Holder of a "bourse postdoctorale France-Québec", 1971–1972.

[4]When R = CH_3, **A**, **B**, and **E** are respectively mirror images of **F**, **I**, and **G**, thus in such a case only six conformers are possible.

Can. J. Chem. Downloaded from www.nrcresearchpress.com by 210.87.254.42 on 09/05/12
For personal use only.

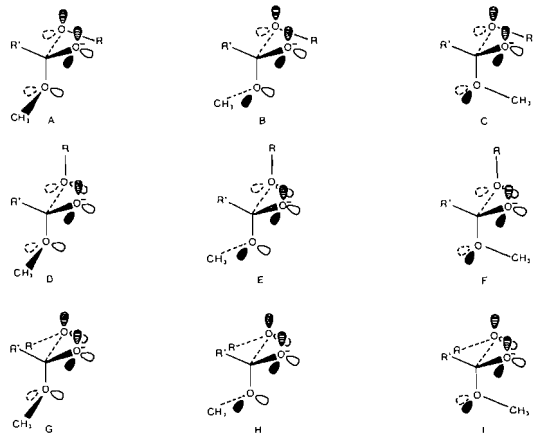

SCHEME 2

in conformer **A** would be a much higher energy process and therefore should not be observed because the departure of the OR group can be assisted by only one electron pair orbital (negative oxygen), the oxygen of the OCH_3 group having no lone pair orbital oriented antiperiplanar to the C—OR bond. Conformer **B** can give either the *transoïde* ester **2B** or the *cisoïde* ester **3A**. The *transoïde* ester **2B** can be obtained since the negative oxygen and the OR oxygen have each an orbital antiperiplanar to the C—OCH_3 bond. The *cisoïde* ester **3A** can also be produced from B since the negative oxygen and the OCH_3 oxygen have each an orbital antiperiplanar to the C—OR bond. In this case, the *cisoïde* ester **3A** is obtained because the C—R′ bond is antiperiplanar to the second orbital of the OCH_3 oxygen, the O—CH_3 bond being in a gauche orientation to the C—R′ bond.

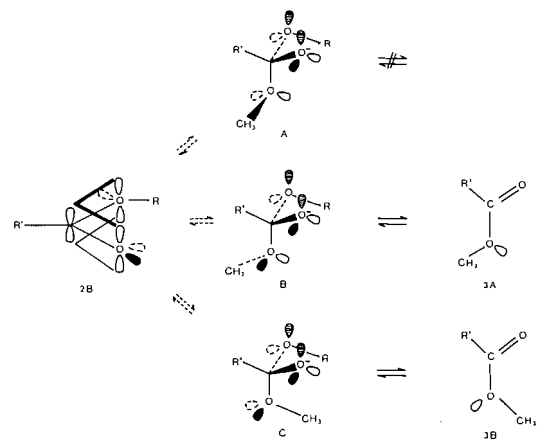

SCHEME 3

TABLE 1. Specific cleavages that should be observed

Ester **2**		Conformer **1**		Ester **3**
Transoïde	⇌	**A**	≠	
Transoïde	⇌	**B**	⇌	*cisoïde*
Transoïde	⇌	**C**	⇌	*transoïde*
	≠	**D***	≠	
	≠	**E**	⇌	*cisoïde*
	≠	**F**	⇌	*transoïde*
Cisoïde	⇌	**G**	≠	
Cisoïde	⇌	**H**	⇌	*cisoïde*
Cisoïde	⇌	**I**	⇌	*transoïde*

*If the rigid conformer such as **D** is produced, it should cleave but the transition state will be of higher energy. Ozonolysis of *trans*-1,8-dioxaoctahydronaphthalene gives an intermediate equivalent to **D** (2).

Conformer **C** can give either the *transoïde* ester **2B** or **3B**. Table 1 describes the specific cleavages that should be observed with all the nine different conformers.

In the reverse reaction, attack of methoxide ion on the *transoïde* ester **2B**, only three tetrahedral conformers (**A**, **B** and **C**) can first be formed (Scheme 3). The energy level of the transition states for reaction of each conformer resembles the energy level of each conformer. Thus, a study of the relative stability of all nine conformers should give information for a more precise knowledge on the general mechanism of ester hydrolysis.

During our study on the ozonolysis of acetals (1, 2) we have observed that the reaction of ozone with simple tetrahydropyranyl ethers (**4**) and with conformationally rigid methyl β-glycopyranosides yielded only the corresponding alkyl 4-hydroxypentanoate derivatives **7** (Scheme 4); lactone formation (**6**) was never observed. Identical results have been obtained with tetrahydrofuranyl ethers. Ozonolysis of 2-methoxy tetrahydrofuran (Ac_2O–AcONa) gave only methyl 4-*O*-acetylbutanoate, the corresponding γ-lactone was not detected.[5] This reaction is apparently therefore kinetically controlled, the transition state leading to the less stable hydroxy-ester **7** being energetically favored over the transition state leading to the

[5]Analogous results have been obtained with 2-ethoxy tetrahydrofuran and with both anomers of methyl 2,3,5-tri-*O*-acetyl-ribofuranoside (2).

Can. J. Chem. Downloaded from www.nrcresearchpress.com by 210.87.254.42 on 09/05/12
For personal use only.

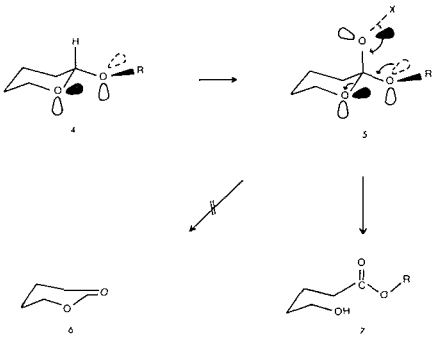

SCHEME 4

lactone **6**. We have postulated (1) that the ozonolysis of acetals proceeds via a hydrotrioxide intermediate such as **5** (X = OOH). This intermediate could also be an analog such as the hemi-orthoester **5** (X = H). By utilizing the preceding stereoelectronic theory, it is easy to understand the preferred specific decomposition of the tetrahedral intermediate **5** into the less stable product, the hydroxy-ester **7**.

We have previously established (2) that in order to react with ozone the acetal function must have a conformation in which each oxygen has an orbital oriented antiperiplanar to the C—H bond. Thus, the most stable conformation (3) for an alkyl β-glycopyranoside which corresponds to **4** should specifically give the tetrahedral conformer **5**, which can give **7** since both oxygens of the OX[6] and the OEt groups have each an orbital oriented antiperiplanar to the ring oxygen–C_2 bond. The conversion of **5** into the lactone **6** is a higher energy process because the ring oxygen atom does not have an orbital antiperiplanar to the C—OR bond in order to assist in its departure. In fact, intermediate **5** is a model for conformer **A** in Scheme 2.

King and Allbutt (4) have recently described the stereoselective hydrolysis of dioxolenium ions and orthoesters fused to anchored six-membered rings. For example, mild acid hydrolysis of the dioxolenium salt **8** or the orthoesters **9** afforded the axial ester – equatorial alcohol **10** with only a very small amount of the isomer **11**

[6]The O—X bond in **5** can also take two other gauche orientations but this is irrelevant. This O—X bond can be considered as a potential lone pair orbital by loss of a proton when X = H or by decomposition of the hydrotrioxide function when X = OOH.

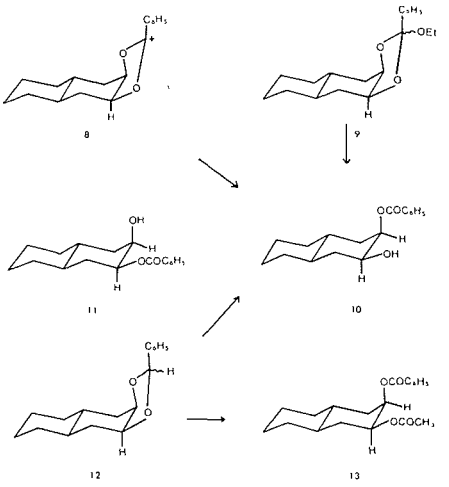

SCHEME 5

(Scheme 5). We have found that the ozonolysis in ethyl acetate of the benzylidenes **12** gave mainly the axial ester – equatorial alcohol **10** (>94%). Ozonolysis of **12** in acetic anhydride – sodium acetate (1) gave only the axial benzoate – equatorial acetate **13**,[7] thus establishing that the ozonolysis of acetals doubtless proceeds via the formation of an intermediate analogous to a hemi-orthoester.

Further evidence that a hemi-orthoester such as **5** (X = H) gives only the hydroxy-ester **7** is apparent from the observation that mild basic hydrolysis (NaOH 0.1 *N*, 10 min, r.t.) of 2-ethoxy-2-dihydropyran (**15**)[8] gave only ethyl 5-hydroxypentanoate (**17**)[9] (Scheme 6). This selective reaction can be explained by the intermediate formation of hemi-orthoester **16**[10] (**5**, X = H) and its subsequent orbital-assisted decomposition to **17**. Formation of ethyl 4-hydroxypentanoate (**17**) was also observed using mild acid hydrolysis (~2 min, r.t., trace of *p*-toluenesulfonic acid in water) from 2,2-diethoxytetrahydropyran (**14**),[8] no δ-valerolac-

[7]The structure of **13** has been confirmed by an alternative synthesis.

[8]This product was synthesized by following the procedure described by McElvain and McKay (5) using ketene diethylacetal (6).

[9]The corresponding acetate gave expected analytical and spectroscopic data.

[10]The O—H bond in **16** can also take two other gauche orientations, but an O—H bond can be considered as a potential lone pair orbital by the loss of the proton.

Can. J. Chem. Downloaded from www.nrcresearchpress.com by 210.87.254.42 on 09/05/12
For personal use only.

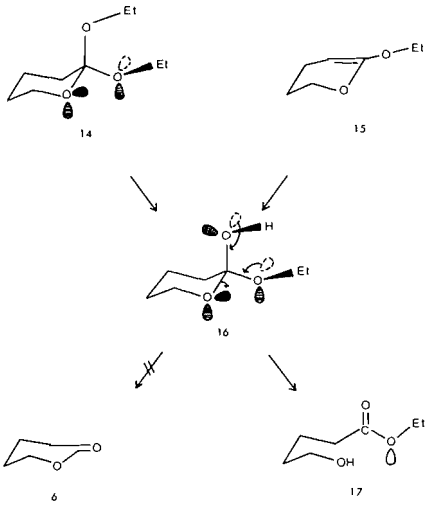

SCHEME 6

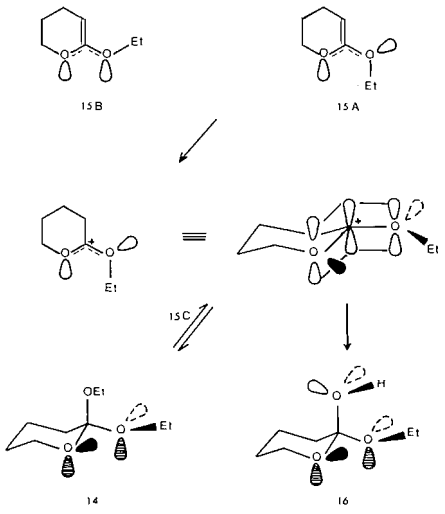

SCHEME 7

tone (**6**) being produced. Acid hydrolysis of **15** gave only **17**.[11]

Keteneketal **15** can have a *transoïde* (**15A**) or a *cisoïde* (**15B**) conformation (Scheme 7). As in an ester, the *transoïde* conformer **15A** must be highly favored (7). Proton capture at C_3 from water leads to the dioxolenium ion **15C**. Attack by hydroxide ion on **15C** should give specifically the conformer **16** in which the ring oxygen and the OEt oxygen have each an orbital antiperiplanar to the C—OH bond which has just been formed. Intermediate **15C** can also be obtained in acidic medium by loss of ethanol from **14**. In **14**, the O—Et bond of the equatorial ethyl group is in the most favored gauche conformation relative to the ring oxygen as in methyl β-glycoside (3). Furthermore, the ring oxygen and the equatorial OEt oxygen have each an orbital antiperiplanar to the axial OEt group which permits the cleavage of this axial OEt group. A good example for such a requirement in orthoester has been reported by Eliel (8).[12]

[11]Analogously, 2,2-diethoxy-4-methyl-tetrahydropyran[8] and 2-ethoxy-4-methyl-dihydropyran[8] gave only ethyl 5-hydroxy-3-methyl pentanoate.[9]

[12]King and Allbutt have considered a combination of steric and stereoelectronic effects to explain their results on the hydrolysis of dioxolenium ions; the stereoelectronic argument proposed being similar to ours (4).

Thus we suggest that the conformation of the tetrahedral intermediate is extremely important in the general mechanism of ester hydrolysis. We believe that it is specially important with regard to the hydrolysis of esters by enzymes, since it is very likely that the tetrahedral intermediate formed in such case possesses a specific conformation. We think that the above results have an attractive new chemical basis and should be given serious consideration (9). Work is now in progress to obtain more rigid chemical models in order to test further this stereoelectronic theory.

1. P. DESLONGCHAMPS and C. MOREAU. Can. J. Chem. **49**, 2465 (1971).
2. P. DESLONGCHAMPS, C. MOREAU, D. FRÉHEL, and P. ATLANI. Can. J. Chem. This Issue.
3. R. U. LEMIEUX. Molecular rearrangements, Pt. 2. *Edited by* Paul de Mayo. Interscience, New York. 1964; R. U. LEMIEUX. Abstract of Papers, Am. Chem. Soc. **135**, 5E (1959); R. U. LEMIEUX. Pure Appl. Chem. **25**, 527 (1971).
4. J. F. KING and A. D. ALLBUTT. Can. J. Chem. **48**, 1754 (1970); Tetrahedron Lett. 49 (1967).
5. S. M. MCELVAIN and G. R. MCKAY. J. Am. Chem. Soc. 77, 5601 (1955).
6. S. M. MCELVAIN and D. KUNDIGER. Organic synthesis. Coll. Vol. III. John Wiley and Sons, Inc., New York, N.Y. 1955. p. 506.
7. R. HUISGEN and H. OTT. Tetrahedron, **6**, 253 (1959).
8. E. L. ELIEL. J. Am. Chem. Soc. **91**, 536 (1969).
9. W. P. JENCKS. Catalysis in chemistry and enzymology. McGraw-Hill. 1969, p. 282.

Can. J. Chem. Downloaded from www.nrcresearchpress.com by 210.87.254.42 on 09/05/12
For personal use only.

^{19}F N.M.R. Study of the Difluorochlorine(III) Cation, ClF_2^+

MORLEY BROWNSTEIN[1] AND JACOB SHAMIR

Department of Inorganic and Analytical Chemistry, The Hebrew University of Jerusalem, Jerusalem, Israel

Received July 25, 1972

The ^{19}F n.m.r. spectrum of ClF_2^+ has been observed for the first time. Solvolysis of the ClF_2^+ cation in neutral anhydrous hydrogen fluoride to give ClF_3 is extremely slight.

On a observé pour la première fois le spectre ^{19}F n.m.r. du ClF_2^+. La solvolyse du cation du ClF_2^+ dans du fluorure d'hydrogène anhydre neutre produisant du ClF_3 est extrêmement faible.

[Traduit par le journal]

Canadian Journal of Chemistry, **50**, 3409 (1972)

Can. J. Chem. Downloaded from www.nrcresearchpress.com by 210.87.254.5 on 09/05/12
For personal use only.

Halogen fluorocations have been a subject of continuing interest (1). 1:1 complexes of ClF_3 with AsF_5 and SbF_5 were first reported by Seel and Detmer (2) who formulated them as ionic compounds (*e.g.* $ClF_2^+.SbF_6^-$) on the basis of the conductivity of $ClF_3.SbF_5$ in ClF_3. Although the vibrational spectra of the solid complexes were initially interpreted on the basis of a purely ionic structure, it has since been conclusively shown by Raman spectroscopy (3) and X-ray crystallography (4, 5) that there is a significant degree of fluorine bridging in the solid between the ions.

Attempts have been made to obtain the ^{19}F n.m.r. spectrum of ClF_2^+ in molten ClF_2BF_4 (6) as well as for the complexes dissolved in BrF_5, SO_3 (7) or excess ClF_3 (6, 7). However, because of rapid fluorine exchange no meaningful results were reported for temperatures down to -80 °C.

We have successfully observed the ^{19}F n.m.r. signal of the ClF_2^+ cation for solutions of ClF_2SbF_6 and ClF_2AsF_6 in anhydrous HF. The complexes were prepared directly in Kel-F n.m.r. tubes with the more volatile component in excess, followed by pumping off the excess starting material. Material handling procedures were similar to those previously described (8). ^{19}F n.m.r. spectra were obtained on a Varian HA-100 n.m.r. spectrometer operating at 94.1 MHz.

At room temperature, the ^{19}F n.m.r. spectrum of ClF_2SbF_6 in HF is a single broad line because of rapid fluorine exchange. On lowering the temperature a broad ClF_2^+ peak at +25 p.p.m. from $CFCl_3$ becomes visible in addition to the solvent peak, and narrows on further cooling of the sample (Table 1). Exchange of fluorine between ClF_2^+ and the solvent can occur via ClF_3 by the reactions

$$[1] \qquad ClF_2^+ + HF_2^- \rightleftharpoons ClF_3 + HF$$

$$[2] \qquad ClF_2^+ + 2HF \rightleftharpoons ClF_3 + H_2F^+$$

With the addition of excess SbF_5, any traces of fluoride are mopped up and the solution is made strongly acidic (9).

$$[3] \qquad SbF_5 + 2HF \rightarrow H_2F^+ + SbF_6^-$$

It is now possible to observe the ClF_2^+ peak even at room temperature (Table 1). N.m.r. signals from fluorine on antimony were observed only with excess SbF_5 present, in agreement with earlier observations of fluorocation SbF_6^- salts in HF (10).

Since merely cooling the solution of ClF_2SbF_6 in HF is enough to allow observation of the ClF_2^+ peak, we conclude that solvolysis of ClF_2^+ in HF must be extremely slight and that the equilibrium position of reaction 2 lies far to the left. This conclusion is reinforced by the

TABLE 1. ^{19}F n.m.r. of ClF_2SbF_6 in HF

		ClF_2^+	
Solute	T (°C)	δ_{CFCl_3}	Width*
ClF_2SbF_6	0	25	2500
	−30	24	120
	−60	24	50
ClF_2SbF_6 + excess SbF_5	35	25	330
	0	23	150
	−30	23	20

*Width in Hz at half height.

[1]To whom correspondence should be addressed. Present address: Department of Chemical Engineering, McMaster University, Hamilton, Ontario.

knowledge that ClF_3 was present in excess during the preparation of ClF_2SbF_6. Thus traces of SbF_5 can not be present to acidify the solution.

ClF_2AsF_6 in HF also has a ClF_2^+ peak at +24 p.p.m. whose behavior as a function of temperature and solvent acidity (*i.e.* addition of excess AsF_5) is the same as that found for ClF_2^+ from ClF_2SbF_6.

1. R. J. GILLESPIE and M. J. MORTON. Q. Rev. **25**, 553 (1971).
2. F. SEEL and O. DETMER. Z. anorg. allg. Chem. **301**, 113 (1959).
3. R. J. GILLESPIE and M. J. MORTON. Inorg. Chem. **9**, 616 (1970).
4. A. J. EDWARDS and R. J. C. SILLS. J. Chem. Soc. A, 2697 (1970).
5. H. LYNTON and J. PASSMORE. Can. J. Chem. **49**, 2539 (1971).
6. A. C. RUTENBERG. ORNL-3832. 45 (1965).
7. K. O. CHRISTE and A. E. PAVLATH. Z. anorg. allg. Chem. **335**, 210 (1965).
8. M. BROWNSTEIN and J. SHAMIR. Appl. Spectrosc. **26**, 77 (1972).
9. R. J. GILLESPIE and K. C. MOSS. J. Chem. Soc. 1170 (1966).
10. M. AZEEM, M. BROWNSTEIN, and R. J. GILLESPIE. Can. J. Chem. **47**, 4159 (1969).

Can. J. Chem. Downloaded from www.nrcresearchpress.com by 210.87.254.5 on 09/05/12
For personal use only.

Can. J. Chem. Downloaded from www.nrcresearchpress.com by 210.87.254.5 on 09/05/12
For personal use only.

Canadian Journal of Chemistry

Published by THE NATIONAL RESEARCH COUNCIL OF CANADA

VOLUME 50 NOVEMBER 1, 1972 NUMBER 21

Étude par spectromètrie i.r. des effets de solvant sur les fréquences fondamentale et harmoniques de l'acide iodhydrique

NGUYEN-VAN-THANH ET INGA ROSSI

Laboratoire d'Infrarouge, Equipe de Recherche Associée au C.N.R.S., Université de Paris VI, 91, Campus d'Orsay, Essonne, France

Reçu le 1 mai 1972

Les fréquences des transitions $(0 \rightarrow 1)$, $(0 \rightarrow 2)$, et $(0 \rightarrow 3)$ de la molécule HI en solution CCl_4 ont été déterminées par spectrométrie i.r. Les calculs des déplacements de fréquence basés sur un modèle cellulaire Lennard–Jones–Devonshire de l'état liquide sont en bon accord avec les résultats expérimentaux.

The wavenumbers of the fundamental, first and second overtones have been measured for HI in liquid CCl_4. The solvent shifts calculated, assuming a Lennard–Jones–Devonshire cell model of the solution, are in good agreement with the experimental data.

Canadian Journal of Chemistry, **50**, 3411 (1972)

Introduction

Dans l'étude des effets de solvant sur les fréquences de vibration des molécules diatomiques Buckingham (1–3) a prévu que le déplacement $\Delta\nu_{0\rightarrow v}$ de fréquence, dû au solvant, est proportionnel au nombre quantique v de vibration du niveau excité, si la constante d'anharmonicité mécanique du soluté est la même pour les états gazeux et dissous. Mais récemment, plusieurs auteurs (4–6) ont montré que pour certains vibrateurs XH, la constante d'anharmonicité dépend de la nature du solvant.

D'autre part, Monson et coll. (7), en utilisant un potentiel intermoléculaire de type Lennard–Jones–Devonshire (LJD), ont pu rendre compte de l'effet de solvant sur les déplacements de fréquence de H_2 et D_2 en solution.

Nous nous proposons de comparer les valeurs théoriques et expérimentales des déplacements de fréquences de vibration des transitions $(0 \rightarrow 1)$, $(0 \rightarrow 2)$, et $(0 \rightarrow 3)$ de la molécule HI en solution CCl_4. L'effet de solvant est interprété à l'aide du potentiel d'interaction LJD (6–12) pour l'état liquide (8, 9).

Conditions expérimentales

L'étude expérimentale a été réalisée à l'aide d'un spectromètre de type Pfund à réseau échelette de 240 traits/mm fonctionnant dans les ordres 1, 2, et 3 correspondant respectivement à 4.50 μ, 2.25 μ, et 1.5 μ. L'étalonnage du domaine spectral est obtenu par la méthode de Poggendorff en utilisant comme repères de nombre d'onde ceux des raies de vibration–rotation des transitions $(0 \rightarrow 1)$, $(0 \rightarrow 2)$, et $(0 \rightarrow 3)$ de la molécule HI à l'état gazeux (10, 11). La fonction d'appareil est une fonction triangle dont la largeur à mi-hauteur est de 0.5 cm^{-1} à 2200 cm^{-1}, de 1.0 cm^{-1} à 4400 cm^{-1} et de 1.5 cm^{-1} à 6500 cm^{-1}.

Les cuves circulaires utilisées pour les trois domaines spectraux ont respectivement les épaisseurs suivantes: 2 mm, 10 mm, et 200 mm. Les solutions saturées de HI s'obtiennent par un simple barbotage du gaz durant une quinzaine de minutes.

Afin d'éviter la formation de couples moléculaires de type $HI–H_2O$, le solvant CCl_4 a été déssèché sur un tamis moléculaire (4 Å). La concentration de HI en solution CCl_4 a été déterminée par acidimétrie. Elle est de l'ordre de 10^{-4} mol/cm^3. Avec une si faible concentration la formation de paires HI–HI semble très peu probable.

Rappels théoriques

Les expressions donnant le terme spectral de vibration pour une molécule diatomique à l'état

Can. J. Chem. Downloaded from www.nrcresearchpress.com by 210.87.254.5 on 09/05/12
For personal use only.

gazeux et à l'état dissous sont données par (6, 12):

$$[1]\quad G_v^{gaz} = \frac{E_v^{gaz}}{hc} = (\omega_e - W)(v+\tfrac{1}{2}) - X(v+\tfrac{1}{2})^2 + Y(v+\tfrac{1}{2})^3 + c$$

et

$$[2]\quad G_v^{sol} = \frac{E_v^{sol}}{hc} = (\omega_e - W - \bar{W})(v+\tfrac{1}{2}) - (X+\bar{X})(v+\tfrac{1}{2})^2 + (Y+\bar{Y})(v+\tfrac{1}{2})^3 + c + \bar{c}$$

D'après ces deux dernières relations, on déduit les relations donnant les nombres d'onde relatifs au déplacement de fréquence $\Delta v_{0\to v}$ des bandes du soluté lors du passage de l'état gazeux à l'état dissous:

$$[3a]\quad \Delta v_{0\to 1} = v_{0\to 1}^{gaz} - v_{0\to 1}^{sol} = \bar{W} + 2\bar{X} - \tfrac{13}{4}\bar{Y}$$

$$[3b]\quad \Delta v_{0\to 2} = v_{0\to 2}^{gaz} - v_{0\to 2}^{sol} = 2\bar{W} + 6\bar{X} - \tfrac{31}{2}\bar{Y}$$

$$[3c]\quad \Delta v_{0\to 3} = v_{0\to 3}^{gaz} - v_{0\to 3}^{sol} = 3\bar{W} + 12\bar{X} - \tfrac{171}{4}\bar{Y}$$

Les quantités $\bar{W}$, $\bar{X}$ et $\bar{Y}$ dépendent du potentiel intermoléculaire U.

Rappelons que l'hamiltonien de vibration de la molécule diatomique à l'état dissous s'écrit

$$[4]\quad H_v = H_v^0 + H_v^a + U$$

où H_v^0 est l'hamiltonien relatif à l'oscillateur harmonique. $(H_v^a + U)$ désigne l'hamiltonien perturbateur avec

$$[5]\quad H_v^a = K_3 q^3 + K_4 q^4 + \ldots$$

et tel que l'on ait $K_3 q^3 \gg K_4 q^4 \ldots$

Le potentiel intermoléculaire U peut être exprimé en fonction de deux variables τ et q

$$[6]\quad U(\tau,q) = U_e(\tau) + \frac{1}{1!}\left(\frac{\partial U(\tau)}{\partial q}\right)_e q + \frac{1}{2!}\left(\frac{\partial^2 U(\tau)}{\partial q^2}\right)_e q^2 + \ldots$$

où τ représente l'ensemble des variables qui permettent de fixer la position et l'orientation de la molécule de soluté par rapport aux molécules environnantes de solvant. La coordonnée normale sans dimension q est définie par

$$[7]\quad q = \left(\frac{\omega_e}{2B_e}\right)^{1/2}\xi$$

avec $\xi = (x - x_e)/x_e$ et x_e étant la distance internucléaire à l'équilibre de la molécule diatomique. Le calcul rigoureux de $U(\tau,q)$ est très laborieux; on peut alors expliciter U seulement en fonction de q, ce qui revient à raisonner sur une valeur moyenne de τ. L'expression du déplacement relatif de fréquence harmonique $\Delta\omega/\omega_e$ est donnée en première approximation par (6, 12):

$$[8]\quad \frac{\Delta\omega}{\omega_e} = \frac{\bar{W}}{\omega_e} \simeq -\frac{1}{2\omega_e}\left(\frac{\partial^2 u}{\partial q^2}\right)_e + \frac{3k_3}{\omega_e^2}\left(\frac{\partial u}{\partial q}\right)_e$$

en posant $(U/hc) = u$ et $K_3/hc = k_3$

Les constantes k_3 et α_e sont reliées par (13):

$$[9]\quad \alpha_e = -\frac{12}{\sqrt{2}}\left(\frac{B_e}{\omega_e}\right)^{3/2} k_3 - \frac{6B_e^2}{\omega_e}$$

Les quantités u, $(\partial u/\partial q)_e$, $(\partial^2 u/\partial q^2)_e$, k_3, α_e, B_e, et ω_e sont exprimées en cm^{-1}. On peut donc calculer la valeur théorique de $\Delta\omega$ si l'on connaît $(\partial u/\partial q)_e$, $(\partial^2 u/\partial q^2)_e$ et k_3.

Expression du potentiel intermoleculaire U

L'énergie d'interaction entre une molécule de soluté polaire 1 et une molécule de solvant 2 non polaire est la somme des énergies de répulsion, de dispersion et d'induction (14):

$$[10]\quad U_{1,2}(r) = 4\varepsilon\left[\left(\frac{\sigma}{r}\right)^{12} - \left(\frac{\sigma}{r}\right)^{6}\right] - \frac{\alpha_2\mu_1^2}{\varepsilon_2 r^6}$$

où ε et σ sont les paramètres du potentiel de Lennard–Jones, et r est la distance intermoléculaire. ε_2 et α_2 sont respectivement la constante diélectrique et la polarisabilité du solvant; μ_1 désigne le moment dipolaire de la molécule de soluté. En introduisant le paramètre r^* défini par $r^* = 2^{1/6}\sigma$, la relation précédente devient

$$[11]\quad U_{1,2}(r) = \varepsilon\left[\left(\frac{r^*}{r}\right)^{12} - 2\left(\frac{r^*}{r}\right)^{6}\right] - \frac{\alpha_2\mu_1^2}{\varepsilon_2 r^6}$$

Pour décrire la distribution moléculaire au sein du liquide, nous pouvons adopter un modèle cellulaire dans lequel la molécule de soluté prend la place d'une molécule de solvant et se trouve ainsi placée dans une enceinte constituée par des molécules de solvant. Les positions moyennes des molécules sont celles des nœuds d'un réseau c.f.c. dans lequel cristallise le solvant CCl_4. Comme l'énergie d'induction est négligeable, l'énergie d'interaction entre la

TABLEAU 1. Fréquences d'absorption $\nu_{0\to1}$, $\nu_{0\to2}$, $\nu_{0\to3}$ et déplacements de fréquence $\Delta\nu_{0\to1}$, $\Delta\nu_{0\to2}$, et $\Delta\nu_{0\to3}$ de HI

HI	$\nu_{0\to1}(cm^{-1})$	$\nu_{0\to2}(cm^{-1})$	$\nu_{0\to3}(cm^{-1})$	$\Delta\nu_{0\to1}(cm^{-1})$	$\Delta\nu_{0\to2}(cm^{-1})$	$\Delta\nu_{0\to3}(cm^{-1})$
Gazeux	2229.581 (10)	4379.225 (10)	6448.034 (10)			
Dissous	2204.4	4327.4	6371.8	25.1	51.8	76.2
(CCl_4)	2204 (16)					

Can. J. Chem. Downloaded from www.nrcresearchpress.com by 210.87.254.5 on 09/05/12
For personal use only.

molécule de soluté et les Z molécules voisines de solvant s'écrit (15)

$$[12]\quad U(a) = Z\varepsilon\left[C\left(\frac{r^*}{a}\right)^{12} - D\left(\frac{r^*}{a}\right)^{6}\right]$$

où a est la distance intermoléculaire obtenue à l'aide de la relation

$$[13]\quad a = \left(\frac{M\sqrt{2}}{Nd}\right)^{1/3}$$

M désigne la masse moléculaire du solvant, d sa densité; N est le nombre d'Avogadro. Pour la molécule CCl_4, la distance intermoléculaire a est égale à 6.09 Å.

C et D sont deux facteurs numériques qui dépendent de la configuration géométrique de la maille considérée. Afin d'introduire l'effet de vibration de la molécule de soluté, nous supposons que la distance r^* (et non ε) seulement dépend de ξ. En posant

$$[14]\quad r^* = r_e^* + \Delta r$$

avec $\Delta r = (x_e\xi/2)$, où r_e^* est le paramètre de Lennard–Jones pour $\xi = 0$.

D'après la relation (8), le calcul du déplacement relatif de fréquence harmonique $\Delta\omega/\omega_e$ nécessite la connaissance des dérivées $(du/dq)_e$ et $(d^2u/dq^2)_e$. En faisant le changement de variables $q = (\omega_e/2B_e)^{1/2}$. ξ nous obtenons les expressions des dérivées de u

$$[15]\quad \left(\frac{du}{dq}\right)_e = \left(\frac{2B_e}{\omega_e}\right)^{1/2} 3Z\varepsilon\left(\frac{x_e}{r_e^*}\right) \times\left[2C\left(\frac{r_e^*}{a}\right)^{12} - D\left(\frac{r_e^*}{a}\right)^{6}\right]$$

$$[16]\quad \left(\frac{d^2\mu}{dq^2}\right)_e = \left(\frac{2B_e}{\omega_e}\right) 3Z\varepsilon\left(\frac{x_e}{r_e^*}\right)^2 \times\left[11C\left(\frac{r_e^*}{a}\right)^{12} - \frac{5}{2}D\left(\frac{r_e^*}{a}\right)^{6}\right]$$

Le déplacement relatif de fréquence harmonique est alors donné par la relation suivante

$$[17]\quad \frac{\Delta\omega}{\omega_e} \simeq -\frac{1}{2\omega_e}\left(\frac{2B_e}{\omega_e}\right) 3Z\varepsilon\left(\frac{x_e}{r_e^*}\right)^2 \times\left[11C\left(\frac{r_e^*}{a}\right)^{12} - \frac{5}{2}D\left(\frac{r_e^*}{a}\right)^{6}\right] + \frac{3k_3}{\omega_e^2}\left(\frac{2B_e}{\omega_e}\right)^{1/2} 3Z\varepsilon\left(\frac{x_e}{r_e^*}\right) \times\left[2C\left(\frac{r_e^*}{a}\right)^{12} - D\left(\frac{r_e^*}{a}\right)^{6}\right]$$

Ainsi, nous trouvons une expression analogue à celle donnée par Monson et coll. (7).

Résultats expérimentaux

Dans le tableau 1 figurent les fréquences d'absorption $\nu_{0\to v}$ et les déplacements de fréquence $\Delta\nu_{0\to v}$ de l'acide iodhydrique.

Etant donné la grande étendue spectrale des bandes ν, 2ν, et 3ν de la molécule HI en solution CCl_4, la détermination des centres de bande est beaucoup moins précise pour l'état dissous que pour l'état gazeux. Les erreurs des déplacements de fréquence $\Delta\nu_{0\to v}$ sont les suivantes

$$\delta(\Delta\nu_{0\to1}) \simeq \delta(\nu_{0\to1}^{sol}) = \pm 0.5\ cm^{-1}$$

$$\delta(\Delta\nu_{0\to2}) \simeq \delta(\nu_{0\to2}^{sol}) = \pm 1.0\ cm^{-1}$$

$$\delta(\Delta\nu_{0\to3}) \simeq \delta(\nu_{0\to3}^{sol}) = \pm 1.5\ cm^{-1}$$

Les valeurs de $\bar{W}$, $\bar{X}$, et $\bar{Y}$ s'obtiennent par résolution du système de trois équations, données par les relations 3*a*, 3*b*, et 3*c*:

$$\bar{W} = 20 \pm 8\ cm^{-1}$$

$$\bar{X} = 3.7 \pm 5.5\ cm^{-1}$$

$$\bar{Y} = 0.6 \pm 1\ cm^{-1}$$

D'après ces résultats les valeurs de $\bar{X}$ et $\bar{Y}$ n'ont

TABLEAU 2. Constantes moléculaires de HI gazeux et dissous*

HI	ω_e (cm^{-1})	$\bar{W}$ (cm^{-1})	X (cm^{-1})	$\bar{X}$ (cm^{-1})	Y (cm^{-1})	$\bar{Y}$ (cm^{-1})
Gazeux	2308.091 (10)		+38.9810 (10)		−0.1980 (10)	
Dissous (CCl_4)		25.5		—		—

*Les valeurs obtenues par Pugh et Rao (10) et Josien et coll. (16) sont également indiquées dans les tableaux 1 et 2.

TABLEAU 3. Constantes du potentiel Lennard–Jones (6–12) (14)

Molécules	σ (Å)	ε/k (°K)
HI	4.123	324
CCl_4	5.881	327

pas de signification. Seule la valeur de $\bar{W}$ peut être obtenue à partir des relations suivantes.

$$\left.\begin{aligned} 25.1 &= \bar{W} \quad (a)\\ 51.8 &= 2\bar{W} \quad (b)\\ 76.2 &= 3\bar{W} \quad (c) \end{aligned}\right\} \quad (3 \text{ bis})$$

d'où

$$\bar{W} = 25.5 \pm 0.5 \text{ cm}^{-1}$$

Dans le tableau 2, nous donnons les constantes moléculaires ω_e, X, et Y (10) et la valeur expérimentale la plus probable de $\bar{W}$. Les quantités $\bar{X}$ et $\bar{Y}$, étant entachées d'erreurs trop élevées, ne peuvent y figurer.

Calcul du deplacement de frequence

En utilisant les constantes suivantes relatives à la molécule HI: $\alpha_e = 0.16886 \text{ cm}^{-1}$ (10) et $B_e = 6.5111 \text{ cm}^{-1}$ (10), nous avons obtenu à partir de la relation (9): $k_3 = -219.544 \text{ cm}^{-1}$. Les constantes caractéristiques du potentiel de Lennard–Jones (6–12) sont données dans le tableau 3.

Avec ces constantes nous pouvons calculer les valeurs théoriques de $(\Delta\omega/\omega_e)^{\text{répulsion}}$ et $(\Delta\omega/\omega_e)^{\text{dispersion}}$ données par la relation (17) (voir tableau 4).

Discussion

D'après le tableau 2, il apparaît que si la valeur expérimentale du terme d'ordre zéro $\bar{W}$ peut être obtenue avec une précision raisonnable, celles des termes d'ordre un $\bar{X}$ et d'ordre deux $\bar{Y}$ sont très imprécises. Ceci s'explique comme nous l'avons vu précedemment par le fait que les bandes v, $2v$, et $3v$ des solutions de HI sont très larges; ce qui entraîne une certaine imprécision dans le pointé des centres de bande.

Le potentiel intermoléculaire (LJD) (6–12) dépend du premier nombre de coordination Z et des deux paramètres C et D. Pour l'état liquide, si nous ne considérons que la couche de molécules de solvant la plus proche de la molécule de soluté, les facteurs C et D prennent les valeurs suivantes: $C = 1$, $D = 2$ (15); le nombre Z peut être réduit de $Z = 12$ (état solide) à $Z = 10$ (état liquide). La "théorie des lacunes" (Hole Theory) permet de rendre compte de la décroissance de Z avec la densité du solvant (17). Par ailleurs, il semble raisonnable d'adopter le modèle de cage pour le solvant CCl_4. Bonamy et coll. (18) ont montré que l'amplitude moyenne $\bar{\rho}$ des oscillations des molécules de solvant CCl_4 reste faible devant la distance a entre deux nœuds du réseau c.f.c.

TABLEAU 4. Valeurs calculées et observées de $\Delta\omega/\omega_e$

Paramètres du potentiel (LJD)			$\frac{\Delta\omega}{\omega_e} \times 10^3$				$\frac{\Delta\omega^{\text{théor}}}{\Delta\omega^{\text{obs}}}$
Z	C	D	Répulsion	Dispersion	Théorique	Observé	
12	1.01	2.41	−19.9	+35.1	15.2	11.0	138%
10	1	2	−16.4	+24.3	7.8	11.0	71%

Can. J. Chem. Downloaded from www.nrcresearchpress.com by 210.87.254.5 on 09/05/12
For personal use only.

En effet, pour $T = 300\ ^{\circ}K$, ils ont obtenu $\bar{\rho} = 0.049$ a.

Ainsi, ayant choisi un potentiel intermoléculaire de type (LJD), nous pouvons déterminer la quantité $\bar{W} = \Delta\omega$ par la relation (8) et ensuite comparer les valeurs théoriques et expérimentales du déplacement relatif $\Delta\omega/\omega_e$. Le tableau 4 montre que la contribution des forces de dispersion est plus importante que celle des forces de répulsion, les forces d'induction étant négligeables. En adoptant les valeurs numériques suivantes: $Z = 12$, $C = 1.01$ et $D = 2.41$ (15), nous observons un écart important entre valeurs théorique et expérimentale de $\Delta\omega/\omega_e$. Cet écart n'est pas surprenant, car la valeur de $Z = 12$, valable pour l'état solide, est probablement trop élevée pour décrire l'état liquide. Par contre, avec les valeurs $Z = 10$, $C = 1$, et $D = 2$, l'accord est très raisonnable.

En conclusion, le choix d'un potentiel intermoléculaire de type LJD (6–12) permet de rendre compte de manière satisfaisante de l'effet d'un solvant non polaire CCl_4 sur les déplacements de fréquence d'une molécule diatomique polaire HI.

Nous tenons à remercier Monsieur le Professeur P. Barchewitz pour l'intérêt qu'il a porté à cette étude.

1. A. D. BUCKINGHAM. Proc. Roy. Soc. A, **248**, 169 (1958).
2. A. D. BUCKINGHAM. Proc. Roy. Soc. A, **255**, 32 (1960).
3. A. D. BUCKINGHAM. Trans. Faraday Soc. **56**, 753 (1960).
4. P. V. HUONG, M. PERROT, et G. TURREL. J. Mol. Spectrosc. **28**, 341 (1968).
5. A. D. MAY, G. VARGHESE, J. C. STRYLAND, et H. L. WELSH. Can. J. Phys. **42**, 1058 (1964).
6. I. ROSSI, NGUYEN-VAN-THANH, C. BRODBECK, et C. HAEUSLER. Can. J. Chem. **48**, 3362 (1970).
7. P. R. MONSON, H. L. CHEN, et G. E. EWING. J. Mol. Spectrosc. **25**, 501 (1968).
8. J. E. LENNARD-JONES et A. F. DEVONSHIRE. Proc. Roy. Soc. A, **163**, 53 (1937).
9. J. E. LENNARD-JONES et A. F. DEVONSHIRE. Proc. Roy. Soc. A, **165**, 1 (1938).
10. L. A. PUGH et K. N. RAO. J. Mol. Spectrosc. **37**, 373 (1971).
11. C. HAEUSLER, NGUYEN-VAN-THANH, et P. BARCHEWITZ. J. Phys. Paris, **24**, 289 (1963).
12. G. DUROCHER et C. SANDORFY. J. Mol. Spectrosc. **22**, 347 (1967).
13. G. HERZBERG. Molecular spectra and molecular structure. Vol. I. D. Van Nostrand Company. 1950.
14. J. HIRSCHFELDER, J. CURTISS, et R. BIRD. Molecular theory of gases and liquids. Wiley, New York. 1954.
15. I. PRIGOGINE. The molecular theory of solutions. North Holland Company, Amsterdam. 1957.
16. M. L. JOSIEN, G. SOURISSEAU, et C. CASTINEL. Bull. Soc. Chim. Fr. 1539 (1955).
17. J. DE BOER. Proc, Roy. Soc. A, **215**, 1 (1952).
18. L. BONAMY, D. ROBERT, et L. GALATRY. J. Mol. Struct. **1**, 91 (1967).

Can. J. Chem. Downloaded from www.nrcresearchpress.com by 210.87.254.5 on 09/05/12
For personal use only.

Infrared Investigation of H_2S Adsorption and Decomposition on Alumina and on Alumina Supported Molybdenum Sulfide[1]

T. L. SLAGER[2] AND C. H. AMBERG

Department of Chemistry, Carleton University, Ottawa, Canada K1S 5B6

Received June 1, 1972

Adsorption and subsequent reaction of H_2S on alumina gave major i.r. bands at 1341, 1568, 1625, and 3400 cm^{-1}. Relative band intensities were used to follow the first order decomposition of adsorbed H_2S and formation of H_2O. Rate constants of the surface reaction at 23, 55, and 80 °C were 0.70, 1.48, and 3.42×10^{-3} s^{-1}, respectively. A mechanism consistent with the observed spectral and kinetic data involved adsorption to an exposed Al ion forming an Al—S surface bond, and hydrogen bonding to neighboring O and OH species. It was assumed that the sulfur remained on the surface as a sulfide. The 1568 cm^{-1} band was discussed in terms of an Al—O species.

With adsorption on MoS_2–Al_2O_3, bands appeared at 1330 and 1575 cm^{-1}. Behavior in all respects was similar to that observed on the alumina support alone.

L'adsorption suivie d'une réaction ultérieure de H_2S sur l'alumine conduisent à des bandes infrarouge majeures à 1341, 1568, 1625, et 3400 cm^{-1}. Les intensités relatives des bandes ont été utilisées pour suivre la décomposition du 1er ordre de H_2S adsorbé et la formation de H_2O. Les constantes de vitesse de la réaction superficielle à 23, 55, et 80 °C sont respectivement de 0.70, 1.48, et 3.42×10^{-3} s^{-1}. Un mécanisme compatible avec les données spectrales et cinétiques observées fait intervenir une adsorption sur un ion Al exposé conduisant à une liaison superficielle Al—S et une liaison hydrogène avec les espèces voisines O et OH— on admet que le soufre reste sur la surface sous forme de sulfure. La bande à 1568 cm^{-1} a été discutée en rapport avec les espèces Al–O. Avec l'adsorption sur MoS_2–Al_2O_3 des bandes apparaissent à 1330 et 1575 cm^{-1}. Le comportement est semblable à tous égards à celui observé pour le support alumina seule.

[Traduit par le journal]

Canadian Journal of Chemistry, **50**, 3416 (1972)

Can. J. Chem. Downloaded from www.nrcresearchpress.com by 210.87.254.42 on 09/05/12
For personal use only.

Introduction

Hydrogen sulfide, a product of the hydrodesulfurization reaction, plays a significant role in the catalytic process in a number of ways. Although activation of hydrodesulfurization catalysts can be accomplished by reduction in hydrogen alone (1), presulfidation is generally preferred (2–5) for obvious practical reasons, and this is generally carried out with H_2S/H_2, thiophene/H_2, or similar mixtures. It might further be cited that H_2S strongly poisons butene hydrogenation on a commercial cobalt molybdate catalyst (6), as well as on unsupported MoS_2 (3), while having a much smaller effect on thiophene desulfurization. Similar behavior was noted in comparing a presulfided with a purely oxidic chromia catalyst (7). A recent critical review of the literature on hydrodesulfurization by Schuman and Shalit (8) should be consulted for further details.

In the following we report an i.r. spectroscopic study of the adsorption of H_2S on a supported MoS_2 catalyst, and on alumina, the support alone. Although it would have been most desirable to examine the adsorption on unsupported MoS_2, this proved to be intractable, as no sample could be made that would transmit sufficient radiation for reliable spectroscopic analysis. Few efforts to examine the adsorption of H_2S by means of i.r. spectroscopy have so far been reported. Blyholder and Bowen (9) saw no evidence of bands arising from adsorbed H_2S on a silica-supported nickel sample. On the other hand, Blyholder and Richardson (9) did note that H_2S adsorption on Fe_2O_3 gave rise to an OH stretching band, and suggested that this might have come about by a surface decomposition of H_2S not unlike that proposed in the present paper. Deo, Dalla Lana, and Habgood (10) were successful in finding i.r. evidence for its adsorption on alumina and on a number of other catalysts active in the Claus reaction, at pressures higher than those used in the present study. Their results and interpretation differed from ours

[1]Abstracted from the thesis of T. L. Slager, which was submitted in partial fulfilment of the requirements for the Ph.D. degree, Carleton University, 1969.

[2]Present address: LECO Corporation, Saint Joseph, Michigan 49085.

Can. J. Chem. Downloaded from www.nrcresearchpress.com by 210.87.254.42 on 09/05/12
For personal use only.

in a number of aspects, but are consistent with them in general. Ratnasamy and Fripiat reported the absence of noticeable effects with unsupported MoS_2 (11).

Experimental

(i) Apparatus

A Beckman IR-7 grating spectrophotometer was used to record all spectra presented. A slit program of two times normal, ranging between 0.85 and 0.24 mm, gave a spectral resolution of 1–2 cm^{-1} in the region 4000 to 900 cm^{-1}. All other instrument parameters were adjusted so that the noise level was less than 1% at 50%T.

The sample and reference cells were similar to those previously described (12). A Cahn RG electro-balance has been substituted for the null-reading quartz spring microbalance. A catalyst sample approximately 19.5 × 35 × 0.1 mm^3 was pressed at 7.0 kg mm^{-2} and mounted in a quartz sample holder. Other modifications to the system were designed to eliminate adsorbate contact with high-vacuum grease. Sodium chloride windows were attached to the flat flange surface of the cell with brass couplings and Viton O-rings. A Teflon retaining ring served to prevent distortion of the O-ring. Another Teflon ring was used to prevent scoring of the sodium chloride disks by the brass couplings.[3] A stainless steel Viton O-ring flange replaced the upper cell opening and the thermocouple joint was replaced by a tungsten-through-glass seal. The balance compartment and sample cell were isolated from the rest of the vacuum system by Teflon stopcocks. The O-rings and Teflon stopcocks were treated at temperatures up to 100 °C prior to mounting the high-area samples in the system. It was possible to maintain a static vacuum in the system of better than 10^{-5} Torr for several days.

(ii) Reagents

Hydrogen sulfide and deuterium sulfide (Matheson Corp.) were purified by bulb-to-bulb distillation and freeze–pump–thaw cycles. The middle third of the resulting liquid H_2S or D_2S was distilled into a 2 l bulb which was equipped with Teflon stopcocks. The purity was checked by mass spectrometry and found to be >99%.

Two alumina samples were used: η-Al_2O_3 as prepared by MacIver *et al.* (13) and γ-Al_2O_3 (Alon C was supplied through the courtesy of Cabot Corp. Boston, Mass.). Three alumina supported molybdenum "disulfide" catalysts were prepared by dissolving molybdenum oxide (Baker Reagent Grade) in 30% hydrogen peroxide. Alon C was added slowly with stirring.[4] The wet mass was dried in a 110 °C oven overnight. It was sulfided *in situ* with a 10:1 hydrogen: hydrogen sulfide mixture for 24 h at 300 °C.

Table 1 shows the surface areas and observed concentrations of molybdenum and sulfur for the various adsorbents. Sulfur was determined gravimetrically by oxidation to a soluble sulfate, and precipitation with barium chloride (14), and molybdenum was determined colorimetrically. Hydrogen peroxide oxidation of the sample was necessary when the sulfur occurred as a sulfide. Whenever possible, the molybdenum content was determined prior to sulfidation. The MoO_3 was dissolved in an ammonia solution buffered with tartaric acid and colored by forming an EDTA complex. The absorbance was measured at 450 mμ and the amount of molybdenum read from a calibration curve.

TABLE 1. Data for the various adsorbates used

Catalyst	Surface area* (m^2g^{-1})	Molybdenum† (wt %)	Sulfur† (wt %)	S/Mo atom ratio‡
η-Al_2O_3	235	—	—	—
γ-Al_2O_3	105	—	—	—
MoS_2–Al_2O_3 (A)	102	7.0	3.5	1.5
MoS_2–Al_2O_3 (B)	103	4.8	2.29	1.4
MoS_2–Al_2O_3 (C)	105	1.66	0.93	1.7

*As determined by nitrogen gas adsorption in a conventional volumetric B.E.T. apparatus.
†±5% absolute.
‡±10% absolute.

(iii) Experimental Procedure

All samples were outgassed at 300 °C and 10^{-6} Torr for 16 h. They were cooled to experimental temperature, the background spectrum determined and the adsorbate admitted. Spectra were recorded at various time intervals. When the system had reached equilibrium, the adsorbed gases were desorbed by condensation into a liquid nitrogen trap, and examined by mass spectrometry (MS-10; Associated Electrical Industries Ltd.).

Results and Discussion

Fifteen minutes after H_2S had been adsorbed onto an alumina sample at various temperatures, a spectrum was determined (*e.g.* Fig. 1*B*). This consisted of five additional i.r. bands whose frequencies are listed in Table 2. No significant differences between η-alumina and Alon C were observed. The two bands at 2568 and 1341 cm^{-1} correspond to the known stretching and bending modes of H_2S (15), within the range expected for adsorbed molecules. The very broad band appearing at about 3400 cm^{-1} can be assigned to an OH-stretching mode formed by hydrogen bonding of hydrogen atoms in H_2S to oxygen atoms in the alumina surface. Assignment to hydrogen bonding was supported by band frequency and shape, as well as by the absence of fine-structure. As the 3400 cm^{-1} band grew on standing, the band at about 3720 cm^{-1} initially present, and arising from alumina surface OH-groups lost its definition, indicating either overlap with the new band, or growth of

[3]Further detail is shown in a scale diagram in the Ph.D. thesis of T. L. Slager.

[4]Care should be taken when adding the alumina to the hydrogen peroxide, because of a tendency of the mixture to spatter.

TABLE 2. Infrared band frequencies for H_2S and D_2S adsorbed on alumina at room temperature*

Compound	Pressure (Torr)	Observed frequencies (cm^{-1})	Gas phase frequencies (cm^{-1})	Assignment
H_2S	24.7	1341	1290	H—S—H (bend)
		1420vw		
		1568		
		2568vw	2684	S—H (stretch)
		3400vb		O—H (hyd.bonded)
(H_2O)		1625		H—O—H (bend)
D_2S	10.6	1860vw	1999	S—D (stretch)
		2700vb		O—D (hyd.bonded)
(D_2O)		1215		D—O—D (bend)

*vw = very weak, vb = very broad.

yet a third type of OH-band at a similar frequency. There was also a shift to somewhat higher frequency of this band during H_2S adsorption, not noted by Deo *et al.* (10), although these authors were able to induce a similar shift by doping their sample with NaOH. The remaining two bands at 1420 and 1568 cm^{-1} will be discussed below.

Hydrogen bonding is presumably the reason for the shifts of -166 cm^{-1} from the gas phase asymmetric stretch of H_2S, and of $+51$ cm^{-1} from the bending mode. This is reasonable in view of the fact that the unperturbed S—H bond will become weakened and the HSH deformation restricted through hydrogen bonding.

In order to determine whether the 1341 cm^{-1} adsorption was, in fact, the bending mode of H_2S or arose from an S—O species of some type, D_2S was used as the adsorbate. If the 1341 cm^{-1} band were due to an S—O stretching mode, as argued by Deo *at al.* (10) in the case of their intense band at 1330 cm^{-1}, then little or no difference in frequency should be expected between adsorbed H_2S and D_2S. In D_2S, the gas phase bending occurs at 934 cm^{-1} (15). Unfortunately, even the estimated positive shift of 50 cm^{-1} due to adsorption is insufficient to place this band outside the region of the very intense Al—O vibrational frequencies occurring between 1050 and 600 cm^{-1}. Thus no bending mode could be observed for D_2S. However, since no other bands occurred with D_2S adsorption near 1341 cm^{-1} which could then have been attributed to an S—O bond, the frequency in question was assumed to be the bending mode of H_2S.

Other bands in the initial spectrum of hydrogen sulfide were observed at 1568 and 1420 cm^{-1}. That at 1420 cm^{-1} was very weak. It was not observed at a pressure of 0.8 Torr, but appeared at pressures of 2 Torr or above (Fig. 1). The absorption at 1568 cm^{-1} was much stronger and its growth was proportional to the intensity of the bending mode of hydrogen sulfide at 1341 cm^{-1}. The ratio between the band areas of the 1341 and 1568 cm^{-1} bands was 1.6 ± 0.1. No sulfur compound containing aluminum, oxygen, and/or hydrogen has been reported with an i.r. absorption at or near 1568 cm^{-1}. This band could be completely removed by placing a liquid nitrogen trap in the closed system. When the surface had been repeatedly exposed to species containing carbon and hydrogen, bands appeared at 1568 and 1460 cm^{-1}. They became more intense with every adsorption–desorption cycle. Parkyns (16) observed very broad intensity bands at 1570 and 1440 cm^{-1} after several adsorption–desorption cycles using CO as the adsorbate and alumina as the adsorbent. Oxygen treatment up to 400 °C did not reduce their intensity, and deuteration did not alter their absorption frequency. He associated these with surface vibrational modes of the alumina. Similarly, Scholten *et al.* (17) found peaks at 1552 and 1473 cm^{-1} after an adsorption–desorption cycle using formic acid as the adsorbate. Evacuation at 450 °C for 20 h did not remove them. Addition of a monolayer of H_2O caused their frequency to shift to 1570 and 1452 cm^{-1}. Mathieu and Bozon (18) also reported seeing peaks at 1580 and 1480 cm^{-1} with the adsorption of ethylene and ethane on alumina. Both Mathieu and Bozon and Scholten *et al.* found

Can. J. Chem. Downloaded from www.nrcresearchpress.com by 210.87.254.42 on 09/05/12
For personal use only.

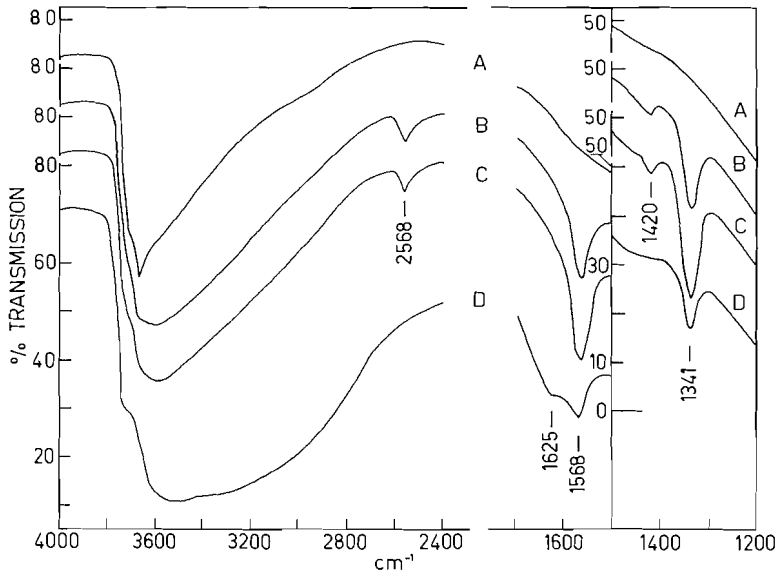

FIG. 1. Infrared bands of H_2S adsorption on Al_2O_3. *A*: background; *B*: 1/2 h; *C*: 2 h; *D*: 24 h; (pressure = 1.9 Torr; temperature = 23 °C).

that the bands in question could be removed by oxygen treatment at 450 °C. All three sets of workers seem to agree that they arise from a surface vibrational mode. No one has hypothesized as to their origin.

In the following we propose an assignment for the 1570 cm^{-1} band, which is consistent with the large variety of compounds producing it. Since it appears with H_2S adsorption, while the one at 1460 cm^{-1} does not, it is assumed that these two arise from different vibrating species. Dorsey (19) found similar bands with alumina films, their exact frequency depending on the conditions under which they were formed. He assigned them to an Al=O vibration and estimated their range to lie between 1345 and 1696 cm^{-1}. It is plausible to interpret the 1570 cm^{-1} band as arising from adsorbates imparting double bond character to aluminum–oxygen bonds; this would also explain both the frequency variation of the band and the broad range of adsorbates which cause it to appear. One could envisage H_2S adsorption through the sulfur atom to the surface, as shown below,

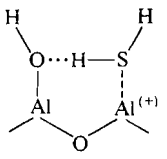

acting in this manner. For the reasons cited we favor this model over that proposed by Deo *et al.* (10), in which the sulfur forms an Al—O—H···SH_2 hydrogen bond with surface hydroxyls. It is also in better accord with the mechanism of surface sulfide formation discussed below.

The absorption in the range 1440–1480 cm^{-1} might arise from some reaction of carbon with the alumina surface, since it appears with CO, H_2COOH, C_2H_4, and C_6H_6 but not with H_2S. More data are necessary to attempt an assignment of this band.

Relatively little work has been done on the adsorption and subsequent decomposition of hydrogen sulfide on alumina. Bayley (20) noted that H_2S could not be quantitatively desorbed during adsorption-desorption cycles. deRosset *et al.* (21) have investigated the same system at low coverages and high temperatures and reached the conclusion, that the formation of Al—S and Al—O bonds on oxygen vacancies following the adsorption of H_2S and H_2O was consistent with bulk thermodynamics.

The decomposition of hydrogen sulfide is readily confirmed using i.r. and gravimetric techniques as outlined below. Extended contact time with alumina (curves *C* and *D* in Fig. 1) resulted in further increase of intensity in the O—H region, and an absorption at 1625 cm^{-1} arising from the H_2O bending mode. This

Can. J. Chem. Downloaded from www.nrcresearchpress.com by 210.87.254.42 on 09/05/12
For personal use only.

Can. J. Chem. Downloaded from www.nrcresearchpress.com by 210.87.254.42 on 09/05/12
For personal use only.

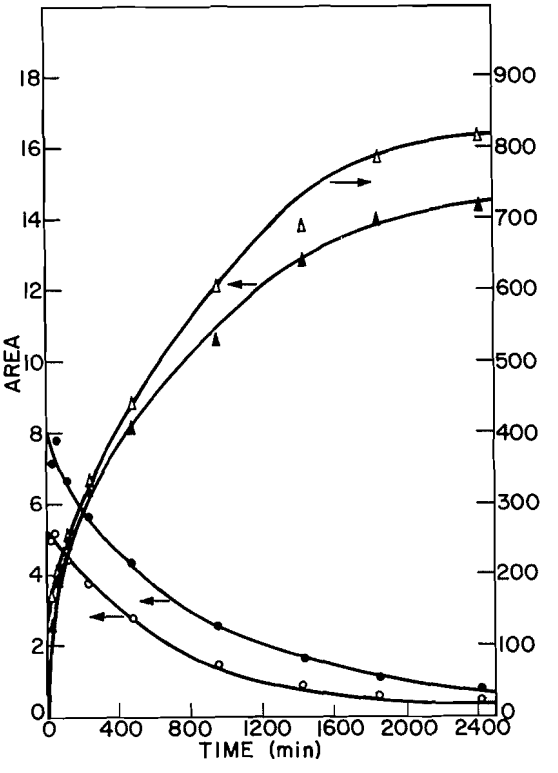

FIG. 2. Time dependence of the area of the i.r. bands appearing during the decomposition of H_2S on Al_2O_3: ●, 1341; ○, 1568; ▲, 1625; △, 3400; (pressure = 0.82 Torr; temperature = 55 °C).

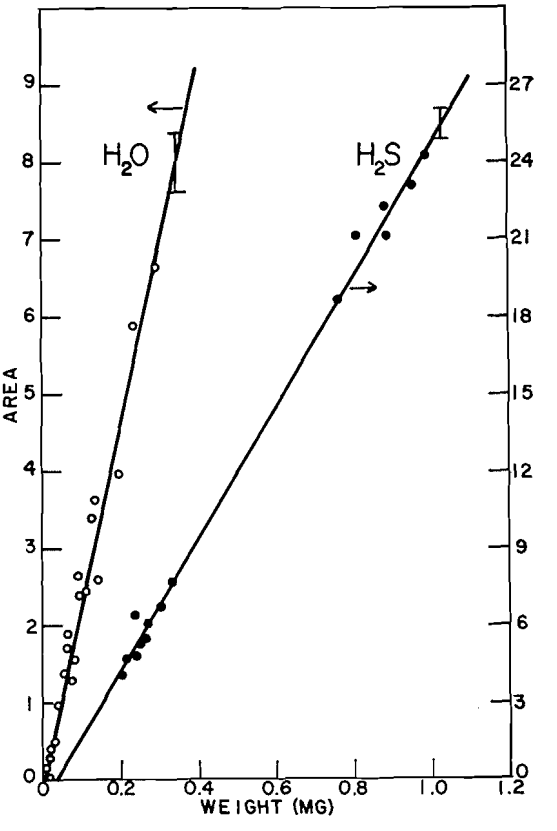

FIG. 3. Relation between the band areas of H_2S and H_2O and the weight of adsorbed material (weight of Al_2O_3 = 100 mg).

establishes that water is one of the decomposition products.

Band areas were determined using a Simpson's rule approximation, and then plotted as a function of time. The graphs of the four major bands at 1341, 1568, 1625, and 3400 cm^{-1} are given in Fig. 2. It was interesting to note that increases in the hydrogen-bonded OH stretching band at 3400 cm^{-1} paralleled the total weight increase with time of the sample. Assuming that weight changes originate exclusively from the addition or removal of H_2O or H_2S molecules, we have attempted further to define the nature of the hydrogen bonding. If one regards the bond (or set of different bonds) as being made up of weighted contributions from each species, the weighting factors remaining constant over the range of surface coverages, then the empirical relation

$$xA_{H_2S} + yA_{H_2O} = A_{O-H}$$

should hold, where the A_i's are the respective band areas of the 1341, 1625, and 3400 cm^{-1} bands, and x and y are the weighting coefficients. By solving for x and y for appropriate sets of values at various time intervals, this relationship was confirmed semiquantitatively (± 20%), as were the assumptions underlying it.

Since we are dealing with reacting species, and since absolute intensities of the deformation bands of neither adsorbed H_2O nor adsorbed H_2S are available from the literature, the following procedure had to be adopted (for a similar case, see Amberg and Seanor (22)). When the area of the 1341 cm^{-1} band is plotted against the weight of adsorbed material, an initial steep rise, essentially due to H_2S alone, is followed by a more gradual decrease as H_2S becomes converted to H_2O. The ascending branch of this curve, shown in Fig. 3, was used

Can. J. Chem. Downloaded from www.nrcresearchpress.com by 210.87.254.42 on 09/05/12
For personal use only.

TABLE 3. Intensity values for the ν_2 deformation modes of adsorbed H_2O, H_2S, and comparable species

Compound	State	Frequency (cm^{-1})	Extinction coefficient (mol^{-1} l cm^{-1})	Integrated intensity (mol^{-1} l cm^{-2})	Reference
H_2O	Adsorbed	1625	87 ± 10	4320 ± 200	
H_2S	Adsorbed	1341	95 ± 7	4460 ± 250	
H_2O	Vapor			4900 ± 490	23
H_2O	Vapor			5940 ± 600	24
HDO	Liquid			3700 ± 200	25

TABLE 4. Rate constants for the reaction of H_2S with Al_2O_3

Experiment number	Catalyst	Temperature (°C)	Rate constant ($s^{-1} \times 10^3$) At 1341 cm^{-1}	At 1568 cm^{-1}	At 1625 cm^{-1}	Pressure (Torr)	Sample weight (mg)
28	η-Al_2O_3	23	0.948	1.55	—	0.82	68.2
29	Alon C	23	0.702	1.08	0.876	0.82*	78.6
31	Alon C	23	0.694	1.13	0.756	0.80	84.8
40	Alon C	23	—	—	1.17	27.40	84.8
60	Alon C	55	1.48	1.57	1.34	0.82	139.6
61	Alon C	23	0.749	0.846	0.597	1.90	139.6
62	Alon C	23	0.720	0.671	0.640	0.21	139.6
63	Alon C	80	3.42	3.52	2.68	0.82	139.6

*A pressure of 0.8 Torr H_2S gives monolayer coverage as calculated from the B.E.T.(N_2) isotherm.

to calculate the weight of H_2O generated on the surface. This in turn was plotted against the band area of the 1625 cm^{-1} band, as seen in the left-hand line of Fig. 3. The molar integrated intensity and the molar extinction coefficient for the bending modes of adsorbed H_2S and H_2O, calculated from the least-squares lines of these plots, are listed in Table 3, together with recent literature values for H_2O and HDO (23–25). From this it appears that the ν_2 mode for H_2O on the alumina surface is slightly less intense than it is in the unperturbed vapor state, and only marginally more so than in liquid HDO.

A logarithmic plot of D against time (Fig. 4), where D = either $A - A_\infty$ or $A_\infty - A$ for decomposition or formation, respectively (A being the area of the i.r. band under consideration), showed that hydrogen sulfide decomposition on alumina followed first order kinetics. The rate constants for the reaction under various experimental conditions are given in Table 4. The following points of interest may be noted: comparison of experiments 29 and 31 will give an indication of the reproducibility of the rate constants; 29, 31, 61, and 62 of the effect of pressure; 29, 60, and 63 of variation with temperature; 28 and 29 of similarity between the two types of aluminas. Estimates of the enthalpy and entropy of activation made on the basis of the usual assumptions gave values of $\Delta H^{\ddagger} = 5.4$ kcal/mol and $\Delta S^{\ddagger} = -58$ e.u.

Examination of Fig. 4 and Table 4 shows that the decomposition rate of hydrogen sulfide and the rate of formation of water were essentially the same. This indicates that no stable entity such as O—H^- or Al—O—H existed as a separate reaction intermediate.

A mechanism in agreement with the preceding data is shown below. Retention of the

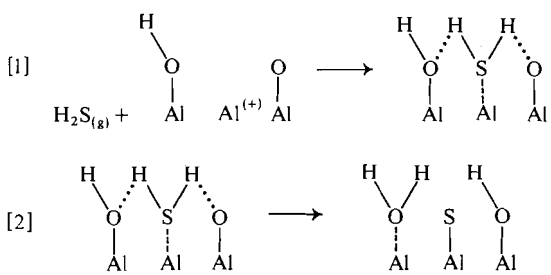

Can. J. Chem. Downloaded from www.nrcresearchpress.com by 210.87.254.42 on 09/05/12
For personal use only.

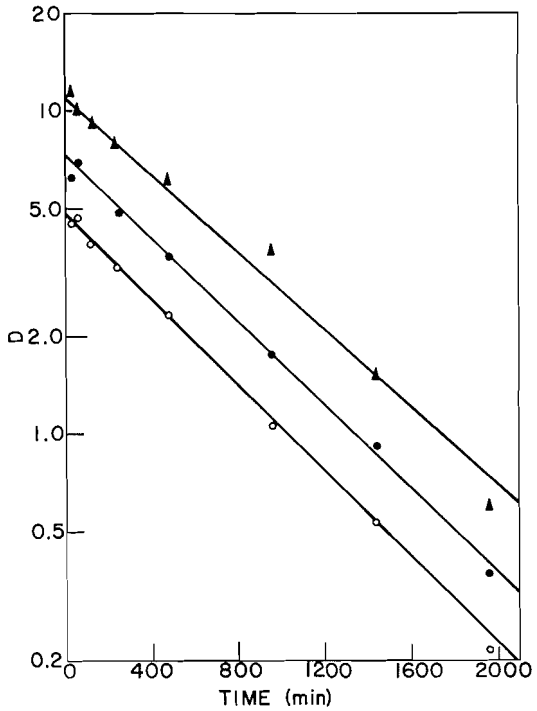

FIG. 4. First order plot of the i.r. band areas of Fig. 2 *vs.* time: ●, 1341; ○, 1568; ▲, 1625; D = either $A - A_\infty$ or $A_\infty - A$.

H_2S bending mode at a frequency of 1341 cm^{-1}, formation of the hydrogen bonded species absorbing at 3400 cm^{-1}, and the formation of the Al—O bond at 1568 cm^{-1} are all consistent with the formation of the adsorbed state as shown in step 1. Examination of Fig. 2 shows that hydrogen sulfide adsorbed fairly rapidly reaching a maximum in 1 to 3 h in contrast to the much slower formation of H_2O. Therefore step 1 must be a fast step in this reaction. Step 2 is consistent with the thermodynamics, and equality of the rate of decomposition and formation reactions. The adsorbed state of hydrogen sulfide was sufficiently perturbed, as shown in the shift of $+51$ cm^{-1} to 1341 cm^{-1}, so as to lower the energy requirements, causing a low value for $\Delta H^{\ddagger}$. The large negative value of $\Delta S^{\ddagger}$ indicated that a large degree of ordering occurred in going from the adsorbed state to the transition state. According to this mechanism, bond breaking in hydrogen sulfide can be thought of as being coincident with the formation of the O—H bond. Rationalization for the O—H lying next to the adsorbed hydrogen sulfide can be made following Peri's work (26) in which a plot of the percent of O—H retained, against evacuation temperature showed that at least 50% of the surface would still be covered by hydroxyl groups after evacuation at 325 °C. Thus it would be improbable that H_2S could adsorb on exposed aluminum ions without having an O—H species as a neighbor.

It is possible to consider the reaction of hydrogen sulfide with an alumina surface in terms of a redox system. Flockhart *et al.* (27) proposed the existence of two alumina sites acting as a redox system. If in the present case the decomposition of hydrogen sulfide were a redox reaction, hydrogen sulfide would have to be the reductant while a surface oxygen or hydroxyl group would have to be the oxidant. This is shown below. Bulk alumina would have to act

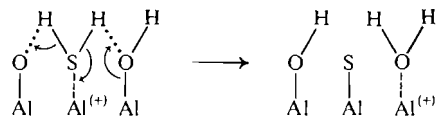

as the charge carrier between the two sites. It is possible that the alumina surface could act in such a fashion; however, there is insufficient evidence to argue conclusively that a redox reaction was operative in the case under discussion. The only evidence comes from the fact that the hydroxyl group has been reduced to water and the hydrogen sulfide oxidized to "aluminum sulfide", no evidence existing as to the final nature of the sulfur atom.

Other conceivable reaction paths could involve the breaking of the hydrogen–sulfur bonds to form H^+, H^0, or H^-, and S^{2-}, S^0, or S^{2+}. Decomposition forming $2\,H^+$ and S^{2-} is a possibility that cannot be discounted, as H^+ would readily react with the O^{2-} on the surface to form OH^- or H_2O. No evidence was found that would eliminate S^{2-} as a product. The formation of $2\,H^0$ and S^0 can also be thought feasible, if it is assumed that H^0 reacts much faster with oxygen species than with itself. This assumption would be necessary, because only H_2O was detected as a product in the decomposition. It is unlikely that H^- would be formed, as subsequent reaction with an OH^- or O^{2-} to form water would be inhibited by like charges. The formation of S^{2+} is also unlikely, but if formed it would probably react with the surface

Can. J. Chem. Downloaded from www.nrcresearchpress.com by 210.87.254.42 on 09/05/12
For personal use only.

O^{2-} to form SO_x. Infrared bands for SO_x or S_x species were not observed, and no pertinent peaks were detected in the mass spectrum. Thus the decomposition to 2 H^- and S^{2+} is improbable. Any of the three other reaction possibilities discussed above (concerted reaction, H^+ ion formation, or hydrogen atom formation) are equally probable.

The adsorption of hydrogen sulfide on supported molybdenum sulfide produced two bands (1330 and 1575 cm^{-1}), as did adsorption on alumina. Note, however, that both frequencies were lower by about 5 to 10 cm^{-1} than those observed on alumina, and thus closer to the gaseous state, indicating that the H_2S molecule was less perturbed by adsorption on the MoS_2–Al_2O_3 catalyst than on Al_2O_3. This was possibly due to the substantial decrease in the concentration of oxygen atoms exposed on the surface. Hydrogen bonding is very much weaker to a sulfide atom than to an oxygen atom, and will not therefore affect the adsorbed H_2S as greatly on a sulfide surface. The decrease in the number of molecules hydrogen bonded to oxygen atoms was evident from the difference between the intensity of the 3400 cm^{-1} band adsorbed on supported molybdenum sulfide and on alumina, at equivalent pressures.

The two hydrogen sulfide bands disappeared upon raising the temperature higher than 110 °C at 0.8 Torr, reproducing the behavior of H_2S adsorbed on alumina. Upon decomposition, water bands again appeared, presumably by reaction with the alumina support. A separate rate study of the decomposition of hydrogen sulfide was not undertaken but, from other experiments, it appears to be of the same order of magnitude as on the alumina surface.

The financial support of the National Research Council of Canada is gratefully acknowledged. The authors are also grateful to Dr. H. W. Habgood and colleagues for making available their manuscript prior to publication, and to Dr. A. W. Ashbrook and J. Arnason for assistance with the molybdenum analysis.

1. J. M. J. G. Lipsch. Ph.D. Thesis. Technische Hogeschool, Eindhoven, The Netherlands. 1968.
2. P. J. Owens and C. H. Amberg. Adv. Chem. Ser. **33**, 182 (1961).
3. S. Kolboe and C. H. Amberg. Can. J. Chem. **44**, 2623 (1966).
4. F. P. Ivanovskiĭ, R. S. Kalvarskaya, G. S. Beskova, and N. P. Sokolova. J. Phys. Chem. USSR, **30**, 1860 (1956).
5. F. W. Kirsch and S. E. Shull. Ind. Eng. Chem. Prod. Res. Develop. **2**, 48 (1963).
6. P. Desikan and C. H. Amberg. Can. J. Chem. **42**, 843 (1964).
7. P. J. Owens and C. H. Amberg. Can. J. Chem. **40**, 941 (1962).
8. S. C. Schuman and H. Shalit. Cat. Revs. **4**, 245 (1971).
9. G. Blyholder and D. O. Bowen. J. Phys. Chem. **66**, 1288 (1962); G. Blyholder and E. A. Richardson. J. Phys. Chem. **66**, 2597 (1962).
10. A. V. Deo, I. G. Dalla Lana, and H. W. Habgood. J. Catal. **21**, 270 (1971).
11. P. Ratnasamy and J. J. Fripiat. Trans. Faraday Soc. **66**, 2897 (1971).
12. D. A. Seanor and C. H. Amberg. Rev. Sci. Instr. **34**, 917 (1963).
13. D. S. MacIver, H. H. Tobin, and R. T. Barth. J. Catal. **2**, 485 (1963).
14. A. I. Vogel. Quantitative inorganic analysis. J. Wiley and Sons, Inc., New York. 1961. p. 462.
15. G. Herzberg. Infrared and raman spectra of polyatomic molecules. D. van Nostrand Co. Inc., Princeton, New Jersey. 1956. p. 283.
16. N. D. Parkyns. J. Chem. Soc. A, 1910 (1967).
17. J. J. F. Scholten, P. Mars, P. G. Menon, and R. Van Hardeveld. Proc. Int. Congr. Catal. 3rd, 881 (1965).
18. M. V. Mathieu and M. Bozon. Proc. Int. Congr. Catal. 3rd, 896 (1965).
19. G. A. Dorsey, Jr. J. Electrochem. Soc. **113**, 169 (1966); **115**, 1053 (1968).
20. C. H. Bayley. Can. J. Res. **10**, 19 (1934).
21. A. J. deRosset, C. G. Finstrom, and C. J. Adams. J. Catal. **1**, 235 (1962).
22. C. H. Amberg and D. A. Seanor. Proc. Int. Congr. Catal. 3rd, 450 (1965); 461 (1965).
23. A. Goldman and U. P. Oppenheim. Appl. Opt. **5**, 1073 (1966).
24. Y. Ben Aryeh. J. Quant. Spectrosc. Radiat. Transfer **7**, 211 (1967).
25. C. A. Swenson. Spectrochim. Acta, **21**, 987 (1965).
26. J. B. Peri. J. Phys. Chem. **69**, 211 (1965); **69**, 220 (1965); **69**, 231 (1965).
27. B. D. Flockhart, I. R. Leith, and R. C. Pink. J. Catal. **9**, 45 (1967).

Electrochemical Fission of Vicinal Diketals to Orthoesters

R. COUTURE
Department of Chemistry, University of Ottawa, Ottawa, Canada
AND
B. BELLEAU[1]
Department of Chemistry, McGill University, Montreal, Quebec
Received May 1, 1972

Anodic methoxylation at a platinum electrode of α,α′-dimethoxystilbene yielded benzil tetramethylketal (**2**) which upon further electrolysis in methanol gave a 62% yield of trimethyl orthobenzoate. The mechanism of this new anodic fission reaction is briefly discussed.

La méthoxylation anodique, sur une électrode de platine, de l'α,α-diméthoxystilbène conduit au benzile tétraméthylcétal (**2**) qui par électrolyse ultérieure dans le méthanol donne le triméthylorthobenzoate, avec un rendement de 62%. Le mécanisme de cette nouvelle réaction anodique de fission est discuté brièvement.
[Traduit par le journal]

Canadian Journal of Chemistry, **50**, 3424 (1972)

During the course of our studies on the electrochemical synthesis of benzoquinone ketals, it was observed that *o*-benzoquinone tetramethyl ketal possessed the remarkable ability to suffer anodic cleavage in alkaline methanol to the corresponding hexamethyl *cis,cis*-orthomuconate (1). Because of the unprecedented nature of the reaction, the question arose as to whether this anodic cleavage is substrate specific or applicable to other types of vicinal diketals. Accordingly, we chose to test the behavior of an open-chain analog such as benzil tetramethyl ketal (**2**) which may be expected to yield methyl orthobenzoate (**3**) upon electrochemical oxidation in alkaline methanol. Unfortunately, the benzil diketal **2** is unknown and could not be prepared by the general methods familiar to the organic chemist. However, by taking advantage of our recent finding that vinyl ethers can be not only dimerized but 1,2-dimethoxylated directly at a platinum anode in methanol (2), an electrochemical synthesis of **2** from α,α′-dimethoxy stilbene (**1**) could be envisaged. The starting stilbene **1** can be prepared by first reacting benzil with sodium followed by reaction of the diketyl anion intermediate with dimethyl sulfate (3). The pure product is obtained in low yield and should have the *cis*-configuration according to Bauld (4).

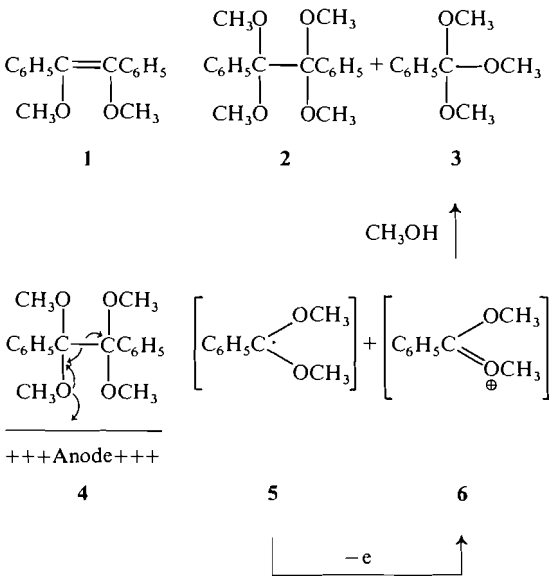

1 **2** **3** **4** **5** **6**

Oxidation of **1** in 1% methanolic potassium hydroxide at a platinum anode following our previously described techniques (1, 2) gave after 1 h (3 A, 12 V) the *bis*-ketal **2** (45% yield) and trimethyl orthobenzoate (**3**) (18% yield). Under the same conditions, the *bis*-ketal **2** underwent electrolytic cleavage to **3** in 62% yield after a reaction time of 1.5–2 h. Optimum conditions for the production of **2** from **1** or **3** from **2** were not determined. The anodic fission of *o*-benzoquinone ketals (1) can thus be

[1]To whom correspondence should be addressed.

Can. J. Chem. Downloaded from www.nrcresearchpress.com by 210.87.254.6 on 09/05/12
For personal use only.

Can. J. Chem. Downloaded from www.nrcresearchpress.com by 210.87.254.6 on 09/05/12
For personal use only.

extended to other vicinal diketals. The question of mechanism is of considerable interest as it bears analogy to the periodate and lead tetraacetate cleavage of vicinal diols and related structures. We have previously shown that adsorbed species at the anode provide the substrate for the solvent methanol (2). In the case of vinyl ethers, the adsorbed species were deduced to consist of radical cations on the basis that dimerization to succindialdehyde acetals is a major reaction pathway. Indeed, radical cations were shown to be generated from methoxybenzenes upon anodic oxidation to quinone ketals (5). However, anodic discharge of **2** cannot yield a resonance stabilized radical cation as is the case with vinyl ethers which benefit from π-conjugation (2). Moreover, we have also eliminated the involvement of methoxy radicals in the production of quinone ketals from methoxybenzenes (5). A mechanism involving initial discharge of a benzene ring to a radical cation subsequently allowing C—C fission through intramolecular electron shifts may also be ruled out since in the absence of methoxy or hydroxy substituents, benzene rings do not suffer anodic oxidation under the experimental conditions (6). A mechanism which might account for the results would consist in an electron discharge from an ether oxygen (as in **4**) to give a stabilized cation **6** readily captured by methanol and a stabilized radical **5** readily oxidized to cation **6**. One factor which may supply part of the driving force for the fission would be the strong steric repulsion between the four ether oxygens of the α-diketal. Of considerable interest is the formal analogy of this new C—C fission reaction to the well-known periodate or lead tetraacetate cleavage of vicinally oxygenated C—C bonds. This new reaction is potentially useful for the synthesis of mixed orthoesters, a class of compounds not accessible by conventional methods.

Experimental

Benzil Tetramethyl Diketal (2) and Trimethyl Orthobenzoate (3)

A solution of 4.8 g of α,α'-dimethoxystilbene (**1**) (3) in 250 ml of methanol containing 2.5 g of potassium hydroxide was electrolyzed for 1 h by passing a 3 A current at 12 V while stirring and cooling to 10–15°. A platinum anode (total surface area of 160 cm^2) and nickel cathode (total surface area of 240 cm^2) were used as previously described (1, 2). The anodic current density was of the order of 0.03 A/cm^2. The solvent was evaporated, the residue taken up in ether, and the extract washed with water. Evaporation of the ether yielded an oil which was distilled *in vacuo* to give 1.20 g (18% yield) of trimethyl orthobenzoate (**3**), b.p. 46–8°/0.25 nm (n.m.r. absorption at 6.99 τ for OCH_3 and 2.68 τ for aromatic protons in a ratio of 9:5) followed by 2.70 g (45% yield) of benzil tetramethyl diketal (**2**), b.p. 112°/0.25 mm (n.m.r. absorption at 6.70 τ for OCH_3 and 3.00 τ for aromatics in a ratio of 12:10; TMS as internal reference; CCl_4 as solvent). The overall current efficiency was approximately 45%. Treatment of **2** in aqueous methanol with a little dilute hydrochloric acid gave a quantitative yield of methyl benzoate (identified by i.r. and n.m.r. spectroscopy).

Further electrolysis of 1 g of **2** under the same conditions for 1.5–2 h gave after work-up and distillation a 62% yield (about 5% current efficiency) of trimethyl orthobenzoate identified as above.

This research was generously supported by the National Research Council of Canada.

1. B. BELLEAU and N. L. WEINBERG. J. Am. Chem. Soc. **85**, 2525 (1963).
2. B. BELLEAU and Y.-K. AU-YOUNG. Can. J. Chem. **47**, 2117 (1969).
3. H. KUNIMOTO. Chem. Abstr. **59**, 11309 (1963).
4. N. L. BAULD. J. Am. Chem. Soc. **87**, 4788 (1965).
5. N. L. WEINBERG and B. BELLEAU. Tetrahedron. In press.
6. N. L. WEINBERG. Ph.D. Thesis. University of Ottawa, Ottawa, Canada. 1963.

The Triplet State of Ketones in Solution: Quenching of Triplet Acetone by Amines[1]

R. W. YIP AND RAFIK O. LOUTFY[2]

Division of Chemistry, National Research Council of Canada, Ottawa, Canada K1A 0R6

AND

Y. L. CHOW AND L. K. MAGDZINSKI

Department of Chemistry, Simon Fraser University, Burnaby, British Columbia

Received May 11, 1972

Rate constants for quenching of triplet excited acetone by primary and tertiary amines in solution have been measured directly by flash and pulsed laser techniques. The rate constants were found to be independent of solvent dielectric constant over the range ε 1.9 to ε 80, but were influenced by amine ionization potential. The results are interpreted as supporting a charge-transfer model for the quenching of triplet ketones by tertiary amines. The intervention of free ions in the quenching process is discussed. Free energy calculations indicate that electron transfer from *N,N*-dimethylaniline to triplet ketones is exothermic but is slightly more favorable for triplet aromatic ketones than for triplet acetone. Evidence for direct hydrogen atom transfer was obtained for quenching of triplet acetone by *n*-hexylamine.

Les constantes de vitesse d'extinction de l'acétone excitée triplet par les amines primaires et tertiaires en solution ont été mesurées directement par les techniques Laser flash et pulsé. On a trouvé que ces constantes de vitesse étaient indépendantes de la constante diélectrique du solvant dans toute l'intervalle ε de 1.9 à 80 mais dépendaient du potentiel d'ionisation de l'amine. L'interprétation de ces résultats vient à l'appui du modèle de transfert de charge dans l'extinction des cétones triplets par les amines tertiaires. L'intervention des ions libres dans le processus d'extinction est discutée. Les calculs d'énergie libre montrent que le transfert d'électron de la *N,N*-diméthylaniline aux cétones triplets est exothermique et légèrement plus favorable pour les cétones aromatiques triplet que pour l'acétone triplet. La preuve du transfert direct de l'atome d'hydrogène a été obtenue dans l'extinction de l'acétone triplet par la *n*-hexylamine.

[Traduit par le journal]

Canadian Journal of Chemistry, **50**, 3426 (1972)

Can. J. Chem. Downloaded from www.nrcresearchpress.com by 210.87.254.105 on 09/05/12
For personal use only.

The recently reported detection and assignment of the triplet state of acetone in liquids (1) enable us to obtain directly quantitative data on its reactivity towards amines and other molecules in solution. Although it is assumed, usually implicitly, that triplet aliphatic ketones and $n\pi^*$ triplet aromatic ketones behave identically, such a comparison has not yet been possible owing to the lack of reliable rate data on the $n\pi^*$ triplet state of acetone and other aliphatic ketones. In this paper, we present results on the triplet state of acetone which bear on the more general quations of $n\pi^*$ triplet ketone reactivity.

Before considering the experimental results on triplet acetone, attention should be drawn to some of the data and their interpretations on the photoreduction of aromatic ketones by amines. Cohen and co-workers (2) and Davidson and co-workers (3) have proposed that the photoreduction process takes place by a step-wise mechanism. It was suggested that the initial step involved the transfer of an electron from the nitrogen atom of the amine to the electron deficient oxygen atom of the excited carbonyl group to form an ion pair. This was then followed by a proton transfer step and electron redistribution. The detailed description of the electron transfer step has undergone some revision since it was first postulated by Cohen. Initially, the species formed by electron transfer were written as separate species (2*a*), which implied the direct formation of free ions. Later, Cohen *et al.* (2*c*–2*i*) favored the formation of a charge-transfer complex or an ion-pair.

Supporting evidence for the postulate of an electron transfer process has come from flash photolysis of benzophenone with tri-*p*-tolylamine in acetonitrile, where a transient which is believed to be the amine radical cation absorbing at 670 nm was observed (4).

[1]NRCC No. 12785.

[2]NRCC Postdoctoral Fellow, 1971–present.

Can. J. Chem. Downloaded from www.nrcresearchpress.com by 210.87.254.105 on 09/05/12
For personal use only.

TABLE 1. Rate constant for quenching acetone phosphorescence by amines in various solvents*

Quencher†	Solvent	ε	k_q (M^{-1} s^{-1})
n-Hexylamine (8.71 eV)	Water	80	$(1.0\pm0.6)\times10^7$
	t-Butanol	10.9	$(1.0\pm0.7)\times10^7$
	Acetonitrile	37.7	$(1.3\pm0.1)\times10^7$
	n-Hexane	1.89	$(1.8\pm0.1)\times10^7$
t-Butylamine (8.64 eV)	Water	80	$(1.9\pm0.4)\times10^6$
Triethylamine (7.50 eV)	Water	80	$(2.7\pm0.5)\times10^8$
	Acetonitrile	37.7	$(3.9\pm0.3)\times10^8$
	t-Butanol	10.9	$(3.3\pm0.1)\times10^8$
N,N-dimethylaniline (7.14 eV)	Water	80	$(2.5\pm0.8)\times10^9$
	n-Hexane	1.89	$(2.0\pm0.1)\times10^9$

*Measured using a flash emission apparatus (ref. 1) except in *n*-hexane, where a Q-switched neodymium glass laser was used. Acetone concentration 0.05 *M*. Experiments carried out at 23°.

†The numbers in parentheses after the amines are first ionization potentials of the amines (ref. 17).

A number of differences between the photoreduction of benzophenone by aliphatic and alkyl aromatic amines have been observed (3*b*), mainly, that reduction with *N,N*-dimethylaniline is insensitive to the addition of naphthalene as quencher while the reduction with 2-butylamine is quenched. On the basis of these observations, the authors suggested that an ion-pair intermediate was not involved in the photoreduction of amines with high ionization potential.

In one instance, it was reported that quenching of a triplet aromatic ketone by tertiary amine did not occur by electron transfer. By indirect quenching method, Wagner and Kemppainen (5) studied the quenching of valerophenone triplet by triethylamine and dimethyl-*t*-butylamine in benzene, acetonitrile, and methanol. The rate constants reported for quenching by the amines were $\sim3\times10^9$ M^{-1} s^{-1} in benzene and in acetonitrile. The values obtained in methanol, however, were roughly a factor of 5 lower. The results were interpreted by these authors as indicating the absence of electron transfer in the quenching step.

In our experiments, we have measured the rate constants for quenching of triplet acetone by the tertiary amines *N,N*-dimethylaniline (E_I 7.14 eV) and triethylamine (E_I 7.50 eV) in solvents ranging in dielectric constants from aqueous solution (ε 80) to *n*-hexane (ε 1.9). For comparison, quenching data were also obtained for the primary amines, *n*-hexylamine (E_I 8.71 eV) and *t*-butylamine (E_I 8.64 eV). Evidence for the occurrence of hydrogen atom transfer in these reactions has been obtained by flash absorption studies (6). From our results, we will draw some general conclusions regarding (*1*) the plausibility of forming free ions, charge-transfer complex, or ion-pair from direct electron transfer, (*2*) the validity of using solvent dielectric constant as a criterion for electron transfer reaction, and (*3*) the role of amine ionization potential on quenching rate.

Results and Discussion

The results recorded in Table 1 show that the rate constants for quenching of acetone triplet by a given amine are, within experimental errors, identical in all of the solvents studied. However, the rate constants are dependent on the ionization potential, E_I, of the amine. With the exception of *n*-hexylamines, a linear correlation was obtained (Fig. 1) on plotting log k_q against E_I.

Apart from direct hydrogen atom transfer to the excited carbonyl group (8), quenching by amines can be described by the following sequence of steps

$$\begin{array}{ccccc} & \mathrm{I} & & \mathrm{II} & \\ \mathrm{A}^* + \mathrm{B} & \underset{k_{-1}}{\overset{k_1}{\rightleftharpoons}} & [\mathrm{A}^*\mathrm{B} \leftrightarrow \mathrm{AB}^* \leftrightarrow \mathrm{A}^-\mathrm{B}^+] & \xrightarrow{k_2} & \mathrm{A}^- + \mathrm{B}^+ \\ \downarrow k_d & & \text{complex} \downarrow k_{d'} & & \end{array}$$

A* is the triplet ketone, and B, the amine.

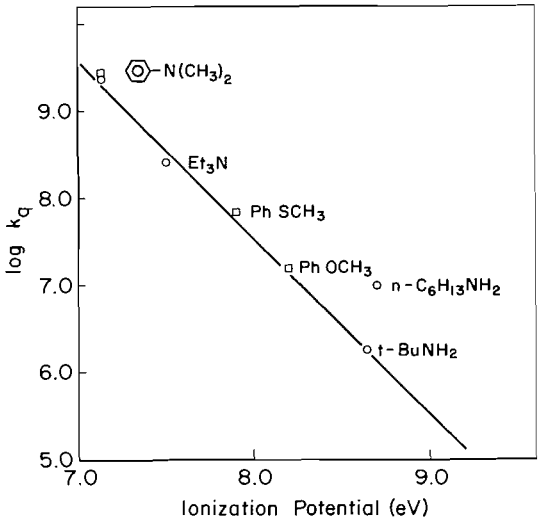

FIG. 1. Correlation between the ionization potential of the quencher and the rate constant for quenching of triplet acetone. ●, this work; □, ref. 3*d*.

A^-B^+ represents the charge-transfer (CT) states of the complex. A*B and AB* are locally excited states of A and B. In step I, A* and B are brought together with an encounter rate constant k_1, and may reversibly dissociate with a value k_{-1}. The rate constants k_d and $k_{d'}$ represent deactivation by all processes of A*, and the complex, respectively. One of these processes would be dissociation of the complex to form A + B*. This is a distinct possibility, but would appear to be excluded from the independence of k_q on solvent viscosity (water, $\eta = 1$ cP; *n*-hexane, $\eta = 0.34$ cP) and from the yield of radical (6). In step II, charge separation to form the free ions (*i.e.*, ions free from the Coulomb field of the countercharge) occurs. The reverse process, k_{-2}, will in general, not occur because of unfavorable energetics.

We do not consider the direct formation of free ions by electron transfer probable except in aqueous solution for reasons which we will describe. If we make the reasonable assumption that electron transfer occurs by an exchange mechanism such as that operative for triplet–triplet transfer, and for the annihilation of two triplet states, then we can expect relatively short-ranged interaction. For instance, the distance of interaction in the latter case is of the order of 9 Å for two phenanthrene triplets (9), while Weller finds 7 Å to be the distance separating the amine and aromatic molecules in the CT complex formed by electron transfer from amine to the singlet excited aromatic molecules (10*a*). However, to form free ions requires that the counter-charges be separated by a distance equal to $R_c > e^2/\varepsilon RT$. For instance in *n*-hexane (ε 1.9), acetonitrile (ε 37), and water (ε 80), $R_c \sim 300$, 15, 7 Å, respectively. It is abundantly clear that for encounter distances of the order of molecular diameter involved in the exchange mechanism, charges formed are still well within the Coulombic field of their countercharge, except in solvents with the highest dielectric constants such as water. We therefore feel that the earlier suggestion by Cohen and Cohen (2*a*) and Davidson and co-workers (3) of ion formation as the process responsible for quenching of the triplet carbonyl excited state unlikely. On the other hand, the formation of a CT complex which has been suggested by Cohen and co-workers (2*c*–2*i*) and Wagner and Kemppainen (5) appears to be reasonable providing certain energetic requirements, which we will discuss later, are met. It should be stressed that to the extent that A^-B^+ contributes to the complex, the encounter process (I) can be legitimately described as an electron transfer process. From this point of view, differences between the interpretations of Wagner and Kemppainen (5) and Cohen and co-workers' later works (2*c*–2*i*) would appear to be more semantic then real.

It would be most useful to estimate if the formation of A^-B^+ in the equilibrium reaction I is favored on thermodynamic grounds or not. Nernst's equation relates the free energy ΔF to the e.m.f. E^0 generated for two coupled half cells according to $\Delta F = -zFE^0$, where F is Faraday's constant, and z, the charge, which is equal to one in our case. If ΔF is expressed in eV and the e.m.f. in V, then F is unity ($F = 1$ eV/V). If for reaction I, we add to E^0 a coulomb energy term $e^2/\varepsilon a$ (where a = the distance between A^- and B^+ in the complex) and the triplet energy E_T, then we obtain an equation which is essentially identical to that previously derived by Weller and co-workers (10).

$$[1] \qquad -\Delta F = E^0 + E_T + \frac{e^2}{\varepsilon a}$$

Can. J. Chem. Downloaded from www.nrcresearchpress.com by 210.87.254.105 on 09/05/12
For personal use only.

TABLE 2. Thermodynamics for the process* $A + B \rightleftharpoons A^- + B^+$

A	$E(A^-/A)$† (V)	E^0 (eV)	E_T (eV)	$-\Delta F$ (eV)
Acetone	−2.305	−3.085	3.38‡	0.37
Acetophenone	−2.12	−2.90	3.21§	0.39
Benzaldehyde	−1.95	−2.73	3.12§	0.43
Benzophenone	−1.84	−2.62	2.99§	0.44

*In acetonitrile. $E(B/B^+)$ for dimethylaniline is equal 0.78 V *vs.* s.c.e. (ref. 4). We assume $e^2/\varepsilon a = 0.07$ eV. ΔF calculated using eq. 1.
†Reference 16, *vs.* s.c.e. in acetonitrile.
‡Reference 11. We have assumed the lower value (11*b*) of the two references.
§Reference 18.

where

$$E^0 = E(A^-/A) - E(B/B^+)$$

The calculated values of $-\Delta F$ recorded in Table 2 indicate that the electron transfer process involving the tertiary amine *N,N*-dimethylaniline is thermodynamically favorable for acetone, and for the aromatic ketones listed. Differences in the calculated ΔF values between acetone and the aromatic ketones are of the order of the uncertainty in the triplet energy of acetone (78–80 kcal mol^{-1} (11)), and is therefore not necessarily significant in the absence of further supporting data. However, the significantly lower rate constant (by an order of magnitude) for quenching of triplet acetone by triethylamine than those reported for triplet benzophenone (2*h*) and valerophenone (5) is consistent with a lower $-\Delta F$ for electron transfer to triplet acetone than for the aromatic ketones.

We now enquire into the role of solvent dielectric constant and amine ionization potential on the quenching rate constant. In terms of the mechanism which we have described, the rate constant for quenching depends on a competition of rate processes.

$$k_q = k_1(1 - \alpha) \quad \text{where} \quad \alpha = \frac{k_{-1}}{k_{-1} + k_2 + k_{d'}}$$

The lower the energy of the CT complex with respect to A* and B, the higher the activation energy for k_{-1}, and therefore k_q will tend to approach the encounter rate constant k_1 ($= 2 \times 10^{10}\ M^{-1}\ s^{-1}$ for acetonitrile solution). Those amines with small $E(B/B^+)$ or low ionization potential (*i.e.*, tertiary amines) can therefore be expected to quench more efficiently than primary amines. Our results (Table 1) are in agreement with this expectation. Despite the large $-\Delta F$ for electron transfer from *N,N*-dimethylaniline to triplet acetone, the value for k_q which we have obtained is less than k_1 by an order of magnitude. This suggests that k_{-1} is not negligible compared to $k_{d'}$ and k_2. Thus far in our discussion of k_q, solvent dielectric constant plays no explicit role. There is, however, one case where ε could affect k_q in an obvious way. If formation of the free ions $A^- + B^+$ were energetically favorable in water, for instance, then we could expect k_2 to be sufficiently large ($6 \times 10^9\ s^{-1}$ (10*b*)) to result in an α being small compared to unity. Under these circumstances, k_q assumes a maximum value of k_1, the diffusion-controlled encounter rate constant. In a solvent with a low ε, the formation of free ions will not be energetically possible. In this case, k_q will be reduced by the factor $(1 - \alpha)$ over the diffusion-controlled rate. But *the absence of a dielectric constant effect on k_q cannot be considered sufficient proof for ruling out the occurrence of electron transfer in a reaction.*

The plausibility of free ion formation in aqueous solution implies that aqueous solution photolysis could differ from those in other solvents. Cohen *et al.* (2*c*) has reported that the photoreduction of aryl ketones by tertiary amines is clean in aqueous but not in non-aqueous solution. The observations could be interpreted that step I and step II are very fast and that there are no side reactions corresponding to k_d and $k_{d'}$. In other words, the complex is a very short-lived species in water.

In the preceding discussion, we have discussed the relationship between k_q and ΔF and had implicitly assumed in our qualitative dis-

Can. J. Chem. Downloaded from www.nrcresearchpress.com by 210.87.254.105 on 09/05/12
For personal use only.

Can. J. Chem. Downloaded from www.nrcresearchpress.com by 210.87.254.105 on 09/05/12
For personal use only.

cussion that the ionization potential of the amine E_I is related to the oxidation potential $E^{ox}_{1/2}$. It can be shown that E_I and $E^{ox}_{1/2}$ are in fact related (12) according to

$$[2] \qquad E^{ox}_{1/2} = E_I + \Delta E_{solv} - C$$

where C is a constant and ΔE_{solv} is the difference in the solvation energies between the ion and neutral molecule. Hence, in order to correlate E_I with $E^{ox}_{1/2}$, we must either know ΔE_{solv} or that it is constant in a given series of compounds. However, the experimental fact that a reasonably good correlation between k_q and E_I was obtained (Fig. 1), independent of the structure of B, suggests the difference in the solvation energy term is small in comparison with differences in ionization potentials in affecting the free energy of the reaction. It should also be pointed out, that as the reaction becomes progressively more endothermic (*i.e.*, as the ionization potential of the amine becomes larger), charge transfer becomes less probable and the possibility of other competing processes intervening in the overall quenching process becomes more likely. We should therefore not be surprised to find that the correlation between $-\Delta F$ (or E_I) and k_q is less than perfect for grossly endothermic CT reactions such as those involving the primary amines.[3]

The deviation in the correlation between k_q and E_I observed for the primary amines (Fig. 1) can either be interpreted in terms of an enhanced k_q for *n*-hexylamine or a reduced rate for *t*-butylamine possibly for steric reasons. If we examine the question more carefully, it can be seen that triethylamine is even more sterically hindered than *t*-butylamine and yet the former amine shows a much larger k_q than *t*-butylamine. Furthermore, the E_I values of both compounds do not deviate from the correlation between E_I *vs.* σ_I or σ^*, indicating the absence of abnormality such as steric effects (14). We therefore believe that k_q for *t*-butylamine is not low but that k_q for *n*-hexylamine is high. The increased reactivity of *n*-hexylamine can be attributed to direct hydrogen atom transfer in addition to complex formation. This supposition was supported by measuring the rate of formation of the $CH_3\dot{C}OHCH_3$ radical (6). Due to scattered light, the measurements were not as accurate as might be desired. However, the value which we obtained for *n*-hexylamine, $(2 \pm 1) \times 10^7\ M^{-1}\ s^{-1}$ was identical with the quenching rate of triplet acetone. It should be noted that because of the stronger C—H bond energies possessed by the primary hydrogens in *t*-butylamine, hydrogen abstraction does not play a significant role in the overall quenching of the triplet ketone. Quenching rate constants which we have obtained for *t*-butyl alcohol and hexamethylethane (both containing primary C—H) (15) are in complete accord with these arguments.

[3]An approximate calculation for *n*-hexylamine shows that ΔF is positive by ~ 0.4 eV ($E^{ox}_{1/2} \simeq +1.5$V *vs.* s.c.f. in acetonitrile as estimated from a correlation between $E^{ox}_{1/2}$ and E_I (13)).

Experimental

Materials

The acetone (spectroscopic grade) used was obtained from Baker Chemicals. Acetonitrile was obtained from Matheson, Coleman and Bell (spectroscopic grade) and was used as received.

n-Hexylamine was obtained from Eastman and was fractionally distilled under reduced pressure. *t*-Butylamine (Eastman Organic Chemicals) was dried over anhydrous calcium chloride and then distilled (under nitrogen atmosphere) from sodium metal. The fraction that boiled at 43 °C was collected. Triethylamine (Aldrich) was distilled under nitrogen from acetic anhydride. The distillate was dried over activated alumina and redistilled three times (b.p. 89 °C). Freshly purified sample has to be prepared just before use since triethylamine oxidized rapidly with the color of the solution changing red. *N,N*-dimethylaniline (B.D.H., AR) was distilled under reduced pressure before use. *n*-Hexane Fisher (spectroscopic grade) was passed through activated silica gel and dried over molecular sieves.

Sample Preparation

Acetone–amine samples were prepared by weighing the appropriate amount of amine with 0.05 *M* acetone in 50 ml volumetric flask. From that solution 30 ml was pipetted into the cells (10 cm path length, cylindrical quartz cells). The quartz cell was joined through graded seal glass to a degassing vessel. The solutions were degassed by the freeze–pump–thaw cycles for four successive cycles. The solution was then transferred to the cell and the sample cell was sealed.

Apparatus

Two apparatus were used to measure the rate constants for quenching of triplet acetone by amines. In relatively inert solvents (water, acetonitrile, and *t*-butanol), a capacitor discharge flash emission apparatus was used as previously described (1). In *n*-hexane solutions, quenching of triplet acetone by hydrogen abstraction from solvent required an apparatus with shorter time resolution than that used for the other solvents. For these studies, a 30 ns pulse at 265 nm from a Q-switched, amplified neodymium-doped glass

laser was used. The amplified laser system consisted of a 1/2 in. × 6 in. oscillator rod, a beam expanding telescope and a 3/4 in. × 14 in. amplifier rod. The laser was operated so as to produce 6 J of energies at 1.06 μ. Second and fourth harmonic frequencies were generated using a KDP and an ADP crystal, respectively. The flash absorption apparatus was essentially the same as previously described (7).

We wish to thank Dr. Willem Siebrand for useful discussion, Dr. Raouf O. Loutfy for generously making available to us reduction potentials for the ketones, and Mr. S. E. Sugamori for his continuing and invaluable assistance in laser instrumentation.

1. G. PORTER, R. W. YIP, J. M. DUNSTON, A. J. CESSNA, and S. E. SUGAMORI. Trans. Faraday Soc. **67**, 3149 (1971).
2. (*a*) S. G. COHEN and J. E. COHEN. J. Am. Chem. Soc. **89**, 164 (1967); (*b*) S. G. COHEN and R. J. BAUMGARTEN. J. Am. Chem. Soc. **89**, 3741 (1967); (*c*) S. G. COHEN, N. STEIN, and H. M. CHAO. J. Am. Chem. Soc. **90**, 521 (1968); (*d*) S. G. COHEN and H. M. CHAO. J. Am. Chem. Soc. **90**, 165 (1968); (*e*) S. G. COHEN and J. E. COHEN. J. Phys. Chem. **72**, 3792 (1968); (*f*) S. G. COHEN and J. B. GUTTENPLAN. Tetrahedron Lett. 5353 (1968); (*g*) S. G. COHEN and N. STEIN. J. Am. Chem. Soc. **91**, 3690 (1969); (*h*) S. G. COHEN and A. D. LITT. Tetrahedron Lett. 837 (1970); (*i*) S. G. COHEN and G. PARSON. J. Am. Chem. Soc. **92**, 7603 (1970).
3. (*a*) R. S. DAVIDSON and P. F. LAMBETH. Chem. Commun. 1265 (1967); (*b*) R. S. DAVIDSON and P. F. LAMBETH. Chem. Commun. 511 (1968); (*c*) R. S. DAVIDSON and P. F. LAMBETH. Chem. Commun. 1098 (1969); (*d*) R. S. DAVIDSON and P. R. STEINER. Chem. Commun. 1115 (1971).
4. R. S. DAVIDSON, P. F. LAMBETH, J. F. MCKELLAR, P. H. TURNER, and R. WILSON. Chem. Commun. 732 (1969).
5. P. J. WAGNER and A. E. KEMPPAINEN. J. Am. Chem. Soc. **91**, 3085 (1969).
6. G. PORTER, R. O. LOUTFY, and R. W. YIP. Unpublished results.
7. R. W. YIP, W. D. RIDDELL, and A. G. SZABO. Can. J. Chem. **48**, 987 (1970).
8. R. W. YIP and W. SIEBRAND. Chem. Phys. Lett. **13**, 209 (1972).
9. (*a*) A. KAWADA and R. C. JARNAGIN. J. Chem. Phys. **44**, 1919 (1966); (*b*) L. P. GARY, K. DE GROOT, and R. C. JARNAGIN. J. Chem. Phys. **49**, 1577 (1968).
10. (*a*) A. WELLER. Nobel Symposium 5, Fast Reactions and Primary Processes in Chemical Kinetics. *Edited by* S. Claesson. Almqvist and Wiksell, Stockholm, 1967; (*b*) H. KNIBBE, D. REHM, and A. WELLER. Ber. Bunsenges. Phys. Chem. **72**, 257 (1968); (*c*) D. REHM and A. WELLER. Ber. Bunsenges. Physik. Chem. **73**, 834 (1969); **73**, 839 (1969); (*d*) D. REHM and A. WELLER. Israel J. Chem. **8**, 259 (1970); (*e*) H. BEENS and A. WELLER. Molecular luminescence. *Edited by* E. C. Lim. Benjamin, New York. 1969. p. 203.
11. (*a*) R. F. BORKMAN and D. R. KEARNS. J. Chem. Phys. **44**, 945 (1966); (*b*) R. B. CUNDALL and A. S. DAVIES. *In* Progress reaction kinetics, vol. 4. Pergamon Press, Oxford. 1967.
12. M. E. PEOVER. Electroanalytical chemistry. Vol. II. *Edited by* A. J. Bard, Dekker, New York. 1967.
13. L. L. MILLER, G. D. NORDBLOM, and E. A. MAYED. J. Org. Chem. **37**, 916 (1972).
14. L. S. LEVITT and B. W. LEVITT. Israel J. Chem. **9**, 71 (1971).
15. G. PORTER, R. W. YIP, and S. E. SUGAMORI. Unpublished results.
16. RAOUF O. LOUTFY and RAFIK O. LOUTFY. J. Phys. Chem. In press.
17. K. WATANABE, T. NAKAYAMA, and J. MOTTL. J. Quant. Spectrosc. Radiative Transfer, **2**, 369 (1962).
18. J. G. CALVERT and J. N. PITTS. Photochemistry. J. Wiley, New York. 1966.

Can. J. Chem. Downloaded from www.nrcresearchpress.com by 210.87.254.105 on 09/05/12
For personal use only.

Oxidations with Potassium *trans*-1,2-Diaminocyclohexanetetraacetatomanganate-(III). I. Composition of the Complex and the Reaction with Methanol[1]

BO LONG POH AND ROSS STEWART

Department of Chemistry, The University of British Columbia, Vancouver 8, British Columbia

Received May 17, 1972

The complex of manganese(III) with *trans*-1,2-diaminocyclohexanetetraacetic acid has been shown to exist as the crystalline monohydrate, $KMn^{III}CyDTA(H_2O)$, where CyDTA represents the ligand *trans*-1,2-diaminocyclohexanetetraacetate.

In aqueous methanol (2.5% water v/v) three forms of the complex exist: $Mn^{III}CyDTA(H_2O)^-$ in neutral solution, $Mn^{III}CyDTA(OH)^{2-}$ in base, and $HMnCyDTA(H_2O)$ in acid. In basic methanol the complex decomposes by disproportionation following first-order kinetics. When the same solvent system contains acid the disappearance of Mn^{III} is first-order in complex and first-order in acid but in this case methanol is oxidized to formaldehyde.

The isotope effects observed in the oxidation of CH_3OD, CD_3OH, and CD_3OD are all small (1.25 or less). This together with the acid dependence indicates that the oxidation proceeds by rate-controlling electron abstraction from methanol by the protonated form of the complex, possibly via an intermediate in which one of the coordinating ligands is replaced by methanol.

Nous démontrons que le complexe de manganèse(III) avec l'acide *trans*-1,2-diaminocyclohexanetétraacétique existe sous forme cristalline monohydratée, $KMn^{III}CyDTA(H_2)$, où CyDTA représente le ligand *trans*-1,2-diaminocyclohexanetétraacétate.

En milieu méthanol aqueux (2.5% H_2O v/v), il existe trois formes du complexe: $Mn^{III}CyDTA(H_2O)^-$ en solution neutre, $Mn^{III}CyDTA(OH)^{2-}$ en solution basique et $HMnCyDTA(H_2O)$ en solution acide. Le complexe se décompose dans le méthanol basique par disproportionnation, selon une cinétique de premier ordre. Lorsque le même système de solvant contient de l'acide Mn^{III} disparaît selon un premier ordre en complexe et un premier ordre en acide, mais dans ce cas, le méthanol est oxydé en formaldéhyde.

Tous les effets isotopiques observés au cours de l'oxydation de CH_3OD, CD_3OH et CD_3OD sont petits (1.25 ou moins). Ceci, combiné avec la dépendance de l'acide, indique que l'oxydation se déroule au moyen d'une abstraction d'électron du méthanol par la forme protonée du complexe, procédé qui contrôle la vitesse, possiblement au moyen d'un intermédiaire dans lequel un des ligands coordonnés serait remplacé par le méthanol. [Traduit par le journal]

Canadian Journal of Chemistry, **50**, 3432 (1972)

Introduction

In 1967 Hamm and Suwyn (1) prepared a complex of manganese(III) with *trans*-1,2-diaminocyclohexanetetraacetic acid to which they assigned the formula $KMn^{III}CyDTA\text{-}(2.5H_2O)$ on the basis of elemental analysis (CyDTA is used as an abbreviation for the *trans*-1,2-diaminocyclohexanetetraacetic acid anion ligand). They found that this complex was stable at room temperature when it was stored in the dark, and that it existed in two forms in solution. In acidic solution, a pink species with a formula believed to be $Mn^{III}CyDTA(H_2O)^-$ predominated, and under basic conditions, the predominant species was yellow in color with a formula believed to be $Mn^{III}CyDTA(OH)^{2-}$.

Manganese(III) is an exclusively one-equivalent oxidant of considerable strength but the value of the uncomplexed ion is impaired by its instability in any but the most acidic systems (2,3). The stability of $Mn^{III}CyDTA$ over a wide p*H* range induced us to use this ion in our study of the factors affecting the oxidation of hindered phenols. The latter is the subject of the accompanying paper; herein we report the results of our study of the composition of the oxidant and its reaction with aqueous methanol, the latter being the medium used in the phenol oxidation studies.

[1]Taken in part from the Ph.D. Thesis of Bo Long Poh, 1972.

Results and Discussion

Composition of Crystalline $KMn^{III}CyDTA$

Hamm and Suwyn (1) assigned the formula $KMn^{III}CyDTA(2.5H_2O)$ to the complex they prepared, on the basis of elemental analysis. We prepared our complex in the same way as Hamm

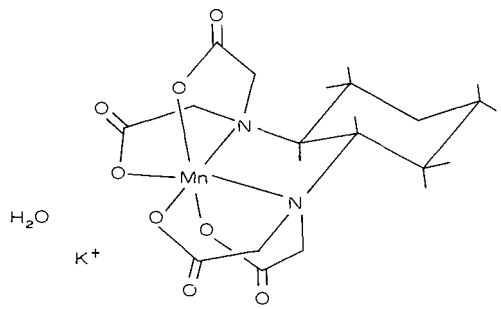

FIG. 1. Structure of potassium *trans*-1,2-diaminocyclohexanetetraacetatomanganate(III).

and Suwyn and recrystallized the crude sample (melting or decomposition point about 170°) from hot methanol–water to a m.p. of 201–203°. Karl Fischer titrations were conducted on crude and recrystallized samples of the complex. When the titrations were carried out as soon as possible after introduction of the samples the percentage of water in the two cases was found to be 6.6 and 0.6%, corresponding to 1.7 and 0.15 mol of water, respectively. It is clear that in the pure complex there is very little, if any, water that is loosely bound. After a sample of the recrystallized complex was kept in anhydrous methanol in the titration vessel for 30 min water was released corresponding to 4.0% of the weight of the complex, that is 1.0 mol of water per mole of complex. It is not certain whether a methanol molecule replaces the water molecule in the Mn^{III} complex or whether the water is released as a result of the slow decomposition of the Mn^{III} complex in the Karl Fischer reagent mixture.

Elemental analysis of the pure complex is in good agreement with the mono-aquo formula (see Experimental section) as are the results of an X-ray crystallographic study conducted by Rettig and Trotter of this department. Their structure indicates a slightly distorted octahedron of Mn^{III}; the cyclohexane ring is in a chair conformation with the two nitrogen atoms attached to the cyclohexane ring in a *trans*-diequatorial conformation (Fig. 1).

The position of the water molecule seems to vary. The major position is at a distance of 3.68 ± 0.02 Å from the Mn^{III} ion and the other position is 4.55 ± 0.02 Å from the Mn^{III} ion. These two values are much longer than a normal metal–water bond (about 2.1 Å), suggesting that the Mn^{III} ion is six-coordinated. However, the results of the Karl Fischer titrations indicate that this water molecule is bound sufficiently tightly to the manganese to remain coordinated even in solution.

The fact that the mono-aquo complex is obtained pure by recrystallization from 60% methanol and 40% water mixed solvent suggests that water is the preferred ligand. Attempts to determine the equilibrium concentration of water and methanol in the complex in the presence of 97% methanol – 3% water (the mixture used in the kinetic studies) failed. Flash evaporation of such solutions produced a solid residue which was partly decomposed and gave variable amounts of water. Throughout this article the complex will be shown containing water as the ligand.

Spectrum of the Mn^{III} Complex in Methanol (2.5% Water v/v)

The pK_a value for the equilibrium in water between the pink and yellow species of the complex was determined by Hamm and Suwyn to be 8.1.

$$\underset{\text{(pink)}}{Mn^{III}CyDTA(H_2O)^-} \overset{K_a}{\rightleftharpoons} H^+ + \underset{\text{(yellow)}}{Mn^{III}CyDTA(OH)^{2-}}$$

In methanol a similar equilibrium exists. In the absence of base, the pink species $Mn^{III}CyDTA(H_2O)^-$ predominates (absorption maximum at 510 nm). When base is added the pink color immediately changes to yellow owing to the formation of $Mn^{III}CyDTA(OH)^{2-}$ (absorption maximum at 466 nm). When acid is added to the yellow solution the color reverts back to pink immediately. We find that another form of the complex exists in methanol in the presence of an excess of acid (Fig. 2). This third species is also pink in color but its visible spectrum shows it to be different from the other two species. Its absorption maximum in the visible is at 520 nm. Addition of excess base immediately changes this species to the yellow species, and when acid is added to the resulting yellow solution, the pink color appears immediately. This third species is probably a protonated form of the Mn^{III} complex with formula $HMn^{III}CyDTA(H_2O)$. (Kinetic evidence presented in this and the accompanying paper (4) indicates the presence of such a protonated form.) Protonation probably occurs

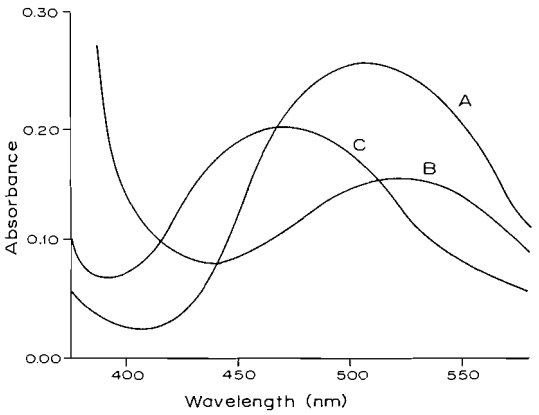

FIG. 2. Visible spectrum of a 6×10^{-4} *M* solution of $KMn^{III}CyDTA(H_2O)$ in methanol containing 2.5% water (v/v); cell width 1 cm. *A*, no acid or base added; *B*, 6.1×10^{-2} *M* in hydrochloric acid; *C*, 1.8×10^{-2} *M* in tetramethylammonium hydroxide.

at a carboxylate arm of the ligand which becomes free from coordination with the Mn^{III} ion. (The following compounds all have a free, protonated, carboxylate arm: $Cr^{III}YH(H_2O)$; $Fe^{III}YH(H_2O)$; $Ga^{III}YH(H_2O)$; $Ni^{III}YH(H_2O)$; where Y is ethylenediaminetetraacetic acid anion (5–8); in the unprotonated form, all these complexes have all the four carboxylate arms coordinated to the central metal ion.)

An attempt to measure the ionization constant of the protonated form of the Mn^{III} complex by spectrophotometry failed because of its rapid reaction with methanol.

No spectral change can be observed when acid is added to an *aqueous* solution of the Mn^{III} complex.

Decomposition of the Mn^{III} Complex in Methanol in the Presence of Base

Hamm and Suwyn reported that the Mn^{III} complex decomposes into manganese dioxide in water above p*H* 11. Similarly, in alkaline methanol the disappearance of the complex with time is due to decomposition, rather than to oxidation of methanol since only a trace of formaldehyde could be detected as a reaction product. Furthermore, when the reaction mixture at the completion of a reaction was oxidized by lead dioxide no spectrum due to the Mn^{III} complex could be obtained, thus indicating the Mn^{II} formed in the reaction mixture was not complexed to CyDTA ligands, unlike the situation in acid solution.

TABLE 1. Effect of base on the rate of decomposition of the manganese(III) complex in methanol at 25°*

Molarity of tetramethylammonium hydroxide	First-order decomposition rate (s^{-1})
0.71×10^{-2}	0.96×10^{-4}
0.90×10^{-2}	1.04×10^{-4}
1.43×10^{-2}	1.49×10^{-4}
1.78×10^{-2}	1.80×10^{-4}
2.65×10^{-2}	2.77×10^{-4}

*$[Mn^{III}]_0 = 5.4 \times 10^{-4}$ *M*.

The reaction has the following stoichiometry.

$$2Mn^{III} + 4OH^- \rightarrow Mn^{II} + MnO_2 + 2H_2O$$

The decomposition of the complex in methanolic base gave excellent first-order kinetics up to about 50% reaction. The reaction is also approximately first-order in base (Table 1). The activation parameters for the decomposition reaction are $\Delta H^* = 16.1 \pm 0.14$ kcal mol^{-1} and $\Delta S^* = -15.0 \pm 1.4$ e.u.

Reduction of the Mn^{III} Complex by Acidic Methanol

In neutral methanol the reduction of the complex is extremely slow. Addition of acid, however, results in reduction of the complex and oxidation of methanol. Three products, Mn^{II} complex, formaldehyde, and carbon dioxide, were identified, one mole of formaldehyde being produced for every 2 moles of the Mn^{III} complex used. Reaction of the Mn^{III} complex with methanol (solvent) was carried out with excess hydrochloric acid present. Plots of logarithm of the Mn^{III} absorbance *vs.* time are linear up to greater than 80% of the reaction, showing the reaction to be first order in Mn^{III}. An increase in the concentration of hydrochloric acid causes the rate to rise and then level off suggesting that the oxidant involved in the rate-determining step is the protonated species $HMn^{III}_{p^0}$. (The subscript p (for pink) identifies the color of the species and its superscript 0 (for zero) identifies the species' charge.)

The following reaction scheme is proposed to explain the kinetic results.

$$Mn^{III}_{p^-} + H^+ \underset{}{\overset{K_b}{\rightleftharpoons}} HMn^{III}_{p^0}$$

$$HMn^{III}_{p^0} + CH_3OH \xrightarrow{k} Mn^{II} + CH_3O\cdot$$

$$Mn^{III} + CH_3O\cdot \xrightarrow{\text{fast}} Mn^{II} + CH_2O$$

TABLE 2. Rates for oxidation of isotopic methanols at 25° $[Mn^{III}]_0 = 5.6 \times 10^{-4}$ *M* [HCl] = [DCl] = 2.05×10^{-2} *M*

Experiment	Acid	Solvent	k' (s^{-1})
A	HCl	CH_3OH*	2.10×10^{-3}
B	DCl	CH_3OD†	2.20×10^{-3}
C	DCl	CD_3OD†	2.03×10^{-3}
D	HCl	CD_3OH*	1.68×10^{-3}

*Containing 2.5% H_2O v/v.
†Containing 2.5% D_2O v/v.

where $Mn_p^{III-} = Mn^{III}CyDTA(H_2O)^-$, $HMn_p^{III} = HMn^{III}CyDTA(H_2O)$.

The rate of disappearance of the Mn^{III} complex is given by eq. 1

$$[1] \quad -d[Mn^{III}]_{tot}/dt = 2k[HMn_{p0}^{III}][CH_3OH]$$

where

$$[Mn^{III}]_{tot} = [HMn_{p0}^{III}] + [Mn_p^{III-}]$$

and

$$[HMn_{p0}^{III}] + [Mn_p^{III-}] = K_b[H^+]$$

This leads to

$$[2] \quad -d[Mn^{III}]_{tot}/dt = k'[Mn^{III}]_{tot}$$

where

$$k' = 2kK_b[H^+][CH_3OH]/(1 + K_b[H^+])$$

Integration of eq. 2 gives the expression $\log [Mn^{III}]_{tot} = -k't/2.303$. The value of k' was obtained from the slopes of plots of the logarithms of the absorption of the complex at 520 nm against time. (Although both Mn_p^{III-} and HMn_{p0}^{III} absorb at this wavelength only the latter makes a significant contribution to the rate.)

Reactions of the Mn^{III} complex with methanol-d_4 (CD_3OD), methan-d_3-ol (CD_3OH), and methanol-O-*d* (CH_3OD) in the presence of deuterium chloride (hydrogen chloride was used for reaction with methan-d_3-ol) were carried out to obtain some information about the mechanism of the reaction between the Mn^{III} complex and methanol.

The values of the rate constant k' for the four isotopically distinct methanols are given in Table 2. It can be seen that the effect of deuterium substitution is small. Comparison of experiments A and D gives an isotope effect k_H/k_D of 1.25 whereas the analogous system (Experiments B and C) gives the somewhat smaller value of 1.08. Evidently a primary isotope effect is absent and the carbon–hydrogen bond in methanol is not being cleaved in the rate-controlling step. The effect of deuteration of the hydroxyl group and of the hydrochloric acid is somewhat harder to assess. A comparison of experiments A and B, and D and C, shows that the observed rate is raised somewhat by deuterium substitution of this sort. Although analysis of these data is complicated by, among other things, the uncertain effect of deuterium substitution on K_b, it is unlikely that such effects are sufficiently large to transform this small negative isotope effect into a positive effect of sufficient magnitude to correspond to rupture of the oxygen–hydrogen bond in the rate-controlling step.

TABLE 3. Effect of anion on rate of oxidation of methanol by Mn^{III} complex in acid solution at 25°*

$[HClO_4]$ 10^2 *M*	[HCl] 10^2 *M*	k' 10^3 s^{-1}
1.63	0	1.14
1.30	0.33	1.30
0.82	0.81	1.52
0.33	1.30	1.49
0	1.63	1.54

*$[Mn^{III}]_0 = 5.9 \times 10^{-4}$ *M*.

The mechanism suggested for the reaction in the presence of acid involves as the rate-controlling step the transfer of an electron from methanol to manganese(III) to produce, after proton loss, a radical $CH_3O\cdot$ (or $\cdot CH_2OH$), which undergoes further, rapid, oxidation by a second mole of oxidant to give formaldehyde. Analysis of the product mixture showed that 1 mol of formaldehyde was indeed produced for every 2 mol of the Mn^{III} complex consumed. This path is further substantiated by the kinetic results obtained for the oxidation of 2,4,6-tri-*t*-butylphenol with the Mn^{III} complex in methanol in the presence of acid (4). (Recently, Wells and Barnes (9) reported the results of a study of the oxidation of methanol by Mn^{III} ion in aqueous perchloric acid. They found that 1 mol of formaldehyde was produced for every 2 mol of Mn^{III} consumed.)

Carbon dioxide was also observed as one of the reaction products. It is probably formed by oxidation of the CyDTA ligands. This is a minor reaction compared with the oxidation of methanol by the Mn^{III} complex since at the conclusion of the reaction the Mn^{II} could be

oxidized back to more than half the original concentration of the Mn^{III} complex with lead dioxide, as shown by the mixture's visible spectrum.

A convenient path for the reaction might be ligand substitution (methanol for either water or carboxylate) with the electron transfer taking place within the complex, thus accounting for the small isotope effects observed. (Indeed, ligand substitution could even be rate-controlling.) The radical that is subsequently formed by proton loss could be either the methoxy radical $CH_3O\cdot$ of the hydroxymethyl radical $\cdot CH_2OH$. The latter is the more easily formed when hydrogen-atom abstraction from methanol occurs directly. However, proton loss from the hydroxyl group of a radical-cation such as CH_3OH^+ should occur with extreme ease and we accordingly write the intermediate radical as $CH_3O\cdot$ rather than as $\cdot CH_2OH$. The results in this and the accompanying paper, however, can equally well be accommodated by the latter species.

The effect of chloride ion on the reaction is rather small, as shown by two pieces of evidence. First, the spectrum of the Mn^{III} complex in methanol containing hydrochloric acid is identical to that in methanol containing an equivalent amount of perchloric acid. Secondly, the rate of oxidation of methanol by the Mn^{III} complex is not greatly affected by the replacement of hydrochloric acid by perchloric acid (Table 3).

The protonated form of the Mn^{III} complex, $HMn^{III}CyDTA(H_2O)$, is a much more powerful oxidant than $Mn^{III}CyDTA(H_2O)^-$. It is not certain whether the slow disappearance of the latter in methanol is due to oxidation of methanol or simply to decomposition of the complex. In the absence of acid the pseudo first-order rate constant in methanol is $2.24 \times 10^{-6}\ s^{-1}$ at 25°, close to the reported rate of decomposition of $Mn^{III}CyDTA(H_2O)^-$ in water, $6.8 \times 10^{-6}\ s^{-1}$ at 25° (1).

Experimental

Potassium *trans*-1,2-diaminocyclohexanetetraacetatomanganate(III) was prepared by the method of Hamm and Suwyn (1) and was purified by recrystallization from methanol–water; m.p. 201–203°. Elemental analysis indicates that this compound has one molecule of water per molecule of compound.

Anal. Calcd. for $KMnC_{14}H_{18}N_2O_8(H_2O)$: C, 37.00; H, 4.40; N, 6.17. Found: C, 36.98; H, 4.46; N, 6.0. (Anal. Calcd. for $KMnC_{14}H_{18}N_2O_8(2.5H_2O)$: C, 34.92; H, 4.78; N, 5.82.)

Spectrophotometry was used to monitor the disappearance of the Mn^{III} complex by following the disappearance of the visible absorption near 500 nm. A $6.92 \times 10^{-2}\ M$ stock solution of $KMn^{III}CyDTA(H_2O)$ in distilled water was prepared and stored under nitrogen in a wrapped vial equipped with a rubber seal. Transfers were made using syringes and all reactions conducted in a nitrogen atmosphere.

Carbon dioxide was detected using the sodium carbonate–phenolphthalein test (10). Formaldehyde was analyzed by the chromotropic acid method (11).

All rate constants and activation parameters were obtained by the method of least squares using a Hewlett–Packard calculator and plotter, model 9125 A. The listed errors in the activation parameters are standard variance estimates (12).

The financial support of the National Research Council of Canada is gratefully acknowledged. B.L.P. is grateful to the Canadian International Development Agency for a scholarship.

1. R. E. Hamm and M. A. Suwyn. Inorg. Chem. **6**, 139 (1967).
2. W. A. Waters and J. S. Littler. *In* Oxidation in organic chemistry. *Edited by* K. B. Wiberg. Academic Press. New York, N.Y. 1965.
3. R. Stewart. *In* Oxidation in organic chemistry. *Edited by* K. B. Wiberg. Academic Press. New York, N.Y. 1965.
4. R. Stewart and B. L. Poh. Can. J. Chem. This issue.
5. J. L. Hoard, G. S. Smith, and M. Lind. *In* Advances in the chemistry of the coordination compounds. *Edited by* S. Kirschner. The Macmillan Co., New York, N.Y. 1961. pp. 296–302.
6. J. L. Hoard, C. H. L. Kennard, and G. S. Smith. Inorg. Chem. **2**, 1316 (1963).
7. J. L. Lambert, C. E. Godsey, and L. M. Seitz. Inorg. Chem. **2**, 127 (1963).
8. G. S. Smith, and J. L. Hoard. J. Am. Chem. Soc. **81**, 556 (1959).
9. C. F. Wells and C. Barnes. J. Chem. Soc. A, 430 (1971).
10. A. I. Vogel. A textbook of macro and semi-micro inorganic qualitative analysis. 4th ed. Longman, 1964. p. 328.
11. C. E. Bricker and H. R. Johnson. Ind. Eng. Chem. Anal. Ed. **17**, 400 (1945); A. P. Allshuller, D. L. Miller, and S. F. Selva. Anal. Chem. **33**, 621 (1961).
12. D. V. Huntsberger. Elements of statistical inference. Allyn and Bacon, Boston. 1967. p. 262.

Oxidations with Potassium *trans*-1,2-Diaminocyclohexanetetraacetatomanganate(III). II. Reaction of the Complex with Hindered Phenols[1]

ROSS STEWART AND BO LONG POH

Department of Chemistry, The University of British Columbia, Vancouver 8, British Columbia

Received May 17, 1972

A series of 4-substituted-2,6-di-*t*-butylphenols has been oxidized with potassium *trans*-1,2-diaminocyclohexanetetraacetatomanganate(III) $KMn^{III}CyDTA(H_2O)$, in methanol containing 2.5% water by volume. Addition of either acid or base greatly accelerates the reaction, acid because it produces $HMn^{III}CyDTA(H_2O)$, and base because it produces both $Mn^{III}CyDTA(OH)^{2-}$ and the phenolate ion.

In acidic methanol $HMn^{III}CyDTA(H_2O)$ reacts with both methanol and the phenol leading to formation of both methoxy and aryloxy radicals. The latter are stable in some instances and in others undergo further reaction. The methoxy radicals produced by the concomitant oxidation of methanol are competed for by Mn^{III} and by phenol; formaldehyde and Mn^{II} being the products in the former case and methanol and aryloxy radicals in the latter case.

In basic methanol $Mn^{III}CyDTA(OH)^{2-}$ converts the hindered phenols to aryloxy radicals, some of which are stable and others of which undergo further reaction.

Isotope effects, k_H/k_D, between 5 and 6 are observed for the oxidation of the phenols in acidic or neutral CH_3OD. Smaller effects (less than 2) are observed in basic solution. Substituents have a large effect on the reaction only in basic solution. The ρ of 2.69 in base probably reflects the effect of substituents on the ionization of the phenol.

Une série de 2,6-di-*t*-butylphénols substitués en position 4 ont été oxydés au moyen du *trans*-1,2-diaminocyclohexanetétraacétatomanganate(III) de potassium, soit $KMn^{III}CyDTA(H_2O)$, dans du méthanol contenant 2.5% d'eau par volume. L'addition d'un acide ou d'une base accélère fortement la réaction: l'acide produit $HMn^{III}CyDTA(H_2O)$ et la base, $Mn^{III}CyDTA(OH)^{2-}$ et l'ion phénolate.

En milieu méthanol acide, $HMn^{III}CyDTA(H_2O)$ réagit à la fois avec le méthanol et le phénol pour former les radicaux méthoxy et aryloxy. Dans certains cas, ces derniers réagissent et dans d'autres cas ils sont stables. Mn^{III} et le phénol entrent en compétition pour réagir avec les radicaux méthoxy produits par l'oxydation du méthanol; la formaldéhyde et Mn^{II} sont les résultats de la première possibilité, le méthanol et les radicaux aryloxy, de la seconde.

En milieu méthanol basique, $Mn^{III}CyDTA(OH)^{2-}$ réagit sur les radicaux phénols gênés pour les transformer en radicaux aryloxy, dont quelques-uns sont stables et d'autres continuent à réagir.

On observe des effets isotopiques, k_H/k_D, entre 5 et 6 pour l'oxydation des phénols en milieu CH_3OD acide ou neutre. Des effets moins importants (moins de 2) apparaissent en milieu basique. Les substituants ont un effet important sur la réaction en solution basique seulement. Le ρ de 2.69 en milieu basique reflète probablement l'effet des substituants sur l'ionisation du phénol. [Traduit par le journal]

Canadian Journal of Chemistry, **50**, 3437 (1972)

Introduction

In the previous paper we reported the results of our studies on the composition and structure of potassium *trans*-1,2-diaminocyclohexanetetraacetatomanganate(III), $KMn^{III}CyDTA(H_2O)$, and its reaction with aqueous methanol (1). This paper reports the results of a study of the reaction of this complex with a series of hindered phenols in methanol containing 2.5% water by volume. Hindered phenols such as 2,4,6-tri-*t*-butylphenol (**1**) are useful substrates for oxidation studies because of their tendency to undergo clean one-equivalent oxidations to give stable aryloxy radicals (2–6).

The oxidants usually used to convert phenols to aryloxy radicals are alkaline ferricyanide (7) and lead dioxide (6). High yields are obtained with the former oxidant only when a large excess of reagent is used, and with the latter only when the reagent is high in active oxygen and when the solution is dilute in phenol. A further drawback to the use of lead dioxide in a kinetic study is its extremely low solubility.

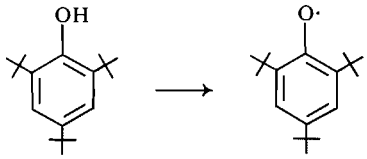

1 **2**

[1]Taken in part from the Ph.D. Thesis of Bo Long Poh, 1972.

Can. J. Chem. Downloaded from www.nrcresearchpress.com by 210.87.254.40 on 09/05/12
For personal use only.

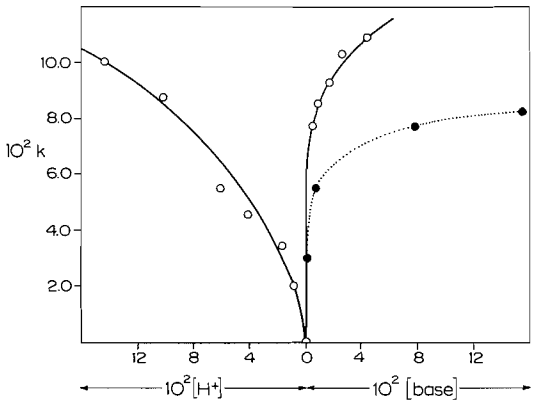

FIG. 1. Effect of added acid or base on the second-order rate of the reaction of $KMn^{III}CyDTA(H_2O)$ with 2,4,6-tri-*t*-butylphenol in methanol containing 2.5% water by volume, $T = 25°$; $[H^+]$ = molarity of hydrochloric acid, [base] = molarity of tetramethylammonium hydroxide (open circles) or *t*-butylamine (closed circles). The values of the rate plotted on the ordinate are the observed pseudo first-order rate constants divided by the concentration of phenol; $[Mn^{III}]_0 = 5.6 \times 10^{-4}$ *M*, $[ArOH]_0 = 2.5\text{–}5.1 \times 10^{-2}$ *M*.

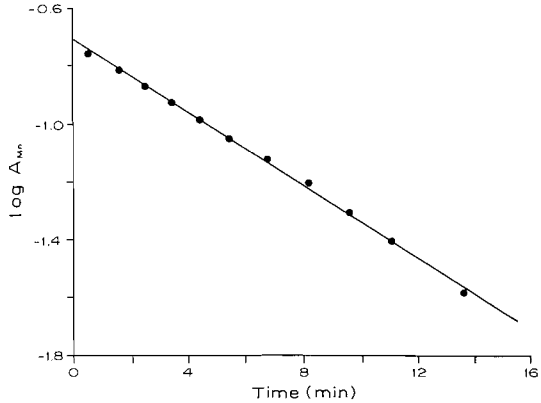

FIG. 2. Rate plot for disappearance of Mn^{III} complex in aqueous methanol containing an excess of 2,4,6-tri-*t*-butylphenol and base. $T = 25°$; $[Mn^{III}]_0 = 5.6 \times 10^{-4}$ *M*, $[ArOH]_0 = 2.52 \times 10^{-2}$ *M*, $[(CH_3)_4N^+OH^-]_0 = 1.78 \times 10^{-2}$ *M*.

We have used the one-equivalent reagent $KMn^{III}CyDTA(H_2O)$ as an oxidant for hindered phenols because this system enables us to follow the rate of the reaction in a homogeneous medium whose acidity can be easily varied. Among other things we hoped to learn was the effect of charge type of the oxidant and reductant on the rate of a reaction that takes place exclusively by one-equivalent paths. Charge type is known to be of importance in other oxidation–reduction systems (8).

Results and Discussion

The effect of acid or base on the rate of conversion of 2,4,6-tri-*t*-butylphenol (**1**) to 2,4,6-tri-*t*-butylphenoxyl (**2**) by the Mn^{III} complex is shown in Fig. 1. The addition of either acid or base causes drastic increases in the rate of the reaction. A quantitative conversion of phenol **1** to radical **2** was observed under all conditions as shown from the visible and e.s.r. spectra of the product.

In both acidic and basic systems the rate of disappearance of the Mn^{III} complex in the presence of excess phenol is first-order in Mn^{III} over several half-lives (Fig. 2). The other reactants, methanol, the phenol, and acid or base were always present in considerable excess and the rate of disappearance of Mn^{III} could be expressed as $-d[Mn^{III}]_{tot}/dt = k'[Mn^{III}]_{tot}$. When no acid or base is added the reaction is very slow and is first-order in Mn^{III} only after the first 7% or so of reaction has taken place, the initial reaction being the more rapid. Presumably this effect is due to the unbuffered nature of the system and the presence of a small amount of the more reactive oxidant Mn^{III}-$CyDTA(OH)^{2-}$. As the reaction proceeds acid is produced and eventually the equilibrium shown in eq. 1 lies far to the left.

$$[1] \qquad Mn_p^{III} \overset{K_a}{\rightleftharpoons} Mn_{y^2}^{III} + H^+$$

where $Mn_p^{III} = Mn^{III}CyDTA(H_2O)^-$, $Mn_{y^2}^{III} = Mn^{III}CyDTA(OH)^{2-}$, $HMn_{p^0}^{III} = HMn^{III}CyDTA(H_2O)$, ArOH = 2,4,6-tri-*t*-butylphenol (**1**).

The Reaction in Acidic Solution

Although doubling the concentration of Mn^{III} doubles the rate of reaction, doubling the concentration of phenol can either speed up or slow down the disappearance of Mn^{III}, depending on the concentrations of phenol that are used. These observations together with the observed activation by acid (Fig. 1) can be accounted for in the following way, where the protonated complex reacts initially with both methanol and the phenol.

$$[2] \qquad Mn_p^{III} + H^+ \overset{K_b}{\rightleftharpoons} HMn_{p^0}^{III}$$

Can. J. Chem. Downloaded from www.nrcresearchpress.com by 210.87.254.40 on 09/05/12
For personal use only.

Can. J. Chem. Downloaded from www.nrcresearchpress.com by 210.87.254.40 on 09/05/12
For personal use only.

[3] $HMn_{p^0}^{III} + CH_3OH \longrightarrow CH_3O\cdot + Mn^{II}$

[4] $HMn_{p^0}^{III} + ArOH \longrightarrow ArO\cdot + Mn^{II}$

[5] $CH_3O\cdot + Mn^{III} \xrightarrow{fast} CH_2O + Mn^{II}$

[6] $CH_3O\cdot + ArOH \xrightarrow{fast} CH_3OH + ArO\cdot$

Since the concentration of the Mn^{III} complex was much smaller than that of either methanol or the phenol, Mn^{III} should disappear at a first-order rate regardless of the relative rates of the steps in the competitive reactions 3 and 4, and 5 and 6. This was found to be so and the pseudo first-order rate constants, k', used to calculate the second-order rate constants shown in Fig. 1 were obtained experimentally from the relation $\log [Mn^{III}]_{tot} = -k't/2.303$ (see Fig. 2).

In the proposed mechanism 2,4,6-tri-*t*-butylphenol and the Mn^{III} complex compete for the methoxy radicals (or hydroxymethyl radicals (1)). If this is true, a plot of k' *vs.* the concentration of 2,4,6-tri-*t*-butylphenol should show a minimum at a certain concentration of the phenol. When the latter's concentration is at or near zero the methoxy radicals are essentially all oxidized to formaldehyde, eq. 5, thus reducing a second mole of manganese(III). Small amounts of added phenol intercept the methoxy radicals giving methanol and inert aryloxy radicals, eq. 6, and the reduction of manganese(III) is slowed. When the concentration of added phenol passes a certain value reaction 4 becomes dominant and the reaction rate then rises as a function of the phenol concentration. Figure 3 is a plot of observed rate against phenol concentration and it, indeed, has the expected shape.

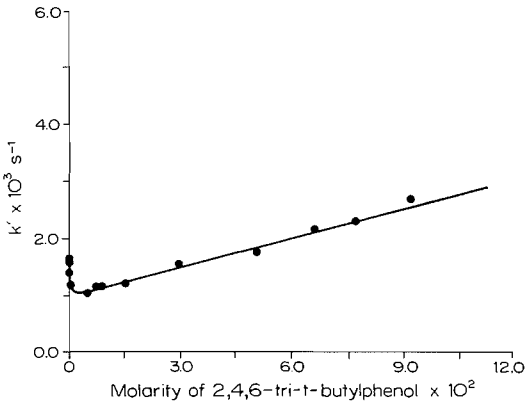

FIG. 3. Effect of changing the concentration of 2,4,6-tri-*t*-butylphenol on the rate of reduction of Mn^{III} complex in aqueous methanol containing acid. $T = 25°$; $[Mn^{III}]_0 = 5.6 \times 10^{-4}$ *M*, $[HCl] = 1.63 \times 10^{-2}$ *M*.

The Reaction in Basic Solution

The activation by base shown in Fig. 1 appears to have two causes: conversion of $Mn_{p^-}^{III}$ to the more active oxidant, $Mn_{y^{2-}}^{III}$, and conversion of the neutral phenol to the more active reductant, the phenoxide ion. The hindered phenol **1** is approximately four p*K* units weaker as an acid than is $Mn_{p^-}^{III}$ and it is possible to study the effect of the change in identity of the oxidant alone by conducting the reaction in the presence of a weak base. *t*-Butylamine was used for this purpose. Addition of small amounts of the amine greatly catalyze the oxidation reaction but the curve of rate *vs.* concentration begins to flatten out at concentrations of amine greater than about 10^{-2} *M* (Fig. 1), when the $Mn_{p^-}^{III}$ to $Mn_{y^{2-}}^{III}$ conversion is more than half complete. (The conversion of the phenol to phenoxide ion has occurred to the extent of less than 0.1% when the amine concentration is 10^{-2} *M*.) A similar effect occurs with added hydroxide ion but there is a much greater conversion of phenol to phenoxide ion and the observed reaction is correspondingly faster (Fig. 1).

In basic solution the reaction could be monitored by following the increase in absorption due to **2** at 400 nm, in addition to following the decrease in absorbance of the manganese(III) complex. Fair agreement was obtained between the two methods, considering that in basic solution some decomposition of the complex accompanies the oxidation.

Kinetic Isotope Effect

In both neutral and acidic solution a substantial isotope effect is obtained when the oxidation of **1** is conducted in methanol-*d*. The values of k_H/k_D at 25° are 4.8 in acid solution (DCl used as acid) and 5.9 in neutral solution. In basic solution the isotope effects are much smaller; less than 2.0 in all cases. An exhaustive analysis of the results in basic solution does not seem worthwhile because of the difficulties encountered in making a meaningful partition of the small effect observed between several processes, *viz.*, decomposition of the complex, oxidation of the neutral phenol, oxidation of

TABLE 1. Effect of substituents on the oxidation of 4-substituted-2,6-di-*t*-butylphenols (Ar'OH) by Mn^{III} complex at 25°*

Substituent	Acidic conditions†	Neutral conditions	Basic conditions‡
OH	>20	—	—
t-Bu	3.4×10^{-2}	2.4×10^{-4}	8.5×10^{-2}
CH_3	7.2×10^{-2}	4.7×10^{-4}	3.2×10^{-1}
CH_2OH	5.4×10^{-2}	—	—
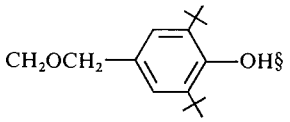	2.0×10^{-2}	—	—
$CH_2N(CH_3)_2$	4.1×10^{-2}‖	—	—
H	2.6×10^{-2}	6.2×10^{-4}	0.71
Cl	3.5×10^{-2}	—	—
Br	3.6×10^{-2}	6.0×10^{-4}	2.0
I	4.2×10^{-2}	5.8×10^{-4}	—
COC_6H_5	8.8×10^{-2}	2.5×10^{-4}	—
COOH	3.1×10^{-2}	—	—
$COOH_3$	10.3×10^{-2}	—	—
CN	6.2×10^{-2}	3.4×10^{-4}	—
CHO	5.0	69.0×10^{-4}	—

*All rates given are the observed pseudo first-order constants divided by the concentration of the particular phenol and are in units of M^{-1} s^{-1}; $[Mn^{III}] = 5.6\times10^{-4}$ *M*, $[Ar'OH] = 0.4\times10^{-2}$ *M* to 5×10^{-2} *M*.
†$[HCl] = 1.63\times10^{-2}$ *M*.
‡$[(CH_3)_4N^+OH^-] = 0.90\times10^{-2}$ *M*.
§Corrected for a statistical factor of 2.
‖The amino group is protonated.

the phenoxide ion, and dissociation of the phenol. The small size of the isotope effects is, however, consistent with electron abstraction from the phenoxide ion being the predominant reaction.

A reasonable route for the reaction of the manganese(III) complex with methanol was considered to be substitution of methanol for the water ligand in the complex followed by electron transfer to manganese and liberation of a methoxy (or hydroxymethyl) radical (1). We do not favor this route for the hindered phenols since their bulk is such as to make substitution difficult. Furthermore, the substantial isotope effect observed in acid solution with **1** (but not with methanol) suggests that abstraction of a hydrogen atom from neutral phenol by the neutral manganese(III) complex may be taking place. In basic solution this appears to be replaced by electron transfer from the phenoxide ion to the dianionic form of the complex as the principal reaction path.

Substituent Effects

The effect of different substituents in the 4-position of 2,6-di-*t*-butylphenols was examined under various conditions (Table 1). In neutral and acidic solution the effect of substituents is slight ($\rho = -0.07$ in neutral solution and $+0.39$ in acidic solution), a condition that is consistent with the transition state having radical character as a result of hydrogen-atom abstraction from the phenolic hydroxyl group. Two groups, —OH and —CHO, cause large deviations from the Hammett plots and in the case of hydroxyl this is due to its being oxidized directly. The formyl case is more difficult to understand. Benzaldehyde is oxidized only one-tenth as fast as is 2,6-di-*t*-butylphenol under the reaction conditions and a very large reaction constant (ρ) for aromatic aldehyde oxidation would be needed to account for direct oxidation of the formyl group in the case of the substituted compound. Furthermore, a substantial kinetic isotope effect ($k_H/k_D = 4.9$) was observed when the formyl compound was oxidized in CH_3OD containing DCl, indicating that attack takes place at the phenolic group.

In basic solution there is a large effect of substituents, consistent with the phenolate

Can. J. Chem. Downloaded from www.nrcresearchpress.com by 210.87.254.40 on 09/05/12
For personal use only.

TABLE 2. Products formed by oxidation of various hindered phenols by Mn^{III} complex

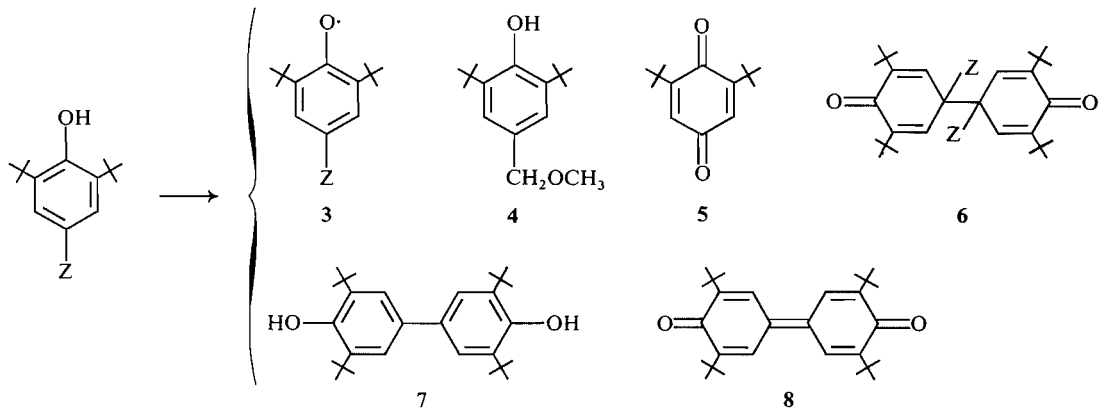

Reactant	Product	Reactant	Product
Z		Z	
$(CH_3)_3C$—	3	HO— —CH_2OCH_2—	4, 8
CH_3—C(=O)—	3	$(CH_3)_2NCH_2$—	7, 8
C_6H_5—C(=O)—	3	Cl—	6 (Z = Cl), 8
CH_3—	3*, 4†	Br—	6 (Z = Br), 8
NC—	3*	I—	8
HO—	5	HO_2C—	7, 8
$HOCH_2$—	7, 8	OHC—	7, 8
H—	7, 8		

*Neutral and basic conditions.
†Acidic conditions.

anion being the principal reactive entity. A value of 2.7 was found for the reaction constant ρ for four substituted phenols under conditions where **1** is only slightly ionized. With most electron-withdrawing substituents the reactions were too fast to measure. The high ρ is probably a reflection, principally, of the effect of substituents on the ionization step, which produces the more reactive reductants, the phenolate anions.

Reaction Products

The initial product of the reaction between the 4-substituted-2,6-di-*t*-butylphenols and Mn^{III} is believed to be the aryloxy radical **3**, and, indeed, in the case of five of the phenols the radicals are sufficiently stable for their e.s.r. spectra to be determined. In other cases further reaction takes place (see Table 2).

Experimental

Preparation of Compounds

The identity of each phenol was checked by examination of its n.m.r. spectrum and by the correspondence of its melting point with that reported in the literature. The following compounds were prepared by standard procedures (literature references in parentheses): 3,3′,5,5′-tetra-*t*-butyl-*p*-diphenoquinone, (**8**), m.p. 246–247°; bis-(1,3,5-tri-*t*-butyl-2,5-cyclohexadiene-4-one)peroxide (**9**), m.p. 148–149 (9); 3,5-di-*t*-butyl-4-hydroxybenzaldehyde[2] m.p. 189–190° (10); 2,6-di-*t*-butyl-4-bromophenol, m.p. 83–83.5° (11); 2,6-di-*t*-butyl-4-chlorophenol, m.p. 74–76° (11, 12); 2,6-di-*t*-butyl-4-iodophenol, m.p. 77–79° (11); 2,6-di-*t*-butyl-4-acetylphenol, m.p. 150–151° (13); 2,6-di-*t*-butyl-4-benzoylphenol, m.p. 124–124.5° (13); 2,6-di-*t*-butyl-4-hydroxyphenol, m.p. 103–104° (2); 2,6-di-*t*-butyl-4-cyanophenol, m.p. 145–146° (14). The other phenols were obtained from commercial sources.

[2]Since this compound reacted at an anomalously high rate it was subjected to a number of rigorous identity checks including elemental analysis.

Anal. Calcd. for $C_{15}H_{22}O_3$: C, 76.82; H, 9.39. Found: C, 76.86; H, 9.48.

Can. J. Chem. Downloaded from www.nrcresearchpress.com by 210.87.254.40 on 09/05/12
For personal use only.

Can. J. Chem. Downloaded from www.nrcresearchpress.com by 210.87.254.40 on 09/05/12
For personal use only.

Product Analysis and Rate Measurements

Radicals were identified by e.s.r. spectrometry using a Varian E-248-1 instrument. The ultraviolet and visible spectrum of non-radical products were compared with those obtained using authentic samples. The extinction coefficient of 3,3′,5,5′-tetra-*t*-butyl-*p*-diphenoquinone (**8**) in methanol was determined at various concentrations of solute and found to obey Beer's law very closely. The slope of the plot of absorbance at 419 nm against concentration gave a slope of 79 000 for the extinction coefficient. In a similar way the extinction coefficient of bis-(1,3,5-tri-*t*-butyl-2,5-cyclohexadiene-4-one)peroxide (**9**) was shown to be 22 010 at 240 nm in methanol, compared to the literature value of 25 800 at 240 nm in benzene (9).

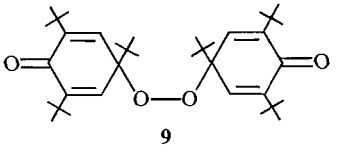

9

It is difficult to prepare a pure sample of 2,4,6-tri-*t*-butylphenoxyl (3) because of its reactivity towards oxygen. The method used here to determine its extinction coefficient avoids the difficult step of isolating a pure solid sample. It involves the generation of **2** from its phenol using lead dioxide as the oxidant, and determining its concentration from the amount of **9** that is formed. A 9.8 mg sample of **1** was mixed with 0.1 g of lead dioxide in a 2 ml centrifuge tube, which was sealed with a rubber cap and the contents flushed with nitrogen. A 1.5 ml aliquot of methanol (which had been flushed with nitrogen) was syringed into the tube through the rubber cap and the contents of the tube were shaken for 1 min. Then, the tube was centrifuged for 2 min, whereupon a clear blue solution of **2** appeared above the lead dioxide layer. A 0.025 ml aliquot of this clear blue solution was syringed into each of: (*a*) two 1 cm cells each containing 3 ml of oxygen-free methanol and capped with a silicon rubber disc, and (*b*) two test-tubes each containing 3 ml of methanol saturated with oxygen. Absorbance readings at 400 nm for **2** in the two oxygen-free cells were recorded. The solutions in the two test-tubes containing oxygen were left to stand for a few hours to ensure that all of **2** was converted to **9** and then the absorbance at 240 nm was recorded for each sample. Since the absorbance of 2,4,6-tri-*t*-butylphenol is at its minimum in this region any unreacted 2,4,6-tri-*t*-butylphenol would make a negligible contribution to the absorbance at 240 nm. Knowing the extinction coefficient of **9**, its concentration could be calculated, and doubling this concentration gives the concentration of **2** and hence the extinction coefficient, assuming that the same quantity of **2** was formed in the two sets of experiments. It was found that all duplicate samples gave results in good agreement with one another. This procedure was followed for three other quantities of 2,4,6-tri-*t*-butylphenol (up to 23.8 mg) with the weight of lead dioxide used being kept at 0.1 g. An average value of 1955 ± 66[3] was obtained for the extinction coefficient of **2** at 400 nm in methanol compared with the value of 2050 at 400 nm reported in benzene (15).

[3]The values calculated for the extinction coefficient of **2** at various initial concentrations of **1** are as follows: 1943 (2.07×10^{-4} *M*), 2049 (3.09×10^{-4} *M*), 1896 (4.03×10^{-4} *M*), 1933 (5.00×10^{-4} *M*). The extinction coefficient, thus, does not appear to be a function of concentration, indicating that Beer's law is obeyed for **2** and that no significant amount of dimerization occurs.

Reaction rates were determined by monitoring the disappearance of Mn^{III}, as previously described (1), and in the case of 2,4,6-tri-*t*-butylphenoxyl the appearance of the spectrum of the radical at 400 nm. All rate constants were obtained using least square calculations.

Effect of Specific Cations on the Oxidation Rate

It was observed that the rate of the oxidation reaction in basic solution varied with the identity of the cation that was used. Taking the rate for the reaction in the presence of tetramethylammonium hydroxide to be unity gives the following values for the relative rates in the presence of other bases: $(C_3H_7)_4NOH$ (1.5), $(n\text{-}C_4H_9)_4NOH$ (1.5), LiOH (1.7), NaOH (2.3), KOH (3.4). The effect of specific cations on oxidation rates has also been noted by other workers (16).

Reversibility of the Reaction

Although there was no indication that the radical-forming reaction studied herein was reversible we have observed that the corresponding reaction with ferricyanide is clearly so. Mixtures of **2** and acidic ferrocyanide produce considerable amounts of ferricyanide ion, which can be identified by its ultraviolet spectrum.

We thank the National Research Council of Canada for financial support and the Canadian International Development Agency for a scholarship support to B.L.P.

1. B. L. Poh and R. Stewart. Can. J. Chem. This issue.
2. C. D. Cook. J. Org. Chem. **18**, 261 (1953).
3. E. Müller and K. Ley. Chem. Ber. **88**, 601 (1955).
4. K. U. Ingold. Chem. Rev. **61**, 563 (1961).
5. W. A. Waters. J. Chem. Soc. (B), 2026 (1971).
6. M. L. Mihailovic and Z. Cekovic. *In* The chemistry of the hydroxyl group. Part 1. *Edited by* S. Patai. Interscience Publishers, Great Britain. 1971. Chapt. 10.
7. B. S. Thyagarajan. Chem. Rev. **58**, 439 (1958).
8. R. Stewart. Oxidation mechanisms. W. A. Benjamin Inc., New York, N.Y. 1964. pp. 60, 67–73.
9. C. D. Cook and R. C. Woodworth. J. Am. Chem. Soc. **75**, 6242 (1953).
10. G. M. Coppinger and T. W. Campbell. J. Am. Chem. Soc. **75**, 734 (1953); T. W. Campbell and G. M. Coppinger. J. Am. Chem. Soc. **74**, 1469 (1952).
11. K. Ley, E. Müller, R. Mayer, and K. Scheffler. Chem. Ber. **91**, 2670 (1958).
12. E. Müller, K. Ley, and W. Kiedaisch. Chem. Ber. **87**, 922, 1605 (1954).
13. C. D. Cook and N. D. Gilmour. J. Org. Chem. **25**, 1429 (1960); T. Matsuura, A. Nishinaga, and H. J. Cahnmann. J. Org. Chem. **27**, 3620 (1960).
14. L. A. Cohen. J. Org. Chem. **22**, 1333 (1957).
15. M. A. DaRooge and L. R. Mahoney. J. Org. Chem. **32**, 1 (1967).
16. M. Shposer, G. Ron, A. Lowenstein, and G. Navon. Inorg. Chem. **4**, 362 (1965); J. C. Sheppard and A. C. Wahl. J. Am. Chem. Soc. **79**, 1020 (1957); R. J. Ward and S. I. Weissman. J. Am. Chem. Soc. **79**, 2086 (1957).

The Infrared Spectrum of Ethylene Oxide Clathrate Hydrate between 360 and 20 cm^{-1}, at 100 °K

J. E. BERTIE AND D. A. OTHEN[1]

Department of Chemistry, University of Alberta, Edmonton 7, Alberta

Received January 11, 1972[2]

The infrared spectra of authenticated samples of ethylene oxide hydrate and deuterate at 100 °K have been measured between 360 and 20 cm^{-1}. The spectra confirm that the water molecules are orientationally-disordered and reorient slowly compared to far-infrared frequencies. An empirical correlation is suggested between the frequencies of strong absorption and the number of non-equivalent hydrogen bonds, their length and distribution. The contribution to the spectrum by the ethylene oxide intermolecular vibrations is discussed.

Les spectres infrarouges d'échantillons authentiques d'hydrate et de deutérate d'oxyde d'éthylène à 100 °K ont été mesurés entre 360 et 20 cm^{-1}. Les spectres confirment une orientation désordonnée des molécules d'eau se réorientant lentement lorsqu'on les compare aux fréquences de l'infrarouge lointain. Une corrélation empirique a été suggérée entre les fréquences de forte absorption et le nombre de liaisons hydrogène non-équivalentes, leur longueur et leur distribution. La contribution au spectre, de vibrations intermoléculaires de l'oxyde d'éthylène, est discutée. [Traduit par le journal]

Canadian Journal of Chemistry, **50**, 3443 (1972)

Introduction

Ethylene oxide hydrate (1, 2) has been studied by X-ray diffraction (2, 3), dielectric relaxation (4–7), and proton magnetic resonance (7–9) techniques. The variation of its stoichiometry with the parent-solution composition (10) and of its lattice dimensions with stoichiometry (11) have also been studied.

X-Ray studies (2, 3) have shown that the hydrate has the 12 Å cubic, Type I clathrate hydrate structure. The 46 water molecules per unit cell form six tetrakaidecahedral and two pentagonal dodecahedral cages, called large and small cages, respectively, hereafter. When the hydrate is formed under equilibrium conditions the large cages each contain one ethylene oxide molecule while the small cages have shown occupancies of 19 to 40%, corresponding to stoichiometries from $6.38\,C_2H_4O{\cdot}46H_2O$ to $6.80\,C_2H_4O{\cdot}46H_2O$ (3, 10). Flash frozen samples have formed (11) with the stoichiometry $1.1\,C_2H_4O{\cdot}46H_2O$ and a lattice parameter 0.4% smaller than for $6.8C_2H_4O{\cdot}46H_2O$. The ethylene oxide (guest) molecules are not hydrogen-bonded to the host, and the X-ray diffraction results showed that the guests in the large holes reorient between two preferred orientations (3). The specific orientations reported (3) have been questioned (12) as a result of calculations of the energy distribution in the cages. The water molecules are hydrogen-bonded with distorted-tetrahedral co-ordination and are orientationally-disordered (3).

Dielectric relaxation studies have shown that the water molecules reorient at about 1 Mc/s at 240 °K, but freeze into disordered orientations below about 140 °K (4). The guest molecules reorient at 6.6 Gc/s at 88 °K (5, 6) and 1 Kc/s at 28 °K (7). The mean activation energy for guest molecule reorientation between 28 and 88 °K is about 1.26 kcal/mol (7). The p.m.r. results (7–9) are consistent with those from the dielectric studies, and suggest that the molecules rotate isotropically above about 230 °K (7). These results do not appear to be consistent with the conclusions drawn from the X-ray analysis (3) concerning the number of preferred positions of the guest molecule in the large cages and the mode of reorientation between these positions, but suggest, as do the energy calculations (12), the existence of several preferred orientations with low energy barriers between them. No evidence exists for preferred positions of the guests in the small cages (3) and no evidence specifically indicates different reorientation behavior of guest molecules in the two types of cages (5–9), although a wide range of behavior does appear to occur (7).

[1]Present address: Atlantic Regional Laboratory, National Research Council of Canada, Halifax, Nova Scotia.

[2]Revision received July 25, 1972.

Can. J. Chem. Downloaded from www.nrcresearchpress.com by 210.87.254.5 on 09/05/12
For personal use only.

Can. J. Chem. Downloaded from www.nrcresearchpress.com by 210.87.254.5 on 09/05/12
For personal use only.

The present work has two aims. First, to observe the spectrum of the water molecules, to give further evidence on the factors influencing the far-infrared spectrum of condensed water. Second, to try to locate absorption due to the intermolecular vibrations of the guest molecules.

This guest-molecule absorption is predicted from theoretical considerations and its presence has been inferred from the dielectric constant studies (7). At 4 °K the dielectric constant at 1 Kc/s is 4.1 ± 0.3 (7), compared to 2.85 ± 0.1 for the isostructural hydrates of the non-dipolar guests argon (13), nitrogen (13), and cyclopropane (14). The orientation relaxation for both guest and host molecules occurs below 1 Kc/s at 4 °K, and does not contribute to the value of 4.1. Therefore the difference of 1.25 must arise from lattice vibrations of the ethylene oxide molecules, probably mainly rotational vibrations. At 100 °K the situation is less clear. The dielectric constant at 1 Kc/s is about 14 (7) and includes the contribution from the orientation polarization of the guest. Part of the orientation relaxation occurs at about 10 Gc/s at 100 °K (6) but the high-frequency limit is not known. It is reasonable to assume that this limit is about 10 cm^{-1}, in which case the absorption above 10 cm^{-1} must account for a low-frequency dielectric constant of about 4.1. Quite strong absorption by the guest molecules must occur in the far-infrared spectrum to account for this value, when the corresponding value for the same water structure but with a non-dipolar guest is about 2.85.

Experimental

Two techniques, based on the work of Wurtz (15), were used to prepare the hydrate. (*i*) Ethylene oxide (Matheson 99.7%, unpurified) was bubbled through 5 ml of distilled water at room temperature for 30 min. The solution was then left in a 5 ± 2 °C cold room in a stoppered flask. When crystallization was complete the crystals were quickly blotted free from mother liquor, in the cold room, and were cooled in liquid nitrogen. The samples were kept at about 100 °K from this point on, using techniques described previously (16). (*ii*) Distilled water (5 ml), in a pre-weighed flask, was outgassed in vacuum and re-weighed. Ethylene oxide, triply-distilled in vacuum from −80 °C and checked for purity by infrared spectroscopy, was condensed into the flask from a vacuum line, and the flask was closed and re-weighed. The procedure then followed that of method (*i*).

The hydrate was ground using a SPEX freezer mill, cooled with liquid nitrogen. The sample does not contact the coolant in this grinder and must be ground in short bursts with re-cooling time between bursts, to avoid excessive heating. One minute of grinding was followed by 5 min cooling times in this work. The ground powder was stored under liquid nitrogen in the inner of two glass bottles.

The ground samples were characterized by powder X-ray methods using techniques previously described (16). The sample temperature on the camera was 130 °K.

Infrared spectra were measured between 360 and 20 cm^{-1} using a Beckman-RIIC model FS 720 interferometer. Interferograms were run from $+x$ to $-x$ cm path difference and were transformed using sine and cosine Fourier transformation, the intensity being obtained from the square root of the sum of the squares of the two transforms. Step and Moiré (continuous) driving mechanisms for the moving mirror were used, the step drive being slightly superior to the Moiré drive below 50 cm^{-1}. High-frequency cut-off filters were purchased from Beckman Instruments Inc. The electronics of the interferometer are non-standard in that the d.c. output is fed into a Hewlett–Packard model 2401C digital voltmeter and the voltage is punched onto cards using an IBM model 026 card punch driven by the voltmeter via a Hewlett–Packard model 2540B coupler. The digitized interferograms were Fourier-transformed on the IBM model 360/67 computer at the University of Alberta using BOBS IV, a program written in Fortran IV in this laboratory, and the spectra were plotted on an off-line Calcomp plotter. The program uses the subroutine RHARM from the IBM scientific sub-routine package, and permits the ratioing of two spectra to eliminate the background and obtain the absorbance of the samples. It also permits the averaging of several spectra to reduce the random noise level. Triangular apodization was used in all transforms. The calibration of the interferometer was checked several times using water vapor (17), hydrogen chloride (18), and methyl chloride (19), and the literature values were reproduced to at least ± 0.2 cm^{-1}. The only exception to this statement occurs above 250 cm^{-1}, where the step-drive gives very large errors, and is not used.

The infrared samples were prepared by mulling the powdered hydrate with liquid propane or Freon-13 using methods described previously (16). For the reference spectra the same procedure was followed except that no hydrate was used. The absence of ice absorption in these reference spectra served as a check on the technique and therefore they were recorded regularly. Two cells were used to maintain the samples at about 100 °K in the interferometer. The first was a stainless steel cell of conventional design with a copper sample holder, in vacuum, soldered to the bottom of the liquid nitrogen reservoir. We did not succeed in determining the actual sample temperature in this cell, and to reduce the doubt on this point, spectra below 120 cm^{-1} were also recorded with the sample held in a Janis model 8 DT variable temperature Dewar, using liquid nitrogen as the coolant. In this cell the sample is surrounded by gas at atmospheric pressure, and the temperature could be well-controlled at 90 ± 1 °K. Polyethylene windows, tapered to reduce interference fringes, were used throughout, except for the cold sample chamber of the Janis cell where crystal quartz windows were used.

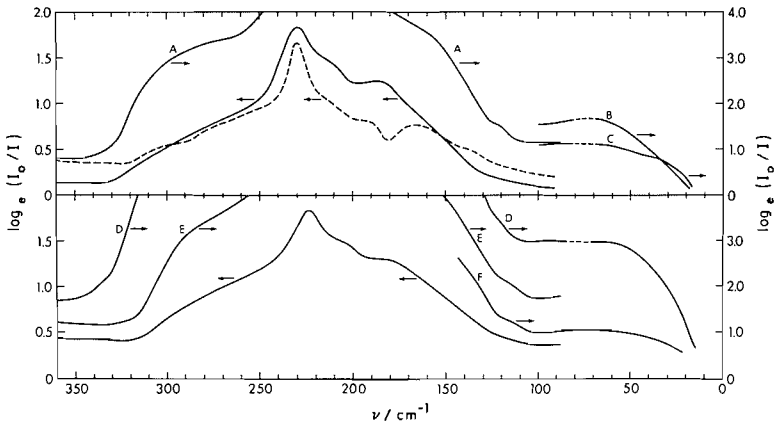

FIG. 1. The far-infrared spectrum of ethylene oxide hydrate (upper box) and deuterate (lower box) at 100 °K. Curves carrying different letters were obtained from different mulls. The arrows indicate the appropriate absorption scale. The dashed curve is the spectrum of H_2O ice I*h*, obtained in the same way as those of the hydrate.

Results

The *d*-spacings and qualitative intensities obtained from the X-ray photographs of the hydrate agreed with those calculated from the single-crystal study (3) and confirmed that the samples were ethylene oxide hydrate. The *d*-spacings differed slightly, of course, because of our lower temperature and different stoichiometry. Photographs of the two samples of ethylene oxide deuterate and one of the three hydrate samples showed very weakly the strongest ice I*h* lines, but no differences were seen between the spectra of the pure and impure hydrate samples, and the spectra of the deuterate were consistent with those of the hydrate.

The stoichiometry of our samples was not measured. One of the hydrate samples was prepared by method (*ii*) from a solution containing 13 mol% of ethylene oxide, and should have the stoichiometry $6.8C_2H_4O{\cdot}46H_2O$ (10). The other samples, prepared by method (*i*) were probably not of uniform stoichiometry. At least 85% of the solution crystallized when these samples were formed, so the solutions must have contained at least 11 mol% ethylene oxide. Using Glew and Rath's results (10), it therefore seems probable that their stoichiometries varied within a sample from about 6.3 to 6.6 or $6.8C_2H_4O$ per $46H_2O$. Unless the spectrum contained absorption specific to guest molecules in the small cages, no clear differences would be expected between the spectra of different samples with such small differences in stoichiometry, and none were observed.

The spectra of ethylene oxide hydrate and deuterate at 100 °K are presented in Fig. 1 at 2 cm^{-1} resolution. The curves shown were obtained by averaging the individual absorbance spectra in groups of about six, and smoothing a few small features that were not reproducible even after averaging. Below 100 cm^{-1} the curves shown are composites of curves, obtained as just described, which covered different frequency regions and which matched well in the overlap regions. A spectrum of ice I*h* between 360 and 100 cm^{-1} obtained in the same way as those of the hydrate is included in Fig. 1 for comparison. In all cases the reference spectrum, I_0, was obtained as discussed in the previous section. The frequencies of the various features of the hydrate spectrum are listed in Table 1. For all features other than the peak the choice of frequency is subjective and it is not useful to assign error limits. The most difficult feature to characterize by a frequency is the low-frequency edge of the plateau below 100 cm^{-1}. This feature is not sharp and its exact shape was found to be very difficult to determine. The curves in Fig. 1 show typical variations. We believe that the variation arises from the difficulty of making good mulls of the 50 to 150 μ thickness required for this region. The existence of the plateau between 100 and about 60 cm^{-1} and of the drop-off below about

Can. J. Chem. Downloaded from www.nrcresearchpress.com by 210.87.254.5 on 09/05/12
For personal use only.

TABLE 1. Frequencies of features in the far-infrared spectrum of ethylene oxide hydrate and deuterate at 100 °K

Hydrate (ν/cm^{-1})	Description	Deuterate (ν/cm^{-1})
~335	Inflection	~320
~300	Shoulder	~290
250	Inflection	240
229.6±0.9	Peak	223.1±0.5
210	Shoulder	203
198	Minimum	
184	Peak (shoulder)	180
120	Shoulder	114
110	Inflection	105
~60	Low-frequency edge of plateau	~60

60 cm^{-1} are not in doubt and no justification exists at present for further work to pin-point the frequency at which the plateau ends.

Discussion

The absorption below 360 cm^{-1} is expected to arise from the translational vibrations of the water molecules and the intermolecular vibrations of the ethylene oxide molecules. Above 100 cm^{-1} the spectrum shifts to low-frequency by about 3% when the water is deuterated, indicating clearly that the dominant absorption arises from the translational vibrations of the water molecules. Below 100 cm^{-1} the spectrum does not permit an isotope shift to be observed and therefore can not be assigned from experimental evidence.

The spectra consist of a broad absorption with well-defined features upon it, but no particularly sharp features occur. Because of theoretical considerations (20) and a knowledge of the spectra of several phases of ice (21–23), the spectra confirm the conclusion drawn from X-ray (3) and dielectric (4) studies that the water molecules are orientationally disordered, and reorient at 100 °K extremely slowly compared to far-infrared frequencies. Theory (20) predicts that the spectrum is a superposition of broad absorption, which approximates the density of states weighted by frequency-squared, and sharp absorption due to transitions allowed under the factor group of the diffraction space group, $Pm3n$, O_h^3. Nine F_{1u} water translational modes are infrared allowed by the diffraction symmetry, but because no sharp-features are

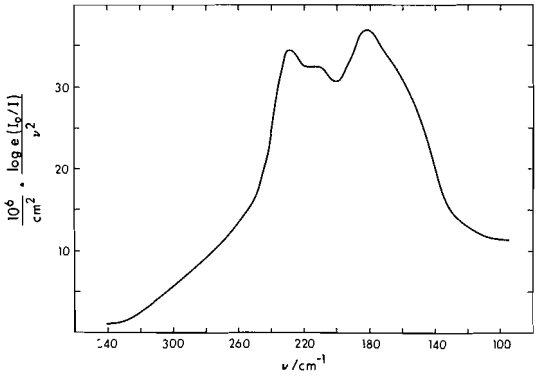

FIG. 2. $(\log_e I_0/I)/\nu^2$ plotted against ν for ethylene oxide hydrate at 100 °K. Calculated from the unlabelled curve in the upper box of Fig. 1.

seen they do not appear to influence the spectrum. The spectrum arises, then, from the disorder-allowed absorption and the curve shown in Fig. 2, representing absorbance-divided-by-frequency-squared, approximates the density of states for the translational modes of the water. Figure 2 does not extend below 100 cm^{-1} because of the possible contribution by the guest molecules in this region.

The spectrum of the hydrate, and its relationship to the spectra of ice Ih and other ice phases, can only be understood in terms of the crystal structures and intermolecular forces through calculations of the dispersion curves and density of state curves. These are not available at present, and the spectrum can therefore not be assigned or understood from a theoretical viewpoint. However, a comparison of the structures and far-infrared spectra of five phases formed by orientationally-disordered water molecules suggests an empirical correlation between the frequencies at which strong absorption occurs and the number, length, and distribution of hydrogen bonds in these phases.

Table 2 presents structural data for ices Ic (24), Ih (25 and references therein), V (26), and VI (27), and ethylene oxide hydrate, at 100 °K. For the hydrate the data of McMullan and Jeffrey (3) was corrected for a 0.8% contraction in unit cell parameter between −30 °C and −173 °C (11), assuming a proportional shortening of each hydrogen bond.

The spectra of ice Ih and ice Ic both contain a strong, rather sharp, peak centered at 229.2

Can. J. Chem. Downloaded from www.nrcresearchpress.com by 210.87.254.5 on 09/05/12
For personal use only.

Can. J. Chem. Downloaded from www.nrcresearchpress.com by 210.87.254.5 on 09/05/12
For personal use only.

TABLE 2. Structural data for several phases at 100 °K

Phase	Hydrogen-bonds	
	O---O distance in Å	Multiplicity
I*c*	2.75	4
I*h*	2.75	8
V	2.766	12
	2.781	8
	2.782	8
	2.798	8
	2.819	8
	2.820	8
	2.867	4
VI	2.773	1
	2.786	1
	2.801	2
	2.803	2
	2.840	4
EO hydrate	2.74	8
	2.75	48
	2.79	24
	2.82	12

cm^{-1} (21). This can be related to one type of hydrogen bond, 2.75 Å long. Both spectra also contain other, weaker features, and it is a weakness of this proposal that we must neglect them. The spectrum of ice V contains a broad peak, centered at 200 cm^{-1}, with a half-width of approximately 50 cm^{-1} (22). The breadth of this peak can be taken to reflect the relatively equal distribution of a wide-range of hydrogen-bond lengths in ice V. The frequency of the maximum, 200 cm^{-1}, can be related to the weighted-mean hydrogen bond length of 2.797 Å. The spectrum of ice VI contains a broad peak centered at 187 cm^{-1}, and a shoulder at 160 cm^{-1} (23). The overall half-width of the peak plus shoulder is about 50 cm^{-1} and, again, a relatively equal distribution of a wide range of bond-lengths exists in ice VI. The peak frequency can be roughly correlated with the weighted mean hydrogen bond length of 2.813 Å. For the hydrate the strongest feature in the spectrum is the peak at 229.6 cm^{-1}. By comparison with the data on ice I this can be related to the 2.75 Å bonds, which constitute 52% of the bonds in the unit cell. This peak is broader than the corresponding peak in ice I, and the broadening on the high-frequency side can be related to the 9% of 2.74 Å bonds in the structure. The hydrate absorbs more strongly relative to the 229 cm^{-1} peak than does ice I between about 185 and 210 cm^{-1}, with definite features at these two frequencies. By comparison with the data on ices V and VI this can be related to the 26% of 2.79 Å bonds and the 13% of 2.82 Å bonds in the structure. This correlation is clearly rather approximate, but the experimental data strongly suggest that a useful correlation does exist.

We wish to emphasize that the above presents an empirical correlation, not a theoretical interpretation of the spectrum. The correlation is by no means unreasonable on theoretical grounds but the detailed assignment of these features undoubtedly is much more complicated than the correlation suggests. For example, the spectrum of ice I*c* (21) contains many features, and two peaks, yet only one type of O---O hydrogen bond exists in the structure (neglecting the small variations due to the disorder). Theoretically this spectrum is quite well understood (21), and the various features arise from features in the density of states, which in turn arise from vibrational coupling (28). The influence of this vibrational coupling on the density of states curve, and hence on the spectrum, is completely unknown for ices V, VI, and for ethylene oxide hydrate, and until the appropriate calculations have been carried out to indicate this, no theoretical interpretation of the spectrum is possible.

A noteworthy difference between the spectrum of the hydrate and that of ice I is the isotope shift of the 229 cm^{-1} peak. The peaks are essentially coincident in the hydrate and in H_2O ice I, but are at 223.1 and 221.7 cm^{-1} in the deuterate and in D_2O ice I, respectively. The ratio of peak frequencies of the hydrate to the deuterate is 1.029, compared to the 1.054 expected from a simple harmonic oscillator model, and the 1.034 found in ice I. It has been argued (21) that the low ratio in ice I can not be entirely due to anharmonicity of the translational lattice vibrations, and must reflect a larger effective harmonic potential constant for D_2O than for H_2O. This effect is clearly even more pronounced in the clathrate hydrate structure, unless the smaller isotope shift in the clathrate arises from interaction between water

Can. J. Chem. Downloaded from www.nrcresearchpress.com by 210.87.254.5 on 09/05/12
For personal use only.

molecule vibrations and guest molecule vibrations. In view of the probable frequency of the guest molecule vibrations (see below), this seems to be unlikely, but it cannot be dismissed.

One of the objects of this work was to seek the absorption by the intermolecular vibrations of the ethylene oxide molecules in the cages. Because of previous experimental results on the far-infrared absorption by non-polar (29) and polar (30) liquids, and considering the dipole moment of ethylene oxide (31), there can be little doubt that most of the absorption intensity will arise from the rotational vibrations, although these are not necessarily distinct from the translational vibrations in this disordered crystal. The experimental results do not dictate the assignment of these vibrations. However, there are experimental and theoretical arguments that are relevant and these will be briefly discussed.

Inelastic neutron scattering studies (32) have shown that the density of states of water translational vibrations below 100 cm^{-1} in sulfur dioxide hydrate is similar to that in ice I, except that the maximum occurs about 20 cm^{-1} higher than in ice I. In ice I at 100 °K the maximum in the density of states shows in the infrared spectrum as a shoulder at about 60 cm^{-1}; between 100 and 60 cm^{-1} the intensity of absorption decreases as the frequency decreases, and below 60 cm^{-1} the intensity decreases even more sharply (21, 33). Using this result and theory (20), the infrared absorption by the water translational modes in sulfur dioxide hydrate is expected to decrease from 100 cm^{-1} to about 80 cm^{-1} and to decrease more sharply below about 80 cm^{-1}. It is reasonable to assume that similar absorption by the water translational vibrations occurs in ethylene oxide hydrate, which is isostructural with sulfur dioxide hydrate. The difference between this expectation and the observed spectrum (Fig. 1) must, then, be due to the absorption by the ethylene oxide intermolecular vibrations. The observed spectrum can be qualitatively reproduced by superimposing on top of this expected water absorption a broad absorption band which extends from about 100 cm^{-1} to low frequency, with a maximum absorption at about 50 cm^{-1}. Thus, if these arguments are correct, the ethylene oxide intermolecular vibrations are centered at about 50 cm^{-1} and contribute to the spectrum from about 100 cm^{-1}, to low frequencies.

Morris and Davidson (34) have shown how the experimental value of $\varepsilon_{\infty 2}$ for the hydrate, and the value calculated by neglecting the atomic polarization of the guest molecules, can be used to calculate an approximate frequency for the two rotational vibrations which cause the guest molecule's dipole to rotate, assuming that they are degenerate. Using their method the frequency is given by

$$\nu = \left[\frac{1}{\Delta n} \cdot \frac{N_m \mu^2}{3\pi c^2 I}\right]^{1/2}$$

where Δn is the difference in the refractive indices corresponding to the two values of $\varepsilon_{\infty 2}$, and c is the velocity of light. For $6.8C_2H_4O \cdot 46H_2O$, the density of guest molecules, N_m, is 3.9×10^{-3} $Å^{-3}$, the dipole moment of ethylene oxide, μ, is 1.89×10^{-18} e.s.u. cm (31), and I, taken as the mean of the two moments of inertia about the axes perpendicular to the symmetry axis, is 45×10^{-40} g cm^2 (35). The value of $\varepsilon_{\infty 2}$ neglecting the atomic polarization is calculated to be 3.2, by using eq. 4 of ref. 34 and the following parameters: $\varepsilon_\infty^0 = 2.80$, $\alpha_M = 4.68$ $Å^3$ (calculated from refractive index and density in ref. 36), $a_m = 2.9$ Å (12, 34), and $\varepsilon_{02} = 13.7$ (7). This value of $\varepsilon_{\infty 2}$ along with the experimental value of 4.1 (7) yields the frequency of the rotational vibrations as 39 cm^{-1}. However, 3.2 appears to be rather high for the calculated value of $\varepsilon_{\infty 2}$, in view of the experimental value of 2.85 for cyclopropane hydrate (14). If 2.85 is taken to be a more probable value, the frequency is calculated as 33 cm^{-1}. These calculations assume that the vibrations absorb at a single frequency. In fact the absorption is expected to be broad (7), but the calculations indicate that it should be centered near to 35 cm^{-1}. It seems likely that the frequency is not significantly temperature dependent (37).

Thus the calculations suggest that the ethylene oxide vibrations are centered at a significantly lower frequency than is obtained from the arguments based on experimental data. It seems clear that they contribute to the observed absorption below 50 cm^{-1}, but the calculations do not appear to support the result, deduced above, that they contribute at frequencies as high as 100 cm^{-1}. It is clear that further

experimental evidence is required before a firm assignment can be made.

NOTE ADDED IN PROOF: Recent work in this laboratory on cyclopropane hydrate (type I) at 100 °K has confirmed that the rotational vibrations of ethylene oxide do contribute to the spectrum of ethylene oxide hydrate at 100 °K from 100 cm^{-1} to low frequency. Full details will later be published.

We thank the National Research Council of Canada for their support of this work. One of us (D.A.O.) thanks the Canadian Kodak Company and the National Research Council of Canada for the award of scholarships. We thank Drs. D. W. Davidson and W. B. Kamb for prepublication information about their work.

1. G. A. JEFFREY and R. K. MCMULLAN. The clathrate hydrates. *In* Progress in Inorganic Chemistry. Vol. 8. *Edited by* F. A. Cotton. Academic Press, New York. 1967. pp. 43–108.
2. M. V. STACKELBERG and B. MEUTHEN. Z. Electrochem. **62**, 130 (1958).
3. R. K. MCMULLAN and G. A. JEFFREY. J. Chem. Phys. **42**, 2725 (1965).
4. D. W. DAVIDSON and G. J. WILSON. Can. J. Chem. **41**, 1424 (1963).
5. D. W. DAVIDSON, M. M. DAVIES, and K. WILLIAMS. J. Chem. Phys. **40**, 3449 (1964).
6. M. M. DAVIES and K. WILLIAMS. Trans. Faraday Soc. **64**, 529 (1968).
7. S. K. GARG, B. MORRIS, and D. W. DAVIDSON. J. Chem. Soc. Faraday II. **68**, 481 (1972).
8. S. BROWNSTEIN, D. W. DAVIDSON, and D. FIAT. J. Chem. Phys. **46**, 1454 (1967).
9. B. L. AFANAS'EV, V. I. KVLIVIDZE, and G. G. MALENKOV. Doklady Akademii Nauk. S.S.S.R. (Engl. Transl.) **183**, 816 (1969).
10. D. N. GLEW and N. S. RATH. J. Chem. Phys. **44**, 1710 (1966).
11. J. A. MCINTYRE and D. R. PETERSEN. J. Chem. Phys. **47**, 3850 (1967).
12. D. W. DAVIDSON. Can. J. Chem. **49**, 1224 (1971).
13. S. R. GOUGH, E. WHALLEY, and D. W. DAVIDSON. Can. J. Chem. **46**, 1673 (1968).
14. Y. A. MAJID, S. K. GARG, and D. W. DAVIDSON. Can. J. Chem. **47**, 4697 (1969).
15. M. A. WURTZ. Ann. Chim. Phys. Ser 3 **69**, 317 (1863).
16. J. E. BERTIE and E. WHALLEY. Spectrochim. Acta, **20**, 1349 (1964); J. E. BERTIE, L. D. CALVERT, and E. WHALLEY. J. Chem. Phys. **38**, 840 (1963).
17. K. N. RAO, R. V. DEVORE, and E. K. PLYLER. J. Res. Natl. Bur. Stand. **67A**, 351 (1963).
18. A. R. H. COLE and F. R. HONEY. Appl. Opt. **10**, 1581 (1971).
19. E. D. PALIK and K. N. RAO. J. Chem. Phys. **26**, 1401 (1957).
20. E. WHALLEY and J. E. BERTIE. J. Chem. Phys. **46**, 1264 (1967).
21. J. E. BERTIE and E. WHALLEY. J. Chem. Phys. **46**, 1271 (1967).
22. J. E. BERTIE, H. J. LABBÉ, and E. WHALLEY. J. Chem. Phys. **49**, 775 (1968).
23. J. E. BERTIE, H. J. LABBÉ, and E. WHALLEY. J. Chem. Phys. **49**, 2141 (1968).
24. L. G. DOWELL and A. P. RINFRET. Nature, **188**, 1144 (1960).
25. R. BRILLE and A. TIPPE. Acta Cryst. **23**, 343 (1967).
26. W. B. KAMB, A. PRAKASH, and C. KNOBLER. Acta Cryst. **22**, 706 (1967).
27. W. B. KAMB, W. C. HAMILTON, S. J. LAPLACA, and A. PRAKASH. Private communication.
28. H. J. SMITH. Phil. Trans. **241A**, 105 (1948).
29. S. K. GARG, J. E. BERTIE, H. KILP, and C. P. SMYTH. J. Chem. Phys. **49**, 2551 (1968).
30. MANSEL DAVIES, G. W. F. PARDOE, J. E. CHAMBERLAIN, and H. A. GEBBIE. Trans. Faraday Soc. **64**, 847 (1968).
31. R. D. NELSON, D. R. LIDE, JR., and A. A. MARYOTT. Selected values of electric dipole moments for molecules in the gas phase. United States Department of Commerce. 1967.
32. A. W. NAUMANN and G. J. SAFFORD. J. Chem. Phys. **47**, 867 (1967).
33. J. E. BERTIE, H. L. LABBÉ, and E. WHALLEY. J. Chem. Phys. **50**, 4501 (1969).
34. B. MORRIS and D. W. DAVIDSON. Can. J. Chem. **49**, 1243 (1971).
35. G. L. CUNNINGHAM, JR., A. W. BOYD, R. J. MYERS, W. D. GWINN, and W. I. LEVAN. J. Chem. Phys. **19**, 676 (1951).
36. The handbook of chemistry and physics. Chemical Rubber Co.
37. J. C. BURGIEL, H. MEYER, and P. L. RICHARDS. J. Chem. Phys. **43**, 4291 (1965).

Can. J. Chem. Downloaded from www.nrcresearchpress.com by 210.87.254.5 on 09/05/12
For personal use only.

Enthalpies of Dissociation of Ammonia and Amine Adducts of some Tetraalkylammonium Pentafluorosilicates

I. WHARF AND M. ONYSZCHUK

Department of Chemistry, McGill University, Montreal, Quebec

Received February 23, 1971[1]

Condensed phase enthalpies of dissociation of $[R_4N][SiF_5(NH_3)]$, in which R = C_2H_5, C_3H_7, and C_5H_{11}, are in the order: $C_2H_5— < C_3H_7— < C_4H_9— > C_5H_{11}—$, and a lower limit of 16.8 ± 0.6 kcal mol^{-1} is suggested for the gas phase interaction of NH_3 with SiF_5^-. Enthalpies of dissociation of the amine adducts, $[(C_5H_{11})_4N][SiF_5L]$, in which L = CH_3NH_2, $(CH_3)_2NH$, and $(CH_3)_3N$ are in the order: $NH_3 \simeq CH_3NH_2 < (CH_3)_2NH \simeq (CH_3)_3N$.

Les enthalpies de dissociation de phase condensée de $[R_4N][SiF_5(NH_3)]$, où R = C_2H_5, C_3H_7, C_4H_9 et C_5H_{11} sont, dans l'ordre: $C_2H_5— < C_3H_7— < C_4H_9— > C_5H_{11}—$; nous proposons une limine inférieure de 16.8 ± 0.6 kcal mol^{-1} pour l'interaction en phase gazeuse de NH_3 avec SiF_5. Les enthalpies de dissociation des groups amines, $[(C_5H_{11})_4N][SiF_5L]$, où L = CH_3NH_2, $(CH_3)_2NH$, et $(CH_3)_3N$ sont, dans l'ordre: $NH_3 \simeq CH_3NH_2 < (CH_3)_2NH \simeq (CH_3)_3N$. [Traduit par le journal]

Canadian Journal of Chemistry, **50**, 3450 (1972)

Introduction

Following a previous article (1 and references therein), in which the acceptor powers of SiF_5^- and GeF_5^- were compared by measuring the condensed phase enthalpies of dissociation of the ammonia adducts of their tetrapropylammonium salts, we now report the enthalpies of dissociation of the salts $[R_4N][SiF_5(NH_3)]$, in which R = C_2H_5, C_3H_7, C_4H_9, and C_5H_{11}. Our aim has been to determine the effect of changes in cation size on the stability of ammonia adducts of SiF_5^-. Enthalpies of dissociation of the amine adducts, $[(C_5H_{11})_4N][SiF_5L]$, in which L = CH_3NH_2, $(CH_3)_2NH$, and $(CH_3)_3N$ have also been measured with the object of determining the relative basicities of the methylamines toward SiF_5^-.

Experimental

The experimental methods were essentially the same as those described previously (1). The tetramethylammonium and tetraethylammonium pentafluorosilicate salts reported in Table 1 were prepared by slowly bubbling silicon tetrafluoride (Matheson) through a well-stirred, ice-cold ethanol solution (60 ml) of the tetraalkylammonium fluoride (Aldrich) for 5 min. Tetramethylammonium pentafluorosilicate precipitated immediately, whereas the addition of benzene (60 ml) was necessary to precipitate the tetraethylammonium salt. Both salts were filtered off, washed with ether and *n*-hexane, and dried in a vacuum at room temperature.

Tetrapropyl- and tetrabutylammonium pentafluorosilicates were prepared as before (1). Tetrapentylammonium pentafluorosilicate (Table 1) was prepared by dissolving silicon dioxide (1.20 g) in a solution of tetrapentylammonium fluoride obtained by stirring silver carbonate (2.8 g) with tetrapentylammonium iodide (8.5 g) (Eastman) in a mixture of methanol (25 ml) and concentrated hydrofluoric acid. The mixture was evaporated down three times, methanol (50 ml) being added each time, to give a brown oil which solidified on stirring after benzene (50 ml) and *n*-hexane (100 ml) were added. The brown solid was recrystallized from a mixture of ethyl acetate and diethyl ether to give white needles which were dried in a vacuum at room temperature, m.p. 100–101°.

The absence of water in the above compounds was confirmed by infrared spectral measurements. Absorption bands typical of the SiF_5^- ion (1) were observed at 880 and 789 cm^{-1}, 878 and 777 cm^{-1}, and 878 and 785 cm^{-1}, for $[(CH_3)_4N][SiF_5]$, $[(C_2H_5)_4N][SiF_5]$, and $[(C_5H_{11})_4N][SiF_5]$, respectively.

Dissociation pressures were measured as described previously (1). The 1:1 interaction of gaseous ligand with each $[R_4N][SiF_5]$ salt was confirmed by *P.V.T.* measurements. Infrared spectral measurements showed that the parent SiF_5^- was reformed after thermal dissociation of each adduct.

Results and Discussion

Dissociation pressure–temperature curves were obtained for the ammonia adducts of several tetraalkylammonium pentafluorosilicates, $[R_4N][SiF_5]$, R = C_2H_5, *n*-C_3H_7, *n*-C_4H_9, and *n*-C_5H_{11}. The resulting data and thermodynamic parameters given in Table 2 show that the cation effect is significant. Interaction of ammonia with tetraethylammonium pentafluorosilicate is small, increases with increasing cation size, and becomes approximately constant for $[(C_4H_9)_4N][SiF_5]$ and $[(C_5H_{11})_4N][SiF_5]$.

[1] Revision received May 16, 1972.

Can. J. Chem. Downloaded from www.nrcresearchpress.com by 210.87.254.5 on 09/05/12
For personal use only.

TABLE 1. Preparations and analyses of new pentafluorosilicate salts

Reactants	Product (yield)	Analysis (%)* C	H	N	Si	F
$SiF_4 + [(CH_3)_4N]F$ (9.3 g)	$[(CH_3)_4N][SiF_5]$ (8.3 g, 42%)	24.36 24.59	6.13 6.41	7.10 7.27	14.24 13.84	48.16 48.28
$SiF_4 + [(C_2H_5)_4N]HF_2$ (8.5 g)	$[(C_2H_5)_4N][SiF_5]$ (4.2 g, 33%)	37.93 38.20	7.96 8.02	5.53 5.81	11.09 11.23	37.30 37.57
$SiO_2 + [(C_5H_{11})_4N]F$ (1.2 g)	$[(C_5H_{11})_4N][SiF_5]$ (4.1 g, 49%)	56.97 56.88	10.52 10.27	3.32 3.10	6.66 6.21	22.53 22.04

*Microanalyses were by Schwarzkopf Microanalytical Laboratory, Woodside, New York. Experimental results are given directly underneath corresponding calculated values.

TABLE 2. Thermodynamic parameters for the reaction
$[R_4N][SiF_5(NH_3)](s) \rightarrow NH_3(g) + [R_4N][SiF_5](s)$

Alkyl group R	Vapor pressure eq. $\log_{10} P\,(mm) = -A/T + C$: $A \times 10^{-2}$	C	Temperature range (°C)	ΔH^0 (kcal mol^{-1})	$\Delta G^0_{298.15}$ (kcal mol^{-1})
C_2H_5	13.0 ± 0.9	5.0 ± 0.7	25 → 80	6.0 ± 0.4	3.0 ± 1.5
C_3H_7	26.3 ± 1.1	10.2 ± 1.1	30 → 70	12.0 ± 0.5	2.0 ± 2
C_4H_9	36.6 ± 1.2	13.1 ± 1.3	25 → 80	16.8 ± 0.6	2.5 ± 1.0
C_5H_{11}	31.7 ± 1.5	12.8 ± 1.5	0 → 35	14.5 ± 0.7	1.0 ± 0.7
	38.3 ± 2.3*	10.6 ± 2.2*	130 → 150*	17.5 ± 1.0*	7 ± 4*

*Data for the reaction
$[(C_3H_7)_4N][GeF_5(NH_3)](s) \rightarrow NH_3(g) + [(C_3H_7)_4N][GeF_5](s)$.

The influence of lattice energy changes can be seen from the cycle in Scheme 1.

For compounds with cations considerably larger than the complex anions SiF_5^- and $SiF_5(NH_3)^-$, lattice geometry and dimensions will be determined principally by cation packing and lattice energies will remain unchanged on formation of the ammonia adduct anion. Thus, in the enthalpy cycle (Scheme 1), $U_1 = U_2$, and experimental dissociation enthalpies (ΔH_1) will equal the gas-phase values (ΔH_2) and be independent of the cation. The tetrabutylammonium and tetrapentylammonium systems are examples of this type and the largest value observed for the enthalpy of dissociation, 16.8 ± 0.6 kcal mol^{-1}, gives a lower limit for the desired gas phase dissociation of the ammonia adduct of the pentafluorosilicate ion. That enthalpies of dissociation of the $(C_5H_{11})_4N^+$ and $(C_4H_9)_4N^+$ salts are not identical is not unexpected since the term $(U_1 - U_2)$ is the difference between two large numbers. Alternatively, the observed difference might be due to a greater range of solid solution behavior with the tetrapentylammonium salt, as suggested by one of the referees.

With smaller cations, lattice dimensions will be determined by the complex anions, SiF_5^- and $SiF_5(NH_3)^-$. As ammonia is absorbed, the crystal lattice of the pentafluorosilicate salt will

$$\begin{array}{ccc} [R_4N][SiF_5(NH_3)](s) & \xrightarrow{\Delta H_1} & NH_3(g) + [R_4N][SiF_5](s) \\ \downarrow U_1 & & \uparrow -U_2 \\ [R_4N]^+(g) + [SiF_5(NH_3)]^-(g) & \xrightarrow{\Delta H_2} & NH_3(g) + [R_4N]^+(g) + [SiF_5]^-(g) \end{array}$$

$$\Delta H_1 = \Delta H_2 + (U_1 - U_2)$$

SCHEME 1

Can. J. Chem. Downloaded from www.nrcresearchpress.com by 210.87.254.5 on 09/05/12
For personal use only.

TABLE 3. Thermodynamic parameters for the reaction
$[(C_5H_{11})_4N][SiF_5L](s) \rightarrow L(g) + [(C_5H_{11})_4N][SiF_5](s)$

Ligand L	Vapor pressure eq. $\log_{10} P\,(mm) = -A/T + C$		Temperature range (°C)	ΔH^0 (kcal mol^{-1})	$\Delta G^0_{298.15}$ (kcal mol^{-1})
	$A \times 10^{-2}$	C			
NH_3	31.7 ± 1.5	12.8 ± 1.5	$0 \rightarrow 35$	14.5 ± 0.7	1.0 ± 0.7
CH_3NH_2	31.3 ± 0.7	11.7 ± 0.7	$15 \rightarrow 65$	14.3 ± 0.3	2.3 ± 1.3
$(CH_3)_2NH$	26.9 ± 0.7	11.4 ± 0.7	$-10 \rightarrow 30$	12.3 ± 0.3	0.8 ± 1.4
$(CH_3)_3N$	27.0 ± 1.5	9.8 ± 1.2	$25 \rightarrow 60$	12.4 ± 0.7	3.0 ± 2.2
	–	–	–	14.3*	2.0*

*Parameter for the reaction

$$SiF_4 \cdot 2(CH_3)_3N(s) \rightarrow (CH_3)_3N(g) + SiF_4(CH_3)_3N(s)$$

calculated from data in ref. 7.

expand to accommodate the larger ammonia adduct anion. Lattice energies will decrease ($U_1 < U_2$), and the measured dissociation enthalpy (ΔH_1) will be less than the gas-phase dissociation enthalpy (ΔH_2). The tetraethylammonium system exemplifies this situation, while $[(C_3H_7)_4N][SiF_5]$ and $[(C_3H_7)_4N][SiF_5(NH_3)]$ perhaps differ only to a small extent in crystal lattice energies. Similar arguments have been used (2, 3) to account for the greater stability of salts of hydrogen dihalide ions with increasing cation size.

Unfortunately it is not presently possible to give a quantitative basis to the above discussion. Tetraalkylammonium ions are too flexible to allow for simple radius ratio arguments, while crystal structure data even for the parent SiF_5^- salts are not yet available. Preliminary X-ray diffraction studies of $[(C_3H_7)_4N][SiF_5]$, $[(C_3H_7)N]_2[SiF_5]Br$, and $[(C_4H_9)_4N][SiF_5]$ have shown that all give disordered crystals (5). Although changes in lattice geometry will occur with changes in cation size, this will not affect the above discussion provided no change occurs on formation of the adduct. However, when cation and anion are of similar size, *e.g.* as in $[(C_2H_5)_4N][SiF_5]$, a change in lattice geometry may well occur on adduct formation, and the above argument becomes irrelevant.

Standard free energy changes, $\Delta G^0_{298.15}$, for the dissociations are positive but small, reflecting the low stabilities of the ammonia adducts. The standard entropy of dissociation, $\Delta S^0_{298.15}$, for both $[(C_4H_9)_4N][SiF_5(NH_3)]$ and $[(C_5H_{11})_4N][SiF_5(NH_3)]$ is ~46 cal deg^{-1} mol^{-1}. Since for ammonia, $S^0_{298.15} = 46.0$ cal deg^{-1} mol^{-1} (4), there is very little difference in entropy between $[R_4N][SiF_5]$ (R = C_4H_9, C_5H_{11}) and its ammonia adduct, supporting the idea that crystal lattices and perhaps lattice energies do not alter significantly on formation of the ammonia adduct in those two cases. The standard entropy of dissociation of the ammonia adduct of $[(C_2H_5)_4N][SiF_5]$ is about 10 cal deg^{-1} mol^{-1}, showing the entropy of the adduct to be greater than the parent SiF_5^- salt. This is consistent with some change in crystal structure on dissociation of the adduct. It is worth noting that for the reaction

$$[(C_3H_7)_4N][MF_5(NH_3)](s) \rightarrow [(C_3H_7)_4N][MF_5](s) + NH_3(g)$$

$\Delta S^0_{298.15}$ is 35 cal deg^{-1} mol^{-1} for M = Ge, and 33 cal deg^{-1} mol^{-1} for M = Si. The similarity of these values supports the idea proposed previously (1) that crystal lattice changes on adduct formation are approximately the same for corresponding silicon and germanium systems.

Results for the thermal dissociation of the adducts of $[(C_5H_{11})_4N][SiF_5]$ with NH_3, CH_3NH_2, $(CH_3)_2NH$, and $(CH_3)_3N$ are given in Table 3. This system was chosen in the hope that with the large cation $(C_5H_{11})_4N^+$, crystal lattice changes on dissociation of the adducts would be minimal. A small decrease in the enthalpy of dissociation of the adducts is noted for the ligands $(CH_3)_2NH$ and $(CH_3)_3N$ compared with NH_3 and $(CH_3)_2NH$, while entropies of dissociation at 25 °C are about 45, 40, 39, and 32 cal deg^{-1} mol^{-1}, for the NH_3, CH_3NH_2, $(CH_3)_2NH$, and $(CH_3)_3N$ adducts, respectively. Since for the ligands $S^0_{298.15}$ values are 46.0 (4),

Can. J. Chem. Downloaded from www.nrcresearchpress.com by 210.87.254.5 on 09/05/12
For personal use only.

TABLE 4. Thermodynamic parameters for the reaction
$2[(CH_3)_4N][SiF_5](s) \rightarrow SiF_4(g) + [(CH_3)_4N]_2[SiF_6](s)$

Line No.	Temperature range (°C)	$\log_{10} P$ (mm) $= -A/T + C$		ΔH^0 (kcal mol^{-1})	$\Delta G^0_{298.15}$ (kcal mol^{-1})
		$A \times 10^{-2}$	C		
1	90–150	7.86 ± 0.47	2.82 ± 0.30	3.6 ± 0.2	3.7 ± 0.6
2	130–210	5.44 ± 0.34	2.29 ± 0.22	2.5 ± 0.2	3.3 ± 0.4

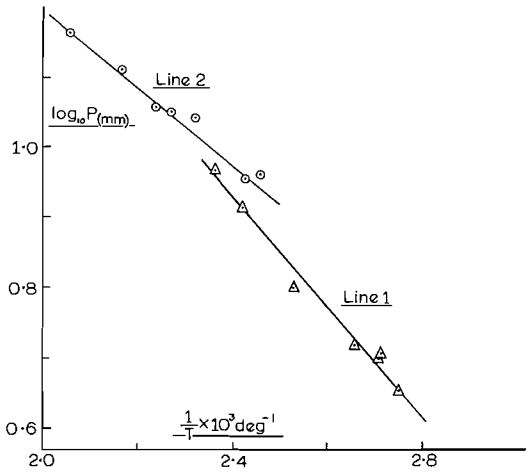

FIG. 1. Plot of $\log_{10} P$ (mm) against $1/T$ °K for the reaction
$2[(CH_3)_4N][SiF_5](s) \rightarrow SiF_4(g) + [(CH_3)_4N]_2[SiF_6](s)$.

57.7, 65.3, and 69.0 cal deg^{-1} mol^{-1} (6), in the same order, it is clear that with increasing substitution the entropies of the adducts increase by comparison with $[(C_5H_{11})_4N][SiF_5]$. Thus on adduct formation using the larger methylamine ligands, some crystal lattice change occurs, and measured dissociation enthalpies will not give approximate gas-phase values. Thermodynamic data for the hypothetical reaction

$$SiF_4 \cdot 2(CH_3)_3N(s) \rightarrow (CH_3)_3N(g) + SiF_4(CH_3)_3N(s)$$

are in Table 3. There is an evident similarity in the acceptor power toward $(CH_3)_3N$ of the five coordinate neutral, $SiF_4 \cdot (CH_3)_3N$ species and the anion, SiF_5^-.

Since the formation of either $[(CH_3)_4N][SiF_5]$ or $[(CH_3)_4N]_2[SiF_6]$ at room temperature depends on the preparative method employed, these systems may differ only slightly in stability. On drying a sample of the pentafluorosilicate at 100 °C under high vacuum, an infrared adsorption at 740 cm^{-1} in the dried material showed SiF_6^{2-} ion had been formed. This suggested that the following disproportionation had occurred.

$$2[(CH_3)_4N][SiF_5](s) \rightarrow SiF_4(g) + [(CH_3)_4N]_2[SiF_6](s)$$

Variation of SiF_4 pressure, P mm Hg, with temperature, T °K, above $[(CH_3)_4N][SiF_5]$ is shown as a plot of $\log_{10} P$ against $1/T$ in Fig. 1. Since only very low SiF_4 pressures were measured, the highest being about 14 mm at 212 °C, complete reversibility was difficult to attain. Two straight lines are identified with the transition occurring over the range 130–150 °C. The two highest points on line 1 were obtained with increasing temperature while the two lowest points on line 2 were measured with decreasing temperature. Vapor pressure equations and values for ΔH^0 and $\Delta G^0_{298.15}$ for the disproportionation reaction are given in Table 4. Small enthalpy changes for the reaction show that ΔH_f^0 for $[(CH_3)_4N][SiF_5](s)$ is close to the average of the values for $SiF_4(g)$ and $[(CH_3)_4N]_2[SiF_6]$. For SiF_4 gas at 25 °C, $\Delta H_f^0 = -373$ kcal mol^{-1} (4) while negative ion spectra (8) give $\Delta H_f^0 < -583$ kcal mol^{-1} for the gaseous SiF_5^- species. Preliminary calculations using an ionic model indicate that SiF_4 and SiF_6^{2-} have similar gas-phase enthalpies of formation. However, the lattice energy of $[(CH_3)_4N]_2[SiF_6]$ should be greater than that of $[(CH_3)_4N][SiF_5]$ and as the energetics of the disproportionation include lattice energy differences and gas-phase enthalpies, it is not possible to discuss them in greater detail at present.

We are grateful for the financial support of the National Research Council of Canada.

1. I. WHARF and M. ONYSZCHUK. Can. J. Chem. **48**, 2250 (1970).
2. D. H. MCDANIEL and R. E. VALLEE. Inorg. Chem. **2**, 996 (1963).

Can. J. Chem. Downloaded from www.nrcresearchpress.com by 210.87.254.5 on 09/05/12
For personal use only.

3. S. A. HARRELL and D. H. MCDANIEL. J. Am. Chem. Soc. **86**, 4497 (1964).
4. JANAF Interim Thermochemical Tables. Dow Chemical Co., Midland, Michigan.
5. P. BIRD. Private communication.
6. Landolt-Bornstein. 6th Auflage, Band 2, Teil 4.
7. J. E. FERGUSON, D. K. GRANT, R. H. WICKFORD, and C. J. WILKINS. J. Chem. Soc. 99 (1959).
8. J. C. J. THYNNE and K. A. G. MCNEIL. Inorg. Chem. **9**, 1946 (1970).

Can. J. Chem. Downloaded from www.nrcresearchpress.com by 210.87.254.5 on 09/05/12
For personal use only.

Total Synthesis of (±)-Ishwarane, a Tetracyclic Sesquiterpenoid

R. B. KELLY, J. ZAMECNIK, AND B. A. BECKETT
Department of Chemistry, University of New Brunswick, Saint John, New Brunswick

Received June 23, 1972

A total synthesis of (±)-ishwarane, a novel tetracyclic sesquiterpenoid possessing a tricyclo[3.2.1.$0^{2,7}$]octane system, is described. Completion of the synthesis of ishwarane firmly establishes the structure assigned to this sesquiterpenoid and provides corroboration of the structure assigned to the related sesquiterpenoid ishwarone. A total synthesis of (±)-isoishwarane, a transformation product of ishwarone, is also described.

Une synthèse totale de la (±)-ishwarane, nouveau sesquiterpène tétracyclique comportant le système tricyclo[3,2,1,$0^{2,7}$]octane, est décrite. L'aboutissement de cette synthèse établit de façon sûre la structure assignée à ce sesquiterpénoide et corrobore celle attribuée à l'ishwarone, sesquiterpène apparenté. Une synthèse totale de la (±)-isoishwarane, produit de transformation de l'ishwarone, est également donnée.

Canadian Journal of Chemistry, **50**, 3455 (1972)

Can. J. Chem. Downloaded from www.nrcresearchpress.com by 210.87.254.6 on 09/05/12
For personal use only.

The closely related pair of sesquiterpenoids ishwarane (**1**) and ishwarone (**2**) were discovered, together with other terpenoids, in the roots of *Aristolochia indica* Linn. (1–5). The isolation of the former (**1**) from the petals of *Cymbopetalum penduliforum*, Baill., a material used for flavoring beverages, has also been reported very recently (6).

The isolation and characterization of ishwarone (**2**) was first reported in 1935 (1). It was not until 34 years later, however, that the novel and biogenetically interesting tetracyclic structure **2** was proposed for ishwarone (2, 5, see also 3). A year later, in 1970, the isolation of ishwarane was reported and, in the same communication, structure **1**, having the same carbon skeleton as ishwarone, was assigned to this sesquiterpenoid (4). The assignment of structure **1** to ishwarane was based mainly on the fact that it could be obtained from ishwarone (**2**) simply by Wolff–Kishner reduction of the keto group (4). The validity of structure **1** for ishwarane is therefore dependent on the correctness of structure **2** for ishwarone. The latter structure (**2**) was adduced from chemical evidence, including the conversion of ishwarone into (+)-nootkatane, and spectral data (2, 3, 5).

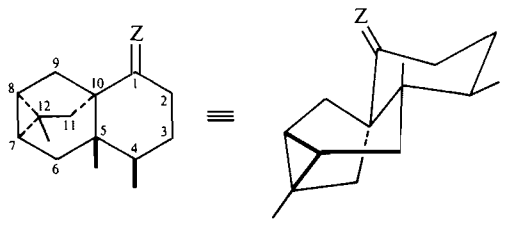

1 Z = H, H
2 Z = O

Recently we completed a total synthesis of ishwarane (**1**) (7, 8), thereby providing proof of the validity of structure **1** for ishwarane and corroboration of structure **2** for ishwarone. We now wish to describe the details of the synthesis of (±)-ishwarane.[1]

A novel structural feature of the carbon skeleton common to ishwarane (**1**) and ishwarone (**2**) is the tricyclo[3.2.1.$0^{2,7}$]octane system. Another important stereochemical aspect of this skeleton is the pair of vicinal *cis* methyl groups at C-4 and -5 and their stereorelationship to the tricyclooctane system.[2] In designing a synthesis of ishwarane these stereochemical aspects must be taken into account.

In planning the synthesis of ishwarane, it was decided that the synthetic route should, at an early stage, proceed through a bicyclic intermediate in which the vicinal *cis* methyl groups had been established. Thus, one of the stereochemical problems associated with the synthesis would be solved early in the sequence of reactions. The octalone **3** was chosen as the intermediate since it not only satisfies the requirements with regard to the *cis* methyl groups but it also possesses functionality, in the form of an α,β-unsaturated ketone, suitable for the development of the tricyclooctane system.

[1]Preliminary reports of some aspects of the work described in this article have appeared (refs. 7 and 8).

[2]The numbering system shown in **1** is adhered to throughout.

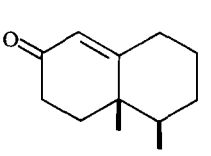

3

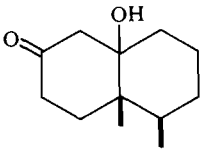

4

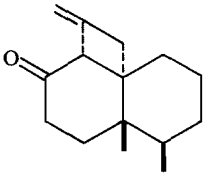

5

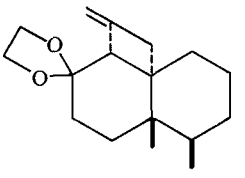

6

The octalone **3** was prepared either by annelation of *cis*-2,3-dimethylcyclohexanone (9) with methyl vinyl ketone and dehydration of the intermediate crystalline alcohol **4** (*cf.* 10 and 11), or by a recently published, more lengthy synthesis (10). The two methods afforded the same octalone for which the stereostructure **3** has been firmly established (10).

Having obtained the required intermediate octalone **3**, the next task was the elaboration of the tricyclooctane system. Briefly, this was accomplished by converting **3** into **5** by photo-addition of allene, skeletal rearrangement of **5**, by a series of transformations, into intermediates possessing a bicyclo[2.2.2]octane system and, finally, the transformation of the bicyclooctane system into the required tricyclooctane system (*vide infra*).

Photo-addition of allene to the octalone **3** afforded the adduct **5** in 75% yield as an oil. Consistent with the assigned structure (**5**), the i.r. spectrum of the adduct showed a keto band at 1695 cm^{-1} and bands at 1660 and 880 cm^{-1} due to the exocyclic methylene; in the n.m.r. spectrum a multiplet appeared at δ 4.96 (2H) attributable to the exocyclic methylene.[3] The stereostructure assigned to the photo-adduct follows from the established stereospecificity of the photo-addition of allene to α,β-unsaturated ketones (12, 13).

Acetalization of **5** in the usual manner converted it into the oily ethylene acetal **6** in 75% yield. In agreement with this conversion, the i.r. spectrum of the acetal was devoid of carbonyl bands and a multiplet (4H) due to the ethylene group of the acetal function appeared in the n.m.r. spectrum at δ 3.91.

Treatment of **6** with perbenzoic acid followed by chromatography on alumina furnished two epoxides **7***a* (m.p. 65°) and *b* (m.p. 30°), each in 39% yield. Both were converted individually, in two steps, to the same mixture of epimeric keto alcohols **9**, thence, in a single step to the common intermediate **10** (Scheme 1). The i.r. spectra of the two epoxides were similar and both were devoid of olefinic bands; the n.m.r. spectra, however, were distinctly different. In the case of **7***a*, the signals for the methylene protons of the oxirane ring appeared as a pair of doublets ($J = 5$ Hz) at δ 2.27 and 2.99 and the signal for the ethylene protons of the acetal function appeared as a 4-proton multiplet at δ 3.78; in contrast, the corresponding signals in the case of **7***b* were found at δ 1.95 and 2.11 (methylene protons of oxirane ring) and at δ 3.71 (ethylene of acetal function).

The stereostructures assigned to the epoxides are based on n.m.r. spectroscopy. An obvious difference in the n.m.r. spectra of the epoxides was the nature of the signal due to the ethylene group of the acetal function. In both spectra this signal appeared at *ca.* δ 3.75. However, in the case of the lower melting epimer, the signal was broader and considerably more complex than the corresponding signal in the spectrum of the other epimer. This difference was attributed to the closer proximity of the oxygen atom of the oxirane ring to the dioxolane ring in the lower melting epimer. Hence, structure **7***b* was assigned to the lower melting epimer and structure **7***a* to the other epimer (**14**). Consistently, a similar, but less pronounced effect was observed on comparison of the tertiary alcohols **8***a* and *b* which were derived from **7***a* and *b*, respectively (*vide infra*).

Corroborative evidence for the validity of the structures assigned to the epoxides (**7***a* and *b*) was found on comparison of the n.m.r. chemical shifts for the methylene protons of the oxirane rings. Models show that the oxirane ring protons in structure **7***a* are significantly closer to the dioxolane ring than in **7***b*. As a consequence of the deshielding effect of the oxygen atoms of the dioxolane ring, it could therefore be expected

[3]Only spectral data pertinent to the discussion will be given in this section; for further details see the Experimental.

Can. J. Chem. Downloaded from www.nrcresearchpress.com by 210.87.254.6 on 09/05/12
For personal use only.

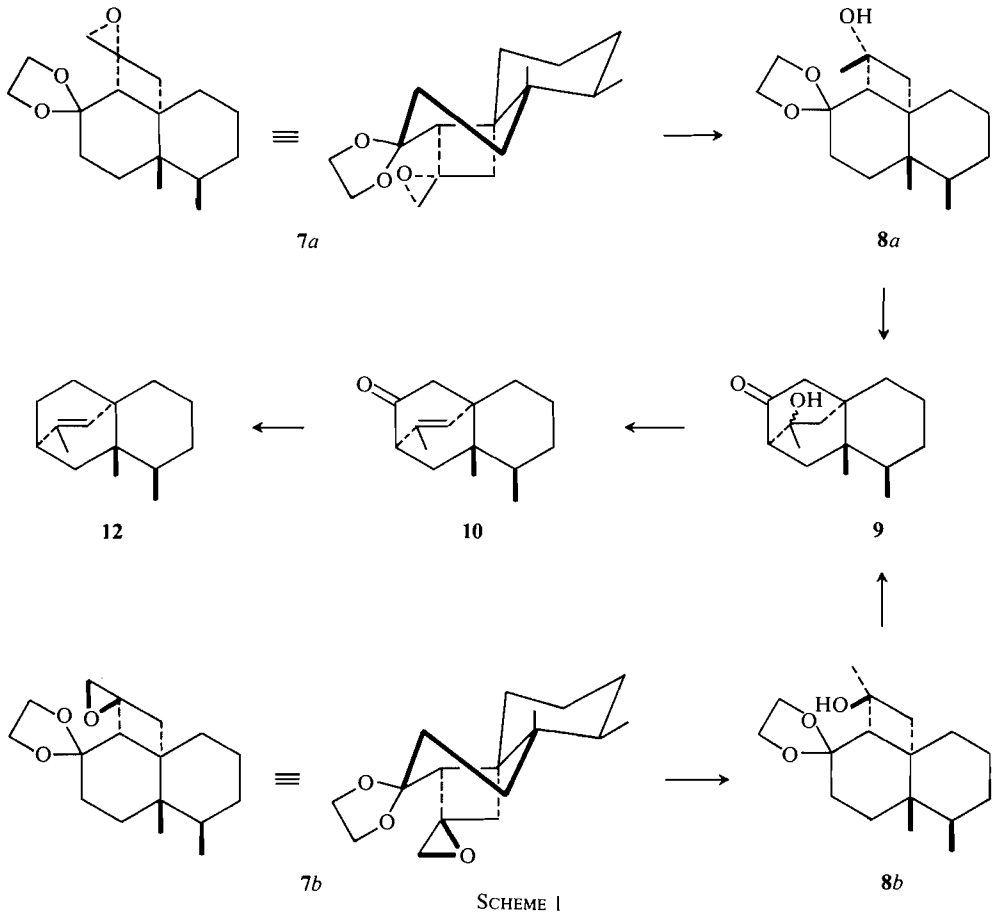

7a 8a 9 10 12 7b 8b

SCHEME I

that the n.m.r. signals for these protons in **7***a* would appear downfield relative to the corresponding signals in the spectrum of **7***b*. In agreement with expectation and the structures assigned to the epoxides, the pertinent signals in the spectrum of **7***a* appeared at δ 2.27 and 2.99 whereas the corresponding signals in the case of **7***b* appeared at δ 1.95 and 2.11.

The epoxides **7***a* and *b* were reduced with lithium aluminum hydride in excellent yield to the corresponding crystalline tertiary alcohols **8***a* and **8***b*, respectively. Stereochemically, the structures assigned to the epimeric tertiary alcohols follow from the stereostructures previously adduced for the precursor epoxides (*vide supra*). The i.r. spectrum of **8***a* showed a hydroxyl band at 3500 cm^{-1} and the corresponding band in the case of **8***b* was observed at 3525 cm^{-1}; singlets due to the methyl group on the cyclobutane ring appeared in the n.m.r. spectra of both alcohols at *ca.* δ 1.30.

Treatment of either of the epimeric alcohols (**8***a* or *b*) with aqueous hydrochloric acid in tetrahydrofuran resulted in deacetalization followed by skeletal rearrangement to a crystalline mixture of epimeric alcohols **9** in 97% yield. Obviously, the conversion of **8***a* and *b* into the same mixture of epimeric alcohols **9** involves deacetalization to give the corresponding keto cyclobutanols, retro-aldolization to give the common intermediate diketone **11**, and, finally,

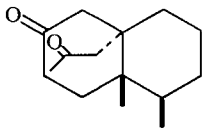

11

Can. J. Chem. Downloaded from www.nrcresearchpress.com by 210.87.254.6 on 09/05/12
For personal use only.

Can. J. Chem. Downloaded from www.nrcresearchpress.com by 210.87.254.6 on 09/05/12
For personal use only.

aldol condensation to give **9**. The mixture of epimeric alcohols **9** was barely separated into two components by t.l.c. but attempts to separate the mixture into two epimers by column chromatography were unsuccessful. The i.r. spectrum of the mixture (**9**) showed broad bands at 3350 (hydroxyl) and 1700 cm^{-1} (ketone); in the n.m.r. spectrum there was a singlet (3H) at δ 1.25 due to the methyl group at C-12.

The failure to resolve the mixture of keto alcohols (**9**) into two epimers had no adverse effect on the synthesis since the mixture, on dehydration with *p*-toluenesulfonic acid in boiling benzene, afforded a single enone **10** as an oil in 89% yield. Consistent with structure **10**, there were bands in the i.r. spectrum of the dehydration product at 1725 (ketone) and at 1650 cm^{-1} (olefin) and, in the n.m.r. spectrum, there was a singlet (3H) at δ 1.81 (vinylic methyl), a multiplet (1H) at 2.80 (methine adjacent to ketone), and a multiplet (1H) at 5.88 (vinylic proton).

At this point it was decided to depart briefly from the main synthetic route in order to convert **10** into the olefinic hydrocarbon **12**. The latter structure had been assigned to isoishwarane, a transformation product of ishwarone (**2**) (2, 3). In terms of structure **2** for ishwarone, the two-step transformation was envisaged as involving a rupture of the cyclopropane ring to give isoishwarone (**13**) which, on reduction of the keto group, afforded **12** (2, 3).

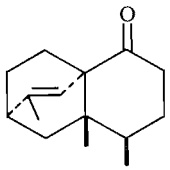

13

The enone **10** was successfully converted, in 74% yield, into the hydrocarbon **12** by a Huang–Minlon reduction (15). The hydrocarbon was obtained as an oil with spectral properties in agreement with structure **12**. The i.r. spectrum was devoid of carbonyl absorption but displayed a band at 1648 cm^{-1} (olefinic); in the n.m.r. spectrum there was a doublet (3H) at δ 1.73 due to the vinylic methyl, a multiplet (1H) at 2.20 due to the allylic proton, and a multiplet (1H) at 5.61 due to the vinylic proton.

The synthetic hydrocarbon **12** was found to be identical with an authentic sample of isoishwarane prepared from ishwarone by comparison of their i.r., n.m.r., and mass spectra fragmentation patterns. Completion of the total synthesis of isoishwarane provided proof of the correctness of structure **12** for this compound and corroboration of structures **1** and **2** for ishwarane and ishwarone respectively. Furthermore, it provided assurance that the synthesis of ishwarane was proceeding along the correct stereochemical lines.

Returning to the main synthetic route, there now remained the task of converting the enone **10** into an intermediate possessing the tricyclooctane system, thence to ishwarane (**1**). This was accomplished by reduction of **10** to the pair of epimeric alcohols **14***a* and *b*, conversion of the alcohols, individually, by a parallel sequence of transformations into the common intermediate cyclopropyl ketone **20**, and reduction of the latter to ishwarane (see Scheme 2).

Reduction of the enone **10** with lithium aluminum hydride and chromatography of the product on silica gel resulted in the isolation of two epimeric alcohols **14***a* (m.p. 116°) and *b* (m.p. 110°), each in 38% yield. The i.r. spectra of the two alcohols were devoid of carbonyl absorption but each displayed an hydroxyl band and a band at 1648 cm^{-1} due to olefinic absorption. In the n.m.r. spectra, the signal for the proton associated with the secondary alcohol appeared as a multiplet at δ 3.93 in the case of **14***a* and at 3.91 in the case of **14***b*.

Stereochemically, the two alcohols could be differentiated by n.m.r. spectroscopy. In the spectrum of the higher melting epimer, the signal for the angular methyl group appeared 12 Hz downfield relative to the corresponding signal in the spectrum of the other epimer. The deshielding effect on the angular methyl group in the case of the higher melting epimer is due to the hydroxyl group (16). Therefore, the epimer melting at 116° was assigned structure **14***a* in which the hydroxyl group is within effective deshielding range of the angular methyl group leaving the alternative structure **14***b* to be assigned to the epimer melting at 110°. A similar deshielding effect, due to the oxygen function at C-8 was observed consistently in the subsequent compounds **15***a* to **18***a* inclusive.

The pair of epimeric alcohols **14***a* and *b* were converted into their respective benzyl ethers **15***a*

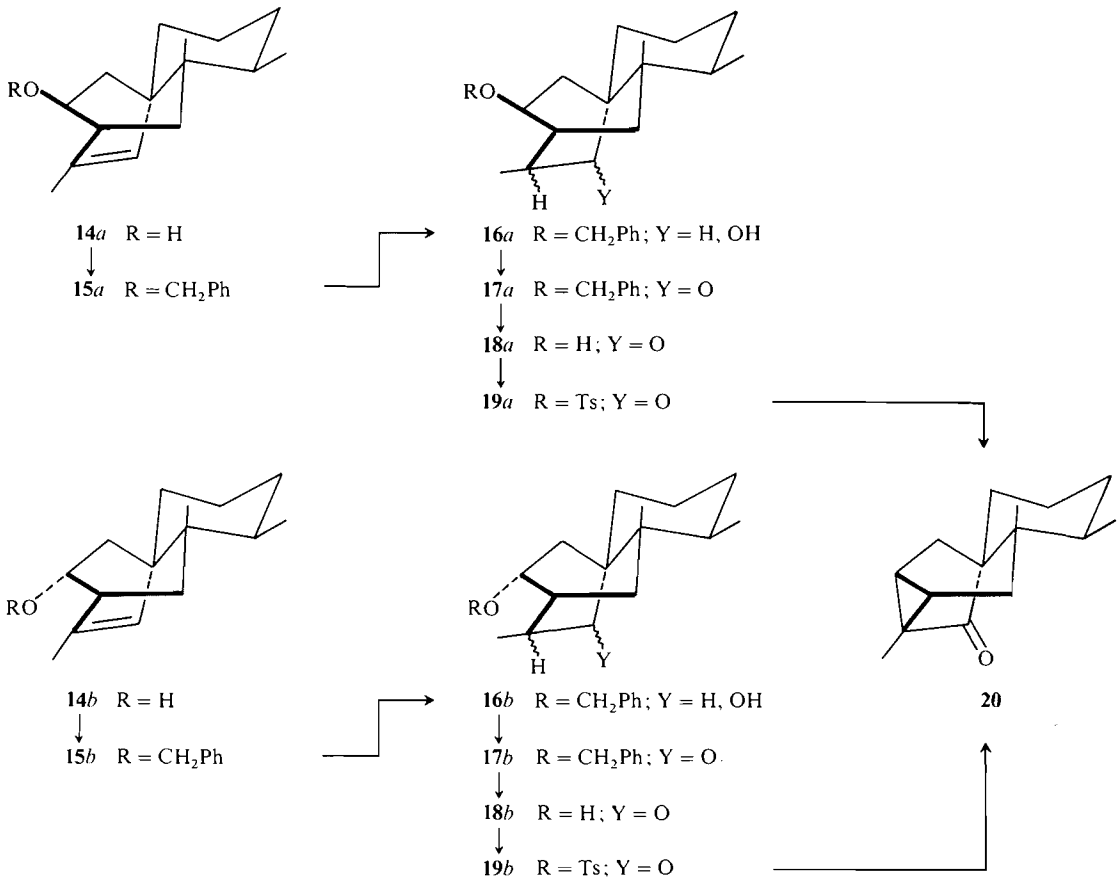

SCHEME 2

and *b*, both of which were obtained as oils. The i.r. spectra of both **15***a* and *b* were devoid of hydroxyl absorption but showed bands due to aromatic absorption; in the n.m.r. spectra of **15***a* and *b*, there was a singlet (2H) at *ca.* δ 4.40 due to the benzylic methylene and a multiplet (5H) due to the aromatic protons.

Hydroboration of **15***a* and *b* gave, in each case, a single crystalline alcohol. The alcohol **16***a*, derived from **15***a*, was obtained in 82% yield. The i.r. spectrum was devoid of olefinic absorption but showed hydroxyl absorption at 3475 cm^{-1}; in the n.m.r. spectrum there appeared two doublets (3H each) at δ 0.78 and 1.20 due to the secondary methyls and a multiplet (1H) at 3.88 arising from the proton at C-11. The alcohol **16***b*, obtained from **15***b* in 71% yield, exhibited spectral properties similar to those of **16***a*.

A study, with the aid of models, of the steric factors relevant to the hydroboration of **15***a* and *b* and an analysis of the spectral data for the resulting alcohols, **16***a* and *b*, revealed no reliable clues as to the precise stereochemical orientation about C-11 and -12 in the latter. This, however, was of no consequence in so far as the synthetic plan was concerned.

Jones oxidation (17) of the alcohols **16***a* and *b* gave the corresponding ketones **17***a* and *b* respectively in 80–90% yield, the former as an oil and the latter as a crystalline compound. The i.r. spectra of both **17***a* and *b* showed ketonic absorption at 1715 cm^{-1}; the n.m.r. spectrum of **17***a* showed a doublet (3H) at δ 1.13 due to the methyl group adjacent to the ketone and, in the case of **17***b*, the corresponding signal was found at δ 1.07.

Hydrogenolysis of the keto benzyl ethers **17***a* and *b* afforded the corresponding keto alcohols **18***a* and *b*, both as crystalline compounds in

Can. J. Chem. Downloaded from www.nrcresearchpress.com by 210.87.254.6 on 09/05/12
For personal use only.

Can. J. Chem. Downloaded from www.nrcresearchpress.com by 210.87.254.6 on 09/05/12
For personal use only.

80–90% yield. The i.r. spectrum of **18***a* showed hydroxyl absorption at 3415 cm^{-1} and ketonic absorption at 1703 cm^{-1}; the n.m.r. spectrum was devoid of signals due to aromatic protons and showed a multiplet (1H) at δ 4.05 due to the proton at C-8. The spectral properties of **18***b* were similar to those of **18***a*: i.r. 3250 (hydroxyl) and 1710 cm^{-1} (ketone); n.m.r. δ 4.20 (multiplet, proton at C-8).

The tosylate **19***a*, derived from the keto alcohol **18***a*, was smoothly transformed in 70% yield, into the cyclopropyl ketone **20** by heating at 60° for 2 h in dimethyl sulfoxide containing a 45% excess of methylsulfinyl carbanion (18). The epimeric tosylate **19***b* was also converted, under identical conditions to **20**, although in somewhat lower yield (60%). The identity of the condensation product (**20**) obtained from the two sources was rigorously established (see Experimental).

The spectral properties of the condensation product were in accord with structure **20**. Thus, there was an absorption maximum in the u.v. spectrum at 208 nm (ε 4000) due to the cyclopropyl ketone moiety; the i.r. spectrum was devoid of bands attributable to a tosyl group or a hydroxyl group but showed a band at 1715 cm^{-1} due to ketonic absorption; the n.m.r. spectrum showed a multiplet (partially obscured) at *ca.* δ 0.60 due to the protons on the cyclopropane ring and a singlet (3H) at 1.17 for the methyl group on the cyclopropane ring.

The fact that the epimeric tosylates **19***a* and *b* were both converted, under identical conditions, to the cyclopropyl ketone **20** invites speculation as to the mechanism of this conversion. The condensation **19***a* → **20** seems unexceptional since the tosylate function in **19***a* is favorably aligned for an S_N2i displacement by the carbanion at C-12. Such is not the case, however, with **19***b*. In the latter case a plausible mechanism involving a double displacement can be envisaged. Thus, the tosylate function in **19***b* could, conceivably, suffer S_N2 displacement either by methyl sulfinyl carbanion or a molecule of solvent to give the intermediates **21** or **22** which could readily undergo a classical S_N2i displacement resulting in the formation of **20**.

Another, less attractive mechanism, which could be envisaged for both **19***a* and *b* would involve an elimination to give the olefin **23**. Attack by the carbanion at C-12 on the double bond would result in the formation of an intermediate **24** in which the carbanion is homoconjugated with the ketone. Protonation of **24** would then give **20**.

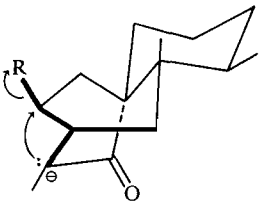

21 R = CH_2SOCH_3
22 R = $O—\overset{\oplus}{S}(CH_3)_2$

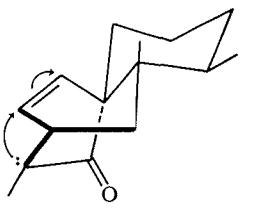

23

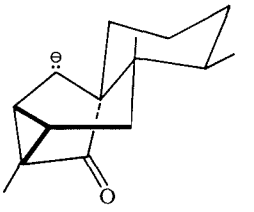

24

The final step in the synthesis of ishwarane was the reduction of the cyclopropyl ketone **20** to the hydrocarbon **1**. This was achieved, in 67% yield, by the Barton modification of the Wolff–Kishner (19) reduction followed by purification of the product by preparative t.l.c. The spectral properties of the hydrocarbon were consistent with structure **1**; the i.r. spectrum showed no carbonyl absorption, and the n.m.r. spectrum showed a multiplet (2H) at δ 0.50 due to the protons on the cyclopropane ring and a singlet (3H) at 1.12 due to the methyl group on the cyclopropane ring.

The synthetic hydrocarbon **1** was identical with a sample of authentic ishwarane by the following criteria: identity of i.r. and n.m.r. spectra; identity of the fragmentation patterns of the mass spectrum; identical retention times on v.p.c.

The completion of the synthesis of ishwarane firmly establishes structure **1** for this sesquiterpenoid and provides corroboration of structure **2** for the related sesquiterpenoid ishwarone.

Experimental

Melting points were determined on a Fisher–Johns apparatus and are uncorrected. The i.r. spectra were recorded on a Perkin–Elmer model 237 B spectrophotometer and u.v. spectra were determined with a Perkin–Elmer

Can. J. Chem. Downloaded from www.nrcresearchpress.com by 210.87.254.6 on 09/05/12
For personal use only.

Coleman model 124 instrument. The n.m.r. spectra were recorded with a Varian T-60 instrument; chemical shifts are expressed in p.p.m. (δ-values) downfield from the signal for tetramethylsilane which is used as an internal standard.

V.p.c. was performed on a Hewlett-Packard model 5750 instrument fitted with a stainless steel column (6 ft × 1/8 in.) packed with 10% of UC-W98 (silicone gum-rubber) on diatoports (80–100 mesh). The t.l.c. was carried out on Silica Gel GF-254 procured from Brinkman Instruments (Canada) Ltd.

Reaction products were isolated by the following procedure. The product was extracted into the specified solvent and the extract was washed two or three times with appropriate aqueous solutions as indicated. The original aqueous layer (if any) and the aqueous washings were extracted three times with the solvent and the combined extracts were dried over anhydrous magnesium sulfate, filtered, and evaporated *in vacuo* on a rotary evaporator.

Petroleum ether refers to the fraction with boiling point range 30–60°.

Brine refers to a saturated solution of sodium chloride.

*9-Hydroxy-5,10-dimethyl-2-decalone (**4**)*

A mixture of 19.2 g of *cis*-2,3-dimethylcyclohexanone (9) and 0.6 ml of an ethanolic 3 *M* solution of sodium ethoxide was cooled to −15°. The mixture was treated, with efficient mechanical stirring and in a nitrogen atmosphere, with 12.1 g of methyl vinyl ketone over a period of 6 h. The reaction mixture was then left, under nitrogen, at −16° for 15 h after which it was dissolved in 200 ml of ether. The ether solution was worked-up in the usual manner by washing with brine. The residue, obtained by evaporation of the ether extract was distilled *in vacuo*. The first fraction (b.p. 71°/20 mm, 12.0 g) was 2,3-dimethylcyclohexanone and was used for recycling as above. The fraction with b.p. 120–150°/0.2 mm, after crystallization from petroleum ether, yielded 3.07 g of **4**, m.p. 134–135°; ν_{max} (Nujol) 3350 (OH) and 1703 cm^{-1} (ketone); n.m.r. ($CDCl_3$), δ 0.90 (d, $J = 6.5$ Hz, 3H, secondary methyl), 0.92 (s, 3H, angular methyl).

Anal. Calcd. for $C_{12}H_{20}O_2$: C, 73.43; H, 10.27. Found: C, 73.39; H, 10.12.

*Octalone (**3**)*

A solution of 10.0 g of the keto alcohol **4** and 1.30 g of *p*-toluenesulfonic acid in 300 ml of benzene was refluxed for 1 h while water was collected in a Dean–Stark adapter. The cooled reaction solution was worked-up in the usual manner by washing with saturated sodium bicarbonate solution followed by brine. Evaporation of the solvent *in vacuo* and distillation of the residue afforded 8.71 g (97%) of **3**, b.p. 95–97°/0.2 mm (lit. (10), 96–97°/0.2 mm); λ_{max} (EtOH) 240 nm (ε, 12 100); ν_{max} (film) 1672 (ketone) and 1605 cm^{-1} (olefin); n.m.r. ($CDCl_3$), δ 0.91 (d, $J = 6$ Hz, 3H, secondary methyl), 1.12 (s, 3H, angular methyl), 5.70 (s, 1H, vinylic H).

The *2,4-dinitrophenyl hydrazone*, crystallized from ethanol, melted at 139–140°.

Anal. Calcd. for $C_{18}H_{22}N_4O_4$: C, 60.32; H, 6.19; N, 15.63. Found: C, 60.56; H, 6.60; N, 15.83.

*Photo-adduct **5***

Photo-addition of allene to the octalone **3** was carried out at −70° using a 450 W mercury vapor immersion lamp with a Corex sleeve. A solution of 6.20 g of **3** and 14 g of allene in 1500 ml of freshly distilled hexane was irradiated for 6 h. After irradiation, the reaction solution was left overnight in a fume hood to allow excess allene to evaporate. The solvent was evaporated *in vacuo* and the residue was chromatographed on a column of 255 g of silica gel with benzene–ether (98:2) as solvent. Distillation of the eluted material afforded 5.70 g (75%) of **5**, b.p. 105–109°/0.18 mm; ν_{max} (film) 1695 (ketone) and 1660 and 880 cm^{-1} (olefin); n.m.r. ($CDCl_3$), δ 0.75 (s, 3H, angular methyl), 0.82 (d, $J = 6.5$ Hz, 3H, secondary methyl), 4.96 (m, 2H, vinylic protons).

Anal. Calcd. for $C_{15}H_{22}O$: C, 82.52; H, 10.16. Found: C, 82.33; H, 10.10.

*Ethylene Acetal **6***

A solution of 10.0 g of **5**, 34.0 g of ethylene glycol, and 1.20 g of *p*-toluenesulfonic acid in 600 ml of benzene was refluxed under a nitrogen atmosphere for 18 h. During reflux, water was separated in a Dean–Stark adapter. The cooled reaction solution was worked-up in the usual manner with sodium bicarbonate solution and brine. The resulting oil was chromatographed on a column of 660 g of basic alumina (activity IV) starting with petroleum ether as solvent followed by gradually increasing proportions of benzene in petroleum ether. Thereby, 9.30 g (77%) of **6** was obtained as an oil, ν_{max} (film) 1665 and 870 cm^{-1} (olefin); n.m.r. ($CDCl_3$) δ 0.75 (poorly developed doublet, 3H, secondary methyl), 1.05 (s, 3H, angular methyl), 4.93 (m, 2H, vinylic protons).

Mol. Wt. Calcd. for $C_{17}H_{26}O_2$: 262. Found (mass spectrum): 262.

Epoxides 7a and b

A solution of 9.00 g of the acetal **6** in 300 ml of dry chloroform was treated with 3.66 g of solid sodium bicarbonate followed by 92.2 ml of a 0.43 *M* chloroform solution of perbenzoic acid. The resulting mixture was stirred at room temperature, in the dark, for 24 h. The reaction solution was shaken with 200 ml of 5% sodium bisulfite solution then worked-up in the usual manner with saturated sodium bicarbonate solution and brine. The crude product, an oil, was chromatographed on a column of 450 g of basic alumina (activity III) with gradually increasing proportions of benzene in petroleum ether as eluant. Two crystalline epoxides were separately eluted from the column.

Epoxide 7a was the first to be eluted from the column. Crystallization from pentane afforded 3.73 g (39%) of this compound, m.p. 65°; i.r. devoid of olefinic absorption; n.m.r. (CCl_4), δ 0.72 (poorly resolved doublet, 3H, secondary methyl), 1.03 (s, 3H, angular methyl), 2.27 and 2.99 (doublets, $J = 5$ Hz, 1H each, methylene of oxirane ring), 3.78 (m, 4H, ethylene of acetal group).

Anal. Calcd. for $C_{17}H_{26}O_3$: C, 73.34; H, 9.41. Found: C, 73.31; H, 9.42.

Epoxide 7b was the more strongly absorbed epoxide. Crystallization from pentane afforded 3.68 g (39%) of this compound, m.p. 29–30°; i.r. no olefinic absorption; n.m.r. (CCl_4), δ 0.77 (poorly resolved doublet, 3H, secondary methyl), 0.91 (s, 3H, angular methyl), 1.95 and 2.11 (doublets, $J = 5$ Hz, 1H each, methylene of oxirane ring), 3.71 (broad complex multiplet, 4H, ethylene of acetal group).

Anal. Calcd. for $C_{17}H_{26}O_3$: C, 73.34; H, 9.41. Found: C, 73.01; H, 9.43.

Tertiary Alcohol 8a

A mixture of 1.00 g of the epoxide **7a**, 250 mg of lithium

Can. J. Chem. Downloaded from www.nrcresearchpress.com by 210.87.254.6 on 09/05/12
For personal use only.

aluminum hydride, and 50 ml of dry ether was refluxed for 15 min. The reaction mixture was cooled on an ice bath and treated with a few drops of brine. The ether solution was decanted from solid material and worked-up in the usual manner with brine. Crystallization of the product from ether–pentane afforded 839 mg (83%) of **8***a*, m.p. 114°; ν_{max} (Nujol) 3500 cm^{-1} (OH); n.m.r. (CCl_4), δ 0.70 (poorly resolved multiplet, 3H, secondary methyl), 0.98 (s, 3H, angular methyl), 1.28 (s, 3H, methyl on cyclobutane ring), 3.80 (s, 4H, ethylene of acetal group).

Anal. Calcd. for $C_{17}H_{28}O_3$: C, 72.82; H, 10.07. Found: C, 73.00; H, 10.20.

Tertiary Alcohol 8b

Reduction of the epoxide **7***b* as described in the preceding experiment and crystallization of the product from pentane afforded, in 93% yield, the tertiary alcohol **8***b*, 69–70°; ν_{max} (Nujol) 3525 cm^{-1} (OH); n.m.r. (CCl_4), δ 0.73 (poorly resolved multiplet, 3H, secondary methyl), 0.93 (s, 3H, angular methyl), 1.27 (s, 3H, methyl on cyclobutane ring), 3.83 (m, 4H, ethylene of acetal group).

Anal. Calcd. for $C_{17}H_{28}O_3$: C, 72.82; H, 10.07. Found: C, 73.07; H, 9.96.

Keto Alcohols 9

(a) From Tertiary Alcohol 8a

A solution of 280 mg of **8***a* in 25 ml of tetrahydrofuran was treated with 20 ml of 1 *M* aqueous hydrochloric acid and left at room temperature under nitrogen for 20 h. Water (50 ml) was added to the reaction solution and it was extracted with chloroform. The chloroform extracts were worked-up in the usual manner by washing with water, saturated sodium bicarbonate solution, and water again. Evaporation of the chloroform extracts left an oil which, on crystallization from pentane, afforded 228 mg (97%) of **9** as a mixture of epimers, m.p. 90–114°; ν_{max} (Nujol) 3350 (OH) and *ca.* 1700 cm^{-1} (broad band, ketone); n.m.r. ($CDCl_3$), δ 0.80 (s, 3H, angular methyl), 0.85 (d, $J = 6.5$ Hz, 3H, secondary methyl), 1.25 (s, 3H, CH_3—C—OH).

The mixture was resolved by t.l.c. with benzene–ether (1:1) as solvent into two, barely separated, components (estimated ratio, 1:1).

Anal. Calcd. for $C_{15}H_{24}O_2$: C, 76.23; H, 10.24. Found: C, 76.41; H, 10.18.

(b) From Tertiary Alcohol 8b

The same mixture of epimeric alcohols (**9**) was obtained, in comparable yield, from **8***b* by the above procedure.

Enone 10

A solution of 250 mg of a mixture of the epimeric alcohols (**9**) and 25 mg of *p*-toluenesulfonic acid monohydrate in 100 ml of benzene was refluxed for 24 h. The cooled reaction solution was worked-up with saturated sodium bicarbonate solution and water. The product, an oil, was chromatographed on a column of 21 g of silica gel with benzene–ether (95:5) as solvent. The purified product was obtained as an oil (205 mg, 89%), ν_{max} (film) 1725 (ketone) and 1650 cm^{-1} (weak, olefin); n.m.r. ($CDCl_3$), δ 0.77 (d, $J = 6.5$ Hz, 3H, secondary methyl), 0.87 (s, 3H, angular methyl), 1.81 (m, 3H, vinylic methyl), 2.80 (m, 1H, methine adjacent to ketone), 5.88 (m, 1H, vinylic H).

Mol. Wt. Calcd. for $C_{15}H_{22}O$: 218. Found (mass spectrum): 218.

(±)-Isoishwarane (12)

The reduction of the enone **10** to isoishwarane (**12**) was carried out in a dry nitrogen atmosphere as follows (*cf.* 15). The enone **10** (150 mg) was dissolved in 6 ml of a stock solution prepared by dissolving 260 mg of dry potassium hydroxide in 26 ml of triethylene glycol. The solution was treated with 1 ml of anhydrous hydrazine (19) and allowed to reflux at 180° for 14 h. An additional 0.5 ml of hydrazine was added and reflux was continued for 1 h after which hydrazine was distilled from the reaction flask until the temperature (inside) of the reaction solution reached 210°. After keeping the reaction solution at 210° for 8 h, it was allowed to cool to room temperature then treated with 5 ml of water followed by 50 ml of ether. The ether solution was worked-up in the usual manner with dilute hydrochloric acid, saturated sodium bicarbonate solution, and brine. Chromatography of the product on a column of 10.7 g of silica gel with pentane as solvent followed by distillation in a small collar flask at 0.5 mm (bath temperature 98°) afforded 103 mg (74%) of (**12**) as an oil, ν_{max} (film) 1648 cm^{-1} (olefin); n.m.r. (CCl_4), δ 0.67 (d, $J = 6.5$ Hz, 3H, secondary methyl), 0.87 (s, 3H, angular methyl), 1.73 (d, $J = 2.0$ Hz, 3H, vinylic methyl), 2.20 (m, 1H, allylic proton), 5.61 (m, 1H, vinylic proton).

The i.r. and n.m.r. spectra and fragmentation pattern of the mass spectrum of synthetic **12** were identical with the corresponding properties of an authentic sample of isoishwarane prepared from ishwarone.

Anal. Calcd. for $C_{15}H_{24}$: C, 88.16; H, 11.84. Found: C, 88.17; H, 11.72.

Enols 14a and b

A solution of 1.07 g of the enone **10** in 100 ml of dry ether was treated with 0.50 g of lithium aluminum hydride and the mixture was refluxed for 4 h. The cooled reaction mixture was treated dropwise with brine until the excess lithium aluminum hydride was deactivated and the ether solution was decanted from solid material. The ether solution was worked-up in the usual manner with brine. Column chromatography of the product on 107 g of silica gel, with gradually increasing portions of ether in benzene as solvent, gave two fractions.

Enol 14a. The first fraction eluted from the column afforded, after crystallization from pentane, 413 mg (38%) of **14***a*, m.p. 115–116°; ν_{max} (Nujol) 3300 (OH) and 1648 cm^{-1} (olefin); n.m.r. ($CDCl_3$), δ 0.72 (d, $J = 6.5$ Hz, 3H, secondary methyl), 0.98 (s, 3H, angular methyl), 1.73 (d, $J = 2$ Hz, 3H, vinylic methyl), 2.26 (m, 1H, allylic methine), 3.93 (m, 1H, H—C—OH), 5.65 (m, 1H, vinylic proton).

Anal. Calcd. for $C_{15}H_{24}O$: C, 81.76; H, 10.98. Found: C, 82.13; H, 11.16.

Enol 14b. Crystallization of the second fraction from the column from pentane afforded 412 mg (38%) of **14***b*, m.p. 110°; ν_{max} (Nujol) 3250 (OH) and 1648 cm^{-1} (olefin); n.m.r. ($CDCl_3$), δ 0.67 (d, $J = 6.5$ Hz, 3H, secondary methyl), 0.77 (s, 3H, angular methyl), 1.77 (d, $J = 2.0$ Hz, 3H, vinylic methyl), 2.29 (m, 1H, allylic methine), 3.91 (m, 1H, H—C—OH), 5.69 (m, 1H, vinylic proton).

Anal. Calcd. for $C_{15}H_{24}O$: C, 81.76; H, 10.98. Found: C, 81.62; H, 11.04.

Benzyl Ether 15a

The enol **14***a* was converted to the benzyl ether **15***a* in a

Can. J. Chem. Downloaded from www.nrcresearchpress.com by 210.87.254.6 on 09/05/12
For personal use only.

dry nitrogen atmosphere by the following procedure. A mixture of 250 mg of **14***a*, 100 mg of sodium hydride, and 8 ml of dry benzene was refluxed for 5 h. After cooling to room temperature the mixture was treated dropwise with 0.5 ml of benzyl chloride and refluxing was continued for 24 h. The cooled reaction mixture was treated dropwise with 2 ml of methanol then poured into a mixture of 150 g of ice and water. The aqueous mixture was extracted with ether and the extracts were washed with water. The product was chromatographed on a column of 86 g of silica gel with increasing proportions of benzene in petroleum ether as solvent. Elution of the column afforded 307 mg (87%) of **15***a* as an oil, ν_{max} (film) 3030–3000, 2000–1600, and 800–680 (multiple bands, aromatic) and 1648 (olefin); n.m.r. ($CDCl_3$), δ 0.70 (d, $J = 6.5$ Hz, 3H, secondary methyl), 1.02 (s, 3H, angular methyl), 1.74 (d, $J = 2.0$ Hz, 3H, vinylic methyl), 2.43 (m, 1H, allylic proton), 3.57 (m, 1H, H—C—O), 4.43 (s, 2H, benzylic methylene), 5.67 (m, 1H, vinylic proton), 7.25 (m, 5H, aromatic protons).

Mol. Wt. Calcd. for $C_{22}H_{30}O$: 310. Found (mass spectrum): 310.

Benzyl Ether ***15b***

The enol **14***b* was converted into the benzyl ether **15***b* by the procedure described in the preceding experiment. The benzyl ether **15***b* was obtained in 82% yield as an oil, ν_{max} (film) 3030–3000, 2000–1600, and 800–680 (multiple bands, aromatic) and 1648 cm^{-1} (olefin); n.m.r. ($CDCl_3$), δ 0.69 (d, $J = 6.5$ Hz, 3H, secondary methyl), 0.73 (s, 3H, angular methyl), 1.77 (d, $J = 2.0$ Hz, 3H, vinylic methyl), 2.50 (m, 1H, allylic proton), 3.70 (m, 1H, H—C—O), 4.40 (s, 2H, benzylic methylene), 7.17 (m, 5H, aromatic protons).

Mol. Wt. Calcd. for $C_{22}H_{30}O$: 310. Found (mass spectrum): 310.

Benzyl Ether Alcohol ***16a***

The following reaction was carried out in a dry nitrogen atmosphere. A solution of 220 mg of the benzyl ether **15***a* in 3 ml of dry tetrahydrofuran was treated with 0.73 ml of a 1 *M* tetrahydrofuran solution of borane and stirred at room temperature for 12 h. The reaction mixture was treated with 0.5 ml of water followed by 1 ml of 1 *M* sodium hydroxide solution. The alkaline solution was treated, with cooling on an ice bath, with 1 ml of 30% hydrogen peroxide then stirred at 45° for 45 min. The reaction mixture was worked-up with ether and brine in the usual manner. Crystallization of the product from pentane afforded 190 mg (82%) of **16***a*, m.p. 104°, ν_{max} (Nujol) 3475 (OH); n.m.r. ($CDCl_3$), δ 0.78 and 1.20 (doublets, $J = 6.5$ Hz, 3H each, secondary methyls), 1.10 (s, 3H, angular methyl), 3.60 (m, 1H, H—C—O), 3.88 (m, 1H, H—C—OH), 4.45 (s, 2H, benzylic methylene), 7.25 (m, 5H, aromatic protons).

Anal. Calcd. for $C_{22}H_{32}O_2$: C, 80.43; H, 9.82. Found: C, 80.11; H, 10.01.

Benzyl Ether Alcohol ***16b***

The benzyl ether **15***b* (550 mg) was converted to the benzyl ether alcohol **16***b* by the procedure described in the preceding experiment. The product was purified by chromatography on a column of 33 g of silica gel in benzene–ether. Crystallization of the eluted product from pentane afforded 413 mg (71%) of **16***b*, m.p. 85–86°; ν_{max} (film) 3410 cm^{-1} (OH); n.m.r. ($CDCl_3$), δ 0.78 and 1.05 (doublets, $J = 6.5$ Hz, 3H each, secondary methyls), 0.85 (s, 3H, angular methyl), 3.73 (m, 2H, H—C—O and H—C—OH superimposed), 4.41 (s, 2H, benzylic methylene), 7.23 (m, 5H, aromatic protons).

Anal. Calcd. for $C_{22}H_{32}O_2$: C, 80.43; H, 9.82. Found: C, 80.26; H, 9.73.

Keto Benzyl Ether ***17a***

A solution of 420 mg of the benzyl ether alcohol **16***a* in 20 ml of acetone was treated drop-wise with Jones reagent (17) until a persistent orange color was observed. The excess oxidizing reagent was then deactivated by dropwise addition of methanol until a permanent green color resulted. The reaction solution was treated with 5 ml of 1 *M* sodium bicarbonate solution and diluted with 150 ml of ether. The ethereal mixture was worked-up in the usual manner with sodium bicarbonate and brine. Purification of the oily product by preparative t.l.c. on silica gel with benzene–ether (95:5) as solvent afforded 340 mg (82%) of **17***a* as an oil, ν_{max} (film) 1715 cm^{-1} (ketone); n.m.r. ($CDCl_3$), δ 0.83 (d, poorly resolved, 3H, secondary methyl), 1.13 (d, $J = 6.5$ Hz, 3H, secondary methyl adjacent to ketone), 1.15 (s, 3H, angular methyl), 3.68 (m, 1H, H—C—O), 4.47 (s, 2H, benzylic methylene), 7.27 (m, 5H, aromatic protons).

Anal. Calcd. for $C_{22}H_{30}O_2$: C, 80.94; H, 9.26. Found: C, 81.03; H, 9.07.

Keto Benzyl Ether ***17b***

The benzyl ether alcohol **16***b* was oxidized to the keto benzyl ether **17***b* by the procedure described in the preceding experiment. Crystallization of the product from pentane afforded **17***b* in 91% yield, m.p. 84–85°; ν_{max} (film) 1715 cm^{-1} (ketone); n.m.r. ($CDCl_3$), δ 0.78 (d, poorly resolved, 3H, secondary methyl), 0.92 (s, 3H, angular methyl), 1.07 (d, $J = 6.5$ Hz, 3H, secondary methyl adjacent to ketone), 3.83 (m, 1H, H—C—O), 4.45 (s, 2H, benzylic methylene), 7.17 (m, 5H, aromatic protons).

Anal. Calcd. for $C_{22}H_{30}O_2$: C, 80.94; H, 9.26. Found: C, 80.81; H, 8.85.

Keto Alcohol ***18a***

The keto benzyl ether (**17***a*, 340 mg) in 50 ml of ethanol was hydrogenated over 180 mg of a palladium–charcoal catalyst (10% Pd) at atmospheric pressure for 1 h. Removal of the catalyst by filtration, evaporation of the solvent *in vacuo*, and crystallization of the product from ether–pentane afforded 218 mg (89%) of **18***a*, m.p. 90–91°; ν_{max} (Nujol) 3415 (OH) and 1703 cm^{-1} (ketone); n.m.r. ($CDCl_3$), δ 0.83 (d, poorly resolved, 3H, secondary methyl), 1.15 (s, 3H, angular methyl), 1.16 (d, $J = 6.5$ Hz, 3H, secondary methyl adjacent to ketone), 4.05 (m, 1H, H—C—OH).

Anal. Calcd. for $C_{15}H_{24}O_2$: C, 76.23; H, 10.24. Found: C, 75.83; H, 10.20.

Keto Alcohol ***18b***

The keto benzyl ether **17***b* was converted to the keto alcohol **18***b* by the procedure described in the preceding experiment. Crystallization of the product from ether–pentane afforded **18***b* in 80% yield, m.p. 111–112°; ν_{max} (Nujol) 3250 (OH) and 1710 cm^{-1} (ketone); n.m.r. ($CDCl_3$), δ 0.80 (d, poorly resolved, 3H, secondary methyl), 0.92 (s, 3H, angular methyl) 1.10 (d, $J = 6.5$ Hz, 3H, methyl adjacent to ketone), 4.20 (m, 3H, H—C—OH).

Anal. Calcd. for $C_{15}H_{24}O_2$: C, 76.23; H, 10.24. Found: C, 75.98; H, 10.54.

Can. J. Chem. Downloaded from www.nrcresearchpress.com by 210.87.254.6 on 09/05/12
For personal use only.

Cyclopropyl Ketone **20**

From Keto Alcohol **18***a*

A solution of 225 mg of **18***a* in 2 ml of dry pyridine was treated with 580 mg of *p*-toluenesulfonyl chloride and the resulting solution was kept under a nitrogen atmosphere at 3° for 3 days. The solution was then cooled on an ice bath, treated with 2 ml of ice-water, and stirred at 0° for 20 min. Ice-cold ether (60 ml) was added to the cold reaction mixture and the ethereal solution was worked-up in the usual manner with ice-cold 2 *M* hydrochloric acid and brine. The semi-crystalline product (370 mg) was used immediately for the next step.

The following reaction was carried out in a dry nitrogen atmosphere. The tosylate (370 mg) was dissolved in 5 ml of dry dimethyl sulfoxide and the solution was treated with 2.8 ml of a 0.5 *M* dimethyl sulfoxide solution of methylsulfinyl carbanion (18). The reaction solution was kept at 60° for 2 h, cooled to room temperature, and treated with 0.5 ml of water then diluted with 60 ml of ether. The ether solution was worked-up with brine in the usual manner. The product was purified by t.l.c. on silica gel with benzene–ether (95:5) as solvent. Elution of the silica gel afforded 147 mg (71%) of **20** as an oil which gave rise to a single peak on v.p.c. having a retention time of 15 min, 40 s (column temperature programmed from 50 to 250° at 10°/mm), λ_{max} (EtOH) 208 nm (ε 4000); ν_{max} (film) 1715 cm^{-1} (ketone); n.m.r. ($CDCl_3$), δ *ca.* 0.60 (m, partially obscured, protons on cyclopropane ring), 0.73 (d, $J = 6.5$ Hz, 3H, secondary methyl), 0.97 (s, 3H, angular methyl), 1.17 (s, 3H, methyl on cyclopropane ring).

Anal. Calcd. for $C_{15}H_{22}O$: C, 82.52; H, 10.16. Found: C, 82.39; H, 9.88.

From Keto Alcohol **18***b*

The keto alcohol **18***b* was converted into the cyclopropyl ketone **20** in 60% yield by the procedure described in the preceding experiment. The product was identical with the cyclopropyl ketone obtained in the preceding experiment (i.r. and n.m.r. spectra, identical retention time on v.p.c. and inseparability on t.l.c. in various solvent systems).

*(±)-Ishwarane (***1***)*

The reduction of the cyclopropyl ketone **20** to ishwarane was carried out in a dry nitrogen atmosphere as follows (*cf.* 19). The cyclopropyl ketone **20** was dissolved in 6 ml of a stock solution prepared by dissolving 690 mg of sodium in 60 ml of ethylene glycol. The resulting solution was treated with 0.2 ml of anhydrous hydrazine (19) and heated with an oil bath until the temperature of the reaction solution reached 180°. More anhydrous hydrazine was added until the reaction solution refluxed freely at 180° and reflux at this temperature was continued for 14 h. Hydrazine was then distilled from the reaction flask until the temperature of the reaction solution reached 210°. After heating the reaction solution at 210° for 24 h, it was allowed to cool to room temperature and diluted with 60 ml of ether. The ether solution was worked-up in the usual manner with ice-cold 1 *M* hydrochloric acid, saturated sodium bicarbonate, and brine. Purification of the product by t.l.c. on silica gel with hexane as solvent afforded 64 mg (67%) of **1** as an oil which gave rise to a single peak on v.p.c. having a retention time of 17 min, 20 s (column temperature programmed from 50 to 250° at 8°/min), i.r., devoid of carbonyl absorption; n.m.r. (CCl_4), δ 0.50 (m, 2H, protons on cyclopropane ring), 0.72 (d, $J = 6.5$ Hz, 3H, secondary methyl), 0.78 (s, 3H, angular methyl), 1.12 (s, 3H, methyl on cyclopropane ring).

Anal. Calcd. for $C_{15}H_{24}$ (mol. wt. 204): C, 88.16; H, 11.84. Found (204 (mass spectrum)): C, 88.31; H, 11.65.

The synthetic hydrocarbon **1** was identical with an authentic sample of ishwarane obtained from natural sources (i.r. and n.m.r. spectra, retention times on v.p.c., fragmentation pattern of the mass spectra).

We are grateful to the National Research Council of Canada for a grant in aid of this work. We also thank Dr. T. R. Govindachari, CIBA Research Centre, Bombay, India for samples and spectra of isoishwarane and ishwarane and Dr. E. Piers, University of British Columbia, Vancouver, B.C., for his cooperation in establishing the stereochemistry of the octalone.

1. U. S. K. Rao, B. L. Manjunath, and K. N. Menon. J. Indian Chem. Soc. **12**, 494 (1935).
2. A. K. Ganguly, K. W. Gopinath, T. R. Govindachari, K. Nagarajan, B. R. Pai, and P. C. Parthasarathy. Tetrahedron Lett. 133 (1969).
3. H. Fuhrer, A. K. Ganguly, K. W. Gopinath, T. R. Govindachari, K. Nagarajan, B. R. Pai, and P. C. Parthasarathy. Tetrahedron, **26**, 2371 (1970).
4. T. R. Govindachari, P. A. Mohamed, and P. C. Parthasarathy. Tetrahedron, **26**, 615 (1970).
5. R. T. Govindachari, K. Nagarajan, and P. C. Parthasarathy. Chem. Commun. 823 (1969).
6. L. C. Teng and J. F. DeBardeleben. Experientia, **27**, 14 (1971).
7. R. B. Kelly and J. Zamecnik. Chem. Commun. 1102 (1970).
8. R. B. Kelly, J. Zamecnik, and B. A. Beckett. Chem. Commun. 479 (1971).
9. H. E. Ulery and J. H. Richards. J. Am. Chem. Soc. **86**, 3113 (1964).
10. E. Piers, R. W. Britton, and W. de Waal. Can. J. Chem. **47**, 4307 (1969).
11. C. Berger, M. Frank-Neumann, and G. Ourisson. Tetrahedron Lett. 3451 (1968).
12. K. Wiesner, L. Poon, I. Jirkovsky, and M. Fishman. Can. J. Chem. **47**, 433 (1969).
13. R. W. Guthrie, Z. Valenta, and K. Wiesner. Tetrahedron Lett. 4645 (1966).
14. N. S. Bhacca and D. H. Williams. Applications of n.m.r. spectroscopy in organic chemistry. Holden-Day, Inc., San Francisco. 1964. pp. 103–104.
15. Huang-Minlon. J. Am. Chem. Soc. **71**, 3301 (1949).
16. Reference 14. Chapt. 2 and refs. cited therein.
17. K. Bowden, I. M. Heilbron, E. R. H. Jones, and B. C. L. Weedon. J. Chem. Soc. 39 (1946).
18. E. J. Corey and M. Chaykovsky. J. Am. Chem. Soc. **87**, 1345 (1965).
19. D. H. R. Barton, D. A. J. Ives, and B. R. Thomas. J. Chem. Soc. 2056 (1955).

Primary Bond Formation in the Addition of Cyclopentenone to Chloroethylenes[1,2]

R. O. LOUTFY[3] AND P. DE MAYO

Photochemistry Unit, Department of Chemistry, The University of Western Ontario, London, Ontario

Received June 21, 1972

The cycloaddition of cyclopentenone to all the halogenated ethylenes has been studied. There is no evidence, as has been previously suggested, that specific β addition takes place as the first step. The details of the two-step closure are discussed and it is concluded that spin relaxation is probably of no relevance for the stereochemical outcome.

La cycloaddition de la cyclopentènone sur tous les éthylènes halogénés a été étudiée. Il n'existe aucune preuve, comme cela a été suggéré antérieurement, pour que l'addition spécifique β ait lieu dans la première étape. La fermeture du cycle en deux étapes a été discutée en détail et on a conclu que la relaxation de spin n'a probablement aucun rapport avec le résultat stéréochimique.

Canadian Journal of Chemistry, **50**, 3465 (1972)

Can. J. Chem. Downloaded from www.nrcresearchpress.com by 210.87.254.40 on 09/05/12
For personal use only.

In recent years there has been much activity in several laboratories on the subject of the addition of photo-excited cyclic enones to olefins (for reviews, see refs. 2, 3), regarding both mechanism and synthetic utility. The broad outlines of the reaction pathway appear to have been elucidated, but several aspects remain unclear. It appears to be generally accepted that, with or without prior complex formation, a tetramethylene intermediate is involved which may either close to the cyclobutane or revert to starting materials.[4] A similar situation is found in other reactions (*inter alia* refs. 5–8 and refs. cited therein).

Amongst the matters remaining obscure at least in part, are the stereochemical features of the reaction; that is, both the question of the orientation of the two moieties with respect to each other and that of the geometry of the resultant fusion. Concerning the first aspect, the early contribution of Corey and coworkers (9) has been remarkably effective in relating orientation with presumed electron distribution in the reactive entities. There are clear indications, however, that this interpretation is not complete (10). With regards to the second question, satisfying interpretations are still lacking to explain, for instance, the occurrence of *trans*-fusions in photo-annelation. Of these the most extraordinary example (though not in an enone) is that reported in the addition of dichloromaleic anhydride to cyclopentadiene (11). Though rationalizations both on the basis of conformational analysis (3) and on speculations as to the geometry of the excited enone (see refs. cited in (2)) have been discussed, the overall picture remains in large measure unsatisfying.

Connected with both these questions is that of which bond, that is, that α or β to the carbonyl group, is formed first in a two-step reaction. Since, in this step the orientation of one of the relevant centers is fixed (to the extent that this particular tetramethylene goes on to give product), it was thought that a complete stereochemical study of one type of addition might shed some light on the problem of the preferred bond formation and, perhaps, on certain stereochemical aspects of the problem.

The structural elucidation of a number of stereoisomers represented a massive problem, and olefins were required, therefore, in which the orientations of the substituents in the products might be elucidated by n.m.r. spectroscopy. For this reason the chloroethylenes were selected, and, in the event, the structures of all adducts were successfully resolved. The synthesis and structural elucidation of these substances will be reported separately (12).

[1]Photochemical Synthesis. Part 45. For Part 44, see ref. 1.

[2]Publication no. 51 from the Photochemistry Unit, The University of Western Ontario.

[3]Present address: Division of Chemistry, National Research Council of Canada, Ottawa, Canada K1A 0R6.

[4]It has been suggested recently (4) that in the addition of 3-phenylcyclohex-2-enone to tetramethylethylene this may be the case whatever the multiplicity of the tetramethylene.

FOR ERRATA SEE
V.54(18)1974....P.3396.

TABLE 1. Product distribution and structures of cyclopentenone *vic*-dichloroethylene adducts*

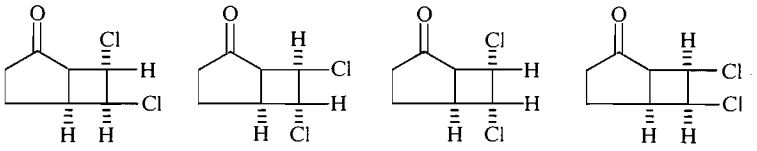

3 **4** **5** **6**

Olefin	Solvent	Temperature (°C)	Product distribution (%)† 3	4	5	6
cis-Dichloro-ethylene	Neat (13.2 *M*)	25	49.30	11.70	19.44	19.56
	Ether	25	50.20	11.17	19.56	19.07
	Ether	−75	55.97	8.03	13.26	22.73
trans-Dichloro-ethylene	Neat (13.2 *M*)	25	17.71	22.10	54.68	5.50
	Ether	25	18.35	23.04	52.62	6.00
	Ether	−75	14.85	10.83	69.94	4.28

*[Cyclopentenone] = 0.3 *M*; [*vic*-dichloroethylene] = 6.1 *M*.
†Each measurement was the average of three runs.

TABLE 2. Product distribution, and structures of cyclopentenone *gem*-dichloroethylene adducts

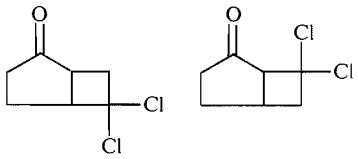

10 **11**

Ketone (*M*)	Olefin (*M*)	Solvent	Temperature (°C)	Product distribution (%) 10	11
0.30	5	Cyclohexane	25	84.55	15.44
0.25	5	Ether	25	84.19	15.81
0.25	5	CH_3CN	25	70.65	29.35
0.25	10	Neat	25	80.51	19.49
0.25	10	Neat	−75	85.38	14.61

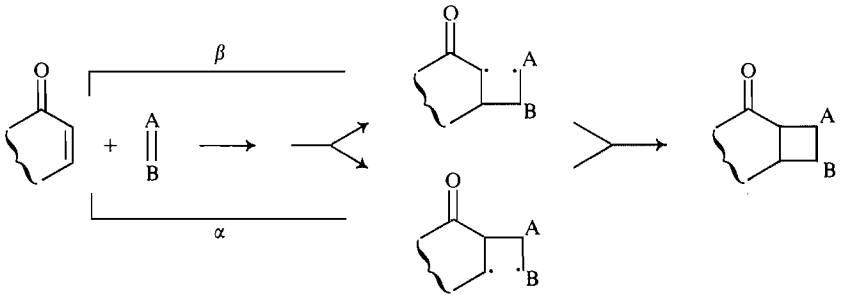

SCHEME 1

Can. J. Chem. Downloaded from www.nrcresearchpress.com by 210.87.254.40 on 09/05/12
For personal use only.

TABLE 3. Product distribution (%), and structures of cyclopentenone trichloroethylene adducts*

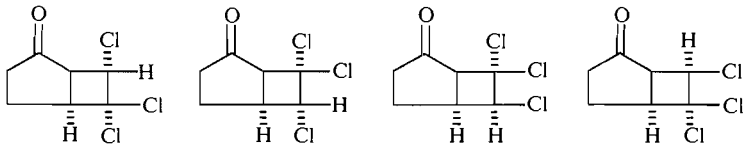

12 **13** **14** **15**

Solvent	Solvent dielectric constant	12	13	14	15
Cyclohexane	2.22	28.00	23.13	32.56	16.31
Ether	4.33	25.92	22.13	35.81	16.12
Acetonitrile	37.5	23.71	21.42	41.15	13.71
Acetic acid	6.5	28.54	16.42	34.58	20.45
Ether (−75 °C)		39.32	13.13	36.94	10.56

*[Cyclopentenone] = 0.25 *M*; [trichloroethylene] = 5 *M*.

TABLE 4. Product distribution (%), and structures of cyclopentenone vinyl chloride adducts*

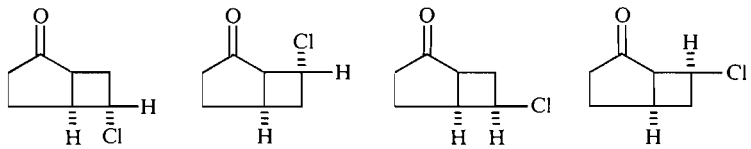

16 **17** **18** **19**

Solvent	16	17	18	19
Ether (−75 °C)	30.80	32.80	30.70	5.67

*[Cyclopentenone] = 0.3 *M*; [vinyl ethylene] = 6 *M*.

Whilst this study was in progress a report appeared of the results of a similar investigation (13). Whilst our results do not, in our opinion, unfortunately, allow the drawing of unequivocal positive conclusions, we believe that a number of possibilities, including that propounded in ref. (13), may be excluded, at least for the system studied.

The composition of the mixtures obtained by the addition of cyclopentenone to vinyl chloride, *cis*- and *trans*-dichloroethylenes (DCE), 1,1-dichloroethylene, and trichloroethylene are listed in Tables 1–4. Since the *cis*- and *trans*-DCE are the source of more information they will be discussed first.

A simplified possible general path for photo-annelation is shown in Scheme 1. It presents the two possible tetramethylene intermediates both of which may close or revert to starting material. We shall discuss the question of multiplicity later, but since the reaction involves the triplet manifold (2) the tetramethylene will probably initially be a triplet.[5] A number of authors have suggested that most of the products from the photo-annelation of $\alpha\beta$-unsaturated ketones derive from a process in which the first bond is formed at C-3 (Scheme 1, path β) (for example, see refs. 18–20). The evidence that this is so in general is not compelling and there are instances which indicate that α addition may occur (21). (The presence

[5]We prefer this description rather than a doublet of doublets since over the distances involved there must be overlap (14–16). For a powerful discussion of this entire problem recourse should be had to the lucid presentation of the physical chemists Salem and Rowland (17).

Can. J. Chem. Downloaded from www.nrcresearchpress.com by 210.87.254.40 on 09/05/12
For personal use only.

Can. J. Chem. Downloaded from www.nrcresearchpress.com by 210.87.254.40 on 09/05/12
For personal use only.

of the appropriate isobutenyl derivatives in the products of isobutene addition to cyclohexenone (9) also suggest this.)

For the DCE's it was proposed (13) that initial bond formation occurred solely at C-3 (β pathway) and that the biradical intermediates were conformationally equilibrated before ring closure. The basis for the conclusion was the analysis of the product distribution. On the assumption of C-3 bond formation, the partitioning of the two tetramethylenes, **1** and **2**,

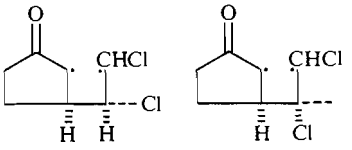

1 **2**

can be calculated. The same tetramethylenes obtained from the isomeric DCE should, with equilibration prior to closure, partition in the same way. Although the original results suggested that this was the case (13), our present results do not confirm this.[6] A similar analysis based on α bond formation was also unsatisfactory leading therefore to the conclusion that one (or more) of the assumptions implicit in this approach was invalid. And in a certain sense, even if the analysis had been satisfactory, the results would have retained an element of ambiguity. Evidently such an analysis could only refer to bond formation leading to product. It is quite conceivable that the fastest primary bond formation (K_r) is by one pathway such as α. A fraction of these, perhaps small, go on to product and the major part reverts to starting material. A slower (K_r') primary bond formation might be by pathway β, but in this case the majority of the tetramethylenes give product. This situation would not be revealed by any product analysis.

One measure of the occurrence of this energy-wasting phenomenon, one which has been observed in thermal addition also (22), and, in fact, the method by which it was revealed (23, 24), is the value of the quantum yield of addition at infinite olefin concentration. The quantum yield has been determined for the DCE's previously (25) in neat liquid, (13 M) but have not been extrapolated to infinite concentration. Previous experience (26) suggests that the difference would not be great and so the values obtained ($\Phi_{cis\text{-DCE}} = 0.35$; $\Phi_{trans\text{-DCE}} = 0.18$)[7] incline us to believe that the *cis* addition is reversing less than the *trans* (provided that no other energy-wasting reversible intermediate lies on the reaction pathway before the tetramethylene). A similar observation has been made by Bartlett and coworkers (27) in the addition of the DCE's to triplet cyclopentadiene. But if the same two species were formed from both isomers the same reversibility would be expected. One must conclude, then, that either the tetramethylenes are not identical because equilibration has not occurred prior to closure, or both α and β bond formation occur to a different degree with the different isomer, or both. In the second and third cases the composition would depend on the rates of formation of the relevant tetramethylenes.

The present results provide another argument against the participation of the same two, and only two, tetramethylenes in DCE addition. Such species, if equilibrated, should be influenced in their partitioning between closing and reverting to starting materials, by temperature in the same way. Assuming α or β bond formation only, analysis using the product distribution obtained at $-75°$ (Table 1) leads to an even worse fit than obtained at room temperature. This would be reasonable if, at the lower temperature, the distribution were further away from equilibrium than at room temperature. Indeed the ratio of *trans* to *cis* products is closer, when approached from the isomeric DCE's, at room temperature than at low temperature. Thus, the *trans*:*cis* ratio for *cis*-DCE decreases from 1.78 at low temperature to 1.58 whilst for *trans*-DCE the ratio increases from 0.35 to 0.71. However the configuration favored at low temperature is the *opposite* of that of the starting olefin. That is, more *trans* products are formed from *cis*-DCE and more *cis* from *trans*-DCE. On the assumption that only β bond formation leads to product then this cannot be interpreted as being due to incomplete equilibration.

[6]One source of error may have been the missing of the fourth isomer (**6**) which has a longer retention time than the other three.

[7]The value given here was based on all four adducts (28, 29).

[1] 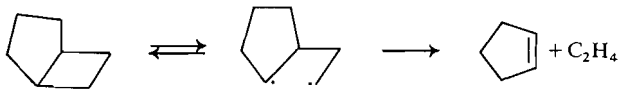

As has been shown (28, 29) a change in temperature in enone photo-annelation leads both to change in K_r (the rate of disappearance of the quenchable species (28)) and to change in the relative partitioning of the tetramethylene. With cyclopentenone and cyclohexene for instance the value of K_r changed from 12×10^8 to 3.2×10^8 M^{-1} s^{-1} with a change of temperature from 27 to -71 °C. Over the same temperature range the fraction of molecules leading to product changed from 0.49 to 0.72. Our conclusion from these observations is that both α and β bond-formation pathways are operative. At present we have no adequate explanation for the preferred stereochemical inversion unless specific interactions between the halogen and the carbonyl group occur.

There has been much speculation as to the nature and behavior of the tetramethylenes formed in cycloaddition, particularly as regards thermally induced processes (*inter alia* 22, 27, 30–32). With photochemical reactions proceeding through the triplet, the additional complexities of spin relaxation are introduced. If in the present reactions spin correlation were the rate-determining step then much of the previous discussion would be void. However there is reason to believe that spin relaxation cannot be the slow step.

The closure of singlet tetramethylene unlike the combination of radicals, implies an activation energy reflecting part of the strain inherent in a cyclobutane. In the present cases the fusion of a cyclopentanone ring to the cyclobutane may increase this activation energy somewhat, and it should be remembered that similar photo-annelations with acetylenes to give cyclobutenes are known (33, 34) and that even additions to cyclobutenes (29) (to give the 2.2.0 bicyclohexane system) are recorded. In the latter the strain is considerably increased and must in part be reflected in the transition state. With activation energies of ~6.6 kcal/mol (35, 36) estimated for the bicyclo[3.2.0]heptane system bond closure must necessarily be slow. Further non-bonded interactions of the halogen substituents with the skeletal atoms may increase this further. With a positive activation as high as 7–8 kcal/mol (and possibly more if *trans* fusions are generated) rate constants at room temperature of the order of 10^8 s^{-1} would be admissible.

On the other hand in the presence of the halogen atoms intersystem crossing should be enhanced. Thus one chlorine atom attached to the naphthalene nucleus can decrease the lifetime of the triplet by about an order of magnitude (37). In the tetramethylenes under discussion the singlet–triplet energy splitting is necessarily small because of the near degeneracy and the tetramethylene must be subject to greater magnetic and electric perturbation than in, for instance, an aromatic hydrocarbon, quite aside from adventitious quenching by impurities such as oxygen that drastically shortens the lifetime of aromatic triplets. Since the latter may have lifetimes as short as 1 μs those for the triplet tetramethylene in solution may well be less. It is interesting that product distribution in several cycloadditions carried out in this laboratory appear to be the same under rigorous degassing (freeze–thaw cycles), nitrogen passage, and occasionally without any precaution. These experiments were not deliberately carried out, the significance at that time not being understood, and so are merely suggestive. But such observations seem to imply that the lifetime of the triplet tetramethylene is not shortened by oxygen.

But although ring closure is, it seems, slower than spin relaxation, it may not be the slowest step. The tetramethylene may well, because of electron repulsion, be formed in a conformation incapable of cyclization (30, 32) which may have to await the attaining of such an appropriate arrangement. The energy barriers to rotation have been discussed elsewhere (22, 30, 38) and if of the order of 5–8 kcal/mol, as seems likely, may well be competitive with bond closure.

We concur, therefore, with the views of Stephenson and Brauman (32) in believing (*a fortiori* in the case of the chlorinated compounds) that the original spin state in these

Can. J. Chem. Downloaded from www.nrcresearchpress.com by 210.87.254.40 on 09/05/12
For personal use only.

Can. J. Chem. Downloaded from www.nrcresearchpress.com by 210.87.254.40 on 09/05/12
For personal use only.

cycloadditions is irrelevant. Wagner and Zapp (8) have very recently reached similar conclusions with regards the Norrish Type II.

A limited amount of further information may be gleaned from adduct formation with the other chloroolefins.

The addition to 1,1-dichloroethylene gave the adduct which was predominantly 6,6-disubstituted. The two tetramethylenes which could give rise to this are **7** and **8**, of which **8** may be estimated to be about 8 kcal/mol more stable than **7** (40). This suggests, but does not conclusively prove, that in this case α addition is predominant. The alternative view would be that β addition is still predominant but that **9**

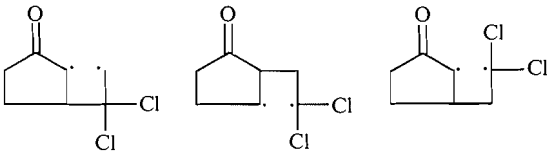

7 **8** **9**

has a high probability of reversal to starting material. In this case the quantum yield must of necessity be low, but the required data are not available.

On the basis of the Corey mechanism the same orientation would be expected as with ketene acetal, but to a lesser degree as is observed (though all orientation effects are contingent on the degree of reversibility). However, the overall dipole–dipole interactions would be expected to lead to the same product (10). This view makes the additional prediction that such specificity may decrease in polar media, and this is in agreement with the present results (Table 2). In acetonitrile the ratio of **10** to **11** changes by about a factor of two as against the value in diethyl ether. The small, but real changes in isomer distribution with change of temperature however imply most probably changes in reversibility and limit the conclusion which can be drawn. It should be noted that in other cases quite small orientation preferences have been observed even with polar substituents on the olefin (39–41) but unfortunately the relevant solvent studies were not made.

The case of the trichloroethylenes would be expected to be more complex. The overall dipole–dipole interaction will be less and will, furthermore, not be directed along the axis of the carbon–carbon double bond. This implies a greater solvent dependence for product distribution. Bartlett concluded that in the addition of cyclopentadiene to trichloroethylene 81.5% passed through the tetramethylene stabilized by two chlorine atoms (27). This assumed terminal addition to the diene. In the present case stabilization of an electron by an adjacent carbonyl is trivial as compared with that by a double bond (42) and it is doubtful that analogy can be made. The major product is now not the 6,6-dihalo compound, but there is little overall preference. The same appears true for the vinyl chloride adducts.

Experimental

The preparation and structure proof for these substances are described elsewhere (12, 29). Analytical gas chromatography was performed on an Aerograph (Hi Fi 600-A) hydrogen flame detector equipped with a 5% FFAP, 9 ft × 1/8 in. column using a Diatoporte S support at 100°. The areas were integrated using a Digital Readout System Model CRS-100 (Infrotronics), and the results were corrected for the differences in flame detector response.

1. R. Lapouyade and P. de Mayo. Can. J. Chem. Submitted.
2. P. de Mayo. Acc. Chem. Res. **4**, 41 (1971).
3. P. G. Bauslaugh. Synth. **2**, 287 (1970).
4. J. J. McCullough and B. R. Ramachandran. Chem. Commun. 1180 (1971).
5. L. K. Montgomery, K. Schueller, and P. D. Bartlett. J. Am. Chem. Soc. **86**, 622 (1964).
6. P. D. Bartlett and N. A. Porter. J. Am. Chem. Soc. **90**, 5317 (1968).
7. N. C. Yang and S. P. Elliott. J. Am. Chem. Soc. **91**, 7550 (1969).
8. P. J. Wagner and R. G. Zepp. J. Am. Chem. Soc. **94**, 287 (1972).
9. E. J. Corey, J. D. Bass, D. Le Mahieu, and R. B. Mitra. J. Am. Chem. Soc. **86**, 5570 (1964).
10. B. D. Challand and P. de Mayo. Chem. Commun. 982 (1968).
11. H-D. Scharf. Tetrahedron Lett. 4231 (1967).
12. M. C. Woods, N. Farid, and R. O. Loutfy. In preparation.
13. W. L. Dilling, T. E. Tabor, F. P. Boer, and P. P. North. J. Am. Chem. Soc. **92**, 1399 (1970).
14. M. C. R. Symons. Nature, **213**, 1226 (1967).
15. P. D. Bartlett and J. M. McBride. Pure App. Chem. **15**, 89 (1967).
16. A. B. Evnin, D. R. Arnold, L. A. Karnischky, and E. Strom. J. Am. Chem. Soc. **92**, 6218 (1971).
17. L. Salem and C. Rowland. Angew. Chem. Int. Ed. **11**, 92 (1972).
18. P. J. Wagner and G. S. Hammond. Adv. Photochem. **5**, 21 (1968); *cf.* p. 118.

19. T. S. CANTRELL, W. S. HALLER, and J. C. WILLIAMS. J. Org. Chem. **34**, 509 (1969).
20. J. W. HANIFIN and E. COHEN. J. Am. Chem. Soc. **91**, 4494 (1969).
21. J. J. MCCULLOUGH, J. M. KELLY, and P. W. W. RASMUSSEN. J. Org. Chem. **34**, 2933 (1969).
22. P. D. BARTLETT, C. J. DEMPSTER, L. K. MONTGOMERY, K. E. SCHUELLER, and G. E. H. WALLBILLICH. J. Am. Chem. Soc. **91**, 405 (1969).
23. P. DE MAYO, A. A. NICHOLSON, and M. F. TCHIR. Can. J. Chem. **47**, 711 (1969).
24. P. J. WAGNER and D. J. BUCHEK. Can. J. Chem. **47**, 713 (1969).
25. P. DE MAYO, J-P. PETE, and M. F. TCHIR. Can. J. Chem. **46**, 2535 (1968).
26. P. DE MAYO, A. A. NICHOLSON, and M. F. TCHIR. Can. J. Chem. **48**, 225 (1970).
27. P. D. BARTLETT, R. HELGESON, and O. A. WERSEL. Pure App. Chem. 187 (1970).
28. R. O. LOUTFY, P. DE MAYO, and M. F. TCHIR. J. Am. Chem. Soc. **91**, 3984 (1969).
29. R. O. LOUTFY. Unpublished observations; Ph.D. Thesis, The University of Western Ontario, London, Ontario, 1972.
30. R. G. BERGMAN and W. L. CARTER. J. Am. Chem. Soc. **91**, 7510 (1969).
31. P. D. BARTLETT. Sci. **159**, 833 (1968).
32. L. M. STEPHENSON and J. I. BRAUMAN. J. Am. Chem. Soc. **93**, 1988 (1971).
33. P. E. EATON. Tetrahedron Lett. 3695 (1964).
34. P. DE MAYO and M. C. USSELMAN. Anales de Quimica. In press.
35. H. E. O'NEAL and S. W. BENSON. Int. J. Chem. Kinet. **11**, 423 (1970).
36. H. E. O'NEAL and S. W. BENSON. J. Phys. Chem. **72**, 1866 (1968).
37. J. B. BIRKS. Photophysics of aromatic molecules. Wiley, New York. 1970. p. 208 *et seq.*
38. J. A. BERSON, D. C. TOMKINS, and G. JONES. J. Am. Chem. Soc. **92**, 5799 (1970).
39. N. J. TURRO and P. A. WRIEDE. J. Am. Chem. Soc. **92**, 320 (1970).
40. S. H. SCHROETER and C. M. ORLANDO. J. Org. Chem. **34**, 1181 (1969).
41. S. H. SCHROETER. Chem. Commun. 12 (1969).
42. S. W. BENSON. Thermochemical kinetics. Wiley, New York. 1968. See also H. E. O'NEAL and S. W. BENSON. Kinetic data on gas phase unimolecular reactions. U.S. Department of Commerce. National Bureau of Standards, 1970.

Can. J. Chem. Downloaded from www.nrcresearchpress.com by 210.87.254.40 on 09/05/12
For personal use only.

Nitration Studies on 2-Isopropylimidazole

R. S. GLASS,[1] J. F. BLOUNT, D. BUTLER, A. PERROTTA, AND E. P. OLIVETO

Chemical Research Department, Hoffmann-La Roche Inc., Nutley, New Jersey 07110

Received March 6, 1972

The nitration of 2-isopropylimidazole has been studied under a variety of conditions involving nitration of the unprotonated imidazole, the imidazole anion, or an imidazole radical. From the reaction of nitronium tetrafluoroborate with 1-trimethylsilyl-2-isopropylimidazole there was isolated a dinitro compound the structure of which was shown by X-ray crystallography to be 1,4-dinitro-2-isopropylimidazole.

On a étudié la nitration de 2-isopropylimidazole sous des conditions diverses y comprenant la nitration de l'imidazole non protoné, l'anion de l'imidazole ou un radical de l'imidazole. De la réaction entre le tétrafluoroborate de nitronium et le 1-triméthylsilyl-2-isopropylimidazole on a isolé un composé dinitro dont la structure s'est montrée d'être le 1,4-dinitro-2-isopropylimidazole avec l'aide de la cristallographie par rayons X.

Canadian Journal of Chemistry, **50**, 3472 (1972)

Can. J. Chem. Downloaded from www.nrcresearchpress.com by 210.87.254.42 on 09/05/12
For personal use only.

In the course of preparing the potent histomonostat (1, 2) and trichomonacide (3) 1-methyl-2-isopropyl-5-nitroimidazole,[2] we found it necessary to study alternate methods of nitrating the intermediate 2-isopropylimidazole, since the standard nitration procedure (4, 5) for 2-substituted imidazoles using a mixture of nitric and sulfuric acids gave only about 50% of the desired 2-isopropyl-4(5)-nitroimidazole. Nitration in the presence of mercuric chloride (6) gave slight improvement. Addition of sulfur trioxide to the nitrating mixture gave inferior results, in contrast to the improvement reported for the nitration of imidazole (7).

To augment these studies three alternate methods of nitrating 2-isopropylimidazole were attempted: (*a*) nitration of unprotonated imidazole derivative, (*b*) nitration of an imidazole anion, and (*c*) nitration of an imidazolium radical.

Katritzky and others (8, 9) have demonstrated that basic pyridines ($pK_a > +1$) are first protonated and then slowly nitrated, while weakly basic pyridines ($pK_a < -2.5$) undergo nitration under mild conditions as free bases. Thus, the difficulty in nitrating 2-substituted imidazoles with nitric–sulfuric acid mixtures might be ascribed to the fact that the protonated species is being nitrated (7).[3]

A procedure in which unprotonated basic nitrogen heterocycles may be nitrated was reported by Olah (11) who found that nitronium tetrafluoroborate nitrates aromatic compounds in solvents such as sulfolane and acetonitrile. However, a possible complicating feature when aromatic heterocycles are nitrated could be the occurrence of C or N nitration. Indeed, Olah and co-workers (12) found that nitronium tetrafluoroborate reacts with pyridine to form the *N*-nitro salt. Other pyridines and a quinoline have shown similar behavior (13).

Nitration of 2-isopropylimidazole with nitronium tetrafluoroborate gave crude 4(5)-nitro-2-isopropylimidazole in 49% yield (31% after recrystallization). Two reasonable mechanisms for this reaction are shown in Schemes 1 and 2.

These mechanisms suggest likely reasons for the low yield of **2**. The *N*-nitro intermediate (like *N*-nitropyridine) (12) may not undergo N to C rearrangement of the nitro group (14) or at least not completely. Ring opening of the *N*-nitro salt would also lead to reduced yields of **2**. Incidentally, a stable *N*-nitro salt could not be isolated from the reaction.

Another possible cause for the low yield of **2**, namely further reaction of this compound with nitronium tetrafluoroborate, is ruled out because **2** may be recovered in good yield after exposure to the nitration conditions.

Both Schemes 1 and 2 involve the formation of fluoroboric acid (or its salt with **2**). If 2-isopropylimidazole reacts with fluoroboric acid instead of nitronium tetrafluoroborate, the

[1]Present address: University of Arizona, Tucson, Arizona 85721.

[2]TM® Ipropran (Hoffmann-LaRoche Inc.)

[3]The pK_a in water of 2-ethylimidazole is 8 (10).

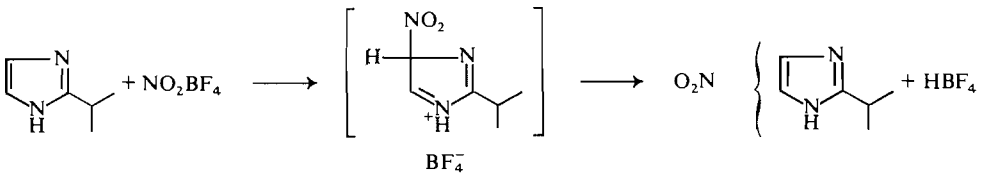

1 2

SCHEME 1

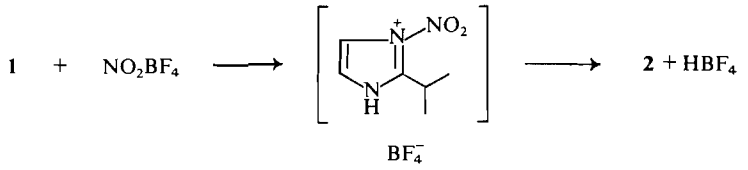

SCHEME 2

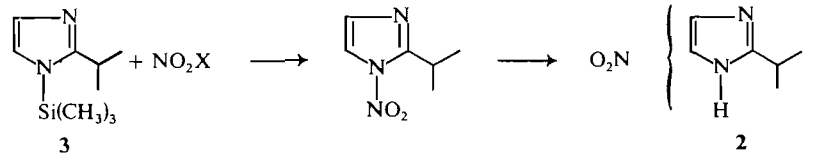

3 2

SCHEME 3

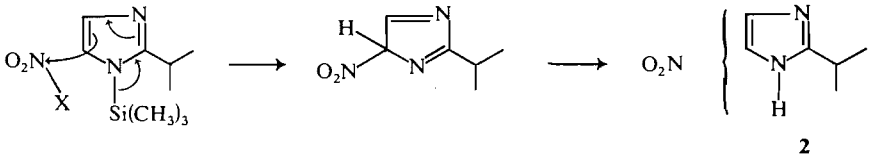

2

SCHEME 4

resulting salt might be stable to the reaction conditions. In this event, some 2-isopropylimidazole would be recovered on work-up, and this was indeed observed.

To avoid the formation of an unreactive 2-isopropylimidazolium salt in the nitration of 2-isopropylimidazole, a derivative which might undergo nitration without loss of a proton was investigated. 1-Trimethylsilyl-2-isopropylimidazole (**3**) might react with a NO_2^+ source according to Schemes 3 or 4. Scheme 3 is analogous to conversion of 1-trimethylsilylimidazole into 1-acetylimidazole (15), *N*,*N*′-thiocarbonyldiimidazole (16), and *N*,*N*′-imidazolesulfide (17) with acetyl chloride, thiophosgene, and sulfur dichloride, respectively. Scheme 4 is analogous to the formation of 1-acetyl-1,2,3-triazole from 2-trimethylsilyl-1,2,3-triazole and acetyl chloride (18). Unfortunately **2** was not obtained on treatment of 1-trimethylsilyl-2-isopropylimidazole with nitryl chloride.[4] The silyl compound **3**, however, afforded a mixture of **2** and a dinitro compound on reaction with nitronium tetrafluoroborate. The spectral data and elemental analysis for the dinitro compound are consistent with structure **4** (Scheme 5).

The u.v. or n.m.r. spectrum (20) of this compound does not unambiguously support one isomer (either **4***a* or **4***b*) over the other. Chemical support for the gross structure was obtained in two ways. Nitrolysis (21) of **4** in concentrated sulfuric acid gave **2**, and catalytic hydrogena-

[4]Nitryl chloride, which may be in equilibrium with nitrogen dioxide and chlorine (19*a*, *b*) has been pictured as a source of free radicals (19*a*, *c*, *d*), chloronium ions (19*d*), and nitronium ions (19*c*).

Can. J. Chem. Downloaded from www.nrcresearchpress.com by 210.87.254.42 on 09/05/12
For personal use only.

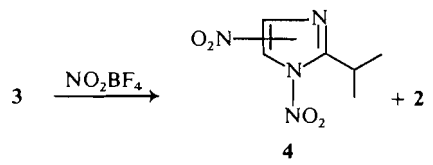

4

a = 4-NO_2
b = 5-NO_2

SCHEME 5

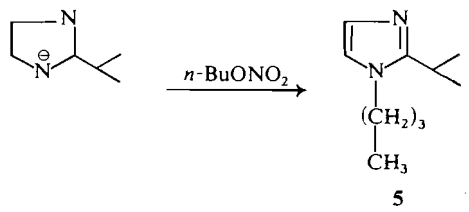

5

SCHEME 6

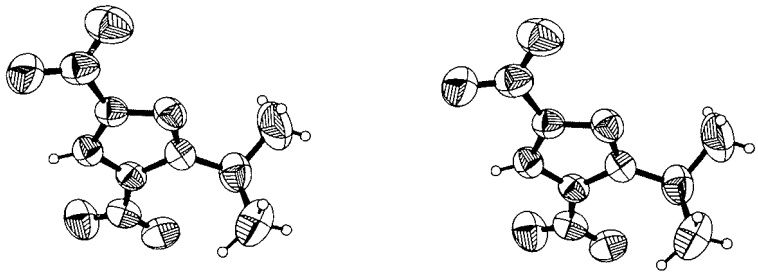

FIG. 1. Stereoscopic view of **4***a*.

tion in acetic anhydride (20*a*, 22) afforded a diacetate which was identical with that prepared by catalytic hydrogenation of **2** in acetic anhydride.

During the progress of this work a report appeared (23) which described the formation of 2-methyl-1 (4 or 5)-dinitroimidazole in high yield from the nitration of 2-methylimidazole with nitric acid in the presence of acetic anhydride. The exact position of the *C*-nitro group could not be determined. Application of these nitration conditions to **1** produced **4** in good yield. With sufficient material now easily available, crystals suitable for an X-ray analysis could be obtained, and the structure was shown to be 2-isopropyl-1,4-dinitroimidazole (**4***a*). (see Fig. 1).

Nitration of 2-isopropylimidazole anion (24) was then investigated. Sodium hydride converted 2-isopropylimidazole into the corresponding sodium salt, and the reaction of this salt with *n*-butyl nitrate in tetrahydrofuran gave only 1-*n*-butyl-2-isopropylimidazole (**5**) (Scheme 6).[5] This material was identical with the compound prepared from *n*-butyl iodide and the sodium salt of 2-isopropylimidazole.

[5]Solvolysis of nitrates has been shown to involve displacement on carbon, displacement on nitrogen, β-hydrogen elimination giving an olefin and α-hydrogen elimination giving a carbonyl compound (25).

For attempted nitration of an imidazole radical,[6] sodium 2-isopropylimidazole was reacted with tetranitromethane (28, 29), but no isolable **2** was formed. Also, decomposition of pernitrous acid (30) in the presence of 2-isopropylimidazole resulted only in the recovery of starting material.

Experimental

All melting points were taken on a Thomas–Hoover capillary melting point apparatus, and are uncorrected. All elemental analyses were performed on samples which were recrystallized an additional time.

Nitration of 2-Isopropylimidazole (1)

(A) Using Nitronium Tetrafluoroborate

To a stirred slurry of nitronium tetrafluoroborate (32) (3.03 g, 0.022 mol) and dried, distilled acetonitrile (6 ml) cooled in an ice bath, a solution of 2-isopropylimidazole (2.02 g, 0.018 mol) in dried, distilled acetonitrile (30 ml) was added dropwise. Stirring and cooling were continued for 30 min after completion of the addition. The solution was then concentrated on a rotary evaporator and added to aqueous sodium bicarbonate solution without delay. The aqueous solution was extracted with chloroform and the extract dried (anhydrous Na_2SO_4) and concentrated to dryness, giving an orange–brown solid (1.38 g, 49%). This material was dissolved in benzene–chloroform, washed through an alumina (5 g) column, and recrystallized from water to give a total of 0.86 g (31%) of **2** in two crops, m.p. 182–183.5° (lit. (3, 31) m.p. 180°).

[6]Unfortunately, very little is known about the reactivity of imidazoles towards radicals (26, 27).

Can. J. Chem. Downloaded from www.nrcresearchpress.com by 210.87.254.42 on 09/05/12
For personal use only.

Can. J. Chem. Downloaded from www.nrcresearchpress.com by 210.87.254.42 on 09/05/12
For personal use only.

(B) Using HNO_3-Ac_2O

To a solution of 4.0 g of **1** in 115 ml of glacial acetic acid was added 26.4 ml of concentrated nitric acid and then 71.2 ml of acetic anhydride was added slowly over a period of 35–40 min while maintaining the temperature at 20–22°. After being stirred at this temperature for an additional hour, the mixture was added to 200 ml of water at 17–20°, stirred for 15 min, and extracted with methylene chloride. The extracts were washed with sodium bicarbonate solution, then with saturated salt solution, and dried over sodium sulfate. Evaporation of the solvent gave 2.8 g of crude **4***a*. Crystallization from ether–hexane gave 2.2 g (44%), m.p. 79–80°, identical (i.r., u.v., n.m.r.) with material obtained by nitration of **3** (see below).

*Nitration (NO_2BF_4) of 1-Trimethylsilyl-2-isopropylimidazole (**3**)*

A solution of 1-trimethylsilyl-2-isopropylimidazole (**3**) (prepared from 2-isopropylimidazole (1.00 g, 9.1 mmol) and hexamethyldisilazane (4.00 g, 31.0 mmol) in acetonitrile (10 ml)) was added dropwise to a stirred slurry of nitronium tetrafluoroborate (1.265 g, 9.5 mmol) and acetonitrile (5 ml) cooled in an ice bath. The solution was stirred for 30 min with ice cooling and benzene (2 ml) was added. It was concentrated on a rotary evaporator, neutralized with aqueous sodium bicarbonate, and extracted with chloroform. These extracts were dried (Na_2SO_4) and concentrated to an orange oil (1.07 g). A sample (150 mg) of this material was chromatographed on a layer of silica gel and eluted with a 4:5 acetone:cyclohexane mixture. Two bands separated from material at the origin and were extracted from the silica gel. Band 1 gave 25 mg of dinitro compound **4***a* (10%). Band 2 gave 36 mg of **2** (18%). Recrystallization of band 1 material from ether–hexane gave **4***a*, m.p. 76–77°.

Anal. Calcd. for $C_6H_8N_4O_4$: C, 36.00; H, 4.03; N, 27.99. Found: C, 35.78; H, 3.99; N, 27.71.

Recrystallization of band 2 material from acetonitrile gave **2**, m.p. 181–183°, identical (i.r., t.l.c., mixed m.p.) with an authentic sample.

*Sulfuric Acid Treatment of **4a***

A sample of **4***a* (41 mg, 0.26 mmol) was dissolved in concentrated sulfuric acid (8 drops). After standing 5 h at room temperature the solution was cooled, neutralized with aqueous sodium bicarbonate solution, and the p*H* adjusted to 2 with 1 *N* hydrochloric acid. This mixture was extracted with chloroform, the aqueous phase adjusted to p*H* 5 and again extracted with chloroform. The chloroform extracts were combined, dried (Na_2SO_4) and concentrated to dryness to give a solid (28.8 mg). This material was purified by t.l.c. to give a solid (28.5 mg, 72%) which was recrystallized from water to give 14 mg (36%) m.p. 181–182.5°, identical with **2** (mixed m.p., t.l.c., i.r.).

Reaction of Sodium 2-Isopropylimidazole with n-Butyl Nitrate

Sodium hydride (2.42 g, 54.5%) mineral oil dispersion, 0.055 mol) was added in small portions to a stirring solution of 2-isopropylimidazole (5.50 g, 0.050 mol) in anhydrous tetrahydrofuran (30 ml) under a nitrogen atmosphere. After stirring the reaction mixture for 2 h a solution of *n*-butyl nitrate (33) (5.95 g, 0.050 mol) in dry tetrahydrofuran (5 ml) was added dropwise and stirring was continued overnight. The reaction mixture was poured into water and the two phases separated. The aqueous solution was extracted with three 100 ml portions of chloroform. The water-insoluble phase was dissolved in chloroform and extracted with two 50 ml portions of dilute aqueous hydrochloric acid. The acidic aqueous solution was brought to p*H* 10 with concentrated ammonia and extracted with three 100 ml portions of chloroform. These chloroform extracts and those previously obtained were combined, dried (Na_2SO_4) and concentrated to a yellow oil which was distilled. A fraction distilling at 65–80° (1 mm) was collected (2.67 g, 32%). This material formed a picrate, m.p. 130.5–132°.

Anal. Calcd. for $C_{16}H_{21}N_5O_7$: C, 48.61; H, 5.32; N, 17.72. Found: C, 48.84; H, 5.49, N, 17.91.

Reaction of Sodium 2-Isopropylimidazole with n-Butyl Iodide

Sodium hydride (4.84 g, 54.5% mineral oil dispersion, 0.110 mol) was added portionwise to a stirred solution of 2-isopropylimidazole (11.0 g, 0.10 mol) in dry tetrahydrofuran (100 ml) under a nitrogen atmosphere. After stirring the reaction mixture for 3 h at room temperature, *n*-butyl iodide (18.0 g) was added dropwise. The reaction mixture was stirred overnight and then diluted with ether and filtered through Celite. The filtrate was concentrated to an oil. A sample of this oil was converted to a picrate, m.p. 131–132°, identical with material prepared from *n*-butyl nitrate.

Anal. Calcd. for $C_{16}H_{21}N_5O_7$: C, 48.61; H, 5.32; N, 17.72. Found: C, 48.58; H, 5.48; N, 17.89.

The remaining oil was distilled to give a fraction, b.p. 47–74° (0.7 mm); 8.7 g (52%).

Crystallography

The crystal data for **4***a* are:

$C_6H_8N_4O_4$ f.w. = 200.15

Monoclinic. $P2_1/c$, $a = 15.488(5)$, $b = 6.072(3)$, $c = 10.030(5)$ Å, $\beta = 99.35(3)°$, $V = 930.7$ Å^3, $\rho_o = 1.34(3)$, $Z = 4$, $\rho_c = 1.428$ g cm^{-3} (21 °C, CuKα, $\lambda = 1.5418$ Å).

The intensity data were measured on a Hilger–Watts model Y290 four circle diffractometer by a moving crystal-moving detector method. Nickel filtered CuKα radiation and pulse height discrimination were used. Of the 1749 accessible reflections in the unique quadrant ($2\theta < 140°$), 1000 had intensities significantly greater than background. The crystal was approximately $0.05 \times 0.2 \times 0.5$ mm.

The structure was solved by straightforward application of the symbolic addition method (34). All of the heavier atoms were located from the first *E*-map except for the three isopropyl carbon atoms, which were found in the subsequent electron density map. The hydrogen atoms were located from a difference Fourier calculated after refinement of the heavier atoms. Full matrix least squares refinement was continued with isotropic temperature factors for the hydrogens and anisotropic temperature factors for the other atoms until the shifts in all parameters were less than 1/6 of their respective standard deviations. A difference Fourier based on the final parameters has no features greater than 0.1 *e* Å^{-3} in magnitude. The final $R = \Sigma||F_o|-|F_c||/\Sigma|F_o| = 0.044$ for the 1000 observed data.

The function minimized in the least squares refinement was $\Sigma w||F_o|-|F_c||^2$ where $w = 1/(3.2 + |F_o| + 0.019|F_o|^2)$ for the observed data and $w = 0$ for the unobserved data.

TABLE 1. Final parameters (e.s.d.'s) × 10^4
T.F. (iso) = $\exp[-B\sin^2\theta/\lambda^2]$
T.F. (aniso) = $\exp[-(h^2\beta 11 + k^2\beta 22 + l^2\beta 33 + \beta hk\beta 12 + 2hl\beta 13 + 2k\beta 23)]$

Atom	x	y	z	$B \times 10$ or $\beta 11$	$\beta 22$	$\beta 33$	$\beta 12$	$\beta 13$	$\beta 23$
N(1)	1783(2)	−6310(4)	−1661(3)	53(1)	280(8)	109(3)	−14(3)	12(1)	−21(4)
C(2)	2573(2)	−5168(6)	−1459(3)	52(2)	355(11)	119(4)	−17(3)	13(2)	4(5)
N(3)	2476(2)	−3370(4)	−787(3)	56(1)	339(9)	127(4)	−24(3)	18(2)	−26(4)
C(4)	1632(2)	−3396(5)	−556(3)	55(1)	282(9)	101(4)	1(3)	14(2)	6(4)
C(5)	1180(2)	−5172(6)	−1079(3)	48(1)	344(10)	109(4)	−8(3)	8(2)	19(5)
N(2)	1558(2)	−8288(5)	−2402(3)	74(2)	337(10)	116(4)	−18(4)	9(2)	−11(4)
O(1)	2142(2)	−9246(4)	−2800(3)	91(2)	384(9)	153(4)	23(3)	12(2)	−52(4)
O(2)	0801(2)	−8788(5)	−2557(3)	75(2)	566(12)	214(5)	−75(4)	12(2)	−104(6)
N(4)	1302(2)	−1676(5)	205(3)	77(2)	315(9)	112(4)	12(3)	23(2)	21(4)
O(3)	1755(2)	−25(5)	464(3)	106(2)	363(8)	154(4)	−25(3)	34(2)	−49(4)
O(4)	591(2)	−1944(5)	539(3)	80(2)	464(10)	207(4)	33(3)	61(2)	28(5)
C(6)	3410(3)	−5904(8)	−1887(5)	61(2)	532(17)	171(6)	−15(5)	37(3)	−46(9)
C(7)	3956(6)	−3887(16)	−2109(13)	77(3)	790(35)	377(17)	−54(10)	92(7)	−22(23)
C(8)	3868(4)	−7530(14)	−820(8)	68(3)	727(29)	274(11)	60(8)	27(5)	−20(14)
H(5)	630(30)	−5620(70)	−1100(40)	66(10)					
H(6)	3280(30)	−6630(70)	−2700(50)	72(11)					
H(7)A	4440(50)	−4260(110)	−2230(70)	117(19)					
H(7)B	3690(50)	−2980(140)	−2710(80)	143(35)					
H(7)C	4090(40)	−3000(100)	−1290(60)	105(21)					
H(8)A	4020(40)	−6450(110)	−90(60)	119(21)					
H(8)B	4340(50)	−7900(100)	−1170(60)	119(19)					
H(8)C	3430(50)	−8810(110)	−750(70)	134(22)					

TABLE 2. Bond lengths (Å) in **4***a* with standard deviations in parentheses

Bond	Length	Bond	Length
N(1)—C(2)	1.392(4)	N(2)—O(2)	1.195(4)
C(2)—N(3)	1.305(4)	C(4)—N(4)	1.435(4)
N(3)—C(4)	1.365(4)	N(4)—O(3)	1.227(4)
C(4)—C(5)	1.344(5)	N(4)—O(4)	1.214(4)
C(5)—N(1)	1.367(4)	C(2)—C(6)	1.497(5)
N(1)—N(2)	1.426(4)	C(6)—C(7)	1.526(8)
N(2)—O(1)	1.198(4)	C(7)—C(8)	1.542(8)

TABLE 3. Bond angles (degrees) in **4***a* with standard deviations in parentheses

Bond	Angle
C(5)—N(1)—C(2)	109.4(3)
N(1)—C(2)—N(3)	108.6(3)
C(2)—N(3)—C(4)	105.8(3)
N(3)—C(4)—C(5)	113.3(3)
C(4)—C(5)—N(1)	103.0(3)
N(2)—N(1)—C(2)	129.1(3)
N(2)—N(1)—C(5)	121.4(3)
O(1)—N(2)—O(2)	127.7(3)
O(1)—N(2)—N(1)	116.6(3)
O(2)—N(2)—N(1)	115.7(3)
N(4)—C(4)—N(3)	121.0(3)
N(4)—C(4)—C(5)	125.8(3)
O(3)—N(4)—O(4)	124.4(3)
O(3)—N(4)—C(4)	117.8(3)
O(4)—N(4)—C(4)	117.8(3)
C(6)—C(2)—N(1)	126.2(3)
C(6)—C(2)—N(3)	125.2(3)
C(7)—C(6)—C(8)	114.3(7)
C(7)—C(6)—C(2)	109.2(5)
C(8)—C(6)—C(2)	108.4(5)

The refinement calculations were made with a local modification of the program ORFLS (35). Standard atomic scattering curves were used for O, C, N (36), and H (37).

The final atomic parameters and their estimated standard deviations are listed in Table 1. Tables 2 and 3 contain the bond lengths and bond angles for the non-hydrogen atoms. A table of the final F_o and F_c values has been placed in the Depository for Unpublished Data.[7]

The imidazole ring is planar to within ±0.005 Å. The 1-nitro nitrogen (N(2) is displaced 0.07 Å from the plane of the ring while N(4) and C(6) lie 0.04 and 0.06 Å, respectively, out of the plane on the opposite side from N(2). The nitro groups are both twisted slightly from the plane of the imidazole ring. The dihedral angles between the plane of the ring and the 1-nitro (N(2), O(1), O(2)) and 4-nitro (N(4), O(3), O(4)) groups are 7.3 and 10.0°, respectively.

[7]These data are available upon request from the Depository for Unpublished Data, National Science Library, National Research Council of Canada, Ottawa K1A 0S2, Canada.

Can. J. Chem. Downloaded from www.nrcresearchpress.com by 210.87.254.42 on 09/05/12
For personal use only.

Can. J. Chem. Downloaded from www.nrcresearchpress.com by 210.87.254.42 on 09/05/12
For personal use only.

1. M. MITROVIC, M. HOFFER, and E. SCHILDKNECHT. Antimicrobial Agents and Chemotherap. 445 (1968).
2. M. HOFFER, M. MITROVIC, A. BEAMAN, and A. BROSSI. J. Med. Chem. **14**, 993 (1971).
3. K. BUTLER, H. L. HOWES, J. E. LYNCH, and D. K. PIRIE. J. Med. Chem. **10**, 891 (1967). TM® Ipropran (Hoffmann-La Roche Inc.).
4. R. FARGHER and F. PYMAN. J. Chem. Soc. **115**, 217 (1919).
5. A. WINDAUS. Chem. Ber. **42**, 758 (1909).
6. (*a*) T. OZAWA, T. YOSHIDA, and K. NAMBA. Kogyo Kayaku Kyokaishi, **27**, 162 (1967). Chem. Abstr. **68**, 48701*k* (1968); (*b*) T. YOSHIDA, M. TAMURA, T. OZAWA, and K. NAMBA. Kogyo Kagaku Zasshi, **70**, 1367 (1967). Chem. Abstr. **68**, 48710*n* (1968).
7. M. W. AUSTIN, J. R. BLACKBOROW, J. H. RIDD, and B. V. SMITH. J. Chem. Soc. 1051 (1965).
8. (*a*) A. R. KATRITZKY and C. D. JOHNSON. Angew. Chem. Intl. Ed. **6**, 608 (1967); (*b*) C. D. JOHNSON, A. R. KATRITZKY, B. J. RIDGEWELL, and M. VINEY. J. Chem. Soc. B, 1204 (1967); (*c*) C. D. JOHNSON, A. R. KATRITZKY, and M. VINEY. J. Chem. Soc. B, 1211 (1967).
9. (*a*) J. GLEGHORN, R. B. MOODIE, K. SCHOFIELD, and M. J. WILLIAMSON. J. Chem. Soc. B, 870 (1966); (*b*) C. D. JOHNSON, A. R. KATRITZKY, N. SHAKIR, and M. VINEY. J. Chem. Soc. B, 1213 (1967), but see also A. R. KATRITZKY and M. KINGSLAND. J. Chem. Soc. B, 862 (1968).
10. A. ALBERT. *In* Physical methods in heterocyclic chemistry. A. R. Katritzky, editor. Vol. I. Academic Press, New York. 1963. p. 97.
11. (*a*). G. A. OLAH and N. A. OVERCHUK. Can. J. Chem. **43**, 3279 (1965) and ref. therein; (*b*) B. M. LYNCH, C. M. CHEN, and Y. WIGFIELD. Can. J. Chem. **46**, 1141 (1968) and refs. therein; (*c*) H. WIN. Diss. Abstr. **28**, 1867-B (1967).
12. G. A. OLAH, J. A. OLAH, and N. A. OVERCHUK. J. Org. Chem. **30**, 3373 (1965).
13. C. A. CUPAS and R. L. PEARSON. J. Am. Chem. Soc. **90**, 4742 (1968).
14. (*a*) W. N. WHITE, C. HATHAWAY, and D. HUSTON. J. Org. Chem. **35**, 737 (1970); (*b*) D. V. BANTHORPE. *In* The chemistry of the amino group. S. Patai, editor. Interscience, New York. 1968. p. 639; (*c*) W. N. WHITE and J. R. KLINK. J. Org. Chem. **35**, 965 (1970).
15. L. BIRKOFER, P. RICHTER, and A. RITTER. Chem. Ber. **93**, 2804 (1960).
16. T. PULLUKAT and G. URRY. Tetrahedron Lett. 1953 (1967).
17. F. FEHÉR and B. DEGEN. Angew. Chem. Intl. Ed. **6**, 703 (1967).
18. L. BIRKOFER and P. WEGNER. Chem. Ber. **100**, 3485 (1967).
19. (*a*) H. F. CORDES and H. S. JOHNSTON. J. Am. Chem. Soc. **76**, 4264 (1954); (*b*) A. TERADA and A. HASSNER. Bull. Chem. Soc. Jap. **40**, 1937 (1967); (*c*) H. SCHECHTER. Rec. Chem. Progr. **25**, 55 (1964); (*d*) J. BEGER. J. prakt. Chem. **307**, 326 (1967); (*e*) K. C. MALHOTRA. Chem. and Ind. 1704 (1967).
20. (*a*) M. HOFFER, V. TOOME, and A. BROSSI. J. Hetero. Chem. **3**, 454 (1966); (*b*) J. S. G. COX, C. FITZMAURICE, A. R. KATRITZKY, and G. J. T. TIDDY. J. Chem. Soc. (B), 1251 (1967); (*c*) V. SUNJIC, F. KAJFFZ, M. SLAMNIK, and D. KOLBAH. Bull. Sci. Cons. Acad. RSF Yougoslavie, **12**, 59 (1967); Chem. Abstr. **68**, 2483*n* (1968).
21. (*a*) G. F. WRIGHT. *In* The chemistry of the nitro and nitroso groups. H. Feuer, editor. Part 1. Interscience, New York. 1969. Chapt. 9; (*b*) P. A. S. SMITH. The chemistry of open chain nitrogen compounds. Vol. II. W. A. Benjamin. 1966. p. 490.
22. (*a*) G. S. REDDY. Chem. and Ind. 1426 (1965); (*b*) I. BUTULA. Ann. **718**, 260 (1968).
23. S. NOVIKOV, L. KHMEL 'NITSKII, O. LEBEDEV, V. SAVAST 'YANOVA, and L. EPISHINA. Khim. Geterotsikl. Soedin. 507 (1970).
24. (*a*) P. B. D. DELAMARE and J. H. RIDD. Aromatic substitution. Academic Press, Inc., New York. 1959. p. 55; (*b*) R. C. KERBER and M. J. CHICK. J. Org. Chem. **32**, 1329 (1967); (*c*) B. LOEV, F. DOWALO, I. M. FRIED, and M. GOODMAN. Tetrahedron Lett. 817 (1968); (*d*) H. FEUER, A. M. HALL, S. GOLDEN, and R. L. REITZ. J. Org. Chem. **33**, 3622 (1968); (*e*) H. FEUER and J. P. LAWRENCE. J. Am. Chem. Soc. **91**, 1856 (1969).
25. (*a*) S. J. CRISTOL, B. FRANZUS, and A. SHADAN. J. Am. Chem. Soc. **77**, 2512 (1955) and refs. therein; (*b*) R. T. M. FRASER. Chem. and Ind. 1117 (1968).
26. D. M. WHITE and J. SONNENBERG. J. Am. Chem. Soc. **88**, 3825 (1966).
27. M. R. GRIMMETT. *In* Advances in heterocyclic chemistry. A. R. Katritzky and A. J. Boulton, editors. Vol. 12. Academic Press. 1970. p. 175.
28. (*a*) E. SCHMIDT and H. FISCHER. Chem. Ber. **53**, 1529 (1920); (*b*) M. SOKOLOVSKY, J. F. RIORDAN, and B. L. VALLEE. Biochem. **5**, 3582 (1966); (*c*) A. G. ANDERSON, R. SCOTONI, E. J. COWLES, and C. G. FRITZ. J. Org. Chem. **22**, 1193 (1957); (*d*) D. H. ILES and A. LEDWITH. Chem. Commun. 364 (1969). Reaction of tetranitromethane with skatole gives an unusual product rather than simple nitration: T. F. SPANDE, A. FONTANA, and B. WITKOP. J. Am. Chem. Soc. **91**, 6199 (1969).
29. T. C. BRUICE, M. J. GREGORY, and S. L. WALTERS. J. Am. Chem. Soc. **90**, 1612 (1968).
30. (*a*) E. HALFPENNY and P. L. ROBINSON. J. Chem. Soc. 928, 939 (1952); (*b*) R. B. HESLOP and P. L. ROBINSON. J. Chem. Soc. 1271 (1954).
31. C. COSAR, C. CRISAN, R. HORCLOIS, R. JACOB, J. ROBERT, S. TCHELITCHEFF, and R. VAUPRÉ. Arzneimittel-Forsch. **16**, 23 (1966).
32. S. J. KUHN and G. A. OLAH. J. Am. Chem. Soc. **83**, 4564 (1961).
33. *n*-Butyl nitrate was prepared using the procedure of A. P. BLACK and F. H. BABERS. Org. Syn. Coll. Vol. II, 412 (1943) but substituting *n*-butyl alcohol for methyl alcohol.
34. I. L. KARLE and J. KARLE. Acta Cryst. **16**, 969 (1963).
35. W. R. BUSING, K. O. MARTIN, and H. A. LEVY. Report ORNL-TM-305, Oak Ridge National Laboratories, Oak Ridge, Tennessee. 1962.
36. D. R. CROMER and J. T. WABER. Acta Cryst. **18**, 104 (1965).
37. R. F. STEWART, E. R. DAVIDSON and W. T. SIMPSON. J. Chem. Phys. **42**, 3175 (1965).

The Thermal Decomposition of *N*-Arylcarbamates of *t*-Alcohols. 2. Effects of Solvent, Temperature, and Substituents

S. J. ASHCROFT[1] AND MELANIE P. THORNE
University of Keele, Keele, Staffordshire, England ST5 5BG

Received May 4, 1972

The influence of solvent, ring substituents, and tertiary carbon atom substituents on the decomposition at 423–473 K of some *N*-arylcarbamates of tertiary alcohols (p-$XC_6H_4NHCO_2C(CH_3)_2R$, where X = CH_3, H, Cl, NO_2, R = C≡CH, C_2H_5, CH=CH_2) has been investigated. In dodecane, diphenyl ether, acetophenone, nitrobenzene, and decanol, the reactions were first order yielding chiefly carbon dioxide, amine, and olefin. *t*-Pentyl carbamates yielded the olefins 2-methyl-1-butene and 2-methyl-2-butene in a 3:1 mixture. Solvent effects are reflected in variations in enthalpies and entropies of activation, but effects on the actual values of the specific rate constants are small. Substituent effects are also small, with changes in R from C≡CH to CH=CH_2 producing only a tenfold rate increase. Variations in X yield Hammett $\sigma\rho$ plots with slopes of about 0.50. These results are consistent with the charge separated cyclic transition state proposed before (1). In ethylene glycol, increased reaction rates and 1:1 yields of the olefins from the *t*-pentyl carbamates indicate a mechanism with greater carbonium ion character.

L'influence du solvant, des substituants du cycle, et des substituants sur le carbone tertiaire; sur la décomposition à 423–473 K de quelques *N*-arylcarbamates d'alcools tertiaires (p-$XC_6H_4NHCOOC(CH_3)_2R$ où X = CH_3, H, Cl, NO_2 et R = C≡CH, C_2H_5, CH=CH_2), a été étudiée. Dans le dodécane, diphényléther, acétophénone, nitrobenzène, et décanol, les réactions sont du premier ordre et conduisent principalement au gaz carbonique, amine et oléfine. Les carbamates de *t*-pentyle donnent les oléfines méthyl-2 butène-1 et méthyl-2 butène-2 dans un rapport 3:1. Les effets de solvants se reflètent sur les variations d'enthalpie et d'entropie d'activation mais ces effets sur les valeurs des constantes de vitesse spécifique sont faibles. Les effets des substituants sont également petits avec des variations lorsque R passe de C≡CH à CH=CH_2 provoquant un accroissement par 10 de la vitesse. Les variations de X conduisent aux courbes $\sigma\rho$ de Hammett avec des pentes de l'ordre de 0.50. Ces résultats sont compatibles avec un état de transition cyclique à charge séparée que l'on propose avant (1). Dans l'éthylèneglycol l'accroissement des vitesses de réactions et des rendements en mélange 1:1 d'oléfines à partir des carbamates de *t*-pentyle, montre un mécanisme à caractère plus accentué en ion carbonium. [Traduit par le journal]

Canadian Journal of Chemistry, **50**, 3478 (1972)

Introduction

N-Phenylcarbamates and meta or para substituted *N*-phenylcarbamates of *t*-butanol have been shown previously (1) to decompose in diphenyl ether at 450 K according to eq. 1.

[1] $ArNHCOOC(CH_3)_3 \rightarrow ArNH_2 + CO_2 + CH_2{=}C(CH_3)_2$

The *N*-phenyl- and *N*-tolyl-carbamates also yielded small quantities of the corresponding diarylurea.

Reaction 1 was shown to follow a first order rate law with electron-withdrawing substituents having a small activating effect. A ρ value of 0.54 was obtained for the Hammett $\sigma\rho$ plot.

On the basis of these results it was postulated that these esters decomposed by a cyclic mechanism similar to that proposed for olefin-forming pyrolytic eliminations of esters of carboxylic acids (2–4) and xanthates (5), with the possibility that some charge separation occurred. Cyclic mechanisms have also been proposed for the liquid-phase decomposition of α-methylbenzyl *N*-phenylcarbamates (6) and for cholesteryl *N*-phenyl- and *N*-benzyl-carbamates (5, 7).

The object of the present work was to extend the investigation to include the effects of solvent, tertiary carbon atom substituents, and temperature on the decomposition reactions in order to provide additional information about the nature of the transition state, with particular reference to the amount of charge separation which occurs. Consequently rates of decomposition of *N*-phenyl- or para-substituted *N*-phenyl-carbamates in selected solvents have been measured over the temperature range 423–473 K.

[1]Present address: Department of Chemical Engineering, University of Exeter, Exeter, England.

Can. J. Chem. Downloaded from www.nrcresearchpress.com by 210.87.254.42 on 09/05/12
For personal use only.

TABLE 1. Product yield from decomposition of *t*-butyl *N*-phenylcarbamate*

Solvent	Temperature (K)	Amine	Urea	Total C_6H_5NH—
Dodecane	453.0	—	16.5	
	463.0	—	16.3	
	473.0		15.3	
Diphenyl ether	450.5	87.0	5.8	98.6
	453.5	88.8	4.9	98.6
	457.6	88.7	5.0	98.7
	465.5	87.9	5.5	98.9
	467.5	87.5	5.1	97.6
Acetophenone	443.0	99.5	0	99.5
Nitrobenzene	453.0	96.9	0	96.9
Decanol	443.0	50.6	0	50.6
Ethylene glycol	433.0	98.7	0	98.7
	451.0	98.5	0	98.5

*Values are given as mol % of reactant.

The results provide support for the suggestion that decomposition occurs via a charge separated cyclic transition state, although it is also evident that, in some instances, an additional mechanism is operating.

Experimental

Materials

The carbamates were prepared as before (1), recrystallized from petroleum ether (b.p. 60–80°) or from a 5:1 heptane–benzene mixture and, finally, sublimed *in vacuo*. Lower-melting *t*-pentyl carbamates, which failed to crystallize out from the solvent on cooling, were obtained as pure solids by vacuum sublimation of the oil remaining after evaporation of the solvent. The compounds were characterized by melting point, elemental analysis, and n.m.r. spectra.

Solvents, either Fisher certified reagent grade or BDH reagent grade, were used without further purification. The purity of these solvents is claimed to be at least 99%.

Kinetic Experiments

The decompositions were carried out in a system similar to that described previously, using vapor phase chromatography to follow the reactions (1). The flow-rate of the helium used to sweep the volatile products into the gas sampling loop of the chromatograph was carefully controlled by Pye gas-flow restrictors. It was shown before that, for a constant helium flow-rate, the rates of evolution of the gases are linearly related to the peak heights obtained when samples from the gas loop are injected into the chromatograph. The chromatograms were obtained on a Wilkens Aerograph with a $\frac{1}{4}$ in. × 10 ft column of 20% Quadrol on Chromosorb P at 323 K, or on a Pye (series 104) chromatograph with a $\frac{1}{4}$ in. × 10 ft column of 20% Squalene on Chromosorb P at 321 K or a $\frac{1}{4}$ in. × 3 ft Poropak Q column at 423 K. 2-Methyl-1-butene could be separated from 2-methyl-2-butene using both the Quadrol and Squalene columns.

Amine and Urea Analyses

Analyses for residual amine and urea were carried out by the methods described previously (1). The potentiometric titrations of the amine with hydrochloric acid in the 1:1 ethylene glycol–isopropanol solvent mixture were done automatically using Radiometer Automatic Titration Equipment.

Results

Reaction Products

Decomposition of the carbamates yielded carbon dioxide, an olefin (identified by comparison of retention times in the g.l.c. with those of pure samples) and a residue which could be titrated with a non-aqueous solution of hydrochloric acid and was assumed to be an amine. Aniline, positively identified by n.m.r., was obtained from decompositions of *t*-butyl *N*-phenylcarbamate in both diphenyl ether and ethylene glycol, by extracting the solvent residue with aqueous acid and ether, in the usual way.

In dodecane and, to a lesser extent in diphenyl ether, decompositions of *N*-phenyl- and *N*-tolylcarbamates also yielded small quantities of diphenyl or ditolyl urea (identified by m.p.). The values for the yields of urea, together with those for amine, for decompositions of *t*-butyl *N*-phenylcarbamate in six solvents at temperatures from 443 to 467 K are given in Table 1. Yields for ureas from *t*-pentyl carbamates were similar to those from the *t*-butyl analogs. Amine analyses were not done for the decompositions in dodecane because of immiscibility of this solvent with the titration solvent. However,

Can. J. Chem. Downloaded from www.nrcresearchpress.com by 210.87.254.42 on 09/05/12
For personal use only.

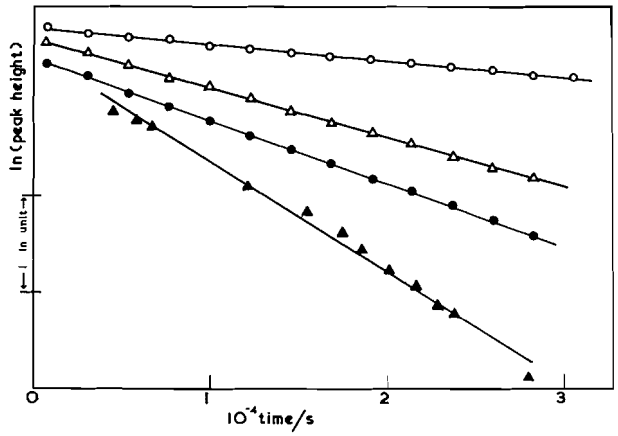

FIG. 1. First order rate plots for evolution of carbon dioxide during decomposition of *t*-butyl *N*-phenylcarbamate at 453 K in dodecane ○, acetophenone △, nitrobenzene ●, and decanol ▲. (The lines have been displaced vertically for clarity.)

decompositions of the *p*-nitro-substituted *N*-phenylcarbamates in dodecane resulted, on cooling the reaction mixture, in precipitation of a yellow solid which was identified by melting point (417–418 K) and elemental analysis as *p*-nitroaniline (lit. m.p. 419 K).

Anal. Calcd. for $C_6H_6N_2O_2$: C, 52.2; H, 4.35; N, 20.3. Found: C, 52.7; H, 4.42; N, 20.5.

Complete precipitation, to give yields of 100 mol %, of the *p*-nitroaniline could be effected by addition of low-boiling petroleum ether. *p*-Nitroaniline was not precipitated from decompositions of the appropriate carbamates in any other solvents and is not sufficiently basic to be estimated by titration.

Those reactions which yielded significant amounts of disubstituted ureas also yielded an additional volatile product. Its presence was detected from the gas chromatograms from the early stages of the reactions and its apparent rate of evolution decreased with time. The product was identified as *t*-butanol, *t*-pentanol, or 3-methyl-butyne-3-ol, depending on the carbamate from which it arose, by comparison of the retention time with that of a pure sample of the appropriate alcohol.

t-Butanol or *t*-pentanol were also produced when the respective carbamates were decomposed in decanol. In this solvent, however, all attempts to precipitate a urea failed, but the aniline determined by titration amounted to only 50% of the possible maximum (Table 1).

Actual yields of volatile products were not ascertained during this study, but it was shown previously (1) that recovery of the carbonyl group as carbon dioxide or as carbon dioxide plus urea was complete for decompositions of *t*-butyl carbamates in diphenyl ether, and that the *t*-butyl entity was not retained in the reaction mixture in any form.

Kinetic Results

The first-order rate constants were determined, as before (1), by computing the slope of the best line through the points obtained from the plot of the logarithm of the peak heights against time, using the method of least squares. The theoretical lines were generated in the computer and both the lines and points printed out using the digital incremental plotter. In all experiments except those in decanol at 453 K and above, the points obtained from measurements of the evolution of carbon dioxide or olefins were linear over at least two or three half-lives. Even in the decanol experiments the non-linearity of the points is so small that rate constants have been calculated assuming a first order rate law. Figure 1 shows the graphs for the evolution of carbon dioxide from the decomposition of *t*-butyl *N*-phenylcarbamate at 453 K in different solvents. Similar graphs were obtained for the other sets of kinetic data.

The rate constants for the decompositions of the carbamates in six different solvents at temperatures between 403 and 473 K are given in Tables 2, 3, and 4. The values quoted are usually

Can. J. Chem. Downloaded from www.nrcresearchpress.com by 210.87.254.42 on 09/05/12
For personal use only.

TABLE 2. Rate constants for the decomposition of *t*-butyl *N*-phenylcarbamate and *t*-butyl *N*-(*p*-nitrophenyl)carbamate in selected solvents

Solvent	Temperature (K)	k_{CO_2}*($s^{-1} \times 10^{-5}$)	k_{ene}†($s^{-1} \times 10^{-5}$)	k_{ene}/k_{CO_2}	d.e.‡
t-Butyl N-phenylcarbamate					
Dodecane	443.0	0.74	0.75	1.0	1.83
	453.0	2.01	2.01	1.0	1.82
	463.0	4.51	4.64	1.0	1.81
	473.0	10.31	11.08	1.1	
Diphenyl ether	443.1	2.20§			2.60
	450.5	4.45	4.44	1.0	2.55
	459.0	8.84§			
	463.0	9.85	9.70	0.99	2.47
	467.6	19.0§			
	479.0	31.70	30.30	0.96	
Acetophenone	443.0	1.89	1.93	1.0	11.8
	453.0	5.21	5.19	1.0	11.0
	463.0	12.23	12.17	1.0	10.6
Nitrobenzene	443.0	3.12	3.44	1.1	21.8
	453.0	6.72	6.75	1.0	20.2
	463.0	22.23	22.55	1.0	19.4
Decanol	423.0	0.93	1.06	1.1	7.78
	443.0	5.03	4.81	0.96	7.65
	453.0	11.59	11.03	0.95	7.62
	463.0	24.40	23.75	0.97	7.59
Ethylene glycol	403.0	9.42	8.53	0.91	
	413.0	22.10	18.30	0.83	
	423.0	42.90	37.10	0.86	
	433.0	69.10	56.38	0.84	
	443.0	86.05	68.63	0.79	17.4
	463.0	154.4	122.4	0.83	15.7
t-Butyl N-(p-nitrophenyl)carbamate					
Dodecane	443.0	2.72	2.99	1.1	
	453.0	7.23	8.05	1.1	
	463.0	16.98	17.80	1.1	
Acetophenone	433.0	4.75	5.30	1.1	
	443.0	12.21	13.37	1.1	
	453.0	28.44	30.65	1.1	
Nitrobenzene	433.0	7.73	9.02	1.2	
	443.0	19.05	21.00	1.1	
	453.0	42.37	43.27	1.0	
Decanol	433.0	8.91	9.28	1.0	
	443.0	18.73	19.16	1.0	
	453.0	36.74	39.85	1.1	

*Rate constant from carbon dioxide evolution.
†Rate constant from isobutene evolution.
‡Dielectric constants at temperatures given calculated from data in ref. 8.
§Rates measured by n.m.r.

the average of duplicate experiments, agreement between which was always within 7%. Rate constants have been calculated using the data for both the evolution of carbon dioxide (k_{CO_2}) and the evolution of olefin (k_{ene}). The values of k usually increase with increasing dielectric constant of the solvent, the reactions in decanol providing the exception. Decomposition of *t*-pentyl carbamates is faster than that of the corresponding *t*-butyl compounds, but the effect of the ring substituents in the *t*-pentyl series is similar to that reported for *t*-butyl carbamates (1). Log k is linearly related to the Hammett σ constants as is seen in Fig. 2, where the lines for log k_{CO_2} against the σ values are given. Similar lines were obtained for log k_{ene} *vs.* σ. The slopes (ρ values) of the lines are given in Table 5.

Can. J. Chem. Downloaded from www.nrcresearchpress.com by 210.87.254.42 on 09/05/12
For personal use only.

Can. J. Chem. Downloaded from www.nrcresearchpress.com by 210.87.254.42 on 09/05/12
For personal use only.

TABLE 3. Rate constants for the decomposition of para-substituted *t*-pentyl *N*-arylcarbamates ($XC_6H_4NHCOOC_5H_{11}$) in selected solvents at 463 K

Solvent	"X"	k_{CO_2}*($s^{-1} \times 10^{-4}$)	$k_{1\text{-ene}}$†($s^{-1} \times 10^{-4}$)	$k_{2\text{-ene}}$†($s^{-1} \times 10^{-4}$)	$k_{1\text{-ene}}/k_{CO_2}$	1-ene/2-ene‡
Dodecane	$-CH_3$	0.66	0.63	0.64	0.96	3.7
	—H	0.72	0.69	0.75	0.96	3.4
	—Cl	1.11	1.06	1.13	0.96	3.8
	$-NO_2$	2.85	2.89	2.89	1.0	3.3
Diphenyl ether	$-CH_3$	1.34	1.39	1.34	1.0	3.8
	—H	1.60	1.59	1.54	0.99	3.4
	—Cl	2.50	2.42	2.49	0.97	3.2
	$-NO_2$	7.46	5.08	4.91	0.68	2.8
Acetophenone	$-CH_3$	1.64	1.62	1.72	0.98	3.6
	—H	1.86	1.67	1.74	0.92	3.1
	—Cl	3.45	3.10	3.12	0.90	3.0
	$-NO_2$	14.37	9.63	9.19	0.67	2.6
Nitrobenzene	$-CH_3$	2.47	2.36	2.37	0.96	3.1
	—H	3.03	2.98	2.78	0.98	3.2
	—Cl	4.84	4.24	4.34	0.88	2.9
	$-NO_2$	13.40	10.05	9.41	0.75	2.5
Decanol	—H	4.33	3.87	3.40	0.90	2.7
Ethylene glycol	$-CH_3$	10.74	7.52	7.79	0.70	1.1
	—H	12.85	8.70	8.65	0.68	1.3
Diphenyl ether (at 449 K)	H	0.44	0.44	0.44	1.0	3.5
Diphenyl ether (at 479 K)	H	6.63	5.54	5.42	0.84	3.5

*Rate constant from carbon dioxide evolution.
†Rate constants from evolution of 2-methyl-1-butene and 2-methyl-2-butene respectively.
‡Ratio of yields of the two substituted butenes.

TABLE 4. Rate constants for the decomposition of *N*-arylcarbamates of unsaturated tertiary alcohols in diphenyl ether at 463 K

Carbamate	k_{CO_2}*($s^{-1} \times 10^{-5}$)	k_{ene}†($s^{-1} \times 10^{-5}$)	k_{ene}/k_{CO_2}
$C_6H_5NHCOOC(CH_3)_2CH{=}CH_2$	66.44	52.61	0.79
$C_6H_5NHCOOC(CH_3)_2C{\equiv}CH$	7.06	6.52	0.92
p-$ClC_6H_4NHCOOC(CH_3)_2C{\equiv}CH$	9.09	9.51	1.0
m-$ClC_6H_4NHCOOC(CH_3)_2C{\equiv}CH$	15.47	13.45	0.87

*Rate constant from carbon dioxide evolution.
†Rate constant from olefin evolution.

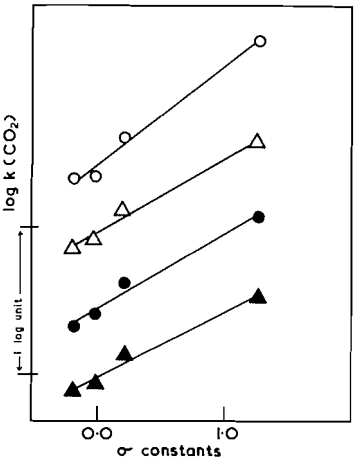

FIG. 2. Correlation between Hammett σ constants and log k_{CO_2} for evolution of carbon dioxide during decomposition at 463 K of para-substituted *N*-phenylcarbamates of *t*-pentanol in acetophenone ○, diphenyl ether △, nitrobenzene ●, and dodecane ▲. (The lines have been displaced vertically for clarity.) σ-Value of 1.27 used for p-NO_2 derivatives (1).

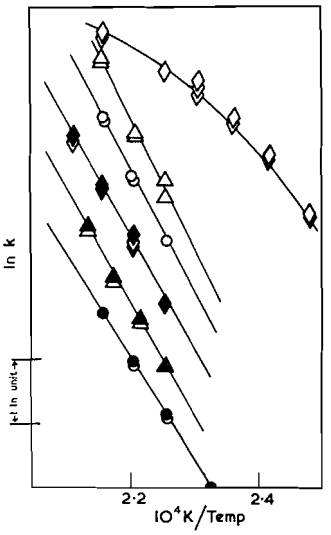

FIG. 3. Arrhenius plots (ln k_{CO_2} *vs.* T^{-1}) for carbon dioxide evolution from decomposition of *t*-butyl *N*-phenylcarbamate in decanol ●, diphenyl ether ▲, dodecane ◆, acetophenone ○, and nitrobenzene △. The non-linear plot for decompositions in ethylene glycol ◇ is also shown. (The lines have been displaced vertically for clarity.)

The values of k_{ene} and k_{CO_2} are usually the same, but in a few systems, particularly those involving ethylene glycol as solvent or *t*-pentyl *N*-(*p*-nitrophenyl)carbamate as reactant, the ratio k_{ene}/k_{CO_2} can be as low as 0.7 (Tables 2–4).

Both the possible butenes, 2-methyl-1-butene and 2-methyl-2-butene, are evolved from the *t*-pentyl compounds. An estimate of the relative proportions in which they are formed was obtained from the average value of the ratio of the two peak heights taken over all the samples in any one run (1-ene/2-ene, Table 3). In most solvents the ratio is about that which would be expected from statistical considerations, but decompositions in ethylene glycol give the two isomers in about equal proportions.

The Arrhenius and thermodynamic quantities of activation for the *t*-butyl carbamates in the different solvents and for the *t*-pentyl *N*-phenylcarbamate in diphenyl ether are listed in Table 6. These quantities were obtained from the least squares fit of the logarithmic forms of the Arrhenius equation and of the absolute rate theory equation (eq. 2), respectively. In the latter case, the transmission coefficient, κ, was taken as unity. Using either the k_{CO_2} or k_{ene} rate constants, the graphs of ln k_r *vs.* T^{-1} and of ln $(k_r \cdot T^{-1})$ *vs.* T^{-1} were linear over the temperature ranges studied, for all solvents except ethylene glycol. The Arrhenius plots for the carbon dioxide rate constants from the decomposition of *t*-butyl *N*-phenylcarbamates (ln k_{CO_2} *vs.* T^{-1}) are given in Fig. 3. Similar graphs were obtained for the other sets of data.

Can. J. Chem. Downloaded from www.nrcresearchpress.com by 210.87.254.42 on 09/05/12
For personal use only.

TABLE 5. Hammett ρ values for decomposition of *t*-pentyl *N*-arylcarbamates in selected solvents at 463 K

Solvent	Dodecane	Diphenyl ether	Acetophenone	Nitrobenzene
ρ	0.48	0.52	0.68	0.50

TABLE 6. Activation parameters for the thermal decomposition of *N*-arylcarbamates of tertiary alcohols in selected solvents

	Carbon dioxide evolution			Butene evolution		
Solvent	E_a (kJ mol^{-1})	$\Delta H^{\ddagger}$ (kJ mol^{-1})	ΔS^* (J mol^{-1} K^{-1})	E_a (kJ mol^{-1})	ΔH^* (kJ mol^{-1})	ΔS^* (J mol^{-1} K^{-1})
(a) t-Butyl N-phenylcarbamate						
Dodecane	148.7	144.8	−18.9	154.5	150.7	−5.94
Diphenyl ether				150.7*	146.9*	−5.73*
Acetophenone	159.5	155.7	13.1	157.1	153.4	7.95
Nitrobenzene	165.5	161.4	27.1	160.7	156.9	19.8
Decanol	134.0	130.3	−36.15	130.8	127.1	−43.5
(b) t-Butyl N-(p-nitrophenyl)carbamate						
Dodecane	155.4	151.7	6.94	149.9	146.1	−4.52
Acetophenone	148.9	145.2	4.64	142.4	138.7	−9.33
Nitrobenzene	138.0	134.3	−16.4	125.6	123.2	−40.7
Decanol	115.5	111.8	−67.4	118.8	115.1	−59.4
(c) t-Pentyl N-phenylcarbamate						
Diphenyl ether	161.4	157.1	18.6	151.2	146.7	−4.14

*Rates measured by disappearance of *t*-butyl group from n.m.r. spectra of aliquots of reaction mixture (ref. 1).

[2] $$k_r \cdot T^{-1} = \kappa \frac{k}{h} \cdot e^{\Delta S^*/R} \cdot e^{-\Delta H^*/RT} s^{-1}$$

Discussion

In most of the systems studied, the decomposition of the carbamate took place almost exclusively according to eq. 3.

[3] $$ArNHCOOR \rightarrow ArNH_2 + CO_2 + Olefin$$

The effects of solvent, substituents, and temperature on the reaction rates are generally consistent with the charge separated cyclic transition state suggested earlier (1) in analogy with mechanisms put forward by Maccoll (4), Smith and co-workers (9) and, more recently, Lum and Smith (10) for the gas-phase pyrolysis of acetates. The reaction scheme was envisaged as depicted in eq. 4.

[4] $ArNHCOOC(CH_3)_2R' \longrightarrow$ 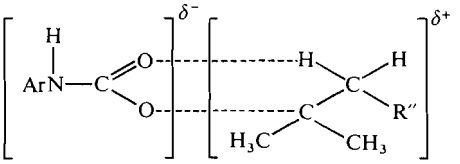 $(R' = CH_2R'')$

$\downarrow$

$[ArNHCOOH] + Olefin$

$\downarrow$ fast

$ArNH_2 + CO_2$

Can. J. Chem. Downloaded from www.nrcresearchpress.com by 210.87.254.42 on 09/05/12
For personal use only.

Can. J. Chem. Downloaded from www.nrcresearchpress.com by 210.87.254.42 on 09/05/12
For personal use only.

The small quantities of urea and alcohol formed when *N*-phenyl- and *N*-tolyl-carbamates were decomposed in dodecane or diphenyl urea can be accounted for by the reaction sequence: eq. 3 followed by [5] and [6] as suggested previously (1).

[5] $$ArNHCOOR \rightarrow ArNCO + ROH$$

[6] $$ArNCO + ArNH_2 \rightarrow ArNHCONHAr$$

This scheme is preferred to eq. 7, also suggested previously (1), since the latter would lead one to predict the rate of alcohol evolution to rise to a maximum and then fall off as the relative concentrations of the amine and carbamate changed.

[7] $$ArNHCOOR + ArNH_2 \rightarrow ArNHCONHAr + ROH$$

Solvent Effects

The specific rate constants for the decomposition of any particular carbamate generally increase as the dielectric constant of the solvent increases. Decanol provides the exception, rates being much higher in this solvent than would be expected from considerations of dielectric constant alone. This may reflect the inadequacy of the macroscopic dielectric constant to provide a good measure of all the interactions of solvent and solute on a molecular scale (11) or it may indicate that the rates in decanol appear to be greater than is actually the case, because transesterification occurs (eq. 8).

[8] $$C_6H_5NHCOOR + C_{10}H_{21}OH \rightarrow C_6H_5NHCOOC_{10}H_{21} + ROH$$

Reports of similar reactions are sparse, but work of Gaylord and Sroog (12) indicates that such a reaction is possible and that it might be reasonably fast. Equation 8 can account for both the observed formation of alcohols and the low yields (50%) of amine, since the decyl carbamate would be unlikely to decompose at the temperatures used (6). The kinetic method used, in which the measured quantity is related to the rate of evolution of a product and not to its concentration in the reaction vessel, means that an additional reaction, such as [8], which consumes reactant, could result in an apparent rate constant which is larger than is actually the case. The degree of error would depend on the relative rates of reaction and the equilibrium constant for reaction 8.

As a measure of solvent polarity the E_T parameters determined by Dimroth *et al.* (13) from the effect of solvent on the molar transition energies of the solvatochromic band of pyridinium *N*-phenolbetaine at 298 K, have been used. The E_T values for the temperature range under consideration will be different from those at 298 K, but since the thermochromic variation of the absorption band is small compared with the solvatochromic variation,[2] the relative values will be substantially the same at the different temperature. E_T values for *n*-dodecane and *n*-decanol have not been published, but have been estimated from data given for *n*-hexane and *n*-heptane and for the C_1—C_4 primary alcohols respectively. The parameters show a reasonably good linear correlation with the free energy ($\log k$) of activation of the decompositions (Figs. 4 and 5) but the slopes are very small (Table 7), indicating that a highly charged transition species is unlikely. The slopes of log k_{CO_2} *vs.* E_T and log k_{ene} *vs.* E_T are usually the same for any one carbamate, and only lines for the effect of solvent on carbon dioxide evolution are given in Figs. 4 and 5. Table 7 shows however that, for *t*-pentyl *N*-(*p*-nitrophenyl)carbamate, where k_{ene} and k_{CO_2} are not equal, the effects of solvent on the two apparent rate constants are not the same.

The rates in ethylene glycol are, on the whole, very much greater than would be predicted

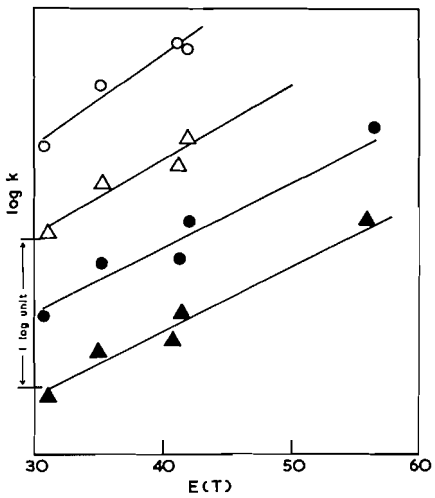

FIG. 4. Plots of log k_{CO_2} *vs.* solvent polarity parameter, E_T for carbon dioxide evolution from decomposition at 463 K of *t*-pentyl *N*-arylcarbamates. Aryl = *p*-tolyl ▲, phenyl ●, *p*-chlorophenyl △, and *p*-nitrophenyl ○. (The lines have been displaced vertically for clarity.)

[2]C. Reichardt. Private communication

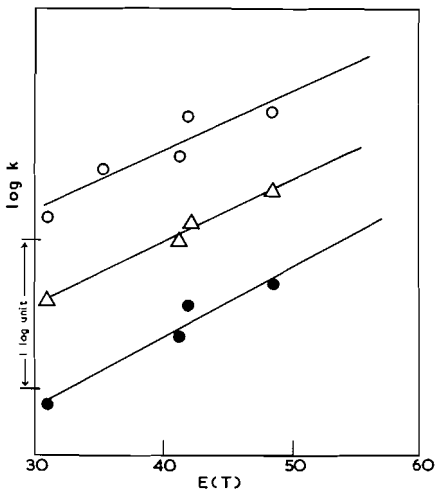

FIG. 5. Plots of $\log k$ *vs.* solvent polarity parameter, E_T for carbon dioxide evolution from decomposition of *t*-butyl *N*-phenylcarbamate at 443 K ●, 453 K △, and 463 K ○. (The lines have been displaced vertically for clarity).

from the solvent polarity plot. This could also be due to transesterification, but no tertiary alcohol was detected in the volatile products and the amine analyses indicated that aniline was formed in stoichiometric quantities. The 1:1 ratio of the two 2-methyl butenes from the *t*-pentyl carbamates instead of an approximately 3:1 ratio, indicates that the decompositions in ethylene glycol proceed in a different fashion.

The individual thermodynamic parameters of activation (Table 6) show considerable variation over the range of solvents. However, Leffler (16) has pointed out that in a series of related reactions, changes in solvent often affect both the entropy and enthalpy of activation in a compensating manner, and $\Delta H^{\ddagger}$ is frequently linearly related to $\Delta S^{\ddagger}$, by the so-called isokinetic relationship $\Delta H^{\ddagger} = \alpha + \beta\Delta S^{\ddagger}$, where α and β are constants. The existence of such a relationship is a much more significant criterion of similar mechanism than a comparison of activation enthalpies alone. Figure 6 shows that plots of $\Delta H^{\ddagger}$ *vs.* $\Delta S^{\ddagger}$ for the two *t*-butyl carbamates are linear, thus suggesting that the reaction mechanisms are similar in the different solvents. Schaleger and Long have pointed out (14) that $\Delta S^{\ddagger}$ values cannot be estimated to within more than ± 10.9 J mol^{-1} K^{-1} (2.6 cal mol^{-1} deg^{-1}) so that the deviations of the points from the lines in Fig. 6 probably represent no more than experimental error.

TABLE 7. Effect of solvent polarity (E_T)* on the decomposition of *t*-butyl and *t*-pentyl *N*-arylcarbamates

Aryl group	Temperature (K)	Slope of E_T *vs.* log k_{CO_2}	Slope of E_T *vs.* log k_{ene}
(a) t-Pentyl carbamates			
p-tolyl	463	0.043	0.043
phenyl	463	0.043	0.043
p-chlorophenyl	463	0.049	0.049
p-nitrophenyl	463	0.060	0.050
(b) t-Butyl carbamates			
phenyl	463	0.040	0.040
phenyl	453	0.043	0.042
phenyl	443	0.048	0.047
p-nitrophenyl	453	0.043	0.044
p-nitrophenyl	443	0.050	0.048

*E_T values: dodecane 30.9, diphenyl ether 35.3, acetophenone 41.3, nitrobenzene 42.0, decanol 48.5, ethylene glycol 56.5.

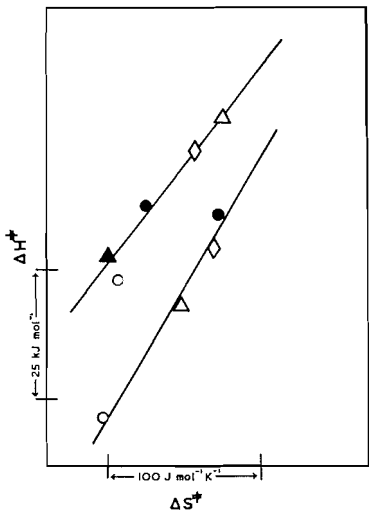

FIG. 6. Plots of $\Delta H^{\ddagger}$ *vs.* $\Delta S^{\ddagger}$ for carbon dioxide evolution from decomposition of *N*-phenylcarbamate (upper line) and *N*-*p*-nitrophenylcarbamate (lower line) of *t*-butanol in decanol ○, diphenyl ether ▲, dodecane ●, acetophenone ◇, and nitrobenzene △. (The lines have been displaced vertically and horizontally for clarity.)

Substituent Effects

The effects of substituents on the tertiary carbon atom are also similar to that in acetate pyrolyses and are quite different from the effects of similar substituents in reactions involving carbonium ion mechanisms. Thus the ratio of rate constants for the decomposition of the carbamates $C_6H_5NHCO_2C(CH_3)_2R'$ at 463 K in diphenyl ether is 1.0:1.6:7.4 when R′ is CH_3,

Can. J. Chem. Downloaded from www.nrcresearchpress.com by 210.87.254.42 on 09/05/12
For personal use only.

Can. J. Chem. Downloaded from www.nrcresearchpress.com by 210.87.254.42 on 09/05/12
For personal use only.

C_2H_5, $CH{=}CH_2$ respectively. These may be compared to the relative rates of 1.0:1.5 (510 K), 2.5 (584 K) : 4.1 (570 K) for gas-phase pyrolysis of the corresponding acetates (17, 15, 10).

In contrast, the relative rates 0.72:1.0:7.4 found for the decompositions of the carbamates when R′ varies in the order $C{\equiv}CH$, CH_3, $CH{=}CH_2$ are very different from those of 2.5×10^{-2}:1.0: 2.5×10^3 estimated by Streitwieser (18) from published data for the solvolysis in 80% aqueous alcohol at 278 K of R′C-$(CH_3)_2Cl$ when R′ is also $C{\equiv}CH$, CH_3, $CH{=}CH_2$. These solvolysis reactions are known to take place via a carbonium ion mechanism, and are clearly much more influenced by β-carbon substituents than the thermal decompositions of *N*-phenylcarbamates or acetates. Furthermore, solvolysis of tertiary halides also leads to some elimination, and those *t*-carbinyl groups capable of eliminating to more than one olefin invariably yield the most substituted olefin (*i.e.* the Saytzeff product) in greatest quantities (19). Thus elimination from *t*-pentyl bromide in 80% ethanol yields 82% 2-methyl-2-butene and 18% 2-methyl-1-butene (20). Thermal decomposition of *t*-pentyl *N*-arylcarbamates, on the other hand, gives rise to an approximately 3:1 (*i.e.* statistical) ratio of 2-methyl-1-butene to 2-methyl-2-butene, in analogy with the pyrolysis of *t*-pentyl acetates (15).

The yield of 2-methyl-2-butene relative to the yield of 2-methyl-1-butene increases slightly with the electron-withdrawing power of the ring substituents, and with the polarity of the solvent. This can be accounted for if a small amount of charge separation in the transition state is assisted by the electronegative substituents and the more polar solvents, producing greater carbonium ion character. In ethylene glycol the large proportion of 2-methyl-2-butene from *t*-pentyl carbamates indicates that a mechanism involving a charged transition state is important, possibly in addition to the cyclic mechanism, in view of the non-linearity of the Arrhenius plot.

The small activating effects of electron-withdrawing substituents in the benzene ring found previously (1) for decomposition of *t*-butyl carbamates, in diphenyl ether, are also apparent in the decompositions of the *t*-pentyl carbamates, and indicate that the nitrogen atom is not directly involved in the cyclic transition state. The ρ values for the solvents dodecane, diphenyl ether, and nitrobenzene are approximately the same and compare well with a value of 0.54 found for the *t*-butyl series in diphenyl ether (Table 5). The value for the decompositions in acetophenone is slightly higher (0.68).

The reason for the low values for k_{ene}/k_{CO_2} in a few systems is not at all clear, since the measurement of the peak heights of the gases effectively measures the concentration of reactant at a given time. Only detailed product analysis will provide the necessary information to ascertain what additional reaction is occurring in these systems.

Some of the research work was done at Memorial University, St. John's, Newfoundland. One of us (M.P.T.) wishes to thank the Chemistry Department of that University for its generous hospitality and assistance for three months in 1970, and Professor J. M. W. Scott for valuable discussions.

Fortran Plotter routines were compiled by Dr. P. Borrell of this Department. We are indebted to him for his assistance and advice in their use.

1. M. P. THORNE. Can. J. Chem. **45**, 2537 (1967).
2. C. D. HURD and F. H. BLUNK. J. Am. Chem. Soc. **60**, 2419 (1938).
3. A. T. BLADES. Can. J. Chem. **32**, 366 (1954).
4. A. MACCOLL. J. Chem. Soc. 3398 (1958).
5. G. L. O'CONNOR and H. R. NACE. J. Am. Chem. Soc. **75**, 2118 (1953).
6. E. DYER and G. C. WRIGHT. J. Am. Chem. Soc. **81**, 2138 (1958).
7. A. F. MCKAY and G. R. VAVASOUR. Can. J. Chem. **31**, 688 (1953).
8. Handbook of Chemistry and Physics. 45th ed. The Chemical Rubber Company, Cleveland, Ohio. 1964.
9. R. TAYLOR, G. G. SMITH, and W. H. WETZEL. J. Am. Chem. Soc. **84**, 4817 (1962).
10. K. K. LUM and G. G. SMITH. Int. J. Chem. Kinet. **1**, 401 (1969).
11. C. REICHARDT. Angew. Chem. Int. Ed. **4**, 29 (1965).
12. N. GAYLORD and C. E. SROOG. J. Org. Chem. **18**, 1632 (1953).
13. K. DIMROTH, C. REICHARDT, T. SIEPMANN, and F. BOHLMANN. Liebigs Ann. Chem. **661**, 1 (1963).
14. L. L. SCHALEGER and F. A. LONG. *In* Advances in physical organic chemistry. Vol. 1. Academic Press, Inc., London. 1963. p. 1.
15. E. U. EMOVAN and A. MACCOLL. J. Chem. Soc. 335 (1962).
16. J. E. LEFFLER. J. Org. Chem. **20**, 1202 (1955).
17. J. C. SHEER, E. C. KOOYMAN, and F. L. J. SIXMA. Rec. Trav. Chim. des Pays-Bas. **82**, 1123 (1963).
18. A. STREITWIESER JR. Chem. Rev. **56**, 571 (1952).
19. D. V. BANTHORPE. Elimination reactions. Elsevier Pub. Co. Ltd., London. 1963. p. 59.
20. K. A. COOPER, E. D. HUGHES, C. K. INGOLD, and B. J. MACNULTY. J. Chem. Soc. 2038 (1948).

Studies of the Metal–Sulfur Bond. Complexes of the Pyridine Thiols

B. P. KENNEDY AND A. B. P. LEVER

Department of Chemistry, York University, Downsview, Toronto, Ontario

Received May 8, 1972

Complexes of 2-pyridine thiol, 4-pyridine thiol, and 2-methyl-6-pyridine thiol, and some of their oxygen analogs with cobalt(II), nickel(II), zinc(II), cadmium(II), mercury(II), platinum(II), bismuth(III), and tin(IV) are characterized. On the basis of vibrational (conventional and far infrared) and electronic spectroscopy, magnetism, conductivity, and X-ray powder diffraction, the structures of these complexes are identified. In the thiol complexes, the bonding occurs, in all cases, through the sulfur, rather than the nitrogen atom. Bonding through oxygen is confirmed for the hydroxypyridine analogs. Tetrahedral MS_4^{2+} chromophores are identified for M = Co(II), Zn(II), and Cd(II), whilst square MS_4^{2+} chromophores occur with M = Ni(II) and Pt(II). The complexes exhibit sulfur-to-metal charge transfer spectra from which the optical electronegativities of the thiol ligands are shown to be near 2.4. Spectroscopic parameters for the complexes are derived and compared, together with their oxygen analogs, against phosphorus and arsenic sulfides and oxides.

Les complexes avec le pyridine-2 thiol, pyridine-4 thiol et méthyl-2 pyridine-6 thiol et quelques uns de leurs analogues oxygénés avec le cobalt(II), nickel(II), zinc(II), cadmium(II), mercure(II), platine(II), bismuth(III), et étain(IV), ont été caractérisés. Sur des bases de spectroscopic vibrationnelle (conventionnelle et infrarouge lointain) et électronique, magnétisme, conductivité et diffraction des rayons X sur les poudres; les structures de ces complexes ont été identifiées. Dans les complexes avec le thiol, la liaison se fait dans tous les cas, par l'intermédiaire du soufre plutôt que par l'atome d'azote. La liaison par l'intermédiaire de l'oxygène a été confirmée sur les analogues hydroxypyridine. Les chromophores tétraédriques MS_4^{2+} ont été identifiés pour M = Co(II), Zn(II), et Cd(II) tandis que les chromophores carrés MS_4^{2+} se font pour M = Ni(II) et Pt(II). Ces complexes donnent des spectres de transfert de charge du soufre au métal, à partir desquels les électronégativités optiques des ligands thiol ont été trouvées voisines de 2.4. Les valeurs spectroscopiques pour ces complexes ont été déduites et comparées ensembles avec leurs analogues oxygénés, avec les sulfures et oxydes de phosphore et d'arsenic. [Traduit par le journal]

Canadian Journal of Chemistry, **50**, 3488 (1972)

Can. J. Chem. Downloaded from www.nrcresearchpress.com by 210.87.254.105 on 09/05/12
For personal use only.

There has been considerable interest in ambidentate ligands, *i.e.* ligands with more than one mode of coordination, because of the light the behavior of such molecules throws on the nature of the metal–ligand bond. In particular ligands which may, in principle, coordinate through either nitrogen or sulfur have been of especial concern (1–16). The complexity of the ligands has in some cases precluded unambiguous definition of the identity of the ligating atoms, whilst in other cases it is difficult to judge whether the coordination behavior derives from steric or electronic phenomena. Furthermore the current interest in metal–sulfur chromophores in biological molecules requires a detailed study of simple metal–sulfur systems which have not been adequately investigated in the past. For these reasons we have studied the complexation behavior of a series of closely related pyridine thiols and compared the results against data for the corresponding hydroxy derivatives. Complexes of 2- and 4-pyridine thiol and 2-methyl-6-pyridine thiol with cobalt(II), nickel(II), zinc(II), cadmium(II), mercury(II), platinum(II), tin(IV), and bismuth(III) are reported. A number of complexes of 2- and 4-hydroxypyridine are also included.

Experimental

2- and 4-pyridine thiol were purchased from Aldrich and used without further purification. Their oxygen analogs were also obtained from Aldrich as brown powders, and were each recrystallized twice from benzene (yielding colorless crystals) before use. 2-Pyridine thiol was also prepared from 2-bromopyridine (which, in turn, was made (17) from 2-aminopyridine) by the method of Thirtle (18). 2-Methyl-6-pyridine thiol was prepared from 2-amino-6-methylpyridine by a similar route (19) (m.p. = 154–6°, lit. (19) m.p. = 152–4°). The abbreviations Py2SH, Py4SH, and 2MePy6SH will be used for 2-pyridine thiol, 4-pyridine thiol, and 2-methyl-6-pyridine thiol, respectively. Similar abbreviations, using O rather than S, will be used for the corresponding hydroxy derivatives.

Co Complexes

CoX_2L_2 (X = Cl, Br; L = Py2SH, 2MePy6SH, Py4SH)

Stoichiometric quantities of $CoX_2.6H_2O$ (0.0025 mol) and L (0.005 mol) were dissolved in EtOH and the solutions

Can. J. Chem. Downloaded from www.nrcresearchpress.com by 210.87.254.105 on 09/05/12
For personal use only.

mixed. A green precipitate formed immediately. It was filtered and washed with ethanol and then diethyl ether.

$CoI_2(Py2SH)_2$

This complex was prepared as above, except that CoI_2 was formed *in situ* by the double decomposition of $CoCl_2.6H_2O$ and NaI in alcohol. The precipitated NaCl was filtered and the solution of CoI_2 was used as in the preparation of CoX_2L_2.

$Co(Py2SH)_4(NO_3)_2$

Py2SH (0.01 mol) in ethanol was slowly added to an ethanolic solution of $Co(NO_3)_2.6H_2O$ (0.0025 mol), giving green, needle-like crystals. The complex was filtered and washed with ethanol and diethyl ether.

CoL_4X_2 ($L = Py2SH, Py4SH$; $X = ClO_4$)

$Co(ClO_4)_2.6H_2O$ (0.0025 mol) was dissolved in *n*-BuOH/EtOH (5:1) (~30 ml), and added to L (0.01 mol) in *n*-BuOH (~30 ml) under a N_2 atmosphere. The solution, which immediately turned green, was stirred for several hours; the green solid was filtered and washed with copious amounts of diethyl ether.

$Co(2MePy6SH)_4(BF_4)_2$

This was prepared as were the CoL_4X_2 compounds, but $Co(BF_4)_2$ was prepared *in situ* by the action of HBF_4 on $CoCO_3$.

$Co(Py2OH)_6.CoX_4$ ($X = Cl, Br$)

Ethanolic solutions of $CoX_2.6H_2O$ and Py2OH were mixed (the stoichiometric ratio being 1:3). The bromide complex started to precipitate about 10 min (at room temperature). The chloride complex came down after storing in a freezer for several days. Both complexes are blue.

$CoX_2(Py4OH)_2$ ($X = Cl, Br$)

These blue complexes were prepared in the same manner as their thio-analogs. The chloride has been reported previously (22).

Most of the above complexes (CoX_2L_2, $CoI_2(Py2SH)_2$, $CoX_2(Py4OH)_2$) were recrystallized with ethanol by soxhlet extraction. All complexes were dried under vacuum, over P_2O_5 and at 80° (excepting the perchlorates, which were dried at room temperature).

Ni Complexes

$NiCl_2(Py2SH)_2$

A green precipitate resulted immediately upon admixture of ethanolic solutions of $NiCl_2.6H_2O$ (0.0025 mol) and Py2SH (0.005 mol). It was filtered off, washed with ethanol and ether, and dried. Attempts at recrystallization gave intractable mixtures of green and yellow forms. Sometimes a yellow compound, rather than a green one, was obtained, with the formulation $NiCl_2L_x$($x = 1.2$–1.5) (based on Ni analysis). This "compound" could also be formed on heating $NiCl_2(Py2SH)_2$ in *n*-butanol.

$NiBr_2(Py2SH)_2$

$NiBr_2$ (anhydrous) (0.005 mol) was dissolved in ethanol (with a few drops of H_2O) added to an ethanolic solution of Py2SH (0.01 mol) and left in the freezer overnight. A negligible amount of fine yellow precipitate came down, and was filtered off. The filtrate was slowly evaporated on a steam bath, giving dark green crystals. As with the chloride analog, attempts at recrystallization gave only a flocculent yellow precipitate.

$NiI_2(Py2SH)_4$

NiI_2 (0.0025 mol) was prepared by metathesis between $NiCl_2$ and NaI. An ethanolic solution was treated with Py2SH (0.01 mol) and left in the freezer overnight; this yielded a thin dark film on the sides of the flask. The solution was filtered and the filtrate left in the freezer another week, giving well formed, very dark green crystals of $NiI_2(Py2SH)_4$.

$Ni(NO_3)_2(Py2SH)_4$

$Ni(NO_3)_2.6H_2O$ (0.0025 mol) and Py2SH (0.0010 mol) were each dissolved in ethanol, and mixed. The resultant green solution was placed in a freezer overnight. The well formed, dark green crystals were filtered, washed with alcohol and ether, and dried.

Zn Complexes

Zinc complexes were prepared by mixing ethanolic solutions of the appropriate Zn salt and the ligand. The resulting precipitate was recrystallized from ethanol by soxhlet extraction. (The oxo-ligand complexes were more soluble than their S counterparts, and required evaporation to a small volume and cooling in a freezer). The zinc halides required addition of the appropriate hydrohalic acid to prevent partial hydrolysis.

$Zn(NO_3)_2L_4$ ($L = Py2SH, Py4SH$)

An ethanolic solution of $Zn(NO_3)_2.4H_2O$ (0.0025 mol) was slowly added to a stirred ethanolic solution of L (0.01 mol). The complex precipitated slowly as the $Zn(NO_3)_2$ was being added.

Other Complexes

$CdX_2(Py2SH)_2$ and $HgX_2(Py2SH)_2$ ($X = Cl, Br$), and *$Cd(NO_3)_2.(Py2SH)_4$*

These were prepared in a similar fashion to the zinc complexes; they could not be recrystallized.

$Hg(Py2S)_2$

This compound could be prepared in two ways:

(*a*) Na^+Py2S^- was prepared in ethanol by addition of NaOEt to the ligand, and this solution was added to $HgCl_2$ (in ethanol). The white precipitate was recrystallized by soxhlet extraction with methanol, giving needle-like crystals.

(*b*) The same white precipitate could also be prepared by reaction of Py2SH with $Hg(OAc)_2$ in ethanol.

HgX_2L ($L = 2MePy6SH, Py4SH, Py2OH$, $X = Cl, Br$)

These were prepared in a similar fashion to the other mercury complexes.

$PtCl_2(Py2SH)_4$

$PtCl_2$ (0.0025 mol) and Py2SH (~0.0125 mol) were mixed intimately and fused together at 130° for 3 h. The resultant mixture was soxhlet extracted with methanol, giving the yellow compound.

$SnCl_4(Py2SH)_2$

On mixing ethanolic solutions of $Sn(II)Cl_2.4H_2O$ and Py2SH, a yellow-orange gum formed; probably due to aerial oxidation of the Sn(II) to Sn(IV). The gum was soxhlet extracted with chloroform to give a yellow-orange complex.

$BiCl_3(Py2SH)_2$

On mixing $Bi(III)Cl_3$ and Py2SH solutions in ethanol a yellow-orange gum formed. It was soxhlet extracted with ethanol, giving an orange solid.

Can. J. Chem. Downloaded from www.nrcresearchpress.com by 210.87.254.105 on 09/05/12
For personal use only.

Physical Measurements

Infrared spectra were obtained from Nujol mulls on a Beckman IR-12 instrument. NaCl, KBr, and polythene plates were used in the regions 4000–1000 cm^{-1}, 1000–400 cm^{-1}, and 400–190 cm^{-1}, respectively.

Electronic spectra were obtained with a Cary 14 spectrometer, from Nujol mulls in the infrared and visible regions. The higher energy region spectra (600–200 nm) were obtained from mulls in Dow-Corning fluid 200 (viscosity = 2.5×10^6 cstokes). The scattering of light was reduced considerably by crushing the compound very finely using a "Wig-L-Bug" (Crescent Dental Mfg. Co., Chicago, Ill., U.S.A.). As a check, the spectrum of naphthalene was recorded in ethanol and as the solid. They were very similar, the solution spectrum having the vibrational bands smeared out.

Conductance measurements were carried out on a Wayne–Kerr Universal Bridge, Model B221A.

Magnetic measurements (room temperature and variable temperature data) were obtained with a fully automatic Faraday balance (21).

X-Ray powder photographs were obtained on a Philips "Norelco" X-ray generator using nickel filtered copper radiation and a Debye–Scherrer type powder camera.

Analyses

(*a*) C, H analyses were carried out by A. B. Gygli (Toronto), Galbraith (Knoxville, Tenn., U.S.A.) and Chemalytics (Tempe, Ariz., U.S.A.).

(*b*) Metals were analyzed by standard techniques (24) after destruction of the complexes with aqua regia. Some mercury determinations were carried out using a Jarrel-Ash "Dial-Atom" atomic absorption spectrophotometer.

(*c*) Halide analyses were carried out by potentiometric titration with $AgNO_3$, after destruction of the complexes by sodium fusion. The data are presented in Table 1.

Results

2- and 4-pyridine thiols, and their oxygen analogs, exist in two tautomeric forms, I and II (using 2-pyridine thiol as an example) with the thione form (II) being dominant in solution (23–25). Metal ions may be expected to coordinate through the nitrogen atom of form I (or less likely II) or through the sulfur atom of form (II) (less likely I). In the case of the four-substituted species, polymerization by bonding through both nitrogen and sulfur may occur. The possibility of the 2-substituted derivatives being involved in chelation with the generation of a four-membered ring must also be considered. Despite the simplicity and ready availability of the pyridine thiols, apart from some studies of $Ru(Py2S)_2(PPh_3)_2$ (26, 27), little definitive complexation information has appeared on these ligands.

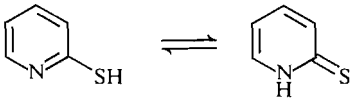

I II

Cobalt(II) Complexes

Cobalt(II) salts react readily with the pyridine thiols in ethanolic media to yield complexes of the formula CoL_2X_2 where X is a halogen and CoL_4X_2 where X is ClO_4^-, BF_4^-, or NO_3^-. The magnetic and electronic spectroscopic data (Table 2) for these complexes leave little doubt that they are all tetrahedral. They exhibit fairly intense structured bands in the visible and near infrared regions typical of tetrahedral or pseudo-tetrahedral cobalt(II) (28) and have magnetic moments in the region 4.3–4.95 B.M. almost independent of temperature (29). The perchlorate and tetrafluoroborate complexes are readily soluble in acetonitrile, yielding solutions whose conductances (Table 3) indicate that they are 1:2 electrolytes, in agreement with the supposition that they contain CoL_4^{2+} cations. The CoL_2X_2 species, on the other hand, are essentially insoluble in common solvents with the exception of the lower alcohols, in which they are extensively solvolyzed. Consideration of the infrared spectra arising from the perchlorate and tetrafluoroborate groups implies that they retain their T_d symmetry and are therefore uncoordinated in the solid state (30–32). The far infrared spectra, considered in detail below, reveal bands in the CoL_2X_2 complexes assignable to νCo—X stretching modes (X = Cl, Br, and I) in the regions anticipated for tetrahedral molecules (33).

In contradistinction to the above, 2-hydroxypyridine reacts with cobalt perchlorate and tetrafluoroborate to yield octahedral complexes containing $Co(Py2OH)_6^{2+}$ cations (34). Attempts to prepare halogen complexes corresponding to the thiol derivatives discussed above led to complexes of empirical formula CoL_3X_2 whose magnetic and spectroscopic data, after comparison of their electronic spectra and magnetism (Table 2) with those of the CoX_4^{2-} ions (35) and the CoL_6^{2+} cations (34), leave little doubt of their formulation as $CoL_6^{2+}.CoX_4^{2-}$. As expected they are 1:1 electrolytes in nitromethane (Table 3). It has previously been reported (20) that 4-hydroxypyridine yielded the neutral chloride species $Co(Py4OH)_2Cl_2$ thereby paralleling the

Can. J. Chem. Downloaded from www.nrcresearchpress.com by 210.87.254.105 on 09/05/12
For personal use only.

TABLE 1. Analytical results

Compound	Metal		X		C		H		Formula
	Calcd.	Found	Calcd.	Found	Calcd.	Found	Calcd.	Found	
$CoCl_2(Py2SH)_2$	16.7	16.6	20.1	20.6	34.1	33.9	2.8	2.6	$C_{10}H_{10}Cl_2CoN_2S_2$
$CoBr_2(Py2SH)_2$	13.4	13.2			27.2	27.4	2.3	2.4	$C_{10}H_{10}Br_2CoN_2S_2$
$CoI_2(Py2SH)_2$	11.0	10.8			22.4	22.2	1.9	1.6	$C_{10}H_{10}CoI_2N_2S_2$
$Co(Py2SH)_4(NO_3)_2$	9.4	9.2			38.3	38.6	3.2	3.1	$C_{20}H_{20}CoN_6O_6S_4$
$Co(Py2SH)_4(ClO_4)_2$	8.4	8.1			34.2	34.3	2.9	2.9	$C_{20}H_{20}Cl_2CoN_4O_8S_4$
$CoCl_2(2MePy6SH)_2$	15.5	15.4	18.6	18.3	37.9	37.9	3.7	3.7	$C_{12}H_{14}CoCl_2N_2S_2$
$CoBr_2(2MePy6SH)_2$	12.6	12.4			30.7	30.8	3.0	2.9	$C_{12}H_{14}Br_2CoN_2S_2$
$Co(2MePy6SH)_4(BF_4)_2$	8.0	8.2			39.3	39.2	3.8	3.8	$C_{24}H_{28}B_2CoF_8N_4S_4$
$CoCl_2(Py4SH)_2$	16.7	17.0			34.1	34.3	2.8	2.7	$C_{10}H_{10}Cl_2CoN_2S_2$
$CoBr_2(Py4SH)_2$	13.4	13.2			27.2	27.3	2.3	2.1	$C_{10}H_{10}Br_2CoN_2S_2$
$Co(Py4SH)_4(ClO_4)_2$	8.4	8.3			34.2	34.4	2.9	2.7	$C_{20}H_{20}Cl_2CoN_4O_8S_4$
$CoCl_4.Co(Py2OH)_6$	14.2	14.2	17.1	16.9	43.4	43.2	3.6	3.6	$C_{15}H_{15}Cl_2CoN_3O_3$
$CoBr_4.Co(Py2OH)_6$	11.7	11.2	31.7	31.5	35.7	35.6	3.0	3.0	$C_{15}H_{15}Br_2CoN_3O_3$
$Co(Py2OH)_6(ClO_4)_2$	7.1	7.1			43.5	43.5	3.7	3.6	$C_{30}H_{30}Cl_2CoN_6O_{14}$
$CoCl_2(Py4OH)_2$	18.4	18.4	22.2	22.3	37.5	37.2	3.1	2.9	$C_{10}H_{10}Cl_2CoN_2O_2$
$CoBr_2(Py4OH)_2$	14.4	14.4			29.4	29.6	2.5	2.7	$C_{10}H_{10}Br_2CoN_2O_2$
$NiCl_2(Py2SH)_2$	16.7	16.3	20.1	20.4	34.1	34.0	2.9	3.2	$C_{10}H_{10}Cl_2N_2NiS_2$
$NiBr_2(Py2SH)_2$	13.3	13.2			27.2	27.3	2.3	2.5	$C_{10}H_{10}Br_2N_2NiS_2$
$NiI_2(Py2SH)_4$	7.8	7.6			31.7	31.6	2.7	2.7	$C_{20}H_{20}I_2N_4NiS_4$
$Ni(NO_3)_2(Py2SH)_4$	9.4	8.9			38.3	38.5	3.2	3.4	$C_{20}H_{20}N_6NiO_6S_4$
$ZnCl_2(Py2SH)_2$	18.2	18.5	19.8	20.2	33.5	32.8	2.8	2.9	$C_{10}H_{10}Cl_2N_2S_2Zn$
$ZnBr_2(Py2SH)_2$	14.6	14.4			26.8	26.9	2.3	2.4	$C_{10}H_{10}Br_2N_2S_2Zn$
$Zn(NO_3)_2(Py2SH)_4$	10.3	10.6			37.9	38.4	3.2	3.05	$C_{20}H_{20}N_6O_6S_4Zn$
$ZnCl_2(2MePy6SH)_2$	16.9	16.5	18.3	18.5	37.3	37.4	3.7	3.8	$C_{12}H_{14}Cl_2N_2S_2Zn$
$ZnCl_2(Py4SH)_2$	18.2	18.2	19.8	19.9	33.5	33.4	2.8	2.7	$C_{10}H_{10}Cl_2N_2S_2Zn$
$Zn(NO_3)_2(Py4SH)_4$	10.3	10.2			37.9	37.6	3.2	2.9	$C_{20}H_{20}N_6O_6S_4Zn$
$ZnCl_2(Py2OH)_2$	20.0	20.0			36.8	36.7	3.1	2.9	$C_{10}H_{10}Cl_2N_2O_2Zn$
$ZnCl_2(Py4OH)_2$	20.0	19.7	21.7	21.0	36.8	37.1	3.1	3.1	$C_{10}H_{10}Cl_2N_2O_2Zn$
$Cd(Py2SH)_4(NO_3)_2$					35.3	35.7	3.0	2.9	$C_{20}H_{20}CdN_6O_6S_4$
$CdCl_2(Py2SH)_2$	27.7	27.4	17.5	17.7	29.6	29.8	2.5	2.4	$C_{10}H_{10}CdCl_2N_2S_2$
$CdBr_2(Py2SH)_2$	22.7	22.3			24.3	24.5	2.0	2.0	$C_{10}H_{10}Br_2CdN_2S_2$
$HgCl_2(Py2SH)_2$	40.6	40.5			24.3	24.1	2.0	1.9	$C_{10}H_{10}Cl_2HgN_2S_2$
$HgBr_2(Py2SH)_2$			27.4	27.3	20.6	20.8	1.7	1.7	$C_{10}H_{10}Br_2HgN_2S_2$
$Hg(Py2S)_2$					28.5	28.7	1.9	2.0	$C_{10}H_8HgN_2S_2$
$HgCl_2(2MePy6SH)$	50.6	51.4			18.2	18.1	1.8	1.6	$C_6H_7Cl_2HgNS$
$HgBr_2(2MePy6SH)$					14.8	15.1	1.5	1.3	$C_6H_7Br_2HgNS$
$HgCl_2(Py4SH)$	52.4	51.7	18.5	18.8	15.7	15.2	1.3	1.2	$C_5H_5Cl_2HgNS$
$HgBr_2(Py4SH)$					12.7	12.5	1.1	1.0	$C_5H_5Br_2HgNS$
$HgCl_2(Py2OH)$	54.7	54.6			16.4	16.1	1.4	2.3	$C_5H_5Cl_2HgNO$
$HgBr_2(Py2OH)$	44.0	44.3			13.2	13.3	1.1	1.0	$C_5H_5Br_2HgNO$
$PtCl_2(Py2SH)_4$	27.5	27.7			33.8	34.0	2.8	2.9	$C_{20}H_{20}Cl_2N_4PtS_4$
$SnCl_4(Py2SH)_2$			29.4	29.1	24.9	24.7	2.1	1.9	$C_{10}H_{10}Cl_4N_2S_2Sn$
$BiCl_3(Py2SH)_2$			19.8	20.0	22.3	22.2	1.9	1.8	$C_{10}H_{10}BiCl_3N_2S_2$

thiol derivatives in behavior. This was confirmed and the corresponding bromide, $Co(Py4OH)_2Br_2$ also prepared. The electronic spectra and magnetism of these complexes are reported in Table 2; they are evidently tetrahedral. We note that our sample of $Co(Py4OH)_2Cl_2$ differs both in its magnetism and electronic spectra from that reported by Wasson *et al.* (20). Possibly two isomers exist; however, repreparation of the complex using the method reported (20) yielded a complex with the same properties as reported in Table 2.

Nickel(II) Complexes

Reaction of 2-pyridine thiol with nickel halides in alcohol yielded the dark green derivatives $Ni(Py2SH)_2X_2$, X = Cl, Br, and $Ni(Py2SH)_4I_2$. Nickel nitrate forms the dark green $Ni(Py2SH)_4(NO_3)_2$. Attempts to recrystallize these complexes led to mixtures of

Can. J. Chem. Downloaded from www.nrcresearchpress.com by 210.87.254.105 on 09/05/12
For personal use only.

TABLE 2. Electronic spectra (d–d transitions, kK) and magnetism of cobalt complexes

Compound	Mull transmittance spectra	Magnetism†			
		χ_g (c.g.s. × 10^6)	χ'_m (c.g.s. × 10^6)	μ_{eff}(B.M.)	Temperature (°K)
$Co(Py2SH)_4(ClO_4)_2$	5.70 6.72 7.97 (13.44) 14.28 14.59 14.99 (18.49)	11.89 [43.21]	8632 [30 630]	4.58 [4.46]	303 [81]
$Co(Py2SH)_4(NO_3)_2$	6.80 8.41 14.20 (14.63) (15.24) (19.05) (19.76)	12.13	7865	4.35	301
$CoCl_2(Py2SH)_2$	5.87 7.34 13.77 15.34 16.16 (17.14) (18.29)	23.80 [81.88]	8527 [28 980]	4.51 [4.41]	298 [84]
$CoBr_2(Py2SH)_2$	5.41 6.00 7.14 13.68 14.43 15.35 (18.74) (19.90) (20.68) 21.34	21.14 [71.16]	9492 [31 560]	4.75 [4.58]	297 [83]
$CoI_2(Py2SH)_2$*	5.49 6.36 6.92 12.82 14.04 15.55 (18.91)	18.72	10210	4.95	300
$Co(2MePy6SH)_4(BF_4)_2$	7.33 13.50 14.24 15.47	10.88 [34.13]	8317 [25 370]	4.45 [4.34]	297 [93]
$CoCl_2(2MePy6SH)_2$	5.75 7.28 13.74 15.39 16.18 (17.06) (18.35) (19.37)	22.14	8588	4.55	301
$CoBr_2(2MePy6SH)_2$	5.61 7.30 13.51 14.79 15.51 (16.00) (16.33) (17.09)	18.97	9092	4.67	301
$Co(Py4SH)_4(ClO_4)_2$	5.95 8.20 12.73 14.06 14.72	11.17 [40.14]	8124 [28 470]	4.43 [4.42]	301 [86]
$CoCl_2(Py4SH)_2$	5.84 7.49 13.83 15.18 16.00 (20.11)	24.51 [79.83]	8777 [28 260]	4.57 [4.42]	298 [87]
$CoBr_2(Py4SH)_2$	5.78 7.00 13.70 14.73 15.37 (19.50)	19.64	8830	4.61	301
$CoCl_2(Py4OH)_2$	5.81 6.51 7.21 (14.33) 15.18 16.27 (16.83) (17.19) (17.83) 19.70 20.59 23.19 23.76	26.83	8699	4.58	301
$CoBr_2(Py4OH)_2$	5.82 6.62 (13.78) 14.41 16.00 (16.52) 16.99 19.10 (20.19) (22.66) 23.22 26.06	21.21	8810	4.61	301
$Co(Py2OH)_6CoCl_4$*	(5.26) 5.54 6.19 (6.34) 8.38 14.42 14.93 15.71 (16.17) (17.57) (18.16) 18.85 (19.47) (21.85)	23.48	9896	4.86	299
$Co(Py2OH)_6CoBr_4$*	5.17 5.65 (6.04) 8.38 13.99 14.23 14.97 15.50 16.53 16.97 17.32 18.93 20.70 21.17 21.50 (21.77) 23.01 23.53	18.84	9667	4.83	301

*Low temperature (~ −190 °C). Shoulders in parentheses.
†Values in square brackets are low temperature data.

TABLE 3. Conductance measurements* (Mho mol^{-1} cm^{-2})

Compound	Solvent	Λ_m	Electrolyte	Concentration (M)
$Co(Py2SH)_4(ClO_4)_2$	CH_3CN	340	2:1	0.980×10^{-3}
$Co(2MePy6SH)_4(BF_4)_2$	CH_3CN	325	2:1	1.15×10^{-3}
$Co(Py4SH)_4(ClO_4)_2$	CH_3CN	314	2:1	0.981×10^{-3}
$CoCl_4.Co(Py2OH)_6$	CH_3NO_2	139	1:1†	2.04×10^{-3}
$CoBr_4.Co(Py2OH)_6$	CH_3NO_2	177	1:1†	2.01×10^{-3}
$PtCl_2(Py2SH)_4$	MeOH	176	2:1	0.979×10^{-4}

*Standard ranges are (ref. 67): in CH_3CN: 1:1 electrolyte, ~140 Mho mol^{-1} cm^{-2}; 1:2 electrolyte, very wide range, 145–336 Mho mol^{-1} cm^{-2}. In CH_3NO_2: 1:1 electrolyte, ~100 Mho mol^{-1} cm^{-2}. In MeOH: 1:1 electrolyte, 90–100 Mho mol^{-1} cm^{-2}; 1:2 electrolyte, ~190 (range 160–220) Mho mol^{-1} cm^{-2}.
†Further solvolysis may be occurring in these cases.

yellow and green products from which neither pure yellow nor green products could be isolated. The bromo and chloro derivatives are paramagnetic and have electronic spectra (Table 4) typical of octahedral nickel(II) (28). They are evidently polymeric in nature. The presence of bands near or above 200 cm^{-1} in their far infrared spectra (see detailed discussion below) assignable to Ni—X stretching vibrations suggests that polymerization is through the sulfur ligand rather than the halides. Bridging halides give rise to Ni—X stretching vibrations well below 200 cm^{-1} (36). The complexes containing four pyridine thiol groups are diamagnetic and have a band in their visible absorption spectrum near 16 700 cm^{-1}, (almost independent of counter ion), characteristic of square planar nickel(II) (28). The nitrate complex exhibits a single band at 1735 cm^{-1} typical of complexes containing ionic nitrate groups (37). There seems little doubt that these complexes contain the NiL_4^{2+} cation.

The observation of an additional band (at 9340 cm^{-1}) in the spectrum of $Ni(Py2SH)_4I_2$ dissolved in pyridine, suggests that the complex becomes octahedral in this solvent (Table 4). With the remaining thiol ligands, difficulties arose in obtaining pure products with nickel salts. Mixed products were often obtained, samples analyzing with non-integral ligand-to-nickel ratios. With 2-hydroxypyridine, nickel perchlorate and tetrafluoroborate yield (34) salts of the $Ni(Py2OH)_6^{2+}$ cation.

Group IIB Complexes

All the thiols and hydroxypyridine derivatives investigated yielded zinc halide complexes of the type ZnL_2X_2 (X = Cl, Br). The hydroxypyridine derivatives exhibit bands readily attributable to Zn—X stretching vibrations within the regions expected for tetrahedral zinc (*vide infra*) suggesting that these complexes are indeed simple monomeric tetrahedral species. The zinc chloride thiol complexes all exhibit a band near 275 cm^{-1}, which is near the lower limit for zinc chloride stretching frequencies in tetrahedral zinc complexes (33).

The complex $Zn(Py2SH)_2Br_2$ exhibits a Zn—Br stretching vibration at 254 cm^{-1}, well within the appropriate range, suggesting that this complex is tetrahedral. The infrared spectra of the nitrate complexes infer the presence of ionic nitrate groups (37) and therefore the existence of tetrahedral ZnL_4^{2+} cations. Similarly CdL_4^{2+} cations occur in the isomorphic cadmium complex.

The cadmium complexes $CdX_2(Py2SH)_2$ (X = Cl, Br) appear to be tetrahedral; the chloride complex exhibits a band at 248 cm^{-1} assignable to νCd—Cl in a tetrahedral complex. In octahedral complexes the νCd—Cl frequency lies below 200 cm^{-1} (38, 39). A band at 221 cm^{-1} is tentatively assigned to the νCd—Br vibration in the tetrahedral bromide derivative, albeit it is somewhat high.

Mercury forms complexes of the type $Hg(Py2SH)_2X_2$ (X = Cl, Br) and $Hg(Py2S)_2$ with 2-pyridine thiol. The chloride and bromide complex differ in that whilst the bromide has a band at 217 cm^{-1} which may be associated with a Hg—Br stretching vibration in a mercury(II) complex (38, 39), no band which may be associated with a Hg—Cl stretching vibration is observed above 200 cm^{-1}. It is likely therefore that the chloride complex contains linear $Hg(Py2SH)_2$ units with long Hg—Cl

Can. J. Chem. Downloaded from www.nrcresearchpress.com by 210.87.254.105 on 09/05/12
For personal use only.

Can. J. Chem. Downloaded from www.nrcresearchpress.com by 210.87.254.105 on 09/05/12
For personal use only.

TABLE 4. Electronic spectra (d–d transitions, kK) and magnetism of nickel complexes*

	Mull transmittance spectra†						
	ν_1	ν_2	ν_3	χ_g (c.g.s. × 10^6)	χ'_m (c.g.s. × 10^6)	μ_{eff}(B.M.)	Temperature (°K)
$NiCl_2(Py2SH)_2$	(8.34) 9.29 (10.32)	13.97 15.03	21.88	13.39 [45.59]	4859 [16 190]	3.41 [3.23]	299 [81]
$NiBr_2(Py2SH)_2$	8.04 8.77 9.79	13.47 14.54	20.28	10.48	4789	3.40	301
$NiI_2(Py2SH)_4$‡	9.34(17)	16.75(18)					
$NiI_2(Py2SH)_4$	16.43					0	
$Ni(NO_3)_2(Py2SH)_4$	16.81					0	

*Values in square brackets are low temperature data.
†Shoulders in parentheses.
‡In pyridine solution, molar intensities in parentheses.

TABLE 5. X-Ray powder data*; *d* spacing (Å)

$Zn(NO_3)_2(Py2SH)_4$	$Co(NO_3)_2(Py2SH)_4$	$Cd(NO_3)_2(Py2SH)_4$
17.9m	17.7m	18.4m
14.3w		14.6w
12.7m	12.6m	13.1ms
11.4w	11.2mw	11.4w
9.62vw		
9.05vs	9.01s	9.19s
8.47w		8.52vw
7.43m		7.65mw
7.03s	7.03w	7.30w 7.02m
6.43ms		6.36mw
6.17m	6.29w	
5.80w		5.85m
5.44ms	5.45w	5.54m
4.87m	4.86w	4.93mw
4.53w		4.59w
4.38vw		
4.27vw		
4.03m	4.04w	4.07mw
3.84mw	3.85w	3.89w
3.59vw		3.56w
3.51w	3.50w	3.42w
3.39vw	3.39w	
3.22vw		3.20w
3.15w		3.08w
3.04w		

$ZnCl_2(Py2SH)_2$	$CoCl_2(Py2SH)_2$	$CdCl_2(Py2SH)_2$	$CoBr_2(Py2SH)_2$	$ZnBr_2(Py2SH)_2$
13.5vw		13.7w		
12.4s	12.4m	12.5m	12.9m	12.7m
10.8vs	10.9s	10.9s	10.7m	10.6m 11.4w
10.0w				9.21w
8.27ms	8.32m	8.42ms	8.50s	8.33s
7.00mw	6.99mw	7.07m		7.29m
6.68w		6.74w	6.81w	6.62mw
6.35vs	6.33ms	6.38m	6.43m	6.34mw
6.06mw		6.12w	6.01m	5.90m
5.73m	5.73w	5.82w		
5.40m	5.38w	5.45w	5.40w	5.46w
4.92w	4.89w	4.94w	4.86w	4.78mw 5.28mw
4.60mw	4.59w	4.66m	4.67w	4.58w
4.37w	4.41w	4.39w	4.43w	4.35w
4.18w		4.13w	4.10w 4.29w	4.21w
3.71w	3.68w	3.76w 3.94w	3.86w 4.00w	3.91w 4.04w
3.51w	3.49w	3.56w	3.70w	3.78w
3.40w		3.45w		3.48w 3.65w
3.27w		3.34w		3.36w
3.17w				
3.10w				
3.04w				
2.91w				

*Relative intensities on a given film are indicated by w = weak, m = medium, s = strong, v = very. The cobalt compounds fluoresce in the X-ray beam, thereby obscuring the weaker lines. Data for $ZnCl_2(Py2OH)_2$, $ZnCl_2(Py4SH)_2$, $ZnCl_2(Py4OH)_2$, $HgCl_2(Py2SH)_2$, and $HgBr_2(Py2SH)_2$ were also obtained (available from the authors upon request). No further isomorphism was noted.

Can. J. Chem. Downloaded from www.nrcresearchpress.com by 210.87.254.105 on 09/05/12
For personal use only.

Can. J. Chem. Downloaded from www.nrcresearchpress.com by 210.87.254.105 on 09/05/12
For personal use only.

contacts, whilst the bromide complex has a distorted octahedral structure probably similar to that exhibited by $Hg(Py)_2Cl_2$ (40). The Hg—Br vibrational frequency is at a somewhat lower energy than would be expected (39) for a tetrahedral complex. The inner complex $Hg(Py2S)_2$ is probably linear but the data thereon are not definitive in this respect.

The complexes $Hg(2MePy6SH)X_2$ (X = Cl, Br) have stoichiometries suggestive of a binuclear tetrahedral structure. The presence of two bands in the chloride complex near 300 cm^{-1}, but only one in the case of the bromide, implies an Hg—Cl terminal stretching vibration above 300 cm^{-1} consistent with this formulation. The chloride complex also has a band at 198 cm^{-1} which can be assigned to a bridging Hg—Cl stretching vibration (39). A binuclear formulation quite common with mercury halide derivatives (39, 41–45) seems highly probable. It seems likely that the corresponding $HgLX_2$ complexes with 4-pyridine thiol and 2-hydroxypyridine also have such a binuclear tetrahedral formulation.

Platinum chloride forms a complex with 2-pyridine thiol of formula $PtCl_2L_4$. This complex is unusual in that most sulfur ligands form complexes of stoichiometry $PtCl_2L_2$ with platinum chloride (46). The complex is diamagnetic and has no electronic absorption below 20 000 cm^{-1}. No absorption attributable to Pt—Cl vibrations are observed in the 300 cm^{-1} region (47) and therefore the complex is believed to contain the PtL_4^{2+}, presumably square planar, cation. The conductance data in methanol, though somewhat low (Table 3), are indicative of a 1:2 electrolyte. Thioacetamide forms a complex of similar stoichiometry (16*b*).

Bismuth trichloride reacts with 2-pyridine thiol to form orange $BiCl_3L_2$ of uncertain stereochemistry. Similarly stannic chloride forms $SnCl_4L_2$. A strong band in the far infrared spectrum of this latter complex at 295 cm^{-1}, identifiable as a Sn—Cl stretching vibration suggests a *trans* octahedral structure for this complex.

X-Ray Powder Data

Table 5 lists the *d* spacings obtained from X-ray powder photographs of some of the complexes. Comparison of the data for the series $M(NO_3)_2(Py2SH)_4$ M = Co, Zn, and Cd, suggests that all are isomorphous. The correlation between the cobalt and zinc complexes is good, but in the case of cadmium there are minor discrepancies which probably arise from the larger size of the cadmium atom. Similarly the series $MCl_2(Py2SH)_2$, M = Co, Zn, and Cd are evidently isomorphous, as are $MBr_2(Py2SH)_2$, M = Co and Zn. Comparison of the data across these series suggests that the chloro and bromo complexes of cobalt, zinc, and cadmium, of formula MX_2L_2 are all isostructural. The mercury derivatives were not found to be isomorphous with analogous cadmium derivatives. No isomorphism was noted between thiol derivatives and the corresponding hydroxypyridine derivative.

Discussion

Infrared Spectra (4000–400 cm^{-1})

Infrared spectra, in the above region, provide little informative data. Bands which may be attributed to the "thioamide I, II, III, and IV" vibrations (48, 49) do not shift in any significant fashion. In simple pyridine metal complexes a shift in the ring breathing mode is used as a guide to metal coordination (11, 50, 51). In the case of 2-pyridine thiol the band at 984 cm^{-1} tentatively assigned (52) to the ring breathing mode increases in energy by some 10–17 cm^{-1} in the various complexes. Similar increases are noted for the 977 and 989 cm^{-1} bands of 2-methyl-6-pyridine thiol and 4-pyridine thiol, respectively. Whilst these data are certainly indicative of coordination by the thiols, they do not provide information concerning the mode of coordination. Extensive coupling within the ring system, as indicated, for example, by a ^{18}O study of 2-hydroxy-pyridine (53), precludes the identification of any band definitively assigned to a C=S stretching vibration, and therefore precludes use of this vibration as a guide to metal sulfur bonding. Whilst bands have been assigned to such a vibration (25, 52), in the light of the previous argument, and the fact that the shifts in this band are small (less than 18 cm^{-1} in the complexes studied), such data cannot be used as a guide to mode of coordination.

The N—H stretching frequency in the metal complexes tends to lie at a higher energy than in the free ligand solid state spectrum (10, 34, 54, 55), but at a lower energy than the ligand

Can. J. Chem. Downloaded from www.nrcresearchpress.com by 210.87.254.105 on 09/05/12
For personal use only.

TABLE 6.
Infrared spectroscopic data, part *a*

Compound	ν(N—H)	"ν(C=S)"	"Ring breathing"	Far infrared (400–190 cm^{-1})			
				Ligand vibrations	ν(M—X)	ν(M—L)	Unassigned
Py2SH ≡ L	3163	1137	984	387w 332s			
$CoCl_2L_2$	3176	1138	1000 993sh	388w 369s 354s	307s 291s	228s	
$CoBr_2L_2$	3172	1139	1002	388w 361s 346sh		234brs	258m
CoI_2L_2	3164	1134	997	390s 356s 346sh 336sh	210s	232s	256mw
$CoL_4(ClO_4)_2$	3194	1136	1001	380ms 252s 335s		233s 227sh	249ms
$CoL_4(NO_3)_2$	3189	1136	987	364vs		232s	
$NiCl_2L_2$	3168	1139	1002	387m 355s 344m	262s	239 ms	297 s
$NiBr_2L_2$	3164	1134	1001	387s 355vs 344m	198 ms	239 vs	
NiI_2L_4		1131	993	384w 403w 363w 340w			
$Ni(NO_3)_2L_4$		1132	1001	386w 402w 375w 363w 343w			
$ZnCl_2L_2$	3178	1140	1002 994sh	387mw 368s 361sh	276vs	213s	
$ZnBr_2L_2$	3171	1139	995	388m 349s	241ms	225sh 212s	
$Zn(NO_3)_2L_4$	3187	1138	992	391vw 362vs		234sh 209s	
$CdCl_2L_2$	3176	1137	1001 993sh	388w 352s	248vs	198ms 194ms	
$CdBr_2L_2$	3172	1135	1000	388w 339s	221s	198m	
$HgCl_2L_2$	3174	1138	1001	386ms 358s		198s	
$HgBr_2L_2$	3168	1134	999	387m 347s	217ms		
$PtCl_2L_4$		1132	994 987sh	385w 407m 398m			234m
$BiCl_3L_2$		1129	1000	388w 350ms			306ms 253sh 243s 211s 207s
$SnCl_4L_2$		1129	1017	390m 329mw	305sh 295vs 275sh		252sh
Py4SH ≡ L	3186	1100	989	312m			
$CoCl_2L_2$	3216	1110	1001	371ms 347ms	298vs 289vs		214s
$CoBr_2L_2$	3226	1107	1001	369ms 348ms	245vs	235vs	214s
$CoL_4(ClO_4)_2$	3242	1108	1004	361m 343m 337ms		234ms	256ms 250ms 198m
$ZnCl_2L_2$	3198	1114	1000	357s 329w	264vs	233s	
$Zn(NO_3)_2L_4$		1112	1001	353s 338s		231s 227sh	248s
$HgCl_2L$			1004	342m 317s 301m	221m	198m	
$HgBr_2L$	3215	1111	999	364w	244ms	201ms	

Can. J. Chem. Downloaded from www.nrcresearchpress.com by 210.87.254.105 on 09/05/12
For personal use only.

TABLE 6 (*Concluded*)
Infrared spectral data, part *b*

Compound	ν(N—H)	"ν(C=S)" or "ν(C=O)"	"Ring breathing"	Far infrared
2MePy6SH ≡ L	3200	1144	977	295wbr 265s 229m 216m
$CoCl_2L_2$	3207	1143	988	323s 305s 298s 295s 286sh 218m 192ms
$CoBr_2L_2$	3209	1142	988	320s 306s 235s 226s 202ms 191ms
$CoL_4(BF_4)_2$	3248	1147	989	329s 322s 312s 294m 255mw 224m 210m
$ZnCl_2L_2$	3205	1149	989	306s 274vs 267s 219m
$HgCl_2L$		1149	996	329vs 300s ~190
$HgBr_2L$	3250 3227	1149	994	318s 211vs
$Cd(NO_3)_2L_2$	3185	1138	993	390w 352s 207m 198m
Py2OH ≡ L	*	1687 1650 1641 1610	1002	395w 231s 222s
$CoL_6(ClO_4)_2$	3279 3220	1648 1612	998	395w 290sh 277vs 235s 230s
$CoCl_4CoL_6$	3280 3247 3214	1645 1609	990	401w 393w 321s 290br 262sh 257s 235sh 229s
$CoBr_4CoL_6$	3275 3245 3203	1650 1606	997	390w 266sh 253sh 242sh 231s 203w
$ZnCl_2L_2$	3283 3250 3205	1643	996	388w 323s 290s 254m 228m 223m
$ZnBr_2L_2$	3254 3229 3207	1645	1000	396w 254s 234m 227sh 216m 197mw
$HgCl_2L$	3245	1702 1654	995	398w 341vs 219m
$HgBr_2L$	3232	1633 1616	1000	398mw 250vs 222s

Infrared spectral data, part *c*

Compound	ν(N—H)	"ν(C=O)"	Ligand bands	ν(M—X)	ν(M—L)
Py4OH ≡ L	3194	1636	304w		
$CoCl_2L_2$	3285	1636		310s 292s	269s 249sh 241sh
$CoBr_2L_2$	3271	1636	301w	254s 226s	273s 270sh
$ZnCl_2L_2$	3290	1638		293s 279s	254s 251sh 241sh

*Solid state: 3080 cm^{-1} (ref. 68), 3100 cm^{-1} (ref. 69); solution (CCl_4): 3413 cm^{-1} (ref. 69).

TABLE 7. Comparison of Dq and B values of CoL_2X_2 complexes

Compound	Dq (cm^{-1})		B(cm^{-1})	
	Observed	Calcd.	Observed	Calcd.
$CoCl_4^{2-}$	312 ± 14	—	710 ± 19	—
$CoBr_4^{2-}$	280 ± 11	—	695 ± 20	—
CoI_4^{2-}	265 ± 6	—	665 ± 25	—
$CoCl_2(Py2SH)_2$	383	354 ± 27	681	672 ± 42
$CoBr_2(Py2SH)_2$	358	338 ± 26	663	665 ± 42
$CoI_2(Py2SH)_2$	363	331 ± 23	634	650 ± 34
$CoCl_2(2MePy6SH)_2$	377	372 ± 29	687	648 ± 39
$CoBr_2(2MePy6SH)_2$	375	356 ± 28	655	641 ± 39
$CoCl_2(Py4SH)_2$	387	365 ± 28	671	635 ± 38
$CoBr_2(Py4SH)_2$	370	349 ± 27	659	628 ± 38

solution spectrum (10, 25). The low frequency in the free ligand spectra undoubtedly arises through extensive hydrogen bonding (55, 56) which is broken upon dissolution in a solvent. It has been suggested (10) that the comparatively sharp N—H band spectrum of some thiazolidine thione metal complexes indicated absence of hydrogen bonding, and therefore that comparison of these energies with the *solution* N—H frequency of the ligand could be used as a guide to M—N coordination. In the complexes studied here there is little difference in bandwidth between the solid state spectra of the ligands (where hydrogen bonding is undoubtedly present) and of the complexes. Thus the N—H stretching vibrations cannot be used as a guide to mode of coordination. Further proof that the perchlorate and tetrafluoroborate complexes contain uncoordinated anions is furnished by their near infrared spectra. The perchlorate complexes show no resolution of the bands near 1100 and 620 cm^{-1} which would be expected were coordination to occur (57). Similarly in the tetrafluoroborate the 1080 cm^{-1} band is unsplit, and no absorption is observed near 360 cm^{-1} (32). The nitrate complexes did not exhibit any splitting of the NO_3 ($\nu_1 + \nu_4$) combination band, indicative of uncoordinated nitrate (37).

The far infrared spectra (below 400 cm^{-1}), whilst they may substantiate a particular mode of bonding which has been deduced by other methods are not in themselves diagnostic. We therefore defer discussion of this region until after the electronic spectra, which are frequently definitive, have been discussed.

Electronic Spectra

Cobalt(II) complexes: analysis of the electronic spectra of the tetrahedral cobalt(II) derivatives described above leads to an unequivocal determination of the mode of bonding. Such analysis leads to values of Dq and B (28) which are reported for the CoL_2X_2 complexes in Table 7 and for the CoL_4^{2+} cations in Table 8. Data are also collected in Table 8 concerning the Dq and B values previously determined for model CoS_4 and CoN_4 tetrahedral chromophores. As may be seen the Dq and B ranges for the CoS_4 chromophores lie within 316–425 and 600–664 cm^{-1}, respectively, while the corresponding ranges for the CoN_4 chromophores are 467–538 and 700–757 cm^{-1}, respectively. From the data in Table 8 it is seen unequivocally that the thiol CoL_4^{2+} cations, described above, fall into the CoS_4 chromophore class. Using the "law of average environment" (28), the Dq and B values for the CoL_2X_2 derivatives may be calculated by taking averages of the Dq and B values of the appropriate CoL_4^{2+} and CoX_4^{2-} ions; Table 7 shows the more than satisfactory agreement between the observed and calculated data confirming, thereby, that the CoL_2X_2 series also contain cobalt–sulfur bonds.

The isomorphism of $ZnCl_2(Py2SH)_2$, $ZnBr_2(Py2SH)_2$, and $Zn(NO_3)_2(Py2SH)_4$ with their cobalt analogs is proof of sulfur bonding (rather than nitrogen) in the zinc derivatives. Furthermore, $CdCl_2(Py2SH)_2$ and $Cd(NO_3)_2(Py2SH)_4$ are also isomorphous with their zinc and cobalt analogs, confirming sulfur bonding in these compounds also. Whilst these com-

Can. J. Chem. Downloaded from www.nrcresearchpress.com by 210.87.254.105 on 09/05/12
For personal use only.

Can. J. Chem. Downloaded from www.nrcresearchpress.com by 210.87.254.105 on 09/05/12
For personal use only.

TABLE 8. Dq and B values for tetrahedral CoS_4 and CoN_4 chromophores

Compound*	Dq (cm^{-1})	B (cm^{-1})	Reference
(a) CoS_4			
CdS:Co	330	610	70
ZnS:Co	375	610	70
CdS:Co	316	664	71
$Co(etu)_4(ClO_4)_2$	378	651	72
$Co(tu)_4(ClO_4)_2$	425	600	73
$Co(DMTA)_4(ClO_4)_2$	387	655	74
$Co(\varepsilon\text{-thiocaprolactam})_4(ClO_4)_2$	391	634	75
$Co(thioacetate)_4$	387	645	76
$Co(pentafluorothiophenoxide)_4$	366	631	76
$Co(thiophenoxide)_4$	387	600	76
$Co(Py2SH)_4(NO_3)_2$	450	587	This work
$Co(Py2SH)_4(ClO_4)_2$	396	635	This work
$Co(2MePy6SH)_4(BF_4)_2$	432	585	This work
$Co(Py4SH)_4(ClO_4)_2$	418	559	This work
(b) CoN_4			
$Co(2\text{-methylimidazole})_4^{2+}$	525	716	77
$Co(benzimidazole)_4^{2+}$	510	716	78
$Co(imidazole)_4^{2+}$	538	750	79
$Co(LE)_2(ClO_4)_2$	526	716	80
$Co(LP)_2(ClO_4)_2$	465	731	80
$Co(Imidazole)_2$	526	700	83

*ety = ethylenethiourea; tu = thiourea; LE = 1,2-bis(2′-imidazoline-2′-yl)ethane; LP = 1,2-bis-(2′-imidazolin-2′-yl)benzene; DMTA = N,N-dimethylthioacetamide.

TABLE 9. Electronic spectra of nickel(II) complexes with sulfur ligands (kK)

Compound*	ν_1	ν_2	ν_3	References
(i) Octahedral complexes				
$NiCl_2(2,5\text{-dithiahexane})_2$	8.85	14.70	24.00	81
$NiBr_2(2,5\text{-dithiahexane})_2$	8.72	14.55	23.60	81
$[Ni(2,5\text{-dithiahexane})_3](ClO_4)_2$	10.60	17.00	28.00	81
$Ni(diethylenethiourea)_6^{2+}$	8.06	13.70	(20.00)	82
$Ni(dtp)_2(py)_2$	9.00	14.00	(22.70)	83
$Ni(exan)_2(py)_2$	9.30	15.90		83
	10.20			
(ii) Square planar complexes (NiS_4)				
$Ni(dtp)_2$	14.50			83
$Ni(dtc)_2$	15.80			83
$Ni(exan)_2$	15.50			83
$Ni(S_2CNH_2)_2$	15.60			83

*dtp = diethyldithiophosphate; exan = ethyl xanthate; dtc = diethyldithiocarbamate.

plexes are not isomorphous with the corresponding mercury derivatives, there seems little doubt, in view of the remarkable affinity mercury(II) has for sulfur, that the mercury complexes are also bonded through sulfur.

Comparison of the electronic spectra of the thiol derivatives with those of octahedral and square planar nickel(II) complexes involving Ni—S bonds (Table 9) also leave little doubt that the thiol complexes are sulfur bonded. Significantly higher band energies would be expected (28) if the bonding were through nitrogen. The far infrared spectrum (*vide infra*) support the contention that bonding is through sulfur in the platinum derivative, but the data are not definitive in the case of the bismuth and tin compounds. The presence of a low energy band near 20 000 cm^{-1} in the bismuth com-

Can. J. Chem. Downloaded from www.nrcresearchpress.com by 210.87.254.105 on 09/05/12
For personal use only.

pound is suggestive of sulfur coordination. Bismuth(III) thiol derivatives are highly colored, red or orange, (58, 59), whilst bismuth(III) amine complexes are colorless. The charge transfer spectrum of the tin complex (*vide infra*) seems definitive of tin–sulfur bonding. Thus all the complexes discussed here involve metal–sulfur rather than metal–nitrogen coordination by the thiol ligands. Reedijk (34) had proposed that bonding was through oxygen rather than nitrogen in the hydroxy derivatives and the additional work presented here lends further support to such a conclusion.

Far Infrared Spectra (400–190 cm^{-1})

The basic procedures for analyzing far infrared spectra, by comparison of ligand and complex spectra, and by varying the counterion, have been adequately discussed in the past (60). Because of the inevitable coupling processes which occur, few if any bands in an infrared spectrum can be regarded as arising from a "pure" vibration. The title "metal–halogen" or "metal–sulfur" vibration used below should be taken to infer that a particular absorption band arises primarily, but not necessarily totally, from such a normal coordinate.

Table 6 lists the far infrared spectra of the ligands and the various complexes. 2- and 4-pyridine thiol each have a single strong band just above 300 cm^{-1} but, with the exception of a weak band near 390 cm^{-1} in the 2-thiol, are otherwise transparent in the region studied. 2-Methyl-6-pyridine thiol, on the other hand, has at least four bands in the pertinent region rendering assignment of the bands in its metal complexes rather difficult.

All the 2-pyridine thiol derivatives have a band, of varying intensity, between 380–390 cm^{-1} which corresponds to the weak band in this region in the free ligand spectrum. In addition one or two bands are found, generally between 340 and 370 cm^{-1}, which probably correspond to the 332 cm^{-1} absorption. The relatively high energy of these bands, and their lack of sensitivity towards change, either of halogen or of metal would seem to preclude their assignment as metal–ligand vibrations. In the tetrahedral cobalt(II), zinc(II), and cadmium(II) complexes of 2-pyridine thiol, the metal–halogen vibration is generally recognizable as a consequence of its sensitivity to change in halogen. The band positions are generally within the ranges expected for such tetrahedral derivatives (33, 47), though in the case of the chloro cobalt and zinc complexes they are observed to be near the lower limits of these ranges. By exclusion, bands near 230 cm^{-1} in the cobalt(II) and zinc(II) complexes, and near 200 cm^{-1} in the cadmium(II) complexes are probably metal–ligand, *i.e.* M—S in origin. Thiourea and thioacetamide complexes exhibit Co—S and Zn—S vibrations in this region (18). Cobalt–sulfur stretching vibrations have frequently been observed above 300 cm^{-1} (8, 9, 61) but the varying electronic demands of sulfur in differing bonding environments (*e.g.* thiol, thioether, thiocarbonyl, thioester, phosphine, or arsine sulfide, etc.) suggest that the metal–sulfur force constant and hence frequency, may vary considerably.

In the octahedral nickel complexes halogen sensitive bands are observed at 262 cm^{-1} for the chloride and at 198 cm^{-1} for the bromide. The band positions and their relative energies are consistent with their assignment as Ni—X stretching vibrations in an octahedral nickel complex (33, 47, 51). In particular the energies reflect the presence of terminal nickel-halogen bonds, rather than bridging bonds (36). Since these complexes are octahedral and necessarily polymeric, it follows that the bridging must be through the thiol ligand, *i.e.* through sulfur. Indeed since bridging through nitrogen would be impossible, these data provide further evidence of sulfur coordination. The possibility of mixed halogen and sulfur bridging cannot, however, be eliminated. A band at 239 cm^{-1} in both complexes may be associated with the Ni—S stretching vibration. In support of the above assignments it is pertinent that the square planar nickel complexes are transparent between 200 and 300 cm^{-1}. Additional bands observed between 300 and 400 cm^{-1} in these diamagnetic derivatives are probably associated with the νNi—S vibrations which should absorb at higher energies than in the octahedral complexes.

Comparison of the data for the 4-pyridine thiol complexes leads to the ready identification in most cases of the metal halogen stretching bands. Bands near 230 cm^{-1} in the cobalt and

Can. J. Chem. Downloaded from www.nrcresearchpress.com by 210.87.254.105 on 09/05/12
For personal use only.

TABLE 10. Charge transfer and ligand electronic spectra

Ligand	Electronic spectra (kK)*
Py2SH ≡ L	35.58 42.02
$CoL_4(ClO_4)_2$	22.72 (23.78) (28.20) 35.52
$CoL_4(NO_3)_2$	22.42 24.04 30.15 35.96
$CoCl_2L_2$	25.06 34.97 40.49
$CoBr_2L_2$	25.64 34.64
CoI_2L_2	(23.31) 24.15 29.94 34.84
$NiCl_2L_2$	25.84 34.84
$NiBr_2L_2$	24.33 34.60 39.68
NiI_2L_4	(22.62) 29.32 36.63
$Ni(NO_3)_2L_4$	21.15 29.21 36.14
$Zn(NO_3)_2L_4$	26.85 (29.15) 35.60
$ZnCl_2L_2$	26.99 (28.05) 35.45
$ZnBr_2L_2$	27.78 (28.82) 35.52 (36.83)
$CdL_4(ClO_4)_2$	26.65 (28.15) 34.67
$CdCl_2L_2$	27.10 (28.01) 36.10 (29.24)
$CdBr_2L_2$	27.55 (28.90) 34.84
$HgCl_2L_2$	27.70 33.00 35.21 41.49
$HgBr_2L_2$	27.00 (28.90) 35.75 32.22
$BiCl_3L_2$	20.89 26.30 35.46
$SnCl_4L_2$	26.59 (30.38) 37.53
$PtCl_2L_4$	24.03 25.03 31.89
$Py2S^-Na^+$	30.96 35.71 42.37
$Hg(Py2S)_2$	30.86 36.10 40.98
Py2SH(H_2O solution)(thione)	28.98 36.63
$Py2S^-$(H_2O solution)	32.25 37.87
2MePy6SH ≡ L	34.20
$CoL_4(BF_4)_2$	22.37 24.07 (29.73) 35.17
$CoCl_2L_2$	(24.39) 25.25 (26.74) 35.09
$CoBr_2L_2$	(22.73) 23.98 24.94 (26.38) 34.48
$ZnCl_2L_2$	26.88 (27.93) 35.46
$HgCl_2L$	27.79 36.27
Py4SH ≡ L	40.82
$CoL_4(ClO_4)_2$	21.90 (23.73) 29.55 35.42
$CoCl_2L_2$	22.22 25.64 (26.81) 32.05 41.84
$CoBr_2L_2$	21.93 (23.36) 25.77 32.15 41.50 (25.19)
$Zn(NO_3)_2L_4$	26.23 35.89 40.16
$ZnCl_2L_2$	28.09 32.15 41.67
$HgCl_2L$	28.64 38.06
Py2OH ≡ L	(30.77) 33.58
$CoL_6(ClO_4)_2$	30.97 (32.14)
$CoCl_4 \cdot CoL_6$	30.43 (31.35)
$CoBr_4 \cdot CoL_6$	30.45 (31.80)
$ZnCl_2L_2$	31.57 (32.35)
$HgCl_2L$	(31.14) 32.53
Py4OH ≡ L	35.88
$CoCl_2L_2$	(29.84) (30.62) 33.90 (42.11)
$CoBr_2L_2$	(29.70) (30.60) 34.14 40.21
$ZnCl_2L_2$	36.27 (37.44)

*Shoulders in parentheses.

TABLE 11. Optical electronegativity data

Compound	ν_{CT} (kK)	B (kK)	$10Dq$ (kK)	χ_{opt} (M)	χ_{opt} (L) M—L	χ_{opt} (L) L—M
$Co(Py2SH)_4(ClO_4)_2$	22.72	0.635	3.96	1.9*	0.9_2	2.4_1
$Co(Py2SH)_4(NO_3)_2$	22.42	0.587	4.50	1.9*	0.9_7	2.40
$CoCl_2(Py2SH)_2$	25.06	0.681	3.83	1.9*	0.8_2	2.4_7
$CoBr_2(Py2SH)_2$	25.64	0.663	3.58	1.9*	0.8_1	2.5_0
$CoI_2(Py2SH)_2$	24.15	0.634	3.63	1.9*	0.8_0	2.4_6
$NiCl_2(Py2SH)_2$	26.31	0.54	9.32	1.8*	0.9	2.4_1
$ZnCl_2(Py2SH)_2$	27.03			1.5	—	2.4_3†
$ZnBr_2(Py2SH)_2$	27.73			1.5	—	2.4_3†
$Zn(Py2SH)_4(NO_3)_2$	26.85			1.5	—	2.4_3†
$CdCl_2(Py2SH)_2$	27.10			1.5	—	2.4_3†
$CdBr_2(Py2SH)_2$	27.55			1.5	—	2.4_3†
$HgCl_2(Py2SH)_2$	27.70			1.5*	0.5_8	2.4_2
$HgBr_2(Py2SH)_2$	27.00			1.5*	0.6_0	2.4_0
$BiCl_3(Py2SH)_2$	20.89			1.7	—	2.4†
$SnCl_4(Py2SH)_2$	26.59			1.5*	0.6_1	2.3_9
$Co(2MePy6SH)_4(BF_4)_2$	22.37	0.585	4.32	1.9*	0.9_7	2.4_1
$Co(2MePy6SH)_2Cl_2$	24.39	0.687	3.77	1.9*	0.8_4	2.4_5
$Co(2MePy6SH)_2Br_2$	23.98	0.655	3.75	1.9*	0.8_7	2.4_5
$Zn(2MePy6SH)_2Cl_2$	26.88			1.5	—	2.3_6†
$Hg(2MePy6SH)Cl_2$	27.79			1.5*	0.5_7	2.4
$Co(Py4SH)_4(ClO_4)_2$	21.90	0.559	4.18	1.9*	0.9_9	2.3_1
$CoCl_2(Py4SH)_2$	22.22	0.671	3.87	1.9*	0.9_2	2.3_8
$CoBr_2(Py4SH)_2$	21.93	0.659	3.70	1.9*	0.9_3	2.2_8
$ZnCl_2(Py4SH)_2$	28.09			1.4	—	2.3_6†
$Zn(Py4SH)_4(NO_3)_2$	26.23			1.5	—	2.3_6†
$HgCl_2(Py4SH)$	28.64			1.5*	0.5_4	2.4_6

*Assumed (see text).

zinc complexes are again assignable as metal–sulfur vibrations. The assignments in the case of the mercury complexes are tentative; they can only be rationalized in terms of a much weaker mercury–chlorine interaction than mercury–bromine as discussed above. Data for the 2-methyl-6-pyridine thiol are presented in Table 6 but are too complicated for unequivocal assignment. The 2-hydroxypyridine data reported in Table 6 are also somewhat complex.

High Energy Absorption and Optical Electronegativities

Whilst the thiols exhibit absorption above 30 000 cm^{-1} as a consequence of internal π–π^* transitions, many of the complexes exhibit absorption between 22 000 and 30 000 cm^{-1} which cannot, since they are observed in the non-transition metal complexes, be associated with crystal field transitions (Table 10). The 2-pyridine thiol complexes generally exhibit a band, usually a shoulder, near 29 000 cm^{-1} which can be associated with a weak ligand absorption (seen in solution but not in the solid state) and an additional moderately intense absorption band at lower energy. These lower energy bands (which are absent in the hydroxypyridine complexes), fall in the sequence

$$Hg(II) \geq Cd(II) \geq Zn(II) > Sn(IV) > Ni(II) \geq Co(II) > Pt(II) > Bi(III)$$

for analogous complexes (where possible). The energies are dependent upon the nature of the other coordinated ligand, but there appears to be no systematic dependence.

There is some doubt that n–π^* transitions are seen in these thiols (62) and in any event such transitions would be expected to shift up in energy, probably beyond 30 000 cm^{-1} upon coordination of the sulfur to a metal. It is therefore probable that these bands are charge transfer in origin. The sequence above does not readily indicate whether the transition is of the metal-to-ligand, or ligand-to-metal variety; the inference is that the transfer is of the metal-to-

Can. J. Chem. Downloaded from www.nrcresearchpress.com by 210.87.254.105 on 09/05/12
For personal use only.

Can. J. Chem. Downloaded from www.nrcresearchpress.com by 210.87.254.105 on 09/05/12
For personal use only.

ligand variety since the highest energy bands occur with those metals which are most difficult to oxidize (28). However, it will be shown that this is not the case. These data represent a rare example of the breakdown of the simple procedure to identify the direction of the electron transfer (28). The electron transfer process is in fact from sulfur to metal and the unusual sequence above arises because of the range of different energies of the acceptor orbitals on the metal.

The procedure for analysis of data in terms of the optical electronegativities of the metal and ligand (62, 63), has been adequately described (28, 62). It may be assumed that in the cases of mercury, cadmium, zinc, and tin, electron transfer occurs from the completed d shell, or into the empty s orbital. In the case of bismuth it is from the 6s level or into the 6p level, whilst for cobalt, platinum, and nickel the transitions will occur from or to, the d shell. Table 11 presents data which have been calculated on the basis, (*a*) that the process is metal to ligand, and (*b*) that it is ligand to metal. In the first instance data were calculated for mercury, tin, nickel, and cobalt since optical electronegativity data are available for these species. Note that the optical electronegativities are defined with respect to the spherical one-electron energy of the unsplit d orbitals (64) and not with respect to the t_{2g} subshell (62, 63) in those cases where transitions involving the d shell are concerned. We deal first with the 2-pyridine thiol complexes. On the assumption that the transition is from metal to ligand, the ligand optical electronegativities fall within the range 0.58 to 0.85 with considerable scatter. With the alternate assumption that the transition is from ligand to metal, the ligand optical electronegativities fall within the narrow range 2.35 to 2.50 with an average of 2.43. Since the data form a consistent set with the second assumption rather than the first, it is concluded that these charge transfer bands do arise through a ligand(sulfur)-to-metal transition. Using the average value of the ligand optical electronegativity, it is possible to calculate values for the optical electronegativities of the metals for which such data have not been available in the past. Thus Table 11 reports values of 1.5 for the optical electronegativities of zinc and cadmium in tetrahedral environments, and 1.7 for bismuth(III). Similar sets of consistent data are also obtained with 2-methyl-6-pyridine thiol and 4-pyridine thiol derivatives (Table 11). The 4-pyridine thiol seems to have a slightly smaller electronegativity than the α-thiols, but the difference is marginal.

TABLE. 12. Comparison of electronic spectroscopic parameters for CoX_2L_2 and CoL_4^{2+} species when L = $(CH_3)_3AsY$, $(CH_3)_3PY$, and PyxYH, Y = O or S, $x = 2, 4$

	Y=O		Y=S	
	Dq (kK)	β	Dq (kK)	β
L ≡ Me_3AsY				
CoL_2Cl_2	0.384	0.76	0.339	0.73
CoL_2Br_2	0.365	0.75	0.331	0.72
CoL_2I_2	0.388	0.76	0.334	0.66
CoL_4^{2+}	0.398	0.81	0.407	0.62
L ≡ Me_3PY				
CoL_2Cl_2	0.373	0.76	0.334	0.74
CoL_2Br_2	0.359	0.76	0.328	0.72
CoL_2I_2	0.345	0.75	0.326	0.66
CoL_4^{2+}	0.380	0.83	0.389	0.65
L ≡ Py4YH				
CoL_2Cl_2	0.376	0.74	0.387	0.69
CoL_2Br_2	0.359	0.72	0.370	0.67
CoL_4^{2+}	—	—	0.418	0.57
L ≡ Py2YH				
CoL_2Cl_2	—	—	0.383	0.70
CoL_2Br_2	—	—	0.358	0.68
CoL_2I_2	—	—	0.363	0.65
CoL_4^{2+}	—	—	0.396	0.65

The sulfide ion itself is believed (63) to have an optical electronegativity near 2.4, whilst species such as the dialkyldithiophosphates and thioethers have somewhat higher electronegativities (near 2.7 and 2.9 respectively (63)). Since amines containing only one lone pair are expected (63) to have electronegativities exceeding 3.0 these data provide further convincing evidence of the proposal that bonding is through sulfur rather than nitrogen in these derivatives. The possibility of observing sulfur-to-metal transitions in a pyridine thiol in which the nitrogen atom is coordinated to the metal is not zero, but the transition probability for such an electron jump would be quite small; it is not reasonable to ascribe the strong bands seen in these derivatives to such a transition, in an *N*-bonded complex. Finally we note that the

TABLE 13. Spectroscopic data and parameters for Me_3PS and Me_3AsS complexes

Complex	Ultraviolet spectrum			$10Dq$*	B*	χ_{opt} Co(II)†	χ_{opt} L
Me_3AsS	38.34						
$CoCl_2(Me_3AsS)_2$	30.58	37.23		3.39	0.706	1.9	2.6_5
$CoBr_2(Me_3AsS)_2$	29.03	33.93	37.37	3.31	0.696	1.9	2.6_1
$HgCl_2(Me_3AsS)_2$	34.75					1.5	2.6_6
$CoCl_2(Me_3PS)_2$	31.67	35.09	37.23	3.34	0.716	1.9	2.6_9
$CoBr_2(Me_3PS)_2$	30.64	37.00		3.28	0.696	1.9	2.6_6

*Calculated from data in ref. 61.
†Assumed.

data suggest that the availability of electron density on the sulfur atom is comparable to that of the free S^{2-} ion and certainly more than that on the thiophosphates and thioethers.

Summary and Conclusions

The identity of the donor atom in these complexes has been defined unequivocally for virtually every complex discussed here, and in all cases bonding appears to be through sulfur rather than nitrogen. There is no positive evidence that in any of the complexes discussed here, the 2-pyridine thiol behaves as a bidentate ligand, as its anionic form does towards ruthenium(II) (26, 27). Such bidentate coordination may possibly occur in $Hg(PyS)_2$ and weak interaction with the nitrogen atom may be responsible for the somewhat low metal chloride stretching frequencies in the "tetrahedral" zinc and cobalt chloro derivatives.

A comparison of the crystal field and nephelauxetic effects of the pyridine thiols and hydroxy pyridines *vs.* arsenic and phosphorus oxides and sulfides is instructive. Table 12 compares the Dq and β (B(complex)/B(free ion)) values for a series of cobalt(II) tetrahedral complexes, of these various oxygen and sulfur donors.

It is noteworthy that the Dq and B values for the pyridine thiol cobalt halides are essentially independent of the thiol used. This is itself strong evidence of sulfur rather than nitrogen bonding. Had nitrogen bonding occurred we would have been dealing with a sterically unhindered ligand (Py4SH), a sterically hindered ligand (Py2SH), and a sterically highly hindered ligand (2-Me-Py6SH); in such circumstances the Dq values and the B values should have changed markedly with ligand (65). If the bonding is through sulfur, however, the steric requirements of the three ligands are essentially the same.

As far as the oxygen ligands are concerned, there is very little difference between the data for the hydroxy-pyridines and for the arsenic and phosphorus oxides. Apparently the electronic characteristics of the donor oxygen atom are little affected by the nature of the rest of the ligand. However, whilst the arsenic and phosphorus oxides yielded CoL_4^{2+} cations, only CoL_6^{2+} species may be obtained with the 2-hydroxy pyridines. In view of the fairly high electronegativity of the oxygen ligands, and the fact that tetrahedral cobalt(II) compounds tend to be covalent, a coordination number of six is probably the norm with oxygen ligands (66). The coordination number of four with the arsenic and phosphorus ligands can then be explained in terms of the bulkiness of these ligands. With sulfur, on the other hand, the much lower electronegativity, and greater polarizability, will indeed favor four coordinate tetrahedral complexes.

In the phosphorus and arsenic complexes of formula CoL_2X_2 the Dq for the oxygen complexes is greater than for the corresponding sulfur complexes as would be anticipated on the basis of the spectrochemical series. In the CoL_4^{2+} complexes of these ligands, however, there is little difference in Dq. The values of the oxide CoL_4^{2+} complexes are clearly too low. If this is a genuine phenomenon (and not an artifact of the method of calculation which may arise because of the multiplicity of the bands concerned), it may reflect the "dislike" of cobalt(II) to form tetrahedral CoO_4^{2+} complexes.

Can. J. Chem. Downloaded from www.nrcresearchpress.com by 210.87.254.105 on 09/05/12
For personal use only.

Can. J. Chem. Downloaded from www.nrcresearchpress.com by 210.87.254.105 on 09/05/12
For personal use only.

In contradistinction to the oxygen series, the pyridine thiol CoL_2X_2 complexes have markedly higher mean Dq values than the phosphorus or arsenic sulfides. In the CoL_4^{2+} series the Dq values are comparable. The lower Dq values in the P=S and As=S systems may reflect increased contribution of sulfur-to-metal bonding arising as a consequence of the softness of the atom (P or As) to which the sulfur is attached. In the thiols, or more correctly, thione compounds, the higher electronegativity of the carbon atom to which the sulfur is attached, and the electron sink character of the pyridine ring, will decrease the capability of the sulfur atom to donate electron density. Notwithstanding this effect, the optical electronegativity data suggest that the availability of electron density in these derivatives exceeds that in, for example, the thioethers and dithiophosphates. Table 13 shows previously unpublished ultraviolet data for some Me_3PS and Me_3AsS complexes originally characterized by Rodley and co-workers (61). These data reveal an optical electronegativity of 2.6–2.7 for these ligands, somewhat higher than for the thiols. Possibly these data are indicative of appreciable P=S and As=S interaction thereby decreasing the availability of the lone pair to the metal atom. Unfortunately the conclusions which may be drawn from consideration of the crystal field and optical electronegativity data for the arsenic and phosphorus sulfides seem mutually contradictory.

We are indebted to the National Research Council of Canada for financial support, and to Dr. G. A. Rodley for the supply of arsenic and phosphine sulfides.

1. J. L. Burmeister. Coord. Chem. Rev. **1**, 205 (1966); **3**, 225 (1968).
2. R. A. Bailey, S. L. Kozak, T. W. Michelson, and W. N. Mills. Coord. Chem. Rev. **6**, 407 (1970).
3. W. J. Eilbeck, F. Holmes, and A. E. Underhill. J. Chem. Soc. A, 757 (1967).
4. J. A. Weaver, P. Hambright, P. T. Talbert, E. Kang, and A. N. Thorpe. Inorg. Chem. **9**, 268 (1970).
5. E. J. Duff, M. N. Hughes, and K. J. Rutt. J. Chem. Soc. A, 2354 (1968).
6. M. N. Hughes and K. J. Rutt. J. Chem. Soc. A, 3015 (1970); E. J. Duff, M. N. Hughes, and K. J. Rutt. J. Chem. Soc. A, 2101 (1969).
7. B. Singh, Lakshmi, and E. Agarwala. Inorg. Chem. **8**, 2341 (1969).
8. S. K. Madan and C. Goldstein. J. Inorg. Nucl. Chem. **28**, 1251 (1966).
9. D. DeFilippo and C. Preti. J. Chem. Soc. A, 1904 (1970).
10. P. P. Singh and R. Rivest. Can. J. Chem. **46**, 2361 (1968).
11. M. Keeton and A. B. P. Lever. Inorg. Chem. **10**, 47 (1971).
12. M. Keeton, A. B. P. Lever, and B. S. Ramaswamy. Can. J. Chem. **48**, 3187 (1970).
13. G. J. Sutton. Aust. J. Chem. **24**, 919 (1971); **22**, 2475 (1969).
14. S. E. Livingstone and J. D. Wolan. Aust. J. Chem. **22**, 1817 (1969); P. S. K. Chia and S. E. Livingstone. Aust. J. Chem. **22**, 1825 (1969).
15. A. Yamaguchi, R. B. Penland, S. Mizushima, J. T. Saul, C. Curran, and J. V. Quagliano. J. Am. Chem. Soc. **80**, 527 (1958).
16. C. D. Flint and M. Goodgame. J. Chem. Soc. A, 744 (1966); 750 (1968).
17. C. F. H. Allen and J. R. Thirtle. Org. Synth. **26**, 16 (1946).
18. J. R. Thirtle. J. Am. Chem. Soc. **68**, 342 (1946).
19. C. L. Bell, R. S. Egan, and L. Bauer. J. Heterocycl. Chem. **2**, 420 (1965).
20. J. R. Wasson, K. K. Ganguli, and L. Theriot. J. Inorg. Nucl. Chem. **29**, 2807, (1967).
21. J. C. Donini, B. R. Hollebone, and A. B. P. Lever. J. Phys. E. **5**, 385 (1972).
22. A. I. Vogel. Quantitative inorganic analysis. Longmans, London. 1961.
23. V. I. Bliznyukov and V. M. Reznikov. J. Gen. Chem. USSR. **25**, 1735 (1955).
24. R. A. Jouls and A. R. Katritzky. J. Chem. Soc. 3610 (1958).
25. E. Spinner. J. Chem. Soc. 1237 (1960); J. Org. Chem. **23**, 2037 (1958).
26. J. D. Gilbert, D. Rose, and G. Wilkinson. J. Chem. Soc. A, 2765 (1970).
27. S. R. Fletcher and A. C. Skapski. J. Chem. Soc. Dalton, 635 (1972).
28. A. B. P. Lever. Inorganic electronic spectroscopy. Elsevier, Amsterdam. 1968.
29. J. Lewis. Sci. Progr. **51**, 452 (1963).
30. B. J. Hathaway and A. E. Underhill. J. Chem. Soc. 3091 (1961).
31. S. F. Pavkovic and D. W. Meek. Inorg. Chem. **4**, 1091 (1965).
32. D. S. Brown, J. D. Lee, B. G. A. Melson, B. J. Hathaway, I. M. Proctor, and A. A. G. Tomlinson. Chem. Commun. 369 (1967).
33. R. J. H. Clark. Halogen chemistry. Vol. 3. *Edited by* V. Gutmann. Academic Press, New York. 1968. p. 85.
34. J. Reedijk. Rec. Trav. Chim. **88**, 1139 (1969).
35. F. A. Cotton, D. M. L. Goodgame, and M. Goodgame. J. Am. Chem. Soc. **83**, 4690 (1961).
36. C. Postmus, J. R. Ferraro, A. Quattrochi, K. Shobatake, and K. Nakamoto. Inorg. Chem. **8**, 1851 (1969).
37. A. B. P. Lever, E. Mantovani, and B. S. Ramaswamy. Can. J. Chem. **49**, 1957 (1971).
38. (*a*) G. E. Coates and D. Ridley. J. Chem. Soc. 166 (1964). (*b*) R. J. H. Clark and C. S. Williams. Inorg. Chem. **4**, 350 (1965).

39. I. S. AHUJA and P. RASTOGI. J. Chem. Soc. A, 2161 (1970).
40. D. GRDENIC and I. KRSTANOVIC. Arkiv. Kemi. **27**, 143 (1955).
41. G. B. DEACON and J. H. S. GREEN. Spectrochim. Acta, **25A**, 355 (1969).
42. G. B. DEACON, J. H. S. GREEN, and D. J. HARRISON. Spectrochim. Acta, **24A**, 1921 (1968).
43. R. C. EVANS, F. G. MANN, H. S. PEISER, and D. PURDIE. J. Chem. Soc. 1209 (1940).
44. R. C. CASS, G. E. COATES, and R. G. HAYTER. J. Chem. Soc. 4007 (1955).
45. I. S. AHUJA and P. RASTOGI. J. Chem. Soc. A, 378 (1970) and references therein.
46. W. P. GRIFFITH. The chemistry of the rarer platinum metals. Interscience, New York. 1967.
47. D. M. ADAMS. Metal-ligand and related vibrations. Edward Arnold, London. 1967.
48. C. N. R. RAO and R. VENKATARAGHAVAN. Spectrochim. Acta, **18**, 541 (1962).
49. C. N. R. RAO, R. VENKATARAGHAVAN, and T. R. KASTURI. Can. J. Chem. **42**, 36 (1964).
50. S. P. SINHA. Spectrochim. Acta, **20**, 879 (1964).
51. D. A. BALDWIN, R. V. PARISH, and A. B. P. LEVER. Inorg. Chem. **8**, 107 (1969).
52. A. R. KATRITZKY and R. A. JONES. J. Chem. Soc. 2947 (1960).
53. G. H. KELLER, L. BAUER, and C. L. BELL. Can. J. Chem. **46**, 2475 (1968).
54. A. W. MCLELLAN and G. A. MELSON. J. Chem. Soc. A, 137 (1967).
55. L. CAVALEA, M. NARDELLI, and G. FAVA. Acta Cryst. **13**, 594 (1960).
56. B. R. PENFOLD. Acta Cryst. **6**, 591 (1953).
57. B. J. HATHAWAY and A. E. UNDERHILL. J. Chem. Soc. 3091 (1961).
58. F. J. ALLDAY. Ph.D. Thesis. Manchester University, Manchester. 1967. T. HARRISON. Ph.D. Thesis. Manchester University, Manchester. 1969.
59. F. J. ALLDAY, T. HARRISON, R. N. HASZELDINE, and A. B. P. LEVER. Unpublished observations.
60. A. B. P. LEVER and E. MANTOVANI. Inorg. Chem. **10**, 817 (1971).
61. A. M. BRODIE, S. G. HUNTER, G. A. RODLEY, and C. J. WILKINS. J. Chem. Soc. A, 987, 2039 (1968).
62. C. K. JØRGENSEN. Orbitals in atoms and molecules. Academic Press, New York. 1962.
63. C. K. JØRGENSEN. Progr. Inorg. Chem. **12**, 101 (1970).
64. W. BYERS, B. FA-CHUN CHOU, A. B. P. LEVER, and R. V. PARISH. J. Am. Chem. Soc. **91**, 1329 (1969).
65. M. KEETON, A. B. P. LEVER, and B. S. RAMASWAMY. Spectrochim. Acta, **26A**, 2173 (1970).
66. R. C. CARLIN. Trans. Met. Chem. **1**, 1 (1966).
67. W. J. GEARY. Coord. Chem. Rev. **7**, 81 (1971).
68. E. SPINNER and J. C. B. WHITE. J. Chem. Soc. **B**, 991 (1966).
69. L. J. BELLAMY and P. E. ROGASCH. Proc. Roy. Soc. **257A**, 98 (1960).
70. R. H. LEE, J. GRISWOLD, and J. KLEINBERG. Inorg. Chem. **3**, 1278 (1964).
71. R. PAPPALARDO and R. E. DIETZ. Phys. Rev. **123**, 1188 (1961).
72. R. L. CARLIN and S. L. HOLT. Inorg. Chem. **2**, 849 (1963).
73. F. A. COTTON, O. D. FAUT, and J. T. MAGUE. Inorg. Chem. **3**, 17 (1964).
74. S. K. MADAN and D. MUELLER. J. Inorg. Nucl. Chem. **28**, 177 (1966).
75. S. K. MADAN and C. GOLDSTEIN. J. Inorg. Nucl. Chem. **28**, 1251 (1966).
76. B. R. HOLLEBONE. J. Chem. Soc. A, 481 (1971).
77. D. M. L. GOODGAME, M. GOODGAME, and G. W. RAYNER-CANHAM. Inorg. Chim. Acta. **3**, 399 (1969).
78. M. GOODGAME and F. A. COTTON. J. Am. Chem. Soc. **84**, 1543 (1962).
79. W. J. DAVIS and J. SMITH. J. Chem. Soc. A, 317 (1971).
80. A. B. P. LEVER and B. S. RAMASWAMY, S. H. SIMONSEN, and L. K. THOMPSON. Can. J. Chem. **48**, 3076 (1970).
81. R. L. CARLIN and E. WEISSBERGER. Inorg. Chem. **3**, 611 (1964).
82. S. L. HOLT and R. L. CARLIN. J. Am. Chem. Soc. **86**, 3017 (1964).
83. C. K. JØRGENSEN. J. Inorg. Nucl. Chem. **24**, 1571 (1962).

Can. J. Chem. Downloaded from www.nrcresearchpress.com by 210.87.254.105 on 09/05/12
For personal use only.

A Positive-Ion Reaction Mechanism for the Radiation Induced Oxidation of Carbon Monoxide in the High Dose Rate Radiolysis of $CO-O_2$ Mixtures [1]

C. WILLIS,[2] A. W. BOYD, AND P. E. BINDNER

Physical Chemistry Branch, Chalk River Nuclear Laboratories, Atomic Energy of Canada Limited, Chalk River, Ontario

Received February 17, 1972

Carbon dioxide and ozone yields have been measured in the irradiation of $CO-O_2$ mixtures with single pulses of electrons. The yields of CO_2 at 2×10^{27} eV g^{-1} s^{-1} are large $G(CO_2) = 15 \pm 1$ from 20–60% O_2. These decrease by ~50% at 10^{28} eV g^{-1} s^{-1}. Although the results are somewhat irreproducible the addition of c-C_4F_8, an electron scavenger, increases these CO_2 yields at both dose rates by up to a factor of 15. They are reduced to $G(CO_2) < 2$ by the addition of positive ion scavengers. These results are consistent with a chain reaction similar to that proposed for low dose rate studies involving O_2^+, CO_3^+, and CO_2^+ as chain carriers.

The ozone yields are consistent with a total oxygen atom yield of $G(O) = 1.4$ in pure CO from neutral processes.

Nous avons mesuré les rendements en dioxyde de carbone et en ozone obtenus par irradiation de mélanges $CO-O_2$ par pulsation simple d'électrons. A partir de 20–60% de O_2, les rendements en CO_2 sont élevés, soit $G(CO_2) = 15 \pm 1$ à 2×10^{27} eV g^{-1} s^{-1}. Ils diminuent de près de 50% à 10^{28} eV g^{-1} s^{-1}. Quoique les résultats soient assez peu reproductibles, l'addition de c-C_4F_8, un piège à électrons, augmente les rendements en CO_2 aux deux vitesses de dose par un facteur de 15. Les pièges à électrons positifs réduisent ces rendements à $G(CO_2) < 2$. Les résultats concordent avec l'hypothèse d'une réaction en chaîne semblable à celle proposée pour les études à faible vitesse de dose, impliquant O_2^+, CO_3^+, et CO_2^+ comme porteurs de chaînes.

Les rendements en ozone sont consistants avec le rendement total d'un atome d'oxygène, $G(O) = 1.4$ en CO pur à partir de procédés neutres. [Traduit par le journal]

Canadian Journal of Chemistry, **50**, 3508 (1972)

Can. J. Chem. Downloaded from www.nrcresearchpress.com by 210.87.254.105 on 09/05/12
For personal use only.

Introduction

In a series of papers (1–7), we have proposed mechanisms and primary yields for radiolysis of CO_2, O_2, CO, and CO_2-O_2 mixtures. These have been based on product yield measurements in these systems at the high dose rates (10^{26}–10^{28} eV g^{-1} s^{-1}) obtainable with Febetron pulses. We have now looked at the high dose rate radiolysis of $CO-O_2$ mixtures.

Low dose rate studies of the $CO-O_2$ system have been reported by Lind and Bardwell (9), by Clay, Johnson, and Warman (8) and by Anderson, Best, and Willet (10). All agree that the yield of CO_2 in these systems is very high. The most detailed study is that of Clay, Johnson, and Warman who studied the γ-radiation induced oxidation of CO from 1–98% O_2 and investigated the effect of dose rate, pressure, and the presence of additives. Yields of CO_2 were highest at 50% O_2 where at 60 Torr pressure $G(CO_2) \simeq 8000$. They observed some effect of pressure but none of dose rate in the range 2×10^{14}–5×10^{15} eV g^{-1} s^{-1}. The reaction scheme they postulated is as follows:

Initiation	$CO^+ + O_2 \rightarrow CO_3^+$
	O_2^+ ($^4\pi_u$ state or higher) + $CO \rightarrow CO_3^+$
Propagation	$CO_3^+ + CO \rightarrow CO_2^+$ ($^2\pi_u$?) + CO_2
	CO_2^+ ($^2\pi_u$?) + $O_2 \rightarrow O_2^+$ ($^4\pi_u$) + CO_2
Termination	$CO_3^+ + CO + M \rightarrow CO_2^+ + CO_2 + M$

They concluded, because of the lack of effect of dose rate, that termination could not be due to charge neutralization but must be due to formation of an unexcited CO_2^+ ion thus precluding the formation of an excited O_2^+ ion which was the chain carrier in their mechanism.

Anderson, Best, and Willet (10) studying the system at higher dose rates, ~10^{23} eV g^{-1} s^{-1}, did observe an effect of dose rate indicating charge neutralization termination of the chain.

The mechanism proposed by Clay, Johnson, and Warman (8), although in agreement with their observations is not unique and is difficult to further substantiate by low dose rate studies. However, work at high dose rates could yield more information and it was for this purpose that the present study was undertaken.

[1] AECL No. 4299.

[2] Present address: Chemistry Department, University of the West Indies, Mona, Kingston 7, Jamaica.

Can. J. Chem. Downloaded from www.nrcresearchpress.com by 210.87.254.105 on 09/05/12
For personal use only.

Experimental

Irradiations

Two pulsed electron accelerators were used in this work, a Febetron 705[3] and a Febetron 706[3]. The 2 MeV Febetron 705 has an effective dose rate for gaseous samples of 2×10^{27} eV g^{-1} s^{-1}. The 600 keV Febetron 706 has a higher dose rate of 1×10^{28} eV g^{-1} s^{-1}.

Two types of irradiation cells were used for the determination of the CO_2 yields: cells of quartz (11) and cells of aluminum (12), both of similar dimensions. In early experiments discharges were observed from the quartz cells after they had been irradiated and it was thought that these might contribute to an "after-effect" yield in the CO–O_2 mixtures. However, the results from the aluminum cells which were well grounded during irradiation were identical to those obtained using the quartz cells, except, perhaps, for the elimination of the odd, very high yield.

The dose absorbed in these cells was determined by irradiating pure N_2O taking $G(N_2) = 12.4 \pm 0.3$ (12–14) for these dose rates.

Ozone yields were determined in a stainless steel cell containing a conventional optical system (15). The dosimetry for these measurements was achieved by irradiation of pure oxygen taking $G(O_3) = 12.8 \pm 0.5$ (5, 6, 16, 17).

Materials

NH_3, c-C_4F_8 (perfluorocyclobutane), SF_6, N_2O, and O_2, Matheson (C.P. Grade) and C_3H_6 and C_3H_8 Phillips (Research Grade) were taken directly from the cylinder. Except for O_2, the gases were subjected to freeze–pump–thaw cycles to remove impurities non-condensible at 77 °K.

The CO used was Matheson (Research Grade). This was further purified by passing through a furnace containing copper turnings at 700 °C. This pyrolyzed traces of carbonyl and also catalyzed combination of traces of O_2 with CO. The gas was then passed through a freshly conditioned column of Linde 13X molecular sieve and finally through a 1 mm i.d. spiral 2 m long immersed in liquid nitrogen. We have previously used a similar purification procedure for CO and obtained satisfactory results (4).

Analyses

CO_2

For CO_2 determinations the irradiated gas (100 ml volume) was expanded into twin cold traps (1.2 l volume) at liquid nitrogen temperatures and left for 5 min. The non-condensed gas was slowly pumped off via a U-tube immersed in liquid nitrogen. The material condensed in the traps and the U-tube was then distilled into the inlet port valve of a Loenco 15C gas chromatograph equipped with a Porapak Q column at 60 °C and thermal conductivity detectors. The scrubbing procedure used here was shown to quantitatively remove carbon dioxide by using synthetic mixtures of CO_2–CO with concentrations similar to those expected in irradiated samples.

O_3

Ozone was determined directly in the optical cell by its absorption at 254.5 nm (18). We have described this procedure previously (2, 7, 19).

[3]Manufactured by Field Emission Corporation, McMinnville, Oregon, USA.

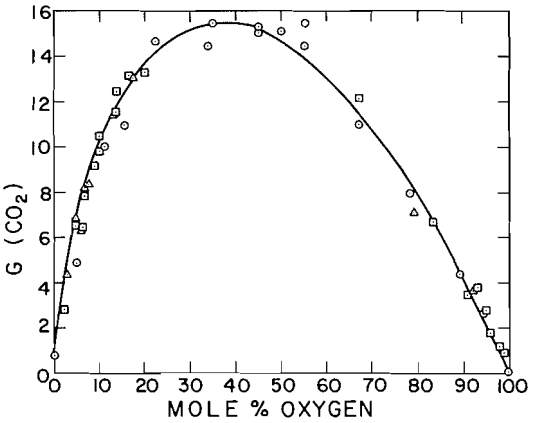

FIG. 1. CO_2 yields from single pulse irradiations of CO–O_2 mixtures at 2×10^{27} eV g^{-1} s^{-1}: ○, 450 Torr Al cell; □, 450 Torr quartz cell; △, 650 Torr quartz cell.

N_2

Nitrogen produced in the dosimetry experiments was analyzed using standard vacuum line techniques and a CEC 610 mass spectrometer.[4]

Results

CO_2 Yields

The yields of carbon dioxide from single pulse irradiations of CO–O_2 mixtures are shown in Fig. 1. As O_2 is added to CO the yield of CO_2 increases to $G(CO_2) \simeq 15 \pm 1$ between 25–55% O_2. Further increases in the O_2 concentration cause the CO_2 yield to decrease.

There is no effect of pressure for the range shown. At 1×10^{28} eV g^{-1} s^{-1} the yields were not as reproducible. In the range 25–55% O_2 they were between 6 and 9. Mixtures of 50% O_2–50% CO were irradiated at various temperatures between 373 and 77 °K. Basically identical results were obtained. There did appear to be a slight decrease in yield going from 273 to 198 °K but this was of the order of the experimental errors.

Effect of Dose

Figure 2 shows the CO_2 yield as a function of the dose for a 50% O_2–50% CO mixture. As can be seen, the yield remains constant up to at least 9×10^{20} eV g^{-1} (9 pulses).

Effect of Positive Ion Scavengers

Figure 3 shows the effect on the CO_2 yield of adding NH_3, C_3H_6, and C_3H_8 to a 45%

[4]Manufactured by Dupont Instrumental Products Division, Monrovia, California, USA.

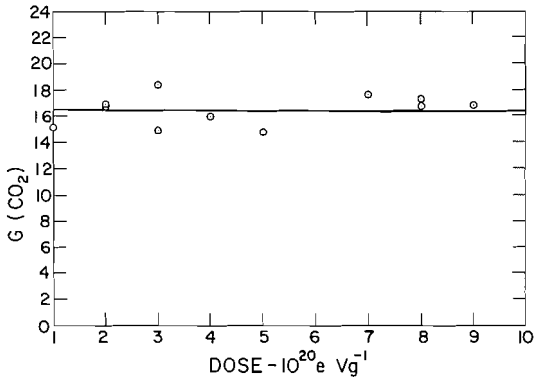

FIG. 2. $G(CO_2)$ as a function of dose at 2×10^{27} eV g^{-1} s^{-1}; 450 Torr pressure, 50%–50% CO–O_2.

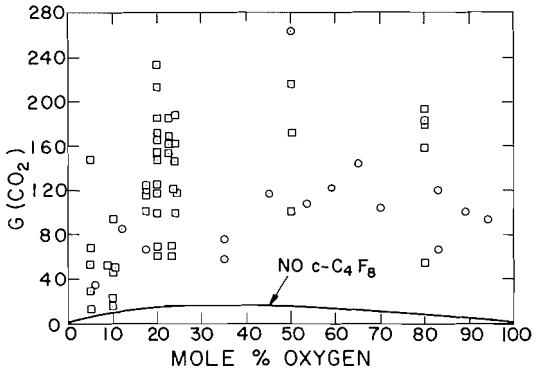

FIG. 4. Effect of c-C_4F_8 addition to CO–O_2 at 2×10^{27}–10^{28} eV g^{-1} s^{-1}: 450 Torr pressure; ○, Al cell; □, quartz cell.

O_2–55% CO mixture. NH_3 and C_3H_6 have virtually identical effects and reduce the CO_2 yield to close to zero above 5% additive. The effect of C_3H_8 is qualitatively the same but its efficiency is an order of magnitude less than that of C_3H_6 or NH_3.

In the CO–O_2–C_3H_6 and CO–O_2–C_3H_8 mixtures some CO_2 is produced from the hydrocarbon. Blank mixtures of O_2–C_3H_8 and O_2–C_3H_6 were irradiated for the experiments. Only for yields of $G(CO_2) < 1$ did the contribution from the hydrocarbon become significant.

Effect of c-C_4F_8

We could not use SF_6 as an electron scavenger where CO_2 was to be determined as we could not separate it from the CO_2 peak on the chromatographic column used. Consequently, we used c-C_4F_8 which can be separated more easily from the CO_2. We have used c-C_4F_8 in oxygen systems previously (6) and found its effect indistinguishable from that of SF_6.

The effect on the radiolytic yields of CO_2 of adding 2–5% perfluorocyclobutane to CO–O_2 mixtures is shown in Fig. 4. The effect is quite dramatic although somewhat irreproducible. For the range 25–55% O_2, the CO_2 yields increase from $G(CO_2) = 15 \pm 1$ in the absence of c-C_4F_8, to $G(CO_2) = 60$–240 in the presence of 2–5% c-C_4F_8.

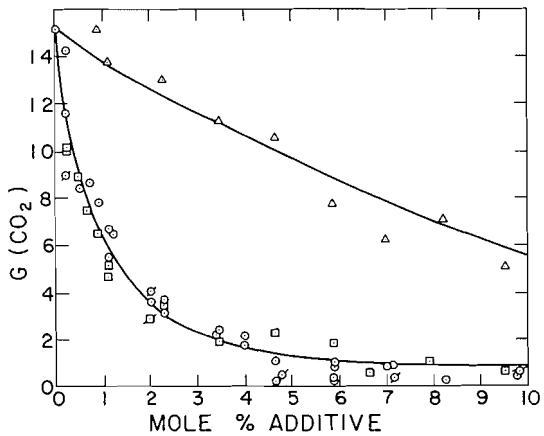

FIG. 3. Effect of adding NH_3, C_3H_6, C_3H_8 to 55% CO–45% O_2 at 2×10^{27}–10^{28} eV g^{-1} s^{-1}; 450 Torr pressure; □, C_3H_6; ○, NH_3; △, C_3H_8 in Al cell; ⊠, C_3H_6; ∅, NH_3 in quartz cell.

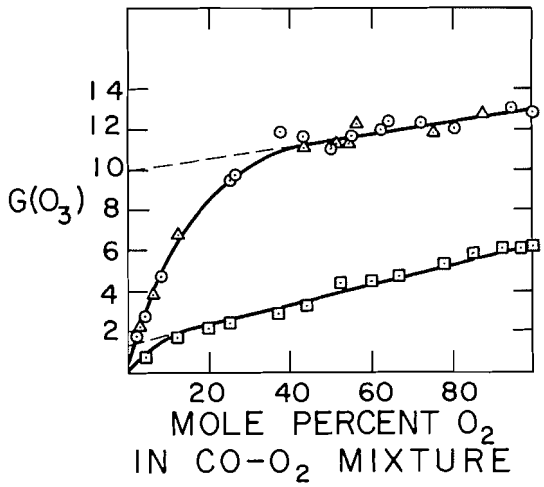

FIG. 5. O_3 yields in CO–O_2 and CO–O_2–2–5% SF_6 at 2×10^{26} eV g^{-1} s^{-1}: ○, 450 Torr, CO–O_2; △, 650 Torr, CO–O_2; □, 650 Torr, CO–O_2–SF_6.

Can. J. Chem. Downloaded from www.nrcresearchpress.com by 210.87.254.105 on 09/05/12
For personal use only.

TABLE 1. Primary yields in CO and O_2 radiolysis

CO			O_2		
Species	Yield	Reference	Species	Yield	Reference
e	3.11	20	e	3.27	see ref. 6
CO^+	2.92		O_2^+	3.17	for
C^+	0.14	21	O^+	0.10	discussion
O^+	0.05				
$C_2O^3\Sigma$	1.40	3, 4			
O^3P	1.41	22, 23	O^3P	3.15	
O^1D	~0.0	23, 4	O^1D	2.75	7
O^1S			O^1S	0.30	

Experiments as a function of temperature for $CO-O_2-2\%$ c-C_4F_8 mixtures were difficult because of the irreproducibility of the system but it appeared that lowering the temperature in the range 273 to 198 °K significantly reduced the CO_2 yield although it should not have led to any condensation of the c-C_4F_8.

In a few isolated experiments, the effects of adding NH_3 and C_3H_6 to $CO-O_2$-c-C_4F_8 mixtures were investigated. The results were very irreproducible but a large decrease in yield was observed. Above ~3% of NH_3 or C_3H_6 the results were indistinguishable from those obtained with $CO-O_2$ mixtures with the same amount of these gases in the absence of c-C_4F_8.

O_3 Yields

The O_3 yields from $CO-O_2$ mixtures with and without SF_6 are shown in Fig. 5. In the presence of 2–5%SF_6, the O_3 yields show an almost linear dependence, decreasing from $G(O_3) = 6.2$ for 100% O_2 to an extrapolated yield of $G(O_3)_{ext} = 1.4 \pm 0.1$ for 100% CO.

The yields in the absence of SF_6 are higher and decrease from $G(O_3) = 12.8$ in 100% O_2 to an apparent intercept of $G(O_3) \sim 10$ for 100% CO. It should be noted that, in the absence of SF_6 the O_3 yield begins to diverge from linear dependence below ~45% O_2 whereas in the presence of SF_6, the yield does not begin to diverge until below ~12% O_2.

Discussion

To facilitate discussion, the primary yields of species in the radiolysis of pure CO and pure O_2 are given in Table 1.

In pure CO, oxygen atoms react to give CO_2 but in the presence of oxygen, ozone will be formed (24–29), reaction 1.

[1] $$O + O_2 (+CO, O_2) \rightarrow O_3 (+CO, O_2)$$

Thus ozone yields can be taken as a measure of the oxygen atom yield. Ozone yields from $CO-O_2$ mixtures with added SF_6, Fig. 5, then, are as would be expected.[5] They go from an extrapolated yield of $G(O_3)_{extrapolated} = 1.4 \pm 0.1$ for pure CO to $G(O_3) = 6.2$ for pure O_2. The extrapolated yield for pure CO agrees very well with earlier estimates of Briggs and Clay (22, 23). In the absence of SF_6 the ozone yields are higher, therefore oxygen atoms must be produced in the charge neutralization step.

Clearly, if oxygen atoms lead to ozone formation they cannot lead to formation of carbon dioxide. Thus charge transfer from CO^+ to O_2, [4], followed by

[4] $$CO^+ + O_2 \rightarrow CO + O_2^+$$

dissociative neutralization of O_2^+, [5],

[5] $$O_2^+ (+e) \rightarrow 2O$$

cannot explain the increase in CO_2 yield on adding O_2 to CO, Fig. 1. We must therefore suppose a mechanism not involving oxygen atoms to explain the CO_2 yield.

Consider now the effect of c-C_4F_8. The direct effect of adding this to $CO-O_2$ mixtures is to scavenge free electrons.

[6] $$e + \text{c-}C_4F_8 \rightarrow \text{c-}C_4F_8^-$$

[5] In the presence of SF_6, contributions from ion-neutralization processes are suppressed (see for example discussion in ref. 6).

[2] $$e + SF_6 \rightarrow SF_6^-$$

[3] Positive ion + $SF_6^- \rightarrow$ dissociation products.

Can. J. Chem. Downloaded from www.nrcresearchpress.com by 210.87.254.105 on 09/05/12
For personal use only.

Can. J. Chem. Downloaded from www.nrcresearchpress.com by 210.87.254.105 on 09/05/12
For personal use only.

This leads to the indirect effect of changing the neutralization step to involve c-$C_4F_8^-$ as the dominant negative species. Addition of c-C_4F_8 to CO–O_2 mixtures does not decrease the CO_2 yield but rather leads to a very significant increase in the yield, Fig. 4. This eliminates the possibility of a negative ion–molecule reaction for CO_2 production. The increase in yield, however, would be consistent with a positive ion–molecule chain reaction with chain termination by charge neutralization. Neutralization of positive ions by c-$C_4F_8^-$ may well be a much slower process than the equivalent reaction with an electron or O_2^- (30) which would allow a longer chain. The decrease in yield on going to a higher dose rate, from 2×10^{27} to 1×10^{28} eV g^{-1} s^{-1}, is consistent with this. Also, since the ionization potentials of NH_3, C_3H_6, and C_3H_8 are lower than those of CO and O_2, the marked reduction in CO_2 yield in the presence of these additives can be explained by positive charge transfer termination of the chain.

Thus we can propose a positive ion–molecule chain oxidation of CO to CO_2 with charge neutralization as chain termination, the neutralization process yielding oxygen atoms.

Initiation

[7] $$O_2 \rightsquigarrow O_2^+ + e$$

[8] $$CO \rightsquigarrow CO^+ + e$$

Propagation

[9] $$O_2^+ + O_2 + M \rightarrow O_4^+ + M$$

[10] $$O_4^+ + CO \rightarrow CO_3^+$$

[11] $$CO^+ + O_2 \rightarrow CO_3^+$$

[12] $$CO_3^+ + CO \rightarrow CO_2^+ + CO_2$$

[13] $$CO_2^+ + O_2 \rightarrow O_2^+ + CO_2$$

[14] $$e + O_2 + M \rightarrow O_2^- + M$$

Termination

[15] $$O_4^+ + e\ (\text{or } O_2^-) \rightarrow 2O\ (+O_2)$$

[16] $$CO_3^+ + e\ (\text{or } O_2^-) \rightarrow 2O + CO\ (+O_2)$$

The mechanism represented by these reactions, 7–16, is consistent with the observations. Reactions 7–13 are, of course, essentially those used by Clay, Johnson, and Warman (8), to explain the low dose rate oxidation of CO by O_2.

Reaction 9 is included because $k_9 = 2.9 \times 10^{-30}$ cm^6 $molecule^{-1}$ s^{-1} (31) and this means that neutralization of O_2^+ cannot compete with its attachment to O_2 ($\alpha_{O_2^+} = 2.2 \times 10^{-7}$ cm^3 s^{-1} (32)).

Reaction 15 is included for the sake of completeness. We are not in a position to eliminate CO_3^+ as a possible chain terminator, however, if reaction 15 does take place it must yield two oxygen atoms to come close to explaining the yield of ozone in the absence of SF_6, Fig. 5. However, the falloff in CO_2 yield ultimately requires a competition between reaction 10 and reaction 15 suggesting that O_2^+ (or O_4^+) is the more important chain terminator.

At low O_2 concentration, *i.e.* high CO concentrations, the decrease in CO_2 yield can be accounted for by formation of $C_2O_2^+$, reaction 17.

[17] $$CO^+ + CO \rightarrow C_2O_2^+$$

$$k_{17} = 1 \times 10^{-10}\ cm^3\ molecule^{-1}\ s^{-1} \quad (33)$$

Presumably $C_2O_2^+$ cannot react to give CO_3^+ and its formation will reduce the concentration of chain carriers. $C_2O_2^+$ will therefore be neutralized directly to give 2CO, reaction 18.

[18] $$C_2O_2^+ + e \rightarrow 2CO$$

As has been pointed out (34), reaction 18 is not unlikely as the ionization potentials of CO and C_2O_2 are not much higher than the bond dissociation energy of CO.[6] Formation of $C_2O_2^+$ will then explain the divergence of the ozone yields from a linear dependence below ~45% O_2 for CO–O_2 mixtures in the absence of SF_6, Fig. 5.

A check on the plausibility of this mechanism, *i.e.* reactions 1–18, has been made by computer calculations. Rate constants in the range $1–2 \times 10^{-10}$ cm^3 $molecule^{-1}$ s^{-1} were assumed for reactions 9–12 and in the range $10^{-7}–10^{-6}$ cm^3 $molecule^{-1}$ s^{-1} for charge neutralization reactions (37–40) along with the primary ion yields in Table 1. These data and the absorbed dose and dose rate values were used with a computer program developed by Schmidt (41, 42). The use of this program in similar calculations has been described previously (43). The computed values

[6] I.P. CO^+ = 14.0 eV (35); I.P. $C_2O_2^+$ = 12.8 eV (36); D(C—O) = 11.1 eV (35).

Can. J. Chem. Downloaded from www.nrcresearchpress.com by 210.87.254.105 on 09/05/12
For personal use only.

of both $G(O_3)$ and $G(CO)$ in pure CO–O_2 mixtures agreed with the observed values within the experimental uncertainties. That is a smooth line joining the calculated CO_2 or O_3 yields fitted the experimental points as well as the lines shown in Figs. 1 and 5. Decreasing the rate constant for charge neutralization from 5×10^{-7} to 5×10^{-8} cm^3 molecule^{-1} s^{-1} (equivalent to c-C_4F_8 addition) resulted in an order of magnitude increase in the calculated yield of CO_2. Although the agreement between the calculated and experimental values supports the plausibility of the mechanism it can hardly be taken as proof as some of the rate constant values had to be assumed. A more detailed fit would not be worthwhile until rate constants are known for nearly all of the reactions.

Although it is difficult to assess the quantitative effect of NH_3, C_3H_6, and C_3H_8 as we do not know the charge transfer reaction involved one further comment is perhaps required. The rates of reactions 19 and 20.

[19] $$O_2^+ + NH_3 \rightarrow NH_3^+ + O_2$$

$$k_{19} = 2.6 \times 10^{-9} \text{ cm}^3 \text{ molecule}^{-1} \text{ s}^{-1} \quad (44)$$

[20] $$O_2^+ + C_3H_8 \rightarrow \text{products}$$

$$k_{20} = 1.8 \times 10^{-9} \text{ cm}^3 \text{ molecule}^{-1} \text{ s}^{-1} \quad (44)$$

would be expected to predict similar quantitative effects for NH_3 and C_3H_8. Clearly NH_3 is much more effective than C_3H_8, Fig. 3. This would suggest that O_2^+ (at least in its ground electronic state) is not the chain carrier. Whether the difference is due to the presence of O_4^+ rather than O_2^+ or whether the charge transfer involves other ions, may be in different electronic states, must await further kinetic data.

Conclusions

The mechanism we have derived is not significantly different to that proposed by Clay, Johnson, and Warman (8) but is based on more experimental observations. In their work (8), it was proposed that CO_3^+, CO_2^+, and O_2^+ were all in excited states. Since we clearly have chain termination by charge neutralization we can draw no firm conclusion on this point.

The major conclusions which can be made from the present work are that a positive chain oxidation of CO does occur, the primary O atom yield in pure CO is $G(\text{O atom}) = 1.4 \pm 0.1$ and that the rate of charge neutralization by c-$C_4F_8^-$ is about ten times slower than by O_2^-.

1. C. Willis, A. W. Boyd, and P. E. Bindner. Can. J. Chem. **48**, 1951 (1970).
2. C. Willis and P. E. Bindner. Can. J. Chem. **48**, 3463 (1970).
3. C. Willis and C. Devillers. Chem. Phys. Lett. **2**, 51 (1968).
4. C. Willis and O. A. Miller. Can. J. Chem. **48**, 3029 (1970).
5. A. W. Boyd, C. Willis, R. Cyr, and D. A. Armstrong. Can. J. Chem. **47**, 4715 (1969).
6. C. Willis, A. W. Boyd, M. J. Young, and D. A. Armstrong. Can. J. Chem. **48**, 1505 (1970).
7. C. Willis, A. W. Boyd, and P. E. Bindner. Can. J. Chem. **50**, 1557 (1972).
8. P. G. Clay, G. R. A. Johnson, and J. M. Warman. Discuss. Faraday Soc. **36**, 46 (1963).
9. S. C. Lind and D. C. Bardwell. J. Am. Chem. Soc. **47**, 2675 (1925).
10. A. R. Anderson, J. V. F. Best, and M. J. Willett. Trans. Faraday Soc. **62**, 595 (1966).
11. C. Willis, A. W. Boyd, and O. A. Miller. Can. J. Chem. **47**, 3007 (1969).
12. C. Willis, O. A. Miller, A. E. Rothwell, and A. W. Boyd. Adv. Chem. Ser. **81**, 539 (1968).
13. C. Willis, A. W. Boyd, and D. A. Armstrong. Can. J. Chem. **47**, 3783 (1969).
14. C. Willis, A. W. Boyd, and O. A. Miller. Radiat. Res. **46**, 428 (1971).
15. W. A. Seddon, C. Willis, M. J. Young, and E. B. Selkirk. Atomic Energy of Canada Limited Report AECL-3853. 1971.
16. J. A. Ghormley, C. J. Hochanadel, and J. W. Boyle. J. Chem. Phys. **50**, 419 (1969).
17. G. M. Meaburn, D. Perner, J. LeCalve, and M. Bourene. J. Phys. Chem. **72**, 3920 (1968).
18. W. B. DeMore and O. Raper. J. Phys. Chem. **68**, 412 (1964).
19. C. Willis, A. W. Boyd, and M. J. Young. Can. J. Chem. **48**, 1515 (1970).
20. G. G. Meisels. J. Chem. Phys. **41**, 51 (1964).
21. A. Cornu and R. Massot. Compilation of mass spectral data. Heyden and Sons, London. 1966.
22. J. P. Briggs and P. G. Clay. Nature, **217**, 947 (1968).
23. J. P. Briggs and P. G. Clay. Int. J. Radiat. Phys. Chem. **1**, 67 (1968).
24. G. Paraskevapoulos and R. J. Cvetanovic. J. Am. Chem. Soc. **91**, 7572 (1969).
25. R. A. Young, G. Black, and T. G. Slanger. J. Chem. Phys. **49**, 4758 (1968).
26. W. B. DeMore and C. Dede. J. Phys. Chem. **74**, 2621 (1970).
27. T. G. Slanger and G. Black. J. Chem. Phys. **53**, 3717 (1970).
28. T. G. Slanger and G. Black. J. Chem. Phys. **53**, 3722 (1970).

29. H. WEBSTER and E. J. BAIR. J. Chem. Phys. **53**, 4532 (1970).
30. S. G. LIAS, R. E. REBBERT and P. AUSLOOS. J. Chem. Phys. **57**, 2080 (1972).
31. D. A. DURDEN, P. KEBARLE, and A. GOOD. J. Chem. Phys. **48**, 509 (1969).
32. M. A. BIONDI. Can. J. Chem. **47**, 1711 (1969).
33. M. SAPOROSCHENKO. J. Chem. Phys. **49**, 768 (1968).
34. A. R. ANDERSON. Fundamental processes in radiation chemistry. *Edited by* P. Ausloos. J. Wiley Publ., New York. 1968. p. 336.
35. J. L. FRANKLIN, J. G. DILLARD, H. M. ROSENSTOCK, J. T. HERRON, K. DRAXL, and F. H. FIELD. NSRDS-NBS-26. 1969.
36. M. S. B. MUNSON, F. H. FIELD, and J. L. FRANKLIN. J. Chem. Phys. **37**, 1790 (1962).
37. E. E. FERGUSON. Space Res. 7. North Holland Pub. Co. Amsterdam. 1967. p. 135.
38. M. A. BIONDI. Can. J. Chem. **47**, 3711 (1969).
39. W. H. KASNER and M. A. BIONDI. Phys. Rev. **174**, 139 (1968).
40. J. R. PETERSON, W. H. ABERTH, J. T. MOSELEY, and J. R. SHERIDAN. Phys. Rev. A**3**, 1651 (1971).
41. K. H. SCHMIDT. USAEC Research and Development Report ANL-7199. 1966.
42. K. H. SCHMIDT. USAEC Research and Development Report ANL-7693. 1966.
43. C. WILLIS, A. W. BOYD, A. E. ROTHWELL, and O. A. MILLER. Int. J. Radiat. Phys. Chem. **1**, 373 (1969).
44. F. C. FEHSENFELD *et al.* E.S.S.A. Technical Report ERL 135-AL3 U.S. Government Printing Office, Washington, D.C. 20402.

Can. J. Chem. Downloaded from www.nrcresearchpress.com by 210.87.254.105 on 09/05/12
For personal use only.

The Hydrate of Hexafluorophosphoric Acid[1]

D. W. Davidson and S. K. Garg

Division of Chemistry, National Research Council of Canada, Ottawa, Canada K1A 0R9

Received May 12, 1972

HPF_6 is said to form a hexahydrate of a unique clathrate structure in which PF_6^- ions occupy truncated-octahedral cages in a framework of hydrogen-bonded water molecules. N.m.r. studies show, however, that appreciable quantities of HF are incorporated in the lattice and that the composition is more properly $H_3O^+PF_6^-\cdot HF\cdot 4H_2O$, a result supported by chemical analysis. H_3O^+ and HF appear to be distributed over the lattice sites previously assigned to water molecules so as to involve all H atoms in the hydrogen bonding. The ^1H resonance line is narrowed by rapid proton diffusion down to 150 °K. The ^{19}F line of encaged PF_6^- is narrowed by rotation above 75 °K and reaches the rigid-lattice shape only below 25 °K.

HPF_6 est reconnu pour former une hexahydrate de structure clathrate unique dans laquelle les ions PF_6^- occupent des cages octaédriques tronquées dans une structure de molécules d'eau liées par des ponts hydrogène. Des études au RMN démontrent toutefois que des quantités appréciables de HF sont incorporées dans le réseau et que la composition serait plutôt $H_3O^+PF_6^-\cdot HF\cdot 4H_2O$, résultat supporté par analyse chimique. H_3O^+ et HF semblent distribués sur des sites du réseau attribués auparavant à des molécules d'eau, de façon à impliquer tous les atomes de H dans des ponts hydrogène. La raie de résonance ^1H est amincie par une diffusion rapide de proton au-dessus de 150 °K. La raie de ^{19}F du PF_6^- en cage est amincie par la rotation au-dessus de 75 °K et atteint la forme caractéristique du réseau rigide seulement au-dessous de 25 °K.

[Traduit par le journal]

Canadian Journal of Chemistry, **50**, 3515 (1972)

Hexafluorophosphoric acid appears not to be stable in isolated form (1), at least at ordinary temperatures. Commercial 65% HPF_6 is an equilibrium mixture which contains (2) about 21 wt.% H_2O, 6% HF, and 8% of the phosphoric acids HPO_2F_2, H_2PO_3F, and H_3PO_4. The PF_6^- ion itself is stable in various salts (1) and is not readily hydrolyzed in dilute solutions of the acid (3).

The solid (m.p. 31.5 °C) which crystallizes from relatively concentrated solutions is considered (4) to be a hexahydrate, apparently on the basis of determination of HPF_6 as the nitron salt. On exposure to the atmosphere at room temperature, hydrate crystals soon become liquid, reputedly because of their hygroscopic character (1). The X-ray study of the hydrate at room temperature by Bode and Teuffer (5) suggested a structure of a unique clathrate type in which each PF_6^- group occupies a truncated-octahedral cage (Fig. 1) composed of mutually hydrogen-bonded water molecules. The positions of the six F atoms were not accurately fixed, but were best represented as disordered over 48 equivalent sites within each cage (5). The position of the extra proton was not determined.

[1]NRCC No. 12786.

The truncated-octahedral structure is the only known 4-coordinated clathrate structure in which polyhedral cages of a single kind fit together to fill all the space in a 3-dimensional lattice (6). In the common clathrates of the gas hydrate type, cages of two different kinds are present (7, 8). All the water molecules of the ideal truncated-octahedral structure occupy crystallographically equivalent sites (symmetry $\bar{4}2m$) and the 24 water molecules at the vertices of the tetrakaidecahedron are equidistant from its center. These features are also unique among the known clathrate hydrates (8).

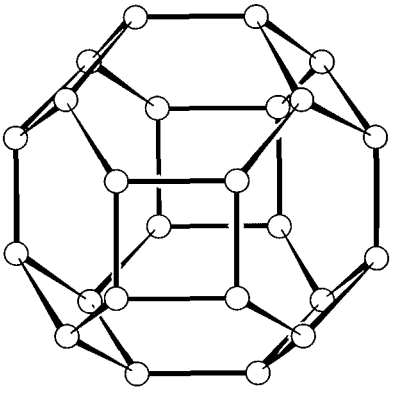

FIG. 1. The truncated-octahedral cage of HPF_6 hydrate.

Can. J. Chem. Downloaded from www.nrcresearchpress.com by 210.87.254.40 on 09/05/12
For personal use only.

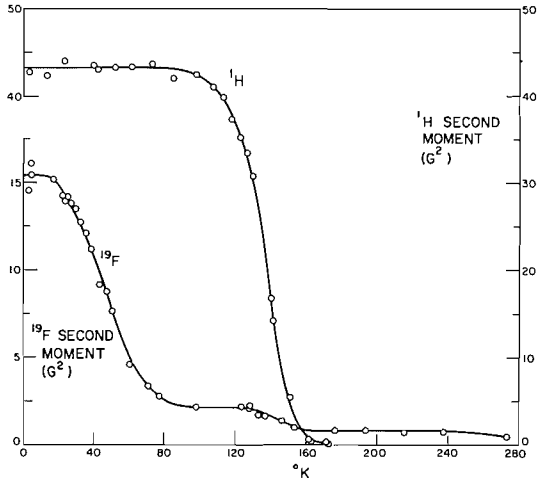

FIG. 2. Second moments of ^{1}H and ^{19}F absorption lines. Below 140 °K the F second moments are for the narrower component only.

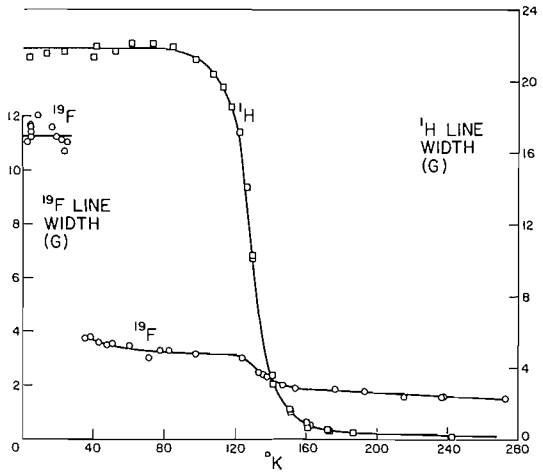

FIG. 3. Line widths as separations of *extrema* of derivative curves.

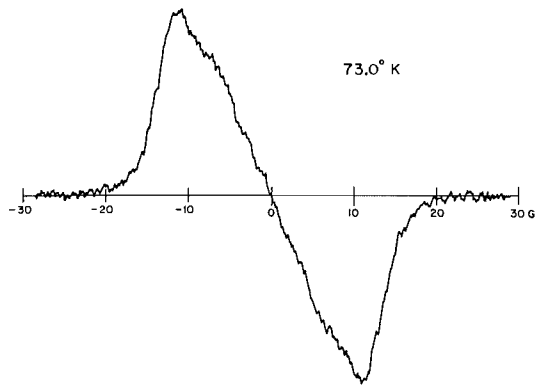

FIG. 4. Characteristic shape of the derivative of the ^{1}H absorption at low temperatures.

Experimental Methods

As part of a study of clathrate hydrates, we have examined the ^{19}F and ^{1}H n.m.r. derivative spectra of HPF_6 hydrate between 2 and 273 °K. Measurements were made at 17 MHz with a single coil probe which formed part of a marginal oscillator circuit. A low-power Robinson oscillator was used for a few measurements at the lowest temperatures. Other experimental details are given elsewhere (9).

Crystals of hydrate were prepared by adding sufficient water to 65% HPF_6 to bring the H_2O/HPF_6 mol ratio to about 6, cooling to nucleate hydrate formation, and storage at ~9 °C for several hours. The powdered crystals were then dried between filter paper, placed in sample tubes of polyethylene (for study of the ^{19}F resonance) and Teflon (for ^{1}H) and stored in liquid nitrogen until used. Subsequently, it was found that larger crops of crystals were obtained from samples containing less than six moles of water per mole of HPF_6.

Results and Discussion

^{1}H Magnetic Resonance

The second moments of the proton resonance lines are given in Fig. 2 and the line widths, as separations between the maximum and minimum points of the derivative curves, in Fig. 3.

Below the line-width transition centered near 135 °K the second moment has a constant value of 43 ± 2 G^2. This rigid-lattice second moment is too high to be consistent with the hexahydrate structure suggested by the X-ray study (5), a structure which cannot lead to a proton second moment much greater than that of ice Ih itself, *viz.* 32.4 ± 1.1 G^2 at 75 °K (10). Likewise, the line shape (Fig. 4) differs considerably from the shape found for the absorption by the water molecules of ice (10) and gas hydrates (9, 11). As was the case for gas hydrates of magnetic guest species (9, 11), no evidence was found at any temperature of saturation of the proton absorption signal by r.f. fields at the 5 mG level. This result is in marked contrast with the serious saturation observed (10) at low temperatures in various ice polymorphs.

Above 175 °K the second moment falls below 0.1 G^2 and the line shape becomes approximately Lorentzian. This behavior is clearly a result of rapid diffusion of the protons and differs from the behavior of ice Ih and of other clathrate hydrates where complete diffu-

Can. J. Chem. Downloaded from www.nrcresearchpress.com by 210.87.254.40 on 09/05/12
For personal use only.

Can. J. Chem. Downloaded from www.nrcresearchpress.com by 210.87.254.40 on 09/05/12
For personal use only.

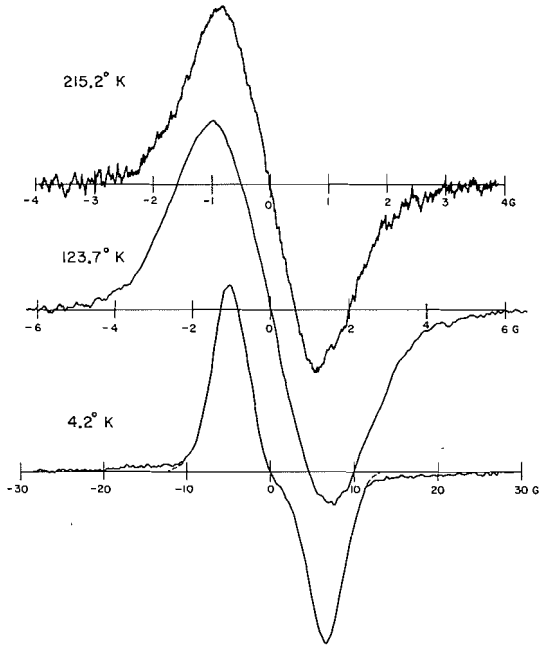

FIG. 5. Derivative line shapes of ^{19}F at three temperatures. The dashed line in the 4.2° spectrum indicates the truncation used to evaluate the second moment of the dominant narrow component.

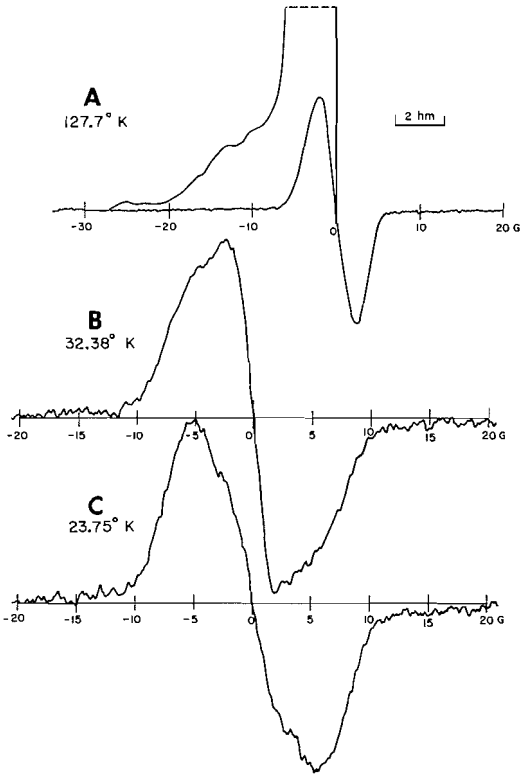

FIG. 6. ^{19}F derivative curves showing (*A*) the presence of the broad component in a half spectrum recorded at 100 times the sensitivity of the "normal" spectrum, and (*B* and *C*) the change of shape during the low-temperature line-width transition.

sional narrowing is only reached at or near the melting point. The acid protons of HPF_6 hydrate are thus very mobile and rapidly exchange with water protons.

^{19}F *Magnetic Resonance*

There are two regions of transition in the ^{19}F second moment (Fig. 2). The broad transition between 25 and 75 °K clearly marks the narrowing which results from increasingly rapid reorientation of the encaged PF_6^- ions. The second region of line narrowing coincides with the proton line-width transition and is probably again the result of proton diffusion. Line shapes in the three plateau temperature regions are shown in Fig. 5.

In the region of 170 to 250 °K the measured second moments lie between 0.7 and 0.8 G^2. These values are much too large to be attributed entirely to PF_6^- groups which are isotropically rotating but not diffusing in a water lattice in which the interactions with the protons are averaged out by proton diffusion. The sole contribution to the ^{19}F second moment in this case would be from inter-guest interactions, which, for the X-ray structure (5), is only 0.28 G^2.

Between 90 and 130 °K the observed second moment is 2.1 ± 0.1 G^2. This value agrees with the value of 2.09 G^2 calculated for isotropic reorientation of PF_6^- groups encaged in a lattice in which the protons are rigid. Under conditions of high sensitivity, however, the spectra (*e.g.* Fig. 6*A*) show additional absorption in the wings which has not been included in the evaluation of the second moment. Thus there is a broad, weak F band in addition to the relatively narrow line from rotating PF_6^- ions.

A similar broad component is also clearly present below 25 °K (see the 4.2 °K spectrum of Fig. 5), where the overlap with the now-broader PF_6^- component is more pronounced. ^{19}F spectra in this temperature region were obtained with the Robinson oscillator since measurements at the higher r.f. levels of the mar-

TABLE 1. Calculated second moments

Resonance	Conditions	Contributing species	Second moments (G^2)* $H_3O^+ \cdot PF_6^- \cdot 5H_2O$	Second moments (G^2)* $H_3O^+ \cdot PF_6^- \cdot HF \cdot 4H_2O$
^1H	Rigid lattice	H_2O	32	33
		H_3O^+	38	39
		HF		130
		total	33	*43*
^{19}F	Rigid lattice	PF_6^-	16.6	*16.7*
		HF		156
		total		36.6
	Isotropic rotation of PF_6^-, other nuclei fixed	PF_6^-	2.09	*2.17*
		HF		155
		total		24.0
	Isotropic rotation of PF_6^-, diffusion of protons but not of F atoms	PF_6^-	0.28	0.49
		HF		2.02
		total		*0.71*

*Second moments in italics are to be compared with experimental values plotted in Fig. 2.

ginal oscillator showed small saturation effects. Second moments of about 15 G^2 were obtained for the narrow component by somewhat arbitrary truncation of the absorption (*cf.* Fig. 5). A value of 16.6 G^2 is calculated for PF_6^- ions (with $r_{P-F} = 1.58$ Å (12)) which are fixed in random orientations about the center of the cage in the rigid hydrate lattice.

The abrupt change in ^{19}F line width near 30 °K shown in Fig. 3 is a result of the change of line shape. As spectra *B* and *C* of Fig. 6 illustrate, the change of second moment with cooling through this transition region is the result of increasing absorption by the broader of two strongly overlapping components.

N.M.R. Evidence for the Presence of HF

The hexahydrate structure is therefore unable to account for (*a*) the large ^1H second moment and the line shape at low temperatures, (*b*) the large ^{19}F second moment above 170 °K, and (*c*) the presence of a very broad ^{19}F band at all temperatures below 130 °K. If it be assumed that the X-ray structure is correct in broad outline, these observations may be accounted for only by the presence of appreciable quantities of HF in the lattice.

Thus observation (*b*) above, which refers to temperatures at which the proton second moment is averaged almost to zero by diffusion, may be attributed to the presence in the lattice of HF molecules in which the F atoms are not rapidly diffusing. If each HF molecule present replaces a water molecule, with the F atom occupying a lattice site assigned to an O atom in the X-ray structure (5), the ^{19}F second moment is given by $[(0.28 + 1.25x) + x(1.40 + 3.7x)]/(1 + x)$, where x is the fraction of water molecules replaced by HF and the two terms are contributed by PF_6^- and HF, respectively. Solution for the observed second moment of 0.75 ± 0.05 G^2 yields the composition $HPF_6 \cdot (1.09 \pm 0.11)HF \cdot (4.91 \mp 0.11)H_2O$; that is, about one water molecule of every six present in the hexahydrate is replaced by HF.

To calculate second moments at lower temperatures we assume the composition $H_3O^+ \cdot PF_6^- \cdot HF \cdot 4H_2O$ and a random distribution of H_3O^+ and HF over the sites of the water molecules of the original unit cell (5). The calculation requires a knowledge of the HF bond length and H_3O^+ geometry in a 4-coordinated environment. For lack of a better value, we take the inter-proton distance in H_3O^+ to be 1.72 Å, the value found (13) in nitric acid monohydrate. The H—F distance may be roughly estimated from the line shape illustrated in Fig. 6*A*. The broad component is expected to have the shape characteristic of the strongly interacting pair of unlike nuclei in HF. In particular, the small peaks at the outermost edges (*e.g.* the one at −25 G in Fig. 6*A*) may be taken to approximately define the values of the field at $\pm 2\mu r^{-3}$ from the line center where the absorption of the ideal Pake doublet drops to zero for the polycrystalline case. Here μ is the proton magnetic

Can. J. Chem. Downloaded from www.nrcresearchpress.com by 210.87.254.40 on 09/05/12
For personal use only.

Can. J. Chem. Downloaded from www.nrcresearchpress.com by 210.87.254.40 on 09/05/12
For personal use only.

moment and r is the H—F bond length. A separation of 50 G gives $r_{H-F} = 1.04$ Å.

Table 1 gives the results of the calculations of the ^1H rigid lattice second moments and of ^{19}F second moments appropriate to the temperatures of the three plateaus in second moment. Values are also given for the original hexahydrate structure. The calculations make use of the methods described elsewhere (9) for the gas–hydrate type of clathrate, including assignments of the disordered positions of the water protons.

The structure in which HF is incorporated in the hydrogen-bonded lattice gives second moments which are in satisfactory agreement with those plotted in Fig. 2. Although no great accuracy can be claimed for the calculated values, a lattice stoichiometry of approximately $H_3O^+ \cdot HF \cdot 4H_2O$ is clearly indicated.

Chemical Analysis

Because of the similarity of the molecular weights of HF and H_2O, determination of HPF_6 as the nitron salt is insensitive to the presence of HF. Thus the observation (5) of 57.2 to 57.6 wt.% of HPF_6 in the hydrate is almost as consistent with the 57.0% of $HPF_6 \cdot HF \cdot 5H_2O$ as with the 57.5% of $HPF_6 \cdot 6H_2O$.

The acid content of the hydrate was determined by titration with phenolphthalein of dilute aqueous solutions of numerous samples of hydrate (including freshly-prepared samples as well as the samples which had been used for the n.m.r. studies) against $N/10$ NaOH and by back-titration against $N/10$ HCl of samples dissolved in cold excess KOH solution. The acid content was 2.13 ± 0.04 and 1.07 ± 0.02 times, respectively, as great as given by $HPF_6 \cdot 6H_2O$ and $HPF_6 \cdot HF \cdot 5H_2O$. Shapes of potentiometric titration curves with NaOH solution were almost identical with those given by equimolar mixtures of HF and HCl, that is, of HF and a strong monobasic acid.

The small but consistent excess acidity over that represented by the stoichiometry $HPF_6 \cdot HF \cdot 5H_2O$ is possibly the result of adsorption of HF by the crystals. Another possible explanation is given below.

Structural Considerations

The stoichiometry $HPF_6 \cdot HF \cdot 5H_2O$ has the structural advantage that each of the species present in the lattice H_2O, H_3O^+, and HF, can participate fully in a four-coordinated scheme of hydrogen bonding, the number of hydrogen bonds being equal to the number of hydrogen atoms. In $HPF_6 \cdot 6H_2O$, however, the H^+ contributed by HPF_6 does not fit into a fully hydrogen-bonded lattice. In the actual hydrate, the HF molecules are probably statistically distributed over all the sites previously assigned (5) to water molecules so as to preserve the original X-ray symmetry.

It is possible to account for the excess acidity noted in the last section by the incorporation into the structure during crystallization of acid "impurities" from the solution. This may be done by allowing, for example, a fraction x of the cages to be occupied by PO_3F^{2-} to give the composition $(1-x)HPF_6 \cdot xH_2PO_3F \cdot (1+x)HF \cdot (5-x)H_2O$, where the HF content is increased sufficiently to maintain full hydrogen bonding. A value of $x \simeq 0.06$ gives formal agreement with the analyses.

The n.m.r. evidence of rapid reorientation of the PF_6^- ion to temperatures below 75 °K is not readily compatible with the presence, at room temperature, of the preferred orientations suggested (5) by the X-ray results. Likewise, the estimation (5) of a P—F bond length of 1.73 Å, based on location of the sites of the F atoms, is unlikely. The magnitude of the PF_6^- contribution to the rigid lattice ^{19}F second moment is much more consistent with the bond length of 1.58 Å found (12) in KPF_6 and supported in a general way by n.m.r. studies (14) of the alkali hexafluorophosphates. If 1.40 Å is allowed for the van der Waals radius of a water molecule, the free diameter of the truncated-octahedral cage is 5.78 Å. A value of 5.86 Å for the van der Waals diameter of PF_6^- is given by $r_{P-F} = 1.58$ Å. This value is more compatible with the cage size than the value of 6.16 Å given by $r_{P-F} = 1.73$ Å.

In the clathrate hydrate of SF_6, a molecule of size and shape very similar to PF_6^- ($r_{S-F} = 1.58$ Å), the ^{19}F resonance line broadens only below 12 °K (15). Here, however, the 16-hedral cage has the relatively large mean free diameter of 6.56 Å.

We are indebted to V. G. Meadors of the Ozark-Mahoning Company, Tulsa, Oklahoma, for helpful correspondence and to A. Desaulniers of the Analytical Chemistry Section of NRCC for chemical analyses.

1. W. LANGE. *In* Fluorine chemistry. Vol. 1. *Edited by* J. H. Simons. Academic Press, New York. 1950. p. 164.

2. J. B. BEAL, JR. *In* Kirk-Othmer Encyclopedia of Chemical Technology. Vol. 9. 2nd ed. Interscience Publishers, New York. 1966. p. 636.
3. E. BAUMGARTNER, M. BUSCH, and R. FERNÁNDEZ-PRINI. J. Phys. Chem. **74**, 1821 (1970).
4. W. LANGE and R. LIVINGSTON. U.S. Patent 2,488,298, Nov. 15, 1949.
5. H. BODE and G. TEUFFER. Acta Cryst. **8**, 611 (1955).
6. A. F. WELLS. The third dimension in chemistry. Clarendon Press, Oxford. 1956. p. 56.
7. M. VON STACKELBERG and H. R. MÜLLER. Z. Elektrochem. **58**, 25 (1954).
8. G. A. JEFFREY and R. K. MCMULLAN. *In* Progress in inorganic chemistry. Vol. 8. *Edited by* F. A. Cotton. 1967. p. 43.
9. S. K. GARG, B. MORRIS, and D. W. DAVIDSON. J. Chem. Soc., Faraday Trans. II, **68**, 481 (1972).
10. S. W. RABIDEAU, E. D. FINCH, and A. B. DENISON. J. Chem. Phys. **49**, 4660 (1968).
11. Y. A. MAJID, S. K. GARG, and D. W. DAVIDSON. Can. J. Chem. **46**, 1683 (1968).
12. H. BODE and H. CLAUSEN. Z. Anorg. Allgem. Chem. **265**, 229 (1951).
13. R. E. RICHARDS and J. A. S. SMITH. Trans. Faraday Soc. **47**, 1261 (1951).
14. G. R. MILLER and H. S. GUTOWSKY. J. Chem. Phys. **39**, 1983 (1963).
15. S. K. GARG and D. W. DAVIDSON. Chem. Phys. Lett. **13**, 73 (1972).

Can. J. Chem. Downloaded from www.nrcresearchpress.com by 210.87.254.40 on 09/05/12
For personal use only.

Infrared Spectra and Structures of Solid CH_4 and CD_4 in Phases I and II

C. CHAPADOS[1] AND A. CABANA

Département de Chimie, Université de Sherbrooke, Sherbrooke, Québec

Received May 4, 1972

This paper reports the results of extensive infrared absorption measurements of CH_4, CD_4, and mixed isotopic crystals containing CH_4, CD_4, CHD_3, and CH_3D at low concentration in matrices of light and heavy methane in crystalline phases I and II. The interpretation of the spectra, based upon the Halford–Hornig approach, provides information on the crystal structures. The spectra indicate that the two solid phases of CH_4 are similar to the two higher temperature phases of CD_4. In phase I, there is apparently considerable motion: either the molecules undergo large angular oscillations or even rotational diffusion. In phase II, there exist two types of sites for the molecules: some molecules undergo quantized rotation similar to that found in noble gas matrices while others order with a local symmetry that is probably slightly distorted from T_d ($\bar{4}$ 3m) to D_{2d} ($\bar{4}$ 2m). Acceptable factor groups are then limited to T_d and O_h, but the former is unlikely for it could yield the f.c.c. lattice found by diffraction experiments only by a particular choice of the parameters, whereas the latter leads to the f.c.c. space group O_h^6 (Fm 3c).

On a enregistré un grand nombre de spectres d'absorption de CH_4, CD_4 et de cristaux constitués de mélanges isotopiques contenant CH_4, CD_4, CHD_3, et CH_3D à basse concentration dans des matrices de méthane et de deutérométhane en phases cristallines I et II. L'interprétation des spectres, basée sur l'approche Halford–Hornig, procure des renseignements sur la structure cristalline. Les spectres indiquent que les deux phases solides du CH_4 sont semblables aux deux phases de plus haute température du CD_4. En phase I il existe apparemment une grande liberté de mouvement: les molécules subissent soit des oscillations angulaires de grande amplitude, soit une diffusion rotationnelle. En phase II, il existe deux types de site pour les molécules: certaines subissent une rotation quantique empêchée semblable à celle qui fut trouvée dans les matrices des gaz nobles, tandis que d'autres sont ordonnées avec une symétrie locale D_{2d} ($\bar{4}$ 2m), bien que la distorsion de T_d ($\bar{4}$ 3m) soit très faible. Seuls les deux groupes facteurs T_d et O_h demeurent acceptables mais le premier est considéré peu probable puisqu'il ne peut correspondre à la structure du cube à faces centrées déterminée par des expériences de diffraction que par un choix particulier des paramètres. Le groupe facteur O_h conduit au groupe d'espace O_h^6 (Fm 3c) lequel correspond à un réseau cube à faces centrées.

Canadian Journal of Chemistry, **50**, 3521 (1972)

Can. J. Chem. Downloaded from www.nrcresearchpress.com by 210.87.254.5 on 09/05/12
For personal use only.

Introduction

Crystalline CH_4 and CD_4 have been extensively studied both experimentally and theoretically. The main references, up to 1969, are collected in the introduction of a paper by Colwell (1). In spite of much effort directed toward the determination of the crystal structures and of the molecular energy levels in the different solid phases of the methanes our understanding of the subject has remained far from satisfactory. Heat capacity measurements (1–3) have shown that there were λ-type anomalies around 27 and 22 °K for CD_4 and one around 20 °K for CH_4. In addition there is, for CH_4, a second anomaly around 8 °K but the existence of a second λ transition for CH_4 at normal pressure has been questioned (4, 5). Measurements of nuclear magnetism (6, 7) have indicated that conversion among the three spin species occurs at low temperature in the crystal. X-Ray diffraction experiments on polycrystalline material (8) have shown that the carbon atoms lie on a face centered cubic lattice in the two phases of CH_4 and in the three phases of CD_4. Coherent neutron diffraction from a single crystal of CD_4 (9) in phase I indicates the space group O_h^5 (Fm 3m) with four molecules occupying randomly sites of C_{3v} (3m) symmetry such that the point symmetry is O_h ($m3m$) on average. After considering two possible structures for CD_4 in phase II, Press (9) selects the space group O_h^6 (Fm 3c) with eight molecules per primitive cell, of which two are orientationally disordered and six are ordered with local symmetry D_{2d} ($\bar{4}$ 2m).

Several investigations of the vibrational spectra of neat CH_4 and CD_4 crystals have been reported in the literature (10–16) with mixed isotopic crystals of these two molecules being

[1]Present address: Département de Chimie–Biologie, Université du Québec à Trois-Rivières, Trois-Rivières, Québec.

TABLE 1. Composition of the five methanes (mol %)

Sample	Component*					
	CH_4	CH_3D	CH_2D_2	CHD_3	CD_4	Other impurities
CD_4			0.5	4.5	94.2	O_2, N_2, ethane, D_2O
CD_4†			0.3	3.5	96.1	O_2, N_2 < 80 p.p.m.
CHD_3			4.3	94.4	0.4	O_2, N_2, ethane
CH_2D_2		2.8	96.4	0.3		O_2, N_2, ethane
CH_3D	2.5	96.9	0.1			O_2, N_2, ethane
CH_4	99.99					O_2, N_2 < 0.01%

*The uncertainty on the percentages of the impurities is ±0.2%, except for CH_4 where the analysis is accurate to the figures given.
†From Morrison.

studied by i.r. absorption only (12, 17). The i.r. (18–20) and Raman (21) spectra of both molecules in noble gas matrices have also been extensively studied.

Unfortunately the information about the crystal structures derived from different experimental techniques is sometimes inconsistent. In the course of our experiments on the i.r. spectra of crystals, we have found that microcrystals obtained from a gaseous spray on a cold target often yield irreproducible spectra. Since this particular technique had been used in some of the previous i.r. studies it seemed worthwhile to reinvestigate the i.r. absorption of the neat crystals, especially in the light of recent theoretical models for the structure of these solids (22–25). New considerations in the analysis of the spectra of mixed isotopic solutions containing partially deuterated species (17, 26, 27) have shown that such spectra provide a new way to specify the site symmetry in the solids. Thus, such results were obtained and are analyzed in the present paper in an attempt to explain the discrepancies between the structures derived from spectral and other measurements.

Experimental

The CH_4 (stated purity 99.99%) used in our experiments was obtained from Matheson of Canada, Ltd., and used without purification. The CD_4, CHD_3, CH_2D_2, and CH_3D purchased at Merck, Sharp, and Dohme of Canada, Ltd., were analyzed by mass spectroscopy and found to contain a few % of isotopic impurities. In the present study, CD_4 was studied as a neat crystal; therefore special efforts were made to obtain a sample isotopically and chemically pure. A sample of CD_4 purified by gas chromatography was kindly given to us by Morrison. The composition of the methanes used in our experiments is given in Table 1. The medium resolution (0.3 to 0.8 cm^{-1}) spectra were recorded on a Perkin–Elmer Model 125 prism-grating spectrometer calibrated with reference to the I.U.P.A.C. tables (28); the frequency accuracy is always better than 0.5 cm^{-1} for sharp peaks. The high resolution spectra were recorded on a 2.5 m Littrow spectrometer, similar in design to that described by McCubbin *et al.* (29), built in our laboratory (30), and equipped with liquid nitrogen cooled PbS and PbSe detectors. The spectra recorded with this spectrometer were obtained with a resolution of 0.03 to 0.09 cm^{-1} and with a frequency accuracy limited by the widths of the peaks, to about 0.05 cm^{-1}. The calibration was made against accurately measured 1–0 vibration–rotation lines of CO (31).

A conventional cryostat equipped with a variable pressure gas exchanger was used to obtain any selected temperature in the range 4 to 120 °K with liquid helium or nitrogen as the coolant. The temperature stability achieved by adjusting the gas pressure in the heat exchanger was relatively good. For example, the sample temperature could be maintained within 0.5 °K by adjusting the pressure every 10 min during the first half hour. At later times the temperature stability was improved if the adjustments of the gas pressure were continued.

A small temperature gradient was created across the sample cell by using the filling tube, which entered the top of the cell as a heating element. The filling tube, 0.030 in. in diameter, was made of thin stainless steel and a current of a few mA from a 6 V a.c. source was circulated through it. This arrangement was found particularly useful in preventing clogging of the tube if it inadvertently touched the nitrogen shield. In addition this small heater has provided fine monitoring of the sample temperature. The temperature gradient thus obtained was not measured but is certainly not very large in view of the good thermal conduction of the cell body which was made of brass.

The rate of cooling at the freezing or transition points was of the order of 0.5 deg per hour. Reproducible spectra were always obtained when the samples were repeatedly cycled through the transition temperatures. The sample thickness was about 1 μ for the neat crystals and 50 μ for the isotopic mixtures.

The gaseous mixtures were prepared in a Pyrex system previously degassed and evacuated to 1×10^{-6} mm Hg. The samples were prepared by condensing the pure gas, or the appropriate isotopic mixture, to the liquid between two circular windows of 1 in. diameter sealed off to a closed

Can. J. Chem. Downloaded from www.nrcresearchpress.com by 210.87.254.5 on 09/05/12
For personal use only.

Can. J. Chem. Downloaded from www.nrcresearchpress.com by 210.87.254.5 on 09/05/12
For personal use only.

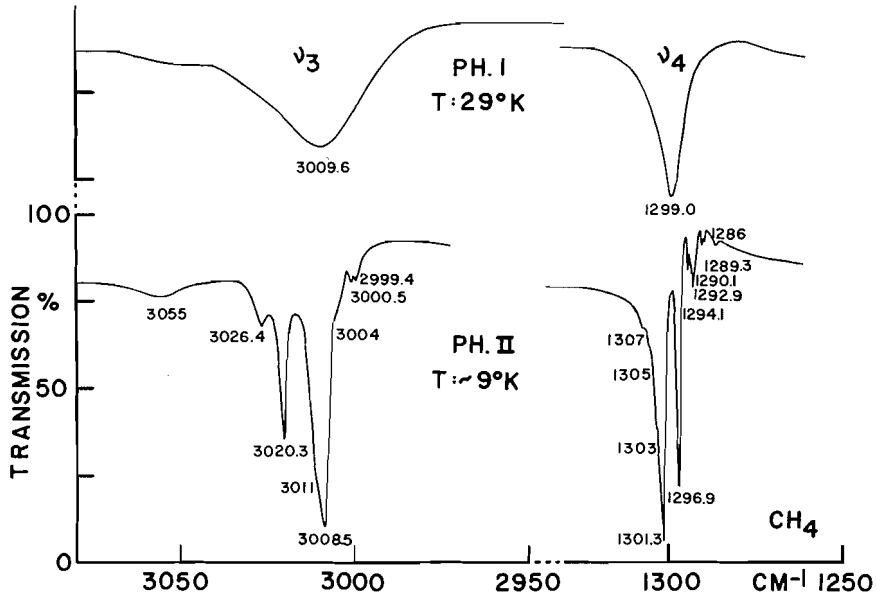

FIG. 1. Infrared absorption spectrum of solid CH_4: upper trace, phase I at 29 °K; lower trace, phase II at 9 °K.

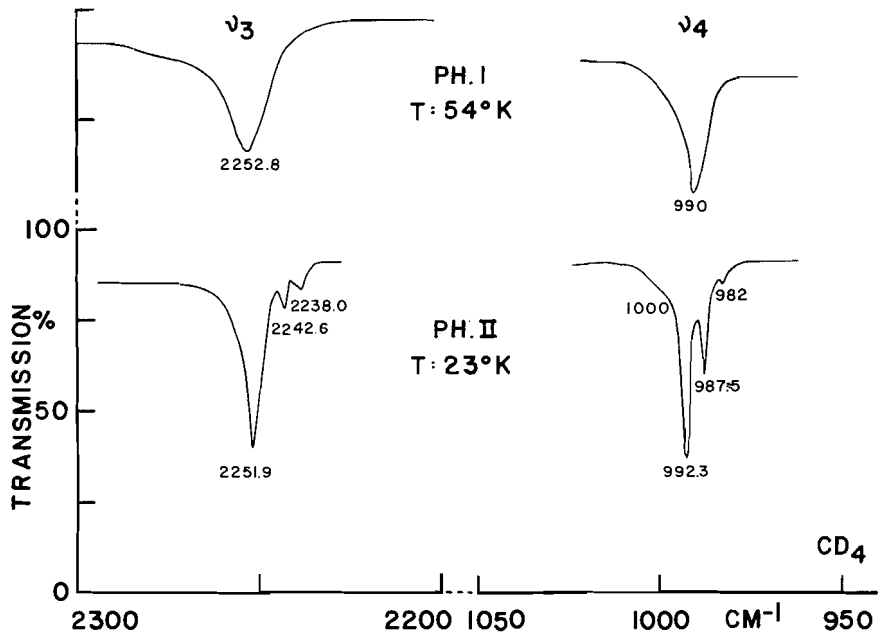

FIG. 2. Infrared absorption spectrum of solid CD_4: upper trace, phase I at 54 °K; lower trace, phase II at 23 °K.

compartment by means of indium gaskets. Two window materials were used: germanium and IRTRAN-II. Because of its lower index of refraction IRTRAN-II is preferred to germanium although the spectra obtained with the two materials are very similar; slight variations in the band shapes need not be considered since they do not alter our discussion of the crystal structures.

Results and Discussion

A. The Infrared Spectra and Structure of Phase I Crystalline CH_4 and CD_4

The spectra of phase I crystals are reproduced in Figs. 1–4: Fig. 1, CH_4; Fig. 2, CD_4; Figs. 3

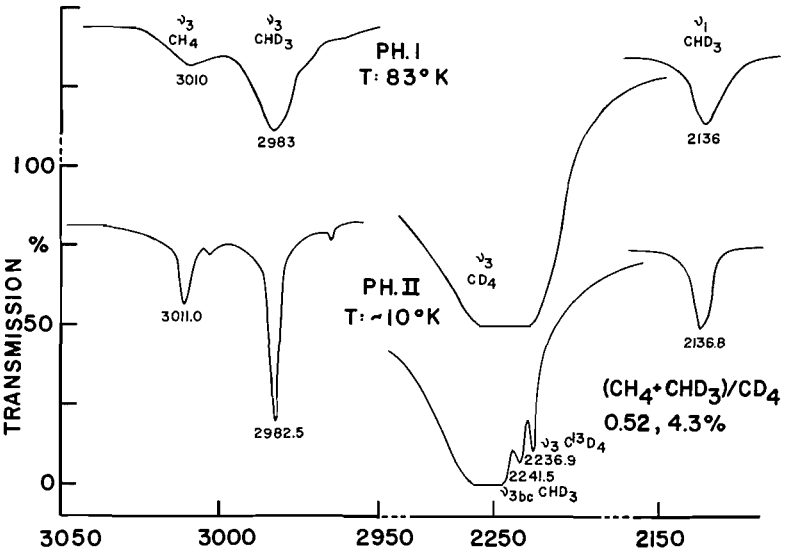

FIG. 3. Infrared absorption spectrum in the region 3050 to 2100 cm^{-1}, of 0.5% CH_4 and 4% CHD_3 in 95% CD_4: upper trace, phase I CD_4 at 83 °K; lower trace phase II CD_4 at 22 °K.

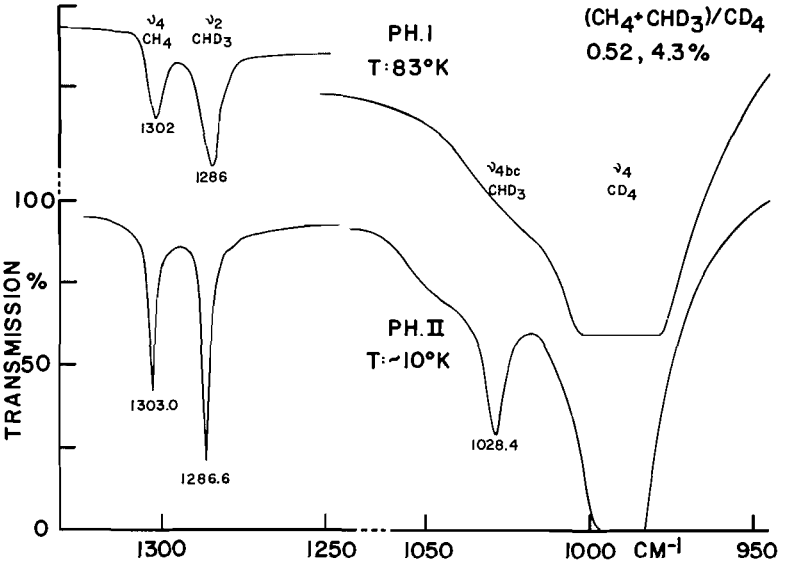

FIG. 4. Infrared absorption spectrum, in the region 1350 to 950 cm^{-1}, of 0.5% CH_4 and 4% CHD_3 in 95% CD_4: upper trace, phase I CD_4 at 83 °K; lower trace, phase II CD_4 at 22 °K.

and 4, CH_4 and CHD_3 at low concentration in CD_4. The frequencies at maximum absorption are collected in Tables 2–4. These spectra are all characterized by unusually broad bands. Although the widths decrease markedly upon lowering the temperature, the bands remain so broad over the complete range for phase I that no site or factor group components may be resolved since the splittings for such van der Waals crystals are always much smaller than the bandwidths observed for these crystals. Therefore it is impossible to carry out an analysis of the spectra, based upon group theory, that could lead to the site and factor groups. How-

Can. J. Chem. Downloaded from www.nrcresearchpress.com by 210.87.254.5 on 09/05/12
For personal use only.

TABLE 2. Vibrational frequencies of CH_4 (in cm^{-1})

Solid I		Solid II			
I.r. (28 °K)	Raman* (77 °K)	I.r. (~9 °K)	Raman* (~12 °K)	Comments and assignments†	
	3050	3058	3056	v w br	$\nu_3 + \nu_L$, $2\nu_2$ Raman
		—	3037	w	
		3026.4	—	w	
		3020.3	—	s	ν_3
3009.8	3030	3011.0	3009	s sh	
		3008.5		v s	
		3004.0	—	w sh	
		3000.5	—	w	$\nu_3{}^{13}CH_4$
		2999.4	—	w	
		—	2907		
—	2905	—	2901	s	ν_1
			1553	m w	
—	1538	—	1530	m w	ν_2
			1526	m w	
		1348		v w, br	$\nu_4 + \nu_L$
		1307		w sh	
		1305		w sh	
		1303		w sh	
		1301.3		v s	
1299.0	—	1296.9	—	s	
		1294.1		w	$\nu_4{}^{13}CH_4$ at 1294.1
		1292.9		w	
		1290.1		v w	$^{13}CH_4$ at 1290.1
		1289.3		v w	
		1286		v w	

*Reference 14.
†Comments and assignments refer to the i.r. spectra unless the i.r. band is inactive.
‡Key: v = very, w = weak, s = strong, sh = shoulder, m = medium, br = broad.

ever, a qualitative discussion of the measured bandwidths and of their behavior with a variation of the temperature of the crystal is interesting.

Several factors may contribute individually or collectively to the width of the bands in these solids, but it is believed that the following are the most important: (*1*) a static orientational disorder of the molecules; (*2*) large angular oscillations of the tetrahedra around their equilibrium position; (*3*) rotational diffusion, and (*4*) large amplitude lattice vibrations. Thus the rapid narrowing of the bands occurring upon cooling the crystal would reflect either a partial ordering of the molecules, or a decrease in the amplitude of the lattice modes, or less rotational diffusion, or a combination of these phenomena. The spectra alone do not permit a choice between these alternatives but recent neutron diffraction experiments are helpful in this matter since they have indicated more ordering at 77 °K than at 35 °K (9). This information permits us to rule out partial ordering upon cooling. We may therefore conclude that the disorder in phase I results from considerable motion of the molecules but it is not possible to specify the type of motion.

B. Effects of the Crystal Site Environment on the Degenerate Vibrations of Guest Molecules in Crystalline Phase II CH_4 and CD_4

The symmetry at the site occupied by the molecules in the crystal may often be determined through the analysis of the vibrational spectrum of a guest isotopic molecule present at low concentration in a crystal of the parent host molecule. The coupling of the vibrations of

Can. J. Chem. Downloaded from www.nrcresearchpress.com by 210.87.254.5 on 09/05/12
For personal use only.

TABLE 3. Vibrational frequencies of CD_4 (in cm^{-1})

Solid I		Solid II			
I.r. (54 °K)	Raman* (77 °K)	I.r. (23 °K)	Raman* (25 °K)	Comments and assignments†	
		—	2305	br v w	$\nu_3 + \nu_L$
		—	2293	br v w	
		2258			
2252.8	2262	2251.9	2253	v str	ν_3
		2242	2243	w	ν_{3bc} CHD_3‡
		2237		v w	$\nu_3{}^{13}CD_4$‡
		—	2094	m w	ν_1
—	2093	—	2090	v s	
		—	1091	m	ν_2
		1000	—	w	ν_{4a} CHD_3
990	—	992.3	—	v s	ν_4
		987.5	—	s	
		982	—	v w	$\nu_4{}^{13}CD_4$

*Reference 14.
†Comments and assignments refer to the i.r. spectrum unless the i.r. band is inactive. Key: same as in Table 2.
‡These bands were previously erroneously assigned to a splitting by the crystal field of ν_3 $^{12}CD_4$ (ref. 12 and 14).

TABLE 4. Infrared absorption frequencies of guest molecules in phase II CD_4: 0.5% CH_4 and 4% CHD_3 in 95.4% CD_4

Gas*	Solid I (83 °K)	Solid II (22 °K)	Comments†	Assignment
3019	3010	3011.0	m	ν_3 CH_4
3013	—	3003.0	w	ν_{3b} CH_2D_2
2993	2983	2982.5	s	ν_{3a} CHD_3
2976	2965	2965.2	w	ν_{3a} CH_2D_2
2263	—	2241.5	s over	ν_{3bc} CHD_3
—	—	2236.9	s over	$\nu_3{}^{13}CD_4$
2142	2136	2136.8	m br	ν_1 CHD_3
1306	1302	1303.0	s sharp	ν_4 CH_4
1291	1286	1286.6	s sharp	ν_2 CHD_3
1036	~1030	1028.4	s br	ν_{4bc} CHD_3
1003	—	1000.0	s over	ν_{4a} CHD_3?

*The gas phase frequencies are taken from ref. 34.
†The comments refer to phase II crystal. Key: m = medium, w = weak, s = strong, s over = strong overlap, br = broad.

guest and host molecules is largely destroyed when the vibrational frequencies of the two molecules are different enough. Thus, the vibrations of the guest molecule are influenced almost exclusively by the site symmetry of the host crystal (32).

The spectra of several mixed isotopic solutions have been recorded with a resolution of 0.5 to 0.8 cm^{-1} and a few selected bands with high resolution (0.03–0.09 cm^{-1}). Selected examples of medium resolution spectra are reproduced in Figs. 3–5 while high resolution spectra are shown in Figs. 6 and 7. The frequencies at maximum intensities are given in Tables 5 and 6. In a previous report (17) we have already shown that CD_4 at low concentration in CH_4 phase II and vice versa yield spectra where the triple degeneracy of the infrared active modes seems completely preserved (see Figs. 3 and 4). Among the sub-groups of the free molecule point group only the local symmetries T or T_d are acceptable if the free molecule F_2 vibrational modes are true singlets in the solids. Since it appeared that the natural bandwidth is smaller than the spectral resolution, a high resolution spectrum of the ν_3 vibration of CD_4 at low concentration in CH_4 was recorded (Fig. 6). The width at half height of the band is 0.50 cm^{-1} and there is a slight asymmetry on the high frequency side revealing that the band might be an unresolved doublet. If it is a doublet, one member would be approximately 4–6 times weaker than the other with a separation of the order of 0.5 cm^{-1}. Each peak may result from molecules lying at different sites but if one

Can. J. Chem. Downloaded from www.nrcresearchpress.com by 210.87.254.5 on 09/05/12
For personal use only.

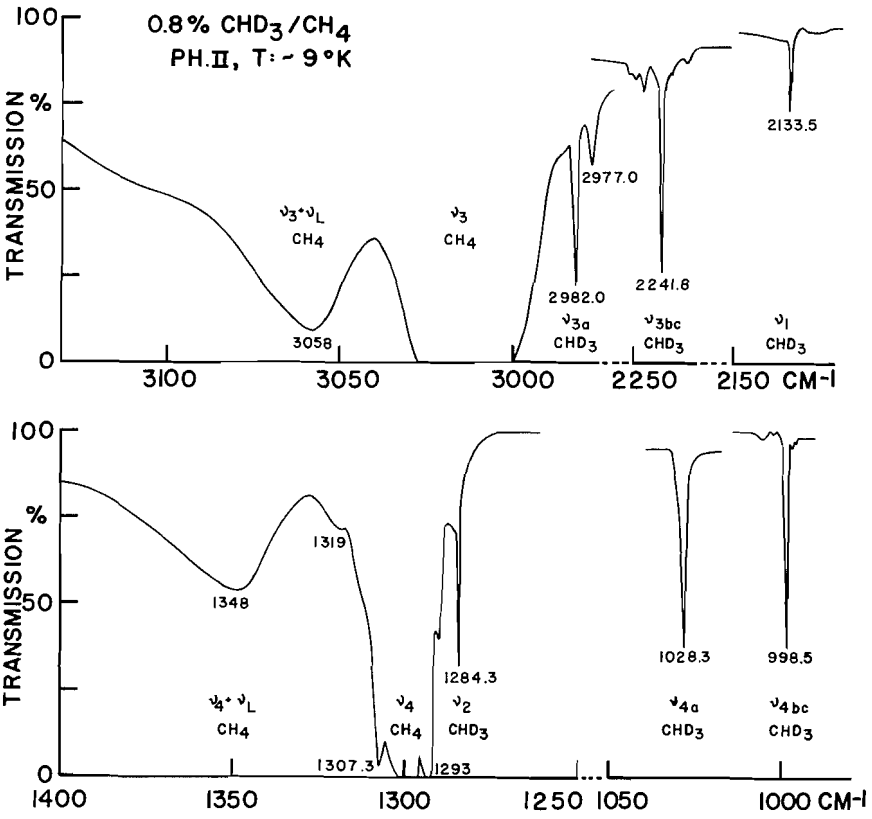

FIG. 5. Infrared absorption spectrum of 0.8% CHD_3 in phase II CH_4 at 9 °K.

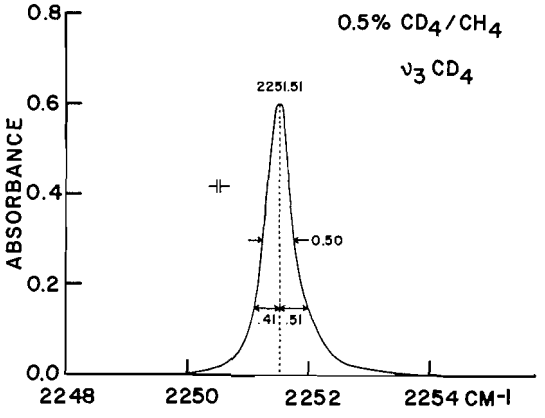

FIG. 6. High resolution infrared absorption of the ν_3 vibration of CD_4 in phase II CH_4. The sample is 0.5% CD_4 and 99.5% CH_4 and the temperature is 6 °K. Note the asymmetry on the high frequency side of the band.

assumes that the band asymmetry results from site splitting, the true local symmetry is one of D_{2d}, S_4, C_{3v}, or C_3. However, the distortion from T or T_d symmetry should then be very small in order to produce such a small splitting. It will be shown later that, although it is unusual for such molecular crystals, two types of sites appear to be occupied in phase II solid methane. Therefore this asymmetry cannot be considered as providing strong evidence for these lower site symmetries. Moreover we hesitate to conclude the presence of a real doublet from the slight asymmetry of a line since we are not certain that lines in the solids ought to be symmetrical. Additional information might be gained from an analysis of the infrared spectra of mixed isotopic solutions of CHD_3 in phase II CH_4 and CD_4 since the E modes should split for D_{2d} and S_4 site symmetries but not for C_3 or C_{3v}. Of course T or T_d symmetry would also leave the E mode degenerate. However, for the partially deuterated methanes the site symmetry may be reflected on the spectra through a multiplicity of the lines corresponding to various orientations of the guest molecules in the host

Can. J. Chem. Downloaded from www.nrcresearchpress.com by 210.87.254.5 on 09/05/12
For personal use only.

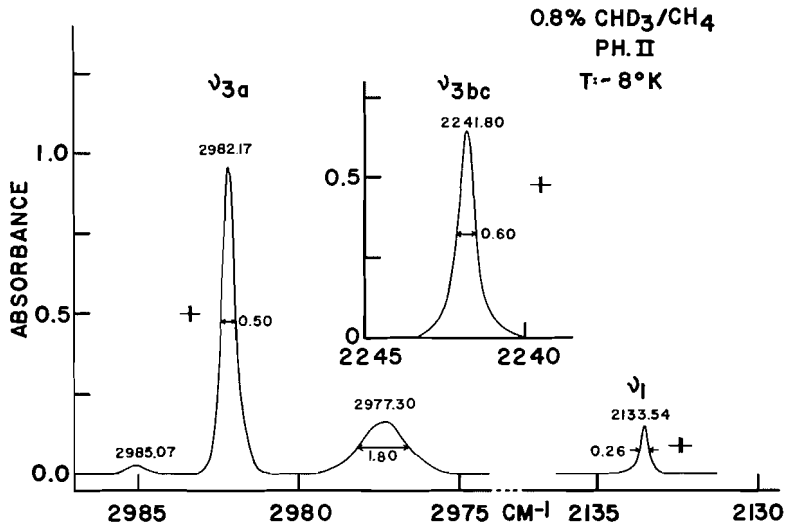

FIG. 7. High resolution infrared absorption bands of 0.8% CHD_3 in 99.2% phase II CH_4 at 8 °K.

TABLE 5. Infrared absorption frequencies of guest molecules in phase II CH_4: (*a*) 0.7% CD_4 in 99.3% CH_4, and (*b*) 0.8% CHD_3 in 99.2% CH_4

Gas*	Solid II 9 °K	Comments	Assignment
(*a*)	2257	w br	?
2259	2251.51†	s (0.50)	$\nu_3{}^{12}CD_4$
	2240.5	w	ν_{3bc} CHD_3
	2235.7	w	$\nu_3{}^{13}CD_4$
	1000	w	ν_{4a} CHD_3
	993.5	v w	
	992.2	s sh	$\nu_4{}^{12}CD_4$
	989.0	v w	
	987.5	v w	$\nu_4{}^{13}CD_4$?
(*b*)	2985.07†	v w	
2993	2982.13†	v s (0.50)	ν_{3a} CHD_3
	2977.30†	w br (1.80)	
	2250	v w	
	2247.7	v w	
	2247.1	v w	
2263	2241.80†	s (0.60)	ν_{3bc} CHD_3
	2240	v w	
	2236.0	v w	
2142	2133.54†	m (0.26)	ν_1 CHD_3
1291	1284.3	s over	ν_2 CHD_3
1036	1028.3	v s	ν_{4bc} CHD_3
	1003	v w	
	1002	v w	
1003	998.5 =	v s	ν_{4a} CHD_3
	997	v w	
	996	v w	

*The gas phase frequencies are taken from ref. 34.
†Bands recorded under very high resolution. Key: w = weak, br = broad, v = very, s = strong, numbers in parentheses = width at half height in cm^{-1}.

crystal. These effects will show up for both the degenerate and nondegenerate modes and will be discussed in the next section.

C. *Effects of the Crystal Site Environment on the Vibrational Modes of Partially Deuterated Guest Molecules in Crystalline Phase II CH_4 and CD_4*

For a space-fixed tetrahedral framework there exists a number of distinguishable orientations that the individual partially deuterated methanes can assume: 6 for CH_2D_2, 4 for CHD_3 or CH_3D, and only one possible orientation for CH_4 and CD_4. The zero point entropies, which are $R \ln 6$ for CH_2D_2, $R \ln 4$ for CHD_3 or CH_3D, and zero for CH_4 and CD_4, as calculated from extrapolation of the heat capacity from 8 to 0 °K, imply that in the crystals the molecules are still randomly oriented in this respect at a temperature as low as 8 °K (1, 3). It is now postulated that partially deuterated methanes in a host crystal of CH_4 or CD_4 will also be free to orient in any of the possible different ways that obviously may or may not correspond to different energies depending upon the point symmetry of the site occupied in the crystal. For example for the trivial symmetry each orientation corresponds to a different physical situation, thus there are 6 possible energies for the CH_2D_2 molecules and 4 for either CH_3D or CHD_3. For higher site symmetries some of the

Can. J. Chem. Downloaded from www.nrcresearchpress.com by 210.87.254.5 on 09/05/12
For personal use only.

TABLE 6. Number of I.R. and Raman bands for possible site and factor groups of crystalline CH_4 and CD_4 in phase II

Site	Factor	F.c.c. space groups*	I.r. A_1	I.r. E	I.r. F_1	I.r. F_2	Raman A_1	Raman E	Raman F_1	Raman F_2	Remark†
T	O_h	O_h^8	0	0	1	1	1	2	1	1	nc
T	T_d	T_d^5	0	0	1	1	1	2	1	1	c
T	O	$O^{3,4}$	0	0	1	1	1	2	1	1	nc
T	T_h	$T_h^{3,4}$	0	0	1	1	1	2	1	1	nc
T	T	T^2	0	0	1	1	1	1	1	1	c
T_d	T_d	T_d^2	0	0	0	1	1	1	0	1	c
T_d	O_h	$O_h^{5,7}$	0	0	0	1	1	1	0	1	nc
D_{2d}	O_h	O_h^6	0	0	1	2	2	3	1	2	nc
D_{2d}	T_d	None	0	0	1	2	2	3	1	2	c
C_{3v}	T_d	T_d^1	1	1	1	2	2	2	2	4	c
C_{3v}	O_h	$O_h^{5,7}$	1	1	1	2	2	2	2	4	nc
S_4	T_d	T_d^5	0	2	1	3	2	4	4	4	c
S_4	O_h	O_h^8	0	2	1	3	2	4	4	4	nc
C_3	O_h	$O_h^{6,7,8}$	1	2	3	3	2	4	6	6	c
C_3	T_d	T_d^5	1	2	3	3	2	4	6	6	c
C_3	T	T^2	1	2	3	3	2	3	5	5	c
C_3	T_h	$T_h^{3,4}$	1	2	3	3	2	3	5	5	nc
C_3	O	$O^{3,4}$	1	2	3	3	2	4	6	6	nc

*Under the heading: "F.c.c. space groups", appear the face centered cubic space groups, consistent with both the site and factor groups.

†c means that the i.r. and Raman bands are necessarily frequency coincident; nc means that the i.r. and Raman bands are different modes that may have different frequencies.

orientations are related by symmetry operations and are therefore equivalent. The case of the C_{3v} molecules will be presented in some detail.

For C_s site symmetry, only three of the four distinct orientations are energetically different since two are related by a reflection through the plane. For C_2 or C_{2v} site symmetries only two of the four space orientations are energetically different. For C_3 and C_{3v} again only two are different but their statistical weights are 1:3 whereas they are 1:1 in the cases of C_2 and C_{2v}. For S_4, D_2, D_{2d}, T, and T_d all the four orientations correspond to the same energy. The cases of D_2 and D_{2d} are not so obvious but they may be understood by observing that the three C_2 axes perpendicular to one another relate the four deuterium or hydrogen atoms. A spectrum complicated with orientational effects is a superposition of spectra each corresponding to molecules in a slightly different environment. These orientational effects were thoroughly investigated for mixed isotopic solutions of the benzenes (27) and were also shown to influence the vibrational spectra of partially deuterated methanes (17).

The medium resolution absorption spectrum of CHD_3 at low concentration (0.8%) in crystalline phase II CH_4 is reproduced in Fig. 5, where all the fundamental vibrations of CHD_3 are observed. The corresponding spectrum for a mixed crystal containing 4.3% CHD_3 in phase II CD_4 is given in Figs. 3 and 4. It shows all the bands of the guest molecule except ν_{4a} which overlaps with the strong absorption of the host molecule. With a resolution of 0.5 cm^{-1}, each vibrational band, degenerate or not, of CHD_3 in both matrices appears as a symmetrical singlet. This is entirely consistent with T or T_d site symmetries, since under these two local symmetries the doubly degenerate bands of CHD_3 should remain degenerate and there should be no orientational effects. As for D_{2d} and S_4 local symmetries, although they would not give rise to orientational effects, they should lift the degeneracy of the E modes but this may be very small as in the case of the F_2 modes of CD_4 at low concentration in CH_4. The two trigonal symmetries should not lift the degeneracy of the E modes but should give rise to orientational effects. It appeared worthwhile to record a few bands under higher resolution in an attempt to check for these two site effects. The CH_4 matrix

Can. J. Chem. Downloaded from www.nrcresearchpress.com by 210.87.254.5 on 09/05/12
For personal use only.

Can. J. Chem. Downloaded from www.nrcresearchpress.com by 210.87.254.5 on 09/05/12
For personal use only.

was used because its phase II exists at lower temperature where the lines are narrower. The ν_{3a}, ν_{3bc}, and ν_1 regions each show one slightly asymmetrical line whose widths are 0.50, 0.60, and 0.26 cm^{-1}, respectively. (The weaker lines in the ν_{3a} region may be disregarded for the moment.) Therefore, even under very high resolution, we have not obtained strong evidence for site splitting or orientational effects. We may again conclude that, although we cannot definitely rule out any of the symmetries considered in the preceding sections, if there is distortion from T or T_d site symmetry it is very small.

D. The Selection of Acceptable Factor Groups

The X-ray and neutron scattering experiments have indicated that the carbon atoms lie on a face centered cubic lattice (8–9). Therefore we will search among the super groups of the point groups previously selected for those which will necessarily place the carbon atoms on a f.c.c. lattice. Table 6 lists all the possible combinations of site and factor groups which were retained including the C_3 and C_{3v} site groups, although these are considered unlikely in view of the absence of observable orientational effects. These two trigonal groups are the only ones predicting the i.r. activity of the totally symmetric ν_1 mode of the free molecule. We have therefore checked for the infrared activity of the free molecule $\nu_1(A_1)$ mode and $\nu_2(E)$ mode with samples about 50 times thicker than those required for the gas phase allowed fundamentals. Since no absorption was found in the appropriate regions, the intensities of ν_1 and ν_2 are at least 2000 times weaker than the intensities of the gas phase allowed fundamentals. Therefore we believe that both vibrations remained symmetry forbidden in the phase II crystal. This excludes C_3 and C_{3v} local symmetries and in addition it is inconsistent with S_4 which predicts i.r. activity of the free molecule E mode. Thus we are left with T_d, T, and D_{2d} site symmetries. The total number of lines in the ν_3 and ν_4 vibration regions appears inconsistent with any of the symmetry groups that survived elimination since as is shown in Table 6 none of the combinations of site and factor groups retained would yield more than three i.r. components. Moreover the site groups T_d, T, and D_{2d} which have survived elimination are consistent with only one (with T or T_d) or two (with D_{2d}) components. Therefore none of the structures listed in Table 6 may be considered correct under the assumption that a single set of sites is occupied in the crystal. However, a visual inspection of the spectra reproduced in Figs. 1 and 2 reveals that among the lines of a given band there is a strong component which is wide and unsymmetrical and that the other lines are sharp and much weaker. This is particularly evident with CH_4 (Fig. 1) whose spectrum has been recorded at a much lower temperature than CD_4 (Fig. 2). This observation suggests that there may be two sets of sites occupied by the molecules in the crystal as was originally proposed by James and Keenan (33). Such a structure has also been recently deduced from a coherent neutron scattering study of CD_4 (9). In this structure there are eight molecules per unit cell of which six are ordered on sites of symmetry D_{2d} ($\bar{4}\,2m$) and two are free to rotate located on sites of symmetry O(432). Since D_{2d} was found an acceptable site group, our spectra will be examined for consistency with this model. For the selection of a factor group, only the main wider components will be considered; the narrower spectral features are believed attributable to quantized rotational levels of the molecules on sites of octahedral symmetry and this will be discussed later in this section. The ν_3 regions of both CH_4 and CD_4 were scanned under high resolution and although the main peaks could not be resolved it appears that they contain two wide components of appreciable intensity and one additional line of lower intensity.

If the strong highly unsymmetrical band is a doublet arising from crystal field effects, the local symmetry is D_{2d} and the factor group is T_d or O_h (see Table 6) but if on the contrary ν_3 and ν_4 are not split, the local symmetry is T or T_d and seven combinations of site and factor groups remain acceptable. Correlation diagrams have been constructed for every possible symmetry and the results of this group theoretical analysis are collected in Table 6. Unfortunately we have not succeeded in obtaining high resolution spectra of the ν_4 bands because we did not have any suitable detectors for these regions.

Further elimination might be possible by comparing the infrared and Raman frequencies,

Can. J. Chem. Downloaded from www.nrcresearchpress.com by 210.87.254.5 on 09/05/12
For personal use only.

for if they are not coincident the factor groups T and T_d are eliminated. Unfortunately the frequencies of the reported Raman bands (14) are not accurate enough ($\pm 2 cm^{-1}$) for this type of comparison to be meaningful.

Two absorption bands were found in the lattice vibration region of both molecules (15). These two bands are consistent with both symmetry combinations involving D_{2d} site symmetry but not with any combination of site and factor groups involving T or T_d site symmetry (see Table 6). It should be noted that if the site symmetry is D_{2d} the factor group T_d is not acceptable since this combination of symmetries does not yield any f.c.c. lattice (see Table 6) and that there remains only one possible factor group, O_h, which yields only the f.c.c. space group O_h^6 ($Fm\,3c$).

Within this structure there could be eight molecules per primitive cell of which six would be ordered on sites of D_{2d} ($\bar{4}\,2m$) symmetry (type A) and two free to rotate on sites of O(432) symmetry (type B). In this arrangement the eight carbon atoms form a f.c.c. lattice by symmetry. Therefore the type B molecules are in a cage surrounded by ordered type A molecules that form the f.c.c. lattice. This arrangement is exactly analogous to that existing when methane occupies a substitutional cavity in a matrix of one of the noble gases since these also crystallize with a f.c.c. structure. The resemblance with krypton is particularly striking since both crystals have cavities of very similar sizes; this was previously discussed by one of us (18, 20, 21). Since quantized molecular rotation of methane was shown to exist in the crystals of the noble gases we will try to assign the sharp lines left unexplained in the spectra of the neat crystals to vibration–rotation transitions of the type B molecules.

Essentially, for CH_4 at 10 °K there were four (and in some cases five) components with a separation somewhat smaller than the separation between the gas phase vibration–rotation lines. From the free rotor predicted intensities and from the variation with time of the intensities of the observed lines in the matrix, the strongest component was assigned to R(0). The same general pattern was found for CD_4 isolated in noble gas matrices except for the greater number of components corresponding to the Boltzmann distribution amongst the more closely spaced energy levels of CD_4 which has a greater moment of inertia. It must be remembered that although the fine structure is well resolved at 8 °K, it broadens very rapidly with temperature and that around 30 °K only the rotational envelope is preserved (20). The spectra of the neat crystals were recorded at 9 °K for CH_4 and 23 °K for CD_4; therefore from the noble gas matrices results it is obvious that the rotational features, if present, will be easier to detect in CH_4 than in CD_4.

Let us now turn our attention to the i.r. spectrum of crystalline methane in phase II and try to reconcile it with the assumption that one out of four molecules in the solid undergoes quantized molecular rotation similar to that shown to exist in noble gas matrices. According to the foregoing discussion two main bands ought to be observed: one corresponding to the R(0) line of molecules that are free to rotate (type B) and the other, about three times as intense, arising from molecules that are not free to rotate (type A). (The other vibration–rotation lines including the Q branch are much weaker since the Q(0) line is forbidden.) The infrared spectrum of phase II CH_4 (Fig. 1) shows the main features we are looking for: the most intense bands (in the ν_3 region at 3008.5 cm^{-1} and in the ν_4 region at 1301.3 cm^{-1}) arise from type A molecules, whereas the bands at 3020.1 and 1296.9 cm^{-1} would be the R(0) lines of type B molecules. The ratio of the intensities of the bands of type A molecules to those of type B molecules is about three to one. This is somewhat accidental because the two types of molecules need not have the same intensity. There are additional weak features which may be assigned to vibration–rotation lines of type B molecules: in ν_3, R(1) at 3026, Q at 3011, P(1) at 3004; in ν_4, R(1) hidden under 1301.3, R(0) at 1296.9, Q at 1292.9, and P(1) at 1289.3. Table 7 illustrates the similarity between the spectrum of neat CH_4 crystals and that of CH_4 isolated in a krypton matrix. The spacings between the various lines are very similar to the spacings found in noble gas matrices (20). The weaker features at 3000.5, 2999.4, 1294.1, 1290.1, and 1286 very likely belong to the $^{13}CH_4$ isotope. The CD_4 spectrum is also consistent with molecular rotation. In

TABLE 7. Infrared absorption frequencies of CH_4 isolated in a krypton matrix and as a neat crystal in phase II

Krypton* 9 °K	Neat crystal 9 °K	Assignment	
3030	3026	R(1)	ν_3
3026.5	3020.3	R(0)	
3018.3	3011	Q	
3010.1	3004	P(1)	
1306.1	~1300	R(1)	ν_4
1302.4	1296.9	R(0)	
1298.9	1292.9	Q	
1294.6	1289.3	P(1)	

*Reference 20.

the ν_4 region (Fig. 2) the band at 987.5 belongs to type B molecules whereas that at 992.3 arises from type A molecules; on the high frequency side, a shoulder is assigned to ν_4 of CHD_3 molecules present as an impurity whereas on the low frequency side the shoulder is due to $^{13}CD_4$ in natural abundance. In the ν_3 region the lines of type B molecules are lost under the wide band of type A molecules, although a shoulder, assigned to the R(0) line, is observed around 2260 cm^{-1}. The smaller rotational constant for CD_4 and, to a greater extent, the higher temperature of the sample are responsible for the apparent differences between the spectra of phase II CH_4 and CD_4. The Raman spectra of the neat crystals (14) may also reveal some features that could arise from molecules which are free to rotate. In the krypton matrix (21) a wide band was observed with a maximum around 3040 cm^{-1}. By comparison the band at 3037 cm^{-1} in the spectrum of neat solid CH_4 could arise frome type B molecules, whereas in the ν_2 region these molecules would be responsible for the band at 1553 cm^{-1} but this cannot be considered established until Raman spectra of higher quality are obtained. In the ν_1 region, 2901 cm^{-1} could be the band of type A whereas 2907 could be the Q(1) transition of type B molecules.

No features easily assigned to molecules free to rotate were found in the spectra of guest molecules of mixed isotopic crystals. It is not impossible that at least some of the weak lines, found close to the main bands of the guest molecules (see for example Fig. 7 of this paper and Fig. 1 of ref. 17), are vibration–rotation lines of molecules lying on sites of octahedral symmetry but it may be that the guest molecules are, in the host crystal, occupying only sites of D_{2d} ($\bar{4}\,2m$) symmetry. This problem is the subject of further studies in this laboratory.

Finally two series of experiments were carried out in an attempt to observe conversion among the various spin species of methane through a variation of the intensities of the vibration–rotation features identified in the spectrum of the neat crystal. In the first series, the spectrum was recorded at various time intervals over a period of 3 h; no time dependance was detected but unfortunately nothing may be said for the first hour where the unexplained phenomenon reported by Blanchard *et al.* (16) was observed. In the second series of experiments, oxygen was added to methane (up to 1%) since Frayer and Ewing (19) had shown that the addition of O_2 to a mixed crystal of CH_4 and noble gases increases the rate of spin equilibration. In our spectra the line width has been noticeably increased by the addition of oxygen such that it is difficult to draw a firm conclusion although it seems that features arising from the $J = 1$ level had lost some intensity but the variation of intensity was within experimental accuracy. The overlapping of the various components is such that no accurate intensity measurement is possible.

E. Conclusions

The i.r. spectra indicate that methane and methane-d_4 have the same crystal structures in phase I as well as in phase II.

In phase I the i.r. absorption bands are so wide that no information on site and factor groups may be derived. The spectra reflect considerable motion of the molecules but it not possible to specify what type of motion is involved.

In phase II the bands are much sharper, and the analysis of the observed features yields more precise information. The analysis of the vibrational bands corresponding to the internal modes of the molecule is consistent with three different site symmetries namely, T_d, T, and D_{2d} and nine different couples of site and factor groups. The diffraction experiments have fixed the carbon atoms on a face centered cubic lattice. Eight of our nine different couples are possible in a total of eleven face centered cubic

Can. J. Chem. Downloaded from www.nrcresearchpress.com by 210.87.254.5 on 09/05/12
For personal use only.

space groups and one of the couples is rejected for it cannot exist in any f.c.c. space group. The D_{2d} local symmetry is the only one compatible both with our spectra and with the existence of the two lattice modes found in the far i.r. region. Therefore it is suggested that, in agreement with recent neutron diffraction experiments, the space group is O_h^6 ($Fm\,3c$). This conclusion could be checked by recording high quality Raman spectra. The lattice vibration region would be particularly useful since, amongst the eleven remaining space groups, O_h^6 ($Fm\,3c$) is the only one yielding two lattice modes. Moreover the i.r. and Raman bands would correspond to different modes and are likely to have different frequencies. It has been clearly shown that quantized rotation of the methane molecules, similar to that found in noble gas matrices, exists in this phase. The proportion of the number of molecules which are free to rotate over that of ordered molecule could be 1:3 as suggested by James and Keenan. The Raman spectra would also provide a good test for our conclusion about molecular rotation for in the A_1 mode only the Q(1) transition will be found at 9 °K since Q(0) as well as the $\Delta J = \pm 1$ transitions are forbidden. The vibrational spectra at much lower temperatures are being investigated in this laboratory. The study will be extended to the complete series of partially deuterated methanes.

The authors wish to express their gratitude to Professor J. A. Morrison for his interest and for helpful discussions concerning this work as well as for providing them with a purified sample of CD_4. Thanks are due to Nguyen Cong Thanh, L. Lambert, and C. Pépin for their assistance in recording the high resolution spectra. Technical assistance with the apparatus from Jules Rousseau is gratefully acknowledged. Financial support was provided by the "Ministère de l'Education de la Province de Québec" and by the National Research Council of Canada.

1. J. H. Colwell. J. Chem. Phys. **51**, 3820 (1969).
2. K. Clusius. Z. Phys. Chem. **B3**, 41 (1929); K. Clusius, L. Popp, and A. Frank. Physica, **4**, 1105 (1937); A. Frank and K. Clusius. Z. Phys. Chem. **B36**, 291 (1937); E. Bartholome, G. Drikos, and A. Eucken. Z. Phys. Chem. **B39**, 371 (1938).
3. J. H. Colwell, E. K. Gill, and J. A. Morrison. J. Chem. Phys. **36**, 2223 (1962); **39**, 635 (1963); **42**, 3144 (1965).
4. H. P. Hopkins, Jr., P. L. Donoho, and K. S. Pitzer. J. Chem. Phys. **47**, 864 (1967).
5. T. Yamamoto and Y. Kataoka. Prog. Theor. Phys. Suppl. **46**, 383 (1970).
6. K. P. Wong, J. D. Noble, M. Bloom, and S. Alexander. J. Mag. Resonance, **1**, 55 (1969).
7. Ö. Runolfsson, S. Mango, and M. Borghini. Physica, **44**, 494 (1969).
8. A. Schallamach. Proc. Roy. Soc. (London), **A171**, 569 (1939); S. C. Greer. Ph.D. Dissertation. The University of Chicago, Chicago, Illinois. 1969; S. C. Greer and L. Meyer. Z. angew. Phys. **27**, 198 (1969); J. Chem. Phys. **52**, 468 (1970).
9. W. Press. J. Chem. Phys. **56**, 2597 (1972).
10. J. A. Glasel. J. Chem. Phys. **34**, 1649 (1961).
11. M. F. Crawford, H. L. Welsh, and J. H. Harrod. Can. J. Phys. **30**, 81 (1952).
12. G. B. Savitsky and D. F. Hornig. J. Chem. Phys. **36**, 2634 (1962).
13. G. E. Ewing. J. Chem. Phys. **40**, 179 (1964).
14. A. Anderson and R. Savoie. J. Chem. Phys. **43**, 3468 (1965).
15. R. Savoie and R. P. Fournier. Chem. Phys. Lett. **7**, 1 (1970).
16. J. Blanchard, L. C. Brunel, and M. Peyron. C. R. Acad. Sci. (Paris), **B273**, 19 (1971).
17. C. Chapados and A. Cabana. Chem. Phys. Lett. **7**, 191 (1970).
18. A. Cabana, G. B. Savitsky, and D. F. Hornig. J. Chem. Phys. **39**, 2942 (1963).
19. F. H. Frayer and G. E. Ewing. J. Chem. Phys. **46**, 1994 (1967); **48**, 781 (1968).
20. A. Chamberland, R. Belzile, and A. Cabana. Can. J. Chem. **48**, 1129 (1970).
21. A. Cabana, A. Anderson, and R. Savoie. J. Chem. Phys. **42**, 1122 (1965).
22. T. Yamamoto. J. Chem. Phys. **48**, 3193 (1968).
23. T. Yamamoto and Y. Kataoka. J. Chem. Phys. **48**, 3199 (1968); Phys. Rev. Lett. **20**, 1(1968).
24. Y. Kataoka and T. Yamamoto. Prog. Theor. Phys. Suppl. 436 (1968).
25. T. Yamamoto and Y. Kataoka. Prog. Theor. Phys. Suppl. **46**, 383 (1970).
26. R. Kopelman. J. Chem. Phys. **47**, 2631 (1967).
27. E. R. Bernstein. J. Chem. Phys. **50**, 4842 (1969).
28. Tables of wavenumbers for the calibration of infra-red spectrometers. Butterworths Inc., Washington, D.C. 1961.
29. T. K. McCubbin, Jr., J. A. Lowenthal, and H. R. Gordon. Appl. Opt. **4**, 711 (1965).
30. J. Giguère. M.Sc. Dissertation. Université de Sherbrooke, Sherbrooke, Quebec. 1969.
31. D. H. Rank, G. Skorinko, D. P. Eastman, and T. A. Wiggins. J. Mol. Spectrosc. 4, 518 (1960); K. Narahari Rao, C. J. Humphreys, and D. H. Rank. Wavelengths standards in the infrared. Academic Press, New York. 1966.
32. G. L. Hierbert and D. F. Hornig. J. Chem. Phys. **20**, 918 (1952).
33. H. M. James and T. A. Keenan. J. Chem. Phys. **31**, 12 (1959).
34. J. K. Wilmhurst and H. J. Bernstein. Can. J. Chem. **35**, 226 (1957).

Can. J. Chem. Downloaded from www.nrcresearchpress.com by 210.87.254.5 on 09/05/12
For personal use only.

Equilibria Studies on Tetraalkylcyclopentenyl Cations. A Steric Origin for a Baker–Nathan Order?

K. Ranganayakulu and T. S. Sorensen

The Department of Chemistry, The University of Calgary, Calgary, Alberta

Received May 15, 1972

The possibilities of using observable cation equilibria to obtain evidence concerning C—H hyperconjugation are discussed. The experimental approach of this paper, using tetraalkylcyclopentenyl cation equilibria, is to vary the structure of the "normal" alkyl series in such a way that the hypothetical C—H hyperconjugative ability remains constant for a given series while the steric bulk of the groups changes. In fact, the observed equilibrium changes are minimal. Other experiments have been performed to measure both the effect of solvents on the equilibrium constants and the rate of the equilibration reaction. Still other experiments were designed to test the ability of H *vs.* CH_3 in stabilizing alkyl cations and a value of ≥ 4.6 kcal/mol favoring CH_3 has been found. Finally, the possibility of using structurally similar cation and anion equilibria to cancel out steric effects in these equilibria is discussed.

Les utilisations possibles des équilibres que l'on peut observer entre les cations pour mettre en évidence l'hyperconjugaison du C—H sont discutées. L'approche expérimentale de cette note qui utilise l'équilibre du cation tétraalkylcyclopentènyle, consiste à faire varier la structure de la série alkyle "normale" de telle manière que la propriété supposée de l'hyperconjugaison du C—H reste constante dans une série donnée tandis que l'encombrement stérique des groupes varie. En fait, les variations observées pour l'équilibre sont minimales. D'autres expériences ont été réalisées pour mesurer à la fois l'effet des solvants sur les constantes d'équilibre et la vitesse de la réaction d'équilibration. Pour vérifier la capacité de stabilisation des cations alkyles de H par rapport au CH_3, d'autres expériences ont donné une valeur ≥ 4.6 kcal/mol en faveur de CH_3. La discussion finale porte sur la possibilité d'utiliser les équilibres entre cations et anions de structures semblables pour éliminer les effets stériques dans ces équilibres.

[Traduit par le journal]

Canadian Journal of Chemistry, **50**, 3534 (1972)

Can. J. Chem. Downloaded from www.nrcresearchpress.com by 210.87.254.42 on 09/05/12
For personal use only.

The tetraalkylcyclopentenyl cations A and B, where R^1 and R^2 are different alkyl groups, fairly rapidly reach an equilibrium situation if the proper acid solvent system is used (eq. 1) (1). The dimethylcyclopentenyl cation substructure serves simply as a vehicle to compare the alkyl groups R^1 and R^2. Previous work (1) has shown that if R^1 = *t*-butyl and R^2 = methyl, then the equilibrium constant is 18. With R^1 = ethyl and isopropyl, respectively, the observed equilibrium constants are 1.6 and 2.6. If one restricts oneself to a comparison of the partial cation structure shown below the dashed lines in structures A and B, then one has an obvious example of the Baker–Nathan order for alkyl groups. This comparison ignores the R groups at C-4 and we have previously suggested (1) that differential inductive effects for different alkyl groups at this position are likely to be negligible. The steric consequences of the R groups at *both* C-1 and -4 are the subject of this paper.

This method for determining the ability of alkyl groups to stabilize a positive charge offers two distinct advantages over a great majority of the previous investigations (mostly solvolytic rate comparisons) (2): (*1*) the energy differences observed in comparisons between the various alkyl groups are much larger, and (*2*) one is comparing isomeric systems so that no assumptions need to be made concerning the bond energies of the extra carbon and hydrogen atoms involved in non-isomeric systems (3).

[1]

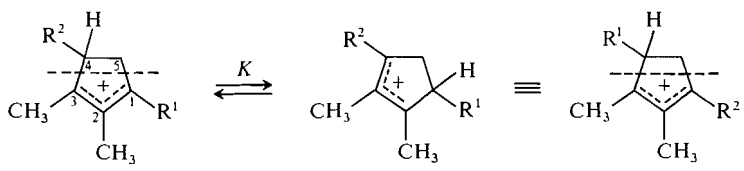

A B

Can. J. Chem. Downloaded from www.nrcresearchpress.com by 210.87.254.42 on 09/05/12
For personal use only.

	Primary	*Secondary*	*Tertiary*
Normal series	CH_3CH_2-	$(CH_3)_2CH-$	$(CH_3)_3C-$
	$(CH_3)_3C-CH_2-$	$CH_3-\overset{H}{\underset{CH_2CH_3}{C}}-$	$(CH_3CH_2)_3C-$
	$(CH_3)_2CH-CH_2-$		$(CH_3)_3C-\overset{CH_3}{\underset{CH_3}{C}}-$

CHART 1

The objectives of the present work are: (*1*) to complete the series A ⇄ B, involving the permutation of all of the standard alkyl groups (methyl, ethyl, isopropyl, and *t*-butyl). The only permutation remaining was the ethyl *vs.* *t*-butyl comparison, *i.e.* R^1 = *t*-butyl and R^2 = ethyl in A ⇄ B.

Objective (2): an unavoidable consequence of testing either the Baker–Nathan or the inductive order of alkyl groups is the problem of a changing steric situation accompanying this process. In the case of ions A and B, it is unlikely that one will have any direct R^1–R^2 interactions. Any difference observed will be due to differences in the interactions of R^1 and R^2 with two nonequivalent sites (shown by arrows) of the testing vehicle, the dimethylcyclopentenyl cation substructure. Briefly, these are (assuming a planar allyl system): at C-4, a staggered (55°) interaction with the C-3 methyl, and an eclipsed interaction with one of the C-5 protons; at C-1, an eclipsed interaction with the C-2 methyl and a staggered interaction with both C-5 protons. One approach to the problem of delineating the cause of the previously observed (1) Baker–Nathan order (hyperconjugation or steric effects?) would be to keep the hypothetical hyperconjugation portion of the alkyl group the same and to vary only the size of the alkyl group. An obvious restriction of this is that structural (steric) changes can only be made at β or higher carbon atoms since the α substitution defines the C–H hyperconjugative properties. Some restrictions on the kind of groups that one can use become apparent when one considers the possible n.m.r. spectra expected from mixtures of A and B. The R^1 groups shown in Chart 1 seemed feasible. For R^2, a methyl or an isopropyl group offered the best chances for obtaining a decipherable n.m.r. spectrum and both were used.

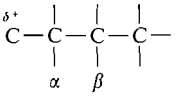

Objective (3): to examine other testing vehicles. In this connection, the previous work can be said to involve a 1,4-alkyl comparison in a cyclopentenyl cation ring. An alternative comparison would involve the 2- and 3-positions.

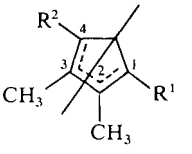

1,4-Comparison

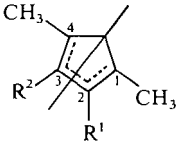

2,3-Comparison

The system where R^2 = isopropyl and R^1 = methyl was chosen.

Objective (4): to attempt to measure the equilibrium constant for a H *vs.* alkyl case. Since a *t*-butyl group appears to be the least stabilizing of the alkyl groups, the system depicted by eq. 2 was chosen.

[2]

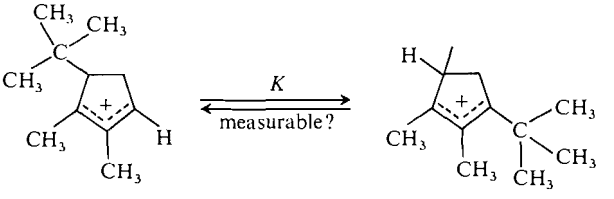

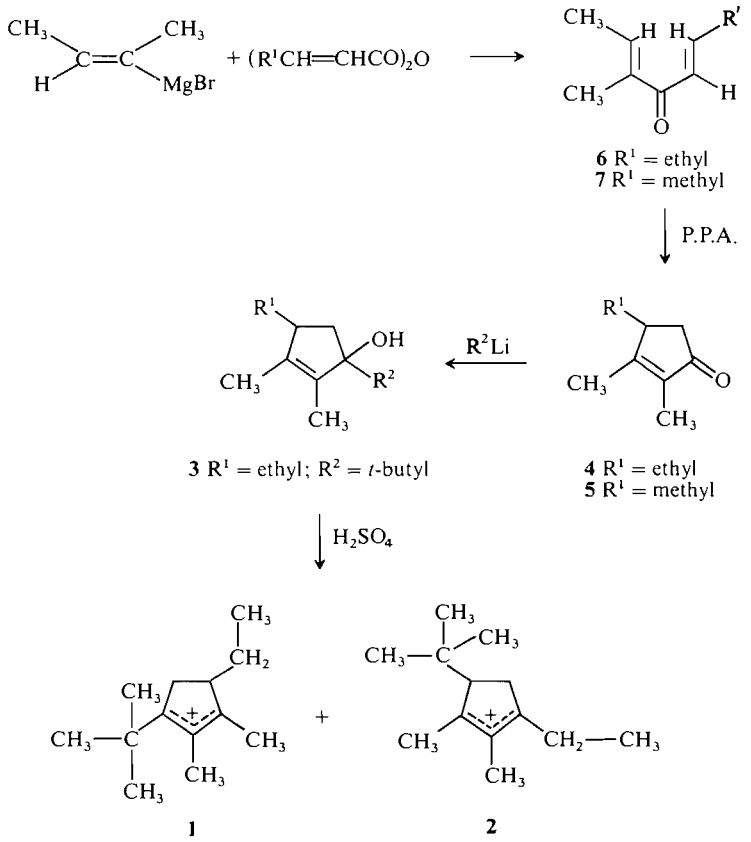

SCHEME 1

Objective (5): the observed free energy difference, $\Delta G = -RT \ln K$, obtained for the A ⇄ B equilibria, can in general be broken down into specific contributions, $\Delta G = \Delta G$ (internal) + ΔG (differential solvation) + ΔG (differential counter ion interaction etc.). One hopes, in this study, that only the first contribution is involved but it seemed desirable to extend the previous work by investigating the position of one of the equilibria in a wider variety of acid solvents and others than was used previously (1). The ion system A ⇄ B, where R was methyl and isopropyl was chosen, since some work had already been done (1) and the n.m.r. analysis for A and B is particularly good.

Objective (6): the proposed approach to all of the above measurements involves the synthesis of only one ion of the A ⇄ B pair. In this circumstance, it became desirable to measure the rate of the equilibration process. It was hoped to measure all of the equilibria in both 93 and 96% H_2SO_4. Rate studies were therefore carried out in both of these solvents as well as in both higher and lower percentages of H_2SO_4. The two systems chosen as representative cases for investigation were the methyl *vs.* isopropyl and the methyl *vs.* *t*-butyl, the latter being particularly suited for study if one starts with the less stable of the pair.

Synthetic Approaches

The Ethyl vs. t-Butyl System

The cations **1** and **2** were prepared from the allylic alcohol **3** which was readily obtained by adding ethyl lithium to the ketone **4**. This ketone was prepared by the reactions outlined in Scheme 1, R^1 = ethyl.

The C-2 methyl groups of **1** and **2** are well separated, τ 7.71 and 7.88 respectively, and these were used, following previously described procedures (1, 4), to determine the equilibrium constant. This has been incorporated with the

Can. J. Chem. Downloaded from www.nrcresearchpress.com by 210.87.254.42 on 09/05/12
For personal use only.

Can. J. Chem. Downloaded from www.nrcresearchpress.com by 210.87.254.42 on 09/05/12
For personal use only.

TABLE 1. Data for the normal alkyl series

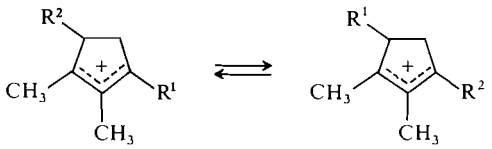

A B

Table no. of cation	Cation[a]	$K = [B]/[A]$	ΔG^b	$\Delta\Delta G^b$
1	R^1 = ethyl; R^2 = methyl	1.6[c]	0.28	
2	R^1 = isopropyl; R^2 = methyl	2.6	0.56	
3	R^1 = *t*-butyl; R^2 = methyl	18	1.70	
4	R^1 = isopropyl; R^2 = ethyl	1.7	0.32	$0.28(2-1)$[d]
5	R^1 = *t*-butyl; R^2 = ethyl	11.4	1.44	$1.52(3-1)$
6	R^1 = *t*-butyl; R^2 = isopropyl	5.5	1.04	$1.14(3-2)$

[a]Taken from ref. 1 except for *5*.
[b]In kcal/mol at 25°.
[c]The error in each value is estimated as ±10%.
[d]From subtraction of the ΔG values.

previously measured systems (1) in Table 1. The ethyl *vs.* *t*-butyl value falls intermediate between the methyl *vs.* *t*-butyl and the isopropyl *vs.* *t*-butyl cases and is, from $\Delta\Delta G$ estimations, close to what might have been calculated.

Systems Employing Other Alkyl Groups

The ketone **7** was prepared as shown in Scheme 1 using crotonic anhydride. The ketone **8** was prepared by the acid-catalyzed rearrangement of thujone, as described in the literature (5). No serious problems were encountered in adding isobutyl or neopentyl lithium to both of these ketones, giving alcohols **9**–**12**. The *sec*-butyl lithium was added only to **7** since it was expected that problems in the n.m.r. analysis would occur with the ions from **8** derived systems. In spite of many attempts using several different procedures, it proved impossible to prepare the lithium derivatives of triethylmethyl chloride or 2-chloro-2,3,3-trimethylbutane. Since these groups (from the above chlorides) represented the simplest tertiary groups which it was felt could be analyzed by n.m.r. spectroscopy, we were left with no representative of this class. In these circumstances, the perdeutero *t*-butyl group was chosen since a deuterium atom is expected to have a smaller size than a proton (6). *t*-Butyl lithium-d_9 was added to both ketones **7** and **8**, yielding the alcohols **14** and **15**.

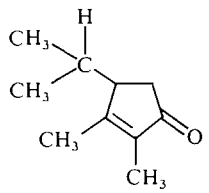

8

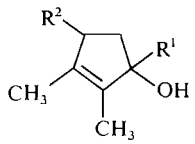

9 R^2 = methyl; R^1 = isobutyl
10 R^2 = methyl; R^1 = neopentyl
11 R^2 = isopropyl; R^1 = isobutyl
12 R^2 = isopropyl; R^1 = neopentyl
13 R^2 = methyl; R^1 = *sec*-butyl
14 R^2 = methyl; R^1 = *t*-butyl-d_9
15 R^2 = isopropyl; R^1 = *t*-butyl-d_9

The pertinent n.m.r. spectral data for all of the ions are given in Table 8 in the Experimental. The actual peaks used to determine the concentrations of the two ions in the equilibrated mixture are noted there. In Table 2, we list the observed equilibrium constants together with a comparison between the ΔG values for these alkyl groups and the "normal" member of the series. The only ion system which proved difficult to analyze was the methyl *vs.* *sec*-butyl case (see below), from alcohol **13**.

Diastereomeric Cations

Each of the cations **22** and **23** exists as a pair of diastereomers and initially this so complicated the spectra that an analysis could not be made. Using 220 MHz n.m.r. spectroscopy however, it has been possible to analyze the equilibrium mixture of all four ions and to definitively assign

Can. J. Chem. Downloaded from www.nrcresearchpress.com by 210.87.254.42 on 09/05/12
For personal use only.

TABLE 2. Equilibrium data for the isohyperconjugative alkyl groups

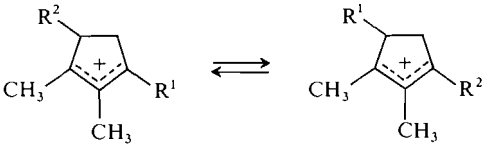

A B

Formula no.		Cation	$K = [B]/[A]^a$	ΔG^b
—	—	R^1 = ethyl; R^2 = methyl	1.6[c]	0.28
16 ⇄	**17**	R^1 = isobutyl; R^2 = methyl	1.4	0.20
18	**19**	R^1 = neopentyl; R^2 = methyl	2.0	0.41
20	**21**	R^1 = isopropyl; R^2 = methyl	2.6	0.56
22	**23**	R^1 = *sec*-butyl; R^2 = methyl	2.0	0.41
24	**25**	R^1 = *t*-butyl; R^2 = methyl	18	1.7
26	**27**	R^1 = *t*-butyl-d_9; R^2 = methyl	17.5	1.7
—	—	R^1 = isopropyl; R^2 = ethyl	1.7	0.32
28	**29**	R^1 = isopropyl; R^2 = isobutyl	2.2	0.47
30	**31**	R^1 = isopropyl; R^2 = neopentyl	2.0	0.41
—	—	R^1 = *t*-butyl; R^2 = isopropyl	5.5	1.05
32	**33**	R^1 = *t*-butyl-d_9; R^2 = isopropyl	6.3	1.1

[a]Values in 96% H_2SO_4. Those in 93% H_2SO_4 were identical within experimental error.
[b]In kcal/mol at 25°.
[c]The error in each value is estimated as ±10%.

the structure of the diastereomers of cation **23**. One optical isomer of each diastereomer is shown below with the probable most stable conformation for the cation **23** diastereomers indicated. Many of the n.m.r. peaks from cations **22** and **23** overlap and only those from the C-4 and C-1 alkyl groups in **22** and from the C-4 alkyl group in **23** are useful for the structure assignments. The observed n.m.r. peaks and the assignments are listed in Table 3. The key n.m.r. features which distinguish **22** from **23** are the

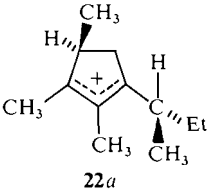

22*a*

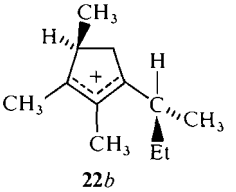

22*b*

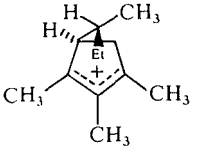

23*a*

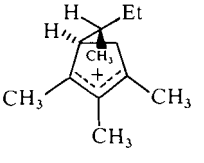

23*b*

TABLE 3. The n.m.r. assignments for the cations **22** and **23**

Ion	C_4-Methyl	*sec*-Butyl group
22 A or B	8.57 (d)[a] $J = 7.4$	8.61 (d) $J = 6.0$ 8.97 (t)[a] $J = 7.0$
22 A or B	8.57 (d)[a] $J = 7.4$	8.65 (d) $J = 6.0$ 8.97 (t)[a] $J = 7.0$
23 A		8.85 (d) $J = 7.0$ 9.14[b]
23 B		9.44 (d) $J = 6.0$ 8.98 (t) $J = 7.2$

[a]These peaks have the same chemical shift in both diastereomers.
[b]This peak appears as a singlet with shoulders on each side separated by about 6 Hz. There appear to be some lower intensity peaks buried nearby (the CH_2 protons of the isobutyl group of this diastereomer).

higher field positions expected for both the CH_3 doublet and the CH_3 triplet of the *sec*-butyl group (further from the cation center in **23**). Although two separate CH_3 doublets are observed for **22***a* and *b*, it is not possible to specifically assign the peaks.

The key n.m.r. feature of the **23** diastereomers is the large chemical shift difference in the CH_3

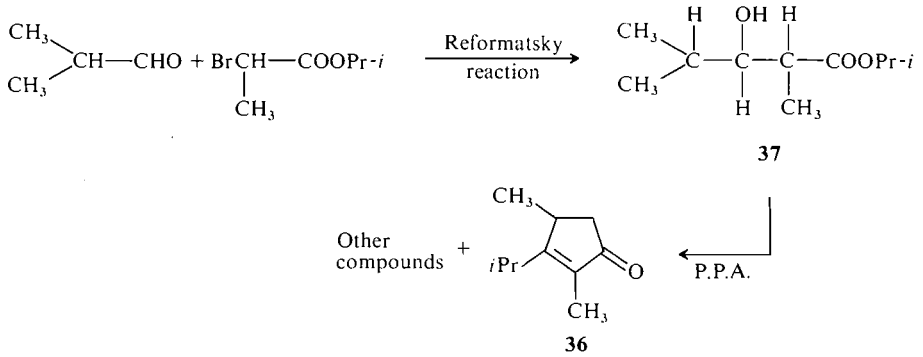

37

36

SCHEME 2

doublets of the *sec*-butyl group, τ 8.85 and 9.44, and the appearance of a methyl group (from the ethyl portion) lacking the usual triplet appearance and in fact resembling a close coupled A_2B_3 pattern. It has been previously found (7) that an isopropyl group in the C-4 position of these cations (analogous to **23**) shows an extremely large non-equivalence of the two methyl groups and this can confidently be attributed to a preferred conformation in which one of the methyl groups lies above and in the shielding region of the allyl cation portion. With the *sec*-butyl compound, the diastereomer with the very high field methyl doublet must be **23***b* and the isomer with the normal methyl doublet but with the abnormally high CH_2 chemical shift (implied from the A_2B_3 spectrum) must be **23***a*, in which the CH_2 protons are now over the allyl cation portion.

The equilibrium constants for these cations are: **22***a* ⇄ **22***b* = 1.20 or 1/1.20, **23***a* ⇄ **23***b* = 2.5 and combined **22** ⇄ combined **23** = 2.0. As will be shown later, interconversions between **22** and **23** proceed by loss of a proton at C-4 and the subsequent addition of one to C-1. This process allows for the interconversions between diastereomers if the proton goes back at C-4 on the opposite face. Interconversion of the diastereomers of **22** can also occur by proton loss from the *sec*-butyl group, destroying the asymetric center, and then reprotonation (eq. 3). The two processes in cation **22** allow inversion of different centers, for example, SR ⇄ SS and SR ⇄ RR, respectively.

Comparison of Alkyl Groups in the 2- and 3-Positions

The cation system desired was **34** ⇄ **35** and the only synthetic problem involved a preparation of the unknown ketone **36**. This was accomplished by the steps shown in Scheme 2.

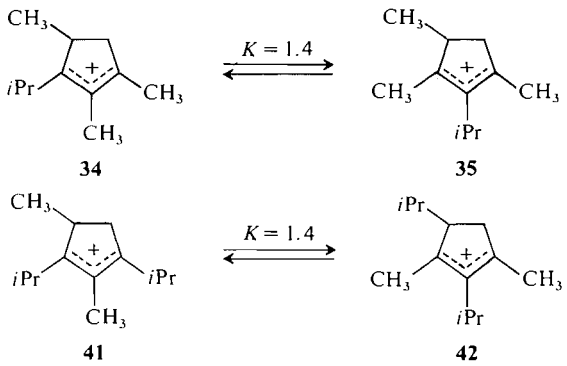

34 35

41 42

In an initial attempt, the polyphosphoric acid ring closure of ethyl 3-hydroxy-2,4-dimethyl-3-isopropylpentane carboxylate (**38**) from diisopropyl ketone and ethyl α-bromopropionate) led to a complex mixture in which none of the desired product could be detected.

[3]

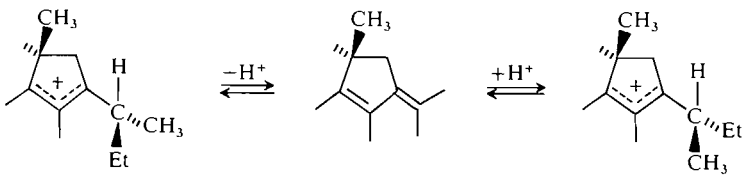

22*b* 22*a*

Can. J. Chem. Downloaded from www.nrcresearchpress.com by 210.87.254.42 on 09/05/12
For personal use only.

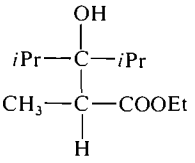

38

Addition of methyl lithium to **36** led to the alcohol **39** and since the ketone was readily available, isopropyl lithium was also added to generate the alcohol **40**. The ions were prepared in the usual way and the pertinent n.m.r. peaks are listed in Table 8. The measured equilibrium constants are shown with the structures.

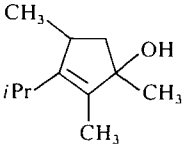

39

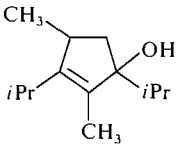

40

The H vs. t-Butyl Comparison. Results and Discussion

The cation **43** was generated from the diene mixture obtained on attempted distillation of the alcohol **45** (eq. 4), which in turn was prepared by the addition of *t*-butyl lithium to the known (8) 2,3-dimethylcyclopentenone. Care was taken in the purification of both the cyclopentenone and the diene since small extraneous n.m.r. peaks can severely limit the scope of the analysis, where in general one wants to be limited at the lower end only by the signal/noise characteristics of the instrument. The solvents used were 93 or 96% H_2SO_4 and the solution was left for a period of time sufficient to cause complete equilibration. The peak searched for was the 9H *t*-butyl peak of **44**, which by analogy to other similar systems, *e.g.*, cations **2** and **25** (Tables 2 and 8), was expected about τ 8.8–8.9. A low concentration reference peak was used to calculate the height of the *t*-butyl peak in ion **43** since this peak was well off-scale at the full amplification used.

Several n.m.r. peaks which were in approximately the correct range were located but these could not be identified unambiguously with **44**. One can however place a minimum value of 120 for the equilibrium constant $\mathbf{44} \overset{k}{\rightleftarrows} \mathbf{43}$ ($\Delta G \geq 2.8$ kcal/mol). The cation **43** is also in equilibrium with a small amount of the cyclohexenyl cation **46**, but the chemical shift positions of this ion

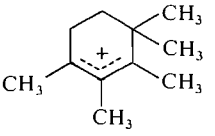

46

are known (9); the *gem*-dimethyl peak is, for example, at a lower field than that expected for the *t*-butyl group in cation **44**. Since a 1-*t*-butyl-substituted cyclopentenyl cation is found to be less stable than the 1-methyl analog (Table 1), it follows, assuming additivity, that the methyl *vs.* H energy difference will be a minimum of 4.6 kcal/mol. Since the energy difference between a secondary and a tertiary alkyl cation is estimated to be 11–14 kcal/mol (10), the value of $\geq$4.6 kcal/mol looks reasonable for an allyl cation case, where the change involved is likely to be less than one-half of that in an alkyl cation. Brouwer and Van Doorn (11), using completely different methods, have estimated this value to be 5.3 kcal/mol in a related cyclopentenyl cation.

Solvent Studies

The equilibrium constant for ions **20** and **21** (see Table 2) was measured in the solvent systems listed in Table 4. These two cations have previously been reported (1). The equilibration reaction is extremely slow in FSO_3H–SbF_5(4:1) and the value reported in Table 4 is possibly not yet the equilibrium one. The aprotic solvent systems were prepared by either evaporating as much FSO_3H as possible from a normal 10% cation – FSO_3H solution and then adding the other solvent or by preparing a very concentrated acid solution and diluting this with the

[4]

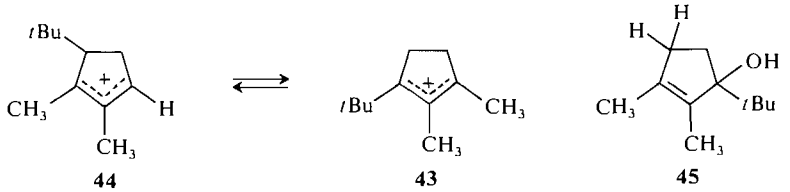

44 43 45

Can. J. Chem. Downloaded from www.nrcresearchpress.com by 210.87.254.42 on 09/05/12
For personal use only.

Can. J. Chem. Downloaded from www.nrcresearchpress.com by 210.87.254.42 on 09/05/12
For personal use only.

TABLE 4. Solvent effects on equilibrium constants[a]

Solvent	K^b
FSO_3H–SbF_5 (4:1)	2.0
FSO_3H	2.5
CF_3SO_3H (95%)	3.0
$FSO_3H + CH_3NO_2$	2.7
$CF_3SO_3H + CH_3NO_2$	2.9
$H_2SO_4 + CH_3NO_2$	2.5
$CF_3SO_3H + CH_2Cl_2$	2.5

[a]For the system $K = \mathbf{21}/\mathbf{20}$.
[b]Estimated error ±10%.

TABLE 5. Sample rate constants for the equilibration reactions at 25.0°

Ions	Solvent % H_2SO_4[a]	$k_r \times 10^4$ (s^{-1})
20 ⇄ **21**	99.4	0.47[b]
	96.3	1.6
	94.4	3.1
	92.9	4–6
	90.6	6–10
24 ⇄ **25**	99.4	1.5[c]
	96.3	3.8
	94.4	7.8
	92.9	15
	90.6	37

[a]These percentages have been corrected to take into account the water produced during the preparation of the ions from the alcohols. The figures are accurate to ±0.10%.
[b]Estimated as ±10% for the first three values.
[c]The error is estimated as ±5% from the scatter obtained in repeated determinations.

other solvent. In the evaporation procedure, it is impossible to remove all of the calculated excess of FSO_3H, an indication of the strength of the solvation forces in these cation salts. In any event, all of the equilibrium constant values are very close to one another and quite possibly identical within the experimental error of the analysis. These results amplify and substantiate those obtained previously (1) and no evidence has yet been found to suggest that differential solvent or counter ion effects are important, although one must concede that the effects in themselves may be important. The subsequent discussion will treat ΔG values as indicative of the internal free energy differences between the cations.

Rate Studies

The rate studies were performed in a similar manner to those previously described (1) and the forward rate constants, using a reversible first order rate expression, for both ions **20** ⇄ **21** and **24** ⇄ **25**, are listed in Table 5. The accuracy of the lower percentage H_2SO_4 rate constants is poor because substantial equilibration occurs during the ion preparation. A plot of the logarithm of the forward rate constants for the *t*-butyl-substituted cations, **24** ⇄ **25** (eq. 5), against the Hammett acidity function, H_0, gives a slope of 0.96, in agreement with the value previously observed for another reaction in which a deprotonation–protonation mechanism has been definitely shown to occur (12). It is possible that other mechanisms are involved in the FSO_3H and related solvent systems.

The equilibrium rate is slightly faster for the *t*-butyl case, reflecting the less stable structure of this ion system. In all of the other ion systems, where no rate studies were made *per se*, the reactions were allowed to stand for periods of time which would have allowed complete equilibration within the practical sense of the word. In all of the *t*-butyl-substituted ions, one must not overdo this since a slow irreversible rearrangement is also occurring. This rearrangement has been described (1).

Discussion

The results may be summarized: (*1*) tetraalkyl-substituted cyclopentenyl cations equilibrate by a deprotonation–reprotonation mechanism; (*2*) the equilibrium constants appear to be a function of only the internal free energy of the two cations involved; (*3*) changes in the steric environment at the β-carbon atom of the alkyl side chain do not significantly affect the equilibrium constants observed. The first two points had previously been assumed in the earlier work (1) and the present results simply provide a sound experimental basis for these assumptions.

[5] 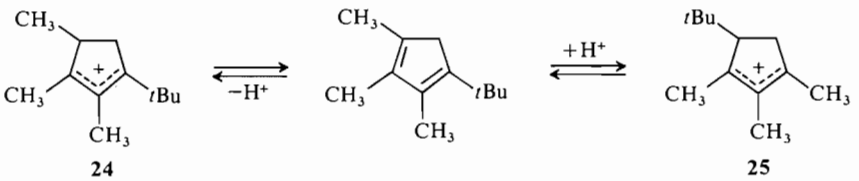

24 **25**

[6] 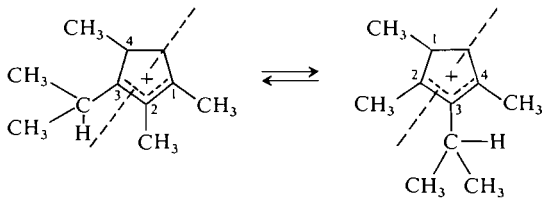

34 35

The "steric effects" experiments in this work have been cast in such a way that positive information would perhaps have proven a steric argument for our Baker–Nathan order. Since the results are basically negative (Table 2), one might examine the converse proposition, namely, that the absence of a demonstrable steric effect shows that differential C—H hyperconjugation[1] is involved. This is doubtful because it is possible by definition only to vary the β-carbon substitution and there is no guarantee that such changes will mimic changes at the α-carbon center. As pointed out previously, any important steric interactions are likely to be between the alkyl groups and the testing vehicle and one obvious extension of the present work would involve the use of other testing vehicles where the steric interactions, although unknown, could be reasonably supposed to be different.

Other Comparison Vehicles

The results from the 2–3-cyclopentenyl comparison (eq. 6) are not in good agreement with the 1–4-comparison although the results are still in the same direction. One drawback in this comparison is the probable presence of some positive charge density at the C-2 position in the cyclopentenyl cations (13). The comparison thus involves two positively changed centers, C-2 and -3, and one can readily see that in the extreme, where δ^+ C-2 = δ^+ C-3, K would be 1 on pure hyperconjugative arguments. In the absence of definitive evidence on the charge density at C-2, one can only surmise that K for this comparison, on hyperconjugation grounds, should be smaller than for a 1–4-comparison. The second compound of this series involves a combined 1–4- and 2–3-comparison and in this case, the result is quite clearly much smaller than expected.

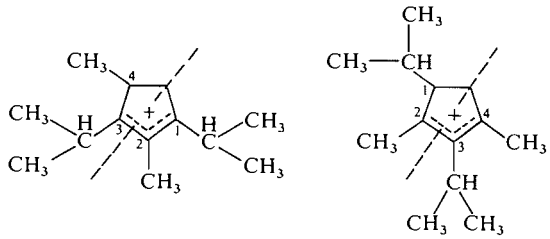

41 42

Still other comparisons of the general type discussed in this work are possible and several of these have been investigated, although not necessarily for the purposes used here. The simplest systems and the ones most likely to show differences in energy because of hyperconjugation would be alkyl cations, where the positive charge is localized. The equilibrium mixtures of the individual isomers in both the *t*-hexyl and *t*-heptyl cations are known and provide no evidence for differential C—H hyperconjugation. Thus, the C-6 system exists at equilibrium with 38% **47**, 30% **48**, and 32% **49**

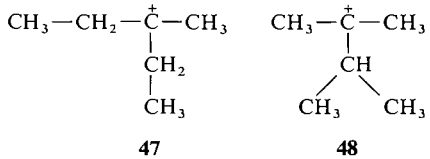

47 48

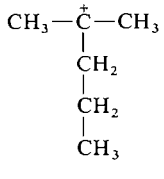

49

[1]On fussy scrutiny, our use of the "big four" alkyl group series to test for C—H hyperconjugation has drawbacks. (*1*) Both the ethyl and isopropyl substituents lack local three-fold symmetry and if this allows preferred rotamers to be formed, an entropy factor could be involved in determining the size of the equilibrium constants. (*2*) ΔH and ΔG are assumed to be equal (*3*) C—C hyperconjugation is generally ignored; and (*4*) even if C—C hyperconjugation were included, the extent of delocalization C—H *vs.* C—C may not be a constant as one varies the change density at the testing position.

Can. J. Chem. Downloaded from www.nrcresearchpress.com by 210.87.254.42 on 09/05/12
For personal use only.

[7]

(14). A more complex procedure would involve comparisons of the type depicted by eq. 7, where for example, $R^1 = R^2 = CH_3$, R^3 = other alkyl. One practical drawback to this experiment is the ease of fragmentation of large alkyl cations (14–16) especially if a *t*-butyl group is present. It also appears likely that direct R—R steric interactions would be involved.

Other allyl cation comparisons are possible in principle. Cations analogous to those studied in this work, in which both the C-2 and -3 positions are substituted by protons, **50** and **51**, are

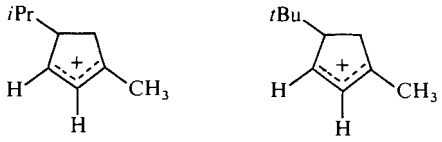

50 **51**

known, (17, 18) and might be thought to be superior systems. However, these ions are not stable in H_2SO_4 and other rearrangements compete with the equilibration reactions in FSO_3H solvent. The same drawback probably applies to a simple allyl cation comparison vehicle, *e.g.* **52** ⇄ **53** (eq. 8). The 1,3,4-trialkylcyclopentenyl cation system has previously been studied (4), but where R = *t*-butyl, **54** ⇄ **55** (eq. 9), only a lower limit for *K* could be obtained because of a competing rearrangement. The 9,10-dialkyl anthracenium ion system has been studied briefly (19) but this system involves too little charge density at the 9- and 10-positions to be particularly suitable. In the following paper (20), a cyclohexenyl cation system has been examined, but even here, other competing rearrangements make the experiments barely possible.

Other Approaches

Arnett and Larsen (21) have reported calorimetric heats of protonation of alkyl benzenes which correlate well with the Baker–Nathan order. The method appears to be very sensitive but suffers from the disadvantage that one is comparing non-isomeric systems; however an advantage is the fact that it directly gives ΔH values. In more recent results by Larsen (22), using substituted β-diketones, the hyperconjugative explanation for the Baker–Nathan order has been discounted and a steric explanation seems more likely.

Comparisons of Equivalent Cation and Carbanion Equilibria

In theory, perhaps the most suitable way to eliminate steric effects would be to compare isomeric cation and carbanion series, *e.g.* eq. 10. Alkyl groups stabilize a positive charge and this ensures that only two isomeric species will be involved in the cation cases. Even alkyl cations which are completely alkylated but partially

[8] 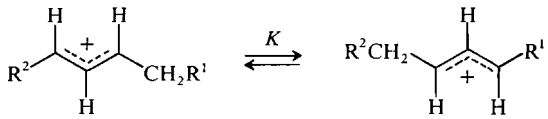

52 **53**

[9] 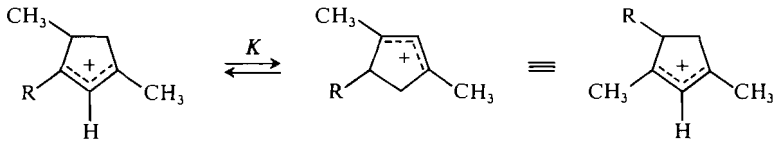

54 **55**

[10] 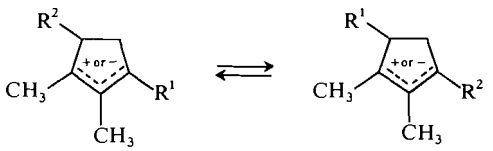

Can. J. Chem. Downloaded from www.nrcresearchpress.com by 210.87.254.42 on 09/05/12
For personal use only.

[11] 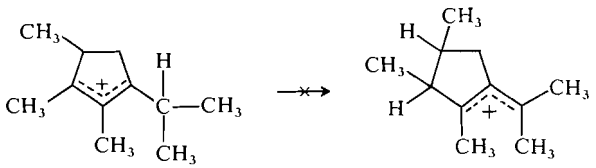

56

[12] 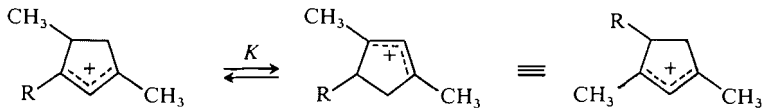

R	K
isopropyl	3
t-butyl	>2.3

[13] 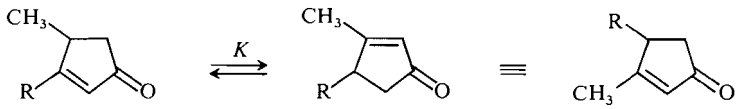

59 R = isopropyl
61 R = *t*-butyl

60 R = isopropyl
62 R = *t*-butyl

R	K
isopropyl	2.8
t-butyl	1.8

exocyclic to the rings are not observed, *e.g.* **56** (eq. 11), where R^1 = isopropyl in the above formulae. Although the requisite experiments have not been attempted, it can be predicted with some certainty (23) that carbanions of the above type would, in fact, prefer to form structures without alkyl substitution, *i.e.* **57** and **58**.

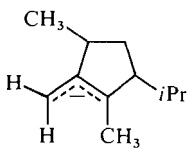

57

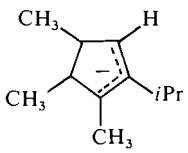

58

It has however been possible in this work to compare cation equilibria with very closely equivalent ketone equilibria, where the charge densities, while not negative, are at least considerably reduced. This involves the comparisons depicted by eqs. 12 and 13. The cation series has previously been reported (4), although the figure for R = *t*-butyl is only a minimum value. The ketones were equilibrated under basic conditions; in the *t*-butyl compound, both pure isomers were available and both were shown to reach the same equilibrium values. The results for the cations and ketones are in the same direction but since the critical *t*-butyl-substituted cation equilibrium constant is not known for certain, the comparisons are rather restricted.

Experimental

General

All boiling points and melting points are uncorrected. Gas chromatography analyses were made on a 6 ft × 1/4 in. 5% SE-30 on Chromosorb W column unless otherwise specified. The n.m.r. spectra of all of the neutral compounds were measured as *ca.* 10% solutions in CCl_4 or $CDCl_3$ either at 60 or 100 MHz. The 220 MHz n.m.r. spectra were recorded by the 220 MHz n.m.r. center, Ontario Research Foundation. All coupling constants are in Hz units, ±0.3 Hz.

3-Methylhepta-2,5-dien-4-one (7)

The general procedure of Normant (24) was used. The Grignard reagent (2-butenyl-2-magnesium bromide), from 136 g (1 mol) of the bromide, was added in a reverse fashion to a solution of crotonic anhydride (184 g, 1.2 mol) dissolved in 1 l of tetrahydrofuran. The tetrahydrofuran solution was cooled to −40° in a Dry-Ice bath (under nitrogen atmosphere), and the Grignard reagent was added through a heated dropping funnel. The addition was carried out over a period of about 2 h. After the addition, the contents of the reaction flask were warmed to 0° in a refrigerator and allowed to stand for 2 days, after which time the reaction mixture was decomposed by pouring it into cold saturated ammonium chloride solution. After work-up, the fraction boiling at 40–90°/8 mm was collected and subsequently refractioned using a spinning band column. Pure 3-methylhepta-2,5-dien-4-one boiled at 72–74°/8 mm, a high boiling

Can. J. Chem. Downloaded from www.nrcresearchpress.com by 210.87.254.42 on 09/05/12
For personal use only.

Can. J. Chem. Downloaded from www.nrcresearchpress.com by 210.87.254.42 on 09/05/12
For personal use only.

fraction containing crotonic anhydride and crotonic acid was discarded. The yield of the ketone was 35 g (28%); i.r.: 1665 and 1618 cm^{-1}; n.m.r.: 3.14–3.66, (m), (3H), vinyl protons; 8.03 and 8.13, (d), $J = 6.6$ Hz, the C-1 methyl group; 8.05, one-half, the other half is buried under 8.19, each of these peaks is further split into a doublet by the C-5 proton, $J = 1$ Hz, (3H), the C-7 methyl group; 8.19, (3H), the methyl group attached to C-3; refractive index, $n_D^{25} = 1.4842$.

Anal. Calcd. for $C_8H_{12}O$: C, 77.38; H, 9.74. Found: C, 77.20, H, 10.06.

*2,3,4-Trimethylcyclopent-2-en-1-one (**5**)*

This preparation follows the standard Nazarov ring closure (25). 3-Methylhepta-2,5-dien-4-one (8 g, 0.66 mol) was mixed with 4 g of polyphosphoric acid and 12 g of formic acid and placed in a 50 ml flask provided with a magnetic stirring bar and calcium chloride drying tube. The contents of the flask were heated in an oil bath with stirring at 90–100° for a period of 6 h. The reaction mixture was cooled and poured into 200 ml of cold water. After work-up, the residue, on fractional distillation, gave 5.5 g (70% yield) of 2,3,4-trimethylcyclopent-2-en-1-one, b.p. 90° (15 mm); i.r.: 1700 and 1650 cm^{-1}; n.m.r.: 7.25–7.75, (b), (3H), CH and CH_2 protons at C-4 and -5; 8.04, (3H), C-3 methyl protons; 8.38, (3H), C-2 methyl protons; 8.78 and 8.89, (d), $J = 6.6$ Hz, C-4 methyl protons.

Anal. Calcd. for $C_8H_{12}O$: C, 77.38; H, 9.74. Found: C, 77.87; H, 9.33.

The refractive index was n_D^{23} 1.4845, the reported constants are: b.p. 77–78°/11 mm, n_D^{20} 1.4836 (26).

*3-Methylocta-2,5-dien-4-one (**6**)*

2-Butenyl-2-magnesium bromide, from 136 g (1 mol) of 2-bromo-2-butene and 24.3 g (1 mol) of magnesium in tetrahydrofuran solvent, was added in reverse fashion through a heated dropping funnel under a nitrogen atmosphere to a solution of 2-pentenoic anhydride, 216 g (1.2 mol), in 1 l of tetrahydrofuran cooled to −40°. After work-up, fractional distillation of the residue gave 25 g (18% yield) of 3-methylocta-2,5-dien-4-one, b.p. 95–97°/14 mm; i.r.: 1690 and 1645 cm^{-1}; refractive index n_D^{23} 1.4835.

Anal. Calcd. for $C_9H_{14}O$: C, 78.21; H, 10.21. Found: C, 78.08; H, 10.35.

N.m.r.: 3.2–3.4, (m), the vinyl protons; 7.6–8.0, (m), (2H), the methylene protons; 8.13, one half of a doublet, the other half is buried under 8.23, and appears as a shoulder at 8.25, the peak at 8.13 is further split into a quartet, $J = 2$ Hz, the C-1 methyl protons; 8.23, (3H), the C-3 methyl protons; 8.79, 8.90, and 9.01, (t), $J = 6.6$ Hz, (3H), the C-7 methyl protons.

*4-Ethyl-2,3-dimethylcyclopent-2-en-1-one (**4**)*

3-Methylocta-2,5-dien-4-one, 9.2 g (0.067 mol), was placed in a 50 ml flask and was treated with a mixture of 4 g of polyphosphoric acid and 12 g of formic acid. The reaction mixture was stirred in a nitrogen atmosphere at 90–100° for 6 h and then worked-up. The ketone boiled at 104–105°/15 mm; yield, 5.9 g (65%). This ketone was further purified through the semicarbazide, m.p. 201–203°, after three recrystallizations from methanol.

Anal. Calcd. for $C_{10}H_{17}ON_3$: C, 61.51; H, 8.19. Found: C, 61.36; H, 8.48.

Hydrolysis with 6*N* sulfuric acid for 4 h, work-up, and distillation of the residue (spinning band column) gave the pure ketone, 10.5 g, b.p. 91–92°/8 mm; i.r.: 1715 and 1660 cm^{-1}; refractive index n_D^{23} 1.4804; 100 MHz n.m.r. in $CHCl_3$: 7.2–7.72, the CH and CH_2 protons at C-4 and -5; 7.84, (shoulder); 7.90, 8.08, one more peak is buried under 8.01, the CH_2 of the ethyl group; 8.01, (3H), the C-3 methyl group; 8.33, (3H), the C-2 methyl group; 9.06, 9.13, and 9.205, (t), $J = 7.2$ Hz, the methyl protons of the ethyl group.

*Ethyl 3-Hydroxy-2,4-dimethyl-3-isopropylpentane Carboxylate (**38**)*

The procedure followed the standard Reformatsky reaction conditions (27). From 31.8 g (0.5 g atoms) of Zn, 90 g (0.5 mol) of ethyl α-bromopropionate, and 57 g (0.5 mol) of diisopropyl ketone there was obtained, after fractionation of the crude residue, pure (by g.l.c.) ethyl 3-hydroxy-2,4-dimethyl-3-isopropylpentane carboxylate, b.p. 88–90°/8 mm; 32 g (30% yield); 60 MHz n.m.r. in CCl_4: 5.68, 5.79, 5.92, and 6.03, (q), $J = 6.6$ Hz, (2H), the CH_2 protons of the ethyl group (ester); 6.43, 6.55, 6.67, and 6.79, $J = 7.2$ Hz, (1H), the CH proton at the C-2 position; 7.24–7.74, (m), (2H), the CH protons of the isopropyl groups; 8.60, one-half of a methyl doublet, the other half is buried under 8.74, the C-2 methyl protons; 8.67, 8.74, 8.78, and 8.85, (two doublets), $J = 6.6$ Hz each, (12H), the methyl protons of the isopropyl groups; 8.87, 8.97, 9.07, (t), $J = 6$ Hz, (3H), the methyl protons of the ethyl group (ester).

*Attempted Conversion of **38** into the Cyclopentenone **36***

Cyclopentenones have been prepared (28) from the acid-catalyzed rearrangement of γ-lactones and on this basis, compound **38** was expected to yield the desired cyclopentenone **36**. Accordingly, 4 g (0.02 mol) of the ester, 1 ml of glacial acetic acid, and 30 g of polyphosphoric acid were mixed together in a 100 ml flask and heated in an oil bath at 120° for 2 h. After work-up, distillation of the residue gave an oily compound, b.p. 85–95°/8 mm. This material on g.l.c. analysis appeared to consist of at least four compounds, none corresponding to the desired ketone, as determined from the n.m.r. spectra of the individual components which were separated in small quantities by preparative g.l.c. No attempt was made to establish the structure of the individual components.

*Isopropyl 3-Hydroxy-2,4-dimethylpentane Carboxylate (**37**)*

The above ester was prepared in 70% yield using the Reformatsky reaction, starting with isobutyraldehyde, isopropyl α-bromopropionate, zinc dust, and dry benzene. The ester boiled at 90–91°/8 mm. The 60 MHz n.m.r. spectrum in CCl_4 solution showed: 4.7–5.34, (m), (1H), the CH proton of the isopropyl group (ester); 6.38–6.92, (m), (1H), the CH proton at the C-3 position; 7.15, the —OH proton; 8.14–8.64, (b), (1H), the CH proton at the C-4 position; 8.71 and 8.81, (d), $J = 6$ Hz, the isopropyl methyl protons in the ester function; one peak buried under 8.81, 8.93, 8.98, 9.06, 9.08, 9.12, 9.15, 9.17 (shoulder), the CH_3 protons at the C-4, -5, and -2 positions.

The compound has two asymetric centers so that one likely has two diastereoisomers present (thus accounting for the "extra" peaks in the methyl region).

*3,4-Dimethylcyclopent-2-en-1-one and 2,4-Dimethyl-3-isopropylcyclopent-2-en-1-one (**36**)*

The synthesis of ketone **36** follows a recent general cyclo-

Can. J. Chem. Downloaded from www.nrcresearchpress.com by 210.87.254.42 on 09/05/12
For personal use only.

TABLE 6. Fractionation of crude **36**

Weight (g)	Fraction	Boiling range (°C)	Pressure (mm)
2	I	57–60	8
1.5	II	60–61	8
2	III	61–63	8
2	IV	64–74	8
4	V	80–85	8
4	VI	85–90	8

pentenone synthesis reported by Conia and Leriverend (29). The other cyclopentenone is produced via the γ-lactone route, which curiously did not work for the preparation of **36** (see above).

The ester **37**, 30 g (0.15 mol), was mixed with 250 g of polyphosphoric acid in a 500 ml flask equipped with a magnetic stirring bar, a condenser, and a drying tube. A few drops of acetic acid were added and the mixture was initially stirred and then allowed to stand at 100–105° in an oil bath for a period of 1.5 h. The contents were cooled and worked-up by pouring into ice-cold water and then extracting the mixture with (3 × 100 ml) ether.

After washing and drying, the solvent was removed under reduced pressure and the residue was quickly distilled in a small distillation apparatus to give a pale yellow oil. Refractionation in a spinning band column resulted in the fractions shown in Table 6.

The first fraction contained mainly 3,4-dimethylcyclopent-2-en-1-one with about 20% of a low boiling impurity (g.l.c.). Fractions II and III were pure 3,4-dimethylcyclopent-2-en-1-one. Fraction IV contained mainly 3,4-dimethylcyclopent-2-en-1-one, with 10% of a high boiling impurity. Fraction V contained two products whose composition could not be established. Fraction VI contained two products which were separated using preparative g.l.c., Carbowax, 30% on Chromosorb W, column diameter 3/8 in., 12 ft. length, operating at 160°. The compounds had retention times of 13 min 12 s, and 20 min 12 s, respectively, at 100 ml/min He flow rate. The compound with retention time 20 min 12 s was the desired ketone, 2,4-dimethyl-3-isopropylcyclopent-2-en-1-one. The structure of the compound with the retention time of 13 min 12 s could not be established.

The 3,4-dimethylcyclopent-2-en-1-one had the following n.m.r. peaks (60 MHz spectrum in CCl_4 solution): 4.17, (b), (1H), the CH proton at the C-2 position; 6.98–7.83, (b), the CH and CH_2 protons of the ring at the C-4 and -5 positions; 7.90, (3H), the C-3 methyl group protons; 8.83, 8.95, (d), $J = 7.2$ Hz, (3H), the C-4 methyl protons.

The ketone **36** had the following n.m.r. peaks (60 MHz spectrum in CCl_4 solution: 6.87–8.06, a complex region comprising the CH and CH_2 protons of the isopropyl group and the C-4 and -5 protons of the ring; 8.32, 8.35, (d), $J = 1.8$ Hz, (3H), the C-2 methyl protons; 8.72, 8.74, 8.83, and 8.85, (two doublets), $J = 6.6$ Hz each, (9H), the CH_3 protons of the isopropyl group and the C-4 methyl protons.

Alkyl Lithium Reagents

Methyl, ethyl, isopropyl, *t*-butyl, and *sec*-butyl compounds were commercially available. Neopentyl, isobutyl, and *t*-butyl-d_9 compounds were prepared from the corresponding chlorides in pentane solution under an argon atmosphere, using lithium ribbon containing 1% sodium. Periods of reflux up to about 18 h were needed for complete

TABLE 7. New alcohols prepared

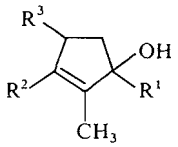

Compound	No.	B.p. (°C/mm)	Analytical (%) C Found	C Calcd.	H Found	H Calcd.
R^1 = isopropyl; $R^2 = R^3$ = methyl		42/0.1	78.74	78.51	12.20	11.98
R^1 = *sec*-butyl; $R^2 = R^3$ = methyl	**13**	52–53/0.3	79.05	79.06	12.32	12.16
R^1 = isobutyl; $R^2 = R^3$ = methyl	**9**	47–48/0.15	79.66	79.06	11.26	12.16
R^1 = neopentyl; $R^2 = R^3$ = methyl	**10**	39–41/0.1	79.08	79.53	12.00	12.32
R^1 = *t*-butyl; $R^2 = R^3$ = methyl		48/0.1	79.56	79.06	12.60	12.16
R^1 = *t*-butyl-d_9; $R^2 = R^3$ = methyl	**14**	38–39/0.05				
R^1 = isobutyl; R^2 = methyl; R^3 = isopropyl	**11**	67–68/0.015	79.92	79.94	12.36	12.46
R^1 = neopentyl; R^2 = methyl; R^3 = isopropyl	**12**	50–55/0.1	80.57	80.29	12.44	12.58
R^1 = *t*-butyl-d_9; R^2 = methyl; R^3 = isopropyl	**15**[a]	48–49/0.05				
R^1 = methyl; R^2 = isopropyl; R^3 = methyl	**39**	49–52/0.075				
$R^1 = R^2$ = isopropyl; R^3 = methyl	**40**	60–62/0.075				

[a]The corresponding proton compound has been reported (1).

TABLE 8. The n.m.r. spectra of the ions[a]

Ion	CH_3 at C-2	CH_3 at C-4 (when present)	Other
1	7.71*[b]		CH_3 of ethyl 9.05 (t) $J = 7.0$ CH_3 of *t*-butyl 8.52
2	7.88*		CH_3 of ethyl 8.59 (t) $J = 7.0$ CH_3 of *t*-butyl 8.92
16	7.85*[c,d]	8.57 (d) $J = 7.5$	CH_3 of isobutyl 8.94 (d) $J = 6.3$
17	7.85*[c]		CH_3 of isobutyl = two (d), 8.90, one-half of one doublet and 9.03, one-half of the other doublet
18	7.82	8.55 (d) $J = 7.5$	CH_3 of neopentyl 8.85*
19	7.85		CH_3 of neopentyl 8.94*
22 and **23**[e]			
26, **27**, **32**, and **33**[f]			
28	7.86[c]		CH_3 of isopropyl = two (d), 8.64* and 8.68* $J = 6.5$ each. CH_3 of isobutyl 9.06, one-half of a doublet
29	7.86[c]		CH_3 of isopropyl = two (d) 8.82* and 9.40* $J = 6.5$ each. CH_3 of isobutyl = two (d) 8.92 and 8.95 $J = 6.0$ each
30	7.83[c]		CH_3 of isopropyl = two (d) 8.74 position of one-half only and 9.40 $J = 6.5$. CH_3 of neopentyl 8.84*
31	7.83[c]		CH_3 of isopropyl = two (d) 8.61 and 8.64 $J = 6.5$. CH_3 of neopentyl = 8.94*
34	7.83*[g]	8.59* (d) $J = 7.0$	CH_3 of isopropyl 8.53* (d) $J = 6.6$
35		*h*	CH_3 of isopropyl 8.69* (d) $J = 7.2$
41	7.84*	8.57 (d) $J = 7.0$	CH_3 of isopropyl = two (d) 8.53 and 8.65[c] $J = 7.0$
42			CH_3 of isopropyl at C-2 = two (d) 8.53 and 8.65[c] $J = 7.0$. CH_3 of isopropyl at C-4 = two (d) 8.82* and 9.44* $J = 6.5$
43	7.74		CH_3 of *t*-butyl 8.56*, Cl methyl 7.18, C-4 methylene 6.60, C-5 methylene 6.54 (b)

[a]Unless specified, centers of multiple peaks are quoted relative to internal tetramethylammonium cation = τ 6.90.
[b]The asterisk (*) refers to peaks used in the area analysis for the two ions.
[c]Peaks overlap completely.
[d]Analysis obtained by difference by subtracting the area of the C-4 methyl from the combined C-2 methyls peak.
[e]See Table 3.
[f]See ref. 1 for the undeuterated spectrum description. In both cases, the C-2 methyl groups were used in the analysis.
[g]Analysis obtained by difference. The area under the isopropyl and C-4 methyl peaks of both isomers corresponds to an area 9H. This area divided by three represents a constant 3H area and subtracting the C-2 methyl area from this gives the concentration of **35**.
[h]Buried under the isopropyl methyl protons.

reaction and after this time, the cooled solutions were filtered under argon through a glass wool plug into the storage bottle and stored in a refrigerator under an argon atmosphere. Analysis of the alkyl lithium solutions was done either by acid titration of decomposed aqueous solutions or by the Gilman procedure (30). Attempts to prepare the corresponding lithium compounds from triethylmethyl chloride and 2-chloro-2,3,3-trimethylbutane failed. The solvents tried were anhydrous ether, pentane, petroleum ether, decalin, and tetrahydrofuran. The temperatures varied from refluxing pentane to refluxing decalin. The lithium was, in several instances, converted to a very fine dispersion prior to the attempted reactions. Finally, mixed solvents like pentane-tetrahydrofuran failed. With the ether solvents, a reaction did occur, but the Gilman double titration showed no alkyl lithium formed and it seems likely that the solvent was cleaved by the lithium (with perhaps the incipient formation of the alkyl lithium).

Allylic Alcohols

The alcohols were prepared in a manner similar to previous descriptions (1, 4). The alcohols are not analyzable by g.l.c. because of a facile dehydration but the n.m.r. spectra generally indicate the presence of both the *cis* and *trans* isomers. The spectra are relatively complex in most cases and are chiefly useful to ascertain that there is no unreacted ketone present (also shown by i.r. spectroscopy) and in a general way to indicate that the chemical shift positions and integrations are reasonable. Descriptions of the n.m.r. and i.r. spectra can be found in ref. 31. The data for the alcohols

Can. J. Chem. Downloaded from www.nrcresearchpress.com by 210.87.254.42 on 09/05/12
For personal use only.

Can. J. Chem. Downloaded from www.nrcresearchpress.com by 210.87.254.42 on 09/05/12
For personal use only.

prepared are summarized in Table 7. The yields varied and no attempt was made to optimize the alcohol recovery since the primary considerations were quality not quantity.

1-t-Butyl-2,3-dimethylcyclopent-2-en-1-ol Dehydration Products

The crude alcohol was prepared by adding *t*-butyl lithium twice to 2,3-dimethylcyclopentenone (8) and working the reaction up in the usual way. An n.m.r. spectrum of the crude product indicated that the desired alcohol had been formed but on attempted distillation through a spinning band column only the dehydrated compounds were obtained, b.p. 38°/0.2 mm.

Anal. Calcd. for $C_{11}H_{18}$: C, 87.93; H, 12.07. Found: C, 87.79; H, 12.27.

This material was however equally suitable for the desired ion preparation. The n.m.r. spectrum showed two low field broad multiplets at 4.28 and 5.46 (area ratio *ca.* 4:1), the latter being characteristic of exocyclic $=CH_2$ protons and thus giving about 12% of the diene total the structure **63**. The remaining cyclopentadiene is probably a mixture of two isomers **64** and **65** since two *t*-butyl peaks were observed at 8.83 and 9.11 with an area ratio of 2.8:1. The minor peak is therefore clearly not from the exocyclic compound **63**. Other absorptions appropriate for the assigned structures were present.

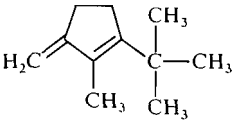

63

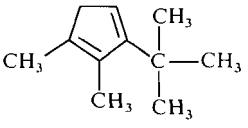

64

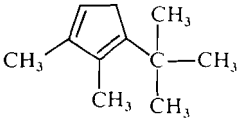

65

Preparation of the Cations

The procedures used to prepare the ions and to obtain the equilibrium constants have been described (1, 4). The n.m.r. spectrum of the cation solution immediately after preparation consists mainly of the isomer expected and it is fairly easy, in the first instance, to assign which peaks belong to which ion after equilibration. Many cyclopentenyl cations have been previously prepared and it is not difficult to specifically assign the peaks in most of the n.m.r. spectra. In Table 8, we report those peaks in the n.m.r. spectrum which are distinctive for a particular ion and also indicate which peaks were used in the area analyses. In general, C-1 and -3 methyl groups are rather broad peaks and where two isomers are present, one generally finds only one broad peak for these groups (when present) from both ions. The same considerations apply to the C-4 methine and C-5 methylene protons. In addition, the methylene and methine protons of some of the complex alkyl groups occur in the same general region. All of these peaks are not included in Table 8 but their positions can be found in ref. 31.

Rate Studies

The procedures used have been described in previous publications (1, 4). The samples were kept in a constant temperature bath at 25.0° except during the measurements, which were conducted at 25 ± 1° in the n.m.r. probe.

Base-catalyzed Equilibration of the Ketones

A 100 μl sample of the ketones **61** and **62** (the preparation of these to be reported) was added separately to two vials containing 1 ml of 30% sodium methoxide in methanol and allowed to stand at room temperature. After 2 days, 200 μl of the methanol solution from each of the vials was separately worked-up by diluting with 1 ml of water and extracting with 2 ml of ether. The ether layer was separated and dried over $CaCl_2$. The ether solution was evaporated to about 200 μl and 50 μl of this was injected onto a g.l.c. column (Carbowax, 12 ft × 3/8 in., 200°, He flow 90 ml/min.). Two peaks were observed corresponding to the ketones **61** and **62**, with retention times of 30.8 and 37.5 min, respectively. Identical results were obtained using either sample. The work-up procedure was repeated at intervals of 2 days, each time checking the concentration ratio by g.l.c. analysis. The relative amounts of the two ketones did not further change in successive work-ups. The ratio of the two ketones was found to be 1:1.8.

On the other system, only one of the ketones, *i.e.* **60**, was available (1) and the procedure adopted was similar to that used for **61–62**. The ketones **59** and **60** had retention times of 35.3 and 40.6 min, respectively, at 182°, above column conditions. The ratio of the two ketones was 1:2.8.

The authors wish to thank the National Research Council of Canada for generous financial support.

1. T. S. Sorensen. J. Am. Chem. Soc. **89**, 3794 (1967).
2. M. J. S. Dewar. Hyperconjugation. The Ronald Press Co., New York. 1962.
3. M. J. S. Dewar. Chem. Eng. News **43** (2), 86 (1965).
4. T. S. Sorensen. J. Am. Chem. Soc. **89**, 3782 (1967).
5. R. H. Eastman and A. V. Winn. J. Am. Chem. Soc. **82**, 5908 (1960).
6. V. F. Raaen, T. K. Dunham, D. D. Thompson, and C. J. Collins. J. Am. Chem. Soc. **85**, 3497 (1963).
7. T. S. Sorensen. Can. J. Chem. **45**, 1585 (1967).
8. D. Varech, C. Quannes, and J. Jaques. Bull. Soc. Chim. Fr. 1662 (1965).
9. P. A. Christensen. Ph.D. Thesis, University of Calgary, Calgary, Alberta, 1971.
10. M. Saunders and E. L. Hagen. J. Am. Chem. Soc. **90**, 2436 (1968).
11. D. M. Brouwer and J. A. Van Doorn. Rec. Trav. Chim. **89**, 333 (1970).
12. T. S. Sorensen, I. J. Miller, and C. M. Urness. Can. J. Chem. **48**, 3374 (1970).
13. N. C. Deno. Prog. Phys. Org. Chem. **2**, 129 (1964).
14. D. M. Brouwer. Rec. Trav. Chim. **87**, 210 (1968).
15. G. A. Olah and J. Lucas. J. Am. Chem. Soc. **89**, 4739 (1967).
16. G. A. Olah, G. Klopman, and R. H. Schlosberg. J. Am. Chem. Soc. **91**, 3261 (1969).

17. T. S. SORENSEN and K. RAJESWARI. J. Am. Chem. Soc. **93**, 4222 (1971).
18. T. S. SORENSEN and K. RANGANAYAKULU. J. Am. Chem. Soc. **92** 6539 (1970).
19. D. M. BROUWER and J. A. VAN DOORN. Rec. Trav. Chim. **89**, 89 (1970).
20. T. S. SORENSEN and K. A. ANANTHANARAYAN. Can. J. Chem. This issue.
21. E. M. ARNETT and J. W. LARSEN. J. Am. Chem. Soc. **91**, 1438 (1969).
22. J. W. LARSEN. J. Am. Chem. Soc. **92**, 5136 (1970).
23. H. KLOOSTERZIEL and J. A. A. VAN DRUNEN. Rec. Trav. Chim. **88**, 1471 (1969).
24. H. NORMANT. Advan. Org. Chem. **2**, 40 (1960).
25. E. A. BRAUDE and J. A. COLES. J. Chem. Soc. 1430 (1952).
26. I. N. NAZAROV and A. I. KUZNETSOVA. Bull. Acad. Sc. U.S.S.R. 392 (1942).
27. Organic synthesis. Coll. Vol. IV. John Wiley and Sons, New York. 1963. p. 444.
28. M. F. ANSELL and M. H. PALMER. Quart. Rev. **18**, 211 (1964).
29. J. M. CONIA and M. L. LERIVEREND. Tetrahedron Lett. 2101 (1968).
30. H. GILMAN and A. H. HAUBEIN. J. Am. Chem. Soc. **66**, 1515 (1944).
31. K. RANGANAYAKULU. Ph.D. Thesis, University of Calgary, Calgary, Alberta, 1971.

Can. J. Chem. Downloaded from www.nrcresearchpress.com by 210.87.254.42 on 09/05/12
For personal use only.

Equilibria Studies on Tetraalkylcyclohexenyl Cations

K. A. ANANTHANARAYAN AND T. S. SORENSEN

The Department of Chemistry, The University of Calgary, Calgary, Alberta

Received May 15, 1972

A cyclohexenyl cation equilibria which effectively "pits" alkyl groups against one another yields equilibrium constants in the hyperconjugative order direction; however the size of the free energy differences are only about 60% of those observed for the identical cyclopentenyl cation member. The rate of the equilibrium reaction was studied, as was the rate of several aberrant ion–ion rearrangements, one on the *t*-butyl substituted ions causing particular problems. Unfortunately, the results appear consistent with either a steric or a hyperconjugation argument.

Les équilibres entre cation cyclohexènyle qui oppose effectivement les groupes alkyles les uns aux autres, conduisent à des constantes d'équilibre de type hyperconjugaison; cependant les grandeurs des différences d'énergie libre ne sont que de 60% environ de celles observées pour le cation cyclopenténylе analogue. La vitesse de l'équilibration a été étudiée ainsi que celle de plusieurs réarrangements aberrants entre ions, l'un d'eux qui s'effectue sur des ions *t*-butyles substitués, cause des problèmes particuliers. Les résultats apparaissent malheureusement compatibles aussi bien avec l'argument stérique que celui de l'hyperconjugaison.

[Traduit par le journal]

Canadian Journal of Chemistry, **50**, 3550 (1972).

Can. J. Chem. Downloaded from www.nrcresearchpress.com by 210.87.254.42 on 09/05/12
For personal use only.

Previously it has been shown (1) that a series of equilibria involving tetraalkyl-substituted cyclopentenyl cations (eq. 1), where R^1 and R^2 are methyl, ethyl, isopropyl, and *t*-butyl groups, give an excellent correlation with the Baker–Nathan order. This result is most directly explained by either differential C—H hyperconjugation or by an unspecified steric effect or perhaps both. If steric effects are involved, then

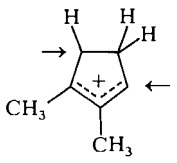

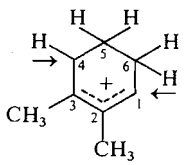

they would most certainly not be direct R^1–R^2 interactions, but in fact, differential interactions of R^1 and R^2 with two non-equivalent sites in the testing vehicle, the 2,3-dimethylcyclopentenyl cation substructure. In the cyclopentenyl system, the two sites are an sp^2 center containing an internal angle smaller than the normal 120° and an sp^3 center flanked by an sp^2 $\overset{\delta+}{C}$—CH_3 center and (assuming a planar molecule) eclipsing protons at C-5. In the corresponding cyclohexenyl ring there are slight differences. The sp^2 center can be substantially closer to 120° and the C-4 and C-5 centers probably involve pseudo axial and equatorial arrangements (2) so that the vicinal interactions are skew. The proposed experiments are not actually dependent on any assumed geometry and the essential point is simply the not unreasonable hope that the steric environment in the two cases will be different. If the various equilibrium constants are due to steric effects, then one would expect the equilibria to be rather sensitive to even small structural changes such as may be involved here. It was of interest therefore to determine whether the equilibrium constants for an analogous series of cyclohexenyl cations would match those of the cyclopentenyl series.

Results

Only one of the cations involved in each equilibrium "pair" was synthesized and this was then allowed to reach an equilibrium with the other isomer. The ions were prepared by the addition of the appropriate allylic alcohol to the strong acid solvents, as described previously for

[1]

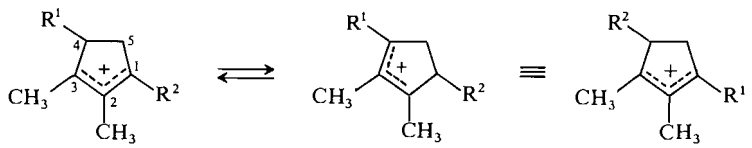

[2] 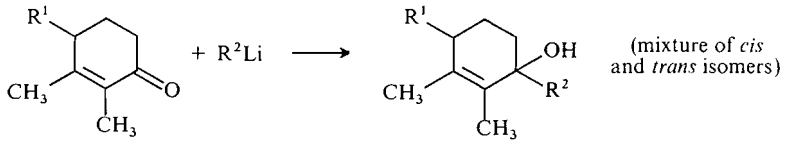

the cyclopentenyl system (1, 3). The standard route to the allylic alcohol was as depicted by eq. 2. To prepare all of the possible combinations of R^1 and R^2 = methyl, ethyl, isopropyl, and *t*-butyl, where $R^1 \neq R^2$, requires the three ketones **1**, **2** and **3**. The trimethyl ketone **1** was known (4) and the synthesis of ketones **2** and **3**

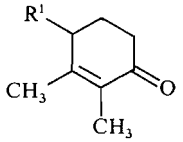

1 $R^1 = CH_3$
2 $R^1 = CH_3CH_2$
3 $R^1 = (CH_3)_2CH$

proceeded in the same manner, starting with Hagemann's ester (see Scheme 1). The first step is well known but only methylation (4) has been tried in the second stage. For the base, the use of sodium hydride in toluene was superior to alkoxide–alcohol mixtures. More forcing conditions are required to introduce the ethyl and isopropyl groups and in all cases, the second alkylation produces mixtures of the 2,2- and the 2,4-dialkyl products. Only the 2,4 product (vinylogous β-keto acid) decarboxylates so the separation of the desired ketone is no problem. In preparing the alcohol, the usual problems were encountered with partial enolization of the ketone on R^2Li addition and with the very easy dehydration of the alcohol product (1, 2). The six alcohols **4**–**9** were prepared.

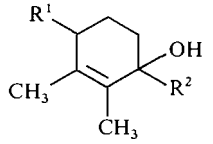

4 $R^1 = Me$; $R^2 = Et$
5 $R^1 = Me$; $R^2 = i$Pr
6 $R^1 = Me$; $R^2 = t$Bu
7 $R^1 = Et$; $R^2 = i$Pr
8 $R^1 = Et$; $R^2 = t$Bu
9 $R^1 = i$Pr; $R^2 = t$Bu

Measurement of the Ion Equilibria

For the equilibrium constant measurements the ions were initially prepared in 95% H_2SO_4 and then allowed to equilibrate at room temperature (< 1 h). As in the cyclopentenyl cation series (1), the analysis involved area measurements of peaks characteristic of each ion and the n.m.r. data for the 12 ions **10**–**21** and the peaks used in the area analyses are reported in Table 1.

Unexpected problems were encountered with all of the *t*-butyl substituted ions. It was anticipated that all of the tetraalkylcyclohexenyl cations would eventually ring-contract to a five-membered cation (2, 5, 6) but this process was

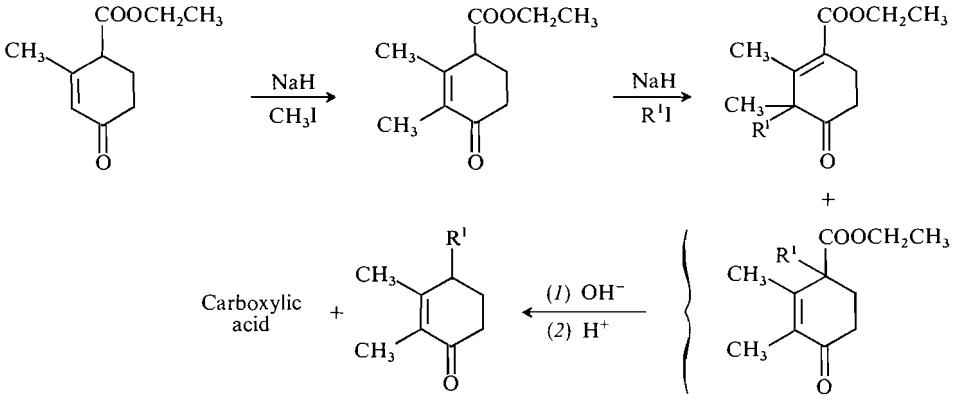

SCHEME 1

Can. J. Chem. Downloaded from www.nrcresearchpress.com by 210.87.254.42 on 09/05/12
For personal use only.

TABLE 1. The n.m.r. spectra of the cations*

Ion (Text no.)	CH_3 at C-2	CH_3 at C-4 (when present)	Other
10	7.82†	8.60 (d),‡ $J = 7.2$	CH_3 of ethyl 8.64 (t),‡ $J = 6.9$
11	7.82†		CH_3 of ethyl 8.89 (t),‡ $J = 7.2$
12	7.82†	8.59 (d),‡ $J = 7.2$	CH_3 of isopropyl 8.665 (d), $J = 6.9$
13	7.82†		CH_3 of isopropyl = two (d), 8.875‡ and 9.095,‡ $J = 6.9$ each
14	7.58	8.51 (d), $J = 7.2$	CH_3 of *t*-butyl 8.42‡
15	7.69		CH_3 of *t*-butyl 8.83‡
16	7.82†		CH_3 of isopropyl 8.68 (d),‡ $J = 6.6$ CH_3 of ethyl 8.89 (t),‡ $J = 6.6$
17	7.82†		CH_3 of isopropyl = two (d), 8.89‡ and 9.12,‡ $J = 6.6$ each CH_3 of ethyl 8.65 (t),‡ $J = 6.6$
18	7.65		CH_3 of *t*-butyl 8.49‡ CH_3 of ethyl 8.76–9.0§
19	7.77		CH_3 of *t*-butyl 8.89‡ CH_3 of ethyl 8.61 (t), $J = 7.2$
20	7.61		CH_3 of *t*-butyl 8.46‡ CH_3 of isopropyl = two (d), 8.745 and 9.035, $J = 6.9$ each
21	7.73		CH_3 of *t*-butyl 8.86‡ CH_3 of isopropyl = two (d), 8.585 and 8.625, $J = 6.9$ each
22	7.83	8.585, $J = 7$	
24	7.86		CH_3 of isopropyl 8.615 (d), $J = 7$
25	7.74	8.62	CH_3 of isopropyl = two (d), 8.90 and 9.08, $J = 6.6$ each
26	7.58		α,α-dimethyl 8.54, CH_3 of isopropyl 8.995 (d), $J = 6.6$

*Unless specified, centers of multiple peaks are quoted relative to internal tetramethylammonium cation = τ 6.90; J in Hz. The solvent is sulfuric acid except for cations **25** and **26** where the solvent was fluorosulfuric acid.
†Peaks overlap completely.
‡Indicates peak used for the area analysis.
§Partially buried.

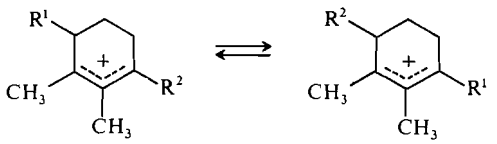

10 $R^1 = Me$; $R^2 = Et$ **11** $R^1 = Et$; $R^2 = Me$
12 $R^1 = Me$; $R^2 = iPr$ **13** $R^1 = iPr$; $R^2 = Me$
14 $R^1 = Me$; $R^2 = tBu$ **15** $R^1 = tBu$; $R^2 = Me$
16 $R^1 = Et$; $R^2 = iPr$ **17** $R^1 = iPr$; $R^2 = Et$
18 $R^1 = Et$; $R^2 = tBu$ **19** $R^2 = tBu$; $R^1 = Et$
20 $R^1 = iPr$; $R^2 = tBu$ **21** $R^1 = tBu$; $R^2 = iPr$

expected to be much slower than the equilibration reactions if sulfuric acid was used as the solvent. To make certain that this reaction was not responsible for the difficulties, we sought first to measure the rate of this reaction and for simplification chose the 1,2,3,4-tetramethyl system **22**, prepared from the allylic alcohol **23** (eq. 3).

At 25.0°, the first order rate constant for **22** → **24** (also prepared unambiguously from 1-isopropyl-2,3-dimethylcyclopent-2-en-1-ol) was 9×10^{-6} s^{-1} in four different sulfuric acid concentrations (91–100%). The reaction is therefore not base-catalyzed. The rate of this reaction is unlikely to be very dependent on the nature of the R^1 and R^2 alkyl groups and where $R^1 \neq R^2$, two different cyclopentenyl cations would be

Can. J. Chem. Downloaded from www.nrcresearchpress.com by 210.87.254.42 on 09/05/12
For personal use only.

Can. J. Chem. Downloaded from www.nrcresearchpress.com by 210.87.254.42 on 09/05/12
For personal use only.

[3] 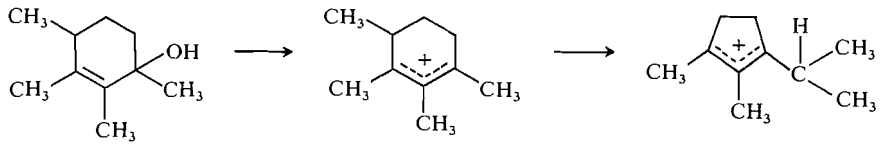

23 22 24

[4] 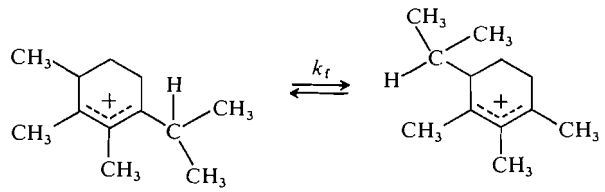

13 12

[5] 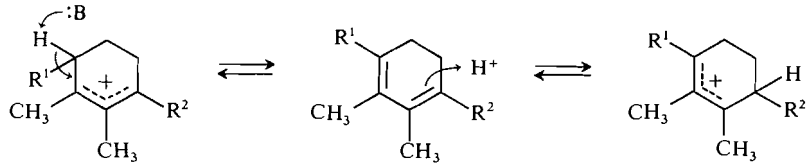

expected under conditions where the equilibration reaction is rapid. Although the rate of the six–five reaction was not measured in the other cases, it was verified that the reaction was very slow on the time scale needed for the six–six equilibration. The rate of this latter equilibration reaction should be dependent on the basicity of the solvent system used (1) and it was desirable to have a rough measure of this. For this study, the rearrangement of ion **13** to the equilibrium mixture of **12** and **13** (eq. 4) was chosen as the representative example since the area analyses are particularly good in this case. The first order rate constants for the forward reaction are reported in Table 2. The results are only approximate for the two weaker acid solvents since substantial rearrangement occurred before the first area measurements could be made. The equilibration reaction is clearly base-catalyzed, thereby implying equilibration mechanism depicted by eq. 5, and in all cases, much faster than the six–five reaction.

TABLE 2. Kinetics of the equilibrium reaction of **13** ⇄ **12** in H_2SO_4 at 25°

% acid	Actual acid concentration*	k_f (s^{-1})	k_f (s^{-1}) for analogous cyclopentenyl members†
100.0	99.4	1.5×10^{-3}	4.7×10^{-5}
97.1	96.5	5.0×10^{-3}	1.6×10^{-4}
95.3	94.7	*ca.* 6×10^{-3}	3.1×10^{-4}
93.8	93.2	*ca.* 7×10^{-3}	$4\text{–}6 \times 10^{-4}$

*Corrected to take into account the water produced during the ion preparation.
†Reference 1.

The fact that the equilibrations are 15–30 times faster in the cyclohexenyl series compared to the cyclopentenyl (Table 2) was expected from the prior results of Deno *et al.* (7) on the pK_a's and H–D substitution rates of both cyclohexenyl and cyclopentenyl cations.

It was clear, therefore, that the problem observed with the *t*-butyl compounds was not due to a six–five reaction. However, this aberrant reaction of the *t*-butyl ions also appeared to be solvent-independent and it proved possible to obtain some equilibrium constant measurements by working in 85% H_2SO_4 at 0°. This percentage of acid is the lowest possible if one wishes to retain relatively sharp peaks for the ion n.m.r. spectra and from extrapolation of the results in Table 2, would be predicted to result in a rapid six–six equilibration, even at 0°. Even so, the aberrant *t*-butyl ion rearrangement eventually causes enough spurious peaks in the n.m.r. spectrum so that one becomes uncertain whether a given peak is in fact a peak of the minor isomer or some other ion peak. Thus, in Table 3, the equilibrium constant figures quoted are minimum values in the case of the *t*-butyl substituted ions.

The aberrant rearrangement was eventually

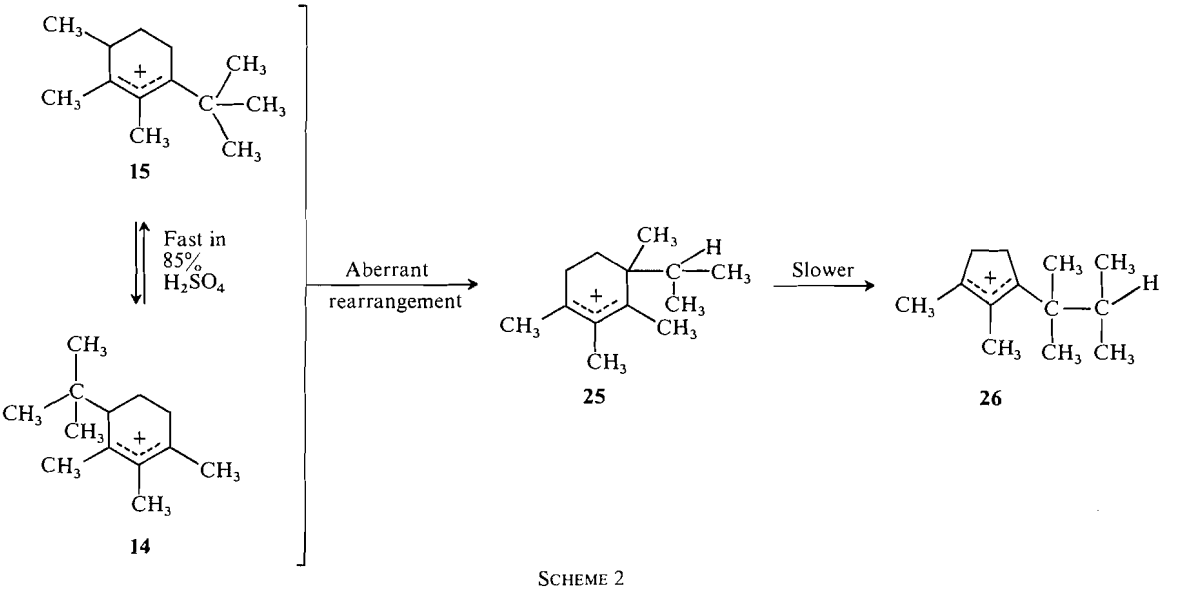

SCHEME 2

TABLE 3. Equilibrium constants for the cations

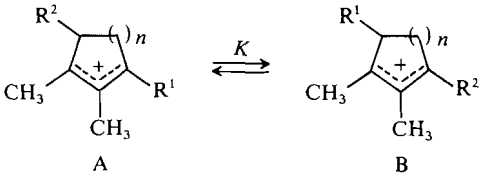

Cation	$K = [B]/[A]$ $n = 1$*	$n = 2$†
R^1 = ethyl; R^2 = methyl	1.6	1.35
R^1 = isopropyl; R^2 = methyl	2.6	2.0
R^1 = *t*-butyl; R^2 = methyl	18	≥6.1‡
R^1 = isopropyl; R^2 = ethyl	1.7	1.2
R^1 = *t*-butyl; R^2 = ethyl	11.4	≥5.3‡
R^1 = *t*-butyl; R^2 = isopropyl	5.5	≥3.4‡

*Taken from ref. 1.
†The error is estimated as ±10% except for the *t*-butyl substituted cations.
‡Obtained in 85% H_2SO_4. The remainder were measured in 95% H_2SO_4.

shown to be as depicted in Scheme 2, using the methyl-*t*-butyl system **14**→**15** as an example. The structural assignments of ions **25** and **26** are based solely on the observed n.m.r. spectra but these are so distinctive that the assignments are unequivocal.

That it is isomer **15** which reacts was shown by dehydrating the alcohol **6** to give the three isomeric dienes **27**, **28**, and **29** (eq. 6), each separated by preparative g.l.c. When these dienes are added to the much stronger acid, FSO_3H, the allylic cations which are formed do not equilibrate with the other isomer. Dienes **28** and **29** produce only ion **15** while diene **27** gives a non-equilibrium mixture of both **15** and **14**. The ion **15** rearranges to the ion **25** with a first-order rate constant of 8.5×10^{-4} s^{-1} at 0°, while ion **14** much more slowly forms a different, unidentified, product, possibly the six–five rearrangement product analogous to ion **24**.

There appears to be an intermediate formed in the conversion of ion **15** to **25** but no definite structural assignment for this ion was possible. The rearrangement reactions in the ethyl–*t*-butyl and isopropyl–*t*-butyl ions are likely to be analogous to **15** but these were not investigated in detail. This rearrangement occurs, however, *only* in the *t*-butyl-substituted ions.

[6] 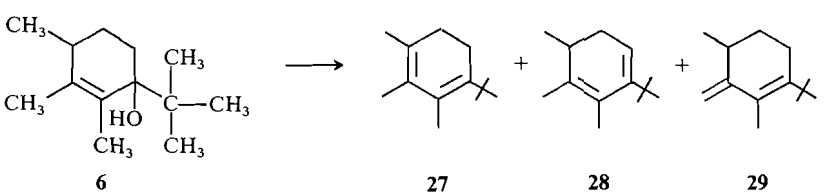

Can. J. Chem. Downloaded from www.nrcresearchpress.com by 210.87.254.42 on 09/05/12
For personal use only.

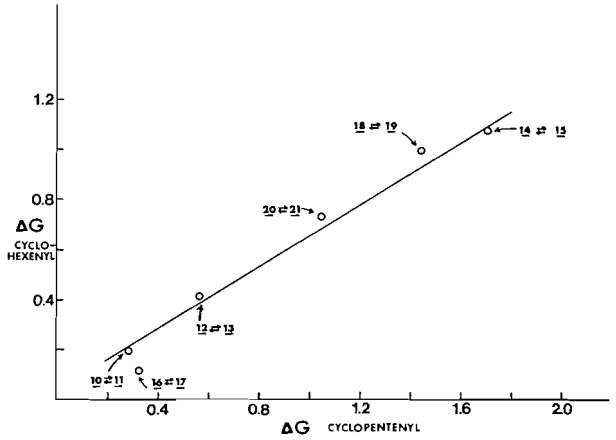

FIG. 1. Linear free energy plot of the related cyclopentenyl and cyclohexenyl cation equilibrium constants.

The aberrant ion **25** further rearranges to the cyclopentenyl cation **26** ($k = 2 \times 10^{-3}$ s^{-1} at 30°), but this process is entirely predictable, based on previous work on very similar systems (2).

Discussion

The equilibrium results for the cyclohexenyl and cyclopentenyl series are compared in Table 3. If one accepts the *t*-butyl-substituted cyclohexenyl ion equilibria as equal to the stated values, then one has an extremely close correlation between the two series and this is shown graphically in Fig. 1. The free energy difference, ΔG, between any two alkyl groups in a cyclohexenyl cation is only about 60% of the value for the corresponding cyclopentenyl series. If all of these equilibrium constants are the result of steric effects, they would have to have occurred because of slightly lower differential steric interactions of the larger alkyl group with the C-1 and -4 positions and to explain the numerical values in both series, the interaction with C-1 would, of necessity, have to be dominant. It is certainly possible that this interaction would be reduced in the cyclohexenyl cations because of the changed situation at C-6 (C-5 in the cyclopentenyl cations).

Simple cyclohexenyl cations are, however, less stable than cyclopentenyl cations for reasons which are not totally understood. One of us has suggested previously (2) that this may be the result of the cyclopentenyl cation possessing a quasi-6π-electron system *or* that direct 1,3 π-overlap stabilization, expected to be stronger in the cyclopentenyl cations, is involved. Paradoxically, if the results of this work are in fact due to differential C—H hyperconjugation, then the cyclohexenyl cations must be less stable because they are less efficient in delocalizing the charge out of the basic allyl cation system into the alkyl substituents, compared to a cyclopentenyl cation.

One has therefore two plausible explanations, admittedly of the assumed cause–expected effect type, each singly based on the effects one is trying to separate. We remain pessimistic that the problem of hyperconjugation can ever be "solved" by using the "big four" alkyl group series, even where the hyperconjugation order is observed.

Experimental

The various instruments and general procedures used in this work are described in the preceding paper (1) together with a description of the various abbreviations used in the text.

Preparation and Analysis of the Cations

The procedures were virtually identical to those used for the cyclopentenyl cations (1). The spectra are actually very similar in many ways and this has helped in assigning the n.m.r. peaks. In Table 1, we report those peaks in the n.m.r. spectrum which are distinctive for the particular cation. In general, the C-1 and -3 methyl groups, where present, absorb about τ 7.2, and since these are broad peaks, they overlap from both isomers of the equilibrium "pair". The same situation exists with the C-4 and -6 protons (*c.a.* 6.5–7.1) and the C-5 protons (*ca.* 8.0).

Kinetic Measurements

The first order cation **22**→ cation **24** rearrangement was

Can. J. Chem. Downloaded from www.nrcresearchpress.com by 210.87.254.42 on 09/05/12
For personal use only.

Can. J. Chem. Downloaded from www.nrcresearchpress.com by 210.87.254.42 on 09/05/12
For personal use only.

followed by periodically measuring the n.m.r. spectra of thermostated (25.0°) solutions. The area analysis is not very accurate since the rather broad C_1–C_3 methyl proton peaks had to be used; the cyclohexenyl cation peak coming at τ 7.25 (6H) and the cyclopentenyl at τ 7.09 (3H). The base-catalyzed equilibration reactions (cation **12** ⇄ cation **13**) were carried out at the same temperature and the data were analyzed for reversible first order kinetics. The area analyses used the high field isopropyl methyl peaks of **13** and the C-4 methyl and C-1 isopropyl methyl peaks of **12**. The first order cation **15** → cation **25** kinetics were measured in fluorosulfuric acid at 0° using the *t*-butyl peak in **15** and either the C-4 methyl or C-4 isopropyl methyl peaks in **25**. The first order cation **25** → cation **26** kinetics were measured in fluorosulfuric acid at 25° using the C-2 methyl peaks of each ion for the area analysis.

4-Carboethoxy-2,3-dimethylcyclohex-2-en-1-one

Hagemann's ester (91.8 g, 0.504 mol) was added with stirring to sodium hydride (28 g in 56% oil dispersion, 0.65 mol) in dry toluene solvent (300 ml) at room temperature. After stirring for 2 h, hydrogen evolution ceased and iodomethane (84.5 g, 0.595 mol) was added dropwise together with 2 drops of ethanol and the reaction mixture was refluxed for 8 h. Work-up in the usual way and distillation of the residue through an 18 in. spinning band column (18:1 reflux ratio) gave 87 g (88%) of the title compound, b.p. 139–140°/8 mm, reported (8), 144–146/13 mm. Partial n.m.r. spectrum: 8.74 (t) $J = 6.9$ Hz (3H); 8.26 (3H); 8.05 (3H); 6.77 (m) (1H); 5.85 (q) $J = 7$ Hz (2H).

*2,3,4-Trimethylcyclohex-2-en-1-one (**1**)*

A second methylation, using 51.0 g, 0.256 mol, of the above ester was carried out, as above, to yield a fraction, b.p. 136–155°, containing both the 2,2- and 2,4-dimethyl adduct. This fraction was hydrolyzed with a refluxing (10 h) 10% alcoholic sodium hydroxide solution, under nitrogen. The solvent was stripped off and the solution acidified with 6 *M* HCl at 0°. This mixture was refluxed until carbon dioxide evolution ceased and then cooled and extracted with ether (3 × 30 ml). The combined ether layers were washed twice with dilute sodium carbonate and then water and finally dried over anhydrous $MgSO_4$. Distillation of the residue through a spinning band column gave 6.2 g (18%) of the title compound, b.p. 93–98°/8 mm. N.m.r.: 8.79 (d) $J = 6.9$ Hz (3H); 8.30 (3H); 8.09 (3H); i.r.: 1675 and 1645 cm^{-1}; semicarbazone 208–210°, reported (4), 210°.

*4-Ethyl-2,3-dimethylcyclohex-2-en-1-one (**2**)*

The preparation of **1** was followed (except that a 36 h reflux was used) using iodoethane. The carboethoxy compound had b.p. 141–148°/8 mm and the title ketone b.p. 98–102°/8 mm. The overall yield was 19%. N.m.r.: 9.00 (t) $J = 7$ Hz (3H); 8.32 (3H); 8.10 (3H); i.r.: 1675 and 1635 cm^{-1}; semicarbazone had m.p. 192–194°.

Anal. Calcd. for $C_{10}H_{16}O$: C, 78.9; H, 10.59. Found: C, 79.02, H, 10.48.

*4-Isopropyl-2,3-dimethylcyclohex-2-en-1-one (**3**)*

The preparation of **1** was followed (72 h reflux) using isopropyl iodide. The carboethoxy compound had b.p. 137–147°/8 mm and the title compound b.p. 48.5–51°/0.05 mm. N.m.r.: 8.98 and 9.15, two (d), $J = 6.2$ Hz each (3H each); 8.28 (3H); 8.08 (3H); i.r. 1678, 1650, 1378, and 1372 cm^{-1}. In another preparation, a very impure product was obtained which necessitated a preparative g.l.c. separation to obtain the pure title compound.

The Allylic Alcohols

These were prepared in a manner similar to previous descriptions (1–3). The n.m.r. spectra of these indicate the presence of both *cis* and *trans* isomers and the n.m.r. spectra are therefore quite complex. Descriptions of the n.m.r. and i.r. spectra can be found in ref. 9.

*1,2,3,4-Tetramethylcyclohex-2-en-1-ol (**23**)*

The compound had b.p. 75–77°/0.5 mm, yield 85%.

Anal. Calcd. for $C_{10}H_{18}O$: C, 77.87; H, 11.76. Found: C, 78.36; H, 11.73.

*1-Isopropyl-2,3,4-trimethylcyclohex-2-en-1-ol (**5**)*

The compound had b.p. 85–92°/0.35 mm, yield 86%.

Anal. Calcd. for $C_{12}H_{22}O$: C, 79.06; H, 12.16. Found: C, 78.79; H, 12.41.

*1-t-Butyl-2,3,4-trimethylcyclohex-2-en-1-ol (**6**)*

The compound had b.p. 75–82°/0.05 mm.

Anal. Calcd. for $C_{13}H_{24}O$: C, 79.53; H, 12.32. Found: C, 79.25; H, 12.23.

*4-Ethyl-1,2,3-trimethylcyclohex-2-en-1-ol (**4**)*

The compound had b.p. 57–59°/0.15 mm.

Anal. Calcd. for $C_{11}H_{20}O$: C, 78.51; H, 11.98. Found: C, 76.17; H, 11.41.

*1-Isopropyl-2,3-dimethyl-4-ethylcyclohex-2-en-1-ol (**7**)*

The compound had b.p. 82–89°/0.2 mm.

Anal. Calcd. for $C_{13}H_{24}O$: C, 79.53; H, 12.32. Found: C, 79.88; H, 11.80.

*1-t-Butyl-2,3-dimethyl-4-ethylcyclohex-2-en-1-ol (**8**)*

The compound had b.p. 87–92°/0.1 mm.

Anal. Calcd. for $C_{14}H_{26}O$: C, 79.94; H, 12.46. Found: C, 80.85; H, 11.88.

*1-t-Butyl-2,3-dimethyl-4-isopropylcyclohex-2-en-1-ol (**9**)*

The compound had b.p. 124–127°/0.8 mm.

Anal. Calcd. for $C_{15}H_{28}O$: C, 80.29; H, 12.58. Found: C, 80.38; H, 12.46.

*Dehydration of Alcohol **6***

Alcohol **6** was dehydrated in the injection port (220°) of a g.l.c. column and the alkenes separated using a 6 ft × 1/4 in. column of 20% SE-30 on Chromosorb W at 124°. He flow 30 ml/min, employing sample sizes of 25 μl. The n.m.r. spectra are definitive in distinguishing the three isomers, one has =CH—, one has $=CH_2$, and the remaining one has no low field peaks.

*Low Retention Product (58 min, 37% of the total): 3-t-Butyl-1,2,6-trimethylcyclohexa-1,3-diene (**28**)*

Partial 100 MHz n.m.r.: 9.185 (d) $J = 6.5$ Hz (3H); 8.85 (9H); 8.24 (b) (3H); 8.12 (b) (3H); 4.5 (m) (1H).

*Middle Retention Product (73 min, 43% of the total): 1-t-Butyl-2,4-dimethyl-3-methylenecyclohex-1-ene (**29**)*

Partial 100 MHz n.m.r.: 8.965 (d) $J = 6.5$ Hz (3H); 8.79 (9H); 8.04–8.14 (b); 5.15 (b) and 5.35 (b) (2H).

*High Retention Product (85 min, 20% of the total): 4-t-Butyl-1,2,3-trimethylcyclohexa-1,3-diene (**27**)*

Partial 100 MHz n.m.r.: 8.81 (9H); 8.26, 8.15, 8.13 (9H).

The authors wish to thank the National Research Council of Canada for financial support.

1. K. RANGANAYAKULU and T. S. SORENSEN. This issue.
2. T. S. SORENSEN. J. Am. Chem. Soc. **91**, 6398 (1969).
3. T. S. SORENSEN. J. Am. Chem. Soc. **89**, 3794 (1967).
4. P. C. MUKHERJI. J. Ind. Chem. Soc. **33**, 99 (1956).
5. N. C. DENO and J. J. HOUSER. J. Am. Chem. Soc. **86**, 1741 (1964).
6. N. C. DENO and R. R. LASTOMIRSKY. J. Am. Chem. Soc. **90**, 4085 (1968).
7. N. C. DENO, N. FRIEDMAN, J. D. HODGE, and J. J. HOUSER. J. Am. Chem. Soc. **85**, 2995 (1963). N. C. DENO, J. BOLLINGER, N. FRIEDMAN, K. HAFER, J. D. HODGE, and J. J. HOUSER. J. Am. Chem. Soc. **85**, 2998 (1963).
8. A. KÖTZ, K. BLENDERMANN, F. MAHNERT, and R. ROSENBUSCH. Ann. **400**, 72 (1913).
9. K. A. ANANTHANARAYAN. M.Sc. Thesis, University of Calgary, Calgary, Alberta. 1971.

Can. J. Chem. Downloaded from www.nrcresearchpress.com by 210.87.254.42 on 09/05/12
For personal use only.

A Nuclear Magnetic Resonance Study of some 4-X-Substituted-2,6-Dinitroanisoles and Related Meisenheimer 1,3- and 1,1-Complexes

M. P. SIMONNIN[1] AND M. J. LECOURT

Laboratoire de Spectrographie, E.N.S.C.P., 11, rue Pierre et Marie Curie, 75005 Paris, France

AND

F. TERRIER[1] AND C. A. DEARING

Laboratoire de Physicochimie des Solutions, E.N.S.C.P., 11, rue Pierre et Marie Curie, 75005 Paris, France

Received May 2, 1972

The structures of transient 1,3-complexes **2** and stable 1,1-complexes **3** formed by the reaction of methoxide ion with various 4-X-2,6-dinitroanisoles in DMSO-d_6 are confirmed by n.m.r. spectroscopy. ^{13}C satellites in the proton spectra of anisoles and 1,1-complexes have been used to obtain $^1J_{^{13}C-H}$ as well as $^4J_{H-H}$ in these symmetrical compounds.

The chemical shifts of the ring protons in 1,3- and 1,1-complexes give some information concerning the influence of the substituent X on the delocalization of the negative charge. In anisoles and 1,1-complexes, $^1J_{^{13}C-H}$ of the ring protons are mainly dependent on the inductive effect of X. Furthermore, a linear relationship is observed in anisoles between the chemical shift as well as $^1J_{^{13}C-H}$ of the methoxyl protons and the Hammett σ_p constant of X, thus suggesting an identical geometry of these molecules at C-2, -1, and -6.

Les structures des complexes -1,3 et -1,1 de Meisenheimer **2** et **3** formés lors de l'interaction des ions CH_3O^- avec divers dinitro-2,6 anisoles X-4 substitués dans le DMSO-d_6 ont été confirmées par r.m.n. Les satellites du ^{13}C des spectres des anisoles et des complexes-1,1 ont permis de déterminer les constantes de couplage $^1J_{^{13}C-H}$ et $^4J_{H-H}$ dans ces composés symétriques.

Les déplacements chimiques des protons du cycle des complexes -1,3 et -1,1 mettent en évidence l'influence du substituant X sur la délocalisation de la charge négative. Dans les anisoles et les complexes-1,1, les couplages $^1J_{^{13}C-H}$ des protons du cycle dépendent principalement de l'effet inductif du substituant X. De plus, les déplacements chimiques et les couplages $^1J_{^{13}C-H}$ des protons méthoxylés des anisoles varient linéairement avec la constante de Hammett σ_p du substituant, ce qui suggère que tous ces composés ont une géométrie identique au niveau des C-2, -1, et -6.

Canadian Journal of Chemistry, **50**, 3558 (1972)

Introduction

Servis first observed by n.m.r. spectroscopy that the reaction of methoxide ion with 2,4,6-trinitroanisole in DMSO results in the fast initial formation of the 1,3-complex followed by the slower appearance of the more stable 1,1-complex (1, 2).

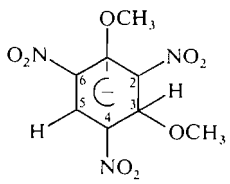

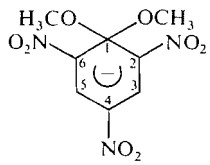

Other workers observed similar results not only with 2,4,6-trinitroanisole but also with 4-cyano-2,6-dinitroanisole and 3,5-dinitro-4-methoxypyridine (3–10). More recently we obtained evidence for the formation of a number of 1,3-complexes from extensive rapid kinetic studies of this reaction with various 4-X-2,6-dinitroanisoles (11–15).

In order to substantiate the structure of the new transient 1,3-complexes thus detected, we have undertaken a thorough n.m.r. study of these reactions. Such an investigation could also be expected to yield interesting information concerning the influence of the substituent X on n.m.r. parameters of anisoles and corresponding 1,3- and 1,1-complexes.

Because of the symmetrical structures of anisoles and 1,1-complexes, the coupling constant $^4J_{H_3-H_5}$ could not be obtained from the proton spectra of these species. So we were led to examine the ^{13}C satellites which could be expected to yield $^1J_{^{13}C-H}$ as well as $^4J_{H_3-H_5}$ coupling constants.

[1]Authors to whom correspondence should be addressed.

Experimental

Materials

Anisoles

2,4,6-Trinitroanisole (Eastman Kodak) was recrystallized from aqueous methanol and dried *in vacuo*, m.p. 68°. Prepared and purified as previously described were 2,6-dinitroanisole (m.p. 118°) (16) and the following 4-X-2,6-dinitroanisoles: 4-chloro (m.p. 65°) (17), 4-cyano (m.p. 114°) (9, 18), 4-fluoro (m.p. 83°) (19), 4-trifluoromethyl (m.p. 60°) (20), 4-benzoyl (m.p. 107°) (21, 22).

4-Trifluoromethylsulfonyl-2,6-dinitroanisole was prepared by adding dropwise a mixture of 4 ml of fuming nitric acid (density 1.52) and 4 ml of concentrated sulfuric acid to a stirred and cooled (*ca.* 20°) solution of 500 mg 4-trifluoromethylsulfonyl-2-nitroanisole (23) in 4 ml concentrated sulfuric acid. The reaction mixture was heated slowly to 70° and maintained at 70–80° for 2 h. After cooling to room temperature, the solution was poured onto crushed ice (100 g) and the precipitated dinitro compound was filtered, washed with cooled water, recrystallized from carbon tetrachloride or chloroform, and dried *in vacuo*, m.p. 59°.

Anal. Calcd. for $C_8H_5F_3N_2O_7S$: C, 29.10; H, 1.52; N, 8.48; S, 9.68. Found: C, 29.54; H, 1.79; N, 8.59; S, 9.39.

The same procedure was used to prepare 4-methylsulfonyl-2,6-dinitroanisole from 4-methylsulfonyl-2-nitroanisole except that the reaction mixture was stirred at 50° for 1 h and the white crystals formed were recrystallized from methanol, m.p. 206°.

Anal. Calcd. for $C_8H_8N_2O_7S$: C, 34.79; H, 2.92; N, 10.14; S, 11.60. Found: C, 34.58; H, 3.25; N, 9.98; S, 11.67.

Isolable 1,1-Complexes

Potassium 1,1-dimethoxy-2,4,6-trinitro- or -4-cyano-2,6-dinitrocyclohexadienates were prepared as previously described by the addition of nearly 1 equiv of 5.85 *M* methanolic potassium methoxide to a solution of corresponding anisoles in a mixture of methanol and dioxane (9). The same procedure was used to prepare analogous adducts from 4-methylsulfonyl and 4-benzoyl-2,6-dinitroanisoles. Since these salts contained some dioxane of crystallization (9) the analyses were found to be rather poor, but their purity was greater than 98% by n.m.r. integration.

Because of its very high stability, we succeeded in preparing potassium 1,1-dimethoxy-4-trifluoromethylsulfonyl-2,6-dinitrocyclohexadienate by the addition of nearly 1 equiv of 1 *M* methanolic potassium methoxide to a solution of the parent molecule (100 mg) in a minimum amount of methanol. The reaction mixture turned immediately deep orange and was allowed to stand at room temperature for 15 min. Then, the solvent was removed under vacuum and the residue, collected as an orange solid, washed with dry benzene (or anhydrous ether), and dried *in vacuo* to constant weight in order to eliminate any associated solvent.

Anal. Calcd. for $C_9H_8F_3KN_2O_8S$: C, 27.00; H, 2.01; N, 7.00; S, 8.01. Found: C, 26.89; H, 2.15; N, 7.05; S, 8.22.

Nuclear Magnetic Resonance Measurements

N.m.r. spectra at 60 MHz were obtained with a Varian A-60 spectrometer at 37° (probe temperature) or between 20 and 25°, using TMS as an internal standard. Chemical shift data were taken from spectra determined at a sweep width of 500 Hz.

The transient 1,3-complexes were generated *in situ* by a dropwise addition of 5.85 *M* methanolic potassium methoxide to solutions of anisoles **1** in DMSO-d_6 (*ca.* 40 mg **1** in 0.6 ml $(CD_3)_2SO$). The spectrum of solutions was determined rapidly after each addition of methoxide ion and scanned repeatedly until no further changes were observed. After the addition of 1 equiv of base, the spectra consisted only of the signals associated with 1,1-complexes **3** and generally remained unchanged for several hours. The half-time of the transient species was often too short for an accurate determination of the $^4J_{H_3-H_5}$ coupling constant, whose order of magnitude, however, has been indicated.

In order to investigate ^{13}C satellites of anisoles and 1,1-complexes the spectra of these compounds were also recorded at 100 Hz on a Varian XL-100-12 spectrometer at the probe temperature (32°) and using TMS for field/frequency lock. ^{13}C satellites of ring protons and methoxyl protons were observed respectively from spectra at sweep widths of 250 and 500 Hz, using various sweep times.

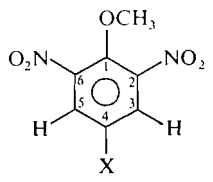

1

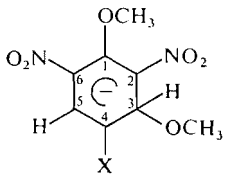

2

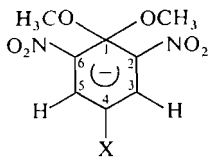

3

Results and Discussion

1,3-Dimethoxy-4-X-2,6-dinitrocyclohexadienates (1,3-Complexes, 2)

Addition of a drop of 5.85 *M* methanolic potassium methoxide to solutions of 4-X-2,6-dinitroanisoles **1** (X = Cl, CO—C_6H_5, CF_3, SO_2CH_3, SO_2CF_3) in DMSO-d_6 results in an immediate decrease in the intensity of the signals due to **1** and the appearance of a transient two proton AX system with weak coupling constant ($^4J_{H_3-H_5}$ = 1.3–1.8 Hz) and two transient methoxyl singlets at higher field (Fig. 1).

Whereas the lower field doublet is consistent with the sp^2 hybrid environment for the proton H-5 of the 1,3-complexes **2**, the higher field doublet is attributed to the proton H-3 attached to the sp^3 hybridized carbon. Similar conclusions can be drawn from a comparison of the chemical shifts of the lower and the higher field

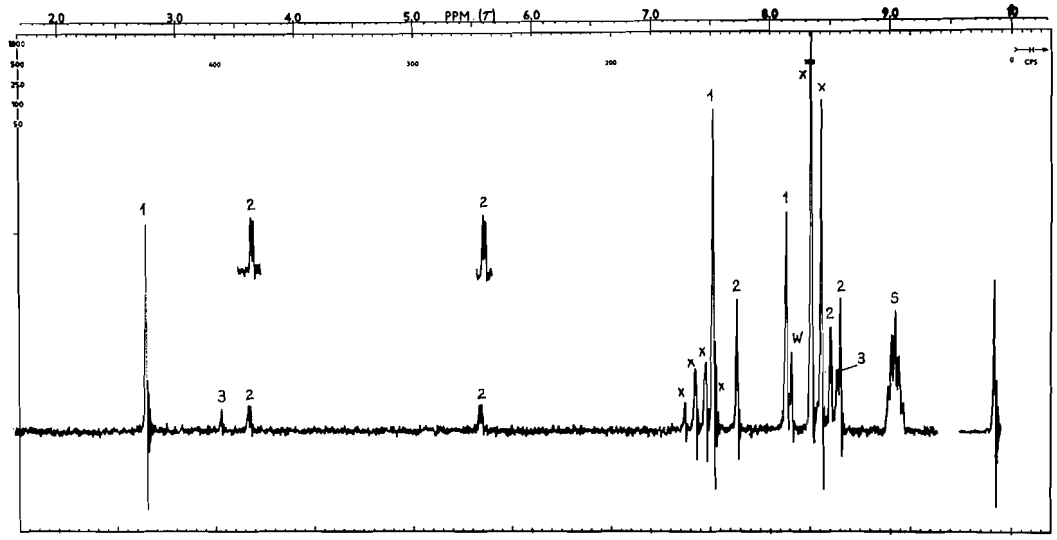

FIG. 1. The n.m.r. spectrum (60 MHz) for the reaction of methoxide ion with 4-methylsulfonyl-2,6-dinitroanisole in DMSO-d_6. Resonance of anisole, 1,3- and 1,1-complexes are identified with structure numbers **1**, **2**, **3**. Other resonances: s, solvent; x, methanol; w, H_2O.

TABLE 1. N.m.r. parameters (60 MHz) for transient 1,3-dimethoxy-2,6-dinitro-4-X-substituted cyclohexadienates **2** (solvent: DMSO-d_6)

	Cl							NO_2					
X	*a*	*b*	$CO—C_6H_5$ [c]	CF_3 [d]	CN [e]	SO_2CH_3 [d]	SO_2CF_3 [c]	*a*	*f*	*g*	*h*	*e*	*b*
$\delta_{OCH_3(1)}$ [j]	3.82	3.81	3.84	3.86	3.78	3.83_7	3.90	3.82	3.85	3.45	3.85	3.47	3.83
$\delta_{OCH_3(3)}$ [j]	3.12	3.10	3.14_6	—	3.08	3.05_3	—	3.17_5	3.20	3.20	3.18	3.18	3.17
$\delta_{H(3)}$ [j]	5.45	5.45	6.04_5	5.70	5.48	5.98	5.83	6.11	6.17	6.17	6.15	6.17	6.13
$\delta_{H(5)}$ [j]	7.13	7.17	7.76_6	7.65	7.75	7.94_4	8.21_3	8.42	8.42	8.42	8.47	8.41	8.48
$^4J_{H_3-H_5}$ [i,k]	1.3	1.5	1.4			1.3	1.8	1.9_5					

[a] At 100 MHz, temperature 32 °C.
[b] Reference 24, temperature 15 °C.
[c] Temperature 37 °C.
[d] Temperature 20–25 °C.
[e] Reference 9, temperature 25 °C.
[f] Reference 1, temperature 30 °C.
[g] Reference 2, temperature 30 °C.
[h] Reference 5, temperature 33.5 °C.
[i] The sign of this coupling constant is unknown.
[j] In p.p.m.
[k] In Hz.

singlets which are assigned respectively to the methoxyl protons of the sp^2 C-1 and the sp^3 C-3 carbons of **2**. Unfortunately, we were not always able to identify both of these methoxyl singlets because of resonances of methanol appearing in the same region of the spectrum.

In agreement with recent kinetic studies (11), this set of transient signals disappears more quickly with decreasing electron-withdrawing power of the substituent X and we detect concurrently the signals due to the formation of the 1,1-complexes **3**. Similar behavior is observed with the addition of a second drop of potassium methoxide, but as soon as the amount of base reaches 1 equiv, only the signals associated with 1,1-complexes **3** can be seen in the spectrum.

The results are summarized in Table 1 which also includes those previously reported for 4-cyano-2,6-dinitroanisole (9) and 2,4,6-trinitroanisole (1, 2, 5, 9, 24). The results for the

chloro derivative are in agreement with those recently published by Crampton *et al.* (24). Concerning 2,4,6-trinitroanisole, it must be noted that the literature indicated very different values for the chemical shift of the methoxyl group on the sp^2 C-1 of the 1,3-complex. As can be seen from Table 1, the values reported by Servis (1), Foster *et al.* (5) and Crampton *et al.* (24) appear consistent with the observed influence of the substituent X on this chemical shift, as opposed to the values reported by Servis (2) and Fendler *et al.* (9). Indeed, by reinvestigating the reaction of CH_3O^- ions with 2,4,6-trinitroanisole, at 100 MHz, we found a value in good agreement with the results of Crampton *et al.* (24).

We were not able to detect by n.m.r. the 1,3-complex from 4-fluoro-2,6-dinitroanisole, although we did succeed in identifying it kinetically (12). The corresponding spectrum appeared broadened, thus suggesting the presence of free radicals. A similar situation was recently encountered with 2-fluoro-4,6-dinitroanisole, and in this case, an e.p.r. signal was detected (25).

With the exception of 1,3-dimethoxy-2,4,6-trinitrocyclohexadienate, the chemical shift of the H-5 proton in 1,3-complexes **2** is found to increase roughly as a function of the Hammett σ_R constant of the substituent X, thus suggesting that the delocalization of the negative charge in **2** occurs mainly through the resonance structure **4**. Indeed, this result is not unexpected because it is in agreement with the very high capacity to resonance of a para nitro group (9, 26, 27). The abnormal behavior of the trinitro derivative with respect to this series would be due to the fact that, if $X = NO_2$, the contribution of the resonance structure **5** should not be neglected.

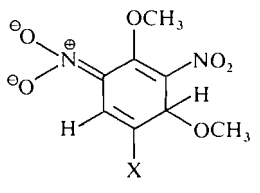

4

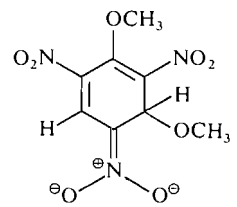

5

4-X-2,6-Dinitroanisoles and 1,1-Dimethoxy-4-X-2,6-dinitrocyclohexadienates

In order to observe ^{13}C satellites, the proton spectra of anisoles and isolable 1,1-complexes ($X = CO—C_6H_5$, CN, SO_2CH_3, NO_2, SO_2CF_3) were recorded at 100 MHz by using somewhat concentrated solutions in DMSO-d_6 (about 100 mg **1** or **3** in 0.6 ml $(CD_3)_2SO$). ^{13}C satellites could also be observed in the 4-trifluoromethyl-1,1-complex ($X = CF_3$) generated *in situ*, but similar attempts with fluoro and chloro derivatives were unsuccessful.

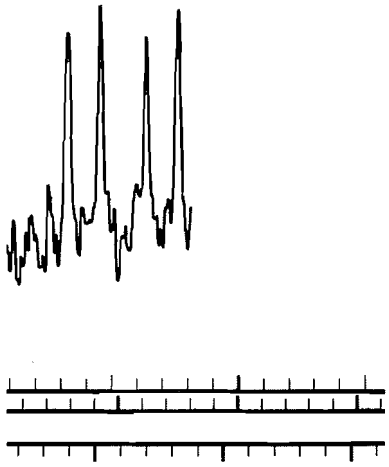

FIG. 2. The downfield ^{13}C satellite of the ring protons of 4-fluoro-2,6-dinitroanisole (100 MHz).

The ^{13}C satellites of methoxyl protons in **1** and **3** consist of a doublet, thus giving directly $^1J_{^{13}C-H}$. On the other hand, the ^{13}C satellites of the two equivalent ring protons H-3,5 in **1** and **3** consist of two doublets (and two quadruplets if X = F, Fig. 2). The two ring protons H-3,5 and the ^{13}C nucleus constitute an AA'X system, which depends on the relative values of $^1J_{^{13}C-H}$, $^3J_{^{13}C-H}$ and $^4J_{H_3-H_5}$. However, as pointed out by Schaefer and co-workers, $^3J_{^{13}C-H}$ and $^4J_{H_3-H_5}$ being much lower than $^1J_{^{13}C-H}$, a first-order analysis neglecting the long range coupling constants gives $^1J_{^{13}C-H}$ with an error of about 0.1 Hz (28).

In agreement with previous findings (29, 30), upfield and downfield positions of the ^{13}C satellites indicate a positive (upfield) ^{13}C isotope effect on the proton chemical shift, of the order of 0.1–0.3 Hz. This effect is small, but it must be noted that the $^1J_{^{13}C-H}$ values which were determined only from the downfield satellites have an additional uncertainty. This was the case for $X = CO—C_6H_5$ in **1** and **3** in which only

TABLE 2. N.m.r. parameters (100 MHz) for anisoles and 1,1-dimethoxy-2,6-dinitro-4-X-substituted cyclohexadienates (solvent: DMSO-d_6)

δ (p.p.m.) and J (Hz)	X	σ-Constants	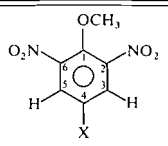	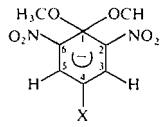
	F	σ_p 0.062 [a]	3.97	—
	Cl	0.227 [a]	3.99	3.04_6 [f]
	$CO—C_6H_5$	0.42 [b]	4.05_2	3.04
	CF_3	0.54 [a]	4.06	3.04_8 [f]
$\delta_{OCH_3(1)}$	CN	0.66 [a]	4.03_5	3.00
	SO_2CH_3	0.72 [a]	4.04	3.00
	NO_2	0.778 [a]	4.09	3.03_4
	SO_2CF_3	0.93 [c]	4.14	3.04_8
	F		148.7	—
	Cl		148.9	—
	$CO—C_6H_5$		149.6	142.5
$^1J_{^{13}C-H}$	CF_3		149.7	142.5 [f]
$[OCH_3]$	CN		149.7	142.6
	SO_2CH_3		149.9	142.3
	NO_2		150.1	143.5
	SO_2CF_3		150.5	143.1_5
	F	σ_R −0.44 [d]	8.34_4 [g]	7.74 [h]
	Cl	−0.24 [d]	8.43_5	7.80_4 [f]
	$CO—C_6H_5$	0.08 [e]	8.55	8.42
	CF_3	0.14 [d]	8.71 [i]	8.11_4 [f,j]
$\delta_{H(3,5)}$	CN	0.07 [d]	8.88	8.05
	SO_2CH_3	0.14 [d]	8.77 [k]	8.18 [l]
	NO_2	0.15 [d]	9.05_7	8.62_4
	SO_2CF_3	0.22 [c]	8.95[m]	8.12 [n]
	F	σ_I 0.50 [d]	174.4	—
	Cl	0.47 [d]	176	—
	$CO—C_6H_5$		172.2 [o]	158.9 [o]
$^1J_{^{13}C-H}$	CF_3	0.41 [d]	173.8	160.4
$[H_{(3,5)}]$	CN	0.59 [d]	177	163.1
	SO_2CH_3	0.59 [d]	175.5	163.2
	NO_2	0.63 [d]	177.9	165.8
	SO_2CF_3	0.69 [c]	177.8	165.1
	F		3.1	—
	Cl		2.6	—
	$CO—C_6H_5$		2.1	2.1
	CF_3		2.4	2.5
$^4J_{H_3-H_5}$	CN		2.1	2.1
	SO_2CH_3		2.3	2.5
	NO_2		2.8	2.8
	SO_2CF_3		2.1	2.3

[a] Reference 31.
[b] Reference 32.
[c] Reference 33.
[d] Reference 34.
[e] Estimated σ_R value for $CO—C_6H_5$ ($\sigma_R \simeq \sigma_p - \sigma_m \simeq 0.08$).
[f] Generated *in situ*.
[g] $|^3J_{F-H}| = 7.6$ Hz; this coupling constant is known to be positive (48).
[h] At 60 MHz. $|^3J_{F-H}| = 8.8$ Hz; this coupling constant is probably positive (25).
[i] $|^4J_{F-H}| = 0.7$ Hz; this coupling constant has been reported to be negative (49).
[j] $|^4J_{F-H}| = 0.4$ Hz; sign unknown.
[k] $\delta_{SO_2CH_3} = 3.40$.
[l] $\delta_{SO_2CH_3} = 2.98_6$.
[m] $|^5J_{F-H}| = 0.5$ Hz; sign unknown.
[n] $|^5J_{F-H}| = 0.5$ Hz; sign unknown.
[o] From low field ^{13}C satellite.

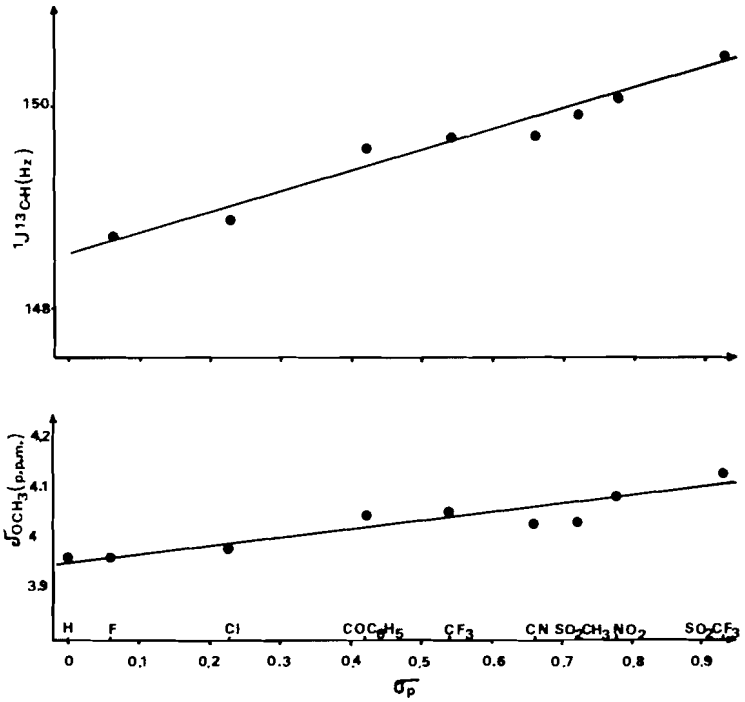

FIG. 3. Plots of δ_{OCH_3} and $^1J_{^{13}C-H}$ of methoxyl protons *vs.* σ_p for 4-X-2,6-dinitroanisoles. The δ value for X = H was taken from ref. 8.

the downfield satellite was observed, the high-field one overlapping with the absorption of the aromatic protons.

The results are listed in Table 2.

4-X-2,6-Dinitroanisoles

As previously observed for monosubstituted anisoles and other systems (35, 36) a rather good linear relationship exists between the Hammett σ_p constant of the substituent X and the chemical shift δ_{OCH_3} as well as the coupling constant $^1J_{^{13}C-H}$ of the methoxyl protons in anisoles **1** (Fig. 3).

Such relations imply that all these 4-X-2,6-dinitroanisoles exhibit a similar geometry at C-2, -1, and -6. More significantly, taking into account the X-ray study reported for 2,4,6-trinitrophenetole (37), it turns out that the methoxyl group lies in the plane of the ring while the nitro groups at the ortho positions are twisted out of this plane.

Furthermore, compared to the value reported for anisole (35) ($^1J_{^{13}C-H}$ = 143 Hz), the value of $^1J_{^{13}C-H}$ appears to be strongly increased. This result can be rationalized by considering the electron-withdrawing capacities of two nitro groups and the X substituent in **1**.

Whereas attempts to correlate the chemical shift of the protons H-3,5 in the ortho positions to X with substituent constants give poor results, the corresponding coupling constant $^1J_{^{13}C-H}$ is found to correlate fairly well with the inductive σ_I constant. This trend indicates that the hybridization of C-3,5 (38) and/or their effective nuclear charge (39) are mainly dependent on the inductive effect of the ortho substituent X.

The value of $^1J_{^{13}C-H}$ for ring protons, higher in anisoles **1** than in benzene (40) ($^1J_{^{13}C-H}$ = 157.5 Hz) appears to be normal, considering the attractive effect of four substituents attached to the ring in **1**.

The meta coupling constant $^4J_{H_3-H_5}$, which is known to be positive (47), varies with the nature of the X substituent from 2.1 Hz (X = SO_2CF_3) to 3.1 (X = F). Castellano and Kostelnik and Schaefer and co-workers have demonstrated the additivity of substituent effects on the proton–proton coupling constants in some di- and tri-substituted aromatic substrates (41, 42). If such an additivity scheme is valid

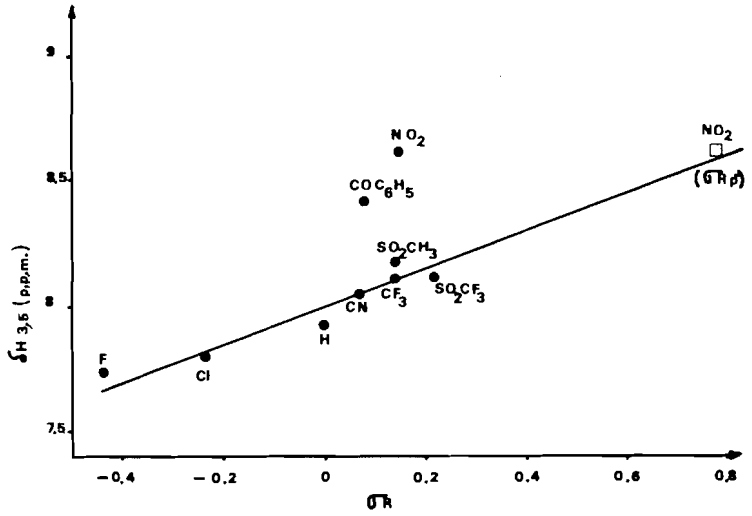

FIG. 4. Plot of $\delta_{H_{3,5}}$ *vs.* σ_R for 1,1-dimethoxy-4-X-2,6-dinitrocyclohexadienates 3. The δ value for X = H was taken from ref. 8.

TABLE 3. Predicted and observed meta coupling constants in 4-X-2,6-dinitroanisoles

X	ΔJ^X_{2-6}	J^m_{3-5} (predicted)	J^m_{3-5} (experimental)	Difference
Cl	0.88	2.20	2.6	-0.4_0
NO_2	1.03	2.35	2.8	-0.4_5
F	1.37	2.69	3.1	-0.4_1

for tetrasubstituted derivatives, such as 4-X-2,6-dinitroanisoles, J^m_{3-5} would be deduced from eq. 1 where J^B_m is the unperturbed coupling

[1] $$J_m = J_{3-5} = J^B_m + \Delta J^{OCH_3}_{3-5} + 2\Delta J^{NO_2}_{2-4} + \Delta J^X_{2-6}$$

constant in benzene and ΔJ values for the substituents are derived from the corresponding monosubstituted aromatic compounds. The ΔJ values are known for Cl, F, NO_2 (42); for OCH_3, it can be deduced from J_m in anisole (43, 44).

As can be seen from Table 3, the predicted values are lower than the experimental ones, but their difference is found to be nearly constant in these three cases. However, changing the substituent X from Cl to NO_2 or F causes a similar increase in ΔJ^X_{2-6} and in the experimental values of J^m_{3-5}. Although the solvent is different, this suggests that the failure of Schaefer's additivity scheme to reproduce J^m_{3-5} in 4-X-2,6-dinitroanisoles arises from the twisting of the nitro groups at C-2 and -6 out of the plane of the ring. Such a twisting would make $\Delta J^{NO_2}_{2-4}$ less negative in eq. 1, thus increasing the value of J^m_{3-5}.

1,1-Dimethoxy-4-X-2,6-dinitrocyclohexadienates (1,1-Complexes, 3)

As could be expected from the tetragonal hybridization of C-1, the chemical shift of methoxyl protons in 1,1-complexes 3 is relatively insensitive to the nature of the X substituent.

On the other hand, except for the nitro and benzoyl groups, a fairly good linear relationship is observed between chemical shift of the H-3,5 protons attached to sp^2 carbons and the Hammett σ_R constant (Fig. 4). Although these chemical shifts could be influenced by the

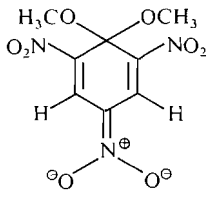

6

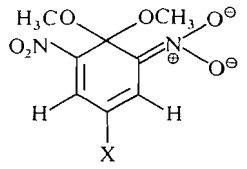

7

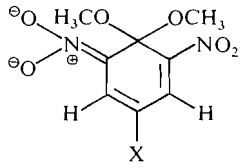

8

anisotropic effects of the substituent, it must be pointed out that the use of the $\sigma_{R_p^-}$ constant (0.78) for the nitro group (45) allows the corresponding value of $\delta_{H_{3,5}}$ to be placed on the linear graph. This result suggests, in agreement with LCAO calculations previously reported by Zollinger and co-workers (27), that the nitro group para to C-1 carries a very large portion of the negative charge in the 1,1-complex derived from 2,4,6-trinitroanisole (resonance structure **6**). In the other 1,1-complexes, delocalization through resonance structures **7** and **8** should not be negligible.

The coupling constant $^1J_{^{13}C-H}$ in **3** changes according to a similar sequence to that found in anisoles **1**, *i.e.* increases with increasing values of σ_I.

In addition, as already observed for 1,1-complexes of 2-X-4,6-dinitroanisoles (25), the magnitude of the coupling $^4J_{H_3-H_5}$ appears to be very close to that found in molecules **1**, thus suggesting that the geometry of the ring at C-3, -4, and -5 is similar in **3** and **1**. This result is consistent with crystallographic studies of 2,4,6-trinitrophenetole and the corresponding diethoxy-1,1-complex (37, 46).

1. K. L. SERVIS. J. Am. Chem. Soc. **87**, 5495 (1965).
2. K. L. SERVIS. J. Am. Chem. Soc. **89**, 1508 (1967).
3. M. R. CRAMPTON and V. GOLD. J. Chem. Soc. B, 893 (1966).
4. R. FOSTER and C. A. FYFE. Rev. Pure and Appl. Chem. **16**, 61 (1966).
5. R. FOSTER, C. A. FYFE, P. H. EMSLIE, and M. I. FOREMAN. Tetrahedron, **23**, 227 (1967).
6. E. BUNCEL, A. R. NORRIS, and K. E. RUSSELL. Q. Rev. **22**, 123 (1968).
7. M. R. CRAMPTON. Adv. Phys. Org. Chem. 7, 211 (1969).
8. M. J. STRAUSS. Chem. Rev. **70**, 667 (1970).
9. J. H. FENDLER, E. J. FENDLER, and C. E. GRIFFIN. J. Org. Chem. **34**, 689 (1969).
10. P. BEMPORAD, G. ILLUMINATI, and F. STEGEL. J. Am. Chem. Soc. **91**, 6742 (1969).
11. F. MILLOT and F. TERRIER. Bull. Soc. Chim. Fr. 2692 (1969).
12. F. TERRIER and F. MILLOT. Bull. Soc. Chim. Fr. 1743 (1970).
13. F. TERRIER, C. DEARING, and R. SCHAAL. Reaction transition states. Proceedings of the 21st meeting of the Société de Chimie Physique. *Edited by* Gordon and Breach. London. 1972.
14. F. TERRIER, A. P. CHATROUSSE, and R. SCHAAL. J. Org. Chem. In press.
15. F. MILLOT, J. MOREL, and F. TERRIER. C. R. Acad. Sc. Paris, **274C**, 23 (1972).
16. A. F. HOLLEMAN and R. TER WEEL. Rec. Trav. Chim. Pays-Bas, **35**, 50 (1916).
17. M. KOHN and R. KRAMER. Monatsh. Chem. **49**, 154 (1928).
18. J. J. BLANSKMA and C. H. WITTE. Rec. Trav. Chim. Pays-Bas, **60**, 811 (1941).
19. G. SCHIEMANN and T. B. MIAU. Ber. **66**, 1179 (1933).
20. L. M. YAGUPOLSKII and V. S. MOSPAN. Ukrain. Khim. Zhur. **21**, 818 (1955).
21. F. ULLMANN. Ann. **366**, 92 (1909).
22. W. BLAKEY, W. I. JONES, and H. A. SCARBOROUGH. J. Chem. Soc. 2865 (1927).
23. L. M. YAGUPOLSKII and M. S. MARENETS. Zh. Obsch. Khim. **29**, 278 (1959).
24. M. R. CRAMPTON, M. A. ELGHARIANI, and H. A. KJAN. Chem. Commun. 834 (1971).
25. F. TERRIER, J. C. HALLE, and M. P. SIMONNIN. Org. Mag. Res. **3**, 361 (1971).
26. C. F. BERNASCONI. J. Am. Chem. Soc. **92**, 4682 (1970); **93**, 6975 (1971).
27. P. CAVENG, P. B. FISHER, E. HEILBRONNER, A. L. MILLER, and H. ZOLLINGER. Helv. Chim. Acta, **50**, 848 (1967).
28. H. M. HUTTON, W. F. REYNOLDS, and T. SCHAEFER. Can. J. Chem. **40**, 1758 (1962).
29. J. M. READ, JR., R. W. CRECELY, and J. H. GOLDSTEIN. J. Mol. Spectrosc. **25**, 107 (1968).
30. L. R. WOMBLE and G. B. SAVITSKY. J. Magn. Res. **4**, 226 (1971).
31. C. G. SWAIN and E. C. LUPTON. J. Am. Chem. Soc. **90**, 4328 (1968).
32. O. EXNER and E. SVATEK. Coll. Czechoslov. Chem. Commun. **36**, 534 (1971).
33. W. SHEPPARD. J. Am. Chem. Soc. **85**, 1314 (1963).
34. R. W. TAFT. J. Am. Chem. Soc. **79**, 1045 (1957).
35. C. H. YODER, R. H. TUCK, and R. E. HESS. J. Am. Chem. Soc. **91**, 539 (1969).
36. F. W. WEHRLI, W. GIGER, and W. SIMON. Helv. Chim. Acta, **54**, 229 (1971).
37. C. M. GRAMMACCIOLI, R. DESTRO, and M. SIMONETTA. Acta Cryst. **B24**, 129 (1968).
38. J. N. SHOOLERY. J. Chem. Phys. **31**, 1427 (1959).
39. D. M. GRANT and W. M. LITCHMAN. J. Am. Chem. Soc. **87**, 3994 (1965).
40. F. J. WEIGERT and J. D. ROBERTS. J. Am. Chem. Soc. **89**, 2967 (1967).
41. S. CASTELLANO and R. KOSTELNIK. Tetrahedron Lett. 5211 (1967).
42. T. SCHAEFER, G. KOTOWYCZ, H. M. HUTTON, and J. W. S. LEE. Can. J. Chem. **46**, 2531 (1968).
43. S. CASTELLANO, C. SUN, and R. KOSTELNIK. Tetrahedron Lett. 5205 (1967).
44. M. D. STEPHENS, J. D. REINHEIMER, and A. H. KAPPELMAN. Can. J. Chem. **49**, 3759 (1971).
45. D. J. CRAM. Fundamentals of carbanion chemistry. Academic Press, Inc., New York. 1965. p. 58.
46. R. DESTRO, C. M. GRAMMACCIOLI, and M. SIMONETTA. Acta Cryst. **B24**, 1369 (1968).
47. J. W. EMSLEY, J. FEENEY, and L. H. SUTCLIFFE. High resolution nuclear magnetic resonance spectroscopy. Pergamon Press, Oxford. 1965. p. 772.
48. P. DIEHL and C. L. KHETRAPAL. NMR-Basic principles and progress. Vol. 1. Springer-Verlag, Berlin. 1969. p. 64.
49. D. J. BLEARS, S. S. DANYLUK, and T. SCHAEFER. Can. J. Chem. **46**, 652 (1968).

Can. J. Chem. Downloaded from www.nrcresearchpress.com by 210.87.254.105 on 09/05/12
For personal use only.

A Nuclear Magnetic Resonance Study of Norbornadiene Partially Oriented in a Nematic Phase

E. E. BURNELL[1] AND P. DIEHL

Department of Physics, University of Basel, Basel, Switzerland

Received May 10, 1972

The n.m.r. spectrum of norbornadiene partially oriented in a nematic phase has been measured, and the geometry of the proton skeleton has been determined. The results are compared with several electron diffraction studies, and are only consistent with those in which the angle $C_1C_7C_4$ is approximately 92°.

Nous avons analysé le spectre r.m.n. du norbornadiène partiellement orienté dans une phase nématique en vue de déterminer la géométrie du squelette protoné. Les résultats ont été comparés à ceux obtenus dans plusieurs études utilisant la diffraction des électrons et concordent uniquement lorsque l'angle $C_1C_7C_4$ vaut approximativement 92°.

Canadian Journal of Chemistry, **50**, 3566 (1972)

Introduction

Small ring cyclic molecules have been of special interest to the theoretical chemist because of their strained geometries. Among this group is norbornadiene (Fig. 1). Many electron diffraction studies have been carried out to determine the molecular geometry (1–5), but this method is inaccurate in the determination of proton coordinates. In addition, Yokozeki and Kuchitsu (5) find that the angle $C_1C_7C_4$ cannot be determined with precision (see caption to Fig. 1). A further difficulty with the electron diffraction studies is that they are not consistent within themselves.

Molecules oriented in nematic solvents give accurate information about the relative proton coordinates (6). Thus, a study of norbornadiene was carried out in an attempt to determine which of the electron diffraction studies is the most plausible, and to obtain values of the angles containing protons. The various effects of nuclear motions (7) are neglected.

Experimental

A spectrum (Fig. 2) of 19 mol % norbornadiene oriented in the nematic phase of *N*-(*p*-ethoxybenzylidene)-*p'*-*n*-butylaniline was recorded on a Varian HR-220 spectrometer

[1]Permanent address: Chemistry Department, University of British Columbia, Vancouver 8, British Columbia.

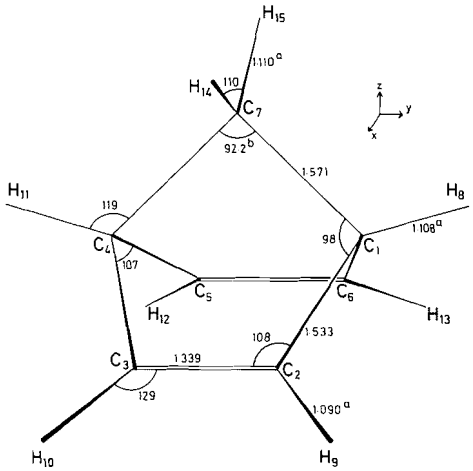

FIG. 1. Norbornadiene (bicyclo [2.2.1] hepta-2,5-diene). The angles (in degrees) and the bond lengths (in Å) are obtained from a combination of the electron diffraction data of case I of ref. 5, and the present n.m.r. study (see text). ⊖, the angle between the $C_1C_2C_3C_4$ plane and the $C_1C_6C_5C_4$ plane, is 114.7°. The angle that the $C_2C_3H_{10}H_9$ plane is bent from the $C_1C_2C_3C_4$ plane is 4°, H_9 and H_{10} moving in the negative *z* direction.

(*a*) Values recalculated from least squares fit (see text). The electron diffraction values are $r_{1,8} = r_{7,15} = 1.109$ Å; $r_{2,9} = 1.0896$ Å (assumed).

(*b*) For the angle $C_1C_7C_4$, other electron diffraction studies give: $96.7 \pm 2.3°$ (1); 96.5° (2); $92.0 \pm 0.8°$ (3); $99.5 \pm 0.6°$ (and other cases, but always >96°) (4); $96.0 \pm 0.2°$ and $94.1 \pm 3.0°$ (5).

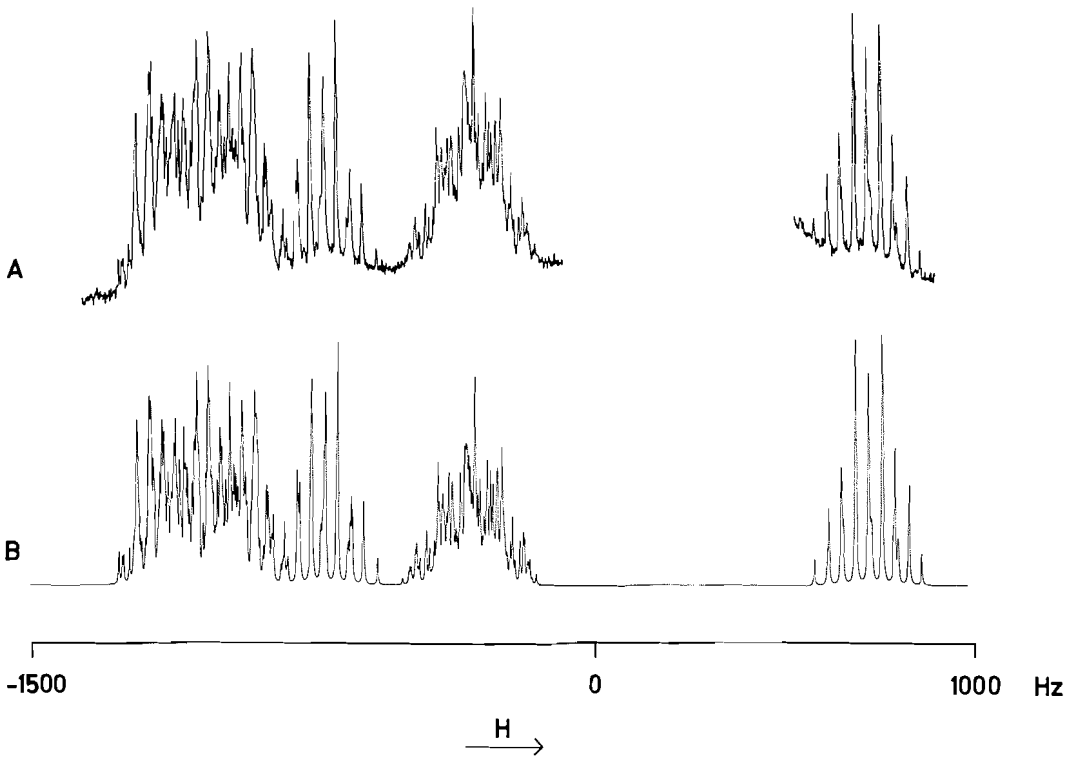

FIG. 2. Observed (A) and calculated (B) 220 MHz n.m.r. spectrum of partially oriented norbornadiene. Concentration 19 mol %; temperature ~ 25 °C; linewidth of (B) = 3 Hz.

operated in the frequency swept mode using a capillary of tetramethylsilane for field-frequency lock. The probe temperature was ~ 25 °C, and rapid spinning was used (8). The sample was left spinning in the probe for approximately 16 h to reach temperature equilibrium. The spectrum, with a linewidth of 3–4 Hz, was run at a scale of 1 Hz = 0.2 mm, and was analyzed with the iterative program LAOCOONOR (9) fitting 125 of 150 observed lines to 304 transitions with an r.m.s. error of 0.9 Hz after two iterations. The spectral parameters obtained are in Table 1.

Results and Discussion

Because of the relatively small orientation of the solute the spectrum appears as distinct groups. These groups also appear at 56.4 and 100 MHz with some overlap; however, only the 220 MHz spectrum had sufficient resolution for an analysis. Consequently, for couplings between chemically shifted nuclei, the spectrum is only sensitive to the sum of $2\,D_{ij} + J_{ij}$. The values and signs of the J_{ij} have, when possible, been taken from the literature (10, 11). The signs of the J_{ij} in Table 1 seem reasonable.

TABLE 1. 220 MHz n.m.r. parameters (in Hz) of partially oriented norbornadiene*

$D_{8,9}$	-34.8 ± 0.1	$J_{8,9}$	(2.85)†
$D_{8,10}$	2.9 ± 0.1	$J_{8,10}$	(0.99)†
$D_{8,11}$	9.5 ± 0.1	$J_{8,11}$	(1.85)†
$D_{8,14}$	33.7 ± 0.1	$J_{8,14}$	(1.65)‡
$D_{9,10}$	37.6 ± 0.1	$J_{9,10}$	(5.28)†
$D_{9,12}$	-16.4 ± 0.1	$J_{9,12}$	(0)†
$D_{9,13}$	-51.2 ± 0.1	$J_{9,13}$	(0)†
$D_{9,14}$	35.7 ± 0.2	$J_{9,14}$	(0)†
$D_{9,15}$	-0.8 ± 0.2	$J_{9,15}$	(0)†
$D_{14,15}$	-475.9 ± 0.1	$J_{14,15}$	(−12)§
$\nu_{14} - \nu_8$	334.9 ± 0.1		
$\nu_{14} - \nu_9$	1040.2 ± 0.1		

*Errors are standard deviations from LAOCOONOR (9); Values in brackets are assumed.
†From ref. 10.
‡From ref. 11.
§$J_{14,15}$ has a negligible effect on the spectrum.

In principle, the signs of the J_{ij} could be determined by studying a spectrum with a different (preferably larger) orientation.

Can. J. Chem. Downloaded from www.nrcresearchpress.com by 210.87.254.105 on 09/05/12
For personal use only.

TABLE 2. Structural parameters of norbornadiene*

	Case A †	Case B ‡
x (8) Å	(0)	(0)
y (8) Å	(2.192)	(2.157)
z (8) Å	1.613±0.003	1.645±0.011
x (9) Å	1.913±0.003	1.930±0.007
y (9) Å	1.354±0.002	1.359±0.004
z (9) Å	(0)	(0)
x (14) Å	0.910±0.0015	0.918±0.003
y (14) Å	(0)	(0)
z (14) Å	3.017±0.010	3.01 ±0.04
S_{xx}	0.0239±0.0001	0.0245±0.0003
S_{zz}	−0.0176±0.0001	−0.0182±0.0002
Weighted r.m.s. error	0.2 Hz	0.13 Hz

*Values in brackets are assumed. The scale is from the least squares fit to the electron diffraction data of case I of ref. 5.

†Case A: Results using weighting factors from the errors of Table 1.

‡Case B: The D_{ij} are given the weights from a calculation of LAOCOONOR where the J_{ij} were also varied. Consequently, $D_{8,9}$, $D_{8,10}$, $D_{8,14}$, $D_{9,14}$, and $D_{9,15}$ have much less weight than in case A.

The relative proton geometry was obtained with the iterative weighted least squares program SHAPE (12), and results are in Table 2 (case A). The weighted r.m.s. error of the experimental and recalculated D_{ij} was 0.2 Hz. However, because the signs of the J_{ij} may be incorrect, another solution is sought and found (case B, Table 2, weighted r.m.s. error = 0.13 Hz) when the D_{ij} are given weights from a calculation with LAOCOONOR where all the J_{ij} are varied. Thus, the D_{ij} between chemically shifted protons are given a much lower weight in the least squares calculation than the remaining D_{ij}. This solution is close to that found when $J_{8,14}$ is set negative.

Because of the two possible solutions, and because of the range of the diffraction data (1–5), it seemed valuable to "fit" our relative proton coordinates to the carbon coordinates of the various electron diffraction studies; this "fit" is a function of the two following parameters: (*i*) the scaling factor for the proton skeleton, and (*ii*) the height of the $C_2C_3C_5C_6$ plane above the $H_9H_{10}H_{12}H_{13}$ plane. We use an iterative least squares procedure, minimizing the difference between experimental and calculated C—H bond lengths, while keeping constant the carbon and the relative proton coordinates. With case A of Table 2, only when the angle $C_1C_7C_4$ is approximately 92° (ref. 3 and case I of ref. 5; see Fig. 1) are reasonable recalculated C—H bond lengths obtained from the least squares "fit". For the other electron diffraction studies, angle $C_1C_7C_4$ is larger than 92° (see Fig. 1), and the recalculated value of r_{18} is too short. To obtain plausible recalculated C—H bond lengths with the solution of case B, angle $C_1C_7C_4$ would have to be even smaller (~90°). Therefore we choose case A, Table 2, as the acceptable proton geometry. Consequently the acceptable electron diffraction studies are ref. 3 and case I of ref. 5. Figure 1 gives the result of combining our case A with the electron diffraction of case I of ref. 5. Errors are not quoted because of the neglect of the various effects of nuclear motions (7). A more reliable solution might be obtainable by analyzing the n.m.r. and electron diffraction spectra simultaneously.

We thank Mr. A. Frey of the E.T.H., Zürich, for the use of the Varian HR-220 spectrometer, and Dr. P. M. Henrichs for taking additional spectra at 56.4 MHz. The authors are grateful to the Swiss National Foundation for the Advancement of Science for financial support.

1. V. SCHOMAKER, and W. C. HAMILTON. Unpublished research, *Cited in* W. G. WOODS, R. A. CARBONI, and J. D. ROBERTS. J. Am. Chem. Soc. **78**, 5653 (1956).
2. T. W. MUECKE and M. I. DAVIS. Trans. Am. Crystallogr. Assoc. **2**, 173 (1966).
3. Y. MORINO, K. KUCHITSU, and A. YOKOZEKI. Bull. Chem. Soc. Jap. **40**, 1552 (1967).
4. G. DALLINGA and L. H. TONEMAN. Rec. Trav. Chim. **87**, 805 (1968).
5. A. YOKOZEKI and K. KUCHITSU. Bull. Chem. Soc. Jap. **44**, 2356 (1971).
6. P. DIEHL and C. L. KHETRAPAL. N.M.R.—Basic principles and progress. Vol. 1. Springer-Verlag. 1969.
7. A. D. BUCKINGHAM, E. E. BURNELL, and C. A. DE LANGE. Mol. Phys. **16**, 299 (1969).
8. A. D. BUCKINGHAM, E. E. BURNELL, and C. A. DE LANGE. Mol. Phys. **15**, 285 (1968).
9. P. DIEHL, C. L. KHETRAPAL, and H. P. KELLERHALS. Mol. Phys. **15**, 333 (1968).
10. E. W. GARBISCH. Chem. Commun. 332 (1968) and refs. therein.
11. F. S. MORTIMER. J. Mol. Spectrosc. **3**, 528 (1959).
12. P. DIEHL, P. M. HENRICHS, and W. NIEDERBERGER. Mol. Phys. **20**, 139 (1971).

Can. J. Chem. Downloaded from www.nrcresearchpress.com by 210.87.254.105 on 09/05/12
For personal use only.

Two Diastereomeric Oxalatobis(*S*-butane-1,3-diamine)cobalt(III) Complexes

M. PARRIS,[1] L. J. DEHAYES, AND D. H. BUSCH
Chemistry Department, The Ohio State University, Columbus, Ohio

Received June 28, 1972

A study of the oxalatobis(*S*-butane-1,3-diamine)cobalt(III) system shows that the dissymmetric ligand imposes uniquely related geometric and configurational selectivity. The selectivity is in agreement with conformational prediction and the magnitudes of the Cotton effects lend some support to recently developed sector rules.

L'étude du système oxalatobis (*S*-butane diamine-1,3)cobalt(III) montre que le ligand dissymétrique impose une sélectivité particulière et appropriée dans la géométrie et la configuration. La sélectivité est en accord avec la conformation prévue et les amplitudes des effets Cotton viennent à l'appui des règles de secteur développées récemment. [Traduit par le journal]

Canadian Journal of Chemistry, **50**, 3569 (1972)

Can. J. Chem. Downloaded from www.nrcresearchpress.com by 210.87.254.42 on 09/05/12
For personal use only.

During the course of an investigation into stereochemistry of the bis and tris(butane-1,3-diamine)cobalt(III) complexes, it had appeared initially that there was little stereoselectivity evidenced by this ligand in forming its *cis* complexes. The absence of stereoselectivity is more apparent than real, however, and a recent report (1) has indicated an analogous situation in the bis(*R*-propylene-diamine)cobalt(III) system which makes an interesting contrast. The following is an account of the findings which lead us to this conclusion.

The apparent circular dichroism of a solution obtained by the action of oxalate ion, under neutral or basic conditions, upon *trans* dichlorobis(*S*-butane-1,3-diamine)cobalt(III) ion is smaller, by a factor of about ten, than that of the oxalatobis(trimethylenediamine)cobalt(III) complex which has been obtained (2) as its pure enantiomer. The steric requirements of the *cis* bis(*S*-butane-1,3-diamine) system indicate that there are *two* preferred geometric isomers which are illustrated in Fig. 1. Each belongs to the C_2 point group, and, while strictly they are diastereomers, they might be described as *pseudo-enantiomers* insofar as their configurations are concerned. There are other possible geometric isomers containing chair rings but these will lead to increased ligand distortion and their contribution to an equilibrated solution may be neglected. There are additionally isomers containing skew rings, but it has been shown (3) that the chair form of trimethylenediamine is favored over the skew form to the extent of about 1.7 kcal mol^{-1}.

In the *cis* bis(*R*-propylenediamine)cobalt(III) system a diastereomeric mirror image is allowed only at the expense of an unfavorable ring conformation, that is, the favored isomer is $\Delta\lambda\lambda$ (or "lel") and the unfavored is $\Lambda\lambda\lambda$ (or "ob") regardless of which of the two possible geometric isomers with equivalent methyl groups these represent. The equilibrium constant (1) appears to be in the order of 6 which is not incompatible with the value of about 5 obtained for the equivalent ethylenediaminebis(*R*-propylenediamine)cobalt(III) system (4). For the *cis* bis(*S*-butane-1,3-diamine)cobalt(III) system, if the figure of 1.7 kcal is accepted, the same type of change is precluded, for the rings will now be in the chair form. There is no conformational

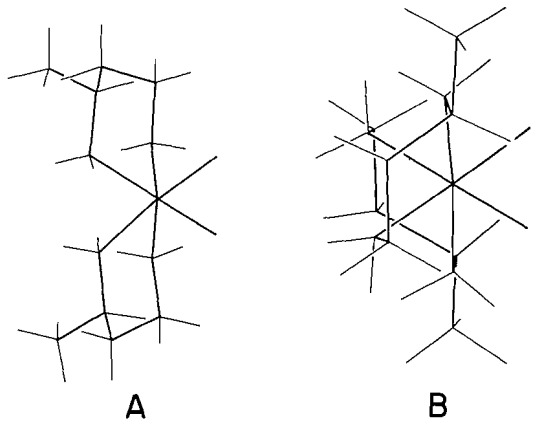

FIG. 1. Configurations of the bis(*S*-butane-1,3-diamine) cobalt(III) isomers: A, Λ; B, Δ.

[1]On sabbatical leave 1970–1971 from the Chemistry Department, Carleton University, Ottawa.

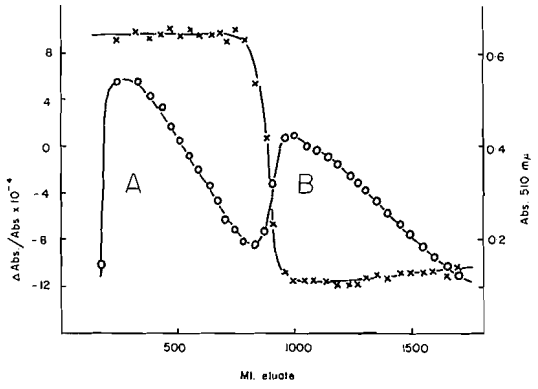

FIG. 2. Ion-exchange separation of the A, B isomers: ○, absorbance at 510 mμ; ×, dissymmetry factor at 510 mμ.

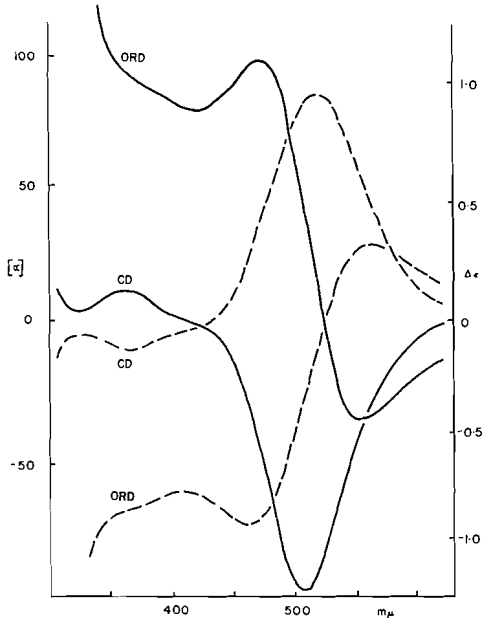

FIG. 3. C.d. and o.r.d. spectra of the A, B isomers: ---, A; —, B.

requirement to favor either Λ or Δ isomer, but it is possible to separate the two *geometric* isomers, each with a preferred absolute configuration, and here there is a marked contrast between the six- and five-membered ring complexes.

Figure 2 illustrates the progress of an ion-exchange separation of two oxalatobis(*S*-butane-1,3-diamine)cobalt(III) isomers from their equilibrium mixture and Fig. 3 shows the c.d. and o.r.d. spectra of the two isolated complexes. The faster-moving isomer, A, shows a positive c.d. in the 500 mμ region and is assigned (5) absolute configuration Λ (as in Fig. 1). Using the apparent differential extinction coefficient of the original solution, $\Delta\varepsilon_{app.} = +0.17$ (510 mμ), together with the observed values for the two separated isomers, $\Delta\varepsilon_A = +0.95$, $\Delta\varepsilon_B = -1.4$, the equilibrium constant is calculated as $K(A/B) = 1.1$, $\Delta G = 0.058$ kcal mol^{-1}.

TABLE 1. Individual contributions (kcal mol^{-1}) to excess free energy for the *cis* dichloro(*S*-butane-1,3-diamine)cobalt(III) isomers

Parameter	Value	
	Isomer A (Λ)	Isomer B (Δ)
Bond stretching	2.67	2.64
Non-bonded interactions	2.62	2.63
Bond angle distortions	6.18	6.18
Torsional distortions	0.19	0.20
Net conformational enthalpy	11.65	11.65
TS	40.35	40.18
Net free energy	−28.70	−28.53

We have carried out an assessment of ΔG using methods of conformational analysis (6–8) recently developed. Table 1 lists individual contributions to a net ΔG of 0.17 kcal mol^{-1}, wholly attributable to the small entropy difference favoring the Λ isomer (A). While the calculations have been carried out for the *cis* dichloro compounds, these results are not expected to be significantly different for the oxalato system.

An interesting feature is the difference in the differential extinction coefficients for the two isomers, +0.95 *vs.* −1.4, whereas $\Delta\varepsilon$ for (+) $[Co(tn)_2ox]^+$ is +1.21. The parent symmetry for these three complexes is C_{2v}, and in this point group the dominant pseudo-scalar function (9, 10) has the form XY, leading to a simple quadrant rule. The methyl groups in *both* isomers lie in negative sectors while the configurational contributions will be positive, for both $\Lambda(bn)_2$ and $\Lambda(tn)_2$ and negative for $\Delta(bn)_2$. Hence the magnitude of the Cotton effect for the trimethylenediamine complex should lie between the magnitudes for the two butane-1,3-diamine complexes as is observed.

Experimental

Butane-1,3-diamine was prepared and resolved by standard methods (11, 12). *Trans* (Co(*S*-butane-1,3-diamine)$_2$

Can. J. Chem. Downloaded from www.nrcresearchpress.com by 210.87.254.42 on 09/05/12
For personal use only.

Cl_2ClO_4 was prepared by an adaptation of Jonassen, Lincoln and Stranks' method (13). A mixture of 1.4 g anhydrous *S*-butane-1,3-diamine and 0.98 g anhydrous $CoCl_2$ in anhydrous ethanol was oxygenated for 4 h. The brown solution was acidified with HCl and dilute $HClO_4$. Fractional crystallization yielded the *trans* dichloro perchlorate as green octahedra, $[\alpha]_D + 8.2°$ ($C = 0.008$ M, nitromethane).

Anal. Calcd. for $C_8H_{12}N_2O_4Cl_3Co$: C, 23.7; H, 5.93; N, 13.8. Found: C, 23.5; H, 6.02; N, 13.7.

Ion-exchange separation of Λ and Δ[Co(*S*-butane-1,3-diamine)ox] oxalates. A solution of *trans*[Co(*S*-bn)$_2$Cl$_2$]-ClO_4 (0.41 g) together with sodium oxalate (1.3 g) in 4 ml H_2O was heated at 50 °C for 30 min. It rapidly developed a pink color, and, after cooling in ice and filtering off excess sodium oxalate, the pink solution was absorbed on a 60 × 1 cm column of Dowex 50W X4 ion-exchange resin (H^+ form). Oxalic acid solution (50 g/l) was used for elution. The components were separated almost completely into two bands and fractions were assessed for optical purity by comparing ratios of $\Delta\varepsilon$ to ε. The separated isomers' solutions were evaporated to small volume and then taken to dryness after filtering off oxalic acid. Extraction with absolute ethanol removed the remaining oxalic acid and the oxalato oxalates were crystallized from water/acetone.

Isomer A (Λ) was contained in the first 750 ml eluate, $[\alpha]_D + 22°$.

Anal. Calcd. for $C_{11}H_{24}N_4O_6Co$: C, 36.0; H, 6.54; N, 15.2. Found: C, 35.8; H, 7.05; N, 15.2.

Isomer B (Δ) was contained in the second 1000 ml eluate, $[\alpha]_D - 29°$.

Anal. Found: C, 36.1; H, 7.70; N, 15.3.

1. R. A. Haines and A. A. Smith. Can. J. Chem. **49**, 3907 (1971).
2. G. R. Brubaker and D. P. Schaefer. Inorg. Chem. **10**, 968 (1971).
3. J. R. Gollogly and C. J. Hawkins. Inorg. Chem. **11**, 156 (1972).
4. T. E. MacDermott. Chem. Commun. 223 (1968).
5. T. E. MacDermott and A. M. Sargeson. Austr. J. Chem. **16**, 334 (1963).
6. R. H. Boyd. J. Chem. Phys. **49**, 2574 (1968).
7. M. R. Snow. J. Am. Chem. Soc. **92**, 3610 (1970).
8. L. J. DeHayes. Ph.D. Dissertation. The Ohio State University, Columbus, Ohio. 1971.
9. F. S. Richardson. J. Phys. Chem. **75**, 692 (1971).
10. J. A. Schellman. J. Chem. Phys. **44**, 55 (1966).
11. T. Kurihara and K. Ro. J. Pharm. Soc. Jap. **75**, 1267 (1955).
12. E. Balieu, P. M. Boll, and E. Larsen. Acta Chem. Scand. **23**, 2191 (1969).
13. I. R. Jonassen, S. F. Lincoln, and D. R. Stranks. Aust. J. Chem. **23**, 2267 (1970).

Can. J. Chem. Downloaded from www.nrcresearchpress.com by 210.87.254.42 on 09/05/12
For personal use only.

Can. J. Chem. Downloaded from www.nrcresearchpress.com by 210.87.254.105 on 09/05/12
For personal use only.

Canadian Journal of Chemistry

Published by THE NATIONAL RESEARCH COUNCIL OF CANADA

VOLUME 50 NOVEMBER 15, 1972 NUMBER 22

The Effect of Aromatic Amines on the Catalyzed Decarboxylation of 3-Oxo-glutaric Acid

K. N. LEONG AND M. W. LISTER

Department of Chemistry, University of Toronto, Toronto, Ontario

Received May 9, 1972

Equilibrium constants have been measured for the formation of MA species, where M is divalent manganese, cobalt, nickel, or zinc, and A^{2-} is the 3-oxo-glutarate ion. Equilibrium constants have also been measured for the reactions $MB^{2+} + A^{2-} \rightleftharpoons MAB$, where B is 2,2′-bipyridyl or 1,10-phenanthroline. These constants were obtained by p*H* measurements at 25 °C and an ionic strength of 0.60. The results are compared with those for similar systems, especially as regards the tendency to form ternary mixed complexes of the type MAB.

The rates of decarboxylation of the various MA and MAB species have been measured. The resulting rate constants follow the Irving–Williams order for stability constants, except that in both MAB species the cobalt compound decomposed slightly faster than the nickel compound. The aromatic base, which had been found earlier to have very little effect in copper complexes, increased the rate constants appreciably with other metals, especially with manganese and zinc. Usually 1,10-phenanthroline has a larger effect than 2,2′-bipyridyl. Some possible explanations of the results are considered.

Nous avons mesuré les constantes d'équilibre dans la formation d'espèces MA, où M est le manganèse, le cobalt, le nickel ou le zinc bivalents et A^{2-}, l'ion 3-oxo-glutarate. Nous avons également mesuré les constantes d'équilibre des réactions $MB^{2+} + A^{2-} \rightleftharpoons MAB$, où B est le 2,2′-bipyridyl ou le 1,10-phénanthroline. Ces constantes furent obtenues au moyen de mesures de p*H* à 25 °C et sous une force ionique de 0.60. Nous comparons les résultats à ceux de systèmes semblables, spécialement en ce qui concerne la tendance à former des complexes ternaires mixtes du type MAB.

Nous avons mesuré les vitesses de décarboxylation des espèces MA et MAB. Les constantes de vitesse obtenues suivent l'ordre d'Irving–Williams des constantes de stabilité, excepté que dans les deux espèces MAB, le composé de cobalt se décompose légèrement plus vite que celui de nickel. La base aromatique, chez qui on a trouvé antérieurement très peu d'effet dans les complexes de cuivre, augmente appréciablement les constantes de vitesse avec d'autres métaux, spécialement le manganèse et le zinc. La 1,10-phénanthroline possède un plus grand effet que le 2,2-bipyridyl. Nous considérons quelques explications possibles des résultats.

[Traduit par le journal]

Canadian Journal of Chemistry, **50**, 3573 (1972)

In recent paper (1), the present authors reported experiments on the effect of two tertiary aromatic amines, 2,2′-bipyridyl and 1,10-phenanthroline, on the decarboxylation of 3-oxo-glutaric acid, catalyzed by copper ions. It was found that complexes of formula CuAB, where A^{2-} is the 3-oxo-glutarate ion and B is the aromatic amine, were responsible for the enhanced rates of decomposition. Kinetic and equilibrium measurements made it possible to compare the rate constants for decarboxylation of CuAB and CuA species. In fact the rate constants do not differ greatly, and the major enhancement of the rate arises from changes in the equilibria, and hence in the concentrations. References to related work are given in the above paper (1), but a recent paper by Hay and Leong (2) may be particularly mentioned.

The present paper extends the measurements to other transition metal ions, particularly to the divalent cations of manganese, cobalt, nickel, and zinc, which were already known to give

Can. J. Chem. Downloaded from www.nrcresearchpress.com by 210.87.254.105 on 09/05/12
For personal use only.

catalytically active species of formula MA (3). Since the catalyzed decarboxylation of ketocarboxylate ions seems to arise from the tendency of the metal to withdraw electrons from the ketocarboxylate ion (4–6), it was hoped that the rate constants could give information on the tendency of the base, B, to withdraw electrons from the metal ion. This will be considered in the discussion of the results.

Experimental

The 3-oxo-glutaric acid, 2,2′-bipyridyl, and 1,10-phenanthroline were obtained as described earlier (1).

Nickel nitrate, cobalt nitrate, zinc nitrate, and manganese nitrate were "Baker-Analyzed" reagents, and were used after recrystallization from water. Sodium nitrate, used to control ionic strength, was also "Baker-Analysed", recrystallized from water. Reagent grade nitric acid and sodium hydroxide, from the Fisher Scientific Company, were used to bring the pH within certain desired ranges. Stock solution of the transition metal nitrates, containing a small, but known, amount of nitric acid to suppress hydrolysis, were prepared, and were analyzed by EDTA titration.

Equilibrium Measurements

Equilibria were measured by means of a Beckman research pH meter, with a glass electrode and calomel reference electrode. All solutions were at 25.00 ± 0.01 °C, and had an ionic strength adjusted to 0.60 M. The pH meter was standardized, as usual, by potassium hydrogen phthalate, which was taken to have a pH of 4.008. The pH meter could be read to 0.0005 pH unit.

As it was necessary to connect pH readings to hydrogen ion concentrations, readings were taken on nitric acid solutions between 12.92 and 0.883×10^{-3} M, also containing sodium nitrate to give an ionic strength of 0.60 M. It was found that the results fitted the equation: $-\log[H^+] = pH + 0.169$, where $[H^+]$ was calculated on the assumption that all the nitric acid was ionized, and pH is the meter reading. The term 0.169 had a root mean square deviation of 0.0027 in nine measurements covering the range of concentrations given above. This gives an indication of the accuracy of the pH measurements.

Two series of measurements of equilibria were made: firstly on the formation of MA; secondly on MAB. In each series known amounts of 3-oxo-glutaric acid, metal nitrate, sodium hydroxide, and an aromatic amine if required, were mixed in solution, and the pH was measured. The equilibrium constants were calculated as described below.

The rates of decarboxylation were followed by the rate of evolution of carbon dioxide, in the apparatus already described (1). Throughout the temperature of the solutions was 25.00 ± 0.01 °C, and the ionic strength was 0.60 M. Measurements were also made on the pH of each reacting solution.

Results

Equilibrium for MA Species

It was assumed that, in solutions containing no aromatic amine, the following species were present: H_2A, HA^-, A^{2-}, M^{2+}, MA, H^+, Na^+, and NO_3^-. Here H_2A is 3-oxo-glutaric acid, and M^{2+} is the transition metal ion. Mass and charge balances and equilibrium expressions for the ionization of the acid give

$$K_{MA} = \frac{T_A - FG}{F(FG - T_A + T_M)}$$

where $K_{MA} = [MA]/[M^{2+}][A^{2-}]$, and is the desired constant, T_A = total 3-oxo-glutaric acid concentration, T_M = total transition metal concentration, T_N = total sodium hydroxide added (after allowing for its reaction with any nitric acid present), $[H^+]$ = hydrogen ion concentration, deduced from the pH reading, K_1, K_2 = successive ionization constants of 3-oxo-glutaric acid and

$$F = \frac{2T_A - T_N - [H^+]}{[H^+]/K_2 + 2[H^+]^2/K_1K_2}$$

$$G = 1 + [H^+]/K_2 + [H^+]^2/K_1K_2$$

The values of K_1 and K_2 used were 1.52×10^{-4} and 9.7×10^{-4}, taken from earlier experiments under the same conditions.

TABLE 1. Formation constant of the manganese(II) 3-oxo-glutarate complex, at 25.0 °C and $I = 0.60$ M

Run	10^2T_N	10^2T_A	10^2T_M	$10^4[H^+]$	K_{MA}
1	2.524	1.527	4.740	0.862	7.6
2	2.641	1.470	5.325	0.467	7.2
3	2.546	1.418	5.869	0.470	6.5
4	2.907	1.654	3.423	0.557	10.4
5	2.789	1.620	3.733	0.659	9.6
6	2.678	1.588	4.108	0.760	8.75
7	4.017_5	2.826	0.983	1.490	11.7
8	2.459	1.369	6.374	0.472	6.2
9	2.377	1.323	6.847	0.476	6.0
10	4.010	2.520	6.012	1.070	6.1

Table 1 gives the results for the manganese(II) complex, the last column being the calculated equilibrium constants. The average value of K_{MA} is 8.0 M^{-1}, with an average deviation of 1.7. A further estimate of the accuracy was obtained by calculating the change in the pH of the solution caused by the formation of the complex. This change for the runs in Table 1 ranged from 0.032 to 0.131, and this may be compared with the root-mean-square deviation of 0.0027 for the nitric acid calibration. It was also calculated that an error of 0.003 in the pH would alter the calculated K_{MA} by 11 to 13%

Can. J. Chem. Downloaded from www.nrcresearchpress.com by 210.87.254.105 on 09/05/12
For personal use only.

TABLE 2. Formation constant of the cobalt(II) 3-oxo-glutarate complex at 25.0 °C and $I = 0.60$ M

Run	10^2T_N	10^2T_A	10^2T_M	$10^4[H^+]$	K_{MA}
11	1.848	1.147	1.487	0.915	19.7
12	1.824	1.126	1.825	0.942	18.8
13	1.792	1.106	2.154	0.953	16.7
14	2.079	1.570	0.973	1.95	19.6
15	2.428_5	1.844	1.749	2.14	19.8
16	2.619_5	1.788	2.847	1.67	21.0
17	2.500	2.537	2.999	4.73	20.2
18	2.647	1.803	2.692	1.66	22.2
19	3.241	1.805	1.867	0.451	19.2

TABLE 3. Formation constant of the nickel(II) 3-oxo-glutarate complex at 25.0 °C and $I = 0.60$ M

Run	10^2T_N	10^2T_A	10^2T_M	$10^4[H^+]$	K_{MA}
20	1.893	1.169	1.136	0.894	22.8
21	1.026	1.162	1.162	5.05	23.8
22	1.700_5	2.184	2.186	7.05	26.9
23	1.955_5	1.583	0.982	2.46	26.1
24	2.772_5	2.416	0.853	2.93	23.0
25	2.312	1.860	1.764	2.60	23.6
26	2.701_5	1.835	2.375	1.64	25.3
27	2.673	1.819	2.535	1.65	23.5
28	2.193	1.876	1.779	3.13	27.7
29	3.316	1.846	1.433	0.447	26.1

TABLE 4. Formation constant of the zinc(II) 3-oxo-glutarate complex at 25.0 °C and $I = 0.60$ M

Run	10^2T_N	10^2T_A	10^2T_M	$10^4[H^+]$	K_{MA}
30	2.090	1.790	1.795	2.86	10.9
31	2.657	1.813	1.720	1.38	11.5
32	3.661	2.377	3.391	1.16	7.2
33	4.542	2.854	2.939	1.02	10.3
34	3.034_5	1.689	3.056	0.455	11.6
35	3.390	2.108	3.110	0.971	9.9
36	2.566	1.556	2.650	0.851	12.2
37	3.032	1.798	3.706	0.706	6.3

depending on the run. Tables 2, 3, and 4 give similar results for the other transition metal ions. The results can be summarized as follows:

In this table, "difference in pH" means the difference between the observed pH and the pH calculated on the assumption that no complex formation occurs; the two values are the largest and smallest differences found in different runs. "Effect of 0.003 error in pH" gives the % change in K_{MA} caused by a change of 0.003 in pH; again the two values are the extremes from various runs.

In any of these measurements, the presence of appreciable amounts of MA_2^{2-} ions would result in an increase in the calculated K_{MA} with increasing $[A^{2-}]$. This is not observed with the exception of a slight drift in K_{MA} for manganese. Hence it was assumed in later experiments that no MA_2^{2-} ions were present. In no case did K_{MA} drift appreciably with pH, so that species such as MAH^+ are not important. The K_{MA} values are decidedly lower than those reported earlier (1) from absorbance measurements. These earlier measurements depended on rather small differences in extinction coefficients, and consequently the values of K_{MA} were not very accurate. The errors involved in the present pH method can be fairly well judged from the data in Tables 1 to 4, and the calculations mentioned above. Since the measurements on MAB complexes, described below, were also done by means of pH, the K_{MA} values derived from pH were used throughout.

Equilibria for MAB Species

These measurements were similar to those already described, except that either 2,2′-bipyridyl or 1,10-phenanthroline was also added in approximately equimolar amounts as compared with the transition metal nitrate. In the calculations it was assumed that the following species were present: H_2A, HA^-, A^{2-}, M^{2+}, MA, MB^{2+}, MB_2^{2+}, MB_3^{2+}, MAB, B, BH^+, H^+, Na^+, and NO_3^-. Data on relevant equilibrium constants are available in literature (7–9) as summarized in Table 5. This table gives the logarithms of the constants, and the three

M^{2+}	Mean K_{MA} (M^{-1})	Average deviation (M^{-1})	Difference in pH	Effect of 0.003 error in pH (%)
Mn^{2+}	8.0	1.7	0.032–0.131	11–13
Co^{2+}	19.7	1.0	0.046–0.136	3–9
Ni^{2+}	24.9	1.5	0.040–0.136	3–9
Zn^{2+}	10.0	1.5	0.054–0.075	4.7–12.7

Can. J. Chem. Downloaded from www.nrcresearchpress.com by 210.87.254.105 on 09/05/12
For personal use only.

TABLE 5. Log (equilibrium constants) for formation of MB_n^{2+} ions

Metal ion	n	2,2′-Bipyridyl	1,10-Phenanthroline
Mn^{2+}	1	2.6	—
	2	4.6	—
	3	5.7	—
Co^{2+}	1	5.7	7.0
	2	11.3	13.7
	3	16.1	19.9
Ni^{2+}	1	7.07	8.6
	2	13.93	16.7
	3	20.13	24.25
Zn^{2+}	1	5.2	6.45
	2	9.6	12.1
	3	13.4	17.4
H^+	1	4.52	4.96

numbers for each metal are for the overall stability constants, $[MB_n^{2+}]/[M^{2+}][B]^n$, with $n = 1$, 2, or 3. The values opposite H^+ are the logarithms of $[BH^+]/[B][H^+]$. The data used in Table 5 are those of Irving and Mellor (7), who made a critical study of the information available on these stability constants, as well as their own measurements by the solvent extraction method. Their data are for 25 °C and an ionic strength of 0.1 M, but since the charge is the same on both sides of the equation in all these equilibria, their values were also used for our higher ionic strength.

In any one solution, a value of $[H^+]$ was found by pH measurement, and since $[Na^+]$ and $[NO_3^-]$ are known from the quantities added, this leaves eleven unknown concentrations and one unknown constant, $K_{MAB} = [MAB]/[MB^{2+}][A^{2-}]$. There are eight equilibrium equations and four mass or charge balance equations, so K_{MAB} can be found. In practice the algebra is difficult, and the simplest method seems to be as follows. If we define G and other symbols as above, and in addition:

$$R = \frac{T_A\left(2 + \frac{[H^+]}{K_2}\right) - G\left\{[H^+]\left(1 + \frac{[B]}{K_{HB}}\right) + T_N\right\}}{[H^+](1 + [B]/K_{HB}) + T_N - 2T_A}$$

$$K_{HB} = [BH^+]/[B][H^+]$$

it can be shown that

$$[M^{2+}] = \frac{(G + R)\left\{T_B - [B]\left(1 + \frac{[H^+]}{K_{HB}}\right) - RT_A\right\}}{(G + R)\{K_{MB}[B] + 2\beta_{MB_2}[B]^2 + 3\beta_{MB_3}[B]^3\} - K_{MA}T_A}$$

and also

$$[M^{2+}] = \frac{(G + R)T_M - RT_A}{(G + R)\{1 + K_{MB}[B] + \beta_{MB_2}[B]^2 + \beta_{MB_3}[B]^3\}}$$

where K_{MB}, β_{MB_2}, and β_{MB_3} are the stability constants given in Table 5, and T_B is the total aromatic base added. The method used was to guess a value of [B], calculate two values of $[M^{2+}]$ from the equations above, and repeat this with other values of [B] until one was found for which the two values of $[M^+]$ differed by less than 0.1%. As $[M^{2+}]$ and [B] were now known, K_{MAB} was calculated from

$$K_{MAB} = \frac{R - K_{MA}[M^{2+}]}{K_{MB}[M^{2+}][B]}$$

It was now possible to calculate the concentrations of all the species present, and to check that the equilibrium and mass balance equations were in fact obeyed.

Table 6 gives the results for manganese(II) with 2,2′-bipyridyl. The mean value of K_{MAB} is 15.1 M^{-1}, with an average deviation of 0.95 M^{-1}. As before, an estimate of the accuracy of the result was made by calculating what would have been the pH of the solution if no MAB were formed, and comparing it with the actual pH. Since this also involved a long calculation

Can. J. Chem. Downloaded from www.nrcresearchpress.com by 210.87.254.105 on 09/05/12
For personal use only.

TABLE 6. Formation constant of manganese(II) 2,2′-bipyridyl 3-oxo-glutarate complex at 25 °C and $I = 0.60$ M

Run	10^2T_N	10^2T_A	10^2T_M	10^2T_B	$10^4[H^+]$	K_{MAB}
40	4.452	2.491	12.51	12.37	0.257	15.4
41	4.437	2.491	9.005	9.008	0.251	15.1
42	4.760	2.510	4.350	4.380	0.110	16.8
43	4.213	2.507	6.003	6.005	0.367	14.1
44	4.477	2.507	10.42	10.31	0.256	16.4
45	3.881	2.100	8.050	8.060	0.151	13.9
46	4.041	2.230	5.100	5.120	0.191	13.9

TABLE 7. Formation constant of the cobalt(II) 2,2′-bipyridyl 3-oxo-glutarate complex at 25 °C and $I = 0.60$ M

Run	10^2T_N	10^2T_A	10^2T_M	10^2T_B	$10^4[H^+]$	K_{MAB}
47	2.652	1.673	2.172	2.179	1.03	20.4
48	2.881	1.862	2.297	2.307	1.19	24.3
49	2.519	1.687	2.190	2.197	1.35	20.3
50	3.008	1.914	2.362	2.371	1.08	18.3
51	2.644	1.716	3.227	3.234	1.26	18.3
52	3.628	2.715	3.227	3.234	2.17	22.5
53	4.479	2.730	4.246	4.254	0.981	19.5
54	3.865	2.530	3.652	3.680	1.36	21.3
55	3.794	2.230	5.673	5.685	0.856	18.3
56	5.175	2.980	5.673	5.685	0.730	18.6

TABLE 8. Formation constant of the nickel(II) 2,2′-bipyridyl 3-oxo-glutarate complex at 25 °C and $I = 0.60$ M

Run	10^2T_N	10^2T_A	10^2T_M	10^2T_B	$10^4[H^+]$	K_{MAB}
57	4.442	2.996	3.001	3.010	1.50	20.6
58	4.030	2.510	3.560	3.560	1.08	18.3
59	4.056	2.524	2.002	2.010	0.950	17.8
60	3.335	2.021	2.560	2.570	0.876	21.5
61	4.023	2.770	4.520	4.530	1.80	20.3
62	4.907	3.105	4.520	4.530	1.25	20.3
63	4.437	2.996	3.001	3.010	1.50	19.6
64	3.245	2.499	3.001	3.010	2.34	18.2

by trial and error for the value of [B], it was only attempted for some selected runs. For run 42 in Table 6 the change of pH arising from MAB formation was 0.155, and for run 44 it was 0.096. Hence an error of 0.003 is 2 to 3% of this. However, the average deviation in K_{MAB} is 6.3%, which of course includes other errors.

Table 7 gives the results for cobalt(II) with 2,2′-bipyridyl. The mean value of K_{MAB} is 20.2 M^{-1}, with an average deviation of 1.58. In run 47, the calculated change of pH arising from MAB formation was 0.073.

Table 8 gives the results for nickel(II) with 2,2′-bipyridyl. The mean value of K_{MAB} is 19.6 M^{-1} with an average deviation of 1.1 M^{-1}. In run 57, the calculated change of pH arising from MAB formation was 0.047.

Table 9 gives the results for zinc(II) with 2,2′-bipyridyl. The mean value of K_{MAB} is 8.0 M^{-1}, with an average deviation of 0.7 M^{-1}. In run 72, the calculated change or pH arising from MAB formation was 0.076.

Table 10 gives the results for cobalt(II) with 1,10-phenanthroline. The mean value of K_{MAB}

Can. J. Chem. Downloaded from www.nrcresearchpress.com by 210.87.254.105 on 09/05/12
For personal use only.

TABLE 9. Formation constant of the zinc(II) 2,2′-bipyridyl 3-oxo-glutarate complex at 25 °C and $I = 0.60$ M

Run	10^2T_N	10^2T_A	10^2T_M	10^2T_B	$10^4[H^+]$	K_{MAB}
65	3.433	2.215	3.071	3.085	1.08	6.8
66	4.896	3.050	3.105	3.121	0.912	7.1
67	4.222	2.525	7.303	7.315	0.850	7.5
68	5.916	3.530	5.015	5.050	0.767	7.5
69	2.375	1.589	5.015	5.050	1.45	9.4
70	3.644	2.574	5.119	5.101	1.70	7.9
71	2.333	1.530	4.050	4.058	1.22	8.1
72	3.261	2.505	8.091	8.062	2.47	8.9
73	3.152	2.512	6.357	6.352	2.60	8.6

TABLE 10. Formation constant of cobalt(II) 1,10-phenanthroline 3-oxo-glutarate complex at 25 °C and $I = 0.60$ M

Run	10^2T_N	10^2T_A	10^2T_M	10^2T_B	$10^4[H^+]$	K_{MAB}
75	2.860	2.385	2.073	2.050	2.85	31.3
76	2.982	2.363	2.054	2.030	2.43	25.7
77	2.292	1.761	2.182	2.158	2.26	28.3
78	3.635	2.259	1.964	1.943	0.946	21.2
79	3.513	2.279	1.981	1.960	1.19	24.8
80	2.419	1.687	2.090	2.068	1.64	28.8
81	4.137	2.701	3.108	3.086	1.32	22.9
82	4.495	2.750	4.358	4.360	1.05	23.5
83	4.177	2.520	2.875	2.880	0.863	22.4
84	5.008	3.150	4.358	4.360	1.21	23.8

TABLE 11. Formation constant of nickel(II) 1,10-phenanthroline 3-oxo-glutarate complex at 25 °C and $I = 0.60$ M

Run	10^2T_N	10^2T_A	10^2T_M	10^2T_B	$10^4[H^+]$	K_{MAB}
85	4.976	4.073	3.372	4.011	2.80	20.2
86	5.240	4.317	2.027	2.016	2.70	21.6
87	4.290	3.301	2.007	2.013	2.24	23.2
88	3.554	2.741	2.007	2.013	2.24	21.4
89	4.490	3.080	3.044	3.036	1.60	18.3
90	4.967	3.080	3.044	3.036	1.02	19.2
91	4.217	2.560	3.548	3.550	0.946	18.8
92	4.771	2.830	3.548	3.550	0.812	18.0
93	5.653	2.580	4.034	4.040	1.21	18.9
94	3.872	2.520	4.034	4.040	1.42	21.5

is 25.3 M^{-1}, with an average deviation of 2.6 M^{-1}. In run 82, the calculated change of pH arising from MAB formation was 0.084.

Table 11 gives the results for nickel(II) with 1,10-phenanthroline. The mean value of K_{MAB} is 20.1 M^{-1}, with an average deviation of 1.47 M^{-1}. In run 85, the calculated change of pH arising from MAB formation was 0.071.

Table 12 gives the results for zinc(II) with 1,10-phenanthroline. The mean value of K_{MAB} is 6.05 M^{-1} with an average deviation of 0.65 M^{-1}. In run 95, the calculated change of pH arising from MAB formation was 0.040.

Kinetic Results

The rates of reaction were first measured in the presence of transition metal ion, but without the addition of a tertiary aromatic amine. It was

Can. J. Chem. Downloaded from www.nrcresearchpress.com by 210.87.254.105 on 09/05/12
For personal use only.

TABLE 12. Formation constant of zinc(II) 1,10-phenanthroline 3-oxo-glutarate complex at 25 °C and $I = 0.60$ M

Run	10^2T_N	10^2T_A	10^2T_M	10^2T_B	$10^4[H^+]$	K_{MAB}
95	3.626	2.587	5.036	5.044	1.72	6.0
96	3.626	2.594	3.137	3.095	1.68	8.3
97	3.673	2.491	4.128	4.142	1.37	5.3
98	3.801	2.512	4.541	4.565	1.25	5.3
99	5.376	3.530	3.451	3.460	1.18	5.7
100	4.602	2.895	2.541	2.565	0.935	6.2
101	4.943	3.010	4.541	4.565	0.842	6.1
102	4.297	2.730	5.036	5.044	1.08	6.5
103	3.133	2.150	3.850	3.850	1.42	5.0

TABLE 13. Manganese catalyzed decomposition of 3-oxo-glutaric acid

Run	10^2T_A	10^2T_M	$10^4[H^+]$	$10^3[H_2A]$	$10^3[HA^-]$	$10^3[A^{2-}]$	$10^3[MA]$	10^5k_{obs}	10^5k_{MA}
1	2.491	20.00	2.20	1.90	8.37	5.79	8.85	2.55	2.05
2	2.505	10.00	1.70	1.60	9.14	8.17	6.13	2.43	1.97
3	2.491	16.66	1.11	0.679	5.93	8.13	10.17	2.10	2.05
4	2.505	13.33	0.990	0.614	6.02	9.24	9.18	2.00	1.98
5	2.491	16.66	2.04	1.81	8.59	6.40	8.11	2.53	2.07
6	2.505	13.33	1.88	1.72	8.89	7.19	7.25	2.52	2.12
7	2.505	16.66	0.851	0.431	4.91	8.75	10.93	1.83	1.83
8	2.491	20.00	0.732	0.300	3.97	8.25	12.38	1.82	1.93

TABLE 14. Cobalt catalyzed decomposition of 3-oxo-glutaric acid

Run	10^2T_A	10^2T_M	$10^4[H^+]$	$10^3[H_2A]$	$10^3[HA^-]$	$10^3[A^{2-}]$	$10^3[MA]$	10^5k_{obs}	10^5k_{MA}
9	2.560	10.03	2.32	1.99	8.31	5.45	9.85	4.27	6.50
10	2.546	8.015	2.15	1.92	8.66	6.13	8.75	4.13	6.67
11	2.569	14.02	1.85	1.19	6.26	5.15	13.08	4.75	6.75
12	2.598	15.99	1.79	1.06	5.76	4.89	14.26	4.93	6.82
13	2.539	12.00	1.78	1.20	6.54	5.59	12.06	4.50	6.57
14	2.560	8.015	1.25	0.818	6.35	7.72	10.72	4.00	6.42
15	2.539	12.00	1.51	0.914	5.87	5.91	12.69	4.75	7.03
16	2.569	10.03	0.867	0.390	4.36	7.64	13.30	4.28	6.58

found that a plot of $\ln (P_\infty - P_t)$ against time was linear up to about 35% of the total reaction. Here P_t is the pressure of evolved carbon dioxide at time t, and P_∞ is the pressure for complete reaction, on the assumption that one CO_2 is evolved by each 3-oxo-glutaric acid. This assumes that the decomposition of the initial product, acetoacetic acid, is relatively slow, as was already known (3, 10). Hence this plot gives a value of k_{obs}, defined by

$$d[CO_2]/dt = k_{obs}T_A$$

The concentrations of all species present were calculated from the usual mass balance and equilibrium expressions, and the observed pH.

In interpreting the results it was assumed that

$$k_{obs}T_A = k_{H_2A}[H_2A] + k_{HA^-}[HA^-] + k_{A^{2-}}[A^{2-}] + k_{MA}[MA]$$

The values of k_{H_2A}, k_{HA^-} and $k_{A^{2-}}$ were already known (3). The relatively long linear part of the plot of $\ln (P_\infty - P_t)$ against time implies that there is no very great change in the relative concentrations of the various species as the reaction proceeds. This must mean that the extent of complexing of the transition metal ion by the acetoacetic acid is not very different from that by 3-oxo-glutaric acid, but detailed information on this is not at present available.

Tables 13 to 16 give the results for various

TABLE 15. Nickel catalyzed decomposition of 3-oxo-glutaric acid

Run	10^2T_A	10^2T_M	$10^4[H^+]$	$10^3[H_2A]$	$10^3[HA^-]$	$10^3[A^{2-}]$	$10^3[MA]$	10^5k_{obs}	10^5k_{MA}
17	1.239	6.001	2.06	0.883	4.16	3.07	4.28	5.12	9.57
18	1.246	8.028	2.08	0.805	3.76	2.74	5.16	5.62	9.63
19	2.601	8.020	2.91	2.83	9.44	4.93	8.81	5.30	9.70
20	2.512	5.981	1.57	1.21	7.49	7.25	9.17	5.20	9.88
21	1.283	10.040	2.32	0.891	3.73	2.44	5.77	5.93	9.68
22	1.249	6.001	0.930	0.242	2.52	4.12	5.61	5.45	9.77
23	2.601	8.028	1.24	0.749	5.86	7.18	12.22	5.60	9.38
24	2.512	8.028	0.851	0.374	4.27	7.62	12.85	5.75	9.47

TABLE 16. Zinc catalyzed decomposition of 3-oxo-glutaric acid

Run	10^2T_A	10^2T_M	$10^4[H^+]$	$10^3[H_2A]$	$10^3[HA^-]$	$10^3[A^{2-}]$	$10^3[MA]$	10^5k_{obs}	10^5k_{MA}
25	2.594	19.98	2.32	1.98	8.27	5.42	10.27	5.25	8.88
26	2.485	9.99	1.39	1.10	7.66	8.37	7.72	4.18	8.20
27	2.577	14.99	2.00	1.75	8.49	6.45	9.08	4.90	8.87
28	2.505	7.493	1.37	1.17	8.32	9.23	6.33	3.88	8.38
29	2.587	12.51	2.00	1.87	9.06	6.88	8.06	4.63	8.82
30	2.519	5.017	1.36	1.28	9.10	10.18	4.63	3.42	8.13
31	2.594	14.99	1.15	0.719	6.07	8.02	11.13	4.82	8.33
32	2.577	9.99	0.880	0.533	5.88	10.15	9.21	4.30	8.65

transition metals. The tables include the concentrations of the reactive species present, and the values of k_{MA}, obtained by taking $k_{H_2A} = 2.08 \times 10^{-5}$, $k_{HA^-} = 4.83 \times 10^{-5}$ and $k_{A^{2-}} = 0.17 \times 10^{-5}\ s^{-1}$ (3). The mean values of k_{MA} and their average deviations are as follows:

M^{2+}	$10^5 k_{MA}$ (s^{-1})	Average deviation (s^{-1})
Mn^{2+}	2.00	0.07
Co^{2+}	6.67	0.15
Ni^{2+}	9.64	0.12
Zn^{2+}	8.53	0.27

Runs were now carried out in which either 2,2′-bipyridyl or 1,10-phenanthroline were added in an amount roughly equimolar as compared with the transition metal. In interpreting the results it was assumed that MAB species were also catalytically active, so that

$$k_{obs}T_A = k_{H_2A}[H_2A] + k_{HA} - [HA^-] + k_{A^{2-}}[A^{2-}] + k_{MA}[MA] + k_{MAB}[MAB]$$

A plot of $\ln(P_\infty - P_t)$ was linear up to about 30% of the total reaction so that k_{obs} could be obtained from these plots. In calculating the concentrations it was assumed that H^+, H_2A, HA^-, A^{2-}, M^{2+}, MA, MB^{2+}, MB_2^{2+}, MB_3^{2+}, MAB, B, BH^+, Na^+, and NO_3^- were present. The pH gave a value of $[H^+]$, and mass balance and equilibrium equations enabled all other concentrations to be calculated.

Tables 17 to 20 give the results when the base was 2,2′-bipyridyl with the various transition metal ions; Tables 21 to 23 similarly give the results when the base was 1,10-phenanthroline. The mean values of k_{MAB} obtained from these tables are collected in Table 24, which also gives the average deviation of each result.

Discussion of Results

Some comments may first be made on the results on stability constants, together with those obtained earlier for copper compounds (1). These are summarized in Table 25, which contains values of log K, as equilibrium constants are often easier to compare in this form. The results in general follow the Irving–Williams order (11), though there is a small drop at nickel in log K_{MAB} values for both aromatic bases. There is no drop in log K_{MA}, but the rise in going from cobalt to nickel is small; it is smaller than the rise for other comparable ligands, chelated

Can. J. Chem. Downloaded from www.nrcresearchpress.com by 210.87.254.105 on 09/05/12
For personal use only.

Can. J. Chem. Downloaded from www.nrcresearchpress.com by 210.87.254.105 on 09/05/12
For personal use only.

TABLE 17. Manganese(II), 2,2′-bipyridyl catalyzed decomposition of 3-oxo-gluraric acid

Run	10^2T_A	10^2T_M	10^2T_B	$10^4[H^+]$	10^5k_{obs}	10^5k_{MAB}
33	2.491	9.005	9.008	0.251	2.77	6.82
34	2.507	6.003	6.005	0.367	2.47	6.67
35	2.491	12.51	12.37	0.257	3.20	6.87
36	2.501	10.42	10.31	0.256	2.90	6.68
37	2.507	10.42	10.31	0.530	3.00	6.52
38	2.491	12.51	12.37	0.841	3.50	7.17
39	2.491	9.005	9.008	1.040	3.30	7.47
40	2.507	6.003	6.005	1.100	2.97	7.33

TABLE 18. Cobalt(II), 2,2′-bipyridyl catalyzed decomposition of 3-oxo-glutaric acid

Run	10^2T_A	10^2T_M	10^2T_B	$10^4[H^+]$	10^5k_{obs}	10^5k_{MAB}
41	2.594	8.213	8.179	3.67	4.77	15.80
42	2.601	7.017	7.109	2.29	4.73	14.98
43	2.519	5.133	5.133	1.64	4.45	15.87
44	2.539	7.581	7.562	3.61	4.58	14.83
45	2.471	6.554	6.507	2.08	4.72	15.32
46	2.505	6.159	6.178	1.25	4.63	14.77
47	2.594	8.213	8.179	0.925	5.50	16.17
48	2.539	7.581	7.562	0.832	5.37	16.37

TABLE 19. Nickel(II), 2,2′-bipyridyl catalyzed decomposition of 3-oxo-glutaric acid

Run	10^2T_A	10^2T_M	10^2T_B	$10^4[H^+]$	10^5k_{obs}	10^5k_{MAB}
49	1.287	5.058	5.013	1.01	4.65	13.66
50	1.253	6.985	7.010	1.21	5.40	13.37
51	1.239	4.014	4.039	1.12	4.32	13.14
52	2.601	8.108	8.091	3.17	5.07	13.66
53	2.526	6.081	6.068	2.20	4.72	12.55
54	2.601	8.108	8.091	0.913	5.75	13.99
55	2.526	6.985	7.010	1.58	5.08	12.82
56	1.287	6.021	6.018	0.745	5.00	12.37

TABLE 20. Zinc(II), 2,2′-bipyridyl catalyzed decomposition of 3-oxo-glutaric acid

Run	10^2T_A	10^2T_M	10^2T_B	$10^4[H^+]$	10^5k_{obs}	10^5k_{MAB}
57	2.574	5.119	5.101	1.70	4.68	28.8
58	2.601	7.100	7.132	2.46	5.17	29.6
59	2.512	6.357	6.352	2.60	4.67	25.9
60	2.601	4.211	4.188	1.76	4.42	29.9
61	2.505	8.091	8.062	2.47	4.93	24.2
62	2.505	8.091	8.062	1.28	5.58	26.8
63	2.601	7.100	7.132	1.05	4.70	21.7
64	2.512	6.357	6.352	0.910	4.78	24.3

Can. J. Chem. Downloaded from www.nrcresearchpress.com by 210.87.254.105 on 09/05/12
For personal use only.

TABLE 21. Cobalt(II), 1,10-phenanthroline catalyzed decomposition of 3-oxo-glutaric acid

Run	10^2T_A	10^2T_M	10^2T_B	$10^4[H^+]$	10^5k_{obs}	10^5k_{MAB}
65	2.587	6.554	6.518	3.40	5.35	19.4
66	2.488	4.027	4.005	1.89	4.98	20.2
67	2.580	6.001	6.016	2.95	5.20	18.3
68	2.505	5.054	5.025	2.21	5.42	20.8
69	2.491	5.449	5.472	1.58	5.97	21.7
70	2.587	6.554	6.518	1.12	7.07	23.3
71	2.580	6.001	6.016	0.948	6.18	20.2
72	2.491	5.449	5.472	0.851	6.30	22.0

TABLE 22. Nickel(II), 1,10-phenanthroline catalyzed decomposition of 3-oxo-glutaric acid

Run	10^2T_A	10^2T_M	10^2T_B	$10^4[H^+]$	10^5k_{obs}	10^5k_{MA}
73	1.301	5.168	5.139	1.90	5.48	18.0
74	1.253	3.101	3.083	0.960	4.63	18.3
75	2.615	4.757	4.754	1.73	5.37	19.3
76	2.560	5.620	5.646	2.76	5.35	19.0
77	2.485	5.118	5.123	2.02	5.28	17.9
78	2.615	4.757	4.754	1.28	5.68	20.5
79	2.560	5.620	5.646	1.06	5.58	16.8
80	2.485	5.218	5.123	0.835	6.13	20.5

TABLE 23. Zinc(II), 1,10-phenanthroline catalyzed decomposition of 3-oxo-glutaric acid

Run	10^2T_A	10^2T_M	10^2T_B	$10^4[H^+]$	10^5k_{obs}	10^5k_{MA}
81	2.587	5.036	5.044	1.72	5.83	51.9
82	2.401	4.128	4.142	1.37	5.55	54.1
83	2.594	3.137	3.095	1.68	4.47	46.2
84	2.512	4.541	4.565	2.35	5.07	47.2
85	2.512	2.229	2.210	1.49	4.00	48.7
86	2.587	5.036	5.044	1.16	5.97	49.3
87	2.491	4.128	4.142	0.943	5.70	53.3
88	2.512	4.541	4.565	0.838	6.27	55.7

TABLE 24. Value of k_{MAB}, and average deviations, for various species*

M	B	10^5k_{MAB} (s^{-1})	10^5(average deviation) (s^{-1})
Mn	bipy	6.94	0.29
Co	"	15.55	0.51
Ni	"	13.2	0.47
Zn	"	26.4	2.4
Co	phen	20.7	1.2
Ni	"	18.8	1.1
Zn	"	50.8	2.9

*bipy = 2,2'-bipyridyl; phen = 1,10-phenanthroline.

through oxygen (such as the malonate ion), where the usual rise in log K is about 0.4 (9). Possibly this irregularity arises from the fact that the metal in the MAB complexes is not in anything close to an octahedral field: the larger ligand field splitting of the base, B, will give a considerable linear component to the field. 3d electrons in a linear field are split in energy so that one orbital is considerably above the average, two are slightly above, and two well below. This would give an increasing crystal field stabilization in going from Mn^{2+} to Co^{2+}, a slight drop to Cu^{2+}, and a larger drop to

Can. J. Chem. Downloaded from www.nrcresearchpress.com by 210.87.254.105 on 09/05/12
For personal use only.

TABLE 25. Logarithms of equilibrium constants

M	log K_{MA}	log K_{MAB} B = 2,2′-bipy	log K_{MAB} B = 1,10-phen
Mn	0.90	1.18	—
Co	1.29	1.31	1.40
Ni	1.40	1.29	1.30
Cu	2.18	2.56	2.43
Zn	1.00	0.90	0.79

Zn^{2+}. Coupled with the usual Jahn–Teller distortion round Cu^{2+}, this might explain the observed trend. However, the main difficulty with this explanation is that the usual Irving–Williams trend is observed for formation constants of MB^{2+}, where such a linear field might be expected to apply.

The values of log K_{MA} in Table 25 are lower than the values reported (3) earlier, and have a wider spread in values in going from one metal to the next. Some support for this wider spread can be obtained by comparison with the stability constants (9) of similar ligands, where a spread in values at least as large as ours is generally found. The earlier values were obtained from relatively small changes in optical absorbance, or in the voltage of a cell using a zinc amalgam electrode, but the cause of the discrepancy is at present uncertain.

A comparison of the log K_{MAB} values in Table 25 shows that cobalt has a somewhat lower value of K_{MAB} if B is 2,2′-bipyridyl, nickel almost equal values, and copper and zinc lower values if B is 1,10-phenanthroline. However, the differences are so small that it is doubtful if a detailed explanation can be attempted at present. It was observed earlier (1) that for copper complexes, the 3-oxo-glutarate ion is much less strongly bound that either of the aromatic bases, though it is nearly as strong a base as they are. This was attributed, at least in part, to back-bonding by 3d electrons on M^{2+} to π^*-orbitals on the base. The same holds for the other metal ions besides copper, presumably for the same reasons. This is also true of attachment of either B or A^{2-} to MA species; in fact, MA_2^{2-} species were not observed in the present work, and were only weakly formed when M is copper.

In contrast to the slight irregularities in the equilibrium constants for the attachment of A^{2-} to MB^{2+}, the constant for the reactions

$$MA + B \rightleftharpoons MAB$$

follow the Irving–Williams order. These equilibrium constants, which are equal to $K_{MAB}K_{MB}/K_{MA}$, are larger for the stronger base 1,10-phenanthroline; this is also true for the reactions $M^{2+} + B \rightleftharpoons MB^{2+}$. A qualitative explanation of the difference between 2,2′-bipyridyl and 1,10-phenanthroline can be found in a simple Hückel molecular orbital treatment of these two molecules. If we take $\alpha_N = \alpha_C + 0.5\beta$, where α_N and α_C are the Coulomb integrals on nitrogen and carbon, and β is the exchange integral for neighboring carbons or carbon–nitrogen, and the factor 0.5 is chosen as being the difference in electronegativities, then the net charge on nitrogen is -0.199 in 2,2′-bipyridyl and -0.244 in 1,10-phenanthroline. This would presumably cause a proton to bond more strongly to 1,10-phenanthroline making it the stronger base. As regards π-backbonding in MB^{2+}, the lowest suitable m.o. in 1,10-phenanthroline is a little higher in energy (by 0.032β) than in 2,2′-bipyridyl but the coefficient of the a.o. on nitrogen is higher in 1,10-phenanthroline (0.396 compared with 0.373), giving better overlap with a 3d orbital on the metal, which would make K_{MB} larger for 1,10-phenanthroline. The Hückel m.o. method is, of course, very approximate, but it can perhaps serve to explain the relative behavior of two similar molecules.

The constants K_{MAB} provide some information on the discriminating behavior of metal ions and ligands, which has been noted in other systems (*e.g.* 12 and references therein). It was found (1) that the equilibrium constant of

$$CuA_2^{2-} + CuB_2^{2+} \rightleftharpoons 2\ CuAB$$

was about 4×10^4 if B is 2,2′-bipyridyl, and about 1.2×10^4 if B is 1,10-phenanthroline. This agrees with the previously observed behavior (13) of copper bonded to two chelating ligands, one attached by two nitrogen atoms, and the other by two oxygen atoms. Owing to the failure to observe MA_2^2 species for M = manganese, cobalt, nickel, and zinc, all that can be said is that for these metals the corresponding constants are also large. A somewhat different comparison is also often made (13) by means

Can. J. Chem. Downloaded from www.nrcresearchpress.com by 210.87.254.105 on 09/05/12
For personal use only.

TABLE 26. Logarithms of rate constants: values of log (10^5k); time in seconds

	log (10^5k)		
		MAB	
M	MA	bipy	phen
Mn	0.30	0.84	—
Co	0.82	1.19	1.32
Ni	0.98	1.12	1.27
Cu	2.29	2.42	2.23
Zn	0.83	1.42	1.71

of values of $\Delta \log K = \log K_{MAB} - \log K_{MA}$, which is the equilibrium constant for

$$M^{2+} + MAB \rightleftharpoons MA + MB^{2+}$$

Small negative values of $\Delta \log K$ would be expected if A^{2-} and B do not affect each other's chance of bonding to a metal ion. Small positive values of $\Delta \log K$ were found for copper (0.38 if B is 2,2′-bipyridyl, and 0.25 if B is 1,10′-phenanthroline). This seems to be a common situation for copper bonded to 2,2′-bipyridyl and another chelating ligand attached through two oxygens (13–15), but negative values of $\Delta \log K$ are also found when a ligand, other than 2,2′-bipyridyl, which chelates through nitrogen is used (16–18). In the present work, the values of $\Delta \log K$ from Table 25 are

	$\Delta \log K$	
M^{2+}	bipy	phen
Mn^{2+}	0.28	—
Co^{2+}	0.02	0.11
Ni^{2+}	−0.11	−0.10
Zn^{2+}	−0.10	−0.22

These values show a trend to more negative $\Delta \log K$ with increasing number of d electrons, but it must be remembered that a positive $\Delta \log K$ had been found for copper. The most that can be concluded at present is that the two bases give very similar trends.

If we now consider the rate constants, values of $\log k$ are collected in Table 26. Two points may be mentioned first. Firstly, as the experiments reported above were carried out without a buffer, it was not necessary to consider species in which the transition metal ion was complexed with the buffer anion. Buffered solutions would have controlled pH better, but would have greatly increased the difficulties of interpretation.

Secondly, 3-oxo-glutaric acid can, in theory, give two types of chelated complexes:

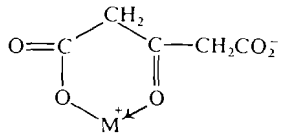

I

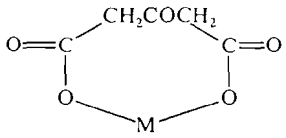

II

The first is more probable on the basis of ring size, and this type of structure has been suggested by other workers (2, 19), though not invariably (20). Recently Yerhoff and Larson (21), on the basis of infrared spectra of solid hydrates, $MA.xH_2O$, have proposed a structure with only unidentate bonding of the metal ion to the carboxylate group. They base this, in part, on the fairly small change observed in the carbonyl stretching frequency in, for instance, $CoA.xH_2O$ as compared with Na_2A. Admittedly some other possibly chelated complexes, such as those of salicylaldehyde with Co^{2+}, Ni^{2+}, and Zn^{2+} (22) or of diethyl oxaloacetate (23) also give a rather small change in frequency when the complex is formed; and it is also possible that the solid compound, even though hydrated, may have a different structure in solution. Yerhoff and Larson suggest a structure which, in solution, would presumably be

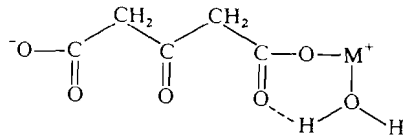

III

Since equilibrium measurements measure the total complexed 3-oxo-glutarate ions, and the rate measurements measure the total rate, it follows that k_{MA} would be an average rate con-

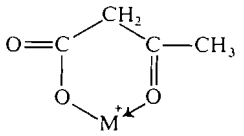

stant, if in fact more than one MA species is present in solution. Structure II would probably not decarboxylate readily, since the copper complex of 3-oxo-butyric acid was found not to decarboxylate (3). In structure III, it seems unlikely that the metal ion would transmit any large effect to the far end of the molecule, so that structure I is probably the most reactive species. Similar uncertainties are, of course, present in interpreting the analogous reactions of other β-ketoacids, such as oxaloacetic acid, which could give two structures analogous to I above:

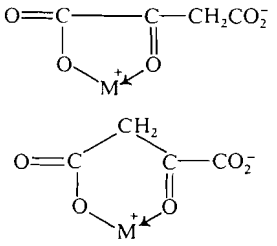

of which the first seems to be the more reactive (24).

The results in Table 26 follow the same order as the Irving–Williams order for stability constants, in the cases of the MA species, but in both MAB series the rate for nickel is slightly below that for cobalt. The similar behavior of the equilibrium constants might lead one to expect that log (rate k) plotted against log (equilibrium K) would give a straight line. No such simple relation seems to exist, the chief deviation coming from the zinc compounds, where the rate constants are relatively high. Prue (19) has noted that the gross catalytic effects, which are proportional to $k_{MA}K_{MA}$, parallel the equilibrium constants for complexing of the metal with malonate: he obtained $\log k_{cat} = 1.3 \log K_{Mal} +$ constant. We have examined the correlation of $\log k_{MA}$ with the logarithm of the stability constants of the metals complexes with various anions (referred to as $\log K_{MX}$). A straight line was drawn by least squares through the points for $\log k_{MA}$ plotted against $\log K_{MX}$, and the root mean square deviations of the points from this line were then

TABLE 27. Correlation of $\log k_{MA}$ with $\log K_{MX}$

Ligand, X	r.m.s. deviation	K_{MX}/K_{MA}: r.m.s. deviation
3-Oxo-glutarate	0.163	—
Oxalate	0.294	0.425
Malonate	0.077	0.148
Succinate	0.330	0.664
Oxaloacetate	0.088	0.273
Acetate	0.303	0.684
Glycinate	0.147	0.211
Ethylenediamine	0.192	0.224
Acetylacetonate	0.110	0.102

calculated. The results are given in Table 27, mostly from data in ref. 9. The best fit is with malonate, and this perhaps means, as Prue originally suggested, that the activated complex is close to a structure resembling a malonate complex, that is

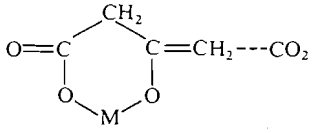

where the CO_2 is almost separated. The slope of the best line is 0.82; *i.e.* $\log k_{MA} = 0.82 \log K_{Mal} +$ constant. However, on this interpretation it would be more precise to attempt a correlation of $\log k_{MA}$ with the ratio of the stability constants of the metal ion combined with 3-oxo-glutarate and with malonate (or other anion), as the rate is determined by the free energy change in going from the ground state to the activated complex. Unfortunately a correlation of $\log k_{MA}$ with $\log (K_{MX}/K_{MA})$ is not as good as with $\log K_{MX}$ alone: the root mean square deviations are given in the third column of Table 27. The fit with the data for malonate is still moderate, but that with the data for acetylacetonate is better. Admittedly the acetyl-acetonate chelate is not very different in structure, but some doubt is cast on conclusions about the nature of the activated complex.

If we consider the change in the rate constant in going from MA to MAB species, we can see that in general MAB species decarboxylate faster. The sole exception is CuA(1,10-phenanthroline). The increase in rate in both series is large for manganese and zinc, and least for

Can. J. Chem. Downloaded from www.nrcresearchpress.com by 210.87.254.105 on 09/05/12
For personal use only.

copper. Thus the aromatic bases chiefly promote the effects of the catalytically least efficient metal ions. The enhanced rates of decarboxylation, which for copper arose largely from changes in equilibrium constant, are largely or completely from increases in the rate constants for cobalt, nickel, and zinc, and to a lesser extent for manganese. Similarly the rate constants for MAB species are larger when B is 1,10-phenanthroline, except when the metal is copper. As was mentioned in connection with equilibrium constants, 1,10-phenanthroline probably accepts electron density into its π-system more easily than 2,2′-bipyridyl, and this would explain the relative sizes of the rate constants except those for copper. The reason for the special position of copper is not clear, though it is possibly connected with the usually non-octahedral arrangement of ligands around it.

1. K. N. Leong and M. W. Lister. Can. J. Chem. In press.
2. R. W. Hay and K. N. Leong. J. Chem. Soc. (A), 3639 (1971).
3. D. W. Larson and M. W. Lister. Can. J. Chem. **46**, 823 (1968).
4. J. V. Rund and R. A. Plane. J. Am. Chem. Soc. **89**, 367 (1964).
5. J. V. Rund and K. G. Claus. Inorg. Chem. **7**, 860 (1968).
6. K. G. Claus and J. V. Rund. Inorg. Chem. **8**, 59 (1969).
7. H. Irving and D. H. Mellor. J. Chem. Soc. 5222 (1962).
8. W. A. E. McBryde. Can. J. Chem. **45**, 2093 (1967).
9. L. G. Sillen and A. E. Martell. Stability constants of metal ion complexes. Special Publication No. 17. The Chemical Society, London. 1964.
10. K. J. Pedersen. J. Am. Chem. Soc. **51**, 2098 (1929).
11. H. Irving and R. J. P. Williams. J. Chem. Soc. 3192 (1953).
12. H. Sigel and D. B. McCormick. Acc. Chem. Res. **3**, 201 (1970).
13. R. Griesser and H. Sigel. Inorg. Chem. **9**, 1238 (1970).
14. G. A. L'Heureux and A. E. Martell. J. Inorg. Nucl. Chem. **28**, 481 (1966).
15. H. Sigel, K. Becker, and D. B. McCormick. Biochim. Biophys. Acta, **148**, 655 (1967).
16. P. R. Huber, R. Griesser, and H. Sigel. Inorg. Chem. **10**, 945 (1971).
17. D. D. Perrin, I. G. Sayce, and V. S. Sharma. J. Chem. Soc. (A), 1755 (1967).
18. W. B. Schaap and D. L. McMasters. J. Am. Chem. Soc. **83**, 4699 (1961).
19. J. E. Prue. J. Chem. Soc. 2331 (1952).
20. I. E. Bukolov, K. V. Astokhov, V. I. Zimin, and V. S. Tairov. Russ. J. Inorg. Chem. **7**, 816 (1962).
21. F. W. Yerhoff and D. W. Larson. Can. J. Chem. **50**, 826 (1972).
22. L. J. Bellamy and R. F. Branch. J. Chem. Soc. (A), 4491 (1954).
23. R. W. Hay. Aust. J. Chem. **17**, 759 (1964).
24. S. Seltzer, G. A, Hamilton, and F. H. Westheimer. J. Am. Chem. Soc. **81**, 4019 (1959).

Can. J. Chem. Downloaded from www.nrcresearchpress.com by 210.87.254.105 on 09/05/12
For personal use only.

Intermediate Binary Carbonyls of Palladium $Pd(CO)_n$ where $n = 1-3$; Preparation, Identification, and Diffusion Kinetics by Matrix Isolation Infrared Spectroscopy

E. P. KÜNDIG, M. MOSKOVITS, AND G. A. OZIN

Lash Miller Chemistry Laboratory and Erindale College, University of Toronto, Toronto, Ontario

Received April 26, 1972

The co-condensation reaction of atomic palladium with a dilute CO–argon mixture (1:1000) at 10 °K yields intermediate carbonyls of palladium $Pd(CO)_n$ where $n = 1-3$ as well as very small amounts of $Pd(CO)_4$. Isotopic substitution experiments using $^{12}C^{18}O$ were used to aid the spectral assignments. The probabilities of forming the various $Pd(CO)_n$ carbonyl species as a function of the CO concentration in Ar are analyzed and compared with the experimental observations. An analysis of the diffusion kinetics demonstrates their usefulness in assigning bands to various species in a series of compounds such as $Pd(CO)_n$. The data make possible the assignment of infrared absorptions at 2070, 2060, 2044, and 2050 cm^{-1} to tetrahedral (T_d) $Pd(CO)_4$, trigonal planar (D_{3h}) $Pd(CO)_3$, linear ($D_{\infty h}$) $Pd(CO)_2$, and linear ($C_{\infty v}$) PdCO, respectively. Cotton–Kraihanzel force constants are calculated for $Pd(CO)_n$ and are compared with those for the analogous intermediate carbonyls of nickel, $Ni(CO)_n$.

La réaction de co-condensation du palladium atomique avec un mélange dilué CO–argon (1:1000) à 10 °K permet de former des carbonyls intermédiaires de palladium, soit $Pd(CO)_n$, où $n = 1-3$ de même que de petites quantités de $Pd(CO)_4$. Nous avons utilisé la substitution isotopique, soit $^{12}C^{18}O$ pour interpréter plus facilement les bandes spectrales. Les probabilités de formation des différentes espèces carbonyl, $Pd(CO)_n$ en fonction de la concentration de CO dans l'argon sont alors analysées et comparées aux observations expérimentales. Une analyse de la cinétique de diffusion s'est avérée très utile dans l'assignation des bandes de différents groupes d'une série de composés, tels $Pd(CO)_n$. Les résultats rendent possible l'assignation des absorptions infrarouges à 2070, 2060, 2044, et 2050 cm^{-1} au $Pd(CO)_4$ tétrahédrique (T_d), au $Pd(CO)_3$ planaire trigonal (D_{3h}), au $Pd(CO)_2$ linaire ($D_{\infty h}$) et au PdCO linéaire ($C_{\infty v}$), respectivement. Nous calculons les constantes de force de Cotton-Kraihanzel pour $Pd(CO)_n$ et les comparons avec celles des carbonyls analogues intermédiaires du nickel, $Ni(CO)_n$. [Traduit par le journal]

Canadian Journal of Chemistry, **50**, 3587 (1972)

Can. J. Chem. Downloaded from www.nrcresearchpress.com by 210.87.254.6 on 09/05/12
For personal use only.

Introduction

Vibrational spectroscopic evidence for the existence and structure of palladium tetracarbonyl has recently been independently reported by two research groups (1, 2). In both cases the experiments involved the co-condensation of atomic palladium with carbon monoxide at cryogenic temperatures (4.2–20 °K). Ozin and co-workers (1) characterized the product of this reaction by using the combined techniques of matrix infrared and Raman spectroscopy including matrix Raman polarization data. Analysis of the spectra proved that the observed lines arose from $Pd(CO)_4$ with T_d symmetry. Ogden and co-worker (2) employed $^{12}C^{18}O$ isotope substitution experiments in order to characterize the carbonyl species. In a mixed $^{12}C^{16}O/^{12}C^{18}O$ matrix infrared experiment a quintet pattern of bands was observed in the CO stretching region, with the isotopic shifts and intensities expected for $Pd(CO)_4$ with T_d symmetry.

We have extended our matrix isolation infrared experiments of the Pd–CO system to dilute CO–argon matrices to prepare and characterize the intermediate carbonyls of palladium $Pd(CO)_n$ where $n = 1-3$. The palladium carbonyls are analogous to DeKock's (3) intermediate nickel carbonyls $Ni(CO)_n$ and are of considerable interest from the point of view of their vibrational spectra, structure, and bonding.

Experimental

The argon (99.99%) and carbon monoxide (99.9%) used in this work were supplied by Matheson. The furnace and cryotip arrangement have been described previously (4). Palladium atoms were produced by evaporation from a palladium filament (99.9%) of dimensions 1.75 in. × 0.375 in. × 0.010 in. The filament was suspended between water-cooled copper electrodes and directly heated within a.c. The rate of deposition was continuously monitored during

Can. J. Chem. Downloaded from www.nrcresearchpress.com by 210.87.254.6 on 09/05/12
For personal use only.

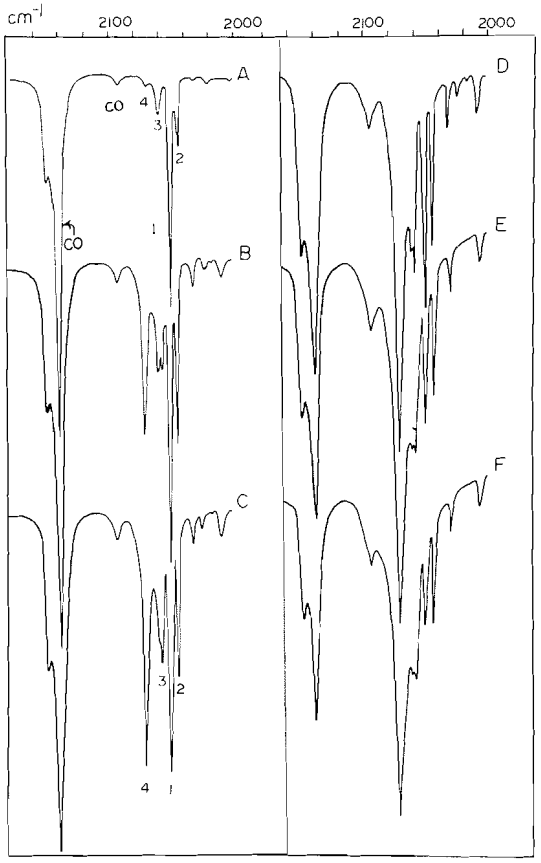

FIG. 1. The matrix isolation i.r. spectrum of the products of the co-condensation reaction between atomic palladium and CO in Ar (1:1000): (*A*), on deposition at 10 °K; (*B–F*) after successive diffusion warm up experiments at 20–30 K.

the course of the experiment using a quartz crystal microbalance with a resolution of 10^{-9} g (5). An average deposition was carried out for 4–6 h onto the cold tip of a Displex closed cycle helium refrigeration system. Infrared spectra were recorded on a Perkin–Elmer 180 spectrophotometer in the region 2400–200 cm^{-1}.

Results and Discussion

A number of experiments in which the matrix gas varied from pure CO to CO diluted in argon (M:A = 1:100–1:1000) as well as the analogous experiments using isotopically enriched carbon monoxide ($^{12}C^{18}O$ 92%, $^{12}C^{16}O$ 8%) were performed. The i.r. spectra for the Pd:CO:Ar ≅ 0.1:1.0:1000 experiments are presented in Fig. 1 and clearly show the presence of one major line (on the initial deposition, Fig. 1*A*) at 2050 cm^{-1} and three much weaker lines at 2070, 2060, and 2044 cm^{-1} (note that the band previously assigned to $Pd(CO)_4$ at 2070 cm^{-1} in pure CO matrices is, as expected, hardly visible in Fig. 1*A*). The order of band intensities at the end of the 10 °K deposition is $I_{2050} \gg I_{2044} > I_{2060} \gg I_{2070}$. Based on its intensity at 10 °K, its behavior during the warmup experiments and the isotopic shift observed with $^{12}C^{18}O$ the line at 2050 cm^{-1} was assigned to the monocarbonyl PdCO.

As can be seen in the annealing experiments, (Fig. 1*B–F*) and from a series of other runs, progressive growth and decay of the bands at 2044 and 2060 cm^{-1} occurs together with the rapid appearance of a band at 2070 cm^{-1}, assigned to the tetracarbonyl, $Pd(CO)_4$. Each of these lines has a counterpart line, with the expected frequency shifts on $^{12}C^{18}O$ substitution, calculated using the Cotton–Kraihanzel force field approximation (6), in which one assumes that the terminal CO stretching vibrations in metal carbonyls are "factored off" from the remaining vibrations of the molecule.

Observed ($^{12}C^{16}O$)	Observed ($^{12}C^{18}O$)	Calculated ($^{12}C^{18}O$)
2070 →	2022	2020
2060 →	2013	2010
2050 →	2005	2001
2044 →	1998	1995

Weak lines are observed at 2031 and 2008 cm^{-1} whose growth patterns do not correlate satisfactorily with any of the lines assigned to $Pd(CO)_n$ where $n = 1$–4 and are probably associated with aggregate carbonyl species formed in the initial diffusion processes during deposition.[1] We note that a similar effect was observed for nickel. These lines appear to be anomalous as their counterparts were not found in the $^{12}C^{18}O$ experiments and remain unaccounted for.

A *prima facie* assignment of the four bands at 2070, 2060, 2050, and 2044 cm^{-1} to the four $Pd(CO)_n$ species can be made on the basis of the

[1]Recent work in our laboratory involving the co-condensation reaction of Pd atoms with N_2/CO/Ar matrices has shown that the lines at 2031 and 2008 cm^{-1} are associated with mixed $Pd(N_2)_m(CO)_n$ species formed from trace impurities of nitrogen in the dilute matrices (E. P. Kündig and G. A. Ozin, unpublished results).

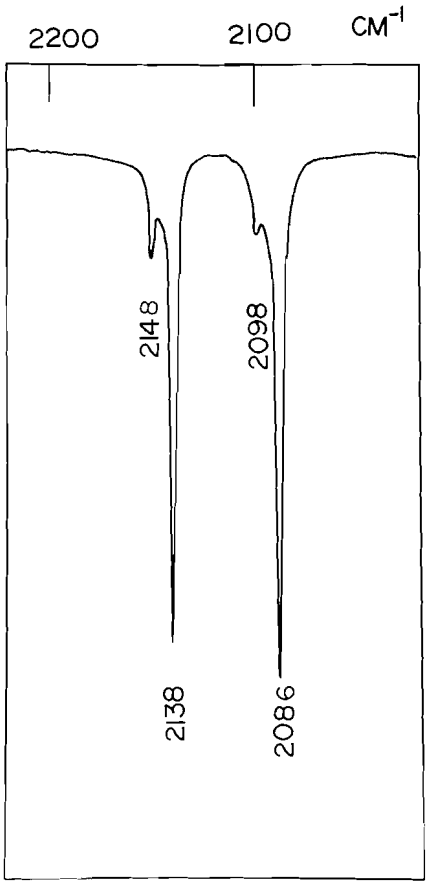

FIG. 2. The matrix i.r. spectrum of an approximately equimolar mixture of $^{12}C^{16}O$ and $^{12}C^{18}O$ in argon (1:1:500) at 10 °K.

relative intensities of the four bands assuming intuitively that at a dilution of CO:Ar = 1:1000 the relative probabilities of forming $Pd(CO)_n$ decreases monotonically with increasing n.

These assignments are strengthened further by the following analysis of the warmup data. Although these data were not obtained with rigorous quantitative analysis in mind sufficient interesting qualitative and semi-quantitative information can be obtained from them to warrant the following discussion.

Before describing the analysis of the warmup data it is necessary to briefly discuss the presently accepted nature of CO in the dilute argon matrices. It has been tacitly assumed in the literature (for example, refs. 3, 7, 8) that the 2138 cm^{-1} of matrix isolated CO belongs to monomeric CO rather than CO dimers. Moreover we have obtained new results which require that the carbon monoxide monomer–dimer problem (9, 10) be re-examined (11). A simple theory, based on a thermodynamic equilibrium between two types of CO argon lattice sites and argon vacancies provides an adequate and alternative explanation for (*a*) the CO/Ar concentration dependence, (*b*) the temperature dependent diffusion characteristics of, and (*c*) the respective matrix shifts from gaseous CO (on the basis of Buckingham's theory (12) for solvent shifts) of the i.r. absorptions at 2148 and 2138 cm^{-1}.

In carefully performed mixed isotope $^{12}C^{16}O:^{12}C^{18}O:Ar = 1:1:500$ matrix i.r. experiments both the lines at 2148 w and 2138 s cm^{-1} and their $^{12}C^{18}O$ counterpart lines were observed at 10 °K (Fig. 2). If the bands at 2138 and 2086 cm^{-1} did in fact belong to CO dimers then one would have expected to observe two additional bands associated with the mixed isotope dimer ($^{12}C^{16}O.^{12}C^{18}O$), one intermediate in frequency and one above them. One of these bands should in fact have been more intense than that of the smaller of the isotopically pure dimer bands on the basis of statistical arguments. The absence of this band makes the assignment of the 2138 cm^{-1} feature to CO dimer most unlikely.

In the present analysis the concentrations of free CO and of the four carbonyls $Pd(CO)_n$ are assumed to be proportional to their respective absorbances according to the Beer–Lambert relationship. Absorbances were calculated using peak height values. Thus

$$[1] \qquad A_n = \varepsilon_n [n] l$$

where A_n, $[n]$, and ε_n are the absorbance, concentration, and extinction coefficient respectively of $Pd(CO)_n$; and l is the matrix thickness. Similarly for the free CO, A_{co} was set equal to $\varepsilon_{co} l[CO]$. If one makes the assumption that

$$[2] \qquad \varepsilon_n = n\varepsilon_1$$

i.e. that each of the CO ligands absorbs independently of the others, and with similar strength in all the various $Pd(CO)_n$, then combining eqs. 1 and 2 one obtains

$$[3] \qquad [n] = \frac{1}{\varepsilon_1 l}(A_n/n)$$

Can. J. Chem. Downloaded from www.nrcresearchpress.com by 210.87.254.6 on 09/05/12
For personal use only.

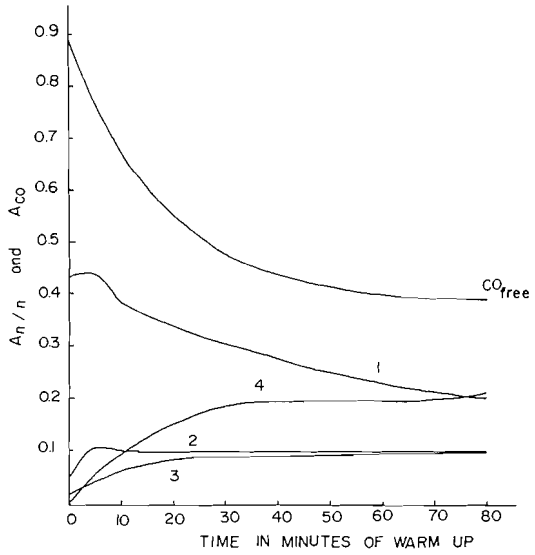

FIG. 3. A_n/n and A_{CO} as a function of warm up time, where A_n is the absorbance of $Pd(CO)_n$. The numbers 1 through 4 refer to the four $Pd(CO)_n$ species.

In the absence of suitable values for ε_1 and l we set the factor $\varepsilon_1 l$ equal to unity and use the quantity A_n/n as a direct measure of $[n]$.

Before beginning the warm ups the concentrations [1], [2], [3], and [4] were found to be in the ratio 1:0.125:0.039:0.009. To see under what circumstances this was compatible with a dilution of CO in Ar of 1:1000 we performed the following calculation.

We assume that the metal atoms are isolated from one another and that they occupy substitutional sites in the f.c.c. lattice of the solid argon. CO molecules are also assumed to occupy substitutional sites in the argon lattice and to react with the metal if it comes within one nearest neighbor distance of it. If there is no diffusion of either species before the matrix is warmed up and if the stabilities of the $Pd(CO)_n$ are in the order

$$Pd(CO)_4 \gg Pd(CO)_3 \gg Pd(CO)_2 \gg PdCO$$

then the probability P_n of finding a $Pd(CO)_n$ molecule is given by

$$[4] \qquad P_n = \binom{12}{n}\alpha^n(1-\alpha)^{12-n}$$

for $n = 1, 2, 3$ and

$$[5] \qquad P_4 = \sum_{n=4}^{12}\binom{12}{n}\alpha^n(1-\alpha)^{12-n}$$

where $\binom{12}{n}$ is the binomial coefficient and α is the CO/argon ratio.

Using formulas 4 and 5, [1], [2], [3], and [4] are found to be in the ratio $1:5.5\times10^{-3}:1.8\times10^{-5}:4.1\times10^{-8}$ for $\alpha = 10^{-3}$. The experimentally determined ratio indicates considerably more $Pd(CO)_{2\to4}$ than would be expected on the basis of this calculation. This suggests that during deposition there is considerable surface diffusion and reaction before the co-condensate is quenched. Based on this calculation alone, therefore, one cannot conclude unequivocably that one is justified in assigning the $Pd(CO)_n$ to the four bands on the basis of their intensities.

Analysis of the Warmup Kinetics

Hannay (13) gives the following equation for the rate of decrease of concentrations of two species A and B which react by diffusion in a solid

$$[6] \qquad \frac{-d[A]}{dt} = \frac{-d[B]}{dt} = 4\pi r_0[D_A + D_B] \times\left(1 + \frac{r_0}{[\pi(D_A + D_B)t]^{1/2}}\right)[A][B]$$

D_A and D_B are the diffusion coefficients of species A and B and r_0 is the radius of sphere within which A and B are assumed to react instantaneously. For typical values of diffusion coefficients in solids and for $r_0 \simeq 3$ Å the term $r_0/[\pi(D_A + D_B)t]^{1/2}$ is negligible for values of t in excess of 1. This, coupled with the assumption that one of the species B, say, diffuses much more slowly than A reduces eq. 6 to the form

$$[7] \qquad \frac{-d[A]}{dt} = 4\pi r_0 D_A[A][B]$$

which is of the form

$$\frac{d[\text{products}]}{dt} = k[A][B]$$

that is, that of second order kinetics. In our own case we assume that only CO diffuses, that trimolecular and higher encounters contribute negligibly to the formation of product and that no decomposition of the product takes place at the temperatures of the warmup experiments.

Accordingly the reactions which take place

Can. J. Chem. Downloaded from www.nrcresearchpress.com by 210.87.254.6 on 09/05/12
For personal use only.

Can. J. Chem. Downloaded from www.nrcresearchpress.com by 210.87.254.6 on 09/05/12
For personal use only.

during warmup are

$$M + CO \rightarrow \mathbf{1}$$
$$\mathbf{1} + CO \rightarrow \mathbf{2}$$
$$\mathbf{2} + CO \rightarrow \mathbf{3}$$
$$\mathbf{3} + CO \rightarrow \mathbf{4}$$

where **1**, **2**, **3**, **4** stand, respectively for the Pd mono, di, tri, tetra carbonyl and M for the free metal. The kinetics are therefore governed by the equations

$$[8] \qquad \frac{d[\mathbf{1}]}{dt} = k[CO]([M] - [\mathbf{1}])$$

$$[9] \qquad \frac{d[\mathbf{2}]}{dt} = k[CO]([\mathbf{1}] - [\mathbf{2}])$$

$$[10] \qquad \frac{d[\mathbf{3}]}{dt} = k[CO]([\mathbf{2}] - [\mathbf{3}])$$

$$[11] \qquad \frac{d[\mathbf{4}]}{dt} = k[CO][\mathbf{3}]$$

where

$$[12] \qquad k = 4\pi r_0 D_{CO}$$

and [M] stands for the free metal concentration. The free CO concentration decreases according to the equation

$$\frac{-d[CO]}{dt} = k[CO]([M] + [\mathbf{1}] + [\mathbf{2}] + [\mathbf{3}])$$

which may be written

$$[13] \qquad \frac{-d[CO]}{dt} = k[CO](N_0 - [\mathbf{4}])$$

where $N_0 = [M] + [\mathbf{1}] + [\mathbf{2}] + [\mathbf{3}] + [\mathbf{4}]$ is a constant equal to the total metal concentration in the matrix in any form. Figure 2 shows the concentration of the various species in the matrix as a function of warmup time. It indicates that with the exception of free CO the concentrations of all species at first increase with time. This indicates that initially the right hand sides of eqs. 8 through 11 are positive, thereby implying that

$$[14] \quad [M]_0 > [\mathbf{1}]_0 > [\mathbf{2}]_0 > [\mathbf{3}]_0 > [\mathbf{4}]_0$$

where the zero subscript indicates initial values.

This vindicates our assignments of the bands to the $Pd(CO)_n$ species on the basis of their relative intensities. It should be pointed out that because the concentrations of the four species are proportional to A_n/n rather than to A_n one requires a tentative assignment of the lines to the various $Pd(CO)_n$ before the concentrations can be evaluated and compared. The initial values of the A_n for the four carbonyl species were such, however, that only the assignment we stated previously is compatible with inequality (14).

Since the free metal concentration decreases monotonically with time, the concentration of the monocarbonyl is expected according to eq. 8 to come to a maximum and then decrease as indicated in Fig. 2. Although the temperature control and the time measurements were not carried out with the precision required in diffusion experiments it is instructive to see if the diffusion coefficient that one must assume for free CO in order to get the observed curves in Fig. 2 is a reasonable one. To do this we make use of the fact that initially $[\mathbf{4}] \ll N_0$ which yields the solution

$$[15] \qquad [CO] = [CO]_0 \exp(-kN_0 t)$$

for eq. 13.

A plot of $\log_e A_{CO}$ *vs.* t shows an initial straight line portion having slope of 3×10^{-4} s^{-1}. Taking N_0 to be approximately 3×10^{-8} atom cm^{-3} as determined from our deposition conditions and r_0 to be 4×10^{-8} cm, we obtain approximately 2×10^{-16} cm^2/s for D_{CO} in argon at a mean temperature of approximately 30 °K.

No literature values were found for the diffusion of CO in solid argon. One can, however, calculate the self-diffusion coefficient at 30 °K of Ar in Ar from the data of Berne *et al.* (14) to be of the order of 10^{-27} cm^2/s. It would appear that CO diffuses through solid argon much more rapidly than does argon itself. Such large differences in diffusivity of different species in the same solid are not uncommon in the solid state (15).

Our main purpose in presenting these calculations was to demonstrate their usefulness in assigning bands to various species in a series of compounds, such as $Pd(CO)_n$. The data prove that each of the observed bands at 2070, 2060, 2050, and 2044 cm^{-1} belong to a separate species since each behaves on annealing in an independent yet predictable manner.

TABLE 1. Cotton–Kraihanzel force constants for $Pd(CO)_n$ where $n = 1$–4.

Molecule	Frequency (cm^{-1}) M = Pd	Frequency (cm^{-1}) M = Ni	C.K. secular equation	Symmetry type	Force constant (mdyn/Å) M = Pd	Force constant (mdyn/Å) M = Ni
MCO	2050	1996	$\lambda_1 = \mu K_{CO}$	Σ^+	$K_{CO} = 16.97$	16.09
$M(CO)_2$	2044	1967	$\lambda_2 = \mu(K'_{CO} - K'_{COCO})$	Σ_u^+	$K'_{COCO} = 17.16$ $K'_{COCO} = 0.29$	16.63 1.00
$M(CO)_3$	2060	2017	$\lambda_3 = \mu(K''_{CO} - K''_{COCO})$	e'	$K''_{CO} = 17.35$ $K''_{COCO} = 0.21$	17.00 0.57
$M(CO)_4$	2070 2122*	2052	$\lambda_4^{t_2} = \mu(K'''_{CO} - K'''_{COCO})$ $\lambda_4^{a_1} = \mu(K'''_{CO} + 3K'''_{COCO})$	t_2 a_1	$K'''_{CO} = 17.54$ $K'''_{COCO} = 0.24$	17.42 0.32

*Observed in the matrix Raman spectrum of Pd in pure CO(1).

Discussion of the Bonding, CO Stretching Frequencies and Force Constants in the Palladium Carbonyls $Pd(CO)_n$ where $n = 1$–4

Kimball (16) has employed a group theoretical approach to determine which orbitals on a metal atom are available for σ and π bonding for various symmetries $M(CO)_n$. For the palladium carbonyls $Pd(CO)_n$ we can associate four i.r. absorptions with the four species $n = 1$–4 the most probable stereochemistries of which are linear ($C_{\infty v}$) PdCO, linear ($D_{\infty h}$) $Pd(CO)_2$, trigonal planar (D_{3h}) $Pd(CO)_3$, and tetrahedral (T_d) $Pd(CO)_4$. These structural assignments for $Pd(CO)_n$ were determined independently of the corresponding $Ni(CO)_n$ data (3) and are the expected shapes which would be favored using the Gillespie–Nyholm (17) electron pair repulsion theory for a d^{10} system and Kettle's (18) overlap-integral arguments.

The assignments for $Pd(CO)_n$ and $Ni(CO)_n$ show some interesting parallelisms. Probably the most striking one is that the order of the observed CO stretching frequencies for $Pd(CO)_n$ is found to be identical to that of $Ni(CO)_n$(3). According to simple M.O. bonding theory one expects that as the coordination number increases, the metal–carbonyl π bond strength should decrease while the CO π bond strength increase, since the d_π–p_π interaction is antibonding in the CO region. This leads to the prediction that the CO π bond strength should follow the order $Pd(CO)_4 > Pd(CO)_3 > Pd(CO)_2 > PdCO$. This order should be reflected by the bond stretching force constants but not necessarily by the frequencies because the frequencies of the $Pd(CO)_{2\to4}$ depend on both stretch and stretch–stretch interaction force constants while that of PdCO depends only on stretch force constants. In fact, the experimentally determined frequencies are in the order $Pd(CO)_4 > Pd(CO)_3 > PdCO > Pd(CO)_2$ with the frequencies of the mono and dicarbonyls reversed, while the bond stretching force constants calculated from these increase monotonically with n in $Pd(CO)_n$.

A comparison of the force constants of the CO bonds in $Pd(CO)_n$ with $Ni(CO)_n$ is also desirable and the Cotton–Kraihanzel approximation is an appropriate starting point (6). In this approximation only the K_{CO} and K_{COCO} force constants are retained in the analysis. The frequencies, symmetry assignments, and secular equations are listed in Table 1 for $Pd(CO)_n$ where $n = 1$–4 together with DeKock's data for $Ni(CO)_n$. As both the i.r. and Raman frequencies of $Pd(CO)_4$ are known, K'''_{CO} and K'''_{COCO} can be determined uniquely (17.54 and 0.24 mdyn/Å respectively) and are in close agreement with Darling and Ogden's values (2) (17.55 and 0.295 mdyn/Å) estimated from their matrix infrared data for the mixed isotopic molecules $Pd(^{12}C^{16}O)_n(^{12}C^{18}O)_{4-n}$ where $n = 0$–4. In order to determine the K_{CO} and K_{COCO} force constants for the lower palladium carbonyls the K_{CO} bond stretching force constant values are assumed to be linear with the coordination number n which is in analogy with the findings of DeKock for $Ni(CO)_n$(3).

The calculations yield a set of K_{CO} force constants which as expected follow the order predicted on the basis of the simple π bonding model. The calculated K_{COCO} stretch–stretch

Can. J. Chem. Downloaded from www.nrcresearchpress.com by 210.87.254.6 on 09/05/12
For personal use only.

Can. J. Chem. Downloaded from www.nrcresearchpress.com by 210.87.254.6 on 09/05/12
For personal use only.

interaction constant for $Pd(CO)_n$ are all quite similar but smaller than the corresponding values for $Ni(CO)_n$.

It is interesting to note that the CO stretching frequencies and corresponding K_{CO} force constants for $Pd(CO)_n$ are all higher values than those for the corresponding $Ni(CO)_n$. One can attempt to rationalize this observation in the light of the following discussion.

Semi-empirical molecular orbital calculations (19) have been performed on $Ni(CO)_4$ and, on the basis of overlap populations, conclude that the nickel 4p orbitals are the major contributions to both σ and π Ni—CO bonding.

If this is also true in the palladium case one can possibly relate the lower stability of palladium carbonyls to the unfavorable energy of the palladium 5p orbitals.

Changes in the charge density in the carbon–oxygen internuclear region have also been examined (20) in a series of isoelectronic and isostructural carbonyls and correlated with infrared CO stretching frequencies. The constancy of the CO interatomic overlap populations for σ bonding orbitals confirmed the proposal that the σ-bond strengths are invarient throughout a series of related carbonyls. However, the corresponding π-overlap populations show distinct changes, implying that changes in CO bond strength which determines the variation in CO stretching frequency, is dominated by a change in the π-orbital overlap population.

Thus the higher CO stretching frequencies in $Pd(CO)_n$ compared to $Ni(CO)_n$ would appear to reflect a decreased M—CO π interaction in palladium relative to the corresponding nickel carbonyls.

It is also noteworthy that we could not detect any Pd—C stretching modes for $Pd(CO)_n$ where $n = 1$–4 in the low frequency region 500–200 cm^{-1} where the corresponding modes of $Ni(CO)_n$ are observed (3, 21). In matrix infrared studies performed independently of our own, Ogden and Darling (2) could not observe a Pd—C stretching mode for $Pd(CO)_4$.

Thus we are forced to conclude that either the vibrational modes of $Pd(CO)_n$ where $n = 1$–4 other than the CO stretching modes have low extinction coefficients and are too weak to observe or that they lie below 200 cm^{-1}.

In summary, the data appear to indicate weaker Pd—C bonds in $Pd(CO)_n$ compared to $Ni(CO)_n$ and this may be one of the contributing factors responsible for the unstable nature of $Pd(CO)_4$ relative to $Ni(CO)_4$.

We wish to thank Mr. H. Huber, Mr. B. Hughes, Mr. B. Torbet, Mr. A. Campbell, and Mr. R. Carter for technical assistance and the National Research Council of Canada and the Research Corporation for financial assistance.

1. E. P. KÜNDIG, H. HUBER, M. MOSKOVITS, and G. A. OZIN. Nat. Phys. Sci. 235, 98 (1972); J. Mol. Struct. In press.
2. J. H. DARLING and J. S. OGDEN. Inorg. Chem. **11**, 666 (1972).
3. R. L. DEKOCK. Inorg. Chem. **10**, 1205 (1971).
4. E. P. KÜNDIG, M. MOSKOVITS, and G. A. OZIN. J. Mol. Struct. 1972. In press.
5. M. MOSKOVITS and G. A. OZIN. J. Appl. Spectrosc. 1972. In press.
6. F. A. COTTON and C. S. KRAIHANZEL. J. Am. Chem. Soc. **84**, 4432 (1962).
7. J. L. SLATER, R. K. SHELINE, K. C. LIN, and W. WELTNER. J. Chem. Phys. **55**, 5129 (1971).
8. A. BOS. Chem. Commun. 26 (1972).
9. J. B. DAVIES and H. E. HALLAM. J. Chem. Soc. Faraday II, 509 (1972).
10. G. LEROI, G. EWING, and G. C. PIMENTEL. J. Chem. Phys. **40**, 2298 (1964).
11. M. MOSKOVITS and G. A. OZIN. J. Chem. Phys. (1972). In press.
12. A. D. BUCKINGHAM. Proc. Roy. Soc. (London), A248, 169 (1958); A255, 32 (1960).
13. N. B. HANNAY. Solid state chemistry. Prentice Hall, New Jersey. 1967. p. 114.
14. A. BERNE, G. BOATO, and M. DEPAZ. Nuovo Cimento, **24**, 1179 (1962).
15. K. HAUFFE. Oxidation of metals. Plenum Press, N.Y. (1965). p. 45.
16. G. E. KIMBALL. J. Chem. Phys. **8**, 188 (1940).
17. R. J. GILLESPIE and R. S. NYHOLM. Q. Rev. Chem. Soc. **11**, 339 (1957). R. J. GILLESPIE. J. Chem. Educ. **47**, 18 (1970).
18. S. F. A. KETTLE. J. Chem. Soc. (A), 420 (1966).
19. A. F. SCHREINER and T. L. BROWN. J. Am. Chem. Soc. **90**, 3366 (1968).
20. K. G. CAULTON and R. F. FENSKE. Inorg. Chem. **7**, 1273 (1968). K. F. PURCELL. J. Am. Chem. Soc. **91**, 3487 (1969).
21. L. H. JONES. Inorg. Chem. **6**, 1269 (1967).

A Low Temperature Infrared Study of Self-association in Thiols

R. BICCA DE ALENCASTRO[1] AND C. SANDORFY

Département de Chimie, Université de Montréal, Montréal, Québec

Received May 24, 1972

The infrared spectra of several aliphatic thiols and of benzenethiol were measured between 2400 and 2700 cm^{-1}, and 4800 and 5300 cm^{-1} in a 1:1 mixture of CCl_3F and $C_2F_4Br_2$, at temperatures ranging from 20 to −190 °C. Dimerization takes place at low temperatures and more highly associated species also appear. Free S—H groups are present in the solutions as well as in the pure liquids, even at the lowest temperatures. The association is of the S—H---S type in aliphatic thiols; both S—H---S and S—H---π bonds are found in the case of benzenethiol and α-toluenethiol. Hydrogen bonding has little effect on the anharmonicity of the S—H stretching vibration.

Les spectres infrarouges d'un certain nombre de thiols aliphatiques est du benzènethiol ont été mesurés entre 2400 et 2700 cm^{-1} et 4800 et 5300 cm^{-1} dans un mélange de CCl_3F et de $C_2F_4Br_2$ à des températures allant de 20 à −190 °C. Quand on abaisse la température, des dimères se forment suivis par des espèces plus associées. Des groupements S—H libres sont présents, toutefois, même aux plus basses températures et même dans les liquides. Les associations sont du type S—H---S dans les thiols aliphatiques alors qu'on trouve des liaisons S—H---S aussi bien que S—H---π chez le benzènethiol et le α-toluènethiol. La formation de la liaison hydrogène n'affecte guère l'anharmonicité de la vibration de valence S—H.

Canadian Journal of Chemistry, **50**, 3594 (1972)

Can. J. Chem. Downloaded from www.nrcresearchpress.com by 210.87.254.42 on 09/05/12
For personal use only.

Introduction

S—H---S type hydrogen bonds are known to exist in dissolved and liquid thiols and thiophenols (1–6). In inert solvents, a free and an associated S—H stretching band can be distinguished at concentrations higher than 0.5–1.0 *M*. The free band is usually located at about 2580–2590 cm^{-1}, and it undergoes a low frequency shift upon hydrogen bond formation. The fundamental of the associated species shows an intrinsic intensity about 10 to 20 times greater than that of the free band (3, 4).

The associated species was usually thought to be a dimer. Infrared and n.m.r. studies of the molecular equilibria (3, 6) led to monomer–dimer equilibria highly displaced in favor of the monomer, at least at room temperature and at moderate concentrations. Some authors considered the possibility of the formation of open or cyclic dimers in both aliphatic and aromatic mercaptans (4, 5, 7). Josien, Dizabo, and Saumagne (1), and Cole, Little, and Michell (7) attributed a band found at 2564 cm^{-1} in liquid benzenethiol to a polymeric species.

We thought it might be interesting to study self-association of sulfhydryl-containing compounds over a wide temperature range and to measure the first S—H overtones as well as the fundamentals. The solvent used was a 1:1 mixture of CCl_3F (Freon 11) and $C_2Br_2F_4$ (Freon 114B2), (FR), which becomes a rigid glass at liquid nitrogen temperature. We hoped (*a*) to be able to follow the changing pattern of self-association from room to liquid nitrogen temperature; (*b*) to determine the anharmonicity constant of the S—H stretching vibration, and (*c*) to make the identification of certain free and associated species easier by exploiting the different intensity ratio of the corresponding bands at the fundamental and at the first overtone level.

Similar studies on the self-association of alcohols and amines were performed in this laboratory (8, 9) and it is hoped that the knowledge gained on the nature of hydrogen bonding of O—H, N—H, and S—H groups will be helpful in the investigation of more complex hydrogen bonded systems.

Results and Discussion

1. *Aliphatic Thiols*

We have chosen propane-1-thiol, propane-2-thiol, and 2-methyl-propane-2-thiol (tert-butylmercaptan) as representatives of primary, secondary, and tertiary aliphatic thiols with varying degrees of steric hindrance affecting

[1]Brazil–Canada exchange fellow. On leave of absence from Instituto de Química, Universidade Federal do Rio de Janeiro, Rio de Janeiro, Brazil.

Can. J. Chem. Downloaded from www.nrcresearchpress.com by 210.87.254.42 on 09/05/12
For personal use only.

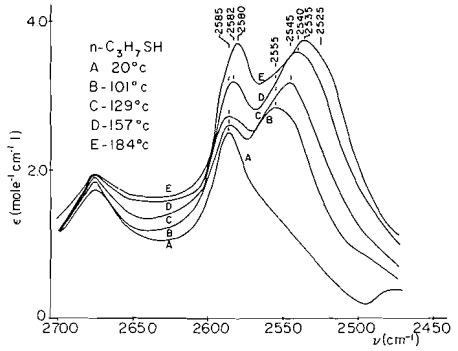

FIG. 1. The infrared spectrum (2400–2700 cm^{-1}) of a 0.69 *M* solution of propane-1-thiol in FR at different temperatures from 20 to −184 °C.

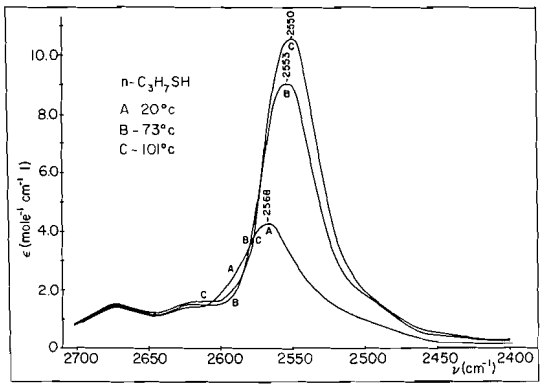

FIG. 2. The infrared spectrum (2400–2700 cm^{-1}) of liquid propane-1-thiol at 20, −73, and −101 °C.

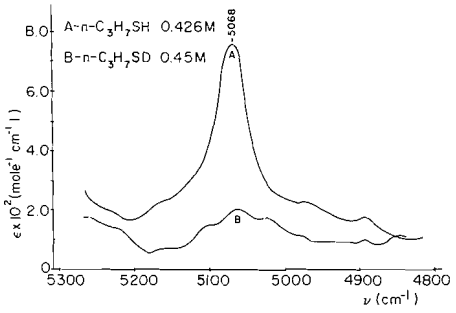

FIG. 3. The infrared spectrum (4800–5300 cm^{-1}) of solutions of propane-1-thiol and propane-1-thiol-d_1 in FR at 20 °C.

the S—H group. These compounds are sufficiently soluble in our solvent (FR). The results are very similar for these three molecules in the region of the fundamental, as well as in the region of the first overtone (Figs. 1–10).

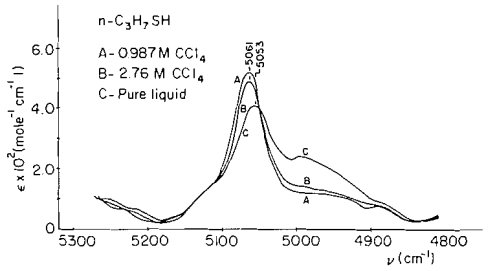

FIG. 4. The infrared spectrum (4800–5300 cm^{-1}) of solutions of propane-1-thiol in carbon tetrachloride and of the pure liquid at 20 °C.

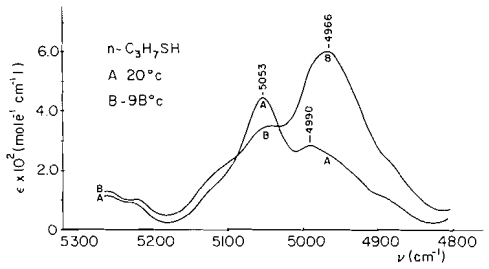

FIG. 5. The infrared spectrum (4800–5300 cm^{-1}) of liquid propane-1-thiol at 20 °C and −98 °C.

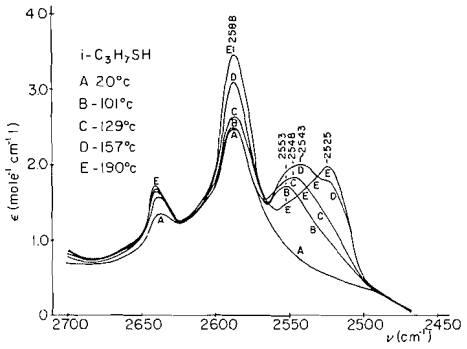

FIG. 6. The infrared spectrum (2400–2700 cm^{-1}) of a 0.47 *M* solution of propane-2-thiol in FR at different temperatures from 20 to −190 °C.

Surprisingly, in dilute solution, the fundamental of the free S—H group has its intensity increased when temperature is decreased (we shall discuss this apparent anomaly in section 2). At the same time, at lower frequencies, a broad and asymmetrical band appears which is very probably due to more than one associated species. In the case of propane-2-thiol (Fig. 6), two distinct associated bands are actually resolved. Both the free and the associated bands

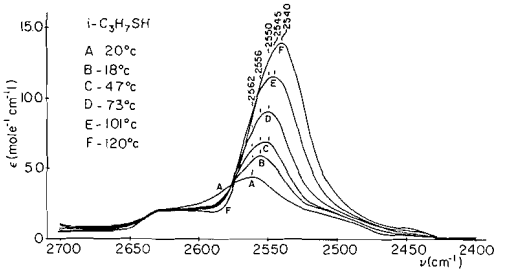

FIG. 7. The infrared spectrum (2400–2700 cm^{-1}) of liquid propane-2-thiol at different temperatures from 20 °C to −120 °C.

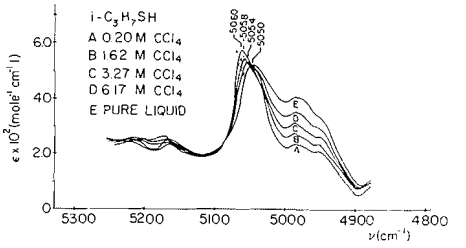

FIG. 9. The infrared spectrum (4800–5300 cm^{-1}) of solutions of propane-2-thiol in carbon tetrachloride and of the pure liquid at 20 °C.

are quite weak. Their apparent molecular extinction coefficients are of the order of $\varepsilon = 3$ l mol^{-1} cm^{-1}, and the approximate half-widths are about 30 cm^{-1} for propane-1-thiol and propane-2-thiol. In order to check our assignments, we measured the spectrum of propane-1-thiol-d_1 at room temperature as well as at low temperatures. The disappearance of both the free and the associated bands demonstrated their S—H character. (There is a weak band between 2675 and 2640 cm^{-1} in the aliphatic thiols. This band does not shift when we deuterate the —SH group, so it is not an SH band. According to Smith, Devlin, and Scott (10) it is a combination of two CH_3 deformation vibrations.)

Following suggestions by previous authors it seems natural to consider the higher frequency band located near 2540 cm^{-1} as the band due to the dimer and the lower frequency component near 2525 cm^{-1} as originating from a more associated species.

The low melting point of propane-1-thiol and propane-2-thiol enabled us to measure the spectra of the pure liquids at low temperatures (Figs. 2 and 7). At room temperature only a broad band can be seen with maximum at 2568 cm^{-1} for propane-1-thiol, and 2562 cm^{-1} for propane-2-thiol. The intensity of these bands increases upon lowering the temperature and their maxima are slightly displaced towards lower frequencies. This is a complex band due to more than one associated species.

The first overtone of the free S—H vibration is located near 5050 cm^{-1} and is split in two in dilute solutions. This splitting has been studied by several authors (10–12) and has been linked to the existence of rotamers. The splitting of the first overtone is roughly double (about 20 cm^{-1}) that of the fundamental. We have also measured the spectrum of propane-1-thiol-d_1 in this region. It contains only much weaker bands, which can be interpreted in terms of combinations involving C—H and S—D motions. This supports our assignment of the band near 5050 cm^{-1} to the free S—H stretching overtone. The corresponding anharmonicity constants can be computed from

$$\omega_e x_e = \nu_{01} - \frac{\nu_{02}}{2}$$

for the free S—H stretching vibration of the aliphatic thiols. It is of the order of 50 cm^{-1}, lower than those of the free OH and NH vibrations which are about 80 and 70 cm^{-1}, respectively (see refs. 9, 13, and references therein).

When the temperature is lowered the intensity of the free band decreases, and a band appears near 4960 cm^{-1} with a shoulder near 4930 cm^{-1}. The relative weakness of these bands is well in line with the similar behavior of the overtones of O—H and N—H associated vibrators (8, 9).

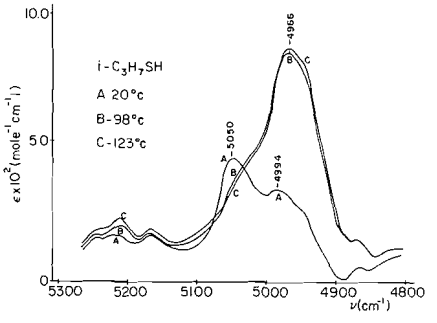

FIG. 8. The infrared spectrum (4800–5300 cm^{-1}) of liquid propane-2-thiol at different temperatures from 20 to −123 °C.

Can. J. Chem. Downloaded from www.nrcresearchpress.com by 210.87.254.42 on 09/05/12
For personal use only.

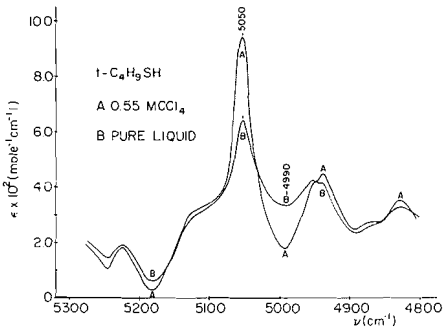

FIG. 10. The infrared spectrum (4800–5300 cm^{-1}) of a 0.55 *M* solution of methyl-2-propane-2-thiol (*t*-butylmercaptan) in carbon tetrachloride and of the pure liquid at 20 °C.

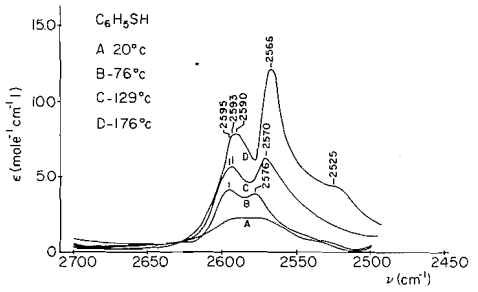

FIG. 11. The infrared spectrum (2400–2700 cm^{-1}) of a 0.29 *M* solution of benzenethiol in FR at different temperatures from 20 °C to −176 °C.

The anharmonicities computed with these overtone frequencies are about the same as that of the free band.

To ascertain the existence of these weak associated overtone bands we measured them at higher concentrations and in the pure liquid (Figs. 4, 5, 8, and 9). At −98 °C the spectrum of the pure liquid shows that the free band is still present, but its intensity is decreased and we observe a pronounced increase in the intensity of the associated bands. This implies that the pure liquid is mostly associated at this temperature, in agreement with the observations made with the fundamental. Again two strongly overlapping bands can be seen and we assign the one at higher frequencies to a dimer and the one at lower frequencies to a more associated species.

Observations made in this laboratory in the case of amines (14) showed that the bromine-containing solvent is capable of diminishing the degree of association. In order to ascertain whether the thiols behave similarly, we measured the spectrum of propane-2-thiol in CCl_3F (Freon 11) only, down to −98 °C, the lowest temperature we could reach with this solvent. The spectra were practically identical with those taken in FR at the same temperatures. It would seem then, that the bromine atoms in the solvent do not modify the association equilibria, (at least down to −98 °C).

The only new feature of the first overtone spectrum of 2-methyl-propane-2-thiol (tert-butylmercaptan) (Fig. 10) is that the free band is sharper and stronger than that of the other mercaptans. This means that in the pure liquid, the free band is less affected by overlap with neighboring bands, indicating that due to steric reasons it is associated to a lesser degree than propane-1-thiol and propane-2-thiol. The differences between the spectra of the pure liquid and dilute solutions nevertheless permit us to locate the associated band near 4990 cm^{-1} at room temperature (Fig. 10). Several weak bands can be seen in Fig. 10 at both higher and lower frequencies, but since they do not change their intensity appreciably with concentration, they must be due to combination tones not involving the S—H vibrator.

2. Benzenethiol and α-Toluenethiol

Several investigations have been carried out on the self-association of benzenethiol and substituted benzenethiols (1–7, and 15). The fundamental region shows a weak free band at 2591 cm^{-1} (for benzenethiol) and a dimer band at 2577 cm^{-1}, in dilute CCl_4 solutions. In the pure liquid the maximum is at 2569 cm^{-1} and this new maximum was attributed to a polymeric species (1).

We have measured the spectrum of a dilute solution (0.29 *M*) of benzenethiol in FR at temperatures ranging from 20 to −176 °C (Fig. 11). The free band is constantly present at about 2590 cm^{-1}, but an associated band at 2566 cm^{-1} (at −176 °C) becomes gradually stronger as the temperature is lowered. The asymmetry of this band and a weak band at 2525 cm^{-1} indicate the existence of other associated species.

As in the case of aliphatic thiols the intensity of the free band increases upon lowering the temperature. This curious fact deserves some discussion at this point. It is probably due to a

Can. J. Chem. Downloaded from www.nrcresearchpress.com by 210.87.254.42 on 09/05/12
For personal use only.

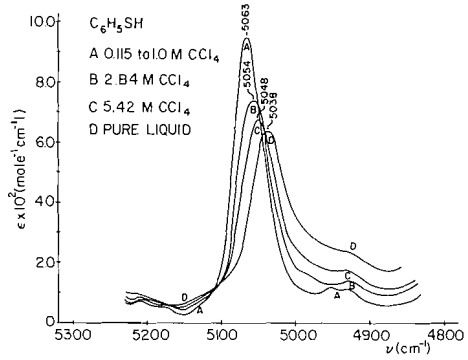

FIG. 12. The infrared spectrum (4800–5300 cm^{-1}) of solutions of benzenethiol in carbon tetrachloride and that of the pure liquid at 20 °C.

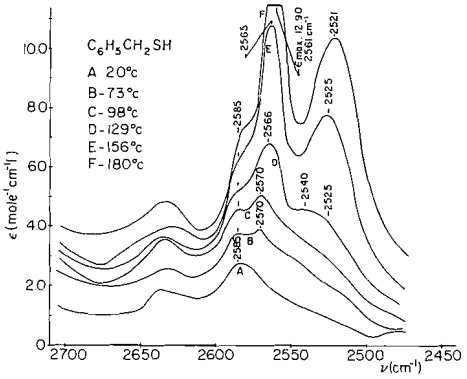

FIG. 13. The infrared spectrum (2400–2700 cm^{-1}) of a 0.37 *M* solution of α-toluenethiol in FR at different temperatures from 20 °C to −180 °C; curves displaced arbitrarily in the vertical axis.

combination of reasons. Firstly, the free and associated bands are close to each other (much more so than in the case of O—H---O or N—H---N bonds) and the apparent intensity of the free band is actually boosted by overlap with the dimer band. Secondly, if the dimer is an open dimer the free S—H endgroup should contribute to the observed intensity of the free band (actually the persistence of the free band could be used as an argument in favor of the open dimer structure). Thirdly, the equilibrium between rotamers and the different intensities of the respective bands could cause intensification of the free band in the case of aliphatic thiols if we suppose that the rotamer favored at lower temperatures has the more intense band.

In the overtone region, in dilute solutions (0.23 *M* in FR), only the free band is found with a maximum at 5076 cm^{-1}, and a half-width of about 50 cm^{-1}. It is slightly asymmetrical at its lower frequency side. At low temperature the intensity of this band decreases and a weak shoulder appears near 5020 cm^{-1}, but there is no detectable increase in intensity in the 4900–5000 cm^{-1} range. We were not able to measure the spectrum of the liquid at low temperatures (it crystallizes near −15 °C), so we studied the concentration dependence at room temperature (Fig. 12). Although only one maximum is seen in the whole range of concentrations (0.115, 1.00, 2.84, 5.42, and 9.76 *M* in CCl_4) the large half-width, the asymmetry, and the observed shifting of the frequency, together with observations made on the fundamental region, indicate that this band is actually composed of two strongly overlapping bands. They would give the usual anharmonicities of the order of 50 to 60 cm^{-1}.

Benzenethiol presents an interesting problem. The frequency of the strongest band at 2566 cm^{-1} (Fig. 11) is closer to that of the free band than the dimer band of the aliphatic thiols, and it is sharper. We are therefore justified in asking whether or not it is due to the same type of hydrogen bond (S—H---S) as in aliphatic thiols. It has been reported that the intensity of this band increases when mesitylene is added to the solution (1), and it has been suggested (5) that it could be due to S—H---π type bonds.

In order to clarify this point, we measured the spectra of α-toluenethiol which should present a spectrum similar to an aliphatic compound if there were only S—H---S type bonds present. The fundamental region of this molecule was measured from 20 to −180 °C in a 0.37 *M* solution of FR. The results are quite interesting: we find bands that correspond to both aromatic and aliphatic thiols (Fig. 13). At room temperature, the free band is at 2585 cm^{-1} which is characteristic of an aliphatic thiol. The associated bands readily appear when the temperature is lowered. At the lowest temperatures the free band is still present as a shoulder of the much more intense band centered at 2561 cm^{-1} and another broad band can be seen with maximum at 2521 cm^{-1}. This last band can be seen at intermediate temperatures to be formed by two overlapping bands (located at 2540 and 2525 cm^{-1} at −129 °C) as

Can. J. Chem. Downloaded from www.nrcresearchpress.com by 210.87.254.42 on 09/05/12
For personal use only.

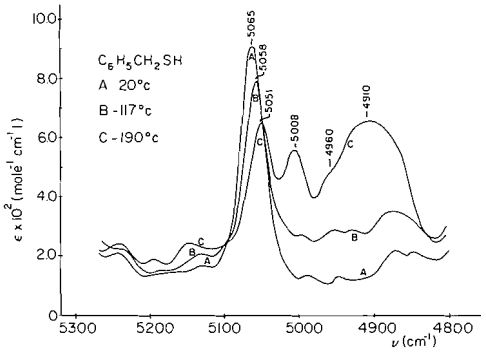

FIG. 14. The infrared spectrum (4800–5300 cm^{-1}) of a 0.37 *M* solution of α-toluenethiol in FR at different temperatures from 20 to −190 °C.

in the case of aliphatic thiols. We therefore interpret the 2561 cm^{-1} band (at −180 °C) as a dimer of the S—H---π type, and the bands found in the normal position for the aliphatic thiols (2540–2520 cm^{-1}) as due to S—H---S type association.

The free, S—H---π, and S—H---S bands (Fig. 14) are also clearly distinguished at the overtone level. It seems natural to assign the bands found at 5065 cm^{-1} (20 °C); 5008 cm^{-1} (−180 °C); and 4910 cm^{-1} (at −180 °C; with a sub-maximum near 4960 cm^{-1}) to the free, S—H---π, and S—H---S types, respectively. The latter band contains evidently several different species, however, and its intensity seems to be higher than that of the S—H---S dimer overtone for either benzenethiol or the aliphatic thiols. It must contain more highly associated species of both the S—H---S or S—H---π types, but we do not have any additional information on this. The computed anharmonicities are of the order of 50 to 60 cm^{-1} as in the previous cases.

Thus, the results obtained with α-toluenethiol help us to have a better understanding of the spectrum of benzenethiol. We interpret the 2566 cm^{-1} band as due to S—H---π type hydrogen bonding. Its overtone is likely to be in the region of 5000–5020 cm^{-1}. The other bands observed at low frequencies must be of the S—H---S type as in the case of α-toluenethiol.

Experimental

The fundamentals were measured on a Perkin–Elmer Model 621 spectrometer and the overtones on a Cary 17 instrument.

In the fundamental region, we used 0.48 and 0.9 mm cells for solutions, and 0.07 mm cells for the pure liquids. The cell windows were either silver chloride or silver bromide. In the overtone region, 1, 3, and 10 cm quartz cells were used. Their design followed conventional lines. No reactions were observed between the windows and the solutions or liquids. Temperatures were measured with a copper–constantan thermocouple.

The solvents were 1:1 mixtures of CCl_3F (Freon 11) and $C_2F_4Br_2$ (Freon 114B2) (FR) obtained from the E.I. Dupont de Nemours Co. of Canada. They were distilled and kept over phosphorus pentoxide. Spectrograde quality carbon tetrachloride from Anachemia Chems. Ltd., Montreal, was dried on molecular sieves type 4A.

The mercaptans were purchased from Aldrich Chem. Co. and were i.r., g.c. or refraction index controlled. Our benzenethiol was an Eastman Kodak Co., b.p.: 62–63/15 mm, chemical reagent quality product. The infrared spectra of all compounds we measured were practically identical with their previously published spectra. All products were handled in inert atmosphere to avoid oxidation or moisture adsorption. Deuterated propane-1-thiol was purchased from Merck, Sharp, and Dohme of Canada Ltd., with a minimum isotopic purity of about 98%, and was handled by conventional vacuum line techniques.

The solutions were prepared gravimetrically in narrow-neck volumetric flasks and the concentration was corrected for solvent contraction, admitting a linear dependence of volume with temperature. All curves were corrected for solvent absorption. Other details of the experimental technique, including calibration of the instruments were given elsewhere (13, 16).

Conclusions

The above results confirm the existence of S—H---S hydrogen bonds as postulated by previous authors. As the temperature is lowered the proportion of the dimer increases, but we find free molecules even at the lowest temperatures. At low temperatures at least one more highly associated species is present.

The S—H stretching overtones exhibit a behavior similar to that already described for alcohols and amines. The free band's relative intensity is much greater than at the fundamental level and makes it easier to identify free molecules, which are thus seen to exist even in the pure liquids, as in liquid water, alcohols, and amines (8, 9).

The anharmonicity constants are low, of the order of 50–60 cm^{-1} and they do not differ much from the free to the associated species. This is another characteristic of all *weakly* self-associated systems of the O—H---O, N—H---N, and S—H---S type.

In the case of benzenethiol and α-toluenethiol the presence of both S—H---π and S—H---S type bonds is strongly indicated.

Can. J. Chem. Downloaded from www.nrcresearchpress.com by 210.87.254.42 on 09/05/12
For personal use only.

We would like to express our thanks to the National Research Council of Canada for financial help. One of us (R.B.A.) would like to express his gratitude to the National Research Council of Canada and the Conselho Nacional de Pesquisas, Rio de Janeiro, Brazil, for financial assistance under the Brazil–Canada Program for Scientific Exchange, and to the Instituto de Química da Universidade Federal do Rio de Janeiro, Rio de Janeiro, Brazil, for a special leave of absence.

1. M.-L. JOSIEN, P. DIZABO, and P. SAUMAGNE. Bull. Soc. Chim. Fr. 423 (1957).
2. M.-L. JOSIEN, C. CASTINEL, and P. SAUMAGNE. Bull. Soc. Chim. Fr. 648 (1957).
3. R. A. SPURR and H. F. BYERS. J. Phys. Chem. **62**, 425 (1958).
4. M. O. BULANIN, G. S. DENISOV, and R. A. PUSHKINA. Opt. Spectrosc. **6**, (6), 491 (1959).
5. J. G. DAVID and H. E. HALLAM. Spectrochim. Acta, **21**, 841 (1965).
6. S. H. MARCUS and S. I. MILLER. J. Am. Chem. Soc. **88**, 3719 (1966).
7. A. R. H. COLE, L. H. LITTLE, and A. J. MICHELL. Spectrochim. Acta, **21**, 1169 (1965).
8. C. BOURDÉRON, J.-J. PÉRON, and C. SANDORFY. J. Phys. Chem. **76**, 864, 869 (1972).
9. M.-C. BERNARD-HOUPLAIN and C. SANDORFY. J. Chem. Phys. **56**, 3412 (1972).
10. D. SMITH, J. P. DEVLIN, and D. W. SCOTT. J. Mol. Spectrosc. **25**, 174 (1968).
11. P. J. KRUEGER, J. JAN, and H. WIESER. J. Mol. Struct. **5**, 375 (1970).
12. T. TORGRIMSEN and P. KLAEBOE. Acta Chem. Scand. **24**, 1139 (1970).
13. M. ASSELIN and C. SANDORFY. J. Mol. Struct. **8**, 145 (1971).
14. M.-C. BERNARD-HOUPLAIN, C. BOURDÉRON, J.-J. PÉRON, and C. SANDORFY. Chem. Phys. Lett. **11**, 149 (1971).
15. P. J. KRUEGER. Tetrahedron, **26**, 4753 (1970).
16. G. DUROCHER and C. SANDORFY. J. Mol. Spectrosc. **20**, 410 (1966).

Can. J. Chem. Downloaded from www.nrcresearchpress.com by 210.87.254.42 on 09/05/12
For personal use only.

Solvent Effects on the Phosphorescent State of Some Aromatic Carbonyls

JAMES B. GALLIVAN

American Cyanamid Company, Central Research Division, Stamford, Connecticut 06904

Received April 17, 1972

Triplet state properties of chromone, 4-chromanone, acetophenone, and several alkyl derivatives of acetophenone were studied in a variety of solvent systems. The phosphorescence excitation method was used to monitor the energies and relative intensities of singlet–triplet absorption bands in the presence and absence of heavy atom solvents. The results, combined with earlier optical and magnetic resonance studies of such systems, illustrate the importance of solvent environment in determining fundamental properties of these excited states. Observed trends are interpreted in terms of contrasting effects of changing solvent polarity on proximate n,π^* and π,π^* triplet states. To describe the relative contribution of each orbital type to the phosphorescent state, the coefficients of each wavefunction must change with solvent. Correspondingly, the solvent environment should be specified whenever orbital designations are made.

Nous avons étudié les propriétés de l'état triplet du chromone, du chromanone-4, de l'acétophénone et de plusieurs dérivés alkylés de l'acétophénone dans plusieurs systèmes de solvants. La méthode d'excitation par phosphorescence a été utilisée pour promouvoir les énergies et les intensités relatives des bandes d'absorption singulet-triplet en présence ou pas de solvants d'atomes lourds. Les résultats, combinés avec ceux provenant de la optique et magnétique résonance ultérieure de tels systèmes, illustrent l'importance de l'environnement du solvant dans la détermination des propriétés fondamentales de ces états excités. Nous interprétons les tendances observées en termes d'effets contrastants provenant du changement de polarité des solvants sur les états triplets n,π^* et π,π^* rapprochés. Afin de décrire la contribution relative de chaque type d'orbitale à l'état phosphorescent, les coefficients de chaque fonction d'onde doivent changer avec le solvant. On doit également spécifier l'environnement du solvant chaque fois qu'on fait les désignations d'orbitales. [Traduit par le journal]

Canadian Journal of Chemistry, **50**, 3601 (1972)

Can. J. Chem. Downloaded from www.nrcresearchpress.com by 210.87.254.42 on 09/05/12
For personal use only.

Introduction

The ability to invert the relative energies of close lying n,π^* and π,π^* triplet states by altering the solvent environment has been demonstrated for certain aromatic carbonyls (1, 2). Problems associated with orbital labelling of the phosphorescent state of such compounds have been discussed (3). In a prior communication (4), zero field splitting (Z.F.S.) values determined from e.p.r. spectra of the triplet state were used to help designate orbital character. In this communication, results obtained by the phosphorescence excitation (P.E.) method are emphasized although a variety of experimental parameters are reported. The P.E. technique, as developed by Kearns and his associates (5), is considered advantageous in that it not only monitors the phosphorescent state, but also reveals the absorption spectra of the singlet–triplet transitions involved. Spectral differences in these transitions, induced by heavy atom solvents and changes in solvent polarity, provide valuable guidelines for orbital classification.

Experimental

Essential experimental details on all aspects of the work reported here, excepting the phosphorescence excitation spectra, have been given previously (3, 4, 6). The acetophenone (Fisher) and 4'-methylacetophenone (Eastman Kodak) were used as received. Eastman ethylene glycol was diluted 1:1 with distilled water to prepare the EG-W glasses. The heavy atom solvents ethyl iodide, carbon tetrabromide, and 1,5-diiodopentane (all from Eastman) and carbon tetrachloride (Baker) were used as received.

Phosphorescence excitation spectra were scanned at 77 °K on a Perkin–Elmer (Hitachi) MPF-2A luminescence spectrophotometer. High concentrations (~ 0.1 *M*) of the various solutes were examined in 3-methylpentane (3-MP), 2-methyltetrahydrofuran (MTHF), ethanol (ETOH), and ethylene glycol–water (EG–W). Spectra were also run in these same solvents containing $\sim 20\%$ ethyl iodide (ETI), or in one of the other heavy atom solvents.

Results

Phosphorescence excitation spectra for ~ 0.1 *M* solutions of acetophenone and 4'-methylacetophenone in ETOH and in ETOH–ETI are given in Figs. 1 and 2, respectively. The lowest energy band observed in each solvent system is indicated by an arrow. The results compare very

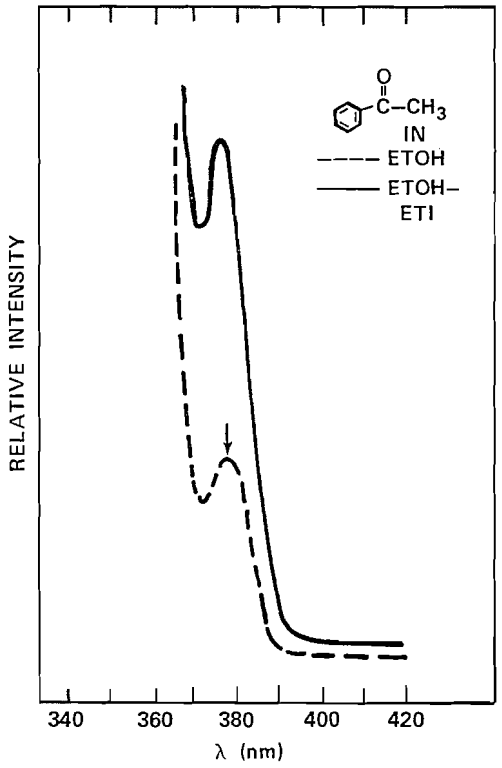

FIG. 1. Phosphorescence excitation spectra of acetophenone in ETOH and ETOH–ETI. The lowest energy band in each solvent system is indicated by an arrow.

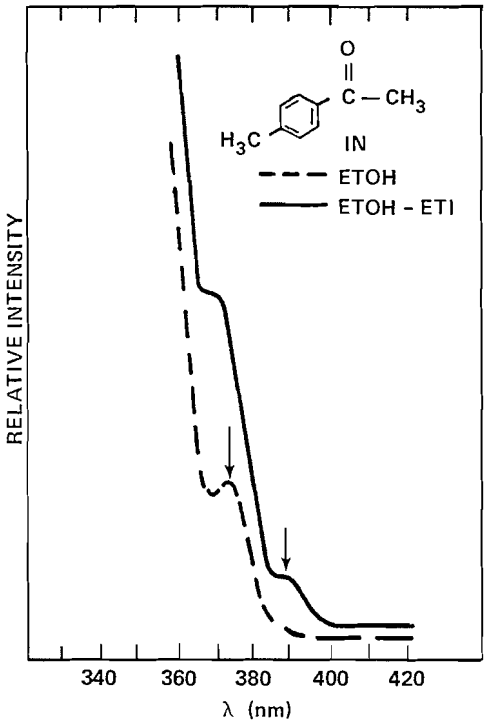

FIG. 2. Phosphorescence excitation spectra of 4′-methylacetophenone in ETOH and ETOH–ETI. The lowest energy band in each solvent system is indicated by an arrow.

favorably with those reported by Yang *et al.* (7) for these same solutes in EPA (ether, isopentane, alcohol in 5:5:2 ratios) glasses. Corresponding spectra for 3′,4′-dimethylacetophenone, chromone, and 4-chromanone are shown in Figs. 3 to 5. The weaker band observed for chromone in ETOH–ETI matches the band reported previously (3), which was observed in chloroform using the Evans oxygen perturbation technique (8). Wavelengths of the O–O bands of phosphorescence and the longest wavelength S→T absorption bands in ETOH and ETOH–ETI are given in Table 1.

In MTHF, the P.E. spectra were similar to those in ETOH, while those in 3-MP and EG–W were complicated by a number of factors. The acetophenones displayed no clearly resolved singlet–triplet absorption bands in 3-MP, although weak shoulders were indicated (*e.g.* ~372 and ~381 nm for 4′-methylacetophenone). In 3-MP–ETI and ETI itself, acetophenone exhibited a single such band, while the methyl derivatives displayed two bands (~372 and ~390 nm for 4′-methylacetophenone). As noted in prior publications (3, 4), chromone and 4-chromanone tend to associate at higher concentrations ($> 10^{-3}$ *M*) in nonpolar solvents at reduced temperatures. Thus, the observations of phosphorescence spectra from aggregates and unresolved singlet–triplet absorption bands in 3-MP were not surprising. In 3-MP–ETI the P.E. spectra of all five compounds were similar to those spectra in ETOH–ETI or in ETI itself. Neither the solutes nor ETI were miscible with EG–W at high concentrations, consequently no S→T bands were resolved in this solvent.

To minimize solvation effects due to polar heavy atom solvents, carbon tetrachloride (CCl_4), carbon tetrabromide (CBr_4), and 1,5-diiodopentane ($C_5H_{10}I_2$) were tried as substitutes for ETI in 3-MP solutions. These efforts were not successful owing to a variety of experimental problems. The CCl_4, even at very high concentrations, did not enhance spin–orbit

Can. J. Chem. Downloaded from www.nrcresearchpress.com by 210.87.254.42 on 09/05/12
For personal use only.

TABLE 1. Phosphorescence emission (0–0 band maxima) and excitation (low energy band maxima) bands of some aromatic carbonyls in ETOH and in 3:1 ETOH–ETI

Compound	ETOH λ_{em} (nm)	ETOH λ_{ex} (nm)	ETOH–ETI λ_{ex} (nm)
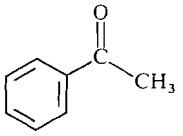	386	377	377
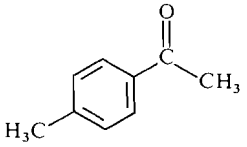	394	374	389
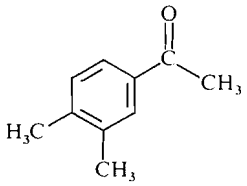	399	372	394
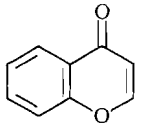	382	364	380
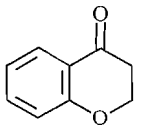	393	374	392

coupling sufficiently to permit observation of the weaker S→T bands. The CBr_4 was not sufficiently soluble to serve as a heavy atom solvent, while the $C_5H_{10}I_2$, although miscible with 3-MP, led to a snowy, non-transparent matrix on cooling with the result that no S→T bands were resolved.

In addition to the phosphorescence excitation spectra other experimental parameters were determined to supplement previously reported data. Spectral and lifetime data on the phosphorescent state of acetophenone and 4′-methylacetophenone in dilute (10^{-3}–10^{-4} *M*) solutions are given in Table 2. At these concentrations, triplet e.p.r. spectra were observed for chromone, 4′-methylacetophenone and 3′,4′-dimethylacetophenone in ETOH and EG–W. At the concentrations used for P.E. studies (~0.1 *M*), a positive e.p.r. spectrum was also observed for

TABLE 2. Phosphorescence spectral and lifetime data of ~10^{-3} *M* acetophenone and 4′-methylacetophenone in different solvent systems at 77 °K*

	Acetophenone		4′-Methylacetophenone	
	λ_{max} (0–0)	τ_m (ms)	λ_{max} (0–0)	τ_m (s)
3-MP	388	2.1	392	0.028
MTHF	385	5.7	393	0.092
ETOH	386	6.6	394	0.15
EG–W†	388	310	398	0.49

*Corresponding data for the other three solutes are given in ref. 4.
†In this solvent system, these results for 3′,4′-methylacetophenone, chromone, and 4-chromanone were 412 nm, 0.52 s; 392 nm, 0.81 s; and 398 nm, 0.74 s, respectively.

Can. J. Chem. Downloaded from www.nrcresearchpress.com by 210.87.254.42 on 09/05/12
For personal use only.

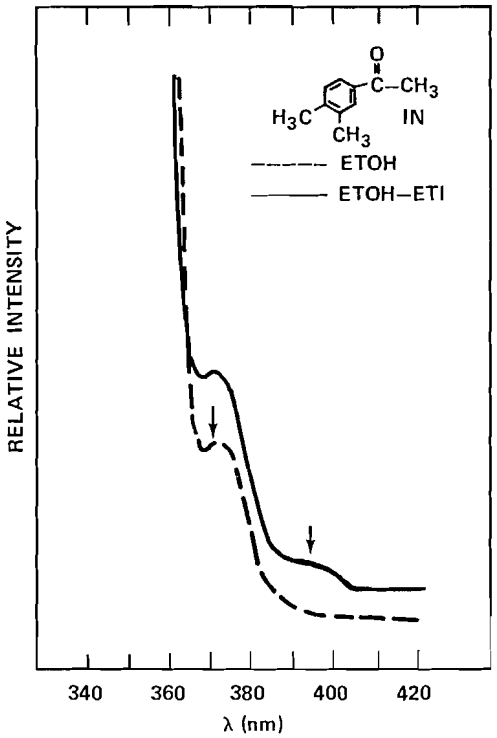

FIG. 3. Phosphorescence excitation spectra of 3',4'-dimethylacetophenone in ETOH and ETOH–ETI. The lowest energy band in each solvent system is indicated by an arrow.

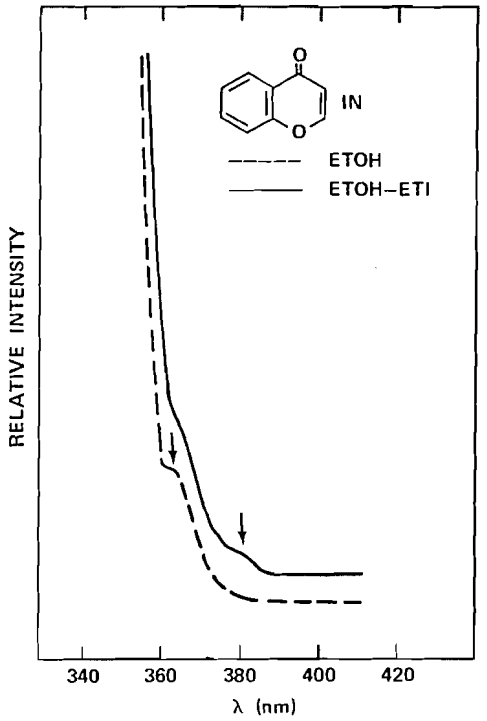

FIG. 4. Phosphorescence excitation spectra of chromone in ETOH and ETOH–ETI. The lowest energy band in each solvent system is indicated by an arrow.

4-chromanone with D^* values of $\sim 0.135\ cm^{-1}$ determined in each solvent.

Discussion

The phosphorescence excitation spectra as shown in Figs. 1 to 5 reveal weak absorption bands which represent direct population of triplet manifolds from singlet ground states. At the high solute concentrations used for these studies, the stronger of these bands is observed for each solute in both polar and non-polar solvents, without the aid of the heavy atom solvent. The weaker of these singlet–triplet (S→ T) bands is observed for all systems, except acetophenone, in the presence of high concentrations of ethyl iodide. Approximate extinction coefficients can be estimated by comparing relative phosphorescence intensities for excitation into each of these bands. In the absence of ETI, relative intensities of the stronger S→T bands and weaker S→S bands can be compared for each solute. Absolute values of ε for the S→S bands can be determined from conventional absorption spectrophotometry.

Values for ε of the stronger S→T bands in these compounds are not enhanced substantially by the addition of the heavy atom solvent. This observation, when coupled with estimated values for ε of $\sim 0.1\ l\ mol^{-1}\ cm^{-1}$, suggests that a primarily $^3n,\pi^*$ designation for these bands is appropriate. The weaker S→T bands are greatly enhanced by the presence of the heavy atom solvent. Values of ε range from $< 10^{-3}\ l\ mol^{-1}\ cm^{-1}$ in the lighter solvents to $> 10^{-2}\ l\ mol^{-1}\ cm^{-1}$ in these same solvents containing $\sim 20\%$ ETI. These observations are consistent with characteristics usually associated with transitions of primarily π,π^* character.

Acetophenone, even in polar solvents with added ETI, did not show a lower energy S→T band than that observed in 3-MP. This is consistent with the viewpoint (1, 2, 7) that the $^3n,\pi^*$ state of this compound lies lower in energy in many solvents covering a wide range of polarity.

Can. J. Chem. Downloaded from www.nrcresearchpress.com by 210.87.254.42 on 09/05/12
For personal use only.

Can. J. Chem. Downloaded from www.nrcresearchpress.com by 210.87.254.42 on 09/05/12
For personal use only.

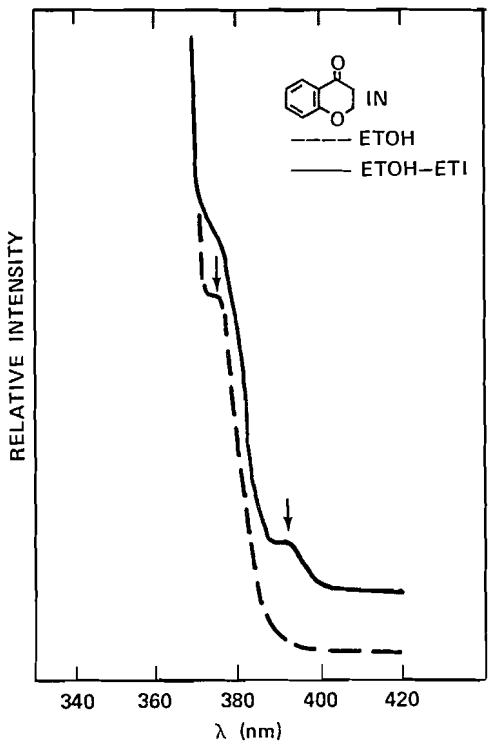

FIG. 5. Phosphorescence excitation spectra of 4-chromanone in ETOH and ETOH–ETI. The lowest energy band in each solvent system is indicated by an arrow.

The phosphorescence lifetime data (Table 2) reflect changes in radiative and/or radiationless rate processes as the solvent changes from 3-MP to MTHF to ETOH. These changes are interpreted in terms of an increasing contribution of π,π^* orbital character to the phosphorescent (n,π^*) state. On the basis of polarization data, Li and Lim (9) drew just the opposite conclusion concerning the relative energy orientation of these two states in acetophenone.

As shown in Fig. 2, 4′-methylactophenone displays one $S \rightarrow T$ absorption band ($^3n,\pi^*$) in ETOH and a second, lower energy band ($^3\pi,\pi^*$) in ETOH–ETI. These designations agree with those of Yang *et al.* (7) and are consistent with the change in relative intensities of these bands from >20:1 in ETOH to <6:1 in ETOH–ETI.

The results for 4′-methylacetophenone in 3-MP illustrate some of the problems associated with obtaining good P.E. spectra on such polar compounds in a non-polar matrix. Not only are solubilities of the samples reduced, but the increased energies of the π,π^* bands, and decreased energies of the n,π^* bands have the effect of merging the weak singlet–triplet transitions. Experimental problems resulted when alternative "non-polar" heavy atom solvents were tried, so that spin–orbit coupling enhancement was not demonstrated without the accompanying solvation effects. That such solvation effects are important is substantiated by the similarity of P.E. spectra in 3-MP–ETI, ETOH–ETI and ETI itself. The prospect of demonstrating the heavy atom role of enhancing spin–orbit coupling without the accompanying solvation effects may still be possible, *e.g.* in a heavy, rare gas matrix.

The P.E. results for 3′,4′-dimethylacetophenone, chromone, and 4-chromanone parallel those for 4′-methylacetophenone, and similar interpretations apply. The aggregation of chromone and 4-chromanone at the higher concentrations in 3-MP made all attempts to resolve $S \rightarrow T$ bands of these compounds in non-polar environments an exercise in futility. The observation of a triplet e.p.r. spectrum at 0.1 *M* 4-chromanone contrasts with our observations at 10^{-3} *M*, and points to the importance of the absolute steady state triplet concentration for e.p.r. detection. This factor must be fully assessed before drawing conclusions on negative e.p.r. results.

Radiative Lifetimes

The results given in Table 2 corroborate previously reported data (4) of generally decreasing energies and increasing lifetimes of the phosphorescent state with increasing solvent polarity. The relatively minor spectral shifts and approximately constant quantum efficiencies contrast with the order of magnitude changes in the phosphorescence lifetimes. These lifetime changes are consistent with significant increases in the radiative lifetime as the contribution of π,π^* character to the phosphorescent state increases. It is possible to estimate radiative lifetimes of these systems by employing different experimental parameters in several familiar expressions.

The first equation (10) expresses the radiative lifetime (τ_p^0) in terms of the measured phosphorescence lifetime τ_p, and measured fluorescence and phosphorescence quantum yields, ϕ_f and ϕ_p, respectively. Since the compounds

studied here show no measurable fluorescence, ϕ_f is assumed to be 0, while the ϕ_p for acetophenone, 0.65 (11), is taken as representative for these compounds; consequently τ_p^0 is simply $\sim 1.5\tau_p$. Interestingly, the compound with the longest lifetime, 3′,4′-DMA has a lowest triplet state which has been designated as n,π^* in a durene host crystal, based on the magnitude of its Z.F.S. parameter D (12*a*). However, in a more recent study of the magnetic resonance properties of the triplet states of some related aromatic carbonyls (12*b*), it is suggested that such clear cut designations may not be warranted.

Radiative lifetimes estimated from integrated intensities of the singlet–triplet absorption spectra (ref. 10, p. 49), yield values of τ_p^0 of <20 ms for the stronger bands and >1.5 s for the weaker bands in these compounds. In solvents containing $\sim 20\%$ ETI, the absorption of the weaker bands is enhanced sufficiently to give τ_p^0 values of ~ 0.1 s. The magnitudes of these τ_p^0's are consistent with n,π^* triplets (<20 ms), π,π^* triplets (>1.5 s), and π,π^* triplets (~ 0.1 s) for which spin–orbit coupling has been enhanced significantly by the presence of the heavy (iodine) atom.

Summary

The accumulated experimental evidence of these and earlier studies suggests that the phosphorescent states of these aromatic carbonyls are described best by an expression such as

$$\psi_T = \alpha\psi\ {}^3n,\pi^* + \beta\psi\ {}^3\pi,\pi^*$$

which includes the variable parameters α and β. The normalized sum $(1/\sqrt{2})(\alpha^2 + \beta^2)$ is unity with values for both α and β ranging between the limits 0 and 1, depending on the solvent environment. Although the solvent dependent luminescence properties of these and related systems have received considerable attention in recent years (1–4, 7, 13), and various interpretations of common phenomena have been offered (14, 15), additional experimental and theoretical effort will be necessary to unravel the complexities of these systems.

The author would like to thank J. S. Brinen for the e.p.r. measurements of the triplet state for the compounds studied. Thanks are also due Dr. Brinen, Dr. M. K. Orloff, and Dr. W. G. Hodsgon for valuable discussions and helpful suggestions.

1. A. A. Lamola. J. Chem. Phys. **47**, 4810 (1967).
2. R. Rusakowicz, G. W. Byers, and P. A. Leermakers. J. Am. Chem. Soc. **93**, 3263 (1971).
3. J. B. Gallivan. Can. J. Chem. **48**, 3928 (1970).
4. J. B. Gallivan and J. S. Brinen. Chem. Phys. Lett. **10**, 455 (1971).
5. (*a*) W. Rothman, A. Case, and D. R. Kearns. J. Chem. Phys. **43**, 1067 (1965). (*b*) R. F. Borkman and D. R. Kearns. Chem. Commun. 446 (1966). (*c*) A. P. Marchetti and D. R. Kearns. J. Am. Chem. Soc. **89**, 768 (1967). (*d*) W. A. Case and D. R. Kearns. J. Chem. Phys. **52**, 2175 (1970).
6. J. B. Gallivan. Mol. Photochem. **2**, 191 (1970).
7. N. C. Yang, D. S. McClure, S. L. Murov, J. J. Houser, and Ruth Dusenbery. J. Am. Chem. Soc. **89**, 5468 (1967).
8. D. F. Evans. J. Chem. Soc. 1351 (1967); 3885 (1957).
9. Y. H. Li and E. C. Lim. Chem. Phys. Lett. **7**, 15 (1970).
10. N. J. Turro. Molecular photochemistry. W. A. Benjamin Inc. N.Y. 1965. p. 54.
11. (*a*) E. H. Gilmore, G. E. Gibson, and D. S. McClure. J. Chem. Phys. **23**, 399 (1955). (*b*) F. Wilkinson and J. T. Dubois. J. Chem. Phys. **39**, 377 (1963).
12. (*a*) N. Hirota. Chem. Phys. Lett. **4**, 305 (1969). (*b*) T. H. Cheng and N. Hirota. Chem. Phys. Lett. **13**, 194 (1972).
13. (*a*) H. W. Pownall and J. R. Huber. J. Am. Chem. Soc. **93**, 6429 (1971). (*b*) S. Hotchandani and A. C. Testa. J. Chem. Phys. **54**, 4508 (1971). (*c*) W. Klopffer. Chem. Phys. Lett. **11**, 482 (1971). (*d*) N. J. Gould and D. J. Morantz. Mol. Crystals, **15**, 247 (1971).
14. M. E. Long, Y. H. Li, and E. C. Lim. Mol. Photochem. **3**, 221 (1971).
15. A. A. Efimov, R. N. Nurmukhametov, J. L. Belaits, and A. I. Tolmacher. Opt. Spectry. **30**, 337 (1971).

Can. J. Chem. Downloaded from www.nrcresearchpress.com by 210.87.254.42 on 09/05/12
For personal use only.

The Structure and Physical Properties of μ-oxo-bis{oxotrichloro(*O*-perrhenyl chloride)rhenium(VI)}, and the Non-existence of β-$ReOCl_3$

C. CALVO, P. W. FRAIS, AND C. J. L. LOCK[1]

Institute for Materials Research, McMaster University, Hamilton, Ontario

Received May 25, 1972

The compound previously reported as β-$ReOCl_3$ has been shown by analysis and single crystal X-ray diffraction to be μ-oxo-bis{oxotrichloro(*O*-perrhenyl chloride)rhenium(VI)}, $(Re_2O_3Cl_6)(ReO_3Cl)_2$. The crystals were triclinic, $a = 6.112(5)$, $b = 12.876(9)$, $c = 6.020(5)$ Å, $\alpha = 88.30(5)$, $\beta = 95.88(5)$, $\gamma = 105.36(5)°$, $P\bar{1}(C_i^2$, No. 2) $Z = 1$. Intensities were measured by a densitometer from photographs recorded on an integrating precession camera. The structure was refined by full matrix least squares to give a final R_2 of 0.072. The molecule is composed of a dimeric $Re_2O_3Cl_6$ unit with a bridging oxygen atom on the center of symmetry and an Re—O (bridge) distance of 1.847(1) Å. The remaining oxo-group on each rhenium is *cis* to the bridge and is strongly bonded (1.69(2) Å), and the position *trans* to the terminal oxo-group is filled by a weak bond to an oxygen atom of a perrhenyl chloride molecule. The infrared spectrum of the compound has been explained in terms of the structure.

Nous démontrons que le composé rapporté précédemment comme étant β-$ReOCl_3$ est le μ-oxo-bis{oxotrichloro(*O*-chlorure de perrhényl)rhénium(VI)}, soit $(Re_2O_3Cl_6)(ReO_3Cl)_2$, par analyse et diffraction de rayons-x d'un cristal unique. Les cristaux sont tricliniques, $a = 6.112(5)$, $b = 12.876(9)$, $c = 6.020(5)$ Å, $\alpha = 88.30(5)$, $\beta = 95.88(5)$, $\gamma = 105.36(5)°$, $P\bar{1}(C_i^2$, No. 2) $Z = 1$. Les intensités ont été mesurées au moyen d'un densitomètre à partir de photographies prises par une caméra de précession d'intégration. Nous raffinons la structure par calcul matriciel de moindres carrés pour obtenir un R_2 final de 0.072. La molécule est composée d'une unité $Re_2O_3Cl_6$ dimérique comprenant un atome d'oxygène faisant pont au centre de symétrie, avec une distance Re—O(pont) de 1.847(1) Å. Le groupe oxo-résiduel sur chaque rhénium est *cis* par rapport au pont et fortement lié (1.69(2) Å); la position *trans* par milieu fragile à l'atome d'oxygène d'une molécule de chlorure de perrhényl. Nous expliquons le spectre infrarouge de la molécule en nous basant sur la structure.

[Traduit par le journal]

Canadian Journal of Chemistry, **50**, 3607 (1972)

Can. J. Chem. Downloaded from www.nrcresearchpress.com by 210.87.254.42 on 09/05/12
For personal use only.

Introduction

We have described previously some products of the reaction of ReO_3 and $ReCl_5$ (1, 2). One of the products was apparently obtained by interconversion from α-$ReOCl_3$, and because of infrared data, and a superficial resemblance of the unit cell parameters of crystals of the product to those of monoclinic $MoOCl_3$, we suggested that the compound might be another form of $ReOCl_3$, which we have designated as "β-$ReOCl_3$". Further studies have shown that this conclusion was arrant nonsense and that "β-$ReOCl_3$" is an adduct of $Re_2O_3Cl_6$ and perrhenyl chloride. A single crystal X-ray diffraction study, analyses, and infrared studies have allowed us to identify the compound as μ-oxo-bis{oxotrichloro(*O*-perrhenyl chloride) rhenium(VI)}, $ClReO_3 \cdot Re_2O_3Cl_6 \cdot O_3ReCl$.

Experiments

Rhenium oxotetrachloride and perrhenyl chloride were prepared by standard methods and Nujol and solvents were purified and dried as previously outlined (3). Analyses of the rhenium to chlorine ratio as well as the oxidation state were done by neutron activation (4).

Infrared spectra were recorded on Perkin-Elmer 337 and 521 instruments. Solid samples were ground into a mull with dry Nujol and mounted between KBr, Irtran 2, or polyethylene plates with edges wrapped in Teflon tape, or crystals of $Re_2O_3Cl_6(ReO_3Cl)_2$ were squeezed between plates of Irtran 2 or polyethylene and the edges wrapped with Teflon tape to keep air and moisture out. X-Ray diffraction photographs of powdered samples were recorded on a Debye-Scherrer camera using nickel-filtered CuKα radiation. Samples were sealed inside fused silica capillary tubes.

Preparation of $Re_2O_3Cl_6(ReO_3Cl)_2$

(*a*) Equimolar amounts of ReO_3 and $ReCl_5$ were heated in a sealed, evacuated reaction vessel at ~300 °C for 24 h. Volatiles were distilled into U-traps by cooling the U-traps with liquid nitrogen. For several weeks, one of the U-traps not containing the volatiles was cooled in ice water while the volatiles were kept at room temperature. A purple frost formed on the sides of the room temperature U-traps and a green liquid formed in the cooled trap. The U-traps were sealed off and, upon standing for weeks, the purple frost decomposed and thin purple plates formed in another part of the tube. These purple plates, previously called "β-$ReOCl_3$" (1), are in fact $Re_2O_3Cl_6(ReO_3Cl)_2$. This

[1]To whom correspondence should be addressed.

Can. J. Chem. Downloaded from www.nrcresearchpress.com by 210.87.254.42 on 09/05/12
For personal use only.

method of preparation yielded only minor amounts of both purple compounds and in addition produced Re_3Cl_9, ReO_2, Re metal, $ReOCl_4$, and ReO_3Cl in varying and non-reproducible amounts.

(*b*) Rhenium oxotetrachloride was sealed in an evacuated Pyrex vessel, and irradiated with 3500 Å light for ~12 h. The yield of both purple products previously referred to as α- and β-$ReOCl_3$ (1), was very variable, and reaction only occurred about 50% of the time. After our previous publication (1), it was discovered that impurities in the $ReOCl_4$ played the major role in determining the extent and usefulness of this reaction in preparing $Re_2O_3Cl_6(ReO_3Cl)_2$.

(*c*) Once the crystal structure was solved and the existence of $ReOCl_4(OH_2)$ was confirmed (2), a reproducible method of preparation was found. One cmol of $ReOCl_4$ (estimated from the volume of the melt) and 1/2 cmol of H_2O (measured by connecting an evacuated, calibrated vessel to a source of water and varying the vapor pressure of the water by varying the temperature) were distilled into a Pyrex reaction tube (equipped with a breakseal) and sealed under vacuum. The tube was heated uniformly at ~200 °C for a few hours and then slowly cooled, taking care to avoid any temperature gradient. To the resulting mixture of $ReOCl_4$ and $ReOCl_4(OH_2)$ (2) was added (by distillation through the breakseal) 1 cmol of ReO_3Cl. The reaction vessel was then bathed in 3500 Å ultraviolet light (Rayonet Photochemical Reactor with 16 RPR 3500 Å lamps) until no further reaction occurred (~24 h) and the vessel was filled with thin purple crystals of $Re_2O_3Cl_6(ReO_3Cl)_2$. Excess $ReOCl_4$ and ReO_3Cl were separated from the product by cooling one end of the reaction tube with icewater or by hand picking the crystals of $Re_2O_3Cl_6(ReO_3Cl)_2$. The latter technique was often better since, because of the instability of $Re_2O_3Cl_6(ReO_3Cl)_2$ in a temperature gradient, it was difficult to free the crystals from impurities "purple frost" and $ReOCl_4(OH_2)$ without causing decomposition. Neutron activation analyses of the thin purple crystals gave chlorine:rhenium ratios of 2.22 and 2.15 (calcd. 2.00) and a ratio of ReO_4^-/ReO_2 in the alkaline hydrolysis of 6.3 (calcd. 5.0 for an oxidation state of $6\frac{1}{2}$). (Note: We consider this good agreement since the ratio is changing rapidly as a function of average oxidation state in this region as shown by the following oxidation states and ratios 6.4: 4:1, 6.5: 5:1, 6.6: 6.5:1, 6.7: 9:1.) Crystals prepared by all three methods were shown to be identical by X-ray powder photography.

Crystallography

Single crystal X-ray studies were done on a crystal prepared by method (*a*). The crystal was sealed in a fused silica capillary tube. All crystal data were obtained from a needle crystal of length 1.03 mm and thickness 0.05 × 0.11 mm^2.

Weissenberg and precession photographs of the crystal showed that it was triclinic. Precession photographs of the (*hk*0) and (*h*0*l*) layers, taken with CuKα radiation, were calibrated with a crystal of TiO_2 (rutile) and accurate cell parameters were obtained using the parameters for TiO_2, $a = 4.5929(5)$, $c = 2.9591(3)$ Å (5). Crystal data were

$Cl_8O_9Re_4$ Mol.wt. = 1172.4

Triclinic, $a = 6.112(5)$, $b = 12.876(9)$, $c = 6.020(5)$ Å, $\alpha = 88.30(5)$, $\beta = 95.88(5)$, $\gamma = 105.36(5)°$, $V = 454.4$ Å^3, $P\bar{1}$ (C_i^2, No. 2), ρ_0 not determined (see text), $Z = 1$, $\rho_c = 4.28$ (22 °C; CuKα, $\lambda = 1.5418$ Å).

Because of the instability of $Re_2O_3Cl_6(ReO_3Cl)_2$, it was not possible to obtain an experimental value for the density. The unit cell used in this work, which reflects the form of the crystal, is not the cell defined by International Tables for Crystallography; the I.T.C. cell is $a = 6.112(5)$; $b = 12.707(9)$; $c = 6.020(5)$ Å; $\alpha = 92.20(5)$; $\beta = 101.83(5)$; $\gamma = 93.20(5)°$ and is derived from our cell by the transformation matrix (100/110/001).

Intensity data for the (*nkl*), $n = 0$, 1, 2 layers were obtained initially from films recorded on an integrating Weissenberg camera using CuKα radiation and for the (*h*0*l*) and (*hk*0) layers on an integrating precession camera using MoKα radiation. No attempts were made to assign standard errors to each intensity measured. Using this data set, the structure was solved and an R_1 factor of 0.15[2] was obtained. Because of the shape of the crystal, considerable absorption errors existed in the CuKα data ($R_1 = 0.18$ as opposed to $R_1 = 0.12$ for MoKα data) and it was therefore decided to obtain a complete data set using MoKα radiation only.

Final intensity data used in the refinement of the structure were obtained from films recorded on an integrating precession camera using MoKα radiation, the layers recorded being (*hnl*), $n = 0$, 1, 2, 3 and (*hkm*), $m = 0$, 1, 2. All intensities were measured using a Joyce–Loebl microdensitometer and then corrected for Lorentz and polarization effects. No absorption corrections were made. This would introduce a maximum error in F_0 of 16%, but more than 90% of the data will not be in error by more than 6% as a result of absorption. Standard errors, σ, were assigned to each intensity measured and weights $w = 1/\sigma^2$ were used throughout the refinement. For each reciprocal lattice layer measured, a minimum value of σ was estimated from the accumulated relative errors of the

[2] $R_1 = \dfrac{\Sigma\| F_o| - |F_c\|}{\Sigma|F_o|}$; $\quad R_2 = \left\{\dfrac{\Sigma w(|F_o| - |F_c|)^2}{\Sigma w F_o^2}\right\}^{1/2}$.

Can. J. Chem. Downloaded from www.nrcresearchpress.com by 210.87.254.42 on 09/05/12
For personal use only.

factors used to scale different films and different wedges on the densitometer. To this minimum value of σ was added an additional value which took account of the intensity and intensity profile of the spot, intensity and irregularity of the background, edges of the beam stop or layer screen shadows, and average reproducibility of each measured intensity. Smallest values of σ were therefore assigned to well defined spots of uniform integrated intensity that could be measured on three or more films. For unobserved reflections, weights calculated from $\sigma = 0.5\,F_{min}$ were used only when the calculated structure factor $|F_c| > 0.8\,F_{min}$, where F_{min} was the local minimum of the observed structure factor; otherwise they were given zero weights.

Solution of the Structure

The unit cell was triclinic with space group $P1$ or $P\bar{1}$. Patterson maps were calculated separately using zero layer Weissenberg data (CuKα) from the (100) zone, and the zero layer precession data (MoKα) from the (010) and (001) zones. The four largest peaks found in the asymmetric unit of each projection were such that two were approximately twice as large as the remaining two. This is characteristic of four rhenium atoms in the unit cell, related in pairs by a center of inversion. The choice of $P\bar{1}$ as the space group at this stage was later confirmed by the successful structure analysis.

Using the initial data set obtained chiefly with an integrating Weissenberg camera using CuKα radiation (see Experiments section), the positions of the two rhenium atoms in the asymmetric unit were easily established. The structure was found to consist of a tetramer of rhenium atoms, with distances of Re1—Re2 = 3.89(1) Å, Re2—Re′2 = 3.72(1) Å and Re1—Re″1 = 4.50(1) Å (where Re′2 indicates the atom related to Re2 by the inversion center and Re″1 indicates Re′1 translated 1 unit cell distance in the y direction). The electron density was calculated based on phases obtained from the heavy atom positions, and it became clear that the structure was not consistent with the assumption that the compound was $ReOCl_3$. Four chlorine atoms and five oxygen atoms were soon located in the asymmetric unit and the structure was found to be an adduct of $Re_2O_3Cl_6$ and two molecules of ReO_3Cl. The structure was refined using a full matrix least-squares program CUDLS written by Stephens for the CDC 6400 computer. Despite the fact that R_1 was 0.15, all bond distances, bond angles, non-bonded distances, and isotropic temperature factors were reasonable and the structure was assumed to be essentially correct. The high value of R_1 was attributed to absorption errors which were especially apparent for the Weissenberg data using CuKα radiation. A completely new set of data was obtained before refinement of the structure was continued (see Experiments section) and R_1 dropped to 0.10 by varying only the overall scale constant. Refinement was terminated when no shift of atom parameters of greater than $\frac{1}{3}\sigma$ was observed and $R_1 = 0.067$ and $R_2 = 0.072$. Of the 1768 independent reflections measured, 1576 were given non-zero weights in the last cycle of least squares refinement. Scattering curves used in the refinement process were obtained from Cromer and Waber (6) for rhenium, chlorine, and oxygen, and anomalous dispersion corrections for rhenium and chlorine were taken from Cromer (7).

A difference Fourier map calculated using the structure factors listed in Table 4 had no residual peaks greater than $+1.5\ e/Å^3$ or less than $-1.7\ e/Å^3$.[3] The final parameters of the atoms are shown in Table 1.

Discussion

$Re_2O_3Cl_6(ReO_3Cl)_2$ consists of one molecule per unit cell of a tetramer of rhenium atoms, joined by two types of bridging oxygen atoms, as illustrated in Fig. 1. One of these lies at a center of inversion. The sixth coordination site of each of the two rhenium atoms in the μ-oxo-bis{oxotrichlororhenium(VI)} portion of the molecule is filled by a weak bond to one of the oxygen atoms of perrhenyl chloride. The resulting adduct is a combination of tetrahedrally coordinated Re(VII) and octahedrally coordinated Re(VI), with an average oxidation state of 6.5, which was confirmed by analysis.

Tables 2 and 3 list bonded distances, bond angles, and non-bonded distances found in $Re_2O_3Cl_6(ReO_3Cl)_2$. An examination of the bonded distances in the $Re_2O_3Cl_6$ portion of

[3]Table 4 is available, at a nominal charge, from the Depository of Unpublished Data, National Science Library, National Research Council of Canada, Ottawa, Canada, K1A 0S2.

Can. J. Chem. Downloaded from www.nrcresearchpress.com by 210.87.254.42 on 09/05/12
For personal use only.

TABLE 1. Final parameters (e.s.d.'s) $\times 10^3$ t_{ij}. $= \exp\{-2\pi^2(a^{*2}h^2U_{11} + \ldots + 2a^*b^*hkU_{12} + \ldots +)\}$

Atom	x	y	z	U_{11}	U_{22}	U_{33}	U_{12}	U_{13}	U_{23}
Re1	473.9(1)	154.58(5)	638.1(1)	33.4(3)	22.3(3)	35.7(5)	9.8(2)	4.7(3)	6.6(4)
Re2	282.1(1)	391.16(4)	348.0(1)	25.4(3)	16.7(3)	21.0(4)	5.6(2)	2.1(2)	1.1(3)
Cl1	68.1(8)	220.6(5)	247(1)	42(2)	38(2)	54(4)	2(2)	−1(2)	−7(3)
Cl2	68.5(6)	307.1(4)	648(1)	32(1)	41(2)	37(3)	9(2)	10(2)	2(3)
Cl3.	168(1)	62.0(5)	782(1)	59(3)	49(3)	70(5)	6(2)	27(3)	13(4)
Cl4	553.5(7)	357.9(4)	142(1)	39(2)	40(2)	33(2)	9(2)	9(2)	−3(3)
O1	155(2)	466(1)	169(3)	40(6)	52(9)	33(8)	23(6)	4(6)	0(10)
O2	473(2)	291(1)	609(2)	39(5)	21(5)	31(8)	9(4)	5(5)	−6(7)
O3	490(3)	102(1)	390(4)	70(10)	47(9)	50(10)	29(8)	11(8)	20(10)
O4	704(3)	143(1)	802(4)	56(8)	50(10)	80(20)	16(7)	0(10)	20(10)
O5†	500(0)	500(0)	500(0)	56(9)	0(5)	40(10)	−8(5)	25(9)	−11(8)

†Non-positive-definite temperature Factor (see text).

Can. J. Chem. Downloaded from www.nrcresearchpress.com by 210.87.254.42 on 09/05/12
For personal use only.

TABLE 2. Bond distances and angles in $Re_2O_3Cl_6(ReO_3Cl)_2$*

Bond	Distance (Å)	Bond	Distance (Å)
Re1—O3	1.70(2)	Re1—O2	1.76(1)
Re1—Cl3	2.182(7)	Re1—O4	1.67(2)
Re2—Cl1	2.303(5)	Re2—O1	1.69(2)
Re2—Cl2	2.305(5)	Re2—O2	2.41(1)
Re2—Cl4	2.301(6)	Re2—O5	1.847(1)

Bonds	Angle (deg)	Bonds	Angle (deg)
O3—Re1—Cl3	109.3(6)	Cl3—Re1—O2	110.5(5)
O3—Re1—O2	111.0(8)	Cl3—Re1—O4	109.5(7)
O3—Re1—O4	106(1)	O2—Re1—O4	109.9(7)
Cl1—Re2—O	100.6(5)	O1—Re2—O2	177.6(5)
Cl1—Re2—O5	159.9(2)	O1—Re2—Cl4	102.2(6)
Cl1—Re2—Cl2	85.7(2)	O5—Re2—Cl2	89.2(1)
Cl1—Re2—O2	81.8(3)	O5—Re2—O2	78.2(3)
Cl1—Re2—Cl4	86.1(2)	O5—Re2—Cl4	90.5(1)
O1—Re2—O5	99.4(5)	Cl2—Re2—O2	77.4(4)
O1—Re2—Cl2	102.6(5)	Cl2—Re2—Cl4	154.9(2)
O2—Re2—Cl4	78.0(4)		

*Estimated standard deviations in parentheses.

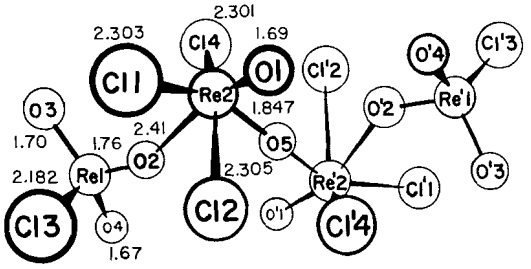

FIG. 1. Geometry of a single molecule of $Re_2O_3Cl_6(ReO_3Cl)_2$ viewed up the a^* axis. Bond distances shown in Å.

the molecule reveals several interesting, although not unexpected, features. The three chlorine–Re2 bond distances (2.303(5), 2.301(6), and 2.305(5) Å) do not differ significantly even though two chlorine atoms are *trans* to each other, whereas the third is *trans* to a bridging oxygen atom. Similar results have been observed previously (8, 9). These Re—Cl distances are shorter than most which have been measured. Typical values are 2.330(5) to 2.370(5) Å but are usually for complexes of Re(III), (IV), and (V), and the Re—Cl distances in our compound are comparable to those found in other Re(VI) (2.29(1) Å for $ReOCl_4 \cdot OH_2$(2)) and Re(VII) compounds (2.230(4) Å for ReO_3Cl(10)).

The Re2—O1 distance of 1.69(2) Å is comparable to those found in $ReOCl_4(OH_2)$ (1.63(2) Å) (2), K_2ReOCl_5 (1.66(3) Å) (11), $ReOCl_3[P(C_2H_5)_2(C_6H_5)]_2$ (1.60(5) Å) (12), $ReOCl_2(C_5H_7O_2)P(C_6H_5)_3$ (1.70(1) Å) (13), $[ReOBr_4(CH_3CN)]^-$ (1.73(6) Å) (14), and $[ReOBr_4(OH_2)]^-$ (1.71(4) Å (15), where the very strongly bonded oxo-group is postulated to be present (14).

The center of symmetry requires either the Re2—O5—Re′2 system be both symmetric and linear or that the system is asymmetric, or bent, or both, and disordered. Refinement of the isotropic temperature factors for O5 gave a value comparable to the O1 and O2 temperature factors, and the value is not abnormally large which suggests no disorder. However, the final anisotropic temperature factors for O5, while of comparable or smaller magnitude than O1 and O2, are markedly anisotropic. One can consider three reasons for this anisotropy as (*i*) absorption errors, (*ii*) disorder, (*iii*) genuine anisotropic motion. We have tested for (*i*) by refining the structure using only reflections which would not show large absorption corrections, but there was little change in the anisotropic temperature factors and no tendency for U_{22} to increase. The thermal parameters suggest the motion is in the *ac* plane and since the force constants for motion along a M—O—M bond are far higher than that for a bending motion (22), we might

Can. J. Chem. Downloaded from www.nrcresearchpress.com by 210.87.254.42 on 09/05/12
For personal use only.

TABLE 3. Non-bonded distances in $Re_2O_3Cl_6(ReO_3Cl)_2$*

(*a*) Intramolecular

Atoms	Distance (Å)	Atoms	Distance (Å)
Cl1–O1	3.10(2)	Cl3–O2	3.25(1)
–O3	3.36(2)	–O4	3.16(2)
–Re1	3.495(6)	Cl4–O1	3.13(2)
–Cl2	3.13(1)	–O5	2.963(6)
–O2	3.09(1)	–O2	2.97(2)
–Cl4	3.143(7)	O1–O5	2.70(1)
Cl2–O1	3.14(2)	O2–O3	2.85(2)
–O5	2.934(4)	–O5	2.72(1)
–O2	2.95(1)	–O4	2.81(2)
Cl3–O3	3.18(2)	O3–O4	2.70(3)
Re1–Re2	3.855(1)	Re2–Re'2‡	3.695(1)

(*b*) Intermolecular

Atoms	Symmetry relationships	Distance (Å)
Cl1–O″4†	$(x-1, y, z-1)$	3.29(2)
Cl2–O″2	$(x-1, y, z)$	3.49(1)
–O″1	$(x, y, z+1)$	3.35(2)
–O″4	$(x-1, y, z)$	3.34(2)
–O″1	$(-1-x, 1-y, 1-z)$	3.08(2)
Cl3–O″4	$(x-1, y, z)$	3.28(2)
Cl4–O″2	$(x, y, z-1)$	3.30(2)
–O″1	$(1-x, 1-x, -1-z)$	3.18(1)
O1–O″1	$(-1-x, 1-x, -1-z)$	2.92(2)
O3–O″4	$(1-x, -1-x, 1-z)$	3.25(3)
–Re″1	$(1-x, -1-y, 1-z)$	3.36(2)
–O″3	$(1-x, -1-y, 1-z)$	2.91(3)

*Estimated standard deviations in parentheses. Except for Re—Re, only distances less than 3.50 Å are included.

†Atoms indicated with a double prime mark are related to the atoms listed in Table 1 (x, y, z) by the symmetry relationships shown in the second column.

‡Atoms indicated with a single prime mark are related to the atoms listed in Table 1 (x, y, z) by the symmetry relations $(1-x, 1-y, 1-z)$, and belong to the same molecule (see Fig. 1).

expect that the bending motion, which will take place roughly in the *ac* plane, would be preferred. It is not possible to decide unambiguously between (*ii*) and (*iii*), but we prefer (*iii*) to (*ii*) since there is no apparent anomaly in the temperature factors of the other groups attached to Re1, which we would expect if a bent Re—O—Re bond were present, since the disorder would cause a movement of the other attached groups. In addition we see no sign of the infrared active M—O—M symmetric stretch at $\sim 500\ cm^{-1}$, which is observed for compounds of this type which have a bent M—O—M bond (22).

The apparent Re2—O5 distance of 1.847(1) Å is comparable to 1.860(5) Å reported for $K_4ReOCl_{10}\cdot H_2O$ (8) where the bridging atom lies on a four-fold axis, but not a center of symmetry. Apparently, however, the Re2—O5 distance is significantly shorter than reported for the Re—O (bridge) distance $[Pt(NH_2)_4]_2$-$Re_2O_3(CN)_4$ (1.9149(4) Å) (16) where again the oxygen atom is in a special position. The errors in the bond lengths, which are probably higher than those reported here, are so low because the atoms involved apparently lie in special positions between the two rhenium atoms, for which the interatomic distance is known with high accuracy. In all the structures reported, bending of the M—O—M system and subsequent disorder, although unlikely, might occur, but would be difficult to detect because of the position of the oxygen atom between the two heavy scatterers. Despite these reservations, the apparent difference in bond lengths is reflected in the M—O—M stretch frequencies (see later) and presumably in bond strength.

$Re_2O_3Cl_6(ReO_3Cl)_2$ is the first compound containing coordinated perrhenyl chloride whose structure has been investigated by X-ray diffraction techniques. The compound $ReOCl_4\cdot ReO_3Cl$, whose structure was postulated to be very similar to that of one of the centrosymmetrically related halves of $Re_2O_3Cl_6$-$(ReO_3Cl)_2$ (17, 18) on the basis of infrared spectroscopy, and another adduct, SO_2Cl_2-$(ReO_3Cl)_2$, whose postulated structure involved coordination through an oxygen of the sulfuryl chloride group resulting in a five coordinate rhenium atom (26) have been reported. In $Re_2O_3Cl_6(ReO_3Cl)_2$, the symmetry of the perrhenyl chloride group is C_1 compared to C_{3v} for free ReO_3Cl. This is reflected by the longer Re1—O2 bond length (1.76(1) Å) for the bridging oxygen atom as compared to the remaining Re1—O distances of 1.70(2) and 1.67(2) Å. These Re1—O distances are, on the average, shorter than those found in perrhenyl chloride (1.761(3) Å (10), and a similar shortening of the Re1—Cl3 distance from 2.230(4) Å to 2.182(7) Å is observed in going from the uncoordinated species to the adduct. The decrease in bond lengths on coordination is not unexpected for the non-bridging atoms, although one would expect a resultant lengthening in the bridging Re1—O2 distance, which is not observed.

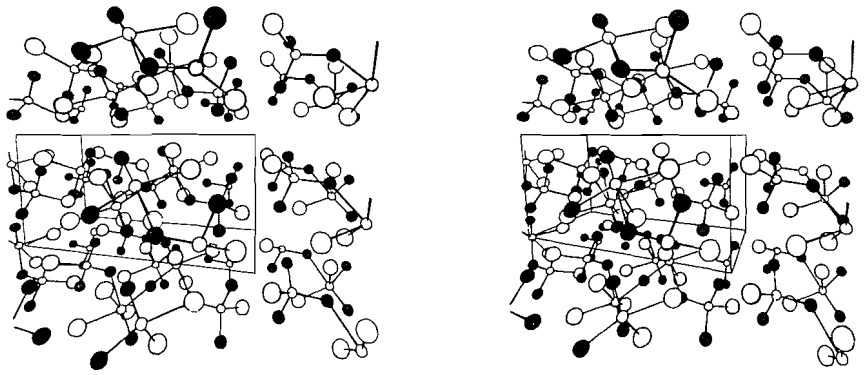

FIG. 2. Stereogram (stereoscopic pair of perspective projections) of $Re_2O_3Cl_6(ReO_3Cl)_2$ viewed down the *a* axis. The origin of the unit cell is at the upper right and the *b* and *c* axis run approximately parallel to the planes described by *a* and the horizontal and vertical edges of the paper, respectively.

The crystal packing is shown in Fig. 2. The molecular units are packed in a layer structure with the layers running parallel to the *ab* plane. Within the layers, the molecules are stacked directly above each other in the *a* direction, and in the *b* direction the molecules are packed end to end such that the chlorine atom and two oxygen atoms of a perrhenyl chloride group in one molecule interleave with the centrosymmetrically related atoms of the next molecule. This means that the rhenium atoms (and thus the framework of the molecules) are arranged almost in a spiral along the *b* direction. The layers are also arranged such that in the *c* direction, a molecule in one layer sits almost directly above another molecule in the next layer.

The measured X-ray data for a powdered sample of $Re_2O_3Cl_6(ReO_3Cl)_2$ are reported in Table 5, with corresponding calculated values of *d* spacings and intensities calculated from the single crystal parameters determined in this work. There is fair agreement between the two sets of values although the ratio I_{calcd}/I_{obs} at low angles is consistently higher than the ratio at high angles. (This is probably caused by I_{obs} being reduced at low angles because of absorption; peaks in this region are strong and are superimposed on an appreciable background scattering caused by the glass capillary containing the sample.) We found that the X-ray powder pattern was the only easy, reliable method of checking the purity of $Re_2O_3Cl_6(ReO_3Cl)_2$. On many occasions, when we thought we had pure samples of crystals, X-ray powder photographs showed that the sample was contaminated with appreciable amounts of "purple frost" (a product which we have not yet characterized), as well as $ReOCl_4(OH_2)$ and the decomposition products noted previously (2). Because of the difficulty of purifying $Re_2O_3Cl_6(ReO_3Cl)_2$, a legitimate question arises as to whether the measured powder data are for a pure sample. The commonest, and most difficult to remove, impurity was "purple frost", and comparison of the X-ray powder photograph of this compound (1), and those of other possible impurities, with our powder photograph of $Re_2O_3Cl_6(ReO_3Cl)_2$, has convinced us that, although the agreement between observed and calculated data is only fair, the observed powder data (Table 5) is that of pure $Re_2O_3Cl_6(ReO_3Cl)_2$.

Initially it proved difficult to obtain an infrared spectrum of $Re_2O_3Cl_6(ReO_3Cl)_2$. When heated *in vacuo*, in a gas cell, the purple crystals decomposed to a yellow liquid and a nonvolatile black residue. The yellow liquid had an infrared spectrum characteristic of a mixture of $ReOCl_4$ and ReO_3Cl, whereas the residue was identified by X-ray powder diffraction as Re_3Cl_9. Similarly, in Nujol as well as $TiCl_4$ and CCl_4, $Re_2O_3Cl_6(ReO_3Cl)_2$ decomposed and infrared spectra showed peaks characteristic of a mixture of $ReOCl_4$ and ReO_3Cl (see Table 6). The Nujol mull, as well as both solutions, became emerald green, typical of solutions of $ReOCl_4$.

As reported previously (1), problems were also encountered in obtaining reproducible infrared data for solid $Re_2O_3Cl_6(ReO_3Cl)_2$ when

Can. J. Chem. Downloaded from www.nrcresearchpress.com by 210.87.254.42 on 09/05/12
For personal use only.

Can. J. Chem. Downloaded from www.nrcresearchpress.com by 210.87.254.42 on 09/05/12
For personal use only.

TABLE 5. A comparison of the powder X-ray diffraction pattern of $Re_2O_3Cl_6(ReO_3Cl)_2$ with values calculated from the single crystal data

d_{obs}	d_{calcd}	hkl	I_{calcd}*		I_{obs}
†	12.42	010	25		
6.22	6.208	020	3		9
5.92‡	5.988	001	100	186	60
	5.942	$1\bar{1}0$	17		
	5.865	100	69		
4.97	4.966	$1\bar{2}0$	9		5
4.83	4.834	110	54		27
4.42‡	4.448	$\bar{1}11$	55	108	25
	4.412	$\bar{1}01$	53		
4.31‡	4.316	021	83	140	42
	4.304	$0\bar{2}1$	57		
	4.139	030	3		
4.02	4.020	$1\bar{1}1$	28	36	12
	3.993	$\bar{1}21$	8		
3.90	3.918	$\bar{1}\bar{1}1$	9	77	38
	3.900	$1\bar{3}0$	68		
3.79	3.794	120	24		18
3.67	3.672	$1\bar{2}1$	35		19
3.62	3.623	111	25		16
3.39	3.400	$0\bar{3}1$	6		7
3.37	3.374	$\bar{1}31$	8		8
3.17	3.171	$1\bar{3}1$	44		31
3.11‡	3.119	121	37	83	100
	3.104	040	41		
	3.102	$1\bar{4}0$	5		
3.02‡	3.039	$2\bar{1}0$	9	25	14
	2.994	002	10		
	2.971	$2\bar{2}0$	6		
2.79	2.789	$\bar{1}12$	10	16	8
	2.780	$\bar{1}02$	6		
2.76‡	2.760	$2\bar{3}0$	13	35	34
	2.759	041	10		
	2.753	$0\bar{4}1$	6		
2.69‡	2.700	022	9	29	25
	2.699	210	8		
	2.694	$0\bar{2}2$	12		
2.66	2.667	$\bar{1}22$	6		5
2.59	2.604	$2\bar{1}1$	14	27	25
	2.602	$\bar{2}31$	13		
2.57§	2.572	$1\bar{1}2$	19		8
2.55‡	2.561	$2\bar{2}1$	6	27	30
	2.548	$\bar{2}11$	21		
2.48	2.486	140	12	19	31
	2.483	050	7		
2.45	2.457	$\bar{1}32$	8		8
2.42	2.424	$\bar{1}\bar{2}2$	12	22	21
	2.423	$0\bar{3}2$	2		
	2.422	$2\bar{3}1$	5		
	2.417	220	3		
2.37	2.377	$\bar{1}51$	12		13
2.33	2.329	$\bar{1}41$	17		17
2.30	2.301	$1\bar{5}1$	3	9	11
	2.296	051	6		
2.25	2.251	$\bar{2}12$	31		22
	2.142	230	3		
2.07	2.079	132	3		7

TABLE 5 (*Concluded*).

d_{obs}	d_{calcd}	hkl	I_{calcd}		I_{obs}
2.02‡	2.031	$2\bar{1}2$	10	26	25
	2.024	$3\bar{2}0$	7		
	2.018	$2\bar{5}1$	7		
	2.015	$3\bar{1}0$	2		
	1.996	003	7		
1.98§	1.981	$\bar{1}52$	9	13	8
	1.980	$\bar{3}21$	4		
1.97‡	1.973	231	10		21
1.95‡	1.959	151	2	20	27
	1.957	061	4		
	1.954	$0\bar{6}1$	2		
	1.951	$\bar{1}\bar{4}2$	2		
	1.950	$2\bar{6}0$	6		
	1.940	$\bar{3}31$	4		
1.91§	1.909	$\bar{1}23$	2	7	6
	1.909	052	5		
1.90‡	1.899	$\bar{1}\bar{1}3$	4	13	25
	1.899	$0\bar{5}3$	2		
	1.895	$1\bar{5}2$	7		
	1.877	142	6		
1.86§	1.859	$\bar{3}41$	5	7	8
	1.858	310	2		
1.84	1.842	$\bar{2}52$	5	20	27
	1.841	$\bar{2}\bar{4}1$	3		
	1.837	$1\bar{7}0$	8		
	1.836	$2\bar{4}2$	2		
	1.836	103	2		
	1.828	$\bar{1}33$	8		
1.82§	1.823	$\bar{3}\bar{1}1$	8	12	13
	1.818	$2\bar{6}1$	4		
1.80‡	1.813	$\bar{1}\bar{2}3$	7	25	25
	1.808	160	7		
	1.807	301	4		
	1.803	$\bar{2}\bar{3}2$	7		
1.76§	1.758	$3\bar{4}1$	6		4
	1.756	$\bar{3}12$	2		
1.74‡	1.753	$\bar{2}13$	5		13
	1.740	$1\bar{7}1$	7		
	1.738	320	2		
	1.730	$1\bar{3}3$	4		
	1.717	161	7		
	1.716	$\bar{3}02$	3		
1.70‡	1.713	$2\bar{5}2$	–		13
	1.699	$0\bar{7}1$	5		
	1.695	$\bar{2}33$	4		

*$I_{calcd} < 3$ were omitted unless they contributed to an observable peak.
†Behind the collimator shadow.
‡Broad line.
§Shoulder on another peak.

ground between NaCl plates. Spectra varied enormously, the only peak observed in all spectra being one at 1018 cm^{-1} which was once observed as the only peak present in the 1100–600 cm^{-1} region. This was one of the factors which led us to believe that $Re_2O_3Cl_6$-

Can. J. Chem. Downloaded from www.nrcresearchpress.com by 210.87.254.42 on 09/05/12
For personal use only.

TABLE 6. Infrared data in cm^{-1}

$ReOCl_4$		ReO_3Cl					$Re_4O_9Cl_8$		
Vapor AgCl gas cell (3)	Nujol mull KBr	Nujol mull KBr	Vapor AgCl gas cell (19)	$ReOCl_4$ and ReO_3Cl (1:1), AgCl gas cell	$ReOCl_4$ and ReO_3Cl, neat liquid KBr	$Re_2O_4Cl_5$, fluorolube mull (17)	Crystals; Irtran 2 polythene	Nujol mull KBr	Assignment
1047 s*						1042 sh			
1040 vs							1039 s		†
1033 sh s	1033 vs			1033 m	1034 vs	1036 s		1036 m	
						1020 sh			
			1011 m	1012 vvw					
				1005 m, sharp	1005 m	1005 a			
		1002 w	1003 m	1002 w, sharp	1001 sh		1003 s	1002	‡
			995 m						
			979 sh	982 sh	977 m				
			971 vs	970 vvs		973 s	970 s	970 m	§
		967 s	965 sh	963 sh	966 w, sh				
				936 m	940 m	931 s	930 s		‖
						890 m, br			¶
							830 m		**
			437 sh			442 s	441 s		††
			429 s		437 m, broad	433 sh	431 sh		
			421 sh						
							350 s, v broad		‡‡

*s = strong, m = medium, w = weak, v = very, sh = shoulder.
†$\nu_{Re=O}$ of free or coordinated $ReOCl_4$ or of the oxo-group of $Re_2O_3Cl_6$ in $(Re_2O_3Cl_6)(ReO_3Cl)_2$.
‡$\nu_{Re=O}$ symmetric stretch of coordinated (*a'* symmetry) or free (a_1) ReO_3Cl.
§$\nu_{Re=O}$ asymmetric stretch of ReO_3Cl (*e* for uncoordinated, *a'* or *a"* for coordinated).
‖$\nu_{Re=O}$ asymmetric stretch of coordinated ReO_3Cl (*a'* or *a"*).
¶Hydrolysis product (see text).
**$\nu_{Re=O-Re}$ asymmetric stretch of linear bridging oxygen atom.
††Symmetric deformation in free and coordinated ReO_3Cl, possibly nearly coincident with Re=O....Re stretch for ReO_3Cl coordinated to $ReOCl_4$ or $Re_2O_3Cl_6$.
‡‡ν_{Re-Cl}.

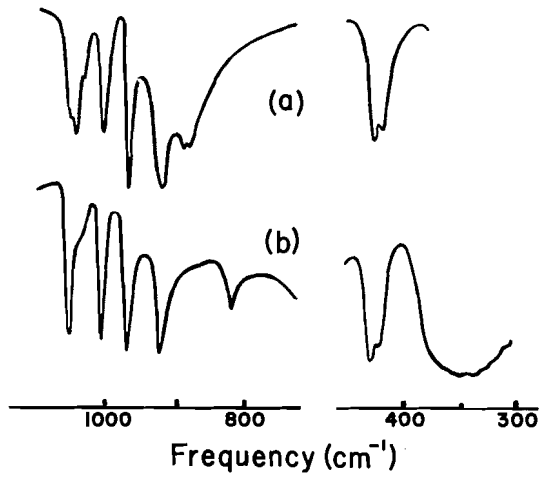

FIG. 3. The infrared spectra of (*a*) $ReOCl_4 \cdot ReO_3Cl$ (from ref. 17), and (*b*) $(Re_2O_3Cl_6)(ReO_3Cl)_2$ (this work).

$(ReO_3Cl)_2$ was β-$ReOCl_3$, but clearly the 1018 cm^{-1} peak arises from one of the impurities often observed in the X-ray powder films of apparently pure $Re_2O_3Cl_6(ReO_3Cl)_2$, possibly $ReOCl_4(OH)_2$ which has an infrared peak at $1016.5 \pm 1\ cm^{-1}$ (2).

Reproducible infrared spectra of $Re_2O_3Cl_6$-$(ReO_3Cl)_2$ were finally obtained by carefully supporting very thin, large plate crystals between Irtran 2 slabs or polyethylene discs with the disc edges wrapped in Teflon tape. The success of this technique for obtaining an infrared spectrum was very dependent on the thickness of the crystals mounted, which were as thin as possible (< 0.1 mm). The infrared spectrum is shown in Fig. 3 with that reported recently for a 1:1 adduct of $ReOCl_4$ and ReO_3Cl (17) where the postulated structure is very similar to that of one of the centrosymmetrically related halves of $Re_2O_3Cl_6(ReO_3Cl)_2$. The frequencies and assignments of these and other infrared spectra are listed in Table 6.

In the gas phase, ReO_3Cl has infrared absorptions at 1003 cm^{-1} (a_1), 971 cm^{-1} (e), and 429 cm^{-1} (a_1) (19). The lowering of symmetry on coordination in $Re_2O_3Cl_6(ReO_3Cl)_2$, results in a splitting of ν_4 (e). The two components (a' and a'') appear for $Re_2O_3Cl_6$-$(ReO_3Cl)_2$ at 970 and 930 cm^{-1} and for $ReOCl_4 \cdot ReO_3Cl$ at 973 and 931 cm^{-1} (17). The peak at 1003 cm^{-1} (a') in ReO_3Cl is unaffected by the lowering of symmetry, and is at 1003 cm^{-1} for $Re_2O_3Cl_6(ReO_3Cl)_2$ and 1005 cm^{-1} for $ReOCl_4 \cdot ReO_3Cl$. The symmetric ReO_3 deformation in ReO_3Cl at 429 cm^{-1} of a_1 symmetry is apparently split in both $Re_2O_3Cl_6(ReO_3Cl)_2$ (441 and 431 cm^{-1}) and $ReOCl_4 \cdot ReO_3Cl$ (442 and 433 cm^{-1}). The splitting cannot arise from the lowering of symmetry from C_{3v} to C_1, and in the former case, where we know the crystal structure, cannot arise from different site symmetries for the two ReO_3Cl groups. Thus the splitting must arise either from coupling between the vibrational modes of the two perrhenyl groups in the same molecule, or in reality there is no splitting, but an accidental near-coincidence between the symmetric ReO_3 deformation mode and an ReO_3Cl–(molecular residue) interaction, perhaps the Re—O stretch of the weakly bonded perrhenyl chloride oxygen atom.

The Re=O stretch in $ReOCl_4$ (gas phase) at 1040 cm^{-1} (3) is shifted to 1036 cm^{-1} for $ReOCl_4 \cdot ReO_3Cl$, and the Re=O stretch for the similar oxo group in $Re_2O_3Cl_6(ReO_3Cl)_2$ is at 1039 cm^{-1}. The very small shift in this stretching frequency implies very little change in the Re=O bond strength, and suggests a very weak bond to the group *trans* to the oxo group, consistent with the long distance to the ReO_3Cl groups in $Re_2O_3Cl_6(ReO_3Cl)_2$. There is no evidence of splitting of the 1039 cm^{-1} peak in $Re_2O_3Cl_6(ReO_3Cl)_2$, as was observed for $ReOCl_4 \cdot ReO_3Cl$ (17). Furthermore, the reported broad peak at $\sim 890\ cm^{-1}$ in the infrared spectrum of $ReOCl_4 \cdot ReO_3Cl$ (17) did not appear in the infrared spectra of pure mixtures of ReO_3Cl and $ReOCl_4$ (see Table 6), whereas evidence of the 1:1 adduct was there in all cases. A broad peak at $\sim 890\ cm^{-1}$ was observed, however, when the neat mixture of ReO_3Cl and $ReOCl_4$ between KBr plates was opened to the atmosphere for a few seconds. We therefore conclude that this absorption in the infrared spectrum of $ReOCl_4 \cdot ReO_3Cl$ is the result of a hydrolysis or oxidation product, and not the result of vibration of the weakly bonded oxygen atom of ReO_3Cl against the rhenium atom of $ReOCl_4$, as was postulated by Petrov *et al.* (17).

The infrared absorption at $\sim 830\ cm^{-1}$ observed for $Re_2O_3Cl_6(ReO_3Cl)_2$ is caused by the Re—O—Re stretching mode of the linear bridge, and is quite similar to 851 cm^{-1}

Can. J. Chem. Downloaded from www.nrcresearchpress.com by 210.87.254.42 on 09/05/12
For personal use only.

Can. J. Chem. Downloaded from www.nrcresearchpress.com by 210.87.254.42 on 09/05/12
For personal use only.

for $Cs_4[Re_2OCl_{10}]$, and 855 cm^{-1} for $K_4[Re_2OCl_{10}]$ (20, 21), which has been shown to contain a linear Re—O—Re system (8).

In passing, it should be noted that Wing and Callahan (22) have tried to relate M—O—M stretching frequencies to the M—O—M angle. It is evident that the group *trans* to the bridging oxygen atom is also important in determining this frequency. For instance, for $[(C_6H_5)_4As]_2Re_2O_3Cl_8$ and $[(C_2H_5)_4N]_2Re_2O_3Cl_8$, which are postulated to contain linear O=Re—O—Re=O systems, the bridging frequencies are at 725 and 740 cm^{-1}, respectively, with the terminal Re=O stretch frequencies at 977, 970, and 977, 955 cm^{-1}, respectively (23). A similar effect is observed for the $Re_2O_3(CN)_8^{4-}$ ion, which is also known to contain a similar linear system (16) where the Re—O—Re stretch frequency is at 720 cm^{-1} and the Re=O stretch frequency is at 1020 cm^{-1} (24). As we have seen above, however, if the oxo group is *cis* to the Re—O—Re system and a chlorine atom is *trans*, the Re—O—Re stretch frequency is at least 100 cm^{-1} higher. We have commented previously on the strong *trans* weakening effect of the Re=O system (25), which is shown clearly here in the lower M—O—M stretch frequencies and, as we have commented above, in the longer Re—O (bridging) bond length in $Re_2O_3(CN)_8^{4-}$ compared to that in $Re_2O_3Cl_6(ReO_3Cl)_2$.

The preparation of $Re_2O_3Cl_6(ReO_3Cl)_2$ is clearly dependent on the co-condensation of $ReOCl_4$, ReO_3Cl, and H_2O, as shown in preparation (*c*). The preparation probably involves a photochemical elimination of HCl from $ReOCl_4(OH_2)$ in the presence of ReO_3Cl (to complete the octahedral coordination) to give $ReOCl_3(OH)\cdot ReO_3Cl$, which quickly condenses with $ReOCl_4\cdot ReO_3Cl$ to yield $Re_2O_3Cl_6(ReO_3Cl)_2$ and another mole of HCl. This mechanism explains why preparation by methods (*a*) and (*b*) was so difficult and irreproducible, since success is obviously dependent on water being present.

The characterization of β-$ReOCl_3$ as a perrhenyl chloride complex of $Re_2O_3Cl_6$ has raised doubts about the nature of α-$ReOCl_3$ (1). Further work by us has shown that the samples prepared by Guest and Lock and used for analysis are different from the samples used by Frais and Lock for infrared and X-ray studies.

The material used by Frais and Lock and called herein "purple frost", has now been analyzed several times, and shows considerable variation in composition. Cl:Re ratios have been determined by neutron activation analysis (4) on different samples and have yielded values of 3.59, 3.19, 3.80, 2.73, 2.50, 3.66, 4.15, and 2.47. The ReO_4^-/ReO_2 ratios obtained on alkaline hydrolysis vary much less (6.0, 6.9, and 5.2) indicating an average oxidation state of ~6.5. The latter results confirm that Frais and Lock's "purple frost" is not α-$ReOCl_3$, and is different from Guest and Lock's material.

Guest and Lock's product had an average Cl:Re ratio of 3.0(1) (4 determinations) and an oxidation state of approximately 5. We were unable to test the variation in the oxidation state analysis because of lack of material, and only one analysis was made rather than the more usual 3 to 5. Clearly, the Re:Cl ratio does not distinguish between $ReOCl_3$ and $Re_2O_3Cl_6$, and the single oxidation state determination is more susceptible to error because of neutron flux variation (4). Guest and Lock's results are consistent with the existence of $ReOCl_3$, but we feel are not conclusive. Confirmation of the existence of $ReOCl_3$ must await further physical measurements.

We thank the National Research Council of Canada for financial support of this work and a scholarship to one of us (P.W.F.).

1. P. W. Frais, C. J. L. Lock, and A. Guest. Chem. Commun. 75 (1971).
2. P. W. Frais and C. J. L. Lock. Can. J. Chem. **50**, 1811 (1972).
3. A. Guest and C. J. L. Lock. Can. J. Chem. **49**, 603 (1971).
4. W. D. Courrier, A. Guest, C. J. L. Lock, and R. H. Tomlinson. Can. J. Chem. **46**, 2965 (1968).
5. D. T. Cromer and K. Herrington. J. Am. Chem. Soc. **77**, 4708 (1955).
6. D. T. Cromer and J. T. Waber. Acta Cryst. **18**, 104 (1965).
7. D. T. Cromer. Acta Cryst. **18**, 17 (1965).
8. J. C. Morrow. Acta Cryst. **15**, 851 (1962).
9. A. McL. Mathieson, D. P. Mellor, and N. C. Stephenson. Acta Cryst. **5**, 185 (1952).
10. E. Amble, S. L. Miller, A. L. Schawlow, and C. H. Townes. J. Chem. Phys. **20**, 192 (1952).
11. L. O. Atovmyan, O. A. D'yachenko, and E. B. Lobkovskii. J. Struct. Chem. (USSR), **11**, 429 (1970).
12. H. W. W. Ehrlich and P. G. Owston. J. Chem. Soc. 4368 (1963).
13. C. Wan. Ph.D. Thesis. McMaster University, Hamilton, Ontario, 1969.

14. F. A. COTTON and S. J. LIPPARD. Inorg. Chem. **5**, 416 (1966).
15. F. A. COTTON and S. J. LIPPARD. Inorg. Chem. **4**, 1621 (1965).
16. R. SHANDLES, E. O. SCHLEMPER, and R. K. MURMANN. Inorg. Chem. **10**, 2785 (1971).
17. K. I. PETROV, V. V. KRAVCHENKO, D. V. DROBOT, and V. A. ALEKSANDROVA. Russ. J. Inorg. Chem. **16**, 928 (1971).
18. D. V. DROBOT, B. G. KORSHUNOV, and V. A. ALEKSANDROVA. Zh. Neorg. Khim. **16**, 2295 (1971).
19. A. GUEST, H. E. HOWARD-LOCK, and C. J. L. LOCK. J. Mol. Spectrosc. **43**, 273 (1972).
20. F. A. COTTON and R. M. WING. Inorg. Chem. **4**, 867 (1965).
21. B. JEZOWSKA-TRZEBIATOWSKA, J. HANUZA, and M. BALUKA. Acta Phys. Pol. A **38**, 563 (1970).
22. R. M. WING and K. P. CALLAHAN. Inorg. Chem. **8**, 871 (1969).
23. B. J. BRISDON and D. A. EDWARDS. Inorg. Chem. **7**, 1898 (1968).
24. C. J. L. LOCK and G. TURNER. Unpublished work.
25. N. P. JOHNSON, C. J. L. LOCK, and G. WILKINSON. J. Chem. Soc. 1054 (1964).
26. K. W. BAGNALL, D. BROWN and R. COLTON. J. Chem. Soc. 3017 (1964).

Can. J. Chem. Downloaded from www.nrcresearchpress.com by 210.87.254.42 on 09/05/12
For personal use only.

Crystal Structure of and Electron Spin Resonance of Mn^{2+} in MgV_2O_6

HOK NAM NG AND CRISPIN CALVO

Department of Chemistry, McMaster University, Hamilton, Ontario

Received June 12, 1972

MgV_2O_6 crystallizes in the monoclinic space group $C2/m$ with lattice parameters $a = 9.279(7)$, $b = 3.502(2)$, $c = 6.731(6)$ Å and $\beta = 111.77(6)^\circ$ with $Z = 2$. The structure was refined, at room temperature, utilizing 593 symmetry independent reflections, by full matrix least squares to a final R value of 0.032. The structure consists of Mg^{2+} lying at a site of $2/m$ symmetry octahedrally coordinated to oxygen atoms with a mean separation of 2.140 Å. All the remaining atoms lie in crystallographic mirror planes with the V ion coordinated to six oxygen atoms with bond distances ranging from 1.666 to 2.671 Å. The spin Hamiltonian parameters for Mn^{2+} were determined at room temperature and again at liquid N_2 temperatures. As these values are invariant with temperature there is no indication of a phase transformation in $Mg(VO_3)_2$ to a lower symmetry space group. The spin Hamiltonian parameters are $g_x = 2.0042$, $g_y = 2.0090$, $g_z = 2.0005$; $D = -459$ G, $E = 65$ G, and $A = -78$ G with one of the principal axes, X, parallel to the b-axis and the Z-axis at an angle of 5° to the c-axis.

MgV_2O_6 cristallise sous une forme possédant le groupe spatial monoclinique $C2/m$, avec les paramètres de réseau $a = 9.279(7)$, $b = 3.502(2)$, $c = 6.731(6)$ Å et $\beta = 111.77(6)^\circ$ et $Z = 2$. La structure a été raffinée, à la température de la pièce, au moyen de 593 réflexions de symétrie indépendante, par moindres carrés de matrice complète, jusqu'à une valeur finale de R de 0.032. La structure consiste en ions Mg^{2+} se situant à des positions de symétrie $2/m$, coordonnés octaédriquement à des atomes d'oxygène à une distance moyenne de 2.140 Å. Les atomes restants se situent dans des plans-miroirs cristallographiques, l'ion V étant coordonné à six atomes d'oxygène, à des distances variant entre 1.666 et 2.671 Å. Nous avons déterminé les paramètres Hamiltoniens de spin pour Mn^{2+} à la température de la pièce et de l'azote liquide. Ces valeurs, étant indépendantes de la température, indiquent l'absence de transformation de phase dans $Mg(VO_3)_2$ en un groupe spatial de symétrie inférieure. Les paramètres Hamiltoniens de spin sont $g_x = 2.0042$; $g_y = 2.0090$, $g_z = 2.0005$; $D = -459$ G, $E = 65$ G et $A = -78$ G, un des axes principaux, X, étant parallèle à l'axe b et l'axe des Z faisant un angle de 5° avec l'axe c. [Traduit par le journal]

Canadian Journal of Chemistry, **50**, 3619 (1972)

Introduction

A number of divalent metal metavanadates, MV_2O_6, have been found to crystallize in the brannerite structure of $ThTi_2O_6$ (1). These include the Cd, Ca, Zn, Hg, and Co metavanadates (2–4). Most crystallize in the monoclinic system with possible space groups $C2/m$, $C2$, or Cm. Only the Cd and Hg metavanadates have been found to be dimorphous. The phase transformation in CdV_2O_6, it has been suggested, involves no change in crystal symmetry, but only a contraction of the high temperature cell dimensions (2), while β-HgV_2O_6 has the space group $Pbca$ (4). The structure of CdV_2O_6 has been refined in the centrosymmetric space group $C2/m$ (2) while that of ZnV_2O_6 in space group $C2$ (4). Except for the fact that the atoms are no longer restricted to mirror planes in the latter case the two structures are nearly identical.

Attempts to grow crystals of CdV_2O_6 large enough for an electron paramagnetic resonance study of the phase transition proved fruitless. Nevertheless Mn^{2+} in magnesium metavanadate was chosen for study since changes in the direction of the principal axes have provided a sensitive technique for detection of subtle transformations. In the system MgO–V_2O_5 compounds with oxide ratios of 3:1, 2:1, and 1:1 have been reported (5) and the crystal structure of the first two, $Mg_3(VO_4)_2$ (6) and $Mg_2V_2O_7$ (7), are now known. A recent study denies the appearance of MgV_2O_6 but claims to have obtained $Mg_3V_4O_{13}$ (8). In $Mg_3(VO_4)_2$ the vanadium ion is tetrahedrally coordinated to oxygen atoms. In one of the polymorphs of the $Mg_2V_2O_7$, half of the vanadium ions are tetrahedrally coordinated while the remainder are coordinated to five oxygen atoms. The metavanadate, MgV_2O_6, has an X-ray powder pattern similar to that of β-CdV_2O_6 (2). However, no α–β transition has been reported for this compound. In this study the structure of MgV_2O_6 has been refined from X-ray diffraction data. The e.p.r. spectra of MgV_2O_6 doped with Mn^{2+} were also examined at ambient and liquid nitrogen temperatures in an attempt to

Can. J. Chem. Downloaded from www.nrcresearchpress.com by 210.87.254.42 on 09/05/12
For personal use only.

Can. J. Chem. Downloaded from www.nrcresearchpress.com by 210.87.254.42 on 09/05/12
For personal use only.

TABLE 1. Positional and thermal parameters of MgV_2O_6*

Atom	Position type	x	y	z	U_{11}†	U_{22}	U_{33}	U_{12}	U_{13}	U_{23}
Mg	2(a)	0	0	0	0.0131(5)	0.0113(5)	0.0085(5)	—	0.0069(4)	—
V	4(i)	0.30514(4)	$\frac{1}{2}$	0.3436(1)	0.0070(2)	0.0045(2)	0.0052(2)	—	0.0042(1)	—
O(1)	4(i)	0.1517(2)	$\frac{1}{2}$	0.1133(3)	0.0100(6)	0.0115(7)	0.0081(6)	—	0.0028(5)	—
O(2)	4(i)	0.4607(2)	$\frac{1}{2}$	0.2764(3)	0.0107(7)	0.0094(7)	0.0104(6)	—	0.0078(5)	—
O(3)	4(i)	0.1930(2)	$\frac{1}{2}$	0.5652(3)	0.0122(6)	0.0047(6)	0.0095(6)	—	0.0071(5)	—

*Estimated standard deviation in parentheses.
†Calculated from $\beta_{ij} = 2\pi^2 b_i b_j U_{ij}$ where $T = \exp[-(\beta_{11}h^2 + 2\beta_{12}hk + \ldots)]$ is the thermal factor appearing in the structure factor expression and b_i's are reciprocal lattice vectors.

Can. J. Chem. Downloaded from www.nrcresearchpress.com by 210.87.254.42 on 09/05/12
For personal use only.

establish whether there is a low temperature phase.

Experiments

A. X-Ray Diffraction Studies

Crystal data

MgV_2O_6 f.w. = 222.194

Space group: $C2/m$, $a = 9.279(7)$, $b = 3.502(2)$, $c = 6.731(6)$ Å, $\beta = 111.77(6)$°, $Z = 2$, $V = 203.12$ Å^3, $\rho_o = 3.66$ g/cm^3, $\rho_c = 3.64$ g/cm^3.

Crystals of MgV_2O_6 were prepared from a mixture of MgO and V_2O_5 in a molar ratio of 37:63. The mixture was melted in a Vitreosil crucible at 850 °C, cooled at 3 °C/h to 640 °C and quenched to room temperature. The yellow crystal plates of MgV_2O_6 were invariably elongated along the *b*-axis. A good quality single crystal was selected and cut to a cube of 0.3 mm in each dimension for X-ray intensity measurements.

Photographic work established the space group as $C2/m$, Cm, or $C2$ as reflections were systematically absent when $h + k = 2n + 1$, n = integer. Accurate lattice parameters were determined by a least squares fit to 15 2θ values measured with the Syntex automatic diffractometer.

Intensity data were collected on a Syntex automatic diffractometer using graphite monochromatized MoKα ($\lambda = 0.71069$ Å) radiation and θ–2θ mode of scan at a variable rate. Reflections whose intensity, corrected for background, exceeded three times the calculated standard deviation were considered observed. Reflections with intensities calculated as negative were left out of the refinement. A total of 593 symmetry-independent reflections were recorded and the data were corrected for Lorentz, polarization, and absorption effects ($\mu r = 1.36$). Symmetry-equivalent reflections differed on average by less than 2% from the mean. Within a sphere defined by $2\theta \leqslant 75°$ there were only 38 unobserved reflections in the data set.

B. Electron Paramagnetic Resonance Studies

For e.p.r. studies about 0.1% of $MnCO_3$ was added to the starting mixture of V_2O_5 and MgO before melting. The resulting MgV_2O_6 crystals were light brown in color. Several crystal plates with dimensions of the order $2 \times 1 \times 0.3$ mm were selected and aligned by X-ray techniques described previously (9). The accuracy in orientation was estimated to be ±3°. A Varian V-4503 EPR spectrometer with a 12 in. rotatable magnet was used. The microwave cavity was operated at 35 GHz in the cylindrical TE_{011} mode. The magnetic field was measured with a Varian Fieldial unit calibrated by n.m.r. techniques utilizing a Li^7 probe. The *g*-values were measured by using a DPPH standard.

Results

A. X-Ray Studies

A full matrix least squares program, written by Stephens for the CDC 6400 computer, was used to refine the structure. The final coordinates and anisotropic temperature factors of CoV_2O_6 (10) were used as initial parameters for the refinement in the centrosymmetric space group

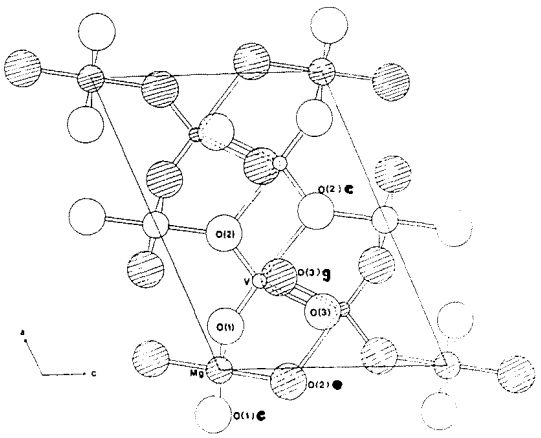

FIG. 1. Projection of the MgV_2O_6 Structure on *ac*-plane, (shaded circles for atoms at $y = 0$, unshaded circles for atoms at $y = 1/2$).

$C2/m$. Since the refinement was satisfactory, no attempt was made to refine the structure in the less symmetric space groups $C2$ or Cm. Atomic scattering curves for Mg^{2+}, V^{5+}, and O^{2-} were taken from Cromer and Waber (11) and those for magnesium and vanadium were corrected for anomalous dispersion (12). A weighting function $\omega = (2.0 + 0.25\,F_o + 0.006\,F_o^2)^{-1}$ was chosen so that $\omega(|F_o| - |F_c|)^2$, the square of the difference between the observed and calculated structure factors, would be independent of the local average of $|F_o|$. Refinement was terminated when the maximum shift in the parameters was less than 15% of the calculated standard deviation. The final R value was 0.032 and the $\omega R = \{\sum\omega|F_o - F_c|^2/\sum\omega F_o^2\}^{1/2}$ was 0.043. Table 1 contains the final atomic parameters while Table 2 compares the observed and calculated structure factors.[1]

This class of crystals can be described as composed of distorted XO_6 octahedra with $X = V^{5+}$ or Ti^{4+} (1). These octahedra share opposite corners forming chains running parallel to the *b*-axis. Octahedra in adjacent chains share edges involving O(2) and O(2)e, as shown in Fig. 1, on one side of the chain. On the other side chains interleaf such that one octahedron shares two edges with two adjacent octahedra in a neighbouring chain. These edges are O(3)a

[1]Photocopies of Table 2 are available, at a nominal charge, from the Depository of Unpublished Data, National Science Library, National Research Council of Canada, Ottawa, Canada, K1A 0S2.

TABLE 3. Bond geometry in MgV_2O_6 with estimated standard deviations in parentheses

Bond	Distance (Å)		Bonds	Angle (deg)	Bonds	Angle (deg)
MgO_6 Group						
Mg—O(1)a*	2.199(2)†	4X	O(1)a—Mg—O(1)c	74.4(1)		
—O(2)e	2.024(3)	2X	—O(1)b	105.6(1)		
			—O(2)e	90.5(1)		
VO_6 Group						
V—O(1)a	1.671(2)		O(1)a—V—O(2)a	105.9(2)	O(2)a—V—O(3)g	100.8(2)
—O(2)a	1.666(3)		—O(3)g	102.0(2)	—O(3)a	153.6(2)
—O(3)g	1.853(2)	2X	—O(3)a	100.5(2)	O(3)g—V—O(3)a	73.3(1)
—O(3)a	2.111(3)		O(2)c—V—O(1)a	176.8(1)	O(2)c—V—O(3)g	77.2(1)
—O(2)c	2.671(3)		—O(2)a	77.3(2)	—O(3)a	76.3(1)
O(1)a—O(2)a	2.663(3)					
—O(3)g	2.741(2)	2X				
—O(3)a	2.921(4)					
O(2)a—O(3)g	2.714(3)	2X				
O(3)g—O(3)a	2.376(2)					
O(2)c—O(3)g	2.895(3)	2X				
—O(2)a	2.821(4)					
—O(3)a	2.986(4)					

*Oxygen atom positions are derived from those listed in Table 1 by symmetry operations designated by a...g in the same order as listed in the International tables for X-ray crystallography, vol. I.
†Estimated standard deviations include uncertainties in the unit cell lengths.

and O(3)g with one octahedron and O(3)a and O(3)g with the next one (translated by a *b* axis length).

Mg^{2+} ions lie in octahedral interstices sharing oxygen atoms with six different V^{5+} ions. MgO_6 groups form chains paralleling the *b*-axis by sharing O(1)a–O(1)c edges with two translation-equivalent MgO_6 groups. The average Mg—O bond length is 2.140 Å and the group shows an angular distortion consistent with a repulsive interaction between vanadium ions separated by a *b*-axis translation and sharing an oxygen atom with the Mg^{2+} ion. The individual bond lengths and angles are found in Table 3.

The VO_6 group has five strong bonds and one weak one. The vanadium ion is displaced by about 0.5 Å along the O(1)a–O(2)c axis towards O(1)a yielding V—O bond lengths of 1.671 and 2.671 Å. The V^{5+} ion is also displaced from the O(1)a–O(2)c axis of the octahedron away from the edges O(3)a–O(3)g shared with neighbouring vanadium ions. This displacement is primarily towards O(2)a and away from O(3)a, thus yielding bonds to these oxygen atoms of 1.666 and 2.111 Å, respectively. The remaining V—O bonds are mirror plane related, involve O(3)g and are 1.853 Å long.

B. Electron Paramagnetic Resonance Studies

The crystal symmetry of MgV_2O_6 is such that it requires one of the principal axes of the **D**-tensor to be parallel to the *b*-axis, if the paramagnetic ion substitutes directly for the magnesium, independent of whether the space group is *C*2, *Cm*, or *C*2/*m*. Furthermore, the remaining two principal axes are constrained in a plane perpendicular to the *b*-axis. One $MgV_2O_6:Mn^{2+}$ crystal was mounted along the b-axis so that the external magnetic field explored the *ac*-plane. For each orientation of the magnetic field in this plane the spectrum consists of five groups of lines corresponding to the five allowed transitions of a ^6S state ion of Mn^{2+} as shown in Figs. 2 and 3. Each group was further split into six lines due to hyperfine interaction with the Mn^{55} nucleus. This hyperfine splitting of 78 ± 5 G was found to be isotropic within experimental errors. A maximum in the fine structure splitting was found when the magnetic field was in a direction about 5° from the *c*-axis towards the *a*-axis. This direction was chosen as the *Z*-axis. As the magnetic field was rotated in the *ac*-plane, the fine structure separation was reduced, but it increased again to another maximum when the

Can. J. Chem. Downloaded from www.nrcresearchpress.com by 210.87.254.42 on 09/05/12
For personal use only.

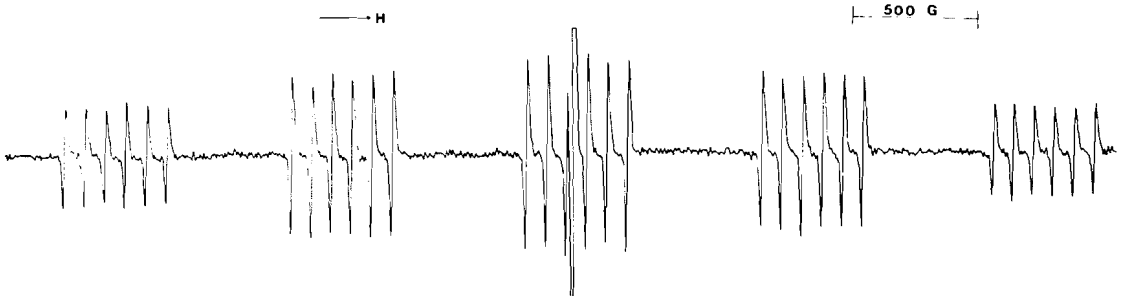

FIG. 2. Electron paramagnetic resonance spectrum of Mn^{2+} in MgV_2O_6 with $H \| Z$ (strong peak due to DPPH indicated by arrow).

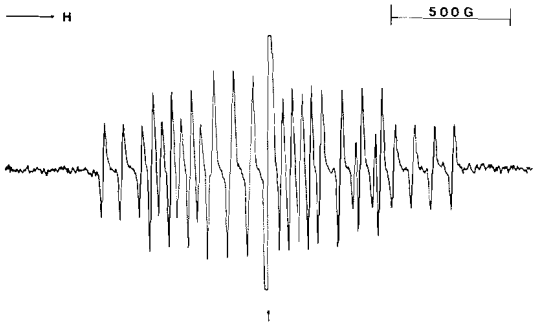

FIG. 3. Electron paramagnetic resonance spectrum of Mn^{2+} in MgV_2O_6 with $H \| Y$ (strong peak due to DPPH indicated by arrow).

magnetic field was 90° from the Z-axis in the ac-plane. This second principal axis direction was labelled the Y-axis of the **D**-tensor. That the b-axis is also a principal axis of the **D**-tensor was verified by locating the maximum in the fine structure splitting by rotating the magnetic field in a plane perpendicular to the c-axis of a second crystal. The principal axes of the **g**-tensor were assumed to coincide with those of the **D**-tensor. The principal g-values along the X, Y, and Z directions were found from the center of the hyperfine lines of the central group in the respective spectra. These parameters are tabulated in Table 4. It was observed from the spectra that D_z should have opposite sign to D_x and D_y. The relative signs of D and A were found by measuring the difference in hyperfine separations at low field and at high field (13). It was concluded that A is of the same sign as D_z but of opposite sign to D_x and D_y. The sign of the Mn^{2+} hyperfine interaction has been found in published literature to be almost always negative. It was assumed to be negative in this case also, thus giving the sign of D as negative. This sign of D was verified from the change in the relative intensity of the fine structure when the temperature was lowered to 77 °K (14).

Similar e.p.r. measurements on the same crystals were also made at 77 °K. The results showed that there was no observable change in the principal directions of the **D**-tensor at low temperature, although there was a slight but definite increase in the axial field parameter, noted in Table 4.

Discussion

The MgV_2O_6 has the brannerite structure at room temperature. The e.p.r. results are consistent with the crystallography if the Mn^{2+} substitutes for Mg^{2+} in the crystal. The crystal field around the cation reflects the same symmetry as its oxygen coordination. The Z-axis lies along the O—Mg—O bond, that is in the axial direction of the distorted octahedron. The Y-axis of the crystal field lies along the direction of projection of the Mg—O(1) bond on the ac-plane. The relatively large value of E indicates a considerable deviation from axial symmetry. This deviation is borne out by the bond angles formed between the cation and the four equatorial oxygens in the XY-plane (105.6 and 74.4°) as shown in Table 3.

The e.p.r. results show there is only one site for the Mn^{2+} ion. Since the two cations in the unit cell of MgV_2O_6 occupy sites related by lattice centering and are therefore magnetically

Can. J. Chem. Downloaded from www.nrcresearchpress.com by 210.87.254.42 on 09/05/12
For personal use only.

TABLE 4. Spin Hamiltonian parameters for Mn^{2+} in MgV_2O_4 with estimated standard deviations in parentheses; $D = \frac{3}{2}D_z$, $E = \frac{1}{2}(D_x - D_y)$, $X \| b$ axis

Component	g	A(G)		D(G)	
		300 K	77 K	300 K	77 K
X	2.0042(5)	−78(5)	−80(5)	+218(5)	+224(15)
Y	2.0090(10)	−78(5)	−80(5)	+87(5)	+98(8)
Z	2.0005(5)	−78(5)	−80(5)	−306(20)	−325(20)

equivalent, the result is consistent with a direct substitution of Mn^{2+} for Mg^{2+}. These two cation sites are all magnetically equivalent in the space groups $C2/m$, $C2$, or Cm and the ambiguity in the space group remains unresolved from the e.p.r. study.

The e.p.r. results at low temperature have to be interpreted with some caution. The cation environment apparently undergoes little change as the temperature is lowered to 77 °K. If a low temperature phase of MgV_2O_6 is the same as that in CdV_2O_6, the principal axis of the crystal field will still be constrained along the b-axis and perpendicular to it. A small change in the environment of the cation, say a rotation of the oxygen octahedron about the b-axis, will not be detected if this rotation is less than 3°, the limit of accuracy in this experiment. The changes in the crystal field parameters at 77 °K indicate a shortened distance between the cation and the axial oxygens (Mg—O(2)e) as suggested by the increased value of D, but the change is hardly significant. The results also indicate a further deviation from axial symmetry of the crystal field around the cation. Although we found no evidence for a low temperature phase of MgV_2O_6 between 77–300 °K, the possibility cannot be ignored that such a phase is present with only small changes in cell dimensions but no drastic change in crystal symmetry. However, a change as large as that indicated for CdV_2O_6, where the volume changes by about 10% (2), seems unlikely. If the structure of α-CdV_2O_6 is isotypic with that of CaV_2O_6 (3) while that of β-CdV_2O_6 is isotypic with the MgV_2O_6, then the major structural change expected is the loss of the long V–O(2) interaction. The consequence of this change in MgV_2O_6 would be stronger V–O interactions and a strengthened Mg–O(2) interaction.

Note should be taken of the enhanced distortion of the VO_6 group compared with that of the TiO_6 group in brannerite. In the latter case the bond lengths range from 1.83 to 2.20 Å. The long V—O(2)c bond length in MgV_2O_6 becomes a Ti—O bond length of 2.06 Å in the brannerite. This illustrates again the unsymmetrical nature of oxygen atom bridges between vanadate groupings.

This research was supported by the National Research Council of Canada through a postdoctoral Fellowship (H.N.N.) and a research grant #A-0948.

1. R. RUH and A. D. WADSLEY. Acta Cryst. **21**, 974 (1966).
2. J. C. BOULOUX and J. GALY. Bull. Soc. Chim. Fr. 736 (1969).
3. G. PEREZ, B. FRIT, J. C. BOULOUX, and J. GALY. C.R. Acad. Sci. Paris, **C270**, 952 (1970).
4. J. ANGENAULT. Rev. Chim. Min. **7**, 651 (1970).
5. V. A. MATVEEVICHEVA, Z. I. EZHKOVA, and B. E. ZAITSEV. Russ. J. Phys. Chem. **43**, 143 (1969).
6. N. KRISHNAMACHARI and C. CALVO. Can. J. Chem. **49**, 1629 (1971).
7. R. GOPAL. Ph.D. thesis, McMaster University, Hamilton, Ontario. 1972.
8. E. I. SPERANSKAYA. Izvestiya Akad. Nauk. SSSR. Neorgan. Mater. **7**, 1804 (1971).
9. C. CALVO, K. Y. LEUNG, and C. V. STAGER. J. Chem. Phys. **49**, 3653 (1968).
10. E. E. SAUERBREI. M.Sc. thesis, McMaster University, Hamilton, Ontario. 1972.
11. D. T. CROMER and J. T. WABER. Acta Cryst. **18**, 104 (1965).
12. D. T. CROMER. Acta Cryst. **18**, 17 (1965).
13. W. LOW. Solid state physics. Supplement 2. Academic Press, New York. 1960. p. 72.
14. A. ABRAGAM and B. BLEANEY. Electron paramagnetic resonance of transition ions. Clarendon Press. 1970. p. 160.

Can. J. Chem. Downloaded from www.nrcresearchpress.com by 210.87.254.42 on 09/05/12
For personal use only.

Cycloaddition and Related Reactions of Some Unsaturated Phosphines with Dimethyl Acetylenedicarboxylate

MAUREEN DAVIES, A. N. HUGHES, AND S. W. S. JAFRY

Department of Chemistry, Lakehead University, Thunder Bay, Ontario

Received December 29, 1971[1]

Diphenylvinylphosphine reacts with dimethyl acetylenedicarboxylate to give either an equilibrium mixture of two cyclic ylidic 1:1 adducts or a strained bicyclic ylidic 1:2 adduct depending upon the reaction conditions. The adducts have been characterized by trapping them as their hydrolysis or deuterolysis products or by their Wittig reactions. *trans*-1,2-Bis(diphenylphosphino)ethylene reacts with the ester to give a 1:1 zwitterionic adduct which exhibits some ylidic properties and hydrolyzes by a very unexpected mechanism. The *cis* isomer of this phosphine reacts with the ester to give the expected 1,4-diphosphorin which has been fully characterized.

La diphénylvinylphosphine réagit avec l'acétylène dicarboxylate de diméthyle pour conduire soit à un mélange à l'équilibre de deux composés d'addition 1:1 de type ylure cyclique soit à un composé d'addition 1:2 de type ylure bicyclique tendu, en fonction des conditions de la réaction. Ces composés d'addition ont été caractérisés en les piègeant en tant que produits issus de l'hydrolyse et deutériolyse ou encore par réaction de Wittig. Le bis-(diphénylphosphino)-1,2 éthylène *trans* réagit avec l'ester en donnant un composé d'addition 1:1 de type zwitterion qui possède quelques propriétés d'ylure et s'hydrolyse selon un mécanisme très inattendu. L'isomère *cis* de cette même phosphine réagit avec l'ester pour conduire à la diphosphorine-1,4 attendue qui a été complètement caractérisée. [Traduit par le journal]

Canadian Journal of Chemistry, **50**, 3625 (1972)

Until quite recently, cyclic phosphonium ylides (apart from the 1,1-disubstituted phosphorins) were relatively little known (1) and little work had been done on convenient and generally applicable syntheses of these systems. Since triphenylphosphine reacts readily with dimethyl acetylenedicarboxylate (2) and benzyne (3), it seemed likely that one possibly general route to cyclic phosphonium ylides of various ring sizes would be the cycloaddition of various unsaturated linkages such as suitable alkynes and arynes to vinylphosphines. Such additions would produce five-membered cyclic phosphonium ylides. Furthermore, by analogy with the insertions of dimethyl acetylenedicarboxylate into the P=C bonds of open-chain ylides (4), these initial products could possibly react further to give larger ylidic rings.

Such reactions would be essentially one-step processes involving relatively easily accessible starting materials. We therefore report here the results of our investigations regarding the reactions of diphenylvinylphosphine (**1**, R = H), *trans*-1,2-bis(diphenylphosphino)ethylene (**2**), *cis*-1,2-bis(diphenylphosphino)ethylene (**3**), and 3,4,5-triphenyl-4-phosphabicyclo[3.1.0]hex-2-ene (**4**) with dimethyl acetylenedicarboxylate. A preliminary communication regarding the reactions of **1** (R = H) with the acetylenic ester has already appeared (5). In addition, certain exploratory experiments involving the generation of benzyne in the presence of **1** and **2** are briefly mentioned. It should also be noted that, during the early stages of this work, Savage and Trippett (6) reported the cycloaddition of acrylonitrile to diphenyl(1-phenylvinyl)phosphine (**1**, R = Ph) to give the ylide **5**.

As expected, diphenylvinylphosphine reacts readily with dimethyl acetylenedicarboxylate in ether or benzene although the nature of the product depends upon the mode of addition and the proportions of the reactants. Thus, dropwise addition of a benzene solution of the ester to an equimolar amount of the phosphine in benzene at room temperature under nitrogen leads immediately to the formation of a very dark solution. Evaporation of the solution yields a tarry material in which the principal product appears to be a dark blue polymeric material. Repeated ethereal extraction of the blue material and crystallization of the residual crude product from ethanol leads to the isolation (in about 23% yield) of colorless crystals, m.p. 130–132°, which analyze well for a mole-

[1] Revision received July 11, 1972.

Can. J. Chem. Downloaded from www.nrcresearchpress.com by 210.87.254.5 on 09/05/12
For personal use only.

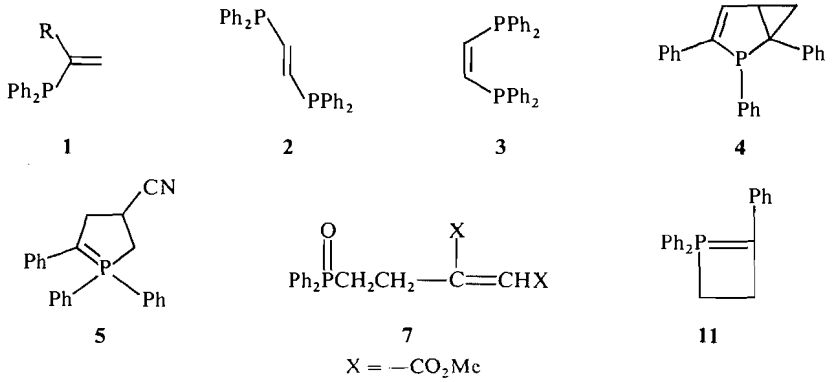

1 2 3 4

5 7 11

X = —CO_2Me

cular formula of $C_{20}H_{21}O_5P$, *i.e.* a 1:1:1 adduct of the phosphine, the ester, and water. The mass spectrum shows a molecular ion at *m/e* 372 which is consistent with the proposed molecular formula. The same product is formed regardless of whether dried or undried solvents are used (although ether containing appreciable amounts of ethanol should be avoided) and this indicates that during the reaction (or during work-up if anhydrous solvents are used), hydrolysis of an initially formed 1:1 adduct of the ester with the phosphine occurs.

The expected initial product of the reaction is the cyclic ylide **6** (a 3*H*-phosphole derivative) and, since most phosphonium ylides are very sensitive to water, this might be expected to hydrolyze to give the phosphine oxide **7** by protonation followed by ring cleavage of the resulting cyclic phosphonium hydroxide by elimination of the most stable carbanion (7). In support of this, the base peak in the mass spectrum of the 1:1:1 adduct occurs at *m/e* 201 which is typical of compounds containing the $Ph_2P(O)$— grouping (6). Furthermore, the i.r. spectrum also shows a typical (8) P=O stretching frequency at 1193 cm^{-1} and a weak substituted C=C vibration at 1664 cm^{-1}. However the ^1H n.m.r. spectrum is inconsistent with structure **7** since, although it shows the presence of two methylene groups, the coupling pattern clearly shows that these two groups are not adjacent. The spectrum shows a ten proton aromatic complex multiplet at τ 2.0–2.6, an olefinic one proton quartet at τ 2.6–3.3, two ester methyl groups at τ 6.30 and 6.37, one methylene group as a doublet of doublets centered on τ 6.69 (with the indication that $J_{HH} = 8$ and $^2J_{PH} = 16$ Hz), and one methylene group as a very closely spaced doublet ($J = ca.$ 1.5 Hz) at τ 6.65 superimposed upon the other methylene signal. One interesting feature of this spectrum is that to some extent it is concentration dependent. For example, at concentrations approaching 50%, the ester peaks are shifted a few cycles upfield while the two methylene signals are shifted very slightly downfield.

This spectrum fits the isomeric structure **9** extremely well and this structure is also consistent with the i.r. and mass spectral data. Thus, the tentatively assigned values of J_{HH} and $^2J_{PH}$ for the methylene group (τ 6.69) adjacent to the phosphorus atom are in excellent agreement with those observed for related structures in the literature (see for example, values for $^2J_{PH}$ for compounds containing the $Ph_2P(O)CH_2$— grouping quoted in ref. 6). Furthermore, the locations of the two methylene groups in the spectrum are as expected for **9**. The methylene group adjacent to the terminal ester group (τ 6.65) presumably occurs as a poorly defined doublet ($J = ca.$ 1.5 Hz) because of long-range coupling with the phosphorus atom. Such long-range couplings are known to give rise to values of $^5J_{PH}$ of the order of 1 Hz (9). On the other hand, it is possible that this methylene group is coupled to the olefinic proton which could account for the broadening of the peaks in the olefinic quartet. The fact that the olefinic signal occurs as a

Can. J. Chem. Downloaded from www.nrcresearchpress.com by 210.87.254.5 on 09/05/12
For personal use only.

Can. J. Chem. Downloaded from www.nrcresearchpress.com by 210.87.254.5 on 09/05/12
For personal use only.

quartet (in the approximate ratio 1:3:3:1) implies that J_{HH} and $^3J_{PH}$ have approximately the same value (7 Hz).

These tentative n.m.r. assignments have been confirmed by ^1H–^1H spin decoupling (field sweep) experiments. In this case, since the couplings in some instances are relatively large and the signal width is therefore considerable, selective decoupling techniques (10*a*) were found to give the best results. Irradiation of the low field doublet of the doublet of doublets of the methylene signal centered on τ 6.69 while scanning the olefinic signal causes the two high field peaks of the olefinic signal to collapse to an intense, sharp singlet centered on the more intense of the original peaks. Likewise, irradiation of the high field doublet of the methylene doublet of doublets causes the low field pair of peaks of the olefinic signal to collapse in a similar fashion. Conversely, irradiating the more intense of the two low field peaks of the olefinic signal while scanning the methylene signal at τ 6.69 causes the high field doublet of this signal to collapse to a singlet. Similar irradiation of the more intense of the two high field peaks of the olefinic signal leads to a collapse of the low field doublet of the methylene signal.

These results clearly show that the olefinic proton is coupled to the methylene protons at τ 6.69 ($J = 8$ Hz) and that the olefinic $^3J_{PH}$ coupling is 7 Hz (the small difference in these couplings accounts for the broadened peaks in the olefinic quartet). Furthermore, the $^2J_{PH}$ coupling of the methylene group adjacent to the phosphorus atom is 16 Hz and these selective decoupling experiments show (10*a*) that $^2J_{PH}$ and $^3J_{PH}$ are of opposite sign.

Very careful scanning of the spectrum in the decoupling mode shows that there is no coupling between the olefinic protons and the methylene group centered on τ 6.65 (assigned to the methylene group adjacent to the terminal ester group) and the narrow splitting of this signal (1.5 Hz) is therefore confirmed as being due to long-range P–H coupling.

Very strong support for structure **9** is also provided by the mass spectrum which shows weak peaks at *m/e* 299 (possibly $M^+ - CH_2CO_2Me$), 215 (possibly $Ph_2\overset{\overset{O}{\|}}{P}CH_2^+$) and 157 (possibly $M^+ - Ph_2\overset{\overset{O}{\|}}{P}CH_2$). These tentative assignments are confirmed by precise mass measurements (*m/e* 299: calcd., 299.0837; found, 299.0839; *m/e* 215: calcd., 215.0626; found, 215.0623; *m/e* 157: calcd., 157.0501; found, 157.0509). These peaks are very weak because cleavage would be preferred in a position allylic to the C=C link, *i.e.* adjacent to the phosphorus atom or the terminal ester group. These expected peaks are very strong in the mass spectrum of the 1:1:1 adduct. Finally, the spectrum shows a peak of medium intensity at *m/e* 340 corresponding to loss of methanol from the $-CH_2CO_2Me$ grouping. The fragmentation is confirmed by a weak metastable peak at *m** 310.7. Such eliminations are common in esters of this type (11).

The i.r. spectrum also shows two ester carbonyl stretching frequencies at 1722 (α,β-unsaturated ester) and 1749 cm^{-1} (saturated ester) and this is in agreement with structure **9**.

Structure **9** could be derived either from **7** by proton migration (a process which seems unlikely) or from hydrolysis of the cyclic ylide **8** (a 2*H*-phosphole derivative) which is a tautomer of **6**. Moreover, in such a tautomeric equilibrium, **8** should be preferred over **6** since in **8** there is more delocalization of the ylidic carbon atom negative charge over the adjacent ester group. Deuterolysis experiments support the suggestion that **9** is derived from **8** by hydrolysis. Thus, when cycloaddition of the vinylphosphine **1** (R = H) and the acetylenic ester was carried out in rigorously dried ether followed by addition of a little D_2O to the reaction mixture, it was found that mainly double deuteration (to give **10**) and some triple deuteration occurs. For example, the mass spectrum shows that the strongest molecular ion peaks occur at *m/e* 374 (double deuteration) and 375 (triple deuteration). The n.m.r. spectrum shows that the narrow doublet due to the methylene group adjacent to the terminal ester group has almost disappeared from the spectrum although there is also a reduction (from 2 to about 1.4 protons) in the intensity of the other methylene signal. The ^1H n.m.r. spectrum therefore shows that deuteration occurs mainly at the site adjacent to the terminal ester group (although some deuteration occurs at the other methylene group) and this is

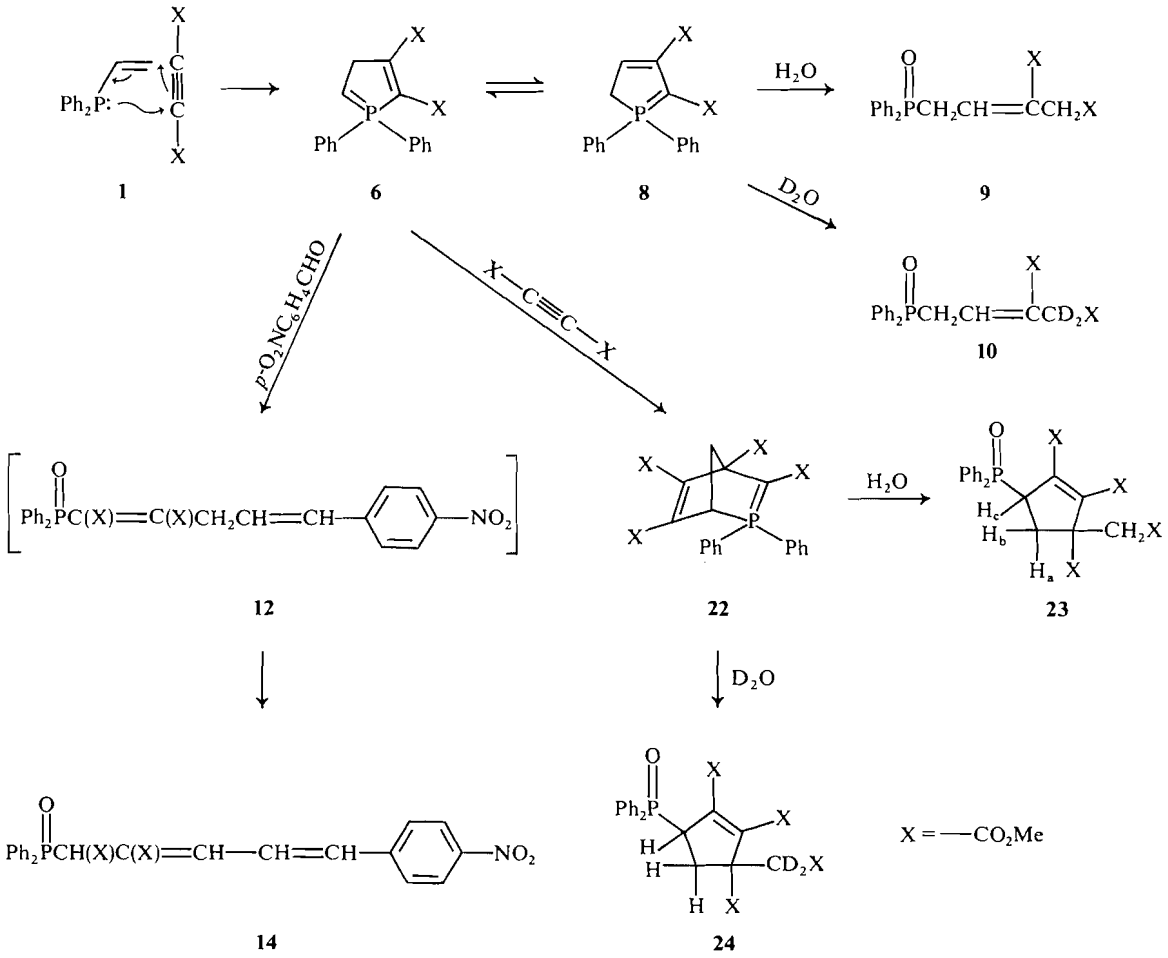

SCHEME 1

consistent with the behavior expected of **8** on hydrolysis.

These observations then are fairly good evidence that the ylide **8** is formed from the initially formed ylide **6** by tautomerization. Furthermore, similar tautomeric equilibria have been observed in the case of the four-membered ylide **11** (6). Several attempts to trap **6** before tautomerization could occur were therefore made. Attempts to trap **6** in a Wittig reaction with acetone and with benzaldehyde were unsuccessful. The use of acetone gave only uncrystallizable materials and use of benzaldehyde gave the adduct **9** as the only isolable product. However, cycloaddition of the ester and phosphine in the presence of *p*-nitrobenzaldehyde leads to the formation of a 1:1:1 adduct of the ester, the phosphine, and the aldehyde for which elemental analyses are in excellent agreement with the formula $C_{27}H_{24}O_7NP$. The mass spectrum confirms the molecular weight as 505 and the base peak is again at *m/e* 201 indicating the presence of the $Ph_2\overset{\overset{\displaystyle O}{\|}}{P}$— grouping. Thus, a Wittig reaction has occurred and the intermediacy of a cyclic ylide is established.

The adduct expected from **6** would be **12** while that from **8** would be **13** but the ^1H n.m.r. spectrum shows that the adduct is neither of these since there are no signals due to methylene groups in the spectrum. The spectrum shows 17 aromatic/olefinic protons as a broad complex multiplet at τ 1.6–3.4, one methine proton as a

Can. J. Chem. Downloaded from www.nrcresearchpress.com by 210.87.254.5 on 09/05/12
For personal use only.

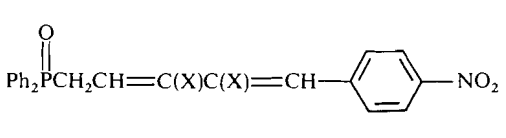

13

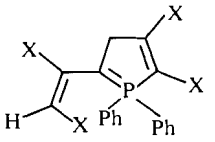

15

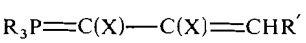

16

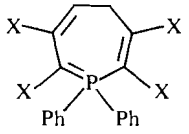

17

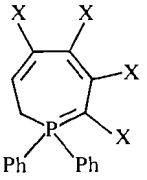

18

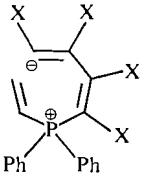

19

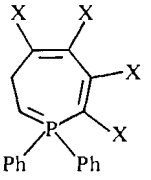

20

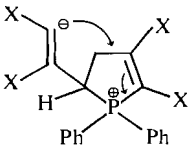

21

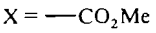

doublet ($J = 15$ Hz) centered on τ 4.38, and two ester methyl group signals at τ 6.33 and 6.38. Of the various possible isomers obtainable by addition of *p*-nitrobenzaldehyde to **6** or **8**, only **14** agrees with all the physical data since it contains no methylene groups and the low field location and the splitting of the methine proton ($J = 15$ Hz) are consistent with its position adjacent to a phosphoryl grouping and two other electron-withdrawing groups. Clearly **14** cannot be derived directly from **6** or **8** and is presumably derived from **12** by a prototropic shift. Such a shift is not surprising since it increases the conjugation in the system and the conditions of the reaction (the ylide **6** would be a strong base) would favor migration of the mildly acidic protons of the methylene group in **12**. A similar prototropic shift in **13** could produce a methine proton adjacent to an ester group (though far removed from the phosphorus atom) but this would decrease the conjugation. Some further, though not conclusive evidence for structure **14** is given by the mass spectrum which shows a peak at *m/e* 273 probably corresponding to the

$$[Ph_2\overset{\overset{O}{\|}}{P}CHCO_2Me]^+$$

fragment (precise mass found: 273.0673; calcd.: 273.0681). This could only be derived from **14** unless major rearrangements occur on electron impact. This peak is comparable in intensity with the molecular ion peak though much weaker than the base peak. In addition, the i.r. spectrum shows both saturated (1745 cm^{-1}) and α,β-unsaturated (1692 cm^{-1}) ester carbonyl stretching frequencies.

As already mentioned, the mode of reaction and proportions of the reactants in the reaction of the phosphine **1** (R = H) with the acetylenic ester can influence the nature of the product. If the phosphine (1 mol) in ether is added to an ethereal solution of the ester (2 mol) under the same reaction conditions as the 1:1 addition, a 1:2:1 adduct of the phosphine, the ester and water is obtained in about 10% yield. Analyses are in excellent agreement with a molecular formula of $C_{26}H_{27}O_9P$ and the mass spectrum shows a molecular ion at *m/e* 514 together with

$$PH_2\overset{\overset{O}{\|}}{P}—$$

the base peak at *m/e* 201 (PH_2P—). On the basis of the arguments used in the case of the 1:1:1 adduct of diphenylvinylphosphine with the ester and water, it is virtually certain that the 1:2:1 adduct is derived from hydrolysis of an ylidic 1:2 adduct of the phosphine and the ester.

There are several possible modes of reaction. For example, Michael addition of the ylide **6** to a second mole of the ester could occur to give

Can. J. Chem. Downloaded from www.nrcresearchpress.com by 210.87.254.5 on 09/05/12
For personal use only.

Can. J. Chem. Downloaded from www.nrcresearchpress.com by 210.87.254.5 on 09/05/12
For personal use only.

the ylide **15** although this type of addition is not possible for the ylide **8**. This type of mechanism was suggested by Trippett (12) for the addition of cyanomethylenetriphenylphosphorane ($Ph_3P{=}CHCN$) to dimethyl acetylenedicarboxylate and would presumably be due to the highly acidic nature of the methine proton in the initially formed zwitterion. On the other hand, Bestmann and Rothe (4) have found that addition of alkylidenephosphoranes to the ester leads (in every case studied by his group), to insertion of the ester into the $R_3P{=}CHR'$ link to give compounds of type **16**. This would suggest that **6** or **8** could react further with the ester to give the seven-membered ylides **17** or **18** respectively (or, possibly, tautomers of these). Another possible mode of reaction is the generation of the zwitterion **19** followed by cyclization to give **20**. A similar reaction path occurs in the reaction of 1,2,5-triphenylphosphole with an excess of the ester (13). Finally, the initially formed ylide **6** could react further with the ester to give **21** which could cyclize by attack at the β-position of a vinylphosphonium grouping to give the strained bicyclic ylide **22** in much the same way as **6** itself is formed.

Examination of the ^1H n.m.r. spectrum of the 1:2:1 adduct shows quite conclusively that it is **23** which is derived from hydrolysis of the bicyclic ylide **22**. Thus, hydrolysis of the other possible intermediates **15**, **17**, **18**, or **20** (or possible tautomers) would lead to a product containing olefinic protons whereas careful integration of the ^1H n.m.r. spectrum of the 1:2:1 adduct shows clearly that the adduct contains no olefinic protons.

The spectrum of the 1:2:1 adduct shows ten aromatic protons as a complex multiplet at τ 1.9–2.7, one methine proton as eight unevenly spaced, poorly defined, and partly overlapping peaks of similar intensity centered on τ 5.72, four ester methyl groups at τ 6.29, 6.32, 6.38, and 6.82, two methylene protons as an *apparent* doublet at τ 6.72 and 6.81, and two other methylene protons as a poorly defined multiplet of at least 12 maxima at τ 6.80–7.70. Since the two ring methylene protons in **23** would be non-equivalent, they would have somewhat different chemical shifts and may couple with each other, the neighboring methine proton, and the phosphorus atom to give up to 16 peaks of which at least 12 are observed. Similarly, the methine proton should appear at a much lower field location as two doublets of doublets through coupling with the phosphorus atom and the non-equivalent ring methylene protons. The side-chain methylene group presumably occurs as an apparent doublet (the inner peaks of a closely spaced AB signal of which the outer peaks are buried under the ester signals and the other methylene signals) in the spectrum because its proximity to an asymmetric center renders the two protons non-equivalent as is the case with the diastereotopic protons of 1,2-dichloropropane (14*a*). The signal separation of the two inner peaks of the AB pattern in such cases normally falls in the range 2–15 Hz (*e.g.* 14*b*). It is unlikely that the splitting of this signal is due to long-range coupling with the phosphorus atom since the value of $J = 5.5$ Hz is rather high compared with other measured values of $^5J_{PH}$ (9).

Again, double resonance and mass spectral studies confirm the proposed structure **23** for the 1:2:1 adduct. Careful scanning of the n.m.r. spectrum in the decoupling mode shows that fairly strong irradiation (*i.e.* full decoupling) at τ 7.00 while scanning the region of the eight peak one-proton signal centered on τ 5.72 causes the latter signal to collapse to a doublet of doublets with one coupling constant of 7 Hz and the other of 12 Hz. Similarly, irradiation at τ 7.32 again causes the one-proton eight peak signal to collapse to a doublet of doublets in which one coupling constant is 4.5 Hz while the other is 12.5 Hz. Designating the proton at τ 7.32 as H_a, the proton at τ 7.00 as H_b, and the proton at τ 5.72 as H_c, it is clear that $J_{H_aH_c} = 4.5$, $J_{H_bH_c} = 7$, and $J_{PH_c} = 12.5$ Hz. Thus, the P–H coupling constant is of the right order of magnitude for $^2J_{PH}$ while the couplings of H_c with H_a and H_b are consistent with the proposed structure **23**.

Irradiation of the proton at τ 5.72 (H_c) while scanning the proton signals at τ 7.00 and 7.32 causes considerable changes in these regions but no clear pattern emerges because of overlap of the H_a and H_b signals. Decoupling of H_a from H_b was not feasible since instrumental limitations did not allow decoupling of two such closely spaced signals.

One fact which did emerge from these de-

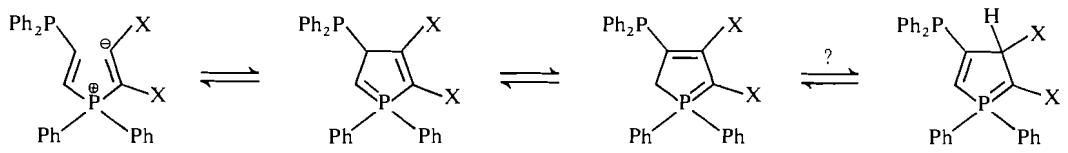

25 26 27 28

SCHEME 2

coupling experiments is that the weak outer peaks of the closely spaced methylene AB signal centered on τ 6.77 appear to be at τ 6.50 and τ 7.02 since irradiations of H_c while scanning H_a or H_b show that these peaks remain unchanged while considerable changes occur in the remaining peaks. Further support for this assignment comes from the fact that the intensity ratio (5.5:1) of the two fairly clearly seen low field peaks of the AB pattern (τ 6.50 and τ 6.72) is as predicted by theory (10*b*).

Mass spectral studies offer further confirmation for the structure **23**. For example, the loss of methanol characteristic of the $—CH_2CO_2Me$ grouping (11) is shown by a peak at *m/e* 482 and the one-step fragmentation is confirmed by a metastable peak at *m** 452. Furthermore, the expected loss of the allylic $—CH_2CO_2Me$ group is shown by a weak peak (25% of the molecular ion peak and 3% of the base peak) at *m/e* 441. Again, this fragmentation is confirmed by a weak metastable peak at *m** 378.3. Unfortunately, precise mass measurements for these peaks were not possible because suitable reference peaks were not available. Similarly, a weak peak at *m/e* 240 suggests the loss of both of the allylic $Ph_2\overset{\overset{\displaystyle O}{\|}}{P}—$ and $—CH_2CO_2Me$ groups and this is confirmed by precise mass studies (calcd.: 240.0634; found: 240.0636). Presumably this peak is weak because the charge would tend to stay with the $Ph_2\overset{\overset{\displaystyle O}{\|}}{P}—$ grouping and the fact that the base peak in the spectrum at *m/e* 201 is due to this grouping offers some support for this suggestion.

As with the 1:1:1 adduct, deuterolysis experiments on the 1:2 adduct offer further confirmation of these n.m.r. assignments since generation of this adduct in rigorously dried solvents followed by treatment of the solution with a little D_2O leads to the formation of **24**. The ^1H n.m.r. spectrum is virtually identical with that of **23** except that the AB pattern due to the side-chain methylene group has vanished from the spectrum. The only other change is a very small reduction in the signal strength of the other methylene multiplet. The heavy deuteration in the side-chain of **24** is strong evidence for the intermediacy of **22**. Reactions of **1** (R = H) with the ester are summarized in Scheme 1.

Attempts to trap the ylide **22** in a Wittig reaction with acetone, benzaldehyde, and *p*-nitrobenzaldehyde were unsuccessful. However, this is not surprising since the ylidic link in **22** would be highly hindered. Attempts to prepare perchlorate salts of **6**, **8**, and **22** were also unsuccessful but this too is not unexpected since recent work on related cyclic ylides (15) has shown that these salts are highly soluble in water and ethanol and are extremely difficult to crystallize even when the ylides themselves are available in considerable quantity.

The experiments already described for the phosphine **1** were extended to other α,β-unsaturated phosphines and, in the case of *trans*-1,2-bis(diphenylphosphino)ethylene (**2**), some quite surprising results were obtained.

When a benzene solution of dimethyl acetylenedicarboxylate is added slowly, with constant stirring under a dry nitrogen stream, to a solution (in a benzene/pentane mixture) of the *trans*-phosphine **2**, keeping the temperature around 8 °C, a light yellow precipitate is obtained. This adduct analyses well for a 1:1 adduct and is obtained in 69% yield. The mass spectrum confirms the 1:1 nature of the adduct and shows a molecular ion peak at *m/e* 538.

The most likely mode of reaction is cycloaddition of the type shown in the sequence **2**→**25**⇌**26**⇌**27**⇌**28** (Scheme 2). This would be very similar to the 1:1 reaction between diphenylvinylphosphine and dimethyl acetylenedicarboxylate already described where similar

Can. J. Chem. Downloaded from www.nrcresearchpress.com by 210.87.254.5 on 09/05/12
For personal use only.

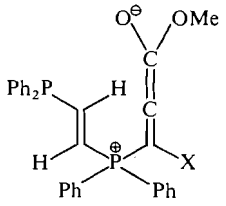

29

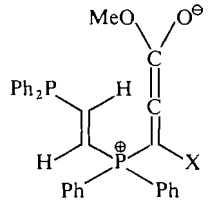

30

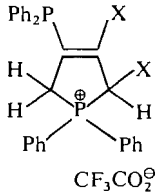

31

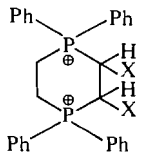

32

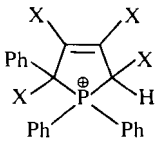

33

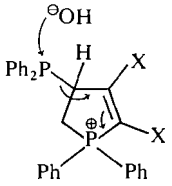

34

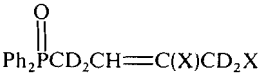

35

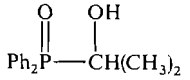

36

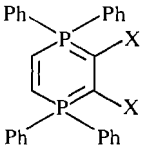

37

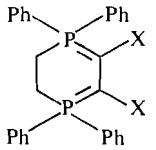

38

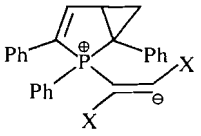

39

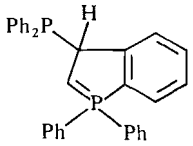

40

X = —CO_2Me

tautomeric equilibria have been observed. Furthermore, Savage and Trippett (6) have suggested equilibria of this type in the reaction of **1** (R = Ph) with acrylonitrile.

The i.r. spectrum shows two distinct carbonyl frequencies. One of these is at 1712 cm^{-1} and is clearly due to a normal unsaturated ester carbonyl stretching vibration, while the other is at 1601 cm^{-1} with a smaller, though still intense, peak at 1585 cm^{-1}. These last peaks are, therefore, probably due to an ester carbonyl group adjacent to a carbon atom with appreciable carbanionic character (16). Superficially, this would suggest that the adduct is either **27** or **28** with **27** the more likely by analogy with the reaction of diphenylvinylphosphine and dimethyl acetylenedicarboxylate.

However, the ^{1}H n.m.r. spectrum of the adduct at −2 °C is definitely not consistent with **27** and probably not consistent with **26** or **28**. The spectrum shows 21 aromatic/olefinic protons as a complex multiplet at τ 2.18–3.32, one apparently olefinic proton as two poorly defined doublets of doublets centered on τ 3.60 and 4.00, respectively, and six methoxy protons as three peaks of unequal area at τ 6.13 (3 protons), 6.23, and 6.56. At −50 °C, the spectrum is much the same apart from small downfield shifts and better definition of the two doublets of doublets except that the three proton methoxy signal which occurs at τ 6.13 in the spectrum at −2 °C appears as a very closely spaced doublet with peaks of unequal intensity at τ 6.01 and 6.03. There is no evidence in the spectrum for a proton on an ylidic carbon atom which would be expected to resonate in the range τ 8–11 (9). At 42 °C, the spectrum is unstable because of sample decomposition but the spectrum of a very freshly prepared sample is much the same as the spectrum at −2 °C except that the olefinic proton signals are very poorly defined.

The ^{1}H n.m.r. spectrum in the methoxy region is consistent with the i.r. spectrum in that it indicates that one of the ester groups is adjacent to a carbanionic center and shows conformational preference as has been observed (16) for

Can. J. Chem. Downloaded from www.nrcresearchpress.com by 210.87.254.5 on 09/05/12
For personal use only.

Can. J. Chem. Downloaded from www.nrcresearchpress.com by 210.87.254.5 on 09/05/12
For personal use only.

certain cyclic phosphonium ylides. However, this would also apply to **25** where the only non-aromatic protons are olefinic and where one ester group is adjacent to a carbanionic center. Major contributors to the resonance hybrid of **25** would be **29** and its rotational isomer **30**.

The multiplicity of the olefinic proton signal is of interest. Presumably the two fairly widely separated doublets of doublets (25 Hz) could be the result of the conformational preference of the methoxycarbonyl group as in **29** and **30** and its effect upon the proton β to the phosphonium center. One might perhaps expect this proton to appear under the aromatic signal but it has been shown that in some related structures such as **2**, *cis*-$Ph_2P(O)CH{=}CH(O)PPh_2$, and *cis*-$Ph_2P(S)CH{=}CH(S)PPh_2$, the ethylene bridge protons resonate (17) between τ 3.0 and 3.5. Further, the close proximity of the carbanion negative charge to this proton would be expected to shield it to some extent. In theory, ignoring different conformational arrangements of the ester groups in **25**, eight peaks would be expected for this proton due to coupling with the other olefinic hydrogen and the two different phosphorus atoms but it is well known (17, 18) that the protons on the bridging carbon atoms of bisphosphines show less than the normal expected multiplicity. In the opinion of the authors, the eight peaks observed are probably due to rotational isomerism of the ester groups although the difference in chemical shift of the two doublets of doublets (25 Hz) is within the normal J_{PH} coupling range for similar (17) bridged phosphines. This suggestion is reinforced by the observation that the olefinic signals become much more poorly defined as the temperature is increased. Furthermore, one ester methyl group appears as a three proton singlet at -2 °C while the other (presumably the one adjacent to the carbanion by analogy with the behavior of similar systems (16)) appears as two peaks (corresponding possibly to two conformational arrangements) at τ 6.23 and 6.56.

Thus, of the possible structures considered so far, only **25** (best represented as **29** or **30**) is fully consistent with both the ^{1}H n.m.r. and i.r. spectra, although the reasons why this tautomer should be preferred over the other possible tautomers in the equilibrium are obscure. Unfortunately, because of the extreme sensitivity of the adduct to trace amounts of water and oxygen and an apparent thermal sensitivity, it was not possible to carry out double resonance studies.

The ^{1}H n.m.r. spectrum of the adduct in trifluoroacetic acid gives further information although the spectrum itself is rather unexpected. The spectrum of a freshly prepared solution in CF_3CO_2H (with TMS added) shows, at room temperature, a ratio of approximately 20 aromatic protons at τ 1.6–2.8 to approximately one proton as a diffuse multiplet at τ 4.3–5.1 to approximately six methoxy and two methylene or methine protons as a complex multiplet between τ 5.60 and 6.65. One interesting feature of this last region is that each of the two methoxy signals (centered on τ 6.98 and 6.42 respectively) is split into two closely spaced and unequal peaks. Clearly, these methoxy signals cannot be due to rotational isomerism relative to a carbanionic center since the solution is strongly acidic. It seems likely then that the spectrum is caused by a mixture of isomers caused by protonation of two (or more) of the tautomers in the previously suggested equilibrium.

The ^{1}H n.m.r. spectrum in CF_3CO_2D is similar except that the multiplet at τ 4.3–5.1 is absent. Presumably these protons are provided by the acid or are rapidly exchanged with the acidic solvent.

Some evidence for the idea that the spectrum is caused by a mixture is given by the observation that if the acid solution is allowed to stand for several days, the spectrum is modified to show 20 aromatic protons as a multiplet at τ 1.5–2.8, one methine proton as a doublet ($J = 13$ Hz) at τ 4.49, two methoxy groups as singlets at τ 5.95 and 6.45, respectively, and two methylene protons as a multiplet partly hidden under the methoxy protons in the range τ 5.6–6.3. All of these peaks are present in the spectrum of the freshly prepared solution.

These observations are consistent with the idea that two or more of the postulated tautomers in the original ylide equilibrium are protonated by the trifluoroacetic acid but that further equilibria between ylide tautomers and protonated ylide tautomers lead to an increasing amount of the more stable protonated form.

Of the various protonated tautomers possible from the originally postulated equilibrium, only

Can. J. Chem. Downloaded from www.nrcresearchpress.com by 210.87.254.5 on 09/05/12
For personal use only.

31 (derived from **27**) agrees in every respect with the ^{1}H n.m.r. spectrum of the solution of the adduct in CF_3CO_2H which has been allowed to stand for several days. Thus the methine proton at τ 4.49 is virtually identical in location and splitting with the similar protons in **32** (15) and **33** (16), while the multiplicity of the methylene protons is very like that of the similar protons in **32**.

To summarize, the i.r. and ^{1}H n.m.r. evidence indicates that the 1:1 adduct of **2** with dimethyl acetylenedicarboxylate is an equilibrium of the structures **25**, **26**, **27**, and possibly **28** in which the zwitterionic form **25** greatly predominates over the other forms. However, in the presence of acid, the ylidic contributors to the equilibrium are protonated more readily than the zwitterionic form. This may also be true in the reactions of diphenyl(1-phenylvinyl)phosphine with acrylonitrile (6) and of diphenylvinylphosphine with dimethyl acetylenedicarboxylate where the initial 1:1 adduct could not be isolated and conclusions regarding the nature of the adducts have been drawn solely on the basis of their chemical reactions.

Chemical reactions indicate that an ylidic contributor is the reactive form present in the equilibrium but, again, very unexpected results were obtained.

If the adduct has appreciable ylidic character, it should hydrolyze in the manner of an ylide to give (7) a phosphine oxide. However, when the adduct was dissolved in aqueous ethanol and warmed with stirring for several hours, the oxide **9** was formed which is identical with the hydrolysis product obtained from the 1:1 adduct of diphenylvinylphosphine with dimethyl acetylenedicarboxylate, *i.e.* one of the diphenylphosphino groups has been lost. The m.p. and the i.r., ^{1}H n.m.r., and mass spectra of this product are identical with those of an authentic sample.

This reaction is completely unexpected and is very difficult to account for. However one possible mechanism is as follows.

Presumably, the first step in the hydrolysis would be protonation of the most reactive tautomer to give a phosphonium hydroxide. In the proposed ylide/zwitterion equilibrium, the most reactive tautomer would probably be **26**, since in this case, the ylidic negative charge is stabilized only by overlap with the d-orbitals of the phosphorus atom and is not delocalized in any way. Protonation of this ylide by water would give **34**.

It would be expected that normal rearrangement of this phosphonium hydroxide would involve attack of hydroxide ion upon the phosphonium grouping followed by apical elimination of the most stable carbanion to give a phosphine oxide. On the other hand, it is well known (19) that in phosphonium compounds, nucleophilic attack may sometimes take place at the atom β to the phosphorus atom as in the sequence $R_3\overset{+}{P}\overset{\curvearrowleft}{\text{—}}X\text{—}Y\ \overset{\curvearrowleft}{\dot{N}u} \rightarrow R_3P{=}X$.

In the structure **34** the diphenylphosphino group is not β to the phosphonium group but is vinylogously β to this group and attack of hydroxide ion on **34** as shown to give **8** and then **9** by hydrolysis could conceivably occur. It is not clear why hydroxide ion should prefer, in this case, to attack by the postulated route rather than by the more conventional route of attack on the phosphonium center.

Deuterolysis experiments using hot D_2O (99.7%) for several hours give some support to this mechanism since the compound **35**, together with some trideuterated material, is produced by treatment of the 1:1 adduct of **2** with the acetylenic ester with deuterium oxide.

Accurate integrations taken by means of signal averaged ^{1}H n.m.r. spectra show clearly that the olefinic hydrogen atom in this compound is not replaced by deuterium since the aromatic/olefinic:ester methyl integration is exactly 11:6. Furthermore, the n.m.r. spectrum shows that the methylene protons adjacent to the terminal ester group have been completely replaced by deuterium whereas traces (much less than one proton on integration) of the other methylene protons remain. This is confirmed by the mass spectrum which shows a molecular ion at *m/e* 376 together with a smaller peak at *m/e* 375 corresponding to the replacement of a maximum of four hydrogen atoms by deuterium. This is consistent with the proposed mechanism since the olefinic proton in the products **9** and **35** is derived from the proton adjacent to the displaced Ph_2P group and is not particularly activated. On the other hand, the other protons in **9** are derived either from the solvent or are adjacent to a phosphonium group and, under the

Can. J. Chem. Downloaded from www.nrcresearchpress.com by 210.87.254.5 on 09/05/12
For personal use only.

basic conditions of the reaction, these protons should be exchangeable with the deuterium oxide solvent which is present in great excess.

In the hydrolysis of the 1:1 adduct, the fate of the missing Ph_2P-group is uncertain. However, in one experiment in which the crude product of hydrolysis had been exposed to acetone, a very small amount of a colorless compound (m.p. 143°) was obtained. This compound showed no significant peaks in the mass spectrum above *m/e* 201 ($Ph_2P{=}O$) and the i.r. and ^1H n.m.r. spectra and analyses are consistent with the known (20) compound **36** (m.p. 137–139°) which can be formed by the addition of $Ph_2P(O)H$ to acetone. The compound is unstable in solution and repeated ^1H n.m.r. scans of the same sample showed that acetone is regenerated over a period of several hours. These observations tend to support attack of $\bar{O}H$ upon the exocyclic Ph_2P-group in **34** on hydrolysis of **25**.

The adduct **25** apparently does not enter into Wittig reactions.

The reactions with dimethyl acetylenedicarboxylate described for the *trans*-bisphosphine **2** were extended to the *cis*-bisphosphine **3** in order to see if addition of the type observed for **1** and **2** would occur or if the second phosphorus atom would attack on the unsaturated ester grouping in the initial zwitterionic intermediate to give the 1,1,4,4-tetraphenyl-1,4-diphosphorin **37**. Additions of this type have been observed (21) in the 1:2 addition of the ester to triphenylphosphine. During the later stages of this investigation, Tebby and co-workers (22) published a brief account of essentially the same work in which he described the cycloaddition of **3** and the acetylenic ester to give **37**.

There are only minor differences between our findings and those of Tebby. Thus, Tebby characterized the adduct mainly from the mass spectrum and the i.r. spectrum (which shows that both ester groups are attached to ylidic carbon atoms) and the behavior of the adduct **37** on hydrolysis which leads to the dioxide of **3**. No analytical data were reported although we were able to obtain reasonable analyses. Tebby was unable to carry out ^1H n.m.r. studies on the adduct because of its sensitivity to hydrolysis but, using freshly prepared samples of the adduct, we have been able to obtain reproducible ^1H n.m.r. measurements which confirm the bis-ylide nature of the adduct. The spectrum shows 22 aromatic and olefinic protons as a broad complex multiplet at τ 1.9–2.9 and six methoxy protons as a very broad unresolved hump at τ 6.2–7.1. The unresolved nature of the methoxy region is probably due to the presence of several interconvertible rotational isomers since the ester groups are adjacent to ylidic carbon atoms. Some support for this is given by the fact that the spectrum in the methoxy region at room temperature is almost identical in appearance to that of the cyclic bis-ylide **38** (23). Also, at −40° (where interconversion should be slow) the methoxy region is resolved into two reasonably sharp peaks of unequal area at τ 6.32 and 7.10 with the peak at τ 6.32 almost twice the area of the other peak. Furthermore both peaks show signs of splitting into doublets with unequal splitting of the two signals.

The adduct **37** also forms a crystalline bisperchlorate confirming its bis-ylide nature and ^1H n.m.r. studies of **37** in trifluoroacetic acid solution also confirm the proposed structure. The spectrum shows 22 aromatic/olefinic protons at τ 1.6–2.5 and six methoxy protons as a singlet at τ 6.27. The two methine protons appear as a broad hump at τ 4.6–5.0 with the broadening presumably due to exchange with the solvent.

One interesting point regarding the i.r. spectrum of **37** is that the main carbonyl absorption is at 1640 cm^{-1} with lesser peaks on either side. This is at a considerably higher location than for the apparently similar ester groups in **38** (ν = 1585 cm^{-1}). This may indicate that perhaps the carbanionic negative charges in **37** are delocalized into the ring to give something approaching an aromatic system whereas in **38** the delocalization is over the ester groups.

The cyclic phosphine **4** is a highly hindered version of **1** and reactions of **4** with dimethyl acetylenedicarboxylate were carried out in an attempt to achieve cycloadditions of the type observed for **1**. The highly strained and hindered ylides which would be produced by such cyclizations would be of considerable interest. However, attempts to carry out the cycloaddition under a wide variety of conditions using rigorously dried ethereal and non-ethereal solvents and even no solvent other than an excess of the ester, gave only the oxide of **4**. The change in

Can. J. Chem. Downloaded from www.nrcresearchpress.com by 210.87.254.5 on 09/05/12
For personal use only.

appearance of the various reaction mixtures clearly indicates that a reaction occurs rapidly but it seems likely that the probable initially formed zwitterion **39** is too hindered to cyclize or react further and hydrolyzes on work-up in the manner observed for similar zwitterions (24) to give the corresponding phosphine oxide.

Finally, as a continuation of the work described in this paper, some preliminary experiments involving the generation of benzyne in the presence of the phosphines **1** and **2** have been carried out and, in some cases, some very unusual results have been obtained. Thus, treatment of **1** with *o*-benzenediazonium carboxylate unexpectedly gives the bisphosphine $Ph_2PCH_2CH_2PPh_2$ in moderate yield while **2** reacts with *N*-nitrosoacetanilide in the presence of potassium acetate to give the expected ylide **40** in very low yield which has been trapped as its hydrolysis product. These reactions are under further investigation and will be reported fully in a later paper.

Experimental

The i.r. spectra were recorded in Nujol mulls using a Beckman IR12 spectrophotometer while n.m.r. measurements were made with a Varian Associates model A60-A spectrometer equipped with a V-6058A spin decoupler using deuteriochloroform or trifluoroacetic acid solutions with tetramethylsilane as internal reference. Signal averaging was carried out using a Varian Data Systems model 620i unit. Mass spectra were determined using an Hitachi–Perkin–Elmer model RMU-7 double focusing mass spectrometer fitted with a direct heated inlet system. Melting points are uncorrected and were recorded using a Mel-Temp high-temperature m.p. apparatus.

Ether was dried by distillation from sodium or lithium aluminum hydride while tetrahydrofuran and benzene were dried by distillation from calcium hydride. Dimethyl acetylenedicarboxylate was freshly distilled under reduced pressure (*ca.* 1 Torr) immediately before use.

3,4,5-Triphenyl-4-phosphabicyclo[3.1.0]hex-2-ene (**4**) was prepared by the method of Hughes and Srivanavit (25).

Addition of Dimethyl Acetylenedicarboxylate to Diphenylvinylphosphine

Dimethyl acetylenedicarboxylate (8.0 g) in benzene (50 ml) was added dropwise with magnetic stirring to diphenylvinylphosphine (12.1 g) in benzene (300 ml) under nitrogen at room temperature. The solution was heated under reflux for a few minutes during which time it turned a dark blue and a tarry precipitate appeared. One or two drops of water were then added and the mixture was again heated under reflux for a few minutes. The mixture was then evaporated under reduced pressure to about 50 ml. Ether (*ca.* 300 ml) was added to the gummy mixture and this dissolved much of the blue material. Repeated washing with small portions (*ca.* 30 ml) of ether left the crude adduct as a greyish crystalline material (7.1 g, m.p. 119–123°). The crystalline material was recrystallized from ethanol to give colorless needles (4.8 g, 23%) of the 1:1:1 adduct **9**, m.p. 130–132°.

Anal. Calcd. for $C_{20}H_{21}O_5P$: C, 64.51; H, 5.64; P, 8.33. Found: C, 64.74; H, 5.81; P, 8.78.

The i.r. spectrum shows ν_{max} at 1749, 1722, 1664, 1450, 1444, 1342, 1310, 1223, 1193, 1130, 1105, 751, 732, and 708 cm^{-1}.

Addition of Dimethyl Acetylenedicarboxylate to Diphenylvinylphosphine in the Presence of D_2O

Ether (dried by distillation from $LiAlH_4$) was shaken with D_2O and again dried with $LiAlH_4$. Dimethyl acetylenedicarboxylate (1.34 g) in ether dried as above (50 ml) was added dropwise at room temperature to diphenylvinylphosphine (2.05 g) again in ether dried as above (50 ml) under nitrogen. When the addition was complete, D_2O (5 ml) was added to the reaction mixture which was then filtered to give a dark blue solid. This solid was recrystallized twice from benzene to give colorless needles of the deuterated adduct **10** (0.07 g), m.p. 132–133°.

Addition of Dimethyl Acetylenedicarboxylate to Diphenylvinylphosphine in the Presence of p-Nitrobenzaldehyde

Dimethyl acetylenedicarboxylate (3.53 g) in dry ether (80 ml, freshly distilled from $LiAlH_4$) was added dropwise over a period of 50 min to a mixture of diphenylvinylphosphine (5.0 g) and *p*-nitrobenzaldehyde (3.21 g) in dry ether (600 ml) under nitrogen at room temperature. The solution became dark green during the addition and was allowed to stand overnight in an atmosphere of dry nitrogen. The mixture was then filtered, the filtrate was evaporated to low bulk, and the mixture was chromatographed on neutral alumina using benzene followed by acetone as eluents. The acetone fractions were collected and evaporated to low bulk to give a crude sample of the adduct **14** (1.145 g, 10%), m.p. 190–194° (dec.). Further purification was effected by dissolution of the solid in chloroform followed by reprecipitation with ether. The pure adduct **14** was obtained as fine yellow crystals, m.p. 194–199° (dec.).

Anal. Calcd. for $C_{27}H_{24}O_7NP$: C, 64.16; H, 4.79; N, 2.77; P, 6.13. Found: C, 63.69; H, 4.98; N, 2.98; P, 6.14.

The i.r. spectrum shows ν_{max} at 1745, 1692, 1630, 1600, 1515, 1440, 1345, 1275, 1249, 1159, 1110, 1020, 991, 731, and 700 cm^{-1}.

Addition of Diphenylvinylphosphine to Dimethyl Acetylenedicarboxylate

Diphenylvinylphosphine (8.8 g) in ether (50 ml) was added dropwise with stirring to freshly distilled dimethyl acetylenedicarboxylate (12.4 g) in ether (1500 ml) at room temperature under nitrogen. After the addition was complete, the dark colored mixture was filtered and the crude adduct **23** obtained as a greyish precipitate (2.3 g, 11%). This product was recrystallized from hot benzene to give the pure adduct **23** as colorless granular crystals, m.p. 198–201°.

Anal. Calcd. for $C_{26}H_{27}O_9P$: C, 60.70; H, 5.29; P, 6.02. Found: C, 60.70; H, 5.29; P, 6.63.

The i.r. spectrum (in $CHCl_3$) shows ν_{max} at 1738 (very broad), 1649, 1605, 1439, 1277, 1220 (very broad), and 1180 (shoulder) cm^{-1}.

Deuterolysis of the 1:2 adduct **22** was carried out as described for the 1:1 adduct to give **24**, m.p. 206–213°.

Can. J. Chem. Downloaded from www.nrcresearchpress.com by 210.87.254.5 on 09/05/12
For personal use only.

The Reaction of trans-1,2-Bis(diphenylphosphino)ethylene (2) with Dimethyl Acetylenedicarboxylate

The *trans*-phosphine (2.4 g) was dissolved in dry benzene (25 ml) and cooled to about 10 °C. To this solution was added dry pentane (35 ml) slowly with constant stirring until the solution became slightly turbid. At this stage a few drops of benzene were added to remove the turbidity.

A mixture of dimethyl acetylenedicarboxylate (0.852 g) and benzene (10 ml) was then added slowly, under a stream of dry nitrogen with constant stirring to the *trans*-phosphine solution while keeping the temperature of the reaction mixture around 8°. When the addition was complete, a light yellow precipitate (2.10 g, 69%) of a 1:1 adduct was obtained. This was filtered under nitrogen and washed several times with dry benzene followed by pentane. The precipitate was then pumped under reduced pressure (*ca.* 2 Torr) and at 55° for several hours.

Recrystallization of the adduct could not be achieved because of its high sensitivity towards water and air.

Anal. Calcd. for $C_{32}H_{28}O_4P_2$: C, 71.4; H, 5.2; P, 11.5. Found: C, 71.1; H, 5.4; P, 11.2.

The compound decomposed over a wide temperature range on heating.

The i.r. spectrum shows ν_{max} at 1712 (normal unsaturated ester C=O stretching), 1601 (stretching of the C=O group adjacent to a carbanionic center), 1445 (P—Ph), 1350, 1240, 1170, 1130, 1120, 1104, 1060, 950, 860, 820, 810, 765, 758, 750, 740, 720, 704, 700, and 670 cm^{-1}.

Hydrolysis and Deuterolysis of the 1:1 Adduct of trans-1,2-Bis(diphenylphosphino)ethylene and Dimethyl Acetylenedicarboxylate

The 1:1 adduct (1.85 g), obtained in the above experiment, was dissolved in aqueous ethanol (30 ml, 1:1 mixture) and heated under reflux for 24 h. A white precipitate was obtained which was filtered and washed with a little benzene followed by pentane. The product was then pumped under reduced pressure (*ca.* 1 Torr) and at 60°. The crude oxide **9** (0.80 g, m.p. 132°) was obtained in 63% yield. The crude product was further recrystallized from benzene and obtained as fine cotton-like crystals.

Anal. Calcd. for $C_{20}H_{21}O_5P$: C, 64.5; H, 5.6; P, 8.3. Found: C, 64.9; H, 5.8; P, 8.8.

Deuterolysis was carried out as above except that pure D_2O was used as the deuterolyzing agent. The oxide **35** (m.p. 136°) was obtained in 70% yield. The i.r. spectrum was almost identical to that of the hydrolysis product **9**.

The ^1H n.m.r. was also found to be very similar to that of **9** except that the aliphatic protons had almost vanished from the spectrum while the mass spectrum shows a molecular ion peak at *m/e* 376 (with a small peak at *m/e* 375) which confirms that mainly tetradeuteration occurred.

The Reaction of cis-1,2-Bis(diphenylphosphino)ethylene (3) with Dimethyl Acetylenedicarboxylate

cis-1,2-Bis(diphenylphosphino)ethylene (**3**) (4.75 g) was dissolved in benzene (500 ml) and to this was added dropwise a solution of dimethyl acetylenedicarboxylate (1.744 g) in benzene (100 ml) under a dry nitrogen stream with constant stirring while maintaining the temperature of the reaction flask around 8°.

After the addition was over, a buff precipitate was formed which was filtered, washed with benzene, and then pumped under reduced pressure (*ca.* 1 Torr) at 50° for 4 h. The dry ylide **37** was obtained as a buff powder (4.76 g, 73%).

The ylide **37** is highly water sensitive and it was therefore not possible to recrystallize it since it hydrolyzed rapidly even in quite rigorously dried solvents. Furthermore, the ylide has no definite m.p. and decomposes slowly above 140°.

Anal. Calcd. for $C_{32}H_{28}O_4P_2$: C, 71.4; H, 5.2; P, 11.5. Found: C, 69.5; H, 5.4; P, 11.1.

The i.r. spectrum shows ν_{max} at 1640, 1600 (ylidic C=O stretching), 1440 (P—Ph), 1340, 1310, 1260, 1160, 1120, 740, 710, 695, and 670 cm^{-1}.

Hydrolysis of Dimethyl 1,1,4,4-Tetraphenyl-1,4-diphosphorin-2,3-dicarboxylate (37)

The ylide **37** (200 mg) was mixed with an excess of 1:1 aqueous ethanol and stirred for 5 h at room temperature. During this time, the dark brown solution became almost colorless. The solution was allowed to stand at room temperature for 2 days and a white precipitate slowly settled down. This was filtered, washed with acetone, and pumped under reduced pressure (*ca.* 1 Torr) to give the dioxide of **3** (110 mg, 68%). The dioxide was further recrystallized from a 1:1 mixture of ethanol and acetone to give colorless crystals, m.p. 244° (lit. (26) m.p. 244–245°).

The i.r. spectrum shows ν_{max} at 1440 (P—Ph) 1230, 1200, 1185, 1175, 1120, 1100, 1030, 1000, 930, 780, 765, 750, 730, 710, 700, and 670 cm^{-1}.

The mass spectrum shows the molecular ion peak at *m/e* 428.

Preparation of the Bisperchlorate of Dimethyl 1,1,4,4-Tetraphenyl-1,4-diphosphorin-2,3-dicarboxylate (37)

To the solid ylide **37** (200 mg) was added, with constant stirring and under a nitrogen stream, perchloric acid (1 ml, 74%) dropwise at room temperature. After about 10 min the solid mass, initially buff, became colorless. The mixture was stirred for another 30 min and then methanol (3 ml) was added. The mixture was warmed briefly to dissolve the solid and the solution then left for crystallization. After 2 days, fine white crystals appeared and these were filtered, washed with a little methanol, then with pentane and finally with ether. The crystals were pumped under reduced pressure (*ca.* 1 Torr) at 50° to remove residual solvent from the bisperchlorate which was obtained in 28% yield (76 mg). The salt decomposed slowly above 200°.

Anal. Calcd. for $C_{32}H_{30}Cl_2O_{12}P_2$: C, 52.0; H, 4.1; Cl, 9.7; P, 8.4. Found: C, 51.3; H, 4.0; Cl, 10.0; P, 8.0.

The i.r. spectrum shows ν_{max} at 1770, 1760, 1740 (normal C=O stretching), 1590, 1440, 1340, 1290, 1240, 1230, 1200, 1170, 1120–1065 (broad typical perchlorate peak), 1000, 900, 850, 800, 760, 740, 700, 690, 670, and 630 cm^{-1}.

We thank the Senate Research Committee of Lakehead University and the National Research Council of Canada for generous financial support of this work.

1. For a review on cyclic phosphonium ylides see M. DAVIES and A. N. HUGHES. J. Heterocycl. Chem. **9**, 1 (1972).
2. A. W. JOHNSON and J. C. TEBBY. J. Chem. Soc. 2126 (1961); and several later papers.

3. G. WITTIG and E. BENZ. Chem. Ber. **92**, 1999 (1959); E. ZBIRAL. Tetrahedron Lett. 1649 (1964).
4. H. J. BESTMANN and O. ROTHE. Angew. Chem. Int. Ed. **3**, 512 (1964).
5. A. N. HUGHES and M. DAVIES. Chem. and Ind. 138 (1969).
6. M. P. SAVAGE and S. TRIPPETT. J. Chem. Soc. C, 591 (1968).
7. A. WILLIAM JOHNSON. Ylid chemistry. Academic Press, New York, N.Y. 1966. p. 88.
8. D. E. C. CORBRIDGE. Top. in Phosphorus Chem. **6**, 235 (1969).
9. J. C. TEBBY. *In* Organophosphorus chemistry. Vol. 1. *Edited by* S. Trippett. The Chemical Society, London. 1970. p. 301.
10. (*a*) E. D. BECKER. High Resolution NMR. Academic Press. New York, N.Y. 1969. p. 192; (*b*) p. 138.
11. H. C. HILL. Introduction to mass spectrometry. Heyden, London. 1966. p. 65.
12. S. TRIPPETT. J. Chem. Soc. 4733 (1962).
13. N. E. WAITE and J. C. TEBBY. J. Chem. Soc. C, 386 (1970); A. N. HUGHES and S. UABOONKUL. Tetrahedron, **24**, 3437 (1968).
14. VARIAN. High resolution N.M.R. spectra catalog. Vol. 1. 1962. (*a*) Spectrum no. 30. (*b*) Spectra nos. 30, 74, 182, 277.
15. S. W. S. JAFRY. M.Sc. Thesis. Lakehead University, Thunder Bay, Ontario, 1971.
16. N. E. WAITE, J. C. TEBBY, R. S. WARD, and D. H. WILLIAMS. J. Chem. Soc. C, 1100 (1969).
17. J. J. BROPHY and M. J. GALLAGHER. Aust. J. Chem. **20**, 503 (1967).
18. A. J. CARTY and R. K. HARRIS. Chem. Commun. 234 (1967).
19. A. J. KIRBY and S. G. WARREN. The organic chemistry of phosphorus. Elsevier, Amsterdam. 1967. p. 207.
20. J. L. WILANS. U.S. Patent 3126416 (1964); Chem. Abstr. **61**, 1894*d* (1964).
21. M. A. SHAW, J. C. TEBBY, R. S. WARD, and D. H. WILLIAMS. J. Chem. Soc. C, 2442 (1967).
22. M. A. SHAW, J. C. TEBBY, R. S. WARD, and D. H. WILLIAMS. J. Chem. Soc. C, 504 (1970).
23. A. N. HUGHES and S. W. S. JAFRY. J. Heterocycl. Chem. **6**, 991 (1969).
24. M. A. SHAW, J. C. TEBBY, R. S. WARD, and D. H. WILLIAMS. J. Chem. Soc. C, 2975 (1968); E. M. RICHARDS, J. C. TEBBY, R. S. WARD, and D. H. WILLIAMS. J. Chem. Soc. C, 1542 (1969).
25. A. N. HUGHES and C. SRIVANAVIT. Can. J. Chem. **49**, 874 (1971).
26. A. M. AGUIAR and D. DAIGLE. J. Am. Chem. Soc. **86**, 2299 (1964).

Can. J. Chem. Downloaded from www.nrcresearchpress.com by 210.87.254.5 on 09/05/12
For personal use only.

2-Aryloxytetrahydrofurans. Their Reductive Cleavage by Ether Solutions of AlH_2Cl and their Cleavage and Rearrangement by Ether Solutions of $AlCl_3$ [1]

P. C. Loewen and R. K. Brown

The Department of Chemistry, University of Alberta, Edmonton, Alberta

Received February 14, 1972

The hydrogenolysis of 2-aryloxytetrahydrofurans by excess AlH_2Cl gave, in excellent yield, only those products expected from *exo* C—O bond cleavage regardless of the nature of the substituent in the aryl ring. None of the 4-aryloxy-1-butanol, the product expected from ring cleavage, was detected. The reaction was very much faster than the corresponding AlH_2Cl hydrogenolysis of 2-alkoxytetrahydrofurans which is known to give only ring cleavage products under similar conditions.

Treatment of 2-aryloxytetrahydrofurans or pyrans with $AlCl_3$ in ether, resulted in acid-catalyzed cleavage to the corresponding phenol and dihydrofuran or dihydropyran, the latter immediately forming polymeric products. For those 2-aryloxytetrahydrofurans or pyrans, unsubstituted, or substituted with electron donor groups in the aryl ring, another product was obtained which resulted from electrophilic attack of one protonated dihydrofuran or pyran on the ortho or para position of the phenol. These rearrangement products were also obtained in small amounts as byproducts when 2-aryloxytetrahydrofurans were hydrogenolyzed with insufficient AlH_2Cl.

L'hydrogène des aryloxy-2 tétrahydrofurannes par un excès de AlH_2Cl donne, avec un rendement excellent, les produits attendus à partir seulement du clivage de la liaison C—O *exo*, quelle que soit la nature du substituant du cycle aryle. Aucun aryloxy-4 butanol-1, produit attendu de l'ouverture de cycle, n'a pu être détecté. La réaction est beaucoup plus rapide que pour l'hydrogénolyse des alkoxy-2 tétrahydrofurannes par AlH_2Cl, connue pour donner seulement des produits d'ouverture de cycle, dans des conditions identiques.

Le traitement des aryloxy-2 tétrahydrofurannes ou pyrannes par $AlCl_3$ dans l'éther entraîne une ouverture acido-catalysée conduisant au phénol correspondant, au dihydrofuranne ou dihydropyranne, ce dernier formant immédiatement des polymères. Pour ces aryloxy-2 tétrahydrofurannes ou pyrannes, substitués ou non par des groupes électrodonneurs sur le cycle aryle, un autre produit est obtenu résultant d'une attaque électrophile du dihydrofuranne ou pyranne protoné sur la position ortho ou para du phénol. Ces produits réarrangés sont également obtenus en petites quantités, en tant que sous-produits, lors de l'hydrogénolyse des aryloxy-2 tétra-hydrofurannes par AlH_2Cl en défaut.

[Traduit par le journal]

Canadian Journal of Chemistry, **50**, 3639 (1972)

Can. J. Chem. Downloaded from www.nrcresearchpress.com by 210.87.254.40 on 09/05/12
For personal use only.

Introduction

It has been reported (1) that the reductive cleavage by a 1:1 mixture of lithium aluminum hydride and aluminum chloride in ether of 2-phenoxytetrahydropyran and of 2-*p*-tolyloxytetrahydropyran provides exclusively tetrahydropyran and the corresponding phenol, products of *exo* C—O bond cleavage. This has been attributed to the electron-withdrawing effect of these aryl substituents strongly destabilizing the transition state leading to the formation of that oxocarbonium ion involved in ring cleavage (route *a*, Scheme 1, $n = 2$, $R' = H$, $R = aryl$), thus permitting exclusive formation and reaction of the oxocarbonium ion involved in ring retention (route *b*, Scheme 1).

This paper describes the results of a study of the hydrogenolysis by a 1:1 mixture of lithium aluminum hydride and aluminum chloride (*i.e.*, AlH_2Cl (2, 3)) of ether solutions of a number of 2-aryloxytetrahydrofurans, and also of the tendency for certain of the 2-aryloxytetrahydrofurans and the homologous pyrans to undergo rearrangement in competition with the normal cleavage reaction in the presence of the Lewis acid $AlCl_3$.

Results and Discussion

Hydrogenolysis of 2-Aryloxytetrahydrofurans with AlH_2Cl

The general hydrogenolysis procedure was the same as that used for the reductive cleavage of 2-alkoxytetrahydrofurans (4), an advantageous modification of the method reported previously (1). Products were found to be stable

[1]Taken in part from the thesis of P. C. Loewen submitted to the Faculty of Graduate Studies and Research, University of Alberta, in partial fulfillment of the requirements for the Ph.D. degree.

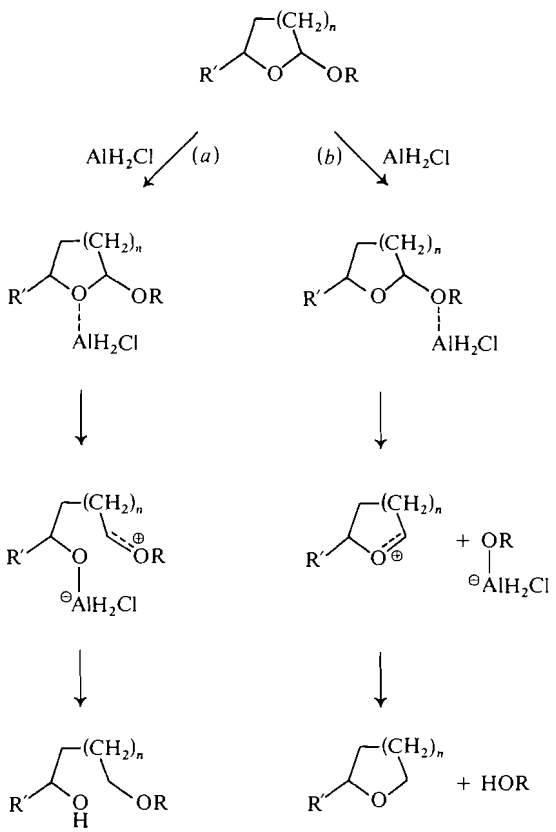

SCHEME 1

under the reaction conditions, and were identified by comparison of their g.l.c. retention times with those of authentic samples, or in cases of doubt, by actual isolation and subsequent identification or characterization, of the products. The results of these reactions are shown in Table 1.

Experiments 1–5 show that regardless of the nature of the substituent or its position in the aromatic ring R, the 2-aryloxytetrahydrofurans are cleaved only at the *exo* C—O bond to produce tetrahydrofuran and the phenol. This agrees with the findings for the hydrogenolysis of the 2-aryloxytetrahydropyrans (1) but is in sharp contrast to the exclusive ring cleavage observed in the hydrogenolysis with AlH_2Cl of 2-alkoxytetrahydrofurans (4), and to the production of both ring and *exo* cleavage products in the hydrogenolysis of 2-alkoxytetrahydropyrans (1).

A second and significant observation from Table 1, and one which is amplified by the results shown in Table 2, is that the reductive cleavage of the 2-aryloxytetrahydrofurans is very fast, completed well within 10 min, and is very much faster than the analogous cleavage of 2-alkoxytetrahydrofurans. The latter fact is clearly demonstrated when mixtures of equimolar quantities of 2-aryloxy- and 2-ethoxytetrahydrofuran are hydrogenolyzed with an amount of AlH_2Cl sufficient to reduce only half of the total amount of this mixture of acetals. In each case, hydrogenolysis of the 2-aryloxytetrahydrofuran occurred exclusively and completely (Table 2), with no evidence (by g.l.c.) of any cleavage of the 2-ethoxytetrahydrofuran.

Although the phenoxy group has electron donor properties ($\sigma = -0.320$, (5); $\sigma^+ = -0.5$, (6)) which would stabilize the transition state leading to the oxocarbonium ion involved in ring cleavage (route *a*, Scheme 1), the absence of any observable ring cleavage products from the hydrogenolysis of *any* of the 2-aryloxytetrahydrofurans (Table 1) regardless of the type of substituent in the aryl ring, indicates quite clearly that such electronic stabilization or destabilization by the 2-aryloxy substituent is insignificant in determining the direction of cleavage (route *a* or *b*, Scheme 1). It is suggested here that the feature which causes only *exo* C—O bond cleavage in the hydrogenolysis of 2-aryloxytetrahydrofurans is the π electron system of the aryl ring which, with its attached oxygen atom provides a region of high electron concentration which attracts the Lewis acid. The aryloxy group with the associated Lewis acid becomes a good "leaving group" whose departure is facilitated by the ability of the ring oxygen to stabilize the positive charge which develops on C-2 (route *b*, Scheme 1). Alternative association of the Lewis acid with the ring oxygen followed by ring C—O bond cleavage, or transfer of the Lewis acid from the aryloxy group to the ring before *exo* C—O bond cleavage takes place, apparently is insignificant. Since C—O bond cleavage of acetals is considered to be the rate determining step in their hydrolysis (7) or hydrogenolysis (8), the stabilization of the aryloxy anion by the associated Lewis acid to provide a good leaving group would account for the much greater rate of hydrogenolysis of the 2-aryloxytetrahydrofurans compared to that of the 2-alkoxytetrahydrofurans.

Can. J. Chem. Downloaded from www.nrcresearchpress.com by 210.87.254.40 on 09/05/12
For personal use only.

TABLE 1. Room temperature hydrogenolysis of ether solutions of 2-aryloxytetrahydrofurans with AlH_2Cl*

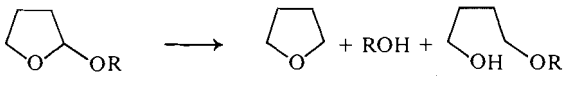

A B C

Experiment no.	Compound A with R as	Total material recovery (%)	B (as % of reduced product)	C
1	C_6H_5—	85	100	0
2	2,6-$Cl_2C_6H_3$—	95	100	0
3	2,6-$(CH_3)_2C_6H_3$—	90	100	0
4	3,5-$(CH_3)_2C_6H_3$—	90	100	0
5	4-*t*-$C_4H_9C_6H_4$—	94	100	0

*Although reduction was fast and generally complete within 10 min, the reduction time was extended to 2 h in each case to ensure complete reaction. Equimolar mixtures of $LiAlH_4$, $AlCl_3$, and the acetal were used, thus ensuring a large excess of reducing agent.

TABLE 2. Competitive hydrogenolysis at room temperature of ether solutions of equimolar mixtures of a 2-aryloxytetrahydrofuran and 2-ethoxytetrahydrofuran with a limited amount of AlH_2Cl*

A B A C

Experiment no.	R in Compound B	Total material recovery (%)	Amount of A reduced (%)	Amount of B reduced (%)†
1	2,6-$(CH_3)_2C_6H_3$—	95	0	100
2	C_6H_5—	95	0	100
3	2,6-$Cl_2C_6H_3$—	82	0	100

*The molar ratio of A:B:AlH_2Cl at the beginning of the reaction was 1:1:0.5. Reaction time was extended to 2 h, to ensure completion of reaction.

†A very small amount of high boiling material was obtained. This was later identified as a rearrangement product from the 2-aryloxytetrahydrofuran (see below).

There are two observations in a previous paper (4) which are in agreement with this view. It was shown that although 2-methoxytetrahydrofuran gave only the ring cleavage product when hydrogenolyzed with AlH_2Cl, 2-methoxy-5-methoxymethyltetrahydrofuran and 2-methoxy-5-phenyltetrahydrofuran each gave both ring cleavage and *exo* C—O bond cleavage products, respectively, in the ratio 93.5:6.5 in the former acetal and 84.3:15.7 in the latter. This could be due to association of the Lewis acid to some extent with the C-5 methoxymethyl group, and especially with the C-5 phenyl group, rather than only with the adjacent ring oxygen atom,[2] sufficiently to allow a second molecule of AlH_2Cl to attack the *exo* oxygen and bring about some reductive cleavage of the *exo* C—O bond. Also, it was shown that AlH_2Cl hydrogenolysis of 2-benzyloxytetrahydrofuran gave in excellent yield *both exo* and *endo* (ring) C—O cleavage products in the ratio 48.5:51.5, respectively (Table 2, experiment 2 in ref. 4). Here also, the 48.5% *exo* cleavage experienced by 2-benzyloxytetrahydrofuran could be attributed to the strong tendency for the Lewis acid to associate with the aryl ring rather than practically completely with the more "basic" ring oxygen atom (a feature considered to be responsible for the exclusive ring cleavage experienced by 2-methoxytetrahydrofuran as well as all the other 2-alkoxytetrahydrofurans (4)), thus markedly improving the "leaving" ability of the

[2]The Lewis acid must associate with the ring oxygen atom if ring cleavage is to occur.

Can. J. Chem. Downloaded from www.nrcresearchpress.com by 210.87.254.40 on 09/05/12
For personal use only.

Can. J. Chem. Downloaded from www.nrcresearchpress.com by 210.87.254.40 on 09/05/12
For personal use only.

TABLE 3. Reactions of 2-aryloxytetrahydrofurans and 2-aryloxytetrahydropyrans in ether with $AlCl_3$*

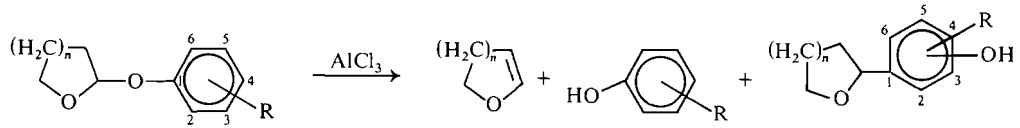

A B C

Experiment no.	Compound A		Reaction time	Total material recovery (%)	Extent of reaction (%)	% of isolated product as	
	n	R				B†	C
1	1	H	2 h	91	100	86.5 (R = H)	13.5 (R = H; 2-OH)
2	1	3,5-diCH_3	10 min	94	100	25 (R = 3,5-diCH_3)	75 (2-OH; R = 4,6-diCH_3)
3	1	2,6-diCl	2 h	95	100	100 (R = 2,6-diCl)	0 (4-OH; R = 3,5-diCl)
4	1	2,6-diCH_3	10 min	88	100	10.5 (R = 2,6-diCH_3)	16.5 (4-OH; R = 3,5-diCH_3)‡
5	2	3,5-diCH_3	10 min	85	100	30 (R = 3,5-diCH_3)	70 (2-OH; R = 4,6-diCH_3)
6	2	4-CH_3	2 h	85	100	90 (R = 4-CH_3)	10 (2-OH; R = 5-CH_3)
7	2	H	2 h	90	77.5	97 (R = H)	3 (2-OH; R = H)
8	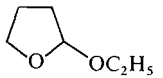		2 h	92	35.6	100 as C_2H_5OH	0 rearranged product

*The proportion of the 2-aryloxy compound and $AlCl_3$ was 1:0.25 equivalents respectively.
†Estimated by g.l.c. measurement of the phenol produced. The dihydrofuran (or pyran) could not be measured since it polymerized immediately.
‡The remainder of the isolated product (73%) was the coupling product 4,4′-dihydroxy-3,3′,5,5′-tetramethylbiphenyl, a type of product not detected in the reactions of the other 2-aryloxy compounds.

Can. J. Chem. Downloaded from www.nrcresearchpress.com by 210.87.254.40 on 09/05/12
For personal use only.

benzyloxy group. As well, the Lewis acid associated with the aryl ring would be in a position to transfer easily to the *exo* oxygen, a position leading to *exo* C—O bond cleavage. The degree of such preferred association of the Lewis acid with the aryl ring system appears to depend on the strength of the Lewis acid, since experiments 1–4, Table 2 of ref. 4 show that the proportion of *exo* cleavage of 2-benzyloxytetrahydrofuran increases from 20.5 to 91.3% as the Lewis acid strength of the hydrogenolyzing reagent is increased.

Reaction of 2-Aryloxytetrahydrofurans and 2-Aryloxytetrahydropyrans with $AlCl_3$ in Ether

In the competitive reaction of equimolar quantities of a 2-aryloxytetrahydrofuran and 2-ethoxytetrahydrofuran with an amount of AlH_2Cl sufficient to reduce only one half of the total amount of the acetal mixture, a very small amount of high boiling material was formed in some of the reactions (Table 2). The retention times of these substances were similar to those of authentic 4-aryloxy-1-butanols, products expected from reductive ring cleavage of the 2-aryloxytetrahydrofurans. However, the amount formed was insufficient for their isolation by g.l.c. and subsequent positive identification. Related to this was the observation that attempts at competitive hydrogenolysis of equimolar mixtures of two 2-aryloxytetrahydrofurans with an amount of AlH_2Cl sufficient only to reductively cleave half of the total acetal mixture, always resulted in reaction of the acetal to the extent of 75 to 100%. Accordingly it was suspected that the 2-aryloxytetrahydrofurans were not only being hydrogenolyzed by the AlH_2Cl but also subjected to a reaction caused by the Lewis acidity of the aluminum species. That this was so is shown by the results of the reaction of ether solutions of 2-aryloxytetrahydrofurans and also of 2-aryloxytetrahydropyrans with $AlCl_3$ (Table 3). The products in each case were analyzed by g.l.c. For those experiments where the g.l.c. yield of the rearranged product was 16% or more, (experiments 2, 4, and 5) it was possible to isolate by chromatography a sufficient quantity of it for purification and positive identification. For the other cases (experiments 1, 6, and 7) of lower yield of the rearrangement products, isolation was very difficult, hence these were assigned structures on the basis of the similarity of their retention times to those of the compounds actually isolated and whose structures were established.

The data shows that in all cases the expected acid-catalyzed cleavage of the acetal occurred at least as part of the reaction, to produce the dihydrofuran (or pyran) and the corresponding phenol. The dihydrofuran or pyran could not be estimated readily since it polymerized under the reaction conditions. However, it was measured indirectly by the g.l.c. analysis of the phenolic product B, formed in an amount equal to the dihydro compound. The other product obtained (C in Table 3) was that resulting from a rearrangement due to an electrophilic attack by the protonated dihydrofuran or pyran on the phenolic material which arose from acid-catalyzed *exo* C—O bond cleavage. The relative amount of C obtained depended upon the type of substituent in the aromatic ring, being greatest when two activating alkyl groups were in the ring (75 and 70%, experiments 2 and 5) and least when deactivating groups (chlorine) were in the ring (0%, experiment 3). Attack by the protonated dihydrofuran (or pyran) occurred on the aromatic nucleus in the position ortho to the hydroxyl substituent, if this position was free (experiments 1, 2, 5–7), but if the ortho position was blocked, then the para position was the point of attack (experiment 4). The retention times of the small amount of high boiling material obtained in the competitive reaction shown in experiments 1 and 2 of Table 2 were identical to those of compound C of experiments 1 and 4 in Table 3, and distinctly different from those of the expected 4-aryloxy-1-butanols. Hence these must have arisen from the Lewis acid property of the reagent AlH_2Cl.

Experimental

Boiling points are uncorrected.

Preparative g.l.c. and g.l.c. analyses were carried out with the columns and instruments described previously (4). Quantitative g.l.c. analyses were made by measuring the signal area directly, uncorrected for detector response, since observed and correct areas usually differed by less than 5%, though in a few cases this difference was as much as, but no more than 10%.

I.r. spectra were recorded with a Perkin–Elmer Model 337 instrument.

P.m.r. spectra were recorded with a Varian Associates A60 instrument operated by Mr. R. Swindlehurst, and an

Can. J. Chem. Downloaded from www.nrcresearchpress.com by 210.87.254.40 on 09/05/12
For personal use only.

HR-100 spectrometer operated by Mr. G. Bigham. The i.r. and p.m.r. spectra, taken for all compounds described, agreed well with the structures proposed.

Elemental analyses were performed by Mrs. D. Mahlow of this Department.

Solvents were removed by rotary evaporator unless otherwise noted.

Preparation of 2-Aryloxytetrahydrofurans and Pyrans

These were prepared by the acid-catalyzed reaction of 2,3-dihydrofuran or 3,4-dihydro-2*H*-pyran with the appropriate phenol, following published directions (9), but with the following modification. Following completion of the reaction, the cooled mixture was diluted with ether and treated with Claisen's alkali (10) which effectively removed the excess phenolic reagent. The ether layers were dried ($MgSO_4$) and separated from solid and solvent and the residue distilled. The products and their physical constants are shown in Table 4.

Preparation of 4-Aryloxy-1-butanols. Possible Ring Cleavage Products from the Hydrogenolysis of 2-Aryloxytetrahydrofurans

The precursors, the *1-aryloxy-3-bromopropanes*, were prepared by the reaction of 1,3-dibromopropane with the appropriate phenol following published directions (11) but using sodium hydride as the base and 1,2-dimethoxyethane as solvent. The products and their physical constants are listed in Table 5. Following published general directions (11), the 1-aryloxy-3-bromopropanes were converted to the corresponding 4-aryloxybutyronitriles, and these in turn were changed to the ethyl 4-aryloxybutyrates. The latter were then reduced with lithium aluminum hydride in ether, as usual, to the 4-aryloxy-1-butanols. The boiling points and refractive indices of these nitriles, esters and alcohols are shown in Table 5.

Hydrogenolysis of 2-Aryloxytetrahydrofurans

The general procedure was the same as that employed for the hydrogenolysis of 2-alkoxytetrahydrofurans (4). The results are shown in Table 1.

$AlCl_3$-Catalyzed Rearrangement of 2-Aryloxytetrahydrofurans and Pyrans. General Procedure

To a vigorously stirred solution of anhydrous aluminum chloride (0.17 g, 0.00125 mol) in 30 ml of dry ether at room temperature was added 0.96 g (0.005 mol) of 2-(3,5-dimethylphenoxy)tetrahydrofuran. The mixture became pale orange while it was stirred for an additional 10 min. An aqueous 15% solution of potassium hydroxide was added to discharge the color (0.25 ml). The ether solution was separated by decantation and freed from solvent by fractional distillation. G.l.c. analysis of the residue (0.90 g, 94%) gave the results shown in Table 3 for experiment 2. Results of the reactions of the other 2-aryloxytetrahydrofurans and pyrans are shown also in Table 3. No 2,3-dihydrofuran was detected in the products of reactions involving the tetrahydrofurans, but a very small amount of 3,4-dihydro-2*H*-pyran was found by g.l.c., in the product mixture arising from the $AlCl_3$ reaction with 2-aryloxytetrahydropyrans.

Isolation of Products of the $AlCl_3$-Catalyzed Rearrangements

(a) From 2-(3,5-Dimethylphenoxy)tetrahydrofuran

The residue (0.9 g) from the reaction of this furan with $AlCl_3$ (see above) was chromatographed on 20 g of acid-washed alumina. A 4:1 mixture of Skellysolve B and chloroform was the eluant, and 75-ml fractions were collected. The first fraction contained no product, whereas a colorless oil was obtained from fractions 2 and 3. The oil solidified on standing. Recrystallization from Skellysolve B gave colorless crystals (0.5 g, 55%) of *2-(4,6-dimethyl-2-hydroxyphenyl)-tetrahydrofuran*, m.p. 65–67°.

Methylation according to general directions (12) gave 2-(4,6-dimethyl-2-methoxyphenyl)tetrahydrofuran, b.p. 98–100° at 0.3 mm; η_D^{20} 1.5388. This was identical with authentic *2-(4,6-dimethyl-2-methoxyphenyl)tetrahydrofuran* prepared below.

(b) From 2-(3,5-Dimethylphenoxy)tetrahydropyran

Rearrangement with $AlCl_3$ as above gave the product *2-(4,6-dimethyl-2-hydroxyphenyl)tetrahydropyran*, m.p. 87–89°.

(c) From 2-(2,6-Dimethylphenoxy)tetrahydrofuran

Rearrangement of this furan with $AlCl_3$ as above gave a residue (88.5%) which deposited an ether-insoluble solid. Trituration of the mixture with ether, followed by filtration, gave a colorless solid in 73% yield, m.p. 213–215°, identical in all respects with authentic *4,4'-dihydroxy-3,3',5,5'-tetramethylbiphenyl* (13). The ether filtrate, freed from solvent, gave a residue which was methylated (12). The product when distilled gave 2,6-dimethylanisole (10%) and a 10% yield of *2-(3,5-dimethyl-4-methoxyphenyl)tetrahydrofuran*, b.p. 105° at 0.5 mm; η_D^{25} 1.5175. This was identical with authentic material prepared below.

Authentic 2-(4,6-Dimethyl-2-methoxyphenyl)tetrahydrofuran

Succinic anhydride (7.8 g, 0.077 mol) was condensed with 3,5-dimethylanisole (10.5 g, 0.077 mol) by the published general procedure (14) to produce *β-(4,6-dimethyl-2-methoxybenzoyl)propionic acid*. The crude acid was crystallized best by solution in chloroform (200 ml) and reducing the volume of the dried ($MgSO_4$) solution to 75 ml. Careful addition of Skellysolve B to cloudiness, and preservation of the mixture in a refrigerator for 18 h, gave pure material (14 g, 78%), m.p. 97–99°.

The acid was converted to 1-(4,6-dimethyl-2-methoxyphenyl)-1,4-butanediol by reduction with lithium aluminum hydride as usual. The crude diol (91% yield) was cyclized by the same method used to convert 1-phenyl-1,4-butanediol to 2-phenyltetrahydrofuran (4). The small amount of contaminating *p*-toluenesulfonyl chloride could be removed only by heating the impure 2-substituted tetrahydrofuran with 15% aqueous potassium hydroxide under reflux. Ether extracts of the cooled mixture were dried ($MgSO_4$) and freed from solvent. The residue on distillation provided a 38% yield of pure *2-(4,6-dimethyl-2-methoxyphenyl)tetrahydrofuran*, b.p. 100–102° at 0.5 mm; η_D^{22} 1.5375.

Authentic 2-(3,5-Dimethyl-4-methoxyphenyl)tetrahydrofuran

The reaction (14) of succinic anhydride with 2,6-dimethylanisole as above gave *β*-(3,5-dimethyl-4-methoxybenzoyl)-propionic acid, yield, 72%, m.p. 108–110°; lit. m.p. 114–115° (15).

Reduction of the acid with lithium aluminum hydride gave the crude oil *1-(3,5-dimethyl-4-methoxyphenyl)-1,4-butanediol* (90%) which was cyclized as above to *2-(3,5-*

Can. J. Chem. Downloaded from www.nrcresearchpress.com by 210.87.254.40 on 09/05/12
For personal use only.

TABLE 4.

(*a*) 2-Aryloxytetrahydrofurans

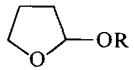

No.	R	Yield (%)	B.p. (°C/mm)	η_D/°C	Elemental analysis (%) C Calcd.	C Found	H Calcd.	H Found	Cl Calcd.	Cl Found
1	C_6H_5	82	86/2.8	1.5217/25	73.12	73.42	7.31	7.45		
2	2,6-$Cl_2C_6H_3$	54	100–102/0.8	1.5469/25	51.53	51.73	4.32	4.72	30.42	30.17
3	2,6-$(CH_3)_2C_6H_3$	75.5	95–96/1.0	1.5160/25	74.96	75.18	8.39	8.70		
4	3,5-$(CH_3)_2C_6H_3$	54	74/0.1	1.5183/25	74.96	75.11	8.39	8.21		
5	4-*t*-$C_4H_9C_6H_4$	69.5	92/0.1	1.5108/25	76.32	76.46	9.15	8.85		

(*b*) 2-Aryloxytetrahydropyrans*

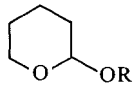

6	3,5-$(CH_3)_2C_6H_3$	66	85–86/0.5	1.5133/23	75.64	75.43	8.79	9.09		

*The compounds *2-phenoxytetrahydropyran* and *2-(p-tolyloxy)-tetrahydropyran* were obtained by published directions (1).

Can. J. Chem. Downloaded from www.nrcresearchpress.com by 210.87.254.40 on 09/05/12
For personal use only.

TABLE 5.

(*a*) 4-Aryloxy-1-butanols and their precursors

Ar	$ArO(CH_2)_3Br$ B.p. (°C/mm)	$ArO(CH_2)_3Br$ η_D/°C	$ArO(CH_2)_3CN$ B.p. (°C/mm)	$ArO(CH_2)_3CN$ η_D/°C	$ArO(CH_2)_3CO_2C_2H_5$ B.p. (°C/mm)	$ArO(CH_2)_3CO_2C_2H_5$ η_D/°C	$ArO(CH_2)_4OH$ B.p. (°C/mm)	$ArO(CH_2)_4OH$ η_D/°C
C_6H_5	105/5.0 (136–142/20)*	1.5454/25	93–97/0.08 (162–166/22)*	1.5177/22	105–107/0.1 (160–165/25)*	1.5016/23 (1.491/22)*	100–102/0.6 (162–164/19)*	1.5260/22 (1.520/27)*
$2,6\text{-}Cl_2C_6H_3$	100–103/0.1	1.5181/23	128–130/0.6	1.5346/22	120–122/0.3	1.5119/23	110–111/0.07	1.5380/22
$2,6\text{-}(CH_3)_2C_6H_3$	105–106/1.5	1.5290/22	109–110/0.2	1.5088/22	113–115/0.7	1.4927/22	116–118/0.9	1.5136/22
$3,5\text{-}(CH_3)_2C_6H_3$	90–93/0.5	1.5343/22	114–115/0.3	1.5150/22	112–115/0.4	1.5016/23	120–123/0.8	1.5205/22

(*b*) Elemental analysis of the 4-Aryloxybutanols ($ArO(CH_2)_4OH$)†

Ar	%C Calcd.	%C Found	%H Calcd.	%H Found	%Cl Calcd.	%Cl Found
C_6H_5	72.26	71.94	8.48	8.73		
$2,6\text{-}Cl_2C_6H_3$	51.08	51.12	5.15	5.32	30.16	30.44
$2,6\text{-}(CH_3)_2C_6H_3$	74.19	74.19	9.34	9.05		
$3,5\text{-}(CH_3)_2C_6H_3$	74.19	74.45	9.34	9.42		

*Reference 11.

†Elemental analyses were not made on the precursors, although they were carefully fractionally distilled. Their i.r. and p.m.r. spectra were clean and agreed completely with the assigned structure.

dimethyl-4-methoxyphenyl)tetrahydrofuran, yield 44%; b.p. 98–100° at 0.7 mm; n_D^{25} 1.5230.

The authors thank the National Research Council of Canada for financial support for a part of this work.

One of us (P. C. Loewen) thanks the National Research Council of Canada for the award of a Bursary, and the Isaac Killam Memorial Fund of the University of Alberta for the award of a Fellowship.

1. U. E. DINER and R. K. BROWN. Can. J. Chem. **45**, 2547 (1967).
2. E. C. ASHBY and J. PRATHER. J. Am. Chem. Soc. **88**, 729 (1966).
3. U. E. DINER, H. A. DAVIS, and R. K. BROWN. Can. J. Chem. **45**, 207 (1967).
4. P. C. LOEWEN, (MISS) L. P. MAKHUBU, and R. K. BROWN. Can. J. Chem. **50**, 1502 (1972).
5. D. H. MCDANIEL and H. C. BROWN. J. Org. Chem. **23**, 420 (1958).
6. H. C. BROWN and Y. OKAMOTO. J. Am. Chem. Soc. **80**, 4979 (1958).
7. M. M. KREEVOY and R. W. TAFT, JR. J. Am. Chem. Soc. **77**, 5590 (1955).
8. B. E. LEGGETTER and R. K. BROWN. Can. J. Chem. **42**, 990 (1964).
9. E. L. ELIEL, B. E. NOWAK, R. A. DAIGNAULT, and V. G. BADDING. J. Org. Chem. **30**, 2441 (1965).
10. L. F. FIESER. Experiments in organic chemistry. Third edition. D. C. Heath and Co., Boston. 1957. p. 310.
11. C. S. MARVEL and A. L. TANENBAUM. J. Am. Chem. Soc. **44**, 2645 (1922).
12. U. E. DINER, F. SWEET, and R. K. BROWN. Can. J. Chem. **44**, 1591 (1966).
13. K. AUWERS and TH. V. MARKOVITS. Chem. Ber. **38**, 234 (1905).
14. J. C. HARLAND and A. ROBERTSON. J. Chem. Soc. 937 (1939).
15. W. COCKER. J. Chem. Soc. 36 (1964).

Can. J. Chem. Downloaded from www.nrcresearchpress.com by 210.87.254.40 on 09/05/12
For personal use only.

Pyrochlores. VIII. Studies of some 2–5 Pyrochlores and Related Compounds and Minerals[1]

FRANÇOIS BRISSE,[2] DAVID J. STEWART,[3] V. SEIDL,[4] AND OSVALD KNOP

Department of Chemistry, Dalhousie University, Halifax, Nova Scotia

Received June 8, 1972

The cubic pyrochlores $Cd_2Nb_2O_7$, $Cd_2Ta_2O_7$, $Sn_2Nb_2O_7$, $Sn_2Ta_2O_7$, $Cd_2Sb_2O_7$, $Ca_2Sb_2O_7$, $Mn_2Sb_2O_7$, $Pb_2Sb_2O_7$, and related compounds were prepared and investigated by a number of methods. On heating above 700°, $Ca_2Sb_2O_7$(pyrochlore) transformed to $Ca_2Sb_2O_7$(weberite), while $Pb_2Sb_2O_7$(pyrochlore) changed to a rhombohedrally distorted $Pb_2Sb_2O_7$ pyrochlore. Refinement of the crystal structures of $Cd_2Nb_2O_7$ and $Cd_2Ta_2O_7$ from powder diffractometer intensities yielded 0.434(2) and 0.434(3) respectively as the best estimates of $x(O_2)$. Specimens of natural bindheimite and stibiconite were also examined. Stibiconite from San Luís Potosí (Mexico) was shown, on the evidence of its Mössbauer ^{121}Sb spectrum, to contain Sb(V) and Sb(III) in the approximate ratio of 0.2.

$BaCd_2Cl_6 \cdot 5H_2O$ and $BaCd_2Cl_6 \cdot 2H_2O$ both give powder diffraction patterns of the pyrochlore type. The chlorine could be partially replaced by Br to give mixed crystals $BaCd_2Cl_{6-z}Br_z \cdot 5H_2O$ almost up to $z = 2$.

The crystal chemistry of 2–5 oxide pyrochlores and the relationship of the weberite to the pyrochlore phases are discussed.

Les composés cubiques de type pyrochlore $Cd_2Nb_2O_7$, $Cd_2Ta_2O_7$, $Sn_2Nb_2O_7$, $Sn_2Ta_2O_7$, $Cd_2Sb_2O_7$, $Ca_2Sb_2O_7$, $Mn_2Sb_2O_7$, $Pb_2Sb_2O_7$ ainsi que quelques autres qui s'y rattachent ont été préparés et examinés par différentes méthodes. $Ca_2Sb_2O_7$(pyrochlore) se transforme au dessus de 700° en $Ca_2Sb_2O_7$(wébérite) alors que $Pb_2Sb_2O_7$(pyrochlore) se transforme en $Pb_2Sb_2O_7$(pyrochlore à déformation rhomboèdrique). L'affinement des structures cristallines de $Cd_2Nb_2O_7$ et de $Cd_2Ta_2O_7$, à partir d'intensités obtenues avec un diffractomètre de poudre, donne comme valeurs les plus probables de $x(O_2)$:0.434(2) et 0.434(3) respectivement. On a aussi examiné les minéraux bindheimite et stibiconite. Le spectre Mössbauer de ^{121}Sb montre que la stibiconite de San Luís Potosí (Mexique) contient Sb(V) et Sb(III) approximativement dans le rapport de 0.2.

Les diagrammes de poudre de $BaCd_2Cl_6 \cdot 5H_2O$ et de $BaCd_2Cl_6 \cdot 2H_2O$ sont du type pyrochlore. Le brome peut partiellement remplacer le chlore pour former des cristaux mixtes $BaCd_2Cl_{6-z}Br_z \cdot 5H_2O$ jusqu'à z presque égal à 2.

On discute de la cristallochimie des pyrochlores oxygénés de type 2–5 ainsi que de la relation entre les phases pyrochlore et wébérite.

Canadian Journal of Chemistry, **50**, 3648 (1972)

As a sequel to our previous investigations of oxide pyrochlores of compositions $A_2^{3+}B_2^{4+}O_7$ (3–4 pyrochlores) and $A_2^{1+}B_2^{5+}O_6$ (1–5 pyrochlores) (1–8), some corresponding 2–5 pyrochlores have been studied.

Minerals of this type (pyrochlore, microlite etc.) have been known for a long time, and the discovery of ferroelectricity in $Cd_2Nb_2O_7$ (9) initiated a search for similar compounds with unusual dielectric properties. This search has proved disappointing in that it has uncovered but a minuscule number of new ferroelectrics of this structure type. It showed, however, that for some combinations of divalent and pentavalent cations the composition of the pyrochlore (*P*) phase is not limited to the ideal $A_2B_2O_7$ stoichiometry, while for other combinations *only* hypostoichiometric *P* phases can be prepared by conventional methods. The 2–5 pyrochlores are then best described by the general formula $A_{1+z}B_2O_{6+z}$. The range of z is determined by the particular combination of A and B, and may include unity.

The stability of the *P* structure can be correlated, for 3–4 pyrochlores, with the ionic size and radius ratio of the cations (10). A similar correlation is less satisfactory for the 2–5 pyrochlores (11). Pentavalent cations of suitable size and chemistry are relatively few, and the absence, among divalent elements, of an extensive sequence of closely related ions, such as that formed by the trivalent lanthanons, makes each of the 2–5 *P* phases more unique. The

[1]For Part VII, see ref. 7. This paper is based in part on the Ph.D. thesis submitted by F. Brisse to the Department of Chemistry, Dalhousie University, March 1967.

[2]Present address: Département de Chimie, Université de Montréal, Montréal, Québec.

[3]Present address: Invermay Research Centre, Private Bag, Mosgiel, New Zealand.

[4]Killam Postdoctoral Fellow, 1967–1969. Present address: Department of Mineralogy, Institute of Chemical Technology, Prague 6, Czechoslovakia.

Can. J. Chem. Downloaded from www.nrcresearchpress.com by 210.87.254.105 on 09/05/12
For personal use only.

Can. J. Chem. Downloaded from www.nrcresearchpress.com by 210.87.254.105 on 09/05/12
For personal use only.

polarizing action of the B ions, and the polarizability of the A ions, are increased in the 2–5 series and therefore more important as structure-determining factors than in the 3–4 series.

Substituted 2–5 pyrochlores analogous to natural pyrochlore, which has the generic formula $NaCaNb_2O_6OH$, can also be prepared with F^- (*cf.* for example refs. 12–14), and very likely also with OH^- (15), substituting for O^{2-} in the ideal pyrochlore formula. For example, replacing even a very small amount of oxygen in $Ca_2Sb_2O_7$, which normally has the weberite (*W*) structure, by F^- causes the antimonate to adopt the *P* structure (12). Thus evidently substitution in the anion sublattice has a strong effect in determining the structure of $A_2^{2+}B_2^{5+}O_7$ oxides. When such substitution is present but not recognized, it may contribute to the poor correlation of stability of the P structure with cation size and $r(A^{2+}):r(B^{5+})$ ratio alone.

The main purpose of this investigation is to establish a more reliable basis for a crystal chemistry of stoichiometric 2–5 oxide pyrochlores, both by attempting to verify and reconcile earlier literature reports, often contradictory, and by obtaining and examining completely new evidence.

Experimental

The purity and source of supply of most of the starting materials have been described elsewhere (1–6). In addition the following compounds were used: black SnO (typical analysis, in p.p.m., 200 Cl, 50 SO_4, 100 Fe), MnO_2, $CaCO_3$, $CdCO_3$, $CdCl_2 \cdot 2\frac{1}{2}H_2O$, $CdBr_2 \cdot 4H_2O$, $SrCl_2 \cdot 6H_2O$ (Fisher Certified Reagents); $BaBr_2 \cdot 2H_2O$ (Fisher Laboratory Chemical); $PbCO_3$ (reagent grade, Anachema Chemicals Ltd.); $MnCO_3$, PbO, $SbCl_5$ (Baker Analyzed Reagents); and Nb_2O_5 and Ta_2O_5 (3N, CIBA "optical grade").

Preparations were carried out essentially as described in previous accounts (1–6) except as noted (Table 1). The dry-mixed reactants were fired either in air or sealed in evacuated quartz-glass ampoules. In the latter case pellets of the dry-mixed powders were sometimes contained in small crucibles of recrystallized alumina (*e.g.* to prepare the Sn(II) pyrochlores). When there was a possibility that oxidation, reduction, or decomposition would occur during firing, preliminary thermogravimetric analysis (t.g.a.) was made to assist in determining optimum conditions for the preparation. T.g.a. of the reactant mixture during reactive firing was also carried out in cases such as the preparation of $Pb_2Sb_2O_7$ from PbO_2 and Sb_2O_3, to verify that no overall weight loss occurs.

A hydrothermal synthesis of lead antimonate from $PbO_2 + Sb_2O_3$ was attempted by placing the reactant mixture together with an excess of water contained in a recrystallized-alumina crucible, in a small steel bomb and keeping the charge at 350° for 24 h.

Ca, Cd, Mn, and Pb antimonates were prepared by a method previously described by Baccaredda (16). The original suggestion called for firing an excess of the appropriate metal salt with antimonic acid and leaching out the unreacted metal salt with boiling water or some other suitable agent. However, to ensure 1:1 ratios of M to Sb in the products, we used stoichiometric proportions of reactants. The antimonic acid was prepared as described in ref. 6 and reacted with $PbAc_2 \cdot 3H_2O$, $CdAc_2 \cdot 3H_2O$, $Ca(NO_3)_2 \cdot 4H_2O$, or $MnAc_2 \cdot 4H_2O$.

"$BaCd_2Cl_6$" and other mixed anhydrous chlorides were prepared by fusing mixtures of the simple chlorides at 550–600° in a platinum crucible. The charge was maintained in the molten state for 10–15 min and cooled in the furnace.

The hydrated mixed chlorides were obtained by dissolving calculated amounts of the simple chlorides in distilled water and allowing the mixed solution to crystallize slowly at room temperature. Alternatively, the mixed solution was heated to saturation, in which case crystals appeared quickly on cooling.

For details of the t.g.a., X-ray, infrared, and dielectric techniques as well as of the structure refinement by least squares refs. 1–3 and 5 may be consulted. Ni-filtered Cu K radiation was used for photographic work and also for powder diffractometry. However, in the concluding stages of this investigation a curved LiF-crystal focussing monochromator became available which gave very low backgrounds with unfiltered Cu K radiation.

Results

Cadmium Niobate and Tantalate

The lattice parameters of $Cd_2Nb_2O_7$ and $Cd_2Ta_2O_7$ agreed well with the values reported earlier by other authors (Table 1).

The permittivity *vs.* temperature curve of the niobate between room temperature and 4.2 °K was in good agreement with a similar curve reported by Jona *et al.* (17). The room-temperature permittivity was 360 and the maximum permittivity, 2420 (at 178 °K).

No ferroelectric transition was observed by permittivity measurements in $Cd_2Ta_2O_7$ between ambient temperature and 4.2 °K.

Calcium Niobate and Tantalate

With one exception (18), attempts by a number of authors to prepare a $Ca_2Nb_2O_7$ pyrochlore have always resulted in a product whose symmetry was eventually determined as monoclinic (19; *cf.* also refs. 20 and 21) and whose lattice parameters resemble remarkably those of $La_2Ti_2O_7$ and $Nd_2Ti_2O_7$ (22). According to a preliminary description (21) the structure of $Ca_2Nb_2O_7$ consists of slabs of nearly regular perovskite structure arranged in a manner dif-

Can. J. Chem. Downloaded from www.nrcresearchpress.com by 210.87.254.105 on 09/05/12
For personal use only.

TABLE 1. Details of preparation and crystallographic data of 2–5 pyrochlores and related compounds

Composition	Preparation and product*	Type	$a_0(P)$, Å	Reference
$Mn_2Sb_2O_7$	$MnO_2 + Sb_2O_3$ (*A*): 400/12, 500/12, 600/12, 700/5: olive-grey	*P*+	10.17(2)	This work
	$MnAc_2 \cdot 4H_2O$ + antimonic acid: 150/5, 200/2, 320/10, 500/14, 550/24	*P*	10.068(3)	This work
$Cd_2Sb_2O_7$	Excess $Cd(NO_3)_2 \cdot 4H_2O$ + antimonic acid: fused and fired to red heat, excess CdO leached out with dilute acetic acid	*P*	10.18†	16
	Details of preparation not given, presumably by firing dry-mixed $CdCO_3 + Sb_2O_3$. Lattice parameters determined from single-crystal photographs: $d_{exp.} = 7.10$ g/cm^3	*W*	—	23
	$CdO + CdSb_2O_6$ (*A*): 950–1000/24, air-quenched in Au tube	*P*	10.270(2)	35
	$CdO + Sb_2O_3$: 690/20, 740/42, 825/19, 880/5	*P*	10.259(1)	This work
	$CdAc_2 \cdot 3H_2O$ + antimonic acid: 150/20, 380/43, 690/23	*P*	10.259(1)	This work
$Cd_2Nb_2O_7$	$CdCO_3 + Nb_2O_5$: 1000/15	*P*	10.37†	23
	1150°	*P*	10.370(6)	9
	Single crystals grown from $Cd_2Nb_2O_7$ + CdO in a closed container at 1470–1420/1: rapid cooling	*P*	10.372(1)	17
		P	10.368	68
	(*i*) $CdCO_3 + Nb_2O_5$: 500/24, 650/24, 750/24, 900/24, 950/48	*P*	10.373(1)	This work
	(*ii*) $CdCO_3 + Nb_2O_5$: 200/24, 400/18, 800/48	*P*	10.372(1)	This work
$Cd_2Ta_2O_7$	$CdCO_3$ + tantalic acid: 1000/15	*P*	10.38†	23
	1200°	*P*	10.376	17
	$CdCO_3 + Ta_2O_5$: 500/24, 700/24, 850/8, 950/48	*P*	10.375(1)	This work
$Yb_2Nb_2O_7$	2/3 Yb_2O_3 + 2/3 Yb + Nb_2O_5 (*A*): 450/24, 550/24, 640/12, 750/24, 850/2 + 1000/12, 1100/24; grey-black	Not *P*	—	This work
$Ca_2Sb_2O_7$	Excess $Ca(NO_3)_2 \cdot 4H_2O$ + antimonic acid: fused and fired to red heat, excess $Ca(NO_3)_2$ washed out with boiling water	*P*	10.32†	16
	$CaCO_3 + Sb_2O_3$: 1200/15	*W*	—	23
	CaO (?) + Sb_2O_3 (?): 620/23, 750/11, 1105/12; sintered	*W*	—	11
	$CaCO_3 + Sb_2O_3$: 400/24, 800/24, 1000/1 wk, 1200/48	*W*	—	This work
	$Ca(NO_3)_2 \cdot 4H_2O$ + antimonic acid: fused at 200 + 400/1, 620/20, 700/35, 700/86	*P*	10.321(8)	This work
$Ca_2Ta_2O_7$	$CaCO_3$ + tantalic acid: 1220/15	*P*	10.37†	23
	$CaO + Ta_2O_5$: 1000/several days	Not *P*	—	27
	CaO (?) + Ta_2O_5: 950/24, 1185/14: slightly sintered, $a(P) = 10.35$ Å; 1365/12, greatly sintered	*P*	10.41	11
		P_{rh} ?	(10.420)	26
	$CaCO_3 + Ta_2O_5$: 1000°, 1500/24, 1500/24	*P*		24
	$CaCO_3 + Ta_2O_5$: 1350/12, 1350/12, 1380/12, 1500/12	*P*+	10.39(1)	This work
	$CaCO_3$ + tantalic acid: 600/2, 1060/15, 1550/15	*P*+	10.399(8)	This work

Can. J. Chem. Downloaded from www.nrcresearchpress.com by 210.87.254.105 on 09/05/12
For personal use only.

TABLE 1 (*Concluded*)

Composition	Preparation and product*	Type	$a_0(P)$, Å	Reference
$Sr_2Sb_2O_7$	Details of preparation not given, presumably by firing dry-mixed $SrCO_3 + Sb_2O_3$	*W*	—	23
	$SrCl_2 \cdot 6H_2O$ + antimonic acid: 300/2, 400/20, 720/17	*W*	—	This work
$Sn_2Sb_2O_7$	$SnO_2 + Sb_2O_3$ (*A*): 400/12, 600/12, 700/12: no apparent reaction	—	—	This work
	SnO_2 + antimonic acid: 150/24, 390/17	Not *P*	—	This work
$Sn_{1.5}Nb_2O_{6.5}$	SnO + Nb_2O_5 (*A*): 400/24, 500/24, 600/24, 750/24: bright orange-yellow	*P*+		This work
$Sn_2Nb_2O_7$	SnO + Nb_2O_5 (*A*): 400/12, temperature then increased at 100°/h: $d_{exp.} = 5.64$ g/cm^3	*P*	10.581(2)	32
	(*i*) SnO + Nb_2O_5 (*A*): 400/24, 500/24, 600/24, 750/24: bright orange-yellow, weak lines of β-Sn	*P*+	10.587(2)	This work
	(*ii*) SnO + Nb_2O_5 (*A*): 100/5 + 200/5 + 300/5 + 400/5 + 500/5 + 650/5, 890/56	*P*	10.588(2)	This work
$Sn_{2.74}Nb_2O_{7.74}$	Same as for $Sn_2Nb_2O_7$	*P*	10.623(2)	32
$SnTa_2O_6$	SnO + Ta_2O_5 (*A*): 1000°. $Sn_2Ta_2O_7$ + ~$SnTa_4O_{11}$			30
$Sn_2Ta_2O_7$	Sn + amorph. $SnO_2 + Ta_2O_5$: high-frequency induction furnace. Multiphase product containing yellow microscopic crystals of *P*	*P*	10.47(5), 10.48	28, 29
	SnO + Ta_2O_5 (*A*): 1000°	*P*	10.562(3)†	30
	SnO + Ta_2O_5 (*A*): forms at 400°, very well crystallized at 1000°: $d_{exp.} = 8.33$ g/cm^3	*P*	10.550(2)	32
	(*i*) SnO + Ta_2O_5 (*A*): 400/24, 500/24, 600/24, 750/24: greenish-white	*P*	10.564(2)	This work
	(*ii*) SnO + Ta_2O_5 (*A*): 100/5 + 200/5 + 300/5 + 400/5 + 500/5 + 635/5, 905/200	*P*	10.565(2)	This work
$Sn_{2.6}Ta_2O_{7.6}$	SnO + Ta_2O_5 (*A*): 100/5 + 200/5 + 300/5 + 400/5 + 500/5 + 600/5, 905/83	*P*	10.579(2)	This work
$Sn_{2.74}Ta_2O_{7.74}$	Same as for $Sn_2Ta_2O_7$	*P*	10.588(2)	32
$Sn_3Ta_2O_8$	SnO + Ta_2O_5 (*A*): 1000°	*P*	10.606(3)†	30
$Pb_{1.5}Sb_2O_{6.5}$	$PbO_2 + Sb_2O_3$: 400/48, 700/48, 900/24: orange-ochre	$PbSb_2O_6$ +	—	This work
$Pb_2Sb_2O_7$	$PbAc_2 \cdot 3H_2O$ + antimonic acid: fused and fired to red heat, excess Pb leached out with boiling NaOH	*P*	10.70†	16
	$PbCO_3 + Sb_2O_3$: 900/20	*P*	10.40†	23
	PbO + $PbSb_2O_6$ (*A*): 950–1000/24, air-quenched in Au tube: $a_{rh} = 10.64(1)$ Å, $\alpha = 87.85(5)°$	P_{rh}		35
	(*i*) $PbCO_3 + Sb_2O_3$: 500/24, 750/24, 900/24: orange-ochre, $a_{rh} = 10.677(1)$ Å, $\alpha = 87.70(5)°$	P_{rh}		This work
	(*ii*) $PbO_2 + Sb_2O_3$: 400/48, 700/24, 800/24, 900/24: orange-ochre, same powder pattern as (*i*)	P_{rh}		This work
	(*iii*) $PbAc_2 \cdot 3H_2O$ + antimonic acid: 250/7, 390/62, 520/11, 680/32, 730/20	*P*	10.529(2)	This work

*400/12 stands for 400° for 12 h. *A*, fired in an evacuated, sealed ampoule; in the present work the sample was fired in a recrystallized-alumina crucible inside a sealed quartz-glass tube *in vacuo*. *P*, cubic pyrochlore; P_{rh}, rhombohedrally distorted pyrochlore; *W*, weberite.
†Converted from kX.

Can. J. Chem. Downloaded from www.nrcresearchpress.com by 210.87.254.105 on 09/05/12
For personal use only.

ferent from other known structures. The cubic $Ca_2Nb_2O_7$ ($a = 10.37$ Å) reported by Lamure and Colas (18) was prepared under rather special conditions and may have been non-stoichiometric or fluorine-stabilized.

However, the corresponding tantalate has been variously described as "pyrochlore" (11, 23, 24), "pyrochlore-type" (25), "distorted pyrochlore" (26), and "not pyrochlore" (27). Despite numerous attempts involving different heat treatments, stoichiometry and reactants we were unable to obtain a single-phase *P* product. Using tantalic acid and $CaCO_3$, which Byström (23) claimed gave a *P* product at 1200°, yielded the same material as we obtained in all other cases. This was apparently the same product as obtained by Aleshin and Roy (11), who described their material as "*P* + trace". However, they claimed to have obtained a single-phase $Ca_2Ta_2O_7(P)$ upon further firing. The only other reference to $Ca_2Ta_2O_7$ being *P* is in a study of the constitution diagram for the $CaO-Ta_2O_5$ system made by Reeve (24).

The strongest lines of the X-ray powder pattern we obtained for $Ca_2Ta_2O_7$ in all preparations can be indexed on a *P* unit cell of 10.399(8) Å. The additional lines could not be accounted for by considering distortion of the cubic *P* cell, since the majority of the lines did not appear to be displaced from their expected positions for the cubic *P* structure. Doubling or tripling of the cubic unit cell also was ineffective in explaining the extra lines. The additional lines should therefore belong to a second phase, possibly originating in incomplete reaction, but we were unable to identify it as any Ca or Ta oxide or any of the other Ca tantalates so far reported.

Tin(II) Niobate and Tantalate

The question whether $Sn_2^{2+}Nb_2^{5+}O_7$ and $Sn_2^{2+}Ta_2^{5+}O_7$ can be prepared as cubic pyrochlores appeared of considerable interest. Successful preparation of these two compounds would enable the effective radius of Sn^{2+} to be estimated for a 6 + 2 oxygen coordination at a centrosymmetric site of relatively high symmetry, $\bar{3}m$, which by itself would be valuable. That $Sn_2Ta_2O_7$ exists was first suggested by Gasperin (28, 29), who found yellow microscopic crystals giving a diffraction pattern of the *P* type among the products of high-temperature reactions involving Sn, SnO_2, and Ta_2O_5, but their quantities were too small for chemical analysis and their composition was surmized from circumstantial evidence. A cubic $Sn_2Ta_2O_7$ pyrochlore was later reported by Trunov *et al.* (30).[5]

Our initial attempt to prepare $Sn_2Nb_2O_7$ resulted in a bright orange-yellow product whose *P* powder pattern contained very weak extra lines ascribable to β-Sn (sample *i*, Table 1). Reducing the Sn:Nb ratio in the reactant mixture still did not yield a single-phase product; on the contrary, foreign lines not belonging to Sn or SnO_2 appeared (intended composition, $Sn_{1.5}Nb_2O_{6.5}$, Table 1). However, a subsequent paper by Bodiot (32) reported the preparation of the niobate by much the same procedure and claimed a single-phase product; the firing schedule was almost identical with ours. A further attempt at preparing the compound using a very gradual increase in temperature *did* produce a single-phase pyrochlore (sample *ii*, Table 1). Considering that sample *i* was not single-phase, the difference between the lattice parameter of its *P* phase and that of Bodiot's product was very small.

Our initial preparation of Sn(II) tantalate produced a greenish-white compound with a powder pattern of the *P* type, with *very* weak extra lines present. The lattice parameter again agreed very well with the value reported subsequently by Bodiot. A second preparation (sample *ii*) yielded a completely homogeneous product.

Bodiot has reported the homogeneity range of the $Sn_{1+z}B_2O_{6+z}$ niobate and tantalate pyrochlores to extend from $z = 1$ to $z = 1.74$, while from the account of Trunov *et al.* $z = 2$ seems to be the upper limit of the range for the tantalate. There is nothing in either paper to suggest that at $z = 1$ the *P* phase is not a normal pyrochlore $Sn_2^{2+}B_2^{5+}O_7$ with a "classical" distribution of the atoms, *i.e.*, analogous to that in $Er_2Ti_2O_7$ (1). However, attempts to refine the structures of our first niobate and tantalate

[5]A mineral, *sukulaite*, stated to be isotypic with microlite and thus of the *P* type ($a = 10.57$ Å), was found as narrow rims or aggregates (grain size approx. 5 μ) in wodginite inclusions in tantalian cassiterite (31). The Sn:Nb:Ta ratio, as determined by microprobe analysis, would correspond to the formula $Sn_2(Nb_{0.22}Ta_{0.78})_2O_7$ if minor Fe and Mn are disregarded and the tin is assumed to be Sn(II).

Can. J. Chem. Downloaded from www.nrcresearchpress.com by 210.87.254.105 on 09/05/12
For personal use only.

preparations from integrated powder diffractometer intensities were unsatisfactory even when allowance was made, in the compositions assumed, for departures from ideal stoichiometry that were thought consistent with the estimated intensities of the foreign-phase powder lines (*vide infra*). This and certain other considerations prompted us to initiate a more detailed investigation of the two pyrochlores by Mössbauer ^{119}Sn spectroscopy and other methods (33).

Antimonates: Method of Preparation

Attempts at synthesizing *P*-type antimonates have been made ever since the discovery of the minerals bindheimite and stibiconite.[6] The products were, however, mostly other than pyrochlores. The only generally successful method by which $M_2Sb_2O_7$ (M = Ca, Cd, Pb) pyrochlores have been obtained is that described by Baccaredda (16): a hydrated salt of M is fused with antimonic acid at low heat followed by calcining at 300–400°. Using dry reactants, such as an MO oxide and an antimony oxide, has usually been found to produce antimonates having structures not of the (cubic) *P* type.

In view of the known ability of OH^- to stabilize the *P* structure and the fact that bindheimite and stibiconite invariably contain OH^- or H_2O (34), it might be thought that the success of Baccaredda's method lies in its use of hydrated reactants. The products obtained by it might therefore contain OH^- or H_2O and would not be stoichiometric $M_2Sb_2O_7$ pyrochlores. However, we were unable to detect any absorption due to hydrogenic species in the infrared spectra of our preparations of antimonates made by the Baccaredda method. Furthermore, using antimonic acid and a nonhydrated metal salt did not always give a *P*-type product. The explanation for the success of the method seems rather to lie in the low temperature required for the reaction (100–200°), and perhaps also in the use of an antimony oxide which already has the *P* structure (*cf.* ref. 7 for details of the structure of antimonic acid). We have found both $Ca_2Sb_2O_7$ and $Pb_2Sb_2O_7$ pyrochlores to be metastable with respect to temperature, so that mild reaction conditions are a necessity if these *P* phases are to be obtained at all.

[6]Bindheimite is an oxide mineral containing mainly Sb and Pb, while stibiconite contains Sb and some Ca. Both give X-ray powder patterns of the *P* type.

Calcium Antimonate

The X-ray powder lines of $Ca_2Sb_2O_7(P)$ were always somewhat diffuse at high angles. Above 700° lines of a *W* pattern developed until finally the yellow-ochre material transformed to give a white powder with a sharp pattern of the *W* type. Our attempts to prepare $Ca_2Sb_2O_7(P)$ from $CaCO_3$ and Sb_2O_3 always resulted directly in the formation of an antimonate with the *W* structure. Other authors have reported the same results (13, 23).

The *P* structure can be stabilized by the substitution of very small amounts of F^- for O^{2-} in the anion sublattice. Thus Butler *et al.* (13) have prepared $Ca_2Sb_2O_{6.5}F$, as well as similar formulations containing less fluorine, all of the *P* type and stable to temperatures of 1000°. Aia *et al.* (12) have reported a similar preparation of $Ca_{1.56}Sb_2O_{6.37}F_{0.44}$ and have carried out an X-ray refinement of its structure (Table 4). The lattice parameter of their material was 10.300(2) Å, which differs only slightly from our value for $Ca_2Sb_2O_7(P)$ (Table 1).

Lead Antimonate

Unlike the Ca compound, $Pb_2Sb_2O_7(P)$ can be prepared with a well-defined X-ray powder pattern. The yellow powder we obtained using Baccaredda's method and after firing to 730° gave sharp, well-resolved lines even at high angles. This is in contrast with Baccaredda's findings for his preparation of $Pb_2Sb_2O_7$: the positions of only eight, low-angle lines of the pattern were measured and these only to poor accuracy. It seems likely that his material was fired to only about 400°, at which temperature the powder pattern is still diffuse. The lattice parameter of our $Pb_2Sb_2O_7(P)$ decreased slightly on heating the compound from 400 to 700°.

When $Pb_2Sb_2O_7(P)$ was heated above 730°, it transformed into a rhombohedrally distorted pyrochlore phase P_{rh} without loss of weight. P_{rh} is also the phase which results by firing dry-mixed oxides: the lattice parameters of a product obtained at 900° (Table 1) were a_{rh} = 10.677(1) Å, $\alpha = 87.70(5)°$. These values are in

Can. J. Chem. Downloaded from www.nrcresearchpress.com by 210.87.254.105 on 09/05/12
For personal use only.

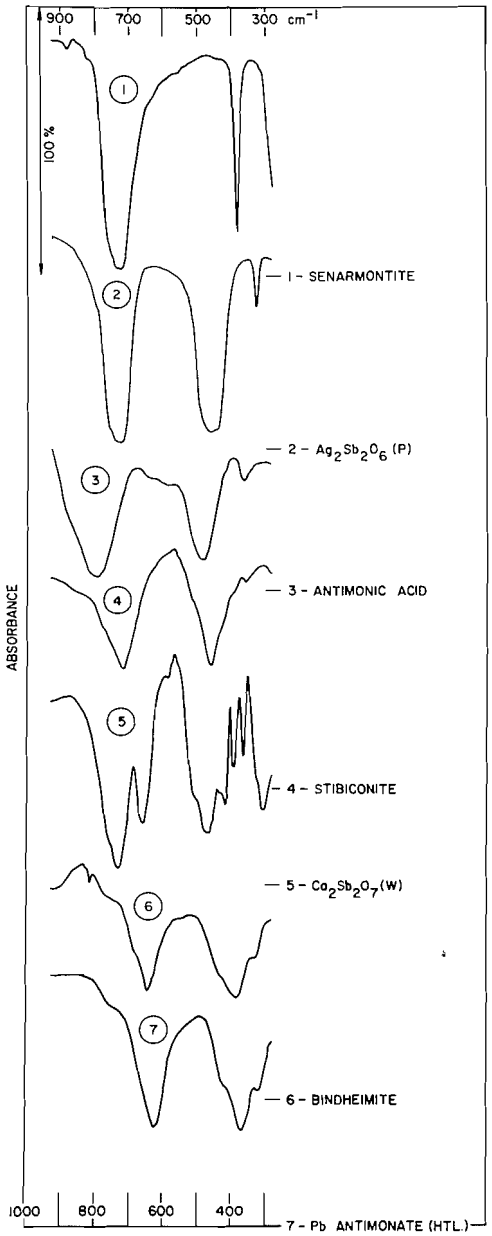

FIG. 1. Infrared spectra of Sb_2O_3 (senarmontite, 1) and antimonates of pyrochlore (2, 3, 4, 6, 7?) and weberite (5) types obtained with compensated KBr pellets. The 100% absorbance values for the individual compounds are indicated by short horizontal lines; HTL, hydrothermal.

reasonable agreement with those reported recently by Moisan *et al.* (35) for a sample fired in a sealed container, 10.64(1) Å and 87.85(5)°, if one takes into account the effect of the small difference in composition which probably existed between their preparation and ours.[7] These authors dispose of the question of existence of $Pb_2Sb_2O_7(P)$ by suggesting that it actually has a formula of $Pb_{2-u}Sb_2O_{7-u}$, in analogy with the defect pyrochlore $Pb_{2-u}Nb_2O_{7-u}$ of ref. 9. Since the transformation $P \rightarrow P_{rh}$ took place without change in weight, this view is not consistent with the observed facts.[8]

We were also able to prepare an ochre-colored fine powder that gave an X-ray pattern of the F (P?) type, by hydrothermal synthesis from $2PbO_2 + Sb_2O_3$ (see Experimental). However, the reflections were only poorly developed.

Bindheimite and Stibiconite

A *bindheimite* specimen from Otjimboyo East, S.W. Africa (BM 1929, 1843) gave a sharp powder pattern of the P type. The lattice parameter, 10.447(2) Å, was in excellent agreement with the value of 10.4480(4) Å reported by Bothwell *et al.* (38).[9] Another specimen (Endellion, Cornwall; BM 26757) gave a fluorite-type pattern resembling that of the product of the hydrothermal synthesis, but the material was not sufficiently crystalline to observe the weak P lines that may have been present. There was no visible change in the pattern on heating the material to 500° for 24 h.

The i.r. spectra of both mineral specimens before heat treatment and of the hydrothermal product were similar. They all contained the two strong bands between 800 and 300 cm^{-1} characteristic of P antimonates (Fig. 1) and a strong OH stretching band centered at 3400 cm^{-1}.

[7]Pb and Sb both begin to volatilize from the antimonate at temperatures of about 800°.

[8]Analogy with $Pb_{2-u}Nb_2O_{7-u}$ would require a substantial loss of weight on transformation or the appearance of a second phase: for the niobate, $u = 0.5$ corresponds to a P phase and $u = 0$ to a P_{rh} phase, but for $0 < u < 0.5$ two-phase mixtures have been reported (37), and a similar situation appears to exist for $Pb_{2-u}Ta_2O_{7-u}$ (15, 36, 37). A preparation intended to yield $Pb_{1.5}Sb_2O_{6.5}$ resulted in a mixture of $PbSb_2O_6$ + another phase (Table 1).

[9]Values quoted for the lattice parameter of bindheimite range from 10.39 Å (converted from kX) (39) to 10.47 Å (34). They are lower than the value for synthetic $Pb_2Sb_2O_7$ (P), reflecting deficiency in the Pb content.

Can. J. Chem. Downloaded from www.nrcresearchpress.com by 210.87.254.105 on 09/05/12
For personal use only.

A specimen of *stibiconite* from San Luís Potosí, Mexico,[10] was well crystallized and gave sharp powder patterns. The value of a_0 was 10.292(2) Å, as compared with 10.321(8) Å for synthetic $Ca_2Sb_2O_7(P)$ (Table 1) and 10.34–10.38 Å for antimonic acid (7). Although there was a weight loss of 6.7% on heating to 950° (t.g.a.), the *P* structure was retained and the crystallinity improved. The i.r. spectrum of the untreated material in the 900–300 cm^{-1} region was of the same type as the spectra of bindheimite, antimonic acid, $AgSbO_3(P)$, and Sb_2O_3 (senarmontite). It did not exhibit the fine structure and splitting evident in the spectrum of $Ca_2Sb_2O_7(W)$ (Fig. 1).

A Mössbauer ^{121}Sb spectrum of this stibiconite contained resonant absorptions of both Sb(III) and Sb(V). Computer-fitting of eight Lorentzian lines gave isomer shifts, relative to InSb at 77 °K, of −6.0(2) mm/s for Sb(III) and +9.57(4) mm/s for Sb(V). The respective quadrupole splittings were +15(3) and ±4(1) mm/s, and the corresponding line widths were 3.4(8) and 3.36(15) mm/s. These values are comparable to those in antimonic acid and Sb_6O_{13} (7). The ratio of the Sb(III):Sb(V) peak areas, 0.18(3), may be taken, approximately, to be the Sb(III):Sb(V) population ratio in the sample.[11] Stibiconite is thus a "reduced" nonstoichiometric pyrochlore rather than a 2–5 pyrochlore. The Mössbauer spectrum provides a direct confirmation of the correctness of the general formula $(Sb^{3+}, Ca)_y Sb^{5+}_{2-z}(O, OH, H_2O)_{6-7}$ which was proposed for stibiconite by Vitaliano and Mason (40) on the basis of their chemical analyses for oxygen. Stibiconite was the only one among the antimonate minerals they examined which these authors considered as containing both valences of antimony (34).

[10]Semiquantitative spectrographic analysis of this material gave the following result: Sb, medium; Ca, medium high; silica, low medium; Na, 0.3%; Al, Mg, 0.05%; Sr, 0.03%; Pb, 0.02%; Ba, Ti, V, Fe, 0.01%; Ni, 0.002%; Mn, Cu, Ag, <0.001%. Examination of thin and polished sections revealed amorphous silica and numerous calcite inclusions. It is probable that most of the calcium is contained in the carbonate.

[11]For comments on the validity of this assumption and for details of apparatus and computer-fitting see refs. 7 and 8. For the Sb(V) absorption equally good fit was obtained with either sign of the quadrupole splitting, *i.e.* within the experimental uncertainty the Sb(V) line is symmetric.

Manganese Antimonate

$Mn_2Sb_2O_7(P)$ is also metastable, though largely owing to the strong tendency of the Mn^{2+} to oxidize. We were able to prepare the grey-green $Mn_2Sb_2O_7(P)$ both from antimonic acid and Mn^{2+} acetate (Baccaredda's method) and from $2MnO_2 + Sb_2O_3$. In air the compound was stable only to about 600°, and its powder pattern was not well defined.

As with $Ca_2Sb_2O_7$, the introduction of F^- into the anion sublattice stabilizes the *P* structure. Aia *et al.* (12) report preparation of a *P*-type manganese fluoantimonate with a_0 of 10.141(3) Å but were unable to determine its precise stoichiometry.

Cadmium Antimonate

The single crystal which Byström (23) found in his $Cd_2Sb_2O_7$ preparation and examined by Weissenberg photography had a structure of the *W* type. However, we did not succeed in preparing such a compound. All our preparations, whether by Baccaredda's method or from $CdO + Sb_2O_3$, gave a green powder having an X-ray powder pattern of the *P* type. The product obtained by Baccaredda's method gave a well-defined powder pattern of a somewhat better quality than the product synthesized from the oxides. There was no indication of any structural transformation, and the material was stable at 900° when slow loss of CdO occurred. Recently Moisan *et al.* (35) have also found $Cd_2Sb_2O_7$ to have the *P* structure (Table 1).

Strontium and Sn(II) Antimonates

Attempts to prepare $Sr_2Sb_2O_7$ and $Sn_2Sb_2O_7$ with the *P* structure were unsuccessful, even when using Baccaredda's method. The $Sr_2Sb_2O_7$ preparation always gave powder patterns of the *W* type, and no single phase could be obtained from reactions intended to yield $Sn_2Sb_2O_7$.

Mixed Antimonates $(Cd,Ca)_2Sb_2O_7$ and $(Cd,Sr)_2Sb_2O_7$

Samples of the overall compositions $Cd_{2-u}M_uSb_2O_7$ ($u = 0.5, 1, 1.5, 2$) were prepared by adding acetic acid to the requisite amounts of dry-mixed carbonates + Sb_2O_3 in a platinum crucible, evaporating to dryness and firing the residues, with intermediate grinding, at successively higher temperatures, ultimately

Can. J. Chem. Downloaded from www.nrcresearchpress.com by 210.87.254.105 on 09/05/12
For personal use only.

at 850–900° for 3 days. Repeated firing at 700° for several days gave powder patterns of poor quality.

In the Ca series *P* reflections plus those of another phase(s) were clearly visible at $u = 0.5$ and 1, with a progressive increase in $a(P)$. The pattern for $u = 1.5$ could not be interpreted with confidence. It appeared to contain neither *P* nor *W* reflections, and the solid-state reaction may have been incomplete. The *W* pattern observed at $u = 2$ was well defined.

In the Sr series the *P* lines were present even at $u = 1.5$. No foreign lines were observed at $u = 0.5$, but the *P* lines were appreciably broadened, indicating possible presence of two or more *P* phases of different compositions as a result of incomplete reaction. Weak lines of an unidentified phase were seen in the $u = 1$ product. At $u = 1.5$ the pattern was essentially that of *W* with very weak *P* lines possibly present, while at $u = 2$ the *W* pattern was sharp and well defined. The $a(P)$ increased with u.

The degree of completeness of reaction and equilibrium in these exploratory experiments is uncertain, but as the variation of $a(P)$ with the overall composition indicates, limited substitution of Cd in $Cd_2Sb_2O_7(P)$ by Ca or Sr is possible, assuming of course that the stoichiometry of the mixed *P* phases remains essentially unchanged.

Chlorides

Ferrari and Cavalca (41; *cf.* also ref. 42) prepared $BaCd_2Cl_6 \cdot 5H_2O$ with a *P*-type powder pattern ($a \sim 13.85$ Å) by crystallization from a mixed solution of the simple chlorides. They reported that the product of dehydration at 200° gave a *P*-type pattern identical with that of the fresh crystal, from which they concluded that the five molecules of water were of zeolitic nature.

Our t.g.a. dehydration curve of the pentahydrate (Fig. 2) indicated the existence, at 110–115°, of a stable dihydrate. The dihydrate also gave a *P*-type pattern, and there was little or no difference between the lattice parameters of the dihydrate, 13.813(2) Å, and the pentahydrate, 13.814(2) Å. The three molecules of water removable at the relatively low temperature are thus probably zeolitic.

When the dihydrate (or the pentahydrate) was kept at 160°, the chloride was completely

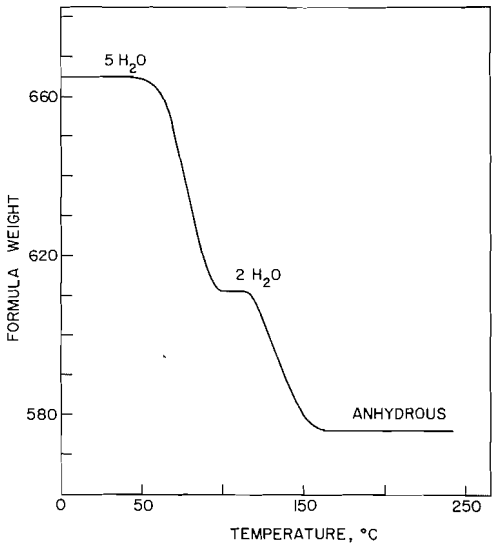

FIG. 2. T.g.a. curve of $BaCd_2Cl_6 \cdot 5H_2O$ in stagnant air. Heating rate, 1°/min.

dehydrated, but contrary to Ferrari and Cavalca's statement the powder pattern of the anhydrous material was not of the *P*-type. It clearly corresponded to a mixture, one of the constituents being $CdCl_2$. The numerous lines of the other phase(s) could not be identified with certainty. A product with the same powder pattern was obtained by fusing $BaCl_2$ and $CdCl_2$ in the requisite proportion. These observations are consistent with Sandonnini's (43) claim that there are no compounds in the system $BaCl_2 - CdCl_2$ and that the system is of the simple eutectic type.

Attempts to replace, by crystallization or by fusion, Ba with Sr or Pb, and Cd with Hg, failed. However, the chlorine could be partially replaced by bromine. This was evident from the change in a_0 of crystals obtained from solutions with different concentrations in Cl^- and Br^-:

Values of $a_0(P)$ for $BaCd_2Cl_{6-z}Br_z \cdot 5H_2O$ (intended compositions)

z	$a_0(P)$, Å
0	13.814(2)
0.5	13.834(3)
1	13.854(2)
1.5	13.882(2)
2	13.919(2)

TABLE 2. Least-squares refinements of $Cd_2Nb_2O_7$ and $Cd_2Ta_2O_7$ (Cu Kα: full matrix)*

Parameter	Value		
	$Cd_2Nb_2O_7$ (sample *ii*)		
	Refinement No. 12	Refinement No. 11*a*†	$Cd_2Ta_2O_7$, Refinement No. 5
Input	$43I_o$	$43I_o$	$42I_o$
Weighting scheme	*W4*	*W4*	*W3*
$x(O_2)$	0.4349(12)	0.4331(16)	0.4346(26)
B(Cd), Å^2	1.23(13)	0.83(10)	0.60(12)
B(B), Å^2	0.62(12)	0.88(12)	0.90(8)
$B(O_1)$, Å^2	0.79(77)	2.21(141)	0.44(137)
$B(O_2)$, Å^2	2.08(36)	1.69(43)	1.55(80)
$D(\Delta I)$, all reflections	1.83	2.23	3.25
$D(\Delta I)$, $I_o > 0.01I_c(222)$	1.39	1.67	2.27
$D(I)$, all reflections	1000	996	997
$D(I)$, $I_o > 0.01I_c(222)$	1001	1000	993

*$D(\Delta I) = 100\ \Sigma|\Delta I|/\Sigma I_o$; $D(I) = 1000\ \Sigma I_c/\Sigma I_o$.
†Focussing monochromator in diffracted beam.

The presence of the slightly larger Br^- ion resulted in an increase of the lattice parameter. For $z = 2$ two kinds of crystals were obtained, which indicated that the acceptable amount of Br^- in the structure had reached a limit. In a plot of $a_0(P)$ against the intended z all five points fall on a smooth curve. This suggests that the limiting value of z is close to 2, but a proper correlation will have to await a more detailed study including determinations of Cl and Br in the solid-solution phase after proper equilibration.

Structure Refinements

The crystal structures of Cd niobate and tantalate were refined from powder diffractometer data using *ad hoc* full-matrix programs and (*i*) individual isotropic temperature factors or (*ii*) an overall temperature factor. Weighting schemes W3 (44) and W4 were used; the latter is defined by $w(hkl) = \varepsilon^{-1}(hkl)$, where $\varepsilon(hkl)$ is the standard deviation of $I_o(hkl)$ obtained from several measurements. The initial values of the parameters were K, 1.000; $x(O_2)$, 0.4200; B(Cd), 0.15 Å^2; $B(B^{5+})$, 0.60 Å^2; $B(O_1) = B(O_2)$, 1.50 Å^2; B(overall), 1.00 Å^2. The ionic scattering factors for Cd^{2+}, Nb^{5+}, Ta^{5+} (45) and O^{2-} (46) were corrected for dispersion (both parts, ref. 47).

Integrated diffractometer intensities were collected at least in quadruplicate. The structures were refined both from $|F_o|$'s of single reflections and from intensities. In the F-refinements all single reflections permitted in *Fd3m* up to and including 10.6.6 were used. The $|F_o|$'s of reflections whose intensities were too weak to be counted were entered at 4/9 of the standard deviation of the local background count over 1°(2θ). A similar procedure was adopted for the I-refinements. The exception was the refinement 11*a* (Table 2) of the niobate, in which *measured* monochromatized intensities of all reflections up to and including 10.6.6 were utilized.

The discrepancy indices of the individual refinements were quite low (Table 2) and the agreement of I_o and I_c was very satisfactory (Table 3). However, the values of $x(O_2)$ varied, for the best refinements, by as much as 0.002, which was also the order of magnitude of $\sigma(x)$. About 60% of the observed intensities were below 1% of $I_c(222) = 100$, and at least one half of these 60% were below 0.1%. The latter category contains almost all those reflections to whose intensity the metal atoms make no contribution. Thus the very reflections on which an accurate determination of $x(O_2)$ depends are of doubtful quality. This situation is rendered even more unfavorable by the large scattering powers of the metal atoms relative to oxygen.

The best estimate of $x(O_2)$ appears to be 0.434(2) for the niobate and 0.434(3) for the tantalate. Any difference that might be expected between the two compounds is completely

Can. J. Chem. Downloaded from www.nrcresearchpress.com by 210.87.254.105 on 09/05/12
For personal use only.

TABLE 3. Observed and calculated intensities for Cd niobate and tantalate (Cu Kα)*

	$Cd_2Nb_2O_7$ (sample *ii*)				$Cd_2Ta_2O_7$,	
	Refinement No. 12		Refinement No. 11*a*†		Refinement No. 5	
hkl	I_o	I_c	I_o	I_c	I_o	I_c
111	0.1‡	0.07	0.1	0.1		
220	0.1‡	0.01	0.00	0.00	0.05‡	0.00
311	0.1‡	0.02	0.2	0.05	5.3	4.6
222	99.9	100	100.3	100	102.0	100
400	31.0	30.5	31.5	30.6	34.9	35.2
331	4.0	4.0	4.1	4.4	0.03‡	0.00
422	0.6	0.5	0.7	0.5	0.03‡	0.3
511, 333	1.4	1.4	1.6	1.6	1.7	1.6
440	41.9	41.6	44.3	44.5	40.2	41.1
531	0.2	0.2	0.3	0.3	0.6	0.9
620	0.3	0.4	0.4	0.3	0.02‡	0.2
533; 622§	37.2	37.5	41.3	41.3	40.5	41.0
444	9.0	9.7	10.1	10.7	10.1	10.5
711, 551	0.05‡	0.09	0.09	0.1	1.0	0.8
642	0.03‡	0.04	0.02	0.03	0.02‡	0.02
731, 553	0.03‡	0.08	0.2	0.1	1.3	1.0
800	5.0	5.2	5.8	6.1	5.5	5.5
733	0.3	0.2	0.4	0.4	0.05‡	0.00
822, 660	0.03‡	0.2	0.6	0.3	0.05‡	0.2
751, 555; 662§	13.0	13.1	15.4	15.8	14.6	14.6
840	11.0	11.1	12.9	13.4	12.3	12.3
911, 753	0.04‡	0.05	0.3	0.2	0.4	0.2
664	0.04‡	0.07	0.2	0.07	0.04‡	0.05
931	0.04‡	0.02	0.00	0.00	0.04‡	0.3
844	8.6	8.7	10.5	10.4	9.8	9.7
933, 771, 755	0.04‡	0.08	0.4	0.3	0.02‡	0.1
10.2.0, 862	0.04‡	0.04	0.3	0.06	0.02‡	0.03
951, 773; 10.2.2, 666§	10.3	10.4	13.0	12.5	12.6	12.0
953	0.07‡	0.01	0.03	0.06	0.03‡	0.07
10.4.2	0.07‡	0.02	0.06	0.01	0.03‡	0.01
11.1.1, 775	0.07‡	0.01	0.04	0.06	0.03‡	0.1
880	3.4	3.5	3.9	4.0	3.8	3.9
11.3.1, 971, 955	0.08‡	0.01	0.09	0.1	0.01‡	0.2
10.6.0, 866	0.2	0.09	0.2	0.09	0.01‡	0.07
11.3.3, 973; 10.6.2§	14.9	14.7	17.1	16.5	18.6	17.1
12.0.0, 884	10.3	9.6	11.0	11.0	11.0	10.8
11.5.1, 777	0.03‡	0.03	0.00	0.03	0.01‡	0.2
12.2.2, 10.6.4	0.03‡	0.09	0.01	0.1	0.01‡	0.07
11.5.3, 975	0.03‡	0.01	0.00	0.1	0.01‡	0.2
12.4.0	10.4	10.0	11.2	10.7	10.8	11.3
991	0.03‡	0.00	0.08	0.04	0.03‡	0.03
10.8.2	0.03‡	0.00	0.00	0.00	0.03‡	0.00
13.1.1, 11.7.1, 11.5.5, 993; 10.6.6§	12.8	13.4	14.0	14.5	15.4	16.0

*The intensities have been normalized to $I_c(222) = 100$.
†Focussing monochromator in diffracted beam.
‡Intensity too weak to be counted. I_o was entered as $(4/9)\sigma$(background).
§Overlapping peaks.

obscured by the large standard deviations, but in both cases the mean value of the parameter is below the ideal value of $7/16 = 0.4375$ required for undistorted BO_6 coordination octahedra. The present $x(O_2)$ values are higher than those reported by earlier workers (Table 4).

The interatomic distances calculated from the final parameter values (Table 5) may be com-

Can. J. Chem. Downloaded from www.nrcresearchpress.com by 210.87.254.105 on 09/05/12
For personal use only.

TABLE 4. Comparison of $x(O_2)$ in 2–5 pyrochlores*

Compound	$x(O_2)$	Refined from	Reference
$Cd_2Re_2O_7$	0.441(7)	Single-crystal photographs (Mo Kα)	50
$Cd_2Nb_2O_7$	0.430(3)	Single-crystal photographs (Mo Kα)	17
	0.434(2)	Powder diffractometry (Cu Kα)	This work
$Cd_2Ta_2O_7$	0.414	Visual powder intensities (Cr Kα)	23
	0.434(3)	Powder diffractometry (Cu Kα)	This work
$Hg_2Sb_2O_7$	(0.429)	Estimated from assumed B—O distances	51
$Hg_2Nb_2O_7$	0.427(2)	Powder diffractometry (Cu Kα)	51
$Hg_2Ta_2O_7$	(0.428)	Estimated from assumed B—O distances	51
$Ca_{1.56}Sb_2O_{6.37}F_{0.44}$	0.412(2)	Powder diffractometry (Cu Kα)	12

*The contents of the *P* unit cell (space group *Fd3m*) are 16 A^{2+} in 16(*c*) [000 etc.], 16 B^{5+} in 16(*d*) [$\frac{1}{2}\frac{1}{2}\frac{1}{2}$ etc.], 8 O_1 in 8(*a*) [$\pm$(1/8, 1/8, 1/8) etc.], 48 O_2 in 48(*f*) [*x*, 1/8, 1/8 etc.] (*cf.* ref. 1). The above values of $x(O_2)$ refer to origin in 16(*c*), *i.e.* Sleight's choice A_0 (51). Close examination of the original papers shows that for $Cd_2Ta_2O_7$ (23) and $Cd_2Nb_2O_7$ (17, 69) the origin was placed in 8(*a*) (Sleight's choice O_0), in accordance with the description of *Fd3m* in ref. 66. The dispute on this point (70, 71) may thus be regarded as settled.

TABLE 5. Apparent interatomic distances and bond angles in $Cd_2Nb_2O_7$ and $Cd_2Ta_2O_7$*

Bond	Distance (Å)	
	$Cd_2Nb_2O_7$	$Cd_2Ta_2O_7$
B—O_2	1.957(22)	1.958(33)
B—O_2	3.756(54)	3.757(81)
Cd—$O_1 = a_0\sqrt{3}/8$	2.246(2)	2.246(2)
Cd—O_2	2.647(45)	2.647(67)
$O_2(5)$—$O_2(6)$	2.734(28)	2.734(42)
$O_2(4)$—$O_2(5)$	2.802(87)	2.802(130)
$O_1(1)$—$O_2(3)$	3.205(62)	3.206(93)
$O_1(1)$—$O_2(2)$	3.718(10)	3.719(15)
O_1—$O_1 = a_0\sqrt{3}/4$	4.492(2)	4.493(2)
B—B, Cd—Cd, B—Cd $= a_0\sqrt{2}/4$	3.667(2)	3.668(2)

Bonds	Angle (deg)	
	$Cd_2Nb_2O_7$	$Cd_2Ta_2O_7$
$O_2(4)$—B(1)—$O_2(5)$	91.4(23)	91.4(35)
$O_2(2)$—Cd(1)—$O_2(3)$	62.2(15)	62.2(23)
$O_1(1)$—Cd(1)—$O_2(3)$	81.4(9)	81.4(14)
$O_2(2)$—$O_1(1)$—$O_2(3)$	45.8(6)	45.8(9)

*For atomic positions see Table 4 of ref. 1 and for relations between bond angles, Table VII of ref. 5. The uncertainty limits are based on $3\sigma(x)$, and on $4\sigma(a_0)$ for distances independent of $x(O_2)$.

pared with corresponding M—O distances in other compounds (Table 6). The B—O_2 distances are not very different from average values of Nb—O and Ta—O distances in NbO_6 and TaO_6 groupings, but the Cd—O_2 distance equals or exceeds the largest Cd—O distance so far reported, that in $Cd(NO_3)_2 \cdot 4D_2O$.

Compared with the results for the two Cd pyrochlores, the Sn(II) phases (samples *i*) refined poorly. The *R* value for $Sn_2Ta_2O_7$ could not be reduced below 7.6% and the $x(O_2) = 0.448$ and *B*(Sn) values were unreasonably high. The niobate refined to 6.9%; $x(O_2) = 0.436$ fell in the expected range, but both *B*(Sn) and *B*(Nb) were too high, and there were considerable discrepancies in the intensity agreement for some of the reflections. Keeping in mind that samples *i* were not completely homogeneous, allowance was made in the overall formula for a decrease in the intended Sn content, but neither this nor attempts to adjust the populations of the 16(*c*) and 16(*d*) sites by assuming reduced or mixed occupancies produced satisfactory results. Since density measurements on the final, homogeneous preparations (samples *ii*) indicated incompletely occupied unit cells, the necessity of determining whether mixed valency states were present became apparent. Results of a Mössbauer ^{121}Sb investigation will be communicated in another paper of this series (33).

Discussion

Lattice Parameters

The lattice parameter of the *P* antimonates varies linearly with the ionic radius $r(A^{2+})$ for 8-coordination (Fig. 3*A*).

The straight line for the *P* niobates and tantalates, drawn parallel to the antimonates lines, is only tentative, for only Cd, Hg, and Sn

Can. J. Chem. Downloaded from www.nrcresearchpress.com by 210.87.254.105 on 09/05/12
For personal use only.

TABLE 6. Metal–oxygen distances in some compounds of Cd, Nb, and Ta

Compound	Coordination	Distance, Å	Reference
	Cd–O distances		
CdO (*B*1)	6 O	2.348	72
CdO_2 (*C*2)	6 O	2.30	73
$Cd_2V_2O_7$ (thortveitite)	2 O + 2 O + 2 O	2.24(2); 2.30(1); 2.39(2)	56
$CdSO_4 \cdot H_2O$	$O + O_w + O + O + O_w + O$	2.21; 2.24; 2.27; 2.33; 2.33; 2.36	94
$Cd(NO_3)_2 \cdot 4D_2O$	$2\ O_w + 2\ O_w + 2\ O + 2\ O$	2.247(22); 2.295(12); 2.438(9); 2.590(11)	74
	Nb—O distances		
$Hg_2Nb_2O_7$ (pyrochlore)	6 O	1.999(8)	51
$NbOPO_4$	O + 4 O + O	1.783(12); 1.969(9); 2.321(12)	75
$LiNbO_3$ (r.t.)	3 O + 3 O	1.889(3); 2.112(4)	76
$KNbO_3$ (r.t.)	2 O + 2 O + 2 O	1.863(7); 1.991(1); 2.180(9)	77
$GaNbO_4$ (monoclinic)	O + O + O + O + O + O	1.797; 1.906; 1.937; 2.000; 2.215; 2.333	78
$SbNbO_4$	O + O + O + O + O + O	1.809(9); 1.879(9); 2.006(9); 2.076(9); 2.125(9); 2.125(9)	79
$CaNb_2O_6$	O + O + O + O + O + O	1.774(9); 1.919(9); 1.947(9); 2.065(9); 2.077(9); 2.342(8)	80
$Na_2Nb_4O_{11}$	2 O + 2 O + 2 O	1.95(2); 1.98(3); 2.00(2)	95
$Ba_3Si_4Nb_6O_{26}$	O + 2 O + 2 O + O	1.918(4); 1.937(4); 2.044(7); 2.056(3)	96
$(NH_4)_3NbO(C_2O_4)_3 \cdot H_2O$	O + O + O + O + O + O + O	1.710(10); 2.114(12); 2.122(7); 2.126(10); 2.137(8); 2.150(13); 2.157(10)	97
	Ta—O distances		
TaO (*B*1)	6 O	2.211–2.220 (depending on stoichiometry)	81
TaO_2 (rutile)	4 O + 2 O	2.02	81
$LiTaO_3$ (r.t.)	3 O + 3 O	1.908(3); 2.073(3)	82
$SnTa_2O_7$ (thorcaulite)	O + O + O + O + O + O	1.80(15); 1.90(16); 1.98(13); 2.13(13); 2.15(13); 2.21(16)	83
$CaTa_4O_{11}$	6 O	1.98(2)	95
$Ba_5Ta_4O_{15}$	3 O + 3 O 3 O + 3 O	1.856(22); 2.219(28) 1.943(27); 2.065(21)	96

have been reported to form cubic pyrochlores. It accommodates the experimental points reasonably well. The point for $(2V)^{1/3}$ of $Ca_2Nb_2O_7$ (19, 20) and the "$a_0(P)$" of $Ca_2Ta_2O_7$ fall only slightly below it. The a_0 values for Cd niobate and tantalate are very similar, as are those for the Hg compounds, but they differ significantly for Bodiot's $Sn_2Nb_2O_7$ and $Sn_2Ta_2O_7$ (both stated to be stoichiometric) and so do the $V^{1/3}$ values for the rhombohedrally distorted pyrochlores $Pb_2Nb_2O_7$ and $Pb_2Ta_2O_7$. Furthermore, the sequence followed by the a_0 values in corresponding Nb–Ta pairs is not the same for the different A^{2+}.

The slope of the line through the points for Cd_2TiWO_7 and Sn_2TiWO_7 (48) is similar to that for the antimonates, but $a_0(Pb_2TiWO_7)$ is too low.

Tentative straight lines have been drawn in Fig. 3*A* through the $V^{1/3}$ (or $(2V)^{1/3}$) points for $Ca_2Nb_2O_7$, $Sr_2Nb_2O_7$, $Sr_2Ta_2O_7$,[12] $Ba_2Nb_2O_7$, and $Ba_2Ta_2O_7$, and for the three uranates. The trends that seem to emerge despite the discrepancies in the descriptions of the unit cells of these compounds must be regarded as provisional.

[12]Whiston and Smith (49) found no evidence for $Sr_2Ta_2O_7$ in their investigation of the system $SrO-Ta_2O_5$, nor do they mention $Ba_2Nb_2O_7$ among the compounds they identified in the system $BaO-Nb_2O_5$.

Can. J. Chem. Downloaded from www.nrcresearchpress.com by 210.87.254.105 on 09/05/12
For personal use only.

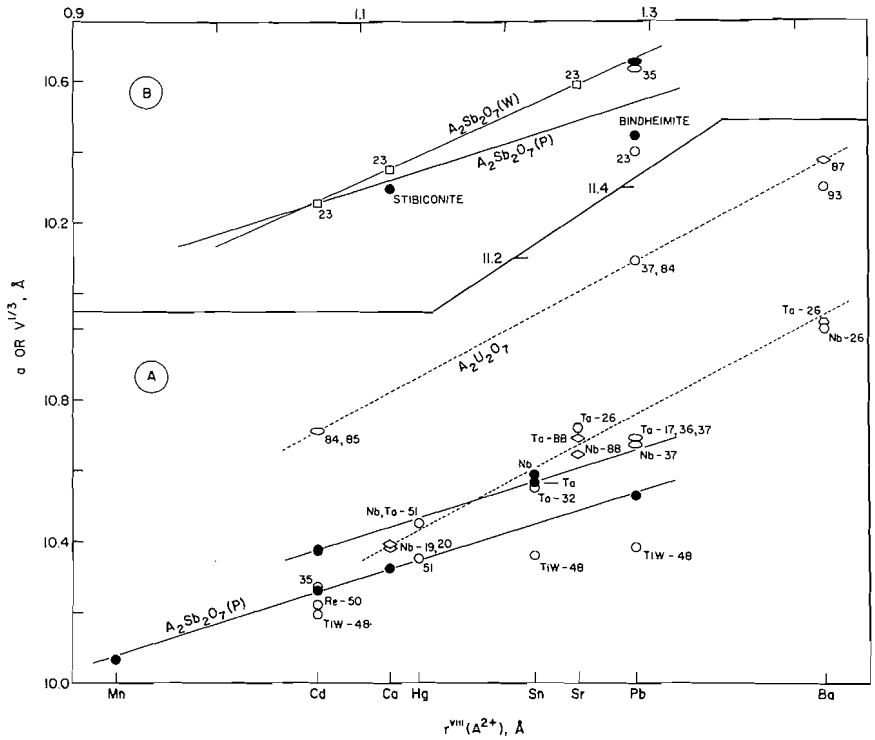

FIG. 3. (*A*) Lattice parameter (or $V^{1/3}$) of stoichiometric $A_2^{2+}B_2^{5+}O_7$ pyrochlores and related compounds plotted against Shannon and Prewitt's (52) ionic radius $r^{VIII}(A^{2+})$. For explanation of symbols see Fig. 4. Full symbols refer to compounds investigated in the present work. Open symbols are for compounds reported in the literature (reference numbers shown): (*B*) Comparison of pyrochlore- and weberite-type $A_2Sb_2O_7$ antimonates.

The Positional Parameter $x(O_2)$

Examination of the $x(O_2)$ values for 2–5 pyrochlores (Table 4) reveals no real evidence that the ideal value of $7/16 = 0.4375$ is exceeded or even reached. The only value greater than 7/16, 0.441(7) for $Cd_2Re_2O_7$, was not regarded as definite evidence for distortion of the ReO_6 octahedra by the authors who reported it (50): by the same token it cannot be viewed as evidence for the *absence* of distortion. The ideal value is, however, approached by our $x(O_2) + \sigma(x)$ values for Cd niobate and tantalate.

While the results available to-date strongly indicate that the BO_6 octahedra in cubic 2–5 pyrochlores (and *a fortiori* in cubic 3–4 oxide pyrochlores; *cf.* refs. 3–5, 10) are never regular, this conclusion is not necessarily definitive. The large disparity of the X-ray scattering factors of the metal and oxygen atoms implies that the appreciable uncertainty in $x(O_2)$ values is inherent in determinations by X-ray diffraction. It is unfortunate that the 2–5 pyrochlores whose reported $x(O_2)$ values are closest to 7/16, and thus most important for resolving the doubt, contain Cd and are therefore unsuitable for neutron diffraction. Methods that are sensitive to site symmetry (Mössbauer and other spectroscopic methods) cannot be expected to decide unambiguously between distorted and regular BO_6 octahedra either: the site symmetry of the B atoms at 16(*d*) is $\bar{3}m$, so for $x(O_2) = 7/16$ the octahedra are only metrically, not crystallographically regular.

The $x(O_2)$ values in 2–5 oxide pyrochlores are higher than in 3–4 pyrochlores. The observed range in the 3–4 series is approximately 0.408–0.428 (and may be expected to extend as high as 0.432 in the high-pressure pyrochlore $Gd_2Ge_2O_7$), whereas the lowest value so far reported for the 2–5 series is 0.427(2) ($Hg_2Nb_2O_7$, Table 4). In $A_2^{3+}B_2^{4+}O_7$ pyrochlores the empirical lower limit coincides

Can. J. Chem. Downloaded from www.nrcresearchpress.com by 210.87.254.105 on 09/05/12
For personal use only.

Can. J. Chem. Downloaded from www.nrcresearchpress.com by 210.87.254.105 on 09/05/12
For personal use only.

approximately with the $x(O_2)$ value at which the electrostatic (Madelung) lattice energy *vs.* $x(O_2)$ curve calculated for the completely ordered *P* structure intersects the corresponding curve for a structure random with respect to A and B (10).[13] However, for 2–5 pyrochlores the two curves do not intersect above $x(O_2) = 0.375$, the value which is appropriate to the defect fluorite structure. It is thus doubtful that the observed $x(O_2)$ range for 2–5 pyrochlores can be derived from a simple electrostatic model which does not take detailed account of cation–anion and anion–anion repulsive forces. In any case the upper limit of the range can be determined from such a model neither for the 2–5 nor for the 3–4 phases.

Attempts to define the existence field of $A_2^{2+}B_2^{5+}O_7$ pyrochlores in terms of the radius ratio $r(A^{2+}):r(B^{5+})$, and to correlate $x(O_2)$ with this ratio, lead to confused results. The structures of only four of the known stoichiometric 2–5 pyrochlores have been refined (Table 4); the $Cd_2Re_2O_7$ phase might contain $Re^{4+} + Re^{6+}$. This leaves Cd niobate and tantalate, and Hg niobate; estimates have been made for Hg tantalate and antimonate (51). A plot of $x(O_2)$ *vs.* radius ratio thus consists of essentially three points (Cd niobate and tantalate have closely similar values) and shows a trend opposite to that observed for 3–4 pyrochlores, *viz.* a decrease of $x(O_2)$ with increasing value of the radius ratio. When Shannon and Prewitt's (52) tentative value of $r(Re^{5+})$ for 6-coordination, 0.52 Å, is used to include $Cd_2Re_2O_7$ in the plot, the trend disappears altogether. On the other hand, a recognizable trend emerges when $x(O_2)$ is plotted against lattice parameter: $x(O_2)$ decreases with increasing a_0. This is again the opposite of what is observed for the A^{3+} titanates and stannates (3, 5), although allowance must be made for the fact that an attempt is being made here to compare on equal basis compounds which belong to different 2–5 composition series.

Similar uncertainties are evident when one tries to delineate the existence field of 2–5 oxide pyrochlores. The only A atoms known to date to form 2–5 pyrochlores are Mn, Cd, Ca, Hg, Sn, and Pb. The number and size range of eligible B atoms are very small: Nb, Ta, Sb, U, and Re (so far only $Cd_2Re_2O_7$ known). Combinations of W^{6+} with B^{4+} (Ti, Sn, Zr) have also been reported (48, 53) to form pyrochlores with A^{2+}, though in ref. 53 the B:W ratios are greater than unity.

An attempt to assess the role of the size factor (at ordinary pressures) is made in Fig. 4. The "ionic" radii of A and B atoms, in 8- and 6-coordination respectively, are those of ref. 52. The exception is the effective radius of Re^{5+}, which is unlikely to be 0.52 Å, as estimated by Shannon and Prewitt from the lattice parameter of $Cd_2Re_2O_7$. Comparison of the *a* (or $V^{1/3}$) values for Cd uranate, tantalate, niobate, antimonate, and Cd_2TiWO_7 points to 0.59(2) Å as a more reasonable value. The average of $r(Re^{4+})$ and $r(Re^{6+})$ is 0.58 Å (52).

The compositions of the stoichiometric cubic *P* phases known to-date fall between the $r^{VIII}(A^{2+}):r^{VI}(B^{5+})$ values of 1.5 and 2.2, and between $r^{VIII}(A^{2+})$ values of *ca.* 0.92 and 1.32 Å (0.83 and 1.18 Å if $r^{VI}(A^{2+})$ is used). Converted to $r^{VI}(A^{2+}):r^{VI}(B^{5+})$ the radius-ratio limits are 1.35 and 2.0, which compares to approximately 1.2 and 1.6 for the stoichiometric 3–4 pyrochlores.[14] These radius-ratio limits in fact accommodate also all the known distorted oxide pyrochlores and weberites with the exception of $Cd_2U_2O_7$ (reported to be P_{rh}), for which the lower limit should be 1.4 rather than 1.5.

Pentavalent vanadium is evidently too small to form *P* phases. Like P(V) and As(V) in pyrophosphates and pyroarsenates (for examples in $Mg_2As_2O_7$, ref. 54), it is present in pyrovanadate structures as the $V_2O_7^{4-}$ ion, as in the thortveitite-type $Mn_2V_2O_7$ (55) and $Cd_2V_2O_7$ (56). No work seems to have been done on Mo^{5+} and W^{5+} compositions.

Niobium and tantalum are 2–5 pyrochlore formers *par excellence*, though the true symmetry of $Ca_2Ta_2O_7$ is yet to be settled and $Ca_2Nb_2O_7$ and the Sr and Ba compounds are not pyrochlores. That $Ca_2B_2^{5+}O_7$ phases should have different crystal structures depending on whether B is Sb, Nb, or Ta, and in spite of the similarity of the effective radii of the three ions, is not peculiar to this stoichiometry. Similar diversity is known to exist for $Li_3B^{5+}O_5$ and, to

[13]The electrostatic lattice energies in ref. 10 are normalized to $a_0 = 10$ Å.

[14]The upper limit would be about 1.72 if the high-pressure pyrochlore $Gd_2Ge_2O_7$ is included.

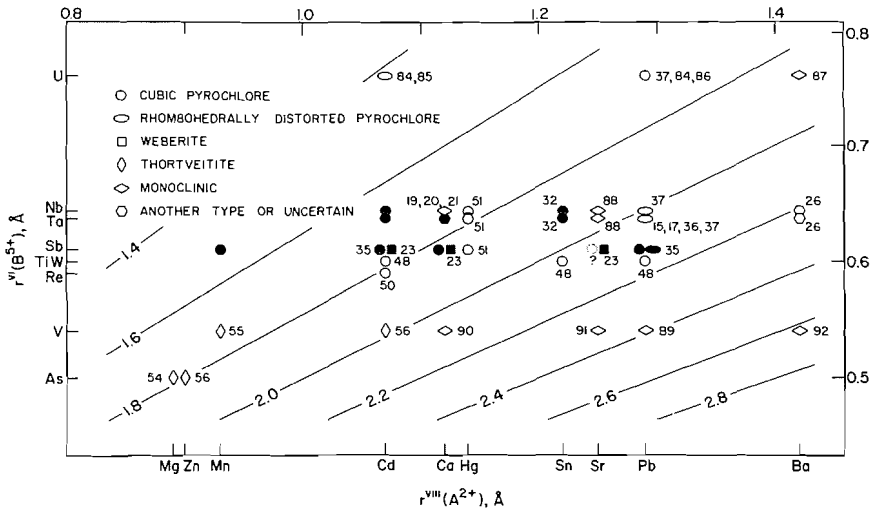

FIG. 4. Existence field of stoichiometric 2–5 oxide pyrochlores in terms of Shannon and Prewitt's ionic radii. The radii of Nb^{5+} and Ta^{5+} are slightly offset relative to one another to separate the points for the niobates and tantalates. The symbol for "thortveitite" implies that the monoclinic crystal structure has been definitely identified as isotypic with thortveitite. The straight lines represent loci of equal $r^{VIII}(A^{2+}):r^{VI}(B^{5+})$ ratios.

a lesser degree, for $A^{2+}B_2^{5+}O_6$ and some other complex oxides; possible reasons for such behavior have been discussed qualitatively by Blasse (57).

Clearly it is significant that in $A_2^{2+}B_2^{5+}O_7$ pyrochlores that form readily and in preference to other structure types the A^{2+} ion has, formally, a d^{10} (or a d^5) configuration, perhaps in relation to polarizability. While $Pb_2Nb_2O_7$ forms a very extensive solid solution with $Cd_2Nb_2O_7$, up to about 90 mol%, the homogeneous $Cd_{2-u}Ca_uNb_2O_7$ *P* phase persists to *u* less than 0.4, in spite of the close similarity of the ionic radii of Cd^{2+} and Ca^{2+} (17). No conclusions can be drawn at present as to possible restrictions on the nature of the B atom. While Sb is the only non-transition B element known to occur in $A_2^{2+}B_2^{5+}O_7$ pyrochlores, there are no other pentavalent non-transition ions of suitable size and existing under ordinary conditions.

Pyrochlore and Weberite Structures as Polymorph Alternatives

A number of observations point to the possibility that the *W* structure is, at least for the stoichiometric antimonates, a dimorph alternative to the *P* structure.

$Cd_2Sb_2O_7$ and $Ca_2Sb_2O_7$ have been reported by some authors to occur with the *P* structure but with the *W* structure by others. In particular, Byström's (23) claim that his $Cd_2Sb_2O_7$ preparation had the *W* structure cannot be discounted, as his conclusion was based on single-crystal diffraction photographs and density of the antimonate. $Ca_2Sb_2O_7(P)$ forms only when antimonic acid and low firing temperatures are employed in the preparation. It transforms into *W* on heating above 700°. However, the existence of $Sr_2Sb_2O_7$ as *W* rather than *P* is undisputed.

When Byström's unit-cell dimensions (converted to Å) of the weberite Cd, Ca, and Sr antimonates are used to calculate "*a*" $= (2V)^{1/3}$ and the resulting values are plotted against $r(A^{2+})$ (Fig. 3*B*), it is seen that the point for $Cd_2Sb_2O_7(W)$ practically coincides with that for $Cd_2Sb_2O_7(P)$, while the points for $Ca_2Sb_2O_7(W)$ and $Sr_2Sb_2O_7(W)$ are significantly above the *P* line. This is true even when an uncertainty as large as ± 0.02 Å is assigned to the $(2V)^{1/3}$ values. Moreover, the three *W* points are on a straight line. The weberites thus have consistently larger (normalized) unit-cell volumes, but the *W* and *P* lines cross at approximately $r(Cd^{2+})$.

The observed facts can be explained if *W* is assumed to be the high-temperature phase of

Can. J. Chem. Downloaded from www.nrcresearchpress.com by 210.87.254.105 on 09/05/12
For personal use only.

Can. J. Chem. Downloaded from www.nrcresearchpress.com by 210.87.254.105 on 09/05/12
For personal use only.

these compounds. The $P \rightarrow W$ transformation temperature of the Ca compound must be above 700° but below 1100° (*cf.* Table 1); under ordinary conditions the transformation may well be irreversible, similar to the perovskite → ilmenite transformation in $CdTiO_3$ (58) and $CdSnO_3$ (59). Unlike for $CdTiO_3$, however, the high-temperature phase, *W*, is less dense than the low-temperature phase, and so increased pressure would tend to convert *W* into *P*, thereby extending the *P* stability field in the *p*–*T* diagram of $Ca_2Sb_2O_7$. For $Cd_2Sb_2O_7$ the $P \rightarrow W$ transformation temperature must be above 1000°: $Cd_2Sb_2O_7$ sealed in a gold tube which was kept for 24 h at 950–1000° and rapidly cooled in air had the *P* structure (35). Unfortunately Byström did not report the firing temperature which produced the *W* phase in his investigation, and the exact stoichiometry of the single crystal he used was not known.

For $Sr_2Sb_2O_7$ the transformation temperature must be well below 700°. Application of high pressure during reactive firing of SrO + $SrSb_2O_6$ or to $Sr_2Sb_2O_7(W)$ at elevated temperatures ought to produce $Sr_2Sb_2O_7(P)$. The latter experiment would verify the assumption of *P* and *W* being polymorphs.

It is not surprising that with ions in the size range of Cd^{2+} and Ca^{2+} both phases occur at ordinary pressures. Cd^{2+} is at the ilmenite–perovskite boundary for $A^{2+}B^{4+}O_3$ compounds, and Ca^{2+} at the calcite–aragonite boundary for $A^{2+}CO_3$ carbonates. However, the fact that we were able to prepare $Pb_2Sb_2O_7(P)$ by Baccaredda's method but not $Sr_2Sb_2O_7(P)$ seems to indicate that factors other than relative ionic size are involved. The readiness with which Pb^{2+} enters pyrochlore structures, in spite of its large size, has occasioned comment already by Aleshin and Roy (11), who suggested the large polarizability of the ion as the reason for this behavior.

The "a" = $V^{1/3}$ of the rhombohedrally distorted P_{rh} dimorph, into which $Pb_2Sb_2O_7(P)$ transforms on heating above 730°, almost falls on the extension of the *W* line in Fig. 3*B*. This would suggest that the P_{rh} structure is an alternative preferred by $Pb_2Sb_2O_7$ to the *W* structure under conditions where the latter might be expected to be stable.

It is odd that the only oxide weberites so far known are the Cd, Ca, and Sr antimonates. Contrary to an earlier claim by Rooksby and White (60), the orthorhombic compounds Ln_3NbO_7 and Ln_3TaO_7 (Ln = La, Nd) are not of the *W* type. Their space group is not *Imm*2, as reported for weberite, but *Pnam* (61; *cf.* also ref. 62). Further representatives of this structure type, $Sm_2B^{3+}NbO_7$ (B = Sm,[15] ... Lu, Y), have recently been reported (63). In addition, the low-temperature forms of La_3SbO_7 and Pr_3SbO_7 have been stated to transform to "highly distorted *P*" structures on heating at 1400°/60 h and 1450°/78 h respectively; neither the low nor the high-temperature structures are of the *W* or thortveitite types (64). However, the spacings and intensities reported for the powder diffraction patterns of these high-temperature forms (64) show strong similarities to those given by Savchenko *et al.* (65) for Ln_3NbO_7 (Ln = La, Ce, Pr).[16] This would suggest that the structures of the two high-temperature antimonates are of the same, or a closely similar, type as those of the orthorhombic niobate phases.

Chlorides

Ferrari and Cavalca's (41) claim that the structure of $BaCd_2Cl_6 \cdot 5H_2O$ is of the *P* type is based on a comparison of photometric powder intensities with those calculated from the model

16(*c*)	16(*d*)	48(*f*)
8 Ba	16 Cd	48 Cl ($x = 0.44$)

(*Fd*3*m*; converted to origin at center in 16(*c*); *B*(overall) = 1.5 Å^2, atomic scattering factors from ref. 66, Vol. 2). The appreciable water content was disregarded. By present-day stan-

[15] Sm_3NbO_7 is stated to be cubic (*F* or *P*) in ref. 60 but orthorhombic (*Pnam*), and transforming to *F* at around 1800°, in ref. 61. While Rooksby and White's (60) standard firing schedule was 1000°/2 h followed by 1400°/2 h, they also mention that in some instances pressed pellets of the ball-milled simple oxides were heated to 1800° and above with an oxyhydrogen flame, without however listing the compositions so treated. It seems likely that their Sm_3NbO_7 was prepared in this way and did not transform to the orthorhombic form, in spite of being possibly annealed at 1300°.

[16] The reported niobate patterns do not contain the weak lines that would correspond to those listed in the antimonate patterns. However, the erratic backgrounds of the diffractograms in Fig. 2 of ref. 65 do not exclude the possibility that additional, weak lines may have been present but escaped notice.

Can. J. Chem. Downloaded from www.nrcresearchpress.com by 210.87.254.105 on 09/05/12
For personal use only.

dards the intensity agreement is poor, but in view of the appreciable scattering powers of Ba and Cd and of the fact that all the Cl atoms are placed in equivalent sites, the approximate correctness of the assumed structure is likely. The water molecules are supposed to be accommodated in the voids of the structure resulting from unoccupied sites (presumably 8(*a*)). No clear suggestion is made as to how as many as 40 H_2O molecules are to be distributed over possible equipoints; this is much the same problem as where to accommodate the water molecules in antimonic acid, which is also of the *P* type (*cf.* ref. 7).

The existence of a dihydrate seems to suggest that the 16 H_2O molecules per unit cell are distributed over the 8(*a*) sites and the available 16(*c*) sites left vacant owing to the incomplete occupancy of 16(*c*) by Ba atoms. Occupancy of 8(*a*) in crystal structures of the *P* type is very common, while mixed Ba + H_2O occupancy of an equipoint has been postulated in the crystal structure of psilomelane, (Ba, $H_2O)_2Mn_5O_{10}$, in which, ideally, Ba:H_2O = 1:2 (67).

It is not obvious where to place the remaining 24 H_2O molecules per unit cell in the structure of the pentahydrate. Eight molecules could be placed in 8(*b*), thus cancelling the contribution to the diffraction intensity from 8(*a*), while 32(*e*) sites might be considered for the last 16 H_2O molecules.

Although single crystals of the pentahydrate were available, a detailed X-ray study was not attempted at this time. The diffuseness of some of the powder reflections led us to believe that crystals for this purpose would have to be grown more slowly and carefully than was the case in the present investigation.

We should like to express our gratitude to the following individuals: Mr. R. Dayal, for examination of polished sections of stibiconite; Dr. P. G. Embrey (British Museum of Natural History), for mineral specimens (marked BM); Dr. M. Falk, for the use of his infrared spectrometer; Dr. C.-H. Huang, for preparing the mixed antimonates; Dr. M. H. Jericho, for making possible the dielectric investigation; Mr. Y. S. Lim, for carrying out the dielectric measurements; and Dr. F. W. D. Woodhams (University of Aberdeen), for obtaining the Mössbauer spectrum of stibiconite.

Financial support by the National Research Council of Canada and by the Geological Survey of Canada through grants to one of us (O.K.) is hereby acknowledged.

1. O. KNOP, F. BRISSE, L. CASTELLIZ, and SUTARNO. Can. J. Chem. **43**, 2812 (1965).
2. F. BRISSE and O. KNOP. Can. J. Chem. **45**, 609 (1967).
3. F. BRISSE and O. KNOP. Can. J. Chem. **46**, 859 (1968).
4. O. KNOP, F. BRISSE, R. E. MEADS, and J. BAINBRIDGE. Can. J. Chem. **46**, 3829 (1968).
5. O. KNOP, F. BRISSE, and L. CASTELLIZ. Can. J. Chem. **47**, 971 (1969).
6. D. J. STEWART and O. KNOP. Can. J. Chem. **48**, 1323 (1970).
7. D. J. STEWART, O. KNOP, C. AYASSE, and F. W. D. WOODHAMS. Can. J. Chem. **50**, 690 (1972).
8. D. J. STEWART, O. KNOP, F. W. D. WOODHAMS, and R. A. HOWIE. To be published.
9. W. R. COOK, JR., and H. JAFFE. Phys. Rev. **88**, 1426 (1952); **89**, 1297 (1953).
10. W. W. BARKER, J. GRAHAM, O. KNOP, and F. BRISSE. Crystal chemistry of oxide pyrochlores. *In* The chemistry of extended defects in non-metallic solids. *Edited by* L. Eyring and M. O'Keeffe. North-Holland Publ. Co., Amsterdam-London, 1970. pp. 198-206.
11. E. ALESHIN and R. ROY. J. Am. Ceram. Soc. **45**, 18 (1962).
12. M. A. AIA, R. W. MOONEY, and C. W. W. HOFFMAN. J. Electrochem. Soc. **110**, 1048 (1963).
13. K. H. BUTLER, M. J. BERGIN, and V. M. B. HANNAFORD. J. Electrochem. Soc. **97**, 117 (1950).
14. R. MAZELSKY. Ph.D. Thesis. University of Connecticut, Storrs, Conn., 1959.
15. B. D. JOYCE. Ph.D. Thesis. Imperial College, University of London, London, England. May 1960.
16. M. BACCAREDDA. Gazz. Chim. Ital. **66**, 539 (1936).
17. F. JONA, G. SHIRANE, and R. PEPINSKY. Phys. Rev. **98**, 903 (1955).
18. J. LAMURE and J.-L. COLAS. C.R. C, **270**, 700 (1970).
19. J. F. ROWLAND, N. F. H. BRIGHT, and A. JONGEJAN. Adv. X-Ray Anal. **2**, 97 (1960); Mines Branch Res. Rept. R48, Dept. Mines Tech. Surveys, Ottawa, Ont. (1959).
20. L. H. BRIXNER and K. BABCOCK. Mater. Res. Bull. **3**, 817 (1968).
21. J. K. BRANDON and H. D. MEGAW. Phil. Mag. [8] **21**, 189 (1970).
22. F. QUEYROUX, M. HUBER, and R. COLLONGUES. C.R. C, **270**, 806 (1970).
23. A. BYSTRÖM. Ark. Kemi Min. Geol. **18A**, No. 21 (1944); **18B**, No. 10 (1944-45).
24. D. A. REEVE. J. Less-Common Met. **17**, 215 (1969).
25. V. A. ISUPOV. Izv. Akad. Nauk SSSR, ser. fiz. **21**, 404 (1957).
26. I. G. ISMAILZADE. Izv. Akad. Nauk SSSR, ser. fiz. **22**, 1485 (1958).
27. O. ROSÉN and A. WESTGREN. Geol. Fören. Stockholm Förhandl. **60**, 226 (1938).
28. M. GASPERIN. C.R. **240**, 2340 (1955).
29. M. GASPERIN. Bull. Soc. franç. Minéral. Crist. **83**, 1 (1960).
30. V. K. TRUNOV, YU. P. SIMANOV, and L. M. KOVBA. Zh. Strukt. Khim. **4**, 277 (1963).
31. A. VORMA and J. SIIVOLA. Bull. Comm. Géol. Finl. **229**, 173 (1967).
32. D. BODIOT. Rev. Chim. Minér. **5**, 569 (1968).

Can. J. Chem. Downloaded from www.nrcresearchpress.com by 210.87.254.105 on 09/05/12
For personal use only.

33. D. J. STEWART, O. KNOP, R. E. MEADS, and W. G. PARKER. To be published.
34. B. MASON and C. J. VITALIANO. Mineral. Mag. **30**, 100 (1953).
35. J.-Y. MOISAN, J. PANNETIER, and J. LUCAS. C.R. C, **271**, 403 (1970).
36. E. C. SUBBARAO. J. Am. Ceram. Soc. **44**, 92 (1961).
37. S. KEMMLER-SACK and W. RÜDORFF. Z. Anorg. Allgem. Chem. **344**, 23 (1966).
38. D. L. BOTHWELL, R. J. DAVIS, and A. A. MOSS. Mineral. Mag. **32**, 664 (1960).
39. G. NATTA and M. BACCAREDDA. Z. Krist. **85**, 271 (1933).
40. C. J. VITALIANO and B. MASON. Amer. Mineral. **37**, 982 (1952).
41. A. FERRARI and L. CAVALCA. Gazz. Chim. Ital. **74**, 117 (1944).
42. A. BENRATH and K. LECHNER. Z. Anorg. Allgem. Chem. **244**, 359 (1940).
43. C. SANDONNINI. Atti R. Accad. Lincei, [5]**20(II)**, 649 (1911).
44. SUTARNO, O. KNOP, and K. I. G. REID. Can. J. Chem. **45**, 1391 (1967).
45. D. T. CROMER and J. T. WABER. Acta Cryst. **18**, 104 (1965).
46. M. TOKONAMI. Acta Cryst. **19**, 486 (1965).
47. D. T. CROMER. Acta Cryst. **18**, 17 (1965).
48. J.-P. MIRANDAY, G. GAUTHIER, and R. DE PAPE. C. R. C, **273**, 970 (1971).
49. C. D. WHISTON and A. J. SMITH. Acta Cryst. **23**, 82 (1967).
50. P. C. DONOHUE, J. M. LONGO, R. D. ROSENSTEIN, and L. KATZ. Inorg. Chem. **4**, 1152 (1965).
51. A. W. SLEIGHT. Inorg. Chem. **7**, 1704 (1968).
52. R. D. SHANNON and C. T. PREWITT. Acta Cryst. **B25**, 925 (1969); **B26**, 1046 (1970).
53. I. N. BELYAEV, L. N. AVER'YANOVA, and I. I. BELYAEVA. Kristallogr. **9**, 280 (1964); Sov. Phys.–Crystallogr. **9**, 220 (1964–65).
54. C. CALVO and K. NEELAKANTAN. Can. J. Chem. **48**, 890 (1970).
55. E. DORM and B.-O. MARINDER. Acta Chem. Scand. **21**, 590 (1967).
56. P. K. L. AU and C. CALVO. Can. J. Chem. **45**, 2297 (1967).
57. G. BLASSE. J. Inorg. Nucl. Chem. **26**, 1191 (1964).
58. J. LIEBERTZ and C. J. M. ROOYMANS. Z. Phys. Chem. N. F. Frankf. **44**, 242 (1965).
59. I. MORGENSTERN-BADARAU, P. POIX, and A. MICHEL. C.R. **256**, 692 (1963); **258**, 3036 (1964).
60. H. P. ROOKSBY and E. A. D. WHITE. J. Am. Ceram. Soc. **47**, 94 (1964).
61. G. TILLOCA, M. PEREZ Y JORBA, and F. QUEYROUX. C.R. C, **271**, 134 (1970).
62. N. S. AFONSKII and M. NEIMAN. Izv. Akad. Nauk SSSR, Neorg. Mater. **3**, 1280 (1967); Inorg. Mater. **3**, 1132 (1967).
63. G. BAUD and J.-P. BESSE. C.R. C, **272**, 1222 (1971).
64. D. K. NATH. Inorg. Chem. **9**, 2714 (1970).
65. E. P. SAVCHENKO, N. A. GODINA, and E. K. KELER. Zh. Priklad. Khim. **39**, 1913 (1966); J. Appl. Chem. USSR **39**, 1797 (1966).
66. Internationale Tabellen zur Bestimmung von Kristallstrukturen. Vol. 1. Gebr. Borntraeger, Berlin. 1935.
67. A. D. WADSLEY. Acta Cryst. **6**, 433 (1953).
68. I. G. ISMAILZADE. Kristallogr. **3**, 85 (1958); Sov. Phys.–Crystallogr. **3**, 78 (1958).
69. F. JONA and G. SHIRANE. Ferroelectric crystals. Pergamon Press, New York. 1962. p. 264.
70. H. R. HOEKSTRA and S. SIEGEL. Inorg. Chem. **8**, 2039 (1969).
71. A. W. SLEIGHT. Inorg. Chem. **8**, 2039 (1969).
72. H. E. SWANSON and R. K. FUYAT. Natl. Bur. Stand. Circular 539, **2**, 27 (1953).
73. C. W. W. HOFFMAN, R. C. ROPP, and R. W. MOONEY. J. Am. Chem. Soc. **81**, 3830 (1959).
74. A. C. MACDONALD and S. K. SIKKA. Acta Cryst. **B25**, 1804 (1969).
75. J. M. LONGO and P. KIERKEGAARD. Acta Chem. Scand. **20**, 72 (1966).
76. S. C. ABRAHAMS, J. M. REDDY, and J. L. BERNSTEIN. J. Phys. Chem. Solids, **27**, 997 (1966).
77. L. KATZ and H. D. MEGAW. Acta Cryst. **22**, 639 (1967).
78. B. MOROSIN and A. ROSENZWEIG. Acta Cryst. **18**, 874 (1965).
79. A. C. SKAPSKI and D. ROGERS. Chem. Commun. 611, (1965).
80. J. P. CUMMINGS and S. H. SIMONSEN. Am. Mineral. **55**, 90 (1970).
81. N. SCHÖNBERG. Acta Chem. Scand. **8**, 240 (1954).
82. S. C. ABRAHAMS, W. C. HAMILTON, and A. SEQUEIRA. J. Phys. Chem. Solids, **28**, 1693 (1967).
83. W. G. MUMME. Am. Mineral. **55**, 367 (1970).
84. W. RÜDORFF, S. KEMMLER, and H. LEUTNER. Angew. Chem. Int. Ed. **1**, 329 (1962).
85. S. KEMMLER-SACK and W. RÜDORFF. Z. Anorg. Allgem. Chem. **354**, 255 (1967).
86. S. KEMMLER-SACK, E. STUMPP, W. RÜDORFF, and H. ERFURTH. Z. Anorg. Allgem. Chem. **354**, 287 (1967).
87. S. KEMMLER-SACK. Z. Naturforsch. **B23**, 1260 (1968).
88. L. H. BRIXNER and J. F. WEIHER. J. Solid State Chem. **2**, 55 (1970).
89. P. BARIAND, F. CHANTRET, R. POUGET, and A. RIMSKY. Bull. Soc. franç. Minéral. Crist. **86**, 117 (1963).
90. V. A. MAKAROV, A. A. FOTIEV, and L. N. SEREBRYAKOVA. Kristallogr. **13**, 333 (1968); Sov. Phys.–Crystallogr. **13**, 268 (1968).
91. A. A. FOTIEV and V. A. MAKAROV. Kristallogr. **14**, 723 (1969); Sov. Phys.–Crystallogr. **14**, 621 (1970).
92. A. A. FOTIEV, V. A. MAKAROV, V. L. VOLKOV, and L. L. SURAT. Zh. Neorg. Khim. **14**, 277 (1969); (Engl. transl.) **14**, 144 (1969).
93. N. M. VORONOV and R. SOFRANOVA. Chem. Abstr. **71**, 25434y, 63708y (1969).
94. J.-M. BRÉGEAULT and P. HERPIN. Bull. Soc. franç. Minér. Crist. **93**, 37 (1970).
95. L. JAHNBERG. J. Solid State Chem. **1**, 454 (1970).
96. J. SHANNON and L. KATZ. Acta Cryst. **B26**, 102, 105 (1970).
97. G. MATHERN and R. WEISS. Acta Cryst. **B27**, 1610 (1971).

Orientational Dependance of Vicinal and Geminal ^{13}C–^{1}H Coupling[1]

J. A. SCHWARCZ[2] AND A. S. PERLIN

Department of Chemistry, McGill University, Montreal, Quebec

Received April 20, 1972

The effect of changes in the relative orientation of vicinal and geminal ^{13}C and ^{1}H nuclei, and in the disposition of adjacent substituents, on coupling between these nuclei has been examined with a variety of ^{13}C-labelled carbohydrates. Compounds synthesized for this purpose include derivatives of D-glucose-1- and -6-^{13}C and L-idose-6-^{13}C, and related lactones, and the measurements have been made with p.m.r. spectra of these compounds. Vicinal ^{13}C–^{1}H coupling, both through C—C and C—O bonds shows an orientational dependance analogous to that for protons: *i.e.*, dihedral angles of 60–100° are associated with smaller coupling (0–3 Hz) than angles of 140–180° (4.5–5.5 Hz); sp^2 carbon produces splittings of almost twice these values. The observed spacing is smaller when an oxygen atom is in the plane of the coupling pathway than when out of plane, both for vicinal and geminal ^{13}C–^{1}H interactions, and the presence of an extra oxygen also may have a notable impact on the geminal interaction. A study of rotational isomerism in these compounds indicates that the characteristics of coupling between ^{13}C and ^{1}H nuclei may fruitfully be compared with those of H–H coupling in the analysis of such dynamic systems.

L'effet du changement d'orientation des noyaux ^{13}C et ^{1}H vicinaux et géminaux et de la disposition des substituants adjacents, sur le couplage entre ces noyaux, a été examiné sur une série de carbohydrates marqués au ^{13}C. Les composés synthétisés dans ce but sont dérivés du ^{13}C-1 et -6 D-glucose, ^{13}C-6 L-idose, les lactones apparantées et les mesures ont été effectuées sur les spectres r.m.n. de ces composés. Le couplage vicinal ^{13}C–^{1}H, à travers les liaisons C—C et C—O, dépend de l'orientation comme dans le cas des protons à savoir, des couplages plus petits pour les angles dièdres de 60–100° (0–3 Hz) que pour les angles de 140–180° (4.5–5.5 Hz), le carbone sp^2 provoquant un dédoublement de presque deux fois ces valeurs. L'écart observé est plus faible lorsqu'un atome d'oxygène se trouve dans le plan du chemin de couplage, à la fois pour les interactions vicinales et géminales ^{13}C–^{1}H et la présence d'un atome supplémentaire d'oxygène peut se répercuter de façon notable sur l'interaction géminale. L'étude de l'isomérie de rotation dans ces composés fournit des caractéristiques de couplage entre ^{13}C et ^{1}H qui peuvent être comparées fructueusement avec les données du couplage H–H dans l'analyse de tels systèmes dynamiques. [Traduit par le journal]

Canadian Journal of Chemistry, **50**, 3667 (1972)

The n.m.r. spectra of ^{13}C-enriched α- and β-D-glucopyranose show that axial H-1 of the β-anomer is much less affected by ^{13}C coupling than is equatorial H-1 of the α-anomer (1). Observed spacings of 5–6 and 1 Hz, attributed respectively to coupling between *anti*-oriented $H_{1\alpha}$–$C_{3\alpha}$ and *gauche* $H_{1\beta}$–$C_{3\beta}$, which are close to values anticipated by Karabatsos *et al.* (2), indicate a steric dependance analogous to that of H–H vicinal coupling in these compounds (3). The current study, which utilizes a variety of sugars and derivatives specifically labelled with carbon-13, furnishes a much more extensive description of orientational influences upon vicinal ^{13}C–H coupling.[3] Also, the suggestion (1) that ^{13}C–H geminal coupling is sterically-dependant now receives verification, and some amplification.

When this study was being undertaken, it appeared that ^{13}C enrichment is essential for satisfactory measurement of vicinal and geminal ^{13}C–H coupling. However, with rapid improvements in Fourier transform n.m.r. spectroscopy such parameters are becoming available from natural abundance ^{13}C n.m.r. (c.m.r.) spectra, and hence potentially should be more widely useful as stereochemical probes.

Synthesis of the ^{13}C enriched carbohydrate derivatives reported herein has been expedited by the methodology of ^{14}C-labelling (4). Accordingly, cyanide-^{13}C has been used in the Kiliani–Fischer reaction to build up the carbon-chain of the sugars from lower homologs. However, a major difference in technique stems from the fact that whereas carrier is usually added to facilitate isolation of the radioactive compound, dilution of the ^{13}C-labelled product has of neces-

[1] Presented at the symposium "Perspectives in NMR for the Seventies", Ottawa, Canada, Feb. 21–23, 1972.

[2] National Research Council of Canada Scholarship Holder, 1969–1972.

[3] A communication (32) that has appeared concurrently with the submission of this paper provides additional examples of this interrelationship, and delineates its significance for the study of nucleoside conformations.

Can. J. Chem. Downloaded from www.nrcresearchpress.com by 210.87.254.42 on 09/05/12
For personal use only.

Can. J. Chem. Downloaded from www.nrcresearchpress.com by 210.87.254.42 on 09/05/12
For personal use only.

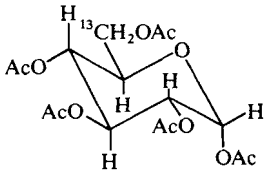

1

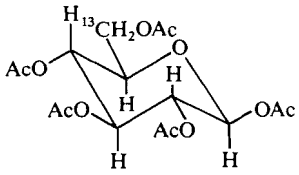

2

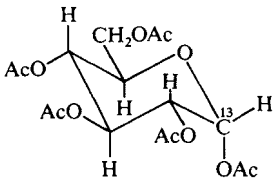

3

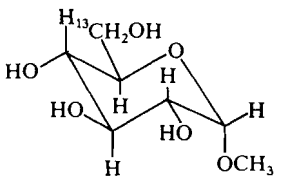

4

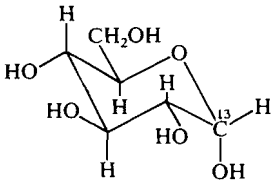

5

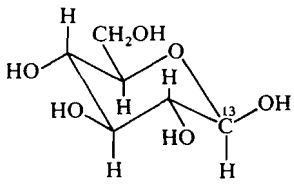

6

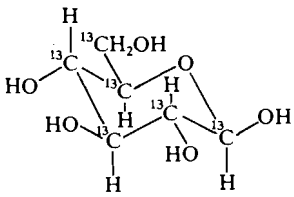

7

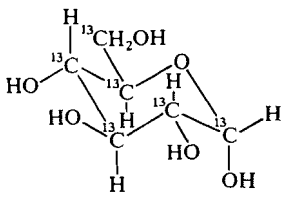

10

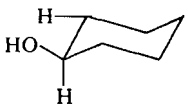

8

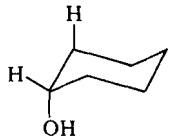

9

sity been avoided and more laborious purification frequently required. Also, in the reduction of intermediate aldonolactones to aldoses, it has been found more satisfactory to use an aluminum chloride-modified hydride reduction (5) than the standard sodium amalgam or other hydride reductions (4). Compounds described below include glucose-1- and -6-^{13}C, and L-idose-6-^{13}C, and a variety of their derivatives. The aldohexosyluronolactones and aldohexonolactones synthesized as intermediates have served to provide comparative information about ^{13}C coupling with hydrogen in systems containing sp^2 hybridized carbon. All spacings were measured from p.m.r. spectra at 100 or 220 MHz, in several instances the higher frequency being

Can. J. Chem. Downloaded from www.nrcresearchpress.com by 210.87.254.42 on 09/05/12
For personal use only.

necessary for adequate separation of the pertinent proton signals from others, including the strong satellite signals (see Experimental).

Vicinal ^{13}C–H Coupling

The compounds used to furnish different examples of vicinal dihedral angle and the ^{13}C–H coupling that they exhibit are listed in Table 1, and angular dependance based on these data is depicted in Fig. 1. It should be emphasized that although the compounds themselves are well-known, angles subtended by the particular bonds under consideration are not known accurately, especially for solutions of these compounds. Proton–proton coupling has, of course, been taken into account wherever possible as a primary point of reference, but since the interpretation of H–H coupling itself sometimes contains substantial uncertainty (6, 7), the approximate nature of the dihedral angles must be recognized. The curve contained in Fig. 1 is incorporated to illustrate that the arrangement of these points bears a resemblance to the type of plot that has been obtained from calculations (8) of vicinal ^{13}C–H coupling in some simpler molecules.

Since the exact solution geometry of the molecules studied is not known, only approximate dihedral angles have been considered. Thus, for compounds **1**–**7** (Table 1) the listed values of 60° are nominal. Within this group of compounds substantial conformational differences may exist, but the range of such variation surely cannot be as large as that observed among the coupling constants *i.e.*, 3.3 to 1 Hz (Table 1). One possible source of such variation is that vicinal ^{13}C–H coupling is exceedingly sensitive in the 60° region of dihedral angle, *i.e.*, analogous to a steeply sloped portion of the Karplus curve for H–H coupling (6, 7, 9). Changes in s-character and/or electronegativity are not likely to account for these differences, because compound **3**, one of those not exhibiting vicinal coupling differs from the others in that the enriched carbon bears an extra oxygen atom; this should give rise to an *increase* rather than a decrease in $J_{^{13}CCCH}$ (10). A more plausible factor appears to be the orientation of oxygen substituents appended to the interaction pathway, as in H–H vicinal coupling (11, 12). Thus the coupling between *gauche* protons is characteristically 2–3 Hz smaller

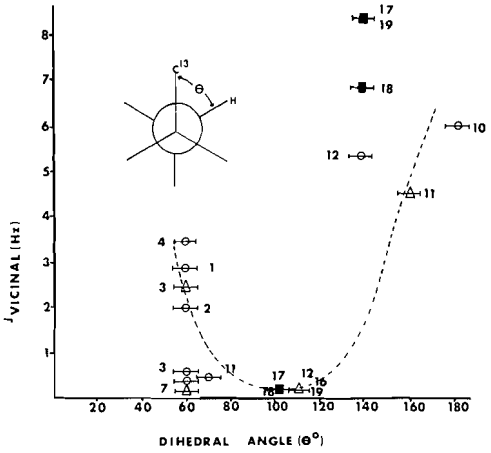

FIG. 1. A plot of ^{13}C–^{1}H vicinal coupling (J, Hz) *vs.* dihedral angle (θ, ±5°) obtained with ^{13}C-labelled carbohydrates (the numbers correspond to compounds listed in Table 1). The broken-line resembles the general shape of the curve plotted from calculated values (8) of J *vs.* θ.

when the O is in the C—C—H plane (as in **9**) than when it is out-of-plane (**8**); *i.e.*, in **9** the O and H are *trans* whereas in **8** they are *gauche*. By analogy, O-3 of **3** is *trans* to ^{13}C-1 and the extent of coupling between ^{13}C-1 and H-5 is correspondingly reduced; the coupling between ^{13}C-3 and H-1 of **7** is similarly affected by virtue of the *trans* relationship between O-1 and ^{13}C-3. Alternatively, O-4 of **1**, **2**, or **4** is *gauche* with respect to ^{13}C-6 and coupling between ^{13}C-6 and H-4 is observed. Additional instances of this kind are given below.

As noted earlier (1) a dihedral angle of nominally 180° is furnished by the spatial relationship between ^{13}C-3 or -5 and H-1 of **10**. The multiplicity of the H-1 signal in this instance shows that more than one interaction of 5–6 Hz is involved. However, the possibility that geminal coupling with ^{13}C-2 also contributes to these broader splittings appears to be small in the light of the discussion presented below.

Other entries in Table 1 deal with five-membered ring, furanose, derivatives. Although these are more flexible than the pyranoses, the fused 1,2-*O*-isopropylidene group that each contains imposes partial rigidity on these rings, and the 3,5,6-tri-*O*-orthoformate (**11**) must have even fewer contributing forms in its conformational itinerary. Especially pertinent in this context is the fact that H_2–H_3 coupling is not ob-

Can. J. Chem. Downloaded from www.nrcresearchpress.com by 210.87.254.42 on 09/05/12
For personal use only.

TABLE 1. ^{13}C–^{1}H spin–spin coupling (Hz) in ^{13}C-enriched carbohydrates

	Compound	Vicinal coupling: Coupling pathway	Vicinal coupling: Dihedral angle (degree)	Vicinal coupling: J_{vic}*	J_{gem}*	Direct coupling	$J_{H,H}$: 4,5	$J_{H,H}$: 5,6	$J_{H,H}$: 5,6′
(1)	1,2,3,4,6-Penta-*O*-acetyl-α-D-glucopyranose-6-^{13}C	$^{13}C_6—C_5—C_4—H_4$	60	2.8	0	148, 150	10	2	4.0
(2)	1,2,3,4,6-Penta-*O*-acetyl-β-D-glucopyranose-6-^{13}C	$^{13}C_6—C_5—C_4—H_4$	60	2	0	148, 150	10	2	4.0
(3)	1,2,3,4,6-Penta-*O*-acetyl-β-D-glucopyranose-1-^{13}C	$^{13}C_1—C_2—C_3—H_3$	60	0	5.0	166			
		$^{13}C_1—O—C_5—H_5$	60	2.5					
(4)	Methyl-α-D-glucopyranoside-6-^{13}C	$^{13}C_6—C_5—C_4—H_4$	60	3.3	0	141, 142	9.5	2.2	5.2
(5)	α-D-Glucose-1-^{13}C	$^{13}C_1—C_2—C_3—H_3$			0	168			
(6)	β-D-Glucose-1-^{13}C	$^{13}C_1—C_2—C_3—H_3$			5.7	160			
(7)	β-D-Glucose-U-^{13}C	$^{13}C_3—C_2—C_1—H_1$	60	0		160			
		$^{13}C_5—O—C_1—H_1$	60	0					
(10)	α-D-Glucose-U-^{13}C	$^{13}C_3—C_2—C_1—H_1$	180	5–6					
(11)	1,2-*O*-Isopropylidene-3,5,6-tri-*O*-orthoformyl-α-D-glucofuranose-6-^{13}C	$^{13}C_6—C_5—C_4—H_4$	70	0	0	148, 154	1.5	0	5.0
		$^{13}C_6—O—C—H$ formyl	160	4.6					
(12)	1,2-*O*-Isopropylidene-α-D-glucofuranose-1-^{13}C	$^{13}C_1—C_2—C_3—H_3$	140	5.5	5.5	186			
		$^{13}C_1—O—C_5—H_5$	110	0					
(13)	1,2-*O*-Isopropylidene-α-D-glucofuranose-6-^{13}C	$^{13}C_6—C_5—C_4—H_4$		2.4	<2	143, 143	8.0	2.7	6.0
(14)	1,2-*O*-Isopropylidene-β-L-idofuranose-6-^{13}C	$^{13}C_6—C_5—C_4—H_4$		0	0	143, 143	7.5	3.5	6.0
(15)	1,2:5,6-Di-*O*-isopropylidene-α-D-glucofuranose-6-^{13}C	$^{13}C_6—C_5—C_4—H_4$		2.7	0	149, 149	8.0	5.5	6.2
(16)	1,2:5,6-Di-*O*-isopropylidene-α-D-glucofuranose-1-^{13}C	$^{13}C_1—C_2—C_3—H_3$	140		5.5	186			
		$^{13}C_1—O—C_5—H_5$	110	0					
(17)	1,2-*O*-Isopropylidene-α-D-glucofuranurono-6,3-lactone-6-^{13}C	$^{13}C_6—C_5—C_4—H_4$	140	9	4.1				
		$^{13}C_6—O—C_3—H_3$	100	0					
(18)	1,2-*O*-Isopropylidene-β-L-idofuranurono-6,3-lactone-6-^{13}C	$^{13}C_6—C_5—C_4—H_4$	140	6.6	0				
		$^{13}C_6—O—C_3—H_3$	100	0					
(19)	D-Mannono-1,4-lactone-1-^{13}C	$^{13}C_1—C_2—C_3—H_3$	140	8.9	4.8				
		$^{13}C_1—O—C_5—H_5$	110	0					

*0 Hz indicates < 1 Hz.

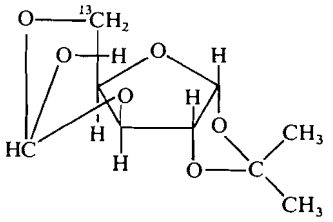

11

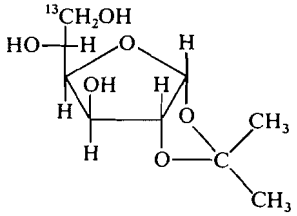

13

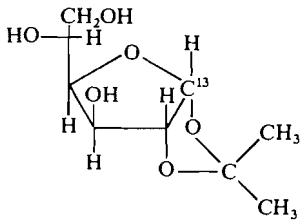

12

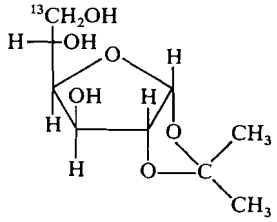

14

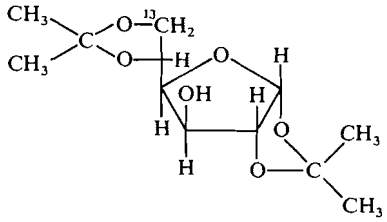

15

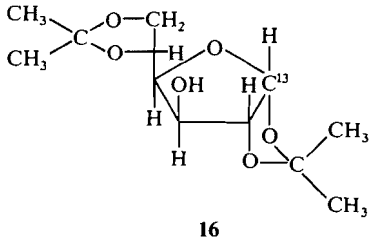

16

served in the spectra of any of these compounds.[4] This is strong evidence that the 2,3-dihedral angle is invariably close to 90°, and that these furanose derivatives may be depicted most satisfactorily by an envelop or twist conformation in which C-3 is above the plane of the ring (14). Such circumstances provide justification for assigning a dihedral angle relationship of about 140° for ^{13}C-1 and H-3 of **12**, and of about 70° for ^{13}C-6 and H-4 of **11**. Little or no coupling is observed in the latter instance, which is consistent with the 60° examples cited above because the ring oxygen of **11** is *anti* with respect to ^{13}C-6.

The introduction of oxygen in place of a carbon along the interaction pathway appears not to alter the general features of these angular dependancies (Table 1). For example, ^{13}C-6 and the ortho-formyl H of **11**, which must be associated through a dihedral angle of close to 160° give rise to a splitting of 4.5 Hz. According to the discussion above on five-membered ring conformations, ^{13}C-1 and H-5 of **12** and **16** are related by a dihedral angle of about 110°, and the observed coupling is ~1 Hz. In **10**, a 180° angle and 5–6 Hz splitting is associated with coupling across the ring oxygen between ^{13}C-5 and H-1 and in **3**, a 60° angle between ^{13}C-1 and H-5 with a splitting of 2.5 Hz. Although the latter value is characteristic of other 60° angles (Table 1), it stands in contrast to the apparent absence of coupling between ^{13}C-1 and H-3 in the same compound. However, it may be noted that the ^{13}C-1–H-5 *gauche* interaction pathway does not contain an in-plane O atom analogous to O-3 and, according to the discussion above, should be expected to generate the size of coupling observed. Another contributing factor could reasonably be differences in the angles C—O—C and C—C—C of the two interaction pathways (10).

An examination (10) of a wide range of com-

[4]The related 3,5,6-tridentate periodate complex of 1,2-*O*-isopropylidene-α-D-glucofuranose also does not show H_2–H_3 coupling (13).

Can. J. Chem. Downloaded from www.nrcresearchpress.com by 210.87.254.42 on 09/05/12
For personal use only.

Can. J. Chem. Downloaded from www.nrcresearchpress.com by 210.87.254.42 on 09/05/12
For personal use only.

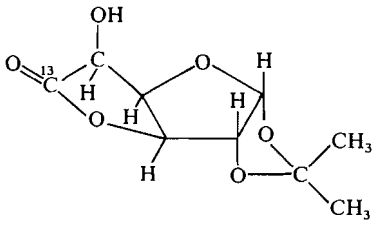

17

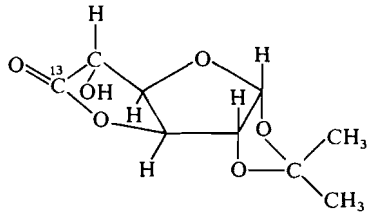

18

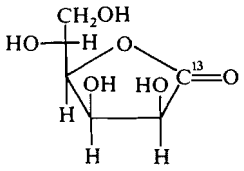

19

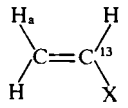

20

pounds has detected no clear correlation between the s-character of a ^{13}C atomic orbital and the magnitude of coupling through three bonds. Hence it is noteworthy that in the current study sp^2 hybridized carbon is found to give rise to much larger values of $J_{^{13}CCCH}$ than encountered previously. Thus, lactones **17**, **18**, and **19** (Table 1), in which the carbonyl carbon is enriched, exhibit vicinal ^{13}C–H coupling that is at least 3–4 Hz larger than observed for sp^3 carbon in this range of dihedral angle. These data provide another indication of the extent to which factors aside from dihedral angle influence the experimentally observed value of J.

Geminal ^{13}C–H Coupling

Geminal coupling also may furnish useful information about the orientation of substituents in cyclic systems. This is suggested by the striking difference between α- and β-D-glucose-1-^{13}C (**5** and **6**), *i.e.* H-2 of the latter anomer exhibits coupling with ^{13}C-1 of 5.7 Hz, whereas H-2 of the α-anomer shows no such coupling (Table 1). Although these findings contrast with the fact that geminal ^{13}C–H splitting of about 4 Hz is seen in the spectra of various acyclic alkyl derivatives (15), it is possible that there is a substantial difference between **5** and **6** in the angle subtended by $^{13}C_1$—C_2—H_2. Furthermore, there appears to be an analogy here to observations (16, 17) made with chloro- or bromoethylene-1-^{13}C (**20**). In **20**, (X = Cl or Br) coupling of −8.3 to −8.5 Hz is found between ^{13}C-1 and the proton *cis* with respect to halogen, but H_a gives rise to a value of +7.1 to +7.5. Similarly, in a series of cyclopropane-1-^{13}C halogen and other derivatives (18) coupling between methylene protons and the geminal ^{13}C is always more negative when the proton and electronegative substituent bear a *cis* relationship, than when *trans*. These geometric differences appear therefore to give rise to opposing contributions to coupling.

^{13}C-1 of β-D-glucose-1-^{13}C (**6**) is strongly coupled with H-2, whereas coupling of this kind is not detected with the α-anomer (**5**). The enriched carbon of these compounds bears two electronegative substituents, the orientation of the ring oxygen relative to the C_2—H_2 bond is the same in both anomers, but OH-1 is either *gauche* or *anti* to H-2 (**21** or 22).[5] Even if the sign of coupling is not known,[6] in view of the data cited above it is reasonable to expect that these orientational differences could account for the widely divergent coupling characteristics observed. As another example, Newman projection **23** shows that the oxygen on ^{13}C-6 of tri-*O*-orthoformate **10** is constrained in a *trans* orientation relative to H-5. Since this arrangement is analogous to that in α-D-glucose-1-^{13}C (**5**) it is pertinent that, again, coupling between the geminal nuclei is not detected.

Compounds **17** and **18** are another pair of epimers that show a striking difference in geminal coupling. In the light of the comments above, the fact that signal H-5 of the D-glucofuranurono-1,4-lactone (**17**) exhibits coupling of 4.1 Hz with

[5]The disposition of the two O atoms relative to each other and their resultant effects on ^{13}C-1 and H-2 would be a more complete description of these geometric relationships.

[6]Although it is more likely to be negative (see refs. 17, 19).

Can. J. Chem. Downloaded from www.nrcresearchpress.com by 210.87.254.42 on 09/05/12
For personal use only.

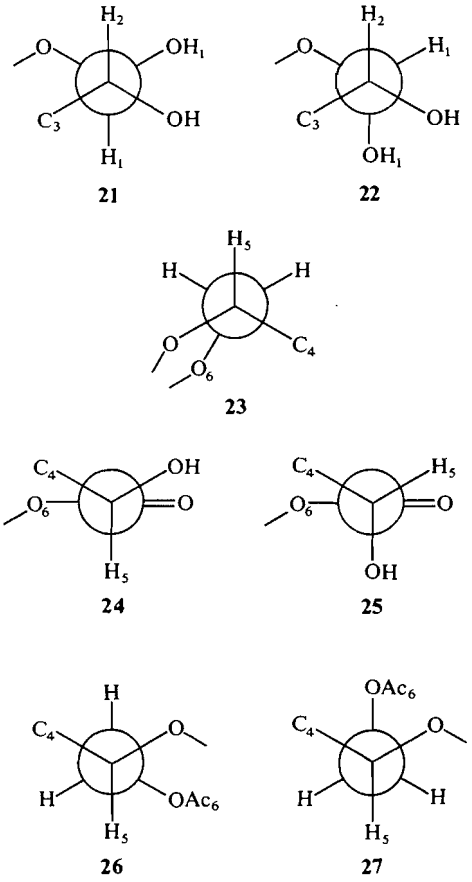

^{13}C-6 whereas H-5 of the L-*ido* isomer (**18**) does not suggests that H-5 cannot be *trans* to O-6 in the favored conformation of **17** (*i.e.*, as in **24**) but approaches that situation in **18** (as in **25**). A geminal coupling of 4.8 Hz is found with the related lactone (**19**). If two projections analogous to **24** and **25** are again envisaged here, this coupling may also be taken as an indication that the arrangement corresponding to **24** predominates.

Geminal coupling is strongly influenced as well by the degree of electronegative substitution on the intervening carbon between the geminal ^{13}C and H nuclei (17). The magnitude of this effect in chloroalkanes is large enough (17) to suggest an explanation for the contrasting impact of labelling at C-1 as compared with C-2 of β-D-glucose. That is, H-1 of β-D-glucose-U-^{13}C (7) is not coupled to ^{13}C-2 whereas, as shown above with **6**, there is coupling between H-2 and ^{13}C-1.[7] However, the presence of the extra O on the carbon (C-1) intervening between ^{13}C-2 and H-1 is expected to strongly reduce coupling relative to the reverse pathway (*e.g.*, an extra chlorine on the intervening carbon in chloroalkanes makes the geminal coupling less negative by about 4 Hz (**17**)). For the same reason, it would be anticipated that ^{13}C-2 is not strongly coupled to H-1 of α-D-glucose-U-^{13}C (**10**) and, as discussed above, that the broad splitting of the H-1 signal produced by this compound is due to vicinal coupling with ^{13}C-3 and -5.

Vicinal and Geminal ^{13}C–H Coupling in Rotamers

Rotational isomerism of carbinol groups exocyclic to five- or six-membered sugar rings has been studied extensively by p.m.r. spectroscopy. However, the interpretation of vicinal H–H coupling within such systems is not straightforward because of time averaging possibilities arising from the rapid interconversion of rotamers. It has been of interest, therefore, to examine vicinal and geminal ^{13}C–H coupling of rotamers of this class as an independant source of information for comparison with the H–H coupling data.

Two preferred rotamers about the 5,6-bond have been advanced for penta-*O*-acetyl-α- or β-D-glucose-6-^{13}C (**1** or **2**): *i.e.*, **26** (20) and **27** (21). Considering possibilities for geminal coupling in the rotamers, a *trans* relationship is found between H-5 and the $^{13}C_6$—O_6 bond in **27**, and a *gauche* one in **26**. Since this corresponds to the inter-relationship described above for β- and α-D-glucose-1-^{13}C (**6** and **5**, respectively), the fact that no geminal coupling is detected between H-5 and ^{13}C-6 appears to be in accord with a preference for **27** rather than **26**.

The p.m.r. spectrum of 1,2-*O*-isopropylidene-α-D-glucofuranose-6-^{13}C (**13**), its L-*ido*-epimer (**14**), or 1,2:5,6-di-*O*-isopropylidene-α-D-glucofuranose-6-^{13}C (**15**), shows that H-4 and -5 are strongly coupled (14) (see Table 1). For each of these compounds, the large value of $J_{H,H}$ observed (7.5–8 Hz) is consistent with a preponderance of either of two rotamers: in one, H-4 and -5 are eclipsed and in the other, antiperi-

[7]The relative orientation of hydrogens and hydroxyl groups is the same in both pathways but, as noted above, the ^{13}C—C—H angles may not be the same.

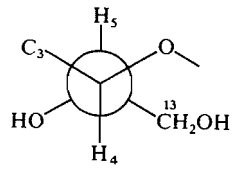

28

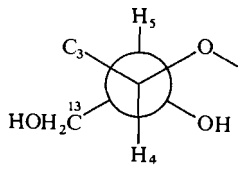

29

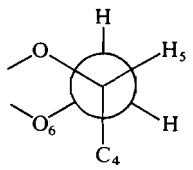

30

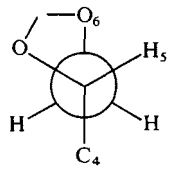

31

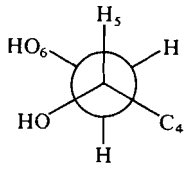

32

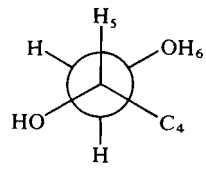

33

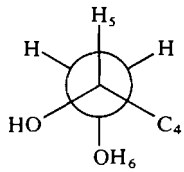

34

planar. On conformational grounds, obviously the latter arrangement (**28**-D-*gluco*, **29**-L-*ido*) is the more likely (14). Hence the small vicinal ^{13}C–H coupling detected (Table 1) agrees with the dihedral angle of nominally 60° relating these two nuclei in **28** or **29**. It is worth noting also that the ring O is *trans* to ^{13}C-6 in **29** but *gauche* in **28** which, according to the data presented above, is consistent in this context with the larger coupling exhibited by the D-*gluco* isomer (**18**).

As to the relative orientation of the 5- and 6-hydroxyl groups in these compounds it is useful to consider the di-*O*-isopropylidene derivative (**15**) because it permits the fewest alternatives: C-5 and C-6 must be constrained in a *gauche* relationship (as in **30** or **31**). Since spin–spin couplings between the 5- and 6-protons are almost equal (Table 1, the smaller value presumably is due to H-6 being *anti* to O-5 (11, 12, 20, 22)), **30** appears to be more favored than **31**. Similarly, from the spectrum of the labelled compound, the fact that geminal coupling between ^{13}C-6 and H-5 is not detectable (Table 1) is more consistent with **30** (in which H-5 is *trans* to O-6), than with **31** (in which they are *gauche*).

$J_{5,6}$ and $J_{5,6'}$ of each of the mono-*O*-isopropylidene derivatives, **13** and **14**, differ substantially (Table 1). However, this does not necessarily mean a preference for rotamers **32** and/or **33**, each of which incorporates an *anti* (6 Hz) and *gauche* (2.7–3.5 Hz) relationship, because the magnitude of the larger spacing (6 Hz) is the same as produced by *gauche* 5,6 orientations in **15** and in "free" rotamers of some other compounds (23, 24). Rotamer **34**, in which O-5 is *trans* to one H-6, is therefore a plausible major contributor. In view of the geminal coupling differences between the anomers of D-glucose-1-^{13}C and of the fact that values for geminal coupling in alkyl derivatives are commonly 4–5 Hz (15–19), the orientations represented by **32** and **33** would both be expected to give rise to perhaps a 4–5 Hz splitting of the H-5 signal due to interaction with ^{13}C-6. Only a small coupling (2 Hz) attributable to the latter source is found in the spectrum of **13**, and none is detected in the spectrum of **14**. Therefore, it appears more likely that an orientation of the primary carbinol group such as shown in **34**, in which H-5 is *trans* to O-6, represents the most highly preferred rotational isomer of these systems.

Directly Bonded ^{13}C–H Coupling

Table 1 lists values measured for coupling between directly bonded ^{13}C and H nuclei. As found earlier with compounds **7** and **10** (1), splitting of the signals produced by anomeric protons (two adjacent O atoms) is substantially larger than that of signals from carbinol protons. Also, there is a difference between anomers (**5** and **10** as compared with **6** and **7**). It is noteworthy that furanose derivatives (**12** and **16**) show much larger anomeric coupling than do the pyranoses. However, a part of this difference may arise from the fact that O-1 of **12** and **16** bears a substituent group, because coupling in other free carbinols is smaller than in substituted carbinols (compare **4**, **13**, **14** with **1**, **2**, **11**, **16**).

Can. J. Chem. Downloaded from www.nrcresearchpress.com by 210.87.254.42 on 09/05/12
For personal use only.

Can. J. Chem. Downloaded from www.nrcresearchpress.com by 210.87.254.42 on 09/05/12
For personal use only.

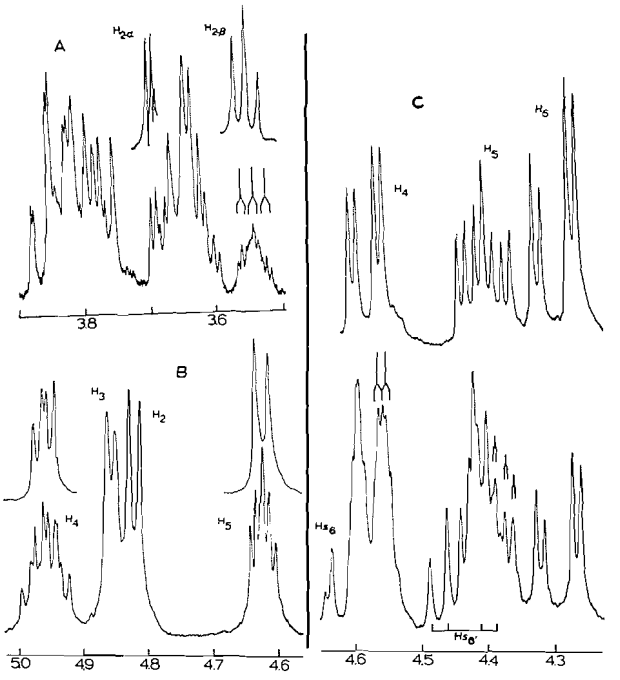

FIG. 2. Partial p.m.r. spectra at 220 MHz of (A) α- and β-D-glucose-1-^{13}C (**5** and **6**) in deuterium oxide; (B) 1,2-*O*-isopropylidene-α-D-glucofuranurono-6,3-lactone-6-^{13}C (**17**) in chloroform-*d*; (C) 1,2-*O*-isopropylidene-α-D-glucofuranose-6-^{13}C (**12**) in deuterium oxide (Hs-satellite signal). In each instance, the upper signals are those produced by the unlabelled compound.

On the other hand, direct coupling is smaller in cyclohexane than in cyclobutane or cyclopropane (25).

Experimental

Measurement of ^{13}C–H Coupling

^{13}C–H coupling was determined by p.m.r. spectroscopy at 100 and/or 220 MHz.[8] In each instance, the spectrum of the unlabelled compound was analyzed with the aid of spin decoupling (aside from those spectra that have been adequately described elsewhere), and extra splitting due to the ^{13}C nucleus then measured from the spectrum of the isotopically-enriched analog. Figure 2 presents some examples of these data:

(*A*) Geminal coupling in α- and β-D-glucose-1-^{13}C (**5** and **6**) in deuterium oxide. The H-2β triplet at 3.3 p.p.m. (inset) (26) becomes a triplet of doublets attributable to coupling of 5.7 Hz with ^{13}C-1; about half of the original triplet remains unaffected because the degree of enrichment is 55% (see below). A comparison of the H-2α quartet (half of which is reproduced in the inset at 3.6 p.p.m.) with the corresponding signal below, shows that the incorporation of isotope at C-1 has no effect.

[8]Recorded at the Canadian 220 MHz NMR Center, Sheridan Park, Ontario, with the helpful assistance of Dr. A. Grey.

(*B*) Vicinal and geminal coupling in 1,2-*O*-isopropylidene-α-D-glucofuranurono-6,3-lactone-6-^{13}C (**17**). Signal H-4 exhibits a splitting of 9.0 Hz ascribable to coupling with $^{13}C_6$ via C-5 and -4, whereas the pathway via O-4 and C-3 does not give rise to a discernible interaction between H-3 and ^{13}C-6. Geminal coupling between H-5 and ^{13}C-6 amounts to 4.1 Hz.

(*C*) Vicinal and geminal coupling in 1,2-*O*-isopropylidene-α-D-glucofuranose-6-^{13}C (**12**). Overlap by satellite signals (centered at 4.45 and 4.62 p.p.m.) produced by the two 6-protons partially obscures this spectrum. Nevertheless, the upfield portion of signal H-4 clearly shows a splitting of 2.4 Hz ascribable to coupling with ^{13}C-6. Similarly, the upfield portion of signal H-5 exhibits a line broadening of 2–2.5 Hz; but it is noteworthy that the component of this signal found at 4.44 p.p.m. is much less influenced by the presence of the isotope, an effect that has not been observed in other spectra of this series.

Synthesis of ^{13}C-Labelled Compounds

In general, syntheses were carried out by procedures closely similar to those that have been described for the corresponding ^{14}C-labelled compound, or by other well-known procedures. Isotope was introduced in all instances by the addition of potassium cyanide-^{13}C, 55% enriched (Merck, Sharpe and Dohme Ltd., Montreal, Quebec), to the appropriate aldose.

The methods of synthesis are summarized below; unless

Can. J. Chem. Downloaded from www.nrcresearchpress.com by 210.87.254.42 on 09/05/12
For personal use only.

otherwise noted, the products were obtained in crystalline form and had correct melting points.

*1,2-O-Isopropylidene-α-*D*-glucofuranurono-6,3-lactone-6-*^{13}*C (17)*: via treatment of 1,2-*O*-isopropylidene-5-aldehydo-α-D-xylodialdo-1,4-furanose with potassium cyanide ^{13}C according to the conditions of Schaffer and Isbell (4, 27).

*1,2-O-Isopropylidene-α-*D*-glucofuranose-6-*^{13}*C (13)*: by reduction of **17** with sodium borohydride in methanol (28).

*1,2:5,6-Di-O-isopropylidene-α-*D*-glucofuranose-6-*^{13}*C (15)*: by acetonation of **13**.

*1,2-O-Isopropylidene-3,5,6-tri-O-orthoformyl-α-*D*-glucofuranose-6-*^{13}*C (11)*: by treatment of **13** with triethyl orthoformate and hydrogen chloride (29).

*Methyl α-*D*-glucopyranoside-6-*^{13}*C (4)*: acid hydrolysis of **13**, followed by treatment of the liberated α,β-D-glucose-6-^{13}C with hot methanolic hydrogen chloride.

*1,2,3,4,6-Penta-O-acetyl-β-*D*-glucopyranose-6-*^{13}*C (1)*: from α,β-D-glucose-6-^{13}C by acetylation with hot acetic anhydride–anhydrous sodium acetate (30).

*1,2,3,4,6-Penta-*D*-acetyl-α-*D*-glucopyranose-6-*^{13}*C (2)*: by treatment of **1** with acetic anhydride–perchloric acid at 40° (31).

*1,2-O-Isopropylidene-β-*L*-idofuranurono-6,3-lactone-6-*^{13}*C (18)*: obtained as the epimeric product in the preparation of **17** (4, 28).

*1,2,-O-Isopropylidene-β-*L*-idofuranose-6-*^{13}*C (14)*: by reduction of **18** with sodium borohydride in methanol (28).

*α- and β-*D*-Glucose-1-*^{13}*C (5 and 6)*: addition of potassium cyanide-^{13}C to D-arabinose, according to the procedure of Schaffer and Isbell (27) yielded crystalline D-glucono-1,5-lactone-1-^{13}C. The latter, on reduction with lithium aluminum hydride–aluminum chloride (5) afforded **5** and **6**. The individual anomers were not isolated in crystalline form, and their p.m.r. spectra were recorded in admixture (see Fig. 2).

*1,2-O-Isopropylidene- and 1,2:5,6-Di-O-isopropylidene-α-*D*-glucofuranose-6-*^{13}*C (12 and 16)*: isolated by fractional crystallization as products of the acetonation of **5** and **6**.

*1,2,3,4,6-Penta-O-acetyl-β-*D*-glucopyranose-1-*^{13}*C (3)*: by treatment of **5** and **6** with hot acetic anhydride–anhydrous sodium acetate (30).

D-*Mannono-1,4-lactone-1-*^{13}*C (19)*: the epimeric product from the cyanohydration of D-arabinose, isolated during the synthesis of **5** and **6** (28).

The authors express their gratitude to the National Research Council of Canada and to the Pulp and Paper Research Institute of Canada for most generous support. They also thank Dr. H. J. Koch, Dr. N. Cyr, and Dr. S. S. Bhattacharjee for helpful discussion and assistance.

1. A. S. Perlin and B. Casu. Tetrahedron Lett. 2921 (1969).
2. G. J. Karabatsos, C. E. Orzech, Jr., and N. Hsi. J. Am. Chem. Soc. **88**, 1817 (1966).
3. R. U. Lemieux, R. K. Kullnig, H. J. Bernstein, and W. G. Schneider. J. Am. Chem. Soc. **79**, 1005 (1957).
4. (*a*) R. Schaffer and H. S. Isbell. *In* Methods in carbohydrate chemistry. Vol. 1. *Edited by* R. C. Whistler and M. L. Wolfrom. Academic Press, N.Y. 1962. pp. 276–285. (*b*) A. C. Neish. Can. J. Chem. **32**, 334 (1954).
5. S. S. Bhattacharjee, A. S. Perlin, and J. A. Schwarcz. Unpublished.
6. M. Karplus. J. Chem. Phys. **30**, 11 (1959).
7. M. Karplus. J. Am. Chem. Soc. **85**, 2870 (1963).
8. N. Cyr, A. S. Perlin, and J. A. Schwarcz. Unpublished.
9. F. A. L. Anet. Can. J. Chem. **39**, 789 (1961).
10. G. J. Karabatsos and C. E. Orzech, Jr. J. Am. Chem. Soc. **87**, 560 (1965).
11. D. H. Williams and N. S. Bhacca. J. Am. Chem. Soc. **86**, 2742 (1964).
12. H. Booth. Tetrahedron Lett. 411 (1965).
13. A. S. Perlin and E. M. von Rudloff. Can. J. Chem. **43**, 2071 (1965).
14. R. J. Abraham, L. D. Hall, L. Hough, and K. A. McLauchlan. J. Chem. Soc. 3699 (1962).
15. G. J. Karabatsos, J. D. Graham, and F. M. Vane. J. Am. Chem. Soc. **84**, 37 (1962).
16. F. J. Weigert and J. D. Roberts. J. Phys. Chem. **73**, 449 (1969).
17. C. J. Jameson and M. C. Damasco. Mol. Phys. **18**, 491 (1970).
18. K. M. Crecely, R. W. Crecely, and J. H. Goldstein. J. Phys. Chem. **74**, 2680 (1970).
19. K. A. McLauchlan and T. Schaeffer. Can. J. Chem. **44**, 321 (1966).
20. L. D. Hall, J. F. Manville, and N. S. Bhacca. Can. J. Chem. **47**, 1 (1969).
21. R. U. Lemieux and J. D. Stevens. Can. J. Chem. **43**, 2059 (1965).
22. B. Coxon. Tetrahedron, **22**, 2281 (1966).
23. A. Maradufu, G. M. Cree, and A. S. Perlin. Can. J. Chem. **49**, 3429 (1971).
24. R. Deslauriers, R. D. Lapper, and I. C. P. Smith. Can. J. Biochem. **49**, 1279 (1971).
25. E. F. Mooney and P. H. Winson. *In* Annual review of n.m.r. spectroscopy. Vol. 2. *Edited by* E. F. Mooney. Academic Press, London. 1969. p. 189.
26. H. J. Koch and A. S. Perlin. Carbohydr. Res. **15**, 403 (1970).
27. R. Schaffer and H. S. Isbell. J. Am. Chem. Soc. **79**, 3867 (1954).
28. H. L. Frush and H. S. Isbell. J. Am. Chem. Soc. **78**, 2844 (1956).
29. K. Freudenberg and W. Jacob. Ber. **80**, 325 (1947).
30. A. P. N. Franchimont. Ber. **12**, 1938 (1879).
31. D. Kruger and W. Roman. Ber. **69**, 1830 (1936).
32. R. U. Lemieux, T. L. Nagabhushan, and B. Paul. Can. J. Chem. **50**, 773 (1972).

The ^{125}Te Mössbauer Absorption Spectra of the Thiourea, Ethylenethiourea, and Tetramethylthiourea Derivatives of Tellurium(II) and Tellurium(IV)

B. M. CHEYNE, C. H. W. JONES, AND P. VASUDEV

Simon Fraser University, Burnaby 2, British Columbia

Received February 17, 1972

The ^{125}Te Mössbauer spectra of a number of Te(II) and Te(IV) complexes of thiourea and related derivatives have been measured. The isomer shifts and quadrupole splittings for several of the compounds are interpreted in terms of a bonding scheme utilizing three-center, two-electron bonds in which the tellurium 5p orbitals participate. The ^{129}I Mössbauer spectrum of *trans*-$TeEtu_2{}^{129}I_2$ is reported and the isomer shift and quadrupole splitting are shown to be consistent with the proposal that the iodine uses only a 5p orbital in bonding to the tellurium.

Nous avons mesuré les spectres Mössbauer, utilisant ^{125}Te de certains complexes de Te(II) et Te(IV) avec la thiourée et de dérivés semblables. Nous interprétons les déplacements d'isomères et les éclatements quadrupolaires de plusieurs de ces composés en termes d'un mécanisme de liaisons à trois centres, deux liaisons électroniques auxquelles participent les orbitales 5p du tellure. Nous rapportons également le spectre Mössbauer utilisant ^{129}I du *trans*-$TeEtu_2{}^{129}I_2$ et montrons qu'il vérifie l'hypothèse que l'iode utilise seulement une orbitale 5p pour sa liaison avec le tellure. [Traduit par le journal]

Canadian Journal of Chemistry, **50**, 3677 (1972)

Introduction

Although the Mössbauer effect for ^{125}Te has been known for some time, relatively few Mössbauer studies of chemical bonding and structure in tellurium compounds have been reported. The bulk of the work which has been carried out to date has been concerned with the metal tellurides (1, 2), tellurium metal (1, 3), the tellurium–oxygen compounds (4–10), and the tellurium hexahalo- and tetrahalo-compounds (4, 6–9, 11, 12). In the present paper we report on the ^{125}Te Mössbauer absorption spectra of a number of thiourea (Tu), ethylene thiourea (Etu), and tetramethylthiourea (Tmtu) derivatives of tellurium.

The compounds investigated contain tellurium in the formal oxidation states of II and IV, and it was of interest to study the dependence of the Mössbauer isomer shift on the oxidation state of the tellurium and also on the nature of the co-ordinated ligands. The geometry around the tellurium atom in these compounds varies from octahedral to square planar and distorted square planar, and the measurement of the quadrupole splitting for these various coordinations was of considerable interest. The presence of *cis–trans* isomerism in some of these complexes was a further point of interest.

Experimental

The Mössbauer spectra (2 × 256 channel mirror image spectra) were recorded using a Nuclear Science and Engineering Corporation AM-1 spectrometer, equipped with a Texas Instruments Inc. CLF-3 cryoflask, and coupled to a Nuclear Data 2200, 512 channel analyzer. The ^{125}Te and ^{129}I spectra were recorded with the source and absorber at 80 °K. For the ^{125}Te studies a 50 mCi ^{125}I/Cu source supplied by New England Nuclear Corporation was used. The 35.5 keV resonant γ-ray was detected, using a Reuter–Stokes Xe/CO_2 proportional detector (2 atm), by monitoring the 6 keV escape peak. The ^{129}I spectrum was recorded using a $Zn^{129m}Te$ source prepared in this laboratory using ^{129m}Te labelled tellurium metal obtained by neutron irradiating ^{128}Te (>99%) at Chalk River Nuclear Laboratories. The $Zn^{129}Te$ source gave an isomer shift of -0.50 ± 0.04 mm s^{-1} against a $Na^{129}I$ absorber.

The velocity scale of the spectrometer was routinely calibrated using an α-Fe_2O_3 absorber and a 5 mCi ^{57}Co/Pd source. The line spacings in the α-Fe_2O_3 spectrum were taken as those given in ref. 13. A National Bureau of Standards $Na_2(Fe(CN)_5NO).2H_2O$ absorber ($\delta = -0.442$ mm s^{-1}, $\Delta = 1.712$ mm s^{-1}) was also measured against the ^{57}Co/Pd source at a number of velocities to determine the zero velocity of the spectrometer. The two absorbers gave consistent values for the velocity calibration. The δ of α-Fe_2O_3 was found to be $+0.20 \pm 0.01$ mm s^{-1}. A number of standard ^{125}Te spectra were also recorded to allow a ready comparison of the data with that of previous work, since Erickson and Maddock (10) have noted that different sources used in ^{125}Te work in the past have resulted in quite different isomer shifts. All ^{125}Te isomer shifts given in the present work are quoted with respect to the ^{125}I/Cu source, while the ^{129}I result is quoted with respect to the ZnTe source.

Can. J. Chem. Downloaded from www.nrcresearchpress.com by 210.87.254.40 on 09/05/12
For personal use only.

TABLE 1. Analytical data

	Compound*	Analysis (%) C† Found	C† Calcd.	N† Found	N† Calcd.	Te‡ Found	Te‡ Calcd.
1	$TeTu_4Cl_2$	8.9	9.6	20.8	22.3	25.2	25.4
2	$TeEtu_4Cl_2$	22.7	22.3	18.5	17.4	20.8	19.8
3	$TeTu_4Br_2$	8.3	8.1	18.3	18.4	21.5	21.6
4	$TeTu_4(SCN)_2$	13.1	12.8	25.7	25.6	23.1	23.3
5	$TeTu_4(NO_3)_2$	8.4	8.6	25.5	25.2	22.7	23.0
6	$[TeTu_3(HF_2)_2]_2$§	8.4	8.3	19.7	19.4		
7	*cis*-$TeTu_2Cl_2$	7.3	6.9	16.1	16.0	36.1	36.4
8	*cis*-$TeTu_2Br_2$	5.4	5.5	12.6	12.8	29.3	29.0
9	*cis*-$TeTu_2I_2$	4.6	4.5	10.6	10.5	23.6	23.9
10	*trans*-$TeEtu_2Br_2$	13.6	14.6	11.0	11.4	26.1	26.0
11	*trans*-$TeEtu_2I_2$	12.5	12.3	9.8	9.6	22.0	21.8
12	$TeTmtuCl_2$	Impure					
13	*trans*-$TeTmtu_2Cl_4$	23.2	22.5	10.6	10.5	23.7	23.9
14	*trans*-$TeTmtu_2Br_4$	Impure					

*Tu = Thiourea, Etu = Ethylenethiourea, Tmtu = Tetramethylthiourea.
†C and N analyses were carried out in this laboratory using a Perkin-Elmer 240, C, H, and N Analyzer.
‡Te analyses were carried out by Bernhardt Microanalytisches Laboratorium.
§The compound $[TeTu_3(HF_2)_2]_2$ was relatively unstable and turned black on standing. Only C and N analyses were performed on this sample.

The mirror-image spectra were independently fitted to Lorentzians using a computer program kindly provided by Stone (Appendix to ref. 14). The ^{125}Te spectra were fitted without any applied constraints, while the ^{129}I spectrum was fitted constraining all the line-widths as being equal. The program generates χ^2 values which provide an estimate of the goodness of fit to the data, and the χ^2 values for the two halves of each spectrum were always in good agreement. The isomer shift and quadrupole splitting values quoted are the mean values obtained from the two halves of the spectrum. The errors in these parameters were calculated from the standard deviations in the line positions. The half-widths quoted are the mean values obtained for the peaks in the first half of each spectrum.

The ^{125}Te compounds were synthesized in high yields using 75% enriched ^{125}Te obtained from Oak Ridge National Laboratories and using the methods described by Foss *et al.* (15–22). Analysis results for sample preparations using unenriched tellurium are shown in Table 1. The samples of $TeTmtu_2Br_4$ and $TeTmtuCl_2$ were found to contain impurities. Foss *et al.* have reported that the former compound contains $TeTmtuBr_2$ as impurity. Because chemical analyses were not carried out on the ^{125}Te-enriched samples, Raman and i.r. spectra were recorded for the isotopically enriched and unenriched samples and were shown to be identical, although Raman spectra were not obtained for $TeTmtu_2Br_4$ and $TeTmtuCl_2$. Where comparisons could be made, the Raman spectra were in reasonable agreement with those of Hendra and Jovic (23, 24). The ^{125}Te absorbers contained 10–15 mg cm^{-2} of ^{125}Te.

The *trans*-$TeEtu_2{}^{129}I_2$ was synthesized using ^{129}I obtained as $Na^{129}I$ in aqueous solution from Oak Ridge National Laboratories. This absorber contained *ca.* 10 mg cm^{-2} ^{129}I.

Results

The ^{125}Te Mössbauer parameters for the thiourea, ethylenethiourea, and tetramethylthiourea compounds investigated are given in Table 2. The computed fits to the spectra were judged statistically acceptable (the 5% limit on χ^2 is 284 for 247 degrees of freedom) for all of the compounds except $TeTmtu_2Br_4$ and $TeTmtuCl_2$, where the samples were known to contain small amounts of impurities. Sample spectra are shown in Fig. 1. The values given in Table 2 for tellurium metal, tellurium dioxide, and zinc telluride are those measured in the present work.

The ^{129}I Mössbauer data for *trans*-$TeEtu_2{}^{129}I_2$ is presented later in the paper.

Discussion

Structures of the Compounds Studied

Before discussing the significance of the measured Mössbauer parameters, it is relevant to briefly review the structures of these compounds. Foss and co-workers (25–29) have made a detailed and systematic study of the structures of many of the thiourea and related derivatives of Te(II) and Te(IV) and the results of their investigations together with those of

Can. J. Chem. Downloaded from www.nrcresearchpress.com by 210.87.254.40 on 09/05/12
For personal use only.

TABLE 2. Mössbauer parameters

	Compound*	δ†,‡ (mm s^{-1})	Δ‡ (mm s^{-1})	2Γ (mm s^{-1})§	χ^2 for 247 degrees of freedom‖
1	$Te^{II}Tu_4Cl_2$	$+0.93 \pm 0.06$	15.62 ± 0.06	7.5	286
2	$Te^{II}Etu_4Cl_2$	$+0.93 \pm 0.12$	16.00 ± 0.21	8.4	289
3	$Te^{II}Tu_4Br_2$	$+1.00 \pm 0.06$	15.65 ± 0.06	7.7	269
4	$Te^{II}Tu_4(SCN)_2$	$+0.86 \pm 0.07$	16.11 ± 0.07	7.1	273
5	$Te^{II}Tu_4(NO_3)_2$	$+0.87 \pm 0.10$	15.19 ± 0.18	7.9	285
6	$[Te^{II}Tu_3(HF_2)_2]_2$	$+0.80 \pm 0.06$	15.55 ± 0.06	7.8	257
7	*cis*-$Te^{II}Tu_2Cl_2$	$+0.74 \pm 0.06$	15.22 ± 0.10	7.9	261
8	*cis*-$Te^{II}Tu_2Br_2$	$+0.74 \pm 0.06$	15.35 ± 0.07	7.7	263
9	*cis*-$Te^{II}Tu_2I_2$	$+0.80 \pm 0.08$	15.39 ± 0.12	6.9	261
10	*trans*-$Te^{II}Etu_2Br_2$	$+1.00 \pm 0.06$	17.37 ± 0.04	7.5	281
11	*trans*-$Te^{II}Etu_2I_2$	$+0.85 \pm 0.08$	16.16 ± 0.12	7.6	255
12	$Te^{II}TmtuCl_2$	$+0.58 \pm 0.08$	17.90 ± 0.12	6.8	318
13	*trans*-$Te^{IV}Tmtu_2Cl_4$	$+1.60 \pm 0.06$	0	9.5	275
14	*trans*-$Te^{IV}Tmtu_2Br_4$	$+1.58 \pm 0.07$	0	6.3	361
15	TeO_2 (nat.)	$+0.91 \pm 0.16$	6.74 ± 0.2	6.9	224
16	Te-metal	$+0.68 \pm 0.08$	7.16 ± 0.11	8.7	285
17	ZnTe (nat.)	-0.07 ± 0.08	0	7.9	264

*Tu = Thiourea, Etu = ethylenethiourea, Tmtu = tetramethylthiourea.
†δ with respect to an ^{125}I/Cu source.
‡δ and Δ are the mean values computed from the two halves of the mirror image spectrum. The errors are calculated from the standard deviations of the line-positions.
§2Γ is the average full width at half-maximum for the first half of the mirror image spectrum.
‖χ^2 are again those for the first half of the mirror-image spectrum.

Husebye and George (30) are presented in condensed form in Table 3. The table shows the geometrical configuration for four different types of compounds, and the bond lengths and bond orders for several specific cases. The bond orders were determined using the formula (31)

$$D(n) - D(1) = -0.60 \log n$$

where $D(n)$ is the bond length, $D(1)$ is the sum of the covalent radii, and n is the bond order.

Compound **6**, $[TeTu_3(HF_2)_2]_2$, does not appear in Table 3 and is reported to contain a dimeric cation, $(TeTu_3)_2^{4+}$, in which each tellurium is bonded to two terminal and two bridging thiourea ligands in an approximately square-planar arrangement (29). The compound $TeTmtuCl_2$, which again is not included in Table 3, is reported (22) to have *trans*-chlorines, with a fourth, long chlorine contact *trans* to the sulfur completing a planar arrangement about the tellurium.

Foss (25) has proposed that the bonding in many of these compounds may be described in terms of three-center, two-electron bonds, in which the tellurium employs one 5p orbital to bond to two ligands at 180° to each other. The common occurrence of bond angles close to 90° and 180° at the tellurium, together with the relatively long, weak Te—S bonds observed in those compounds containing the *trans*-S—Te—S configuration, are cited (25) as evidence for such a bonding scheme. For *cis*-$TeTu_2Br_2$, where the Te—S bond is much shorter than that in $TeTu_4^{2+}$ while the Te—Br bond is much longer than that in *trans*-$TeEtu_2Br_2$, it is apparent that as one bond increases in strength the bond *trans* to it weakens, further supporting the three-center, two-electron model. Finally, Foss (25) points out that Hendra and Jovic (23) have interpreted the Raman and i.r. spectra of the $TeTu_4^{2+}$ complexes as showing that the Te—S bond is weaker than the I—Cl bond in the isoelectronic ICl_4^- ion, where three-center bonds involving the iodine 5p orbitals have previously been proposed.

The Isomer Shifts

We may now turn to a discussion of the ^{125}Te isomer shifts. The results of Table 1 show that in all the $Te^{II}Tu_4X_2$, *cis*-$Te^{II}Tu_2X_2$, and *trans*-$Te^{II}Etu_2X_2$ compounds, the Mössbauer isomer shifts span a small range from 0.74 to 1.00 mm s^{-1}, while in the *trans*-$Te^{IV}Tmtu_2X_4$ com-

Can. J. Chem. Downloaded from www.nrcresearchpress.com by 210.87.254.40 on 09/05/12
For personal use only.

Can. J. Chem. Downloaded from www.nrcresearchpress.com by 210.87.254.40 on 09/05/12
For personal use only.

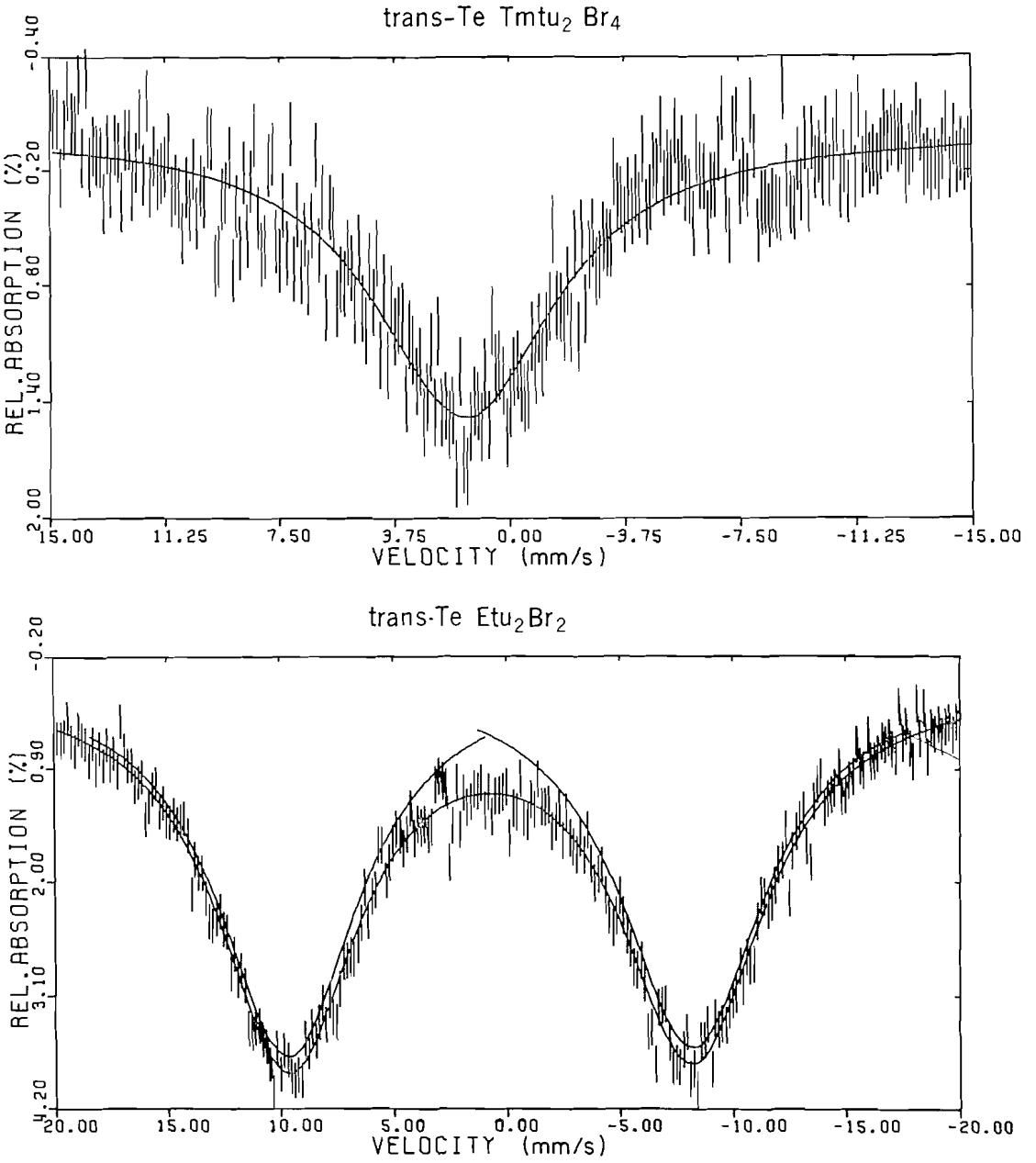

FIG. 1. The ^{125}Te Mössbauer spectra of some of the thiourea complexes as measured at 80 °K.

pounds the isomer shifts are about 1.6 mm s^{-1}. Thus there is a clear differentiation between the isomer shifts for the Te(II) and Te(IV) compounds, the values being more positive for the higher oxidation state. Assuming (32) that $\Delta R/R$, the change in nuclear radius divided by the radius of the ground state, is positive for ^{125}Te, the observed trend in isomer shifts may be readily understood in terms of the bonding scheme proposed by Foss. Thus if the bonding in these compounds occurs principally through the tellurium 5p orbitals, the 5s^2 electrons forming

TABLE 3. The structures of the tellurium–thiourea compounds

	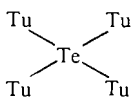	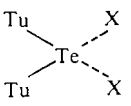	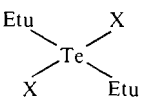	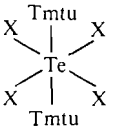
	$TeTu_4X_2$ (**1–5**) Square planar	*cis*-$TeTu_2X_2$ (**7–9**) Square planar with 2 short contacts and 2 long contacts	*trans*-$TeEtu_2X_2$ (**10–11**) Square planar	*trans*-$TeTmtu_2X_4$ (**13–14**) Octahedral
Te—S	2.69 Å(0.34), X = Cl*	2.48 Å(0.97), X = Cl† 2.47 Å(0.97), X = Br	2.69 Å(0.34), X = Br, I‡	2.70 Å(0.34), X = Cl§ 2.71 Å(0.34), X = Br
Te—X		2.92 Å(0.12), X = Cl		2.54 Å, 2.52 Å } (0.54), X = Cl
		3.05 Å(0.13), X = Br	2.78 Å (0.36), X = Br 2.92 Å (0.47), X = I	2.71 Å, 2.69 Å } (0.53), X = Br

*Reference 26.
†Reference 27.
‡Reference 28.
§Reference 30.

a stereochemically inactive lone-pair, then the removal of 5p electrons would result in deshielding of the $5s^2$ electrons from the nucleus. This would correspond to an increase in $|\psi_s(0)|^2$ and a more positive Mössbauer isomer shift for the higher oxidation states on the tellurium. This is certainly consistent with the trend in isomer shifts observed for the Te(II) and Te(IV) compounds.

The compounds $TeTu_4X_2$ are observed to have the same isomer shift within the error of the measurement, consistent with the presence of the $TeTu_4^{2+}$ cation in each case. As would be expected, the anions X have little influence on the isomer shift. The *trans*-$TeEtu_2X_2$ compounds have the same isomer shift as that for $TeTu_4^{2+}$ and thus there is no measurable effect on δ of substituting the *trans*-X—Te—X three-center bond for the *trans*-S—Te—S configuration. (This point is further borne out by the fact that the *trans*-$TeTmtu_2X_4$ compounds do not have a measurable quadrupole splitting, as will be discussed below.) The Etu ligand and the Tu ligand play an identical role in bonding to the tellurium, as demonstrated by the close agreement of the parameters for $TeTu_4Cl_2$ and $TeEtu_4Cl_2$.

In *cis*-$TeTu_2Cl_2$ and -Br_2 the isomer shifts appear to be less positive than those for $TeTu_4X_2$ and *trans*-$TeEtu_2X_2$, although this difference may not be statistically significant. In the case of *cis*-$TeTu_2X_2$, the Te—S bond order approaches one, and the p-electron density on the tellurium is evidently about the same as that in the $TeTu_4^{2+}$ cation, thus resulting in approximately the same isomer shift. This is certainly consistent with the three-center, two electron bonding scheme, two short, strong Te—S bonds contributing about the same 5p electron density as four long, weak Te—S bonds.

The question arises as to whether the small variations in the isomer shifts for the Te(II) compounds are significant. It may be noted that in *cis*-$TeTu_2Cl_2$ and -Br_2 the geometry around the tellurium shows significant deviations from a regular square-plane (27). Thus the Te—S and Te—X planes intersect at an angle of 11 to 12°, while the S—Te—S bond angles are 93 to 95°. This may indicate the presence of some tellurium 5s character in the bonding, which would tend to make the isomer shift more negative. It is unfortunate that the errors in the isomer shifts do not allow any firm conclusion to be drawn on this point. In the case of $TeTmtuCl_2$ the isomer shift is certainly much less positive than in $TeTu_4^{2+}$ and this would be consistent with the presence of a small amount of s-character. This point will be referred to again following a discussion of the quadrupole splittings.

Before concluding this section, it is of interest to extend the above discussion of the pure p-bonding model a little further. The bonding

Can. J. Chem. Downloaded from www.nrcresearchpress.com by 210.87.254.40 on 09/05/12
For personal use only.

Can. J. Chem. Downloaded from www.nrcresearchpress.com by 210.87.254.40 on 09/05/12
For personal use only.

scheme proposed above is analogous to that which has previously been used to describe the bonding in the interhalogen compounds. In the ^{129}I and ^{127}I Mössbauer studies of the alkali iodides and the iodine interhalogen compounds (33–35), the isomer shifts have been shown to be directly related to the electron populations of the 5p orbitals on the iodine, the $5s^2$ electrons again forming a non-bonding lone-pair. The iodine 5p electron populations have been independently obtained from n.m.r. and dynamic quadrupole resonance data and this has led to the establishment of a relationship between $\delta(^{129}I)$ and *hp*, where *hp* is the number of p-holes in the closed $5p^6$ configuration of the iodine (34):

$$\delta(^{129}I)_{ZnTe} = 1.50\,hp - 0.54$$

A similar analysis (36, 37) for tellurium has been attempted, using the halogen n.q.r. data of Nakamura *et al.* (38) for the TeX_6^{2-} (X = Cl, Br, I) ions to determine the charge on tellurium. However, this approach is dependent on certain assumptions regarding the bonding s-character of the tellurium and the halogen in these ions (36). A more direct approach is to relate the isomer shift/*hp* plot for ^{129}I to that for ^{125}Te through the ratio of the isomer shifts for these two isotopes (36, 39), $\delta(^{125}Te)/\delta(^{129}I) = +0.29$. This leads to the proposed expression (36, 37) for tellurium

$$\delta(^{125}Te)_{I/Cu} = 0.44\,hp - 0.23$$

where $\delta(^{125}Te)$ is in mm s^{-1}. This expression may be used to examine the *hp* values for the Te(II) and Te(IV) compounds.

The average isomer shift for the $TeTu_4^{2+}$ cation obtained from compounds **1–5** is $+0.92 \pm 0.05$ mm s^{-1}. This corresponds to an *hp* value of 2.5 ± 0.2, where the error includes an estimate of the error in the above isomer shift expression. For the *trans*-$TeTmtu_2X_4$ compounds, since there is no measurable quadrupole splitting the three 5p orbitals on the tellurium must have very similar populations. It may then be proposed that *hp* for these compounds should be just 3/2 times that of the *hp* value for $TeTu_4^{2+}$, *i.e.* 3.9 ± 0.3. The isomer shift of *ca.* 1.6 mm s^{-1} for $TeTmtu_2X_4$ corresponds to an *hp* value of 4.0 ± 0.2, in good agreement with the predicted value. In this admittedly naïve approach, it is assumed that the change in formal oxidation state of the tellurium does not lead to a change in the effective population of the bonding 5p orbitals. In support of such a proposal we may note the following: (*1*) The Te—S bond lengths in $Te^{II}Tu_4^{2+}$ and in *trans*-$Te^{IV}Tmtu_2X_4$ are essentially the same (30). (However, it must be noted that the Te—Br bond in *trans*-$TeTmtu_2Br_4$ is somewhat shorter than that in *trans*-$TeEtu_2Br_2$.) (*2*) For $I^{I}Cl_2^-$, $I^{III}Cl_4^-$, and $I^{V}Cl_6^-$, the bonding 5p orbital populations on the iodine in the three-center Cl—I—Cl configurations were found to be very similar in all three cases, despite the increase in charge on the central atoms (40).

On the basis of the above we may conclude that the values of the isomer shifts for the Te(II) and Te(IV) compounds are consistent with a three-center two-electron bonding scheme utilizing the tellurium 5p orbitals.

The Quadrupole Splittings

Turning to a discussion of the quadrupole splittings, Δ, the immediate point to note is the very large value of Δ for compounds **1–12**. The very large electrostatic field gradient present in all these instances is consistent with the square planar structure for these compounds, and has its origin in the unequal population of the $5p_x$, $5p_y$, and $5p_z$ orbitals.

The similarity in the quadrupole splittings for compounds **1–12** indicates that a similar imbalance in the 5p orbital populations exists in all cases. Within the context of the bonding scheme discussed above, this would imply a similar occupancy of the in-plane $5p_x$ and $5p_y$ orbitals in each case, the $5p_z$ orbital defining the axis of the electrostatic field gradient and containing two, non-bonding electrons.

Thus the similarity in quadrupole splittings for $TeTu_4^{2+}$, *cis*-$TeTu_2X_2$, and *trans*-$TeEtu_2X_2$ is quite consistent with the similarity in isomer shifts for these compounds.

For the case of the $TeTu_4^{2+}$ ion it is possible to examine the significance of the quadrupole splitting in more detail. The quadrupole splitting for a molecule, e^2qQ mol, is related to the imbalance in the p orbital populations through the following expressions (34)

$$e^2qQ \text{ mol} = -Upe^2qQ \text{ atom}$$

Can. J. Chem. Downloaded from www.nrcresearchpress.com by 210.87.254.40 on 09/05/12
For personal use only.

where e^2qQ atom is the quadrupole splitting which would arise in the electrostatic field gradient generated by one $5p_z$ electron, Q is the nuclear quadrupole moment of the 3/2 excited state, and Up is defined by:

$$Up = -Uz + \frac{Ux + Uy}{2}$$

where Ux, Uy, and Uz are the populations of the $5p_x$, $5p_y$, and $5p_z$ orbitals, respectively.

Thus an interpretation of e^2qQ mol in terms of Ux, Uy, and Uz requires a knowledge of e^2qQ atom. A value for e^2qQ atom is available through the calculation of Barnes and Smith (41) of q for one $5p_z$ electron, and through the calculated value of Q, reported by Shikazono (1), Violet *et al.* (3), and Pasternak and Bukshpan (5). These calculations yield

$$e^2qQ \text{ atom} = 570 \pm 60 \text{ Mc s}^{-1}$$

For the centrosymmetric $TeTu_4^{2+}$ ion the asymmetry parameter, η, is zero and

$$e^2qQ_{mol} = 2\Delta = 31.4 \pm 0.3 \text{ mm s}^{-1}$$
$$= 880 \pm 10 \text{ Mc s}^{-1}$$

Then

$$Up = -1.5 \pm 0.2$$

If it is assumed that $Uz = 2$, and $Ux = Uy$, then

$$Ux = Uy = 0.5 \pm 0.2$$

The large uncertainty in Ux and Uy arises from the large uncertainty in e^2qQ atom.

It is of interest to determine whether the isomer shift data are consistent with the above value of Up. Since

$$hp = 6 - (Ux + Uy + Uz)$$

then, if $Uz = 2$ and $Ux = Uy$

$$hp = 4 - 2Ux$$
$$= -2Up$$

The analysis of the isomer shift data presented above yielded a value of $hp = 2.6 \pm 0.2$, and this would lead to $Up = -1.3 \pm 0.1$. Within the very large error, the values of Up obtained from the quadrupole splittings (-1.5 ± 0.2) and isomer shifts (-1.3 ± 0.1) for the $TeTu_4X_2$ compounds are reasonably consistent, providing further support for a pure p-bonding model in these compounds. It may be noted that the above analysis also indicates that the quadrupole splittings observed here are reasonably consistent with the previously reported (1, 3, 5) value of Q of *ca.* 0.2 barn.

Returning to the discussion concerning the compound $TeTmtuCl_2$, in this instance it cannot be assumed that $Ux = Uy$ and thus it is not possible to calculate Up from δ. However, simple inspection of the data shows that while the value of Δ is large, and consistent with a square planar configuration about the tellurium with a large imbalance in 5p electron density between the z axis and x–y plane, the value of δ is significantly smaller than in the other square planar compounds. A rationale for the low value of δ in this compound may lie in the participation of a small amount of tellurium 5s character in the bonding. This would make δ significantly smaller, since as in iodine compounds the participation of even a small fraction of the 5s electrons in bonding would have a direct, large effect in decreasing $|\psi_s(0)|^2$. Thus, the bonding may be principally 5p in character, leading to the large value of Δ, with a small amount of 5s character leading to a small δ. That the bonding in this compound differs from that in the other thiourea derivatives may also explain the formation of an essentially 3-coordinate tellurium with *trans*-chlorines in this instance, the *trans*-$TeEtu_2X_2$ compounds being fully 4-coordinate.

For the compounds *trans*-$TeTmtu_2X_4$ where the Te^{IV} is fully octahedrally co-ordinated, a quadrupole splitting would be expected if the Te—S and Te—X bonds had different bonding characteristics. The absence of a measurable quadrupole splitting in these compounds clearly points to the very similar populations of the $5p_x$, $5p_y$, and $5p_z$ orbitals on the tellurium.

The ^{129}I Mössbauer Absorption Spectrum of trans-$TeEtu_2{}^{129}I_2$

As a further extension of this work, the ^{129}I Mössbauer absorption spectrum of $TeEtu_2{}^{129}I_2$ was measured against a $Zn^{129m}Te$ source. The spectrum was fitted (constraining the linewidths as being equal) to the independent Lorentzians shown in Fig. 2 and the isomer shift and quadrupole coupling calculated using the standard expressions (34). The values ob-

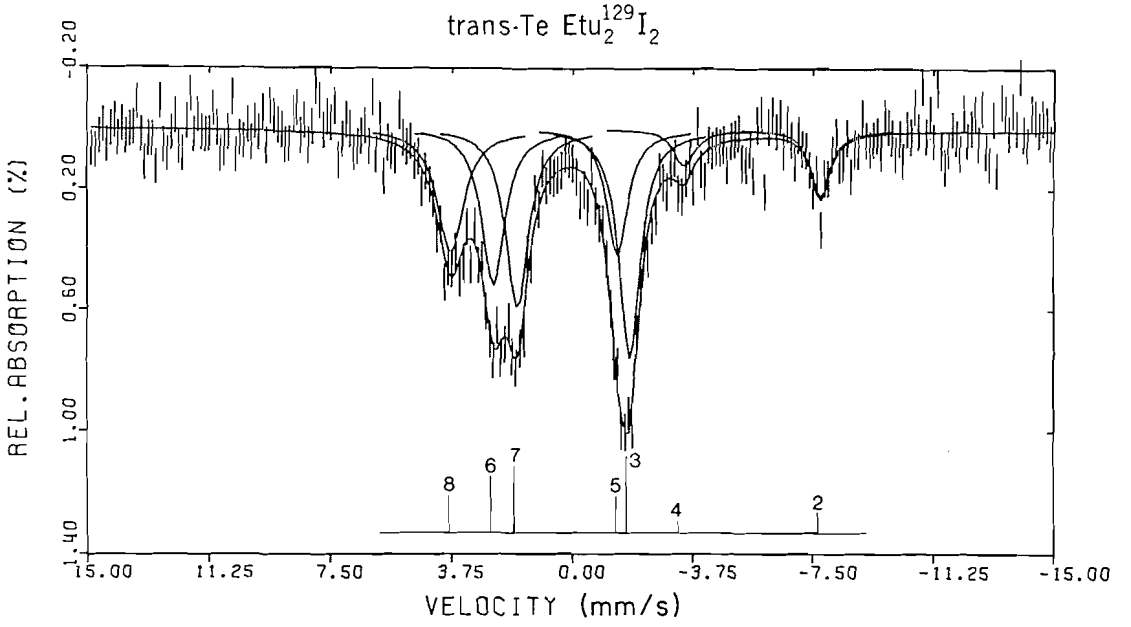

FIG. 2. The ^{129}I Mössbauer spectrum of *trans*-TeEtu$_2{}^{129}$I$_2$ at 80 °K. The computed lines shown had intensities in good agreement with the theoretically predicted values (5).

tained were $\delta = +0.010 \pm 0.001$ mm s^{-1} with respect to ZnTe and $e^2qQ^{129} = -597.7 \pm 6.2$ Mc s^{-1}, $\eta = 0$. The computed line-width was 1.1 mm s^{-1}. The small percent absorption in this experiment derives from the fact that a ^{129m}Te source was used rather than a ^{129}Te source.

If the iodine employs pure p electrons in bonding to the tellurium then the expression (34)

$$\delta = 1.50\,hp - 0.54$$

may be used to calculate hp on the iodine. This yields a value of $hp = 0.37 \pm 0.01$. Furthermore, a value of Up for the iodine may be calculated from e^2qQ^{129}

$$Up = \frac{-e^2qQ^{129}\ \text{mol}}{e^2qQ^{129}\ \text{atom}} = +\frac{597.7}{1605} = +0.37 \pm 0.01$$

where e^2qQ^{129} atom $= e^2qQ^{127}$ atom $\times$ 0.7.

For the case of pure σ-bonding through an iodine p orbital to the tellurium, Up should be equal to hp since

$$hp = 6 - (Ux + Uy + Uz)$$
$$= 2 - Uz \qquad \text{if } Ux = Uy = 2$$

while

$$Up = -Uz + \frac{Ux + Uy}{2}$$
$$= 2 - Uz \qquad \text{if } Ux = Uy = 2$$

Thus, since $hp = Up$, δ and e^2qQ are consistent with the proposal that iodine bonds to the tellurium through an iodine 5p orbital. If there was significant iodine 5s character in the bond then δ would yield a value of hp significantly smaller than Up, while if π-bonding was present Up would be smaller than hp.

The authors wish to thank the National Research Council of Canada for a grant supporting this research, and Dr. F. Brown, Head, Solid State Research Branch, A.E.C.L. Chalk River, for assisting in the production of the Zn^{129m}Te source.

1. N. SHIKAZONO. J. Phys. Soc. Jap. **18**, 925 (1963).
2. G. ALBANESE, C. LAMBORIZIO, and I. ORTALLI. Nuovo Cimento (B), **50**, 65 (1967).
3. C. E. VIOLET, R. BOOTH, and F. WOOTEN. Phys. Lett. **5**, 230 (1963).
4. C. E. VIOLET and R. BOOTH. Phys. Rev. **144**, 225 (1966).
5. M. PASTERNAK and S. BUKSHPAN. Phys. Rev. **163**, 297 (1967).

Can. J. Chem. Downloaded from www.nrcresearchpress.com by 210.87.254.40 on 09/05/12
For personal use only.

6. P. JUNG and W. TRIFTSHÄUSER. Phys. Rev. **175**, 512 (1968).
7. M. L. UNLAND. J. Chem. Phys. **49**, 4514 (1968).
8. S. L. RUBY and G. K. SHENOY. Phys. Rev. **186**, 326 (1969).
9. T. C. GIBB, R. GREATREX, N. N. GREENWOOD, and A. C. SARMA. J. Chem. Soc. (A), 212 (1970).
10. N. E. ERICKSON and A. G. MADDOCK. J. Chem. Soc. (A), 1665 (1970).
11. S. E. GUKASYAN, B. Z. IOFA, A. N. KARASEV, S. I. SEMENOV, and V. S. SHPINEL. Phys. Stat. Sol. **37**, 91 (1970).
12. V. S. SHPINEL, V. A. BRYUKHANOV, V. KOTHEKAR, B. Z. IOFA, and S. I. SEMENOV. Symp. Faraday Soc. **1**, 69 (1967).
13. Mössbauer Effect Data Index 1958-1965, *Edited by* A. M. Muir, K. J. Ando, and H. M. Coogan. Interscience, New York. 1966. p. 26.
14. G. M. BANCROFT, W. K. ONG, A. G. MADDOCK, R. H. PRINCE, and A. J. STONE. J. Chem. Soc. (A), 1966 (1967).
15. O. FOSS and S. HAUGE. Acta Chem. Scand. **13**, 1252 (1959).
16. O. FOSS and S. HAUGE. Acta Chem. Scand. **15**, 1615 (1961).
17. O. FOSS and S. HAUGE. Acta Chem. Scand. **15**, 1616 (1961).
18. O. FOSS and S. FOSSEN. Acta Chem. Scand. **15**, 1618 (1961).
19. O. FOSS and S. FOSSEN. Acta Chem. Scand. **15**, 1620 (1961).
20. O. FOSS and S. HAUGE. Acta Chem. Scand. **15**, 1623 (1961).
21. O. FOSS and W. JOHANNESSEN. Acta Chem. Scand. **15**, 1939 (1961).
22. O. FOSS and W. JOHANNESSEN. Acta Chem. Scand. **15**, 1940 (1961).
23. P. J. HENDRA and Z. JOVIC. J. Chem. Soc. (A), 735 (1967).
24. P. J. HENDRA and Z. JOVIC. J. Chem. Soc. (A), 911 (1968).
25. O. FOSS. Pure and Appl. Chem. **24**, 31 (1970).
26. K. FOSHEIM, O. FOSS, A. SCHEIE and S. SOLHEIMSNES. Acta Chem. Scand. **19**, 2336 (1965).
27. O. FOSS, K. JOHNSEN, K. MAARTMANN-MOE, and K. MARØY. Acta Chem. Scand. **20**, 113 (1966).
28. O. FOSS, H. M. KJØGE and K. MARØY. Acta Chem. Scand. **19**, 2349 (1965).
29. O. FOSS and S. HAUGE. Acta Chem. Scand. 2395 (1965).
30. S. HUSEBYE and J. W. GEORGE. Inorg. Chem. **8**, 313 (1969).
31. L. PAULING. The nature of the chemical bond. University Press, Ithica, N.Y. 1960. p. 255.
32. K. V. MAKARIUNAS, R. A. KALINAUSKAS, and R. I. DAVIDONIS. Sov. Phys. JETP. **33**, 848 (1971).
33. D. W. HAFEMEISTER, G. DE PASQUALI, and H. DEWAARD. Phys. Rev. **135**, B1089 (1964).
34. S. BUKSHPAN and T. SONNINO. J. Chem. Phys. **48**, 4442 (1968).
35. G. J. PERLOW and M. R. PERLOW. J. Chem. Phys. **45**, 2193 (1966).
36. J. J. JOHNSTONE, C. H. W. JONES, and P. VASUDEV. In press.
37. B. M. CHEYNE, J. J. JOHNSTONE, and C. H. W. JONES. Chem. Phys. Lett. **14**, 548 (1972).
38. D. NAKAMURA, K. ITO, and M. KUBO. J. Am. Chem. Soc. **84**, 163 (1962).
39. J. L. WARREN, C. H. W. JONES, and P. VASUDEV. J. Phys. Chem. **75**, 2867 (1971).
40. C. H. W. JONES and J. L. WARREN. J. Chem. Phys. **53**, 1740 (1970).
41. R. G. BARNES and W. V. SMITH. Phys. Rev. **93**, 95 (1954).

Can. J. Chem. Downloaded from www.nrcresearchpress.com by 210.87.254.40 on 09/05/12
For personal use only.

The Influence of the Substrate on Hydrogen – Water Deuterium Exchange over Carbon Supported Platinum[1]

NORMAN HENRY SAGERT AND RITA MARY LOUISE POUTEAU

Research Chemistry Branch, Whiteshell Nuclear Research Establishment, Atomic Energy of Canada Limited, Pinawa, Manitoba, R0E 1L0

Received May 19, 1972

Rate data for hydrogen – water deuterium isotope exchange are reported for a number of platinum on carbon catalysts whose carbon supports were graphitized to varying degrees before the metal was deposited on the support. The exchange over platinum black was studied for comparison. Over carbon supported catalysts, the rate was almost independent of hydrogen pressure and increased approximately linearly with water pressure. The rate controlling step seems to be the transfer of deuterium between chemisorbed hydrogen atoms and physisorbed HDO.

Activation energies for the rate determining step decreased from 14 kcal/mol over unsupported platinum to as low as 2 kcal/mol over highly graphitized supports. Rates increased with heat treatment temperatures up to 2100 °C. These effects are ascribed to electron transfer from the carbon support to the metal, resulting in a weaker Pt—H bond, and faster exchange. However they may be partially the result of non-linear adsorption of water.

Nous rapportons les données de vitesse d'échange isotopique hydrogène–deutérium dans l'eau pour certains catalyseurs de platine sur carbone dont les supports de carbone furent préalablement traités au graphite à différents degrés, avant que le métal soit déposé sur le support. Pour comparer, nous avons étudié l'échange sur noir de platine. Avec des catalyseurs sur carbone, la vitesse est à peu près indépendante de la pression d'hydrogène et croît approximativement linéairement avec la pression de l'eau. L'étape limitante semble être le transfert de deutérium entre les atomes d'hydrogène chemisorbés et le HDO physisorbé.

Les énergies d'activation pour l'étape limitante diminuent de 14 kcal/mol pour le platine sans support jusqu'à des valeurs aussi faibles que 2 kcal/mol pour les supports à haute teneur en graphite. On remarque une augmentation de vitesse lors de traitements par la chaleur, à des températures allant jusqu'à 2100 °C. Ces effets sont imputés à un transfert d'électron du support de carbone vers le métal, résultant en un lien Pt–H plus faible et un échange plus rapide. Ils peuvent toutefois résulter partiellement de l'adsorption non-linéaire de l'eau. [Traduit par le journal]

Canadian Journal of Chemistry, **50**, 3686 (1972)

Introduction

The role of the support in reactions catalyzed by supported metal catalysts has become an active field of research in recent years (1, 2). While it was previously thought that the support only provided a physical base for the small metal crystallites and also provided some stability against sintering, more recent studies have shown that the support can change the chemical nature of the metal, and thus affect the reaction being studied (1–3). This is an effect on the reaction catalyzed by the metal and is not to be confused with the role of the support in dual function catalysis (4). Since the metal function is being studied, data must be interpreted on a unit metal surface area basis, so these studies have only become possible with the development of methods for measuring metal surface areas in the presence of supports (5).

We previously reported a study of the particle size effect for the catalysis of hydrogen–water deuterium exchange over silica supported platinum (6). The present work is an examination of the role of the support on the same reaction. The reaction was chosen because it is a simple deuterium exchange and no chemical changes occur in the catalyst bed with time. Heat effects can be entirely neglected. If the amount of D_2O is kept low, the only product is HD. This simplifies the kinetics and makes the reaction easy to follow by measuring HD (6, 7). The reaction is also of interest as a method of producing heavy water commercially. Carbons were used as supports because the electronic properties of carbons can easily be varied over a wide range by heat treating to different temperatures (8, 9).

Early in the work, some very unusual temperature dependences were noted. Thus it was necessary to study the kinetics in somewhat more detail than in our previous work on silica supported platinum (6).

[1]AECL No. 4317.

Can. J. Chem. Downloaded from www.nrcresearchpress.com by 210.87.254.5 on 09/05/12
For personal use only.

Can. J. Chem. Downloaded from www.nrcresearchpress.com by 210.87.254.5 on 09/05/12
For personal use only.

Experimental Procedures

Kinetic Studies

Rate measurements were carried out in a flow system at atmospheric pressure as previously described (6). To investigate the rates as a function of hydrogen pressure, provision was made for mixing argon with the hydrogen before the combined stream was saturated with water containing 4% D_2O. Hydrogen and argon flow rates were measured using rotameters calibrated at the pressure of operation with a positive displacement flow meter. Purified argon did not interfere with the gas chromatographic determination of HD. The catalyst reduction procedures were identical to those used earlier (6) except that the final reduction was done at 300 °C.

Materials

The sources and purification of water, D_2O, and hydrogen have been described (6). High purity argon (99.999% min) was passed over copper turnings at 450 °C to remove oxygen and through a Dry Ice trap to remove water.

Platinum black was prepared by reducing an alkaline solution of sodium hexachloroplatinate with formaldehyde at 12 °C. The precipitate was washed carefully to remove sodium, dried at 100 °C, and pre-reduced in a hydrogen stream at 250 °C.

Graphon, which is highly graphitized Spheron 6 (2800 °C) and Thermax, a medium thermal black, were obtained commercially and sieved to 60–80 mesh unless otherwise stated. The Thermax was graphitized to various degrees by heating at different temperatures for 60 min in pure graphite containers in a furnace fitted with graphite heating elements. The heat treatments were done in the presence of 100 Torr of helium. Temperatures were measured with thermocouples or with an optical pyrometer. Catalysts were prepared from the graphitized carbons by wetting with a solution containing the required amount of chloroplatinic acid, followed by evaporating to dryness with stirring. The catalysts were then dried overnight at 100 °C and pre-reduced in 15 g batches at 250 °C. Most catalysts contained 0.5% platinum by weight. The exact amount was determined by atomic absorption spectroscopy (10).

Surface Areas

Total surface areas were measured by adsorption of nitrogen at 77 °K as previously described (6). Metal surface areas were measured by Boudart's hydrogen titration technique (11). To do these titrations, catalysts were subjected to the reduction used for kinetic studies and were then evacuated to 2×10^{-6} Torr while cooling to room temperature. Dry air was slowly admitted to the system and left in contact with the metal for 30 min. The sample was pumped at room temperature until pressures well below 10^{-5} Torr were attained. A hydrogen chemisorption isotherm was then measured volumetrically (6). Techniques used for electron microscopy have been described earlier (6).

Results

With water containing 4% deuterium, the deuterium is virtually all present as HDO and only reaction 1 need be considered.

[1] $$HDO + H_2 \rightleftarrows H_2O + HD$$

Under these conditions the reaction rate k, in moles of D_2 per gram of catalyst per second is given (6, 7) by eq. 2,

[2] $$k = \frac{F}{(\alpha + \gamma)W} \ln \frac{n_e - n_0}{n_e - n}$$

where F is the hydrogen flow rate in mol/s, W is the catalyst weight in g, α is the reciprocal of the equilibrium constant for reaction 1, and γ is the ratio of the hydrogen pressure to the water pressure. The n's refer to deuterium concentrations, before reaction (n_0), after reaction (n), and at equilibrium (n_e). The methods for calculating n_e and α have been given previously (6). Thus k may be calculated from the initial slope of a plot of $\ln (n_e - n_0)/(n_e - n)$ against W/F and unless otherwise noted, all the k's quoted are calculated from such plots, which were generally linear to fairly high conversions (6). This linearity is usually considered to show that the data is not affected by external diffusion, although Chambers and Boudart (12) have shown that this is not a conclusive proof.

At reaction temperatures of 100 °C the catalysts lost about 15% of their activity during a day. The activity was restored by reactivating at 300° for 12 h in a hydrogen stream. At lower temperatures the losses in activity were higher, but were also restored by reactivating at 300 °C. Over half the loss in activity occurred in the first hour, so catalysts were generally conditioned in the water–hydrogen stream for about 40 min. At temperatures over 100 °C the loss in activity was small.

Calculations based on equations given by Satterfield (13) showed that the efficiency factor for pore diffusion was probably close to unity. To confirm this, the particle diameter was varied over a threefold range. Figure 1 shows results obtained for 0.5% Pt on Graphon catalysts. Within experimental error no significant change in rate with particle size was observed even for the fastest rates. Thus the efficiency factor is probably greater than 0.9 (ref. 13, p. 143).

The variations of the rates with hydrogen and water pressure are shown in Figs. 2 and 3 for 0.5% Pt on ungraphitized Thermax and Thermax graphitized at 2100 °C. Figure 2 shows the dependence on the partial pressure of hydrogen, measured at 80 °C with 175 Torr of water vapor. The range and precision of this data were limited by experimental restrictions. Only a

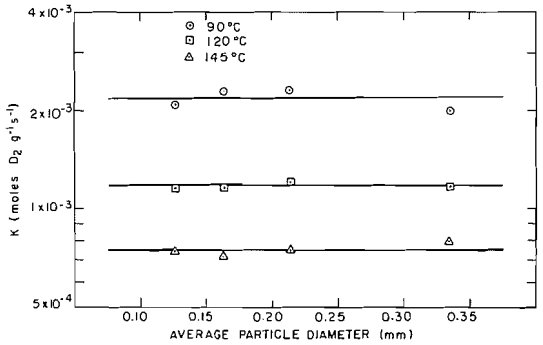

FIG. 1. Influence of catalyst particle size on the reaction rate over $\frac{1}{2}\%$ Pt on Graphon: $P_{H_2O} = 175$ Torr.

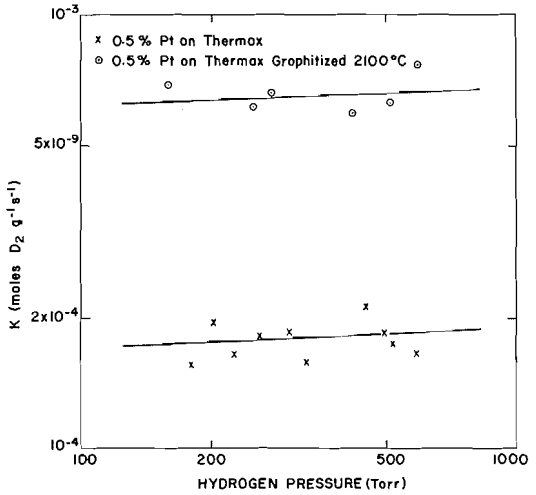

FIG. 2. Variation of rate with changing hydrogen pressure for the two catalysts indicated: reaction temperature = 80 °C; $P_{H_2O} = 175$ Torr.

fourfold variation in hydrogen pressure was possible. Furthermore data could only be obtained at a single hydrogen flow, so the precision is not as good as for other data presented. The reaction order with respect to hydrogen, given by the slope of the lines, is 0.0 ± 0.2. Figure 3 shows the dependence of the rate on water pressure at 100 °C for the same two catalysts. An eightfold range of water pressures was covered and total flow rates could be varied. The order for the 0.5% Pt on ungraphitized Thermax is 0.92. With the graphitized support, the order at lower pressures, as given by the line through the points, is 1.15. In the range of conditions studied, the rate equation is well represented by eq. 3.

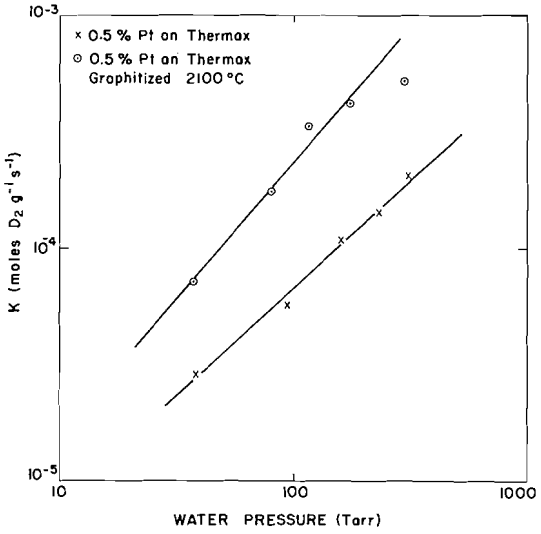

FIG. 3. Variation of rate with changing water pressure for the two catalysts indicated: reaction temperature = 100 °C.

$$[3] \qquad k = k' P_{H_2O}^{1.0 \pm 0.2} \, P_{H_2}^{0.0 \pm 0.2}$$

The lack of hydrogen pressure dependence probably means that a full coverage of hydrogen is maintained. This would be expected from hydrogen chemisorption experiments on supported platinum (5, 11, 14). The dependence on water pressure can be accounted for in terms of variations of adsorbed water coverage. Let us assume that the rate is proportional to water coverage and that this water coverage can be represented by a Langmuir isotherm.

$$[4] \qquad k = k_0 \theta_{H_2O} = k_0 \left(\frac{b P_{H_2O}}{1 + b P_{H_2O}} \right)$$

By plotting k^{-1} *vs.* $P_{H_2O}^{-1}$ an estimate of θ_{H_2O} is obtained which, at 100 Torr H_2O, is 0.1 for platinum on the ungraphitized support and 0.06 for platinum on the graphitized support. Thus water coverages are low and hence proportional to water pressure as observed.

Surface areas were determined using the titration technique of Benson and Boudart (11).

$$[5] \qquad PtO + \tfrac{3}{2}H_2 \rightarrow PtH + H_2O$$

It has been shown recently that eq. 5 is an excellent approximation to the stoichiometry (15). Results of these titrations are shown in Fig. 4. The flat portion of the isotherm was extrapolated

Can. J. Chem. Downloaded from www.nrcresearchpress.com by 210.87.254.5 on 09/05/12
For personal use only.

TABLE 1. Platinum surface areas and total surface areas of catalysts

Support	Heat treatment temperature (°C)	% Platinum	Platinum surface area (m^2/g)	Platinum particle diameter (Å)	Total surface area (m^2/g)
Thermax	—	0.512	0.239	60.9	13.1
Thermax	750	0.479	0.207	64.4	—
Thermax	1000	0.580	0.343	47.3	8.0
Thermax	1400	0.504	0.171	82.9	7.4
Thermax	1800	0.428	0.152	78.8	7.2
Thermax	2100	0.525	0.112	131.1	7.2
Graphon	2800	0.460	0.239	53.8	45.6
Platinum Black	—	~100	0.877	~3000	—

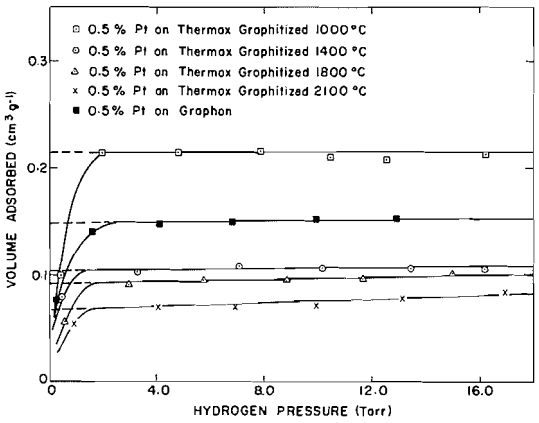

FIG. 4. Hydrogen "PtO Titrations" for Pt areas of a number of catalysts.

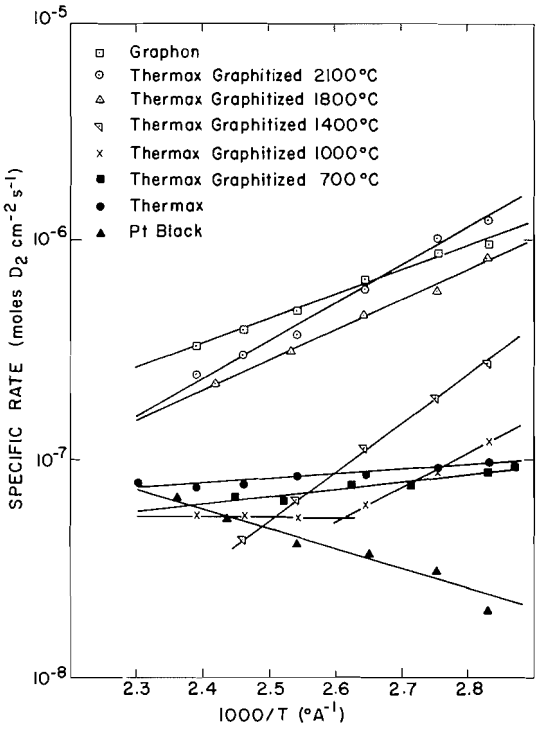

FIG. 5. Arrhenius plots for the catalysts studied: P_{H_2O} = 175 Torr.

to zero pressure and the value for the volume of hydrogen adsorbed was used to calculate the surface area, assuming each platinum atom has an area of 8.9 $Å^2$ (16). The areas correspond to spherical platinum particles with diameters in the range 65 ± 15 Å (Table 1), with the exception of the catalyst prepared over Thermax graphitized at 2100 °C, which has platinum particles of 130 Å diameter. These diameters were verified from electron micrographs which also showed the particles to be approximately spherical on ungraphitized substrates, but to be elongated on graphitized ones. Total surface areas of the Thermax supports are decreased slightly by graphitizing.

Arrhenius plots of the temperature dependence of the rates are shown in Fig. 5. The rates are expressed as specific rates by dividing the rate per gram of catalyst by the platinum area per gram as determined from the hydrogen titrations. For comparison, specific rates are shown over unsupported platinum black, which had been heated in hydrogen to reduce and stabilize its surface area. The unsupported platinum black shows an apparent activation energy of 4.0 kcal/mol, whereas the activation energies over platinum supported on ungra-

Can. J. Chem. Downloaded from www.nrcresearchpress.com by 210.87.254.5 on 09/05/12
For personal use only.

Can. J. Chem. Downloaded from www.nrcresearchpress.com by 210.87.254.5 on 09/05/12
For personal use only.

TABLE 2. Activation energies for hydrogen–water deuterium exchange on supported platinum

Support	E_{app}	Reference	E_0
Al_2O_3	6.5	20	~16.5
SiO_2	7.5	6	17.5
None	4.0	This work	14.0
Thermax	−1.0	This work	9.0
Graphon	−5.1	This work	4.9
Thermax (2100)	−7.9	This work	2.1

phitized carbon were in the range zero to about 1 kcal/mol negative. With graphitized supports the activation energies become progressively more negative. The results are summarized in Table 2. With supported catalysts no large differences in rate (±30%) and no significant changes in activation energies (±2 kcal/mol) were noted when the inert glass beads were replaced with Teflon or with unplatinized Graphon. Therefore the diluent does not seem to be playing any large part in the reaction, and Graphon is catalytically inert. Similarly, with unsupported platinum no changes in rates were noted within ±20%, and no changes in apparent activation energies within ±1 kcal/mol were noted when the beads were replaced with Teflon or Graphon. Thus whatever the mechanism which produces the changes in rates and activation energies, it does not operate over the distances involved in a mechanical mixture of platinum and Graphon.

Discussion

We have shown above that the rate expression over the region of pressures and temperatures investigated can be satisfactorily expressed by eq. 4. This dependence can be explained in terms of a mechanism involving surface exchange between hydrogen chemisorbed on the platinum and weakly adsorbed water. Hydrogen is adsorbed to the extent of a full monolayer at the temperatures and pressures used (5, 11, 14), and water vapor is not expected to prevent hydrogen chemisorption on platinum (17, 18). The heat of adsorption of water vapor has been shown to be 11 kcal/mol on reduced unsupported platinum (17, 19), whereas the heat of vaporization of water is 10.6 kcal/mol. Thus the net heat of adsorption of water is small on unsupported platinum, and probably fairly small in our system as well. Following Rolston and Goodale (20), we will assume that adsorption of hydrogen and water take place on different sites, I and II, and write the following mechanism

[6] $$H_2(g) + 2(I) \rightleftarrows 2H_{ads}$$

[7] $$HDO(v) + (II) \rightleftarrows HDO_{ads}$$

[8] $$HDO_{ads} + H_{ads} \rightleftarrows H_2O_{ads} + D_{ads}$$

[9] $$H_{ads} + D_{ads} \rightleftarrows HD(g) + 2(I)$$

[10] $$H_2O_{ads} \rightleftarrows H_2O(v) + (II)$$

Rolston and Goodale (20) have derived the rate expression for this scheme, assuming reaction 8 to be rate limiting. They noted that if the transfer rate per gram can be expressed in terms of coverage, then the differential rate (7, 20) is

[11] $$\text{Rate/g} = k(N - \alpha n) = \tfrac{1}{2}(k_8\theta_{HDO}\theta_H - k_{-8}\theta_{H_2O}\theta_D)$$

where N is the mole fraction of deuterium in the water leaving the reactor. If equilibria between the gas and surface phases are established then

[12] $$\theta_{HDO} = \theta_{H_2O}K_7K_{10}\frac{P_{HDO}}{P_{H_2O}}$$

$$\theta_D = \frac{\theta_H}{K_6K_9}\frac{P_{HD}}{P_{H_2}}$$

Since $P_{HDO} = 2NP_{H_2O}$ and $P_{HD} = 2nP_{H_2}$, then noting that $\alpha^{-1} = K_6K_7K_8K_9K_{10}$

[13] $$k = k_8K_7K_{10}\theta_{H_2O}\theta_H$$

An alternative mechanism using reaction 9 as the rate limiting step does not lead to a dependence of k on θ_{H_2O}, as is required.

If equilibrium is maintained between the gas and the surface K_7K_{10} will be constant, and will probably be unity to within a few percent. At high hydrogen pressures θ_H will be constant and almost unity. Thus

[14] $$k \simeq k_8\theta_{H_2O}$$

Rolston and Goodale (20) showed that a Langmuir isotherm was applicable for water coverages in the platinum–alumina system. Our data are not sufficiently precise or extensive to determine if a Langmuir isotherm is applicable. However, we will assume that such is the case. At low coverages the approximation should be sufficiently accurate. If a Langmuir

Can. J. Chem. Downloaded from www.nrcresearchpress.com by 210.87.254.5 on 09/05/12
For personal use only.

isotherm for water adsorption is used in eq. 14 and the logarithm of the resulting expression is differentiated with respect to $1/T$, then the activation energy is given by eq. 15.

$$[15] \qquad E_{app} = E_0 - (1 - \theta_{H_2O})\lambda_{H_2O}$$

where E_{app} is the measured apparent activation energy, E_0 is the chemical activation energy and λ_{H_2O} is the heat of desorption of water. The true chemical activation energy E_0 will be largely a reflection of the activation energy for reaction 8, the hydrogen isotope switch reaction. We have shown that a reciprocal plot of the data from Figs. 2 and 3 leads to estimates of θ_{H_2O} at 100° of 0.1 for an ungraphitized Thermax support and 0.06 for a Thermax support graphitized at 2100 °C. Taking λ_{H_2O} as 11 kcal/mol, then $(1 - \theta_{H_2O})\lambda_{H_2O}$ has a value close to 10 kcal/mol.

To obtain a comparison with values for other supports we note that Rolston and Goodale (20) have shown that the reaction over a platinum–alumina catalyst is also dependent on water pressure, although in the region in which they worked the power of θ_{H_2O} was between zero and one. Unpublished work from this laboratory has shown that over platinum silica catalysts, the rate is proportional to water pressure from 30 to 200 Torr H_2O. Although it has not been conclusively proven in these cases that eq. 12 holds or that $(1 - \theta_{H_2O})\lambda_{H_2O} \simeq 10$ kcal/mol, we will assume that these conditions hold and obtain E_0 by adding 10 kcal/mol to the reported activation energies over these catalysts.

The resulting E_0 values for carbon and these other supports are shown in Table 2. It is seen that changing the support results in a lowering of E_0 from about 15 kcal/mol for inert supports, or unsupported platinum to about 9 for low temperature carbons and to 3.5 ± 1.5 for high temperature carbons.

The remarkable lowering of E_0, which may be taken as equivalent to a lowering of E_8, is evidence of some type of metal–support interaction. The cause of this metal–support effect has not been completely established. It will be discussed first of all in terms of electron transfer to the platinum. The work function of platinum has been variously measured as 4.1 to 6.3 eV (21). Reference 21 gives 5.36 eV as the preferred value. A recent determination by Bouwman and Sachtler gives 5.7 eV (22). For this discussion it is adequate to take 5.5 eV. The work function of graphite is about 4.6 eV (21). For carbons heated to 400 °C there is a band gap, the energy gap between the bottom of the conduction band and the top of the valence band, of about 1.7 eV. As the carbon is heated to higher and higher temperatures, the valence band rises and the energy gap disappears at a heat treatment temperature (HTT) of about 1100 °C. Generally, impurity levels are thought to exist at an energy of 0.2 to 0.5 eV below the conduction band (9). The present state of knowledge of the band structure of heat-treated carbons has been summarized recently by Mrozowski (8). A totally satisfactory description is not available but it has been well established that for carbon heat-treated above 1000 °C, a large concentration of free carriers is available.

If platinum is put on a graphite surface the platinum should acquire a negative charge because of the difference in work functions of graphite and platinum. The extent to which this charge transfer can occur will not be limited by a corresponding positive charge in the vicinity of the particle since the carriers are free. On the less highly graphitized carbons, the donor impurity levels near the bottom of the conduction band may allow a small charging of the platinum. Some electrons from these donor levels will migrate into the metal until an equilibrium is set up. This results in a positive space charge in the carbon, and a negative charge on the metal, limiting the number of transferable electrons (2).

If the proposed mechanism (reactions 6 to 10) holds, the observed lowering of E_0 is associated in some way with a lowering of the activation energy for reaction 8, the hydrogen switching step. Water is assumed to be weakly bound to the metal with a low net heat of adsorption. Hence it is most reasonable to assume that the major way in which the activation energy E_8 can be lowered is by a change in the Pt—H bonding.

For uncharged platinum, the details of the bonding to hydrogen are somewhat confusing particularly at low temperatures, where both positive and negative changes in film resistance and work function are noted depending on coverage (23). However, at room temperature and above, Mignolet (24) found only an increase

Can. J. Chem. Downloaded from www.nrcresearchpress.com by 210.87.254.5 on 09/05/12
For personal use only.

in the work function of platinum when hydrogen was adsorbed and Geus (25) states that Offret observed only an increase in film resistance. This is consistent with the polarization of the platinum–hydrogen bond being $Pt^{\delta+}—H^{\delta-}$ (26).

If the hydrogen is negatively charged, then charging the platinum metal negatively should weaken the platinum–hydrogen bond. In hydrido–platinum complexes, it has been noted that adding electronegative ligands, which withdraw electrons from the platinum atom, significantly strengthens the platinum–hydrogen bond (27). A weakening of the platinum–hydrogen bond will lower the activation energy for reaction 8, particularly if the hydrogen has sufficient hydride character for an encounter complex to be formed similar to that examined by Ritchie and King (28).

It is of interest that this same hydrogen switch mechanism has been proposed by Holleck and Flanagan (29) for the exchange between aqueous solutions and deuterium gas on palladium surfaces at pH greater than 5. In neutral solutions (0.1 N NaCl) they found that keeping the palladium anodic decreased the exchange rate considerably. Thus positively charging the platinum appears to decrease the rate of reaction 8, in agreement with our postulate. Furthermore part of the promoting effect of chromia on the nickel catalyzed hydrogen–water deuterium exchange (7) has been interpreted in terms of the negative charging of nickel by electrons donated from chromia (30).

An entirely different reason for the changes in activation energies must be considered. On the more hydrophilic supports, water adsorption is primarily on the support and this adsorbed water is in equilibrium with water adsorbed on the platinum. As the carbon is graphitized it becomes less hydrophilic and a large decrease in water affinity is noted at a HTT of 1000 °C (31). If decreases in the E_0 and increases in the rate can be attributed to a lowering of the affinity for water, it would be expected that a completely hydrophobic support should give the smallest E_0 and the highest rate. Under these conditions the support would be relatively inert and the reaction should resemble that on unsupported platinum. In fact, with unsupported platinum a high E_0 was observed regardless of the nature of the diluent. Thus the loss of hydrophilic sites on the support is probably not responsible for the observed phenomena. It should be recalled, however, that the transfer of other species from support to metal is possible. Furthermore non-linear adsorption of water on the metal may greatly affect our results. Unfortunately it is difficult to study the adsorption of water on the metal alone in the presence of the support.

We would like to thank D. Faulkner and E. E. Sexton of the Materials Science Section, WNRE, for taking the electron micrographs, N. S. McIntyre of the Analytical Science Branch, WNRE, for the platinum analyses, and A. G. Wikjord and C. F. Musick of the same branch for determining the BET surface areas. Helpful discussions with G. G. Strathdee are gratefully acknowledged.

1. J. H. Sinfelt. Catal. Rev. **3**, 175 (1970).
2. F. Solymosi. Catal. Rev. **1**, 233 (1968).
3. R. F. Baddour and M. C. Deibert. J. Phys. Chem. **70**, 2173 (1966).
4. G. C. Bond. Catalysis by metals. Academic Press London. 1962. pp. 437–446.
5. M. Boudart. Adv. Catal. Rel. Subj. **20**, 153 (1969).
6. N. H. Sagert and R. M. L. Pouteau. Can. J. Chem. **49**, 3411 (1971).
7. P. Margineanu and A. Olariu. J. Catal. **8**, 359 (1967).
8. S. Mrozowski. Carbon, **9**, 97 (1971).
9. P. L. Waters. *In* Proceeding of the Fifth Conference on Carbon. Vol. 2. MacMillan, New York. 1963. pp. 131–148.
10. M. M. Schnepfe and F. S. Grimaldi. Talanta, **16**, 591 (1969).
11. J. E. Benson and M. Boudart. J. Catal. **4**, 704 (1965).
12. R. P. Chambers and M. Boudart. J. Catal. **6**, 141 (1966).
13. C. N. Satterfield. Mass transfer in heterogeneous catalysis. M.I.T. Press, Cambridge, Mass. 1970.
14. C. E. Hunt. J. Catal. **23**, 93 (1971).
15. M. A. Vannice, J. E. Benson, and M. Boudart. J. Catal. **16**, 348 (1970).
16. T. A. Dorling, C. J. Burlace, and R. L. Moss. J. Catal. **12**, 207 (1968).
17. H. Chon, R. A. Fisher, and J. G. Aston. J. Am. Chem. Soc. **82**, 1055 (1960).
18. E. S. J. Tomezsko and G. T. Furukawa. J. Catal, **8**, 386 (1967).
19. H. D. F. Cole. Ph.D. Thesis. The University of Texas, Austin, Texas, 1964.
20. J. H. Rolston and J. W. Goodale. Can. J. Chem. **50**, 1900 (1972).
21. Handbook of chemistry and physics. 49th ed. Chemical Rubber Co., Cleveland. 1960. pp. E77–E78.
22. R. Bouwman and W. M. H. Sachtler. J. Catal. **19**, 127 (1970).
23. R. V. Culver and F. C. Tomkins. Adv. Catal. Rel. Subj. **11**, 67 (1959).
24. J. C. P. Mignolet. J. Chim. Phys. **54**, 19 (1957).

25. J. W. GEUS. The influence of adsorption on metal films. *In* Chemisorption and reactions on metallic films. Vol. 1. *Edited by* J. R. Anderson. Academic Press, London. 1971. pp 416–417.
26. G. PARRAVANO. J. Catal. **22**, 96 (1971).
27. A. P. GINSBERG. *In* Transition metal chemistry, Vol. I. *Edited by* R. L. Carlin. Marcel Dekker, New York. 1965. p. 214.
28. C. D. RITCHIE and H. F. KING. J. Am. Chem. Soc. **90**, 833 (1968).
29. G. L. HOLLECK and T. B. FLANAGAN. J. Phys. Chem. **73**, 285 (1969).
30. D. TARINA, E. WEISSMANN, and D. BARB. J. Catal. **11**, 348 (1968).
31. W. H. WADE. J. Colloid and Interface Sci. **31**, 111 (1969).

Can. J. Chem. Downloaded from www.nrcresearchpress.com by 210.87.254.5 on 09/05/12
For personal use only.

Hydroxy Complexes of Platinum(II) and Palladium(II)

GORDON WILLIAM BUSHNELL, KEITH ROGER DIXON, ROBERT GEORGE HUNTER, AND JOHN JAMES MCFARLAND

Department of Chemistry, University of Victoria, Victoria, British Columbia

Received June 15, 1972

The preparation of hydroxy bridged complexes, $[M_2(OH)_2L_4][BF_4]_2$, where M = Pt and L = triethylphosphine, triphenylphosphine or pyridine, or where M = Pd and L = triphenylphosphine, is described. The structures are unambiguously established by infrared, nuclear magnetic resonance, and X-ray crystallographic studies. The complexes are surprisingly stable, and in particular, resist bridge cleavage by tertiary phosphines under conditions which easily cleave analogous chloro bridged complexes.

La préparation de complexes pontés hydroxylés $[M_2(OH)_2L_4][BF_4]_2$, où M = Pt et L = triéthylphosphine, triphénylphosphine ou pyridine, ou encore M = Pd et L = triphénylphosphine, est décrite. Les structures ont été établies sans ambiguité par infrarouge, résonance magnétique nucléaire et cristallographie aux rayons-X. Les complexes sont étonamment stables et en particulier, résistent au clivage du pont par les phosphines tertiaires dans des conditions où les analogues chlorés sont facilement clivés.

[Traduit par le journal]

Canadian Journal of Chemistry, **50**, 3694 (1972)

Can. J. Chem. Downloaded from www.nrcresearchpress.com by 210.87.254.105 on 09/05/12
For personal use only.

Platinum(II) and palladium(II) may be regarded as soft (class B) acids whereas hydroxide is a hard (class A) base (1). Consequently hydroxy complexes of platinum(II) and palladium(II) are expected to be relatively uncommon and unstable and the paucity of reports of such complexes is consistent with this view. The older literature (see, for example, ref. 2 and references therein) contains references to a number of platinum(II) and palladium(II) hydroxy complexes, especially species containing amine ligands, *e.g.* $M(OH)_2(NH_3)_2$, but prior to the commencement of our work the only detailed modern study was the characterization of $[Pt_2(OH)_2(PPh_2O)_2(PEt_3)_2]$, Ph = phenyl, Et = ethyl, by Chatt and Heaton (3). The reports by Cross and Glockling (4) of $[Pt(OH)(GePh_3)(PEt_3)_2]$ and by Bailar and Itatani (5) of $[PtCl(OH)(PPh_3)_2]$ have subsequently been shown to be incorrect (3, 6). No other tertiary phosphine stabilized hydroxy complexes of platinum(II) or palladium(II) and no hydroxy bridged complexes of these metal ions had been reported. We now report the synthesis and characterization of hydroxy bridged, tertiary phosphine complexes of platinum(II) and palladium(II).

During the progress of our work the complexes $[Pt(OH)(NHSO_2R)(PPh_3)_2]$ (7) and $[Pt_2(OH)_2(PPh_3)_4][BF_4]_2$ (8) have been mentioned in the literature but no detailed characterization has been given. The latter was obtained as a product of oxidation of a platinum azo complex, a quite different preparation to that described below.

Results and Discussion

Reactions of the complexes, $[PtCl_2(PEt_3)_2]$, $[PtCl_2(PPh_3)_2]$, and $[PdCl_2(PPh_3)_2]$, with $AgBF_4$ (1 mol) are known (9) to give chloro bridged complexes, $[M_2Cl_2(PR_3)_4][BF_4]_2$. We now find that reaction of the $[MCl_2(PR_3)_2]$ complexes with 2 mol of $AgBF_4$ (or reaction of the bridged complexes with 1 mol) in moist acetone ($\sim 0.5\%$ H_2O) results in precipitation of AgCl and formation of hydroxy complexes of the type

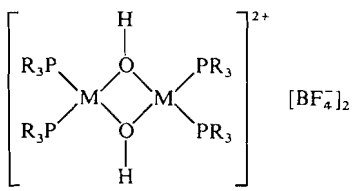

Structures

Analytical data confirming the stoichiometry of the products are given in Table 1 together with the molar conductance, infrared, and nuclear magnetic resonance data referred to in the following discussion.

The presence of co-ordinated hydroxy groups

Can. J. Chem. Downloaded from www.nrcresearchpress.com by 210.87.254.105 on 09/05/12
For personal use only.

TABLE 1. Characterization data

Complex	Melting point (°C)	%C		%H		Molar conductance[a] (ohm^{-1} cm^2)	Infrared (cm^{-1})[b]		^1H Magnetic resonance τ(O—H)
		Calcd.	Found	Calcd.	Found		ν(O—H)	ν(O—D)	
$[Pt_2(OH)_2(PEt_3)_4][BF_4]_2$	194–196 dec.	26.9	27.1	5.84	5.78	183	3450 s[c]	2250	7.15[d]
$[Pt_2(OH)_2(PPh_3)_4][BF_4]_2$	253–255	52.5	52.3	3.79	3.95[e]	181	3550 w	2620	7.9[f]
$[Pt_2(OH)_2(PPh_3)_4][BPh_4]_2$	~185 dec.	68.2	67.9	4.87	4.68	229	3550 w	—	—[g]
$[Pt_2(OH)_2(Py)_4][BF_4]_2$	~170 dec.	26.3	27.1	2.43	2.61[h]	142	3450 m[i]	—	7.15[d]
$[Pd_2(OH)_2(PPh_3)_4][BF_4]_2$	~170 dec.	58.8	59.3	4.25	4.54	190	3590 m	2650	8.0[f]

[a] 10^{-3} *M* solutions in nitromethane.
[b] w = weak, m = medium, s = strong.
[c] ν(Pt—O) = 480 s.
[d] Acetone-d_6 solution.
[e] %F, calcd. = 9.2, found = 9.3.
[f] Nitromethane solution.
[g] Not sufficiently soluble.
[h] %N, calcd. = 6.1, found = 6.4.
[i] ν(Pt—O) = 480 w

Can. J. Chem. Downloaded from www.nrcresearchpress.com by 210.87.254.105 on 09/05/12
For personal use only.

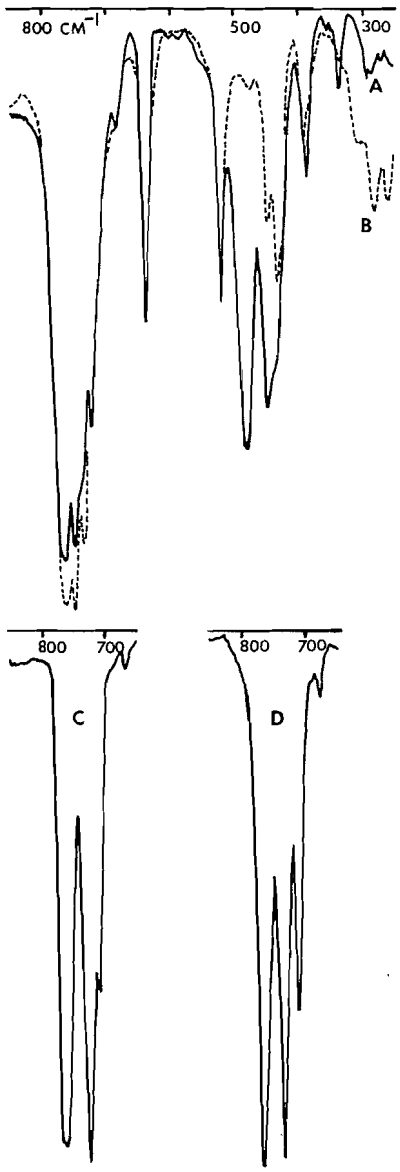

FIG. 1. Infrared spectra, $A = [Pt_2(OH)_2(PEt_3)_4][BF_4]_2$, $B = [Pt_2Cl_2(PEt_3)_4][BF_4]_2$, $C = cis\text{-}[PtCl_2(PEt_3)_2]$, $D = trans\text{-}[PtCl_2(PEt_3)_2]$.

is confirmed by relatively sharp (width at 1/2 height, 30–100 cm^{-1}) infrared absorptions at about 3500 cm^{-1}, shifting to about 2600 cm^{-1} on deuteration. These frequencies are similar to those reported previously for $\alpha\text{-}[Pt_2(OH)_2(PPh_2O)_2(PEt_3)_2]$, 3520 cm^{-1} shifting to 2600 cm^{-1} (3), and for $[(CH_3)_3PtOH]_4$, 3595 cm^{-1} shifting to 2655 cm^{-1} (10), and the value of 3550 cm^{-1} for $[Pt_2(OH)_2(PPh_3)_4][BF_4]$ agrees within experimental error with the previous report (8) of 3545 cm^{-1}. That these bands are due to hydroxyl and not to water is confirmed by the absence of absorption at 1630 cm^{-1} corresponding to the HOH bending mode of water (11). A bridging hydroxyl group is also expected (11, 12) to absorb in the ranges 950–1200 cm^{-1} (MOH bending) and 400–600 cm^{-1} (M—O stretching). In the triphenylphosphine complexes both regions are obscured by BF_4^- and ligand absorptions, respectively, but $[Pt_2(OH)_2(PEt_3)_4][BF_4]_2$ (Fig. 1) shows a strong band at 480 cm^{-1} which does not occur in the spectrum of the well-known (13) chloride bridged complex, $[Pt_2Cl_2(PEt_3)_4][BF_4]_2$, and is therefore assigned to ν(Pt—O). $[Pt_2Cl_2(PEt_3)_4][BF_4]_2$ and $[Pt_2(OH)_2(PEt_3)_4][BF_4]_2$ have essentially identical spectra except for the PtOH bands described above and the Pt—Cl bands at 260 and 280 cm^{-1}. This comparison is evidence for the dimeric structure of the hydroxy complexes especially since we find the contour of the ligand absorption bands at 700–800 cm^{-1} to be characteristic of the complex type. Spectra of *cis*- and *trans*-$[PtCl_2(PEt_3)_2]$ in this region are included in Fig. 1 to illustrate the type of changes observed.

Further structural evidence comes from the nuclear magnetic resonance spectra. Resonances at 7–8 τ are assigned to the hydroxylic protons and, although these are generally too weak to permit accurate integration or observation of coupling to ^{195}Pt, the relative integrated intensities are approximately correct in all cases. The chemical shifts show considerable solvent dependence but are in general agreement with the previous report (8) of 8.4 τ for the hydroxyl protons of $[Pt_2(OH)_2(PPh_3)_4][BF_4]_2$ in $CDCl_3$ solution. The presence of *cis*-PEt_3 ligands in $[Pt_2(OH)_2(PEt_3)_4][BF_4]_2$ is confirmed by the appearance of the methyl resonance as an approximately 1:2:2:2:1 quintet centered at 8.85 τ (13).

Attempts to confirm the dimeric structures by conductance measurements proved inconclusive. The molar conductances (Table 1) of 10^{-3} *M* solutions in nitromethane are in the range expected for 2:1 electrolytes (14) but plots of equivalent conductance against square root of

TABLE 2. Crystallographic results

Parameter	Value	
	$[PtCl(PEt_3)_2(BF_4)]_n$	$[Pt(OH)(PEt_3)_2(BF_4)]_n$
Space Group	*Pbcn* No. 60	$P2_1/c$ No. 14
Unit cell *a* (*nm*)	1.996	1.605
b (*nm*)	1.382	1.852
c (*nm*)	1.438	1.337
β (°)	—	101.5
Volume (nm^3)	3.967	3.894
Crystal density ($g\ cm^{-3}$)	1.845	1.821
Number of monomer units per unit cell	7.96	7.98

equivalent concentration had slopes of about 1000, suggestive (15) of 3:1 electrolytes. In order to check the possibility of a trimeric structure we undertook molecular weight determinations by crystal density and unit cell measurements. The results are shown in Table 2. Both $[Pt_2Cl_2(PEt_3)_4][BF_4]_2$ and $[Pt_2(OH)_2(PEt_3)_4][BF_4]_2$ have 8 platinum atoms per unit cell and this clearly excludes the possibility of a trimeric cation. Tetrameric and octameric structures can also be excluded by consideration of the translational elements of the space group symmetry and this leaves only a dimeric structure or the chemically unlikely possibility of monomers. For the chloro complex the Weissenberg photographs of the layers perpendicular to *c* can be divided into two sets (*l* even and *l* odd). All the films in each set have approximately the same intensity distribution and the strong areas in one set correspond to the weak areas in the other. The *Z* co-ordinates of the heavy atoms are therefore 0 and 1/2, giving the crystallographic problem a two dimensional aspect, and suggesting a very plausible trial structure based on four dimeric molecules per unit cell. We therefore consider that the above crystallographic and infrared evidence clearly establishes our formulation of both hydroxy and chloro complexes as containing bridged dimeric cations.

Reactivity

These hydroxy complexes are surprisingly stable. They are non-hygroscopic, air-stable solids which can be recovered unchanged from a variety of organic solutions including those in halogenated solvents such as chloroform and dichloromethane. The hydroxy protons are rather non-labile and deuteration requires prolonged stirring (15 h) in D_2O/acetone solution and for the platinum complexes a piperidine catalyst is also necessary. Attempts to determine K_a values for the hydroxy protons by potentiometric titration with hydroxide in nitromethane or methanol resulted in formation of red or brown precipitates, presumably because of reduction to cluster complexes (16), and amine bases such as piperidine did not give satisfactory titration curves.

Reactions of $[Pt_2(OH)_2(PEt_3)_4][BF_4]_2$, $[Pt_2(OH)_2(PPh_3)_4][BF_4]_2$, or $[Pd_2(OH)_2(PPh_3)_4][BF_4]_2$ with excess triphenylphosphine (5 mol) give no evidence of bridge cleavage to form complexes having terminal hydroxy ligands whereas the corresponding chloro bridged complexes cleave easily under similar conditions (9). Generally the hydroxy complexes are recovered unchanged although the product of reaction of $[Pt_2(OH)_2(PEt_3)_4][BF_4]_2$ with triphenylphosphine shows nuclear magnetic resonance evidence for some replacement ($\sim 10\%$) of triethylphosphine by triphenylphosphine. The ν(OH) absorption in the infrared spectrum of this product is unchanged in frequency but slightly decreased in intensity whereas ν(Pt—O) is unchanged, suggesting that some deprotonation may have occurred. The product of reaction of $[Pt_2(OH)_2(PEt_3)_4][BF_4]_2$ with triethylphosphine shows similar infrared evidence of deprotonation but in neither case could new complexes be isolated and there was no evidence for bridge cleavage.

Can. J. Chem. Downloaded from www.nrcresearchpress.com by 210.87.254.105 on 09/05/12
For personal use only.

Can. J. Chem. Downloaded from www.nrcresearchpress.com by 210.87.254.105 on 09/05/12
For personal use only.

The failure of these attempted cleavage reactions suggests an unusual stability for the hydroxy bridge relative to terminal hydroxy complexes, especially since kinetic studies (17) show tertiary phosphines to be among the best nucleophiles for platinum(II). This stability of the bridge is further demonstrated by the reaction of $[PtCl(PEt_3)_2(PPh_3)][BF_4]$ with $AgBF_4$ in moist acetone to yield $[Pt_2(OH)_2(PEt_3)_4][BF_4]_2$ and triphenylphosphine. In this case formation of the bridge involves actual displacement of triphenylphosphine which is very surprising in view of the expected "hard" character of the hydroxy group and "soft" character of the phosphine and platinum(II).

Reaction of $[Pt_2(OH)_2(PEt_3)_4][BF_4]_2$ with Cl^- (2 mol) also fails to yield a complex having a terminal hydroxy group, the products being $[PtCl_2(PEt_3)_2]$ (1 mol) and the starting complex (1/2 mol). $[Pt_2(OH)_2(PEt_3)_4][BF_4]_2$ does not react with piperidine whereas $[Pt_2Cl_2(PEt_3)_4][BF_4]_2$ cleaves easily under similar conditions.

Other Complexes

Syntheses of several other hydroxy complexes were attempted to investigate the generality of the synthetic procedure. A small yield of $[Pt_2(OH)_2(Py)_4][BF_4]_2$, Py = pyridine, was obtained but reactions of $AgBF_4$ with *trans*-$[PdCl_2(PEt_3)_2]$ or $[Pt_2Cl_4(PEt_3)_2]$ did not yield isolable hydroxy complexes.

Experimental

Silver tetrafluoroborate was from City Chemical Corporation, New York, and was used as received. Complexes, *trans*-$[PdCl_2(PR_3)_2]$ (18), *cis*-$[PtCl_2(PEt_3)_2]$ (19), *cis*-$[PtCl_2(PPh_3)_2]$ (5), *cis*-$[PtCl_2(Py)_2]$ (20), $[Pt_2Cl_4(PEt_3)_2]$ (21), and $[Pt_2Cl_2(PEt_3)_4][BF_4]_2$ (9) were prepared as previously described. Solvents were reagent grade and were dried over molecular sieves (type 4A) before use. All reactions were conducted in an atmosphere of dry nitrogen and those involving $AgBF_4$ were conducted in the dark but the products were stable and were isolated and purified in the atmosphere. All products were dried *in vacuo* at 70–80° before recrystallization and spectroscopic study.

Microanalyses were by Schwartzkopf Microanalytical Laboratory, New York. Conductance measurements were made on $\sim 10^{-3}$ *M* solutions in nitromethane using a dip-type cell connected to a Radiometer Model CDM3 Conductivity bridge. Nuclear magnetic resonance spectra were recorded on Perkin–Elmer R12A or Varian HA60 spectrometers with tetramethylsilane as external reference. Infrared spectra were recorded, with accuracy $\pm 5\ cm^{-1}$ from 4000 to $250\ cm^{-1}$, for all products described below, using a Beckman IR 20 spectrophotometer calibrated against polystyrene films or water vapour. Solid samples were examined as Nujol mulls between caesium iodide plates. Where additional characterization is not given these infrared spectra served to identify the products.

Crystal densities were determined by floatation in a mixture of *n*-propyl iodide and 1,2-dibromoethane. Unit cell parameters were determined by Weissenberg and precession photography.

1. Preparations

$[Pt_2(OH)_2(PEt_3)_4][BF_4]_2$

A solution of $AgBF_4$ (0.58 g, 3.0 mmol) in acetone (15 ml) was added dropwise to a stirred solution of *cis*-$[PtCl_2(PEt_3)_2]$ (0.72 g, 1.43 mmol) in moist acetone (~0.5% H_2O) (50 ml) at 25°. After 15 min had elapsed, filtration gave AgCl (0.36 g, 2.5 mmol). Addition of the filtrate to diethyl ether (300 ml) gave an oily precipitate. On standing overnight this precipitate darkened and extraction with acetone left a further quantity of Ag/AgCl mixture.[1] Addition of the acetone extract to stirred diethyl ether gave $[Pt_2(OH)_2(PEt_3)_4][BF_4]_2$ (0.65 g, 0.61 mmol) as a white precipitate which was recrystallized from acetone by dropwise addition of diethyl ether to give colorless needles.

$[Pt_2(OH)_2(PPh_3)_4][BF_4]_2$

A similar procedure using $AgBF_4$ (0.047 g, 0.24 mmol) and $[Pt_2Cl_2(PPh_3)_4][BF_4]_2$ (0.20 g, 0.12 mmol) in a dichloromethane–acetone solvent mixture gave AgCl (0.032 g, 0.22 mmol) and $[Pt_2(OH)_2(PPh_3)_4][BF_4]_2$ (0.17 g, 0.10 mmol). The product was a white precipitate recrystallized from dichloromethane–diethyl ether.[2]

$[Pd_2(OH)_2(PPh_3)_4][BF_4]_2$

A similar procedure using $AgBF_4$ (0.57 g, 2.93 mmol) and *trans*-$[PdCl_2(PPh_3)_2]$ (1.02 g, 1.45 mmol) in a dichloromethane–acetone solvent mixture gave AgCl (0.39 g, 2.72 mmol) and $[Pd_2(OH)_2(PPh_3)_4][BF_4]_2$ (1.0 g, 0.68 mmol). The product was a white precipitate recrystallized from dichloromethane–diethyl ether.[3]

$[Pt_2(OH)_2(Py)_4][BF_4]_2$

A similar procedure using $AgBF_4$ (0.27 g, 1.39 mmol) and *cis*-$[PtCl_2(Py)_2]$ (0.29 g, 0.68 mmol) in a dichloromethane–acetone solvent mixture gave AgCl (0.19 g, 1.33 mmol) and $[Pt_2(OH)_2(Py)_4][BF_4]_2$ (0.10 g, 0.11 mmol). The product was a white precipitate recrystallized from nitromethane–diethyl ether. The low yield may have been due to formation of $Pt(OH)_2(Py)_2$ as the product was very difficult to crystallize and the slightly high C, H, and N analyses and low conductance figure (Table 1) are consistent with contamination of the product by this complex.

$[Pt_2(OH)_2(PPh_3)_4][BPh_4]_2$

$NaBPh_4$ (0.31 g, 0.91 mmol) and $[Pt_2(OH)_2(PPh_3)_4][BF_4]_2$ (0.067 g, 0.041 mmol) were stirred in 1:1 acetone–dichloromethane solution from 3 h at 25°. The resulting cream precipitate of $[Pt_2(OH)_2(PPh_3)_4][BPh_4]_2$ (0.053 g, 0.025 mmol) was recrystallized from dichloromethane–diethyl ether.

[1]This procedure was found to give cleaner products than prolonged stirring of the original reaction mixture.

[2]This recrystallization gave purer products when carried out in the presence of 1–2 mol of triphenylphosphine.

[3]This recrystallization gave purer products when carried out in the presence of 1–2 mol of triphenylphosphine.

Reactions of $[Pt_2Cl_4(PEt_3)_2]$ or trans-$[PdCl_2(PEt_3)_2]$ with $AgBF_4$

These were carried out by similar techniques to those described above but failed to yield isolable hydroxy complexes. Precipitation of AgCl did occur but the Pt- and Pd-containing products were intractable oils.

2. Reactions with Lewis Bases

Reactions of the bridged complexes with potassium chloride, piperidine, triethylphosphine, or triphenylphosphine were conducted in polar organic solvents (CH_3OH, CH_2Cl_2, CH_3NO_2 or $(CH_3)_2CO$) at 25° for reaction times of 5–15 h. Solid products were recovered by addition of diethyl ether to the resulting solutions.

3. Reaction of $[PtCl(PEt_3)_2(PPh_3)][BF_4]$ with $AgBF_4$

$[PtCl(PEt_3)_2(PPh_3)][BF_4]$ was prepared in almost quantitative yield by reaction of PPh_3 with $[Pt_2Cl_2(PEt_3)_4][BF_4]_2$ in a procedure similar to that described previously for $[PtCl(PPh_3)_3][BF_4]$ (9). It was characterized by comparison of its infrared and nuclear magnetic resonance spectra with those of the known complexes, $[PtCl(PPh_3)_3][BF_4]$ and $[PdCl(PEt_3)_2(PPh_3)][BPh_4]$ (18).

$AgBF_4$ (0.052 g, 0.27 mmol) and $[PtCl(PEt_3)_2(PPh_3)][BF_4]$ (0.20 g, 0.25 mmol) were stirred in acetone solution at 25° for 2 h. Filtration gave AgCl (0.026 g, 0.18 mmol) and addition of diethyl ether to the filtrate gave $[Pt_2(OH)_2(PEt_3)_4][BF_4]_2$ (0.10 g, 0.09 mmol).

We thank the National Research Council of Canada and the University of Victoria for research grants and the University of Victoria for a postgraduate fellowship (to J.J.M.).

1. S. AHRLAND, J. CHATT, and N. R. DAVIES. Q. Rev. **12**, 265 (1958). R. G. PEARSON. Chem. Br. **3**, 103 (1967).
2. Gmelins Handbuch der Anorganische Chemie. Vol. 65, 1942, and Vol. 68, 1957.
3. J. CHATT and B. HEATON. J. Chem. Soc. A, 2745 (1968).
4. R. J. CROSS and F. GLOCKLING. J. Chem. Soc. 5422 (1965).
5. J. C. BAILAR and H. ITATANI. Inorg. Chem. **4**, 1618 (1965).
6. R. J. D. GEE and H. M. POWELL. J. Chem. Soc. A, 1956 (1971).
7. W. BECK, M. BAUDER, G. LA MONICA, S. CENINI, and R. UGO. J. Chem. Soc. A, 113 (1971).
8. S. CENINI, R. UGO, and G. LA MONICA. J. Chem. Soc. A, 3441 (1971).
9. K. R. DIXON and D. J. HAWKE. Can. J. Chem. **49**, 3252 (1971).
10. P. A. BULLINER and T. G. SPIRO. Inorg. Chem. **8**, 1023 (1969).
11. K. NAKAMOTO. Infrared spectra of inorganic and co-ordination compounds. 2nd ed., Wiley-Interscience, New York. 1970.
12. V. BARAN. Co-ord. Chem. Rev. **6**, 65 (1971).
13. H. C. CLARK, K. R. DIXON, and W. J. JACOBS. J. Am. Chem. Soc. **90**, 2259 (1968).
14. W. J. GREARY. Co-ord. Chem. Rev. **7**, 81 (1971).
15. R. D. FELTHAM and R. G. HAYTER. J. Chem. Soc. 4587 (1964).
16. R. UGO, F. CARIATI, and G. LA MONICA. Chem. Commun. 868 (1966). R. D. GILLARD, R. UGO, F. CARIATI, S. CENINI, and F. BORATI. Chem. Commun. 869 (1966).
17. R. G. PEARSON, H. SOBEL, and J. SONGSTAD. J. Am. Chem. Soc. **90**, 319 (1968).
18. H. C. CLARK and K. R. DIXON. J. Am. Chem. Soc. **91**, 596 (1969).
19. K. A. JENSEN. Z. Anorg. Allgem. Chem. **229**, 238 (1936).
20. G. B. KAUFFMAN. Inorg. Synth. **7**, 250 (1963).
21. J. CHATT and L. M. VENANZI. J. Chem. Soc. 2787 (1955).

Can. J. Chem. Downloaded from www.nrcresearchpress.com by 210.87.254.105 on 09/05/12
For personal use only.

The Crystal Structure of Caesium Oxotetrafluorovanadate(V)

G. W. BUSHNELL AND K. C. MOSS

Department of Chemistry, University of Victoria, Victoria, British Columbia

Received June 22, 1972

The crystal structure of caesium oxotetrafluorovanadate(V) has been solved and refined to an *R*-value of 0.070 using diffractometer measurements. The cell dimensions are: $a = 548.4(2)$ pm, $b = 634.2(2)$ pm, $c = 1403.4(3)$ pm. The space group is *Pnma* (No. 62) with four formula units per cell. Each vanadium atom lies 32.6 pm above the base of a tetragonal pyramid with oxygen at the apex (V=O length = 152.9 pm) and fluorine at the four base corners (mean V—F length = 178.8 pm). The tetragonal pyramids are linked by *cis*-fluorine bridges involving a long V—F bond (V—F(2^1) = 231.2 pm) to give an anionic chain structure. Structural relationships with other fluorides and oxide-fluorides are noted, and the bond lengths are discussed.

Nous avons résolu la structure cristalline de l'oxotétrafluorovanadate(V) de césium et l'avons raffinée jusqu'à obtenir une valeur de *R* de 0.070, au moyen de mesures au diffractomètre. Les dimensions de la maille sont: $a = 548.4(2)$ pm, $b = 634.2(2)$ pm, $c = 1403.4(3)$ pm. Le groupe spatial est *Pnma* (No. 62) avec quatre unités de formule par maille. Chaque atome de vanadium se trouve à 32.6 pm au-dessus de la base d'une pyramide tétragonale, l'oxygène étant au sommet (V=O, longueur = 152.9 pm) et le fluor aux quatre coins de la base (longueur moyenne V—F = 178.8 pm). Les pyramides tétragonales sont reliées au moyen de ponts de fluor *cis*, impliquant un long lien V—F (V—F (2^1) = 231.2 pm), résultant en une structure de chaîne anionique. Nous remarquons les relations de structure existant avec les autres fluorures et oxyde-fluorures et discutons de la longueur des liaisons. [Traduit par le journal]

Canadian Journal of Chemistry, **50**, 3700 (1972)

Can. J. Chem. Downloaded from www.nrcresearchpress.com by 210.87.254.6 on 09/05/12
For personal use only.

Introduction

Recently the preparation and spectroscopic properties of $CsVOF_4$ were described by Howell and Moss (1). From ^{51}V and ^{19}F n.m.r. studies in aqueous and non-aqueous HF they concluded that the anion VOF_4^- undergoes rapid rearrangement in solution between C_{4v} and C_{2v} symmetries. Raman and infrared spectra on solid $CsVOF_4$ (200–4000 cm^{-1}) did not give an unequivocal assignment of the stereochemistry of VOF_4^- in the solid state. The spectra were interpreted on the basis that the ion was essentially monomeric, with C_{4v} symmetry, but the possibility of F bridging between the anions was also suggested. This paper reports the crystal structure of $CsVOF_4$ and confirms the tentative suggestions of Howell and Moss.

Experimental

The preparation and analysis of the crystals have already been described (1). Preliminary photographic work was done on a Weissenberg camera with CuK_α radiation. The crystal data are given in Table 1. The crystal dimensions are given in the directions of *a*, *b*, and *c*, respectively. From the systematic absences the space group might have been the noncentrosymmetric $Pn2_1a$ (No. 33 with non-standard setting). No piezoelectric effect was found using a Wooster Mark III piezoelectric test apparatus. Use of the $Pn2_1a$ space group in the middle stages of the refinement did not produce significant departure from the atomic arrangement conforming to *Pnma*, and the refinement was completed satisfactorily in terms of the latter. The cell dimensions were calculated by least squares analysis of 23 2θ measurements made on a Picker 4-circle diffractometer with MoK_α radiation. The density was observed to be too high for flotation type measurements in all the non-aqueous media available. Other methods requiring large quantities of material were not attempted. Ionic volume calculations strongly suggested four formula units per cell. In *Pnma* under these circumstances, the VOF_4^- anion must have the point group symmetry *m*.

Intensity measurements were completed up to $2\theta = 60°$ using MoK_α radiation ($\lambda = 71.069$ pm) and a manually operated 4-circle diffractometer. The instrument was operated in the bisecting position with $\omega = 0$. Reflections were scanned in the $\theta/2\theta$ mode for 1 min at a rate of 2°/min in 2θ. The background counts were measured daily for orientation

TABLE 1. Crystal data for $CsVOF_4$

Crystal dimensions in mm	0.70 × 0.18 × 0.08
System	Orthorhombic
Space group	*Pnma* (No. 62)
Formula weight	275.84
Cell dimensions	$a = 548.4 \pm 0.14$ pm
	$b = 634.2 \pm 0.16$ pm
	$c = 1403.4 \pm 0.31$ pm
Cell volume	488.1×10^{-24} cm^3
Density (calcd.)	3.75 g cm^{-3}
No. of formula units/cell	4
Absorption coefficient (MoK_α)	96.0 cm^{-1}

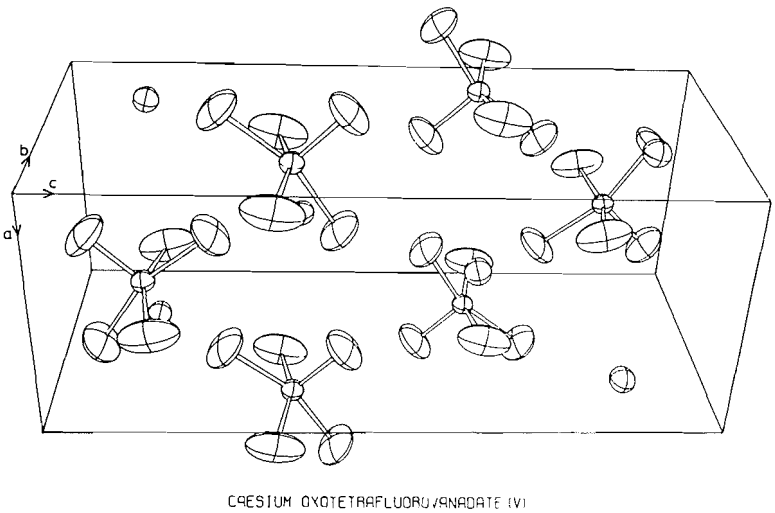

FIG. 1. Stereoscopic view of the cell.

checking, and a standard reflection 2,2,4 was examined after every batch of 50 reflections. Of the 770 reflections measured, 660 were classified as observed using the criterion that the net count must exceed the standard deviation of the background count (σ). The measurements between $-\sigma$ and $+\sigma$ were squeezed by a factor of 0.5 into the 0 to $+\sigma$ range. Measurements below $-\sigma$ were given a value very close to zero. The unobserved reflections were included in the structure factor calculations but not in the least squares refinement. Lorentz and polarization factors were applied to all measurements. Absorption corrections were done with a program utilizing a Gaussian grid numerical integration procedure. The number of points used in the a, b, and c directions were 12, 8, and 4, respectively.

Structure Determination

A set of programs supplied by Penfold was used for this investigation (2). The structure was solved from the three dimensional Patterson function. In choosing the scattering factor curves all atoms were assumed to be uncharged. The curves were obtained from the work of Cromer and Waber (3), and the anomalous dispersion corrections of Cromer (4) were used for caesium and vanadium. At first all the light atoms were treated as fluorine. The first structure factor calculation gave an R-value of 0.45. The first Fourier map showed the structure quite clearly. The positions of the light atoms were improved by difference synthesis. The light atom closest to the vanadium atom was assumed to be oxygen. The refinement was by minimization of $w(|F_o| - |F_c|)^2$ using full matrix least squares.[1] The weights were derived from counting statistics and an experimentally determined instrument instability factor using the formulae given by Stout and Jensen (5). A supplementary refinement was done using a suitable algebraically derived weighting scheme. All atoms except F(1) lay on the mirror planes and had their y-coordinates fixed and their B_{12} and B_{23} temperature factors equal to zero in the least squares calculations. The final lowering of the conventional R-value was in the sequence 0.108, 0.071, 0.070, 0.070 (all reflections included).

Results

The fractional atomic coordinates of caesium oxotetrafluorovanadate(V) are listed in Table 2. Figure 1 is an illustration of the unit cell. All atoms except those labelled F(1) lie on the mirror planes at $Y = 0.25$ and $Y = 0.75$. The F(1) atoms occur in mirror pairs. The oxygen atom is at the apex of the approximately tetragonal pyramids drawn. Extra atoms have been added in the a direction to show the connectivity along this axis through assymmetric *cis*-bridging by the fluorine atom F(2). Only the shorter of the two bridge bonds has

[1]The structure factor table is available, at a nominal charge, from the Depository of Unpublished Data, National Science Library, National Research Council of Canada, Ottawa, Canada K1A 0S2.

Can. J. Chem. Downloaded from www.nrcresearchpress.com by 210.87.254.6 on 09/05/12
For personal use only.

Can. J. Chem. Downloaded from www.nrcresearchpress.com by 210.87.254.6 on 09/05/12
For personal use only.

TABLE 2. Fractional atomic coordinates*

Atom	X	Y	Z
Cs	0.0371(2)	0.75	0.1306(1)
V	0.5166(4)	0.25	0.1416(1)
F(1)	0.5453(14)	−0.0264(9)	0.1639(7)
F(2)	0.3163(21)	0.25	0.2426(8)
F(3)	0.7918(20)	0.25	0.0740(7)
O	0.3225(26)	0.25	0.0634(9)

*Estimated standard deviations in parentheses.

TABLE 3. Interatomic distances*

(*a*) Vanadium coordination

Bond	Length (pm)	Bond	Length (pm)
V—F(1)	178.8(6)	V—O	152.9(12)
V—F(2)	179.3(10)	V—F(2^{I})	231.2(10)
V—F(3)	178.3(10)		

(*b*) Caesium coordination

Bond	Length (pm)	Bond	Length (pm)
Cs—F(1^{II})	316.2(7)	Cs—F(3^{V})	302.1(10)
Cs—F(1^{III})	308.3(7)	Cs—O^{VI}	336.1(12)
Cs—F(1^{IV})	321.4(9)		

*Estimated standard deviations are given in tenths of a pm.

Superscript	Position	Position
I	$\frac{1}{2}+X, \frac{1}{2}-Y, \frac{1}{2}-Z$	—
II	$X, 1+Y, Z$	$X, 1\frac{1}{2}-Y, Z$
III	$X-1, 1+Y, Z$	$X-1, \frac{1}{2}-Y, Z$
IV	$X-\frac{1}{2}, \frac{1}{2}-Y, \frac{1}{2}-Z$	$X-\frac{1}{2}, 1+Y, \frac{1}{2}-Z$
V	$1-X, \frac{1}{2}+Y, -Z$	—
VI	$-X, \frac{1}{2}+Y, -Z$	—

been drawn. This arbitrarily produces five coordinate vanadium atoms. Alternatively the structure might be regarded as containing polymeric ribbons of distorted octahedra. The atoms F(3) are not involved in the bridging.

The bond lengths associated with the vanadium coordination are given in Table 3*a*. From the compilation of effective ionic radii by Shannon and Prewitt (6) we obtain, for the coordination number of six, the values $R(V) = 54$ pm, $R(F) = 133$ pm, $R(O) = 140$ pm, $R(Cs) = 170$ pm. The F(1) pair, F(2), and F(3) make up the square base of the pyramid. Their bond lengths to vanadium are all equal, with the mean value of 178.8 pm only slightly less than the sum of the radii (187 pm). The V—O bond to the apex is short (152.9 pm), whereas the V—F bond *trans* to the oxygen atom is very long (231.2 pm).

The caesium coordination is quite complicated, there being 16 adjacent atoms in the range 302–386 pm. The short end of this range is approximately equal to the sum of the caesium and fluorine radii (303 pm). In Table 3*b* we give the 8 nearest neighbors and their distances from the caesium ion which has the coordinates given in Table 2. Each F(1) entry describes a pair of bonds since there is a mirror plane containing the caesium ion at $Y = 3/4$. Thus, six of the eight nearest neighbors to the caesium ion are space group relatives of F(1).

Table 4 gives the angles subtended at the vanadium atom. Row 1 shows a linear O—V—F(2^{I}) group, but considerable bending from linearity for F(1)—V—F(1) and F(2)—V—F(3). The bending is away from the V—O bond by approximately 10° as shown by the angles of approximately 100° in row 2. The bending is toward F(2^{I}), so that row 3 shows angles of approximately 80°. The mean of the remaining two entries is slightly less than 90°.

A least squares plane calculation was done for the group of four equatorial fluorine atoms (around the polar O—V—F(2^{I}) axis). The quantity minimized was $R = \sum_i W_i P_i^2$ where the weight W_i for atom i is given by $3/[\sigma^2(x_i) + \sigma^2(y_i) + \sigma^2(z_i)]$ and P_i is the perpendicular distance of atom i from the plane. The quantity $\chi^2 = \sum_i P_i^2/\sigma^2(P_i)$ was calculated as an index of the planarity of the group. Using the crystal axis system the equation of the plane was found to be $0.673\,x + 0.740\,z = 3.702$ with $\chi^2 = 7.14$. The group is close to planarity, with F(1), F(2), and F(3) lying −1.1, +1.6, and +1.4 pm from the plane. The vanadium atom lies 32.6 pm from this mean plane.

The bond lengths and angles of the vanadium complex can be described approximately in terms of an octahedron formed by the oxygen and five fluorine atoms. The eight independent values for the length of the octahedral edge have a mean of 258 pm and are contained in the range ±18 pm. The octahedron is elongated by 26 pm along the O—V—F(2^{I}) axis and the vanadium atom is displaced 32.6 pm from the center toward the oxygen atom.

Table 5 gives the anisotropic temperature parameters. The corresponding thermal ellip-

TABLE 4. Angles subtended at the vanadium atom*

Bonds	Angle (deg)	Bonds	Angle (deg)	Bonds	Angle (deg)
O—V—F(2^{I})	178.8 (7)	F(1)—V—F(1)	157.4 (6)	F(2)—V—F(3)	159.9 (6)
O—V—F(1)	100.8 (3)	O—V—F(2)	98.1 (7)	O—V—F(3)	102.0 (7)
F(1)—V—F(2^{I})	79.3 (3)	F(2)—V—F(2^{I})	83.1 (1)	F(3)—V—F(2^{I})	76.9 (5)
F(1)—V—F(2)	85.1 (3)	F(1)—V—F(3)	91.1 (3)		

*Estimated standard deviations are given in tenths of a degree.

TABLE 5. Anisotropic temperature parameters*

Atom	β_{11}	β_{22}	β_{33}	β_{12}	β_{13}	β_{23}
Cs	184 (3)	247 (3)	32 (1)	0	3 (1)	0
V	133 (8)	130 (5)	25 (1)	0	−2 (3)	0
F(1)	391 (32)	124 (15)	156 (8)	22 (19)	−56 (13)	−11 (8)
F(2)	327 (46)	696 (45)	63 (6)	0	88 (15)	0
F(3)	318 (45)	688 (50)	60 (7)	0	78 (15)	0
O	427 (64)	508 (52)	62 (8)	0	−97 (20)	0

*$T = \exp[-(h^2\beta_{11} + k^2\beta_{22} + l^2\beta_{33} + 2hk\beta_{12} + 2hl\beta_{13} + 2kl\beta_{23})]$. The parameters have been multiplied by 10^4. Estimated standard deviations are given in parentheses.

TABLE 6. V—O bond lengths (pm)*

Compound	V(IV) = O length (pm)	Reference	Compound	V(V) = O length (pm)	Reference
1	158	10	**3**	153	This work
2	157	11, 12	**4**	157	13
2	156	11, 12	**5**	164	9
			6	159	14
			7	156	15

*1 = bis(acetylacetonato)4-phenylpyridineoxovanadium(IV); 2 = bis(acetylacetonato)oxovanadium(IV); 3 = caesium oxotetrafluorovanadate(V); 4 = vanadium oxide trifluoride; 5 = potassium dioxotrifluorovanadate(V); 6 = vanadium pentoxide; 7 = vanadium oxide trichloride.

soids scaled to include 50% probability are shown in Fig. 1.

Discussion

The work of Edwards and collaborators (7, 8) has established a set of pentafluoride and oxidetetrafluoride chain structures with *cis*-bridging fluorine atoms. The compounds are VF_5, CrF_5, TcF_5, ReF_5, $MoOF_4$, $ReOF_4$, and $TcOF_4$ (the latter has an alternative trimeric form). Ryan, Mastin, and Reisfeld (9) point out the structural relationship between the doubly charged anionic chain structure of $K_2VO_2F_3$ and the structure of the neutral chains in the compounds mentioned. Caesium oxotetrafluorovanadate(V) has singly charged anionic chains of the same type.

Various V=O bond length measurements are given in Table 6. Vanadium(IV) compounds are included as well as those of vanadium(V). Although the V(V) compounds might be expected to give slightly shorter V=O bonds, no difference is evident. The V=O length in $CsVOF_4$ is a little shorter than usual but not unreasonable. The length was unaltered by the change in the weighting scheme which we tried.

In Table 7 we present an analysis of the V—F bond lengths in $CsVOF_4$ and closely related compounds. We find it necessary to allow for charge, bridging, and a *trans* effect, and have separated these factors as far as possible. Some normal terminal V—F lengths are given in Table 7*a*. They illustrate the charge effect and stand for comparison with the lengths lower in the Table. V—F lengths in two kinds of F-bridge are given in Table 7*b*. The increase is 20–30 pm. Next we examine in Table 7*c* the V—F bonds which are *trans* to a V=O bond. The value of

Can. J. Chem. Downloaded from www.nrcresearchpress.com by 210.87.254.6 on 09/05/12
For personal use only.

Can. J. Chem. Downloaded from www.nrcresearchpress.com by 210.87.254.6 on 09/05/12
For personal use only.

TABLE 7. V—F bond lengths (pm)

(*a*) Terminal bonds

Compound	V—F length (pm)	Charge	Reference
8	171	0	7
9	170	0	13
10	179	−1	This work
11	186, 191	−2	9
12	192	−2	16

(*b*) Fluorine bridges

Compound	V—F length (pm)	Bridge type	Increase (pm)	Reference
8	193, 200	*cis*	21, 29	7
9	193, 195	double	23, 25	13

(*c*) Bonds *trans* to a short bond

Compound	V—F length (pm)	*Trans* group and length (pm)	Reference
9	234	V=O, 157	13
10	231	V=O, 153	This work
12	229	V—F, 161	16

(*d*) Bridge bonds *trans* to V=O

Compound	V—F length (pm)	Bridge type	*Trans* group length (pm)	Reference
11	219	Symmetric *cis*	164	9

*8 = vanadium pentafluoride; 9 = vanadium oxide trifluoride; 10 = caesium oxotetrafluorovanadate(V); 11 = potassium dioxotrifluorovanadate(V); 12 = caesium hexafluorovanadate(IV).

231 pm in $CsVOF_4$ agrees well with the 234 pm found in VOF_3. Both these bonds are similarly involved in assymmetric *cis*-bridging, the shorter arms of the bridges being 181 and 179 pm, respectively. The *trans* effect presumably causes the assymmetry if not all of the lengthening. Since the *trans* and bridging effects are not clearly separated in these two cases, we have given also the example of the vanadium(IV) compound, Cs_2VF_6, which has recently been reported (16) in an orthorhombic form. Previously the compound was known in cubic, hexagonal, and trigonal forms (17). The crystal structure of orthorhombic Cs_2VF_6 contains isolated VF_6^{2-} ions in which a pure *trans* effect can be seen. Separation of the *trans* and bridging effects is quite impossible for $K_2VO_2F_3$. Each bridging F atom is *trans* to two V=O bonds. The V—F length is given in Table 7*d*, and applies to both arms of the bridge.

The published crystal structure of Cs_2VF_6 (16) is of concern to us, in that the short V—F length of 161 pm challenges the validity of our method of recognizing the oxygen atom in $CsVOF_4$. The evidence published (16) for the identity of the compound Cs_2VF_6 consists of a density determination, a fluorine analysis with a specific ion electrode, and a well refined crystal structure. The latter would not distinguish F from O, nor would it necessarily detect hydrogen atoms which might be present. The orthorhombic structure is very unusual for the A_2MF_6 type of compound for which there is a well developed crystal chemistry (18). The method of preparation using aqueous hydrofluoric acid, in contrast to the fluorine preparations of Liebe, Weise, and Klemm (17), also leaves open the possibility that oxygen may be present in the compound. We therefore assert the correctness of the method by which we have assigned V=O as the short bond in $CsVOF_4$.

Operating funds were obtained from the National Research Council of Canada and the Committee for Research Leave and Travel of the University of Victoria. A major equipment grant and computing facilities were provided by the University of Victoria. Dr. A. Tweedale of the University of Victoria Computing Centre has generously given assistance. The authors gratefully acknowledge all these contributions.

1. J. A. S. HOWELL and K. C. MOSS. J. Chem. Soc. (A), 270 (1971).
2. B. R. PENFOLD. University of Canterbury Crystallographic Programs, Christchurch, New Zealand.
3. D. T. CROMER and J. T. WABER. Acta Cryst. **18**, 104 (1965).
4. D. T. CROMER. Acta Cryst. **18**, 17 (1965).
5. G. H. STOUT and L. H. JENSEN. X-Ray structure determination. Macmillan, New York, 1968, p. 456.
6. R. D. SHANNON and C. T. PREWITT. Acta Cryst. ***B25***, 925 (1969).
7. A. J. EDWARDS and G. R. JONES. J. Chem. Soc. (A), 1651 (1969).
8. A. J. EDWARDS and B. R. STEVENTON. J. Chem. Soc. (A), 2503 (1968).
9. R. R. RYAN, S. H. MASTIN, and M. J. REISFELD. Acta Cryst. ***B27***, 1270 (1971).
10. M. R. CAIRA, J. M. HAIGH, and L. R. NASSIMBENI. Inorg. Nucl. Chem. Lett. **8**(1), 109 (1972).

11. P. HON, R. BELFORD, and C. E. PFLUGER. J. Chem. Phys. **43**, 3111 (1965).
12. R. P. DODGE, D. H. TEMPLETON, and A. ZALKIN. J. Chem. Phys. **35**, 55 (1961).
13. A. J. EDWARDS and P. TAYLOR. Chem. Commun. 1474 (1970).
14. H. G. BACHMANN, F. R. AHMED, and W. H. BARNES. Z. Kristallogr. **115**, 110 (1961).
15. K. J. PALMER. J. Am. Chem. Soc. **60**, 2360 (1938).
16. A. CARPY and K. WALTERSSON. C.R. Acad. Sc. Paris (Série C), **274**, 405 (1972).
17. W. LIEBE, E. WEISE, and W. KLEMM. Z. Anorg. Chem. **311**, 281 (1961).
18. K. R. DIXON. Ph.D. Thesis. University of Strathclyde, Glasgow, Scotland. 1966.

Can. J. Chem. Downloaded from www.nrcresearchpress.com by 210.87.254.6 on 09/05/12
For personal use only.

E.S.R. Studies of γ-Ray Irradiated Single Crystals of D-Tartaric Acid

J. K. MULCHINOCK[1] AND F. R. HALLETT
Department of Physics, University of Guelph, Guelph, Ontario

AND

F. C. ADAM
Department of Chemistry, University of Calgary, Calgary, Alberta

Received May 8, 1972

Electron spin resonance (e.s.r.) studies on single crystals of normal and deuterated D-tartaric acid have been carried out as part of a larger investigation of radical production and migration in biologically related single crystals. The D-tartaric acid system is especially interesting since the second and third carbon atoms of the molecule, which are chemically identical in solution, become conformationally non-equivalent in the unit cell. The effects of this conformational difference on the e.s.r. spectra are discussed. The radicals identified in this study are consistent with the work of others on similar systems.

Nous avons entrepris des études de résonance paramagnétique électronique (r.p.e.) sur des cristaux uniques d'acide D-tartrique normal et deutéré; ces études font partie d'un programme élaboré d'études sur la production et la migration radicalaires dans les cristaux uniques reliés à la biologie. Nous nous intéressons plus particulièrement à l'acide D-tartrique puisque les second et troisième atomes de carbone de la molécule, chimiquement identiques en solution, deviennent de conformation non équivalente dans la maille. Nous discutons des effets de cette différence conformationnelle sur les spectres r.p.e. Les radicaux identifiés dans cette étude sont consistants avec les travaux d'autres auteurs sur des systèmes semblables.

[Traduit par le journal]

Canadian Journal of Chemistry, **50**, 3706 (1972)

Can. J. Chem. Downloaded from www.nrcresearchpress.com by 210.87.254.5 on 09/05/12
For personal use only.

Introduction

Previous electron spin resonance (e.s.r.) studies by Rao and Gordy (1) and by Moulton and Cernansky (2, 3) have identified some of the radiation-produced free radicals in single crystals of deuterated DL-tartaric acid. The latter workers pointed out that the radicals which they identified were consistent with those proposed by Schwartz, Hanna, and Bales (4) in a mechanism formulated to explain the production and reactions of radicals in single crystals of carboxylic acids after X- or γ-irradiation. However, several of the radicals predicted by this mechanism were not identified in the DL-tartaric acid spectra and some uncertainty as to the validity of the mechanism remained. Much of this uncertainty is removed in our work which is a detailed study of the D-tartaric acid system.

D-Tartaric acid is chemically similar to DL-tartaric acid, but has a substantially different crystal structure. In addition, the interpretation of e.s.r. spectra is greatly aided by the X-ray crystallographic work that has been done on this system by Beevers and Stern (5) and by Okaya, Stemple, and Kay (6). The dimensions of the unit cell axes are $a = 7.71$ Å, $b = 6.00$ Å, and $c = 6.23$ Å. b corresponds to a two-fold screw axis and the a–c angle is 100°. As may be seen from Fig. 1, the five oxygen and carbon atoms at each end of the molecule are located in two planes set at an angle of 54.6° to each other.

Using the numbering system shown in the figure, it may be observed that carbon atoms 1 and 1′, 2 and 2′, 3 and 3′, 4 and 4′ are symmetrically related pairs. Carbon atoms 2 and 3 are indistinguishable when the molecule is in solution; but are conformationally non-equivalent in the crystal and there is no way that they can be related by symmetry operations. This also applies to carbon atoms 1 and 4. Because of this non-equivalence unpaired electron density created at sites 2 and 3 can lead to radicals which have different e.s.r. spectra. Likewise, distinct e.s.r. spectra may also be expected from radicals whose unpaired spin is centered on positions 1 and 4. These observations are of particular importance in the arguments which follow. In the following pages the nature of the radicals observed at −196 °C, −20 °C, and room temperature are discussed and a subjective

[1]Present address: St. Andrew's College, Aurora, Ontario, Canada.

Can. J. Chem. Downloaded from www.nrcresearchpress.com by 210.87.254.5 on 09/05/12
For personal use only.

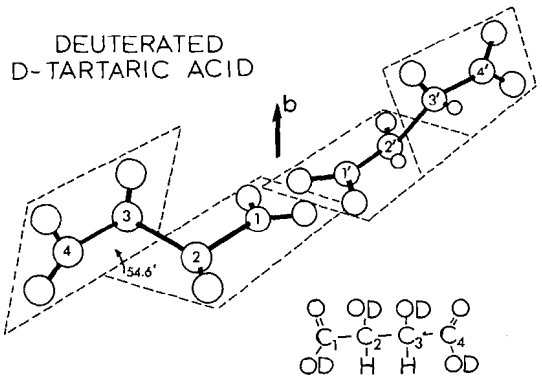

FIG. 1. Positions of atoms in the unit cell in a monoclinic crystal of D-tartaric acid. Deuterated positions are also shown.

interpretation of radical distributions at similar sites is made on the basis of some of the known physical properties of the unit cell. Finally, a mechanism is proposed which explains some of the steps in the radical migration process.

Experimental Procedure

Monoclinic ($P2_1$) single crystals of both normal (Nutritional Biochemical Corporation) and deuterated D-tartaric acid were grown by slow cooling of saturated solutions. Deuteration was accomplished by successive recrystallizations from D_2O to ensure that all exchangeable protons were 99.9% deuterated.

The crystals, which were checked by a polarizing microscope to be single crystals, were irradiated at -196 °C with a ^{60}Co γ-ray source (Gammacell 220, Atomic Energy of Canada Ltd) to a dosage of approximately one Mrad at a dose rate of about 1 Mrad per hour.

All e.s.r. measurements were made on a Varian E-12 X-band spectrometer equipped with Fieldial and a variable temperature apparatus. With the exception of a few room temperature spectra, only first order lines were observed and the corresponding first order spin Hamiltonian

$$\mathcal{H} = \beta\, \mathbf{S.g.H} + \mathbf{S.A.I}$$

was used in calculations. Hyperfine tensors (**A**) and **g** tensors were obtained from data taken at 10° intervals about three mutually perpendicular axes which were chosen to be the *a'bc* axes of the crystal (Fig. 2). Tensors were diagonalized by computer using a method based on the theoretical work of Schonland (7).

Results

Three different radicals were apparent in spectra of normal and deuterated crystals when observation and irradiation were carried out at liquid nitrogen temperatures. Figure 3 shows two typical spectra taken with *b* parallel to the external magnetic field; the lines are numbered to correspond to the three radical types. Experimental hyperfine (A) values and g-values in the $a'b$ plane are given in Fig. 4 for each set of lines. The principal values and direction cosines of the **A** and **g** tensors of these and all radicals appearing at higher temperatures are given in Tables 1 and 2, respectively.

As the crystals were slowly warmed there was a dramatic change in the spectra beginning at approximately -90 °C and tapering off at -20 °C. The strong doublet of Fig. 3*a* began to

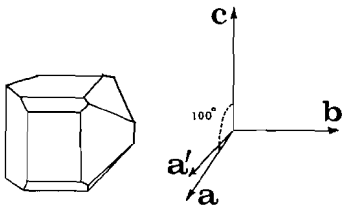

FIG. 2. The crystal habit of monoclinic crystals of D-tartaric acid.

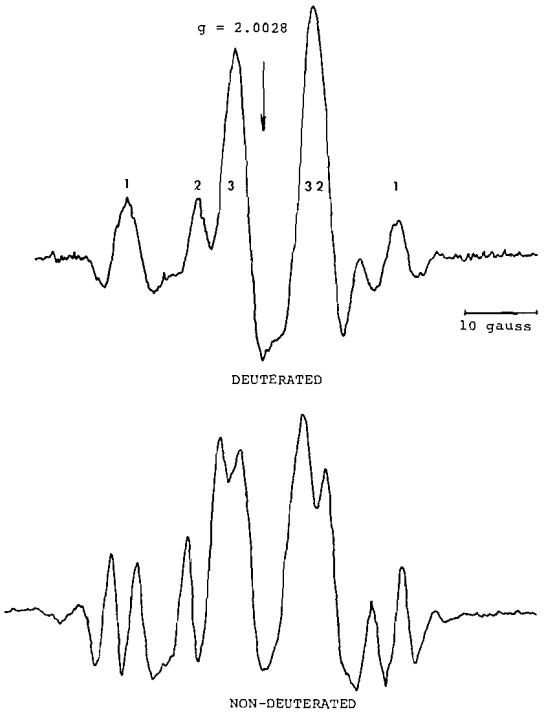

FIG. 3. Second-derivative spectra of deuterated and non-deuterated D-tartaric acid crystals irradiated and observed at -196 °C with *b* parallel to the external magnetic field.

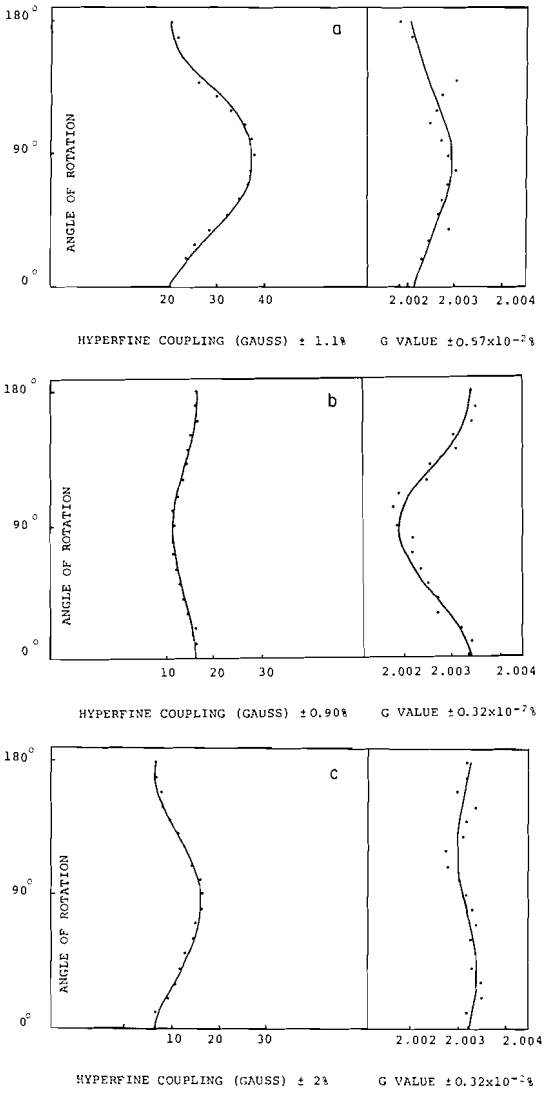

FIG. 4. Experimental (dots) and least squares fit (solid line) data for (*a*) spectral lines 1 in the *a'b* plane; (*b*) spectral lines 2 in the *a'b* plane and (*c*) spectral lines 3 in the *a'b* plane. See Fig. 3 for numbering system. *b* is parallel to the external magnetic field at 0°. Samples were irradiated and observed at −196 °C.

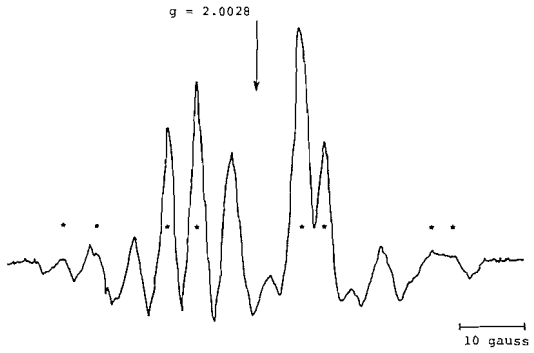

FIG. 5. Typical spectrum obtained after warming to −20 °C. The eight new lines are starred.

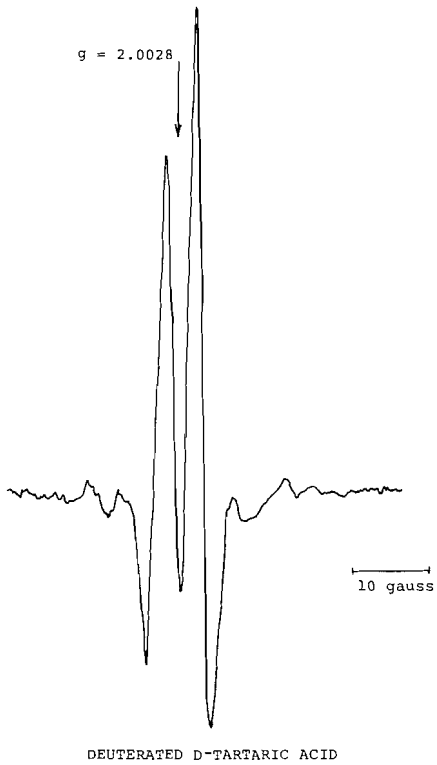

FIG. 6. Typical spectrum obtained after warming to room temperature. Observed at −196 °C.

decrease and eight new lines appeared as shown in Fig. 5. The changes were irreversible and all data was taken after recooling to −196 °C.

The spectra obtained from samples irradiated at liquid nitrogen temperature and warmed to room temperature for several hours and then recooled to liquid nitrogen temperature for observation were identical to spectra resulting from irradiation at room temperature and observation at liquid nitrogen temperature. A typical spectrum resulting from these procedures is shown in Fig. 6 and appears to result from two different radicals. Lines having the characteristics of second order effects were observed in these particular spectra.

Can. J. Chem. Downloaded from www.nrcresearchpress.com by 210.87.254.5 on 09/05/12
For personal use only.

TABLE 1. Principal A-values and direction cosines

Sample treatment	Proposed radical	Principal A-values (G)	Direction cosines with respect to $a'bc$ axes		
Irradiated and observed at −196 °C	"A" on site 4 (lines 1, Fig. 3)	$A_{xx} = 35.6$	0.99	0.04	0.06
		$A_{yy} = 29.0$	−0.03	−0.01	0.99
		$A_{zz} = 20.0$	0.06	0.99	0.04
		error ±1.0*			
	"A" on site 1 (lines 3, Fig. 3)	$A_{xx} = 16.3$	0.96	−0.07	−0.27
		$A_{yy} = 11.1$	0.06	0.99	−0.03
		$A_{zz} = 9.8$	0.28	0.01	0.96
		error ±0.5*			
	"B" on site 1 (lines 2, Fig. 3)	$A_{xx} = 19.4$	−0.01	0.06	0.99
		$A_{yy} = 16.2$	0.10	0.99	−0.06
		$A_{zz} = 5.8$	0.99	−0.10	0.02
		error ±0.8*			
Warmed to −20 °C	"C" on site 2	$A_{xx} = 33.5$	0.96	0.10	−0.26
		$A_{yy} = 21.8$	−0.07	0.99	0.12
		$A_{zz} = 12.1$	0.27	−0.10	0.96
		error ±1.5*			
Warmed to 22 °C	"D" on site 2	$A_{xx} = 5.7$	0.95	−0.11	0.28
		$A_{yy} = 4.4$	−0.18	0.52	0.83
		$A_{zz} = 3.5$	0.24	0.84	−0.48
		error ±0.5*			
	"D" on site 3	$A_{xx} = 31.0$	0.99	−0.09	−0.09
		$A_{yy} = 24.2$	0.01	−0.62	0.78
		$A_{zz} = 23.2$	0.13	0.78	0.62
		error ±1.0*			

*Error based on quality of fit.

Discussion

The primary feature of the spectra observed in deuterated D-tartaric acid single crystals after irradiation at liquid nitrogen is a strong doublet (labelled doublet 3 in Fig. 3) with a splitting of approximately 12 G. This spectrum could arise from any one of a total of the ten possible radicals shown in Fig. 7. Because the strong doublet is weakly anisotropic, it most likely arises from a single β-hydrogen coupling or in other words from a hydrogen situated on the carbon atom adjacent to the site of the unpaired spin. The only radicals that have single β-hydrogens are "A", "B", "D", "G", "H", and "I". In spectra of the non-deuterated crystals these two lines are split by a second isotropic β-hydrogen so that possibilities "B", "G", "H", and "I" are eliminated. Radicals "G" and "H" can also be discounted as these species have never before been reported in single crystal studies and are believed to be extremely unstable. Consequently only radicals "D" and "A" have arrangements of β-protons which are consistent with the observed spectra. Other evidence that will be considered later suggests that radical "D" is observed at room temperature, but not at liquid nitrogen temperature. Thus we ascribe the strong doublet observed at liquid nitrogen to radical "A". Moulton and Cernansky (2) have observed the same radical in DL-tartaric acid.

There are two possible sites for radical "A" in each molecule, *i.e.* positions 1 and 4. The direction cosines of the minimum g-value corresponding to the intense doublet are 0.05, 0.99, 0.08 which suggest that the principal axis of the p-orbital is essentially along b. Consideration of the atomic coordinates of the molecule indicates that p-orbitals on 4 and 4′ are along a whereas p-orbitals on 1 and 1′ should be along b. It may be concluded from this that the intense doublet arises from the carboxyl radical "A" with the unpaired electron primarily on carbon 1 of the D-tartaric acid molecule.

The spectrum shown in Fig. 3 contains another doublet (labelled doublet 1) which demonstrates site splitting at certain orientations. This site splitting arises from symmetrically related sites which become non-equivalent at certain

Can. J. Chem. Downloaded from www.nrcresearchpress.com by 210.87.254.5 on 09/05/12
For personal use only.

TABLE 2. Principal g-values and direction cosines

Sample treatment	Proposed radical	Principal g-values	Direction cosines with respect to $a'bc$ axes		
Irradiated and observed at −196 °C	"A" on site 4 (lines 1, Fig. 3)	$g_{xx} = 2.0047$	−0.209	−0.045	0.977
		$g_{yy} = 2.0026$	0.041	0.998	0.055
		$g_{zz} = 2.0020$	0.977	0.051	−0.208
		error ±0.0004*			
	"A" on site 1 (lines 3, Fig. 3)	$g_{xx} = 2.0035$	−0.388	−0.062	0.919
		$g_{yy} = 2.0033$	0.920	−0.081	0.383
		$g_{zz} = 2.0017$	0.051	0.995	0.088
		error ±0.0002*			
	"B" on site 1 (lines 2, Fig. 3)	$g_{xx} = 2.0041$	−0.107	−0.051	0.993
		$g_{yy} = 2.0033$	0.828	0.548	0.117
		$g_{zz} = 2.0029$	−0.549	0.835	−0.016
		error ±0.0002*			
Warmed to −20 °C	"C" on site 3	$g_{xx} = 2.0029$	−0.208	0.793	−0.573
		$g_{yy} = 2.0025$	−0.644	0.552	0.529
		$g_{zz} = 2.0021$	0.208	0.793	−0.573
		error ±0.0003*			
	"C" on site 2	$g_{xx} = 2.0046$	0.512	−0.139	0.848
		$g_{yy} = 2.0035$	0.613	0.751	−0.246
		$g_{zz} = 2.0033$	0.602	−0.645	−0.469
		error ±0.0003*			
Warmed to 22 °C	"D" on site 2	$g_{xx} = 2.0048$	0.839	0.017	0.544
		$g_{yy} = 2.0034$	−0.533	0.233	0.813
		$g_{zz} = 2.0023$	0.113	0.972	−0.205
		error ±0.0002*			
	"D" on site 3	$g_{xx} = 2.0048$	−0.509	0.305	0.805
		$g_{yy} = 2.0028$	0.818	−0.119	0.562
		$g_{zz} = 2.0019$	0.267	0.945	−0.189
		error ±0.0003*			

*Errors based on quality of fit.

angles of rotation with respect to the external magnetic field. Normals to the planes containing sites 4 and 4′ are not parallel and hence site splitting should be observed with this set. Such site splitting is not expected with sites 1 and 1′ as their corresponding normals are parallel. Spectra from non-deuterated samples showed that the lines from the deuterated crystals were further split by a second β-hydrogen. This evidence plus the fact that the direction cosines of the minimum g-values are approximately along a' suggests that these lines probably arise from type "A" radicals situated on sites 4 and 4′. The large difference observed in the doublet splitting and anisotropy between type "A" radicals on sites 1 and 4 (see Table 1) is thought to be a result of differences in both electron densities and bond angles at these two sites. While we prefer this argument we cannot exclude the possibility that doublet 1 arises from the single α-proton of radical "F". In view of all the research done in organic acids this radical seems to be an unlikely candidate. Isotopic labelling studies will probably be necessary to remove the ambiguity.

There is finally another poorly resolved and weakly anisotropic doublet (labelled doublet 2 in Fig. 3) which appears in the liquid nitrogen spectra. This doublet is not additionally split in the non-deuterated crystals. The only radicals which have a β-hydrogen but no adjacent hydroxyl protons are radicals "B" and "G". Since "G" is highly unlikely, we ascribe doublet 2 in Fig. 3 to radical "B". Analysis of the **g**-tensor of the species is somewhat uncertain but it appears that the direction of the orbital containing the unpaired spin is along b.

Conclusive statements regarding the stabilities of radicals "A" and "B" are also difficult because lines due to product radicals formed

Can. J. Chem. Downloaded from www.nrcresearchpress.com by 210.87.254.5 on 09/05/12
For personal use only.

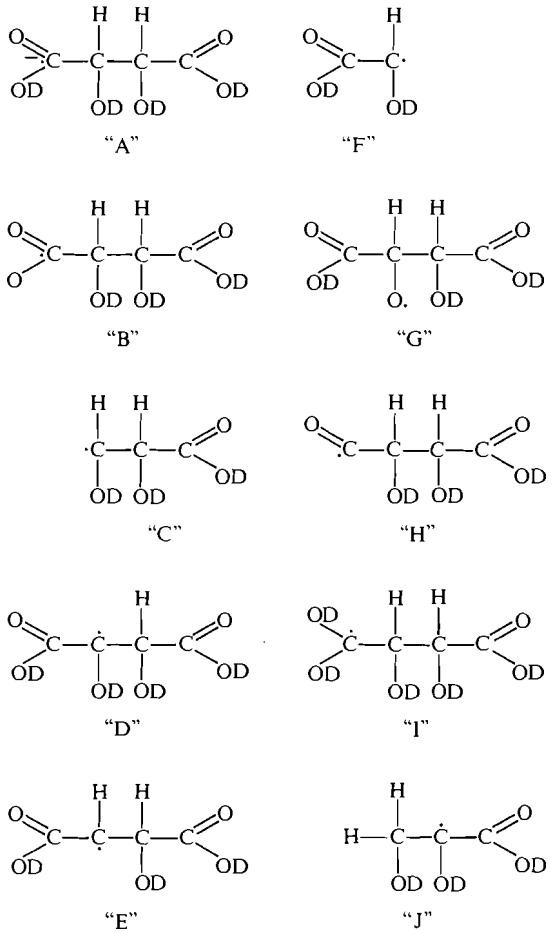

FIG. 7. Possible radicals from D-tartaric acid. Positions that can be deuterated are indicated by the letter D.

by heating mask their decay. Nevertheless, it appears that radical "A" is more stable than radical "B" and lines due to "A" are visible at -20 °C. No trace of the doublet ascribed to radical "B" was found at temperatures greater than -90 °C.

The eight new lines arising after warming to -20 °C are shown in Fig. 5 and are of two types. One set of four lines is typical of α- and β-hydrogen splitting. Radicals types "C" and "E" are the only ones that can give this type of splitting. It is generally believed that decarboxylation by electron transfer is energetically more favorable than hydroxyl radical abstraction. Radical "E" is eliminated because of this argument. Moulton and Cernansky (3) also have concluded that radical "C" is present at -20 °C in DL-tartaric acid.

The minimum g value of this radical is almost along the b axis indicating that the radical probably is situated at sites 2 and 2′. The outside four lines demonstrate site splitting, and are anomalous in that the isotropic hyperfine splitting between them is 50 G. This number is too large for the type of radicals that can occur in this system. Thus two additional lines must exist under the more intense lines found at the center of the spectra. This set of lines is believed to arise from type "C" radicals situated on sites 3 and 3′. The site splitting is consistent with radicals situated on 3 and 3′. Also observed is a single line that is hidden under the right hand line of the intense doublet. This line is thought to be due to a CO_2^- radical that is produced on decarboxylation of the carboxyl groups. We estimate the average g-value of this line to be 2.000 with an uncertainty of 0.002. This agrees with values of $\langle g \rangle$ for the CO_2^- radical obtained by Janecka, Vyas, and Fujimoto (8) and Schwartz, Hanna, and Bales (4). The species is very stable and exists in single crystals at room temperature where it absorbs in the same position in the spectrum.

As deuterated D-tartaric acid was further warmed to room temperature the spectra changed once more with the lines at -20 °C disappearing and eight new lines appearing. Again an intense doublet is seen in the spectra in Fig. 6. These two lines are split by 8 G and are characteristic of a β-hydrogen interaction with the unpaired electron. If one considers all the remaining possibilities in Fig. 7 only radical "D" could give the β-hydrogen splitting observed. The direction cosines associated with the minimum g-value indicate that the p-orbital is along b and resides on sites 2 and 2′. Further evidence that this is radical "D" is observed in the non-deuterated sample where the strong doublet does not split. This would be expected if the β-hydrogen on the oxygen is in the nodal plane of the p-orbital containing the unpaired electron. A model of the unit cell based on atomic positions given by Okaya, Kay and Stemple (6) agrees with this.

The pair of lines next to this intense doublet are believed to be second order lines. Evidence for this is that the intensities are angularly de-

Can. J. Chem. Downloaded from www.nrcresearchpress.com by 210.87.254.5 on 09/05/12
For personal use only.

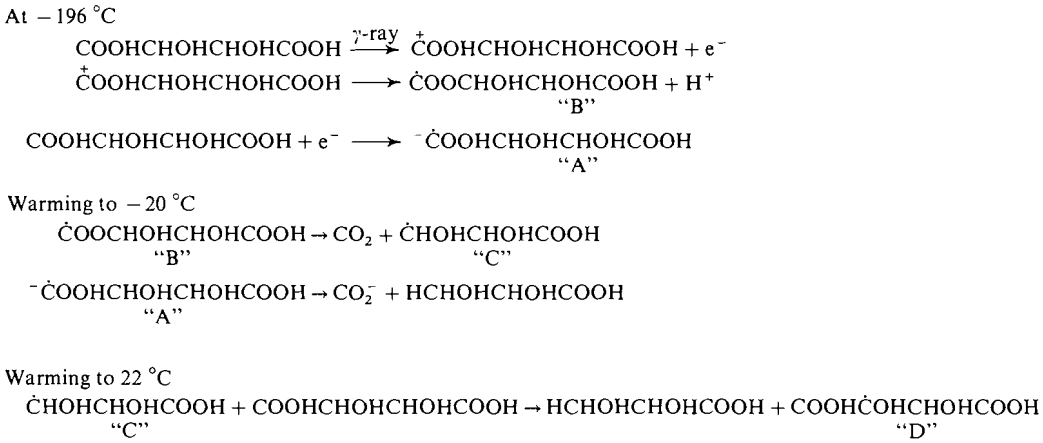

FIG. 8. Mechanism for radical production and migration in D-tartaric acid.

pendent, with virtually no deviation from the constant splitting of 8 G from the major doublet. Rao and Gordy (1) have observed the intense doublet of radical "D" in DL-tartaric acid at room temperature. They also observed a pair of lines separated by 8 G from the intense doublet which were proved to be second order lines by measuring the crystal spectra at two different microwave frequencies.

Also observed in the wings of the room temperature spectra are a set of poorly resolved lines with an isotropic hyperfine splitting of approximately 30 G. These are attributed to radical "D" where the unpaired electron is situated on sites 3 and 3′. These outer lines are broad, which may be due to the site splitting expected for such radicals. The inability to resolve this site splitting leads to an averaging of the *a* and *c* components of the **g** tensor and hence the minimum *g*-value falsely appears to be aligned along *b* instead of the calculated direction *c*. The two outermost lines are believed to be the second order lines arising from radical "D" situated on sites 3 and 3′ since they demonstrate all the required characteristics of second order effects.

Because of the peculiar symmetry properties of D-tartaric acid crystals, it is possible to observe the distribution of radicals at chemically similar, but conformationally different sites. The effect was observed at room temperature where type "D" radicals predominated at site 2 relative to site 3. Similarly, there was a higher concentration of type "C" radicals on position 2 than on position 3 in crystals which had been warmed from −196 to −20 °C. Finally in the spectra observed at −196 °C with no warming of the sample, type "A" anion radicals were identified at site 1 and possibly at site 4. From a crude observation of line widths and intensities it was apparent that there were significantly more radicals on position 1 than on position 4.

There are few apparent reasons for these observations. All that can be suggested at the present time is that the preferred sites, namely 1 and 2 are better able to stabilize radicals. If one considers the positions of atoms in the unit cell as determined by Okaya, Stemple, and Kay (see Fig. 1), the plane containing sites 1 and 2 is somewhat more planar than the plane containing sites 3 and 4 and better able to delocalize the unpaired spin. This plus small differences in bond angles and lengths may account for the radical distributions which we observe.

The radicals previously discussed must all be accounted for not only in terms of spectral identification but also the ease of formation by some sort of chemical mechanism in the solid state.

Because of the high energy of the cobalt 60 γ rays (1.33 MeV) the initial radiation damage should be completely random throughout the crystal. The primary event at this energy is due to Compton scattering which leads to the ejection of energetic electrons from molecular orbitals. These electrons can have sufficient energy to eject other electrons from molecular orbitals. The electron density of tartaric acid is

Can. J. Chem. Downloaded from www.nrcresearchpress.com by 210.87.254.5 on 09/05/12
For personal use only.

greatest at the carboxyl groups and therefore electron ejection should predominate at these sites. Once the electron has been ejected from the carboxyl group it can migrate through the lattice until it is trapped. The large electron affinity of the carboxyl groups also makes them best candidates for trapping sites. If an electron is knocked out of the carboxyl group then the anion species can be formed easily and further decays to the neutral species radical "B". This mechanism is proton migration over a hydrogen bridge and is shown in Fig. 8.

As the sample is warmed a decarboxylation reaction on radical "A" occurs at approximately $-90\,^{\circ}C$ and is complete at $-20\,^{\circ}C$. In this process hydrogen atom migration occurs from the carboxyl species to the adjacent carbon atom. The neutral radical "B" also decarboxylates to give radical "C" and carbon dioxide. At room temperature these secondary radicals are able to abstract hydrogen from positions 2 and 3 of other molecules in the lattice to give the tertiary species "D", which is stable even to temperatures approaching the melting point of the crystal.

These studies support the observation of Moulton and Cernansky on the DL-tartaric acid system, and those of Schwartz, Hanna, and Bales on the succinic acid system. Further work is underway on the *meso*-tartaric acid systems to provide additional confirmation of the mechanism.

This work was supported by Ontario Department of University Affairs grant #640-60. We are indebted to W. A. Bernhard for the use of his computer program and to M. Fujimoto for many valuable discussions.

1. D. V. G. L. N. RAO and W. GORDY. J. Chem. Phys. **36**, 1143 (1962).
2. GRACE C. MOULTON and B. CERNANSKY. J. Chem. Phys. **51**, 2283 (1968).
3. GRACE C. MOULTON and B. CERNANSKY. J. Chem. Phys. **53** 3022 (1970).
4. R. N. SCHWARTZ, N. W. HANNA, and B. L. BALES. J. Chem. Phys. **51**, 4336 (1969).
5. C. A. BEEVERS and F. STERN. Acta Cryst. **3**, 341 (1950).
6. Y. OKAYA, N. R. STEMPLE, and M. I. KAY. Acta Cryst. **21**, 237 (1966).
7. D. S. SCHONLAND. Proc. Roy. Soc. (London), **A**73, 788 (1959).
8. J. JANECKA, H. M. VYAS, and M. FUJIMOTO. J. Chem. Phys. **54**, 3229 (1971).

Can. J. Chem. Downloaded from www.nrcresearchpress.com by 210.87.254.5 on 09/05/12
For personal use only.

Rhodium(I) and (III) Complexes of Some Phospholes and Their Behavior as Homogeneous Hydrogenation Catalysts

DAVID G. HOLAH, ALAN N. HUGHES, AND BENJAMIN C. HUI
Department of Chemistry, Lakehead University, Thunder Bay, Ontario

Received June 20, 1972

Reactions between rhodium(III) chloride hydrate and certain phospholes are described; these result in the formation of both Rh(III) and Rh(I) complexes. The phospholes also react with Rh(I) carbonyl and ethylene complexes. The products of these reactions were investigated as homogeneous catalysts in the hydrogenation of 1-hexene, and some show relative rates of hydrogenation comparable with that of hydridocarbonyltris(triphenylphosphine)rhodium(I) but slower than that of tris(triphenylphosphine)rhodium (I) chloride.

Les réactions entre le chlorure de rhodium(III) hydraté et certains phospholes sont décrites et conduisent aux complexes de Rh(III) et Rh(I). Les phospholes réagissent aussi avec les complexes de Rh(I) carbonyle et éthylène. Les produits de ces réactions ont été étudiés comme catalyseurs en phase homogène dans l'hydrogénation de l'hexène-I et certains d'entre eux donnent des vitesses relatives d'hydrogénation comparables à celles de l'hydrure carbonyltris(triphénylphosphine) rhodium(I) mais inférieures à celles du chlorure de tris(triphénylphosphine)rhodium(I). [Traduit par le journal]

Canadian Journal of Chemistry, **50**, 3714 (1972)

Can. J. Chem. Downloaded from www.nrcresearchpress.com by 210.87.254.40 on 09/05/12
For personal use only.

Introduction

We have previously reported transition metal complexes of 1,2,5-triphenylphosphole (TPP) (a derivative of the aromatic phosphole system) and its oxide (TPPO), sulfide (TPPS), and selenide (1, 2). Coordination of the ligands to the metal ions occurs through the donor atoms in all cases except for the TPPO complexes of Rh(I) where the π-diene system of the ligand is involved (2). In view of the interesting complexes obtained from the rhodium system, a study of reactions between some other unsaturated cyclic phosphines and rhodium halides was undertaken. In this paper, we report some substituted phosphole complexes of Rh(I) and Rh(III), together with preliminary data on the catalytic properties of these compounds.

Results and Discussion

(A) Rhodium(III) Complexes

Rhodium(III) chloride trihydrate in ethanol or butanol reacts almost instantly with up to 6-fold excesses of DBP (9-phenyl-9-phosphafluorene) and, under reflux for short periods, PP (1-phenylphosphole) to produce yellow, air-stable solids of composition $RhCl_3L_3$ (L = DBP or PP) which can be recrystallized from methylene chloride. With a similar excess of TPP, the complex $RhCl_3(TPP)$ is formed first (3) in solution, but when the reaction mixture is heated under reflux for at least 24 h, the stable, yellow-brown hydrido complex $RhHCl_2(TPP)_2$ is produced. There appears to be no change in the composition of the $RhCl_3L_3$ complexes when suspensions of these are heated under reflux for long periods.

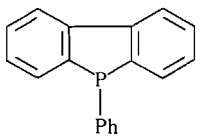

DBP

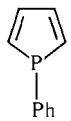

PP

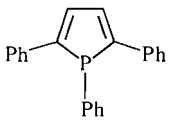

TPP

Little structural information is available from infrared spectra which are very similar to those of the ligands, but it appears that DBP and PP behave in a rather similar manner to some other tertiary alkyl or arylalkyl phosphines (*e.g.* Et_3P, Me_2PhP, Bu^n_3P) which also form (4–6) stable Rh(III) complexes of the type RhX_3L_3. On the other hand the behavior of TPP parallels that of more bulky phosphines which form (6, 7) analogous hydrido species $RhHCl_2L_2$ (L = $Bu^tPr^n_2P$, Bu^i_2MeP, Bu^i_2EtP, or $Bu^i_2Pr^nP$) from $RhCl_3.3H_2O$ and the ligands L. In contrast $RhHCl_2(Ph_3P)_2$ has only been prepared (8) from $RhCl(Ph_3P)_3$ and HCl. The far infrared spectrum of $RhHCl_2(TPP)_2$ shows only one Rh—Cl stretching frequency at 285 cm^{-1}, and vibrations of Rh—Cl containing compounds in

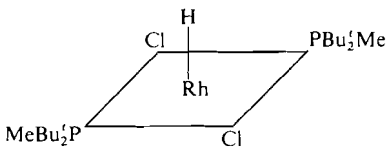

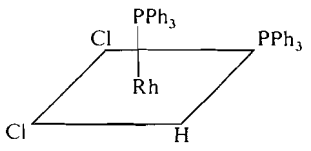

this frequency range have been interpreted (7) as indicating the presence of mutually *trans* chlorine atoms (*cf. cis* chlorine atoms show two Rh—Cl stretching frequencies (7)). The Rh—H stretching frequency in $RhHCl_2(TPP)_2$ occurs at 1990 cm^{-1} compared with 1938 cm^{-1} for $RhHCl_2(Bu^t_2MeP)_2$ (7). These spectral data (as well as n.m.r. data on the latter compound), together with the close similarity in the methods of synthesis of the $RhHCl_2L_2$ complexes (L = TPP, Bu^t_2MeP), suggest that the two complexes have similar structures. In contrast, the $RhHCl_2(Ph_3P)_2$ complex has been assigned (8) a *cis*-chloride structure.

(B) Rhodium(I) Complexes

The products of the reaction between Rh(III) and TPP are very dependent on the solvent and when ethanol is replaced by certain other solvents (in which TPP has a higher solubility), reduction of the Rh(III) occurs. Thus, TPP in chloroform reacts with $RhCl_3.3H_2O$ in methanol (6:1) under reflux conditions to produce an orange solid of composition RhCl(TPPO)(TPP). The infrared spectrum of this complex in the 1100–1200 cm^{-1} region shows that the TPPO is π-bonded to the rhodium (*cf.* ref. 2), and the complex is analogous to $RhCl(TPPO)(Ph_3P)$ which has been previously reported (2). That the rhodium has a stronger affinity towards the π-system of the TPPO in the presence of an excess of TPP again emphasizes the relatively poor donor properties (1) and probably aromatic nature of the substituted phosphole system.

$RhCl_3.3H_2O$ in ethanol reacts with TPPS under reflux to give a brown solid which can be recrystallized from methylene chloride as $RhCl(TPPS).CH_2Cl_2$. The phosphole sulfide, in contrast to TPPO (2), is believed to be bonded to the rhodium through the sulfur atom as shown by a shift in the P—S stretching frequency from 637 cm^{-1} in the free ligand to either 625 or 595 cm^{-1} in the complex. This difference in behavior of the metal towards the O and S donor atoms is not unexpected since rhodium falls into the "class b" acceptor category (9).

Rhodium carbonyl chloride $[RhCl(CO)_2]_2$, in alcoholic solutions, reacts smoothly with an excess of TPP, DBP, or TPPS (1:3) to produce yellow solids characterized as $RhCl(CO)(TPP)_2$, and $RhCl(CO)_2(DBP)$, and black $RhCl(CO)_2$-(TPPS). $RhCl(CO)(TPP)_2$ is also formed from the reaction of $RhCl_3.3H_2O$ with TPP in ethanol under reflux with the subsequent introduction of formaldehyde (10). The carbonyl complexes are likely to have monomeric square planar structures.

The chlorobis(ethylene)rhodium(I) dimer, $[RhCl(C_2H_4)_2]_2$, in methanol solutions reacts with DBP or TPP in a 1:3 ratio under reflux to yield the dimeric complexes $[RhCl(DBP)_2]_2$ and $[RhCl(TPP)_2]_2$. These complexes are air sensitive, apparently taking up oxygen which appears in the form of a broad P=O stretching frequency at 1150 cm^{-1} (*cf.* $[RhCl(Ph_3P)_2]_2$ (11)). Addition of $[RhCl(DBP)_2]_2$ to an excess of DBP (1:6) in methanol under reflux produces an orange-red air-stable solid of composition $RhCl(DBP)_3$. The analogous complex RhCl-$(TPP)_3$ is produced when a 6-fold excess of TPP is heated under reflux with $[RhCl(C_2H_4)_2]_2$ in $CHCl_3$/EtOH (1:1) solution. These complexes are generally similar to other rhodium(I) complexes of tertiary phosphines (5, 6, 11–13).

(C) Catalytic Properties

The activities of the complexes were examined in the homogeneous hydrogenation of 1-hexene. Thus, in a benzene solution and in the presence of Et_3N, $RhHCl_2(TPP)_2$ is an extremely active catalyst for this process at less than 1 atm pressure of hydrogen at 20 °C. There is no activity in the absence of the amine which appears to be essential in stabilizing the proton released as the hydrogen is cleaved heterolytically. This phosphole complex catalyzes the reaction at a rate (Table 1) which is comparable to that at which $RhH(CO)(Ph_3P)_3$ catalyzes this hydrogenation. The similar Rh(III) complexes containing bulky ligands, $RhHCl_2(PBu^tPr^n_2)_2$ and $RhH_2Cl(PBu^t_3)_2$, have recently been reported to be active catalysts for the hydrogena-

Can. J. Chem. Downloaded from www.nrcresearchpress.com by 210.87.254.40 on 09/05/12
For personal use only.

TABLE 1. Relative rates of hydrogenation of 1-hexene (0.5 *M*) in benzene (25 ml total volume) at 60 cm partial pressure of H_2 at 20 °C

Complex	Concentration (m*M*)	Relative rate*
$RhCl(PPh_3)_3$	0.70	42.0
$RhH(CO)(PPh_3)_3$	1.00	10.0
$RhHCl_2(TPP)_2$†	1.00	6.7
$RhCl(DBP)_3$	0.75	4.2
$[RhCl(DBP)_2]_2$	0.42	2.0
$[RhCl(C_2H_4)_2]_2$/DBP‡	1.03 in Rh	2.3
$[RhCl(C_2H_4)_2]_2$/TPP§	0.89 in Rh	~1.0
$RhCl(TPP)_3$	0.71	~0.1

*Rate for $RhH(CO)(PPh_3)_3$ is arbitrarily set at 10.
†In the presence of 2.15 m*M* Et_3N.
‡DBP/Rh = 2.
§TPP/Rh = 2.

tion of olefins (7), but the other Rh(III) complexes prepared in this work are not active under similar conditions.

The Rh(I) complexes, $RhCl(DBP)_3$, and $[RhCl(DBP)_2]_2$ in benzene solutions also catalyze the 1-hexene hydrogenation at 20 °C; the former being about twice as fast as the latter. The presence of a base is not required and the solutions containing the catalysts generally turned yellow before addition of the olefin, indicative of the formation of a dihydride (11). *In situ* production of a catalytically active species can be achieved by adding $Rh_2Cl_2(C_2H_4)_4$ to a 2-fold excess of DBP (or TPP) in benzene. Instantaneous reaction between the Rh(I) species and the ligand occurs and the rate of hydrogenation by the $Rh_2Cl_2(C_2H_4)_4$/DBP system is the same as when $Rh_2Cl_2(DBP)_4$ itself is used. When Ph_3P is replaced by DBP or TPP, the rate decreases and this is possibly due to the interaction of the phosphorus lone pair electrons with the π-system which results in decreasing the electron density on the Rh atom. Alternatively, steric effects may be responsible for this decrease in activity.

The other Rh(I) complexes, *e.g.* $RhCl(CO)(TPP)_2$, RhCl(TPPO)(TPP), and $[RhCl(TPPO)]_2$ (2), show no activity at 20 °C, and less than 1 atm pressure of hydrogen but the last compound shows a slight activity at 60 °C.

Detailed kinetic studies have been carried out on certain of these systems and will be published separately.

Experimental

1-Phenylphosphole (14), the other phosphole ligands (1), hydridocarbonyltris(triphenylphosphine)rhodium(I) (15), chlorobis(carbonyl)rhodium(I) (16), and chlorobis(ethylene)rhodium(I) (17) were prepared as described in the literature. Rhodium trichloride hydrate was obtained from Engelhard Industries. Reactions generally involved the appropriate rhodium compound in quantities corresponding to ~50 mg Rh in ~100 ml of solvent, and the products were dried by heating under vacuum (10^{-6} Torr) at 30–50 °C.

Microanalyses (Table 2) were carried out on a Perkin–Elmer 240 Elemental Analyzer at this institution. Chloride analyses (2) and physical measurements were made as described previously (18).

For the catalysis experiments, 1-hexene was treated with iron(II) salts, distilled over calcium hydride and stored under nitrogen at all times. Reagent grade benzene was used without further purification. In a typical run (11) the catalyst was weighed into a Teflon basket which was then suspended from a side arm of a 100 ml 3-necked flask. The olefin was contained in a burette fitted to the other side arm and the reaction flask was connected to a standard vacuum system by a condenser.

$RhCl_3(DBP)_3.0.5CH_2Cl_2$

To a solution of DBP in hot ethanol was added a solution of $RhCl_3.3H_2O$ in ethanol (6:1 mole ratio). Precipitation of the product occurred almost immediately and the solution was heated under reflux for $\frac{1}{2}$ h. The hot solution was filtered and the yellow crystals washed with ethanol and ether (95% yield). The product was recrystallized from methylene chloride as $RhCl_3(DBP)_3.0.5CH_2Cl_2$.

The same product was obtained by heating the reaction mixture for 24 h by using 3:1 mole ratio of reactants, or by using butanol as solvent.

$RhCl_3(PP)_3$

PP was added dropwise to $RhCl_3.3H_2O$ (6:1) in hot ethanol and the mixture heated under reflux for $\frac{1}{2}$ h. The yellow solid was filtered off and washed with ethanol and ether (yield 60%).

$RhHCl_2(TPP)_2$

A mixture of $RhCl_3.3H_2O$ and TPP (1:3) in ethanol was heated under reflux for at least 40 h after which the hot solution was filtered. The yellow-brown solid was washed with ethanol and ether (yield 75%).

$RhCl(CO)(TPP)_2$

(*a*) An ethanol solution of $RhCl_3.3H_2O$ was added to a suspension of TPP in hot ethanol (1:4) and the mixture heated under reflux for 10 min during which time the solution turned brown. An excess of formaldehyde was added and a yellow precipitate quickly formed. The mixture was heated under reflux for a further 1 h, filtered, and the yellow crystals washed with chloroform and ether and recrystallized from benzene (yield 75%).

(*b*) TPP suspended in ethanol was added to an ethanol solution of $Rh_2Cl_2(CO)_4$ (3:1) and the mixture heated under reflux for 1 h during which time yellow crystals were formed. These were filtered off and washed with chloroform and ether (yield 85%).

Can. J. Chem. Downloaded from www.nrcresearchpress.com by 210.87.254.40 on 09/05/12
For personal use only.

Can. J. Chem. Downloaded from www.nrcresearchpress.com by 210.87.254.40 on 09/05/12
For personal use only.

TABLE 2

Compound	Color	Melting point (°C)	Analyses*			Infrared spectra (cm^{-1})			
			C	H	Cl	νRh—H	νC=O	νP=S or νP=O	νRh—Cl
$RhCl_3(DBP)_3 0.5CH_2Cl_2$†	yellow	275–278	63.1 63.40	3.9 3.91	10.5‡ 10.30				290, 308, 345
$RhCl_3(PP)_3$	yellow	decomp 254	52.8 52.24	4.3 3.95	14.9 15.42				288, 310
$RhHCl_2(TPP)_2$	yellow-brown	decomp 224–226	65.4 66.10	4.3 4.41	8.9 8.87	1990			285
$RhCl(CO)(TPP)_2$	yellow	288	68.4 68.32	4.4 4.33	4.2 4.48		1985		320
$RhCl(CO)_2(DBP).MeOH$†	yellow	165	51.8 51.83	3.5 3.52	7.3 7.28		1988 1960		315
$RhCl(TPPS).CH_2Cl_2$†	green-brown	decomp 255	49.8 48.66	3.3 3.37	6.6‡ 6.25			625 595?	275
$RhCl(CO)_2(TPPS).CH_2Cl_2$†	black	283–285	47.4 48.14	3.0 3.07	5.4‡ 5.68		2020 1983	625 592	300
$Rh_2Cl_2(DBP)_4$	red-brown	153	65.9 65.62	4.1 3.98	5.3 5.38				275
$Rh_2Cl_2(TPP)_4$	orange-brown	151–153	68.4 69.26	4.4 4.49	4.6 4.65				275
$RhCl(DBP)_3$	orange-red	154–155	70.0 70.56	4.3 4.28	3.9 3.86				300
$RhCl(TPP)_3$	brown	140–143	73.9 73.71	4.9 4.78	3.1 3.30				300, 280?
$RhCl(TPPO)(TPP)$	orange	122–125	67.8 67.84	4.9 4.40	4.5 4.55			1205s 1185sh	280

*Calculated values below found.
†Presence of solvent confirmed from n.m.r./mass spectral data.
‡Not including methylene chloride.

$RhCl(CO)_2(DBP).MeOH$

DBP was added to a methanol solution of $Rh_2Cl_2(CO)_4$ (3:1) and the mixture heated under reflux for 2 h. Yellow crystals of the adduct formed and these were collected and washed with methanol and ether (yield 80%).

$RhCl(TPPS).CH_2Cl_2$

A solution of $RhCl_3.3H_2O$ in ethanol was added to TPPS in ethanol (1:2) and the mixture heated under reflux for 15 h. The hot solution was filtered and the resulting brown solid washed with ethanol and ether (yield 90%). The product was recrystallized from methylene chloride/*n*-hexane solution as the methylene chloride adduct.

$RhCl(CO)_2(TPPS).CH_2Cl_2$

TPPS was added to an ethanol solution of $Rh_2Cl_2(CO)_4$ (2:1) and the mixture heated under reflux for 2 h. The black solid was collected, washed with ethanol and ether (yield 50%) and recrystallized from methylene chloride.

$Rh_2Cl_2(DBP)_4$

A mixture of $Rh_2Cl_2(C_2H_4)_4$ and DBP (1:3) in methanol was heated under reflux for 1 h. The solution was filtered at room temperature and the red crystals washed with methanol and ether (yield 85%).

$Rh_2Cl_2(TPP)_4$

A mixture of $Rh_2Cl_2(C_2H_4)_4$ and TPP (1:3) in ethanol was heated under reflux for 2 h. The solution was concentrated, the orange-brown solid filtered off and recrystallized twice from ethanol (yield 65%).

$RhCl(DBP)_3$

The complex $Rh_2Cl_2(DBP)_4$ and DBP (1:6) in methanol were heated under reflux for 1 h and the orange-red crystals which formed were collected and washed with methanol and ether (yield 80%).

$RhCl(TPP)_3$

A mixture of $Rh_2Cl_2(C_2H_4)_4$ and TPP (1:6) in $CHCl_3$/EtOH (1:1) was heated under reflux for 1.5 h. The brown solution was filtered at room temperature, *n*-hexane added and the product was obtained by concentrating the solution. The product was recrystallized from EtOH (yield 60%).

$RhCl(TPPO)(TPP)$

A mixture of $RhCl_3.3H_2O$ (0.13 g) in methanol (10 ml) and TPP (0.84 g) in chloroform (15 ml) (1:6) was heated under reflux for 15 h, the solvent removed and the orange-brown residue extracted into benzene (15 ml). The benzene was removed, the residue extracted into methanol/benzene (1:1) and the solution concentrated to ~10 ml and filtered. The solvent was again removed yielding an orange solid which was recrystallized from ethanol (yield 60%).

We gratefully acknowledge the assistance of the personnel of the Science Instrumentation Laboratory in obtaining micro analytical data.

We also thank the Senate Research Committee of Lakehead University and the National Research Council of Canada for generous financial support.

1. D. Budd, R. Chuchman, D. G. Holah, A. N. Hughes, and B. C. Hui. Can. J. Chem. **50**, 1008 (1972).
2. D. G. Holah, A. N. Hughes, and B. C. Hui. Can. J. Chem. **50**, 2442 (1972).
3. R. A. Walton. J. Chem. Soc. A, 365 (1966).
4. J. Chatt, N. P. Johnson, and B. L. Shaw. J. Chem. Soc. 2508 (1964).
5. R. G. Hayter. Inorg. Chem. **3**, 301 (1964).
6. G. M. Intille. Inorg. Chem. **11**, 695 (1972).
7. C. Masters, W. S. McDonald, G. Raper, and B. L. Shaw. Chem. Commun. 210 (1971).
8. M. C. Baird, J. T. Mague, J. A. Osborn, and G. Wilkinson. J. Chem. Soc. A, 1347 (1967).
9. S. Ahrland, J. Chatt, and N. R. Davies. Quart. Rev. **12**, 265 (1958).
10. D. Evans, J. A. Osborn, and G. Wilkinson. Inorg. Synth. **11**, 99 (1968).
11. J. F. Young, J. A. Osborn, F. H. Jardine, and G. Wilkinson. J. Chem. Soc. A, 1711 (1966).
12. J. T. Mague and G. Wilkinson. J. Chem. Soc. A, 1736 (1966).
13. S. Montelatici, A. van der Ent, J. A. Osborn, and G. Wilkinson. J. Chem. Soc. A. 1054 (1968).
14. F. Mathey, R. Mankowski-Favelier, and R. Maillet. Bull. Soc. Chim. Fr. 4433 (1970).
15. D. Evans, G. Yagupsky, and G. Wilkinson. J. Chem. Soc. A, 2660 (1968).
16. J. A. McCleverty and G. Wilkinson. Inorg. Synth. **8**, 211 (1966).
17. R. Cramer. Inorg. Chem. **1**, 722 (1962).
18. P. R. Heckley, D. G. Holah, and D. Brown. Can. J. Chem. **49**, 1151 (1971).

Can. J. Chem. Downloaded from www.nrcresearchpress.com by 210.87.254.40 on 09/05/12
For personal use only.

Photolysis and Thermolysis of Ethyl Diazomalonanilate and of 5-Hydroxy-1,4-diphenyl-1,2,3-triazole in Various Alcohols

NGUYEN THANH BUU AND J. T. EDWARD

Department of Chemistry, McGill University, Montreal, Quebec

Received March 2, 1972

Ethyl diazomalonanilate was photolyzed in three alcohols (methanol, ethanol, and isopropanol) to produce the corresponding ethyl α-alkoxymalonanilates, ethyl alkyl α-*N*-phenylaminomalonates, and ethyl malonanilate. Thermolysis of the diazoanilide in ethanol and isopropanol yielded the same products as photolysis, but in lower yields. The yield of ethyl malonanilate increased with benzophenone sensitization.

Photolysis and thermolysis of 5-hydroxyl-1,4-diphenyl-1,2,3-triazole in isopropanol produced α-isopropoxy-α-phenylacetanilide, isopropyl α-*N*-phenylamino-α-phenylacetate, and 2,5-diketo-1,3,4,6-tetraphenylpiperazine.

Possible mechanisms for the decomposition of both compounds are discussed; an α-lactam may be an intermediate in the formation of the α-*N*-phenylamino esters.

La photolyse du diazomalonanilate d'éthyle dans les trois alcools (méthanol, éthanol, et isopropanol) fournit les trois produits suivants: α-*N*-alkoxymalonanilates d'éthyle, α-*N*-phénylaminomalonates d'éthyle et d'alkyle, et malonanilate d'éthyle. La thermolyse du diazoanilide dans l'éthanol et l'isopropanol produit les mêmes composés que ce de la photolyse, mais avec rendement inférieur. Le rendement du malonanilate d'éthyle s'augmente grandement avec la sensitization par benzophénone.

La photolyse et la thermolyse du 5-hydroxy-1,4-diphényl-1,2,3-triazole dans l'isopropanol fournissent α-isopropoxy-α-phénylacetanilide, α-*N*-phénylamino-α-phénylacetate d'isopropyle, et 2,5-dicéto-1,3,4,6-tetraphénylpiperazine.

Des possibles mécanismes pour la décomposition des deux composés sont discutés; un intermédiaire du genre de α-lactam peut être impliqué dans la formation des esters α-*N*-phénylamino.

Canadian Journal of Chemistry, **50**, 3719 (1972)

Can. J. Chem. Downloaded from www.nrcresearchpress.com by 210.87.254.105 on 09/05/12
For personal use only.

Introduction

The photochemical and thermal decomposition of α-diazoesters have recently received considerable attention (1–5). In particular, the photolysis of ethyl diazoacetate in alcohols (2, 3) has led to products resulting from novel reaction paths. The photolysis of α-diazoamides, on the other hand, has been virtually ignored (3), perhaps because of the difficulties encountered in the preparation of these compounds (6).

The most general method for the preparation of α-diazoamides consists of diazotizing an α-amino ester, and then converting the ester into an amide (7). The feasibility of this method is limited by the availability and reactivity of α-amino esters (3).

We have used a second method, due to Dimroth (8), in which an azide reacts with the carbanion of an ester to yield a triazole (see Scheme 1). These triazoles are in equilibrium to varying extents with the tautomeric α-diazoamides (9). In the case of the triazole (**1***a*) obtained by reaction of ethyl malonate with phenyl azide, the equilibrium lies to the extent of 99.7% on the side of ethyl diazomalonanilate (**2***a*), because of the electron-withdrawing character of the carbethoxy group. In contrast, diazoacetamide exists to the extent of more than 99% in the form of the triazole tautomer (10), and 5-hydroxy-1,4-diphenyl-1,2,3-triazole (**1***b*), obtained by the reaction of ethyl phenylacetate with phenylazide (11), exists almost completely as the triazole tautomer.

We now report studies of the products from the thermal and photochemical decomposition of the diazoamide **2***a* and of the triazole **1***b*.

Experimental

General Procedures

Photolyses were carried out at temperatures between 10 and 25 °C in a Rayonnet photochemical reactor equipped with eight low-pressure mercury lamps of 2537 Å wavelength, unless otherwise noted. A stream of nitrogen was bubbled through the solution before each irradiation, and photolysis was continued until there was no further change in the i.r. spectrum of the reaction mixture. Solvents were evaporated at reduced pressure, at room temperature, and residues were chromatographed on plates coated with a 1 mm layer of silica containing a fluorescent indicator (Silica Gel H_F254 acc. to Stahl, Canlab, Montreal), using

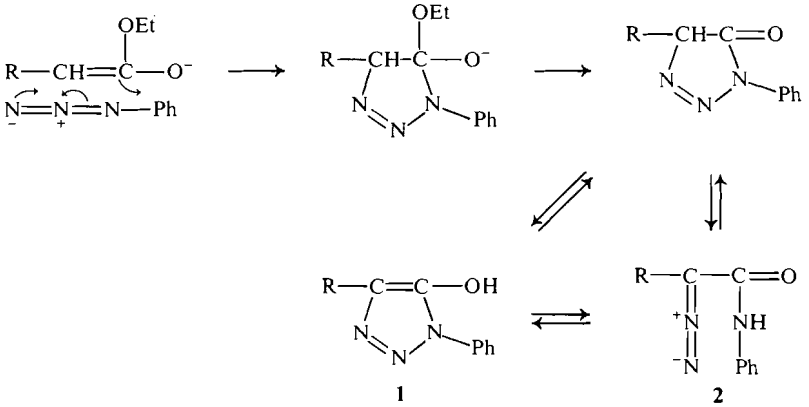

1

2

a R = EtOCO
b R = Ph

SCHEME 1

chloroform–ether (8:1) as eluant. Products were extracted from the adsorbent by chloroform (Fisher, spectrograde) to which a few drops of methanol had been added to increase polarity. The extracts were dried over sodium sulfate, and concentrated at reduced pressure. I.r. spectra were determined in carbon tetrachloride solution with a Perkin–Elmer 257 (Grating) or a Perkin–Elmer 337 (Prism) spectrophotometer. N.m.r. spectra were obtained using a Varian T-60 or a Varian A-60 instrument, with carbon tetrachloride as solvent and tetramethylsilane as internal standard, unless otherwise stated. Mass spectra were measured on an AEI-MS 902 instrument at an inlet temperature of approximately 150°. Elemental analyses were performed by C. Daesslé, Montreal.

Ethyl Diazomalonanilate (2a)

The procedure of Dimroth (8) was followed with little modification, using phenyl azide prepared by the method of Lindsay and Allen (12). The crude product, after recrystallization twice from petroleum ether (b.p. 30–60°) or pentane, was obtained as yellowish crystals, m.p. 72–73° (lit. 71–72° (8)). The i.r. spectrum (in CCl_4) showed characteristic bands at 3300 (N—H), 2130 ($=\overset{+}{N}=\overline{N}$) 1700 (ester C=O), and 1670 cm^{-1} (amide C=O). The n.m.r. spectrum showed a broad singlet at δ 9.5 (1H, amide), a multiplet at 7.4 (5H, phenyl), a quartet at 4.3 (2H, ethoxy methylene), and a triplet at 1.4 (3H, ethoxy methyl).

When a sample reacted with sodium ethoxide, a white precipitate, m.p. 185–189°, of the sodium salt of **1***a* appeared, as reported by Dimroth (8). On acidification this reverted to **2***a*.

5-Hydroxy-1,4-diphenyl-1,2,3-triazole (1b)

This triazole was prepared in 40% yield by the method of Dimroth and Letsche (11) from ethyl phenylacetate and phenyl azide, and had a melting point of 135–136° (reported m.p. 135° (11)). The i.r. spectrum showed absorption peaks at 3340 (OH), 3030, and 1600 cm^{-1} (phenyl). The mass spectrum showed a molecular-ion peak at *m/e* 237 and a peak of medium intensity at *m/e* 209 corresponding to the loss of nitrogen.

Photolysis of Ethyl Diazomalonanilate in Isopropanol

A solution of ethyl diazomalonanilate (120 mg) in isopropanol (60 ml) was photolyzed for 5 h. The crude residue on thin-layer chromatography showed three major spots having R_f 0.82, 0.67, and 0.48. Separation of the major spots by preparative thick-layer chromatography yielded: (*a*) ethyl α-isopropoxy malonanilate (**3**; R = *i*-Pr), an oil (32 mg, 23% yield) which crystallized slowly in *n*-hexane; (*b*) ethyl isopropyl α-*N*-phenylaminomalonate (**4**; R = *i*-Pr), an oil (34 mg, 25%); and (*c*) ethyl malonanilate (**5**) (42 mg, 36%).

Ethyl α-isopropoxy malonanilate, recrystallized from *n*-hexane, was obtained as white crystals (25 mg), m.p. 42–43°.

Anal. Calcd. for $C_{14}H_{19}NO_4$: C, 63.4; H, 7.2; N, 5.3. Found: C, 63.2; H, 7.3; N, 5.4.

Ethyl isopropyl α-N-phenylaminomalonate was an uncrystallizable oil.

Anal. Calcd. for $C_{14}H_{19}NO_4$: C, 63.4; H, 7.2; N, 5.3. Found: C, 63.4; H, 7.1; N, 5.4.

Ethyl malonanilate was obtained as an oil which in benzene slowly deposited crystals (32 mg), m.p. 36–38°. It had a parent peak at *m/e* 207 in its mass spectrum, and had n.m.r. and i.r. spectra identical to those of an authentic sample prepared from ethyl malonate and aniline by the method of Chattaway and Almstead (13).

When ethyl diazomalonanilate (233 mg) in isopropanol (50 ml) was irradiated at 2537 Å wavelength for 12 h, the proportions of the three major products were almost unchanged (ethyl-α-isopropoxymalonanilate, 22%; ethyl isopropyl α-*N*-phenylaminomalonate, 23%; and ethyl malonanilate, 26%).

Photolysis of Ethyl Diazomalonanilate in Isopropanol in the Presence of Oxygen

A solution of **2***a* (231 mg) in isopropanol (50 ml) was flushed with oxygen for 10 min before being irradiated. A small positive pressure of oxygen was maintained over the solution throughout the irradiation period (8 h). Evapora-

Can. J. Chem. Downloaded from www.nrcresearchpress.com by 210.87.254.105 on 09/05/12
For personal use only.

Can. J. Chem. Downloaded from www.nrcresearchpress.com by 210.87.254.105 on 09/05/12
For personal use only.

tion of the solvent left a dark yellow residue, shown on thin-layer chromatography to contain spots corresponding to diethyl α-*N*-phenylaminomalonate and ethyl α-ethoxymalonanilate, but no spot corresponding to ethyl malonanilate. The n.m.r. spectrum of the residue did not reveal any singlet at δ 3.4 characteristic of the methylene protons of the malonanilate.

Benzophenone-sensitized Photolysis of Ethyl Diazomalonanilate in Isopropanol

A solution of **2***a* (233 mg) and benzophenone (92 mg) in isopropanol (50 ml) was photolyzed as described above. Thin-layer chromatography of the reside showed two spots corresponding to benzophenone and ethyl malonanilate. No effort was made to determine the percentage yield of the ester.

Thermolysis of Ethyl Diazomalonanilate in Isopropanol

A solution of ethyl diazomalonanilate (230 mg) in isopropanol (10 ml) in a pressure bottle was heated to 160–170° by an oil bath. After 12 h the solvent was removed at reduced pressure and the crude product separated by preparative thick-layer chromatography into ethyl α-isopropoxymalonanilate (68 mg, 6%), ethyl isopropyl α-*N*-phenylaminomalonate (47 mg, 18%), and ethyl malonanilate (52 mg, 25%).

Photolysis of Ethyl Diazomalonanilate in Ethanol

A solution of ethyl diazomalonanilate (115 mg) in absolute ethanol (50 ml) was photolyzed for 6 h. The crude residue on thin-layer chromatography showed three major products having R_f 0.84, 0.70, and 0.49. Separation of the major products by preparative thick-layer chromatography yielded: (*a*) ethyl α-ethoxymalonanilate, an oil which crystallized from hexane (34 mg, 27%), m.p. 32–35°; (*b*) diethyl α-*N*-phenylaminomalonate, an oil (23 mg, 18%), and (*c*) ethyl malonanilate (34 mg, 32%) identified by comparison with an authentic sample.

Ethyl α-ethoxymalonanilate, recrystallized from pentane (25 mg), had m.p. 31–32°.

Anal. Calcd. for $C_{13}H_{17}NO_4$: C, 62.1; H, 6.8; N, 5.6. Found: C, 61.8; H, 6.7; N, 5.6.

Ethyl α-N-phenylaminomqlonate was an uncrystallizable oil.

Anal. Calcd. for $C_{13}H_{17}NO_4$: C, 62.1; H, 6.8; N, 5.6. Found: C, 62.0; H, 6.9; N, 5.6.

A second irradiation of ethyl diazomalonanilate (230 mg) in absolute ethanol (50 ml) under the same conditions yielded ethyl α-ethoxymalonanilate (60 mg, 24%), diethyl α-*N*-phenylaminomalonate (40 mg, 16%), and ethyl malonanilate (60 mg, 33%).

Photolysis of Ethyl Diazomalonanilate in Ethanol at Low Temperature

A solution of ethyl diazomalonanilate (235 mg) in absolute ethanol (50 ml), cooled by a Dry Ice–acetone mixture, was irradiated by a 450 W Hanovia lamp, contained in a quartz jacket immersed in the reaction mixture. Magnetic stirring of the solution was maintained throughout the photolysis. Aliquots were taken at 20 min intervals to be tested quickly for the presence of α-lactam by i.r. spectroscopy (characteristic C=O absorption at 1835 cm^{-1}). The temperature of the solution was −50 °C at the start of the irradiation, and −5 °C after 20 min of irradiation. No α-lactam was detected. The photolysis was complete after 2 h of irradiation. Evaporation of the solvent left a residue which on thin-layer chromatography showed three major spots R_f 0.84, 0.69, 0.49, corresponding to ethyl α-*N*-phenylaminomalonate, ethyl α-ethoxymalonanilate, and ethyl malonanilate, and three minor spots at lower R_f. Separation by thick-layer chromatography yielded diethyl α-*N*-phenylaminomalonate (36 mg, 14%), ethyl α-ethoxymalonanilate (46 mg, 18%), and ethyl malonanilate (42 mg, 20%), all identified by t.l.c. and i.r. spectra.

Benzophenone-sensitized Photolysis of Ethyl Diazomalonanilate in Ethanol

A solution of **2***a* (232 mg) and benzophenone (92 mg) in absolute ethanol (50 ml), magnetically stirred in a Pyrex vessel, was flushed with a stream of nitrogen and then irradiated by eight high-pressure 3500 Å wavelength Rayonnet lamps for 8 h. Evaporation of the solvent left a yellow oil, shown by thin-layer chromatography to contain benzophenone and ethyl malonanilate. Separation of the residue by preparative thick-layer chromatography yielded ethyl malonanilate (154 mg, 75%) identified by i.r. and n.m.r. spectra.

Thermolysis of Ethyl Diazomalonanilate in Ethanol

A solution of **2***a* (220 mg) in absolute ethanol (10 ml) in a pressure bottle of 100 ml capacity was heated to 160–170° by an oil-bath. After 12 h the solvent was evaporated at reduced pressure. Thin-layer chromatography of the residue showed three major spots and two minor spots. Separation of the major spots by preparative thick-layer chromatography yielded ethyl α-ethoxymalonanilate (51 mg, 20%), ethyl α-*N*-phenylaminomalonate (36 mg, 15%), and ethyl malonanilate (30 mg, 15%).

Photolysis of Ethyl Diazomalonanilate in Methanol

A solution of ethyl diazomalonanilate (120 mg) in methanol (60 ml) was photolyzed for 5 h. The crude residue, on thin-layer chromatography, showed three main spots (R_f at 0.80, 0.73, and 0.47). Separation of the major products by preparative thick-layer chromatography yielded ethyl malonanilate (R_f 0.47, 13 mg, 12%) and an oil (31 mg, 25%) which on a thin-layer plate showed a mixture of two spots (R_f 0.80 and 0.73). A second preparation of this oil after thick-layer chromatography yielded ethyl methyl α-*N*-phenylaminomalonate (R_f 0.73), an uncrystallizable oil (5 mg).

Photolysis of Ethyl Diazomalonanilate in the Presence of Styrene

A solution of ethyl diazomalonanilate (467 mg), styrene (2.1 g), and trinitrobenzene (*ca.* 1.0 mg) in anhydrous ether (60 ml) was photolyzed with radiation of 2537 Å wavelength for 8 h. Evaporation of the solvent left an uncrystallizable yellow oil which on thin-layer chromatography showed five spots. The n.m.r. of the crude residue did not reveal a triplet at δ 4.5 and a doublet at 3.5 and 3.3 characteristic of the corresponding cyclobutanone. No effort was made to isolate and characterize the products.

Photolysis of Ethyl Diazomalonate in Ethanol

A solution of ethyl diazomalonate (377 mg), prepared by the method of Doering and Knox (14), in absolute ethanol

Can. J. Chem. Downloaded from www.nrcresearchpress.com by 210.87.254.105 on 09/05/12
For personal use only.

(50 ml) was irradiated with lamps of 2537 Å wavelength. Thin-layer chromatography of the residue showed five products but did not show any spot corresponding to that of ethyl malonate. The n.m.r. of the crude residue did not show any peak at δ 3.4 corresponding to that of the methylene proton of ethyl malonate. No effort was made to isolate the products.

Benzophenone-sensitized Photolysis of Ethyl Diazomalonate in Isopropanol

The photolysis of a solution of ethyl diazomalonate (168 mg) and benzophenone (90 mg) in isopropanol (50 ml) was carried out as above. The reaction mixture was concentrated at room temperature. Thin-layer chromatography of the residue showed two major spots corresponding to benzophenone and ethyl malonate. Separation of the major spots by preparative thick-layer chromatography yielded 98 mg (61%) of ethyl malonate, identified by comparison of the i.r. spectrum with that of an authentic sample.

Attempted Photolysis of Ethyl Malonanilate in Ethanol

A solution of ethyl malonanilate (210 mg) in ethanol (50 ml) was photolyzed for 8 h. Thin-layer chromatography of the solution revealed little change in the composition of the solution. Irradiation for another 8 h period, and evaporation of the solvent left ethyl malonanilate (187 mg) in 90% yield.

Photolysis of 5-Hydroxy-1,4-diphenyl-1,2,3-triazole in Isopropanol

A solution of the triazole **1***b* (238 mg) in isopropanol (100 ml) was irradiated by eight low pressure mercury lamps of 2537 Å wavelength for 12 h. The solvent was evaporated at reduced pressure and the oily residue was extracted with 100 ml of hot *n*-hexane. A brown residue remained which was removed by filtration. Wasteful recrystallization of the residue three times from glacial acetic acid yielded 10 mg (5%) of 2,5-diketo-1,3,4,6-tetraphenylpiperazine (**13**), a white solid, m.p. 275–276° (lit. m.p. 277.5–278° (15)). The i.r. spectrum showed absorption peaks at 3338, 3100, 3030, and 1670 cm^{-1}. The mass spectrum showed a molecular-ion peak at *m/e* 418 with a base peak at *m/e* 209.

The filtrate from the brown residue was concentrated to give a yellow oily residue, which on t.l.c. showed two major spots of R_f 0.76 and 0.59, and three minor spots of lower R_f. Separation of the two major spots by preparative thick-layer chromatography yielded: *(1)* *α-Isopropoxy-α-phenylacetanilide* (**11**) (56 mg), a white solid; m.p. 72–74°; ν_{max} 3300 (N—H), 3100 (phenyl), and 1680 cm^{-1} (amide C=O); mass spectral peaks at *m/e* 150, 120, and 77.

Anal. Calcd. for $C_{17}H_{19}NO_2$: C, 75.8; H, 7.1; N, 5.2. Found: C, 75.8; H, 7.3; N, 5.1.

(2) Isopropyl α-N-phenylamino-α-phenylacetate (**12**), an uncrystallizable oil (20 mg, 7%); ν_{max} 3350 (N—H), 3100 (phenyl), 1720 cm^{-1} (ester C=O), mass spectral peaks at *m/e* 269 and 182.

Anal. Calcd. for $C_{17}H_{19}NO_2$: C, 75.8; H, 7.1; N, 5.2. Found: C, 76.1; H, 7.2; N, 5.3.

Thermolysis of 5-Hydroxy-1,4-diphenyl-1,2,3-triazole (1b) in Isopropanol

The thermolysis of this triazole (233 mg) in isopropanol (15 ml) was carried in a pressure bottle immersed in an oil bath heated to 150° for 12 h. Working-up the residue by the procedure described above yielded: the diketopiperazine (16 mg, 8%), α-isopropoxy-α-phenylacetanilide (42 mg, 18%), and isopropyl α-*N*-phenylamino-α-phenylacetate (11 mg, 4%). The products were identified by t.l.c. and i.r. spectra.

Thermolysis of 1,3-Di-tert-butylaziridinone in Methanol

A solution of 1,3-di-tert-butylaziridinone (**18**) (500 mg), was decomposed in boiling methanol (10 ml), following the procedure of Sheehan and Beeson (16), and afforded methyl 2-(*N-t*-butylamino)-3,3-dimethylbutyrate (**19**) (88 mg, 15%) and 2-methoxy-3,3-dimethyl-*N-t*-butylbutyramide (**20**) (176 mg, 30%). The physical constants and the i.r. and n.m.r. spectra of the products were in agreement with those reported by Sheehan and Beeson, but these authors reported different yields (26% of the butyrate and 45% of the butyramide).

Photolysis of 1,3-Di-tert-butylaziridinone in Various Alcohols

The photolyses of this α-lactam (0.553) in methanol, ethanol, and isopropanol (100 ml) were carried out in a Pyrex vessel equipped with an immersion high-pressure Hg lamp (450 W, Hanovia). The reactor was cooled in an ice-water bath to minimize the effects of a possible thermolysis. In all three cases photolysis yielded an oily residue which was shown by n.m.r. to contain no starting material, but also none of the butyrate or butyramide resulting from thermal reaction of the alcohol with the aziridinone. This was confirmed by failure to isolate these products by the procedures which were successful in isolating them from the thermolysis mixture.

Results and Discussion

Structures of Reaction Products

The photolyses and thermolyses of **2***a* in methanol, ethanol, and isopropanol produced in each case three major products: an ethyl α-alkoxymalonanilate (**3**), an α-*N*-phenylaminomalonic ester (**4**), and ethyl malonanilate (**5**) (eq. 1).

The yields of these products isolated by preparative thick-layer chromatography varied only slightly with duration of the photolysis, and are given in Table 1.

The products **3** (R = Et, *i*-Pr) and **4** (R = Me,

[1] $EtOOC-\underset{\underset{N^-}{\overset{\|}{N^+}}}{\overset{\|}{C}}-CONHPh \xrightarrow{ROH} EtOOC-\underset{OR}{CH}-CONHPh + EtOOC-\underset{NHPh}{CH}-COOR + EtOOC-CH_2-CONHPh$

2*a* **3** **4** **5**

Can. J. Chem. Downloaded from www.nrcresearchpress.com by 210.87.254.105 on 09/05/12
For personal use only.

TABLE 1. Yields (%) of products isolated from photolysis and thermolysis of **2***a* in alcohols

	Photolysis			Thermolysis		
	3	**4**	**5**	**3**	**4**	**5**
Methanol	25		12	—	—	—
Ethanol	24–27	16–18	32–33	20	14	15
i-Propanol	22–23	23–25	26–36	26	18	25

TABLE 2. Chemical shifts (in δ) of n.m.r. signals* from protons of different groups in ethyl α-alkoxymalonanilates **3** (R = Et and *i*-Pr)

Group	R = Et	R = *i*-Pr
N—H	8.5 (s, 1H)†	8.4 (s, 1H)†
Phenyl	7.4 (m, 5H)	7.4 (m, 5H)
Methine	4.3 (s, 1H)	4.3 (s, 1H)
Ethoxy	4.2 (q, 2H) 1.4 (t, 3H)‡	4.2 (q, 2H) 1.3 (t, 3H)‡
Alkoxy	3.8 (q, 2H) 1.4 (t, 3H)‡	3.9 (m, 1H) 1.3 (d, 6H)‡

*s = Singlet; d = doublet; t = triplet; q = quartet; m = multiplet.
†Abolished by treatment with D_2O and a trace of triethylamine.
‡Overlapping.

TABLE 3. Tentative identification of peaks in mass spectra of ethyl α-alkoxymalonanilates **3** (R = Et and *i*-Pr)

	R = Et	R = *i*-Pr
Identity	*m/e* (intensity)	*m/e* (intensity)
M^+	251 (12)	265 (30)
$M^+ - CH_3CHO$	207 (10)	
$M^+ - CH_3COCH_3$		207 (17)
$M^+ - COOEt$	178 (10)	192 (10)
$\overset{+}{HO}=CH-CONPh$	150 (12)	150 (25)
$M^+ - PhNCO$	132 (100)	146 (100)
$PhNHCO^+$	120 (25)	120 (35)
$Ph-N\equiv CH^+$	104 (52)	104 (60)
$Ph-NH_2^+$	93 (51)	93 (65)
Ph^+	77 (35)	77 (40)

TABLE 4. Characteristic i.r. absorption peaks (in cm^{-1}) of ethyl alkyl α-*N*-phenylamino-malonates **4** (R = Me, Et, and *i*-Pr)

	R		
Vibrational mode ν	Me	Et	*i*-Pr
N—H	3380	3350	3350
C=O (ester)	1720	1730	1730
C=O (ester)	1710	1727 (sh)	1710

Et, and *i*-Pr) are all new compounds; the structures assigned them are based on elemental analyses and spectral properties. Considering first ethyl α-ethoxy- (**3**; R = Et) and α-isopropoxymalonanilates (**3**; R = *i*-Pr), their i.r. spectra showed absorption peaks at 1730 (ester C=O), 1680 (amide I band), 1535 (amide II band), and 3370–3380 cm^{-1} (N—H stretch). Their n.m.r. spectra also showed the peaks expected for the structures **3** (R = Et) and **3** (R = *i*-Pr) (Table 2). Finally, the mass spectra of the two compounds both showed a similar pattern of fragmentation (Table 3), with a molecular-ion peak of small intensity and a parent peak at M − 119 due to the loss of CONPh, perhaps as Ph—N=C=O. The presence of the phenylcarbamoyl group was revealed by a peak of medium intensity at *m/e* 120, due to the characteristic ion $CONHPh^+$ (17), and the elimination of neutral PhNCO which may be visualized to proceed through a six-membered intermediate (Scheme 2). In addition, a peak at *m/e* 93 is also characteristic of anilides (18), and is probably due to the ion $PhNH_2^+$. The other peaks (Table 3) are also readily accommodated by the structures **3** (R = Et and *i*-Pr).

Turning now to the three products assigned the structures **4** (R = Me, Et, and *i*-Pr), these all exhibited *two* i.r. absorption peaks above 1700 cm^{-1} (Table 4) and hence contained two ester groups. The N—H group gave rise to i.r. peaks at approximately δ 4.6, overlapping the methine proton (Table 5). When D_2O was added, exchange took place readily, and the area of the signal at δ 4.6, previously integrating to two

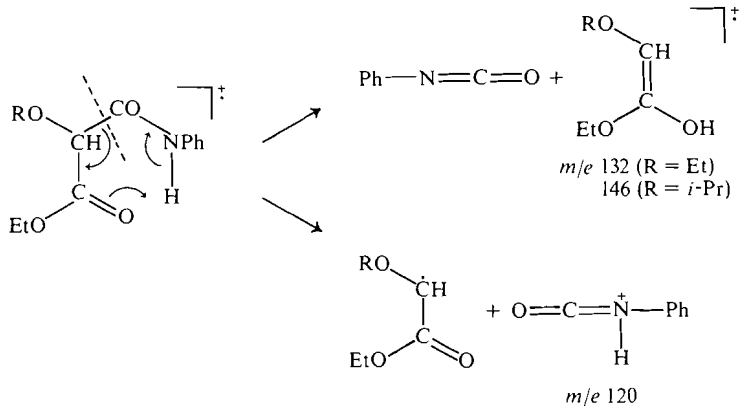

SCHEME 2

TABLE 5. Chemical shifts (δ) of n.m.r. signals from protons in different groups of ethyl alkyl α-*N*-phenylaminomalonates (**4**; R = Me, Et, and *i*-Pr)

	R		
Group	Me	Et	*i*-Pr
Phenyl	7.0 (m, 5H)	7.0 (m, 5H)	7.0 (m, 5H)
N—H, Methine	4.6 (s, 2H)	4.8 (s, 2H)	4.7 (s, 2H)
Ethoxy	4.2 (q, 2H) 1.2 (t, 3H)	4.4 (q, 2H) 1.4 (t, 3H)*	4.3 (q, 2H) 1.3 (t, 3H)*
Alkoxy	3.7 (s, 3H)	4.4 (q, 2H) 1.4 (t, 3H)*	5.1 (m, 1H) 1.3 (d, 6H)*

*Overlapping.

hydrogen atoms, now integrated to one. However, most informative were the mass spectra (Table 6), which showed the familiar fragmentation pattern of α-amino esters (19) with prominent peaks corresponding to the loss of the carbalkoxy groups (fission *a* and *b* in Scheme 3). The base peak in the mass spectra of all three compounds was the ion of *m/e* 104 which resulted from further decomposition of one of these fission fragments by a familiar route (20), as shown in Scheme 3.

The third product obtained in both thermolyses and photolyses of ethyl diazomalonanilate in the three different alcohols was ethyl malonanilate (**5**), identified by comparison with an authentic sample.

Strausz and co-workers (2) found that thermolysis and photolysis of ethyl diazoacetate (**6**; R = H) in isopropanol produced isopropyl α-isopropoxyacetate (**7**; R = H), and proposed that an ion-pair was formed by light-induced heterolysis and exchange with solvent (Scheme 4).

However, we found no trace of the exchanged product **7** (R = PhNHCO) when **2** (= **6**; R = PhNHCO) was heated or photolyzed in isopropanol. Similarly, we found no evidence of exchange of ethyl for methyl when the reaction was carried out in methanol. It seems likely that

TABLE 6. Tentative assignment of peaks in mass spectra of ethyl alkyl α-*N*-phenylaminomalonates (**4**; R = Me, Et, and *i*-Pr)

	Me	Et	*i*-Pr
Assignment	*m/e* (intensity)	*m/e* (intensity)	*m/e* (intensity)
M^+	237 (25)	251 (20)	265 (22)
$M^+ - COOEt$	164 (62)	178 (85)	192 (80)
$M^+ - COOR$	178 (37)	178 (85)	178 (90)
$M^+ - COOR—C_2H_4$	150 (5)	150 (5)	150 (38)
$PhNH{=}C{=}C{=}O$	132 (5)	132 (75)	132 (8)
$HC{=}NPh^+$	104 (100)	104 (100)	104 (100)
Ph^+	77 (50)	77 (80)	77 (45)

Can. J. Chem. Downloaded from www.nrcresearchpress.com by 210.87.254.105 on 09/05/12
For personal use only.

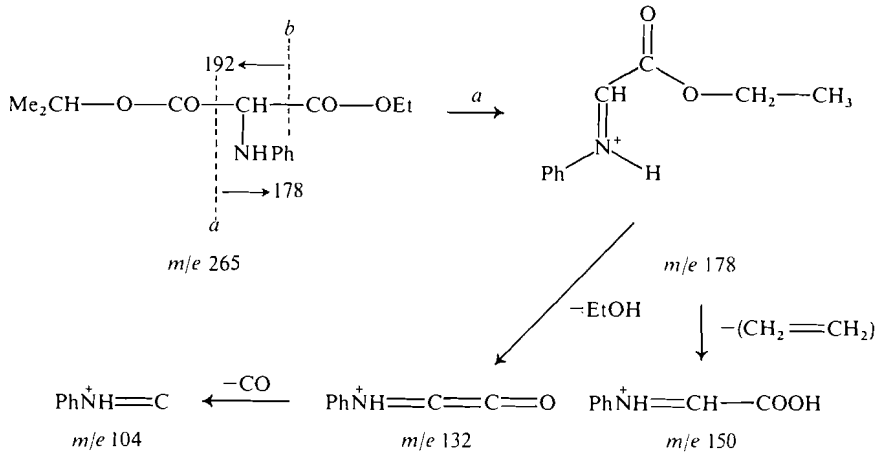

SCHEME 3

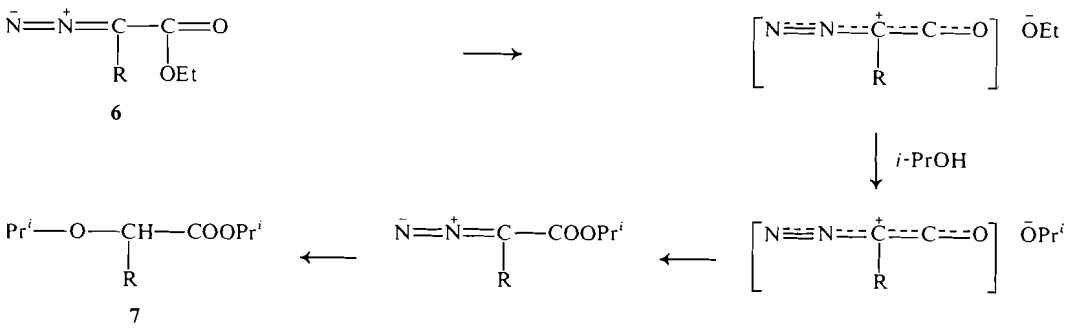

SCHEME 4

heterolysis in these cases is prevented by the electron-withdrawing effect of the PhNHCO group, which would destabilize the intermediate carbonium ion.

We also found no evidence of Fries-like rearrangement products (21) from ethyl malonanilate in the product mixture resulting from photolysis of ethyl diazomalonanilate in alcohols, and no reaction took place when a solution of ethyl malonanilate (**8**; R = EtOCO) was photolyzed in ethanol. Photolysis of acetanilide (**8**; R = H) in ethanol is known to give *o*-amino- (**9**; R = H) and *p*-aminoacetophenone (**10**; R = H) (19) (eq. 2), and we confirmed these results in our apparatus, so that the failure of ethyl malonanilate to undergo photolysis cannot be regarded as adventitious.

The photolysis and thermolysis of 5-hydroxy-1,4-diphenyl-1,2,3-triazole (**1***b*) in isopropanol yielded two isomeric products (**11** and **12**) analyzing for $C_{17}H_{19}NO_2$, and a small amount of the crystalline diketopiperazine **13** (eq. 3).

The structure **11** is indicated for one of the isomeric products by its i.r. spectrum, which shows a carbonyl amide absorption at 1675 cm^{-1}, and by its n.m.r. spectrum, which shows a singlet at δ 8.4 (N—H amide). Other n.m.r. peaks at δ 7.4 (multiplet, 10H, phenyl), 4.8 (singlet, 1H, methine), 3.8 (multiplet, 1H, isopropyl), and 1.3 (doublet, 6H, isopropyl methyl)

[2] 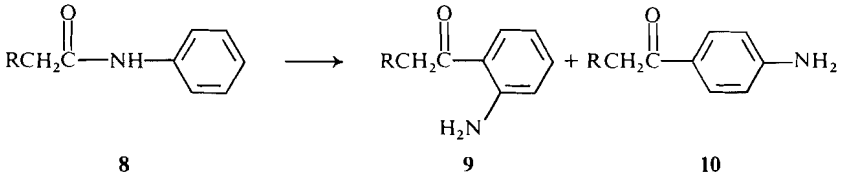

8 **9** **10**

Can. J. Chem. Downloaded from www.nrcresearchpress.com by 210.87.254.105 on 09/05/12
For personal use only.

[3] 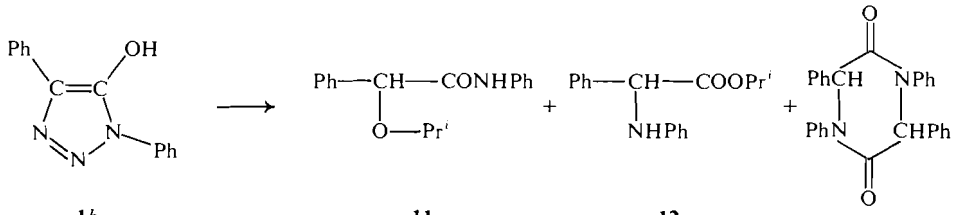

1b **11** **12** **13**

Can. J. Chem. Downloaded from www.nrcresearchpress.com by 210.87.254.105 on 09/05/12
For personal use only.

also point to this structure, as does the mass spectrum, with a molecular-ion peak at *m/e* 269, a base peak at 150 (M – PhNCO), and a peak at 120 (Ph—NHCO) (*cf.* Scheme 2).

The structure **12** was assigned to the isomeric product because its i.r. spectrum exhibited an ester carbonyl absorption peak at 1720 cm^{-1}. Its n.m.r. spectrum showed a multiplet at δ 7.2 (10H, phenyl), a broad singlet at 6.4 (1H, N—H) amine, exchangeable with D_2O), a multiplet at 5.1 (1H, isopropyl), a singlet at 4.6 (1H, methine), and a doublet at 1.1 (6H, methyls of isopropyl). Its mass spectrum had a molecular-ion peak at *m/e* 269 and strong peaks at *m/e* 192 and 182 as expected for the structure **12** (*cf.* Scheme 3).

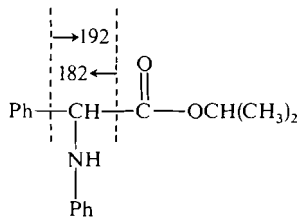

12

The third product was 2,5-diketo-1,3,5,6-tetraphenylpiperazine (**13**) with melting point and i.r. spectrum (CO absorption at 1665 cm^{-1}) corresponding to values in the literature (15). The mass spectrum showed the expected molecular-ion peak at *m/e* 418 and a base peak at *m/e* 209 due to a symmetrical fission, the most likely being the following:

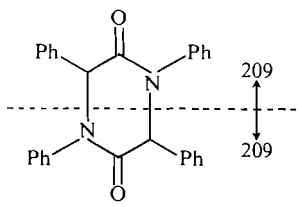

13

which allows for delocalization of charges and odd electrons by the benzene rings.

Spin States of Intermediates Giving the Different Reaction Products from **2***a*

Photolysis or thermal decomposition of ethyl diazomalonanilate (**2***a*) would be expected to cause loss of nitrogen and formation of the singlet carbene **14** which could then drop down to the longer-lived, lower energy triplet **15** (22).

The products **3** (R = Et and *i*-Pr) and **4** (R = Me, Et, and *i*-Pr) probably arise from reaction of the singlet **14** with solvent alcohol, and are formed in the presence of oxygen (a triplet scavenger). The ethers **3** (R = Et and *i*-Pr) could result from insertion of the singlet carbene into the O—H bond of the alcohol, which is an unexceptional reaction (23). The mechanism of formation of the α-*N*-phenylaminomalonic esters (**4**; R = Me, Et, and *i*-Pr) is less obvious and is discussed below.

Ethyl malonanilate (**5**) is not formed by photolysis in the presence of oxygen, but is the only product in the absence of oxygen when benzophenone is used as a sensitizer. These facts point to the triplet **15** as an intermediate, which would have to abstract two hydrogen atoms from the solvent alcohols to form **5**. Similarly the triplet state of carbethoxymethylene, from the benzophenone-sensitized photolysis of ethyl diazoacetate, abstracts two protons from cyclohexene to yield ethyl acetate (4), and we have found that the benzophenone-sensitized photolysis of ethyl diazomalonate in isopropanol produced ethyl malonate in good yield. Thus abstraction of two hydrogen atoms from solvent molecules by the triplet carbene seems to go well in the presence of an α-carbonyl group. A tentative mechanism for the formation of ethyl malonanilate (**5**) is shown in Scheme 5.

Mechanism for the Formation of α*-N-Phenylaminomalonates* **4** *from* **2***a*

We may now consider the mechanism for the

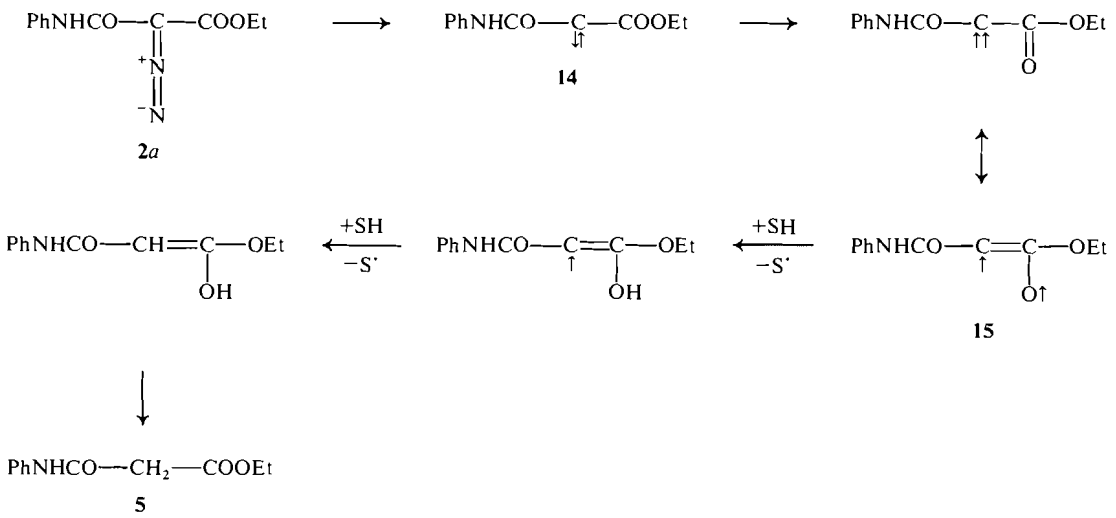

SCHEME 5

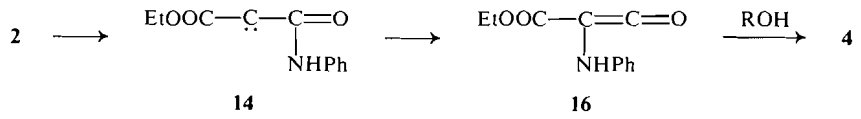

SCHEME 6

migration of the phenylamino group from its terminal linkage in **2***a* to its attachment to the α-carbon atom in **4** (R = Me, Et, and *i*-Pr). A possible mechanism (which does not specify the precise manner of this migration) would involve the ketene intermediate **16** and is depicted by Scheme 6. Similar ketene intermediates have been postulated to explain the products obtained in the photolysis of phenyl diazoacetate (3) and of ethyl diazoacetate (4). However, efforts to trap the intermediate ketene **16** with styrene did not give any detectable amount of the corresponding cyclobutanone. In any case, this particular rearrangement occurs only with certain diazo-esters: ethyl trifluoroacetyl diazoacetate (24) and diethyl diazomalonate (1) yield the products of methylene attack on solvents rather than rearrangement products. It therefore appears that the presence of electron-withdrawing groups inhibits formation of ketene intermediates.

An alternative and perhaps preferable mechanism to explain the formation of α-*N*-phenylaminomalonic esters (**4**) involves the α-lactam intermediate **17** (Scheme 7). The insertion of the methylene into the N—H bond would yield the α-lactam, which would then react with solvent to give the α-amino ester, corresponding to an acyl-

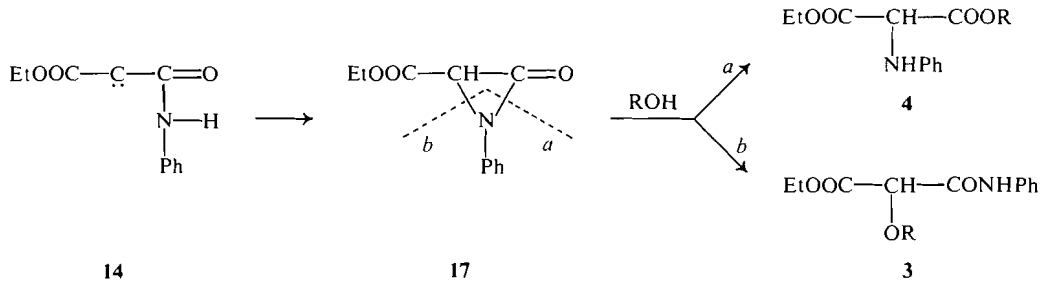

SCHEME 7

Can. J. Chem. Downloaded from www.nrcresearchpress.com by 210.87.254.105 on 09/05/12
For personal use only.

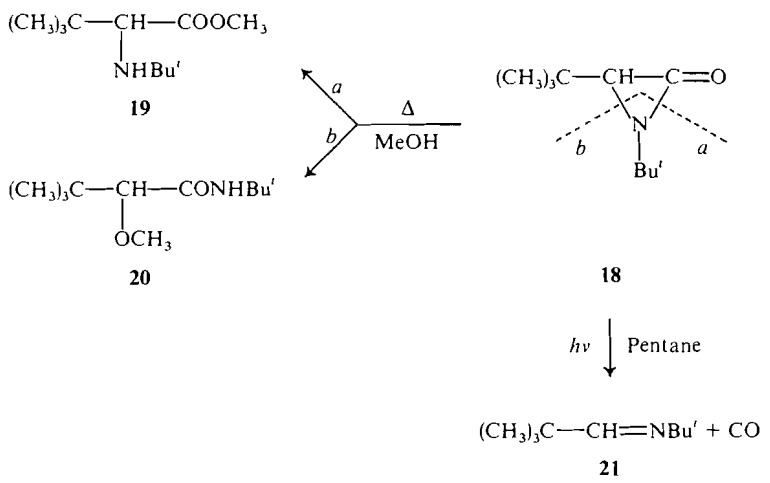

SCHEME 8

nitrogen bond cleavage (*a*), and an α-alkoxyamide, corresponding to an alkyl-nitrogen bond cleavage (*b*). These two types of ring-opening are known to occur readily. Sheehan and Beeson (16) have reported (and we have confirmed) that 1,3-di-tert-butylaziridinone (**18**) reacts in boiling methanol to give the ester **19** (cleavage *a*) and the amide **20** (cleavage *b*):

Attempts to obtain evidence for such an α-lactam, which would then react with solvent to examination of the reaction mixture obtained when photolysis in ethanol was carried out at a relatively low temperature (−5 °C) were unsuccessful, probably because the α-lactam **17** can be expected to be much less stable than **18** for steric and electronic reasons (16).

Sheehan and Nafissi-V (25) reported that photolysis of **18** in pentane gave carbon monoxide and the imine **21** (see Scheme 8). We found that photolysis of **18** in methanol gave an oily product which contained no **19** or **20**; photolysis in ethanol and isopropanol gave similar results. If the lactam **17** is an intermediate in the formation of **3** and **4**, its subsequent reaction is thermal rather than photolytic.

Mechanism for the Thermolysis and Photolysis of 1b

The thermolysis and photolysis of the triazole **1***b* gave **11** and **12**, completely analogous to the products **3** and **4** obtained by thermolysis or photolysis of the diazoanilide **2***a*. A possible explanation would be that in alcohols the tautomerization **1***b* → **2***b* is very rapid, and that the reactive species is **2***b* rather than **1***b*.[1] Further work is required on the photolysis and thermolysis of **1***b* and **2***a* in solvents in which tautomerization is slow.

It should be noted that the thermal and photochemical products from **2***a* and **1***b* show differences as well as similarities. In the reaction mixture from **1***b* we were unable to detect the presence of α-phenylacetanilide (analogous to **5**, obtained from **2***a*); on the other hand, the diketopiperazine **13** from **1***b* finds no analogue in the products isolated from **2***a*. Sarel and Greenberger (15) obtained this diketopiperazine by a different route, in which they assumed an α-lactam to be an intermediate. We were unable to detect the presence of any appreciable quantity of α-lactam in the reaction mixtures from the photolysis of **1***b* (no i.r. band at 1835 cm^{-1} (26)), but this α-lactam would be expected to be particularly unstable (16).

Grateful acknowledgment is made to the National Research Council of Canada for financial support.

1. W. VON E. DOERING and L. H. KNOX. J. Am. Chem. Soc. **83**, 1989 (1961).
2. THAP DOMINH, O. P. STRAUSZ, and H. E. GUNNING. J. Am. Chem. Soc. **90**, 1660 (1968); **91**, 1261 (1969).
3. HERMAN CHAIMOVICH, R. J. VAUGHAN, and F. H. WESTHEIMER. J. Am. Chem. Soc. **90**, 4088 (1968).

[1]Equally, it could be maintained that the similarity in reaction products arises because in both cases triazoles (**1***a* and *b*) are the reactive species.

Can. J. Chem. Downloaded from www.nrcresearchpress.com by 210.87.254.105 on 09/05/12
For personal use only.

4. THAP DOMINH and O. P. STRAUSZ. J. Am. Chem. Soc. **92**, 1766 (1970).
5. D. E. THORNTON, R. K. GOSAVI, and O. P. STRAUSZ. J. Am. Chem. Soc. **92**, 1768 (1970).
6. H. ZOLLINGER. Azo and diazo chemistry. Interscience Publishers Inc., New York, N.Y. 1961. p. 21.
7. C. D. GUTSCHE. Org. React. **8**, 364 (1954).
8. O. DIMROTH. Ber. **35**, 4051 (1902).
9. O. DIMROTH. Ann. **336**, 143 (1905).
10. TH. CURTIUS and J. THOMPSON. Ber. **39**, 4140 (1906).
11. O. DIMROTH and E. LETSCHE. Ann. **335**, 93 (1904).
12. R. O. LINDSAY and C. F. H. ALLEN. Organic syntheses. Coll. Vol. III, John Wiley and Sons, Inc., New York, N.Y. 1955. p. 710.
13. F. D. CHATTAWAY and J. M. D. OLMSTEAD. J. Chem. Soc. **97**, 938 (1910).
14. W. VON E. DOERING and L. H. KNOX. J. Am. Chem. Soc. **78**, 4947 (1956).
15. S. SAREL and A. GREENBERGER. J. Org. Chem. **23**, 330 (1958).
16. J. C. SHEEHAN and J. H. BEESON. J. Am. Chem. Soc. **89**, 366 (1967).
17. J. A. GILPIN. Anal. Chem. **31**, 935 (1959).
18. J. A. COTTER. J. Chem. Soc. 5477 (1964).
19. K. BIEMANN. Mass spectrometry. McGraw-Hill Book Company, Inc., New York, N.Y. 1962. p. 262.
20. K. BIEMANN, J. SEIBL, and F. GAPP. J. Am. Chem. Soc. **83**, 3795 (1961).
21. D. ELAD. Tetrahedron Lett. 873 (1963).
22. R. BRESLOW. Organic reaction mechanisms. W. A. Benjamin, New York. 1966. p. 124.
23. W. KIRMSE, L. HORNER, and H. HOFFMANN. Ann. **614**, 19 (1958). R. HUISGEN and G. JUPPE. Chem. Ber. **94**, 2332 (1961).
24. F. WEYGAND, H. DWORSHAK, K. KOCH and S. KONSTAS. Angew. Chem. **73**, 409 (1961).
25. J. C. SHEEHAN and M. MEHDI NAFISSI-V. J. Am. Chem. Soc. **91**, 1176 (1969).
26. H. E. BAUMGARTEN. J. Am. Chem. Soc. **84**, 4975 (1961).

Can. J. Chem. Downloaded from www.nrcresearchpress.com by 210.87.254.105 on 09/05/12
For personal use only.

Photolysis of Ethyl Diazomalonanilate in Acetonitrile

NGUYEN THANH BUU AND J. T. EDWARD

Department of Chemistry, McGill University, Montreal, Quebec

Received March 2, 1972

Photolysis of ethyl diazoacetate and of ethyl diazomalonate in acetonitrile gave oxazoles. Photolysis of ethyl diazoacetate in the presence of benzophenone gave an oxazoline incorporating the elements of carbethoxymethylene, benzophenone, and acetonitrile. Photolysis of ethyl diazomalonanilate gave 5-ethoxy-2-methyl-4-phenylcarbamoyloxazole, 5-ethoxy-3-methyl-4-phenylcarbamoylisoxazole, and ethyl α-hydroxymalonanilate. With 2537 Å wavelength radiation the oxazole was formed predominantly; on the other hand, with benzophenone-sensitization, the isoxazole was formed (among other products) but no oxazole. The oxazole was isomerized to the isoxazole when irradiated in the presence of a sensitizer, while the isoxazole was isomerized to the oxazole when irradiated with radiation of 2537 Å wavelength. A tentative mechanism is advanced to explain formation of the different products.

La photolyse du diazoacétate et du diazomalonate d'éthyle dans l'acétonitrile fournit oxazoles, tandis que la photolyse du diazoacétate d'éthyle dans l'acétonitrile en presence du benzophénone fournit une oxazoline incorporant les élements du carbéthoxyméthylène, du benzophénone, et de l'acétonitrile. La photolyse du diazomalonanilate d'éthyle fournit les produits suivants: 5-éthoxy-2-méthyle-4-phénylcarbamoyloxazole, 5-éthoxy-3-méthyle-4-phénylcarbamoylisoxazole, et α-hydroxymalonanilate d'éthyle. Avec des lampes de 2537 Å longeur d'ondes, l'oxazole se forme principalement; par contre, avec la sensitisation par benzophénone l'isoxazole est formé à l'exclusion de l'oxazole. En presence du benzophénone l'irradiation de l'oxazole fournit l'isoxazole, tandis que l'irradiation de l'isoxazole avec des lampes de 2537 Å longeur d'ondes fournit l'oxazole. On propose un possible mécanisme gouvernant la formation des produits différents.

Canadian Journal of Chemistry, **50**, 3730 (1972)

Can. J. Chem. Downloaded from www.nrcresearchpress.com by 210.87.254.40 on 09/05/12
For personal use only.

Introduction

The products of the photolysis of ethyl diazomalonanilate in methanol and other alcohols point to the following mechanism: decomposition of the diazo compound into nitrogen and a singlet carbene, which can then (*a*) react with solvent; (*b*) rearrange to an unstable intermediate (α-lactam?) which then reacts with solvent; (*c*) decay to a triplet, which then reacts with solvent. Each of these routes gives a different product (1). An alternative, less probable mechanism involved the prototropic tautomerization of ethyl malonanilate to 4-ethoxycarbonyl-5-hydroxy-1-phenyltriazole, which then lost nitrogen to give a 1,3-diradical. In an attempt to distinguish between these mechanisms, the photolysis of ethyl diazomalonanilate was carried out in a number of aprotic solvents (dioxane, benzene, ether, cyclohexene) in which tautomerization would be expected to be very slow. In all cases a complex mixture of products was obtained, from which no pure compound could be isolated. However, in acetonitrile, a solvent used successfully in other photolyses (2), crystalline products were obtained. These are discussed below; their formation is more readily rationalized by the photolysis of the diazo compound, rather than of its triazole tautomer. Furthermore, photolysis of the simpler esters, ethyl diazoacetate and ethyl diazomalonate, which are incapable of tautomerization to triazoles, was also investigated briefly, and found to give similar products.

Experimental

Photolyses of diazo compounds in acetonitrile were carried out according to the procedure described in ref. 1. Three sets of lamps giving radiation of different wavelengths (2537, 3000, and 3600 Å) were used. When irradiated by lamps giving 2537 Å radiation, the solutions were contained in quartz vessels; when irradiated by lamps giving 3000 or 3600 Å radiation, Pyrex vessels were used.

Photolysis of Ethyl Diazoacetate with 2537 Å Wavelength Radiation

A solution of ethyl diazoacetate (Eastman Chemicals, highest purity, 342 mg) in acetonitrile (Fisher spectrograde, 50 ml) was irradiated for 5 h. Evaporation of the solvent at reduced pressure left an oily residue, shown by i.r. (absence of $=\overset{+}{N}=\overset{-}{N}$ band at 2130 cm^{-1}) and by t.l.c. to contain no starting material ($R_f = 0.70$) but six or seven compounds of R_f between 0.70 and 0.30. These compounds were separated by preparative thick-layer chromotography. The n.m.r. spectrum of only one compound ($R_f = 0.63$) showed the presence of a methyl peak at δ 2.2 (singlet, 3H), as well as

Can. J. Chem. Downloaded from www.nrcresearchpress.com by 210.87.254.40 on 09/05/12
For personal use only.

peaks at 5.8 (singlet, 1H), at 4.0 (quartet, 2H), and at 1.30 (triplet, 3H). Purification by t.l.c. gave approximately 10 mg of 5-ethoxy-2-methyloxazole (**5**; R = H, R′ = Me), a clear viscous oil whose mass spectrum showed a molecular ion peak at *m/e* 127.

Benzophenone-sensitized Photolysis of Ethyl Diazoacetate

A solution of ethyl diazoacetate (335 mg) and benzophenone (91 mg) in acetonitrile (50 ml) was irradiated for 8 h by eight 3500 Å Rayonnet lamps. Evaporation of the solvent left a yellow viscous residue which on t.l.c. showed seven small spots and a major spot at R_f 0.32. Separation of the latter material by thick-layer chromatography, followed by extraction of the silica gel with chloroform containing a trace of methanol, yielded ethyl 2-methyl-5,5-diphenyloxazolin-4-carboxylate (**10**) as an oil (85 mg). Treatment of the oil with 6 *N* HCl solution (5 ml) at room temperature produced, after 1 h of stirring, a precipitate of ethyl 2,2-diphenyl-2-hydroxy-1-acetamidopropionate (**11**) (78 mg), m.p. 158–162°. Recrystallization of **11** from a solution of chloroform–hexane (1:10) yielded 68 mg of yellowish crystals, m.p. 160–161°.

Anal. Calcd. for $C_{19}H_{21}NO_4$: C, 69.7; H, 6.5; N, 4.3. Found: C, 69.4; H, 6.5; N, 4.3.

Diphenyldiazomethane

This red crystalline compound was prepared in 80% yield from benzophenone hydrazone according to the procedure of Miller (3), and had a m.p. of 31–34° (lit. 29–32° (3)).

Photolysis of Diphenyldiazomethane with 2537 Å Wavelength Radiation

The photolysis of diphenyldiazomethane (582 mg) in acetonitrile (50 ml) was carried out for 8 h. After removal of solvent, the residue was extracted with hot ethanol, leaving an insoluble portion (103 mg) of tetraphenylazine (**8**) m.p. 165–167° (lit. 163–163.5° (4)). Its mass spectrum showed a molecular ion peak at *m/e* 360. On cooling, the ethanol solution yielded two further crops (20 mg) of crude **8**, m.p. 172–178°. The mother liquors were concentrated, and a few drops of ether were added. The solution was then allowed to stand overnight at −5 °C, and yielded 32 mg of yellow crystals of tetraphenylethane (**7**), m.p. 208–210° (lit. 209–211° (4)).

Ethyl Diazomalonate

Ethyl malonate was converted into ethyl diazomalonate in three steps, according to procedures in the literature (5, 6). The i.r. spectrum of the crude product revealed a strong absorption at 2140 cm^{-1} due to the diazo group. Efforts to purify the compound by distillation at reduced pressure were unsuccessful.

Photolysis of Ethyl Diazomalonate with 2537 Å Wavelength Radiation

The photolysis of ethyl diazomalonate (531 mg) in acetonitrile (50 ml) was carried out according to the procedure described above for ethyl diazoacetate. The crude product showed five spots on thin-layer chromatography, which were eluted and examined by n.m.r. Only the fraction of R_f 0.62 showed the presence of an isolated methyl group (singlet at δ 2.3). This oily product (53 mg, 10% yield) was isolated by preparative thick-layer chromatography. Its n.m.r. spectrum had two quartets which partly overlapped each other at δ 4–4.6 (4H), a singlet at 2.3 (approximately 3H) and a quartet (overlapping of two triplets) at 1.2–1.6 (6H). Purification of this compound twice by thick-layer chromatography yielded 6 mg of 5-ethoxy-4-ethoxycarbonyl-2-methyloxazole (**5**; R = CO_2Et, R′ = Me), an oil whose mass spectrum revealed a parent peak at *m/e* 199, and a fragmentation pattern as follows: *m/e* (intensity): 199 (33), 171 (40), 154 (45), 126 (33), 125 (100), 101 (55), 43 (100).

Photolysis of Ethyl Diazomalonanilate with 2537 Å Wavelength Radiation

A solution of this diazo compound (230 mg) in acetonitrile (50 ml) was irradiated for 6 h, by which time the i.r. spectrum of the reaction mixture showed that the diazo absorption at 2130 cm^{-1} had disappeared. Evaporation of the solvent at reduced pressure yielded 240 mg of a yellow viscous oil which on t.l.c., with chloroform–ether 10:1 as eluant, showed three major spots, at R_f 0.68, 0.60, and 0.37, and some minor spots. Separation of the major spots by preparative thick-layer chromatography yielded three products: 5-ethoxy-2-methyl-4-phenylcarbamoyloxazole (**12**), R_f 0.68, an oil (85 mg, 35% yield) which crystallized slowly in hexane; 5-ethoxy-3-methyl-4-phenylcarbamoylisoxazole (**13**), R_f 0.60, an oil (25 mg, 10% yield) which crystallized from pentane; and ethyl α-hydroxymalonanilate (**14**), R_f 0.37, an oil (8 mg; 4% yield).

5-Ethoxy-2-methyl-4-phenylcarbamoyloxazole (12) recrystallized twice from pentane, was obtained as white crystals (41 mg), m.p. 64–65°, ν_{max} 3370, 1690, 1670, 1600, and 1550 cm^{-1}.

Anal. Calcd. for $C_{13}H_{14}N_2O_3$: C, 63.4; H, 5.7; N, 11.4. Found: C, 63.6; H, 5.9; N, 11.4.

The mass spectrum had a molecular ion peak of medium intensity at *m/e* 246, and a fragmentation pattern as follows: *m/e* (intensity): 246 (45), 200 (78), 126 (60), 93 (100), 77 (78), 43 (100).

The oxazole **12** (15 mg) dissolved in 59% perchloric acid solution (5 ml). In about 15 min a yellowish perchlorate salt was removed by filtration. On recrystallization from water this gave 17 mg of white crystals, m.p. 178–185° (dec.), whose n.m.r. spectrum in deuterated DMSO showed a singlet at δ 8.3 (1H), a doublet at 7.3 (5H), a singlet at 6.0 (1.5 H, exchangeable with D_2O), a quartet at 4.2 (2H), a singlet at 2.3 (3H), and a triplet at 1.2 (3H).

The perchlorate (12 mg) was dissolved in 2 *N* sodium hydroxide (5 ml) and the solution was extracted with ether. Evaporation of the ether yielded the oxazole **12** as a yellow oil (6 mg), identified by thin-layer chromatography and i.r. spectrum.

5-Ethoxy-3-methyl-4-phenylcarbamoylisoxazole (13) crystallized from pentane in white crystals (16 mg), m.p. 37–39°, ν_{max} 3370, 1690, 1650 (shoulder), 1640, 1545, and 870 cm^{-1}; δ 8.5 (s, 1H), 7.0–7.9 (m, 5H), 2.4 (s, 3H), 4.7 (q, 2H), 1.5 (t, 3H).

Anal. Calcd. for $C_{13}H_{14}N_2O_3$: C, 63.4; H, 5.7; N, 11.4. Found: C, 63.4; H, 5.7; N, 11.4.

The mass spectrum revealed a molecular-ion peak at *m/e* 246, and a fragmentation pattern identical to that of **12**.

The isoxazole dissolved in 59% perchloric acid, but a crystalline perchlorate could not be obtained. When the acidic solution was neutralized with sodium hydroxide and extracted with ether, the isoxazole (identified by i.r. spectrum and thin-layer chromatography) was recovered unchanged.

Can. J. Chem. Downloaded from www.nrcresearchpress.com by 210.87.254.40 on 09/05/12
For personal use only.

Ethyl α-Hydroxymalonanilate (14) was an uncrystallizable oil, ν_{max} 3400, 3350, 1710 cm^{-1}; n.m.r. δ 8.7 (s, 1H), 7.2–7.8 (m, 5H), 4.5 (s, 2H), 4.4 (q, 2H), and 1.5 (t, 3H).

Anal. Calcd. for $C_{11}H_{13}NO_4$: C, 59.2; H, 5.9; N, 6.3. Found: C, 59.4; H, 5.9; N, 6.2.

The mass spectrum showed the following peaks (*m/e*; intensity in parentheses): 223 (50), 182 (12), 150 (16), 135 (12), 120 (25), 103 (100), 93 (90), 77 (50), 43 (30).

Photolysis of Ethyl Diazomalonanilate with 3000 Å Wavelength Radiation

A solution of the diazo compound (224 mg) in acetonitrile (50 ml) was irradiated by eight 3000 Å wavelength Rayonnet lamps for 48 h. Evaporation of the solvent left a yellow residue (215 mg) which slowly crystallized. Thin-layer chromatography of the residue showed that the starting material and compounds **12**, **13**, and **14** were present. Separation by preparative thick-layer chromatography yielded **12** (28 mg, 25% yield), **13** (24 mg, 21%), **14** (32 mg, 35%), and starting material (97 mg).

Repetition of the photolysis with a more dilute solution of ethyl diazomalonanilate (120 mg) in acetonitrile (50 ml) yielded **12** (18 mg, 30% yield), **13** (15 mg, 27%), **14** (16 mg, 30%), and starting material (71 mg).

Photolysis of Ethyl Diazomalonanilate with 3000 Å Wavelength Radiation in the Presence of Oxygen

A solution of ethyl diazomalonanilate (231 mg) in acetonitrile (50 ml) was flushed with oxygen for 10 min before being irradiated by 3000 Å lamps. A small positive pressure of oxygen was maintained over the solution throughout the irradiation period (24 h). Evaporation of the solvent left a dark yellow residue, shown by thin-layer chromatography and n.m.r. spectrum to contain starting material and **12**, but no **13**. The residue was dissolved again in acetonitrile, the solution was flushed with oxygen, and was irradiated for another 24 h in the presence of oxygen. Again evaporation of the solvent left a dark yellow oil residue, shown by thin-layer chromatography to contain starting material, **12**, four unidentified products, but no **13**. The absence of **13** was also evident from the n.m.r. spectrum of the crude mixture, which exhibited the methyl absorption of oxazole **12** (singlet at δ 2.5) but no corresponding methyl absorption of isoxazole **13** at higher field.

Benzophenone-sensitized Photolysis of Ethyl Diazomalonanilate

A solution of the diazo compound (237 mg) and benzophenone (91 mg) in acetonitrile (50 ml), magnetically-stirred in a Pyrex vessel, was flushed with a stream of nitrogen and then irradiated by eight 3500 Å wavelength Rayonnet lamps for 8 h. Evaporation of the solvent left a yellow oil, shown by thin-layer chromatography to contain benzophenone, isoxazole **13** and four other compounds of lower R_f. Separation of the mixture by preparative thick-layer chromatography yielded benzophenone (81 mg) and isoxazole **13** (28 mg), identified by n.m.r. and i.r. spectra. The presence of the oxazole **12** could not be detected.

Another solution of the diazomalonanilate (82 mg) in acetonitrile (50 ml) contained in a Pyrex vessel, was irradiated under similar conditions but in the absence of benzophenone. Thin-layer chromatography of the residue showed only starting material and a trace of unidentified compound, R_f 0.21. The residue was recrystallized from petroleum ether (30–60°) to yield 76 mg of starting material.

Irradiation of 5-Ethoxy-3-methyl-4-phenylcarbamoylisoxazole (13) at 2537 Å

A solution of the isoxazole **13** (5 mg) in acetonitrile (4 ml) was irradiated for 8 h. Evaporation of the solvent left a residue which showed on t.l.c. a major spot corresponding to the oxazole **12**, and three other spots of lower R_f, but no starting material. Separation of the major spot by thick-layer chromatography yielded **12** (1 mg), identified by its i.r. spectrum.

Irradiation of 5-Ethoxy-2-methyl-4-phenylcarbamoyloxazole (12) at 2537 Å

A solution of the oxazole **12** (6 mg) in acetonitrile (4 ml) was irradiated for 8 h. The residue on t.l.c. showed starting material and two other spots, but no spot corresponding to the isoxazole (**13**).

Benzophenone-sensitized Isomerization of 5-Ethoxy-2-methyl-4-phenylcarbamoyloxazole (12)

A solution of the oxazole **12** (13 mg) and benzophenone (1 mg) in acetonitrile (4 ml) in a Pyrex tube was irradiated at 3500 Å for 8 h. The residue on t.l.c. showed spots corresponding to isoxazole **13** and benzophenone and two other spots at lower R_f, but no starting material.

Benzophenone-sensitized Irradiation of 5-Ethoxy-2-methyl-4-phenylcarbamoylisoxazole (13)

A solution of the isoxazole **13** (2 mg) and benzophenone (1 mg) in acetonitrile (4 ml) was irradiated at 3500 Å for 8 h. The residue showed on t.l.c. starting material **13** but no spot corresponding to that of oxazole **12**.

Results and Discussion

Reactions of Ethyl Diazoacetate

Huisgen *et al.* (7) have shown that a mixture of ethyl diazoacetate (**1**, R = H) and benzonitrile (**3**, R′ = Ph), heated to 140°, gives 5-ethoxy-2-phenyloxazole (**5**, R = H, R′ = Ph). We found that ethyl diazoacetate, photolyzed in acetonitrile (**3**, R = Me), gave (along with several unidentified products) a small yield of a compound of mass 127, which was undoubtedly 5-ethoxy-2-methyloxazole (**5**, R = H, R′ = Me). Thus the n.m.r. spectrum showed a singlet at δ 5.8 (1H), assigned to the olefinic proton, a singlet at 2.2 (3H), assigned to the 2-methyl protons, and the characteristic quartet at 4.0 (2H) and triplet at 2.3 (3H) of the ethoxy group. The mass spectrum showed a molecular ion peak of medium intensity at *m/e* 127, and a base peak at *m/e* 72 due to the loss of OEt.

In both the thermal and the photolytic reactions leading to oxazoles it seems likely that the carbethoxymethylene **2** is first formed by

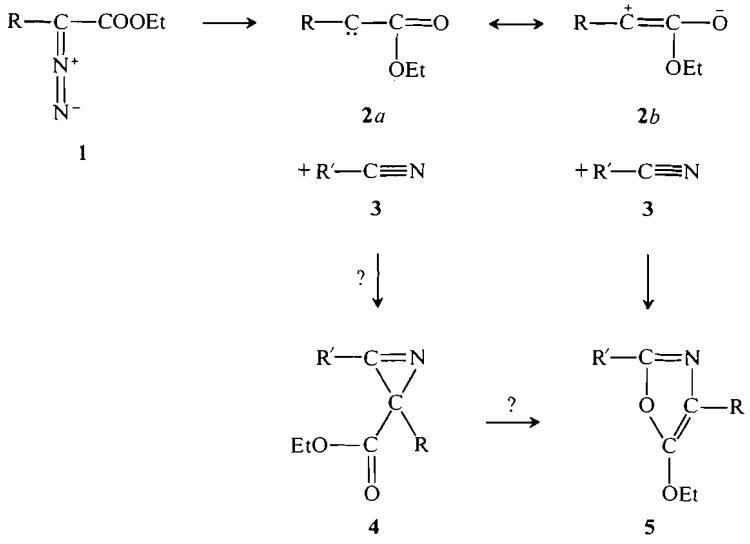

SCHEME 1

decomposition of the diazo ester; Huisgen (8) has suggested that this could then add to the nitrile triple bond to give the acylazirine **4**, which can then rearrange to **5** (see Scheme 1). Such a mechanism seems less likely than the 1,3-dipolar addition (8) of **2** (in its dipolar form **2***b*) to the nitrile to form the oxazole **5** directly, since simple carbenes show little tendency to add to nitrile to form azirines. For example, in the photoreaction of diazomethane with acrylonitrile, methylene adds to the carbon–carbon double bond and not to the nitrile triple bond (9); further, we have found that photolysis of diphenyldiazomethane (**6**) in acetonitrile gave tetraphenylethane (**7**) and tetraphenylazine (**8**), (see Scheme 2), products previously obtained by the decomposition of this diazo compound in aprotic solvents such as benzene (4). No products resulting from the addition of diphenylcarbene to the triple bond could be isolated.

Since the direct photolysis of diazoesters usually produces singlet carbene (10), it is reasonable to assume that the formation of the oxazole **5** is accomplished through reaction of the singlet carbethoxymethylene. In an attempt to confirm this point, the benzophenone-sensitized photolysis of ethyl diazoacetate in acetonitrile was studied. The reaction failed to produce any observable amount of the oxazole **5** (R = H, R = Me). Instead, the oily oxazoline **10** was formed, presumably by the addition of triplet carbethoxymethylene to benzophenone

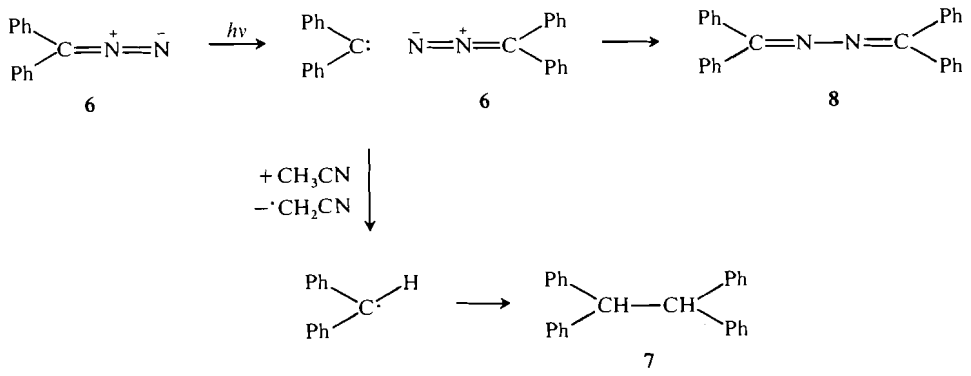

SCHEME 2

Can. J. Chem. Downloaded from www.nrcresearchpress.com by 210.87.254.40 on 09/05/12
For personal use only.

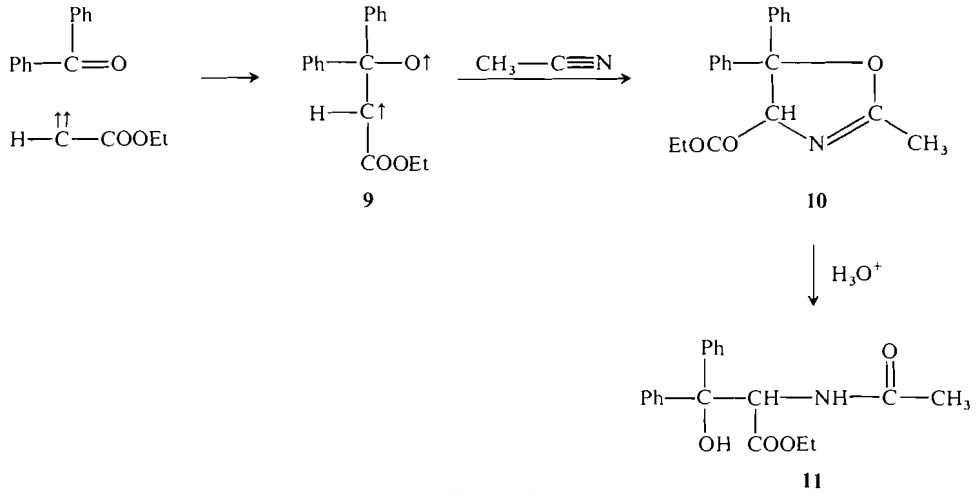

SCHEME 3

and further addition of the diradical intermediate **9** to acetonitrile (Scheme 3).

The oxazoline structure **10** for the oily product was supported by its n.m.r. spectrum, which showed the presence of phenyl groups (multiplet at δ 7.4–8.0), a hydrogen atom at the 4-position (singlet at δ 5.5), a methyl at the 2-position (singlet at δ 2.4), and an ethoxy group (quartet at δ 4.0 and triplet at 1.2). However, more important evidence for the structure **10** came from the hydrolysis of the oil in hydrochloric acid to a crystalline product having the combustion analysis and spectral properties expected for ethyl 2,2-diphenyl-2-hydroxy-1-acetamidopropionate (**11**). Thus its i.r. spectrum showed characteristic absorption peaks at 3680, 3590 (O—H), 3400 (N—H), 1710 (ester C=O) and 1660 cm^{-1} (amide (C=O). Its n.m.r. spectrum showed a multiplet at δ 7.3–8.0 (10H, aromatic protons), a broad singlet at 4.7 (1H, hydroxyl, exchangeable with D_2O), a sharp singlet at 2.0 (3H, acetyl), a quartet at 4.1 (2H, ethoxy methylene), a triplet at 1.0 (3H, ethoxy methyl), a broad doublet at 6.85 (1H, amide, $J = 8.5$ Hz), and a sharp doublet at 5.85 (1H, methine, $J = 8.5$ Hz). The amide hydrogen did not exchange with neutral deuterium oxide, but when deuterium oxide containing a drop of triethylamine was added to a solution of **11** in deuterated DMSO, the signal assigned to the amide proton disappeared, and the methine doublet at δ 5.85 was replaced by a singlet. Finally, the mass spectrum of the compound, besides showing a molecular-ion peak at *m/e* 327 and M + 1 peak at 328, showed a base peak at 183 and strong peaks at 254, 195, and 145, all readily accommodated by the structure **11**:

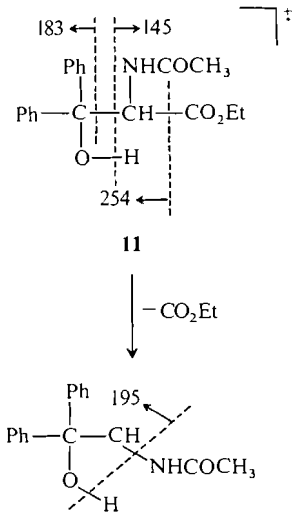

Reaction of Ethyl Diazomalonate

Ethyl α-diazomalonate (**1**; R = COOEt), photolyzed in acetonitrile, gave a small yield of oily product which was most probably the oxazole **5** (R = COOEt, R′ = CH_3). Thus the n.m.r. spectrum had a singlet at δ 2.3 (3H, 2-methyl), two quartets at 4–4.6 which partly overlap each other (4H, ethoxy methylenes), and a quartet at 1.2–1.6 due to the overlap of two triplets (6H, ethoxy methyls). The mass spectrum

Can. J. Chem. Downloaded from www.nrcresearchpress.com by 210.87.254.40 on 09/05/12
For personal use only.

Can. J. Chem. Downloaded from www.nrcresearchpress.com by 210.87.254.40 on 09/05/12
For personal use only.

of the compound gave the molecular-ion peak at *m/e* 199 required for **5** (R = COOEt, R′ = Me), with a base peak at *m/e* 154 (M − OEt) and a peak of moderate intensity at *m/e* 125 (M − CO_2Et—H).

Reaction of Ethyl Diazomalonanilate: Structure of Products

The photolysis of ethyl diazomalonanilate (**1**; R = CONHPh) with light of 2537 Å wavelength in acetonitrile yielded two isomeric crystalline products, m.p. 64–65° and m.p. 37–39°, analyzing as $C_{13}H_{14}N_2O_3$, and an oily product analyzing as $C_{11}H_{13}NO_4$.

The first compound, m.p. 64–65°, was undoubtedly the expected oxazole **5** (R = CONHPh, R′ = Me). In agreement with this formulation, its i.r. spectrum showed absorption peaks at 3370 and 3300 (N—H), 1690 (amide-I), 1670 (ring C=N), 1620 (C=C), 1600 (phenyl), and 1550 cm^{-1} (amide-II). Its n.m.r. spectrum showed a broad singlet at δ 8.5 (1H; amide N—H, exchangeable with D_2O), an unsymmetrical doublet at 7.6 (5H; phenyl), a singlet at 2.5 (3H, ring methyl), a quartet at 4.3 (2H, ethoxy methylene), and a triplet at 1.45 (3H, ethoxy methyl). The mass spectrum showed, besides a parent peak (*m/e* 246) of medium intensity, a strong M − 46 peak due to the loss of ethanol and a M − 120 peak of medium intensity due to the loss of C_6H_5NHCO. When treated with D_2O containing a trace of triethylamine, the amide proton was readily replaced by deuterium. The mass spectrum then showed a parent peak at *m/e* 247, a M − 121 peak due to loss of C_6H_5NDCO, and a strong M − 47 peak due to the loss of C_2H_5OD. This would seem to indicate that the ethoxyl group is split off with the amide hydrogen or deuterium, possibly from the hydrogen-bonded structure **12**:

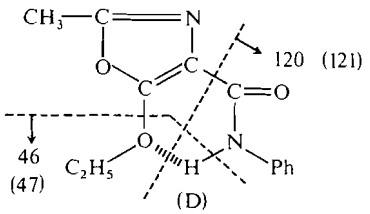

12

Oxazoles are fairly strong bases (11), and so the photoproduct formed a crystalline perchlorate, from which it could be recovered on treatment of the salt with sodium hydroxide.

The isomeric product, m.p. 37–39°, was assigned the isoxazole structure **13** because its

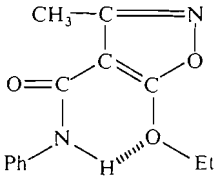

13

i.r. spectrum exhibited a characteristic absorption band at 870 cm^{-1} (absent in the i.r. spectrum of the oxazole **12**) which may be assigned to the stretching of the N—O linkage (12). Its i.r. spectrum also showed absorption peaks at 3370 cm^{-1} (N—H stretching), 1690 (amide-I), 1650 (shoulder, C=N ring), 1640 (C=C), and 1545 cm^{-1} (amide-II). Its n.m.r. spectrum exhibited a broad singlet at δ 8.5 (1H, amide, exchangeable with D_2O), a multiplet at 7–7.9 (5H, aromatic), a singlet at 2.4 (3H, ring methyl), a quartet at 4.7 (2H, ethoxy methylene), and a triplet at 1.5 (3H, ethoxy methyl).

Isoxazoles, like oxazoles, are moderately strong bases (13). The basicity of the photoproduct was indicated by its solubility in acid solution, from which it was precipitated unchanged on basification.

The mass spectrum showed an almost identical fragmentation pattern with that of compound **12**, with a molecular-ion peak of medium intensity at *m/e* 246, a strong M − 46 peak, and a medium M − 120 peak.

The oily product is most plausibly formulated as ethyl α-hydroxymalonanilate (**14**). Its mass

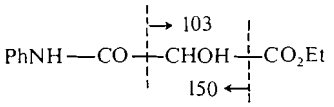

14

spectrum showed, besides the molecular ion peak at *m/e* 223, strong peaks at *m/e* 150 and 103, accounted for by the loss of $COOC_2H_5$ and C_6H_5NHCO. The i.r. spectrum exhibited peaks at 3400 and 3350 (O—H and N—H), 1710 (ester C=O), and 1685 cm^{-1} (shoulder, amide C=O). The n.m.r. spectrum showed a singlet at δ 8.7 (1H, amide), a multiplet at 7.27–7.8 (5H, aro-

Can. J. Chem. Downloaded from www.nrcresearchpress.com by 210.87.254.40 on 09/05/12
For personal use only.

TABLE 1. Yields of products from the photolysis of ethyl diazomalonanilate in acetonitrile under different conditions

Conditions (wavelength, additives, etc.)	12 (%)	13 (%)
2537 Å	35	10
3000 Å	28	25
3000 Å + O_2	Present	Absent
3000 Å + benzophenone	Absent	Present

matic), a singlet at 4.5 (2H, overlapping hydroxyl and methine), a quartet at 4.4 (2H, ethoxy methylene), and a triplet at 1.5 (3H, ethoxy methyl). When deuterium oxide was added to a solution of the compound in carbon tetrachloride, the signal at δ 4.5 (hydroxyl and methine) became a sharp singlet (1H, methine).

Effect of Reaction Conditions on Proportions of Products

The formation of **14** probably results from abstraction of hydrogen from the solvent by the carbene **2** (R = CONHPh) to form a radical, which then reacts with dissolved oxygen to form a hydroperoxide and ultimately an alcohol. No attempts were made to study the effect of reaction conditions on its formation.

The formation of the isoxazole **13**, relative to that of the oxazole **12**, is dependent on the wavelength of the radiation employed, and on the spin-states of the intermediates, as can be seen from Table 1.

We further found that the two isomers can be interconverted in acetonitrile, and that the conversion depends on the wavelength of the radiation used. Thus with radiation of 2537 Å wavelength, a solution of **13** yielded **12** (among other products), while under these conditions a solution of **12** did not yield **13**. On the other hand, with benzophenone-sensitization **12** was converted into **13**, but not *vice versa*.

Such a wavelength-controlled interconversion has precedent in the work of Ullman and Singh (14), who demonstrated that irradiation of 3,5-diphenylisoxazole (**15**) in ether with radiation of 2537 Å wavelength resulted in the formation of 2,5-diphenyloxazole (**17**), but not when a sensitizer was present. The intermediate in this isomerization was shown to be 3-benzoyl-2-phenylazirine (**16**). This azirine could rearrange to either oxazole or isoxazole, depending on the wavelength of the radiation employed. Thus with radiation having a wavelength of 3100 Å or shorter, the azirine rearranged almost quantitatively to the oxazole **17**, while with radiation having a wavelength of 3340 Å or longer the azirine rearranged to the isoxazole **15**. These results were explained in terms of a selective ring cleavage of the azirine, the triplet state of the excited azirine opening at *b* (see Scheme 4) to yield the isoxazole **15**, and the singlet state opening at *a* to yield the oxazole **17**.

We may postulate a similar intermediate **18** for the interconversion of **12** and **13**, although our attempts to isolate it have been unsuccessful, and a possible scheme for the formation of **12** and **13** is depicted by Scheme 5. The primary product is the oxazole **12**, formed by the 1,3-dipolar addition of singlet **2** (R = PhNHCO) to **3**, and this would account for the fact that photolysis of **1** (R = PhCONH) in acetonitrile in the presence of oxygen, a triplet quencher, gave the oxazole **12** (among the other products), but no **13**.

Reaction with solvent **3** of "hot" **2** (R = PhNHCO), carrying over some of the excess energy resulting from the extrusion of molecular nitrogen from **1** (R = PhNHCO), could give **12** in an excited singlet state, which could decay to a triplet and thence give **13** via **18**. This would account for the small amount of isoxazole **13** formed when ethyl diazomalonanilate (**1**, R =

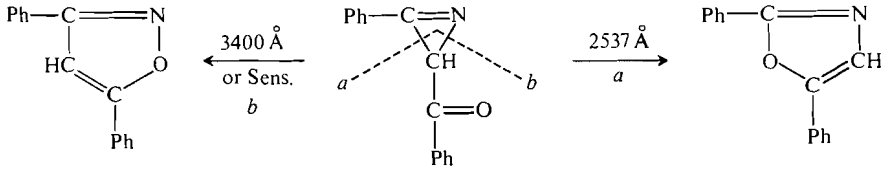

15 **16** **17**

SCHEME 4

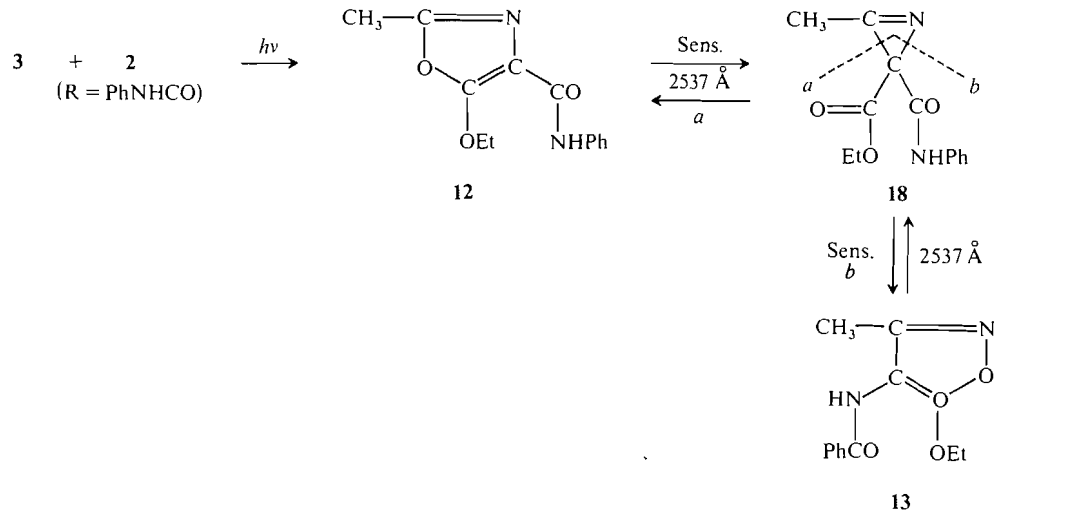

SCHEME 5

PhNHCO) was photolyzed in acetonitrile with 2537 Å wavelength radiation, and its formation (to the exclusion of **12**) when the photolysis was carried out in the presence of benzophenone.

We gratefully acknowledge the financial support of the National Research Council of Canada.

1. N. G. BUU and J. T. EDWARD. Can. J. Chem. This issue.
2. E. M. BURGESS, R. CARIUTHERS, and L. MCCULLOGH. J. Am. Chem. Soc. **90**, 1923 (1968).
3. J. B. MILLER. J. Org. Chem. **24**, 560 (1959).
4. W. KIRMSE. Ann. **614**, 20 (1958).
5. (*a*) H. R. SNYDER and C. N. SMITH. J. Am. Chem. Soc. **66**, 350 (1944). (*b*) E. SCHIPPER and A. R. DAY. J. Am. Chem. Soc. **74**, 350 (1952).
6. W. VON E. DOERING and L. H. KNOX. J. Am. Chem. Soc. **83**, 1898 (1961).
7. R. HUISGEN, H. KONIG, G. BINSCH, and H. I. STURM. Angew. Chem. **73**, 368 (1961).
8. R. HUISGEN. Angew. Chem. Intern. Ed. Engl. **2**, 633 (1963).
9. F. D. POPP and A. CATALA. J. Org. Chem. **26**, 2738 (1961). D. GOTKIS and G. B. CLOKE. J. Am. Chem. Soc. **56**, 2710 (1934).
10. W. VON E. DOERING and T. MOLE. Tetrahedron, **10**, 65 (1960).
11. J. W. CORNFORTH. Heterocyclic compounds. *Edited by* R. C. Elderfield. Vol. V. John Wiley and Sons, Inc., New York, N.Y. 1957. p. 324.
12. R. M. SILVERSTEIN and G. C. BASSLER. Spectrometric identification of organic compounds. 2nd ed. John Wiley and Sons, Inc., New York, N.Y. 1968. p. 99.
13. R. A. BARNES. Heterocyclic compounds. *Edited by* R. C. Elderfield. Vol. V. John Wiley and Sons, Inc., New York, N.Y. 1957. p. 464.
14. E. F. ULLMANN and B. SINGH. J. Am. Chem. Soc. **88**, 1844 (1966). B. SINGH, A. ZWEIG, and J. B. GALLIVAN. J. Am. Chem. Soc. **94**, 1199 (1972).

Can. J. Chem. Downloaded from www.nrcresearchpress.com by 210.87.254.40 on 09/05/12
For personal use only.

Can. J. Chem. Downloaded from www.nrcresearchpress.com by 210.87.254.6 on 09/05/12
For personal use only.

On the Rate Constant for *n*-Pentyl Radical Isomerization

K. W. WATKINS

Department of Chemistry, Colorado State University, Fort Collins, Colorado 80521

Received May 23, 1972

A new interpretation of the mechanism used by Endrenyi and LeRoy for the calculation of the rate constant for *n*-pentyl isomerization is proposed. The addition of one step to the scheme makes possible a recalculation of the Arrhenius parameters. Significantly different values are found which eliminate the previously reported low *A*-factor.

Une nouvelle interprétation du mécanisme utilisé par Endrenyi et LeRoy pour calculer la constante de vitesse de l'isomérisation du *n*-pentyle, est proposée. L'addition d'une étape au schéma rend possible un nouveau calcul des paramètres d'Arrhénius. Des différences significatives de valeurs ont été trouvées éliminant ainsi le faible facteur *A* rapporté antérieurement. [Traduit par le journal]

Canadian Journal of Chemistry, **50**, 3738 (1972)

A discrepancy has long been recognized (1) between the reported *A*-factors and those estimated from reasonable entropies of activation for the thermal isomerization of *n*-pentyl (2) and *n*-hexyl (3) radicals.

[1] $$n\text{-}C_5H_{11} \rightarrow sec\text{-}C_5H_{11}$$

[2] $$n\text{-}C_6H_{13} \rightarrow sec\text{-}C_6H_{13}$$

The reported *A*-factors were about $10^7\ s^{-1}$, whereas the theoretical *A*-factors for *n*-pentyl and *n*-hexyl isomerization were estimated to be $10^{10.5-11.0}\ s^{-1}$ (1*b*, 1*c*) and $10^{10}\ s^{-1}$ (4) respectively. The purpose of this communication is to suggest a resolution of this dilemma for *n*-pentyl radical isomerization.

In the case of isomerization of *n*-pentyl radicals by 1,4-hydrogen atom migration, a reinterpretation of the original data of Endrenyi and LeRoy (2) suggests a suitable solution. These workers carried out their kinetic runs at temperatures between 165 and 230°. They assumed that the only reactions of *sec*-pentyl were isomerization back to *n*-pentyl, and combination with methyl. In other reports of *n*-pentyl radical isomerization, both Gordon and McNesby (5) and Wijnen (6) observed that *sec*-pentyl radicals formed from *n*-pentyl isomerization at 300° decomposed. Also, Morganroth and Calvert (7) in a study of the photolysis of *n*-azobutane observed that *n*-butyl radicals began to decompose into ethylene and ethyl radicals at about 157°.

[3] $$CH_3CHCH_2CH_2CH_3 \rightarrow CH_3CH{=}CH_2 + \cdot CH_2CH_3$$

This work proposes that in the calculations of Endrenyi and LeRoy a significant fraction of *sec*-pentyl radicals was not accounted for because they decomposed by reaction 3. A propene balance on their data (8) shows this suggestion to be a reasonable one. The three most important propene forming reactions (excluding 3) are

[4] $$C_3H_7 + CH_3 \rightarrow C_3H_6 + CH_4$$

[5] $$C_3H_7 + C_3H_7 \rightarrow C_3H_6 + C_3H_8$$

[6] $$C_3H_7 + CH_2COCH_3 \rightarrow C_3H_6 + CH_3COCH_3$$

Other reactions yielding C_3H_6 can be imagined but their contribution is relatively unimportant. The rate of formation of propene from these reactions can be estimated by the following expression where known or estimated disproportionation to combination ratios can be used.

$$R'(C_3H_6) = k_4^d R(C_4H_{10}) + k_5^d R_4(C_6H_{14}) + k_6^d R(\text{MBK})$$

$R_4(C_6H_{14})$ is the rate of formation of $n\text{-}C_6H_{14}$ from propyl radical combination. It is estimated from expression (*iv*) (8), $k_5^d = \Delta(n\text{-Pr}, n\text{-Pr}) = 0.15$ (9); k_4^d was estimated to be 0.04, from

TABLE 1. Contributions to $R'(C_3H_6)$

Run (8)	R_4	0.15 R_4	0.04 $R(C_4H_{10})$	0.06 R(MBK)	$R'(C_3H_6)$	$R(C_3H_6)$	Δ
25	2.26	0.34	0.77	0.65	1.76	6.70	4.94
26	1.97	0.30	0.90	0.68	1.88	5.14	3.26
30	1.53	0.23	0.88	0.50	1.61	2.75	1.14
27	1.12	0.17	0.82	0.30	1.29	1.39	0.10
31	0.67	0.10	0.62	0.19	0.91	0.82	−0.09
28	0.41	0.06	0.55	0.10	0.71	0.66	−0.05
29	0.19	0.03	0.37	0.06	0.46	0.37	−0.09

Δ(Me, *n*-Pr) = 0.058 (9), 0.033 (10), and Δ(Me, *n*-Bu) = 0.030 (11). k_6^d was estimated to be 0.06; similar to the value of Δ(Et, *n*-Pr) = 0.065 (9).

Table 1 lists the individual contributions and compares them to $R(C_3H_6)$ from ref. 8. $\Delta = R(C_3H_6) - R'(C_3H_6)$. From Table 1, it can be seen that $R'(C_3H_6)$ accounts well for the observed $R(C_3H_6)$ in runs at temperatures below 186°, but in runs above this temperature, much more propene is produced than $R'(C_3H_6)$ predicts. If this excess propene is attributed to reaction 3, then the rate constant for isomerization can be recalculated. Let R(*sec*-pentyl products) = $R_f(i\text{-}C_6H_{14}) + \Delta$, and substitute it for $R_f(i\text{-}C_6H_{14})$ in the calculation of $k_7k_3^{1/2}/k_8$ (2). This has the effect on an Arrhenius plot of raising the high temperature (502 °K) rate constants by a factor of three, while leaving the low temperature (438 °K) rate constant unchanged. The plot is slightly curved, but a least squares treatment gives $\log (k_7k_3^{1/2}/k_8) = 4.8 - 21/\theta$, where $\theta = 2.3\,RT$ in kcal mol^{-1}. Assuming that $\log A_3 = 13.34$ (12 and references therein), $\log A_8 = 13.64$, and that E_3 and E_8 are zero, one gets $\log k_7 = 11.7 - 21/\theta$.

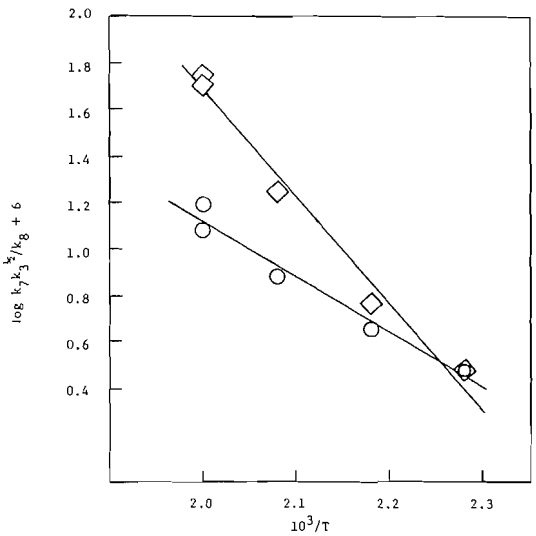

FIG. 1. Arrhenius plot for the isomerization of *n*-pentyl radicals: ○, original data of ref. 2; □, recalculated.

These rate parameters are significantly different from those originally published (2). They are similar to those that agree with the activated complex model, and threshold energy used by Watkins and Lawson (1*a*) to get agreement between their R.R.K.M. theoretical rate constant and the experimental rate constant. The R.R.K.M. theory of unimolecular reactions has been established as a means to correlate chemical activation and thermal data (13). The complex frequencies correspond to $\Delta S^{\ddagger} = 12.2$ cal deg^{-1} mol^{-1}, and $\log A$ (s^{-1}) = 10.6 at 53°. The threshold energy of 19 kcal mol^{-1} corresponds to an activation energy of 18 kcal mol^{-1} (14).

Recently, Watkins (15) reported lower limits to the *A*-factor and activation energy for *n*-pentyl isomerization of $\log A = 8.3$ and $E = 15$ kcal mol^{-1}, respectively. Since complications arose in this work also, the author suggests taking the rate constant at 160° where the complications were least important, and substituting in an activation energy of 20 kcal mol^{-1} to find the *A*-factor. Since k (160°) = 8.1 s^{-1}, $\log A = 11.0$. The agreement between these three independent results is now satisfactory. The Arrhenius parameters for *n*-pentyl isomerization are summarized in Table 2.

TABLE 2. Summary of *n*-pentyl isomerization rate parameters

Rate constant	Reference
$\log k = 11.7 - 21/\theta$	(2) Recalculated
$\log k = 10.6 - 18/\theta$	Complex model in (1*a*)
$\log k = 11.0 - 20/\theta$	(15) Recalculated

Can. J. Chem. Downloaded from www.nrcresearchpress.com by 210.87.254.6 on 09/05/12
For personal use only.

1. (*a*) K. W. WATKINS and D. R. LAWSON. J. Phys. Chem. **75**, 1632 (1971); (*b*) H. M. FREY and R. WALSH. Chem. Rev. **69**, 103 (1969); (*c*) E. A. HARDWIDGE, C. W. LARSON, and B. S. RABINOVITCH. J. Am. Chem. Soc. **92**, 3278 (1970); (*d*) S. W. BENSON. Advances in chemistry series, No. 97. American Chemical Society, Washington, D.C. 1970. p. 1.
2. L. ENDRENYI and D. J. LEROY. J. Phys. Chem. **70**, 4081 (1966).
3. K. W. WATKINS and L. A. OSTREKO. J. Phys. Chem. **73**, 2080 (1969).
4. D. M. GOLDEN, R. K. SOLLY, and S. W. BENSON. J. Phys. Chem. **75**, 1333 (1971).
5. A. S. GORDON and J. R. MCNESBY. J. Chem. Phys. **31**, 853 (1959).
6. M. H. J. WIJNEN. J. Am. Chem. Soc. **83**, 3752 (1961).
7. W. E. MORGANROTH and J. G. CALVERT. J. Am. Chem. Soc. **88**, 5387 (1966).
8. L. ENDRENYI and D. J. LEROY. J. Phys. Chem. **71**, 1334 (1967).
9. J. O. TERRY and J. H. FUTRELL. Can. J. Chem. **45**, 2327 (1967).
10. J. GROTEWOLD and J. A. KERR. J. Chem. Soc. 4324 (1963).
11. K. W. WATKINS. Unpublished results.
12. N. BASCO, D. G. L. JAMES, and R. D. STUART. Int. J. Chem. Kinet. **2**, 215 (1970).
13. W. L. HASE, R. L. JOHNSON, and J. W. SIMONS. Int. J. Chem. Kinet. **4**, 1 (1972).
14. S. GLASSTONE, K. J. LAIDLER, and H. EYRING. The theory of rate processes. McGraw-Hill Book Company, Inc., New York, N.Y. 1941. p. 195.
15. K. W. WATKINS. J. Am. Chem. Soc. **93**, 6355 (1971).

Dethioacetalization with Thallium(III) Trifluoroacetate[1]

TSE-LOK HO AND C. M. WONG

Department of Chemistry, University of Manitoba, Winnipeg, Manitoba R3T 2N2

Received July 13, 1972

Thioacetals undergo facile hydrolysis on treatment with thallium(III) trifluoroacetate.

Les thioacétals s'hydrolysent facilement lorsqu'on les traite par le trifluoroacétate de thallium(III).
[Traduit par le journal]

Canadian Journal of Chemistry, **50**, 3740 (1972)

Of the numerous existing protecting groups for the carbonyl (1), acetals and thioacetals are most commonly used. The acetal group is stable towards basic conditions but it is extremely labile in the presence of mineral acids. Although it is usually believed that it is suitable for masking the carbonyl when a molecule is exposed to organometallic reagents, this is not always true (2, 3). Thioacetals have been utilized only sporadically, mainly because they are obnoxious in smell, and more difficult to hydrolyze. However, besides the facts that thioacetals are easier to prepare, much more stable under a variety of experimental conditions, the development of a versatile synthetic method by Corey and Seebach (4 and references therein), based on nucleophilic attack of 2-lithio-1,3-dithianes, has stimulated a search for better ways of regenerating the carbonyl function.

Burgeoning activities are recorded in the recent literature, outlining different approaches to solving the problem. Thus, dethioacetalization has been effected by chloramine T (5), ceric ammonium nitrate (6), and *via* S-alkylation (7). In this paper, we wish to describe another novel procedure for oxidative hydrolysis of dithioacetals to regenerate the parent carbonyl compounds. This method, utilizing thallium(III) trifluoroacetate, was prompted by our fascination of thallium compounds in mediating organic reactions (Taylor–McKillop reactions) (ref. 8 and previous papers), as well as the consideration that thallium salts may act as soft acids (9), therefore they should combine with sulfur atoms readily.

We observed that the mildly exothermic reaction between thallium(III) trifluoroacetate and a thioacetal in tetrahydrofuran is complete almost instantaneously at room temperature, as indicated by the rapid fading of the initially brown solution to a milky white color. The

[1]Support of this research by the National Research Council of Canada is gratefully acknowledged.

Can. J. Chem. Downloaded from www.nrcresearchpress.com by 210.87.254.6 on 09/05/12
For personal use only.

1. (*a*) K. W. WATKINS and D. R. LAWSON. J. Phys. Chem. **75**, 1632 (1971); (*b*) H. M. FREY and R. WALSH. Chem. Rev. **69**, 103 (1969); (*c*) E. A. HARDWIDGE, C. W. LARSON, and B. S. RABINOVITCH. J. Am. Chem. Soc. **92**, 3278 (1970); (*d*) S. W. BENSON. Advances in chemistry series, No. 97. American Chemical Society, Washington, D.C. 1970. p. 1.
2. L. ENDRENYI and D. J. LEROY. J. Phys. Chem. **70**, 4081 (1966).
3. K. W. WATKINS and L. A. OSTREKO. J. Phys. Chem. **73**, 2080 (1969).
4. D. M. GOLDEN, R. K. SOLLY, and S. W. BENSON. J. Phys. Chem. **75**, 1333 (1971).
5. A. S. GORDON and J. R. MCNESBY. J. Chem. Phys. **31**, 853 (1959).
6. M. H. J. WIJNEN. J. Am. Chem. Soc. **83**, 3752 (1961).
7. W. E. MORGANROTH and J. G. CALVERT. J. Am. Chem. Soc. **88**, 5387 (1966).
8. L. ENDRENYI and D. J. LEROY. J. Phys. Chem. **71**, 1334 (1967).
9. J. O. TERRY and J. H. FUTRELL. Can. J. Chem. **45**, 2327 (1967).
10. J. GROTEWOLD and J. A. KERR. J. Chem. Soc. 4324 (1963).
11. K. W. WATKINS. Unpublished results.
12. N. BASCO, D. G. L. JAMES, and R. D. STUART. Int. J. Chem. Kinet. **2**, 215 (1970).
13. W. L. HASE, R. L. JOHNSON, and J. W. SIMONS. Int. J. Chem. Kinet. **4**, 1 (1972).
14. S. GLASSTONE, K. J. LAIDLER, and H. EYRING. The theory of rate processes. McGraw-Hill Book Company, Inc., New York, N.Y. 1941. p. 195.
15. K. W. WATKINS. J. Am. Chem. Soc. **93**, 6355 (1971).

Dethioacetalization with Thallium(III) Trifluoroacetate[1]

TSE-LOK HO AND C. M. WONG

Department of Chemistry, University of Manitoba, Winnipeg, Manitoba R3T 2N2

Received July 13, 1972

Thioacetals undergo facile hydrolysis on treatment with thallium(III) trifluoroacetate.

Les thioacétals s'hydrolysent facilement lorsqu'on les traite par le trifluoroacétate de thallium(III).
[Traduit par le journal]

Canadian Journal of Chemistry, **50**, 3740 (1972)

Of the numerous existing protecting groups for the carbonyl (1), acetals and thioacetals are most commonly used. The acetal group is stable towards basic conditions but it is extremely labile in the presence of mineral acids. Although it is usually believed that it is suitable for masking the carbonyl when a molecule is exposed to organometallic reagents, this is not always true (2, 3). Thioacetals have been utilized only sporadically, mainly because they are obnoxious in smell, and more difficult to hydrolyze. However, besides the facts that thioacetals are easier to prepare, much more stable under a variety of experimental conditions, the development of a versatile synthetic method by Corey and Seebach (4 and references therein), based on nucleophilic attack of 2-lithio-1,3-dithianes, has stimulated a search for better ways of regenerating the carbonyl function.

Burgeoning activities are recorded in the recent literature, outlining different approaches to solving the problem. Thus, dethioacetalization has been effected by chloramine T (5), ceric ammonium nitrate (6), and *via* S-alkylation (7). In this paper, we wish to describe another novel procedure for oxidative hydrolysis of dithioacetals to regenerate the parent carbonyl compounds. This method, utilizing thallium(III) trifluoroacetate, was prompted by our fascination of thallium compounds in mediating organic reactions (Taylor–McKillop reactions) (ref. 8 and previous papers), as well as the consideration that thallium salts may act as soft acids (9), therefore they should combine with sulfur atoms readily.

We observed that the mildly exothermic reaction between thallium(III) trifluoroacetate and a thioacetal in tetrahydrofuran is complete almost instantaneously at room temperature, as indicated by the rapid fading of the initially brown solution to a milky white color. The

[1]Support of this research by the National Research Council of Canada is gratefully acknowledged.

Can. J. Chem. Downloaded from www.nrcresearchpress.com by 210.87.254.42 on 09/05/12
For personal use only.

TABLE 1. Dethioacetalization with Tl(III) trifluoroacetate

	Aldehyde or ketone	Yield of parent cpd.	Boiling point*
1,3-Dithiolans	Acetophenone	84%	200–205°
	Benzophenone	95%	(45–48°)
	Benzil (mono-)	95%	(93–96°)
	Benzaldehyde	83%	176–180°
1,3-Dithians	Phenylacetone	77%	212–218°
	Cycloheptanone	80%	173–180°

*Boiling points are heating block temperature; melting points in parentheses.

consistently high yields and simple operation involved in this reaction should be of great value to organic synthesis.

Finally, it is of interest to note that unsuccessful attempt of using thallium(I) salts to catalyze dethioacetalization has been reported (10).

Experimental

Infrared spectra were taken in dichloromethane using a Perkin–Elmer 710 Spectrophotometer. N.m.r. spectra were recorded on a Varian A56/60A spectrometer in carbon tetrachloride with tetramethylsilane as internal standard. Melting points are uncorrected.

General Procedure for Dethioacetalization with Thallium(III) Trifluoroacetate

To a solution of the dithioacetal (1.0 mmol) in tetrahydrofuran (2 ml) was added thallium(III) trifluoroacetate (600 mg, *ca.* 1.1 mmol; purchased from Aldrich Chemical Co.). The reaction became mildly exothermic as the thallium salt went into solution, and the brownish mixture soon faded to milky white. After 5 min at room temperature, it was poured into water (10 ml) and extracted with benzene (2 × 15 ml). The combined extracts were washed with dilute sodium bicarbonate, dried over anhydrous magnesium sulfate, and evaporated *in vacuo*. The crude product was purified by passing through a short neutral alumina column and recrystallized or evaporatively distilled. Identification of the carbonyl compounds was performed by comparison of their infrared, n.m.r. spectra with authentic samples.

Yields are listed in Table 1.

1. J. F. W. McOmie. *In* Advances in organic chemistry: methods and results. Vol. 3. Interscience Publishers, New York-London, 1962, p. 191.
2. J. N. Hines, M. J. Peagram, G. H. Whitham, and M. Wright. Chem. Commun. 1593 (1968).
3. H. C. Ho, T. L. Ho, and C. M. Wong. Can. J. Chem. **50**, 2718 (1972).
4. D. Seebach. Synthesis, 17 (1969).
5. W. F. J. Huurdman, H. Wynberg, and D. W. Emerson. Tetrahedron Lett. 3449 (1971).
6. T.-L. Ho, H. C. Ho, and C. M. Wong. Chem. Commun. 791 (1972).
7. (*a*) T. Oishi, K. Kamemoto, and Y. Ban. Tetrahedron Lett. 1085 (1972); (*b*) T. L. Ho and C. M. Wong. Synthesis. In press; (*c*) M. Fetizon and M. Jurion. Chem. Commun. 382 (1972).
8. E. C. Taylor, R. L. Robey, and A. McKillop. Angew. Chem. Intern. Ed. **11**, 48 (1972).
9. R. G. Pearson and J. Songstad. J. Am. Chem. Soc. **89**, 1827 (1967).
10. E. Vedejs and P. L. Fuchs. J. Org. Chem. **36**, 366 (1971).

The Oxidation of Organic Compounds by Sodium Ruthenate

Donald G. Lee, David T. Hall, and James H. Cleland

Department of Chemistry, The University of Saskatchewan, Regina Campus, Regina, Saskatchewan

Received July 20, 1972

The preparation of sodium ruthenate and its use as an oxidant for a variety of organic compounds is decribed.

La préparation du ruthenate de sodium et son utilisation comme oxydant d'une variété de composés organiques sont décrites. [Traduit par le journal]

Canadian Journal of Chemistry, **50**, 3741 (1972)

The oxidation of organic compounds by ferrate(VI) ion has recently been described (1, 2). The procedure is useful because of its "specificity, mild conditions, and speed of reaction". However, the preparation of ferrate(VI) is difficult and laborious, and the reagent is not particularly stable. The corresponding ruthenate(VI) ion, on the other hand, is extremely stable under basic conditions and very easy to prepare. Consequently we have examined

Can. J. Chem. Downloaded from www.nrcresearchpress.com by 210.87.254.42 on 09/05/12
For personal use only.

TABLE 1. Dethioacetalization with Tl(III) trifluoroacetate

	Aldehyde or ketone	Yield of parent cpd.	Boiling point*
1,3-Dithiolans	Acetophenone	84%	200–205°
	Benzophenone	95%	(45–48°)
	Benzil (mono-)	95%	(93–96°)
	Benzaldehyde	83%	176–180°
1,3-Dithians	Phenylacetone	77%	212–218°
	Cycloheptanone	80%	173–180°

*Boiling points are heating block temperature; melting points in parentheses.

consistently high yields and simple operation involved in this reaction should be of great value to organic synthesis.

Finally, it is of interest to note that unsuccessful attempt of using thallium(I) salts to catalyze dethioacetalization has been reported (10).

Experimental

Infrared spectra were taken in dichloromethane using a Perkin–Elmer 710 Spectrophotometer. N.m.r. spectra were recorded on a Varian A56/60A spectrometer in carbon tetrachloride with tetramethylsilane as internal standard. Melting points are uncorrected.

General Procedure for Dethioacetalization with Thallium(III) Trifluoroacetate

To a solution of the dithioacetal (1.0 mmol) in tetrahydrofuran (2 ml) was added thallium(III) trifluoroacetate (600 mg, *ca.* 1.1 mmol; purchased from Aldrich Chemical Co.). The reaction became mildly exothermic as the thallium salt went into solution, and the brownish mixture soon faded to milky white. After 5 min at room temperature, it was poured into water (10 ml) and extracted with benzene (2 × 15 ml). The combined extracts were washed with dilute sodium bicarbonate, dried over anhydrous magnesium sulfate, and evaporated *in vacuo*. The crude product was purified by passing through a short neutral alumina column and recrystallized or evaporatively distilled. Identification of the carbonyl compounds was performed by comparison of their infrared, n.m.r. spectra with authentic samples.

Yields are listed in Table 1.

1. J. F. W. McOmie. *In* Advances in organic chemistry: methods and results. Vol. 3. Interscience Publishers, New York-London, 1962, p. 191.
2. J. N. Hines, M. J. Peagram, G. H. Whitham, and M. Wright. Chem. Commun. 1593 (1968).
3. H. C. Ho, T. L. Ho, and C. M. Wong. Can. J. Chem. **50**, 2718 (1972).
4. D. Seebach. Synthesis, 17 (1969).
5. W. F. J. Huurdman, H. Wynberg, and D. W. Emerson. Tetrahedron Lett. 3449 (1971).
6. T.-L. Ho, H. C. Ho, and C. M. Wong. Chem. Commun. 791 (1972).
7. (*a*) T. Oishi, K. Kamemoto, and Y. Ban. Tetrahedron Lett. 1085 (1972); (*b*) T. L. Ho and C. M. Wong. Synthesis. In press; (*c*) M. Fetizon and M. Jurion. Chem. Commun. 382 (1972).
8. E. C. Taylor, R. L. Robey, and A. McKillop. Angew. Chem. Intern. Ed. **11**, 48 (1972).
9. R. G. Pearson and J. Songstad. J. Am. Chem. Soc. **89**, 1827 (1967).
10. E. Vedejs and P. L. Fuchs. J. Org. Chem. **36**, 366 (1971).

The Oxidation of Organic Compounds by Sodium Ruthenate

Donald G. Lee, David T. Hall, and James H. Cleland

Department of Chemistry, The University of Saskatchewan, Regina Campus, Regina, Saskatchewan

Received July 20, 1972

The preparation of sodium ruthenate and its use as an oxidant for a variety of organic compounds is decribed.

La préparation du ruthenate de sodium et son utilisation comme oxydant d'une variété de composés organiques sont décrites. [Traduit par le journal]

Canadian Journal of Chemistry, **50**, 3741 (1972)

The oxidation of organic compounds by ferrate(VI) ion has recently been described (1, 2). The procedure is useful because of its "specificity, mild conditions, and speed of reaction". However, the preparation of ferrate(VI) is difficult and laborious, and the reagent is not particularly stable. The corresponding ruthenate(VI) ion, on the other hand, is extremely stable under basic conditions and very easy to prepare. Consequently we have examined

Can. J. Chem. Downloaded from www.nrcresearchpress.com by 210.87.254.40 on 09/05/12
For personal use only.

Can. J. Chem. Downloaded from www.nrcresearchpress.com by 210.87.254.40 on 09/05/12
For personal use only.

TABLE 1. Products obtained from sodium ruthenate oxidations

Substrate	Product	Conditions	Yield (%)
Cyclohexanol	Cyclohexanone	1 h, 25°	85
Benzyl alcohol	Benzoic acid	1 h, 25°	97
Cinnamyl alcohol	Cinnamic acid	1 h, 10°	70
Cinnamic acid	No reaction	1 h, 25°	—
	Benzoic acid	4 h, 55°	91
Benzylamine	Benzaldehyde	1 h, 25°	14
Di-*n*-butyl ether	No reaction	11 h, 55°	—

its usefulness as an oxidant and wish here to report a summary of our observations.

Sodium ruthenate was prepared by stirring a solution of ruthenium tetroxide in carbon tetrachloride with aqueous sodium hydroxide. Under these conditions ruthenium tetroxide is reduced (reaction 1) and the highly polar perruthenate ion migrates to the aqueous solution where it slowly converts to ruthenate ion (reaction 2) (3, 4). At sodium hydroxide concentrations greater than 0.4 *M* the ruthenate solution is indefinitely stable at room tempera-

$$[1] \quad 4RuO_4 + 4OH^- \rightarrow 4RuO_4^- + 2H_2O + O_2$$

$$[2] \quad 4RuO_4^- + 4OH^- \rightarrow 4RuO_4^{2-} + 2H_2O + O_2$$

ture and may safely be stored in solution for long periods of time. In less basic solutions it is not completely stable as evidenced by the slow precipitation of ruthenium dioxide. The concentration of ruthenate ion in these solutions can be easily determined spectrophotometrically from its known absorption spectrum (5), and the reaction can then be carried out by dropwise addition of the appropriate quantity of oxidant to a vigorously stirred aqueous suspension of the organic compound. When a 50% excess of organic reductant was used the yields reported in Table 1 were obtained.

A comparison between these results and those reported for the ferrate reaction indicate that ruthenate is a more vigorous oxidant. For example, it gives an 85% yield of cyclohexanone from cyclohexanol, while under comparable conditions ferrate gave a yield of only 20–30% (1). The greater vigor of ruthenate is also illustrated by noting that it oxidizes benzyl alcohol to benzoic acid whereas benzaldehyde is obtained using ferrate ion.

It also appears that ruthenate will attack carbon–carbon double bonds only when high temperatures and longer reaction times are used. This fact makes it an ideal reagent for the oxidation of unsaturated alcohols such as cinnamyl alcohol.

It is also of interest to note that the low reactivity of ruthenate toward carbon–carbon double bonds and ethers is in contrast to the reaction of ruthenium tetroxide which very readily oxidizes compounds containing such functional groups (6).

Experimental

Preparation of Sodium Ruthenate

Five grams of ruthenium dioxide were added to an aqueous solution of sodium periodate (20 g). The solution was stirred vigorously for 10 min and then extracted with 6 × 70 ml of carbon tetrachloride. The aqueous solution remaining was a very pale yellow color indicating that only a small amount of ruthenium tetroxide remained, while the carbon tetrachloride layer was a bright greenish-yellow.

This ruthenium tetroxide solution was added to an equal volume of 1.0 *M* sodium hydroxide and shaken continuously for 2 h. At the end of this time the carbon tetrachloride layer was clear while the upper layer was a very dark orange color. The two layers were separated and the aqueous layer was extracted with 100 ml of carbon tetrachloride to remove any ruthenium tetroxide that might be present. (Ruthenium tetroxide is more soluble in carbon tetrachloride than water with a partition coefficient of 60:1) (7). On standing at room temperature for 2 days the solution became a bright orange color, and exhibited a visible–ultraviolet spectrum characteristic of ruthenate ion. The concentration of the RuO_4^{2-} was estimated by measuring the absorbance at a wavelength of 385 nm; at this wavelength the molar extinction coefficient is known to be 1030 (5).

The Oxidation Reaction

To 100 ml of 1.0 *M* sodium hydroxide 1.5 g of substrate was added. While stirring vigorously sufficient sodium ruthenate to oxidize approximately 1 g of the substrate was added drop by drop. Stirring was continued at room temperature for 1 h after all of the oxidant had been added.

In the cases of cyclohexanol, benzyl alcohol, cinnamyl alcohol, and benzylamine the reaction went to completion in this length of time as shown by the disappearance of the orange color and the appearance of a black precipitate of ruthenium dioxide. However, cinnamic acid and di-*n*-butyl ether were not oxidized under these conditions as evidenced by the persistance of the orange color. When the cinnamic acid solution was heated at 55 °C for 4 h the orange color did, however, disappear indicating that a reaction had taken place. Di-*n*-butyl ether on the other hand did not react even when heated at 50 °C for 11 h.

The solutions obtained from those substrates which reacted were filtered using a fine-fritted funnel to separate ruthenium dioxide (which could then be reused) from the organic products. The products were extracted into diethyl ether with 5 extractions of 75 ml each. The solutions were

dried for 1 h over anhydrous $MgSO_4$, concentrated to approximately 2 ml by rotary evaporation and the products identified by use of g.l.c. and n.m.r.

The aqueous solutions were then acidified with concentrated H_2SO_4 and again extracted with diethyl ether. The ether was evaporated and any non-volatile products were separated and identified using standard techniques.

The authors are grateful to the National Research Council of Canada and to Imperial Oil Enterprises Ltd. for research grants which supported this work.

1. R. J. AUDETTE, J. W. QUAIL, and P. J. SMITH. Tetrahedron Lett. 279 (1971).
2. R. J. AUDETTE, J. W. QUAIL, and P. J. SMITH. Chem. Commun. 38 (1972).
3. F. A. COTTON and G. WILKINSON. Advanced inorganic chemistry. 2nd ed. Interscience Publishers, New York. 1966. p. 1006.
4. G. NOWOGROCKI and G. TRIDOT. Bull. Soc. Chim. Fr. 684 (1965).
5. R. E. CONNICK and C. R. HURLEY. J. Amer. Chem. Soc. **74**, 5012 (1952).
6. D. G. LEE. Oxidation, techniques and applications in organic synthesis. *Edited by* R. L. Augustine. Marcel Dekker, Inc. New York. 1969. pp. 17, 54.
7. P. J. BEYNON, P. M. COLLINS, D. GARDINER, and W. G. OVEREND. Carbohyd. Res. **6**, 431 (1968).

Can. J. Chem. Downloaded from www.nrcresearchpress.com by 210.87.254.40 on 09/05/12
For personal use only.

Can. J. Chem. Downloaded from www.nrcresearchpress.com by 210.87.254.40 on 09/05/12
For personal use only.

The Elucidation of the Coupling Constants for the Cyclobutane Ring of the *trans*-Fused 2-Oxabicyclo[4.2.0]octane System

M. PAUL SERVÉ

Department of Chemistry, Wright State University, Dayton, Ohio 45431

Received July 26, 1972

The coupling constant for the fusion hydrogens of a bicyclo[4.2.0]octane ring system has been found using the shift reagent $Eu(fod)_3$.

La constante de couplage pour les hydrogènes au point de jonction du système bicyclo[4.2.0] octane a été trouvée, en utilisant le chélate de terre rare $Eu[fod]_3$.

Canadian Journal of Chemistry, **50**, 3744 (1972)

The size of the coupling constant J is an important tool in the elucidation of the stereochemistry of organic molecules. This is especially true for fused ring systems. The *trans*-fused bicyclo[4.2.0]octane system has been synthesized many times (1). However, the J for the fusion hydrogens on such a system has never been reported either because the splitting pattern was too complex or because one of the fusion hydrogens had been replaced by another substituent.

The molecule 1R*,6S*,7R*,8S*-7,8-diphenyl-2-oxabicyclo[4.2.0]octane (1) has recently been isolated by t.l.c. as a minor product ($< 10\%$ yield) from the photocycloaddition of *cis*-stilbene to 2,3-dihydropyran at 2537 Å. Mass spectral analysis of **1** indicated a 1:1 adduct of the two starting materials. The n.m.r. spectrum of **1** was quite complex. However, addition of the shift reagent $Eu(fod)_3$ (2) sufficiently spread out the spectrum so that spin decoupling experiments could be performed (Fig. 1). The following coupling constants were found: $J_{1,6} = 4.0$; $J_{1,8} = 4.2$; $J_{6,7} = 9.5$; $J_{7,8} = 9.5$ Hz.

The size of $J_{6,7}$ and $J_{7,8}$ indicated a *cis* arrangement for H-7 and -8 (3). Further evidence to support this assignment was obtained by heating **1** in a potassium-*t*-butoxide–*t*-butanol solution for 12 h. Since H-7 and -8 are each benzylic hydrogens, equilibration in strong base should result in their conversion into a *trans*-orientation. There are two *trans*-arrangements possible for H-7 and -8 and each would be expected to give rise to a separate peak in the g.l.p.c. chromatogram. G.l.p.c. analysis showed that as the peak for **1** disappeared two new peaks formed and grew during the 12 h period.

Since the J for the fusion hydrogens of the *cis*-fused bicyclo[4.2.0]octane system has been reported to be greater than 7 Hz (4), a *trans*-ring fusion **1** is indicated. A *trans* arrangement for H-1 and -8 is also indicated by the size of the coupling constant (5).

Thus, thanks to the substitution on the four-membered ring of **1** and the presence of the oxygen atom which enabled the use of the shift reagent, all the coupling constants on the four-membered ring could be elucidated.

1. M. P. CAVA and E. MOROZ. J. Am. Chem. Soc. **84**, 115 (1962); J. MEINWALD, G. G. CURTIS, and P. G. GASSMAN. J. Am. Chem. Soc. **84**, 116 (1962); K. B. WIBERG, J. E. HIATT and K. HSEIH. J. Am. Chem. Soc. **92**, 544 (1970); K. B. WIBERG and J. G. PFEIFFER. J. Am. Chem. Soc. **92**, 553 (1970).
2. R. E. RONDEAU and R. E. SIEVERS. J. Am. Chem. Soc. **93**, 1522 (1971).
3. M. KARPLUS. J. Am. Chem. Soc. **85**, 2870 (1963).
4. L. PAOLILLO, H. ZIFFER, and O. BUCHARDT. J. Org. Chem. **35**, 38 (1970).
5. I. FLEMMING and D. H. WILLIAMS. Tetrahedron, **23**, 2747 (1967).

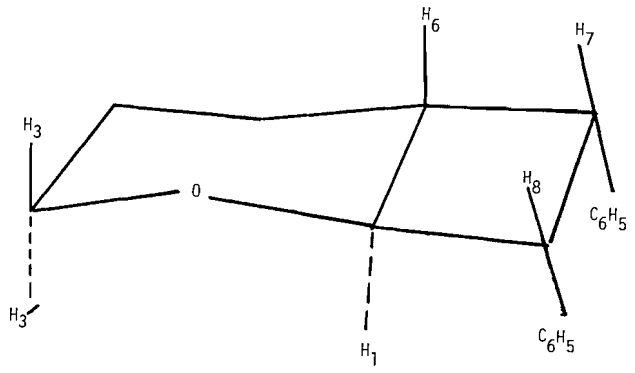

1

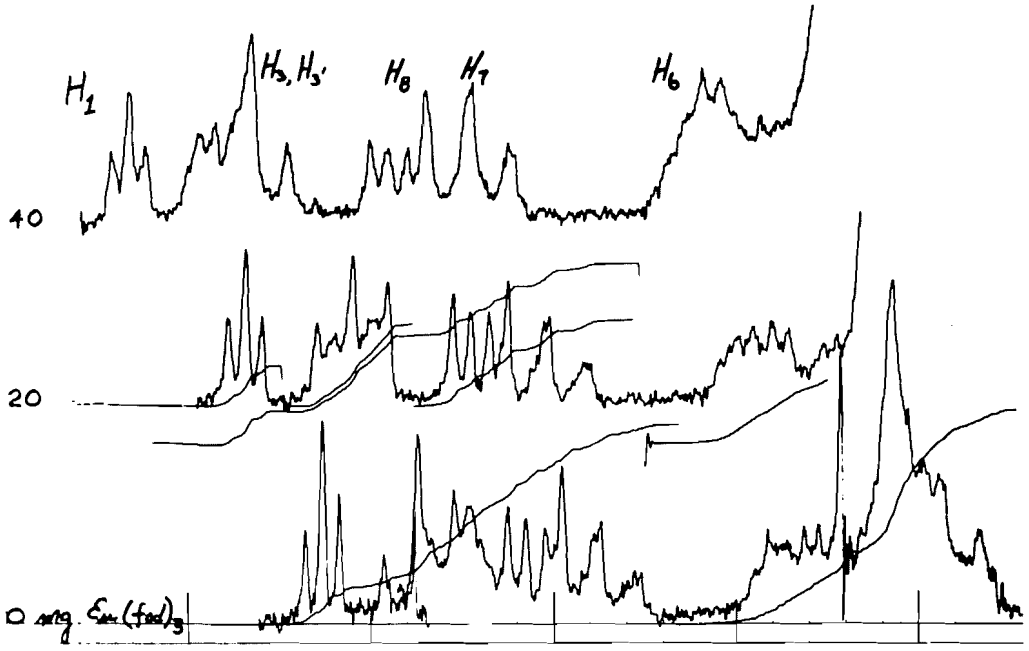

FIG. 1. Effect of adding $Eu(fod)_3$ to the n.m.r. spectrum of **1**.

Can. J. Chem. Downloaded from www.nrcresearchpress.com by 210.87.254.40 on 09/05/12
For personal use only.

Binary Dioxygen Complexes of Nickel; Infrared Spectroscopic Evidence for $Ni(O_2)$ and $(O_2)Ni(O_2)$ in Low Temperature Matrices

H. HUBER AND G. A. OZIN[1]

Lash Miller Chemistry Laboratory and Erindale College, University of Toronto, Toronto, Ontario

Received July 26, 1972

The cocondensation reaction of nickel atoms with oxygen or dilute oxygen–argon matrices at 4.2–10 °K gives rise to the first examples of binary transition metal dioxygen complexes. Variable concentration and diffusion controlled warm up studies and $^{16}O_2$, $^{16}O^{18}O$, $^{18}O_2$ isotope substitution studies establish the stoichiometries of the dioxygen complexes of nickel to be $Ni(O_2)$ and $(O_2)Ni(O_2)$. Both complexes have the dioxygen molecule(s) coordinated to the nickel atom in a "sideways" fashion.

La réaction de cocondensation d'atomes de nickel avec des matrices d'oxygène ou d'oxygène dilué-argon à 4.2–10 °K donne lieu aux premiers exemples de complexes de dioxygène métalliques de transition binaire. Les études de réchauffage contrôlées à concentration et à diffusion variables et les études de substitution d'isotopes $^{16}O_2$, $^{16}O^{18}O$, $^{18}O_2$ indiquent que les stoechiométries des complexes de dioxygène du nickel sont $Ni(O_2)$ et $(O_2)Ni(O_2)$. La ou les molécules de ces deux complexes sont coordonnées à l'atome de nickel de façon "latérale". [Traduit par le journal]

Canadian Journal of Chemistry, **50**, 3746 (1972)

Several complexes of low valency transition metals such as iridium (1), rhodium (2), ruthenium (3), cobalt (4), and the platinum triad (5) react with oxygen to give adducts, sometimes reversibly.

Dioxygen complexes of this type have recently become of considerable interest to chemists because of their relationship to naturally occurring dioxygen carriers and the reactivity of coordinated dioxygen to various reductants.

However, in most of the complexes reported so far, it appears that the presence of other ligands in the complex in addition to dioxygen is a necessary prerequisite for the isolation of a stable compound. The involvement of these other ligands in the overall bonding scheme is often difficult to assess which can make discussions of the bonding of the O_2 to the metal atom somewhat open to criticism.

In this communication we present data which show for the first time that *binary* dioxygen complexes of nickel are capable of existence under conditions of matrix isolation.

Briefly our experiments consisted of cocondensing nickel atoms (McKay 99.99%) with pure $^{16}O_2$ (Matheson 99.99%); $^{16}O_2$/Ar (1:20; 1:100; 1:200; and 1:500) and $^{16}O_2/^{16}O^{18}O/^{18}O_2$/Ar (1:2:1:800) onto a CsI window cooled to 4.2 or 10 °K by either a liquid helium transfer system or a closed cycle helium refrigerator. The rate of nickel atom deposition was controlled by using a quartz crystal microbalance incorporated into the evaporation furnace (6). The concentration of nickel atoms in the matrix was arranged to be such that the probability of a nickel atom having another nickel atom as a nearest neighbor was 10^{-3}. Matrix gas flows were kept in the range 0.5–2.0 mmol/h, using micrometer needle valves. Matrix infrared spectra were recorded on a Perkin–Elmer 621 spectrophotometer over the frequency range 2000–200 cm^{-1}.

When nickel atoms are cocondensed with dilute $^{16}O_2$/Ar (1:200 or 1:500) matrices a single, strong sharp infrared absorption is observed at 966.2 cm^{-1}, which in a $^{16}O_2/^{16}O^{18}O/^{18}O_2$/Ar (1:2:1:800) matrix splits into a characteristic 1:2:1 *triplet* of bands at 966.2, 940.1, and 913.6 cm^{-1}.

The number and intensity ratio of the bands in this multiplet together with the excellent agreement between their observed and calculated ^{18}O isotopic shifts provide convincing evidence for a molecule containing a *single* dioxygen molecule bonded in a "sideways" fashion to a single nickel atom; that is, the lines at 966.2, 940.1, and 913.6 cm^{-1} are assigned to $Ni(^{16}O_2)$, $Ni(^{16}O^{18}O)$ and $Ni(^{18}O_2)$, respectively. Low frequency bands assignable to Ni–O stretching modes were not observed probably because of

[1]To whom correspondence should be addressed.

Can. J. Chem. Downloaded from www.nrcresearchpress.com by 210.87.254.5 on 09/05/12
For personal use only.

Can. J. Chem. Downloaded from www.nrcresearchpress.com by 210.87.254.5 on 09/05/12
For personal use only.

their low extinction coefficients or their occurrence below the low wavenumber limit of our spectrometer (200 cm^{-1}).

In a number of diffusion controlled warm up experiments of the dilute $Ni/^{16}O_2/Ar$ matrices in the temperature range 10–15 °K a sharp infrared absorption at 1062.0 cm^{-1} grows in at the expense of the band previously assigned to $Ni(^{16}O_2)$.

When nickel atoms are cocondensed with pure $^{16}O_2$ matrices at 4.2–10 °K an infrared absorption at 1064 cm^{-1} is found to be the strongest feature in the spectrum and the absorption at 966 cm^{-1} is completely absent. At no stage of the diffusion-controlled warm up experiments in pure $^{16}O_2$ matrices does the absorption at 966 cm^{-1} appear.

We conclude from the warm up data in dilute $^{16}O_2/Ar$ matrices and from the data in pure $^{16}O_2$ matrices that the infrared absorption at 1062.0 cm^{-1} is the O—O stretching mode of a dioxygen complex of nickel containing more than a single molecule of dioxygen.

The stoichiometry of this complex is established from a diffusion-controlled warm up experiment in a $^{16}O_2/^{16}O^{18}O/^{18}O_2/Ar$ (1:2:1:800) matrix, which shows in addition to the infrared absorption at 1062 cm^{-1}, *six* other absorptions at 1052.2, 1045.2, 1035.2, 1018.2, 1016.0, and 1001.4 cm^{-1} which can be assigned to the O—O stretching modes of the various isotopic oxygen molecule permutations of a complex of nickel containing *two* dioxygen molecules, that is $(O_2)Ni(O_2)$.

The multiplets observed in this experiment indicate that two equivalent O_2 molecules are arranged such that the O atoms are equivalent. The simplicity of the multiplet spectrum also indicates that the dioxygen molecules are bonded to the nickel atom in a "sideways" fashion in $(O_2)Ni(O_2)$, thereby filling four coordination sites around the nickel atom. In this context it is worth noting that the four coordination sites around nickel in the complex $Ni(N_2)_4$ are filled by four N_2 molecules bonding to the nickel in an "end-on" fashion (7).

At this stage in our investigations it is not possible to prove whether the dioxygen molecules in $(O_2)Ni(O_2)$ are arranged in a tetrahedral (D_{2d}) or planar (D_{2h}) configuration about the nickel atom, although the observation of a septet rather than a sextet tends to favor the latter.

This work is presently being extended to include Raman, u.v.–visible, and e.s.r. matrix isolation studies, the data from which should yield considerable information concerning the nature of the bonding of the dioxygen molecule to the nickel atom and the electronic structures of $Ni(O_2)$ and $(O_2)Ni(O_2)$.

We thank the National Research Council of Canada and the Research Corporation for financial support.

1. (*a*) L. VASKA. Science, **140**, 809 (1963). (*b*) L. VASKA and D. L. CATONE. J. Am. Chem. Soc. **88**, 5324 (1966). (*c*) M. S. WEININGER, I. F. TAYLOR, and E. L. AMMA. Chem. Commun. 1172 (1971).
2. (*a*) J. T. MAGUE and G. WILKINSON. J. Chem. Soc. A, 1736 (1966). (*b*) M. C. BAIRD, D. N. LAWSON, J. T. MAGUE, J. A. OSBORNE, and G. WILKINSON. Chem. Commun. 129 (1966). (*c*) K. HIROTA, M. YAMAMOTO, S. OTSUKA, A. NAKAMURA, and Y. TATSUNO. Chem. Commun. 533 (1968).
3. (*a*) K. R. LAING and W. R. ROPER. Chem. Commun. 568 (1968). (*b*) B. E. CAVIT, K. R. GRUNDY, and W. R. ROPER. Chem. Commun. 60 (1972). (*c*) S. CENINI, A. FUSI, and G. CAPARELLA. Inorg. Nucl. Chem. Lett. **8**, 127 (1972). (*d*) J. VALENTINE, D. VALENTINE, and J. P. COLLMAN. Inorg. Chem. **10**, 219 (1971).
4. (*a*) A. L. CRUMBLISS and F. BASOLO. J. Am. Chem. Soc. **92**, 55 (1970). (*b*) G. A. RODLEY and W. T. ROBINSON. Nature, **235**, 438 (1972). (*c*) N. W. TERRY, E. L. AMMA, and L. VASKA. J. Am. Chem. Soc. **94**, 653 (1972).
5. (*a*) S. TAKAHASHI, K. SONOGASHIRA, and A. HAGIHAR. Nippon Kagaku Zasshi, **87**, 610 (1966). (*b*) G. WILKE, H. SCHOTT, and P. HEIMBACK. Angew. Chem. **79**, 62 (1967). (*c*) S. OTSUKA, A. NAKAMURA, Y. TATSUNO, and M. MIKI. J. Am. Chem. Soc. **94**, 3761 (1972).
6. M. MOSKOVITS and G. A. OZIN. J. App. Spectrosc. In press.
7. H. HUBER, E. P. KUNDIG, M. MOSKOVITS, and G. A. OZIN. J. Am. Chem. Soc. In press.

Can. J. Chem. Downloaded from www.nrcresearchpress.com by 210.87.254.105 on 09/05/12
For personal use only.

Canadian Journal of Chemistry

Published by THE NATIONAL RESEARCH COUNCIL OF CANADA

VOLUME 50 DECEMBER 1, 1972 NUMBER 23

Synthesis of Lambertianic Acid

R. A. BELL, M. B. GRAVESTOCK, AND V. Y. TAGUCHI

Department of Chemistry, McMaster University, Hamilton, Ontario

Received July 5, 1972

A synthesis of lambertianic acid **2***a* starting from podocarpic acid is described. The central intermediate, diester-ketone **4***b*, is obtained by ozonolysis and hydrogenation, and the exocyclic methylene group in ring B generated via a Reformatsky reaction. The furan ring is attached by nucleophilic attack of 3-lithiofuran, for which an improved preparation is described, on either the acid chloride **7***b* or the aldehyde **16**. The 12-oxygen atom is removed by mesylation of the alcohols **12***a* and *b* and Li–liquid ammonia reduction.

Nous avons dècrit la synthèse de l'acide Lambertianique **2***a* à partir de l'acide podocarpique. La cétone diester, intermédiaire central, est obtenue par ozonolyse et hydrogénation et le groupe méthylene exocyclique du cycle B géneré par une réaction de Réformatsky. Le cycle furannique est lié par l'attaque nucléophile du lithio-3-furanne, pour lequel une meilleure préparation est donnée, au chlorure d'acide **7***b* ou à l'aldehyde **16**. L'atome d'oxygène 12 est éliminé par mésylation des alcools **12***a* et *b* et réduction par le lithium dans l'ammoniac liquide.

Canadian Journal of Chemistry, **50**, 3749 (1972)

The synthesis of diterpenoids based on the labdane, **1**, skeleton[1] has been founded on the initial construction of a bicyclic intermediate with the side chain (carbons 11→16) being added in the final stages. The bicyclic intermediate has either been directly generated (1) or engineered from a preformed tricyclic species (2). We have chosen the latter course for a synthesis of the furano-diterpene, lambertianic acid[2] **2***a*, because it has the advantage of generating an intermediate with carbon atoms 11 and 12 attached to the bicyclic nucleus and also because the oft-synthesized (5) and readily available[3] podocarpic acid, **3***a*, formed a convenient starting material.

The ready transformation in high yield of **3***b* into the bicyclic keto-acid **4***a* by low temperature

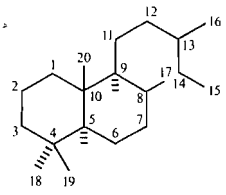

1

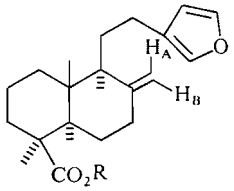

2
a R = H
b R = Me

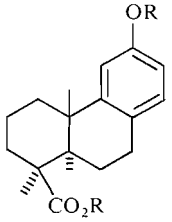

3
a R = H
b R = Me

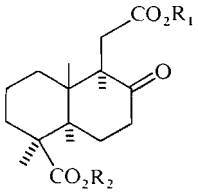

4
a R_1 = H; R_2 = Me
b R_1 = R_2 = Me

[1]The numbering system employed here is that proposed by the informal IUPAC committee on Diterpene Nomenclature, London, July, 1968.

[2]Lambertianic acid (3) is the (+) enantiomer of the naturally occurring daniellic acid (4). Since we use the (+) enantiomer of podocarpic acid **3** (absolute stereochemistry as shown) as a starting material, the final product is optically pure lambertianic acid.

[3]Available from New Zealand Timber Products Ltd., P.O. Box 5784, Auckland, New Zealand.

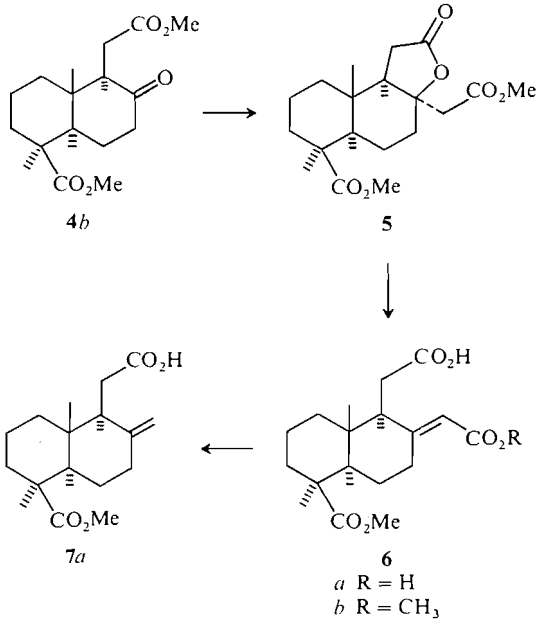

SCHEME 1

ozonolysis and hydrogenation has already been described (6). The remaining problems to complete a synthesis of lambertianic acid are therefore generation of the exocyclic methylene at C-8 and attachment of the furan ring at C-12. The synthetic intermediates used in the solution of these two problems are shown in Scheme 1, and in Schemes 2 and 4.

The generation of the exocyclic methylene at C-8 was first attempted by means of a direct Wittig reaction. There is a literature precedent (7) for the methylenation of an 8-ketone in the manool series, but in the case of either **4***a* or *b* exhaustive attempts under a wide variety of experimental conditions proved fruitless. The use of methylene magnesium iodide (8) likewise failed and in view of the experience of other workers (9) in similar systems further efforts to introduce the exocyclic methylene directly were abandoned, and consideration was given to the use of the ethoxyacetylene decarboxylation sequence of Stork *et al.* (9), which had already been used by Pelletier *et al.* in the synthesis of polyalthic acid (2*c*). However, before this sequence was attempted, the ester–ketone **4***b* was subjected to the little used, but highly convenient Reformatsky reaction (10) with methyl bromoacetate and active zinc, and it was with some

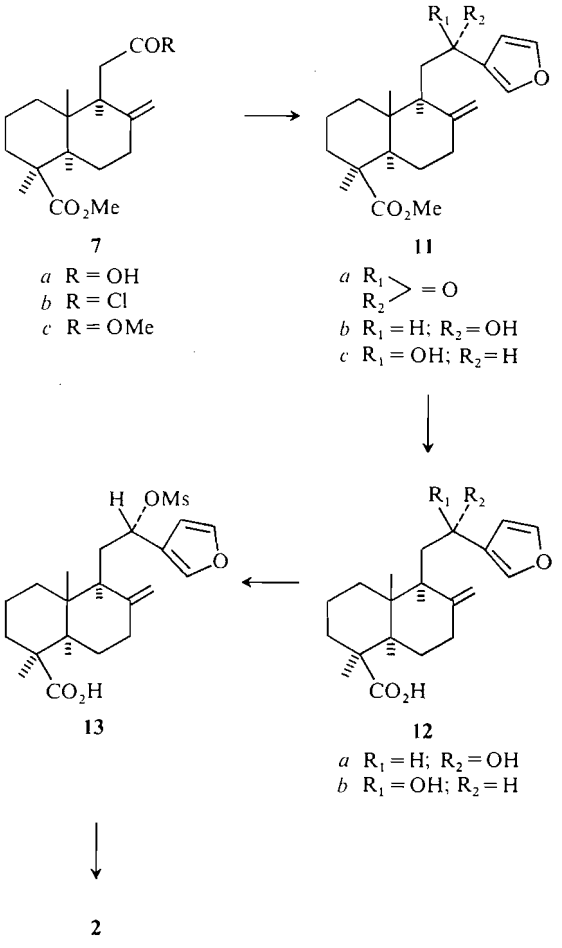

SCHEME 2

pleasure that we observed the formation in reasonable yield of the lactone-diester **5**. Further experimentation showed that a benzene–dimethoxyethane (DME) solvent mixture (3:1) led to production of **5** in over 90% yield. The presence of DME was mandatory since its absence led to inferior yields of **5** and the simultaneous formation of variable quantities of the known (6) lactone **8**. This latter unsaturated derivative presumably arose through $ZnBr_2$ Lewis acid-catalyzed lactonization of **4***b* to give **9** followed by proton rearrangement from C-11 to C-8 via the lactone enol. When DME is present, the $ZnBr_2$ is strongly solvated and therefore its Lewis acid activity is greatly diminished. The α-configuration at C-8 is assigned on the basis of preferred nucleophilic

Can. J. Chem. Downloaded from www.nrcresearchpress.com by 210.87.254.105 on 09/05/12
For personal use only.

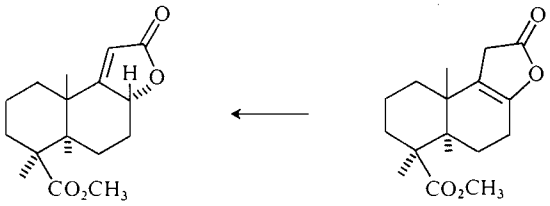

8 9

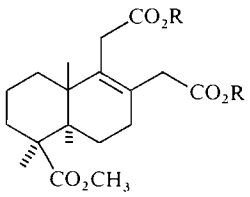

10
a R = H
b R = CH_3

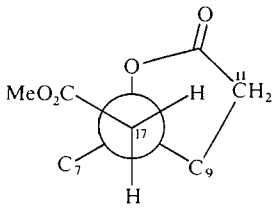

FIG. 1. Newman projection of preferred conformation of lactone **5** that permits facile *trans*-elimination leading to the E-olefin **6**.

attack of the zinc reagent from the less hindered underside of the molecule. Support is found for this in the Grignard reaction of a similar 8-ketone used as an intermediate in the synthesis of manool by Bigley *et al.* (2*a*) and also the behavior of **4***b* with methyl lithium and $NaBH_4$ (11).

The lactone ring of **5** could be opened by treatment with sodium methoxide in methanol, or, more conveniently, with sodium hydroxide in methanol since this reagent led directly to the desired unsaturated diacid **6***a* in 95% yield. There was present in this reaction product a small percentage (*ca.* 3%) of a compound which was assigned the β,γ-unsaturated acid structure **10***a* on evidence which is discussed below. The major diacid was assigned the E-configuration on the basis of the most likely conformation about the C_8—C_{17} bond which would lead to a *trans*-elimination. The conformation (shown in Fig. 1 in Newman projection) with the carbomethoxy group over ring B should be of lowest energy since it minimizes dipolar interactions by placing the carbomethoxy group as far away as possible from the developing carboxylate anion of the lactone ring. No clear evidence for the presence of the 8(17)-Z double bond isomer of **6** could be obtained by either p.m.r. spectroscopy or t.l.c., but the wide-range melting point of even repeatedly crystallized samples of **6** led to the suspicion that there probably was 2–3% of the Z-isomer present. However, the occurrence of this isomer in the elimination product was of secondary importance as both E- and Z-isomers should give the same product on subsequent reaction.

The pyrolytic decarboxylation of the diacid **6** to the monoacid **7***a* was effected in 80% yield following the normal procedure of thermolysis in quinoline (9). However, it was noted that the intermediate β,γ-unsaturated acid, **10***a*, had the double bond in the 8,9- rather than the 7,8-position, since aliquots of the decarboxylation reaction mixture showed an initial rise and then fall in intensity of the C-20 CH_3 (δ 0.80 p.p.m.) absorption of **10***a* in its p.m.r. spectrum. In one large scale run, chromatography of the crude methylated reaction product gave a sample of the triester **10***b* which showed the absence of any vinylic protons. Thus with **10***a* as the pre-decarboxylation intermediate it is possible, *a priori*, for either the C-12 or the C-17 carboxyl group to be lost. Close scrutiny of the p.m.r. spectra and chromatographic fractions of crude decarboxylation reaction mixtures did not show any significant traces of the 9,11-olefin. From the inspection of molecular models, it was concluded that a transition state involving a stereospecific introduction of the 12-carboxyl proton at C-8 in an axial (β) manner to permit continuous overlap of the developing sp^3 orbital at C-8 with the incipient C-11 methylene group (9), would result in severe steric interactions between the C-11 and -1 hydrogens. The corresponding stereoelectronically controlled axial (α) proton transfer from the C-17 carboxyl to C-9 was subject to no steric constraints and the decarboxylation therefore was able to proceed rapidly. The crude acid **7***a* was contaminated with 10–15% of the C-19 carboxylic acid derived from quinoline hydrolysis of the 19-methyl ester and

Can. J. Chem. Downloaded from www.nrcresearchpress.com by 210.87.254.105 on 09/05/12
For personal use only.

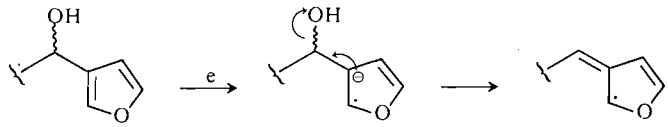

12 14

SCHEME 3

it was found convenient to methylate the crude products with excess diazomethane and isolate the pure diester **7***c* by chromatography on Florisil. In this way the keto-ester **4***b* could be routinely transformed into the olefin-ester **7***c* in overall yields of 40–50% and this compares more than favorably with the 30% yield obtained from the lithium ethoxyacetylide route (2*c*).

The attachment of the furan ring was initially undertaken by condensation of the acid chloride **7***b* with 3-lithiofuran[4] in ether at −78° (see Scheme 2). The mono-furan derivative **11***a* was obtainable in yields up to 80% and it was anticipated that reductive removal of the C-12 keto group could be readily achieved by one of the many available methods. However, in the sequel all the usual procedures resulted in either recovery of starting material or severe degradation of the furan ring. Thus the Wolf–Kishner reaction, conducted at lower than normal temperatures (14) on the supposedly reactive α-furyl ketone (15) gave an intractable mixture wherein the furan rings had been destroyed in the majority of the product. Indeed, **11***a* was so resistant to derivative formation that even the elegant tosylhydrazone reduction sequence (16) failed. The stubborn and unreactive behavior of the 12-ketone, apparently caused by the steric congestion forced upon it by the exocyclic methylene group at C-8, demanded that an alternative process for the removal of the 12-oxygen function be found. An early paper by Birch (17) had shown that 2-furfuryl alcohol could be reduced to 2-methyl furan by sodium in liquid ammonia and this precedent led to the hope that the 12-oxygen might be removed in a similar manner. Moreover, the methyl ester of methyl desoxypodocarpate had been reported (18) to undergo reductive hydrolysis with Li–liquid ammonia to give the corresponding acid, and it was therefore hoped to obtain lambertianic acid in one step from the isomeric 12-hydroxy-esters, **11***b* and *c*. However, a mixture of the 12-alcohols (obtained from $NaBH_4$ treatment of the 12-ketone[5]) with a moderate excess of Na or Li metal (4–5 equiv) in liquid ammonia showed no reduction of the 12-alcohol, but showed that reduction of the C-19 ester to the alcohol competed with reductive hydrolysis. Indeed, when the analogous reaction of methyl *O*-methylpodocarpate **3***b* with Li–liquid ammonia was repeated under identical reaction conditions, reduction of the ester to alcohol was more than competitive with reductive hydrolysis. It is possible here that some additional factor or contaminant (proton source?) was responsible for the reaction course, but despite exhaustive efforts, the hydrolysis procedure was never satisfactory in our hands. In a further effort to induce removal of the 12-hydroxyl group and minimize reduction at C-19, the free hydroxy-acids **12***a* and *b* (obtained from early trial reductions) were subjected to a massive excess of Li metal (25 equiv). Again the 12-hydroxyl was completely retained, and some reduction of the C-19 acid was noted. This behavior is difficult to rationalize, particularly when it was noted from molecular models that a strong steric interaction exists between C-12 and the exocyclic methylene group. Such steric congestion would be expected to greatly favor formation of the C-12 sp^2 hybridized intermediate **14**, which is a reasonable intermediate (20) following the expulsion of the OH from the furanoid radical-anion (see Scheme 3).

[4]In our hands a modification (see Experimental, and note warning) of the procedure of Gronowitz and Sorlin (12) proved most satisfactory. Other procedures involving the reduction of polyiodo-furans (13) were less convenient.

[5]The 12(R) and 12(S) alcohols were obtained from the $NaBH_4$ reduction in a ratio of 2:3. They were readily separated by column chromatography and their configurations were assigned by analogy with the corresponding 12-hydroxylabdan-19-oic acids (19). Since the present work was aimed at destroying the asymmetry at C-12, the detailed conformational arguments for the configurational assignments are not present here but may be found in ref. 19.

Can. J. Chem. Downloaded from www.nrcresearchpress.com by 210.87.254.105 on 09/05/12
For personal use only.

Can. J. Chem. Downloaded from www.nrcresearchpress.com by 210.87.254.105 on 09/05/12
For personal use only.

A straightforward solution to this problem would be the transformation of the 12-hydroxyl into a better leaving group in order to facilitate its expulsion during the Li–liquid ammonia reduction stage. However, before this proposal could be reduced to practice, some improvement was necessary in the hydrolysis step of **11** to **12**. Potassium tertiary butoxide in dimethylsulfoxide (DMSO) has been shown (21) to be an especially useful reagent for the hydrolysis of hindered esters; the *t*-butoxide anion effecting an S_N2 displacement on the CH_3 of a methyl ester to give methyl *t*-butyl ether and a carboxylate anion. In our hands the C-19 ester of **11***b* or *c* was cleanly hydrolyzed, but unfortunately the reaction conditions necessary and the strength of the *t*-butoxide base coupled to make elimination of the pseudo-benzylic 12-hydroxyl group a competing process. Moreover the 8(17)-double bond appeared susceptible to migration, and the net result of these competing reactions was to make the overall yields of **12** highly variable. For example, in one medium scale reaction only a 40% yield of combined **12***a* and *b* was obtained after silica gel chromatography. The *t*-butoxide–DMSO reagent was therefore not as satisfactory as had been anticipated, and at this point no highly selective method for achieving the **11** to **12** transformation has been determined. However, from a practical standpoint, adequate supplies of both **12***a* and *b* were available from the *t*-butoxide–DMSO experiments, and the main task of generating a better leaving group at C-12 could be undertaken. The preparation of the mesylate of **12***a* was attempted via the methanesulfonyl chloride–triethylamine procedure (22).[6] Reaction proceeded readily as evidenced by the p.m.r. spectrum of the crude product (upfield shift of the C-17 H_A proton), but the mesylate **13** was exceedingly sensitive to thermal decomposition and could not be isolated in a pure state. It was therefore necessary to prepare the mesylate and immediately subject it to Li–liquid ammonia reduction. When this sequence was carried out using 5 equiv of Li metal a 36% yield of lambertianic acid **2***a* was obtained. This material was identical in its chromatographic and spectral properties with an authentic sample provided by Professor W. G. Dauben. A small sample of the acid was transformed into the ester **2***b* and shown to be identical with the methyl ester derived from natural sources.

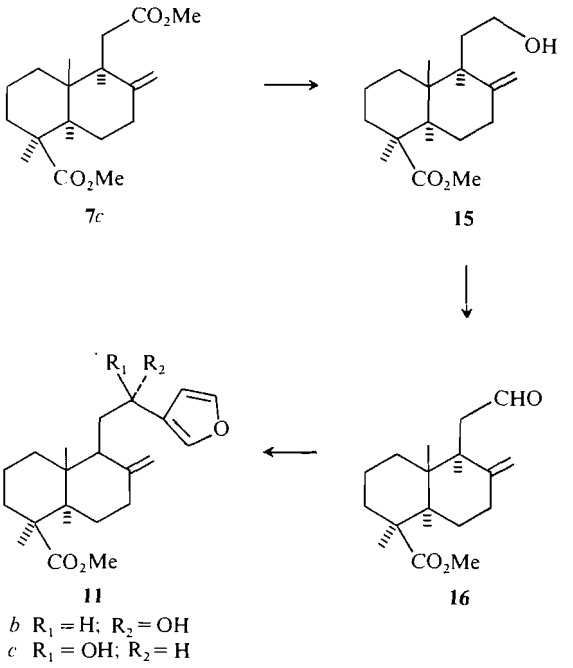

b $R_1 = H$; $R_2 = OH$
c $R_1 = OH$; $R_2 = H$

SCHEME 4

In view of the necessity of removing the 12-oxygen atom as the alcohol, it was clear that alternative approaches to **11***b* and *c* could be envisaged. One route which was found to be particularly convenient in practical terms is shown in Scheme 4. The entire sequence, when carried out without purification of the intermediates, gave the alcohols **11***b* and *c* in an overall yield of 52% from the diester **7***c*. The selective reduction of the primary C-12 ester over the highly hindered, axial C-19 ester was readily accomplished with excess $LiAlH_4$ in ether for 45 min at temperatures below 0°. The alcohol **15** was routinely obtained in better than 90% yields. Oxidation of **15** to the aldehyde[7] **16**, was carried out with either the Collins reagent (24) (CrO_3–pyridine in CH_2Cl_2) or the Fetizon reagent (25) (Ag_2CO_3–Celite) in quantitative yield, and the

[6]Attempts to prepare the toluenesulfonate of **12***a* met with no success whatsoever and we interpret this as being a further attestation to the steric crowding at C-12. The ready formation of the mesylate is evidently a consequence of the very high activity of the sulfene precursor (22).

[7]Attempts to prepare the aldehyde **16** in one step from the diester **7***c* with sodium bis(2-methoxyethoxy)aluminum hydride (Vitride) (23) were unsuccessful.

addition of the furan ring effected again with 3-lithiofuran in THF at −78°. In this instance minor stereoselectivity was noted in the generation of the alcohols as the ratio of **11***b* to *c* was 2:1 (from isolation by chromatography).

Summary

A formal total synthesis of lambertianic acid **2***a* has been achieved using podocarpic acid as a relay. The exocyclic methylene at C-8 was introduced via a Reformatsky reaction carried out in benzene–dimethoxyethane as solvent to avoid Lewis acid-catalyzed rearrangements. Decarboxylation of the α,β-unsaturated acid **6** led to excellent yields of the key keto-acid **7***a*. The furan ring of lambertianic acid was introduced by nucleophilic attack of 3-lithio-furan on either the acid chloride **7***b* or the aldehyde **16**. Serious difficulty was encountered in removal of the 12-oxygen function either as the ketone **11***a* or the alcohols **11***b* and *c* and only Li–liquid ammonia reduction of the 12-mesylate **13** afforded reasonable yields of lambertianic acid.

Experimental

Melting points were determined on a Kofler micro hot-stage apparatus and are uncorrected. Spectra were recorded in the following solvents and instruments: i.r. ($CHCl_3$) Perkin–Elmer 337 and Beckman IR5; p.m.r. ($CDCl_3$) Varian Associates A-60, T-60, and HA-100, tetramethylsilane as internal standard; mass spectra, Hitachi Perkin–Elmer RMU-6A (at 80 eV) and C.E.C. 21-110. Carbon and hydrogen microanalyses were performed by Spang Microanalytical Laboratories, Ann Arbor, Michigan. In the experimental descriptions to follow, the organic substrates were isolated via extraction with the appropriate solvent (2×) followed by washing of the combined solvent layer with water, saturated brine, and finally drying with anhydrous Na_2SO_4. The solvents were removed by evaporation at reduced pressure on a Buchi Rotavapor.

17-Carbomethoxy-8β-hydroxy-(13→16)-tetranorlabda-12, 19-dioic Acid

19-Methyl Ester 8β → 12-Lactone (5)

(i) Method using benzene as solvent. Granulated zinc (20 mesh) was activated by the procedure of Johnson and Fieser (26). After the metal had been heated in concentrated sulfuric acid containing a few drops of nitric acid at 100° for about 10 min, the majority of the acid was decanted off, and water added. After vigorous H_2 evolution for a few minutes all traces of acid were removed by repeated washing with water, followed by acetone, ether, and then drying at 110°.

The keto-acid **4***a*, m.p. 171–172°, 5.00 g (16.9 mmol) was dissolved in 250 ml anhydrous benzene in a dry 500 ml three-necked flask fitted with a mechanical stirrer and reflux condenser (a magnetic stirrer bar gave adequate agitation in smaller scale runs). Then 5.20 g (34 mmol) of methylbromoacetate (R) (Eastman), 5 g activated zinc, and 50 mg iodine were added, and the stirred mixture brought rapidly to reflux under nitrogen. Two further additions of 2.60 g methyl bromoacetate, 5 g zinc, and a crystal of iodine, were made after 6 and 12 h reflux. After 24 h total reflux, the reaction mixture was cooled, the zinc complex destroyed in 2 *N* sulfuric acid, and the acidified mixture extracted with benzene (2 × 100 ml) after removal of the initial benzene layer. The combined benzene extracts on usual work-up gave 6.25 g dark yellow oil. P.m.r. analysis indicated some 5% of non-diterpenoid reagent condensation products, 75–80% lactone-ester **5**, 10% starting material, 5% of unsaturated lactone **8**, and a few percent of an unknown compound with a C-20 methyl absorption at 0.63 p.p.m. Extraction of an ethereal solution of the product with saturated $NaHCO_3$ solution served to remove starting material and the unknown component. Two crystallizations of a portion from 2:1 hexane–ethyl acetate gave the analytical sample as colorless needles, m.p. 104.5–105°; i.r. ν_{max} 3025, 3000, 2955, 2855, 1775, 1735, 1720, 1440, 1220(b), 1142, 985, 940, 925 cm^{-1}; p.m.r. δ 0.74 (s, 3H, C-20 CH_3), 1.22 (s, 3H, C-18 CH_3), 3.65 and 3.72 (s and 3H each, C-19 and -21 $COOCH_3$'s) p.p.m.

Anal. Calcd. for $C_{19}H_{28}O_6$: C, 64.75; H, 8.01. Found: C, 64.71; H, 8.01.

(ii) Method using benzene and dimethoxyethane as co-solvent. The keto-acid **4***a*, 3.50 g (12.5 mmol, *ca.* 95% pure) was dissolved in 160 ml dry benzene and 40 ml dry dimethoxyethane (distilled from calcium hydride) and 3.80 g (25 mmol) of methylbromoacetate, 3 g zinc, and a crystal of iodine added. The mixture was mechanically stirred under reflux and a nitrogen atmosphere for 12 h and then a further 3.0 g (20 mmol) methylbromoacetate, 3 g zinc, and crystal of iodine added. After a further 6 h reflux the reaction mixture was cooled and worked-up in similar manner to (*i*), to give 3.97 g yellow oil. The p.m.r. spectrum revealed no discernible unsaturated lactone **8**, 90–95% pure lactone-ester **5** and some 5% starting material.

The oil was chromatographed on 160 g Florosil in 50:50 benzene–petroleum ether (30–60°) and the chromatogram developed with benzene and 5% ethyl acetate–benzene which yielded *ca.* 100 mg of yellow oil which by odor and p.m.r. analysis appeared to be methyl phenylacetate. Further elution with 10% ethyl acetate–benzene gave a total of 2.98 g (75%) of pure (>98%) lactone-ester **5**, m.p. 103–105°.

19-Ethyl Ester 8β → 12-Lactone

Precisely the same procedure was followed as above in (*i*) for the carbomethoxy ester, utilizing 5.70 g (2 mol equiv) ethyl bromoacetate initially and two subsequent additions of 2.85 g (1 mol equiv). However, the extent of conversion was poorer than in (*i*) and p.m.r. analysis indicated some 70% product, 20–25% starting material, and 5% of unsaturated lactone **8**.

Sodium bicarbonate extraction and two crystallizations gave an analytical sample of the ethyl ester of **5**, m.p. 74–75°; i.r. ν_{max} 3025, 3000, 2955, 2855, 1778, 1732, 1722, 1455, 1230(b), 1142, 985, 940, 925 cm^{-1}; p.m.r. δ 0.76 (s, 3H, C-20 CH_3), 1.22 (s, 3H, C-18 CH_3), 1.28 (t, J = 7.0 Hz, 3H, ester $-CH_2 \cdot CH_3$), 3.65 (s, 3H, C-19 $COOCH_3$); 4.20 (q, J = 7.0 Hz, 2H, ester $-CH_2 \cdot CH_3$) p.p.m.

Anal. Calcd. for $C_{20}H_{30}O_6$: C, 65.55; H, 8.25. Found: C, 65.72; H, 8.09.

Can. J. Chem. Downloaded from www.nrcresearchpress.com by 210.87.254.105 on 09/05/12
For personal use only.

Can. J. Chem. Downloaded from www.nrcresearchpress.com by 210.87.254.105 on 09/05/12
For personal use only.

17-Carbomethoxy-(13→16)-tetranorlabd-8(17)E-ene-12,19-dioic Acid

*19,21-Dimethyl Ester (**6b**)*

The lactone-ester **5**, 3.00 g (8.5 mmol, 95% pure) obtained by direct bicarbonate washing and one crystallization from ethyl acetate–hexane (1:3, at −20°) was dissolved in 50 ml of methanol (dried over $Mg(OCH_3)_2$), and added to a solution of 0.50 g clean sodium metal (22 mmol, 2.5 equiv) in 50 ml of dry methanol under N_2. The solution was heated at reflux under N_2 for 2 h, cooled, and poured into 1 l of 0.5 *N* sulfuric acid, and extracted with benzene (3 × 150 ml). The extracts on usual work-up gave 2.90 g pale yellow "foam" (96.5%). The p.m.r. spectrum indicated a product of 90–95% purity with traces of a component with C-20 methyl absorption at 0.66 p.p.m. Recrystallization from methyl acetate–hexane (1:2) gave 2.63 g of off-white needles, m.p. 150–160°. A second recrystallization gave the analytical sample of the C-17 methyl ester of **6** as colorless needles, m.p. 152–160; i.r. ν_{max} 3600–2400, 2950, 1725, 1715, 1705, 1640, 1425, 1250, 1170 cm^{-1}; u.v. λ_{max} 227 (16 000) (calcd. 224 (+5)) mμ; p.m.r. δ 0.527 (s, 3H, C-20 CH_3), 1.22 (s, 3H, C-18 CH_3), 2.51 (s, broad, $w_{h/2}$ = 3 Hz, 2H, C-11 CH_2), 3.64 and 3.69 (s and 3H each, C-19 and -21 $COOCH_3$'s), 5.55 (s, broad, $w_{h/2}$ = 2.5 Hz, 1H, C-17 vinylic), 9–11 (s, broad, $w_{h/2}$ = 10–60 Hz, C-12 COOH) p.p.m.

Anal. Calcd. for $C_{19}H_{28}O_6$: C, 64.75; H, 8.01. Found: C, 64.58; H, 8.11.

The m.p. range is apparently due to small quantities, *ca.* 3% of the Z-$\Delta^{8,17}$ double bond stereoisomer which is not resolvable by p.m.r. analysis or t.l.c. at this concentration.

*19-Methyl Ester (**6a**)*

*(i) By hydrolysis of αβ-unsaturated ester **6b**.* The αβ-unsaturated ester **6b**, 2.00 g (5.65 mmol) m.p. 150–160° (containing a minimum of 90% of the E-double bond isomer) was dissolved in 150 ml (R) methanol together with 50 ml of 1 *N* sodium hydroxide solution and refluxed under nitrogen for 2 h. The majority of the methanol was removed *in vacuo* and the residue poured into 250 ml of 1 *N* sulfuric acid. The liberated acid was extracted with benzene (3 × 75 ml) and the extracts worked-up in the usual way to give 1.94 g (100%) of an off-white crystalline solid. The p.m.r. spectrum showed at least 90% E-double bond isomer, unsaturated diacid **6a**, with 2–3% **10a** (see below).

*(ii) By hydrolysis of lactone–ester **5**.* The lactone–ester, 2.98 g (m.p. 103–105°, 98% pure, direct from chromatography of the reaction product) was dissolved in 225 ml (R) methanol and 75 ml 1 *N* sodium hydroxide added. The whole was refluxed under N_2 for 2 h. The majority of the methanol was removed *in vacuo* and the residue diluted with water, washed twice with ether, and the aqueous extracts acidified with 2 *N* sulfuric acid. The acidified solution was extracted with benzene (3 × 100 ml) which on usual work-up gave 2.85 g (99%) of a near colorless "foam". The p.m.r. spectrum indicated some 95% of unsaturated diacid **6a**, plus 2–3% of the βγ-unsaturated isomer **10a**. This latter compound was also present as a decarboxylation intermediate and the crude reaction mixture could thus be used directly for decarboxylation (see below). Two crystallizations of a portion from ethyl acetate–hexane (1:2) gave the analytical sample as colorless crystalline clusters m.p. 216–220° (dec. at 205°); i.r. ν_{max} 3500–2500(b), 3010, 1705, 1690, 1640, 1250, 1240(b), 1155, 930 cm^{-1}; u.v. λ_{max} 220 (12 800) mμ; p.m.r. δ 0.54 (s, 3H, C-20 CH_3), 1.22 (s, 3H, C-18 CH_3), 2.52 (s, broad $w_{h/2}$ = 4 Hz 2H, C-11 CH_2), 3.60 (s, 3H, C-19 $COOCH_3$), 4.05 (m, 1H, C-7 H), 5.52 (s, broad $w_{h/2}$ = 3 Hz, 1H, C-17 vinylic), 9–11 (s, broad (15 Hz), 2H, C-12 and -21 COOH's) p.p.m.

Anal. Calcd. for $C_{18}H_{26}O_6$: C, 63.88; H, 7.74. Found: C, 63.60; H, 7.81.

*(13→16)-Tetranorlabd-8(17)-ene-12,19-dioic Acid 19-Methyl Ester (**7a**)*

The αβ-unsaturated diacid **6a** (containing 2–3% βγ-isomer **10a**), 2.00 g (5.90 mmol), was dissolved in 20 ml quinoline (distilled and degassed under nitrogen) together with 50 mg of copper chromite catalyst (see below) in a dry 50 ml flask containing a magnetic stirring bar. The flask was sealed with a reflux (air) condenser and a three-way trap to nitrogen and a water pump. The flask was evacuated with stirring at room temperature, flushing the contents twice with nitrogen, and then finally evacuated while the temperature was raised to 100°. It was then filled with nitrogen and the temperature raised to 230° (silicone oil bath). The mixture was stirred under nitrogen at 230° (±2°) for 1.25 h and then withdrawn from the bath and allowed to cool to room temperature. After diluting the contents of the flask with 200 ml of 1:4 benzene–ether, the whole was extracted with 10% sodium hydroxide solution (4 × 25 ml) and 25 ml water. The extracts were poured onto crushed ice, acidified with 80 ml of 2 *N* sulfuric acid and benzene extracted (3 × 100 ml). Usual work-up of the extracts gave 1.54 g (88%) of a pale yellow oil. The p.m.r. spectrum indicated 80% methylene vinylic absorption at 4.45 and 4.80 p.p.m. due to **7a** (C-20 CH_3 absorption at 0.53 p.p.m.), and also the corresponding C-19 demethylated compound (C-20 CH_3 absorption at 0.63 p.p.m.). In addition there was 10% of unreacted intermediate **10a**, and 10% of other minor components. In the main synthetic sequence the product was purified and fully characterized as the methyl ester **7b**, (see below). However, material from one run was isolated by two crystallizations from (1:3) ethyl acetate–hexane, giving off-white flakes m.p. 153–155° (>98% pure); i.r. ν_{max} 3500–2400(b), 2940, 2855, 1715, 1645, 1460, 1150, 890, 680 cm^{-1}; p.m.r. δ 0.53 (s, 3H, C-20, CH_3), 1.20 (s, 3H, C-18 CH_3), 3.60 (s, 3H, C-19 $COOH_3$), 4.45 and 4.80 (s, and 1H each, both $w_{h/2}$ = 3 Hz, C-17 vinylic CH_2), 9–11 (s, broad $w_{h/2}$ = 10 Hz, 1H, C-12 COOH) p.p.m.

Preparation of Copper Chromite Catalyst

The method of Sherrill and Mellock (27) was essentially used. Concentrated ammonium hydroxide was added to a solution of 63 g (0.25 mol) of ammonium dichromate in 250 ml water until the solution was yellow (chromate). A solution of 120.8 g (0.5 mol) of cupric nitrate dihydrate in 150 ml water was then added in a slow stream to the well-stirred chromate solution. The orange-brown precipitate was filtered off under pressure and dried overnight at 110°.

After pulverizing to a fine powder it was then heated slowly in a porcelain basin over a small flame. After spontaneous decrepitation had ceased it was then roasted strongly so that a fine black powder was finally produced. The powder was suspended in 10% acetic acid in water, filtered, and the process repeated three times in water. The product was finally dried at 110° to give 65 g of "$CuCrO_4$" as a fine black powder.

Can. J. Chem. Downloaded from www.nrcresearchpress.com by 210.87.254.105 on 09/05/12
For personal use only.

Dimethyl(13→16)-tetranorlabd-8(17)ene-12,19-dioate (7b)

The crude unsaturated acid **7a** (from the decarboxylation of 2 g of diacid **6a**), 1.54 g, was esterified with ethereal diazomethane, to give 1.60 g (87% from **6a**) of crude methyl ester **7b**, containing some 80% of the desired compound, as a dark yellow oil. The oil was chromatographed on 64 g of Florisil in 50:50 benzene–petroleum ether (30–60°) and the chromatogram developed with the same solvent. Elution with benzene yielded a total of 1.12 g (61% from **6a** of pure (>98%) crystalline unsaturated ester **7b**. The sample for analysis was crystallized from 1:9 ethyl acetate–hexane giving colorless prisms, m.p. 109–110°; i.r. ν_{max} 3020, 2950, 2850, 1735, 1720, 1645, 1440, 1225(b), 1160, 910, 710 cm^{-1}; p.m.r. δ 0.53 (s, 3H, C-20 CH_3), 1.19 (s, 3H, C-18 CH_3), 2.40 (s, 2H, C-11 CH_2), 3.60 and 3.625 (s, and 3H each, C-19 and -12 $COOCH_3$'s), 4.46 and 4.75 (s, and 1H each, both broad $w_{h/2}$ = 3 Hz, C-17 vinylic CH_2) p.p.m.; mass spectrum (high resolution), *m/e* calcd. for $C_{18}H_{28}O_4$, 308.198747; found: 308.200294 (mol. ion).

Anal. Calcd. for $C_{18}H_{28}O_4$: C, 70.10; H, 9.15. Found: C, 70.28; H, 9.24.

Preparation of 3-Iodofuran

The basic procedure of Gronowitz and Sorlin (12) was used, with further modifications due to the work of Wrobel and Dabrowski (28) and as a result of present investigations.

2-Furoic acid, 224 g (2 mol), was dissolved in 3 l of warm (35°) water and added dropwise over 1 h to a well-stirred solution of 320 g (1 mol) mercuric acetate in 5 l water at room temperature. The precipitated solid resulting was filtered under pressure and dried at 0.1 mm room temperature for 2 days to give 316 g (0.81 mol) of 2-(acetoxymercuric)-furoate as a buff powder (81%). This material was pyrolyzed following an adaption of Wrobel's (28) procedure.

WARNING: The mercuric salts should not, under any circumstances, be pyrolyzed in the absence of a solvent as severe and unpredictable explosions can occur.

2-(Acetoxymercuric)-furoate, 200 g (0.512 mol) was suspended in 350 ml xylene in a 1 l three-necked flask, fitted with a Herschberg stirrer, thermometer and a Dean–Stark trap with reflux condenser. The mixture was stirred and heated over 30 min to reflux temperature (*ca.* 140°), and kept at reflux for 1 h, when the trap contained water, xylene/water azeotrope and acetic acid. The temperature was then reduced to 135° and heating and stirring continued for 23 h. After cooling in an ice-bath, 250 ml of 95% acetic acid was added and stirring continued at room temperature for 3 h *only*. By this time nearly all solid matter had dissolved to a dark brown solution which was then poured into 1.7 l water and sodium chloride added until no further precipitation took place. After stirring overnight the mixture was filtered under pressure to give a tan solid which was washed well with water and dried at 0.1 mm room temperature for 36 h, to give 133 g of a tan solid (crude 3-(chloromercuric)-furan, plus a little 2-isomer and mercuric acetate).

The crude material was extracted with ether in a Soxhlet apparatus. The results of the extraction were examined in lots. Thus after 48 h, 34 g of 3-(chloromercuric)-furan was obtained, the p.m.r. spectrum of which showed the presence of 5–6% of the 2-isomer. Another 24 h gave 7.5 g material containing 7–8% 2-isomer. Another 36 h gave 7 g material containing 8–9% of 2-isomer. Further prolonged extraction gave only 3 g containing 30–40% 2-isomer. Batches one to three, combined thus gave 48.5 g of 3-(chloromercuric)-furan containing *ca.* 6% of the 2-isomer, p.m.r. (DMF, p.p.m. relative to center of DMF doublet) δ 3.8 (1H, d, β-H), 4.7 (1H, d, α-H) 5.0 (1H, m, α'-H to O and Hg). This was of a purity comparable to that previously obtained by crystallization of the extracted product (12) and is of adequate purity for final reaction by iodine oxidation. The overall yield from 2-(acetoxymercuric)-furan is thus 51% (assuming initial disproportionation to mercuric acetate and mercuric difuroate) and 31% from starting material. This represents twice the yield previously obtained (12).

3-(Chloromercuric)-furan, 33.5 g (0.11 mol), from the above was suspended in 400 ml water and a solution of 28.0 g (0.11 mol) iodine (I_2), in 36.5 g potassium iodide and 400 ml water was added dropwise to the stirred suspension at room temperature. After the addition was complete, excess iodine was destroyed with sodium thiosulfate and the 3-iodofuran present steam distilled from the reaction mixture by boiling for *ca.* 2 h, (500 ml distillate). The distillate was extracted with ethanol-free ether (3 × 100 ml), and the extracts washed twice with brine, filtered through anhydrous sodium sulfate and evaporated in vacuo at 35° (maximum temperature) to give 16.16 g (75%) of 3-iodofuran as a pale yellow oil. The p.m.r. spectrum indicated 5% of the 2-isomer (12). The substance can be redistilled *in vacuo* but was sufficiently pure for purposes of the present synthesis. It is stable indefinitely at −20° in the dark, p.m.r. (see also ref. 12), δ 6.55 (m, 1H, β-H), 7.3–7.6 (7.45 center) (2H, m, α-H's).

*Methyl 15,16-Epoxy-12-ketolabda-8(17),13(16),14-trien-19-oate (**11a**)*

(a) Preparation of the Acid Chloride 7b

The crystalline unsaturated ester **7c**, 565 mg (1.83 mmol, >98% pure) was refluxed in 90 ml methanol together with 30 ml 1 *N* sodium hydroxide solution for 3 h under nitrogen. The methanol was removed *in vacuo*, the residue diluted with 300 ml water, washed once with 20% benzene in ether, and then acidified with cold 2 *N* sulfuric acid. Benzene extraction and usual work-up gave 530 mg (98%) of 98% pure unsaturated acid **7a**. A portion of the product 235 mg (0.80 mmol) was dissolved in 3 ml methanol in a 10 ml flask and 74 mg (0.88 mmol) (R) sodium bicarbonate added, together with 2 ml of water. After stirring at room temperature for 2 h, when all carbon dioxide evolution had ceased, solvent was removed *in vacuo* on the rotary evaporator and the residue finally dried overnight at 0.1 mm at room temperature.

The product (255 mg sodium salt (0.80 mmol), plus *ca.* 8 mg sodium bicarbonate) was covered with 5 ml benzene containing 1% pyridine in the same 10 ml flask, cooled to partial freezing in an ice-bath, and treated dropwise with 340 mg (2.6 mmol) oxalyl chloride (Eastman) in 3 ml dry benzene. The mixture was stirred at the same temperature for 15 min and then allowed to warm to room temperature with stirring for a further 1.5 h. The solvent and the bulk of the oxalyl chloride were removed *in vacuo* at 30°, the residue flushed with a further 5 ml benzene, and this was also removed in the same way. Finally the residue was dried at 0.1 mm room temperature for 15 min, and taken up in 2 ml anhydrous benzene–3 ml anhydrous ether, for addition to the furyl lithium solution prepared below.

(b) Preparation of 3-Lithiofuran

Methyl lithium (2.40 *M* in ether), 0.50 ml (1.20 mmol), was syringed into a dry 20 ml flask equipped with septum inlet, under an atmosphere of nitrogen. Anhydrous ether,

Can. J. Chem. Downloaded from www.nrcresearchpress.com by 210.87.254.105 on 09/05/12
For personal use only.

2 ml, was also syringed in, and the flask cooled to $-70°$ in a Dry Ice–acetone bath. 3-Iodofuran, 235 mg (1.22 mmol) was then added dropwise by syringe in 5 ml of anhydrous ether and the solution stirred at $-70°$ for 1 h, by which time 3-furyl lithium formation was complete. (*n*-Butyl lithium can also be used (12), when the formation time is faster, but the reagent is more difficult to keep at stable concentration.)

At this time the acid chloride **7***b* solution (from (*a*), above) was taken up in a 10 ml syringe (size 19 needle to prevent possible blockage by precipitated sodium chloride present) and introduced into the 3-furyl lithium solution in a fast stream over 1–3 s. The resultant mixture was then stirred at $-70°$ for a further 30 min and allowed to warm to room temperature over 1–2 h by removal of the cold bath. The product was quenched in 5% sodium dihydrogen phosphate solution, benzene extracted (3 × 75 ml) and worked-up in the usual manner to give 260 mg (95%) of a dark yellow oil. The p.m.r. spectrum showed 80% of the desired keto-furan **11***a*, (furanoid and C-20 methyl absorption), 10% starting material **7***a*, and 10% of minor components (the principal contaminant has a C-20 methyl absorption at 0.50 p.p.m.).

The product was eluted onto 10.5 g Florisil in 50:50 benzene–petroleum ether (30–60°) and developed with the same solvent, finally eluting with pure benzene, giving a total of 182 mg (66%) of 97% pure keto-furan **11***a* as a near-colorless oil. (The oil resisted all attempts at crystallization which is not unexpected since methyl lambertianate **2***b* itself is an oil.) I.r. ν_{max} 2970, 2940, 2875, 1720, 1680, 1645, 1560, 1500, 1210 (broad), 1156, 888, 872 cm^{-1}; u.v. λ_{max} 251 (245) (π–π^*, B); 210 (7200) (end absorption, π–π^*, K); n–π^*, R, band too small to measure; p.m.r. δ 0.59 (s, 3H, C-20 CH_3), 1.18 (s, 3H, C-18 CH_3), 3.65 (s, 3H, C-19 $COOCH_3$), 4.31 and 4.66 (s, 1H each, broad $w_{h/2} = 3$ Hz, C-17 vinylic CH_2), 6.66 (m, 1H, C-14 β-furanoid H), 7.29 (m, 1H, C-15 α-furanoid H), 7.98 (m, 1H, C-16 α-furanoid H) p.p.m.; high resolution mass spectrum *m/e*: calcd. for $C_{21}H_{28}O_4$: 344.198747; found: 344.199064 (mol. ion), 249 (M-95, β-ketone cleavage).

*Attempts to Form C-12 Ketone Derivatives of (**11***a*)

(a) p-Toluenesulfonyl Hydrazone

The ketone **11***a* was kept with excess *p*-toluenesulfonyl hydrazine in solutions of dry dimethoxyethane–ethanol at room temperature, 50 and 80°. Even when these mixtures were left for up to 10 days at room temperature no reaction occurred, as evidenced by direct *in situ* reaction of the products with sodium borohydride which gave only the alcohols **11***b*/**11***c* resulting from reduction of the starting material. At ethanol reflux temperature, extensive reduction of the 8(17)-double bond took place apparently due to diimide production (29).

Use of *p*-toluenesulfonic acid as a catalyst and isolation of the product revealed two components as judged by p.m.r. inspection, one of which showed a new (31.0 Hz) C-20 methyl absorption. However, sodium borohydride at 60° failed to produce any effect on the mixture. Prolonged refluxing with sodium borohydride in isopropanol overnight gave a complex mixture, probably as a result of Bamford–Stevens (30) reaction via the diazo compound.

(b) Semicarbazone

Heating the ketone at 45° with semicarbazide hydrochloride in methanol–DMF with sufficient sodium bicarbonate to provide the right p*H* (31), produced an ill-defined product resulting from apparent degradation of the furan ring. No reaction occurred overnight at room temperature with this reagent.

(c) Oxime

Boiling hydroxylamine hydrochloride in aqueous pyridine at 110° for 20 h (conditions shown to give reaction with very hindered 11-keto steroids (32)) gave a superficially homogeneous product which appeared to contain oximated material (i.r. evidence), but the p.m.r. spectrum showed a greatly reduced intensity of the furan absorptions indicating destruction of the furan ring.

(d) Thioketal

The ketone **11***a*, 20 mg (0.058 mmol), was placed in 5 ml "pear"-tube and 5 drops (116 mg, 1.12 mmol) ethandithiol added together with 2 drops (20 mg) of boron trifluoride ethereate. The solution was held at room temperature overnight. The product was diluted with benzene washed with 5% sodium hydroxide solution, water, brine, and evaporated to give a dark-pink oil, 22 mg. P.m.r. showed species containing mixed furanoid absorption, and the vinylic protons had shifted downfield, each showing a 4 Hz splitting. When the product was added to 400 mg W-2 Raney nickel (deactivated by refluxing for 1 h in acetone) and stirred at room temperature for 30 min, the final result showed some sulfur removal but considerable double bond reduction.

*Methyl 15,16-Epoxy-12-hydroxylabda-8(17),13(16),14-trien-19-oate (**11***b and c)*

Ketone **11***a* 50 mg, was stirred with excess sodium borohydride in aqueous ethanol overnight at room temperature. The solution was then poured into 5% NaH_2PO_4 solution and benzene extracted. Usual work-up gave 49 mg colorless oil which p.m.r. inspection showed to be a mixture of the two alcohols **11***b* and *c* in the approximate ratio of 3:2 (this same mixture was obtained from borohydride reaction in the abortive tosylations above); i.r. ν_{max} 3620, 3400, 2920, 2850, 1720 (1730 sh), 1640, 1470, 1230, 1160, 1025, 895, and 875 cm^{-1}.

The mixture was chromatographed at 100:1 on Florisil in 50:50 petroleum ether (30–60°)–benzene. Elution with benzene gave 15 mg of the 12(R)-alcohol **11***c* as a colorless oil, p.m.r. δ 0.515 (s, 3H, C-20 CH_3), 1.18 (s, 3H, C-18 CH_3), 3.58 (s, 3H, C-19 $COOCH_3$), 4.48 (H_A) and 4.86 (H_B) (s and 1H each, broad $w_{h/2} = 3$ Hz, C-17 vinylic H's), 4.71 (m, C-12H), 6.37 (m, 1H, C-14 furanoid H), 7.3 (m, 2H, C-15/16 furanoid) p.p.m. Ethyl acetate (5%)–benzene gave 20 mg of crystalline solid, 12(S)-alcohol **11***b*, p.m.r. δ 0.530 (s, 3H, C-20 CH_3), 1.18 (s, 3H, C-18 CH_3), 3.55 (s, 3H, C-19 $COOCH_3$) 4.72 (H_A), and 4.88 (H_B) (s and 1H each, $w_{h/2}$ = 3 Hz (H_B) or 4.5 Hz (H_A), C-17 vinylic H's), 4.78 (m, 1H, C-12H, 6.37 (m, 1H, C-14H furanoid), 7.3 (m, 2H, C-15/16H furanoid) p.p.m.

*Methyl 12-Hydroxy-(13→16)-tetranorlabd-8(17)-en-19-oate (**15**)*

A solution of 198 mg (5.21 mmol) of $LiAlH_4$ in 10 ml dry THF was stirred for 30 min at room temperature under a nitrogen atmosphere and then cooled to $-60°$ in a Dry Ice–acetone bath. To this solution was added dropwise a solution of 1.046 g (3.39 mmol) of the diester **7***c* in 15 ml dry THF. Upon completion of the addition, the solution was allowed to warm to $-4°$ and was kept at $-4 \pm 3°$ for 45 min. The reaction was then cooled to $-60°$, quenched with 2.0 ml (20.8 mmol) of EtOAc added dropwise, and allowed

Can. J. Chem. Downloaded from www.nrcresearchpress.com by 210.87.254.105 on 09/05/12
For personal use only.

to warm to 0°. At 0°, the mixture was diluted with H_2O (10 ml) and allowed to warm to room temperature. The mixture was acidified to p*H* 6, further diluted with H_2O (150 ml), extracted with 10% benzene–Et_2O (4 × 50 ml) and worked-up in the usual way to give 919 mg (97%) of a colorless oil which showed: p.m.r. δ 0.52 (s, 3H, C-20 CH_3), 1.18 (s, 3H, C-18 CH_3), 3.60 (s, 3H, C-19 $COOCH_3$), 3.33–3.93 (3H, C-12H's and C-12 OH), 4.53 (s, 1H, $w_{h/2} = 3$ Hz, C-17H_A), 4.85 p.p.m. (s, 1H, $w_{h/2} = 3$ Hz, C-17H_B); i.r. ν_{max} 3630 (non-bonded), 3500 (broad, bonded), 2950, 1710 (C=O), 1640 (C=C), 1440, 1220, 1157, 1094, 1037, 984, 893 cm^{-1}; mass spectrum (80 eV) *m/e* 280 (M^+, calcd. for $C_{17}H_{28}O_3$: 280.2038; found: 280.2048), 249 (M − CH_2OH, calcd. for $C_{16}H_{25}O_2$: 249.1854; found: 249.1848).

*Methyl 12-Oxo-(13→16)-tetranorlabd-8(17)-en-19-oate (**16**)*

(a) Via Dipyridine Chromium(VI) Oxide (24)

Chromium(VI) oxide (8.3 g, 0.083 mol) (dried *in vacuo* over P_2O_5) was added in small portions to 60 ml pyridine (dried over CaH_2) stirred with a mechanical stirrer as nitrogen was passed over it. The mixture became very viscous and after 30 min, petroleum ether was added and the reddish-brown solid was filtered through a Buchner funnel while nitrogen was passed over it via an inverted funnel. The solid was dried *in vacuo* and a quantitative yield of the complex was obtained.

A solution of 56 mg (0.19 mmol) of the ester-alcohol **15** in 5 ml dry methylene chloride was prepared under a nitrogen atmosphere. Similarly, a suspension of 340 mg (1.32 mmol, 7:1 molar ratio) of the dipy–CrO_3 complex in 15 ml dry CH_2Cl_2 was prepared under a nitrogen atmosphere in a flask with a septum inlet. The ester-alcohol solution was syringed into the flask containing the oxidizer and the mixture was stirred for 15 min after which it was poured onto a short column of Florisil. The product was eluted with 50 ml 1:1 benzene–ethyl acetate. Evaporation of the solvent gave 52 mg (100%) of the aldehyde as a colorless oil which showed: p.m.r. δ 0.53 (s, 3H, C-20 CH_3), 1.18 (s, 3H, C-18 CH_3), 3.58 (s, 3H, C-19 $COOCH_3$), 4.40 (s, 1H, $w_{h/2}$ = 3 Hz, C-17H_A), 4.82 (s, 1H, $w_{h/2} = 3$ Hz, C-17H_B) 9.52 p.p.m. (m, 1H, CHO); i.r. ν_{max} 2950, 2850 (aldehyde C—H) 2725 (aldehyde C—H), 1720 (ester and aldehyde), 1645 (C=C), 1470, 1450, 1435, 1385, 1248, 1225, 1156, 1136, 1094, 1040, 984, 900 cm^{-1}; mass spectrum (80 eV) *m/e* 278 (M^+, calcd. for $C_{17}H_{26}O_3$: 278.1882; found: 278.1894).

(b) Via Ag_2CO_3–Celite (25)

A well-stirred suspension of 56 g (97.9 mmol, 10 equiv) of the reagent in 225 ml benzene was refluxed for 30 min with a Dean–Stark trap. A solution of 2.74 g (9.79 mmol) of the alcohol **15** in 20 ml benzene was added dropwise through an equilibrating separatory funnel. After refluxing for 18 h, the mixture was filtered through a short column of "Celite". Evaporation of the solvent gave 2.62 g (96%) of the aldehyde **16** as a colorless oil which was identical to the aldehyde obtained in (*a*).

*Methyl 15,16-Epoxy-12-hydroxylabd-8(17),13(16),14-trien-19-oate (**11***b and c)*

(a) 3-Lithiofuran

The system composed of a three-necked flask (50 ml), equipped with a nitrogen inlet, equilibrating separatory funnel (25 ml), condenser and drying tube, and magnetic stirrer bar, was flushed with nitrogen and then cooled in a Dry Ice–acetone bath. To this system were added 21 ml (5.24 mmol) of a 2.43 *M* solution of methyllithium in ether and 5 ml dry ether. After sufficient cooling a solution of 0.66 ml (7.00 mmol) of 3-iodofuran in 2 ml dry ether and 2 ml additional ether were added dropwise and the mixture was stirred for 1½ h at −70°.

*(b) Reaction with Aldehyde **16***

To the solution of 3-lithiofuran prepared above was added dropwise a solution of 972 mg (3.50 mmol) of the aldehyde **16** in 7 ml dry ether and 2 ml additional ether and the resulting mixture was stirred for 30 min at −70°. The reaction was quenched with 15 ml of 5% NaH_2PO_4 added dropwise at −70°. After 10 min, the mixture was allowed to warm to room temperature. The reaction mixture was then diluted with water (30 ml) and extracted with ether (3 × 40 ml) and worked-up in the usual way to give 998 mg of a mixture of the two epimeric alcohols which was chromatographed at 50:1 on Florisil in 50:50 petroleum ether (30–60°)–benzene. The alcohols **11***b* and *c* were obtained in a ratio of 2:1 and in 56% total yield from the chromatography. Elution with 15% petroleum ether–benzene gave the (R)-alcohol **11***c* as a colorless oil which showed: p.m.r. δ 0.517 (s, 3H, C-20 CH_3), 1.18 (s, 3H, C-18 CH_3), 3.58 (s, 3H, C-19 $COOCH_3$), 4.48–4.85 (m, 1H, C-12H), 4.47 (H_A) and 4.87 (H_B) (s and 1H each, broad $w_{h/2}$ = 4 and 3 Hz, C-17 vinylic H's), 6.37 (m, 1H, C-14H furanoid), 7.35 p.p.m. (m, 2H, C-15/16H furanoid): i.r. ν_{max} 3676 (non-bonded), 3448 (broad, bonded), 2941, 2857, 1715 (C=O), 1645 (C=C), 1466, 1449, 1227, 1205, 1160, 1023, 894, 875 cm^{-1}; mass spectrum (80 eV) *m/e* 346 ($M^+ - H_2O$, calcd. for $C_{21}H_{28}O_3$: 328.2038; found: 328.2005). Elution with benzene gave the (S)-alcohol **11***b* as a crystalline solid which showed: p.m.r. δ 0.517 (s, 3H, C-20 CH_3), 1.12 (s, 3H, C-18 CH_3), 3.57 (s, 3H, C-19 $COOCH_3$), 4.48–4.85 (m, 1H, C-12H), 4.72 (H_A) and 4.88 (H_B) (s, and 1H each, broad $w_{h/2}$ = 5 and 4 Hz, C-17 vinylic H's), 6.38 (m, 1H, C-14H furanoid), 7.35 p.p.m. (m, 2H, C-15/16H furanoid); i.r. identical to **11***c*; mass spectrum (80 eV) *m/e* 346 (M^+, calcd. for $C_{21}H_{30}O_4$: 346.2144; found: 346.2141).

15,16-Epoxy-12-hydroxylabda-8(17),13(16),14-trien-19-oic Acid (12a and b)

A solution of 998 mg (2.88 mmol) of the mixed alcohols **11***b* and *c* in 5 ml dry dimethylsulfoxide (DMSO) was prepared under a nitrogen atmosphere in a three-necked flask equipped with a nitrogen inlet, condenser, and an equilibrating separatory funnel. The reaction mixture was warmed to 56° and 43 ml (43.0 mmol) of a 1.0 *N* solution of potassium *t*-butoxide in DMSO was added dropwise. After 2 h at 55–56°, the mixture was poured into 200 ml of rapidly stirred ice-water. This was followed by the addition of 1:1 ether–benzene (80 ml), acidification to p*H* 3, and extraction with additional 1:1 ether–benzene (2 × 80 ml). The combined ethereal layers were worked-up in the usual way to give 823 mg (86%) of the crude acid as a yellow oil. The crude acid was chromatographed on a silica gel column (50:1) in hexane to give the mixed alcohols **12***b* and *c* in 40% yield. The (R)-alcohol **12***b* was eluted with 10% EtOAc–hexane and isolated as a colorless oil which showed: p.m.r. δ 0.60 (s, 3H, C-20 CH_3), 1.25 (s, 3H, C-18 CH_3), 4.48–4.85 (m, 1H, C-12H), 4.48 (H_A) and 4.90 (H_B) (s and 1H each, broad $w_{h/2}$ = 5 Hz, C-17 vinylic H's), 6.00 (broad, 2H,

Can. J. Chem. Downloaded from www.nrcresearchpress.com by 210.87.254.105 on 09/05/12
For personal use only.

—OH's), 6.40 (m, 1H, C-14H furanoid), 7.35 p.p.m. (m, 2H, C-15/16H furanoid); i.r. ν_{max} 3600, 2972, 2938, 2850, 1689 (C=O), 1639 (C=C), 1461, 1444, 1256, 1201, 1021, 891, 871 cm^{-1}; mass spectrum (80 eV) *m/e* 332 ($M^+ - H_2O$, calcd. for $C_{20}H_{26}O_3$: 314.1882; found: 314.1876). The (S)-alcohol was eluted with 25% ethyl acetate–hexane and was isolated as a colorless oil which showed: p.m.r. δ 0.617 (s, 3H, C-20 CH_3), 1.18 (s, 3H, C-18 CH_3), 4.48–4.85 (m, 1H, C-12H), 4.73 (H_A) and 4.90 (H_B) (s and 1H each, $w_{h/2} = 5$ and 4 Hz, C-17 vinylic H's), 6.40 (m, 1H, C-14H furanoid), 7.35 p.p.m. (m, 2H, C-15/16H furanoid); i.r. identical with the (R)-alcohol **12***b* above.

Methyl 15,16-Epoxy-12-hydroxylabda-8(17),13(16),14-trien-19-oate 12(S)-Methanesulfonate

A solution of 45 mg (0.13 mmol) of the alcohol **11***b* in 3 ml dry CH_2Cl_2 was prepared under nitrogen. To this solution was added 91 μl (0.65 mmol) of Et_3N and 0.5 ml CH_2Cl_2 and the resulting mixture was cooled in an ice–salt bath. To this mixture was added 31 μl (0.39 mmol) of mesyl chloride and 0.5 ml CH_2Cl_2 and the whole was stirred for 1.5 h. The reaction mixture was diluted with 60 ml CH_2Cl_2, washed with ice-water, cold 1% HCl, saturated brine, and filtered through Na_2SO_4. Evaporation of the solvent gave 52 mg of a colorless oil whose p.m.r. spectrum showed *ca.* 70% mesylate: p.m.r. δ 0.517 (s, 3H, C-20 CH_3), 1.18 (s, 3H, C-18 CH_3), 3.58 (s, 6H, C-19 $COOCH_3$ and CH_3SO_2—), 4.37 (H_A) and 4.87 (H_B) (s and 1H each, broad, $w_{h/2} = 3$ and 5 Hz, C-17 vinylic H's), 4.43–4.85 (m, 1H, C-12 H), 6.40 (m, 1H, C-14 H furanoid), 7.33 p.p.m. (m, 2H, C-15/16 H furanoid).

15,16-Epoxy-12-hydroxylabda-8(17),13(16),14-trien-19-oic Acid 12(S)-Methanesulfonate (13)

A solution of 63 mg (0.19 mmol) of the alcohol **12***a* in 3 ml dry CH_2Cl_2 was prepared under nitrogen. To this solution was added 317 μl (2.28 mmol) of Et_3N and the resulting mixture was cooled in an ice–salt bath. To this mixture was added 119 μl (1.52 mmol) of mesyl chloride and 1 ml CH_2Cl_2 and the whole was stirred for 1.5 h. The reaction mixture was diluted with 60 ml CH_2Cl_2, washed with ice-water, cold 1% HCl, saturated brine, and filtered through Na_2SO_4. Evaporation of the solvent gave 57 mg of a yellow oil which decomposed rapidly on standing at room temperature.

Lambertianic Acid (2a)

To a solution of 47 mg (0.14 mmol) of the (S)-alcohol **12***a* in 5 ml dry methylene chloride under nitrogen was added 0.2 ml (1.42 mmol) of triethylamine and the resulting mixture was cooled in an ice–salt bath. After sufficient cooling, 66 μl (0.85 mmol) of mesyl chloride was added and the solution was stirred for $1\frac{1}{2}$ h at $-5°$. The reaction mixture was diluted with 50 ml methylene chloride and washed with cold 2% hydrochloric acid, ice-water, saturated brine, and filtered through anhydrous sodium sulfate. Evaporation of the solvent *in vacuo* gave a brown oil which was immediately redissolved in dry tetrahydrofuran and added to a freshly prepared solution of 10 mg (1.42 mmol) of lithium in 10 ml liquid ammonia. After 1 h, the reaction was quenched with 5 ml saturated NH_4Cl solution and stirred for a further 15 min before the ammonia was allowed to evaporate. Dilution with water gave a solution of p*H* 11. The neutral fraction was extracted with 1:1 ether–benzene (2 × 25 ml) and worked-up in the usual way to give 5 mg of hydrocarbon material. The aqueous layer was acidified to p*H* 1 and extracted with 1:1 ether–benzene (2 × 25 ml) and worked-up in the usual way to give 16 mg (36%) lambertianic acid as a colorless oil which showed: p.m.r. δ 0.60 (s, 3H, C-20 CH_3), 1.22 (s, 3H, C-18 CH_3), 4.57 (H_A) and 4.90 (H_B) (s and 1H each, $w_{h/2} = 4$ Hz, C-17 vinylic H's), 6.27 (m, 1H, C-14 H furanoid), 7.20 (m, 1H, C-16H furanoid), 7.35 p.p.m. (m, 1H, C-15H furanoid); i.r. ν_{max} 2944, 2856, 1694 (C=O), 1644 (C=C), 1467, 1450, 1263, 1233, 1179, 1168, 1063, 1026, 894, 874 cm^{-1}; mass spectrum (80 eV) *m/e* 316 (M^+, calcd. for $C_{20}H_{28}O_3$: 316.2038; found: 316.2004).

Lithium–Liquid Ammonia Reductions

(i) On 11b and c

A three-necked flask fitted with a Dry Ice condenser, septum inlet, and gas inlet was flushed with nitrogen and filled with 20 ml liquid ammonia. To this system was added 27 mg (2.4 mmol, 3.8 equiv) of Li and a solution of 110 mg (0.32 mmol) of a mixture of the alcohols **11***b* and *c* in 5 ml THF. After 30 min, the reaction was quenched with the dropwise addition of 10 ml saturated NH_4Cl. After the bulk of ammonia had evaporated, the mixture was diluted with 50 ml H_2O, acidified to p*H* 4, extracted with 1:1 ether–benzene (2 × 50 ml), and worked-up in the usual way to give 103 mg of an oil. The p.m.r. spectrum showed complete retention of the 12-OH, and partial reduction of the C-19 methyl ester to the alcohol. The i.r. spectrum showed the presence of an acid due to partial hydrolysis of the methyl ester to the acid.

(ii) On Methyl O-Methyl Podocarpate

A solution of 145 mg (0.48 mmol) of methyl O-methyl podocarpate in 5 ml dry THF was added to a freshly-prepared solution of 40 mg (5.76 mmol, 6 equiv) of Li in 15 ml liquid NH_3. The mixture was stirred for 30 min and then quenched with the dropwise addition of 20 ml saturated NH_4Cl solution. The ammonia was allowed to evaporate and the remainder was acidified to p*H* 2 and extracted with 3:1 ether–benzene and worked-up in the usual way to give 118 mg of an oil whose p.m.r. spectrum showed >80% of the reduction product O-methyl podocarpinol.

We wish to thank the National Research Council of Canada for financial support of this work and for a Fellowship to Dr. M. B. Gravestock.

1. For a recent example see L. MANGONI, M. ADINOLFI, G. LAONIGRO, and R. CAPUTO. Tetrahedron, **28**, 611 (1972).
2. See *inter alia* (*a*) D. B. BIGLEY, N. A. J. ROGERS, and J. A. BARLTROP. J. Chem. Soc. 4613 (1960); (*b*) E. WENKERT, J. R. MAHAAJAN, M. NUSSIM, and F. SCHENKER. Can. J. Chem. **44**, 2575 (1966); (*c*) S. W. PELLETIER, L. B. HAWLEY, JR., and K. W. GOPINATH. Chem. Commun. 96 (1966); 97 (1966).
3. W. G. DAUBEN and V. F. GERMAN. Tetrahedron, **22**, 679 (1966).
4. J. HAEUSER, R. LOMBARD, F. LEDERER, and G. OURISSON. Tetrahedron, **12**, 205 (1961).
5. See *inter alia* F. E. KING, T. J. KING, and J. G. TOPLISS. Chem. and Ind. 113 (1956); W. L. MEYER and K. K.

MAHESHWARI. Tetrahedron Lett. 2175 (1964); T. A. SPENCER, R. J. FRIARY, W. W. SCHMIEGEL, J. F. SIMEONE, and D. S. WATT. J. Org. Chem. **33**, 719 (1968).
6. R. A. BELL and M. B. GRAVESTOCK. Can. J. Chem. **48**, 1105 (1970).
7. O. E. EDWARDS and B. S. MOOTOO. Can. J. Chem. **47**, 1189 (1969).
8. G. CAINELLI, F. BERTINI, P. GRASSELLI, and G. ZUBIANI. Tetrahedron Lett. 5153 (1967).
9. G. STORK, A. MEISELS, and J. E. DAVIES. J. Am. Chem. Soc. **85**, 3419 (1963).
10. R. L. SHRINER. Org. React. **1**, 1 (1942).
11. R. A. BELL and V. Y. TAGUCHI. Unpublished results.
12. S. GRONOWITZ and G. SORLIN. Arkiv Kemi, **19**, 515 (1962).
13. H. GILMAN and G. F. WRIGHT. J. Am. Chem. Soc. **55**, 3302 (1933).
14. M. GATES and G. TSCHUDI. J. Am. Chem. Soc. **78**, 1380 (1956).
15. D. DODD. Org. React. **4**, 378 (1948).
16. L. CAGLIOTI and P. GRASSELLI. Chem. Ind. 153 (1964).
17. A. O. BEDENBAUGH, J. H. BEDENBAUGH, J. D. ADKINS, and W. A. BERGIN. J. Org. Chem. **35**, 543 (1970); A. J. BIRCH. J. Chem. Soc. 809 (1945).
18. E. WENKERT and B. G. JACKSON. J. Am. Chem. Soc. **80**, 217 (1958).
19. R. A. BELL, M. B. GRAVESTOCK, and V. Y. TAGUCHI. In preparation.
20. H. O. HOUSE. Modern synthetic reactions. W. A. Benjamin, Inc., New York. 1965. p. 75.
21. F. C. CHANG and N. F. WOOD. Tetrahedron Lett. 2969 (1964).
22. R. K. CROSSLAND and K. L. SERVIS. J. Org. Chem. **35**, 3195 (1970).
23. J. VIT. Eastman Org. Chem. Bull. **43**, No. 3 (1970).
24. J. C. COLLINS, W. W. HESS, and F. J. FRANK. Tetrahedron Lett. 3363 (1968).
25. V. BALOGH, M. FÉTIZON, and M. GOLFIER. J. Org. Chem. **36**, 1339 (1971).
26. W. S. JOHNSON and L. F. FIESER. J. Am. Chem. Soc. **62**, 575 (1940).
27. M. L. SHERRILL and E. S. MELLOCK. J. Am. Chem. Soc. **59**, 2134 (1937); W. A. LAZIER and H. R. ARNOLD. Org. Syn. Coll. Vol. **2**, 142 (1943).
28. J. T. WROBEL and Z. DABROWSKI. Roczniki. Chemii Ann. Soc. Chim. Polonanim. **39**, 1239 (1965); **40**, 503 (1966).
29. R. S. DEWEY and E. E. VAN TAMELEN. J. Am, Chem. Soc. **83**, 3729 (1961).
30. W. R. BAMFORD and T. S. STEVENS. J. Chem. Soc. 4735 (1952).
31. M. F. GRUNDON, H. B. HENBEST, and M. D. SCOTT. J. Chem. Soc. 1855 (1963).
32. E. B. HERSHBERG, E. P. OLIVETO, and R. RAUSSER. Chem. Ind. 1477 (1958).

Can. J. Chem. Downloaded from www.nrcresearchpress.com by 210.87.254.105 on 09/05/12
For personal use only.

The Reactions of Organometallic Compounds Involving Silicon. Reactions of Triphenyl-, Diphenylmethyl-, and Phenyldimethylsilyl-lithium with 9-Phenylfluorene in Tetrahydrofuran

M. A. HAMID

Department of Chemistry, University of Manchester Institute of Science and Technology, Sackville Street, Manchester, M60 1QD, England

Received March 27, 1972

Triphenyl-, diphenylmethyl-, and phenyldimethylsilyl-lithium react very rapidly with 9-phenylfluorene in tetrahydrofuran (THF) but the reaction can be followed spectroscopically using the stop-flow technique at low temperatures. The order of reaction, found from the dependence of the initial rate of reaction on the initial reactant concentrations, is unity in both 9-phenylfluorene and the relevant organosilyl-lithium reagent. The thermodynamic constants of activation for the reaction between 9-phenylfluorene and triphenylsilyl-lithium (Ph_3SiLi), diphenylmethylsilyl-lithium ($Ph_2MeSiLi$), and phenyldimethylsilyl-lithium ($PhMe_2SiLi$), respectively, are: $\Delta H^* = 4.5$, 4.0, and 4.0 kcal mol^{-1}; $\Delta G^* = 13.0$, 12.5, and 12.5 kcal mol^{-1}; $\Delta S^* = -34.9$, -34.8, and -34.9 cal mol^{-1} deg^{-1}.

Le triphényl-, diphénylméthyl-, et phényldiméthylsilyl-lithium réagissent très rapidement avec le phényl-9 fluorène dans le tétrahydrofurane (THF) et la réaction peut être suivie par spectroscopie en utilisant la technique d'arrêt d'écoulement à basses températures. L'ordre de la réaction, trouvé à partir de la relation entre la vitesse initiale de la réaction et les concentrations initiales du réactant, est de un à la fois pour le phényl-9 fluorène et pour le réactif organosilyllithium correspondant. Les constantes thermodynamiques d'activation pour la réaction entre le phényl-9 fluorène et le triphénylsilyl-lithium (Ph_3SiLi), diphénylméthylsilyl-lithium ($Ph_2MeSiLi$), et phényldiméthylsilyl-lithium ($PhMe_2SiLi$) sont respectivement $\Delta H^* = 4.5$, 4.0 et 4.0 kcal mol^{-1}; $\Delta G^* = 13.0$, 12.5, et 12.5 kcal mol^{-1}; $\Delta S^* = -34.9$, -34.8, et -34.9 cal mol^{-1} deg^{-1}.

[Traduit par le journal]

Canadian Journal of Chemistry, **50**, 3761 (1972)

Can. J. Chem. Downloaded from www.nrcresearchpress.com by 210.87.254.40 on 09/05/12
For personal use only.

The metalation of fluorene by ethyl-lithium (1), *n*-butyl-lithium (2), and *t*-butyl-lithium (3) has been studied in benzene. The reactions were fairly slow and could be studied by any suitable conventional method. The order of reaction in fluorene was found to be unity in each case, and in alkyl-lithium was always fractional due to the alkyl-lithium existing as aggregates. The reactions of Ph_3SiLi, $Ph_2MeSiLi$, and $PhMe_2SiLi$ with fluorene (4) and 9-methylfluorene (5) in THF have already been reported; the results for the reaction of 9-phenylfluorene with Ph_3SiLi, $Ph_2MeSiLi$, and $PhMe_2SiLi$ in THF are now presented.

Experimental

Materials

9-Phenylfluorene was prepared by the reaction of crystallized phosphoric acid with triphenylcarbinol as described by A. Kliegl (6). The 9-phenylfluorene thus obtained was purified by crystallizing three times from pure benzene; the final product, m.p. 145.5–146.5 °C, was collected, and dried under high vacuum (10^{-5} Torr). Hexaphenyldisilane (K & K Laboratories, Inc.) was recrystallized three times from pure xylene and dried under high vacuum conditions; m.p. 369–370 °C.

1,1,2,2-Tetraphenyl-1,2-dimethyldisilane was prepared by the reaction of sodium with diphenylmethylchlorosilane (K & K Laboratories, Inc.) in toluene as described by Gilman *et al.* (7), and was recrystallized three times from ethanol:benzene solution and finally dried and sublimed under high vacuum conditions; m.p. 145.5–146.5 °C.

1,2-Diphenyl-1,1,2,2-tetramethyldisilane was also prepared by the reaction of sodium with phenyldimethylchlorosilane (K & K Laboratories, Inc.) in xylene as described by Gilman *et al.* (7). The 1,2-diphenyl-1,1,2,2-tetramethyldisilane thus prepared was fractionally distilled twice, the middle fraction, b.p. 290–300 °C, was collected and was further purified twice by fractional distillation under high vacuum conditions (10^{-5} Torr).

Tetrahydrofuran (B.D.H. Laboratory Reagent) was purified and dried as described by Evans *et al.* (8).

All the compounds used in this work are known. However, samples obtained were identified and confirmed by their melting points, elemental analyses and n.m.r. spectra. The purity was finally established by g.l.c. using a column of Apiezon L.

Ph_3SiLi, $Ph_2MeSiLi$ and $PhMe_2SiLi$ were prepared by the cleavage of corresponding symmetrical disilanes with lithium in THF as described earlier (9).

Kinetic Measurements

The rates of reaction between organosilyl-lithium and 9-phenylfluorene compounds in tetrahydrofuran were measured by mixing the reagents under high vacuum at low temperatures and using the stop-flow technique (10) to follow the change of optical density at 490 nm, and hence

Can. J. Chem. Downloaded from www.nrcresearchpress.com by 210.87.254.40 on 09/05/12
For personal use only.

TABLE 1. Spectral values for 9-phenylfluoren-9-yl-lithium

Temperature (°C)	λ_{max} (nm)	$10^{-3}\,\varepsilon_{\lambda max}$	λ_{max}	$10^{-3}\,\varepsilon_{\lambda max}$
20	490	3.90	527	3.52
−20	490	4.01	527	3.66
−80	490	4.04	527	3.77

the formation of the product 9-phenylfluoren-9-yl-lithium, with time. The technique used to study the order of reaction in 9-phenylfluorene was to keep the organosilyl-lithium initial concentration and the reaction temperature constant, while varying the 9-phenylfluorene concentration approximately in the ratios 1:2 to 2:1; for the order of reaction in the organosilyl-lithium, the initial concentration was varied while keeping the 9-phenylfluorene and the reaction temperature constant.

Spectra

In the determination of the spectra and the extinction coefficients for the products of the reaction between organosilyl-lithium and 9-phenylfluorene in THF, the organosilyl-lithium was used in slight excess to convert all the 9-phenylfluorene into 9-phenylfluoren-9-yl-lithium. Before mixing the two reactants, the apparatus was evacuated thoroughly and baked while pumping. It was then sealed off from the vacuum line and the reactants were mixed by breaking the internal seals with a glass breaker. A yellow color developed immediately when the two reactants made contact with each other. To ensure that reaction was complete the reaction mixture was shaken and kept at room temperature for a few minutes before sealing the silica optical cells.

To determine the electronic spectra of the compounds at different temperatures, the sealed silica cell containing the sample was placed in a Dewar flask fitted with silica windows and used in conjunction with a Unicam SP 800 spectrophotometer. The temperature of the sample was controlled by passing a jet of cold nitrogen through the Dewar flask. A resistance-type temperature sensor near the sample monitored the gas stream temperature. The gas was cooled by passing it through a coil in liquid nitrogen held in a larger Dewar. The sample was placed approximately 1 in. above the sensor in the gas stream and required about 10–15 min to reach the temperature of the gas. The temperature range studied was from +20 to −80 °C.

Results

The spectra of R_3SiLi reagents in THF showed an absorption maximum at 335 nm. The values obtained for $\varepsilon_{\lambda max}$ were in agreement with those previously (4) reported for R_3SiLi reagents within the experimental error of ±2%. In spite of the intense brown–yellow color of R_3SiLi reagents they do not give any significant absorption in the wavelength region above 450 nm even at a concentration as high as 5×10^{-2} mol l^{-1} (1 mm cell).

The spectrum in THF of 9-phenylfluoren-9-yl-lithium, prepared by mixing the organosilyl-lithium and 9-phenylfluorene reagents at +20 °C, showed two distinct absorption peaks in the visible region, λ_{max} 490 and 527 nm, shoulders at 458 and 550 nm. The estimated extinction coefficients at different temperatures are given in Table 1.

TABLE 3. Reaction data in THF at −30 °C

	10^3[9-Phenylfluorene]$_i$ (mol l^{-1})	10^3[R_3SiLi]$_i$ (mol l^{-1})	k* (l mol^{-1} s^{-1})
Ph_3SiLi	3.11	2.65	10.2
	3.11	3.96	10.5
	3.11	5.71	9.8
	3.11	7.48	10.6
$Ph_2MeSiLi$	2.65	1.65	26.5
	2.65	2.82	27.5
	2.65	4.02	26.9
	2.65	5.72	27.3
$PhMe_2SiLi$	3.05	1.87	24.5
	3.05	3.12	25.2
	3.05	4.23	25.1
	3.05	6.25	24.8

$$*k = \frac{\text{Initial rate}}{[R_3SiLi]_i[9\text{-phenylfluorene}]_i}$$

Kinetics

All the experiments using the stop-flow technique were carried out at −30 °C. The reaction of R_3SiLi with 9-phenylfluorene in THF to give 9-phenylfluoren-9-yl-lithium and silane shows second order kinetics up to at least 90% of the reaction (see Table 2 and Fig. 1). The reaction of R_3SiLi with 9-phenylfluorene in THF is of irreversible nature under the conditions used.

TABLE 2. Data for the second order rate constant k at −30 °C

	Curve No.	10^3 [R_3SiLi]$_i$ (mol l^{-1})	10^3[9-Phenylfluorene]$_i$ (mol l^{-1})	k (l mol^{-1} s^{-1})
Ph_3SiLi	A	3.52	2.45	9.4
$Ph_2MeSiLi$	B	3.05	2.82	26.4
$PhMe_2SiLi$	C	3.49	2.82	25.8

Can. J. Chem. Downloaded from www.nrcresearchpress.com by 210.87.254.40 on 09/05/12
For personal use only.

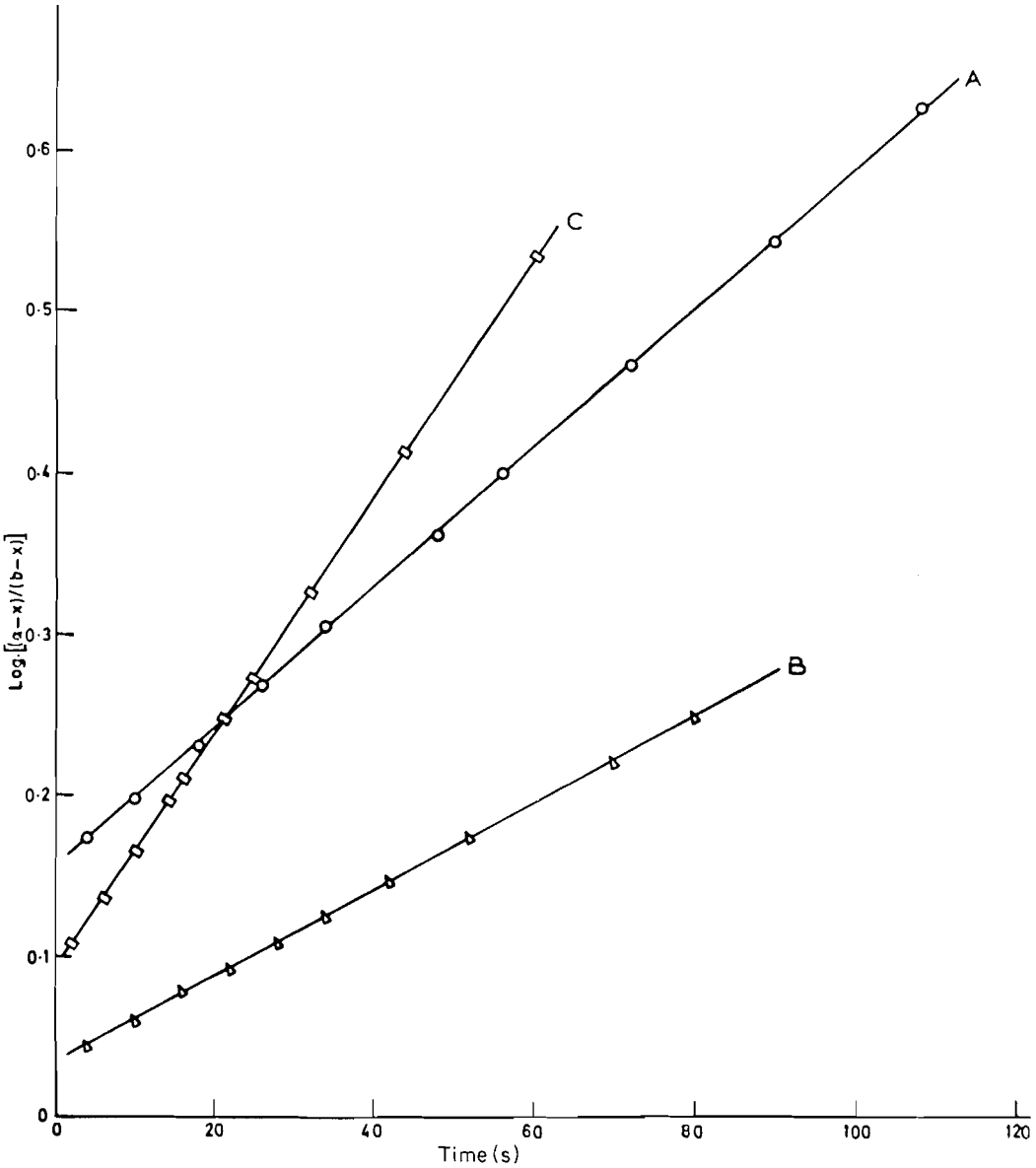

FIG. 1. Second order dependence of reaction rate for the system: R_3SiLi + 9-phenylfluorene in THF at $-30\,^{\circ}C$. (A) $[Ph_3SiLi]_i = 3.52 \times 10^{-3}\ M$; [9-phenylfluorene]$_i = 2.45 \times 10^{-3}\ M$. (B) $[Ph_2MeSiLi]_i = 3.05 \times 10^{-3}\ M$; [9-phenylfluorene]$_i = 2.82 \times 10^{-3}\ M$. (C) $[PhMe_2SiLi]_i = 3.49 \times 10^{-3}\ M$; [9-phenylfluorene]$_i = 2.82 \times 10^{-3}\ M$.

The orders of reaction found from the dependence of the initial rate of reaction on the initial reagent concentration were 1.01 in Ph_3SiLi, 1.02 in $Ph_2MeSiLi$, and 1.01 in $PhMe_2SiLi$. For this sequence of R_3SiLi the order in 9-phenylfluorene was 0.98, 0.98, and 1.1 (see Tables 3 and 4).

The temperature dependence of the initial rate of reaction at constant initial 9-phenylfluorene and R_3SiLi concentrations was measured in the range -6 to $-45\,^{\circ}C$ (see Table 5). The Arrhenius plots gave the following apparent activation energies (kcal mol^{-1}): Ph_3SiLi, 5.0; $Ph_2MeSiLi$, 4.5; $PhMe_2SiLi$, 4.5. The thermodynamic

Can. J. Chem. Downloaded from www.nrcresearchpress.com by 210.87.254.40 on 09/05/12
For personal use only.

TABLE 4. Reaction data in THF at −30 °C

	$10^3[R_3SiLi]_i$ (mol l^{-1})	10^3[9-Phenylfluorene]$_i$ (mol l^{-1})	k^* (l mol^{-1} s^{-1})
Ph_3SiLi	3.52	2.45	9.9
	3.52	3.61	10.5
	3.52	5.27	10.2
	3.52	7.01	9.7
$Ph_2MeSiLi$	3.05	1.82	27.4
	3.05	2.82	26.8
	3.05	3.89	27.3
	3.05	5.41	26.4
$PhMe_2SiLi$	3.49	1.95	24.9
	3.49	2.82	25.6
	3.49	3.89	26.4
	3.49	6.21	27.4

$$^*k = \frac{\text{Initial rate}}{[R_3SiLi]_i[\text{9-phenylfluorene}]_i}$$

TABLE 5. Temperature dependence of rate constants

	Temperature (°C)	k ($l\,mol^{-1}\,s^{-1}$)
Ph_3SiLi	−6	25.4
	−15	18.4
	−25	12.8
	−30	10.5
	−38	7.1
	−45	5.1
$Ph_2MeSiLi$	−8	60.2
	−18	41.0
	−25	32.7
	−30	27.3
	−38	19.7
	−45	14.8
$PhMe_2SiLi$	−8	54.2
	−18	42.4
	−25	31.6
	−30	26.4
	−38	19.3
	−45	13.6

constants of activation for the reaction between R_3SiLi and 9-phenylfluorene are given in Table 6. The results quoted have the following estimated systematic errors: k, ±7%; $\Delta H^{\ddagger}$ and $\Delta G^{\ddagger}$, ±5%; and $\Delta S^{\ddagger}$, ±9%.

Products of Reactions

For product analysis, three experiments were carried out at −30 °C with varying amounts of Ph_3SiLi and 9-phenylfluorene in THF. On completion of the reaction, the mixtures were quenched with deuterium oxide.

The products formed when a reaction mixture was quenched with D_2O were isolated by distilling off THF; the residue was dissolved in *n*-hexane, washed with water, and dried over $MgSO_4$. The *n*-hexane was then distilled off under reduced pressure and the solid product isolated by fractional crystallization or preparative t.l.c., depending on the ratio of the reactants used. All the compounds obtained were identified by their melting points, n.m.r. spectra, and elemental analyses. The n.m.r. values for 9-phenylfluorene and 9-phenylfluoren-9-yl-deuterium are 1.6–2.8 (m, Ph), 4.55–4.75 (t, CH), and 1.6–2.8 τ (m, Ph), respectively. The results obtained for the remaining components agree with the previously reported values (5).

Discussion

Spectra

The results show that R_3SiLi reacts rapidly with 9-phenylfluorene to give products of 9-phenylfluoren-9-yl-lithium and silane.

Comparison of the values of λ_{max} and $\varepsilon_{\lambda max}$ at 20 °C for 9-phenylfluoren-9-yl-lithium with the corresponding values for 9-fluorenyl-lithium (4) suggests that the substitution of the 9-hydrogen atom by a phenyl group results in bathochromic shift of *ca.* 5–9 nm. However, this shift is in

TABLE 6. Thermodynamic constants of activation for the reaction of R_3SiLi and 9-phenylfluorene in THF at −30 °C*

	Ph_3SiLi	$Ph_2MeSiLi$	$PhMe_2SiLi$
k ($l\,mol^{-1}\,s^{-1}$)	10.2 (1.1)	27.0 (2.9)	25.4 (2.9)
$\Delta H^{\ddagger}$ (kcal mol^{-1})	4.5 (6.1)	4.0 (6.6)	4.0 (6.2)
$\Delta G^{\ddagger}$ (kcal mol^{-1})	13.0 (14.0)	12.5 (13.6)	12.5 (13.6)
$\Delta S^{\ddagger}$ (cal mol^{-1} deg^{-1})	−34.9 (−32.5)	−34.8 (−28.8)	−34.9 (−30.3)

*The figures in parentheses are the corresponding values for the reaction of R_3SiLi with fluorene (4) in THF calculated for −30 °C.

Can. J. Chem. Downloaded from www.nrcresearchpress.com by 210.87.254.40 on 09/05/12
For personal use only.

marked contrast to the bathochromic shift of *ca.* 30 nm reported in the case of a 9-fluorenyl-lithium and 9-methylfluoren-9-yl-lithium (5). Streitweiser and Brauman (11) have reported the visible spectrum of 9-phenylfluorene-9-yl-lithium in cyclohexylamine. The slight red shift and the relatively higher $\varepsilon_{\lambda max}$ found in the spectrum of the product obtained by the reaction of R_3SiLi and 9-phenylfluorene in THF could be due to the change of the solvent.

The spectra of 9-phenylfluoren-9-yl-lithium at different temperatures (20 to -80 °C) in THF reveal that $\varepsilon_{\lambda max}$ increases slightly with decrease in temperature (see Table 1). This increase in ε suggests that there is formation of new solvent separated ion-pairs of 9-phenylfluoren-9-yl-lithium, having ε greater than the parent contact ion-pairs, as the temperature decreases. It is surprising that there is no significant change in the spectrum of 9-phenylfluoren-9-yl-lithium with temperature if a new species (solvent separated ion-pairs of 9-phenylfluoren-9-yl-lithium) is forming. It has been suggested however, by Hogen-Esch and Smid (12, 13) that the contact and solvent separated ion-pairs of fluorenyl-lithium are likely to have values of λ_{max} differing by as little as 1 nm which would be difficult to resolve. The spectral changes occurring as the temperature is lowered are reversible.

Dilution of the 9-phenylfluoren-9-yl-lithium reagent and addition of a common ion salt (tetraphenylboron-lithium) have no significant effect on the spectrum.

A relatively small increase with decreasing temperatures in $\varepsilon_{\lambda max}$ for 9-phenylfluoren-9-yl-lithium as compared with 9-fluorenyl-lithium (4) (75% solvent separated ion-pairs at 25 °C (12)) and 9-methylfluoren-9-yl-lithium (5) may be due to the fact that the successive replacement of H or CH_3 by C_6H_5 does lead to a more solvated 9-phenylfluoren-9-yl-lithium at 20 °C. All the experimental results suggest that the new species formed at low temperature is the solvent separated 9-phenylfluoren-9-yl-lithium ion-pairs.

Mechanism of Reaction

Since the orders of reaction observed were unity in both 9-phenylfluorene and the relevant organosilyl-lithium reagents, the rate of formation of 9-phenylfluoren-9-yl-lithium is given by the simple second order expression

$$\text{Initial rate} = k\,[\text{9-phenylfluorene}]_i[R_3SiLi]_i$$

The first order dependence in organosilyl-lithium reagent suggests that the Ph_3SiLi, $Ph_2MeSiLi$, and $PhMe_2SiLi$ species are in the monomeric form in THF. It is known that *n*-butyl-lithium exists as a hexamer in benzene (2) and as a dimer in THF (14). Furthermore, it has been established that organo-lithium reagents form etherates in diethylether (15) and in THF (16). It seems reasonable to suggest that because the organosilyl-lithium reagents are bulky molecules compared to *n*-butyl-lithium the formation of dimers or trimers is inhibited due to steric hindrance; they prefer to remain as solvated monomers rather than self-associated aggregates in THF.

The values of second order rate constant k obtained by the methods of curve analysis and initial rate agree reasonably well with each other (see Tables 2–4), and the values of thermodynamic constants of activation calculated at -30 °C indicate the following order of decreasing reactivity: $Ph_2MeSiLi \geqslant PhMe_2SiLi > Ph_3SiLi$. The order of reactivity observed for $Ph_2MeSiLi$, and $PhMe_2SiLi$ is not that which would be expected from a consideration of the electronic effects of methyl and phenyl groups. This order of relative reactivities has been reported elsewhere (4, 5, 9, 17–19) and can be interpreted using the arguments suggested by Evans *et al.* (17). However, the exceptionally broad absorption peak exhibited for $PhMe_2SiLi$ (4) reagent may be partly due to interaction between $PhMe_2SiLi$ and THF. It could be suggested in the light of this that $PhMe_2SiLi$ should be more reactive than $Ph_2MeSiLi$ but the former has a stronger interaction with the solvent than the latter, which may be due to the structure of $PhMe_2SiLi$. In other words, steric hindrance may be responsible for the lower reactivity of $PhMe_2SiLi$.

The relative reactivities of organosilyl-lithium with fluorene (4) and 9-phenylfluorene are consistent with the fact that the replacement of a 9-hydrogen atom by a phenyl group enhances the acidity of the hydrocarbon.

The products obtained after the completion of reaction between R_3SiLi and 9-phenylfluorene

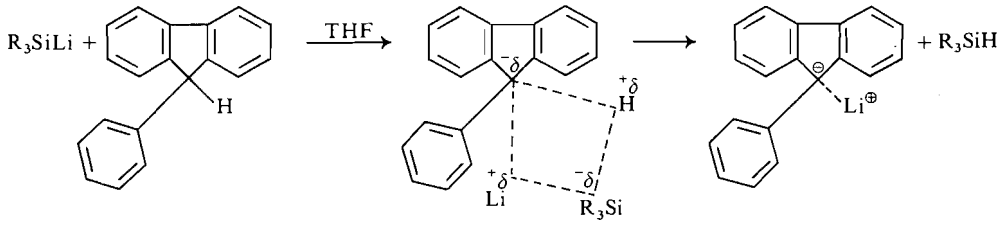

Initial state Transition state Final state

SCHEME 1

in THF were treated with D_2O to replace lithium by deuterium for product analysis. The results obtained from product analysis suggest that no disubstituted phenylfluorene or biphenylfluorene was produced during the reaction regardless of relative concentrations of reactants used. Thus the results from product analysis agree with the second order kinetics obtained.

The reaction mechanism which could be postulated on the practical evidence probably involves a four-membered ring transition state as shown in Scheme 1. This transition state may be formed by the interaction of a 9-phenylfluorene molecule with a molecule of R_3SiLi in which case the reaction is second order.

1. A. G. EVANS, C. R. GORE, and N. H. REES. J. Chem. Soc. 5110 (1965).
2. A. G. EVANS and N. H. REES. J. Chem. Soc. 6039 (1963).
3. R. A. H. CASLING, A. G. EVANS, and N. H. REES. J. Chem. Soc. B, 519 (1966).
4. A. G. EVANS, M. A. HAMID, and N. H. REES. J. Chem. Soc. B, 1110 (1971).
5. A. G. EVANS, M. A. HAMID, and N. H. REES. J. Chem. Soc. B, 2164 (1971).
6. A. KLIEGL. Ber. **38**, 284 (1905).
7. H. GILMAN, R. K. INGHAM, and A. G. SMITH. J. Org. Chem. **18**, 174 (1953).
8. J. E. BENNETT, A. G. EVANS, J. C. EVANS, E. D. OWEN, and B. J. TABNER. J. Chem. Soc. 3953 (1963).
9. A. G. EVANS, M. LL. JONES, and N. H. REES. J. Chem. Soc. B, 961 (1967).
10. D. DADLEY and A. G. EVANS. J. Chem. Soc. B, 418 (1967).
11. A. STREITWEISER, JR. and J. I. BRAUMAN. J. Am. Chem. Soc. **85**, 2033 (1963).
12. T. E. HOGEN-ESCH and J. SMID. J. Am. Chem. Soc. **88**, 307 (1966).
13. T. E. HOGEN-ESCH and J. SMID. J. Am. Chem. Soc. **88**, 318 (1966).
14. J. G. CARPENTER, A. G. EVANS, C. R. GORE, and N. H. REES. J. Chem. Soc. 908 (1969).
15. Z. K. CHEEMA, G. W. GIBSON, and J. F. EASTHAM. J. Am. Chem. Soc. **85**, 3517 (1963).
16. S. BYWATER and D. J. WORSFOLD. Can. J. Chem. **40**, 1564 (1962).
17. A. G. EVANS, M. LL. JONES, and N. H. REES. J. Chem. Soc. B, 894 (1969).
18. H. GILMAN and F. K. CARTLEDGE. J. Organomet. Chem. **1**, 8 (1963).
19. F. K. CARTLEDGE. Diss. Abs. **25**, B, 622 (1965).

Can. J. Chem. Downloaded from www.nrcresearchpress.com by 210.87.254.40 on 09/05/12
For personal use only.

Thiohydantoins. X. Kinetic Studies of the Acid Hydrolysis of 1-Acyl-2-thiohydantoins

WAYNE IRVINE CONGDON[1] AND JOHN THOMAS EDWARD
Department of Chemistry, McGill University, Montreal, Quebec

Received December 13, 1971[2]

The rates of hydrolysis of 22 1-acyl-2-thiohydantoins in aqueous sulfuric acid to give 2-thiohydantoin and a carboxylic acid have been determined. In 0–90% sulfuric acid, hydrolysis takes place by an A-2 mechanism, and the rate reaches a maximum in about 70% acid. In acid more concentrated than about 90%, hydrolysis takes place by an A-1 mechanism, and the rate increases monotonically. Evidence for the two mechanisms comes from Yates r and Bunnett-Olsen ϕ parameters; from entropies of activation; from $\rho\sigma$ and $\rho\sigma^+$ relations; and from steric effects.

On a déterminé les vitesses de l'hydrolyse de 22 acyle-1 thiohydantoïnes-2 dans l'acide sulfurique, fournissant le thiohydantoïne-2 et une acide carboxylique. Dans la zone de concentration de 0–90% d'acide sulfurique, la réaction se passe par un mécanisme A-2, et la vitesse de la reaction atteint un maximum dans une concentration de 70% acide environ. Entre 90–100% concentration d'acide, la réaction suit un mécanisme A-1 et la vitesse de la réaction s'augmente continuellement avec la concentration d'acide. La dualité des mécanismes est supportée par: les paramètres r de Yates et ϕ de Bennett et Olsen; les entropies d'activation; les relations $\rho\sigma$ ou $\rho\sigma^+$; et les effets stériques.

Canadian Journal of Chemistry, **50**, 3767 (1972)

Can. J. Chem. Downloaded from www.nrcresearchpress.com by 210.87.254.105 on 09/05/12
For personal use only.

1-Acyl-2-thiohydantoins (B in Scheme 1) are hydrolyzed in aqueous acid exclusively to a carboxylic acid and 2-thiohydantoin (see review in ref. 1); reports to the contrary have been found incorrect (2). The mechanism of this hydrolysis is of interest because of its use in certain modifications (3) of Schlack and Kumpf's procedure (4) for identifying the C-terminal amino acid residue of peptides. In the present paper we show that hydrolysis in aqueous sulfuric acid may take place by an A-2 or an A-1 mechanism, depending on the concentration of acid; the mechanism of the reaction proves to be very similar to that of the acid-catalyzed hydrolysis of *N*-acylthioureas (5).

As a first step it was necessary to study the protonation of 1-acyl-2-thiohydantoins in sulfuric acid. 2-Thiohydantoin itself undergoes mono- and then partial diprotonation as the concentration of sulfuric acid increases from 0 to 100%. Over the range 50 to 80% sulfuric acid changes in the u.v. spectrum indicate protonation to be taking place on the thiocarbonyl sulfur ($pK_{BH^+} = -4.83$), the extent of protonation depending on the H_0 value of the solution (6). We have observed that the spectral changes taking place as the acid concentration is increased above 90% indicate the beginning of a second protonation, this time on the carbonyl oxygen (5). In 100% acid 2-thiohydantoin is about half converted into the diprotonated species.[3]

We have found that 1-acyl-2-thiohydantoins show very similar changes in their u.v. spectra when they are dissolved in varying concentrations of acid. However, a quantitative determination of the extent of their protonation was made difficult by their rapid hydrolysis. Eventually, it was found that 1-*o*-iodobenzoyl-2-thiohydantoin was sufficiently stable in different concentrations of acid at 25.3 °C to give the spectra shown in Fig. 1. The character of the spectral changes indicated protonation to be taking place first on the sulfur atom (5) to give the cation BH^+ (see Scheme 1). Analysis of the spectral changes by conventional methods (7, 8) showed that the ionization ratio ($[BH^+]/[B]$) was proportional to h_0 (Fig. 2), and that the pK_{BH^+} was -6.8.

By lowering the temperature of the solutions to 9.4 °C, and by extrapolating absorbance readings back to the time of mixing, it was possible to measure the u.v. absorbance of 1-ben-

[1]Holder of NRCC Studentship, 1968–1970.

[2]Revision received July 26, 1972.

[3]R. J. Gillespie, in unpublished cryoscopic and conductometric studies, found a mean ν value of 2.5 and a mean γ of 1.4 for 2-thiohydantoin in 100% sulfuric acid.

Can. J. Chem. Downloaded from www.nrcresearchpress.com by 210.87.254.105 on 09/05/12
For personal use only.

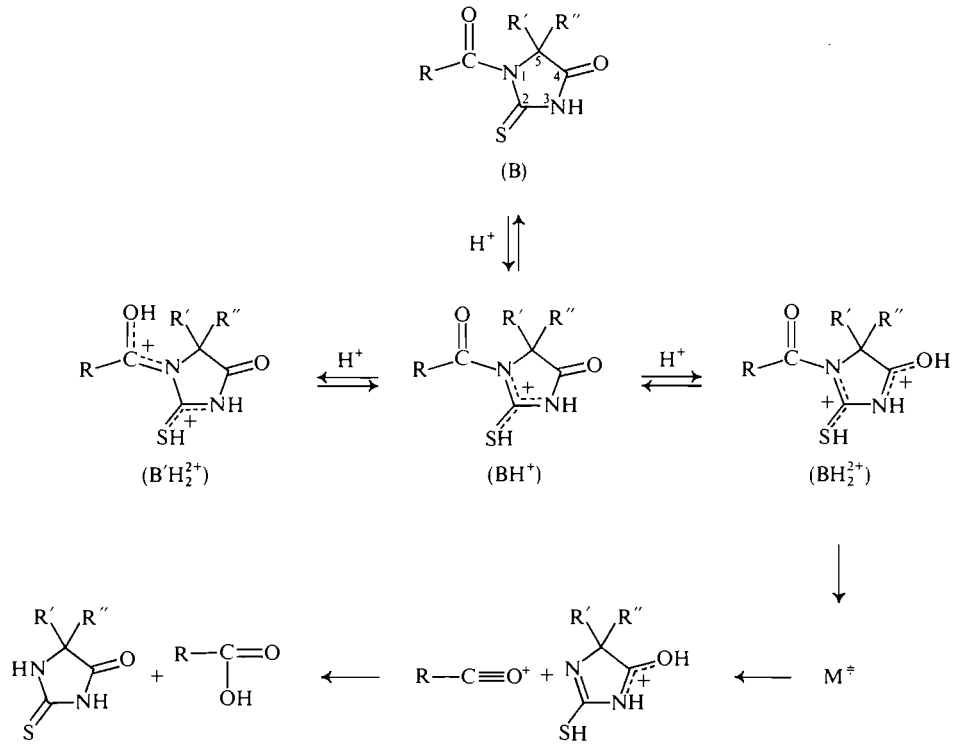

SCHEME 1

zoyl-2-thiohydantoin and of 1-*m*-trifluoromethylbenzoyl-2-thiohydantoin in different concentrations of acid. Again, the ionization ratio was found to follow h_0 (Fig. 2), and the pK_{BH^+} values of -6.6 and -6.7, respectively, were obtained. The similarity of these values indicates that the basicity at the sulfur atom is little affected by substitution in the benzene ring. A more precise analysis (*e.g.* a $\rho\sigma$ analysis) is not warranted, in view of the limited accuracy

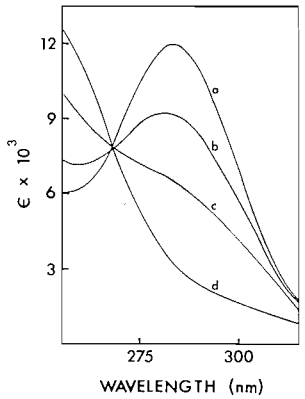

FIG. 1. The u.v. absorption spectra of 1-*o*-iodobenzoyl-2-thiohydantoin in (*a*) 0.0; (*b*) 74.9; (*c*) 78.1; (*d*) 96.3% sulfuric acid.

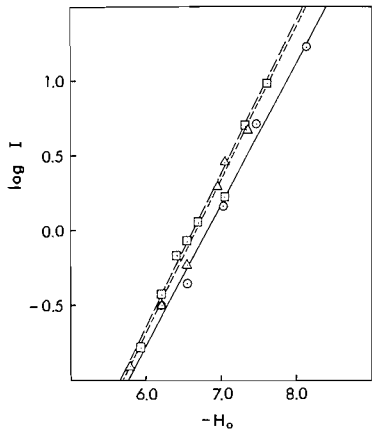

FIG. 2. A plot of log I ($\equiv [SH^+]/[S]$) *vs.* $-H_0$ for 1-benzoyl-2-thiohydantoin (slope = 1.02, $pK_{BH^+} = -6.6$; □); 1-*m*-trifluoromethyl-benzoyl-2-thiohydantoin (slope = 1.03, $pK_{BH^+} = -6.7$; Δ); 1-*o*-iodobenzoyl-2-thiohydantoin (slope = 0.95, $pK_{BH^+} = -6.8$; ○).

Can. J. Chem. Downloaded from www.nrcresearchpress.com by 210.87.254.105 on 09/05/12
For personal use only.

TABLE 1. Experimental and calculated rates of hydrolysis of 1-acetyl-5,5-dimethyl-2-thiohydantoin in sulfuric acid at 25.3 °C

% Sulfuric acid	Experimental $10^4 k_\psi$ (s^{-1})	Calculated $10^4 k_\psi$ (s^{-1})
6.1	1.6*	†
24.2	7.5*	5.0
39.6	26.0 ± 0.05	23.0
53.5	78.5 ± 0.50	78.0
58.0	127.5 ± 4.60	120.0
62.4	178.0 ± 1.10	170.0
66.1	231.0 ± 5.70	214.0
68.0	253.5 ± 0.50	220.0
70.1	290.0 ± 4.40	240.0
72.7	254.0 ± 5.70	220.0
74.9	238.0 ± 3.50	180.0
77.5	175.0 ± 4.50	120.0
80.0	49.6 ± 1.80	60.0
84.2	13.6 ± 0.40	14.0
88.4	4.4 ± 0.10	4.4
91.2	3.0 ± 0.12	1.5
94.4	3.5 ± 0.16	0.4
96.3	5.9 ± 0.20	0.2
97.1	7.6 ± 0.12	†
97.9	12.2 ± 0.36	†
98.9	22.6 ± 0.48	†

*Values measured by Liu (26).
†H_A is unmeasured for this acid concentration.

of the pK_{BH^+} values, but obviously ρ for the reaction approaches zero.

In acid concentrations above about 94%, spectral changes similar to those accompanying the diprotonation of *N*-acylthioureas (5) were observed, suggesting the formation of the cations BH_2^{2+} and $B'H_2^{2+}$ (Scheme 1); however, no systematic study of these changes was made because hydrolysis of the 1-acyl-2-thiohydantoins was too rapid. The kinetic results described below were best accommodated by postulating the formation of the *O*-protonated AH^+ in addition to the *S*-protonated BH^+ in dilute acid (Scheme 2), but the character of the spectral changes (*cf.* ref. 5) indicated only BH^+ to contribute significantly to the acid-base equilibrium.

The hydrolysis, followed by u.v. absorbance changes, was found to follow first-order kinetics in the large excess of acid used. The pseudo-first-order rate constants (k_ψ) for the hydrolysis of 1-acetyl-5,5-dimethyl-2-thiohydantoin in 6–99% sulfuric acid are given in Table 1. The rate constants increased with acid concentration up

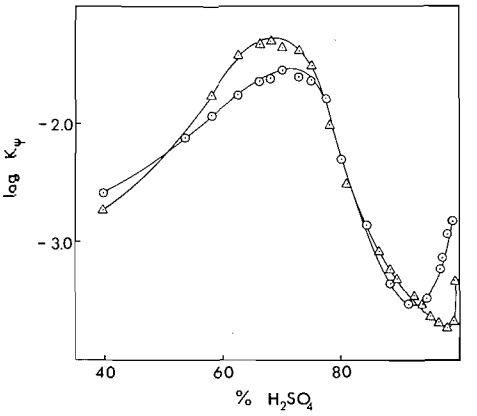

FIG. 3. Plot of log k_ψ at 25.3° *vs.* percent sulfuric acid for 1-acetyl-5,5-dimethyl-2-thiohydantoin (○) and 1-acetyl-2-thiohydantoin (△).

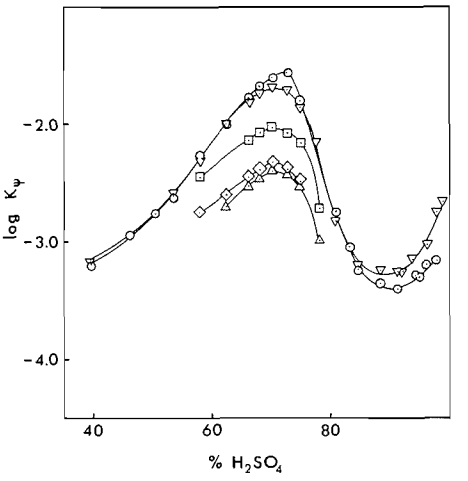

FIG. 4. A plot of log k_ψ at 25.3 °C *vs.* concentration of sulfuric acid for 1-benzoyl-3-phenyl-2-thiohydantoin (○); 1-benzoyl-2-thiohydantoin (▽); 1-benzoyl-5-methyl-2-thiohydantoin (□); 1-benzoyl-5-sec-butyl-2-thiohydantoin (◇); and 1-benzoyl-5-isopropyl-2-thiohydantoin (△).

to a maximum in about 70% acid, then decreased to a minimum in about 92% acid, and then increased again, as shown in Fig. 3. Also shown in this figure is the rate profile for 1-acetyl-2-thiohydantoin, which is fairly similar to that of the 5,5-dimethyl derivative over most of the range of acid concentrations, but has a rate minimum in about 98% acid. Other 1-acyl-2-thiohydantoins showed somewhat similar rate-concentration profiles, as shown in Figs. 4 and 5, with maximum rates in about 70% acid.

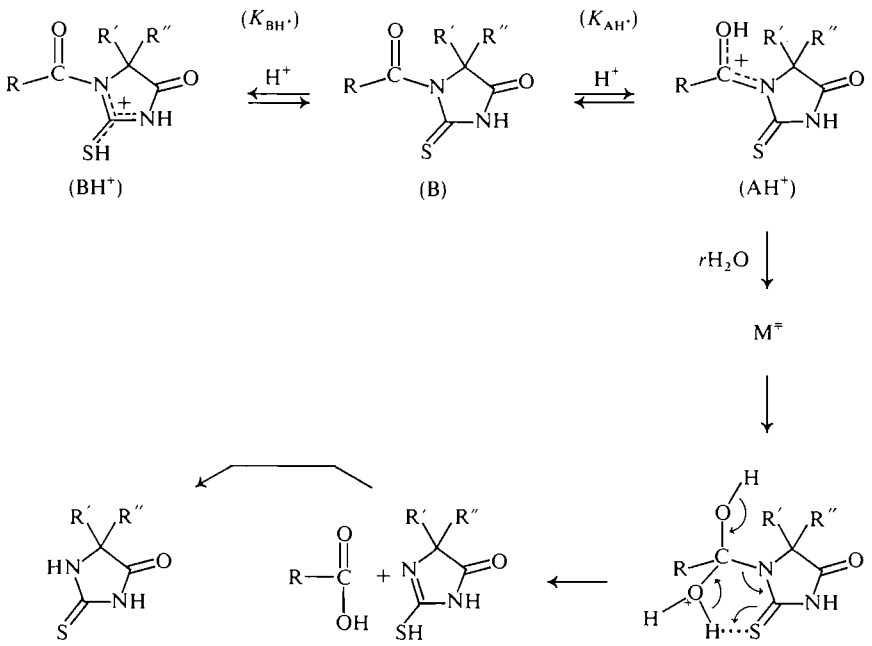

SCHEME 2

However, the positions of the minima varied considerably, and none could be observed for the hydrolysis of 1-*m*-trifluoromethylbenzoyl-2-thiohydantoin (see Fig. 5).

From analogy with similar rate profiles already reported (9), these results suggest an A-2 mechanism for hydrolysis in approximately 0–90% acid, followed by an A-1 mechanism for hydrolysis of most (but not all) of the 1-acyl-2-thiohydantoins in higher concentrations of acid. This dualism of mechanism would explain most of the qualitative features of the rate profiles, if it is assumed that the A-2 hydrolysis takes place by the mechanism outlined in Scheme 2, and the A-1 hydrolysis by the mechanism outlined in Scheme 1. Geminal dimethyl substitution at the 5-position should not affect

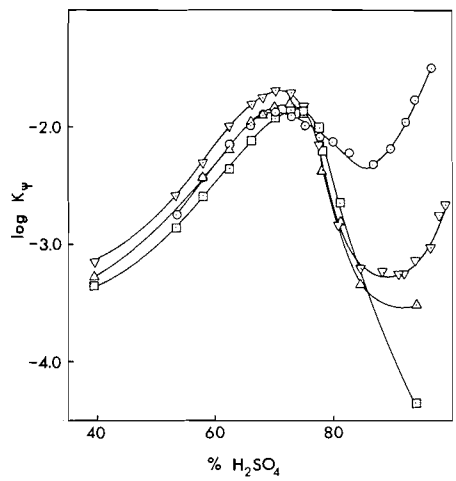

FIG. 5. A plot of log k_ψ at 25.3 °C *vs.* concentration of sulfuric acid for 1-benzoyl-2-thiohydantoin (▽); 1-*p*-chlorobenzoyl-2-thiohydantoin (△); 1-*p*-methoxybenzoyl-2-thiohydantoin (○); and 1-*m*-trifluoromethylbenzoyl-2-thiohydantoin (□).

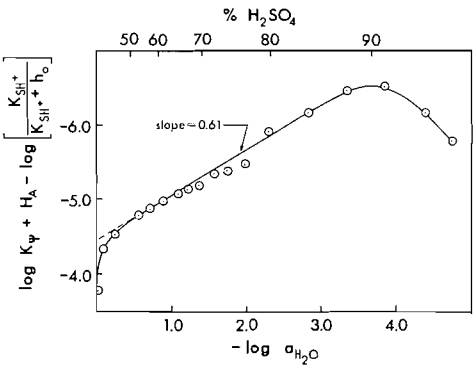

FIG. 6. A plot of log $k_\psi + H_A - \log\{K_{SH^+}/(K_{SH^+} + h_0)\}$ *vs.* $-\log a_{H_2O}$ for 1-acetyl-5,5-dimethyl-2-thiohydantoin sulfuric acid at 25.3 °C.

Can. J. Chem. Downloaded from www.nrcresearchpress.com by 210.87.254.105 on 09/05/12
For personal use only.

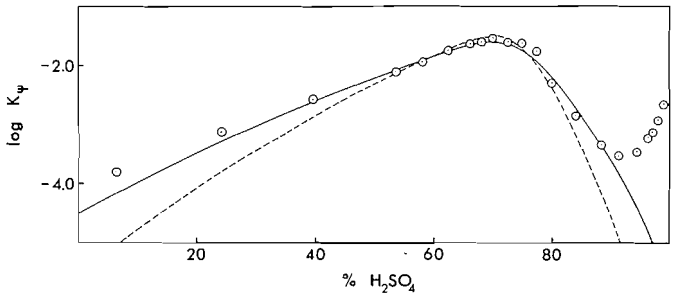

FIG. 7. Rate–acidity dependence for the hydrolysis of 1-acetyl-5,5-dimethyl-2-thiohydantoin in aqueous sulfuric acid at 25.3 °C. Points: experimental k_ψ (in s^{-1}).——The theoretical curve derived from eq. 1.---The theoretical curve derived from eq. 2.

appreciably the basicity of the various centers, but should slow down the A-2 reaction (by steric hindrance in the step: $AH^+ + rH_2O \rightarrow$ intermediate), and should accelerate the A-1 reaction (by steric acceleration of the *N*-acyl fisson). This would account for the change in the position of the minimum in the rate profile on going from 1-acetyl-2-thiohydantoin to 1-acetyl-5,5-dimethyl-2-thiohydantoin (Fig. 3). The general effect of 5-substitution in decreasing the rate of the A-2 reaction is illustrated in Fig. 4. Electron-withdrawing substituents on the benzene ring of substituted 1-benzoyl-2-thiohydantoins should, from analogy with the behavior of substituted benzamides (10), shift the maximum of the rate profile to higher acidities, and this effect is shown to a very slight extent (Fig. 5); much more dramatic is the effect in inhibiting the A-1 reaction (see Fig. 5) by destabilizing the acylium ion. The stability of 1-*o*-iodobenzoyl-2-thiohydantoin arises from both the steric effect of the large iodine atom in slowing the A-2 reaction, and its electronic effect in slowing the A-1 reaction.

The duality of mechanism is supported by various quantitative analyses of the kinetic data. This evidence is as follows:

(1) Hydration Parameters

Yates and his coworkers (11) have modified the original Bunnett hydration parameter treatment (12) to take account of the correct acidity function to apply to the protonation of the substrate being hydrolyzed. In the present case it is most reasonable to assume that the extent of protonation of B to give the reactive intermediate AH^+ (Scheme 2) is governed by the acidity function H_A (13), and that $[AH^+] \ll [BH^+]$ (*cf.* ref. 5). In such a case, the mechanism of Scheme 2 necessitates the following rate expression:

$$[1] \quad k_\psi = \{(k_1 h_A a_{H_2O}^r f_{AH^+})/(K_{AH^+} f_+)\} \times \{K_{BH^+}/(K_{BH^+} + h_0)\}$$

where k_1 is the rate constant for the reaction: $AH^+ + rH_2O \rightarrow$ products; a_{H_2O} is the activity of water; the f's are activity coefficients; and the other symbols can be understood by reference to Scheme 2. A plot against log a_{H_2O} of $(\log k_\psi + H_A - \log \{K_{BH^+}/(K_{BH^+} + h_0)\})$ for 1-acetyl-5,5-dimethyl-2-thiohydantoin, assuming $pK_{BH^+} = -6.4$,[4] gives a fairly good straight line between 24.2 and 88.4% sulfuric acid (correlation coefficient 0.9977) (see Fig. 6), as required by eq. 1 if (f_{AH^+}/f_+) is invariant with acid concentration. The r value of 0.61 given by the slope of this line is considerably lower than usual for amide hydrolyses (11); however, r values are found to become lower for hydrolyses in more concentrated acids (5). In any case, the change in slope above 84.2% acid is clearly indicative of a change from an A-2 to an A-1 mechanism (9). The intercept shown in Fig. 6 gives $\log (k_1 f_{AH^+}/K_{AH^+} f_+) = -4.45$ (if we make the usual assumption that the activity coefficient ratio is invariant with acid concentration (14)). Use of this value, and $r = 0.61$, gives the theoretical curve for the rates of hydrolysis of 1-acetyl-5,5-dimethyl-2-thiohydantoin shown in Fig. 7.

[4]1-Benzoyl-2-thiohydantoin has a pK_{BH^+} of -6.6; substitution of methyl groups at the 5-position should affect the basicity very little, but substitution of the phenyl by a methyl group would be expected to strengthen the basicity slightly. The results of the calculations are not greatly affected by small variations in the precise pK_{BH^+} assumed.

Can. J. Chem. Downloaded from www.nrcresearchpress.com by 210.87.254.105 on 09/05/12
For personal use only.

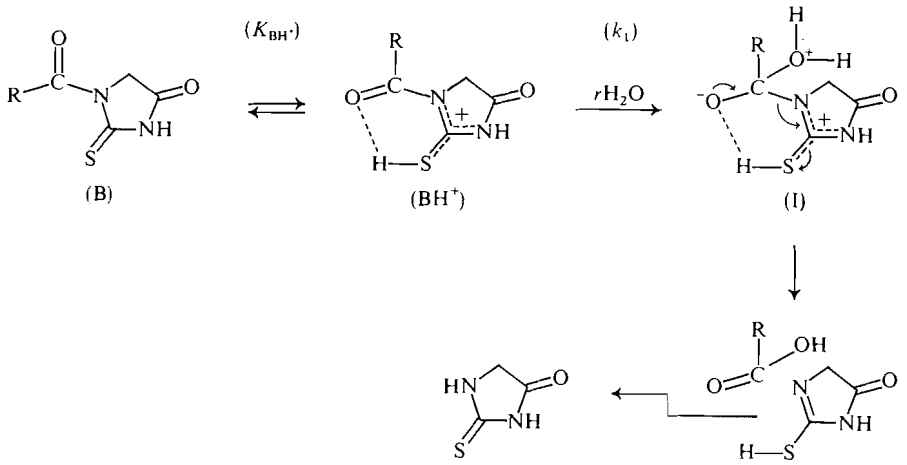

SCHEME 3

The agreement with the experimental points is reasonably good in view of the various assumptions, and offers strong support for the A-2 mechanism outlined in Scheme 2. An alternative mechanism would be that of Scheme 3, which would lead to the following rate equation:

$$[2] \quad k_\psi = \{k_1 a^r_{H_2O} f_{BH^+}/f_\ddagger\}\{h_0/(K_{BH^+} + h_0)\}$$

Analysis of the kinetic data by this equation yields $r = 1.65$ and $\log (k_1 f_{BH^+}/f_\ddagger) = -1.0$, but the fit with the experimental results is much poorer, as shown in Fig. 7.

Bunnett and Olsen (15) have produced an equation, based on a modification of the original hydration hypothesis (12), which has proved highly successful in predicting the variation of the rates of acid-catalyzed reactions with acid concentration. Applied to the kinetic situation of Scheme 2, this equation becomes

$$[3] \quad \log k_\psi + H_0 - \log\{K_{BH^+}/(K_{BH^+} + h_0)\} = \Phi(H_0 + \log[H^+]) + \text{constant}$$

A plot of $(\log k_\psi + H_0 - \log\{K_{BH^+}/(K_{BH^+} + h_0)\}$ against $(H_0 + \log[H^+])$ (assuming $[H^+] = [H_2SO_4]$ (16)) gives a curve of gratifying linearity up to 88% sulfuric acid, having a slope $\Phi = 0.81$, normal for an amide hydrolysis by an A-2 mechanism. Again, the change to a slope of $\Phi = -0.98$ in acid concentrations above 88% is indicative of a change to an A-1 mechanism. (see Fig. 8).

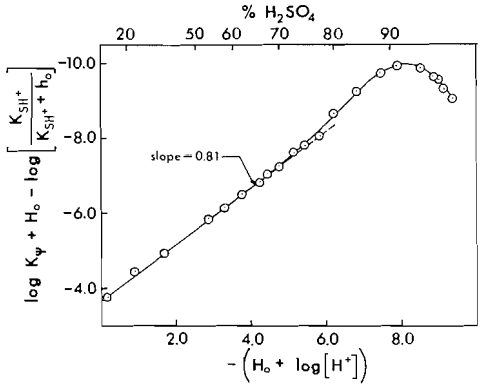

FIG. 8. A plot of $\{\log k_\psi + H_0 - \log [K_{SH^+} + (K_{SH^+} + h_0)]\}$ *vs.* $\{H_0 + \log [H^+]\}$ for 1-acetyl-5,5-dimethyl-2-thiohydantoin.

It is not possible to deduce a kinetic expression for the A-1 hydrolysis based on Scheme 1, because the required h_A values of strong sulfuric acid solutions are not available.

(2) Entropies of Activation

Plots of $\log k_\psi$ against $1/T$ for 1-acetyl-, 1-benzoyl-, and 1-acetyl-5,5-dimethyl-2-thiohydantoin gave straight lines from which entropies of activation ($\Delta S^\ddagger$) were calculated (Table 2). For hydrolyses in 39.6 and 84.9% sulfuric acid, these had about the values (near -20 e.u.) expected for an A-2 reaction (17); the marked increase in $\Delta S^\ddagger$ for hydrolyses in more concentrated acids was indicative of a change to an A-1 mechanism. In 96.4% sulfuric acid hydrolysis of 1-acetyl-5,5-dimethyl-2-thiohydantoin would be expected to take place

Can. J. Chem. Downloaded from www.nrcresearchpress.com by 210.87.254.105 on 09/05/12
For personal use only.

TABLE 2. Temperature dependence of the rate of sulfuric acid catalyzed hydrolysis of 1-acyl-2-thiohydantoins

Compound (% sulfuric acid)	Temperature (°C)	$10^4 k_\psi$ (s^{-1})	log A (s^{-1})	ΔS^* (e.u.)	E_a (kcal/mol)
1-Acetyl-2-thiohydantoin	25.3	19.3 ± 1.50	9.4 ± 0.2	−18 ± 2	17 ± 2
(39.6)	35.9	48.8 ± 0.50			
	45.6	109.7 ± 1.50			
1-Acetyl-5,5-dimethyl-	11.0	7.2 ± 0.03	8.3 ± 0.1	−22 ± 1	14 ± 1
2-thiohydantoin	25.3	26.0 ± 0.04			
(39.6)	35.5	54.7 ± 0.43			
	49.6	170.0 ± 7.22			
1-Acetyl-2-thiohydantoin	25.3	12.0 *	9.9 ± 0.2	−15 ± 2	18 ± 2
(84.9)	35.9	28.5 ± 0.75			
	45.6	70.7 ± 2.40			
1-Acetyl-2-thiohydantoin	25.3	2.1 ± 0.07	12.0 ± 0.2	−5 ± 2	22 ± 2
(96.4)	35.5	6.7 ± 0.12			
	45.6	19.6 ± 0.50			
1-Acetyl-5,5-dimethyl-	10.8	1.15 ± 0.04	12.8 ± 0.2	−2 ± 2	22 ± 2
2-thiohydantoin	20.1	3.1 ± 0.04			
(96.4)	35.5	24.2 ± 0.60			
	49.6	124.0 ± 4.00			
	58.1	266.0 ± 12.0			
1-Benzoyl-2-thiohydantoin	25.3	6.9 ± 0.10	8.6 ± 0.2	−21 ± 2	16 ± 2
(39.6)	35.5	16.8 ± 0.20			
	45.6	37.1 ± 0.72			

*Value obtained by interpolation from the rate profile.

nearly completely by the A-1 mechanism (see Table 1 and Figs. 3 and 7), and ΔS^* was −2 e.u., while hydrolysis of 1-acetyl-2-thiohydantoin would be expected, from inspection of Fig. 3, to be about 70% A-2 and 30% A-1, and ΔS^* was −5 e.u. Lack of information on the extent and position of diprotonation prevents a further interpretation of these values.

(3) Hammett $\rho\sigma$ and $\rho\sigma^+$ Relations

The rate profile for 1-benzoyl-2-thiohydantoin (Fig. 5) suggests an A-2 mechanism of hydrolysis in 0–90% acid and an A-1 mechanism in 90–100% acid. The rate constants (k_ψ) for the hydrolysis of 13 substituted 1-benzoyl-2-thiohydantoins in 58.0% sulfuric acid, of 10 substituted 1-benzoyl compounds in 84.6% sulfuric acid, and of 10 substituted 1-benzoyl compounds in 93.8% acid are given in Table 3 and Figs. 9 and 10.

An A-2 mechanism would be expected to result in log k_ψ varying as σ rather than σ^+; and this indeed is found for hydrolyses in 58.0% sulfuric acid, as shown in Fig. 9. The ρ given by the slope of the line is −0.41. A small value of ρ would be expected from the mechanism of Scheme 2 because of the compensating effects of substituents on the various pre-equilibria as well as on the rate-determining step; an exact estimate of the separate ρ values is difficult in the present case.[5] The mechanism of Scheme 3 might be expected to lead, however, to a larger ρ value than −0.41: ρ_1 for the step $B \rightleftharpoons BH^+$ should approach zero, but ρ_2 for the step $BH^+ + rH_2O \rightarrow$ products would be expected to be about +1 (19), so that the overall ρ_{ov} ($= \rho_1 + \rho_2$) should be about +1.

An A-1 mechanism would be expected to result in log k_ψ varying as σ^+ rather than σ: this is observed for hydrolysis in 93.8% acid (Fig. 9). The value of ρ (−2.51) thus obtained has about the magnitude observed for other A-1 reactions yielding acylium ions (21).

In 84.6% sulfuric acid, the plot of log k_ψ *vs.* σ changes slope at $\sigma \approx 0$ (Fig. 10). This is con-

[5]Models indicate that for the conformation of B shown in Scheme 1, the benzene ring cannot be coplanar with the carbonyl group (in such cases the carbonyl group is generally coplanar with trigonal nitrogen in preference to phenyl (18)). This would result in ρ values different from those of analogous substituted phenyl compounds in which the benzene ring approached coplanarity with the carbonyl group.

Can. J. Chem. Downloaded from www.nrcresearchpress.com by 210.87.254.105 on 09/05/12
For personal use only.

TABLE 3. Rates of hydrolysis (k_ψ, in 10^{-4} s^{-1}) of substituted 1-benzoyl-2-thiohydantoins in three different concentrations of sulfuric acid at 25.3 °C

Substituent	58.0% H_2SO_4	84.6% H_2SO_4	93.8% H_2SO_4
p-Methoxy	37.20 ± 0.20	55.00*	171.20 ± 1.50
p-tert-Butyl	50.60 ± 0.15	—	33.00 ± 0.65
p-Methyl	49.80 ± 0.17	23.30 ± 1.20	32.70 ± 0.45
m-Methyl	52.00 ± 0.35	9.00 ± 0.36	11.85 ± 0.01
—	49.80 ± 0.50	6.04 ± 0.21	7.40 ± 0.30
p-Fluoro	35.10 ± 0.10	4.43 ± 0.18	5.32 ± 0.06
m-Methoxy	42.10 ± 0.80	—	1.44 ± 0.24
p-Chloro	35.50 ± 0.30	4.28 ± 0.09	2.87 ± 0.03
p-Bromo	35.60 ± 1.05	3.76 ± 0.15	2.54 ± 0.07
p-Iodo	36.50 ± 0.60	4.00 ± 0.24	—
m-Chloro	32.60 ± 0.14	4.10 ± 0.08	1.06 ± 0.15
m-Bromo	31.60 ± 0.10	3.70 ± 0.24	—
m-Trifluoromethyl	26.00 ± 0.05	—	0.44 ± 0.03
p-Nitro	21.53 ± 0.08	—	—

*Value obtained by interpolation from the rate profile.

Can. J. Chem. Downloaded from www.nrcresearchpress.com by 210.87.254.105 on 09/05/12
For personal use only.

sonant with a mechanism dependent on the nature of the substituents in the benzoyl group: electron-releasing groups promote reaction by an A-1 mechanism (hence the steep slope of the line on the left-hand side of Fig. 10); electron-withdrawing groups ensure that the A-2 mechanism still predominates at this acid concentration (hence the small slope of the line on the right hand side of Fig. 10). This evidence can also be construed in support of the mechanism of Scheme 2 rather than that of Scheme 3.

(4) C-5 Substituent Effects

As shown in Fig. 4, substituents at the 5-position reduce the height but do not greatly alter the position of the rate maximum in plots of log k_ψ *vs.* acid concentration. From Fig. 3 it is apparent, however, that they do alter the position and depth of the minimum. The effect of C-5 substituents on the height of the maximum is interpretable in terms of steric hindrance to attack of water on the protonated substrate, as might be expected for an A-2 mechanism. Comparison of the entropy and enthalpy values for 1-acetyl- and 1-acetyl-5,5-dimethyl-2-thiohydantoin in 39.6% acid (Table 2) (bearing in mind the error discussion in ref. 17) leads to the following relative values: $T\Delta\Delta S^{\ddagger} = 1.5$ kcal; $\Delta\Delta H^{\ddagger} = 1.6$ kcal. The results are similar to those for formation and hydrolysis of semicarbazones (22) of substituted ketones. This decrease in $\Delta S^{\ddagger}$ is in agreement with the modified Hammett–Price rule for a reaction in a

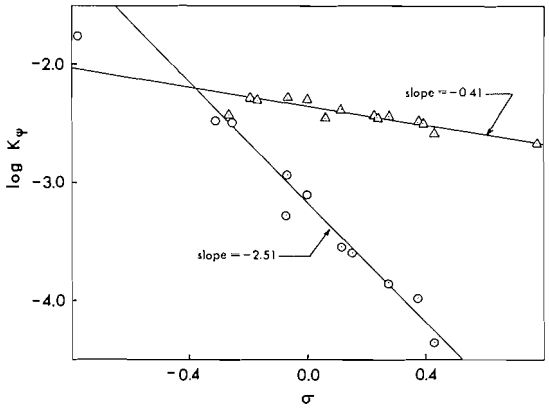

FIG. 9. A plot of log k_ψ *vs.* σ, for substituted 1-benzoyl-2-thiohydantoins in 58.0% sulfuric acid at 25.3 °C (c.c.: 0.950; s.d.: 0.04) (Δ); and *vs.* σ^+, for substituted 1-benzoyl-2-thiohydantoins in 93.8% sulfuric acid at 25.3 °C (c.c.: 0.992; s.d.: 0.11) (○). (σ^+ values of ref. 20 used for *m*- and *p*-methoxyl group in strong acid).

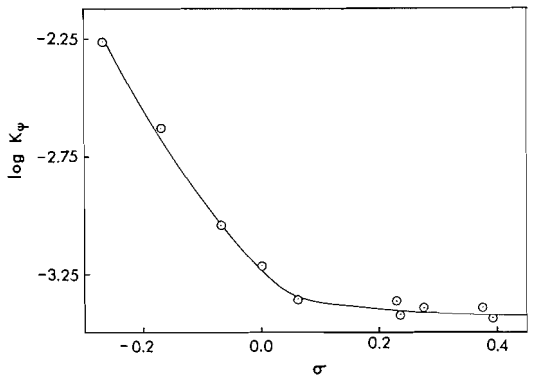

FIG. 10. A plot of log k_ψ *vs.* σ for substituted 1-benzoyl-2-thiohydantoins in 84.6% sulfuric acid at 25.3 °C.

TABLE 4. (*a*) Pseudo-first-order rate constants (k_ψ, in 10^{-4} s^{-1}) for substituted 1-benzoyl-2-thiohydantoins (substituent shown) at 25.3 °C

Sulfuric acid (%)	1-Benzoyl-	1-*p*-Methoxybenzoyl-	1-Benzoyl-3-phenyl-	1-*p*-Chlorobenzoyl-	1-*m*-Trifluoromethylbenzoyl
39.6	6.92 ± 0.09	—	6.41 ± 0.14	5.34 ± 0.15	4.44 ± 0.05
46.2	—	—	11.53 ± 0.36	—	—
50.4	—	—	17.68 ± 0.27	—	—
53.5	26.50 ± 0.55	18.30 ± 0.21	24.34 ± 0.40	—	14.00 ± 0.18
58.0	49.80 ± 0.50	37.20 ± 0.20	50.90 ± 1.70	35.50 ± 0.30	26.00 ± 0.05
62.4	100.90 ± 2.00	67.80 ± 1.05	98.10 ± 2.40	66.50 ± 1.50	45.30 ± 0.63
66.1	158.00 ± 0.80	103.90 ± 2.80	168.20 ± 1.80	106.90 ± 1.10	76.70 ± 1.65
68.0	180.80 ± 9.50	127.20 ± 2.25	210.60 ± 3.30	126.00 ± 1.50	—
70.1	205.70 ± 4.00	131.70 ± 3.90	250.20 ± 8.10	151.00 ± 2.80	118.20 ± 2.10
72.7	195.40 ± 7.90	127.10 ± 5.70	277.50 ± 11.7	157.30 ± 4.00	141.50 ± 3.18
74.9	139.20 ± 4.80	103.80 ± 5.00	159.00 ± 4.50	136.10 ± 4.20	136.30 ± 1.00
77.5	70.30 ± 3.30	83.35 ± 0.15	—	—	98.10 ± 1.60
78.1	—	—	—	43.10 ± 2.10	65.70 ± 2.40
79.8	—	75.30 ± 1.70	—	—	—
80.9	14.90 ± 0.75	—	18.70 ± 0.54	14.80 ± 0.33	22.90 ± 0.45
82.4	—	61.60 ± 1.80	—	—	—
83.1	—	—	9.05 ± 0.14	—	—
84.6	6.04 ± 0.21	—	5.80 ± 0.25	4.28 ± 0.08	—
86.4	—	48.50 ± 2.10	—	—	—
88.4	—	—	4.43 ± 0.14	—	—
89.4	—	66.20 ± 1.00	—	—	—
91.2	5.63 ± 0.18	—	3.92 ± 0.18	—	—
92.1	5.69 ± 0.12	105.30 ± 3.60	—	—	—
93.8	7.40 ± 0.30	171.20 ± 1.50	—	2.87 ± 0.03	0.44 ± 0.03
94.4	—	—	5.16 ± 0.17	—	—
94.9	—	—	5.05 ± 0.12	—	—
96.4	9.40 ± 0.27	324.00 ± 11.0	6.46 ± 0.30	—	—
97.1	—	—	7.02 ± 0.16	—	—
97.9	17.90 ± 0.21	—	—	—	—

(*b*) Pseudo-first-order rate constants (k_ψ, in 10^{-4} s^{-1}) for substituted 2-thiohydantoins at 25.3 °C

Sulfuric acid (%)	1-Acetyl	1-Benzoyl-5-methyl-	1-Benzoyl-5-isopropyl-	1-Benzoyl-5-sec-butyl-
39.6	19.30 ± 1.50	—	—	—
58.0	—	35.50 ± 0.63	—	17.90 ± 0.40
62.4	380.00 ± 11.7	—	19.60 ± 0.40	24.80 ± 0.36
66.1	470.00 ± 18.0	71.80 ± 0.90	29.80 ± 0.42	35.50 ± 0.60
68.0	487.00 ± 9.00	84.90 ± 1.83	33.60 ± 0.66	40.80 ± 0.90
70.1	463.00 ± 33.6	93.10 ± 3.24	39.70 ± 1.20	47.30 ± 0.66
72.7	414.00 ± 15.0	84.10 ± 2.70	36.60 ± 1.15	41.60 ± 0.78
74.9	325.00 ± 5.70	70.20 ± 2.30	29.30 ± 0.78	32.40 ± 1.32
78.1	102.00 ± 2.55	19.10 ± 1.00	10.30 ± 0.48	—
80.9	31.60 ± 0.45	—	—	—
86.4	8.74 ± 0.18	—	—	—
88.4	5.78 ± 0.06	—	—	—
89.4	4.90 ± 0.03	—	—	—
92.2	3.55 ± 0.03	—	—	—
93.8	3.05 ± 0.10	—	—	—
94.9	2.41 ± 0.09	—	—	—
96.4	2.09 ± 0.08	—	—	—
97.9	1.89 ± 0.05	—	—	—
98.9	2.23 ± 0.05	—	—	—
99.1	4.69 ± 0.15	—	—	—
96.1	—	5.08 ± 0.18	8.91 ± 0.27	10.30 ± 0.23

Can. J. Chem. Downloaded from www.nrcresearchpress.com by 210.87.254.105 on 09/05/12
For personal use only.

Can. J. Chem. Downloaded from www.nrcresearchpress.com by 210.87.254.105 on 09/05/12
For personal use only.

TABLE 5. Physical properties of 1-acyl-2-thiohydantoins

Substituents	Melting point (°C)	U.v. absorption peaks* Type I λ_{max} (nm)	Type I ε_{max}	Type II λ_{max} (nm)	Type II ε_{max}	Type III λ_{max} (nm)	Type III ε_{max}
1-*p*-Anisoyl	169–170†	368	390	281	18 200	237	21 000
1-*m*-Anisoyl	176–178	370	190	284	11 900	238	21 300
1-*p*-Toluoyl	153–155	372	180	275	11 500	241	20 600
1-*m*-Toluoyl	162–164	370	145	281	10 300	241	21 300
1-*p*-tert-Butyl-benzoyl	165–168	370	190	278	11 800	241	20 800
1-Benzoyl	159–161‡	372	140	283	11 000	242	21 500
1-*p*-Fluorobenzoyl	196–198	374	140	279	11 100	240	22 100
1-*p*-Chlorobenzoyl	204–206	376	301	277	11 200	242	22 700
1-*m*-Chlorobenzoyl	197–198	375	130	286	14 000	241	32 600
1-*p*-Bromobenzoyl	194–195	376	200	276	15 900	241	22 900
1-*m*-Bromobenzoyl	203–205	378	140	284	11 100	240	22 600
1-*o*-Iodobenzoyl	212–214	384	60	284	11 800	234	23 300
1-*p*-Iodobenzoyl	207–209	370	305	275	16 200	239	21 200
1-*m*-Trifluoromethylbenzoyl	194–196	374	125	287	10 400	241	23 500
1-*p*-Nitrobenzoyl	230–231§	370	291	285	11 100	243	21 200
1-Acetyl	176–177‖	365	34	277	18 200	233	16 000
1-Acetyl-5,5-dimethyl	186–187¶	366	30	279	19 000	233	16 000
1-Benzoyl-5-methyl	161–163**	370	180	280	9 800	241	24 800
1-Benzoyl-5-isopropyl	179–180	373	180	283	9 200	243	23 200
1-Benzoyl-5-sec-butyl	167–169	369	200	280	8 700	242	18 000
1-Benzoyl-3-phenyl	132–133	375	120	285	9 200	245	18 300

*Ethanol or ethanol–water 1:24 (v/v) used as solvent. See ref. 1 for explanation of band types.
†Johnson and Scott report m.p. 166° (27).
‡Johnson and Nicolet report m.p. 165° (24).
§Liu reports m.p. 230–231° (26).
‖Johnson and Nicolet report m.p. 175° (24).
¶Carrington reports m.p. 186–187° (28).
**Schlack and Kumpf report m.p. 158–159° (4).

TABLE 6. Analytical data for previously unreported 1-acyl-2-thiohydantoins

1-Substituent	Calculated (%)			Found (%)		
	C	H	N	C	H	N
1-*m*-Anisoyl	52.8	4.0	11.2	53.1	3.7	11.4
1-*p*-Toluoyl	56.4	4.3	12.0	56.3	4.2	12.2
1-*m*-Toluoyl	56.4	4.3	12.0	56.2	4.3	12.0
1-*p*-tert-Butyl-benzoyl	60.9	10.2	5.8	61.2	10.4	6.0
1-*p*-Fluorobenzoyl	50.4	2.9	11.8	50.4	2.9	11.5
1-*p*-Chlorobenzoyl	47.1	2.8	11.0	46.7	2.7	10.9
1-*m*-Chlorobenzoyl	47.1	2.8	11.0	47.3	2.9	11.2
1-*p*-Bromobenzoyl	40.2	2.3	9.7	40.5	2.5	9.3
1-*m*-Bromobenzoyl	40.2	2.3	9.7	40.4	2.6	9.4
1-*o*-Iodobenzoyl	34.7	2.0	8.1	35.1	1.7	7.8
1-*p*-Iodobenzoyl	34.7	2.0	8.1	35.0	2.3	7.9
1-*m*-Trifluoromethylbenzoyl	45.8	2.4	9.7	46.1	2.3	10.0
1-*p*-Nitrobenzoyl*	45.3	2.6	15.9	45.4	2.8	15.7
1-Benzoyl-5-sec-butyl	61.0	5.8	10.1	61.2	6.0	9.8
1-Benzoyl-5-isopropyl	59.5	5.3	10.7	59.7	5.5	10.5

*Analysis reported by Liu (26).

highly polar solvent having a highly polar transition state (23), in that the more highly complex molecule (with substituents adjacent to the reaction center) has a lower activation entropy.

(5) N-3 Substituents

As seen in Fig. 4, replacement of hydrogen by a phenyl group at the N-3 position increases the height of the maximum but does not affect its position in a plot of log k_ψ *vs.* percent acid. Also it may be noted that it decreases the minimum rate but not the position of the minimum. The phenyl group as noted earlier is more electron-withdrawing than hydrogen ($pK_{BH^+} = -4.83$ for 2-thiohydantoin and -5.18 for 3-phenyl-2-thiohydantoin (6)) so that one might expect a higher maximum for the A-2 mechanism, since the 3-phenyl-2-thiohydantoin would be a better leaving group. The result in concentrated acid is more important. For the A-1 hydrolysis of *m*- and *p*-(anilide) substituted mesitoylanilides in 96.2% sulfuric acid at 25 °C (which proceeds by *N*-protonation of the anilide) $\rho = 2.3$ (6). If one were to assume a similar mechanism for the A-1 hydrolysis of 1-acyl-2-thiohydantoins, one would expect the 3-phenyl group to enhance the rate. Instead, it decreases it by 30% (Table 4). This can be interpreted as support for an A-1 mechanism involving protonation of the C-4 carbonyl to give BH_2^{2+} (Scheme 1), since the basicity of this carbonyl should be appreciably affected by substituting a phenyl group at the N-3 position.

Experimental

Materials

1-Acyl-2-thiohydantoins were synthesized according to the method of Johnson and Nicolet (24), and were recrystallized from methanol or ethanol. 1-Benzoyl-3-phenyl-2-thiohydantoin (2) was a gift of J. K. Liu. Melting points (Table 5) were determined on a hot stage microscope and are uncorrected. Analyses were done by A. Bernhardt of West Germany, and are recorded in Table 6.

Basicity Measurements

Ultraviolet absorbance measurements were conducted in thermostatted 1 cm quartz cells in a Unicam recording SP-800 spectrophotometer following the general procedures of ref. 25, and are given in Table 7. Calculation by the usual procedures (25) gave the data shown plotted in Fig. 2.

Rate Measurements

Acid (3.00 ml) of known concentration was allowed to come to thermal equilibrium in a thermostatted (±0.1 °C) spectrophotometer cell with a Teflon stopper. Methanolic stock solution (8–10 μl) of the 1-acyl-2-thiohydantoin was then injected into the solution using a Hamilton syringe with a Chaney adaptor. The cell was shaken, placed back in the thermostatted cell block, and spectra were recorded after 3–10 min (shown in separate experiments to be sufficient to re-establish thermal equilibrium). Absorbance (A) measurements were made, most often at about 300 nm, but calculated rates were unaffected by the wavelength chosen. Rates were followed for at least two half-lives, and absorbance values for complete hydrolysis (A_∞) taken after 6–10 half-lives. Products were stable under reaction conditions, and in all cases the final spectrum was identical to that of an equimolar mixture of 2-thiohydantoin and the carboxylic

Can. J. Chem. Downloaded from www.nrcresearchpress.com by 210.87.254.105 on 09/05/12
For personal use only.

TABLE 7. Ultraviolet absorbance at 285 nm of substituted 2-thiohydantoins in varying concentrations of sulfuric acid

% H_2SO_4	1-Benzoyl*	1-*m*-Trifluoromethylbenzoyl†	1-*o*-Iodobenzoyl‡
0	1.090§	—	1.342§
65.0	—	1.093§	—
70.0	—	1.020	—
71.0	1.022	—	—
72.7	0.957	0.931	1.092
74.0	0.895	—	—
74.9	0.870	0.846	1.020
76.0	0.835	0.830	—
77.5	—	0.649	—
78.1	0.740	0.595	0.720
80.0	0.690	0.541	—
80.9	—	—	0.469
81.8	0.655	—	—
84.9	—	—	0.366
85.5	0.610‖	—	—
86.4	—	0.424‖	—
94.4	—	—	0.302‖

*Concentration c of 2-thiohydantoin, 9.8×10^{-5} M; at 9.4 °C.
†$c = 10^{-4}$ M; at 9.4 °C.
‡$c = 10^{-4}$ M; at 25.3 °C.
§Taken as absorbance of unprotonated substrate.
‖Taken as absorbance of protonated substrate.

acid in the concentration of sulfuric acid used. Rate coefficients were calculated on an IBM-360 computer by a least squares program for log $(A_t - A_\infty)$ *vs.* time. Duplicate kinetic runs agreed to within 4%, and in nearly all cases correlation coefficients better than 0.998 for eight points were obtained. It was found that k_ψ was unaffected by substrate concentration over the range $5 \times 10^{-5} - 2 \times 10^{-3}$ M. Detailed numerical data for each run are recorded in ref. 29.

The financial support of the National Research Council of Canada is gratefully acknowledged. We are also most grateful to Dr. J. K. Liu for much preliminary experimentation, and to Professor R. J. Gillespie for informing us of his cryoscopic and conductometric studies of the ionization of 2-thiohydantoin in 100% sulfuric acid.

1. J. T. EDWARD. *In* The chemistry of organic sulfur compounds. Vol. II. *Edited by* N. Kharasch and C. Y. Meyers. Pergamon Press, Oxford. 1966. p. 295.
2. J. T. EDWARD and J. K. LIU. Can. J. Chem. **46**, 71 (1968).
3. V. H. BAPTIST and H. B. BULL. J. Am. Chem. Soc. **75**, 1727 (1953). L. D. CROMWELL and F. R. STARK. Biochem. **8**, 4735 (1969).
4. P. SCHLACK and W. KUMPF. Z. physiol. Chem. **154**, 125, (1926).
5. W. I. CONGDON and J. T. EDWARD. J. Am. Chem. Soc. **94**, 6096, 6099 (1972).
6. G. D. DERDALL. Ph.D. Thesis. McGill University, Montreal, Quebec, 1971.
7. L. FLEXSER, L. P. HAMMETT, and A. DINGWALL. J. Am. Chem. Soc. **57**, 2103 (1935).
8. C. T. DAVIS and T. A. GEISSMAN. J. Am. Chem. Soc. **76**, 3507 (1954).
9. K. YATES and R. A. MCCLELLAND. J. Am. Chem. Soc. **89**, 2686 (1967).
10. J. T. EDWARD and S. R. C. MEACOCK. J. Chem. Soc. 2000 (1957).
11. K. YATES and J. B. STEVENS. Can. J. Chem. **43**, 529 (1965). K. YATES and J. C. RIORDAN. Can. J. Chem. **43**, 2328 (1965).
12. J. F. BUNNETT. J. Am. Chem. Soc. **83**, 4956 (1961).
13. K. YATES, J. B. STEVENS, and A. R. KATRITZKY. Can. J. Chem. **42**, 1957 (1964). C. D. JOHNSON, A. R. KATRITSKY, and N. SHAKIR. J. Chem. Soc. B, 1235 (1967).
14. E. M. ARNETT. *In* Progress in physical organic chemistry. *Edited by* S. G. Cohen, A. Streitwieser, Jr. and R. W. Taft. Interscience, New York, 1963. p. 223.
15. J. F. BUNNETT and F. P. OLSEN. Can. J. Chem. **44**, 1899, 1917 (1966).
16. J. F. BUNNETT. J. Am. Chem. Soc. **83**, 4965 (1961).
17. L. L. SCHALEGER and F. A. LONG. *In* Advances in physical organic chemistry. *Edited by* V. Gold. Academic Press Inc., London. 1963. p. 25.
18. R. HUISGEN, I. UGI, H. BRADE, and E. RAUENBUSCH. Ann. **586**, 30 (1954).
19. J. T. EDWARD, H. S. CHANG, K. YATES, and R. STEWART. Can. J. Chem. **38**, 2271 (1960).
20. R. STEWART and K. YATES. J. Am. Chem. Soc. **80**, 6355 (1958).
21. M. L. BENDER and M. C. CHEN. J. Am. Chem. Soc. **85**, 30, 37 (1963).
22. F. P. PRICE and L. P. HAMMETT. J. Am. Chem. Soc. **63**, 2387 (1941).

Can. J. Chem. Downloaded from www.nrcresearchpress.com by 210.87.254.105 on 09/05/12
For personal use only.

23. R. W. TAFT, JR. *In* Steric effects in organic chemistry. *Edited by* M. S. Newman. John Wiley and Sons, London. 1956. p. 652–655.
24. T. B. JOHNSON and B. H. NICOLET. J. Am. Chem. Soc. **33**, 1973 (1911).
25. J. T. EDWARD and H. STOLLAR. Can. J. Chem. **41**, 721 (1965).
26. J. K. LIU. Ph.D. Thesis. McGill University, Montreal, Quebec, 1968.
27. T. B. JOHNSON and W. M. SCOTT. J. Am. Chem. Soc. **35**, 1134. (1913).
28. H. C. CARRINGTON. J. Chem. Soc. 681 (1947).
29. W. I. CONGDON. Ph.D. Thesis. McGill University, Montreal, Quebec, 1970.

Can. J. Chem. Downloaded from www.nrcresearchpress.com by 210.87.254.105 on 09/05/12
For personal use only.

Thiohydantoins. XI. Kinetic Studies of the Alkaline Hydrolysis of 1-Acyl-2-thiohydantoins

WAYNE I. CONGDON[1] AND JOHN T. EDWARD
Department of Chemistry, McGill University, Montreal, Quebec

Received April 10, 1972

1-Acyl-2-thiohydantoins ionize in alkaline solution ($pK \sim 7$). In solutions more alkaline than $pH > 11$ they are rapidly hydrolyzed to 2-thiohydantoin and a carboxylic acid, by attack of a hydroxide ion on the conjugate base of the 1-acyl-2-thiohydantoin. Possible mechanisms to accord with the entropy of activation, which is less negative than usual for base-catalyzed amide hydrolyses, are discussed. 1-Benzoyl-2-thiohydantoin hydrolyzes more rapidly than 1-acetyl-2-thiohydantoin, possibly because the ground state of the former molecule is destabilized by steric effects.

Les acyl-1 thiohydantoïnes-2 s'ionisent en milieu alcalin ($pK \sim 7$). En milieu plus alcalin ($pH > 11$) ils s'hydrolisent rapidement aux acides carboxyliques et à thiohydantoïne-2, par l'attaque de l'ion hydroxide à la base conjuguée de l'acyl-1 thiohydantoïne-2. On réfléchit sur les mécanismes qui peuvent être en accord avec l'entropie de l'activation, qui est moins négative que les entropies de l'activation pour les amides plus ordinaires. Le benzoyl-1 thiohydantoïne-2 s'hydrolyse plus vite que l'acétyl-1 thiohydantoïne-2, peut-être parce que le premier est déstabilisé par les effets stériques.

Canadian Journal of Chemistry, **50**, 3780 (1972)

Can. J. Chem. Downloaded from www.nrcresearchpress.com by 210.87.254.5 on 09/05/12
For personal use only.

The study of the deacylation of 1-acyl-2-thiohydantoins (**1**) by acid or alkali (1) is of interest in connection with the procedure of Schlack and Kumpf (2) for the stepwise degradation of peptides or proteins. This procedure received only desultory attention for many years (3), but lately has been the focus of renewed interest (4). It consists of reacting the C-terminal amino acid of a polypeptide (RCO—NHCH$_1$R″—COOH) or protein with ammonium thiocyanate to give a 2-thiohydantoin derivative, attached to the remainder of the peptide chain by a 1-acyl linkage, as in **1** (R = polypeptide, R′ = H). This 1-acyl linkage can then be selectively cleaved by acid or alkali under unusually mild conditions (1) to give the polypeptide (**2**) minus its original C-terminal amino acid, the latter being now incorporated in a 2-thiohydantoin (**3**) (see eq. 1). This facility of hydrolysis is shared by other amides (5–7) and esters (8) having electron-attracting groups attached to the nitrogen or oxygen atom which separates from the acyl group in hydrolysis; there is a very rough correlation between the rate of the reaction and the stability of the anion A^- derived by ionization of the amino or alcohol moiety HA formed in the hydrolysis (as measured by the pK_{HA} of HA (9–11)).

The mechanisms for the alkaline hydrolysis of various amides differ with regard to the timing of various proton-transfers (see DeWolfe and Newcomb (12) for an excellent, brief review), and reference to them will be made later. However, we should first note that *p*-nitroacetanilide (pK_{HA} 13.8 (6)) and diacetylimine (**6**) (pK_{HA} 12.9 (7)) ionize as acids in dilute aqueous sodium hydroxide. Kinetic studies (6, 7) indicate that the hydrolysis of both of these compounds takes place by attack of hydroxide ion on the unionized compound (*e.g.*, **6**), and not on the anion (*e.g.*, **5**), presumably because the negative charge of the latter is delocalized over the amide

[1] 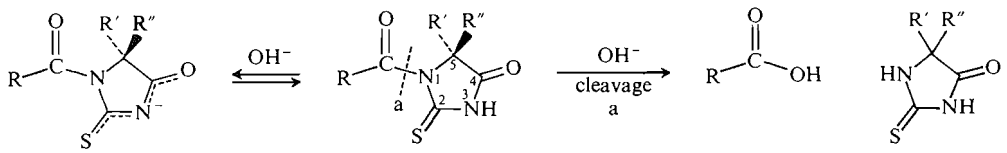

4 **1** **2** **3**

[1]Holder of NRCC Studentship, 1968–1970.

[2] 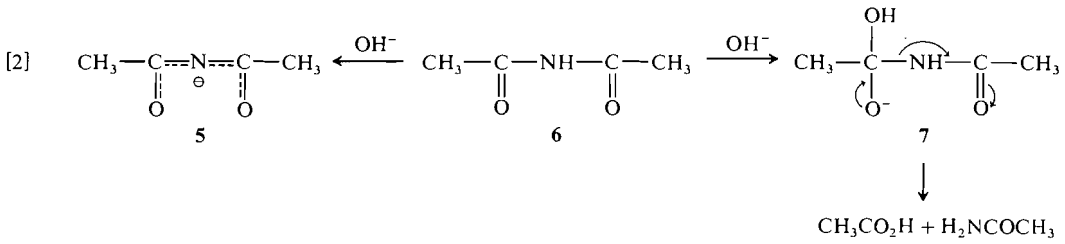

carbonyl group and decreases its electrophilic character drastically (see eq. 2).

1-Acyl-2-thiohydantoins also ionize as weak acids ($\mathbf{1} \rightarrow \mathbf{4} + H^+$), and have pK_a values of 6.5–7.0 (Table 1). Consequently, in the solutions more alkaline than pH 9, in which they begin to be hydrolyzed at appreciable rates, they must be more than 99% in the ionized form **4**. However, the negative charge of **4** is not delocalized over the 1-acyl carbonyl group which is attacked in hydrolysis, and so this charge might be expected to reduce its reactivity by a factor of about 10^2 (*cf.* ref. 13) or less. In such a case the greater reactivity of **1** would not be expected to compensate for the greater abundance of **4**. This expectation is realized: the rates for the hydrolysis of various 1-acyl-2-thiohydantoins in a large excess of buffer or alkali (at constant ionic strength) is first-order in hydroxide ion concentration, as shown by the invariance of the second order rate constants k_b ($=k_\psi/[OH^-]$) in Table 2. Consequently, hydrolysis must proceed mainly by attack of

TABLE 1. pK_{HA} values of 1-acyl-2-thiohydantoins in water at 25°

Compound	pK_{HA}
1-Acetyl-2-thiohydantoin*	7.03
1-Acetyl-5-methyl-2-thiohydantoin†	6.95
1-Acetyl-5,5-dimethyl-2-thiohydantoin‡	6.93
1-Benzoyl-2-thiohydantoin*	6.50
1-*p*-Anisoyl-2-thiohydantoin†	6.65
1-*p*-Nitrobenzoyl-2-thiohydantoin†	6.45

*Unpublished work by I. C. Wang.
†Reference 28.
‡Unpublished work by I. Lantos.

TABLE 2. The effect of pH and ionic strength on the rate of base-catalyzed hydrolysis of 1-acetyl-5,5-dimethyl-2-thiohydantoin at 25.4 °C

Buffer composition*	pH	Ionic strength	$k_\psi \times 10^4$ (s^{-1})	k_b ($l\ mol^{-1}\ s^{-1}$)
0.03 *M* K_2HPO_4, 0.01 *M* K_3PO_4	10.95†	1.0000	1.57 ± 0.05	0.176
0.0025 *N* NaOH	11.40‡	0.0025	2.04 ± 0.04	0.081
0.04 *M* K_2HPO_4, 0.04 *M* K_3PO_4	11.47†	1.0000	5.13 ± 0.08	0.174
0.08 *M* K_2HPO_4, 0.08 *M* K_3PO_4	11.56†	1.0000	6.25 ± 0.05	0.172
0.01 *M* K_2HPO_4, 0.03 *M* K_3PO_4	11.88†	1.0000	12.10 ± 0.15	0.159
0.01 *N* NaOH	12.00‡	0.0100	8.94 ± 0.23	0.089
0.01 *N* NaOH	12.00‡	0.0400	10.41 ± 0.01	0.104
0.01 *N* NaOH	12.00‡	0.0900	11.23 ± 0.23	0.112
0.01 *N* NaOH	12.00‡	0.1600	12.00 ± 0.20	0.120
0.0175 *N* NaOH	12.25‡	1.0000	25.60 ± 0.45	0.144
0.025 *N* NaOH	12.40‡	1.0000	41.40 ± 0.20	0.165
0.063 *N* NaOH	12.80‡	1.0000	102.40 ± 0.15	0.162
0.1 *N* NaOH	13.00‡	0.5000	136.50 ± 0.50	0.136
0.1 *N* NaOH	13.00‡	1.0000	148.00 ± 0.70	0.149
0.2 *N* NaOH	13.30‡	1.0000	302.00 ± 0.05	0.151
0.5 *N* NaOH	13.70‡	1.0000	764.00 ± 11.00	0.152
0.8 *N* NaOH	13.90‡	1.0000	1340.00 ± 13.00	0.169
1.0 *N* NaOH	14.00‡	1.0000	1740.00 ± 40.00	0.174

*Plus KCl to make up to ionic strength indicated.
†pH measured in quintuplicate (±0.04 pH units) with a Radiometer 202-C glass electrode. *vs.* a saturated calomel electrode on a Radiometer TTT-1 recording pH meter.
‡Calculated from $pH = 14.00 + \log [NaOH]$.

Can. J. Chem. Downloaded from www.nrcresearchpress.com by 210.87.254.5 on 09/05/12
For personal use only.

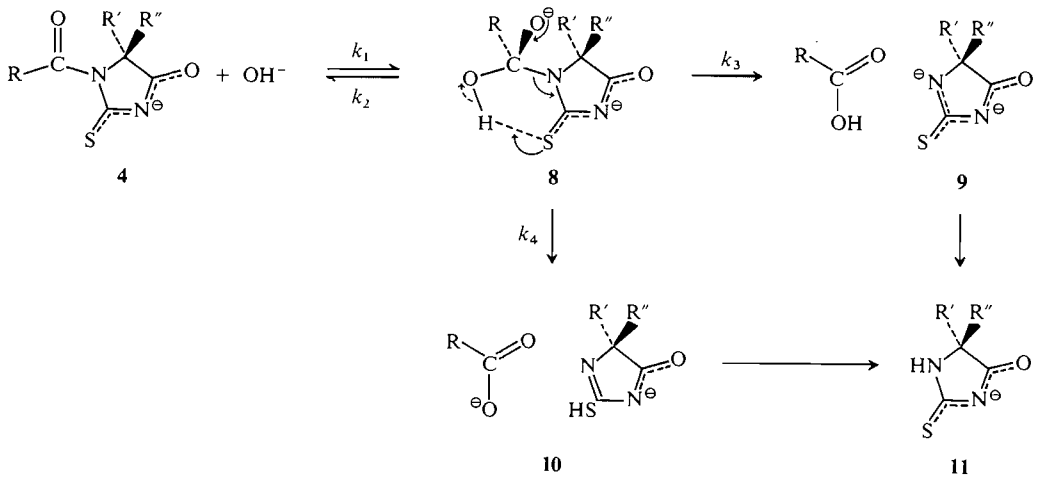

SCHEME 1

hydroxide ion on the anion **4** (*cf.* discussion in ref. 7).

This accords with observations of the effect of ionic strength on the rate of the reaction. For a reaction between two charged ions the observed rate will be given by:

$$[3] \quad \log k_b = \log k_0 + 1.02\, Z_a Z_b \sqrt{\mu}/(1+\sqrt{\mu})$$

where k_0 is the second order rate constant at zero ionic strength, and μ is the ionic strength (14*a*). In the present instance the ionic charges $Z_a = Z_b = -1$, so that k_b increases with ionic strength. The plot of $\log k_b$ for the hydrolysis of 1-acetyl-5,5-dimethyl-2-thiohydantoin *vs.* $\sqrt{\mu}/(1+\sqrt{\mu})$ gives a curve similar to that obtained for the base-catalyzed hydrolysis of a series of dicarboxylic acid half esters EtO—CO—$(CH_2)_n$—CO_2^- ($n = 0$–4) (15), with the slope approaching unity as $\mu \to 0$. This is shown in Fig. 1, which indicates that the second-order rate constant more than doubles on going from $\mu = 0$ to $\mu = 1$.

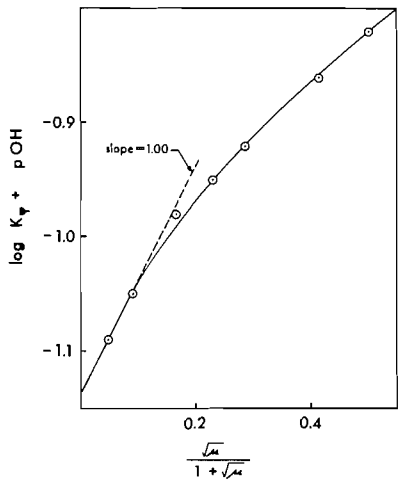

FIG. 1. A plot of $\log k_b$ ($\equiv \log k_\psi + pOH$) (in l mol^{-1} s^{-1}) against $\sqrt{\mu}/(1+\sqrt{\mu})$ for 1-acetyl-5,5-dimethyl-2-thiohydantoin at 25.4 °C.

The mechanisms which best accommodate these and other experimental facts discussed below are outlined in Scheme 1. Formation of the tetrahedral intermediate **8** (*cf.* refs. 5, 6, 12) will be hindered by bulky groups at the 5-position, particularly if hydrogen-bonding between the new hydroxyl group and the strongly basic sulfur atom, as shown in **8**, causes eclipsing of the groups at the 5-position with groups in the newly-tetrahedral atom. Steric hindrance will be especially severe for the solvated anionic oxygen. This may explain the retardation of alkaline hydrolysis by substitution, and more especially by geminal disubstitution, at the 5-position, as shown in Table 4. Substitution at this position is less effective in retarding acid-catalyzed hydrolysis, as can be seen by comparing the last two columns of Table 3, although it has usually been thought that steric effects on both base- and acid-catalyzed hydrolyses are the same (16). The

Can. J. Chem. Downloaded from www.nrcresearchpress.com by 210.87.254.5 on 09/05/12
For personal use only.

TABLE 3. Effects of C-5 substituents on the hydrolysis rates of 1-benzoyl-2-thiohydantoin

Substituent	$10^4 k_\psi$*	$10^4 k_\psi$†	Relative rates: Base	Relative rates: Acid
Unsubstituted	31.40±0.40	49.8±0.50	1.00	1.00
5-Methyl	12.70±0.21	35.5±0.60	0.41	0.71
5-Phenyl	10.20±0.66	22.8±0.36	0.33	0.46
5-Isopropyl	4.77±0.18	—	0.15	—
5-Isobutyl	6.64±0.15	18.4±0.54	0.21	0.37
5-sec-Butyl	4.65±0.16	17.9±0.40	0.15	0.36
5,5-Dimethyl	2.38±0.06	29.4±1.32	0.08	0.60

*Pseudo-first-order rate constants (s^{-1}) measured at 25.3 °C in a phosphate buffer at an ionic strength of 0.45 and a pH = 11.2.
†Pseudo-first-order rate constants (s^{-1}) measured at 25.3 °C in 58.0% sulfuric acid.

TABLE 4. Temperature dependence of the rate of alkaline hydrolysis of 1-acyl-2-thiohydantoins

Compound and buffer solution	Temperature (°C)	$10^4 k_\psi$ (s^{-1})	log A_1[a] (l mol^{-1} s^{-1})	ΔS^{+}[b,c] (e.u.)	E_a (kcal mol^{-1})
1-Acetyl-2-thiohydantoin;	20.0	3.98±0.13	10.9±0.2	−11±2	18±2
pH = 10.95; μ = 1.0;	25.4	6.97±0.41			
0.03 M K_2HPO_4, 0.01 M K_3PO_4	30.4	11.50±0.15			
	35.6	18.20±0.90			
	41.5	30.80±1.40			
1-Benzoyl-2-thiohydantoin;	20.0	8.83±0.06	10.4±0.2	−13±2	16±2
pH = 10.95; μ = 1.0;	25.4	16.40±0.30			
0.03 M K_2HPO_4, 0.01 M K_3PO_4	30.4	25.60±0.06			
	35.6	39.10±1.20			
	41.5	65.80±0.50			
1-Acetyl-5,5-dimethyl-2-	11.0	3.65±0.02	10.1±0.2	−14±2	15±2
thiohydantoin	25.3	12.90±0.04			
pH = 11.95; μ = 0.55;	49.6	95.80±0.93			
0.1 M Na_2HPO_4, 0.075 M NaOH	58.1	177.00±2.10			

[a]Based on $k_b = k_\psi/[OH^-]$ in l mol^{-1} s^{-1}.
[b]The standard state for ΔS^+ utilizing k_b is 1 mol per liter and Δn^+ in the Arrhenius equation is assumed small since this is a bimolecular reaction in solution (14*b*).
[c]These values have been corrected for the effect of ionic strength at one temperature (25.3 °C).

difference in the present instance may reflect the difference in the proximity of the 5-substituents to the charged centers in **8** and in **12**, the tetrahedral intermediates for alkaline- and acid-catalyzed hydrolysis (17) respectively, and hence their different effects on the solvation required to stabilize these charged intermediates (see eq. 4).

The mechanism of Scheme 1 also takes account of measurements of the Arrhenius parameters for the base-catalyzed hydrolysis, which show its rapidity to be determined chiefly

[4] 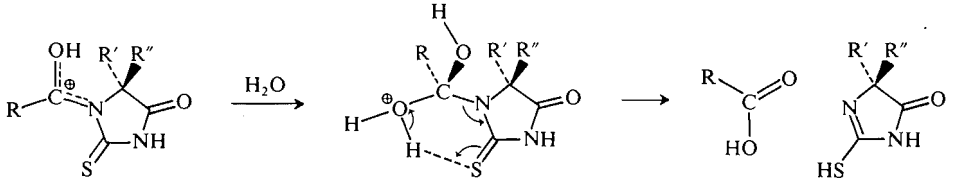

12

Can. J. Chem. Downloaded from www.nrcresearchpress.com by 210.87.254.5 on 09/05/12
For personal use only.

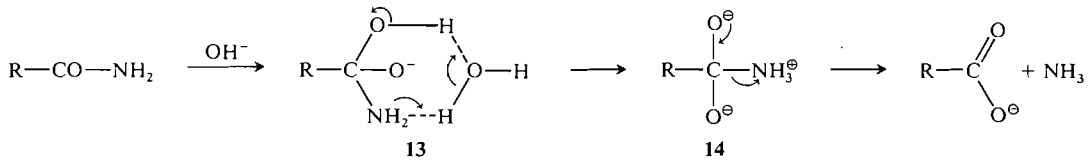

SCHEME 2

by favorable entropy factors. Plots of log $(k_\psi/[OH^-])^2$ against $1/T$ (shown in Fig. 2) give straight lines, the slopes of which give the activation energy ($E_a/2.3R$) in kcal mol^{-1} and the intercept, the logarithm of the frequency factor, log A_t, in 1 mol^{-1} s^{-1} (Table 4). This must be modified for the effect of ionic strength at one temperature to obtain meaningful entropy values.

The results in Table 4 show that the very rapid hydrolyses of 1-acetyl-2-thiohydantoin (**1**; R = Me, R′ = R″ = H) and of 1-benzoyl-2-thiohydantoin (**1**; R = Ph, R′ = R″ = H) are due to favorable entropy factors, as measured by the A_t values for the reactions, and not to low energies of activation. (For comparison,

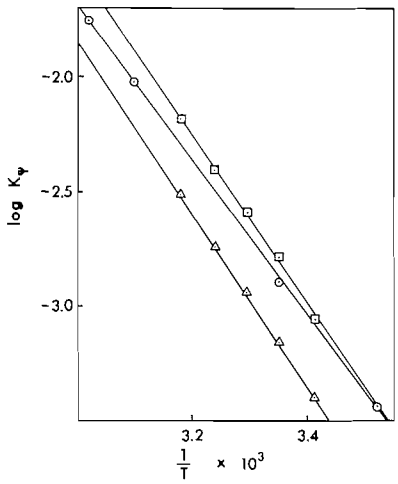

FIG. 2. Arrhenius plots for the hydrolysis of 1-acetyl-5,5-dimethyl-2-thiohydantoin (○), 1-benzoyl-2-thiohydantoin (□), and 1-acetyl-2-thiohydantoin (△) in phosphate buffer (see Table 5).

[2]Hydroxide ion concentration was calculated from pH measurements of buffer solutions at 25°. However, the hydroxide ion activity (or concentration) will not be constant for the same buffer composition but different temperatures, so the activation parameters must be regarded as only approximate. We are indebted to a referee for making this point.

log A_t for the alkaline hydrolysis of acetamide and benzamide is 4.4 and 4.2 l mol^{-1} s^{-1}, respectively, and E_a is 14.3 and 12 kcal^{-1} mol^{-1}, respectively (18)). The A_t values are derived from the overall rate constant k_b, which according to the steady-state principle applied to the mechanism of Scheme 1, should be given by

$$[5] \qquad k_b = \frac{k_1(k_3 + k_4)}{k_2 + k_3 + k_4}$$

In such a case the frequency factor A_t should depend on the individual frequency factors for the different reactions k_1, k_2, k_3, and k_4 (19). In general, the frequency factor is reduced by about 10^2 by electrostatic effects between two particles each bearing a charge of -1 (14*c*). If in the present instance the frequency factor for k_1 is so reduced, the high values of A_t must result from compensation by very high values for the frequency factors for k_3 and k_4, as compared with the frequency factor for the corresponding step in the hydrolysis of acetamide or benzamide (19). The latter is expected to be low because of stringent requirements for the ordering of solvent if, as seems probable (*cf.* refs. 5, 12), the mechanism for the hydrolysis is given by Scheme 2 with the formation of the zwitterion **14** (or something closely similar). On the other hand, the breakdown of the tetrahedral intermediate **8** for the hydrolysis of 1-acyl-2-thiohydantoins either does not require a proton-transfer (in the k_3 route), and leads to a dianion (**9**) with low solvation requirements (unlike **14**) because of the dispersal of the double charge, or else requires a proton-transfer (in the k_4 route) which can be effected internally without the necessity for ordering of solvent (as required in **13** → **14**).

While both routes (k_3 and k_4) of Scheme 1 are compatible with the evidence to date, it is difficult to know whether in fact both are kinetically significant, or whether the hydrolysis

Can. J. Chem. Downloaded from www.nrcresearchpress.com by 210.87.254.5 on 09/05/12
For personal use only.

TABLE 5. Ratio of pseudo-first-order rate constants for the hydrolysis of acetyl (k_ψ^a) and benzoyl (k_ψ^b) derivatives in alkaline and acid solutions

Compounds	k_ψ^a/k_ψ^b in base	k_ψ^a/k_ψ^b in acid
Ethyl acetate/ethyl benzoate	11.5(16)	384(16)
Acetamide/benzamide	4.1(18)	—
N-Acetylthiourea/*N*-benzoylthiourea	38.5*	22†
1-Acetyl-2-thiohydantoin/1-benzoyl-2-thiohydantoin	0.68‡	4.1§
1-Acetyl-5-methyl-2-thiohydantoin/1-benzoyl-5-methyl-2-thiohydantoin	0.95‡	4.8§
1-Acetyl-5,5-dimethyl-2-thiohydantoin/1-benzoyl-5,5-dimethyl-2-thiohydantoin	0.88‡	4.3§

*In aqueous 1 *N* NaOH at 25.3 °C.
†In 39.6% sulfuric acid at 49.1 °C.
‡In aqueous phosphate buffer, pH = 11.2, μ = 0.45.
§In 58.0% sulfuric acid at 25.3 °C.

proceeds by essentially only one route. Further investigations (*e.g.* of solvent isotope effects) would seem to be required.

A second factor promoting the rapid hydrolysis of 1-acyl-2-thiohydantoins in alkali is steric. This is shown up by an examination of the relative rates of hydrolysis of 1-acetyl- and of 1-benzoyl-2-thiohydantoin. In general, one expects amides and esters of acetic acid to be hydrolyzed more rapidly than the corresponding esters and amides of benzoic acid, and this is usually found true, as shown in Table 5. Thus ethyl acetate is saponified 11 times more rapidly than ethyl benzoate: the latter is stabilized by resonance interaction (admittedly weak (20)) between the benzene ring and the ester carbonyl group, and this resonance stabilization is lost in forming the tetrahedral intermediate. (The difference in rates becomes less for the amides, to the extent that the nitrogen atom releases electrons to the carbonyl group more readily than the oxygen atom, and so lessens the importance of phenyl–carbonyl resonance interaction.) However, surprisingly, the 1-benzoyl-2-thiohydantoins are found to hydrolyze in alkaline solution more *rapidly* than the corresponding 1-acetyl-2-thiohydantoins (Table 5).

Obviously a new factor is at work which is missing from the first three pairs of compounds of Table 5, and an examination of models suggests that this factor is steric. The 1-acyl group can be expected to be as much as possible coplanar with the thiohydantoin ring in order to maximize its amide-type resonance interaction with N-1 (21). For 1-acetyl-2-thiohydantoin, two coplanar conformations are possible: that in which the acyl carbonyl and the thiocarbonyl groups are aligned parallel; and that shown in Fig. 3, in which the acyl oxygen and thiocarbonyl sulfur are separated as much as possible. The former conformation involves very strong dipolar repulsions, and is expected to be strongly disfavored (22). However, for 1-benzoyl-2-thiohydantoin, the conformation which maintains the coplanarity of the acyl group with the thiohydantoin ring, and which avoids the dipolar repulsions, requires the benzene ring to be twisted about 90° out of the plane of the acyl group in order to avoid steric interference between the bulky sulfur atom and the ortho-hydrogens of the benzene ring (see Fig. 4).

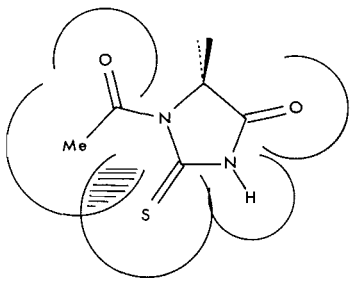

FIG. 3. Scale drawing of 1-acetyl-2-thiohydantoin, using bond-lengths and van der Waals radii from crystallographic studies of related compounds (32). The van der Waals radii for hydrogen and for the methyl group may be somewhat too large (33), and hence the overlap of methyl and sulfur would not seriously affect coplanarity of the acetyl group with the rest of the molecule.

Can. J. Chem. Downloaded from www.nrcresearchpress.com by 210.87.254.5 on 09/05/12
For personal use only.

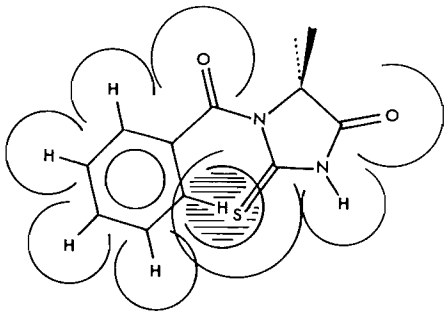

FIG. 4. Scale drawing of 1-benzoyl-2-thiohydantoin.

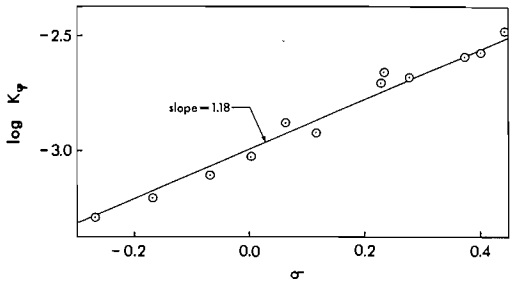

FIG. 5. A plot of log k_ψ against σ for *m*- and *p*- substituted 1-benzoyl-2-thiohydantoins (c.c.: 0.9902; s.d.: 0.05) in aqueous phosphate buffer, p*H* 10.75, $\mu = 0.42$, at 25.3 °C.

In fact, it seems likely that the steric congestion in 1-benzoyl-2-thiohydantoin is relieved by some rotation about *both* the phenyl—CO and the CO—N_1 bonds,[3] because the Hammett reaction constant ρ, given by the slope (1.18) of the plot of log k_ψ against σ for 12 *m*- and *p*-substituted 1-benzoyl-2-thiohydantoins (Table 7 and Fig. 5), has a value very close to that (1.055 (23)) reported for the alkaline hydrolysis of *m*- and *p*- substituted benzamides. This closeness is probably due to the operation of two opposing sets of factors. The lessening of electron-release from N-1 because of the juxtaposed thiocarbonyl, and because of twisting about the CO—N_1 bond, should increase ρ above 1.055; the lessening of resonance interaction between *m*- and *p*- substituents and the carbonyl group, by twisting about the phenyl—CO bond, should decrease ρ below 1.055 (24). The twisting about both Ph—CO and CO—N_1 should make the formation of the tetrahedral intermediate less costly (in terms of the loss of resonance energy), and should explain why the hydrolysis of 1-benzoyl-2-thiohydantoin goes faster than the hydrolysis of 1-acetyl-2-thiohydantoin.

It can be seen from Fig. 3 that any increase in size beyond that of the methyl group of 1-acetyl-2-thiohydantoin will lead to steric congestion between thiocarbonyl sulfur and the acyl group. This will be true for the acyl group derived from any amino acid, and so the 2-thiohydantoin derivative formed from the C-terminal amino acid of any peptide should be expected to be hydrolyzed in alkali at a greater rate than is 1-acetyl-2-thiohydantoin. It would seem, then, that the facility of Schlack and Kumpf's procedure for degrading peptides depends on favorable entropy and steric effects in the hydrolysis of the 2-thiohydantoin intermediates.

TABLE 6. Pseudo-first-order rate constants (k_ψ) for the hydrolysis of *m*- and *p*-substituted 1-benzoyl-2-thiohydantoins in alkaline phosphate buffer (p*H* 10.75, $\mu = 0.42$) at 25.3 °C

Substituent	$10^4 k_\psi$ (s^{-1})
p-Methoxy	5.12±0.15
p-Methyl	6.17±0.16
m-Methyl	7.61±0.23
(H)	9.31±0.18
p-Fluoro	13.30±0.30
m-Methoxy	11.90±0.30
p-Chloro	19.40±0.20
p-Bromo	21.90±0.28
p-Iodo	20.80±0.30
m-Chloro	25.90±0.45
m-Bromo	27.10±0.32
m-Trifluoromethyl	32.90±0.41

It is evident from Table 5 that the greater ease of acid-catalyzed hydrolysis of acetyl as compared with benzoyl derivatives extends to the hydrolysis of 1-acyl-2-thiohydantoins, in spite of the steric effects destabilizing the benzoyl derivatives. These effects would be expected to increase the rate of attack of water on the protonated 1-acyl-2-thiohydantoin to form the tetrahedral intermediate **12**; however, it is

[3]Alternatively, coplanarity of the benzene ring and the carbonyl group can be maintained if the alternative conformation having parallel carbonyl and thiocarbonyl groups is adopted. This conformation would explain the greater reactivity of 1-benzoyl- as compared with 1-acetyl-2-thiohydantoin, but is made less likely by the Hammett ρ value for the reaction.

Can. J. Chem. Downloaded from www.nrcresearchpress.com by 210.87.254.5 on 09/05/12
For personal use only.

TABLE 7. Physical properties of 5-substituted 1-acyl-2-thiohydantoins

Substituents	M.p. (°C)	Ultraviolet absorption bands* Type I λ_{max} (nm)	ε	Type II λ_{max} (nm)	ε	Type III λ_{max} (nm)	ε
1-Benzoyl-5-phenyl-	205–207†	372	130	282	9 600	242	21 900
1-Benzoyl-5-isobutyl-	169–170‡	365	220	273	11 600	242	20 200
1-Benzoyl-5,5-dimethyl-§	170–172	366	160	275	12 000	243	21 800
1-Acetyl-5-methyl-	167–168‖	366	28	277	18 800	233	14 300

*See ref. 3 for an explanation of band types.
†Kjaer reports m.p. 200–201 °C (29).
‡Cornforth reports m.p. 167–169 °C (30).
§Anal. Calcd. for $C_{12}H_{12}N_2O_2S$: C, 58.1; H, 4.8; N, 11.3. Found: C, 57.8; H, 5.0; N, 11.0.
‖Johnson reports m.p. 166° (31).

TABLE 8. Pseudo-first-order rate constants k_ψ (in s^{-1}) for hydrolysis of acetyl and benzoyl derivatives in an excess of acid or base

Compound	Base k_ψ	Acid k_ψ
N-Acetylthiourea	142.00±2.7*	8.69±0.18†
N-Benzoylthiourea	3.69±0.30*	0.39±0.01†
1-Acetyl-2-thiohydantoin	21.4 ±0.4‡	202.0 ±4.3§
1-Benzoyl-2-thiohydantoin	31.4 ±0.4‡	49.8 ±0.5§
1-Acetyl-5-methyl-2-thiohydantoin	12.0 ±0.5‡	171.0 ±1.5§
1-Benzoyl-5-methyl-2-thiohydantoin	12.7 ±0.2‡	35.5 ±0.6§
1-Acetyl-5,5-dimethyl-2-thiohydantoin	2.10±0.10‡	127.5 ±4.6§
1-Benzoyl-5,5-dimethyl-2-thiohydantoin	2.38±0.06‡	29.4 ±1.3§

*In 1 *N* NaOH at 25.3 °C.
†In 39.6% H_2SO_4 at 49.1 °C.
‡In phosphate buffer, $\mu = 0.45$, p*H* = 11.2 at 25.3 °C.
§In 58.0% H_2SO_4 at 25.3 °C.

apparent that this is more than offset by the decrease in the basicity of the 1-acyl group resulting from diminished Ph—CO and CO—N_1 resonance interaction (*cf.* refs. 25, 26).

Experimental

All compounds were made and purified according to the procedure of Johnson and Nicolet (27). Most were known compounds; physical properties are listed in Table 7 for compounds not described in ref. 17. Buffer solutions were made using Fisher reagent grade KCl, K_2HPO_4, K_3PO_4 and distilled water. p*H* values were measured at 25.4 °C using a TTT-1 automatic titrator and a Radiometer 202-C electrode *vs.* a saturated calomel electrode. p*H* values were found to remain constant during the reaction. For buffer solutions above p*H* of 12, standard B.D.H. sodium hydroxide (1 *N*) was used with KCl to prepare solutions; the p*H* values reported were calculated from the relation: $pH = 14 + \log [OH^-]$.

For the kinetic runs, 3.00 ml of buffer was allowed to come to thermal equilibrium in a stoppered u.v. cell contained in a thermostatted cell compartment. A methanolic solution (10 μl) of 1-acyl-2-thiohydantoin was then injected, using a Hamilton syringe with Chaney adaptor, the cell was vigorously shaken, and the absorbance (D) at constant wavelength was recorded by a Unicam SP 800 recording u.v. spectrophotometer fitted with scale expander and slave recorder attachments. Measurements were always made in the region 300–330 nm, because the 2-thiohydantoin has no appreciable absorption in this region, and so its further hydrolysis has no spectral consequences. Results were analyzed by a linear least squares program using log $(D_t - D_\infty)$ *vs.* time. D_∞ was taken after 7–10 half-lives, and for several slow reactions Guggenheim's method was used. Correlation coefficients for individual runs were generally greater than 0.999 for 8 points, and separate runs were found to be reproducible to within 3–4%. The experimental data on which some of the entries of Table 6 are based are given in Table 8.

We acknowledge gratefully much preliminary experimentation by Dr. J. K. Liu, helpful criticism by Professor R. Stewart, and financial support from the National Research Council of Canada.

Can. J. Chem. Downloaded from www.nrcresearchpress.com by 210.87.254.5 on 09/05/12
For personal use only.

1. J. T. EDWARD and J. K. LIU. Can. J. Chem. **46**, 71 (1968).
2. P. SCHLACK and W. KUMPF. Z. Physiol. Chem. **154**, 125 (1926).
3. J. T. EDWARD. *In* The chemistry of organic sulfur compounds. Vol. II. *Edited by* N. Kharasch and C. Y. Meyers. Pergamon Press, Oxford. 1966. p. 295.
4. L. D. CROMWELL and G. R. STARK. Biochem. **8**, 4735 (1969).
5. M. L. BENDER and R. J. THOMAS. J. Am. Chem. Soc. **83**, 4182 (1961).
6. R. M. POLLACK and M. L. BENDER. J. Am. Chem. Soc. **92**, 7190 (1970).
7. J. T. EDWARD and K. A. TERRY. J. Chem. Soc. 3527 (1957).
8. E. SACHER and K. J. LAIDLER. Can. J. Chem. **42**, 2404 (1964).
9. D. J. CRAM. Fundamentals of carbanion chemistry. Academic Press, New York. 1965. p. 4; K. BOWDEN. Chem. Rev. **66**, 119 (1966).
10. J. T. EDWARD and S. NIELSEN. J. Chem. Soc. 5075, 5090 (1957).
11. F. G. BORDWELL and G. D. COOPER. J. Am. Chem. Soc. **74**, 1058 (1952).
12. R. H. DEWOLFE and R. C. NEWCOMB. J. Org. Chem. **36**, 3870 (1971).
13. T. C. BRUICE and B. HOLMQUIST. J. Am. Chem. Soc. **89**, 4028 (1967).
14. K. J. LAIDLER. Chemical kinetics. McGraw-Hill Book Co. New York. 2nd Ed. 1965. (*a*) p. 219–222, and refs. therein; (*b*) p. 90; (*c*) p. 216.
15. J. I. HOPPE and J. E. PRUE. J. Chem. Soc. 1775 (1957).
16. R. W. TAFT. *In* Steric effects in organic chemistry. *Edited by* M. S. Newman. John Wiley and Sons, London. 1956. pp. 587–590, 603–604, 670–672.
17. W. I. CONGDON and J. T. EDWARD. Can. J. Chem. This issue. Part X.
18. J. PACKER, A. L. THOMSON, and J. VAUGHAN. J. Chem. Soc. 2601 (1955).
19. M. L. BENDER, R. D. GINGER, and J. D. UNIK. J. Am. Chem. Soc. **80**, 1044 (1958).
20. G. W. WHELAND. Resonance in organic chemistry. John Wiley, New York. 1955. pp. 108, 159.
21. L. PAULING, R. B. COREY, and H. R. BRANSON. Proc. Nat. Acad. Sci. **37**, 205 (1951).
22. M. CALVIN and C. L. WOOD. J. Am. Chem. Soc. **62**, 3152 (1940). R. BRESLOW. Organic reaction mechanisms. W. A. Benjamin, Inc., New York. 1965. p. 163.
23. L. P. HAMMETT. Physical organic chemistry. McGraw-Hill Book Co. New York. 1940. p. 184.
24. H. L. GOERING, T. RUBIN, and M. S. NEWMAN. J. Am. Chem. Soc. **76**, 787 (1954).
25. R. HUISGEN, I. UGI, H. BRADE, and E. RAUENBUSCH. Ann. **586**, 30 (1954).
26. H. C. BROWN, D. H. MCDANIEL, and O. HAFLIGER. Determination of organic structures by physical methods. *Edited by* E. A. Braude and F. C. Nachod. Academic Press, New York. 1955. p. 567.
27. T. B. JOHNSON and B. H. NICOLET. J. Am. Chem. Soc. **33**, 1973 (1911).
28. J. K. LIU. Ph.D. Thesis. McGill University, Montreal, Quebec, 1968.
29. A. KJAER. Acta Chem. Scand. **1**, 889 (1953).
30. J. W. CORNFORTH. The chemistry of penicillin. *Edited by* H. T. Clark, J. R. Johnson, and Sir R. Robinson, Princeton University Press, 1949. p. 688.
31. T. B. JOHNSON. J. Biol. Chem. **11**, 97 (1913).
32. (*a*) P. J. WHEATLEY. Acta Cryst. **6**, 369 (1953); (*b*) B. R. PENFOLD. Acta Cryst. **6**, 707 (1953); (*c*) N. C. KUNCHUR and M. R. TRUTER. J. Chem. Soc. 2551 (1958); (*d*) L. PAULING. The nature of the chemical bond. 2nd ed. Cornell University Press, Ithaca, N.Y. 1948. pp. 160, 187.
33. E. A. BRAUDE and F. SONDHEIMER. J. Chem. Soc. 3754 1955).

Can. J. Chem. Downloaded from www.nrcresearchpress.com by 210.87.254.5 on 09/05/12
For personal use only.

The Trifluoroacetic Acid Solvent System. Part IV. Triple Ions

M. G. HARRISS AND J. B. MILNE

Department of Chemistry, University of Ottawa, Ottawa, Canada K1N 6N5

Received June 5, 1972

Electrolytes studied in 100% trifluoroacetic acid exhibit a minimum in equivalent conductivity with increasing solute concentration. This behavior is accounted for by the formation of triple-ions at higher concentrations. Triple-ion dissociation constants, k, have been evaluated and, in general, they show the opposite trend with changing ion size to that of the ion-pair dissociation constants; that is the triple-ions of smaller ions are more dissociated. The experimentally observed trend is accounted for by using a partial ionic charge instead of unit charge for the ion-pair charges in the theoretical Fuoss expression for k.

The excellent extrapolation of the triple-ion data to give a value of $\Lambda^0 K_d$ for the ion-pair, which agrees well with that determined from a Fuoss plot, permits an estimate of Λ^0 for LiO_2CCF_3 from the triple-ion data.

Les électrolytes étudiés dans l'acide trifluoroacétique à 100% montrent un minimum, à conductivité équivalente, pour une concentration croissante en soluté. Ce phénomène s'explique par la formation d'ions triples en concentrations élevées. Les constantes de dissociation des ions triples k ont été évaluées; elles varient généralement en sens contraire, par rapport aux constantes de dissociation des paires d'ions, avec le changement dans la taille de l'ion. Cette tendance, observée expérimentalement, a été interpretée en utilisant une charge ionique partielle, au lieu de l'unité pour les charges des paires d'ions dans l'expression théorique de Fuoss pour k.

L'excellente extrapolation des données sur l'ion triple pour la valeur $\Lambda^0 K_d$ de la paire d'ion, en bon accord avec la valeur tirée de la courbe de Fuoss, permet une estimation de Λ^0 pour LiO_2CCF_3 à partir des données sur l'ion triple. [Traduit par le journal]

Canadian Journal of Chemistry, **50**, 3789 (1972)

Can. J. Chem. Downloaded from www.nrcresearchpress.com by 210.87.254.42 on 09/05/12
For personal use only.

Introduction

A plot of equivalent conductivity *vs.* concentration for electrolytes in solvents of dielectric constant <20 exhibits a minimum if sufficiently high concentrations are studied. This has long been known for many of the classical non-aqueous solvents of interest to inorganic chemists such as ammonia (1), sulfur dioxide (2), acetic acid (3) and, more recently, 100% hydrogen chloride (4). The effect was accounted for by the proposal of Fuoss and Kraus that triple-ions are formed in these solutions (5). The equilibria concerned account for the initial decrease in concentration of current-carrying species per mole of added solute, followed by the subsequent increase with the formation of triple-ions

$$3A^+ + 3B^- \rightleftarrows 3AB \rightleftarrows A_2B^+ + AB_2^-$$

The mathematical treatment of the electrical conductivity data in the concentration region of triple-ion formation has been presented often (5–8) and will not be repeated here. The treatment accounts very well for the experimental observations.

Davies (9) has put forward another theory to account for the minimum in solvents of $\varepsilon \sim 12$ or greater which is based upon activity effects. He suggests that, in the expression for the thermodynamic equilibrium constant for ion-pair dissociation

$$K_D = \frac{f^2 c\gamma^2}{f_{i,pr}(1-\gamma)}$$

if the function $f^2 c/f_{i,pr}$ passes through a maximum with increasing concentration, γ and Λ will exhibit a minimum.

On the basis of the knowledge acquired for the concentration region where simple ion-pair equilibria are involved (10, 11), extension of the interpretation to higher concentrations, more usual in the use of this solvent for preparative purposes and kinetic studies (12–14) is possible and forms the subject of this work.

Experimental

Details of the purification of materials and procedure for the measurement of electrical conductivities are given in Parts I and III (10, 11). Triple-ion dissociation constants, k, were evaluated by a least-mean-squares plot of eqs. 2 and 3 (see below), which was conducted

Can. J. Chem. Downloaded from www.nrcresearchpress.com by 210.87.254.42 on 09/05/12
For personal use only.

and extrapolated by computer. The evaluation of the limiting equivalent conductivity of the single-ions, Λ^0, from specific conductances in the triple-ion region and a single point in the ion-pair region was performed by computer also.

Results and Discussion

Evaluation of Triple-Ion Dissociation Constants

The results of conductivity measurements for solutes in the triple-ion concentration region are given in Table 1. A minimum in Λ is observed in all cases except for $B(O_2CCF_3)_3$. A curve of Λ *vs.* $\sqrt{c}$, synthesized for any of the electrolytes using the data from the ion-pair concentration region and the extended Debye–Hückel expression for the activity coefficient, shows no minimum; this eliminates Davies' "Dissociation Minimum" theory (9) as a possible explanation of the results. However the data are readily interpreted in terms of triple-ion formation.

The triple-ion dissociation equilibria are

$$A_2B^+ \overset{k_+}{\rightleftarrows} AB + A^+$$

$$AB_2^- \overset{k_-}{\rightleftarrows} AB + B^-$$

In no instance has a complete solution for k_+, k_- and the individual λ_T^0 for the triple-ions in any solvent ever been accomplished; the simplifying assumption that $k_+ = k_- = k$ is required to effect a solution. The simple treatment (8), which ignores long range interionic effects, yields the expression

$$[1] \qquad c^{1/2}\Lambda = \sqrt{K_D}\Lambda^0 + \frac{\sqrt{K_D}\Lambda_T^0}{k}\, c$$

where K_D is the ion-pair dissociation constant and Λ_T^0 is the equivalent conductivity of the hypothetical electrolyte $[M_2A^+][MA_2^-]$. According to this expression, a plot of $c^{1/2}\Lambda$ *vs.* c will yield a straight line with an intercept, $\sqrt{K_D}\Lambda^0$ and slope, $\sqrt{K_D}\Lambda_T^0/k$. A more sophisticated equation which introduces a blanket correction for long range interionic effects (5–7) is given by:

$$[2] \qquad \frac{c^{1/2} f\Lambda}{\left\{1 - \dfrac{(B_1\Lambda^0 + B_2)\sqrt{c\Lambda}}{(\Lambda^0)^{3/2}}\right\}\left(1 - \dfrac{\Lambda}{\Lambda^0}\right)^{1/2}} = \sqrt{K_D}\Lambda^0 + \frac{\sqrt{K_D}\Lambda_T^0}{k}\, 1\left(-\frac{\Lambda}{\Lambda^0}\right)c$$

where B_1 and B_2 are defined as in (8) and the other parameters are defined as above. A plot of this expression yields the same slope and intercept as for the simpler expression. Elimina-

TABLE 1. Specific conductances (K_{sp}) and equivalent conductivities (Λ) at 25 °C in the region of the conductivity minimum

Solute	$10^3\ C$ (mol l^{-1})	$10^6\ K_{sp}$ (ohm^{-1} cm^{-1})	Λ (ohm^{-1} cm^2 equiv^{-1})
LiO_2CCF_3	0.3165	0.6516	2.059
	0.4004	0.7334	1.832
	0.5166	0.8352	1.616
	0.6506	0.9407	1.446
	0.7714	1.028	1.332
	0.8890	1.107	1.245
	1.010	1.183	1.171
	1.114	1.245	1.117
	1.241	1.318	1.062
	1.370	1.388	1.014
	1.536	1.476	0.9605
	1.692	1.552	0.9177
	3.466	2.301	0.6637
	7.985	3.719	0.4657
	25.64	7.901	0.3081
	43.77	11.92	0.2725
	66.72	17.34	0.2600
	*83.95	21.82	0.2599
	103.6	27.43	0.2648
	124.3	33.99	0.2735
	153.8	44.62	0.2901
	210.2	69.32	0.3298
	289.3	114.0	0.3940

TABLE 1 (*Continued*).

Solute	$10^3 C$ (mol l^{-1})	$10^6 K_{sp}$ (ohm^{-1} cm^{-1})	Λ (ohm^{-1} cm^2 equiv^{-1})
NaO_2CCF_3	0.6764	1.335	1.974
	1.403	1.990	1.418
	2.695	2.864	1.063
	5.420	4.282	0.7901
	12.42	7.093	0.5713
	25.94	11.66	0.4496
	37.07	15.26	0.4116
	58.61	22.89	0.3906
	*70.96	27.70	0.3903
	81.78	32.23	0.3941
	100.6	40.88	0.4064
	130.6	57.00	0.4364
KO_2CCF_3	0.3085	1.777	5.760
	0.5498	2.459	4.472
	0.9791	3.412	3.485
	2.624	6.085	2.319
	5.425	9.560	1.762
	9.722	14.14	1.455
	13.87	18.33	1.321
	17.81	22.28	1.251
	21.36	25.91	1.213
	24.77	29.45	1.189
	28.05	32.96	1.175
	31.10	36.33	1.168
	34.12	39.75	1.165
	*36.12	42.99	1.164
	39.63	46.27	1.167
	42.29	49.56	1.172
	47.49	56.11	1.182
	54.17	65.18	1.203
$NH_4O_2CCF_3$	0.2120	1.779	8.394
	0.6239	3.327	5.333
	1.391	5.299	3.908
	2.146	6.864	3.197
	4.293	10.60	2.470
	8.373	16.64	1.987
	11.45	20.90	1.826
	15.75	26.82	1.703
	19.74	32.40	1.642
	22.88	36.93	1.614
	27.15	43.27	1.594
	*31.51	50.01	1.587
	35.43	56.34	1.590
	39.30	62.90	1.600
RbO_2CCF_3	0.5003	3.042	6.080
	1.143	4.965	4.344
	2.315	7.624	3.294
	6.590	15.08	2.288
	11.97	23.36	1.952
	17.16	31.34	1.826
	21.55	38.31	1.778
	26.40	46.36	1.756
	*30.11	52.81	1.754
	33.80	59.54	1.762
	39.46	70.42	1.785
	44.80	81.35	1.816
	54.47	103.0	1.890
	67.32	135.0	2.005

Can. J. Chem. Downloaded from www.nrcresearchpress.com by 210.87.254.42 on 09/05/12
For personal use only.

TABLE 1 (*Concluded*).

Solute	$10^3 C$ (mol l^{-1})	$10^6 K_{sp}$ (ohm^{-1} cm^{-1})	Λ (ohm^{-1} cm^2 equiv^{-1})
CsO_2CCF_3	0.2019	2.357	11.68
	0.8139	5.526	6.789
	1.832	9.143	4.990
	6.241	20.83	3.337
	11.31	32.92	2.909
	17.92	49.05	2.738
	*22.50	60.96	2.710
	25.96	70.41	2.712
	28.71	78.20	2.723
	31.84	87.41	2.745
	37.27	104.3	2.798
	42.43	121.4	2.862
$CsB(O_2CCF_3)_4$	0.3395	3.947	11.63
	0.6348	5.840	9.200
	1.343	9.248	6.886
	2.977	14.84	4.985
	5.075	21.00	4.137
	8.387	29.86	2.560
	13.08	42.30	3.235
	18.31	56.09	3.063
	23.24	69.51	2.990
	27.42	81.31	2.963
	*31.23	92.45	2.960
	34.48	102.2	2.963
SbF_5	0.2862	1.396	4.876
	0.3349	1.551	4.631
	1.031	3.218	3.121
	2.251	5.210	2.314
	3.568	6.935	1.944
	4.767	8.334	1.748
	9.704	13.29	1.370
	18.34	20.97	1.144
	29.67	30.78	1.037
	37.35	37.63	1.008
	43.57	43.36	0.9948
	*51.98	51.45	0.9898
	57.02	56.45	0.9899
	62.56	62.13	0.9932
	71.55	71.79	1.003
	84.41	86.56	1.026
	99.94	105.8	1.059
$B(O_2CCF_3)_3$	0.3848	0.4545	1.181
	0.9063	0.5957	0.6573
	1.822	0.7387	0.4053
	6.438	1.200	0.1864
	13.28	1.692	0.1274
	22.83	2.230	0.0977
	40.55	2.999	0.0740
	56.12	3.535	0.0630
	70.87	3.968	0.0560
	83.56	4.299	0.0514
	95.66	4.587	0.0480
	106.7	4.828	0.0452

*Concentration at the lowest observed conductivity.

Can. J. Chem. Downloaded from www.nrcresearchpress.com by 210.87.254.42 on 09/05/12
For personal use only.

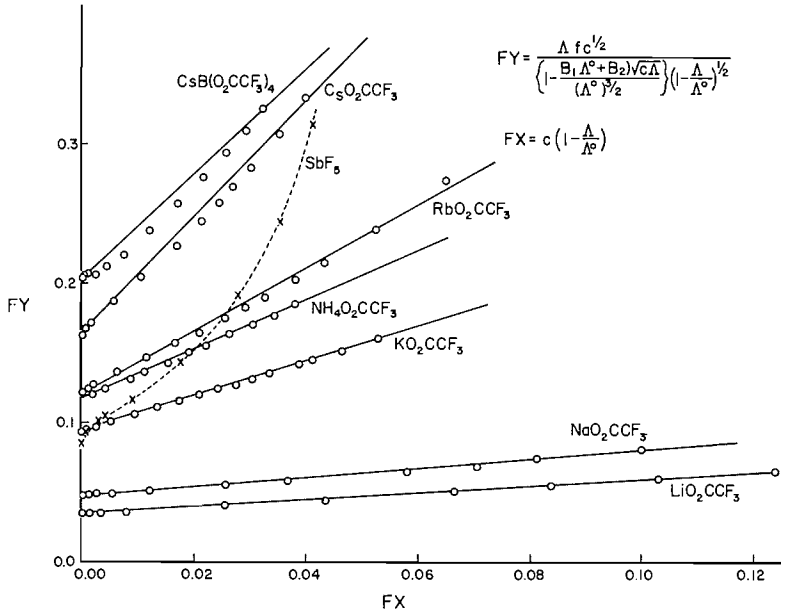

FIG. 1. Triple-ion plots with long-range interionic effects allowed for (eq. 2).

tion of $\sqrt{K_D}$ between the slope and intercept gives

$$\frac{\text{Intercept}}{\text{Slope}} = \frac{\Lambda}{\Lambda_T^0} k$$

and a knowledge of the ratio of $\Lambda^\circ/\Lambda_T^0$ permits evaluation of the triple-ion dissociation constant, k. Various assumptions and estimates of this ratio ranging from 0.33 to 0.82 have been used (5, 7, 15).

The results of the plot by the method of least squares of both eqs. 1 and 2 are given in Table 2 and the plots for eq. 2, are shown in Fig. 1. In the evaluation of eq. 2, the extended Debye–Hückel expression for the activity coefficient was used with "a", the distance of closest approach, set at the value for the ion-pair (10). Since the proportion of single ions to triple-ions will change with concentration, "a" will be a function of concentration but this effect will be small and has been ignored in this treatment. Both K_D from the Fuoss plot (ion-pair region) (10) and that calculated from the triple-ion plot intercept, using Λ° from the Fuoss extrapolation (10), (K_D') are given in Table 2 as well as the % error in K_D' as determined from the mean % deviation of the experimental points from the line. The triple-ion dissociation constants have been determined assuming $\Lambda_D^0/\Lambda^0 = 0.43$. This ratio is arrived at by assuming Stoke's law dependence of mobility on ion diameter and taking the average triple-ion diameter to be 7/3 that of the single ions, that is the average for the three orientations of the triple ion along the Cartesian coordinates. From the data in Table 2 it may be seen that for all but the solutes $B(O_2CCF_3)_3$ and SbF_5, the more refined treatment (eq. 2) gives a better description of the behavior as judged by the % error in K_D' and the excellent agreement between the ion-pair dissociation constant calculated from the triple-ion plot (K_D') and that from the Fuoss extrapolation (K_D). From Fig. 1, however, it may be seen that serious departures from straight line behavior occur for some of the solutes, especially those with low single ion mobilities. Positive deviations of FY (see Fig. 1) are expected for solutes with small Λ^0 since in such cases the denominator of FY will approach zero at relatively low concentrations; that is when

$$\frac{(B_1\Lambda^0 + B_2)\sqrt{c\Lambda}}{(\Lambda^0)^{3/2}} \approx 1$$

For example the denominator of FY becomes zero for SbF_5 when $c = 0.067$ M. The source of

Can. J. Chem. Downloaded from www.nrcresearchpress.com by 210.87.254.42 on 09/05/12
For personal use only.

Can. J. Chem. Downloaded from www.nrcresearchpress.com by 210.87.254.42 on 09/05/12
For personal use only.

TABLE 2. Triple-ion and ion-pair dissociation constants calculated from plots of eqs. 1 and 2

Solute	Λ°* ($ohm^{-1} cm^2 equiv^{-1}$)	$10^5 K_D$* ($mol l^{-1}$)	Plot of eq. 1			Plot of eq. 2		
			$10^5 K_D'$ ($mol l^{-1}$)	% error on K_D'	k ($mol l^{-1}$)	$10^5 K_D'$ ($mol l^{-1}$)	% error on K_D'	k ($mol l^{-1}$)
LiO_2CCF_3	112	0.0098	0.0099	27.8	0.0268	0.0092	3.8	0.0563
NaO_2CCF_3	73.79	0.0398	0.0498	8.5	0.0289	0.0398	3.8	0.0600
KO_2CCF_3	63.73	0.219	0.286	4.9	0.0146	0.218	1.6	0.0326
$NH_4O_2CCF_3$	54.73	0.455	0.614	6.7	0.0125	0.456	0.9	0.0286
RbO_2CCF_3	58.60	0.422	0.585	6.0	0.0110	0.422	4.3	0.0232
CsO_2CCF_3	52.41	1.01	1.35	8.9	0.0086	1.00	5.7	0.0172
$CsB(O_2CCF_3)_4$	48.56	1.72	2.38	7.6	0.0109	1.67	4.8	0.0229
$B(O_2CCF_3)_3$	22.34	0.122	0.0629	17.2	−ve	0.0524	19.0	−ve
SbF_5	18.77	1.75	2.94	12.9	0.0185	12.5	46.0	−ve

*As determined by Fuoss extrapolation (10) except in the case of LiO_2CCF_3.

Can. J. Chem. Downloaded from www.nrcresearchpress.com by 210.87.254.42 on 09/05/12
For personal use only.

these departures may be traced back to the use of the Limiting Law for electrical conductance in the derivation of eq. 2.

No minimum in equivalent conductivity is observed for the solute $B(O_2CCF_3)_3$ up to 0.1 *M*. This solute is known to weakly ionized (as opposed to dissociated) (11) and the concentration of ions and ion-pairs is probably not sufficiently high to permit triple-ion formation at the concentrations studied.

Evaluation of Λ^0 from Electrical Conductivity Measurements in the Triple-ion Region

For most of the solutes studied the agreement between K_D, calculated from the Fuoss extrapolation and that determined from the intercept of the triple-ion plot using eq. 2, was sufficiently good that an attempt was made to evaluate Λ^0 for LiO_2CCF_3, for which Fuoss extrapolation was not possible (10), in the following way. A series of K_D were generated for various values of "*a*" by use of the theoretical Fuoss equation for ion-pair dissociation (ref. 6, p.213). From these, using the highest concentration specific conductance point in the ion-pair region (10^3 $c = 0.1797$ mol l^{-1}; 10^6 $K_{sp} = 0.4906$ ohm^{-1} cm^{-1}), which should be the least affected by solvent self-dissociation or impurity ions (see (10)), a series of Λ^0 were calculated, using the expressions for Λ and K_D applicable in the ion-pair region (10). The Λ^0 were then used to extrapolate the data for the triple-ion region and to evaluate K_D' from the intercepts. The best Λ^0 was that which gave the closest agreement between the K_D assumed and that calculated from data in the triple-ion region. Table 3 gives a list of Λ^0 for the univalent trifluoroacetates calculated in this way. Λ^0 from Fuoss extrapolations are given for comparison. The data show that the procedure gives a reasonably accurate estimate of Λ^0. The Li^+ ion is more mobile than the Na^+ ion in trifluoroacetic acid, continuing the trend of greater mobility for the smaller cation and emphasizing further the low solvating capacity of this solvent for cations (10).

Comparison with the Theoretical Expressions for k_T

The order of the triple-ion dissociation constants in Table 2 as determined by either eq. 1 or 2, in relation to ion size, is interesting. The triple-ions of the univalent trifluoroacetates from

TABLE 3. Comparison of Λ^0 (ohm^{-1} cm^2 equiv^{-1}), calculated from the ion-pair (Λ^0) and triple-ion ($\Lambda^{0\prime}$) regions

Solute	Λ^0	Λ^0
LiO_2CCF_3	—	112
NaO_2CCF_3	73.79	73
KO_2CCF_3	63.73	66
$NH_4O_2CCF_3$	54.73	54
RbO_2CCF_3	58.60	59
CsO_2CCF_3	51.76	56

NaO_2CCF_3 to CsO_2CCF_3 are more dissociated the smaller the cation; exactly the opposite to the change in degree of dissociation of the ion-pair to single ions and to that predicted on electrostatic grounds alone. The trend in k is reversed, however, for LiO_2CCF_3 and $CsB(O_2CCF_3)_4$ in as much as the triple-ions of LiO_2CCF_3 are less dissociated than those of NaO_2CCF_3 and those of $CsB(O_2CCF_3)_4$ are more dissociated than for CsO_2CCF_3.

Two theoretical expressions for the triple-ion dissociation constant have been derived. The Fuoss–Kraus expression (5) is given by

$$[3] \qquad k^{-1} = \frac{2\pi Na^3}{1000} I(b)$$

where "*a*" is the distance of closest approach of the ion to the ion-pair and $I(b)$ is a tabulated function. This expression is analogous to that for ion-pair dissociation derived by Bjerrum and suffers from the same objections in ignoring the molecularity of the solvent. Fuoss has derived an expression for triple-ion dissociation based upon a molecular approach

$$[4] \qquad k^{-1} = \frac{\pi Na^3}{1000} \exp\,(b/2 - 3 - E_s/kT)$$

$$b = \frac{z_1 z_2 e^2}{\varepsilon kTa}$$

and E_s is the solvation energy change occurring on association of the ion-pair and the ion (other constants are defined above or in (8)). The -3 in the exponential function allows for the entropy change associated with the solute species (6).

Table 4 gives a comparison of calculated k with experimental values. For evaluation of the theoretical expression "*a*" has been set equal

Can. J. Chem. Downloaded from www.nrcresearchpress.com by 210.87.254.42 on 09/05/12
For personal use only.

TABLE 4. Comparison of observed and theoretical triple-ion dissociation constants

Solute	b	a^3 (Å^3)	$I(b)$	$10^2 k(I(b))$ (mol l^{-1})	$e^{b/2}$	$e^{b/2-3}$	Partial Z (e)	$e^{b/2}$ (partial Z)	$10^2\, k_{b/2}$ (mol l^{-1})	$10^2\, k_{b/2-3}$ (mol l^{-1})	$10^2\, k_{b/2}$ (partial Z) (mol l^{-1})	Observed $10^2\, k$ (mol l^{-1})
LiO_2CCF_3	12.76	144	1.895	0.968	590.0	28.9	0.65	62.8	0.62	12.7	5.85	7.86
NaO_2CCF_3	11.01	223	1.665	0.711	244.7	12.2	0.67	40.1	0.97	18.6	5.95	8.38
KO_2CCF_3	9.63	333	1.480	0.535	124.0	6.17	0.76	38.5	1.28	25.8	4.13	4.56
$NH_4O_2CCF_3$	9.00	408	1.387	0.449	90.0	4.48	—	—	1.44	29.0	—	4.00
RbO_2CCF_3	9.07	399	1.400	0.772	93.0	4.66	0.79	35.9	1.43	28.5	3.70	3.24
CsO_2CCF_3	8.82	517	1.282	0.398	64.0	3.19	0.83	31.5	1.60	31.1	3.25	2.40
$CsB(O_2CCF_3)_4$	7.82	623	1.203	0.352	49.9	2.48	0.83*	25.8	1.70	34.3	3.30	3.20

*This may be an underestimate depending upon the electronegativity of $[B(O_2CCF_3)_4]$ which has been assumed equal to that of Cl.

Can. J. Chem. Downloaded from www.nrcresearchpress.com by 210.87.254.42 on 09/05/12
For personal use only.

to 1.5 × the value of "a" for the ion-pair. It may be seen that the earlier theoretical expression (eq. 3) predicts the observed general trend in k with increasing cation size although the behavior of LiO_2CCF_3 and $CsB(O_2CCF_3)_4$ is not accounted for.

For the evaluation of the Fuoss expression (eq. 4) a value for E_s is required and this has been determined in only one instance (ref. 6, p. 262). Table 4 shows, however, that, calculation using eq. 4 with exp ($b/2$) or exp ($b/2 - 3$) gives changes in k with the opposite general trend to that observed. E_s for association would very probably be positive, since there is a change from solvation of two species, one a relatively small single ion, to solvation of a large triple-ion. Moreover, E_s would be small in comparison to $b/2$ and therefore, the use of exp ($b/2 - 3 - E_s/kT$) would not have a large effect on k and, if anything, would exaggerate the trend towards greater dissociation with large ions since the magnitude of the exponential term would be smaller. It should be noted, however, that E_s would be larger in the smaller ion case and this effect, while small, would offset the general trend towards greater association for the smaller ion predicted.

The basis of the derivation of eq. 4 provides some insight into the trend of change in k with ion size and suggests a possible modification of the expression to account for the trend. The triple-ion dissociation constant is an inverse function of the collision volume of the ion pair and the Boltzmann factor associated with the energy change upon association (6):

$$k^{-1} \propto [\text{collision volume}][e^{b/2}]$$

Thus as ion size increases: (a) the collision volume increases and triple-ion dissociation decreases; (b) working in the opposite direction, the energy released upon association decreases and the triple-ion dissociation increases. Obviously, the general trend in Table 4 shows that collision volume is predominant and the exponential factor has a smaller effect than allowed for in the Fuoss expression.

The Boltzmann factor is determined assuming the ions in the contact ion-pair have unit charge; however, mutual polarization will result in a net reduction in charge. Allowance for this effect reduces the sharp fall-off in the exponential term with increasing ion size and the volume factor becomes predominant in determining k. Estimation of the partial ionic charge on the ions in an ion-pair may be made by considering the relative electronegativities of the cation and anion (16). No experimental value for the electronegativity of the $[CF_3CO_2]$ group is available in the literature but the comparable acid strengths of HO_2CCF_3 and HCl and comparable electronegativities of Cl and the average of the atoms making up the $[CF_3CO_2]$ group, suggest that the electronegativity of Cl should be a fair approximation. The partial charges, $e^{b/2}$ factors and k from this calculation are listed in Table 4. It may be seen that consideration of partial charge reproduces the relative order of k observed experimentally. The observed and theoretical k differ in magnitude, but better agreement would be achieved if the entropy change in both solute and solvent and the enthalpy change upon dissociation were considered since these would have the effect of making the exponential term smaller and, thus, k larger. Completely satisfactory agreement would also require improvements in the treatment of the electrical conductivity data such as allowance for different triple-ion dissociation constants, k_+ and k_-, use of a conductance equation other than the Limiting Law, consideration of the variation in "a" with concentration and evaluation of the ratio, Λ_T^0/Λ^0.

Conclusion

The dissociation behavior of triple-ions in trifluoroacetic acid is, in general, opposite to that of their respective ion-pairs; that is, the triple-ions formed with the smaller cation are more dissociated. That this is so is readily seen by comparing Λ at comparable concentrations in the triple-ion region for different solutes in Table 1. A plot of Λ *vs.* c for acetates in acetic acid from data in the literature (3, 17) shows analogous behavior. For trifluoroacetic acid, at the two ends of the scale of ion size (LiO_2CCF_3 and $CsB(O_2CCF_3)_4$), in terms of the Fuoss expression for k (eq. 4), the Boltzmann factor predominates and the solute triple-ions containing Li are less dissociated than those of Na with the larger cation; similarly, the triple-

ions of CsO_2CCF_3 are less dissociated than those of $CsB(O_2CCF_3)_4$, which has the larger anion. However for the remaining solutes, excluding SbF_5 which is an acid and not readily compared to the others, the size of the solute species and their collision probability predominates; thus, the triple-ions containing the larger cation are the least dissociated.

The National Research Council of Canada is thanked for financial assistance and M.G.H. thanks the Council for the award of a bursary.

1. E. C. FRANKLIN. Z. Phys. Chem. **69**, 272 (1909).
2. E. C. FRANKLIN. J. Phys. Chem. **15**, 675 (1911).
3. K. HOPFGARTNER. Monatsh. **33**, 123 (1912).
4. M. E. PEACH and T. C. WADDINGTON. J. Chem. Soc. 69 (1963).
5. R. M. FUOSS and C. A. KRAUS. J. Am. Chem. Soc. **55**, 2387 (1933).
6. R. M. FUOSS and F. ACCASCINA. Electrolytic conductance. Interscience, New York. 1959.
7. R. J. L. MARTIN. Aust. J. Chem. **16**, 84 (1963).
8. R. A. ROBINSON and R. H. STOKES. Electrolyte solutions. Butterworths, London. 1965.
9. C. W. DAVIES. Ion association. Butterworths, London. 1962. p. 105.
10. M. G. HARRISS and J. B. MILNE. Can. J. Chem. **49**, 1888 (1971).
11. M. G. HARRISS and J. B. MILNE. Can. J. Chem. **49**, 3612 (1971).
12. C. EABORN, P. M. JACKSON, and R. TAYLOR. J. Chem. Soc. B, 613 (1966).
13. H. C. BROWN and R. A. WIRKKALA. J. Am. Chem. Soc. **88**, 1447 (1966); **88**, 1453 (1966); **88**, 1456 (1966).
14. A. HIMOE and L. M. STOCK. J. Am. Chem. Soc. **91**, 1452 (1969).
15. G. S. BIEN, C. A. KRAUS, and R. M. FUOSS. J. Am. Chem. Soc. **56**, 1860 (1934).
16. R. T. SANDERSON. Inorganic chemistry. Reinhold, New York. 1967. p. 82.
17. I. M. KOLTHOFF and A. WILLMAN. J. Am. Chem. Soc. **56**, 1007 (1934).

Can. J. Chem. Downloaded from www.nrcresearchpress.com by 210.87.254.42 on 09/05/12
For personal use only.

Some Mixtures of Carbon Tetrachloride with Several *n*-Alkanes: Enthalpies and Energies of Mixing[1]

JAMES M. BERRYMAN[2] AND E. L. HERIC[3]

Department of Chemistry, University of Georgia, Athens, Georgia 30601

Received June 14, 1971[4]

Molar enthalpies of mixing for the five *n*-alkanes from pentane through nonane with carbon tetrachloride at 298.15 K have been measured. The maximum values are, with increasing chain length, 295, 315, 339, 373, and 417 J. Energies calculated from the enthalpies are compared with the lattice theory of mixtures. The comparison is also extended through hexadecane, using previously reported results.

Nous avons mesuré les enthalpies molaires de mélange de cinq *n*-alcanes, du pentane au nonane, avec le tétrachlorure de carbone à 298.15 K. Avec la longueur de chaîne croissante, les valeurs maximales sont, 295, 315, 339, 373 et 417 J. Nous comparons les énergies calculées à partir des enthalpies avec la théorie des réseaux de mélanges. Nous étendons la comparaison à l'hexadécane au moyen de résultats publiés antérieurement.

[Traduit par le journal]

Canadian Journal of Chemistry, **50**, 3799 (1972)

Can. J. Chem. Downloaded from www.nrcresearchpress.com by 210.87.254.42 on 09/05/12
For personal use only.

Introduction

Previous workers have considered Guggenheim's lattice theory of mixtures (1) for binary systems of *n*-alkanes and a dissimilar common second component. For example, Gainey and Young (2) found that the activity coefficients of benzene at infinite dilution in the alkanes from *n*-C_5 through *n*-C_{32} were adequately explained by this approach. Vesely (3) reported, however, that the theory agreed to a degree with experimental molar energies of mixing of cyclohexane with *n*-alkanes which ranged from very good to semi-quantitative as the chain length increased from *n*-C_6 to *n*-C_{16}.

Everett and Swinton (4), commented in 1963 on possible "genuine departures" of their results from lattice theory behavior. The theory continues to be examined, both in its originally intended application to *r*-meric mixtures and in extensions to nonhomologous mixture components.

We report here molar enthalpies of mixing of carbon tetrachloride with the *n*-alkanes from *n*-C_5 through *n*-C_9. (For brevity in this paper we shall label a carbon tetrachloride–*n*-alkane system by identifying only the alkane.) Molar energies of mixing have been calculated therefrom, and the lattice theory has been applied to these data, as well as to the results of others from *n*-C_6 through *n*-C_{16} (5–7). This represents the extent to which the theory may reasonably be considered now relative to these systems.

Experimental Section

Calorimetric Apparatus

The design of the calorimeter was essentially the same as that of Adcock and McGlashan (8). Two liquids are mixed under mercury so that no vapor phase is present. The temperature was followed with a ten-junction copper–constantan difference couple and a reflecting galvanometer. The heater was constructed of about 40 cm of B and S No. 38 constantan wire wound noninductively onto a glass bell. The amount of heat introduced was determined by measuring the voltage drop across the calorimeter heater, the current through the heating circuit, and the time of heating. A Leeds and Northrup K-1 potentiometer and one circuit of an L and N x_1–x_2 recorder were used for the voltage measurements. A 1-ohm standard resistor, another K-1 potentiometer, and the other circuit of the recorder were used to measure the current.

Procedure

The two liquids were mixed as previously described (8). Typically the total mixture volume was 1 to 2 ml. A measured amount of heat was added as soon as possible after mixing to compensate for, as nearly as possible, the heat absorbed on mixing. The heat capacity of the loaded calorimeter was then determined by measuring the temperature rise caused by the addition of another measured quantity of heat. This heat capacity was used to correct for the off-balance of the opposing heat effects occurring during the simultaneous mixing and heater operation. Possible errors of the design have been described (8).

The calorimeter was tested with the system benzene + carbon tetrachloride at 298.15 K. Larkin and McGlashan summarized heats of mixing for this system reported prior

[1]Presented, in part, at the combined Southeast-Southwest Meeting, ACS, New Orleans, Louisiana, December 1970.

[2]Present address: Department of Chemistry, West Georgia College, Carrollton, Georgia.

[3]To whom correspondence should be addressed.

[4]Revision received August 21, 1972

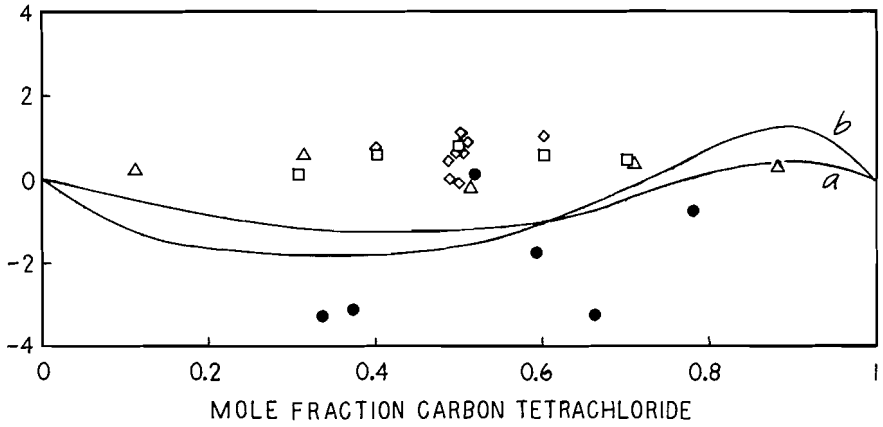

FIG. 1. Deviations (J mol^{-1}) of heats of mixing of carbon tetrachloride + benzene at 298.15 K from the values of Larkin and McGlashan (9). ●, this work; □, Larkin and McGlashan, added in proof in ref. 9; ◇, Larkin and Scott (10); △, Lewis and Johnson (11). Curves are the smoothed results reported in (*a*), ref. 12 and (*b*), ref. 13.

to their own work (9). The latter is generally several J mol^{-1} higher than prior work. In Fig. 1, our calibration results are compared with those of Larkin and McGlashan, and with other values subsequently reported for this system (10–13). Our results fall somewhat below the others, although the disagreement is not considerable. It may be due to incomplete mixing, which is a hazard of the calorimeter design. A smooth curve through our calibration results shows that $(\Sigma d^2/n)^{1/2}$ is 1.2 J mol^{-1}, where d is the difference between a smoothed H^E and the corresponding unsmoothed value, and n is the number of results.

Materials

All of the components were purified by double distillation through a four-foot Vigreux column at atmospheric pressure over CaH_2. The middle third of the product of each distillation was recovered. The final product was tested for reactivity with mercury. No color change on the mercury surface was evident after 48 h of stirring in contact with the final product.

The refractive indices of the compounds were determined at 298.15 K with a Bausch and Lomb Precision Refractometer with the Na-D line. For carbon tetrachloride the value was 1.45729 (lit., 1.45704 (14)), and for benzene, 1.49760 (lit., 1.49792 (15)). For the *n*-alkanes in order of increasing chain length, the values were 1.35457, 1.37216, 1.38495, 1.39521, and 1.40304 (lit., 1.35472, 1.37226, 1.38511, 1.39505, and 1.40311 (15)). A gas chromatogram was also obtained for each liquid and no significant amounts of impurities were detected.

Results and Discussion

Experimental H^E at 298.15 K are listed in Table 1. They were fitted by the method of least-squares to

$$[1] \quad \frac{H^E}{x_1 x_2} = A + B(x_1 - x_2) + C(x_1 - x_2)^2 + \ldots$$

with a digital computer. Each datum was statistically weighted on the basis of the uncertainty in the product $x_1 x_2$ (16). Two coefficients were sufficient to fit each system, although more might be required with measurements of greater precision and over a greater range of mixture compositions. The values of the coefficients and the standard deviations are given in Table 1. Throughout this work x_1 is the mole fraction of carbon tetrachloride.

Table 1 shows that the quality of H^E data in the alkane systems is considerably less than what would be predicted from the calibration results. Several factors may account for this. (*1*) The calorimeter design, in which stirring results from the turbulence during the rise of the less dense through the more dense liquid, is decreasingly effective as the viscosities of the alkanes increase with increasing chain length. (*2*) Extrapolation of the time-temperature curves is increasingly uncertain as H^E grows larger with greater alkane chain length. (*3*) Manipulation of the shorter-chained alkanes involves risk of error through their high volatility.

Experimental H^E were also fitted to a volume fraction equation analogous to eq. 1. This also required two coefficients and yielded essentially the same percent deviation as eq. 1.

Present results are briefly compared with previous values in Table 2, all smoothed with with eq. 1. Tabular, rather than graphical, comparison has been used to provide a more incisive basis for noting the effect of these disagreements

Can. J. Chem. Downloaded from www.nrcresearchpress.com by 210.87.254.42 on 09/05/12
For personal use only.

Can. J. Chem. Downloaded from www.nrcresearchpress.com by 210.87.254.42 on 09/05/12
For personal use only.

TABLE 1. Heats of mixing for carbon tetrachloride + *n*-alkanes, unsmoothed results (298.15 K)

System*	(X_1)	H^E (J mol^{-1})	U^E (J mol^{-1})
CCl_4–pentane	0.2232	196	188
	0.3875	262	250
	0.4992	297	284
	0.6223	287	274
	0.7500	222	211
	0.8506	158	150
CCl_4–hexane	0.1438	144	124
	0.2621	230	198
	0.3867	280	239
	0.4709	316	272
	0.4939	316	272
	0.7486	260	224
CCl_4–heptane	0.1520	137	114
	0.2522	215	177
	0.3849	306	251
	0.6422	332	264
	0.7560	273	212
CCl_4–octane	0.1548	153	117
	0.3904	317	237
	0.5095	369	277
	0.5131	361	269
	0.6394	378	284
	0.8066	286	214
CCl_4–nonane	0.1423	120	79
	0.2431	220	152
	0.3692	311	214
	0.6326	420	300
	0.7251	403	291
	0.7785	335	234
	0.8408	273	190

*For the systems in order of increasing chain length, the coefficients of eq. 1 as A, B J mol^{-1} ± standard per cent deviation in H^E are: 1168, 108, 2.4; 1257, 152, 4.1; 1339, 341, 2.5; 1458, 593, 4.2; 1576, 799, 3.1.

on lattice theory calculations below. The systems *n*-C_5 and *n*-C_9 have not previously been reported.

In the *n*-C_6 system present results, within experimental error, agree with those of Bissell *et al.* (6) up to $x_1 \sim 0.6$ and with those of Jain *et al.* (5) beyond. For *n*-C_7, present results and those of Bissell agree up to $x_1 \sim 0.75$ and are generally greater than those of Jain *et al.* For this system the results of Vilcu and Stanciu (7) agree so poorly with the other three sources that that work was excluded from further consideration here. For *n*-C_8 present results agree with those of Jain *et al.* up to $x_1 \sim 0.8$. In summary, while there are some regions of agreement between the three data sources retained, there are significant differences.

From lattice theory with the zeroth approximation (1),

$$[2] \qquad U^E = x_1 x_2 ru/(x_1 + x_2 r)$$

where U^E is the molar energy of mixing at constant volume, r is a molecular size ratio, and u is the interaction energy parameter. U^E have been calculated from H^E with Scatchard's equation (17)

$$[3] \qquad U^E = H^E - T\alpha V^E/\beta$$

where T is absolute temperature, α the thermal expansion coefficient, β the isothermal compressibility, and V^E the molar excess volume of mixing. For mixtures, α and β were obtained with

$$[4] \qquad \alpha = \phi_1'\alpha_1 + (1 - \phi_1')\alpha_2$$

TABLE 2. Comparison of present enthalpies of mixing with some previously reported results, smoothed values (298.15 K)

		Enthalpies of mixing (J mol^{-1})			
System	x_1	This work	Reference 5	Reference 6	Reference 7
	0.2	187	162	183	
CCl_4–hexane	0.5	314	296	316	
	0.8	216	215	231	
	0.2	182	149	192	232
CCl_4–heptane	0.5	335	301	339	398
	0.8	240	230	256	226
	0.2	176	181		
CCl_4–octane	0.5	364	355		
	0.8	289	315		

TABLE 3. Some physical properties of carbon tetrachloride and *n*-alkanes and their equimolar mixtures (298.15 K)*

Compound	V (ml mol^{-1})	$10^3\alpha$† (deg^{-1})	$10^4\beta$ (atm^{-1})	V^E ($x_1 = 0.5$) (ml mol^{-1})
Carbon tetrachloride	86.903[14]	1.221	1.091[18]	
Pentane	116.104[15]	1.557	2.17[19]	0.05§
Hexane	131.600[15]	1.388	1.627[20]	0.16[24]
Heptane	147.459[15]	1.247	1.475[21]	0.23[25]
Octane	163.534[15]	1.150	1.307[21]	0.32[25]
Nonane	179.675[15]	1.064	1.175‡	0.39§
Dodecane	228.597[15]	0.945	0.996[21]	0.52[25]
Hexadecane	294.105[15]	0.902	0.881[21]	0.62[24]

*Superscripts denote reference numbers.
†Obtained with $\alpha = \Delta V/V\Delta T$, using source cited for V and $\Delta T = 5$ °C.
‡Obtained by extrapolation to 298.15 K of a plot (22) of log β *vs.* T (23).
§Obtained with a procedure described in text.

[5] $$\beta = \phi_1'\beta_1 + (1 - \phi_1')\beta_2$$

where α_i and β_i are those of the pure components and

[6] $$\phi_1' = x_1V_1/(x_1V_1 + x_2V_2)$$

is the volume fraction (ideal). V_i is the molar volume of pure component *i*. V_i, α_i, and β_i, and V^E at equimolarity are given in Table 3. U^E for the present work are given in Table 1. $T\alpha V^E/\beta$ increases with alkane chain length, becoming 158 and 198 J mol^{-1} for the *n*-C_{12} and *n*-C_{16} systems, respectively, at equimolarity.

The uncertainty in $T\alpha V^E/\beta$ in the seven systems is largely due to that in V^E values, which in some instances can only be estimated. Alternative values of β_i for *n*-C_6 (21) and *n*-C_8 (20), differing from those in Table 3 by about 10^{-5} atm^{-1} and of apparently equal dependability, exist, but they lead to conclusions agreeing with those given below.

For the *n*-C_6 and *n*-C_{16} systems V^E were calculated from equations given by Heric and Brewer (24)

[7] $$V^E = x_1x_2[A' + B'(x_1 - x_2) + C'(x_1 - x_2)^2 + \ldots]$$

For the *n*-C_7, *n*-C_8, and *n*-C_{12} systems V^E reported by Jain *et al.* (25) were smoothed with eq. 7. Bissell *et al.* (6) have also reported V^E for the systems of *n*-C_6 and *n*-C_7. Their results for the latter are in good agreement with those of Jain *et al.*, but for the former are over 0.1 ml mol^{-1} at equimolarity below values reported in the above two sources.

V^E have not been reported for the systems of *n*-C_5 and *n*-C_9. These were estimated by a procedure adapted from Desmyter and van der Waals (26), who found that for *n*-alkane + *n*-alkane mixtures V^E at equimolarity were linearly related to a function of the chain lengths of the components n_i and n_i', $[1/(n_i + 1) - 1/(n_i' + 1)]^2$. The plot is also linear for the present type of system from *n*-C_6 through *n*-C_{16}, using the combined equimolar data of Heric and Brewer (24) and Jain *et al.* (25), with $n_i = 1$ for carbon tetrachloride and n_i' as the alkane chain length. For the eight systems plotted, equimolar V^E are randomly distributed about the least-squares line, with $[\sum d^2/n]^{1/2} = \pm 0.03$ ml/mol, where d is the deviation of equimolar V^E for the n systems. A' for use in eq. 7 were obtained from this plot for the systems of *n*-C_5 (extrapolation) and *n*-C_9 (interpolation).

B' values for these two systems were obtained with a plot B' *vs.* alkane chain length in the systems from *n*-C_6 through *n*-C_{12}. Over this range B' is distributed randomly about a monotonic curve increasing with alkane chain length, with $[\sum d^2/n]^{1/2} = \pm 0.15$ ml mol^{-1} in B values. This is equivalent to a maximum effect of ± 0.01 ml mol^{-1} in V^E. These procedures yield $V^E = x_1x_2$ [0.20] and $V^E = x_1x_2[1.56 + 0.51\ (x_1 - x_2)]$ for the *n*-C_5 and *n*-C_9 systems, respectively.

We estimate that the uncertainty in V^E at equimolarity is no greater than ± 0.03 ml mol^{-1} for the systems from *n*-C_5 through *n*-C_{16}, and is generally less. This produces an uncertainty in $T\alpha V^E/\beta$ at equimolarity which varies from about 6 to 10 J mol^{-1} over the range of alkanes listed in Table 3.

Can. J. Chem. Downloaded from www.nrcresearchpress.com by 210.87.254.42 on 09/05/12
For personal use only.

TABLE 4. Values of r and u in eq. 2 (298.15 K)

System	$r \pm$ std. dev.; $u \pm$ std. dev. (J mol^{-1})			Ratio of component molar volumes
	This work	Reference 5	Reference 6	
CCl_4–pentane	1.16±0.07; 1037±42			1.20
CCl_4–hexane	1.35±0.07; 948±40	1.64±0.17; 797±56	1.52±0.03; 904±11	1.35
CCl_4–heptane	1.58±0.13; 861±66	2.23±0.28; 669±80	1.45±0.05; 939±19	1.52
CCl_4–octane	2.04±0.07; 812±35	2.67±0.18; 745±53		1.68
CCl_4–nonane	3.15±0.22; 668±35			1.85
CCl_4–dodecane		5.26±0.24; 581±35		2.35
CCl_4–hexadecane		13.89±1.32; 445±82		3.03

In calculating r and u from U^E and x in eq. 2, we have followed the method of Everett and Swinton (4), which is iterative. Values of r are adjusted to obtain the parameter u independent of concentration. It has been shown (4, 27) that u varies linearly with $\phi_1 = x_1/(x_1 + x_2 r)$ for r values near that sought. Thus the "best" r is that for which $du/d\phi_1 = 0$ in the linear plot of $du/d\phi_1$ *vs.* r. From the best r value, the mean value of u is obtained with eq. 2. $du/d\phi_1$, the r for which $du/d\phi_1 = 0$, and the mean value of u were all obtained here using the method of least-squares.

Values of r and u and their uncertainties, for both the present data and those of the two previous works (5, 6) are given in Table 4, along with the ratio of molar volumes of each component pair. The data of Bissell *et al.* (6) exhibit the least uncertainty in r and u, and they indicate almost the same values of r and of u in the *n*-C_6 and *n*-C_7 systems. The data of Jain *et al.* (5) show the greatest scatter, but indicate a trend of increasing r and decreasing u with increasing chain length. In treating Jain *et al.*'s results we have omitted several data which were statistically atypical in a system. The trend of r and u in Jain *et al.*'s results is confirmed by our data, although there is significant difference between the two works.

Table 4 shows that r from our work change from equality with to greater than the ratio of molar volumes as chain length increases; that is, as the difference between the component molar volumes increases. This trend is continued in the work of Jain *et al.* for the *n*-C_{12} and *n*-C_{16} systems. Cutler and Morrison (27) found $r = 1.79$ for the system methane + propane, which exceeded the ratio of molar volumes by 0.1. An increase in r with increasing chain length is plausible, but the increasing rate of change of r is less easily justified. The true rate may actually be considerably less at the longest chain length, because the available data in the *n*-C_{16} system covers a range of ϕ_1 of only about 0.3. This is undesirably small for the method used to determine r and u.

Williamson and Scott (28) have shown that treatment of mixtures of homologs with lattice theory leads to equivalent relations obtained through van der Waals theory. Although lattice theory is extended here to non-homologous pairs, if u is considered to be related to the difference between the cohesive energy densities of a component pair, a concept which has received prominent attention in van der Waals

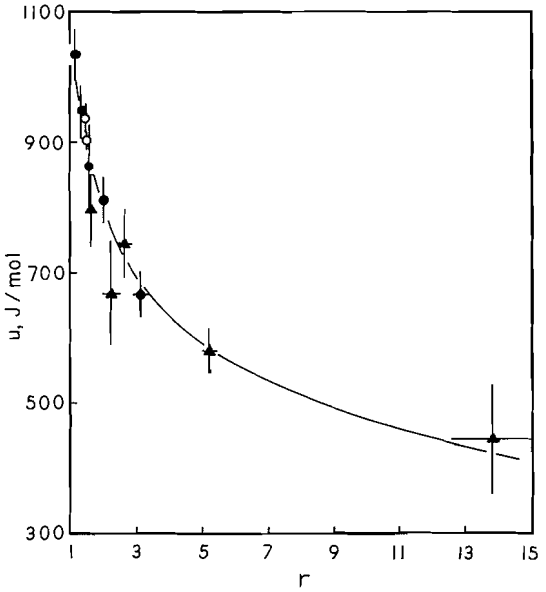

FIG. 2. The variation of u with r in eq. 2. ●, this work; △, Jain *et al.* (5); ○, Bissell *et al.* (6).

Can. J. Chem. Downloaded from www.nrcresearchpress.com by 210.87.254.42 on 09/05/12
For personal use only.

theories (29), then a decrease of u with increasing alkane chain length is tenable. The cohesive energy density of n-C_{16} is less than that of carbon tetrachloride, and it decreases for n-alkanes with decreasing chain length.

The relation between u and r is plotted in Fig. 2. The curve has been drawn by inspection through our results from n-C_5 to n-C_9 and extended through Jain *et al.*'s results for n-C_{12} and n-C_{16}. The scatter of points for the systems n-C_6, n-C_7, and n-C_8, for which more than one data source is available, shows the sensitivity of u and r toward differences in the heats of mixing shown in Table 2. Conclusions which can be drawn from Fig. 2 must clearly be considered tentative. Whereas Jain *et al.*'s data and our own include a considerable range of chain length, they are of lesser precision than those of Bissell *et al.*, whose data treat only two adjacent alkanes. Moreover systematic errors in the data for any of the systems can have a considerable effect on the r and u values there. Resolution of the questions raised by Fig. 2 must await highly precise measurements of H^E and V^E for this series of systems. Studies such as that of Vesely (3), where the total concentration range was observed, represent a much more stringent test of the theory than those like that of Gainey and Young (2), where the concentration range was restricted.

1. E. A. GUGGENHEIM. Mixtures. Oxford Univ. Press, Oxford. 1952. Chap. 11.
2. B. W. GAINEY and C. L. YOUNG. Trans. Faraday Soc. **64**, 349 (1968).
3. F. VESELY. Collect. Czech. Chem. Commun. **36**, 2881 (1971).
4. D. H. EVERETT and F. L. SWINTON. Trans. Faraday Soc. **59**, 2476 (1963).
5. D. V. S. JAIN, O. P. YADAV, and S. S. GILL. Indian J. Chem. **9**, 339 (1971).
6. T. G. BISSELL, G. E. OKAFOR, and A. G. WILLIAMSON. J. Chem. Thermodyn. **3**, 393 (1971).
7. R. VILCU and F. STANCIU. Analele Univ. Bucaresti Ser. Stiint. Nat. **12**, 87 (1963).
8. D. S. ADCOCK and M. L. MCGLASHAN. Proc. Roy. Soc. **A226**, 266 (1954).
9. J. A. LARKIN and M. L. MCGLASHAN. J. Chem. Soc. 3425 (1961).
10. J. A. LARKIN, D. V. FENBY, T. S. GILMAN, and R. L. SCOTT. J. Phys. Chem. **70**, 1959 (1966).
11. G. LEWIS and A. F. JOHNSON. J. Chem. Eng. Data, **14**, 484 (1969).
12. C. G. SAVINI, D. R. WINTERHALTER, L. H. KOVACH, and H. C. VANNESS. J. Chem. Eng. Data, **11**, 40 (1966).
13. G. W. LUNDBERG. J. Chem. Eng. Data, **9**, 193 (1964).
14. R. R. DREISBACH and R. A. MARTIN. Ind. Eng. Chem. **41**, 2875 (1949).
15. API Research Project 44, Selected values of physical and thermodynamic properties of hydrocarbons and related compounds. Carnegie Press, Pittsburgh. 1953. pp. 34, 69.
16. E. L. HERIC. J. Chem. Eng. Data, **11**, 66 (1966).
17. G. SCATCHARD. Trans. Faraday Soc. **33**, 160 (1937).
18. G. A. HOLDER and E. WHALLEY. Trans. Faraday Soc. **58**, 2095 (1962).
19. K. SHINODA and J. H. HILDEBRAND. J. Phys. Chem. **65**, 183 (1961).
20. H. E. EDULJEE, D. M. NEWITT, and K. E. WEALE. J. Chem. Soc. 3086 (1951).
21. J. H. VAN DER WAALS. Trans. Faraday Soc. **52**, 916 (1956).
22. M. L. MCGLASHAN, K. W. MORCOM, and A. G. WILLIAMSON. Trans. Faraday Soc. **57**, 601 (1961).
23. J. W. M. BOELHOUWER. Physica, **26**, 1021 (1960).
24. E. L. HERIC and J. G. BREWER. J. Chem. Eng. Data, **12**, 574 (1967).
25. D. V. S. JAIN, B. S. LARK, S. S. CHAMAK, and P. CHANDER. Indian J. Chem. **8**, 66 (1970).
26. A. DESMYTER and J. H. VAN DER WAALS. Rec. Trav. Chem. Pays-Bas. **77**, 53 (1958).
27. A. J. B. CUTLER and J. A. MORRISON. Trans. Faraday Soc. **61**, 429 (1965).
28. A. G. WILLIAMSON and R. L. SCOTT. Trans. Faraday Soc. **66**, 335 (1970).
29. J. H. HILDEBRAND and R. L. SCOTT. Regular Solutions, Prentice-Hall, Inc., Englewood Cliffs, N.J. 1962. Chap. 7.

Can. J. Chem. Downloaded from www.nrcresearchpress.com by 210.87.254.42 on 09/05/12
For personal use only.

Synthesis and Structural Investigation of *cis*-8-Oxabicyclo[4.3.0]nonan-3-ols

KOICHI KIMOTO, TA-YAN LEONG, TAKESHI IMAGAWA, AND MITUYOSI KAWANISI[1]

Department of Industrial Chemistry, Kyoto University, Kyoto, Japan 606

Received March 2, 1972

A variety of methods of synthesis of hitherto unknown isomeric *cis*-8-oxabicyclo[4.3.0]nonan-3-ols were studied, and the best method for obtaining *cis*-8-oxabicyclo[4.3.0]nonan-3β-ol (**2**) was hydroboration of *cis*-8-oxabicyclo[4.3.0]non-3-ene (**1**). *cis*-8-Oxabicyclo[4.3.0]nonan-3α-ol (**3**) could be obtained highly stereoselectively by the hydrogenation of *cis*-8-oxabicyclo[4.3.0]nonan-3-one (**4**) over platinum oxide in an acidic medium. The configurations of **2** and **3** were deduced mainly from the chemical and spectral similarity with the known *cis*-bicyclo[4.3.0]nonan-3-ols. The preferred conformations of the two isomeric alcohols were discussed in terms of i.r. as well as n.m.r. spectroscopy using paramagnetic shift reagents. There is almost no difference in the coordination abilities of europium ions with the alcoholic and ethereal oxygen atoms in these compounds.

Des méthodes variées de synthèse des *cis* oxa-8 bicyclo[4,3,0] nonanols-3 isomères, inconnus jusqu'ici, ont été étudiées et la meilleure méthode pour obtenir le *cis* oxa-8 bicyclo[4,3,0] nonanol-3β (**2**) est l'hydroboration du *cis* oxa-8 bicyclo[4,3,0] nonène-3 (**1**); le *cis* oxa-8 bicyclo[4,3,0] nonanol-3α (**3**) peut être obtenu de façon hautement stéréosélective par hydrogénation du *cis* oxa-8 bicyclo[4,3,0] nonanone-3 (**4**), en présence de l'oxyde de platine en milieu acide. Les configurations de **2** et **3** ont surtout été déduites à partir des propriétés chimiques et spectrales similaires aux *cis* bicyclo[4,3,0] nonanols-3 connus. Les conformations préférentielles des deux alcools isomères ont été discutées à partir des données de la spectroscopie i.r. et de la r.m.n. utilisant les chélates de terres rares. Il n'y a pratiquement aucune différence dans la coordination des ions europium avec les atomes d'oxygène des groupes alcool ou éther pour ces composés.

[Traduit par le journal]

Canadian Journal of Chemistry, **50**, 3805 (1972)

In connection with the studies of steroids, there have been many reports on the studies of synthesis and stereochemistry of bicyclo[4.3.0]-nonanes (1, 3). However, in the field of their oxa-analogs (8-oxabicyclo[4.3.0]nonanes) (2), research has not been so active. In order to gain an insight into the properties of the compounds in which a methylene group of the five-membered ring in bicyclo[4.3.0]nonanes is replaced by an oxygen atom, the synthesis of the hitherto unknown alcohols, *cis*-8-oxabicyclo[4.3.0]nonan-3β-ol (**2**)[2] and *cis*-8-oxabicyclo[4.3.0]nonan-3α-ol (**3**) has been undertaken (see Scheme 1). The configurations of the resulting alcohols **2** and **3** were deduced from the stereochemical consideration similar to the determination of the configurations of *cis*-bicyclo[4.3.0]nonan-3-ols (3) and cyclohexanols (4).

Granger *et al.* had determined the conformations of bicyclo[4.3.0]nonan-3-ols with i.r. and n.m.r. spectroscopic methods (3). In the present investigation we have employed additionally the recently developed technique of n.m.r. paramagnetic shift reagent which enabled us to deduce the preferred conformations of **2** and **3** in more detail, as well as to certify the configurational assignment.

Results and Discussion

(a) Syntheses and Configurations

As shown in Table 1, hydroboration of **1** with diborane gave mainly **2**, but hydroboration with diisopinocamphenylborane did not improve the ratio of **2**. Lithium aluminum hydride (LAH) reduction of the epoxide of **1**[3] obtained by the reaction of **1** with *m*-chloroperbenzoic acid also gave **2** as major product. The reduction of **4** with sodium in ethanol yielded mainly **2** whereas reduction with LAH afforded the isomer **3** predominantly. Compound **3** was obtained stereoselectively by the hydrogenation of **4** over platinum oxide in acetic acid with a small amount of hydrochloric acid. Summarizing these results, the hydroboration of **1** with diborane seems to be the method of choice for the synthesis of isomer **2**, and the hydrogenation

[1]To whom correspondence should be addressed.

[2]A hydroxyl group oriented *cis* to the angular hydrogens at C-1 and -6 is termed β; the *trans* orientation is termed α.

[3]Formation of epoxide of **1** was confirmed by i.r., and the ring opening of the epoxide was immediately effected without further purification (see Experimental). This epoxide was described in the literature (5) without isolation.

Can. J. Chem. Downloaded from www.nrcresearchpress.com by 210.87.254.42 on 09/05/12
For personal use only.

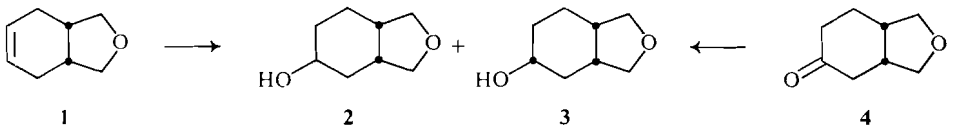

1 2 3 4

SCHEME 1

TABLE 1. Reactions of **1** and **4**

Starting materials	Methods of preparation	Alcohol ratio* 2 (%)	3 (%)
1	(A) B_2H_6, H_2O_2	86	14
	(B) DICB†, H_2O_2	75	25
	(C) MCPBA, LAH‡	85	15
	(D) Oxymercuration§, Demercuration	22	78
4	(E) LAH‡	15	85
	(F) PtO_2, H_2/AcOH	<2	>98
	(G) Na/EtOH	61	39
		β-ol (%)	α-ol (%)
cis-Bicyclo[4.3.0]non-3-ene (3)	(E) LAH‡	18	82
	(F) PtO_2, H_2/AcOH‖	25	75
	(G) Na/EtOH	62	38

*Percentage of ratio of alcohols **2** and **3** was determined by g.l.c. analysis, conversion in all cases was 100%.
†DICB stands for diisopinocamphenylborane.
‡MCPBA stands for *m*-chloroperbenzoic acid and LAH stands for lithium aluminum hydride.
§Oxymercuration of **1** was described in ref. 6 without a specific ratio.
‖No hydrochloric acid was added during hydrogenation.

of **4** in an acidic medium provides the most convenient route to **3**.

It is generally accepted that the reduction of cyclohexanone derivatives with sodium in alcohol yields the more stable alcohols whereas hydrogenation in an acidic medium gives the less stable alcohols (4). Judging from the above tendency and from the agreement of the results of the reduction of **4** with those of *cis*-bicyclo-[4.3.0]nonan-3-one (3) (Table 2), it can be safely stated that the hydroxyl group of **2** is *trans* to the five-membered ring, that is, it has a β-configuration and that of **3** has an α-configuration. From this close resemblance in stereochemical relationships, there seems to be no difference in the reactivities of the ketones in reductions even when one methylene group of the five-membered ring is substituted by an oxygen atom.

During the hydroboration of **1**, chiefly due to the steric hindrance of the methylene groups in the five-membered ring, and probably due, to a certain extent, to the direct participation (6), if any, of the ethereal oxygen orbitals towards the C_3—C_4 double bond, **2** should be formed predominantly as the boron atom attacks preferably from the *exo*-face, and actually the

TABLE 2. Infrared spectral data of **2** and **3**

Compounds		I.r. cm^{-1}* (7% CCl_4 solutions)
3		3368 (s), 3618 (w),
	ν_{C-O}†	1065 (s), 1040 (s), 1020 (s), 993 (m)
	ν_{C-O-C}†	1080 (s)
2		3380 (s), 3616 (w)
	ν_{C-O}†	1025 (s), 1009 (m) 987 (m)
	ν_{C-O-C}†	1080 (s), 1055 (s)

*s, Strong; m, medium; and w, weak absorptions.
†ν_{C-O} represents the bands for cyclic secondary alcohols and ν_{C-O-C} represents the bands for the cyclic ether moieties. The latter is assigned by comparing with the spectrum of **1**.

Can. J. Chem. Downloaded from www.nrcresearchpress.com by 210.87.254.42 on 09/05/12
For personal use only.

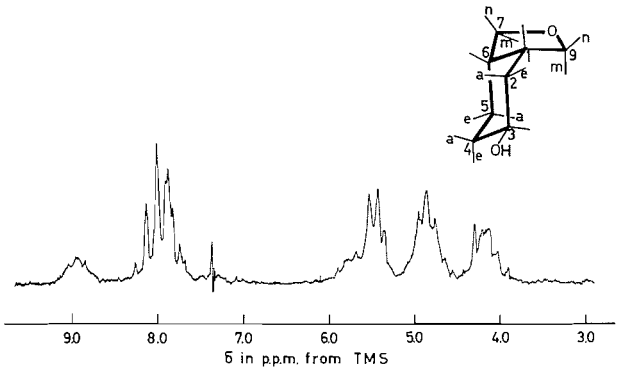

FIG. 1. 60 MHz spectrum of **2** in $CDCl_3$ after addition of 0.38 mol of $Eu(DPM)_3$

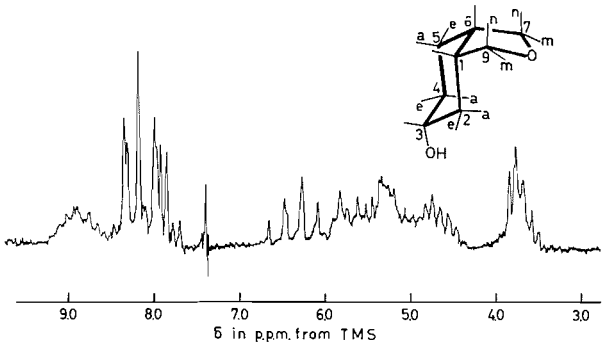

FIG. 2. 60 MHz spectrum of 3 in $CDCl_3$ after the addition of 0.32 mol of $Eu(DPM)_3$

result was as expected. This steric hindrance also accounts for the higher yield of **2** in the reductive ring opening of the epoxide of **1**. The hydroboration with the bulky diisopinocamphenylborane is unexpectedly lower in stereoselectivity than that with diborane, and the reason for this is not clear yet.

(b) Nuclear Magnetic Resonance Studies Using the Shift Reagent, Eu(DPM)$_3$.

The lanthanide complex-induced n.m.r. shift effect has become a valuable aid for the structural analysis of organic molecules having substituents with lone-pair electrons (7). To obtain conformational evidence, we have applied this technique to the n.m.r. study of the isomers of *cis*-8-oxabicyclo[4.3.0]nonan-3-ols (**2** and **3**), which are bifunctional compounds with two coordination sites[4] (8) (see Figs. 1 and 2).

The relationship between the variation of chemical shifts (δ_E) and $Eu(DPM)_3$/substrate (molar ratio) and the shift parameters, the *S* values[5] (9) for the two isomers of **2** and **3** is shown in Figs. 3 and 4, demonstrating the linearity between δ_E and $Eu(DPM)_3$/substrate for different protons in both isomers.

The linearities even at a high concentration of 1.2 molar ratio for the carbinyl protons and the four methylene protons adjacent to the oxygen atom of the five-membered rings indicate that there is no great difference in the equilibrium constants of complex formation for the alcoholic and the ethereal oxygen atoms.

Since Sanders and Williams (10) reported

[4]One of the referees has recommended the more recently developed shift reagent, tris-(1,1,1,2,2,3,3-heptafluoro-7,7-dimethyl-4,6-octanedione)-europium(III), $Eu(fod)_3$, because of its superior complexing properties for ethers (22). As expected, we obtained the following three results: (*i*) the signals of the carbinyl proton (H-3) and the α-protons of ether (H_7 and H_9) overlapped in all molar ratios of $Eu(fod)_3$/substrate, (*ii*) the other signals showed a pattern similar to the case of $Eu(DPM)_3$, (*iii*) the gradients of the signals shifted by $Eu(fod)_3$ are *ca.* 1.6 times greater than those of signals shifted by $Eu(DPM)_3$.

[5]*S* represents the shift parameters and is defined in (9) as $\delta_E = \delta + S \cdot Eu(DPM)_3$/substrate, where δ is the chemical shift in the uncomplexed substrate.

Can. J. Chem. Downloaded from www.nrcresearchpress.com by 210.87.254.42 on 09/05/12
For personal use only.

Can. J. Chem. Downloaded from www.nrcresearchpress.com by 210.87.254.42 on 09/05/12
For personal use only.

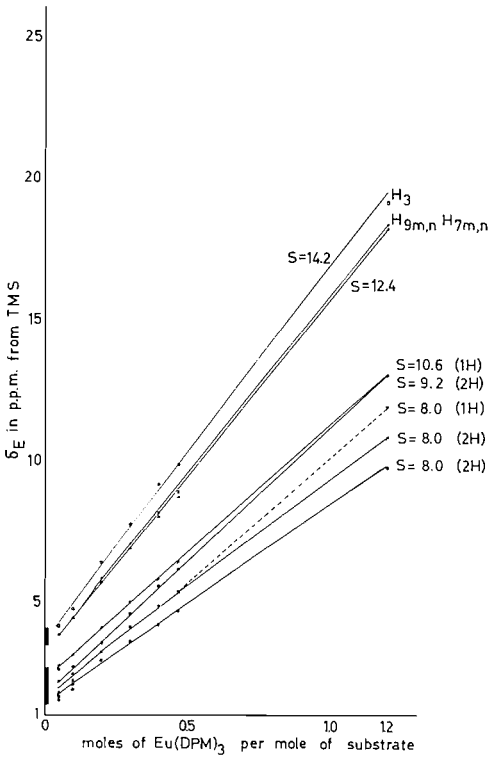

FIG. 3. Variation of chemical shift with molar ratio of Eu(DPM)$_3$/substrate for **2** in $CDCl_3$ solution.

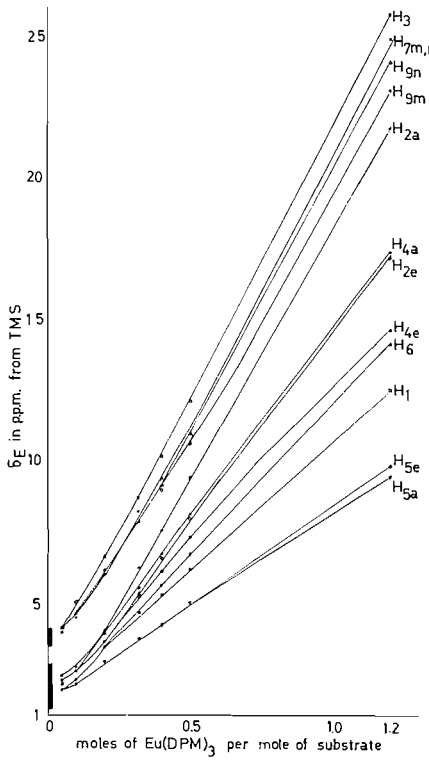

FIG. 4. Variation of chemical shift with molar ratio of Eu(DPM)$_3$/substrate for **3** in $CDCl_3$ solution.

that the gradients for RCH_2OH and RCH_2OCH_2R are $20 \sim 25$ and 10 (in CCl_4), respectively, it is generally accepted that the carbinyl protons are shifted much more than the protons situated α to the ethereal oxygen atom; however, no qualitative competition experiment in this respect has ever been reported. Hart and Love (11) reported the gradients, ΔEu values of $25 \sim 29$ for the α protons of cyclic ethers (probably in $CDCl_3$). This contradiction demonstrates the difficulty of comparing the gradients directly from one compound to another. As examples of intramolecular competition, there are two reports: Farid *et al.* indicated that the ethereal oxygen and not the sterically hindered hydroxyl group is involved in complex formation (12); whereas on the other hand, judging from the n.m.r. charts in Horton and Thomson's report (13) on carbohydrates, we can deduce that complex formation occurs mainly at the hydroxyl group, although the compound contains two ethereal oxygen atoms.

We have carried out an intermolecular competitive experiment on an equal molar mixture of tetrahydrofuran and cyclohexanol and the results are shown in Fig. 5. The $S_{-CH-OH}/S_{-CH-O-CH-}$ for the mixture is 1.19 and is compatible with the average values of **2** and **3** (1.16 and 1.14 respectively), indicating a similar degree of competitive coordination for the two sites in these three cases.

We could obtain a reasonably satisfactory linear relationship between S values and the values of $r_A^{-2} + r_E^{-2}$ (where r_A stands for the distance of the proton from the alcoholic oxygen atom and r_E represents the distance of the proton from the ethereal oxygen atom) (Table 3) for the protons of **3***a*,[6] but not **3***b*. Unfortunately, however, the tentatively assigned S and $r_A^{-2} + r_E^{-2}$ for **2***a* and *b* both displayed a fairly good linearity and the differentiation between **2***a* and *b* as the preferred conformation is impossible.

[6]Even if the value of a/b for $a \cdot r_A^{-2} + b \cdot r_E^{-2}$ is changed, the linearity cannot be improved.

Can. J. Chem. Downloaded from www.nrcresearchpress.com by 210.87.254.42 on 09/05/12
For personal use only.

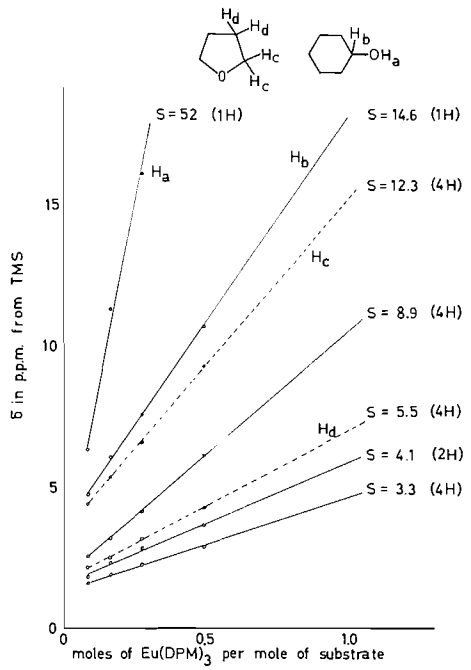

FIG. 5. Variation of chemical shift with molar ratio of $Eu(DPM)_3$/substrate and *S*-values for an equal molar mixture of cyclohexanol and tetrahydrofuran in $CDCl_3$. Dotted lines represent protons of tetrahydrofuran, solid lines represent protons of cyclohexanol.

However, these satisfactory r–S relationships show clearly that the equilibrium constants of complex formation for the alcoholic oxygen atom and the ethereal oxygen atom with the shift reagent are almost equal.

The spectral pattern for H_{2a} of **3** is clearly discernible in Fig. 2. The spacings of the four-line multiplet indicate the coupling constants of $J_{1,2a} \sim J_{3,2a} \sim J_{2e,2a} = ca.$ 12 Hz. These values clearly indicate that the cyclohexanol ring in **3** adopts a regular chair conformation and the hydroxyl group exists in an equatorial arrangement. When the $Eu(DPM)_3$/substrate (molar ratio) is increased to 0.5, in the case of **3**, the spectral pattern of $H_{7m,n}$ and $H_{9m,n}$[7] are simplified to such an extent that analysis becomes possible. The signals of H_{9n} and H_{9m} feature the AB portion ($J_{AB} = 8.9$ Hz) of the ABX system and the approximately calculated values (14) of $J_{AX} = 4.9$ Hz, (A = H_{9n}, X = H_1); $J_{BX} = 1.9$ Hz (B = H_{9m}, X = H_1) are obtained.[8] Judging from the molecular model with a conformation of **3***a* as shown in Fig. 6, the dihedral angles between the hydrogen C-1 and the hydrogens m,n at C-9 are nearly 90 and 30°, respectively. The above

[7]A hydrogen atom oriented *trans* to the angular hydrogens at C-1 and -6 is termed m; the *cis* orientation is termed n. Refer to Figs. 1 and 2 for a detailed description.

TABLE 3. The values of $r_A^{-2*} + r_E^{-2*}$ for **2** and **3**

		3		**2**	
		$r_A^{-2} + r_E^{-2}$		$r_A^{-2} + r_E^{-2}$	
Protons	*S*†	**3***a*	**3***b*	**2***a*	**2***b*
1	8.8	0.150	0.177	0.163	0.211
2a	17.8	0.261	0.140	0.192	0.211
2e	14.2	0.203	0.204	0.197	0.203
3	17.4	0.280	0.301	0.309	0.267
4a	14.2	0.200	0.132	0.168	0.165
4e	12.0	0.180	0.171	0.181	0.175
5a	7.0	0.112	0.289	0.179	0.136
5e	7.0	0.105	0.110	0.112	0.190
6	10.4	0.156	0.151	0.134	0.181
7m	16.4	0.285	0.297	0.266	0.281
7n	16.4	0.266	0.278	0.262	0.271
9m	14.2	0.282	0.445	0.276	0.281
9n	14.2	0.268	0.307	0.300	0.278

*r_A, distance of proton from alcoholic oxygen atom; r_E, distance of proton from ethereal oxygen atom, measured by using Dreiding models.

†*S*, the shift parameter, obtained from 0.1 molar ratio to 0.5 molar ratio.

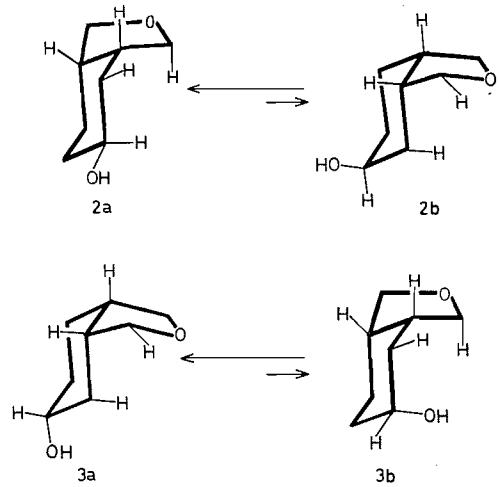

FIG. 6. Molecular models of **2** and **3**.

[8]The spectral pattern of $H_{7m,n}$ shows the AB portion of the deceptively simple ABX pattern for the relationship of $1/2(J_{AX} - J_{BX}) = 0$ or $\delta_{AB} = 0$. (A = B = $H_{7m,n}$), (X = H_6) (15), and information on n.m.r. parameter cannot be obtained.

Can. J. Chem. Downloaded from www.nrcresearchpress.com by 210.87.254.42 on 09/05/12
For personal use only.

coupling constants are in good agreement with the values calculated according to the Karplus equation (16) with the above angles.

On the other hand, in the case of **2**, even when the concentration of the shift reagent is increased to 1.2 equiv, the degeneracy of signals, except those of the carbinyl proton and the methylene protons adjacent to the ethereal oxygen atom, cannot be altered (Fig. 3); that is, three clusters of signals consisting of three protons, three protons, and two protons each are shifted together as groups.

Based on the $r_A^{-2} + r_E^{-2}$ in Table 3, the groups of complex multiplets are tentatively assigned in the order of chemical shifts as follows: (H_{5a}, H_{2a}, H_{2e}); (H_{4a}, H_{4e}, H_1); (H_6, H_{5e}).

These assignments are partially supported by irradiation at the signals of the carbinyl proton causing remarkable changes in both the three-proton multiplets and none in the two-proton multiplet, although the decoupling experiments in other cases are rendered difficult by the inherent degeneracies of the signals.

(c) Conformations

To determine the axial or equatorial nature of protons adjacent to the hydroxyl or the acetate moieties, it is helpful to observe the half-band widths of the proton signal. The half-band widths of the carbinyl protons of **2** and **3** cannot be observed directly owing to the overlapping with the signals of the protons α to the ethereal oxygen, but the widths of the respective acetates of **2** and **3** are observed to be 14 and 17 Hz, respectively, indicating the equatorial arrangement of the acetoxy groups in both acetates.

The half-band widths of the carbinyl protons (H_3) of **2** and **3** are observed, however, after addition of the n.m.r. shift reagent as described earlier, the values being about 16 and 17 Hz, respectively. These band widths would seem to confirm that the preferred conformations for **2** and **3** are **2***a* and **3***a* in Fig. 6, when we consider additionally the information[9] about the total ring-systems of **2** and **3** described in the previous section.

The i.r. spectra of CCl_4 solutions of **2** and **3** (Table 2) show absorptions due to the stretching vibration ν_{C-O-} at 1025, 1009, and 987 cm^{-1} for compound **2** and at 1020, 993 cm^{-1} for compound **3**, respectively. When the stronger intensities of the equatorial bands are compared with those described for bicyclo[4.3.0]nonan-3-ols (3), the above conformational assignments are further supported. The i.r. spectra of highly diluted solutions of **2** and **3** indicate no intramolecular hydrogen bonding resulting from the hydroxyl group and the ethereal oxygen; therefore, a boat form or a skewed boat form stabilized by intramolecular hydrogen bonding might be excluded.

These conclusions on conformational assignments are consistent with the deduction using the concept of conformational analysis as described for *cis*-bicyclo[4.3.0]nonan-3-ols by Dauben and Jiu (1*b*).

[9]Although the evidence for **2** might be less convincing than that for **3**, the conclusion will not be unchanged in light of the fact that the *r*–*S* relationships for **2** were not obtained in terms of its boat or skewed boat conformations.

Experimental

The i.r. spectra were recorded on a Shimadzu IR-27C spectrometer with the exception of the investigation of the intramolecular hydrogen-bonding spectra which were run on a Shimadzu IR-27G spectrometer using CCl_4 solutions of various concentrations from 0.01–0.002 *M* in a cell of 1 cm in path length. The n.m.r. spectra were determined on a JEOL C-60H spectrometer using tetramethylsilane as an internal standard, and $CDCl_3$ as solvent. Tris(dipivalomethanato)europium(III), $Eu(DPM)_3$, was prepared in a manner similar to that of Eisentraut and Sievers (17), and had a m.p. 189.5–190° (lit. m.p. 190–191° (18)). The g.l.c. analyses and separations were carried out on a Shimadzu GC-4APT using a 3 m × 3 mm column with 15% polyethyleneglycol on 60/80 Chromosorb W operating at 150° with a He flow rate of 40 cc/min. For preparative t.l.c., a 1.0 mm thickness of Merck GF-254 Silica Gel was employed with the solvent system of diethyl ether–benzene (50:50). Microanalyses were performed by Mrs. K. Fujimoto of our laboratory. Mass spectra were recorded with a Hitachi RMS-4 mass spectrometer with a nominal ionizing energy of 70 eV, and a source temperature of 150 °C. All melting points and boiling points were uncorrected.

Reaction of cis-8-Oxabicyclo[4.3.0]non-3-ene (1)

(a) Hydroboration with Diborane

Diborane generated by adding a solution of 14 g of $BF_3 \cdot Et_2O$ in 25 ml of diglyme to 1.9 g of sodium borohydride in 50 ml of diglyme was passed during 75 min into a stirred solution of 5.9 g of **1** (19) in 50 ml of THF, cooled in an ice bath. The solution was then left for 75 min at room temperature, excess diborane was decomposed with water (15 ml), and 15 ml of 3 *N* sodium hydroxide was added, and subsequently, 15 ml of 30% hydrogen peroxide was added dropwise. The reaction mixture was stirred for an additional hour at room temperature and extracted with dichloromethane. After evaporation of the solvent, distillation yielded 4.2 g of a mixture of **2** and **3**, b.p. 115°/9 mm; the isomeric ratio of **2** to **3** was shown to be 86:14 by g.l.c.

Can. J. Chem. Downloaded from www.nrcresearchpress.com by 210.87.254.42 on 09/05/12
For personal use only.

(b) Hydroboration with Diisopinocamphenylborane

Hydroboration with diisopinocamphenylborane was carried out with 6.8 g of **1** according to the method of Brown *et al.* (20), and 5.8 g of a mixture of **2** and **3** was obtained, the isomeric ratio of which was shown to be 75:25 by g.l.c.

*(c) Reaction of **1** with m-Chloroperbenzoic Acid Followed by Reduction with Lithium Aluminum Hydride (LAH)*

A solution of 5.4 g of 85% *m*-chloroperbenzoic acid in 120 ml of dry chloroform was added dropwise to a stirred solution of 3 g of **1** in 50 ml of dry chloroform. The reaction mixture was stirred overnight at room temperature. The solution was then washed twice with 100 ml of 10% sodium sulfite solution, twice with 100 ml of 5% sodium bicarbonate solution, and finally with saturated sodium chloride solution, and dried (Na_2SO_4). Chloroform was driven off at reduced pressure, and the i.r. of the reaction product (3.2 g) showed no absorption of olefin, but bands at 3008 and 810 cm^{-1}, confirming the presence of epoxide. G.l.c. analysis also showed that the starting material **1** had disappeared; however, it was impossible to determine the isomeric ratio of the epoxide under the above-mentioned g.l.c. condition, and the following reaction with LAH was carried out without further purification of the epoxide. The solution of 3.2 g of the above epoxide in 50 ml of dry ether was added dropwise to a stirred slurry of LAH in 50 ml of ether, and the mixture was stirred overnight at room temperature. Aqueous hydrochloric acid (10%) was added to destroy the excess hydride, the aqueous phase extracted with ether, and dried (Na_2SO_4). On concentration, 2.44 g of a mixture of **2** and **3** was obtained, which was shown by g.l.c. to have an isomeric ratio of 85:15.

*(d) Reduction of cis-8-Oxabicyclo[4.3.0]nonan-3-one (**4**)*

The ketone (**4**) was prepared by oxidizing the mixture of **2** and **3** obtained in the hydroboration (with diborane) of **1**. A solution of 2.84 g of a mixture of **2** and **3** in a small volume of dichloromethane was oxidized with chromium trioxide–pyridine complex as described by Ratcliffe and Rodehorst (21) to yield 1.68 g of **4**, b.p. 118–119°/19 mm, i.r.: 1718, 1710, 1060, 1035 cm^{-1}; n.m.r.: (CCl_4) δ 4.03–3.22 (4H, m), 2.84–1.34 (8H, m); *m/e*: 140 (M^+, 10%), 82 (100%).

Anal. Calcd. for $C_8H_{12}O_2$: C, 68.54; H, 8.63. Found: C, 68.66; H, 8.83.

A solution of **4** (200 mg) in 10 ml of ether was added dropwise to a stirred slurry of 70 mg of LAH in 10 ml of ether. The mixture was stirred overnight at room temperature, dilute hydrochloric acid was added to destroy excess hydride, the aqueous phase was extracted with ether, and dried (Na_2SO_4). The solvent was removed and the alcohols **2** and **3** were formed in the ratio of 15:85 and no trace of **4** could be detected.

*(e) Hydrogenation of **4** over Platinum Oxide*

A sample (100 mg) of **4** in 5 ml of glacial acetic acid was added to 50 mg of platinum oxide in 10 ml of glacial acetic acid, three drops of concentrated hydrochloric acid was added, and hydrogenation was carried out under a normal atmosphere of hydrogen at room temperature. A rapid uptake of hydrogen occurred and the theoretical amount of hydrogen was absorbed in 20 min. The reaction mixture was neutralized with aqueous sodium bicarbonate, extracted with ether, and dried (Na_2SO_4). Analysis of the reaction product with g.l.c. showed that **3** was obtained at an isomeric ratio of over 98%. This method was employed to obtain a pure sample of **3** by separating the trace of **2** with preparative t.l.c. (*vide infra*).

*(f) Reduction of **4** with Sodium in Ethanol*

A solution of 32 mg of **4** in 10 ml of absolute ethanol was placed in a flask fitted with a reflux condenser and 175 mg of small pieces of sodium were added to maintain reflux. After the addition of sodium was finished, the reaction mixture was refluxed for an additional hour, then cooled and acidified with 10% aqueous hydrochloric acid. Ethanol was removed under diminished pressure and the aqueous phase extracted with ether, and dried (Na_2SO_4). Analysis of the reaction product with g.l.c. showed that the isomers **2** and **3** were formed in a ratio of 61:39.

*Preparation of Pure Specimens of **2** and **3***

Pure samples of **2** and **3** were isolated from the reaction mixtures obtained in methods (*a*) and (*e*), respectively, purified after separation by preparative t.l.c. and g.l.c., and showed the following properties.

Compounds **2** and **3**: i.r. and n.m.r. spectral data: shown in Table 2; *m/e* for **2**: 142 (M^+, 9%), 124 ($M^+ - 18$, 47%), 79 (100%); *m/e* for **3**: 142 (M^+, 5%), 124 ($M^+ - 18$, 30%), 69 (100%).

Anal. Calcd. for $C_8H_{14}O_2$: C, 67.57; H, 9.93. Found for **2**: C, 67.35; H, 9.65. **3**: C, 67.37; H, 10.17.

Acetate of **2**: i.r.: (neat) 1741, 1245, 1060, 1020 cm^{-1}: n.m.r.: (CCl_4) δ 5.12–4.66 (m, *w*/2: 14 Hz, 1H), 4.04–3.33 (m, 4H), 2.64–1.14 (m, 11H); *m/e*: 184 (M^+, 2%), 141 ($M^+ - 43$, 30%), 124 ($M^+ - 60$, 30%), 43(100%).

Acetate of **3**: i.r.: (neat) 1756, 1742, 1255, 1236, 1083, 1050, 1034, 1016 cm^{-1}; n.m.r.: (CCl_4) δ 5.01–4.52 (m, *w*/2: 17 Hz, 1H), 3.91–3.40 (m, 4H), 2.51–1.09 (m, 11H); *m/e*: 184 (M^+, 2%), 141 ($M^+ - 43$, 25%), 124 ($M^+ - 60$, 28%), 43 (100%).

*Decoupling Experiments for the Nuclear Magnetic Resonance Spectral Assignment of **3***

Decoupling experiments were done with a Varian HA-100 spectrometer operating at a 100 MHz field in the frequency-swept and tetramethylsilane (TMS) locked mode.

The spectrum of **3** shows a one-proton multiplet at δ 9.10 assignable to the carbinyl proton (H_3) and two AB portions of ABX systems at δ 8.15 ~ 9.05 (sharp 2 × 6 lines) due to the four methylene protons adjacent to the oxygen of the five-membered ring.

Decoupling on H_3 resulted in changes of the one-proton quartet centered at δ 6.95 into a broad triplet, of the complex two-proton multiplet at δ 5.7 ~ 6.6 into a more complex but sharper multiplet, and of the broad multiplet at δ 5.58 into a relatively sharper pattern.

Irradiation at the center of the six-line pattern (AB portion of ABX system) centered at δ 8.87 made the broad triplet at δ 5.24 relatively narrower, and double irradiation at the other AB portion of ABX system changed the six-line multiplet at δ 4.87 into a five-line multiplet.

Then, the complex multiplet (two protons) at δ 3.55 ~ 4.20 which showed no change on these three decoupling experiments is assignable to H_{5a} and H_{5e} (refer to formula in Fig. 2).

Double irradiation (to cover the wide resonance frequencies) at the multiplets of H_{5a} and H_{5e} at δ 3.55 ~ 4.20 changed the broad triplet at δ 5.24 into a relatively narrower quartet, which was assignable to H_6, and the two-proton

multiplet at δ 5.7 ~ 6.6 into a much broader and featureless pattern, which might be due to H_{4a} and H_{4e}. Accordingly, the signals at δ 6.95 and 5.58 may be assignable to H_{2a} and H_{2e}, respectively, based on their signal widths (base-line; 40 and 30 Hz, respectively), and on the spacing of 11.8 Hz for the quartet at δ 6.95.

On irradiation on H_6, the six-line pattern at δ 8.87 collapsed to a broad AB pattern of the case where δ_{AB} is small relative to J_{AB}; therefore this AB pattern is ascribed to H_{7m} and H_{7n}. On irradiation on the six-line multiplet at δ 4.87 now assignable to H_1, the six-line multiplet at δ 8.26–8.70 was changed into an AB quartet, which is due to H_{9m} and H_{9n}.

The authors are grateful to Prof. H. Nozaki for help and encouragement.

1. (*a*) K. H. Baggaley, S. G. Brooks, J. Green, and B. T. Redman. J. Chem. Soc. C, 2671, 2678 (1971). (*b*) W. G. Dauben and J. Jiu. J. Am. Chem. Soc. **76**, 4426 (1954).
2. L. J. Dolby and M. J. Schwarz. J. Org. Chem. **28**, 1456 (1963).
3. R. Granger, J.-P. Chapat, J. Crassous, and J.-P. Girard. Bull. Soc. Chim. Fr. 2662 (1971) and refs. cited therein.
4. D. H. R. Barton. J. Chem. Soc. 1027 (1953).
5. B. Rickborn and S.-Y. Lwo. J. Org. Chem. **30**, 2212 (1965).
6. B. P. Mundy, A. R. DeBernardis, and R. D. Otzenberger. J. Org. Chem. **36**, 3830 (1971); **37**, 677 (1972).
7. W. D. Horrock, Jr., J. P. Sipe, III, and J. R. Luber. J. Am. Chem. Soc. **93**, 5258 (1971), and refs. cited therein.
8. I. Fleming, S. W. Hanson, and J. K. M. Sanders. Tetrahedron Lett. 3733 (1971).
9. A. F. Cockerill and D. M. Rackham. Tetrahedron Lett. 5149, 5153 (1970).
10. J. K. M. Sanders and D. H. Williams. J. Am. Chem. Soc. **93**, 641 (1971).
11. H. Hart and G. M. Love. Tetrahedron Lett. 625 (1971).
12. S. Farid, A. Ateya, and M. Maggio. Chem. Commun. 1285 (1971).
13. D. Horton and J. K. Thomson. Chem. Commun. 1389 (1971).
14. J. W. Emsley, J. Feeney, and L. H. Sutcliffe. High resolution nuclear magnetic resonance spectroscopy. Vol. 1. Pergamon Press, Oxford. 1965. p. 357.
15. *cf.* Reference 14. p. 364, Fig. 8.20.
16. L. M. Jackman and S. Sternhell. Applications of nuclear magnetic resonance spectroscopy in organic chemistry. 2nd ed. Pergamon Press, Oxford. 1969. p. 281.
17. K. J. Eisentraut and R. E. Sievers. J. Am. Chem. Soc. **87**, 5254 (1965).
18. J. Selbin, N. Ahmad, and N. Bhacca. Inorg. Chem. **10**, 1383 (1971).
19. E. L. Eliel and C. Pillar. J. Am. Chem. Soc. **77**, 3600 (1955).
20. H. C. Brown, N. R. Ayyangar, and G. Zweifel. J. Am. Chem. Soc. **86**, 397 (1964).
21. R. Ratcliffe and R. Rodehorst. J. Org. Chem. **35**, 4000 (1970).
22. R. E. Rondeau and R. E. Sievers. J. Am. Chem. Soc. **93**, 1525 (1971).

Can. J. Chem. Downloaded from www.nrcresearchpress.com by 210.87.254.42 on 09/05/12
For personal use only.

Chemical Reactions of Methane in a Triboelectric Discharge

W. G. ALCOCK, E. J. HAYWARD, B. MILE, AND B. WARD

Shell Research Ltd., Thornton Research Centre, P.O. Box 1, Chester CH1 3SH, England

Received March 27, 1972

Methane can be converted into C_2 hydrocarbons and hydrogen in a triboelectric discharge arising from the intermittent contacting of mercury with a glass surface. The discharge is a result of the accumulation of high densities of static charge at the interface by the transfer of electrons from the mercury to the glass. Excited species with energies up to 20 eV above their ground states have been detected by spectroscopic examination of the discharge. The effects of physical parameters such as surface area and surface nature on the triboelectrification process have been examined. Both the area and nature of the solid surface influence the extent of breakdown and discharge. The rates of conversion are virtually invariant with pressure from 760 to 200 Torr, but at 200 Torr they increase sharply before gradually falling off again as the pressure is further reduced. This behavior is explained in terms of the opposite effects of pressure on the electrical breakdown of the gas and on the rates of the chemical reactions accompanying the discharge. The pressure at which the rise in yield occurs has been used to estimate the production of an average static charge density of 2 e.s.u. cm^{-2} by contact electrification at a mercury/glass interface. The effects of inert gases and oxygen have also been studied and the results of these experiments together with a comparison of the products formed in other decomposition processes suggest that CH_2 and CH_3 are important intermediates in the triboprocess occurring in methane.

On peut convertir le méthane en hydrocarbures C_2 et en hydrogène au moyen d'une décharge triboélectrique provenant du contact intermittent du mercure avec une surface de verre. La décharge est le résultat d'une accumulation de charge statique de forte densité à l'interface provoquée par le transfert d'électrons du mercure au verre. Nous avons détecté des espèces excitées possédant des énergies allant jusqu'à 20 eV au-dessus de leur état fondamental, au moyen d'un examen spectroscopique de la décharge. Nous avons examiné des effets de paramètres physiques, tels la grandeur et la nature de la surface sur le procédé de triboélectrification. Ces deux facteurs influent sur la brisure et la décharge. Les vitesses de conversion sont virtuellement indépendantes de la pression de 760 à 200 Torr, mais à 200 Torr, elles augmentent brusquement avant de retomber graduellement lorsqu'on diminue de plus la pression. On explique ce comportement en termes d'effets antagonistes de la pression sur la brisure électrique du gaz et sur les vitesses des réactions chimiques accompagnant la décharge. Nous avons utilisé la pression à laquelle augmente le rendement pour estimer la production d'une densité de charge statique moyenne de 2 u.s.e. cm^{-2} par électrification de contact à une interface mercure/verre. Nous avons aussi étudié les effets de gaz inertes et d'oxygène et les résultats de ces expériences, combinés à une comparaison des produits formés dans d'autres procédés de décomposition, suggèrent que CH_2 et CH_3 sont d'importants intermédiaires dans la triboélectrification du méthane.

[Traduit par le journal]

Canadian Journal of Chemistry, **50**, 3813 (1972)

Introduction

The term 'triboluminescence' describes the emission of light when certain materials are rubbed, or otherwise intermittently contacted. A particularly vivid example in which heat is converted, via mechanical motion, into light is the sporadic flashing and sparking of a glass/mercury diffusion pump during operation. More generally, it seems that photons are emitted whenever mercury moves along the surface of an insulating material.

The luminescence is a result of a weak gas discharge which itself must result from the generation of high electric fields by the movement of mercury over an insulating material such as glass. These high fields probably arise from the transfer of ions or electrons across the mercury/glass interface, followed by the separation of the statically charged surfaces (1).

Spectroscopic examinations of the light emitted when mercury moves over quartz or glass surfaces in the presence of inert gases at various temperatures and pressures have been made by de Walden (2), Ikenoue and Sasada (3), Dybwad and Mandeville (4), and Schoen (5). The results indicate that excited species with energies up to 20 eV above the ground state are produced by the simple mechanical agitation of liquid mercury in glass vessels.

Since the strength of most chemical bonds is below 8 eV, the production of species with 20 eV excess energy during the triboprocess should result in appreciable chemical change when complex molecules rather than inert

Can. J. Chem. Downloaded from www.nrcresearchpress.com by 210.87.254.6 on 09/05/12
For personal use only.

Can. J. Chem. Downloaded from www.nrcresearchpress.com by 210.87.254.6 on 09/05/12
For personal use only.

gases are present in the system. For this reason we decided to investigate tribodischarging in the presence of methane. Initial experiments showed that methane could be converted into C_2 and C_3 hydrocarbons and hydrogen in a tribodischarge, and here we report a detailed study of some of the factors that influence the rates of conversion.

There were no reported studies of the chemical aspects of triboluminescence when we started our investigations but very recently Johnson *et al.* (6), and de Paoli and Strausz (7) have briefly reported their observations of such chemical changes in a range of compounds.

Experimental

Two types of reactor were used which we refer to as the 'bubbler' reactor and the 'rotator' reactor. In the bubbler reactor, methane was circulated continuously through a vertical glass column (packed and unpacked) containing some 600 g of mercury. Teflon stopcocks were used in the circulating system, which was grease-free. In the simpler but less efficient rotator reactor the movement of surfaces was achieved by rotating a cylindrical glass vessel containing methane and a pool of mercury (200 g). Rotation speeds of 150 r.p.m. were used giving a linear velocity of 3100 cm/min at the mercury edge.

Since the triboprocess is likely to be very surface-dependent, a rigorous procedure was adopted for cleaning the glassware both in the rotator and in the bubbler experiments. This involved washing with permanganic acid, 100-volume hydrogen peroxide, and distilled water, followed by drying at 120 °C and pumping on a high vacuum line for 12 h.

Samples were withdrawn from both reactors into a gas syringe by using a serum cap which was isolated from the reaction systems except for the time of sampling. The gases were analyzed by g.l.c., a Porapak T column being used for hydrocarbon analysis and a molecular sieve 5A column for hydrogen.

A Hilger Medium Raman Spectrograph was used to make spectroscopic measurements with the bubbler. The spectra were photographed using an exposure of about 2 days and were calibrated with the spectral lines from a mercury arc.

Results

Spectroscopic Studies

The spectra observed from different gases confirm the results of Schoen and unequivocally demonstrate that highly excited species can be formed by simple mechanical agitation of mercury in glass vessels. A new feature was the observation of a CH emission (431.2 nm, $^2\Delta \rightarrow {}^2\pi$) with methane which provides striking evidence for the decomposition of methane. Interestingly, the triboluminescence spectrum from methane differs from that observed in a spark discharge (8) at atmospheric pressure in that emission from C_2 was not observed. One can infer from this that the conditions in a triboelectric discharge are not identical with those in a spark discharge.

Chemical Studies

(a) Products and Time Dependence

Simple agitation of mercury in either reactor at ambient temperatures results in the conversion of methane into acetylene, ethylene, ethane, hydrogen and traces of C_3 hydrocarbons. The yield of hydrogen corresponded closely to that expected from its concurrent production with the C_2 hydrocarbons, *i.e.*

$$[H_2] = [C_2H_6] + 2[C_2H_4] + 3[C_2H_2]$$

Similar products and product ratios were observed by de Paoli and Strausz (7) in their experiments at 10 Torr.

The growth curves for the production of C_2 hydrocarbons depend on the type of reactor used and on other factors discussed below but Fig. 1 for the rotator at 200 Torr gives the general shape of such curves for unpacked reactors. It can be seen that the rates of conversion decreased with increasing time. C_3 hydrocarbons were present in small amounts but were not produced during the early stages of reaction.

(b) Reactor Material

The effect of the nature of the surface of the reactor material was examined by using reactors made of different materials. Although the differences found were small, the order of efficiency was quartz > Pyrex > nylon. No reaction occurred in a steel reactor. Pyrex vessels were used in all the other experiments described here.

(c) Surface Area

In the unpacked bubbler reactor the intermittent contacting between the mercury and the glass is small. If the triboprocess is dependent on the making and breaking of the mercury/glass interface then any way of increasing this interface should increase the rate of decomposition of methane. The simplest way of increasing the contact area is to pack the reactor. The best packing material was found to be that of Pyrex helices of 3 mm diameter; this had a large

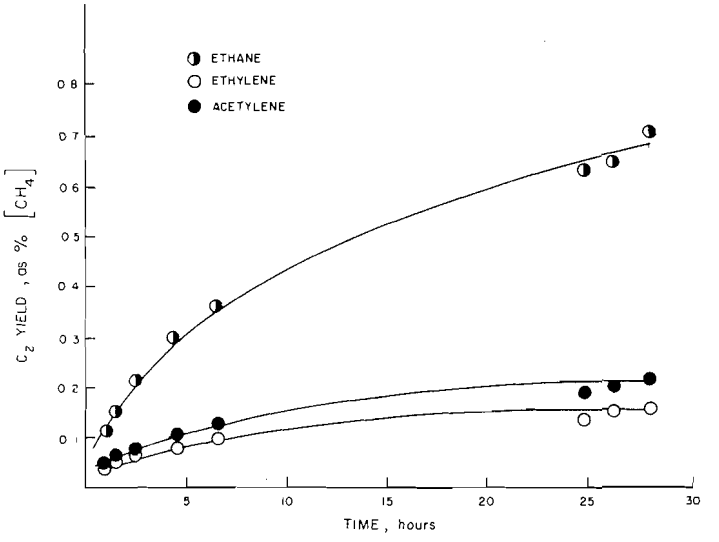

FIG. 1. C_2 hydrocarbon formation in rotator, CH_4 pressure = 200 Torr.

surface area and did not impede the flow of mercury, and vigorous agitation could be seen to be occurring. With this packing the rates of C_2 production increased approximately four-fold as illustrated in Fig. 2. Unlike the case of the unpacked reactor the rates of conversion did not fall off after a few hours operation but were maintained even after 200 h. It is probable that the fall-off in rates is due to the contamination of the glass surface. The agitation of the packing scours and keeps the surface free from contaminant. Indeed, with a packing of 5-mm diameter spheres distinct bands of contaminant built up only where the packing was not rubbing against the reactor wall.

(d) Pressure Effects

The rotator was used for detailed studies of the effect of pressure. The results for the initial rates of production of C_2 hydrocarbons are shown in Fig. 3. Despite some scatter in the results (due probably to the difficulty of obtaining reproducible surface conditions in the reactor) it is clear that the effect of pressure is not simple and monatonic but complex, the most significant feature being the sharp rise in rates as the pressure was reduced below 200 Torr. Many experiments were carried out in the region of 200 Torr to show that there was indeed a very sharp change, almost a discontinuity in behavior, at this pressure. Below 200 Torr there was a more gradual fall-off in rates. A similar discontinuity at 200 Torr was also found in experiments with the bubbler reactor.

(e) Gas Additives

We have used the rotating vessels to study the effect of the addition of helium, argon, krypton, xenon, nitrogen, and oxygen to methane at a total pressure of 200 Torr. The results are summarized in Table 1.

Discussion

The present results show that methane, characterized by its extremely low reactivity, can be decomposed and converted into higher hydrocarbons at room temperature by the simple mechanical agitation of mercury against glass and other insulator surfaces. The results are most conveniently discussed in terms of two aspects of the triboprocess; (*a*) the excitation process involving the conversion of mechanical into electrostatic energy; and (*b*) the chemical reactions occurring in the gas discharge arising from this excitation. The overall chemical changes and the effects of experimental conditions result from the interaction of these two aspects.

Excitation Mechanism

It is probable that the reactions are initiated by excited species produced in the gas discharge. The occurrence of the discharge shows that high electric fields of several 1000 V/cm must be

Can. J. Chem. Downloaded from www.nrcresearchpress.com by 210.87.254.6 on 09/05/12
For personal use only.

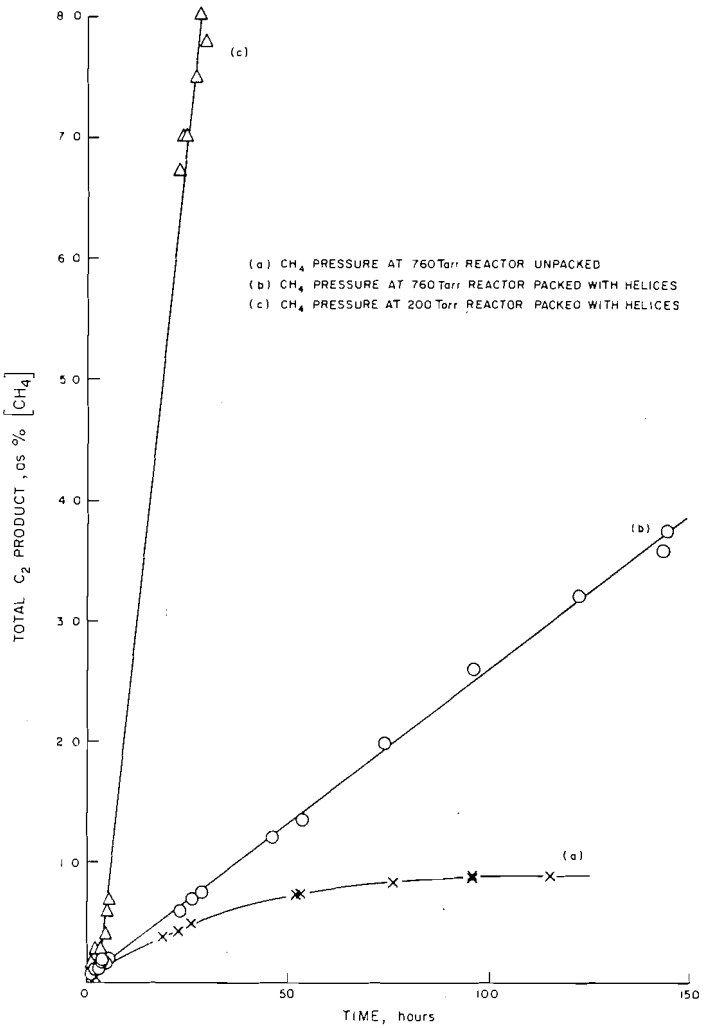

FIG. 2. Production of C_2 hydrocarbons in bubbler reactor.

created as mercury makes intermittent contact with the glass surface. Three mechanisms for the creation of such high fields are possible in the circumstances of the present experiments, contact, frictional, and spray electrification (9). Our results show that contact and/or frictional electrification are the predominant mechanisms for the following reasons.

(*a*) The rates of production of C_2 hydrocarbons depend on the reactor material. Thus there was a definite decrease in rate in the series quartz, Pyrex, and nylon, and no conversion at all occurred in the stainless-steel reactor even though bubble and spray formation must have taken place. Such effects can only be explained in terms of a mechanism involving liquid/solid interactions.

(*b*) The fall-off in the rates of conversion with time found in the case of the rotator and unpacked bubbler experiments is probably associated with the build-up of deposits on the vessel surfaces. This again shows that it is the liquid/solid interaction that is the most important.

(*c*) The use of a sinter to break up the gas stream, though leading to more bubble formation and disintegration, did not increase the efficiency of the bubbler. Furthermore, no spray or droplets were produced in the rotator and

Can. J. Chem. Downloaded from www.nrcresearchpress.com by 210.87.254.6 on 09/05/12
For personal use only.

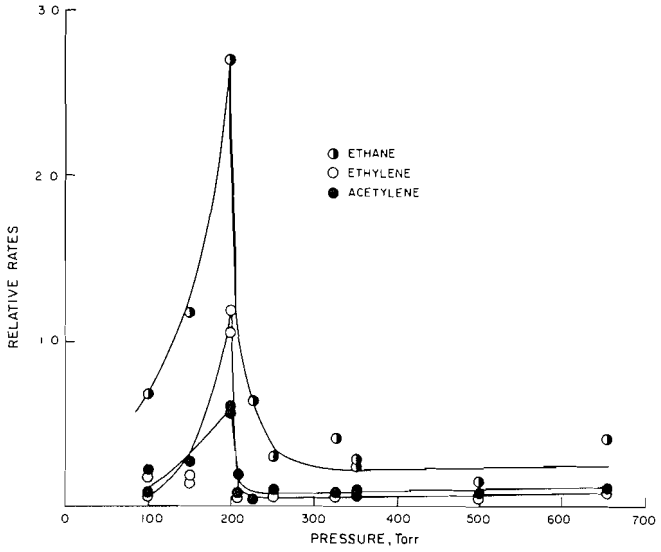

FIG. 3. Effect of pressure on relative rates of C_2 hydrocarbon formation.

TABLE I. Effects of added gases on the yields of C_2 and C_3 hydrocarbons. % Product compared with methane after 5 h reaction time in the rotator*

Added gas (Torr)	Methane (Torr)	Ethane (%)	Ethylene (%)	Acetylene (%)	C_3 products (%)	Total methane† decomposed (%)
0	200	0.161 ± 0.017 (100)	0.056 ± 0.013 (34 ± 6)	0.051 ± 0.013 (32 ± 6)	0.039 ± 0.010 (24 ± 6)	0.653 ± 0.033
Argon 20	180	0.171 (100)	0.058 (34)	0.062 (36)	0.048 (28)	0.726
Krypton 20	180	0.177 (100)	0.069 (39)	0.067 (38)	0.051 (29)	0.728
Xenon 20	180	0.182 (100)	0.064 (35)	0.060 (33)	0.053 (29)	0.771
Helium 100	100	0.163 ± 0.018 (100)	0.051 ± 0.015 (31)	0.064 ± 0.014 (39)	0.072 ± 0.010 (44)	0.672 ± 0.033
Argon 100	100	0.140 (100)	0.059 (42)	0.082 (59)	0.058 (41)	0.836
Krypton 100	100	0.196 (100)	0.073 (37)	0.061 (31)	0.062 (32)	0.846
Xenon 100	100	0.279 (100)	0.103 (37)	0.077 (28)	0.088 (32)	1.182
			Oxygen addition			
Oxygen 20	180	0.055 (100)	0.080 145	0.046 83	0.0003 5	0.0362

*Figures in parentheses normalize the product distribution to ethane at 100.
†Calculated on the basis of $-\Delta CH_4 = 2C_2H_6 + 2C_2H_4 + 2C_2H_2 + 3C_3$ hydrocarbons.

yet appreciable conversions occurred in this reactor. Thus spray electrification, if it occurs at all, plays only a minor role in the triboprocess.

Nature of Reactor Surface

The observed order of efficiency, quartz > Pyrex > nylon > steel correlates directly with

Can. J. Chem. Downloaded from www.nrcresearchpress.com by 210.87.254.6 on 09/05/12
For personal use only.

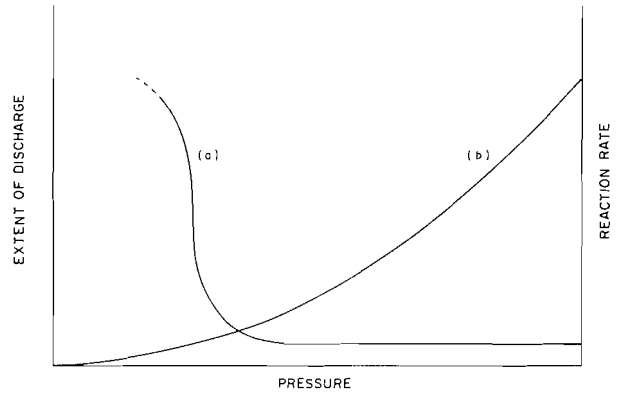

FIG. 4. Possible effects of pressure on (*a*) extent of discharging and (*b*) rate of chemical reaction.

the increasing conductivity along this series as expected, since an increase in surface conductivity will result in the accumulation of lower surface charge densities. However, other factors such as the potential depth of the electron traps in the insulator and the topology of the energy barrier to electron transfer also change along the series and these also will be important.

The Effect of Pressure

The complex dependence of the rate on the methane pressure is probably due to the result of the opposite effects of pressure on the two stages of the triboprocess; (*1*) initiation of the discharge; and (*2*) the reactions occurring in the discharge.

Consider first the effect of pressure on the breakdown of the gas. The field created by the separation of the mercury and glass will be proportional to the charge density, σ, on the two surfaces. Because one of the surfaces is a non-conductor, and further because the electron traps will be localized, there will be some spread in the value of the charge density and hence in the value of the field, E. At any one pressure, discharges will only occur near those sites where the critical breakdown field at this pressure is exceeded.

At high pressures very few sites will have fields sufficiently high to allow discharge to occur. No great change will take place on decreasing the pressure until the breakdown field required corresponds to the field created by the majority of sites. Further reduction in pressure will allow those sites with fields lower than the average to discharge. These changes are represented schematically by curve *a* of Fig. 4.

Consider now the effect of pressure on the rate of formation of C_2 hydrocarbons. Although no detailed mechanism can be formulated at present it is reasonable to assume that the rates of the reactions producing C_2 hydrocarbons will increase with increase in pressure. A second-order pressure dependence is shown in curve *b* of Fig. 4 for the purpose of discussion.

The overall influence of pressure on the yield of C_2 hydrocarbons will be the resultant of these two effects. The sharp discontinuity in the experimental curve occurs at that pressure of methane whose breakdown field corresponds to the field produced by most of the surface sites. The value of the pressure at which the discontinuity occurs can be used to give an order of magnitude estimate of the average charge density. The value of the breakdown field for methane at 200 Torr is estimated (10) to be 6800 V cm^{-1}. If the two surfaces are planar the field is given by $E = 4\pi\sigma/\varepsilon_0$ and thus $\sigma = E\varepsilon_0/4\pi$, where ε_0 is the dielectric constant for methane (4π will be replaced by different constants for different geometries). The value of σ so calculated is approximately 2 e.s.u. cm^{-2}, which is close to that found by other, more direct, methods (1, 11). The maximum number of surface sites will be given by the number of atoms in the surface (12) (10^{15} cm^{-2}) and hence if one electron is transferred to each site the

Can. J. Chem. Downloaded from www.nrcresearchpress.com by 210.87.254.6 on 09/05/12
For personal use only.

TABLE 2. Relative yields of products from methane decomposed by different processes

Process	Pressure (Torr)	Ethane	Ethylene	Acetylene	References
Triboprocess	200	100	34	32	This work*
Electrons (15 eV)	10^{-2}	100	49	46	19
Glow discharge (600 V cm^{-1})	6.84	100	83	76	21
Photolysis (121.6 nm)	350	100	<3	10	18
Photolysis (58.4 nm)	1.95	100	500	6.25	15, 16
X-rays (50 kV)	760	100	14	Very small	14

*Ratios of the C_2 products are essentially unchanged down to 0.05% decomposition of CH_4.

maximum charge density will be 5×10^5 e.s.u. cm^{-2}. The value of 2 e.s.u. cm^{-2} shows that very few surface sites are charged.

Addition of Inert Gases

Inert gases were added to the methane in order to determine whether energy transfer and sensitization could affect the rates of production of C_2 hydrocarbons. The addition of 10% of inert gas to methane did not result in any pronounced change in the C_2 hydrocarbon yields or affect the product distribution significantly (Table 1). This shows that charge transfer from inert gas ions or excitation by long-lived metastable states of the inert gases (*e.g.* He^3S) are not effective at the 10% level.

In the case of a 1:1 mixture of the inert gases and methane at 200 Torr total pressure there are significant and specific effects on the rate of C_2 production. Consideration of the ionization potentials and the ionization cross-sections of the inert gases and methane allows at least a phenomenological explanation of the effect of the inert gas additives to be given. The cross-sections for electronic excitation will probably be of a similar magnitude and follow the same order as those for ionization.

The absence of any real effect in the case of helium can probably be attributed to the much smaller cross-section of helium compared with that of methane.

There is a real increase in rates in the presence of argon which is probably associated with two factors: (*1*) the cross-section for argon is close to that for methane; and (*2*) argon has a metastable state, ^3S, at 11.55 eV above the ground state. Indeed, the argon does have a significant effect on the product distribution (the acetylene yield is doubled with respect to that of ethane) and this could arise because ionized or excited argon favors those routes which lead to acetylene.

The progressive increase in rates, argon < krypton < xenon, correlates with the increase in cross-section in this series. If is of interest that the ionization potential of xenon is below that of methane, since this suggests that the first excited state of the xenon ion with energy of 13.43 eV may be an important participant (13).

Possible Reaction Intermediates

The present results allow some conclusions to be drawn about the relative importance of intermediates such as radicals, ions or carbenes in the triboprocess.

Radicals

Oxygen produces a dramatic reduction in the ethane yield but is almost without effect on the ethylene and acetylene yields (Table 2). The C_3 yields are also reduced to near zero. This shows that ethane is produced principally from intermediates not involved in producing ethylene and acetylene. The reaction between radicals and oxygen (*e.g.*, $CH_3 + O_2 + M \rightarrow CH_3O_2$) is known to be very fast so that the decrease in ethane yield in the presence of oxygen indicates that methyl radical combination could be an important source of ethane. The localized nature of the discharge will favor radical–radical reactions. The fall in yield of the C_3 hydrocarbons also indicates that they are formed by free radical reactions. The absence of any large effect in the case of ethylene and acetylene shows that these products are formed via non-radical intermediates.

Can. J. Chem. Downloaded from www.nrcresearchpress.com by 210.87.254.6 on 09/05/12
For personal use only.

Can. J. Chem. Downloaded from www.nrcresearchpress.com by 210.87.254.6 on 09/05/12
For personal use only.

Ions

In the X-ray radiolysis (14) and vacuum u.v. photolysis (58.4 nm (15, 16)) the products are considered to arise from the reactions of the intermediates CH_4^+, CH_3^+, and $C_2H_3^+$. Since the product distribution from these processes (Table 2) is so different from that found in the present work under similar conditions, it is unlikely that these intermediates are important in the triboprocess. The participation of the CH_5^+ cannot be excluded but Field and Munson (17) have shown that this ion does not react rapidly with methane.

Carbenes

Mahan and Mandal (18), Ausloos and Lias (19) (photolysis at 123.6 nm), and Manton and Tickner (20) (15 eV electron irradiation), all suggest that singlet methylene (ground or excited state) may be an important precursor of the C_2 hydrocarbons in these cases. If this conclusion is correct the similar product distribution found in the triboprocess suggests that methylene may participate here also. The absence of any effect of oxygen on the yields of ethylene and acetylene is evidence for the formation of these hydrocarbons from a precursor that does not react appreciably with oxygen. Singlet methylene satisfies this requirement and the following reactions of this species can explain most of the present results.

$$CH_2 + CH_4 \rightarrow C_2H_6^*$$
$$C_2H_6^* \rightarrow C_2H_4 + H_2$$
$$\rightarrow C_2H_2 + 2H_2$$
$$\rightarrow 2CH_3$$
$$C_2H_6^* + M \rightarrow C_2H_6 + M$$

Methylene could be produced by electron excitation or by a recombination process:

$$CH_4 \xrightarrow{e} CH_4^* \rightarrow CH_2 + H_2$$
$$CH_4^+ + e \rightarrow CH_4^* \rightarrow CH_2 + H_2$$

Acetylene could also be produced from the reaction of C (^{1}D) atoms with methane (22),[1]

$$C(^1D) + CH_4 \rightarrow C_2H_2 + H_2$$

though we suspect that the relatively small effect of oxygen on the acetylene yield suggests that carbon atom reactions are not important in this system (23).

The C_3 hydrocarbons were not produced during the early stages of the triboprocess and are thus most likely to result from secondary reactions of the C_2 hydrocarbons.

[1]We are indebted to one of the referees for pointing out this possibility.

1. W. R. HARPER. Contact and frictional electrification. Clarendon Press, Oxford. 1967.
2. S. DE WALDEN. Acta Phys. Polon. **1**, 223 (1932).
3. K. IKENOUE and Y. SASADA. Mem. Def. Acad. Japan. II, No. 2, 49 (1962); II, No. 2, 57 (1962).
4. G. L. DYBWAD and C. E. MANDEVILLE. Phys. Rev. **161**, 527 (1967).
5. L. J. SCHOEN. Can. J. Phys. **38**, 967 (1960).
6. J. H. JOHNSON, R. H. KNIPE, and A. S. JORDAN. Can. J. Chem. **48**, 3604 (1970).
7. S. DE PAOLI and O. P. STRAUSZ. Can. J. Chem. **48**, 3756 (1970).
8. L. W. SIECK and R. H. JOHNSEN. J. Phys. Chem. **67**, 2281 (1963).
9. L. B. LOEB. Sci. **102**, 573 (1945).
10. H. RAETHER. Electron avalanches and breakdown in gases. Butterworths, London. 1964.
11. J. W. PETERSON. J. Appl. Phys. **25**, 907 (1954).
12. W. SHOCKLEY. Phys. Rev. **56**, 317 (1939).
13. R. E. FOX, W. M. HICKAM, and T. KJELDAS. Phys. Rev. **89**, 555 (1953).
14. G. G. MEISELS, W. H. HAMIL, and R. R. WILLIAMS. J. Phys. Chem. **61**, 1456 (1957).
15. P. AUSLOOS and R. E. REBBERT. J. Am. Chem. Soc. **90**, 7370 (1968).
16. C. A. JENSEN and W. F. LIBBY. J. Chem. Phys. **40**, 2831 (1968).
17. F. H. FIELD and M. S. B. MUNSON. J. Am. Chem. Soc. **87**, 3289 (1965).
18. B. H. MAHAN and R. MANDAL. J. Chem. Phys. **37**, 207 (1962).
19. P. AUSLOOS and S. G. LIAS. J. Chem. Phys. **38**, 2207 (1963); **48**, 392 (1968).
20. J. A. MANTON and A. W. TICKNER. Can. J. Chem. **38**, 858 (1960).
21. L. M. YEDDANAPALLI. J. Chem. Phys. **10**, 249 (1942).
22. E. TSCHUIKOW-ROUX, Y. INEL, S. KODAMA, and A. W. KIRK. J. Chem. Phys. **56**, 3238 (1972).
23. M. PANDOW, C. MACKAY, and R. WOLFGANG. J. Inorg. and Nucl. Chem. **14**, 153 (1960).

Metal–Amino Polycarboxylic Acid Complexes. IV. A Polarographic Study of Lead (II) Complexes with Diethylenetriaminepentaacetic Acid in Aqueous Solution[1]

P. LETKEMAN

Department of Chemistry, Brandon University, Brandon, Manitoba

AND

J. B. WESTMORE

Department of Chemistry, University of Manitoba, Winnipeg, Manitoba

Received June 5, 1972

Can. J. Chem. Downloaded from www.nrcresearchpress.com by 210.87.254.42 on 09/05/12
For personal use only.

The polarographic behavior of the lead ion in the presence of excess DTPA was studied over the pH range 2–10. Three different polarographic waves can be distinguished. The wave occurring at the most negative potentials and highest pH values is assigned to an irreversible reduction of $PbHA^{2-}$. The kinetic current treatment gives the results

$$PbHA^{2-} \underset{k \leqslant 8.7 \times 10^{8}\ M^{-1}\ s^{-1}}{\overset{k \geqslant 8.7 \times 10^{4}\ s^{-1}}{\rightleftharpoons}} PbA^{3-} + H^{+}$$

The wave occurring at intermediate potentials and pH values is also assigned to an irreversible reduction of $PbHA^{2-}$. The kinetic current treatment gives the results

$$PbHA^{2-} \underset{k = 2.6 \times 10^{4}\ M^{-1}\ s^{-1}}{\overset{k = 0.79\ s^{-1}}{\rightleftharpoons}} PbA^{3-} + H^{+}$$

Protonation is assumed to occur at different coordination sites. In the former case it occurs at the center carboxyl group; in the latter case it occurs at a terminal nitrogen atom. The reversible wave occurring at the most positive potentials and lowest pH values can be interpreted in either of two ways

$$Pb^{2+} + H_2A^{3-} \underset{k = 1.5 \times 10^{6}\ M^{-1}\ s^{-1}}{\overset{k = 2.5 \times 10^{10}\ M^{-1}\ s^{-1}}{\rightleftharpoons}} PbHA^{2-} + H^{+}$$

$$Pb^{2+} + H_2A^{3-} \underset{k = 1.6 \times 10^{4}\ s^{-1}}{\overset{k = 2.5 \times 10^{10}\ M^{-1}\ s^{-1}}{\rightleftharpoons}} PbH_2A^{-}$$

For the stability constant we obtained $\log K_{PbA} = 19.1$. All values above were obtained at 25° and an ionic strength of 0.2.

Nous avons étudié le comportement polarographique de l'ion plomb en présence d'un excès de DTPA, sur une gamme de pH de 2–10. On a pu distinguer trois vagues polarographiques différentes. La vague se produisant aux potentiels les plus négatifs et aux valeurs les plus élevées de pH est assignée à une réduction irréversible de $PbHA^{2-}$. Le traitement de courant cinétique donne les résultats suivants

$$PbHA^{2-} \underset{k \leqslant 8.7 \times 10^{8}\ M^{-1}\ s^{-1}}{\overset{k \geqslant 8.7 \times 10^{4}\ s^{-1}}{\rightleftharpoons}} PbA^{3-} + H^{+}$$

La vague située aux valeurs de pH et de potentiel intermédiaires est aussi assignée à une réduction irréversible de $PbHA^{2-}$. Le traitement de courant cinétique permet d'obtenir

$$PbHA^{2-} \underset{k = 2.6 \times 10^{4}\ M^{-1}\ s^{-1}}{\overset{k = 0.79\ s^{-1}}{\rightleftharpoons}} PbA^{3-} + H^{+}$$

On suppose que la protonation se produit à différents sites de coordination. Dans le premier cas, elle se produit en groupement carboxyl central; dans le dernier cas, à l'atome d'azote terminal.

[1]We thank the National Research Council of Canada for financial support of this work.

La vague réversible située aux potentiels les plus positifs et aux pH les plus bas peut s'interpréter de deux façons différentes

$$Pb^{2+} + H_2A^{3-} \underset{k = 1.5 \times 10^{6}\ M^{-1}\ s^{-1}}{\overset{k = 2.5 \times 10^{10}\ M^{-1}\ s^{-1}}{\rightleftharpoons}} PbHA^{2-} + H^{+}$$

$$Pb^{2+} + H_2A^{3-} \underset{k = 1.6 \times 10^{4}\ s^{-1}}{\overset{k = 2.5 \times 10^{10}\ M^{-1}\ s^{-1}}{\rightleftharpoons}} PbH_2A^{-}$$

Nous obtenons pour la constante de stabilité log $K_{PbA} = 19.1$ Toutes les valeurs précédentes ont été obtenues à 25° et à une force ionique de 0.2. [Traduit par le journal]

Canadian Journal of Chemistry, **50**, 3821 (1972)

Can. J. Chem. Downloaded from www.nrcresearchpress.com by 210.87.254.42 on 09/05/12
For personal use only.

Introduction

Information on the thermodynamics and kinetics of equilibria between metal ions and aminopolycarboxylic acids in aqueous solution is of importance from both a theoretical viewpoint and because of the wide use of aminopolycarboxylic acids in analytical applications. In favorable circumstances the polarographic method can be used to obtain such information and has been applied, for example, to the study of solutions of Cd^{2+} with NTA (1, 2), with EDTA (3), and with TTHA (4). In this paper we describe a systematic study of solutions of Pb^{2+} with diethylenetriaminepentaacetic acid (DTPA) by the polarographic method. These results complement and extend those obtained in our earlier proton magnetic resonance study of this system (5).

Experimental

DTPA (J. T. Baker) was recrystallized from hot water, dried, weighed, and dissolved in distilled water containing sufficient sodium hydroxide to affect solution. This was made up to a sufficient volume to give a 0.01 *M* stock solution. A stock solution of Pb^{2+} was prepared from lead nitrate (Fisher Scientific Co.). Chloroacetic acid – chloroacetate buffers were used for the p*H* range 2–4 and acetic acid – acetate buffers for the range 4–8. Sodium perchlorate was used to adjust the ionic strength of the test solution to 0.2. Triton X-100 was obtained from Rohm and Hass. All solutions were stored in polyethylene bottles. Test solutions were prepared by taking appropriate aliquots of the stock, buffer and sodium perchlorate solutions, then diluting to nearly the volume required. The p*H* was measured (Radiometer type PH28 p*H* meter calibrated at p*H* = 2.00, 4.01, and 6.86 with Beckman buffers), then adjusted by addition of sodium hydroxide or perchloric acid as required. The solution was then made up to its final volume with distilled water.

The test solutions were placed in one arm of an H-cell (6) immersed in a water thermostat, deoxygenated with nitrogen, and polarograms recorded with a Sargent model XXI polarograph. The potential of the dropping electrode was recorded against a saturated calomel electrode contained in the other arm of the H-cell. When accurate potential measurements were required a Rubicon type B precision potentiometer was used.

Capillary characteristics were measured at open circuit at a number of mercury heads (corrected for the interfacial tension at the mercury drop). For the most frequently used conditions the characteristics were: $h = 50$ cm, $h_{corr} = 48.4$ cm, $m = 1.733$ mg/s, $t = 5.02$ s, $m^{2/3}t^{1/6} = 1.887$; $h = 60$ cm, $h_{corr} = 58.4$ cm, $m = 2.071$ mg/s, $t = 4.20$ s, $m^{2/3}t^{1/6} = 2.064$; $h = 70$ cm, $h_{corr} = 68.4$ cm, $m = 2.396$ mg/s, $t = 3.63$ s, $m^{2/3}t^{1/6} = 2.217$; where the symbols have their conventional meanings.

Results

In the p*H* range 2–4 polarograms of solutions containing Pb(II) and DTPA exhibited strong maxima. These maxima could be suppressed by the addition of small amounts of gelatin or Triton X-100. Detailed studies showed the latter compound to perform better as a maximum suppressor than the former. Figure 1 shows the effect of various concentrations of Triton X-100 on the polarograms of a 1:2, Pb(II):DTPA solution at p*H* = 4.0. Low concentrations of Triton X-100 suppress the maximum and reveal that at least three waves are present in the polarogram. Higher concentrations of Triton X-100 shift the waves to more negative potentials and reduce the heights of the waves. Triton X-100 (up to 0.003%) had little effect on the reduction of free Pb^{2+} other than to suppress the maximum. Above p*H* = 4 the addition of a maximum suppressor was unnecessary.

Figure 2 shows the effect of addition of increasing amounts of DTPA added to a given amount of Pb^{2+} at p*H* = 4.0. As the DTPA concentration increases the height of the original wave decreases and a second wave appears at more negative potentials. Polarograms obtained at higher ligand concentrations show a third

Can. J. Chem. Downloaded from www.nrcresearchpress.com by 210.87.254.42 on 09/05/12
For personal use only.

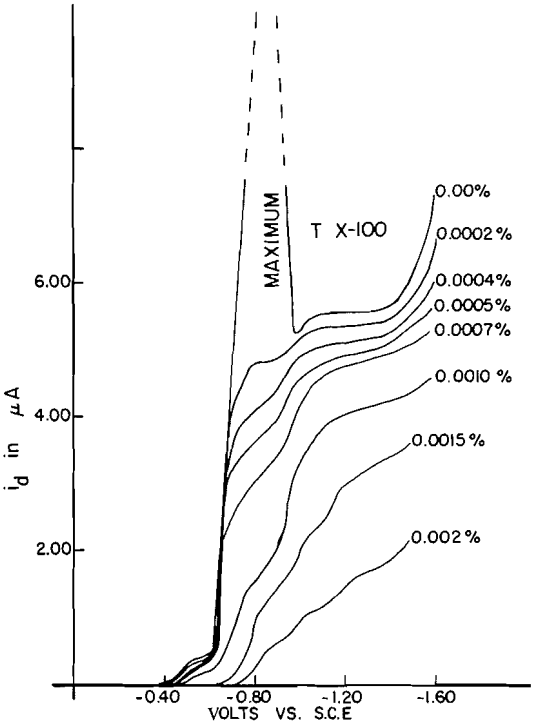

FIG. 1. Effect of Triton X-100 on the polarogram. Experimental conditions: [lead] = 1.0×10^{-3} M; [DTPA] = 2.0×10^{-3} M; pH = 4.0; h = 60 cm; t = 4.20 s; μ = 0.2; T = 25°.

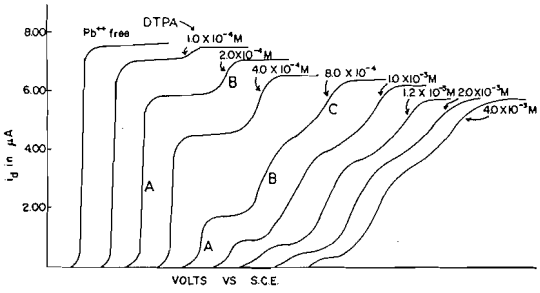

FIG. 2. Effect of DTPA concentrations on the polarograms. Experimental conditions: [lead] = 1.0×10^{-3} M; pH = 4.0; h = 60 cm; t = 4.20 s; μ = 0.2; T = 25°; Triton X-100 = 0.0001%. (For clarity, successive polarograms are displaced along the abscissa.)

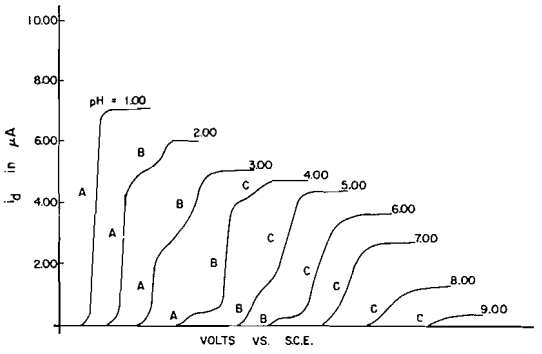

FIG. 3. Effect of pH on the polarograms. Experimental conditions: [lead] = 1.0×10^{-3} M; [DTPA] = 2.0×10^{-3} M; h = 60 cm; t = 4.20 s; μ = 0.2; T = 25°; Triton X-100 = 0.0001% (pH ≤ 4.0), 0% (pH > 4.0). (For clarity, successive polarograms are displaced along the abscissa.)

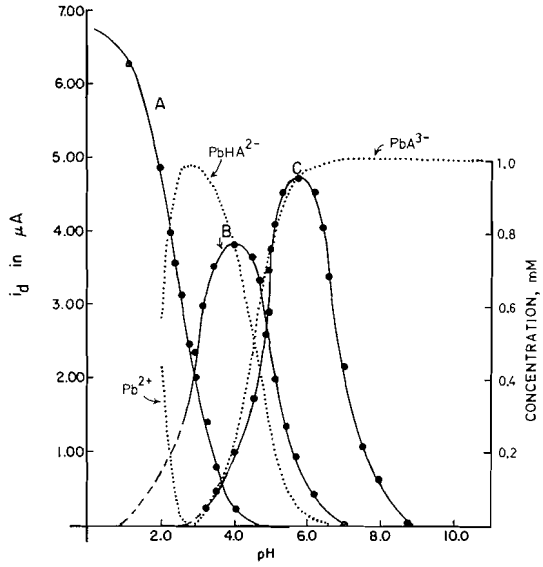

FIG. 4. Limiting currents of waves A, B, and C as a function of pH (solid line) and calculated concentrations of lead-containing species (dotted line). Conditions: [lead] = 1.0×10^{-3} M; [DTPA] = 2.0×10^{-3} M; h = 60 cm; t = 4.20 s; μ = 0.2; T = 25°.

wave, at yet more negative potentials. In subsequent discussion the three waves will be referred to as waves A, B, and C, respectively. As the concentration of ligand is increased, the height of wave A decreases, but wave A is still detectable up to the highest ligand concentrations shown. The heights and positions of the three waves were strongly pH dependent, as verified by studies on solutions with metal:ligand concentration ratios of 1:2 and 1:8. Results obtained for the 1:2 ratio are shown in Figs. 3, 4, and 5.

The characteristics of the three waves are summarized in Table 1. It is appropriate to recall the following properties of polarographic waves: (i) for a reversible two-electron reduction at 25°

Can. J. Chem. Downloaded from www.nrcresearchpress.com by 210.87.254.42 on 09/05/12
For personal use only.

TABLE 1. Characteristics of the polarographic waves of Pb(II) – DTPA solutions

Wave	Total metal ion concentration in mM	Total ligand concentration in mM	Ionic strength in M	pH	Suppressor Triton X-100	Reciprocal slope of log $i/(i_l - i)$ *vs.* E plot at 25 °C	Dependence of i_l on mercury head	Temperature coefficient between 20° and 50° in % per °C
A, $i_l > 25\%\ i_d$	1.0	2.0	0.2	3.0	0.001%	-29 ± 2 mV	$i_l \propto h_{corr}^{1/2}$	—
A, $i_l < 10\%\ i_d$	1.0	2.0	0.2	4.0	0.001%	—	partially dependent*	4.1
A	1.0	8.0	0.2	4.0	0.001%	-30 ± 2 mV	nearly independent†	4.2
B	1.0	2.0	0.2	6.0	0	-56 ± 2 mV	nearly independent†	3.9
B	1.0	8.0	0.2	6.0	0	-62 ± 2 mV	nearly independent†	4.0
C	1.0	2.0	0.2	7.0	0	-99 ± 4 mV	nearly independent†	4.0
C	1.0	8.0	0.2	7.0	0	-91 ± 2 mV	nearly independent†	4.0

*i_l increases but by less than required for diffusion control.
†i_l increases slightly as h increases.

Can. J. Chem. Downloaded from www.nrcresearchpress.com by 210.87.254.42 on 09/05/12
For personal use only.

a reciprocal slope of -29.5 mV for the plot of $\log \{i/(i_l - i)\}$ *vs.* E is required. An irreversible reduction will give a value numerically greater than 29.5 mV; (*ii*) for a diffusion controlled reduction $i_l \propto h_{corr}^{1/2}$, whereas for a kinetically controlled reduction i_l is independent of h_{corr}; (*iii*) diffusion controlled waves typically have wave height temperature coefficients of about 1.5%/°C. Kinetically controlled reduction waves usually have temperature coefficients significantly greater than this. Table 1 allows the following conclusions about the waves to be drawn:

Wave A

This wave changes from a diffusion controlled to a kinetically controlled reduction wave as the pH increases, *e.g.* at p$H = 4.00$ when i_l was less than 10% of the total diffusion current its properties resemble those of a kinetic wave. The electrochemical reduction step is however reversible.

Waves B and C

At small wave heights, *e.g.* at p$H = 6.0$ and p$H = 7.0$, respectively, the properties of these waves are consistent with those of irreversible, kinetically controlled reduction waves.

Supplementary Studies

To supply data required for the mathematical interpretation of the characteristics of wave A, the diffusion currents and half-wave potentials of the lead ion were measured in solutions identical to those of the test solutions except that they did not contain DTPA. The values of the half-wave potentials in the buffer solutions are shown in Fig. 5.

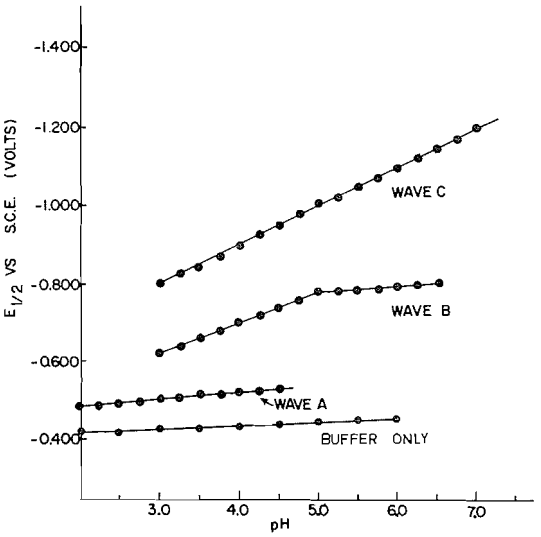

FIG. 5. Half-wave potentials of waves A, B, and C as a function of pH, and of free lead in the same buffer. Conditions: [lead] = 1.0×10^{-3} M; [DTPA] = 2.0×10^{-3} M; $h = 60$ cm; $t = 4.20$ s; $T = 25°$; $\mu = 0.2$.

Discussion

The polarographic method of determining formation constants from half-wave potentials requires a reversible electron-transfer electrode reaction. Hence only wave A could yield information of this type. Although waves B and C could not be used to obtain formation constants the waves can be analyzed by the kinetic wave treatment (see Appendix 2) to obtain data on the rates of chemical equilibria in the solutions. The species in solution can be deduced from equilibrium constant data and are shown in Fig. 4 using the values $K_{PbA} = 10^{18.9}$, $K^{H}_{PbHA} = 10^{4.52}$ (7), where DTPA is represented by H_5A, and allowing for the complexing effect of the buffer. (Throughout this paper, published equilibrium constants are used without any attempt to correct for effects of ionic strength. We used a constant ionic strength of 0.2 throughout.) The waves are discussed in order of increasing complexity of interpretation, *i.e.* in reverse order.

Wave C

Potentiometric (7) and n.m.r. (5) measurements on solutions containing Pb^{2+} and DTPA have been interpreted by the existence of pH dependent equilibria involving the complex species $PbHA^{2-}$ and PbA^{3-} in solution. When p$H > 6$, in presence of excess DTPA, the only metal-containing species present in solution in significant concentration is PbA^{3-}. If this species is non-reducible at the dropping mercury electrode, this would account for the disappearance of all reduction waves when p$H > 9$. The assumption that wave C is due to the reduction of $PbHA^{2-}$ results in a successful application of the kinetic wave theory. We can write the reactions as

$$PbHA^{2-} \underset{k_p}{\overset{k_d}{\rightleftharpoons}} PbA^{3-} + H^+ \quad \text{(rate determining)}$$

$$PbHA^{2-} + Hg + 2e^- \rightleftharpoons Pb(Hg) + HA^{4-} \quad \text{(fast when mean limiting current reached)}$$

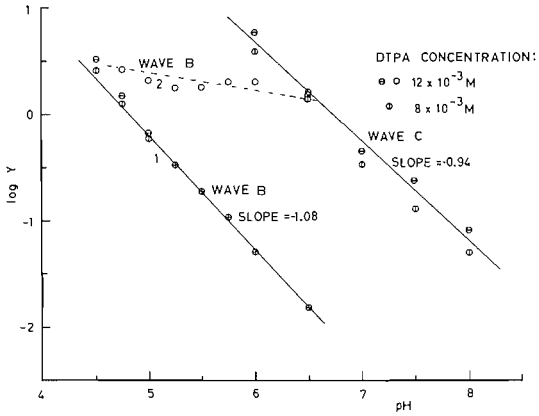

FIG. 6. Test of kinetic current theory for waves B and C. Wave B: 1 (solid line), $\log Y = \{\log i_l/(i_d - i_l)\} + \log \alpha_{PbA(H)}$. Wave B: 2(broken line), $\log Y = \log \{i_l/(i_d - i_l)\} + \log \alpha_{PbHA(H)}$. Wave C: $\log Y = \log \{i_l/(i_d - i_l)\}$. Conditions: [lead] = 1.0×10^{-3} M; [DTPA] = 2.0×10^{-3} M, and 8.0×10^{-3} M; $h = 60$ cm; $t = 4.20$ s; $\mu = 0.2$; $T = 25°$.

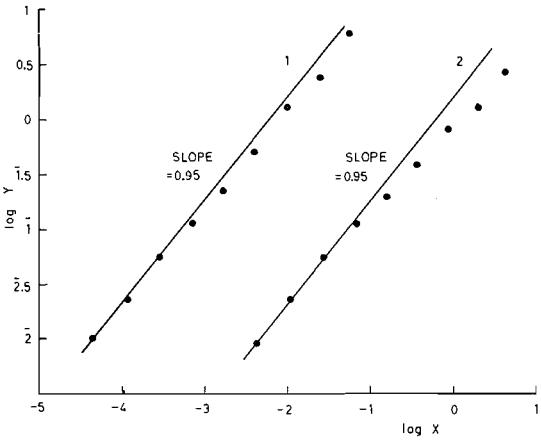

FIG. 7. Test of kinetic current theory for wave A. Plot 1: $\log Y = \log\{i_l/(i_d - i_l)\} + \log\{1 + (i_l C_M \alpha_{H_2A(H)})/(i_d C_L \alpha_{PbHA(H)})\}$; $\log X = \frac{1}{2}\{\log \alpha_{Pb(B)} + \log \alpha_{H_2A(H)}\} - \log \alpha_{PbHA(H)} - \text{pH}$. Plot 2: $\log Y = \log \{i_l/(i_d - i_l)\} + \log \{1 + (i_l C_M \alpha_{H_2A(H)})/(i_d C_L \alpha_{PbH_2A(H)})\}$; $\log X = \frac{1}{2}\{\log \alpha_{Pb(B)} + \log \alpha_{H_2A(H)}\} - \log \alpha_{PbH_2A(H)}$. Conditions: [lead] = 1.0×10^{-3} M; [DTPA] = 8.0×10^{-3} M; $h = 60$ cm; $t = 4.20$ s; $\mu = 0.2$; $T = 25°$.

For this reaction (see appendix 2) a plot of $\log\{i_l/(i_d - i_l)\}$ *vs.* pH should yield a straight line with slope = -1.0 (see eq. A2.2). This is verified in Fig. 6 where the value of $i_d = 5.4$ μA (the maximum value of the sum of the heights of wave B and wave C) was used at $t = 4.2$ s. We return to discussion of this reaction after some discussion of wave B.

Wave B

The reaction that was expected to produce this wave was:

$$\underset{\text{reducible}}{PbH_2A^-} \underset{k_p}{\overset{k_d}{\rightleftharpoons}} PbHA^{2-} + H^+ \quad \text{(rate determining)}$$

provided that the equilibrium concentration of PbH_2A^- is insignificant. In fact, potentiometric (7) and n.m.r. (5) studies have failed to detect the species PbH_2A^- when p$H > 2$ suggesting that its concentration in solution never exceeds an upper limit of about 5–10% of other complex species, *i.e.* $K^H_{PbH_2A} \leqslant 10^{2.0}$. Thus, $[PbH_2A^-]$ should certainly be insignificant at pH = 5–6.5. Equation A2.4 given as a solution to the above reaction scheme must be modified to include the pH dependence of $[PbHA^{2-}]$ to give

$$[1] \qquad \frac{i_l}{i_d - i_l} = \frac{0.886\ [H^+]}{\alpha_{PbHA(H)}} \sqrt{k_p t K^H_{PbH_2A}}$$

where $\alpha_{PbHA(H)} = 1 + K^H_{PbHA}/[H^+]$ (see eq. A1.6). A plot of $\log\{i_l/(i_d - i_l)\} + \log \alpha_{PbHA(H)}$ *vs.* pH is shown in Fig. 6. A straight line with a slope of -1.0 should be obtained but the observed slope (-0.15 approx.) is significantly different from this. The reaction scheme

$$\underset{\text{reducible}}{PbH_2A^-} \rightleftarrows PbHA^{2-} \rightleftarrows PbA^{3-}$$

where the equilibria involve reactions of comparable rates was also considered. The solution to this problem has been given by Koutecky (8). It was found that wave B did not correspond to this reaction scheme. The only reaction that was found to give a satisfactory response to the kinetic wave theory was

$$\underset{\text{reducible}}{PbHA^{2-}} \underset{k_p}{\overset{k_d}{\rightleftharpoons}} PbA^{3-} + H^+ \quad \text{(rate determining)}$$

as for wave C. The corrected form of eq. A2.2 is

$$[2] \qquad \frac{i_l}{i_d - i_l} = \frac{0.886\ [H^+]}{\alpha_{PbA(H)}} \sqrt{k_p t K^H_{PbHA}}$$

A plot of $\log\{i_l/(i_d - i_l)\} + \log \alpha_{PbA(H)}$ *vs.* pH has a slope close to -1.0 (see Fig. 6). The implication of this result is that the protonated complex giving rise to wave B has a different structure from the protonated complex giving rise to wave C.

Can. J. Chem. Downloaded from www.nrcresearchpress.com by 210.87.254.42 on 09/05/12
For personal use only.

Can. J. Chem. Downloaded from www.nrcresearchpress.com by 210.87.254.42 on 09/05/12
For personal use only.

Interpretation of Waves B and C

Application of the kinetic wave theory to these waves leads to rate expressions of the same kinetic form, namely, rate $= k_p[PbA^{3-}][H^+]$, with different values of k_p for each wave. Thus, the waves can be interpreted as the reduction of protonated complexes of different structures. The slower protonation reaction leads to the more readily reduced complex. Previously, we have interpreted the structure of PbA^{3-} from n.m.r. studies (5) and suggest that the present observation can be explained by the scheme

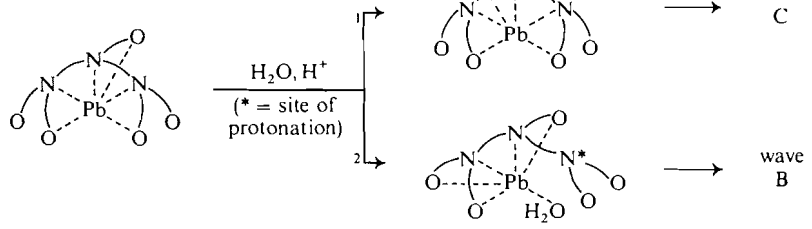

This scheme makes no implication as to the rate-determining steps in what are certainly multi-step reactions. The slow step in each reaction is likely to be the breakage of the appropriate metal ligand bond, and entry of a water molecule into the coordination shell of the metal ion; this is followed by rapid proton transfer equilibria. Protonation of the ligating atoms would block their reentry into the coordination shell. The lability of the metal–water bonds in the protonated complexes would provide an opportunity for electron transfer to occur at the electrode surface.

Although reaction 1 is assumed to be much faster than reaction 2 the equilibrium constant is such that its product is not detectable by the n.m.r. studies, *i.e.* the measured equilibrium constant $K^H_{PbHA} = 10^{4.52}$ (7) corresponds to that for reaction 2 and the corresponding equilibrium constant for reaction 1 will be smaller than this. If we assume an upper limit of $10^{4.0}$ for this equilibrium constant then the wave C data lead to a lower limit for reaction 1 for k_p of 8.7×10^8 l mol^{-1} s^{-1} and an upper limit for k_d of 8.7×10^4 s^{-1}. For reaction 2, using the wave B data, we obtain $k_p = 2.6 \times 10^4$ l mol^{-1} s^{-1} and $k_d = 0.79$ s^{-1}. Furthermore, it is reasonable to expect reaction 2 to be slower than reaction 1 because more extensive reorganization of the coordination shell of the metal ion is necessary. In addition, in aminopolycarboxylate complexes the metal–oxygen bonds are more labile than the metal–nitrogen bonds (see ref. 5 and references therein).

Wave A

Wave A is due to a reversible electrochemical reduction. Its height is much greater than expected from the equilibrium concentration of uncomplexed Pb^{2+} (see Fig. 4). Wave A can be explained by the reduction of uncomplexed Pb^{2+} produced by a rate determining dissociation of its DTPA complex in the diffusion layer. Application of the kinetic current treatment in the pH region where the equilibrium concentration of Pb^{2+} is insignificant, *i.e.* when p$H \geqslant 3$ (Fig. 4) shows that the major contribution to production of wave A under kinetic control conditions comes from the sequence:

$$\underset{\text{reducible}}{Pb^{2+}} + H_2A^{3-} \rightleftarrows PbH_2A^- \rightleftarrows PbHA^{2-} + H^+$$

where it is not possible to determine mathematically which reaction is rate determining. If the reaction $PbHA^{2-} + H^+ \rightarrow PbH_2A^-$ is rate determining, followed by a rapid dissociation of PbH_2A^- at the electrode surface to give free Pb^{2+}, the reaction reduces to

$$\underset{\text{reducible}}{Pb^{2+}} + H_2A^{3-} \underset{k_2}{\overset{k_1}{\rightleftharpoons}} PbHA^{2-} + H^+$$

The species Pb^{2+}, H_2A^{3-}, and $PbHA^{2-}$ also participate in other equilibria. After applying the necessary corrections (see appendix 1) to eq. A2.6 the expected limiting current for wave A

Can. J. Chem. Downloaded from www.nrcresearchpress.com by 210.87.254.42 on 09/05/12
For personal use only.

is given by

$$[3]\quad \left(\frac{i_l}{i_d - i_l}\right)\left(1 + \frac{i_l}{i_d}\cdot\frac{C_M}{C_L}\cdot\frac{\alpha_{H_2A(H)}}{\alpha_{PbHA(H)}}\right)^{1/2} = \frac{0.886\,[H^+]}{\alpha_{PbHA(H)}}\sqrt{\frac{k_2 t \alpha_{Pb(B)}\alpha_{H_2A(H)}}{K_{eq}C_L}}$$

where C_L is the overall concentration of ligand not bound up in complex formation, and C_M is the overall concentration of metal. Hence, a plot of log (l.h.s.) *vs.* $\frac{1}{2}(\log \alpha_{Pb(B)} + \log \alpha_{H_2A(H)}) - \log \alpha_{PbHA(H)} - pH$ should yield a straight line with a slope = 1.0. This plot is shown in Fig. 7.

Alternatively, if the rate determining step in supplying Pb^{2+} to the electrode surface is dissociation of PbH_2A^- the reaction reduces to

$$\underset{\text{reducible}}{Pb^{2+}} + H_2A^{3-} \underset{k_4}{\overset{k_3}{\rightleftharpoons}} PbH_2A^-$$

$$K^{Pb}_{PbH_2A} = k_3/k_4$$

The expected limiting current for wave A is given by

$$[4]\quad \left(\frac{i_l}{i_d - i_l}\right)\left(1 + \frac{i_l}{i_d}\cdot\frac{C_M}{C_L}\cdot\frac{\alpha_{H_2A(H)}}{\alpha_{PbH_2A(H)}}\right)^{1/2} = \frac{0.886}{\alpha_{PbH_2A(H)}}\sqrt{\frac{k_4 t \alpha_{Pb(B)}\alpha_{H_2A(H)}}{K^{Pb}_{PbH_2A}C_L}}$$

This equation was obtained by modifying eq. A2.9 to allow for participation by Pb^{2+}, H_2A^{3-}, and PbH_2A^{2-} in other equilibria. A plot of log (l.h.s.) *vs.* $\frac{1}{2}(\log \alpha_{H_2A(H)} + \log \alpha_{Pb(B)}) - \log \alpha_{PbH_2A(H)}$ should yield a straight line with a slope = 1.0. To test this plot, values $\alpha_{PbH_2A(H)}$ are required. These were calculated using an upper limit, discussed earlier, for $K^{H}_{PbH_2A}$ of $10^{2.0}$. Use of this value does not greatly affect values of $\alpha_{PbHA(H)}$ when $pH \geqslant 2.5$, as used in the previous test plot. The plot is shown in Fig. 7. The two plots shown in Fig. 7 are very similar in form because $\alpha_{PbHA(H)} = [H^+]K^{Pb}_{PbH_2A}\alpha_{PbH_2A(H)}$. The slopes of the plots at the high pH end are close to the required value of 1.0 but deviations occur at the low pH end, where uncertainties in data used in calculating α functions probably lead to greater inaccuracies, and the conditions desired for true kinetic currents hold less rigorously.

Approximate rate constants for these reactions were calculated using the data for pH = 4.50. For the first case, using eq. A2.6 to evaluate $K_{eq} = 10^{4.5} \times 10^{18.9} \times 10^{-8.7} \times 10^{-10.5} = 10^{4.2}$, we obtain $k_2 = 1.5 \times 10^6$ l mol^{-1} s^{-1} and $k_1 = 2.5 \times 10^{10}$ l mol^{-1} s^{-1}. For the second case, using eq. A2.9 to evaluate $K^{Pb}_{PbH_2A} = 10^{2.0} \times 10^{4.5} \times 10^{8.9} \times 10^{-8.7} \times 10^{-10.5} = 10^{6.2}$ as an upper limit, we obtain $k_4 = 1.6 \times 10^4$ s^{-1} (lower limit) and $k_3 = 2.5 \times 10^{10}$ l mol^{-1} s^{-1} (not dependent on value of $K^{Pb}_{PbH_2A}$). If the first case is rate determining then a higher value for k_4 is implied. If the second case is rate-determining then a higher value for k_2 is implied. We suggest that the slow step in each case would be the breakage of a metal–ligand bond as the complex further unwraps after the first metal–nitrogen bond is broken. In the first case breakage of the second metal–nitrogen bond (probably that involving the center nitrogen atom) is rate-determining; in the second case breakage of the third metal–nitrogen bond is rate-determining.

Calculation of Equilibrium Constants

Since wave A corresponds to a reversible reduction of lead ions the half-wave potentials may be used for the calculation of equilibrium constants. For a reversible diffusion-controlled reduction of a metal complex the dependence of the half-wave potential on the stability constant has been given (9), and for a 1:1 metal:ligand complex at 25°, simplifies to

$$[5]\quad E^c_{1/2} = E^s_{1/2} - \frac{0.0591}{n}\log K_{app}C^0_L$$

where $E^c_{1/2}$ and $E^s_{1/2}$ are the half-wave potentials of the complex and simple ions, respectively, K_{app} is the apparent stability constant of the complex under the prevailing conditions, and C^0_L is the concentration of ligand at the electrode surface. For a kinetically controlled reversible reduction at 25 °C $E^c_{1/2}$ is related to $E^k_{1/2}$, the measured half-wave potential of the kinetic wave (10) by

$$[6]\quad E^c_{1/2} = E^k_{1/2} + \frac{0.0591}{n}\log\frac{i_l}{i_d}$$

where i_l is the limiting kinetic current. Also

$$C^0_L = C_L + C_M\cdot\frac{i_l}{i_d}$$

where C_L is the free ligand concentration and C_M is the overall metal ion concentration.

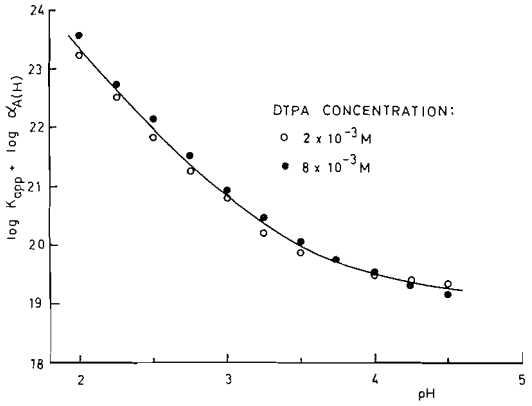

Fig. 8. Values of $\log K_{app} + \log \alpha_{A(H)}$ as a function of pH. Conditions: [lead] = 1.0×10^{-3} M: [DTPA] = 2.0×10^{-3} M and 8.0×10^{-3} M; $h = 60$ cm; $t = 4.20$ s; $\mu = 0.2$; $T = 25°$.

Combining and rearranging eqs. 1 and 2 we obtain

$$[7] \quad \log K_{app} = \frac{n}{0.0591}(E^{k}_{1/2} - E^{s}_{1/2}) - \log \frac{i_l}{i_d} - \log C^{0}_{L}$$

Values of $\log K_{app}$ were calculated from the wave A data (Fig. 5) over the pH range 2.0–4.5. The effect of the buffer on half-wave potentials is cancelled out by taking $E^{s}_{1/2}$ as the value for the free lead ion in the same buffer at the same pH.

Using the methods of appendix 1 it is now readily shown that

$$[8] \quad K_{app} = K_{PbA}\alpha_{PbA(H)}/\alpha_{A(H)}$$

or

$$[9] \quad \log K_{app} + \log \alpha_{A(H)} = \log K_{PbA} + \log \alpha_{PbA(H)}$$

If we assume that a series of protonated complexes is possible then using the methods of appendix 1, it can be shown that

$$[10] \quad \alpha_{PbA(H)} = [1 + 10^{\log K^{H}_{PbHA} - pH} + 10^{\log K^{H}_{PbH_2A} + \log K^{H}_{PbHA} - 2pH} + \ldots]$$

an expression which is convenient for graphical interpretation. In Fig. 8, $\log K_{app} + \log \alpha_{A(H)}$ is plotted against pH. Assuming that singly, doubly, and triply protonated complexes are possible the best fit to the experimental data was obtained from

$$[11] \quad \log K_{app} + \log \alpha_{A(H)} = 19.10 + \log (1 + 10^{4.05 - pH} + 10^{7.45 - 2pH} + 10^{10.20 - 3bH})$$

which gives $\log K_{PbA} = 19.10$, $\log K^{H}_{PbHA} = 4.05$, $\log K^{H}_{PbH_2A} = 3.40$, and $\log K^{H}_{PbH_3A} = 2.75$. The first of these equilibrium constants is in good agreement with the literature value (7) used earlier and supports our interpretation of wave A. The other values are inaccurate since other reliable evidence (5, 7) fails to detect doubly and triply protonated complexes when p$H \geqslant 2$. Reasons for the failure of the polarographic method here are not obvious but may be associated with the necessity to use a maximum suppressor when p$H < 4.0$.

Appendix 1

Use of Alpha Coefficients

The nature of the solutions studied in this report is complex. Several species participate in many side reactions and to simplify the equations used in other parts of the paper we have adopted the use of alpha coefficients introduced by Schwarzenbach (11) and further described by Ringbom (12). For example, for a ligand L which can complex with a metal but also participate in various side reactions we have

$$[A1.1] \quad \alpha_L = \frac{[L']}{[L]}$$

where [L] denotes the concentration of the free active form of the ligand in solution and [L′] denotes the concentration not only of the free ligand but also all the concentrations of the complexing agent not bound to the metal. Thus, for DTPA, which can be represented as H_5A, we can write

$$[A1.2] \quad \alpha_{A(H)} = ([A^{5-}] + [HA^{4-}] + [H_2A^{3-}] + [H_3A^{2-}] + [H_4A^{-}] + [H_5A])/[A^{5-}]$$

where $\alpha_{A(H)}$ is a coefficient accounting for the influence of the side reaction between A^{5-} and H^{+} on the reaction between A^{5-} and the metal

Can. J. Chem. Downloaded from www.nrcresearchpress.com by 210.87.254.42 on 09/05/12
For personal use only.

Can. J. Chem. Downloaded from www.nrcresearchpress.com by 210.87.254.42 on 09/05/12
For personal use only.

ion. Equation A1.2 can be rewritten as

$$[A1.3]\quad \alpha_{A(H)} = 1 + \frac{[H^+]}{K_5} + \frac{[H^+]^2}{K_4K_5} + \frac{[H^+]^3}{K_3K_4K_5} + \frac{[H^+]^4}{K_2K_3K_4K_5} + \frac{[H^+]^5}{K_1K_2K_3K_4K_5}$$

where K_1, K_2, K_3, K_4, and K_5 are the successive ionization constants of DTPA. Values of $\alpha_{A(H)}$ were calculated using the following values of the ionization constants: $pK_1 = 1.92$, $pK_2 = 2.66$, $pK_3 = 4.34$, $pK_4 = 8.67$, $pK_5 = 10.50$, which are an average of literature values (12–15). If required, values of $\alpha_{HA(H)}$, $\alpha_{H_2A(H)}$, etc. can be obtained by similar methods.

Metal ions which are not complexed to L may be involved in complex formation reactions with buffer components, and we can write

$$[A1.4]\quad \alpha_{M(B)} = \frac{[M^{z+}] + [MB]}{[M^{z+}]} = 1 + \frac{[MB]}{[M^{z+}]}$$

where [MB] represents the sum of concentrations of complexes between buffer and metal ions. For a buffer containing the components of a monobasic acid, such as acetic or chloroacetic acid, equation A1.4 becomes

$$[A1.5]\quad \alpha_{M(B)} = 1 + K_{MB}[B^-] = 1 + \frac{K_{MB}C_B}{(1 + [H^+]K_a^{-1})}$$

where K_{MB} is the stability constant of the complex of the metal ion with B^-, K_a is the ionization constant of HB, and C_B is the overall concentration of the buffer. Values of $\alpha_{M(B)}$ can usually be found from tabulated values (12) or calculated from published equilibrium constants (16).

Complexes between metal ions and complexing agent may also exist in a number of protonated forms, and we can write, for example

$$[A1.6]\quad \alpha_{MHL(H)} = \frac{[ML] + [MHL] + [MH_2L] + \ldots}{[MHL]}$$

which can be rewritten

$$[A1.7]\quad \alpha_{MHL(H)} = \frac{1}{[H^+]K^H_{MHL}} + 1 + [H^+]K^H_{MH_2L} + \ldots$$

where

$$K^H_{MHL} = \frac{[MHL]}{[ML][H^+]}$$

and

$$K^H_{MH_2L} = \frac{[MH_2L]}{[MHL][H^+]} \quad \text{etc.}$$

Expressions for $\alpha_{ML(H)}$, $\alpha_{MH_2L(H)}$ can be obtained by similar methods.

Appendix II

Treatment of Polarographic Kinetic Currents

The theoretical treatment of polarographic kinetic currents was developed and described in numerous publications, mainly by Koutecky, and by Koryta, and by Brdicka. References to this work are contained in reviews by Brdicka, Hanus, and Koutecky (17) and by Koryta (18). The equations summarized below can be derived from those in the former review.

The reaction

$$[A2.1]\quad \underset{\text{reducible}}{MHA^{2-}} \underset{k_p}{\overset{k_d}{\rightleftharpoons}} MA^{3-} + H^+$$

where k_d and k_p are the overall proton dissociation and protonation rate constants, respectively, belongs to reaction scheme III*a* (17). Under kinetic control conditions the relationship of the mean limiting current, i_l, to the mean current, i_d, expected for a diffusion controlled process is given by

$$[A2.2]\quad \frac{i_l}{i_d - i_l} = 0.886[H^+]\sqrt{k_p t K^H_{MHA}}$$

where t is the drop time, and

$$K^H_{MHA} = \frac{[MHA^{2-}]}{[MA^{3-}][H^+]} = \frac{k_p}{k_d}$$

Similarly, for the reaction

$$[A2.3]\quad \underset{\text{reducible}}{MH_2A^-} \underset{k_p}{\overset{k_d}{\rightleftharpoons}} MHA^{2-} + H^+$$

$$[A2.4]\quad \frac{i_l}{i_d - i_l} = 0.886[H^+]\sqrt{k_p t K^H_{MH_2A}}$$

where

$$K^H_{MH_2A} = \frac{[MH_2A^-]}{[MHA^{2-}][H^+]} = \frac{k_p}{k_d}$$

A reaction of the type

$$[A2.5]\quad \underset{\text{reducible}}{M^{2+}} + H_2A^{3-} \underset{k_2}{\overset{k_1}{\rightleftharpoons}} MHA^{2-} + H^+$$

belongs to the reaction scheme V*a* (17). The solution is

$$[A2.6]\quad \left(\frac{i_l}{i_d - i_l}\right)\left(1 + \frac{[MHA^{2-}]}{[H_2A^{3-}]}\cdot\frac{i_l}{i_d}\right)^{1/2} = 0.886[H^+]\sqrt{\frac{k_2 t}{K_{eq}[H_2A^{3-}]}}$$

where the equilibrium constant is given by

$$[A2.7]\quad K_{eq} = K^H_{MHA}K_{MA}K_4K_5$$

A reaction of the type

$$[A2.8]\quad \underset{\text{reducible}}{M^{2+}} + H_2A^{3-} \underset{k_4}{\overset{k_3}{\rightleftharpoons}} MH_2A^-$$

leads to the result

$$[A2.9]\quad \left(\frac{i_l}{i_d - i_l}\right)\left(1 + \frac{[MH_2A^-]}{[H_2A^{3-}]}\cdot\frac{i_l}{i_d}\right)^{1/2} = 0.886\sqrt{\frac{k_4 t}{K^M_{MH_2A}[H_2A^{3-}]}}$$

where the equilibrium constant, $K^M_{MH_2A}$, is given by

$$[A2.10]\quad K^M_{MH_2A} = \frac{[MH_2A^-]}{[M^{2+}][H_2A^{3-}]} = K^H_{MH_2A}K^H_{MHA}K_{MA}K_4K_5$$

1. J. KORYTA. Coll. Czech. Chem. Commun. **24**, 2903 (1959).
2. C. V. D'ALKAINE and J. KORYTA. Coll. Czech. Chem. Commun. **34**, 2138 (1969).
3. R. W. SCHMID and C. N. REILLEY. J. Am. Chem. Soc. **80**, 2101 (1958).
4. G. CONRADI, M. KOPANICA, and J. KORYTA. Coll. Czech. Chem. Commun. **30**, 2029 (1965).
5. P. LETKEMAN and J. B. WESTMORE. Can. J. Chem. **49**, 2073 (1971).
6. L. MEITES. Polarographic techniques. 2nd ed. Interscience. 1965. p. 321.
7. G. ANDEREGG, P. NÄGELI, F. MÜLLER, and G. SCHWARZENBACH. Helv. Chim. Acta, **42**, 827 (1959).
8. J. KOUTECKY. Chem. Listy, **48**, 360 (1954); Coll. Czech. Chem. Commun. **19**, 1093 (1954).
9. H. IRVING. *In* Advances in polarography. Vol. 1. *Edited by* I. S. Longmuir. Pergamon Press. 1960. p. 42.
10. J. KORYTA. *In* Progress in polarography. Vol. 1. *Edited by* P. Zuman and I. M. Kolthoff. Interscience. 1962. p. 291.
11. G. SCHWARZENBACH. Complexometric titrations. Interscience, New York. (1957).
12. A. RINGBOM. Complexation in analytical chemistry. Interscience, New York. 1963.
13. E. WANNINEN. Svomen Kemistilehti B, **28**, 146 (1955).
14. E. J. DURHAM and E. P. RYSKIEWICH. J. Am. Chem. Soc. **80**, 4812 (1958).
15. A. E. FROST. Nature, **178**, 322 (1956).
16. L. G. SILLEN and A. E. MARTELL. Stability constants of metal–ion complexes. Special Publication No. 17. The Chemical Society, London. 1964.
17. R. BRDICKA, V. HANUS, and J. KOUTECKY. *In* Progress in polarography. Vol. 1. *Editors*. P. Zuman and I. M. Kolthoff. Interscience. 1962. p. 145.
18. J. KORYTA. *In* Advances in electrochemistry and electrochemical Engineering. Vol. 6. *Edited by* P. Delahay. Interscience. 1967. p. 289.

Can. J. Chem. Downloaded from www.nrcresearchpress.com by 210.87.254.42 on 09/05/12
For personal use only.

The Master Equation for the Dissociation of a Dilute Diatomic Gas. VII. Vibration–Dissociation Coupling in an Expansion Nozzle

N. I. LABIB, D. L. S. MCELWAIN, AND H. O. PRITCHARD

Centre for Research in Experimental Space Science, York University, Downsview, Ontario

Received February 16, 1972

The normal-mode approach to the solution of the vibration–dissociation coupling problem for a dilute diatomic gas, which was described in Part III of this series, has been extended to the treatment of recombination in a steady supersonic nozzle expansion. This method of solution did not suffer from the familiar instabilities associated with parasitic eigenvalues which have so far impeded solution of this problem. We report a calculation on $H + H + M \rightarrow H_2 + M$ (*without* V–V coupling) yielding simultaneously the temperature, density, velocity, and the populations of *each individual* vibrational level from 3900–1500 °K which was completed with acceptable accuracy along the zero-streamline in a few minutes of computer time.

In the absence of V–V coupling effects, although grossly distorted vibrational population distributions were found, the populations were always monotonic with vibrational quantum number; however, it was possible to generate absolute overpopulations of one vibrational state with respect to another by simulating vibrational coupling effects.

The main conclusions of the calculation are that under these conditions (*i*) the rate constant for recombination is the normal phenomenological recombination rate constant; (*ii*) the vibrational relaxation time τ_{vib} appears to vary over several orders of magnitude depending on the approximation used to define the vibrational energy content, but if a proper measure of the vibrational energy is used, τ_{vib} can be correlated with the second eigenvalue of the relaxation matrix, and is therefore the same as that which would have been found in a shock-tube measurement.

Nous avons étendu l'approche du mode normal à la solution du problème de couplage dissociation–vibration d'un gaz diatomique dilué, décrit dans la partie III de cette série, à la solution de recombinaison dans une expansion constante de gicleur supersonique. Cette méthode de solution ne souffre pas des instabilités inhérentes aux valeurs propres parasites qui nuisent habituellement à trouver la solution de ce problème. Nous rapportons un calcul de $H + H + M \rightarrow H_2 + M$ (*sans* couplage V–V) aboutissant à la température, la densité, la vitesse et les populations de chaque niveau vibrationnel *individuel*, de 3900–1500 °K, complété avec une précision acceptable le long de la ligne zéro pendant un court temps d'ordinateur.

Nous constatons qu'en l'absence de couplage V–V, que les populations sont toujours monotones avec le nombre quantique vibrationnel, quoique apparaissent certaines distortions dans les distributions des populations vibrationnelles; il est toutefois possible de susciter des surpopulations absolues d'un état vibrationnel par rapport à un autre en simulant des effets de couplage vibrationnel.

A partir de ce calcul, nous concluons principalement que sous ces conditions (*i*) la constante de vitesse de recombinaison est la constante de vitesse de recombinaison phénoménologique normale; (*ii*) le temps de relaxation vibrationnel τ_{vib} semble varier sur plusieurs ordres de grandeur, dépendant de l'approximation utilisée pour définir la quantité d'énergie vibrationnelle, mais si on utilise une mesure appropriée de l'énergie vibrationnelle, τ_{vib} peut être relié à la deuxième valeur quantifiée de la matrice de relaxation et par conséquent est le même que celui qui aurait été trouvé au moyen d'une mesure dans des tubes de choc.

[Traduit par le journal]

Canadian Journal of Chemistry, **50**, 3832 (1972)

Introduction

The problems associated with the calculation of vibration–dissociation coupling in a gas flowing at supersonic speeds are well known, and have been well documented (1, 2 and references therein). Briefly, the internal (vibrational) relaxation times are very much shorter than the chemical relaxation time, but in order to obtain an accurate numerical solution of the problem it is necessary to use an integration step length which is short compared to the fastest of the internal relaxation times, which means that integrations spanning chemically interesting relaxation times are prohibitive in computer time (2, 3). The differential equations are said to be stiff, and the system of equations is said to have parasitic eigenvalues (2). In Part III of this series (3), we described a method of integration which overcame these difficulties in the special case of a highly dilute diatomic gas (*i.e.* one in which there is no vibration–vibration coupling) and the method was shown to give accurate results in the simple example of a vibration–dissociation relaxation taking place at constant

Can. J. Chem. Downloaded from www.nrcresearchpress.com by 210.87.254.5 on 09/05/12
For personal use only.

Can. J. Chem. Downloaded from www.nrcresearchpress.com by 210.87.254.5 on 09/05/12
For personal use only.

volume and constant temperature. In this paper we describe the extension of this method to the coupling of the vibration–dissociation relaxation and the gas dynamic equations of flow. Hitherto, this has been impossible because of the difficulties noted above: many calculations have been performed (4–6) but they all fall into one of two broad general classes. The first are calculations in which, following on from the early work of Lighthill (7) and Freeman (8), there is proper coupling between the dissociation rate and the flow but the vibrations of the molecule are all assumed to be in equilibrium with each other, in the sense that the vibrational population distribution is Boltzmann for some temperature which is not the local translational temperature. There has been some suspicion (devastatingly confirmed by the results of our calculations below) that this could be a poor assumption, and at least one calculation (9) has been done in which the vibrational population distribution is described by two effective temperatures, one for the lower vibrational levels and another for the higher vibrational levels. Unfortunately, the all too ready acceptance by experimenters (10) of the elegant harmonic-oscillator result that a system of oscillators will relax through a series of Boltzmann distributions (11) has impeded a proper interpretation of the experimental results; the application of this concept to anharmonic oscillators should be eradicated from such discussions as quickly as possible. The second class consists of calculations in which the dissociation is ignored *i.e.* there is coupling between the flow and the vibrational degree of freedom only: these calculations have become quite sophisticated recently because of interest in lasers, and the equations include terms representing V–V coupling between both like and unlike molecules and radiation coupling (12 and references therein): it is usually assumed in these calculations that as far as T–V transfers are concerned only nearest-neighbor transitions occur (12), which is moderately acceptable (13); however, the concept of conservation of vibrational quanta in V–V collisions clearly cannot be justified for anharmonic molecules with any significant degree of vibrational excitation (14), except on grounds of convenience.

The analysis in this paper is concerned *only* with the solution of the vibration–dissociation–gasdynamic flow problem, and for this reason the numerical experiment is a somewhat artificial one in several respects; it is therefore to be regarded only as the first step towards the complete solution of the vibration–dissociation–gasdynamic flow problem for a real system. We begin by assuming, as in our previous calculations (3, 13), that we have a mixture consisting of He and H_2 in 1000 to 1 proportions, and that only T–V transitions occur with transition probabilities given as a function of temperature by eq. III(1) (a Roman numeral prefix denotes an equation taken from an earlier paper in this series). In order to avoid the problems associated with integrating through the throat of the nozzle from the reservoir (5, 15), when the gas flow changes from subsonic to supersonic, our calculation begins with the gas already in the divergent section of the nozzle, flowing with a slightly supersonic velocity. The initial conditions are taken to be $[He] = 3.5 \times 10^{19}$ atoms cc^{-1}, $[H_2] + \frac{1}{2}[H] = 3.5 \times 10^{16}$ molecules cc^{-1}, with the system at complete thermodynamic equilibrium at 3900 °K, moving at a velocity of $U = 4.0 \times 10^5$ cm s^{-1}; the nozzle parameters are those used previously by Emanuel and Vincenti (16) with the integration beginning at $x_0 = 1.651$ cm, about 1 mm from the throat which is located at $x = 1.55$ cm. The reasons for choosing these initial conditions are as follows. At 3900 °K, H_2 is almost completely dissociated ($\alpha \approx 0.96$) whereas at 1500 °K at equilibrium at the same density, it is almost completely recombined ($\alpha < 10^{-4}$); hence this is an interesting temperature range, at least as far as chemical disequilibrium is concerned. The initial choice of thermodynamic equilibrium at 3900 °K is simply a matter of convenience: since the velocity is only just sonic (Mach number ≈ 1.08)[1] the populations will not be grossly different from those in the reservoir. Thus, not only is equilibrium at 3900 °K convenient, but it is moderately realistic, and in fact for our purposes any arbitrary initial distribution could have been chosen. The other feature of our

[1]To the extent that even ignoring the vibrational relaxation problem altogether the NASA (Lewis Research Center) General Chemical Kinetics Computer Program prints out flags to warn that one is too near the singularity at the sonic point (17).

Can. J. Chem. Downloaded from www.nrcresearchpress.com by 210.87.254.5 on 09/05/12
For personal use only.

initial conditions is that they correspond to an enormously fast initial rate of temperature change, of about 10^4 °K per cm (or 4×10^9 °K per s!): the advantage of this choice is that it is possible, in an hour or so's computer time, to integrate the necessary equations of flow by Runge–Kutta methods and span a temperature drop of about 200 °K, thereby providing a valuable check on our own method which takes much longer steps; we well appreciate that under these conditions a real flow would not be ideal, that the assumption of quasi-one-dimensional flow is unrealistic, that boundary-layer separation would occur, and so on. However, once it is established that the parasitic eigenvalue problem can be overcome, all of these features can be accommodated in future calculations.

Brute-Force Integration: Nineteen Equations

In Parts II and III of this series (13, 3) it was shown that using an asymptotic expansion technique, it was possible to take integration steps as much as 10^6 larger than is possible with conventional *e.g.* Runge–Kutta methods: in those calculations however, both the temperature and therefore the transition probabilities were regarded as constants, independent of time. In order to check on the accuracy of our technique when the gas was considered to be flowing, and therefore the temperature and the transition probabilities were changing with time, we felt it was necessary to perform an integration by standard techniques, and extending over as large a temperature range as possible. Our choice of initial conditions, as noted above, meant that a 200 °K range was accessible without consumption of inordinate amounts of computer time, thereby providing a valuable direct check on our results: otherwise, only circumstantial evidence of accuracy, such as conservation, rate constants, entropy production, etc., would be available, and would have to suffice.

We consider a mass element m of gas, having an initial density ρ_0, and containing a total number of particles N of which N_{He} are helium atoms, N_H are hydrogen atoms and N_{H_2} are hydrogen molecules, with $\frac{1}{2}N_H + N_{H_2} = N^0_{H_2}$; it will be a convenient notation to write $\rho_0/\rho_x = V_x$. Our previous formulation of the master equation for H_2 was in terms of changes taking place in 1 cc (3, 18), but must now be recast to refer to changes taking place within the mass element, whatever its density may be. The N_i now represent the number of molecules in vibrational state i, with N_n the number of dissociated molecules ($N_H = 2N_n$) in the mass element m; a tilde, *e.g.* $\tilde{N}_i$, implies the equilibrium value of N_i for the translational temperature and the density at the point in question. The probabilities of endothermic processes are assumed to be given by eq. III(1), with P_{ji} being the probability per collision of a transition from state i to state j, and $\bar{P}_{ni}$ being the probability per collision of a direct dissociation from state i: probabilities of deactivation processes are related to those of the activation processes by the usual detailed-balancing relationships, which now become

$$P_{ij}\tilde{N}_j = P_{ji}\tilde{N}_i$$

$$\bar{P}_{in}\tilde{N}_n^2/V_x = \bar{P}_{ni}\tilde{N}_i$$

If $Z_{1,1}$ is the number of collisions *per cc* per second when there is one helium atom and one hydrogen molecule in that cc, then the master equation for the mass element m is

$$[1]\quad \frac{dN_i}{dt} = \frac{(Z_{1,1})N_{He}}{V_x} \times \left\{ \sum_{j=0}^{14} (P_{ij}N_j - P_{ji}N_i) + \bar{P}_{in}N_n^2/V_x - \bar{P}_{ni}N_i \right\} \qquad i = 0, 1, \ldots, 14$$

$$[2]\quad \frac{dN_n}{dt} = \frac{(Z_{1,1})N_{He}}{V_x} \sum_{j=0}^{14} (\bar{P}_{nj}N_j - \bar{P}_{jn}N_n^2/V_x)$$

These sixteen equations have to be solved simultaneously with the equations of flow of the gas, and here we follow standard procedures for the description of quasi-one-dimensional flow (2, 4–12, 15, 16). We have first the Bernoulli equation

$$[3]\quad H = E + PV + \tfrac{1}{2}mU^2 = \text{stagnation enthalpy} = \text{constant}$$

or in differential form

$$[3']\quad dE + PdV + VdP + mUdU = 0$$

second, the mass-conservation equation

$$[4]\quad \rho UA = \text{constant}$$

where A is the cross-sectional area of the nozzle,

Can. J. Chem. Downloaded from www.nrcresearchpress.com by 210.87.254.5 on 09/05/12
For personal use only.

or in differential form

$$[4'] \qquad d\rho/\rho + dU/U + dA/A = 0$$

and third, the momentum-conservation equation for quasi-one-dimensional flow

$$[5] \qquad -\rho U dU = dP$$

After considerable algebraic manipulation (19), and assuming the perfect-gas laws, one can reduce these three equations to one of the form

$$[6] \quad dE + \frac{kTN}{(mU^2 - kTN)} \times \{mU^2 dA/A - kN dT - kT dN\} = 0$$

Now consider the conservation of energy

$$[7] \quad E = N_{He}\varepsilon^{He}_{trans} + N_{H_2}(\varepsilon^{H_2}_{trans} + \varepsilon^{H_2}_{rot} + \varepsilon^{H_2}_{vib}) + N_H(\varepsilon^{H}_{trans} + \tfrac{1}{2}D_0)$$

where ε denotes an average energy per molecule, and all internal energies are measured with respect to $H_2(v = 0)$. Using the gas laws, it is a simple matter to assign values to the ε_{trans} terms, and $N_{H_2}\varepsilon^{H_2}_{vib}$ is just

$$\sum_{i=0}^{14} \varepsilon_i N_i$$

where the ε_i are the vibrational energy levels assumed for the molecule (13). However, since we chose to use the *experimental* equilibrium constant (20), one cannot maintain strict conservation and assume that the rotational energy of H_2 is simply the kinetic-theory value of $N_{H_2}kT$, as we have noted previously (13), but one has to make a correction which becomes more severe as the temperature becomes higher (21). Thus, denoting for the moment the rotational energy per molecule by R_{H_2} and remembering that the rotational specific heat (dR_{H_2}/dT) is not exactly equal to k, one finds after extensive manipulation (19) that dE can be eliminated between [6] and the differential form of [7] to give

$$[8] \qquad \frac{dT}{T} = \frac{\dfrac{dN}{N} - \dfrac{2\bar{\varepsilon}_u}{kT}\dfrac{dA}{A} + \left\{\dfrac{2\bar{\varepsilon}_u}{kT} - 1\right\}\left\{-\dfrac{1}{2}\dfrac{D_0}{kT}\dfrac{dN_H}{N} - \dfrac{3}{2}\dfrac{dN}{N} - \dfrac{R_{H_2}}{kT}\dfrac{dN_{H_2}}{N} - \sum_i \dfrac{\varepsilon_i}{kT}\dfrac{dN_i}{N}\right\}}{\left\{\dfrac{2\bar{\varepsilon}_u}{kT} - 1\right\}\left\{\dfrac{3}{2} + \dfrac{1}{k}\left(\dfrac{dR_{H_2}}{dT}\right)\dfrac{N_{H_2}}{N}\right\} - 1}$$

where $\bar{\varepsilon}_u$ is the mean (per particle) kinetic energy of the flow *i.e.*

$$\bar{\varepsilon}_u = mU^2/2N$$

In order to avoid cancellation difficulties in the numerical evaluation of the rotational heat capacity, one has to write

$$[9] \qquad K_c = K^* e^{-D_0/kT}$$

where, as was noted above, K_p (from which K_c is derived) is tabulated in the JANAF Tables every 100 °K; thus, before proceeding K^* was fitted to a fifth-order polynomial in T. Then

$$R_{H_2} = \left[\frac{3kT}{2} - \frac{\sum_{i=0}^{14} \varepsilon_i e^{-\varepsilon_i/kT}}{Q^{H_2}_{vib}(T)} - kT^2\frac{d \ln K^*}{dT}\right]$$

follows from the standard relationship between K_c and the relevant partition functions $Q(T)$: thus

$$\frac{dR_{H_2}}{dT} = \left[\frac{3k}{2} - \frac{1}{Q^{H_2}_{vib}(T)}\cdot\frac{d}{dT}\left(\sum_{i=0}^{14} \varepsilon_i e^{-\varepsilon_i/kT}\right) + \frac{\sum_{i=0}^{14} \varepsilon_i e^{-\varepsilon_i/kT}}{\{Q^{H_2}_{vib}(T)\}^2}\cdot\frac{dQ^{H_2}_{vib}(T)}{dT} - \frac{2kT\, d \ln K^*}{dT} - \frac{kT^2\, d^2 \ln K^*}{dT^2}\right]$$

If one inspects eq. 8, it is written in a completely dimensionless form. The normal procedure is to solve the equations, advancing x, the distance down the nozzle, for which the quantity dA/A is always specified by the polynomial (16) describing the nozzle shape. The terms in dN_H/N, dN_{H_2}/N,

dN_i/N, and therefore dN/N change only as the result of vibrational and chemical relaxations embodied in the sixteen eqs. 1 and 2, and it is therefore convenient to convert these equations into distance-dependent instead of time-dependent ones by substituting dx/U for dt, *viz.*

$$[1x] \qquad \frac{dN_i}{dx} = \frac{(Z_{1,1})N_{He}}{UV_x}\left\{\sum_{j=0}^{14}(P_{ij}N_j - P_{ji}N_i) + \bar{P}_{in}N_n^2/V_x - \bar{P}_{ni}N_i\right\} \qquad i = 0, 1, \ldots, 14$$

$$[2x] \qquad \frac{dN_n}{dx} = \frac{(Z_{1,1})N_{He}}{UV_x}\sum_{j=0}^{14}(\bar{P}_{nj}N_j - \bar{P}_{jn}N_n^2/V_x)$$

Common practice at this stage is to construct one more differential equation, *e.g.* by substituting $-P\,dV$ for dE (from equations [3′] and [5] into [6] whence

$$[10] \qquad \frac{d\rho}{\rho} = \left\{\frac{dT}{T} + \frac{dN}{N} - \frac{2\bar{\varepsilon}_u}{kT}\frac{dA}{A}\right\}\Big/\left(\frac{2\bar{\varepsilon}_u}{kT} - 1\right)$$

giving eighteen equations in all, *i.e.* (1x], [2x], [8], and [10] which can be solved simultaneously using the auxiliary algebraic eq. [4] to find U. However, for the normal-mode solution which we describe below, this procedure is inadequate because one cannot regard U as being constant over the very large steps used in that method: therefore, one more equation is needed for a complete solution, *viz.*

$$[11] \qquad \frac{dt}{dx} = \frac{1}{U}$$

Thus, to set up the standard test-solution, these nineteen equations were solved by a fifth-order Runge–Kutta procedure (22), paying considerable attention to conservation. For example, at each of the six points within the fifth-order Runge–Kutta routine, new transition probabilities were calculated according to eq. III(1), a new value of K^* was calculated, new rotational heat contents and heat capacities were generated, and so on. The result was that even with the very rapid rates of change that exist in this system, a calculation covering the temperature range 3900–3710 °K was achieved in about 2 h of computer (IBM360/50) time, in which both the stagnation enthalpy and the total number of H atoms (*i.e.* H_2^0) were conserved to 13 decimal places. This solution was used as the standard against which to test the normal-mode procedure described below; discussion of the results will be deferred until the comparison of the two methods has been described.

Normal-mode Integration: Five Equations

Following exactly our previous derivation (3), the sixteen eqs. 1 and 2 can be transformed, at constant mass instead of at constant volume, to the sixteen normal-mode equations analogous to III(9a) and III(9b)

$$[12] \qquad \frac{d\Psi_i}{dt} = D_i\Psi_i(t) + \Gamma_i\Phi_n^2(t)$$

$$[13] \qquad \frac{d\Phi_n}{dt} = \frac{\tilde{N}_n^{1/2}}{V_x}\left\{V_x\sum_{i=0}^{14}\Gamma_i\Psi_i(t) + \Gamma_n\Phi_n^2(t)\right\}$$

where the capital-letter symbols refer to the mass element m, as opposed to the lower case symbols used previously to describe the relaxation at constant volume ($V = 1$). As before,

$$[14] \qquad \Psi_i = \sum_{j=0}^{14}\tilde{S}_{ij}\tilde{N}_j^{-1/2}N_j \qquad i = 0, 1, \ldots, 14$$

$$[15] \qquad \Phi_n = \tilde{N}_n^{-1/2}N_n$$

i.e., eq. III(10); note the omission of a tilde from the $\tilde{S}_{ij}$ in ref 3. Then, transcribing the derivation of the asymptotic expansion solution, eqs. III(13) and III(14) to constant-mass but variable-volume, we have

$$[16] \qquad \frac{d\Psi_{n-1}}{dt} = D_{n-1}\Psi_{n-1}(t) + \Gamma_{n-1}\Phi_n^2(t)$$

$$[17] \qquad \frac{d\Phi_n}{dt} = \frac{\tilde{N}_n^{1/2}}{V_x}\left\{\sum_{i=0}^{13}V_x\Gamma_i[\Psi_i(t_0) - \Gamma_iD_i^{-1}\Phi_n^2(t_0)]\,e^{D_i(t-t_0)} + V_x\Gamma_{n-1}\Psi_{n-1}(t) + \left[\Gamma_n - V_x\sum_{i=0}^{13}\Gamma_i^2D_i^{-1}\right]\Phi_n^2(t)\right\}$$

Finally, we form [16x] and [17x] by multiplying the right hand sides of [16] and [17] by U^{-1}, and changing the denominators on the left-hand sides to dx instead of dt. It is implicit in writing equations [16x] and [17x], and attempting to solve them simultaneously by Runge–Kutta

Can. J. Chem. Downloaded from www.nrcresearchpress.com by 210.87.254.5 on 09/05/12
For personal use only.

Can. J. Chem. Downloaded from www.nrcresearchpress.com by 210.87.254.5 on 09/05/12
For personal use only.

methods with [8], [10], and [11], that we must know the eigenvalues D_i and the eigenvectors S_{ij} of the relaxation matrix at every integration step. Once it has been established that large steps can be taken, these can probably be calculated as and when needed for the density and temperature in question, as already described (3), and we hope to undertake a shock-wave calculation where the temperature change is less violent by this approach in the near future. However, since part of our testing procedure in this work was to compare solutions for the same distance x obtained by using a variety of step-lengths, it would have been prohibitive to calculate the D_i and the S_{ij} anew each time. Hence, the d_i and s_{ij} for the initial density ρ_0 (*i.e.* $N_{He} = 3.5 \times 10^{19}$ atoms cc^{-1}; $N^0_{H_2} = 3.5 \times 10^{16}$ molecules cc^{-1}) were calculated every 100° from 1500 to 4000 °K: then each element of s_{ij} and the d_i were fitted to an eighth-order polynomial in T, d_{n-1} being treated separately like the equilibrium constant (eq. 9) because of its very rapid change with T; nevertheless, four sets of polynomials had to be used to give adequate representation, covering the ranges 4000–3000, 3200–2500, 2600–2000, and 2200–1500 °K respectively. Thus, to obtain the correct values at the density in question for the quantities in eqs. 16 and 17 from the corresponding values interpolated for the same temperature, but at density ρ_0, one needs the following scaling

$$D_i = d_i/V_x$$
$$\Gamma_i = \gamma_i/V_x^{3/2}$$
$$\Gamma_n = \gamma_n/V_x$$
$$S_{ij} = s_{ij}$$

The five equations [8], [10], [11], [16x], and [17x] can now be solved by a fifth-order Runge–Kutta procedure: hence, instead of generating transition probabilities and detailed-balancing relationships at each point within the integration, the D_i, Γ_i, etc. have to be generated from the standard sets of polynomials already stored in the machine.

It is important to realize that eqs. 16 and 17 are not exact. Two terms have been omitted (19), one in $d\tilde{N}_i/dT$ and the other in dS_{ij}/dT. In other words, [16] and [17] are only correct (as were III(13) and III(14)) if the temperature does not change during the step. By ignoring these two terms, we are implying that the $\tilde{N}_i$ and the S_{ij} do not change appreciably across each integration step. Clearly, then, we are not going to be able to take the very large steps characteristic of our earlier work (3), but making use of the exact solution found by the nineteen-equation method, can find how big a step-length is possible whilst still retaining acceptable accuracy.

Results

(a) Comparison of the Two Methods

For the particular flow chosen as the subject of the calculation described in this paper, the longest integration step that was possible with the nineteen-equation method whilst maintaining stability, conservation of particles, and conservation of stagnation enthalpy (eq. 3) was about 10^{-5} cm *i.e.* 2×10^{-11} s; this is more-or-less consistent with the fact that the largest eigenvalue of the relaxation matrix is always of the order of 10^{11} s^{-1} (2, 3). The five-equation method was then used over the same temperature range and with a step-length of 8×10^{-5} cm there was agreement at 3711 °K as follows: stagnation enthalpy, 10 decimal places; flow parameters, 8 decimal places; atom concentration, 8 decimal places; ground vibrational state population, 5 decimal places; topmost vibrational state population, 4 decimal places. Our interpolations of d_i, K^*, s_{ij}, etc. are not consistent with each other and with the assumed transition probabilities to better than 10 decimal places, hence, about 10 figures is the best agreement that would be possible. For convenience, therefore, the total hydrogenic population was readjusted after each integration cycle to be exactly $N^0_{H_2} = 3.5 \times 10^{16}$ molecules. Integrations were then continued down to about 3000 °K with a variety of step-lengths 8, 64, 128, and 256×10^{-5} cm, and thence down to 1500 °K in steps of 256×10^{-5} cm. At 2000 °K the stagnation enthalpy still agreed with the initial starting value to 7 decimal places, but the agreement deteriorated towards 1500 °K due to increasing inaccuracy in the eigenvectors S_{ij} at the lower temperatures. From our experiments with varying step-length, we conclude that using the longest step, which is 256 times as long as that allowed in the nineteen-equation method, the

TABLE 1. Gasdynamic properties of the model flow*

x (cm)	t (s)	$10^{-5}\,U$ (cm s^{-1})	$10^{4}\,\rho_x$ (g cm^{-3})	T (°K)	$10^{16}\,N_H$	$10^{16}\,\tilde{N}_H$	$10^{15}\,N_{H_2}$	$10^{15}\,\tilde{N}_{H_2}$
1.651	0	4.000	2.327	3900	6.726796	6.727	1.36602	1.366
1.662	2.753×10^{-8}	4.123	2.238	3800	6.726788	6.638	1.36606	1.811
1.678	6.479×10^{-8}	4.252	2.150	3700	6.726756	6.515	1.36622	2.423
1.698	1.107×10^{-7}	4.372	2.064	3600	6.726699	6.348	1.36650	3.261
1.721	1.643×10^{-7}	4.490	1.979	3500	6.726620	6.122	1.36690	4.389
1.749	2.258×10^{-7}	4.604	1.894	3400	6.726522	5.822	1.36739	5.890
1.781	2.943×10^{-7}	4.716	1.811	3300	6.726410	5.436	1.36795	7.818
1.817	3.690×10^{-7}	4.825	1.730	3200	6.726287	4.965	1.36856	10.177
1.857	4.507×10^{-7}	4.932	1.649	3100	6.726158	4.409	1.36921	12.954
1.900	5.374×10^{-7}	5.034	1.571	3000	6.726027	3.806	1.36986	15.970
1.949	6.330×10^{-7}	5.137	1.493	2900	6.725891	3.162	1.37055	19.192
2.002	7.366×10^{-7}	5.240	1.415	2800	6.725752	2.524	1.37124	22.379
2.059	8.431×10^{-7}	5.336	1.341	2700	6.725619	1.959	1.37191	25.207
2.123	9.619×10^{-7}	5.435	1.266	2600	6.725481	1.444	1.37260	27.779
2.189	1.083×10^{-6}	5.528	1.195	2500	6.725351	1.038	1.37324	29.809
2.263	1.216×10^{-6}	5.621	1.124	2400	6.725220	0.709	1.37390	31.456
2.343	1.357×10^{-6}	5.712	1.055	2300	6.725094	0.466	1.37453	32.669
2.430	1.508×10^{-6}	5.802	0.987	2200	6.724970	0.291	1.37515	33.543
2.527	1.674×10^{-6}	5.893	0.919	2100	6.724846	0.171	1.37577	34.147
2.632	1.851×10^{-6}	5.981	0.854	2000	6.724733	0.095	1.37633	34.526
2.745	2.038×10^{-6}	6.066	0.792	1900	6.724636	0.050	1.37682	34.750
2.870	2.243×10^{-6}	6.151	0.730	1800	6.724540	0.024	1.37730	34.879
3.011	2.470×10^{-6}	6.236	0.669	1700	6.724446	0.011	1.37777	34.947
3.165	2.715×10^{-6}	6.319	0.611	1600	6.724356	0.004_2	1.37822	34.979
3.336	2.985×10^{-6}	6.399	0.555	1500	6.724270	0.001_5	1.37865	34.993

*Equilibrium populations denoted by $\tilde{N}$ refer to thermodynamic equilibrium at the stated temperature, not to an "equilibrium" calculation, see text.

final accuracies on the population distributions are: atoms, 5–6 figures; ground vibrational state, 4 figures; topmost vibrational state, 2 figures, the latter quantity always being the most sensitive to error (23). However, since the population distributions observed are so very non-Boltzmann, 2-decimal place accuracy on the topmost level is a very considerable advance on previous assumptions of an effective vibrational temperature which could place the topmost level at 1500 °K perhaps seven or eight orders of magnitude different from what we find, depending upon how closely the vibrational temperature followed the translational temperature. In our earlier calculations (3), in which the temperature did not change, we found it was possible to take very large steps whilst still maintaining excellent accuracy on all populations. The poorer performance of the method described here is due in the main to the neglect of the terms in $d\tilde{N}_i/dT$ and dS_{ij}/dT noted above: the step length of 256×10^{-5} cm corresponds to a temperature drop of about 20 °K at early times in the flow; the S_{ij} are very insensitive to temperature, but the $\tilde{N}_i$, particularly $\tilde{N}_n$ the number of dissociated molecules, change appreciably over a 20° range. From the evidence available, it would appear that the present five-equation approximation will be highly satisfactory for integrations in which there is a change of not much more than (say) 1° over the integration cycle. Smaller errors arise from the imperfections in interpolating the d_i, etc., also noted above: for example, one of the thermodynamic quantities monitored in the flow was the total entropy, which rose gradually from 9.28810582 cal deg^{-1} g^{-1} 3900 °K to 9.28810858 cal deg^{-1} g^{-1} at 1500 °K, but with discernible steps when the polynomials were changed at 3000, 2500, and 2000 °K; the entropy was calculated as described previously (13, 19). Had there been no non-equilibrium effects present, the flow would have been isentropic (24) and the smallness of the observed increase is due to the fact that the mixture is quite dilute in H_2. In a previous paper (13) we examined successive time derivatives of the

Can. J. Chem. Downloaded from www.nrcresearchpress.com by 210.87.254.5 on 09/05/12
For personal use only.

Can. J. Chem. Downloaded from www.nrcresearchpress.com by 210.87.254.5 on 09/05/12
For personal use only.

entropy, but in this approximate calculation, the accuracy of the total entropy is too low for us to derive any meaningful information on the higher derivatives and on monotonicity.

(b) Population Distributions

The principal gasdynamic quantities for the flow are tabulated at 100° intervals in Table 1. In the sixth and seventh columns we compare the actual atom population and the value it would have at equilibrium at the listed temperature; likewise for molecules in columns eight and nine. Note that the equilibrium populations are *not* the populations that would have been obtained in an "equilibrium" calculation, since through the energy conservation relationships, the temperature would have been altered slightly. Nevertheless, they are quite close to what would have been obtained in such a calculation, as are the flow parameters (17), since the mixture is very dilute in H_2. It is clear that on this time scale, the recombination reaction appears to be almost frozen, which is to be expected under the chosen conditions.

Table 2 shows the evolution of the vibrational population distributions at 100° intervals: at the same time, Table 2 also shows what would be the equilibrium vibrational population distribution based on the same number of ground-state molecules (figures underlined). Comparison of the actual and equilibrium values reveals immediately that down to about 2000 °K, states $v = 1$ and $v = 2$ remain very closely coupled to the ground state, $v = 0$, but that by 1500 °K, $v = 2$ is no longer coupled to $v = 0$, and $v = 1$ is beginning to depart strongly from the equilibrium value. On the other hand, the topmost vibrational levels remain in very close equilibrium with the free atoms: this is not immediately obvious from the data presented in Table 2, where N_{14} appears to be changing much more rapidly than N_H; however, when one allows for the density change which is occurring in the flow, the mass-action ratio n_H^2/n_{14} hardly changes at all throughout the calculation.

The sudden onset of freezing of successive vibrational levels is shown very clearly in Table 2: if we use as a rough-and-ready criterion for freezing that the actual population is about three (or more) times what it would be if it were in equilibrium with N_0 at the list temperature, then one can see that levels $v = 11, 12, 13$, and 14 suddenly freeze between 3700 and 3500 °K; at 3700 °K, no actual value exceeds the equilibrium value by as much as a factor of two, whereas at 3500 °K, the topmost four levels have clearly failed to remain in any sort of rough equilibrium with the ground state. As time goes on, more and more levels freeze suddenly, so that at 3000 °K, $v = 8$ and above are no longer strongly coupled to the ground-state population, at 2500 °K, $v = 6$ and above are frozen, at 2000 °K the freezing point is around $v = 3$ or 4, and at 1500 °K, the first vibrational level is about to freeze. An interesting second-order effect occurs for $v = 6$, 7, 8, and 9 around 2100 °K, and by 1500 °K has spread to levels $v = 4$ to 10 inclusive; these levels were originally much more strongly coupled to the ground state than to the atoms but, these levels having failed to keep step with the ground-state population, now become somewhat better coupled to the atoms than to the ground state, and their populations begin to rise again.

It is interesting that the initial onset of freezing takes place at and around $v = 11$, which is about the position where we have previously suggested that a bottleneck occurs with the particular set of transition probabilities used in this calculation (3). However, as the flow progresses, the freezing point moves to progressively lower vibrational levels, thereby amplifying our earlier conclusion (27) that any vibrational bottleneck is basically a very complex manifestation.

(c) Generating Population Inversions

It seems likely that if, under these severe conditions, one cannot generate a vibrational population inversion, then one is not going to be able to do so in this temperature range if only T–V processes are allowed. This statement refers, of course, to gross vibrational populations (there may be overpopulations of optically coupled J-substates, as is often discussed in treatments of nozzle lasers (12, 25)); also, H_2 is homonuclear and will not radiate, but the behavior of heteronuclear molecules will not be very different (26) unless atom exchange reactions are important. It is, however, possible to generate an absolute vibrational overpopulation by simulating V–V processes in our flow. As we noted above, our method of solution is applicable only to T–V processes, and V–V processes cannot be properly included; however, their

Table 2. Comparison of the computed vibrational population distribution (n.b. the underlined figures represent that would be in equilibrium with the actual number calculation)

$T^{\circ}K$	N_{14}	N_{13}	N_{12}	N_{11}	N_{10}	N_9	N_8
3900	$\underline{1.83\times10^{9}}$	$\underline{2.30\times10^{9}}$	$\underline{3.39\times10^{9}}$	$\underline{5.71\times10^{9}}$	$\underline{1.08\times10^{10}}$	$\underline{2.29\times10^{10}}$	$\underline{5.33\times10^{10}}$
3800	1.76×10^{9} $\underline{1.30\times10^{9}}$	2.20×10^{9} $\underline{1.65\times10^{9}}$	3.20×10^{9} $\underline{2.45\times10^{9}}$	5.25×10^{9} $\underline{4.19\times10^{9}}$	9.63×10^{9} $\underline{8.09\times10^{9}}$	1.98×10^{10} $\underline{1.74\times10^{10}}$	4.56×10^{10} $\underline{4.15\times10^{10}}$
3700	1.69×10^{9} $\underline{9.13\times10^{8}}$	2.11×10^{9} $\underline{1.16\times10^{9}}$	3.02×10^{9} $\underline{1.75\times10^{9}}$	4.77×10^{9} $\underline{3.03\times10^{9}}$	8.36×10^{9} $\underline{5.95\times10^{9}}$	1.65×10^{10} $\underline{1.31\times10^{10}}$	3.70×10^{10} $\underline{3.19\times10^{10}}$
3600	1.63×10^{9} $\underline{6.26\times10^{8}}$	2.03×10^{9} $\underline{8.02\times10^{8}}$	2.87×10^{9} $\underline{1.22\times10^{9}}$	4.40×10^{9} $\underline{2.15\times10^{9}}$	7.38×10^{9} $\underline{4.30\times10^{9}}$	1.39×10^{10} $\underline{9.67\times10^{9}}$	3.02×10^{10} $\underline{2.42\times10^{10}}$
3500	1.57×10^{9} $\underline{4.21\times10^{8}}$	1.95×10^{9} $\underline{5.43\times10^{8}}$	2.75×10^{9} $\underline{8.36\times10^{8}}$	4.11×10^{9} $\underline{1.49\times10^{9}}$	6.61×10^{9} $\underline{3.05\times10^{9}}$	1.19×10^{10} $\underline{7.02\times10^{9}}$	2.48×10^{10} $\underline{1.80\times10^{10}}$
3400	1.51×10^{9} $\underline{2.75\times10^{8}}$	1.89×10^{9} $\underline{3.58\times10^{8}}$	2.64×10^{9} $\underline{5.57\times10^{8}}$	3.88×10^{9} $\underline{1.01\times10^{9}}$	6.01×10^{9} $\underline{2.12\times10^{9}}$	1.03×10^{10} $\underline{4.99\times10^{9}}$	2.04×10^{10} $\underline{1.32\times10^{10}}$
3300	1.46×10^{9} $\underline{1.75\times10^{8}}$	1.83×10^{9} $\underline{2.30\times10^{8}}$	2.55×10^{9} $\underline{3.63\times10^{8}}$	3.70×10^{9} $\underline{6.73\times10^{8}}$	5.56×10^{9} $\underline{1.44\times10^{9}}$	9.06×10^{9} $\underline{3.47\times10^{9}}$	1.71×10^{10} $\underline{9.44\times10^{9}}$
3200	1.41×10^{9} $\underline{1.09\times10^{8}}$	1.77×10^{9} $\underline{1.44\times10^{8}}$	2.47×10^{9} $\underline{2.30\times10^{8}}$	3.55×10^{9} $\underline{4.35\times10^{8}}$	5.22×10^{9} $\underline{9.50\times10^{8}}$	8.16×10^{9} $\underline{2.36\times10^{9}}$	1.46×10^{10} $\underline{6.62\times10^{9}}$
3100	1.36×10^{9} $\underline{6.53\times10^{7}}$	1.72×10^{9} $\underline{8.70\times10^{7}}$	2.41×10^{9} $\underline{1.42\times10^{8}}$	3.44×10^{9} $\underline{2.73\times10^{8}}$	4.96×10^{9} $\underline{6.12\times10^{8}}$	7.50×10^{9} $\underline{1.57\times10^{9}}$	1.27×10^{10} $\underline{4.54\times10^{9}}$
3000	1.31×10^{9} $\underline{3.82\times10^{7}}$	1.67×10^{9} $\underline{5.13\times10^{7}}$	2.35×10^{9} $\underline{8.49\times10^{7}}$	3.35×10^{9} $\underline{1.67\times10^{8}}$	4.78×10^{9} $\underline{3.85\times10^{8}}$	7.03×10^{9} $\underline{1.02\times10^{9}}$	1.13×10^{10} $\underline{3.05\times10^{9}}$
2900	1.26×10^{9} $\underline{2.12\times10^{7}}$	1.62×10^{9} $\underline{2.88\times10^{7}}$	2.30×10^{9} $\underline{4.85\times10^{7}}$	3.28×10^{9} $\underline{9.78\times10^{7}}$	4.64×10^{9} $\underline{2.32\times10^{8}}$	6.70×10^{9} $\underline{6.32\times10^{8}}$	1.03×10^{10} $\underline{1.97\times10^{9}}$
2800	1.22×10^{9} $\underline{1.12\times10^{7}}$	1.57×10^{9} $\underline{1.54\times10^{7}}$	2.25×10^{9} $\underline{2.64\times10^{7}}$	3.22×10^{9} $\underline{5.46\times10^{7}}$	4.55×10^{9} $\underline{1.33\times10^{8}}$	6.48×10^{9} $\underline{3.78\times10^{8}}$	9.66×10^{9} $\underline{1.23\times10^{9}}$
2700	1.17×10^{9} $\underline{5.78\times10^{6}}$	1.52×10^{9} $\underline{8.05\times10^{6}}$	2.20×10^{9} $\underline{1.41\times10^{7}}$	3.17×10^{9} $\underline{2.99\times10^{7}}$	4.49×10^{9} $\underline{7.54\times10^{7}}$	6.36×10^{9} $\underline{2.22\times10^{8}}$	9.26×10^{9} $\underline{7.53\times10^{8}}$
2600	1.13×10^{9} $\underline{2.75\times10^{6}}$	1.48×10^{9} $\underline{3.88\times10^{6}}$	2.15×10^{9} $\underline{6.93\times10^{6}}$	3.12×10^{9} $\underline{1.52\times10^{7}}$	4.44×10^{9} $\underline{3.97\times10^{7}}$	6.28×10^{9} $\underline{1.22\times10^{8}}$	9.03×10^{9} $\underline{4.34\times10^{8}}$
2500	1.08×10^{9} $\underline{1.27\times10^{6}}$	1.43×10^{9} $\underline{1.82\times10^{6}}$	2.11×10^{9} $\underline{3.33\times10^{6}}$	3.07×10^{9} $\underline{7.52\times10^{6}}$	4.39×10^{9} $\underline{2.04\times10^{7}}$	6.24×10^{9} $\underline{6.55\times10^{7}}$	8.92×10^{9} $\underline{2.45\times10^{8}}$
2400	1.03×10^{9} $\underline{5.41\times10^{5}}$	1.39×10^{9} $\underline{7.85\times10^{5}}$	2.06×10^{9} $\underline{1.47\times10^{6}}$	3.03×10^{9} $\underline{3.44\times10^{6}}$	4.37×10^{9} $\underline{9.74\times10^{6}}$	6.23×10^{9} $\underline{3.28\times10^{7}}$	8.91×10^{9} $\underline{1.30\times10^{8}}$
2300	9.89×10^{8} $\underline{2.17\times10^{5}}$	1.34×10^{9} $\underline{3.19\times10^{5}}$	2.02×10^{9} $\underline{6.15\times10^{5}}$	3.00×10^{9} $\underline{1.49\times10^{6}}$	4.35×10^{9} $\underline{4.41\times10^{6}}$	6.25×10^{9} $\underline{1.57\times10^{7}}$	8.96×10^{9} $\underline{6.56\times10^{7}}$
2200	9.44×10^{8} $\underline{7.90\times10^{4}}$	1.29×10^{9} $\underline{1.18\times10^{5}}$	1.98×10^{9} $\underline{2.35\times10^{5}}$	2.96×10^{9} $\underline{5.93\times10^{5}}$	4.33×10^{9} $\underline{1.84\times10^{6}}$	6.27×10^{9} $\underline{6.93\times10^{6}}$	9.06×10^{9} $\underline{3.10\times10^{7}}$
2100	8.99×10^{8} $\underline{2.54\times10^{4}}$	1.25×10^{9} $\underline{3.89\times10^{4}}$	1.93×10^{9} $\underline{7.98\times10^{4}}$	2.92×10^{9} $\underline{2.10\times10^{5}}$	4.32×10^{9} $\underline{6.92\times10^{5}}$	6.32×10^{9} $\underline{2.77\times10^{6}}$	9.21×10^{9} $\underline{1.33\times10^{7}}$
2000	8.55×10^{8} $\underline{7.42\times10^{3}}$	1.21×10^{9} $\underline{1.16\times10^{4}}$	1.89×10^{9} $\underline{2.46\times10^{4}}$	2.89×10^{9} $\underline{6.82\times10^{4}}$	4.32×10^{9} $\underline{2.38\times10^{5}}$	6.38×10^{9} $\underline{1.02\times10^{6}}$	9.40×10^{9} $\underline{5.34\times10^{6}}$
1900	8.11×10^{8} $\underline{1.95\times10^{3}}$	1.16×10^{9} $\underline{3.12\times10^{3}}$	1.85×10^{9} $\underline{6.90\times10^{3}}$	2.86×10^{9} $\underline{2.02\times10^{4}}$	4.32×10^{9} $\underline{7.51\times10^{4}}$	6.45×10^{9} $\underline{3.48\times10^{5}}$	9.61×10^{9} $\underline{1.98\times10^{6}}$
1800	7.68×10^{8} $\underline{4.34\times10^{2}}$	1.12×10^{9} $\underline{7.13\times10^{2}}$	1.81×10^{9} $\underline{1.65\times10^{3}}$	2.83×10^{9} $\underline{5.10\times10^{3}}$	4.32×10^{9} $\underline{2.04\times10^{4}}$	6.54×10^{9} $\underline{1.03\times10^{5}}$	9.85×10^{9} $\underline{6.45\times10^{5}}$
1700	7.24×10^{8} $\underline{7.86\times10}$	1.07×10^{9} $\underline{1.33\times10^{2}}$	1.77×10^{9} $\underline{3.23\times10^{2}}$	2.80×10^{9} $\underline{1.07\times10^{3}}$	4.33×10^{9} $\underline{4.66\times10^{3}}$	6.64×10^{9} $\underline{2.59\times10^{4}}$	1.01×10^{10} $\underline{1.81\times10^{5}}$
1600	6.81×10^{8} $\underline{1.19\times10}$	1.03×10^{9} $\underline{2.07\times10}$	1.73×10^{9} $\underline{5.32\times10}$	2.78×10^{9} $\underline{1.90\times10^{2}}$	4.36×10^{9} $\underline{9.06\times10^{2}}$	6.77×10^{9} $\underline{5.61\times10^{3}}$	1.05×10^{10} $\underline{4.41\times10^{4}}$
1500	6.38×10^{8} $\underline{1.39}$	9.87×10^{8} $\underline{2.52}$	1.69×10^{9} $\underline{6.88}$	2.75×10^{9} $\underline{2.67\times10}$	4.38×10^{9} $\underline{1.41\times10^{2}}$	6.91×10^{9} $\underline{9.88\times10^{2}}$	1.09×10^{10} $\underline{8.91\times10^{3}}$

Can. J. Chem. Downloaded from www.nrcresearchpress.com by 210.87.254.5 on 09/05/12
For personal use only.

Can. J. Chem. Downloaded from www.nrcresearchpress.com by 210.87.254.5 on 09/05/12
For personal use only.

distribution with an equilibrium vibrational

the populations of vibrationally excited molecules

N_0 of ground-state molecules found in the flow

N_7	N_6	N_5	N_4	N_3	N_2	N_1	N_0
1.36×10^{11}	3.80×10^{11}	1.16×10^{12}	3.83×10^{12}	1.38×10^{13}	5.38×10^{13}	2.291×10^{14}	1.064×10^{15}
1.17×10^{11}	3.29×10^{11}	1.02×10^{12}	3.44×10^{12}	12.7×10^{13}	5.09×10^{13}	2.233×10^{14}	1.074×10^{15}
1.09×10^{11}	3.12×10^{11}	9.77×10^{11}	3.33×10^{12}	1.24×10^{13}	5.02×10^{13}	2.226×10^{14}	
9.43×10^{10}	2.69×10^{11}	8.53×10^{11}	2.97×10^{12}	1.13×10^{13}	4.73×10^{13}	2.164×10^{14}	1.087×10^{15}
8.58×10^{10}	2.53×10^{11}	8.18×10^{11}	2.89×10^{12}	1.11×10^{13}	4.68×10^{13}	2.154×10^{14}	
7.60×10^{10}	2.19×10^{11}	7.10×10^{11}	2.55×10^{12}	1.01×10^{13}	4.39×10^{13}	2.093×10^{14}	1.100×10^{15}
6.68×10^{10}	2.03×10^{11}	6.78×10^{11}	2.48×10^{12}	9.90×10^{12}	4.34×10^{13}	2.084×10^{14}	
6.11×10^{10}	1.77×10^{11}	5.86×10^{11}	2.18×10^{12}	8.94×10^{12}	4.05×10^{13}	2.020×10^{14}	1.112×10^{15}
5.13×10^{10}	1.61×10^{11}	5.55×10^{11}	2.11×10^{12}	8.76×10^{12}	4.00×10^{13}	2.013×10^{14}	
4.91×10^{10}	1.42×10^{11}	4.80×10^{11}	1.84×10^{12}	7.86×10^{12}	3.72×10^{13}	1.944×10^{14}	1.125×10^{15}
3.86×10^{10}	1.25×10^{11}	4.49×10^{11}	1.77×10^{12}	7.68×10^{12}	3.67×10^{13}	1.934×10^{14}	
3.94×10^{10}	1.13×10^{11}	3.88×10^{11}	1.54×10^{12}	6.85×10^{12}	3.39×10^{13}	1.865×10^{14}	1.138×10^{15}
2.86×10^{10}	9.63×10^{10}	3.58×10^{11}	1.47×10^{12}	6.68×10^{12}	3.35×10^{13}	1.855×10^{14}	
3.19×10^{10}	8.94×10^{10}	3.11×10^{11}	1.27×10^{12}	5.92×10^{12}	3.08×10^{13}	1.784×10^{14}	1.152×10^{15}
2.08×10^{10}	7.27×10^{10}	2.82×10^{11}	1.21×10^{12}	5.76×10^{12}	3.03×10^{13}	1.773×10^{14}	
2.61×10^{10}	7.06×10^{10}	2.46×10^{11}	1.04×10^{12}	5.07×10^{12}	2.78×10^{13}	1.700×10^{14}	1.165×10^{15}
1.48×10^{10}	5.38×10^{10}	2.18×10^{11}	9.81×10^{11}	4.91×10^{12}	2.73×10^{12}	1.688×10^{14}	
2.19×10^{10}	5.63×10^{10}	1.95×10^{11}	8.50×10^{11}	4.33×10^{12}	2.50×10^{12}	1.618×10^{14}	1.178×10^{15}
1.03×10^{10}	3.92×10^{10}	1.66×10^{11}	7.87×10^{11}	4.15×10^{12}	2.44×10^{13}	1.602×10^{14}	
1.86×10^{10}	4.47×10^{10}	1.52×10^{11}	6.77×10^{11}	3.62×10^{12}	2.21×10^{13}	1.528×10^{14}	1.191×10^{15}
6.97×10^{9}	2.77×10^{10}	12.4×10^{11}	6.17×10^{11}	3.45×10^{12}	2.16×10^{13}	1.512×10^{14}	
1.63×10^{10}	3.60×10^{10}	1.17×10^{11}	5.31×10^{11}	2.98×10^{12}	1.94×10^{13}	1.436×10^{14}	1.205×10^{15}
4.54×10^{9}	1.90×10^{10}	8.95×10^{10}	4.74×10^{11}	2.82×10^{12}	1.88×10^{13}	1.418×10^{14}	
1.48×10^{10}	3.00×10^{10}	9.13×10^{10}	4.15×10^{11}	2.44×10^{12}	1.70×10^{13}	1.345×10^{14}	1.217×10^{15}
2.92×10^{9}	1.29×10^{10}	6.40×10^{10}	3.60×10^{11}	2.29×10^{12}	1.64×10^{13}	1.326×10^{14}	
1.38×10^{10}	2.56×10^{10}	7.10×10^{10}	3.17×10^{11}	1.96×10^{12}	1.46×10^{13}	1.249×10^{14}	$1.231.10^{15}$
1.77×10^{9}	8.28×10^{9}	4.39×10^{10}	2.64×10^{11}	1.80×10^{12}	1.40×10^{13}	1.229×10^{14}	
1.33×10^{10}	2.28×10^{10}	5.68×10^{10}	2.43×10^{11}	1.56×10^{12}	1.24×10^{13}	1.157×10^{14}	1.243×10^{15}
1.06×10^{9}	5.25×10^{9}	2.97×10^{10}	1.92×10^{11}	1.41×10^{12}	1.18×10^{13}	1.134×10^{14}	
1.30×10^{10}	2.11×10^{10}	4.65×10^{10}	1.84×10^{11}	1.21×10^{12}	1.04×10^{13}	1.061×10^{14}	1.256×10^{15}
5.96×10^{8}	3.16×10^{9}	1.92×10^{10}	1.34×10^{11}	1.07×10^{12}	9.85×10^{12}	1.036×10^{14}	
1.30×10^{10}	2.02×10^{10}	3.98×10^{10}	1.41×10^{11}	9.34×10^{11}	8.66×10^{12}	9.671×10^{13}	1.268×10^{15}
3.22×10^{8}	1.83×10^{9}	1.21×10^{10}	9.16×10^{10}	8.01×10^{11}	8.07×10^{12}	9.401×10^{13}	
1.32×10^{10}	1.99×10^{10}	3.57×10^{10}	1.09×10^{11}	7.07×10^{11}	7.07×10^{12}	8.731×10^{13}	1.280×10^{15}
1.63×10^{8}	1.01×10^{9}	7.22×10^{9}	6.01×10^{10}	5.79×10^{11}	6.48×10^{12}	8.435×10^{13}	
1.35×10^{10}	2.01×10^{10}	3.36×10^{10}	8.70×10^{10}	5.25×10^{11}	5.64×10^{12}	7.785×10^{13}	1.292×10^{15}
7.63×10^{7}	5.13×10^{8}	4.05×10^{9}	3.73×10^{10}	4.02×10^{11}	5.06×10^{12}	7.459×10^{13}	
1.39×10^{10}	2.07×10^{10}	3.31×10^{10}	7.31×10^{10}	3.89×10^{11}	4.30×10^{12}	6.876×10^{13}	1.303×10^{15}
3.33×10^{7}	2.47×10^{8}	2.16×10^{9}	2.23×10^{10}	2.70×10^{11}	3.86×10^{12}	6.517×10^{13}	
1.43×10^{10}	2.15×10^{10}	3.36×10^{10}	6.55×10^{10}	2.92×10^{11}	3.43×10^{12}	6.018×10^{13}	1.313×10^{15}
1.35×10^{7}	1.11×10^{8}	1.09×10^{9}	1.27×10^{10}	1.75×10^{11}	2.88×10^{12}	5.623×10^{13}	
1.49×10^{10}	2.25×10^{10}	3.50×10^{10}	6.22×10^{10}	2.23×10^{11}	2.60×10^{12}	5.910×10^{13}	1.322×10^{15}
4.92×10^{6}	4.55×10^{7}	5.05×10^{8}	6.74×10^{9}	1.08×10^{11}	2.06×10^{12}	4.756×10^{13}	
1.55×10^{10}	2.38×10^{10}	3.72×10^{10}	6.25×10^{10}	1.78×10^{11}	1.93×10^{12}	4.403×10^{13}	1.331×10^{15}
1.56×10^{6}	1.64×10^{7}	2.11×10^{8}	3.28×10^{9}	6.18×10^{10}	1.41×10^{12}	3.926×10^{13}	
1.63×10^{10}	2.53×10^{10}	3.99×10^{10}	6.54×10^{10}	1.52×10^{11}	1.42×10^{12}	3.691×10^{13}	1.340×10^{15}
4.35×10^{5}	5.31×10^{6}	7.99×10^{7}	1.48×10^{9}	3.34×10^{10}	9.28×10^{11}	3.172×10^{13}	
1.71×10^{10}	2.71×10^{10}	4.32×10^{10}	7.05×10^{10}	1.42×10^{11}	1.04×10^{12}	3.047×10^{13}	1.347×10^{15}
1.02×10^{5}	1.48×10^{6}	2.66×10^{7}	5.96×10^{8}	1.66×10^{10}	5.75×10^{11}	2.486×10^{13}	

Can. J. Chem. Downloaded from www.nrcresearchpress.com by 210.87.254.5 on 09/05/12
For personal use only.

effect can be surmized as follows. We consider a distribution such as that occurring in the middle of Table 1: we actually chose 2490 °K for this calculation. It is considered that *from this point on*, the heat-bath molecules M have the special property that they can deactivate H_2 in state i to H_2 in state j with high probability (*e.g.*, because M now has some degree of freedom which can be excited and which is closely resonant with $(\varepsilon_i - \varepsilon_j)$) and that the excitation transferred to M is rapidly degraded to heat: thus $P_{ji} = 0.5$ was substituted for the normal value, with P_{ij} following from detailed-balancing. The calculation was then continued by the nineteen-equation method, since such a change in one specific pair of transition probabilities is sufficient to change both the d_i and the s_{ij}. The general effect is to depress the population of state i and augment state j: it is obviously not possible to overpopulate state j with respect to state $(j-1)$ because of the large numbers involved, but it may be possible to depopulate state i by this wide-open channel to the extent that N_{i+1} would exceed N_i, and this is in fact the case. Three examples were examined. One was across the bottleneck (3, 27) with $P_{2,11} = 0.5$ and this generated a small overpopulation of state $v = 12$ with respect to $v = 11$. In a second experiment, $P_{2,5}$ was set equal to 0.5, but there was no overpopulation of $v = 6$ with respect to $v = 5$, presumably because $v = 2$ and $v = 6$ are slightly too closely coupled by T–V processes. However, with $P_{2,6} = 0.5$, a significant overpopulation of $v = 7$ with respect to $v = 6$ was observed. Before switching on the V–V simulation, N_7 and N_6 were 1.32×10^{10} and 2.26×10^{10} molecules respectively, but after quite a short time ($\sim 2 \times 10^{-9}$ s), a strong reversal to $N_7 = 1.15 \times 10^{10}$ molecules and $N_6 = 5.64 \times 10^9$ molecules had developed. Whilst this is no more than an illustrative calculation, it is clear that under the right conditions, such overpopulations should occur in simple nozzles, since if the "V–V" process had been switched on from the beginning of the flow, the overpopulation would have been more marked than is shown here.

(d) The Rate Constant for Recombination

We have already shown (3) that under non-flowing conditions, the rate constant for recombination $k_{r,M}$ can be found from the smallest eigenvalue d_{n-1} of the relaxation matrix by eqs. III(21) and III(22) *viz.*

$$[18] \quad k_{r,M} = K_c^{-1} k_{d,M} = -K_c^{-1}[M]^{-1} d_{n-1}$$

where $k_{d,M}$ is the dissociation rate constant. The quantity d_{n-1} is used at every step throughout the five-equation method, and it is therefore a simple matter to say what the true recombination rate constant should be at any instant. From the transition probabilities that were assumed together with the calculated population distribution function, it is also possible to write down the recombination flux by eq. II(11*b*) (analogous to eq. 2 but in n_i (per cc) instead of N_i) and obtain the phenomenological rate constant for recombination via

$$[19] \quad (Z_{1,1})[M] \sum_{j=0}^{n-1} \{\bar{P}_{jn} n_n^2 - \bar{P}_{nj} n_j\} = k_{r,M}[M]\left\{(2n_n)^2 - K_c \sum_{j=0}^{n-1} n_j\right\}$$

At very early times, when the system is not very far from the 3900 °K equilibrium distribution, the results are inaccurate because of severe cancellation in the left-hand side of eq. 19. However, once the temperature has fallen 200–300°, the cancellation difficulties subside, and thereafter, all the way down the flow, the values of $k_{r,M}$ calculated by eq. 18 and by eq. 19 agree excellently, as shown in Table 3 (note also that there are small "kinks" in the agreement at 3000 and 2500 °K where the eigenvalue and eigenvector polynomials were changed). Hence, since our nozzle flow is an extremely severe one, generating grossly non-Boltzmann distributions, we regard this result as conclusive evidence that the recombination rate constants measured in nozzle flows should agree with those deduced from shock-wave dissociation measurements via the rate-quotient law.

(e) The Vibrational Relaxation Time

There has been considerable discussion recently over the question as to whether the vibrational relaxation time measured in an expanding flow (*i.e.* in deactivation) is the same as that measured in excitation in a shock wave (10, 28, 29). These experimental flows are very much more complicated than that described in this paper, being dominated by V–V transitions,

TABLE 3. Correlation of the two smallest eigenvalues of the relaxation matrix with the rate constant for recombination and the vibrational relaxation time

T (°K)	$10^{35}k_{r,M}$ (cm^6 molecule^{-2} s^{-1})	$-10^{35}K_c^{-1}[M]^{-1}d_{n-1}$ (cm^6 molecule^{-2} s^{-1})	$10^8\tau_{vib}\rho_x/\rho_0$ (s)	$-10^8 d_{n-2}^{-1}$ (s)
3800	6.88	8.22	0.50	0.50
3700	7.81	8.31	0.56	0.53
3600	8.17	8.42	0.63	0.56
3500	8.39	8.55	0.69	0.60
3400	8.58	8.68	0.76	0.63
3300	8.75	8.82	0.83	0.68
3200	8.94	8.99	0.91	0.73
3100	9.14	9.17	0.99	0.78
3000	9.23	9.37	1.25	0.84
2900	9.48	9.59	1.33	0.91
2800	9.75	9.85	1.42	1.00
2700	10.04	10.13	1.54	1.09
2600	10.35	10.44	1.66	1.20
2500	10.66	10.75	1.82	1.33
2400	11.03	11.11	2.02	1.47
2300	11.42	11.50	2.23	1.65
2200	11.86	11.93	2.45	1.87
2100	12.36	12.42	2.81	2.12
2000	12.91	12.97	3.35	2.44
1900	13.51	13.56	3.87	2.82
1800	14.18	14.23	4.53	3.31
1700	14.96	15.00	5.41	3.92
1600	15.81	15.86	6.54	4.71
1500	16.73	16.77	8.07	5.73

and perhaps plagued by impurity effects (28). Nevertheless, an examination of the vibrational relaxation time in our flow may throw some light on the interpretation of the experimental findings. The standard experimental approach is to assume that a vibrational temperature can be defined, and then an attempt is made to measure it. This has been done in some cases (*e.g.* CO) by the measurement of direct emission intensity from the $0 \leftarrow 1$ transition (30, 31) which can be interpreted to yield the ratio N_1/N_0. This ratio can be used to define a vibrational temperature which, if it can be assumed to represent the complete vibrational population distribution, gives the mean vibrational energy content of the molecule ε_{vib}. In other cases, reversal measurements have been made (10, 32): the resulting vibrational temperature is less easy to define, but is clearly characteristic of some part of the upper-level population distribution of the molecule. One can also conceive, in principle, of other possible methods of measuring population ratios of pairs of levels, and so we have taken a general approach in examining the problem, that of taking the data in Table 2 and for each value of T, calculating the effective vibrational temperature from the population ratio of *every possible pair* of levels. Early in the flow, the calculated temperatures do not depart disastrously from the translational temperature. For example, at 3700 °K, N_0 taken together in turn with each other N_i gives temperatures rising monotonically from 3711 °K (from N_1/N_0) to 3870 °K (from N_{14}/N_0). However, once pairs of high levels are used, the discrepancy is larger, and the trend is no longer monotonic, with N_{12}/N_{11} yielding the highest apparent vibrational temperature of 4455 °K. Towards the end of the calculation, however, below $T = 2100$ °K, the situation has become very exaggerated, with some population ratios, *e.g.* N_8/N_7, yielding "temperatures" of around 10 000 °K. Then each value of $(T_{vib})_{ij}$ was used to generate a vibrational energy content ε_{vib} on the assumption that equilibrium existed amongst all the vibrational levels. By repeating the calculation for adjacent points in the flow (usually one step upstream or down-

Can. J. Chem. Downloaded from www.nrcresearchpress.com by 210.87.254.5 on 09/05/12
For personal use only.

Can. J. Chem. Downloaded from www.nrcresearchpress.com by 210.87.254.5 on 09/05/12
For personal use only.

stream), values for $d\varepsilon_{vib}/dt$ were established, since the velocity U was also known. Hence the vibrational relaxation time τ_{vib} follows by substitution in the standard equation (24, 33)

$$[20] \qquad -\frac{d\varepsilon_{vib}}{dt} = \frac{\varepsilon_{vib} - \tilde{\varepsilon}_{vib}}{\tau_{vib}}$$

where $\tilde{\varepsilon}_{vib}$ would be the vibrational energy content at equilibrium at the bath temperature T. In many of the cases, of course, this cannot be done since as we have just noted, if i and j are both high, $(T_{vib})_{ij}$ rises as the gas cools, giving *negative* values of $(\tau_{vib})_{ij}$.

It is however possible to solve eq. 20 exactly for τ_{vib} since our solutions for each value of T contain all the populations N_i, all the dN_i/dt, and of course the ε_i are given. Values of τ_{vib} calculated in this way are listed in Table 3, where they are compared with the quantity $-d_{n-2}^{-1}$, which we have previously identified (3) as the vibrational relaxation time that should be observed in the perfect shock-wave experiment; the comparison requires of course that the τ_{vib} be scaled by ρ_x/ρ_0 so that they refer to the same density as do the d_{n-2}. It can be seen that the agreement is remarkably good, and in our view, the fact that the two columns of numbers do not coincide more precisely arises from the limited accuracy of our solutions a long way down the flow. The basic reason for this agreement seems to be that the highly overpopulated vibrational levels are strongly coupled to the atoms, but that their contribution to ε_{vib} is only of the order 0.1% of the total vibrational energy content; on the other hand, those molecules which contain the bulk of the vibrational energy, *i.e.* $i(=v) = 1, 2, 3$, and 4 have $(T_{vib})_{0i} \approx T$, and so eq. 20 may be expected to hold reasonably well. It would have been interesting to continue on to lower temperatures still, but we cannot yet generate satisfactory eigenvectors S_{ij} below 1500 °K.

The question then arises, do any of the non-negative values of $(\tau_{vib})_{ij}$ calculated from population ratios give the correct vibrational relaxation time? The answer appears to be yes; if $(\tau_{vib})_{ij}$ is calculated from N_1/N_0, it appears to be consistently about 20% too low, or if it is calculated from the ratio N_2/N_0 it is usually within 2–3% of the correct answer (this statement only holds above 2000 °K, since below that, $v = 2$ and then $v = 1$ begin to freeze, thereby making the population ratios meaningless as "temperature"). However, using other ratios N_i/N_0, $(\tau_{vib})_{ij}$ rapidly diverges from the correct answer to something about 10^3 too long, and then may become negative as described above. In the current terminology (28, 29), $\phi \approx 10^{-3}$, which is considerably smaller than anything so far found experimentally. However, using N_i/N_j ratios where neither i nor j is zero, much faster relaxation times are also calculated, the fastest in our particular calculation being $\phi \approx 20$ which is similar to some of the controversial experimental values (29). This occurred when the system was not very far from equilibrium and when both levels used to define $(T_{vib})_{ij}$ were above the bottleneck, *i.e.* $i,j \geqslant 10$ and $T > 3800$ °K. Thus it would seem that the derived value of ϕ is rather sensitive to any imperfection there may be in the representation of the non-equilibrium vibrational population distribution by a "vibrational temperature", and whilst this result is only valid in the T–V regime, it does point to a possible source of difficulty in the more general case.

(f) Future Calculations

It should be possible in the foreseeable future to extend this method to the study of the vibrational activation and dissociation of a dilute diatomic gas as it flows at hypersonic speed over an aerodynamically interesting object, obtaining population distributions at least as reliable as those found in this work. Here again, assumptions of vibrational equilibrium can be rejected for the first time. If better accuracy is required than was achieved in this calculation, it will follow automatically if the change in temperature per integration step is reduced. This will be acceptable where temperature changes are small, but for a proper treatment of very large and rapid temperature changes, it will be necessary to modify eqs. 12 and 13 to include terms dS_{ij}/dT and $d\tilde{N}_n/dT$. That will leave, apart from the problem of calculating transition probabilities which we have argued (3, 13) is not crucial, the problem of including V–V coupling in such calculations; until such time as this can be achieved, it seems that we will have to rely on perturbation simulations applied to the T–V solutions, such as that described in section (*c*) above, together with a large measure of insight

(14) and guidance from experimental observation.

1. H. LOMAX. Stable implicit and explicit numerical methods for integrating quasi-linear differential equations with parasitic-stiff and parasitic-saddle eigenvalues. NASA TN D-4703. 1969.
2. H. E. BAILEY. Phys. of Fluids. **12**, 2292 (1969).
3. D. L. S. MCELWAIN and H. O. PRITCHARD. Thirteenth Symp. (Int.) on Combust. The Combustion Institute. 1971. p. 37. Part III of this series.
4. J. G. HALL and C. E. TREANOR. Nonequilibrium effects in supersonic nozzle flows. Cornell Aeronautical Laboratory, Report No. 163. 1968; J. W. RICH and C. E. TREANOR. Annu. Rev. Fluid Mech. **2**, 355 (1970).
5. J. D. ANDERSON. AIAA J. **8**, 545 (1970).
6. H. K. CHENG and R. S. LEE. AIAA J. **6**, 823 (1968); **6**, 831 (1968).
7. M. J. LIGHTHILL. J. Fluid Mech. **2**, 1 (1957).
8. N. C. FREEMAN. J. Fluid Mech. **4**, 407 (1958).
9. W. A. REINHARDT. A simplified molecular model for studying vibration–dissociation coupling in fluid flows. NASA TR R-324. 1969.
10. I. R. HURLE and A. L. RUSSO. J. Chem. Phys. **43**, 4434 (1965).
11. E. W. MONTROLL and K. E. SHULER. J. Chem. Phys. **26**, 454 (1957); A. I. OSIPOV. Dokl. Akad. Nauk. S.S.S.R. **130**, 523 (1960).
12. R. E. CENTER and G. E. CALEDONIA. Appl. Opt. **10**, 1795 (1971).
13. D. L. S. MCELWAIN and H. O. PRITCHARD. J. Am. Chem. Soc. **91**, 7693 (1969). Part II of this series.
14. D. L. S. MCELWAIN and H. O. PRITCHARD. J. Am. Chem. Soc. **92**, 5027 (1970).
15. P. A. BLYTHE. Phil. Trans. Roy. Soc. (London), **A262**, 203 (1967).
16. G. EMANUEL and W. G. VINCENTI. Method for calculation of the one-dimensional nonequilibrium flow of a general gas mixture through a hypersonic nozzle. Arnold Engineering Development Center. TDR-62-131. 1962.
17. R. A. CRAIG. Personal communication. *c.f.* D. A. BITTKER and V. J. SCULLIN. General chemical kinetics computer program for static and flow reactions, with application to combustion and shock-tube kinetics. NASA TN D-6586. 1972.
18. V. A. LODATO, D. L. S. MCELWAIN, and H. O. PRITCHARD. J. Am. Chem. Soc. **91**, 7688 (1969). Part I of this series.
19. N. I. LABIB. Ph.D. Thesis. York University, Downsview, Ontario. 1972.
20. JANAF Thermochemical Tables. Dow Chemical Co., Midland, Michigan. 1965.
21. S. H. LUI, K. H. LAU, and H. EYRING. J. Chem. Phys. **55**, 5657 (1971).
22. J. D. LAWSON. SIAM J. Num. Anal. **3**, 593 (1966).
23. D. G. RUSH and H. O. PRITCHARD. Eleventh Symp. (Int.) on Combust. The Combustion Institute. 1967. p. 13.
24. W. G. VINCENTI and C. H. KRUGER. Introduction to physical gas dynamics. John Wiley, New York. 1965.
25. G. E. CALEDONIA and R. E. CENTER. J. Chem. Phys. **55**, 552 (1971).
26. D. L. S. MCELWAIN and H. O. PRITCHARD. Can. J. Chem. **50**, 897 (1972). Part VI of this series.
27. E. KAMARATOS and H. O. PRITCHARD. Can. J. Chem. **49**, 2617 (1971). Part IV of this series.
28. C. W. VON ROSENBERG, R. L. TAYLOR, and J. D. TEARE. J. Chem. Phys. **54**, 1974 (1971).
29. T. I. MCLAREN and J. P. APPLETON. J. Chem. Phys. **53**, 2850 (1970).
30. A. P. BLOM and N. H. PRATT. Nature, **223**, 1052 (1969); A. P. BLOM, K. N. C. BRAY, and N. H. PRATT. Astronaut. Acta, **15**, 487 (1970); K. N. C. BRAY and N. H. PRATT. J. Chem. Phys. **53**, 2987 (1970).
31. T. JUST and P. ROTH. J. Chem. Phys. **55**, 2395 (1971).
32. I. R. HURLE, A. L. RUSSO, and J. G. HALL. J. Chem. Phys. **40**, 2076 (1964); A. L. RUSSO. J. Chem. Phys. **47**, 5201 (1967).
33. T. L. COTTRELL and J. C. MCCOUBREY. Molecular energy transfer in gases. Butterworths, London. 1961.

Can. J. Chem. Downloaded from www.nrcresearchpress.com by 210.87.254.5 on 09/05/12
For personal use only.

Préparation simple et configuration de dérivés des bicyclo[3.3.1]nonanol-2 ones-9 *endo* et *exo*. Utilité de la fonction trichloro-2,2,2 éthoxycarbonyle comme groupe protecteur d'aldols

D. GRAVEL, S. RAHAL,[1] ET A. REGNAULT[2]

Département de Chimie, Université de Montréal, C.P. 6128, Montréal, Québec

Reçu le 2 mars 1972

Des modes de préparation simples et efficaces de paires d'épimères *endo* et *exo* en série bicyclo[3.3.1]nonanol-2 one-9 sont décrits. La configuration de chacun des isomères est établie par voie spectroscopique et par corrélation chimique. Il est montré que le groupe trichloro-2,2,2 éthoxycarbonyle peut être employé pour protéger ces aldols et que leur régénération n'entraîne aucune épimérisation.

Simple and efficient preparations of some *endo* and *exo* epimeric pairs in the bicyclo[3.3.1]nonan-2-ol-9-one series are described. The configuration of each isomer is established spectroscopically and by chemical correlation. It is shown that the 2,2,2-trichloroethoxycarbonyl group may be used to protect these aldols and that regeneration of the latter does not give rise to epimerization.

Canadian Journal of Chemistry, **50**, 3846 (1972)

Can. J. Chem. Downloaded from www.nrcresearchpress.com by 210.87.254.42 on 09/05/12
For personal use only.

Introduction

Depuis la parution en 1961 des travaux de Murray *et al.* (1), les dérivés bicyclo[3.3.1]-nonanes ont connu une période très féconde des points de vue synthèse, mécanismes réactionnels, et analyse conformationnelle. A l'examen des travaux, on remarque que la paire d'isomères: *endo* (**1***a*) et *exo* (**2***a*), quoique préparée plusieurs fois (2–8) n'a été séparée qu'une seule fois (7) sur une base préparative et ce par une méthode laborieuse impliquant: chromatographie, cristallisation, et sublimation.

En relation avec des travaux en cours dans notre laboratoire, nous avons mis au point deux méthodes simples d'obtention de quantités importantes des paires d'isomères *endo* et *exo*: **1**, **2** et **3**, **4**. Etant donné l'importance de ces paires d'épimères dans l'étude de la réactivité du système bicyclo[3.3.1]nonane nous rapportons ici les détails de préparation ainsi que les preuves de structure.

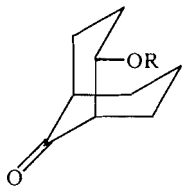

1

a R = H

b R = —C(=O)—OCH_2CCl_3

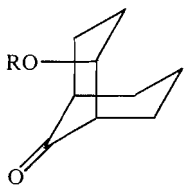

2

a R = H

b R = —C(=O)—OCH_2CCl_3

Résultats et discussion

La méthode de Allan *et al.* (6) a été empruntée pour préparer le mélange des alcools **1***a* et **2***a*. L'analyse par c.p.g. montra que le céto–alcool *exo* (**2***a*) est formé à 40% et que le céto–alcool *endo* (**1***a*) constitue 60% du mélange. Ces proportions sont en accord avec celles trouvées par Kraus *et al.* (7) ainsi que par Dean *et al.* (5).

Au cours de notre étude, nous avons remarqué que lorsqu'on acétalise le mélange des céto–alcools **1***a* et **2***a*, les proportions relatives de ces deux isomères se trouvent *inversées*. De plus, ce qui s'avère très utile, ces deux isomères sont faciles à séparer: l'isomère *exo* (**4***a*) étant très soluble dans l'hexane.

L'acétal–alcool *endo* (**3***a*), montre en r.m.n. le proton carbinolique comme un massif centré à 4.1 p.p.m., largeur à la mi-hauteur ($L_{\frac{1}{2}}$): 24 Hz; l'isomère *exo* (**4***a*) présente ce proton à 4.15 p.p.m. avec un $L_{\frac{1}{2}}$ de 5 Hz, conformément à la stéréochimie postulée (7). D'autre part, le spectre i.r. de solutions diluées de chaque épimère montre: pour l'*endo* (**3***a*): une bande fine à 3625 cm^{-1} (OH libre) alors que l'*exo* (**4***a*) présente une bande large à 3530 cm^{-1}, indiquant un pont hydrogène intramoléculaire (3). Finalement, les tosylates **3***b* et **4***b* ont été préparés et seul le tosylate **4***b* conduit à l'oléfine **5** (9) con-

[1]Boursier de l'Agence Canadienne de Développement International (ACDI).

[2]Boursier post-doctoral 1969–1970.

Can. J. Chem. Downloaded from www.nrcresearchpress.com by 210.87.254.42 on 09/05/12
For personal use only.

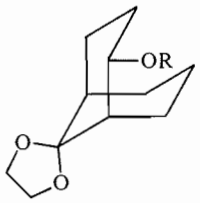

3

a R = H
b R = Ts

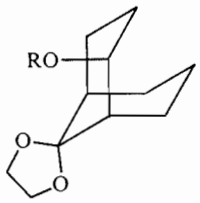

4

a R = H
b R = Ts

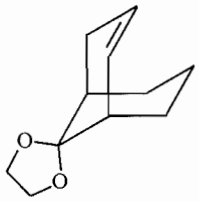

5

firmant la position axiale du groupement hydroxyle dans **4***a* (3).

La méthode exposée plus haut permet donc d'une façon simple d'obtenir les isomères *endo* et *exo* du bicyclo[3.3.1]nonanol-2 one-9 mais bloqués sous forme d'acétal. Etant donné qu'il n'est pas possible de débloquer celui-ci sans isomériser l'alcool en position 2, nous avons mis au point une seconde méthode d'obtention des alcools mais cette fois en modifiant la fonction hydroxyle du mélange.

Celle-ci consiste à préparer le dérivé trichloro-2,2,2 éthoxycarbonyle (**1***b* + **2***b*) (10) du mélange des céto–alcools qui, par trituration dans le *n*-hexane, laisse précipiter l'isomère *exo* (**2***b*). Par chromatographie simple du résidu, on obtient l'isomère *endo* (**1***b*). Contrairement à l'acétalisation qui favorisait l'isomère *exo* par équilibration, la formation des dérivés "*carbonates*", conserve le rapport *endo–exo* (60:40) du mélange de départ.

Comme dans le cas précédent, l'isomère *exo* (**2***b*) présente en r.m.n. à 5.25 p.p.m. un singulet, dû au proton carbinolique ayant un $L_{\frac{1}{2}}$ de 7 Hz alors que l'isomère *endo* (**1***b*) montre à 4.80 p.p.m. un massif ayant un $L_{\frac{1}{2}}$ de 30 Hz. Une corrélation de configuration de chacun des isomères fut apportée en les transformant respectivement en alcool *endo* (**1***a*) et *exo* (**2***a*) décrits par Kraus *et al.* (7). La transformation se fait dans de l'acide acétique glacial en présence de poudre de zinc. Le céto–alcool *exo* (**2***a*) obtenu a le point de fusion et les propriétés spectroscopiques décrits (7).[3] De même, l'alcool *endo* (**1***a*) possède des propriétés spectroscopiques décrites (7).

Enfin, il est important de noter que la réaction est stéréospécifique ce qui suggère l'application de ce dérivé comme groupe protecteur de la fonction aldol.

Partie éxperimentale

Les points de fusion, déterminés à l'aide d'un appareil "Buchi", ne sont pas corrigés. Les spectres i.r. ont été pris dans le chloroforme sur un spectrophotomètre "Beckman" modèle IR-8. Les spectres de r.m.n. ont été pris dans le $CDCl_3$, sauf indication contraire, sur un spectromètre "Jeol" de 60 MHz modèle C60-H. Les déplacements chimiques ($-\delta$) sont exprimés en p.p.m. et la référence interne est le TMS. Les analyses par c.p.g. ont été faites sur un appareil "Varian Aerograph", modèle 90 P. Colonne: 6 pd. × 1/4 po., adsorbant: 10% U.C.W. 98 sur diatoport 80–100 S. Température: 170°. Les indices de réfraction ont été mesurés à l'aide d'un réfractomètre "Abbé" de la compagnie Karl–Zeiss. Les analyses élémentaires ont été confiées à "Midwest Microlab Inc.", Indianapolis, Indiana.

*Bicyclo[3.3.1]nonanol-2 one-9 (**1***a* + **2***a*) (6)*

Un mélange de 31 g (0.20 mol) d'(oxo-2 cyclohexyl)-3 propanal (6), 45 ml de Rexyn 101 et 150 ml d'eau distillée est porté à reflux pendant 2–3 h. Après extraction à l'éther la masse gommeuse obtenue est recristallisée d'un mélange acétate d'éthyle–*n*-hexane. Le solide obtenu (22–25 g, 73–83%, litt. (6) 90–95%) est un mélange de **1***a* et **2***a*. I.r.: 1720, 3450, et 3640 cm^{-1}. R.m.n. 3.2 singulet, (échangeable avec D_2O); 4.1 p.p.m. massif (protons carbinoliques).

*Analyse par c.p.g. du mélange des épimères (**1***a* + **2***a*)*

(A) Ethers silylés (11)

Un mélange de 10 mg des épimères, 1 ml de pyridine, 0.2 ml d'hexaméthyldisilazane, et 0.1 ml de triméthylchlorosilane est agité 30 s, puis laissé reposer pendant 1 h. Résultat: le rapport *endo*:*exo* est de 60:40.

(B) Acétates

Un mélange de 10 mg des épimères, 5 gouttes de pyridine, 2 ml d'acide acétique, et 4 ml d'anhydride acétique est mis à reflux pendant 1 h. Le mélange est laissé à reposer 1 h. Résultat: le rapport *endo*:*exo* est de 60:40.

*Ethylènedioxy-9,9 bicyclo[3.3.1]nonanol-2 endo (**3***a*) et exo (**4***a*)*

Une solution de 15.4 g (0.10 mol) de bicyclo[3.3.1]-nonanol-2 one-9 (**1***a* + **2***a*), 12.5 g (0.20 mol) d'éthylène glycol, 0.05 g d'acide *p*-toluène sulfonique dans 150 ml de benzène est refluée jusqu'à élimination de 1.8 ml d'eau. Après le traitement habituel et distillation, un liquide visqueux est isolé (19 g). Celui-ci traité par 150 ml d'hexane permet de précipiter 7.2 g (36.4%) de cristaux d'acétal–

[3]Ce céto–alcool fut aussi isolé en bas rendement par Martin *et al.* (3) lors de la réduction d'une énol–lactone bicyclique appropriée.

alcool *endo* (**3***a*): p.f. 101–102° (hexane). I.r.: 1000, 1100, et 3640 cm^{-1}.

Anal. calc. pour $C_{11}H_{18}O_3$: C, 66.66; H, 9.09. Trouvé: C, 66.74; H, 9.18.

L'huile résiduelle, distillée, donne 11 g (55.6%) d'acétal-alcool *exo* (**4***a*): p.f. 34–35°. I.r.: 1010, 1110, et 3520 cm^{-1}.

Anal. calc. pour $C_{11}H_{18}O_3$: C, 66.66; H, 9.09. Trouvé: C, 66.59; H, 9.06.

Etude de dilution en i.r. des épimères **3***a et* **4***a*

L'appareil utilisé est un spectrophotomètre Perkin-Elmer modèle 621. Résultats: isomère *endo*, pour $c = 0.15$ *M* (cellules 0.2 mm): bande OH libre à 3625 cm^{-1}, bande OH lié de 3250 à 3550 cm^{-1} et non symétrique. Pour $c = 0.15 \times 10^{-2}$ *M* (cellules 2 cm): bande OH libre à 3625 cm^{-1} seulement. Isomère *exo*, pour $c = 0.15$ *M*: bande OH lié intramoléculairement à 3530 cm^{-1}, et bande OH lié intermoléculairement chevauchant la précédente et allant jusqu'à 3250 cm^{-1}. Pour $c = 0.15 \times 10^{-2}$ *M*: bande OH lié intramoléculairement à 3530 cm^{-1} seulement.

*(Trichloro-2,2,2 éthoxycarbonyl)-oxy-2 bicyclo[3.3.1]nonanone-9 endo (***1***b) et exo (***2***b) (10)*

Dans 20 ml de pyridine on agite pendant une nuit à température ambiante 1 g (0.065 mol) de céto-alcool (**1**a et **2**a), et 3 g (0.14 mol) de chloroformiate de trichloro-2,2,2 éthyle. Le mélange est dilué dans 20 ml d'eau et extrait à l'éther. Celle-ci est lavée, séchée, et évaporée pour donner 3.2 g d'une huile. Triturée dans le *n*-hexane, cette huile donne 0.9 g de cristaux qui après recristallisation dans un mélange acétate d'éthyle–hexane donnent 0.8 g (38%) de produit *exo* (**2***b*). P.f.: 110–111°. I.r.: 1730 et 1750 cm^{-1}.

L'huile restante (2.3 g) est chromatographiée sur gel de silice, en éluant avec du *n*-hexane; les premières fractions donnent un solide blanc issu du réactif. Les fractions suivantes, éluées avec 5% d'acétate d'éthyle dans l'hexane, contiennent 1.2 g (56%) d'une huile limpide qui est le produit *endo* (**1***b*). I.r.: 1720 et 1750 cm^{-1}.

*Bicyclo[3.3.1]nonanol-2 one-9 endo (***1***a) et exo (***2***a) (10)*

Une portion de 1 g de dérivé *exo* (**2***b*) est agitée à la température ambiante avec un même poids de poudre de zinc dans 10 ml d'acide acétique pendant 2 h. Après filtration, la solution est reprise par du chloroforme, lavée à l'eau, séchée, et évaporée. Le résidu est un solide cotonneux qui, après recristallisation dans un mélange *n*-hexane–acétate d'éthyle donne 400 mg (85%) d'alcool *exo* (**2***a*). P.f.: 175–176° (litt. (7) 175–176°). I.r.: 955, 1720, et 3450 cm^{-1}. R.m.n. (CCl_4): 3.25, singulet (1 H) échangeable avec D_2O; 4.3 p.p.m. singulet élargi (1H).

Le même procédé est utilisé pour le dérivé *endo* (**1***b*), sauf que l'agitation dure une nuit. Le résidu obtenu est une huile qui cristallise partiellement mais qui, sublimée à 150° sous 0.5 Torr donne 320 mg (70%) d'alcool *endo* (**1***a*). P.f.: 199–200° (litt. (7) 192–193.5°). I.r.: 1050 et 1700 cm^{-1}. R.m.n. (CCl_4): 3.9 p.p.m., massif (1H).

*p-Toluènesulfonates des éthylènedioxy-9,9 bicyclo[3.3.1]nonyl-2 endo (***3***b) et exo (***4***b) (12)*

Une solution de 2 g (0.01 mol) d'acétal-alcool (**3***b*) ou (**4***b*) dans de la pyridine (20 ml) est traitée par 2.20 g de chlorure de *p*-toluènesulfonyle pendant une nuit à 0°. Après traitement habituel, le tosylate *endo* (**3***b*) est obtenu sous forme d'un solide blanc. Rendement 88%. P.f.: 100–101° (*n*-hexane). I.r.: 1040, 1120, 1180, 1350 et 1600 cm^{-1}. R.m.n.: 2.46, singulet (3H); 3.90, singulet (4H); 4.90, massif (1H), et 7.60 p.p.m., quadruplet déformé (4H).

Anal. calc. pour $C_{18}H_{24}O_5S$: C, 61.36; H, 6.82; S, 9.09. Trouvé: C, 61.20; H, 7.02; S, 9.39.

Le tosylate *exo* (**4***b*) est obtenu sous forme d'un solide blanc qui se décompose avec le temps; rendement 60%. P.f.: 79–80° (pentane). I.r.: 1040, 1130, 1180, 1360, et 1600 cm^{-1}. R.m.n. 2.46, singulet (3H); 3.94, singulet (4H); 4.75, singulet élargi (1H), et 7.60 p.p.m., quadruplet déformé (4H).

*Ethylènedioxy-9,9 bicyclo[3.3.1]nonène-2 (***5***)*

Une solution de 1.30 g (0.004 mol) de tosylate *exo* (**4***b*) dans 25 ml d'éthanol en présence d'éthylate de sodium (0.17 g de Na dans 25 ml d'éthanol absolu) est chauffée à reflux pendant 2 h. Le mélange est extrait au *n*-hexane, et la phase organique est lavée à l'eau séchée et évaporée pour donner l'oléfine **5** (9) sous forme d'huile incolore avec un rendement de 67%. I.r.: 1040, 1120, et 1650 cm^{-1}. R.m.n.: 3.87, singulet (4H), et 5.5 p.p.m., massif (2H).

Nous remercions tout particulièrement le Conseil National de Recherches du Canada pour l'aide financière apportée à D.G. sous forme d'octroi de recherche et l'Agence Canadienne de Développement International pour une bourse d'étude accordée à S.R. Notre reconnaissance s'adresse également à Mme M. Bernard pour sa collaboration lors de l'étude de dilution en i.r. Enfin, nous remercions le Dr R. J. Wells de nous avoir fourni des détails supplémentaires sur la cyclisation en présence de résine acide.

1. R. D. H. Murray, W. Parker, et R. A. Raphael. Tetrahedron, **16**, 74 (1961).
2. A. C. Cope, D. L. Nealy, P. Scheiner, et G. Wood. J. Am. Chem. Soc. **87**, 3130 (1965).
3. J. Martin, W. Parker, B. Shroot, et T. Stewart. J. Chem. Soc. C, 101 (1967).
4. W. Kraus et W. Rothenwöhrer. Tetrahedron Lett. 1007 (1968).
5. C. S. Dean, J. R. Dixon, S. H. Graham, et D. O. Lewis. J. Chem. Soc. C, 1491 (1968).
6. R. D. Allan, B. G. Gordiner, et R. J. Wells. Tetrahedron Lett. 6055 (1968).
7. W. Kraus, W. Rothenwöhrer, et R. Chassin. Tetrahedron Lett. 4581 (1969).
8. H. Kato et M. Kawanisi. Synth. 256 (1970).
9. C. S. Foote et R. B. Woodward. Tetrahedron, **20**, 687 (1964).
10. T. B. Windholz et D. B. R. Johnston. Tetrahedron Lett. 2555 (1967).
11. Handbook of silylation. Pierce Chemical Co., Rockford, Ill. 1970. Handbook GPA-3.
12. Reagents for organic synthesis. L. F. Fieser and M. Fieser, Editors. John Wiley and Sons, Inc., New York. 1967. p. 1180.

Can. J. Chem. Downloaded from www.nrcresearchpress.com by 210.87.254.42 on 09/05/12
For personal use only.

Photooxidation and Decarboxylation of Tyrosine Studied by E.P.R. and C.I.D.N.P. Techniques

MICHA TOMKIEWICZ,[1] ROBERT D. MCALPINE,[2] AND MICHAEL COCIVERA

Department of Chemistry, University of Guelph, Guelph, Ontario

Received June 21, 1972

The photooxidation of deoxygenated solutions of tyrosine in water at p*H* 8.5–12.6 has been studied at room temperature using e.p.r. spectroscopy. By means of e.p.r., four radicals were detected during irradiation with the full spectrum of a Hg–Xe arc lamp. These were identified as the tyrosyl radical, CO_2^- and two radicals derived from dopa. A tentative mechanism suggested for CO_2^- formation involves the reaction of tyrosine with the hydrated electron, which has been ejected from another tyrosine molecule in one of its excited electronic states. A mechanism similar to the one proposed for the photooxidation of phenol has been suggested for the formation of the radicals derived from dopa. Support for this mechanism is provided by the observation of proton nuclear spin polarization during irradiation.

La photooxydation des solutions desoxygénées de tyrosine dans l'eau, à des p*H* de 8.5–12.6, a été étudiée à la température ambiante au moyen de la spectroscopie r.p.e. Quatre radicaux ont été détectés pendant l'irradiation par la totalité du spectre d'arc de la lampe Hg–Xe. Ils ont été identifiés aux radicaux tyrosyle, CO_2^- et deux dérivés du dopa. Une tentative pour expliquer le mécanisme de la formation de CO_2^- fait intervenir la réaction de la tyrosine avec l'électron hydraté, éjecté d'une autre molécule de tyrosine dans un de ses états électroniques excités. Un mécanisme, semblable à celui proposé dans la photooxydation du phénol, a été suggéré pour la formation des radicaux dérivés du dopa. A l'appui de ce mécanisme, la polarisation de spin nucléaire du proton a été observée durant l'irradiation. [Traduit par le journal]

Canadian Journal of Chemistry, **50**, 3849 (1972)

Can. J. Chem. Downloaded from www.nrcresearchpress.com by 210.87.254.5 on 09/05/12
For personal use only.

Introduction

The use of e.p.r. spectroscopy to detect radical intermediates resulting from the irradiation of aromatic amino acids has been mainly confined to the solid state (1). Without the use of special techniques, such as ENDOR (Electron Nuclear Double Resonance), the broad nature of solid state e.s.r. lines makes the identification of hyperfine interactions difficult. However, in the liquid state, molecular motion tends to sharpen the lines of the spectrum, and isotropic hyperfine coupling constants can be obtained to a high degree of precision. Often the details of the hyperfine structure of a radical spectrum are sufficient to assign the structure of the radical. One additional motivation for carrying out liquid phase studies is the fact that variables, such as p*H*, ionic strength, and concentrations may be more easily controlled in liquid than in solid state. We have undertaken an e.p.r. study of the irradiation of tyrosine and several related compounds in water solution using the full spectrum (quartz optics) of a 1000 W mercury–xenon high pressure lamp. Subsequently, we will attempt to extend these studies to polypeptides.

Since tyrosine is a building block of polypeptides and proteins, it is our hope that information about the photochemistry of this and other aromatic amino acids will lead to some understanding of u.v. irradiation processes in the larger molecules. Tyrosine consists of a phenol attached to an alanine residue. Consequently, in this article, we will show that most of the photochemical oxidation of tyrosine in basic solution, and in the absence of molecular oxygen, may be understood in terms of the known photochemical oxidation of phenol, a study which has been carried out in this laboratory (2). Under the conditions described, the tyrosyl radical **1**, and an *o*-benzosemiquinone **2** derived from dopa can be detected. The formation of these radicals can be understood in terms of photoelectron ejection via an excited state of tyrosine (3) followed by a hydroxide ion attack on the tyrosyl radical to form dopa, which is subsequently further oxidized to the *o*-benzosemiquinone radical **2**. Additional evi-

[1]Present address: Lawrence Radiation Laboratory, University of California, Berkeley, California.

[2]Postdoctoral support by Department of University Affairs, 1969–1972.

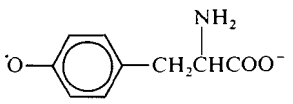

1

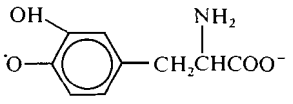

2

dence in favor of this mechanism was obtained from the n.m.r. spectrum of the solution obtained during irradiation. Under these conditions nuclear spin polarization, which is consistent with the proposed mechanism, is obtained.

Experimental

Solutions of 10^{-2} *M* L-tyrosine (Cyclo Chemical Co.) were irradiated at various p*H* values between 8.5–12.6, in the microwave cavity of a Varian E-12 e.p.r. spectrometer. The irradiation consisted of the full spectrum of a Hanovia 1000 W mercury–xenon lamp using quartz optics. Closed, continuous flow systems were used as described previously (2*b*). Solutions were maintained oxygen free by passing nitrogen (Canox) or argon (Canox) through the reservoir of the flow system. For several experiments the nitrogen gas was replaced by N_2O (Canox).

In a few experiments tyrosine α-d_1, or tyrosine α-d_1, *o*-d_2 (both prepared specially for us by Merck, Sharpe and Dohme, Montreal) were irradiated in the place of tyrosine.

N.m.r. studies were carried out on a Varian HA100 spectrometer which was equipped with a special probe which allowed the n.m.r. spectrum to be observed during irradiation. The details have been described previously (2*b*).

Results and Discussion

Electron Paramagnetic Resonance Spectroscopy

Figure 1 illustrates the e.p.r. spectrum obtained during irradiation of a deoxygenated solution of 0.01 *M* tyrosine in water at p*H* 11 and room temperature. For this spectrum, the flow rate was 5 ml/min. Variation in the flow rate (5–20 ml/min) has very little effect on the absolute, but no effect on the relative intensities of the lines. Variation in the p*H* affects both the absolute and the relative intensities of the lines. Maximum absolute intensities occur around p*H* 11.4. Below p*H* 8.5 and above p*H* 12.6, the radicals could not be detected at the flow rates employed (5–20 ml/min).

The spectrum in Fig. 1 can be analyzed as a superposition of the spectra of four radicals. In the first (*g*, 2.0041), the hyperfine interactions involve six protons in equivalent sets 2:2:1:1 with coupling constants 6.15, 1.5, 15.4, and 0.4 G, respectively. Borg and Elmoro (4) have observed the same spectrum with less resolution during chemical oxidation of tyrosine in alkaline water. They did not observe the 0.4 G splitting. They assigned this spectrum to the tyrosyl radical with the ortho and meta protons having the coupling constants 6.5 and 1.5 G, respectively. They suggested that the CH_2-protons were unequivalent due to hindered rotation with one having a coupling constant of 15.4 G and the other having one too small to resolve. They base this conclusion on the fact that these protons appear to be equivalent in acidic water solutions but become unequivalent again when a NH_2- or a COOH-proton is substituted by a bigger

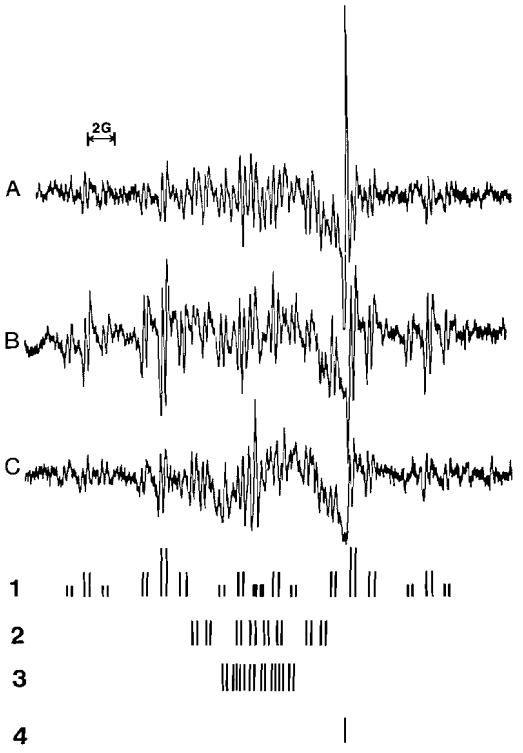

FIG. 1. (A) E.p.r. spectrum obtained during the irradiation of a deoxygenated water solution of 0.01 *M* tyrosine at p*H* 11 and ambient temperature. Flow rate is 5 ml/min. (B) E.p.r. spectrum under the same conditions as part A except the solution is saturated with N_2O. (C) E.p.r. spectrum under the same conditions as part B except the solution contains 1 *M* methanol.

Can. J. Chem. Downloaded from www.nrcresearchpress.com by 210.87.254.5 on 09/05/12
For personal use only.

TABLE 1. Observed hyperfine coupling constants

Radical	g	α-H*	β-H*	o-H†	m-H†
Tyrosyl (**1**)	2.0041	0.4	7.7‡	6.15	1.5
Tyrosyl α-d_1,o-d_2	2.0041	<0.1	7.6‡	0.9	1.5
Tyrosyl o-d_1	2.0041	<0.1	7.6‡	6.0	1.3
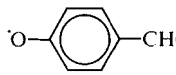	—	0.35	8.2	6.4	1.4
Dopa semiquinone, acid form (**2**)	2.0021	<0.1	2.7‡	(3.55,	1.12, 0.32)§
Dopa semiquinone, base form (**3**)	2.0021	<0.1	1.85‡	(1.55,	0.91, 0.39)§
CO_2^- (**4**)	2.0001	—	—		—

*α, β are defined relative to the —COOH group.
†o, m are defined relative to the —OH group.
‡The β hydrogens are assumed to undergo hindered rotation.
§The assignments of hyperfine constants for the three unequivalent ring protons of radicals 2 and 3 cannot be specified with the present information.

group. While we agree that hindered rotation probably is responsible for the occurrence of a doublet rather than a triplet splitting due to the methylene protons, we prefer to assign the doublet splitting to both methylene protons rather than to one of them. Thus, although a triplet is expected, a doublet is observed because the hindered rotation occurs at a rate which broadens the central line to the extent that it cannot be detected. This alternating linewidth effect has been observed for a number of radicals (5). Thus, according to our interpretation, the hyperfine coupling constant for the methylene protons is 7.7 G. Support for this interpretation is the fact that these methylene protons have a coupling constant of 7.8 G when the tyrosyl radical is formed under conditions in which hindered rotation is unimportant and the triplet is observed (4). Additional evidence in favor of this assignment is given below.

To obtain a more conclusive assignment of the hyperfine interactions, we have repeated our experiments using two types of partially deuterated tyrosine: tyrosine o-d_2,α-d_1 and tyrosine α-d_1. These were obtained under the same conditions as Fig. 1. The effect of the deuteration on the spectra of the other radicals will be discussed below. The spectrum for radical **1** obtained from tyrosine o-d_2,α-d_1 indicates that the two equivalent protons with the hyperfine constant of 6.15 G observed in Fig. 1 have been replaced by two deuterons. Furthermore, the 0.4 G splitting has disappeared. The absence of the 0.4 G splitting occurred for tyrosine α-d_1, also. These results indicate that the 6.15 G splitting is due to the ortho-protons and the 0.4 G splitting is due to the α-CH-proton. To check the possibility that the aliphatic side-chain has undergone an elimination reaction to give the phenoxyl radical derived from *p*-hydroxycinnamic acid, we have studied the irradiation of this acid under the same conditions. We detected the phenoxyl radical derived from this acid with the following hyperfine coupling constants for the α-H, β-H, *o*-H, and *m*-H, respectively: 0.35, 8.2, 1.4, and 6.4 G. Thus since the doublet splitting due to the β-H of this radical is about half the value of 15.4 G observed for the β-H of the tyrosyl radical, this alternative is unlikely. Combining these conclusions with those made in the previous paragraph, the assignment of the hyperfine coupling constants for tyrosyl radical are given in Table 1.

Since we feel that the second and third radicals are closely related, we will discuss them together. The spectrum for the second radical in Fig. 1 can be analyzed in terms of four doublet splittings with values of 5.30, 3.55, 1.12, and 0.32 G, and $g = 2.0021$. The third radical also has a spectrum which can be analyzed in terms of four doublet splittings having values of 1.55, 3.70, 0.91, and 0.39 G, and $g = 2.0021$. We suggest that the second and third radicals have structures **2** and **3**, respectively. As can be seen,

Can. J. Chem. Downloaded from www.nrcresearchpress.com by 210.87.254.5 on 09/05/12
For personal use only.

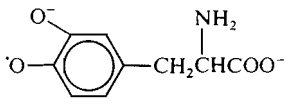

3

3 is the conjugate base of **2**. As in the case of the tyrosyl radical, the observation of a doublet rather than a triplet splitting for the CH_2-protons of **2** and **3** is explained in terms of hindered rotation at a rate which broadens the central line of the triplet to the extent that it cannot be detected. The spectra for these radicals obtained from tyrosine o-d_2,α-d_1 exhibited broad lines with insufficient detail for an adequate analysis. This result is not unexpected since deuteration at the ring should cause overlap of lines. On the other hand, the spectra for radicals **2** and **3** obtained from tyrosine α-d_1 are identical to the spectra in Fig. 1, indicating the absence of a measurable hyperfine interaction for the α-CH proton. The assignments of the hyperfine coupling constants are given in Table 1. These assignments are arbitrary, and the choice of the largest splitting for the methylene protons is made to be consistent with the similar assignment made for the tyrosyl radical.

Another reason for the choice of **2** and **3** is that the relative concentrations of these radicals depend on the pH of the solution. From this pH dependence, the pK_a value for the acid dissociation of **2** is determined to be about 12.4. This value can only be considered approximate since it is based on measurements at only seven pH values ranging from 9.6 to 12.6. Gorton and Jameson (6) have obtained a value of 13.4 for the same acid dissociation step involving the corresponding diamagnetic molecule, dopa (3-[3,4-dihydroxyphenyl]alanine). Thus, the pK_a value appears to decrease when an electron is removed from dopa. A decrease is not unexpected since Carrington and Smith (7) have found a similar but larger effect for pyrogallol.

Additional support for the assignment of **2** and **3** is the fact that L-dopa forms these radicals, also, as can be seen in Fig. 2. The spectrum given in Fig. 2 is obtained in water at pH 11 in the absence of irradiation. If the solution is made acidic, the radicals cannot be detected. Oxidation of L-dopa by molecular oxygen seems unlikely since the same spectrum was observed, also, in a static solution which had been evacu-

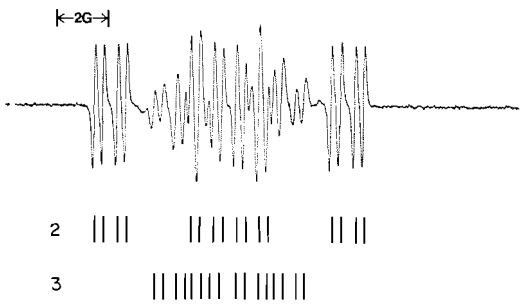

FIG. 2. E.p.r. spectrum of a deoxygenated water solution of L-dopa at pH 11 in the absence of irradiation. The intensity of the spectrum is enhanced during irradiation and no additional signals are observed.

ated to 2 μ Hg. This degassed solution was prepared by dissolving L-dopa in water after the evacuation had been completed. At this pressure, the concentration of O_2 in water is about 10^{-9} M whereas the concentration of radicals is about 10^{-5} M. As a result, we believe that dopa is being oxidized by a small amount of its corresponding o-quinone which is present as an impurity. Upon irradiation, no new radicals are observed, but the concentrations of **2** and **3** are increased. Thus, in the absence of molecular oxygen, oxidation of L-dopa beyond its corresponding o-benzosemiquinone cannot be detected. A similar result was obtained for o- and p-hydroquinone (2*b*).

Borg (8) has studied the oxidation of dopa in alkaline water using $K_3Fe(CN)_6$ as an oxidizing agent. Apparently his experiment involved air-saturated solutions, and he observed a radical different from **2** and **3**. As a check, we have repeated his experiment under anaerobic conditions. The resultant spectrum is identical to Fig. 2.

We have ruled out the possibility of ring formation via nitrogen addition to the phenyl ring (9) because no nitrogen hyperfine interaction is observed. Furthermore, lactone formation (10) would result in structures which are not consistent with the observed hyperfine interactions. Thus, we suggest structures **2** and **3**.

The fourth radical observed during the irradiation of tyrosine solution has a spectrum consisting of one line as indicated in Fig. 1. The g factor, which is 2.0001, is very close to the one determined (11) for CO_2^- (2.0003). The mech-

Can. J. Chem. Downloaded from www.nrcresearchpress.com by 210.87.254.5 on 09/05/12
For personal use only.

Can. J. Chem. Downloaded from www.nrcresearchpress.com by 210.87.254.5 on 09/05/12
For personal use only.

anism for the formation of this radical seems to involve the hydrated electron because the resonance line is not observed when the solution is saturated with N_2O, as indicated in Fig. 1B. N_2O is a good scavenger of the hydrated electron via reaction 1 (12). Tyrosine is known to react

$$[1] \qquad N_2O + e^-_{aq} \rightarrow N_2 + OH^- + OH$$

with the hydrated electron (13) also, although the details of the reaction have not been specified. Thus, it is possible that CO_2^- is formed via a reaction between the hydrated electron and tyrosine. The presence of N_2O reduces the extent of this reaction by competing for the hydrated electron. The possibility that the CO_2^- radical disappears because it reacts directly with N_2O is ruled out because of the results obtained by Neta *et al.* (12). These workers generated CO_2^- by two different reactions as indicated in eqs. 2 and 3. In eq. 3 the OH radical

$$[2] \qquad CO_2 + e^-_{aq} \rightarrow CO_2^-$$

$$[3] \qquad HCO_2^- + OH \rightarrow CO_2^- + H_2O$$

is formed by reacting N_2O with the hydrated electron according to eq. 1. Consequently, N_2O was present in the system when reaction 3 was used to generate CO_2^-. The rate of decay of CO_2^- was found to be the same whether reaction 2 or 3 was used to generate the radical. This result indicates that N_2O does not affect the lifetime of CO_2^-. Thus, we conclude that the N_2O results indicate that the hydrated electron is involved in the formation of CO_2^-. A possible reaction path is depicted by eq. 4. It is interesting to note that we were unable to detect CO_2^- during the irradiation of 3-[*p*-hydroxyphenyl]propionic acid under the same conditions. Apparently an α-amino group facilitates the decarboxylation.

$$[4] \qquad \underset{\text{dianion}}{\text{Tyrosine}} + e^-_{aq} \xrightarrow[H_2O]{} \text{Tyramine} + CO_2^- + OH^-$$

Comparison of Fig. 1A with 1B indicates that the presence of N_2O enhances the concentrations of radicals **1**, **2**, and **3**. Since the reaction of N_2O with the hydrated electron results in the formation of the OH radical (eq. 1), much of the enhancement is probably due to the reaction of this radical with the anions of tyrosine and dopa to form **1**, **2**, and **3**. This conclusion is based on the fact that addition of 1 *M* methanol to the tyrosine–N_2O solution causes the enhancement to disappear (compare Fig. 1C with 1A). Methanol is known to be a scavenger of the OH radical (14). That methanol is scavenging this radical under these conditions is confirmed by the observation of the CH_2OH radical.

The presence of 0.1 *M* H_2O_2 in a solution of tyrosine at p*H* 11 causes an enhancement in the concentration of radicals **1**, **2**, and **3** during irradiation. The enhancement is smaller for **1** than for the other radicals. Most likely several reactions are responsible for these enhancements. First, OH, which is formed from the irradiation-induced cleavage of H_2O_2, could add to the phenyl ring of tyrosine to form **2** and **3** since OH addition to the phenyl ring has been observed in studies of phenol (13*a*, 15). Second, the reaction of the OH radical (16) and H_2O_2 (17) with the hydrated electron would result in a slower rate of removal of **1**, **2**, and **3** via recombination with the hydrated electron. Third, OH may react with tyrosine to form **1** (13*a*). With our present results, it is not possible to decide on the importance of each of these reactions.

However, in the absence of N_2O, H_2O_2, and O_2, we feel that the addition of the OH radical to the phenyl ring is not an important path in the formation of **2** and **3** because the addition of methanol to the solution has little effect on the intensity of the spectrum observed under these conditions. Therefore, we propose the mechanism depicted by Scheme 1 for the formation of **1**, **2**, and **3**. In this scheme, R represents the allanyl group ($CH_2CHNH_2COO^-$). The tyrosine dianion absorbs a photon and subsequently ends up in an electronic excited state from which an electron is ejected to form **1** in its ground state. These steps are consistent with the formation of the hydrated electron observed during the flash photolysis of tyrosine and other substituted phenols (3, 18). Although the excited state involved has not been determined for tyrosine, Joschek and Grossweiner (18) have suggested that the electron ejection step for phenol involves a charge-transfer-to-solvent state which is produced via an excited singlet state. The next step in Scheme 1 is the addition of the hydroxide ion to the phenyl ring to form **4** from which a hydrogen atom is removed by **1** to form tyrosine and the dianion of dopa. The

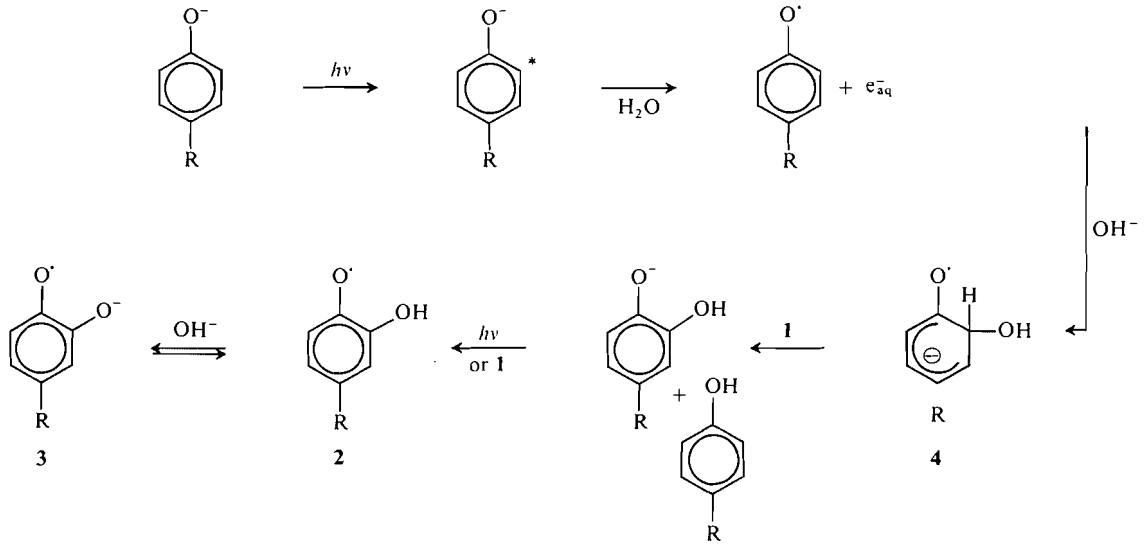

SCHEME 1

oxidation of dopa to form **2** may be accomplished either with **1** or with a photon; we cannot distinguish between these steps with our results. These steps are identical to the ones proposed to explain the oxidation of phenol to *o*- and *p*-benzosemiquinone (2) under similar conditions. In the case of phenol, the oxidation proceeds beyond *o*- and *p*-benzosemiquinone to oxy- and dioxybenzosemiquinone. Finally, as indicated in Scheme 1, we suggest that the equilibration between **2** and **3** occurs after the electron has been removed from dopa because the pK_a for dopa (6) is larger than the one for **2**. However we do not mean to imply that only **2** is formed from dopa.

As just mentioned, the photooxidation of dopa does not proceed as far as the photooxidation of phenol under the same conditions. For example at p*H* 12, oxy- and dioxybenzosemiquinone can be detected during the irradiation of phenol (2) but not during the irradiation of tyrosine. The manner in which the side-chain inhibits further oxidation is not clear at this time.

Nuclear Magnetic Resonance Spectroscopy

We have studied the irradiation of tyrosine in deoxygenated water by means of proton n.m.r. spectroscopy, also, and the results support the mechanism given in Scheme 1. In these experiments, an evacuated solution of 10^{-2} *M* tyrosine in D_2O at p*H* 11 is irradiated in the n.m.r. probe. Because tyrosine is sparingly soluble in water, its concentration could not be increased significantly above 10^{-2} *M* under these conditions. Consequently, the n.m.r. lines due to the protons of tyrosine could not be detected with our spectrometer. As a result, the spectrum of the D_2O solution in the absence of irradiation consists of one line due to a small amount (0.2%) of HDO present in the solvent. During irradiation, this line changes from absorption to emission as can be seen in Fig. 3. This emission indicates that the HDO-proton is spin polarized, *i.e.* the populations of the nuclear spin states differ from those expected for a Boltzmann distribution. Nuclear spin polarization has been observed for a number of systems involving radical reactions (19), and a rather convincing body of evidence is available to indicate that the nuclear spin polarization occurs via a radical pair. Since this phenomenon has been discussed in detail elsewhere (19), a general presentation of the mechanism for nuclear spin polarization is unnecessary in this paper. Instead, we will show only that the observed nuclear spin polarization is qualitatively consistent with the mechanism proposed in Scheme 1. The mechanism proposed to explain the spin polarization of the HDO-proton is given in Scheme 2 which simply describes some of the steps in Scheme 1 in more detail. In

Can. J. Chem. Downloaded from www.nrcresearchpress.com by 210.87.254.5 on 09/05/12
For personal use only.

Can. J. Chem. Downloaded from www.nrcresearchpress.com by 210.87.254.5 on 09/05/12
For personal use only.

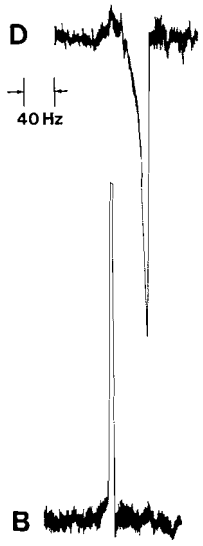

FIG. 3. The n.m.r. line of the HDO-proton for a deoxygenated D_2O solution of 0.01 *M* tyrosine at p*H* 11 and ambient temperature; B: before irradiation, D: during irradiation. The field strength increases from left to right. The shift in the HDO line during irradiation is due to local heating of the sample.

Scheme 2, **1**, and **4**, which start out as non-interacting radicals in the bulk, diffuse together to form a radical pair symbolized as [**1** **4**]. The radicals in the radical pair can diffuse apart or undergo a disproportionation reaction to form tyrosine and dopa having nuclear spin polarization. The proton of interest is the tyrosine OH-proton which is labelled with an asterisk. The removal of this proton by OD^- to form HDO is probably more rapid than its spin relaxation rate. This conclusion is based on the rate constant for reaction of phenol with OH^- (20). Thus, Scheme 2 provides a mechanism for the observed spin polarization of the HDO-proton.

The HDO-proton is polarized in the same manner during the irradiation of phenol under the same conditions (2). The mechanism used to explain this polarization is identical to Scheme 2. For this system, it was possible to present additional evidence in favor of Scheme 2. Because of the close similarity between the results for phenol and tyrosine it seems reasonable that they would be oxidized via the same mechanism under these conditions.

Thus according to Scheme 1, after tyrosine has been oxidized to the tyrosyl radical **1**, it can act as an oxidizing agent for subsequent oxidation to dopa and **2** or **3**. In other words, once the tyrosyl radical is formed no other oxidizing agent is needed to form dopa. It will be interesting to determine if enzymatic oxidation of tyrosine can be accomplished in the same manner. In addition, this work is being extended to other aromatic amino acids and to polypeptides containing tyrosine to determine the feasibility of investigating the irradiation of proteins using these techniques.

Finally, in Scheme 1, the formation of the hydrated electron is suggested, but a mechanism for its disappearance has not been discussed. The e.p.r. and n.m.r. results give us no information concerning the reaction of this species. Probably it disappears by way of various paths which do not alter the mechanism proposed in Scheme 1. For example, the hydrated

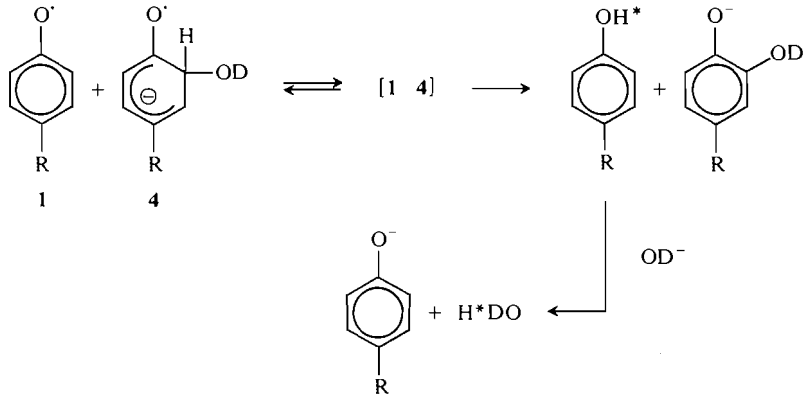

SCHEME 2

electron could combine with any of the observed radicals or react with water.

We are grateful to Dr. M. Fujimoto for allowing the use of the e.p.r. spectrometer and to the referee for pointing out the alternating linewidth effect. This work has been supported in part by the Petroleum Research Fund administered by the American Chemical Society, the Department of University Affairs (Ontario), and the Defence Research Board of Canada.

1. (*a*) R. JOHNS, F. LOONEY, and D. WHELAN. Photochem. Photobiol. **7**, 65 (1968); Biochim. Biophys. Acta, 147, 369 (1967); (*b*) A. MEYBECK and J. WINDLE. Photochem. Photobiol. **10**, 1 (1969); (*c*) A. VAN DE VORST. Photochem. Photobiol. **13**, 321 (1971); (*d*) E. FASANELLA and W. GORDY. Proc. Natl. Acad. Sci. (U.S.), **64**, 1 (1969); **62**, 299 (1969).
2. (*a*) M. TOMKIEWICZ, A. GROEN, and M. COCIVERA. J. Chem. Soc. **93**, 7102 (1971); (*b*) M. COCIVERA, M. TOMKIEWICZ, and A. GROEN. J. Am. Chem. Soc. **94**, 6598 (1972).
3. L. GROSSWEINER, G. SWENSON, and E. ZWICKER. Sci. **141**, 805 (1963).
4. D. BORG and J. ELMORE, JR. Magnetic resonance in biological systems. Proc. 2nd Int. Conf., Stockholm, 1966. Pergamon Press, Oxford. 1967. p. 341.
5. P. SULLIVAN and J. BOLTON. Advances in magnetic resonance. J. Waugh, Editor. Academic Press, New York. 1970. p. 39.
6. J. GORTON and R. JAMESON. J. Chem. Soc. A, 2615 (1968).
7. A. CARRINGTON and I. SMITH. Mol. Phys. **8**, 101 (1964).
8. D. BORG. Proc. Natl. Acad. Sci. (U.S.) **53**, 633 (1965).
9. J. WERTZ, D. REITZ, and F. DRAVNIEKS. Free radicals in biological systems. M. S. Blois, Editor. Academic Press, New York. 1961. p. 183.
10. T. SPANDE, B. WITKOP, Y. DEGANI, and A. PATCHORNIK. Advances in protein chemistry. Vol. 24. Academic Press, New York. 1970. p. 193.
11. A. BECKWITH and R. NORMAN. J. Chem. Soc. B, 400 (1969).
12. P. NETA, M. SIMIC, and E. HAYON. J. Phys. Chem. **73**, 4207 (1969).
13. (*a*) J. CHRYSOCHOOS. Rad. Res. **33**, 465 (1968); (*b*) R. BRAAMS. Rad. Res. **27**, 319 (1966).
14. G. ADAMS, J. BOAG, and B. MICHAEL. Trans. Faraday Soc. **61**, 1417 (1965).
15. E. LAND and M. EBERT. Trans. Faraday Soc. **63**, 1181 (1967).
16. M. MATHESON and J. RABANI. J. Phys. Chem. **69**, 1324 (1965).
17. S. GORDON, E. HART, M. MATHESON, J. RABANI, and J. THOMAS. J. Am. Chem. Soc. **85**, 1375 (1963).
18. H. JOSCHEK and L. GROSSWEINER. J. Am. Chem. Soc. **88**, 3261 (1966).
19. (*a*) R. KAPTEIN and L. OOSTERHOFF. Chem. Phys. Lett. **4**, 195, 214 (1969); (*b*) G. CLOSS and A. TRIFUNAC. J. Am. Chem. Soc. **92**, 2183 (1970); (*c*) H. FISCHER. Z. Naturforsch. **25**a, 1957 (1970); (*d*) M. TOMKIEWICZ, A. GROEN, and M. COCIVERA. Chem. Phys. Lett. **10**, 39 (1971); (*e*) M. TOMKIEWICZ, A. GROEN, and M. COCIVERA. J. Chem. Phys. **56**, 5850 (1972).
20. Z. LUZ and S. MEIBOOM. J. Am. Chem. Soc. **86**, 4766 (1964).

Can. J. Chem. Downloaded from www.nrcresearchpress.com by 210.87.254.5 on 09/05/12
For personal use only.

Phosphonitrilic Chloride — The Dehydration of Amides to Nitriles

JOHN C. GRAHAM[1] AND DAVID H. MARR
Hooker Chemical Corporation, Research Center, Grand Island, N.Y. 14072

Received June 12, 1972

Phosphonitrilic chloride is found to dehydrate amides to nitriles rapidly and in high yields. A mechanism for the dehydration is proposed.

Le chlorure de phosphonitrile convertit les amides en nitriles, par une réaction de deshydratation rapide, avec de bons rendements. Un mécanisme pour cette réaction a été proposé.

[Traduit par le journal]

Canadian Journal of Chemistry, **50**, 3857 (1972)

Can. J. Chem. Downloaded from www.nrcresearchpress.com by 210.87.254.105 on 09/05/12
For personal use only.

The dehydration of amides to nitriles has been accomplished by a variety of agents (1). Many of these have been summarized recently (2). We have found that 1,1,3,3,5,5-hexachlorocyclophosphazatriene (**1**), commonly called phosphonitrilic chloride can also be used to convert amides to nitriles rapidly and in excellent yields.[2] Ideally, the reaction is carried out on a mixture of the amide and **1** at temperatures above 100 °C and the nitrile distilled from the reaction mixture on formation. Although in our investigations we preferred a 1:3 mole ratio of **1** to amide, we found in many cases that a ratio of 1:6 could be used, and in the case of acetamide, a 1:12 mole ratio was effective.

In addition to the nitrile, an amorphous, hy-

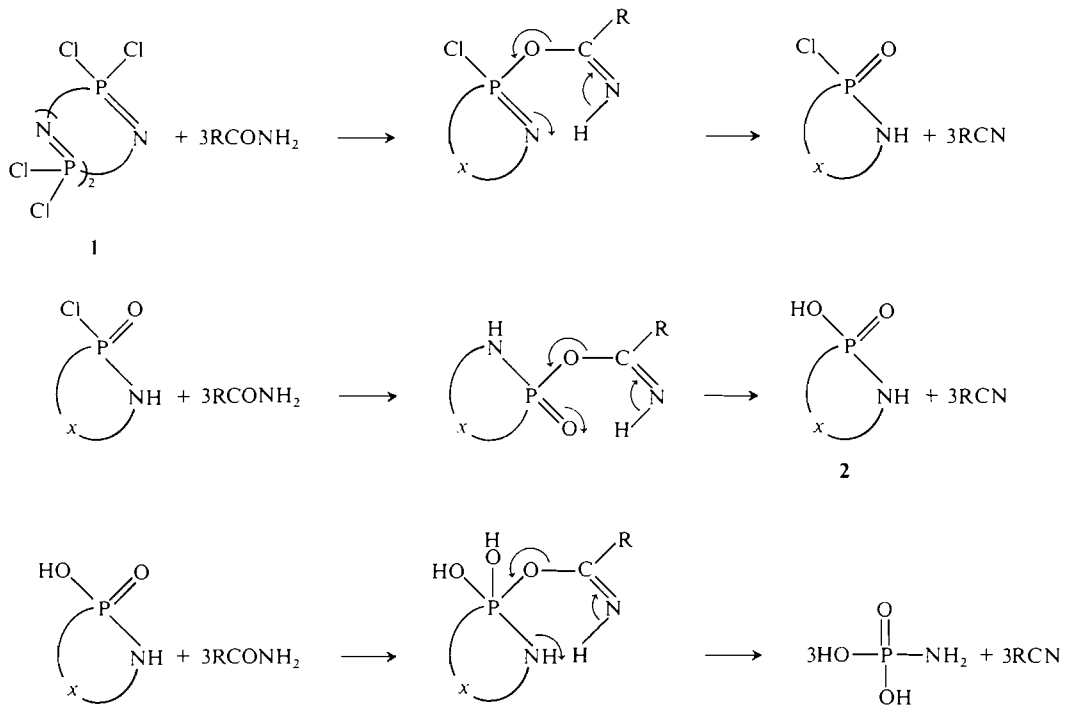

1

2

[1]Author to whom all correspondence should be addressed.

[2]The high amide to $(PNCl_2)_3$ ratios employed, combined with minimum handling difficulties, makes this reagent competitive with other commonly employed dehydrating agents. Although pure **1** is expensive, **1** admixed with higher cyclic and linear material is inexpensive and commercially available (5). Dehydration reactions using this mixture gave similar results.

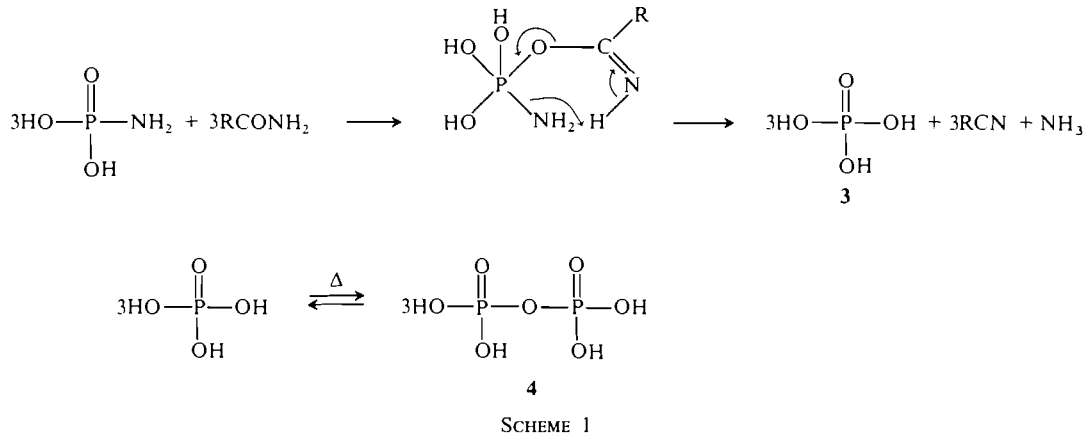

SCHEME 1

groscopic, water-soluble material is recovered. ^{31}P n.m.r. analysis of this amorphous residue gave singlets at +11.0 and 0.0 p.p.m. relative to H_3PO_4. The former is consistent with pyrophosphoric acid (**4**) (3) or its monoammonium salt and the latter signal has been assigned to pyrophosphimic acid ($HOPO_2NHPO_2OH$) or its monoammonium salt. It is important to note that the absence of orthophosphoric acid (**3**) was established by the addition of authentic material. The proposed trimetaphosphimic acid intermediate (**2**) was not observed (3, 4). Neutralization of the amorphous residue with aqueous sodium hydroxide followed by evaporation yielded $Na_4P_2O_7$ as evidenced by X-ray diffraction.

Discussion

The discovery of $Na_4P_2O_7$ in the neutralized residue and the ^{31}P n.m.r. singlet at 0.0 p.p.m. indicative of pyrophosphimic acid suggests the reaction path outlined in Scheme 1.[3] Preliminary investigations regarding the mechanism of the dehydration have shown the intermediate phosphorous moieties to be better dehydrating agents than **1**. In controlled reactions using various ratios of **1** to acetamide, the theoretical amount of excess **1** was recovered based on a mole equivalent ratio of 1:12. The results are summarized in Table 1. This is not surprising since sulfonic acid amides (SO_3HNH_2) (6) as well as alkyl phosphates and phosphoramides (which are similar to the intermediates proposed for this reaction) are known to dehydrate amides in good to excellent yields. This dehydration reaction has been applied to a number of amides and appears to be quite general except for α-chloroacetamide which did not react and hydroxyamides which yield, not unexpectedly, high molecular weight materials via nucleophilic displacement of chloride (7). The results are summarized in Table 2.

Sonobe (8) has proposed a mechanism for the reaction of ammonium salts of carboxylic acids with $(PNCl_2)_x$ to form nitriles and acid chlorides, based on the nucleophilic attack of the salt on $(PNCl_2)_x$. This proposal is analogous to those of Bezman and Reed (9) and Caglioti *et al.* (10) for the reaction of sodium salts of carboxylic acids with $(PNCl_2)_x$ where nitriles and anhydrides are isolated. However, at the temperatures involved in Sonobe's investigation, it is likely that the ammonium carboxylates are converted to amides which then react as outlined in Scheme 1. Consequently, in light of the present work, it appears that at least two mechanistic pathways may be involved; the

[3]A referee has pointed out that a more logical first step in the mechanism involves nucleophilic attack by nitrogen instead of oxygen. However, a number of investigators have established that amides behave as weak nucleophiles with oxygen as the most reactive site (excellent reviews on this aspect can be found in ref. 2*a*, Chapts. 3 and 13). This argument cannot in itself preclude the possibility of intramolecular rearrangements which would lead to the same intermediate obtainable directly from nucleophilic attack by nitrogen. Similar rearrangements are well-documented in the field of amide chemistry, but in this instance, the 4-centered intermediate required for the rearrangement would be in direct competition with the 6-centered intermediate postulated in step 2 of Scheme 1. Intuitively, the authors favor the latter.

Can. J. Chem. Downloaded from www.nrcresearchpress.com by 210.87.254.105 on 09/05/12
For personal use only.

TABLE 1. Amount of $(PNCl_2)_3$ recovered from controlled reactions with acetamide*

Reactants (mol)		Ratio	Recovered $(PNCl_2)_3$ (mol)	
$(PNCl_2)_3$	CH_3CONH_2	$(PNCl_2)_3/CH_3CONH_2$	Experimental	Theoretical
0.021	0.252	1:12	0	0
0.042	0.252	1:6	0.023	0.021
0.042	0.126	1:3	0.032	0.031
0.042	0.084	1:2	0.036	0.035

*Using chlorobenzene as the solvent; yield of nitrile was nearly quantitative by ^1H n.m.r. analysis.

TABLE 2. Dehydration of amides

Amide	Amide/$(PNCl_2)_3$ (mol)	Solvent	Temperature (°C)	Nitrile yield (%)
Acetamide	6	None	120	100
Acetamide	6	Chlorobenzene	132	92
Acetamide	12	Chlorobenzene	132	95
Thioacetamide	6	None	120	52
Thioacetamide	3	Chlorobenzene	132	100
Acrylamide	6	None	120	44
Acrylamide	3	Chlorobenzene	132	84
Phenylacetamide	3	Chlorobenzene	132	76
p-Methoxyphenylacetamide	3	Chlorobenzene	132	100
Benzamide	3	Chlorobenzene	132	75
Benzamide	6	None	200	93
o-Bromobenzamide	2	Chlorobenzene	132	92

reaction of ammonium carboxylates directly with $(PNCl_2)_x$ to yield nitrile, acid chloride, and anhydride or first its conversion to the amide with subsequent reaction via Scheme 1 to give solely the nitrile. Since the source of nitrilic nitrogen is different for the two pathways, ^{15}N labeling experiments should resolve this question.

Experimental

Trimeric phosphonitrilic chloride $(PNCl_2)_3$ was obtained by distillation of a commercially obtainable material, m.p. 112–114° (lit. 112–113°) (11).

Commercially available chlorobenzene was used as the solvent. Identification of compounds was by i.r. and n.m.r. techniques. Boiling points and melting points were used where applicable. Two methods were used in the synthetic approach as follows.

Method A

The amide and phosphonitrilic chloride were heated in a flask to above the boiling point of the nitrile. Almost immediately, the nitrile began to distill with liberation of HCl and after 30 min, the required amount of nitrile had been recovered. Gas chromatographic analysis showed the nitrile to be extremely pure with no anomalous peaks.

Method B

The amide and phosphonitrilic chloride were dissolved or suspended in a suitable solvent such as chlorobenzene. The mixture was then heated at reflux for a few hours. The mixture in the flask was filtered and the nitrile recovered from the filtrate by evaporation of the solvent or from the filtered solid by dissolving the solid nitrile in a suitable solvent and filtering off the inorganic residue.

Nuclear Magnetic Resonance Analysis

The ^{31}P n.m.r. chemical shifts of saturated aqueous solutions were obtained on a Varian HA-100 spectrometer operating at 40.5 MHz with baseline stabilization. An external capillary of 85% H_3PO_4 was used as a reference and chemical shifts were obtained by interpolation between reference and sample side bands. Calibration was provided by the known sideband separation in Hz. An average of five separate determinations were taken and the values obtained are estimated to be accurate to ± 0.5 p.p.m.

The authors wish to thank the Hooker Chemical Corporation for permission to publish this work.

1. (*a*) D. J. CRAM and P. HABERFIELD. J. Am. Chem. Soc. **83**, 2363 (1961). (*b*) M. SCALERA and R. E. BROUILLARD. U.S. Pat. 2 525 620 (1950). (*c*) C. R. STEPHANS, E. J. BIANCO, and F. J. PILGRIM. J. Am. Chem. Soc. **77**, 1701 (1955). (*d*) W. E. DENNIS. J. Org. Chem. **35**, 3253 (1970). (*e*) R. BACALOGLU and G. OSTROGOVICH. Rom. Pat. 51 080 (1968). (*f*) J. DEVILLERS, M. WILLSON, and R. BURGADA. Bull. Soc. Chim. Fr. 4670 (1968);

Can. J. Chem. Downloaded from www.nrcresearchpress.com by 210.87.254.105 on 09/05/12
For personal use only.

K. KANAOKA, T. KUGA, and K. TANIZAWA. Chem. Pharm. Bull. **18**, 397 (1970); L. HORNER, H. OEDIGER, and H. HOFFMANN. Ann. **626**, 26 (1959); R. I. HOAGLIN, H. C. SCHULTZ, and C. E. HODGES. U.S. Pat. 2 910 502 (1959). (*g*) L. G. HUMBER and M. A. DAVIS. Can. J. Chem. **44**, 2113 (1966); N. W. YOON and H. C. BROWN. J. Am. Chem. Soc. **90**, 2927 (1968). (*h*) S. E. ELLZEY, C. H. MACK, and W. J. CONNICK. J. Org. Chem. **32**, 846 (1967). (*i*) E. M. KAISER, R. L. VAULX, and C. R. HAUSER. J. Org. Chem. **32**, 3640 (1967).

2. (*a*) J. F. BIERON and F. J. DINAN. The chemistry of functional groups—amides. J. Zabicky, Editor. John Wiley & Sons, N.Y. 1970; (*b*) L. F. FIESER and M. FIESER. Reagents for organic synthesis. John Wiley & Sons, N.Y. 1967.
3. V. MARK, C. H. DUNGAN, M. M. CRUTCHFIELD, and J. R. VANWAZER. Topics in phosphorus chemistry. Vol. 5. M. Grayson and E. J. Griffith, Editors. Interscience, N.Y. 1967.
4. M. L. NIELSEN. Inorganic synthesis. Vol. 6. 79.
5. Available from Hooker Chemical Corporation, M.P.O. Box 8, Niagara Falls, N.Y. 14302.
6. A. V. KIRSANOV and Y. M. ZOLOTOV. Zhur. Obshchei Khim. **20**, 284 (1950); W. J. KLAPPROTH. U.S. Pat. 2 783 264 (1957); G. LOHAUS. Chem. Ber. **100**, 2719 (1967).
7. R. A. SHAW. Rec. Chem. Progr. **28**, 243 (1967).
8. K. SONOBE. Kogyo Kagaku Zasshi, **70**, 2305 (1967).
9. I. I. BEZMAN and W. R. REED. J. Am. Chem. Soc. **82**, 2167 (1960).
10. L. CAGLIOTI, M. POLONI, and G. ROSINI. J. Org. Chem. **33**, 2979 (1968).
11. H. R. ALLCOCK and R. L. KUGEL. J. Am. Chem. Soc. **91**, 5452 (1969).

Can. J. Chem. Downloaded from www.nrcresearchpress.com by 210.87.254.105 on 09/05/12
For personal use only.

Kinetics of the Anation Reaction of Nickel(II) and 1,10-Phenanthroline in Ethanol

M. L. SANDUJA AND W. MACF. SMITH

Department of Chemistry, Queen's University, Kingston, Ontario.

Received June 13, 1972

The kinetics of formation of the monophenanthroline complex of nickel(II) in ethanol has been studied using stopped-flow methods over the temperature range 7 to 35 °C. Tetrabutyl ammonium perchlorate in concentration 0.044 *M* does not affect the rate appreciably, sodium perchlorate at the same concentration depresses the rate significantly. Most measurements were made in the absence of electrolytes other than nickel perchlorate and a trace of perchloric acid. The second order rate constant is not significantly dependent on the nickel(II) concentration over a four-fold change in value indicating that the concentration of encounter pairs is small relative to the concentration of the free reactants. The rate constant at 25 °C ($31 \times 10^3\ M^{-1}\ s^{-1}$) is consistent with a dissociative interchange mechanism and the rate constant for ethanol exchange on nickel. However, the value of $\Delta H^{\ddagger}$ for the overall reaction (15.9 ± 1.0 kcal mol^{-1}) is about 5 kcal mol^{-1} higher than that reported for ethanol exchange.

Nous avons étudié la cinétique de formation du complexe monophénanthroline du nickel(II) dans l'éthanol au moyen de méthodes à débit arrêté, dans un domaine de température de 7 à 35 °C. Le perchlorate de tétrabutyl ammonium en concentration de 0.044 *M* n'affecte pas appréciablement la vitesse; le perchlorate de sodium, par contre, à la même concentration ralentit cette vitesse de façon significative. La plupart des mesures ont été effectuées sans d'autres électrolytes que le perchlorate de nickel et une trace d'acide perchlorique. La constante de vitesse d'ordre deux ne dépend pas de la concentration de nickel(II) de façon significative pour un changement de la valeur par un facteur de quatre, indiquant que la concentration de paires voisines est petite relativement à la concentration des réactifs libres. La constante de vitesse à 25 °C ($31 \times 10^3\ M^{-1}\ s^{-1}$) est conciliable avec un mécanisme d'échange dissociatif et avec la constante de vitesse d'échange d'éthanol sur le nickel. Toutefois la valeur de $\Delta H^{\ddagger}$ pour la réaction globale (15.9 ± 1.0 kcal mol^{-1}) est environ de 5 kcal mol^{-1} plus élevée que celle rapportée pour l'échange d'éthanol.

[Traduit par le journal]

Canadian Journal of Chemistry, **50**, 3861 (1972)

Kinetic behavior in the anation reactions of nickel(II) in the hydroxylic solvents water (1) and methanol (2) is consistent with a dissociative interchange (I_d) (3) mechanism [1].

$$[1]\qquad \begin{aligned} NiS_6^{2+} + L &\overset{K_0}{\rightleftharpoons} NiS_6^{2+}.L \\ NiS_6.L^{2+} &\xrightarrow{k} NiS_5L^{2+} + S \end{aligned}$$

where NiS_6^{2+} represents the solvated nickel ion and NiS_6^{2+}. L the encounter complex and L is the entering ligand which is represented here as neutral and monodentate and k is the rate constant for collapse of the encounter complex which in the case of an I_d mechanism relates to the rate constant for solvent exchange on nickel(II). For reactions of nickel(II) with bidentate ligands the reaction involving the first solvent molecule appears to be rate controlling (4) although formation of the final product involves replacement of two solvent molecules. If the concentration of the encounter complex is close to the equilibrium value and is substantially less than those of the free reactants, the overall rate of reaction would be second order with rate constant $k_f = kK_0$. However, Bennetto and Caldin (5) consider that the results of investigations on the reactions of nickel(II) with 2,2′-bipyridyl and 2,2′,2″-terpyridyl in a variety of solvents, predominantly non-hydroxylic, are not consistent with a simple I_d mechanism. Also, the data of Langford and Tsiang (6) on the reaction of $Ni(DMSO)_6^{2+}$ with thiocyanate and murexide imply a value for the rate constant which is less than anticipated on the basis of an I_d mechanism if a value of K_0 of the order expected from the Fuoss–Eigen equations (8) is assumed to apply. Cock, Cottrell, and Boyd (9) on the basis of their results on the reactions of 2,2′,2″-terpyridyl with $Ni(DMSO)_6^{2+}$ and a species they believe to be $[Ni(terpy)Cl(DMSO)_2]^{2+}$ consider that the mechanisms are of I_d character although the values obtained for the rate constants are substantially less than anticipated on the basis of commonly accepted interpretations.

To expand information about the as yet unresolved kinetic behavior of nickel(II) in various classes of solvents we are investigating the reactions of nickel(II) in ethanol, a hydroxylic

Can. J. Chem. Downloaded from www.nrcresearchpress.com by 210.87.254.42 on 09/05/12
For personal use only.

Can. J. Chem. Downloaded from www.nrcresearchpress.com by 210.87.254.42 on 09/05/12
For personal use only.

solvent relating to the commonly used solvents water and methanol. The rate of ethanol exchange on nickel(II) has been investigated by Breivogel (10) but studies of other anation reactions in this solvent do not appear to have been reported. Although the ionizing power of this solvent is greater than implied by simple electrostatic considerations and its dielectric constant (11), complications in interpreting data due to outer ion pairing between reactant and nonreactant species and to corresponding uncertainties in the nature of the ion environment may be expected when ligands are charged. However, the reaction between nickel(II) and phenanthroline, upon which we report here, involves an uncharged ligand, a large association constant, a probable lack of sensitivity on ionic strength and in consequence complications associated with ion pairing involving reactant and nonreactant species should not be serious.

Experimental

Hydrogen chloride was of electronic grade from Matheson of Canada. Anhydrous nickel chloride of analytical grade from Alfa-Inorganics and silver perchlorate of reagent grade from G. Frederick Smith were heated at 100 °C under reduced pressure over phosphorus pentoxide for 48 h before use. Absolute ethanol was subjected to standard purification procedures with magnesium turnings and iodine (12) and the middle fraction from distillation with a Widmer column was stored in colored bottles in a dry box and used within a few days of preparation. All other substances were of reagent grade from Fisher Scientific Company, G. Frederick Smith or British Drug Houses and apart from drying over silica gel or drierite were subjected to no further purification.

The preparation and transfer of solutions were carried out in a dry box under an atmosphere of dry nitrogen, and freshly prepared solutions were used in all kinetic runs. Nickel chloride, silver perchlorate, sodium perchlorate, and tetrabutyl ammonium perchlorate, stored in vacuum desiccators were transferred to the dry box for weighing at the time of their use in the preparation of solutions. All glassware used for measurement or storage of solutions was dried at 115 to 120 °C for several hours prior to use. Solutions of nickel perchlorate were prepared from solutions of nickel chloride and silver perchlorate of known concentrations with the precipitated silver chloride removed by filtration through a glass frit. The nickel content of the nickel chloride solution was estimated using EDTA and murexide as indicator (13, 14). Perchloric acid solution was prepared from ethanolic solutions of known concentrations of hydrogen chloride and silver perchlorate. The solution of perchloric acid was tested for the presence of excess silver ion by addition of a little hydrogen chloride solution to some test solution and was standardized using B.D.H. standard sodium hydroxide solution.

Spectrophotometric measurements relating to equilibria were made with a DK1 spectrophotometer. Kinetic measurements were made using a model D-150 Durrum–Gibson stopped-flow spectrophotometer with thermostatic control of the solution maintained to ± 0.1 °C. The oscilloscope traces of transmission against time which were photographed were the overlay of the traces of four or five kinetic runs carried out with the same reactant solutions under given conditions. Near $\lambda 295$ mμ the extinction coefficient of the complex is in optimal excess over that of phenanthroline and light of this wavelength was used to monitor the course of the reaction.

The majority of kinetic runs was made at a concentration of nickel(II) of 2.0×10^{-3} M and a concentration of phenanthroline of 2.0×10^{-5} M but some measurements were made over the ranges of 1.0×10^{-3} to 8.0×10^{-3} M in nickel(II) and 2.0×10^{-5} to 5.0×10^{-5} M in phenanthroline to check the order of the reaction. To avoid possible complications associated with the solvolysis of nickel(II) ions, a trace of perchloric acid was added to all solutions to a concentration 4×10^{-7} M. A further four-fold increase in acidity yielded no significant change in rate. The spectrophotometric properties of the slightly acidified solution of phenanthroline were identical with those of solutions of the free base, implying that at the concentration of acid used in the kinetic runs the phenanthroline is substantially all in the basic form. At higher acidities there is an increase in optical density of the solutions at wavelengths less than $\lambda 360$ mμ, with a nearly five-fold increase in absorbance occurring, to reach a plateau where presumably monoprotonated phenanthrolinium ion is the dominant species. Some kinetic runs were made with solutions containing tetrabutyl ammonium perchlorate or sodium perchlorate but in the majority of runs no electrolyte beyond nickel perchlorate and the trace of perchloric acid were added and the values of the kinetic parameters reported below are based on measurements on solutions in which there was no electrolyte additional to nickel perchlorate and the trace of perchloric acid. That reaction was substantially complete is attested by the independence of the change in optical density over the course of a run on nickel(II) concentration when it was varied four-fold at constant phenanthroline concentration. Measurements at 25 °C using as solvent the center cut of absolute ethanol which had been distilled through a Widmer column yielded results which were not significantly different from those obtained using ethanol subjected to treatment with magnesium and iodine prior to distillation. However, the addition of 0.6 wt. % of water was found to increase the rate by a factor of almost two with the implied rate constant greater than those applying to purely ethanolic or purely aqueous solvents.

In interpreting our data we have provisionally assumed that the rate controlling step in the formation of the complex is the formation of a monodentate intermediate. If an interchange mechanism is dominant and the concentration of encounter pairs is small relative to that of the reactants, the relation [2] should apply where NiL^{2+} represents NiS_4L^{2+}.

$$[2] \quad \frac{d}{dt}[NiL^{2+}] = kK_0[Ni^{2+}][L] = k_f[Ni^{2+}][L]$$

As the nickel(II) was present in substantial excess over phenanthroline the reaction should be pseudo first order, and as the phenanthroline exists almost entirely as the free

TABLE 1. Values for the rate constant k_f for the formation of $Ni(phen)^{2+}$ in ethanol

Temperature (°C)	Added electrolyte	I (M)	[Ni(II)] $M \times 10^3$	$[Phen]_0$ $M \times 10^5$	$k_f \times 10^{-3}$ (M^{-1} s^{-1})
7	None	0.006	2.0	2.0	4.7 ± 2.2
		0.024	8.0	2.0	4.6 ± 0.4
15	None	0.006	2.0	2.0	11.2 ± 2.2
25	None	0.006	2.0	2.0	31.3 ± 3.1
	None	0.006	2.0	5.0	32.7 ± 5.6
	None	0.012	4.0	2.0	29.8 ± 2.9
	TBA ClO_4	0.050	2.0	2.0	29.2 ± 1.8
	TBA ClO_4	0.050	2.0	2.0	28.4 ± 3.2*
	$NaClO_4$	0.050	2.0	2.0	13.7 ± 0.7
35	None	0.003	1.0	2.0	65.4 ± 13.8
		0.006	2.0	2.0	67.6 ± 2.9
		0.012	4.0	2.0	60.6 ± 4.7†

*Solvent was absolute ethanol which was subjected to Widmer column distillation but was not treated with magnesium and iodine.
†Based on two evaluations only.

base and the change in absorbance (A) of the solution is proportional to the concentration of the complex (NiL) formed, the slope of the plot of log $(A - A_\infty)$ against time is identifiable with $-k_f[Ni]_0/2.303$ where $[Ni]_0$ represents the initial concentration of nickel(II) which remains essentially at this value throughout the course of the run.

Results and Discussion

Values for the rate constants k_f with a summary of the conditions to which they apply are given in Table 1. Each value for k_f is the mean of several estimates, and each estimate is derived from a record of transmission against time which was the overlay of the records of four or five runs. Included with the value for k_f is the standard error associated with the estimates (three to five in number unless otherwise indicated). Under the heading I are values obtained from the relation $I = \frac{1}{2}\sum c_i z_i^2$ where c_i is the initial concentration of the ions assuming that the electrolytes are completely dissociated and z_i is the ionic charge number. In view of the possibility of significant ion association these values may not accurately summarize the ionic environmental conditions existing in solutions.

It is apparent that the influence of tetrabutyl ammonium perchlorate on rate is barely significant but that sodium perchlorate has a significant effect. If ion pairing between nickel(II) ion and perchlorate ion is occurring to a significant degree, the kinetic activity of the ion pairs must be close to that of free nickel(II) ion. The depressive effect of sodium ion was unexpected but is possibly associated with the formation of associates between sodium ion and phenanthroline. The near independence of rate constant on concentration of reactants implies that the concentration of encounter pairs (NiS_6.Phen) is low relative to the concentration of free phenanthroline. Otherwise a fall-off in rate constant with increase in the concentration of nickel(II) would be expected. A plot of $\log k_f/T$ *vs.* $1/T$ based on data applying to $[Ni(II)] = 2 \times 10^{-3}$ M and $[Phen]_0 = 2 \times 10^{-5}$ M is presented in Fig. 1. The values of the kinetic parameters implied by this plot are $\Delta H^{\ddagger} = 15.9 \pm 1.0$ kcal mol^{-1} $\Delta S^{\ddagger} = 15.4 \pm 3.2$ cal deg^{-1} mol^{-1}.

If, as we are provisionally assuming, the formation of a monodentate complex is rate controlling and if an interchange mechanism is dominant and the concentration of encounter pairs is not marked then $k_f = kK_0$. The value for the first order rate constant for ethanol exchange on nickel(II) at 25 °C has been reported as 6.6×10^4 sec^{-1} (10) and on the basis of an interchange model $k = k_f/K_0$ should relate closely to this value. The value for K_0 implied by the Fuoss relation (7) for non-interacting encounter pairs is dependent only on the value of a, the distance between centers of the members of an encounter pair. We assume that the value applicable to this reaction in ethanol is somewhat larger than the value 5 Å which has been assumed for reaction in water and 6 Å which has been assumed for reaction in methanolic solutions (2). For a value

Can. J. Chem. Downloaded from www.nrcresearchpress.com by 210.87.254.42 on 09/05/12
For personal use only.

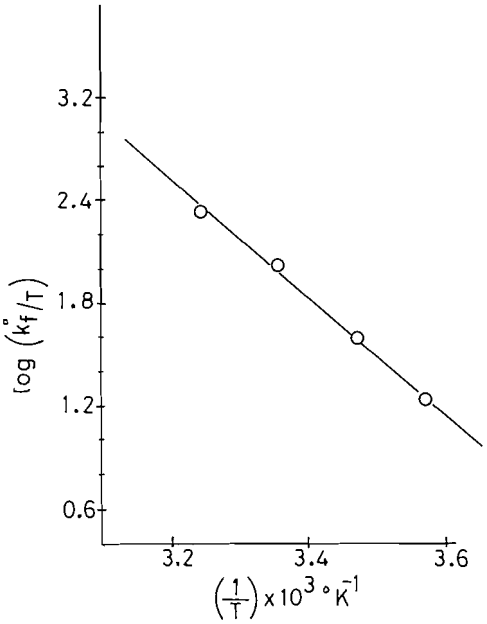

FIG. 1. Modified Arrhenius plot for the reaction of nickel(II) with 1,10-phenanthroline in ethanol.

of $a = 7$ Å, K_0 (Fuoss) is 0.87 M^{-1}, for $a = 9$ Å it is 1.84 M^{-1}. The corresponding values of k are then 3.4×10^4 s^{-1} and 1.6×10^4 s^{-1} which may be compared with the value 6.6×10^4 s^{-1} for the first order rate constant (k_{ex}) for ethanol exchange on nickel(II). In view of the possibility of some attractive interaction between the nickel(II) ion and phenanthroline the above estimates of K_0, which are based on an application of the Fuoss relation which assumes no interaction, may be somewhat low and the values for k correspondingly high. Taken in isolation our data for 25 °C suggest the applicability of the dissociative interchange mechanism. The value of $\Delta H^{\ddagger}$ of 15.9 kcal mol^{-1} for the overall reaction does differ significantly from the value for $\Delta H^{\ddagger}$ of 10.8 kcal mol^{-1} which has been reported for ethanol exchange on nickel (10) and it is improbable that the difference of 5 kcal mol^{-1} would be attributed to ΔH^0 for the formation of the encounter complex. However, in view of the range of values for $\Delta H^{\ddagger}$ for solvent exchange which have been reported for other processes (*e.g.* for the exchange of dimethyl sulfoxide on nickel(II) values ranging from 6.2 to 13.1 kcal mol^{-1} have been reported (9, 15)) we suggest that a mechanism which is essentially dissociative interchange is an acceptable interpretation for the reaction between nickel(II) and phenanthroline in ethanol on the basis of presently available evidence.

Bennetto and Caldin (5) consider that mechanisms such as I_d are too simplistic to describe the behavior of ligand substitution reactions in a variety of solvents and present a model in which the change in structural features in the solvent zones surrounding the reacting species as well as the breaking of the metal–solvent bond on the cation are specifically influential in controlling the magnitude of $\Delta H^{\ddagger}$ and $\Delta S^{\ddagger}$ for the overall process. In this model a difference between the values of $\Delta H^{\ddagger}$ for solvent exchange and for foreign ligand entry may occur even when there is little direct interaction between the entering ligand and the cation up to the attainment of the transition state. They suggest that a ligand which loosens the bulk solvent structure will lead to values of $\Delta H^{\ddagger}$ (and $\Delta S^{\ddagger}$) which are higher than those for solvent exchange. This in turn implies a dependence of kinetic character on ligand type which in fact is not very marked for the reactions of nickel(II) in water and methanol. For reactions in water they suggest that the structural "stiffness" of water confers on the liquid an ability to preserve its structure during the attainment of the transition state, that little net structural work is done for a variety of ligands and consequently there is little ligand specificity and $\Delta H^{\ddagger}$ would be about the same for solvent exchange and foreign ligand entry. The degree to which there is ligand specificity in the various anation reactions of nickel(II) in ethanol and how such specificity, if any, relates to solvent structure must await the results of further investigation.

We thank the National Research Council of Canada for financial support of this work.

1. K. KUSTIN and I. SWINEHART. Prog. Inorg. Chem. **13**, 107 (1970).
2. R. G. PEARSON and P. ELLGEN. Inorg. Chem. **6**, 1379 (1967).
3. C. H. LANGFORD and H. B. GRAY. Ligand substitution processes. W. A. Benjamin, New York, 1966.
4. R. H. HOLYER, C. D. HUBBARD, S. F. A. KETTLE, and R. G. WILKINS. Inorg. Chem. **4**, 929 (1965).
5. H. P. BENNETTO and E. F. CALDIN. J. Chem. Soc. A2191 (1971).

Can. J. Chem. Downloaded from www.nrcresearchpress.com by 210.87.254.42 on 09/05/12
For personal use only.

6. C. H. LANGFORD and H. G. TSIANG. Inorg. Chem. **9**, 2346 (1970).
7. R. M. FUOSS. J. Am. Chem. Soc. **80**, 5059 (1958).
8. M. EIGEN. Z. Phys. Chem. NF **1**, 176 (1954).
9. P. A. COCK, C. E. COTTRELL, and R. K. BOYD. Can. J. Chem. **50**, 402 (1972).
10. F. W. BREIVOGEL. J. Phys. Chem. **73**, 4205 (1969).
11. C. W. DAVIES. Ion association. Butterworth, London, 1962, Chap. 9.
12. D. D. PERRIN, W. L. AMEREGO, and D. R. PERRIN. Purification of laboratory chemicals. Pergamon. 1966.
13. G. SCHWARTZENBACH and H. FLASCHKA. Complexometric titrations. *Translated by* H. Irving. Methuen, London. 1957.
14. A. I. VOGEL. A textbook of quantitative inorganic analysis. 3rd ed. Longman's Green, London. 1956.
15. L. S. FRANKEL. Chem. Commun. 1254 (1969).

Can. J. Chem. Downloaded from www.nrcresearchpress.com by 210.87.254.42 on 09/05/12
For personal use only.

Isotopic Studies of the Metal–Ligand Bond. Part I. Further Spectroscopic Studies of Copper Ethylenediamine Complexes: Copper–Nitrogen Vibrations

G. W. RAYNER CANHAM AND A. B. P. LEVER
Department of Chemistry, York University, Toronto, Ontario

Received June 6, 1972

Confirmation of the far infrared (500–200 K) spectroscopic assignments of the metal–ligand vibrations in the complexes $Cu(N-N)_2X_2$ and $Cu(N-N)X_2$((N–N) = ethylenediamine, symmetric and asymmetric *N,N*-dimethyl- and *N,N*-diethylethylenediamine, X = Cl, Br, NO_3) has been obtained from copper isotopic substitution measurements. Extension of the series Cu(ethylenediamine)$_2X_2$ has provided some exceptions to the straight line correlation between $[\nu(Cu—N)]^2$ and mean electronic d–d band energy. These are discussed.

A l'aide de mesures de la substitution d'isotopes du cuivre, on a confirmé les attributions spectroscopiques infrarouges lointaines (500–200 K) des vibrations métal–groupe coordiné dans les complexes $Cu(N-N)_2X_2$ et $Cu(N-N)X_2$((N–N) = éthylènediamine, *N,N*-diméthyléthylènediamine et *N,N*-diéthyléthylènediamine symétriques et asymétriques, X = Cl, Br, NO_3). L'extension de la série Cu(éthylènediamine)$_2X_2$ a fourni quelques exceptions à la corrélation en ligne droite entre $[\nu(Cu-N)]^2$ et l'énergie de bande d–d électronique moyenne. Celles-ci sont discutées. [Traduit par le journal]

Canadian Journal of Chemistry, **50**, 3866 (1972)

Can. J. Chem. Downloaded from www.nrcresearchpress.com by 210.87.254.42 on 09/05/12
For personal use only.

Introduction

Previous studies (1, 2) have indicated a relationship between values of a far infrared vibrational band and the d–d band envelope maximum for series of copper(II) ethylenediamine complexes. This infrared absorption was assigned as predominantly a metal–nitrogen stretching mode for the copper (1, 2) and related cobalt (1, 3) and nickel (1, 3) complexes. Metal isotopic substitution is now well established as a means of identifying asymmetric metal–ligand vibrations (4), thus the principle was applied to the conclusive identification of most of those vibrations which were predominantly copper–nitrogen in character.

It had been observed that the complex $Cu(en)_2(NO_3)_2$ was an exception to the straight line correlation (1). To elucidate this observation, spectroscopic studies of the series $Cu(en)_2X_2$ were extended to the anions NO_2^-, N_3^-, NCS^-, $SeCN^-$, SO_4^{2-}, HgI_4^{2-}, and $Hg(SCN)_4^{2-}$.

Experimental

^{65}CuO and ^{63}CuO were obtained from Oak Ridge National Laboratory, Tennessee. *N,N'*-Diperdeutero-methylethylenediamine was prepared by the method of Johnson and Bailey (5); however, the initial synthesis of the tosylate was performed by the Schotten–Baumann procedure. N-Deuteration was undertaken as described previously (1). Mass spectrometry was used to check the isotopic purity of the deuterated ligand.

TABLE 1. Copper analyses and bibliography

Complex	% Cu Found	% Cu Calcd.	Reference
$Cu(en)_2[Hg(SCN)_4]$	10.3	10.3	36
$Cu(en)_2(HgI_4)$	7.1	7.1	37
$Cu(en)_2SO_4$	22.6	22.7	—
$Cu(en)_2(N_3)_2$	21.7	21.5	38
$Cu(en)_2(NO_2)_2$	23.0	23.0	39
$Cu(en)_2(SeCN)_2$	15.85	16.1	39
$[Cu(en)_2(NCS)]ClO_4$	18.4	18.6	24

Anion exchange methods were employed for the isolation of the complexes $Cu(en)_2X_2$ with X as N_3^-, NO_2^-, $SeCN^-$, HgI_4^{2-}, and $Hg(SCN)_4^{2-}$. $Cu(en)_2(NCS)(ClO_4)$ was prepared from the reaction of stoichiometric quantities of $Cu(en)_2(SCN)_2$ and $Cu(en)_2(ClO_4)_2$ in aqueous methanol. All the complexes have been reported previously. Copper analyses (to ensure purity) and references are presented in Table 1.

Far infrared spectra were obtained with a Beckman IR-12 instrument using high density polythene plates with petroleum jelly as a mulling agent. Slow, repeated scanning enabled isotopic shift measurements, accurate to within ±0.3 K. A Cary 14 spectrophotometer was utilized for transmittance electronic spectroscopic studies.

Results and Discussion

In a recent review, Durig and Wertz (6) reported a profusion of values of ν(M—N) for ethylenediamine complexes. They concluded that the vibration lay between 400 and 600 K.

Can. J. Chem. Downloaded from www.nrcresearchpress.com by 210.87.254.42 on 09/05/12
For personal use only.

TABLE 2. 2:1 Complexes: isotopic studies of the far infrared spectra*

Complex	Ring	νCu—N vibration	Other bands†
$Cu(en)_2Cl_2$	472s	403.5s,326s	(237vs),(218s)
^{65}Cu	472s	402s,324.5s	(237vs),(218s)
$Cu(en)_2(NO_3)_2$	485m	420m,331m	315w,(225vs)
^{65}Cu	485m	419m,328.5m	315w,(225vs)
N-deuterated	449m	407m,319m	296w,sh,(198vs)
$Cu(en)_2(AgI_2)_2$	472s	414.5s	332w, 309w, 197m
^{65}Cu	472s	412s	197m
sym-Me_2enH_2.2Cl	479w	—	298vs,214s
N-deuterated	459w	—	283vs,196s
Me-deuterated	479w	—	273vs,210vs
$Cu(sym\text{-}Me_2en)_2Cl_2$	(460vs,br)	378s,301.5m	(401s,br),(283w),(257w),(233m)
^{65}Cu	(460vs,br)	375.5s,300m	(401s,br),(283w),(257w),(233m)
Me-deuterated	(471vs,br)	359s,301m	429m,390m,370m,265m,209w,194s
$Cu(sym\text{-}Me_2en)_2(NO_3)_2$	459s	376s,301.5m	407s,(277w),231m
^{65}Cu	459s	375s,300s	406.5s,(277w),231m
Me-deuterated	439s,429s	359m,300s	395s,327m,br,289w,261m,218m,196w
$Cu(asym\text{-}Me_2en)_2Cl_2$	459m	376w,296.5m	432.5m,(418w),265s,(231s),(213m)
^{65}Cu	459m	375w,295.5m	432m,(418w),264s,(231s),(213m)
$Cu(asym\text{-}Me_2en)_2(NO_3)_2$	465.5s	394.5s,301s	439s,221s
^{65}Cu	465s	393s,300s	438s,221s
$Cu(sym\text{-}Et_2en)_2Br_2$	497m	388m,291s	220m
^{65}Cu	497m	387m,289.5s	220m
$Cu(sym\text{-}Et_2en)_2(NO_3)_2$	454m	— 307s	433m,291.5m,(263w),(221s)
^{65}Cu	454m	— 305.5s	432.5m,290m,(262w),(221s)
$Cu(asym\text{-}Et_2en)_2Cl_2$	472s	386w,301m	408.5m,356w,(258.5sh),220s
^{65}Cu	472.5s	385w,300m	408.5m,356w,(258.5sh),220s
$Cu(asym\text{-}Et_2en)_2(NO_3)_2$	478s	367.5s,285m	416s,317m,295.5m,252.5m
^{65}Cu	478s	367s,284m	416s,317m,295.5m,252.5m

*Natural copper contains 69% ^{63}Cu and 31% ^{65}Cu; this will lead to some broadening in the spectra and to *underestimation* of the isotopic shift. Some isotopically pure ^{63}Cu data are cited in Table 3.
†Bands in parentheses are too broad or too weak for accurate determination of isotopic shift.

Subsequent values of ν(M—N) obtained range from 360 K (M = Lanthanide) (7) through 400, 320 K (M = Cu) (1, 2) to 518, 470 K (M = Pt) (8) and 570, 550 K (M = Pt, Pd) (9–11). A recent normal coordinate analysis suggested that four bands above 200 K in ethylenediamine complexes have metal–ligand character (12). In the case of $Cu(en)_2(SCN)_2$, the absorptions at 472 and 412 K were assigned as ν(Cu—N) and those at 330 and 230 K as (N—Cu—N) deformations (12).

Assignments of the low energy ligand bands themselves are not definitive (13–15). Isotopic substitutions of $enH_2.2X$ lead to the assignments; C—N torsion at 331 K and C—C—N deformation at 244 K (15). On complexation, the former appears to become only weakly active (1, 12), and the latter adopts the character of a ring mode (12). The greatest uncertainty concerned the CH_3 torsional mode in the *N*-alkylated ethylenediamines. This particular vibration has been assigned to bands between 280 and 180 K in other systems (16–19). On a deductive basis the band at about 300 K in the *N*-alkyl ethylenediamine hydrochlorides was ascribed to the methyl vibration (14); however the same authors did not assign any absorption to this vibration in the corresponding metal complexes (9). Subsequently the vibration was reported to be between 280 and 320 K (13). Considerable shifting or inactivation of this mode upon coordination has been reported in the case of *N*-methyl imidazole (20).

Table 2 shows the results of ^{65}Cu isotopic substitution for the series of bis(ethylenediamine) copper(II) chlorides and nitrates, and

Can. J. Chem. Downloaded from www.nrcresearchpress.com by 210.87.254.42 on 09/05/12
For personal use only.

their alkylated congeners. In addition some deuteration studies are included. Values in parentheses indicate bandwidths too great for observation of shifts. In each case two or more bands were shifted by measurable amounts. (NOTE: Because of the inherent limitations of the metal isotopic shift method, we do not exclude the possibility of metal–ligand contributions to other vibrations.) According to the Teller Redlich direct product rule (21), shifts of up to 3 K are expected for the metal–ligand vibrations; values of up to 2.5 K are observed, indicative of a substantial contribution of metal–ligand character.

For the ethylenediamine complexes, the two bands previously assigned as ν(Cu—N) (1) were found to be isotopically sensitive, thereby confirming the assignments. The alkyl substituted complexes in each case have bands at ca. 300 K and ca. 380 K which shift, and correspond to the isotopically sensitive bands at ~330 and 410 K in the non-alkylated complexes. Previously the 300 K band was assigned to a CH_3 torsional vibration. The complexes Cu(asym-Me_2en)$_2$-$(NO_3)_2$ and Cu(sym-Et_2en)$_2(NO_3)_2$ also have metal sensitive bands at 439 and 433 K respectively, which appear to correspond to the ν(Cu—N)(*b*) of Omura *et al.* (12). Apparently in these complexes there is a ν(Cu—N) contribution (small in the other complexes studied) to this basically ring breathing mode (9). Earlier (1) it had been supposed that the sensitivity of certain of the ring vibrations towards deuteration implied possible coupling between these modes and the metal–nitrogen vibrations. It now appears that with the exception of the two compounds indicated above, such coupling does not occur to any appreciable extent. Presumably there is coupling between the ring modes and some N—H vibrations. Discussion of assignments of the few other bands where shifts are observed would be purely speculative at this time.

The above assignments cast doubt on the position of the CH_3 torsional mode. To clarify the matter, perdeuteromethyl and deuteronitrogen sym-dimethylethylenediamines were prepared. The 298 K band of the ligand hydrochloride shifts 15 K upon N-deuteration and 25 K upon methyl deuteration. The methyl torsional mode is expected to shift considerably upon deuteration (19), thus the 300 K band in the alkylated ethylenediamines is more likely to be a skeletal mode. The bands in the 2:1 *complexes* could generally be correlated with their non-deuterated congeners on the basis of band shapes and relative intensities. All but one of the medium to strong bands in the CD_3 substituted complexes showed shifts in energy of 10–20 K, confirmatory evidence of the vibrational coupling in these systems. The exception, the band at 300 K, appeared unshifted. That this band does not shift upon methyl or nitrogen (1) deuteration and yet is the most strongly affected by metal isotopic substitution (1, 3) would indicate that it is a relatively "pure" Cu—N vibration. The CH_3 torsional mode itself would appear to be below 200 K.

Isotopic substitution data for the 1:1 complexes are shown in Table 3. Isotopically pure ^{63}Cu complexes were prepared in two cases to maximize isotopic shift values obtained. Although assignments are more tentative, in that both ν(Cu—Cl) and ν(Cu—N) vibrations appear in the same region and are both sensitive to copper isotopic substitution, meaningful conclusions may be drawn. The lower energy metal–nitrogen and the metal–chlorine stretching vibration both lie close to 300 cm^{-1}; they are generally distinguished by the following criteria: (*i*) in the corresponding bromo complex the ν(Cu—N) vibration should lie at approximately the same energy whilst the ν(Cu—Cl) vibration will, of course, disappear, and be replaced by a lower energy ν(Cu—Br) vibration, with ν(Cu—Br)/ν(Cu—Cl) ≃ 0.77 (22), (*ii*) upon methyl or nitrogen deuteration the ν(Cu—N) vibration should be more affected than the ν(Cu—Cl) vibration. Coupling between the Cu—Cl and Cu—N vibrations undoubtedly occurs such that the distinction drawn above may be somewhat arbitrary. Considering the limiting *cis*-CuN_2X_2 structure, two ν(Cu—X) are to be expected (23); however, as previously reported (2), only one is conclusively identified in this series.

Previous assignments of the copper–nitrogen bands (2) appear, in general, to be correct though with the reclassification of the CH_3 torsion as predominantly a copper–nitrogen mode.

Having confirmed the assignments of the metal–ligand vibrations, a further study of the

Can. J. Chem. Downloaded from www.nrcresearchpress.com by 210.87.254.42 on 09/05/12
For personal use only.

TABLE 3. 1:1 Complexes: isotopic studies of the far infrared spectra (K)*

Complex	Ring	Cu—N vibration	ν(Cu—X)	Other bands
$Cu(en)Cl_2(^{63}Cu)$	478m	375s,317.5s	265m	284m,(221s)
^{65}Cu	478m	373s,315s	264m	284m,(218.5s)
N-deuterated	—	361s,312s	264m	220s
$Cu(en)Br_2$	472s	368.5s,300.5s	196m	277.5m
^{65}Cu	473s	367.5s,299s	196m	277.5m
$Cu(sym\text{-}Me_2en)Cl_2(^{63}Cu)$	449s	353.5s,285.5s	307s	487s,426w,394.5m,(263m),(207s)
^{65}Cu	449s	352s,280.5s	304.5s	486.5w,425w,393m,(263m),(207s)
Me-deuterated	416s	342s,269s	309s	467w,428m,376m,(—),195s
$Cu(asym\text{-}Me_2en)Cl_2$	453m	380s,(285sh)	299vs	429m,(392sh),248s,197m
^{65}Cu	453m	379s,(285sh)	297.5vs	429m,(392sh),248s,197m
N-deuterated	451m	372s,(285sh)	299vs	429m,(392sh),248s,197m
$Cu(sym\text{-}Et_2en)Cl_2$	491.5s	397.5s,300s	(310sh)	270.5m,252m
^{65}Cu	491.5s	397.5s,298s	(308sh)	270.5m,252m
$Cu(asym\text{-}Et_2en)Cl_2$	468s	399.5s,307.5m	281.5s	427.5m,352m,242.5s,(226w)
^{65}Cu	468s	399s,306m	279.5s	427.5m,352m,242.5s,(226w)

*The copper bromine stretching frequencies are: $Cu(sym\text{-}Me_2en)Br_2$, 227 K; $Cu(asym\text{-}Me_2en)Br_2$, 233 K; $Cu(sym\text{-}Et_2en)Br_2$, 229 K; $Cu(asym\text{-}Et_2en)Br_2$, 198 K. These data and those of the N-deuterated complexes are taken from ref. 2.

TABLE 4. Spectroscopic data of $Cu(en)_2X_2$ complexes

		Far infrared (500–200 K)		
Complex	d–d (kK)	Ring	Cu—N vibration	Other bands
$Cu(en)_2[Hg(SCN)_4]$	18.52	474s	411s,323w	453s,436s,243s
$Cu(en)_2(HgI_4)$	19.76	470m,br	408m,328vw	293w,br,194s
$Cu(en)_2SO_4$	17.82	473s	407s,325w	332m,256s,247s,228vs
$Cu(en)_2(N_3)_2$	18.12	467s,br	407s,327w	301m,235s
$Cu(en)_2(NO_2)_2$	18.30	478s	412s,327m	245vs
$Cu(en)_2(SeCN)_2$	18.90	469m	408m,327m	219s
$Cu(en)_2(SCN)_2$*	19.41	475s	412s,331w	484†s,233s
$[Cu(en)_2NCS]ClO_4$	18.59	478s	406s,326w	490†s,463m,290w,228vs
$Cu(en)_2(ClO_4)_2$*	19.19	472s	408s,328w	464m,206s

*Previously reported in ref. 1.
†δ(SCN).

relationship between the electronic and vibrational bands (1, 2) was undertaken.

The series of $Cu(en)_2X_2$ complexes was extended to include the terminal anions NCS^-, N_3^-, and NO_2^- and the bridging SO_4^{2-}, HgI_4^{2-}, $Hg(SCN)_4^{2-}$, and SCN^- (this last complex, $[Cu(en)_2NCS]ClO_4$ has been shown to have N-bridging thiocyanate and ionic perchlorate groups (24)). Spectroscopic data are shown in Table 4. A plot of ν_{d-d} against $[\nu(Cu—N)]^2$ (higher energy band, near 400 K) gave a poorer correlation than previously reported (1) (coefficient of variation, 2.85%); a plot of ν_{d-d} against $[\nu(Cu—N)]^2$ (lower energy band, near 330 K) yielded comparatively better agreement (coefficient of variation, 2.16%). There appears to be a similar correlation between the ν_{d-d} band and the lower energy ν(Cu—N) vibration, near 300 K, in the sym-dimethylethylenediamine complexes but no such correlation is observed with the other substituted ethylenediamines (1). In these circumstances the lower energy correlation will not be pursued.

There seems little doubt that the correlation of $[\nu(Cu—N)]^2$ (higher energy) with ν_{d-d} is valid. Indeed the correlation has now been extended to the copper tetraammine complexes (25) and to the charge transfer spectra of the ethylenediamine complexes (26). However, as indicated above, there are a number of apparent excep-

Can. J. Chem. Downloaded from www.nrcresearchpress.com by 210.87.254.42 on 09/05/12
For personal use only.

tions to this correlation. These may arise through the difficulty in accurately assessing the in-plane crystal field transition energy.

An approximation in the previous work (1) was to take the maximum of the d–d band envelope as a measure of the in-plane bond strength (*i.e.*, the transition $x^2 - y^2 \leftarrow xy$) (23). Single crystal studies of the $Cu(en)_2X_2$ series (27) show one transition to be dominant in the spectrum, namely, $x^2 - y^2 \leftarrow xz,yz$. The $x^2 - y^2 \leftarrow xy$ transition lies close to, or under, this band and cannot generally be accurately located. Variations in intensity and position of each component will diminish the accuracy of the approximation used, and may well explain the poorer correlation found for this extensive series.

The sulfate complex is intriguing in that the position of the d–d band maximum is considerably lower than that expected for such a conventionally weak ligand. By previous arguments (1) such a ligand should lead to a strong in-plane field. The crystal structures of $Cu(NH_3)_4SO_4$ (28) and Cu(1,3-diaminopropane)$_2SO_4$ (29) both show considerable inequalities in the Cu—O bond distances. The low energy of the band might thus be explained by loss of center of symmetry of the CuN_4O_2 chromophore, causing a bathochromic shift similar to, but of course smaller than, observed upon addition of 1 mol of ammonia to $Cu(en)_2X_2$ complexes (30). This explanation, unfortunately, does not hold for the nitrate complex as the copper–oxygen bond lengths are identical within experimental error (31).

The azide complex is interesting in that two equal intensity components of $\nu(N{\equiv}N)$ are observed at 2030 and 2007 K. Before dismissing this as a solid state effect, it is worth noting that a similar phenomenon has been observed in *trans* bis-azide complexes of platinum, both in the solid state and in solution (32). A splitting of this order has been found for non-centrosymmetric molecules (33).

The assignment of $\delta(SCN)$ in $Cu(en)_2(SCN)_2$ to the band at 484 K rather than that at 475 K (34) is preferable by comparison with the isomorphous selenocyanate complex (35).

Conclusion

The vibrations of the complexes $Cu(en)_2X_2$ and $Cu(en)X_2$ and of the alkylated ethylenediamine congeners at *ca.* 300–300 K and *ca.* 380–420 K are metal isotope sensitive. These bands are assigned as predominantly copper–nitrogen in character.

In those cases where the relationships between ν_{d-d} and vibrational bands do not appear to be valid, this may arise because of the difficulty in locating the $x^2 - y^2 \leftarrow xy$ transition.

We thank Miss M. F. Rushton for valuable preparative assistance and the National Research Council of Canada for financial support.

1. A. B. P. Lever and E. Mantovani. Inorg. Chem. **10**, 817 (1971).
2. A. B. P. Lever and E. Mantovani. Inorg. Chem. Acta, **5**, 429 (1971).
3. A. B. P. Lever and E. Mantovani. To be published.
4. C. Udovich, J. Takemoto, and K. Nakamoto. J. Coord. Chem. **1**, 89 (1971).
5. T. B. Johnson and G. C. Bailey. J. Am. Chem. Soc. **38**, 2135 (1916).
6. J. R. Durig and D. W. Wertz. Appl. Spectrosc. **22**, 627 (1968).
7. J. H. Forsberg and T. Moeller. Inorg. Chem. **8**, 883 (1969).
8. T. G. Appleton and J. R. Hall. Inorg. Chem. **9**, 1800 (1970).
9. R. J. Mureinik and W. Robb. Spectrochim. Acta, **24A**, 837 (1968).
10. P. Uguagliati, B. Crociani, and U. Belluco. J. Chem. Soc. (A), 363 (1970).
11. B. Crociani, T. Boschi, R. Pietropaolo, and U. Belluco. J. Chem. Soc. (A), 531 (1970).
12. Y. Omura, I. Nakagawa, and T. Shimanouchi. Spectrochim. Acta, **27A**, 2227 (1971).
13. A. Sabatini and S. Califano. Spectrochim. Acta, **16**, 677 (1960).
14. R. J. Mureinik and W. Robb. Spectrochim. Acta, **24A**, 377 (1968).
15. R. W. Berg and K. Rasmussen. Spectry. Lett. 4, 285 (1971).
16. N. T. McDevitt, A. L. Rozek, F. F. Bentley, and A. D. Davidson. J. Chem Phys. **42**, 1173 (1965).
17. J. F. Jackovitz, J. A. Durkin, and J. L. Walter. Spectrochim. Acta, **23A**, 67 (1967).
18. B. D. Park and E. Wyn-Jones. J. Chem. Soc. (A), 422 (1969).
19. J. Bracjin, K. L. Kizer, and J. R. Durig. J. Mol. Spectry. **38**, 289 (1971).
20. D. M. L. Goodgame, M. Goodgame, and G. W. Rayner Canham. Inorg. Chim. Acta, **3**, 406 (1969).
21. G. Herzberg. Infrared and Raman spectra of polyatomic molecules. Van Nostrand, N.J., 1945. p. 231.
22. R. J. H. Clark and C. J. Williams. Inorg. Chem. **4**, 350 (1965).
23. A. B. P. Lever. Inorganic electronic spectroscopy. Elsevier, Amsterdam. 1968.
24. M. Cannas, G. Carta, and G. Marongiu. J. Chem. Soc. (D), 1462 (1971).

25. R. J. DUDLEY, B. J. HATHAWAY, P. G. HODGSON, and A. A. G. TOMLINSON. Chemical Society (London) Autumn Meeting. 1971. Abstract B28.
26. B. P. KENNEDY, A. B. P. LEVER, and E. MANTOVANI. To be published.
27. B. J. HATHAWAY, D. E. BILLING, P. NICHOLLS, and I. M. PROCTOR. J. Chem. Soc. (A), 319 (1969).
28. B. MOROSIN. Acta Cryst, **B25**, 19 (1969).
29. B. MOROSIN and J. HOWATSON. Acta Cryst. **B26**, 2062 (1970).
30. A. A. G. TOMLINSON and B. J. HATHAWAY. J. Chem. Soc. (A), 1685 (1968).
31. Y. KOMIYAMA and E. C. LINGAFELTER. Acta Cryst. **17**, 1145 (1964).
32. K. BOWMAN and Z. DORI. Inorg. Chem. **9**, 395 (1970).
33. I. AGRELL. Acta Chem. Scand. **25**, 2965 (1971).
34. R. BARBUCCI, G. CIALDI, G. PONTICELLO, and P. PAOLETTI. J. Chem. Soc. (A), 1775 (1969).
35. M. E. FARAGO and J. M. JAMES. Inorg. Chem. **4**, 1706 (1965).
36. G. SPACU and G. GRECU. Bul. soc. stiinte Cluj, **5**, 422 (1931); H. SCOULOUDI. Acta Cryst. **6**, 651 (1953).
37. G. SPACU and G. SUCIU. Z. anal. Chem. **78**, 329 (1929).
38. W. STRECKER and E. SCHWINN. J. Prakt. Chem. **152**, 205 (1939).
39. G. T. MORGAN and F. H. BURSTALL. J. Chem. Soc. 1259 (1927).

Can. J. Chem. Downloaded from www.nrcresearchpress.com by 210.87.254.42 on 09/05/12
For personal use only.

Identification and Thermal Stability of Copper(I) Sulfate

KIM VO VAN AND FATHI HABASHI

Department of Mining and Metallurgy, Laval University, Quebec 10, Quebec

Received May 10, 1972

Anhydrous Cu_2SO_4 was prepared and its X-ray diffraction pattern was established. Differential thermal analysis, thermogravimetric analysis, and X-ray diffraction methods were used to study the effect of heating in different atmospheres. The formation of Cu_2SO_4 as an intermediate in chemical processes has been discussed.

Le sulfate cuivreux anhydre a été préparé et son spectre de diffraction de rayons-X établi. L'analyse thermique différentielle, l'analyse thermogravimétrique et les méthodes de diffraction de rayons-X ont été utilisées pour étudier l'effet de la chaleur sous des atmosphères différentes. La formation de Cu_2SO_4 comme intermédiaire dans des processus chimiques a été discutée. [Traduit par le journal]

Canadian Journal of Chemistry, **50**, 3872 (1972)

Can. J. Chem. Downloaded from www.nrcresearchpress.com by 210.87.254.6 on 09/05/12
For personal use only.

Introduction

While extensive literature exists for $CuSO_4$, very little is known about Cu_2SO_4 (1). Druce and Fowles (2) reported that Cu_2SO_4 was formed during the dissolution of metallic Cu in hot concentrated H_2SO_4 (2). Schenck (3) concluded from vapor pressure measurements on the system Cu_2S–$CuSO_4$ at 300–500 °C the possible formation of Cu_2SO_4 according to the equation

$$Cu_2S + 4CuSO_4 \rightarrow 3Cu_2SO_4 + 2SO_2$$

Cu_2SO_4 was identified indirectly by quenching the samples in water and filtering; the appearance of metallic copper was indication of the presence of Cu_2SO_4 since it disproportionates in water according to:

$$Cu_2SO_4 \xrightarrow{H_2O} Cu + CuSO_4$$

Recent work (4) showed that Cu_2SO_4 is formed during the reduction of $CuSO_4$ by H_2.

$$2CuSO_4 + 2H_2 \rightarrow Cu_2SO_4 + SO_2 + 2H_2O$$

Cuprous ion can be readily formed in aqueous sulfate solutions (1). For example, metallic copper dissolves in $CuSO_4$ solution in absence of air to form Cu^+ ions. $CuSO_4$ solutions can be reduced by SO_2 or CO under pressure at about 90 °C to generate Cu^+. However, it is not possible to crystallize Cu_2SO_4 from aqueous solutions. The present investigation was undertaken to acquire more information on anhydrous Cu_2SO_4.

Experimental

Preparation and Identification of Cu_2SO_4

The starting material for preparing Cu_2SO_4 is Cu_2O. Reagent grade Cu_2O was not suitable for this purpose because it contained CuO. Therefore, Cu_2O was freshly prepared from Fehling's solution (5). The other method described by Brauer (6) and involving the reduction of cupric acetate by hydrazine was not convenient because Cu_2O obtained was extremely fine powder and was difficult to wash. The purity of Cu_2O was ascertained by X-ray diffraction and thermogravimetric analysis.

Cu_2SO_4 was then prepared according to Recoura's method (7) by the reaction of Cu_2O with dimethyl sulfate:

$$Cu_2O + (CH_3)_2SO_4 \rightarrow Cu_2SO_4 + (CH_3)_2O$$

Cu_2SO_4 so prepared was washed with ether and dried at 60 °C in a stream of argon for 24 h; it was pale beige in color. According to Recoura, this material disproportionates in water to give metallic copper and pure cupric sulfate solution in equimolecular amounts, thus indicating that copper existed in the cuprous form. Because of its sensitivity to moisture it was stored in a desiccator. Reaction of Cu with hot concentrated H_2SO_4 did not yield any Cu_2SO_4 as claimed by Druce and Fowles (2).

Since the X-ray diffraction pattern of Cu_2SO_4 is not described in the literature, we present it in Table 1 as obtained by powder diffractometry counter method from the sample we prepared. Two hours were needed for obtaining a diffractogram. The diffractogram showed the presence of $CuSO_4$, the amount of which was estimated from thermogravimetric analysis in argon to be 25% as described later. The presence of $CuSO_4$ in the sample seems to be inherent to the method of preparation and not due to deterioration by exposure to the air, because a sample exposed to the air for 10 h contained the same amount of $CuSO_4$ as a freshly prepared sample and no metallic copper.

Studies on Cu_2SO_4

Differential thermal analysis (DTA) and thermogravimetric analysis (TGA) were used to study the effect of heating Cu_2SO_4 in different atmospheres. The DTA instrument was a Stanton model Standata 6-25 with stainless steel sample holder; weight of sample was about 200 mg. The TGA instrument was a Fisher Series 100 TGA System; weight of sample was about 20 mg. In both instruments a continuous gas flow was maintained, and a heating rate of 10 °C/min was used.

Can. J. Chem. Downloaded from www.nrcresearchpress.com by 210.87.254.6 on 09/05/12
For personal use only.

TABLE 1. X-ray diffraction pattern of Cu_2SO_4, copper target (K_{α_1} radiation), θ in degrees, d in Ångstrom units, I/I_1 refer to height of peaks, $\lambda = 1.5405$ Å

θ	d	I/I_1
8.90	4.98	2
9.30	4.77	3
9.45	4.69	3
10.55	4.21	4
12.93	3.44	3
13.13	3.39	4
13.45	3.31	4
14.10	3.16	100
16.64	2.69	23
18.50	2.43	11
19.30	2.33	11
20.24	2.22	4
20.90	2.16	11
21.28	2.12	11
23.35	1.94	3
25.20	1.81	16
26.23	1.74	5
27.50	1.66	3
27.78	1.65	4
28.68	1.60	4
29.10	1.58	2
29.43	1.57	2
31.85	1.46	2
32.15	1.45	2
32.50	1.43	5
32.75	1.42	5
33.05	1.41	3
33.35	1.40	5
34.65	1.35	2
38.88	1.23	2

Samples of $CuSO_4.5H_2O$ were heated in both DTA and TGA apparatus and the thermograms so obtained were compared. Since the sample in DTA apparatus is in intimate contact with the thermocouple, the temperatures at which dehydration and decomposition take place were considered precise enough for calibrating the TGA.

Reaction products were identified by interrupting the heating of samples under investigation at a certain temperature and examining the residue by X-ray powder diffractometry. Sulfur dioxide liberated during the tests was detected by absorption in KI solution acidified by 1% HCl and containing starch as indicator. The solution was continuously titrated during a test by KIO_3 solution to maintain a constant color (8).

Results and Discussion

Heating in Argon

The TGA thermogram presented in Fig. 1 shows that the first decomposition takes place at about 300 °C followed by two other overlapping steps at about 560 and 650 °C. DTA curves shown in Fig. 2, however, revealed peaks at 400, 610, 720, and 805 °C. SO_2 produced in this case was first detected at 350 °C. Heating was interrupted at different temperatures (marked *a* to *e* in Fig. 2) in the DTA instrument and the samples obtained were examined by X-ray diffraction. The products identified by this method are shown in Table 2. It can be concluded from this information that the drifting of the base line in the endothermic region in DTA curve starting at about 220 °C may be attributed to the partial decomposition of Cu_2SO_4 according to

$$Cu_2SO_4 \rightarrow Cu + CuSO_4$$

The first stage of decomposition then follows the following reaction

$$3Cu_2SO_4 \rightarrow 2CuSO_4 + 2Cu_2O + SO_2$$

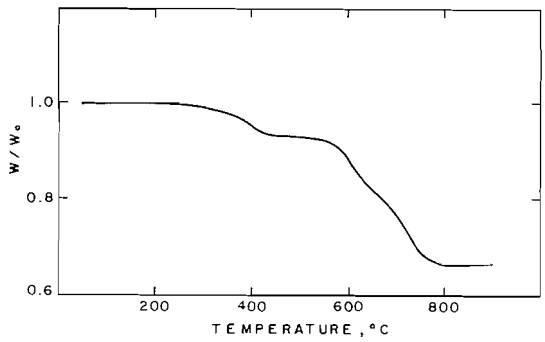

FIG. 1. TGA curve showing the decomposition of Cu_2SO_4 in argon. Heating rate 10 °C/min, gas flow 80 ml/min.

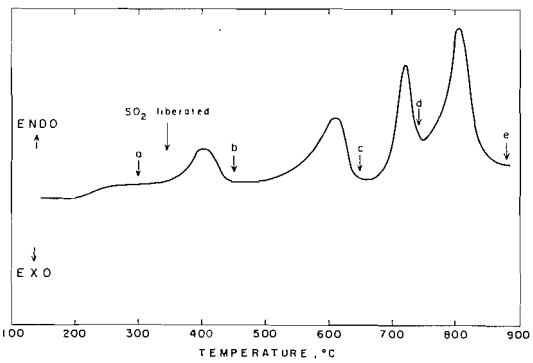

FIG. 2. DTA curve showing the decomposition of Cu_2SO_4 in argon. Heating rate 10 °C/min, gas flow 80 ml/min. Letters *a* to *e* indicate the temperatures at which heating was interrupted and samples obtained were examined by X-ray diffraction (see Table 2).

TABLE 2. Identification of products of decomposition of Cu_2SO_4 in argon by X-ray diffraction

Point on DTA curve	Temperature of interruption in DTA (°C)	Product		
		Major	Minor	Trace
a	300	Cu_2SO_4	$CuSO_4$	Cu
b	450	$CuSO_4$, Cu_2O	—	Cu
c	650	$CuO.CuSO_4$, Cu_2O	—	Cu
d	740	$CuO.CuSO_4$, CuO	—	Cu
e	880	CuO	—	Cu

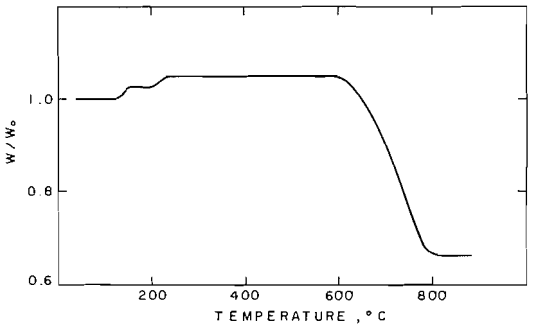

FIG. 3. TGA curves showing the behavior of Cu_2SO_4 when heated in air. Heating rate 10 °C/min, gas flow 100 ml/min. Letters *a* to *d* indicate the temperatures at which heating was interrupted and samples obtained were examined by X-ray diffraction (see Table 3).

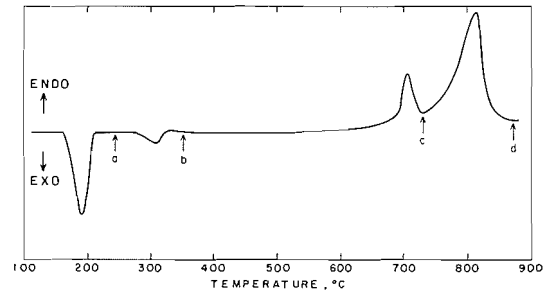

FIG. 4. DTA curves showing the behavior of Cu_2SO_4 when heated in air. Heating rate 10 °C/min, gas flow 100 ml/min.

The weight change according to this equation is 9.6% while data in Fig. 1 indicate 7.2%. The discrepancy between these two values is due to the presence of $CuSO_4$ in the sample which remains undecomposed in the low temperature range. The amount of $CuSO_4$ in the sample can be calculated as 25% of its weight.

TABLE 3. Identification of products of decomposition of Cu_2SO_4 in air by X-ray diffraction

Point on DTA curve	Temperature of interruption in DTA (°C)	Product		
		Major	Minor	Trace
a	250	$CuSO_4$, Cu_2O	—	—
b	350	$CuSO_4$, CuO	—	—
c	740	$CuO.CuSO_4$, CuO	—	—
d	880	CuO	—	—

Data in Table 2 suggest that the above reactions are followed by

$$4CuSO_4 + Cu_2O \rightarrow 3CuO.CuSO_4 + SO_2$$

$$CuO.CuSO_4 + Cu_2O \rightarrow 4CuO + SO_2$$

$$CuO.CuSO_4 \rightarrow 2CuO + SO_2 + \tfrac{1}{2}O_2$$

which correspond to the last three DTA peaks in Fig. 2. The liberation of SO_2 in each step was confirmed.

Heating in Air

Figure 3 shows the TGA curves for the behavior of Cu_2SO_4 when heated in air. It can be seen that there are two steps indicating a weight increase at 120 and 200 °C, and a loss in weight at 600 °C. Figure 4 shows the DTA curves for the same process. It can be seen that the first two reactions are exothermic while the last two are endothermic. X-ray diffraction analysis after each step (Table 3) and the percentage change in weight conform to the following reaction scheme

$$2Cu_2SO_4 + \tfrac{1}{2}O_2 \rightarrow 2CuSO_4 + Cu_2O$$

$$Cu_2O + \tfrac{1}{2}O_2 \rightarrow 2CuO$$

$$2CuSO_4 \rightarrow CuO.CuSO_4 + SO_2 + \tfrac{1}{2}O_2$$

$$CuO.CuSO_4 \rightarrow 2CuO + SO_2 + \tfrac{1}{2}O_2$$

These reactions can therefore be assigned to the DTA peaks in Fig. 4.

Heating in H_2

Figure 5 shows that the change in weight during reduction by H_2 is gradual in the temperature range 120 to 340 °C. X-ray diffraction analysis of residues obtained when heating was interrupted at 250 °C showed the presence of $CuSO_4$ and Cu. It seems that reduction takes place according to the equation

$$Cu_2SO_4 + 2H_2 \rightarrow 2Cu + SO_2 + 2H_2O$$

Can. J. Chem. Downloaded from www.nrcresearchpress.com by 210.87.254.6 on 09/05/12
For personal use only.

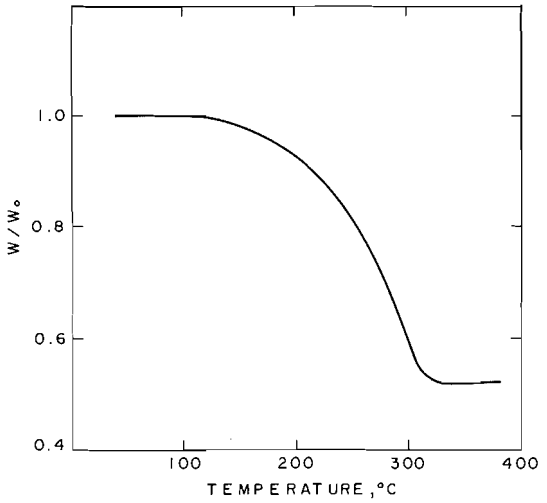

FIG. 5. TGA curves showing the reduction of Cu_2SO_4 by H_2. Heating rate 10 °C/min, gas flow 360 ml/min.

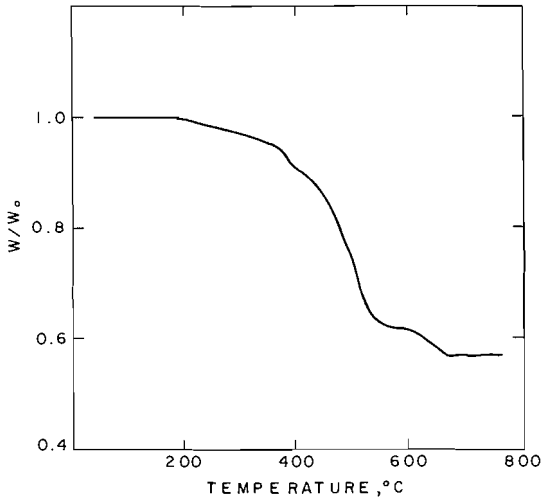

FIG. 6. TGA curves showing the reduction of Cu_2SO_4 by CO. Heating rate 10 °C/min, gas flow 100 ml/min.

and the H_2O vapor liberated reacts with the remaining Cu_2SO_4 to form Cu and $CuSO_4$

$$Cu_2SO_4 \xrightarrow{H_2O} CuSO_4 + Cu$$

$CuSO_4$ is then reduced to Cu_2SO_4

$$2CuSO_4 + 2H_2 \rightarrow Cu_2SO_4 + SO_2 + 2H_2O$$

These three reactions proceed simultaneously until all Cu_2SO_4 is reduced to Cu. DTA curves did not yield any significant data because the heat liberated or absorbed is the sum of the above reactions.

Heating in CO

Figure 6 shows the TGA curve for reduction by CO. In the temperature range 200 to 400 °C the behavior is the same as in the case when heating in argon. At 400 °C, X-ray diffraction revealed the presence of $CuSO_4$ and Cu_2O, *i.e.*, the following reaction takes place

$$3Cu_2SO_4 \rightarrow 2CuSO_4 + 2Cu_2O + SO_2$$

Above 400 °C, $CuSO_4$ is reduced in two steps, namely to Cu_2O then to Cu as follows (4)

$$2CuSO_4 + 3CO \rightarrow Cu_2O + 2SO_2 + 3CO_2$$
$$3Cu_2O + 3CO \rightarrow 6Cu + 3CO_2$$

Conclusions

Anhydrous Cu_2SO_4 can be readily prepared in about 75% purity by the action of dimethyl sulfate on Cu_2O; the remaining 25% is $CuSO_4$. The material is fairly stable in dry air at room temperature but decomposes rapidly in presence of moisture or on heating. In air or in H_2, decomposition starts at 120 °C while in argon or in CO decomposition takes place at 200 °C. It is doubtful that Cu_2SO_4 can exist above 300 °C under any circumstances.

The financial support of the National Research Council of Canada is gratefully acknowledged.

1. Gmelin. Handbuch der anorganischen Chemie. Vol. 60. Kupfer. Part B. Weinheim. 1958. pp. 487–551.
2. J. G. F. DRUCE and G. FOWLES. Chem. News, **137**, 385 (1928).
3. R. SCHENCK. Z. Elektrochem. **43**, 438 (1937).
4. F. HABASHI, K. VO VAN, and R. DUGDALE. To be published.
5. J. W. MELLOR. Comprehensive treatise on inorganic and theoretical chemistry. Vol. 3. Longman, London. 1928. p. 120.
6. G. BRAUER. Handbook of preparative inorganic chemistry. Academic Press, New York. 1965. p. 1011.
7. A. RECOURA. C. R. **148**, 1105 (1909).
8. Annual book of ASTM standards, Part 32. American Society for Testing and Materials. Easton, Md., U.S.A. 1971. p. 839.

Can. J. Chem. Downloaded from www.nrcresearchpress.com by 210.87.254.6 on 09/05/12
For personal use only.

A Conformational Study of Lysergic Acid and *iso*-Lysergic Acid Dialkylamides by Proton Magnetic Resonance Spectroscopy

K. BAILEY

Research Laboratories, Health Protection Branch, Department of National Health and Welfare, Ottawa, Canada K1A 0L2

AND

A. A. GREY

Ontario Research Foundation, Sheridan Park, Ontario

Received May 19, 1972

The 220 MHz p.m.r. spectra of the dimethylamides of D-lysergic acid (**3**) and D-*iso*-lysergic acid (**4**) are reported. Extensive use of double resonance experiments and the presence of four long-range coupling constants provide an unambiguous assignment for the conformation of **3** in $CDCl_3$. Its D ring is shown to exist in a half-chair form in which the 8-β amide function is pseudo-equatorial. Its epimer essentially exists in the other half-chair form with a pseudo-equatorial 8-α amide function. Data from the p.m.r. spectra of a series of *N*,*N*-dialkylamides of these acids are also presented.

The spectrum of protonated **3** at 23 °C shows two forms of the 6-NCH_3 and 8-$CON(CH_3)_2$ groups but only one for the epimer **4**.

Les spectres de r.m.n. à 220 MHz des diméthylamides de l'acide D-lysergique (**3**) et de l'acide D-*iso*-lysergique (**4**) sont rapportés. L'usage extensif de la double résonance et la présence de quatre constantes de couplage à longue distance ont permis d'attribuer sans ambiguité la conformation de **3** dans le $CDCl_3$. On a montré que le cycle D de ce dernier existe sous la forme demi-chaise dans laquelle la fonction amide-8β est pseudoéquatoriale. Son épimère existe essentiellement sous l'autre forme demi-chaise avec la fonction amide-8α pseudo-équatoriale. Les données des spectres de r.m.n. d'une série de *N*,*N*-dialkylamides de ces acides sont également présentés. Le spectre de **3** sous forme protonée à 23 °C montre deux formes pour les groupes NCH_3-6 et $CON(CH_3)_2$-8 alors que l'épimère **4** n'en donne qu'une. [Traduit par le journal]

Canadian Journal of Chemistry, **50**, 3876 (1972)

Introduction

Interest in possible similarities in the mode of action of LSD, tryptamines, and the hallucinogenic phenylethylamines (1–5) prompted us to study the solution conformation of LSD and other amides (**3–12**) of lysergic and *iso*-lysergic acids (**1** and **2**) (6) by p.m.r. spectroscopy (7). Stoll *et al.* (8) have presented evidence that ring D in both acids is in a ψ-chair form, the carboxyl function being equatorial in lysergic acid and axial in the *iso*-acid.

Experimental

The p.m.r. spectra of **3** and **4** were obtained on a Varian HR-220 spectrometer (Canadian 220 MHz n.m.r. centre, Ontario Research Foundation, Sheridan Park, Ontario). Double resonance experiments were carried out under track-field sweep decoupling conditions with a Wavetek, Model 101, voltage-controlled generator calibrated to the sweep widths of the spectrometer recorder. Other spectra were obtained on Varian A 60-A and XL-100 spectrometers.

The synthesis employed (9) gives a mixture of the isomeric amides of both acids, column chromatography on alumina readily separating the faster-running lysergamide from the *iso*-lysergamide (10). The p.m.r. spectral assignments in Table 1 are based primarily on chemical shift values and are supported by the decoupling experiments described below.

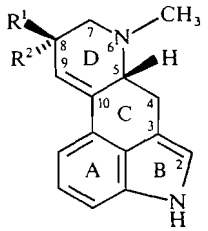

1 $R^1 = CO_2H$; $R^2 = H$
2 $R^1 = H$; $R^2 = CO_2H$
3 $R^1 = CON(CH_3)_2$; $R^2 = H$
4 $R^1 = H$; $R^2 = CON(CH_3)_2$
5 $R^1 = CONCH_3 \cdot C_3H_7$; $R^2 = H$
6 $R^1 = H$; $R^2 = CONCH_3 \cdot C_3H_7$
7 $R^1 = CONC_2H_5 \cdot C_3H_7$; $R^2 = H$
8 $R^1 = H$; $R^2 = CONC_2H_5 \cdot C_3H_7$
9 $R^1 = CON(C_3H_7)_2$; $R^2 = H$
10 $R^1 = H$; $R^2 = CON(C_3H_7)_2$
11 $R^1 = CONC_3H_7 \cdot C_4H_9$; $R^2 = H$
12 $R^1 = H$; $R^2 = CONC_3H_7 \cdot C_4H_9$

Can. J. Chem. Downloaded from www.nrcresearchpress.com by 210.87.254.40 on 09/05/12
For personal use only.

TABLE 1. P.m.r. data* for amides of D-lysergic and D-*iso*-lysergic acids

Compound, conditions†		$H_{12,13,14}$	H_2	H_9	H_8	N-CH_3
3	220	7.15	6.86	6.36	3.98	2.59
5	60	7.15	6.85	6.35	*ca.* 3.90	2.55
7	100	7.14	6.86	6.34	3.90	2.58
9	60	7.15	6.88	6.35	*ca.* 3.90	2.57
11	100	7.14	6.84	6.34	3.94	2.59
LSD‡	60	7.15	6.85	6.32	?	2.57
4	220	7.09	6.79	6.30	3.78	2.59
6	60	7.05	6.78	6.28	*ca.* 3.75	2.58
8	100	7.08	6.82	6.24	3.72	2.60
10	60	7.02	6.77	6.23	*ca.* 3.75	2.58
12	100	7.02	6.77	6.24	3.75	2.60

*δ-Values in p.p.m. downfield from internal TMS, solutions *ca.* 15% in $CDCl_3$; these signals are singlets or largely unresolved multiplets, H_8 is broad (*ca.* 20 Hz).
†Frequency of examination in MHz (see Acknowledgments).
‡Data made available by Dr. G. A. Neville, N.H. & W. laboratories.

TABLE 2. P.m.r. data* for D-lysergic acid N,N-dimethylamide (**3**)

δ ($CDCl_3$) (p.p.m.)	δ (C_6D_6) (p.p.m.)	Δ (p.p.m.)	J($CDCl_3$) (Hz)	Assignment	δ Irradiation ($CDCl_3$): observation
3.98	3.83	+0.15	10.5, 5.0, 3.5, *ca.* 2	$H_{8\alpha}$	6.36: Lose $J \approx 2$; 10.5, 5.0, 3.5 apparent
					3.08: Lose $J \approx 5$
					2.89: Lose $J \approx 11$
3.54	3.40	+0.14	5.5, 14.8	$H_{4\beta}$	6.86: No change
					6.36: No change
3.20	3.15	+0.05	11.5, 5.5, 3.8, 1.0	$H_{5\beta}$	6.36: Lose $J \approx 1.0$; 11.5, 5.5, 3.8 apparent
3.15	2.33	+0.82		$CONCH_3$	
3.08	*ca.* 2.97	$\approx$ +0.1	11.2, 5.3, 1.0	$H_{7\alpha}$	6.36: Lose $J \approx 1.0$
					3.98: Lose $J \approx 5.5$
3.02	2.31	+0.71	singlet	$CONCH_3$	
2.89	*ca.* 2.97	≈ -0.1	11.2, 10.4	$H_{7\beta}$	3.98: Lose $J \approx 10$–11
2.68	2.84	−0.16	14.8, 11.5, 1.6	$H_{4\alpha}$	6.86: Lose $J \approx 1.5$
2.59	2.66	−0.07	singlet	N-CH_3	

*Measured at 220 MHz, with internal TMS, additional data in Table 1. J Values are first order, in Hz.

Results and Discussion

The assignment of signals other than those in Table 1 was not attempted with homologues higher than N,N-dimethyl, because the NCH_2-multiplets (doubled for every compound because of the partial double-bond character of the amide C—N link) extensively overlap multiplets derived from the basic ergoline system. The methyl resonances from compounds **3** and **4** provided the minimum interference and their spectra were determined at 220 MHz. The results are shown in Tables 2 and 3. Axial and equatorial positions are indicated parenthetically by a and e respectively and the designation α or β is made with respect to the proton at C-5 being termed β; see conformations **I**–**III**.

D-*Lysergic Acid Dimethylamide (3)*

The pertinent 220 MHz spectra are reproduced in Figs. 1 and 2. Double irradiation of the H_2 resonance at 6.86 p.p.m. (11) affected only the multiplet at 2.68 p.p.m. ($J = 1.6$ Hz). The magnitude of the coupling is typical of a *cisoid*-allylic coupling (12) and must involve H_2 and H_4 where the estimated dihedral angle $\theta_{2,4\alpha}$ between these hydrogens measures about 80°. The magnitude of geminal coupling constants adjacent to a π bond system is also known to be orientation dependent (12, 13). The observed −14.8 Hz splitting in $H_{4\alpha}$ at 2.68 p.p.m. therefore is also consistent with an estimated $\theta_{2,4\alpha} = 80°$ where the indole π-bond lobes are more or less aligned with $H_{4\alpha}$ and are expected to exert

Can. J. Chem. Downloaded from www.nrcresearchpress.com by 210.87.254.40 on 09/05/12
For personal use only.

TABLE 3. P.m.r. data* for D-*iso*-lysergic acid *N*,*N*-dimethylamide (**4**)

δ ($CDCl_3$) (p.p.m.)	δ (C_6D_6) (p.p.m.)	Δ (p.p.m.)	J($CDCl_3$) (Hz)	Assignment	δ Irradiation ($CDCl_3$): observation
3.78	3.48	+0.30	mult., W = 19 Hz	$H_{8\beta}$	6.30: Lose $J \approx 2$, complex multiplet remains
3.42	3.37	+0.05	11.5, 5.5, 2.5, *ca.* 1	$H_{5\beta}$	6.30: Lose $J \approx 1$; 11.5, 5.5, 2.5 apparent
3.25	3.14	+0.11	14.1, 5.5	$H_{4\beta}$	6.30, 6.70: No change
ca. 3.18	3.28	−0.10	12.0, 7.5	$H_{7\alpha}$	6.30, 6.70: No change apparent
3.19	2.36	+0.83	singlet	$CONCH_3$	
3.00	2.36	+0.64	singlet	$CONCH_3$	
2.86	2.69	+0.17	12.0, 5.2, *ca.* 1?	$H_{7\beta}$	6.30: Sharpening of peaks
2.82	2.83	−0.01	14.2, 12.0, 1.5	$H_{4\alpha}$	6.70: Lose $J \approx 1.5$; 14.2, 12.0 remain
2.59	2.65	−0.06	singlet	N-CH_3	

*See footnote Table 2; band-width (W) of multiplet (mult.) in Hz.

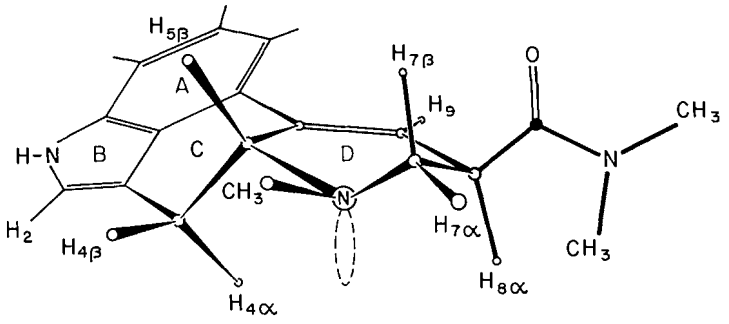

I

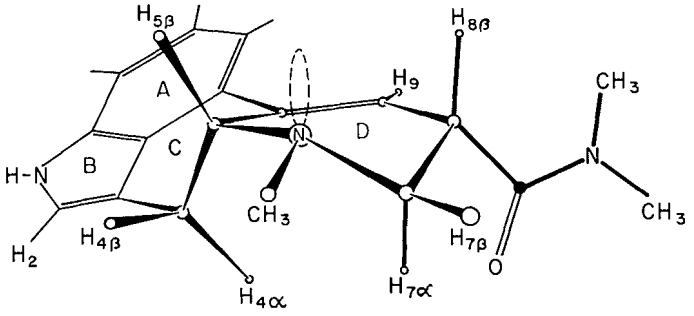

II

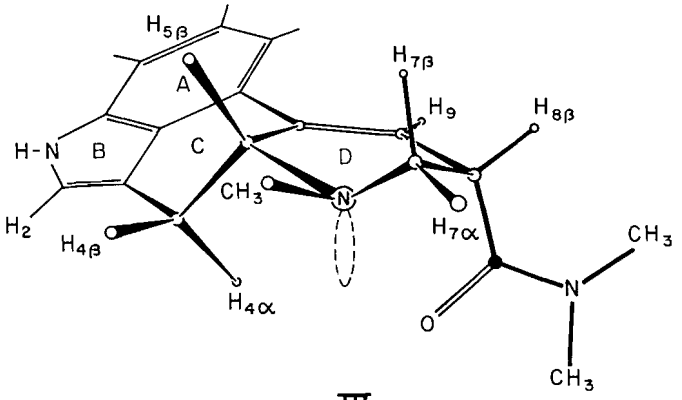

III

Can. J. Chem. Downloaded from www.nrcresearchpress.com by 210.87.254.40 on 09/05/12
For personal use only.

Can. J. Chem. Downloaded from www.nrcresearchpress.com by 210.87.254.40 on 09/05/12
For personal use only.

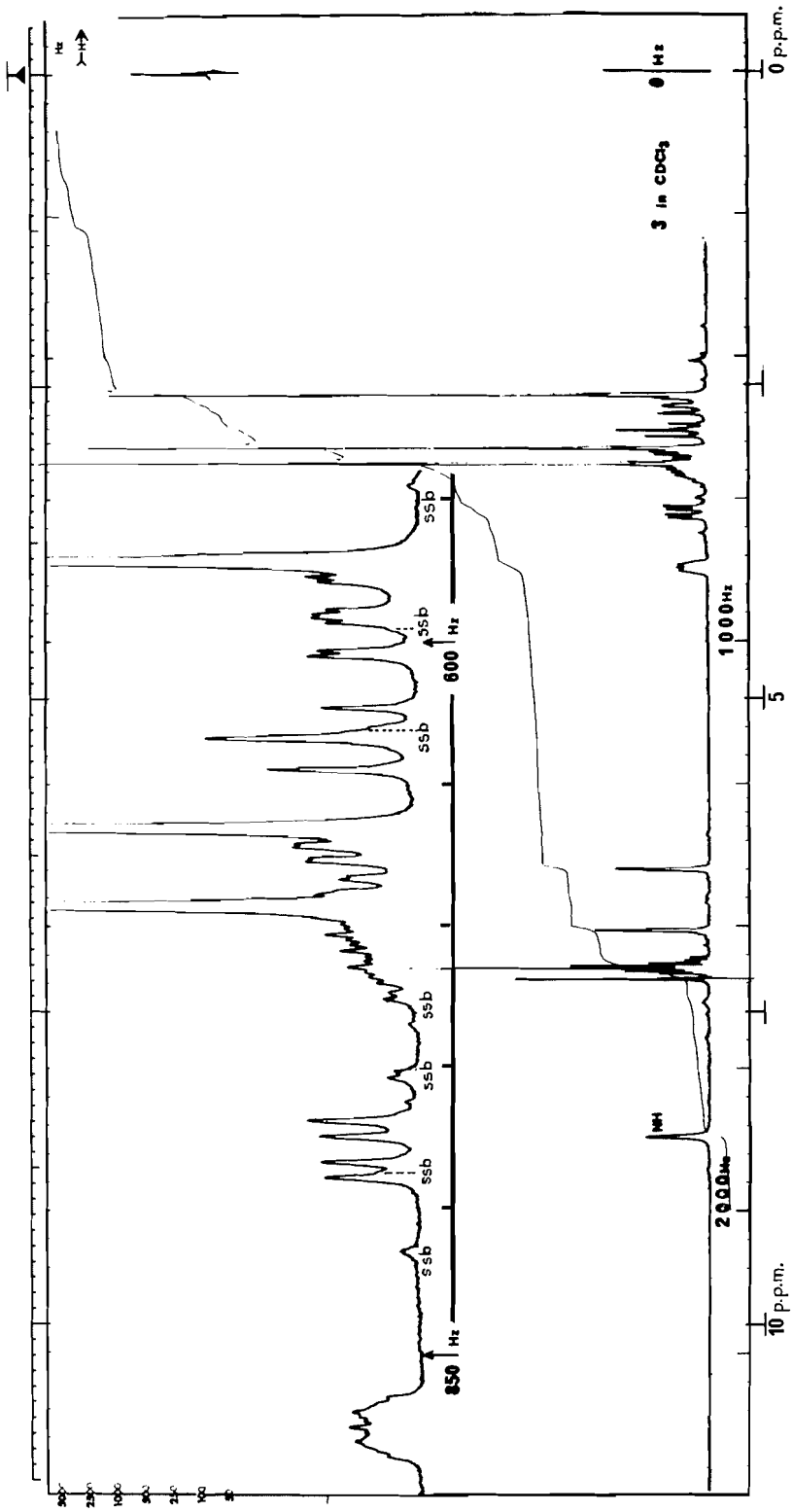

FIG. 1. 220 MHz spectrum of 3 in $CDCl_3$ solution. Lower trace: sweep width 2500 Hz. Insert: 5 × expansion of signals from δ 2.59–3.98 p.p.m., spinning side-bands are indicated by s.s.b.

Can. J. Chem. Downloaded from www.nrcresearchpress.com by 210.87.254.40 on 09/05/12
For personal use only.

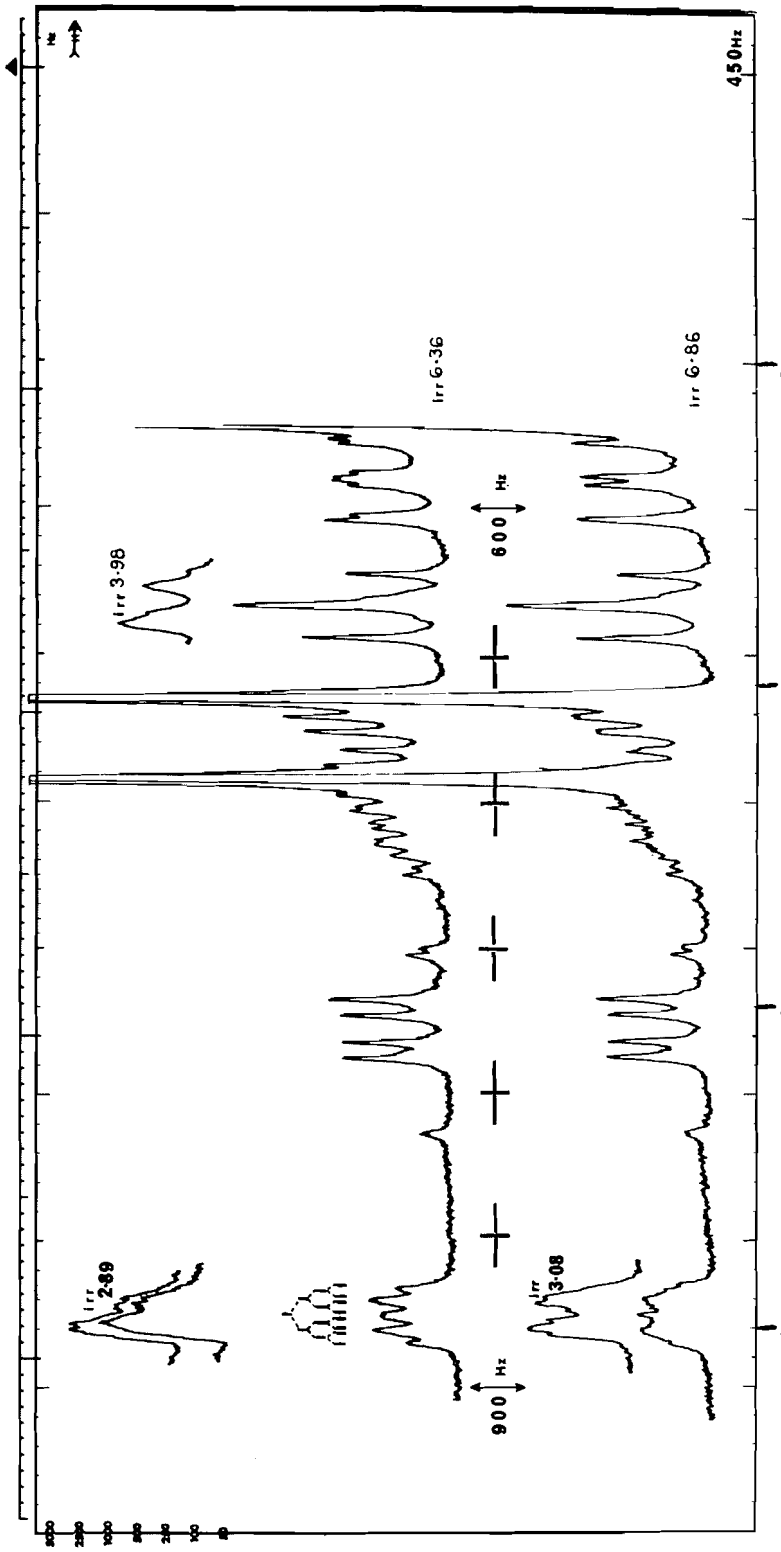

FIG. 2. 220 MHz spectrum of **3** in $CDCl_3$ solution, sweep width 500 Hz, signals from δ 2.59–3.98 p.p.m. Upper main trace with irradiation at δ 6.36 p.p.m.; lower trace with irradiation at δ 6.86 p.p.m. Inserts of signals demonstrate the effect upon them of irradiation of the signals indicated.

Can. J. Chem. Downloaded from www.nrcresearchpress.com by 210.87.254.40 on 09/05/12
For personal use only.

a near-maximum effect on J_{gem}. The well defined geometry for $H_{4\beta}$ necessitates that its resonance be deshielded relative to $H_{4\alpha}$ by virtue of its almost planar orientation with the aromatic B ring while showing a very small (0.5 Hz) $J_{2,4\beta}$ allylic coupling. Indeed, $H_{4\beta}$ is 0.86 p.p.m. to low field of $H_{4\alpha}$ and displays only two observable couplings of 5.5 and −14.8 Hz, the latter being $J_{4\alpha,4\beta}$.

Models indicate that the methine hydrogen $H_{5\beta}$ is rigidly fixed by virtue of its bridgehead position at C-5 which is at the puckered end of the half-chair ring C. This unique arrangement places H_5 above the aromatic ring plane of rings A and B with C_5—H_5 bond more or less perpendicular to these as well as to the olefinic double bond in ring D: an ideal position for allylic coupling with H_9. Double resonance experiments on H_9 at 6.36 p.p.m. clearly reduce the heavily coupled multiplet at 3.40 p.p.m. to an eight-line pattern with splittings of 11.4, 5.5, and 3.8 Hz. The former two are those observed in $H_{4\alpha}$ and $H_{4\beta}$ respectively, allowing the assignment of H_5 at 3.40 p.p.m. In addition, $H_{5\beta}$ is uniquely situated at a bridgehead position which is attached to nitrogen which permits an assessment of its environment with respect to the nitrogen lone pair of electrons (14); methine hydrogens in structurally related fragments which are *gauche* to the nitrogen lone pair are deshielded by about 0.6–0.8 p.p.m. relative to those oriented *trans*-axially which are found at ~3.2 p.p.m. The observed chemical shift of $H_{5\beta}$ at 3.20 p.p.m. suggests it to be the latter with the N-lone pair directed in a *trans*-axial relationship with H_5. Such an arrangement can only be realized if ring D exists in that half-chair conformation in which C-5, -10, -9, and -8 are more or less in the same plane. Carbon-7 is above this plane on the same side as H_5; the heterocyclic nitrogen and its lone pair are directed below.

The remaining 3.8 Hz splitting associated with $H_{5\beta}$ can be related to the broad unresolved multiplet at 3.98 p.p.m. This resonance is transformed on double irradiation at 6.36 p.p.m. (H_9) into a symmetrical first-order eight-line multiplet of splittings J = 3.5, 10.5, and 5.0 Hz.

The larger couplings are also found in the mutually coupled (J_{gem} = −11.2 Hz) signals at 2.89 and 3.08 p.p.m. respectively. The analysis of the $H_{8\alpha}$, $H_{7\alpha}$, $H_{7\beta}$ subsystem indicates that $J_{7\beta,8\alpha}$(a–a) = 10.5, $J_{7\alpha,8\alpha}$(e–a) = 5.2, and $J_{7\alpha,7\beta}$ (*gem*) = (−)11.3 Hz. The common 3.8 Hz coupling between H_5 and H_8 is a homoallylic long-range interaction (13) which clearly portrays their relative orientations with each other and the olefinic double bond. For appreciable coupling, both dihedral angles involved for maximum σ–π overlap (15) must approach 90°. The dihedral angles $\theta_{5,9}$ and $\theta_{8,9}$ measured from models in the conformation depicted in Fig. 1 are 90 and 75° respectively. The latter is of such magnitude as to expect a small vicinal coupling between the sp^2–sp^3 bonded hydrogens on C-9 and -8. Its presence is responsible for the unresolved appearance of the unperturbed $H_{8\alpha}$ resonance at 3.98 p.p.m.

The only remaining unaccounted coupling is evident in $H_{7\alpha}$ at 3.08 p.p.m. This multiplet also loses a coupling of about 1 Hz on irradiating H_9 and is compatible with a long-range W coupling between H_9 and H_7. These are more or less in one plane because of the half-chair conformation imposed on ring D. A self-consistent analysis could not be obtained if the other ψ-chair form (compare conformation **II**) were present to any great extent.

The spectrum of **3** measured in C_6D_6 gave chemically shifted resonances (16) as summarized in Table 2, where $\Delta = \delta(CDCl_3) - \delta(C_6D_6)$. Consideration of the data for H_5, H_7, H_8, and 6-NCH_3 suggests that the rotameric conformation of the amide function is possibly as shown in conformation **I**.

These results support conformation **I** proposed by Chothia and Pauling (17) for LSD, and for lysergic acid by Stoll *et al.* (8) at least in the solvents considered here.

iso-Lysergic Acid Dimethylamide (4)

The pertinent 220 MHz n.m.r. spectra are reproduced in Figs. 3 and 4. In $CDCl_3$, the dimethylamide singlets overlap with those of H_4 and H_7 but are preferentially shifted upfield in C_6D_6 thereby allowing the complete coupling data for the ring hydrogens to be extracted. The assignments were confirmed by double resonance experiments in $CDCl_3$ solution.

The assignments of $H_{4\alpha}$, $H_{5\beta}$, and $H_{8\beta}$ follow arguments similar to those presented for **3**; however, the identification of $H_{7\alpha}$ and $H_{7\beta}$ in the *iso*-compound is less clear. Conformations **II** and **III** represent **4** with ring D in a ψ-chair form

Can. J. Chem. Downloaded from www.nrcresearchpress.com by 210.87.254.40 on 09/05/12
For personal use only.

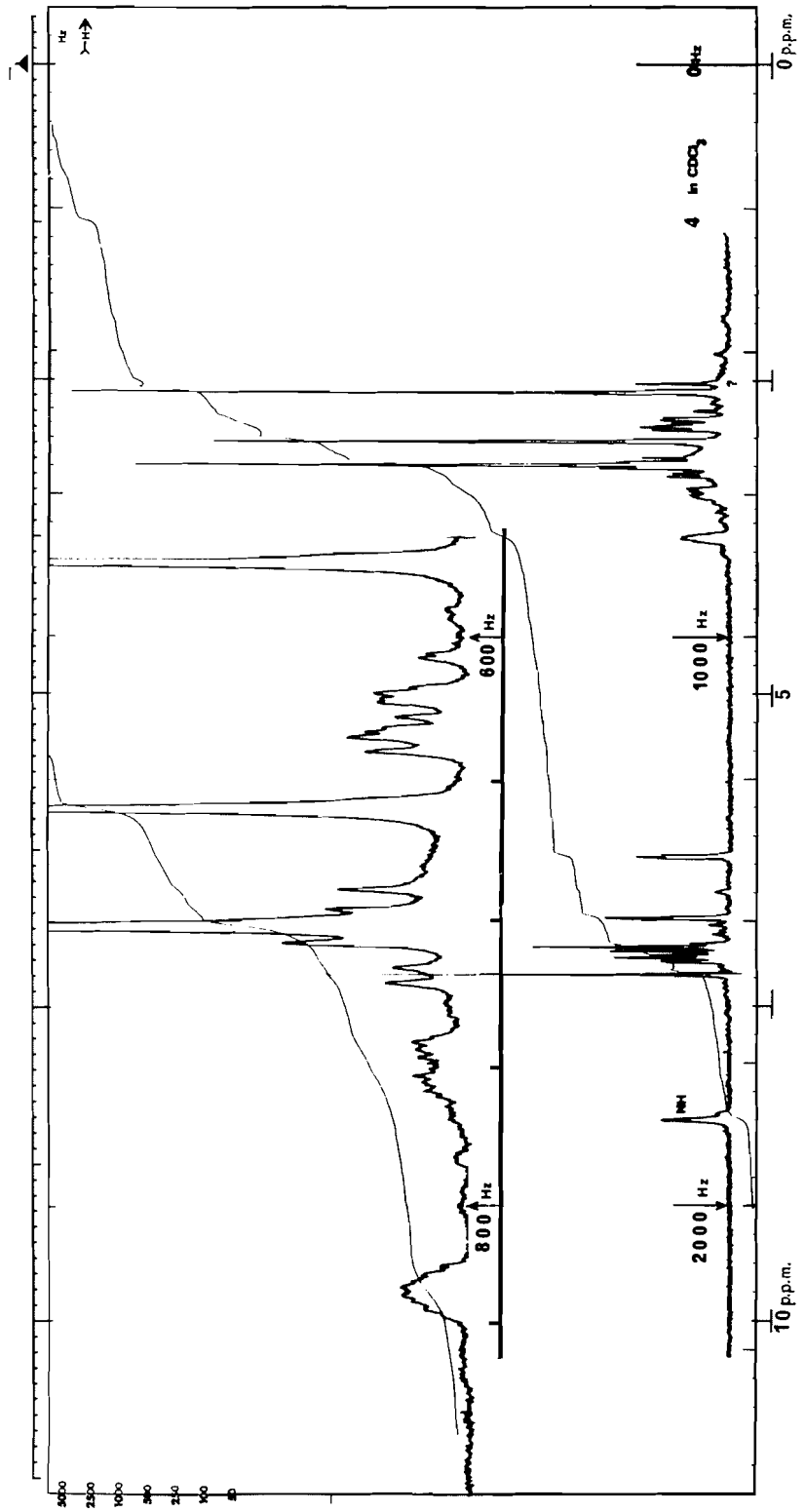

FIG. 3. 220 MHz spectrum of 4 in $CDCl_3$ solution. Lower trace: sweep width 2500 Hz. Insert: 5 × expansion of signals from δ 2.59–3.78 p.p.m.

Can. J. Chem. Downloaded from www.nrcresearchpress.com by 210.87.254.40 on 09/05/12
For personal use only.

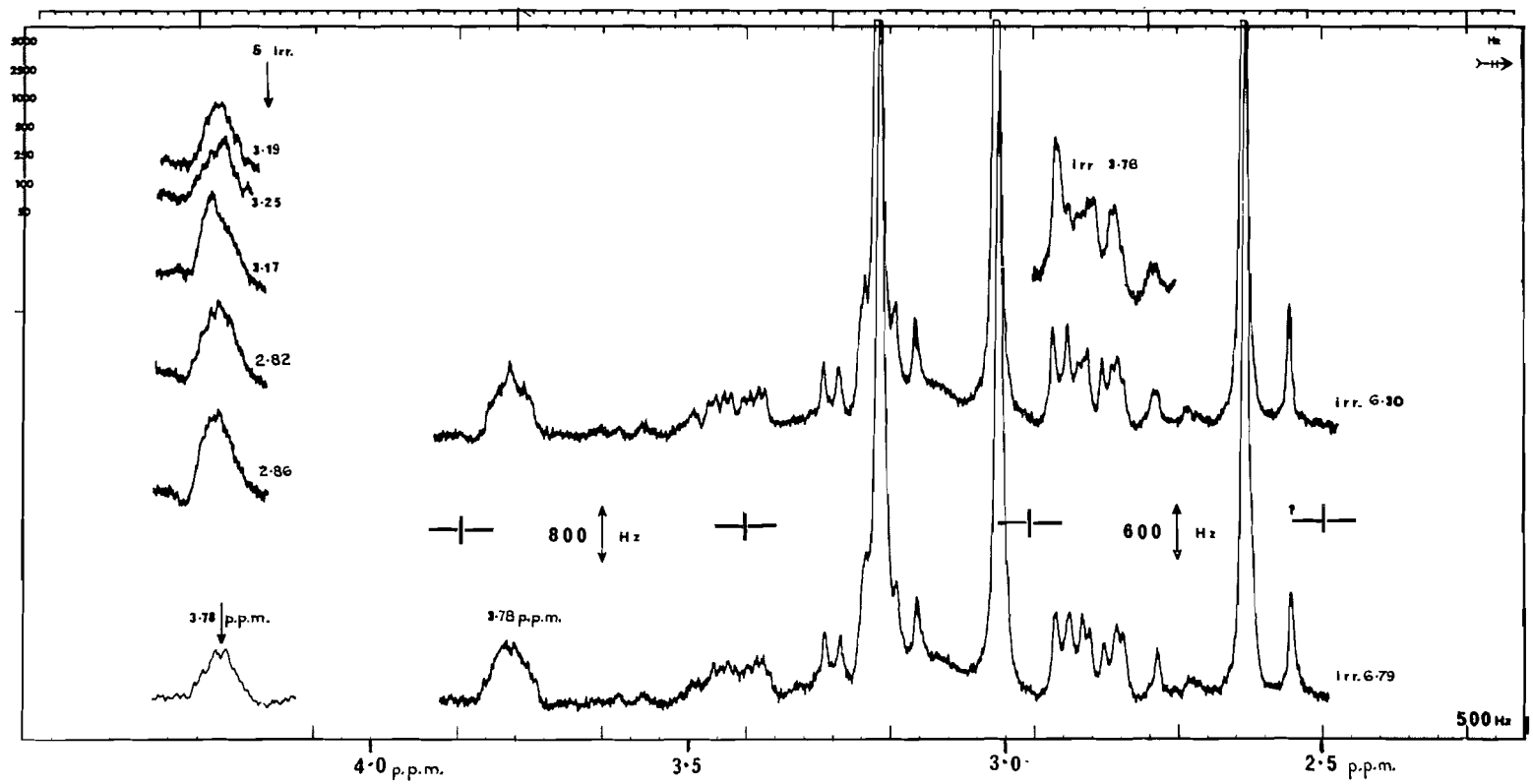

FIG. 4. 220 MHz spectrum of **4** in $CDCl_3$ solution, sweep width 500 Hz, signals from δ 2.59–3.78 p.p.m. Upper main trace with irradiation at δ 6.30 p.p.m.; lower trace with irradiation at δ 6.79 p.p.m. Inserts as in Fig. 2.

Can. J. Chem. Downloaded from www.nrcresearchpress.com by 210.87.254.40 on 09/05/12
For personal use only.

in which $H_{8\beta}$ is axial and equatorial, respectively. The 6-NCH_3 is considered equatorially displaced for minimum steric interaction in both conformers, only the 7 and 8 hydrogens interchange their axial or equatorial positions.

Consideration of the ψ-chair form illustrated in conformation **II** shows that only one realistic assignment can be made. The resonance at 2.86 p.p.m. is attributed to $H_{7\beta}$ (equatorial) with $J_{7\beta,8\beta}$(e–a) = 5.2 Hz while that at 3.18 p.p.m. to $H_{7\alpha}$ (axial) with $J_{7\alpha,8\beta}$(a–a) = 7.5 Hz.[1] The geminal coupling $J_{7\alpha,7\beta} = (-)12.1$ Hz is common to both resonances. The observed slight sharpening of the proposed $H_{7\beta}$ resonance at 2.86 p.p.m. on double irradiation of the olefinic H_9 at 6.36 p.p.m. may be ascribed to a long-range W coupling as was observed in **3**. Since the 6, 7, 8, 9 system possesses almost the same relative geometry to that of **3** in conformation **I**, similar vicinal couplings constants are expected in this 7, 8 subsystem. The smaller 7.5 Hz *trans*-axial vicinal coupling constant appears to be anomalous compared to that in **3**; however, it is not unlike that obtained from a similar arrangement found in shikimic acid (19) and other systems (20) which display $J_{aa} = 6.2$–8.4 Hz in half-chair conformations.

The alternative conformer, **III**, can be assigned as follows: $H_{7\alpha}$ (equatorial) at 2.86 p.p.m. and $H_{7\beta}$ (axial) at 3.18 p.p.m. with $J_{7\alpha,8\beta}$(e–e) = 5.2, $J_{7\beta,8\beta}$(a–e) = 7.5 Hz. Molecular models suggest that $\theta_{7\alpha,8\beta} = 80$ and $\theta_{7\beta,8\beta} = 40°$. An interchange of assignments for the 7-hydrogens forces an unrealistic set of J_{vic} which does not conform with the general view of the Karplus relationship. As before, this assignment also accounts for the decoupling of the equatorial $H_{7\alpha}$ while irradiating H_9. The fact that only one of these H_7 protons shows an observable long-range coupling does not negate the possibility of a dynamic equilibrium between conformations **II** and **III**, since the averaging process is expected to reduce $J_{7,9}$ perhaps making it too small to detect in the signal at 3.18 p.p.m. Rough calculations from coupling constants expected in frozen conformations ($J_{ae} = 5.3$, $J_{aa} = 10.4$ Hz in **II** (see **3**); $J_{ae} = 3$–4, $J_{ee} = 1.5$–3.0 Hz in **III**) for the observed $J_{7,9}$ couplings indicate that **II**:**III** $\simeq 2:1$ if $H_{7\beta}$ is at 2.86 and $H_{7\alpha}$ is at 3.18, but self-consistent results cannot be obtained with the reverse assignment. Although the case here is less clear than for the lysergamides, the analysis thus supports conformation **II** for the *iso*-lysergamides in the solutions examined here.

The solvent-shift Δ values suggest that the amide–carbonyl bond is directed as shown in **II** (pointing towards the $H_{4\alpha}$ bond projection). Comparing the chemical shifts of **3** and **4**, H_9, 6-NCH_3, and Δ6-NCH_3 are very similar and indicate that the anisotropic amide group disposition with respect to H_9 and 6-NCH_3 is much the same on epimerization at C-8 (the conformations **I**, **II**, and **III** all satisfy this condition.)

Spectra of **3** and **4** in $CDCl_3$ with an added excess of trifluoracetic acid were not very useful because of the complexities of protonation at different sites, peak broadening, and poor resolution. However, the amide **3** clearly displayed two protonated forms (21) at 23 °C for each of its methyl groups and the complex aromatic region; each amide methyl group displayed a doublet ($\delta = 3.0$ and 3.2 p.p.m., $J = 10$ Hz) and the two $CH_3\overset{+}{N}H$ doublets at 3.05 and 3.10 p.p.m. ($J_{CH_3\overset{+}{N}H} = 4.8$ Hz) collapsed to singlets on irradiation of the broad $\overset{+}{N}H$ peaks at 9.91 and 10.05 p.p.m. The amide **4** displayed only one doublet for each of its CH_3 groups, the doublet $CH_3\overset{+}{N}H$ ($J = 5$ Hz) collapsing on irradiation of the $\overset{+}{N}H$ at 9.21 p.p.m.

Conclusion

The D ring of the *N*,*N*-dimethylamide of D-lysergic acid and its 8-epimer exist in different conformations in $CDCl_3$. The gross stereochemical features of these amides are essentially the same in that the N_6-methyls as well as the *N*,*N*-dimethylamide groups are in pseudo-equatorial positions. The different biological activities of the two series of amides may be in part

[1]This analysis stems from a generalization of the Karplus equation (18) that when both vicinal coupling constants are greater than about 5 Hz in a $—CH_2—CH_x—$ system where the geminal "dihedral" angle is 120°, then H_x must lie outside the *gem* protons. The only conformation consistent with this is that shown in conformation **II** and possibly the less favored boat form in which both 6-NCH_3 and the amide group assume pseudo-equatorial positions. However, J_0 values required to calculate J's from estimated dihedral angles are unrealistic, see ref. 19.

due to the relative orientation of the 6-nitrogen lone pair of electrons. In LSD, the latter is *trans*-axial to $H_{5\beta}$ and on the concave α-face while for the *iso*-compounds, it is essentially *gauche* and on the β-face of the molecule.

Spectra at 60 MHz were determined by Mr. H. W. Avdovich using a Varian A 60-A, Department of National Health and Welfare, Health Protection Branch, Research Laboratories, Ottawa; at 100 MHz on a Varian XL-100 through the courtesy of Dr. G. Buchanan, Department of Chemistry, Carleton University, Ottawa; and at 220 MHz with a Varian HR-220 at the Canadian 220 MHz n.m.r. Centre. Mlle. D. Verner and Monsieur D. Legault of the Department of National Health and Welfare are thanked for assistance in the preparation and purification of the amides examined.

1. A. Bebbington and R. W. Brimblecombe. Br. Med. Bull. **25**, 293 (1969).
2. Drugs and the brain (Part 1). P. Black, Editor. The Johns Hopkins Press, Baltimore. 1969.
3. A. Balestrieri and D. Fontanari. Arch. Gen. Psychiatr. **1**, 279 (1959); A. Balestrieri. *In* Psychotropic drugs. S. Garattini and V. Ghetti, Editors. Elsevier Publishing Co., Amsterdam. 1957.
4. H. Isbell, A. B. Wolbach, A. Wikler, and E. J. Miner. Psychopharmacol. **2**, 147 (1961); A. B. Wolbach, H. Isbell, and E. J. Miner. Psychopharmacol. **3**, 1 (1962).
5. S. Garattini and L. Valzelli. Serotonin. Elsevier Publishing Co., New York. 1965.
6. H. G. Leemann and S. Fabbri. Helv. Chim. Acta, **42**, 1696 (1959).
7. F. A. Bovey. Nuclear magnetic resonance spectroscopy. Academic Press, New York, N.Y. 1969.
8. A. Stoll, T. Petrzilka, J. Rutschmann, A. Hofmann, and H. H. Gunthard. Helv. Chim. Acta, **37**, 2039 (1954).
9. R. P. Pioch. U.S. Pat. 2 736 728. Chem. Abstr. **50**, 10 803 (1956).
10. A. Stoll and A. Hofmann. Helv. Chim. Acta, **38**, 421 (1955).
11. L. A. Cohen, J. W. Daly, H. Kny, and B. Witkop. J. Am. Chem. Soc. **82**, 2184 (1960).
12. L. M. Jackman and S. Sternhell. Applications of nuclear magnetic resonance spectroscopy in organic chemistry. Pergamon Press, Oxford. 1969.
13. S. Sternhell. Quart. Rev. **23**, 236 (1969).
14. T. A. Crabb, R. F. Newton, and D. Jackson. Chem. Rev. **71**, 109 (1971).
15. M. Karplus. J. Chem. Phys. **33**, 1842 (1960); J. Am. Chem. Soc. **82**, 4431 (1960).
16. N. S. Bhacca and Dudley H. Williams. Applications of NMR spectroscopy in organic chemistry. Holden Day Inc., San Francisco. 1966. Chapt. 7.
17. C. Chothia and P. Pauling. Proc. Natl. Acad. Sci. **63**, 1063 (1969).
18. R. J. Abraham and J. S. E. Holken. J. Chem. Soc. 806 (1963).
19. L. D. Hall. J. Org. Chem. **29**, 297 (1964).
20. B. Coxon, H. J. Jennings, and K. A. McLauchlan. Tetrahedron, **23**, 2395 (1967).
21. J. C. N. Ma and E. W. Warnhoff. Can. J. Chem. **43**, 1849 (1965).

Can. J. Chem. Downloaded from www.nrcresearchpress.com by 210.87.254.40 on 09/05/12
For personal use only.

A New Synthesis of 5-Phenyl-2,3-dihydro- and 2,3,4,5-Tetrahydro-1*H*-2-benzazepin-1-ones

K. ACKERMAN,[1] D. E. HORNING, AND J. M. MUCHOWSKI[2]
Bristol Laboratories of Canada, Candiac, Quebec

Received June 26, 1972

It was shown that 3-phenyl-3-(2-aminoethyl)phthalide (**6**, R = H) and its *N*-methyl analog (**6**, R = CH_3) existed in the amino lactone form in solution at room temperature. In the absence of solvents, however, these compounds underwent a spontaneous transformation into the 5-phenyl-2,3,4,5-tetrahydro-1*H*-2-benzazepin-1-ones (**8**, R = H, CH_3) which suffered dehydration in sulfuric acid with the formation of 5-phenyl-2,3-dihydro-1*H*-2-benzazepin-1-ones (**9**, R = H, CH_3).

This benzazepine synthesis can be considered to be analogous to the known (12–15) conversion of 1-aminomethylphthalides (**11**) to 4-hydroxy-3,4-dihydroisocarbostyrils (**13**).

Il a été montré que la phényl-3 (amino-2 éthyl)-3 phtalide (**6**, R = H) et son analogue *N*-méthyle existent en solution sous forme d'aminolactone à la température ambiante. En l'absence de solvants cependant, ces composés subissent une transformation spontanée en phényl-5 tétrahydro-2,3,4,5-1*H*- benzazépine-2 ones-1 (**8**, R = H, CH_3) qui se déshydratent en milieu sulfurique en formant des phényl-5 dihydro-2,3-1H- benzazépine-2 ones-1 (**9**, R = H, CH_3).

Cette synthèse de benzazépine peut être considérée comme l'analogue de la conversion (12–15) connue des aminométhyl-1 phtalides (**11**) en hydroxy-4 dihydro-3,4 isocarbostyryles (**13**).

[Traduit par le journal]

Canadian Journal of Chemistry, **50**, 3886 (1972)

In connection with a synthetic program the purpose of which was to prepare compounds structurally related to Diazepam[3] (**1**) we required a method whereby certain 4-aryl-2,3-dihydro-1*H*-2-benzazepin-1-ones (**2**) would be available in large quantities. The Schmidt or Beckmann expansions of 4-aryl-1-tetralones, which in principle might provide access to precursors of the above compounds, are in practice of little synthetic value because of the predominant formation of 5-aryltetrahydro-1-benzazepin-2-ones (2). With the possible exception of the acid-catalyzed cyclization of the acid chlorides of *o*-carboxycinnamonitriles (4), the other known 2-benzazepin syntheses (3, 5–7) did not appear to be readily adaptable to the preparation of **2** or derivatives thereof.

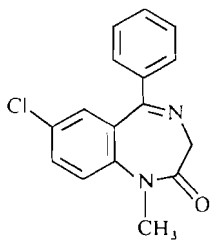

1

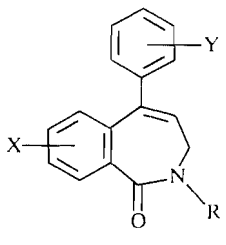

2

It occurred to us that a straightforward synthesis of compounds of type **2** might be based on an intramolecular variant of the aminolysis of esters. An examination of Dreiding models revealed that the benzobicyclo[3.2.1] transition state (intermediate (?), see ref. **8**, pp. 1164–1166) **7** (Scheme 1) would be especially favorable. Therefore, to test the feasibility of the above approach, the anion generated from 3-phenylphthalide (**3**), using sodium hydride in dimethylformamide (9), was alkylated with 2-(tetrahydropyran-2-yloxy)ethyl bromide and the product thus obtained was hydrolyzed to the alcohol **4**, (X = OH). The bromo compound **4** (X = Br), prepared from the alcohol and phosphorous tribromide, was converted without purification to the azide **5**, which was subjected to catalytic reduction in 2-propanol solution. If this solution was diluted with ether and then treated with gaseous hydrogen bromide, the amino lactone **6** (R = H) was isolated as its stable hydrobromide salt. If the solvent was

[1]Present address: F. H. Hoffman-LaRoche, A. G., Basel, Switzerland.

[2]To whom enquiries should be addressed at: Syntex, S.A., Division de Investigacion, Calle Carretera Mexico-Toluca No. 2822, Apartado Postal 10-820, Mexico 10, D.F.

[3]Diazepam is a widely used tranquilizer and muscle relaxant (1).

Can. J. Chem. Downloaded from www.nrcresearchpress.com by 210.87.254.42 on 09/05/12
For personal use only.

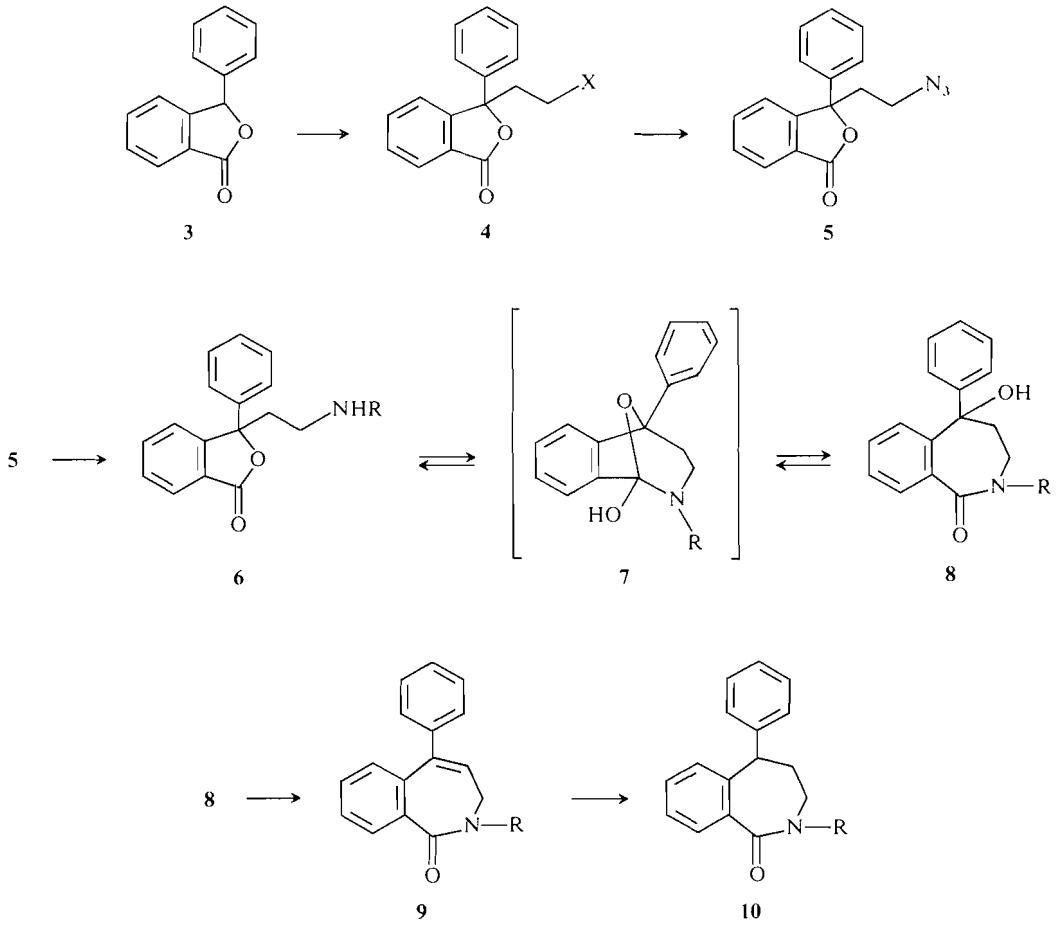

SCHEME 1

removed, however, an oil (strong i.r. band at 1765 cm^{-1}) was obtained, which underwent a spontaneous transformation into a crystalline, non-basic compound, isomeric with the starting material, and having an intense absorption at 1672 cm^{-1} in the i.r. spectrum. The 2-benzazepin-1-one structure **8** (R = H) was assigned to this compound on the basis of its spectral properties (see Table 1) and on the chemical evidence cited below. Solution of the above alcohol in concentrated sulfuric acid at 0°, and subsequent quenching of the reaction with ice, resulted in the formation of 5-phenyl-2,3-dihydro-1*H*-2-benzazepin-1-one (**9**, R = H). The structure of this substance was strongly supported by the n.m.r. spectrum, and fully substantiated by palladium-catalyzed hydrogenation to the tetrahydro derivative **10** (R = H) identical to the minor product[4] obtained from the Schmidt expansion of 4-phenyl-1-tetralone (2).

The process depicted by formulae **6** → **8** → **9** was also applicable when the amine function in **6** was secondary. Thus, the methyl amine **6** ($R = CH_3$), prepared by alkylation of the iminophosphorane **4** ($X = N^-P^+(C_6H_5)_3$) with methyl iodide followed by aqueous acidic hydrolysis of the phosphiniminium salt (10), rearranged when neat to the hydroxy lactam **8** ($R = CH_3$), which underwent dehydration in the expected manner to the olefin **9** ($R = CH_3$). The last-mentioned compound was identical to the product obtained by *N*-alkylation of the sodium salt of **9** (R = H) with methyl iodide.

The compounds represented by structures **6**

[4]We thank Dr. I. Monkovic of these laboratories for providing us with a specimen of this compound.

Can. J. Chem. Downloaded from www.nrcresearchpress.com by 210.87.254.42 on 09/05/12
For personal use only.

TABLE 1. Spectral properties of some substituted phthalides and 2-benzazepin-1-ones

Compound	Infrared[a] (cm^{-1})	Nuclear magnetic resonance δ(p.p.m.)[b]
4 (X = H)	3445, 1770[c]	1.83 (s, 1H)[d], 2.66 (m, 2H)[e], 7.28–7.69(m, 8H), 7.82–7.98 (m, 1H)[f]
6 (R = H)	3440[g], 3370[g], 1758	1.22 (d, 4.6H)[g], 2.72 (m, 4H), 3.80 (sept., 0.8H)[g], 5.0–7.0 (3H)[d], 7.30–7.94 (m, 9H)
6 ($R = CH_3$)	1759	—
8 (R = H)	3375, 3215, 1668	2.20 (m, 1H), 2.93 (m, 1H), 3.08 (m, 2H), 5.78 (s, 1H)[d], 7.17–7.97 (m, 10H)
8 ($R = CH_3$)	3200, 1632	2.23 (m, 1H), 2.85 (s, 3H), 3.18 (m, 1H), 3.33 (m, 2H), 5.80 (s, 1H)[d], 7.44 (d, 9H)[h]
9 (R = H)	3415, 3290, 3200[i] 1650	3.52 (t, 2H; $J = 7.2$)[j], 6.55 (t, 1H; $J = 7.2$), 7.07–7.26 (m, 1H), 7.31–7.65 (m, 8H), 7.93–8.15 (m, 1H)[k]
9 ($R = CH_3$)	1629[i]	3.25 (s, 3H), 3.70 (d, 2H; $J = 7.4$), 6.58 (t, 1H; $J = 7.4$), 7.08–7.64 (m, 8H), 8.05–8.21 (m, 1H)[f]
10 ($R = CH_3$)	3415, 3281, 3207[i], 1660	2.45 (m, 2H), 3.12 (m, 2H), 4.34 (t, 1H; $J = 9$), 6.57–6.76 (m, 1H), 7.12–7.34, (m, 7H), 7.40–7.59 (m, 1H), 7.83 (s, 1H)[d,l]

[a]Recorded as dispersions in Nujol unless specified otherwise.
[b]Recorded as solutions in perdeuteriodimethylsulfoxide; d, doublet; m, multiplet; s, singlet; sept., septuplet; t, triplet. J values in Hz.
[c]Liquid film.
[d]Exchangeable with D_2O.
[e]AB quartet at δ 2.45 and 2.86 ($J = 14.6$) with each signal split into triplets ($J = 6.8$)
[f]Recorded in deuteriochloroform.
[g]Absorptions due to 2-propanol of crystallization.
[h]Two broad singlets at δ 7.38 and 7.50.
[i]Recorded in chloroform.
[j]Coupled equally to NH and olefinic CH.
[k]Measured in deuteriochloroform containing 50% perdeuteriodimethylsulfoxide.
[l]Recorded in deuteriochloroform containing 30% perdeuteriodimethylsulfoxide.

and **8** can be considered as the reactant and the product in an ester aminolysis reaction (see ref. 11, p. 330). They may also be regarded as the two extreme forms of a ring chain tautomeric equilibrium (see ref. 8, pp. 802–805). In either case, **6** and **8** ought to be interconvertible. After 24 h at room temperature a chloroform solution of **6** (R = H) showed neither diminution of the integrated intensity of the i.r. carbonyl absorption at 1765 cm^{-1}, nor the presence of the lactam tautomer ($\nu_{(C=O)} = 1672\ cm^{-1}$). Removal of the solvent gave an oil which was soon converted to the crystalline hydroxylactam **8** (R = H) as described previously. When a solution of the lactam in various solvents was heated, a rapid reversion to the amino lactone took place; indeed, even the most rapid recrystallization of this compound did not prevent considerable conversion to the lactone tautomer. The compounds in the *N*-methyl series displayed essentially the same behavior as the parent members.

When this study was completed, we became aware of the work of Ullyot *et al.* (12–14) and Szeki (15),[5] which demonstrated that the liberation of 1-aminomethylphthalides (**11**, Scheme 2) from their salts (2 or 3 equiv of hot sodium hydroxide was used) resulted in the formation of stereoisomeric mixtures of 3-alkyl-3,4-dihydroisocarbostyrils (**13**) which were dehydratable with hot, concentrated sulfuric acid to 3-alkylisocarbostyrils (**14**).[6] On the basis that the above reaction occurred more readily[7] in the presence of an excess of alkali, Ullyot *et al.* (12, 13) concluded that the reaction was base-catalyzed and proceeded through the open chain intermediate (**15**) which cyclized to **13** with the loss of an hydroxide ion. We suggest that this intermediate is unlikely in view of the observations described herein, and of the known mechanisms of ester aminolysis (ref. 11, p. 330) and amide hydrolysis (ref. 11, pp. 327–329).

Experimental

The melting points were recorded in a Gallenkamp melting point apparatus and are not corrected. The i.r. spectra were measured with a Unicam SP-200G i.r. spectro-

[5]We are grateful to a referee for directing our attention to references 13–15.

[6]The benzazepine synthesis described herein must therefore be considered to be an extension of the observations of these investigators.

[7]The cyclization also occurred in the absence of an external base, but at a rate 1/3 to 1/5 of that in the presence of alkali.

Can. J. Chem. Downloaded from www.nrcresearchpress.com by 210.87.254.42 on 09/05/12
For personal use only.

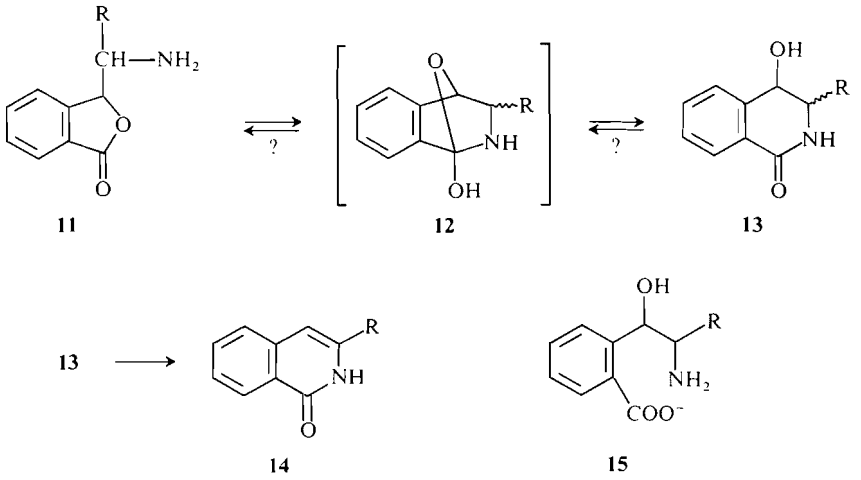

SCHEME 2

photometer. The n.m.r. spectra were recorded with a Varian A-60A spectrometer and are expressed in p.p.m. (δ) from internal tetramethylsilane.

The tetrahydropyranyl ether of bromoethanol was prepared according to the method of Parham and Anderson (16). 3-Phenylphthalide was prepared from 2-benzoylbenzoic acid by the method of Mole (17).

*3-Phenyl-3-(2-hydroxyethyl)phthalide (**4**, X = OH)*

A 55% dispersion of sodium hydride in mineral oil (3.50 g) was washed free of the carrier with petroleum ether (b.p. 30–60°), layered with anhydrous DMF (400 ml), and then 3-phenylphthalide (15.73 g, 75 mmol) was added. The mixture was heated to 50° in an atmosphere of dry nitrogen until hydrogen evolution had ceased (45 min), the solution was then cooled to room temperature and the tetrahydropyranyl ether of 2-bromoethanol (16.8 g, 80 mmol) was added. After stirring at room temperature for 7 h, the solution was poured into a large amount of cold water, the product was extracted into benzene, the extract was washed well with water and dried over sodium sulfate. The solvent was removed *in vacuo* and the residual oil was dissolved in a solution made up of methanol (180 ml) and 10% hydrochloric acid (20 ml). After 10 min at reflux temperature the solution was concentrated to a small volume *in vacuo*, the residue was diluted with water, and the mixture was extracted with ethyl acetate. The extract was washed with water, dried over sodium sulfate, and evaporated *in vacuo*. The alcohol was obtained as a very viscous oil in quantitative yield. A small portion was twice evaporatively distilled at 130°/0.005 mm. A satisfactory analysis could not be obtained, but the n.m.r. spectrum (See Table 1) indicated a purity of at least 95%.

Anal. Calcd. for $C_{16}H_{14}O_3$: C, 75.57; H, 5.55. Found: C, 75.10; H, 5.69.

*3-Phenyl-3-(2-azidoethyl)phthalide (**5**)*

The crude alcohol from above (7.82 g, 30.8 mmol) was treated, in a dropwise manner with stirring at 0°, with phosphorous tribromide (9.5 g, 35.1 mmol). The cooling bath was removed, and after 18 h at room temperature and 1 h on a steam bath, the oil was treated with a large amount of ice–water. The product was extracted into benzene, the extract was washed with sodium carbonate solution (100 g/l), then with water, and finally it was dried over sodium sulfate. Removal of the solvent *in vacuo* left an oil (6.83–7.52 g, 70–77%) the i.r. spectrum (neat) of which was devoid of absorptions in the 3600–3200 cm^{-1} region but which had a strong band at 1772 cm^{-1}. This material partially decomposed on distillation and therefore it was used in the next step without purification.

The crude bromo compound (3.31 g, 10.5 mmol) in dimethylsulfoxide (80 ml), was mixed with a solution of sodium azide (6.3 g, 97 mmol) in water (30 ml), and the resultant was heated on a steam bath for 92 h. The solution was poured into a large amount of water, and the product was extracted into ethyl acetate. The extract was washed well with water, dried over sodium sulfate, and evaporated *in vacuo*. The residual oil (2.52–2.84 g, 86–97%) had strong i.r. absorptions (neat) at 2105 and 1768 cm^{-1}, and was used without purification.

*3-Phenyl-3-(2-aminoethyl)phthalide hydrobromide (**6**, R = H)*

A solution of the above azide (8.00 g, 28.7 mmol) in 2-propanol (250 ml) containing 10% palladium-on-charcoal (800 mg), was hydrogenated at room temperature and a hydrogen pressure of 55 p.s.i.g. for 1.5 h. The catalyst was removed by filtration through Celite and the filtrate was concentrated to a volume of *ca.* 50 ml, diluted with ether, and dry hydrogen bromide was bubbled into the solution. The solid was collected by filtration and crystallized from 2-propanol–ether. There was obtained a solid (8.7 g, m.p. 113–116°) which after crystallization from 2-propanol had m.p. 116–118°. The elemental analysis and the n.m.r. spectrum (DMSO-d_6) showed that the salt crystallized with 0.75 mol of 2-propanol.

Anal. Calcd. for $C_{16}H_{15}NO_2$:HBr:0.75 C_3H_8O:C, 57.80; H, 5.85; N, 3.69. Found: C, 57.46; H, 6.09; N, 3.69.

*5-Phenyl-5-hydroxy-2,3,4,5-tetrahydro-1H-2-benzazepin-1-one (**8**, R = H)*

If the 2-propanol solution obtained from the reduction

Can. J. Chem. Downloaded from www.nrcresearchpress.com by 210.87.254.42 on 09/05/12
For personal use only.

Can. J. Chem. Downloaded from www.nrcresearchpress.com by 210.87.254.42 on 09/05/12
For personal use only.

of the azide was evaporated to dryness there was obtained an oil (i.r. (neat) bands at 1765 and 1672 cm^{-1}) which solidified on standing. After 14 h the residue was slurried with benzene and the insoluble solid (71–82% yield), m.p. 129–134° was collected by filtration. A small specimen was rapidly crystallized from acetonitrile to give compound **8** with m.p. 145–147°.

Anal. Calcd. for $C_{16}H_{15}NO_2$: C, 75.87; H, 5.97; N, 5.53. Found: C, 76.13; H, 6.00; N, 5.55.

*3-Phenyl-3-(2-methylaminoethyl)phthalide (**6**, R = CH_3)*

The crude azide **5** (4.94 g, 17.6 mmol) described previously, in dry benzene (130 ml), containing triphenylphosphine (4.62 g, 17.6 mmol) was heated at reflux temperature for 1.5 h. To the cooled solution was added methyl iodide (5.0 g, 35.2 mmol), and reflux temperature was maintained for an additional 2 h. The solvent was removed *in vacuo*, glacial acetic acid (50 ml) and 48% hydrobromic acid (50 ml) were added to the residue, and boiling under reflux was resumed (2.5 h). The solution was concentrated to a small volume *in vacuo*, ice–water was added to the residue, and the mixture was extracted with benzene. The aqueous phase was made basic with sodium carbonate solution (200 g/l), the product was extracted into benzene, the extract was dried and evaporated to a small volume (10–20 ml) *in vacuo*. The solution was diluted with ether and the hydrobromide salt was formed in the usual manner. The salt was crystallized from acetonitrile to give material (3.7 g), m.p. 176–177°.

Anal. Calcd. for $C_{17}H_{17}NO_2$: HBr: C, 58.63; H, 5.21; N, 4.02. Found: C, 58.64; H, 5.13; N, 4.10.

*2-Methyl-5-phenyl-5-hydroxy-2,3,4,5-tetrahydro-1H-2-benzazepin-1-one (**8**, R = CH_3)*

If the benzene solution from the above experiment, containing the secondary amine, was evaporated *in vacuo*, an oil remained (i.r. bands at 1766 and 1636 cm^{-1}) which completely solidified after 24 h. The solid was slurried with ether and collected by filtration. The product, m.p. 136–138°, was obtained in 61% yield. One crystallization from benzene gave material with m.p. 140–141°.

Anal. Calcd. for $C_{17}H_{17}NO_2$: C, 76.38; H, 6.41; N, 5.24. Found: C, 76.43; H, 6.30; N, 5.29.

*5-Phenyl-2,3-dihydro-1H-2-benzazepin-1-one (**9**, R = H)*

Crystalline 5-phenyl-5-hydroxy-2,3,4,5-tetrahydro-1*H*-2-benzazepin-1-one (**8**, 1.2 g, 4.84 mmol) was added all at once at 0° with efficient stirring to concentrated sulfuric acid (40 ml). After 25 min, solution of the solid had been achieved and this was poured slowly with good stirring onto a large amount of ice. The solid was collected by filtration, dried, and then crystallized from benzene. The product **9** (R = H, 795–861 mg, 70–76%) was obtained in two crops, m.p. 230–233° and 227–230°. One additional crystallization gave material with m.p. 233–235°.

Anal. Calcd. for $C_{16}H_{13}NO$: C, 81.67; H, 5.57; N, 5.95. Found: C, 81.37; H, 5.67; N, 5.66.

*2-Methyl-5-phenyl-2,3-dihydro-1H-2-benzazepin-1-one (**9**, R = CH_3)*

(a) By Dehydration of the Corresponding Tetrahydro Alcohol

The dehydration was performed in the same manner as described above for the *N*-unsubstituted compound. Crystallization of the crude product from hexane: benzene (2:1) gave the product (60–64%) in two crops, m.p. 136–137.5° and 131–133°. After recrystallization and then sublimation at 110°/0.001 mm the product had m.p. 136.5–138°.

Anal. Calcd. for $C_{17}H_{15}NO$: C, 81.90; H, 6.06; N, 5.62. Found: C, 81.98; H, 6.02; N, 5.72.

(b) By Alkylation of 5-Phenyl-2,3-dihydro-1H-2-benzazepin-1-one with Methyl Iodide

A 55% suspension of sodium hydride in mineral oil (110 mg) was washed free of the carrier with hexane, layered with dry DMF (15 ml), and cooled with stirring to 0°. The unsubstituted lactam (353 mg) was added all at once, the cooling bath was removed, and when gas evolution was complete, methyl iodide (675 mg, 4.8 mmol) was added. The solution was stirred at room temperature under a slight positive pressure of nitrogen for 18 h, then diluted with water, and extracted with benzene. The extract was dried, evaporated *in vacuo*, and the residue was crystallized from hexane: benzene (2:1). The product **9** (R = CH_3, 283 mg, 76%), m.p. 136–138° was identical in every respect (i.r., n.m.r., mixed melting point) to the product obtained in method (*a*).

*5-Phenyl-2,3,4,5-tetrahydro-1H-2-benzazepin-1-one (**10**, R = H)*

A solution of 5-phenyl-2,3-dihydro-1*H*-2-benzazepin-1-one (**9**, R = H, 235 mg, 1 mmol) in glacial acetic acid (37 ml) containing 60% perchloric acid (1.5 ml) and 10% palladium-on charcoal (50 mg) was hydrogenated at room temperature and an initial hydrogen pressure of 59 p.s.i.g. ($2\frac{1}{4}$ h). The catalyst was removed by filtration through Celite, the filtrate was diluted with water, the product (195 mg) was collected by filtration and dried. After crystallization from benzene:hexane it had m.p. 224–225° (undepressed on admixture with an authentic specimen) and was identical in all respects with the minor product of the Schmidt rearrangement on 4-phenyl-1-tetralone (reported (2) m.p. 226–228°).

1. W. C. CUTTING. Handbook of pharmacology. Third ed. Appleton–Century–Crofts, New York. 1967. p. 570.
2. L. H. WERNER, S. RICCA, A. ROSSI, and G. DESTEVENS. J. Med. Chem. **10**, 575 (1967).
3. M. H. SHERLOCK. U.S. Pat. 3 225 031 (1965); Chem. Abstr. **64**, 9696 (1966). U.S. Pat. 3 242 164 (1966); Chem. Abstr. **64**, 19576 (1966).
4. G. SIMCHIN. Angew. Chem. Intern. Ed. Engl. **7**, 464 (1968).
5. J. R. BROOKS and D. N. HARCOURT. J. Chem. Soc. (C). 625 (1969).
6. H. FUJIMURA and M. HORI. U.S. Pat. 3 409 607 (1968); Chem. Abstr. **70**, 77827*c* (1969).
7. G. N. WALKER and D. ALKALAY. J. Org. Chem. **36**, 461 (1971).
8. C. K. INGOLD. Structure and mechanism in organic chemistry. Second ed. Cornell University Press, Ithaca. 1969.
9. H. E. ZAUGG, D. A. DUNNIGAN, R. J. MICHAELS, I. R. SWETT, T. S. WANG, A. H. SOMMERS, and R. W. DENET. J. Org. Chem. **26**, 644 (1961).
10. H. ZIMMER and G. SINGH. J. Org. Chem. **28**, 483 (1963).

11. E. S. GOULD. Mechanism and structure in organic chemistry. Holt, Rinehart and Winston, New York. 1959.
12. G. E. ULLYOT, J. J. STEHLE, C. L. ZIRKLE, R. L. SHRINER, and F. J. WOLF. J. Org. Chem. **10**, 429 (1945).
13. J. W. WILSON, E. L. ANDERSON, and G. E. ULLYOT. J. Org. Chem. **16**, 800 (1951).
14. G. E. ULLYOT. U.S. Pat. 2 538 431 (1951); Chem. Abstr. **45**, 4271 (1951).
15. T. SZEKI. Ber. ungar. pharm. Ges. **13**, 680 (1937); Chem. Abstr. **31**, 6643 (1937).
16. W. E. PARHAM and E. L. ANDERSON. J. Am. Chem. Soc. **70**, 4187 (1948).
17. T. MOLE. J. Chem. Soc. 2132 (1960).

Can. J. Chem. Downloaded from www.nrcresearchpress.com by 210.87.254.42 on 09/05/12
For personal use only.

The Conformation of Racemic 4,6-Dimethyl Trimethylene Sulfite by Gas Phase Electron Diffraction

FRANK J. MUSTOE AND J. LAWRENCE HENCHER
Department of Chemistry, University of Windsor, Windsor, Ontario

Received December 21, 1971[1]

The molecular geometry of the racemate *trans*-4,6-dimethyl trimethylene sulfite has been studied in the gas phase by electron diffraction. Six trial conformations were examined by least squares fitting of the intensity data. A significance test applied to the fits obtained for each of the six static models tested indicate that the best single representation of the molecule has a chair conformation, although a mixture containing other conformations could not be definitely eliminated. It was not possible to conclusively discriminate between an axial or an equatorial S=O bond, although the axial position is favored. The following bond distances (r_g values) and angles were determined: C—H = 1.119 ± 0.020, C—C = 1.505 ± 0.014, C—O = 1.413 ± 0.013, S=O = 1.480 ± 0.022, S—O = 1.622 ± 0.009 Å; ∠CCO = 111.1 ± 1.3, ∠OS=O = 116.7 ± 1.4, ∠COS = 114.1 ± 1.0, ∠OSO = 100.7 ± 2.0°. The following angles were assumed to be tetrahedral: ∠CCC, ∠HCH, ∠CCH. The errors are estimated to be at the 95% confidence level. The molecular parameters are in agreement with those of trimethylene sulfite.

La géométrie moléculaire du *trans* diméthyl-4,6 triméthylène sulfite racémique a été étudiée en phase gazeuse par diffraction électronique. Six conformations ont été testées par la méthode des ajustements aux moindres carrés sur les données des intensités. Un test significatif appliqué aux ajustements obtenus sur chacun des six modèles statiques montre que l'unique et la meilleure représentation de la molécule possède une conformation chaise, bien qu'un mélange d'autres types de conformations n'ait pu être écarté définitivement. Il n'a pas été possible de trancher de façon concluante entre une liaison S=O axiale ou équatoriale, malgré une position axiale favorisée. Les valeurs suivantes pour les distances et les angles ont été déterminées: C—H = 1.119 ± 0.020, C—C = 1.505 ± 0.014, C—O = 1.413 ± 0.013, S=O = 1.480 ± 0.022, S—O = 1.622 ± 0.009 Å; ∠CCO = 111.1 ± 1.3, ∠OS=O = 116.7 ± 1.4, ∠COS = 114.1 ± 1.0, ∠OSO = 100.7 ± 2.0°. Les angles suivants ont été supposés tétrahédraux: ∠CCC, ∠HCH, ∠CCH. Les erreurs ont été estimées à 5%; les paramètres moléculaires sont en accord avec ceux du triméthylène sulfite.

[Traduit par le journal]

Canadian Journal of Chemistry, **50**, 3892 (1972)

Can. J. Chem. Downloaded from www.nrcresearchpress.com by 210.87.254.42 on 09/05/12
For personal use only.

Introduction

The considerable controversy in recent literature prompted this study of a dimethyl substituted six-membered cyclic sulfite in which steric interactions might be expected to play an important role in determining the conformation. The early literature of trimethylene sulfite and its derivatives is mainly concerned with the orientation of the exocyclic oxygen atom (1–6), although equilibrium mixtures of conformers are suggested (7, 8). The positioning of the exocyclic oxygen has since been shown to be axial in solution studies (9–12), in X-ray diffraction of solid crystals (13, 14), and in the gas phase by electron diffraction (15).

The first isomers of trimethylene sulfite substituted in the 4- and 6-positions were isolated by Lauterbur *et al.* (3) who, on the basis of i.r. and n.m.r. spectra assigned the racemic isomer a chair form with equatorial S=O. Overberger *et al.* (8) concluded from temperature dependance of the n.m.r. and i.r. spectra that a conformational mixture of chair forms (S=O axial and S=O equatorial) was present with S=O axial predominating. From spectral studies and dipole moments, Wucherpfennig (16) proposed a mixture of twist and perhaps chair forms. A previous spectral study (17) of the analogous racemic 4,6-diisopropyl trimethylene sulfite was in favor of the twist form. Wyn-Jones and coworkers (18–21) have used ultrasonic techniques to study various sulfites and have concluded that anancomeric equilibria of inverting chair conformations are present. Finally, Wood and Miskow (22) favor a distorted chair or flexible form for the racemic isomer and have reinterpreted the ultrasonic results to agree with that viewpoint (23, 24).

Experimental

A gas chromatographically pure sample of the racemic compound was provided by Dr. M. H. Miskow (23).

[1]Revision received August 15, 1972.

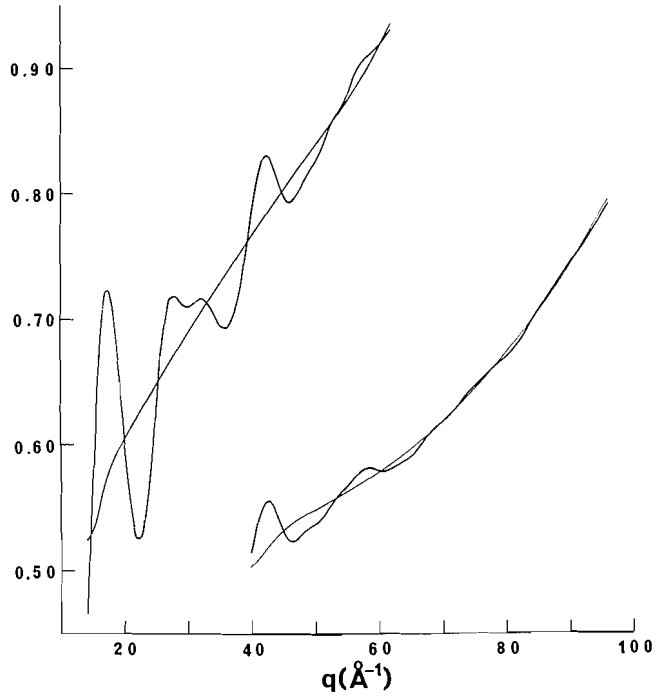

FIG. 1. The experimental intensity and background curves for racemic 4,6-dimethyl trimethylene sulfite, data set I.

Can. J. Chem. Downloaded from www.nrcresearchpress.com by 210.87.254.42 on 09/05/12
For personal use only.

Sectored electron diffraction photographs were recorded on the Cornell apparatus (25). A suitable vapor pressure was obtained with the sample at a temperature about 10 °C lower than that of the nozzle which was at 130 °C as measured by an attached thermocouple. Optical densities as a function of radial position were obtained with a digitized microphotometer (27). The data reduction procedure was that of Bauer and co-workers (26, 27), using the Hartley modification to the least square procedure (28) and a weight matrix that includes the first off-diagonal terms (29). Anharmonicity corrections were made for bonded atom pairs (30).

Results

Experimental relative intensities of four plates were obtained, covering the ranges $q = 14$–96 Å^{-1} (data set I) and $q = 6$–93 Å^{-1} (data set II), where $q = (40/\lambda) \sin(\theta/2)$, λ is the electron wavelength, and θ the scattering angle. Both sets of data have been placed in the Depository of Unpublished Data[2], and the intensities for data set I are plotted with the refined backgrounds in Fig. 1.

Six conformations, described using Hilderbrandt's algorithm (31), were tested against the experimental reduced intensity $(\pi/10)(qM_{expt}(q))$ by the method of least squares. The conformations were labelled **A** through **F** and are presented in Fig. 2. A larger drawing of model **A** with numbered atoms is shown in Fig. 3. The endocyclic carbon atoms and their attached hydrogen atoms were positioned routinely by means of C—C, C—H, and $\angle$CCH = $\angle$CCC = $\angle$HCH. The endocyclic oxygens were positioned by means of C—C, C—O, $\angle$CCC, $\angle$CCO and the angle τOCC (*e.g.* the nonvalence angle between C_4—C_5 and C_6—O_1. A value of zero for τOCC would correspond to these oxygens lying in the plane formed by $C_4C_5C_6$). The position of the sulfur atom was obtained using the distance $C_5 \ldots S_2$ (parameter C ... S) and angle $H_1C_5S_2$ (parameter $\angle$SCH). This ensures that both S—O lengths are equivalent and conveniently allows the boat or chair conformations to be determined primarily by the value of $\angle$SCH. The twist forms were obtained by rotating the C—O bonds against each other by means of τOCC (See Fig. 2). Due to the complexity of the molecule it was assumed

[2]Both sets of data are available at a nominal charge, from the Depository of Unpublished Data, National Science Library, National Research Council of Canada, Ottawa, Canada K1A 0S2.

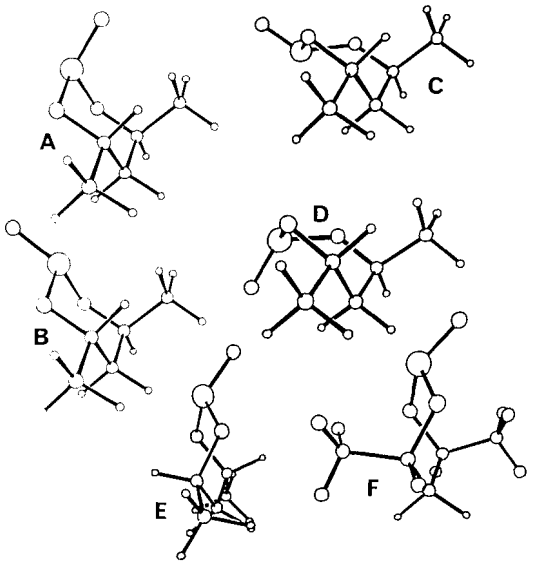

FIG. 2. The six different conformations analyzed by least square fitting of the reduced experimental molecular scattering curve.

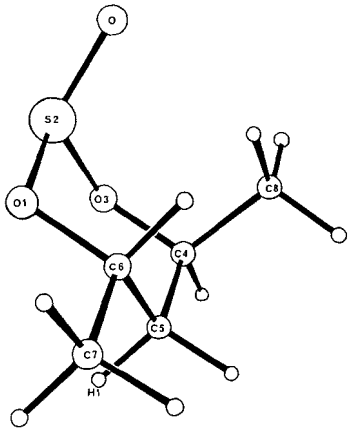

FIG. 3. The conformation, with numbered atoms, for model A.

that all CCH, HCH, and CCC angles were tetrahedral, and that the endo- and exocyclic CCO angles were equivalent.

The selection of initial parameter values for

TABLE 1. The structural parameters* and standard deviations obtained from independent least squares fits to data set I (q = 14–96 Å^{-1}) and data set II (q = 6–93 Å^{-1}) for model **A**

	Data set I		Data set II		
Parameter	Value	σ	Value	σ	Weighted value†
C—H	1.125	0.0058	1.106	0.0090	1.119
C—C	1.505	0.0044	1.505	0.0049	1.505
C—O	1.411	0.0035	1.417	0.0058	1.413
S=O	1.479	0.0068	1.481	0.0081	1.480
∠CCO	111.2	0.3956	110.9	0.5199	111.1
∠OS=O	116.8	0.3942	116.4	0.6247	116.7
C...S	3.002	0.0185	3.011	0.0106	3.009
∠SCH	101.8	0.7508	101.2	0.2356	100.3
∠OCC	58.8	0.9246	59.8	0.2847	59.7
Redundant parameters					
S—O	1.621	0.0032	1.623	0.0026	1.622
∠COS	114.0	0.2481	114.9	0.5894	114.1
∠OSO	100.7	0.5815	100.8	0.8304	100.7
R‡	0.0646		0.1010		

*Bond lengths are r_g values in Å, angles are in degrees. The following angles were constrained to be tetrahedral: ∠CCC, ∠CCH, ∠HCH.

†The values are weighted by the standard deviations:

$$x = \frac{\sum_i (x_i/\sigma_i^2)}{\sum_i (1/\sigma_i^2)}$$

‡
$$R = \left[\frac{\sum_q \left(\frac{\pi}{10} qM(q)_{\text{expt}} - \frac{\pi}{10} qM(q)_{\text{theor}} \right)^2 \cdot W_q}{\sum_q \left(\frac{\pi}{10} qM(q)_{\text{expt}} \right)^2 \cdot W_q} \right]^{1/2}$$

Can. J. Chem. Downloaded from www.nrcresearchpress.com by 210.87.254.42 on 09/05/12
For personal use only.

TABLE 2. Interatomic distances* and mean square amplitudes† for model A‡

	O	O-1	S-2	O-3	C-4	C-5	C-6	C-7	C-8
O	0.0	2.642 (0.060)	1.479 (0.047)	2.642 (0.060)	3.247 (0.121)	3.875 (0.121)	3.247 (0.121)	4.587 (0.121)	2.965 (0.121)
O-1		0.0	1.621 (0.049)	2.497 (0.070)	2.850 (0.121)	2.406 (0.075)	1.411 (0.050)	2.406 (0.750)	3.493 (0.121)
S-2			0.0	1.621 (0.049)	2.546 (0.083)	3.002 (0.121)	2.546 (0.083)	3.892 (0.121)	2.996 (0.121)
O-3				0.0	1.411 (0.050)	2.406 (0.075)	2.850 (0.121)	4.250 (0.121)	2.406 (0.075)
C-4					0.0	1.505 (0.050)	2.455 (0.082)	3.786 (0.121)	1.505 (0.050)
C-5						0.0	1.505 (0.050)	2.458 (0.082)	2.458 (0.082)
C-6							0.0	1.505 (0.050)	2.928 (0.121)
C-7								0.0	4.273 (0.121)
C-8									0.0

*These are r_g values, in Å.

†The *lij* values presented in this table were determined during previous least squares analysis and were constrained during the later stages of refinement. Mean square amplitudes involving hydrogen were as follows: C—H = 0.080; H... H = 0.120; with geminal C or O atom = 0.100; with all other heavy atoms = 0.150; all long H... H distances = 0.200. All values are in Å.

‡The conformation and designation of the atoms corresponds to Fig. 3. The distances presented above were calculated for this conformation using the parameter values listed for data set I in Table 1.

least squares refinement was straight forward for the bond lengths and valence angles. However, initial values of ∠SCH, C... S, and τOCC had to be found by trial and error in order that the redundant parameters ∠COS, ∠OSO, and S—O would have reasonable starting values, as calculated from the interatomic distance matrix. In order to test each conformation it was necessary to attempt a refinement of as many parameters as possible, although under these conditions large correlation coefficients were found between the parameters and convergence was difficult to obtain.

Radial distribution curves were calculated using a value of 0.0025 for the Degard damping constant. Only the contributions due to C—H and S—O were clearly resolved. By fitting the intensity curves we find two solutions for each of the chair models, placing the S—O distance at 1.62 Å. The parameter values obtained when both sets of data were treated independently for the preferred chair form of model **A** are given in Table 1. The corresponding interatomic distances and mean square amplitudes of vibration for the heavy atoms are given in Table 2 and the correlation coefficients between the parameters in this solution are listed in Table 3. Some of the parameters are highly correlated, and although convergence was not obtained, the parameter values were oscillating with amplitudes less than the given uncertainties.

The alternate form of model **A**, again refined independently from the two sets of data, gave valence parameter values in close agreement with each other, and within the errors given for the preferred model, with the exceptions of ∠OS=O, ∠COS, and ∠OSO. For these respective parameters we determined the values 107.9, 117.9, and 106.9° from data set I ($R = 0.0846$) and 108.6, 118.3, and 106.1° from data set II ($R = 0.0986$). Although the fit to data set II for this form is better than that given in Table 1, it is not significantly so (32, 33), and the values for ∠OS=O are smaller than expected.

A similar result was obtained for model **B**, the chair form with equatorial S=O bond, although the best fits to both data sets were obtained with parameter values similar to those discussed above for the alternate form of model **A**. These results are presented in Table 4. On comparing

Can. J. Chem. Downloaded from www.nrcresearchpress.com by 210.87.254.42 on 09/05/12
For personal use only.

TABLE 3. Correlation matrix for model A*

	C—H	C—C	C—O	∠CCO	τOCC	C...S	∠SCH	S=O	∠OS=O
σ	0.0058	0.0044	0.0035	0.3956	0.9246	0.0185	0.7508	0.0068	0.3942
C—H	1	−0.01	0.05	0.10	−0.02	0.00	−0.01	0.04	−0.02
C—C		1	0.36	−0.86	−0.70	0.77	−0.69	−0.89	0.53
C—O			1	−0.51	−0.25	0.41	−0.26	−0.44	0.30
∠CCO				1	0.60	−0.78	0.58	0.84	−0.37
τOCC					1	−0.94	0.98	0.69	−0.20
C...S						1	−0.90	−0.74	0.17
∠SCH							1	0.68	−0.24
S=O								1	−0.64
∠OS=O									1

*The individual standard deviations are given by

$$\sigma = \left[\frac{B_{ii}^{-1} V' W V}{n - m}\right]^{1/2}$$

and the correlation coefficients by

$$\rho_{ij} = \frac{B_{ij}^{-1}}{(B_{ii}^{-1} B_{jj}^{-1})^{1/2}}$$

TABLE 4. The structural parameters and standard deviations obtained from independent least square fits to data set I and data set II for model **B**

	Data set I		Data set II		
Parameter	Value	σ	Value	σ	Weighted value
C—H	1.117	0.0075	1.101	0.0083	1.110
C—C	1.512	0.0036	1.514	0.0039	1.513
C—O	1.427	0.0060	1.428	0.0062	1.427
S=O	1.469	0.0070	1.473	0.0078	1.471
∠CCO	108.8	0.4288	109.1	0.4726	108.9
∠OS=O	108.3	0.4747	109.3	0.5645	108.7
C...S	2.983	0.0120	2.992	0.0139	2.987
∠SCH	89.9	0.7228	88.9	0.8770	89.5
τOCC	66.1	0.7332	65.9	0.8805	66.0
Redundant parameters					
S—O	1.621	0.0024	1.626	0.0028	1.623
∠COS	119.3	0.5833	120.3	0.6766	119.7
∠OSO	105.8	0.8430	106.0	0.9095	105.9
R	0.0746		0.0863		

Tables 1 and 4 it is evident that the differences in the chair forms are due largely to the parameters ∠SCH and τOCC. Transferring the parameters given in Table 1 as an initial structure for model **B**, we find that allowing the valence and conformational determining parameters to vary results in solutions with valence parameters as given in Table 1, within the given errors, with the exception of ∠OSO. Data sets I and II yield values of 92.4 and 91.0° respectively for ∠OSO, values which are approximately 10° less than the similar angle determined in trimethylene sulfite (13, 15) and 2,2′-dichloro trimethylene sulfite (14).

The boat forms **C** and **D** were analyzed using data set I only. The best fits obtained for these conformations had *R* values of 0.1878 and 0.2186 respectively, and the hypothesis that they were significant compared to A was rejected at the 99% confidence level (32, 33). Partially twisted boat conformations did not successfully refine, hence the completely twisted forms **E** and **F** were assumed by constraining the sulfur atom to the position shown in Fig. 2 by means of ∠SCH = 125.25°. Model **E** was analyzed using data set I only and refined to a set of valence parameter values consistent with those of Table 1, ($R = 0.1701$) but was likewise re-

Can. J. Chem. Downloaded from www.nrcresearchpress.com by 210.87.254.42 on 09/05/12
For personal use only.

Can. J. Chem. Downloaded from www.nrcresearchpress.com by 210.87.254.42 on 09/05/12
For personal use only.

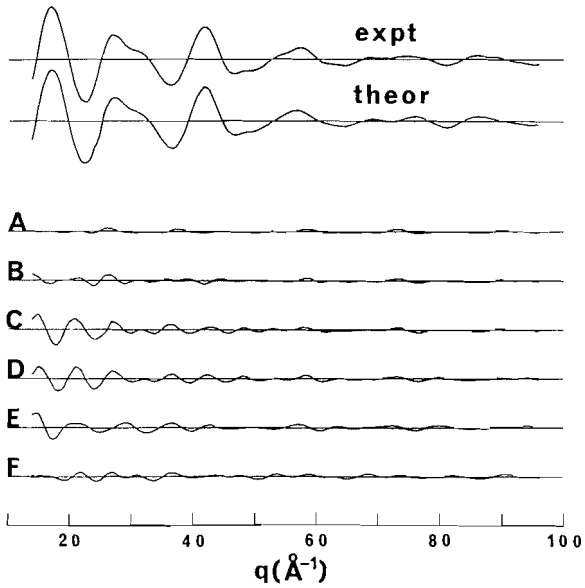

FIG. 4. The reduced experimental molecular scattering curve, the corresponding theoretical curve calculated for model A, and the difference curves (experimental – theoretical) for models **A** through **F**, data set I.

jected. Model **F** was analyzed using both data sets, ($R = 0.1101$ for set I and $R = 0.1469$ for set II) and was also rejected at the 99% confidence level (32, 33).

The experimental reduced intensity $(\pi/10)(qM_{expt}(q))$ is compared with $(\pi/10)(qM_{theor}(q))$ for **A** in Fig. 4 along with the difference curves for **A** through **F**. The corresponding radial distribution curves calculated from the reduced intensity curves are presented in Fig. 5 for the region of structural interest. The full experimental radial distribution curve is compared with that calculated for model A in Fig. 6.

Discussion

While the analyses of the two sets of data are consistent in that the parameter values obtained for models **A**, **B**, and **F** are the same, within calculated errors, the normalized standard deviations for models **A** and **B** are not consistent: for data set I the lowest value for R is given by model **A**, the chair form with axial S=O bond, while for data set II the lowest value for R is given by model **B**, a chair form having different ring valence angles than those of model **A**, with an equatorial bond. However, the R factor ratio

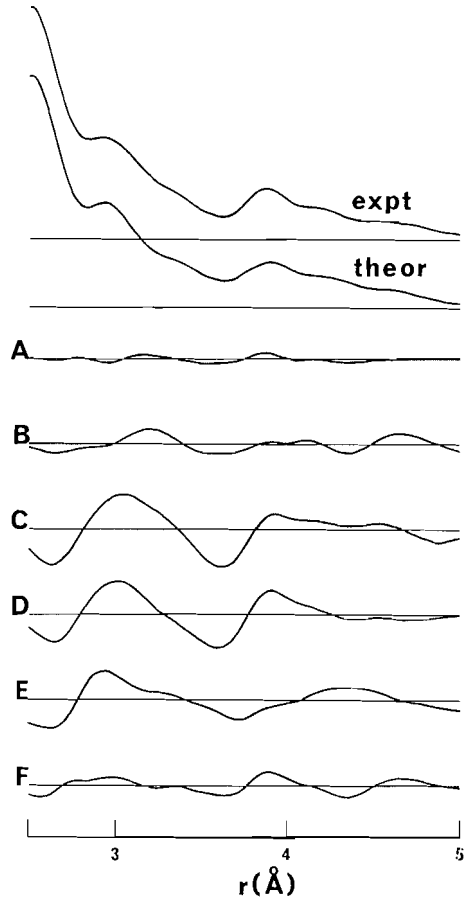

FIG. 5. The experimental radial distribution function in the region of structural interest, together with the corresponding theoretical function for model **A** and the difference curves (experimental – theoretical) for models **A** through **F**.

$0.0746/0.0646 = 1.155$ for the two fits to data set I does not allow us to statistically reject the hypothesis that model **B** is an acceptable solution at the 1% level of significance for this data (32, 33).

We tested the tetrahedral constraint on ∠CCC for model **A** and data set I. Using the parameters of Table 1 as an initial model, we found a minimum ($R = 0.0585$) with the exocyclic ∠CCC = 111.1° and the endocyclic angle = 106.6°. As a second test we constrained ∠CCC at 110.5° and obtained a fit with $R = 0.0704$. In both cases the other parameters were unchanged, within the estimated errors, and the addition of ∠CCC to the varied parameters, or the change in the value of the constraint, does not make a

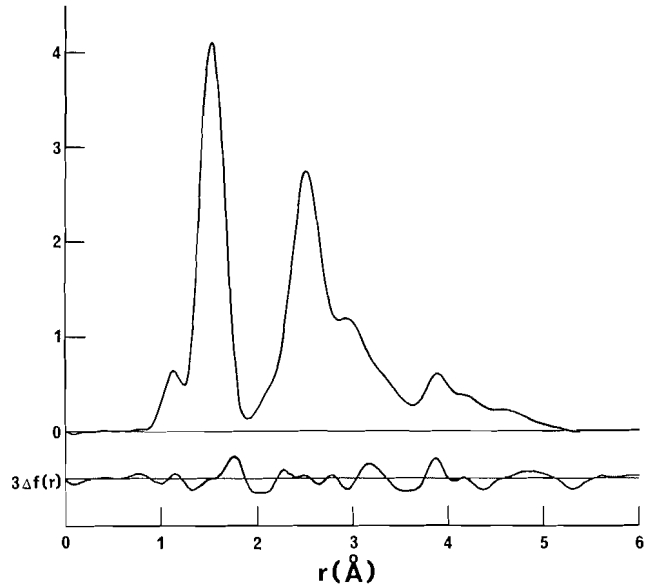

FIG. 6. The refined experimental radial distribution curve. $\Delta f(r) = [f(r)_{expt} - f(r)_{theor}]$.

TABLE 5. Comparison of the molecular parameters* for racemic 4,6-dimethyl trimethylene sulfite with trimethylene sulfite (TMS) and 2,2′-dichlorotrimethylene sulfite (DTA)

Parameter	Model **A**	Model **B**	Electron diffraction TMS (15)	X-Ray TMS (13)	X-Ray DTS (14)
C—H	1.119±0.020(0.08)	1.110±0.023	1.12 (assumed) (0.08)	—	—
C—C	1.505±0.014(0.05)	1.513±0.011	1.52±0.02(0.049)	1.52±0.018	1.523±0.008
C—O	1.413±0.013(0.05)	1.427±0.018	1.42±0.02(0.049)	1.46±0.015	1.462±0.007
S=O	1.480±0.022(0.05)	1.471±0.022	1.45±0.02(0.049)	1.45±0.011	1.442±0.006
S—O	1.622±0.009(0.05)	1.623±0.007	1.62±0.01(0.055)	1.60±0.008	1.622±0.004
∠CCC	109.5 (assumed)	109.5 (assumed)	110±3	110±1.3	110.6±0.6
∠CCO	111.1±1.3	108.9±1.3	112±3	109±1.2	108.8±0.4
∠OSO	100.7±2.0	105.9±2.6	99±2	100±0.6	97.8±0.3
∠COS	114.1±1.0	119.7±1.9	113±2	116±0.7	116.2±0.3
∠OS=O	116.7±1.4	108.7±1.5	113.5±3	107±0.4	107.2±0.2

*Bond lengths in Å, angles in degrees. The mean square amplitudes of vibration are given in parentheses.

significant difference to the fit obtained. We therefore conclude that ∠CCC might well be a degree or so larger than tetrahedral.

A more serious constraint in our analysis was the use of the same mean square amplitudes of vibration for all the models. The mean square amplitudes given in Table 2 are certainly not unique, and we would expect different results depending on the values used. However, it is beyond the capabilities of our experiment to determine the non-bonded amplitudes for this molecule, so we have assumed a reasonable set of values and admit that an alternate set might give an improved fit to any of the models tested, although it is highly unlikely that the rejected models would become statistically significant.

The parameter values for models **A** and **B** are again listed and compared with the values in trimethylene sulfite (13, 15) and 2,2′-dichlorotrimethylene sulfite (14) in Table 5. The errors given for the two models in the present work are three times the calculated uncertainties and are estimated to be at the 95% confidence level and to include systematic errors. It can be seen that

Can. J. Chem. Downloaded from www.nrcresearchpress.com by 210.87.254.42 on 09/05/12
For personal use only.

model **A** agrees reasonably well with the electron diffraction results for the unsubstituted molecule, while model **B** compares more favorably with the X-ray results, particularly in that ∠COS is much larger than ∠OS=O. This is an unexpected trend, and we note that in model **A** the peak in the radial distribution curve just less than 4 Å is due to the exocyclic oxygen to carbon distances. When this oxygen is placed in the equatorial position, as in model **B**, it is precisely these distances which change the most. It is therefore reasonable to assume, as Naumov and co-workers have pointed out (15), that the ∠OS=O would tend to become much smaller than that determined for an axial S=O model in an effort to make these distances the same as before.

In summary, the electron diffraction data are not consistent with a static boat, or fully twisted conformation for racemic 4,6-dimethyl trimethylene sulfite. Although the available evidence favors a chair form with an axial S=O bond, the equatorial form, or mixture of conformers, could not be definitely eliminated.

We extend our thanks to Professor S. H. Bauer for the use of experimental facilities, and to Dr. M. H. Miskow for providing a sample of the compound. The financial support of the National Research Council of Canada is gratefully acknowledged.

1. P. B. D. DE LA MARE, W. KLYNE, D. J. MILLEN, J. G. PRITCHARD, and D. WATSON. J. Chem. Soc. 1813 (1956).
2. J. G. PRITCHARD and R. L. VOLLMER. J. Org. Chem. **28**, 1545 (1963).
3. P. C. LAUTERBUR, J. G. PRITCHARD, and R. L. VOLLMER. J. Chem. Soc. 5307 (1963).
4. D. G. HELLIER, J. G. TILLETT, H. F. VAN WOERDEN, and R. F. M. WHITE. Chem. Ind. (London), 1956 (1963).
5. R. S. EDMUNDSON. Tetrahedron Lett. 1649 (1965).
6. H. F. VAN WOERDEN. Tetrahedron Lett. 2407 (1966).
7. B. A. ARBUZOV. Bull. Soc. Chim. Fr. 1311 (1960).
8. C. G. OVERBERGER, T. KURTZ, and S. YAROSLAVSKY. J. Org. Chem. **30**, 4363 (1965).
9. H. F. VAN WOERDEN. Ph.D. Thesis. Leiden, 1964.
10. H. F. VAN WOERDEN and E. HAVINGA. Rec. Trav. Chim. **86**, 341 (1967).
11. H. F. VAN WOERDEN and E. HAVINGA. Rec. Trav. Chim. **86**, 353 (1967).
12. D. G. HELLIER. Ph.D. Thesis. University of London, London, England, 1966.
13. C. ALTONA, H. J. GIESE, and C. ROMERS. Rec. Trav. Chim. **85**, 1197 (1966).
14. J. W. L. VAN OYEN, R. C. D. E. HASEKAMP, G. C. VERSCHOOR, and C. ROMERS. Acta Cryst. **B24**, 1471 (1968).
15. V. A. NAUMOV, N. M. ZARIPOV, and L. F. SHATRUKOV. Zh. Strukt. Khim. **8**, 291 (1967).
16. W. WUCHERPFENNIG. Justus Liebigs Ann. Chem. **737**, 144 (1970).
17. L. CAZAUX and P. MARONI. Tetrahedron Lett. 3667 (1969).
18. R. PETHRICK, E. WYN-JONES, P. HAMBLIN, and R. WHITE. J. Mol. Struct. **1**, 333 (1967–1968).
19. (*a*) R. A. PETHRICK, E. WYN-JONES, P. HAMBLIN, and R. WHITE. Trans. Faraday Soc. **66**, 310 (1970); (*b*) E. WYN-JONES and R. A. PETHRICK. *In* Topics in stereochemistry. Vol. 5. *Edited by* E. L. Eliel and W. L. Allinger. Interscience, New York, N.Y. 1970. p. 205.
20. R. A. PETHRICK, E. WYN-JONES, P. C. HAMBLIN, and R. F. M. WHITE. J. Chem. Soc. *A*, 2552 (1969).
21. R. A. PETHRICK and E. WYN-JONES. Quart. Rev. (London), **23**, 304 (1969).
22. G. WOOD and M. H. MISKOW. Tetrahedron Lett. **14**, 1109 (1969).
23. M. H. MISKOW. Ph.D. Thesis. University of Windsor, Windsor, Ontario, 1971.
24. G. W. WOOD, J. M. MCINTOSH, and M. H. MISKOW. Can. J. Chem. **49**, 1202 (1971).
25. S. H. BAUER and K. KIMURA. J. Phys. Soc. Jap. **17**, 300 (1962).
26. J. L. HENCHER and S. H. BAUER. J. Am. Chem. Soc. **89**, 5527 (1967).
27. W. HARSHBARGER, G. LEE, R. F. PORTER, and S. H. BAUER. Inorg. Chem. **8**, 1683 (1969).
28. T. G. STRAND, D. A. KOHL, and R. A. BONHAM. J. Chem. Phys. **39**, 1307 (1963).
29. Y. MURATA and Y. MORINO. Acta Cryst. **20**, 605 (1966).
30. L. S. BARTELL. J. Chem. Phys. **23**, 1219 (1955).
31. R. L. HILDERBRANDT. J. Chem. Phys. **51**, 1654 (1969).
32. W. C. HAMILTON. Statistics in physical science. The Ronald Press Company, New York. 1964.
33. W. C. HAMILTON. Acta Cryst. **18**, 502 (1965).

Can. J. Chem. Downloaded from www.nrcresearchpress.com by 210.87.254.42 on 09/05/12
For personal use only.

Cancentrine. IV. Acetolysis Products of Cancentrine Methiodide

R. RODRIGO AND R. H. F. MANSKE
Department of Chemistry, University of Waterloo, Waterloo, Ontario
AND
V. SMULA, D. B. MACLEAN, AND L. BACZYNSKYJ
Department of Chemistry, McMaster University, Hamilton, Ontario
Received August 2, 1972

Treatment of cancentrine methiodide with boiling acetic anhydride in the presence of sodium acetate gave two highly unsaturated products formed in rearrangement reactions. One of the products retained all the original carbon and both nitrogen atoms of cancentrine while the other formed with loss of three carbon atoms and one nitrogen atom. The structures of the two compounds were deduced through analysis of their p.m.r. spectra and through comparison of their p.m.r. and u.v. spectra with those of model compounds synthesized in this study. A mechanism for the formation of the rearrangement products is proposed and discussed.

Le traitement du méthyliodure de la cancentrine par l'anhydride acétique bouillant, en présence d'acétate de sodium, conduit à deux produits hautement insaturés issus de réactions de réarrangement. L'un des produits conserve tous les atomes de carbone originaux et les deux atomes d'azote de la cancentrine tandis que l'autre perd trois atomes de carbone et un d'azote. Les structures des deux composés ont été déduites à partir de leurs spectres r.m.n. et par comparaison de leurs spectres r.m.n. et u.v. avec ceux de composés modèles synthétisés au cours de cette étude. Un mécanisme pour la formation de produits réarrangés a été proposé et discuté. [Traduit par le journal]

Canadian Journal of Chemistry, **50**, 3900 (1972)

Can. J. Chem. Downloaded from www.nrcresearchpress.com by 210.87.254.40 on 09/05/12
For personal use only.

The structure of cancentrine (**1**) a novel dimeric alkaloid from *Dicentra canadensis* Walp. was recently determined by a combination of physical and chemical methods (1). One of the first items of chemical evidence obtained concerning its structure came from the reaction of cancentrine methiodide with acetic anhydride and sodium acetate. We now report the results of our investigation of this acetolysis reaction and the structures of the products obtained.

Cancentrine methiodide, when refluxed with acetic anhydride and sodium acetate for *ca.* 48 h, produced two compounds to which we assign structures **3** and **4**. The i.r. spectrum of **3** lacked the characteristic carbonyl absorption of cancentrine and its derivatives at 1660 ± 5 cm^{-1} but had strong absorption at 1765 cm^{-1} indicative of a phenyl acetate. The u.v. spectrum was complex and bore no similarity to the now familiar spectra of cancentrine and its derivatives. The mass spectrum of **3** provided little structural information but had intense ions at *m/e* 615 (58),[1] 573 (44), 531 (100), and 43 (50). The mass of the molecular ion at *m/e* 615 corresponds in composition to $C_{37}H_{29}NO_8$ (h.r.m.s.) and this formula was confirmed by elemental analysis of **3**. The ions at *m/e* 573 and 531 arise from the successive loss of ketene from the molecular ion and merely indicate the presence of two acetate groups in the molecule.

The p.m.r. spectrum of **3**, to be examined in detail later, confirmed the presence of two phenyl acetate groups and also indicated that the molecule contained three methoxyl groups and ten aromatic protons. Besides these absorptions there were two triplets of two protons each, centered at 2.92 and 4.16 δ constituting an A_2X_2 system (confirmed by decoupling).

Compound **3** upon hydrolysis with potassium hydroxide and methylation with diazomethane yielded a pentamethoxy compound **5** with the expected p.m.r. properties. The mass spectrum of **5** had the molecular ion at *m/e* 559 (100) corresponding in mass to the formula, $C_{35}H_{29}NO_6$ (h.r.m.s.) and an intense *m/2e* ion at 279.5 but nothing else of significance.

Thus it was clear from the preliminary data on **3** that extensive changes have taken place in the reaction of the methiodide with acetic anhydride – sodium acetate. These changes may

[1]Ion intensities are in parentheses.

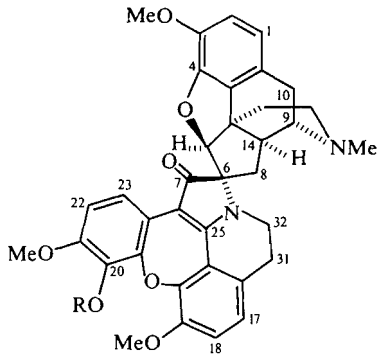

1 R = H
2 R = Ac

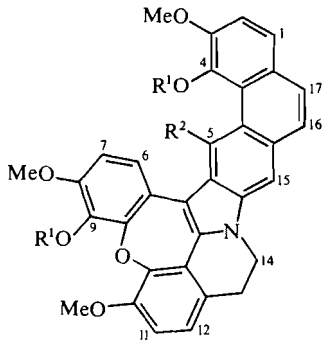

3 R′ = Ac; R^2 = H
4 R′ = Ac; R^2 = $CH_2CH_2N(Me)Ac$
5 R′ = Me; R^2 = H

be summarized as follows: (*i*), the carbonyl group and the characteristic chromophore of cancentrine of which it was a part had been destroyed; (*ii*), extensive aromatization had taken place; and (*iii*), cancentrine, $C_{36}H_{34}N_2O_7$, had been converted to the equivalent of $C_{33}H_{25}NO_6$ (*i.e.* **3** less two acetyl groups) in the overall process indicating that the elements of C_3H_9NO had been lost in the conversion. A search was therefore launched for other products of the reaction and *N*-methylethanolamine was successfully isolated from the aqueous extract after a prior saponification, and characterized as its chloroaurate. Since the acetolysis had been carried out with cancentrine methiodide this result meant that an *N*-demethylation had also been effected under the conditions. Such *N*-demethylations of quaternary metho salts by acetate ion have been studied (2) in many systems. These findings suggested the presence of a morphine-like moiety in cancentrine because the loss of the *N*-methyl ethanamine bridge (C_3H_7N) and a suitably placed oxygen function (as the equivalent of H_2O) is normally observed during the acetolysis of most morphine alkaloids (3). Meanwhile the structure of cancentrine was established by other methods (4) so that it was possible to proceed with the investigation of the structures of **3** and **4**.

The aromatic region of the p.m.r. spectrum of **3** determined at 220 MHz showed the presence of four AB quartets and two singlets (Fig. 1). One of the singlets at extremely low field (9.90 δ in **3** and 10.26 δ in **5**) is crucial to the structural arguments subsequently presented for both **3** and **4**. Previous studies of the p.m.r. spectra of condensed polycyclic benzenoid aromatic systems have shown that "bay" protons absorb at unusually low fields due to ring current effects and/or a variety of local influences. Some of the latter possibilities that have been explored are mutual van der Waals interactions, deshieldings due to σ-bond anisotropies, and electric field effects (5 and references therein). In any event, the 4- and 5-protons of phenanthrene (**6**) resonate at *ca.* 8.7 δ (5) while the 14-hydrogen of benz(*a*,*j*)anthracene (**7**) appears at 9.97 δ (6). This prompted the idea that the low field proton of **3** is in a similar environment. Cancentrine *O*-acetate (**2**) contains three pairs of ortho aromatic protons which appear as AB quartets in its p.m.r. spectrum (1); the presence of a fourth AB quartet in the product is easily accounted for by aromatization at the 9,10 position of **2**. Thus structure **3** can be derived for the first acetolysis product, the singlets at 9.90 and 7.72 δ being ascribed to C-5 and -15 protons, respectively, and the $—CH_2—CH_2—$ unit at C-13, -14 being responsible for the A_2X_2 system. The structure is supported by the detection of significant nuclear Overhauser effects (n.O.e.) in the C-5 proton when the acetate methyl groups of **3** (14%) and the *O*-methyl groups of **5** (18%) were saturated.

The second acetolysis product **4** had the molecular formula $C_{42}H_{38}N_2O_9$ (h.r.m.s., elemental analysis) which is greater than **3** by C_5H_9NO. This suggests the presence of an acetylated *N*-methylethanamine side chain in **4**.

Can. J. Chem. Downloaded from www.nrcresearchpress.com by 210.87.254.40 on 09/05/12
For personal use only.

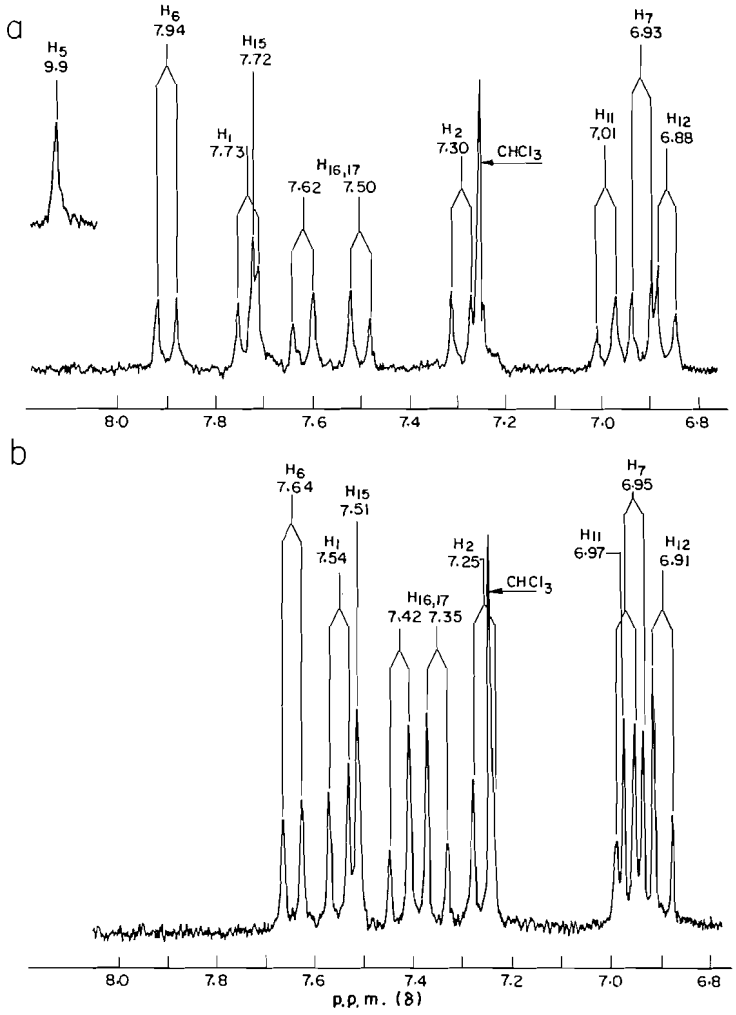

FIG. 1. The aromatic region of the 220 MHz p.m.r. spectrum of (*a*) **3**, (*b*) **4** (at 95°).

The mass spectrum of **4** contained ions corresponding to the presence of precisely such a structural unit as well as two *O*-acetyl groups. Thus there were ions at *m/e* 714 (12), 672 (20), 630 (42), 544 (50), 542 (100), 100 (11), 86 (10), and 44 (36). These correspond to M^+, $[M - CH_2CO]^+$, $[M - 2 \times CH_2CO]^+$, $[M - 2 \times CH_2CO - CH_2N(Me)Ac]^+$, $[M - 2 \times CH_2CO - CH_2N(Me)Ac - 2H]^+$, $[CH_2CH_2N(Me)Ac]^+$, $[CH_2{=}N^+MeAc]$, and $[CH_2{=}\overset{+}{N}HMe]$ respectively. Again, as in **3** there were no significant fragments corresponding to the fission of the ring system. The i.r. spectrum, in accord with the foregoing evidence, showed absorption corresponding to the presence of phenyl-acetate (1765 cm^{-1}) and amide (1630 cm^{-1}) carbonyl groups.

The room temperature p.m.r. spectrum of **4** was very complex. The spectrum was dramatically simplified however when determined at higher temperature. This behavior is attributable to conformational isomerism, and complete coalescence of peaks due to the various conformers takes place only at about 95° indicating that a considerable barrier to rotation about the C—N bond exists in this compound. Similar behavior has been observed before, in a related phenanthrene **8** (7).

Can. J. Chem. Downloaded from www.nrcresearchpress.com by 210.87.254.40 on 09/05/12
For personal use only.

Can. J. Chem. Downloaded from www.nrcresearchpress.com by 210.87.254.40 on 09/05/12
For personal use only.

The spectrum of **4** (at 95°) had seven three-proton singlets, six of which were readily assigned to three *O*-methyl (3.88, 3.94, and 3.96 δ) two *O*-acetyl (2.26 and 2.44 δ), and one *N*-acetyl group (2.15 δ). The other singlet at unusually high field (1.30 δ) was tentatively attributed to the *N*-methyl group. The p.m.r. spectrum also indicated the presence of eight aliphatic and nine aromatic protons. The aromatic region of the spectrum was very similar to that of **3** with the significant exception that it lacked the low field singlet of the latter (Fig. 1).

The ethanamine side chain was therefore placed at C-5 and in a model of **4** so constructed it is found that the *N*-methyl group is forced into the shielding zone of the aromatic system accounting for its unusually high chemical shift.

It is possible to assign the signals in the aromatic regions of the p.m.r. spectra of **3** and **4** by comparison with the spectra of phenanthrene (5) and cancentrine-*O*-acetate (1). In both compounds every aromatic signal had been unambiguously assigned.

Thus signals in the dibenzoxepine part of **3** and **4** are assigned by comparison with cancentrine-*O*-acetate (**2**) and signals of the phenanthrene part by comparison with phenanthrene (**6**). The results are recorded in Table 1. Good qualitative correspondence is found for the signals of the phenanthrene part of **3** and **4** with **6** when allowance is made for the increasing substitution of the phenanthrene moiety in the order **6** < **3** < **4**. The assignment of the resonances of H_{16} and H_{17} in **3** and **4** is based on the small separation between them ($\Delta\nu = 0.12$ and 0.07 p.p.m. respectively). In many phenanthrenes the corresponding H_9 and H_{10} protons have identical chemical shifts and appear in the spectra as two-proton singlets (5). There is excellent agreement between the values for H_{11} and H_{12} of **3** and **4** with the corresponding values of H_{18} and H_{17} of **2**. However, discrepancies are found in the resonances of H_6 and H_7. The reasons for these are not immediately apparent but must be related to the serious crowding that occurs in this region of the molecules of **3** and **4**.

The formation of **3** and **4** from cancentrine methiodide is rationalized in Scheme 1. The first step is *O*-acetylation of the enaminoketone for which a precedent exists (8). The *N*-demethylation is also included at this stage for convenience. This is followed by the key ring-expansion step for which there are two *a priori* possibilities. Thus migration of the C_5—C_6 bond with loss of a C-8 proton may take place leading ultimately to **3** (and **4**), or alternatively, migration of the C_6—C_8 bond with loss of a C-5 proton can lead through similar intermediates to **9**. Structure **3** is supported by the p.m.r. data discussed above but most notably by the detection of a strong n.O.e. (32%) between the signals at 9.90 and 7.94 δ assigned to H_5 and H_6 respectively. Structure **9** is clearly excluded by this observation. The reason for the preferred migration of C_5—C_6 may lie in the geometry of the transition state for this step. $H_{8\alpha}$ is much closer to being *trans* and coplanar to the C_5—C_6 bond than $H_{5\alpha}$ is to the C_6—C_8 bond. There is a further point of interest about this reaction. The retention of the ethanamine side chain during acetolysis has no precedent in the chemistry of morphinan, promorphinan, and related alkaloids with the sole exception of the acetolysis of two closely related compounds, sinomeninone (**10**) and 1-bromosinomeninone (**11**). In these instances both products **12** and **13** were formed from **10**, and **14** and **15** from **11** (9). The location of the second acetoxy group in **13**

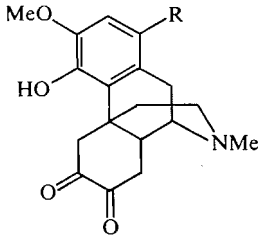

10 R = H
11 R = Br

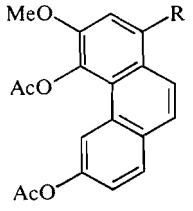

12 R = H
14 R = Br

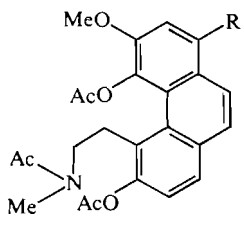

13 R = H
15 R = Br

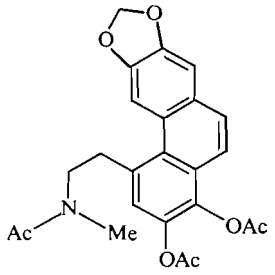

8

Can. J. Chem. Downloaded from www.nrcresearchpress.com by 210.87.254.40 on 09/05/12
For personal use only.

TABLE 1. A comparison of corresponding signals in the p.m.r. spectra of **2**, **3**, **4**, and **6**

	Chemical shift δ (p.p.m.)								Coupling constants J (Hz)			
Compound	H_1	H_2	H_6 (H_{23} in **2**)	H_7 (H_{22} in **2**)	H_{11} (H_{18} in **2**)	H_{12} (H_{17} in **2**)	H_{15} (H_1 in **6**)	$H_{16,17}$ ($H_{9,10}$ in **6**)	1,2	6,7 (23,22 in **2**)	11,12 (18,17 in **2**)	16,17 (9,10 in **6**)
2(1)			7.88	6.68	6.98	6.85	—	—	—	8.0	8.5	—
3	7.73	7.30	7.94	6.93	7.01	6.88	7.72	7.50, 7.62	9.0	8.5	8.5	9.0
4	7.54	7.25	7.64	6.95	6.97	6.91	7.51	7.35, 7.42	9.0	8.5	8.5	9.0
6(5)	7.88	7.57	—	—	—	—	7.88	7.72*	7.7	—	—	0†

*Two-proton singlet.
†9.1 Hz in 1-methylphenanthrene.

Can. J. Chem. Downloaded from www.nrcresearchpress.com by 210.87.254.40 on 09/05/12
For personal use only.

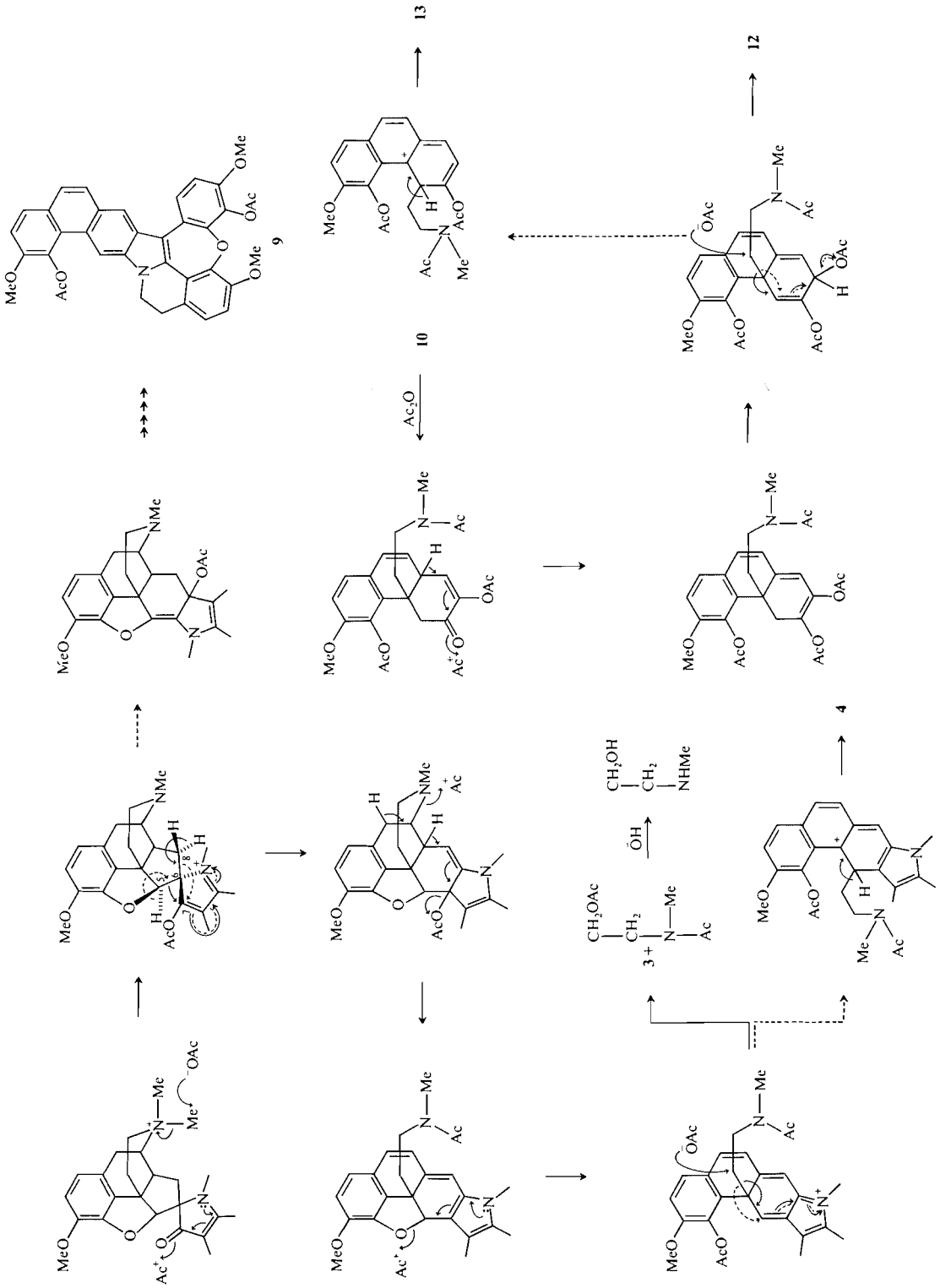

SCHEME 1

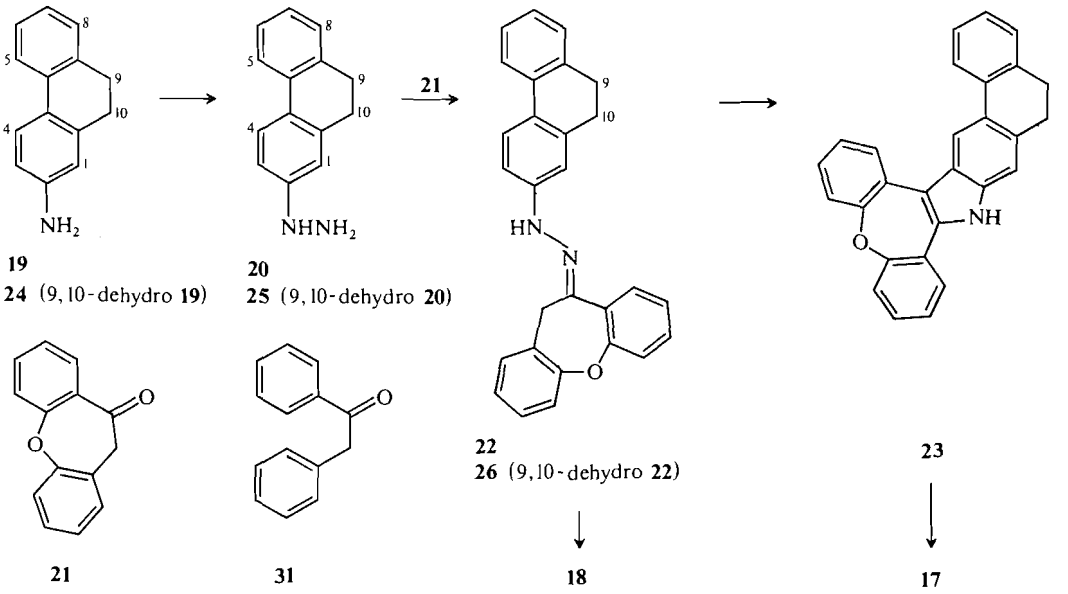

19
24 (9,10-dehydro **19**)
20
25 (9,10-dehydro **20**)
22
26 (9,10-dehydro **22**)
23
21
31
18
17

SCHEME 2

and **15** was not absolutely certain but position C-6 was preferred over C-7 on the basis of some color reactions. The acetolysis of morphine alkaloids containing a C_4—C_5 oxide bridge is believed to involve concerted ring opening of the bridge and *trans*-elimination of the ethanamine side chain (3). In all such cases no retention of the side chain has been observed. In the case of promorphinan compounds that do not possess an oxide bridge the loss of the side chain obviously cannot take place in this way. It is therefore proposed that in the acetolysis of cancentrine methiodide the presence of the second nitrogen atom induces opening of the oxide ring independently of the loss of the side chain by stabilizing the incipient carbonium ion thus leading to both products **3** and **4**. Moreover, this nitrogen atom is in a situation exactly analogous to the oxygen of the carbonyl group at C-7 of sinomeninone. A companion mechanism is proposed for the acetolysis of sinomeninone to emphasize these similarities (Scheme 1).

The second acetolysis product, **4**, is an isomer of compound **16** that would result from a thebenine rearrangement (3) and we therefore wish to propose the name "isothebenine" rearrangement for the process leading to **4**. Indeed the evidence adduced thus far in support of the structure of **4** does not rigorously exclude the alternative structure **16**. The synthesis of model compounds **17** and **18** which correspond to the ring systems of **3** (**4**) and **16**, respectively, was therefore undertaken in order that the u.v. and p.m.r. comparisons could be made. The syntheses (Scheme 2) starting from the dihydrodibenzoxepinone (**21**) and 2-amino-9,10-dihydrophenanthrene (**19**) and 2-aminophenanthrene (**24**), respectively, made use of the Fischer indole procedure for completing the fusion of the two tricyclic halves. It had previously been observed that in the Skraup synthesis with **19** ring closure occurs at C-3 whereas with **24** the same procedure produces ring closure at C-1 (10). In this case therefore **22** is expected to yield **23**, and **26** to give **18** when subjected to the conditions of the Fischer indole synthesis.

The u.v. spectra of **3**, **4**, and **17** were very similar. There were only slight shifts in the absorption maxima which were qualitatively consistent with the degree of substitution of the chromophore in the three compounds. The u.v. spectrum of **18** was substantially different (Fig. 2).

The p.m.r. spectrum of **17** was very complex but showed the presence of singlets at 7.93, 9.39, and 10.86 δ. The latter signal was relatively broad and D_2O exchangeable. It is therefore assigned to the indole proton. The signal at

Can. J. Chem. Downloaded from www.nrcresearchpress.com by 210.87.254.40 on 09/05/12
For personal use only.

Can. J. Chem. Downloaded from www.nrcresearchpress.com by 210.87.254.40 on 09/05/12
For personal use only.

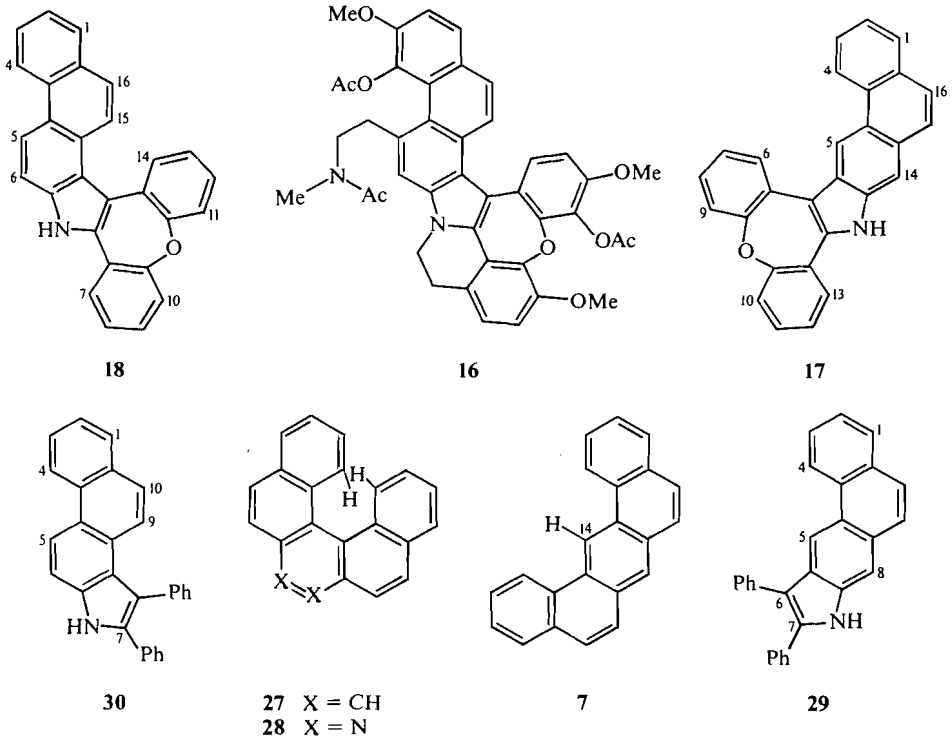

18 **16** **17**

30 **27** X = CH **28** X = N **7** **29**

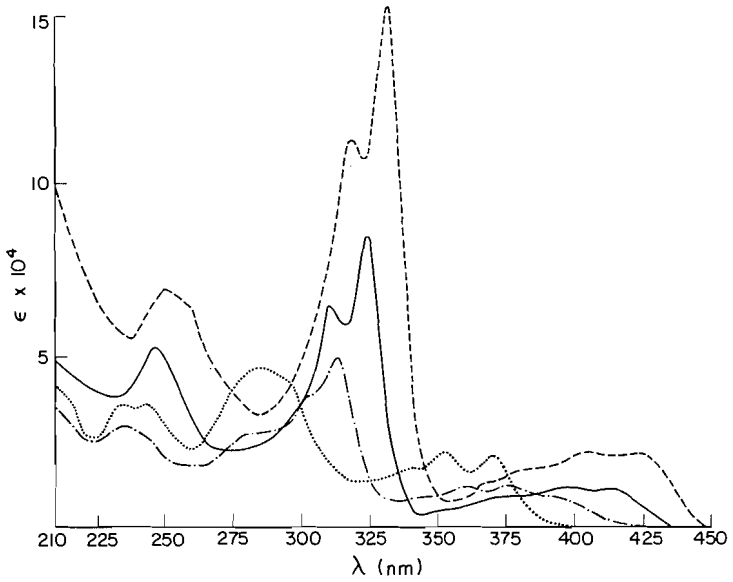

FIG. 2. The u.v. and visible spectra of **3** (——), **4** (----), **17** (·-·-·-), and **18** (·····) in ethanol solution.

9.39 δ is attributed to the C-5 proton which is in a "bay" situation like H_5 in **3** (9.9 δ) and H_{14} in **7** (9.97 δ). The singlet at 7.93 δ is assigned to H_{14} in **17** because of its close correspondence to H_8 in **6** (7.88 δ). The p.m.r. spectrum of **18**, also very complex, contained no singlets, except for

Can. J. Chem. Downloaded from www.nrcresearchpress.com by 210.87.254.40 on 09/05/12
For personal use only.

the indole proton appearing at 11.3 δ and similarly exchangeable with D_2O. There were two other complex but well-separated regions of absorption in the spectrum, 7.10–7.95 δ and 8.45–8.85 δ. The latter (four protons) may be ascribed in part to the "bay" protons H_{14} and H_{15}, since protons in a similar environment in **27** (8.50 δ) and **28** (8.80 δ) appear at similar frequencies (11). The rest of the absorption in the region must be due to H_4 and H_5 of the phenanthrene system.

It is clear that much of the foregoing argument is based upon the previously described de-shielding influences to which protons in a "bay" situation in polycyclic aromatic compounds are exposed. The comparisons made may be validated by an examination of the p.m.r. spectra of **29** and **30** which are related to the systems **17** and **18**, respectively, but lack the oxygen bridge which forces the latter systems into near planarity. In these cases it may be expected that the phenyl substituents of the indole will no longer be coplanar with the rest of the aromatic system and significant changes should be observed in their p.m.r. spectra. These compounds were synthesized by a procedure identical with that described before (Scheme 2) using desoxybenzoin (**31**) in place of the dihydrodibenzoxepinone **21**.

The p.m.r. spectrum of **29** again showed the expected singlets due to H_5 and H_8. The latter appears at 8.00 δ and corresponds well with H_{14} in **17** (7.93 δ). However, the H_5 absorption in **29** is found at 8.95 δ, an upfield shift of 0.44 p.p.m. from its position in **17**, and this must represent the decrease in deshielding at H_5 due to non-coplanarity of the 6-phenyl substituent with the rest of the aromatic system.

The spectrum of **30** also had the two regions of absorption at 7.10–7.95 and 8.50–8.85 δ just like that of **18**. The significant difference however between the two spectra was that the latter region now only integrated for two protons and not four as in the case of **18**. These two protons can be assigned to H_4 and H_5 of the phenanthrene system and once more it appears that the non-coplanarity of the C_8-phenyl substituent with the rest of the aromatic system is responsible for the upfield shift of protons (H_{14} and H_{15} in **18**) now no longer in a "bay" situation.

Experimental

Methods

Melting points were determined in a Fisher Mel-Temp apparatus and are uncorrected. Mass spectra were recorded on a CEC 21-110B double focussing mass spectrometer. Accurate mass measurements were made either by the peak matching technique (12) or by recording spectra on photo plates (13). In both cases appropriate peaks of perfluorokerosene were used for reference (14). The p.m.r. spectra were recorded using the frequency sweep mode of a Varian HA-100 spectrometer. Samples were dissolved in $CDCl_3$ (unless otherwise stated) and added TMS was used as the internal locking signal. Chemical shifts were measured relative to TMS using a V315 frequency counter incorporated in the instrument and are reported in p.p.m. (δ) from TMS. Double irradiation was achieved by employing a Hewlett Packard 201C audiogenerator at the desired frequency. The 220 MHz spectra of **3** and **4** were determined at the Canadian 220 N.M.R. Centre at Sheridan Park, Ontario. A Beckmann IR10 spectrometer was used to record the i.r. spectra and a Cary 14 spectrophotometer was used for the u.v. spectra.

The Acetolysis of Cancentrine Methiodide

Cancentrine methiodide (1.767 g) and anhydrous sodium acetate (4.6 g) were refluxed in acetic anhydride (75 ml) for 48 h under nitrogen. The liquids were removed *in vacuo*, water added, and the mixture extracted with chloroform. The chloroform extracts were dried ($MgSO_4$) and the solvent removed. The residue was purified on a silica gel column. Elution of the column with benzene–acetone (2.5%) yielded **3** (245 mg) crystallized from methanol, m.p. 269°. The u.v. spectrum: λ_{max} (EtOH) 246, 310, 324, 369, 397, and 415 nm; log ε_{max} 4.72, 4.81, 4.94, 3.97, 4.06, and 4.03 respectively. The i.r. spectrum: ν_{max} ($CHCl_3$) 1765 cm^{-1}. The 220 MHz p.m.r. spectrum: 2.52(s) 3H, and 2.55(s) 3H, 2 × OAc; 3.07 (t) 2H and 4.32 (t) 2H (J_{AX} = 6.0 Hz), $—CH_2—CH_2$; 3.67 (s) 3H, 3.70 (s) 3H, 3.78 (s) 3H, 3 × OMe, 6.8–9.9, 10H see text for analysis.

Anal. Calcd. for $C_{37}H_{29}NO_8$ (mol. wt 615.189): C, 72.20; H, 4.74; N, 2.28. Found (615.189 (h.r.m.s.)): C, 72.50; H, 4.94; N, 2.24.

Elution of the silica gel column with chloroform–methanol (2%) yielded **4** (408 mg) crystallized from methanol, m.p. 198°. The u.v. spectrum: λ_{max} (EtOH) 250, 256 (sh), 318, 332, 384, 406, and 424 nm; log ε_{max} 4.84, 4.83, 5.06, 5.19, 4.24, 4.34, and 4.34, respectively. The i.r. spectrum: ν_{max} ($CHCl_3$) 1765 and 1630 cm^{-1}. The 220 MHz p.m.r. spectrum (95°): 1.3 (s) 3H, *N*-Me; 2.15 (s) 3H, *N*-Ac; 2.26 (s) 3H, and 2.44 (s) 3H, 2 × OAc; 2.97 (m) 4H, 3.77 (m) 2H, 4.45 (br.m) 2H; 3.88 (s) 3H, 3.94 (s) 3H, and 3.96 (s) 3H, 3 × OMe; 6.8–7.7, 9H see text for analysis.

Anal. Calcd. for $C_{42}H_{38}N_2O_9 \cdot \frac{1}{2}H_2O$ (mol. wt. 714.258): C, 69.69; H, 5.43; N, 3.87. Found (714.255 (h.r.m.s.)): C, 69.73; H, 5.73; N, 4.16.

The aqueous phase after chloroform extraction was basified with 10% sodium hydroxide and the mixture distilled in a slow current of nitrogen into dilute hydrochloric acid. The distillate was evaporated to dryness and the residue dissolved in a small volume of water and added to a solution of gold chloride in 2 *N* hydrochloric acid. Yellow crystals (18 mg) separated out m.p. 143° (lit. 145–146° (15)).

Can. J. Chem. Downloaded from www.nrcresearchpress.com by 210.87.254.40 on 09/05/12
For personal use only.

Anal. Calcd. for $C_3H_{10}ONAuCl_4$: C, 8.69; H, 2.43; N, 3.38. Found: C, 8.78, 8.76; H, 2.11, 2.30; N, 3.43, 3.78.

Hydrolysis and Methylation of ***3***

Compound **3** (58 mg) and potassium hydroxide (1.5 g) were refluxed for 4.5 h with methanol–*n*-butanol (30 ml, 2:1). The solution was saturated with carbon dioxide and the solvent removed *in vacuo*. Water was added and the mixture extracted with dichloromethane. The latter extract was treated with excess ethereal diazomethane at room temperature for 2 days and a fresh batch of ethereal diazomethane added and the mixture allowed to stand again for 4 days. The solvents were removed and the product purified by chromatography on silica gel (benzene–acetone, 17:3), and crystallized from ethanol–ligroin, m.p. 216–218° (18 mg). The u.v. spectrum: λ_{max} (EtOH) 247, 310, 323, 368, 392, and 405–415 nm; log ε_{max} 4.90, 4.97, 5.07, 4.24, 4.32, and 4.28 respectively. The i.r. spectrum: no absorption between 1600 and 1800 cm^{-1}. The p.m.r. spectrum: 2.94 (t), 2H and 4.20 (t), 2H ($J_{AX} = 6.0$ Hz), $-CH_2-CH_2-$; 3.77 (s) 3H, 3.82 (s) 3H, 3.86 (s) 3H, 3.88 (s) 3H, and 3.96 (s) 3H, 5 × OMe; 6.6–7.6 (9H aromatic), and 10.26 (s) 1H.

Mol. Wt. Calcd. for $C_{35}H_{29}NO_6$: 559.199. Found (h.r.m.s.): 559.197.

*2-Hydrazino-9,10-dihydrophenanthrene (****20****)*

An ice-cold, magnetically stirred suspension of 2-amino-9,10-dihydrophenanthrene hydrochloride (16) (5.172 g) in aqueous hydrochloric acid (40 ml, 20%) was diazotized by the dropwise addition of aqueous sodium nitrite (1.7 g in 3.5 ml). The stirring was continued for 1 h and a small amount of urea added to decompose the excess nitrous acid (until negative to starch-iodide paper). The yellow solution of the resulting diazonium salt was treated in the cold (−5 to 0°) with a solution of stannous chloride ($SnCl_2 \cdot 2H_2O$ 10.3 g) in the minimum quantity of concentrated hydrochloric acid and the stirring continued for 2 h. The precipitated hydrochloride of **20** was filtered, washed with cold water, and crystallized from ethanol–ether, m.p. 218–220°.

Anal. Calcd. for $C_{14}H_{15}N_2Cl$: C, 68.14; H, 6.13. Found: C, 68.13; H, 6.00.

The hydrochloride was treated with 10% aqueous sodium hydroxide and the solution extracted with benzene. The benzene extracts were dried (NaOH) and the solvent removed to yield a red-brown solid (4.50 g).

Preparation of ***17***

To a suspension of the hydrazine **20** (601 mg) in absolute ethanol (10 ml) there was added the dihydrodibenzoxepinone **21** (17) (560 mg) in absolute ethanol (5 ml) and glacial acetic acid (1 ml). The mixture was heated on a steam bath for 10–15 min and the solvent was then removed under reduced pressure. The hydrazone so obtained was dissolved in 1-butanol (10 ml) and the solution was heated to reflux for 20 min while hydrogen chloride gas was bubbled through the mixture. The deposition of ammonium chloride indicated the progress of the reaction. The mixture was washed twice with water, made basic with ammonium hydroxide, rinsed again with water, dried ($MgSO_4$), and evaporated to yield crude **23** (1.182 g). Purification was effected on a silica gel column using benzene–petroleum ether (60°) (1:1) as eluant affording pure **23** (523 mg), crystallized from methanol, m.p. 278–280°.

The pure indole **23** (62 mg) with Pd/C (40 mg of 5%) in naphthalene (720 mg) was heated under dry nitrogen at 220–230° for 3 h. The cold mixture was then dissolved in acetone, filtered, and evaporated. The excess of naphthalene was sublimed off under vacuum to leave crude **17**. Purification of the residue by chromatography on a silica gel plate developed with benzene–petroleum ether (2:1) afforded pure **17** (51 mg), crystallized from ethanol–ether, m.p. 198–200°. The u.v. spectrum: λ_{max} (EtOH) 234, 241(sh), 283(sh), 303(sh), 313, 343, 359, 371, and 391(sh) nm; log ε_{max} 4.47, 4.44, 4.44, 4.57, 4.69, 3.94, 4.06, 4.08, and 3.96, respectively.

Mol. Wt. Calcd. for $C_{28}H_{17}NO$: 383.131. Found: (h.r.m.s.) 383.129.

*2-Hydrazinophenanthrene (****25****)*

2-Aminophenanthrene (18) (993 mg) was converted to 2-hydrazinophenanthrene (900 mg) by the same procedure as that employed in the preparation of **20**; M.p. of hydrochloride (from methanol) 176–178°.

Anal. Calcd. for $C_{14}H_{13}N_2Cl$: C, 68.71; H, 5.35; N, 11.45. Found: C, 68.45; H, 4.99; N, 11.63.

Preparation of ***18***

The hydrazine **25** (293 mg) was treated with the dihydrodibenzoxepinone (**21**) (284 mg) in the manner described above to yield the hydrazone **26** which was subjected to the Fischer-indole conditions as before to yield **18** (348 mg). The product was purified by preparative t.l.c. on silica gel (benzene–ligroin, 3:1), crystallized from methanol, and recrystallized from benzene m.p. 260–262°.

The u.v. spectrum: λ_{max} (EtOH) 235, 243, 284, 292(sh), 336(sh), 352 and 369 nm; log ε_{max} 4.56, 4.55, 4.67, 4.65, 4.21, 4.33 and 4.32, respectively.

Mol. Wt. Calcd. for $C_{28}H_{17}NO$: 383.131. Found (h.r.m.s.): 383.133.

Preparation of ***29***

The procedure was identical to that employed in the preparation of **17**. Thus 2-hydrazino-9,10-dihydrophenanthrene **20**, (100 mg) was treated with desoxybenzoin **31** (52 mg) to yield the hydrazone which was subjected to the Fischer-indole process to give the corresponding indole (67 mg) which was dehydrogenated as before to **29** (56 mg). The product was purified by preparative t.l.c. (silica gel, benzene–ligroin, 3:1) and crystallized once from ethanol and then twice from ligroin. M.p. 224–225°. The u.v. spectrum: λ_{max} (EtOH) 234, 281(sh), 309, 347(sh), 361, and 380 nm; log ε_{max} 4.63, 4.63, 4.91, 4.15, 4.28, and 4.25 respectively.

The molecular formula was determined by h.r.m.s.

Mol. Wt. Calcd. for $C_{28}H_{19}N$: 369.152. Found (h.r.m.s.): 369.154.

Preparation of ***30***

The procedure was identical to that employed in the preparation of **18**. Thus, 2-hydrazinophenanthrene, **25** (116 mg) was treated with desoxybenzoin, **31** (109 mg) to yield the hydrazone which was subjected to the Fischer-indole process to give the indole **30** (169 mg). The product was purified by preparative t.l.c. (silica gel, benzene–ligroin, 3:1) and crystallized from ethanol–ligroin, M.p. 184–186°.

The u.v. spectrum: λ_{max} (EtOH) 241, 269(sh), 281, 291(sh), 341, 350, and 370 nm; log ε_{max} 4.62, 4.68, 4.73, 4.68, 4.39, 4.37, and 4.33 respectively.

Mol. Wt. Calcd. for $C_{28}H_{19}N$: 369.152. Found (h.r.m.s.): 369.153.

Appendix

Systematic names for the ring systems prepared in the study are as follows:

3 (**4**): 9,10-dihydrobenzo[2,3][1]benzoxepino-[6,5,4-*ghi*] phenanthro[3,2,-*b*]indolizine;

17: 10*H*-dibenz[2,3:6,7]oxepino[4,5-*b*]naphth-[1,2-*f*]indole;

18: 7 *H*-dibenz[2,3,:6,7]oxepino[4,5-*b*]naphth-[2,1-*e*]indole;

29: 8*H*-naphth[1,2-*f*]indole;

30: 7*H*-naphth[2,1-*e*]indole.

The names of **3**, (**4**), **17**, and **18** were kindly provided by Dr. Kurt L. Loening, Director of Nomenclature, Chemical Abstracts Service, Columbus, Ohio.

The systematic names were not used in the text because comparison of corresponding protons of ring systems with different numbering might be confusing to the reader.

We wish to thank the National Research Council of Canada for financial support.

1. R. Rodrigo, R. H. F. Manske, D. B. MacLean, L. Baczynskyj, and J. K. Saunders. Can. J. Chem. **50**, 853 (1972).
2. N. D. V. Wilson and J. A. Joule. Tetrahedron, **24**, 5493 (1968).
3. G. Stork. Alkaloids, **2**, 189 (1952).
4. G. R. Clark, R. H. F. Manske, G. J. Palenik, R. Rodrigo, D. B. MacLean, L. Baczynskyj, D. E. F. Gracey, and J. K. Saunders. J. Am. Chem. Soc. **92**, 4998 (1970).
5. K. D. Bartle and J. A. S. Smith. Spectrochim. Acta, **23A**, 1689 (1967); K. D. Bartle and D. W. Jones. J. Chem. Soc. A, 437 (1969).
6. P. Durand, J. Parello, N. P. Buu-Hoi, and L. Alais. Bull. Soc. Chim. Fr. 2438 (1963).
7. W. Dopke, H. Flentje, and P. W. Jeffs. Tetrahedron, **24**, 4459 (1968).
8. A. I. Meyers and S. Singh. Tetrahedron Lett. 5319 (1967).
9. K. Goto, H. Shishido, and K. Takubo. Ann. **497**, 289 (1932).
10. J. W. Krueger and E. Mosettig. J. Org. Chem. **3**, 317 (1939).
11. R. H. Martin, N. Defay, F. Geerts-Erraad, and D. Bogaert-Verhogen. Tetrahedron, Suppl. 8, Part I, 181 (1966).
12. K. S. Quisenberry, T. T. Scotman, and A. O. Nier. Phys. Rev. **102**, 1071 (1956).
13. K. Biemann. Pure Appl. Chem. **9**, 95 (1964).
14. F. W. McLafferty. Anal. Chem. **28**, 306 (1956).
15. L. Knorr and H. Mathes. Ber. **31**, 1069 (1898).
16. H. O. Wirth, K. H. Gonner, and W. Kern. Makromol. Chem. **63**, 53 (1963).
17. R. H. F. Manske and A. E. Ledingham. J. Am. Chem. Soc. **72**, 4797 (1950).
18. W. E. Bachmann and C. H. Boatner. J. Am. Chem. Soc. **58**, 2097 (1936).

Can. J. Chem. Downloaded from www.nrcresearchpress.com by 210.87.254.40 on 09/05/12
For personal use only.

Can. J. Chem. Downloaded from www.nrcresearchpress.com by 210.87.254.42 on 09/05/12
For personal use only.

Ruthenium and Arsenic Electrode Potentials in Fused LiCl–KCl Eutectic

T. FOLKMAN AND JAMES A. PLAMBECK

Department of Chemistry, University of Alberta, Edmonton, Alberta

Received June 1, 1972

Electrode potentials of the Ru(III)/Ru(0) and As(III)/As(0) systems were measured in dilute solutions of the ionic species in fused LiCl–KCl eutectic at 450 °C. Standard molar electrode potentials of these couples of -0.107 ± 0.007 V and -0.460 ± 0.017 V against a standard molar platinum electrode were calculated. The As(V)/As(III) potential was found to be beyond the potential range of the melt.

Les potentiels électrochimiques des systèmes Ru(III)/Ru(0) et As(III)/As(0) ont été mesurés à 450 °C en solutions diluées des ions dans l'eutectique LiCl–KCl fondu. Les potentiels normaux molaires, par rapport au potentiel de l'electrode de platine normale à l'échelle molaire, ont été calculés à -0.107 ± 0.007 V et -0.460 ± 0.017 V. Le potentiel electrochimique du système As(V)/As(III) se trouve outre le domaine des potentiels utilisables du mélange fondu LiCl–KCl.

Canadian Journal of Chemistry, **50**, 3911 (1972)

Introduction

The oxidation states and potentials of most metals have been established in one of the fused halide systems, but arsenic and ruthenium have not yet been extensively studied. No data exist regarding the behavior of arsenic in fused alkali halides. Fung and Johnson (1) studied Ru(III) in the fused LiCl–KCl melt spectrophotometrically and reported a stable $RuCl_6^{3-}$ species in the melt. They report the Ru(III) species to be electrochemically inactive. Spectral measurements on Ru(III) have also been made in this solvent by Suzuki and Tanaka (2), who confirm the species as $RuCl_6^{3-}$.

In this work we report standard potentials of the As(III)/As(0) and Ru(III)/Ru(0) couples in a form compatible with an extensive review of redox potentials in this melt (3).

Experimental

Apparatus

Potentials were measured with a Model 3440A digital voltmeter (Hewlett–Packard) and metal ions were generated using a Model IV coulometric current source (E. H. Sargent and Co.).

The electrolytic cell and glassware preparation procedure used has been previously described (4). The outer glass jacket was heated with a vertical tube furnace equipped with a 59344 Lindberg-Hevi-Duty temperature controller. The temperatures were recorded using a calibrated chromel–alumel thermocouple and the above digital voltmeter.

Solvent

The solvent used was prepared from certified reagent grade LiCl (Fisher Scientific Co.) and KCl (J. T. Baker Chem. Co.) made up as the LiCl 59 mole%–KCl 41 mole% eutectic. The method of purification used was that of Maricle and Hume (5).

Electrodes

For the reduction of Ru(III), purified ruthenium chloride, $RuCl_3 \cdot xH_2O$ (Fisher Scientific Co.) was used. For the oxidation of arsenic, 99.999 + % pieces (lot #08058, Alfa Inorganics, Inc.) connected to a gold wire were used. Gold was used in both cases because arsenic and ruthenium do not alloy with it at these temperatures (6).

Counter electrodes used in coulometric generation were 0.120 × 12 in. carbon rods (AGKSP spectrographic graphite electrodes, National Carbon Co. Div. of Union Carbide) connected to copper leads inside the furnace but above the melt. Standard potential measurements were made against a Pt(II)/Pt electrode (4). All electrodes were dried before entering the melt and each was kept in a separate fritted-glass compartment.

Procedure

The cell was maintained under a slight positive pressure of dry argon to prevent contamination by water vapor. The procedure for arsenic was similar to that described previously for rhodium (4) with additional precautions due to the toxicity of $AsCl_3$. The procedure for ruthenium differed; a weighed amount of $RuCl_3 \cdot xH_2O$ was added to the solvent and Ru(III) plated cathodically on a gold wire. Stable potentials were obtained within a few minutes after cessation of the current and agitation of the electrode to stir the contents of the compartment. This procedure, which is less satisfactory than anodic oxidation, was necessary due to the authors' inability to obtain proper coherent metallic ruthenium.

Can. J. Chem. Downloaded from www.nrcresearchpress.com by 210.87.254.42 on 09/05/12
For personal use only.

The potentials reported in this paper are with reference to the Pt(II) (1.0 *M*), LiCl–KCl/Pt standard molar platinum electrode (s.m.p.e.) of Laitinen and Liu (7) and the calculations were as outlined in that paper. They conform to the I.U.P.A.C. "Stockholm" sign convention.

Results and Discussion

Arsenic (III)/Arsenic(0) Couple

A total of 13 concentration–potential data points were taken at 450 ± 4 °C in two separate experiments. Stable potentials were not obtained at concentrations of As(III) lower than about 1×10^{-3} *M*. At concentrations above 1×10^{-2} *M*, bubbles of $AsCl_3$ became noticeable and continuous negative drifting of the potentials was observed. For the points in the concentration range 10^{-3} to 10^{-2} *M*, the slope of a Nernst plot corresponded to 3.1 electrons. Using a three-electron slope and each individual point, the mean standard potential (molarity scale) of the As(III)/As(0) couple was calculated to be -0.460, standard deviation ± 0.017 V, with respect to the s.m.p.e. This corresponds to values of -0.465 and -0.495 V, with the same standard deviation, on the molal and mole fraction scales, respectively.

Attempts to further oxidize As(III) by replacing the arsenic metal in the compartment with a carbon rod and continuing anodization were unsuccessful; chlorine evolution occurred. This indicates that the As(V)/As(III) potential is beyond the range of the melt. An attempt to cathodize arsenic into solution was also unsuccessful.

There are no literature data with which the arsenic potential measured here is directly comparable, but the standard potentials of the analogous antimony and bismuth couples (7–9) are both -0.635 V on the same scale. A value for arsenic some 150 mV more positive is reasonable.

Ruthenium(III)/Ruthenium(0) Couple

In four separate experiments, a weighed amount of the solid ruthenium trichloride was added to a compartment in the melt, a gold wire was inserted, and ruthenium metal cathodically deposited on the gold using the coulometer. An adherent dark plate, which became silver-shiny after polishing, was obtained. Stable potentials were always obtained a few minutes after completion of the deposition and stirring with Ru(III) concentrations greater than 1×10^{-3} *M*, and a total of 27 such measurements were made.

The ruthenium content of the compartments was analyzed by the method of Ayres and Young (10). Analysis of the ruthenium chloride by the method of Gilchrist and Wichers (11) showed that it contained three to four waters of hydration which were not removable by evacuation or by treatment with HCl gas, and a significant fraction of the ruthenium was not platable, remaining in the compartment as black insoluble material, presumably an oxide or mixed oxide chloride. After correction for this loss, the standard electrode potential of the Ru(III)/Ru(0) couple was calculated as -0.1065, standard deviation ± 0.0067 V against s.m.p.e. In view of the approximate three-electron Nernst slope obtained in these runs, especially those in which the amount of added $RuCl_3$ (and hence water) was comparatively low, it is felt that a value of -0.107 ± 0.007 V against s.m.p.e. is realistic for this couple. This corresponds to values of -0.112 and -0.142 V, with the same standard deviation, on the molal and mole fraction scales, respectively.

The authors are grateful to the National Research Council of Canada for support of this work by an Operating Grant. This work is taken in part from a report of T. Folkman, submitted in partial fulfillment of the requirements for a B.Sc. Honours degree, University of Alberta. The authors are indebted to J. T. Chapman for preliminary studies of ruthenium.

1. K. W. Fung and K. E. Johnson. Inorg. Chem. **10**, 1347 (1971).
2. S. Suzuki and K. Tanaka. Nippon Kinzaku Gakkaishi **34**, 461 (1970); Chem. Abstr. **73**, 30356.
3. J. A. Plambeck. J. Chem. Eng. Data, **12**, 77 (1967).
4. H. A. Laitinen and J. A. Plambeck. J. Am. Chem. Soc. **87**, 1202 (1965).
5. D. L. Maricle and D. N. Hume. J. Electrochem. Soc. **107**, 354 (1960).
6. M. Hansen and K. Anderko. Constitution of binary alloys. 2nd ed. McGraw-Hill, New York. 1958. pp. 154, 230.
7. H. A. Laitinen and C. H. Liu. J. Am. Chem. Soc. **80**, 1015 (1958).
8. H. A. Laitinen and B. B. Bhatia. J. Electrochem. Soc. **107**, 705 (1960).
9. H. A. Laitinen, R. P. Tischer, and D. K. Roe. J. Electrochem. Soc. **107**, 546 (1960).
10. G. H. Ayres and F. Young. Anal. Chem. **22**, 1277 (1950).
11. R. Gilchrist and E. Wichers. J. Am. Chem. Soc. **57**, 2565 (1935).

P.M.R. Spectroscopy of Trimethylsilyl Derivatives of Hydroxy Acids

GUY GORDON STUDDY DUTTON, NORMAN FUNNELL AND KELLY BLAIR GIBNEY[1]

Department of Chemistry, The University of British Columbia, Vancouver 8, British Columbia

Received July 24, 1972

P.m.r. spectroscopy at 60 MHz of trimethylsilyl ethers and esters, prepared from hydroxy acids, gives well resolved sharp singlets in the range τ 9.8–9.9. These signals may be used to determine the ratio of hydroxyl to carboxyl groups in a molecule. Measurements may be made directly on fractions isolated by gas–liquid chromatography. The influence of the solvent on the resolution is demonstrated.

La spectroscopie r.m.n. (60 MHz) des éthers et esters triméthylsilyl, derivés des acides hydroxylés, donne des pics bien résolus (τ 9.8–9.9). On peut utiliser ces signaux pour déterminer le rapport entre les groupements hydroxyles et carboxyles dans une molécule. On peut faire les mesures directement sur les fractions isolées par chromatographie en phase gaseuse. L'influence du solvant sur la résolution des pics est démontrée.

Canadian Journal of Chemistry, **50**, 3913 (1972)

Can. J. Chem. Downloaded from www.nrcresearchpress.com by 210.87.254.40 on 09/05/12
For personal use only.

Trimethylsilyl derivatives have been prepared from many different types of compounds and the silylation reaction has been reviewed (1). These derivatives are commonly prepared mainly for the purpose of separations by gas–liquid chromatography and also for mass spectrometry (1). In contrast to the wealth of literature available on these two applications of trimethylsilyl derivatives much less has been reported on the physical properties of such compounds and, in particular, their uses in p.m.r. spectroscopy.

We have shown recently that the protons of the $—OSi(CH_3)_3$ group in trimethylsilyl ethers give a sharp singlet in the range τ 9.8 and that non-equivalent ethers have distinct chemical shifts (2). Thus, the trimethylsilyl ether of glycerol gives two such singlets (integral ratio 1:2), and the derivatives of methyl α-D-galactopyranoside and of α-D-glucopyranose give four and five well resolved signals of equal magnitude, respectively. Carboxylic acids readily form trimethylsilyl esters and thus hydroxy acids give derivatives which are both trimethylsilyl ethers and esters. The present note shows how p.m.r. spectroscopy of these derivatives may be used to determine the relative numbers of carboxyl and hydroxyl groups per molecule and, in certain cases, the absolute number.

Trimethylsilyl (TMS) derivatives were prepared by reaction of the hydroxy acid in pyridine with hexamethyldisilazane (HMDS) alone or with the addition of chlorotrimethylsilane. Figure 1 shows the p.m.r. spectrum (60 MHz) in carbon tetrachloride of the derivative of citric acid ($HOOC—CH_2—C(OH)(COOH)—CH_2-COOH$) which forms a triester (TMS ester) monoether (TMS ether). Figure 1 utilizes two scales: the signals due to the TMS esters and ethers are shown in Hz downfield from tetramethylsilane (TMS), which was used as internal standard, while those due to the methylene protons are shown on the τ scale (TMS, τ 10). The former were obtained at a sweep width of

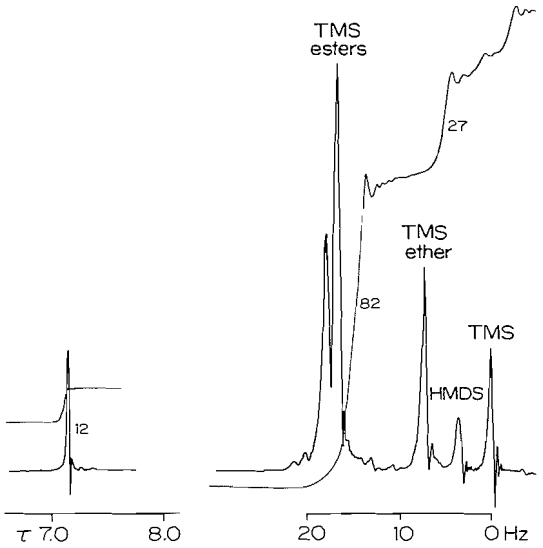

FIG. 1. Citric acid. P.m.r. spectrum at 60 MHz in carbon tetrachloride. Trimethylsilyl ether and esters shown in Hz downfield from tetramethylsilane and methylene protons on the τ scale.

[1]Present address: Department of Cellulose Research, Columbia Cellulose Ltd., 852 Derwent Way, Annacis Island, New Westminster, British Columbia.

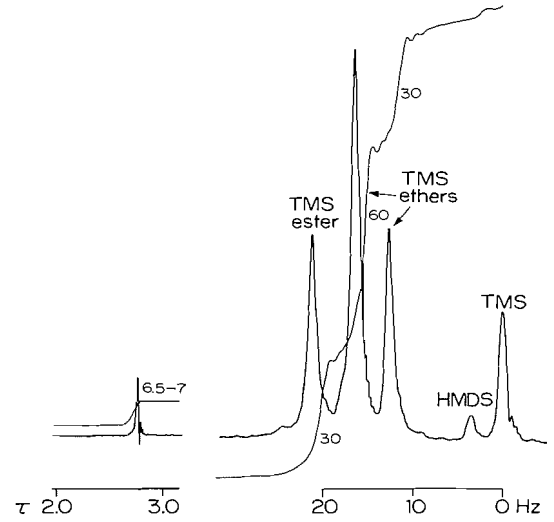

FIG. 2. Gallic acid. P.m.r. spectrum at 60 MHz, as Fig. 1.

100 Hz and the latter at 500 Hz. A small peak due to residual hexamethyldisilazane is also visible. The expanded scale clearly shows that hydroxyl and carboxyl groups are present in the ratio of 1:3. When the spectrum is run at a sweep width of 500 Hz the TMS ether and TMS ester signals are not clearly resolved but are sufficiently well separated from the hexamethyldisilazane and internal standard signals to permit integration and thus comparison with the integral due to the methylene protons. Values of 86:9 (arbitrary units) were obtained in this manner; in Fig. 1 the methylene integral has been increased proportionately to accord with the expanded scale. Figure 2 represents the spectrum, similarly presented, for gallic acid (3,4,5-trihydroxybenzoic acid). Table 1 shows the other compounds studied and gives, in Hz downfield from tetramethylsilane, the chemical shifts of the TMS ether and TMS ester peaks.

In certain cases the resolution of the trimethylsilyl ether signals was better in benzene than in carbon tetrachloride (2) and the effect of solvent was therefore studied for the derivatives of hydroxy acids. To illustrate this Fig. 3 shows the high field portion of the spectra, obtained in different solvents, of the derivative of malic acid. In benzene (Fig. 3*A*) all three signals, although resolved, have similar chemical shifts and in pyridine (Fig. 3*B*), the TMS ester

TABLE 1. Chemical shifts of trimethylsilyl ethers and esters

Acid	Chemical shift (Hz)* TMS ether	TMS ester	Solvent
Malonic	—	20.0	pyr.
Succinic	—	17.0	pyr.
Fumaric	—	18.8	CCl_4
D-Tartaric	9.0	19.7	pyr.
Salicylic	14.4	22.2	CCl_4
m-Hydroxybenzoic	15.6	21.0	CCl_4
p-Hydroxybenzoic	17.2	25.6	pyr.
2,6-Dihydroxybenzoic	15.0	26.0	pyr.
3,4-Dihydroxybenzoic	14.4, 15.7	21.2	CCl_4

*Hz downfield from internal tetramethylsilane (60 MHz).

signals are barely distinguished. In chloroform (Fig. 3*C*) the signal due to the TMS ether is well separated from those of the esters but these, in turn, are poorly resolved. Of the solvents studied carbon tetrachloride (Fig. 3*D*) appears to give the best results. The change in chemical shift of the HMDS signal in the different solvents may also be seen.

It should be noted that these spectra were all obtained at 60 MHz. When working with compounds containing only hydroxyl groups, *e.g.* carbohydrates, it was necessary to run spectra at 100 MHz in order to resolve the four or five TMS ether signals obtained (2).

When a hydroxyl or a carboxyl group is converted to the corresponding trimethylsilyl derivative one proton is effectively replaced by nine protons. The advantage of this in behaving as a built-in signal multiplier and thus permitting p.m.r. spectra to be obtained on small quantities of material, such as individual fractions isolated by gas–liquid chromatography, has been previously illustrated and discussed and is not here repeated (2). The choice of compounds used in this note was influenced by the fact that acids of the tricarboxylic acid cycle have been separated by g.l.c. of their trimethylsilyl derivatives (3–5) and difficulty has been reported in achieving complete silylation of aromatic hydroxy acids (ref. 1, p. 161). The method is clearly extendable, as an aid in structural elucidations and particularly where separations are made by g.l.c. to other naturally occurring hydroxy acids or such acids obtained in degradation studies, for example, urinary acids (6) and alkaline degradation products of flavonoids

Can. J. Chem. Downloaded from www.nrcresearchpress.com by 210.87.254.40 on 09/05/12
For personal use only.

Can. J. Chem. Downloaded from www.nrcresearchpress.com by 210.87.254.40 on 09/05/12
For personal use only.

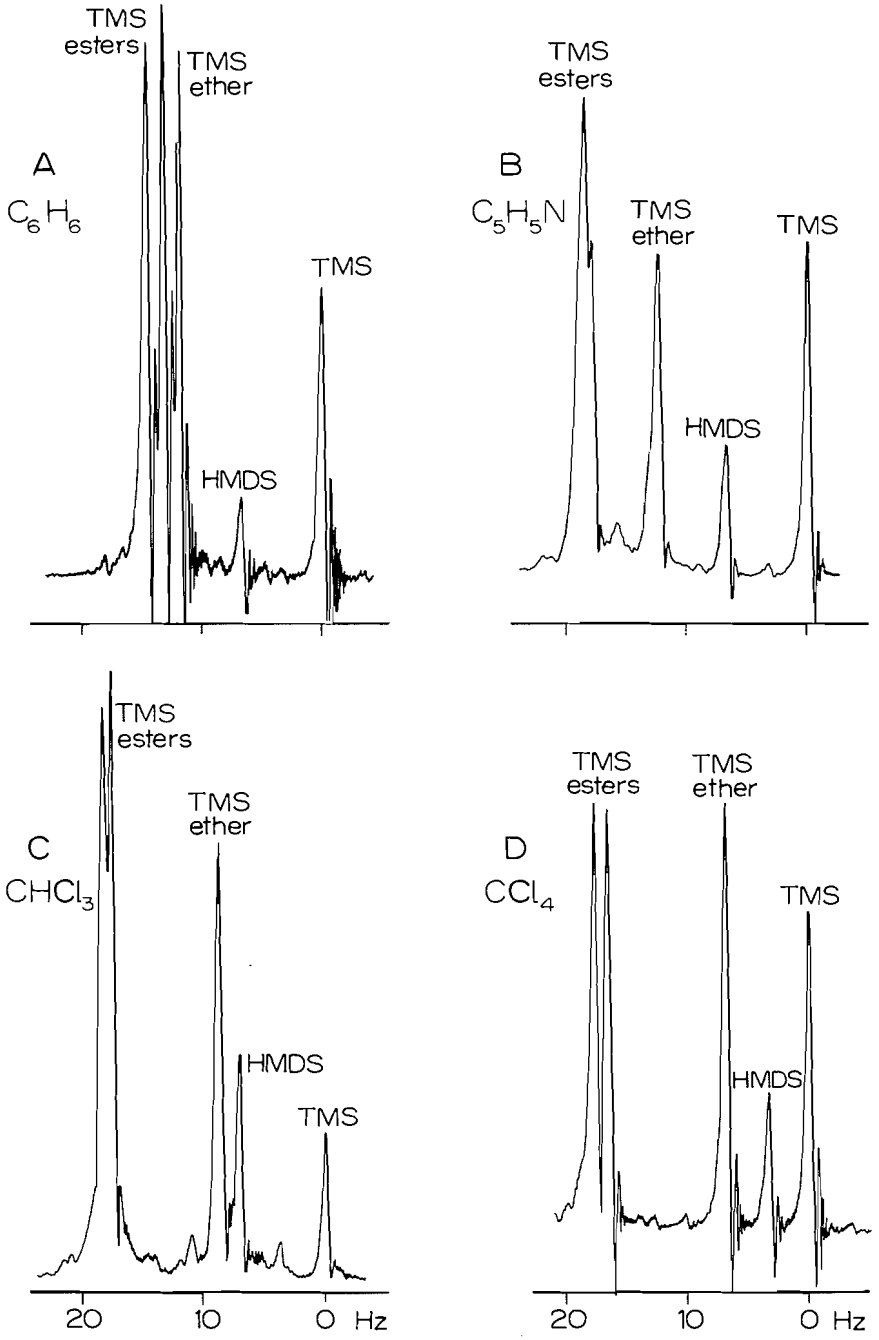

FIG. 3. Malic acid. P.m.r. spectra at 60 MHz in *A*, benzene; *B*, pyridine; *C*, chloroform; *D*, carbon tetrachloride. High field portion only shown (as Fig. 1).

(7). Measurement of the TMS ester and TMS ether signals affords a convenient check on the completeness of trimethylsilylation of hydroxy acids and the former signal may also be used as a means of following the kinetics of hydrolysis of such esters.

Experimental

Trimethylsilylation

The acid (10–50 mg) was dissolved in pyridine (1 ml); for some acids this required several hours of warming at 45°. When solution was complete hexamethyldisilazane (1 ml) was added and the solution was heated at 45° for a further 1–2 h. These conditions gave fully trimethylsilylated derivatives for all the acids used in the present study except for gallic and citric acids. For these compounds chlorotrimethylsilane (0.1 ml) was added in addition to the hexamethyldisilazane and the solution was heated under reflux and protected from moisture for 1 h. Solvents and excess reagents were removed *in vacuo* by an oil pump. Evaporation using a water aspirator gave variable results for the TMS ester signals due, presumably, to hydrolysis. The residual syrups were dissolved in the solvents indicated for p.m.r. measurements.

P.m.r. Spectroscopy

Spectra were obtained on a Varian T60 instrument using a sweep width of 500 Hz. The high field portion was re-run at a sweep width of 100 Hz. Tetramethylsilane (TMS) was used as an internal standard (τ, 10).

We thank Phyllis Watson for running the spectra and Beatrix Krizsan for the drawings. The continued financial support of the National Research Council of Canada and the award of an NRCC scholarship to N.F. are gratefully acknowledged.

1. A. E. PIERCE. Silylation of organic compounds. Pierce Chemical Co., Rockford, Illinois. 1968.
2. G. M. BEBAULT, J. M. BERRY, G. G. S. DUTTON, and K. B. GIBNEY. Anal. Lett. **5**, 413 (1972).
3. H. ROSENQVIST, H. KALLIO, and V. NURMIKKO. Anal. Biochem. **46**, 224 (1971).
4. Z. HORII, M. MAKITA, and Y. TAMURA. Chem. Ind. (London), 1494 (1965).
5. M. G. HORNING, E. A. BOUCHER, A. M. MOSS, and E. C. HORNING. Anal. Lett. **1**, 713 (1968).
6. M. G. HORNING. *In* Biomedical applications of gas chromatography. Vol. 2 *Edited by* H. A. Szymanski. Plenum Press, New York. 1968. p. 53.
7. T. J. MABRY, K. R. MARKHAM, and M. B. THOMAS. Systematic identification of flavonoids. Springer Verlag, New York, 1970.

Can. J. Chem. Downloaded from www.nrcresearchpress.com by 210.87.254.40 on 09/05/12
For personal use only.

Location of Energy Barriers. V. Scaling the Energy-Surface for AB + CD → AC + BD

D. S. PERRY AND J. C. POLANYI

Department of Chemistry, University of Toronto, Toronto 5, Ontario

Received July 19, 1972

In order to make use of the sliding-mass analogy for AB + CD four-center exchange reactions it is necessary to know how to scale the "diagnostic" potential-energy surface. This note describes the method of scaling, and exemplifies it for the case of $H_2 + I_2$.

Afin de pouvoir utiliser l'analogie de la masse glissante pour les réactions d'échange à quatre centres de type AB + CD, on doit savoir graduer la surface "diagnostique" d'énergie potentielle. Cette communication décrit la méthode de graduation et donne l'exemple dans le cas de $H_2 + I_2$.

[Traduit par le journal]

Canadian Journal of Chemistry, **50**, 3916 (1972)

The dynamics of four-center exchange reactions AB + CD → AC + BD continue to be the subject of considerable experimental and theoretical interest (for a review, see ref. 1). Three classical trajectory calculations have been reported (2–4); another is being readied for publication (5). In trajectory studies of three-atom exchange reactions, A + BC → AB + C, the analogue of the sliding mass on a scaled and skewed surface has assisted notably in the interpretation of the findings.[1] The path of the sliding mass can be pictured, hence the solution of the equations of motion for collinear reaction can often be rationalized. As a predictive device the method must be used with caution. Its success depends upon the extent to which a collinear (1D) trajectory can be regarded as being representative of the outcome of a statis-

[1]For a description of the scaling and skewing appropriate to collinear reaction A + BC → AB + C, see ref. 6.

Experimental

Trimethylsilylation

The acid (10–50 mg) was dissolved in pyridine (1 ml); for some acids this required several hours of warming at 45°. When solution was complete hexamethyldisilazane (1 ml) was added and the solution was heated at 45° for a further 1–2 h. These conditions gave fully trimethylsilylated derivatives for all the acids used in the present study except for gallic and citric acids. For these compounds chlorotrimethylsilane (0.1 ml) was added in addition to the hexamethyldisilazane and the solution was heated under reflux and protected from moisture for 1 h. Solvents and excess reagents were removed *in vacuo* by an oil pump. Evaporation using a water aspirator gave variable results for the TMS ester signals due, presumably, to hydrolysis. The residual syrups were dissolved in the solvents indicated for p.m.r. measurements.

P.m.r. Spectroscopy

Spectra were obtained on a Varian T60 instrument using a sweep width of 500 Hz. The high field portion was re-run at a sweep width of 100 Hz. Tetramethylsilane (TMS) was used as an internal standard (τ, 10).

We thank Phyllis Watson for running the spectra and Beatrix Krizsan for the drawings. The continued financial support of the National Research Council of Canada and the award of an NRCC scholarship to N.F. are gratefully acknowledged.

1. A. E. PIERCE. Silylation of organic compounds. Pierce Chemical Co., Rockford, Illinois. 1968.
2. G. M. BEBAULT, J. M. BERRY, G. G. S. DUTTON, and K. B. GIBNEY. Anal. Lett. **5**, 413 (1972).
3. H. ROSENQVIST, H. KALLIO, and V. NURMIKKO. Anal. Biochem. **46**, 224 (1971).
4. Z. HORII, M. MAKITA, and Y. TAMURA. Chem. Ind. (London), 1494 (1965).
5. M. G. HORNING, E. A. BOUCHER, A. M. MOSS, and E. C. HORNING. Anal. Lett. **1**, 713 (1968).
6. M. G. HORNING. *In* Biomedical applications of gas chromatography. Vol. 2 *Edited by* H. A. Szymanski. Plenum Press, New York. 1968. p. 53.
7. T. J. MABRY, K. R. MARKHAM, and M. B. THOMAS. Systematic identification of flavonoids. Springer Verlag, New York, 1970.

Can. J. Chem. Downloaded from www.nrcresearchpress.com by 210.87.254.40 on 09/05/12
For personal use only.

Location of Energy Barriers. V. Scaling the Energy-Surface for AB + CD → AC + BD

D. S. PERRY AND J. C. POLANYI

Department of Chemistry, University of Toronto, Toronto 5, Ontario

Received July 19, 1972

In order to make use of the sliding-mass analogy for AB + CD four-center exchange reactions it is necessary to know how to scale the "diagnostic" potential-energy surface. This note describes the method of scaling, and exemplifies it for the case of $H_2 + I_2$.

Afin de pouvoir utiliser l'analogie de la masse glissante pour les réactions d'échange à quatre centres de type AB + CD, on doit savoir graduer la surface "diagnostique" d'énergie potentielle. Cette communication décrit la méthode de graduation et donne l'exemple dans le cas de $H_2 + I_2$.

[Traduit par le journal]

Canadian Journal of Chemistry, **50**, 3916 (1972)

The dynamics of four-center exchange reactions AB + CD → AC + BD continue to be the subject of considerable experimental and theoretical interest (for a review, see ref. 1). Three classical trajectory calculations have been reported (2–4); another is being readied for publication (5). In trajectory studies of three-atom exchange reactions, A + BC → AB + C, the analogue of the sliding mass on a scaled and skewed surface has assisted notably in the interpretation of the findings.[1] The path of the sliding mass can be pictured, hence the solution of the equations of motion for collinear reaction can often be rationalized. As a predictive device the method must be used with caution. Its success depends upon the extent to which a collinear (1D) trajectory can be regarded as being representative of the outcome of a statis-

[1]For a description of the scaling and skewing appropriate to collinear reaction A + BC → AB + C, see ref. 6.

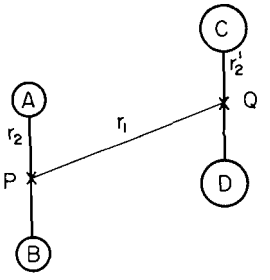

FIG. 1. Coordinate system.

tical group of trajectories in 3D. Most of the trajectory work up to the present has been concerned with potential-energy hypersurfaces that to some degree favor collinear reaction (for a review, see ref. 7). For potential-energy surfaces of this type the collinear surface constitutes a useful "diagnostic" cut through the hypersurface (for a review, see ref. 8).

In a 3D trajectory study of the effect on the dynamics of reactions $AB + CD \rightarrow AC + BD$ of changes in barrier location, it has been found that the potential-energy surface for coplanar rectangular reaction constitutes an instructive diagnostic-cut through the full hypersurface $U(r_{AB},r_{AC},r_{AD},r_{BC},r_{BD},r_{CD})$. It is important to bear in mind, however, that the diagnostic cut in this case gives a still more restricted view of the hypersurface than for the three-center reaction (3).

Consider the coplanar collision of AB + CD in Fig. 1; P and Q are the centers-of-mass of AB and CD. The reagents approach along r_1 and the products separate along $r_2(=r_2')$. The kinetic energy can be written

$$[1] \qquad T = T_{AB} + T_{CD} + T_{AB,CD} = \tfrac{1}{2}(\mu_{AB}\dot{r}_2^2 + \mu_{CD}\dot{r}_2^2 + \mu_{AB,CD}\dot{r}_1^2)$$

where

$$\mu_{AB} = \frac{m_A m_B}{m_A + m_B}$$

$$\mu_{CD} = \frac{m_C m_D}{m_C + m_D}$$

$$\mu_{AB,CD} = \frac{(m_A + m_B)(m_C + m_D)}{m_A + m_B + m_C + m_D}$$

We wish to make an analogy with a sliding mass, whose kinetic energy is

$$[2] \qquad T = \tfrac{1}{2}(\dot{x}^2 + \dot{y}^2)$$

The transformation of coordinates is therefore given by

$$[3] \qquad \begin{pmatrix} r_1 \\ r_2 \end{pmatrix} = \begin{pmatrix} \left(\dfrac{(m_A + m_B)(m_C + m_D)}{m_A + m_B + m_C + m_D}\right)^{-1/2} & 0 \\ 0 & \left(\dfrac{m_A m_B}{m_A + m_B} + \dfrac{m_C m_D}{m_C + m_D}\right)^{-1/2} \end{pmatrix} \begin{pmatrix} x \\ y \end{pmatrix}$$

$$[4] \qquad = \begin{pmatrix} b & 0 \\ 0 & a \end{pmatrix} \begin{pmatrix} x \\ y \end{pmatrix}$$

where a and b are mass-dependent constants. Since r_1 depends only on x, and r_2 on y the Cartesian coordinates, x and y, already provide a "diagonalized" representation of $T(r_1,r_2)$. This result merely constitutes a particular example of a general principle due to Jepsen and Hirschfelder (9),[2] namely that any coordinate system, for n particles, which is analogous to a dangling "mobile" will have the property of expressing the relative kinetic energy without cross-terms.

[2]Their diagonalization applies to motion in 3D.

The constants b and a in eq. 4 correspond to the "scaling factors" required in order that the motion of a sliding mass $T(x,y)$ (eq. 2) shall represent $T(r_1,r_2)$ (eq. 1). The significant parameter is the scaling ratio, $S = b/a$. If $S > 1$ then the exit valley of the energy-surface (along r_1) must be plotted on a larger scale, *i.e.* it must be stretched relative to the entry valley. If $S < 1$ the converse distortion must be applied. It is evident that for the equal-mass case, for example $H_2 + H_2$ studied in ref. 2, $S = 1$. The saddle point configuration for this reaction was square, that is to say it was located symmetrically on the

Can. J. Chem. Downloaded from www.nrcresearchpress.com by 210.87.254.40 on 09/05/12
For personal use only.

Can. J. Chem. Downloaded from www.nrcresearchpress.com by 210.87.254.40 on 09/05/12
For personal use only.

$r_1 = r_2$ diagonal of the coplanar rectangular cut through the potential-energy hypersurface.

Barrier-location has an important bearing on the relative effectiveness of reagent translation and vibration in carrying the system over an energy-barrier; barriers with their crests in the approach coordinate are most-effectively surmounted if the reagents are translationally-excited, conversely barriers with their crests in the retreat coordinate are best surmounted if the reagents have vibration (10, 11). These generalizations regarding the effect of barrier-location are best applied to the location of the barrier on a scale diagnostic energy-surface (11).

It is evident from the preceding discussion that the surface for $H_2 + H_2$ needs no scaling ($S = 1$), consequently the symmetrical location of the barrier-crest, mid-way between the approach and retreat coordinates, leads to the expectation that both reagent translation and reagent vibration will be effective in bringing about reaction. The 3D trajectory calculations of Morokuma *et al.* (2) showed that this was the case.[3]

The effects of "early" and "late" energy-barriers (characterized as "surface I" and "surface II", respectively) have been explored in a 3D trajectory study of hypothetical reactions $AB + CD \rightarrow AC + BD$ (3). The diagnostic surface was the potential-energy surface for reaction through coplanar rectangular configurations. Specimen coplanar trajectories, computed numerically for the equal-mass case, were shown superimposed on the diagnostic energy surfaces I and II (Fig. 2 of ref. 3). Despite the lack of skewing or scaling, the trajectories could be understood, *qualitatively*, in terms of the path expected for a sliding point-mass. In fact the unskewed unscaled surface, as has been shown here, is the surface that causes the sliding mass to mimic the motions involved in coplanar rectangular reaction, $AB + CD \rightarrow AC + BD$.

It should be noted that the sliding-mass analogy for $AB + CD$ was developed here on the assumption that $r_{AB} = r_{CD}$ and $r_{AC} = r_{BD}$ throughout the course of the reactive encounter. In reality the vibration of AB and CD may be out of phase, and so may that of AC and BD; the configuration of the four atoms could deviate from a parallelogram for this reason (if not for others). This did occur in the trajectories recorded in Fig. 2 of ref. 3 (the mean of r_{AB},r_{CD} and the mean of r_{AC},r_{BD} was plotted). Nonetheless the sliding mass analogy retained its value as a qualitative guide to the behavior of the reacting system.

It is important to consider the effect of changing mass-combination on the barrier location. A barrier that is symmetrically-placed on the unscaled surface could be rendered significantly asymmetric on the scaled surface. For reactions $A + BC \rightarrow AB + C$ the two extremes of scaling were achieved for $L + HH$ (L symbolizes a light atom, H a heavy atom), and $H + HL$. The former gave $S \gg 1$ (extended exit valley), the latter $S \ll 1$ (extended entry valley). The corresponding mass-combinations for the exchange reaction $AB + CD \rightarrow AC + BD$ are (eq. 3) $LL + HH$ and $HL + HL$. If $L = 1$ a.m.u., $H = 80$ a.m.u., then $LL + HH$ has $S = 4.5$, $HL + HL$ has $S = 0.22$. (By contrast the other two possible combinations of these atomic masses have for $LL + HL$, $S = 1.2$, and for $HH + HL$, $S = 0.9$.)

It may be significant that the most extreme scaling should apply to the mass combinations appropriate to the celebrated reaction $H_2 + I_2 \rightarrow 2HI$ and its reverse. Noyes (13) has suggested that for the $H_2 + I_2$ reaction H_2 may approach so rapidly that the iodine atoms have insufficient time to separate as r_1 decreases. Trajectory calculations indicate the existence of special behavior due to a kinematic effect (termed the "light atom anomaly") when atomic hydrogen collides with molecular halogens; this has been interpreted as being due to the approach of H before the halogen atoms can separate (14). In the case of $H_2 + I_2$, for which there is a substantial energy-barrier, Noyes suggested that the rapid approach of H_2 might allow too little time for an interaction to occur that could lead to reaction. Reagent vibration, it was felt, would also fail to give rise to bimolecular exchange; instead it would dissociate I_2 (13).

Consideration of the probable path of a sliding mass on an appropriately scaled surface could perhaps shed some light on the effects postulated by Noyes. It should be pointed out, however, that our previous success in using the

[3]For recent, novel, experiments indicative of a requirement for vibrational excitation in the reaction $H_2 + D_2$, see ref. 12.

Can. J. Chem. Downloaded from www.nrcresearchpress.com by 210.87.254.40 on 09/05/12
For personal use only.

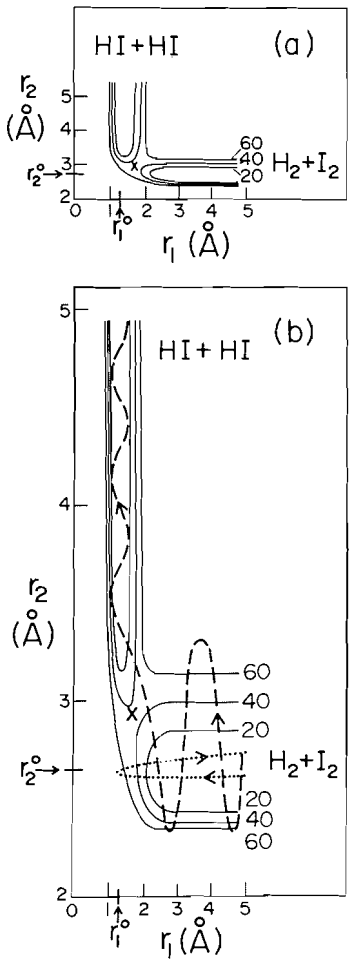

FIG. 2. (*a*) A planar rectangular (or trapezoidal) "cut" through the H_2I_2 potential-energy hypersurface obtained by Raff *et al.* (15). The contours are in kcal mol^{-1}, × is the location of the barrier crest. (*b*) The same surface drawn with scaling appropriate to the $H_2 + I_2$ mass combination. The dashed line is a hypothetical coplanar rectangular reactive trajectory with the reagent energy present as vibration. The dotted line indicates schematically the contrasting non-reactive case, in which the reagent energy is present as translation.

coplanar rectangular cut through the potential-energy surface for AB + CD as a diagnostic device was for a case (3) in which the equilibrium internuclear separations were identical ($r_1^0 = (r_1^0)'$; $r_2^0 = (r_2^0)'$), the normal force constants in the two bonds were the same ($f_1^0 = (f_1^0)'$; $f_2^0 = (f_2^0)'$), and there was no reagent rotation (the effect of reagent rotation was examined only for the case A + BC (11)). In the case of $H_2 + I_2$ reaction these restrictions will not apply.

Figure 2(*a*) shows the semi-empirical potential-energy surface obtained by Raff *et al.* for the $H_2 + I_2$ reaction (15).[4] The crest of the 42 kcal mol^{-1} energy barrier is almost symmetrically located along the reaction coordinate, since the extension in the bonds being formed and those being broken is very similar; $r_1^{\ddagger} - r_1^0 = 0.4$ Å and $r_2^{\ddagger} - r_2^0 = 0.3$ Å. Figure 2 shows the effect of applying the appropriate scaling factor, $S = 5.7$, to this $H_2 + I_2$ surface. The crest of the barrier is shifted significantly into the exit valley to give $(r_2^{\ddagger} - r_2^0)_S/(r_1^{\ddagger} - r_1^0)_S \sim 4$ (the subscript S indicates that these are *distances* measured along the scaled surface).

On the basis of our earlier model studies (3) using the mass-combinations $LL + LL$ and $LL + HH$ ($L = 1$ a.m.u., $H = 35$ a.m.u., corresponding to hydrogen and chlorine) we would anticipate (*a*) that the reactive cross-section would be detectable ($\gtrsim 0.1$ Å^2) only when the reagent energy significantly exceeded the barrier height, (*b*) that reagent vibration would be essential for barrier-crossing in the reaction $H_2 + I_2 \rightarrow 2HI$, and, by contrast, reagent translation for the reverse reaction. In each case the "disfavored" degree of freedom (translation in the former case, vibration in the latter) would further enhance the cross-section, provided that the essential threshold energy of the favored degree of freedom was present.

The first of these anticipations is based on the fact that for *both the mass-combinations* used in the model calculations on AB + CD, on both types of surface, a reagent energy of almost double the classical barrier height was required in order to obtain significant reaction. A further (25%) reduction in cross-section was noted for the unequal mass case $LL + HH$ compared with the equal mass case $LL + LL$. The latter reduction in cross-section has also been observed for the case of three-atom exchange reaction $L + HH$, as compared with $H + HL$ (11) and $H + LH$ (16). This mass-dependant reduction in cross-section is probably con-

[4]The coordinate r_1 in ref. 15 and Fig. 2 is that shown in Fig. 1. The coordinate r_2 in ref. 15 and Fig. 2 is the separation between the centers-of-mass of the two product molecules, HI. Since $m_I \gg m_H$ this means that r_2 is virtually identical to that shown in Fig. 1.

nected with the fact that the sliding mass-point (on a surface of type I *or* II) must find its way from a broad entry valley into a narrow lateral exit valley; see Fig. 2(*b*). The second of these anticipations ((*b*) above) is based on the fact that the scaled surface for $H_2 + I_2$ (Fig. 2(*b*)) is of type II, *i.e.* the barrier crest is displaced toward the exit valley. A pair of purely hypothetical trajectories have been sketched in Fig. 2(*b*) to indicate the anticipated behavior.

A recent detailed Monte Carlo study of the bimolecular reaction $H_2 + I_2$ confirms the first of these anticipations but not the second (4). The reaction cross-section was found to exhibit a threshold 10 kcal mol^{-1} in excess of the 42 kcal mol^{-1} potential-energy barrier for H_2 $(v = 0) + I_2$ $(v = 0)$. If one quantum of vibrational excitation $(E(v = 1) - E(v = 0) = 11.9$ kcal $mol^{-1})$ was introduced into the H_2, the threshold collision energy dropped from $T = 52$ kcal mol^{-1} to $T = 38.4$ kcal mol^{-1}, *i.e.* the *total* reagent energy at threshold for H_2 $(v = 1) + I_2$ $(v = 0)$ was reduced by only 1.7 kcal mol^{-1}, to 50.3 kcal mol^{-1}. For H_2 $(v = 2) + I_2$ $(v = 0)$ the *total* reagent threshold energy rose again to 58.9 kcal mol^{-1}. Vibration instead of being notably more efficient than translation in promoting reaction is at first marginally more efficient and then significantly less efficient. For the reasons already indicated $(r_1^0 \ll (r_1^0)', f_1^0 \gg (f_1^0)'$, and perhaps the rapid rotation of H_2) the scaled diagnostic surface based on coplanar rectangular reaction appears, on the present evidence, to be insufficiently representative of the actual reaction dynamics to assist more than marginally in the interpretation of the findings for the reaction $H_2 + I_2$. Our previous model studies on surfaces with early and late barriers, combined with the discussion of the sliding-mass analogy presented here, strongly suggest that there will be reactions $AB + CD \rightarrow AC + BD$ (less pathological than $H_2 + I_2$) for which the coplanar rectangular diagnostic cut can serve as an aid to interpretation.

D.S.P thanks the National Research Council of Canada for the award of a scholarship. This work was supported by grants from the National Research Council of Canada, the National Aeronautics and Space Administration (Grant NGR 52-026-028), and the Defence Research Board of Canada (Grant 9530-104, U.G.).

1. L. D. SPICER and D. S. RABINOVITCH. Ann. Rev. Phys. Chem. **21**, 349 (1970).
2. K. MOROKUMA, L. PEDERSEN, and M. KARPLUS. J. Am. Chem. Soc. **89**, 5064 (1967).
3. M. H. MOK and J. C. POLANYI. J. Chem. Phys. **53**, 4588 (1970).
4. L. M. RAFF, D. L. THOMPSON, L. B. SIMS, and R. N. PORTER. J. Chem. Phys. **56**, 5998 (1972).
5. J. B. ANDERSON. Private communication.
6. S. GLASSTONE, K. J. LAIDLER, and H. EYRING. The theory of rate processes. McGraw-Hill, New York. 1941. p. 100.
7. D. L. BUNKER. *In* Methods in computational physics. Vol. 10. *Edited by* B. Alder, S. Fernbach, and M. Rotenberg. Academic Press, New York. 1971. p. 287.
8. J. C. POLANYI. Acc. Chem. Res. **5**, 161 (1972).
9. D. W. JEPSEN and J. O. HIRSCHFELDER. Proc. Nat. Acad. Sci. **45**, 249 (1959).
10. J. C. POLANYI and W. H. WONG. J. Chem. Phys. **51**, 1439 (1969).
11. B. A. HODGSON and J. C. POLANYI. J. Chem. Phys. **55**, 4745 (1971).
12. S. H. BAUER, D. M. LEDERMAN, E. L. RESLER, JR., and E. R. FISHER. Int. J. Chem. Kin. To be published.
13. R. M. NOYES. J. Chem. Phys. **48**, 323 (1968).
14. P. J. KUNTZ, E. M. NEMETH, J. C. POLANYI, S. D. ROSNER, and C. E. YOUNG. J. Chem. Phys. **44**, 1168 (1966).
15. L. M. RAFF, L. STIVERS, R. N. PORTER, D. L. THOMPSON, and L. B. SIMS. J. Chem. Phys. **52**, 3449 (1970).
16. C. A. PARR, J. C. POLANYI, and W. H. WONG. J. Chem. Phys. In press.

Can. J. Chem. Downloaded from www.nrcresearchpress.com by 210.87.254.40 on 09/05/12
For personal use only.

Thiohydantoins. XII. Secondary Deuterium Isotope Effects in the Acid- and Base-catalyzed Hydrolysis of 1-Acetyl-5,5-dimethyl-2-thiohydantoin

WAYNE I. CONGDON[1] AND JOHN T. EDWARD
Department of Chemistry, McGill University, Montreal, Quebec

Received June 7, 1972

The rates of hydrolysis of 1-acetyl-5,5-dimethyl-2-thiohydantoin and of 1-acetyl-d_3-5,5-dimethyl-2-thiohydantoin in acid and base over the temperature range 11–58 °C have been measured. For the A-1 hydrolysis in 96.3% sulfuric acid, k_H/k_D decreased from 1.31 at 10.8° to 1.05 at 58.1°; these results accord with the proposed mechanism. For A-2 hydrolysis in 39.6% sulfuric acid and for base-catalyzed hydrolysis in dilute sodium hydroxide, k_H/k_D *vs.* temperature passed through a minimum at about 40 and 25° respectively. Some possible reasons for the temperature effect are discussed.

On a observé les vitesses de l'hydrolyse de l'acétyl-1 diméthyl-5,5 thiohydantoïne-2 et de l'acétyl-1-d_3 diméthyl-5,5 thiohydantoïne-2 dans les solutions acides et basiques entre les températures 11–58 °C. Pour l'hydrolyse A-1 en acide sulfurique de 96.3%, k_H/k_D decroisse de 1.31 à 10.8° à 1.05 à 58.1°, en accord avec autres réactions de mécanisme semblable. Cependant, pour l'hydrolyse A-2 en acide sulfurique de 39.6% et pour l'hydrolyse en hydroxide de sodium dilué, k_H/k_D *vs.* température passe par un minimum. On discute des causes possibles pour cet effet.

Canadian Journal of Chemistry, **50**, 3921 (1972)

Possible mechanisms for the hydrolysis of 1-acyl-2-thiohydantoins in aqueous acid (*1*) and base (2) have been derived from a consideration of several well-established criteria (acidity effects, entropies of activation, Hammett $\rho\sigma$ relations, etc.). It accordingly became of interest to consider yet another criterion, that of secondary deuterium isotope effects. For this reason, we synthesized 1-acetyl-d_3-5,5-dimethyl-2-thiohydantoin (**1**), and compared its rates of hydrolysis to acetic acid-d_3 (**2**) and 5,5-dimethyl-2-thiohydantoin (**3**) in aqueous acid and alkali with the corresponding rates for the protio-compound (see eq. 1). We report below (in order) the results for hydrolysis in 96.3% sulfuric acid, in dilute sodium hydroxide, and in 39.6% sulfuric acid, since this probably represents the order of increasing complexity of mechanisms. Rates were determined in a large excess of acid or base, and rate constants k are pseudo-first-order constants for the disappearance of the 1-acyl-2-thiohydantoin.

In 96.3% sulfuric acid $k_H/k_D > 1$ (Table 1) and increased as the temperature was lowered; extrapolation to $-22°$ indicated that the isotope effect at this temperature would be roughly that found by Bender and Feng (3) for the hydrolysis of acetyl chloride in 10% aqueous acetone. Bender and Feng advance reasons for believing that hydrolysis of acetyl chloride under these conditions proceeds by a rate-determining ionization to chloride ion and acylium ion (CH_3CO^+ or CD_3CO^+). The secondary isotope effects support this view: the formation of carbonium ions is known to be retarded by β-deuterium substitution (4), although there is no unanimity on the explanation. Hyperconjugation (4, 5) and steric effects (6) have been invoked, and in very

[1] 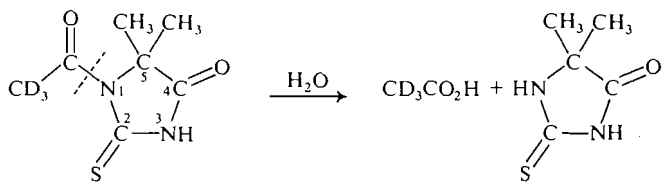

1 **2** **3**

[1]Holder of NRCC Scholarship, 1968–1970.

Can. J. Chem. Downloaded from www.nrcresearchpress.com by 210.87.254.105 on 09/05/12
For personal use only.

TABLE 1. The effect of temperature on the pseudo-first-order rates (k) of hydrolysis of 1-acetyl-d_3-5,5-dimethyl-2-thiohydantoin and 1-acetyl-5,5-dimethyl-2-thiohydantoin

Reaction conditions	Temperature (°C)	k for 1-CH_3 (10^4 s^{-1})	No. of runs	k for 1-CD_3 (10^4 s^{-1})	No. of runs	k_H/k_D	Average error
96.3% sulfuric acid	10.8	1.15± 0.04	2	0.88±0.03	2	1.31	0.10
	20.1	3.11± 0.04	2	2.57±0.04	2	1.22	0.03
	35.5	24.20± 0.60	3	21.30±0.60	3	1.14	0.05
	49.6	124.00± 4.00	3	114.00±2.40	3	1.08	0.05
	58.1	266.00±12.00	3	235.00±7.30	3	1.05	0.08
39.6% sulfuric acid	11.0	7.15± 0.03	3	7.52±0.12	3	0.95	0.02
	25.3	26.00± 0.04	2	28.10±0.19	2	0.93	0.01
	35.5	54.70± 0.43	3	56.70±0.86	3	0.96	0.02
	49.6	170.00± 7.22	5	150.00±1.54	2	1.13	0.06
$pH = 11.95$ $\mu = 0.55$	11.0	3.65± 0.02	2	3.64±0.13	3	1.00	0.04
	25.3	12.90± 0.04	3	13.20±0.02	2	0.97	0.004
	49.6	95.80± 0.93	3	98.30±0.83	3	0.97	0.02
	58.1	177.00± 2.10	3	177.00±1.30	3	1.00	0.02

aqueous solutions the latter effects may be manifest in altered entropies of activation (7). The increase in the isotope effect as the temperature is lowered is in line with calculations by Miller (8). These results support the A-1 mechanism already advanced for the hydrolysis of 1-acyl-2-thiohydantoins in concentrated sulfuric acid (1).

Halevi and Margolin (9) found that k_H/k_D for the hydrolysis of ethyl acetate-d_3 in dilute aqueous sodium hydroxide varied with temperature, going through a minimum ($\sim$0.90) at about 25°. We found evidence for a similar but very much smaller, effect of temperature on the alkaline hydrolysis of 1-acetyl-d_3-5,5-dimethyl-2-thiohydantoin; the effect is scarcely greater than experimental error (see Table 1).

Thornton (10) suggested that Halevi and Margolin's results might be explained by a change of mechanism with temperature. However, this would lead to a non-linear Arrhenius plot; this we do not observe for the hydrolysis of 1-acetyl-5,5-dimethyl-2-thiohydantoin in alkaline solution (or in the two concentrations of acid). Halevi and Margolin point out that the secondary isotope effect observed by them (and observed by others in highly aqueous solutions) is probably caused by small differences in energy and entropy of solvation, resulting from isotopic differences in average charge distribution. In the hydrolysis of 1-acetyl-d_3-5,5-dimethyl-2-thiohydantoin certain special steric effects should additionally be considered, which would preferentially destabilize the protio compound (2). Hence the data displayed in Table 1 can be considered as compatible with (if not convincing evidence for) a similarity in mechanism for the two reactions, both involving formation of a tetrahedral intermediate.

The A-2 acid hydrolysis of esters, in contrast to their alkaline hydrolysis, is relatively unaffected by the electronic effects of changing substitution in the acyl moiety, the effect of the substituent on the preequilibrium protonation being counterbalanced by its effect on the rate of the subsequent attack by a water molecule (11). Consequently, we might expect steric and solvation effects to become predominant in the hydrolysis of 1-acetyl-d_3-5,5-dimethyl-2-thiohydantoin in 39.6% sulfuric acid, which has been shown to proceed most probably by A-2 mechanism (1). However, it is difficult to guess in what direction steric effects caused by the greater "size" of the CH_3 group (6) should operate because of the possibility of destabilization of the ground state by interference between methyl and sulfur (2). In the event, the isotope effect proved to be temperature dependent and k_H/k_D showed a minimum at about 25° (Table 1). The isotope effect is close to that found by Halevi and Margolin for the alkaline hydrolysis of methyl acetate in dilute aqueous solution. This is interesting, because solvation effects in 39.6% sulfuric acid should be quite different

Can. J. Chem. Downloaded from www.nrcresearchpress.com by 210.87.254.105 on 09/05/12
For personal use only.

from those in water (12). While we can offer no plausible explanation, the difference in isotope effects for the hydrolysis in 39.6 and in 96.3% acid points to a difference in mechanism, in agreement with arguments based on other criteria (1).

Experimental

Acetic anhydride-d_6 and acetic acid-d_4 were purchased from Stohler Isotope of Canada and used in the general procedure of Johnson and Nicolet (13) for the preparation of 1-acyl-2-thiohydantoins. 1-Acetyl-5,5-dimethyl-2-thiohydantoin was characterized by m.p. (uncorrected) 186–187 °C, in agreement with Carrington (14), and by n.m.r. (3H-singlet at 7.33 and 6H-singlet 8.5 τ). 1-Acetyl-d_3-5,5-dimethyl-2-thiohydantoin had the same m.p. and n.m.r. spectrum, except that the peak at 7.33 τ was missing. Both compounds in water showed the same u.v. absorption spectrum. Experimental methods for following the hydrolysis and for working-up the data have been described (1, 2).

Grateful acknowledgement is made to the National Research Council of Canada for financial support.

1. W. I. CONGDON and J. T. EDWARD. Can. J. Chem. This issue. Part X.
2. W. I. CONGDON and J. T. EDWARD. Can. J. Chem. This issue. Part XI.
3. M. L. BENDER and M. FENG. J. Am. Chem. Soc. **82**, 6318 (1960).
4. E. S. LEWIS and C. E. BOOZER. J. Am. Chem. Soc. **74**, 6306 (1952).
5. E. A. HALEVI. Prog. Phys. Org. Chem. **1**, 109 (1963).
6. L. S. BARTELL. J. Am. Chem. Soc. **83**, 3567 (1961); Tetrahedron, **17**, 177 (1962).
7. K. T. LEFFEK, R. E. ROBERTSON, and S. E. SUGAMORI. Can. J. Chem. **39**, 1989 (1961).
8. S. I. MILLER. J. Phys. Chem. **66**, 978 (1962).
9. E. A. HALEVI and Z. MARGOLIN. Proc. Chem. Soc. 174 (1964).
10. E. R. THORNTON. Ann. Rev. Phys. Chem. **17**, 365 (1966).
11. R. W. TAFT. Steric effects in organic chemistry. *Edited by* M. S. Newman. John Wiley and Sons, London, 1956. p. 588.
12. E. M. ARNETT and J. J. BURKE. J. Am. Chem. Soc. **88**, 2390 (1966).
13. T. B. JOHNSON and B. H. NICOLET. J. Am. Chem. Soc. **33**, 1973 (1911).
14. H. C. CARRINGTON. J. Chem. Soc. 681 (1947).

A New Photochemical Reaction of Unconjugated Thioketones[1,2,3]

JAMES J. WORMAN,[4] MASON SHEN, AND PATRICK C. NICHOLS
Department of Chemistry, South Dakota State University, Brookings, South Dakota 57006

Received April 5, 1972

Tetramethyl-3-thio-1,3-cyclobutanedione (**1**) and tetramethyl-1,3-cyclobutanedithione (**6**) react with oxygen in the presence of light to yield tetramethyl-1,3-cyclobutanedione (**2**). A mechanism involving singlet oxygen is suggested. 1,3-Diphenyl-2-propanethione (**3**) undergoes accelerated dimerization in the presence of visible radiation to yield tetrabenzyl-1,3-dithietane (**4**).

La tétraméthylthio-3 cyclobutanedione-1,3 (**1**) et la tétraméthylcyclobutanedithione-1,3 (**6**) réagissent avec l'oxygène en présence de lumière pour conduire à la tétraméthylcyclobutanedione-1,3 (**2**). Un mécanisme faisant intervenir l'oxygène singulet est suggéré. La diphényl-1,3 propanethione-2 (**3**) subit une dimérisation accélérée en présence de radiation visible pour conduire au tétrabenzyldithiétane-1,3 (**4**).

[Traduit par le journal]

Canadian Journal of Chemistry, **50**, 3923 (1972)

In a continuing attempt to understand the chemical differences between unconjugated ketones, imines and thioketones, (1) we have investigated the photochemistry of compounds containing the thiocarbonyl chromophore. There were no documented photochemical reports in the literature concerning this unconjugated chromophore until adamantanethione very recently (2) was shown to dimerize and add to alkenes probably through an $n \rightarrow \pi^*$ triplet state.

[1]Presented in part at the Regional Midwest ACS Meetings, Kansas City, Mo., October 1969, Abstr. No. 403 and St. Louis, Mo., October 1971, Abstr. No. 521.

[2]Taken in part from the M.S. Thesis of Mason Shen, South Dakota State University, January 1972.

[3]Taken in part from the M.S. Thesis of Patrick C. Nichols, South Dakota State University, June 1970.

[4]Author to whom correspondence should be addressed.

Can. J. Chem. Downloaded from www.nrcresearchpress.com by 210.87.254.105 on 09/05/12
For personal use only.

from those in water (12). While we can offer no plausible explanation, the difference in isotope effects for the hydrolysis in 39.6 and in 96.3% acid points to a difference in mechanism, in agreement with arguments based on other criteria (1).

Experimental

Acetic anhydride-d_6 and acetic acid-d_4 were purchased from Stohler Isotope of Canada and used in the general procedure of Johnson and Nicolet (13) for the preparation of 1-acyl-2-thiohydantoins. 1-Acetyl-5,5-dimethyl-2-thiohydantoin was characterized by m.p. (uncorrected) 186–187 °C, in agreement with Carrington (14), and by n.m.r. (3H-singlet at 7.33 and 6H-singlet 8.5 τ). 1-Acetyl-d_3-5,5-dimethyl-2-thiohydantoin had the same m.p. and n.m.r. spectrum, except that the peak at 7.33 τ was missing. Both compounds in water showed the same u.v. absorption spectrum. Experimental methods for following the hydrolysis and for working-up the data have been described (1, 2).

Grateful acknowledgement is made to the National Research Council of Canada for financial support.

1. W. I. CONGDON and J. T. EDWARD. Can. J. Chem. This issue. Part X.
2. W. I. CONGDON and J. T. EDWARD. Can. J. Chem. This issue. Part XI.
3. M. L. BENDER and M. FENG. J. Am. Chem. Soc. **82**, 6318 (1960).
4. E. S. LEWIS and C. E. BOOZER. J. Am. Chem. Soc. **74**, 6306 (1952).
5. E. A. HALEVI. Prog. Phys. Org. Chem. **1**, 109 (1963).
6. L. S. BARTELL. J. Am. Chem. Soc. **83**, 3567 (1961); Tetrahedron, **17**, 177 (1962).
7. K. T. LEFFEK, R. E. ROBERTSON, and S. E. SUGAMORI. Can. J. Chem. **39**, 1989 (1961).
8. S. I. MILLER. J. Phys. Chem. **66**, 978 (1962).
9. E. A. HALEVI and Z. MARGOLIN. Proc. Chem. Soc. 174 (1964).
10. E. R. THORNTON. Ann. Rev. Phys. Chem. **17**, 365 (1966).
11. R. W. TAFT. Steric effects in organic chemistry. *Edited by* M. S. Newman. John Wiley and Sons, London, 1956. p. 588.
12. E. M. ARNETT and J. J. BURKE. J. Am. Chem. Soc. **88**, 2390 (1966).
13. T. B. JOHNSON and B. H. NICOLET. J. Am. Chem. Soc. **33**, 1973 (1911).
14. H. C. CARRINGTON. J. Chem. Soc. 681 (1947).

A New Photochemical Reaction of Unconjugated Thioketones[1,2,3]

JAMES J. WORMAN,[4] MASON SHEN, AND PATRICK C. NICHOLS
Department of Chemistry, South Dakota State University, Brookings, South Dakota 57006

Received April 5, 1972

Tetramethyl-3-thio-1,3-cyclobutanedione (**1**) and tetramethyl-1,3-cyclobutanedithione (**6**) react with oxygen in the presence of light to yield tetramethyl-1,3-cyclobutanedione (**2**). A mechanism involving singlet oxygen is suggested. 1,3-Diphenyl-2-propanethione (**3**) undergoes accelerated dimerization in the presence of visible radiation to yield tetrabenzyl-1,3-dithietane (**4**).

La tétraméthylthio-3 cyclobutanedione-1,3 (**1**) et la tétraméthylcyclobutanedithione-1,3 (**6**) réagissent avec l'oxygène en présence de lumière pour conduire à la tétraméthylcyclobutanedione-1,3 (**2**). Un mécanisme faisant intervenir l'oxygène singulet est suggéré. La diphényl-1,3 propanethione-2 (**3**) subit une dimérisation accélérée en présence de radiation visible pour conduire au tétrabenzyldithiétane-1,3 (**4**).

[Traduit par le journal]

Canadian Journal of Chemistry, **50**, 3923 (1972)

In a continuing attempt to understand the chemical differences between unconjugated ketones, imines and thioketones, (1) we have investigated the photochemistry of compounds containing the thiocarbonyl chromophore. There were no documented photochemical reports in the literature concerning this unconjugated chromophore until adamantanethione very recently (2) was shown to dimerize and add to alkenes probably through an $n \rightarrow \pi^*$ triplet state.

[1]Presented in part at the Regional Midwest ACS Meetings, Kansas City, Mo., October 1969, Abstr. No. 403 and St. Louis, Mo., October 1971, Abstr. No. 521.

[2]Taken in part from the M.S. Thesis of Mason Shen, South Dakota State University, January 1972.

[3]Taken in part from the M.S. Thesis of Patrick C. Nichols, South Dakota State University, June 1970.

[4]Author to whom correspondence should be addressed.

Can. J. Chem. Downloaded from www.nrcresearchpress.com by 210.87.254.6 on 09/05/12
For personal use only.

[1] 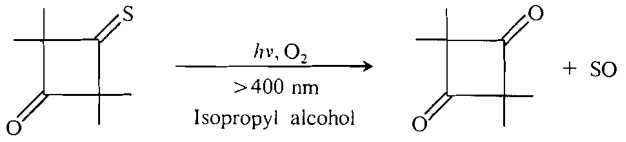

1 2

[2] 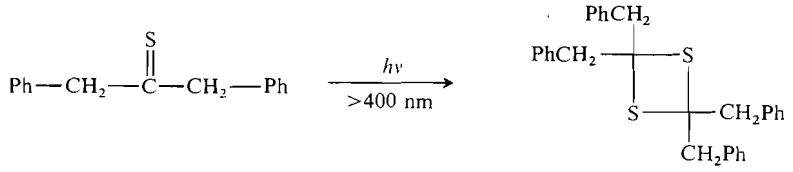

3 4

We wish to report the first example of an unconjugated thioketone reacting photochemically with oxygen. Tetramethyl-3-thio-1,3-cyclobutanedione (**1**) (3) when irradiated in isopropyl alcohol at wavelengths >400 nm in the presence of oxygen gave tetramethyl-1,3-cyclobutanedione (**2**) and most likely sulfur monoxide (eq. 1). The reaction was complete in 3 days and there was no evidence for the formation of a dimer even in the absence of oxygen. It would appear the resulting dimer is structurally unfavorable in this case.

Dibenzyl thione (**3**) photochemically does give tetrabenzyl-1,3-dithietane (**4**) in quantitative yield (eq. 2). This dimerization also occurs in the dark but is definitely accelerated by light. These results are consistent with those reported on the dark reactions of cyclohexanethione (4), in which it was shown that the ground state reaction possessed both ionic and free radical character.

In an attempt to determine the mechanism for the photochemical reaction of the monothione (**1**) with oxygen we encountered once again the importance of singlet oxygen. Because the reaction occurs in the absence of a dye photosensitizer it might be suggested that the reaction proceeds via the triplet $n \rightarrow \pi^*$ state of the thione and triplet oxygen to give a cyclic intermediate (**5**), which then collapses to give the desired products. Our kinetic data obviate this pathway. The reaction is first order in monothione, at low concentration of **1** (0.01–0.1 *M*), and yet the rate decreases dramatically at high concentrations of **1** (1 *M*). This suggests a competitive excited state reaction, photochemical quenching, or substantially decreased oxygen solubility. We are hypothesizing that the excited state thione itself photosensitizes the formation of singlet oxygen from triplet oxygen in a spin forbidden process (5). Singlet oxygen then reacts with ground state thione to give the cyclic intermediate (**5**) which collapses to give

[3] 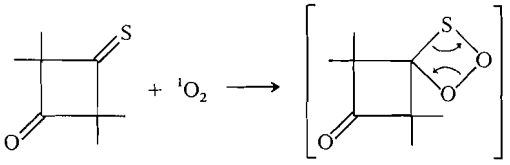

1 5

the products (eq. 3). Ground state thione (**1**) does react in the dark with singlet oxygen generated thermally (6) to give the same products. This reaction occurs at a faster rate than the photochemical reaction and this is consistent with our hypothesis. A mechanism similar to ours has been shown to occur in the dye-photosensitized photooxygenation of 4*H*-pyran-4-thiones and 4*H*-thiopyran-4-thiones (7).

We examined the photochemistry of tetramethyl-1,3-cyclobutanedithione (**6**) under identical conditions to those used for the monothione (**1**) and the same products resulted (eq. 4). Experimental evidence suggests that there is no transannular participation in the dithione (**6**) or in (**1**) (8). We feel therefore that the presence of the carbonyl chromophone has no significant effect when irradiation is carried out on (**1**) at wavelengths greater than 400 nm.

Although only a few examples are present in the literature, it would appear that simple unconjugated thioketones are to some extent unlike their oxygen or nitrogen analogs. The thiones absorb light and react through an

Can. J. Chem. Downloaded from www.nrcresearchpress.com by 210.87.254.6 on 09/05/12
For personal use only.

[4] 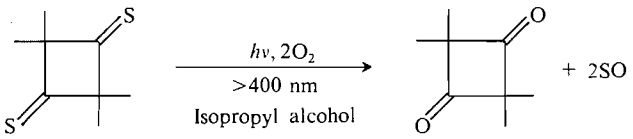

6 2

$n \rightarrow \pi^*$ state to add to alkenes or dimerize in the absence of alkenes if the spirothietane is sterically favorable. A third reaction results in the formation of ketones by reaction of the excited state thione with oxygen.

The mechanisms of these reactions are somewhat aberrant. We are presently investigating the feasibility of the monothione (**1**) acting as a dye type photosensitizer for the production of singlet oxygen.

Experimental

Melting points are uncorrected. The i.r. spectra were recorded with a Perkin–Elmer 521 grating i.r. spectrometer. Visible and u.v. spectra were run on a Beckman DK-2A ratio recording spectrophotometer. The n.m.r. spectra were obtained from a Varian A-60A instrument. Samples were dissolved in CCl_4 solution using tetramethylsilane as the internal standard. Molecular weight data were obtained by use of a Mechrolab Model 301A vapor phase osmometer. Samples were run as solutions in benzene. Mass spectra were run on both the Varian CH-5 and CEC-103-C mass spectrometers at the University of Wyoming, Laramie, Wyoming. Vapor phase chromatography was performed on an Aerograph Autoprep Model A-700 using 30% SE30 on 45/60 Chrom-P. The aluminum column dimensions were 3/8 in. × 20 ft and the operating temperature was 100 °C. Analytical v.p.c. was performed on a Beckman GC-2A using 15% SE-30 on 45/60 Chrom-P. The dimensions of the column were 1/4 in. × 10 ft and the operating temperature was 160 °C. Chemical analyses were performed by Galbraith Laboratories Inc., Knoxville, Tennessee.

*Tetramethyl-3-thio-1,3-cyclobutanedione (**1**) and Tetramethyl-1,3-cyclobutanedithione (**6**)*

The procedure used here was a modification of the one described by Elam and Davis (3).

To 210 g (1.50 mol) of tetramethyl-1,3-cyclobutanedione (**2**) (Aldrich Chemical Co.) dissolved in 500 ml of pyridine was added 150 g (0.67 mol) of phosphorus pentasulfide (Fisher Scientific Co.) and the mixture refluxed for 40 min. After cooling to room temperature the pyridine was decanted and saved. The remaining solid was heated to boiling with 125 ml of fresh pyridine and once again decanted. The combined pyridine solutions were distilled rapidly without fractionating *in vacuo* (35–50 mm Hg). The pyridine was then removed *in vacuo* (30 mm Hg) by fractional distillation until the temperature reached 60 °C. The resulting residue was extracted with 150 ml of warm hexane and then cooled to 20 °C. At this point the majority of unreacted **2** would crystallize. The compound was collected on a Büchner and washed with hexane to remove the last traces of red color. The mother liquor and the hexane washings were combined and distilled and a fraction collected at 160–170 °C. This heavy red liquid was subjected to column chromatography on silicic acid (Matheson Coleman and Bell) with hexane as the eluting solvent. Column dimensions were 80 cm long × 3 cm diameter and the column was packed about half full. After 1 h, three distinct layers appeared. The layers were collected, solvent evaporated, and the compound identified.

Tetramethyl-1,3-cyclobutanedithione (**6**), the first layer, was an orange solid, m.p. 123–125° (lit. 124–125°) (3); i.r.: 1460, 1256, and 1075 cm^{-1}; n.m.r.: 1.40 δ (12H, S); visible and u.v. absorptions in hexane, λ_{max} 227 (ε 21 600), 298 (409), 500 nm (22.4); *m/e* 172; yield 10%.

Tetramethyl-3-thio-1,3-cyclobutanedione (**1**), the second layer, was a red solid, m.p. 57–58° (lit. 57–58°) (3); i.r.: 1800, 1700, 1450, 1290, and 1125 cm^{-1}; n.m.r.: 1.33 δ (12H, S); visible and u.v. absorptions in hexane, λ_{max} 228 nm (ε 8700), 270 (300), 318 (100), and 520 nm (9.65); *m/e* 156; yield 50%.

The third layer was unreacted tetramethyl-1,3-cyclobutanedione.

*Photolysis of Tetramethyl-3-thio-1,3-cyclobutanedione (**1**)*

A solution of **1**, 0.096 *M* in isopropyl alcohol was irradiated through a Kimax sleeve using a 250 W R40/3 Westinghouse lamp. The reaction was followed by u.v. spectroscopy and v.p.c. There was no apparent reaction after 10 days.

Any oxygen stream was introduced and after 3 days the monothione **1** had completely reacted. The hexane solution was evaporated to give a white solid which was purified by sublimation. The compound was identical in all respects to that of an authentic sample of tetramethyl-1,3-cyclobutanedione (**2**); yield 75%.

The effluent oxygen stream from the photoreaction was trapped using 100 ml of 1% sodium hydroxide. The excess sodium hydroxide was neutralized with hydrochloric acid and the solution titrated with iodine to indicate the presence of sodium sulfite, thus the presence of SO_2 in the oxygen stream.

A second method for the detection of sulfur dioxide was to precipitate and identify barium sulfite from a portion of the non-neutralized sodium hydroxide solution.

The photolysis was carried out in hexane and in carbon tetrachloride and the times for complete reaction were 5 and 1 days respectively.

*Reaction of Tetramethyl-3-thio-1,3-cyclobutanedione (**1**) with Singlet Oxygen*

Tetramethyl-3-thio-1,3-cyclobutanedione (**1**), 0.10 *M* in isopropyl alcohol was placed in a 250 ml separatory funnel and 50 ml of 5.25% sodium hypochlorite solution (Hilex) was placed in another separatory funnel. Both funnels were attached to a 250 ml three-neck flask containing 50 ml of 30% hydrogen peroxide (J. T. Baker) which was being stirred magnetically. The sodium hypochlorite solution was added slowly and completely, followed by the dropwise

Can. J. Chem. Downloaded from www.nrcresearchpress.com by 210.87.254.6 on 09/05/12
For personal use only.

addition of the monothione **1** solution. The reaction was complete in 5 min. The gas evolving from the reaction was trapped using 100 ml of 1% sodium hydroxide. A positive analysis for SO_2 was obtained as described above. The diketone **2** was obtained by evaporation of the isopropyl alcohol, yield 90%.

There was no apparent reaction (by visible spectroscopy or v.p.c.) when the monothione **1** was added separately to hydrogen peroxide or to sodium hypochlorite solution.

Photolysis of Tetramethyl-1,3-cyclobutanedithione (6)

A 0.10 *M* solution of the dithione **6** in hexane was irradiated under identical conditions as reported for the monothione **1**. Sulfur dioxide and the diketone **2** were identified as reported above. The reaction was complete in 3 days.

1,3-Diphenyl-2-propanethione (3)

Modified procedure of Mayer and Berthold (9).

To 27.2 g (0.10 mol) of 2,2-diethoxy-1,3-diphenylpropane (10) was added 0.05 g of *p*-toluenesulfonic acid. Hydrogen sulfide gas was passed through the solution for 8 h or until the solution was a consistent brilliant red. The solution was evaporated *in vacuo* to remove excess ketal, hydrogen sulfide, and ethanol. The condensate was a viscous red liquid, n.m.r.: 4.17 (4H, S), 7.19 δ (10H, m), visible absorptions in cyclohexane, λ_{max} 510 nm (ε 10); *m/e* 226, P + 2 228 (1 sulfur).

Tetrabenzyl-1,3-dithietane (4)

1,3-Diphenyl-2-propanethione (**3**) was irradiated using direct sunlight and a Pyrex container. The red color began to disappear and a white precipitate began to form after 2 h. The red color was completely gone after 2 days. The solution was filtered with solution and the precipitate washed with ethanol and acetone. The crude product was then recrystallized from carbon tetrachloride collected and dried in an oven at 120° for 24 h; m.p. 247–248°; i.r.: 3080, 3050, 3025, 2925, 2900, 2825, 1947, 1880, 1810, 1765, 1600, 1577, 1488, 1449, 1426, 1379, 1321, 1309, 1211, 1172, 1150, 1141, 1075, 1039, 1025, 1000, 992, 982, 970, 954, 911, 900, 879, 850, 827, 808, 752, 740, 702, 690, 608, 590, 565, 510 and 460 cm^{-1}; n.m.r.: 7.25 δ (20H, S); *m/e* 452 P + 2 454 (2 sulfur); v.p.o. 442 g/mol.

Anal. Calcd. for $C_{30}H_{28}S_2$: C, 79.59; H, 6.23. Found: C, 79.18; H, 6.39.

1,3-Diphenyl-2-propanethione (**3**) will also dimerize in the dark to give tetrabenzyl-1,3-dithietane (**4**) but the reaction is not nearly complete even after 8 days.

1. J. J. WORMAN, G. L. POOL, and W. P. JENSEN. J. Chem. Ed. **47**, 709 (1970).
2. C. C. LIAO and P. DE MAYO. Chem. Commun. 1525 (1971).
3. E. U. ELAM and H. E. DAVIS. J. Org. Chem. **32**, 1562 (1967).
4. A. KATRITZKY, R. MAYER, J. MORGENSTERN, and M. J. SEWELL. J. Chem. Soc. 5953 (1965).
5. D. R. KEARNS. Chem. Rev. **71**, 395 (1971).
6. C. S. FOOTE, S. WEXLER, W. ANDO, R. HIGGINS. J. Am. Chem. Soc. **90**, 975 (1968).
7. N. ISHIBE, M. ODANI, and M. SUNAMI. J. Chem. Soc. B, 1837 (1971).
8. R. E. BALLARD and C. H. PARK. Spectrochim. Acta, **26**A, 43 (1970).
9. R. MAYER and H. BERTHOLD. Ber. **96**, 3096 (1963).
10. C. D. HURD and M. A. POLLACK. J. Am. Chem. Soc. **60**, 1905 (1938).

The Investigation of Cation–Anion Interactions by ^{39}K Nuclear Magnetic Resonance

E. G. BLOOR[1]

Cariboo College, Kamloops, British Columbia

AND

R. G. KIDD

Department of Chemistry, University of Western Ontario, London 72, Ontario

Received December 17, 1968[2]

The ^{39}K chemical shifts in a number of aqueous electrolyte solutions have been determined. These arise from the overlapping of the outer electron orbitals of the anion and cation during random ionic collisions. The magnitudes of the chemical shifts are shown to be directly proportional to the effectiveness of this overlap interaction.

Nous avons déterminé les déplacements chimiques du ^{39}K dans différentes solutions électrolytiques aqueuses. Ceux-ci proviennent du recouvrement des orbitales des électrons externes de l'anion et du cation lors de collisions ioniques aléatoires. Nous avons montré que l'importance de ces déplacements chimiques est directement proportionnelle à cette interaction de recouvrement.

Canadian Journal of Chemistry, **50**, 3926 (1972)

[1]Present address: Department of Chemistry, Simon Fraser University, Burnaby 2, British Columbia.

[2]Revision received June 23, 1972.

Can. J. Chem. Downloaded from www.nrcresearchpress.com by 210.87.254.6 on 09/05/12
For personal use only.

addition of the monothione **1** solution. The reaction was complete in 5 min. The gas evolving from the reaction was trapped using 100 ml of 1% sodium hydroxide. A positive analysis for SO_2 was obtained as described above. The diketone **2** was obtained by evaporation of the isopropyl alcohol, yield 90%.

There was no apparent reaction (by visible spectroscopy or v.p.c.) when the monothione **1** was added separately to hydrogen peroxide or to sodium hypochlorite solution.

Photolysis of Tetramethyl-1,3-cyclobutanedithione (6)

A 0.10 *M* solution of the dithione **6** in hexane was irradiated under identical conditions as reported for the monothione **1**. Sulfur dioxide and the diketone **2** were identified as reported above. The reaction was complete in 3 days.

1,3-Diphenyl-2-propanethione (3)

Modified procedure of Mayer and Berthold (9).

To 27.2 g (0.10 mol) of 2,2-diethoxy-1,3-diphenylpropane (10) was added 0.05 g of *p*-toluenesulfonic acid. Hydrogen sulfide gas was passed through the solution for 8 h or until the solution was a consistent brilliant red. The solution was evaporated *in vacuo* to remove excess ketal, hydrogen sulfide, and ethanol. The condensate was a viscous red liquid, n.m.r.: 4.17 (4H, S), 7.19 δ (10H, m), visible absorptions in cyclohexane, λ_{max} 510 nm (ε 10); *m/e* 226, P + 2 228 (1 sulfur).

Tetrabenzyl-1,3-dithietane (4)

1,3-Diphenyl-2-propanethione (**3**) was irradiated using direct sunlight and a Pyrex container. The red color began to disappear and a white precipitate began to form after 2 h. The red color was completely gone after 2 days. The solution was filtered with solution and the precipitate washed with ethanol and acetone. The crude product was then recrystallized from carbon tetrachloride collected and dried in an oven at 120° for 24 h; m.p. 247–248°; i.r.: 3080, 3050, 3025, 2925, 2900, 2825, 1947, 1880, 1810, 1765, 1600, 1577, 1488, 1449, 1426, 1379, 1321, 1309, 1211, 1172, 1150, 1141, 1075, 1039, 1025, 1000, 992, 982, 970, 954, 911, 900, 879, 850, 827, 808, 752, 740, 702, 690, 608, 590, 565, 510 and 460 cm^{-1}; n.m.r.: 7.25 δ (20H, S); *m/e* 452 P + 2 454 (2 sulfur); v.p.o. 442 g/mol.

Anal. Calcd. for $C_{30}H_{28}S_2$: C, 79.59; H, 6.23. Found: C, 79.18; H, 6.39.

1,3-Diphenyl-2-propanethione (**3**) will also dimerize in the dark to give tetrabenzyl-1,3-dithietane (**4**) but the reaction is not nearly complete even after 8 days.

1. J. J. WORMAN, G. L. POOL, and W. P. JENSEN. J. Chem. Ed. **47**, 709 (1970).
2. C. C. LIAO and P. DE MAYO. Chem. Commun. 1525 (1971).
3. E. U. ELAM and H. E. DAVIS. J. Org. Chem. **32**, 1562 (1967).
4. A. KATRITZKY, R. MAYER, J. MORGENSTERN, and M. J. SEWELL. J. Chem. Soc. 5953 (1965).
5. D. R. KEARNS. Chem. Rev. **71**, 395 (1971).
6. C. S. FOOTE, S. WEXLER, W. ANDO, R. HIGGINS. J. Am. Chem. Soc. **90**, 975 (1968).
7. N. ISHIBE, M. ODANI, and M. SUNAMI. J. Chem. Soc. B, 1837 (1971).
8. R. E. BALLARD and C. H. PARK. Spectrochim. Acta, **26**A, 43 (1970).
9. R. MAYER and H. BERTHOLD. Ber. **96**, 3096 (1963).
10. C. D. HURD and M. A. POLLACK. J. Am. Chem. Soc. **60**, 1905 (1938).

The Investigation of Cation–Anion Interactions by ^{39}K Nuclear Magnetic Resonance

E. G. BLOOR[1]

Cariboo College, Kamloops, British Columbia

AND

R. G. KIDD

Department of Chemistry, University of Western Ontario, London 72, Ontario

Received December 17, 1968[2]

The ^{39}K chemical shifts in a number of aqueous electrolyte solutions have been determined. These arise from the overlapping of the outer electron orbitals of the anion and cation during random ionic collisions. The magnitudes of the chemical shifts are shown to be directly proportional to the effectiveness of this overlap interaction.

Nous avons déterminé les déplacements chimiques du ^{39}K dans différentes solutions électrolytiques aqueuses. Ceux-ci proviennent du recouvrement des orbitales des électrons externes de l'anion et du cation lors de collisions ioniques aléatoires. Nous avons montré que l'importance de ces déplacements chimiques est directement proportionnelle à cette interaction de recouvrement.

Canadian Journal of Chemistry, **50**, 3926 (1972)

[1]Present address: Department of Chemistry, Simon Fraser University, Burnaby 2, British Columbia.

[2]Revision received June 23, 1972.

Can. J. Chem. Downloaded from www.nrcresearchpress.com by 210.87.254.5 on 09/05/12
For personal use only.

Can. J. Chem. Downloaded from www.nrcresearchpress.com by 210.87.254.5 on 09/05/12
For personal use only.

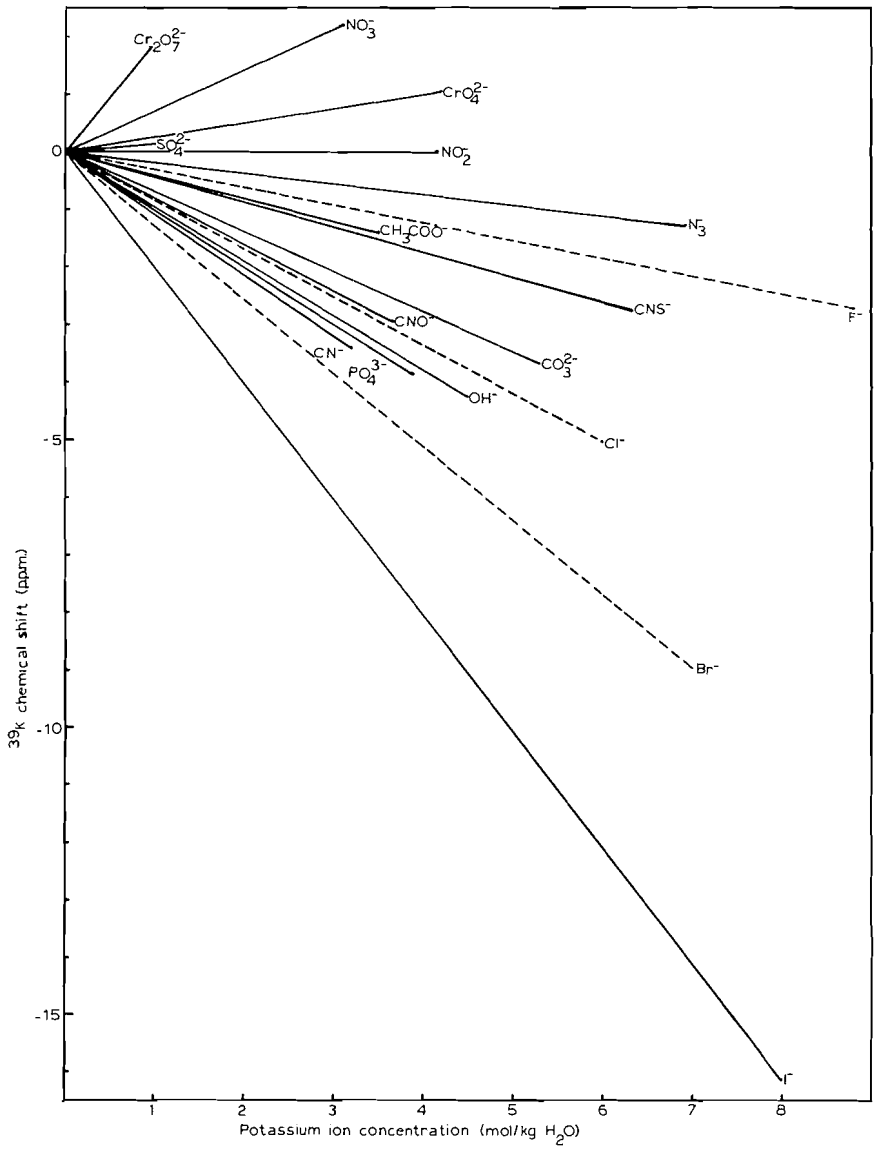

FIG. 1. Anion dependence of ^{39}K chemical shifts in aqueous solutions. The solid lines are the results of our study while the broken lines are from ref. 8.

The dynamic state of electrolyte solutions has been the subject of a great deal of interest amongst n.m.r. spectroscopists (1–4). Most of these studies have monitored the ^1H or ^{17}O chemical shift of the solvent water while systematically varying the constituent ions. As a continuation of our studies of cation–solvent interactions by ^{23}Na n.m.r. (5), we now wish to report a study of cation–anion interactions in aqueous solutions by ^{39}K n.m.r.

In order to isolate the cation–anion interactions, a common cation (K^+) and solvent (H_2O) were used throughout while only the nature of the anion was varied. The ^{39}K n.m.r. spectrum of each of the aqueous solutions of a number of different potassium salts thus investigated consisted of a single line. The position of this line was found to be dependent on both the nature of the anion and concentration of the salt. This dependence is illustrated in Fig. 1. The

TABLE 1. Concentration dependence of the ^{39}K chemical shift* for aqueous solutions of potassium salts

Anion	δ/c (p.p.m./m)	δ_0 (p.p.m.)	$\delta_{corr.}/c$† (p.p.m./m)	$\delta_0$corr. (p.p.m.)
I^-	−2.015	14.84		
I^-	−2.92‡			
Br^-	−1.28‡			
CN^-	−1.061	15.10	−1.114	15.88
PO_4^{3-}	−0.992	14.60		
OH^-	−0.946	15.53	−0.999	16.31
Cl^-	−0.84‡			
CNO^-	−0.805	15.38	−0.868	16.15
CO_3^{2-}	−0.696	14.98	−0.754	15.75
CNS^-	−0.435	15.31	−0.505	16.06
CH_3COO^-	−0.400	15.48		
F^-	−0.31‡			
N_3^-	−0.185	14.20		
NO_2^-	0.00	14.42		
SO_4^{2-}	0.13	15.01		
CrO_4^{2-}	0.248	16.16		
NO_3^-	0.712	15.63		
$Cr_2O_7^{2-}$	1.88	16.19		
		15.20±0.56		16.03±0.22

*Chemical shifts relative to 7.47 m aqueous KI as external reference.
†$\delta_{corr.} = \delta + 2\pi/3\,(\chi_{v(ref.)} - \chi_v)$.
‡From ref. 8.

slope of each line, δ/c, is defined as the "concentration shift" for that particular ion and is the parameter which is most useful in correlating the ^{39}K chemical shifts with known properties of the ions. The concentration shifts are listed in column 2 of Table 1.

All the salts used were AR grade and in most cases these were recrystallized and dried under a partial vacuum with heating. A Varian HR-60 NMR Spectrometer, equipped with the Varian V4200-B wide line accessories, operating at 2.800 MHz was employed. The sample was contained in a 15 mm i.d. cylindrical Pyrex tube fitted with a concentric 6 mm i.d. cylindrical insert for the 7.47 m aqueous KI reference solution. The ^{39}K chemical shifts for each of the electrolyte solutions at infinite dilution are approximately the same, *i.e.* $\delta_0 = 15.20 \pm 0.56$ p.p.m. (column 3, Table 1). The contribution of bulk susceptibility differences to the chemical shift were calculated and these were found to be small and to affect each concentration shift approximately equally (columns 4 and 5, Table 1). In this case then little is to be gained from this correction and only the uncorrected values will be considered further. Chemical shifts were determined at 0.5 m intervals from potassium ion concentrations of 0.5 m to the solubility limit of the salt.

Chemical shifts of alkali metal resonances in alkali metal halide crystals have been best accounted for in terms of the overlapping of the outer electron shells of the oppositely charged ions (6). Since these orbitals are fully occupied, a strong, short-range repulsive force arises due mainly to the Pauli exclusion principle. This results in an increase in the paramagnetic shielding of the nucleus (7) and the resonance is thus shifted to a lower magnetic field. Identical reasoning has been employed (1, 8, 9) to interpret the chemical shifts of the ions in alkali metal halide solutions. Short-range repulsive interactions occur during the random cation–anion collisions which distort the spherical symmetry of the electron distribution and a downfield shift of the resonance results. The larger the halide ion, the larger was the cation paramagnetic shift that was found. This was interpreted as being due to an increased collision probability (8).

The results of this study, however, indicate quite the opposite dependence of cation chemical shift on anion size. Instead, the order of the anions, arranged in the order of their ability

Can. J. Chem. Downloaded from www.nrcresearchpress.com by 210.87.254.5 on 09/05/12
For personal use only.

Can. J. Chem. Downloaded from www.nrcresearchpress.com by 210.87.254.5 on 09/05/12
For personal use only.

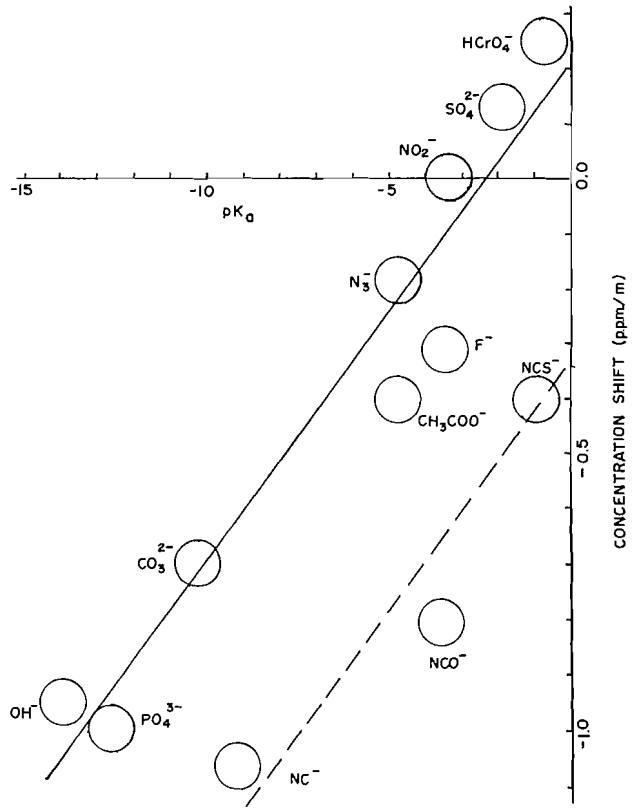

FIG. 2. Correlation of ^{39}K concentration shifts with the basicities of the counterions. The pK_a is the negative $\log_{10}$ of the association constant for the equilibrium which exists between the anion and its parent monoprotic acid. It is inversely proportional to the basicity of the anion.

to increase the paramagnetic shielding, (*i.e.*, $I^- > Br^- > CN^- > PO_4^{3-} > OH^- > Cl^- > CNO^- > CO_3^{2-} > CNS^- > CH_3COO^- > F^- > N_3^- > NO_2^- = H_2O > SO_4^{2-} > CrO_4^{2-} > NO_3^- > Cr_2O_7^{2-}$) bears a striking resemblance to the *nephelauxetic series* (10). The common feature of the two series is the ability of the constituent ions to effect overlap between themselves and a central metal ion. Furthermore, there exists a correlation of the concentration shifts with the basicities of the interacting species (Fig. 2) which is similar to what was found in the earlier ^{23}Na work (5). The greater availability of the electrons on the more basic anions results in a proportionately greater perturbation of the spherical symmetry of the outer electron cloud of the potassium ion. The magnitude of the paramagnetic shift caused by the induction of a net orbital angular momentum in the vicinity of the nucleus is thus a measure of the strength of the cation–anion interaction. The upfield shift of the ^{39}K resonance produced by some anions simply indicates that the overlap interaction between these anions and K^+ is weaker than the water $-K^+$ overlap interaction. The pseudo-halogen ions fall well off the regression line for the other anions in Fig. 2. This is probably because these anions are the only ones among the group studied which have two potential non-identical sites for coordination to the metal ion. Because the second coordination site in these anions depends largely upon a π-type interaction, this additional coordinating ability will not be reflected in the pK_a which reflects only the ability to coordinate protons.

The financial assistance of the National Research Council of Canada throughout the course of this research is gratefully acknowledged.

1. J. D. HALLIDAY, R. E. RICHARDS, and R. R. SHARP. Proc. Roy. Soc. Lond. A313, 45 (1969).
2. C. DEVERELL. Progress in nuclear magnetic resonance spectroscopy. Vol. 4. *Edited by* J. W. Emsley, J. Feeney, and L. H. Sutcliffe. Pergamon Press, Oxford, 1969. Chapt. 4.
3. J. BURGESS and M. C. R. SYMONS. Quart. Rev. **22**, 276 (1968).
4. J. F. HINTON and E. S. AMIS. Chem. Rev. **67**, 367 (1967).
5. E. G. BLOOR and R. G. KIDD. Can. J. Chem. **46**, 3425 (1968).
6. J. KONDO and J. YAMASHITA. J. Phys. Chem. Solids, **10**, 245 (1959).
7. N. F. RAMSEY. Phys. Rev. **78**, 699 (1950).
8. C. DEVERELL and R. E. RICHARDS. Mol. Phys. **10**, 551 (1966).
9. C. DEVERELL and R. E. RICHARDS. Mol. Phys. **16**, 421 (1969).
10. C. E. SCHAFFER and C. K. JORGENSEN. J. Inorg. Nucl. Chem. **8**, 143 (1958).

Isomérisation des épisulfures

KRZYSZTOF JANKOWSKI ET RONALD HARVEY

Département de chimie, Université de Moncton, Moncton, Nouveau-Brunswick

Reçu le 2 mai 1972

La stéréoisomérisation de quelques épisulfures a été realisée par le traitement avec le thiocyanate de potassium en DMF ou en milieu éthanol–eau. La stéréoisomérisation a été suivie par r.m.n.

Stereoisomerisation of some episulfides was observed using the reaction of potassium thiocyanate in DMF or water–ethanol. The stereoisomerisation was followed by n.m.r.

Canadian Journal of Chemistry, **50**, 3930 (1972)

En continuant les travaux précédents (1, 2) sur l'isomérisation des époxydes, nous avons démontré que l'isomérisation peut également être réalisée sur les épisulfures (3). En effet les épisulfures, par exemple, stéroidaux (3–6) ou sur le cyclohexane ayant la stéréochimie voulue ont été synthétisé en une étape. La réaction de l'isomérisation est facilement contrôlée par r.m.n. La différence entre les déplacements chimiques des protons α et β du noyau thiranique des épisulfures isomères reste constante.

La comparaison de la stéréochimie de l'hydroxy-3 épithio-1,2 cyclohexane[1] de départ avec le produit obtenu après le chauffage avec le thiocyanate de potassium (en solution éthanol–eau ou DMF) révèle qu'en partant d'un produit *cis* (**1***c*) (l'hydroxyle et le cycle thiranique *cis*) on obtient le produit *trans* (**1***t*) majoritaire (l'hydroxyle et le cycle thiranique *trans*). En partant d'un mèlange d'épisulfures *cis* et *trans*, on obtient un mélange mais de rapport *cis*/*trans* renversé. Finalement en partant d'un *trans*-hydroxy-3 épithio-1,2 cyclohexane (**1***t*) on obtient le *cis*-hydroxy-3 épithio-1,2 cyclohexane (**1***c*) majoritaire. La série de l'acétoxy-3 épithio-1,2 cyclohexane (*trans* **2***t* et *cis* **2***c*) donnent les résultants semblables (voir tableau 1).

Le controle par r.m.n. de la stéréoisomérisation est basé sur le déplacement chimique des signaux observés pour les protons du noyau thiranique. Nous observons que le signal pour les protons thiraniques des épisulfures *trans* est déplacé vers un champ plus bas par rapport aux épisulfures *cis*. Par exemple, pour le *trans*-hydroxy-3 épithio-1,2 cyclohexane (**1***t*) ce signal est à 3.60 p.p.m. et pour l'isomère *cis* (**1***c*) il est à 3.15 p.p.m. Le $\Delta\delta$ *trans*/*cis* de 0.45 p.p.m. a également été observé pour la série acétoxy-3. Il faut admettre que dans la série méthyle-3 épithio-1,2 cyclohexane cette différence n'est que de 0.06 p.p.m. seulement (les spectres enrégistrés dans les mêmes conditions) (3). Les diphenyl-1,2 épithio-1,2 éthane (épisulfure de stilbène) *trans* et *cis* donnent les signaux des protons thiraniques à 3.98 et 4.40 p.p.m. respectivement, ce que fait une différence de 0.42 p.p.m. (7). Les constantes de couplage sont de $J_{23} \approx 5$ Hz pour les épisulfures *cis* et $J_{23} \approx 0$ Hz pour les épisulfures *trans*. Ces valeurs s'accordent avec des calculs théoriques

[1]Les produits racémiques ont été employés.

Can. J. Chem. Downloaded from www.nrcresearchpress.com by 210.87.254.5 on 09/05/12
For personal use only.

1. J. D. HALLIDAY, R. E. RICHARDS, and R. R. SHARP. Proc. Roy. Soc. Lond. A313, 45 (1969).
2. C. DEVERELL. Progress in nuclear magnetic resonance spectroscopy. Vol. 4. *Edited by* J. W. Emsley, J. Feeney, and L. H. Sutcliffe. Pergamon Press, Oxford, 1969. Chapt. 4.
3. J. BURGESS and M. C. R. SYMONS. Quart. Rev. **22**, 276 (1968).
4. J. F. HINTON and E. S. AMIS. Chem. Rev. **67**, 367 (1967).
5. E. G. BLOOR and R. G. KIDD. Can. J. Chem. **46**, 3425 (1968).
6. J. KONDO and J. YAMASHITA. J. Phys. Chem. Solids, **10**, 245 (1959).
7. N. F. RAMSEY. Phys. Rev. **78**, 699 (1950).
8. C. DEVERELL and R. E. RICHARDS. Mol. Phys. **10**, 551 (1966).
9. C. DEVERELL and R. E. RICHARDS. Mol. Phys. **16**, 421 (1969).
10. C. E. SCHAFFER and C. K. JORGENSEN. J. Inorg. Nucl. Chem. **8**, 143 (1958).

Isomérisation des épisulfures

KRZYSZTOF JANKOWSKI ET RONALD HARVEY

Département de chimie, Université de Moncton, Moncton, Nouveau-Brunswick

Reçu le 2 mai 1972

La stéréoisomérisation de quelques épisulfures a été realisée par le traitement avec le thiocyanate de potassium en DMF ou en milieu éthanol–eau. La stéréoisomérisation a été suivie par r.m.n.

Stereoisomerisation of some episulfides was observed using the reaction of potassium thiocyanate in DMF or water–ethanol. The stereoisomerisation was followed by n.m.r.

Canadian Journal of Chemistry, **50**, 3930 (1972)

En continuant les travaux précédents (1, 2) sur l'isomérisation des époxydes, nous avons démontré que l'isomérisation peut également être réalisée sur les épisulfures (3). En effet les épisulfures, par exemple, stéroidaux (3–6) ou sur le cyclohexane ayant la stéréochimie voulue ont été synthétisé en une étape. La réaction de l'isomérisation est facilement contrôlée par r.m.n. La différence entre les déplacements chimiques des protons α et β du noyau thiranique des épisulfures isomères reste constante.

La comparaison de la stéréochimie de l'hydroxy-3 épithio-1,2 cyclohexane[1] de départ avec le produit obtenu après le chauffage avec le thiocyanate de potassium (en solution éthanol–eau ou DMF) révèle qu'en partant d'un produit *cis* (**1***c*) (l'hydroxyle et le cycle thiranique *cis*) on obtient le produit *trans* (**1***t*) majoritaire (l'hydroxyle et le cycle thiranique *trans*). En partant d'un mèlange d'épisulfures *cis* et *trans*, on obtient un mélange mais de rapport *cis*/*trans* renversé. Finalement en partant d'un *trans*-hydroxy-3 épithio-1,2 cyclohexane (**1***t*) on obtient le *cis*-hydroxy-3 épithio-1,2 cyclohexane (**1***c*) majoritaire. La série de l'acétoxy-3 épithio-1,2 cyclohexane (*trans* **2***t* et *cis* **2***c*) donnent les résultants semblables (voir tableau 1).

Le controle par r.m.n. de la stéréoisomérisation est basé sur le déplacement chimique des signaux observés pour les protons du noyau thiranique. Nous observons que le signal pour les protons thiraniques des épisulfures *trans* est déplacé vers un champ plus bas par rapport aux épisulfures *cis*. Par exemple, pour le *trans*-hydroxy-3 épithio-1,2 cyclohexane (**1***t*) ce signal est à 3.60 p.p.m. et pour l'isomère *cis* (**1***c*) il est à 3.15 p.p.m. Le $\Delta\delta$ *trans*/*cis* de 0.45 p.p.m. a également été observé pour la série acétoxy-3. Il faut admettre que dans la série méthyle-3 épithio-1,2 cyclohexane cette différence n'est que de 0.06 p.p.m. seulement (les spectres enrégistrés dans les mêmes conditions) (3). Les diphenyl-1,2 épithio-1,2 éthane (épisulfure de stilbène) *trans* et *cis* donnent les signaux des protons thiraniques à 3.98 et 4.40 p.p.m. respectivement, ce que fait une différence de 0.42 p.p.m. (7). Les constantes de couplage sont de $J_{23} \approx 5$ Hz pour les épisulfures *cis* et $J_{23} \approx 0$ Hz pour les épisulfures *trans*. Ces valeurs s'accordent avec des calculs théoriques

[1]Les produits racémiques ont été employés.

Can. J. Chem. Downloaded from www.nrcresearchpress.com by 210.87.254.6 on 09/05/12
For personal use only.

Can. J. Chem. Downloaded from www.nrcresearchpress.com by 210.87.254.6 on 09/05/12
For personal use only.

TABLEAU 1. Données physiques des produits

	Rendement (%)			P.é. (°C/mm Hg)	R.m.n. δ (p.p.m.)			Spectroscopie de masse	
	Isomérisation	Obtention méthode*							
		a	*b*			$\Delta\delta$t/c	Autres	*m/e*	*I*%
trans-Hydroxy-3 épithio-1,2 cyclohexane (**1***t*)	35	30	35	97/0.01	3.60	0.45	OH 2.2†	130	11 (M$^+$)
							C*H*—OH 3.96	88	12
								72	100
								58	62
								30	42
cis-Hydroxy-3 épithio-1,2 cyclohexane (**1***c*)	40	40	—	60/0.01	3.15	—	OH 3.5†	130	7 (M$^+$)
							C*H*—OH 3.94	88	14
								72	47
								58	100
								30	22
trans-Acétoxy-3 épithio-1,2 cyclohexane (**2***t*)	40	42	35	110/0.03	3.58	0.46	CH_3 2.1	172	10 (M$^+$)
							CH—O 5.2	130	25
								114	22
								58	32
								43	100
cis-acétoxy-3 épithio-1,2 cyclohexane (**2***c*)	42	32	20	102/0.025	3.12	—	CH_3 2.1	172	12 (M$^+$)
							CH—O 5.0	130	27
								114	41
								58	100
								43	62

*Voir la partie expérimentale.
†Échange D_2O.

(l'équation de Karplus (8)). Il est bon de noter que ces produits représentent des systèmes conformationellement homogènes.

Les épisulfures **1***c* et **1***t* d'une part et **2***c* et **2***t* de l'autre, donnent le spectre de masse qui se compose de pics a *m/e* identique mais de l'intensité différente. Les ions moléculaires sont d'une intensité de 7–12%. Les produits *cis* démontrent les ions 100% provenant de l'ionisation du soufre tandis que les produits *trans* démontrent les ions 100% provenant de l'ionisation de l'oxygène.

Partie éxperimentale

Les spectres de r.m.n. ont été enrégistrés à l'aide de spectrophotomètres Varian A-60 et EM-300 en $CDCl_3$ (concentration 5%); les spectres de masse-Varian EM-600. Les points d'ébullition n'ont pas été corrigés. Les époxydes ont été obtenus par nous mêmes (2). Nous avons utilisé deux méthodes pour l'obtention des épisulfures à partir des époxydes: (*a*) l'action de thiocyante de potassium (par exemple, l'époxyde *trans* donne l'épithio *cis*); (*b*) l'action de la thiourée en milieu H_2SO_4 (par exemple, l'époxyde *cis* donne l'épithio *cis*) (7). Seuls les produits racémiques ont été employés.

Episulfuration des époxydes

Méthode a

L'époxyde (1 mol) est ajouté en deux portions à une solution de thiocyanate de potassium (1.25 mol) dans 100 ml d'eau et 75 ml d'éthanol (ou 175 ml de DMF). Après avoir laissé au repos pendant 3–4 h la solution est vigoureusement agitée pendant 36 h à la température de la pièce dans l'obscurité. Le produit est extrait à l'éther, lavé avec une solution de chlorure de sodium à 10%, séché puis le solvant évaporé *in vacuo*. Le produit est purifié par distillation.

Méthode b

L'époxyde (1 mol) est agité avec de l'eau (50 ml), de l'acide sulfurique (3 equiv), et de la thiourée (3 mol) à la température de la pièce. La solution résultante est agitée 12–24 h et le sulfate est filtré et lavé avec de l'éther, pour ensuite être suspendu dans l'eau. Cette dernière suspension est rendue alcaline (p*H* 9) avec du carbonate de sodium et agitée pour 30 min. L'épisulfure est extrait avec de l'éther puis purifié par distillation.

Isomérisation des épisulfures

L'épisulfure (1 mol) est ajouté à une solution de thiocyanate de potassium dans un mélange éthanol–eau (1:1) (ou dans la diméthylformamide); cette solution est chauffée à reflux et agitée vigoureusement pour 24 h. Le produit est extrait à l'éther, lavé avec une solution de chlorure de sodium à 5%, séché, et le solvant évaporé sous vide. Le produit pur est obtenu par distillation. Le résidue (20–40%) est composé des goudrons sulfurés.

Auteurs remercient le Conseil National de Recherches du Canada et le Conseil de Recherches de l'Université de Moncton pour l'aide financière.

1. K. JANKOWSKI et J. Y. DAIGLE. Synth. 32 (1971).
2. K. JANKOWSKI et J. Y. DAIGLE. Can. J. Chem. **49**, 2594 (1971).
3. K. JANKOWSKI et R. HARVEY. Synth. Sous presse.
4. D. A. LIGHTNER et C. DJERASSI. Tetrahedron, **21**, 583 (1965).
5. L. A. PAQUETTE. Principle of modern heterocyclic chemistry. Benjamin, New York. 1968. p. 57.
6. L. GOODMAN, A. BENITEZ, et B. R. BAKER. J. Am. Chem. Soc. **80**, 1680 (1958).
7. R. KETCHAM et V. P. SHAH. J. Org. Chem. **28**, 229 (1963).
8. M. KARPLUS. J. Chem. Phys. **30**, 11 (1959).

Can. J. Chem. Downloaded from www.nrcresearchpress.com by 210.87.254.6 on 09/05/12
For personal use only.

Erratum: A Synthetic Study in the Tricyclovetivene Series

A. DELJAC, W. D. MACKAY, CONNIE S. J. PAN, KAREL J. WIESNER, AND K. WIESNER
Natural Products Research Center, University of New Brunswick, Fredericton, New Brunswick

Received August 14, 1972
(Ref.: Can. J. Chem. **50**, 726 (1972)

Canadian Journal of Chemistry, **50**, 3933 (1972)

Can. J. Chem. Downloaded from www.nrcresearchpress.com by 210.87.254.42 on 09/05/12
For personal use only.

In the process of abbreviating the Experimental section, the description of the conversion of the alcohol (**31**) to tricyclovetivene (**1***a*) was shortened in a way which made it misleading and in apparent contradiction to a statement in the Theoretical part.

The full description of the experiment should read as follows:

Conversion of the Alcohol (**31**) *to Tricyclovetivene* (**1***a*)

A solution of the "natural" alcohol (**31**) (90 mg) in acetic anhydride (0.7 ml) and pyridine (0.7 ml) was heated to 120 °C for 60 h. After cooling, the reaction mixture was chromatographed on a silica gel column (light petroleum ether) to give the starting alcohol (56 mg) and a mixture of exocyclic and endocyclic olefins (25 mg, 92% based on the starting material consumed) in a ratio of 3.5:1 which was established by analytical g.l.p.c. (15 ft × 1/4 in. column of 30% SE-30 at 225 °C).

The mixture of olefins was then separated by preparative g.l.p.c. to yield a peak fraction of pure "natural" tricyclovetivene (**1***a*) (7.5 mg) as an oil, homogeneous in t.l.c. All analytical data (i.r., n.m.r., mass, t.l.c., and g.l.c.) for "natural" tricyclovetivene were superimposable with those of natural tricyclovetivene.

By the same method synthetic alcohol (**31**) (5.6 mg) was converted to racemic tricyclovetivene (**1***a*) (1.5 mg.).

Mol. Wt. Calcd. for $C_{15}H_{24}$: 204.1878. Found (mass spectroscopy): 204.1876.

The remaining recorded data (i.r. and g.l.c.) were completely identical to those of natural tricyclovetivene.

Can. J. Chem. Downloaded from www.nrcresearchpress.com by 210.87.254.105 on 09/05/12
For personal use only.

Canadian Journal of Chemistry

Published by THE NATIONAL RESEARCH COUNCIL OF CANADA

VOLUME 50 DECEMBER 15, 1972 NUMBER 24

Solvation of the Sodium Ion. Quadrupolar Broadening of the ^{23}Na Nuclear Magnetic Resonance

R. D. GREEN[1] AND JOHN S. MARTIN

Department of Chemistry, The University of Alberta, Edmonton, Alberta T6G 2G2

Received May 28, 1971[2]

Sodium ion preferentially forms long lived complexes with dimethylsulfoxide or *N,N*-dimethylformamide, in mixtures of either of these solvents with either ethanenitrile or propanone. No long lived complexes are observed in solvent mixtures of water or methanol with ethanenitrile or propanone.

L'ion sodium forme de préférence des complexes d'une longue durée de vie avec le diméthylsulfoxyde et le *N,N*-diméthylformamide, dans des mélanges d'un des solvants précédants avec l'éthanenitrile ou le propanone. Il ne forme pas des tels complexes dans des mélanges de l'eau ou le méthanol avec le diméthylsulfoxyde ou le propanone.

Canadian Journal of Chemistry, **50**, 3935 (1972)

Of several spectroscopic methods which have been used to determine the nature of the microscopic environment of ions in solution, one of the more successful has been nuclear magnetic resonance. This usually involves deducing the influence of the ions on the solvent from the change in the solvent ^{1}H or ^{17}O spectrum as a salt is added (1). A complementary approach is to observe the nuclear shielding (2, 3) or linewidth (4–6) of the ion's nucleus as a function of solvent composition. This method has the advantage of allowing observation of small concentrations of ions without masking of the spectral changes by the bulk of the solvent.

The linewidth of the ^{23}Na nuclear resonance in solutions of sodium salts is usually determined by nuclear relaxation by coupling of the nuclear quadrupole, eQ, to transitory field gradients. These may arise from two mechanisms.

(*1*) If no persistent solvation complexes form, and neighboring molecules undergo unrestricted motion, then the reorientation of the electric dipoles of molecules near an ion will lead (7) to a linewidth dependence of the form

$$[1] \qquad \Delta\nu \propto (T_2)^{-1} \propto \left(\frac{eQ}{\hbar}\right)^2 \frac{\mu^2}{r_0^5} N\tau_s$$

where N is the number density of solvent molecules, μ is the solvent molecule dipole moment, and r_0 the distance of closest approach. τ_s, the solvent reorientation correlation time, is usually proportional to the viscosity.

(*2*) If sodium ions are involved in complexes of significant lifetime, then the net electric field gradient in the complex, eq, on thermal reorientation leads to a linewidth dependence (8) of the form

$$[2] \qquad \Delta\nu \propto (T_2)^{-1} \propto \left(\frac{e^2qQ}{\hbar}\right)^2 \tau_c$$

In this case, τ_c is the reorientation correlation time of the complex.

In a mixed solvent, if no complexes form, the first mechanism should yield linewidths intermediate between those in the two pure solvents, unless there are anomalies in the viscosity.

On the other hand, if long-lived complexes form involving a total of n solvent molecules (n

[1]Present address: Department of Chemistry, University of Malaya, Kuala Lumpur, Malaysia.

[2]Revision received July 20, 1972.

TABLE 1. ^{23}Na linewidths in 0.2 *M* solutions of $NaClO_4$, and observed viscosities of solvents at 302 K

Solvent	Linewidth (Hz)	Viscosity $\times 10^4$ (kg $m^{-1} s^{-1}$)	Dipole moment (D)	Donor number (ref. 12)
Propanone	26.8 ± 0.7	2.3	2.9	17
Ethanenitrile	25.0 ± 1.0	2.7	4.0	14
Water	25.3 ± 0.4	8.2	1.8	18
Dimethylsulfoxide	54.3 ± 1.7	19.5	3.9	30
N,N-dimethylformamide	41.7 ± 1.3	7.7	3.8	27

usually being of the order of six), we have contributions to the linewidth from all complexes present of the general formula $NaS_mS'_{n-m}^{+}$ where S and S′ are the two solvents. If the mean lifetime τ_l of a complex is in the range $\tau_c \ll \tau_l \ll T_2$, where T_2 is the relaxation time of a nucleus in that complex (8, 9), the width of the single observed line will be a population-weighted average of the linewidths of all complexes at equilibrium.

Of all possible complexes involving dissimilar solvents, the symmetric ones ($m = 0$ or n) should produce minimum linewidth, since the net field gradient will be small (it is zero for octahedral symmetry). The field gradient and linewidth contributions should increase to a maximum for some mixed complex containing both solvents. Consequently, the possibility exists of a maximum appearing in the curve of linewidth *vs.* concentration when a second solvent is added, if the second mechanism is significant.

Such observations are particularly interesting in the cases of alkali metal ions, whose solvation shells are too labile for their nature and composition to be determined. We have measured the linewidth of the ^{23}Na resonance in 0.2 *M* sodium perchlorate solutions in several pure and mixed solvents. The spectra were obtained at 15.86 MHz, using dispersion mode. The linewidths reported are the separations between the turning points of the signals. Viscosities of the pure and mixed solvents were measured by standard methods (10) using an Ostwald viscosimeter calibrated with water and benzene at ambient probe temperature (302 K).

Table 1 gives observed linewidths of ^{23}Na in several pure solvents. It is apparent that the linewidths do not correlate simply with either viscosity or dipole moment. However, dimethylsulfoxide and *N,N*-dimethylformamide, both strongly basic solvents of relatively high viscosity, produce the greatest linewidths. It has been shown (11) that $NaClO_4$ exhibits no significant ion pairing in these solvents, so interionic contributions to the linewidth should be negligible.

Ideally, to study mixed solvent systems, one would dissolve the salt in an "inert" solvent, S, and monitor the linewidth of the ion's resonance as small quantities of a second solvent, S′, are added. If persistent complexes form as S molecules are displaced by S′ molecules in the solvation shell, the linewidth would increase, pass through a maximum corresponding to the presence of asymmetric complexes, and ultimately decrease to the value characteristic of solvation entirely by S′.

The most nearly "inert" solvents which afford adequate solubility of sodium perchlorate are ethanenitrile (CH_3CN) and propanone (CH_3COCH_3). They appear not to interact strongly with sodium ion; the small change of linewidth between ethanenitrile and propanone occurs uniformly as the composition is varied.

There is no evidence of persistent complexes with water or methanol. The addition of small quantities of either of these solvents to an ethanenitrile solution produced no significant change in the sodium linewidth. This appears to confirm the previous finding (5, 9) that no persistent hydrates of sodium occur in mixed solvents. This is particularly interesting in view of the observation by Bloor and Kidd (2) that water preferentially solvates sodium ion in ethanenitrile–water systems. Thus, it appears that relaxation in these systems is entirely by the first of the two mechanisms discussed previously.

On the other hand, when dimethylsulfoxide or *N,N*-dimethylformamide is added to $NaClO_4$ in ethanenitrile, the linewidth, as shown in Fig. 1, increases rapidly with added solvent S′ con-

Can. J. Chem. Downloaded from www.nrcresearchpress.com by 210.87.254.105 on 09/05/12
For personal use only.

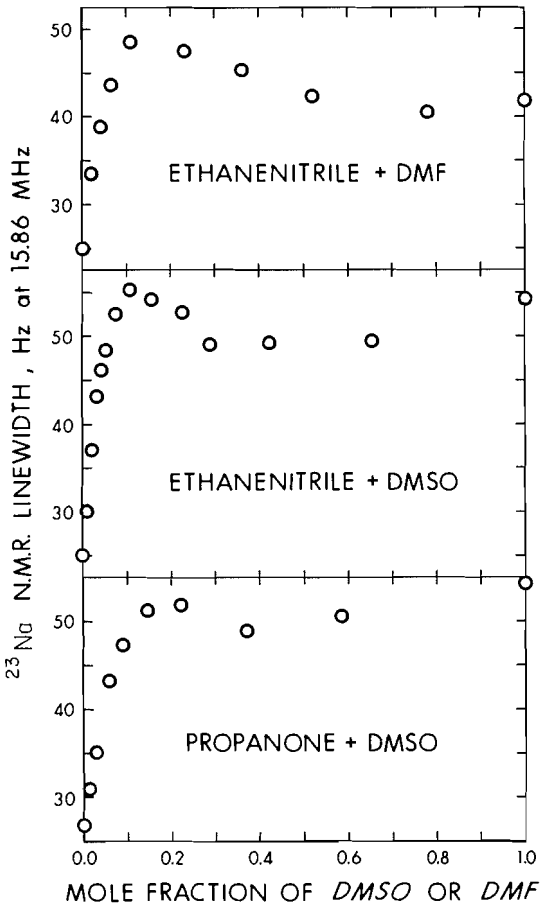

FIG. 1. Variation of ^{23}Na linewidth with solvent composition.

centration, reaching a maximum at a ratio $[S']/[Na^+]$ of about 10 to 15. On further addition of DMSO or DMF, the linewidth decreases again and passes through a slight minimum before reaching the value appropriate to solvent S'. Similar behavior is observed when DMSO is added to $NaClO_4$ in propanone. The linewidth maximum occurs at higher DMSO concentration, but the form of the curve is much the same. The measured viscosities of these solvent pairs showed no corresponding features. A smooth, monotonic variation of viscosity with composition was observed in all cases, with no maxima or minima.

The observed quadrupolar broadening of the ^{23}Na resonance and its dependence on solvent composition have several implications with regard to sodium ion solvation. The maxima in the linewidth curves of systems involving DMSO and DMF imply that the second relaxation mechanism is operative, and thus that complexes of these solvents with Na^+ have lifetimes significantly longer than their reorientation correlation times. It is also evident from the curves of Fig. 1 that the mixed solvation shells, which occur in the neighborhood of the linewidth maxima, predominate when DMSO or DMF is the minor constituent of the mixed solvent. This is evidence that DMSO and DMF preferentially solvate sodium ion, in competition with ethanenitrile or propanone.

Thus dimethylsulfoxide and *N*,*N*-dimethylformamide appear to form complexes which are thermodynamically more stable than those of the other solvents with sodium ion. These complexes also appear to have a significantly greater lifetime when DMSO or DMF is in the solvation shell. This experiment affords no evidence for persistent solvation by ethanenitrile, propanone, water, or methanol. These observations are in accord with the basicities of the various solvents, as measured by their Gutmann donor numbers (12) given in Table 1. The most basic solvents, DMSO and DMF, form the most stable and long-lived complexes with sodium ion.

This work was supported in part by a grant from the National Research Council of Canada.

1. J. F. HINTON and E. S. AMIS. Chem. Rev. **67**, 367 (1967).
2. E. G. BLOOR and R. G. KIDD. Can. J. Chem. **46**, 3425 (1968).
3. M. HERLEM and A. I. POPOV. J. Am. Chem. Soc. **94**, 1431 (1972).
4. O. JARDETZKY and J. E. WERTZ. J. Am. Chem. Soc. **82**, 318 (1960).
5. R. E. RICHARDS and B. A. YORKE. Mol. Phys. **6**, 289 (1963).
6. M. EISENSTADT and H. L. FRIEDMAN. J. Chem. Phys. **44**, 1407 (1966).
7. H. G. HERTZ. Z. Elektrochem. **65**, 20 (1961).
8. T. R. STENGLE and J. D. BALDESCHWIELER. Proc. Nat. Acad. Sci. **55**, 1020 (1966).
9. K. A. VALIEV. Sov. Phys. J.E.T.P. **11**, 883 (1960).
10. F. DANIELS. Experimental physical chemistry. 7th ed. McGraw–Hill, New York. 1970.
11. R. H. ERLICH, E. ROACH, and A. I. POPOV. J. Am. Chem. Soc. **92**, 4989 (1970).
12. V. GUTMANN. Coordination chemistry in non-aqueous solutions. Springer–Verlag, New York. 1968.

Can. J. Chem. Downloaded from www.nrcresearchpress.com by 210.87.254.105 on 09/05/12
For personal use only.

The Vacuum Ultraviolet Photolysis of Cyclopentanone

ALFRED A. SCALA AND DANIEL G. BALLAN
Department of Chemistry, Worcester Polytechnic Institute, Worcester, Massachusetts 01609

Received March 23, 1972

In the vacuum ultraviolet photolysis of cyclopentanone, the major modes of fragmentation of the electronically excited ketone are:

[6] 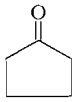 → $CO + (CH_2)_4$ → A: $2C_2H_4$; B: C_4H_8

[8] → $CH_2 + CO + C_3H_6$

[4] → $H + C_5H_7O$

[5] → $H_2 + C_5H_6O$

The sum of the quantum yields for reactions A and B is 0.87 at 147.0 nm and these reactions become less important as the incident energy is increased. A pressure study at 147.0 nm of the partitioning of the tetramethylene diradical between paths A and B indicates that the ratio k_A/k_B is approximately 8. The quantum yield for reaction 8 is only 0.02. The remainder of the decomposition of cyclopentanone is accounted for by reactions 4 and 5, which appear to become more significant as the incident energy increases. The mechanisms for reactions 6 and 8 are best interpreted in terms of diradicals of structure $(CH_2)_n$ where $n = 1$, 3, and 4. The lack of non-acyl σ-cleavage at 147.0 nm is an indication that the absorption of energy occurs at the carbonyl group.

Dans la photolyse ultraviolet sous vide de la cyclopentanone les modes de fragmentation majoritaire pour la cétone électroniquement excitée sont:

[6] 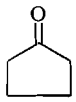 → $CO + (CH_2)_4$ → A: $2C_2H_4$; B: C_4H_8

[8] → $CH_2 + CO + C_3H_6$

[4] → $H + C_5H_7O$

[5] → $H_2 + C_5H_6O$

La somme des rendements quantiques pour les réactions A et B est de 0.87 à 147.0 nm et celle-ci deviennent moins importantes lorsque l'énergie incidente augmente. L'étude sur la pression à 147.0 nm du partage du diradical tétraméthylène entre les voies A et B, indique que le rapport k_A/k_B est approximativement de 8. Le rendement quantique pour la réaction 8 n'est que de 0.02. Le restant de la décomposition de la cyclopentanone est expliqué par les réactions 4 et 5 qui apparaissent plus importantes lorsque l'énergie incidente croît. Les mécanismes des réactions 6 et 8 sont interprétés de la meilleure façon par les diradicaux de structure $(CH_2)_n$ où $n = 1$, 3, et 4. L'absence de clivage σ non acyle à 147.0 nm est une indication que l'absorption d'énergie a lieu sur le groupe carbonyle. [Traduit par le journal]

Canadian Journal of Chemistry, **50**, 3938 (1972)

Introduction

The near ultraviolet photochemistry of cyclopentanone has been extensively investigated and is characterized by reactions 1–3 (for a review, see refs. 1 and 2)

[1] 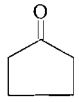 → $CH_2CH(CH_2)_2CHO$

[2] → $CO + 2C_2H_4$

[3] → $CO + c\text{-}C_4H_8$

At 313 nm reaction 1 is the major reaction, while reactions 2 and 3 occur to about the same extent as reaction 1. Lee (3) has shown that in the benzene sensitization of cyclopentanone reaction 1 is the result of triplet energy transfer while reactions 2 and 3 occur by way of singlet energy transfer. Dunion and Trumbore (4) have shown that in the liquid phase γ-radiolysis of cyclopentanone, the first excited triplet state ($n-\pi^*$)

Can. J. Chem. Downloaded from www.nrcresearchpress.com by 210.87.254.6 on 09/05/12
For personal use only.

TABLE 1. Photolysis of cyclopentanone*

	Quantum yield†					
	147.0 nm		123.6 nm		106.7–4.8 nm	
Product	A	B	A	B	A	B
H_2	0.20	0.11	0.22	0.12	0.25	‡
CO	0.87	0.87	0.74	0.74	0.60	0.57
CH_4	0.013	0.0009	0.016	0.0008	0.025	‡
C_2H_4	1.76	1.53	1.41	1.30	0.84	0.70
C_2H_2	0.0049	0.0044	0.0067	0.0063	0.050	0.050
C_2H_6	0.0076	<0.0001	0.0081	<0.0001	0.023	<0.0001
C_3H_6	0.014	0.0096	0.015	0.011	0.013	0.011
c-C_3H_6	0.0054	0.0044	0.0036	0.0044	0.0008	0.0007
C_3H_4	0.0007	0.0009	0.0070	0.0069	0.033	0.027
C_3H_8	0.0058	<0.0001	0.0033	<0.0001	0.0090	<0.0001
1-C_4H_8	0.021	0.0060	0.023	0.015	0.044	0.034
c-C_4H_8	0.019	0.017	0.019	0.018	0.0084	0.0057
n-C_4H_{10}	0.003	<0.0001	‡	<0.0001	0.0047	<0.0001

*Pressure, 7.0 Torr.
†A for no additive, B for 5% NO additive.
‡Not determined.

is the precursor in reaction 1. The present study was undertaken with the expectation that on the basis of product analysis and by making use of cyclopentanone-α-d_4 we would be able to establish some of the primary processes which occur when cyclopentanone is photolyzed in the gas phase with vacuum ultraviolet radiation.

Experimental

The experimental procedures were essentially the same as those used in the vacuum ultraviolet photolysis of cyclohexanone (5). Cyclopentanone obtained from Matheson Coleman Bell was purified by distillation on a thirty theoretical plate spinning band column. Only the middle 1/5, which was outgassed by several trap-to-trap distillations, was used in these experiments and no impurities were discernable by gas chromatography using both diisodecyl phthalate and Poropak Q-S columns. Cyclopentanone-α-d_4 was obtained from Merck, Sharp and Dohme, Ltd., of Canada. It was outgassed and passed through a column of Linde molecular sieves, type 13X. After this treatment, the only discernable impurity was *ca.* 1% of 4-pentenal. According to the mass spectral cracking pattern of cyclopentanone-α-d_4, it contained about 12% cyclopentanone-α-d_3. In calculating the isotopic compositions of the ethylenes formed during photolysis, corrections have been made to compensate for the presence of cyclopentanone-α-d_3. No correction was made in calculating the hydrogen isotopic compositions.

Results

The product distributions obtained when cyclopentanone is photolyzed at 147.0, 123.6, and 106.7–4.8 nm, both in the presence and absence of nitric oxide, are given in Table 1. The conversion in most experiments was 0.1–0.05%. However, even changes by a factor of 10 in the conversion had little effect on the relative yields of the products. The only noticeable effect was a slight increase in the ethane, propane, and butane yields at higher conversions. In Table 2 are the isotopic compositions of the ethylene and hydrogen formed when cyclopentanone-α-d_4 is photolyzed at 147.0 and 123.6 nm. Isotopic compositions were not determined at 106.7–4.8 nm because the low intensity of the argon lamp made the accumulation of enough products for this analysis almost impossible. It can be reported however that the isotopic compositions of both the ethylene and the hydrogen formed in the γ-radiolysis are similar to those reported in Table 2.

In addition to the results reported above, a number of high pressure photolyses were conducted at 147.0 nm in order to determine if 4-pentenal was a product at these energies. In none of these experiments was any 4-pentenal observed, even at conversions as high as 2%. In a further attempt to increase the pressure and stabilize any 4-pentenal which might be formed and undergo secondary decomposition, cyclopentanone was photolyzed in the solid phase at 77 °K. In this case also no 4-pentenal was observed. The analysis for 4-pentenal was capable of detecting as little as a quantum yield of

Can. J. Chem. Downloaded from www.nrcresearchpress.com by 210.87.254.6 on 09/05/12
For personal use only.

TABLE 2. Photolysis of cyclopentanone-α-d_4 (Isotopic composition of hydrogen and ethylene)*

		% distribution						
	Additive	H_2	HD	D_2	C_2H_4	$C_2H_2D_2$	C_2D_4	Other
147.0 nm	None	42	44	14	1.9	85.2	6.5	6.4
147.0 nm	NO(5%)	58	31	11	4.1	84.0	5.9	6.0
123.6 nm	None	†	†	†	4.6	82.0	6.3	7.1
123.6 nm	NO(5%)	51	39	10	3.2	86.7	6.3	4.8

*Total pressure, 7 Torr.
†Not determined.

0.025 of this compound. The ratios C_2H_4/c-C_4H_8 and 1-C_4H_8/c-C_4H_8 observed in these high pressure experiments are presented in Fig. 1. When cyclopentanone was photolyzed in the presence of 2% added ethylene the yields of ethane, propane, and butane relative to carbon monoxide were increased by factors of 2.1, 3.1, and 8.4, respectively. Except for a 20% reduction in the yield of 1-butene, the yields of other products were essentially unchanged. When the xenon photolysis was conducted in the presence of 25% hydrogen sulfide, the methane yield increased from 1.5 in the absence of hydrogen sulfide, to 4.3 relative to carbon monoxide. The quantum yields reported in Table 1 for 123.6 and 106.7–4.8 nm are based upon the measured ionization efficiencies for cyclopentanone of 0.28 and 0.23, respectively. These ionization efficiencies were determined as previously described using the well established ionization efficiencies of nitric oxide as the standard (6). The quantum yield of CO at 147.0 nm is based upon carbon dioxide actinometry (7).

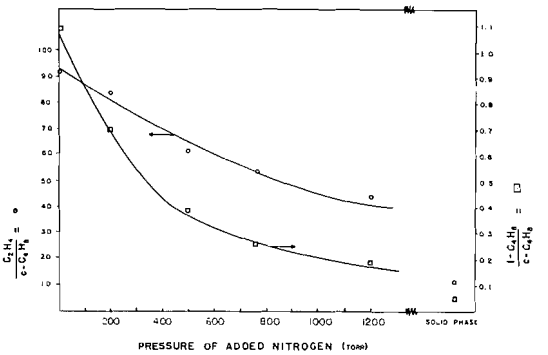

FIG. 1. The dependence of the ratios C_2H_4/c-C_4H_8 and 1-C_4H_8/c-C_4H_8 upon the pressure of added nitrogen at 147.0 nm.

Discussion

There is no evidence to the occurrence of reaction 1 in the vacuum ultraviolet photolysis of cyclopentanone. This observation is consistent with previous work which has shown that intramolecular rearrangements do not occur in

[1] 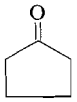 $\rightarrow$ $CH_2=CHCH_2CH_2CHO$

the vacuum ultraviolet photolysis of ketones (5, 8, 9). Although the possibility exists that 4-pentenal is formed and undergoes secondary decomposition, this is unlikely since no trace of 4-pentenal was ever observed, even when 1.5 atmospheres of nitrogen was present to collisionally deactivate the 4-pentenal. The effectiveness of nitrogen in stabilizing vibrationally excited cyclobutane can be seen in Fig. 1.

From the product distributions given in Table 1 it may be seen that ethylene is by far the most abundant hydrocarbon product and that the ratio C_2H_4/CO is very close to 2.0 as required by reaction 2. As the incident energy increases, the importance of ethylene diminishes and the C_2H_4/CO ratio becomes less than 2. The divergence of the quantum yield of carbon monoxide from unity is the result of the occurrence of reactions 4 and 5 which become more important

[4] 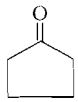 $\rightarrow$ $H + C_5H_7O$

[5] $\rightarrow$ $H_2 + C_5H_6O$

as the incident energy increases. These reactions are not observed in the near ultraviolet photolysis of cyclopentanone, since hydrogen is not a product. If sizeable fractions of the C_5H_7O and C_5H_6O produced in reactions 4 and 5 do not undergo secondary decomposition to produce carbon monoxide, then the difference between the carbon monoxide quantum yield and unity

Can. J. Chem. Downloaded from www.nrcresearchpress.com by 210.87.254.6 on 09/05/12
For personal use only.

Can. J. Chem. Downloaded from www.nrcresearchpress.com by 210.87.254.6 on 09/05/12
For personal use only.

should be reflected in the hydrogen yield. This is in fact what is observed, as the incident energy is increased the quantum yield of carbon monoxide decreases, while the quantum yield of hydrogen increases. A similar observation has been made in the vacuum ultraviolet photolysis of cyclohexanone (5).

At 123.6 and 106.7–4.8 nm ion–molecule reactions may also contribute to the production of hydrogen. The divergence of the ratio C_2H_4/CO from 2.0 at these wavelengths indicates that reactions are occurring which do not produce two molecules of ethylene and a molecule of carbon monoxide. This is also indicated by the slight increases in the C_3 and C_4 products when the incident energy is sufficient to ionize cyclopentanone. The elucidation of the detailed photolytic mechanism at 123.6 and 106.7–4.8 nm is more difficult than at 147.0 nm because although approximately 25% of the incident photons result in ionization we have not been able to clearly demonstrate the occurrence of any ion–molecule reaction.

The photolytic mechanism at 147.0 nm is best interpreted in terms of the initial decomposition of the excited cyclopentanone to carbon monoxide and a tetramethylene diradical. The major reaction products as well as the pressure de-

[6] 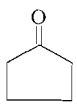 $\rightarrow$ CO + $(CH_2)_4$

pendence of the products (Fig. 1) is then determined by the secondary reactions of the tetramethylene diradical as shown in Scheme 1.

$$(CH_2)_4 \longrightarrow 1\text{-}C_4H_8^* \rightleftharpoons CH_3 + CH_2CHCH_2$$
$$\xrightarrow{k_d} 2\text{-}C_2H_4$$
$$\underset{}{\overset{k_c}{\rightleftharpoons}} c\text{-}C_4H_8^* \xrightarrow[(M)]{} c\text{-}C_4H_8$$

SCHEME 1

At 147.0 nm reaction 6 occurs with a quantum yield of 0.87. The postulation of a tetramethylene diradical is consistent with our interpretation of the vacuum ultraviolet photolysis of cyclohexanone in terms of a pentamethylene diradical. The slight reduction in the ethylene quantum yield observed when 5% nitric oxide is added to the ketone is attributed to the inefficient scavenging of the diradical by nitric oxide. This hypothesis is consistent with the following observations: cyclobutane is a product and it is also inefficiently scavenged by nitric oxide; the trimethylene diradical which must be the precursor of the cyclopropane formed in this system and in the photolysis of cyclohexanone (5) is also slightly scavenged by nitric oxide in both of these systems. McKnight, Lee, and Rowland (10) have observed that the triplet trimethylene diradical produced by the addition of methylene to ethylene is scavenged slightly by oxygen.

Scheme 1 explains the greater susceptibility of the 1-butene to nitric oxide scavenging by the secondary decomposition of vibrationally excited 1-butene to methyl and allyl radicals, a relatively large fraction of which will recombine to form 1-butene (11). The pressure dependence of the $C_2H_4/c\text{-}C_4H_8$ and $1\text{-}C_4H_8/c\text{-}C_4H_8$ ratios shown in Fig. 1 are the result of the decomposition of vibrationally excited cyclobutane. Both the solid phase photolysis and the isotopic composition of the ethylene produced in the photolysis of cyclopentanone-α-d_4 indicate that at most 20% of the ethylene produced in a 7.0 Torr photolysis arises by way of the decomposition of a vibrationally excited cyclobutane molecule. This result would indicate that the ratio k_d/k_c is approximately 8. Considering the likelihood that the tetramethylene diradical is produced with excess vibrational energy this estimate is in good agreement with the experimental results of Gerberick and Walters (12) on the thermal isomerization of *cis*- and *trans*-1,2-dimethylcyclobutane, which respectively indicate this ratio to be 4.6 and 2.8 and with the calculated value of O'Neal and Benson (13) which is 1.9.

The preference of the tetramethylene diradical to undergo cleavage to two molecules of ethylene compared to the preference of the trimethylene diradical to undergo cyclization

[7] $(CH_2)_4 \rightarrow 2C_2H_4$

rather than cleavage is due in part to the more favorable entropy of cyclization of the trimethylene diradical, but mainly to the less favorable enthalpy for the cleavage of the trimethylene to ethylene and methylene (14). The trimethylene diradical shows no tendency to undergo fragmentation in thermal systems and little tendency to undergo this reaction when

Can. J. Chem. Downloaded from www.nrcresearchpress.com by 210.87.254.6 on 09/05/12
For personal use only.

it is produced in the vacuum ultraviolet photolysis of cyclohexanone (5). The trimethylene diradical is an intermediate in the present system since it is necessary to include reaction 8 in the mechanism in order to account for the presence of cyclopropane and propylene among the

[8] 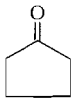 $\rightarrow CH_2CO + (CH_2)_3$

products. The intermediacy of the trimethylene diradical in a number of reactions is well documented (10, 13, 15). Although reaction 8 indicates the production of ketene, at these energies any ketene produced will certainly decompose to methylene and carbon monoxide. Both the total C_3H_6 yield and the C_1 yield indicate that reaction 8 accounts for approximately 3% of the carbon monoxide. If we make the assumption that reaction 8 occurs entirely by way of initial cleavage of the α–β σ bond, we can still conclude that non-acyl σ bond cleavage is certainly a relatively unimportant reaction. Since α–β σ cleavage, which should be statistically favored by a factor of 2 over β–β' σ cleavage, is unimportant and since non-acyl σ cleavage should be a relatively nonselective reaction, we therefore conclude that initial β–β' σ cleavage reaction 9 is insignificant and does not contribute to the production of ethylene. Since

[9] 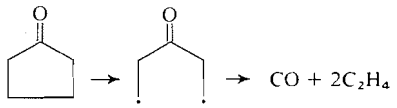 $\rightarrow CO + 2C_2H_4$

1

non-acyl σ cleavage reactions are expected to be more important at higher energies, it seems justified to conclude that **1** which has been suggested as a possible intermediate in reaction 2 is not a source of ethylene in the near ultraviolet photolysis of cyclopentanone (16).

The methylene produced by the decomposition of the ketene formed in reaction 8 probably inserts into the cyclopentanone, followed by the decomposition of a fraction of the methylcyclopentanone to produce methyl radicals and cyclo-

[10] $CH_2 +$ 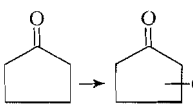 $CH_3^* \rightarrow CH_3 + C_5H_7O$

pentanonyl radicals. The minor contribution of reaction 8 is also indicated by the fact that when the xenon photolysis is conducted in the presence of 25% hydrogen sulfide the methane yield is still only 4.3% of the carbon monoxide yield. Hydrogen sulfide has been shown to be an efficient scavenger of methylene, resulting in the production of methane (15*e*).

The small amounts of acetylene and allene present in the 147.0 nm photolysis products, probably result from the unimolecular decomposition of vibrationally excited C_2H_4 and C_3H_6. These reactions are consistent with the insensitivity of these products to the presence of nitric oxide. The dramatic increase in the yields of both C_2H_2 and C_3H_4 at 106.7–4.8 nm we believe may be due to a proton transfer reaction between $C_2H_3^+$ and $C_3H_5^+$ and cyclopentanone as shown in reaction 11, where R is either C_2H_2 or C_3H_4. The $C_2H_3^+$ and $C_3H_5^+$ ions account

[11] $RH^+ + K \rightarrow R + KH^+$

for 4 and 12% of the total ionization in the 70 eV mass spectrum of cyclopentanone (17, 18). Since the appearance potentials of these ions formed from cyclopentanone are not known, it is not possible to say with certainty that reaction 11 does occur.

The remaining products, methane, ethane, propane and butane are clearly formed in free radical reactions as demonstrated by their almost complete scavenging by nitric oxide. These products can be accounted for by the usual abstraction, disproportionation, and combination reactions of methyl and ethyl radicals. That ethyl radicals originate by hydrogen atom addition to ethylene is demonstrated by the observation that the yields of ethane, propane, and butane are increased by factors of 2.1, 3.1, and 8.4, respectively, when 2% ethylene is added to the ketone prior to photolysis at 147.0 nm. The isotopic compositions of the hydrogen formed in the photolysis of cyclopentanone-α-d_4 as well as the effect of nitric oxide on the hydrogen yield indicate that a sizeable fraction of the hydrogen is produced from hydrogen atoms.

The results of the present study clearly indicate that diradicals are intermediates in the photolysis of cyclopentanone in the vacuum ultraviolet. The broad applicability of diradical intermediates in explaining many experimental

observations on cyclic compounds has been demonstrated by Benson (14). Another interesting aspect of the present study is the insignificance of non-acyl carbon–carbon σ cleavage, particularly at 147.0 nm. This result requires that even at these energies most of the energy is absorbed in the carbonyl group. This is consistent with McMurry's assignment of the 150 nm absorption band of ketones to the $\pi-\pi^*$ transition (19).

We would like to express our sincere appreciation to Dr. Peter Ausloos for his gracious gift of a number of the deuterated compounds which were necessary to complete this study. This research was supported by the U.S. Atomic Energy Commission (AT(30-1)-3945).

1. R. SRINIVASAN. Advances in photochemistry. Vol. 1. *Edited by* W. A. Noyes, Jr., G. S. Hammond, and J. N. Pitts, Jr. Interscience, New York. 1963. p. 83.
2. J. CALVERT and J. N. PITTS, Jr. Photochemistry. John Wiley and Sons, New York. 1968.
3. E. K. C. LEE. J. Phys. Chem. **71**, 2804 (1967).
4. P. DUNION and C. N. TRUMBORE. J. Am. Chem. Soc. **87**, 4211 (1965).
5. A. A. SCALA and D. G. BALLAN. J. Phys. Chem. **76**, 615 (1972).
6. P. AUSLOOS and S. G. LIAS. Radiation Res. Rev. **1**, 75 (1968).
7. J. Y. YANG and F. M. SERVEDIO. Can. J. Chem. **46**, 338 (1968).
8. A. A. SCALA and P. AUSLOOS. J. Phys. Chem. **70**, 260 (1966).
9. A. A. SCALA. J. Phys. Chem. **74**, 2639 (1970)
10. C. MCKNIGHT, E. K. C. LEE, and F. S. ROWLAND. J. Am. Chem. Soc. **89**, 469 (1967).
11. M. AVRAHAMI and P. KEBARLE. J. Phys. Chem. **67**, 354 (1963); J. Chem. Phys. **38**, 700 (1963).
12. H. R. GERBERICK and W. D. WALTERS. J. Am. Chem. Soc. **83**, 3935 (1961); **83**, 4884 (1961).
13. H. E. O'NEAL and S. W. BENSON. J. Phys. Chem. **72**, 1866 (1968).
14. S. W. BENSON. J. Chem. Phys. **34**, 521 (1961).
15. (*a*) O. P. STRAUSZ, P. J. KOZAK, G. N. C. WOODALL, A. G. SHERWOOD, and H. E. GUNNING. Can. J. Chem. **46**, 1317 (1968), (*b*) G. R. DEMARE, L. G. WALKER, O. P. STRAUSZ, and H. E. GUNNING. Can. J. Chem. **44**, 457 (1966). (*c*) E. G. SPITTLER and G. W. KLEIN. J. Phys. Chem. **72**, 1432 (1968). (*d*) P. AUSLOOS, R. E. REBBERT, and S. G. LIAS. J. Phys. Chem. **72**, 3904 (1968). (*e*) A. A. SCALA and P. AUSLOOS. J. Chem. Phys. **49**, 2282 (1968). (*f*) R. J. CVETANOVIC, H. E. AVERY, and R. S. IRWIN. J. Chem. Phys. **46**, 1993 (1967). (*g*) P. DOWD and K. SACHDER. J. Am. Chem. Soc. **89**, 715 (1967).
16. F. E. BLACET and A. MILLER. J. Am. Chem. Soc. **79**, 4327 (1957).
17. P. NATALIS. Bull. Soc. Chem. Belges. **67**, 599 (1958).
18. J. H. BEYNON, R. A. SAUNDERS, and A. E. WILLIAMS. Appl. Spectrosc. **14**, 95 (1960).
19. H. L. MCMURRY. J. Chem. Phys. **9**, 231 (1941).

Can. J. Chem. Downloaded from www.nrcresearchpress.com by 210.87.254.6 on 09/05/12
For personal use only.

Crystal Structure of a New Form of $Cu_3V_2O_8$

ROBERT D. SHANNON[1] AND CRISPIN CALVO
Institute of Materials Research, McMaster University, Hamilton, Ontario

Received June 30, 1972

A new form of $Cu_3V_2O_8$ was prepared at 30 kbar and 900 °C. The unit cell has dimensions $a = 6.2493(9)$, $b = 7.9936(9)$, $c = 6.3776(10)$ Å, $\beta = 111.49(1)°$, and the space group is $P2_1/c$. The crystal structure, refined by least-squares to a final $R = 0.054$, using 848 reflections, is similar to that of $Mg_3V_2O_8$. Chains of edge-shared M2 octahedra run along the c axis at about $y = \pm 1/4$ with M1 octahedra sharing two edges with the M2 octahedra. These octahedral networks at about $y = \pm 1/4$ are linked by corner-shared V–O tetrahedra. The distortion from the $Mg_3V_2O_8$ structure can be explained on the basis of the Jahn–Teller effect in which four of the octahedral Cu—O distances shorten to 1.93–1.99 Å and two Cu—O distances lengthen to 2.3–2.6 Å.

Nous avons préparé une nouvelle forme de $Cu_3V_2O_8$, à 30 kbar et 900 °C. La maille a les dimensions suivantes: $a = 6.2493(9)$, $b = 7.9936(9)$, $c = 6.3776(10)$ Å, $\beta = 111.49(1)°$; le groupe spatial est $P2_1/c$. La structure cristalline, raffinée par moindres carrés jusqu'à une valeur finale de $R = 0.054$ au moyen de 848 réflexions, est semblable à celle de $Mg_3V_2O_8$. Les chaînes d'octaèdres M2 à arêtes communes suivent l'axe des c, à environ $y = \pm 1/4$; les octaèdres M1 partagent deux arêtes avec les octaèdres M2. Ces réseaux octàdriques, aux environs de $y = \pm 1/4$, sont reliés par des tetraèdres V–O à coins communs. La distortion de la structure de $Mg_3V_2O_8$ peut s'expliquer en se basant sur un effet Jahn–Teller où quatre distances octaédriques Cu—O raccoursissent jusqu'à 1.93–1.99 Å et deux distances Cu—O allongent jusqu'à 2.3–2.6 Å.

[Traduit par le journal]

Canadian Journal of Chemistry, **50**, 3944 (1972)

Introduction

Brisi and Molinari (1) reported the preparation of a variety of copper vanadates having the composition nCuO:V_2O_5 where $n = 1$, 2, 3, 4, and 5. Fleury (2, 3) confirmed the compositions with $n = 1$, 2, 3, and 5 but was unable to prepare $Cu_4V_2O_9$. Fleury found $Cu_3V_2O_8$ to decompose at 780 °C. We were interested in $Cu_3V_2O_8$ and $Cu_5V_2O_{10}$ because they are examples of vanadates containing a large percentage of the highly electronegative cation Cu^{2+}. Such compounds were expected to show average V—O distances greater than vanadates containing highly electropositive cations, *e.g.* Li_3VO_4, Ca_2VO_4Cl, and $Ca_3V_2O_8$. Although we were not able to prepare crystals of the $Cu_3V_2O_8$ phase reported by Brisi and Molinari (1) we were able to stabilize a new form of $Cu_3V_2O_8$ at elevated pressures. In this paper we report the synthesis and crystal structure of this new form of $Cu_3V_2O_8$, and compare the structure with that of other compounds having the stoichiometry $M_3V_2O_8$ where M = Co, Ni, Zn, and Mg.

Experiments

Stoichiometric quantities of spectrographic grade CuO and V_2O_5 (Johnson–Matthey) were carefully mixed and heated in air at 700 °C for 24 h. The product was identified as the $Cu_3V_2O_8$ prepared by Brisi and Molinari. This material was heated at a temperature of 900 °C and a pressure of 30 kbar for 2 h and quenched according to a procedure described earlier (4). Small irregular crystals with a dark red color were obtained. Powder diffraction patterns obtained from these crystals indicated a phase different from the starting material. Although the majority of the crystals were badly twinned, a crystal suitable for the structure determination was eventually obtained. The space group was found from precession photographs to be $P2_1/c$. X-Ray powder diffraction photographs were taken with a Hägg–Guinier camera using a KCl internal standard. The d values were obtained using λ (CuKα_1) = 1.54051 Å and a (KCl) = 6.2531 Å. Cell dimensions determined by least squares refinement are $a = 6.2493(9)$, $b = 7.9936(9)$, $c = 6.3776(10)$ Å, $\beta = 111.49(1)°$ at $T = 20$ °C. Other crystal data are: formula wt. = 420.50, $Z = 2$, $d_x = 4.66$ g/cc. Differential thermal analysis performed on the starting material showed two endotherms on heating, one at 500 °C and one at 725°. Apparently there is a phase transition at 500° followed by decomposition at 725 °C. Because of this phase transition at 500 °C it is not possible to say whether the phase reported in this paper is indeed a high-pressure phase or a high-temperature polymorph.

A single crystal of irregular shape and approximate dimensions, 0.19 × 0.14 × 0.18 mm was used to obtain the intensity data. Intensities were collected on a Syntex automatic diffrometer using MoKα radiation, a graphite monochromator ($2\theta = 12°$) and a scintillation detector. Reflections were scanned in the 2θ–θ mode at variable rates from 2.0°–24.0°/min, depending on the peak count, through an angle of 2° plus the α_1–α_2 separation. Background counts were made at the extremes of each scan for

[1]On leave of absence from the Central Research Department, E. I. Du Pont De Nemours, Wilmington, Delaware.

Can. J. Chem. Downloaded from www.nrcresearchpress.com by 210.87.254.40 on 09/05/12
For personal use only.

Can. J. Chem. Downloaded from www.nrcresearchpress.com by 210.87.254.40 on 09/05/12
For personal use only.

times equal to the peak count. The $\bar{1}30$ reflection was chosen as an internal standard and monitored every 50 reflections. No significant deviation in its intensity was noted. The average deviation in intensity of the 60 $0kl$ pairwise equivalent reflections measured was approximately 9% with about 10% of these deviating by as much as 25%. These variations are to be anticipated from the shape of the crystal and imply some systematic error. A total of 848 independent reflections were measured of which 710 were observed. A reflection was considered to be unobserved if the intensity was less than three times the standard deviation of the background $\sigma^2 = \sigma^2_{peak} + \sigma^2_{B1} + \sigma^2_{B2}$. The maximum 2θ was 60°. The intensities were corrected for Lorentz and polarization factors and for absorption assuming a sphere of radius 0.008 cm ($\mu r = 1.18$) using X-ray 67 Program System for X-ray Crystallography written by J. M. Stewart, University of Maryland and adapted to the CDC 6400 computer by H. D. Grundy.

The positions of the metal atoms were obtained from $h0l$ and $0kl$ Patterson projections and the knowledge that Cu(1) must be in a special position. Electron density difference maps were used to locate the four oxygen atoms. Cu(1) was placed at the origin and all other atoms in equipoint 4e. Several cycles of refinement using the full-matrix least squares program CUDLS (5) reduced

$$\omega R = \left\{ \frac{\sum \omega ||F_o| - |F_c||^2}{\sum \omega |F_o|^2} \right\}^{1/2}$$

to 0.109, with isotropic temperature factors. At this stage the isotropic U values were 0.008 for both Cu ions, 0.005 for V, and 0.010, 0.009, 0.009, and 0.009 for O(1), O(2), O(3) and O(4), respectively. A Cruickshank weighting scheme was used in which $\omega = (9.95 - 0.303|F_o| + 0.0141|F_o|^2)^{-1}$. The weights ω were chosen so as to make $\omega||F_o| - |F_c||^2$ independent of the variation in F_o. Unobserved reflections were assigned a maximum possible intensity of 3σ and these were given zero weight if $F_c < F_o$. Further refinement using anisotropic temperature factors and the secondary extinction coefficients calculated according to Zachariasen (6) reduced R to 0.054 and ωR to 0.067 for all reflections. The standard deviation of a reflection of unit weight was 1.00. The last cycle of refinement had a maximum shift over error of 0.02 and an average of 0.004. The secondary extinction parameter refined according to the method of Larson (7) was found to be $c = 3.11 \times 10^{-7}$. Scattering factors for neutral Cu, V, and O were taken from Cromer and Waber (8) with real and imaginary anomalous dispersion terms given by Cromer (9). Table 1 lists the observed and calculated structure factors[2] and Table 2 lists the atomic coordinates with anisotropic temperature factors.

Results and Discussion

Figure 1 shows a perspective view of $Cu_3V_2O_8$ looking along the c axis. The structure is similar to that of $Ni_3V_2O_8$ (10, 11), $Co_3V_2O_8$ (11, 12),

[2]Table 1 is available, at a nominal charge, from the Depository of Unpublished Data, National Science Library, National Research Council of Canada, Ottawa, Canada K1A 0S2.

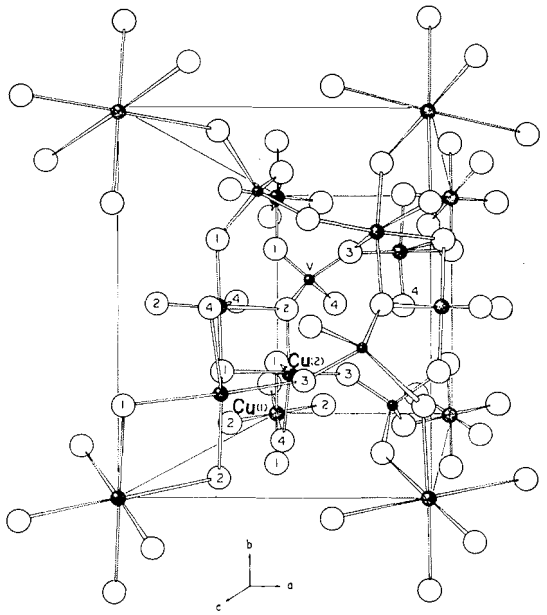

FIG. 1. Perspective view of $Cu_3V_2O_8$ along the c axis. Solid black spheres are V, shaded spheres are Cu, and open spheres are O.

$Zn_3V_2O_8$ (13), and $Mg_3V_2O_8$ (14). These structures are characterized by chains of edge-shared M(2) octahedra running along the a axis near $y = 1/8$, $z = 1/4$ and $y = 3/8$, $z = 3/4$ as shown in Fig. 2a. The M(1) octahedra are situated at $y = 0$, $z = 0$ and $y = 1/2$, $z = 1/2$ and each shares 2 edges with the M(2) octahedra. The network of octahedra containing M(2) ions at $y = 1/8$ is linked to the network of octahedra at $y = 3/8$ by corner-sharing V—O tetrahedra.

In $Cu_3V_2O_8$ the same network of Cu—O octahedra linked by V—O tetrahedra can be seen. The chains of edge-shared octahedra run along the c axis approximately at $y = 1/4$ and 3/4 (see Figs. 1 and 2b). However the Jahn–Teller effect typical of Cu^{2+} which frequently results in four short bonds and two longer bonds has distorted the structure, reducing the symmetry from $Cmca$ to $P2_1/c$. Figure 2b shows the relationship between the two unit cells. The approximate corresponding cell dimensions are $Cu_3V_2O_8$: $a \cos\beta = 5.8$, $b = 8.0$, $c = 6.4$ Å; $Mg_3V_2O_8$: $b/2 = 5.7$, $c = 8.3$, $a = 6.1$ Å. Table 3 contains pertinent bond lengths and angles for $Cu_3V_2O_8$. The octahedra in $Mg_3V_2O_8$ (14) are relatively undistorted: around Mg(1), 2.034 Å ×

Can. J. Chem. Downloaded from www.nrcresearchpress.com by 210.87.254.40 on 09/05/12
For personal use only.

TABLE 2. Final atom parameters for $Cu_3V_2O_8$*

Atom	x	y	z	U_{11}†	U_{22}	U_{33}	U_{12}	U_{13}	U_{23}
Cu(1)	0	0	0	0.0139(6)	0.0048(5)	0.0131(5)	0	0.0118(4)	0
Cu(2)	0.2638(2)	0.2454(1)	0.3915(1)	0.0110(5)	0.0060(5)	0.0109(5)	0.0005(3)	0.0091(3)	0.0004(3)
V	0.2510(1)	0.6185(1)	0.1418(1)	0.0081(5)	0.0048(5)	0.0072(5)	−0.0002(3)	0.0059(4)	0.0000(3)
O(1)	0.0151(8)	0.7622(6)	0.0351(8)	0.0093(18)	0.0086(19)	0.0145(19)	−0.0010(13)	0.0093(16)	−0.0012(14)
O(2)	0.2324(8)	0.4923(6)	0.3573(7)	0.0143(20)	0.0100(21)	0.0102(19)	0.0022(13)	0.0110(16)	0.0029(13)
O(3)	0.5024(8)	0.7261(6)	0.2382(7)	0.0121(19)	0.0108(18)	0.0111(19)	−0.0030(15)	0.0091(15)	−0.0022(14)
O(4)	0.7518(8)	0.5024(6)	0.0727(7)	0.0154(20)	0.0069(18)	0.0087(17)	0.0001(13)	0.0076(15)	−0.0012(14)

*Standard deviations are given in parentheses.
†Calculated from $\beta_{ij} = 2\pi^2 b_i b_j U_{ij}$ where $T = \exp -(\beta_{11}h^2 + 2\beta_{12}hk + \ldots)$ is the temperature factor appearing in the structure factor equation and b_i's are the reciprocal lattice vectors.

TABLE 3. Bond lengths and angles in $Cu_3V_2O_8$*

Bond	Distance (Å)	Bonds	Angles (°)	Bonds	Angles (°)
V—O(1)	1.795(4)	O(1)—V—O(2)	112.8(2)	O(2)—V—O(3)	109.2(2)
O(2)	1.742(5)	O(1)—V—O(3)	109.6(2)	O(3)— O(4*b*)	108.7(2)
O(3)	1.697(4)	O(1)—V—O(4*b*)	107.4(2)		
O(4*b*)	1.670(5)	O(2)—V—O(4*b*)	109.1(2)		
Cu(1)—O(1),(1*b*)	1.912(4)	O(1)—Cu(1)—O(1*b*)	180.0(3)	O(1)—Cu(1)—O(4*c*)	95.8(2)
—O(2*a*),(2*c*)	1.978(5)	—O(2*a*)	85.9(2)	O(2*a*)— —O(4*a*)	77.0(2)
—O(4*a*),(4*u*)	2.595(4)	—O(2*c*)	94.1(2)	—O(4*c*)	103.1(2)
		—O(4*a*)	84.2(2)		
Cu(1)—Cu(2)	2 × 2.859(1)				
Cu(1)—Cu(2)	2 × 3.128(1)				
Cu(2)—O(1*a*)	1.967(5)	O(1*a*)—Cu(2)—O(1*b*)	86.5(2)	O(1*b*)—Cu(2)—O(3*b*)	175.4(2)
O(2)	1.988(5)	—O(2)	84.2(2)	O(2)— —O(3*a*)	95.3(2)
O(3*a*)	1.931(5)	—O(3*a*)	169.2(2)	—O(4*a*)	171.4(2)
O(4*a*)	1.962(4)	—O(4*a*)	87.4(2)	—O(3*b*)	90.8(2)
O(3*b*)	2.288(4)	—O(3*b*)	92.0(2)	O(3*a*)— —O(4*a*)	92.8(2)
O(1*b*)	2.640(4)	O(1*b*)— —O(2)	84.7(2)	—O(3*b*)	98.8(2)
		—O(3*a*)	82.7(2)	O(4*a*)— —O(3*b*)	91.1(2)
Cu(2)—Cu(2)	2 × 3.190(1)	—O(4*a*)	93.1(2)		

*Symmetry transformations: $a = -x, 1/2 + y, 1/2 - z$; $b = -x, -y, -z$; $c = x, 1/2 - y, 1/2 + z$.

Can. J. Chem. Downloaded from www.nrcresearchpress.com by 210.87.254.40 on 09/05/12
For personal use only.

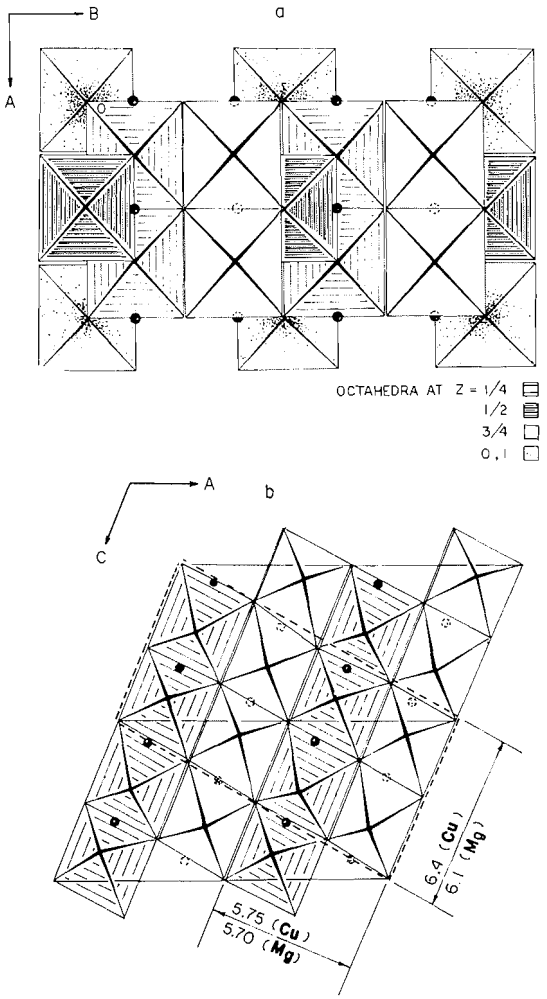

FIG. 2 (*a*) An *ab* projection of $Mg_3V_2O_8$ showing the arrangement of the MgO_6 octahedra. Small spheres represent V atoms. (*b*) An *ac* projection of 4 unit cells of $Cu_3V_2O_8$ showing an octahedral arrangement similar to that of $Mg_3V_2O_8$. The dotted line corresponds to one unit cell of $Mg_3V_2O_8$. Only the edge-shared octahedra at about $y = 1/4$ and 3/4 are shown.

2 and 2.130 Å × 4 and around Mg(2), 2.022 Å × 2, 2.135 Å × 2, and 2.118 Å × 2. In $Cu_3V_2O_8$ the octahedra are greatly distorted: around Cu(1), 1.912 Å × 2, 1.978 Å × 2, and 2.595 Å × 2 and around Cu(2) 1.931, 1.962, 1.967, 1.988, 2.288, and 2.640 Å. The oxygen ions around both Cu(1) and Cu(2) in approximate (201) planes of $Cu_3V_3O_8$ have shortened whereas the oxygen atoms perpendicular to (201) have lengthened. This results in $b(Cu_3V_2O_8) < c(Mg_3V_2O_8)$ and a shortening along a 110 diagonal of $Mg_3V_2O_8$.

The CuO_6 groups sharing an edge have the axially elongated Cu—O bonds nearly parallel. If $Cu_3V_2O_8$ were to crystallize in the $Mg_3V_2O_8$ structure these bonds would necessarily lie parallel to the *c* axis of $Mg_3V_2O_8$ in order that the 2/*m* site symmetry at cation (1) be preserved. However, in $Cu_3V_2O_8$ we find that these elongated bond lengths run parallel to $a + 2c$ rather than the *b* axis. In this manner O(1), which is the only oxygen atom bonded to three Cu ions and the vanadium ion, can reduce its bond strength whereas in the $Mg_3V_2O_8$ structure a comparable weakening of the bonds to this over-bonded oxygen atom cannot occur.

The VO_4 tetrahedron is distorted with distances varying from 1.670 to 1.795 Å. These variations, however, are consistent with distances anticipated from a consideration of the number and strength of cation bonds to each anion. Baur (15) has demonstrated this relationship for a number of tetrahedral oxyanions and Gopal (16) has extended this to vanadates. Gopal (16) derived a relation for tetrahedrally-coordinated V^{5+}, $d(V^{5+}—O) = 1.384 + 0.1602\ p_0$, where p_0 = the sum of electrostatic bond strengths around oxygen. Using the slope of this line and a mean V^{5+}—O value from Shannon and Calvo (17) to calculate V—O distances according to Baur's procedure, we have listed in Table 4 observed and predicted V—O distances in $Cu_3V_2O_8$. Note that his prescription arbitrarily redistributes the valency units so that short Cu—O bond lengths contribute twice as much as do the longer ones. The agreement between observed and calculated distances is rather poor.

Using the relations:

$$[1] \qquad s_{Cu^{2+}} = 0.333\left(\frac{2.084}{R}\right)^{5.3}$$

$$[2] \qquad s_{V^{5+}} = 1.25\left(\frac{1.714}{R}\right)^{5.1}$$

derived from a number of Cu- and V-containing oxides (18) to calculate the strengths of Cu—O bonds and determining the V—O bond strengths as the difference between 2.0 and the sum of the Cu—O bond strengths, there is a fairly good correlation between V—O lengths calcu-

TABLE 4. Bond strength sums around oxygen atoms and V—O distances

Bond	p_0*	Δp_0	s_{V-O}†	d_{obs} (Å)	d_{calc} (Å)‡	d_{calc} (Å)§
V—O(1)	2.25	+0.26	0.92	1.795	1.761	1.820
V—O(2)	2.05	−0.08	1.13	1.742	1.729	1.748
V—O(3)	1.85	−0.08	1.30	1.697	1.697	1.701
V—O(4)	1.85	−0.08	1.44	1.670	1.697	1.667
mean	1.99			1.725		

*p_0 = sum of all O-cation bond strengths.
†$s_{V-O} = 2.0 - \sum s_{O-Cu}$ where s_{O-Cu} were taken from Table 5.
‡$d(V—O) = 1.721 + 0.1602(\Delta p_0)$.
§From eq. 2 in Table 5.

TABLE 5. Bond strengths (s) in $Cu_3V_2O_8$*

Atom	Cu(1)	Cu(2)	V	$\sum s_i$
O(1)	0.53 (0.33)†	0.45 (0.33)†	0.99 (1.25)†	2.06 (2.25)
	0.53 (0.33)	0.10 (0.33)		
O(2)	0.44 (0.33)	0.43 (0.33)	1.15 (1.25)	2.02 (1.91)
	0.44 (0.33)			
O(3)		0.50 (0.33)	1.31 (1.25)	2.02 (1.91)
		0.20 (0.33)		
O(4)	0.10 (0.33)	0.46 (0.33)	1.43 (1.25)	1.99 (1.91)
	0.10 (0.33)			
$\sum s_i$	2.14 (2.00)	2.13 (2.00)	4.88 (5.00)	

*Calculated from

[1] $$s_{Cu^{2+}} = 0.333\left(\frac{2.084}{R}\right)^{5.3}$$

[2] $$s_{V^{5+}} = 1.25\left(\frac{1.714}{R}\right)^{5.1}$$

†Values in parentheses are average bond strengths calculated from s = valence/coordination no.

lated from eq. 2 and the observed V—O lengths. Table 5 lists the results of the calculation of bond strength sums around all atoms using (*1*) eqs. 1 and 2, and (*2*) using Pauling's system (results given in parentheses) which takes average cation coordination number only into account. Using the analytical expressions 1 and 2, the Pauling electrostatic valence rule is satisfied with an average deviation of about 4% from the ideal values of 2.0 for Cu^{2+}, 5.0 for V^{5+}, and 2.0 for O^{2-}.

The mean V—O distance of 1.725 Å agrees well with the value of 1.721 ± 0.012, the grand mean derived from 21 other well-refined vanadate structures (17). The effective ionic radius of V^{5+} in $Cu_3V_2O_8$ (0.365 Å) obtained by subtracting an appropriate oxygen radius (19) is significantly larger than that obtained from Li_3VO_4 (0.337 Å) (17), $Ca_3V_2O_8$ (0.335 Å) (20), Ca_2VO_4Cl (0.327) (21), and KVO_3 (0.344 Å) (22). In ternary $M_xV_yO_z$ systems this behavior can be correlated with the relative strengths of the M—O bonds. Because individual V—O distances show a strong correlation with the total strength of the M—O bonds (see column 4 in Table 4) it is not surprising to find that the average V—O distance is similarly affected. Thus, stronger bonds such as Cu^{2+}—O (as estimated from electronegativity or electrostatic bond strength criteria) result in longer average corrected V—O distances than weaker bonds such as Li—O, Ca—O, or K—O.

The thermal ellipsoid for all the atoms, shown in Table 6, are remarkably similar. The maximum amplitudes range from 0.100 to 0.136 Å and the minima lie between 0.040 and 0.069 Å. These maxima lie in the direction of the long bond Cu—O bonds for the copper

Can. J. Chem. Downloaded from www.nrcresearchpress.com by 210.87.254.40 on 09/05/12
For personal use only.

TABLE 6. Thermal ellipsoid for the atoms $Cu_8V_2O_8$

Atom	r_i	Root-mean-square amplitude	Angle (°) of r_i with a	b	c
Cu(1)	1	0.136	54.3	90	57.2
	2	0.069	90	0	90
	3	0.051	144.3	90	32.8
Cu(2)	1	0.121	55.3	86.3	56.3
	2	0.077	90.4	4.3	93.8
	3	0.054	34.7	92.1	146.1
V	1	0.100	128.4	88.7	120.1
	2	0.069	87.4	175.4	94.5
	3	0.053	141.5	94.4	30.5
O(1)	1	0.128	110.8	80.6	136.5
	2	0.092	88.6	9.7	81.6
	3	0.059	159.1	92.1	47.8
O(2)	1	0.136	51.8	70.3	64.3
	2	0.095	108.9	21.2	91.8
	3	0.040	135.7	97.5	25.8
O(3)	1	0.130	123.1	61.9	116.4
	2	0.096	77.9	28.9	71.0
	3	0.062	144.2	95.2	33.4
O(4)	1	0.126	146.7	89.1	101.8
	2	0.088	107.1	149.0	59.9
	3	0.069	62.4	121.0	147.2

atoms and the minima for the oxygen atoms lie roughly in the direction of the strong V—O bond.

The authors would like to thank Mrs. C. M. Foris and Dr. J. F. Whitney of the Central Research Department, E. I. du Pont de Nemours, Wilmington, Delaware for the Guinier photographs and R. Faggiani for assistance in obtaining the intensity data. This research was supported by a grant from the National Research Council of Canada.

1. C. BRISI and A. MOLINARI. Ann. Chim. **48**, 263 (1958).
2. P. FLEURY. C. R. Acad. Sci. Paris, **C263**, 1375 (1966).
3. P. FLEURY. Rev. Chim. Mineral, **6**, 819 (1969).
4. R. D. SHANNON. Inorg. Chem. **6**, 1474 (1967).
5. J. S. STEPHENS. Unpublished results.
6. W. H. ZACHARIASEN. Acta Cryst. **16**, 1139 (1963).
7. A. C. LARSON. Acta Cryst. **23**, 664 (1967).
8. D. T. CROMER and J. T. WABER. Acta Cryst. **18**, 104 (1965).
9. D. T. CROMER. Acta Cryst. **18**, 17 (1965).
10. A. DURIF and E. F. BERTAUT. J. Phys. Radium, **20**, 455 (1959).
11. H. FUESS, E. F. BERTAUT, R. PAUTHENET, and A. DURIF. Acta Cryst. **B26**, 2036 (1970).
12. E. SAUERBREI. M.Sc. Thesis, McMaster University, Hamilton, Ontario. 1972.
13. R. GOPAL and C. CALVO. Can. J. Chem. **49**, 3056 (1971).
14. N. KRISHNAMACHARI and C. CALVO. Can. J. Chem. **49**, 1629 (1971).
15. W. H. BAUR. Trans. Am. Cryst. Assn. **6**, 129 (1970).
16. R. GOPAL. Ph.D. Thesis. McMaster University, Hamilton, Ontario, 1972.
17. R. D. SHANNON and C. CALVO. Can. J. Chem. In press.
18. I. D. BROWN and R. D. SHANNON. To be published.
19. R. D. SHANNON and C. W. PREWITT. Acta Cryst. **B25**, 925 (1969).
20. R. GOPAL and C. CALVO. Zeit. Krist. In press.
21. E. BANKS, M. GREENBLATT, and B. POST. Inorg. Chem. **9**, 2259 (1970).
22. H. T. EVANS, JR. Zeits. Krist. **114**, 257 (1960).

Can. J. Chem. Downloaded from www.nrcresearchpress.com by 210.87.254.40 on 09/05/12
For personal use only.

Coordination Compounds of Indium. Part XIX[1]. Ligand Exchange Studies with Indium(III) Complexes of Trifluoromethyl-β-diketonates

MRS. G. M. TANNER, D. G. TUCK,[2] AND E. J. WELLS

Department of Chemistry, Simon Fraser University, Burnaby 2, British Columbia

Received, March 7, 1972

The ligand exchange reaction between InL_3 con plexes ($L = CF_3.CO.CH.CO.R^-$ anion; R = methyl, *i*-butyl, phenyl, 2-naphthyl, and 2-thienyl) and excess free ligand (HL) has been studied in the solvents di-isopropyl ketone, acetonitrile, benzene, and dimethylsulfoxide. Studies of the lifetimes of the reactants as obtained from their ^{19}F n.m.r. line-widths show that the exchange is first order in InL_3 concentration, but zero order in free ligand concentration. The coalescence temperature for the collapse of the n.m.r. ^{19}F chemical shift between free and complexed ligand (~50 Hz) yields ΔG^* for the exchange. The results are in agreement with the known stereochemical properties of indium(III) complexes. The rate-controlling process in the exchange is identified as the rotation of one monodentate ligand about a partial double bond prior to intramolecular proton transfer to a second monodentate ligand.

La réaction d'échange de ligand entre les complexes de InL_3 (L = anion $CF_3.CO.CH.CO.R^-$; R = méthyle, isobutyle, phényle, naphtyl-2, et thiényl-2) et un excès de ligand libre (HL) a été étudiée dans les solvants di-isopropylcétone, acétonitrile, benzène, et diméthylsulfoxyde. Les durées de vie des réactants, obtenues à partir des largeurs de raies RMN du ^{19}F, montrent que l'échange est du premier ordre par rapport à la concentration en InL_3 et d'ordre zéro par rapport au ligand libre. La température de coalescence du déplacement chimique du ^{19}F entre le ligand libre et le ligand complexé (~50 Hz) conduit à ΔG^* pour l'échange. Les résultats sont en accord avec les propriétés stéréochimiques connues pour les complexes du l'indium(III). Le processus contrôlant la vitesse de l'échange à été identifié à la rotation d'un ligand monodentate autour d'une double liaison partielle avant le transfert intramoléculaire de proton à un second ligand monodentate.
[Traduit par le journal]

Canadian Journal of Chemistry, **50**, 3950 (1972)

Introduction

In recent years, a number of papers have appeared on the kinetics and mechanism of the exchange reactions between metal chelate complexes of various β-diketonates and the free ligand. In some experiments (1, 2), the ligand has been labelled with ^{14}C radioactive tracer, in which case the final separation of ligand and complex is a critical experimental step. Alternatively, differences in the proton magnetic resonance spectra of free and complexed ligand can be utilized in these kinetic studies (3), and both diketonate and organometal–acetylacetonate (4) complexes have been investigated in the latter way.

We now report the results of ^{19}F n.m.r. studies of ligand exchange between chelates of indium(III) and ligands of the type $CF_3.CO.CH_2.CO.R$ in a number of organic solvents. Indium complexes were selected in order to extend the knowledge of the stereochemistry of the coordination complexes of this element (5) to include kinetic systems. Use of the partially fluorinated diketones allows the ^{19}F resonances of free and complexed ligand to be used to explore the exchange; the fact that the ^{19}F chemical shifts are significantly larger than in the analogous proton experiments is of some advantage in this respect. The availability of a group of these diketonates allowed a range of complexes with varying substituents R to be investigated; InL_3 complexes with R = methyl, *i*-butyl, phenyl, 2-naphthyl, 2-furyl, and 2-thienyl were prepared and studied. The compound R = 2-thienyl is the well-known analytical reagent TTA (thenoyltrifluoroacetone), which leads to some interesting comparisons between the present results and previous reports of mixed chelate–neutral donor complexes of TTA and tri-*n*-butyl phosphate with trivalent metal cations (6, 7).

Experimental

Preparative

In a typical procedure, indium metal (0.62 g) was dissolved in concentrated nitric acid and the solution evaporated to give indium trinitrate hydrate (8). This was dissolved

[1]For Part XVIII see ref. 30.

[2]Present address: Department of Chemistry, University of Windsor, Windsor 11, Ontario.

Can. J. Chem. Downloaded from www.nrcresearchpress.com by 210.87.254.6 on 09/05/12
For personal use only.

Can. J. Chem. Downloaded from www.nrcresearchpress.com by 210.87.254.6 on 09/05/12
For personal use only.

TABLE 1. Analytical and n.m.r. results for indium(III) chelate complexes of diketonates $CF_3.CO.CH_2.CO.R$

R	Melting point (°C)	Indium (%)		Molecular Weight†	^{19}F Chemical shift in $CHCl_3$‡	
		Observed	Calcd.*		L	InL_3
CH_3	119	19.6	19.9	574	4.342	4.268
i-C_4H_9	82	16.5	16.3	700	4.298	4.245
Phenyl	139	14.8	15.0	760	4.334	4.281
2-Naphthyl	183	12.8	12.7	910	4.297	4.235
2-Furyl	204	15.2	15.6	730	4.304	4.251
2-Thienyl	159	14.8	14.7	778	4.269	4.246

*For $In(CF_3.CO.CH.CO.R)_3$.
†From the main parent peak in the mass spectrum; these values agree in each case with the value required for $^{115}In(CF_3.CO.CH.CO.R)_3$.
‡kHz, upfield from $CFCl_3$, at 56.4 Mhz.

TABLE 2. ^{19}F resonance line-widths at half-height as a function of concentration in the system $In(tfac)_3$/Htfac/di-isopropyl ketone

(*a*) Varying $In(tfac)_3$, constant Htfac(1 mmol), at 36 °C

$In(tfac)_3$ added (mmol)	Line-width (Hz)*	
	Htfac	$In(tfac)_3$
0	0.8 ± 0.1	—
1.00	3.6 ± 0.2	12.5
2.37	8.2 ± 0.5	12.0
4.05	13.0 ± 1.0	12.5
6.50	26.0 ± 5.0	13.0

(*b*) Varying Htfac constant $In(tfac)_3$ (0.261 mmol), 42 °C

Htfac added (mmol)	$[Htfac]^{-1}$ (M^{-1})	Line-width (Hz)*	
		Htfac	$In(tfac)_3$
0.82	0.92	17.5	14.0
1.61	0.53	10.5	15.0
2.44	0.39	7.5	14.0
3.28	0.32	6.0	13.0

*Estimated accuracy on individual values ±1 Hz.

in water, the p*H* of the solution adjusted to 6, a solution of TTA (3.2 g) in chloroform added, and the two-phase mixture refluxed for 2 h. Evaporation of the separated chloroform phase yielded a pink solid which was recrystallized from chloroform–petroleum ether as white needles. This procedure yielded the compounds listed in Table 1; reactions were also carried out in this way with the R = 3-pyridyl diketone, but we were unable to obtain the expected crystalline indium complex.

Indium analysis was by titration against EDTA, using pyridine-2-azo-4-resorcinol as indicator (9). Molecular weights were obtained from the parent peak in the mass spectrum, using a Hitachi Perkin–Elmer RMU-6E instrument operating in the single focussing mode at an excitation energy of 80 V, and a sample temperature of 250 °C. Analytical results are given in Table 1.

Nuclear Magnetic Resonance Studies

All ^{19}F n.m.r. spectra were obtained in standard capped 5 mm sample tubes with a Varian A56/60 spectrometer, operating at an oscillator frequency of 56.4 MHz. Resonance frequencies were measured with reference to an external standard of liquid trichlorofluoromethane (see Table 1).

Temperature variation experiments were carried out over the range −40 to 100 °C, unless otherwise restricted by the physical properties of the solvent. Sample temperatures were determined by the usual proton shift n.m.r. thermometers using methanol or ethylene glycol separations at 60 MHz, and are believed to be accurate to within 2 °C. Solutions for the temperature dependence studies contained the InL_3 complex at concentrations in the range 0.4–0.7 *M* (depending on solubility, molecular weight, etc.), and an exactly threefold concentration of free ligand, in order to maintain the nuclear exchange process between chemically shifted sites of identical nuclear population (10, 11).

Solvents

Solvents were Reagent Grade materials. Acetonitrile was distilled from phosphorus pentoxide before use.

In addition to the solvents shown in Table 2, we also investigated 1-propanol and nitromethane. With the former, the compounds proved insufficiently soluble for meaningful spectra to be recorded. With nitromethane, results could only be obtained with $In(CF_3.CO.CH.CO.CH_3)_3$; insolubility again prevented investigation of the other complexes.

Results and Discussion

Theory

For an exchange in a system at equilibrium

$$[1] \qquad aA + bB \underset{k}{\overset{k}{\rightleftharpoons}} aA + bB$$

the average lifetime τ_A of a single reactant

Can. J. Chem. Downloaded from www.nrcresearchpress.com by 210.87.254.6 on 09/05/12
For personal use only.

molecule A is given by (12)

$$[2] \qquad \tau_A^{-1} = \frac{1}{[A]} \cdot \frac{d[A]}{dt} = k[A]^{a-1}[B]^b$$

An exactly analogous equation gives τ_B. In the slow exchange limit (τ_A^{-1}, $\tau_B^{-1} \ll 2\pi\Delta\nu_{AB}$), the width of the n.m.r. resonance line due to A (or some group characteristic of A) is simply related to τ_A^{-1}, and hence can yield the order of the reaction.

Experiments of this type reported below establish that the overall order of reaction in the exchange systems studied is unity. In this case, the reciprocal lifetime of one of the species is just the rate constant k. For chemical exchange of equivalent nuclei between two distinct sites of equal nuclear population, and equal transverse relaxation rates R_2 separated by a chemical shift difference $\Delta\nu = \Delta\omega/2\pi$ Hz, coalescence of the individual site resonances occurs when the chemical exchange rate constant k (s^{-1}) reaches the value (13, 14)

$$[3] \qquad k_c = \Delta\omega/\sqrt{2} = \sqrt{2}\pi\Delta\nu$$

which occurs at a temperature T_c, the coalescence temperature. Thus the observation of the temperature dependence of the n.m.r. spectrum, together with independent measurement of the chemical shift parameters, leads to the chemical exchange rate k_c at the single temperature T_c. This information, together with the well-known Eyring rate equation based on the assumptions of the theory of absolute reaction rates (15, 16)

$$[4] \qquad k_c = \kappa \frac{\boldsymbol{k}T_c}{h} \exp\left(-\Delta G^{\ddagger}/RT_c\right)$$

or

$$[5] \qquad \Delta G^{\ddagger} = RT_c \ln \frac{hk_c}{\kappa \boldsymbol{k} T_c}$$

allows the determination of the activation parameter $\Delta G^{\ddagger}$. In eqs. 4 and 5, the transmission coefficient κ may be arbitrarily assigned the value 0.5 without introducing appreciable error; $\boldsymbol{k}$ is the Boltzmann constant, and the other symbols have their usual significance. A feature of eq. 4 is that for the conditions used in the present work the derived values of $\Delta G^{\ddagger}$ are quite insensitive to errors in both T_c and $\Delta\nu$. Thus for T_c in the region of 330 °K, an error of $\pm 10°$ in T_c introduces an error of only ± 0.5 kcal mol^{-1} in a derived $\Delta G^{\ddagger}$ of about 15 kcal mol^{-1} (*i.e.*, $\sim 3\%$ error); similarly an error of $\pm 20\%$ in the measurement of $\Delta\nu$ leads to an error of ± 0.12 kcal mol^{-1} in $\Delta G^{\ddagger}$ at the same temperature. This might seem to imply that $\Delta G^{\ddagger}$ cannot be measured with any certainty by this technique, but in fact the coalescence method can only be used for $\Delta G^{\ddagger}$ values in the limited range of approx. 8–18 kcal mol^{-1}, and within this range the results are quite reliable.

While $\Delta G^{\ddagger}$ alone is less informative than independent measurements of $\Delta H^{\ddagger}$ and $\Delta S^{\ddagger}$, the above simple method, where applicable, obviates the notorious problems associated with n.m.r. determinations of $\Delta H^{\ddagger}$ and $\Delta S^{\ddagger}$ independently (11). For a comparative study of exchange in related systems, or of the solvent dependence of a common exchange process, one may expect that little is lost by consideration of $\Delta G^{\ddagger}$ alone.

^{19}F n.m.r. *Lifetime Measurements*

As noted above, the order of the exchange reaction can be established by following the life-times of the individual species as a function of reactant concentration, measuring the n.m.r. line widths below coalescence (eq. 2). We chose to investigate the reaction order for the system $In(tfac)_3$/Htfac in di-isopropyl ketone (Htfac = 1,1,1-trifluoromethyl-2,4-pentadione; **1**, R = CH_3), since in this case the ^{19}F resonances are well-resolved below coalescence at the temperature of the probe of the n.m.r. spectrometer, with $\Delta\nu$ at 36 °C = 50 Hz. It is worth noting here the contrast between the ^{19}F and ^1H spectra. The ^1H spectrum of Htfac in carbon tetrachloride consists of sharp singlets at 132 (CH_3) and 353 Hz (γ—CH) downfield from internal TMS; for $In(tfac)_3$ these frequencies are 136 and 352 Hz, while a 3:1 mixture of Htfac and $In(tfac)_3$ show singlets at 133 and 352 Hz. The ^{19}F spectra clearly give rise to more reliable data over a convenient temperature range than could be the case in studies of proton resonances in such systems.

The results reported in Table 2*a* show the ^{19}F line-width for $In(tfac)_3$ and Htfac as a function of the amount of solid complex added to a solution containing a constant quantity of

Can. J. Chem. Downloaded from www.nrcresearchpress.com by 210.87.254.6 on 09/05/12
For personal use only.

ligand. Since the volume changes involved in this case are small the results establish that τ_{Htfac} is a linear function of the complex concentration within experimental error. The only point which deviates from a linear plot is that for the highest InL_3 concentration; here the spectral line for the complex is broad, and non-Lorentzian, overlapping significantly with the free ligand peak, so that the slow exchange limit approximation is not valid.

The half-width of the ^{19}F resonance of the complex in Table 2*a* is sensibly constant. A similar result was obtained in experiments using constant amounts of $In(tfac)_3$ and varying quantities of added ligand. For 0.31 mmol $In(tfac)_3$ and 0.27, 0.55, and 1.04 mmol Htfac at 36 °C, the complex line-widths were 11.5, 12.5, and 12.5 Hz; similarly with 0.22 mmol $In(tfac)_3$, and 0.27, 1.15, and 2.57 mmol Htfac the line-widths were 12.5, 13.0, and 12.5 Hz, so that the line-width is sensibly constant at 36 °C at 12.5 ± 0.5 Hz. A final series of measurements at 42 °C gave the results in Table 2*b*, which show that the line-width for tfac is inversely dependent on [Htfac]; the line-width for $In(tfac)_3$ is once again constant within experimental error. The two expressions for the average life-times are then

$$[6] \qquad \tau_{tfac}^{-1} = k[\text{Htfac}]^{-1}\,[\text{complex}]^{1}$$

$$[7] \qquad \tau_{complex}^{-1} = k[\text{Htfac}]^{0}\,[\text{complex}]^{0}$$

and the rate law for the exchange in di-isopropyl ketone must be of the form

$$[8] \qquad R = k[InL_3]^{1}\,[HL]^{0}$$

It is important in terms of the subsequent discussion to emphasize that the experiments just described were with concentrations similar to those used in the $\Delta G^{\ddagger}$ determinations, and that the range of mole ratios studied spanned the condition $[InL_3] = 3[HL]$ used in those measurements.

Finally we note that since the stability constants of the InL_3 species studied are all very similar, and since the pK_a values of the individual ligands fall within a small range (5.8–6.7) (17), a rate law of the same form, and hence a similar mechanism, should apply in all the InL_3/HL systems studied in the present work.

Experimental Free Energies of Activation

Table 3 shows the experimentally observed coalescence temperatures for a number of complex–ligand systems in a variety of solvents, together with the relevant changes in the ^{19}F resonance frequency between the complex and the free ligand. In a number of systems, complete coalescence of the complex and ligand resonance peaks could not be observed because of limitations imposed by the boiling point of the solvent, but in some of these cases it was possible to estimate an approximate coalescence temperature. Since the calculation of $\Delta G^{\ddagger}$ from $\Delta\nu$ (eq. 3) involves T_c predominantly in a linear term (see above), the errors introduced in this way are not large. With solutions in dimethylsulfoxide (dmso), separate complex and free ligand resonances could not be observed in the available temperature range (*i.e.* even down to the freezing point of the solvent, 18.5 °C), and the chemical shift $\Delta\nu$ was therefore estimated from separate solutions of the individual species in dmso. This procedure may introduce some small errors because of possible differences in the bulk susceptibilities of the two solutions being compared, but the values for solutions are in any case estimated upper limits, so that these susceptibility problems can be neglected. We can also neglect errors which might arise from possible changes in $\Delta\nu$ on changing the temperature from ambient (say 36 °C) to T_c; as emphasized above, the derived values of $\Delta G^{\ddagger}$ are relatively insensitive to errors in $\Delta\nu$.

Solubility restrictions prohibited meaningful measurements in a number of cases (see Experimental). The only complex–ligand pair that could be investigated in nitromethane was for the ligand $CF_3.CO.CH_2.CO.CH_3$, for which we estimate $T_c \sim 110°$ (the b.p. of CH_3NO_2 is 101°); $\Delta\nu$ is 47 Hz, leading to an approximate value of 17.9 kcal mol^{-1} for $\Delta G^{\ddagger}$.

Reaction Mechanism

The results obtained show that rapid ligand exchange occurs in all the InL_3/HL systems studied in the present work. We base our discussion of the mechanism of the reaction on the scheme originally proposed by Adams and Larsen (3) for ZrL_4 and HfL_4 systems, and subsequently adopted by other workers (1, 2, 4).

Can. J. Chem. Downloaded from www.nrcresearchpress.com by 210.87.254.6 on 09/05/12
For personal use only.

TABLE 3. Free energies of activation for ligand exchange in $In(CF_3.CO.CH.CO.R)_3$ complexes

	Di-iso-propylketone			Acetonitrile			Benzene			Dimethylsulfoxide		
R	$\Delta\nu(^{19}F)$ (Hz)	T_c (°C)	ΔG^* (kcal mol^{-1})	$\Delta\nu(^{19}F)$ (Hz)	T_c (°C)	ΔG^* (kcal mol^{-1})	$\Delta\nu(^{19}F)$ (Hz)	T_c (°C)	ΔG^* (kcal mol^{-1})	$\Delta\nu(^{19}F)$ (Hz)	T_c (°C)	ΔG^* (kcal mol^{-1})
Me	50	85	18.3	48.5	>80	>18.1	53	>80 (~85)	≳18.3		†	
i-Bu	34	92*	17.3	30	>80	>16.8	39	>80 (~95)	≳17.3		†	
Ph	48.5	54*	15.3	49.5	50	15.1	52	>80	>18.0	26	<20 (~10)	≲13.4
2-Naphthyl	51	97	19.0	—	†	—	59	>80 (~85)	≳16.6	34	<20	<14.0
2-Thienyl	5	25*	15.2	4.5	40*	16.1	18	>80* (~85)	≳17.4	6	<20	<15.9

*Asymmetric peak at coalescence.
†Insufficient solubility for measurement.

For a six coordinate complex, the reactions are:

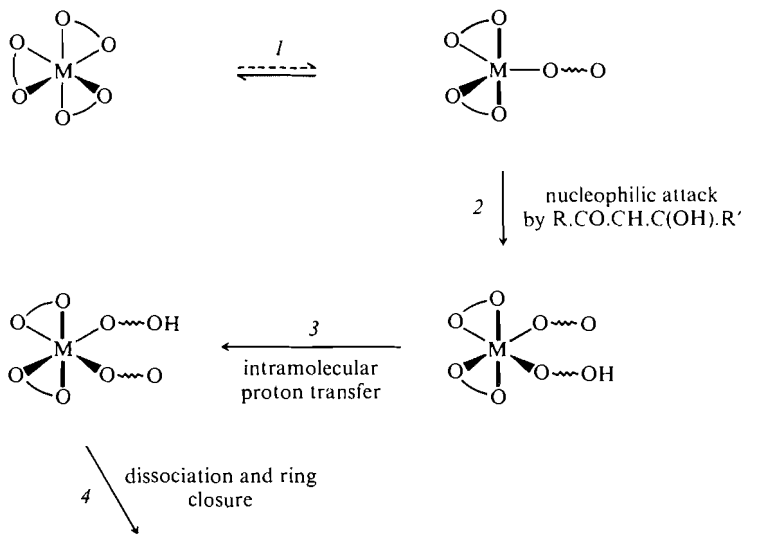

The diketone form of the free ligand does not undergo exchange (3). Various pieces of evidence support different aspects of this scheme for InL_3 complexes.

(*A*) In the light of the known stereochemical behavior of indium(III) complexes, a mechanism requiring a change of coordination number is readily acceptable. Coordination numbers of two, three, four, five, and six have been reported (5, 18), and both preparative work, and studies of solutions in aqueous and non-aqueous solvents (5, 19, 20), have shown that four, five, and six-coordinate neutral and anionic species may co-exist, and readily interchange. The high rate of exchange at the coalescence temperature ($k_c \sim 10^2$ s^{-2}) is in keeping with the known tendency of indium(III) complexes to establish the appropriate equilibrium situation very rapidly in solution (5).

(*B*) The thermodynamic stability of the InL_3 complexes (17) argues against any mechanism involving complete dissociation into free ligand and a charged or neutral residue. At the same time, coordination numbers greater than six are rare for indium(III), so that a dissociative step of some sort must be assumed (*i.e.* step 1). Fay and Piper (21) have reported studies of intramolecular rearrangements in a number of ML_3 chelate complexes, including $In(tfac)_3$, and conclude that such reactions require a five-coordinate intermediate with one monodentate ligand, in equilibrium with the normal tris-chelated form (*i.e.* equilibrium 1 above). This equilibrium is very fast, with ΔG^* for $In(tfac)_3$ below 11.0 kcal mol^{-1}. Fay and Piper were not able to obtain n.m.r. evidence to establish the existence of significant concentrations of the five-coordinate species, and the spectrum of $In(tfac)_3$ was a sharp singlet at all temperatures down to their temperature limit of -57 °C.

We have confirmed this result for the following $In(CF_3.CO.CH.CO.R)_3$ complexes in $CDCl_3$: R = 2-thienyl to -50°; R = 2-furyl to -37°; R = *i*-butyl to -43°; R = *t*-butyl to -25°, and for $In(acac)_3$ to -56°. These temperatures represent limits set by freezing or solubility factors, and do not imply that multiplets appear at lower temperatures. Such results, together with the extensive studies by Fay and Piper (21) show that the rapid formation of a five-coordinate intermediate is a likely step in the intermolecular exchange mechanism. Equally, because of its rapidity, this cannot be the rate-controlling step in the intermolecular process at issue here.

Can. J. Chem. Downloaded from www.nrcresearchpress.com by 210.87.254.6 on 09/05/12
For personal use only.

Can. J. Chem. Downloaded from www.nrcresearchpress.com by 210.87.254.6 on 09/05/12
For personal use only.

(*C*) An interesting piece of supporting evidence for one aspect of this mechanism comes from work on the crystal structure of $[(Meen)_2Cu(CF_3.CO.CH.CO.CF_3)_2]$, where Meen = $(CH_3)_2NC_2H_4NH_2$ (22). In this molecule, the copper atom is six-coordinate, with two bidentate *N,N*-dimethylethylenediamine ligands and two monodentate hexafluoropentane-2,4-dionate ligands; the non-coordinated oxygens of the latter are each hydrogen-bonded to a hydrogen atom of an amino group. This structure confirms that monodentate diketonate ligand can indeed exist, and it seems reasonable that such a structure could be involved in the exchange mechanism described above. The bond lengths show that delocalization is important in the O—C—C—C—O system of the monodentate dionate ligand.

While the general scheme receives support, the present results are in marked contrast with those of Adams and Larsen (3) in one important respect, namely, reaction orders. These authors found that the rate of exchange was first order in both ML_4 and HL, and identified the rate-controlling step as the loss of the monodentate ligand from the ML_5 intermediate (M = Hf or Zr). The analogous process in the above scheme (step 4) cannot be rate-controlling in the InL_3/HL system, and in fact the only step which would give the correct order if rate-controlling is step 3, the intramolecular proton transfer reaction between the two monodentate ligands. The barrier here is presumably not the transfer itself, but the rotation of the monodentate ligand required to bring the —C—OH group of one ligand into the correct orientation with the C=O group of the other. Such a rotation will be hindered by the partial double bond character of the O—C—C—C—O system (see (*C*) above). The free energies of activation of 15–20 kcal mol^{-1} (Table 3) are in keeping with this argument, since such values are typical of the activation barrier to rotation in various well-studied simple carbonyl systems; E_a = 14–16 kcals mol^{-1} for *N,N*-dimethyl carbamyl chloride (23–26), and 18.3 kcal mol^{-1} in the analogous fluoride (27); $\Delta G^{\ddagger}$ is 18 kcal mol^{-1} at room temperature in dimethyl trifluoroacetamide, 17.3 in dimethyl acetamide, and 14.8 in dimethyl benzamide (28), and near 20.5 kcal mol^{-1} in dimethyl formamide (24, 29).

Effects of Solvent, and of the Group R

The results in Table 3 indicate that the order of increasing $\Delta G^{\ddagger}$ of the various ligands in the four solvents used is: dimethylsulfoxide < di-isopropyl ketone < acetonitrile < benzene, so that $\Delta G^{\ddagger}$ increases with decreasing ability of the solvent to act as a hydrogen-bond acceptor. In terms of the intramolecular hydrogen transfer mechanism proposed above, we conclude that the transfer is facilitated by hydrogen-bonding of the transition state to the solvent. This could result from the solvent acting as a protonating bridge from the enol unidentate ligand to the keto unidentate ligand, reducing the strict orientation requirements, or from a lowering of the rotation barrier of the enol form by H-bonding to the solvent.

There is no apparent dependence of the $\Delta G^{\ddagger}$ values on the stability constants (K_1) for the InL_3 complexes, nor on the pK_a values of the parent ligands (17). This is not surprising, since $\Delta G^{\ddagger}$ must involve not only pK_a, but also important $\Delta S^{\ddagger}$ terms such as those for the solvation of the species in question.

We note finally in this respect that in detailed studies of the $In(tfac)_3$/Htfac/di-isopropyl ketone systems, the addition of solvent saturated with water caused no significant change in the ^{19}F n.m.r. spectrum. This result is in contrast to the very marked effect of traces of water found by Adams and Larsen (3) in the $Hf(tfac)_4$/Htfac/benzene system.

Other Studies

Attempts were made to confirm the reaction scheme set out earlier for $In—O_6$ complexes by some further experiments, in which we examined the u.v./visible spectra of InL_3 (R = phenyl) species in solution, arguing that if monodentate diketonate groups containing an aromatic substituent are present, light absorption by a highly conjugated system such as

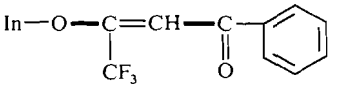

might be observed. We could find no detectable light absorption by solutions in organic solvents such as chloroform or methanol, nor were any n.m.r. signals additional to those of the free ligand and the complex detected on cooling solutions of 3:1 mixtures to −55 °C.

The synergistic extraction of iron(III) and cobalt(III) with mixtures of acetylacetone (acac) and tri-octylphosphine oxide (TOPO) has been discussed in terms of mixed $[M(acac)_3TOPO]$ complexes, implying one monodentate acetylacetone ligand (7). We therefore examined solutions of InL_3 (R = phenyl) in the presence of added TOPO, but again no light absorption could be detected. We therefore conclude that the steady-state concentration of complexes containing monodentate ligand in such systems is extremely small.

This work was supported in part by Operating Grants from the National Research Council of Canada.

1. K. SAITO and K. MASUDA. Bull. Chem. Soc. Jap. **41**, 384 (1968).
2. K. SAITO and M. TAKAHASHI. Bull. Chem. Soc. Jap. **42**, 3462 (1969).
3. A. C. ADAMS and E. M. LARSEN. Inorg. Chem. **5**, 814 (1966).
4. G. E. GLASS and R. S. TOBIAS. J. Organometal. Chem. **15**, 481 (1968).
5. D. G. TUCK. Proceedings of C.N.R.S. Conference No. 191, Editions du C.N.R.S. 1970. p. 159.
6. T. SEKINE and D. DYRSSEN. J. Inorg. Nucl. Chem. **29**, 1489 (1967).
7. J. AGGETT. Chem. Ind. 27 (1965).
8. D. G. TUCK, E. J. WOODHOUSE, and P. CARTY. J. Chem. Soc. 1077 (1966).
9. L. SOMMER and M. HNILICKOVA. Naturwiss. **45**, 544 (1958).
10. H. S. GUTOWSKY, R. L. VOLD, and E. J. WELLS. J. Chem. Phys. **43**, 4107 (1965).
11. A. ALLERHAND, J. S. GUTOWSKY, J. JONAS, and R. MEINZER. J. Am. Chem. Soc. **88**, 3185 (1966).
12. A. LOEWENSTEIN and T. M. CONNOR. Ber. Bunsenges J. Phys. Chem. **67**, 280 (1963).
13. J. A. POPLE, W. G. SCHNEIDER, and H. J. BERNSTEIN. High resolution nuclear magnetic resonance. McGraw-Hill, New York. 1959. p. 223.
14. H. S. GUTOWSKY and C. H. HOLM. J. Chem. Phys. **25**, 1228 (1956).
15. H. EYRING. J. Chem. Phys. **3**, 107 (1935).
16. S. GLASSTONE, K. J. LAIDLER, and H. EYRING. Theory of rate processes. McGraw-Hill, New York. 1941.
17. KEITH BOWDEN, G. M. TANNER, and D. G. TUCK. Can. J. Chem. **50**, 2622 (1972).
18. C. W. HOBBS and R. S. TOBIAS. Inorg. Chem. **9**, 1998 (1970).
19. J. GISLASON, M. H. LLOYD, and D. G. TUCK. Inorg. Chem. **10**, 1907 (1971).
20. P. DOBUD, H. M. LEE, and D. G. TUCK. Inorg. Chem. **9**, 1990 (1970).
21. R. C. FAY and T. S. PIPER. Inorg. Chem. **3**, 348 (1964).
22. M. A. BUSH, D. E. FENTON, R. S. NYHOLM, and M. R. TRUTER. Chem. Commun. 1335 (1970).
23. A. ALLERHAND and H. J. GUTOWSKY. J. Chem. Phys. **41**, 2115 (1964).
24. P. T. INGLEFIELD, E. KRAKOWER, L. W. REEVES, and R. STEWART. Mol. Phys. **15**, 65 (1968).
25. S. O. CHAN and E. J. WELLS. Unpublished results.
26. B. W. RICHARDSON and H. S. GUTOWSKY. Unpublished results.
27. L. W. REEVES and K. N. SHAW. Can. J. Chem. **49**, 3671 (1971).
28. L. W. REEVES, R. L. SHADDICK, and K. N. SHAW. Can. J. Chem. **49**, 3683 (1971).
29. M. RABINOWITZ and A. PINES. J. Am. Chem. Soc. **91**, 1585 (1969).
30. J. J. HABEEB and D. G. TUCK. J. Chem. Soc. (Dalton). In press.

Can. J. Chem. Downloaded from www.nrcresearchpress.com by 210.87.254.6 on 09/05/12
For personal use only.

Synthesis and Reactions of Strained Hydrocarbons Possessing Inverted Carbon Atoms. Tetracyclo[3.3.1.1^{3,7}.0^{1,3}]decanes

R. E. PINCOCK, J. SCHMIDT, W. B. SCOTT, AND E. J. TORUPKA

Department of Chemistry, University of British Columbia, Vancouver 8, British Columbia

Received June 26, 1972

Tetracyclo[3.3.1.1^{3,7}.0^{1,3}]decane (*i.e.*, 1,3-dehydroadamantane or DHA) and its 5,7-dimethyl derivative may be synthesized from the corresponding 1,3-dibromoadamantane compounds with sodium–potassium alloy in ether or heptane. These highly strained cyclopropyl compounds are very reactive towards free radical and electrophilic reagents. They homopolymerize 140–160° to thermally resistant, insoluble materials and spontaneously copolymerize with oxygen in solvents at room temperature. Reaction with bromine in ether at −70° yields an intermediate bromoadamantyloxonium tribromide which decomposes to 1-bromo-3-ethoxyadamantane on warming. Other rapid reactions of these strained 1,3-dehydroadamantanes are reported.

La tétracyclo[3.3.1.1.^{3,7}0^{1,3}]décane (c'est-à-dire le déhydro-1,3 adamantane ou DHA) et son dérivé diméthyl-5,7 peuvent être synthétisés à partir des dibromo-1,3 adamantanes correspondants par traitement à l'alliage sodium–potassium dans l'éther ou l'heptane. Ces composés cyclopropyles hautement tendus sont très réactifs envers les radicaux et les réactifs électrophiles. Une homopolymérisation se produit à 140–160° avec formation de matériaux thermorésistants et insolubles; en présence d'oxygène dans les solvants et à la température ambiante, il y a copolymérisation spontanée. La réaction avec le brome à −70° dans l'éther conduit à l'intermédiaire tribromure de bromoadamantyloxonium qui se décompose par chauffage en bromo-1 éthoxy-3 adamantane. D'autres réactions rapides de ces déhydro-1,3 adamantanes tendus sont raportées.

[Traduit par le journal]

Canadian Journal of Chemistry, **50**, 3958 (1972)

Introduction

Many properties of cyclopropyl compounds and small ring polycyclic compounds can be related to the presence of hybridized carbon atoms possessing high p-character in the constrained C—C bonds. It is of interest to further increase the constraints at bridgehead atoms by incorporating more short bridges between atoms in small rings. This could possibly lead to even greater p-character at the bridgeheads of a polycyclic ring system and to new reactivity characteristics. This possibility has been considered with some hypothetical compounds, *e.g.*, tricyclo[2.2.2.0]octane (1–4), and some special reactivity has been demonstrated in related tricyclo[3.2.1.0]octane compounds **1** (3). This latter ring structure possesses an internal C—C cyclopropyl bond which is essentially formed by sigma bonding of two p-orbitals. The configuration of carbon at the bridgehead may be termed "inverted" (3) since, with respect to the plane defined by three of the attached atoms (see dotted lines in diagram of structure **2**), the quaternary bridgehead atom lies on the opposite side from the fourth attached atom.

1

2

We present here the synthesis and some reactions of two readily accessible compounds of this type,[1] tetracyclo[3.3.1.1^{3,7}.0^{1,3}]decane (**4**, Y = H) and its 5,7-dimethyl derivative, (**4**, Y = CH_3) commonly named 1,3-dehydroadamantanes or DHA's. These compounds are highly reactive in unusual ways and they may be used to form various derivatives of adamantane including polymeric materials.

Results and Discussion

Preparations

A relatively inconvenient preparation of 1,3-dehydroadamantane has been briefly described in a communication (6). The reaction of 1,3-dibromoadamantane (**3**; X = Br, Y = H) with Na–K alloy in refluxing heptane (6) was sensitive to reaction conditions. The reaction sometimes refused to start unless various additives were present. It is not clear whether traces of

[1]Crystallographic data show that 1,3-dehydroadamantanes possess inverted carbon atoms at the bridgeheads (5).

Can. J. Chem. Downloaded from www.nrcresearchpress.com by 210.87.254.40 on 09/05/12
For personal use only.

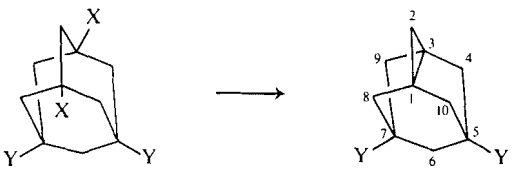

3 4

water (perhaps "cleaning" the surface of the alloy) were necessary for reaction to occur, but, in any case, addition of small amounts of *t*-butyl alcohol or hexamethylphosphoramide promoted rapid reaction. The DHA **4** (Y = H) produced was always accompanied by some adamantane. It was separately shown that the alloy reduces DHA slowly in heptane solvent, and rapidly in hexamethylphosphoramide, to adamantane.

Dehydroadamantane may be separated in small quantities from the heptane solvent by g.l.p.c. However, for larger scale preparations, ether as a solvent is more convenient. This allows isolation of DHA by evaporation of solvent followed by vacuum sublimation. The dimethyldehydro derivative **4** ($Y = CH_3$) was produced from the corresponding dibromide **3** ($X = Br$, $Y = CH_3$) in a similar manner. Some physical characteristics of DHA have been previously reported (6); a comparison of chemical shifts of the cyclopropyl hydrogens of dimethyl–DHA (1.47 δ) with those of DHA (1.66 δ) showed an upfield shift just as predicted by additivity factors of -0.10 for each CH_3 group on the adamantane ring structure (7). On the other hand, all the hydrogens on the DHA structure are greatly affected by the anisotropic field of the cyclopropyl ring so that no simple relationship of n.m.r. spectra with those of adamantanes is possible. For example, the chemical shift difference of the two C-4 hydrogens in dimethyldehydroadamantane is 0.59 p.p.m. whereas no difference shows up in dimethyladamantane itself. Even the C-6 hydrogens of dimethyladamantane, which lie in the plane of the cyclopropyl group but farthest from the cyclopropyl system, are 0.77 p.p.m. lower field than the corresponding hydrogens in dimethyladamantane. This is consistent with "aromatic" ring current effects extending from the cyclopropyl ring across the inside of the DHA skeleton.

Homopolymerization of cyclopropyl compounds is relatively rare, but examples with bicyclobutanes have recently been published (8). DHA, which dissolves readily in common solvents, does not melt when heated but transforms at *ca.* 130–160° to a white polymeric solid, 1,3-polyadamantane. This material is insoluble in all solvents tried including high boiling hydrocarbons, amides, and alcohols. Differential scanning calorimetry of this polymer showed no phase transformations to 500° and the polymer appeared quite thermally stable. Samples held in air yellowed slowly at 400° but remained essentially white under nitrogen for $\frac{1}{2}$ h at this temperature. 1,3-Poly-5,7-dimethyladamantane, prepared by heating molten monomer, m.p. 44–45.5°, showed similar thermal characteristics and lack of solubility.

Polyadamantane possesses a structural relationship to polymethylene in that the four bridgehead positions of adamantane have the same symmetry as methane. 1,3-Polyadamantane is then an analog in which a 1,3-$C_{10}H_{14}$ unit takes the place of a $—CH_2—$ unit in polymethylene. This analogy points to a similar formal relationship of the diamond structure to an adamantane polymer formed by bonding $C_{10}H_{12}$ units at all four bridgehead positions. Such 1,3–5,7-polyadamantane network would be formed by polymerization of double-dehydroadamantane, **5** (pentacyclo[3.3.1.$1^{3,7}$.$0^{1,3}$.$0^{5,7}$]-

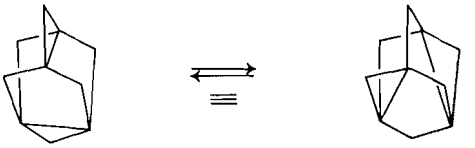

5 5

decane). This compound is also of interest with regards to expected high strain and the possibility of interaction of the internal cyclopropyl bonds leading to a new type of valence tautomerization. Unfortunately, attempts to prepare double-DHA **5** have so far been unsuccessful: 1,3,5,7-tetrabromoadamantane (**3**, X = Y = Br) reacts with Na–K alloy at room temperature in ether to give only DHA as the major detectable product. If double-dehydroadamantane is an intermediate, it is rapidly reduced by the sodium–potassium alloy with apparent hydrogen transfer from the solvent. 1,3,5-Tribromoadamantane similarly gives DHA as the major product accompanied by bromoadamantane and adamantane.

Can. J. Chem. Downloaded from www.nrcresearchpress.com by 210.87.254.40 on 09/05/12
For personal use only.

TABLE 1. Rates of oxygen uptake by 1,3-dehydroadamantane at 22°

Solvent	Inhibitor*	[DHA] (M)	Inhibitor / O_2 DHO (mol)	O_2 DHA (mol)	$k \times 10^5$ (s^{-1})
n-Heptane	—	.086	—	1.38	11.3
"	DBPC	.056	.80	1.46	3.63
n-Octane	—	.231	—	1.17	15.0
"	DBPC	.081	4.00	1.29	3.58
"	"	.158	1.00	1.22	4.22
"	"	.188	.50	1.19	4.10
"	"	.205	.25	1.26	3.98
"	"	.125	.159	1.24	3.98;22.4†
"	"	.238	.139	1.21	3.38
"	"	.254	.086	1.32	3.10;18.7†
"	"	.262	.042	1.35	2.75;18.2†
"	HMBP	.174	.475	1.20	3.38
"	DBHQ	.174	.50	1.52	3.52
"	1-Dodecanethiol	.198	.50	1.25	6.68‡
Xylene	—	.484	—	1.20	32.8
"	DBPC	.185	.333	1.23	12.7
"	"	.278	.167	1.29	12.5
"	"	.345	.083	1.25	13.3;26.3†
"	HMBP	.246	.80	1.24	13.8
"	"	.326	.167	1.20	15.3
"	"	.345	.083	1.23	16.2
"	*p*-Quinone	.088	.289	.96	209.3‡
"	"	.326	.307	.90	20.8‡
"	1-Dodecanethiol	.246	.504	1.11	16.5‡
"	"	.169	.980	.96	17.8‡

*DBPC = 2,6-di-*t*-butyl-*p*-cresol, HMBP = 4-hydroxymethyl-2,6-di-*t*-butyl phenol, DBHQ = 2,5-di-*t*-butyl-4-hydroquinone, *p*-quinone = 1,4-benzoquinone.

†The first figure is the rate constant of the reaction while under the influence of inhibitor, the second figure is the rate constant after all inhibitor was consumed.

‡Inhibitor used reacted directly with DHA in the absence of oxygen.

Free Radical Reactions of Dehydroadamantane

In the absence of oxygen, DHA is thermally quite stable with a half-life of *ca.* 4 h at 0.08 *M* in *n*-octane at 195°. However, exposure of such solutions to air causes loss of DHA in a few hours at room temperature with precipitation of polyperoxyadamantane. This material, explosion point 146–180°, is only partially soluble in benzene and the most insoluble fraction analyzed for close to a 1:1 copolymer with oxygen $(—O—C_{10}H_{14}—O—)_x$. Reduction of the polymer with LAH gave 1,3-dihydroxyadamantane as the major product.

For a formally saturated hydrocarbon, such a rapid reaction with oxygen is unusual and gives rise to the following questions: how is the copolymerization with oxygen initiated at such low temperatures and what is the relative contribution of free radical propagation steps in the overall loss of DHA? Under 1 atm of oxygen the rate of oxygen uptake of DHA was measured at 22° in heptane, octane, and *p*-xylene, with and without various inhibitors present. Without inhibitors the rate of oxygen consumption is first order in DHA with a half-life of *ca.* 90 min in heptane or octane and *ca.* 35 min in xylene. No induction period for oxygen uptake was apparent.

In the presence of inhibitors no precipitation of insoluble polymer occurred and, as shown in Table 1, there was a decreased rate of oxygen consumption. With 0.1 to 4.0 mol ratio of 2,6-di-*t*-butyl-*p*-cresol to DHA the rate was decreased to about one-fourth that of the uninhibited reaction, and as long as sufficient inhibitor was present the reaction remained first order in DHA (with $k = 3.76 \pm 0.35 \times 10^{-5}\ s^{-1}$ at 22° in octane). Those inhibitors which did not react directly with DHA (see Table 1) also decreased the rate of loss of DHA

Can. J. Chem. Downloaded from www.nrcresearchpress.com by 210.87.254.40 on 09/05/12
For personal use only.

Can. J. Chem. Downloaded from www.nrcresearchpress.com by 210.87.254.40 on 09/05/12
For personal use only.

down to about the same spontaneous rate of oxygen uptake. The molar ratio of oxygen to DHA consumed was approximately 1.25. If the reaction exclusively formed long-chain polymers of the type $(—O—C_{10}H_{14}—O—)_x$ the ratio would be 1; if all the peroxyradicals were stopped immediately by hydrogen transfer the product would be $HOO—C_{10}H_{14}—OOH$ and the ratio would be 2. A ratio of only 1.25 indicated that some oligomers were forming even in the presence of inhibitors. If the oligomers were of the type $HO(—O—C_{10}H_{14}—O—)_xOH$, x would average out to four.

The small difference between the inhibited and uninhibited rate of oxygenation and the O_2/DHA ratio indicate that the polymerization chain length is short (*ca.* 3–4 units) and that direct loss of DHA by free radical formation, rather than chain propagation, is a major reaction. The absence of an induction period and the nearly identical rate of oxygenation with various inhibitors suggests that DHA is a direct source of free radicals. Perhaps the high activation energy for ring opening of unencumbered cyclopropanes (9), is reduced in the especially strained DHA cyclopropyl group so that spontaneous ring opening near room temperature is possible, *i.e.*, $DHA \rightleftarrows \cdot C_{10}H_{14} \cdot \xrightarrow{O_2}$ peroxy radicals. In the absence of a free radical scavenger, a rapid ring closure back to DHA would be encouraged by the polycyclic structure. If oxygen is completely effective in trapping out any diradical present, the value of $k_{obs} = 3.7 \times 10^{-5}\ s^{-1}$ is the maximum possible rate constant in octane for formation of the diradical from DHA. A direct reaction of dehydroadamantane with oxygen, *i.e.*, $DHA + O_2 \rightarrow$ peroxy radicals, seems less likely but cannot be eliminated at present. However, radical character of DHA is further indicated by rapid reactions, in the absence of oxygen, with both galvinoxyl radical and with *p*-quinone to give dark, uncharacterized products.

Ionic Addition Reactions of Dehydroadamantane

Dehydroadamantanes react extremely rapidly with electrophilic reagents; for example, in heptane at room temperature acetic acid adds immediately to give 1-adamantyl acetate. Other 1-adamantyl esters may be similarly prepared under mild conditions. Halogenation of DHA in heptane rapidly produces 1,3-dihalo compounds. However, at low temperatures ($-70°$) in ether, the uptake of bromine by DHA occurs immediately but does not directly yield the 1,3-dibromide. A flocculent, lemon-yellow precipitate is formed which, after washing with fresh ether at $-70°$, may be decomposed at room temperature to yield 30% of 1,3-dibromoadamantane. The major product (68%) was identified as 1-bromo-3-ethoxyadamantane by its n.m.r. spectrum and by conversion to 1,3-dibromide with HBr/H_2SO_4. Formation of ethoxy product indicates an oxonium tribromide structure **6** for the yellow precipitate. The initial

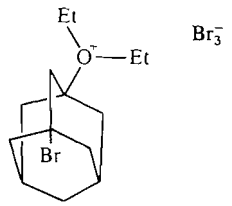

6

addition of bromonium ion to the cyclopropyl ring of DHA leads to a tertiary carbonium ion stabilized by bonding with ether and then precipitation as the tribromide. If the yellow complex is allowed to decompose in CCl_4, 1 mol of bromine is liberated for every mole of DHA used in the preparation. The complex decomposes in ethanol/K_2CO_3, acetone/KI, or acetone/NaCN solutions to give only the 1-bromo-3-ethoxyadamantane. In acetone/water/H_2SO_4 the complex yields 1-bromo-3-hydroxyadamantane (60%) accompanied by 30% of the 1-bromo-3-ethoxy product.

A freshly prepared solution of the complex in acetone at $-65°$ shows a low field quartet ($J = 7$ Hz) at 5.19 δ. This is 1.8 p.p.m. downfield from a corresponding quartet for the methylene group next to oxygen in 1-bromo-3-ethoxyadamantane and is just as expected for an oxonium ion structure (10). Cleavage of the salt at the tertiary center occurs to about 60% in acidic solution, but bases like K_2CO_3, KI, or NaCN cleave an ethyl group from the complex to give rise to bromoethoxyadamantane. A similar complex is obtained by iodination of DHA in ether at $-70°$; decomposition of the dark red precipitate at room temperature gave 1-iodo-3-ethoxyadamantane. Other types of

Can. J. Chem. Downloaded from www.nrcresearchpress.com by 210.87.254.40 on 09/05/12
For personal use only.

ionic additions which occur readily with dehydroadamantane are reaction with methanol/BF_3 to give 1-methoxyadamantane, with benzene/$AlCl_3$ to give predominately 1-phenyladamantane, and with $Hg(OAc)_2$ followed by $NaBH_4$ to give 1-hydroxyadamantane in low yields.

It is apparent that 1,3-dehydroadamantanes are much more reactive than simple cyclopropyl compounds and that the weak 1,3-bond readily undergoes free radical or electrophilic attack. Similar reactivity has been shown with tricyclic-[3.2.1.0] structures (3, 4). Although 1,3-dehydroadamantanes are basically a larger [3.3.1.0] ring system, they still show the high reactivity which seems associated with an inverted carbon at a bridgehead. More quantitative knowledge of relative stabilities and strains can perhaps be attained by thermochemical methods.

Although explicit theoretical suggestions concerning the hybridization of bridgehead atoms in the DHA system have not been made, the reactivity is distinctive enough to suggest an increased p-character in the central cyclopropyl bond over that in a simple cyclopropyl compound. As suggested (2) for related compounds, considerable electron density lies in the region of space most exposed to external attack, the backside of the 1,3-bridgehead bond of the inverted carbon atoms. This promotes attack by electrophilic reagents, while low-lying unoccupied orbitals aid reactions with electron donors and free radical reagents. As both free radical and ionic electrophilic reagents easily react with dehydroadamantanes under mild conditions, they may be quite synthetically useful in forming a variety of adamantyl derivatives and polymers.

Experimental

Adamantane, 1-bromoadamantane, and 1-hydroxyadamantane were obtained from commercial sources. 1,3-Dimethyladamantane and 1,3-dihydroxy-5,7-dimethyladamantane were kindly supplied by Sun Oil Company, Philadelphia, Pa.

General Procedure for the Preparation of Dehydroadamantanes

A typical procedure is the preparation of 5,7-dimethyldehydroadamantane (**4**, $Y = CH_3$).

To 1.0 g of 1,3-dibromo-5,7-dimethyladamantane in 50 ml of ether under nitrogen was added 0.83 g of Na–K alloy (1:5 w/w). The alloy was dispersed by high speed stirring, 25 μl of *t*-butanol and/or hexamethylphosphoramide was added, and the mixture stirred until completion of the reaction (*ca.* 2 h). The appearance of product was monitored by g.l.p.c. using a Carbowax 20M (10% on Chromosorb W) column. The gas inlet, stirrer, and condenser were replaced by a vacuum sublimation assembly of the cold finger type. The diethyl ether was removed under vacuum at autogenous temperatures. A Dry Ice – acetone mixture was then placed in the cold finger and the product sublimed at about 0.5 mm pressure and 25–30°. The yield was 0.35 g (78%) with a ratio of **4**, ($Y = CH_3$) and **3** ($X = H$, $Y = CH_3$) of 1:1. Better ratios of products were often obtained; careful monitoring of the reaction progress can aid prevention of further reduction of **4** to **3** ($X = H$). 1,3-Dichlorides may be used in the preparations; use of 1,3-dichloro-5,7-dimethyladamantane gave 75% yields of the dehydroadamantane derivative and dimethyladamantane (ratio 10:1).

Compound **4** ($Y = CH_3$) was purified by g.l.p.c. and had m.p. 44.0–45.5° (sealed capillary). N.m.r. δ (degassed benzene): singlet 0.91 methyl groups, doublet $J = 10$ Hz 1.01, four of the hydrogens of type C-4, doublet $J = 10$ Hz, 1.60, four other hydrogens at C-4 positions, broad multiplet 1.47, two hydrogens of C-2, singlet 1.92, two hydrogens of C-6. I.r. spectrum (cm^{-1}) in CCl_4: 3030 shoulder, 2900, 1445, 1360, 1280, 890. The absorptions at 3030, 1280 and 890 rapidly disappear in several minutes. Rapid reaction with oxygen also prevented obtaining of consistent C and H analyses.

A similar preparation of 1,3-dehydroadamantane using 1.0 g of 1,3-dibromoadamantane, 0.52 g of Na–K alloy, and 25 μl of hexamethylphosphoramide in 50 ml of ether over 5 h gave after sublimation 0.35 g (77%) of a 9:1 DHA:adamantane mixture.

The physical characteristics of dehydroadamantane **4** ($Y = H$) have been reported (6).

Similar reactions using 1,3,5-tribromo- or 1,3,5,7-tetrabromoadamantane in ether or heptane gave dehydroadamantane with adamantane (ratio *ca.* 8:1) in isolated yield of 40–72%. Some monobromoadamantane was also present. Di-, tri-, and tetrabromoadamantanes and 1,3-dibromo-5,7-dimethyladamantane were made by $AlBr_3$-catalyzed brominations of adamantane or dimethyladamantane (11).

Polymers

Bulk polymerization was effected by heating 1,3-dehydroadamantane overnight at 140° in a sealed vial. The material remained solid throughout the polymerization. At 160° polymerization was complete in *ca.* 10 min. Vacuum sublimation removed the adamantane leaving only a white solid polymer which did not melt to 330°.

Anal. Calcd. for $C_{10}H_{14}$: C, 89.49; H, 10.51. Found: C, 89.31; H, 10.43.

I.r. spectrum (cm^{-1}) as a Nujol mull: 2930, 2640, 1440, 1340, 1000, and 960.

Molten dimethyldehydroadamantane was polymerized similarly at 90–145° to give material with generally the same physical characteristics as polyadamantane. X-ray powder diffraction patterns showed no lines, only halos indicating non-crystallinity.

Anal. Calcd. for $C_{12}H_{18}$: C, 88.82; H, 11.18. Found: C, 88.94; H, 11.19.

The polymeric materials were insoluble in all common solvents. Differential scanning colorimetry showed no transitions up to 500°. Under nitrogen the samples remained

Can. J. Chem. Downloaded from www.nrcresearchpress.com by 210.87.254.40 on 09/05/12
For personal use only.

visibly unchanged; under air, the samples darkened at temperatures above 400°.

Copolymerization with oxygen occurs simply on dissolving dehydroadamantane in pentane at room temperature. The white precipitate was washed with benzene and dried. When heated it exploded at 140–180°. The material was partially soluble in benzene and the benzene insoluble fraction was analyzed.

Anal. Calcd. for $C_{10}H_{14}O_2$: C, 72.26; H, 8.49. Found: C, 72.55; H, 8.28.

Another fraction, more soluble in benzene, was analyzed giving 70.68% C and 8.37% H corresponding to roughly $HO(OC_{10}H_{14}O)_{10}OH$. A suspension of the polyperoxide was refluxed with LAH in ether for 12 h. The predominate product (*ca.* 80–90%) was 1,3-adamantanediol identified by g.l.p.c. comparisons with authentic samples.

Addition Reactions

Hydration

Addition of dilute sulfuric acid to a solution of dehydroadamantane in THF immediately yields 1-hydroxyadamantane (90 ± 5%) by g.l.p.c. comparisons with an authentic sample.

Methanolysis

To 1,3-dehydroadamantane (0.6 g) in 10 ml of methanol and 20 ml of ether under nitrogen at room temperature was added 0.2 ml of boron trifluoride etherate. After 2 min, 0.2 ml of water was added and the solution dried with Na_2SO_4. G.l.p.c. comparisons with authentic solutions of 1-methoxyadamantane showed that 90% yields were obtained together with 6% of an unidentified by-product. Authentic 1-methoxyadamantane was prepared by refluxing 1-hydroxyadamantane with 40 ml of methyl iodide, 10.8 g of sodium hydride and 75 ml of ether for 24 days. Addition of ethanol, then water, followed by extraction and distillation gave, in 69% yields, 1-methoxyadamantane, b.p. 95–100°/1.4 mm.

Anal. Calcd. for $C_{11}H_{18}O$: C, 79.46; H, 10.91. Found: C, 79.56; H, 10.94.

N.m.r. δ (CCl_4): singlet 3.12 methyl group, broad singlet 2.11 three bridgehead hydrogens, and unresolved multiplet 1.67 for 12 CH_2 hydrogens.

Mercuric Acetate Oxidation

A solution of 1.35 g of $Hg(OAc)_2$ in 4 ml of water was added to 0.58 g of DHA in 4.3 ml of THF. After *ca.* 3 min, 4 ml each of 3 *N* NaOH and 1 *N* $NaBH_4$ were added successively and the mixture stirred 5 min before work-up. G.l.p.c. analysis showed that 47% of 1-hydroxyadamantane and *ca.* 9% of 1,3-dihydroxyadamantane was produced. The largest percentage of the several unidentified by-products was *ca.* 18%.

Phenylation

A solution of 0.67 g of DHA in 300 ml of benzene was treated with 2.0 g of $AlCl_3$ at 60° for 10 min. The reaction mixture was cooled and worked-up by normal extractions. 1-Phenyladamantane (40% yields) was identified by g.l.p.c. comparisons with authentic compound. Polymeric material was also produced and was formed in larger amounts in more concentrated solutions.

Ester Formation

Stirring 0.14 g of DHA with 0.3 g of *p*-nitrobenzoic acid in 25 ml of ether under nitrogen for 6 h gave 82% of 1-adamantyl-*p*-nitrobenzoate, m.p. 182–183°, characterized by its reported n.m.r. spectrum (7).

Anal. Calcd. for $C_{17}H_{19}O_4N$: C, 67.75; H, 6.32; N, 4.65. Found: C, 67.62; H, 6.41; N, 4.63.

Halogenation

The iodination product of DHA has been reported (6). 5,7-Dimethyldehydroadamantane immediately decolorizes iodine in ether at room temperature or lower and yields 1,3-diiodo-5,7-dimethyladamantane which, after crystallization from CCl_4, gave m.p. 102–103.2°.

Anal. Calcd. for $C_{12}H_{18}I_2$: C, 34.64; H, 4.36; I, 61.00. Found: C, 34.66; H, 4.68; I, 61.58. N.m.r. δ ($CDCl_3$); singlets at 0.85 for the methyl hydrogens, 1.34 for two hydrogens β to the methyl groups, 2.30 for eight hydrogens β to both CH_3 and iodine, and 3.11 for the two hydrogens β to both iodines. In benzene, corresponding singlets occurred at δ 0.42, 0.75, 1.88, and 3.0.

To a rapidly stirred solution of 0.17 g of DHA in 25 ml of ether at −70° was added dropwise *ca.* 0.7 g of bromine. A flocculent, lemon-yellow precipitate was instantly formed. The solvent was removed with a pipet after centrifugation. The precipitate was washed at −70° with several portions of ether until the supernatant was colorless. The suspension from similar preparations was treated with various reagents and then decomposed by bringing to room temperature. In 250 ml of ether with 4 g K_2CO_3 a 28% yield of 1,3-dibromoadamantane was obtained together with 68% of 1-bromo-3-ethoxyadamantane. These compounds were separated by chromatography on Woelm grade I neutral alumina. 1-Bromo-3 ethoxyadamantane, m.p. 39.5–41.5° (sealed tube), was reacted with 47% HBr in H_2SO_4 to give 1,3-dibromoadamantane.

Anal. Calcd. for $C_{12}H_{19}OBr$: C, 55.70; H, 7.34; Br, 30.83. Found: C, 55.50; H, 7.21; Br, 30.79.

N.m.r. δ (benzene): quartet (J = 7 Hz) 3.18 for —CH_2O— hydrogens, singlet 2.29 for two hydrogens β to EtO and Br, unsymmetrical doublet 2.03 for four hydrogens β to Br; unresolved multiplet 1.79 for two hydrogens at bridgeheads, unsymmetrical doublet 1.47 for four hydrogens β to EtO, poorly resolved triplet 1.17 for two hydrogens δ to both substituents, and triplet (J = 7 Hz) 1.06 for three hydrogens of CH_3.

The precipitated yellow complex in 95% ethanol with powdered K_2CO_3, or acetone–potassium iodide, or acetone–sodium cyanide gave only 1-bromo-3-ethoxyadamantane as shown by g.l.p.c. analysis. In acetone – 10% water the complex decomposed on warming to yield 22–33% of the bromoethoxy compound and 61–43% of 1-bromo-3-hydroxyadamantane, m.p. 157–158° (sealed tube). This compound was purified by sublimation at 70°/1 mm and characterized by its n.m.r. spectrum and by base-promoted ring opening to 3-methylene-bicyclo[3.3.1]nonanone-7 (12).

Anal. Calcd. for $C_{10}H_{15}BrO$: C, 51.96; H, 6.54; Br, 34.57. Found: C, 52.00; H, 6.60; Br, 34.90.

N.m.r. δ (benzene): singlet 2.17 for two hydrogens β to OH and Br, doublet (J = 3 Hz) for four hydrogens β to Br, broad multiplet 1.75 for two hydrogens at bridgehead, unsymmetrical doublet (J = 3 Hz) 1.35 for four hydrogens β to OH, singlet 1.19 for OH, triplet (J = 3 Hz) 1.08 for two hydrogens δ to OH and Br.

Addition of a solution of iodine in ether to DHA in ether at −70° gave a dark red precipitate which was dissolved in

acetone containing solid NaCN and stirred at $-70°$ for 24 h. After warming to room temperature, chromatography on Woelm neutral alumina gave 1-iodo-3-ethoxyadamantane, m.p. 35–37° (sealed tube).

Anal. Calcd. for $C_{12}H_{19}OI$: C, 47.07; H, 6.25; I, 41.45. Found: C, 47.29; H, 6.33; I, 41.31.

N.m.r. δ (benzene): similar to the 1-bromo-3-ethoxy compound above, the corresponding absorptions are quartet ($J = 7$ Hz) 3.17, singlet 2.57, unsymmetrical doublet 2.25, singlet with a lower-field broad shoulder 1.59 (total of six hydrogens), unresolved multiplet 1.35, and triplet ($J = 7$ Hz) 1.05.

The yellow precipitate prepared from 0.157 g of DHA was washed with ether at $-70°$ to remove unbound bromine and decomposed in 50 ml of CCl_4. After dilution to 100 ml the solution was compared spectrophotometrically to a freshly prepared standard solution of bromine in CCl_4. The absorbance at 415 mμ corresponded to 0.9 mol of bromine released per mol of DHA. Because of instability the yellow complex did not give consistent C and H analyses.

The n.m.r. spectrum at *ca.* $-65°$ of the complex in deuterioacetone showed a quartet at 5.19 δ ($J = 7$ Hz) for four hydrogens, a quartet at 3.37 ($J = 7$ Hz) for residual diethyl ether, a singlet at 3.07 for two hydrogens, a broad singlet at 2.59 for six hydrogens, a broad singlet at 2.36 for four hydrogens, a triplet-like absorption at 1.71 for eight hydrogens, and a triplet at 1.10 for residual ether. On warming to $-25°$ the complex decomposes as indicated by the loss of absorptions, especially the prominent low field quartet. Less well defined peaks arise in positions expected for product.

Kinetic Measurements

The volume of oxygen taken up by DHA in rapidly stirred solutions was measured in a simple constant pressure apparatus. Plots of

$$\log (\Delta V_\infty/(\Delta V_\infty - \Delta V_t))$$

against time, where ΔV_∞ is the total volume taken up and ΔV_t is the volume taken up at time t, were straight lines to over two half-lives. Rate constants were obtained from 2.303 times the slope of the plots. With the higher concentration of inhibitors (see Table 1), the plots were also straight lines, while at lower concentrations the curve separated into a straight inhibited portion and another largely straight portion of greater slope (corresponding to some radical chain reaction).

Support of this work by the National Research Council of Canada is gratefully acknowledged.

1. M. D. NEWTON and J. M. SCHULMAN. J. Am. Chem. Soc. **94**, 773 (1972); J. M. SCHULMAN and G. J. FISANICK. J. Am. Chem. Soc. **92**, 6653 (1970).
2. W.-D. STOHRER and R. HOFFMANN. J. Am. Chem. Soc. **94**, 779 (1972).
3. K. B. WIBERG, J. E. HIATT, and G. BURGMAIER. Tetrahedron Lett. 5855 (1968); K. B. WIBERG and G. J. BURGMAIER. Tetrahedron Lett. 317 (1967); K. B. WIBERG, E. C. LUPTON, JR., and G. J. BURGMAIER. J. Am. Chem. Soc. **91**, 3372 (1969).
4. P. G. GASSMAN, A. TOPP, and J. W. KELLER. Tetrahedron Lett. 1093 (1969).
5. J. TROTTER and C. GIBBONS. Unpublished data.
6. R. E. PINCOCK and E. J. TORUPKA. J. Am. Chem. Soc. **91**, 4593 (1969).
7. R. C. FORT, JR., and P. VON R. SCHLEYER. J. Org. Chem. **30**, 789 (1965).
8. H. K. HALL, JR., E. P. BLANCHARD, JR., S. C. CHERKOFSKY, J. B. SIEJA, and W. A. SHEPPARD. J. Am. Chem. Soc. **93**, 110 (1971); H. K. HALL, JR., C. D. SMITH, E. P. BLANCHARD, JR., S. C. CHERKOFSKY, and J. B. SIEJA. J. Am. Chem. Soc. **93**, 121 (1971); T. D. SWARTZ and H. K. HALL, JR. J. Am. Chem. Soc. **93**, 137 (1971).
9. *Cf.* R. G. BERGMAN and W. L. CARTER. J. Am. Chem. Soc. **91**, 7411 (1969); D. W. SETSER and B. S. RABINOVITCH. J. Am. Chem. Soc. **86**, 564 (1964).
10. D. A. TOMALIA and H. HART. Tetrahedron Lett. 3389, 3383, (1966); G. A. OLAH and J. M. BOLLINGER. J. Am. Chem. Soc. **89**, 2993 (1967).
11. B. SCOTT. Unpublished results. See also E. R. TALATY, A. E. CANCIENNE, JR., and A. E. DUPUY, JR. J. Chem. Soc. (C) 1902 (1968).
12. H. STETTER, J. GÄRTNER, and P. TACKE. Chem. Ber. **98**, 3888 (1965).

Can. J. Chem. Downloaded from www.nrcresearchpress.com by 210.87.254.40 on 09/05/12
For personal use only.

Sterically Hindered Aromatic Compounds. V. Solvolysis of *p*-Methyl-, 2,4,6-Trimethyl-, and 2,4,6-Tri-*t*-butylbenzyl Chloride. Effect of Solvent and α-Deuterium Substitution

L. R. C. BARCLAY, J. R. MERCER, AND J. C. HUDSON

Department of Chemistry, Mount Allison University, Sackville, New Brunswick

Received June 7, 1972

Rates, activation parameters, and kinetic α-deuterium isotope effects are reported for solvolysis of *p*-methylbenzyl chloride in 80% trifluoroethanol–water, and in ethanol–water and *t*-butyl alcohol–water of varying solvent compositions. The α-deuterium isotope effect in trifluoroethanol–water ($k_H/k_D = 1.14$ per D) indicates approximately limiting behavior. Results in the other solvents ($k_H/k_D = 1.04$–1.08) indicate considerable nucleophilic participation by solvent in the transition state. 2,4,6-Trimethylbenzyl chloride gave $k_H/k_D = 1.09$ in 80% ethanol–water but $k_H/k_D = 1.16$ in 80% trifluoroethanol–water. 2,4,6-Tri-*t*-butylbenzyl chloride showed k_H/k_D effects of 1.13–1.15 in *t*-butyl alcohol–water and 1.15–1.16 in ethanol–water. The higher kinetic isotope effects for solvolysis of these trialkylbenzyl chlorides are discussed in terms of steric hindrance to nucleophilic participation by solvent. N.m.r. chemical shifts give evidence for steric compression of the benzylic protons in 2,4,6-tri-*t*-butylbenzyl chlorides.

Les vitesses, les paramètres d'activation, et les effets isotopiques sur la cinétique du deutérium α sont rapportés pour la solvolyse du *p*-méthylbenzyle chlorure dans les systèmes trifluoroéthanol 80%–eau et éthanol–eau, *t*-butanol–eau de compositions variables. L'effet isotopique de deutérium α dans le trifluoroéthanol–eau ($k_H/k_D = 1.14$ par D) correspond approximativement à un comportement limite. Les résultats dans les autres solvants ($k_H/k_D = 1.04$–1.08) indiquent une participation nucléophile considérable du solvant dans l'état de transition. Le triméthyl-2,4,6 benzyle chlorure donne un $k_H/k_D = 1.09$ dans l'éthanol 80%–eau mais 1.16 dans le trifluoroéthanol 80%–eau. Le tri-*t*-butyl-2,4,6 benzyle chlorure donne des valeurs de k_H/k_D de 1.13–1.15 dans le *t*-butanol–eau et 1.15–1.16 dans l'éthanol–eau. Les effets isotopiques sur la cinétique les plus élevées dans la solvolyse de ces trialkylbenzyle chlorures sont interprétés en fonction de l'empêchement stérique à la participation nucléophile du solvant. Les déplacements chimiques en r.m.n. fournissent la preuve d'une compression stérique des protons benzyliques dans les tri-*t*-butyl-2,4,6 benzyle chlorures.

[Traduit par le journal]

Canadian Journal of Chemistry, **50**, 3965 (1972)

Can. J. Chem. Downloaded from www.nrcresearchpress.com by 210.87.254.40 on 09/05/12
For personal use only.

Introduction

Our previous publication in this series (1) reported on the effect of the proximity and size of alkyl substituents on the solvolysis of substituted benzyl chlorides in 80% ethanol–water. In the 2,4,6-trialkylbenzyl chlorides, the solvolytic behavior of 2,4,6-tri-*t*-butylbenzyl chloride was of particular interest. This compound exhibited an unexpected high reactivity and an abrupt increase in the entropy of activation (ΔS^*) term. These results were rationalized in terms of steric acceleration in the S_N1 mechanism for solvolysis of this compound.

The main purpose of the present investigation was to apply α-deuterium kinetic isotope effects as a probe for establishing with more certainty the mechanism of solvolysis of 2,4,6-tri-*t*-butylbenzyl chloride. The two bulky *o*-*t*-butyl groups in this chloride place rather severe steric restrictions on the solvation of its transition state. The compound might prove to be an interesting model system for testing ideas of specific solvation or solvent sorting in solvolysis using binary solvent mixtures (2). Thus it was also desirable to determine the effect of different solvent systems on the activation parameters, kinetic isotope effects, and product compositions. It was desirable to find some ground state properties in the sterically hindered benzyl chlorides that indicate more directly the steric effect. The n.m.r. chemical shifts of the benzylic protons are examined in this regard.

Experimental

(a) Preparations

p-Methylbenzyl-α-d_2 Chloride

p-Methylbenzyl-α-d_2 alcohol was prepared by reduction of methyl *p*-toluate with lithium aluminum deuteride according to the procedure used to prepare *p*-methylbenzyl alcohol (1). The crude labelled alcohol was converted into *p*-methylbenzyl-α-d_2 chloride by treatment with thionyl

Can. J. Chem. Downloaded from www.nrcresearchpress.com by 210.87.254.40 on 09/05/12
For personal use only.

TABLE 1. Major mass spectral peaks of 2,4,6-trimethylbenzyl chloride and -α-d_2 chloride

	Peak	Relative intensity	Assignment
2,4,6-Trimethyl-benzyl chloride	168	17	M^+ (parent mass)
	133	100	M − Cl
2,4,6-Trimethyl-benzyl-α-d_2 chloride	170	17	M^+ (parent mass)
	135	100	M − Cl

TABLE 2. Solvolysis of 2,4,6-tri-*t*-butylbenzyl chloride and -α-d_2 chloride in 80% *t*-butyl alcohol–water at 70.05°

Compound	Rate constants ($k_1 \times 10^3$ s^{-1})	Average	% deviation
2,4,6-Tri-*t*-butyl-benzyl chloride	2.267	2.26_1[a]	0.23
	2.255		
	2.262		
	2.262		
2,4,6-Tri-*t*-butyl-α-d_2 chloride	1.773	1.78_1[a]	0.34
	1.785		
	1.787		
	1.781	($k_H/k_D = 1.26_9$)	

[a]In reproducibility checks, average rate constants of 2.249×10^{-3} s^{-1} for 2,4,6-tri-*t*-butylbenzyl chloride and 1.778 for the α-d_2 chloride were obtained ($k_H/k_D = 1.26_5$).

chloride (1). The percent deuterium in the methylene group of this *p*-methylbenzyl-α-d_2 chloride was estimated from its n.m.r. spectrum to be approximately 95%.

2,4,6-Trimethylbenzyl-α-d_2 Chloride

2,4,6-Trimethylbenzyl-α-d_2 alcohol was prepared by reduction of mesitoic acid with lithium aluminum deuteride. The alcohol was converted into the chloride by chlorination with thionyl chloride (1). The n.m.r. spectrum of this 2,4,6-trimethylbenzyl-α-d_2 chloride showed that substitution of benzylic hydrogen for deuterium was essentially complete. This conclusion was confirmed by comparative mass spectroscopic analyses of the labelled and the ordinary chlorides. The data for the major peaks in the spectra and their assignments are summarized in Table 1.

2,4,6-Tri-t-butylbenzyl Chloride and -α-d_2 Chloride

The synthesis and spectroscopic analyses of 2,4,6-tri-*t*-butylbenzyl chloride and -α-d_2 chloride were described earlier (1).

(b) Solvents

The binary solvents were prepared by mixing accurately measured volumes of triply distilled, deionized water and freshly fractionated anhydrous alcohols. Trifluoroethanol (Eastman Chemicals) was purified by the method of Shiner and coworkers (3) and the fraction boiling at 73.4–74.5° used.

(c) Kinetic Measurements

Kinetic measurements were made by the precision conductance method using stirred cells as described previously (1). The data were treated as before and a computer used to calculate the rate constants by means of a least squares program. High accuracy was required to determine the α-deuterium kinetic isotope effects. Computer plots of the first order rate constants were examined for linearity. In all cases the correlations were 0.999. The standard deviations between the four rate constants measured simultaneously in four conductivity cells were less than 1% and usually less than 0.5%. A sample of the data for solvolysis of 2,4,6-tri-*t*-butylbenzyl chloride and α-d_2 chloride is outlined in Table 2.

(d) Product Analysis

Attempts were made to determine the product composition of solvolysis of 2,4,6-tri-*t*-butylbenzyl chloride by v.p.c. Test runs were made on this chloride and the corresponding alcohol on Carbowax, Apiezon and silicon columns at various temperatures. Some decomposition of these compounds during v.p.c. analysis was always observed. The cyclization product, 1,1-dimethyl-4,6-di-*t*-butylindane, reported earlier (4) was produced during the v.p.c. analysis. The product analyses were, therefore, carried out using the n.m.r. method as before (1).

Results and Discussion

(a) Solvolysis of p-Methylbenzyl Chloride

p-Methylbenzyl chloride has been extensively investigated both with regard to solvolytic activation parameters (5–7) and precision α-deuterium kinetic isotope effects (3, 8). This compound was selected as a convenient *reference system* for our studies. It provides a convenient comparison of our rate constants, activation parameters, and α-deuterium isotope effects with reported literature values. At the same time it was desirable to study the variation of these solvolytic data with different alcohol–water binary solvent systems.

(1) Rates and Activation Parameters

The first order rate constants and activation parameters for solvolysis of *p*-methylbenzyl chloride in various binary solvent mixtures are given in Table 3. The rate constant and activation parameters for 45% ethanol–water are in good agreement with the data reported by Hyne and coworkers (6). There was an increase in rates

TABLE 3. Rates and activation parameters of solvolysis of *p*-methylbenzyl chloride in binary solvents

Solvent	Temperature (°C)	Rate ($k_1 \times 10^5$ s^{-1})	ΔE^* (kcal/mol)	ΔS^* (e.u./mol)
80% Ethanol–water[a]	44.89	0.728	21.0	−18.2
	60.09	3.31		
45% Ethanol–water (0.203 mol fraction ethanol)	22.44	0.933[b]	20.7[b]	−13.4[b]
	31.72	2.82		
	44.89	11.2		
	60.09	45.3		
80% TFE[c]–water	45.04	8.35	20.5	−14.8
	60.09	36.2		
80% TBA[d]–water	60.01	0.538	22.4	−17.6
	70.05	1.45		

[a]Results taken fron ref. 1.
[b]Rate constant calculated from results at higher temperatures. Under these conditions, reported results (6) were $k_1 = 0.917$, $\Delta E^* = 20\,830$ cal/mol, $\Delta S^* = -13.1$.
[c]TFE = trifluoroethanol.
[d]TBA = *t*-butyl alcohol.

on going from 80% ethanol–water (or 80% *t*-butyl alcohol–water) to the more highly ionizing binary mixtures of 45% ethanol–water or 80% trifluoroethanol–water. There was an increase in the ΔS^* term of the order of 3–5 e.u. in these more highly ionizing solvent mixtures. Various factors could contribute to variations in activation parameters with such changes in solvent composition. Some of these factors are:

(i) Changes in ground state solvation

Arnett and coworkers (9) provided convincing evidence and arguments for the importance of solvation effects on the ground states as indicated in endothermic maxima behavior of the partial molal heats of solution for a variety of salts and nonelectrolytes. These extrema were limited to the behavior of solutes in the region of high water content of binary solvents (above 0.8 mol fraction H_2O). On the more alcoholic side of these solvent–solute effects, where our measurements are concerned, the situation may be "unmanageably complex" (9) but it should be acknowledged that such effects may play an, as yet, unpredictable role.[1]

[1]A referee points out that initial state solvation differences have a significant kinetic effect with reference to one chosen standard only if the transition state differences are significantly less; a reasonable expectation in the high water range where quasi-aqueous structure is maintained. Conversely in the high alcohol range, one might expect that ground state solvation effects would not have a significant effect.

(ii) Specific solvation of the transition state

p-Methylbenzyl chloride exhibited a very large change in entropy of activation in ethanol–water solvolysis, as the alcohol content of the medium was increased (7) ($\Delta\Delta S = 15.0$ e.u. in the range of 0.00–0.125 mol fraction ethanol). This was interpreted in terms of changes in specificity of solvation or solvent sorting; that is, differences in the activation parameters can be related to variations in specific demand for selective solvation of the ionic transition state by the more polar component (water) in the binary solvent system. It was further argued that, in the case of *p*-methylbenzyl chloride, "the greatest unmixing of the solvent must take place in order to achieve persistence of specific hydration of the transition state as ethanol is added to the solvent" (7). These observations were made in low alcohol content (0.00–0.203 mol fraction ethanol) of the binary solvent mixtures. We recently extended the Hyne hypothesis on specific solvation in an attempt to account for the variation in activation entropy for solvolysis of other alkyl- and phenylbenzyl chlorides in 80% ethanol–water (1).

Specific solvation effects may also in part account for variations in activation parameters shown for *p*-methylbenzyl chloride (Table 3) during changes in the high alcohol content of solvent mixtures. For example, the larger $-\Delta S^*$ values for 80% alcohol(s)–water could, in part,

Can. J. Chem. Downloaded from www.nrcresearchpress.com by 210.87.254.40 on 09/05/12
For personal use only.

TABLE 4. α-Deuterium isotope effects in solvolysis of *p*-methylbenzyl chloride in mixed solvents

Solvent	Temperature (°C)	Rate ($k_1 \times 10^5$ s^{-1}) α-H_2 compound	Rate ($k_1 \times 10^5$ s^{-1}) α-D_2 compound	k_H/k_D	k_H/k_D corrected[a]	k_H/k_D[d] per D
80% Ethanol–water	70.05	7.08	6.56	1.07_9	1.08_4	1.041
50% Ethanol–water	45.04	7.04[b]	6.12	1.15	1.16	1.077[b]
80% TFE–water	60.09	36.2	28.4	1.28	1.29	1.136[c]
80% TBA–water	70.05	1.45	1.32	1.10	1.11	1.054
60% TBA–water	70.05	8.77	7.65	1.15	1.16	1.077

[a]The deuterated compound contained approximately 5.4% benzylic hydrogens, ratios were corrected for complete deuteration.
[b]Shiner and coworkers (3) reported $k_H = 6.999 \times 10^{-5}$ s^{-1} and isotope effect per D = 1.080 at 45° in 50% ethanol–water.
[c]Reported values (3) for k_H/k_D (per D) were 1.140 in 70% TFE–water and 1.145 in 94% TFE–water at 25°.
[d]$(k_H/k_D)^{1/2}$. The third decimal is retained only for comparison purposes.

be a consequence of more solvent "unmixing" required to maintain specific hydration of the transition state in the higher alcohol–water mixtures. This effect is not so noticeable for 80% trifluoroethanol–water. This is understandable because trifluoroethanol is itself a very effective ionizing medium (8). These arguments relating activation parameters to specific solvation effects are admittedly very qualitative and incomplete. They have ignored in this instance the important changes in the structuring of solvent molecules that must take place as the composition of the binary mixture is changed.

(iii) Nucleophilic participation by solvent

Nucleophilic covalent participation by solvent at the reaction site generally will raise the $-\Delta S^*$ value. The ΔS^* parameter together with heat capacities of activation (ΔC_p^*) have been used to give an indication of mechanism for solvolysis (10). These parameters are of doubtful value to diagnose mechanisms in mixed solvents.

In view of the multiplicity of factors affecting activation parameters, it was highly desirable to use other criteria also, notably kinetic isotope effects, as a probe to study the mechanism of solvolysis of hindered benzyl chlorides.

(2) α-Deuterium Isotope Effects

α-Deuterium secondary isotope effects are well recognized as providing a criterion for the mechanism of solvolytic reactions (11). Solvent influences *per se* on α-D effects are small (12), so these effects provide one of the most definitive criteria for the extent of nucleophilic involvement by solvent in the transition state. Shiner and Fisher indicated that α-D effects provide the "best probe" for the degree of nucleophilic attachment (13), although there may be limitations in their use in detecting nucleophilic participation by solvent near the limiting end of solvolysis (14). From highly accurate conductivity rate measurements, Shiner and coworkers (3, 13) were able to place an upper limit of $k_H/k_D = 1.15$ per deuterium for chlorides (including *p*-methylbenzyl-α-d_2 chloride) for S_N1 solvolysis.

Our kinetic isotope effects data for *p*-methylbenzyl-α-d_2 chloride are given in Table 4. Our rate constant in 50% ethanol–water and kinetic isotope effects in this solvent and in trifluoroethanol–water are in very good agreement with the results of Shiner and coworkers (3). The k_H/k_D values were in the range 1.04–1.08 per deuterium for solvolysis in ethanol–water, and *t*-butyl alcohol–water. The magnitude of the isotope effect was rather sensitive to the alcohol content of the binary solvent mixture, at least in these high alcohol content ranges. On the other hand, in 80% trifluoroethanol–water, a solvent system of low nucleophilic power and high ionizing capacity, the isotope effect ($k_H/k_D = 1.14$) approaches that for limiting behavior as observed under similar conditions by Shiner and coworkers (3). The lower kinetic isotope effects in ethanol–water and *t*-butyl alcohol–water indicate that there is undoubtedly considerable nucleophilic participation by solvent (S_N2), especially in the 80% alcohol–water mixtures. We showed earlier (1) that the solvolysis rates in 80% ethanol–water for para and meta *t*-butyl, phenyl, and *p*-methylbenzyl chloride correlated well in a linear free energy relationship provided that σ^+ constants were used. This was taken as evidence that an S_N1

Can. J. Chem. Downloaded from www.nrcresearchpress.com by 210.87.254.40 on 09/05/12
For personal use only.

TABLE 5. Rates and activation parameters of solvolysis of 2,4,6-tri-*t*-butylbenzyl chloride in *t*-butyl alcohol–water

Solvent	Temperature (°C)	Rate ($k_1 \times 10^5$ s^{-1})	ΔE^* (kcal/mol)	ΔS^* (e.u./mol)
80% TBA–water	60.01	78.8	23.8	−3.6
	70.05	226		
60% TBA–water	45.15	106	24.5	2.8
	60.01	599		

TABLE 6. α-Deuterium isotope effects in solvolysis of 2,4,6-trimethylbenzyl chloride

Solvent	Temperature (°C)	Rate ($k_1 \times 10^5$ s^{-1}) Undeuterated	Rate ($k_1 \times 10^5$ s^{-1}) α-D_2 compound	$k_H/k_{\alpha\text{-}D_2}$	k_H/k_D per D
80% Ethanol–water	44.89	39.4	33.1	1.19	1.091
80% Ethanol–water	55.01	89.8	75.6	1.19	1.091
80% Ethanol–water	60.09	171	144	1.19	1.091
80% TFE–water	30.06	1077	800	1.34_6[a]	1.161
80% TFE–water	30.06	1078	797	1.35_3[a]	1.163

[a]Results from two different runs by different investigators. The third decimal point is retained only for comparison purposes.

mechanism applied throughout the series. The present α-deuterium isotope effect shows that this conclusion was not justified. There is considerable nucleophilic participation by solvent, even in 50% ethanol–water, for solvolysis of *p*-methylbenzyl chloride according to the isotope effect (1.08). Thus the solvolyses of other monosubstituted benzyl chlorides examined earlier (1) in ethanol–water most certainly have a significant amount of bimolecular nucleophilic component as well. It appears that the α-deuterium isotope effects provide a much more sensitive and definitive measure of nucleophilic participation by solvent, at least for solvolysis of substituted benzyl chlorides, than do activation parameters or linear free energy relationships.

(b) Solvolysis of 2,4,6-Trimethyl- and 2,4,6-Tri-t-butylbenzyl Chloride

We earlier reported (1) that solvolysis of 2,4,6-tri-*t*-butylbenzyl chloride in 80% ethanol–water gave an abrupt increase in the entropy of activation term compared to other mono- and trialkylbenzyl chlorides, such as *p*-methylbenzyl chloride or 2,4,6-trimethylbenzyl chloride. The results were interpreted in terms of steric hindrance to solvent reorganization at the reaction center due to the two ortho-*t*-butyl groups. It was desirable to study the α-deuterium isotope effect on solvolysis of 2,4,6-tri-*t*-butylbenzyl chloride relative to this effect for typical mono and trialkylbenzyl chlorides such as *p*-methyl- and 2,4,6-trimethyl-. In this way we hoped to determine the degree of nucleophilic participation by solvent when the —CH_2Cl group has two *t*-butyl groups in close proximity.

(1) Solvolysis of 2,4,6-Tri-t-butylbenzyl Chloride in t-Butyl Alcohol–Water

Solvolysis results on 2,4,6-tri-*t*-butylbenzyl chloride in *t*-butyl alcohol–water (Table 5) show again the abrupt increase in entropy of activation (compare ΔS^* in 80% *t*-butyl alcohol–water for *p*-methylbenzyl chloride, Table 3). This is in agreement with the reported results in ethanol–water (1) and is probably due to steric hindrance to solvation. The sizable difference in ΔS^* for 2,4,6-tri-*t*-butylbenzyl chloride in 60% *t*-butyl alcohol–water could be due to a temperature dependance effect on ΔS^* and/or some specific solvation effect as the alcohol content of the medium is changed.

(2) α-Deuterium Isotope Effects

α-Deuterium isotope effects for solvolysis of 2,4,6-trimethylbenzyl chloride in 80% ethanol–water and 80% trifluoroethanol–water are given in Table 6. The results in 80% ethanol–water

Can. J. Chem. Downloaded from www.nrcresearchpress.com by 210.87.254.40 on 09/05/12
For personal use only.

TABLE 7. α-Deuterium isotope effects in solvolysis of 2,4,6-tri-*t*-butylbenzyl chloride

Solvent	Temperature (°C)	Rate ($k_1 \times 10^5$ s^{-1}) Undeuterated	Rate ($k_1 \times 10^5$ s^{-1}) α-D_2 compound	$k_H/k_{\alpha-D_2}$	k_H/k_D per D
80% Ethanol–water	44.89	298	225	1.32	1.149
80% Ethanol–water	45.04	243	181	1.34	1.158
80% TBA–water	70.05	226	178	1.27	1.127
80% TBA–water	60.01	78.8	61.3	1.29	1.136
60% TBA–water	45.15	106	79.6	1.33	1.153

average $k_H/k_D = 1.09$ per deuterium.[2] This is somewhat higher than the α-D effect on *p*-methylbenzyl chloride under these conditions. It is apparent that solvolysis of neither of these compounds approaches limiting behavior (requiring an α-D effect of 1.15) in 80% ethanol–water. In other words there is a significant nucleophilic participation by solvent in the solvolysis of these compounds in ethanol–water, although somewhat less in the case of 2,4,6-trimethylbenzyl chloride.

The α-deuterium isotope effect for 2,4,6-trimethylbenzyl chloride in 80% trifluoroethanol–water ($k_H/k_D = 1.16$) actually exceeded the "upper limit" established by Shiner and Fisher for solvolysis of benzyl chlorides (13). The isotope effects for 2,4,6-tri-*t*-butylbenzyl chloride (Table 7) are also of considerable interest. The values in 80% *t*-butyl alcohol – water (1.13–1.14) indicate that solvolysis in this medium was approaching the limiting character. The results in 60% *t*-butyl alcohol – water and in 80% ethanol–water of 1.15 and 1.16 respectively are unusually high for such solvents. Unfortunately the reaction rate for solvolysis of this chloride in trifluoroethanol–water was too fast for accurate measurement in our apparatus, even at lower temperatures.

These somewhat higher values of isotope effects in the range of 1.15–1.16 for 2,4,6-trimethyl- and 2,4,6-tri-*t*-butylbenzyl chloride are of interest, especially in view of some recent publications on the magnitude of α-deuterium isotope effects (13, 14). Our results are not of the high accuracy of those of Shiner and coworkers. Nevertheless, some preliminary suggestions to account for the high values are in order. One possibility would be to attribute the enhanced isotope effects to a steric contribution due to different nonbonded interactions between the deuteriums of the benzylic group and the hydrogens of the benzylic group, and the di-ortho alkyl groups. The case for a steric contribution to secondary isotope effects has been made by Bartell (15). However, a number of inadequacies have been pointed out in the steric explanation (12) and later calculations have shown the steric contribution to be only a small fraction of the isotope effect (16). There is the possibility of such a direct steric effect in the case of the isotope effect in solvolysis of 2,4,6-tri-*t*-butylbenzyl chloride because of the very close proximity of the two ortho *t*-butyl groups to the deuteriums or hydrogens in the benzylic group. On the other hand, it is unlikely that this is a satisfactory explanation for the results in the case of trimethylbenzyl chloride in 80% trifluoroethanol–water. It seems more reasonable to attribute the higher isotope effects for 2,4,6-trimethyl- and 2,4,6-tri-*t*-butylbenzyl chloride to steric inhibition of nucleophilic participation by solvent in the solvolysis. This means that the reactions would approximate more closely the "free" carbonium ion mechanism. The 2,4,6-tri-*t*-butylbenzyl system provides an interesting model for further work in this field. In particular it is an interesting substrate for studying the magnitude of the α-deuterium isotope effect for different leaving groups under conditions of limiting behavior.

(3) Product Analysis

Comparative product analyses results from solvolysis of trimethyl- and tri-*t*-butylbenzyl

[2]It appears from these data that our results are not sufficiently accurate to detect small differences in k_H/k_D due to temperature effects. The isotope effect is reported (3) to decrease by approximately 0.005 per D for a 20° rise in temperature.

Can. J. Chem. Downloaded from www.nrcresearchpress.com by 210.87.254.40 on 09/05/12
For personal use only.

TABLE 8. Product analysis of solvolysis of 2,4,6-trimethyl- and 2,4,6-tri-*t*-butylbenzyl chloride

Substituted benzyl chloride	Solvent	Mole fraction alcohol	% $ArCH_2$—O—R	% $ArCH_2OH$
Trimethyl-	Ethanol–water[a]	0.553(80%)	66	34
Tri-*t*-butyl-	Ethanol–water[a]	0.553(80%)	58	42
Trimethyl-	TBA[b]–water	0.434(80%)	52	48
Tri-*t*-butyl-	TBA–water	0.434(80%)	0	100
Tri-*t*-butyl-	IPA[b]–water	0.434(76.5%)	63	37

[a]Data taken from ref. 1.
[b]TBA = *t*-butyl alcohol, IPA = isopropyl alcohol.

TABLE 9. Chemical shifts of benzylic protons in trialkylbenzyl chlorides and of aryl methyls in related hydrocarbons

Substituted benzyl chloride	τ Benzyl protons[a] (p.p.m.)	$\Delta\tau$[b]
Parent	5.50	
p-*t*-Butylbenzyl	5.53	
2,4,6-Trimethyl-	5.51	—
2,4,6-Triisopropyl-	5.35	0.15
2-Methyl-4,6-di-*t*-butyl-	5.16	0.34
2,4,6-Tri-*t*-butyl-	4.72	0.78
Toluene	7.72	
2-Methyl-4,6-di-*t*-butyltoluene	7.68[c]	0.04
2,4,6-Tri-*t*-butyltoluene	7.37[c]	0.35

[a]Chemical shifts were measured in carbon tetrachloride containing tetramethylsilane.
[b]$\Delta\tau$ values refer to the chemical shift difference (downfield) relative to the benzylic hydrogens of benzyl chloride or the methyl hydrogens of toluene.
[c]τ values are for the aryl methyl group at position 1.

chloride in ethanol–water and in *t*-butyl alcohol–water are summarized in Table 8. As reported in Part IV of this series (1), the products are the expected corresponding alcohols and ethers. These were obtained in similar amounts in the cases of solvolysis in ethanol–water. The most significant result was obtained in the case of the solvolysis product from tri-*t*-butylbenzyl chloride in *t*-butyl alcohol–water, which was only the corresponding alcohol, there being none of the ether formed. This is an interesting example of the effect of "solvent sorting" on product formation. It appears that the bulky nucleophile (*t*-butyl alcohol) in this case is excluded from the competition with water for the reaction center by the steric requirements of the two ortho-*t*-butyl groups. Despite the usual high reactivity of this chloride, it failed to react with pure *t*-butyl alcohol even after heating at 70° for 98 h. The steric inhibition of ether formation did not appear to be important in the case of solvolysis in isopropyl alcohol–water. In this case, both ether and alcohol were formed.[3]

(c) Compression Chemical Shifts of Hindered Benzylic Protons

It was desirable to discover some ground state property of our hindered 2,4,6-trialkylbenzyl chlorides which might relate to the solvolysis data, especially the "steric acceleration" (1) and limiting behavior of 2,4,6-tri-*t*-butylbenzyl chloride. Protons in a highly congested environment of closely situated C—H bonds are known to undergo low field n.m.r. chemical shifts (17, 18). These so-called compression shifts have been attributed to intramolecular van der Waals-type forces (18) and it is possible that they may give some indication of the degree of steric compression in the ground state of tri-*t*-butylbenzyl compounds.

The downfield compression shifts of benzylic protons in hindered trialkylbenzyl chlorides summarized in Table 9 support the idea of steric congestion in 2,4,6-tri-*t*-butylbenzyl chloride (1). This chloride showed the largest downfield chemical shift of the benzylic protons relative to benzyl chloride. The compression shift does not occur in 2,4,6-trimethylbenzyl chloride. *p*-*t*-Butylbenzyl chloride showed nearly the same chemical shift as benzyl chloride. This indicates that the electronic effect of a *t*-butyl influences the chemical shifts of the benzylic protons comparatively slightly and such effects could be ignored in this qualitative discussion. The compression shift was also exhibited in the methyl

[3]Reaction of 2,4,6-tri-*t*-butylbenzyl chloride with anhydrous isopropyl alcohol yielded the corresponding isopropyl ether in high yield.

Can. J. Chem. Downloaded from www.nrcresearchpress.com by 210.87.254.40 on 09/05/12
For personal use only.

group of 2,4,6-tri-*t*-butyltoluene (Table 9). The shift was considerably less than for the tri-*t*-butylbenzyl chloride. This is presumably due to the smaller size of the aryl—CH_3 group in contrast to the —CH_2Cl group with resulting lower steric congestion in the former.

Financial support of this research provided by the National Research Council of Canada is gratefully acknowledged.

1. L. R. C. BARCLAY, H. R. SONAWANE, and J. C. HUDSON. Can. J. Chem. **50**, 2318 (1972).
2. J. B. HYNE. J. Am. Chem. Soc. **82**, 5129 (1960).
3. V. J. SHINER, W. DOWD, R. D. FISHER, S. R. HARTSHORN, M. A. KESSICK, L. MILAKOFSKY, and M. W. RAPP. J. Am. Chem. Soc. **91**, 4838 (1969).
4. L. R. C. BARCLAY, H. R. SONAWANE, and M. C. MACDONALD. Can. J. Chem. **50**, 281 (1972).
5. R. A. CLEMENT, J. N. NAGHIZADEH, and M. R. RICE. J. Am. Chem. Soc. **82**, 2449 (1960).
6. J. B. HYNE, R. WILLS, and R. E. WONKKA. J. Am. Chem. Soc. **84**, 2914 (1962).
7. J. B. HYNE and R. WILLS. J. Am. Chem. Soc. **85**, 3650 (1963).
8. V. J. SHINER, M. W. RAPP, and H. R. PINNICK. J. Am. Chem. Soc. **92**, 232 (1970).
9. E. M. ARNETT, W. G. BENTRUDE, J. J. BURKE, and P. MCC. DUGGLEBY. J. Am. Chem. Soc. **87**, 1541 (1965).
10. G. KOHNSTAM. Adv. Phys. Org. Chem. **5**, 121 (1967); L. L. SCHALEGER and F. A. LONG. Adv. Phys. Org. Chem. **1**, 1 (1963).
11. E. A. HALEVI. Prog. Phys. Org. Chem. **1**, 109 (1963).
12. V. J. SHINER, W. E. BUDDENBAUM, B. L. MURR, and G. LAMATY. J. Am. Chem. Soc. **90**, 418 (1968).
13. V. J. SHINER and R. D. FISHER. J. Am. Chem. Soc. **93**, 2553 (1971).
14. J. M. HARRIS, R. E. HALL, and P. V. R. SCHLEYER. J. Am. Chem. Soc. **93**, 2551 (1971).
15. L. S. BARTELL. J. Am. Chem. Soc. **83**, 3567 (1961).
16. G. J. KARABATSOS, G. C. SONNICHSEN, C. G. PAPAIOANNOU, S. E. SCHEPPELE, and R. L. SHONE. J. Am. Chem. Soc. **89**, 463 (1967).
17. L. R. C. BARCLAY, G. R. NIXON, H. M. FOOTE, and S. L. BARCLAY. Can. J. Chem. **47**, 4313 (1969), and references reported therein.
18. W. A. GIBBONS and V. M. S. GIL. Mol. Phys. **8**, 199 (1964); **9**, 163 (1965).

Can. J. Chem. Downloaded from www.nrcresearchpress.com by 210.87.254.40 on 09/05/12
For personal use only.

Free Radicals by Mass Spectrometry. XLV. Ionization Potentials and Heats of Formation of C_3H_3, C_3H_5, and C_4H_7 Radicals and Ions[1]

F. P. LOSSING

Division of Chemistry, National Research Council of Canada, Ottawa, Canada

Received June 15, 1972

Using an energy-resolved electron beam, appearance potentials for $C_3H_3^+$, $C_3H_5^+$, and $C_4H_7^+$ fragment ions from hydrocarbons of formula C_3H_4, C_3H_6, C_4H_6, C_4H_8, and C_5H_{10} have been measured. In each case the fragment appears to have a common structure, corresponding to $\Delta H_f(C_3H_3^+) = 256 \pm 2$ kcal/mol, $\Delta H_f(C_3H_5^+) = 226 \pm 2$ kcal/mol, and $\Delta H_f(C_4H_7^+) = 206 \pm 2$ kcal/mol. Ionization potentials have been measured for propargyl radical (8.68 V), methallyl radical (7.54 V), and 2-methylallyl radical (7.89 V). Corresponding ionic heats of formation are propargyl 281 ± 3 kcal/mol, methallyl 204 ± 3 kcal/mol, and 2-methylallyl 211 ± 5 kcal/mol. The $C_3H_3^+$ fragment ion is 25 kcal/mol more stable than propargyl ion, and is almost certainly cyclopropenyl ion. Ionization potentials for propyne, allene, cyclopropene, 1- and 2-butyne, and fifteen isomers of formula C_nH_{2n} have also been measured by monoenergetic electron impact.

En utilisant un faisceau d'électrons d'énergie résolue, les potentiels d'apparition des ions fragments $C_3H_3^+$, $C_3H_5^+$, et $C_4H_7^+$ à partir des hydrocarbures de formule C_3H_4, C_3H_6, C_4H_6, C_4H_8 et C_5H_{10}, ont été mesurés. Dans chaque cas le fragment semble posséder une structure commune correspondant à $\Delta H_f(C_3H_3^+) = 256 \pm 2$ kcal/mol, $\Delta H_f(C_3H_5^+) = 226 \pm 2$ kcal/mol, et $\Delta H_f(C_4H_7^+) = 206 \pm 2$ kcal/mol. Les potentiels d'ionisation ont été mesurés pour les radicaux propargyle (8.68 V), méthallyle (7.54 V), et méthyl-2 allyle (7.89 V). Les chaleurs de formation ionique correspondantes sont, pour le propargyle 281 ± 3 kcal/mol, le méthallyle 204 ± 3 kcal/mol et le méthyl-2 allyle 211 ± 5 kcal/mol. L'ion fragment C_3H_3 est plus stable de 25 kcal/mol que l'ion propargyle et correspond très certainement à l'ion cyclopropenyle. Les potentiels d'ionisation pour le propyne, l'allène, le cyclopropène, les butyne-1 et -2 et pour quinze isomères de formule C_nH_{2n} ont été mesurés par impact électronique monoénergétique. [Traduit par le journal]

Canadian Journal of Chemistry, **50**, 3973 (1972)

Can. J. Chem. Downloaded from www.nrcresearchpress.com by 210.87.254.42 on 09/05/12
For personal use only.

Introduction

Positive ions of mass 55 ($C_4H_7^+$), mass 41 ($C_3H_5^+$), and mass 39 ($C_3H_3^+$) are generally prominent features in the mass spectra of hydrocarbons. Although these ionic species and their uncharged free radical counterparts have been frequently studied by mass spectrometric methods, the structural identities and heats of formation of the ions are by no means well-established, as revealed by a recent data compilation (1). The $C_3H_3^+$ ion, in particular, has been the subject of considerable speculation, in view of the possibility that it could have the cyclopropenyl structure

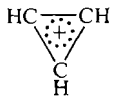

This structure is of special interest, as reviewed by Krebs (2), since it is the smallest aromatic system (3) on the basis of the $(4n + 2)$ π-electron rule, where in this case $n = 0$. The great stability predicted (3) on these grounds has been confirmed experimentally (4–6).

Mass spectral studies on $C_3H_3^+$ formation from deuterium-labelled propyne (7) and 1,3-butadiene (8) have shown that these processes involve complete randomization of H-atoms. The earlier mass spectrometric work on $C_3H_3^+$ attempted to distinguish between cyclo-$C_3H_3^+$ and propargyl ion $HC \equiv \overset{+}{C}CH_2$ on the basis of appearance potentials of $C_3H_3^+$ fragment from hydrocarbons (7–9) including cyclopropene (10), combined with the ionization potential of propargyl radical (11). Although the evidence pointed to a common structure for all $C_3H_3^+$ fragment ions, the data did not permit a clear differentiation between the energies of the two structures. In the present work improved measurements of appearance potentials and of the ionization potential of propargyl radical show that the $C_3H_3^+$ fragment ion from hydrocarbons is at least 1 eV more stable than an ionized propargyl radical, and is therefore almost certainly a cyclopropenyl ion.

Assignment of the allyl structure to the

[1]NRCC No. 12800.

Can. J. Chem. Downloaded from www.nrcresearchpress.com by 210.87.254.42 on 09/05/12
For personal use only.

$C_3H_5^+$ fragment ion seems to have been more-or-less taken for granted. Alternative structures such as cyclopropyl ion or propenyl ($CH_3\overset{+}{C}=CH_2$) ion lack resonance stabilization and are consequently appreciably less stable. An earlier electron impact study (12) showed that the $C_3H_5^+$ fragment ion from six C_4H_8 isomers had nearly the same heat of formation, and one which was close to that for allyl ion. In the present work these appearance potentials have been more precisely re-determined using a monoenergetic electron impact method, and compared with a revised value for ΔH_f (allyl$^+$) (13). There seems from this to be no doubt that the $C_3H_5^+$ fragment ion is in all cases an allyl ion, regardless of the structure of the parent molecule.

Similarly, the heat of formation of $C_4H_7^+$ ion as a fragment from thirteen C_4H_8 and C_5H_{10} isomers is investigated in the present work. Again a common ionic structure appears to be involved. Comparison with the heats of formation and the re-measured ionization potentials for methallyl and 2-methyl allyl radicals suggest that the first of these structures is favored.

In addition to the fragment ion measurements, the molecular ionization potentials for selected C_3, C_4, and C_5 hydrocarbons have also been obtained by monoenergetic electron impact.

Experimental

Measurements of ionization efficiency curves for fragment ion formation and for direct ionization of propargyl, methallyl, and 2-methyl allyl radicals were carried out using an electron energy selector, ionization chamber, ion extractor, and quadrupole mass filter previously described (14). The energy dispersion in the electron beam was about 0.07 V at half-maximum. The free radicals were produced by pyrolysis of suitable compounds at pressures of about 10^{-3} Torr in a fused-silica capillary furnace (11).

Propargyl iodide was prepared from a commercial sample of the bromide by reaction with sodium iodide in acetone. After separation the iodide was purified by bulb-to-bulb distillation at reduced pressure. Propargyl methyl nitrite ($HC{\equiv}CCH_2CH_2ONO$) was prepared from 3-butyn-1-ol through reaction with $NaNO_2$ and H_2SO_4. The nitrites $CH_3CH{=}CHCH_2CH_2ONO$ and $CH_2{=}C(CH_3)CH_2CH_2ONO$, and cyclopropyl methyl nitrite, were prepared similarly from the corresponding alcohols.

Cyclopropene was prepared by the method of Closs and Krantz (15). A propylene impurity was removed by bulb-to-bulb distillation at $-130°$.

Cyclopropylcarbonyl peroxide $\triangleright\text{—}\overset{O}{\overset{\|}{C}}\text{—OO—}\overset{O}{\overset{\|}{C}}\text{—}\triangleleft$ was prepared from cyclopropylacetyl chloride by the method of Sheldon and Kochi (16). After purification it was a white solid apparently stable indefinitely at 20°, and easily sublimed at 30°.

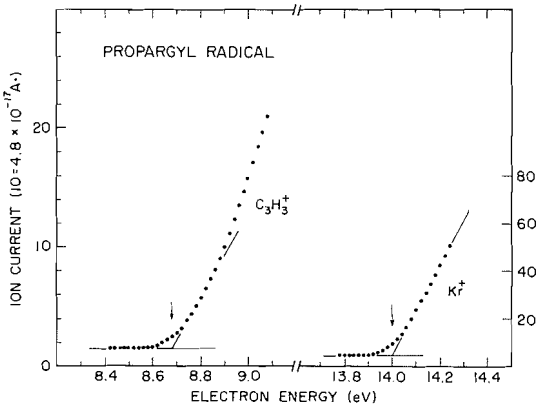

FIG. 1. Ionization efficiency curves for propargyl radical and for krypton standard.

The hydrocarbon samples employed were commercial samples of high purity. The heats of formation at 25° were taken from Cox and Pilcher (17) except for methylcyclopropane (5.7 kcal/mol), ethylcyclopropane (0.7 kcal/mol), and 1,1-dimethylcyclopropane (−1.9 kcal/mol) from Benson and O'Neal's data compilation (18).

Results and Discussion

Propargyl Radical and Ion

In an earlier measurement of the ionization potential, the propargyl radical was produced by the thermal decomposition of propargyl iodide at 1000°–1100° (11). In the present work a better yield was obtained at a much lower temperature by the thermal decomposition (19) of propargyl methyl nitrite.

$$HC{\equiv}CCH_2CH_2ONO \rightarrow HC{\equiv}CCH_2CH_2\dot{O} + NO$$

$$HC{\equiv}CCH_2CH_2\dot{O} \rightarrow HC{\equiv}C\dot{C}H_2 + CH_2O$$

The ionization efficiency curve for propargyl radical is shown in Fig. 1, along with that of krypton for energy calibration. The average of several determinations gave 8.68 V for the ionization potential of this radical. This is appreciably higher than the earlier result of 8.25 V (11), contrary to the usual experience that the older measurements with low energy resolution gave values which were several tenths of a volt too high. Repeat measurements in the original apparatus on propargyl radical from pyrolysis of propargyl iodide, propargyl bromide, and propargyl methyl nitrite all gave ionization potentials of 8.8–8.9 V, consistent with the present results but not with 8.25 V. It

TABLE 1. $C_3H_3^+$ ion: appearance potentials and heat of formation

Process	AP (V) This work	AP (V) Lit. (PI)	$\Delta H_f(C_3H_3^+)$ (kcal/mol) This work	$\Delta H_f(C_3H_3^+)$ (kcal/mol) Lit. (PI)
$CH_3C{\equiv}CH \rightarrow C_3H_3^+ + H$	11.60	11.55*, 11.56†	259.8	258.7
$CH_2{=}C{=}CH_2 \rightarrow C_3H_3^+ + H$	11.47	11.48*†	258.1	258.3
cyclo-$C_3H_4 \rightarrow C_3H_3^+ + H$	10.54	—	257.2	—
$CH_2{=}CHCH{=}CH_2 \rightarrow C_3H_3^+ + CH_3$	—	11.40*, 11.39†, 11.35‡	—	255±1
$CH_3CH{=}C{=}CH_2 \rightarrow C_3H_3^+ + CH_3$	—	10.86*	—	255.2
$CH_3CH_2C{\equiv}CH \rightarrow C_3H_3^+ + CH_3$	10.84	—	255.5	—
$CH_3C{\equiv}CCH_3 \rightarrow C_3H_3^+ + CH_3$	11.04	—	255.3	—
$HC{\equiv}C\dot{C}H_2 \rightarrow HC{\equiv}C\overset{+}{C}H_2$	IP = 8.68	$\Delta H_f(HC{\equiv}C\overset{+}{C}H_2)$	≥ 281§	

*Reference 21.
†Reference 22.
‡Reference 20.
§See text.

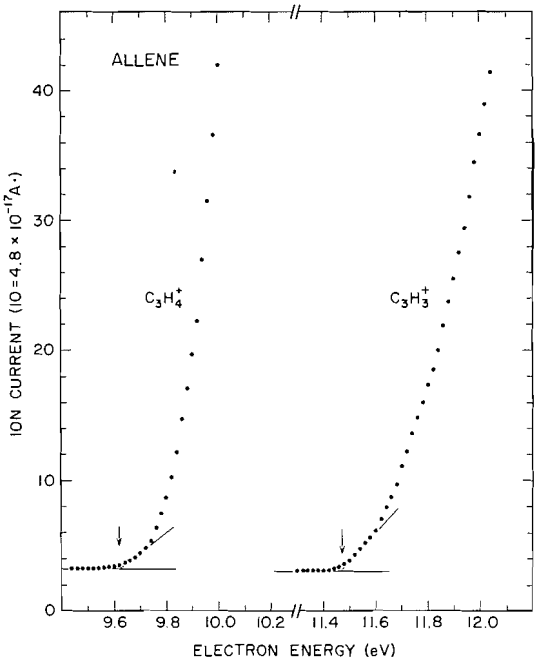

FIG. 2. Ionization efficiency curves for $C_3H_4^+$ parent and $C_3H_3^+$ fragment ions from allene.

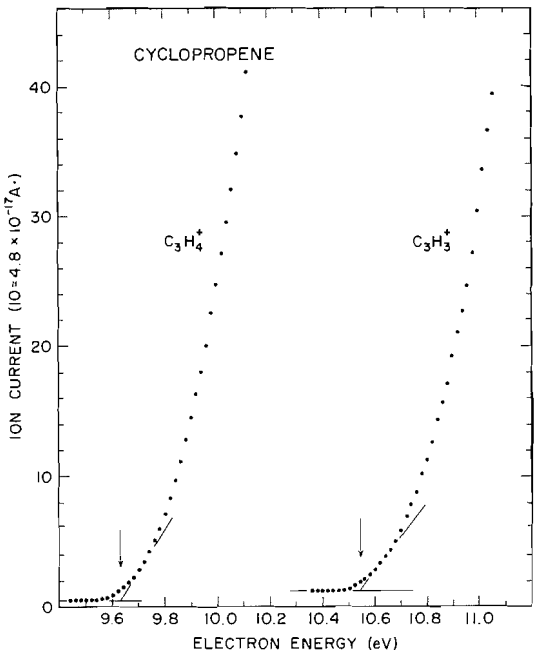

FIG. 3. Ionization efficiency curves for $C_3H_4^+$ parent and $C_3H_3^+$ fragment ions from cyclopropene.

would appear that the voltage scale calibration must have been in error in the earlier work.

$C_3H_3^+$ Fragment Ion

Recent energetics data on $C_3H_3^+$ fragment ions, from the present work and from photoionization studies (20–22) are shown in Table 1. The earlier electron impact results are not included. Typical curves for $C_3H_3^+$ ion production are shown in Figs. 2 and 3. The photoionization data and the present results are in excellent agreement, giving $\Delta H_f(C_3H_3^+) = 256$ kcal/mol with an uncertainty of about ±2 kcal/mol. This value, which is nearly identical with that recommended by Franklin *et al.* (1) will be too high by the difference between the "thermal" shift (23) and the "kinetic" shift (24), which may amount to 2–3 kcal/mol. In this respect it is worth noting

Can. J. Chem. Downloaded from www.nrcresearchpress.com by 210.87.254.42 on 09/05/12
For personal use only.

Can. J. Chem. Downloaded from www.nrcresearchpress.com by 210.87.254.42 on 09/05/12
For personal use only.

from Table 1 that H-loss from C_3H_4 molecules gives $\Delta H_f(C_3H_3^+)$ about 3 kcal/mol higher than does CH_3-loss from C_4H_6, indicating a slightly larger kinetic shift for H-atom loss. This heat of formation almost certainly refers to a common ionic species which can be formed with little or no excess energy from parent ions of widely different structure. The identity of this ion, as mentioned above, has been much discussed, the two most probable configurations being cyclopropenyl and propargyl. A third possible $C_3H_3^+$ structure, methylethynyl $CH_3C{\equiv}C^+$, would have a much higher heat of formation than the propargyl ion, since the neutral radical, unlike propargyl, will not possess resonance stabilization. In addition, the ionization potential for $CH_3C{\equiv}\dot{C}$ radical would be much higher than for propargyl radical.[2]

One can estimate $\Delta H_f(HC{\equiv}CCH_2^+)$ from the ionization potential of the radical and a recent measurement of its heat of formation, $\Delta H_f(HC{\equiv}C\dot{C}H_2) = 80.7$ kcal/mol (25). Adding $IP(HC{\equiv}C\dot{C}H_2) = 8.68$ V gives $\Delta H_f(HC{\equiv}CCH_2^+) = 281$ kcal/mol. This is 25 kcal/mol higher than the heat of formation of the common $C_3H_3^+$ species, which clearly rules out the $HC{\equiv}CCH_2^+$ structure for this fragment ion, at least near the dissociation threshold. It seems probable, therefore, that the $C_3H_3^+$ fragment is a cyclopropenyl ion, even when extensive skeletal rearrangement is necessary. The loss of identity of H-atoms in the dissociative ionization of propyne (7) and 1,3-butadiene (8) would be most easily understood on this basis. The formation of cyclo-$C_3H_3^+$ ion appears to be analogous to the well-known dissociative ionization of benzyl derivatives (26), which detailed labelling experiments have shown to involve an easily-scrambled $C_7H_8^+$ precursor dissociating to symmetrical cycloheptatrienyl cation (tropylium). In this case the loss of positional identity has been demonstrated for both H-atoms (26) and C-atoms (27).

Although the present results indicate that $\Delta H_f = 256$ kcal/mol should be attributed to the cyclopropenyl ion, a much lower heat of formation, < 200 kcal/mol, has been proposed (28, 29) to account for the appearance of $C_3H_3^+$ ion as a result of chemi-ionization in shock-tube oxidation of hydrocarbons. However, an alternative mechanism consistent with $\Delta H_f(C_3H_3^+) \sim 256$ kcal/mol has been suggested (22). Evidence for a lower value comes also from observations of $C_3H_3^+$ ion which is formed in an ion-molecule reaction in butadiene (30):

$$C_4H_6^+ + C_4H_6 \rightarrow C_3H_3^+ + C_5H_9$$

For this proposed CH_3-transfer reaction to be exothermic $\Delta H_f(C_3H_3^+)$ would have to be < 240 kcal/mol, which is not consistent with the present result.

Finally, it should be noted that the appearance potential data for $C_3H_3^+$ ion are concerned only with the identity of the ions produced at minimum energies in the region of the dissociation limit. It is possible that at higher energies $C_3H_3^+$ fragment ions with less stable structures, such as propargyl ion, can be formed, which may have lifetimes before isomerization long enough to be of importance in ion-molecule reactions or in metastable transitions. It may be that there are two stable structures for $C_3H_3^+$ fragment ions as has been proposed (31) to explain fine structure in the metastable transition

$$C_3H_5^+ \rightarrow C_3H_3^+ + H_2$$

There is no supporting evidence for this from appearance potentials, however; the divergence in $\Delta H_f(C_3H_3^+)$ values found in the literature (1, 7) almost certainly can be explained on the basis of the well-known difficulties in measuring appearance potential thresholds by low energy-resolution methods. It might be noted also that photoionization curves for $C_3H_3^+$ fragment from 1,2-butadiene and allene (21) show no indication of a second upward break in the region of ~ 25 kcal/mol above the threshold, which would correspond to formation of $HC{\equiv}CCH_2^+$ ion. There are upward breaks at 1.8 V and 1.5 V, respectively, above the thresholds, but these correspond to breaks at the same energies for both parent ions and for other peaks, suggesting the onset of formation of an excited state of the parent ion (21), rather than a new species of $C_3H_3^+$ fragment ion.

$C_3H_5^+$ Fragment Ion

The appearance potentials obtained for $C_3H_5^+$ ion from C_3H_6 and C_4H_8 isomers are listed in

[2]Note that from $\Delta H_f(HC{\equiv}C^+) = 399$ kcal/mol and $\Delta H_f(HC{\equiv}\dot{C}) = 112$ kcal/mol (1) one obtains $IP(HC{\equiv}\dot{C}) \simeq 12.4$ V. This is 2–3 V higher than the ionization potential of any hydrocarbon radical of the form $R{-}\dot{C}H_2$.

TABLE 2. $C_3H_5^+$ ion: appearance potentials and heat of formation

Process	AP (V) This work	AP (V) Lit.	$\Delta H_f(C_3H_5^+)$ (kcal/mol) This work
cyclo-$C_3H_6 \rightarrow C_3H_5^+ + H$	11.49	12.06*	225.6
$CH_3CH{=}CH_2 \rightarrow C_3H_5^+ + H$	11.88	12.11†	226.7
cyclo-$C_4H_8 \rightarrow C_3H_5^+ + CH_3$	11.00	11.2‡, 11.3§	226.5
cyclo-$C_3H_5{-}CH_3 \rightarrow C_3H_5^+ + CH_3$	11.02	11.2†	225.8
$CH_2{=}CHCH_2CH_3 \rightarrow C_3H_5^+ + CH_3$	11.28	11.4†	225.9
cis-$CH_3CH{=}CHCH_3 \rightarrow C_3H_5^+ + CH_3$	11.33	11.6†	225.4
$(CH_3)_2C{=}CH_2 \rightarrow C_3H_5^+ + CH_3$	11.45	11.8†	225.8
$\Delta H_f(\text{allyl}) + \text{IP} = \Delta H_f(\text{allyl}^+)$ =			226 ± 2

*Reference 33.
†Reference 32.
‡Reference 12.
§Reference 37.

Table 2, together with literature electron impact data (12, 32, 33), which is generally 0.2–0.4 V higher. No photon impact data is available. The ionization efficiency curves for these processes were all of the same general form already reported (13) for $C_3H_5^+$ ion production from propylene. Heats of formation for $C_3H_5^+$ derived from these appearance potentials are also listed in Table 2, and provide further support for the value of $\Delta H_f(C_3H_5^+) = 226$ kcal/mol found earlier (13). As noted in this reference, the heat of formation of allyl ion of known structure is also 226 kcal/mol as derived from $\Delta H_f(\text{allyl}) + \text{IP(allyl)}$. The alternative structure for $C_3H_5^+$, the cyclopropyl ion, has a heat of formation considerably higher than this, as estimated below from the same relationship. Although the heat of formation of cyclopropyl radical is known, 61 ± 3 kcal/mol (34), the ionization potential is not known; an earlier measurement (33) refers almost certainly to cyclopropyl radicals which had largely isomerized to allyl radicals. An attempt was made in the present work to measure the ionization potential of cyclopropyl radical on radicals of mass 41 produced by the thermal decomposition of cyclopropylcarbonyl peroxide (16) at a relatively low furnace temperature, around 250°, with a contact time of 1 ms. The ionization efficiency curves for $C_3H_5^+$ were found, however, to be almost exactly superimposable on those for allyl radical obtained from the pyrolysis of allylmethyl nitrite (13). Either all the cyclopropyl radicals are rapidly isomerized to allyl at this temperature, or the ionization potential of cyclopropyl radical is higher than that of allyl, and the threshold for ionization of any cyclopropyl radicals retaining their identity is obscured by allyl ions. It can be assumed, however, either from calculation (35) or from naïve consideration of cyclopropyl ion as a "secondary" alkyl ion, that its ionization potential will be about the same as, or a few tenths of a volt lower than, that of allyl radical. Assuming, then, that IP(cyclopropyl) > 7.8 V one obtains $\Delta H_f(\text{cyclopropyl}^+) > 241$ kcal/mol, clearly larger than $\Delta H_f(\text{allyl}^+)$.

It appears therefore that the minimum energy path for $C_3H_5^+$ production from all the compounds in Table 2 corresponds to allyl formation with little or no excess energy required, even when extensive skeletal rearrangements are necessary. Although the only $C_4H_8^+$ isomer which can dissociate to allyl ion and CH_3 by a simple bond rupture without rearrangement is the parent ion of 1-butene, the minimum energy dissociation path is not lower for this than for the other isomers. This is consistent with the findings of Meisels *et al.* (12) that complete skeletal randomization occurs in $C_3H_5^+$ production from 1-butene at energies close to the dissociation threshold. Regardless of which isomer one starts with, whenever the total energy content reaches the level of $\Delta H_f(\text{allyl}^+) + \Delta H_f(CH_3)$ (*i.e.* 226 + 34 kcal/mol or 11.27 V), these products can be formed. This implies a facility for isomerization which appears at first sight to be at odds with evidence from ion–molecule studies that various $C_4H_8^+$ isomeric ions lose their identity relatively slowly (36–39).

Can. J. Chem. Downloaded from www.nrcresearchpress.com by 210.87.254.42 on 09/05/12
For personal use only.

TABLE 3. $C_4H_7^+$ ion: appearance potentials and heat of formation

Process	AP (V) This work	AP (V) Lit.	$\Delta H_f(C_4H_7^+)$ (kcal/mol) This work
cyclo-$C_4H_8 \rightarrow C_4H_7^+ + H$	10.91	11.24*, 11.3†	206.3
cyclo-C_3H_5—$CH_3 \rightarrow C_4H_7^+ + H$	11.02	—	207.7
CH_2=$CHC_2H_5 \rightarrow C_4H_7^+ + H$	11.26	12.01‡	207.4
cis-CH_3CH=$CHCH_3 \rightarrow C_4H_7^+ + H$	11.32	11.20‡	207.1
$(CH_3)_2C$=$CH_2 \rightarrow C_4H_7^+ + H$	11.41	—	206.8
cyclo-C_3H_5—$C_2H_5 \rightarrow C_4H_7^+ + CH_3$	10.34	—	205.2
cyclo-C_3H_4—$(CH_3)_2 \rightarrow C_4H_7^+ + CH_3$	10.47	11.38§	205.5
CH_2=$CHC_3H_7 \rightarrow C_4H_7^+ + CH_3$	10.64	—	206.0
trans-CH_3CH=$CHC_2H_5 \rightarrow C_4H_7^+ + CH_3$	10.68	—	204.4
CH_2=$CHCH(CH_3)_2 \rightarrow C_4H_7^+ + CH_3$	10.74	—	207.1
$(CH_3)_2CH$=$CHCH_3 \rightarrow C_4H_7^+ + CH_3$	10.84	—	205.8
CH_2=$C(CH_3)C_2H_5 \rightarrow C_4H_7^+ + CH_3$	10.85	—	207.7
cyclo-$C_5H_{10} \rightarrow C_4H_7^+ + CH_3$	11.14	—	204.5
$CH_3\dot{C}HCH$=$CH_2 \rightarrow C_4H_7^+$	IP = 7.54	$\Delta H_f(CH_3\overset{+}{C}HCH$=$CH_2) = 204 \pm 3$‖	
CH_2=$C(CH_3)\dot{C}H_2 \rightarrow C_4H_7^+$	IP = 7.89	$\Delta H_f(CH_2$=$C(CH_3)\overset{+}{C}H_2) = 211 \pm 5$‖	

*Reference 33.
†Reference 37.
‡Reference 32.
§Reference 40.
‖See text.

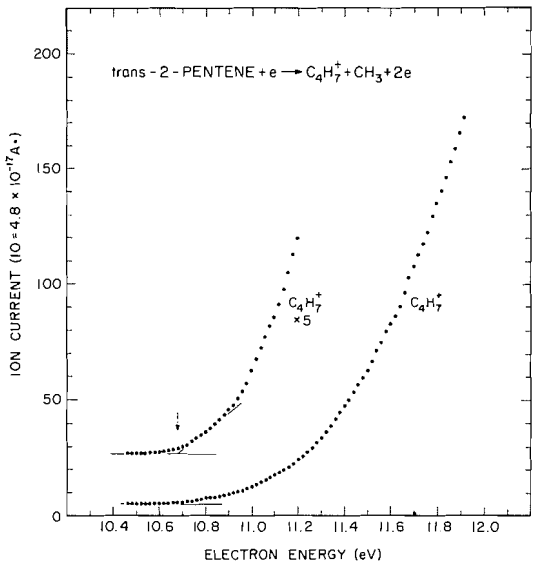

FIG. 4. Ionization efficiency curve for $C_4H_7^+$ fragment ion from *trans*-2-pentene.

In the present experiments, however, we are concerned only with reaction rates along the minimum energy path for dissociation, for which the time-scale will be considerably longer than for isomerization (12). Moreover, as a result of an unusually small ion draw-out potential, the ion residence time in the present apparatus is quite long, around 3×10^{-5} s. This favors the detection of low-energy processes, and reduces the kinetic shift associated with the detectable threshold for dissociation.

The formation, at higher electron energies, of $C_3H_5^+$ fragment ions having a structure other than allyl, which is retained long enough to undergo ion-molecule reactions, cannot of course be ruled out on the basis of the present work.

$C_4H_7^+$ Fragment Ion

The appearance potentials for $C_4H_7^+$ fragment ion from five C_4H_8 isomers and eight C_5H_{10} isomers are listed in Table 3. A few electron impact values are available from the literature (32, 33, 40), but no photoionization results have appeared. The efficiency curves for $C_4H_7^+$ were generally of the form shown in Fig. 4, having no significant structural features other than a low probability near the onset and curving strongly upward over a 1-V interval. The thresholds were not well-defined, so the appearance potentials in Table 3 are probably uncertain to at least ± 0.1 V. Corresponding ionic heats of formation are also given in Table 3, from

Can. J. Chem. Downloaded from www.nrcresearchpress.com by 210.87.254.42 on 09/05/12
For personal use only.

TABLE 4. Ionization potentials and ionic heats of formation for C_3H_4 and C_4H_6 molecules

Species	Ionization potential (V)			$\Delta H_f(C_nH_{2n-2}^+)$ kcal/mol
	This work	PI	PS	This work
Allene	9.62	9.62*, 9.53†	9.83‡	267.5
Propyne	10.36	10.36§, 10.37‖, 10.38*	—	283.3
Cyclopropene	9.64	—	9.70¶	288.5
1-Butyne	10.18	10.18§	—	274.3
2-Butyne	9.56	—	—	255.2

*Reference 21.
†Reference 22.
‡Reference 44.
§Reference 45.
‖Reference 46.
¶Reference 47.

Can. J. Chem. Downloaded from www.nrcresearchpress.com by 210.87.254.42 on 09/05/12
For personal use only.

which it appears that the $C_4H_7^+$ fragment ion from all these isomers has a common structure, with $\Delta H_f = 206 \pm 2$ kcal/mol. The most probable structures are the two allylic forms corresponding to the resonance stabilized free radicals $CH_3\dot{C}HCH{=}CH_2$ and $CH_2{=}C(CH_3)\dot{C}H_2$. To clarify this point these two radicals were generated thermally by the pyrolysis of the appropriate nitrites RCH_2ONO and their ionization efficiency curves were obtained. The ionization potentials, which are about 0.2 V lower than earlier measurements (41), are given in Table 3. Taken with the heat of formation of $CH_3\dot{C}HCH{=}CH_2$ (methallyl) radical, 30.2 kcal/mol (42), the ionization potential gives 204 kcal/mol for the heat of formation of this ion, with an estimated uncertainty of ± 3 kcal/mol. No heat of formation is available for $CH_2{=}C(CH_3)\dot{C}H_2$ radical, but an estimate can be made on the assumption that the bond dissociation energy $D(CH_2{=}C(CH_3)CH_2{-}H) \sim$ 85 kcal/mol, *i.e.* lower than D(allyl—H) = 88 kcal/mol (43) but not as low as $D(CH_3CH{=}CHCH_2{-}H) = 82.5$ kcal/mol (42). This estimate gives $\Delta H_f(CH_2{=}C(CH_3)CH_2) \sim 28.6$ kcal/mol and an ionic heat of formation of 211 kcal/mol for this structure, with an estimated uncertainty of ± 5 kcal/mol. Taking into account a presumed kinetic energy shift in the appearance potential, these values suggest that the $C_4H_7^+$ ion at the energy threshold has more probably the non-branched form, regardless of the structure of the parent ion. Evidently the situation is similar to that for allyl and cyclopropenyl ions, in that isomerization leads to complete loss of parent ion identity on the time-scale involved in dissociation near the energy threshold.

It is interesting to note that for each of the C_4H_8 isomers in Tables 2 and 3, the appearance potentials for the $C_3H_5^+$ and the $C_4H_7^+$ fragment ions are equal within the experimental error; the largest difference, 0.09 V, is found for cyclobutane. It is doubtful if any special significance should be attributed to this fact, other than that, by coincidence, the heats of formation of the two sets of products $C_3H_5^+ + CH_3$ and $C_4H_7^+ + H$ are nearly identical. The exact coincidence of the appearance potential curves for $C_3H_5^+$ and $C_4H_7^+$ from cyclobutane, from the threshold up to 50 V, and the resulting insensitivity of the ratio $C_3H_5^+/C_4H_7^+$ to internal energy, have been noted by Hughes and Tiernan (37).

Molecular Ionization Potentials

The ionization potentials of allene, propyne, cyclopropene, and 1- and 2-butyne, as measured by monoenergetic electron impact, are given in Table 4, together with values obtained by photoionization (PI) and photoelectron spectroscopy (PS) (21, 22, 44–47). The ionization efficiency curves for allene and cyclopropene molecular ions are shown in Figs. 2 and 3, respectively. The allene curve has a short segment at the foot, which appears also in the photoionization curve (21). The cyclopropene curve shows no resolvable structure, but is slightly curved over the first 0.2 V. The agreement of the data for these molecules is satisfactory, except possibly for allene.

The ionization potentials obtained for C_nH_{2n} isomers are given in Table 5, along with photo-

Can. J. Chem. Downloaded from www.nrcresearchpress.com by 210.87.254.42 on 09/05/12
For personal use only.

TABLE 5. Ionization potentials and ionic heats of formation for C_nH_{2n} molecules

Species	Ionization potential (V) This work	PI	PS	$\Delta H_f(C_nH_{2n}^+)$ (kcal/mol) This work
C_3				
Propylene	9.72	9.73*	9.69†	229
Cyclopropane	⩽9.93	10.06*	10.06†, 9.96‡	⩽242
C_4				
cis-2-Butene	9.10	9.13*	9.12†	208
1-Butene	9.58	9.58*, 9.61§	9.59†	221
Isobutene	9.19	9.23*‖	9.17†	208
Methylcyclopropane	9.46	—	9.52‡	224
Cyclobutane	10.06	10.3¶	—	239
C_5				
trans-2-Pentene	8.92	—	—	198
1-Pentene	9.48	9.50*	—	213
2-Methyl-1-butene	9.12	9.12*	—	202
3-Methyl-1-butene	9.52	9.51*	9.52†	213
2-Methyl-2-butene	8.70	8.67*, 8.68‖	—	190
Ethylcyclopropane	9.50	—	—	220
1,1-Dimethylcyclopropane	9.08	—	—	207
Cyclopentane	10.49	10.53*	10.49†, 10.50‡	223

*Reference 45.
†Reference 44.
‡Reference 48.
§Reference 49.
‖Reference 50.
¶Private communication from P. Natalis, B. Steiner, and M. G. Inghram, reported in ref. 37.

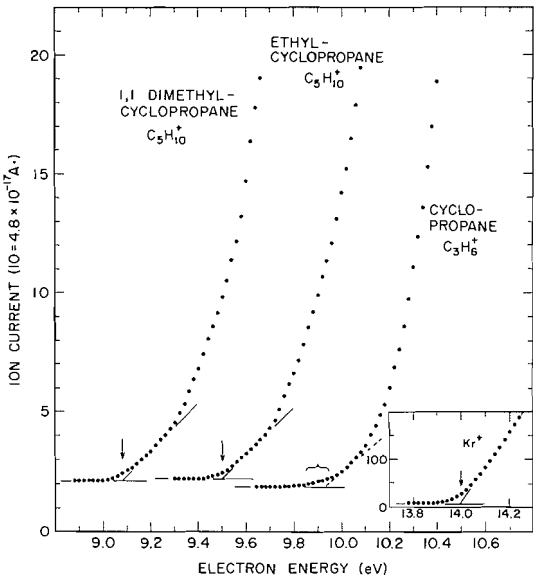

FIG. 5. Ionization efficiency curves for parent ions of 1,1-dimethylcyclopropane, ethylcyclopropane, and cyclopropane. The latter has a nearly asymptotic threshold, corresponding to a low probability for the adiabatic ionization process.

ionization and photoelectron spectroscopy values from the literature (44–50). The ionization efficiency curves were generally of the shape shown by 1,1-dimethylcyclopropane and ethylcyclopropane in Fig. 5, with a moderately abrupt onset, exhibiting possibly a short linear section, as for the latter compound. The curve for cyclopropane itself (Fig. 5) was more nearly asymptotic in shape, and the 9.93 V reported is undoubtedly only an upper limit for the adiabatic ionization potential. The agreement of the data is satisfactory, with the possible exception of cyclopropane and cyclobutane. It is interesting to note that the ionization potential of cyclopropane is lower than that of cyclobutane, which is in turn lower than that of cyclopentane. Methyl- and ethylcyclopropane have essentially the same ionization potential, rather surprisingly lower than that of 1-butene, while 1,1-dimethylcyclopropane is even lower by about 0.4 V, as might be expected from the double substitution.

1. J. L. FRANKLIN, J. G. DILLARD, H. M. ROSENSTOCK, J. T. HERRON, K. DRAXL, and F. H. FIELD. Ionization potentials, appearance potentials, and heats of forma-

Can. J. Chem. Downloaded from www.nrcresearchpress.com by 210.87.254.42 on 09/05/12
For personal use only.

tion of gaseous positive ions. Nat. Stand. Ref. Data Ser. NBS-26. National Bureau of Standards, Washington. 1969.
2. A. W. KREBS. Angew. chem. Int. Ed. **4**, 1 (1965).
3. J. D. ROBERTS, A. STREITWIESER, JR., C. M. REGAN. J. Am. Chem. Soc. **74**, 4579 (1952).
4. R. BRESLOW, J. T. GROVES, and G. RYAN. J. Am. Chem. Soc. **89**, 5048 (1967).
5. G. FARNUM, G. MEHTA, and R. S. SILBERMAN. J. Am. Chem. Soc. **89**, 5049 (1967).
6. R. BRESLOW and J. T. GROVES. J. Am. Chem. Soc. **92**, 984 (1970).
7. J. COLLIN and F. P. LOSSING. J. Am. Chem. Soc. **79**, 5848 (1957); **80**, 1568 (1958).
8. A. B. KING. J. Phys. Chem. **68**, 1409 (1964).
9. F. H. COATS and R. C. ANDERSON. J. Am. Chem. Soc. **79**, 1340 (1957).
10. K. B. WIBERG, W. J. BARTLEY, and F. P. LOSSING. J. Am. Chem. Soc. **84**, 3980 (1962).
11. J. B. FARMER and F. P. LOSSING. Can. J. Chem. **33**, 861 (1955).
12. G. G. MEISELS, J. Y. PARK, and B. G. GIESSNER. J. Am. Chem. Soc. **91**, 1555 (1969); **92**, 254 (1970).
13. F. P. LOSSING. Can. J. Chem. **49**, 357 (1971).
14. K. MAEDA, G. P. SEMELUK, and F. P. LOSSING. Int. J. Mass Spectrom. Ion Phys. **1**, 395 (1968).
15. G. L. CLOSS and K. D. KRANTZ. J. Org. Chem. **31**, 638 (1966).
16. R. A. SHELDON and J. K. KOCHI. J. Am. Chem. Soc. **92**, 4395 (1970).
17. J. D. COX and G. PILCHER. Thermochemistry of organic and organometallic compounds. Academic Press. London. 1970.
18. S. W. BENSON and H. E. O'NEAL. Kinetic data on gas phase unimolecular reactions. Nat. Stand. Ref. Data. Ser. NBS-21, National Bureau of Standards, Washington. 1970.
19. F. P. LOSSING and J. B. DE SOUSA. J. Am. Chem. Soc. **81**, 281 (1959).
20. B. BREHM. Z. Naturforsch. **21***a*, 196 (1966).
21. A. C. PARR and F. A. ELDER. J. Chem. Phys. **48**, 2659 (1968).
22. C. S. MATTHEWS and P. WARNECK. J. Chem. Phys. **51**, 854 (1969).
23. W. A. CHUPKA. J. Chem. Phys. **54**, 1936 (1971).
24. W. A. CHUPKA. J. Chem. Phys. **30**, 191 (1959).
25. WING TSANG. Int. J. Chem. Kinet. **2**, 23 (1970).
26. H. M. GRUBB and S. MEYERSON. Mass spectra of alkylbenzenes. *In* Mass spectrometry of organic ions. F. W. McLafferty, *Editor*. Academic Press, London. 1963. Chap. 10.
27. K. L. RINEHART, A. C. BUCHHOLZ, G. E. VAN LEAR, and H. L. CANTRELL. J. Am. Chem. Soc. **90**, 2983 (1968).
28. G. B. KISTIAKOWSKY and J. V. MICHAEL. J. Chem. Phys. **40**, 1447 (1964).
29. G. P. GLASS and G. B. KISTIAKOWSKY. J. Chem. Phys. **40**, 1448 (1964).
30. I. KOYANO, I. OMURA, and I. TANAKA. J. Chem. Phys. **44**, 3850 (1966).
31. P. GOLDBERG, J. A. HOPKINSON, A. MATHIAS, and A. E. WILLIAMS. Org. Mass Spectrom. **3**, 1009 (1970).
32. I. OMURA. Bull. Chem. Soc. Jap. **34**, 1227 (1961); **35**, 1845 (1962).
33. R. F. POTTIE, A. G. HARRISON, and F. P. LOSSING. J. Am. Chem. Soc. **83**, 3204 (1961).
34. J. A. KERR. Chem. Rev. **66**, 465 (1966).
35. J. J. KAUFMAN. J. Am. Chem. Soc. **84**, 4393 (1962).
36. R. D. DOEPKER and P. AUSLOOS. J. Chem. Phys. **43**, 3814 (1965); I. KOYANO. J. Chem. Phys. **45**, 706 (1966); F. P. ABRAMSON and J. H. FUTRELL. J. Phys. Chem. **72**, 1994 (1968); S. G. LIAS and P. AUSLOOS. J. Am. Chem. Soc. **92**, 1840 (1970); P. S. GILL, Y. INEL, and G. G. MEISELS. J. Chem. Phys. **54**, 2811 (1971).
37. R. M. HUGHES and T. O. TIERNAN. J. Chem. Phys. **51**, 4373 (1969).
38. J. M. S. HENIS. J. Chem. Phys. **52**, 282 (1970); **52**, 292 (1970).
39. L. W. SIECK, S. G. LIAS, L. HELLNER, and P. AUSLOOS. J. Res. Nat. Bur. Standards. In press; S. G. LIAS and P. AUSLOOS. J. Res. Nat. Bur. Standards. In press.
40. P. NATALIS and J. LAUNE. Bull. Soc. Chim. Belges, **73**, 944 (1964).
41. C. A. MCDOWELL, F. P. LOSSING, I. H. S. HENDERSON, and J. B. FARMER. Can. J. Chem. **34**, 345 (1956).
42. D. M. GOLDEN and S. W. BENSON. Chem. Rev. **69**, 125 (1969).
43. D. M. GOLDEN, A. S. RODGERS, and S. W. BENSON. J. Am. Chem. Soc. **88**, 3196 (1966).
44. M. J. S. DEWAR and S. D. WORLEY. J. Chem. Phys. **50**, 654 (1969).
45. K. WATANABE, T. NAKAYAMA, and J. MOTTL. J. Quant. Spectro. Radiat. Transfer, **2**, 369 (1962).
46. D. FROST, F. G. HERRING, C. A. MCDOWELL, and I. A. STENHOUSE. Chem. Phys. Lett. **4**, 533 (1970).
47. P. BISCHOF and E. HEILBRONNER. Helv. Chem. Acta, **53**, 1677 (1970).
48. D. W. TURNER. Adv. Phys. Org. Chem. **4**, 31 (1966).
49. B. STEINER, C. F. GIESE, and M. G. INGHRAM. J. Chem. Phys. **34**, 189 (1961).
50. R. BRALSFORD, P. V. HARRIS, and W. C. PRICE. Proc. Roy. Soc. (London), **A 258**, 459 (1960).

Structure of Radicals Produced by γ-Radiolysis. Part 2. Radicals Derived from 5-Membered Alicyclic Molecules

RON E. LINDER AND A. CAMPBELL LING[1]

Department of Chemistry, West Virginia University, Morgantown, W.V. 26506

Received December 29, 1971[2]

Data are presented for the results of γ-radiolysis on cyclopentane, methyl cyclopentane, cyclopentene, and cyclopentadiene, held as solutes in adamantane matrices. Data from this particular matrix isolation technique are in accord with liquid phase studies for cyclopentane and cyclopentene, and indicate that tertiary hydrogen loss occurs in methyl cyclopentane, and that cyclopentadiene yields at least three radicals. Two of the radicals derived from cyclopentadiene have been identified as the C_5H_5· entity with five equivalent protons, and the allylic-type radical formed by hydrogen atom addition to molecular C_5H_6.

Les résultats de la radiolyse γ du cyclopentane, méthycyclopentane, cyclopentène, et cyclopentadiène, retenus comme solutés dans des matrices adamantane, sont présentés. Cette technique particulière d'isolement par matrice donne des résultats en accord avec ceux de la phase liquide pour le cyclopentane et cyclopentène, et montre que la perte de l'hydrogène tertiaire se produit dans le méthylcyclopentane tandis que le cyclopentadiène conduit au moins à trois radicaux. Parmi ceux ci deux ont été identifiés: c'est l'entité C_5H_5· avec cinq protons équivalents et le radical de type allylique formé par addition d'hydrogène atomique sur C_5H_6 moléculaire. [Traduit par le journal]

Canadian Journal of Chemistry, **50**, 3982 (1972)

Introduction

As part of an investigation involving radiolysis of five-membered heterocyclic molecules it was felt that data from equivalent alicyclic compounds would prove useful. Cyclopentane has been studied previously by Fessenden and Schuler (1) in the liquid phase using continuous flow radiolytic production techniques below room temperature and by Fischer (2) using chemical generation in the liquid phase. The major radical was shown to be that resulting from C—H bond cleavage with a structure that is either planar or rapidly inverting in a "chair–boat" vibration analogous to that undergone by cyclohexane. In this context, it is interesting to note that the cyclohexyl radical resulting from radiolysis of cyclohexane does *not* exhibit four equivalent protons at the β-position relative to the unpaired electron and cannot be planar (1). Ohnishi and Nitta (3) have shown that radiolysis of cyclopentadiene as a crystalline solid at 77 °K leads to the production of two different radicals, one of which was identified as the C_5H_5· radical with five equivalent protons, but the second radical could not be identified from the observed e.s.r. spectrum. Similarly, Kuri and co-workers (4) obtained a broad, and poorly resolved, e.s.r. spectra following radiolysis of cyclopentadiene at 77 °K and assigned it to two different radical species, one of which was probably the C_5H_5· radical. Pyrolysis experiments on ferrocene were shown to lead to the production of C_5H_5· radicals (5), although radiolysis and photolysis of metallocene solutes in glassy 2-methylpentane matrices at 77 °K gave no evidence for C_5H_5· radical production (6). However, photolysis of cyclopentadiene itself as a crystalline solid at 77 °K does lead to C_5H_5· generation, but no other radical (7). Analogously, photolysis of a dilute solution of hexachloro-cyclopentadiene in carbon tetrachloride in a flow system leads to the production of C_5Cl_5· radicals and no others (8). In contrast to these predominantly solid phase studies, Krusic and Kochi (9) studied the chemical generation of C_5H_5· from cyclopentadiene in the liquid state at low temperature. E.s.r. data for the γ-radiolysis of cyclopentene in adamantane has now been reported by Wan and co-worker (10).

[1]To whom correspondence should be addressed.

[2]Revision received July 18, 1972.

Can. J. Chem. Downloaded from www.nrcresearchpress.com by 210.87.254.40 on 09/05/12
For personal use only.

Can. J. Chem. Downloaded from www.nrcresearchpress.com by 210.87.254.40 on 09/05/12
For personal use only.

Experimental

Cyclopentane (CP), cyclopentene (CPE), methyl cyclopentane (MCP), cyclopentadiene dimer, and adamantane, were obtained from commercial sources in the purest grade available and used as received. Cyclopentadiene (CPDE) was prepared from its dimer by standard distillation procedures, collected at −78 °C, degassed, and stored at −78 °C on a vacuum line. Incorporation of CP, CPE, and MCP, into the adamantane matrix was done by multiple recrystallization of adamantane crystals from small aliquots (*ca.* 25 ml) of solvent (CP, CPE, and MCP, respectively), using fresh portions of the solvent each time (3–4 repetitions). Incorporation of CPDE into adamantane required a slightly different technique due to the risk of dimerization at room temperatures and above. Adamantane was recrystallized from methyl cyclohexane[3] to remove solvent impurities contained in the cavity on receipt from the vendor. It was transferred to a container on the vacuum line and degassed, using an ice-bath to restrict sublimation. Freshly prepared CPDE from its storage reservoir (at 195 °K) on the vacuum line was transferred to the adamantane vessel using liquid N_2 to condense the vapor and allowing the reservoir to warm to 273 °K. The container with adamantane was allowed to warm from 77 to 273 °K, thus permitting the adamantane to dissolve in the CPDE liquid. After 60 min the CPDE was transferred out of the adamantane container to a new vessel, and fresh CPDE transferred into the adamantane from the reservoir. Using standard vacuum line techniques and controlling the temperature with ice, Dry-Ice, and liquid N_2, the adamantane was thoroughly washed four to five times with CPDE monomer, where at no time was the temperature allowed to exceed 0 °C for liquid CPDE monomer, so curtailing dimer formation. All adamantane samples containing the requisite solute were dried in an oven at *ca.* 35–40 °C for 15 min, and then irradiated at room temperature in a Pyrex tube utilizing a ^{60}Co source (dose rate 3.5×10^{16} eV g^{-1} min^{-1} via Fricke solution dosimetry). Irradiated adamantane samples containing solute were transferred to quartz e.s.r. tubes and monitored at room temperature using a Varian E-3 e.s.r. spectrometer (typically; 0.5–50 mW power, 0.5–2.0 G modulation amplitude, 16 min scans at 3390 ± 100 G). Saturation effects were noted for radicals derived from CPDE as low as 10 mW, typical γ-doses were *ca.* 10^{18} eV g^{-1}, radical lifetimes varied widely but were all in excess of 2 h. Particularly for radicals derived from CPDE, serious degeneration of the low power spectrum was noted after only 90–120 min. Re-irradiation of the same adamantane sample invariably led to shorter lifetimes, more rapid degeneration, and poorer resolution, of the observed e.s.r. spectrum. Computer simulations of e.s.r. spectra were carried out by a modified program supplied by Quantum Chemistry Program Exchange[4] utilizing an IBM-360/75 computer system and Cal-Comp Plotter accessory.

[3]Recrystallization of adamantane from methyl cyclohexane followed by γ-radiolysis in the usual manner does not lead to any recognizable e.s.r. spectrum attributable to methyl cyclohexane itself. The only noted feature is a broad singlet, typical of polycrystalline e.s.r. studies, and characteristic of 1-adamantyl radicals, rather than of 2-adamantyl radicals which lead to distinctly different signals (11). It is interesting to note that sublimation techniques do *not* necessarily lead to adamantane samples free from impurities. A very characteristic e.s.r. spectrum is obtained by radiolysis of adamantane directly from samples supplied by the vendor. This characteristic spectrum persists even after sublimation, and is attributed to trapped solvent molecules used in the synthesis of adamantane originally.

Results and Discussion

Experimental spectrum, stick spectrum, and computer simulated spectrum for γ-irradiated MCP are shown in Fig. 1. Low power and high power e.s.r. spectra of γ-irradiated cyclopentadiene together with the spectrum obtained from γ-radiolysis of cyclopentene are shown in Fig. 2. Hyperfine coupling constants for the radicals studied are shown in Table 1. Resolution of spectra using adamantane as the trapping matrix is adequate for unambiguous assignments (line widths in the range 0.8–3.0 G), but line widths in general are inferior to those obtained in the liquid state (*e.g.*, 0.08 G (9), 0.5 G and less (1, 12).[5]

Cyclopentane and Cyclopentene

These data from the solid state at room temperature agree well with that previously recorded for low temperature liquid phase studies (see Table 1). In the case of CP, temperature dependent studies in adamantane matrices between 77 and 373 °K proved ambiguous, and did not resolve the question of whether the radical was planar or undergoing vibratory inversion through the ring center.

Methyl Cyclopentane

Data obtained are consistent with tertiary hydrogen loss as previously postulated for alkane molecules (13). The e.s.r. spectrum being assigned to a radical

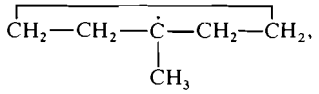

coupling constants are given in Table 1. Again,

[4]Quantum Chemistry Program Exchange, Indiana University, Bloomington, Indiana. Program originally written by C. S. Johnson and M. K. Ahn of Yale University, QCPE Catalog Number 83.

[5]R. W. Fessenden and R. H. Schuler (14) report isotropic spectra in SF_6 matrices with ^{19}F line widths *ca.* 2G.

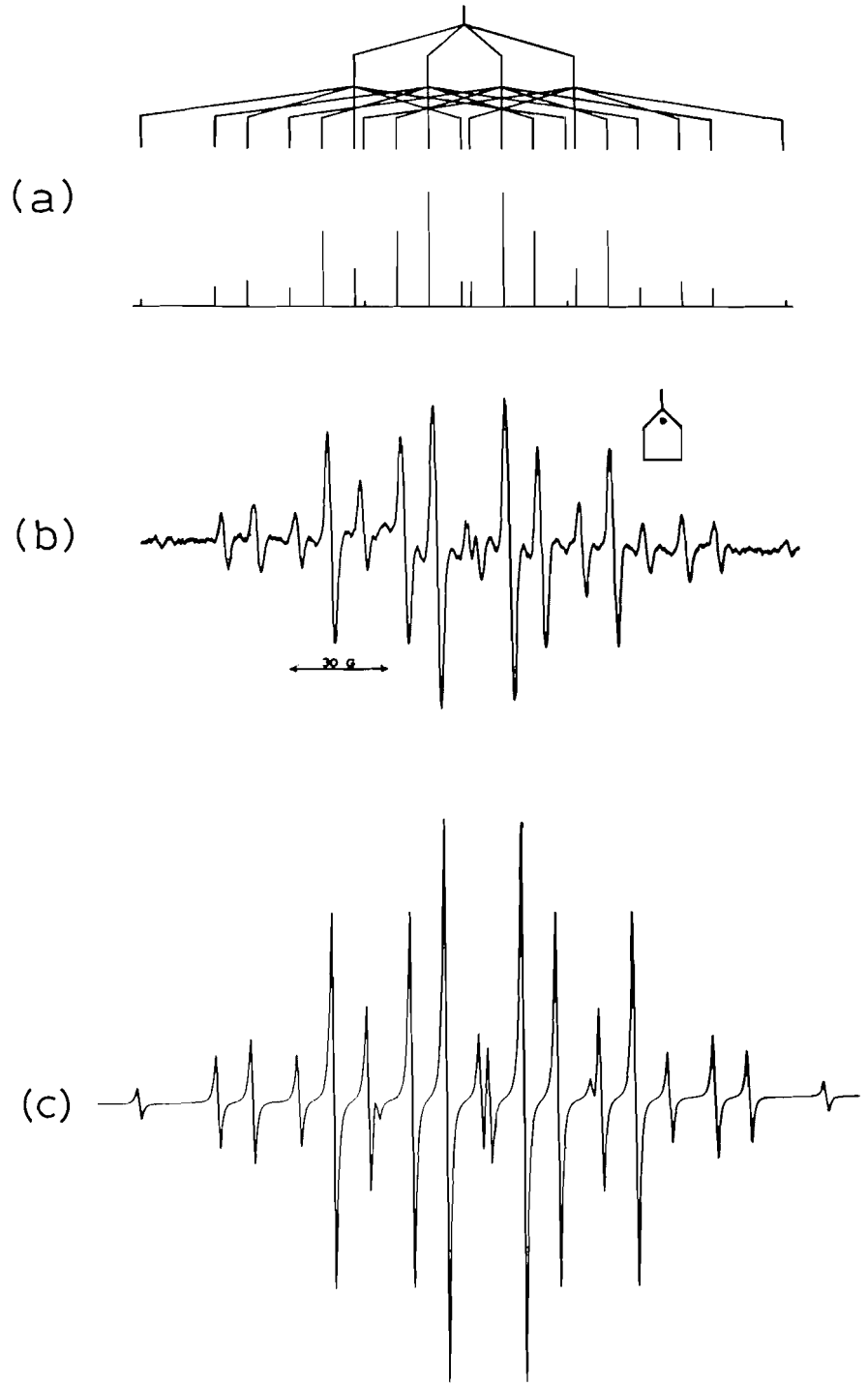

FIG. 1. Stick spectrum: (*a*), experimentally observed spectrum; (*b*), computer simulated spectrum; (*c*), for γ-irradiated methyl cyclopentane in an adamantane matrix at room temperature.

Can. J. Chem. Downloaded from www.nrcresearchpress.com by 210.87.254.40 on 09/05/12
For personal use only.

Can. J. Chem. Downloaded from www.nrcresearchpress.com by 210.87.254.40 on 09/05/12
For personal use only.

temperature dependent studies were unable to answer the question as to whether the radical is planar, or rapidly inverting at room temperature.

Cyclopentadiene

The experimental data are given in Table 1 and in Fig. 2. Power saturation experiments demonstrated that above approximately 20 mW, the e.s.r. spectrum of one radical could be enhanced significantly at the expense of others. The spectrum obtained at 32 mW is shown in Fig. 2*a*, and exhibits a well defined sextet with intensities close to the theoretical 1:5:10:10:5:1 required for five equivalent protons, and a coupling constant of 6.1 ± 0.1 G. The significant features of the underlying spectrum, both at high power and low power, are matching sets of doublets to the outside of the sextet. This is characteristic of the spectrum obtained from the radiolysis of cyclopentene, as demonstrated by the published spectrum of Wan and co-worker (10) and the experimentally obtained spectra in this work (displayed in Fig. 2*c*). Comparison on a peak-by-peak basis, via direct overlay of one spectrum on top of the other, shows complete agreement between the cyclopentenyl spectrum and the peaks in the low-power observed spectrum from cyclopentadiene. However, this low-power spectrum displays more peaks than can be accounted for by the sum of the cyclopentadienyl spectrum and the cyclopentenyl spectrum. There are, therefore, *at least* three radicals produced by γ-radiolysis of cyclopentadiene in adamantane matrices. Both of these observed and assigned radicals can be accounted for simply; the cyclopentadienyl radical $C_5H_5\cdot$ by loss of a hydrogen atom from the $-CH_2-$ group in the five-membered ring, and the cyclopentenyl allylic structure

by addition of a hydrogen atom to a molecule of cyclopentadiene at one of the double bonds (as shown in the scheme below).

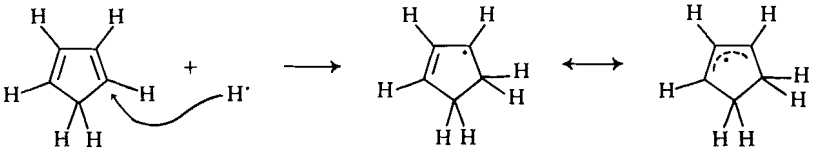

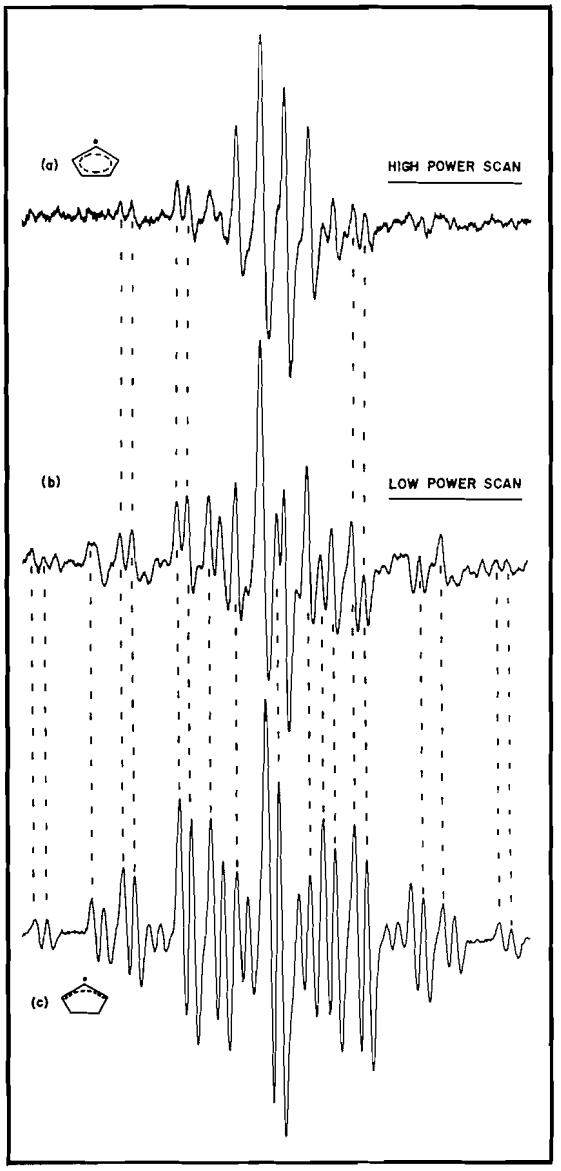

FIG. 2. Experimental e.s.r. spectra for γ-irradiated cyclopentadiene and cyclopentene in adamantane matrices at room temperature: (*a*) high power spectrum of cyclopentadiene (32 mW); (*b*) low power spectrum of cyclopentadiene (2 mW); (*c*) spectrum of the allylic-type radical derived from cyclopentene in adamantane (2 mW).

TABLE 1. E.s.r. coupling constants for radicals derived from 5-membered alicyclic molecules

Radical	Coupling constants observed*† (G)		Coupling constants reported (G)		Reference
	$a_\alpha = 22.5$	$a_\beta = 34.0$	$a_\alpha = 21.48$ 21.05	$a_\beta = 35.16$ 34.86	1 2
	$\alpha_{CH_3} = 23.0$	$\alpha_\beta = 33.0$			
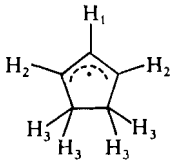	$a_1 = 3.0$ $a_2 = 21.5$	$a_3 = 14.0$	$a_1 = 3.1$ $a_2 = 21.6$	$a_3 = 14.0$	10
	$a = 6.1$‡		$a = 5.61$ $a = 5.98$ $a = 6.2$‡ $a = 6.04$		3 5 7 9

*9 GHz instrument.
†±0.2 G.
‡±0.1 G.

It is tempting to assign the third radical to the structure $\overset{\cdot}{C}H_2—CH_2—CH—CH_2—CH_2$ (*i.e.*, the cyclopentyl radical) corresponding to hydrogen atom addition at the other end of the double bond, but there are insufficient data from the e.s.r. spectrum to support this hypothesis. Hydrogen atom addition to alkenes in conventional matrices is well documented, and Wan[6] reports that γ-radiolysis of cyclooctatetraene in adamantane leads to two radicals, one of which can be explained by hydrogen atom addition to one of the double bonds in this molecule. Finally, in an attempt to elucidate further the mode of decay of adamantane isolated species, the rate of decay of the sextet attributed to the $C_5H_5\cdot$ radical was determined over a period of 110 h at room temperature. Radical concentrations, as measured by the height of the high-field central line of the sextet, were determined for fourteen different times between 0 and 110 h. Plots of concentration against time (correlation coefficient 0.979_2), log (concentration) against time (correlation coefficient 0.980_2), and concentration^{-1} against time (correlation coefficient 0.979_2), were all reasonably linear, with a half-life for the radical species of *ca.* 142 h at room temperatures. It is not possible, therefore, to draw any meaningful conclusions concerning the order of the kinetic rate, since data spanned less than one half-life for the process.

[6]Private communication from J.K.S. Wan of Queen's University, Kingston, Ontario.

One of us (R.E.L.) thanks the National Aeronautics and Space Administration for a pre-doctoral fellowship; we thank the Research Corporation of New York for partial support of this work, the Chemical Engineering Department of this University for use of their facilities, and Professor J. K. S. Wan of Queen's University, Kingston, Ontario, for a chance to read a preprint of his concerning the radiolysis of cyclooctatetraene in adamantane matrices.

1. R. W. FESSENDEN and R. H. SCHULER. J. Chem. Phys. **39**, 2147 (1963).
2. H. FISCHER. J. Phys. Chem. **73**, 3834 (1969).
3. S. -I. OHNISHI and I. NITTA. J. Chem. Phys. **39**, 2848 (1963).
4. S. ARAI, S. SHIDA, Y. YAMAGUCHI, and Z. KURI. J. Chem. Phys. **37**, 1885 (1962).

Can. J. Chem. Downloaded from www.nrcresearchpress.com by 210.87.254.40 on 09/05/12
For personal use only.

5. P. J. ZANDSTRA. J. Chem. Phys. **40**, 612 (1964).
6. A. CAMPBELL LING. J. Inorg. Nucl. Chem. **34**, 2978 (1972).
7. G. R. LIEBLING and H. M. MCCONNELL. J. Chem. Phys. **42**, 3931 (1965).
8. F. GRAF and Hs. H. GUNTHARD. Chem. Phys. Lett. **7**, 25 (1970).
9. P. J. KRUSIC and J. K. KOCHI. J. Am. Chem. Soc. **90**, 7155 (1968).
10. D. R. GEE and J. K. S. WAN. Can. J. Chem. **49**, 20 (1971).
11. G. J. HYFANTIS and A. CAMPBELL LING. To be published.
12. R. W. FESSENDEN and S. OGAWA. J. Am. Chem. Soc. **86**, 3591 (1964).
13. S. W. KANICK, R. E. LINDER, and A. CAMPBELL LING. J. Chem. Soc. (A), 2971 (1971).
14. R. W. FESSENDEN and R. H. SCHULER. J. Chem. Phys. **45**, 1845 (1966).

Can. J. Chem. Downloaded from www.nrcresearchpress.com by 210.87.254.40 on 09/05/12
For personal use only.

Adduct Intermediates in the Side-chain Nitration of 1,4-Dimethylnaphthalene

ALFRED FISCHER AND ALAN LESLIE WILKINSON
Department of Chemistry, University of Victoria, Victoria, British Columbia

Received June 5, 1972

cis and *trans* isomers of 1,4-dimethyl-4-nitro-1,4-dihydro-1-naphthyl acetate (**1**) have been isolated from a mixture of 1,4-dimethylnaphthalene and nitric acid in acetic anhydride by quenching at −40°. At room temperature only 1-methyl-4-nitromethylnaphthalene (**4**) is obtained. The conversion of 1,4-dimethylnaphthalene to **4** and of the *cis* (**1***a*) and *trans* (**1***b*) adducts to **4**, by nitric acid in acetic anhydride, has been followed by n.m.r. 1,4-Dimethyl-4-nitro-1,4-dihydro-1-naphthyl nitrate (**5**) appears to be the immediate product from nitration of 1,4-dimethylnaphthalene in acetic anhydride, methylene chloride, or nitromethane. In acetic anhydride **5** is converted into **1**. Decomposition of **1** in acetic acid gives 1,4-dimethyl-2-naphthyl acetate and some **4**. The formation of **4** in this reaction is suppressed by urea.

Les isomères *cis* et *trans* de l'acétate de diméthyl-1,4 nitro-4 dihydro-1,4 naphtyl-1 (**1**) ont été isolés d'un mélange de diméthyl-1,4 naphtalène et d'acide nitrique dans l'anhydride acétique, après trempage à −40°. A la température ambiante, seul le méthyl-1 nitrométhyl-4 naphtalène (**4**) est obtenu. La conversion par l'acide nitrique dans l'anhydride acétique, du diméthyl-1,4 naphtalène en **4** et des adduits *cis* (**1***a*) et *trans* (**1***b*) en **4**, a été suivie par r.m.n. Le nitrate de diméthyl-1,4 nitro-4 dihydro-1,4 naphtyl-1 (**5**) apparait être le produit immédiat lors de la nitration du diméthyl-1,4 naphtalène dans l'anhydride acétique, chlorure de méthylène ou nitrométhane. Dans l'anhydride acétique, **5** est transformé en **1**. La décomposition de **1** dans l'acide acétique donne l'acétate de diméthyl-1,4 naphtyl-2 et un peu de **4**. La formation de **4** dans cette réaction est supprimée par l'urée. [Traduit par le journal]

Canadian Journal of Chemistry, **50**, 3988 (1972)

Can. J. Chem. Downloaded from www.nrcresearchpress.com by 210.87.254.105 on 09/05/12
For personal use only.

Introduction

There are a number of reported cases of abnormal electrophilic substitution reactions in which substitution occurs in the side-chain of alkyl derivatives of aromatic and heteroaromatic compounds. For example, hexamethylbenzene gives pentamethylbenzyl halide on halogenation under electrophilic conditions (1) and 2,3-dimethylbenzothiophene gives the 2-nitromethyl derivative on reaction with nitric acid in acetic anhydride (2). It seems likely, and has been well established in at least some of the examples (3), that these reactions involve as the first step the normal nuclear electrophilic attack to generate the expected σ-complex (phenonium ion). However, the mechanism by which the σ-complex is converted into the side-chain substitution product has not been established in any of the examples, although almost every report of this type of abnormal substitution includes a speculative mechanism. Formation of 1-methyl-4-nitromethylnaphthalene on nitration of 1,4-dimethylnaphthalene is clearly an example of this type of abnormal substitution.

Nitration of 1,4-dimethylnaphthalene in acetic anhydride, nitromethane, aqueous suspension (4), and in methylene chloride (5) gives 1-methyl-4-nitromethylnaphthalene (**4**). Davies and Warren (6) isolated a pale yellow crystalline substance, m.p. 47–48°, when nitration was carried out in acetic anhydride at −10° using equimolar amounts of nitric acid and 1,4-dimethylnaphthalene. They suggested on the basis of its u.v. spectrum that this compound was 1,4-dimethyl-5-nitronaphthalene, and that it was an intermediate in the formation of **4**. Subsequently Robinson (7) pointed to the absence of the 310–350 nm band expected for a nitronaphthalene in the u.v. spectrum of the yellow substance, and he suggested that it had structure **2**. He also suggested the mechanism outlined in Scheme 1 for the conversion of 1,4-dimethylnaphthalene into **4**. Formation of acetyl nitrate adducts, of which **1** is an example, has been observed from a variety of aromatic compounds on reaction with nitric acid in acetic anhydride (8). In particular, the formation has been reported (8*d*), of 1,4-adducts from some tetracyclic naphthalene derivatives, which are closely related to **1**. However, none of the intermediates, including **1**, depicted in Scheme 1 have been isolated and characterized. Indeed, considering the ambiguity as to the structure of Davies and Warren's yellow compound, none

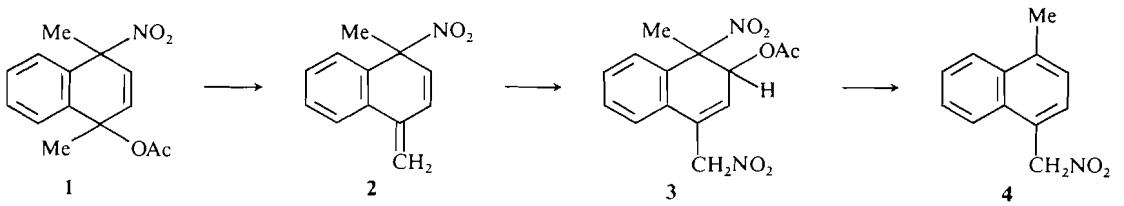

1
a *cis*
b *trans*

2 3 4

SCHEME 1

of the intermediates in Scheme 1 can be properly claimed to have been detected. We now report the investigation of the reaction between nitric acid and 1,4-dimethylnaphthalene in acetic anhydride at −40°, and the detection and isolation of a pair of diastereoisomeric adducts corresponding to structure **1**.

Results and Discussion

Nitration in acetic anhydride of 1,4-dimethylnaphthalene, both at room temperature and at −40°, with the product being isolated by extraction after pouring the reaction mixture onto ice, gave only 1-methyl-4-nitromethylnaphthalene. However, when nitration was carried out at −40° and the reaction mixture was quenched with ammonia at that temperature the diastereoisomeric adducts **1***a* and *b* were formed as the major reaction products, together with **4** and small amounts of 1,4-dimethyl-2-nitronaphthalene and other substances. The diastereoisomers **1***a* and *b* were separated from each other and from the other constituents of the product mixture by low temperature chromatography on alumina.

The structures of the adducts were unambiguously established by their spectra. The presence of the nitro and acetoxy groups was revealed by the i.r. spectra and supported by the mass spectra. The loss of the low field α-naphthyl proton n.m.r. absorption, and the appearance of the E_2 and B bands in the u.v. spectrum in the regions characteristic of the benzenoid system rather than at the longer wavelengths characteristic of a naphthalenic system, is consistent with adduct formation. The n.m.r. spectra also showed that the adducts each contain four aromatic protons and two vinylic protons. It follows that addition must have occurred to the disubstituted rather than the unsubstituted ring. The two vinylic protons exhibited a 10 Hz coupling and must therefore be *cis* and adjacent as in structure **1**.

The *cis* configuration was assigned to **1***a* and the *trans* to **1***b* on the basis of their dipole moments which are 3.54 and 3.79 D, respectively. The difference between the two moments is small but, since the measurements were made under the same conditions and the compounds are of close structural similarity, the conclusion that **1***b* has a larger dipole moment than **1***a* should be valid. The calculated moments are 3.34 (*cis*) and 4.10 (*trans*), for a planar cyclohexadiene ring, and 3.43 (*cis*) and 3.82 (*trans*), for a boat cyclohexadiene ring with equal populations of the two conformations of each isomer. The isomer of lower measured dipole moment was thus assigned the *cis* configuration.

Both **1***a* and *b* decomposed slowly ($t_{\frac{1}{2}} \simeq 45$ min) in acetic acid at 30° and gave as the main product 1,4-dimethyl-2-naphthyl acetate and a lesser amount of the side-chain nitration product **4**. In the presence of urea the formation of **4**, from **1***b*,[1] was completely suppressed and only the acetate was formed, the rate of decomposition being unaffected.

Isolation of **1***a* and *b* allowed a systematic study of the reaction of each with nitric acid in acetic anhydride and made it possible to interpret the behavior of 1,4-dimethylnaphthalene. At −60° 1,4-dimethylnaphthalene was converted into a species which absorbed in the vinylic region and which, like **1**, exhibited a 10 Hz coupling between the vinyl protons and did not absorb in the α-naphthyl proton region. This species was neither **1***a* nor *b*, since both the vinyl protons and the aromatic protons absorbed at lower fields than in either of these

[1]The effect of urea was not investigated in the case of **1***a*. In the absence of urea, **1***a* gives only 15% of **4** whereas **1***b* gives 35% of **4**.

Can. J. Chem. Downloaded from www.nrcresearchpress.com by 210.87.254.105 on 09/05/12
For personal use only.

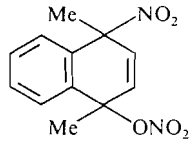

5

adducts. The general similarity of the spectra indicates that it was an adduct similar in structure to **1***a* and *b* and we suggest that it was the nitronium nitrate adduct **5**. At −40° the adducts **1***a* and *b* appeared, their olefinic protons absorbing at higher fields but with the same 10 Hz coupling. At −10° the olefinic peaks of **1***a* and *b* declined and were eventually replaced by the methylene peak of the nitromethyl compound **4**. Simultaneously the low field absorption of the α-naphthyl protons of **4** appeared. At 25° the only prominent peaks were those of **4**.[2] Smaller amounts of other unidentified components were formed at various times but at no stage were there any major peaks observed which could be attributed to the exocyclic diene **2** postulated by Robinson (7). This does not rule out the possibility of **2** being an essential intermediate in the reaction but does imply that if **2** is formed it is more reactive than other intermediates in the sequence.

Both **1***a* and *b* interconverted and formed the species assumed to be the nitronium nitrate addition compound **5** when reacted with nitric acid in acetic anhydride at −30°. The conversion of either isomer to **5** was more rapid than the interconversion of the isomers and **1***b* reacted more rapidly than **1***a*. In both cases an equilibrium concentration ratio of **1***a*:**1***b* = 3.5:1 was reached.

The reaction between 1,4-dimethylnaphthalene and nitric acid in the absence of acetic anhydride was investigated in deuterated methylene chloride and deuterated nitromethane. In methylene chloride the characteristic vinylic AB pattern ($J = 10$ Hz) appeared when the temperature was raised to −40°, and it is presumed the diastereoisomeric nitronium nitrate adducts **5** formed. The aliphatic methyl groups, which in acetic anhydride were obscured by the anhydride methyl proton peak, were observed. The isomeric ratio indicated by these was 6:1. At −20° the adducts began to be converted to the nitromethyl compound **4** and another unidentified transient species. At 25° **4** remained as the major reaction product. Similar behavior was observed in nitromethane.[3]

It is clear that the acetyl nitrate adducts **1** are formed during the side-chain nitration of 1,4-dimethylnaphthalene. It is not possible to demonstrate that these are necessary intermediates since they are in equilibrium with the initially formed nitronium nitrate adducts and it may be the latter that are converted directly to the next intermediate in the sequence rather than the former. Formation of **4** as the minor constitutent of the product when decomposition of the adducts **1***a* and *b* was carried out in acetic acid suggests that the shift of the nitro group from the ring to the side-chain is an intermolecular process. The higher yields of **4** obtained when decomposition occurred in the original nitrating mixture are attributed to the greater amount of nitric acid present (as acetyl nitrate) which can compete more effectively, for the precursor to **4**, with the process leading to the naphthyl acetate.[4] Further support for the conclusion that the **1** → **4** process is intermolecular is provided by the observation that urea suppressed the formation of **4** from the decomposition of **1***b*, presumably because the urea competed effectively for the released nitric acid.

Decomposition of the acetyl nitrate adducts from *o*-xylene (8*a*), 1,2,3-trimethylbenzene (8*b*), indane (8*c*), and tetralin (8*d*), occurs by loss of nitrous acid and leads to the appropriate aryl acetate. Decomposition of the *p*-xylene adduct (8*b*) gives, via loss of nitrous acid and an intramolecular rearrangement, 1,4-dimethyl-2-phenyl acetate. The acetate group must migrate in order for the ring to rearomatize. In the case of the adduct of 1,4-dimethylnaphthalene rearomatiz-

[2]Normally the nitric acid was in excess of the hydrocarbon but some runs were made using excess hydrocarbon and **4** was again the predominant product.

[3]Suzuki and Nakamura (5) have investigated the nitration of 1,4-dimethylnaphthalene in methylene chloride. They claim to have observed addition products but do not give the structure of these. They include **5** as an intermediate in a proposed sequence for the formation of 1-methyl-4-nitromethylnaphthalene. Their suggested mechanism is essentially analogous to Robinson's mechanism (Scheme 1).

[4]No naphthyl acetate was isolated from the nitration reaction in acetic anhydride carried out under conditions under which the adducts decomposed. As indicated, the amount of naphthyl acetate which would form under the conditions would not be large and any which did form would react further with the excess nitric acid present.

Can. J. Chem. Downloaded from www.nrcresearchpress.com by 210.87.254.105 on 09/05/12
For personal use only.

Can. J. Chem. Downloaded from www.nrcresearchpress.com by 210.87.254.105 on 09/05/12
For personal use only.

ation occurs in two ways: loss of nitrous acid and (probably intramolecular) migration of the acetoxy group to give the naphthyl acetate and loss of acetic acid and (intermolecular) migration of the nitro group to give **4**.

Experimental

U.v. spectra were determined on a Unicam SP 700 spectrometer. I.r. spectra were determined on a Beckman IR 20 spectrometer calibrated with polystyrene. N.m.r. spectra were determined on Varian HA-60-IL, and Perkin–Elmer R12A spectrometers with tetramethylsilane as internal standard unless specified otherwise. Mass spectra were determined on a Perkin–Elmer Hitachi RMU-7 spectrometer. Molecular weights were determined in methylene dibromide using a Perkin–Elmer Hitachi Model 115 molecular weight apparatus. Micro-analyses were by Mr. M. Yang, Simon Fraser University, Burnaby, B.C. Melting points are uncorrected. Nitric acid was purified by distilling fuming acid (300 cm^3) at 1 mm from urea (10 g) and sulfuric acid (500 cm^2). Alumina was deactivated with 3% of 10% acetic acid.

Nitration of 1,4-Dimethylnaphthalene in Acetic Anhydride

A cold solution of nitric acid (11 g, 0.26 mol) in acetic anhydride (55 cm^3) was added slowly with stirring to a solution of 1,4-dimethylnaphthalene (20 g, 0.13 mol) in acetic anhydride (25 cm^3) cooled in solid carbon dioxide–acetone. The mixture was allowed to warm to −40° and maintained at that temperature for 30 min. It was then cooled in solid carbon dioxide–acetone, ether (100 cm^3) was added, and ammonia condensed into the solution. Excess ammonia was removed with an aspirator, more ether added, and the mixture poured onto ice. The combined etheral layer and ether extract of the aqueous layer was dried over magnesium sulfate and the ether subsequently evaporated at 14°. The n.m.r. spectrum of the residue (18.2 g) indicated that 30% of the starting material had been reacted, the product consisting mainly of acetyl nitrate adduct with some side-chain nitro compound and considerably smaller amounts of other compounds. Chromatography on alumina at −40° and elution with ether–pentane mixtures gave **1***a* (1.8 g) in the 75% ether fraction and a mixture (3.2 g) of **1***a* and *b* in the 100% ether fraction. Recrystallization of the residue of the 75% ether fraction from ether–pentane gave *cis-1,4-dimethyl-4-nitro-1,4-dihydro-1-naphthyl acetate* (**1***a*), m.p. 61–62°, u.v. (95% ethyl alcohol) 219 (ε 610), 262 nm (shoulder, ε 119 m^2 mol^{-1}); i.r. (Nujol) 1738 and 1239 ($OCOCH_3$), 1538 and 1344 cm^{-1} (NO_2); n.m.r. ($CDCl_3$) τ 8.31 (s, 3, 1-CH_3), 8.04 (s, 3, $OCOCH_3$), 7.93 (s, 3, 4-CH_3), 4.03 (nq, 1, J = 10.3 Hz, 2-*H*), 3.80 (nq, 1, J = 10.3 Hz, 3-*H*), 2.58 p.p.m. (m, 4, C_6H_4); mass spectrum (70 eV) *m/e* (relative intensity) 215.109 (5, $M - NO_2$: $^{12}C_{14}{}^1H_{15}{}^{16}O_2$ requires 215.107), 214 (15), 201.076 (10, $M - CH_3CO_2H$: $^{12}C_{12}{}^1H_{11}{}^{14}N^{16}O_2$ requires 201.079), 184 (7), 173 (72), 172 (82), 157 (47), 156 (100), 155 (95), 141 (90).

Anal. Calcd. for $C_{14}H_{15}NO_4$ (M_r 261): C, 64.36; H, 5.79. Found (262): C, 64.41; H, 5.79.

Chromatography of the residue from the 100% ether fraction and recrystallization of the residue of the new 100% ether fraction gave *trans-1,4-dimethyl-4-nitro-1,4-dihydro-1-naphthyl acetate* (**1***b*), m.p. 91–92°; i.r. (Nujol) 1748 and 1231 ($OCOCH_3$), 1542 and 1344 cm^{-1} (NO_2); n.m.r. ($CDCl_3$) τ 8.39 (s, 3, 1-CH_3), 8.05 (s, 3, 4-CH_3), 7.99 (s, 3, $OCOCH_3$), 3.89 (nq, 1, J = 10.3 Hz, 2-*H*), 3.66 (nq, 1, J = 10.3 Hz, 3-*H*), 2.57 p.p.m. (m, 4, C_6H_4); *m/e* 215.111 ($M - NO_2$: $^{12}C_{14}{}^1H_{15}{}^{16}O_2$ requires 215.107).

Anal. Calcd. for $C_{14}H_{15}NO_4$ (M_r 261): C, 64.36; H, 5.79; N, 5.36. Found (266): C, 64.18; H, 5.98; N, 5.18.

The residue from the 25% ether fraction of the original column gave an unknown compound, m.p. 43°, which decomposed before identification. The decomposition product was also present in the 10% ether fraction and these were combined and chromatographed. The residue of the fraction eluted with 8% ether–pentane from this new column was a mixture of two nitronaphthalenes in a 5:1 ratio. *1,4-Dimethyl-2-nitronaphthalene*, the major component, was crystallized and had m.p. 67–68°; i.r. (CCl_4) 1538 (NO_2), 1369, 1351, 887, 873 cm^{-1}; n.m.r. (CCl_4) τ 7.35 (s, 3, 4-CH_3), 7.29 (s, 3, 1-CH_3) 2.52 (s, 1, 3-*H*), 2.50 (m, 2, 6-*H* and 7-*H*), 2.01 p.p.m. (m, 2, 5-*H* and 8-*H*); mass spectrum (70 eV) *m/e* (relative intensity) 201.081 (100, M_r ($^{12}C_{12}{}^1H_{11}{}^{14}N^{16}O_2$) = 201.079), 184 (97), 171 (22, M − NO), 156 (84), 129 (81), metastable peaks were observed at 168.5, 132.3, and 106.7 corresponding to the successive losses of OH, CO, and HCN in the sequence 201 → 184 → 156 → 129 and confirm the presence of adjacent nitro and methyl groups (9). The sixth fraction of this column gave *1,4-dimethyl-2,3-dinitronaphthalene*, m.p. 260°; i.r. (Nujol), 1540 (NO_2), 1361, 1331, 861, 760, 735 cm^{-1}; n.m.r. ($CDCl_3$) τ 7.30 (s, 6, 1-CH_3 and 4-CH_3); 2.15 (m, 2, 6-*H* and 7-*H*), 1.90 (m, 2, 5-*H* and 8-*H*); mass spectrum (70 eV) *m/e* (relative intensity) 246 (100, M_r ($^{12}C_{12}{}^1H_{10}{}^{14}N_2{}^{16}O_4$) = 246), 229 (41, M − OH), 201 (18), 199 (22, $M - HNO_2$), 198 (21), 155 (26), 154 (44, $M - (NO_2)_2$), 153 (50), 152 (41), metastable peak at 213.2 for 246 → 229 (loss of OH). The highly symmetric n.m.r. spectrum is consistent with the 2,3-dinitro isomer rather than with any other dinitro 1,4-dimethylnaphthalene.

When the initial reaction mixture was worked-up by pouring it onto ice and extracting the product with carbon tetrachloride the only product isolated was 1-methyl-4-nitromethylnaphthalene, m.p. 105° (107° (4)); i.r. (CCl_4) 1561 (NO_2), 1368 cm^{-1}; n.m.r. ($CDCl_3$) τ 7.39 (s, 3, CH_3), 4.26 (s, 2, CH_2), 2.60 (m, 4, 2-*H*, 3-*H*, 6-*H*, 7-*H*), 2.08 (m, 2, 5-*H* and 8-*H*); mass spectrum (70 eV) *m/e* (relative intensity) 201 (3, M_r ($^{12}C_{12}{}^1H_{11}{}^{14}N^{16}O_2$) = 201), 156 (17), 155 (100, $M - NO_2$) 153 (9), 128 (6).

Attempts were made to isolate **1** by pumping the acetic anhydride off the reaction mixture at < −10° but in each case n.m.r. showed that the initially formed adduct **1** was converted into **4**.

Nuclear Magnetic Resonance Study of the Nitration of 1,4-Dimethylnaphthalene

A solution of the hydrocarbon (50 mg, 0.32 mmol) in acetic anhydride (0.13 cm^3) was put into an n.m.r. tube and frozen. A solution of nitric acid (29 mg, 0.46 mmol) in acetic anhydride (0.6 cm^3) was added to the cold tube and the tube placed in the probe of the spectrometer at −60°. The spectrometer was locked on the absorption peak of the acetic anhydride methyl group. The temperature of the probe was raised in 10° increments and the spectrum taken several times at each temperature. A similar procedure was used to investigate the reaction of the adducts **1***a* and *b* with nitric acid

TABLE 1. Measured and calculated dipole moment values

Compound	μ*	μ†	μ_{calcd}‡	μ_{calcd}§	μ_{calcd}‖
1*a*	3.54	3.46	3.34	3.43	3.52
1*b*	3.79	3.73	4.10	3.82	3.82

*Derived using Halverstadt and Kumler's formulae (11).
†Derived using Higasi's formula (12, 13).
‡Calculated assuming a planar hexadiene ring.
§Calculated assuming a boat hexadiene ring with equal populations of each conformer and free rotation about the C—O bond.
‖Calculated assuming a boat hexadiene ring with equal populations of each conformer and free rotation about the C—O bond in both *trans* conformers and in that *cis* conformer with an equatorial acetate group.

in acetic anhydride and also the nitration of 1,4-dimethylnaphthalene in methylene chloride-d_2 and nitromethane-d_3.

Decomposition of the Acetyl Nitrate Adducts of 1,4-Dimethylnaphthalene

Decomposition was followed by n.m.r. 1,4-Dimethyl-2-naphthyl acetate was isolated from the product mixture, m.p. 70–71°; i.r. (CCl_4) 1766 and 1208 ($OCOCH_3$) 1468, 1169, 1082 cm^{-1}; n.m.r. (CCl_4) τ 7.78 (s, 3, $OCOCH_3$), 7.66 (s, 3, 1-CH_3), 7.42 (s, 3, 4-CH_3), 3.18 (s, 1, 3-*H*), 2.68 (m, 2, 6-*H* and 7-*H*), 2.19 p.p.m. (m, 2, 5-*H* and 8-*H*); the methyl groups were assigned from the weak coupling to the 3-H which broadened the 4-CH_3, and to a smaller extent the 1-CH_3, singlets: the relative heights of the 4-CH_3, 1-CH_3, and acetate CH_3 singlets were 59:64:100. On irradiation of the 3-*H* the coupling was reduced and the 4-CH_3 and 1-CH_3 peak heights increased and became more nearly equal at 76:77:100; mass spectrum (70 eV) *m/e* (relative intensity) 214 (20, M_r ($^{12}C_{14}{}^{1}H_{14}{}^{16}O_2$) = 214), 173 (14), 172 (100), 157 (12), 128 (13), 43 (5). **1***a* gave 15% of **4** and 85% of the acetate. **1***b* gave 35% of **4** and 65% of the acetate.

Dipole Moment Measurements and Calculations

Measurements were made in benzene solution following the procedure described previously (8*c*). Dreiding models of the *cis* and *trans* adducts **1***a* and *b* suggest that there are two rigid boat forms which are interconvertible by a ring flip. However, the planar nature of the 1,4-cyclohexadiene ring seems to be well established (10). Dipole moments were calculated for both planar and boat forms and both sets of calculations predicted the *trans* isomer to have the larger moment. The calculations assume that (*i*) the group moment of the C—$OCOCH_3$ fragment is the same as the dipole moment of methyl acetate (1.70 D) with the moment orientated at 66° to the C—O bond with the negative end towards carbon, the acetoxy group is in the *s-trans* configuration and there is free rotation about the C—O bond; (*ii*) the group moment of the C—NO_2 fragment is the same as the dipole moment of nitromethane (3.01 D) directed along the C—N bond with the positive end towards carbon; (*iii*) contributions from the other groups to the overall dipole moment are negligible; (*iv*) the C—O and C—N bonds are coplanar; (*v*) the angle between 1,4-diaxial bonds in the boat forms is 10°; (*vi*) each pair of boat conformers is populated equally; (*vii*) in the planar forms the angle between the exterior pair of bonds at 1-C (and at 4-C) is 108°. Dipole moments are given in Table 1.

The assumption that there is free rotation about the C—O bond is likely to fail in the case of the *cis* diaxial boat form where in one orientation the diaxial $OCOCH_3$ and NO_2 groups would be brought into close proximity. Accordingly the calculations were repeated assuming that only that rotamer was allowed in which the $OCOCH_3$ group was remote from the NO_2 group. This raised the moment calculated for the *cis* form from 3.43 to 3.52 D but did not vitiate the conclusion that the *trans* form has the higher dipole moment.

We thank the National Research Council of Canada and the University of Victoria for financial support.

1. E. BACIOCCHI and G. ILLUMINATI. Tetrahedron Lett. 637 (1962); E. BACIOCCHI and G. ILLUMINATI. Ric. Sci. Rend. 467 (1964).
2. L. J. ANDREWS and R. M. KEEFER. J. Am. Chem. Soc. **86**, 4158 (1964).
3. E. BACIOCCHI, A. CIANA, G. ILLUMINATI, and C. PASINI. J. Am. Chem. Soc. **87**, 3953 (1965).
4. R. ROBINSON and H. W. THOMPSON. J. Chem. Soc. 2015 (1932).
5. H. SUZUKI and K. NAKAMURA. Bull. Chem. Soc. Jap. **44**, 303 (1971).
6. A. DAVIES and K. D. WARREN. J. Chem. Soc. B 873 (1969).
7. R. ROBINSON. J. Chem. Soc. B 1289 (1970).
8. (*a*) D. J. BLACKSTOCK, A. FISCHER, K. E. RICHARDS, J. VAUGHAN, and G. J. WRIGHT. Chem. Commun. 641 (1970); (*b*) D. J. BLACKSTOCK, J. CRETNEY, A. FISCHER, M. P. HARTSHORN, K. E. RICHARDS, J. VAUGHAN, and G. J. WRIGHT. Tetrahedron Lett. 2793 (1970); (*c*) A. FISCHER, C. C. GREIG, D. R. A. LEONARD, and A. L. WILKINSON. Can. J. Chem. **50**, 2211 (1972); (*d*) A. FISCHER and D. R. A. LEONARD. Can. J. Chem. **50**, 3367 (1972).
9. H. BUDZIKIEWICZ, C. DJERASSI, and D. H. WILLIAMS. Mass Spectrom. Org. Compounds. Holden-Day Inc., San Francisco. 1967. p. 516.
10. E. W. GARBISCH, JR. and M. G. GRIFFIN. J. Am. Chem. Soc. **90**, 3590 (1968).
11. I. F. HALVERSTADT and W. D. KUMLER. J. Am. Chem. Soc. **64**, 2988 (1942).
12. K. HIGASI. Bull. Inst. Phys. Chem. Res. (Tokyo), **22**, 805 (1943).
13. B. KRISHNA and K. SRIVASTAVA. J. Chem. Phys. **32**, 663 (1960).

Can. J. Chem. Downloaded from www.nrcresearchpress.com by 210.87.254.105 on 09/05/12
For personal use only.

The Synthesis of 17β-(4(5)imidazolyl)-5α-androstane-3β,11β-diamine: a Water Soluble Steroid with a Potentially Catalytic Substituent

J. PETER GUTHRIE

Department of Chemistry, University of Western Ontario, London, Ontario

Received June 12, 1972

The title compound, **9**, has been synthesized in an eight-step process, starting with corticosterone (**1**). The Weidenhagen reaction on **1** converted the 17-$COCH_2OH$ to an imidazole. Reduction with lithium–ammonia–methanol gave 17β-(4(5)-imidazolyl)-5α-androstane-3β, 11β-diol (**3**) which could be selectively oxidized to the 3β-ol, 11-one, which was then converted to the oxime and hydrogenated to the 3β-ol, 11β-amine, **6**. Oxidation of the 3β-ol to the 3-one, oximation and sodium–propanol reduction gave **9**.

Le produit **9** a été synthétisé en huit étapes en partant de la corticostérone (**1**). La réaction de Weidenhagen sur **1** convertit le $COCH_2OH$-17 en un imidazole. La réduction par le lithium–ammoniac–methanol conduit à l'(imidazolyl-4(5))-17β 5α-androstane diol-3β,11β (**3**), qui peut être oxydée sélectivement en ol-3β one-11, cette dernière étant transformée ensuite en oxime puis hydrogénée en ol-3β amine-11β **6**. L'oxydation du ol-3β en one-3, l'oximation et la réduction par le sodium dans le propanol donnent **9**.

[Traduit par le journal]

Canadian Journal of Chemistry, **50**, 3993 (1972)

Can. J. Chem. Downloaded from www.nrcresearchpress.com by 210.87.254.40 on 09/05/12
For personal use only.

Introduction

There has been considerable interest (1–13) in the study of enzyme models which show both substrate binding and catalytic properties. Such compounds can provide information bearing on two questions of crucial importance to the development of a full understanding of enzymic catalysis: (*1*) the requirements for non-covalent binding of substrate from aqueous solution (14); (*2*) the orientational requirements for efficient catalysis (15–19). The latter question has traditionally been investigated using intramolecular systems (15, 20, 21), but suffers from the limitation that if the reaction is very rapid, the reactive form of the compound must be generated in solution; already cases are known where even stopped flow techniques are barely adequate to follow the kinetics of the intramolecular reaction (22). Thus it would be preferable to study questions of orientation by looking at reactions of two compounds held together in a non-covalent complex, provided that complex formation was favorable, so that reaction occurred only within the complex, *and* provided that complex formation was specific enough that one could be assured of the orientation of the two molecules within the complex. This should be attainable if one uses relatively large, rigid molecules.

As a step towards the goals outlined above, I wish to report the preparation of 17β-(4(5)-imidazolyl)-5α-androstane-3β,11β-diamine (**9**), which was designed to be water-soluble at p*H* below 10, by virtue of the two amino groups, and to have a quasi-equatorial imidazolyl group, which can act as a catalyst for the hydrolysis of active esters. The steroid nucleus provides a large rigid framework, and has the additional advantage that one can draw upon the immense body of synthetic chemistry performed on steroids. With two ionic substituents, micelle formation should not occur (23). The α surface of **9** is unhindered, and available for hydrophobic binding.

Discussion

The approach used for the preparation of **9** is outlined in Schemes 1 and 2. Corticosterone (**1**) was smoothly converted in excellent yield into 11β-hydroxy-17β-(4(5)-imidazolyl)-4-androsten-3-one (**2**) using a procedure based on the imidazole synthesis devised by Weidenhagen and co-workers (24). The stereochemistry at C-5 was established by reduction of **2** using lithium–ammonia–methanol, to give the diol **3**. This reduction is expected to give the 5α-isomer; the stereochemistry was proved unambiguously by comparison of the ^{13}C n.m.r. spectrum (25) of the corresponding dione **10** with the ^{13}C spectra of the known compounds 5α- and 5β-pregnane-3,11,20-trione. The signal from the 19-methyl carbon is strikingly dependent on the stereochemistry at C-5 (25).

Oxidation of the 11β-hydroxyl was expected

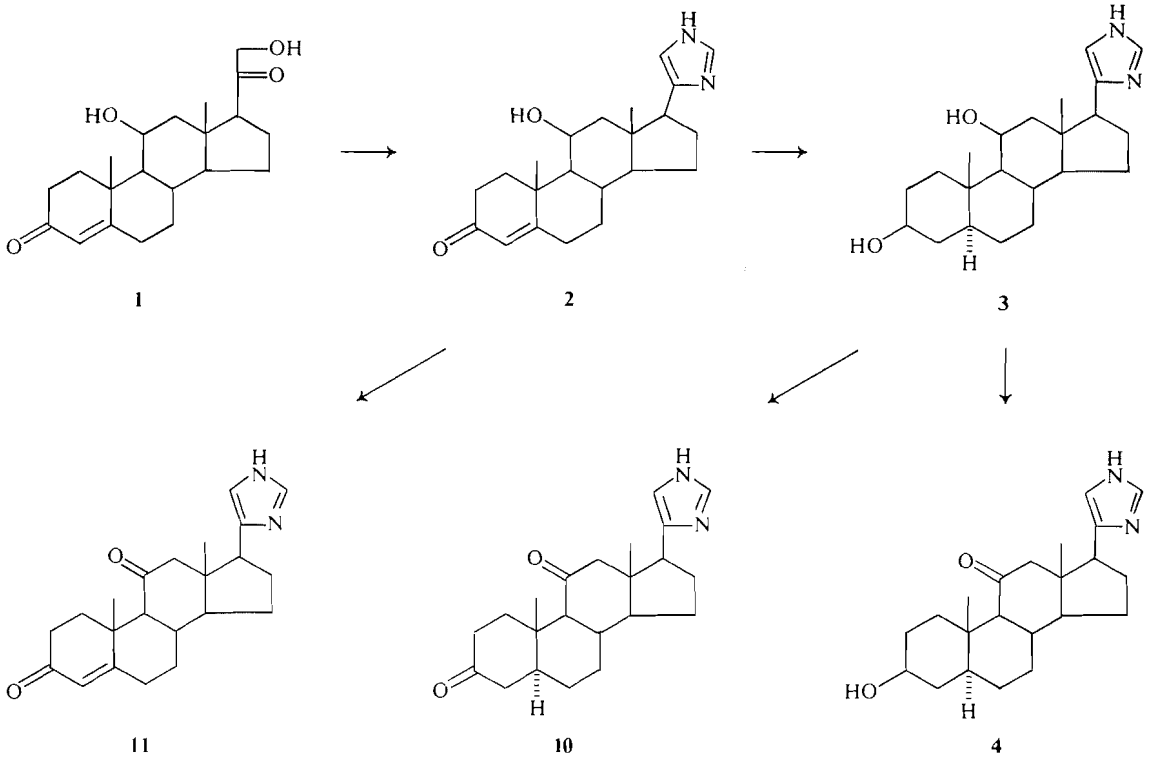

1 2 3 11 10 4

SCHEME 1

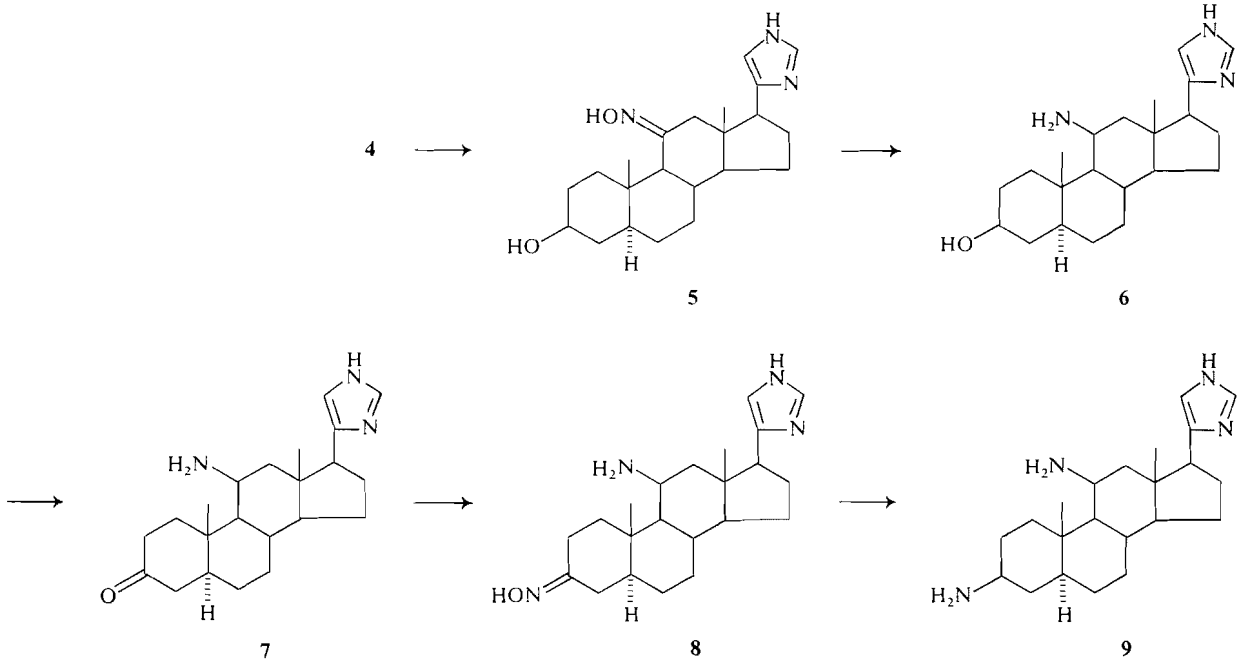

4 5 6 7 8 9

SCHEME 2

Can. J. Chem. Downloaded from www.nrcresearchpress.com by 210.87.254.40 on 09/05/12
For personal use only.

Can. J. Chem. Downloaded from www.nrcresearchpress.com by 210.87.254.40 on 09/05/12
For personal use only.

to be much faster than for the 3β-hydroxyl, on the basis of the kinetic studies of Rocek *et al.* (26). In fact, selective oxidation of **3** to **4** was readily achieved. Crude **4**, containing traces of **3** and **10** (t.l.c. analysis), was converted, via its oxime, **5**, to the 11β-amine by hydrogenation with PtO_2 in acetic acid. This hydrogenation proved to be very slow, requiring high pressure, prolonged reaction time, and large amounts of catalyst. However, the desired 11β-amino compound could be obtained in modest yield. Metal hydride reduction, which would also be expected to give the 11β-amine could not be employed because **5** was insoluble in solvents compatible with $LiAlH_4$. That the stereochemistry was indeed 11β is shown by the n.m.r. spectrum, since the methyne signal attributed to the hydrogen on C-11 has the width expected for an equatorial hydrogen.

Finally, the alcohol at C-3 was converted to an amino group, again by way of an oxime. However, since in this case the *equatorial* amine was desired, it was necessary to use sodium–propanol as the reducing agent. Ordinarily the sequence from **6** to **9** was carried out without purifying intermediates, and **9** was crystallized as the trishydrochloride. The n.m.r. spectrum showed a new signal at 3.20 δ, $\Delta\nu_{\frac{1}{2}} = 20$ Hz attributed to the C-3 proton with the width expected for the equatorial amino group.

The overall synthesis requires purifications at only three stages, **3**, **6**, and **9**. Further optimization is almost certainly possible; however the synthesis as reported here makes **9** available in gram quantities, by a route which gives complete control of stereochemistry. Compound **9** is indeed water soluble, to better than 0.1 *M*, at p*H* 8, where the imidazole group is free to act as a nucleophile.

Active esters of 3-(2-naphthyl)-propionic acid (**12**) and 3-(3-phenanthryl)-propionic acid (**13**) react more rapidly with **9** than with imidazole, and the rate enhancement is larger for derivatives of **13**, as would be expected, since the binding area is larger for **13**. Details of these studies of the catalytic properties of **9** will be published shortly.

Experimental

Materials and Methods

Mallinckrodt 2847 silicic acid was used for column chromatography and Camag silica gel was used for t.l.c. Proton n.m.r. spectra were recorded on a Varian HA100. ^{13}C n.m.r. spectra were recorded on a Varian XL100 with noise decoupling of protons; methyl groups were identified by recording off-resonance decoupled spectra. Imidazole-containing compounds were detected using diazotized sulfanilic acid (Pauly reagent (27)).

11-Hydroxy-17β-(4(5)-imidazolyl)-4-androsten-3-one (2)

Corticosterone (**1**) (Sigma Chemical Corp., m.p. 180–183°) (10 g, 28.9 mmol) was dissolved in 800 ml warm 95% ethanol; to this was added 50 ml formalin (Shawinigan, 37% CH_2O) and a solution of 12 g $Cu(OAc)_2 \cdot H_2O$ (60 mmol) in 30 ml water plus 174 ml concentrated ammonia. The solution was refluxed for 3 h, at which time the solution had turned from blue to green, and t.l.c. (80:20, $CHCl_3$:CH_3OH) showed that the reaction was over. The reaction mixture was allowed to cool and then worked-up by partitioning between saturated aqueous sodium chloride and ethyl acetate. The combined ethyl acetate extracts (total volume about 2 l) were dried over Na_2SO_4, and then evaporated to dryness. The residue was extracted with 46 ml of hot methanol, made alkaline with ammonia, and brought to saturation with water. The first crop was 5.44 g. The residue was extracted with methanol till no more Pauly positive material dissolved. These extracts and the crystallization mother liquors were pooled and evaporated. Similarly using 23 ml of hot methanol a second crop of 2.11 g was obtained. The process was repeated to give 1.89 g in the third crop. Total yield of crude product: 9.43 g (92%). Recrystallization from methanol–water (with a few drops of concentrated ammonia added) gave material of m.p. 177° (dec.); n.m.r. (as HCl salt) δ (D_2O), 0.76 (C-18 methyl), 1.37 (C-19 methyl), 4.30 ($\Delta\nu_{\frac{1}{2}} = 9$ Hz, C-11 methine), 5.58 (singlet, —C*H*=C), 7.14, 8.46 (C—H protons of the imidazolium ring).

Anal. Calcd. for $C_{22}H_{30}N_2O_2 \cdot CH_3OH$: C, 71.46; H, 8.86; N, 7.24. Found: C, 71.33; H, 8.78; N, 7.32.

17β-(4(5)-Imidazolyl)-5α-androstane-3β,11β diol (3)

A solution of **2** (9 g, 25.4 mmol) in 100 ml methanol was added to 1000 ml of liquid ammonia (giving a turbid suspension). To the stirred suspension was added in portions over 2 h, 15 g lithium metal. The solution was allowed to evaporate overnight under nitrogen. The residue was partitioned between ethyl acetate and saturated aqueous sodium chloride, and the combined ethyl acetate extracts were evaporated to dryness. The residue was dissolved in 250 ml of methanol, cooled, and filtered. Repeated concentration of filtrates led to further crops, giving a total of 4.9 g, 13.8 mmol, 54%. Chromatography of the mother liquors on silicic acid, and crystallization of fractions rich in **3** gave a further 0.583 g, making a total of 5.52 g or 61%. Recrystallization of **3** from methanol–water–ammonia gave material of m.p. 263.5–267.5°; n.m.r. (as HCl salt) δ (D_2O): 0.67 (C-18 methyl), 0.94 (C-19 methyl), 3.50 ($\Delta\nu_{\frac{1}{2}} = 21$ Hz, C-3 methine), 4.25 ($\Delta\nu_{\frac{1}{2}} = 8$ Hz, C-11 methine), 7.11, 8.40 (C—H protons of the imidazolium ring).

Anal. Calcd. for $C_{22}H_{34}N_2O_2$: C, 73.71; H, 9.55; N, 7.82. Found: C, 73.67; H, 9.45; N, 7.72.

3β-Hydroxy-17β-(4(5)-imidazolyl)-5α-androstan-11-one (4)

Crude **3**, (4.50 g, 12.5 mmol) was dissolved in a mixture of 23 ml water and 5.7 ml 6 *N* H_2SO_4. To this was added

Can. J. Chem. Downloaded from www.nrcresearchpress.com by 210.87.254.40 on 09/05/12
For personal use only.

225 ml glacial acetic acid. The solution was stirred in an ice bath and 4.3 ml of Jones reagent (2 *M* in CrO_3, 3.3 *M* in H_2SO_4) was added. After 10 min stirring, analytical t.l.c. (80:20 $CHCl_3$:CH_3OH) showed that only traces of starting material remained. Sodium acetate, 4.5 g, in methanol was added to neutralize the excess mineral acid, and the solution was evaporated to dryness. The residue was taken up in water, basified with 50 ml concentrated ammonia, and extracted with ethyl acetate. The extracts were washed with water and the aqueous wash solution was extracted with ethyl acetate. Evaporation of the combined ethyl acetate fractions gave 3.72 g of crude product (10.4 mmol, 84%). Recrystallization of **4** from methanol–water–ammonia gave material of m.p. 301–303°; n.m.r. (as HCl salt) δ (D_2O): 0.41 (C-18, methyl), 0.89 (C-19 methyl); 3.48 ($\Delta\nu_{\frac{1}{2}} = 25$ Hz, C-3 methine), 7.13, 8.40 (C—H protons of the imidazolium ring).

Anal. Calcd. for $C_{22}H_{32}N_2O_2$: C, 74.12; H, 9.05; N, 7.86. Found: C, 74.21; H, 8.88; N, 7.96.

*17β-(4(5)-Imidazolyl)-11-oximido-5α-androstan-3β-ol (**5**)*

Crude **4** (3.73 g, 10.5 mmol) and hydroxylamine hydrochloride, 3.7 g, in refluxing anhydrous pyridine, 25 ml, were allowed to react for 24 h. The reaction mixture was cooled, and poured into 50 ml of water; 1 *N* sodium hydroxide solution was added until the p*H* was 12. The resulting suspension was stirred until the product solidified to a fine powder, and then filtered; yield 3.64 g, 93%.

*11β-Amino-17β-(4(5)-imidazolyl)-5α-androstan-3β-ol (**6**)*

Crude **5**, 5.68 g, in glacial acetic acid, 100 ml, with 5.2 ml of 3 *N* HCl and 2.0 g PtO_2 was hydrogenated at 800 p.s.i. for 48 h. The hydrogenation was twice interrupted and 1.0 g PtO_2 and 2.6 ml 3 *N* HCl were added; after each addition hydrogenation was continued at 1800 p.s.i. for 48 h. After filtering off the catalyst, the solution was evaporated to dryness, taken up in methanol, and adsorbed into 10 g of silicic acid. This material was placed on a column of 60 g of silicic acid, poured in ether. The column was developed with 20% methanol in ether, then 20% 1 *M* ammonia in methanol – 80% ether, then 30% methanolic ammonia, then 40%, finally 100% 1 *M* ammonia in methanol. Elution was followed by t.l.c. Three major bands eluted: 2.50 g of a by-product of unknown constitution, 2.98 g of **6**, and 0.55 g of a more polar material. The n.m.r. of **6** (as HCl salt) δ (D_2O): 0.72 (C-18 methyl), 0.98 (C-19 methyl), 3.18 ($\Delta\nu_{\frac{1}{2}} = 18$ Hz, C-3 methine), 4.02 ($\Delta\nu_{\frac{1}{2}} = 10$ Hz, C-11 methine), 7.34, 8.64 (C—H protons of the imidazolium ring).

*11β-Amino-17β-(4(5)-imidazolyl)-5α-androstan-3-one (**7**)*

Chromatographically purified **6** (0.400 g) was dissolved in 40 ml 6 *N* H_2SO_4. To the stirred solution was added 0.35 ml Jones reagent. After 1 h, an analytical t.l.c. was run to check on the extent of reaction; an appropriate amount of Jones reagent was added and the process was repeated. Reaction was stopped when the ratio of 3-keto to 3-hydroxy-steroid was about 10:1 (attempting to carry the reaction to completion incurs excessive loss of material through over-oxidation). The solution was transferred to a separatory funnel, and basified by the addition of 25 ml of concentrated ammonia solution. Ice was added to cool the solution, which now showed the pink color of ammonia Cr(III) complexes. The solution was extracted four times with 100 ml portions of ethyl acetate; the organic layers were filtered and evaporated to dryness, giving 0.261 g, 67%. Compound **7** was converted to its hydrochloride salt and crystallized from methanol – *n*-propanol; n.m.r. (as HCl salt) δ (D_2O): 0.71 (C-18 methyl), 1.15 (C-19 methyl), 3.94 ($\Delta\nu_{\frac{1}{2}} = 11$ Hz, C-11 methine), 7.13, 8.34 (C—H protons of the imidazolium ring).

Anal. Calcd. for $C_{22}H_{35}N_3OCl_2 \cdot H_2O$: C, 59.18; H, 8.35; N, 9.41. Found: C, 58.87; H, 8.20; N, 9.31.

*17β-(4(5)-Imidazolyl)-3-oximido-5α-androstan-11β-amine (**8**)*

Crude **7** (0.742 g, 2.09 mmol) and 0.75 g of hydroxylamine hydrochloride in 7 ml dry pyridine were heated at *ca.* 90° for 1 h, cooled, poured into 21 g of ice, basified with sodium hydroxide (to p*H* 12), and extracted with ethyl acetate; yield, 0.707 g, 91%.

*17β-(4(5)-Imidazolyl)-5α-androstane-3β,11β-diamine (**9**)*

Crude **8**, 1.16 g, was dissolved in 140 ml refluxing *n*-propanol, under nitrogen. Sodium metal, 4.5 g, was added in portions. After all the sodium was consumed, t.l.c. showed no remaining **8**. The solution was cooled, concentrated to 50 ml, and then poured into 100 ml half-saturated aqueous sodium chloride solution. This solution was extracted with four portions of ethyl acetate and the combined organic layers were washed with saturated sodium chloride solution, filtered and evaporated to give 1.13 g of crude product. This crude material was converted to its hydrochloride which was crystallized from methanol – *n*-propanol to give 0.674 g of trishydrochloride. A second crop, 0.128 g, was obtained from the mother liquor. The yield of crystallized product was 55%; n.m.r. (as HCl salt) δ (D_2O): 0.73 (C-18 methyl), 0.98 (C-19 methyl), 3.20 ($\Delta\nu_{\frac{1}{2}} = 20$ Hz, C-3 methine), 4.00 ($\Delta\nu_{\frac{1}{2}} = 10$ Hz, C-11 methine), 7.40, 8.71 (C—H protons on imidazolium ring).

Anal. Calcd. for $C_{22}H_{39}N_4Cl_3 \cdot H_2O$: C, 54.60; H, 8.54; N, 11.58; Cl, 21.98. Found: C, 54.73; H, 8.76; N, 11.63; Cl, 22.88.

*17β-(4(5)-Imidazolyl)-5α-androstane-3,11-dione (**10**)*

Crude **3** from lithium–ammonia–methanol reduction of 1 g of **2** was oxidized with excess Jones reagent in 90% acetic acid. The solution was treated with water and concentrated ammonia and then extracted with ethyl acetate. The organic layer was extracted four times with 1 *M* HCl, the aqueous extracts were basified with concentrated NH_3, and then extracted five times with ethyl acetate. Evaporation of the combined ethyl acetate extracts gave 619 mg of crude product, m.p. 230–233°. Two recrystallizations from methanol–water gave material with m.p. 232.5–235°; n.m.r. (on HCl salt) δ (D_2O): 0.46 (C-18 methyl), 1.14 (C-19 methyl), 7.30, 8.61 (C—H protons of the imidazolium ring). ^{13}C n.m.r., δ (pyridine): 11.2, C-19; 14.2, C-18.

Anal. Calcd. for $C_{22}H_{30}N_2O_2$: C, 74.54; H, 8.53; N, 7.90. Found: C, 74.35; H, 8.54; N, 7.89.

*17β-(4(5)-Imidazolyl)-4-androstene-3,11-dione (**11**)*

Compound **2** (2 g, 5.7 mmol) in a mixture of 10 ml H_2O, 1.9 ml 3 *M* HCl and 50 ml acetic acid was cooled to 6° and treated with 2.9 ml Jones reagent in two portions. After 10 min 1 ml of isopropanol was added to destroy excess oxidant. The reaction mixture was poured into 500 ml of water, neutralized with Na_2CO_3, and extracted repeatedly with methylene chloride. The combined extracts were

evaporated to dryness and crystallized from hot methanol, giving 0.929 g of product. After recrystallization from methanol–water–ammonia, this material had m.p. 152–155° (dec.); n.m.r. (on HCl salt) δ (D_2O): 0.47 (C-18 methyl), 1.32 (C-19 methyl), 5.67 (—C*H*=C, C-4), 7.14, 8.40 (C—H protons of the imidazolium ring). ^{13}C n.m.r., δ (pyridine): 17.2, C-19; 14.2, C-18.

Anal. Calcd. for $C_{22}H_{28}N_2O_2 \cdot CH_3OH$: C, 71.89; H, 8.38; N, 7.34. Found: C, 71.53; H, 8.41; N, 7.41.

5α- and 5β-Pregnane-3,11,20-triones

These compounds were prepared from 4-pregnene-3,11,20-trione (Sigma) by hydrogenation and separated by crystallization following the procedure of Schmitt *et al.* (28). 5α-pregnane-3,11,20-trione had m.p. 208–215° (lit. m.p. 212–216° (29)); ^{13}C n.m.r., δ (pyridine): 11.1 (C-19) and 14.3 (C-18) p.p.m. 5β-Pregnane-3,11,20-trione had m.p. 155–156° (lit. m.p. 158–160° (30)); ^{13}C n.m.r., δ (pyridine): 14.3 (C-18) and 22.5 (C-19) p.p.m.

Financial support from the National Research Council of Canada, and the University Research Council of the University of Western Ontario is gratefully acknowledged. I wish to thank Dr. J. B. Stothers of this Department for the ^{13}C n.m.r. spectra.

1. J. R. KNOWLES and C. A. PARSONS. Chem. Commun. 755 (1967).
2. C. A. BLYTH and J. R. KNOWLES. J. Am. Chem. Soc. **93**, 3017, 3021 (1971).
3. R. HERSHFELD and M. L. BENDER. J. Am. Chem. Soc. **94**, 1376 (1972).
4. R. BRESLOW and L. E. OVERMAN. J. Am. Chem. Soc. **92**, 1075 (1970).
5. C. ASO, T. KUNITAKE, and S. SHINKAI. Chem. Commun. 1483 (1968).
6. I. M. KLOTZ, G. P. ROYER, and I. S. SCARPA. Proc. Natl. Acad. Sci. U.S. **68**, 263 (1971).
7. D. L. VANDER JAGT, F. L. KILLIAN, and M. L. BENDER. J. Am. Chem. Soc. **92**, 1016 (1970).
8. N. HENNRICK and F. CRAMER. J. Am. Chem. Soc. **87**, 1121 (1965).
9. D. E. TUTT and M. A. SCHWARTZ. J. Am. Chem. Soc. **93**, 767 (1971).
10. R. L. VAN ETTER, J. M. SEBASTION, G. A. CLOWER, and M. L. BENDER. J. Am. Chem. Soc. **89**, 3242, 3253 (1967).
11. C. G. OVERBERGER, M. MORIMOTO, I. CHO, and J. C. SALAMON. J. Am. Chem. Soc. **93**, 3228 (1971).
12. C. G. OVERBERGER and M. MORIMOTO. J. Am. Chem. Soc. **93**, 3222 (1971).
13. R. G. SHORENSTEIN, C. S. PRATT, C. J. HSU, and T. E. WAGNER. J. Am. Chem. Soc. **90**, 6199 (1968).
14. W. P. JENCKS. Catalysis in chemistry and enzymology. McGraw-Hill, New York. 1968. Chapt. 8.
15. D. R. STORM and D. E. KOSHLAND, JR. Proc. Natl. Acad. Sci. U.S. **66**, 445 (1970).
16. A. DAFFORN and D. E. KOSHLAND, JR. Proc. Natl. Acad. Sci. U.S. **68**, 2463 (1971).
17. M. I. PAGE and W. P. JENCKS. Proc. Natl. Acad. Sci. U.S. **68**, 1678 (1971).
18. T. C. BRUICE, A. BROWN, and D. O. HARRIS. Proc. Natl. Acad. Sci. U.S. **68**, 658 (1971).
19. B. CAPON. J. Chem. Soc. B, 1207 (1971).
20. T. C. BRUICE and S. J. BENKOVIC. Biorganic mechanism, Vol. 1. W. A. Benjamin Inc., New York. 1966. pp. 119–201.
21. A. J. KIRBY and A. R. FERSHT. Progr. Bioorg. Chem. **1**, 1 (1971).
22. T. C. BRUICE and S. J. BENKOVIC. J. Am. Chem. Soc. **85**, 1 (1963).
23. G. STAINSKY and A. E. ALEXANDER. Trans. Faraday Soc. **46**, 587 (1950).
24. R. WEIDENHAGEN and R. HERRMANN. Ber. **68**, 1953 (1935); R. WEIDENHAGEN, R. HERRMANN, and H. WEGNER. Ber. **70**, 570 (1937).
25. J. L. GOUGH, J. P. GUTHRIE, and J. B. STOTHERS. Chem. Commun. 979 (1972).
26. J. ROCEK, F. H. WESTHEIMER, A. ESCHENMOSSER, L. MOLDOVANYI, and J. SCHREIBER. Helv. Chim. Acta, **45**, 2554 (1962).
27. H. PAULY. Z. Physiol. Chem. **42**, 508 (1904).
28. J. SCHMITT, J. J. PANOUSSE, P.-J. CORNU, H. PLUCHET, A. HALLOT, and P. COMOY. Bull. Soc. Chim. Fr. 753 (1964).
29. M. STEIGER and T. REICHSTEIN. Helv. Chim. Acta, **21**, 161 (1938).
30. O. MANCERA, H. J. RINGOLD, C. DJERASSI, G. ROSENKRANTZ, and F. SONDHEIMER. J. Am. Chem. Soc. **75**, 1286 (1953).

Can. J. Chem. Downloaded from www.nrcresearchpress.com by 210.87.254.40 on 09/05/12
For personal use only.

Synthesis and Stereochemistry of Some Diastereoisomeric 2-Amino-4-*t*-butylcyclohexanols and Related Compounds

A. F. CASY,[1] E. S. C. WU, AND B. D. WHELTON

Faculty of Pharmacy and Pharmaceutical Sciences, University of Alberta, Edmonton, Alberta

Received April 26, 1972

The synthesis of four RS diastereoisomeric analogs of acetylcholine based on 2-amino-4-*t*-butylcyclohexanol is described. Preferred conformations of these derivatives, their intermediates, and analogs lacking a *t*-butyl substituent, are assigned on the basis of 1- and 2-methine and other p.m.r. characteristics. In general, major deviations from preferred chair conformations arise only in quaternary salts which require an axial trimethylammonium group. Certain p.m.r. signals of *t*-2-amino-*c*-4-*t*-butylcyclohexanol (base and hydrochloride) and *t*-2-dimethylamino-*t*-5-*t*-butylcyclohexanol hydrochloride are duplicated at 30°, a result attributed to a slow interconversion of conformational isomers.

La synthèse de quatre analogues RS diastéréoisomères de l'acétyl choline à partir de l'amino-2 *t*-butyl-4 cyclohexanol est décrite. Les conformations préférentielles de ces dérivés, leurs intermédiaires et les analogues où manque le substituant *t*-butyle, sont attribuées à partir de la r.m.n. du méthine-1 et -2 et des autres caractéristiques. En général, les déviations majeures aux conformations chaises préférentielles se produisent pour les sels quaternaires qui font intervenir un groupe triméthyl-ammonium axiale. Certains signaux r.m.n. du *t*-amino-2-*c*-*t*-butyl-4 cyclohexanol (base et chlorhydrate) et du chlorhydrate de *t*-diméthylamino-2 *t*-butyl-5 cyclohexanol sont dédoublés à 30°, résultat qu'on attribue à une interconversion lente entre les isomères de conformation. [Traduit par le journal]

Canadian Journal of Chemistry, **50**, 3998 (1972)

Can. J. Chem. Downloaded from www.nrcresearchpress.com by 210.87.254.6 on 09/05/12
For personal use only.

This work forms part of our studies of the stereochemistry of muscarinic agonists and their antagonists (1–3). There is considerable interest in the influence of the relative orientations of the acetoxy and trimethylammonium functions of acetylcholine (ACh) upon cholinergic activity and to this end cyclic analogs of ACh based on cyclopropane (4), cyclobutane (5), cyclohexane (6), and decalin (7) have been examined. An extension of work upon six-membered ring analogs to those incorporating a *t*-butyl substituent was considered of value because the isomers **1***b* provide a greater range of N—C—C—O dihedral angle variations than is found in the corresponding disubstituted cyclohexyl derivatives **1***a*.

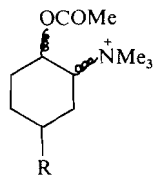

1

a R = H
b R = *t*-Bu

[1]Present address: School of Pharmacy, Liverpool Polytechnic, Byron Street, Liverpool, England L3 3AF.

Synthesis

The 2-dimethylaminocyclohexanol precursors of *trans* **1***a* and *b*[2] (N^aO^a series) were prepared via the *N*-benzyl derivatives **3** rather than directly from the epoxide **2** and dimethylamine. The sequence **2** through **5** (Scheme 1) avoided the need for pressure reactions and facilitated separation of positional isomers (fractional crystallization of the *N*-tosyl derivative of **4***b* and the 5-*t*-butyl analog was readily achieved, monitored by p.m.r. spectroscopy). This route also provided the primary amine **4***a* which could be converted to the *cis* analog by an

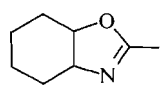

6

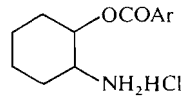

7

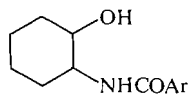

8

Ar = *p*-$NO_2 \cdot C_6H_4$

[2]Following Sicher *et al.*, (8), the configurations of **1***b* and analogs are conveniently represented by the symbols N^aO^a, N^eO^e, N^eO^a, and N^aO^e denoting N and O axial or equatorial substituents in a cyclohexane chair anchored by equatorial *t*-butyl at C-4.

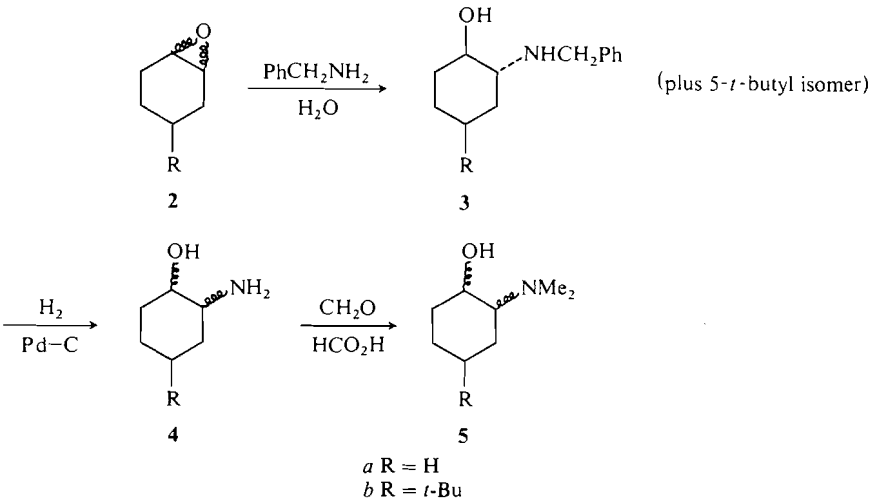

SCHEME 1. *Note*: Configuration is not specified in **4** and **5** so that these structures may serve generally.

inversion procedure (9). The intermediate *cis* oxazoline, **6** (from *N*-*p*-nitrobenzoyl **4***a* and thionyl chloride), and the derived ester hydrochloride **7** and amide **8**, all proved more resistant to acid hydrolysis than was anticipated from the literature (9); high yields of *cis* 2-aminocyclohexanol followed treatment of **7** or **8** with hot ethanolic potash.[3] In the similar inversion of *t*-2-amino-*t*-4-*t*-butylcyclohexanol **9**, the final hydrolysis step was performed on the

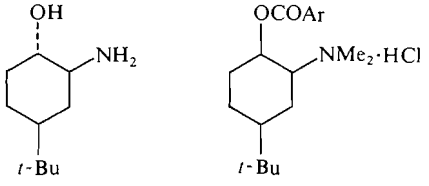

dimethylamino ester salt **10** (N^eO^a) in which O to N acyl migration was blocked. The aminocyclohexanol **9** (N^eO^e) was obtained from *t*-4-*t*-butylcyclohexanol-*t*-2-carboxylate **11** by the method of Sicher *et al.* (8); the acid **11** was made conveniently by carbethoxylation of 4-*t*-butylcyclohexanone. The aminocyclohexanol **14** (N^aO^e) was obtained from 4-*t*-butylcyclohexene following a literature method used for the decalin analog (7) (see Scheme 2).

[3]Inversion of *trans* **4***a* via the acetamide followed by acid hydrolysis has recently been recommended as the best procedure for this interconversion (10).

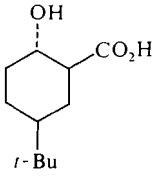

The aminocyclohexanols **4** etc. were *N*,*N*-dimethylated with formaldehyde and formic acid and the resultant tertiary amines acetylated with acetyl chloride. Most of the acetates formed methiodide salts without difficulty; exceptions were the N^aO^e analog **1***b*, isolated as a tosylate, and the N^aO^a derivative **1***b* which was deliquescent. The N^eO^a acetate methiodide **1***b* was made by treating the corresponding cyclohexanol methiodide with acetic anhydride and pyridine.

Stereochemistry

Information about the conformation of the cyclohexyl derivatives **5** and related compounds has been obtained chiefly from the dimensions of the 1- and 2-H methine p.m.r. signals (Table 1). While the 1-H signals were resolved in all spectra and lowest field in esters as a result of the acylation shift (11), isolated 2-H signals were largely confined to spectra of quaternary ammonium salts. The four combinations of vicinal coupling possible for the methine protons of 1,2-disubstituted cyclohexanes are shown

Can. J. Chem. Downloaded from www.nrcresearchpress.com by 210.87.254.6 on 09/05/12
For personal use only.

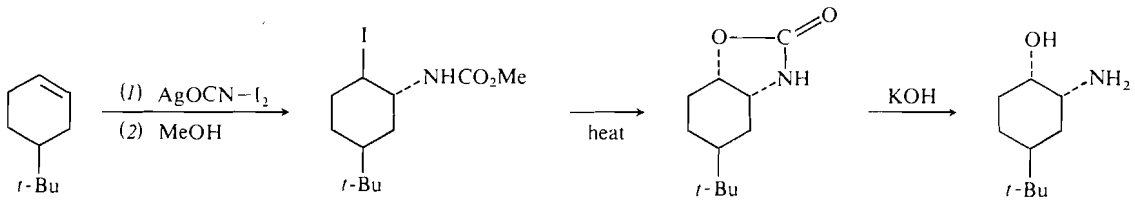

12 13 14

SCHEME 2

below together with their ranking in terms of

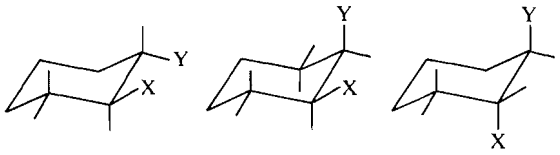

2aa + 1ae > 1aa + 2ae(X) > 2ea + 1ee(Y) ≅ 2ee + 1ea

outer line separations based on ^3J values for six-membered alicycles (12). Model values for the 2aa,1ae and 2ea,1ee types were provided by the 4-H methine signals of derivatives of the *t*- and *c*-3-methyl-4-piperidinols **15** and **16** respectively (1*a*). Some of the present cyclohexyl

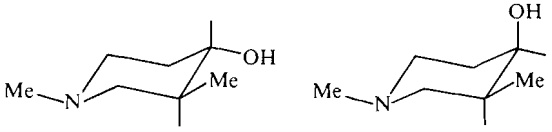

15 16

derivatives themselves provided model spectra when there was little doubt of their preferred conformation; examples are the N^eO^e derivatives (2aa, 1ae type) and N^eO^a quaternary ammonium salts **17** (1-H: 2ea,1ee; 2-H: 1aa,2ae

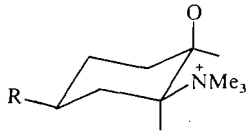

17

type) where the *N*-substituent is markedly larger than the oxygen function. No model was available for the 2ee,1ea type but it is reasonable to assume that signal dimensions in these cases would be similar to or slightly narrower than those of the 2ea,1ee type.

The applicability of first order treatment of model methine resonances and those under investigation could not be judged even when a well resolved methine signal was obtained (Fig. 1*a*) because the 3- and 6-methylene resonances were not resolved. Signal dimensions therefore had to be gauged by measuring the separations of terminal lines (b.w.*)(13) or widths at half the maximum height ($w_{1/2}$) (14). Difficulties arose when outer lines could not be identified with certainty (*cf.* Figs. 1*b* and *c*) while $w_{1/2}$ values were unreliable standards for signals of pronounced asymmetry (*cf.* Figs. 1*d* and *e*). Full base widths (b.w.) are recorded in Table 1 but they provide only very approximate yardsticks because the extremes of a resonance band are generally ill-defined. The appearance of a 1aa,2ae methine signal was characteristic, forming a pair of humps at low amplitude as a result of the single aa exceeding the two ae couplings (Fig. 1*f*). Methine signal dimensions for the model compounds are summarized in Table 2. For 2aa,1ae signals measurements of terminal line separations were possible in all cases and these values (confined to a narrow range) provide a better criterion than the $w_{1/2}$ values which vary from 12 to 21.5 Hz although most lie in the upper end of this range. For the 1aa,2ae type, a $w_{1/2}$ value near 18 Hz together with the characteristic signal appearance seems a reliable standard, while most of the 2ea,1ee signals display $w_{1/2}$ values close to 8 Hz.

In the conformational analyses which follow, conclusions reached on the basis of 1- and 2-methine signal dimensions are corroborated by chemical shift data on these and other proton groups. Generally axial (a) are higher field than equatorial (e) methine resonances in cyclohexane derivatives by about 0.5 p.p.m. (15) and the same order of difference holds for the present

Can. J. Chem. Downloaded from www.nrcresearchpress.com by 210.87.254.6 on 09/05/12
For personal use only.

TABLE 1. Methine proton p.m.r. characteristics of some 2-amino-4-*t*-butylcyclohexanols and related compounds

No.	Structure	Configuration	Solvent	Methine p.m.r. features[a] 1-H	2-H
1	**4***a*	*trans*	$CDCl_3$	δ 3.08 $w_{1/2}$ 13 b.w.* 23	$\delta \sim 2.4$[b] b.w. 34
			D_2O	δ 3.18 $w_{1/2}$ 16 b.w.* 22.5	δ 2.43 $w_{1/2}$ 21 b.w.* 23
2	**4***a* HCl	*trans*	D_2O	δ 3.63 $w_{1/2}$ 19.5 b.w.* 24	δ 2.98 $w_{1/2}$ 21.5 b.w.* 25
3	**4***a*	*cis*	D_2O	δ 3.77 $w_{1/2}$ 11 b.w. 27	δ 2.75 $w_{1/2}$ 13 b.w. 28
4	**4***a* HCl	*cis*	D_2O	δ 4.12 $w_{1/2}$ 7 b.w. 18	δ 3.37 $w_{1/2}$ 17 b.w.* 23
5	**5***a*	*trans*	D_2O	δ 3.52[c] $w_{1/2}$ 16 b.w.* 23	$\delta \sim 2.3$[b]
	5*a* HCl	*trans*	D_2O	δ 3.68 $w_{1/2}$ 20 b.w.* 25	$\delta \sim 3.0$[b]
6	**5***a* MeI	*trans*	D_2O	δ 3.95 $w_{1/2}$ 21 b.w. 29	$\delta \sim 3.3$[b]
7	**5***a* acetate HCl	*trans*	D_2O	δ 4.92[d] $w_{1/2}$ 14 b.w.* 25	3.47 $w_{1/2}$ 26.5[e] b.w.* 26
8	**5***a* acetate MeI	*trans*	DMSO-d_6[f]	δ 5.0 $w_{1/2}$ 17 b.w.* 24	δ 3.85 $w_{1/2}$ 17.5 b.w.* 24.5
9	**5***a* HCl	*cis*	D_2O	δ 4.4[c] $w_{1/2}$ 7 b.w. 14	$\delta \sim 3.2$[b]
10	**5***a* MeI	*cis*	DMSO-d_6	δ 4.47 $w_{1/2}$ 7[g] b.w. 14	δ 3.5[h] $w_{1/2} \sim 18$ b.w. 23
11	**5***a* acetate MeI	*cis*	D_2O	δ 5.4[d] $w_{1/2}$ 7.5 b.w. 13	δ 3.28[h] $w_{1/2}$ 20 b.w. 30
12	**5***a* acetate MeI	*cis*	DMSO-d_6[f]	δ 5.47 $w_{1/2}$ 8 b.w. 15	δ 3.79[h] $w_{1/2}$ 19 b.w. 23
13	**4***b*	N[e]O[e]	$CDCl_3$	δ 3.08 $w_{1/2}$ 20 b.w. 35	$\delta \sim 2.45$[b]
			DMSO-d_6	δ 3.05 $w_{1/2}$ 20 b.w. 33	$\delta \sim 2.45$[b]

Can. J. Chem. Downloaded from www.nrcresearchpress.com by 210.87.254.6 on 09/05/12
For personal use only.

TABLE 1 *(Continued)*.

No.	Structure	Configuration	Solvent	Methine p.m.r. features[a] 1-H	2-H
14	**5***b* HCl	N^eO^e	D_2O	δ 3.70 $w_{1/2}$ 21 b.w. 30	$\delta \sim 3.13^b$
15	**5***b* MeI	N^eO^e	DMSO-d_6	δ 3.79 $w_{1/2}$ 21[g] b.w.* 25	$\delta \sim 3.39^b$
16	**5***b* acetate MeI	N^eO^e	DMSO-d_6	δ 5.0 $w_{1/2}$ 21.5 b.w.* 25	δ 3.86 $w_{1/2}$ 14[e] b.w.* 25
17	**5***b* HCl	N^eO^a	D_2O	δ 4.37 $w_{1/2}$ 8 b.w. 16	$\delta \sim 3.2^b$
18	**5***b* MeI	N^eO^a	DMSO-d_6	δ 4.4 $w_{1/2}$ 9 b.w. 25	$\delta \sim 3.55^b$
			D_2O	$\delta \sim 4.73^b$	$\delta \sim 3.3^b$
19	**5***b* acetate HCl	N^eO^a	D_2O	δ 5.33 $w_{1/2}$ 7.5 b.w. 19	δ 3.35[h] $w_{1/2}$ 19
20	**5***b* acetate MeI	N^eO^a	DMSO-d_6[f]	δ 5.38 $w_{1/2}$ 8 b.w. 20	δ 3.76[h] $w_{1/2}$ 18.5 b.w. 27.5
21	4*b*	N^aO^e	$CDCl_3$	δ 3.5 $w_{1/2}$ 19 b.w. 24	δ 3.15 $w_{1/2}$ 8 b.w. 16
			DMSO-d_6	δ 3.32 $w_{1/2}$ 20[g] b.w. 19.6	δ 2.98 $w_{1/2}$ 5.5 b.w.* 10
22	**5***b*	N^aO^e	$CDCl_3$–TFA	δ 3.73 $w_{1/2}$ 20.5 b.w. 28	$\delta \sim 2.8^b$
	HCl		DMSO-d_6	δ 3.97 $w_{1/2}$ 19	δ 3.47[b] $w_{1/2} \sim 12$
23	**5***b* MeI	N^aO^e	DMSO-d_6	δ 4.4 $w_{1/2}$ 10[g] b.w. 23	$\delta \sim 3.5^b$
24	**5***b* acetate HCl	N^aO^e	DMSO-d_6	δ 5.07 $w_{1/2}$ 19 b.w.* 18	δ 3.59 $w_{1/2}$ 17.5 b.w. 25
			D_2O	δ 5.2 $w_{1/2}$ 17	δ 3.7 $w_{1/2}$ 12
			$CDCl_3$	δ 5.1 $w_{1/2}$ 19 b.w. 28	δ 3.1 $w_{1/2}$ 18 b.w. 25
25	**5***b* acetate Me Ts[i]	N^aO^e	D_2O	δ 5.54 $w_{1/2}$ 9.8 b.w. 18	δ 3.64 $w_{1/2}$ 20.8
			DMSO-d_6	δ 5.36 $w_{1/2}$ 10.5 b.w. 20	δ 3.72 $w_{1/2}$ 20.5 b.w. 30

Can. J. Chem. Downloaded from www.nrcresearchpress.com by 210.87.254.6 on 09/05/12
For personal use only.

TABLE 1 *(Concluded)*.

No.	Structure	Configuration	Solvent	Methine p.m.r. features[a] 1-H	2-H
26	**4***b*	N^aO^a	$CDCl_3$	δ 3.62 $w_{1/2}$ 4.5 b.w.* 9	δ 3.03 $w_{1/2}$ 5.5 b.w.* 10
27	**4***b* HCl	N^aO^a	D_2O	δ 4.16 $w_{1/2}$ 4.5 b.w.* 10	δ 3.70 $w_{1/2}$ 6.3 b.w.* 10
28	**5***b* HCl	N^aO^a	D_2O	δ 4.2 $w_{1/2}$ 8 b.w. 17	δ 3.32 $w_{1/2}$ 8 b.w. 20
			DMSO-d_6	δ 4.0 $w_{1/2}$ 7 b.w.* 12	δ 3.1 $w_{1/2}$ 14.5 b.w.* 20
29	**5***b* MeI	N^aO^a	DMSO-d_6	δ 4.11 $w_{1/2}$ 15.5 b.w. 32.5	$\delta \sim 3.35$[b]
30	**5***b* acetate HCl	N^aO^a	D_2O	δ 5.47 $w_{1/2}$ 7 b.w.* 10	δ 3.71 $w_{1/2}$ 6.7 b.w.* 12.5
31	**5***b* acetate MeI	N^aO^a	DMSO-d_6	δ 5.30 $w_{1/2}$ 8.5 b.w.* 15 b.w. 24	δ 3.64 $w_{1/2}$ 9.5 b.w.* 19 b.w. 32.5
			D_2O	δ 5.58 $w_{1/2}$ 10.5 b.w. 22.5	δ 3.99 $w_{1/2}$ 8.5 b.w.* 19.5 b.w. 27.5
			$CDCl_3$	δ 5.37 $w_{1/2}$ 9.5 b.w. 22.5	δ 3.96 $w_{1/2}$ 9.0 b.w.* 18 b.w. 25
32	**4***b* acetate HCl	N^aO^a	DMSO-d_6	δ 4.1 $w_{1/2}$ 8 b.w. 22.5	δ 2.6 $w_{1/2}$ 8.5 b.w. 28.5
33	**3***a*	*trans*	$CDCl_3$	δ 3.2 $w_{1/2}$ 12.5 b.w.* 23	—
34	**3***a*	*cis*	$CDCl_3$	$\delta \sim 3.8$[b]	δ 2.58 $w_{1/2}$ 14.5 b.w. 23
35	**3***b* HCl	N^aO^a	DMSO-d_6[g]	δ 3.98 $w_{1/2}$ 8.5 b.w. 15	δ 3.12 $w_{1/2}$ 8.5 b.w. 17.5

[a] δ Values are centers of multiplets rather than true chemical shifts and are approximate for obscured signals; $w_{1/2}$ are signal widths at half the maximum height, b.w.* terminal line separations, and b.w. full base width estimations, ± 2 Hz (see text); chemical shifts in p.p.m., all other parameters in Hz.

[b] Signal partly obscured.

[c] Literature (6) $\delta \sim 3.1$, $w_{1/2}$ 24 (*trans* **5***a* base in CCl_4); δ 3.8, $w_{1/2}$ 8 (*cis* **5***a* base in CCl_4).

[d] Literature (6) δ 4.6, $w_{1/2}$ 19 (*trans* **5***a* acetate base in CCl_4); δ 5.15, $w_{1/2}$ 6 (*cis* **5***a* acetate base in CCl_4).

[e] Artefact due to non-symmetrical signal.

[f] Similar spectrum in D_2O.

[g] After D_2O added (HCOH coupling removed).

[h] Characteristic "double humped" signal (Fig. 1*f*).

[i] Tosylate.

Can. J. Chem. Downloaded from www.nrcresearchpress.com by 210.87.254.6 on 09/05/12
For personal use only.

Can. J. Chem. Downloaded from www.nrcresearchpress.com by 210.87.254.6 on 09/05/12
For personal use only.

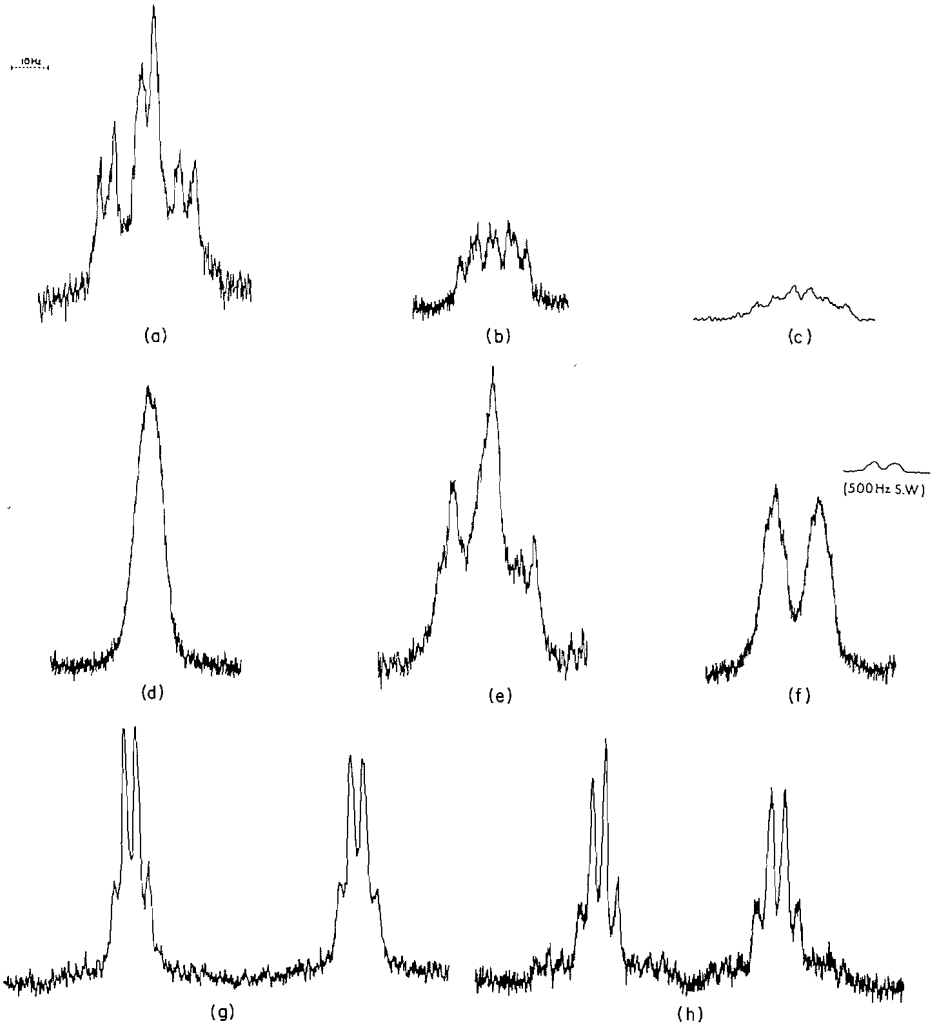

FIG. 1. Methine proton p.m.r. signals: (*a*) 2-H of *trans* **1***a* iodide; (*b*) 1-H of N^aO^e **5***b* acetate hydrochloride; (*c*) 1-H of *trans* **1***a* iodide in D_2O at 60 MHz; (*d*) 1-H of N^eO^a **1***b* iodide; (*e*) 2-H of N^eO^e **1***b* iodide; (*f*) 2-H of N^eO^a **1***b* iodide; (*g*) 1- and 2-H of N^aO^a **4***b* base in $CDCl_3$; (*h*) 1- and 2-H of N^aO^a **4***b* hydrochloride in D_2O. All signals recorded at 100 MHz, sweep width 250 Hz, and in DMSO-d_6 unless otherwise stated.

derivatives as is clear, for example, from δ 1-H values for **18** (axial 1-H) and **19** (equatorial 1-H) (Δ 0.38 p.p.m.). When the OH (or OCOMe) substituent is axial, the resonance of an axial 2-H proton is not significantly higher field than an equatorial 2-H signal because of the deshielding influence of the oxygen function in this orientation (16).

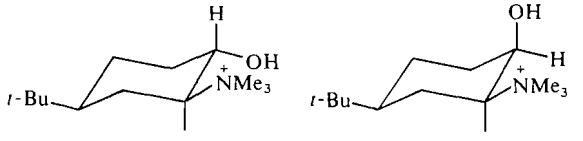

	18	**19**
δ_{1-H}	5.0	5.38
		in DMSO-d_6

The polar solvents deuterium oxide (D_2O) and deuterated dimethylsulfoxide (DMSO-d_6) were mostly employed in these studies; with certain exceptions (discussed below) changes in solvent had little influence upon the dimensions of 1- and 2- p.m.r. signals and, by inference, solute conformation.

TABLE 2. Dimensional parameters of methine p.m.r. signals from spectra of model compounds[a]

Type of ^3J coupling	Models	$w_{1/2}$	b.w.*	b.w.
2aa,1ae	Table 1, nos. 1, 2, 5–8, 13, 15, 16, 33	13, 16, 21, 19.5, 21.5, 21, 14, 17, 24, 20, 21, 21.5, 12.5	23, 22.5, 23, 24, 25, 25, 26, 17.5, 24.5, 25, 25, 25, 23	34, 29, 35
	t-3-Methyl-4-piperidinols[b]	17, 17, 16.5, 16	23, 24, 25, 27	31, 31.5, 32, 34
1aa,2ae	Table 1, nos. 10, 12, 18, 20[c]	18, 19, 18.5	—	23, 23, 27.5
2ea, 1ee	Table 1, nos. 10, 12, 18, 20[d]	7, 8, 9, 8	—	14, 15, 25, 20
	c-3-Methyl-4-piperidinols[b]	7.5, 8.5, 7.5, 6.5, 7.0, 8.0, 6.0	—	16, 18, 16, 17, 16, 16, 13

[a]Footnote *a* of Table 1 applies.
[b]Reference 1*a*.
[c]All 2-H signals with double-humped appearance.
[d]1-H signals.

(1) cis 2-Aminocyclohexanol and Derivatives

The 1- and 2-methine signal dimensions clearly show that the a-OH conformer **20** is

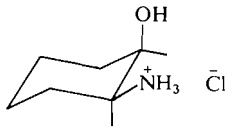

20

preferred for *cis* **4***a* hydrochloride in D_2O (no. 4)[4] as do also the corresponding chemical shifts; note that the 2-H signal is lower field than 2-H of *trans* **4***a* hydrochloride (Δ 0.39 p.p.m.) as a result of deshielding by the axial 1-OH as mentioned above. In contrast, *cis* **4***a* base exists in D_2O as a mixture of the two chair conformers **21** and **22** on the evidence of both 1- and 2-methine signal $w_{1/2}$ magnitudes being intermediate between axial and equatorial values

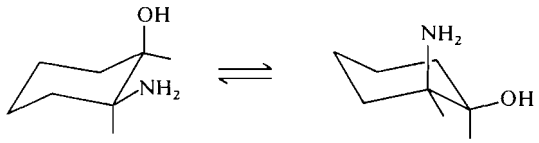

21 **22**

[4]All numbers in parentheses refer to the first column of Table 1.

(no. 3). Methine resonance dimensions and chemical shifts for the hydrochlorides and methiodides of *cis* **5***a* and derived acetate were consistent with a-O, e-N chairs as the preferred conformations (nos. 9–12).

(2) N^eO^a Series

P.m.r. data upon the methine resonances of *c*-4-*t*-butyl-*c*-2-dimethylaminocyclohexanol **5***b* hydrochloride, the corresponding acetate hydrochloride, and methiodide **1***b* likewise establish N^eO^a chairs as the preferred conformations (nos. 17–20).

(3) N^aO^e Series

Methine signal dimensions for *c*-2-amino-*t*-4-*t*-butylcyclohexanol clearly reveal its N^aO^e conformation **23** (no. 21). The $\delta_{2\text{-H}}$ chemical

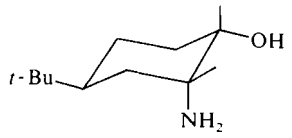

23

shift in $CDCl_3$ is 0.7 p.p.m. lower field than that of axial 2-H in the N^eO^e analog (no. 13) in accord with its equatorial assignment ($\delta_{1\text{-H}}$ (no. 13) is higher field than $\delta_{1\text{-H}}$ (no. 21) because it is shielded by the 2-e-NH_2 group). The $w_{1/2}$ value of the 1-H resonance of the related di-

Can. J. Chem. Downloaded from www.nrcresearchpress.com by 210.87.254.6 on 09/05/12
For personal use only.

Can. J. Chem. Downloaded from www.nrcresearchpress.com by 210.87.254.6 on 09/05/12
For personal use only.

methylamino analog **5***b* is that expected of an axial proton (no. 22) and the 1-H chemical shift (δ 3.73, base in $CDCl_3$–TFA) is consistent with that of an axial proton deshielded by an adjacent axial ammonium function ($\delta_{1\text{-H}}$ for *trans* 2-dimethylaminocyclohexanol in the same solvent is 3.60). The 2-H signal (δ 3.5 in D_2O) is distinctly lower field than that of axial 2-H in *trans* **5***a* and *b* (nos. 5 and 14). In the spectrum of the N^aO^e acetate hydrochloride of **5***b*, in DMSO-d_6 both 1-H and 2-H signals have typically axial $w_{1/2}$ values (no. 24). Chemical shifts of the 1- and 2-protons ($\delta_{1\text{-H}}$ 5.07, $\delta_{2\text{-H}}$ 3.59) are both close to those of the axial methine signals of N^eO^e **5***b* acetate hydrochloride ($\delta_{1\text{-H}}$ 4.92, $\delta_{2\text{-H}}$ 3.5 in DMSO-d_6). Conformations most consistent with this evidence are either a skew-boat of type **24** in which the *N*- and *O*-substituents have

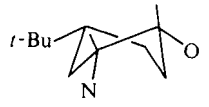

24

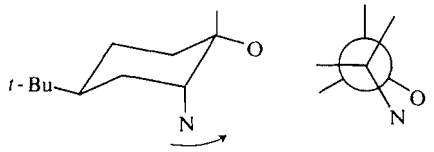

25

pseudo equatorial orientations or a flattened chair (**25**) in which the H—C_1—C_2—H dihedral angle approaches zero with a concomittant increase in $^3J_{H_1H_2}$ (12). Evidence indicative of significant populations of such conformations is also found from p.m.r. data upon N^aO^e **5***b* hydrochloride in DMSO-d_6 and the acetate salt in D_2O (nos. 22 and 24). A flattened chair has previously been proposed as a preferred conformational form in this series for N^aO^e **5***b* free base on the basis of i.r. studies (17). In the spectrum of the methiodide of N^aO^e **5***b* (no. 23) $w_{1/2}$ for the 1-H resonance approaches the typical equatorial value and $\delta_{1\text{-H}}$ (4.4 p.p.m.) is close to equatorial 1-H in spectra of *cis* **5***a* and N^eO^a **5***b* methiodides (nos. 10 and 18). The 2-H signal is obscured but its chemical shift (δ 3.5) corresponds with that of axial 2-H of the same model compounds. Similar results are obtained for the N^aO^e acetate methotosylate (no. 25); both 1- and 2-H signals are well resolved with the methiodides (nos. 12 and 20) serving as the appropriate models. Conformations of the two N^aO^e methiodides favored on the basis of the p.m.r. evidence are the inverted chair **26** and the

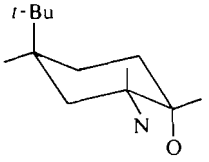

26

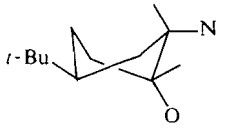

27

skew-boat **27**; the former is unlikely because of its axial *t*-butyl substituent but the latter is a reasonable formulation since there are precedents for *t*-butylcyclohexyl derivatives with skew-boat geometry (18).

(4) N^aO^a Series

Magnitudes of $w_{1/2}$ for 1- and 2-H methine signals of *t*-2-amino-*c*-4-*t*-butylcyclohexanol establish **28** as the preferred conformations of

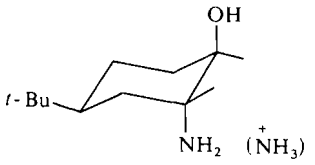

28

both base and hydrochloride form (nos. 26 and 27); in confirmation, the chemical shifts of these protons are both significantly lower field of the signals of corresponding axial protons of model analogs (nos. 13 and 2 respectively). The methine signal dimensions are distinctly smaller than those of the 2ea,1ee type (Table 2) as anticipated from the generally smaller values of $^3J_{ee}$ compared with $^3J_{ea}$ coupling (12); the sum of the ^3J values is about 9 Hz and the signal a near-symmetrical quartet (Figs. 1*g* and *h*). The dimensions of these signals provide no evidence of contributions from skew-boat forms (like **29**) identified as present in solutions of N^aO^a **4***b*

29

Can. J. Chem. Downloaded from www.nrcresearchpress.com by 210.87.254.6 on 09/05/12
For personal use only.

from i.r. studies (19). It is noted, however, that the methine "quartets" are superimposed on broad bands of low but distinct intensity and particularly clear in the spectrum of N^aO^a **4***b* hydrochloride (Fig. 1*h*). These bands are attributed to skew-boat species, probably stabilized by intramolecular hydrogen bonds (19);[5] the rate of interconversion of such forms with N^aO^a conformers (intermolecular bonded and/or solvated molecules) must be slow on the n.m.r. time scale because distinct rather than averaged methine signals are observed. Clearer evidence on this point follows from p.m.r. studies of *t*-2-dimethylamino-*t*-5-*t*-butylcyclohexanol hydrochloride (the N^aO^a 5-*t*-butyl isomer of **5***b*) because chemical shift differences between conformers are greater. Distinct NH (δ 10.4 major, 9.6 minor) and OH (δ 5.77 minor, 5.36 major) signals were apparent in DMSO-d_6 (absent after D_2O) while major and minor 1- and 2-H signals were also present. The two OH signals merged together when the temperature was raised and formed a broad band at 80–90° (other signals were poorly resolved at higher temperatures). In one spectrum at 30°, both signals showed coupling to the 1-H proton ($^3J = 4$ Hz for the higher and 5.5 Hz for the lower field signal); this is good evidence that both signals are due to sec-OH of the cyclohexanol derivative. In $CDCl_3$ at 30° duplicate $\overset{+}{H}N\ Me_2$ (doublets $^3J = 5$ Hz, δ 5.02 major, 4.88 minor) and *t*-Bu (δ 0.96 major, 0.92 minor) signals were clear and minor 1-H and 2-H multiplets could be assigned with reasonable confidence. Further conformational studies of these compounds will be reported elsewhere.

Methine p.m.r. data likewise support N/O *trans* diaxial orientations as the favored conformations of hydrochlorides of the corresponding dimethylaminocyclohexanol **5***b* and derived acetate in D_2O (nos. 28 and 30). The 1- and 2-methine signals of the alcohol salt are 0.3 to 0.5 p.p.m. to lower field of the appropriate axial signals of *trans* 2-dimethylaminocyclohexanol hydrochloride (no. 5). The fact of the chemical shift difference between equatorial 2-H in no. 30 and axial 2-H in no. 7 being less than expected for an *a*–e pair, is accounted for by the known shielding influence of an axial acetyl substituent upon the equatorial proton of an adjacent carbon atom in six-membered saturated rings (16). When D_2O is replaced by DMSO-d_6 as solvent for the N^aO^a hydrochloride **5***b*, the $w_{1/2}$ value of the 2-H resonance increases from 8 to 14.5 Hz while the 1-H signal is little changed (no. 28). This result is evidence that the cyclohexane ring is flattened in a similar manner to that proposed for some of the N^aO^e analogs (see **25**), whence $^3J_{2,3}$ but not $^3J_{1,2}$ couplings increase in magnitude. The 1-H resonance of the methiodide of N^aO^a **5***b* resembles the axial 1-H signals of methiodides of *trans* **5***a* and N^eO^e **5***b* in both dimensions and chemical shift (nos. 6, 15, and 29); the 2-H signal is poorly resolved but its chemical shift correlates with $\delta_{2\text{-H}}$ of the same two standards. Hence the skew-boat **29** is probably the chief contributor to the conformational equilibrium of N^aO^a **5***b* methiodide. The 1-H p.m.r. signal of the N^aO^a acetate methiodide **1***b* was of the equatorial type in spectra recorded in DMSO-d_6, D_2O, and $CDCl_3$ (no. 31), and chemical shift values confirm this assignment (*cf.* nos. 8, 16 (axial 1-H), and 12, 20, 25 (equatorial 1-H); $\delta_{1\text{-H}}$ for no. 12 in D_2O is 5.62). The $w_{1/2}$ values of the 2-H signal in these solvents are also indicative of an equatorial orientation but the dimensions of the signals (all are well resolved four-line resonances of b.w.* near 20 Hz) invalidate a genuine equatorial assignment as in nos. 26 and 27. Hence the preferred conformation of N^aO^a **1***b* iodide is probably a flattened chair of the type **25** with an axial rather than equatorial acyl substituent, and analogous to that of N^aO^a 3-dimethylamino-2-acetoxy-*trans*-decalin methiodide (methine signal $w_{1/2}$ values 8 (2-H) and 10 Hz (3-H)) the solid state conformation of which is known (7).

Differences in chemical shift and extent of $^3J_{HCOH}$ coupling between the methiodides *trans* **5***a*/N^eO^e **5***b* (δ 5.5, $^3J = 5$ Hz and δ 5.48, $^3J = 4.8$ Hz respectively) and *cis* **5***a*/N^eO^a **5***b* (δ 5.18, $^3J = 4.0$ and δ 5.2, $^3J \sim 3.0$ Hz respectively) are typical of those seen between e- and a-O*H* signals in six-membered alicylic sec-alcohols examined in DMSO-d_6 (1*a*, 21). The fact that the p.m.r. features of O*H* in the N^eO^e **5***b* methiodide (δ 5.2, $^3J = 3.8$ Hz) correspond with the axial type seems to support the skew-boat conformation **27** proposed for this salt. The applicability of such data to non-chair con-

[5]Intramolecular hydrogen bonding occurs in amino-alcohol hydrochlorides as well as in the corresponding free bases (20).

Can. J. Chem. Downloaded from www.nrcresearchpress.com by 210.87.254.6 on 09/05/12
For personal use only.

formations is doubtful however, since the O*H* signal of the N^aO^a **5***b* methiodide combines an axial type chemical shift (δ 5.21) with a $^3J_{HCOH}$ value (4.8 Hz) typical of an equatorial group.

It follows from this conformational study that chair conformations (probably flattened somewhat by the *t*-butyl substituent) are preferred for most of the aminoalcohols **5***b* and their acetates. Apart from the case of N^aO^e **5***b* acetate hydrochloride, major deviations arise in formally N^a derivatives only when the 2-substituent is a fully methylated onium group; in this form its steric demands are comparable with those of *t*-butyl. A precedent for the skew-boat forms proposed for methiodides of the N^aO^e and N^aO^a series is that of ring A of the bisquaternary steroid **30***a* (pancuronium iodide) in the solid state as established by X-ray crystallography (22). The 3- and 17-methine signals overlap in the spectrum of the diacetate **30***a*,

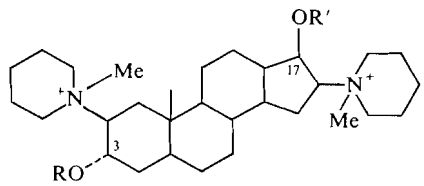

30
a R = R′ = COMe
b R = COMe; R′ = H

but the 3-H signal of the monoacetate **30***b* (dacuronium iodide) in DMSO-d_6 is resolved at δ 5.15 as a typical axial-type resonance ($w_{1/2}$ 20.5, b.w. 35 Hz). N^aO^a forms of **30** are seriously destabilized by 1,3-diaxial interactions between onium and angular methyl groups, a factor absent in the N^aO^a acetate methiodide **1***b* which does not prefer a skew-boat conformation.

The muscarinic activities and other pharmacological properties of the ACh analogs **1** will be reported elsewhere.

Experimental

Melting points (uncorrected) were taken in a Thomas–Hoover capillary apparatus. Hydrochloride and methiodide salts were recrystallized from ethanol–ether unless otherwise stated. Petroleum ether refers to the 30–60° b.p. fraction. P.m.r. spectra were recorded on Varian HA-100 or A-60D spectrophotometers in $CDCl_3$ or DMSO-d_6 (TMS internal standard) or D_2O (DSS internal or TMS external standard) at the ambient temperature. I.r. spectra were recorded (Nujols mulls) on a Beckman IR-10 instrument.

cis- and trans-2-Dimethylaminocyclohexanol and Derivatives

A mixture of cyclohexene oxide (100 g), benzylamine (109 g) and water (15 ml) was heated under reflux for 5 h, then cooled and extracted with ether. The dried (Na_2SO_4) extract was evaporated and the residue recrystallized from ligroin to give *trans*-2-benzylaminocyclohexanol (205 g), m.p. 71–73° (lit. (23) 73°). A mixture of the benzylaminoalcohol **3***a* (205 g), palladium-on-carbon (20 g, 10%), and ethanol (300 ml) was stirred with hydrogen at room temperature and pressure until uptake of gas ceased. The product was filtered and the filtrate concentrated; the residue on distillation gave *trans*-2-aminocyclohexanol (110 g), b.p. 111–112°/17 mm, m.p. 65° (base), 177° (hydrochloride), (lit. (24) b.p. 102–107°/9 mm, m.p. 68° (base), 176–177° (hydrochloride)). The *trans*-dimethylamino alcohol **5***a*, b.p. 91–92°/17 mm, m.p. 186° (hydrochloride) (lit. (25) b.p. 78–80°/11 mm, m.p. 186–188° (hydrochloride)), was obtained from **4***a* by the reported method; it was converted to the corresponding acetate *hydrochloride*, m.p. 187–189°, by stirring with an equimolar proportion of acetyl chloride in toluene for 1 h.

Anal. Calcd. for $C_{10}H_{20}ClNO_2$: C, 54.21; H, 9.03. Found: C, 54.38; H, 9.04.

It formed a methiodide, m.p. 148–149°.

Anal. Calcd. for $C_{11}H_{22}INO_2$: C, 40.38; H, 6.78. Found: C, 40.27; H, 6.75.

Literature reports of the m.p. of this methiodide are inconsistent: 210–211° for monohydrate (26), 134–135° (25), 161–165° hygroscopic (6). Our material was anhydrous and its m.p. was little changed when the salt was crystallized from ethanol–ether containing water.

The *cis-p*-nitrobenzoyl ester hydrochloride **7**, m.p. 231–233° (dec.) (lit. (9) 230–232°), and the *cis-p*-nitrobenzamide **8**, m.p. 173–175° (as lit. (9)), were obtained by the reported methods. The amide **8** (13.1 g) in ethanolic potash (300 ml, 5%) was heated under reflux for 36 h. The cooled mixture was filtered, the filtrate concentrated and the residue extracted with ether. The dried (Na_2SO_4) ether was evaporated to leave *cis*-2-aminocyclohexanol (5.2 g, 90%), m.p. 74–75° (lit. (24) 72–73°). Similar treatment of the ester hydrochloride **7** (3 g) gave the same aminoalcohol (1 g, 87%). *cis*-2-Dimethylaminocyclohexanol, b.p. 102–104°/17 mm, m.p. 42–44° (base), 183–184° (hydrochloride) (lit. (25) b.p. 95–97°/15 mm, m.p. 40–42° (base), 182–183° (hydrochloride)), was converted to the corresponding acetate *hydrochloride*, m.p. 137–138°, by the method described for the *trans*-isomer.

Anal. Calcd. for $C_{10}H_{20}ClNO_2$: C, 54.21; H, 9.03. Found: C, 54.50; H, 8.98.

It formed a methiodide, m.p. 182–184° from methanol–ether (lit. 182–183° (26), 185–186° (25)).

cis-2-Benzylaminocyclohexanol, m.p. 62–63° (base), 245–246° (hydrochloride) (lit. (23) 67° (base), 248–250° (hydrochloride)), was prepared by treating *cis* **4***a* in ether with benzyl chloride and K_2CO_3 at the reflux temperature.

N^aO^a Series

c-4-t-Butyl-t-2-benzylamino- (3b) and t-5-t-Butyl-t-2-benzylaminocyclohexanol

Peracetic acid (40%) (FMC Corporation) (22 g) con-

Can. J. Chem. Downloaded from www.nrcresearchpress.com by 210.87.254.6 on 09/05/12
For personal use only.

taining a small amount of sodium acetate was added dropwise to a stirred mixture of 4-*t*-butylcyclohexene (13.8 g) (8) and Na_2CO_3 (32 g) in methylene chloride (200 ml) cooled in ice–water. The mixture was stirred at room temperature until it gave a negative test with moist starch–iodide paper; further 40% peracetic acid (3 g) was then added and the mixture stirred for a further 24 h (positive test maintained). The filtered solution was evaporated and the residue distilled to give the epoxide mixture **2***b* (12.5 g), b.p. 80–94°/16 mm (lit. (8) 78–80°/9 mm). A mixture of the epoxides (**2***b*) (12 g), benzylamine (8.4 g), and water (10 ml) was heated under reflux for 24 h. The product was extracted with ether and the ether dried (Na_2SO_4) and evaporated; the residue was distilled to give the benzylaminocyclohexanol **3***b* and the 5-*t*-butyl analog (14.5 g), b.p. 146–150°/2 mm, δ (DMSO-d_6): 0.83 (s, *t*-Bu), 3.7 (s, CH_2N). These gave a hydrochloride mixture, m.p. 150–160° from *n*-hexane, δ ($CDCl_3$): 0.83, 0.87 (s, *t*-Bu) which on repeated fractional crystallization from ethanol, ether, and *n*-hexane gave the *c-4-t-butyl isomer* **3***b hydrochloride*, m.p. 185–186° (19 g from 122 g mixture), δ ($CDCl_3$): 0.83 (s, *t*-Bu).

Anal. Calcd. for $C_{17}H_{28}ClNO$: C, 68.55; H, 9.48; N, 4.7. Found: C, 68.41; H, 9.43; N, 5.0.

Treatment of **3***b* hydrochloride (3 g) with acetyl chloride (5 ml) in chloroform (50 ml) (3 h at reflux) gave the corresponding *acetate* of 3*b* hydrochloride (2.9 g), m.p. 232–233°, δ (DMSO-d_6): 5.14 (m, $w_{1/2}$ 8 Hz, 1-H), 4.2 (bs, CH_2Ph), 3.28 (m, 2-H), 1.98 (s, OCOMe), 0.82 (s, *t*-Bu).

Anal. Calcd. for $C_{19}H_{30}ClNO_2$: C, 67.1; H, 8.8; N, 4.1. Found: C, 67.3; H, 8.97; N, 3.9.

t-2-Amino-c-4-t-butylcyclohexanol

A mixture of the benzylaminocyclohexanols **3***b* and isomer (26 g), palladized carbon (2.6 g, 10%), and ethanol (75 ml) containing a few ml water, was stirred with hydrogen at room temperature and pressure until gas absorption ceased. The product was filtered and the filtrate evaporated to give a mixture of aminocyclohexanols N^aO^a **4***b* and isomer. The mixture from 46.5 g of **3***b* and isomer in benzene (120 ml) was stirred for several hours with tosyl chloride (32.1 g) in benzene (120 ml), and aqueous sodium hydroxide (29 ml, 10%). The solid which formed was collected, washed with water, and recrystallized twice from 95% ethanol to give the *N*-tosyl derivative of N^aO^a **4***b* (24.5 g), m.p. 190–191° (lit. (8) 192–193°), δ (DMSO-d_6): 0.72 (s, *t*-Bu). The mother liquors were evaporated and the residue recrystallized first from benzene and then from ethanol to give the *N*-tosyl derivative of the 5-*t*-butyl analog of N^aO^a **4***b* (18 g), m.p. 176°, (lit. (17) 178–178.5°), δ (DMSO-d_6): 0.80, (s, *t*-Bu). The *N*-tosyl derivative of N^aO^a **4***b* (5.7 g) was treated with sodium (2 g) in liquid ammonia (120 ml) as reported (8), and gave the crude aminocyclohexanol N^aO^a **4***b* (2.2 g), m.p. 108–109° from ethyl acetate–petroleum ether, hydrochloride, m.p. 237–238° from ethanol–ether (lit. (8) 108.5–109.5° (base) and 239–240° (hydrochloride)). The amino alcohol N^aO^a **4***b* hydrochloride (1.9 g), m.p. and mixed m.p. 236–238°, was also obtained by hydrogenolysis of **3***b* hydrochloride (3 g) in ethanol (10 ml) with palladized carbon (0.3 g, 10%) as catalyst. Treatment of the *N*-tosyl derivative of the 5-*t*-butyl analog of N^aO^a **4***b* with Na–NH_3 similarly gave *t*-2-amino-*t*-5-*t*-butylcyclohexanol.

c-4-t-Butyl-t-2-dimethylaminocyclohexanol (5b) and Corresponding Acetate

A mixture of the aminoalcohol N^aO^a **4***b* (0.85 g), formalin (6 ml), and formic acid (4 g, 88%) was heated under reflux for 24 h. The product was evaporated under reduced pressure, the residue treated with water, re-evaporated and then made alkaline (NaOH) and extracted with ether. The dried extract (Na_2SO_4) was evaporated and the residual base acidified with ethanolic HCl and diluted with ether; N^aO^a **5***b* hydrochloride, m.p. 186–187° separated on storage at 5°.

Anal. Calcd. for $C_{12}H_{26}ClNO$: C, 61.1; H, 11.1; N, 5.9. Found: C, 61.33; H, 11.25; N, 6.02.

The base formed a methiodide, m.p. 197–198°.

Anal. Calcd. for $C_{13}H_{28}INO$: C, 45.7; H, 8.2. Found: C, 45.82; H, 8.35.

A mixture of N^aO^a **5***b* (1 g), liberated from the hydrochloride, acetyl chloride (1.2 g), and benzene (25 ml) was heated under reflux for 8 h and then evaporated. The residue in ethanol was diluted with ether when N^aO^a **5***b acetate hydrochloride* (1 g) separated, m.p. 183–184° from ethanol–ether, ν_{max} 1750 cm^{-1} (C=O).

Anal. Calcd. for $C_{14}H_{28}ClNO_2$: C, 60.52; H, 10.16. Found: C, 60.42; H, 10.08.

The **5***b* acetate hydrochloride, m.p. and mixed m.p. 182°, was also obtained by reductive methylation of the acetate of N^aO^a **4***b* (mixture of the ester hydrochloride (1 g), formalin (1.25 ml), ethanol (60 ml), and palladized carbon (1 g) stirred with hydrogen until gas absorption ceased). The **4***b* acetate was obtained by catalytic debenzylation of **3***b* acetate hydrochloride (1.5 g) using palladized carbon (1 g, 10%) as catalyst. It had m.p. 254–256° (dec.), δ (DMSO-d_6): 4.95 (m, $w_{1/2}$ 8 Hz, 1-H), 3.35 (m, $w_{1/2}$ 8.5 Hz, 2-H), 2.02 (s, OCOMe), 0.84 (s, *t*-Bu).

N,N-Dimethylation of *t*-2-amino-*t*-5-butylcyclohexanol was similarly performed to yield the *hydrochloride* of the N^aO^a *5-t-butyl analog* of **5***b*, m.p. 212°.

Anal. Calcd. for $C_{12}H_{26}ClNO$: C, 61.1; H, 11.1; N, 5.9. Found: C, 61.33; H, 11.25; N, 6.02.

A mixture of the N^aO^a base **5***b* (1 g) and acetic anhydride (10 ml) was stirred at room temperature for 4 days and then concentrated; the residue was stirred with acetone (5 ml) and methyl iodide (2 g) for 2 days. The solvents were removed and the residual salt recrystallized twice from acetone–benzene to give N^aO^a **1** iodide (0.8 g), m.p. 43–46° (approximate only because of hygroscopic nature), ν_{max} (in $CHCl_3$) 1745 cm^{-1} (C=O).

Anal. Calcd. for $C_{15}H_{30}INO_2$: C, 47.0; H, 7.9. Found: C, 47.38; H, 8.2.

N^aO^c Series

c-4-t-Butyl-t-2-carbomethoxyaminocyclohexyl Iodide (12)

Silver cyanate (47 g) and iodine (50.7 g) were added portionwise to a cold (−40°) solution of 4-*t*-butylcyclohexene (27.7 g) in ether (500 ml). After the addition the mixture was stirred at room temperature for 48 h when it formed a greenish yellow slurry. The mixture was filtered and the filtrate mixed with methanol (50 ml) and heated under reflux for 6 h and the reddish-brown solution left overnight. The solution was washed with aqueous sodium sulfite (150 ml, 10%) and then with water and finally dried (Na_2SO_4). Ether and unreacted 4-*t*-butylcyclohexene were removed by distillation and the residue cooled when a pale yellow solid (10 g) separated. A second crop (5 g) formed when the filtrate was diluted with methanol (few ml) and the combined crops were recrystallized twice from chloroform–methanol to give the acyclic urethane **12** (14 g), m.p.

Can. J. Chem. Downloaded from www.nrcresearchpress.com by 210.87.254.6 on 09/05/12
For personal use only.

154–155°, ν_{max} 3260, 3120 cm^{-1} (NH), 1700 cm^{-1} (C=O), δ ($CDCl_3$): 5.17, 4.6, 4.1 (broad bands $w_{1/2}$ 17.5, 6.5 and 14.5 Hz, respectively 1-H, 2-H, NH) 3.7 (s, OMe), 0.9 (s, *t*-Bu).

Anal. Calcd. for $C_{12}H_{22}INO_2$: C, 42.49; H, 6.53. Found: C, 42.18; H, 6.37.

*t-4-t-Butyl-c-2-aminocyclohexanol (**14**)*

The acyclic urethane **12** (5 g) was heated in an oil bath at 150° under reduced pressure (0.01 mm) for 20 min. The yellow residue was recrystallized from ethyl acetate to give colorless crystals of the *cyclic urethane* **13** (2 g), m.p. 140–142° (lit. (8) 145–146°), ν_{max} 3220, 3120 cm^{-1} (NH), 1750 cm^{-1} (C=O), δ ($CDCl_3$): 5.92 (NH), 4.63, 4.12 (broad bands, 1-H and 2-H), 0.87 (s, *t*-Bu).

Anal. Calcd. for $C_{11}H_{19}NO_2$: C, 66.96; H, 9.7. Found: C, 67.16; H, 9.62.

A mixture of cyclic urethane **13** (1.3 g) and 1 *N* potassium hydroxide in 10% aqueous ethanol (100 ml) was heated under reflux for 12 h. The ethanol was distilled and the residue extracted with chloroform which was dried (Na_2SO_4) and evaporated to give the aminocyclohexanol **14** (0.9 g), m.p. and mixed m.p. 112–113° (lit. (8) 112–113°); its m.p. was depressed to 85–86° when mixed with authentic *c*-4-*t*-butyl-*c*-2-aminocyclohexanol (samples kindly supplied by Dr. M. Tichý). It gave a hydrochloride, m.p. 242–244° (lit. (27) 249–250°).

Anal. Calcd. for $C_{10}H_{12}NO$ (base): C, 70.12; H, 12.36. Found: C, 70.39; H, 12.23.

t-4-t-Butyl-c-2-dimethylaminocyclohexanol and Derivatives

A mixture of the aminoalcohol **14** (9.5 g), formalin (75 ml), and formic acid (50.3 g, 88%) was heated under reflux for 24 h and treated as described for the isomer N^aO^a **5***b* to give the crude dimethylaminoalcohol (11.2 g), isolated as a *hydrochloride*, m.p. 190–192°.

Anal. Calcd. for $C_{12}H_{26}ClNO$: C, 61.1; H, 11.1; N, 5.9. Found: C, 61.2; H, 10.98; N, 5.80.

A mixture of N^aO^e **5***b* hydrochloride (5.7 g), chloroform (100 ml) and acetyl chloride (10 ml) was heated under reflux for 3 h. The solvents were evaporated and the residue recrystallized from ethanol–ether to give the corresponding *acetate hydrochloride* (5.8 g), m.p. 146–148°, ν_{max} 1745 cm^{-1} (C=O).

Anal. Calcd. for $C_{14}H_{28}ClNO_2$: C, 60.5; H, 10.1; N, 5.0. Found: C, 60.63; H, 10.02; N, 5.2.

The alcohol N^aO^e **5***b* with excess of methyl iodide in ether gave a *methiodide*, m.p. 160–162° from ethanol–ether.

Anal. Calcd. for $C_{13}H_{28}INO$: C, 45.7; H, 8.2; N, 4.1. Found: C, 45.79; H, 8.32; N, 4.06.

A mixture of the N^aO^e **5***b* acetate (0.42 g), methyl tosylate (0.28 g) and acetone (30 ml) was heated under reflux for 7 days. The solvent was evaporated and the residue dried in a vacuum desiccator over concentrated sulfuric acid for 2 days, then dissolved in acetone and diluted with ether. The oil which separated solidified on storage at 5° and this solid (0.56 g) was recrystallized from acetone–ether to give the *methyl tosylate* of N^aO^e **1***b*, m.p. 61–64° (hygroscopic), ν_{max} 1740 cm^{-1} (C=O), 700–600 cm^{-1} (SO_3).

Anal. Calcd. for $C_{22}H_{37}NO_5S$: C, 61.8; H, 8.72. Found: C, 61.76; H, 8.87.

Treatment of the acetate base with methyl iodide gave oils which could not be purified.

N^eO^e Series

4-t-Butyl-2-carbethoxycyclohexanone

Sodium hydride dispersion (12 g) (freed from mineral oil by several rinses with benzene) was mixed with benzene (120 ml) and diethyl carbonate (23.6 g). The mixture was heated to reflux and then 4-*t*-butylcyclohexanone (15.4 g) in benzene (50 ml) added over a period of 4 h. When addition was complete the mixture was kept at reflux for a further 1.5 h until gas evolution ceased (detected by a mercury trap connected to the condenser). Then glacial acetic acid (20 ml), followed by ice–cold water (100 ml) was added, the benzene separated and the aqueous phase extracted with more benzene. The combined benzene was washed with water and dried (Na_2SO_4). The benzene and excess of diethylcarbonate were removed under water-pump pressure and the residue distilled to give a fraction, b.p. 90–115°/1 mm. This was redistilled to give an isomeric mixture of the *2-carbethoxycyclohexanones* (16 g), b.p. 99°/0.8 mm, ν_{max} 1745 and 1725 cm^{-1} (C=O of keto form), 1655 and 1615 cm^{-1} (enol), δ (CCl_4): 4.17, 4.05 (q, OCH_2), 1.37, 1.3 (t, CH_3), 0.92, 0.87 (s, *t*-Bu) (paired signals of equal intensities).

Anal. Calcd. for $C_{13}H_{22}O_3$: C, 68.99; H, 9.8. Found: C, 69.24; H, 10.03.

*t-4-t-Butylcyclohexanol-2-t-carboxylate (**11**)*

A mixture of the previous ester (22.6 g), sodium borohydride (1.89 g), and ethanol (250 ml) was stirred for 4 h (ice bath); it was then acidified to p*H* 4–6 by addition of dilute hydrochloric acid and the solvent evaporated. The residue in ether was dried (Na_2SO_4) and the ether evaporated to give a mixture of the ethyl ester of **11** and other isomers (21 g). An analytical sample distilled at 86°/0.05 mm.

Anal. Calcd. for $C_{13}H_{24}O_3$: C, 68.38; H, 10.58. Found: C, 68.41; H, 10.34.

The ethyl esters so obtained (12 g) were treated with sodium methoxide in methanol followed by 50% aqueous sodium hydroxide as reported (8) to give the cyclohexane carboxylic acid **11** (7 g), m.p. 144–145° from acetone (lit. (8) 146–147°).

*t-2-Amino-t-4-t-butylcyclohexanol (**9**)*

The carboxylic acid **11** was methylated with diazomethane or dimethylsulfate–Na_2CO_3 in methanol to give the methyl ester of **11**, m.p. 76–77.5° (lit. (8) 79–80°). By reported procedures (8) the ester was successively converted to the corresponding acid hydrazide, m.p. 178–179° (lit. 177–178°), the cyclic urethane, m.p. 112–115° (lit. 124–125°), and the 2-aminocyclohexanol **9**, m.p. 93–94° from ethyl acetate–petroleum ether (lit. 94.5–95.5°).

t-4-t-Butyl-t-2-dimethylaminocyclohexanol and Derivatives

The aminocyclohexanol **9** (10.5 g) was treated with formalin (83 ml) and formic acid (45.6 ml, 88%) in the usual manner to give the N^eO^e 2-dimethylaminocyclohexanol **5***b* (12 g) isolated as a *hydrochloride*, m.p. 216–217.5°.

Anal. Calcd. for $C_{12}H_{26}ClNO$: C, 61.1; H, 11.1; N, 5.9. Found: C, 61.27; H, 11.09; N, 6.0.

Treatment of the base (2.5 g) with acetyl chloride (6 ml) and chloroform (30 ml) (1.5 h at reflux) gave the acetate hydrochloride of N^eO^e **5***b*, m.p. 231–232.5° from chloroform–ether.

Anal. Calcd. for $C_{14}H_{28}ClNO_2$: C, 60.5; H, 10.1; N, 5.0. Found: C, 60.08; H, 9.94; N, 4.95.

Can. J. Chem. Downloaded from www.nrcresearchpress.com by 210.87.254.6 on 09/05/12
For personal use only.

The same isomer of **5***b* formed a *methiodide*, m.p. 237.5–238.5°.

Anal. Calcd. for $C_{13}H_{28}INO$: C, 45.75; H, 8.27. Found: C, 45.52; H, 8.0.

This methiodide (3 g) was heated under reflux with acetic anhydride (25 ml) for 2 h; on cooling the N°O° *acetate* **1** *methiodide* separated, m.p. 193–194°, from ethanol–ether, ν_{max} 1745 cm^{-1} (C=O).

Anal. Calcd. for $C_{15}H_{30}INO_2$: C, 47.0; H, 7.88; N, 3.6. Found: C, 47.20; H, 7.84; N, 3.9.

N°O° Series

c-4-t-Butyl-c-2-dimethylaminocyclohexanol and Derivatives

p-Nitrobenzoyl chloride (0.92 g) in warm benzene (25 ml) was added to a suspension of the aminocyclohexanol **9** (0.85 g) in water (50 ml) followed by 5% aqueous sodium hydroxide (4 ml). The whole was stirred for several hours, then the solid collected, washed, and recrystallized from 95% ethanol to give the *N-p*-nitrobenzoyl derivative of **9** (1 g), m.p. 176°, ν_{max} 3310, 3210 (OH, NH), 1630 cm^{-1} (C=O), δ (DMSO-d_6): 4.7 (d, J = 4.5 Hz, OH) absent after D_2O.

Anal. Calcd. for $C_{17}H_{24}N_2O_4$: C, 63.75; H, 7.5. Found: C, 63.80; H, 7.69.

A mixture of the amide (10 g) so obtained and thionyl chloride (125 ml) was stirred at room temperature for 2 days. Excess of reagent was evaporated under reduced pressure and the residual crude oxazoline heated under reflux with aqueous hydrochloric acid (75 ml, 10%) and ethanol (75 ml). The product was concentrated and extracted with chloroform; this extract was evaporated and the residual crude ester hydrochloride (a 4-*t*-butyl analog of **7**) treated with formalin (100 ml), formic acid (50 ml, 88%), and solid potassium hydroxide (4 pellets). This mixture was heated under reflux for 4 days then evaporated, made alkaline with aqueous potassium hydroxide, and extracted with benzene. The filtered extract was shaken with 10% aqueous hydrochloric acid and the aqueous phase plus solid in suspension extracted with chloroform. The chloroform extract was evaporated to give the *dimethylamino ester hydrochloride monohydrate* **10** (11.9 g), m.p. 208–212° from chloroform–ether, ν_{max} 3400 (H_2O), 1720, 1730 (CO), δ (DMSO-d_6): 8.38 (s, $C_6H_4NO_2$), 5.7 (m, $w_{1/2}$ 7 Hz, 1-H), 2.8 (s, NMe_2), 0.93 (s, *t*-Bu).

Anal. Calcd. for $C_{19}H_{29}ClN_2O_4H_2O$: C, 56.65; H, 7.7; N, 6.96. Found: C, 56.42; H, 7.54; N, 7.28.

A mixture of the ester hydrochloride **10** (1.6 g), potassium hydroxide (2.8 g), ethanol (50 ml), and water (20 ml) heated under reflux for 18 h and then concentrated under reduced pressure. The residue was diluted with water (50 ml) and extracted with benzene. The N°O° dimethylaminocyclohexanol **5***b* (0.6 g) recovered from the extract was isolated as a *hydrochloride*, m.p. 224° from ethanol–ether.

Anal. Calcd. for $C_{12}H_{26}ClNO$: C, 61.1; H, 11.1. Found: C, 60.90; H, 11.20.

It formed a *methiodide*, m.p. 238–239°.

Anal. Calcd. for $C_{13}H_{28}INO$: C, 45.7; H, 8.2; N, 4.1. Found: C, 45.22; H, 8.24; N, 3.97.

A mixture of the methiodide of N°O° **5***b* (1 g), acetic anhydride (1 ml) and pyridine (2 ml) was stirred at room temperature for 28 h, then evaporated under reduced pressure. The residue was washed with ether and then stored in a vacuum desiccator over concentrated sulfuric acid. The partially solid product was dissolved in acetone then diluted with ether and stored at 5°. The solid which separated was recrystallized from acetone to give the N°O° acetate methiodide **1**, m.p. 222–223°, ν_{max} 1740 cm^{-1} (C=O).

Anal. Calcd. for $C_{15}H_{30}INO_2$: C, 47.0; H, 7.8; N, 3.6. Found: C, 47.5; H, 7.60; N, 3.60.

The authors thank the Medical Research Council of Canada for financial support, Dr. D. S. Savage for samples of dacuronium and pancuronium iodides, and Mr. Ih Chu, M.Sc. for assistance in final stages of the synthetic work.

1. (*a*) A. F. CASY and W. K. JEFFERY. Can. J. Chem. **50**, 803 (1972); (*b*) D. F. BIGGS, A. F. CASY, and W. K. JEFFERY. J. Med. Chem. **15**, 506 (1972).
2. D. F. BIGGS, A. F. CASY, I. CHU, and R. T. COUTTS. J. Med. Chem. **15**, 642 (1972).
3. A. F. CASY, M. M. A. HASSAN, and E. C. WU. J. Pharm. Sci. **60**, 67 (1971).
4. C. Y. CHIOU, J. P. LONG, J. G. CANNON, and P. D. ARMSTRONG. J. Pharmacol. Exp. Ther. **166**, 243 (1969).
5. J. G. CANNON, A. B. REGE, and T. L. GRUEN. J. Med. Chem. **15**, 71 (1972).
6. J. B. KAY and J. B. ROBINSON. J. Chem. Soc. C, 248 (1969); J. B. KAY, J. B. ROBINSON, B. COX, and D. POLKONJAK. J. Pharm. Pharmacol. **22**, 214 (1970).
7. E. E. SMISSMAN, W. L. NELSON, J. B. LA PIDUS, and J. L. DAY. J. Med. Chem. **9**, 458 (1966); E. SHEFTER and E. E. SMISSMAN. J. Pharm. Sci. **60**, 1364 (1971).
8. J. SICHER, F. SÍPOŠ, and M. TICHÝ. Coll. Czech. Chem. Commun. **26**, 847 (1961).
9. G. E. MCCASLAND and D. A. SMITH. J. Am. Chem. Soc. **72**, 2190 (1950).
10. R. A. B. BANNARD, N. C. C. GIBSON, and J. H. PARKKARI. Can. J. Chem. **49**, 2064 (1971).
11. C. C. J. CULVENOR. Tetrahedron Lett. 1091 (1966).
12. S. STERNHELL. Quart. Rev. **23**, 236 (1969).
13. E. W. GARBISCH. J. Am. Chem. Soc. 86, 1780 (1964).
14. H. BOOTH. Tetrahedron, **20**, 2211 (1964); N. C. FRANKLIN and H. FELTKAMP. Angew. Chem. Int. Ed. Engl. **4**, 774 (1965).
15. F. A. L. ANET and A. J. R. BOURN. J. Am. Chem. Soc. **87**, 5250 (1965); J. B. LAMBERT, R. G. KESKE, R. E. CAHART, and A. P. JOVANOVICH. J. Am. Chem. Soc. **89**, 3761 (1967).
16. R. U. LEMIEUX and J. D. STEVENS. Can. J. Chem. **44**, 249 (1966).
17. M. TICHÝ, J. SÍPOŠ, and J. SICHER. Coll. Czech. Chem. Commun. **27**, 2907 (1962); M. TICHÝ, S. VAŠÍČKOVÁ, A. VÍTEK, and J. SICHER. Coll. Czech. Chem. Commun. **36**, 1436 (1971).
18. R. D. STOLOW, A. A. GALLO, and J. L. MARINI. Tetrahedron Lett. 4655 (1969); M. M. A. HASSAN and A. F. CASY. Tetrahedron, **26**, 4517 (1970).
19. M. TICHÝ, S. VAŠÍČKOVÁ, S. V. ARAKELIAN, and J. SICHER. Coll. Czech. Chem. Commun. **35**, 1522 (1970).
20. A. F. CASY and M. M. A. HASSAN. Can. J. Chem. **47**, 1587 (1969).
21. C. P. RADER. J. Am. Chem. Soc. **88**, 1713 (1966); **91**, 3248 (1969).

22. D. S. SAVAGE, A. F. CAMERON, G. FERGUSON, C. HANNAWAY and I. R. MACKAY. J. Chem. Soc. B, 410 (1971).
23. J. KOVAR. Chem. Listy. **52**, 283 (1958).
24. G. E. MCCASLAND, R. K. CLARK, and H. E. CARTER. J. Am. Chem. Soc. **71**, 637 (1949).
25. K. ADANK and W. G. STOLL. Helv. Chim. Acta, **42**, 887 (1959).
26. H. D. BALDRIDGE, W. J. MCCARVILLE, and S. L. FRIESS. J. Am. Chem. Soc. **77**, 739 (1955).
27. J. SICHER, M. TICHÝ, F. SÍPOŠ, M. SVOBODA, and J. JONÁŠ. Coll. Czech. Chem. Commun. **29**, 1561 (1964).

Can. J. Chem. Downloaded from www.nrcresearchpress.com by 210.87.254.6 on 09/05/12
For personal use only.

A Model Compound for Anhydroryanodol

BRIAN G. BROWNLEE, PAK-TSUN HO, and K. WIESNER
Natural Products Research Center, University of New Brunswick, Fredericton, New Brunswick

Received July 17, 1972

The synthesis of the acetoxy lactone **17** by a method potentially suitable for anhydroryanodine is described.

In the course of the synthesis several mechanistically unusual reactions were observed. One of them was an attack of Cl^+ on an exocyclic double bond in a benzobicycloheptane system from the *endo* side. Another was a S_N2 type displacement of chlorine by chloride or acetate ions in a six-membered ring.

La synthèse de l'acétoxy lactone **17** par une méthode pouvant convenir à celle de l'anhydroryanodine est décrite.

Au cours de cette synthèse, plusieurs réactions inhabituelles quant au mécanisme ont été observées. L'une d'entre elles est l'attaque de Cl^+ sur la double liaison exocyclique d'un système benzobicycloheptane par la face *endo*. L'autre concerne le déplacement de type S_N2 d'un chlore par des ions chlorure ou acétate dans un cycle à six membres. [Traduit par le journal]

Canadian Journal of Chemistry, **50**, 4013 (1972)

Introduction

The structure and absolute stereochemistry of anhydroryanodol portrayed by the formula **I** was proposed by us in 1962 (*1*), and in 1966 we deduced (*2a*) the structure of its parent compound ryanodine **II**. When a year later **II** was finally corroborated by X-ray crystallography (*2b*),[1] it became clear to all our critics that the original proposal **I** was in fact correct in every detail. As our laboratory was committed to the development of synthetic methods for various types of diterpene alkaloids we had no plans to synthesize ryanodine or its derivatives. It was only when we realized that the methods developed by us for the synthesis of songorine (*3*) could be readily adapted to the synthesis of **I** that we decided to perform a model study (*4*) to this end.

Scheme 1 (**III** → **IV** → **V** → **VI**) formed the backbone of our plan. In the present communication we wish to describe the synthesis of compound **VI** by an expansion of this scheme, which in its original form did not work.

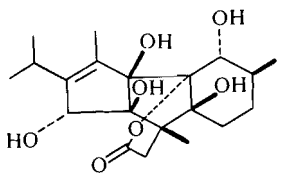

I

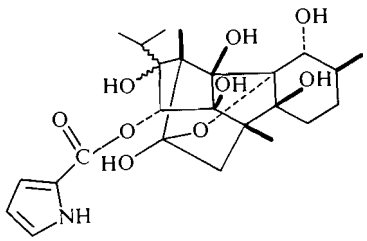

II

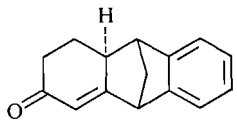

III

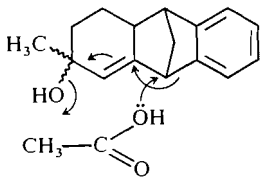

IV

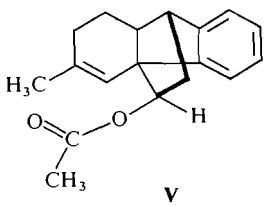

V

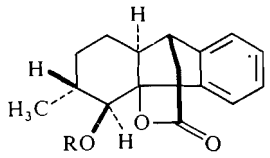

VI

SCHEME 1

[1]The X-ray work has shown the isopropyl group to be *trans* to the adjacent methyl.

Can. J. Chem. Downloaded from www.nrcresearchpress.com by 210.87.254.42 on 09/05/12
For personal use only.

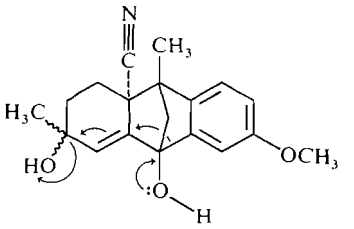

VII

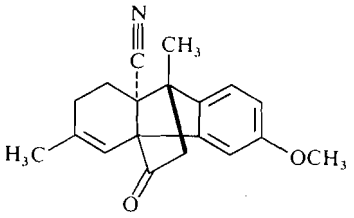

VIII

The failure of the original proposal was due to the fact that the one step rearrangement **IV** → **V** did not take place as planned.

However, in a second generation synthesis now under way the rearrangement **VII** → **VIII** was just accomplished in an almost quantitative yield.

Discussion

The starting material for the synthesis was benzonorbornadiene (5). A Diels–Alder reaction of this compound with an excess of butadiene gave the crystalline adduct **1** in a yield of 76%.

The n.m.r. spectrum of **1** contained a two-proton multiplet at $\tau = 4.12$ p.p.m. for the vinylic hydrogens. The mass spectrum of **1** had a molecular ion at *m/e* 196. The most intense peak was at *m/e* 116 corresponding to a reverse diene addition. At this point the stereochemistry of compound **1** was assumed on the basis of precedent (6), at a later stage conclusive stereochemical evidence will be presented.

Hydroboration of **1** gave the alcohol **2** as a mixture of epimers. Jones oxidation of this mixture yielded the single crystalline ketone **3** in a crude yield of 99%. Bromination of **3** with pyridine hydrobromide perbromide in acetic acid gave an oily mixture from which the crystalline bromoketone **4** was isolated in a yield of 52%. The i.r. carbonyl absorption of **4** was shifted by 25 cm^{-1} to higher wave numbers with respect to the position of the carbonyl maximum in the i.r. of **3** (1715 cm^{-1}). Such a shift indicates a conformation of the bromine in which this substituent is coplanar with the carbonyl group (7). The hydrogen deshielded by the bromine atom appeared in the n.m.r. spectrum of **4** as a doublet ($J = 12$ Hz) at $\tau = 5.3$ p.p.m. This is in agreement with the dihedral angle of about 180° between the two hydrogens marked by asterisks in formula **4**. If we assume that the preferred conformation of the ring is a boat, then the above data are in agreement with the configuration portrayed in the formula **4**.

Dehydrobromination of **4** in boiling pyridine gave an 80% yield of the crystalline unsaturated ketone **5***a*. The u.v. spectrum of **5***a* had an absorption maximum at 236 nm ($\log \varepsilon = 4.19$) and the i.r. displayed a band at 1675 cm^{-1} for the α,β-unsaturated ketone function. A one-proton singlet at $\tau = 4.0$ p.p.m. in the n.m.r. spectrum of the product further confirmed the structure **5***a* assigned to it.

On reflux with methanolic sodium hydroxide compound **5***a* was converted into an equilibrium mixture (2:8) of the starting material and the epimer **5***b* (8). The u.v. maximum of **5***b* (253 nm, $\log \varepsilon = 4.15$) was shifted significantly to high wavelength. This is undoubtedly due to orbital overlap between the α,β-unsaturated ketone and the benzene ring made possible by the stereochemistry of **5***b* but not present in **5***a*. Further support for the configuration of **5***b* came from the n.m.r. spectrum of this compound. A one-proton multiplet at $\tau = 8.8$–9.5 p.p.m. was located upfield from all proton resonances in both **5***b* and *a*. The molecular model of **5***b* shows clearly that the hydrogen marked with the arrow (in **5***b*) is located in the shielding region of the benzene ring.

Treatment of the conjugated ketone **5***a* with methylmagnesium bromide in ether gave in high yield a mixture of two crystalline epimers (3:1) represented by the formula **6**. When this mixture was heated with dilute hydrochloric acid in aqueous tetrahydrofuran a new crystalline alcohol was formed in a yield of 53%. We, of course, hoped that under these conditions the initially formed delocalized allylic carbonium ion would further delocalize by participation of the benzene ring and yield ultimately **7***b*.

Can. J. Chem. Downloaded from www.nrcresearchpress.com by 210.87.254.42 on 09/05/12
For personal use only.

Can. J. Chem. Downloaded from www.nrcresearchpress.com by 210.87.254.42 on 09/05/12
For personal use only.

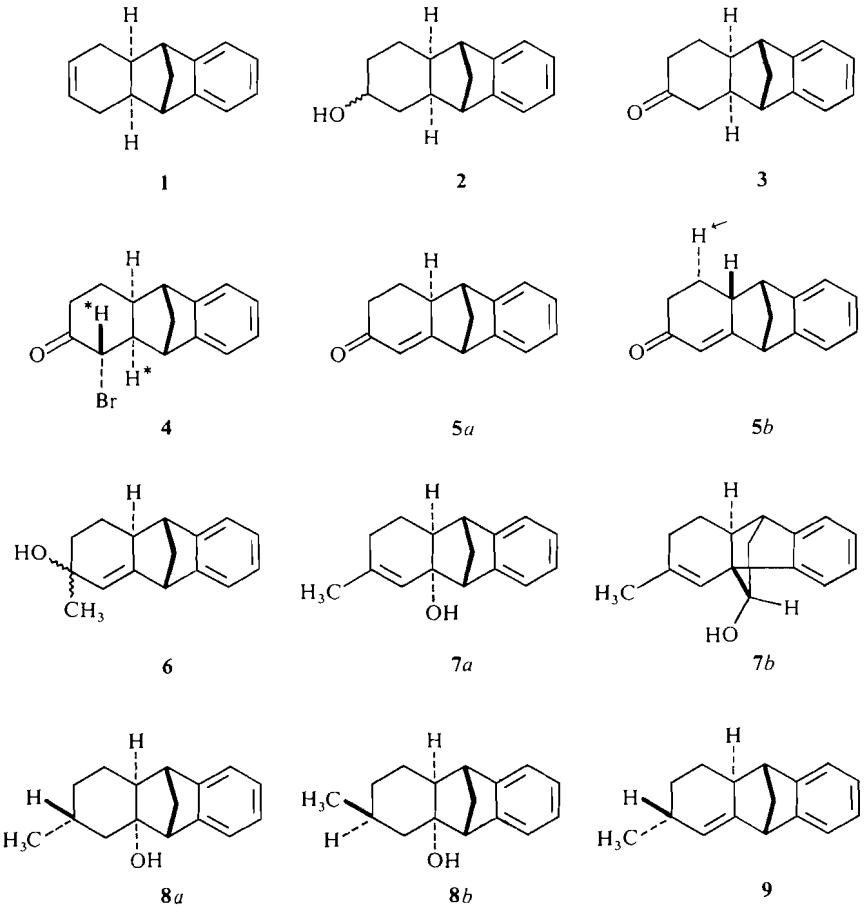

However, it soon became clear that the product of the reaction was, in fact, 7*a*. After many changes of experimental conditions and leaving groups attempts to achieve a reaction of the type **6** → 7*b* were abandoned and the synthesis was continued with 7*a*.

The n.m.r. spectrum of compound 7*a* was in agreement with the formula (see Experimental) and the tertiary nature of the hydroxyl was corroborated by its resistance to oxidation.

The configuration of the hydroxyl is probably as shown in formula 7*a*. The epimeric configuration involves considerable strain and the product was obtained under equilibriating conditions. Moreover, no spectral anomalies were found to indicate orbital overlap between the double bond and the benzene ring.

Hydrogenation of compound 7*a* with palladium on calcium carbonate gave two crystalline epimeric products **8***a* (55%) and *b* (23%). The epimer **8***a* showed in the n.m.r. spectrum a methyl doublet ($\tau = 8.92$ p.p.m., $J = 6$ Hz) at lower field than the epimer **8***b* ($\tau = 9.00$ p.p.m., $J = 6$ Hz). This seems to indicate an interaction between the hydroxyl and methyl group in compound **8***a* and consequently the configurations of the two products were assigned preliminarily as shown. The higher R_f value of **8***a* as compared to **8***b* in t.l.c. led to the same conclusion.

Dehydration of the alcohol **8***a* with thionyl chloride in pyridine gave the compound **9** as an unstable oil. A broad one-proton singlet at $\tau = 4.38$ p.p.m. in the n.m.r. spectrum of this product indicated the presence of a trisubstituted double bond.

When the olefin **9** was subjected to the action of *N*-chlorosuccinimide in glacial acetic acid, the

Can. J. Chem. Downloaded from www.nrcresearchpress.com by 210.87.254.42 on 09/05/12
For personal use only.

highly crystalline compound **10** was isolated in a yield of 48%. This acetoxy-chloro-derivative could be assigned a structure possessing the rearranged carbon skeleton on the basis of the following data. The mass spectrum had molecular ion peaks at *m/e* 306 and 304 in the ratio 1:3 as calculated for $C_{18}H_{21}ClO_2$. The base peak was at *m/e* 183 corresponding to a loss of HCl and $CH_3—CO_2—\underset{|}{CH}—CH_2—$. The n.m.r. spectrum of **10** had a one-proton doublet (J = 3.5 Hz) at $\tau = 5.12$ p.p.m. for the hydrogen deshielded by chlorine, a one-proton quartet (ABX) at $\tau = 5.27$ p.p.m. for the hydrogen deshielded by the acetoxy group, and a broad one-proton singlet at $\tau = 6.86$ p.p.m. for a lone bridgehead hydrogen. The acetoxy group was assigned the *exo* configuration on mechanistic grounds in view of the known preference for *exo* attack of solvent on bridged benzo bicycloheptane carbonium ions. On the other hand the configuration of the chlorine was assigned only on the basis of the small coupling constant (in the n.m.r. spectrum) of the hydrogen unshielded by this substituent.

As a matter of fact we have expected the chlorine to have the opposite configuration (as in **12**) since this epimer could be formed by a fully concerted attack of Cl^+ and acetic acid on **9** with simultaneous rearrangement. However, the fragmentation of compound **10** discovered subsequently corroborated unambiguously the configuration of this product. Treatment of the acetoxychloride **10** with methanolic sodium hydroxide gave the unstable oily aldehyde **11**. This material showed absorption peaks in the i.r. at 2710 and 1730 cm^{-1} in agreement with the presence of the aldehyde group. A u.v. absorption maximum at 255 nm ($\log \varepsilon = 4.27$) indicated the conjugation of the double bond and the benzene ring. The n.m.r. spectrum contained a one-proton triplet (J = 1 Hz) at $\tau = 0.25$ p.p.m. for the aldehyde hydrogen, a one-proton multiplet at $\tau = 4.15$ p.p.m. for a vinylic hydrogen, a one-proton quartet (apparent J = 7 Hz) at τ = 6.30 p.p.m. for the benzylic hydrogen, and a two-proton double triplet (J = 6 and 1 Hz) at $\tau = 7.60$ p.p.m. for the methylene group adjacent to the aldehyde carbonyl.

The facile formation of the aldehyde **11** from **10** and the subsequent finding that the epimer **12** only hydrolyzes to the corresponding chloroalcohol under the same conditions clearly defines the configuration of the chlorine in both compounds.

Treatment of **10** with an excess of lithium chloride in dimethylformamide gave the crystalline compound **12**. The mass and n.m.r. spectra of this material (see Experimental) have shown that it is a diastereoisomer of **10**. The only significant difference in the spectral properties of both diastereoisomers may be seen in the n.m.r. spectrum. The hydrogen unshielded by the chlorine in compound **12** gives a one-proton doublet (J = 10.5 Hz) typical for *trans* diaxial splitting. Thus, compound **12** was produced by a chlorine–chlorine displacement with inversion of configuration and the spectral data combined with the fragmentation of the epimer **10** provide rigorous evidence of the entire stereochemistry for all products involved.[2] Treatment of the acetoxychloride **10** with tetraethylammonium acetate in DMF at 120° yielded the crystalline diacetate **13** by a displacement of the chlorine with inversion of configuration. The n.m.r. of compound **13** had a one-proton doublet at τ = 4.55 p.p.m. (J = 10 Hz) for the proton deshielded by the acetate and adjacent to the methyl group. As in compound **12** (and in ryanodine) this splitting is characteristic for the *trans* diequatorial stereochemistry of the acetoxy and methyl groups.

Selective hydrolysis of **13** gave the crystalline acetoxy alcohol **14** in a yield of 64%.

Oxidation of this product by the Jones reagent yielded quantitatively the crystalline ketone **15**. The i.r. spectrum of **15** had a carbonyl band at 1745 with a shoulder at 1735 cm^{-1}. The n.m.r. showed a one-proton doublet (J = 10 Hz) at $\tau = 4.72$ p.p.m. for the hydrogen deshielded by the acetate and an acetate methyl singlet at $\tau = 7.73$ p.p.m. Hydrolysis of the acetoxy ketone **15** gave the crystalline alcohol **16** which was prepared to characterize the carbonyl absorption of the keto group. Compound **16** showed in the i.r. spectrum as expected a single carbonyl band at 1735 cm^{-1} in agreement with a ketone in a five-membered ring.

[2]The doublet of the hydrogen unshielded by chlorine in compound **12** is exactly the same as the doublet of the proton unshielded by the ring-carbon oxygen in various ryanodine derivatives *cf.* ref. 1.

Can. J. Chem. Downloaded from www.nrcresearchpress.com by 210.87.254.42 on 09/05/12
For personal use only.

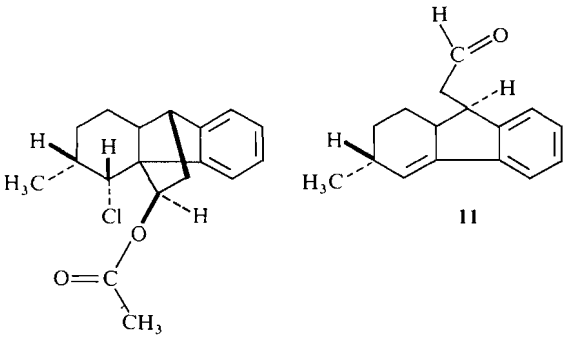

10

11

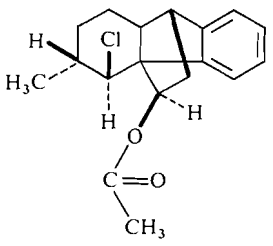

12

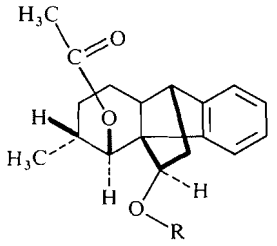

13 R = $C(=O)CH_3$
14 R = H

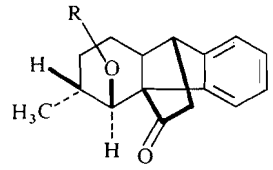

15 R = $C(=O)CH_3$
16 R = H

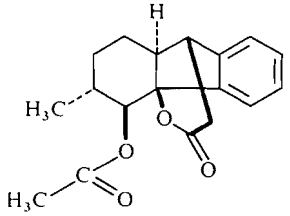

17

Finally, a Baeyer–Villiger oxidation of the acetoxy ketone **15** gave the crystalline lactone **17** in a yield of 67% (based on consumed starting material).[3] The mass spectrum of lactone **17** had a molecular ion at $m/e = 300$ ($C_{18}H_{20}O_4$). The base peak was at $m/e = 196$ ($C_{15}H_{16}$) for the loss of acetic acid and CO_2. The i.r. spectrum had carbonyl absorptions at 1735 and 1720 cm^{-1} for the ester and Δ-lactone functions. The n.m.r. spectrum had a one proton doublet ($J = 10$ Hz) at $\tau = 4.78$ p.p.m. for the hydrogen deshielded by the acetoxyl, a one-proton multiplet at $\tau = 6.7$ p.p.m. for the bridgehead hydrogen, a one-proton doublet ($J = 4$ Hz) at $\tau = 7.18$ p.p.m., and a one-proton doublet ($J = 2$ Hz) at $\tau = 7.3$ p.p.m. for the two hydrogens adjacent to the lactone carbonyl, a three-proton singlet at $\tau = 7.70$ p.p.m. for the acetate methyl, and a three-proton doublet ($J = 6.5$ Hz) for the secondary *C*-methyl. The alternative structure in which the oxygen and the carbonyl groups of the lactone are interchanged is ruled out since it would show the presence of two hydrogens deshielded by the lactone oxygen.

[3]Experiments involving the construction of the anhydroryanodine lactone by a Baeyer–Villiger oxidation of a bicyclo(2.2.1)heptanone derivative were conducted with an entirely different system by P. Cavanagh and K. Wiesner in 1965.

The same construction of the lactone is also envisaged in the synthetic approach of P. Deslongchamps (9).

Experimental

Preparation of the Diels–Alder Adduct **1**

Benzonorbornadiene (5) (8.6 g), hydroquinone (0.1 g), and excess butadiene (25 ml, measured at −70 °C) in dry benzene (100 ml) were heated to 200–220 °C for 40 h in a steel bomb. Evaporation of solvent and volatile by-products left 24 g of crude product which was purified by chromatography on silica gel (720 g). Elution with petroleum ether (b.p. 30–60 °C, 10 l) removed unwanted by-products from the column. Elution with petroleum ether–benzene (9:1, v/v) gave 9.0 g (76%) of **1**, homogeneous by t.l.c. Recrystallization from ethanol three times gave pure material as colorless plates m.p. 62–63 °C.

Anal. Calcd. for $C_{15}H_{16}$ (mol. wt. 196): C, 91.78; H, 8.22. Found (196 (mass spectroscopy)): C, 91.37; H, 8.21.

N.m.r. ($CDCl_3$)τ: unresolved multiplet (2H) 4.12 (vinylic hydrogens), unresolved multiplet (2H) 7.03 p.p.m. (bridgehead hydrogens).

Hydroboration of **1** *to* **2**

The olefin **1** (9.1 g) in dry tetrahydrofuran (100 ml) was stirred 2 h under a dry nitrogen atmosphere with a solution of borane in tetrahydrofuran (1 *M*, 17 ml). Excess borane was decomposed by dropwise addition of water (15–20 drops). Sodium hydroxide solution (2.5 *M*, 5.6 ml) was added and the organoborane was oxidized by addition of 30% hydrogen peroxide (5.6 ml) in small portions at a rate sufficient to maintain a temperature of 40–50 °C in the reaction mixture. After 1 h the solution was poured into ice-water (500 ml) and extracted with three portions of methylene chloride (100 ml). The aqueous phase was rendered slightly acidic with dilute hydrochloric acid to facilitate separation of the organic phase. The combined methylene chloride extracts were washed with water (100 ml), dried over anhydrous magnesium sulfate, and evaporated to give 9.2 g (92%) of a mixture of epimeric alcohols **2**. A small portion of the material was purified by crystallization from ether–hexane and preparative t.l.c. and had m.p. 120–130 °C.

Anal. Calcd. for $C_{15}H_{18}O$ (mol. wt. 214): C, 84.07; H, 8.47. Found (214 (mass spectroscopy)): C, 83.72; H, 8.46.

Can. J. Chem. Downloaded from www.nrcresearchpress.com by 210.87.254.42 on 09/05/12
For personal use only.

I.r. (CCl_4): 3620 cm^{-1} (hydroxyl); n.m.r. ($CDCl_3$)τ: several peaks 5.7–6.5 (H—C—O), broad singlet (2H) 7.10 p.p.m. (bridgehead hydrogens).

Oxidation of Alcohol **2** *to Ketone* **3**

Jones' reagent (10 ml) was added dropwise to a well-stirred, ice-cold solution of alcohol **2** (8.56 g) in acetone (100 ml). The acetone solution was decanted from precipitated chromium salts into 500 ml of ice-water and extracted with three portions of methylene chloride (100 ml). The precipitated chromium salts were dissolved in water and the solution was extracted with methylene chloride (50 ml). The combined methylene chloride extracts were washed with dilute sodium chloride solution, dried over anhydrous magnesium sulfate, and evaporated to give 8.4 g (99%) of crude ketone **3**. After three recrystallizations from carbon tetrachloride–hexane (1:2, v/v), the pure material had a m.p. 134–134.5 °C.

Anal. Calcd. for $C_{15}H_{16}O$ (mol. wt. 212): C, 84.87; H, 7.60. Found (212 (mass spectroscopy)): C, 84.81; H, 7.48.

I.r. (CCl_4): 1715 cm^{-1} (ketone); n.m.r. ($CDCl_3$)τ: broad singlet (2H) 6.93 p.p.m. (bridgehead hydrogens).

Preparation of Bromoketone **4**

The ketone **3** (4.25 g) was dissolved in glacial acetic acid (100 ml). Pyridine hydrobromide perbromide (6.7 g) was added in small portions to the stirred solution. After 0.25 h the solution was poured into ice-water (600 ml) and extracted with three portions of chloroform (100 ml). The combined extracts were washed with water (100 ml), dried over anhydrous magnesium sulfate, and evaporated to give an oil which still contained some acetic acid. This was conveniently removed by azeotropic distillation with two portions of benzene (25 ml). The yield of thick yellow oil was 5.70 g. Analysis by t.l.c. showed this material to consist of three components (approximate ratio, 60:30:10).

This oil was dissolved in hot carbon tetrachloride (15 ml) and the solution was diluted with hexane. Upon cooling there was deposited 3.00 g (52%) of crystalline bromoketone **4**, m.p. 120–132 °C. Material of this purity was used in the subsequent step. Further recrystallizations gave pure material, m.p. 136–137.5 °C.

Anal. Calcd. for $C_{15}H_{15}BrO$ (mol. wt. 290 and 292): C, 61.86; H, 5.19; Br, 27.45. Found (290 and 292 (mass spectroscopy)): C, 61.51; H, 4.88; Br, 30.24.

I.r. (CCl_4): 1740 cm^{-1} (ketone); n.m.r. ($CDCl_3$)τ: doublet (J = 12 Hz, 1H) 5.30 (BrC—H), broad singlet (1H) 6.40 (bridgehead hydrogen), broad singlet (1H) 6.81 p.p.m. (bridgehead hydrogen).

Preparation of α,β*-Unsaturated Ketone* **5***a*

The bromoketone **4** (9.0 g) was heated under reflux with dry pyridine (100 ml) for 6 h. The cooled reaction mixture was poured into ice-water (1000 ml) containing concentrated hydrochloric acid (120 ml), and extracted with two portions of methylene chloride (200 ml). The combined extracts were washed once with dilute hydrochloric acid, dried over anhydrous magnesium sulfate, and evaporated to give 5.7 g of crude product. Chromatography on a column of neutral alumina (175 g, activity grade II) gave 5.2 g (80%) of pure **5***a* eluted with benzene. For analysis, the material was recrystallized from ether–hexane to a m.p. of 99–100 °C.

Anal. Calcd. for $C_{15}H_{14}O$ (mol. wt. 210): C, 85.67; H, 6.71. Found (210 (mass spectroscopy)): C, 85.35; H, 6.67.

I.r. (CCl_4): 1675 cm^{-1} (α,β-unsaturated ketone); u.v. (EtOH): λ_{max} 236 nm (log ε 4.19); n.m.r. ($CDCl_3$)τ: broad singlet (1H) 4.00 (vinylic hydrogen), broad singlet (1H) 6.06 (bridgehead hydrogen), broad singlet (1H) 6.76 p.p.m. (bridgehead hydrogen).

Isomerization of **5***a* *to* **5***b*

The α,β-unsaturated ketone **5***a* (0.210 g, 1.00 mmol) and 1% sodium hydroxide in 90% aqueous methanol were heated to reflux under nitrogen. Analysis by t.l.c. showed the appearance of a new compound **5***b* of lesser mobility. After 30 h it appeared that equilibrium had been obtained (ratio of **5***a* to *b* about 1:5). The reaction mixture was poured into ice-water and extracted with two portions of ether (25 ml). The ether extracts were washed twice with water (25 ml), saturated sodium chloride solution (25 ml), then combined and dried over anhydrous magnesium sulfate. Evaporation of the solvent gave 0.204 g of an oily mixture of α,β-unsaturated ketones **5***a* and *b*. This mixture was separated by preparative t.l.c. on silica gel using hexane–ether 1:1 (v/v). Recovered starting material (0.024 g) had m.p. 89–95 °C and i.r. and n.m.r. spectra identical to authentic **5***a*. The new isomer **5***b* was obtained as a colorless oil (0.140 g).

Mol. Wt. Calcd. for $C_{15}H_{14}O$: 210. Found (mass spectroscopy): 210.

The entire mass spectra of **5***a* and *b* were practically identical.

I.r. (CCl_4): 1675 cm^{-1} (α,β-unsaturated ketone); u.v. (EtOH): λ_{max} 253 nm (log ε 4.15); n.m.r. ($CDCl_3$)τ: doublet (J = 2.5 Hz, 1H) 4.05 (vinylic hydrogen), broad singlet ($w_{1/2h}$ = 3.5 Hz, 1H) τ = 6.03 (bridgehead hydrogen), broad singlet ($w_{1/2h}$ = 7.5 Hz, 1H) 6.56 (bridgehead hydrogen), multiplet (1H) 8.8–9.5 p.p.m. (methylene hydrogen shielded by aromatic ring).

Preparation of Tertiary Allylic Alcohol **6**

A solution of unsaturated ketone **5***a* (2.0 g) in dry ether (80 ml) was added dropwise (0.5 h) to a stirred solution of excess methyl-magnesium bromide (30 mmol) in dry ether (50 ml) under a dry nitrogen atmosphere. The reaction mixture was stirred for 3 h at room temperature and 2 h at reflux. The reaction mixture was cooled (ice-bath) and poured into cold 5% ammonium chloride solution (100 ml). The ether layer was separated, washed with ice-water (100 ml), saturated sodium chloride solution (100 ml), and dried briefly over anhydrous magnesium sulfate. Removal of the solvent *in vacuo* at 20–25 °C gave 2.0 g (93%) of **6** as a waxy, white solid. This material appeared as a 3:1 mixture when examined by t.l.c. on silica gel using pentane–ether (1:1, v/v) as developing solvent.

A portion (100 mg) of this mixture was separated by preparative t.l.c. There was obtained 63 mg of the isomer of higher mobility as white needles m.p. 112–114 °C (stage preheated to 100 °C).

Anal. Calcd. for $C_{16}H_{18}O$: C, 84.92; H, 8.02. Found: C, 84.75; H, 7.69.

I.r. (CCl_4): 3610, 3450 (hydroxyl); 1675 cm^{-1} (—CH=C<); n.m.r. ($CDCl_3$)τ: broad singlet (1H) 4.48 (vinylic hydrogen), broad singlet (1H) 6.31 (bridgehead hydrogen), broad

Can. J. Chem. Downloaded from www.nrcresearchpress.com by 210.87.254.42 on 09/05/12
For personal use only.

singlet (1H) 6.90 (bridgehead hydrogen), singlet 8.55 (hydroxyl), and singlet 8.70 p.p.m. (C—CH_3).

The isomer of lower mobility (19 mg) was obtained as a slightly waxy material, m.p. 121–123 °C (stage preheated to 115 °C).

Anal. Calcd. for $C_{16}H_{18}O$: C, 84.92; H, 8.02. Found: C, 84.67; H, 7.71.

I.r. (CCl_4): 3610, 3450 (hydroxyl); 1675 cm^{-1} (—HC=C<); n.m.r. ($CDCl_3$)τ: broad singlet (1H) 4.46 (vinylic hydrogen), broad singlet (1H) 6.30 (bridgehead hydrogen), broad singlet (1H) 6.86 (bridgehead hydrogen), singlet 8.44 (hydroxyl), and singlet 8.77 p.p.m. (C—CH_3).

Rearrangement of Alcohol **6** *to Alcohol* 7*a*

The alcohol **6** (2.94 g) was dissolved in tetrahydrofuran (130 ml) and to this solution was added 0.02 *N* hydrochloric acid (130 ml). The solution was stirred at room temperature for 18 h, diluted with saturated sodium chloride solution and extracted twice with ether (200 ml). The combined ether extracts were washed with two portions of saturated sodium chloride solution (250 ml) and dried over anhydrous magnesium sulfate. Evaporation of the solvent gave 3.0 g of a thick oil which was chromatographed on silica gel (120 g). Elution with 5–10% ether in petroleum ether (b.p. 30–60 °C) removed less polar material. Pure 7*a* was eluted with 20–25% ether in petroleum ether. The yield was 1.55 g (53%). Two recrystallizations from ether–hexane gave an analytical sample as white needles m.p. 82.5–83 °C.

Anal. Calcd. for $C_{16}H_{18}O$ (mol. wt. 226): C, 84.92; H, 8.02. Found (226 (mass spectroscopy)): C, 85.38; H, 7.95.

I.r. (CCl_4): 3610, 3560 (hydroxyl), and 1670 cm^{-1} (—HC—C<); n.m.r. ($CDCl_3$)τ: broad singlet (1H) 4.34 (vinylic hydrogen), unresolved multiplet (1H) 6.95 (bridgehead hydrogen), unresolved multiplet (1H) 7.10 (bridgehead hydrogen), doublet ($J = 1$ Hz) 8.25 (vinylic —CH_3), and singlet 8.92 p.p.m. (hydroxyl).

Hydrogenation of Alcohol 7*a to the Dihydro Alcohols* **8***a and b*

The allylic alcohol 7*a* (1.55 g) was hydrogenated in absolute ethanol (150 ml) with 10% palladium on calcium carbonate (1.5 g) for 12 h. The product (1.56 g) was a mixture of two compounds which could be separated by chromatography on silica gel (75 g). Epimer **8***a* (0.860 g, 55%) was eluted with 5% ether in petroleum ether (b.p. 30–60 °C). Elution with 6% ether in petroleum ether gave 0.157 g of a mixture of **8***a* and *b*, and epimer **8***b* (0.365 g, 23%) was eluted with 10% ether in petroleum ether.

In a small-scale experiment using 0.200 g of 7*a*, 20 ml of ethanol and 0.20 g of catalyst there was obtained, after purification by preparative t.l.c., 0.115 g (57%) of **8***a* as long white needles m.p. 51–53 °C, and 0.073 g (36%) of **8***b* as fine white needles m.p. 99–101 °C.

After sublimation epimer **8***a* had m.p. 52–53 °C.

Anal. Calcd. for $C_{16}H_{20}O$ (mol. wt. 228): C, 84.18; H, 8.83. Found (228 (mass spectroscopy)): C, 84.11; H, 8.67.

I.r. (CCl_4): 3630, 3575 cm^{-1} (hydroxyl); n.m.r. ($CDCl_3$)τ: unresolved multiplet (2H) 7.04 (bridgehead hydrogens), doublet ($J = 6$ Hz) 8.92 (C—CH_3), singlet 9.07 p.p.m. (hydroxyl).

After sublimation epimer **8***b* had m.p. 102–103 °C.

Anal. Calcd. for $C_{16}H_{20}O$ (mol. wt. 228): C, 84.18; H, 8.83. Found (228 (mass spectroscopy)): C, 83.93; H, 8.73.

I.r. (CCl_4): 3630, 3575 cm^{-1} (hydroxyl); n.m.r. ($CDCl_3$)τ: unresolved multiplet (2H) 7.04 (bridgehead hydrogens), doublet ($J = 6$ Hz) 9.00 p.p.m. (C—CH_3).

Dehydration of **8***a to Olefin* **9**

The alcohol **8***a* (1.14 g) dissolved in dry pyridine (25 ml) was cooled to −10 °C (methanol–ice bath) and treated with excess thionyl chloride (0.50 ml, 0.82 g). The reaction mixture was stirred 1 h at −10 °C and then warmed to 25–30 °C. The excess thionyl chloride and most of the pyridine were removed by water aspirator suction. The residue was treated with ice-water (50 ml) and extracted with ether (50 ml and 25 ml). The ether extracts were washed four times with water (50 ml), saturated sodium chloride solution (50 ml), then combined and dried over anhydrous magnesium sulfate. Evaporation of the solvent gave 1.05 g of a pale-yellow oil showing 15–20% of impurities in the n.m.r. spectrum.

A small sample was purified by preparative t.l.c. on silica gel (hexane as solvent) to give pure **9** as a colorless oil.

Mol. Wt. Calcd. for $C_{16}H_{18}$: 210. Found (mass spectroscopy): 210.

I.r. (CCl_4): 1675 cm^{-1} (—HC=C<); n.m.r. (CCl_4)τ: broad singlet (1H) 4.38 (vinylic hydrogen), broad singlet (1H) 6.38 (bridgehead hydrogen), broad singlet (1H) 6.93 (bridgehead hydrogen), doublet ($J = 6.5$ Hz) 9.05 p.p.m. (C—CH_3).

Preparation of Rearranged Chloro-acetate **10**

The olefin **9** (2.13 g of crude material of about 80% purity) was dissolved in glacial acetic acid (25 ml) and treated with *N*-chlorosuccinimide (1.07 g). The reaction mixture was stirred 3 h at room temperature and most of the acetic acid was removed *in vacuo*. The residue was treated with ice-water and extracted with ether (100 ml and 50 ml). The ether extracts were washed with three portions of water (50 ml), saturated sodium chloride solution (50 ml), combined, and dried over anhydrous magnesium sulfate. The solvent was evaporated and traces of acetic acid were removed from the residue by azeotropic distillation with two portions of benzene (25 ml). The yield of crude product was 2.77 g. Chromatography on silica gel (80 g) and elution with benzene removed less polar impurities. Elution with benzene–ether (9:1, v/v) gave 1.73 g of **10**. Pure **10** m.p. 158–159 °C was obtained by crystallization from ether–hexane. The yield was 1.45 g (48% based on **8***a*).

Anal. Calcd. for $C_{18}H_{21}ClO_2$ (mol. wt. 304 and 306): C, 70.92; H, 6.94; Cl, 11.63. Found (304 and 306 (mass spectroscopy)): C, 71.00; H, 6.94; Cl, 11.72.

I.r. (CCl_4): 1740 (ester carbonyl), 1225, 1030 cm^{-1} (ester —C—O—); (KBr): 1735 (ester carbonyl), 1240, 1045 cm^{-1} (ester—C—O—); n.m.r. ($CDCl_3$)τ: doublet ($J = 3.5$ Hz, 1H) 5.13 (—CHCl—); quartet, X portion of ABX (1H) 5.27 (secondary acetate); broad singlet (1H) 6.86 (bridgehead hydrogen); singlet 7.94 (acetate methyl); doublet ($J = 7$ Hz) 8.90 p.p.m. (C—CH_3).

Alkali Cleavage of **10**

The acetoxychloride **10** (34 mg) was dissolved in methanol (3.8 ml) and 10% sodium hydroxide solution (0.2 ml) was added. The solution was stirred 2 h at room temperature, then poured into ice-water (50 ml) and extracted with two portions of ether (25 ml and 10 ml). The ether extracts were washed with two portions of water (25 ml), saturated

Can. J. Chem. Downloaded from www.nrcresearchpress.com by 210.87.254.42 on 09/05/12
For personal use only.

sodium chloride solution (25 ml), combined and dried over anhydrous magnesium sulfate. Evaporation of the solvent gave 22 mg (89%) of **11** as a colorless oil homogeneous by t.l.c. (hexane–ether 4:1, v/v).

Mol. wt. for $C_{16}H_{18}O$: 226. Found (mass spectrometry): 226.

I.r. (CCl_4): 2710 (aldehyde C—H) and 1730 cm^{-1} (aldehyde carbonyl); u.v. (EtOH): λ_{max} 255 nm (log ε 4.27); n.m.r. (CCl_4)τ: triplet ($J = 1$ Hz, 1H) 0.25 (aldehyde H), multiplet (1H) 4.15 (vinylic hydrogen), quartet ($J = 7$ Hz, 1H) 6.30 (benzylic hydrogen), double triplet ($J = 6$ Hz and 1 Hz, 2H) 7.60 (—CH_2—$\overset{O}{\overset{\|}{C}}$—), and doublet ($J = 6.5$ Hz, 3H) 8.92 p.p.m. (C—CH_3).

Preparation of Acetoxychloride ***12***

A solution of acetoxychloride **10** (0.155 g) and lithium chloride (0.105 g, dried at 160°) in dry *N*,*N*-dimethylformamide (DMF) (5 ml) was stirred for 24 h at 140–145 °C under a nitrogen atmosphere. The cooled reaction mixture was poured into ice-water (100 ml) and extracted with ether (50 ml and 25 ml). The ether extracts were washed with two portions of water (50 ml), saturated sodium chloride solution (50 ml), combined and dried over anhydrous magnesium sulfate. Evaporation of the ether gave 0.27 g of a colorless oil which still contained some DMF. Analysis by t.l.c. showed the presence of a small amount of starting material. This oil was subjected to preparative t.l.c. on silica gel using benzene–chloroform (1:1, v/v) and the resulting solid product was crystallized from ether–hexane to give 64 mg (41%) of pure acetoxychloride **12** as white needles m.p. 125–126.5 °C. The analytical sample obtained after one recrystallization had m.p. 125.5–126.5 °C.

Anal. Calcd. for $C_{18}H_{21}ClO_2$ (mol. wt. 304 and 306): C, 70.92; H, 6.94; Cl, 11.63. Found (304 and 306 (mass spectroscopy)): C, 70.95; H, 6.93; Cl, 11.65.

I.r. (KBr): 1730 (ester carbonyl), 1235, 1035, 1030 cm^{-1} (ester —C—O—); n.m.r. ($CDCl_3$): multiplet (1H) 2.43 (aromatic hydrogen); doublet (3H) 2.90 (aromatic hydrogens); quartet, X portion of ABX (1H) 5.03 (secondary acetate); doublet ($J = 10.5$ Hz, 1H) 5.80 (—CHCl—); broad doublet (1H) 6.82 (bridgehead hydrogen); singlet (3H) 7.92 (acetate methyl); doublet ($J = 6.5$ Hz, 3H) 8.85 p.p.m. (C—CH_3).

Saponification of Compound ***12*** *to the Corresponding Chloroalcohol*

The acetoxychloride **12** (78 mg) was dissolved in methanol (4.5 ml) and 10% sodium hydroxide solution (0.5 ml) was added. The solution was stirred under nitrogen for 24 h at room temperature. The methanol was removed *in vacuo*, ice-water (25 ml) was added to the residue, and the product was extracted into ether (two portions of 20 ml). The ether extracts were washed with two portions of water (25 ml), saturated sodium chloride solution (25 ml), combined and dried over anhydrous magnesium sulfate. Evaporation of the solvent gave 66 mg of a colorless oil. Purification by preparative t.l.c. ($CHCl_3$) gave 50 mg (77%) of the pure chloroalcohol as a colorless oil homogeneous by t.l.c.

Mass spectrum: parent ion less HCl at *m/e* 226; i.r. (CCl_4): 3600 cm^{-1} (hydroxyl); n.m.r. ($CDCl_3$)τ: multiplet (1H) 2.50 (aromatic hydrogen); multiplet (3H) 2.92 (aromatic hydrogens); doublet ($J = 10.5$ Hz, 1H) 5.66 (—CHCl—); quartet, X portion of ABX (1H) 5.85 (secondary alcohol); multiplet (1H) 6.84 (bridgehead hydrogen); doublet ($J = 7$ Hz, 3H) 8.84 p.p.m. (C—CH_3). The material was characterized by oxidation to the corresponding ketone. The chloroalcohol (50 mg) in acetone (2 ml) was oxidized at 0 °C with Jones' reagent. The acetone solution was poured into ice-water (25 ml) and extracted with ether (two portions of 10 ml). The ether extracts were washed with two portions of water (10 ml), saturated sodium chloride solution (10 ml), combined and dried over anhydrous magnesium sulfate. Evaporation of the solvent gave 49 mg of a white solid. After preparative t.l.c. ($CHCl_3$) and crystallization of the product from ether–hexane, the pure chloroketone (45 mg, 91%) was obtained as white needles, m.p. 147–147.5 °C. The analytical sample had m.p. 147.5–148 °C after one recrystallization.

Anal. Calcd. for $C_{16}H_{17}ClO$ (mol. wt. 260 and 262): C, 73.70; H, 6.57; Cl, 13.59. Found (260 and 262 (mass spectroscopy)): C, 73.83; H, 6.63; Cl, 13.59.

I.r. (KBr): 1735 cm^{-1} (ketone in five-membered ring); n.m.r. ($CDCl_3$)τ: multiplet (1H) 2.25 (aromatic hydrogen), multiplet (3H) 2.85 (aromatic hydrogens), doublet ($J = 10$ Hz, 1H) 6.05 (—CHCl—), multiplet (1H) 6.73 (bridgehead hydrogen), doublet ($J = 6$ Hz, 3H) 8.89 p.p.m. (C—CH_3).

Preparation of the Diacetate ***13***

The acetoxychloride **10** (0.183 g), tetraethylammonium acetate (0.57 g, five-fold excess), and dry DMF (6 ml) were heated to 120–125 °C for 18 h under a dry nitrogen atmosphere. The cooled reaction mixture was poured into ice-water (150 ml) and extracted with ether (50 ml and 25 ml). The ether extracts were washed with two portions of water (50 ml), saturated sodium chloride solution (50 ml), combined and dried over anhydrous magnesium sulfate. Evaporation of the solvent gave 0.182 g of a brown oil. The pure diacetate **18** was isolated by preparative t.l.c. ($CHCl_3$) and crystallization of the product from hexane. The yield of white needles, m.p. 147–148 °C, was 63 mg (32%).

Anal. Calcd. for $C_{20}H_{24}O_4$ (mol. wt. 328): C, 73.14; H, 7.37. Found (328 (mass spectroscopy)): C, 73.48; H, 7.61.

I.r. (KBr): 1735 (acetate carbonyl), 1240, 1220, 1045, 1035, 1020 cm^{-1} (acetate —C—O—); n.m.r. ($CDCl_3$)τ: doublet ($J = 10$ Hz, 1H) 4.55 (secondary acetate); quartet, X portion of ABX (1H) 5.00 (secondary acetate); multiplet (1H) 6.82 (bridgehead hydrogen); singlet (3H) 7.86 (acetate methyl); singlet (3H) 7.91 (acetate methyl); doublet ($J = 6$ Hz, 3H) 9.05 p.p.m. (C—CH_3).

Partial Hydrolysis of Diacetate ***13*** *to Monoacetate* ***14***

The diacetate **13** (0.108 g) was dissolved in 90% aqueous methanol containing 0.2% sodium hydroxide (10.0 ml, 1.5 equiv of NaOH). The reaction mixture was stirred at room temperature and the course of the reaction was followed by t.l.c. (benzene–methanol 19:1, v/v). As the starting material was consumed a product of intermediate R_f (monoacetate) appeared, followed more slowly by a product of low R_f (diol). After 12 h the reaction mixture was poured into ice-water (100 ml) and extracted with ether (25 ml and 20 ml). The ether extracts were washed with two portions of water (25 ml), saturated sodium chloride solution (25 ml), combined and dried over anhydrous magnesium sulfate. Evaporation of the solvent gave 0.100 g of a colorless oil. Separation by preparative t.l.c. gave 24 mg of recovered

Can. J. Chem. Downloaded from www.nrcresearchpress.com by 210.87.254.42 on 09/05/12
For personal use only.

starting material, 60 mg (64%) of monoacetate **14** as a white solid homogeneous by t.l.c., and 12 mg of the material of low R_f (diol) as a white solid. The monoacetate crystallized from hexane as slender needles m.p. 169–169.5 °C.

Anal. Calcd. for $C_{18}H_{22}O_3$ (mol. wt. 286): C, 75.49; H, 7.74. Found (286 (mass spectroscopy)): C, 75.88; H, 7.65.

I.r. (CCl_4): 3610 (hydroxyl), 1740 (acetate carbonyl), 1230 cm^{-1} (—C—O—); (KBr): 3490 (hydroxyl), 1710 (acetate carbonyl), 1260 cm^{-1} (—C—O—); n.m.r. ($CDCl_3$)τ: doublet ($J = 10.5$ Hz, 1H) 4.45 (secondary acetate); multiplet, X portion of ABX, sharpened by D_2O exchange (1H) 6.00 (secondary alcohol); broad singlet (1H) 6.87 (bridgehead hydrogen); singlet (3H) 7.79 (acetate methyl); doublet ($J = 6.5$ Hz, 3H) 9.05 p.p.m. (C—CH_3); the signal for the hydroxyl proton was obscured by signals from the methylene protons and its presence could only be inferred from a decrease in the integrated peak area for signals in the range τ 7.3–8.1 after D_2O exchange.

The diol was identified by conversion to the diacetate **13** in a 96% yield by acetylation with acetic anhydride in pyridine for 5 days at 50 °C.

*Oxidation of the Monoacetate **14** to the Acetoxyketone **15***

The monoacetate **14** (68 mg) dissolved in acetone (4 ml) was oxidized at 0 °C with Jones' reagent (0.1 ml) for 0.25 h. The reaction mixture was poured into ice-water (100 ml) and extracted with ether (20 and 10 ml). The ether extracts were washed with two portions of water (25 ml), saturated sodium chloride solution (25 ml), combined and dried over anhydrous magnesium sulfate. Evaporation of the solvent gave 66 mg (98%) of acetoxyketone **15** as a white solid homogeneous by t.l.c. (benzene–methanol 19:1, v/v). The acetoxyketone crystallized from hexane as white needles, m.p. 146–147 °C.

Mol. Wt. Calcd. for $C_{18}H_{20}O_3$: 284.1413. Found (mass spectroscopy): 284.1407.

I.r. (CCl_4): 1745 with a shoulder at 1735 cm^{-1} (carbonyl), 1240, 1030 cm^{-1} (acetate —C—O—); (KBr): 1735 with a shoulder at 1725 (carbonyl), 1240, 1040 cm^{-1} (acetate —C—O—); n.m.r. ($CDCl_3$)τ: doublet ($J = 10$ Hz, 1H) 4.72 (secondary acetate), multiplet (1H) 6.62 (bridgehead hydrogen), singlet (3H) 7.73 (acetate methyl), doublet ($J = 6$ Hz, 3H) 9.07 p.p.m. (C—CH_3).

*Hydrolysis of the Acetoxyketone **15** to the Hydroxyketone **16***

The acetoxyketone **15** (30 mg) was hydrolyzed (3 days) in boiling 1 *N* hydrochloric acid in 90% aqueous methanol (3 ml). The cooled reaction mixture was diluted with ice-water (50 ml) and extracted with ether (20 and 10 ml). The ether extracts were washed with two portions of water (25 ml), saturated sodium chloride solution (25 ml), combined and dried over anhydrous magnesium sulfate. Evaporation of the solvent gave 28 mg of a white solid. The hydroxyketone **21** (22 mg, 86%) was isolated by preparative t.l.c. ($CHCl_3$) as a white solid m.p. 100–102 °C.

Mol. Wt. Calcd. for $C_{16}H_{18}O_2$: 242. Found (mass spectroscopy): 242.

I.r. (CCl_4): 3530 (hydroxyl), 1735 cm^{-1} (ketone in five-membered ring); (KBr): 3500 (hydroxyl), 1720 cm^{-1} (ketone); n.m.r. ($CDCl_3$)τ: multiplet (1H) 2.32 (aromatic hydrogen); multiplet (3H) 2.80 (aromatic hydrogens); multiplet (2H) 6.30–6.53 (secondary alcohol and hydroxyl) changing to a doublet ($J = 9$ Hz, 1H) 6.40 (secondary alcohol) after D_2O exchange; multiplet (1H) 6.60 (bridgehead hydrogen); doublet ($J = 6$ Hz, 3H) 8.90 p.p.m. (C—CH_3).

*Baeyer–Villiger Oxidation of Acetoxyketone **15** to Acetoxylactone **17***

The acetoxyketone **15** (58 mg), sodium acetate (0.10 g), acetic acid (1.5 ml), and 28% peracetic acid in acetic acid (0.5 ml, ten-fold excess) were stirred in the dark for 90 h. Analysis by t.l.c. (benzene–methanol 19:1, v/v) showed some starting material and a new component of lower R_f (ratio about 1:1). The reaction mixture was poured into ice-water (100 ml) containing sodium bisulfite (0.5 g) and extracted with ether (20 and 10 ml). The ether extracts were washed with three portions of water (25 ml), saturated sodium chloride solution (25 ml), combined and dried over anhydrous magnesium sulfate. Evaporation of the solvent and removal of remaining acetic acid from the residue by azeotropic distillation with benzene (2 ml) gave 62 mg of a colorless oil. This oil was fractionated by preparative t.l.c. to give recovered starting material (27 mg) and acetoxylactone **17** (22 mg, 67% based on reacted starting material) as a white solid m.p. 183–185 °C. Crystallization from ether–hexane gave 17 mg of white needles m.p. 187–188 °C. The analytical sample crystallized from absolute ethanol as white rhombs m.p. 189 °C.

Anal. Calcd. for $C_{18}H_{20}O_4$ (mol. wt. 300): C, 71.98; H, 6.71. Found (300 (mass spectroscopy)): C, 72.08; H, 6.62.

I.r. (KBr): 1735, 1720 (ester and lactone carbonyls), 1255, 1240, 1220, 1210, 1030 cm^{-1} (—C—O—); n.m.r. ($CDCl_3$)τ: doublet ($J = 10$ Hz, 1H) 4.78 (secondary acetate), multiplet (1H) 6.70 (bridgehead hydrogen), doublet ($J = 4$ Hz, 1H) 7.18 and doublet ($J = 2$ Hz, 1H) 7.30 (methylene group adjacent to lactone function), singlet (3H) 7.70 (acetate methyl), doublet ($J = 6.5$ Hz, 3H) 9.03 p.p.m. (C—CH_3).

We wish to thank the National Institutes of Health, Bethesda, Maryland, and the National Research Council of Canada for a grant in support of this investigation.

1. K. WIESNER. Pure Appl. Chem. **7**, 285 (1963).
2. (*a*) K. WIESNER, Z. VALENTA, and J. A. FINDLAY. Tetrahedron Lett. 221 (1967); K. WIESNER. Coll. Czech. Chem. Commun. **33**, 2656 (1968). (*b*) S. N. SRIVASTAVA and M. PRZYBYLSKA. Can. J. Chem. **46**, 795 (1968).
3. K. WIESNER and A. PHILIPP. Tetrahedron Lett. 14, 1467 (1966).
4. B. G. BROWNLEE. Ph.D. Thesis. University of New Brunswick, Fredericton, New Brunswick, 1971.
5. G. WITTIG and E. KNAUSS. Chem. Ber. **91**, 895 (1958).
6. J. G. MARTIN and R. K. HILL. Chem. Rev. **61**, 537 (1961).
7. L. J. BELLAMY. The infrared spectra of complex molecules. Wiley, New York. 1958.
8. G. STORK, S. D. DARLING, J. T. HARRISON, and P. S. WHARTON. J. Am. Chem. Soc. **84**, 2018 (1962).
9. D. BERNEY and P. DESLONGCHAMPS. Can. J. Chem. **47**, 515 (1969).

The Chromyl Chloride Oxidation of α-Pinene[1]

FRANK WILLIAM BACHELOR AND UKKEN OUSEPH CHERIYAN
Department of Chemistry, The University of Calgary, Calgary, Alberta, T2N 1N4

Received June 22, 1972

The oxidation of α-pinene with chromyl chloride has been investigated and 11 compounds amounting to 81% of the total reaction have been isolated and identified. Besides a small amount of recovered α-pinene these compounds have been found to be products of acid-catalyzed rearrangement (bornyl chloride, borneol, and limonene); products of allylic oxidation (myrtenal, myrtenol, and verbenone); and products of oxidative addition–rearrangement (pinocamphone, pinocarveol, campholenaldehyde, and pinol). In addition, *p*-cymene was isolated which may arise from several oxidation sequences. The isolation of optically active pinol suggests that at least part of the oxidation of α-pinene is initiated by attack of the chromyl chloride on the same side of the double bond as the dimethyl substituted bridge. An attack by a positive chromium atom on the double bond is ruled out by a deuteration study.

L'oxydation de l'α-pinène par le chlorure de chromyle a été étudiée; onze composés correspondant à 81% de la réaction totale ont été isolés et identifiés. En plus d'une petite quantité d'α-pinène retrouvée, ces composés proviennent de réarrangement acido-catalysé (chlorure de bornyle, bornéol, et limonène), d'oxydation allylique (myrtenal, myrtènol, et verbènone) et de réarrangement d'addition oxydante (pinocamphone, pinocarvéol, campholènaldéhyde, et pinol). On a isolé de plus du *p*-cymène qui pourrait provenir de plusieurs séquences d'oxydation. L'isolement du pinol optiquement actif laisse penser qu'une partie au moins de l'oxydation de l'α-pinène a été initiée par une attaque du chlorure de chromyle sur la même face de la double liaison que le pont diméthyle substitué. L'attaque par un atome de chrome positif sur la double liaison a été écartée par une étude de deutériation. [Traduit par le journal]

Canadian Journal of Chemistry, 50, 4022 (1972)

The oxidation of monoterpenes by chromyl chloride has been an exercise in futility as far as obtaining controlled reactions or identification of products. These reactions lead to a multitude of compounds which result not only from oxidation but from acid-catalyzed rearrangements and often compounds which arise from conditions in the work-up procedure and are not the results of the chromyl chloride reagent at all (see refs. 1 and 2 for reviews of this reaction).

We have reinvestigated the oxidation of α-pinene (**1**) with chromyl chloride with the hope that some modification of the procedure might lead to a more useful reaction and also to attempt to throw some light on the mechanism of the reaction or reactions involved. We have not achieved the former to any practical degree but an investigation of the products has given some clues as to possible mechanisms for this oxidation.

The first treatment of α-pinene with chromyl chloride was by Henderson and coworkers (3, 4) who reported only that among other products there was produced a saturated aldehyde, an unsaturated ketone, and a chlorinated oil. Work done some 50 years later by Okuda (5) identified as the major product *d*-pinocamphone (**2**) and some isocamphenilanaldehyde (**3**). No further work has been reported. The original workers were undoubtedly handicapped by impure α-pinene. Okuda reported that he started with commercial material and, considering that gas chromatography was not yet available in 1951, it is also probable that his α-pinene was not pure.

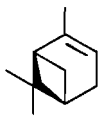

1

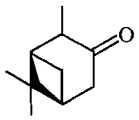

2

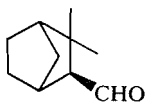

3

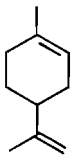

4

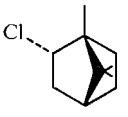

5

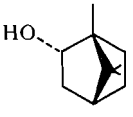

6

[1]Presented at the 55th Canadian Chemical Conference of the Chemical Institute of Canada, Quebec, Quebec, June, 1972.

Can. J. Chem. Downloaded from www.nrcresearchpress.com by 210.87.254.6 on 09/05/12
For personal use only.

Can. J. Chem. Downloaded from www.nrcresearchpress.com by 210.87.254.6 on 09/05/12
For personal use only.

The standard procedure for oxidizing olefins with chromyl chloride was to add either one or two molar equivalents of chromyl chloride to the olefin which produced a precipitate of a complex. The complex was then added to cold water and the products isolated either by steam distillation or ether extraction of the aqueous mixture. Later variations include adding the complex to aqueous sodium bisulfite solution which reduces any higher oxidation states of chromium still remaining. Both of these methods have obvious drawbacks, the first being a highly acidic solution which still contains a strong oxidizing agent, and the second contains a nucleophile which readily opens epoxides, a long sought for intermediate in chromyl chloride oxidations. Considering the penchant of monoterpenes to rearrange under acidic conditions, it is not surprising that a large number of components are found in these reactions, many of which are artifacts from work-up conditions.

We have modified the work-up procedure by adding the complex formed, together with the reaction solvent in which much of the complex is still soluble, to an ice-cold 10% sodium bicarbonate solution. This avoids subsequent acid-catalyzed rearrangements, nucleophilic substitutions, or opening of epoxides and the excess oxidizing agents are relatively weak in such alkaline media. Using this procedure we have been able to reduce the number of components from over 30 distinguishable peaks in a gas chromatograph to 11 readily separable and identifiable components. In addition to these, there is still some 19% of the reaction products which has not been identified. This is mostly polymeric material and probably represents products from allylic oxidations. Only a small amount (6%) of α-pinene is recovered from the reaction.[2]

The products of this reaction can be classified into three groups: those from non-oxidative rearrangements, products of allylic oxidation, and products from oxidation by addition followed by rearrangement. These products and their percentages of the total material are listed in Table 1. All of these compounds were identified by comparison with authentic specimens or by the preparation of derivatives.

TABLE 1. Yields and relative retention times of products from treatment of α-pinene with chromyl chloride

Product	r.r.t.*	Yield†
Bornyl chloride (**5**)	6.6	13.5
Pinocamphone (**2**)	10.0	11.4
Pinol (**14**)	4.2	9.4
Myrtenol (**10**)	42.6	9.4
α-Pinene (**1**)‡	1.0	6.3
Campholenaldehyde (**13**)	9.0	6.3
p-Cymene (**7**)	3.3	5.8
Verbenone (**8**)	27.3	5.6
Pinocarveol (**12**)	20.0	4.2
Borneol (**6**)	25.3	4.2
Myrtenal (**9**)	17.6	3.5
Limonene (**4**)	2.3	3.1
Unidentified polymer	—	18.8

*Relative retention time compared to α-pinene on a 6 ft × 1/8 in. column packed with 20% Carbowax 20M on chromosorb W at a temperature of 90 °C.

†Percentages calculated from areas under the analytical g.l.c. curves, and based on distillable material. The 18.8% polymer represents the non-distillable residue.

‡Recovered unreacted.

Three products were isolated which had the same oxidation state as α-pinene: limonene (**4**), bornyl chloride (**5**), and borneol (**6**). The formation of these products is undoubtedly catalyzed by the hydrochloric acid or intermediate chromium acids formed by the allylic oxidations. The formation of bornyl chloride is straight-forward and is a normal rearrangement product from the action of hydrochloric acid on α-pinene (6). Limonene is also a known rearrangement product from the treatment of α-pinene with strong acids (7), so that it is not too surprising to find it in this medium. Subsequent oxidation of limonene with 1 equiv of chromyl chloride gives primarily *p*-cymene (**7**) (1), also a component of this reaction. The presence of borneol is somewhat more difficult to explain. It certainly does not arise from solvolysis of bornyl chloride during the aqueous work-ups because this reaction does not lead to borneol (8). The most logical explanation would appear to be that the protonated intermediate from α-pinene reacts with some chromium

[2]It has been suggested that perhaps some of the products could arise by the basic conditions of the work-up. We have found no noticeable differences in the products from work-up with bicarbonate or carbonate, with the exception of the epoxide. We believe that the products here reported are those resulting from the reaction of chromyl chloride and its intermediates followed by hydrolysis of these products with water, and that none of them result from nucleophilic attack or elimination caused by the weak bases used here. These products are also those found in bisulfite work-ups.

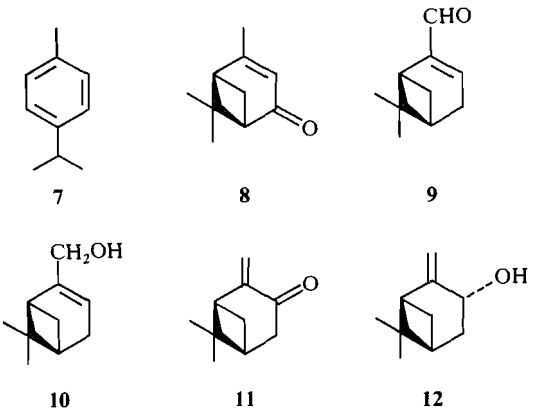

7 8 9

10 11 12

oxide species to give an ester which is subsequently hydrolyzed. All three of these compounds are optically active, bornyl chloride and borneol showing essentially no racemization. The limonene formed is about 50% racemic. This implies a high degree of concertedness to these rearrangements in contrast to other reactions which give, for example, racemic limonene (*7a*).

A possible alternative to the proton-catalyzed formation of these products would be attack on the double bond by a positive chromium ion. In order to check this possibility, a chromyl chloride α-pinene complex was decomposed with D_2O. Should any chromium–carbon bond be present it would be broken and the chromium atom would be replaced by deuterium. Isolation and examination of the bornyl chloride formed showed no incorporation of deuterium. This rules out the attack of any species other than a proton as the initiator for these rearrangements.

Three products from allylic oxidation of α-pinene were obtained. These were verbenone (**8**), myrtenal (**9**), and myrtenol (**10**). These arise from straightforward oxidations of α-pinene in a process which is presumably related to the Etard reaction (9). The nature of these products speaks strongly against the proposals of Stairs *et al.* (10) and Nenitzescu and coworkers (11) both of whom proposed that the α,β-unsaturated carbonyl compounds formed in chromyl chloride oxidations of olefins could arise from the elimination of HCl from an α-chloroketone. This rather unlikely process would yield α,β-unsaturated derivatives of pinocamphone (**2**) but none of these products are found. Although we searched for a chloroketone we were unable to detect any, nor was any pinocarvone (**11**) found.

Finally, the products which result from oxidative attack on the double bond were found to be pinocamphone (**2**), pinocarveol (**12**), campholenaldehyde (**13**), and pinol (**14**). All of these are the products from initial attack on the C-2 position of α-pinene followed by rearrangements. One is tempted to invoke the intermediacy of pinene oxide (**15**) in the formation of these products since all four of them are known to be formed from the oxide from reaction conditions which could be simulated during the oxidation. The rearrangement of oxides to the corresponding ketones with Lewis acids is a common preparative procedure (12). Acid-catalyzed opening of the epoxide also readily leads to pinocarveol (**12**) (13). The treatments of α-pinene oxide with zinc bromide (14) or *p*-toluenesulfonic acid (15) are both known to give campholenaldehyde (**13**) along with other products including *p*-cymene (**7**).

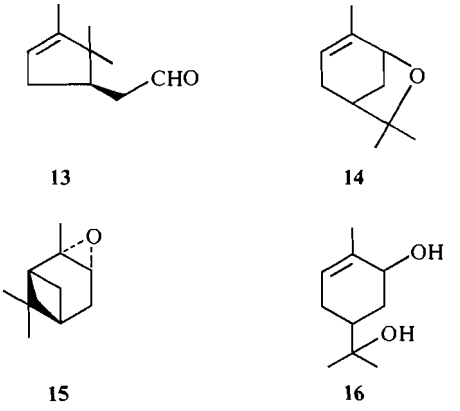

13 14

15 16

The formation of pinol (**14**) is of more than passing interest since it is approximately one-quarter optically active. Pinol may be obtained from α-pinene oxide by heating with water (16) or by treating it with acids (17). These two methods go through an intermediate, sobrerol (**16**), which is optically inactive in both cases. Pinol can also be obtained by treating *cis*-1,2-pinane glycol (**17**) (18) or *trans*-1,2-pinane glycol (**18**) with aqueous oxalic acid (19). From the latter compound optically active pinol was produced. An examination of the formation of

Can. J. Chem. Downloaded from www.nrcresearchpress.com by 210.87.254.6 on 09/05/12
For personal use only.

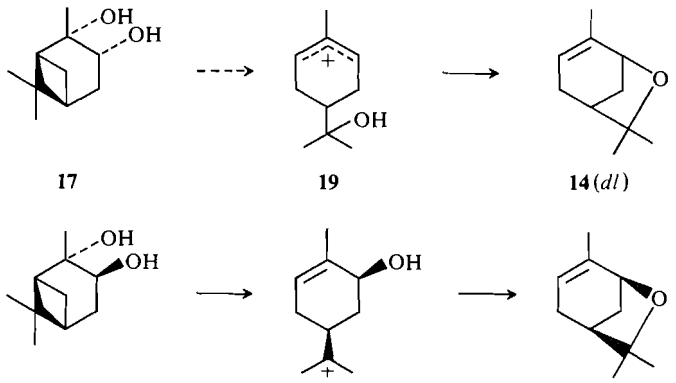

17 19 14(*dl*)

18 20 14 (active)

SCHEME 1

pinol from these two glycols suggests that the *cis*-glycol (**17**) or pinene oxide probably go through the allylic carbonium ion (**19**). This intermediate also would explain the formation of optically inactive sobrerol (**16**). From the *trans*-glycol (**18**), the C_2-hydroxyl group is on the same side of the ring as the migrating bridge in the carbonium ion intermediate (**20**) and can react directly to give optically active pinol. These reactions are depicted in Scheme 1. All of this implies that in order to produce optically active pinol from a pinene derivative the oxygen function at C-2 must be *cis* to the rearranging bridge. Therefore, the chromyl chloride must be attacking the double bond of α-pinene from both sides. This appears to be the first example of a reagent attacking the α-pinene double bond *cis* to the dimethyl substituted bridge.

In contrast to the report by Okuda (5) that isocamphenilanaldehyde (**3**) is formed by the action of chromyl chloride on α-pinene, we were unable to detect any in our reactions. This compound is a natural oxidation product of camphene and is characteristic of the chromyl chloride oxidation of terminal olefins (2). We can only suppose that his α-pinene was contaminated with camphene or, more likely, that camphene was produced from α-pinene in the aqueous work-up and subsequently oxidized.

In spite of the similarity of the oxidation products from chromyl chloride and the rearrangement products from α-pinene oxide, we do not believe that this is a major pathway in the formation of these products. Although it may well be formed to some extent, and probably is, several other intermediates or transition states could readily explain all of the results. We are in the process of examining these possibilities in simpler systems.

Experimental

Melting points were determined on a Kofler hot stage and are uncorrected. N.m.r.'s were run on a Varian A-60 and are reported in τ values relative to internal tetramethylsilane. Mass spectra were run on a Varian-MAT CH-5 mass spectrometer. Analytical gas chromatography was carried out on a Hewlett–Packard Biomedical 402 gas chromatographic instrument using a 6 ft glass column packed with 20% Carbowax 20M on chromosorb W. Preparative gas chromatography was carried out using a Varian Aerograph 90-P gas chromatograph using an 8 ft column, 3/8 in. diameter, packed with 20 or 30% Carbowax 20M on chromosorb W. Optical rotations were measured on a Durrum–Jasco ORD-UV/5 spectropolarimeter.

α-Pinene

Commercially available α-pinene (99+% pure) obtained from Aldrich Chemical Co. was distilled through a Nester–Faust annular Teflon distillation column. The distillate was shown to be better than 99% pure by analytical gas chromatography.

Chromyl Chloride

Chromyl chloride (Alfa Inorganics) was purified by passing a stream of dry nitrogen through it to expel any dissolved hydrogen chloride or chlorine. It was then freshly distilled before each oxidation.

Solvents

Methylene chloride was used throughout in these experiments and was purified by drying over anhydrous calcium chloride and distillation.

Oxidation of α-Pinene with Chromyl Chloride

α-Pinene (136 g, 1 mol, $[\alpha]_D^{25}$ +34.4, neat) was dissolved in 2 l of freshly distilled methylene chloride and cooled in

Can. J. Chem. Downloaded from www.nrcresearchpress.com by 210.87.254.6 on 09/05/12
For personal use only.

Can. J. Chem. Downloaded from www.nrcresearchpress.com by 210.87.254.6 on 09/05/12
For personal use only.

TABLE 2. Column chromatogram of crude oxidation mixture from chromyl chloride on α-pinene

Fraction	Solvent	Solvent ratio	Material eluted (g)
1	Hexane		5.2
2	Hexane–Benzene	19:1	9.9
3	Hexane–Benzene	3:1	4.8
4	Hexane–Benzene	1:1	7.8
5	Hexane–Benzene	1:3	8.1
6	Benzene		6.5
7	Benzene–Chloroform	1:1	10.1
8	Chloroform		13.8

an ice–salt bath to 0 to −5 °C. To this was added dropwise, with stirring, chromyl chloride (160 g, 1 mol) in 1 l of methylene chloride over a period of 6 h. Without isolation, the complex was decomposed by adding it, with vigorous stirring, to 1600 ml of 10% sodium bicarbonate solution containing 500 g of crushed ice. The mixture was placed in a large separatory funnel and ether was added until two clearly separable layers were obtained. The lower aqueous layer was removed, saturated with sodium chloride, and exhaustively extracted with ether. The combined ether extracts were washed with water and dried over anhydrous magnesium sulfate. The solvents were removed by distillation on a steam bath and the last traces were removed by distillation through a spinning band column. The residue amounted to 102 g of crude products.

The crude product (80 g) was fractionated by chromatography on silica gel (2.4 kg, Hopkins and Williams, column diameter, 9 cm) and eluted successively with 10 l of each solvent mixture (see Table 2).

Isolation of p-Cymene and Limonene

The solvent was removed from fraction 1 *in vacuo*. The residue showed two major peaks on analytical g.l.c. with relative retention times (r.r.t.) of 2.3 and 3.3 with respect to α-pinene. These two compounds were separated by preparative g.l.c. (20% Carbowax 20M, column temperature 140 °C). These were found to be limonene (r.r.t. 2.3) $[\alpha]_D^{25}$ +62.5 ($c = 1$, $CHCl_3$), lit. (20) $[\alpha]_D^{25}$ +111.6 (methanol), and *p*-cymene (r.r.t. 3.3) by comparison of their i.r. and n.m.r. spectra with authentic specimens.

Isolation of Bornyl Chloride

Removal of solvent from fraction 2 *in vacuo* left a liquid which showed two major peaks on analytical g.l.c. One of these peaks corresponded to α-pinene (r.r.t. 1) and the second had an r.r.t. of 6.6. Separation of this second component by preparative g.l.c. (20% Carbowax 20M, column temperature 140 °C) yielded a white solid, m.p. 130–131 °C, $[\alpha]_D^{25}$ +31.2 ($c = 0.28$, $CHCl_3$), lit. (20), m.p. 132 °C, $[\alpha]_D^{25}$ +30.96 (ethanol); n.m.r. ($CDCl_3$) 5.82 (1 H, d, $J = 3$ Hz each doublet split into a quartet, $J < 1$ Hz), 9.08 (3 H, s), 9.12 (6 H, s). The i.r. and n.m.r. spectra of this compound were identical to a synthetic sample of bornyl chloride.

Isolation of Campholenaldehyde

Removal of solvent from fraction 3 yielded a yellow oil which, on distillation at 20 mm, gave a colorless liquid. This was found to contain two major components with r.r.t.'s of 6.6 and 9.0 on analytical g.l.c. The former corresponds to bornyl chloride. The compound with r.r.t. 9.0 was collected by preparative g.l.c. (30% Carbowax 20M, column temperature 160 °C). This compound showed prominent bands in the i.r. ($CHCl_3$) at 2725, 1740, 1390, and 1370 cm^{-1}. N.m.r. ($CDCl_3$) 0.24 (1 H, t), 5.2 (1 H, m), 8.3 (1 H, m), 8.98 (3 H, s), 9.2 (3 H, s). A mass spectrum showed a molecular ion at *m/e* 152. The i.r. and n.m.r. spectra of this compound were superimposable on those of an authentic sample of campholenaldehyde.

Isolation of Pinocamphone

The residue after removal of solvent from fraction 4 was distilled at reduced pressure (20 mm). This yielded a colorless liquid which showed only one major component on analytical g.l.c. with r.r.t. 10.0. Purification of this component by preparative g.l.c. (30% Carbowax 20M, column temperature 160 °C) yielded a colorless liquid with the following spectral properties: $[\alpha]_D^{25}$ +28° ($c = 0.18$, $CHCl_3$), lit. (21) $[\alpha]_D^{25}$ +22.5; i.r. 1715, 1390, 1375 cm^{-1}; n.m.r. (CCl_4) 8.66 (3 H, s), 8.97 (3 H, d, $J = 7$ Hz), 9.1 (3 H, s) (see ref. 22).

Semicarbazide hydrochloride (1 g) and sodium acetate (1.5 g) were dissolved in 100 ml of H_2O. To this was added a few drops of the above compound and the mixture shaken. A white precipitate started to appear after about 1 h. The reaction mixture was kept overnight and the crystalline derivative was collected by filtration. Recrystallization from ethanol yielded white crystals, m.p. 226–227 °C, lit. (21) 227 °C, for the semicarbazone of *d*-pinocamphone.

Isolation of Pinol and Myrtenal

Analysis of the residue obtained after removal of the solvent from fraction 5 showed that it contained two major components with r.r.t.'s of 4.25 and 17.6 on analytical g.l.c. The two compounds were obtained pure by preparative g.l.c. (20% Carbowax 20M, column temperature 140 °C).

The compound with r.r.t. 4.25 was a colorless liquid with the following spectral properties: $[\alpha]_D^{25}$ +8.3 ($c = 0.24$, $CHCl_3$); i.r. (CCl_4) 3015, 1380, 1370, 1215, 1115, 1010 cm^{-1}; n.m.r. ($CDCl_3$) 4.78 (1 H, m), 5.98 (1 H, d), 8.27 (3 H, q, $J = 1$ Hz), 8.68 (3 H, s), 8.79 (3 H, s). The mass spectrum showed a molecular ion at *m/e* 152, lit. for pinol (19), $[\alpha]_D^{25}$ +34.8°.

A dibromide was prepared by dissolving 10 drops of the compound in CCl_4 and adding a dilute solution of bromine in the same solvent dropwise until a permanent yellow color was obtained. On addition of water a pale yellow solid precipitated which was collected by filtration and recrystallized from benzene–chloroform, m.p. 92–93 °C, lit. (23) 94 °C. The molecular weight was found to be 312 by mass spectral analysis.

The compound with r.r.t. 17.6 showed the following spectral properties: i.r. (film) 2720, 1690, 1385, 1370 cm^{-1}; n.m.r. (CCl_4) 0.72 (1 H, s), 3.43 (1 H, m, $J = 1$ Hz), 8.62 (3 H, s), 9.22 (3 H, s). The i.r. and n.m.r. spectra were identical to that of an authentic specimen of myrtenal.

Isolation of Borneol and Verbenone

Removal of solvent from fraction 6 left a viscous brown liquid. Two grams of this residue was absorbed on a column of silica gel (100 g, Hopkins and Williams, column diameter

Can. J. Chem. Downloaded from www.nrcresearchpress.com by 210.87.254.6 on 09/05/12
For personal use only.

2.8 cm) and eluted with 1:1 benzene–hexane. The column was eluted with 1.5 l of this solvent and removal of the solvent yielded 1.5 g of a viscous yellow liquid. This contained two major components by analytical g.l.c. with r.r.t.'s 25.3 and 27.3. These were separated by preparative g.l.c. (30% Carbowax 20M, column temperature 170 °C).

The compound with r.r.t. 25.3 was a white solid, m.p. 206–207 °C; $[\alpha]_D^{25}$ +31.6 ($c = 0.21$, $CHCl_3$); i.r. (CCl_4) 3640, 3510, 1385, 1375, 1055 cm^{-1}; n.m.r. (CCl_4) 6.02 (1 H, d, $J = 4$ Hz, each doublet split into a quartet, $J < 1$ Hz), 8.5 (1 H, s, exchanges with D_2O), 9.12 (9 H, s). These spectra were identical to those of an authentic specimen of borneol.

The compound with r.r.t. 27.3 was initially a colorless liquid which turned yellow on standing. It had the following spectral properties: i.r. (CCl_4) 1690, 1390, 1380, 1040, 870 cm^{-1}; n.m.r. (CCl_4) 4.38 (1H, m), 7.98 (3 H, q), 8.48 (3 H, s). These spectra were identical to those of an authentic sample of verbenone obtained from the Glidden–Durkee Co. of Jacksonville, Florida.

Isolation of Pinocarveol and Myrtenol

The solvent was removed from fraction 7 and 2 g of the residue was absorbed on silica gel (100 g, Hopkins and Williams, column diameter 2.8 cm) and eluted with benzene. Elution with 1.5 l of solvent yielded 1.3 g of a viscous yellow oil. Analysis by analytical g.l.c. showed that it was a mixture of two major compounds with r.r.t.'s 20.0 and 42.6, and a minor component with r.r.t. 25.3. The components were separated by preparative g.l.c. (30% Carbowax 20M, column temperature 160 °C).

The compound with r.r.t. 20.0 had the following spectral properties: i.r. (CCl_4) 3614, 3490, 1645, 1385, 1370, 1020, 995, and 865 cm^{-1}; n.m.r. (CCl_4) 5.08 (1 H, d, $J < 1$ Hz), 5.25 (1 H, d, $J < 1$ Hz), 8.5 (1 H, s, exchanges with D_2O), 8.71 (3 H, s), 9.37 (3 H, s). These spectra were identical to those of authentic *trans*-pinocarveol.

The compound with r.r.t. 42.6 was a viscous liquid with the following spectral properties: i.r. (film) 3330, 3040, 1375, 1365, 1060, 890, 800 cm^{-1}; n.m.r. (CCl_4) 4.6 (1 H, m), 6.11 (2 H, s), 7.37 (1 H, s, exchanges with D_2O), 8.7 (3 H, s), 9.15 (3 H, s). These spectra were identical with those of authentic myrtenol.

Analysis of Fraction 8

This fraction was semi-solid and failed to yield any pure compounds.

Quantitative Estimations of Constituents from Oxidation of α-Pinene with Chromyl Chloride

The percentages of the constituents from oxidation of α-pinene with chromyl chloride were estimated by measuring the area of the peaks from analytical g.l.c. chromatography of the crude residue. It was assumed that the sensitivity of the detector was proportional to the amount of compound present, however, it is recognized that this is not necessarily true. All peaks were sufficiently resolved to calculate areas. Unidentified and nonvolatile material accounted for 18.8% of the total residue.

Bornyl Chloride

Bornyl chloride was prepared by the method of Frankforter and Frary (6) and yielded a gas chromatographically pure compound, m.p. 130–131 °C.

Myrtenol and Myrtenal

A mixture of myrtenol and myrtenal was prepared by the oxidation of α-pinene with selenium dioxide according to the procedure of Dupont and Zacharewics (24). The myrtenal was separated by treatment with aqueous sodium bisulfite and the myrtenol extracted with ether. The myrtenal was recovered from the aqueous solution by treating with 8% sodium hydroxide and extraction with ether.

Attempted Isolation of Isocamphenilinaldehyde

The crude oxidation product of α-pinene (15 g) was agitated for 1 h with 100 ml of 20% sodium bisulfite solution and the unreactive components removed by extraction with ether. The aqueous layer was then treated with 100 ml of 8% sodium hydroxide solution and was exhaustively extracted with ether. The ether extracts were combined, dried over anhydrous magnesium sulfate, and the solvent removed by distillation. A colorless liquid (1.2 g) remained. Analytical g.l.c. showed only two components present with r.r.t.'s 9.0 and 17.6. Preparative g.l.c. of this mixture showed these components to be campholenaldehyde and myrtenal respectively.

Examination of Deuterium Incorporation into Bornyl Chloride on Work-up of the α-Pinene–Chromyl Chloride Complex with D_2O

α-Pinene (13.6 g, 0.1 mol) dissolved in 200 ml of dry methylene chloride was cooled in an ice–salt bath to 0 to −5 °C. A solution of chromyl chloride (15.5 g, 0.1 mol) in 125 ml of methylene chloride was added dropwise with stirring over a period of 1 h. The reaction was stirred for an additional 10 min and then decomposed by adding with stirring to a mixture of 10 g of anhydrous sodium carbonate in 20 ml of deuterium oxide (99.7% D_2O). The products were exhaustively extracted with ether, the ether extracts combined, dried over anhydrous $MgSO_4$, and the solvent removed by distillation to yield 10.5 g of crude products.

The crude product mixture was fractionally distilled under reduced pressure (20 mm) and the fraction boiling at 85–95 °C collected for analysis. This fraction contained most of the bornyl chloride produced in this reaction. Purification of the bornyl chloride was accomplished by preparative gas chromatography.

A mass spectral analysis of the pure bornyl chloride showed no significant increase in the *m/e* 173 peak corresponding to the incorporation of one deuterium atom, over that of normal isotopic bornyl chloride.

We wish to thank Dr. E. E. von Rudloff for samples of pinocarveol and campholenaldehyde. We also wish to thank The University of Calgary for a University of Calgary Dissertation Fellowship (UOC) and the National Research Council of Canada for financial support.

1. W. H. Hartford and M. Darrin. Chem. Rev. **58**, 1 (1958).
2. K. B. Wiberg. Oxidation by chromic acid and chromyl compounds. *In* Oxidation in organic chemistry. *Edited by* K. B. Wiberg. Academic Press, New York. 1965. pp. 69–185.
3. G. G. Henderson and R. W. Smith. J. Chem. Soc. **55**, 45 (1889).

4. G. G. HENDERSON and I. M. HEILBRON. J. Chem. Soc. **93**, 288 (1908).
5. O. OKUDA. J. Pharm. Soc. Jap. **71**, 563, 566, 569 (1951).
6. G. B. FRANKFORTER and F. C. FRARY. J. Am. Chem. Soc. **28**, 1461 (1906).
7. (*a*) O. WALLACH. Ann. **239**, 35 (1887). (*b*) R. W. CHARLTON and A. R. DAY. Ind. Eng. Chem. **29**, 92 (1937). (*c*) J. REISMAN. Bull. Soc. Chim. (Fr.), **41**(IV), 94 (1927). (*d*) M. DELÉPINE, J. REISMAN, and E. SUAU. Bull. Soc. Chim. (Fr.), **47**(IV), 966 (1930).
8. O. ASCHAN. Ber. **49**, 4918 (1907).
9. See ref. 2, p. 94.
10. R. A. STAIRS, D. G. M. DIAPER, and A. L. GATZKE. Can. J. Chem. **41**, 1059 (1963).
11. C. N. RENTEA, I. NECSOIU, M. RENTEA, A. GHENCIULESCU, and C. D. NENITZESCU. Tetrahedron, **22**, 3501 (1966).
12. H. O. HOUSE. Modern synthetic methods. 2nd ed. W. A. BENJAMIN, Inc., New York. 1972. pp. 318–320.
13. M. P. HARTSHORN, D. N. KIRK, A. F. A. WALLIS. J. Chem. Soc. 5494 (1964).
14. J. B. LEWIS and G. W. HENDRIK. J. Org. Chem. **30**, 4271 (1965).
15. L. CARROLL and H. FARBER. J. Org. Chem. **26**, 3261 (1961).
16. S. S. NAMETKIN and A. G. YARTZEVA. J. Russ. Phys.-Chem. Soc. **55**, 521 (1924). See Chem. Abstr. **19**, 2818 (1925).
17. G. FARGESS and A. KERGOMARD. Bull. Soc. Chim. Fr. 51 (1963).
18. G. WAGNER. Ber. **27**, 2270 (1894).
19. M. DELÉPINE, A. HOREAU, and M. GRANDPERRIN-Harispe. Ann. Chim. (Paris), **18**(XI), 250 (1943).
20. Dictionary of organic compounds. 4th ed. Eyre and Spottiswoode Publishers, Ltd., London. 1965.
21. H. SCHMIDT. Ber. Schimmel and Co. Akt.-Ges., 50 (1941). See Chem. Abstr. **37**, 4380^2 (1943).
22. N. NAKAGAWA and S. SAITO. Tetrahedron Lett. **11**, 1003 (1967).
23. O. WALLACH and A. OTTO. Ann. **253**, 249 (1889).
24. G. DUPONT and W. ZACHAREWICS. Bull. Soc. Chim. (5)**2**, 533 (1935).

Can. J. Chem. Downloaded from www.nrcresearchpress.com by 210.87.254.6 on 09/05/12
For personal use only.

Reactions of Ozonides. IX. A Radioisotopic Dilution Study of Ozonide Methanolysis

DUNDAPPA R. KERUR AND DENNIS G. M. DIAPER

Department of Chemistry and Chemical Engineering, Royal Military College of Canada, Kingston, Ontario

Received October 5, 1971[1]

A radioisotopic dilution study indicates that no significant amounts of $HOOCH(OCH_3)-(CH_2)_9-{}^{14}CO_2CH_3$ are produced by reacting 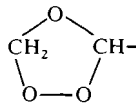 with methanol.

Une étude par dilution radioisotopique montre que des quantités non importantes de $HOOC(OCH_3)-(CH_2)_9-{}^{14}CO_2CH_3$ sont formées dans la réaction de 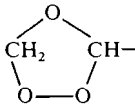 avec le méthanol.

[Traduit par le journal]

Canadian Journal of Chemistry, **50**, 4029 (1972)

A key intermediate in the Criegee mechanism for the ozonolysis reaction is the zwitterion **2** which is produced by cleavage of the primary ozonide **1** (1, 2). Among other reactions, the zwitterion may react with a carbonyl component to form an ozonide **3**, or if a reactive solvent such as methanol is present, the corresponding methoxyhydroperoxide **4** may be produced (see Scheme 1).

While investigating the thermal breakdown of 1-hexene ozonide, Razumovskii and Yurev (3) noted that prolonged holding of the ozonide in methanol at ordinary temperatures did not convert it to the methoxyhydroperoxide. However, thermal decomposition of either the ozonide in methanol or the methoxyhydroperoxide gave similar product distribution. On the basis of their observations, they proposed that at low temperatures, equilibrium in solution between ozonide, zwitterion, and carbonyl fragment was on the side of the ozonide. But with rising temperatures, equilibrium was shifted to the opposite direction leading to fragmentation of the ozonide. The zwitterion thus formed

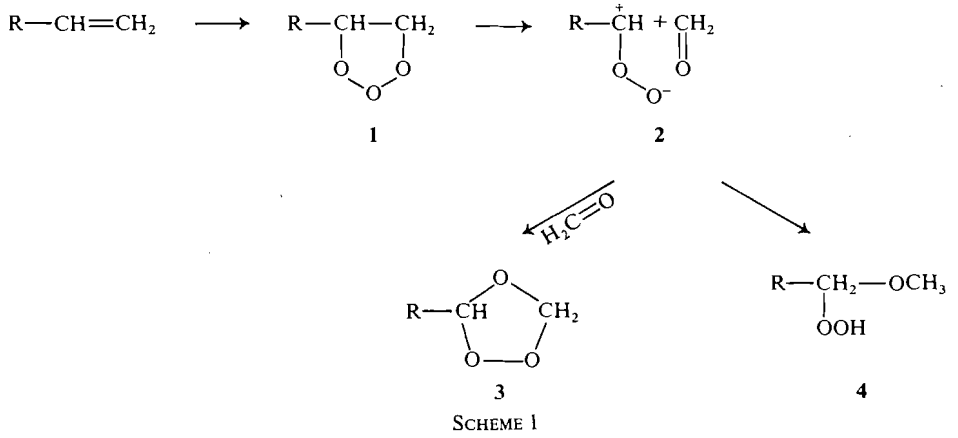

SCHEME 1

[1]Revision received July 25, 1972.

Can. J. Chem. Downloaded from www.nrcresearchpress.com by 210.87.254.105 on 09/05/12
For personal use only.

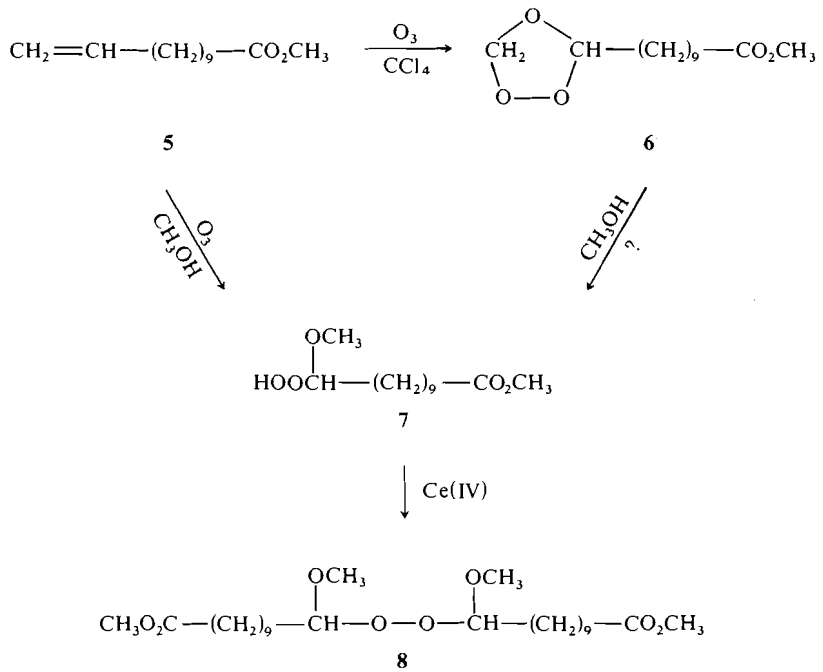

SCHEME 2. Structures **5*** and **6*** represent compounds where the ester function is $^{14}CO_2CH_3$.

reacted with methanol to give the methoxyhydroperoxide which in turn eliminated a molecule of water to produce a methyl ester.

Pryde *et al.* (4), in a study of pyrolytic decomposition of selected ozonolysis products, proposed that an ozonide in the presence of methanol and hydrogen ion produced an ester via a methoxyhydroperoxide. In their investigation, they ozonized 1-decene in water emulsions, conditions under which one would expect formulation of some hydroxyhydroperoxide in addition to the ozonide.

Neither pure ozonides nor pure methoxyhydroperoxides were used in the two reports just cited. Only gross reaction mixtures obtained after ozonation were employed.

In our own experience, methyl 10-undecenoate ozonide (5) could be recovered unchanged and in good yields after prolonged dissolution in methanol at room temperature.

Recently, Criegee and Korber (6) have recorded the fragmentation of several ozonides by methanol. Depending on the substitution pattern on the trioxolane ring, acids and aldehydes or ketones have been identified.

If methanolysis of the ozonide ring proceeds through the methoxyhydroperoxide, failure to isolate this product (3) is explicable by (*a*) rapid further reaction giving the ester, or (*b*) failure to interrupt the reaction before completion of the sequence: ozonide, methoxyhydroperoxide, ester. If on the other hand, methanolysis of the ozonide ring is a concerted process (6) without a methoxyhydroperoxide intermediate, failure to isolate methoxyhydroperoxide products of ozonide methanolysis is also explicable. Sensitivity of detection of methoxyhydroperoxide can be greatly increased using an isotopic dilution method, and the present study was undertaken using this analytical method. Methanolysis of an ozonide and the corresponding methoxyhydroperoxide were performed under comparable conditions to obtain some idea of the relative rates of reaction.

The results support the proposed methanolysis mechanism (6) of ozonide and indicate that intermediate formation of methoxyhydroperoxide plays a negligible part (see Scheme 2).

Experimental

Counting of radioactive samples was done on a Nuclear–Chicago counter.

A Coleman Model 33 Carbon–Hydrogen Analyzer was used for microanalyses.

Can. J. Chem. Downloaded from www.nrcresearchpress.com by 210.87.254.105 on 09/05/12
For personal use only.

Can. J. Chem. Downloaded from www.nrcresearchpress.com by 210.87.254.105 on 09/05/12
For personal use only.

I.r. spectra were recorded on a Perkin–Elmer Infracord spectrophotometer.

N.m.r. spectra were recorded on a Varian A-60A model spectrometer. Tetramethylsilane was used as internal reference.

"Baker Analyzed" reagent grade silica gel powder was used for column chromatography.

T.l.c. was performed on Eastman Chromagram sheets without fluorescent indicator. T.l.c. plates (20 × 20 cm, 100 μ thick) were made on a Shandon Unoplan leveller using silica gel powder containing 5% calcium sulfate.

Two spray reagents were employed in this work. One was a 3% solution of potassium iodide in 5% aqueous acetic acid. The other was prepared by dissolving 1 g of 2,4-dinitrophenyl hydrazine (DNP) in 7.5 ml of concentrated sulfuric acid and diluting the solution to 250 ml with 95% ethanol.

Petroleum ether refers to the fraction boiling between 30 and 60°.

Ceric ammonium nitrate (ammonium hexanitrato cerate) was obtained from the A. Frederick Smith Chemical Co., Columbus, Ohio.

Methyl 11-dodecenoate (**5**), b.p. 138–154° at 4 mm pressure, was prepared by carbonation of undecenylmagnesium bromide and subsequent esterification. Methyl carboxyl-^{14}C-11-dodecenoate (**5***) was similarly prepared using $^{14}CO_2$. Barium carbonate-^{14}C (specific activity 5.0 mCi/mmol) from New England Nuclear Corp., Boston, Massachusetts was used to generate the radioactive carbon dioxide.

*Methyl-carboxyl-^{14}C-11-dodecenoate Ozonide (**6***)*

A solution of methyl carboxyl-^{14}C-11-dodecenoate (**5***) in carbon tetrachloride was treated with a stream of ozone–oxygen at ice-water temperature. The reaction mixture was evaporated and the residue was chromatographed on a silica gel column using 5% ether in petroleum ether as eluant. Fractions were tested for purity by t.l.c. using a potassium iodide–acetic acid spray. Fractions which contained pure ozonide as evidenced by single spots were pooled and evaporated. The ozonide isolated had a specific activity of 220.20 ± 0.69 counts/min mg. N.m.r. spectrum of a similarly prepared non-radioactive sample has been described by us before (5).

Methyl 11-Hydroperoxy-11-methoxyundecanoate (7)

A solution of methyl 11-dodecenoate (**5**) in methanol was ozonized at ice-water temperature. The residue after evaporation was purified on a silica gel column using 50% ether in petroleum ether as eluant.

N.m.r. spectrum of an undiluted sample showed peaks at δ 1.32 (chain CH_2), triplet centered at 2.28 $\left(-CH_2-C(=O)-O\right)$, 3.45 ($-OCH_3$), 3.63 $\left(-C(=O)-OCH_3\right)$, and multiplet between 4.67–4.85 p.p.m. (—O—CH—O—).

In a cognate preparation for methyl 10-hydroperoxy-10-methoxydecanoate the yield of purified product was 74.2%.

*Di(methyl 11-methoxyundecanoate) Peroxide (**8**)*

To a solution of methyl 11-hydroperoxy-11-methoxyundecanoate (**7**) in methanol, solid ceric ammonium nitrate was added at room temperature until a slight orange color persisted. Dilution of the reaction mixture with ether led to separation of a white precipitate. The ether layer was extracted with aqueous sodium bicarbonate and the excess alkali was removed by repeated washing with water. After drying over anhydrous sodium sulfate, the ether solution was evaporated to obtain the diperoxide. It was purified by silica gel column chromatography using 50% ether in petroleum ether. Its i.r. spectrum showed no hydroxyl peak.

N.m.r. spectrum of a carbon tetrachloride solution showed peaks at δ 1.32 (chain CH_2), triplet centered at 2.27 $\left(-CH-C(=O)-O\right)$, 3.24 ($-OCH_3$), 3.62 $\left(-C(=O)-OCH_3\right)$, and triplet centered at 4.27 p.p.m. (—CH).

In a cognate preparation of di(methyl 10-methoxydecanoate) peroxide, the yield of purified material was 77.3%. Due to premature detonation of this diperoxide in the combustion tube, no satisfactory elemental analysis could be obtained.

Anal. Calcd. for $C_{24}H_{46}O_8$: C, 62.31; H, 10.02. Found: C, 62.66, 63.33, 63.20, 62.99; H, 11.09, 10.77, 10.73, 9.29.

It gave a single spot thin layer chromatogram.

In general, the radioactive ozonide **6*** was heated in about 5 ml of methanol for varying periods of time. If necessary, the alcohol was evaporated and the residue was diluted with a measured quantity of unlabelled methoxyhydroperoxide (**7**). The latter was isolated by column or thin layer plate chromatography and submitted to radioactive counting. Further details are listed in Table 1.

In order to facilitate additional purification of the isolated methoxyhydroperoxide it was converted to a diperoxide using ceric ammonium nitrate (8). The diperoxide was subjected to fractionation on an Eastman Chromagram sheet and the major regions of the chromatogram were examined for radioactivity. Details concerning purification of the diperoxide are listed in Table 2.

Stability Studies of Representative Methoxyhydroperoxides

The following experiments were conducted to assess the stability of the methoxyhydroperoxide involved in this study.

Methyl 10-hydroperoxy-10-methoxy-nonanoate (250 mg) was dissolved in 5 ml of methanol and the solution was refluxed vigorously on a steam bath for 1 h. N.m.r. and i.r. spectra of the residue obtained after evaporation of the reaction mixture were identical with those of unheated samples. A peak at 2.9 μ due to the —OH of the hydroperoxy group and a multiplet between δ 4.65–4.85 p.p.m. confirmed that not all of the methoxyhydroperoxide had been destroyed on refluxing.

Similarly, 9-hydroperoxy-9-methoxynonane was submitted to the same treatment as described above. In general, the i.r. and n.m.r. spectra were similar to those of unheated samples. I.r. investigation revealed the presence of an —OH group at 2.8–2.9 μ. In addition, a small peak due to $-C(=O)-$ absorption at 5.8 μ could be observed indicating some decomposition of the methoxyhydroperoxide to carbonyl bearing compounds. N.m.r. revealed the presence of $-OCH_3$ peak at δ 3.48 p.p.m. and absorption due to —O—CH—O— was centered in a multiplet around δ 4.70 p.p.m.

Quantitative assay by i.r. spectroscopy using the carbonyl peak at 5.8 μ and methyl nonanoate as standard revealed that at the end of 1 h refluxing, only 2.8% of the methoxyhydroperoxide had decomposed. Although results varied

TABLE 1. Experimental details of reaction of ozonide **6*** with methanol[a]

Experiment no.	Weight of ozonide **6*** used (mg)	Reaction conditions	Weight of methoxyhydroperoxide **7** added (mg)	Chromatographic separation technique	Specific activity of recovered methoxyhydroperoxide (counts/min mg)
1	145.0	45 min reflux	253.1	Column	104.86 ± 0.48 (recovery 237.5 mg)
2	258.7	45 min reflux	259.9	T.l.c. plate	104.4 ± 0.45 95.76 ± 0.57 108.80 ± 1.00
3	249.5	15 min heat, 30 min reflux	245.6	Column	109.70 ± 0.50 38.41 ± 0.55 15.08 ± 0.12 10.93 ± 0.32
4	250.0	1 h reflux	500.0	Column	104.00 ± 0.50 (recovery 475.0 mg)

[a]Specific activities have been corrected for background, geometry, and self absorption. Counting errors are listed as standard deviations (7). Where several figures are listed, these represent assays after successive chromatographic purifications.

TABLE 2. Fractionation of diperoxide by t.l.c. chromatography

Region of plate	Weight of material isolated (mg)	Specific activity (counts/min mg)	Reaction to spray reagent[a]
Top	5	77.36 ± 0.74	–
Middle	16.6	2.34 ± 0.2	+
Bottom	1.6	0	–

[a]$KI-CH_3CO_2H$ spray.

with different samples in no case did we observe extensive decomposition of the methoxyhydroperoxide after refluxing it for 1 h.

Results and Discussion

After short reflux periods of the radioactive ozonide in methanol, t.l.c. (5% methanol in petroleum ether, $KI-CH_3CO_2H$ spray) revealed considerable amounts of unreacted ozonide together with a blank region at the point of spotting. Further refluxing reduced the intensity of the ozonide spot but showed two additional clear spots slightly above the origin. DNP spray revealed a yellow ozonide spot on the top, a yellow spot in the middle and two blank spots, one at the origin and another slightly above it.

When column chromatography was attempted, methanol was evaporated on a rotary evaporator and the residue was diluted with unlabelled methoxyhydroperoxide (**7**).[2] When thin layer plates were used, the methoxyhydroperoxide was added directly to the cooled reaction mixture and the solution was streaked across the plate. Any unreacted ozonide which was faster moving than the methoxyhydroperoxide was removed by elution with 5% methanol or ether in petroleum ether. In one experiment, refluxing of 250 mg of the ozonide for 1 h left behind 43 mg of it unreacted. To expedite collection of the methoxyhydroperoxide after removal of the ozonide, in some cases 50% ether in petroleum ether was used for elution purposes.

The methoxyhydroperoxide which was used for counting showed several impurities. On careful t.l.c. these were easily discernible with either of the spray reagents. A small amount of

[2]The stability of this methoxyhydroperoxide is such that it could have been refluxed together with the ozonide. But such a procedure only aggravated the problems encountered in its recovery and subsequent purification. The heat stability of methoxyhydroperoxides of this type is in sharp contrast to the stability of α-alkoxy-α-hydroperoxyacetophenones reported by Bailey and Chang (9). Obviously in the latter case, the $-\overset{\overset{O}{\|}}{C}-$ function adjacent to the hydroperoxy group exerts a decidedly destabilizing effect.

Can. J. Chem. Downloaded from www.nrcresearchpress.com by 210.87.254.105 on 09/05/12
For personal use only.

Can. J. Chem. Downloaded from www.nrcresearchpress.com by 210.87.254.105 on 09/05/12
For personal use only.

immovable material registered as a blank circle around the original point of spotting. On extended standing, a blank area developed on top of the methoxyhydroperoxide spot. These impurities could not be eliminated even after extensive attempts at purification. Repeated fractionation on a silica gel column (Table 1, expt. 3) led to continuous lowering of specific activity after each purification. There was thus none or only negligible amounts of ^{14}C labelled methoxyhydroperoxide formed during the reaction. The methoxyhydroperoxide assayed was obviously contaminated with ^{14}C bearing impurities and these were progressively being removed on repeated column chromatography.

It was thus deemed advisable to convert the methoxyhydroperoxide to a derivative which was produced by it alone and not by any of the impurities. Conversion to a diperoxide by action of ceric ammonium nitrate seemed appropriate.

From 475 mg of crude methoxyhydroperoxide (specific activity 104 ± 0.49 counts/min mg, expt. 4 in Table 1) after treatment with ceric ammonium nitrate and dilution with 49.1 mg of unlabelled diperoxide **8**, a total of 426.7 mg of impure diperoxide was obtained. It registered a specific activity of 58.73 ± 0.31 counts/min mg. Elution with 50% ether in petroleum ether on a silica gel column yielded 259.3 mg of nonperoxidic material, specific activity 50.54 ± 0.22 counts/min mg and 67.4 mg of partially pure diperoxide, specific activity 43.89 ± 0.51 counts/min mg.

The diperoxide on further careful examination by t.l.c. revealed the presence of impurities. With iodide spray, these usually showed up as blank spots crowning the diperoxide region and as a blank smear extending from the point of origin to the diperoxide spot. The diperoxide was therefore submitted to further fractionation (Table 2). About 22 mg of it was streaked across an Eastman Chromogram sheet and developed in 50% ether in petroleum ether. Spraying with $KI-CH_3CO_2H$ spray revealed a brown streak due to the diperoxide and a blank area adjacent to it on the top. The sheet was cut into three portions, one covering the diperoxide region, another covering the blank area on top, and a third covering the area from the point of streaking to the diperoxide region. The adsorbent layer from these cuttings was scraped off and washed thoroughly with ether. The ether solutions were evaporated and specific activities of the residues were determined.

The blank area on top of the chromatogram yielded about 5 mg of material with a specific activity of 77.36 ± 0.74 counts/min mg. The diperoxide region gave 16.6 mg of material with a specific activity of 2.34 ± 0.2 counts/min mg. The third fraction covering the region from the point of streaking to the diperoxide zone gave 1.6 mg of material which was nonradioactive. The concentration of radioactivity in the nonperoxidic region as opposed to only minor amounts in the diperoxide region again indicates that under the experimental conditions employed, no substantial amounts of ozonide were converted to the methoxyhydroperoxide. Indeed, Criegee and Korber (6) have drawn attention to the fact that the mechanism of fragmentation of ozonides by alcohols is similar to the cleavage of ozonides by alkalis as proposed by Kornblum and de la Mare (10).

Because the ozonide methanolysis route proposed by Razumovskii and Yurev (3) ozonide → methoxyhydroperoxide → ester makes only a negligible ($\not> 1\%$) contribution, the arguments of these authors concerning ozonide–zwitterion equilibria are not supported.

The authors wish to thank Prof. S. N. Naldrett of this Department for the use of counting facilities. Financial support through Defence Research Board Grant No. 9530-17 is gratefully acknowledged.

1. R. CRIEGEE. Record Chem. Progr. Kresge-Hooker Sci. Lib. **18**, 111 (1957).
2. P. S. BAILEY. Chem. Rev. **58**, 925 (1958).
3. S. D. RAZUMOVSKII and YU. N. YUREV. Zh. Org. Khim. **3**(2), 251 (1967); Chem. Abstr. **66**, 115220*b* (1967).
4. E. H. PRYDE, D. J. MOORE, and J. C. COWAN. J. Am. Oil Chem. Soc. **45**, 888 (1968).
5. D. R. KERUR and D. G. M. DIAPER. Can. J. Chem. **47**, 43 (1969).
6. R. CRIEGEE and H. KORBER. Preprints of the American Chemical Society Symposium on Ozone Chemistry. Los Angeles. March 28–April 2, 1971. p. A31.
7. M. CALVIN, C. HEIDELBERGER, J. C. REID, B. M. TOLBERT, and P. F. YANKWICH. Isotopic carbon. John Wiley and Sons, Inc., New York. 1949. p. 283.
8. D. G. M. DIAPER. Can. J. Chem. **46**, 3095 (1968).
9. P. S. BAILEY and Y. CHANG. J. Org. Chem. **27**, 1192 (1962).
10. N. KORNBLUM and H. E. DE LA MARE. J. Am. Chem. Soc. **73**, 880 (1951).

Deuterium Isotope Effects in the Oxidation of 2,3-Dimethyl-2-butene via the Bromohydroperoxide, by Singlet Oxygen and by Triphenyl Phosphite Ozonide[1,2]

KARL R. KOPECKY AND JOHAN H. VAN DE SANDE[3]

Department of Chemistry, University of Alberta, Edmonton, Alberta T6G 2G2

Received June 2, 1972

The partially deuterated alkenes $(CH_3)_2C{=}C(CD_3)_2$ (**1***b*) and $CH_3CD_3C{=}CCH_3CD_3$ (**1***c*) were prepared and converted to the corresponding allylic hydroperoxides by the routes shown in the title. Two bromohydroperoxides were formed from **1***b* in a 1.6:1 ratio with the major isomer having the OOH group on the carbon bearing the CH_3's. On treatment with base at 0° this mixture formed two allylic hydroperoxides in a 2.2:1 ratio with the major isomer having the OOH group on the carbon bearing the CD_3's, showing migration of the OOH group. This isomer predominated in a 1.4:1 ratio when **1***b* was oxidized with singlet oxygen at 15 or −52° and in a 1.6:1 ratio when **1***b* was oxidized with triphenyl phosphite ozonide at −70°. Under the same conditions C—H bond breaking also predominated in the oxidation of **1***c*, by 2.1:1 via the bromohydroperoxide, by 1.4:1 with singlet oxygen, and by 1.3:1 with triphenyl phosphite ozonide. Migration of the OOH group in the reaction of the bromohydroperoxide of **1***b* does not occur by way of a 1,2-dioxetane. A perepoxide may be the intermediate. Neither perepoxides nor 1,2-dioxetanes are involved in the singlet oxygen oxidation of **1***b* and *c*. At −70° the triphenyl phosphite ozonide oxidations do not proceed by way of these intermediates, either, or by way of singlet oxygen. The intermolecular deuterium isotope effect in the singlet oxygen oxidation of both *cis*- and *trans*-2,3-diphenyl-2-butene was found to be 1.1.

Les alcènes partiellement deutériés $(CH_3)_2C{=}C(CD_3)_2$ (**1***b*) et $CH_3CD_3C{=}CCH_3CD_3$ (**1***c*) ont été préparés puis convertis en hydropéroxydes allyliques correspondants, selon le schéma exposé dans le titre de ce mémoire. Deux hydropéroxydes bromés sont obtenus à partir de **1***b* dans le rapport 1.6:1, l'isomère prépondérant ayant le groupe OOH sur le carbone portent du CH_3. Par traitement basique à 0°, ce mélange conduit à deux hydropéroxydes allyliques, dans le rapport 2.2:1; avec l'isomère possédant le groupe OOH sur le carbone du CD_3, en majorité, montrant ainsi la migration du groupe OOH. Cet isomère prédomine dans le rapport 1.4:1 lorsque **1***b* est oxydé par l'oxygène singulet à 15 ou −52° et dans le rapport 1.6:1 lorsque cette oxydation est effectuée par l'oxyde de la triphénylphosphite à −70°. Dans les mêmes conditions, la cassure de la liaison C—H prédomine aussi dans l'oxydation de **1***c*, dans le rapport 2.1:1 via le bromohydropéroxyde, 1.4:1 dans le cas de l'oxygène singulet, et 1.3:1 avec l'ozonide de la triphénylphosphite. La migration du groupe OOH dans la réaction du bromohydropéroxyde de **1***b* ne se produit pas par l'intermédiaire du dioxétane-1,2. Une perépoxyde serait l'intermédiaire. Ni les perépoxydes, ni les dioxétanes-1,2 n'interviennent dans l'oxydation par l'oxygène singulet de **1***b* et *c*. A −70° les oxydations par l'ozonide de la triphénylphosphite ne passent pas par ces intermédiaires, ni par oxygène singulet. L'effet isotopique intermoléculaire de deutérium dans l'oxydation par l'oxygène singulet des *cis* et *trans* diphényl-2,3 butène-2 a été trouvé égal à 1.1.

[Traduit par le journal]

Canadian Journal of Chemistry, **50**, 4034 (1972)

Introduction

β-Halohydroperoxides derived from a variety of tetrasubstituted ethylenes are converted rapidly at 0° by base to allylic hydroperoxides in good to excellent yields (1, 2). The reaction sequence shown in Scheme 1 represents an alternate synthesis of allylic hydroperoxides which are usually prepared by the oxidation of alkenes with singlet oxygen (3). Indeed, essentially the same distributions of products are formed from the β-halohydroperoxides of 1,2-dimethylcyclohexene (1) and 2-methyl-3-(4-methoxyphenyl)-2-butene (2*b*) as are formed by the oxidation of these alkenes by singlet oxygen.

[1]Presented in part at the 51st Canadian Chemical Conference of the Chemical Institute of Canada, Vancouver, B.C., June, 1968, Abstracts p. 41; at the Symposium on Cyclic Peroxides at the Regional Meeting of the New York, New Jersey, and Puerto Rico Sections of the American Chemical Society, San Juan, Puerto Rico, April 30, 1971; and at the Symposium on Oxidations by Singlet Oxygen sponsored by the Division of Petroleum Chemistry Inc., 162nd National Meeting of the American Chemical Society, Washington, D.C., September, 1971, Petroleum Preprints **16**, No. 4, A65 (1971).

[2]Based on a dissertation submitted by J. H. van de Sande to the Faculty of Graduate Studies of the University of Alberta, Edmonton, Alberta, in partial fulfillment of the requirements of the Ph.D. degree, 1968.

[3]Holder of an NRCC Studentship, 1964–1967, and a University of Alberta Dissertation Fellowship, 1967–1968.

Can. J. Chem. Downloaded from www.nrcresearchpress.com by 210.87.254.5 on 09/05/12
For personal use only.

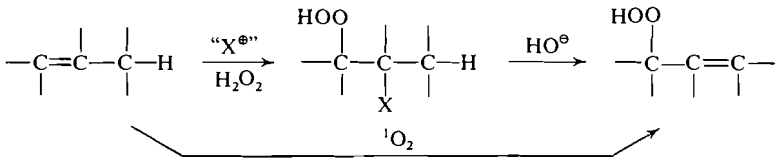

SCHEME 1

However, the formation of allylic hydroperoxides from β-halohydroperoxides is not a general reaction. In sharp contrast to the results outlined above no trace of allylic hydroperoxides could be found among the products of reaction, under similar conditions, between base and a number of less highly substituted ethylenes. A variety of products is formed (1). Carbon–carbon bond cleavage occurs in some cases (1, 4) which indicates that cyclic peroxides may be formed as intermediates, eq. 1. Trimethyl-

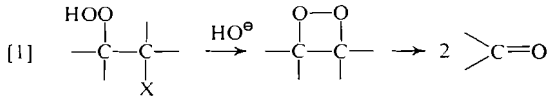

[1]

1,2-dioxetane (5, 6) and 3-methyl-3-phenyl-1,2-dioxetane (6) have been isolated recently from such reactions and are cleaved to carbonyl compounds on heating. No such cleavage products have yet been observed in the reactions between the β-halohydroperoxides of tetrasubstituted ethylenes and base.

The present study was made in an attempt to distinguish between the several possible mechanisms that could be envisaged for the transformation of β-halohydroperoxides to allylic hydroperoxides and, in particular, to determine if the transformation also involves 1,2-dioxetanes as intermediates. In addition, it was of interest to determine whether this reaction and the reaction between singlet oxygen and tetrasubstituted ethylenes have common intermediates as well as common products. Two partially deuterated 2,3-dimethyl-2-butenes, 1,1,1-trideuterio-2-methyl-3-trideuteriomethyl-2-butene (**1***b*) and 2,3-bis(trideuteriomethyl)-2-butene (**1***c*) were prepared. The intramolecular deuterium isotope effects were determined for the conversion of these alkenes to allylic hydroperoxides by the routes (*1*) reaction between their β-bromohydroperoxides and base, (*2*) by oxidation with singlet oxygen generated by a variety of sensitizers and from the hydrogen peroxide–

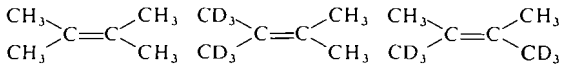

1*a* **1***b* **1***c*

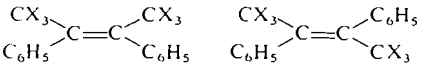

cis-**2** *trans*-**2**

a X = H *a* X = H
b X = D *b* X = D

sodium hypochlorite reactions (3*b*), and (*3*) by oxidation with triphenyl phosphite ozonide (7). Also, *cis*- and *trans*-1,1,1,4,4,4-hexadeuterio-2,3-diphenyl-2-butene (*cis*- and *trans*-**2***b*) were prepared and the intermolecular deuterium isotope effects in the singlet oxygen oxidation of *cis*- and *trans*-2,3-diphenyl-2-butene (*cis*- and *trans*-**2***a*) were determined.

Results

Preparation of the Deuterated Alkenes

The syntheses of the deuterated alkenes **1***b*, **1***c*,[4] and *cis*- and *trans*-**2***b* are outlined in Schemes 2, 3, and 4, respectively.[5] The deuterated methyl hydroxyisobutyrate (Scheme 2) was prepared by addition of deuterium cyanide to hexadeuterioacetone followed by hydrolysis of the resulting product and then treatment of the hydroxy acid so obtained with diazomethane.

[4]Although only the *cis* isomer of **1***c* is shown as the product of the reaction sequence, nearly equimolar amounts of the *cis* and *trans* isomers undoubtedly are formed (8).

[5]In principle, a simpler route to **1***b* would involve addition of trideuteriomethylmagnesium iodide to an ester of isobutyric acid followed by dehydration of the resulting alcohol. However, in numerous exploratory experiments dehydration of 2,3-dimethyl-2-butanol by various methods in the absence of strong acid produced mainly 2,3-dimethyl-1-butene and only small amounts of the desired internal alkene. Acid-catalyzed dehydration of the alcohol gives predominantly the internal alkene, but extensive isotopic exchange would have occurred in the dehydration of the appropriate partially deuterated alcohol (9).

Can. J. Chem. Downloaded from www.nrcresearchpress.com by 210.87.254.5 on 09/05/12
For personal use only.

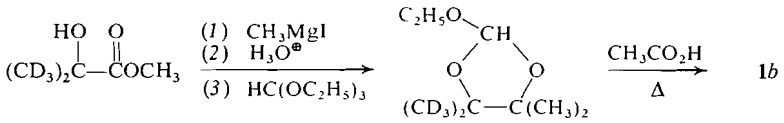

SCHEME 2

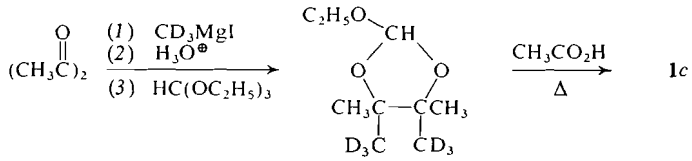

SCHEME 3

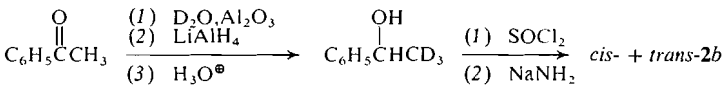

SCHEME 4

Only two points concerning the reactions will be made here. We found the preparation and subsequent decomposition (without isolation) of the orthoformate ester derivative of 2,3-dimethyl-2,3-butanediol to be a more convenient route (10) for the preparation of 2,3-dimethyl-2-butene (**1***a*) than the preparation and decomposition of the thionocarbonate derivative (11). Also, 2,2,2-trideuterioacetophenone could be prepared quickly and on a large scale by passing a solution of acetophenone through a long column of alumina pretreated with deuterium oxide.

Mass spectral analysis (12) at low ionizing voltage (9.5–12 eV) showed that the trideuteriomethyl groups of **1***b* are 99.4% deuterated, those of **1***c* are 95.3% deuterated, and those of *cis*- and *trans*-**2***b* are 92% deuterated. Analysis of the $M^{\oplus} - CX_3$ (X = H or D) region of the mass spectrum taken at 70 eV of **1***b* and *c* showed that very little, if any, exchange of deuterium between the CD_3 and the CH_3 groups had occurred during the preparation of these materials.

Isotope Effect in Elimination of Hydrogen Bromide from 3-Bromo-2,3-dimethyl-2-butyl Hydroperoxide

The alkenes **1***b* and *c* were converted to the bromohydroperoxides, **3***b* + *c* and **3***d*, respectively, by adding 1,3-dibromo-5,5-dimethylhydantoin (dibromantin) to solutions of the alkenes and excess 98% hydrogen peroxide in ether at −40° and then allowing the temperature to rise to 0° (1). The two products from **1***b*, 3-bromo-4,4,4-trideuterio-3-trideuteriomethyl-2-methyl-2-butyl hydroperoxide (**3***b*) and 3-

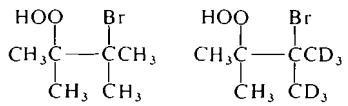

3*a* **3***b*

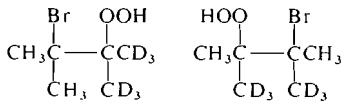

3*c* **3***d*

bromo-1,1,1-trideuterio-2-trideuteriomethyl-2-butyl hydroperoxide (**3***c*) were formed in unequal amounts. The material containing the hydroperoxy group on the carbon bearing the CH_3 groups, **3***b*, made up 61.5% of the product mixture. The product ratio was determined from the n.m.r. spectrum (CCl_4) of the product mixture by comparing the area of the signal at τ 8.57, due to the CH_3 groups of **3***b*, with the area of the signal at τ 8.20, due to the CH_3 groups of **3***c*. The assignments are made on the basis that a bromine atom causes a greater deshielding of β-protons than does a hydroxyl or an alkoxy group (13) and that the hydroperoxy group causes a deshielding similar in magnitude to that of the latter groups. For example, the n.m.r.

Can. J. Chem. Downloaded from www.nrcresearchpress.com by 210.87.254.5 on 09/05/12
For personal use only.

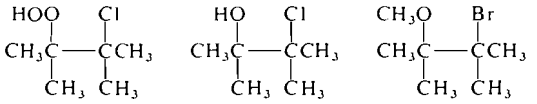

4 5 6

spectra (CCl_4) of 3-chloro-2,3-dimethyl-2-butyl hydroperoxide (**4**) and 3-chloro-2,3-dimethyl-2-butanol (**5**) show signals for the methyl groups at τ 8.38 and 8.60, and at τ 8.36 and 8.69, respectively (1), and the *gem*-dimethyl groups of 3-bromo-2-methoxy-2,3-dimethylbutane (**6**), prepared by the addition of dibromantin to **1***a* in methanol, absorb at τ 8.26 and 8.67.

Freshly prepared samples of the bromohydroperoxides **3***b* + *c* and **3***d* were converted to allylic hydroperoxides by allowing them to react at 0° for 6 h with a five-fold excess of sodium deuteroxide in methanol-d_4, eqs. 2 and 3. Benzene was added as an internal standard so as to be able to obtain material balances for the reactions. A material balance was also obtained in this way for the conversion of the undeuterated bromohydroperoxide **3***a* to 2,3-dimethyl-3-hydroperoxy-1-butene (**7***a*) under similar conditions, eq. 4. The reaction mixtures were analyzed directly by n.m.r. spectroscopy. The relative intensities of the signals at τ 8.70, due to the CH_3 groups attached to the carbon bearing the hydroperoxy group, and at τ 8.22, due to the allylic CH_3 group, of the allylic hydroperoxides were measured by careful integration and the ratios **7***c*/**7***b* and **7***d*/**7***e* were determined as described in the Experimental. Integration of methanolic solutions of **7***a* made from freshly prepared samples of **3***a* gave area ratios for the peaks at τ 8.70 and 8.22 of 2.02 ± 0.06 to 1.00, so no corrections were applied to the area ratios obtained from the runs using the deuterated bromohydroperoxides. However, this area ratio was somewhat larger than 2.0 to 1.0 when samples of **3***a* which had been stored for several weeks at 5° were used to prepare solutions of **7***a*. It was found that this was due to the formation of some 2,3-epoxy-2,3-dimethylbutane whose n.m.r. absorption in methanol solution is almost superimposable upon that of the *gem*-dimethyl group of **7***a*, see below.

The results in Table 1 show that in each case conversion to allylic hydroperoxide is essentially quantitative. Furthermore, it is clear that in the case of the bromohydroperoxides **3***b* and *c* a shift of the hydroperoxy group occurs during the reaction. The compound with the hydroperoxy group on the carbon bearing the CH_3 groups, **3***b*, predominates in the starting mixture while in the product mixture the compound with the hydroperoxy group on the carbon bearing the CD_3 groups, **7***c*, predominates. Clearly, the reaction does not proceed by a direct elimination of the elements of HBr or DBr. In this case the product ratio, **7***c*/**7***b* would have been the same as the ratio, **3***c*/**3***b*, of the starting materials, namely, 0.63. The actual product ratio, **7***c*/**7***b*, is about 2.2.

Further evidence that a C—H or C—D bond is not broken in the rate-determining step of the elimination was obtained by carrying out the elimination reactions on the mixture of **3***b* and *c* with less than one equivalent of base. The relative amounts of **3***b* and *c* remaining at various conversions were determined by n.m.r.

[2] 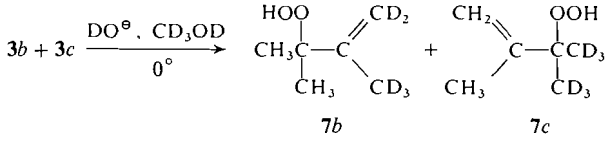

7*b* **7***c*

[3] 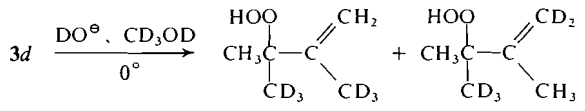

7*d* **7***e*

[4] 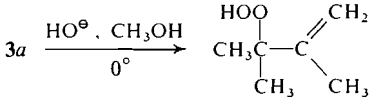

7*a*

Can. J. Chem. Downloaded from www.nrcresearchpress.com by 210.87.254.5 on 09/05/12
For personal use only.

TABLE 1. Yield and product distribution in the reaction between the β-bromohydroperoxides 3*a–d* and base in methanol*

Starting material	Temperature (°C)	% Yield	7*c*/7*b*	7*d*/7*e*†
3*a*‡	25	100		
	2	104		
	−19	100		
3*b* + 3*c*§	0	96±2	2.20±0.04	
		103±3	2.17±0.06	
3*d*§	0	102±2		2.16±0.06
		98±1		2.04±0.03

*Determined by n.m.r. spectroscopy with benzene as an internal standard. Errors are average errors from three integrations per run.

†Corrected to 100% isotopic purity of the trideuteriomethyl groups of 3*d* using the expression

$$\frac{7d}{7d(1-z)+7e(z)} = (7d/7e)$$

observed where z is the fraction of deuterium atoms in the trideuteriomethyl groups.

‡Concentrations: 0.13 *M* 3*a* and 0.81 *N* sodium hydroxide in methanol.

§Concentrations: 0.11 *M* substrate and 0.55 *N* sodium deuteroxide in methanol-d_4.

TABLE 2. Relative rates of disappearance of 3*b* and *c* in basic CD_3OD at 0°

Run	% Conversion*	3*b*/3*c*†	7*c*/7*b*‡
—	0	1.45	—
1	15	1.42	—
2	31	1.46	1.4
3	57	1.43	1.7

*Sufficient 0.55 *N* NaOD was added in each case to 0.11 *M* solutions of 3*b* + *c* to give the conversions shown.

†Measured by n.m.r. spectroscopy from relative peak heights of the signals at τ 8.19 of 3*c* and at τ 8.58 of 3*b*. The ratio of 3*b*/3*c* formed from 1*b* as determined by integration of these signals is 1.6.

‡Measured by n.m.r. spectroscopy from relative peak heights (normalized) of signals of 7*c* at τ 8.22 and of 7*b* at τ 8.70. On complete conversion this ratio is 2.2 as measured by integration of these signals (Table 1).

spectroscopy. The results in Table 2 show that the two bromohydroperoxides 3*b* and *c* both react at essentially the same rate. The ratio, 3*b*/3*c*, changes hardly at all up to 57% reaction. Isotope effects, k_H/k_D, of from 5–9 have been found in a variety of base-promoted elimination reactions of alkyl bromides (14). Thus, if the C—H or C—D and C—Br bonds were being broken simultaneously in the reaction of 3*b* and *c* then 3*c* should be consumed more rapidly than 3*b*, in contrast to what is observed.

The product ratio, 7*c*/7*b*, even at 31% conversion, shows that a migration of the hydroperoxy group has occurred. The ratios of 7*c*/7*b* given in Table 2 differ from those given in Table 1 because the former were determined from the relative peak heights of the signals due to the CH_3 groups of 7*c* and *b*. It was necessary to use the less accurate peak height method of analysis because the absorption of the allylic CH_3 group of 7*c* was too near that of the CH_3 groups at τ 8.20 of the starting material 3*c* for accurate integrations of the signals to be made.

The results suggest that 3*b* and *c* are converted by base to the same reactive bromine-free intermediate which can then lose either a proton or deuteron equally well, except for an isotope effect, to give the allylic hydroperoxides 7*b* and *c*.

The results obtained from the reaction between 3*d* and base are consistent with this. The major product of the reaction is 7*d*, formed by loss of hydrogen bromide, rather than 7*e*, formed by loss of deuterium bromide, and the product ratio, 7*d*/7*e*, is essentially the same as the ratio, 7*c*/7*b*, of products obtained from the mixture of 3*b* and *c*, Table 1.

The results above were obtained before it was discovered that some 2,3-epoxy-2,3-dimethylbutane was formed under these conditions from samples of 3*a* which had been stored for some time. As a result of the method of analysis of the reaction mixtures the ratios, 7*c*/7*b* and 7*d*/7*e*, given in Table 1 are minimum and maximum values, respectively. For example, had 5% of epoxide actually been present in the reaction mixtures obtained from 3*b* + *c* and 3*d*, the corrected value for the ratio, 7*c*/7*b*, would be 2.6 and that for the ratio, 7*d*/7*e*, would be 1.8.

Can. J. Chem. Downloaded from www.nrcresearchpress.com by 210.87.254.5 on 09/05/12
For personal use only.

Can. J. Chem. Downloaded from www.nrcresearchpress.com by 210.87.254.5 on 09/05/12
For personal use only.

It is not known how much epoxide was formed during reaction of the deuterated bromohydroperoxides with base, but the amounts formed, if any, are probably quite small because fresh samples of the deuterated bromohydroperoxides were used so the ratios, *7c*/*7b* and *7d*/*7e*, are uncorrected. Barely detectable amounts, less than 1%, of epoxide were formed from fresh samples of *3a*, while a maximum of about 12% was formed from some of the older samples of *3a*, see below.

Spectroscopic Search for an Intermediate

At the time that these results were obtained it was thought that the intermediate formed during the conversion of the β-bromohydroperoxide, *3a*, to the allylic hydroperoxide, *7a*, might be tetramethyl-1,2-dioxetane (**8**), eq. *5a*. The

[5a] 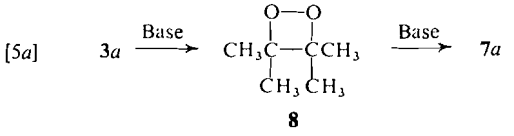

8

formation of **8** from *3a* would be consistent with evidence which was accumulating (1, 4, 15) which suggested that 1,2-dioxetanes were formed in reactions between other suitably substituted hydroperoxides and base. Attempts were made to detect **8** by following the reaction between *3a* and base in methanol between −17.5 and −37.5° by n.m.r. spectroscopy in the thermoregulated probe of a 100 MHz n.m.r. spectrometer. The reaction is rapid enough so that it can be monitored conveniently in this way at temperatures as low as −40°, Table 3. The rate of disappearance of *3a* obeyed second order kinetics over the first 50–60% of reaction during which the reactions were followed.

Besides absorptions for starting material *3a* and product *7a*, a new absorption, a sharp singlet, appeared about 3 Hz downfield from the absorption of the *gem*-dimethyl group of the allylic hydroperoxide and increased in intensity as the reaction progressed until about 40% reaction, after which the intensity of this signal remained constant. It was determined that this signal was due to a compound having 12 equivalent protons by careful integration of the starting material and products before and during reaction using tetramethylsilane as internal standard. The signal was shown to be due to

TABLE 3. Rate of reaction between 3-bromo-2,3-dimethyl-2-butyl hydroperoxide (*3a*) and hydroxide ion in methanol*

Temperature (°C)	$[3a]_0$	$[NaOH]_0$	k_2(graphical) × 10^4 (M^{-1} s^{-1})
−37.5	0.22	0.83	1.0
−27.5	0.15	0.82	1.7
−17.5	0.23	0.58	3.5

*At −17.5° $\Delta H^{\ddagger}$ = 6.9 kcal/mol, $\Delta S^{\ddagger}$ = −47 e.u. for disappearance of *3a*.

2,3-epoxy-2,3-dimethylbutane by comparing the chemical shift of authentic material in methanol solution at the temperatures used and by peak enhancement on addition of small amounts of authentic material to reaction mixtures at low temperatures. About 12% of the epoxide was formed from the samples of bromohydroperoxide used for the rate studies. These samples had been stored for several weeks at 5°. When fresh samples of *3a* were used in the reaction the signal due to the epoxide was barely detectable; less than 1% was formed. The epoxide presumably is formed from the corresponding bromohydrin which may be formed by the slow decomposition of the bromohydroperoxide, *3a*.

No signals other than those due to *3a*, *7a*, and the epoxide could be detected above τ 8 in the n.m.r. spectrum of the reacting mixtures at low temperature. Careful integration indicated that there was no significant absorption other than those due to *3a* and *7a* at around τ 8.20.

Authentic tetramethyl-1,2-dioxetane (**8**) was prepared some time after these experiments were carried out (5). It is not converted to *7a* by base in methanol even in the presence of added bromide ion and in methanol solution it shows absorption at τ 8.53, so that it clearly is not the intermediate which is formed in the reaction between *3a* and base.

There are two other routes involving symmetrical intermediates that appear to be plausible by which the allylic hydroperoxide may be formed from *3a*. One route is fragmentation of the anion of *3a* to give the alkene **1***a*, singlet oxygen, and bromide ion followed by reaction between **1***a* and singlet oxygen, eq. *5b*. This

[5b] 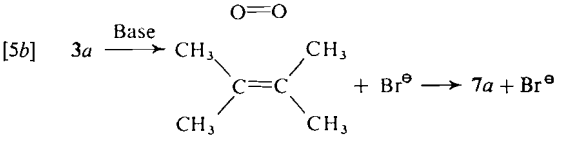

Can. J. Chem. Downloaded from www.nrcresearchpress.com by 210.87.254.5 on 09/05/12
For personal use only.

route to the formation of **7***a* can be ruled out on two grounds. First, the reaction between singlet oxygen and **1***a* is not a diffusion controlled reaction (16) so that a significant amount of the singlet oxygen would be deactivated before it could react and the conversion of **3***a* to **7***a* by this route could not be quantitative. In fact, the yield is essentially quantitative. Second, if the reaction between **3***a* and base proceeded as in eq. 5*b* the singlet oxygen oxidation of the deuterated analogs of **1***a*, *b*, and *c* would give the same distributions of products as are obtained from the reactions of **3***b* + *c* and **3***d* with base. As is shown below, the actual product distributions are quite different from each other.

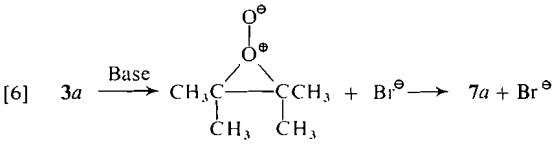

9

The remaining plausible route, and one which we have not yet ruled out, for formation of **7***a* from **3***a* proceeds by way of the perepoxide **9**, eq. 6. Attempts to trap the intermediate **9** with added azide ion have been unsuccessful. A reaction between **3***a* and base in 40% water – 60% CD_3OD saturated with sodium azide (about 0.4 *N*) at 0° formed **7***a* exclusively as judged by the n.m.r. spectrum of the solution after reaction.

Intramolecular Isotope Effects in the Singlet Oxygen and Triphenyl Phosphite Ozonide Oxidation of 2,3-Dimethyl-2-butene

The partially deuterated alkenes **1***b* and *c* were oxidized in methanol to the corresponding mixtures of allylic hydroperoxides with singlet oxygen generated by dye photosensitization (3) and by the reaction between sodium hypochlorite and hydrogen peroxide (3*a*, 3*b*, 17). Mixtures of allylic hydroperoxides were produced whose compositions were analyzed directly by n.m.r. spectroscopy, as described above for the bromohydroperoxide reactions, after extraction into ether and subsequent complete removal of the ether under reduced pressure or after preparative isolation. In these oxidations the allylic hydroperoxides formed by loss of hydrogen rather than deuterium from carbon predominate only to a slight extent. The product ratios, expressed as isotope effects, k_H/k_D, in Table 4 show only a small variation with the source[6] of singlet oxygen and temperature. Indeed, all the values of k_H/k_D for the singlet oxygen oxidations are within 8% of 1.40.[7] The variations of k_H/k_D with temperature and solvent, which are undoubtedly present, are too small to be distinguishable in these experiments. However, the method of product analysis used is accurate enough to show clearly that the observed isotope effects in the singlet oxygen oxidations of the unsymmetrically deuterated alkene **1***b* and the symmetrically deuterated alkene **1***c* differ by no more than 8%. It is also clear that there is a significant difference between the ratios of allylic hydroperoxides formed in these oxidations of **1***b* and *c* and the ratio of allylic hydroperoxides formed by the reactions between base and the bromohydroperoxides of **1***b* and *c*, Table 1, even when the photooxygenation was carried out in the presence of base at −52° (run 8, Table 4). This shows that if any intermediates are formed in the singlet oxygen oxidation of the alkenes **1***b* and *c* they must be different from the intermediates formed in the reactions between base and the bromohydroperoxides of these alkenes.

Triphenyl phosphite ozonide (23) has been shown to oxidize **1***a* to the allylic hydroperoxide **7***a* at −30° and to decompose to triphenyl phosphate and singlet oxygen at −15° (27). It was suggested that **1***a* was oxidized by the singlet oxygen released. In an attempt to distinguish between this mode of oxidation and

[6]A variety of sensitizers was used in order to test the then recent suggestion (18) that sensitizers with high triplet state energies produced more $^1\Sigma_g^+$ than $^1\Delta_g$ oxygen molecules and that these had different reactivities. The suggestion was made to explain the observed (19) sensitizer dependence of product distribution in oxidation of cholest-4-en-3β-ol. It has since been shown that this variation in product distribution is probably due to a direct reaction between sensitizer and substrate which competes with the singlet oxygen ($^1\Delta_g$) reaction and produces a different product (20), and that $^1\Sigma_g^+$ oxygen molecules are deactivated so rapidly by solvent that no reaction with substrate could take place (21).

[7]It has been reported briefly that isotope effects of 1.2 to 2.1 were obtained in the singlet oxygen oxidation of **1***b*, *c*, and 2,2,6,6,2′,2′,6′,6′-octadeuteriocyclohexylidenecyclohexane, unpublished work cited in ref. 22.

NOTE ADDED IN PROOF: These results have now been published (55) and those for **1***b* and *c* are in excellent agreement with the results presented here.

TABLE 4. Intramolecular deuterium isotope effects in the oxidation of **1***b* to **7***b* + *c* and of **1***c* to **7***d* + *e**

Alkene	Run	Reagent (sensitizer)†	Solvent	Temperature (°C)	k_H/k_D‡
1*b*	1	$^1O_2$(MB)	CH_3OH	14	1.35±0.01
	2			14	1.31±0.01
	3			−52	1.35±0.02
	4	$^1O_2$(RB)		14	1.38±0.04
	5	$^1O_2$(Fl)		14	1.36±0.03
	6	$^1O_2$(EY)		14	1.41±0.01
	7			−52	1.44±0.05
	8		CH_3OH–NaOH§	−52	1.30±0.00
	9	H_2O_2–NaOCl	CH_3OH–H_2O	0	1.47±0.01
	10	$(C_6H_5O)_3P{\cdot}O_3$	CH_2Cl_2	−28	1.45±0.01
	11			−70	1.60±0.04
	12			−70	1.65±0.02
1*c*	13	$^1O_2$(MB)	CH_3OH	14	1.32±0.03
	14			14	1.42±0.05
	15			−52	1.53±0.07
	16	$^1O_2$(RB)		14	1.37±0.07
	17	$^1O_2$(Fl)		14	1.34±0.06
	18	$^1O_2$(EY)		14	1.28±0.06
	19			−52	1.46±0.05
	20	$(C_6H_5O)_3P{\cdot}O_3$	CH_2Cl_2	−28	1.27±0.00
	21			−70	1.31±0.03
	22			−70	1.28±0.05

*Alkene concentrations 0.045 *M* except in runs 1, 8–13, and 20–22. Runs 1, 8–10, 13, and 20 were preparative runs beginning with higher concentrations of alkene: 0.44 *M* in runs 1 and 13, 0.089 *M* in run 8, 0.2 *M* in run 9, and 0.1 *M* in runs 10 and 20. Runs 11, 12, 21, and 22 were made with 0.2 *M* olefin.

†MB = Methylene Blue, RB = Rose Bengal, Fl = Fluorescein, EY = Eosin-Y.

‡Determined by n.m.r. $k_H/k_D = 7c/7b$ in oxidation of **1***b* and **7***d*/**7***e* in oxidation of **1***c*. The latter ratio is corrected to 100% isotopic purity as indicated in Table 1. Errors are average errors obtained from at least three integrations per run.

§0.83 *N* NaOH.

a possible direct reaction between the alkene **1***a* and the ozonide, the alkenes **1***b* and *c* were allowed to react with the triphenyl phosphite ozonide at −28° in dichloromethane and the products isolated. The isotope effect in each case is not significantly different from those observed in the oxidations of these alkenes by singlet oxygen generated by unambiguous routes. The oxidations with triphenyl phosphite ozonide were repeated[8] at −70° after it was shown that there is a direct reaction between the ozonide and **1***a* at this temperature which produces **7***a* (24). The reactions were carried out in duplicate with each alkene at the same time. The difference in isotope effects between the two alkenes is somewhat larger in the reactions at −70° than it is at −28° and we feel that at −70° this difference is greater than the probable experimental error of about 8%.

[8]We thank Dr. J.-Y. Ding for performing these experiments.

Intermolecular Deuterium Isotope Effects in the Singlet Oxygen Oxidation of cis- and trans-1,2-Dimethylstilbene

The intramolecular isotope effects in the singlet oxygen oxidation of **1***b* and *c* are quite small. This is not unexpected in view of the high reactivity of **1***a* toward singlet oxygen (16, 25). The energy of activation for the reaction between singlet oxygen and **1***a* is reported to be 0.5 kcal/mol (25*c*). A brief study was made to determine whether the magnitude of the isotope effect would be greater in the oxidation of a less reactive alkene than it is in the oxidation of **1***b* and *c*. The dimethylstilbenes, *cis*- and *trans*-**2***a*, were chosen as substrates for this study as they are readily prepared and were expected to be less reactive toward singlet oxygen than is **1***a*. This expectation was substantiated qualitatively by finding that the methylene blue photosensitized oxidation of 0.014 mol of *cis*-**2**, the more reactive of the two isomers, required 2 h while the oxidation, under identical conditions, of

Can. J. Chem. Downloaded from www.nrcresearchpress.com by 210.87.254.5 on 09/05/12
For personal use only.

TABLE 5. Isotope effects in the singlet oxygen oxidation of *cis*- and *trans*-1,2-dimethylstilbene in methanol at 14°

Isomer	Sensitizer*	% Reaction†	Ratio 2*a*/2*b* Initial	Ratio 2*a*/2*b* Final	k_H/k_D‡
cis	MB	73	1.05	0.97	1.07
	EY	69	1.05	0.95	1.09
trans	MB	49	1.10	1.02	1.13

*MB = Methylene Blue, EY = Eosin-Y.
†Of undeuterated starting material.
‡Calculated by the method of ref. 27.

0.012 mol of **1***a*, required 45 min. After reduction of the intermediate hydroperoxide a 48% yield of 2,3-diphenyl-3-butene-2-ol (**10**) was isolated from the oxidation of *cis*-**2***a*, eq. 7.

[7] *cis*-**2***a* $\xrightarrow[(3)\ NH_4Cl]{(1)\ {}^1O_2,\ (2)\ LiAlH_4}$ $CH_3C(OH)(C_6H_5)C(=CH_2)C_6H_5$

10

In a competitive oxidation (25*a*) it was found that *cis*-**2***a* was about 10 times as reactive as *trans*-**2***a* toward singlet oxygen, in agreement with a previous report that *cis*-**2***a* is more reactive than *trans*-**2***a* (26).

The intermolecular isotope effects in the singlet oxygen oxidations were determined by oxidizing mixtures of *cis*-**2***a* and *cis*-**2***b* and of *trans*-**2***a* and *trans*-**2***b* to partial completion in methanol. The unreacted alkenes were isolated by column chromatography. The composition of the initial and final mixtures of alkenes was determined by mass spectrometry using an ionizing voltage of 9.5 eV. The mass spectrometric analysis of weighed mixtures of *cis*-**2***a* and *b* and of *trans*-**2***a* and *b* reproduced the synthetic ratios to within 2% so it is felt that the isotope effects determined in this way should be accurate to within about 10% or less. The isotope effects, Table 5, are even smaller than those obtained in the singlet oxygen oxidations of **1***b* and *c*. Also, they are the same for both *cis*- and *trans*-**2***a* even though *trans*-**2***a* is less reactive than *cis*-**2***a* toward singlet oxygen.

Discussion

Conversion of **3** *to* **7**

The product distribution observed in the conversion of the mixture of **3***b* + *c* to **7***b* + *c* indicates that migration of the hydroperoxy group occurs in the reaction. This migration cannot occur by fragmentation to singlet oxygen and alkene followed by recombination, eq. 5, or by way of tetramethyl-1,2-dioxetane (5). This appears to leave, as a result of this process of elimination, formation and subsequent reorganization of the perepoxide **9** as the pathway for migration of the hydroperoxy group. The perepoxide **9** must be a short-lived species, at least in the reaction medium used, as attempts to detect it by n.m.r. spectroscopy at temperatures as low as −37° gave no evidence for its existence. Attempts to trap **9** with azide ion also failed. Under the reaction conditions used **9** could be converted to **7** either by an intramolecular reorganization or by reaction with base.

Although the intermediate under discussion has been formulated as a perepoxide the migration of the hydroperoxy group in the present system can also be formulated as proceeding by way of a pair of rapidly interconverting open chain zwitterions, eq. 8, in which case the

[8] $CH_3C(O^{\ominus})(O)C(CH_3)_2C^{\oplus}H_2 \rightleftharpoons$ **9** $\rightleftharpoons CH_3C^{\oplus}(O)C(CH_3)_2O^{\ominus}$

perepoxide would represent a transition state or an intermediate between the two zwitterions.

Evidence that such open chain zwitterions do not play a role in the conversion of bromohydroperoxides to allylic hydroperoxides comes from the reaction between base in methanol and 3-bromo-3-methyl-2-(4-methoxyphenyl)-2-butyl hydroperoxide (**11**), eq. 9, in which migration of the hydroperoxy group also clearly occurs. A mixture of the allylic hydroperoxides **12** and **13** is formed in a 6.3:1 ratio (2*b*). One would

Can. J. Chem. Downloaded from www.nrcresearchpress.com by 210.87.254.5 on 09/05/12
For personal use only.

[9] 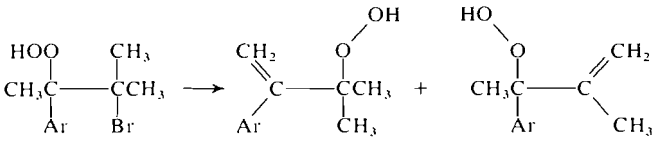

11 12 13

Ar = 4-Methoxyphenyl

expect such a great difference in the stabilities of the two possible open chain zwitterions that might be derived from **11** that **12** should be the exclusive product. A perepoxide intermediate might be more likely to lead to the observed product distribution.

The perepoxides derived from **3** and **11** must form allylic hydroperoxides by a process with a very low activation energy and which may be concerted. This would account for the relatively small magnitude of the isotope effect observed in the conversion of **3** to **7** and the perhaps smaller than expected ratio of **12**:**13** formed from **11**. If the perepoxides rearranged in an intramolecular, concerted reaction the carbon, hydrogen, and oxygen atoms involved in the hydrogen transfer could not be colinear. This would also result in the formation of products with little discrimination as discussed below for the singlet oxygen reactions. In fact, if the perepoxide reaction is concerted the transition state geometry for this reaction must resemble quite closely that of the singlet oxygen reaction.

Until recently there appeared to be no authentic examples of compounds which had structures and which gave reactions analogous to those of **9**. Now, two classes of such "strained dipolar species" have been characterized definitively: the episulfoxides (28) and the aziridine *N*-oxides (29). When suitably substituted these materials rearrange thermally at relatively low temperatures to give allylic sulfenic acids and allylic hydroxylamines, respectively. Further, aziridine *N*-oxides do not rearrange to the four-membered ring compounds, 1,2-oxazetidines (29). In these respects the behavior of the proposed intermediate **9** parallels that of the above materials very closely.

It is possible to compare the neighboring group effect of the hydroperoxy anion with that of the oxide ion in the 2,3-dimethyl-3-bromo-2-butyl system. Because the bromohydroperoxide **3***a* is stable in neutral methanol for several days, at least, the perepoxide **9** must be formed from the conjugate base of **3***a*. Since no evidence was obtained for the formation of any of the dioxetane **8**, cyclization by the neighboring hydroperoxy anion with participation of the disubstituted oxygen to give **9** is at least 50 times faster than is cyclization with participation of the anionic oxygen to give **8**. This is the reverse of what occurs in the reactions between base and 3-bromo-2-methyl-2-butyl hydroperoxide (5) and 1-chloro-2-methyl-2-propyl hydroperoxide (30) in which only 1,2-dioxetanes are formed initially. Apparently, in a system such as **3***a* where a tertiary halide is to be displaced by the hydroperoxy anion, only a small amount of nucleophilic assistance is required so that the inherently more favorable cyclization to form a three-membered ring can compete effectively with the cyclization to form a four-membered ring. Even so, the disubstituted oxygen atom of the hydroperoxy anion is a much less effective neighboring group than is the oxide ion in the present system. From the observation, that in the reaction between base and samples of **3***a* which were contaminated with bromohydrin, epoxide formation was essentially complete by the time 50% of **3***a* had been consumed together with the estimate that the pK_a's of **3***a* ($pK_a \approx 13$ (31)) and the corresponding bromohydrin ($pK_a \approx 18$ (32)) differ by about five pK_a units, it can be reckoned that cyclization of oxide ion to epoxide is 10^4–10^6 times as fast as cyclization of hydroperoxy anion to **9**.

Mechanism of Singlet Oxygen Oxidation

Three mechanisms have been proposed for the oxygenation of alkenes to allylic hydroperoxides by singlet oxygen: (*1*) formation and subsequent reorganization of a perepoxide intermediate which was initially proposed to account for the large rate enhancement caused by increasing substitution of the double bond by alkyl groups (25*a*, 33); (*2*) formation and subsequent reorganization of a 1,2-dioxetane which was proposed when cleavage products were observed in photooxygenation of indene (34); (*3*) a concerted reaction in which the C—O

Can. J. Chem. Downloaded from www.nrcresearchpress.com by 210.87.254.5 on 09/05/12
For personal use only.

Can. J. Chem. Downloaded from www.nrcresearchpress.com by 210.87.254.5 on 09/05/12
For personal use only.

and C—H bonds are formed simultaneously in a cyclic transition state. This latter mechanism was proposed to explain the geometric requirements of the photooxygenation reactions in steroids (35) and the lack of solvent and substituent effects on product distribution (3*a*, 3*b*, 36). Intervention of 1,2-dioxetanes as intermediates in the conversion of alkenes to allylic hydroperoxides by singlet oxygen can be disregarded as a general phenomenon as it has been shown that trimethyl- and tetramethyl-1,2-dioxetane are not converted to allylic hydroperoxides even when treated with base (5). The results of the present study certainly provide no evidence against a concerted mechanism and provide strong evidence that perepoxides are not formed in this reaction.

The perepoxide mechanism had appeared to receive experimental support when it was reported that photooxygenation of **1***a* and of 1,2-dimethylcyclohexene in the presence of azide ion resulted in the formation of high yields of hydroperoxy azides (37). It was suggested that azide ion trapped perepoxides formed by reaction of singlet oxygen with these alkenes. It has now been shown (38) that the formation of hydroperoxy azides is a radical reaction which has nothing to do with the allylic oxygenation reaction. Furthermore, the present work shows that the perepoxide derived from **7***a* cannot be trapped by azide ion anyway under reaction conditions similar to those which gave hydroperoxy azides from **1***a* (37).

Evidence has existed for some time that supports strongly a concerted mechanism for the singlet oxygen oxygenation of alkenes. It is difficult to explain the conformational requirements of the allylic hydrogen which is to be removed by singlet oxygen (35) and the complete lack of reactivity of norbornene, methylenecyclopentene, and methylenecyclohexane towards singlet oxygen (39) in terms of either a dioxetane or a perepoxide mechanism without invoking an extremely unlikely reversible formation of these species. Such arguments have been made already (22).[9]

The magnitudes of the deuterium isotope effect in the photooxygenation of **1***b* and *c* and of **2***a* and *b* might appear to be rather small for a reaction in which a C—H or a C—D bond is broken in the rate determining step. There can be several reasons for this small isotope effect. The reaction has a very small energy of activation so that a large isotope effect is not to be expected. In the transition state for the concerted reaction, it is unlikely that the oxygen, hydrogen, and carbon atoms involved in the hydrogen transfer are colinear. It has been pointed out that in such a situation the isotope effect should be smaller than for a process in which all these atoms can be colinear (41). Finally, it is theoretically possible to have small and even inverse isotope effects for reactions in which hydrogen is transferred from carbon to oxygen (42).

Oxygenation by Triphenyl Phosphite Ozonide

The isotope effects observed on oxygenation of **1***b* and *c* by triphenyl phosphite ozonide at $-70°$ in methylene chloride are quite similar to those observed on oxygenation of **1***b* and *c* by singlet oxygen at $-52°$ in methanol which indicates that a perepoxide intermediate cannot be involved. Also, it has been shown that singlet oxygen does not intervene in the triphenyl phosphite ozonide oxygenation at low temperatures (24) so that still another mechanism is required for oxygenation by this reagent. This reaction gives a higher proportion of the product of C—H bond breaking with **1***b* than with **1***c* which suggests the formation of a transition state or intermediate in which the oxygen is bonded more strongly to the carbon bearing the CD_3 groups of **1***b* than to the other carbon atom than is the case in the singlet oxygen reaction. The difference in isotope effects between **1***b* and *c* is quite small, however, and may not be outside experimental error although it is reproducible.

It is remarkable that there are so many different routes for the conversion of **1***a* to **7***a*.

Experimental

General

Boiling points and melting points are uncorrected. The latter were taken on a Gallenkamp melting point apparatus. I.r. spectra were taken on Perkin–Elmer Model 421 and 337 spectrophotometers and only characteristic absorption bands are cited. Refractive indices were measured on a Bausch and Lomb Abbe-34 refractometer. N.m.r. spectra were determined in carbon tetrachloride and with tetra-

[9]The argument made against a perepoxide intermediate in terms of *syn* and *anti* isomers (22) probably is not valid. These would undoubtedly interconvert rapidly by inversion about the tricoordinated oxygen atom (40).

Can. J. Chem. Downloaded from www.nrcresearchpress.com by 210.87.254.5 on 09/05/12
For personal use only.

methylsilane as internal standard, unless otherwise noted, using Varian analytical spectrometers Models A-60 and HR-100. Abbreviations used in reporting the n.m.r. spectra are b, broad; s, singlet; d, doublet; m, multiplet. Gas chromatography was carried out on an Aerograph A-90-P3 gas chromatograph using a 5 ft × 1/4 in. stainless steel column packed with 20% SF-96 on 60/80 Chromosorb P. Mass spectra were obtained on an A.E.I. MS-2-H mass spectrometer. Organic extracts were dried with magnesium sulfate unless otherwise indicated. Elemental analyses were performed by Mrs. Darlene Mahlow of this Department.

All preparations of β-bromohydroperoxides were carried out behind shields. Apparatus containing these compounds was manipulated with the aid of tongs and hands were protected with heavy canvas gloves.

Materials

Deuterium oxide (99.8 atom %D) and acetone-d_6 (99.5 atom %D) were obtained from Merck, Sharp & Dohme of Canada, Ltd.

Deuteriosulfuric acid was prepared by the addition of anhydrous sulfur trioxide to deuterium oxide.

Trideuterioiodomethane (96.5 atom %D) was prepared by pyrolysis of perdeuteriotrimethyloxosulfonium iodide obtained by isotopic exchange of the undeuterated salt with deuterium oxide (43).

Perdeuterioacetone Cyanohydrin (3,3,3-Trideuterio-2-trideuteriomethyl-2-hydroxypropanenitrile)

The synthesis was patterned after the procedure used for the preparation of acetone cyanohydrin (44). A solution of 28 ml deuteriosulfuric acid in 79 ml of deuterium oxide was added to a cooled (ice-bath) solution of 25 g (0.39 mol) of acetone-d_6 and 22 g (0.45 mol) sodium cyanide in 48 ml deuterium oxide at such a rate as to keep the temperature of the reaction mixture below 15°. The solution was stirred for 15 min after the addition was complete and then continuously extracted with ether for 36 h. The dried ether extract was freed of solvent and the residue distilled to give 32 g (93%) of product, b.p. 78–80° (17 mm), n_D^{25} 1.3966 (lit. (44) for acetone cyanohydrin, b.p. 78–82° (15 mm), n_D^{19} 1.4002); i.r. ($CHCl_3$): 2400 to 2700, 2250 cm^{-1}; n.m.r. (neat) no absorption from τ 0–10.

Methyl 3,3,3-Trideuterio-2-trideuteriomethyl-2-hydroxyproponoate

Perdeuterioacetone cyanohydrin was hydrolyzed using a modification of the procedure for the hydrolysis of a related cyanohydrin (45). A solution of 32.5 g (0.35 mol) of the cyanohydrin and 35 ml concentrated hydrochloric acid in 14 ml water was heated at 95° for 2 h. Sodium sulfate, 12 g, was then added and the mixture cooled to −15°. The resulting mixture was filtered and both the precipitate and the filtrate were extracted continuously with ether for 2 days. The extracts were combined, dried, and a small sample of 3,3,3-trideuterio-2-trideuteriomethyl-2-hydroxypropanoic acid, m.p. 75–76° (lit. (46) for 2-methyl-2-hydroxypropanoic acid, m.p. 79°), was isolated from a portion of the extracts; i.r. ($CHCl_3$): 2500 to 3600, 2230, 1730 cm^{-1}; n.m.r. ($CDCl_3$): τ 3.24 (s).

The remainder of the extracts was treated with 0.4 mol diazomethane in ether at 0°. Excess diazomethane was destroyed by addition of acetic acid in small portions. Removal of solvent and distillation of the residual oil gave 33.0 g (74%) of product, b.p. 133–134° (710 mm), n_D^{25} 1.4069 (lit. (47) for methyl 2-methyl-2-hydroxypropanoate, b.p. 137–139° (760 mm), $n_D^{19.3}$ 1.4112); i.r. ($CHCl_3$): 3250 to 3600, 2230, 2210, 1745 cm^{-1}; n.m.r. τ 6.31 (s, 3.10H), 6.67 (s, 1.0H).

3-Methyl-1,1,1-trideuterio-2-trideuteriomethyl-2,3-butanediol

A solution of 33 g (0.27 mol) of the above ester in 150 ml ether was added to a solution of methylmagnesium iodide prepared from 26.4 g (1.1 mol) magnesium and 200 g (1.45 mol) iodomethane in 1 l ether. The reaction mixture was stirred 4 h after the addition was complete and then poured into a mixture of ice and 1.1 mol hydrochloric acid. The ether layer was separated and the aqueous layer continuously extracted with ether for 2 days. The combined ether extracts were dried thoroughly, first with magnesium sulfate, then with molecular sieves (4 A) and finally poured through a column (4 × 20 cm) of molecular sieves. The solution was concentrated and the residue distilled to give 20 g (88%) of colorless oil, b.p. 164–167° (710 mm) (lit. (48) for pinacol, b.p. 172°); n.m.r.: τ 7.23 (s, 2.0H), 8.82 (s, 6.10H).

1,1,1-Trideuterio-2-trideuteriomethyl-3-methyl-2-butene (1b)

The procedure (10) for the preparation of 2,3-dimethyl-2-butene was adapted. This reaction gave a poor yield of product if the pinacol was not dried thoroughly as described. The above deuterated pinacol, 27.0 g (0.218 mol) was heated with 32.2 g (0.218 mol) of freshly distilled ethyl orthoformate under a 10 cm Vigreux column for 10 h after which the slow distillation of ethanol ceased. Two drops of acetic acid were added and the mixture was heated at 175° until no more product distilled (8 h) into the ice-cooled receiver. The product was redistilled to give 10.9 g (54%) of an oil, b.p. 69.5–70.5° (710 mm) (lit. (49) for 2,3-dimethyl-2-butene, b.p. 73°); i.r. (CCl_4): 2250, 2180, 2060 cm^{-1}; n.m.r.: τ 8.40 (s). Mass spectral analysis (12) at 12 eV, mol % d_n: 0.51 d_3, 0.10 d_4, 2.5 d_5, 96.88 d_6. The mass spectrum taken at 70 eV had the following peaks in the $M^{\oplus} - CX_3$ (X = D or H) region, *m/e* (% relative intensity): 69 (2), 70 (5), 71 (6), 72 (100), 73 (11), 74 (6), 75 (93), 76 (5).

2,3-Bis(trideuteriomethyl)-2,3-butanediol

A solution of 28 g (0.33 mol) dry, freshly distilled 2,3-butanedione in 200 ml ether was added at a rate to maintain mild reflux to a solution of trideuteriomethyl magnesium iodide prepared from 120 g (0.83 mol) trideuterioiodomethane and 18 g (0.75 mol) magnesium in 1500 ml ether contained in a Morton flask. High speed stirring was used during the addition and for 8 h afterwards. Work-up and drying of the product was carried out as described above for the preparation of the other deuterated pinacol to give 34 g (79%) of product, b.p. 163–168° (710 mm); n.m.r.: τ 6.49 (s, 2.0H), τ 8.78 (s, 6.1H).

In exploratory runs using undeuterated materials the yield of pinacol was found to be 30% or less when ordinary stirring was used in the Grignard reaction.

2,3-Bis(trideuteriomethyl)-2,3-dimethyl-2-butene (1c)

This reaction was carried out as described for the preparation of 1*b*. From 34 g (0.28 mol) of the above pinacol and 41 g (0.28 mol) ethyl orthoformate 14 g (56%) of product was obtained, b.p. 69–70.5° (710 mm); i.r. (CCl_4): 2235,

Can. J. Chem. Downloaded from www.nrcresearchpress.com by 210.87.254.5 on 09/05/12
For personal use only.

2180, 2130, 2060 cm^{-1}; n.m.r.: τ 8.41 (s). Mass spectral analysis (12) at 9.5 eV, mol % d_n: 0.31 d_2, 0.77 d_3, 3.09 d_4, 18.4 d_5, 77.43 d_6. The mass spectrum taken at 70 eV had the following peaks in the $M^+ - CX_3$ (X = D or H) region, *m/e* (% relative intensity): 67 (2), 68 (2), 69 (4), 70 (9), 71 (16), 72 (100), 73 (11), 74 (22), 75 (79), 76 (3).

cis- and trans-1,2-Bis(trideuteriomethyl)-stilbene (cis- and trans-2b)

The adsorbed water on 300 g basic alumina was replaced by deuterium oxide with a series of exchanges (50) which involved heating the alumina to 200° under 1 mm pressure followed by cooling and shaking the alumina with 18 g deuterium oxide. This process was repeated until the moisture collected on heating the alumina contained 0.4% protium (four exchanges). The resulting alumina was placed into two long (5 ft × 17 mm) chromatography columns and a solution of 30 g acetophenone in pentane was passed through the columns. The methyl group of the recovered acetophenone was 93% deuterated as determined by n.m.r. spectroscopy. Treatment of this material with lithium aluminum hydride in ether and hydrolysis of the reaction mixture gave 2,2,2-trideuterio-1-phenylethanol in 91% yield, b.p. 97–98° (18 mm), n_D^{25} 1.5245 (lit. (51) for 1-phenylethanol, b.p. 103–104° (20 mm), n_D^{25} 1.5251). This product was treated with a 5% excess of thionyl chloride in benzene to give 2,2,2-trideuterio-1-chloro-1-phenylethane in 90% yield, b.p. 76–77° (13 mm), n_D^{25} 1.5235 (lit. (52) for 1-chloro-1-phenylethane, b.p. 75° (14 mm), n_D^{19} 1.5275), and then converted to the deuterated 1,2-dimethylstilbenes, *cis-* and *trans-***2***b*, with sodium amide using the procedure described (53) for the preparation of the undeuterated analogs. The products were fractionally crystallized from methanol. Samples of both isomers were obtained in pure form as determined by g.c. and n.m.r. spectroscopy, *cis-***2***b*, m.p. 63–64°, *trans-***2***b*, m.p. 103–104° (lit. (53) for *cis-***2***a*, m.p. 65–66°, *trans-***2***a*, m.p. 105–106°); i.r. (CCl_4): *cis-***2***b*, 2230, 2210, 2115, 2060 cm^{-1}, *trans-***2***b*, 2230, 2210, 2110, 2060 cm^{-1}; n.m.r.: *cis-***2***b*, τ 3.09 (s), *trans-***2***b*, τ 2.50 (s); mass spectral analysis (12) at 9.5 eV, mol % d_n: *cis-***2***b*, 0.17 d_0, 0.14 d_1, 0.09 d_2, 0.90 d_3, 6.45 d_4, 30.68 d_5, 61.60 d_6; *trans-***2***b*, 0.07 d_0, 0.03 d_1, 0.09 d_2, 0.90 d_3, 6.65 d_4, 30.80 d_5, 61.47 d_6.

*2,3-Diphenyl-1-butene-3-ol, (**10**)*

A solution of 3 g (0.013 mol) of *cis-***2***a* (53) in 30 ml methanol was photooxidized at 14° using methylene blue as sensitizer in the apparatus previously described (1). Oxygen uptake became very slow after 2 h when 350 ml (112%) had been consumed. The solution was poured into 100 ml ice-water and the resulting mixture extracted twice with 50 ml ether. The combined extracts were washed with water and with saturated aqueous sodium chloride solution. After drying, the ether solution was added to a stirred slurry of 0.5 g lithium aluminum hydride in 25 ml ether. The mixture was heated under reflux for 30 min and then hydrolyzed with 15% potassium hydroxide. The precipitate was stirred several times with ether and the combined ether solutions dried and concentrated. The residue was distilled to give 1.5 g (48%) of a colorless oil, b.p. 101–104° (0.1 mm), n_D^{25} 1.5809; i.r. ($CHCl_3$): 3560, 3300–3500, 3060, 1640, 905 cm^{-1}; n.m.r.: τ 2.5–3.2 (m, 10.4H), 4.55 (d, J = 1.5 Hz, 0.94H), 4.82 (d, J = 1.5 Hz, 1.01H), 8.05 (s, 0.90H), 8.40 (s, 2.80H).

Anal. Calcd. for $C_{16}H_{16}O$: C, 85.67; H, 7.19. Found: C, 85.63; H, 7.00.

3-Bromo-2,3-bis(trideuteriomethyl)-2-butyl Hydroperoxide (3d)

This material was prepared from the corresponding deuterated alkene **1***c*, 98% hydrogen peroxide, and 1,3-dibromo-5,5-dimethylhydantoin according to the procedure described for the preparation of 3-bromo-2,3-dimethyl-2-butyl hydroperoxide (**3***a*) (1), m.p. 90–92° (lit. (1) for **3***a*, m.p. 93–94°); i.r. (CCl_4): 3550, 3200–3500, 2250 and 2160 cm^{-1}; n.m.r.: τ 2.4 (bs, 0.90H), 8.20 (s, 3.0H), 8.57 (s, 3.0H). Iodometric titration indicated that **3***d* contained 97.0% of the theoretical amount of active oxygen.

3-Bromo-4,4,4-trideuterio-3-trideuteriomethyl-2-methyl-2-butyl Hydroperoxide (3b) and 3-Bromo-1,1,1-trideuterio-2-trideuteriomethyl-3-methyl-2-butyl Hydroperoxide (3c)

A mixture of **3***b* and *c* was prepared from the corresponding alkene **1***b* by the procedure described for the preparation of **1***a* (1), m.p. 91–93°; i.r. (CCl_4): 3550, 3200–3500, 2240, 2130 cm^{-1}; n.m.r.: τ 2.1 (bs), 8.20 (s), 8.53 (s). The ratio of the areas of the latter signals was 1:1.60 as determined by careful integration. From four integrations the average ratio of the areas of the corresponding signals in the spectrum of the undeuterated compound **1***a* was 1.00 ± 0.02. Iodometric titration indicated that the mixture of **3***b* and *c* contained 97.4% of the theoretical amount of active oxygen.

*2-Bromo-2,3-dimethyl-3-methoxybutane (**6**)*

To a stirred solution of 5 g (0.06 mol) **1***a* and 9.6 g (0.3 mol) of methanol in 50 ml ether at −40° was added 8.1 g (0.03 mol) of 1,3-dibromo-5,5-dimethylhydantoin in small portions over 10 min. The resulting mixture was allowed to warm to 23° and then was shaken four times with 50 ml water. The organic layer was dried and concentrated and the residue distilled to give 9.2 g (79%) of colorless oil, b.p. 75–77° (15 mm), which crystallized on standing. The solid was recrystallized from methanol to give 7.3 g white needles, m.p. 71–73°; n.m.r.: τ 6.70 (s, 3.0H), 8.26 (s, 6.0H), and 8.67 (s, 6.1H).

*Material Balance and Rate of Reaction Between Base and **1**a*

Material Balance

A methanol solution 0.39 *M* in **1***a* and 0.25 *M* in benzene was made up and the areas of the n.m.r. signals due to benzene and to the methyl groups of **1***a* were carefully measured. Three n.m.r. tubes were prepared at −70° with one part of this solution and two parts of a 1.22 *M* solution of sodium hydroxide in methanol. The tubes were sealed and individual tubes were warmed to −19, 2, and 25°. After standing for 28 h, long enough for complete reaction to occur at −19°, the areas of the n.m.r. signals due to benzene and to the methyl groups of the product allylic hydroperoxide **7***a* were carefully measured. The results are given in Table 1.

Reaction Rates

Volumetric solutions of **1***a* and tetramethylsilane and of sodium hydroxide in methanol were prepared. Aliquots of these solutions were transferred to n.m.r. tubes at −78° and mixed. The tubes were placed in the temperature con-

Can. J. Chem. Downloaded from www.nrcresearchpress.com by 210.87.254.5 on 09/05/12
For personal use only.

trolled probe of the 100 MHz n.m.r. spectrometer. The areas of the signals due to the *gem*-dimethyl group on the carbon bearing the hydroperoxy group of the starting material **1***a*, the *gem*-dimethyl group of product **7***a*, and tetramethylsilane were determined periodically. The apparent second order rate constants for the disappearance of **1***a* were determined from the slopes of plots of $1/(a-b)\ln b(a-x)/a(b-x)$ *vs.* time (54) where a and b represent the initial concentrations of hydroxide ion and **1***a*, respectively, and x is the instantaneous concentration of **1***a*. Reactions were followed to *ca.* 60% completion and the plots gave good straight lines. The results are given in Table 3.

Reaction between Deuterated Bromohydroperoxides **3***b* + *c and* **3***d and Base*

To n.m.r. sample tubes at $-70°$ were added 0.15 ml of a solution made from 0.07 g deuterated bromohydroperoxide, 0.018 g benzene, 1.0 ml methanol-d_4, and 0.30 ml of a solution made from 0.038 g sodium, 0.046 g deuterium oxide, and 2.0 ml methanol-d_4. The contents of the tubes were mixed at $-70°$ and then the tubes were placed in an ice bath for 6 h. The relative amounts of the deuterated allylic hydroperoxides were determined by integration of the n.m.r. signals at τ 8.2 (allylic CH_3) and 8.7 (*gem*-CH_3's). The ratio, **7***c*/**7***b*, was obtained by dividing twice the area of the signal at τ 8.2 by the area of the signal at τ 8.7. To account for the fact that the trideuteriomethyl groups of **1***c* were only 95.3% deuterated the ratio, **7***d*/**7***e*, was obtained using the expression

$$\frac{\text{area at } \tau 8.7}{\text{area at } \tau 8.2} = \frac{3a(100-y)+0.14a(100-y)+3ay+0.14ay}{3a(100-y)+0.141ay} = \frac{314}{2.86y}$$

where a is the area due to one proton and y is the % **3***d* in the product mixture. The results are given in Table 1.

Photosensitized Oxidation of the Deuterated Alkenes **1***b and c*

The photosensitized oxidation of the alkenes **1***b* and *c* was carried out using the apparatus previously described (1). In preparative reactions, a solution of 1 g (0.01 mol) of the alkene and 15 mg methylene blue in 25 ml methanol was irradiated at 14° until oxygen uptake became very slow (*ca.* 45 min, *ca.* 120% oxygen uptake). The solution was then poured into 100 ml ice-water and the resulting mixture extracted with ether, 3 × 50 ml. The combined ether extracts were dried and concentrated and the residual oil distilled. From **1***b* there was obtained 0.65 g (48%) of a mixture of the deuterated allylic hydroperoxides **7***b* and *c*, b.p. 57–59° (17 mm); n_D^{29} 1.4375 (lit. (1) for **1***a*, b.p. 55° (12 mm); n_D^{20} 1.4428). From the oxidation of **1***c* there was obtained 0.70 g (56%) of a mixture of the deuterated allylic hydroperoxides **7***d* and *e*, b.p. 58–60° (17 mm), n_D^{29} 1.4379.

A series of oxidations with various sensitizers was carried out in the same apparatus using solutions 0.044 *M* in alkene **1***b* or *c*. The solutions were irradiated for 15 min, long enough for complete reaction to occur. For the runs at $-52°$ the solutions were cooled by blowing cold nitrogen gas through the jacket of the apparatus. The temperature of the solution was checked just before and just after irradiation. One oxidation of **1***b* was carried out at $-52°$ in the presence of 0.83 *M* sodium hydroxide. This reaction mixture was kept at $-65°$ for 1.5 h after irradiation and then warmed to 0° over a 2 h period before work-up. After irradiation the reaction mixtures were worked-up as described above, except that the ether extracts were concentrated to a film under reduced pressure. Carbon tetrachloride (2 ml) was then added and the resulting solution was again concentrated to a film under reduced pressure. The residue was taken up in 0.5 ml carbon tetrachloride and the relative amounts of the deuterated allylic hydroperoxides were determined as described for the reaction between the deuterated bromohydroperoxides and base. In the analysis of the product of oxidation of the undeuterated alkene **1***a* carried out in this way, it was found that the ratio of twice the area of the signal at τ 8.2 divided by the area of the signal at τ 8.7 was 1.01 ± 0.03 so no correction was applied to the results obtained from deuterated materials which are given in Table 4.

Oxidation of the Deuterated Alkenes **1***b and c with Triphenyl Phosphite Ozonide*

A stream of ozone was introduced into a solution of 2.2 g (0.007 mol) of redistilled triphenyl phosphite in 40 ml methylene chloride at $-75°$ until a blue color persisted in the solution. Excess ozone was flushed out with a stream of nitrogen and a solution of 0.6 g (0.006 mol) of deuterated alkene **1***b* or *c* in 5 ml methylene chloride was added. The resulting solution was mixed and then allowed to stand at $-28°$ for 2.5 h. The methylene chloride was removed through a short fractionating column and the residue was distilled to give the corresponding allylic hydroperoxides. From **1***b* there was obtained 0.36 g (49%) of product, b.p. 50–56° (12 mm), n_D^{25} 1.4398, and from **1***c* 0.28 g (40%) of product, b.p. 49–53° (15 mm), n_D^{25} 1.4395. The composition of each mixture was determined as in the photooxidation reactions.

These reactions were repeated later at lower temperatures. One-milliliter solutions 0.4 *M* in triphenyl phosphite ozonide and 0.2 *M* in deuterated alkene, made up as described above, were allowed to stand at $-70°$ for 4 h (24) and then analyzed directly by n.m.r. spectroscopy at 100 MHz. A run with undeuterated alkene **1***a* was made under these conditions and it was found on n.m.r. analysis that twice the area of the signal at τ 8.2 divided by the area of the signal at τ 8.7 was 1.05 ± 0.03. The results shown in Table 4, runs 11, 12, 21, and 22, are corrected for this.

*Deuterium Isotope Effects in Photosensitized Oxidation of cis- and trans-1,2-Dimethylstilbene (cis- and trans-***2***a)*

A solution of 0.520 g (2.5 mmol) of *trans*-1,2-dimethylstilbene (*trans*-**2***a*) (53) and 0.534 g (2.5 mmol) of *trans*-1,2-bis-(trideuteriomethyl)-stilbene (*trans*-**2***b*) in 40 ml methanol was prepared. Solvent was removed from an aliquot of this solution and the residue analyzed by mass spectrometry at 9.5 eV. The remainder of the solution, after addition of 15 mg methylene blue, was irradiated at 14° in the apparatus described (1) until 49% of *trans*-**2***a* had been consumed as determined by n.m.r. spectroscopy. The reaction mixture was then worked-up as described for the preparation of 2,3-diphenyl-1-butene-3-ol above. The concentrated residue obtained from the lithium aluminum hydride reduction was

absorbed on a 1 cm × 15 cm column of basic alumina. Elution of the column with 50 ml pentane and removal of the pentane from the element left the mixture of unreacted alkenes of which the relative amounts of deuterated and undeuterated materials were determined by analysis (12) of the parent region of the mass spectrum taken at 9.5 eV. There were only traces of ions formed with *m/e* ratios below those of the parent ions at this voltage. The isotope effect, k_H/k_D, was calculated from the relative amounts of the alkenes remaining (25*b*, 27). The same procedure was used in the oxidation of mixtures of *cis*-**2***a* and *cis*-**2***b*. The results are presented in Table 5.

*Relative Rates of Photosensitized Oxidation of cis- and trans-1,2-Dimethylstilbene (cis- and trans-***2***a)*

A solution of 0.253 g *cis*-**2***a*, 0.251 g *trans*-**2***a*, 0.204 g bibenzyl, and 15 mg methylene blue was made up in 40 ml methanol and analyzed by g.c. (165°). Solvent was removed from an aliquot and the residue analyzed by n.m.r. spectroscopy. The methanol solution was irradiated in the apparatus described (1). Aliquots were removed after 25, 30, and 35 min and analyzed by g.c. The hydrocarbons remaining in each aliquot were isolated using the procedure described in the intermolecular isotope effect experiments, above, and their relative amounts also determined by n.m.r. spectroscopy. The relative rates of oxidations, k_{cis}/k_{trans}, were calculated from the relative amounts of materials remaining (25*b*, 27), and were determined at 25, 30, and 35 min to be 9, 11, and 13 by g.c. analysis and 6, 7, and 8 by n.m.r. spectroscopic analysis.

*Reaction between 2,3-Dimethyl-3-bromo-2-butyl Hydroperoxide (***3***a) and Base in the Presence of Azide Ion*

To a heterogeneous mixture of 9.5 mg (0.24 mequiv) of sodium hydroxide and 35.7 mg (0.55 mequiv) of sodium azide in 1.0 ml of 40:60 water–methanol-d_3 solution at 0° was added 25 mg (0.13 mmol) of **3***a*. The resulting mixture was allowed to stand at 0° for 6 h with occasional shaking and then filtered. The n.m.r. spectrum of the filtrate was identical to that from a reaction carried out under identical conditions in the absence of sodium azide. There was no evidence for the formation from **3***a* of any material in addition to the allylic hydroperoxide **7***a*.

This work was supported in part by a grant from the National Research Council of Canada.

1. K. R. KOPECKY, J. H. VAN DE SANDE, and C. MUMFORD. Can. J. Chem. **46**, 25 (1968).
2. (*a*) J. H. VAN DE SANDE. Dissertation. University of Alberta, Edmonton, Alberta, 1968; (*b*) C. MUMFORD. Dissertation, University of Alberta, Edmonton, Alberta, 1970; (*c*) J. E. FILBY. Unpublished results.
3. (*a*) C. S. FOOTE. Acc. Chem. Res. **1**, 104 (1968); (*b*) C. S. FOOTE, S. WEXLER, W. ANDO, and R. HIGGINS. J. Am. Chem. Soc. **90**, 975 (1968); (*c*) G. O. SCHENCK. Angew. Chem. **69**, 579 (1957). (*d*) K. GOLLNICK and G. O. SCHENCK. Pure Appl. Chem. **9**, 507 (1964).
4. W. H. RICHARDSON, J. W. PETERS, and W. P. KONOPKA. Tetrahedron Lett. 5531 (1966).
5. K. R. KOPECKY, C. MUMFORD, J. Y. DING, and J. FILBY. In preparation.
6. E. H. WHITE, J. WIECKO, and C. C. WEI. J. Am. Chem. Soc. **92**, 2167 (1970).
7. (*a*) R. W. MURRAY and M. L. KAPLAN. J. Am. Chem. Soc. **90**, 537 (1968); (*b*) E. WASSERMAN, R. W. MURRAY, M. L. KAPLAN, and W. A. YAGER. J. Am. Chem. Soc. **90**, 4160 (1968).
8. (*a*) D. J. CRAM and K. R. KOPECKY. J. Am. Chem. Soc. **81**, 2748 (1959). (*b*) G. J. KARABATSOS. J. Am. Chem. Soc. **89**, 1367 (1967).
9. V. GOLD and L. C. GRUEN. J. Chem. Soc. B, 600 (1966).
10. G. CRANCK and F. W. EASTWOOD. Aust. J. Chem. **17**, 1392 (1964).
11. E. J. COREY and R. A. E. WINTER. J. Am. Chem. Soc. **85**, 2677 (1963).
12. K. BIEMANN. Mass spectrometry. Organic chemical applications. McGraw-Hill, New York, N.Y. 1962. p. 223.
13. L. M. JACKMAN. Applications of nuclear magnetic resonance spectroscopy in organic chemistry. Pergamon, London. 1959. p. 53.
14. (*a*) V. J. SHINER and M. L. SMITH. J. Am. Chem. Soc. **83**, 593 (1961); (*b*) A. F. COCKERILL. J. Chem. Soc. B, 964 (1967); (*c*) W. H. SAUNDERS and T. A. ASCHE. J. Am. Chem. Soc. **91**, 4473 (1969).
15. (*a*) M. SCHULZ, A. RIECHE, and K. KIRSCHKE. Chem. Ber. **100**, 370 (1967); (*b*) L. DULOG and W. VOGHT. Tetrahedron Lett. 5169 (1966).
16. T. WILSON. J. Am. Chem. Soc. **88**, 2898 (1966).
17. C. S. FOOTE and S. WEXLER. J. Am. Chem. Soc. **86**, 3879 (1964).
18. (*a*) K. KAWAOKA, A. U. KHAN, and D. R. KEARNS. J. Chem. Phys. **46**, 1842 (1967); (*b*) D. R. KEARNS, R. A. HOLLINS, A. U. KHAN, R. W. CHAMBERS, and P. RADLICK. J. Am. Chem. Soc. **89**, 5455 (1967); (*c*) D. R. KEARNS, R. A. HOLLINS, A. U. KHAN, and P. RADLICK. J. Am. Chem. Soc. **89**, 5457 (1967).
19. A. NICKON and W. L. MENDELSON. J. Am. Chem. Soc. **87**, 3921 (1965).
20. C. S. FOOTE and S.-Y. WONG. Abstracts. 157th National Meeting of the American Chemical Society, Minneapolis, Minn., April, 1969. PETR 012.
21. S. J. ARNOLD, M. KUBO, and E. A. OGRYZLO. Adv. Chem. Ser. **77**, III, 133 (1968).
22. F. A. LITT and A. NICKON. Adv. Chem. Ser. **77**, III, 118 (1968).
23. Q. E. THOMPSON. J. Am. Chem. Soc. **83**, 845 (1961).
24. P. D. BARTLETT and G. D. MENDENHALL. J. Am. Chem. Soc. **92**, 210 (1970).
25. (*a*) K. R. KOPECKY and H. J. REICH. Can. J. Chem. **43**, 2265 (1965); (*b*) R. HIGGINS, C. S. FOOTE, and H. CHENG. Adv. Chem. Ser. **77**, III, 102 (1968); (*c*) E. KOCH. Tetrahedron, **24**, 6295 (1968).
26. K. H. SCHUTTE-ELTE. Dissertation. Göttingen University, Germany, 1961. Cited in ref. 3*d*.
27. C. K. INGOLD and F. R. SHAW. J. Chem. Soc. 2918 (1927).
28. J. E. BALDWIN, G. HOFLE, and S. C. CHOI. J. Am. Chem. Soc. **93**, 2810 (1971).
29. J. E. BALDWIN, A. K. BHATNAGAR, S. C. CHOI, and T. J. SHORTRIDGE. J. Am. Chem. Soc. **93**, 4082 (1971).
30. W. H. RICHARDSON and V. F. HODGE. J. Am. Chem. Soc. **93**, 3996 (1971).

Can. J. Chem. Downloaded from www.nrcresearchpress.com by 210.87.254.5 on 09/05/12
For personal use only.

31. W. H. RICHARDSON and V. F. HODGE. J. Org. Chem. **35**, 4012 (1970).
32. (*a*) D. J. CRAM. Fundamentals of carbanion chemistry. Academic Press, New York. 1965. p. 41; (*b*) P. BALLINGER and F. A. LONG. J. Am. Chem. Soc. **82**, 795 (1960).
33. D. B. SHARP. Abstracts. 139th Meeting of the American Chemical Society, New York, Sept., 1960. p. 79.
34. W. FENICAL, D. R. KEARNS, and P. RADLICK. J. Am. Chem. Soc. **91**, 3396 (1969).
35. (*a*) A. NICKON and J. F. BAGLI. J. Am. Chem. Soc. **81**, 6330 (1959); (*b*) A. NICKON and J. F. BAGLI. J. Am. Chem. Soc. **83**, 1498 (1961); (*c*) A. NICKON, N. SCHWARTZ, J. B. DI GIORGIO, and A. D. WIDDOWSON. J. Org. Chem. **30**, 1711 (1965).
36. (*a*) C. S. FOOTE and R. W. DENNY. J. Am. Chem. Soc. **93**, 5162 (1971); (*b*) C. S. FOOTE and R. W. DENNY. J. Am. Chem. Soc. **93**, 5168 (1971).
37. W. FENICAL, D. R. KEARNS, and P. RADLICK. J. Am. Chem. Soc. **91**, 7771 (1971).
38. (*a*) C. S. FOOTE, T. FUJIMOTO, and Y. C. CHANG. Tetrahedron Lett. 45 (1972); (*b*) N. HASTY, P. B. MERKEL, P. RADLICK, and D. R. KEARNS. Tetrahedron Lett. 49 (1972); (*c*) K. GOLLNICK, D. HAISCH, and G. SCHADE. J. Am. Chem. Soc. **94**, 1747 (1972).
39. E. KLEIN and W. ROJAHN. Tetrahedron, **21**, 2173 (1965).
40. J. B. LAMBERT and D. H. JOHNSON. J. Am. Chem. Soc. **90**, 1349 (1969).
41. (*a*) M. F. HAWTHORNE and E. S. LEWIS. J. Am. Chem. Soc. **80**, 4296 (1968); (*b*) E. S. LEWIS and M. C. R. SYMONS. Quart. Rev. Chem. Soc. **12**, 230 (1968).
42. (*a*) F. H. WESTHEIMER. Chem. Rev. **61**, 265 (1961); (*b*) J. BIGELEISEN. Pure Appl. Chem. **8**, 217 (1964).
43. F. A. COTTON, J. H. FASSNACHT, W. D. HORROCKS, JR., and N. A. NELSON. J. Chem. Soc. 4138 (1959).
44. R. F. B. COX and R. T. STORMONT. Organic synthesis. Coll. Vol. II. John Wiley and Sons, Inc., New York. 1963. p. 7.
45. W. G. YOUNG, R. T. DILLON, and H. J. LUCAS. J. Am. Chem. Soc. **51**, 2528 (1939).
46. L. O. BINDER. J. Chem. Ed. **23**, 285 (1946).
47. H. MEERWEIN. Ann. **396**, 251 (1913).
48. J. AYERS. J. Am. Chem. Soc. **60**, 2958 (1938).
49. F. D. ROSSINI, *et al.* Selected values of chemical thermodynamic properties. U.S. Government Printing Office. Washington, D.C. 1955. p. 55.
50. K. MISLOW, M. A. W. GLASS, H. B. HOPES, E. SIMON, and G. H. WAHL, JR. J. Am. Chem. Soc. **86**, 1710 (1964).
51. H. ADKINS and H. R. BILLICA. J. Am. Chem. Soc. **70**, 695 (1948).
52. W. GERRARD. J. Chem. Soc. 218 (1940).
53. W. R. BRASEN, S. W. KANTOR, P. S. SKELL, and C. R. HAUSER. J. Am. Chem. Soc. **79**, 397 (1957).
54. A. A. FROST and R. G. PEARSON. Kinetics and mechanism. 2d ed. John Wiley and Sons. Inc., New York. 1961. p. 17.
55. A. NICKON *et al.* J. Am. Chem. Soc. **94**, 5517 (1972).

Can. J. Chem. Downloaded from www.nrcresearchpress.com by 210.87.254.5 on 09/05/12
For personal use only.

Can. J. Chem. Downloaded from www.nrcresearchpress.com by 210.87.254.5 on 09/05/12
For personal use only.

Correlation of π,π^* Triplet Energy of some Cyclic α,β-Unsaturated Ketones with Electroreduction Potentials[1]

RAFIK O. LOUTFY
Division of Chemistry, National Research Council of Canada, Ottawa, K1A 0R6

AND

RAOUF O. LOUTFY
Chemistry Department, University of Guelph, Guelph, Ontario

Received July 14, 1972

The half-wave reduction potentials, $E_{1/2}$'s, of some cyclic enones have been determined in acetonitrile. A linear free-energy relationship was obtained between $E_{1/2}$ and the lowest π,π^* triplet state of the enones studied. This correlation enabled an estimate to be made of the triplet energy of the cyclohexenone, which was found to be ~70 kcal/mol.

Nous avons déterminé les potentiels de réduction de demi-vague $E_{1/2}$ de quelques énones cycliques dans l'acétonitrile. Nous obtenons une relation linéaire de l'énergie libre entre $E_{1/2}$ et l'état triplet π,π^* des énones considérées. Cette corrélation rend possible l'estimation de l'énergie du triplet de la cyclohexanone, soit ~70 kcal/mol. [Traduit par le journal]

Canadian Journal of Chemistry, **50**, 4050 (1972)

Cyclic enones (α,β-unsaturated ketones) undergo a variety of photochemical reactions (1–3). Generally most of them, such as cycloaddition, rearrangement, and H-abstraction proceed via triplet states (1, 2 and references therein). Correlation of the energy of the lowest triplet state with physical parameters are therefore of great interest.

In previous reports (4, 5), we demonstrated the existence of a linear free-energy relationship between the n,π^* triplet energy of some benzophenones, thiobenzophenones, aromatic, and aliphatic ketones and aldehydes and the corresponding reduction half-wave potentials, $E_{1/2}$'s. Expansion of the above relationship to include cyclic enone's π,π^* triplet states may bring better understanding of the reactivity of this system and provide a correlation which could be utilized to estimate the triplet energy of compounds of known electrochemistry. Such correlation is illustrated in Fig. 1.

The reduction of all cyclic enones in acetonitrile at the dropping mercury electrode exhibited two a.c. waves, which is in general agreement with that reported by Wawzonek and others (6, 7). The first a.c. wave is of interest in this study. Therefore, the following discussion will mainly pertain to it. The procedure used for the polarographic measurements was the same as described previously (4).

The acceptance of a single electron in a reversible reduction results in the formation of the corresponding radical anion. It is well established that the electron normally enters the lowest unoccupied π molecular orbital and the potential at which the molecule is reduced should thus be related to the energy of π^* level. Hence, the triplet excitation energy can simply be given as

$$[1] \qquad E_{^3(\pi,\pi^*)} = \varepsilon_\pi - \varepsilon_{\pi^*} - J_{\pi,\pi^*} - E_{\text{c.i.}}$$

where ε_π and ε_{π^*} are the energies of the π bonding and anti-bonding orbital respectively. The term J_{π,π^*} represents the appropriate exchange integral, and $E_{\text{c.i.}}$ is the term resulting from the configuration interaction (a second order perturbation term). The latter two terms for first approximation can be assumed constant throughout the series, and therefore, can be neglected. Thus, one would expect a linear relationship between the π,π^* triplet energy of

[1]NRCC No. 12887.

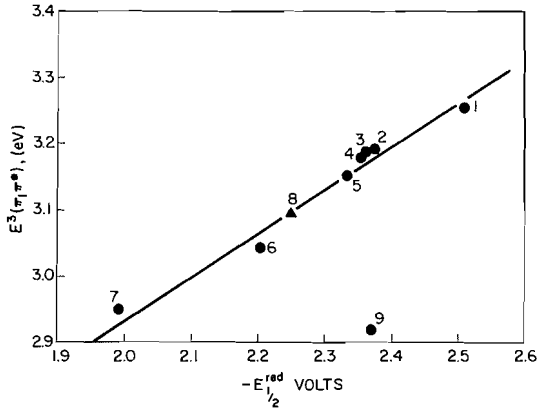

FIG. 1. A plot of $E_{3(\pi,\pi^*)}$ of cyclic enones and the corresponding $E_{1/2}$'s.

TABLE 1. Half-wave potentials and π,π^* triplet energies of some cyclic enones

	Compounds	$E_{3(\pi,\pi^*)}$ eV	$-E_{1/2}$, V (± 0.005 V)
1	Bicyclo[3.3.0]oct-5-en-2-one	3.25*	2.51
2	Cholestenone	3.19†	2.38
3	Cyclopentenone	3.184‡	2.36
4	Testosterone propionate	3.18†	2.35
5	Tricyclo [3.3.2.$0^{1,5}$]dec-3-en-2-one	3.15§	2.33
6	4-Acetoxytestosterone acetate	3.04†	2.20
7	4-Chlorotestosterone acetate	2.95†	1.99
8	Cyclohexenone	(3.08)	2.25
9	4-Methyltestosterone acetate	2.92†	2.37

*Reference 12.
†Reference 13.
‡Reference 14.
§It was predicted that the $^3(\pi,\pi^*)$ of this compound is not more than one kcal/mol above the lowest $^3(n,\pi^*)$, the triplet energy of the latter being 71.6 kcal/mol; see ref. 15.

cyclic enone and the corresponding $E_{1/2}$'s if the energy of the highest occupied MO(π-orbital) is the same throughout the series, or if it is a constant function of π^* level energy.

The location of the main peak of the singlet or triplet (n,π^*) band of α,β unsaturated ketones appears to be displaced to a shorter wavelength by alkyl substitution. For example, in the case of cyclohexenone, one α or β alkyl substituent caused a hypsochromic shift of about $\sim$6 nm (8). This probably means that alkyl substitution on the ethylenic bond raises the energy of the π^* orbital, since the non-bonding orbital is considered to be practically unaffected. Similarly, electron withdrawing substituents would lower the energy of the π^* orbital. On the other hand, alkyl substitution at α or β positions would cause bathochromic shifts of the $^1(\pi,\pi^*)$ band. In steroid system the magnitude of the shift per an α-alkyl and β-alkyl substitution are about 10 and 12 nm respectively (9, 10). This must indicate therefore, that alkyl substitution raises the energy of both π and π^* orbital, where the effect on the ε_π is more pronounced than on ε_{π^*}.

The $E_{1/2}$ data for the cyclic enones studied are shown in Table 1. The compounds studied can be divided into two groups: (*a*) cyclic enones, where cyclopentenone represents the parent compound; (*b*) those where cyclohexenone is the parent compound. In both cases alkyl substitutions at α and/or β position render reduction more difficult, while electron withdrawing groups lower $E_{1/2}$ as predicted. The state correlation is emphasized by a plot of half-wave potentials *vs.* triplet energies which is presented in Fig. 1 with a slope of 0.7. From the previous discussion, it is obvious that the energy of the π-orbital for these cyclic enones is not constant. This linear free energy relationship, therefore, indicates that the change of energy of the π orbital on substitution should be a function of that for the π^* orbital.

This is not, however, surprising since a set of empirical rules for determining the effect of a substituent on the position of the first $^1(\pi,\pi^*)$ band of cyclic enones has been proposed by Woodward (9) and Fieser and Fieser (10) which implies that substitution at the α or β position of cyclic enones causes a systematic shift of both π and π^* orbital.

The triplet energy of cyclohexenone can be estimated, using the relationship in Fig. 1, and it was found to be $\sim$70 kcal/mol which is in very good agreement with the predicted value of 68 kcal/mol reported by de Mayo *et al.* (11).

The deviation of 4-methyl testosterone acetate from the linear correlation obtained, represents a case where the relation between the energy of π and π^* orbital breaks down due to the marked effect of the second-CH_3 group on the π^*-orbital energy (8).

In conclusion, the existence of correlation between the $^3(\pi,\pi^*)$ energy of cyclic enones and $E_{1/2}$'s indicates the presence of useful and meaningful relations between the spectroscopic and electrochemical properties of molecules.

Can. J. Chem. Downloaded from www.nrcresearchpress.com by 210.87.254.5 on 09/05/12
For personal use only.

The authors wish to express their sincerest thanks and deepest gratitude to Dr. W. R. Fawcett, Chemistry Department, University of Guelph, Guelph, Ontario, Canada, for making available the instrumentation to determine the reduction potentials.

1. P. DE MAYO. Acc. Chem. Res. **4**, 41 (1971).
2. O. L. CHAPMAN and D. S. WEISS. Photochemistry of cyclic ketones. In press.
3. P. E. EATON. Acc. Chem. Res. **1**, 50 (1968).
4. R. O. LOUTFY and R. O. LOUTFY. J. Phys. Chem. **76**, 1650 (1972).
5. R. O. LOUTFY and R. O. LOUTFY. J. Phys. Chem. Submitted for publication.
6. S. WAWZONEK and A. GRUNDERSON. J. Electrochem. Soc. **111**, 324 (1964).
7. M. L. ASH, F. L. O'BRIEN, and D. W. BOYKIN, JR. J. Org. Chem. **37**, 106 (1972).
8. (*a*) H. SUZUKI. Electronic absorption spectra and geometry of organic molecules. Academic Press, New York. 1967. (*b*) R. L. CARGILL, W. A. BUNDY, D. M. POND, A. B. SEARS, J. SALTIEL, and J. WINTERLE. Mol. Photochem. **3** (2), 123, 1971.
9. R. B. WOODWARD. J. Am. Chem. Soc. **63**, 1123 (1941); **64**, 72, 76 (42).
10. L. F. FIESER and M. F. FIESER. Steroids. Reinhold, New York. 1959.
11. P. DE MAYO, A. A. NICHOLSON, and M. F. TCHIR. Can. J. Chem. **48**, 225 (1970).
12. R. L. CARGILL, A. C. MILLER, D. M. POND, P. DE MAYO, M. F. TCHIR, K. R. NEUBERGER, and J. SALTIEL. Mol. Photochem. **1**, 301 (1969).
13. G. MARCH, D. R. KEARNS, and K. SCHAFFNER. J. Am. Chem. Soc. **93**, 3129 (1971).
14. R. O. LOUTFY and P. DE MAYO. Chem. Commun. 1040 (1970).
15. R. O. LOUTFY. Ph.D. Thesis. University of Western Ontario, London, Ontario. 1972.

Triplet Charge Transfer Complex between Excited Electron Acceptor and Ground State Electron Donor[1]

RAFIK O. LOUTFY

Division of Chemistry, National Research Council of Canada, Ottawa, Canada K1A 0R6

AND

RAOUF O. LOUTFY

Chemistry Department, University of Guelph, Guelph, Ontario

Received July 14, 1972

The half-wave reduction and oxidation potentials, $E_{1/2}$'s, of carbonyl compounds and amines, respectively, are used to estimate the location of triplet charge transfer states (CT). A linear free-energy relationship between the calculated CT triplet energies and the corresponding carbonyl molecules triplet energies was obtained. It has also been found that the free energy change (ΔF) for CT complex formation correlate with the triplet carbonyl quenching rate constant k_q.

Nous utilisons les potentiels d'oxydation et de réduction de demi-vague, $E_{1/2}$, de carbonyls et d'amines pour estimer les endroits où se trouvent les états triplets de transfert de charge (CT). Nous obtenons une relation linéaire d'énergie libre entre les énergies de triplet CT calculées et les énergies de triplets correspondants pour les molécules de carbonyles. Nous trouvons aussi que le changement d'énergie libre (ΔF) pour la formation de complexes CT est en accord avec la constante de vitesse d'amortissement du triplet carbonyl k_q.

[Traduit par le journal]

Canadian Journal of Chemistry, **50**, 4052 (1972)

In recent years there has been much activity on the subject of quenching of excited aromatic and aliphatic ketones by amines (1–5). It appears to be generally accepted that phosphorescence quenching and photoreduction of the excited carbonyl molecule by amines involved charge transfer (c.t.) complex formation (4, 5). However, several aspects remain unclear: (*1*) the absence of phosphorescence emission from the c.t. state; (*2*) the position of the complex maximum emission frequency; and (*3*) factors influencing the formation of the c.t. complex.

In a large number of cases it has been possible

[1]NRCC No. 12888.

Can. J. Chem. Downloaded from www.nrcresearchpress.com by 210.87.254.5 on 09/05/12
For personal use only.

The authors wish to express their sincerest thanks and deepest gratitude to Dr. W. R. Fawcett, Chemistry Department, University of Guelph, Guelph, Ontario, Canada, for making available the instrumentation to determine the reduction potentials.

1. P. DE MAYO. Acc. Chem. Res. **4**, 41 (1971).
2. O. L. CHAPMAN and D. S. WEISS. Photochemistry of cyclic ketones. In press.
3. P. E. EATON. Acc. Chem. Res. **1**, 50 (1968).
4. R. O. LOUTFY and R. O. LOUTFY. J. Phys. Chem. **76**, 1650 (1972).
5. R. O. LOUTFY and R. O. LOUTFY. J. Phys. Chem. Submitted for publication.
6. S. WAWZONEK and A. GRUNDERSON. J. Electrochem. Soc. **111**, 324 (1964).
7. M. L. ASH, F. L. O'BRIEN, and D. W. BOYKIN, JR. J. Org. Chem. **37**, 106 (1972).
8. (*a*) H. SUZUKI. Electronic absorption spectra and geometry of organic molecules. Academic Press, New York. 1967. (*b*) R. L. CARGILL, W. A. BUNDY, D. M. POND, A. B. SEARS, J. SALTIEL, and J. WINTERLE. Mol. Photochem. **3** (2), 123, 1971.
9. R. B. WOODWARD. J. Am. Chem. Soc. **63**, 1123 (1941); **64**, 72, 76 (42).
10. L. F. FIESER and M. F. FIESER. Steroids. Reinhold, New York. 1959.
11. P. DE MAYO, A. A. NICHOLSON, and M. F. TCHIR. Can. J. Chem. **48**, 225 (1970).
12. R. L. CARGILL, A. C. MILLER, D. M. POND, P. DE MAYO, M. F. TCHIR, K. R. NEUBERGER, and J. SALTIEL. Mol. Photochem. **1**, 301 (1969).
13. G. MARCH, D. R. KEARNS, and K. SCHAFFNER. J. Am. Chem. Soc. **93**, 3129 (1971).
14. R. O. LOUTFY and P. DE MAYO. Chem. Commun. 1040 (1970).
15. R. O. LOUTFY. Ph.D. Thesis. University of Western Ontario, London, Ontario. 1972.

Triplet Charge Transfer Complex between Excited Electron Acceptor and Ground State Electron Donor[1]

RAFIK O. LOUTFY

Division of Chemistry, National Research Council of Canada, Ottawa, Canada K1A 0R6

AND

RAOUF O. LOUTFY

Chemistry Department, University of Guelph, Guelph, Ontario

Received July 14, 1972

The half-wave reduction and oxidation potentials, $E_{1/2}$'s, of carbonyl compounds and amines, respectively, are used to estimate the location of triplet charge transfer states (CT). A linear free-energy relationship between the calculated CT triplet energies and the corresponding carbonyl molecules triplet energies was obtained. It has also been found that the free energy change (ΔF) for CT complex formation correlate with the triplet carbonyl quenching rate constant k_q.

Nous utilisons les potentiels d'oxydation et de réduction de demi-vague, $E_{1/2}$, de carbonyls et d'amines pour estimer les endroits où se trouvent les états triplets de transfert de charge (CT). Nous obtenons une relation linéaire d'énergie libre entre les énergies de triplet CT calculées et les énergies de triplets correspondants pour les molécules de carbonyles. Nous trouvons aussi que le changement d'énergie libre (ΔF) pour la formation de complexes CT est en accord avec la constante de vitesse d'amortissement du triplet carbonyl k_q.

[Traduit par le journal]

Canadian Journal of Chemistry, **50**, 4052 (1972)

In recent years there has been much activity on the subject of quenching of excited aromatic and aliphatic ketones by amines (1–5). It appears to be generally accepted that phosphorescence quenching and photoreduction of the excited carbonyl molecule by amines involved charge transfer (c.t.) complex formation (4, 5). However, several aspects remain unclear: (*1*) the absence of phosphorescence emission from the c.t. state; (*2*) the position of the complex maximum emission frequency; and (*3*) factors influencing the formation of the c.t. complex.

In a large number of cases it has been possible

[1]NRCC No. 12888.

Can. J. Chem. Downloaded from www.nrcresearchpress.com by 210.87.254.5 on 09/05/12
For personal use only.

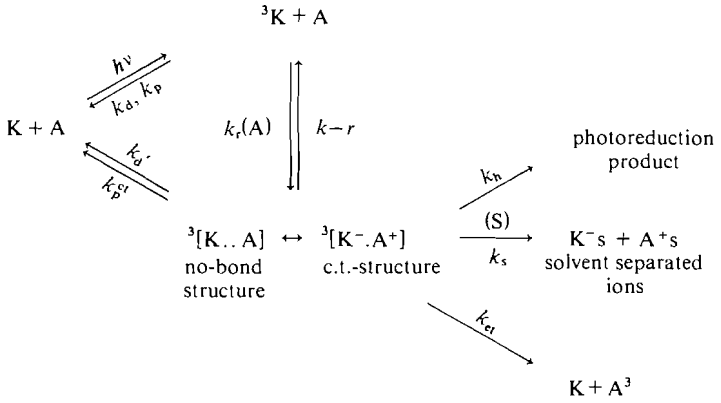

SCHEME I

to observe the formation of the electronically excited singlet c.t. state of aromatic hydrocarbon and amine complexes (6–9). On the other hand, little is known about the lowest triplet excited c.t. state particularly of ketone–amine complexes. In this report, from the polarographic oxidation and reduction potentials measured in acetonitrile, the energies of the triplet c.t. states were estimated and correlated with the experimental triplet quenching rate constants.

Quenching of excited carbonyl groups by amines with low ionization potentials can be described by Scheme 1, where K and A stand for the ketone and amine respectively. $(K^+ \cdot A^-)$ represents the initially formed charge-transfer state, which may undergo proton transfer and electron redistribution to give the photoreduction product by a reaction which proceeds with a rate k_h (1–3 and references therein). Furthermore, when there is sufficient energy gain through solvation, the excited c.t. state may readily dissociate into ions, with rate k_s. The excited c.t. complex may also undergo intercombinative conversion to a triplet state (with rates $k - r$ and/or k_{et}), or be deactivated to the ground state (k_d'). The latter possibility has been discussed in detail by Kuz'min and Guseva (7). Finally, radiative deactivation of the excited c.t. complex competes with all the previously mentioned deactivation processes. In general, radiationless deactivation of the triplet c.t. complex is predominant, and even more pronounced in polar solvents (7) which makes the observation of phosphorescence emission from that state in fluid media rather difficult. In a rigid matrix where all diffusion processes are suppressed there should be greater chance of observing the emission.[2]

The energy of the charge-transfer state is expressed (11) as

$$[1] \qquad E_{c.t.} = I_A - A_K - C - \Delta$$

I_A represents the ionization potential of donor, A_K the electron affinity of the acceptor; $C = e^2/\varepsilon r$ is the columbic interaction between the positive and negative ions, and Δ is an interaction term (12). MacColl (13) suggested that the polarographic reduction half-wave potential ($E_{1/2}^{red}$) is directly related to the electron affinity (eq. 2). Similarly, the oxidation half-wave potential ($E_{1/2}^{oxid}$) is related to I_A (eq. 3) (14),

$$[2] \quad E(K^-/K) \simeq E_{1/2}^{red} = A_A + \Delta E_{K^-}(s) - K$$

$$[3] \quad E(A/A^+) \simeq E_{1/2}^{oxid} = I_D + \Delta E_{A^+}(s) - K$$

where $E(K^-/K)$ and $E(A/A^+)$ represent the standard reduction and oxidation potential which can be taken as equal to $E_{1/2}^{red}$ and $E_{1/2}^{oxid}$, respectively. $\Delta E_{K^-}(s)$ and $\Delta E_{A^+}(s)$ are the differences in free energy of solvation of the neutral molecule and ion, these are almost equal for the systems studied. K is a constant which depends on the reference cell (14). Substituting for the values of I_A and A_k in eq. 1, the following useful form can be derived:

$$[4] \quad E_{c.t.} = [E(A/A^+) - E(K^-/K) - C] - \Delta$$

The half-wave potentials for the compounds studied were obtained from cathodic sweeps

[2]Recently emission from excited states of EDA-complexes of benzophenone with aromatic amines at 77 °K was observed (10).

Can. J. Chem. Downloaded from www.nrcresearchpress.com by 210.87.254.5 on 09/05/12
For personal use only.

TABLE 1. The half-wave reduction and oxidation potential of the studied systems measured in acetonitrile

No.	Substance	$-E_{1/2}^{red}$ (V)*	No.	Substance	$E_{1/2}^{oxid}$
1.	Formaldehyde	2.02	11.	*N,N*-Dimethylaniline	0.78‡
2.	Acetaldehyde	2.14	12.	Triethylamine	0.96†
3.	Acetone	2.305	13.	*t*-Butylamine	1.45§
4.	Benzaldehyde	1.95	14.	*N,N*-Dimethyl *p*-tolyl amine.	0.75‖
5.	Acetophenone	2.12	15.	Phenylmethylsulfide	1.35§
6.	Benzophenone	1.84	16.	*n*-Butylmercaptane	1.34‖
7.	Acrolein	1.71			
8.	Fluorenone	1.45			
9.	Benzonitrile	2.50†			
10.	*s*-Triazine	2.10†			

*This work.
†Reference 19.
‡Reference 18.
§Calculated from the formula $E_{1/2}^{oxid} = 0.43\ IP - 2.25$.
‖Reference 20.

TABLE 2. Data on Complexes between triplet carbonyl molecules and *N,N*-dimethylaniline

No.	Substance	$[E(A/A^+) - E(K^-/K)]$ (kK)	Δ (kK)	$^3E_{c.t.}$	$^3\Delta E_{0,0}$*
1.	Formaldehyde	22.76	1.86	20.90	25.20‡
2.	Acetaldehyde	23.75	2.66	21.09	26.10
3.	Acetone	24.88	3.40	21.48	27.00
4.	Benzaldehyde	22.02	1.30	20.72	25.19
5.	Acetophenone	23.40	2.40	21.00	25.84
6.	Benzophenone	21.13	0.70	20.43§	24.24
7.	Acrolein	20.25	−0.10	20.35	24.20
8.	Benzonitrile†	25.00	3.40	21.60	27.20
9.	*s*-Triazine†	22.40	1.30	21.10	26.00

*References 21 and 22.
†Reference 16.
‡Reference 23.
§This value is in very good agreement with the emission maximum observed recently by Arimitsu and Tsubomura (10).

of the a.c. wave; the procedure for the measurement is the same as that described in ref. (15). The data are given in Table 1 along with the oxidation half-wave potentials of the donors, which were obtained from the literature.

From eq. 4 the energy of the ^{3}c.t. state can be determined if the term Δ is known. This term represents the difference in the energy of formation of c.t. complex in the excited ($\Delta E_{K^-A^+}$) and ground state (ΔE_{KA}) (12). Since no c.t. complex formation was observed in the ground state between ketones and amines the latter term can be neglected. In other words $\Delta = \Delta E(K^-A^+)$ which should be a function of $(E(A/A^+) - E(K^-/K))$. Indeed, from Weller's results (16), a linear relationship between Δ and $[E(D/D^+) - E(A^-/A)]$ has been found, where

$$[5]\quad \Delta = (0.65 \pm 0.06)[E(A/A^+) - E(K^-/K)] - (13.0 \pm 1.3)$$

From this relation Δ's for our systems can be calculated, and the results are given in Table 2. Using the experimentally measured $E_{1/2}^{red}$ of the ketones, the $E_{1/2}^{oxid}$ of *N,N*-dimethyl aniline and the calculated values of Δ the triplet energy of the c.t. complex can be obtained using eq. 4. The data are listed in Table 2.

The calculated ^{3}c.t. energies are about 5000 cm^{-1} to the red of the molecular phosphorescence, compatible with the results obtained for fluorescent quenching of aromatic hydrocarbons by *N,N*-dimethyl aniline (17).

Interestingly, a linear free-energy relationship between the carbonyl molecule triplet energy

Can. J. Chem. Downloaded from www.nrcresearchpress.com by 210.87.254.5 on 09/05/12
For personal use only.

TABLE 3. Data of the quenching rate constant of triplet ketones by chosen donors

	Ketone	E_T (eV)	Quencher	$[E(D/D^+) - E(A^-/A)]$ (V)	ΔF (kcal/mol)	k_q (M^{-1} s^{-1})*
1.	Benzophenone	2.99	**11**	2.62	−8.5	2.7×10^9†
2.			**12**	2.80	−4.37	2.3×10^9†
3.			**13**	3.29	+6.9	7.0×10^7†
4.			**14**	2.59	−9.20	4.3×10^9†
5.			**15**	3.19	+4.60	7.5×10^7‡
6.	Acetophenone	3.21	**16**	3.46	+5.75	1.7×10^7§
7.	Acetone	3.35	**11**	3.085	−6.21	2.7×10^9‖
8.			**12**	3.265	−1.84	3.0×10^8‖
9.			**13**	3.755	+9.20	2.0×10^6‖
10.	Fluorenone	2.30	**11**	2.23	−1.60	6.0×10^8 ¶
11.			**14**	2.20	−2.30	1.6×10^9 ¶

*Amines with relatively high I_D and possessing active α-hydrogen tend to give a higher quenching rate than expected. This could be due to the fact that other chemical reactions (*e.g.* direct H-abstraction) become more favorable than c.t. complex formation. Therefore, these data were omitted.

†Reference 24.
‡Reference 3.
§Reference 25.
‖Reference 5*a*.
¶Reference 2.

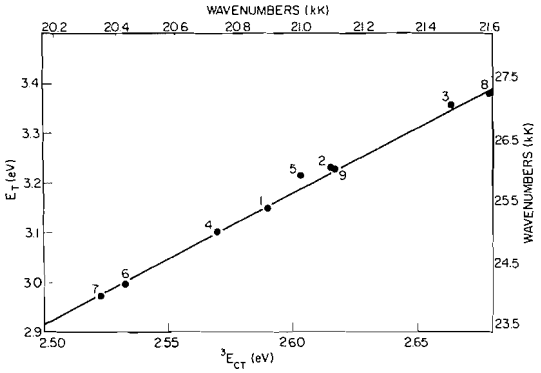

FIG. 1. A plot of the carbonyl compounds triplet energies E_T's *vs.* the corresponding triplet energy of c.t. complex of *N*,*N*-dimethylaniline with : *1*, formaldehyde; *2*, acetaldehyde; *3*, acetone; *4*, benzaldehyde; *5*, acetophenone; *6*, benzonitrile; *7*, acrolein; *8*, benzonitrile; and *9*, *s*-triazine.

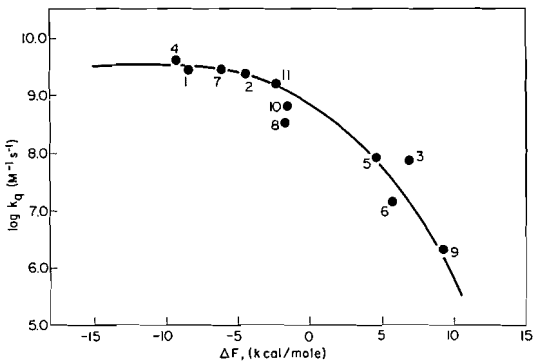

FIG. 2. Plot of the quenching rate constant *vs.* the free energy change (ΔF) of the reaction of triplet: benzophenone with: *1*, *N*,*N*-dimethylaniline; *2*, triethylamine; *3*, *t*-butylamine; *4*, *N*,*N*-dimethyl-*p*-tolylamine; *5*, phenylmethylsulfide, acetophenone with *6*, *N*-butylmercaptane, acetone with *7*,*N*,*N*-dimethylaniline; *8*, triethylamine; *9*, *t*-butylamine and fluorenone with *10*, *N*,*N*-dimethylaniline; *11*, *N*,*N*-dimethyl-*p*-tolylamine.

(E_T) and the corresponding triplet c.t. complex energy was obtained (Fig. 1). The slope of the plot was found to be slightly larger than 2. These results are in very good agreement with those of Azumi and McGlynn (11). These authors found a linear correlation between ($I_D - A_A$) and the singlet energy of the aromatic hydrocarbon excimer with a slope greater than 2.

The free-energy change, ΔF, for charge transfer formation in a triplet excited state may be represented by eq. 6 (16):

$$[6]\quad \Delta F = E(A/A^+) - E(K^-/K) - \frac{e^2}{\varepsilon r} - {}^3\Delta E_{0,0}$$

In the present application the calculated ΔF for triplet ketone–amine, ether, sulfide and thiol c.t. formation are listed in Table 3 along with the experimental quenching rate. From a plot of the calculated ΔF *vs.* the triplet quenching rate constant (Fig. 2) we obtained a curve similar to that reported earlier by Weller and co-worker (18) for the singlet state in which k_q tended to level off at $\Delta F < -4$ kcal/mol. Cohen and co-worker (5*b*) recently applied eq. 2 for a special case,

Can. J. Chem. Downloaded from www.nrcresearchpress.com by 210.87.254.5 on 09/05/12
For personal use only.

where he used common acceptor. In such case, $E(K^-/K)$ and $^3\Delta E_{0,0}$ are constant and ΔF depend only on oxidation potential of the donor or the ionization potential can be used if the solvation energy differences between the various donors are small.

In conclusion, the correlation obtained between the triplet energy of organic carbonyl molecules and the estimated triplet energy of carbonyl molecule–amine c.t. complexes indicates the existence of a direct and useful relation which could be utilized coupled with the electrochemical data to predict the energy of ^{3}c.t. complexes.

The authors wish to express their sincere thanks to Dr. R. W. Yip of National Research Council of Canada, Ottawa for his useful discussions.

1. S. G. COHEN and J. B. GUTTENPLAN. Tetrahedron Lett. 5353 (1968).
2. S. G. COHEN and G. PARSON. J. Am. Chem. Soc. **92**, 7603 (1970).
3. R. S. DAVIDSON and P. R. STEINER. Chem. Commun. 1115 (1971).
4. P. J. WAGNER and A. E. KEMPPAINEN. J. Am. Chem. Soc. **91**, 3085 (1969).
5. (*a*) R. W. YIP, R. O. LOUTFY, Y. L. CHOW, and L. K. MAGDZINSKI. Can. J. Chem. In press.; (*b*) J. B. GUTTENPLAN and S. G. COHEN. J. Am. Chem. Soc. **94**, 4040 (1972).
6. A. WELLER. Nobel Symposium 5. Fast reactions and primary processes in chemical kinetics. *Edited by* S. Claesson, Almqvist and Wiksell, Stockholm. 1967. p. 413.
7. M. A. KUZ'MIN and L. J. GUSEVA. Dak. Phys. Chem. USSR. **200**, 779 (1972).
8. D. REHM and A. WELLER. Ber. Bunserges, Physik. Chem. **73**, 834, 839 (1969).
9. S. IWATA, J. TANAKA, and S. NAGAKURA. J. Chem. Phys. **47**, 2203 (1967).
10. S. ARIMITSU and H. TSUBOMURA. Bull. Chem. Soc. Jap. **45**, 1357 (1972).
11. T. AZUMI and S. P. MCGLYNN. J. Chem. Phys. **41**, 3131 (1964).
12. J. B. BIRKS. Photophysics of aromatic hydrocarbons. Wiley Interscience, New York. 1970. p. 407.
13. A. MACCOLL. Nature, **163**, 178 (1949).
14. M. E. PEOVER. Adv. Electroanal. Chem. **2**, 40 (1967).
15. R. O. LOUTFY and R. O. LOUTFY. J. Phys. Chem. **76**, 1650 (1972).
16. H. BEENS and A. WELLER. Molecular luminescence. E. C. Lim *editor*. Benjamin, New York. 1969. p. 203.
17. BRIAN STEVENS. Adv. Photochem. **8**, 167 (1970).
18. A. WELLER and D. REHM. Isr. J. Chem. **8**, 259 (1970).
19. C. K. MANN and K. K. BARNES. Electrochemical reactions in non-aqueous systems. Marcel-Dekker, Inc., New York. 1970
20. L. L. MILLER, G. D. NORDBLOM, and E. A. MAYEDA. J. Org. Chem. **37**, 916 (1972).
21. P. S. EGEL and B. M. MONROE. Adv. Photochem. **8**, 302 (1970).
22. G. HERZBERG. Electronic spectra and structure of polyatomic molecules. D. Van Nostrand Co., New Jersey. 1966.
23. A. M. NISHIMURA and J. S. VINCENT. Chem. Phys. Lett. **13**, 89 (1972).
24. S. G. COHEN and A. D. LITT. Tetrahedron Lett. 837 (1970).
25. P. J. WAGNER and R. G. ZEPP. Chem. Commun. 167 (1972).

Can. J. Chem. Downloaded from www.nrcresearchpress.com by 210.87.254.5 on 09/05/12
For personal use only.

Structure and Reactions of Cuprous Thiobenzoate

ALDO FERRETTI

Dairy Products Laboratory, Eastern Marketing and Nutrition Research Division, A.R.S., U.S. Department of Agriculture, Washington, D.C. 20250

Received June 30, 1972

Cuprous thiobenzoate is capable of displacing I^- from aliphatic and activated aromatic iodides, in alcoholic or alcohol–pyridine solution, with formation of thiolbenzoates in excellent yield. The reaction fails with other halogenated substrates. In these cases, the products of prolonged heating of the reaction mixture are ethyl benzoate, dibenzoyl disulfide, benzoic acid, thiobenzoic acid, hydrogen sulfide, and cuprous sulfide.

Le benzoate de cuivre(I) est capable de déplacer I^- des iodures aromatiques activés et aliphatiques, en solution alcoolique ou de alcool–pyridine, avec la formation de thiolbenzoates avec un excellent rendement. La réaction ne procéde pas avec autres substrats halogénés. Dans ces cas les produits de chauffage prolongé du mélange de réaction sont le benzoate d'éthyle, le bisulfure de benzoyle, l'acide benzoïque, l'acide thiobenzoïque, acide sulfhydrique et le sulfure de cuivre(I).

Canadian Journal of Chemistry, **50**, 4056 (1972)

where he used common acceptor. In such case, $E(K^-/K)$ and $^3\Delta E_{0,0}$ are constant and ΔF depend only on oxidation potential of the donor or the ionization potential can be used if the solvation energy differences between the various donors are small.

In conclusion, the correlation obtained between the triplet energy of organic carbonyl molecules and the estimated triplet energy of carbonyl molecule–amine c.t. complexes indicates the existence of a direct and useful relation which could be utilized coupled with the electrochemical data to predict the energy of ^{3}c.t. complexes.

The authors wish to express their sincere thanks to Dr. R. W. Yip of National Research Council of Canada, Ottawa for his useful discussions.

1. S. G. COHEN and J. B. GUTTENPLAN. Tetrahedron Lett. 5353 (1968).
2. S. G. COHEN and G. PARSON. J. Am. Chem. Soc. **92**, 7603 (1970).
3. R. S. DAVIDSON and P. R. STEINER. Chem. Commun. 1115 (1971).
4. P. J. WAGNER and A. E. KEMPPAINEN. J. Am. Chem. Soc. **91**, 3085 (1969).
5. (*a*) R. W. YIP, R. O. LOUTFY, Y. L. CHOW, and L. K. MAGDZINSKI. Can. J. Chem. In press.; (*b*) J. B. GUTTENPLAN and S. G. COHEN. J. Am. Chem. Soc. **94**, 4040 (1972).
6. A. WELLER. Nobel Symposium 5. Fast reactions and primary processes in chemical kinetics. *Edited by* S. Claesson, Almqvist and Wiksell, Stockholm. 1967. p. 413.
7. M. A. KUZ'MIN and L. J. GUSEVA. Dak. Phys. Chem. USSR. **200**, 779 (1972).
8. D. REHM and A. WELLER. Ber. Bunserges, Physik. Chem. **73**, 834, 839 (1969).
9. S. IWATA, J. TANAKA, and S. NAGAKURA. J. Chem. Phys. **47**, 2203 (1967).
10. S. ARIMITSU and H. TSUBOMURA. Bull. Chem. Soc. Jap. **45**, 1357 (1972).
11. T. AZUMI and S. P. MCGLYNN. J. Chem. Phys. **41**, 3131 (1964).
12. J. B. BIRKS. Photophysics of aromatic hydrocarbons. Wiley Interscience, New York. 1970. p. 407.
13. A. MACCOLL. Nature, **163**, 178 (1949).
14. M. E. PEOVER. Adv. Electroanal. Chem. **2**, 40 (1967).
15. R. O. LOUTFY and R. O. LOUTFY. J. Phys. Chem. **76**, 1650 (1972).
16. H. BEENS and A. WELLER. Molecular luminescence. E. C. Lim *editor*. Benjamin, New York. 1969. p. 203.
17. BRIAN STEVENS. Adv. Photochem. **8**, 167 (1970).
18. A. WELLER and D. REHM. Isr. J. Chem. **8**, 259 (1970).
19. C. K. MANN and K. K. BARNES. Electrochemical reactions in non-aqueous systems. Marcel-Dekker, Inc., New York. 1970
20. L. L. MILLER, G. D. NORDBLOM, and E. A. MAYEDA. J. Org. Chem. **37**, 916 (1972).
21. P. S. EGEL and B. M. MONROE. Adv. Photochem. **8**, 302 (1970).
22. G. HERZBERG. Electronic spectra and structure of polyatomic molecules. D. Van Nostrand Co., New Jersey. 1966.
23. A. M. NISHIMURA and J. S. VINCENT. Chem. Phys. Lett. **13**, 89 (1972).
24. S. G. COHEN and A. D. LITT. Tetrahedron Lett. 837 (1970).
25. P. J. WAGNER and R. G. ZEPP. Chem. Commun. 167 (1972).

Structure and Reactions of Cuprous Thiobenzoate

ALDO FERRETTI

Dairy Products Laboratory, Eastern Marketing and Nutrition Research Division, A.R.S., U.S. Department of Agriculture, Washington, D.C. 20250

Received June 30, 1972

Cuprous thiobenzoate is capable of displacing I^- from aliphatic and activated aromatic iodides, in alcoholic or alcohol–pyridine solution, with formation of thiolbenzoates in excellent yield. The reaction fails with other halogenated substrates. In these cases, the products of prolonged heating of the reaction mixture are ethyl benzoate, dibenzoyl disulfide, benzoic acid, thiobenzoic acid, hydrogen sulfide, and cuprous sulfide.

Le benzoate de cuivre(I) est capable de déplacer I^- des iodures aromatiques activés et aliphatiques, en solution alcoolique ou de alcool–pyridine, avec la formation de thiolbenzoates avec un excellent rendement. La réaction ne procéde pas avec autres substrats halogénés. Dans ces cas les produits de chauffage prolongé du mélange de réaction sont le benzoate d'éthyle, le bisulfure de benzoyle, l'acide benzoïque, l'acide thiobenzoïque, acide sulfhydrique et le sulfure de cuivre(I).

Canadian Journal of Chemistry, **50**, 4056 (1972)

Can. J. Chem. Downloaded from www.nrcresearchpress.com by 210.87.254.105 on 09/05/12
For personal use only.

Can. J. Chem. Downloaded from www.nrcresearchpress.com by 210.87.254.105 on 09/05/12
For personal use only.

Introduction

In a recent article Nair and Nair (1) concluded, chiefly on the basis of infrared measurements, that in cuprous thiobenzoate, copper is linked to the oxygen, rather than to the sulfur, as in **1**. This article prompted an investigation

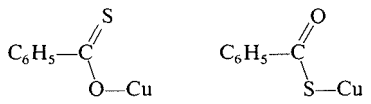

1 **2**

on the potential usefulness of this salt for the direct synthesis of thionbenzoate esters by reaction with aliphatic and aromatic halides according to reaction 1. All the presently avail-

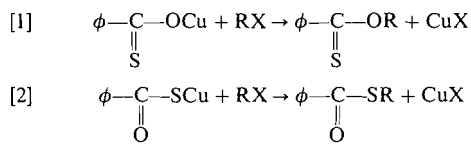

ϕ = phenyl; R = alkyl or aryl; X = halogen

able methods for thionesters are indirect (2, 3). If, however, **2** should prove to be the correct structure of cuprous thiobenzoate, thiolbenzoate esters should result instead, according to reaction 2. Since thiolesters, by acid or alkaline hydrolysis, always yield a carboxylic acid and a thiol (2), the formation of thiolbenzoates with cuprous thiobenzoate would afford a simple two-step method for the synthesis of aromatic and aliphatic thiols and polythiols starting from the corresponding halides.

Results and Discussion

The reaction of cuprous thiobenzoate with the following organic halides has been studied: bromobenzene, fluorobenzene, *p*-iodotoluene, *p*-chlorobenzoic acid, *o*-iodobenzoic acid, iodomethane, 1,2-dichlorotetrafluorocyclobut-1-ene, 1-bromopropane, and 2-chloroethanol. Apparently, cuprous thiobenzoate is not as versatile as cuprous thiophenolate and aliphatic mercaptides (4, 5) in displacing halogens from organic substrates. In fact, only *o*-iodobenzoic acid and iodomethane reacted. However, thiolbenzoates were obtained rather than thionbenzoates.

Iodomethane failed to react in alcohol at reflux temperature. However, when two molar equivalents of pyridine per mole of cuprous thiobenzoate was added, methyl thiolbenzoate formed with 90% yield. Its infrared and mass spectra are identical with those of an authentic sample of *S*-methyl thiobenzoate prepared from benzoyl chloride and methyl mercaptan. When one half molar equivalent of pyridine was used, the yield dropped to 50%. In both cases a small amount of ethyl benzoate was present in the crude product.

The reaction of *o*-iodobenzoic acid with cuprous thiobenzoate proceeded smoothly and quantitatively in absence of pyridine with formation of a thioester. Its infrared spectrum shows a band at 1682 cm^{-1} ($\nu C{=}O$) consistent with a thiolbenzoate structure (6). The high-resolution mass spectrum of the thioester (molecular ion at *m/e* 258, elemental composition $C_{14}H_{10}O_3S$) has the base peak at *m/e* 105 ($C_7H_5O^+$), and shows two intense rearrangement ions at *m/e* 122 ($C_7H_6O_2^{+\cdot}$) and *m/e* 136 ($C_7H_4OS^{+\cdot}$). These fragments are consistent with a thiolbenzoate structure only. Chemical confirmation was obtained by alkaline hydrolysis which afforded benzoic acid and diphenyl disulfide 2,2′-dicarboxylic acid (after $FeCl_3$ oxidation).

In cases in which the halogen compound failed to react, the starting material was recovered along with the following: ethyl benzoate, dibenzoyl disulfide, benzoic acid, thiobenzoic acid, hydrogen sulfide, and cuprous sulfide. These are products of decomposition of the copper salt and were all present each time the reaction was unsuccessful, except in the case of 1,2-dichlorotetrafluorocyclobut-1-ene, where ethyl benzoate was the only identifiable product.

The formation of thiolesters, instead of the thionesters one would expect on the basis of Nair and Nair's conclusion (1), does not necessarily settle the problem of the structure of the salt. The formation of *S*-thiobenzoates can be explained if one admits the existence of an equilibrium mixture of the two tautomeric forms **1** and **2**, the latter reacting much faster than the former (3).

The behavior of cuprous thiobenzoate is somewhat reminiscent of that of cuprous benzylmercaptide, *t*-butylmercaptide, and xanthate (5); namely, with certain substrates it decomposes before the reaction temperature is reached. Unlike cuprous benzylmercaptide (7), the thiobenzoate fails to react with 1,2-dichlorotetra-

Can. J. Chem. Downloaded from www.nrcresearchpress.com by 210.87.254.105 on 09/05/12
For personal use only.

fluorocyclobut-1-ene, even in the presence of pyridine.

On the basis of the above experiments, it appears that cuprous thiobenzoate has a good potential for the synthesis of *S*-thioesters from halides. However, its usefulness is limited to the reaction with aliphatic and activated aromatic iodides.

Experimental

General Conditions

The i.r. spectra were recorded on a Beckman IR 5A instrument, and were calibrated with polystyrene. The mass spectra were determined on a CEC 21-110B double-focusing spectrometer (ionizing energy 70 eV). Accurate mass measurements were made by the peak-matching method using a perfluorokerosene reference. Gas-liquid chromatographic separations were performed with a 240 cm × 6 mm column packed with Chromosorb W coated with 20% Silicone SE-30, and with a 420 cm × 6 mm column packed with Chromosorb W coated with 15% Triton X305. The instrument was a 5750 Hewlett–Packard equipped with a thermal conductivity cell. The reactions were carried out in alcohol or alcohol–pyridine.

Methyl Thiolbenzoate

Two grams (0.01 mol) of cuprous thiobenzoate was suspended in 20 ml of ethanol and 1.6 ml (0.02 mol) of pyridine, and the mixture was heated to mild reflux. Methyl iodide (3.55 g, 0.025 mol) was added, and heating continued for 45 min with magnetic stirring. The reaction mixture was then poured into ice-water containing 2 ml of concentrated hydrochloric acid, and extracted with chloroform. After drying, evaporation of the solvent afforded 1.44 g of crude methyl thiolbenzoate which was contaminated with 5% of ethyl benzoate, as calculated by peak area measurement of the gas chromatogram. Therefore, the actual yield was 90%.

2-(Benzoylthiol)benzoic Acid

Two grams (0.01 mol) of cuprous thiobenzoate and 2.48 g (0.01 mol) of *o*-iodobenzoic acid were heated at gentle reflux in 20 ml of ethanol for 90 min with stirring. The color of the suspended solid changed from brick-red to tan in 45 min. No pyridine was added as the change in color was indicative of reaction. An excess of alcohol was added, and the suspension was filtered hot through a 2 cm layer of Celite 245. The crude material (2.50 g) was recrystallized from ethanol; m.p. 160–161° (Fisher–Johns, uncorrected). This compound has not been previously reported in the literature. Its i.r. spectrum (Nujol) shows bands at 2500 ~ 2800(w), 1698(sh), 1682(s), 1585(m), 1418(m), 1316(m), 1292(w), 1212(m), 1185(m), 1152(w), 1059(w), 963(w), 910(s), 800(m), 772(m), 748(s), 697(m), 687(s), 648(w), 639(m) cm^{-1}. In the mass spectrum, the ten most intense peaks (*m/e*) are (percentage of the base peak and elemental composition in parentheses): 50(9%, $C_4H_2^{+\cdot}$), 51(21%, $C_4H_3^+$), 77(57%, $C_6H_5^+$), 105(100%, $C_7H_5O^+$), 106(9%, $C_6{}^{13}CH_5O^+$), 108(9%, $C_6H_4S^{+\cdot}$), 122(18%, $C_7H_6O_2^{+\cdot}$), 136(37%, $C_7H_4OS^{+\cdot}$), 153(3%, $C_7H_5O_2S^+$), 258(3%, $C_{14}H_{10}O_3S^{+\cdot}$). All the above elemental compositions are the result of accurate mass measurements.

The author thanks Dr. John M. Ruth, Entomology Research Division, A.R.S., U.S. Department of Agriculture, Beltsville, Maryland, for the mass spectral measurements, and Mr. Vincent P. Flanagan of this laboratory for the gas–liquid chromatographic separations.

Mention of brand or firm names does not constitute an endorsement by the Department of Agriculture over others of a similar nature not mentioned.

1. K. P. NAIR and C. G. R. NAIR. Indian J. Chem. **9**, 706 (1971).
2. A. SCHÖBERL and A. WAGNER. Thiosäuren und ihre Derivate. *In* Methoden der Organischen Chemie. (Houben-Weyl). 4th ed. Vol. 9. G. Thieme Verlag, Stuttgart. 1955. p. 741.
3. E. E. REID. Thioacids. *In* Organic chemistry of bivalent sulfur. Vol. 4. Chemical Publishing Co., New York, N.Y. 1962. p. 11.
4. R. ADAMS, W. REIFSCHNEIDER, and M. D. NAIR. Croatica Chem. Acta, 29 (1957).
5. R. ADAMS and A. FERRETTI. J. Am. Chem. Soc. **81**, 4927 (1959).
6. K. NAKANISHI. Infrared absorption spectroscopy–practical. 2nd ed. Nankodo Co. Ltd. Tokyo. 1964.
7. A. FERRETTI and G. TESI. Chem. Ind. (London), **48**, 1987 (1964).

The Preparation and Paramagnetic Susceptibility of β-MnSe

RITCHIE MACLAREN MURRAY, BRIAN CHARLES FORBES, AND ROBERT DONALD HEYDING
Department of Chemistry, Queen's University, Kingston, Ontario

Received July 25, 1972

A procedure is given for the preparation of β-MnSe by precipitation from solution. The cubic B3 zinc blende type structure has a unit cell dimension of 5.88 ± 1 Å. The magnetic susceptibility obeys the Curie–Weiss law above 110 °K with $C = 3.64 \pm 14$ and $\theta = 444 \pm 13$, equivalent to an effective moment of 5.40 μ_B.

Un mode opératoire est donné pour la préparation du β-MnSe par précipitation à partir d'une solution. La structure cubique B3 du type zinc blende possède une maille élémentaire de dimension égale à 5.88 ± 1 Å. La susceptibilité magnétique obéit au-dessus de 110 °K, à la loi de Curie–Weiss avec $C = 3.64 \pm 14$ et $\theta = 444 \pm 13$ ce qui équivaut à un moment effectif de 5.40 μ_B. [Traduit par le journal]

Canadian Journal of Chemistry, **50**, 4059 (1972)

Can. J. Chem. Downloaded from www.nrcresearchpress.com by 210.87.254.5 on 09/05/12
For personal use only.

Introduction

Although manganese sulfide and selenide normally crystallize with the B1 rock salt structure, metastable zinc blende (B3) and wurtzite (B4) modifications have been prepared (1, 2). Baroni prepared β-MnSe (B3) by treating a solution of manganese acetate with hydrogen selenide (2). The hexagonal B4 modification, γ-MnS, was obtained from an ammoniacal solution of manganese chloride or sulfate. Both modifications transformed rapidly to the B1 α-MnSe form when dried.

α-MnSe is antiferromagnetic with a Néel temperature T_N between 145 and 170 °K (3–5). Observation of the magnetic transformation is complicated by a phase transition at *ca.* 245 °K which is sluggish and gives rise to hysteresis effects in the magnetic susceptibility. The low temperature phase has the hexagonal nickel arsenide ($B8_1$) structure (5, 6). The additional neutron diffraction lines observed by Sirota and Makovetskii at 115 °K and believed to be due to a B3 zinc blende type phase (7) are almost certainly due to the formation of the $B8_1$ phase. Baroni's modifications, β- and γ-MnSe, do not appear to be associated with low temperature equilibrium transformations in α-MnSe as had been suggested earlier (3).

In general the addition of H_2Se to any divalent manganese solution produces α-MnSe rather than the metastable forms. Control of the p*H* during the addition of H_2Se is of considerable importance in determining the form of the precipitate. In this Note a recipe for the preparation of β-MnSe is given, and the magnetic properties of this modification are recorded.

Experimental

β-MnSe may be prepared as follows: A solution 0.74 *M* in NaOAc and containing 10 mmol of manganese acetate is outgassed on a vacuum line and exposed at 298 °K to 7 mmol of hydrogen selenide at *ca.* 0.5 atm. The gas dissolves rapidly, and a precipitate begins to appear after 2 h. The reaction is complete in 12 h. The product, a finely divided brown powder, is recovered on a sintered disc under nitrogen, washed with water and ethanol, also under nitrogen, finally washed with ether and air dried. The yield is about 50% of theoretical.

Selenium precipitates at the same time, sometimes in an amorphous form, and may constitute as much as 15% by weight of the total precipitate. Some of this contaminant can be removed by extraction with carbon disulfide.

Traces of γ-MnSe may also appear. Larger quantities may be obtained by increasing the $Mn(OAc)_2$ concentration by a factor of two, but this polymorphic form was never more than a minor constituent in any of the precipitates we recovered, regardless of the recipe.

Magnetic susceptibilities were determined from 85 to 450 °K in a Curie apparatus at field gradients of 19.5, 22, and 23.5×10^6 Oe cm^{-1} (8). The susceptibility of α-MnSe was redetermined using a specimen prepared by direct interaction between the elements in the usual way. Products were identified by Debye–Scherrer X-ray powder diffraction patterns using copper radiation and a nickel screen between specimen and film.

Results and Discussion

The powder diffraction pattern of β-MnSe is given in Table 1. The unit cell dimension, 5.88 ± 1 Å, agrees well with Baroni's value of 5.82 Å obtained by electron diffraction. The manganese–selenium distance in four-coordinated

TABLE 1. X-Ray powder diffraction pattern of β-MnSe cubic, $F\bar{4}3m$, B3 zinc blende, $a = 5.88 \pm 1$ Å Cu K_α radiation, Ni filter, Al screen, $\lambda = 1.5418$ Å I/I_M from integrated Debye Scherrer films

d (Å)	I/I_M	hkl
3.36	100	111
2.99	7	200
2.07	68	220
1.79	43	311
1.47	5	400
1.347	10	331
1.199	12	422
1.131	7	511
1.040	3	440
0.994	7	531
0.930	3	620
0.824	4	551
0.788	6	642

β-MnSe (2.54 Å) is 7% shorter than the interionic distance in six-coordinated α-MnSe (2.73 Å). A similar difference is observed in the manganese–sulfur distance in α- and β-MnS (1). In both systems the molar volume of the β form is 24% greater than that of the α form.

β-MnSe is stable at room temperature and requires no special storage precautions. On heating in a sealed ampoule, transformation to the α form takes place relatively slowly, and at the same time the elemental selenium present in the product reacts with the monoselenide to form the diselenide, $MnSe_2$. The transformation and reaction are complete in 3 days at 625 °K.

The results of the susceptibility studies are summarized in Fig. 1 and in Table 2. Hysteresis in the susceptibility behavior of α-MnSe was again observed below 250 °K. The susceptibility

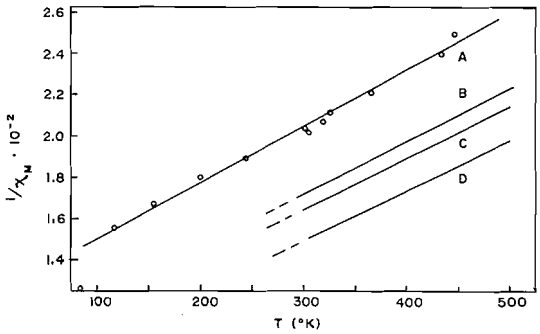

FIG. 1. Paramagnetic susceptibilities of MnSe: *A*, β-MnSe, corrected for 15 weight % Se in sample; *B*, α-MnSe, prepared by direct combination of the elements; *C*, α-MnSe, ref. 12; *D*, α-MnSe, ref. 13.

of β-MnSe obeys the Curie–Weiss law above 110 °K. Positive deviation from the law below 110 °K may indicate the onset of magnetic ordering, but because of the temperature limit of 85 °K in our balance this possibility could not be confirmed. It is surprising that a magnetic transformation does not occur above 110 °K, since the Néel temperature of the corresponding sulfide, β-MnS (~160 °K), is greater than that of α-MnS (~130 °K) (9).

Like the other monsulfides and selenides of manganese, the effective Bohr magneton number, p_{eff}, of β-MnSe is less than expected for a d^5 ion assuming spin only contributions. The exception is γ-MnS, which according to data given by Corliss *et al.*, has an effective moment of 6.15 μ_B (9), and all three dichalcogenides have moments greater than the theoretical value (11).

The susceptibility constants of β-MnSe above

TABLE 2. Paramagnetic susceptibility constants of manganese monochalcogenides (c.g.s./e.m.u.)

Compound	C	θ (°K)	Temperature range (°K)	P_{eff}	Reference
α-MnS	3.49	454	293–773	5.28	12
	3.94 ± 2	397 ± 6	675–1250	5.61	13
	4.10 ± 10*	438 ± 10	195–405	5.73	9
β-MnS	4.03 ± 14*	846 ± 13	295–440	5.68	9
γ-MnS	4.73 ± 13*	951 ± 11	295–471	6.15	9
α-MnSe	4.02	297	600–1200	5.67	10
	3.94 ± 4*	347 ± 9	293–773	5.62	12
	3.89 ± 9	366 ± 7	303–433	5.58	This study
β-MnSe	3.64 ± 14	444 ± 13	110–450	5.40	This study
MnTe	4.46	584	600–1150	5.97	10

*Recalculated using the data given in the reference. Uncertainty limits are the standard deviations in the least squares calculations.

Can. J. Chem. Downloaded from www.nrcresearchpress.com by 210.87.254.5 on 09/05/12
For personal use only.

100 °K are comparable to those of α-MnSe and α-MnS. The remarkably large Weiss constants obtained for β- and γ-MnS which one might have attributed to the effect of a tetrahedral environment as compared to an octahedral environment are not duplicated in β-MnSe.

We are indebted to a number of colleagues, including Brenda Wharton, J. B. M. Johnston, and R. A. Zelonka, who, at one time or another, undertook long and unsuccessful programs designed to repeat Baroni's syntheses. All of these studies were supported by operating grants from the National Research Council of Canada.

1. H. SCHNAASE. Z. phys. Chem. **B20**, 89 (1933).
2. A. BARONI. Z. Krist. **A99**, 336 (1938).
3. R. LINDSAY. Phys. Rev. **84**, 569 (1951).
4. I. G. KERIMOV and T. A. MAMEDOV. Fiz. metal. metalloved. **26**, 188 (1968).
5. A. J. JACOBSON and B. E. F. FENDER. J. Chem. Phys. **52**, 4563 (1970).
6. A. TAYLOR. Appl. Spectrosc. **14**, 116 (1960).
7. N. N. SIROTA and G. I. MAKOVETSKII. Doklady Akad. Nauk. Belorussk, S.S.R. **10**, 542 (1966).
8. R. D. HEYDING, J. B. TAYLOR, and M. L. HAIR. Rev. Sci. Instrum. **32**, 161 (1961).
9. L. CORLISS, N. ELLIOTT, and J. HASTINGS. Phys. Rev. **104**, 924 (1956).
10. J. J. BANEWICZ, R. F. HEIDELBERG, and A. H. LUXEM. J. Phys. Chem. **65**, 615 (1961).
11. J. M. HASTINGS, N. ELLIOTT, and L. M. CORLISS. Phys. Rev. **115**, 13 (1959).
12. A. SERRES. J. Phys. Radium, **8**, 146 (1947).
13. J. J. BANEWICZ, R. F. HEIDELBERG, and R. LINDSAY. Phys. Rev. **117**, 736 (1960).

Can. J. Chem. Downloaded from www.nrcresearchpress.com by 210.87.254.5 on 09/05/12
For personal use only.

The Synthesis of 1-Benzyl-2-carbomethoxy-3,3-dimethyl Aziridine and its Ring Opening with Excess Acids

CASIMIR BERSE AND PIERRE BESSETTE
Department of Chemistry, Université de Montréal, Montreal, Quebec

Received June 27, 1972

The synthesis of 1-benzyl-2-carbomethoxy-3,3-dimethyl aziridine and its ring opening with various excess acids such as hydrogen chloride, acetic, propionic, and thioacetic acids and benzyl mercaptan are herein described.

La synthèse du benzyl-1 méthoxycarbonyl-2 diméthyl-3,3 aziridine et de ses ouvertures, par différents acides en excès tels que: le chlorure d'hydrogène, les acides acétique, propionique, et thiolacétique, et par le benzyl mercaptan, est décrite.

Canadian Journal of Chemistry, **50**, 4061 (1972)

In our attempt to synthesize penicillamine via the aziridine route (1), the preparation and reactions of 1-benzyl-2-carbomethoxy-3,3-dimethylaziridine (**2**) were undertaken. Due to the failure, in our case, of the synthesis of such a highly substituted aziridine by the methods of Cromwell and Huisgen (2, 3), the use of triphenylphosphine dibromide (4) on methyl *N*-benzyl-β-hydroxyvalinate (**1**) was attempted and permitted the formation of aziridine (**2**), b.p. 95–100°/0.05 mm, yield 76%.

Reaction of aziridine (**2**) with anhydrous hydrogen chloride in benzene at 25 °C gave a white solid identified as methyl 3-benzylamino-2-chloro-3-methylbutyrate hydrochloride (**3**), m.p. 174–175°; yield 87%. Structure **3** was differentiated, from its possible 2-benzylamino-3-chloro-isomer, by the fact that its mass spectrum showed a large fragment at *m/e* 148

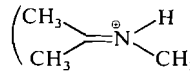

When aziridine **2** was heated at reflux in benzene with acetic acid, the product obtained was methyl 2-(*N*-benzylacetamido)-3-methylcrotonate (**4***a*); b.p. 133–136°/0.15 mm; yield 41%. The n.m.r. of product **4***a* showed a marked non-equivalence between the two methyls on the double bond which appeared as two singlets at τ (CCl_4) 8.60 and 7.90. To distinguish the

100 °K are comparable to those of α-MnSe and α-MnS. The remarkably large Weiss constants obtained for β- and γ-MnS which one might have attributed to the effect of a tetrahedral environment as compared to an octahedral environment are not duplicated in β-MnSe.

We are indebted to a number of colleagues, including Brenda Wharton, J. B. M. Johnston, and R. A. Zelonka, who, at one time or another, undertook long and unsuccessful programs designed to repeat Baroni's syntheses. All of these studies were supported by operating grants from the National Research Council of Canada.

1. H. SCHNAASE. Z. phys. Chem. **B20**, 89 (1933).
2. A. BARONI. Z. Krist. **A99**, 336 (1938).
3. R. LINDSAY. Phys. Rev. **84**, 569 (1951).
4. I. G. KERIMOV and T. A. MAMEDOV. Fiz. metal. metalloved. **26**, 188 (1968).
5. A. J. JACOBSON and B. E. F. FENDER. J. Chem. Phys. **52**, 4563 (1970).
6. A. TAYLOR. Appl. Spectrosc. **14**, 116 (1960).
7. N. N. SIROTA and G. I. MAKOVETSKII. Doklady Akad. Nauk. Belorussk, S.S.R. **10**, 542 (1966).
8. R. D. HEYDING, J. B. TAYLOR, and M. L. HAIR. Rev. Sci. Instrum. **32**, 161 (1961).
9. L. CORLISS, N. ELLIOTT, and J. HASTINGS. Phys. Rev. **104**, 924 (1956).
10. J. J. BANEWICZ, R. F. HEIDELBERG, and A. H. LUXEM. J. Phys. Chem. **65**, 615 (1961).
11. J. M. HASTINGS, N. ELLIOTT, and L. M. CORLISS. Phys. Rev. **115**, 13 (1959).
12. A. SERRES. J. Phys. Radium, **8**, 146 (1947).
13. J. J. BANEWICZ, R. F. HEIDELBERG, and R. LINDSAY. Phys. Rev. **117**, 736 (1960).

Can. J. Chem. Downloaded from www.nrcresearchpress.com by 210.87.254.42 on 09/05/12
For personal use only.

The Synthesis of 1-Benzyl-2-carbomethoxy-3,3-dimethyl Aziridine and its Ring Opening with Excess Acids

CASIMIR BERSE AND PIERRE BESSETTE
Department of Chemistry, Université de Montréal, Montreal, Quebec

Received June 27, 1972

The synthesis of 1-benzyl-2-carbomethoxy-3,3-dimethyl aziridine and its ring opening with various excess acids such as hydrogen chloride, acetic, propionic, and thioacetic acids and benzyl mercaptan are herein described.

La synthèse du benzyl-1 méthoxycarbonyl-2 diméthyl-3,3 aziridine et de ses ouvertures, par différents acides en excès tels que: le chlorure d'hydrogène, les acides acétique, propionique, et thiolacétique, et par le benzyl mercaptan, est décrite.

Canadian Journal of Chemistry, **50**, 4061 (1972)

In our attempt to synthesize penicillamine via the aziridine route (1), the preparation and reactions of 1-benzyl-2-carbomethoxy-3,3-dimethylaziridine (**2**) were undertaken. Due to the failure, in our case, of the synthesis of such a highly substituted aziridine by the methods of Cromwell and Huisgen (2, 3), the use of triphenylphosphine dibromide (4) on methyl *N*-benzyl-β-hydroxyvalinate (**1**) was attempted and permitted the formation of aziridine (**2**), b.p. 95–100°/0.05 mm, yield 76%.

Reaction of aziridine (**2**) with anhydrous hydrogen chloride in benzene at 25 °C gave a white solid identified as methyl 3-benzylamino-2-chloro-3-methylbutyrate hydrochloride (**3**), m.p. 174–175°; yield 87%. Structure **3** was differentiated, from its possible 2-benzylamino-3-chloro-isomer, by the fact that its mass spectrum showed a large fragment at *m/e* 148

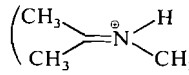

When aziridine **2** was heated at reflux in benzene with acetic acid, the product obtained was methyl 2-(*N*-benzylacetamido)-3-methylcrotonate (**4***a*); b.p. 133–136°/0.15 mm; yield 41%. The n.m.r. of product **4***a* showed a marked non-equivalence between the two methyls on the double bond which appeared as two singlets at τ (CCl_4) 8.60 and 7.90. To distinguish the

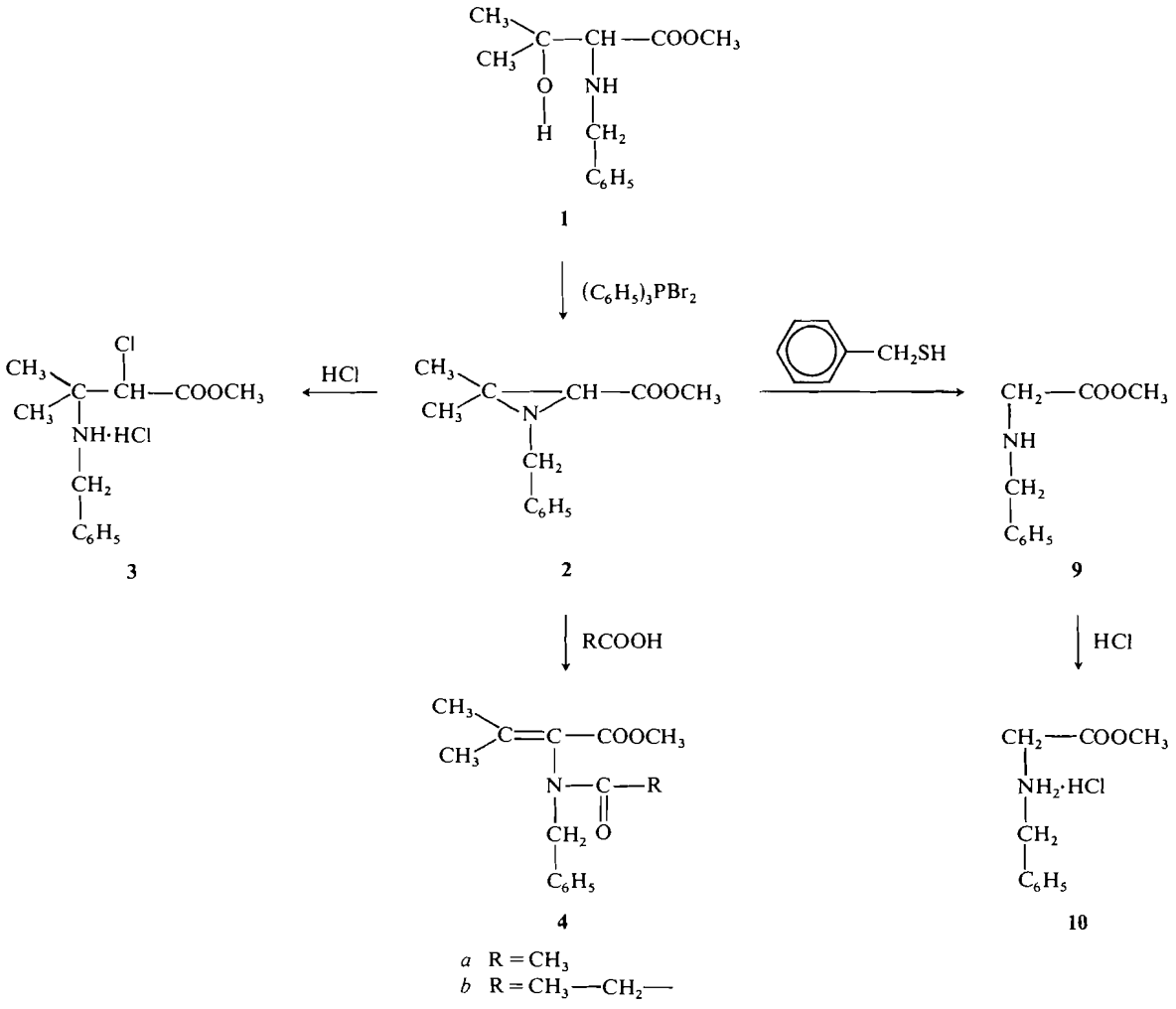

SCHEME 1

two methyl groups from the acetamido group at τ (CCl_4) 8.20, the methyl 2-(*N*-benzylpropionamido)-3-methylcrotonate (**4***b*) was prepared. Product **4***b* showed an almost identical spectrum, except that the singlet of the acetamido group was replaced by a triplet and a quadruplet at τ (CCl_4) 8.97 and 8.00 (Scheme 1).

In the case of reaction of aziridine (**2**) with thioacetic acid in benzene at 25 °C, at least four products could be obtained depending upon the concentration of thioacetic acid used.

At low concentration of thioacetic acid, two products were obtained: (*i*) methyl 3-methyl-2-thioacetoxycrotonate (**5**), b.p. 65–70°/0.05 mm, yield (23%), and (*ii*) methyl 3-(*N*-benzylacetamido)-3-methyl-2-thiobutyrate (**6**), yield (54%), whose mass spectrum showed a high peak at *m/e* 190

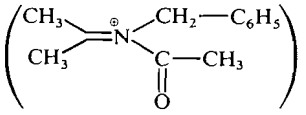

Product **6** which is unstable was further proved by acetylation with acetyl chloride to give a white solid identified as methyl 3-(*N*-benzylacetamido)-3-methyl-2-thioacetoxybutyrate (**7**), m.p. 118–119°, yield (56%).

Use of higher concentration of thioacetic

Can. J. Chem. Downloaded from www.nrcresearchpress.com by 210.87.254.42 on 09/05/12
For personal use only.

Can. J. Chem. Downloaded from www.nrcresearchpress.com by 210.87.254.42 on 09/05/12
For personal use only.

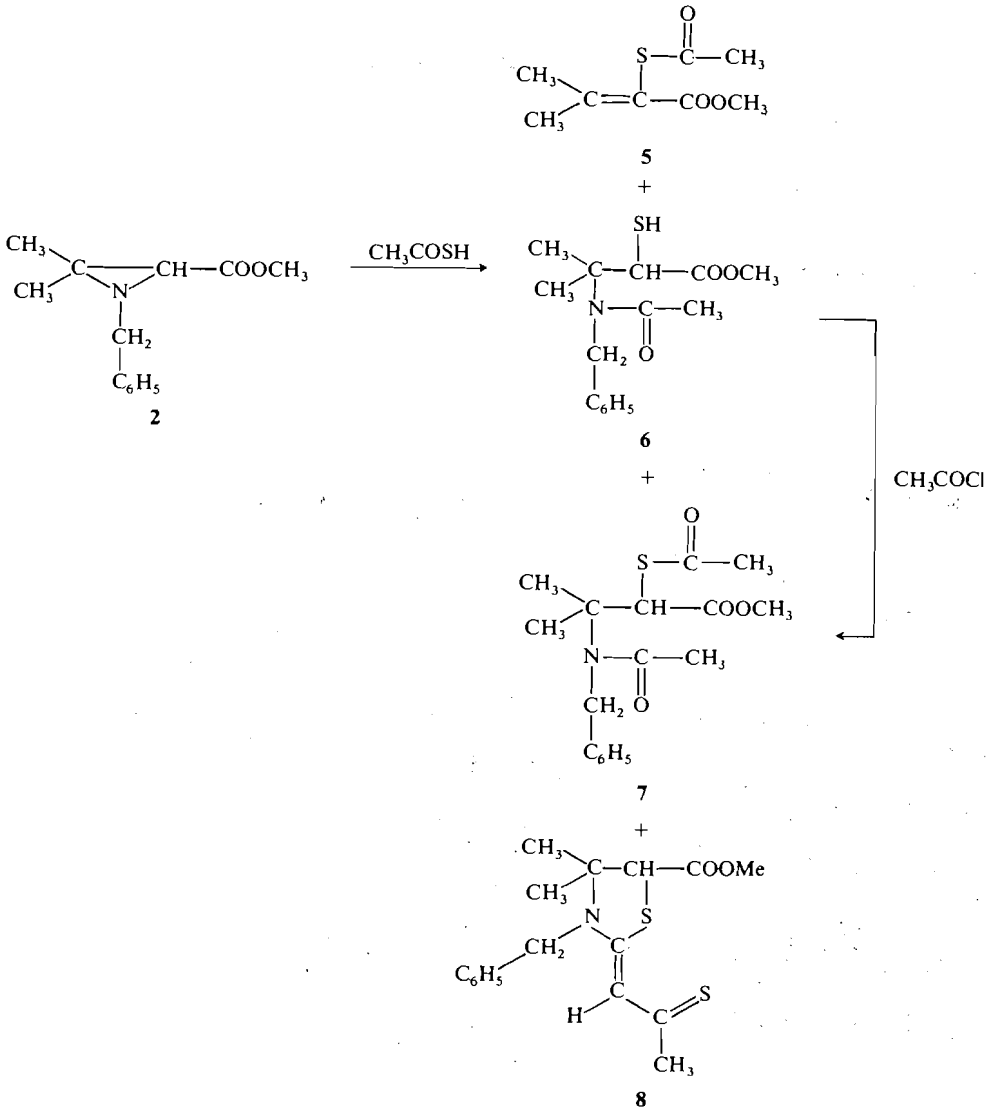

SCHEME 2

acid with aziridine **2** gave, beside product **5** and **7**, an orange solid suspected to be 3-benzyl-5-methoxycarbonyl-4,4-dimethyl-2-(2′-thioxopropylidene)thiazolidine (**8**), m.p. 175–176°, yield (12%).

Finally, when aziridine **2** was heated at reflux in toluene with benzylmercaptan, a breakdown of aziridine **2** occurred and the only product which could be isolated was methyl *N*-benzylglycinate (**9**) which was characterized as its hydrochloride (**10**), m.p. 127–128° (lit. 128° (5)), yield 17% (Scheme 2).

Experimental

All solvents used were thoroughly dried by the conventional methods. All melting and boiling points are uncorrected.

The i.r. spectra were recorded on a Beckman IR-8 double beam spectrometer. The n.m.r. spectra were recorded on a Varian A-60 spectrometer. High resolution mass-spectra were done on an A.E.I. MS902 coupled with a PDP-8

Can. J. Chem. Downloaded from www.nrcresearchpress.com by 210.87.254.42 on 09/05/12
For personal use only.

computer. Elemental analyses were performed by Midwest Microlab. Inc., Indianapolis, Indiana.

Methyl N-Benzyl-β-hydroxyvalinate (1)

To a solution of *N*-benzyl-β-hydroxyvaline (6) (4.005 g, 0.0179 mol) in methanol (50 ml) an ethereal solution of diazomethane was added. The solution was evaporated *in vacuo* and chromatographed on silica gel and eluted with ether–hexane (50:50 v/v) to give product **1**; yield 3.715 g (87%), b.p. 104–106°/0.05 mm Hg. I.r. bands (CCl_4) at 3540, 3360 and 1735 cm^{-1}; τ (CCl_4): 8.96 and 8.80 (6H, singlet), 7.35 (2H, hump), 7.00 (1H, singlet), 6.36 (5H, singlet and AB system for $—CH_2—$ of benzyl, $J = -10$ Hz), 2.76 (5H, singlet).

Anal. Calcd. for $C_{13}H_{19}NO_3$: C, 65.80; H, 8.08. Found. C, 65.88; H, 8.35.

1-Benzyl-2-carbomethoxy-3,3-dimethylaziridine (2)

To a 0 °C cooled solution of triphenylphosphine (7.62 g, 0.0282 mol) in acetonitrile (50 ml) a solution of bromine (4.45 g, 0.0282 mol) in acetonitrile (30 ml) was added dropwise under stirring. The addition finished, product **1** (6.61 g, 0.0279 mol) in acetonitrile (40 ml) was added dropwise during 1/2 h. To the solution obtained, triethylamine (5.69 g, 0.0564 mol) in acetonitrile (40 ml) was added during 1/2 h. The solution was stirred at 0 °C for 2 h and an additional 2 h at 20 °C.

Triethylamine hydrobromide was filtered off. The solution was concentrated *in vacuo* and ether (100 ml) was added. Triphenylphosphine oxide was filtered off, and the ethereal solution evaporated *in vacuo*. The oily residue was chromatographed on silica gel and eluted with ether 20%/hexane to give pure aziridine **2**; yield 4.63 g (76%); b.p. 95–100°/0.05 mm Hg; i.r. bands (CCl_4) at 3090, 3050, 2980, 1750, 1725, 1600 cm^{-1}; τ (CCl_4): 8.75 (6H, singlet), 8.04 (1H, singlet), 6.43 (3H, singlet), 6.34 (2H, singlet (broad)), 2.76 (5H, multiplet).

Anal. Calcd. for $C_{13}H_{17}NO_2$: C, 71.20; H, 7.81. Found: C, 70.99; H, 7.89.

Methyl 3-Benzylamino-2-chloro-3-methylbutyrate Hydrochloride (3)

Product **2** (0.330 g, 0.00151 mol) in anhydrous benzene (5 ml) was bubbled at 20 °C with anhydrous hydrogen chloride for 5 min. The solution was stirred for 2 h. The white solid was filtered and recrystallized in a dichloromethane/ether mixture.

Product **3**, 0.384 g (87%); m.p. 174–175°; i.r. bands (Nujol) at 2740, 2360, 1755, 1740, and 1565 cm^{-1}; τ (D_2O): 8.40 and 8.32 (6H, singlet), 6.07 (3H, singlet), 5.65 (2H, singlet), 5.20 (2H, DHO singlet), 4.82 (1H, singlet), 2.47 (5H, singlet).

Anal. Calcd. for $C_{13}H_{19}NO_2Cl_2$: C, 53.43; H, 6.55. Found: C, 53.14; H, 6.84.

Methyl 2-(N-Benzylacetamido)-3-methylcrotonate (4a)

Product **2** (0.324 g, 0.00148 mol) and acetic acid (2.00 g, 0.033 mol) in benzene (10 ml) were heated at reflux for 14 h. Benzene was evaporated *in vacuo* and ether (50 ml) added. The solution was washed with 5% sodium carbonate dried on magnesium sulfate and chromatographed on silica gel and eluted with ether 40%/hexane.

Product **4***a*, 0.156 g (45%); b.p. 133–135°/0.15 mm Hg; i.r. bands (CCl_4) 2960, 1720, 1665, 1640; τ (CCl_4): 8.60 (3H, singlet), 8.20 (3H, singlet), 7.90 (3H, singlet), 6.45 (3H, singlet), 5.11 and 5.97 (2H, doublet, $J_{gem} = -14$ Hz), 2.78 (5H, singlet).

Anal. Calcd. for $C_{15}H_{19}NO_3$ (mol. wt. 261.1364): C, 69.32; H, 7.34. Found (261.1361 (mass spectrum)): C, 69.75; H, 7.30.

Methyl 2-(N-Benzylpropionamido)-3-methylcrotonate (4b)

Prepared as **4***a*. Reaction of product **2** (0.333 g, 0.00152 mol) with propionic acid (2.79 g, 0.0377 mol) was followed by chromatography on silica gel and pure product **4***b* 0.152 g (37%) was obtained. I.r. bands (CCl_4) at 3000, 2960, 1720, 1665 and 1635 cm^{-1} (shoulder); τ (CCl_4): 8.97 (3H, triplet, $J = 7.5$ Hz), 8.65 (3H, singlet), 8.00 (2H, quadruplet, $J = 7.5$ Hz), 7.91 (3H, singlet), 6.47 (3H, singlet), 5.09 and 5.99 (2H, AB system, $J_{gem} = -14$ Hz) 2.80 (5H, singlet).

Anal. Calcd. for $C_{16}H_{21}NO_3$: C, 69.79; H, 7.68. Found: C, 69.50; H, 7.62.

Methyl 3-Methyl-2-thioacetoxycrotonate (5) and Methyl 3-(N-Benzylacetamido)-2-mercapto-3-methylbutyrate (6)

To a solution of aziridine **2** (0.345 g, 0.00158 mol) in benzene (3 ml) a solution of thioacetic acid (0.360 g, 0.0047 mol) in benzene (3 ml) was added dropwise. The solution was stirred at 20 °C for 2 h and then evaporated *in vacuo*. The yellow oil was chromatographed on silica gel and eluted first with ether 20%/hexane to give **5** and then with ether 50%/hexane to give **6** which gave a positive test for the mercapto group.

Product **5**, 0.070 g(23%); b.p. 65–70°/0.05 mm; i.r. bands (CCl_4) at 2970, 1720, and 1700 cm^{-1} (shoulder); τ (CCl_4): 7.97 (3H, singlet), 7.75 (3H, singlet), 7.68 (3H, singlet), 6.31 (3H, singlet).

Anal. Calcd. for $C_8H_{12}O_3S$: C, 51.04; H, 6.42. Found: C, 50.72; H, 6.41.

Product **6**, 0.250 g (54%); i.r. bands (CCl_4) at 2970, 2350, 1730, and 1650 cm^{-1}; τ (CCl_4): 8.50 (6H, singlet), 8.02 (3H, singlet), 7.7 (1H, broad), 6.30 (3H, singlet), 5.42 (2H, singlet), 5.02 (1H, doublet (broad)), 2.75 (5H, multiplet). Mass spectrum: fragments at *m/e* 277, 190, and 148.

Methyl 3-(N-Benzylacetamido)-3-methyl-2-thioacetoxybutyrate (7)

To a solution of product **6** (0.050 g, 0.00017 mol), and acetyl chloride (0.014 g, 0.00017 mol) in benzene (0.5 ml), a solution of triethylamine (0.018 g, 0.00017 mol) in benzene (0.5 ml) was added dropwise. The solution was stirred at 25 °C for 24 h. The triethylamine hydrochloride was filtered off and the solution evaporated and the residue was crystallized in an ether–hexane mixture.

Product **7**, 0.032 g (56%), m.p. 117–118°; i.r. bands ($CHCl_3$) at 2970, 1730, 1700, and 1645 cm^{-1}; τ ($CDCl_3$): 8.54 (6H, singlet), 8.01 (3H, singlet), 7.68 (3H, singlet), 6.32 (3H, singlet), 5.45 (2H, singlet), 4.42 (1H, singlet), 2.74 (5H, singlet).

Anal. Calcd. for $C_{17}H_{23}NO_4S$: C, 60.51; H, 6.87. Found: C, 60.45; H, 6.66.

3-Benzyl-5-methoxycarbonyl-4,4-dimethyl-2-(2′-thioxopropylidene)thiazolidine (8)

To a stirred solution of aziridine **2** (0.844 g, 0.00386 mol)

thioacetic acid (3.00 g, 0.040 mol) was added dropwise during 10 min. The solution was stirred 1/2 h and excess thioacetic acid was evaporated *in vacuo*. The red oil obtained was chromatographed on silica gel and eluted with ether 10%/hexane, ether 20%/hexane, and ether 30%/hexane to give product **5**, 0.319 g (43%), **8**, 0.161 g (12%), and **7**, 0.144 g (11%), respectively.

Products **5** and **7** were identified by comparison of their spectra, t.l.c., b.p., and m.p., which proved identical in every way to those obtained earlier.

Product **8** had the following characteristics: m.p. 175–177°; i.r. bands ($CHCl_3$) at 2960, 1735, 1500 cm^{-1}; τ ($CDCl_3$): 8.58 and 8.48 (6H, singlet), 7.48 (3H, singlet), 6.20 (3H, singlet), 6.01 (1H, singlet), 5.40 (2H, singlet), 3.58 (1H, singlet), 2.60 (5H, singlet). Mass spectrum: *m/e* 335 (two sulfurs, P + 2/P = 12%); u.v. (EtOH 95%): λ 235 (ε 25 000); λ 288 (ε 5200).

Anal. Calcd. for $C_{17}H_{21}NO_2S_2$: C, 60.86; H, 6.33. Found: C, 60.61; H, 6.35.

*Methyl N-Benzylglycinate Hydrochloride (**10**)*

Product **2** (0.266 g, 0.00192 mol), benzylmercaptan (1.80 g, 0.0121 mol), and toluene (2 ml) were heated at reflux for 20 h. The solution was then chromatographed on silica gel and eluted first with hexane to get rid of the unreacted mercaptan and then with ether–hexane (50–50 v/v). The fraction was evaporated and ether (25 ml) added. The ethereal solution was saturated with hydrogen chloride and the precipitate crystallized in a dichloromethane–ether mixture.

Product **10**, 0.045 g (17%), m.p. 127–128 °C (lit. (5) 128°), fused m.p. with an authentical sample, 127–128 °C; i.r. bands (CH_2Cl_2) at 3100–2200 (broad), 1750 and 1560 cm^{-1}; τ (D_2O): 6.22 (3H, singlet), 6.00 (2H, singlet), 5.70 (2H, singlet), 5.20 (2.7H, singlet DHO), 2.50 (5H, singlet).

1. Casimir Berse and Pierre Bessette. Can. J. Chem. **49**, 2610 (1971).
2. Kenneth R. Henery-Logan and Aline M. Limburg. Tetrahedron Lett. **38**, 4615 (1966).
3. L. Wartski, C. Wakselman, and A. Sierra Escudero. Tetrahedron Lett. **48**, 4193 (1970).
4. Itaru Okada, Kunihiro Ichimura, and Rokuro Sudo. Bull. Chem. Soc. Jap. **43**, 1185 (1970).
5. E. Hardegger, F. Szabo, P. Liechti, Ch. Rostetter, and W. Zankowska-Jasinska. Helv. Chim. Acta, **51**, 78 (1968).
6. Jun-Ichi Oh-Hashi and Kaoru Harada. Bull. Chem. Soc. Jap. **39**, 2287 (1966).

Can. J. Chem. Downloaded from www.nrcresearchpress.com by 210.87.254.42 on 09/05/12
For personal use only.

Can. J. Chem. Downloaded from www.nrcresearchpress.com by 210.87.254.5 on 09/05/12
For personal use only.

Oxidation of *p*-Dimethylaminobenzaldehyde Semicarbazone. Novel Conversion of an Aromatic Aldehyde to an Aroyl Cyanide

PETER KNITTEL AND JOHN WARKENTIN
Department of Chemistry, McMaster University, Hamilton, Ontario

Received July 31, 1972

Oxidation of the semicarbazone of *p*-dimethylaminobenzaldehyde with lead tetraacetate affords *p*-dimethylaminobenzoyl cyanide. Probable intermediates are an iminooxadiazoline and an iminooxirane.

L'oxydation de la semicarbazone de la *p*-diméthylaminobenzaldéhyde par le tetraacétate de plomb conduit au cyanure de *p*-diméthylaminobenzoyle. Les intermédiaires probables sont un iminooxadiazoline et une iminooxirane. [Traduit par le journal]

Canadian Journal of Chemistry, **50**, 4066 (1972)

Oxidative cyclization of carbohydrazones (1) and semicarbazones (2) of ketones with lead tetraacetate (LTA) appears to be a general method for the synthesis of the 2-imino-Δ^3-1,3,4-oxadiazoline ring system, eq. 1.

Corresponding derivatives of aldehydes have

[1] 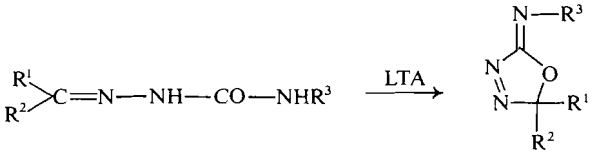

R^1, R^2 = alkyl or aryl; R^3 = alkyl, aryl or $N{=}CR^1R^2$

also been cyclized (3–7) but ring closure is followed by tautomerization; aminooxadiazoles being the products isolated, eq. 2. We wish to

[2] 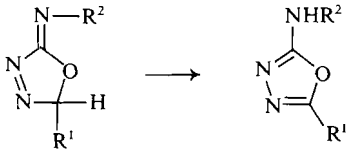

report a novel, efficient conversion of an aromatic aldehyde to an aroyl nitrile (ArCHO → ArCO(CN)) through oxidation of its semicarbazone.

p-Dimethylaminobenzaldehyde semicarbazone (5.0 g, 0.024 mol) in 300 ml of methylene chloride at 0° under pure nitrogen was stirred for 2 h with LTA (10 g, 0.023 mol). Addition of more LTA (12 g, 0.027 mol) and further stirring for 2 h at 0°, followed by addition of water (500 ml), filtration through Celite, separation, and drying of the organic layer gave a greenish-brown solid (3.7 g) which was recrystallized from alcohol and sublimed (100°, 10^{-2} Torr) to afford *p*-dimethylaminobenzoyl cyanide (**1**) as a yellow solid (3.0 g, 71%), m.p. 170–171°, lit. (8) m.p. 170°. Analyses, spectra, and molecular weight consistent with the assigned structure were obtained. Treatment of **1** with aqueous alkali lead to its dissolution with loss of the yellow color. Acidification afforded *p*-dimethylaminobenzoic acid, m.p. 240–242°, lit. (9) m.p. 242.5–243.5°; i.r. and n.m.r. spectra identical with those of an authentic sample. The residual aqueous solution gave a strong Prussian blue test for cyanide ion (10).

Formation of **1** can be rationalized in terms of cyclization of the semicarbazone to the 2-imino-Δ^3-1,3,4-oxadiazoline which, instead of tautomerizing, loses nitrogen to form the iminooxirane **2***a*. The latter may be oxidized to **1**, either by

[3]

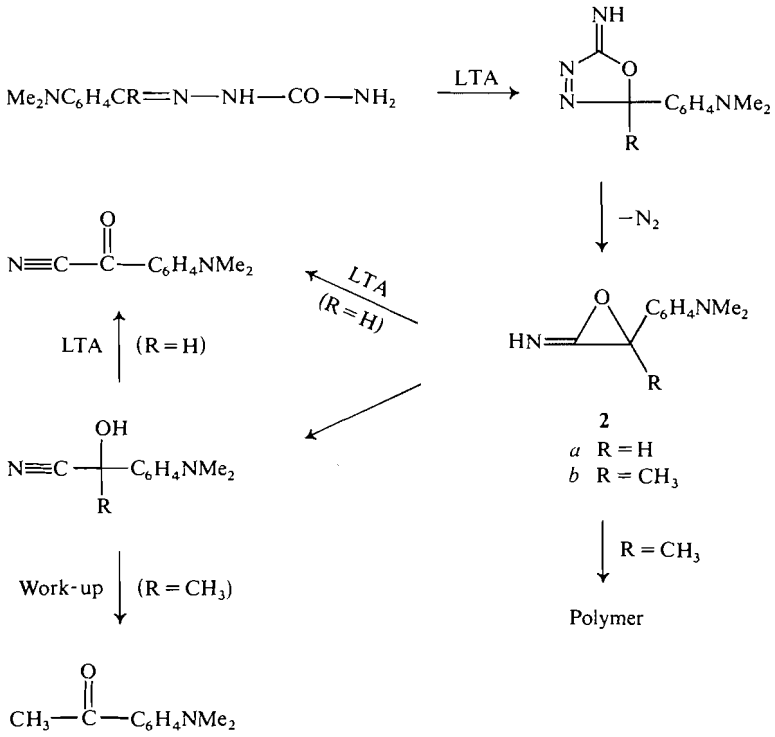

direct action of LTA, or by prior isomerization to aldehyde cyanohydrin, which is then oxidized by LTA, eq. 3.

The same treatment of the semicarbazone of *p*-dimethylaminoacetophenone gave *p*-dimethylaminoacetophenone (*ca.* 15%) and a polymer. With $R = CH_3$ (eq. 3), oxidation of both the iminooxirane and the cyanohydrin is stopped and polymerization, a very facile reaction of α-lactones (11, 12), appears to compete with cyanohydrin formation.

Semicarbazones of benzaldehydes substituted with groups (*e.g.* CH_3O) of lower donor capability than NMe_2 give very little, if any, aroyl nitrile but lead instead to aminooxadiazoles (eq. 2) and their oxidation products. Furfural semicarbazone also follows the latter course.

Work aimed at isolation of iminooxiranes from this novel route is in progress.

This work was supported by the National Research Council of Canada.

1. P. R. WEST and J. WARKENTIN. J. Org. Chem. **33**, 2089 (1968).
2. A. M. CAMERON, P. R. WEST, and J. WARKENTIN. J. Org. Chem. **34**, 3230 (1969).
3. G. VALENTI and F. MAGGIO. Ann. Chim. (Rome), **42**, 13 (1952).
4. F. MAGGIO, G. WERBER, and G. LOMBARDO. Ann. Chim. (Rome), **50**, 491 (1960).
5. H. GEHLEN and K. MÖCKEL. Liebigs Ann. Chem. **651**, 133 (1962).
6. M. S. GIBSON. Tetrahedron, **18**, 1377 (1962).
7. T. M. LAMBE, R. N. BUTLER, and F. L. SCOTT. Chem. Ind. 996 (1971).
8. A. DORNOW and H. GRABHÖFER. Chem. Ber. **91**, 1824 (1958).
9. Handbook of chemistry and physics. *Edited by* R. C. Weast. 49th Ed. The Chemical Rubber Company, Cleveland, Ohio. 1968–1969.
10. A. I. VOGEL. Elementary practical organic chemistry. Part II. Qualitative organic analysis. Longmans, Green and Co., Ltd. London. 1962. pp. 478–481.
11. R. WHELAND and P. D. BARTLETT. J. Am. Chem. Soc. **92**, 6057 (1970).
12. O. L. CHAPMAN, P. W. WOJTKOWSKI, W. ADAM, O. RODRIQUEZ, and R. RUCKTÄSCHEL. J. Am. Chem. Soc. **94**, 1365 (1972).

Can. J. Chem. Downloaded from www.nrcresearchpress.com by 210.87.254.5 on 09/05/12
For personal use only.

The Photocyclization of Aromatic Thioketones[1]

R. LAPOUYADE[2] AND P. DE MAYO

Photochemistry Unit, The University of Western Ontario, London, Ontario

Received August 16, 1972

Certain aromatic thioketones, having an adjacent vacant *peri* position to the thiobenzoyl group cyclize on irradiation. This rearrangement, unknown in the ketonic series, leads to thiophane derivatives.

Certaines thiocétones aromatiques ayant, par rapport au groupe thiobenzoyle, une position *péri* adjacente vacante se cyclisent par irradiation. Ce réarrangement, inconnu en série cétonique conduit à des dérivés du thiophane. [Traduit par le journal]

Canadian Journal of Chemistry, **50**, 4068 (1972)

Can. J. Chem. Downloaded from www.nrcresearchpress.com by 210.87.254.5 on 09/05/12
For personal use only.

Although the photochemistry of aromatic ketones has been studied at very great length, the corresponding thioketones have received very little attention. Such photochemical reactions as have been reported have been concerned, essentially, with cycloaddition (1–3) or reduction (3*a*, 4). We wish to report here a new class of reaction which does not fall into these categories and which has presently (5) no equivalent in the ketonic series.

Aromatic thiones so far described have a lowest n,π^* triplet state (6). In connection with attempts to prepare an aromatic thione with a lowest energy state other than triplet n,π^* lowest in energy, we have prepared a number of substances having an aromatic nucleus substituted by a thiobenzoyl grouping, *i.e.* of the general formula Ar·CS·C_6H_5 (**1**). These substances were prepared from the corresponding ketones by the classical reaction with hydrogen chloride and hydrogen sulfide.[3]

We have observed that irradiation of these substances having a vacant *peri* position to the thiocarbonyl function leads to chemical reaction. With light of wavelength >520 nm, cyclization occurred to give derivatives of thiophane. For instance, in benzene or acetonitrile solution **1**, Ar = 1-naphthyl, 1-pyrenyl, 6-chrysenyl, and 3-perylenyl, gave compounds **2**–**5**, respectively. The yields of crystallized products were of the order of 60%. In contrast, the similar irradiation of **1**, Ar = 2-naphthyl which does not have a free *peri* position, did not lead to any product over comparable time periods.

The carbon skeletons of the products were shown by desulfurization to the benzylic derivatives. In all cases the benzylic hydrogen was detectable in the n.m.r. spectrum, and there was the corresponding loss of one aromatic proton signal. In the case of **2**, the corresponding sulfone was identical in properties with that described in the literature (7). Irradiation of **1**, Ar = 1-naphthyl in acetonitrile solution containing deuterium oxide leads to complete incorporation of one deuterium atom at the benzylic position as indicated by the disappearance of this proton signal from the n.m.r. spectrum. This indicates that the required hydrogen transfer can be intermolecular and suggests the intermediacy of ionic species which would be more in keeping with a reacting singlet state. In keeping with this it was found impossible to quench the photochemical reaction of **1**, Ar = 1-naphthyl by the addition of perylene ($E_T \sim 36$ kcal/mol) which has a triplet below that of the naphthyl derivative ($E_T \sim 39$ kcal/mol[4]).

It is interesting to note that ketonic substances corresponding to these thioketones would be expected to have π,π^* lowest singlets (or, in the case of the naphthalene derivatives very close-lying states which would be expected

[1]Photochemical Synthesis, part 44. Publication No. 52 from the Photochemistry Unit, University of Western Ontario, London, Ontario.

[2]NATO Postdoctoral Fellow, 1971–1972. Present address: Laboratoire de Chimie organique, Université de Bordeaux, Bordeaux, France.

[3]The preparation of the substances and their spectroscopic properties will be reported in full in the complete report. Proper analyses have been obtained for all new substances.

[4]From the emission in EPA at 77 °K.

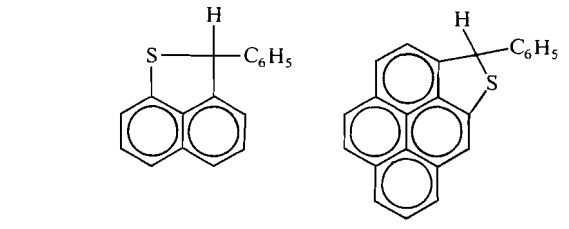

2 3

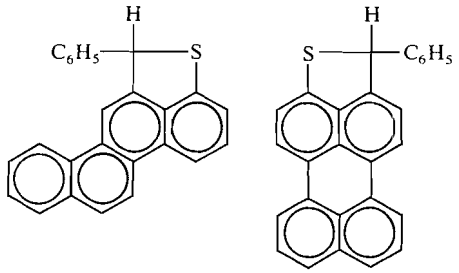

4 5

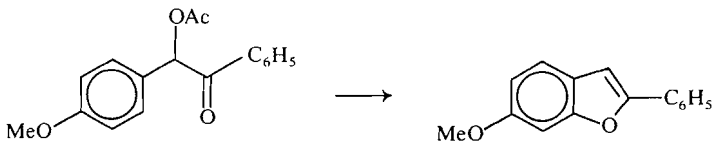

6

to modify chemical behavior). The thioketones, in contrast all have lowest n,π^* singlet states (6*b*). When an aromatic carbonyl group is in the correct spatial relationship and does have the n,π^* singlet state lowest, as in **6**, it does behave appropriately.[5] For these conditions to be met the benzoyl group cannot be directly attached to the aromatic nucleus.

The mechanism of the reaction is under study, but the quantum yields appear to be low. The 1-naphthyl derivative, for instance, reacts with $\Phi \sim 10^{-3}$ depending on the solvent. This may be because of the ready reversibility of an intermediate in which the new C—S bond is already formed. If this is so this decay process is essentially a chemical self-quenching mode.

[5]Reference 8. It is not certain what state is involved in this reaction since the reaction of **6** is quenched with piperylene, but not that of related substances.

1. E. T. KAISER and T. F. WULFERS. J. Am. Chem. Soc. **86**, 1897 (1964); A. OHNO, T. KOIZUMI, Y. OHNISHI, and G. TSUCHIHASHI. Tetrahedron Lett. 2025 (1970) and earlier papers in this series; K. YAMADA, M. YOSHIOKA, and N. SUGIYAMA. J. Org. Chem. **33**, 1240 (1968).
2. H. J. T. BOS, H. SCHINKEL, and TH. C. M. WIJSMAN. Tetrahedron Lett. 3905 (1971); H. GOTTHARDT. Tetrahedron Lett. 2345 (1971).
3. (*a*) D. R. KEMP, A. H. LAWRENCE, C. C. LIAO, R. O. LOUTFY, P. DE MAYO, A. A. NICHOLSON, and S. PASZYC. Pure Appl. Chem. 367 (1971); (*b*) A. A. NICHOLSON and P. DE MAYO. Israel J. Chem. **10**, 341 (1972).
4. (*a*) G. OSTER, L. CITAREL, and M. GOODMAN. J. Am. Chem. Soc. **84**, 703 (1962); (*b*) D. R. KEMP and P. DE MAYO. J. Chem. Commun. 233 (1972); (*c*) N. KITO and A. OHNO. Chem. Commun. 1338 (1971).
5. P. DE MAYO. Acc. Chem. Res. **4**, 41 (1971), footnote 10.
6. (*a*) D. S. L. BLACKWELL, C. C. LIAO, R. O. LOUTFY, P. DE MAYO, and S. PASZYC. Mol. Photochem. In press; (*b*) D. R. KEMP. Unpublished observations.
7. A. G. SCHULTZ and R. H. SCHLESSINGER. Chem. Commun. 1294 (1970).
8. J. C. SHEEHAN, R. M. WILSON, and A. W. OXFORD. J. Am. Chem. Soc. **93**, 7222 (1971).

Can. J. Chem. Downloaded from www.nrcresearchpress.com by 210.87.254.5 on 09/05/12
For personal use only.